UNIVERSITY OF ILLINOIS AT
CHICAGO CIRCLE
801 SO. MORGAN
CHICAGO, IL. 60607

P
1
S3
V.80-83
1977-80
SUB.
INDEX
PER-SOF
N/C
SOI

Physics Abstracts

Volumes 80-83 1977-1980

Cumulative Subject Index
Per—Sof

28 July 1982

inspec
The Institution of Electrical Engineers

© 1981 The Institution of Electrical Engineers

CUMULATIVE SUBJECT INDEX 1977-80

Coverage

The present index provides a subject key to all papers abstracted in *Physics Abstracts* for the years 1977–80. It therefore comprises all relevant entries included in the six monthly subject indexes for the same period.

Subject Headings

In the course of the four years covered by this index the list of subject headings has been revised and new headings have been added. The present index uses the latest (i.e. 1980) version of the list. Entries for articles abstracted in the 1977, 1978 and 1979 volumes have been examined and, where appropriate, re-indexed under the new headings.

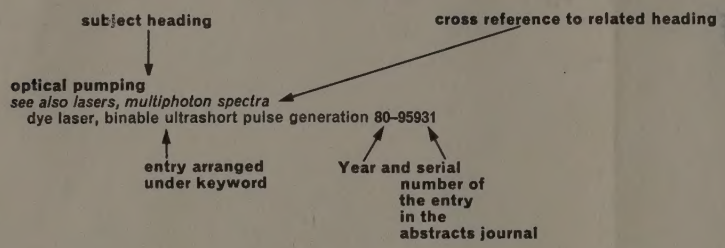
Arrangement

The subject headings are arranged in alphabetical order. The entries under each are prepared so that the most significant or 'key' words appear first and thus determine the position and grouping of entries in the alphabetical sequence under each heading.

Where the names of specific inorganic substances are significant under a given heading, the entries relating to them are found as a second alphabetical listing arranged by the chemical formulae of the particular elements or compounds.

Form of entry

The information contained in the subject index may be illustrated by an example.



How to use the index

The Subject index provides an alphabetical subject key to the articles included in the abstracts journal. Some general guidance on its use is given below:

1. Look in the index for the name of the specific subject in which you are interested. In most cases this name will be a heading in the index and you will find relevant articles listed under it. The majority of the subject headings fall into the following categories: property, phenomena, substance or named objects, instrument, device, theory, method, process, application, event.
2. Occasionally you will be directed from the subject heading chosen to a different heading under which the relevant or additional articles are listed.
3. If you do not find the subject heading you first chose, try a more general heading.
4. Each entry under the heading relates to an article appearing in the abstracts journal and gives the serial number of that article in the journal preceded by the last two digits of the current year, e.g. 78–12345; i.e. Abstract number 12345 in the abstracts journal for 1978.

   The language of the article, if it is not in English, is also indicated, e.g. optical fibre, three-wave stimulated Raman scattering (French) 0–78902.

   Each entry starts with a Keyword or Keyphrase considered to be most relevant to the heading. On sorting these Keywords, the qualifying prefixes are usually ignored (e.g. n-Ge is sorted under Ge).

   There are three main keyword lists; arabic numerals, alphabetical A–Z, and chemical symbols (organic substances are written and not given as chemical formula). More than one Keyword list may be present under each subject heading.

   For document on, say 'photoemission of silicon' at least two access points 'photoemission' and 'elemental semiconductors' are provided. Under the heading 'photoemission' the Keyword will be 'Si' and under 'elemental semiconductors' the Keyword will also be 'Si'.

   In a case like this, it is advisable and quicker to use the heading 'photoemission' and go straight to the chemical symbol list for 'Si' because there are few entries listed under 'photoemission'.

Printed by Unwin Brothers Limited, The Gresham Press, Old Woking, Surrey

Abbreviations and Acronyms

Abbreviations and acronyms are used in the modifiers in all INSPEC Cumulative Subject Indexes. Individual terms should be readily understood in the context of the subject headings. **Inorganic substances** are usually given by their chemical formulae. Iron and aluminium garnets appear in the formulae lists as MIG and MAG (where M is metal element, e.g. YIG and YAG); $(Pb,La)(Zr,Ti)O_3$ and $Ce_2Mg_3(NO_3)_{12}$ appear as PLZT and CMN respectively. **Organic substances** including **liquid crystals** are not given as formulae but common abbreviations are used.

ABS resin	acrylonitrile-butadiene-styrene
AC	alternating current
ACV	air cushion vehicle
A/D	analogue-to-digital
ADP	administrative data processing
AES	Auger electron spectra(oscopy)
AF	audio frequency
AFC	automatic frequency control
AFL	abstract family of languages
AGC	automatic gain control
AGR	advanced gas-cooled reactor
AM	amplitude modulation
ANS	Astronomical Netherlands Satellite
APACHE	accelerator for physics and chemistry of heavy elements
APR	acoustic paramagnetic resonance
APS	appearance potential spectra(oscopy)
APW	augmented plane wave
ATR	attenuated total reflection
ATS	applications technology satellite
ATWS	anticipated transients without scram
AVC	automatic volume control
BARITT	barrier injection transit time
BBEA	4-butoxybenzal-4'-ethylaniline
BCC	body centred cubic
BCD	binary-code decimal
BFO	beat-frequency oscillator
BWO	backward wave oscillator
BWR	boiling water reactor
BWT	backward wave tube
CAD	computer aided design
CAI	computer assisted instruction
CARS	coherent antiStokes Raman scattering (spectra)
CATV	community antenna TV
CB	citizen band
CBOOA	cyanobenzylidene octyloxyaniline
C-CD	charge-coupled device
CDI	collector diffusion isolation
CDM	code division multiplexing
CDW	charge-density wave
CEM	channel electron multiplier
CEPA	coupled electron pair approximation
CERN	Conseil Européen pour la Recherche Nucléaire
CESR	conduction electron spin resonance
CGTO	contracted Gaussian-type orbital
CHF	coupled Hartree-Fock
CI	configuration interaction
CIEH	charge iterated extended Huckel
CIHY	configuration interaction Hylleras
CNDO	complete neglect of differential overlap
COC	cholesteryl oleyl carbonate
COM	computer output to microform (fiche or film)
COOB	4,4'-cyano-octyloxy-biphenyl
CP	charge, parity
CPA	coherent potential approximation
CPSK	coherent phase shift keying
CPT	charge, parity, time
CRO	cathode ray oscilloscope
CRT	cathode ray tube
CS	coupled states
CSM	continuous slowing down models
CTR	controlled thermonuclear reactor
CVD	chemical vapour deposition
CW	continuous wave
D/A	digital-to-analogue
DBR	distributed Bragg reflector
DC	direct current
DDC	direct digital control
DDL	diode-diode logic
DECENT	distribution of exact classical energy transfer
DESY	Deutsches Electron Synchrotron
DF	Dirac-Fock
DFB	distributed feedback
DH	double heterostructure
DIL	dual-in-line
DITE	divertor in torus experiment
DLTS	deep level transient spectra(oscopy)
DM	delta modulation
DMSO	dimethyl sulphoxide
DMSS	Defence Meteorological Satellite System
DOBAMBC	p-decyloxybenzylidene p'-amino 2-methyl butyl cinnamate
DODS	different orbitals for different spins
DORIS	Dopple-ring-Speicher
DOVETT	double velocity transit time
DP	data processing
DPCM	differential pulse code modulation
DPPH	diphenylpicrylhydrazyl
DPSK	differential phase shift keying
DSC	differential scanning calorimetry
DTA	differential thermal analysis
DV-Xα	discrete variational Xα method
E1,E2	electric dipole, quadrupole
EAS	extensive air shower
EB	exponential Born
EBBA	4-ethoxybenzylidene-4'n-butylaniline
EBR	experimental breeder reactor
EBT	Elmo Bumpy Torus
ECC	emergency core cooling
ECELR	epithermal critical experiment laboratory reactor
ECG	electrocardiography (-gram)
EDA	ethylene diamine
EDP	electronic data processing
EDTA	ethylene diamine tetra-acetic acid
EEBAC	ethyl-4-(4'ethoxy-benzylidene-amino) cinnamate
EEG	electroencephalography (-gram)
EELS	electron energy loss spectra
EFM	extended Flygare method
EHD	electrohydrodynamics
EHF	extremely high frequency
EHP	electron-hole potential method
EHT	extended Huckel theory
EHV	extra high voltage
ELDOR	electron electron double resonance

ELF	extremely low frequency
EM	electromagnetic
EMC	electromagnetic compatibility
EMF	electromotive force
EMG	electromyography(-gram)
ENDOR	electron nuclear double resonance
EOS	earth observatory satellite
EPEN	empirical potential energy function based on interactions of electrons and nuclei
EPMA	electron probe microanalysis
EPR	electron paramagnetic resonance
ERG	electroretinography(-gram)
ERPS	extramolecular relaxation polarisation shift
ERTS	earth resources technology satellite
ESCA	electron spectroscopy for chemical analysis
ESCAR	experimental superconducting accelerating ring
ESFI	epitaxial silicon film on insulator
ESS	electronic switching system
EUV	extreme ultraviolet
EXAFS	extended X-ray absorption fine structure
FBR	fast breeder reactor
FCC	face centred cubic
FDM	frequency division multiplex(ing)
FDNC	frequency dependent negative conductance
FDNR	frequency dependent negative resistance
FEM	field emission microscopy
FET	field effect transistor
FFHR	fusion-fission hybrid reactor
FFT	fast Fourier transform
FFTF	fast flux test facilities
FIM	field ion microscopy
FM	frequency modulation
FPT	finite perturbation theory
FSK	frequency-shift keying
FSGO	floating spherical Gaussian orbitals
FTR	fast test reactor
GAMBIT	gate modulated bipolar transistor
GANIL	grand accelerateur national a ions Lourds
GARP	global atmospheric research programme
GATE	GARP Atlantic tropical experiment
GCFR	gas-cooled fast breeder reactor
GCM	generator coordinate method
GHF-NO-CI	generalised Hartree-Fock/natural orbital/ configuration interactions
GIAO	gauge-invariant atomic orbitals
GO	Gaussian orbitals
GOO	generalised Overhauser orbitals
GPM	ground potential model
GSO	general spin orbitals
GTO	Gaussian-type orbitals
GVB	generalised valence bond
HAM	hydrogenic atoms in molecules
HBAB	hexyloxybenzylidene-p' aminobenzonitrile
HBT	N-(p-hexyloxybenzylidene)-p-toluidene
HCDA	hypothetical core disruptive accident
HCP	hexagonal close packed
HEED	high energy electron diffraction
HF	high frequency or Hartree-Fock
HFB	Hartree-Fock-Bogoliubov
HFER	hot fuel examination facility
HFIR	high flux isotope reactor
HFO	Hartree-Fock-Overhauser
HFS	hyperfine structure
HLW	high level waste (radioactive)
HMO	Huckel molecular orbitals
HOAB	heptyloxyazoxybenzene
HOBHA	p-n-heptyloxy-benzylidene-p-n heptylaniline
HOMO	highest occupied molecular orbitals
HORM	hybrid orbital rehybridisation method
HTGR	high temperature gas-cooled reactor
HV	high voltage
HVEM	high voltage electron microscopy
HWR	heavy water reactor
IAEA	International Atomic Energy Authority Agency
IBPBAC	isobutyl-4-(4'-phenylbenzylideneamino) cinnamate
IC	integrated circuit
ICDF	intermediate coupling Dirac-Fock
IDT	interdigital transducer
IEPA	independent electron pair approximation
IF	intermediate frequency
IGFET	insulated gate field effect transistor
IKO	Institute v. Kernph Ouder Amsterdam
I^2L	integrated injection logic
I^3L	isoplanar I^2L
ILS	instrument landing system
IMPATT	impact avalanche transit time
INDO	intermediate neglect of differential overlap
INDOR	internuclear double resonance
ING	intense neutron generator
INO	iterative natural orbital
INTELSAT	international telecommunications satellite consortium
I/O	input/output
IOC-ω	inclusion of the overlap charges in the omega
IR	infrared
IRDO	intermediate retention of differential overlap
ISABELLE	intersecting storage and acceleration
ISR	intersecting storage ring
ISX	impurity study experiment
ITEP	Institute of Theoretical and Experimental Physics
IU	Indiana University
IVO	improved virtual orbitals
JET	Joint European torus
JAERI	Japan Atomic Energy Research Institute
JINR	Joint Institute for Nuclear Research
KEK	Japan National Laboratory for High Energy Physics
KKR	Korringa-Kohn-Rostoker
LAMPF	Los Alamos meson physics facility
LC	inductance-capacitance
LCAO	linear combination of atomic orbitals
LCBO	linear combinations of (semi-localised) band orbitals
LCGO	linear combination of Gaussian orbitals
LCP	large coil program
LCRO	linear combination of Rydberg orbitals
LEC	liquid encapsulated Czochralski
LED	light emitting diode
LEED	low energy electron diffraction
LEP	large electron positron
LET	linear energy transfer
LF	low frequency
LMC	Large Magellanic Cloud
LMFBR	liquid metal fast breeder reactor
LMTO	linear combination of muffin tin orbitals
LOCA	loss of coolant accident
LOCE	loss of coolant experiment
LOFT	loss of flow test facility
LPE	liquid phase epitaxy
LSA	limited space charge accumulation

LSD	local spin density
LSI	large-scale integration
LTE	local thermodynamic equilibrium
LUMO	lowest unoccupied molecular orbitals
LV	low voltage
LWR	light water reactor
MADO	Mulliken approximation for differential overlap
M1,M2	magnetic dipole, quadrupole
MBBA	4-methoxybenzylidene-4'-n-butyl-aniline
MBE	molecular beam epitaxy
MBPT	many body perturbation theory
MCD	magnetic circular dichroism
MCPESCF	multiconfiguration paired excitation SCF
MCZDO	multi-centre zero differential overlap
MEDO	multipole expansion of diatomic overlap
MESFET	metal-semiconductor field effect transistor
MF	medium frequency
MFP	mean free path
MHD	magnetohydrodynamics
MIC	microwave integrated circuit
MIEHM	modified iterative extended Huckel method
MIM	metal-insulator-metal
MIS	metal-insulator-semiconductor or management information system
MIT	Massachusetts Institute of Technology
MMF	magnetomotive force
MNOS	metal-nitride-oxide-semiconductor
MO	molecular orbitals
MOCIC	molecular orbital constraint of interaction coordinates
MODPOT	model potential
MOS	metal-oxide-semiconductor
MOSFET	metal-oxide-semiconductor field effect transistor
MOST	metal-oxide-semiconductor transistor
MRD	multi-reference double excitation
MRINDO	modified Rydberg INDO
MSI	medium scale integration
MSR	molten salt reactor
MSU	Michigan State University
MTBF	mean-time between failures
MTF	modulation transfer function
MTXα	muffin-tin Xα
MUF	maximum usable frequency
MWH	Mulliken-Wolfsberg-Helmholz-semi-empirical method
NAL	National Accelerator Laboratory
NAND	not-and(logic)
NC	numerical control
NCMET	non-closed shell many electron theory
NDDO	neglect of diatomic differential overlap
NDT	nondestructive testing
NEMO	non-empirical molecular orbitals
NEVE	non-empirical valence-electron
NIC	negative impedance convertor
NMR	nuclear magnetic resonance
NNNDO	neglect of non-neighbour differential overlap
NOR	not-or(logic)
NPOST	non-perturbative open-shell theory
NPSO	non-paired spatial orbitals
NQR	nuclear quadrupole resonance
NRC	nuclear regulatory committee
NRM	natural remanent magnetisation
NTO	natural transition orbitals
OAO	orbiting astronomical observatory
OCR	optical character recognition
ODMR	optical detection of magnetic resonance
OER	oxygen enhancement ratio
OGO	orbiting geophysical observatory
OPHF	orbital polarised Hartree-Fock
OPW	orthogonal plane wave
OR	operations research
ORELA	Oak Ridge electron linear accelerator
ORNL	Oak Ridge National Laboratory
OSO	orbiting solar observatory
OTF	optical transfer function
PAA	paraazoxyanisole
PABX	private automatic branch exchange
PAC	perturbed angular correlation
PAHR	post accident heat removal
PAM	pulse amplitude modulation
PAMPUS	photons for atomic and molecular processes and universal studies
PAP	paraazoxyphenetole
PBF	power bursts facility
PBR	pebble bed reactor
PBX	private branch exchange
PC	printed circuit
PCAC	partially conserved axial currents
PCB	printed circuit board
PCGVB	pairwise correlated generalised valence bond
PCILOCC	perturbative configuration interaction using localised orbitals for crystal calculation
PCM	pulse code modulation
PCX	plasma confinement experiment
PDX	poloidal divertor experiment
PEP	positron electron proton
PETRA	positron electron tandem ringbeschle-uniger anlage
PF	power factor
PFM	pulse frequency modulation
PHWR	pressurised heavy water reactor
PID(PI,PD)	proportional+integral+differential (derivative)
PLA	phase locked arrays
PLC	programmable logic control
PLL	phase locked loops
PLT	Princeton Large Torus
PM	pulse modulation
PMMA	polmethylmethacrylate
PMDR	phosphorescence microwave double resonance
PNDO	partial neglect of differential overlap
PNO-CI	pair natural orbital configuration interaction
POL	pair orthogonalised Lowdin
POPAE	protons on protons and electrons
POPOP	phenyl-oxazolyl-phenyl-oxazolyl-phenyl
POS	point of sale
PPDP/S	Pariser-Parr-Del Bene-Pople/Segal calculations
PPI	plan position indicator
PPM	pulse position modulation or parts per million
PPP	Pariser-Parr-Pople
PRDDO	partial retention of diatomic differential overlap
PRF	pulse recurrence (repetition) frequency
PROM	programmable read-only-memory or Pockels readout optical modulator
PS	proton synchrotron (CERN)
PSK	phase shift keying
PTFE	polytetrafluoroethylene
PTM	pulse time modulation
PVC	polyvinyl chloride
PWM	pulse width modulation
PWR	pressurised water reactor

QCD	quantum chromodynamics
QDMBPT	quasi-degenerate many-body perturbation theory
QED	quantum electrodynamics
QPSK	quaternary phase shift keying
RAM	random access memory
RBE	relative biological effectiveness
RC	resistance-capacitance
RCNDO	Rydberg CNDO
R & D	research and development
RF	radio frequency
RFI	radio frequency interference
RHEED	reflection high energy electron diffraction
RINDO	Rydberg INDO
RKKY	Rudermann-Kittel Kasuya-Yosida
RLC	resistance-inductance-capacitance
RMS	root-mean-square
ROM	read-only memory
RPA	random phase approximation
RPM	relaxation potential model
SAMO	simulated ab initio molecular orbitals
SAS	small astronomy satellite
SAW	surface acoustic waves
SCF	self consistent field
SCL	space charge limited
SCPT	self consistent perturbation theory
SCR	silicon controlled rectifier
SDM	space division multiplexing
SDO	shielded diatomic orbitals
SEHF	spin extended Hartree-Fock
SEM	scanning electron microscope
SFE	solar-flare effect
SGHWR	steam generating heavy water reactor
SHF	superhigh frequency
SHG	second harmonic generation
SIMS	secondary ion mass spectrometer
SIN	Swiss Institute of Nuclear Research
SINDO	scaled INDO
SISAM	spectrometer with interference selective amplitude modulation
SMC	Small Magellanic Cloud
SMS	synchronous meteorological satellite
S/N	signal-to-noise
SOG	strongly orthogonal geminal
SOS	silicon on sapphire
SPA	separated pair approximation
SPC	stored program control
SPEAR	Stanford positron electron asymmetric ring
SPHF	spin polarised Hartree-Fock
SPIN-CIPSI	spin symmetry adapted generalisation of CIPSI
SPS	super proton synchroton (CERN)
SQUID	superconducting quantum interference device
SRMCASE	symmetry-restricted-multiconfiguration annihiliation of single excitations
SSB	single sideband
SSC	sudden storm commencement
SSI	supersonic transport
STD	salinity-temperature-depth or subscriber trunk dialling
STEM	scanning transmission electron microscopy
STO	Slater-type orbitals
STOL	short take-off and landing
STP	Slater-transfer Preuss
SUHFC	spin unrestricted Hartree-Fock with local approximation for correlations
SW	short wave
SWR	standing wave ratio
SXAPS	soft X-ray appearance potential spectrum
TBBA	terephthal-butylaniline
TCNE	tetracyanoethylene
TCNQ	tetracyanoquinodimethane
TCR	temperature coefficient of resistance
TDHF	time dependent Hartree-Fock
TDM	time division multiplex(ing)
TDMA	time division multiple access
TDPAC	time differential perturbed angular correlation
TE	transverse electric
TEA	transversely excited atmospheric
TEM	transverse electromagnetic or transmission electron microscopy
TEXT	Texas Experimental Tokamak
TFTR	Tokamak fusion test reactor
TGFB	triglycine fluoroberyllate
TGS	triglycine sulphate
TGSe	triglycine selenate
TJS	transverse junction stripe
TLD	thermoluminescent dosimeter(-ry)
TM	transverse magnetic
TMMC	tetramethylammonium manganese chloride
TOP	transient overpower accident
TNS	The next step
TRAPATT	trapped plasma avalanche triggered transit
TREAT	transient reactor test facility
TRM	thermoremanent magnetisation
TSC	thermally stimulated currents
TSEE	thermally stimulated exo-electron emission
TTF	tetrathiofulvalinium
TTL	transistor transistor logic
TTT	tetrathiotetracene
TUCA	transient undercooling accident
TV	television
TW	travelling wave
TWT	travelling wave tube
UCHF	uncoupled Hartree-Fock
UHF	ultra high frequency unrestricted Hartree-Fock
UHV	ultra high voltage
UKAEA	United Kingdom Atomic Energy Authority
ULF	ultra low frequency
UMD	unitised microwave devices
UPS	ultraviolet photoelectron spectra
US	ultrasonic
UV	ultraviolet
VB	valence bond
VCR	video cassette recorder
VDM	vector dominance model
VDU	visual display unit
VHF	very high frequency
VLBI	very long base line interferometry
VLF	very low frequency
VLSI	very large scale integration
VOR	VHF omnidirectional range
VPE	vapour phase epitaxy
VRC	visual record computer
VRDDO	variable retention of diatomic differential
VSB	vestigial sideband
VSEPR	valence shell electron pair repulsion
VSWR	voltage standing wave ratio
VTOL	vertical take-off and landing
VTR	voltage transformation ratio or video tape recorder
VUV	vacuum ultraviolet
VVER	water moderated water cooled reactors
WWER	water moderated water cooled reactors
XPS	X-ray photoelectron spectra
ZEBRA	zero energy breeder reactor assembly
ZGS	zero gradient synchrotron
ZPPR	zero power plutonium reactor

permittivity continued
plastics and reinforced plastics, tabulated data as design guide 77−21087
PLZT ceramics, ferroelec., special props. 79−42916
PMMA, shock induced polarisation, dielec. const., dipole lifetime rel. to particle velocity *(French)* 77−69776
PMMA-wood polymer composite, dielec. prop. at low temp. *(Japanese)* 78−31545
Poisson's equation, linear and nonlinear numerical solution including spatially variable dielectric const. 80−6825
polar fluid, dielectric saturation theory 77−59507
polar fluid, molecular pair effects, Onsager dielec. theory breakdown 80−75917
polar fluid, translationally invariant correlation function, thermodynamic and dielectric props. 77−35457
polar fluid of heteronuclear molecules, dielectric const. 78−84514
polar fluids, rigid, dielectric relaxation theory 80−60495
polar gas, dielec. permeability, spherical approx. *(French)* 77−45786
polar lattices, dielectric constant, Monte Carlo results 77−4594
polar liqs. permittivity, computer simulation with hard sphere point dipole pot. 80−103911
polar liquid, dielec. props. in far IR range 77−85639
polar liquid, integrated absorpt., microstruct. effect *(French)* 78−10823
polar liquid, nonlinear effects, permittivity, dipolar pot. 78−39493
polar liquid, relative permittivity, dielectric and Kerr effect relaxation in alternating elec. fields 78−80284
polar liquids, dielectric behaviour in far IR spectral range, theory 77−28509
polar liquids, elec. polarisation theory 77−4596
polar liquids, submillimetre region, Poley absorption interpretation 77−36167
polar liquids soln., mol. electric dipole moments, extrapolation formula 79−38437
polar molecules, in nonpolar solvent, dipole moments and relax. times 78−43782
polar molecules in liq. state, dielec. relax. time, dielec. const. 78−19408
polar molecules with fluctuating polarisability, dielec. theory 80−97178
polar semiconductor, exciton-dispersion 80−6741
polar solvents, solvated electron absorpt. spectra, intrasolvent and intersolvent correls. 80−93840
polar-polar liquid mixture, significant structure model applic. to dielec. const. correl. 77−8487
polar/nonpolar mixtures, pot. of mean force, approx. theories, clustering of solute mols. 78−26401
poly(1,3-dioepane), dipole moments, dielectric const. meas 80−66099
poly(4-chlorostyrene, 4-methylstyrene) copolymer, time-depend. ang. correls. 79−73881
poly(vinylidene fluoride) films, poled, piezoelec. activity and field-induced cryst. struct. transitions 80−20592
poly (4-chlorosytrene, styrene), linear copolymers ang. correls., dipole moments and dielec. consts. 77−61884
poly-4-chlorostyrene, undiluted, dielec. relax. spectrum above Tg 80−97194
poly-γ-benzyl-L-glutamate, synthetic polypeptide, nonlinear dielectric effect in nonpolar medium 80−84682
poly-L-proline, TSC and dielec. study of multiple relaxations 77−55748
polyacene quinone radical copolymer, reversal of usual electric field effect and nomadic polarisation 77−12304
polyacenequinones, dielec. polarisation, role of conducting mol. chains *(Russian)* 79−65794
polyacetylene:I, dc microwave cond., permittivity 80−107843
polyacetylene:I, electric props. in semicond. and metallic regions 80−29432
polyacetylene, room temp. dielec. const. 79−73979
polyacetylene film, anisotropy of dielec. const. 80−108146
polyacrylate solutions, dielec. relaxation 80−40045
polyacrylonitrile, pyrolyzed, elec. cond. and dielec. const. in AC regime 78−60173
polyamide 6 (polycaproamide), temp. depend. of complex permittivity rel. to moisture content 80−50251
polycarbonate, γ-irradiated, dielec. behaviour and glass transition 80−97182
polycarbonate, plastic insulation for cryogenic power cable, exam. of dielectric, tensile props. 80−25823
polydiethylene terephthalate chains, dipole moment, config. props. 78−9288
polydiethylsiloxane chains, dipole moments 78−78844
polydimethylsiloxane, crystalline and amorphous, characterised by DTA, polarised light microscopy, dielectric relax. 80−25295
polydimethylsiloxane fluid permittivity and dielectric loss 78−6621
polydimethylsiloxane liquid film, non-pure, dielec. behaviour 80−29672
polyester (Mylar), plastic insulation for cryogenic power cable, exam. of dielectric, tensile props. 80−25823
polyethylene, dielec. props. rel. to mol. struct. 80−29681
polyethylene, gamma radiation effects on dielect. parameters, expt. *(Hungarian)* 78−59836
polyethylene, low-density natural, at elevated temps. 80−97185
polyethylene, plastic insulation for cryogenic power cable, exam. of dielectric, tensile props. 80−25823
polyethylene oxide, dil. soln., chain dipole moment, dielec. const. meas. 77−40169
polyethylene-terephthalate, field-controlled photogeneration and carrier trapping 80−25285
polyferrocene film, plasma polymerised, dielec. props., 40 kHz to 50 MHz, 30-400°C 78−52439
polyhexamethylene oxide, dil. soln., chain dipole moment, dielec. const. meas. 77−40169
polyhydroxyl alcohols, H-bonded solns., microwave dielec. relax. 79−33599
polymer, complex dielectric const. determ. from polarisation current 77−66451
polymer, generation mechanism and charact. *(Japanese)* 80−60488
polymer coatings for corrosion protection, electrochem. techniques for performance monitoring 80−3234
polymer complex dielec. permittivity and compliance, algorithm for calc. freq. dependence 78−68442
polymer-TiO_2 composite, dielec. props. *(Japanese)* 78−95540
polymers, book 80−7257
polymers, conversion of dielectric to viscoelastic data 78−48109
polymers, elec. props. and morphology, correl. review 78−43786
polymers, electrical phenomena, nature and appl., book contrib. 80−50254
polymers, flexible, solns., shear flow, dielec. anisotropy, appls. 79−15393
polypeptide lyotropic liq. crystals, van der Waals-Lifshitz forces 77−84624
polypropylene, plastic insulation for cryogenic power cable, exam. of dielectric, tensile props. 80−25823
polypropylene sulphide, atactic chains, dipole moments, dielec. const. meas. 80−23584
polystyrene, in butan-1-ol, colloidal particles, dispersion force interactions calcs. 79−24842
polystyrene film formed by RF electrodeless excitation, dielec. props. 77−24795
polystyrene foam, X-band microwave dielectric spectra 79−87376
polystyrene-wood, polymer composite, dielec. props. at low temperature range *(Japanese)* 78−95541
polysulphone, plastic insulation for cryogenic power cable, exam. of dielectric, tensile props. 80−25823
polytetrahydrofuran film, electrochemically prepared between Pt and Au electrodes, AC elec. props. 80−40062
polytrimethylene oxide, soln., chain dipole moment, dielec. const. meas. 77−81043
polyvinyl alcohol, hydrocarbon suspension, temp. depend. of electroviscous effect and dielectric parameters 79−79299
polyvinyl fluoride, dielectric support for glass transition 78−2239
polyvinylcarbazole, Coloumb trap controlled hopping mobility model tests, mobility and permittivity meas. 79−56226
polyvinylidene fluoride, correlated mol. motion in dielec. props. 77−55749
polyvinylidene fluoride, dielec. props. and phase transitions *(French)* 80−55008
polyvinylidene fluoride, piezoelectric and dielectric consts. rel. to suitability for underwater transducers 78−1531
polyvinylidene fluoride, thermodynamic model and appl. 80−75955
polyvinylidene fluoride magnetoelectret, AF and RF charge and dielectric charact. 80−40038
polyvinylidene fluoride-tetrafluoroethylene, ferroelectric props. 79−42929
prefired substrate, acid treatment, improvement in as-fired surface finish 79−24636
prefluorinated polymer, DuPont Krytox 143-AB, viscoelastic and dielectric props. 80−1503
1,2-propane diol-dipropylene glycol, dielec. dispersion charact. 80−75932
propanes, substituted, dielec. relax. in liquid state 77−8500
propanes, substituted, liq., microwave absorpt., dielectric relax., loss, permittivity, moments and reorientation 77−63362
2-propanol, dielec. time domain spectroscopy, total transmission method study 80−27323
propyl acetate-propyl alcohol, dielec. dispersion charact. 80−75932
n-propyl trichloroacetate, soln., dielectric props. and relax. mechanisms at microwave freqs. 78−15089
propylene glycols, dielec. props., chain length effect 80−44995
PTFE, in butan-1-ol, colloidal particles, dispersion force interactions calcs. 79−24842
PTFE films, plasma-polymerized, cond. mechanism, AC cond. and capacitance meas. 79−24093
PVC, gamma radiation effects on dielect. parameters, expt. *(Hungarian)* 78−59836
PVC, magnetoelectret form., RF thermomagnetic treatment, dielectric aftereffects 78−6625
PVC, plasticised, thermomechanical and dielec. relax. props. rel. to degree of processing 79−70124
PVC, reduced, dielec. props. rel. to mol. struct. 80−29681
pyridines, substituted and N-oxides, dielectric relax. in solns. 78−6627
PZT ceramics, ferroelec. energy conversion under shock loading 80−108163
α-quartz, complex dielec. const. at audio freqs., 5.5 to 380K 80−25272
quartz, cryst. and fused, far UV optical consts. 77−81078
quartz, effect of neutrons on electr. charact. *(Russian)* 77−48119
quartz, electron irradiation effects on optical, dielec., elastic props. 80−59521
quartz, fused, dielec. const. meas. at 40-1500 MHz *(Japanese)* 77−87780
quartz, pure, fused, optical consts. in far IR, 20 to 120 cm^{-1} 78−79080
quartz, X-band permittivity/temp. charact. obs. 77−2664
quasi one dimensional charge transfer salts, soliton model for dielectric permeability 80−40036
quasi one dimensional organic materials, microwave cond., dielectric const. *(Hungarian)* 78−26850
quasi one-dimensional charge transfer salts, soliton model for dielec. permeability 79−91338
quasi-one-dimensional solids, nomadic polarisation 77−63357
radiation of uniformly moving charge on nonstationary layer 80−32893
random dielectric, mean pot. and field 78−55271
random heterogeneous materials, statistical theory of effective elec. thermal and mag. props. 77−48118
rare earth aluminate, scandate and zironate film coatings, electrophys. props. w.r.t. prep. technology 80−60781
rare earth arsenates, $RAsO_4$, ferroelectricity, dielec. meas. 80−60515
rare earth oxide film, transmission of refl. spectra, opt. consts. and parameters 79−95864
rare earth oxides, dielec. const. and loss at low temp. 80−93229
relaxation time distrib. function, first order moments from permittivity data *(French)* 80−88918
trans-retinal, ground and excited state dipole moments, permittivity, solvent effects, spectrophotometry 78−27883
trans-retylidene-n-butylamine, ground and excited state dipole moments, permittivity, solvent effects, spectrophotometry 78−27883
rigid-dipole fluid, dielectric const., functional-derivative approach 77−63353
(Rochelle salt)$_{1-x}$(ammonium Rochelle salt)$_x$, phase transitions, hydrostatic press. effects 80−93246
rock formations of limited thickness, permittivity rel. to saturation determ. by dielectric wave logging *(Russian)* 79−74990
rocks texture heterogeneity, study via dielectric const. and elec. resistance *(Russian)* 78−96195
rotational swings of colliding dipoles, contrib. to nonlinear dielectric constant 78−27171
rubber, styrene butadiene, dielectric const. and loss, lignin content depend. 80−29670
rubber mixtures, synthetic, natural ageing effects on dielec. props. 77−24778

permittivity continued
rubber-channel black mixtures, natural ageing effects on dielec. props. 77−24777
sapphire, complex dielec. const. at audio freqs., 5.5 to 380K 80−25272
schlieren method for the determination of electric field distributions in dielectrics 80−31720
sea ice, complex dielec. const., 0.1-40 GHz 78−61430
seawater, microwave freqs., improved model 77−17113
seawater at microwave freqs., modelling 77−25690
SELFOC fibre, non-Gaussian laser beam propag. 78−1335
semiconducting film, exciton oscillator strength, EM wave-polaritan propagation, reflective power *(Russian)* 79−99491
semiconductor, crystalline, local field effects on static dielec. const. 77−59264
semiconductor, n-type, donor-polarizability enhancement as the insulator-metal transition is approached from the insulating side 80−80184
semiconductor, noncentrosymmetric cubic cryst., electrooptic effect, dispersion of permittivity 79−69812
semiconductor, optical non-locality phenomena near exciton reson. 79−95794
semiconductor, p-type, infrared absorption and plasma reflection 80−97284
semiconductor, photodielectric effect associated with impurity excitation 79−82630
semiconductor, with spatially varying dielec. const., impurity ion pot., variational calc. 79−7800
semiconductor and semimetal powders, EPR, effect of mag. field depend. of elec. parameters 79−99749
semiconductor plasma, longitudinal oscillations 80−88583
semiconductor substrate-semicond. epitaxial layer, doping profile using ellipsometric meas. 79−99453
semiconductor thin film, Coulomb interaction depend. on film thickness, exciton binding energies *(Russian)* 79−78027
semiconductor thin film, dispersive props., effect of multilayer dielec. medium, anal. *(Russian)* 78−31004
semiconductors, degenerate, acoustodielectric effect, permittivity modulation by acoustic wave in resonance conditions 80−92944
semiconductors, doped, insulator-metal transition, dielec. const. enhancement on insulating side 80−20087
semiconductors, doped, insulator-metal transition, dielec. constant enhancement on insulating side 80−20088
semiconductors, photoconductivity measurement at UHF and at high excitation levels 80−65627
semiconductors, role of excitons in dispersion effects, band gap determ. 79−65393
semiconductors with diamond and zinc-blende struct., refractive index dispersion 79−24280
semimetallic thin film, Coulomb interaction depend. on film thickness, exciton binding energies *(Russian)* 79−78027
serum albumin, bovine, hydrated, dielec. and elec. props. 80−97854
serum low density lipoprotein, human, anomalous permittivity behaviour 80−81540
shadow methods for studying turbulence using reflection from a mirror in the medium 80−95801
shallow impurity centres near Curie point, influence of dielec. nonlinearity on temp. depend. of ionisation energy 80−10916
shear SAW in high permittivity three-layer system *(Russian)* 80−80048
silicone, film deposition, glow discharge polymerisation, elec. and thermal characts. 78−6467
smectic helixing crystal, dielec. props., temp. and freq. depends. *(Russian)* 78−60380
smectic liquid crystal, A phase, dielec. permittivity 78−71673
smectic liquid crystal, C-phase, optical props. *(French)* 77−43959
smectic phases, dielectric constant theory 79−78604
smectic phases, long mol. axis reorientation, LF dielec. dispersion 80−70124
snow, dielectric breakdown characteristics *(Japanese)* 78−40669
snow, permittivity and attenuation, 4-12 GHz 80−85692
soda glass, ageing effect of HF discharge on conductivity and dielec. const. 78−39138
sodium acetylacetonate, anomalous dielec. behaviour, evidence for ferroelectricity 79−91390
sodium benzoylacetonate, dielec. props. and cryst. struct. 79−8099
soil, complex dielectric permittivity, semidisperse model 77−29288
solid, absorption band struct. resolution by using complex dielectric const. 78−72546
solid-liquid interfaces, permittivity matching on flashover 78−1945
solids and liquids, dielectric loss characterisation 78−88252
solution, of polar mols., local order and vibr. coupling, Raman bands, dielec. const. 79−99868
solution, polar solute dipole moment determ. 77−6956
solvation, classical mean space charge model 78−76841
space charge effect 77−63366
spatial dispersion exponential model, boundary conditions *(Russian)* 80−75994
spheroids, in streaming suspension, dynamics, dielectric consts. 78−76374
spin-phonon system, transition to self-trapping 80−10606
squaric acid, dielec. const. and PMR near struct. phase transition 79−10946
squaric acid, dielec. props., press. and temp. depend. 79−99815
squaric acid, hydrostatic press. effect on phase transition, dielec. and dilatometric meas. 78−55941
squaric acid, layered, antiferroelec., phase transition mechanism 80−97210
squaric acid-d_0,-d_2, 2-dimens. antiferroelec., dielec. props. and phase transitions, press. effects 79−95700
starch, hydrocarbon suspension, temp. depend. of electroviscous effect and dielectric parameters 79−79299
stearic acid film, using varying gap immersion method 78−6620
steel, polymer coated, electrolyte permeation and elect. permittivity rel. to metal substrate corrosion 79−96175
stibiotantalite type structure ferro- and antiferroelectrics, props. and crit. points 79−38460
Stockmayer fluids, static dielec. props. 80−93231
Stockmayer fluids with dipoles and quadrupoles, spherical harmonic coeffs., dielec. const. and Kerr factor calcs. 80−84678
Stockmayer molecular fluid, 2-dimens., permittivity and dynamic props. 80−103910
Stockmayer molecules, two dimens. fluid, static props., dielec. const. mol. dynamics calcs. 80−54094
permittivity continued
strain tensor depend. *(Ukrainian)* 79−32254
stripe lasers, twin-transverse junction, dielec. const. of inbuilt waveguide, injection current effect 79−50294
structuring dispersions, meas. device for dynamic dielectric behaviour 78−31710
styrene-butadiene-styrene triblock copolymers, dielec. props. 78−95545
styrene-butyl vinylpyridinium-TCNQ copolymer, dielectric const. *(Japanese)* 78−60375
styrene/n-butyl-2-vinylpyridinium-TCNQ copolymer, dielec. permittivity *(Japanese)* 78−56416
succinonitrile, plastic cryst. with steric hindrance, dielectric const. 77−24779
suspension, of ideally polarisable spherical particles, low-frequency dielectric dispersion 79−61912
suspensions, concentrated, of shell-spheres, dielectric theory, interfacial polarisation, anal. of biological cell suspensions 80−45563
suspensions, dielectric separation of solid particles 80−16213
suspensions of ellipsoidal particles covered with shell, dielec. behaviour, rel. to biological cells 80−51057
Tanane, dielec. and electrooptic meas. near ferroelec. transition 79−33587
TBBA, dielec. const. in cryst. and smectic phases 79−78607
TCNQ salt, acridizinium, one-dimens. cond., permittivity 25 to 60 GHz, 4.2K 78−88248
TCNQ salt, K-TCNQ, high and low temp. phases, dielec. const. 80−34844
TCNQ salt, MeDABCO$(TCNQ)_2$, optical, elec., and mag. props. 80−65539
TCNQ salt, MEM$(TCNQ)_2$, dielec. const. obs., DC and microwave cond. obs. 80−59963
TCNQ salt, N-propyl-quinolinium$(TCNQ)_2$, defect conc. depend. phase transition 80−44577
TCNQ salt., NMeQn$(TCNQ)_2$, role of solvent in phase transition, thermal anal. and transport props. 79−33312
TCNQ salt, NMP-TCNQ, realisation of disordered Hubbard model, dielec. props. 78−79917
TCNQ salt, NPQn $(TCNQ)_2$, neutron irrad. induced defect concentration depend. phase transition 80−29449
TCNQ salt, pyridine $(TCNQ)_2$, phase transition at 80K investig. and interpret. 78−6530
TCNQ salt, Qn$(TCNQ)_2$, decrease of electronic coherence length by impurities 79−69501
TCNQ salt, Qn$(TCNQ)_2$, defect depend. of dielec. permeability and cond. 79−78608
TCNQ salt, Qn$(TCNQ)_2$, defect depend. of dielec. permeability and conductivity 79−91340
TCNQ salt, quinilinium, one-dimens. cond., permittivity 25 to 60 GHz, 4.2K 78−88248
TCNQ salts, Qn$(TCNQ)_2$, NMeAd$(TCNQ)_2$, dielec. const. and cond. 78−79985
TCNQ salts, Qn$(TCNQ)_2$ and NMeAd$(TCNQ)_2$, dielec. const. and elec. cond. 78−60116
TCNQ salts, Qn$(TCNQ)_2$ impurity effects on electronic coherence length 79−73500
TCNQ salts with asymmetric donors, transport props. 78−60115
TDOBAMBCC, chiral smectic C liq. cryst., dielec. consts., electroclinic effect 78−94980
teflon, γ-irradiated, rel. to positron lifetimes 78−76550
1,1,2,2-tetrabromoethane, dil. soln. in benzene, dielec. relax. study 80−29679
tetrabutylammonium iodide, in aq. proline soln., elec. conductance investigation 80−10692
tetraethylene glycol dodecyl ether-H_2O, binary micellar solns. and emulsions, dielec. behaviour 80−44994
tetraethylene glycol dodecyl ether-H_2O-heptane, binary micellar solns. and emulsions, dielec. behaviour 80−44994
tetraglycine, aq. soln., density, viscosity and dielectric const., 0-60°C 78−47462
N,N,N′,N′-tetramethyl-p-phenylenediamine-p-chloranil, soln., optical spectra, temp. and environment effects 79−54861
tetramethylammonium hydrogen bis-trichloracetate $(-d_n)$, ^{35}Cl NQR study 80−66064
tetramethylammonium iodide, in aq. proline soln., elec. conductance investigation 80−10692
tetramethylammonium tetrachlorocobaltate, ferroelec., pressure-temp. phase diagrams 80−97205
tetramethylammonium tetrachlorocuprate crystal, incommensurate-ferroelastic (commensurate) phase transition obs. 80−75352
tetramethylammonium tetrachloroferrate, press. induced ferroelectricity, dielec. and DTA meas. 80−80722
tetramethylammonium tetrachlorozincate, ferroelec., pressure-temp. phase diagrams 80−97205
tetraselenotetracene bromide, positive microwave dielectric const. 78−47771
tetrathiotetracene iodide, positive microwave dielectric const. 78−47771
textured surface reflectance and transmission props. rel. to complex permittivity variation in boundary layer 78−1165
TGS:α-alanine, single crysts., dielec. spectrum in RF range *(Russian)* 80−66097
TGS: nitroaniline, dielec. and pyroelec. props. 80−75916
TGS:Cr single cryst., lattice defect influence on critical behaviour 80−25315
TGS:nitroanilines, permittivity, elec. cond. and Curie temp. 80−25273
TGS, γ-irrad., lattice defect effects on ferroelec. dispersion 79−51904
TGS, characts. of dispersion of permittivity near phase transition 79−28695
TGS, complex dielec. permitt. near Curie temp., ferroelec. polarisation mechanism interpretation 78−43808
TGS, correlation between domain struct. and dielec. props. 79−42927
TGS, critical behaviour in thermal expsn. coeff. and dielectric const. 79−91334
TGS, deuterated, undoped and alanine-doped, growth by rotating disc method and elec. props. 79−47611
TGS, deuterated and undeuterated, pyroelectric, dielectric and thermal props., temp. depend. 78−43809
TGS, dielec. behaviour near transition temp. 78−15127
TGS, domain wall dynamics and small signal permitt., loss mechanism absence 78−43825
TGS, effect of Fe^{3+} admixture on phys. props. 80−76052
TGS, elastic and dielec. consts. from Brillouin scatt. 77−48180

permittivity continued
TGS, gamma irrad. effects on heat capacity, Curie temp., permittivity 78−67737
TGS, L-α-alanine disordered regions, dielec. prop. changes in transition region 80−108159
TGS, monocrystalline, ferroelectric, domain boundary dynamics contrib. to permittivity near Curie point *(Russian)* 79−73875
TGS, pyroelec. IR detectors, permanent polarisation due to X-rays, optimum non-ferroelec. behaviour 77−41684
TGS, static crit. phenomena, lattice defect influence 80−71336
TGS, thermal expansion and dielec. const. near ferroelec. crit. temp. 77−40188
TGS, with radiation defects, dielec. dispersion 79−42882
TGS family, change of order of phase transition under hydrostatic pressure 78−52452
TGS powder, complex dielectric const. temp. depend. 79−47379
TGS powders, dielec. dispersion 80−97180
TGS-TGSe solid soln., phase transitions under hydrostatic press. 79−99840
TGSe, deuterated, thermal and dielectric props. at high hydrostatic press. 80−34864
TGSe, dielectric const. near ferroelec. transition temp., effect of surface capacitance 78−56438
TGSe, ferroelec., effect of gamma irradiation on dielec., piezoelec. and elastic props. 77−43943
TGSe, low freq. dielec. dispersion near Curie point 79−38432
TGSe, surface layers effect on coercive field, spontaneous polarisation, and dielec. const. 79−61321
thermodynamic properties of permanent dipoles on lattice 78−88246
thermoplastic layers with fast heating, discharge process 78−49920
thin ferroelectric layers, permittivity tensor at microwaves 79−42883
thin films, dielec. props. meas., student expt. 79−40323
thiourea, dielec. const. and IR spectra in ferroelec. and antiferroelec. phases 79−33589
thiourea, ferroelec., soft mode and Debye relax., IR reflection spectra 77−90111
thiourea, IR reflectivity study of ferroelec. and antiferroelec. phases, dielec. function model 79−33686
thiourea formaldehyde polymer, pyroelectricity and dielec. props. 79−91379
thiourea monocrystals, γ-irrad. effects on dielec. props. 79−91391
thiourea single cryst., γ-irrad. effect on elec. permittivity 78−64311
time domain reflectometry, index profile determ. 79−26075
tissue, RF mag. field penetration, phase shift and power dissipation, rel. to NMR imaging 78−73189
tissue microwave dielectric props. rel. to rot. mobility of tissue water 77−29092
TMBP.HCNB and TMBTP.HCNB complexes, elec. and mag. props. 78−6512
toluene, dielec. const. meas. using 3-terminal meas. cell 78−21170
trans-p-n-alkoxy-α-methyl p′-cyanophenyl cinnamates, liq. cryst. of strong positive dielec. anisotropy, static dielec. consts. meas. 78−2790
transition metal oxide films, dielec. dispersion and polarization 78−2803
transition metal oxides, dielec. and thermophys. props. 77−52009
transition radiation in nucl. dispersive medium, nucl. levels and permittivity meas. *(Russian)* 77−59635
tremolite asbestos, fibrous, elec. anisotropy 78−80273
tri-n-butylammonium picrate, complex permitt. meas. by time-domain spectroscopy 77−49741
trichloracetonitrile, IR dispersion, complex refractive index and permittivity, time correl. function 80−45057
1,1,1-trichloroethane, in nonpolar solvents, permanent dipole moment determ. 77−43125
trifluoroacetates, methyl and ethyl, intramol. relax. at microwave freqs. 80−55020
trifluoromethane, dielectric const. near critical point 79−15394
trifluoromethane, dielectric constant effect on nuclear spin-spin coupling constants, INDO approx. 79−72240
triglycine, aq. soln., density, viscosity and dielectric const., 0-60°C 78−47462
triglycine fluoberyllate, pyroelectric, dielectric and thermal props., temp. depend. 78−43809
triglycine sulphate, paraelec. phase, thermal expansion coeff. and dielec. constant 79−8100
tris-sarcosine calcium chloride, ferroelec., US attenuation and vel., elastic consts., and permitt. near Curie temp. 79−37761
tris-sarcosine calcium chloride, phase transition, hydrostatic press. effect, dielec. const. meas. 80−71327
trisarcosine calcium chloride crystals, ferroelec., electrooptic and ferroelastic props. 80−34865
trissarcosine calcium chloride, ferroelec. transition, press. effect 80−84681
TSCC ferroelastic monodomain crysts., dielec. behaviour 79−42888
TTF-TCNQ, interchain tunnelling effect on nucl. spin-lattice relax. time, interchain coupling of CDW 80−20163
TTF-TCNQ, positive microwave dielectric const. 78−47771
tungstates, hexagonal bronze type struct., cryst. struct. and props. 77−39574
two phase mixtures, prediction formula 78−48107
undirectional fibre composites, anisotropic constituents, effect elastic moduli and other props. 80−58911
uniaxial crystal with scalar permittivity, optical activity 77−4614
DL-α-valine in aq. soln., dielectric dispersion 78−20141
vinyl acetate, oligomers, dielectric relax., end-group effects 78−92019
vinylidene fluoride-trifluoroethylene film, cryst. phase transition 80−66120
volume hologram two-dimens. theory, incl. varying average dielec. const. effect 78−78960
water, complex permittivity meas. and microwave heating for specific purities and salt. soln. 80−60480
water, dielectric constant of bonded lattice model 78−23386
water, Earth surface forms, at frequencies below 1000 GHz 78−24310
water, heavy water, and ionic solns., high-field nonlinear effect, Piekara factor meas. 78−68441
water, liquid, zeroth order random network model, dielec. const. calc. 79−68993
water, normal and heavy, glass-transition temp., crystn. temp., and dielec. const. 80−15229
water, reflectivity meas. at mm wavelengths 80−66098
water, struct. effect of small additions of nonelectrolyte, dielec. const. obs. 78−9937
permittivity continued
water, supercooled emulsified droplets, relative permitt. and cond., Maxwell-Wagner interfacial polarisation 78−52423
water, Van der Waals interaction, Kramers-Kronig eqn. with full spectral data vs. oscillator model approx. 78−5998
water emulsions, dielec. props. obtained after crystallisation/melting cycle 77−86381
water vapour dielectric constant, rotational part, engineering method of calc. 78−40717
water-in-dodecane microemulsions, dielec. study of phase transition 79−28668
water-in-dodecane microemulsions, struct. transitions in liq. cryst. phase, dielec. props. 79−28669
water-oil microemulsions, optical matching 80−61157
waveguide, inhomogeneous planar, profile determ. from mode spectrum *(Czech)* 80−28312
waveguide dielectric variable permittivity (real part), eqns. for mode attenuation phase const. 77−50768
X- and γ-ray region dielectric permittivity, review 80−44998
zeolite-S layers, high-temp. activated dipole moments in S clusters *(Russian)* 80−20575
X-zeolites, dielectric relax. anal. 80−108153
Ag, adsorption of O, dielec. perm., plasma surface vibr., modulation spectroscopy 77−48198
Ag halides, correlation between electronic dielec. constant and ionic separation 79−4758
Ag halides, static dielec. constant, strain derivatives 80−100629
Ag halides, static dielectric const. strain derivatives, using extended many body lattice theory 79−56710
Ag, halides, strain derivatives of elastic and dielectric consts. 79−60421
Ag, thin layer on Al surface, surface plasmon ATR spectroscopy 79−78770
Ag_3AsS_3, proustite, light effects on dielec. props., elec. resist. 80−49816
Ag_3AsS_3, proustite crystals, stoichiometric composition derivation influence on phase transition 79−95715
AgBr, dielectric behaviour under hydrostatic press. 78−52420
AgBr, exchange charge polarisation 78−92016
AgCl, dielectric behaviour under hydrostatic press. 78−52420
AgCl, exchange charge polarisation 78−92016
$AgCl:OH^-$, dielec. meas., defect reorientation 77−19947
AgCl(Br), electronic dielec. const., vol. depend., Clausius-Mossotti model 80−100630
$AgNO_2$, single crystal, dielec. const., low temp. meas. 80−71290
$AgNa(NO_2)_2$, crit. dynamics, hydrostatic press. effect, dielec. props. meas. 80−71328
$AgNa(NO_2)_2$, order-disorder ferroelec., influence of hydrostatic press. on polarisation dynamics 80−103913
$AgNbO_3$, cryst. growth and phase transitions 80−40243
$Ag_2O-Na_2O-B_2O_3$ mixed cation glasses, electric conduction *(Japanese)* 77−24432
β-$AgSbS_2$, phase transitions, electrophysical props. 80−44316
Ag_3SbS_3, IR refl. spectra, permittivity, lattice vibrs. 79−65862
Ag_3SbS_3, pyrargyrite, order-disorder phase transition and elec. polarisation 79−38468
Ag_5SbS_4, dielec. and acoustic props. *(German)* 78−64335
Al-stearic acid-Al, low-loss thin film capacitor 80−71317
Al-TeO_2-Al, field-assisted cond. mechanism 80−11105
AlF_3 film, dielec. characts. 77−85650
AlF_3 in Al-AlF_3-Al MIM thin film structures, dielec. and elec. props. *(Slovak)* 80−100536
$Al_xGa_{1-x}As$:Mg doping characteristics, elec. props., effective hole masses 79−78117
$Al_2In_{12}S_{21}$, dielec. const., temp. depend. 79−82909
Al_2O_3, DC reactively sputtered, in MIS structs. optical and elec. props. 79−19486
α-Al_2O_3, dielectric constant, effect of degree of purity and perfection 77−48117
Al_2O_3, film, CVD on Si, chem., phys. and elec. props. 77−12543
Al_2O_3 film, dielec. props., AC and DC elec. characts. 78−68445
Al_2O_3 film, RF sputtered by planar magnetron, phys. props. 77−43448
β-Al_2O_3, Na, K and Ag substitued, lattice vibrs., ion transport spectra 77−20121
β-Al_2O_3-Na_2O, electrolytes, electric modulus spectroscopy 77−84974
β-Al_2O_3-Na_2O, microwave absorpt., low-temp. dielectric props. anomalies, ion tunnelling states 78−92013
Ar, Clausius-Mossotti function, exam. of variation with gas density 78−52418
Ar, gas, liquid, solid, refractive index, density and dielectric const. 80−66138
Ar, liq., dielec. const. meas. by reson. method *(Russian)* 77−28511
Ar-H_2(Ne) liquid solution, dielectric props., intermolecular interactions *(Russian)* 80−88904
Ar-O_2 liquid mixture, dielectric polarisation and permittivity *(Russian)* 77−90095
As-Ge-Te, chalcogenide glass, elec. cond. and dielec. const. 80−75567
As-Ge-Te glass, dielectric meas. 79−87382
As-Se-Te system glasses, AC cond. and permittivity; freq. and temp. depend. 77−76857
$As_xGe_{10}Te_{90-x}$ glass, cond. and dielec. const. from 77 to 383K and from DC freq. to 5 MHz 79−23964
$As_{10}Ge_{15}Te_{75}Ag_x$ glass, elec. and dielec. props., Ag additions effect 80−65558
As_2O_3, vitreous, Raman and IR spectra 79−73933
As_2S_3:Te glasses, doping influence on AC conductivity, electron transport by hopping 79−78106
$As_{1-x}Se_x$, ave. energy gap, optical freq. dielec. const. and refr. index 77−76739
As_2Se_3 glass, rel. to microwave elec. cond. 80−49793
As_2Se_3, glassy, dielectric const. determ. 78−72449
As_2Se_3, glassy, influence of oxygen added in As_2O_3 and SeO_2 forms on phys. props. 77−76314
$As_{10}Te_{75}Ge_{15}$, dielec. props. 77−63355
Au, dielectric const. by multiangle reflection meas., optical props. 79−95723
Au film growth, optical and elec. prop. meas. during deposition *(French)* 77−70007
Au small particles in glass, transition cluster-solid state 79−33593
Au-Cu, dielectric const. by multiangle reflection meas., optical props. 79−95723
Au-MgO cermet film, dielectric const. and selective solar absorption 78−2937

permittivity continued
BN film, high temp. reactive plasma deposition, struct., resist., and dielec. const. meas. 77−7988
B_2O_3-CaO-Fe_2O_3 glasses, semicond., cond. models, electronic props., 77−800K 80−54688
B_2O_3-SiO_2 (95.5 wt.%) glass, dielec. relaxation 79−78620
$B_{14}Si$, β rhombohedral, conduction mechanism, thermoelectric props. 80−24932
(Ba, Ca)(Ti, Zr)O_3, segregation of $CaTiO_3$ and effect on dielec. props. 78−38849
(Ba,Sr)TiO_3, ferroelec. props., press. depend., anharmonic oscillator model 80−80716
BaBrF, reacted flux growth, dislocation density, dielec. const. and loss, IR spectra 77−36214
$Ba_{0.92}Ca_{0.08}TiO_3$ ceramic, uniaxial stress effects, US dilatometric and dielec. meas. 78−52454
BaF_2, dielec. const., 5.5 to 400K 80−50249
BaF_2, electronic polarizability and dielectric const., strain derivatives 78−19406
$BaFe_{12}O_{19}$, ferrite, DC cond., dielec. props., lattice consts. 80−80272
$Ba(H_2PO_4)_2$, dielectric const. and polarisation, antiferroelectricity 77−59526
$BaM_2(PO_4)_2$, M=Co, Ni, Mg, Zn, dielec. permittivity and elec. resist., temp. depend. 77−59502
Ba_2MgTeO_6, ferroelec. behaviour, microwave dielec. props. meas. 77−43948
$BaMn_{0.99}Co_{0.01}F_4$, magnetoelec. phenomena, dielec. behaviour near Neel temp. 80−71151
$BaMnF_4$, antiferromag., dielec. anomalies at low temp. obs. 77−20791
$BaMnF_4$, dielec. anomaly, mechanism, spin canting 78−10744
$BaMnF_4$, dielectric props. near 250K phase transition 77−12335
$BaMnF_4$, low temp. dielec. props. and phase transitions 77−20790
$BaMnF_4$, phase transitions review 79−78378
$BaMnF_4$, pure and Co doped, ferroelec. antiferromag., dielec. anomalies 80−71288
$Ba(NO_3)_2$, low temp. struct. changes, elec. props. 79−87377
$Ba_2NaNb_5O_{15}$, low temp. ferroelectric transitions, birefr. and dielec. meas. 79−38499
$Ba_2NaNb_{5-x}Ti_xO_{15-x}F_x$ and $Ba_{2-x}Na_{1+x}Nb_5O_{15-x}F_x$, ferroelectric props., F substitution effect 77−12331
$Ba_3Nb_{10}O_{28}$, diffuse ferroelec. phase transition, dielec. const. and X-ray diffr. meas. 78−23419
BaO-Nd_2O_3-TiO_2-Bi_2O_3 system ceramics, high stability low loss dielectric preparation 80−81008
BaO-TiO_2-Nd_2O_3, exam. of compositional and dielectric props. 79−33601
$(Ba_xSb_{1-x})TiO_3$ 80−60514
$(Ba_xSb_{1-x})TiO_3$, ferroelectric films, dielectric and semicond. props. 79−91388
$Ba_{1.35}Sr_{0.65}NaNb_5O_{15}$ crystals, struct., dielec. and pyroelectric characts. 79−51913
$Ba_{0.54}Sr_{0.46}Nb_2O_6$:Y(La)(Tm), dielectric and electrooptic props. 78−68466
$Ba_xSr_{1-x}Nb_2O_6$ (x=0.27 to 0.54) exam. of freq. dependence of permittivity diffuse ferroelectric phase transition kinetics 80−2703
$Ba_xSr_{1-x}Nb_2O_6$ crystals, struct., dielec. and pyroelectric characts. 79−51913
$Ba_xSr_{1-x}Nb_2O_6$, struct. and dielec. props., isomorphic substitution effect 78−27165
(BaSr)TiO_3 film, ferroelec., dielec. props. in strong elec. fields 78−27163
$Ba_{0.4}Sr_{0.6}TiO_3$, ferroelec. thin film, fabrication, props. 77−28521
$Ba_xSr_{1-x}TiO_3$, disordered ferroelec., dielec. const. and spontaneous polarisation meas. 78−48130
$Ba_2TiGe_2O_8$-$Ba_2TiSi_2O_8$, pseudobinary system, pyroelectricity and related props. 78−95553
$BaTiO_3$, A_1 and E optical phonons obs. in temp. range 10 to 132°C 77−27963
$BaTiO_3$ a-domain crystals, domain struct. influence on physical consts. 79−69798
$BaTiO_3$, c-domain cryst., HF dispersion of permittivity 78−60379
$BaTiO_3$, ceramic, effect of grain size on nonlinear dielec. props. 77−8522
$BaTiO_3$ ceramic dielectric capacitor, processing prop. relations, hysteresis, permittivity 80−80730
$BaTiO_3$, Co substituted, ferroelec., diffuse behaviour 79−38475
$BaTiO_3$ crystals, mechanically compressed, dielec. const. 79−56711
$BaTiO_3$, dielec. and elastic consts., temp. depend. *(Russian)* 78−64307
$BaTiO_3$, dielec. consts. at 5 MHz and Raman frequency region 78−76006
$BaTiO_3$, dielectric const. and polarisation, fluctuations, catastrophes 77−8491
$BaTiO_3$, doped, loss mechanism and domain stabilisation 78−84542
$BaTiO_3$, ferroelec. thin films, r.f. sputtering, X-ray and microprobe obs. 79−47627
$BaTiO_3$, ferroelectric polydomain crysts., piezoresonance effects, appl. as transducer 79−4779
$BaTiO_3$ film, dielectric props. depend. on sinusoidal elec. field 80−71318
$BaTiO_3$ film, sputtered, elec. props. 79−42676
$BaTiO_3$ film, struct. and dielec. props. 80−60514
$BaTiO_3$ film, surface layer nature, AES obs., and effect on permittivity 77−24498
$BaTiO_3$ films, ferroelec., effect of elec. field on dielec. props. 79−33642
$BaTiO_3$, low freq. and lattice contribs. 78−15105
$BaTiO_3$, nonstoichiometry of vac. condensates, effect on dielectric props. 77−16260
$BaTiO_3$, paraelectric crystal, nonlinear props. 80−84699
$BaTiO_3$, permittivity, temp. depend., submm. spectroscopy 77−176
$BaTiO_3$ polydomain crystals, dielec. props. 78−43827
$BaTiO_3$, pure, dielec. behaviour at ultralow freq. 79−38425
$BaTiO_3$, pure, dielectric const. and elastic compliance temp. depend. for various phases 79−19830
$BaTiO_3$, RF sputtered amorphous films, phys. and elec. characterisation 79−83119
$BaTiO_3$ RF sputtered ferroelectic film on Si substrate, ferroelectric props. 80−80697
$BaTiO_3$, RF-sputtered tetragonal films on Si, ferroelec. and insulating props. 79−78888
$BaTiO_3$, single cryst., dielec. const., var. with applied AC field and temp. 78−2787
$BaTiO_3$, single crysts., dielec. spectrum 80−25275
$BaTiO_3$, soft mode exam. 79−37799

permittivity continued
$BaTiO_3$, struct. changes due to cubic-tetragonal phase transition 78−60407
$BaTiO_3$, tetragonal, model for temp. depend. of dielec. const., ferro-paraelectric transition 78−43771
$BaTiO_3$, tetragonal, over-damped soft E-polariton and dielec. dispersion 78−15111
$BaTiO_3$ thin film microwave complex permittivity meas. 79−73879
$BaTiO_3$, transform. of cryst. struct., at cubic-to-tetragonal phase transitions 79−37827
$BaTiO_3$ type perovskite ferroelectric, neutron irradiated, amplification of freq. dispersion of permittivity *(Russian)* 78−52419
$BaTiO_3$, vacuum condensates on US irrad. substrates, props. 77−66466
$BaTiO_3$, X-ray irrad. effect on dielec. props. 78−15082
$BaTiO_3$:Al, 0.05-0.3 wt.%, ceramic dielectric, dielec. and mech. props. 79−8091
$BaTiO_3$:$BaTi_3O_7$, dielec. props. and microstruct. 80−60481
$BaTiO_3$:Co, charact. behaviour of spontaneous polarisation and dielec. const. 78−60382
$BaTiO_3$:Dy ceramic, sintering, grain size, characterisation and props. 77−55923
$BaTiO_3$:La_2O_3 and $BaTiO_3$:La_2O_3.$3TiO_2$ capacitor, permittivity ageing obs. *(Korean)* 80−25325
$BaTiO_3$:Nb, elec. props., contact material influence 80−70848
$BaTiO_3$:Nb, ferroelec. and paraelec. phases, props. 79−42919
$BaTiO_3$:ZrO_2, dielec. loss tangent and const. 79−4769
$BaTiO_3$-$BaNb_2O_6$ system, solid solns. of tungsten bronze struct. of type $BA_{5+x/2}Nb_{10-x}Ti_xO_{30}$ 77−52021
$BaTiO_3$-$BaNbO_3$ system, solid solns., thermal ionic relaxation, vacancy form. 77−8499
$BaTiO_3$-PbO-B_2O_3, liquid phase sintering, effect on props. *(German)* 79−33980
$Ba(Ti_xSn_{1-x})O_3$ film, struct. and dielec. props. 80−60514
$Ba(Ti_xSn_{1-x})O_3$ thick film, ferroelec., phase transitions and dielec. props. 80−97215
$BaZrO_3$-$LaAlO_3$ systems, sintering conditions, elec. props. 79−43184
BeF_3, water free vitreous, preparation and props. 79−66033
Bi complex oxides, antiferroelec. and ferroelec., pyrochlore struct., dielec. and structural study 79−38488
Bi mixed-layer type cpds., $Bi_4A_{2m-1}B_{2m+1}O_{6m+9}$, cryst. struct. and dielec. const. 77−47428
Bi-NbO_2-Bi system, Schottky barrier effects in transport and dielec. props. 80−29486
Bi-Sb, semiconducting, lattice dielec. const., comp. depend. 80−39516
$Bi_2Bi_4Fe_2Ti_3O_8$, dielec. and magnetoelec. props. 78−95562
$Bi_{12}GeO_{20}$, electrophys., props. determ. *(Russian)* 78−51987
Bi_3GeVO_9, dielec. props. and twin struct. 77−12350
BiI_3 film, exciton-phonon interaction, optical consts., Faraday effect., permitt. 80−59884
Bi_2MoO_6 ceramic, permittivity, ferroelec. T_c and hysteresis 79−82932
Bi_2O_3 film, dielec. meas. 80−2696
Bi_2O_3, thin film, struct. and dielec. meas. 79−78622
Bi_2O_3-Mo(W)O_3 system, elec. cond. and dielec. const. obs. 77−89816
Bi_2O_3-ZnO(CdO), elec. cond., dielec. const., mag. susceptibility meas., effect of melting transition 77−7849
Bi_2S_3-$CuPbBi_5S_9$, solid solution, semiconductor and dielectric props. 79−69511
$Bi_xSb_{1-x}SI$, atomic substitution and ferroelec. phase transition 78−68464
$(Bi_{0.25}Sb_{0.75})_2Te_3$, opt. props. of bulk and films 78−27206
Bi_2Si_3, cryst., RI anisotropy obs., polarised light effects 77−12354
$Bi_{12}SiO_{20}$ crystal, piezoelec. and SAW props. 80−75949
$Bi_4Ti_3O_{12}$ ceramics, ferroelectric, hot-forged, grain orientation and dielectric props. 80−40076
$Bi_2TiO_4F_2$, one-layer perovskite-like ferroelec., dielec. study 79−38486
Bi_2WO_6, ferroelectric, dielectric props., elec. cond. and relaxation phenomena obs. 80−80692
Bi_2WO_6, ionic cond. and relaxation polarisation, capacitance, losses 80−24657
$Bi_2W_2O_9$, struct., dielec. props., melting character and thermal stability 79−23572
β-AgI, ionic cond. and dielec. meas., Frenkel defect formation energy 78−87814
C, arc evap. film, optical props., 0.6-3.8 eV 77−81166
$CH_3NH_3Ga(SeO_4)_2.12H_2O$, dielec. relax. near transition temp. 80−60493
CO group, NMR chem. shift, solvent's dielectric const. effect, mag. anisotropy 79−42847
CS_2, emulsion theory, appl. to the permittivity of nonpolar dielectrics *(French)* 78−39497
$CaCO_3$, calcite, complex dielec. const. at audio freqs., 5.5 to 380K 80−25272
$CaCo_2(PO_4)_2$, dielectric permittivity and elec. resist., temp. depend. 77−59502
CaF_2, dielec. const., 5.5 to 400K 80−50249
CaF_2, electronic polarizability and dielectric const., strain derivatives 78−19406
CaF_2, hot pressed, dielectric, optical props. 79−56720
CaF_2, rare-earth-doped, cluster-associated relax., 5.5-400K 78−31153
CaF_2:Er, near-Debye dielectric responses 80−71291
CaF_2:Eu^{3+}, dielec. spectrum 77−36171
CaF_2:Li(Na)(K)(Rb), dielec. relax., activation energy, rel. to vacancy pair reorientation 80−88917
CaF_2:Na, vacancy motion activation vol., complex dielec. const. meas. 80−39356
CaF_2:Y(La), dielec. relax. spectrum, ion size trends 78−72460
$Ca_2Nb_2O_7$, ferroelectric phase transitions, dielec. constant and thermal expansion rel. to temp. 80−88934
CaO, dielec. const., temp. and press. depend. 79−65789
CaO-B_2O_3-Fe_2O_3 glass, electronic and dielec. props. meas. 77−24574
CaO-B_2O_3-Fe_2O_3 glasses, effect of heat treatment on electronic props. 78−2480
CaO-MgO-Al_2O_3-SiO_2, shale glass, glass forming and dielec. props. 78−22660
CaS, dielectric props., effective ionic change 79−65783
$Ca_{1-y}Sr_{y/2}Ba_{y/2}Zr_{1-x}Ti_xO_3$, ceramic system, dielectric props., microwave resonator application 80−80674
$CaTiO_3$-$CaTiSiO_5$, sintering and dielectric props. 80−40307
$CaTiO_3$-TiO_2, ceramic, phys. props. 78−43784
$CdAs_2$ based glasses, cond. and permittivity, freq. depend. 77−76859

permittivity continued
Cd_3As_2, ionised-impurity mobility and static dielec. const. at 4.2K 77−32017
$CdCr_2Se_4$, optical reflectivity, dielectric const. by expt. data Kramers-Kronig anal., spinel struct. 79−99903
$CdGa_2S_4$, IR refl. spectra 80−60604
CdI_2, dielec. props. rel. to polytypically modulated structs. 79−94971
CdI_2, polytypes, periodicity and disorder depend. 77−28506
$Cd(NO_3)_2$, phase transition, SHG, optical and dielec. meas. 80−71334
CdS, elastic, piezoelec. and dielec. props. 80−108157
CdS, elastic, piezoelectric, and dielec. props., 4.2 to 300K 80−60508
CdS, elastic wave propag., in hexagonal piezoelec. crysts. *(Russian)* 77−69777
CdS:Cu binder layer, photoactive, AC impedance meas. 80−25299
CdS:Li film, optical props. 80−2886
$CdSnAs_2(P_2)$ single crysts., refl. spectra, band struct., dielec. consts. 77−44022
CdTe, dielec. const. and loss tangent, temp. depend., 15.95 GHz 77−69763
CdTe, microwave cond. and dielec. permittivity using reson. cavity method 79−51620
$CdTl_2Se_4(Te_4)$:Au, elec. cond., density, dielectric const., changes on fusion 80−88553
CeF_3 film, in MIM struct., dielec. props. *(Czech)* 80−25309
CeO_2, elec. cond. and dielectric props. at low temp. 78−72447
$Ce_2(SO_4)_3.9H_2O$, grown from solution, exam. of Raman spectra and physical props. 79−52104
ClO_3F, heat capacity, permittivity, thermodynamic props., 2.7 to 160K 77−35713
$Co_{0.83}(Pt(C_2O_4)_2).6H_2O$, cond., dielec. const., microwave obs. 80−44636
$Co_xZn_{1-x}Fe_2O_4$, ferrite, DC cond., dielec. props., lattice consts. 80−80272
Cr_2O_3, dielec. const. in mag. field, nonlinear magnetoelec. effect in Neel pt. region 80−66006
Cr_2O_3, dielectric const. and loss, cond., 10^2-10^7 Hz, 30-450°C 77−59504
Cs halides, dielectric const. meas. at 1 MHz 77−16238
$Cs(B_xW_{3-x})O_9$ (B=Na, Ca, Co, Ni, Cd, Ga, Bi, Nb, Ta) cryst. struct., temp. dielec. anomalies 80−1998
$CsBi(MoO_4)_2$, low temp. phase transition, permittivity meas. 79−28698
CsBr, crystal, short range interaction polarization, dielectric const. loss, and elec. cond. 10^2 to 10^7 Hz 79−99814
CsBr, lattice statics and dynamics, deformation shell model 77−20034
CsCl(Br)(I), dielectric const. meas. at 1 MHz by immersion method *(Japanese)* 77−90087
$CsCuCl_3$, phys. props. 77−62511
CsD_2PO_4, dielec. props., press. and temp. depend. 80−25317
$CsFeF_4$, two dimensional structural phase transitions, sp. ht., optical, dielec., X-ray diffr. meas. 79−69240
CsH_2AsO_4 crystals, dielectric radiation effects, γ-radiation 80−93234
CsH_2AsO_4, influence of γ-radiation on dielec. props. 79−46703
$Cs(H_{1-x}D_x)_2PO_4$, dielec. props., temp. meas. 80−71335
CsH_2PO_4 and CsD_2PO_4, dielectric props. and ferroelec. transition temp. 77−12335
CsH_2PO_4, dielec. props., press. and temp. depend. 80−25317
CsH_2PO_4, ferroelec., X-ray and dielec. studies on phase transition 79−38477
CsH_2PO_4, ferroelec., critical behaviour of dielec. constant 80−34845
CsH_2PO_4, lattice consts., temp. depend. of dielec. const. and birefringence, high temp. phase transitions 79−56746
CsH_2PO_4-d, antiferroelec. under hydrostatic press. 79−91384
$CsH_2PO_4(CsD_2PO_4)$, permittivity temp. depend., pseudo one-dimens. ferroelectric ordering and critical props., NMR 79−78635
CsI, far-IR optical props., shell-model calcs. 77−28557
$Cs_8Nb_{22}O_{59}$, melt growth and struct., dielec. and optical characterisation 78−35294
$CsR(MoO_4)$ R=Dy, Ho, Er, permittivity temp. depend., polymorphic transition 80−92670
Cs_2SO_4-$(NH_4)_2SO_4$ mixed cryst., ferroelec. transition, structural and dielec. props., proton spin-lattice relax. 78−39512
Cu, dielectric const. by multiangle reflection meas., optical props. 79−95723
Cu halides, correlation between electronic dielec. constant and ionic separation 79−4758
Cu suspension, determination of dielectric constant 77−40579
$Cu_3B_7O_{13}Cl$, dielec. const. and elec. resist. 77−69783
$Cu_3B_7O_{13}Cl(Br)$, piezoelectric, elastic and electromechanical coefficients *(French)* 78−39504
CuCl, optical consts. in exciton absorption region, spectral depend. *(Russian)* 77−81125
CuCl(Br), electronic dielec. const., vol. depend., Clausius-Mossotti model 80−100630
$CuFeS_2$ single crystal, optical reflectivity spectrum 80−40129
$CuInSe_2$, dielectric const. from capacitance meas. 79−61292
CuPbBiS, ferroelec. semicond., elec. cond., photocond. permittivity, phase transitions 77−47822
$CuWO_4$, elec. cond., thermoelectric power and dielectric constant temp. depend. 80−96886
D-T, liq., dielectric constant and elec. cond. 80−84680
$DyAsO_4$, cooperative Jahn-Teller phase transitions, dielec. anomalies 78−64312
$Dy_2(MoO_4)_3$, cryst. growth and props. 79−55727
$DyVO_4$, cooperative Jahn-Teller phase transitions, dielec. anomalies 78−64312
$DyVO_4$, dielec. anomaly and improper antiferroelectricity at Jahn-Teller transition 77−24802
Er_2O_3, mag. susceptibility, elec. cond. and dielectric const., hopping cond. 77−12083
ethanol-water system, complex dielec. permitt. in UHF region and NMR spectra *(Japanese)* 80−100620
EuO, mag. semicond., dielec. and optical props. 78−10824
EuO, microwave and DC cond., dielec. const., 1.7 to 300K 77−20347
Eu_2O_3, elec. cond., thermoelec. power, dielectric const. 79−69763
Eu_xO_y film, dielec. props. rel. to annealing 79−99636
EuO(Se), complex elec. cond. anomalies 80−107812
EuSe, annealed, AC conductivity and dielectric anomaly 80−34445
EuSe, mag. semicond., dielec. and optical props. 78−10824
EuSe, microwave and DC cond., dielec. const., 1.7 to 300K 77−20347
EuSe, polarisability of shallow donors, permittivity meas. 80−24833
$Eu_2(WO_4)_3$, mag. susceptibility, elec. cond. and dielec. const. meas. 77−11916

permittivity continued
Fe complex, $K_3[Fe(SCN)_6].4H_2O$, optical reflection spectrum, mag. suscept., permittivity, dehydration temp. 79−56809
Fe-Ge, characteristic energy losses and optical props. 80−29834
$Fe(BF_4)_2.6H_2O(6D_2O)$, phase transition, mag. susceptibility and anisotropy and permittivity meas. 79−23718
$Fe_3B_7O_{13}I$, improper ferroelectric, dielectric props., IR radiation pyroelectric detection 80−80711
$Fe_3B_7O_{13}I$, spontaneous polarisation, dielec. const., d.c. resist., sp. ht. 77−1643
$FeCl_3$, nonaq. solns., solvent-solute interactions, Mossbauer investig. of equilib. consts. 79−1729
FeF_2, dielectric properties, IR spectra, lattice dynamics *(French)* 80−76026
$Fe_{0.95}^{2+}Fe_{2.05}^{3+}O_4^{2-}$, magnetite, elec. resistivity above 300K 79−78099
FeI boracite single crystals, dielectric, pyroelectric props., vapour phase transport growth 80−80673
FeO_x-P_2O_5 glass, semicond., dielec. props., thermally stimulated depolarisation meas. 79−95704
Fe_3O_4, dielec. props. of low temp. phase, at microwave freq. 78−64309
$FePb_4Sb_6S_{14}$, photosensitive semiconductor, with high permittivity, elec. props. 79−65518
FeS_2, dielec. constant meas. 79−15395
$FeSO_4.7H_2O$, single cryst., elec. and dielec. props., temp. depend. 79−19826
$FeSb_2S_4$, berthierite cryst., anomalies in elec. and dielec. props. 77−47821
$FeSiF_6.6H_2O$, dielec. props., 100-270K, rel. to $NiSiF_6.6H_2O$ 78−35088
GaAs, electrooptic effect, birefr. harmonics, permittivity dispersion 77−52044
GaAs, noncentrosymmetric cubic cryst., electrooptic effect dispersion of permittivity 79−69812
GaAs, permittivity at laser transitions freq., excess carriers effect 77−14719
GaAs, Schottky barrier diodes, strain sensitivity mechanism 79−38165
GaAs, semi-insulating 80−60479
GaAs:Cr, semi-insulating, complex permittivity, 2.5-36 GHz, 300-400K 77−69763
GaAs-Al_2O_3, MOS struct. dielec. const. dispersion 79−60927
GaAs-$Ga_{1-x}Al_xAs$ stripe geometry lasers 79−94245
GaN, preparation variables rel. to dielectric data, GaAs conversion 78−60591
GaP, Thomas-Fermi theory, dielectric functions, screening, dielectric constants 79−99497
n-GaP:N,O,S,C end, dielec. const. from S-C donor acceptor pair spectra 79−65788
GaS, refr. index in far IR, permitt. meas. 78−64360
GaSe, long wavelength IR refl. spectra 80−11401
$Gd_3Ga_5O_{12}$, dielectric constant, effect of degree of purity and perfection 77−48117
Gd_2O_3, B-type monoclinic, DC(AC) elec. cond., thermoelectric power, dielectric const., temp. depends. 80−59980
Gd_2O_3, elec. cond., thermoelec. power, dielectric const. 79−69763
c-Gd_2O_3, electrical cond., dielectric const. mag. susceptibility, polymorphic transition 77−59505
Ge, amorphous film, optical consts. in near IR range *(Korean)* 79−8137
Ge:Sb, low-freq., low temp. dielec. behaviour below metal-insulator transition 80−50250
Ge-S-Se system, glass-forming, struct. and props. 80−19713
GeH_4, heat capacity, dielectric const., thermodynamic props. 78−83967
$Ge_{1-x}Se_x$, ave. energy gap, optical freq. dielec. const. and refr. index 77−76739
Ge_xSe_{1-x} glasses, DC cond. and static dielectric const. meas. *(French)* 77−62925
H_2, liq., normal and para-, dielectric props. *(Russian)* 79−87374
H_2, solid, dielec. const., 4.2-15K 77−8488
H_3BO_3, aq. soln., dielec. props. and struct. 77−89369
HCN crystals, polarition spectra and lattice dynamics 80−49313
H_2SO_4, solns., static permittivity, kinetic depolarisation, time-domain spectroscopy 78−68440
He, Clausius-Mossotti function, exam. of variation with gas density 78−52418
He, dielec. const. gas thermometry, 4-27K, and eqn. of state 79−63222
He, equations of state, 3.3 to 14K *(Russian)* 78−83912
^{3}He, dielec. constant, static, near liq.-vapour crit. point 78−56016
^{3}He, equations of state, 3.3 to 14K *(Russian)* 78−83912
^{3}He-^{4}He equimolar mixtures, excess vol., temp. and density depend. *(Russian)* 80−39380
^{3}He-^{4}He liquid solution films, thickness calc. from dielec. const. data *(Russian)* 79−11003
^{4}He, liq. and solid, dielec. const. meas. 77−20143
^{4}He, P-ρ-T data near vaporisation crit. point *(Russian)* 80−88373
^{4}He, solid, dielec. const., 0.8-4.3K 77−8488
^{4}He, superfluid, quantized vortices and dielec. const. splashes in crossed fields *(Russian)* 79−19410
Hf, electronic excitations, charact. energy loss meas. up to 50 eV 80−60723
HfO_2, electronic excitations, charact. energy loss meas. up to 50 eV 80−60723
HfO_2 film, CVD growth, struct., elec. and optical prop. characterisation 77−55891
$Hg_{1-x}Cd_xTe$, anodic oxide films, formation and props. 80−3212
Hg_2Cl_2, elec., dielec., and thermophysical props. 79−10989
HgI_2, dielectric const., up to 500 bar, press. depend. 78−27153
$HgSb_4S_8$, photosensitive semiconductors with high permittivity, elec. props. 79−65518
InP, MIS diode prep. by anodic oxidation 79−74270
InSb, current-voltage characteristics at room temperature and high hydrostatic pressure 80−88560
InSb lattice, static dielec. const. and carrier conc. meas. via gyrotropic sphere reson. 80−97143
n-InSb, microwave helicon resonances, carrier density, mobility, dielectric const. 80−96930
$InVO_4.2H_2O$, $In_4(V_2O_7)_3.14H_2O$, physicochem. props. 77−85702
(K,Na)NbO_3 ceramic, hot pressed, dielec. props. 79−87375
$K_xAl_xTi_{8-x}O_{16}$, $1.6 \leq x \leq 2.0$, dielec. response in freq. range 10^{-3} to 10^6 Hz 79−65785
$K(B_xW_{3-x})O_9$ (B=Na, Ca, Co, Ni, Cd, Ga, Bi, Nb, Ta) cryst. struct., temp. dielec. anomalies 80−1998

permittivity continued
$K_2Ba(NO_2)_4$, new ferroelastic, phase transitions, optical and electrical props. 79−55887
KCN-KCl mixed system, order-disorder transition, dielec. props. meas. 78−15112
$K_2Cd_2(SO_4)_3$, ferroelastic phase transition, X-ray diffr. and dielec. temp. depend. meas. 79−55882
$K_2Cd_2(SO_4)_3$, langbeinite type cryst., search for ferroelec. phase transition 77−59535
KCl aqueous solution emulsions, complex permittivity meas., dielec. relax. 78−72459
KCl, colloidal suspension, radiowave dielec. dispersion 80−11311
KCl, γ-irradiation effect on dielectric const. *(Japanese)* 79−51896
KCl, measurement of dielectric constant using transformer ratio arm bridge, 10^2 to 10^6 Hz 79−80641
KCl_xBr_{1-x}, dielectric const. determ. 80−108145
KDP-type crystals, polarisation, dielec. const. thermodyn. props. 77−59527
KD_2PO_4, attenuation const. meas. by SHF dielec. resonance 79−47406
KD_2PO_4, high temp. phase transition, dielec. const., elec. cond. and IR refl. meas. 78−43118
KD_2PO_4, order-disorder type ferroelec., HF dynamics 77−39657
$KD_3(SeO_3)_2$, optical and dielec. props. near ferroelastic phase transition 79−38518
$KDy(WO_4)_2$, Jahn-Teller transition, permittivity behaviour 80−55012
$K_4Fe(CN)_6.3H_2O$, ferroelec. and paraelec. phases, dielec. props. meas. 80−60494
$KFeF_4$, struct. phase transitions obs. by dielec. const. and X-ray diffr. studies 79−95161
KH_2AsO_4, high temp. phase transition, dielec. const., elec. cond. and IR refl. meas. 78−43118
$K(H_{1-x}D_x)_2PO_4$, ferroelec., complex dielec. const., mm wave meas. 77−1633
$K(H_{1-x}D_x)_2PO_4$, static dielec. props., and Curie temp., press. depend. 79−87405
KH_2PO_4, amplitude depend. of permittivity and losses 79−99842
KH_2PO_4, and isomorphs, dielec. props. and birefr., simultaneous obs. 78−15130
KH_2PO_4, attenuation const. meas. by SHF dielec. resonance 79−47406
KH_2PO_4, central components in ferroelec. phase 78−56436
KH_2PO_4, critical and tricritical phenomena, susceptibility, exponents 80−75976
KH_2PO_4, dielec. functions above and below ferroelec. transition 79−33588
KH_2PO_4, dielectric const. and polarisation, fluctuations, catastrophes 77−8491
KH_2PO_4, dispersion of permittivity, 6 to 12 cm^{-1} 79−33616
KH_2PO_4 family of crystals, proton modes, dielec. spectroscopy 80−75915
KH_2PO_4, initial dielec. const. in ferroelec. phase by thermal noise method 77−16267
KH_2PO_4, Landau-Devonshire coeffs. 78−15116
KH_2PO_4-KD_2PO_4 mixed crystals, static and dynamic props., proton-lattice coupled mode model 78−64328
KH_2PO_4-KD_2PO_4 mixed crysts., dielec. spectra, sub-mm wavelengths 80−80724
KH_2PO_4-type ferroelectrics, dielec. props., four-cluster approx. 80−97202
$K_3H(SO_4)_2$, and $K_3D(SO_{42})_2$, dielec. props. and phase transitions 80−60482
$KH_3(SeO_3)_2$, optical and dielec. props. near ferroelastic phase transition 79−38518
$(K_{0.5}La_{0.5})_xBa_{1-x}TiO_3$, cryst. struct., dielec. and IR spectral meas. 79−46614
$K_3Li_2Nb_5O_{15}$ films for optical waveguides epitaxial growth and characterisation 80−79016
$K_2Mg_2(SO_4)_3$, langbeinite type cryst., search for ferroelec. phase transition 77−59535
$K_xMg_{x/2}Ti_{8-x/2}O_{16}$, $1.6 \leq x \leq 2.0$, dielec. response in freq. range 10^{-3} to 10^6 Hz 79−65785
$K_2Mn_2(SO_4)_3$, langbeinite type cryst., ferroelec., phase transitions, dielec., elastic and pyroelec. meas. 77−59535
$K_2Mn_2(SO_4)_3$, phase transition press. effect, dielectric const. meas. 79−37834
$K_{1-x}Na_xTaO_3$, quantum ferroelec., elastic compliance, impurity effects 79−99835
$KNbO_3$, dielec. spectrum rel. to polarisation effects 80−15984
$KNbO_3$, elec. and thermoelec. props., influence of O defects 80−29401
$KNbO_3$, photoferroelectric effects 78−92029
$KNbW_2O_9$, crystallography, polymorphism and phys. props. 78−79599
$K_5Nd(MoO_4)_4$, dielec. and optical props. 79−33590
K_2OsCl_6, single cryst. with H^+ interstitials, protonic cond. from dielec. meas. 80−107515
K_2SO_4, phase transform., mech. of thermal hysteresis, DTA, dilatometry and dielec. meas. 80−75353
$K_2SbNb_5O_{15}$, dielec. and pyroelec. props. 79−99841
K_2SeO_4, dielec. dispersion, 5-900 MHz, near incommensurate-commensurate transition 80−60522
K_2SeO_4, Raman scatt. and dielec. props. 80−11313
$K(Ta,Nb)O_3$ ceramic, prep. and electro-optical props. 80−25620
$KTa_{0.9}Nb_{0.1}O_3$, ferroelec. , dipolar behaviour, crit. exponent of dielec. const. 77−4604
$KTa_{1-x}Nb_xO_3$, holographic storage using photorefractive effect, dielectric const. 80−78800
$KTa_{1-x}Nb_xO_3$, quantum limit of ferroelec. transitions, dielec. and elastic consts. meas. 78−15128
$KTa_{1-x}Nb_xO_3$, quantum ferroelec., elastic compliance, impurity effects 79−99835
$KTaO_3$, dielec. nonlinearity and parametric interactions at low temps. 79−38430
$KTaO_3$, relax. effects, electret state 77−12302
$KTaO_3$:Li, susceptibility extrinsic peak, dielectric const. meas. 79−11394
$KTiF_4$, struct. phase transitions obs. by dielec. const. and X-ray diffr. studies 79−95161
KVF_4, struct. phase transitions obs. by dielec. const. and X-ray diffr. studies 79−95161
K_2ZnCl_4, ferroelec. props. 79−4772
$K_2Zn_2(SO_4)_3$, langbeinite type cryst., ferroelec., phase transitions, dielec., elastic and pyroelec. meas. 77−59535
Kr, Clausius-Mossotti function, exam. of variation with gas density 78−52418

permittivity continued
Kr, gas, liquid, solid, refractive index, density and dielectric const. 80−66138
La, $(SO_4)_3.9D_2O$, soln. growth, struct., props. 77−77363
$La_{0.9}Ca_{0.7}CrO_3$ polar semiconductor, elec. props., slight reduction effect 80−20183
LaF_3 films, electron beam evaporated, dielec. props. 79−91375
La_2O_3, elec. cond. and dielec. const., 400-1180K, phase transition 79−56224
LaOF, features of formation of band structure 79−33232
$La_4(TiO_4)_3$, electrical props., effect of initially used La_2O_3 *(Polish)* 77−59508
(Li,Na,K) (Nb,Ta)O_3, pseudo-binary and ternary systems quenched metastable glassy and cryst. phases 80−29935
(Li, Na)NbO_3 ceramic, dielectric and electromechanical props. 77−40183
(Li,Na)NbO_3, polycryst. disc, temp. and time dependent dielec. props. 77−81060
$Li_2Ag_{2-x}In_x$, optical props., struct., energy bands, interband transitions 78−72539
$Li_2B_4O_7$, ferroelectric glass, phase transition, permittivity, electrochromism, photochromism 80−80719
LiCd ferrite, dielec. const. and loss meas., 50-10^6 Hz 77−77135
$Li_2Cd_{2-x}In_x$, optical props., struct., energy bands, interband transitions 78−72539
LiCl, colloidal suspension, radiowave dielec. dispersion 80−11311
$LiClO_4$, organic solns., complex permittivity meas., dielec. relax. spectrum *(French)* 78−27154
$LiCsSO_4$, thermal and dielec. props. 80−34860
LiF films, polycrystalline and single-cryst., comparative study of phonons by electron spectroscopy 80−25505
$Li_2Gd_4(MoO_4)_7$, ferroelec. and paramag. props. 78−39517
Li_2GeO_3, components of elastic, piezoelec. and permittivity tensors meas. 77−8518
Li_2GeO_3 piezoelectric glass ceramic, recrystallisation, pyroelectric response, permittivity 80−80703
$Li_{1-x}H_xIO_3$, dielec. behaviour, Raman and IR spectra 77−32357
$LiIO_3$ crystal elastic, piezoelec., dielectric and acoustic props. 79−46740
α-$LiIO_3$, depolarisation current, dielectric const. relaxation behaviour *(Chinese)* 80−88905
α-$LiIO_3$, dielectric constant and elec. cond. of single crystals *(Chinese)* 77−77134
α-$LiIO_3$, ion migration polarisation phenomena, current correlation function *(Chinese)* 80−6539
α-$LiIO_3$ single crystals, electrical conduction and dielectric behaviour *(Chinese)* 78−30783
α-$LiIO_3$, statistical theory of relaxation current and low-freq. dielectric dispersion 78−60391
$LiIO_3$, Stokes and antiStokes scatt. by LF polaritons 77−77202
α-$LiIO_3$, surface polariton spectroscopy, frustrated total reflection method *(Russian)* 80−49628
$LiKSO_4$, thermal and dielec. props. 80−34860
$(Li_{0.5}La_{0.5})_xBa_{1-x}TiO_3$, cryst. struct., dielec. and IR spectral meas. 79−46614
Li_3N, superionic conductor, local ionic motion, anisotropic dielec. behaviour 78−87817
Li_3N, superionic conductor, far IR absorption, temp. and isotope effects 79−51969
$LiNH_4SO_4$ and $LiND_4SO_4$, dielec. pyroelec., and thermal props. 80−60509
$LiNbO_3$, amorphous ribbons, prep., electron and X-ray diffr. obs., dielec. const. temp. depend. 79−50993
$LiNbO_3$, polydomain, nonstoichiometric crysts., elastic, piezoelec., dielec. constants. 77−8513
$LiNbO_3$, Raman spectra and dielec. props. near Curie point 79−38530
$LiNbO_3$, single crystal, dielectric const., dispersion, loss tangent and susceptibility 77−16245
$LiNbO_3$ single crystals, growth from melt, Czochralski method *(Chinese)* 80−76171
$LiNbO_3$, vitreous, anomalous dielectric behaviour and reversible pyroelectricity 77−85658
$LiNbO_3$:$3Li_2O.Nb_2O_5$ eutectic, dielectric props. 79−1743
$LiNb_{1-y}Ta_yO_3$, Czochralski growth and basic props. 77−63556
Li_2O-B_2O_3 glass, conductivity, permittivity, and dielectric loss obs., mixed isotope effect 78−95182
$Li_2SO_4.H_2O$, far IR spectra, H_2O flipping motion, lattice modes 80−84258
Li_2SiO_4, piezoelectric glass ceramic, recrystallisation, pyroelectric response, permittivity 80−80703
$LiTaO_3$, Raman spectra and dielec. props. near Curie point 79−38530
$LiTaO_3$, vitreous, anomalous dielectric behaviour and reversible pyroelectricity 77−85658
$Li_{1+y}Ta_{1.5y}Ti_{6y}O_3$ ($0 \leq y \leq 0.028$), non-stoichiometric phase, crystallographic and dielec. props. 80−75212
LiZn ferrite, dielec. const. and loss meas., 50-10^6 Hz 77−77135
Lu_2O_3, elec. cond. and dielec. const., 400-1180K 79−56224
$MNbO_3$, tetragonal, electronic struct., optical anisotropy 80−70599
MgF_2, complex dielec. const. at audio freqs., 5.5 to 380K 80−25272
MgF_2, rutile structure, dielectric props., neutron and Raman scatt. exam. 78−79684
MgO, dielec. const., 5.5 to 400K 80−50249
5 wt.% MgO-Si_3N_4, hot-pressed, dielec. props. 78−10822
Mg_2SiO_2:SiO_2, elec. and dielec. props. 400-900°C 80−104953
$Mg_{0.25}Zn_{0.75}Fe_2O_4$, ferrite, DC cond., dielec. props., lattice consts. 80−80272
$Mn(ClO_4)_2.6H_2O$-polyacrylonitrile, complex permitt. meas. by time-domain spectroscopy 77−49741
$MoSi_2$ oxide film, dielec. props. and growth kinetics 80−81215
N_2, Clausius-Mossotti function, exam. of variation with gas density 78−52418
N_2-Ar(methane)(ethane) binary and ternary mixtures, dielec. const., excess vol. 80−7254
$ND_4D_2PO_4$, cryst., transverse and longit. elec. susceptibilities, modified Ising model calcs. 80−97203
ND_4DSeO_4, crystals, struct., IR spectra, dielec. props. 80−75919
NH_3, liq., relax. time and activation energy 79−91335
NH_4 halides dielectric const. meas. at 1 MHz 77−16238
$(NH_4)_2BeF_4$, far-infrared and submillimetre dielectric response 80−80782
$(NH_4)_2BeF_4$, gamma-ray effects obs. *(Japanese)* 80−11349

permittivity continued
$(NH_4)_2BeF_4$, polycrystalline, surface layer effects on dielec. behaviour 78−39494
$NH_4Cl(Br)$, effect of NH_4^+ internal motion on elec. and optical props. 80−100454
$NH_4Cl_{1-x}Br_x$, dielectric const. meas. at 1 MHz by immersion method *(Japanese)* 77−90087
$NH_4Cl(Br)(I)$, dielectric const. meas. at 1 MHz by immersion method *(Japanese)* 77−90087
$NH_4H_2AsO_4$-$NH_4H_2PO_4$ solid soln., Curie temp. and permittivity comp. depend. 77−59533
$NH_4H_2PO_4$, cryst., transverse and longit. elec. susceptibilities, modified Ising model calcs. 80−97203
$NH_4H_2PO_4$, Mn^{3+} doping effect on Curie temp. and dielec. permittivity 77−59532
NH_4HSO_4, dielectric relax. in ferroelectric and paraelectric phases 77−16246
NH_4HSO_4, ferroelec., critical slowing down of dielec. relax. *(Japanese)* 77−90109
NH_4HSO_4, ferroelectric powder dielectric behaviour particle size depend. 80−55046
$(NH_4)_3H(SO_4)_2$, phase transitions, dielec. study at low temps. 80−88902
$(NH_4)_3H(SO_4)_2$, press.-induced ferroelectricity, dielec. const. meas. 77−12328
$(NH_4)_3H(SO_4)_2$, pressure-induced ferroelectricity, dielec. const. meas. 78−23412
NH_4HSeO_4, cryst. struct., dielec. and ferroelec. props. 80−60528
NH_4HSeO_4, ferroelec., phase transitions, permittivity and pyroelectricity meas. 80−71350
NH_4HSeO_4, para- to ferroelectric transition obs. by permittivity meas. 79−51916
$(NH_4)_3H(SeO_4)$, ferroelec. transition, press. and temp. effects on dielec. props. 78−23413
$(NH_4)_3H(SeO_4)_2$, ferroelec. phase transition, dielec. meas. 77−63376
NH_4IO_3, effect of hydrostatic press. on ferroelec. phase transition 79−51917
$NH_4IO_3.2HIO_3$, dielec. constant, elec. cond. phase transition and cryst. struct. 80−1999
NH_4LiSO_4, ferroelec., phase transition points, hydrostatic press. effect 77−77155
NH_4LiSO_4, ferroelec., hydrostatic press. effect on I-II phase transition, dielec. meas. 79−38496
$(NH_4)_2SO_4$, pure and Rb doped, ferroelec. transition, light scatt. meas., dielec. and elastic props. 78−43822
$(NH_4)_2SO_4$, static and dynamic dielec. behaviour 80−71337
$(NH_4)_6Sb_4(SO_4)_3F_{12}$, dielec. props. and phase transitions 79−69765
(Na,Li)NbO_3 ceramic, optimum prep. conditions and characterisation 78−3079
Na vapour, induced optical anisotropy *(Russian)* 80−38526
$NaAl(MoO_4)_2$, domain struct., phase transition, and dielec. props. 79−56748
$NaBi(MoO_4)_2$, low-temp. paraelectric, permittivity meas., 4.2-400K 79−95702
$Na_{0.5}Bi_{0.5}TiO_3$, dielectric const. thermal hysteresis, ferroelectric-antiferroelectric transitions 80−50281
$NaBrO_3$, surface polariton spectroscopy, frustrated total reflection method *(Russian)* 80−49628
NaCl, calc. of migration volume of vacancies from macroscopic parameters 78−75872
NaCl, monoelectrolyte, highly mineralised salt soln., dielec. and radiation characts. 80−97184
NaCl(Br) (F) (I), lattice dynamics and statics, three-body-force shell model 80−49323
Na_2CoGeO_4, single cryst. growth and study of their piezoelec. and elastic props. 79−4906
$NaFe(MoO_4)_2$, domain struct., phase transition, and dielec. props. 79−56748
Na_2HAsO_4, hydrogen bonded, ^{75}As NQR study 79−38399
$NaH_3(SeO_3)_2$, dielec. props. 78−43764
$(Na_{0.5}La_{0.5})_xBa_{1-x}TiO_3$, dielec. and IR spectra exam., ferroelec. transition 78−23418
$Na_{1-x}Li_xNbO_3$, dielec. const. and X-ray diffr., for Curie temp. and phase diagrams 78−72768
$Na_{1-x}Li_xNbO_3$ mixture, ferroelec.-paraelec. transitions, dielec. props. meas. 80−66125
$NaNH_4SeO_4.2H_2O$, ferroelectric crystal, effect of hydrostatic pressure on phase transition 78−52453
$NaNO_2$, complex dielectric constant, sinusoidal phase in ferroelectric material 79−11376
$NaNO_2$, compressed powder, dielec. props., surface layer effects 78−76413
$NaNO_2$, ferroelec., dielec. and thermal behaviour 80−80680
$NaNO_2$, incommensurate-and-antiferroelectric phase transition, amplitude mode, ultrasonic study 80−39227
$NaNO_2$, nonlinear dielec. anomaly in paraelec. phase 78−39495
$NaNO_2$, optical harmonic generation near ferroelec. transition 80−91858
$NaNO_2$ powder, surface layer effects on dielec. props. 77−1631
$NaNO_3$, low temp. struct. changes, elec. props. 79−87377
$NaNbO_3$, elec. and thermoelec. props., influence of O defects 80−29401
$NaNbO_3$, hydrostatic press. effect on permittivity, phase transition, hysteresis 80−80670
$NaNbO_3$, photoferroelectric effect 78−35108
$NaNbO_3$-$BaTiO_3$ solid soln. form. and props. *(Russian)* 78−48378
$NaNbO_3$-$SrNb_2O_6$, phase diagram, props. meas. 79−11576
Na_2O-TiO_2-SiO_2 glass, elec. props. and energy gap 78−26921
Na_2SO_4, high temp. phase, DTA and dielec. meas. 79−82333
$Na_3Sc_2(PO_4)_3$, ferroelectric props., X-ray diffr. study 79−69789
$Na_{0.33}V_2O_5$, dielec. const. and microwave cond. 78−60378
$Na_5W_3O_9F_5$, single cryst., prep., optical and dielec. studies *(French)* 80−15994
Nb, anodic oxidation, open circuit transient anal., dielec. and elec. props. of oxide film 80−3245
NbN, opt. consts. and physicochem. spectra 77−85677
$NbSe_3$, freq. depend. conductivity 80−107838
$NdAlO_3$ films, preparation, electrophys. props. in MIM structs. 77−24956
Nd_2O_3, A-type, elec. cond. and dielec. const. 4.2-1200K 77−4340
Nd_2O_3, elec. cond., thermoelec. power, dielectric const. 79−69763
$Nd_2(WO_4)_3$, elec. transport and mag. props. meas. 77−24668
Ne, dielectric constant near liquid-vapour critical point 80−50252
Ne, solid, dielec. const., 4.2-15K 77−8488

permittivity continued
Ni suspension, deermination of dielectric constant 77−40579
Ni-I single crystals, mag. and dielectric props. 80−93095
$Ni_3B_7O_{13}I$, nonlinear magnetoelec. and dielec. props. 79−65704
NiBr boracite single crystals, dielectric, pyroelectric props., vapour phase transport growth 80−80673
$Ni_{0.51}{}^{2+}Fe_{0.46}{}^{2+}Fe_{1.95}{}^{3+}O_4{}^{2-}$, elec. resistivity above 300K 79−78099
$Ni_{0.89}{}^{2+}Fe_{0.13}{}^{2+}Fe_{2.11}{}^{3+}O_4{}^{2-}$, elec. resistivity above 300K 79−78099
$NiSiF_6.6H_2O$, dielec. loss and relax., 100-270K, reorient. mech. 78−35088
$NiWO_4$, AC elec. conductivity, thermoelec. power and dielec. const. 80−70736
NiZn ferrite, dielec. props., Jahn-Teller ion effects 80−97181
P-As-Se glasses, mag. susceptibility, dielec. const., opt. props. 78−64184
P-Se-Tl system glasses, polarisation, refr. index and dielec. const. meas. 80−20608
PLZT ceramic, ageing, dielec. props. 80−88940
PLZT ceramic, dielectric anisotropy, role of 90° domain processes 77−63384
PLZT ceramic, optical gate, dielec., optical props., electro-optical effect meas. 78−42418
PLZT ceramics, diffuse phase transitions and thermodynamics 80−29694
PLZT ceramics, ferroelectric and struct. transitions, crystallographic, thermal, and dielec. anal. 80−29693
PLZT ceramics, modified by $Ca^{2+}(Sr^{2+})(Nd^{3+})(Y^{3+})$, dielec. behaviour 80−60519
PLZT ceramics, phase transitions induced by elec. fields 80−29695
PLZT, effect of ageing on temp. depend. of permittivity, for ferroelectric and antiferroelectric compositions 78−48121
PLZT modified high voltage dielectric, permittivity, Curie temp., loss meas. 80−80720
PLZT, phase transitions, permittivity, birefr. and light scatt. meas. 77−81074
PLZT, RF sputtered thin film, ferroelectric props. 79−69780
PLZT, reduced, exam. of ageing phenomena, using dielectric hysteresis *(German)* 79−33647
PLZT, transparent ferroelec., RF sputtering and film characterisation 78−72727
PLZT, with broad phase transition, birefr., electro-optic and dielec. props. 77−16280
PZT, ferroelec. film, elec. props., composition anal., AES 78−84530
$(Pb,Ba)_5Ge_3O_{11}$ ferroelectric crystals, influence of Pb replacement by Ba on props. 79−87402
$(Pb,La)TiO_3$, paraelec. phase, anomalous dielec. behaviour 78−23387
$(Pb,Sr)_5Ge_3O_{11}$, single crysts., growth and X-ray and dielec. investigations 80−88127
$(Pb,Sr)TiO_3$, ferroelec. props., press. depend., anharmonic oscillator model 80−80716
$Pb_{2-}Sr_{1-z}(Zr_x\text{-}Ti_{1-x})O_3{:}Cr_2O_3$, ferroelec. ceramic, reversible characts. and dielectric losses *(Russian)* 78−84517
$(Pb_{1-x}Ba_x)_5Ge_3O_{11}$, ferroelec. phase transition, dielec. const. and quasi-elastic light scatt. 80−71289
$(Pb_xBa_{1-x})_5Ge_3O_{11}$, electrogyration, and dielectric props. 78−19444
$Pb_{2-x}Ba_xLi_{0.5}Nb_{1.5}O_6$, dielectric const., temp. and Ba conc. 78−64308
$(Pb_{1-x}Bi_x)_5Ge_3O_{11}$, spontaneous and induced electrogyration 79−42946
$PbBi_2Nb_2O_9$ ceramic, grain oriented, dielectric and piezoelectric props. 79−42896
$PbBi_4Ti_4O_{15}$ ceramic, dielec. props., temp. depend. 78−95561
$PbCo_{0.33}Nb_{0.66}O_3$, ferroelectric, exam. of permittivity and dielectric props. 79−1742
$PbCo_2(PO_4)_2$, mag. susceptibility, elec. cond. and optical refl. 79−56495
$PbCo_{1/2}Te_{1/2}O_3$, antiferroelec., high-frequency permittivity, temp. depend. 80−71325
β-PbF_2, complex impedance exam. 78−47579
PbF_2, cubic, dielec. const., ionic cond., soft modes 78−14427
$Pb(Fe_{1/2}Nb_{1/2})O_3$-$La_2O_3(CeO_2)$ ferroelec. ceramics, electrophysical props. 78−35099
$2PbFe_{1/2}Nb_{1/2}O_3$-Pb_2FeReO_6, comp., struct., dielec. and mag. props. 80−2704
$2PbFe_{1/2}Ta_{1/2}O_3$-Ba_2FeReO_6, comp., struct., dielec. and mag. props. 80−2704
$2PbFe_{1/2}Ta_{1/2}O_3$-Pb_2FeReO_6, comp., struct., dielec. and mag. props. 80−2704
$Pb(Fe_{2/3}U_{1/3})O_3$-$PbZrO_3$ solid solns., phase transition 77−48138
$PbFe_{2/3}W_{1/3}O_3$-$BaTiO_3$ system ferroelec., antiferromag., ESR and dielec. props. meas. 77−40172
$PbFe_{(2/3}W_{1/3)}O_3$-$Pb(Co_{1/2}W_{1/2})O_3$ solid soln., crystallographic, dielectric, magnetic props., Mossbauer spectra 78−43807
$Pb_3Fe_2WO_9$, perovskite ferroelec., dielec. permittivity and loss meas. 77−8496
$Pb_3(Ge,Si)_2O$, growth from melt, struct. and dielec. props. 77−44148
$Pb_5(Ge,Si)_3O_{11}$, dielec. and elec. props., 20 to 250°C 80−29697
$PbGeO_3$, cryst. struct., dielec. and optical props. 77−1118
$PbGeO_3$, single cryst. films growth, temp. depend. of dielec. constant 79−100066
Pb_3GeO_5, cryst. struct. dielec. and optical props. 77−1118
$Pb_3Ge_2O_7$, dielectric thin film, obtained by sedimentation, exam. of dielectric props. and structure 80−2282
$Pb_3Ge_2O_7$, vacuum condensates on US irrad. substrates, props. 77−66466
$Pb_3Ge_3O_{11}$, uniaxial ferroelec., thermal expansion and dielec. permittivity in vicinity of transition points 77−66459
$Pb_5Ge_3O_{11}$ bonded Pb(Zr,Ti)O_3 composites, piezoelec. props. 79−78629
$Pb_5Ge_3O_{11}$, dielec. behaviour, 60 Hz-100 kHz, particle size effects 79−33638
$Pb_5Ge_3O_{11}$, dielec. functions above and below ferroelec. transition 79−33588
$Pb_5Ge_3O_{11}$, ferroelec., induced and spontaneous optical activity, permittivity 79−33661
$Pb_5Ge_3O_{11}$, ferroelec., surface capacitance effect on dielec. props., DC cond. and dielec. const. meas. 79−91333
$Pb_5Ge_3O_{11}$, freq. and damping of ferroelec. soft mode, permittivity meas. 77−52027
$Pb_5Ge_3O_{11}$, photodielectric effects, Curie temp., permittivity and polarisation 80−40034
$Pb_5(GeO_4)(VO_4)_2$, elastic and dielectric props. 77−7782
$Pb_5(Ge_{1-x}Si_x)_3O_{11}$, dielec. spectra, ferroelec. behaviour 78−60406
$Pb_5(Ge_{1-x}Si_x)_3O_{11}$, electrogyration, phase transition and dielectric props. 80−93269

permittivity continued
$Pb_5(Ge_{1-x}Si_x)_3O_{11}$ solid solutions, dielec. props., ferroelec. phase transitions 80−15988
$Pb_{1-x}Ge_xTe$, dielec. const. determ. near ferroelec. transition 78−88269
$Pb_{1-x}Ge_xTe$, p-n junctions, elec. characts., effect of ferroelec. phase transition 79−33338
$PbHAsO_4$, ferroelec., far IR and microwave dielec. props. 80−55108
$PbHPO_4$, microwave permitt. and far IR refl. spectra in paraelec. and ferroelec. phases 80−40033
$PbHPO_4$, single cryst., dielec. props. 79−38426
PbI_2, dielectric props., elec. cond., space charge polarisation 80−100631
PbI_2, film, fundamental absorption edge, complex dielec. const. *(Russian)* 77−40266
PbI_2, visible exciton spectrum, exciton-phonon interactions, dielectric const. and oscill. strengths 80−25405
$PbIn_{0.5}Nb_{0.5}O_3$, ferroelectric, dielectric props. 80−103923
$Pb_2KNb_{5-x}Ta_xO_{15}$, ferroelastic-ferroelectric coupling, dielec. props. 79−38433
$Pb_{0.9}K_{0.1}(Zn_{1/3}Nb_{2/3})O_{2.95}$-$PbZrO_3$-$PbTiO_3$, morphotropic tetragonal-rhombohedral phase boundary 78−48129
$PbLaZrNbO_7$, dielectric with zero temp. coeff. of dielect. consts., electrophys. props. 77−52010
$Pb_2Li_{1/2}Nb_{3/2}O_6$, antiferroelec. cryst. growth and props. 77−36189
Pb_2MTeO_6, (M=Ca,Cd,Mg), ferroelec. behaviour, microwave dielec. props. meas. 77−43948
$PbMg_{1/3}Nb_{2/3}O_3$, dielec. props. under high hydrostatic pressure near phase transition point 80−44997
$Pb(Mg_{1/3}Nb_{2/3})O_3$, electrostrictive effect 80−66113
$PbMg_{1/3}Nb_{2/3}O_3$, ferroelec., crit. electron-phonon phenomena and diffuse phase transition in elec. field 79−38497
$PbMg_{0.33}Ta_{0.66}O_3$, ferroelectric, exam. of permittivity and dielectric props. 79−1742
$Pb(Mn_{1/2}Ta_{1/2})O_3$, ceramic, for thermal and dielectric isolation at low temp. 80−39365
$Pb(NO_3)_2$, low temp. struct. changes, elec. props. 79−87377
$PbNbO_3$ thin film microwave complex permittivity meas. 79−73879
$PbNb_2O_6$, O defects and elec. props. anomalies 79−42898
$PbNb_2O_6$, permittivity and elec. cond. meas., first order transition 79−24270
$Pb_2Nb_2O_7$, electric cond. and dielect. props. of cathodic-sputtered films *(French)* 79−33371
$PbNb_{0.5}Sc_{0.5}O_3$, ceramic, dielec. props. 79−11392
PbO, disordered photoconductor, dielec. props., temp. depend. anomalies 78−43765
$4PbO.GeO_2$, X-ray phase and thermal anal., new antiferroelectric 79−1744
$15PbO.3B_2O_3.2WO_3$, struct. and electrophys. characts. 77−84716
$Pb_3(PO_4)_2$ ferroelastic, dielec. consts. and birefringence meas. 78−2793
$Pb_3(PO_4)_2$, ferroelastic, dielectric anomalies, phase transitions, permittivity, relaxation *(Russian)* 80−71293
$Pb_3(PO_4)_2$, phase transition at 180°C, dielectric meas. 79−37831
$Pb_{1-\alpha x}R_xTiO_{3+x(1.5-\alpha)}$, R=La or Sm exam. of permittivity as function of temp. 79−33586
n-PbS, natural galenite, function of wavelength in range 10 to 40 μm 79−42975
PbS(Se)(Te), energy gap and dielec. props., 77 to 373K 80−66100
$Pb(Sb_{1/3}Mn_{2/3})O_3$-$PbTiO_3$-$PbZrO_3$, remanent dielec. polarisation of poled ceramic, heat treatment 79−87390
$Pb_5Sb_8S_{17}$, dielectric props. 78−72452
$PbSc_{0.5}Nb_{0.5}O_3$, single cryst., dielec. props. 80−66126
$PbSc_{2/3}Te_{1/3}O_3$, ferroelec., high-frequency permittivity, temp. depend. 80−71325
$PbSc_{2/3}Te_{1/3}O_3$-$PbSc_{2/3}W_{1/3}O_3$($PbFe_{2/3}Te_{1/3}O_3$) ferroelec. props. and lattice consts. 80−60520
$Pb_{1-x}Sn_xSe$, thin film, opt. props. *(Japanese)* 77−1750
$Pb_{1-x}Sn_xTe$, (x<0.35), permittivity and soft modes, carrier density and comp. effects 80−7256
$Pb_{1-x}Sn_xTe$, soft mode, ferroelec. phase transition crit. temp. and dielec. const. calcs. 77−8530
$Pb_{0.94}Sr_{0.06}(Ti_{0.47}Zr_{0.53})O_3$-NiO, modified, dielec. and piezoelec. props. 80−11342
$Pb_{0.95}Sr_{0.05}(Ti_xZr_{1-x})O_3$, solid solns., parameters of Curie Weiss law, permittivity meas. 78−15129
$(Pb_{0.97}Sr_{0.03})Zr_{0.51}Ti_{0.49}O_3$, ferroelec. phase transition under high press. 77−36188
$Pb_{0.95}Sr_{0.05}(Zr_{0.53}.Ti_{0.47})O_3$, low temp. internal friction in ferroelectric ceramic 77−21200
$Pb_2Ta_{2-x}M_xO_{7-x}$, (M=Ti, Sn Zr), oxygen deficient, form., IR spectra, dielec. const. *(Japanese)* 77−48171
Pb_2TaMnO_6, reaction of form. from oxides, ferroder. props. 80−55326
p-PbTe, lattice dielectric const. in far IR region, magnetotransmission meas. 79−78605
PbTe, lattice permittivity determ. by magnetoplasma waves method 78−19075
n-PbTe, low temperature electrical transport, Hall effect 80−84478
PbTe, TO phonon softening, free carriers and defects effects 78−79720
PbTe very thin epitaxial films, transmission and refl. spectra, 1 to 5 eV, dielec. const. calc. 80−7430
PbTe-SnTe compound semiconductors, lattice instability by mm-wave magnetoplasma refl. 80−54336
$PbTiO_3$, $(PbTiO_3)_{0.9}(B_2O_3)_{0.1}$ amorphous ribbons, prep., electron and X-ray diffr. obs., dielec. const. temp. depend. 79−50993
$PbTiO_3$, anomalies in elec., photoelectric and mechanical props. 80−55051
$PbTiO_3$ ferroelec. thin film, prep. by RF sputtering and dielec. props. 79−100052
$PbTiO_3$ ferroelectric thin films, fabrication by RF sputtering, characts. 80−40261
$PbTiO_3$ single crystals, dielectric permittivity meas., permittivity tensor component determ. 79−99817
$PbTiO_3$-$CaFe_{2/3}W_{1/3}O_3$, solid solutions 78−43816
$PbTiO_3$-$La_2O_3.3TiO_2$, struct. and dielec. props. 80−54200
$PbTiO_3$-$PbZrO_3$-$PbNb_{2/2}Zn_{1/3}O_3$(-$PbNb_{2/3}Co(Mg)_{1/3}O_3$) solid solutions, dielec. and piezoelec. props. 79−87393
$PbTiO_3$-$Pb(Ni_{1/2}W_{1/2})O_3$ system, solid soln. form., struct., dielec. props. and thermal expansion *(Japanese)* 78−27501
$xPbTiO_3+(1-x)PbCd_{1/3}Nb_{2/3}O_3$, phase transition spread, polarisation relaxation, dielectric susceptibility *(Russian)* 80−75922
$Pb_3(VO_4)_2$-$Pb_3(PO_4)_3$ solid solutions, ferroelastic, dielec. consts. and birefringence meas. 78−2793
$Pb_3(VO_4)_3$, ferroelastic, dielec. consts. and birefringence meas. 78−2793

permittivity continued
$Pb(Z,Ti,Mg,W)O_3$, low-Q ceramics, props. and transducer appl. 80−75944
$Pb_{1.8}Zn_{0.15}Na_{0.05}Nb_2O_{6.95}F_{0.05}$, electric cond. and dielect. props. of cathodic-sputtered films *(French)* 79−33371
$Pb(Zn_{1/3}Nb_{2/3})O_3$, diffuse phase transition, electro-optical and dielec. obs. 79−82933
$Pb(Zr,Ri)O_3$:Ni-silicon rubber flexible composite pyroelectric, dielectric props. 80−80704
$Pb(Zr,Ti,Nb)O_3$ ceramics, rel. dielec. const. and piezoelec. props. rel. to porosity 79−11388
$Pb(Zr,Ti,Sn)O_3$ ceramics, ferroelec., doped with tri- and pentavalent oxides, piezoelectric props. 78−19413
$Pb(Zr,Ti)O_3$ ceramic, permittivity and resonant frequency ageing, space charge field effects 77−85657
$Pb(Zr,Ti)O_3$ ceramic-polyvinylidene fluoride composite film, complex piezoelec. props. 78−64323
$Pb(Zr,Ti)O_3$ ceramic/polymer, composite systems, piezoelec. props. 79−99823
$Pb(Zr,Ti)O_3$ ceramic, interconnected porous, props. 80−43579
$Pb(Zr, Ti)O_3$ ceramics, low temp. sintering, elec. and mech. props. 80−71616
$Pb(Zr,Ti)O_3$ ceramics with ladder type struct., prep. and props. 80−75945
$Pb(Zr,Ti)O_3$ ceramics, DC field sintering preparation, piezoelectric props., ageing behaviour 80−81211
$Pb(Zr,Ti)O_3$, dielectric response in solid-medium high-pressure device 78−43766
$Pb(Zr, Ti)O_3$, ferroelectric ceramics in solid matrix, temp. and quasi-hydrostatic pressure effects 77−16259
$Pb(Zr,Ti)O_3$ film, ferroelec. and optical props. 77−85674
$Pb(Zr,Ti)O_3$ films, ion beam sputtering, dielec. and ferroelec. props. 79−78881
$Pb(Zr,Ti)O_3$ films, ferroelec., ion beam deposition sputtered from multi-component targets 80−80974
$Pb(Zr,Ti)O_3$ internally electroded multilayers, piezoelectric props., permittivity, transducers 80−80672
$Pb(Zr,Ti)O_3$, internally electroded with Pt, resonance behaviour 80−84701
$Pb(Zr,Ti)O_3$, porosity-permittivity relations, depolarising factors determ. and pore effects *(Japanese)* 80−97189
$Pb(Zr,Ti)O_3$ thin films, fabrication and characterisation electron-beam deposition 80−16188
$Pb(Zr,Ti)O_3$ thin film, ferroelec., fabrication by RF sputtering *(Japanese)* 80−25560
$Pb(Zr,Ti)O_3$:Cr_2O_3 ceramic, electrical cond. and dielectric const. meas. 80−2389
$Pb(Zr,Ti)O_3$:Fe(Nb) ceramic, elec. and electromechanical props., depend. on dopants 80−81212
$Pb(Zr,Ti)O_3$:$PbTiO_3$ (up to 5%), dielec. props. and ferroelec. transitions 77−20806
$Pb(Zr,Ti)O_3$-$Pb_3Ge_5O_{11}$ ceramic, sintering conditions rel. to piezoelec., dielec. props., microstruct. 77−16252
$PbZr_{1-x}Ti_xO_3$, paraelec. phase, first-order phase transition 77−89540
$PbZrO_3$ based ferroelec. ceramic, pressure-temp. phase diagrams 79−24273
$PbZrO_3$, phase transitions, X-ray, dielec., and thermal anal. 80−45020
$PbZrO_3$ pyroelectric detector, low temp. behaviour, expt. 80−31869
$PbZrO_3$, struct. phase transition 79−61312
$PbZrO_3$-monocryst., elec. cond., permittivity, polarisation, para- and ferro- to antiferroelec. phase transistions 78−60402
$PbZrO_3$-$PbCd_{0.5}W_{0.5}O_3$, phase transitions 78−43817
1-x$PbZrO_3$-x$PbSc_{0.5}Nb_{0.5}O_3$, $0\leq x\leq 1$, phase transitions, X-ray, dielec., and thermal anal. 80−45020
$PbZr_xTi_{1-x}O_3$ ceramics, morphotropic phase boundary 80−81035
$Pb(Zr_xTi_{1-x})O_3$, elec. props. temp. and composition depend. 78−47817
$Pb(Zr_xTi_{1-x})O_3$ films, ion beam deposition, struct., dielec. and ferroelec. props. 80−20788
$PbZr_xTi_{1-x}O_3$ solid solutions, tricritical behaviour 78−80296
$Pb(Zr_{0.47}Ti_{0.43}Sn_{0.10})O_3$:$Cr_2O_3$, ferroelec. ceramic, reversible characts. and dielectric losses *(Russian)* 78−84517
$Pn_2Nb_2O_7$, relax. phenomena, meas. of dielec. const., polarisation and sp. ht. 77−4597
$PrCl_3$, cooperative Jahn-Teller ordering of elec. dipoles in non-Kramers doublets 78−15115
$PrCl_3$, one and three dimensional antiferroelec. ordering 77−4607
$Pr(NbO_3)_3$ form. mechanism, struct., dielec. props. 77−16235
Pr_6O_{11}, mag. and transport props., multiphonon hopping conduction 78−19211
RTiNbO$_6$, R=rare earth, electrophys. props. 78−23388
$Rb(B,W_{3-x})O_9$ (B=Na, Ca, Co, Ni, Cd, Ga, Bi, Nb, Ta) cryst. struct., temp. dielec. anomalies 80−1998
RbCN, molecular motion and ordering from dielec. and Raman techniques 79−73932
$Rb_2Cd_2(SO_4)_3$, pyroelectric and dielectric props., ferroelectric transitions 79−38458
RbCl:Li^+, new off-centre defect system, studied with dielec. techniques under hydrostatic press. 79−19834
$RbFeF_4$, two dimensional structural phase transitions, sp. ht., optical, dielec., X-ray diffr. meas. 79−69240
RbH_2AsO_4, attenuation const. meas. by SHF dielec. resonance, Curie point 79−47406
RbH_2AsO_4, phase transition, dielec. pyroelec. and internal friction meas. 77−16261
RbH_2PO_4, attenuation const. meas. by SHF dielec. resonance 79−47406
RbH_2PO_4, critical and tricritical phenomena, susceptibility, exponents 80−75976
RbH_2PO_4, high temp. phase transition, dielec. const., elec. cond. and IR refl. meas. 78−43118
RbH_2PO_4, static dielec. props., and Curie temp., press. depend. 79−87405
$RbHSO_4$, acoustic and dielectric props. near phase transition 80−55053
$RbHSO_4$, compressed powder, dielectric const. and particle size, 77-335K 78−76371
$RbHSO_4$, dielec. dispersion near ferroelec. phase transition 80−2684
$RbHSO_4$, ferroelec., Curie-Weiss behaviour, dielec. const. meas. *(Japanese)* 77−43940
$RbHSO_4$, ferroelec. with small Curie-Weiss const., dielec. props. 78−39496
$RbHSO_4$, ferroelec., dielec. dispersion 80−97179

permittivity continued
$RbHSO_4$, isotope effect, dielec. const. and spin polarisation investigation 80−20574
$RbHSO_4$, phase transition, sp. ht. and dielec. permittivity meas. 77−85672
$Rb_3H(SO_4)_2$, and $Rb_3D(SO_4)_2$, dielec. props. and phase transitions 80−60482
$Rb_3H(SO_4)_2$, phase transitions at 56°C and 126°C, dielec. const. meas. 78−76405
$RbHSeO_4$, ferroelec. props. and domain struct. 79−78637
$RbHSeO_4$, successive phase transitions 80−15985
$RbH_3(SeO_3)_2$, dielec. relax. near ferroelec. Curie temp. 80−97207
$Rb_3H(SeO_4)_2$, phase transitions, dielec. behaviour 79−90777
$RbLiSO_4$, thermal and dielectric props., ferrielectricity 79−28688
$Rb_2Mg_2(SO_4)_3$, langbeinite type cryst., search for ferroelec. phase transition 77−59535
$RbNO_3$, permittivity and dielec. cond. press. up to 5 kbar, antiferroelec. transition obs. 77−36183
$RbNO_3$, single cryst., DC cond., dielec. and thermophys. props., temp. depend., transitions interpret. 78−26682
$RbNbW_2O_9$ crysts., growth and props. 80−104054
Rb_2SO_4-$(NH_4)_2SO_4$ mixed cryst., ferroelec. transition, structural and dielec. props., proton spin-lattice relax. 78−39512
$Rb_6Sb_4(SO_4)_3F_{12}$, dielec. props. and phase transitions 79−69765
Rb_2ZnBr_4, dielectric const. and ferroelectric hysteresis 78−84535
Rb_2ZnBr_4, ferroelectricity, hysteresis loops and dielec. const. meas. 78−23416
Rb_2ZnCl_4, dielec. dispersion, 5-900 MHz, near incommensurate-commensurate transition 80−60522
Rb_2ZnCl_4, ferroelectricity, hysteresis loops and dielec. const. meas. 78−23415
rubber, gamma radiation effects on dielect. parameters, expt. *(Hungarian)* 78−59836
SF_6, critical isochore, dielectric const. critical anomaly upper bound 80−84679
$Sb_{1-x}Bi_xSI$, mixed cryst., ferroelec. phase transition 79−33629
$SbNbO_4$, ferroelec. film characts. 77−48127
$SbNbO_4$ single crystals, pure and doped, growth and pyroelec. and ferroelec. props 80−40248
$SbNbO_4$:$CoO(Fe_2O_3)(TiO_2)$, growth, pyroelectric and ferroelectric props. 79−73886
Sb_2S_3, amorphous and crystalline thin films, optical consts. 79−91518
Sb_2S_3, phase transitions and improper photoconductivity, effect of growth conditions *(German)* 78−39515
Sb_2S_3, thin film, dielectric props. 79−15392
SbSI, aggregates of needle-like crystals, nonstoichiometric, ferroelectric properties *(Japanese)* 78−43821
SbSI, central mode, microwave freqs. 79−19852
SbSI, cryst., low temp. dielec. anomalies and domain struct. 80−40035
SbSI, domain struct. relaxation 78−48135
SbSI, dynamic dielectric nonlinearity, in microwave band 78−35109
SbSI, ferroelec., dielec. props. 79−38428
SbSI ferroelectric, dielectric behaviour, particle-size dependence 78−2811
SbSI, free energy function, temp. depend. and anisotropy of dielec. const., ferro- and paraelec. phases 78−64330
SbSI, paraelec. phase, microwave reson. dielec. dispersion, near T_c 79−99839
SbSI single crysts., nonlinear dielec. effects and microelectronic applics. 77−43944
SbSI, single- and poly-domain, complex permitt. and dielec. relax. losses 79−28699
$SbSI_xBr_{1-x}$, T-p-x phase diagram *(Russian)* 77−16241
Sb_2Se_3 single crysts., phys. prop. anomalies, 400-450K *(German)* 79−38072
Sc, electronic excitations, charact. energy loss meas. up to 50 eV 80−60723
Sc_2O_3, electronic excitations, charact. energy loss meas. up to 50 eV 80−60723
Se, trigonal, electronic props. under press. 77−31939
Se-Ge-Te, chalcogenide glass, elec. cond. and dielec. const. 80−75567
Se-Ge-Te glass, dielectric meas. 79−87382
Si, complex permittivity and cond., microwave meas. 79−65784
Si oxide film, porous Si layer oxidation, dielec. props. 80−55556
Si p-channel MOS structure, stress effects on elec. props., press. transducer props. 80−100526
Si powder semicond., microwave propagation, Rayleigh limit 79−78126
Si-CaF_2 film, dielectric const. and selective solar absorption 78−2937
Si-MgO film, dielectric const. and selective solar absorption 78−2937
$Si_{(6-z)}Al_zO_zN_{(8-z)}$, sialons, hot-pressed, dielec. props. 78−10822
$Si_{6-x}Al_xO_xN_{8-x}$, x=1.5, 3, 4, Sialon ceramics, elec., thermal cond. 79−33124
$Si_{100-x}Au_x$, amorphous, dielec. anomaly, rel. to nonmetal-metal transition 78−2791
Si_3N_4, hot-pressed, dielec. props. 78−10822
SiO_2, chem. bond and rel. props. 77−43199
SiO_2 film formed by ion implantation, dielectric props. 78−35090
SiO_2 films, DC plasma Si anodisation, dielectric const., O_2 pressure influence 80−70564
SiO_2 films, thickness and dielectric const., elec. cond. mech. *(Japanese)* 79−8084
SiO_2, fused, as-received and irrad., dielectric props. 79−65786
SiO_2 gel, hydrocarbon suspension, temp. depend. of electroviscous effect and dielectric parameters 79−79299
SiO_2, hydrated vitreous, spectrum of low-energy dipolar states, dielec. const., dielec. losses and relax. 77−90098
SiO_2, thin film, prep. from low-temp. oxidation of tetraisopropoxysilane, dielec. props. 77−8759
SiO_2, vitreous, effect of neutron irrad. on low temp. dielec. susceptibility 79−73878
SiO_2-Al_2O_3-R_2O_3-MgO-TiO_2, T=rare earth of Ce group, glass-ceramic permittivity comp. depend. 77−43928
SiO_2-B_2O_3-Li_2O-Al_2O_3 (28, 2, 1 wt.%) glass, dielec. const. at 3 GHz 80−93233
Sm_2O_3, B-type monoclinic, DC(AC) elec. cond., thermoelectric power, dielectric const., temp. depends. 80−59980
Sm_2O_3, elec. cond., thermoelec. power, dielectric const. 79−69763
SmS, optical props. and electronic struct., Kramers-Kronig model anal. 79−69859
Sn, liq., optical props., 0.62-3.7 eV 80−75996

permittivity continued
$SnCl_2.2H_2O$, layered, dielectric anomaly calc. using Ising model, possibility of antiferroelectricity 77−12341
$Sn_2P_2S_6$, illumination effect on soft mode and dielectric props., luminesc. study *(Russian)* 80−50420
$Sn_2P_2S_6$, investigation of p-T diagram near a singular point *(Russian)* 80−88937
Sn_2S_3, mixed valence semicond., long wavelength phonons, full space group theoretical anal. 79−65873
Sr-Ti-O system, perovskite oxides, nonstoichiometry rel. to dielectric const. 77−80628
$Sr_{0.5}Ba_{0.5}Nb_2O_3$ piezoelectric transducer, SAW props. 80−79037
$Sr_{0.5}Ba_{0.5}Nb_2O_6$ crystals, ferroelec., dislocation free, pyroelec. props. 79−42907
$Sr_{0.61}Ba_{0.39}Nb_2O_6$, electromechanical props., permittivity, elastic compliance, piezoelectric moduli 80−29691
$Sr_{0.75}Ba_{0.25}Nb_2O_6$, ceramic ageing dielec. props. 80−88940
SrClF, SrBrF, reacted flux growth, dislocation density, dielec. consts. and losses IR spectra 77−36214
SrF_2, dielec. const., 5.5 to 400K 80−50249
SrF_2, electronic polarizability and dielectric const., strain derivatives 78−19406
SrF_2:Er, activation vol. for interstitial motion, dielec. const. meas. 80−49412
SrF_2:La, type-I dipole reorientation, activation vol. determ. from dielec. const. 80−88916
SrF_2:rare earth, dipolar complex exam. 79−38435
$SrGa_2Si_2O_8$-$SrGa_2Ge_2O_8$, solid solution, exam. of elastic and electrical props. 79−96057
$Sr_2KNb_{5-x}Ti_xO_{15-x}F_x$ and $Sr_{2-x}K_{1+x}Nb_5O_{15-x}F_x$, ferroelectric props., F substitution effect 77−12331
$Sr(NO_3)_2$, low temp. struct. changes, elec. props. 79−87377
$Sr_{1.8}Na_{0.1}Nd_{0.1}Ta_2O_7$, solid soln., ferroelectric phase transitions, dielec. constant and thermal expansion rel. to temp. 80−88934
$Sr_2Nb_2O_7$, ferroelectric phase transitions, dielec. constant and thermal expansion rel. to temp. 80−88934
$Sr_2Nb_2O_7$, phase transition at 215°C, physical props. obs. 79−56744
SrO, dielec. const., temp. and press. depend. 79−65789
$Sr_2Ta_2O_7$, ferroelectric phase transitions, dielec. constant and thermal expansion rel. to temp. 80−88934
$SrTeO_3$, ferroelec. vacuum condensates 77−40180
$Sr_6Ti_2Nb_4O_{20}$, new class of layer ferroelectrics. X-ray anal. and permittivity meas. 77−16266
$Sr_nTi_{n-4}Nb_4O_{3n+2}$ layer ferroelectrics, physical props. 78−10854
$SrTiO_3$, dielec. nonlinearity and parametric interactions at low temps. 79−38430
$SrTiO_3$, dielec. props. in microwave region, 4.2-78K 77−16239
$SrTiO_3$ film, behaviour of ferroelecs. in strong elec. microwave field 79−42884
$SrTiO_3$ film, surface layer nature, AES obs., and effect on permittivity 77−24498
$SrTiO_3$ glass ceramics, polarisation and dielec. const., 4-77K 77−32319
$SrTiO_3$, intrinsic quantum paraelec. below 4K, dielec. const. meas. 79−73877
$SrTiO_3$, permittivity, temp. depend., submm. spectroscopy 77−176
$SrTiO_3$, undispersive nonlinear dielectric, third harmonic generation *(Russian)* 80−95955
$SrTiO_3$, vacuum condensates on US irrad. substrates, props. 77−66466
$SrTiO_3$-$Bi_2Ti_2O_7$-$CaTiO_3$ system, solid solns., elec., optical props. 79−11375
$SrTiO_{3-x}$-In contacts, differential capacitance, elec. field depend. permittivity effect 80−54779
TGS, ferroelec. cryst., complex permittivity at microwave freq. and high press. 80−2685
TGSe, ferroelec. cryst., complex permittivity at microwave freq. and high press. 80−2685
TGSe:D,L-α-alanine crysts. with large unipolarity, dielec., piezoelec., elastic props. and internal friction 79−33615
Ta-Ta_2O_5-Au capacitive system, freq. depend. of dissipation factor, dielectric const., conductance *(Spanish)* 77−69426
Ta-Ti-O, reactive sputtered film, elec. props. 78−84336
Ta_2O_5, elec. props. as dielec. in Ta solid dielectric capacitor *(Spanish)* 78−19405
Ta_2O_5, film, dielec. props. meas., two layer Maxwell-Wagner model 78−76373
Ta_2O_5 film, for MIS device, CVD and characterisation 77−4742
Ta_2O_5 film, reactively sputtered on SI, dielectric and optical props. obs *(Bulgarian)* 80−89144
Ta_2O_5, reactive DC sputtering deposited films with magnetron-plasmatron, mechanical elec., optical props. 80−25566
Ta_2O_5-TiO_2, anodic film, Rutherford backscatt., capacitance 77−16734
$Tb_2(MoO_4)_3$, improper ferroelectric, dielectric props., IR radiation pyroelectric detection 80−80711
Tb_2O_3, B-type monoclinic, DC(AC) elec. cond., thermoelectric power, dielectric const., temp. depends. 80−59980
$Tb_{1-x}Sn_xTe$, ferroelectric transition calc., effect on carrier density 77−85673
$TbVO_4$, dielec. meas. at Jahn-Teller transitions 77−24802
Te, Faraday-type microwave Kerr effect 79−23998
TeO_2, ferroelectric glass, phase transition, permittivity, electrochromism, photochromism 80−80719
TeO_2 thin films, dielec. props. rel. to fabrication conditions 80−97199
TeO_2-WO_2 glass, dipole correlations, capacitances and TSC meas. 79−28670
ThO_2 ceramics, CaO and Y_2O_3 stabilised density, elec. cond., permittivity 78−47838
Ti, electropolished, optical props. from 1.8 to 3 eV 80−85088
Ti loaded composite, X-band permittivity/temp. characts. obs. 77−2664
Ti-Al_2O_3 system mixed films, prep., phase comp., struct. and elec. props. 79−37930
TiN, opt. consts. and physicochem. spectra 77−85677
TiO_2 based ceramic dielec. materials, medium permittivity, elect. charact. 78−35086
TiO_2 film, RF sputtering, dielec. props. and X-ray phase analysis 78−80288
TiO_2, nonstoichiometric rutile, dielec. props. 10 Hz to 30 kHz 77−28507
TiO_2, porosity-permittivity relations, depolarising factors determ. and pore effects *(Japanese)* 80−97189
TiO_2, reactive DC sputtering deposited films with magnetron-plasmatron, mechanical elec., optical props. 80−25566
TiO_2 rutile, dielec. const., 10^2-10^7 Hz, DC bias effect 79−78603

permittivity continued
TiO_2, sintered ceramic, props. rel. to additives, impurities 78−35329
TiO_2-Fe_2O_3-CaO-V_2O_5 system ferrites, TiO_2 content and thermomag. effects on dielec. props. 77−43927
TiO_2-Ti_2O_3-P_2O_5, glass form., struct. and elec. props. 80−44592
TiO_3:Cr_2O_3, dielec. consts., AC and DC resist. 80−20186
$(Tl,NH_4)_2Cd_2(SO_4)_3$, langbeinite type mixed cryst., ferroelec. transitions, dielec. and elastic meas. 78−2810
Tl halides, static dielec. constant, strain derivatives 80−100629
Tl halides, strain derivatives of elastic and dielectric consts. 79−60421
TlBr, CsCl and NaCl phases, atomic interactions and lattice statics and dynamics 78−83889
TlBr, dielectric behaviour under hydrostatic press. 78−52420
TlCl, dielectric behaviour under hydrostatic press. 78−52420
TlD_2PO_4, antiferroelectricity, permittivity, electric field double hysteresis loops 80−60512
$TlGaS_2$, mechanism of cond., AC cond. and permittivity meas. 78−14754
$TlGaS_2(Se_2)$ film, elec. and photoelec. props. *(Russian)* 78−52109
$TlGaSe_2$, mechanism of cond., AC cond. and permittivity meas. 78−14754
TlH_2PO_4 and TlD_2PO_4, press. effect on dielec. props. 79−99832
TlH_2PO_4 and TlD_2PO_4, dielec. props. under hydrostatic press. up to 7 kbar 80−29696
TlH_2P0_4, calorimetric and dielectric exam. of phase transition, nearly crit. case. 77−40171
TlI, magnetoabsorption, exciton effective dielec. const. 77−28593
$TlNbO_3$, ceramics, hysteresis loops and dielec. props. 79−42885
$TlTaO_3$, ceramics, hysteresis loops and dielec. props. 79−42885
Tl_2TaO_6, Tl I lone pair stereochem. activity rel. to ferroelectricity 78−15131
$Tl_2Ti_4O_9$ ceramics, hysteresis loops and dielec. props. 79−42885
Tm_2O_3 film, between Al electrodes, prep. and elec. props. 80−60103
Tm_2O_3 film, electron beam deposition, elec. props., and struct. 79−87580
$TmVO_4$, dielec. meas. at Jahn-Teller transitions 77−24802
V, energy gap determ. by optical methods *(Russian)* 78−30867
VN, opt. consts. and physicochem. spectra 77−85677
VO_2, elec. cond. and dielec. props. 79−11379
V_2O_5, dielec. polarisation, permittivity meas., 50-200K *(Russian)* 78−39498
V_2O_5-In(Tl)$_2O_3$, ceramic, elec. resist., dielec. props., porosity 77−8093
V_2O_5-MoO_3-P_2O_5 glass, semicond., DC cond., dielec. props 79−91044
V_3Si film, optical props. *(Russian)* 80−93418
VTe, mag. and elec. transport props. 80−92897
W, anodic oxidation, effect of electrostriction, ellipsometry meas. 78−92394
W, anodic oxidation, open circuit transient anal., dielec. and elec. props. of oxide film 80−3245
W-MgO cermet film, dielectric const. and selective solar absorption 78−2937
WO_3 amorphous anodic film growth on W in acidic soln. 80−81232
WO_3 amorphous film, elec. cond. and dielec. const. 78−60238
WO_3-P_2O_5 glass, AC cond. and dielec. props. 80−92717
Xe, gas, liquid, solid, refractive index, density and dielectric const. 80−66138
Y, electronic excitations, charact. energy loss meas. up to 50 eV 80−60723
Y_2O_3, electronic excitations, charact. energy loss meas. up to 50 eV 80−60723
Y_2O_3-AlN-SiO_2 oxynitride glasses, elec. props. 80−80267
Y_2O5d3 films, preparation, electrophys. props. in metal-oxide-metal structs. 77−24956
Yb_2O_3 film, amorphous, electron beam deposited, dielec. props. 79−91339
$Zn_{1-x}Cd_xS$ films, polycryst., reactively sputtered, MSM struct. obs. of dielec. props. and cond. mechanism *(French)* 78−14841
ZnO ceramic varistors, trapping by localized states, effect on dielec. and elec. props. *(Russian)* 79−28671
ZnO, elastic, piezoelec. and dielec. props. 80−108157
ZnO film, sputtering using Zn target, technique and characterisation 78−3040
ZnO particles, average dielectric const. generalised theory, appl. to IR spectra 79−28667
ZnO, photodielectric effect, space-charge polaris. 79−60872
ZnO, varistor, low temp. AC props. 79−38434
ZnO-Bi_2O_3-CoO-MnO-Sb_2O_3 (97.5, 0.5, 0.5, 1.0 mole%), exam. of elec. props. at different annealing temps. 80−3099
ZnO-SnO_2-M_xO_y, M_xO_y=glass-forming additive, I-V charact., heat treatment effects 77−43595
ZnS, natural and stress induced birefringence dispersion 78−6651
ZnS:Cu powder exam. of dielectric constant anomaly, in terms of polarisation catastrophe phenomena 79−51897
$ZnSiF_6.6H_2O$, dielec. props., 100-270K, rel. to $NiSiF_6.6H_2O$ 78−35088
$ZnSnAs_2(P_2)$ single crysts., refl. spectra, band struct., dielec. consts. 77−44022
Zr, electronic excitations, charact. energy loss meas. up to 50 eV 80−60723
ZrF_4 based glass, elec. and dielec. props. in freq. and temp. ranges 5-500 kHz and 130-280°C *(French)* 79−23772
ZrN, opt. consts. and physicochem. spectra 77−85677
ZrO_2, electronic excitations, charact. energy loss meas. up to 50 eV 80−60723
ZrO_2 film, CVD from organometallic cpds. and characterisation 78−23626

permittivity measurement
aggressive liquids, cell for meas. of dielec. props. 78−21170
agricultural materials, determination using time-domain reflectometer 79−71482
allyl ether, dielectric relaxation obs. at millimetric wavelengths 80−71311
anisotropic dielectrics parameter meas. using resonance of waveguide-dielectric system 80−27274
anisotropy meas. at microwave freq., experimental results 80−52279
anistropic specimen, dielectric const., NDT 80−35475
apparatus for measuring dielec. const. of solids at 40 to 1500 MHz *(Japanese)* 77−87780
aqueous solutions, using HF time domain spectroscopy, problems 77−74440
automatic dielcometer for polymers dielec. relax. meas. 77−45864
permittivity measurement continued
automatic equipment, for solid and liquid dielectrics meas., temp. dependence *(Polish)* 78−32836
automatic system for meas. with high interference rejection *(German)* 80−90864
biological liquids at microwave freqs. 80−26424
biological specimen complex permittivity meas. bench for 2-10 GHz at 77-300K *(Russian)* 77−32966
biological substances at RF and microwave frequencies 80−52275
biomaterial microwave complex permittivity meas., noninvasive selective exposure 79−20729
1-butanol, permitt. meas. by transmission time domain spectroscopy 77−67462
capacitor for wide-range dielectric constant meas. on fluids 80−4737
cavity method of dielectric constant meas., freq. and mode errors 80−13103
cavity perturbation measurements, elimination of influence of non-ideal microwave circuit 79−88979
ceramic low-loss foils, microwave meas. method *(Polish)* 78−37028
chlorobenzene, permitt. meas. by transmission time domain spectroscopy 77−67462
coal, bituminous, meas. as function of freq., polarisation, EM wave direction and temp. 79−12113
coaxial line resonator used for complex dielectric data measurement 78−8419
coaxial lumped capacitance resonators design for dielec. material investigs. 77−67460
complex, at microwave freq. of nonmagnetic materials, rapid determ. *(German)* 78−21161
complex, of dielec. materials, at microwave, two coupler method 78−21167
complex, of liquid dielec., meas. method 77−82558
complex, transformation of, use in determ. LF dispersions in solids *(German)* 77−90089
complex dielec. const., wide-range dynamic measurements using microcomputer control techniques 80−22383
complex dielectric constant meas. of thin foils in mm-wave region, method *(German)* 79−58755
complex dielectric permittivity, lumped-capacitance method time domain spectrosc. obs. 79−85149
complex permittivity, accurate meas. for wide range of materials in H_{01n} mode cylindrical resonator *(Polish)* 80−73383
complex permittivity, real part meas. apparatus *(German)* 79−67338
complex permittivity determ. for wide range of materials in coaxial cavity resonator with lumped capacitance *(Polish)* 80−73382
complex permittivity meas. using cylindrical cavity resonator in H_{01n} mode, approx. method *(Polish)* 80−73384
complex permittivity of liquids at mm/cm wavelengths, quadratic convergence curve fitting technique 80−13097
complex permittivity on liquid and solid dielectrics at mm and sub mm wavelengths 77−18011
conducting solns., highly, using transformer ratio arm bridge, 10^2 to 10^6 Hz 79−80641
conductive liquids, measurement using coaxial line system 79−93164
conductive materials, Sh2-3 dielectric constant meter (USSR) 80−62689
cylindrical TE_{01n} cavity, measurement of complex permittivity using approx. anal. method 79−49254
Dextrane in aqueous solution, dielec. relaxation at microwave study 77−77143
dielectric constant meter, Tangens-2M, sensitivity and static charact. anal. 78−45651
dielectric cylinders, microwave meas. of permittivity using retarded waves *(Czech)* 80−95111
dielectric detector in LF freq. range 78−29126
dielectric discs in rectangular waveguides *(Russian)* 77−18050
dielectric films and plates, nondestructive method 78−57987
dielectric loss measurements at microwave frequencies of rectangular waveguides *(Russian)* 79−2788
dielectric material, microwave freq. using open transmission line resonator 77−26333
dielectric props. of biological substances, physical meas. 80−94417
dielectric sheet materials, at 35 GHz, free-space transmission technique 78−62208
dielectric spectroscopy, combined total reflection-transmission method 78−86295
dielectric thin film permittivity calc. in partly-filled resonator cavity 78−45652
dielectric time domain spectroscopy, transmission method 77−74441
dielectric time domain spectroscopy, transmission methods 77−67462
dielectrics, UHF, using waveguide-dielectric resonances 77−55760
dielectrics, using resonator terminated by infinite sample 79−21777
dielectrophoretic, effects of sample size 80−13094
dielectrophoretic levitation method 80−52264
dispersive Fourier transform spectrometry, dielec. meas. on low-loss materials at millimetre and submillimetre wavelengths 77−37916
dispersive Fourier transform spectroscopy, submillimetre wave, with variable thickness variable temp. liquid cells 77−37915
electrolyte solution, HF elec. cond. and dielec. const., determ. in RF region 77−21396
electrophotographic liquid developer, permittivity and conductivity meas. *(German)* 78−62257
electrostatic force meter, device for undergraduate laboratory 79−17164
EM waves, parallel polarised, equal reflectance at normal and oblique incidence, dielec. const. meas. 80−1119
extended standing wave method, for low dielec. loss meas., permittivity, loss angle calc. *(Japanese)* 77−45869
ferrite rods in mode E_{010} resonators 79−71483
ferroelectrics, dielec. props. in vicinity of phase transition, microwave method 78−74022
film and slab-like materials, open transmission line UHF CW phase technique 79−35778
glass-plastic, engineering, nondestructive structural identification 78−92422
ground, determination using EM methods, review 80−22382
hemispherical dielectric permittivity cell for low temps. 78−70161
heterogeneous dielectric, resistivity and static dielec. permittivity determ. in linearly time depend. elec. field 80−52268
high precision measuring device 80−4742
high-field meas. at VLF *(French)* 80−98933
high-loss dielectrics, applic. of cavity perturbation method 78−24815

permittivity measurement continued
homopolar devices, rotation of DC glow discharge, Doppler shift of spectral lines 80−33838
human serum and erythrocyte microwave complex permittivity meas. 80−3889
immersion method for meas. of dielec. const. of solids *(Japanese)* 77−90087
insulating materials, three-terminal cell for meas. over wide freq. and temp. ranges 80−37053
lanoline emulsion of KCl aqueous solutions, 1 MHz to 70 GHz 77−77144
liquid, complex permittivity measurement by node displacement method *(Russian)* 78−27155
liquid, dielec. spectroscopy at microwave freqs. 77−41646
liquid and solid complex permittivity meas., rectangular waveguide method 80−15941
liquid and spherical particle permittivity meas. by dielectrophoretic levitation 79−17447
liquid chromatography detector based on dielec. const. meas. 77−21436
liquid complex permittivity meas., 100 GHz to 18 THz 77−8490
liquid dielec., sub-mm wave, using laser- and Fourier transform-spectrometry 78−95568
liquid dielectrics, method and apparatus 78−241
liquid drops, size and dielectric const. determ., active microwave system 78−54339
liquids, complex dielectric const., modified Hippel method *(German)* 80−31801
liquids, dielec. const. meas., student experiment appl. 77−37696
liquids, modified microwave cavity perturbation techniques 80−42239
liquids under shear, Couette cell for birefringent, viscous and dielectric props. meas. 78−37034
liquids with high dielectric losses, 300 MHz to 6 GHz *(German)* 80−13106
loss angle/permittivity meas. as function of temp. at 9-10 GHz 77−82559
lossy dielectrics, at millimetre wave freq. 79−30492
lossy high dielec. constant materials, method, biological appl. 78−93732
lossy waveguide attenuation and phase meas. 77−26343
low-loss dielectric microwave measurement in the E_{010} resonator, numerical error analysis *(Polish)* 78−70153
low-loss solid dielectric meas., automated resonance substitution systems 80−15957
low-loss solids, at 1 GHz, coaxial resonator method *(German)* 78−32834
lumped-capacitance method, fringing field effect anal. 78−54392
magnetic suspension densitometer for cryogenic meas. 79−12805
magnetodielectric materials in waveguide, resonance method 79−17449
material testing, nonuniformity of dielec. props., at mm wavelengths, method of determining 78−40001
micrometer electrode for improved meas. in 1-200 MHz range 78−49864
microwave, von Hippel's method, appl. to Eccosorb HF-2050, 500-2000 MHz 77−32314
microwave freqs., two coupler method modification 80−100632
microwave IC substrate permittivity meas. in cylindrical cavity 78−77942
microwave measurement of materials with high permittivity wing waveguide measuring line 80−47080
microwave measurement using cavity perturbation technique 80−31802
microwave Michelson interferometer improvement operating at 140 GHz 80−31854
miniaturised cell for permittivity meas., appl. to o-carborane *(French)* 79−71480
multilayers, solid, liquid, dielec. consts. meas. at microwave freqs. 79−2791
noninvasive beam-wave reflectometer for complex permittivity meas. at microwave freqs. 78−74030
noninvasive beam-wave spectrometric instrumentation for measuring dielectric constant at microwave frequencies 79−70728
nonlinear permitt. and Piekara factor using oscillator and calibration capacitor 78−82002
nonuniform dielectric regions, remote probing wave impedances 77−13781
oil composition analysis by means of cracking, permittivity thermal dependences obs. *(Czech)* 80−46289
one-dimensional conductor, microwave permittivity measurement techniques 78−10825
open resonator methods for microwave permittivity meas. 80−15942
piezoelectric film, third-order piezoelec. and dielec. consts. meas. using surface acoustic waves *(Japanese)* 80−55042
plasma cylinder short-wave probe, inverse diagnostics problem formation 78−67423
plastics, coaxial samples, rapid determination using freq. variation *(German)* 79−26078
polar liqs. using a lumped-capacitance method for coaxial lines 78−77936
polymer films, dielectric constant meas. parallel to film surface 80−97183
ponderomotive forces determ., digital simulation 79−215
precision waveguide cells, for lossy liquids meas. at 70 GHz 78−37032
pseudo-random noise dielectric spectrometry *(Japanese)* 79−17445
pseudorandom noise dielectric spectrometer, appl. of Fourier synthesis 78−16813
reference materials, dm wavelength appl. 79−6143
refrigerated hydrocarbon liquid, capacitance density meas. method 77−26273
relative dielectric constant for insulators in range 1-10 GHz, State Special Standard 80−13037
remote sensing of stratified media, pulse-spectrum technique, permittivity determ. 79−8722
rocks, elec. resistance and dielectric const. meas. method, appl. to Ukrainian shield *(Russian)* 77−73721
seawater and wet soil, at microwave, method 77−45184
seawater at microwave freqs., modelling 77−25690
semiconductor, complex dielectric permittivity meas., in H_{01n} cylindrical cavity 79−93160
semiconductor, waveguide method of measuring electric parameters at microwave frequencies review 79−93170
semiconductor materials, high-resistivity, using EM methods with capacitance sensing element, computer-aided evaluation 79−80647
semiconductors, SHF waveguide methods 78−95542

permittivity measurement continued
small liquid biological sample microwave complex permittivity meas. 80−17222
soil, moist, dielec. relaxation model, complex permitt. meas. 77−43930
soil, SW measurement of dielec. const. and conductivity 80−22388
solid electrolyte, polycryst., impedance and modulus spectroscopy 77−12309
solid electrolyte cells, inductive effects and AC meas. 78−6623
solids and liquids, dielec. characts., temp. depend., laboratory installation for meas. 80−37051
solution dielectric constant meas., cell, student, research laboratory appls. 80−62433
standard specimens, class 1_f for dielectric constant, certification methods 80−13036
student experiment, dielectric consts. and capacitor dissipation meas., RLC ccts. 77−82339
submillimetre region, in polar liquids, Poley absorption interpretation 77−36167
substrate dielectric constants, standard specimens 80−13038
test scheme design 80−13101
thin film complex permittivity in VLF range, meas. apparatus and method 79−21782
thin film permittivity and thickness determ. using differential-gap varying method *(Japanese)* 80−4739
thin film permittivity standard certification 77−74444
thin samples, microwave measurement of plant leaves, method 79−57825
time domain spectroscopy, transmission method 77−43926
time-domain dielectric spectroscopy, multiple refl. method 77−57350
time-domain spectroscopy, complex permitt. meas., 10^6-10^{10}Hz 77−49741
time-domain spectroscopy, for dielec. materials 77−18015
tissue dielectric loss and permittivity spectrometer 79−57743
transducer, capacitive, three-electrode, for sheet material meas. *(Russian)* 77−10047
tubular dielectric, complex permittivity and loss angle meas. in X-band using H_{011} cavity resonator method *(German)* 80−62690
USSR state standard for 0.2-1 GHz range 80−9004
variable frequency method 79−93169
VHF/UHF complex relative permittivity meas., lumped capacitance technique 77−74460
water film, between muscovite sheets, permittivity change meas. method, 20-70°C 80−55009
X-band measurement technique 77−2664
$CsFeF_4$, struct. phase transition at 250K 80−10663
KCl far IR complex permittivity meas. by dispersive Fourier transform spectroscopy, 7 to 300K 80−15940
$LiNbO_3$ piezoelectric coeff. and permittivity meas., small-sample method 80−15981
Mn-Zn ferrites, permittivity anal. and meas. *(Russian)* 79−15391
NaCl, capacitance determination of dielectric constant 79−80573
$NaNO_3$ crystals 79−97403

personal computing
see also microcomputers; sports and entertainment
microcomputer use at University of Michigan 80−62431
physics tutoring feasibility with personal computers 79−30174

personnel
see also education; management; teaching; training
BWR power plant, routine checks and radiation protection 78−74462
BWR power plant turbine building, radiation protection, calc. and obs. 78−74461
coal workers, localised-field magnetopneumographic meas. 80−104714
computer-assisted-learning agency, staffing needs and position in vertical organisational struct. of educational institution 80−42007
consumer electricity supply demands fulfilment and ensuring full employment *(German)* 80−36831
diagnostic ultrasonics, electronic techniques, present applications and future developments *(German)* 79−100683
direct reading pen dosimeters, radiation exposure meas. aspects *(German)* 78−5050
engineering, educational courses, for professional engineers, economic costs and course contents considerations 79−80414
fission reactors, BWR, Enrico Fermi-2, system turnover, test and startup program 80−63338
health hazard due to RF EM waves radiation from high power electronic systems *(Italian)* 77−21561
ionising radiation, personnel exposures, dose limits 80−99350
nuclear plants in developing country, development of local engineering capability 77−65350
nuclear power plant, occupational radiation exposure minimisation at Yankee Atomic, USA 77−18712
nuclear power plant, radiation monitoring systems, review 78−33292
nuclear power plant, Virgil C., startup, conduct of operations, organisation and personnel 80−63340
nuclear power plant operator training, simulator 77−367
nuclear power plants, startup, staffing program, scope, tasks, resources, constraints, anal., implementation 80−63341
nuclear power station, radiation safety 77−71701
nuclear power stations, radiation dosage determination, monitoring and control for personnel safety *(German)* 80−842
nuclear sites, workers' protection against radiation hazards 79−59267
Phenix plant operations and modifications *(French)* 80−47615
power industry, need for continuing education 77−45633
power line elec. field effect on communication line maintenance personnel 78−40353
Project Manager organisation in nuclear plant turnover and startup 80−63339
PWR, Spanish nuclear power program, technology transfer 77−65353
PWR station, radiation safety 77−71700
radiation worker health registry for AECL employees 79−88201
social effects of microelectronics *(Dutch)* 80−20
Swedish State Power Board nuclear power stations, training of emergency organisation 78−50412
West German nuclear fuel element factory licensing legislation *(German)* 79−89469

PERT
see also project engineering
fusion reactor, plasma divertor expt., management techniques and procedure 78−54891

perturbation techniques
see also control system analysis; control system synthesis
ϵ-expansion technique, appl. to integral evaluation in critical dynamics 80−57187
$\epsilon XY(dY/dX)=X-Y(Y+1)$, exact perturbation soln., stellar struct. theory 78−32439
't Hooft Polyakov monopoles, force between widely separated interacting monopoles 77−87895
acoustic nonlinear hyperbolic waves, comparison of three perturbation methods 77−7236
acoustics, echo time delay detection, effect of zero singularity smoothing 78−90605
alkali metal atoms, calc. of Van der Waals energies, variation-perturbation method 77−510
angular momentum expressions reduction by matrix arithmetic, computer method, perturbation calcs. 77−26126
artificial satellite, Vinti problem, extended phase space representation, luni-solar perturbations 79−35101
artificial viscosity, nine-point, for two-dimens. hydrodynamics 79−3989
asymmetric-slab optical waveguide losses due to refractive index inhomogeneities 78−1381
atom, relativistic calcs., perturbation theory approach 79−31422
atom, Sturm expansions in the Hartree-Fock method 78−25409
atomic configuration interactions, appl. of unitary group methods 80−27958
atomic HF and correlation energies, relativistic corrections and dipole matrix, calc. 77−26981
atomic hyperfine interactions, modified delta-function pot. 79−3378
atomic inner shell bound-bound radiative transitions, analytical description 78−82684
atoms, photoionisation cross sections, electron correl. reson. struct., relax. effects many body perturbation calcs. 80−47852
axisymmetric torus electrostatic problem, perturbation method soln. 78−78851
benzene, $^1A_{1g}\rightarrow{}^1B_{2u}$ absorption band, Franck-Condon factors calc. 79−36701
bifurcations, singular perturbations 78−16626
biological systems, containing Fe, electronic and mag. struct., semiempirical MO cluster calcs. 78−62733
blast wave, variable energy, perturbation solns. 78−51192
boundary layer problems, singular perturbations, stability and convergence 78−90827
bounded water bodies finite amplitude waves, dynamics study 78−77273
BWR dynamics, multivariable autoregressive identification 78−94107
celestial mechanics, mathematical methods, conf., Oberwolfach, Germany (Aug. 75) 77−25916
channel flows, slowly varying in 3-D 79−92948
charged current Fermi four field point interaction, weak interaction theory, rescatt. graphs consequences 77−67555
chemically coupled equilibria, thermodynamic theory of solvent-jump relax. method 79−39186
circular crystal plate thickness-shear resonance frequencies, acceleration effects 77−39136
classical mechanics, invariants, stability, KAM theorem 78−41
classical one-component plasma, correl. functions, perturbation calcs. 77−68747
classical thermodynamical fluid n-dimensional reductive perturbation method *(French)* 79−44891
computation with correlated sampling, nuclear reactor neutron transport 79−588
conservative elastic continua, stability anal. with adjacent equilibrium method 78−28951
conservative systems, perturbation expansion validity 79−12587
convection, forced, laminar, wedge flow with separation 80−1523
convection, natural, over uniform heat flux vertical surface, higher-order approx. 78−59388
convective fin, with internal heat generation and temp.-depend. cond., perturbation approx. soln. 78−5633
convergence of perturbation method and boundary conditions at noncanonical surfaces *(Russian)* 78−77696
Couette flow stability, transformation of perturbation eqns. 77−7474
coupled singular eqns., solns. for shell containing crack 77−50997
coupled-core nuclear reactor, distributed parameters identification, pseudorandom perturbation and correlation anal. 80−86966
coupling of elastic surface waves in piezoelectric crystals 77−85045
cross section requirements, for CTR design program 77−23294
crystal growth from vapour, morphological stability analysis 78−92200
cylindrical light beam diffr. on wideband US signal 78−50698
diamond, tetrahedrally bonded valence crystals, SCF perturbation theory appl. 79−37658
differential equations solution, Carson-Cambi, periodic, second-order 77−67207
diffusion equation, derivation from Fokker Planck equation using perturbation methods 78−54117
Dirichlet problem for semilinear eqn. $\Delta^k u=f$ on a disc, approx. techniques 79−40377
dynamic loading of thick rectangular membrane, viscous damping effect 78−46906
elastic plate sealing incompressible liquid, finite deflections 77−50915
electrodynamics, covariant formulation for charges of finite extension 78−77731
electrogravitational conversion cross sections in static EM background fields 78−24711
electron correlation calculations, scaling and Pade approximants rel. to perturbation series 80−5487
electron optics aberrations, algorithm computation using Chebyshev polynomials 79−27156
electrons in logarithmic pots., Dirac eqn. soln. 78−41448
electrostatic two-dimensional problem anal. 77−31043
elliptic operator, perturbation algebra 77−17774
EM plane wave, vertically polarized, refl. from periodic rough surface 78−22073
EM wave propagation in fluctuating medium, mean energy flux calc. *(Russian)* 77−88622
EM wave scatt. from dielectric infinite cylinder embedded into another 79−59620
epidemic models for malaria progress 77−22397
EPR and saturation transfer EPR, fast computation, perturbation approach 78−62212
EPR and saturation transfer EPR, fast computation, perturbation approx. extension for overmodulation 78−82754

perturbation techniques continued
Euclidean ϕ_3^4 theory, phase space cell expansion, Borel summability 78−8501
factorized wave function, appl. to He 79−3355
fast reactor, HCDA, heat conduction calc., method of weighted residuals 79−635
fibre optics theory, first-order correction to weak-guidance approx. 78−90519
fixed-point interactions with wave vector depend. struct. 77−65000
flow, plane parallel, finite amplitude stability, perturbative and iterative methods 78−38293
fluid, atomic, classical, with repulsive pair pot., perturbation method 79−68997
fluids in steep field gradients and near critical points, hydrostatic density distrib. 77−76523
frozen shock wave in two-dimensional steady flow past thin wedge *(Japanese)* 78−26212
gas, rapidly rotating, spin-up problem, perturbation calcs. 78−75147
geothermal reservoir, effect of magma dike intrusion on free convection 78−7599
gravitational wave EM detector, anal. as perturbed boundary-value problem 77−13677
heavy ion-induced multistep multinucleon transfer reactions, grazing collisions, quantal theory 79−6698
heavy-ion collisions, electron slip effects on quasimolecular X-ray emission 77−19040
highly nonlinear oscillation equation, perturbation soln. 78−33938
highly prestressed anisotropic plates, numerical perturbation technique 78−18214
homopolar crystals, imperfect, lattice dynamics 80−59601
Hubbard model, ground state energy, using degenerate perturbation theory 78−18938
human head EM induced field and power absorption, ellipsoidal model 80−3724
hydrocarbon, conjugated, nonlinear susceptibility, extended basis set calcs. 79−27107
hydrocarbons, proton NMR chem. shifts, mag. shielding effect of neighbouring C atoms 77−27094
inertial confinement pellet fusion, perturbation theory for sensitivity and uncertainty anal. 80−68946
invariant perturbation theory as alternative to Hamilton-Jacobi approach in classical mechanics 79−12588
ion-ion optical potls., and Coulomb barrier radius 77−3039
ionisation potential, vertical, inner and valence shells, ab initio SCF MO CI perturbation calc. method 78−74800
itinerant electron ferromagnetic alloys, magnon energy, effect of ordering 79−7986
jet, liq., breakup, 3rd perturbation Cosserat soln. 79−32615
Josephson junction, extended, I-V charact. perturbation calc. 79−69632
laminar flow in 2-D nonlinear perturbations, secondary flow existence *(Russian)* 78−22326
laminar non-Newtonian flow in porous annulus 77−72333
laser rangefinder radiometric efficiency, optomechanical tolerance analysis 79−21705
linear differential eqns. with periodic coefficients, stability conditions, energy expressions *(German)* 77−53746
linear oscillatory system response to shock impact *(Russian)* 79−9096
liquid jet breakup, second perturbation soln. for one-dimensional Cosserat theory 79−86478
LMFBR, space time dynamics for localized disturbances 78−21674
magnon elementary excitations damping *(Russian)* 79−28515
matrix Pade approximants, Fortran IV calc. subroutine 77−9877
melting/freezing interface, annular region, perturbation soln. 78−59286
membrane, prestressed, dynamic loading 78−51068
methane+Ar, rot. compound state resons. 80−28090
micropolar fluids, stability of laminar flows between parallel walls 79−1160
mixed boundary conditions in half-space, stochastic resolution *(French)* 77−9866
mixtures of reacting gases, extension of Chapman Enskog method *(Russian)* 78−57878
molecular configuration interactions, appl. of unitary group methods 80−27958
molecular polarisability, CNDO calcs. including polarisation functions in the basis set 79−6891
molecule, incomplete basis set correction, HF approx., differential eqn. formulation 79−63890
moment method in stochastic perturbation of angular correlations 77−3268
motor output response to applied torque perturbations in man, nonlinearities evaluation 80−76771
multimode optical fibre transmission, perturbation soln. 78−1380
multiple scales method, asymmetric responses of circular plates, nonlinear resonances 79−3951
neutron streaming along fusion reactor ducts, perturbation and variational corrections 80−23143
Newtonian viscous fluid, flow through thin pipe, with thin linear elastic wall 78−42664
non-Abelian gauge fields and nonrelativistic bound states 77−71425
non-hermitian potls., completeness relns. in scatt. theory 77−17854
non-Newtonian fluid, boundary-layer flow in convergent channel 78−30322
nonholonomic system, constrained perturbation procedures 78−16637
nonlinear elastic rods, shear and necking instabilities 77−65682
nonlinear elastic stability problems using a finite difference perturbation method 78−83273
nonlinear post-buckling anal., perturbation approach to imperfect structs. and snap-buckling 78−79244
normal modes of laterally homogeneous Earth, one dimens. example 78−88797
nuclear matter theory, technical aspects, review of theoretical techniques, nuclear interaction investigation 78−62497
nuclear reactor, fast, multiple control rod worth estimation, strong interaction effect 77−46302
nuclear reactor system fixed end-point problem suboptimal control, appl. *(Japanese)* 78−33259
nuclear spin-spin coupling consts., finite perturbation-CI calcs. 80−5563
oxyhaemoglobin dissociation curve direct obs. in man in vivo, computer investigation 78−85433
plasma, obliquely propagating nonlinear Alfven wave, perturbation method approach 77−15176

perturbation techniques continued
plasma, trapped-electron cyclotron instability, in Tokamak, 2-dimens. eigenvalue problem, analytic soln. 78−30434
plasma, Vlasov, mathematical model 79−55503
plate temp. dependent props. under linear temp. distrib., thermoelastic problem for crack 80−48579
polyatomic molecules, isotopic reduced partition function ratio approx., by polynomial perturbation method 78−66530
polymers, linear and ring, intrinsic viscosities, perturbation calc. 79−55914
polytrope n=3, poloidal mag. field effect on linear and adiabatic oscills. 78−24505
porous catalyst pellets, singular perturbation anal. of boundary value problems modelling reactions 78−76906
predissociation, laser-induced, nonreson., quantum theory, selection rules 78−82796
PWR reliability prediction in design, empirical and Monte Carlo techniques 78−54827
QCD, IR struct. of quark-antiquark scatt. kernel, quark binding pot. 78−8588
quadrupole distorted NMR powder patterns, simulation, Fortran program 77−77105
quartz, electroded doubly-rotated thickness-mode resonators, temp.-induced frequency 79−55298
quartz crystal resonator nonlinear analysis 79−55299
quartz SAW velocity/temperature dependence calc. 79−56062
radiative transfer equation perturbation soln. for stellar atm. 77−45404
random fields, lowering of dimensionality in phase transitions 77−17923
randomly perturbed one dimens. wave eqn., multiple-scales space-time anal. 78−8247
rapidly rotating gases, thermally-driven axially antisymm. geostrophic flows, flow field calc. 79−90259
Rayleigh wave scatt. by thin surface layers, singular perturbation anal. 78−58
resistive MHD instabilities, diffuse pinch configs., numerical study 77−58853
Reynolds equation, asymptotic soln. 79−14369
rotating flexible rods, unstable vibration and buckling 78−79242
scattering amplitude at high energies, corrections to geom. optics in quasi-classical limit *(Russian)* 77−2760
second order perturbed energies, coupled HF iterative procedure 79−9991
semiclassical stochastic radiation theory 78−21010
shuttle reentry trajectory optimisation method 77−67021
Signorini's perturbation procedure in elasticity, branching of solutions 80−27134
Signorinis perturbation scheme for a general reference config. in finite elastostatics 78−83241
soil diffusion eqn. soln. with exponential diffusivity comparison of iterative and perturbation techniques 77−41097
soil infiltration eqn. soln., comparison of perturbation and iterative techniques 77−41096
soliton perturbations, variational calcs. 80−46825
solution of a highly non-linear oscillation equation, single particle analogue of field equations of chiral Lagrangian theories of pion interactions 80−62470
spherical shell of variable Young's modulus, radial vibr. 78−94607
stagnation flow, two-dimens., stability, longit. vortices, perturbation method 78−75146
stellar rapidly rotating models with radiation press., struct. parameters calc. 80−67697
stratified fluid with free surface, near field disturbance due to slender body 78−59443
streaming, of vel. and temp., in oscill. boundary layers 78−83358
stretch-receptor organs, crayfish, effects of length-steps with and without perturbations 79−25003
sub-optimal graded index optical fibre analysis using perturbation calculus 80−87480
T-matrix, perturbation formalism for complex poles and widths, appl. to intermediate struct. 78−66255
thermoelasticity, half space subjected to a heat flux step, perturbation anal. *(French)* 79−90130
three-nucleon system, Faddeev eqns. perturbation, nucleon-nucleon interaction with tensor force 78−70463
tidal periodic flow anal. by finite element perturbation method 77−70690
transformation group and limit cycle containing nonlinear differential eqns., connection with perturbation techniques 78−20941
transition metals, 1st period, at. correlation energies, perturbation calc. 79−36508
transition T-matrix complex widths and poles, perturbation formalism 77−26646
transonic flow, two- and three-dimens., perturbation soln. method 79−1208
two-dimensional pattern distortion analysis, biproportional matrix projection method 79−88229
undamped linear elastic systems, stability under follower forces, perturbation study 79−1110
US tomography based on perturbation solns. of wave eqn. 79−70593
vapour deposition process, mass diffusion in two-dimens., perturbation method 79−2737
viscoelastic liquid steady flow about porous rotating disc 79−32586
viscous flow in constricted or widened tube, analytic solns. 79−18959
viscous fluid flow through slot between fixed and rotating surfaces of revolution *(Polish)* 78−79300
von Zeipel, satellite motion in eccentric orbit appl. 77−45295
weather stochastic prediction, stochastic dynamic method, perturb. approx. 79−58060
Wien dissociation in weak electrolytes 78−23950
Yang-Mills theory, large order calcs. 78−8511
BN tetrahedrally bonded valence crystals, SCF perturbation theory appl. 79−37658
BeO, tetrahedrally bonded valence crystals, SCF perturbation theory appl. 79−37658
Fe complexes, electronic and mag. struct., semiempiricial MO cluster calcs. 78−62733
HF, nuclear spin-spin coupling const., finite perturbation calcs. 78−78616
HgI_2, relativistic effects, photoelectron spectra, Hartree-Fock-Slater method, perturbation theory approach 80−27962

perturbation techniques continued
I_2, relativistic effects, photoelectron spectra, Hartree-Fock-Slater method, perturbation theory approach 80−27962
N_2, solid, gamma-phase, anharmonic lattice vibr. 79−33705
NaK, $a^3\Sigma^+$ state, laser induced fluorescence, $D^1\Pi$ to $a^3\Sigma^+$ transition, molecular constants, dissociation energies 79−98143

perturbation theory
see also quantum theory
1/N perturbation theory, large orders by inverse scatt. in 1-dimens., anharmonic oscillators 80−22214
3d-shell, pair correl. energies calcs. 79−31417
β-function in noncovariant Yang Mills theory from perturbation theory 79−247
$(\theta^4)_4$ field, Borel summability, renormalization group, perturbation theory 78−16922
$\lambda{:}\Phi^4{:}/4!$ massive Euclidean field theory, perturbation expansion, cutoff bounds on n-point Schwinger function 79−71630
$\lambda\phi^4$ theory, renormalised perturbation theory, skeleton eqns. and R operation 78−54570
$\lambda P(\phi)_2$ weakly coupled model, spectral props. and bound-state scatt. 77−22629
π-electron, effective Hamiltonians, formal theory 79−59333
σ models, nonlinear, perturbative approach to symmetry restoration 80−37163
Σ perturbation method using Green's functions for mol. calcs. 78−55123
ϕ^4, large order behaviour of perturbation theory and mass terms 79−45018
ϕ^4 model, four-loop approx. 79−89070
$g\phi^4$ theory, asymptotic series sum of perturbation theory, Green's function method *(Russian)* 79−54271
ϕ^4 theory, renormalisation anal. and methods of calc. many loop diagrams 79−58885
$A_0=0$ gauge canonical formalism, gauge degrees of freedom, external charges, quark confinement 79−2936
A=18, shell-model interaction, convergence in reaction matrix G 78−50102
Abelian spontaneously broken gauge model, perturbation expansions *(Chinese)* 78−8500
abstract Hilbert space generalisation of Feenberg's theory, elec. cond. of disordered alloys 77−24542
acetaldehyde, Coriolis resonance bands in IR spectrum 80−47995
acetonitrile, mol. pair correl. functions, scatt. intensities, statistical mechs. calcs. 79−1382
acrylonitrile, dielectric constant effect on nuclear spin-spin coupling constants, INDO approx. 79−72240
actinide ions, tetrapositive, nucl. hexadecapole antishielding factors 79−26909
adiabatic perturbation theory, mol. fixed moving coord. system, review 78−62687
adiabatic perturbation theory for quasilevels 79−40457
adiabatic perturbations of solitons and shock waves 80−46830
adiabatic potential energy of molecules and solids, perturbation expansions *(Japanese)* 77−69205
adiabatic S-matrix and perturbation theory for systems in a periodically-varying external field 79−9133
adsorbed atoms, surface band splitting, theory, with appl. to He/graphite 80−60058
Aharonov-Bohm effect, first-order perturbation theory, for teachers 79−21497
Aitken's δ^2 transformation generalisation, summing perturbation series 78−24652
algebraic aspects of perturbation theories 80−31539
algebraic methods, so(4,2) algebraic soln. of H ground state in strong mag. field 80−47845
alicyclic compounds, nucl. spin-spin coupling via nonbonded interactions, γ-substituent effects 80−69078
aliphatic compounds, nucl. spin-spin coupling via nonbonded interactions, γ-substituent effects 80−69078
alkali atom+alkali atom, laser-induced ionis. collisions 78−5333
alkali halide, static and dynamic props., appl. to KCl 77−7798
alkali metal atoms, laser three-photon absorpt., ionisation cross-sections *(French)* 78−5182
alkali metal atoms, resonance interaction, resonance lines self-broadening, adiabatic pot. curves 77−83676
alkali metal ion, with filled shell, dipole polarisability 80−9501
alkali metals, phonon dispersion curves using second-order perturbation theory 80−79893
n-alkanes, longitudinal acoustic modes, Raman intensities 80−32718
alkanes, nucl. spin-spin coupling via nonbonded interactions, conformational and substituent effects 80−69077
alkenes, 1,1-, 1,2-disubstituted, fragmentation modes in perturbational MO anal. 80−58138
alloys, short-range order, electronic theory using pseudopot. approx., review 79−47004
alloys, thermoelectric props., effect of electron-impurity and electron-phonon interactions 79−33282
almost degenerate, partitioning type treatment 78−32701
amorphous ferromagnet, localised spin and phonon excitations, theory 79−7979
analytic continuation of a group of eigenvalues 79−6010
Anderson model, asymmetric 80−6766
Anderson model, perturbation expansion in infinite conduction bandwidth limit, Kondo temp. 79−28506
anharmonic crystals, neutron scatt. cross-section, sublattice displacement effects 79−77460
anharmonic oscill., classical versus quantum case *(Spanish)* 80−73210
anharmonic oscill., ground state energy calc. infinite coupling limit 77−74582
anharmonic oscill., residue-squaring diagonalisation meth. 77−49635
anharmonic oscillator, computation of energy eigenvalues of Hamiltonian 80−12925
anharmonic oscillator, convergent perturbation series 79−88836
anharmonic oscillator, energy level calcs., double well potential summable series 80−17819
anharmonic oscillator, modified perturbation theories using Riccati eqn., energy eigenvalues 79−12644
anharmonic oscillator, multipseudoparticles, perturbation theory in ground state energy calcs. 79−17622
anharmonic oscillator, perturbation series 80−57137

perturbation theory continued
anharmonic oscillator, perturbation theory, hypervirial theorems 80−105535
anharmonic oscillator, perturbation theory higher orders and struct. *(Russian)* 79−25904
anharmonic oscillator, perturbative approach 79−80464
anharmonic oscillator, strong coupling regime, appl. to $\Phi_4{}^4$ model 78−89622
anharmonic oscillators, divergence of perturbation theory 79−75393
anharmonic oscillators, large order perturbation expansion coeffs. of ground state energy 79−9139
anharmonic oscillators, partition function, statistical variation perturbation method 80−77648
anisotropic crystal impurity states, perturbative theory 80−34390
anisotropic superconductors, upper critical field theory, perturbation theory study 80−75692
annulus, spherical, rot., forced thermal convection of viscous fluid 79−27634
aromatic compounds, electrophilic substitution sites, perturbation theory calcs. 77−30800
asymmetric Anderson Hamiltonian, perturbation expansion 80−6687
asymmetric Anderson model, ground state, perturbation approach 80−65504
asymmetric top molecules, collisional selection rules, perturbation calcs. 77−6838
asymptotic estimate of perturbation theory at large orders, anharmonic oscillator, Φ field theory 80−4585
asymptotic estimates in perturbation theory, Yukawa and $g0^4$ theory 80−4873
asymptotic estimates in perturbation theory and complex instantons 79−6273
asymptotic estimates in quantum field theory, Lipatov method 79−21895
asymptotic estimates of perturbation theory at large orders 79−21901
asymptotic expansion in coupling const. 79−71595
asymptotic solution of a nonlinear singular perturbation problem 79−12576
asymptotic solution of a particular boundary operator in perturbation theory *(German)* 79−54015
asymptotically free massless field theory, self-consistent β functions 78−16911
atom, dynamic multipole polarisability, hydrodynamic model, variational approximations 80−23340
atom, HFS, many-body and relativistic effects 78−37565
atom, hyperfine shift and interatomic pots. in inert buffer gas, alkali atoms and H 80−5491
atom, multiphoton ionis., probability rates 79−13686
atom, nucl. quadrupole coupling const., relativistic many-body perturbation theory 78−37566
atom, open-shell, effective electron-electron interaction, many-body perturbation theory, C appl. 80−47843
atom, radiative decay with time depend. perturbation 77−18834
atom, relativistic, level shifts, transition probabilities, perturbation theory 79−10067
atom, screened Coulomb pots., anal. perturb. theory for relativistic case 78−21861
atom, spontaneous radiation, near field calcs. 80−99493
atom, two-electron, dynamic polarisability calc. 77−14599
atom+charged particle, autoionisation state decay 80−9565
atom+harmonic oscillator, classically forbidden transitions, classical and classical path methods 77−520
atom+ion slow collisions, K-shell excitation of relativistic atoms 80−48073
atom+molecule collisions, differential cross section, classical perturbation scatt. theory 78−5319
atom and mol. excitation, many-body perturbation theory, eqns. of motion formulation 77−88373
atom with partially-filled shell, relativistic theory, secular operator renormalisation *(Russian)* 80−52896
atom-solid surface scattering, quantum theory 78−27357
atom-surface diffraction, perturbation theory calcs. 77−85862
atomic and mol. reson. states, electrostatically induced, 1-D model 77−75077
atomic binding energies, determ. from fund. theorems involving electron density, $\langle r^{-1}\rangle$ and Z^{-1} perturbation expansion 80−63521
atomic bound-state energy, $1/Z$ perturbation expansion, analytic behaviour 77−50344
atomic bound-state energy, $1/Z$ perturbation expansion, singularity 77−50343
atomic collisional ionisation, Penning ionisation, laser induced, two step optical collisional perturbation sequence 80−63778
atomic collisions, diabatic molecular orbitals 78−62901
atomic collisions, quasiclassical theory, transition between spatially degenerate levels 80−43150
atomic collisions, two-state approximation in the adiabatic and sudden-perturbation limits 79−22780
atomic correlation energies calc., Wilson's scaling parameter evaluation 80−5486
atomic double vacancy states, correl. photon and electron transition, perturbation theory 80−27968
atomic doubly ionised K-shell system, radiative decay of excited state, branching ratio calcs. 77−54521
atomic electron (positron) elastic (inelastic) scatt., 5-500 eV, perturbations treatments, review 77−30997
atomic electron elastic scatt., perturbation theory calc., computer program 78−50637
atomic interaction dipoles, perturbation theory 80−78680
atomic interactions, retarded energy shift and pair polarisability, field theoretical perturbation theory 80−102560
atomic interactions, short-range, symmetry and similarity transform. for perturbation theory 77−10722
atomic level shift and width in light field, higher order perturbation theory *(Russian)* 79−3414
atomic many-body perturbation theory with radially restricted basis functions 80−78526
atomic model potentials, constructive theory 79−26869
atomic pair polarisabilities, continuum electrostatic theory 78−86769
atomic photoionisation, many-body perturb. calcs. 79−59406
atomic photoionisation anal. using relativistic random phase approximation and multichannel quantum defect theory 80−63602
atomic pressure broadening, adiabatic theory, low density approxs. 79−22628
perturbation theory continued
atomic quadrupole shielding factors calc. using elec. field variant orbitals 80−106276
atomic spectrum, perturbation by strong light field 79−10073
atomic systems, many-electron autoionisation states, transition probability and autoionisation rate, perturbation theory Z-expansion 80−52863
atomic systems, many-electron autoionising states, Z-expansion energy calcs. 80−909
atoms, heavy, parity non-conservation, relativistic many-body perturbation theory 78−923
atoms, identical, dispersion intermolecular pot. anomaly prod. by intense radiation field 80−58336
atoms, in const. elec. field, rigorous theory of complex scaling 78−70785
atoms, ionisation pots., electron affinities, Rayleigh-Schrodinger and Green's function calcs. 77−75075
atoms, perturbation var. calc. with contact interaction, effect of approx. zero order wavefunctions 80−58107
atoms, relativistic energies, perturbation calcs. 80−102453
atoms, two photon excitation, time depend. emitted light spectra, perturbation theory 80−63605
avoided-crossings, spurious, variationally calc., perturbation theory approach 78−5295
axial vector matrix elements, chiral limit, renormalisation effects 79−17190
Barker-Henderson, appl. to sound prop. vel. in simple liquids *(Russian)* 77−15500
baryon 70, 1^-, multiplet, transition mixing, mass splitting, degenerate perturbation theory model 77−2832
baryon-quark phase transition, asymptotic freedom studied using renormalised coupling constant 78−4830
Be, Rayleigh-Schroedinger perturbation calculations 78−9064
beam-plasma system, wave interaction, dispersion and higher order nonlinear effects 78−71502
beams, plates with varying thickness, fundamental freqs. 79−32324
benzene, π electron system, excitation energy, appl. of MBPT 80−52876
benzene, dynamic polarisabilities, calcs., superposition method of excited config., nonstationary perturbation theory eqns. 80−69257
benzene, substituted cations, spectroscopy, substituent effects 78−58709
benzene, van der Waals interaction energy calc., perturbation theory, MO LCAO method 77−42373
benzene+bromomethane, microwave line width and quadrupole moments, perturbation theory 80−69190
benzene+OCS, microwave line width and quadrupole moments, perturbation theory 80−69190
Bethe lattice, vibration 78−30706
binary alloy, electron theory of short range order 78−10390
binary alloys, FCC, with short-range order, electron theory, pair interaction and third-order perturbation theory 79−69404
binary solutions of dense liquids and gases, isothermal eqn. of state calcs. *(Russian)* 80−88292
biomembranes, excitable, bursting phenomena 79−66455
black holes, gravitational and EM perturbation functions, Reissner Nordstrom geometry 78−49472
black holes, rotating, electromagnetic perturbations 78−12279
Bloch equations solution in presence of varying B_1 field, selective pulse analysis 80−25222
block diagrams, divergence cancellation in energy level perturbation theory 79−80751
Block-Siegert shifts and multi-quantum transitions, spin-one systems, RF and DC fields 77−75103
blood flows, oscill. freq. effects in plane wavy conduit flows 78−20209
bodies disposed from aircraft, dynamic flight characteristics *(Polish)* 78−18311
bond order matrix differentiation, in nonorthogonal basis, density matrix perturbation theory 78−887
Borel summability, improvement on Watsons theorem, $\phi_2{}^4$ appl. 80−52394
Borel summation of perturbation series 78−16683
Born-Oppenheimer approx., IR absorption, circ. dichroism using vibronic gauge function 78−967
Born-Oppenheimer approx., IR absorption, vibr. intensity using vibronic gauge function 78−966
Born-Oppenheimer approx., perturbation theory 77−26988
Bose fluid, interacting excitations 77−43401
boson condensation, solvable quantum field theoretic model 77−57447
boson quantum thermodynamical system in one space dimension, high-order perturbation expansion 80−4636
bound excitons, ground state energies for all mass ratios 79−60729
bound s-state of electron in screened Coulomb field 78−58581
bound state energy levels, quantum mechanical formalism, convergent perturbation theory *(Russian)* 80−4573
bound states, continuum states contribution for teaching 77−33803
bound states, of particle in static screened Coulomb pot., anal. calc. 79−10633
bound states, semiclassical, in one-dimension, perturbation formalism 80−12937
bound-state properties calcs., theoretical error estimates 80−102425
branched polymer molecules, second virial coeff., chain length effects calcs. 78−37775
bremsstrahlung of vector particle in nucl. field 80−37198
Brillouin-Wigner perturbation expansion, convergence props. 78−45491
Brillouin-Wigner theory and quasi-bound states 78−70011
Brillouin-Wigner type perturbation series summation 79−81149
Brownian particles, independent, multiple light scatt. calcs. 78−22087
Brueckner approach to Sutherland one-dimens. many body problem 77−87660
C*-dynamical systems, small perturbations 79−80458
caffeine, semi-empirical excited state Morokuma's EHP calc., geometry and order of states 78−46256
Callan-Symanzik $\beta(g)$ function in perturbation theory around gauge theory instanton 79−2931
Callan-Symanzik equation, perturbation analysis, crit. indices 78−52294
carbonyl compounds, ^{13}C chem. shifts, approximate SCF perturbation theory 77−6804
carbonyl compounds, metastable triplet states, var. and perturbational calcs. 77−61680
CARS in condensed phases, perturbation theory of third-order nonlinear susceptibility 80−14393
catalysed reaction theory applic. 77−1923
catalysis, orbital perturbation approaches 78−80783
celestial mechanics, elementary derivation of perturbation eqns. 77−6

perturbation theory continued
celestial mechanics, perturbation theory in rectangular coordinates 79−21158
CERN School of Physics, Austerlitz-Zeist, Holland (June 1978) 79−30857
changed field, electromagnetic self-energy, in non-minkowskian spacetime, gauge depend. of mass renormalisation 79−85214
chaotic motion theories with appl. to controlled fusion research, review 78−93605
linear Chapman-Enskog procedure, evolution equations of hydrodynamic variables 80−49075
charge equations of motion in perturbation theory quadratic approx., betatron oscills. 80−37661
charged hard spheres in uniform neutralising background, Monte Carlo and perturbation theories 77−55223
charged particles in external fields, classical Dirac, Klein-Gordon eqns. 77−49829
charged particles in single wave fields, adiabatic and stochastic motion 80−9795
charmonium models, energy perturbation series from Schrodinger eqn. 79−6005
chemical bond theory, perturbation expansions, convergence calcs. 77−6662
chemical kinetics, eigenvalue and eigenfunction anal. of Kramer's theory 79−29330
chemical reactions, symmetry correl. and perturbation calcs. methods 80−104427
chemically reacting system, thermodynamic perturbation theory 77−70325
chemisorption on metals, self consistent jellium+adatom calc. 77−66093
chiral field model diagram techniques for low temp. phase 79−58882
chloroform, CNDO approx. 79−72240
circuit based graphs for renormalized perturbation theory 79−71266
classical, of good action-angle variables, applic. to semiclassical eigenvalues and collisional energy transfer 80−23481
classical fluids, correl. functions, perturbation theory for soft sphere systems 77−72536
classical fluids in crit. region, generalised perturbation theory 79−77474
classical mechanics, numerical methods, Newtonian, Lagrangian and Hamiltonian mechanics, book 79−63024
classical mechanics perturbation expansion method, calcs. 77−33741
classical one-dimens. Hamiltonian system, perturbation expansion 77−26167
classical trajectories, use of perturbation theory in asymptotic region, appl. to HF+HF 79−98199
Clebsch-Gordan coefficient summing, appl. to mag. monopole theory 77−41505
clock random perturbations, absolute continuity theorem *(French)* 78−62150
closed-shell system, polarisability and mag. susceptibility calc. by SCF and CI method 80−99443
closed-shell systems, effective Hamiltonian for excitation energies, convergence props. 79−3346
closure approximation, appl. to perturbation theory, muon capture and pion electroproduction 78−16680
coherent averaging, and its appls. 78−73887
coherent multiphoton intense interactions, convergent perturbation anal. 80−1037
coherent two-photon reson. and Doppler free population inversion, perturbation anal. 77−643
collapsing pre-galactic H gas cloud, local stability, linear perturbation anal. 80−82513
collective motion frictional and conservative forces, frictional Schrodinger eqn. 79−85357
collision processes, time-dependent, adiabatic perturbation approx., semi-classical theory 77−71242
complex ϕ^4 theory, Euclidean path integrals and Feynman-Dyson-Wick perturbation expansion 78−49957
computational atomic and molecular physics, conf., Nottingham, England, (Sept. 1978) 79−59567
conducting crystals, kinematical and dynamical inelastic light scatt. 78−80368
conducting mol. crystal, electron-phonon interaction, effect on electron energy level, calc. to second order 79−4499
cone and plate oscillatory motion, secondary flow effects, perturbation anal. 78−1618
conference on hadron struct. and lepton-hadron interactions, Cargese, France (July 1977) 80−4473
conference proceedings, nonlinear dynamics, tribute to Sir Edward Bullard 78−93603
configuration interaction, perturbation theory, partial transformation 78−37562
conjugated compounds, mol. polarisability additive scheme, CNDO approximation calcs. 77−50363
conservation laws, infinite set for Thirring model, massive and quantum sine Gordon model 78−29226
continued fraction solutions to systems of linear eqns. 77−2506
continuum shell model, convergence problems, separation expansion and perturbative continuum treatment 79−17827
contracted orbital formulation of many-body perturbation theory 80−87026
convection natural, in porous medium, singular perturbation problem 79−94715
convection-diffusion problem, singular perturbation problem with nearly resonant operator 78−22352
convergent integral representation for summing of perturbation theory 79−9146
convolutionless master equation, perturbation expansion 78−70047
correlation energy, many-body Rayleigh-Schrodinger perturbation theory calcs., exclusion principle violation 80−52890
Coulomb centres at small separation when (Z_2-Z_1) is large *(Russian)* 78−12583
Coulomb Green's function Sturmian expansion, Goldstone diagrams and reduction theorems 78−898
Coulomb potentials, screened, energy approximants and perturbation theory 80−106368
Coulomb scatt., perturbation theory, renormalised half-off-shell T-matrix 78−32996
Coulombic systems, charged hard sphere system, rel. to restricted primitive model 80−64854
perturbation theory continued
coupled anharmonic oscillators, coherent state representation, perturbative soln. 79−17270
coupled field theory, classical perturbation theory appl. 78−57799
coupled HF-perturbation theory of atomic and mol. props., correl. corrections 80−106269
coupled multiconfiguration SCF perturbation theory, analytic techniques 78−17550
coupled neutron-nuclide problems, time depend. generalised perturbation theory 80−32322
coupled oscillators, approx. and exact quantum energies and eigenfunctions 79−26961
covalent bonding, pseudopot. theory 77−51345
covariant theory for gravitation 77−49661
cranking model, perturbation theory and Dalgarno Lewis method 77−45640
creep buckling of long cylindrical shell 77−11134
critical dynamics in Fokker-Planck formalism 77−22514
critical exponents and large-order behavior of perturbation theory 79−30397
critical phenomena, modern theory, graduate level text 77−102
crystal spectra, intercombination transition intensities in strong crystal fields, symmetry reduction method 78−84175
current conservation in perturbative sine-Gordon and massive Thirring models 79−9273
currents and continuous symmetry restoration in two dimens. 79−21910
curved elastic arcs, perturbation analysis for calculating inextensional natural freqs. 79−23242
cut vertices and their renormalisation, generalisation of Wilson expt. 79−21929
cut-off paths and forms extensions 77−33898
cyanoacetylene, and isotopic forms, $^{13}C/^{12}C$ effects on partition function 79−29352
cyclone development along weak thermal fronts, model soln. 80−81994
cytosine, vertical interaction evaluation methods 79−54772
Davidson's algorithm with and without perturbation ocrrections 80−27570
decoupled eqn. solns., EM and gravitational perturbation eqn. soln. construction 78−70029
deep inelastic scatt., covariant parton model, Feynman integrals of perturbation theory 78−82221
deformation of bar elements, derivatives of deformation parameters, appl. to buckling and post buckling anal. 77−89047
deformation potential polaron, perturbation theory breakdown 80−84440
degenerate, continued fraction solutions 77−17840
degenerate, energy shifts and S-matrix 79−75693
degenerate discrete levels, periodical perturbation *(Russian)* 80−86152
degenerate energy levels, adiabatic and time-independ. perturbation theory diagrammatic anal. 79−2642
degenerate perturbation theory 78−65799
dense Fermi systems, generalised perturbation theory, ground and low excited states 80−22741
dense liquids and gases, one-component systems, isothermal eqn. of state using thermodynamic perturb. theory *(Russian)* 80−49335
dense stellar matter in asymptotically free gauge theories, high density limit 77−53421
density matrix approach to problems in time-dependent perturbation theory 79−92973
derivative-coupling model, 2 dimens., zero mass limit and induced interactions 79−49397
desorption, relaxation time approach limitations 80−93795
diacetylhydrazine, ^{14}N NQR lines fine structure 80−63667
diagrammatic, correlation energy, triply excited state contrib., water appl. 80−18774
diagrammatic many-body perturbation expansion, computer program 78−50454
diagrammatic many-body perturbation expansion, ladder energies, computer program 78−50455
diagrammatic many-body perturbation expansion, ring energies, computer program 78−50456
diagrammatic many-body perturbation theory applicable to arbitrary model spaces 80−47844
diagrammatic many-body perturbation theory for general model spaces 80−18780
diagrammatic perturbation expansion of at. and mol. electronic energy, 4th-order terms 79−85882
diagrammatic perturbation theory, appl. to N_2, CO_2, BF 80−58131
diagrammatic perturbation theory, energy terms calcs. of closed-shell mol. systems 79−22582
diatomic molecule, rot. perturbed Morse oscillator, eigenfunctions and Franck-Condon factors 77−42309
diatomic molecule, Stark effect calcs., rigid rotator rotational levels in asymmetric potential well 80−5580
diatomic molecules, force consts. evaluated in first order of perturbation theory 77−34781
diatonic molecules, Stark effect variational and perturbational calcs. 80−1022
diblock copolymer solution, second virial coeff., perturbation theory 80−29148
dichloromethane, dielectric constant effect on nuclear spin-spin coupling constants, CNDO approx. 79−72240
dielectric, fast electron transfer, in external electric field, appl. of higher-order perturbation theory *(Russian)* 79−23662
dielectric response of solids, approxs. for treatment of local field effects 79−47033
difference approx. for singular perturbation problems 77−33850
differentially rotating gaseous polytropes, second-order perturb. theory 80−21990
diffused waveguide, gaussian index profile, modes, perturbation anal. 77−3671
difluoromethane, dielectric constant effect on nuclear spin-spin coupling constants, INDO approx. 79−72240
diformylhydrazine, ^{14}N NQR lines fine structure 80−63667
dilute alloy, perturbation expansion for the asymmetric Anderson Hamiltonian 80−80202
dilute gas, Boltzmann-Langevin eqn., light scatt. and density correlation function 77−11307
dilute gas, kinetic perturbation theory 80−100051
dilute gas transport props., logarithmic term in softness expansion 80−83872
dimensional anal. in renormalised perturbation theory 78−24950

perturbation theory continued
dimensionally renormalised Green's functions, massless particles theories 77−13839
dimensionally renormalised Green's functions, massless particles theories 77−13840
dipolar liquids, hypernetted-chain eqn., perturbation theory soln. 80−49072
dipole interaction of an oscillator with scalar field 80−94
dipole sum rules for products of 3-j symbols 78−65803
dipole-dipole elastic scatt., second-order perturbation theory 78−5317
Dirac's time dependent perturbation theory, appearance of singularities 79−21984
Dirac equation, approx. soln. using partitioning technique, appl. to H(1s, 2s, 2p) 80−23284
Dirac type essentially self adjoint operators 78−16957
direct-gap crystals, one-photon absorpt., Keldysh and perturbation formulas 80−20607
discontinuous perturbations in singular dynamical systems 77−10169
discrete spectral operators, perturbation theory *(Chinese)* 79−12638
disordered electronic system, scaling theory of localization and non-ohmic effects in two dimensions 80−44539
disordered transition alloys, generalized perturbation calcs. of ordering energies 77−4282
displacement of molecular orbitals due to interaction with charged species 79−63926
displacive phase transition, S ion spin Hamiltonian parameter dependence on order parameter 80−70356
distorted wave Glauber approximation, Pauli eqn. soln. 78−57809
distorted wave perturbation theory, higher order, accuracy and convergence 78−74731
DNA hypochromic effect, oscillator strength, perturbation theory calc. 79−96515
DNA hypochromism anal. *(Russian)* 77−56339
double anharmonic oscillator, asymptotic estimates and Borel resummation 79−85002
double charge transfer and two to one charge transfer adducts, energetics 79−82561
double perturbation theory, generator coord. description of collective vibrs. 77−79031
double scattering struct. in old-fashioned perturbation theory 79−9310
double sine-Gordon equation, perturbation theory 79−75403
doublet with singlet ground state electronic system, long range interaction energy, CNDO approx. 80−53089
Drell-Yan formula in perturbation theory, Abelian gluons 79−30702
Drell-Yan formula in QCD, lepton pair prod. 78−33025
Drell-Yan processes, perturbative QCD corrections 79−22035
Drell-Yan processes, perturbative versus asymptotic freedom convections 79−63446
Drude oscillator model, atomic and molecular props. for different oscillator freq. 80−37846
dynamic conductivity in metals, generalised linear Boltzmann eqn. perturbation soln. 78−34818
dynamic multipole polarisability 80−74252
dynamic potential barrier and tunneling 78−62740
education, EM wave interaction with matter, gauge invariant formulation 78−62006
education, Na Rydberg states, anomalous fine struct., perturbation model 80−57035
education, normalisation of states 77−33770
education, plane rotator, degenerate perturbation theory, Zeeman and Stark effects 79−9059
education, quantum mechanics and perturbation theory, perturbed harmonic oscillator *(Spanish)* 78−36786
education, two-electron atom, 1snl excited levels, ionisation energy calc., perturbation, Schrodinger eqn. methods 80−17728
effective operators in nuclei, nuclear shell model 78−12990
effective shell model interaction, effect of singular part on perturbation theory 77−6265
effective valence shell Hamiltonians, generalised perturbation theory 79−36509
eigenvalue perturbation theory, remarkable examples 78−93558
eigenvalue perturbation theory divergence, quantum mechanical counterexample 79−92982
elastic rod, perturbation methods for soln. of linear eigenvalue problem *(German)* 78−18175
electric dipole allowed transitions, long-range dispersion-induced circular dichroism 79−81196
electrode-redox system electron transfer reacts. time-depend. perturbation theory 78−61027
electrodynamics, asymptotic estimates of higher approx. *(Russian)* 78−12584
electron+atom potential scatt. in low freq. laser field, perturbation theory 80−43191
electron correl., second-order perturbation energy, modified HF operator, virtual MOs perturbation anal. 77−18797
electron correlation energy, approx. 4th-order perturbation theory 79−6876
electron diffraction, dynamical theory, perturbation calcs. 78−83665
electron exchange perturbation theory, direct spatial localisation 77−79668
electron gas, exchange and correlation effects, self consistent theory 77−85161
electron gas, jellium model, dynamic correlations, first-order perturbation theory 80−44527
electron gas, momentum distrib. function, perturbation theory calcs. 77−13693
electron gas, spin polarised, exchange and correl. energy 77−85163
electron in strong mag. field, degenerate perturbation theory example for teaching 77−33801
electron motion in one-dimens. periodic pot. under influence of uniform elec. and mag. fields 78−75972
electron optics, paraxial eqn. asymptotic solns., singular perturbation theory, chromatic aberrations of cathode electron optics 79−41320
electron plasma waves in cylindrical waveguide, Krylov-Bogoliubov-Mitropolsky method 79−4134
electron propagator theory for mol. electron binding energies and photoionis. intensities 80−47848
electron self-energy in non-local QED and correspondence principle 77−22671
electron transfer cross-section, second Born approx. 80−48080
electron-ion system, effective ion interaction and force consts. 80−65185
perturbation theory continued
electronic energy of atoms and mols., (N+1/N) Pade approximants in Rayleigh-Schrodinger perturbation theory 77−71738
electronic struct., two-four body contributions, third order, algebraic approx. 77−18776
electronic transition matrix elements based on local atomic environment 77−39758
electrons in helical mag. fields, quantum theory 79−80470
electrostatic ion cyclotron wave, nonlinear propag. and modulational instability 78−1823
elementary excitations damping, theory of many-particle processes *(Russian)* 79−56522
EM wave scattering from random rough-surface model, comparison of variational, perturbational and exact solns. 78−66724
e.m. waves reflected by rotating cylinder, amplification calc. *(Russian)* 77−3523
ENDOR, multiplet HFS, energy level non-crossing, second order perturbation theory 79−72341
energies, bounds, from perturbative approximations to Bloch-Horowitz effective Hamiltonian, ^{18}O calcs. 78−70466
energy calculation, converging approximations, in terms of Planck's constant 79−25889
energy eigenvalue problem, adiabatic perturbation theory using QFT techniques 78−93551
energy transfer and two-centre optical transitions in OH^- and rare earth double-doped solid 80−7398
envelope wave stability 80−43410
enzymatic catalysis, orbital perturbation anal. 78−31623
EPR spin Hamiltonian, perturbation treatment, M=0 electronic state, HFS of triplet state EPR 80−25185
Epstein-Nesbet partitioning of full Hamiltonian, second-quantisation representation 77−3254
Epstein-Nesbet Rayleigh-Schrodinger perturbation theory, modified H_0 79−49925
equivalent nuclei, ENDOR fine struct., exact solns. 77−6811
error bounds, comparison theorem 77−13574
ethane, nuclear spin-spin coupling consts., vicinal proton-proton coupling calcs. 80−32737
ethylidene, rearrangement to ethylene, barriers, ab initio MO calcs. 80−104424
Euclidean (super $\phi^3)_4$, Wess-Zumino model, asymptotic behaviour in perturbation theory 79−30645
exchange, intermolecular forces, primitive function 78−37701
exchange interactions between atoms or mols., generalised Jansen's perturbation theory 79−6981
exchange perturbation theory for electron scatt., appl. elastic scatt. from H 80−78709
excited states, perturbation and SCF calcs. 80−102455
excitonic molecule, two-photon excitation of first vibr. state probability 79−7789
excitons, Wannier-Mott, interaction with screw dislocations *(Russian)* 79−4513
Fabry-Perot resonators, second-order perturbation theory 79−18451
Faraday's law problem, including nonlinear term, rel. to perturbation theory, for teaching 79−35470
Federbush model, perturbation theory, induced interaction terms 77−13853
Fermi's 'golden rules' and exact long-term transition probability 77−30037
Fermi system, perturbation theory, system exhibiting dynamic symmetry breaking 79−143
fermion self-energy calculation, covariant formulation of relativistic Hamiltonian theory *(Russian)* 80−9087
fermion-instanton coupling in two dimens., using perturbation theory for fermion sector 79−67475
fermions, quantum field theory, large order perturb. theory, more than one coupling constant 80−77940
ferromagnetic materials, EM field penetration, perturbation calc. *(Russian)* 79−59617
ferromagnetic metal, two-site interaction model 79−82744
ferromagnetic metals, s-d exchange interactions, effect on attenuation of spin waves *(Russian)* 79−19730
ferromagnetic resonance in anisotropic Heisenberg model, magnon-magnon, phonon-magnon interactions *(Russian)* 80−11274
ferromagnetic semiconductor, theory review 80−20369
ferromagnets, Heisenberg and planar, exact results for spin-wave renormalisation 79−69660
Feynman path integrals, conference, Marseille, France, 1978 80−31422
Feynman path integrals, generalised meas. 78−384
fifth order perturbation theory prod. amplitudes, pions, nucleons, isobar model 77−54088
film, stability and rupture using perturbation analysis 78−79911
fission reactor, one-group model, convergence acceleration in perturbation theory problems 78−37406
fission reactor calcs., convergence criterion and error estimate 77−14216
fission reactor theory, ratios in linear and nonlinear problems 77−23175
FitzHugh-Nagumo equations, perturbation anal. of slow periodic wave soln. 78−24060
flame propagation, applic. of perturbation theory for eqns. having an invariance group 77−60067
Floquet's theorem, general temporally periodic Hamiltonians 77−57939
flow between porous walls, 2-dimens, laminar 79−14477
flow of viscous imcompressible fluid, singular perturbation theory 77−3803
fluid, (12-6-n), thermodynamic perturbation theory 78−26414
fluid, anisotropic, transport coeffs. 77−7497
fluid, hard dumbbell mols., reference pot., perturbation theories, spherical reference systems 80−28898
fluid, hard-core plus Yukawa tail pot., eqn. of state 78−26410
fluid, one-dimensional, macroscopic and local compressibility, free energy, perturbation calc. 77−35455
fluid, perturbation expansion using hard core with attractive part reference pot. 77−19856
fluid mixtures, analytic and perturbation theories 78−18516
fluid of rod-like mols. interacting via Kihara potential 77−11291
fluid phase, statistical thermodynamics, review 78−83703
fluid with nearly spherically symmetric molecules, thermodynamic perturbation theory 80−14985
fluids, perturbation theory and thermodynamic props., CRIS model 80−92430

perturbation theory continued
fluids, perturbation theory and thermodynamic props., inverse power and 6-12 pots. 80−92431
fluids, perturbation theory and thermodynamic props. 80−92429
fluids with polar, quadrupolar, octupolar mols., thermodynamics, vapour-liq. equilibria 78−95127
fluorene conjugate bases, chem. shift, ring-current and excess-charge effects, semi-empirical calc. 78−33523
fluxon dynamics, perturbation anal. 79−11280
focusing of waves in anisotropic plane-layered medium, analytical solns. of Maxwell's eqns. 80−32890
Fokker-Planck dynamics, perturbation expansion 79−88879
formaldehyde, semi-empirical excited state Morokuma's EHP calc., geometry and order of states 78−46256
formaldehyde+formaldehyde, medium distance interaction, SCF LCAO MO, supermol., perturbation and MCF calc. 79−837
formamide, $^1\pi\pi^*$ state, perturbation theory calcs. 78−62705
formamide+formamide, medium distance interaction, SCF LCAO MO, supermol., perturbation and MCF calc. 79−837
formyl radical, electronic struct., dissoc. energy and pot. energy surface many body perturbation theory and couple cluster doubles calc. 80−23296
fourth order perturbation theory, triple substitutions to electron correl. energy 80−74133
fragmentation functions beyond leading order in QCD 80−13282
free electron lasers, classical theory, saturation, perturbation calcs. 80−83580
free polaron spectrum and convergence radius 80−70626
freezing in finite domains not initially at fusion temp., singular perturbation theory 77−66014
Frenkel-Kontorova system, discreteness effects, perturbation formalism, Peierls pot. and kink vel. reduction 80−34001
Froelich Hamiltonian, perturbation theory calcs. 79−33247
fully coupled SCF perturbation theory in matrix form, simultaneous perturbations 77−34548
fusion reactor eddy currents, 3-dimens., perturbation-polynomial expansion calcs. 78−66372
$g\phi^4$ model perturbation theory, anal. continuation to $g \geq 1$ region 79−97525
gas-solid turbulent suspension flow, frictional pressure drop Prandtl's mixing length anal. 79−14458
gaseous ion transport theory, perturbation treatment of thermal motions 79−64820
gauge copies, Abelian and non-Abelian cases 80−47170
gauge fields, quantisation, renormalisation, and fluctuations 79−30670
gauge invariance and pseudoperturbations 80−22545
gauge invariance in operator-product expansion in non-Abelian gauge theory 77−2751
Gaussian profile diffused waveguides, perturbation analysis for modes 79−18529
Gell-Mann Low function calc., for scalar theory with strong nonlinearity 77−13639
Gell-Mann Low function expansion coeffs., quasiclassical theory *(Russian)* 77−30272
general relativity, type-D metrics 77−64975
generalised Federbush model, current definition, perturbation calcs., gauge transformations 79−6297
generalised Glauber-Ising chain, dynamics in a mag. field, biopolymer appl. 79−155
generalised perturbation theory, new developments in nuclide field 77−23180
generalised perturbation theory, quality of first order wave function 77−67963
generalized bound-state perturbation theory 80−17748
generalized Liouville equation, entropy, and dynamic systems containing limit cycles 79−21648
geometrical spacetime perturbation theory: regular first-order structures 79−2678
glow discharge in diatomic molecular gas, electronic excitation rate, vibr. temp. influence 80−19633
gr^{2N} anharmonic oscillator, perturbation theory 80−90712
graded-index fibres, evanescent theory and perturbation theory comparison 79−32033
Grassman functional Schrodinger equation appl. to perturbation theory 79−21915
gravit. wave propagation calcs., perturbations of analytic background metric 78−8302
gravit.-EM perturbations, Reissner-Nordstrom geometry, forced perturbations 78−8303
gravitational perturbations of quantised EM radiation in cavity 78−54268
gravitational perturbations Vaidya background 77−74292
gravitational waves, Bianchi type-I universe, tensor perturbation equations, derivation 79−124
Green's function, effective mass formalism 78−28915
Green's functions in quantum theory, book 79−65147
gribov ambiguity, perturbation theory, and confinement 79−21934
Gross-Neveu and nonlinear σ-model, scatt. amplitudes in $1/N^2$ perturbation theory 78−70261
halogen ion, with filled shell, dipole polarisability 80−9501
Hamiltonian, zero-order, for many-body perturbation theory 80−9483
Hamiltonian expectation values for time-depend. Foldy-Wouthuysen transformations 77−49633
hard dumbbell fluid, RAM perturbation theory 79−72980
hard dumbbell fluids, RAM and BLIP function theories 80−79658
hard quadrupolar diatomics, free energy, perturbation theory and Monte Carlo calc. 79−90361
hard sphere system, second-order perturbation theory 78−79516
hard-sphere fluids, dipolar and quadrupolar, radial distrib. functions, perturbation theory 78−59727
harmonic oscillator with λx^M perturbation 80−27161
harmonic time depend. oscillator with damping and perturbative force 80−82
Hartree-Fock calculations, with reduced Green's functions, theory 77−14338
Hartree-Fock perturbation theory, first-order, symmetry calcs. 79−6854
heat conduction in solid with random conductivity, perturbation method, temperature field 79−46162
heat conduction quasisteady mode with asymmetric boundary conditions 78−83208
perturbation theory continued
heavy atom substitution, vibr. freqs. and anharmonicity consts., general isotopic rules 77−75122
heavy ion collision, K-shell vacancy sharing, variation-perturbation mol. model 79−31665
heavy ion collisions, perturbed stationary state method, low energy collision and mol. resons. 80−78320
heavy quark systems, spin dependent interactions, QCD perturbation theory anal. 79−36019
heavy-ion collisions, perturbation theory of nucl. friction, strong energy damping 77−67766
Heisenberg classical nearest-neighbour chain, dynamics, exact perturbative results 78−10700
HF equations, instability threshold and peculiar solns. 79−85881
HF subsystems, long range induction and dispersion interactions 80−53092
HF theory, 1st-order, perturbed, use of symmetry in mol. props. calcs. 79−85916
higher order, appls. to quantum mech. and field theory *(Russian)* 78−36886
higher order perturbation methods, implicit and explicit, for reactor anal. 78−78444
higher order time depend. theory, appl. to nuclear reactors 78−58333
holonomic character and local monodromy struct. of Feynman integrals 77−54038
homonuclear diatomic molecule, united-atom projected perturbation theory 78−37705
hot nonuniform magnetised plasma wave propag. theory, Vlasov eqn. perturbation expansion 80−33768
Hubbard model, canonical perturbation expansion 79−38296
hydrides, single-centre perturbation theory calcs. 80−5470
hydrocarbon, ^{13}C NMR shielding constants and tensors, finite perturbation calcs. 77−27092
hydrocarbons, alternant, perturbational MO calcs., appls. 78−74565
hydrocarbons, average elec. polarisabilities and mag. susceptibilities, ab initio valence electron calcs. 80−87033
hydrocarbons, conjugated, ^1H chem. shifts calc. 79−98121
hydrocarbons, thermodynamic props. correls., third parameters 79−95184
hydrogenic atom, model perturbation theoretic calculations with finite continuum basis sets 78−25412
hyperpolarizability, freq. depend., time depend. HF eqn., second order LCAO SCF pertubation theory 79−31388
III-V semiconductors, k.p perturbation theory 77−43484
improved uncoupled Hartree-Fock perturbation methods, 2nd-order energy bounds in UCHF perturbation theory 79−85884
incomplete basis set problem, virtual orbitals and CIBS expansion of HF energies 80−52844
incompletely optimized variational parameters, corrections, perturbation theory anal. 78−41180
incompressible viscous fluid, homogeneous turbulence, systematic perturbation method 77−31282
induction energy, coupled Hartree-Fock calcs. 80−43139
inert gas, thermodynamic properties, perturbation calcs., density depend. 77−7504
inert gas atom, first excited config., intermediate coupling coeff. 80−83450
inert gases, collision induced polarisabilities, perturbation treatment 78−86778
inert gases, mean force constants and rectilinear law of mean force calcs. 78−33414
infinite order, by transformation of Schrodinger eqn. 78−12589
inorganic molecules with polytopic bonds, motion of nuclei 79−41125
instanton effects in pure Yang-Mills theory, perturbation theory rules 78−58125
instanton singularities, Borel summing, method introduction 79−71624
intense field QED in continuous medium, appl. to Thomson scatt. and Cherenkov radiation 80−27435
intensity fluctuations and fourth-order coherence function in random media 80−78774
interactions, point, periodic, one particle theory, polymers, monomolecular layers and crystals 80−105576
interdoublet EPR spectrum ang. depend. for ions with arbitrary electron and nuclear spins in strong axial cryst. field 80−93164
intermediate valence system, local polaron model 80−107717
intermolecular forces, ab initio calcs. applicability and accuracy 80−18898
intermolecular interactions perturbation theory, Pade approximants and convergence 79−31635
interruption function in perturbation theory for molecular collisions 77−23528
intramolecular electron transfer rate, purely electronic effects, simple model Hamiltonian 77−10592
invariant tores, Galerkin's method *(Russian)* 77−53744
inverse matrix diagonal and off diagonal elements, self energy perturbation theory 78−82607
3×3 inverse scattering transform, soliton perturb. scheme 80−27151
inverse theory, nucl. reactor appl. 79−93691
ion+molecule, classical differential cross-sections, anisotropic pots. 78−66627
ionic crystal, quadrupole antishielding factors and polarisabilities 77−51346
ionic crystal, Sternheimer antishielding factors of F^-, Cl^-, Br^- and I^-, approx. free- and cryst.-ion pot. influence 80−39544
ionisation potential, closed shell systems, including electronic relax. and correlations 78−906
ions, electron impact excitation, close-coupling formalism, perturbative treatment 80−48091
ions, H-, He-like, Z=4 to 34, wavelengths, radiative transition probabilities, autoionisation rates 79−25776
ions, ionisation potentials, electron affinities, perturbation theory-CI calcs. 78−9084
ions, multiply charged, level lifetimes relativistic calc., S-matrix approach 80−47942
ions in $1s^22s^n2p^{4-n}$ configurations, term-energy calcs. using perturbation theory 77−42229
ions resembling Li, Be and B, spectra calcs., fine struct., transition energies 77−42260
Ising chain, random bond, low temp. behaviour 80−57211
Ising model, cluster of two spins, time-depend., perturbation theory 77−45799

perturbation theory continued
Ising model, random, $\epsilon^{1/2}$ expansion of crit. behaviour, higher order corrections 78−27050
Ising spin glass, replica symm. and massless modes 79−33486
isostructural phase transitions due to core collapse, one-dimens. model 77−2599
isotropic magnet, Goldstone mode singularities eqn. of state, magnetisation curve, perturbation theory calcs. 78−43607
isotropic medium, elastic wave scatt. from flaws, long-wave approx., appl. to ellipsoidal voids and inclusions 79−86368
iterative natural orbitals for CI using peturbation theory 77−79549
Jahn-Teller linear E-e effect, canonical transformation 78−67993
Jansen-Byers Brown exchange perturbation theory, transformation operator 77−28380
Jeziorski-Piela perturbation theory 77−65523
Jupiter, and Saturn natural vibration spectrum, rot. effects, calc. 80−8583
Keldysh's perturbation formalism 80−13217
Keplerian orbital motion, Lagrange parenthesis and perturbation eqns. *(Spanish)* 77−49280
Keplerian orbital motion, systematic formulation of perturbation formulae *(Spanish)* 77−49279
Kerr black hole, gravit. perturbations in spin coeffs and Weyl tensor components 78−12273
Kerr black hole, gravit. perturbations of quantities finite in stationary state 78−12274
ketene, UHF-INDO perturbation calc., localised spin orbitals, spin anomaly and second order substituent effect 79−68191
kinetic equations for system with weak interaction *(Russian)* 77−64992
Klein-Gordon charged particles, perturbation theory for non-equilibrium stat. Green's functions 80−31994
Kolmogorov Arnold Moser theorems, appl. to struct. problems in condensed matter 80−59878
Kondo alloy, dil., thermoelec. power in asymmetric single-orbital Anderson model, perturbation calc. 79−99534
Koopman's theorem, corrections using energy shifted perturbation theory 79−6845
Korteweg de Vries equation, Pade approximants, soliton solns. 80−42071
Korteweg-de Vries eqns., perturbed solns. and soliton production 80−42074
Korteweg-de Vries equation, perturbation theory 77−33852
Kramers theory of friction and vel. in chemical kinetics 80−50826
Kramers-Heisenberg dispersion formula, Dirac transformation generalisation 78−16960
lagrangian multipliers in frozen core Dirac-Fock calculations 78−73881
Lamb dip, transit time broadening, perturbation theory calcs. 77−647
Landau-Ginzberg ferromagnet, static and dynamic correl. functions near magnetization curve 79−15318
Langmuir solitons, non-neutral soln. 80−33763
lanthanide ions, tripositive nucl. hexadecapole antishielding factors 79−26909
large order, ϕ^{2N} interaction, anharmonic oscillators in quantum mechanics 77−45735
large order, choice of integration contour 79−6263
large order, role of vacuum instability 77−41504
large order behaviour for potential with degenerate minima 78−4516
large order estimates 79−26237
large order expansions in perturbation theory 78−54525
large transverse momentum behaviour of Compton scatt., Moller scatt., and quark-quark scatt. 77−71429
lattice gauge theories, improved strong coupling expansions and matrix Pade approximants 79−71628
lattice gauge theory continuum limit, renormalised perturbation theory, lattice Lagrangian 79−6283
lattice Schwinger model, form factors of dipole states 78−66029
lattice soliton, scatt. by mass interface, reductive perturbation method 78−18889
Lennard-Jones fluid, 2-D, radial distrib. function, integral eqn. perturbation theory 78−26409
Lennard-Jones fluid, 6-12 pot., press. calcs., using integral eqn. and perturbation theory 79−4224
Lennard-Jones fluid, eqn. of state, Monte Carlo and perturbation theory 77−76519
Lennard-Jones fluid, equation of state 79−73083
Lennard-Jones fluid, two-centre, perturbation theory appl. using spherically averaged reference potential 80−64860
Lennard-Jones low temp. gas, eqn. of state, integral eqn. and perturbation method 78−26228
Lennard-Jones system, thermodynamic functions in liq. and vapour region 79−10910
lenslike medium, mode degeneracy removal by x^2y^2 term in index distrib. 77−83812
lepton bound in Coulomb field of nucleus 79−94115
Lie transform, approach to classical perturbation theory, plasma physics appl. 78−93510
lifting-line theory, alternative treatment as perturbation problem 79−27663
light hydrogen-like atoms, nuclear size corrections to energy levels 79−36549
light quark mass spectrum in QCD 79−63427
light scattering by a pair of conjugate nonspherical particles 80−32912
limit cycle, symmetric bifurcation to asymmetric limit cycle, simple model 80−57080
linear polymer molecules, second virial coeff., chain length effects calcs. 78−37775
linear randomly perturbed systems, mean-square stability 77−9870
linear zero-spin fields in external gravit. and scalar fields, perturbation theory 80−31969
linearisation stability and globally singular change of variables 80−31629
Lippmann-Schwinger type integral eqn. of motion, quantum corrections 78−62318
liquid, hard sphere mixture, nonadditive dias., perturbation theory, double reference system 78−38597
liquid, ionic and multipolar, thermodynamic perturbation theory 77−47316
liquid, perturbation theory for soft core pot., radial distrib. function 80−6333
liquid, possible modifications *(Russian)* 77−1056
liquid, props. of optimisation condition 78−38598
liquid crystals, correlation in statistical theory 78−75536

perturbation theory continued
liquid metal, electron momentum density, perturbed Green's function method 78−60052
liquid metal, electronic density of states, pseudopotential calcs. 80−70578
liquid metal, extension to dense partially ionised plasmas 80−75500
liquid metals, radial distrib. function and thermodynamic characts., interparticle interaction pot. *(Russian)* 80−49086
liquid metals, structure, perturbation calcs. using Percus-Yevick equation 78−42889
liquid mixtures, intermol. forces effect on phase diagram and excess props., perturbation theory 80−39287
liquid-vapour phase diagrams, renormalised one-chain approx., square mound reference system 77−11663
liquids, perturbation theory and triangular well pot. 77−47310
liquids, simple, surface tension and density profile from expression for excess free energy 77−80681
liquids, simple, thermodynamically self-consistent theories, radial distrib. function, functional derivative 80−92435
liquids and mixtures, statistical thermodynamics, book 80−90616
liquids with noncentral interactions, struct. contrib., perturbation method and partition function separation 80−24341
LMFBR heterogeneous core, sensitivity anal. 80−22935
localised perturbation theory for projected states, two element group 78−24685
localised spin orbitals, spin anomaly and second order substituent effect 79−68191
logarithmic perturbation expansions, appl. to H in multipole field 80−37720
long wavelength spin susceptibility from particle-particle scattering, logarithmic temp. control 80−7124
long-wave oscillation damping calc. *(Russian)* 78−75302
Lorenz equation in high Rayleigh number limit, periodic soln. using perturbation theory of nonlinear oscills. 79−68681
lower bounds to ground state eigenvalues, Pade approximants 78−49722
lubrication, asymptotic approximation to class of regular perturbation problems 78−18258
LWR, first order perturbation methods in sensitivity anal. 80−37425
Lyman-α line wings, contribution of proton perturbers 78−67325
macromolecular multicomponent system, phase separation, thermodynamic perturbation theory, calculus 78−18778
macromolecules, cluster expansion 80−106408
magnetic elastic system, one-Fermion-one-Boson model 78−43539
Mandelstam graph, deep inelastic asymptotics 79−85244
many body perturbation calculations and coupled electron pair models 79−59363
many body perturbation expansion, fourth order linked diagrams for quadruply-excited states 79−59364
many body perturbation theory fourth order calc. of correl. energy 80−14087
many body systems, Anderson model, localisation phenomena, state variable randomness, perturbation theory 80−29297
many channel Marchenko transform. operator, upper bounds 79−63091
many fermion systems, asymptotic nature of perturbation theory 80−46967
many-atom system, coherent radiation processes, renormalisation calcs. 77−3560
many-body perturbation theory, modified pots., 3- and 4-body contribs. 77−88376
many-body perturbation theory, symmetry-adapted, wave operator matrix elements 80−23311
many-shell SCF theory, convergence, first order perturbation anal. 79−9999
mass divergences in annihilation processes, cut vac. polarisation diagrams 78−70285
mass divergences in annihilation processes, cut vac. polarisation processes, diagrams 78−74157
massive quark pot. scatt., cancellation of infrared divergences 79−71707
massive Thirring model, localised solns. in presence of external electrostatic field 77−13864
massive Thirring model, particle scatt. in perturbation theory 77−82674
massive Thirring-Schwinger model, convergence of perturbation theory and particle structure 77−10173
massless field theory observables, infrared finiteness proof for all perturbation theory orders 79−21917
massless spinor field/massive pseudoscalar field interaction, mass perturbation around exact soln. 79−63368
Mayer cluster function and quantum two-body t matrix 80−17859
Mayer equations for Bose field theoretical models 79−71593
MBBA/EBBA, nematic, mol. interaction energy 80−33881
mean field perturbation theory, path integral formulation 78−12803
mechanics of deformable media, perturbation method in 3-D problems *(Russian)* 78−49660
melting in finite domains not initially at fusion temp., singular perturbation theory 77−66014
meson+meson cross sections in QCD *(Russian)* 80−4968
meson resonances in nuclear field *(Russian)* 78−78424
metal, FCC, covalent component of electron density and energy *(Russian)* 80−28945
metal, impurity effects on cond. electrons, perturbation theory 79−60763
metal, lattice stability, perturbation formalism for comparison of crysts. with different lattices 77−51631
metal, multiplication photoemission in strong field 77−85891
metal, simple, non muffin-tin corrections to eqn. of state *(French)* 80−59906
metal, third order perturbation theory self consistency 78−76014
metal, vacancy formation energies and volumes, exam. of models 78−47349
metal, valency electron density and total energy, weak pseudopotential calc. *(German)* 77−59241
metal surface, band effects and dipole interaction between two adatoms 79−33323
metal surface, perturbative calc. of elec. field 80−45108
metal surface interaction with external mol. complex 79−47140
metal-ligand 3-orbital-4-electron, 4-orbital-4-electron bonding, perturbation theory 79−98000
metals, atomic displacements near impurities and many-particle interactions *(Russian)* 80−24553
metals, electron spin-transverse phonon interaction, spin lifetime perturbation calc. 77−12189
metals, localised dynamic perturbations 80−73262

perturbation theory continued
metals, localised moment interaction, Alexander-Anderson model, perturbation expansion 80−29524
metals, simple, electron-electron interaction, self-consistent perturbation theory based on Hartree-Fock theory 79−95357
metals, X-ray photoemission spectroscopy, anomalous, frequency dependence of exponents 80−71563
metastable liquid, instability and freezing, theory 78−18746
methane, freq. depend. polarizability, LCAO SCF perturbation theory 79−31387
methane, ionisation pot., quasidegenerate many-body perturbation theory calcs. 77−50346
methane, mag. susceptibility, HF perturbation method 77−79702
methane, mol. nuclear spin-spin coupling, ab initio SCF perturbation theory 78−33525
methane, nucl. elec. shielding tensor calcs. 80−83296
methane, proton mag. shielding const., HF perturbation theory 78−46258
methyl isocyanide, unimol. isomerisation to methyl cyanide 79−24725
methylene, triplet ground state, var. and perturbational calcs. 77−61680
MIM diodes, negative differential resistance, stimulated inelastic tunnelling theory 80−49951
MISIM struct. inversion layer, symmetrical, carrier conc. calc. 80−75651
model-space effective operators construction 78−4508
modified virtual orbitals, HF calcs. of second order perturbation energy 80−102437
modulated perturbation theory, mol. interactions, STO expansions nonlinear parameter minimisation 77−57871
moisture horizontal absorption in unsaturated soils, infiltration analysis 77−29345
molecular conformational props., internal rot. barriers, PCILO-CNDO calcs. 77−75056
molecular correlation energy calc. by many-body diagrammatic perturbation theory 78−9087
molecular crystal, surface exciton energy calc. 77−20400
molecular electrical props., chem. substitution effect, LCAO calc. 79−41103
molecular electron correlation, valence bond perturbation theory 79−18120
molecular electron scatt., semiclassical theory 78−58825
molecular energy levels, isotropic rules for heavy atom substitution 77−83660
molecular fluid, computer simulation of liquid-vapour surface 80−54478
molecular fluid, pair correlation function, perturbation theory 78−55799
molecular fluid perturbation theory, Pople expansion third order term, anisotropic pot. 78−79510
molecular fluids, angular pair correl. function, second order perturbation theory 79−86662
molecular fluids, ref. system selection and average Mayer-function perturbation theory 80−38891
molecular gas, low density, transverse nucl. mag. relax. 79−59490
molecular geometry optimisation with explicit inclusion of electron correl. 80−37748
molecular hyperpolarisabilities, HF calc. with correlation method, appl. to HF mol. 80−23342
molecular isotope partition function ratios, perturbation calcs., convergence 80−87239
molecular model potentials, constructive theory 79−26869
molecular multipole magnetisability, mag. shielding, multiple SCF perturbation theory 77−34549
molecular nuclear spin-spin couplings between ^{1}H, ^{13}C, or ^{19}F, LCAO-MO-SCF-MINDO/3 approx. calcs. 79−94019
molecular orbitals, counterintuitive orbital mixing, SCF perturbation methodology 78−74564
molecular polarisabilities calcs., superposition method of excited config., nonstationary perturbation theory eqn. 80−69257
molecular polarisability, ground and excited state, perturbation treatment 78−5144
molecular polarisability, scaling and Pade approximants, many-body perturbation theory 80−42952
molecular rot.-vibr. anal. by finite difference perturbation method 77−50420
molecular rotational spectra, doublet splittings caused by tunnelling, perturbation treatment 80−91541
molecular spectra, IR, operator perturbation method, effective Hamiltonians *(Russian)* 77−79599
molecular spectra, IR, operator perturbation method, effective Hamiltonians *(Russian)* 77−83563
molecular spectroscopy, third order perturbation theory, simplification 79−98064
molecular static polarisability, ab initio SCF wave functions 80−74106
molecular vibr. mean square amplitudes of mol. internal coords., perturbation theory 79−89659
molecular vibration, low-symm. mol., vibr. Hamiltonian 79−22687
molecular vibration excitation on resonant electron scatt., time-perturbation method *(Russian)* 80−14242
molecules, direct CI calcs. with multiconfigurational reference state 80−63506
molecules, excitation to coherent state, resonant energy transfer calcs. 79−98178
molecules, ground state props., coupled cluster and MBPT methods appl. 80−47881
molecules, identical, dispersion intermolecular pot. anomaly prod. by intense radiation field 80−58336
molecules, ionisation potentials, electron affinities, perturbation theory-CI calcs. 78−9084
molecules, ionisation pots., electron affinities, Rayleigh-Schrodinger and Green's function calcs. 77−75075
molecules, isotopically tagged, normal vibr. freq. calc., eigenvalue behaviour, perturbation theory obs. 80−52973
molecules, monochromatic wave perturbation, time depend. HF calcs. *(French)* 80−63516
molecules, pair energy, perturbative corrections, incomplete basis set problem 80−78507
molecules, two criteria for labelling approx. treatments as fully quantal ones 80−23289
monolayer mobile adsorption, 2-D hard disc model, perturbational method 78−38932
Mossbauer line shape, in presence of ionic charge relax., perturbation calc. 77−28495
perturbation theory continued
Mossbauer relaxation theory 80−39954
multicentre electron systems, Eisenschitz-London perturbation theory 78−41915
multicentre electron systems, exchange perturbation theory 78−41914
multicentre electron systems, Hirschfelder-Silbey exchange perturbation theory 78−41916
multicomponent fluid mixtures, renormalised one-chain approx. 77−11452
multiconfiguration reference states, perturbation theory calcs. 79−13644
multiphoton excitation, collisionless, of large mol. kinetic eqns. 79−54914
multiphoton transitions, perturbation theory, atomic ionisation and intermediate reson., dissoc., review 79−41145
multiple well anharmonic oscillators and perturbation theory 79−49086
multiple-scale for anharmonic oscillator 77−74211
multiply charged ions, relativistic perturbation theory appls. 80−23323
muonic atoms, light, finite nucl. size corrections to energy levels 79−18321
$N_2H_5[Fe(N_2H_3COO)_3].H_2O$, elec. field gradient at Fe^{2+}, perturbation theory calcs. 78−19002
N-level system, generator of completely positive dynamical semigroups 78−45513
n-vector model, stochastic, dynamic critical props. 77−24362
naphthalene, singlet and triplet excimer interactions, exciton resons. 80−95535
nearly free electron metal surface, at. chemisorption 78−14588
nematic liq. cryst., nonlinearities and fluctuations at hydrodynamic instability threshold 78−87614
nematic liquid crystals, equation of state, anistropic props., perturbation theory 78−67645
nematic ordering in a system of rods 79−60271
neutrino, Maxwell, and scalar fields in the cylindrical magnetic or plasm universe 80−120
neutron diffusion calcs., appl. to reactor design and anal. 77−79427
neutron diffusion modelisation, optimal design and eigenvalue problems 78−66329
neutron hot perfect fluid relativistic stars, asymptotic eigenfrequency distrib. for even parity perturbations 78−49668
neutron transport eqn., homogenised diffusion approx. 80−47522
Newtonian cosmologies, homogeneous, review 78−16584
NMR spectra in semi-mean interaction regime *(Russian)* 78−80231
noble metal, cubic close-packed struct. anal., interplanar interactions from degenerate perturbation theory 77−58971
noble metal dilute alloy, residual resist. calc. 77−28156
non-Condon approximation calcs. of theory of radiationless processes *(Russian)* 78−72599
non-Minkowskian space-times, mass generation by self-interaction 79−45014
non-standard perturbation theory for Green functions, nuclear spin eqns. appl. *(Russian)* 79−45
nonelectrolyte solutions, liq. theory, review, book contrib. 77−39523
nonideal system, thermodynamic variables, irreducible cluster integrals 77−67394
nonlinear, stochastic differential eqn., perturbation theory, projection operator method, statistical linearisation 78−41229
nonlinear 3-D field model, perturbation theory, UV divergence free 78−54567
nonlinear diffusion-reaction with autocatalysis and saturation law, single perturbation approach 80−35502
nonlinear dispersive and dissipative wave propagation 77−74231
nonlinear field theory, spherical symmetric solution stability, influence of weak perturbations *(French)* 78−16904
nonlinear harmonic oscillator, perturbation theory 80−19272
nonlinear ion-acoustic cnoidal waves, propag., perturbation theory calcs. 79−86581
nonlinear O(3) invariant theory, quantisation in neighbourhood of classical soln. 79−97522
nonlinear periodic waves stability in plasmas 80−38615
nonlinear resonance in quantum system, perturbation and quasiclassical theory 77−13640
nonlinear Schrodinger equation, perturbation expansion, nonlinear Landau damping influence 78−62110
nonlinear singular diffusion eqn., perturbation soln. 79−71387
nonlinear singular perturb. problems, asymptotic equiv. 77−9875
nonlinear singular perturbation problem on a semi-infinite interval 78−94631
nonlinear system, kink-phonon interaction 79−73262
nonlinear systems, canonical perturbation theory 79−17338
nonlinear systems, functional integrals, perturbation expressions 79−97255
nonlinear wave eqns. in n-dimensional space, periodic solns. 78−93540
nonlocal nonpolynomial interactions, strong coupling in quantum field theory 78−21319
nonpolar liquids, soft nonspherical repulsions, effect on props. 77−68903
nonrelativistic one-dimensional problems, perturbation theory algorithm 80−82671
nonrelativistic persistent model, Schrodinger and Klein Gordon interacting fields with Chew-Low coupling, renormalisation props. 79−54250
nonrelativistic perturbation theory, new approach 79−71289
nonrelativistic quantum mechanics and anomalous part of g-factor 77−74238
nonrenormalisable QFT models, summing of perturbation theory 78−74129
nonseparable wave equations, multidimensional perturbation theory 79−58576
nonstationary physical systems, mathematical model 79−84985
nonuniform simple hard-sphere fluid, interface props., statistical mech., perturbation theory 77−84607
nuclear effective charge evaluation using perturbation theory 78−78250
nuclear field theory of three-particle system outside closed-shell nuclei 78−25129
nuclear field theory perturbation expansion for strongly anharmonic systems, convergence, phonons 78−62490
nuclear fuel lattice eigenvalue as function of buckling, perturbation theory correction 79−59118
nuclear matter, third-order calcs. for realistic potentials 77−6281
nuclear matter theory, review, comparison of perturbative to variational techniques 78−33136
nuclear optical model parameter searches, minimisation procedures, use of derivatives 77−10379

perturbation theory continued
nuclear pairing force model, perturbation theory for projected states 78−33126
nuclear reaction cross sections, perturbative calc., eigenchannel and Barrett-Delsanto methods 79−63638
nuclear reactor core reactivity and space-domain noise effects of randomly dispersed materials 78−94071
nuclear spin-spin coupling constants in series of related mols., orbital model, perturbational approach 79−81217
nuclear struct., cf. with degenerate many fermion theory 77−6254
nuclear two-body effective interactions from large matrix diagonalisations 78−41644
nuclei, transitional, pairing rotations and quadrupole modes 80−18165
nuclei acid base stacked dimer, origin of excimer states in extended Huckel method 80−35832
ocean surface gravity waves, nonlinear theory, derivations 77−60387
ocean surface gravity waves, nonlinear theory, interp. and appls. 77−60388
odd anharmonic oscillators, perturbation theory 80−86106
one-dimensional band calculations using perturbation theory 80−44460
one-dimensional molecular crystals, electronic struct., mol. orbital theory 80−54588
one-dimensional particle-in-the-box problem, perturbation theory illustration using champagne bottle situation 80−36816
open resonator with aperture in reflector, theoretical anal. 79−31955
open resonators, diffraction losses for symmetrically tilted plane reflectors 80−58598
open shell excited states, perturbation effects, restricted Hartree-Fock calcs. 78−86770
open shell polarisation propagator, for doublet-doublet transitions calcs. 80−27939
open-shell system, polarisability and mag. susceptibility calc. by SCF and CI method 80−99443
open-shell systems, many-body perturbation theory, coupled cluster approach 79−31360
operator ordering and perturbation expansion, path integral formalism 78−16682
operator polynomials, divisors, perturbation theory 80−36905
optic fibre light propagation, review of analytic methods of study *(French)* 79−90001
optical fibre, low-V, with dip in refractive index, perturbation theory 79−37012
optical fibre, quasiparabolic index profile, propag. characts., perturbation anal. *(French)* 80−33189
optical fibre, step or graded index, refr. index dip effect on propag. 78−18053
optical fibre birefringence, in limit of weak guidance and slight ellipticity 80−1309
optical fibres, evaluation of normalised cutoff frequencies in radially inhomogeneous fibres, perturbation theory 80−43434
optical fibres with power-law core profile, perturbation theory 79−7211
optical graded index fibre propag., expt. and theory 78−90496
optical nuclear polarisation, field and orientation depend., non-crossing rule, perturbation anal. 77−42337
optical nuclear polarisation, the non-crossing rule, electronic relax. perturbation anal. 77−42338
optical plane wave intensity fluctuations in turbulent medium *(Russian)* 78−1156
optical rotary echoes, Bloch eqns. perturbative solns. 80−43407
optical waveguide, asymmetric dielectric-slab, beam mode scatt. characts. 80−38114
optical waveguides, index profile determ. methods 80−1337
optically pumped laser three-photon transition theory 80−102690
orbit-orbit interaction, new tensor expansion, matrix and graphical forms 80−14064
orbital perturbation of tethered satellite systems 78−96381
orbital perturbations of space structures, effect of solar radiation, analysis 79−5723
organic molecular crysts., charge carrier generation by exciton-exciton collisions 80−88568
organic molecules, quadrupole moments, dipole quadrupole A and C polarisabilities, perturbation theory anal. 80−27934
organic mols., NMR coupling consts., MINDO/3 and perturbation theory 77−79630
organic ring mol., INDO finite perturbation theory, contact proton spin-spin coupling 77−50361
orthonormalization, polar decomposition, and transformation to an effective Hamiltonian 79−6811
oscillations in chemical systems, Oregonator concept 77−16784
oscillations in chemical systems, Oregonator concept 77−16785
oscillator, x^{p+2} nonlinear damped, first order perturbation soln. 77−17807
oscillator strengths calcs. in length and rel. forms 79−72275
oxoniomethylene cation, rearrangement to hydroxymethyl cation, barriers, ab initio MO calcs. 80−104424
PAA, nematic, equation of state, anistropic props., perturbation theory 78−67645
Pade and Pade-Borel perturbation theory series summation methods *(Russian)* 79−2663
Pade-Borel summation of perturbation series, Gell-Mann-Low function 78−86416
particle in EM field, group formulation *(Russian)* 78−12627
particle motion in two waves, numerical study 80−8914
particle system in rot. frames, rigid flow impossibility 78−45497
path integral formalism of perturbation theory, simple mols. and atoms 79−6841
PCILO method, modified, second-order energy using CNDO/2 and INDO Hamiltonian approxs. 79−36533
pentofuranosyl nucleosides, isomeric, ^{1}H NMR coupling consts., SCF FPT INDO approx. calc. 80−14156
percolation problem, high order behaviour in 0^3 field theories 78−65883
Percus Yevick eqn. for square mound pot., perturbation soln. 78−22619
Percus-Yevick equation, perturbation treatment, liq. structure factors 77−7641
Percus-Yevick equation, square-well pot., perturbation version 78−63648
Percus-Yevick integral eqn. perturbative soln. for of intermolecular pot. 79−30348
periodic potential energy levels, late terms, asymptotic expansions 79−25895
perturbational MO analysis of ab initio SCF-MO wave functions 77−57867
perturbation theory continued
perturbative numerical methods, local and accumulated truncation methods 80−62536
perturbative QCD, large p_T hadronic collision jet struct. 79−75721
perturbed boundary conditions, for differential equations in theory of atoms 78−33432
perturbed eigenvalues, perturbation expansions and variational constraints 78−16670
perturbed ladder operator method, analytical determ. of generalised central field energies and wavefunctions 78−32704
perturbed ladder operator method, wavefunctions, matrix elements, closed form expressions 80−73203
perturbed stationary state, improved approach 78−90282
phase grating, 3-dimens., electrodynamic perturbation theory for light diffr. 80−28327
phase separation kinetics, Boltzmann's transport eqn. calcs. 80−79952
phase transitions, with random fields, lowering of dimensionality 77−47999
phonon scattering by spherical defect aggregates 80−24552
photon splitting into three components by electron in quantised plane EM field 80−18101
photon-photon, dimensional scatt. amplitude and gauge invariance in lowest order 77−71471
photonuclear sum rules from continuum calcs., dependence on residual interactions 80−22807
pion mass difference, Bars-Halpern-Yoshimura unified gauge model, perturbative calc. 77−10251
pion-nucleon field interactions, covariant perturbative expansion in SU(2)×SU(2) model 77−5983
planar Feynman diagrams in perturbation theory 77−61189
plane SH waves, linearised direct and inverse problems for two-dimensional heterogeneities *(French)* 79−84131
plane wave set, orthogonalised, construction method, bound states 79−25894
plasma, drift waves and trapped particle modes, non-Hermitian radial eqns. 77−89244
plasma, ion-acoustic solitary wave, third-order corrections, reductive perturbation method 80−43898
plasma, ion-acoustic waves, Korteweg-de Vries soliton, higher order terms in reductive perturbation theory 78−1824
plasma column, inhomogeneous, magnetised, RF elec. field 78−83522
plasma ion wave, nonlinear propag., reductive perturbation theory 77−72444
plasma ion waves, nonlinear Schrodinger eqn., perturbation method 78−75301
plasma nonlinear wave phenomena, collisional and weakly collisional cases 77−11346
plasma wave propagation, nonlinear Schrodinger equation, modified Zakharov-Shabat inverse scatt. problem 80−59200
plasma wave trapped particles, resonance interactions *(Russian)* 78−26236
point charge models, magnetic susceptibilities, Frost-model Lewis basis sets calcs. 79−54761
point transformations and non-linear system quantisation, S-matrix from perturbation theory 79−109
polar fluid, thermodynamics and thermodynamics perturbation theory 79−41919
polar molecule, electron scatt., momentum transfer cross-sections, semi-classical perturbation theory 78−58848
polar molecule electron scatt., excitation and scatt. cross sections 78−58826
polarisability and London coeff., ab initio variation perturbation calc. 79−13635
polarisation spectroscopy, Doppler free intracavity 80−52335
polarised nucleus mixed parity radiation, third-order approxs. in ang. distrib. 77−6288
polaron, small hopping, reaction rate treatment, role of vibrational relaxation 78−72092
Polyakov-'t Hooft monopole and dyon, quantum theory *(Russian)* 78−392
polyatomic fluid mixtures, thermodynamics, phase equilib. calcs. 79−1485
polyatomic molecule, sextic centrifugal distortion consts., Watson Hamiltonian, perturbation method 77−10785
polyatomic molecules, radiationless conversion processes, regularities 80−14171
polyatomic molecules, triplet states, var. and perturbational calcs. 77−61680
polyatomic mols., nuclear charge model and valence force consts. prediction 80−43022
polycrystalline materials, macroscopic elec. cond. determ. 79−99521
polyene, infinite, electronic states under local perturbation 77−57878
polymer branched chains, chain length, mol. architecture rel. to second virial coeff. 78−94964
polymer chain, irregular, lattice distortions, SCF perturbation calcs. 78−6018
polymers, statistical theoretical methods 78−18535
positive atomic ions, orbital SCF energies, rel. to total SCF energies 79−3350
positron+H(He), second-order nonadiabatic polaris. pot. for elastic scatt. 79−22836
postbuckling of elastic structs., mode imperfection anal., imperfection sensitivity 77−89048
potential reconstruction by differential scatt. cross section, perturbation theory *(Russian)* 78−45818
potential scattering, classical, small-ang., anisotropic, for Lennard-Jones (2n, n) pot. 80−1043
potential scattering , perturbation methods for local and nonlocal pots. 78−16696
principal value collision integrals, reduction scheme 77−57234
prism bending to helical form, formal perturbation scheme 78−55558
proton magnetic shielding, chem. substitution effect on chem. shift, LCAO perturbation method 77−68064
pulse dispersion in a clad lens-like medium 80−53445
pulsed neutron source, use of perturbation theory for exptl. study 78−66328
pure Yang-Mills perturbation theory, instanton sector renormalisation, zeroth sector comparison 80−105775
QCD_2, fermionic Green function and functional determinant, closed representation 80−13269

perturbation theory continued
QCD, dynamical chiral symmetry breaking and explicit breaking due to current quark masses 79−71717
QCD, e^+e^- annihilation energy, asymptotically free perturbation theory 78−66045
QCD, factorisation and the parton model 78−93848
QCD, four jet prod. in e^+e^- annihilation 79−49459
QCD, gauge invariance and perturbative calcs. 79−63417
QCD, gluon bremsstrahlung by confined sources 79−45067
QCD, hard semi-inclusive processes 78−93862
QCD, high energy behaviour of jet and lepton pair production 79−2932
QCD, jets, deep inelastic scatt., renormalisation group 79−26287
QCD, parton primordial transverse momentum 79−40728
QCD, perturbation theoretic parameter Λ 78−89667
QCD, quark liberation and finite temp. renormalisation group, hadron-quark phase transition *(Russian)* 79−67515
QCD, struct. functions, perturbation theory *(Russian)* 78−8595
QCD, two jet process noncollinearity in first order perturbation theory 80−22567
QCD calc. of three-jet processes in leptoprod. and hadronic μ-pair prod. 78−21338
QCD interactions, perturbation theory and the parton model 79−58927
QCD of highly condensed matter 78−70267
QCD perturbation expansions in coupling const. renormalisation by momentum space subtraction 79−63416
QCD perturbation theory, asymmetries in inclusive hadron prod. 78−50057
QCD perturbation theory, nonperturbative effects on factorisation in high momentum processes 79−36016
QCD perturbation theory, quark decay functions, heavy hadron prod. 78−62364
QCD perturbation theory for confined quarks and gluons 80−401
QCD perturbation theory test for various processes, review 79−326
QCD predictions of deep inelastic scaling violations, non-perturbative effects 79−40732
QCD $q\bar{q}$ running coupling constant, β-function from string model, Pade approx. 79−343
QED, A_0=0 gauge, propagation of fermions 79−71669
QED, asymptotic estimates 78−8564
QED, energy-momentum-tensor trace anomaly calc. 77−46002
QED, IR divergence, rearranged perturbation theory 77−67602
QED, perturbation series, asymptotic estimates and guage invariance 77−87925
QED perturbation series, Dyson instability, asymptotics 78−62342
QFT, perturbation theory at large orders 80−32022
quadrupole perturbation of harmonic oscill. pot. 77−60978
qualitative methods in problem solving, graduate text book 77−71239
quantum chromodynamics, IR struct. perturbation theory calcs. 77−74577
quantum diffusion, particle in fluctuating medium, memory effects 79−49180
quantum Dirac field, scatt. automorphisms, external field perturbations 78−58112
quantum dynamics in effective system states basis, not in radiation field, perturbation theory 78−33499
quantum expectation values variational calc., second order error 77−33894
quantum fermion thermodynamic system, high-order perturbation expansion 80−4635
quantum field theories with homogeneous interactions 77−49836
quantum field theory, asymptotic estimates 77−30241
quantum field theory, asymptotic series summing *(Russian)* 77−82683
quantum field theory regularisation schemes in perturbation calcs., comparisons 77−82663
quantum Hamiltonian on lattice, estimation of eigenvalues 79−40669
quantum mechanical kinetics problems, averaging principle, degenerate states and reson. effects 78−19996
quantum mechanical kinetics problems, averaging principle appls. 78−19995
quantum mechanical perturbation problems, resolution using integral eqn. 80−58112
quantum mechanical perturbation theory, convergence props., energy series 78−80
quantum mechanics, perturbation formulas for energy, derivation 78−86051
quantum molecular crystal, quantum quadrupolar phase theory *(Russian)* 78−22929
quantum statistical mechanics, boundary-value problems *(Rumanian)* 78−86219
quantum system, jarring and corresponding stimulated transitions 80−17839
quantum systems, continuous and discontinuous perturbations 78−62113
quantum theory of solitons, review 78−70288
quark binding, QCD and perturbation theory 77−71444
quark confinement, infrared struct. of QCD, perturbation theory 77−71443
quark form factor, non leading contribs. to asymptotic behaviour 78−8586
quark high momentum transfer scatt., perturbation theory *(Russian)* 78−45883
quark stars, possible existence, 2nd order perturbation theory 80−26889
quarkonium decay into heavy quark flavours, ψ (J) energy distrib., QCD perturbation theory 78−82146
quasi-degenerate Rayleigh-Schrodinger perturbation theory, calc. of effective Hamiltonians 79−71284
quasi-periodic motion, asymptotic expansion method 80−17877
quasibound state energy calc. 78−41191
quasimolecules, intermediate, relax. times 78−42170
radial distribution function, perturbation theory, three-body pot. 77−35456
radial equation perturbation theory 78−49691
radial reduced Coulomb Green's function 80−31559
radial Schrodinger eqn. global numerical soln. by second order perturbation theory 80−68079
radial Schrodinger equation, solns., inversion formulae by expansions by squares *(Russian)* 79−12629
radiation shielding, cross section sensitivity analysis 78−21778
radiative mass generation in perturbation theory and the renormalization group 80−86611
radical+radical reactions, reaction path calc. using perturbation expansion *(German)* 79−34300
perturbation theory continued
radical pair recombination reactions, short time behaviour 77−81393
radius perturbation theory, appl. to NN system and pionic atoms 78−21007
Raman scattered light, Hanle effect influence 80−83323
random heterogeneous materials, statistical theory of effective elec. thermal and mag. props. 77−48118
random Ising magnet, phase diagrams 80−7065
random processes, classical, with arbitrary preparation, perturbation theory 79−54057
randomly rotating rigid body, computation of functionals over sample paths 77−74212
rare gas clusters, small, structure, thermodynamic properties 80−88341
Rayleigh wave scattering from topographical irregularities at oblique incidence 78−38927
Rayleigh-Schrodinger, appl. of Pade approximants 78−65806
Rayleigh-Schrodinger, formal treatment 79−18103
Rayleigh-Schrodinger many-body theory, up to 3rd order, appl. to H_2O, BH, HF, Ne 78−894
rays calculation in inhomogeneous magnetoactive ionosphere by perturbation method 80−21874
reaction-diffusion eqns., axi-symmetric time periodic solns. 78−81930
reactor boundary changes, generalised perturbation theory 78−4980
reactor core, uniform infinite lattice eigenvalue as function of buckling 79−609
reactor materials burnup anal., depletion pertubation theory for coupled neutron-nuclide field 79−45339
reactor physics, perturbation theory developments, review 77−14227
real-photon spectra weight functions, imaginary part of vacuum polarization, and electromagnetic vertices 79−21997
rectification string, pulsation states *(Russian)* 79−30260
Regge field theory, divergence of perturbation series 77−2754
Reggeisation of meson trajectories quark-gluon gauge theories 78−25005
Reggeon field theory, perturbation theory at large orders 78−8510
Reissner-Nordstrom black hole, coupled gravit.-EM perturbation anal. 77−26022
Reissner-Nordstrom black hole, stationary interacting fields 78−24710
relativistic atomic systems, perturbation theory appls. 80−23323
relativistic infinite-component wave eqns., perturbation theory 77−61184
relativistic many-body theory, quantum chromodynamics and neutron stars/supernova 79−40752
relativistic two-electron atom, level shifts, transition probabilities, perturbation theory 79−22001
relaxation phenomena, general treatment 78−44398
renormalisation group eqn., algebraic anal, 77−74575
renormalisation group eqns. and analytic renormalisation 80−82865
renormalisation group eqns. and analytic renormalisation 80−82866
renormalisation theory, perturbative, general features, quantum action principles, pure Yang-Mills theory 80−105794
renormalised perturbation theory, operator-product light-cone expansion 77−82680
renormalized operator form of quantum action principle 80−42314
rescaling Schrodinger eigenvalue problem perturbation series 79−92980
resistivity of grain-boundary joint by pseudopot. method *(French)* 79−51539
resistor, metallic, nonlinear current fluctuations, microscopic calc., heating, perturbation theory 79−69484
resolvent operator expansion, generalised method, Schrodinger eqn. soln. appl. 80−86126
resonance Raman scattering, polariton theory, book contrib. 79−38551
resonant multiphoton ionisation, line profile as Fano profile with background struct. 79−72290
RF, average specific absorpt. rate in ellipsoidal conductor and dielec. models of humans and monkeys 78−40349
rigid rotor in electric field, energy eigenvalues, Brillouin-Lowdin perturbation expansion 78−62690
rigorous lower bounds to energy levels, Brillouin Wigner perturbation theory, finite summations 78−54216
ring laser diffraction theory, perturbation method 80−95919
Robertson-Walker spacetime, vacuum expectation values, perturbation technique in curved space 79−97286
rod, current-carrying, steady-state heat conduction, perturbation soln. 78−5629
rotating black holes, instabilities of massive scalar perturbations 79−54026
rotating disc, laminar boundary layer heat transfer, Prandtl no. effects calcs. 77−31306
rotating fermion systems, quantum mech. treatment 79−17337
rotating stars, perturbs. and stability, eigenvalues and perturb. theory 80−46538
RS perturbation theory, E_3 variational principles 78−58570
s-d electron model, finite temp. diagram technique, perturbation theory 78−67932
S-matrix asymptotic perturbation expansion, time ordered functions in relativistic quantum field theory 77−6039
S-matrix factorisation, analogy of 2-dimens. perturbation theory structural props. in higher dimens. 78−70293
S-matrix theory, determinant and its relation to number of eigenvalues due to perturbation 78−58132
S-matrix theory appl. to perturbation theory in 1/Z expansion *(Russian)* 79−1565
sapphire rod, mode perturbation expansions for wave propag. 77−51434
sapphire rod, numerical description of torsional vibrs. 77−51435
Sato's conjecture, validity using concrete expressions for Feynman amplitudes 78−74123
SAW attenuation due to thin film finite conductivity and air loading 77−31154
scalar electrodynamics, Green's function perturbative expansion higher orders 77−87923
scalar electrodynamics, IR divergences, rearranged perturbation expansion 77−67601
scalar field interacting with Yang-Mills field, higher order perturbation theory *(Russian)* 78−62316
scalar field theories, finite amplitudes in perturbation theory, ϕ^n models, pass. renormalisation 78−93794
scalar field theory with Gaussian propagator, perturbation series 78−70268
scalar theories, perturbation theory divergence, pseudoparticles *(Russian)* 77−30273
scalar Yukawa$_2$ field theory, vacuum energy density in large order perturbation theory 79−17620

perturbation theory continued
scaling and Pade approximants 80−91429
scattered wave focusing in periodically inhomogeneous layers *(Russian)* 78−1158
scattering theory, nonsingular potential, scatt. length by iterative-perturbation method 80−27160
Schrodinger eqn., nonlinear, perturbed, soliton interactions 77−87661
Schrodinger equation, applications of perturbation theory to numerical integration methods 80−12926
Schrodinger equation, energy approximants and perturbation theory 80−22232
Schrodinger equation, nonlinear, perturbation expn. 78−47124
Schrodinger equation, perturbation problem, two-level atom interacting with EM field 80−52056
Schrodinger equation, perturbed nonlinear, inverse problem method 77−60968
Schrodinger equation, radial one-dimens., second order perturbative numerical calcs. 80−31580
Schrodinger equation, rearranged perturbation theory, nonlinear transformation 80−105542
Schrodinger equation, soln. for $\lambda x^2/(1+gx^2)$ interaction with g small and λ large 79−92967
Schrodinger equation, step sizes for perturbative methods of solution 80−86110
Schrodinger equation, systems of coupled equations, piecewise constant reference potential 80−86111
Schrodinger equation eigenvalues, perturbation theory calc. without complete set of eigenfunctions 80−105519
Schrodinger equation with double exponential pot. and large coupling consts. 77−87662
Schrodinger nonlinear eqn., soliton-like soln. 79−44790
Schwarzschild black hole, master differential eqn. for perturbations 77−26214
screened Coulomb pot., perturbation theory and hypervirial theorem, sixth order atom energy levels 80−14071
screened Coulomb pot. full continuum wavefunction, analytic perturbation theory 79−64065
screened Coulomb potentials, energy levels, perturbation theory appl. 78−25406
screened Coulomb pots., perturbation theory approach 80−63524
sd-shell nuclei, large scale shell model calcs. compared with perturbation theory in SU(3) basis 77−57613
second order matrix element eval., trial function linear transformation 80−62529
second-order matrix elements, variational methods 80−12936
second-order optical processes, time-dependent perturbation calculations 79−68417
second-order perturb. theory of distrib. of materials throughout radiation protective shield 79−54608
second-row atoms, static dipole polarisabilities, finite perturbation calcs. 77−6690
second-row elements, nucl. spin-spin coupling consts. to H, INDO calcs. 77−83621
second-row hydrides, nucl. spin-spin coupling consts., ab initio calcs. 80−95647
self oscillating system with small periodic perturbations, perturbation theory 79−57224
self-consistent perturbation theory, generalisation for perturbation-dependent nonorthogonal basis set 78−17563
self-similar space-times, perturbation scheme 78−54099
selfgravitating systems, strongly interacting, perturbation methods 80−73234
semiconductor, dielectric response, local field effects in phonon-induced density change 79−51510
semiconductor, multiplication photoemission in strong field 77−85891
semiconductor, zinc blende struct., cond. band nonparabolicity and cyclotron reson. linewidth *(German)* 78−75993
semiconductor surface space charge layers, subband struct., perturbation theory 80−84497
semiconductor wires, size-quartised, two-photon interband absorpt. 80−93256
semiconductors, binding energy in exciton-impurity systems, Haynes rule 79−15112
semiconductors, deep defects, contrib. to binding energy 80−70634
semiconductors, degenerate, acoustodielectric effect, permittivity modulation by acoustic wave in resonance conditions 80−92944
semiconductors, doped, light diffr. by sound 79−11404
semiconductors, heavily doped, hopping cond. activation energy, percolation method 80−70703
semiconductors, IR absorpt. of light by polarons 79−56799
semiconductors, radiative two-electron transitions 79−43026
semiconductors with direct band gaps, exciton-polariton interactions, Green's function approach 80−92831
shell of variable thickness, thermoelastic problem, perturbation method 79−32272
shell-model interaction, convergence in reaction matrix G 78−50102
shielding problems, higher order generalized theory 80−47731
short gravity-capillary waves modulation by longer-scale periodic flows 80−57106
short-crested waves, third order approx. calcs. 79−50741
short-distance and light-cone expansions for products of currents 79−17638
short-range interparticle interaction potential, thermodynamic perturbation theory 77−43124
short-range order, electronic theory, pseudopotential approach 77−80717
silyl radical, conform., hyperfine struct., nonempirical calcs., vibr., effects 79−97998
simple fluids, semiempirical calcs. using perturbation theory 80−28892
simple liqs. with repulsive forces, thermodynamically selfconsistent theory 80−75139
sine-Gordon breather soliton dynamics, rel. to special relativity 80−46801
sine-Gordon soliton, adiabatic behavior in presence of perturbations 79−49093
sine-Gordon solitons, dynamics, in presence of perturbations 77−37751
single-particle density matrix, perturbation expansion 80−54635
singlet states with two open shells of equal symmetry, orthogonality constrained SCF theory 77−26962
singular perturbation of an Exterior Dirichlet problem 79−12613
singular perturbation of elliptic equation *(Chinese)* 79−35525
singular perturbation pots. 77−60952
perturbation theory continued
singular perturbation theory, eigenvalues that do not tend to unperturbed values 79−92976
singular perturbation theory for suboptimal control of reactors with distributed parameters, computer model 77−6530
singular perturbations for initial value problems, hyperbolic nonlinear partial differential eqns. 78−58111
singular potentials and perturbation theory 79−63060
small gyromagnetic sphere, EM excitations 78−15030
small overdense plasma particle Thomson-like RF scatt., linear perturbation theory 80−48858
soil water, vertical infiltration analysis and perturbation methods 77−29346
solid mechanics application of the method 77−46911
soliton equations, perturbed, variational approach 78−89366
soliton evolution, perturbation effects 80−46824
soliton formation in warm magnetised Vlasov plasma 79−90396
soliton lattice stability in coupled linear chain system 80−73282
solitons, evolution, tail struct. after perturbation *(Russian)* 78−86197
solitons, evolution eqns. for nonlinear waves, perturbation theory *(Russian)* 77−79005
solitons, in dispersive media, nonlinear evolution eqns. soln., review 78−60
solitons as particles, oscills., singular perturbation theory 78−73882
solubility of gases in liquids, Weeks-Chandler Andersen theory 77−84931
spectral analysis of wave perturbations in D-layer and F-layer 80−21873
spectral and scatt. theory for class of non-selfadjoint operators 77−60972
spectral density, time-depend. perturbation theory calcs. 77−13525
spectral distribution methods in effective interaction theory 78−86489
spectral line breadth, press. broadened quantum-path theory 79−31470
spherical mirror resonator, misaligned, open, spatial struct., phase and amplitude distrib. 78−46676
spherically symmetric space-times, even parity junction conditions for perturbations 80−31628
spin adapted configurations, incorporation in many-body perturb. theory formalism 77−88374
spin-1 system, periodic perturbation, analogue of Shirley's eqn. 77−3248
spin-1/2 system, mag. resonance in arbitrarily oriented fields 77−42263
spin-Hamiltonian perturbation energies and state vectors calc., diagrammatic technique 78−65810
spontaneous generation of renormalisation invariant mass in IR stable theories 78−86411
square-well+Sutherland (∞,6) fluid, perturbation theory 77−11455
standardisation operator for projected states, simple non-hermitian choices 77−33903
Stark effect, perturbation and variation treatments, appl. to H(1s) reson. 80−14105
Stark effect in 1-D, resonances and continued fractions 79−59395
stars, tidally distorted, oscill. freq. via perturbation method 77−22206
stationary, commutator possible appl., nth order expectation values 80−86116
stationary state function ambiguity resolution; for teaching 78−24603
statistical mechanics, nonequilib., memory function formalism 77−26234
statistical mechanics, nonequilib., time-displacement operator 77−26233
Stieltjes moment problem, Borel summability and indeterminacy, anharmonic oscills. 78−62094
stiff reactor model, exponential collocation using perturbation technique appl. 78−40032
stochastic acceleration of particle in random pot., renormalised canonical perturbation theory 77−27233
stochastic action integral interpretation of quantum mechanical transformation function 80−77644
stochastic behaviour of quantum pendulum under periodic perturbations 80−8834
stochastic dynamical systems, kinetic eqn. derivation based on cumulant function props. 80−12995
stochastic fields, functional integral methods 79−25973
stochastic properties of complex nonlinear oscillation regimes 80−8919
Stockmayer fluid, mol. dynamics and thermodynamic perturbation theory, mol. polarisability effects 78−71419
Stockmayer fluids with dipoles and quadrupoles, spherical harmonic coeffs., dielec. const. and Kerr factor calcs. 80−84678
storage rings, beam-beam interactions, perturbation method solns. 80−37667
stroboscopic method, higher-order approx., appl. to satellite dynamics 79−66913
strong interaction, appl. to molecular crystals *(Russian)* 77−15528
strongly dispersive system, higher order approx., reductive perturbation method 78−73926
structural vibration modes, inverse perturbation calcs., minimal change theory 79−18691
SU(2)×U(1) hybrid models, divergence cancellations and renormalisaion 77−38083
SU(2)-flavour Schwinger model on the lattice, Hamiltonian lattice perturbation exam. 78−16747
super $(\phi^2)_2$ model, large order perturbation theory 80−82876
super Riemannian space quantisation, perturbation theory rule derivation 78−77790
superconducting small metal particles ground state energy and orbital mag. susceptibility 80−49983
superconductivity proximity effect, McMillan tunnelling model 79−73639
superconductor, EM wave nonlinear absorpt. near one-photon threshold 80−60142
superconductor type II, perturbation series for crit. behaviour near H_{c2} 77−8233
superexchange interactions in cryst. with many-electron paramag. ions and strong cryst. field 77−59402
supergraphs, loop calculations 80−13229
superionic conductors, correlation functions theory 78−79674
superoperator formalism, applic. to mag. field effects on delayed fluoresc. 77−30913
superoperator perturbation theory of density operators of generalized Liouville eqns. 77−26235
superposed Yukawa and inverse square potentials, eigenenergy expansion 79−30281
supersymmetry spontaneous breakdown inducing IR anomaly 77−38095
surface waves, perturbation anal. of attenuation and dispersion 78−47653

perturbation theory continued
symmetry adapted Rayleigh-Schrodinger theories 78−70012
symmetry breaking perturbation technique, tensor operators 79−12975
syndnone, semi-empirical excited state Morokuma's EHP calc., geometry and order of states 78−46256
system influenced by time dependent electric field, fourth order variation perturbation theory 80−22230
ten-electron systems, correl. energy, fourth order diagrammatic, many body Rayleigh Schrodinger perturbation theory 80−63556
tensor contrib. to nuclear matter in first order perturbation theory, binding energy 77−18410
tetrafluoromethane, IR spectrum, Fermi reson. sequences, cubic pot. energy, anharmonicity consts. 77−10674
thermodynamic correlation function perturbation theory for non-ideal system 77−30087
thermodynamic Green's function, perturbation theory 77−26266
Thirring model, massive, with internal U(n) symmetry, zero mass limit 77−57466
Thirring model S-matrix, exact soln., agreement with perturbation theory 77−54049
three-body, elliptic three-dimens. restricted problem, recurrence relations in integration 79−48656
three-body problems, Schrodinger perturbation theory in adiabatic rep. *(Russian)* 77−60976
three-body scatt. in coordinate space, perturbative approach to Faddeev eqns. 79−30682
three-electron atom systems with two vacancies in K-shell excited states and autoionis. state energies *(Russian)* 79−31429
three-electron atomic systems, autoionising states decay calcs. 78−78670
three-electron atoms, ground state third-order energy, Z-depend. perturb. calcs. 77−46484
three-level system, rel. tuned two- and three-photon processes 77−68198
three-nucleon bound state, perturbation approach to Faddeev eqn. 78−54691
three-nucleon bound state, soln., perturbational approach to Faddeev eqn. 79−30793
three-particle scatt., on-shell prescription 78−8559
three-photon coalescence at electron 80−91026
tidal flow, periodic, anal. by finite element perturbation method 78−24290
time dependent generalised perturbation theory burnup calculations 77−23176
time-dependent convergence range 78−68
time-ordered products and Schwinger functions 79−26216
Toda lattice, scatt. of solitons from mass impurity 79−12739
Toda periodic lattice, perturbations 77−13703
Tokamak plasma, confinement time meas. 80−87945
total electronic energy, atoms and mols., SCF binding energy, Z^{-1} perturbation theory 80−83268
trace identity and self-stress in QED 79−97547
transition density matrices, spin variables separation by Fock coordinate function and spin Hamiltonian methods 80−63513
transition metal alloys, disordered, generalised perturbation theory, appl. to self-consistent calc. of ordering energies 78−75975
transition metal complexes, octahedral substituted, ligand-fluid splittings, accidental degeneracy origin 80−10932
transition metal ion, in inert medium, electronic relax., coupling mechanism 79−76466
3d transition metal ions in crystals, Jahn-Teller coupling constants calcs. 80−49679
transition metals, correlation effects, perturb. treatment within Hubbard model 80−70582
transition metals, correlation effects, perturbation treatment 80−59897
transition moments, vibrational, of diatomic and polyatomic mols., elec. and mech. anharmonicity influences 80−23459
transition probability, second order, time-independent perturbation asymptotic formalism 80−27159
transparency, self-induced, perturbed soliton solns., finite relax. time 80−58643
transverse wave packet, 3-dimens., nonlinear evolution in hot plasma, ion-acoustic wave effect 80−43899
triangular well fluid, Helmholtz free energy, Barker-Henderson perturbation theory 79−4218
triangular-potential fluid, Zwanzig's perturbation theory, appl. to thermodynamic props. 79−41920
trifluoromethane, dielectric constant effect on nuclear spin-spin coupling constants, INDO approx. 79−72240
trimolecular interaction, multiple site reactivity, perturbation theory 79−52639
two electron atom, energy levels, classical first order perturbation theory 80−58118
two level system interacting with two optical fields, perturbation soln. from effective two level Hamiltonian 79−36866
two photon absorption, time varying perturbation theory *(Rumanian)* 78−46311
two photon absorptivities, CNDO/S-CI calc. with second order time depend. perturbation eqns. 80−74122
two photon absorptivity, ion cyclotron reson. photodissoc. spectra, CNDO/S-CI-perturbation theory 80−74123
two state two mode vibronic coupling model, Born-Oppenheimer and crude adiabatic perturbation methods 80−87036
two time procedure for anal. of third order nonlinear differential eqns. 77−82369
two-body scatt. T matrix in real-time formalism 78−41230
two-centre Lennard-Jones liquids, free energy, perturbation theory 80−79656
two-dimensional gauge model perturbation theory, Schwinger and massive vector meson models 79−6269
two-dimensional square well fluid, anal. eqns. for compressibility factor 79−77664
two-electron atoms, ground-state energy, Darboux functions, perturbative theory 77−23402
two-electron ions, ground state, quadratic Stark effect 80−37775
two-electron systems, pair function calcs. 80−32590
two-k-shell-vacancy systems, excited states, radiationless decay probability calcs. 78−41993
two-level system, power broadened Doppler-free saturation resons., transit time effects 77−79657
two-nucleon interaction isobar contributions from noncovariant perturbation theory 79−478
two-particle interactions, new variation-perturbation principle 79−10006

perturbation theory continued
two-state quantum system, time-dependent perturbation by sinusoidal field 77−5703
UHF orbitals, ionisation energy calcs. appls. 80−58141
UHFS model, CI, CC, and MBPT approaches, appl. to weak δ-δ bonds and δ-δ^* excitation 80−32585
unimolecular reactions, pot. energy surfaces, SCF perturbation theory 79−91918
unitary transformations theory, vector generalisation of square summable power series 77−49621
unsaturated porous media, one dimens. flow, two parameter singular perturbation soln. 79−23361
unsteady transonic flow about oscillating airfoil, perturbation soln. 77−23985
urea, electro-optical coeffs. meas., rel. to nonlinear optics calcs. 80−34889
UV convergence and analytic properties of manifestly finite perturbation theory 79−71600
vacuum copies and perturbation theory 79−17612
vacuum copies and perturbation theory in the 't Hooft-Veltman gauge of QED 79−21989
vacuum polarisation in intense EM fields, perturbation theory, renormalisation group calcs. *(Russian)* 80−52444
valence correlation energies, contributions of triply- and quadruply excited states determ. using perturbation theory 80−78545
Van der Pol oscillator, renormalised perturbation theory 80−27225
van der Waals forces in QCD colour singlets 78−86441
vapour-liquid equilib., perturbation theory of convex end mol. fluids 79−90769
variable basis sets, numerical finite perturbation vs. analytic approach 79−59330
variable direction method, choice of optimal variant for 2-D reactor models 79−97751
variable thermal properties systems, perturbation methods calcs. 77−58522
variable-thickness conical shell, transient stresses in clamped section 77−89051
variation method, perturbation analysis 77−82404
variational bounds to excited states from generalised Brillouin-Wigner eqn. 78−45507
variational perturbation theory, Hyleraas type base *(Russian)* 77−37775
variational principle for spinning liquid-filled solid bodies 80−43609
vector perturbation series based upon a representation in a finite Banach space 79−63893
vector resonator mode synthesis, from scalar results 80−43374
velocity dependent nuclear potential, matrix soln. of Schrodinger eqn. 79−25892
vertical ionisation energies, finite order perturbation theory 78−33630
vibrating piezoelectric solid, perturbation theory for linear electroelastic eqns. 79−1739
vibration of beams and plates with varying thickness, perturbation method for fundamental freqs. 77−31238
vibrationally inelastic scattering, 3-dimens., adiabatic semiclassical perturbation theory 79−94065
vibrationally inelastic scattering, collinear, adiabatic semiclassical perturbation theory 79−94064
virial theorem and Born-Oppenheimer approx. at different order of perturbation *(French)* 77−49617
viscous fluid magnetic throughflow in slot, inertia effect 79−37418
void swelling, rate theory, effect of recombination on sink strengths 78−87712
water, NMR shielding constants of ^1H and ^{17}O, paramag. contrib., triple perturbation theory 79−10127
water, proton affinity, many-body Rayleigh-Schrodinger perturbation theory 78−92497
water molecule, nucl. spin-spin coupling consts. geometric approx. 79−59380
wave modulation in multi-dimens. space, reductive perturbation method *(Japanese)* 77−41472
waveguide, clad parabolic-index square-law dielectric, perturbation anal. 80−33190
waveguide scattering problem, comparison of two perturbation theories 80−83662
weak coupling superconductors, single particle excitation decay theory 78−52147
weakly bound particle ionisation, perturbation theory series convergence in alternating field 80−4575
weakly dispersive system, higher order approx., reductive perturbation method 78−73925
weakly dissipative system, higher order approx. in reductive perturbation method, shock wave appl. 80−14743
weakly interacting particle system, quantum field divergence disappearance in modified quantum dynamics 80−62537
Wick's theorem, relation between canonical and Fokker-Planck dynamics 79−17329
Wicks theorem and Fokker Planck dynamics 77−87715
Wigner's (2n+1) rule in MBPT 80−42095
Wilson and Wegner-Houghton generators, equivalence at arbitrary anisotropic fixed points 77−22507
X-ray scattering by electrons, basic theory 78−71623
X-Y model, one-dimens., zero temp., transverse time depend. spin correlation functions 78−65876
xanthine, planar autoassoc. energy 80−53086
Yang-Mills field, isodoublet-scalar field coupled, large order estimates for perturbation theory 79−71632
Yang-Mills theory, IR stability in zero-instanton sector 77−30244
Yang-Mills theory gauge symmetries, perturbation theory 78−359
Yukawa fluid used as reference system in perturbation theory 80−6334
Yukawa interaction among fermions, asymptotic estimates 77−30092
Z_1^3 effect, asymptotic, particle ionisation losses, perturbation theory *(Russian)* 80−101735
Z-expansion scheme, generalisation 79−36500
zero frequency modes in perturbation expansion about classical field theory configs. 77−18169
zeroth approximation, formally exact perturbation theory, transition energies calc. 77−42259
d charge form factors, π-contrib., unity of relativistic corrections and meson exchange currents 79−67553
e scatt., in presence of intense EM field 78−33014
e^-e^+ prod. from two photons in nucl. field *(Russian)* 78−45819

perturbation theory continued
e^+e^- annihilation, event shapes, QCD perturbation theory calcs. 79−36056
e^+e^- annihilation, zero mass limit for class of jet-related cross sections 79−71736
e^+e^- annihilation and other processes, event shape anal., QCD perturbation theory 79−13140
$e^+e^-\rightarrow$hadrons, asymptotically free QCD perturbation theory for multijet final states 78−74267
$e^+e^-\rightarrow$hadrons, energy correls. in QCD, asymptotically free perturbation theory 79−63497
$e^+e^-\rightarrow q\bar{q}q\rightarrow$jets, ang. energy flow in perturbative QCD 79−49455
ep, sea quark and gluon momentum distribs., perturbative vs. asymptotic freedom corrections 79−17736
ep deep inelast. scatt., QCD perturbative corrections 78−74263
(γ,n), preequilibrium exciton model with evaporative component, photoneutron spectra, giant resonances 80−57762
ν mass, four component Dirac particles, perturbation theory model for massless ν 79−435
$p(\bar{p}p)\rightarrow W^{\pm}X$, QCD perturbative predictions 79−40812
$pp\rightarrow\pi X$, crucial spin tests of QCD approaches to large transverse momentum processes 79−63558
$\pi^-p\rightarrow\gamma\gamma n$, near threshold, perturbation theory estimates, branching ratio and ang. distrib. 79−89183
$\phi\psi\psi\psi$ model, two dimens., relationship with Yukawa-type model 79−35948
$\Upsilon\rightarrow$photons+gluons, QCD perturbation theory 78−33028
AF_a^{z-} compounds, A-F nucl. spin-spin coupling, ligand influence 77−14454
AgBr, exciton absorpt. at high excitation rates 80−2343
AgBr, luminesc. band shape of free excitons, at high exciton density, calc. 77−81148
AgBr:$Li^+(Na^+)$, impurity induced IR absorpt. 80−7386
Al, chemisorption of H_2, effects of substrate pseudopotential lattice 79−46953
Al, liquid, electron momentum density, correlations and ionic potentials 78−60052
AlH, $X^1\Sigma^+$ states, many body effects, diagrammatic perturbation theory 77−79547
AlSb, indirect exciton dispersion, 'camel's back' 79−73447
Ar, double photoionis. cross section, calc. 77−14397
Ar, double photoionisation, many-body perturbation approach 78−17634
Ar, inner electron energy characteristics, validity of Hartree-Fock-Pauli approx. 80−42957
Ar, liq., struct. factor calc., perturbation treatment using Lennard Jones (6, 12) pot. 80−10483
Ar-He, liq. soln., sound vel., perturbation theory *(Russian)* 77−47512
Ar+HCl, inelastic scatt. exponential perturbation theories 80−74217
Ar+N_2, inelastic scatt. exponential perturbation theories 80−74217
Ar+N_2(O_2, CO), molecular fluid mixtures, equilibrium props. 80−64867
ArH^+, transition moments, perturbation calcs. 80−102542
As_3, 3-body nonadditive interaction, nodal struct. 78−1049
As_2O_3, amorphous, network dynamics, vibr. band splittings 79−42199
As_2S_3, network dynamics, vibr. band splittings 79−42199
$As_2S_3(Se_3)$, amorphous, network dynamics, vibr. band splittings 79−42199
B, atomic correlation energies, perturbations and near degeneracy 79−3371
BF, $X^1\Sigma^+$ state, many-body effects, HF STO calcs., diagrammatic perturbation theory 77−50355
BH, elec. polarisabilities and dipole moments, var. perturbation obs. 80−63527
BH, PE curve, spectroscopic consts., perturbation theory appl. 80−23341
BH, susceptibility and mag. screening calcs. 77−57861
BH, variation-perturbation minimal Gaussian geminal basis sets correl. energy calc. 78−78629
BH, $X^1\Sigma^+$ states, many body effects, diagrammatic perturbation theory 77−79547
BH^{5+}, spurious avoided-crossings, variationally calc., perturbation theory approach 78−5295
BNC⇌BCN, isomerisation energy/barrier correlation, rel. to HNC(LiNC) 80−50840
Ba, 4d subshell spectra, strong interaction regime 79−18165
Be, atomic correlation energies, perturbations and near degeneracy 79−3371
Be, Auger transitions, fluoresc. yield calcs., correl. effects 77−18869
Be, electric dipole polarisabilities and hyperpolarisabilities, perturb. theory calcs. 78−17563
Be, second order correlation energies, variational-perturbation method, radial basis saturation errors 79−97985
Be-like system, numerical many-body perturbation calcs. using multiconfig. model space 80−47907
Be+Be(Li) 78−5310
Be_2, pot. curve of ground-state, many-body perturbation theory and SCF-CI method 79−36563
Be_3, 3-body nonadditive interaction, nodal struct. 78−1049
C, atomic correlation energies, perturbations and near degeneracy 79−3371
CH^+, electron correl. energies, Pade approximants and many-body perturbation theory 79−59366
CN^-, ionisation pot., CI and perturbation methods 79−31734
CO, energy levels for perturbed Morse oscillators 80−78676
CO, ground state, third-order many-body perturbation theory 79−10015
CO, intermolecular pot. parameters from WCA perturbation calc. 79−90770
CO, nucl. elec. shielding tensor calcs. 80−83296
CO, one-electron props., corrections, Moller-Plesset perturbation theory calc. 80−95519
CO, $X^1\Sigma^+$ state, diagrammatic many-body perturbation theory, pot. curves 79−10014
CO_2, rot.-vibr. bands, absorpt. coeff. calc. method, Fermi reson. effect on spectral lines 80−32696
CO_2, vibration, Rayleigh-Schrodinger and contact transform. techniques *(French)* 77−3340
CS, $X^1\Sigma^+$ ground state, diagrammatic perturbation theory calcs. 78−29737
Ca XV, transition probabilities, energy spectra calcs. 78−70791
$CaCO_3:Mn^{2+}$, calcite, on axis half-field forbidden lines, numerical prediction 77−16161

perturbation theory continued
Cd, photoionisation cross section, many-body perturbation theory, dipole length and vel. calc. 78−78674
Cd, quadrupole antishielding factors, Hartree-Fock perturbation theory 78−62723
$CdCl_2$, deformation densities, relativistic effect 80−42928
CdMnTe, exciton ground state, magnetic field influence 80−54616
Ce, isostructural solid-solid phase transitions, core collapse, cell theory 80−59620
Cl I, photoionisation cross section, calc. by many-body perturbation theory 78−62771
Cl, photoionisation cross section and reson. theory, many body perturbation theory, 3p and 3s subshells 80−69114
Cl^-, atomic core states, antishielding effects calcs. 80−83299
Cs, elec. dipole approx. and elec. quadrupole resons. allowed in multiphoton absorpt. *(French)* 78−5190
Cs, two-photon photoionisation theory 77−6741
Cs_2MX_6(M=Se, Te, X=Cl, Br), $\Gamma_4^-(^3T_{1g})$ state, Jahn-Teller effect, luminesc. obs. 80−60650
$Cs(8^2P)$+He(Ar)(Xe), fine-struct. transition cross sections, semiclassical calcs. 77−30972
Cu, electrical resistance of edge dislocations *(German)* 80−96859
Dy, magnetocrystalline anisotropy, perturbation theory 78−2675
Eu, HFS, many-body and relativistic effects 78−37565
F_2, mag. shielding and susceptibility, finite perturbation mol. orbitals calcs. 77−46513
F_2, PE curve, spectroscopic consts., perturbation theory appl. 80−23341
Fe XXI, transition probabilities, energy spectra calcs. 78−70791
Fe^{2+}, nuclear quadrupole interaction, theory, including many-body effects 78−34813
Fe^{3+}, quadrupole antishielding factors, Hartree-Fock perturbation theory 78−62723
Fe^{26+}+H, electron removal by collision 79−76508
GaAs, impurity states and core excitons, binding energies, perturb. theory 80−49659
GaP, indirect exciton dispersion, 'camel's back' 79−73447
Ge, amorphous, molecular liquid model and electronic structure 80−54133
Ge, dispersion law of indirect excitons 80−24805
H atom, energy level calcs. in superstrong mag. field 80−37737
H atom, ground state props., polynomial perturbation problem 78−73878
H atom, Stark effect, second order correction for energy *(Rumanian)* 80−74147
H, atom in strong mag. field, relativistic corrections to binding energies using perturbation calc. 79−68186
H atom perturbation λr, hypervirial relations, energy values without perturbed wavefunctions 78−33416
H, bond energy, chem. substitution influence 80−37718
H, degenerate 3s-3d levels, in mag. field, eigenvalues, Bender-Wu formulas 80−83275
H, eigenvalue resonances in Stark effect and perturbation theory 78−90118
H, electron elastic scatt. phaseshifts H continuum, frozen-core Hartree-Fock approx. perturbation theory 77−75295
H, excited states, Rayleigh-Schrodinger perturbation theory, Pade approximants calcs. 79−98024
H, highly excited, multiphoton ionisation rates, perturb. theory calcs. 77−54542
H, hyperfine shift in He buffer, exchange perturbation theory 77−6736
H, in static multipole field, logarithmic perturbation expansion 80−91431
H, maser response to coherent Zeeman perturbations 78−58972
H, multipole polaris. and shielding factors Wiener Askar perturbation treatment 77−34774
H, nonrelativistic high order perturbation theory corrections to energy levels, infinite series representation 77−34564
H, parity mixing, relativistic neutral current interactions and nonrelativistic pots. 79−26908
H, perturbation theory and Pade approx. in electric field 80−91493
H, quadratic Zeeman effect, perturbative approach 79−22649
H, quasi-stationary states in field of strong monochromatic wave, perturbation theory calcs. *(Russian)* 80−58145
H, Stark effect, dispersion relation, asymptotic formulae, ionis. rate, perturbation theory calc. 80−14106
H, Stark effect, high orders of perturbation theory 79−98025
H, Stark effect, high orders of perturbation theory for excited states 80−87079
H, Stark effect, perturbation theory 79−22652
H^-, many-body perturbation theory with radially restricted basis functions 80−78526
H^-, photodetachment cross section, perturbation-variation method 79−6921
H^+ chemical shifts, INDO calcs. 80−32743
H-like atoms, Stark effect and perturbation approxs. 80−52932
H+H, interaction energy, modified perturbation theory calc. 78−9217
$H+H^+$, interaction energy, perturbation expansion, symmetry forcing 79−22785
H^-+2HF, interaction pot., monopole approx., supermol. SCF and perturbation schemes 77−27139
H_2, Bender-Wu formula, SO(4,2) dynamical group and Zeeman effect, perturbation coeffs. determ. 80−95674
H_2, dynamic polarisabilities, variation-perturbation calcs. 80−87243
H_2, electric dipole polarisabilities and hyperpolarisabilities, perturb. theory calcs. 78−17563
H_2, electric dipole polarisability, many-body perturbation theory calcs. 78−21839
H_2, FCC solid, first-order shifts in electronic states 79−82510
p-H_2, liq., equil. bulk props., perturbation theory approach and quantum effects *(Russian)* 77−89551
H_2, liquid, effect of ortho-para composition *(Russian)* 78−34419
H_2, liquid, perturbation theory and quantum effects, thermodynamic props. and quantum stat. corrections *(Russian)* 78−22867
H_2, metallic, eqn. of state determ. *(Russian)* 77−89519
H_2, octapole magnetisability, multiple SCF perturbation calc. with STO basis set 77−34550
H_2, pair equations, perturbation contribs. to correl. energy 79−6874
H_2, polarisability, finite field MC SCF calcs. 80−14075
H_2 predissociation probabilities of $4p\pi^1\Pi_u^+ v\geq 1$ levels, dissoc. channels interference 80−28074

perturbation theory continued
H_2, triplet state, pot. curve van der Waals region, MS-MA calcs. 77−79551
H_2^+, dynamic dipole polarisability, variational perturbation theory 78−94330
H_2^+, exchange perturbation theory 80−63518
H_2^+, ground state, asymptotic primitive function, symmetry adapted perturbation calcs. 79−6855
H_2^+, intramol. interaction energy, convergence of perturbation expansions 78−17745
H_2^+, modulated perturbation theory variational calc., ground state second order energy 77−57872
H_2^+, nonadiabatic vibrational energies, ab initio calcs. 78−90142
H_2^+, polarisability, internuclear distance depend., excluding continuous spectrum 77−10581
H_2^+, spurious avoided-crossings, variationally calc., perturbation theory approach 78−5295
$(H_2)_2$, ab initio calcs., perturbation dispersion energy versus CI treatment 77−26976
H_3^+, dipole polarisabilities, variational perturbation theory calcs. 78−70765
HCN, semi-empirical excited state Morokuma's EHP calc., geometry and order of states 78−46256
HCNO, vertical ionisation pot., Koopmans' theorem, perturbation connnections calcs. 80−42966
HCl, one-electron props., corrections, Moller-Plesset perturbation theory calc. 80−95519
HCl, second order mag. props., coupled Hartree-Fock perturbation theory 80−87042
HCl, $X^1\Sigma^+$ states, many body effects, diagrammatic perturbation theory 77−79547
HCl-inert gas rot.-vibr. line pressure broadening and shift calc. 80−69124
HCl+iert gas, weak collisions, HCl spectral line broadening of IR spectra 80−74161
HD, dipole moment and rot. spectrum, perturbation theory calcs. 77−65454
HD, nucl. spin coupling const., MBPT theory calcs. 80−28035
HD, spin-spin coupling constant convergence, comparative study 80−63536
HD^+, Hellmann-Feynman theorem anomaly 80−63510
HD^+, nonadiabatic vibrational energies, ab initio calcs. 78−90142
$HD^+ + HD^+$, 0.1-1 eV, rot. transitions and reson. transfer, first-order perturbation theory 77−83698
HF, ab initio HF-STO perturbation Auger transition rate calc. 79−72368
HF, mol. hyperpolarisability, second-order SCF perturbation method, coupled Hartree-Fock calc. 78−33422
HF, nucl. spin-spin coupling consts., finite perturbation and sum-over-states calcs. 79−85893
HF, nuclear spin-spin coupling, ab initio SCF perturbation theory 78−33525
HF, pot. curves, diagrammatic perturbation theory, spectrosc. consts. 78−25458
HF, variation-perturbation minimal Gaussian geminal basis sets correl. energy calc. 78−78629
HF, $X^1\Sigma^+$ state, many-body effects, HF STO calcs., diagrammatic perturbation theory 77−50355
HF, $X^1\Sigma^+$ states, many body effects, diagrammatic perturbation theory 77−79547
HF, $X^2\Sigma^+$ state, 3- and 4-body perturbation theory modified pots. 77−88376
HF+HF, interaction energy, MCF and perturbation calculations 77−27139
HF+HF, medium distance interaction, SCF LCAO MO, supermol., perturbation and MCF calc. 79−837
HF_2^-, mag. shielding and susceptibility, finite perturbation mol. orbitals calcs. 77−46513
HN_3, vertical ionisation pot., Koopmans' theorem, perturbation connnections calcs. 80−42966
HNCO, vertical ionisation pot., Koopmans' theorem, perturbation connnections calcs. 80−42966
HNC⇌HCN, isomerisation energy/barrier correlation, rel. to LiNC(BNC) 80−50840
HNF_2, vertical ionisation pot. calc. by perturbation corrections to Koopmans' theorem 80−83520
H_2NO, hyperfine coupling const. calc., double perturb. theory and CI methods 79−59362
HO_2 free radical, dipole moments and Stark effects from microwave spectra 80−63623
H_2O CI, high-order many-body perturbation theory 77−88397
H_2O, elec. and mag. props. in static fields, perturbed Hartree-Fock calcs. 78−50462
H_2O, ground state, energy, bond parameters, diagrammatic perturbation theory calcs. 78−25414
H_2O, ionisation pot., quasidegenerate many-body perturbation theory calcs. 77−50346
H_2O, iterative natural orbitals for CI using perturbation theory 77−79549
H_2O, mag. susceptibility, HF perturbation method 77−79702
H_2O, many body perturbation theory fourth order calc. of correl. energy 80−14087
H_2O, mol., ionisation pot., CI and perturbation methods 79−31734
H_2O, nucl. elec. shielding tensor calcs. 80−83296
H_2O, nucl. spin-spin coupling consts., finite perturbation and sum-over-states calcs. 79−85893
H_2O, nuclear spin-spin coupling, ab initio SCF perturbation theory 78−33525
H_2O, polarisabilities, finite-field calc., perturbation correlation 79−72249
H_2O, polarisability and mag. susceptibility calc. by SCF and CI method 80−99443
H_2O, proton mag. shielding const., HF perturbation theory 78−46258
H_2O, vertical ionis. pot., many-body Rayleigh-Schrodinger perturbation theory 78−9063
H_2O, vertical valence ionis. pot. calc. by perturbation, CI and CPA techniques 80−69263
H_2O+D_2O⇌2HDO, vibr. anharmonicity effect on equilib. 79−74410
H_2O+H_2O, interaction energy, MCF and perturbation calculations 77−27139
H_2O+H_2O, medium distance interaction, SCF LCAO MO, supermol., perturbation and MCF calc. 79−837
perturbation theory continued
H_2O_2, struct. and barrier to internal rot., HF and Rayleigh-Schrodinger perturbation calcs. 79−13636
H_2O_3, struct., barrier to int. rot., HF and RS-MP perturb. calcs. 79−13637
$H_3O^+ + 2HF$, interaction pot., monopole approx., supermol. SCF and perturbation schemes 77−27139
HOCN, vertical ionisation pot., Koopmans' theorem, perturbation connnections calcs. 80−42966
H_2S, gas-phase, states in valence photoelectron spectrum 78−94284
H_2S, second order mag. props., coupled Hartree-Fock perturbation theory 80−87042
He, ^1S ground state, variational perturbation calc., teaching 78−41129
He, 2p3d $^{1,3}L^0$ doubly excited state, soln. of Hartree-Fock eqns. 77−75072
He, autoionising resons., complex rot. method, non- and degenerate perturbation theory 79−72283
He, dynamic polarisability, 2^3S_1 and 2^1S_0 states var. perturbation calcs. 77−54507
He, elastic electron scatt. phaseshifts, 2s2p ^3P autoionisation, 1s2s $^3S \rightarrow 1sep\ ^3P$ triplet continuum photoionisation 79−31480
He, electric dipole polarisabilities and hyperpolarisabilities, perturb. theory calcs. 78−17563
He energy levels, classical first order perturbation theory 80−58118
He, film, Brownian motion, boundary layers and quantised vortex prod. 80−6579
He, freq. depend. polarizability, LCAO SCF perturbation theory 79−31387
He, ground state radial limit, piecewise polynomial basis functions 78−37560
He, Hartree-Fock energy, perturbative corrections, incomplete basis set problem 78−70744
He, isoelectronic series, ground state specific mass shift, HF variation perturbation calc. 80−47889
He, metastable $1s2s\ ^1S$ state, photoionisation, perturbation theory calcs. 78−78759
He metastable state, two- and three-photon ionisation 80−91518
He, photoionisation, frozen-core HF perturbation theory, oscillator strength, dipole length and vel. calc. 78−78672
He, second order correlation energies, variational-perturbation method, radial basis saturation errors 79−97985
He sequence, 2p3d $^{1,3}L^0$ doubly excited state, soln. of Hartree-Fock eqns. 77−75072
He, transition probabilities in constant electric field, general perturbation theory 78−13466
He, two-photon ionisation cross-section calcs. 78−21888
He^+, electron scatt., elastic, ^1P continuum phaseshift, autoionis. state 77−88561
He+CO, nuclear mag. shielding consts., interaction geometry depend., chemical shift, gauge invariant method 78−62866
He+Cs(Rb), interatomic pots., hyperfine shifts, diffusion coeffs., perturbation exchange theory 79−41220
$He+H_2$, inelastic scatt. exponential perturbation theories 80−74217
He+He, weak intermol. interactions, intramol. correl. effects, perturbation anal. 79−86038
$He+He^{2+}$, single and double electron capture, high vels., independent electron approx. calc. 80−18923
He_2, ground state, interaction energy, many-body perturbation theory calcs. 80−69210
He_3, 3-body nonadditive interaction, nodal struct. 78−1049
He_3, dipole moment, large separation, perturbation theory 78−62946
^{3}He bound state, perturbation approach with Reid soft core pot. 79−67675
^{3}He, liq., interface with nonmag. solid, Kapitza resist., quantum perturbation treatment 80−88385
^{3}He, superfluid A-phase, longitudinal mag. relax. 80−59751
^{3}He-^{4}He, liq., excitation spectrum and quasiparticle interactions 78−10250
^{4}He, liq., elementary excitations, Brillouin-Wigner perturbation theory with correlated basis functions 78−2319
^{4}He, liquid, perturbation corrections to ground-state energy 77−7918
^{4}He, superfluid, roton-roton interaction for large and zero momentum 80−84336
Hg atoms, elastic electron scatt., relativistic effects 80−102568
Hg, liq., long wavelength limit, triplet and higher correls., Percus-Yevick eqn., perturbative anal. 79−37613
$HgCl_2$, deformation densities, relativistic effect 80−42928
$I^2P_{1/2} \rightarrow {}^2P_{3/2}$, collision induced emission (Ar)(Xe), dipole transition moment by perturbation theory 77−83528
In, lattice dynamics, pseudopot. computation *(Russian)* 80−92617
In pnictides, mixed, impurity induced Raman scatt. spectra 80−88983
In, quadrupole antishielding factors, Hartree-Fock perturbation theory 78−62723
In($^2P_{3/2}$), at. quadrupole shielding factor 79−10222
K-Rb, liq., form factors and transport coeffs., pseudopot. perturb. theory 80−44561
KH_2PO_4 type crystals, low lying ferroelec. modes, cluster dynamical theory 78−80305
KH_2PO_4-type crystal, LF dynamics 80−10602
Kr, inner electron energy characteristics, validity of Hartree-Fock-Pauli approx. 80−42957
La, 4d subshell spectra, strong interaction regime 79−18165
Li, $2s^2$2p double Auger rate 80−99489
Li, Auger widths of core levels using renormalised many-body perturbation theory 79−74033
Li, autoionisation states, config. decays and excitation energies 78−13475
Li I, $2s^2$sp and $1s2s^2$ decay rates many-body perturbation theory calc. 79−59376
Li isoelectronic sequence, Hartree-Fock eqns., perturbation calcs. 79−6846
Li isoelectronic sequence of three electron atoms, pair correlation study 80−74096
Li, two-photon ionis., many-body perturbation theory 79−22679
Li^+ 2p3d $^{1,3}L^0$ doubly excited state, soln. of Hartree-Fock eqns. 77−75072
Li+Li(Be), London coeffs. for long range interaction, CI variation-perturbation method 78−5310
$Li^+ + CO_2$, collisional excitation, quasiclassical trajectory calcs. 80−83467

perturbation theory continued
LiF, $X^1\Sigma^+$ state, many-body effects, HF STO calcs., diagrammatic perturbation theory 77−50355
LiH, correlation energy, perturbation calc. using Gaussian-type geminals 79−10042
LiH, correlation energy calc. by many-body diagrammatic perturbation theory 78−9087
LiH, electric dipole polarisabilities and hyperpolarisabilities, perturb. theory calcs. 78−17563
LiH, iterative natural orbitals for CI using perturbation theory 77−79549
LiH, many body perturbation theory fourth order calc. of correl. energy 80−14087
LiH, mol. elec. polarisabilities and dipole moments calcs. 78−41976
LiH, variation-perturbation minimal Gaussian geminal basis sets correl. energy calc. 78−78629
LiH, $X^1\Sigma^+$ states, many body effects, diagrammatic perturbation theory 77−79547
LiNC type molecules, Born-Oppenheimer approx. applicability 80−32603
LiNC⇌LiCN, isomerisation energy/barrier correlation, rel. to HNC(BNC) 80−50840
Li(^{2}S), open shell polarisation propagator, for doublet-doublet transitions calcs. 80−27939
^{6}Li, Coulomb disintegration in field of heavy target nucleus, perturbation theory 78−66319
Mg, chemisorption of H_2, effects of substrate pseudopotential lattice 79−46953
Mg, polarisability and London coeff., ab initio variation perturbation calc. 79−13635
Mg^{2+} atomic core states, antishielding effects calcs. 80−83299
Mg_2, pot. energy curve for $X^1\Sigma_g^+$ state, many-body perturbation calcs. 78−55216
Mn, HFS, many-body and relativistic effects 78−37565
Mn^{2+} EPR of doped powder samples, hyperfine line intensities and axial cryst. field 79−78511
Mo XIII and XVII, spectra, perturbation theory with model pot. 78−58579
Mo XV, electronic struct. of complex ion, relativistic perturbation theory 79−22610
molecular pair polarisabilities, continuum electrostatic theory 78−86769
N, nucl. quadrupole coupling const., relativistic many-body perturbation theory 78−37566
N-containing cpds., ^{13}C chem. shift calcs. using approx. SCF perturbation theory 77−18945
N_2, electronic ground state correl. energy, many-body diagrammatic perturbation theory calc. 78−917
N_2, liq., thermodynamic props., perturbation theory with hard dumbbell reference system 80−14991
N_2, PE curve, spectroscopic consts., perturbation theory appl. 80−23341
α-N_2, solid, anharmonic lattice vibrations calcs. 78−71812
N_2, vertical valence ionis. pot. calc., by perturbation, CI and CPA techniques 80−69263
N_2+O_2, molecular fluid mixtures, equilibrium props. 80−64867
NH_3, freq. depend. hyperpolarisability, time-depend. Hartree-Fock calcs. 79−36559
NH_3, mag. susceptibility, HF perturbation method 77−79702
NH_3, mol. nuclear spin-spin coupling, ab initio SCF perturbation theory 78−33525
NH_3, nucl. elec. shielding tensor calcs. 80−83296
NH_3, proton mag. shielding const., HF perturbation theory 78−46258
^{14}N, spherical ground state nuclear quadrupole interaction, Breit interaction, relativistic perturbation theory 80−42939
^{15}N, spin-lattice relax. time, quantum effect of NH_4-ion rot. 80−75875
Na, Auger widths of core levels using renormalised many-body perturbation theory 79−74033
Na, chemisorption of H_2, effects of substrate pseudopotential lattice 79−46953
Na, equilibrium struct. and phys. props., pseudopot. method 80−96778
Na, photoionisation cross-section, electron correls. Brueckner-Goldstone calcs. 77−6742
Na^+, atomic core states, antishielding effects calcs. 80−83299
Na-K(Cs), liq., form factors and transport coeffs., pseudopot. perturb. theory 80−44561
NaCl, polarisation mechanism and lattice mechanics, microscopic approach 78−59888
NaH, $X^1\Sigma^+$ states, many body effects, diagrammatic perturbation theory 77−79547
Nd ions recoiling in vac. or low press. He, nuclear deorientation, perturbation mech. model 77−50105
Ne, at. struct. by many-body perturbation method, algebraic approx. 77−18776
Ne, atomic struct. calc., symmetry adapted pair functions, Rayleigh Schrodinger HF variational perturbation theory 80−42944
Ne, double photoionisation, many-body perturbation approach 78−17634
Ne isoelectronic series, second order correl. energy, Z depend. of irreducible-pair energies 80−91417
Ne, liquid, effective pair pot. from perturbation approach 77−68908
Ne, liquid, higher order struct. functions in long wavelength limit, improved perturbation approx. 79−37606
Ne, second-order correl. energy calcs. 78−33436
Ne, triply-excited states contributing to correl. energy, diagrammatic perturbation theory 79−81161
Ne, vertical ionis. pot., many-body Rayleigh-Schrodinger perturbation theory 78−9063
Ne, vertical valence ionis. pot. calc. by perturbation, CI and CPA techniques 80−69263
Ne-H_2 liq. mixtures, phase equilib. effects, thermodynamic perturb. theory *(Russian)* 80−92663
Ne_3, 3-body nonadditive interaction, nodal struct. 78−1049
Ni, correlation effects, perturbation treatment 80−59897
Ni, correlation effects, perturb. treatment within Hubbard model 80−70582
O_2, singlet state radiative lifetime, perturbation-variation calc. 77−14496
OH+H_2→H_2O+H, reaction product vibr. distribs, quasiclassical trajectory, calcs. 80−85162
P_2 radical, $b^3\Pi_g$-$a^3\Sigma_u^+$ transition, perturbed by $1^5\Sigma_g^+$ state *(French)* 80−18855
PH_3, second order mag. props., coupled Hartree-Fock perturbation theory 80−87042
Pb+Pb quasimolecules ab initio calc. of K X-ray spectra 78−21941
perturbation theory continued
$Pb_{1-x}Sn_xTe$, lattice instability and phonon-width, perturbative model 79−14906
Pd, liq., Percus-Yevick equation, perturbation theory calcs. 78−75515
Pr^{3+}, correlation contributions to nuclear antiscreening factor, many-body calc. 79−56153
Pr^{3+}, elec. multipole polarisabilities, discrete basis set calcs. 80−91456
Pr^{3+}, nuclear quadrupole screening parameter, many-body perturbation theory calcs. 78−47751
Pt, liq., Percus-Yevick equation, perturbation theory calcs. 78−75515
Rb, ground state, hyperfine struct., relativistic many-body calcs. 80−23322
Rb, HFS, many-body and relativistic effects 78−37565
Rb, liq., long wavelength limit, triplet and higher correls., Percus-Yevick eqn., perturbative anal. 79−37613
Rb, liquid, higher order struct. functions in long wavelength limit, improved perturbation approx. 79−37606
Rb maser response to coherent Zeeman perturbations 78−58972
Rb, photoionis. cross section, elec. field depend. 80−37796
$RbAl(SO_4)_2.12H_2O$, spin-Hamiltonian with trigonal S^3I terms for describing $^{57}Fe^{3+}$ ENDOR spectra 80−75885
$RbGa(SO_4)_2.12H_2O$, spin-Hamiltonian with trigonal S^3I terms for describing $^{57}Fe^{3+}$ ENDOR spectra 80−75885
Rb(6^2P)+He(Ar)(Xe), fine-struct. transition cross sections, semiclassical calcs. 77−30972
S^-, photodetachment in mag. field 79−41143
SF_6, ν_3 band high-J manifolds, eigenvalues use second-order perturbation theory 79−36702
SeH($X^2\Pi$), IR LMR spectrum, spin-orbit coupling const. direct determ. 79−76429
Si, amorphous, molecular liquid model and electronic struct. 80−54133
Si, dispersion law of indirect excitons 80−24805
Si, impurity states and core excitons, binding energies, perturb. theory 80−49659
SiH_4, second order mag. props., coupled Hartree-Fock perturbation theory 80−87042
SiO, interaction between $G^1\Pi$ and $I^1\Pi$ states 79−50040
Tb_6 magnetocrystalline anisotropy, perturbation theory 78−2675
$Te^{VI}O_6$ ion in $A_2B^{II}B^{VI}O_6$ perovskites vibr. anal. using isotope shifts and perturbation theory 77−59073
V_2O_5, energy band structure, tight-binding method 80−70602
Xe, inner electron energy characteristics, validity of Hartree-Fock-Pauli approx. 80−42957
Xe, liq. struct. factor calc., perturbation treatment using Lennard Jones (6, 12) pot. 80−10483
Zn, Zn^{2+}, quadrupole antishielding factors, Hartree-Fock perturbation theory 78−62723
Zn^{2+}, closed shell ion, 3d electron pair correl. energies calcs. 79−31417
Zn^{2+}, electron pair correlation energies 79−93927
$ZnCl_2$, deformation densities, relativistic effect 80−42928
ZnF_2:Co^{2+}, Raman tensor calcs. of isolated impurity in diamagnetic matrix 80−76025
ZnO/SOS monolithic SAW amplifier 78−6205
Zr XI and XV, spectra, perturbation theory with model pot. 78−58579
Zr XIII, electronic struct. of complex ion, relativistic perturbation theory 79−22610

petrol engines *see internal combustion engines*

petroleum industry
acoustic logging in cased wells, effect of excited wave freq. on results *(Russian)* 78−40707
Alaska oil pipeline, induced elec. currents meas. by gradient fluxgate and SQUID magnetometers 80−98231
Alaska pipeline, auroral zone elec. currents induction 79−39645
automation level analysis 78−28327
borehole, obliquely bored, washing fluid temp. calc. method *(Russian)* 79−68555
feedstocks and cokes, graphitisability 80−93580
fluid mixtures, perturbed hard chain theory, thermodynamic props. 79−34343
furnace tube HK40 alloy remaining creep life testing *(Japanese)* 77−28950
Grand Banks drilling rigs, danger from drifting icebergs 78−81200
heat transfer in polymeric and disperse Bingham fluids during forced convection in ultradeep boreholes 79−68762
materials, plant, service failure modes gen. review 78−95904
Newfoundland, offshore oil and gas production, associated problems 79−87946
oil and gas well profiles, appl. of combined well-logging techniques *(Russian)* 78−40705
oil prerefining, shale, in situ, hydrotreatment at 1500 and 2200 psig 79−48047
petro-chemical industrial plants, piping networks, noise abatement 80−28381
petrochemical industry, prevention of water pollution 77−70705
pipline supervisory control systems, implementation guidelines for promotion of electronics in oil and gas sector 79−80039
pollution monitoring in petroleum refinery 77−41163
process heat from nuclear steam supply systems, appl. to prod. and treatment of liquid and gaseous prime movers *(German)* 79−87944
refineries, air pollution data interpretation via pollution roses 78−81379
reservoirs, steady water cone in well, free boundary problems *(Chinese)* 79−50699
shale oil refining, jet fuels production, by surface and in situ technology 79−48048
solar enhanced oil recovery; an assessment of economic feasibility 80−40832
stream anal. using process liquid chromatography 79−16110
US flowmeters, petroleum and similar fluids 80−43804
USSR fields petroleum fractions, isobaric integral heats of condensation *(Russian)* 79−65181
well mud logging, online data processing *(Russian)* 78−40706
worldwide energy prospects, synthesis of studies published in 1976 and 1977 *(French)* 79−29443

petroleum refining *see oil refining*

p.f.m. *see pulse frequency modulation*

pH
acid rain, Pittsburgh (Pennsylvania) area 80−94129
aerobic Escherichia coli cells, metabolism, high resolution ^{31}P NMR studies 77−90741

pH continued
aerosol of Sudan Gezira airstream, chem. composition and pH 80−51518
air pollutants, particle acid content determ. method 77−37448
airborne man-made acidity, determ. using Gran's titration method 79−5606
Alberta forests, acidity of open and intercepted precipitation and effects on soil 77−73844
albumin, adsorption on SiO_2 80−10777
alkali borate glass networks, π-electron distrib. SCF INDO LCAO-MO calc., O basicity 78−79924
alkaline snowfalls in Ottawa and Winnipeg, Canada 79−12175
6-amino-7-hydroxy-4-methylcoumarin solutions, additions effect on fluoresc. 80−2833
aminobenzoic acid, aqueous and dioxane solns. with nonfluoresc. impurity, fluoresc. and pH *(Russian)* 77−83635
anions in snow cover of Adirondack Mountains, meas. 79−12149
artificial membranes, transport regulation by environmental H^+ conc. 80−89725
atmosphere, acid rain and cation leaching in Douglas fir ecosystem 77−78392
atmospheric acid precipitation, 1920 onwards in E. North America 77−37334
atmospheric acid precipitation and acidification of Canadian lakes, effects on fish populations 77−37259
atmospheric acid precipitation and forest ecosystem, symposium (Columbus, Ohio, 1975, May 12-15) 77−37322
atmospheric acid precipitation effects, Norwegian SNSF-project on forest and fish 77−37411
atmospheric acid precipitation effects, on aquatic ecosystems, review 77−37257
atmospheric acid precipitation effects on freshwater ecosystems in Norway 77−37258
atmospheric acid precipitation in central Texas 77−37329
atmospheric acid precipitation in N.E. United States, H ion speciation 77−37336
atmospheric acid precipitation in N.E. United States 77−37328
atmospheric acid precipitation in Norway 77−37371
atmospheric acid precipitation meas., interpretation and review 77−37323
atmospheric acid precipitation meas. in Norway 77−37324
atmospheric acid precipitation rel. to S and N oxide emissions over Canada 77−37338
atmospheric precipitation, pH and acidity over N.E.United States 77−53184
atmospheric precipitation over Iowa, nutrient content and acidity 77−37330
automatic range-changing amplifier, ionisation current pH and vacuum measurement appls. *(French)* 79−63262
basalt, cement reinforcing fibre, alkali resist. 80−89377
blood, gas valves, anal. in mice following pulmonary irrad. 80−104673
calcium phosphates, seeded growth, effect of solid/soln. ratio, calcification 78−15303
catheter tip pH electrodes for continuous intravascular recording 80−81755
cell lethality due to hyperthermia, 41 to 44°C 77−64014
cell nuclei structural change in the physiological pH interval 79−79492
cells, photo-depdnd. ^{14}C-alanine transport into H.halobium cells 77−70439
cetyl pyridinium bromide, adsorpt. on Aerosil, pH depend., mechanism 79−20466
chemical composition, of river water, in northern Okinawa Honto, Japan *(Japanese)* 79−96782
chemical durability, thermodyn. approach 78−7063
chemical reactions, in molten salts, acidity effects 78−73039
chemical water treatment pH value calc. for district heating power station, computer-aided analysis *(Russian)* 79−43572
chlorophyll-duroquinone photochemical interaction, photopot. 77−16903
chloroplast, EPR signal II and Mn-water splitting, factors influencing stability 78−24038
chloroplast membrane proton gradient and osmotic vol. determ. 78−28143
chloroplasts, isolated, effect of temp. on photo-induced pH gradient 80−81566
cloud water acidity rel. to SO_4^{2-} prod. 79−5546
computations in terms of hyperbolic functions 77−25354
coumarin 102, excited state protonation kinetics, laser pH jump and picosecond spectroscopy 80−25992
crosslinked collagen membranes, transport props., physical props. effects 78−77028
crystallisation kinetics, soln. pH effect 79−99095
cutting fluid, hydrolysed polyacrylonitrile based, operational characteristics 80−89359
cytochrome *a* interaction with mitochondrial matrix H^+ ions 79−43806
cytosine monohydrate single crystal growth, effect of pH 79−34473
2,3-dioxogulonic acid, reversible transformation to enol, kinetics, pH effects 79−5152
DNA-Au (III) interaction, rate consts., activation energies, pH, spectrophotometric obs. 80−30228
electrolyte, effect on Cu electrolytic coating, adsorption of surface-active additives 80−100963
erythrocyte membrane, cooperative pH-sensitive state transition, Raman spectroscopy 77−36881
freshwater acidification meas. 79−43802
Gran's plot, acid-base titration 79−79432
haemoglobin, human, liganded, kinetics of alkaline tetramer-dimer dissoc., laser scatt. obs. 78−48749
haemoglobin, O_2 linked Cl^- binding sites, pH dependence 79−62174
Halobacterium halobium R_1 cells, photogeneration of two-vector transmembrane gradient of protons 78−80845
heart physiology, ^{31}P NMR investigations of metabolism, pH and contractile performance 78−69018
Hubbard Brook Experimental Forest, H ion input and precipitation pH 77−37337
hydrometeors, pH detailed struct. 79−92111
8-hydroxy, 1,3,6-pyrene trisulphonate, picosec. proton ejection, ultrafast pH jump 79−83475
3-hydroxy-2-methyl-1,4-naphthaquinone, pH indicator *(Rumanian)* 78−23947
Incoloy 800, stress corrosion cracking in NaOH solns., electrochem. aspects, peening treatment 80−97618
Inconel 600, stress corrosion cracking in NaOH solns., electrochem. aspects, peening treatment 80−97618
Inconel 600 alloys, stress corrosion cracking, prediction in 10% NaOH soln. at 315°C 80−97616
indole, pH dependent fluoresc., quenching by histidine *(Russian)* 78−90209
indole soln. containing histidine, fluoresc. rel. to soln. pH 80−2826
intestinal epithelium, effect of Ca ions and pH on osmotic pot. 78−20156
intestine, small, effect of pH on permeability and mech. props. of intercellular contacts 79−57613
jute, cement reinforcing fibre, alkali resist. 80−89377
Lake Shlavantas, deep autumnal cooling and freezing *(Russian)* 78−36213
Lake Toya, Japan, acid mine drainage, pH effect 79−34449
liquid phase duration in large diameter bubble columns *(German)* 79−32632
liquids for cooling and index matching of Nd:glass laser systems 80−33015
lysine, aq. solns., $H^+(D^+)$ exchange rates, ^{17}O NMR linewidths, pH depend. 80−91661
lysozyme effect of pH on dimorphic crystal growth 79−14728
maleic acid-styrene copolymer, aq. soln., conform. transition 78−75526
methanol-water (propylene glycol), proton medium effects, ferrocene redox couple reference obs. 77−77786
motor reactivity, isolated heart of grass snake, pH and temp. effects 80−26219
muscle Na channel use-depend. block by local anaesthetic, pH effect, frog 78−20160
2-naphthol-3,6-disulphonate, picosec. proton ejection, ultrafast pH jump 79−83475
nerve ionic permeability of K, Na and Cl, regulation by fixed charges and pH, crayfish 77−66809
nerve terminal Ca channel selectivity regulation by weak acid site 79−62231
neurons, Aplysia, effects of NH_4^+ and HCO_3CO_2 on intracellular Cl^- level 78−44485
ocean, pH depend. of low-freq. sound absorpt. 77−84052
peptides and derivatives, mol. electron acceptor groups 80−30637
phenylalanine, hydrated electron impact dissoc., laser flash photolytic investig. 80−58396
plant sieve tube sucrose loading, role of pH gradient and membrane ATPase 77−52757
poly (N^{ε},N^{ε}-terephthaloyl-L-lysine) membrane for artificial red blood cells, interaction with serum proteins *(Japanese)* 80−12061
poly-L-ornithine solution, ^{15}N NMR, coil-helix transition, solvent effects and pH depend. 80−74275
polydicarboxylic acids, electrophoretic and viscometric props. 80−66811
potential-pH diagram, improved algorithms for computer generation, max. constriction method 80−26019
precipitation chemical composition around Tokyo, 1967-68 obs. *(Japanese)* 78−49120
propylene glycol-water (methanol), proton medium effects, ferrocene redox couple reference obs. 77−77786
protein membranes, immobilised, H^+ ion transport, assoc.-dissoc. time-scale factor 79−34529
protein titrations by NMRk pH depend. of internal reference 77−86727
proton transfer reactions, excited state, laser pH jump analysis method 79−47922
proton transport across charged membrane and pH oscillations 80−61516
purple membrane suspensions, light-induced conductivity changes, pH and temp. effects 80−51157
quartz glass-water suspensions, electrolytes effect on viscosity, pH and zeta pot. props. 79−34365
radioactive effluent monitoring problems, loss and error reduction procedures 78−89987
rain, contrib. of SO_4^{2-}, NO_3^- and NH_4^+ ions to acidity 79−2327
rain and snow, release of S and nitrogen oxides by burning fossil fuels 80−26590
rain interacting with rock partially covered by lichen 80−17302
rainfall, amount and pH in Michigan 77−37332
rainfall acidity, natural variance of pH time dependence 80−61840
rainwater, pH and S content in rural areas of England and Wales 79−16562
rainwater chemistry and multiple H ion donor systems, obs. in Minnesota 77−37335
rainwater convective storms over St. Louis 77−37333
rhabdom spectral absorption, crayfish visual pigment, photoproduct and pH sensitivity 78−65008
rhodamine 6G, aqueous soln., absorpt. spectra, ground and triplet state photoprotonation pH depend. 80−42961
rhodamine B, acid-base equilib., photophys., fluoresc. lifetime meas. 78−82762
rhodamine B in aq. LiCl soln., absorpt., pH, electric conductance 77−27079
rivers, O_2 and pH fluctuations, math. model 78−92866
seawater, computerised high-precision titrations of major constituents 77−66926
seawater, pH distrib. rel. to transparency 80−31057
seawater effect on low-freq. sound absorpt. 77−49072
serum albumin, human hydration, pH depend., water self-diffusion obs. *(French)* 79−34475
silver thioamides, precip., electron microscope and potentiometric studies, growth of photosensitive crysts. 80−33107
skin tissue pH electrodes for clinical applications 80−36175
soil, limestone bedrock erosion due to percolating acid waters 77−45023
soil acidity in Alberta, SO_2 effects 77−73843
solution, ^{89}Y spin-spin relax. times, no pH depend. 80−2657
steel, austenitic type 304, sensitised, intergranular stress corrosion cracking inhibition study 80−100939
steel, C, corrosion by wet elemental S, exam. as function of pH and particle size 78−92388
steel, C, corrosion inhibition by 2-ethylamino-ethanol in aerated 3% NaCl soln., pH effect 80−21160
steel, low C, corrosion fatigue strength, soln. pH effects *(Japanese)* 77−52545
steel, martensitic stainless, in SO_4 solns., activation pH and susceptibility to H_2 assisted stress corrosion cracking 80−97619
sulphides, direct leaching 77−29033

pH continued
sulphononaphthols, rapid pH and $\Delta\mu H^+$ jump by short laser pulse 80−16709
superacids, props. and appls. *(French)* 79−74482
thiazolidine, IR spectroscopy of mol. association *(French)* 79−50178
tropocollagen macromolecule form., effect of soln. pH 78−95999
tryptophan, pH dependent fluoresc., quenching by histidine *(Russian)* 78−90209
tryptophan soln. containing histidine, fluoresc. rel. to soln. pH 80−2826
tumour cells, depend. of hyperthermic effect on environmental pH 77−86465
umbelliferones, 3-substituted, fluoresc. spectra, pH depend. 77−88492
voltage/pH convertor, using operational amplifiers *(French)* 79−63267
water quality monitoring, modular system *(German)* 80−26186
$^{18,19}F$ ion diffusion in dental enamel at pH 7, obs. 79−29553
AgBr, adsorption of cyanine 78−62254
Al alloy anodic oxide film hardness, effect of pH and metallic additives *(Japanese)* 77−56146
Al anodic oxidation, in H_2SO_4, pH-values effect *(German)* 80−76419
η-Al_2O_3 outgassed at 400, 650°C, heat of adsorpt. of pyridines from soln., surface acidity 80−61154
As, migration capacity, effect of acid-alkaline conditions on hydrogeochem. 77−37244
C, black, surface acidity effects on work function 78−2548
C blacks, surface polarity, surface activity, slurry pH, oxidation effects 78−68915
C-H bond, acidity in organic mols. and anions, SCF MO calcs. 77−83497
CO_2 outgassing during pH meas., effects on groundwater chemistry and C isotopic comp. 79−66718
$Ca_{10}(PO_4)_6(OH)_2$, hydroxyapatite, aq. solution system, interfacial props. and equilibria 79−77751
Cd, high purity, passivity breakdown pH effect on pitting potential 80−100947
$ClSO_2OH$, superacid, props. and appls. *(French)* 79−74482
Cu complex, polyacrylic acid-polyethyleneimine-Cu(II), struct. *(Russian)* 79−55018
Cu-Be(2 wt.%), tarnish surface films, formed in ammoniacal Cu(II) solns. 80−97624
Cu-Ti (4 wt.%), aged, stress corrosion cracking in Cu-NH_3 solutions, effect of pH, Cu and NHz conc. 78−88562
D_2O, $H^+(D^+)$ exchange rates, ^{17}O NMR linewidths, pH depend. 80−91661
Fe, anodic behaviour in 1M H_2SO_4, influence of straining 80−97612
Fe, corrosion inhibition in pH range 9.3 to 12.6, tartrate ion effect on oxide film thickening 78−44251
Fe, passive film form. in phosphate soln., intensity-following ellipsometry study 80−104345
Fe-Ni-Co coating electrodeposition optimum conditions *(Russian)* 79−83292
Fe-SO_4-H_2O suspension system at 90°C, potential-pH diagram 78−61068
FeO based slag, thermophysical props., effect of basicity, rate of heating *(Russian)* 77−25009
$Fe(OH)_3$-$Fe(OH)_2$ suspension system, potential-pH diagram 80−55728
H_2O, $H^+(D^+)$ exchange rates, ^{17}O NMR linewidths, pH depend. 80−91661
HS_n^-, n=1-4, electronic struct., ab initio Hartree-Fock-Slater calcs. 80−74107
HS_n^{2-}, n=1-4, electronic struct., ab initio Hartree-Fock-Slater calcs. 80−74107
H_2S_n, n=1-4, electronic struct., ab initio Hartree-Fock-Slater calcs. 80−74107
IrO_x film, anodic, electrochromism, pH effects on corrosion stability, coloration and bleaching mech. 80−2726
K^+ transport of squid axon membrane, internal pH effects 79−62221
MgO, catalytic behaviour, rel. to XPS obs. 79−24820
$Mg(OH)_2$, cryst. growth from aq. soln. at 60°C, pH effects 78−23591
$NH_4H_2PO_4$, cryst. growth, pH effect, H_3O^+ inclusions 79−55682
$NH_4H_2PO_4$, cryst. growth in presence of Mn ions 80−93468
$(NH_4)_2SO_4$:Cu^{2+}, ESR parameters, effect of pH of mother soln., trapping sites 80−15791
Na_2O-(CaO)-SiO_2, diffusion controlled attack by aq. solns. 80−81218
Na_2O-SiO_2, aqueous solns., Raman and IR spectra, pH depend., species at equilib. identification 79−87866
Ni, corrosion and passivation in phosphate soln., pH depend., ellipsometric study 80−104448
Ni-Fe-Cd, ternary alloy, electrodeposition from acetate bath 79−95950
$PbCO_3$, cryst. growth, Liesegang ring form., pH effect 80−49140
SO_2-seawater, thermodynamics 77−52660
Si_3N_4, aqueous suspension rheological and processing props. 77−23928
Ti, anodic film structure, intensiostatically formed, pH and current density influence, TEM study *(French)* 79−66217
$Zr(HPO_4)_2$, cryst., heat treated, acid strength distrib. 78−92377
ZrO_2, isoelec. points, effect of pH on electrophoretic mobility 80−35548

pH control
boiler feedwater pH meas. apparatus improvements 79−79341
development of pH monitoring systems, limitations 80−3421
drum boilers, working at 11.0 to 15.5 MPa, pH control by addition of caustic soda *(Russian)* 80−89420
electrical conductivity meas. of crystalline materials, high press. and temp. using buffer techniques *(German)* 79−93162
electrochemical pH-stat and controlled current coulometric acid-base analyser 77−36801
electrolysis, automatic pH control, instrumentation, appls. 77−63928
instrument research, stability, buffering and electrode designs 77−81438
neutralisation process, self-tuning control 80−30242
trace element analysis, pH adjustment by gaseous reagents 78−73094
Fe, mechanism of action of weak acids and their salts on passivation by O_2 80−50886
Pt 79−48340

pH factor *see pH*

pH measurement
aliphatic amine mixtures, ionis. consts. determ. by gas-chromatographic anal. *(Russian)* 79−61921
atmospheric precipitation acidity measurement, error anal. applied to indirect methods 80−72108
automatic potentiometric monitoring station, for examining industrial wastewater 78−56932
biomedical ion sensitive FET micro pH sensor 78−44643

pH measurement continued
biomedical pH measurement techniques, equipment 78−77158
blood gas analysers, review 78−69238
blood gas microanalyser, calomel electrode efficiency restoration 77−25575
boiler feedwater pH meas. apparatus improvements 79−79341
component selection for continuous pH measurement, pollution abatement appl. 77−73767
development of pH monitoring systems, limitations 80−3421
differential electrode method appl. 77−25353
digital, Schott, 1978 exhibition in Munich *(German)* 79−20482
digital pH meter, manual, automatic temp. compensation, laboratory appl. *(Rumania)* 77−74453
digital voltmeter appl., with high input impedance *(Spanish)* 78−20133
dilute polymer solution viscosity/pH meas. 79−68831
electrode, rapid response, cardiac output and ventricular residual fraction determ. 77−40860
electrolysis, automatic pH control, instrumentation, appls. 77−63928
electronics appl. in chemical technology *(German)* 77−77841
enamel electrode design for continuous meas. *(German)* 79−34413
endogastric probe for telemetric pH meas. *(German)* 78−85452
equipment for the measurement of ions in solution, review 80−71983
equipment selection and installation, accurate calibration, proper maintenance 79−16108
FET transducer, H^+, Ca^{++} and K^+-sensitive, biomedical appls. 78−28117
fibre optic pH sensor, miniature, for physiological use 80−109074
glass microelectrode, for pH meas. 80−21291
instrument research, stability, buffering and electrode designs 77−81438
instruments and appls. *(Dutch)* 79−29435
ion selective electrodes for dissolved gas detection *(French)* 79−100472
irradiated nuclear fuel reprocessing streams, remote anal. techniques 79−13510
liver cells, rat, isolated, ^{31}P NMR studies 78−61150
meter constructio for amateurs 77−57321
meter construction, standardisation, and use 77−63995
meter for student laboratory 79−35510
meter selection 77−56271
meters, laboratory, revised British Standard BS3145 77−70371
miniature pH-sensitive polymer membrane electrode 79−100781
model for potential difference across membrane, pH measurements using polarizable electrodes 80−76514
monitor, EIL model 7680, for low conductivity waters 79−74473
monitoring, complete laboratory, installation 78−61123
multi-purpose instrument for biochemical and related undergraduate studies 78−73816
multichannel measurement apparatus for pH of upper gastrointestinal tract 79−57781
muscle pH percutaneous microsensing during haemorrhagic shock and resuscitation 77−52907
muscle surface pH meas., significance of impedance changes 77−52908
ocean water quality instrumentation system test 77−41066
online, installation, calibration and maintenance 78−53282
operational amplifier pH meter circuit 79−21735
oxyhaemoglobin dissociation curve analyser, devel. and improvement 77−13019
pH/ion meter, automated 79−100464
physiological monitoring, by integrated FET micro ion sensor 78−44641
reference electrode liquid junction, press.- and flow-insensitive 77−4906
reference ion sensitive FET for compensation, biomedical appl. 78−44642
spectrophotometer/fluorimeter for university biochem. courses 77−33807
thick film hybrid fabrication of pH-sensitive implantable bioelectrode *(German)* 78−40369
tissue microelectrode design for skin pH meas. 79−100780
water quality meas., continuous, in tubular columns, probes utilisation *(French)* 78−3836
water sample, automated anal., pH, conductivity, alkalinity 79−12287
Al_2O_3 surface, acidity, rel. to topochem., IR determ., adsorption method 80−35611
Cu-Ni alloy, in 0.1 M NaCl, electric pot. and pH meas., crevice corrosion 78−31564
H^+ concentration meas. *(German)* 79−16083
K_2O-B_2O_3:Cu II, glass, O basicity, ESR study 78−80199
K_2SO_4-$ZnSO_4$:Cu II, glass, O basicity, ESR study 78−80199
Li_2SiO_3 glass pH meter electrode performance *(German)* 80−40695
Na_2O-P_2O_5:Cu II, glass, O basicity, ESR study 78−80199
Na_2SiO_3 glass pH meter electrode performance *(German)* 80−40695
PdO-Pd miniature pH electrode description and use 80−89886
Sb thin film, pH sensitivity and electrode potential *(Japanese)* 79−39159
Sb-Sb_2O_3 pH electrode improvement 79−53270
Si ion-controlled diodes, acid-base exposure effects, Si-SiO_2 interface state density 80−96984

phase angle meters *see phase meters*

phase changers *see phase convertors*

phase changing circuits
see also phase convertors; phase shifters
lock-in null detectors, phaser design 77−79122
pulsed NMR spectrometer incorporating phase-splitting circuit 80−62704

phase comparators
77.5 kHz transmitter signal, derivation of standard frequencies *(German)* 77−53928
alternated double time base oscilloscope design and applications *(French)* 77−87784
capacitor loss-angle and capacitance checking cct. 77−61085
digital phase detection used for computing phase angle averages 78−21163
digital picosecond event timer, phase detection system 77−9988
quantum frequency store and Cs atomic transition frequency comparison system 77−79064
stable frequency standards comparison by TV carrier beat note transmission 78−57909

phase conjugation (optical) *see optical phase conjugation*

phase-contrast microscopy *see microscopy*

phase control
AC voltage lead-lag and sequence, monitoring system 78−65942
assisted blood circulation, biological triggering signals 77−78044

phase control continued
cardiac assist devices, in-series, digital afterload phase angle controller 77−44843
flow visualisation holography, generalised phase control during reconstruction 79−50246
gas lasers, mechanical cavity length modulation technique 78−46571
IR phase conjugation adaptive array 77−46790
laser pulse timing by combined passive and active mode-locking, anal. 78−55391
N-loop ensemble reference phase control system, stability 77−46794
noncoherent optical processing, temporal frequency carrier methods 79−76623
quantum oscillator, phase automatic freq. control parameters, optimal values *(Russian)* 80−77814
λ 8-cm radioheliograph at Toyokawa, new local oscillator system phase stability 79−101073
λ 8-cm radioheliograph at Toyokawa, sensitivity and phase stability improvement project 79−101066
RF frequency standard transmission, phase instability due to effect of ionosphere 78−41279
servo system for phase-locking HF chemical lasers 79−72580
synchronous machine phase shift control cct. 78−22054
two-wavelength optical phase control system 80−33140
HF chemical laser phase control servo system 80−33063
He-Ne low-gain laser amplifier, phase control 80−64059

phase convertors
see also phase changing circuits; phase shifters
VLF radio station phase reception/processing convertor for time-freq. secondary standard service 77−87739

phase diagrams
see also phase equilibrium; phase transformations
A15 compound formation by diffusion from ternary bronzes, thermodynamics 78−84740
AB-type compounds, high-press. and high-temp. behaviour, review 78−22850
acenaphthene-α-nitronaphthalene, binary mol. system, phase diagram 77−39664
acetone-chloroform-methyl isobutyl ketone, ternary phase diagrams, interactive computer program 80−71629
p′-acryloyloxyozoxybenzenes, substituted 79−1494
actinides, struct. props. rel. to F electrons 78−83951
actinides and alloys, metallurgical props. rel. to electronic struct., energies calc. method 77−20221
adenine-H_2SO_4-H_2O system, phase diagram, rel. to cryst. growth 79−32929
adsorbed layers, two dimensional incommensurate crystal theory, thermodynamics *(Russian)* 80−49524
alloy, binary, atomic roughness and chemical adsorption at solid-liquid interface *(French)* 78−51787
alloy, binary, crystallisation kinetics, temperature dependence, kinetic phase diagrams 80−16294
alloy, binary, with arbitrary mole fraction, order disorder transition in case of FCC lattice 80−88295
alloy, complex, phase stability diagram 77−90322
alloy, disperse state formation *(Russian)* 78−52757
alloy, multicomponent phase diagram calc., NPL alloy data bank 78−92243
alloy, solidified, thermophysical charact. in region of special points of phase diagram *(Russian)* 78−44082
alloy, solidus temperature determ. by method of moving specimen boundary projected on screen 78−35353
alloy, surface segregation prediction from bulk melting curve shape 77−12597
alloy, ternary, general theory 77−32558
alloy, used in electric power industry, high temp. phenomena 79−11575
alloy between ferromag. and antiferromag. species, competing order parameters, Bethe-Peierls approx. 77−48003
alloy colour and colour stability as alloy design criteria 80−101005
alloy systems assessment of accuracy of cryoscopic calcs. from fusibility diagrams 77−25010
alloys, binary, BCC, order-disorder transform., three-body interaction effects 80−39257
alloys, binary, constitution diagrams, computer calc. *(Russian)* 80−84909
alloys, binary, kinetic crystallisation diagrams, given finite diffusion coeff. *(Russian)* 80−40341
alloys, binary metallic systems, calc. of isomorphous and simple eutectic phase diagrams 79−11570
alloys, exam. of compilation activity 79−8274
alloys, $L1_2$ and $L1_0$ superstructure atomic ordering phase diagrams, order-disorder transition 80−38989
alloys, metastable, determination and representation of phase diagram features 79−11568
alloys, non-ferrous, exam. of props. with aid of phase diagrams 79−11573
alloys, phase analysis by Mossbauer spectra 80−15922
alloys, phase diagrams, prediction using nonthermodynamic approaches 79−8281
alloys ternary and binary, phase diagrams and transition temp., correl. function approach 79−95164
alloys with competing interactions, phase diagrams and crit. props. 79−40514
antiferroelectric transition, phenomenological theory 79−4771
Approximation of the phase diagrams of complex binary systems with unlimited solid solutions and peritectic transitions 78−23680
azeotropic and two terminal solid solution type binary diagrams, synthesis 80−19901
benzene, tables of thermodynamic props. 77−24419
benzene-hexa-n-alkanoates and benzene mixture, disc-like mesogens, thermotropic mesophases 79−86699
benzene-hexa-n-alkylanoates, disc-like molecules, miscibility studies of mesophases 80−19696
binary alloy, ordered BCC to disordered FCC transition 77−43327
binary alloys, diagrams of state, component interaction parameters *(Russian)* 80−55354
binary alloys, diagrams of state, component interaction parameters, computer calcs. *(Russian)* 80−55355
binary alloys, mag. interactions effects on phase separation 78−27047
binary and ternary, calc. by computers using thermodynamic data 79−7672

phase diagrams continued
binary mixture, Van der Waals model, global phase diagram 78−59928
binary mixtures, liq. and solid, spinodal decomposition theory 78−71863
binary solid-liquid equilibria, student experiment, phase diagram computer program 78−89285
binary system with degenerate eutectic and monotectic transition approx. 78−3101
binary systems of eutectic type, phase diagrams, approximations, appls. 78−43094
bis-(p-toluene-sulphonate) of 2,4 hexadiyne 1,6 diol, X-ray scattering obs. of polymerisation mechanism and phase transition *(French)* 80−70399
Blume-Emery-Griffiths model in 2-D, renormalisation group studies 78−54311
bond percolation in anisotropic square lattice 80−46989
bromides, and mixtures, molten, elec. cond., density, viscosity, surface tension, review 77−80638
butyl rubber ethylene propylene ternary copolymer mixture, permeability, diffusion of gases and solvents 79−95217
$Ca_3(VO_4)_2$-$Zn_3(VO_4)_2$, exam. of phase composition and phase diagrams 79−1851
CaO-SiO_2-CO_2, subsolidus and liquidus phase relationships to 30 kbar 80−85643
carbon tetrachloride, emulsion dispersed, metastable phases at high press. *(French)* 77−56253
carbon tetrachloride, liq. and plastic cryst. phases, thermodynamic props., light scatt., US propag. 78−2863
carbon tetrachloride, thermal cond. and phase diagram under pressure 78−75893
3-carboxy-2,2,5,5-tetramethylpyrrolidinyl 1-oxyl system, enantiomer solid soln., cryst. struct. and phase diagram 79−86778
catastrophe theory, phase diagram classification 80−22313
CBOOA/4-cyanobenzylidene-4′-n-octyloxybiphenyl mixture, reentrant nematic phases 79−41953
cemented carbides, physical and chem. nature 80−76265
ceramic, rational molecular engineering 78−11179
ceramic fission reactor fuels, high temperature chemistry, nonstoichiometry, review 77−14238
ceramics, exam. of compilation activities 79−8287
ceramics, high temp. structural, use of equilibria in development 79−11595
ceramists users 78−15380
chalcogenide glass, partial values and structure features 79−41969
chalcopyrite compounds, ternary, review 79−70048
chalcopyrites, for electrolum. device appl., props. and technology, book contrib. 77−73175
chemisorbed layers, surface defects and thermodynamics 80−80068
p-chloronitrobenzene-p-bromonitrobenzene system, growth rate depend. of solid soln. supersaturation 77−1804
cholesteric liquid crystal, phase transitions and critical phenomena *(Russian)* 79−4407
cholesteryl acetate-cholesteryl octanoate system, phase transitions, thermoanalytical microscopy obs. 79−55871
cholesteryl vinyl succinate (fumarate), polymer+monomer systems, liq. cryst. phase states 79−1494
classical lattice systems, contour models 77−30114
classification by catastrophe theory 80−17905
cluster variation method of calc. 79−10916
commensurate and incommensurate charge-density wave states, nearly half-filled Frohlich model 80−107723
commensurate-incommensurate transition and melting in two-dimensions 80−75339
complex oxide crystal flux growth, starting comp. prediction 77−48331
computer coupling of phase diagrams and thermochemistry, conf., Gaithersberg, USA (Aug. 1975) 77−77458
computer generated phase diagrams 78−83928
computerised thermodynamic data treatment centre, facility for chem. thermodynamics anal. 79−10918
condensation point, thermodynamic function singularities, vapour fluctuations 77−41558
conference, 6th CALPHAD meeting, Harwell, England (18-21 Apr., 1977) 78−35350
construction, use of NMR, Mossbauer effect, and gamma ray perturbed angular correlation 79−8417
critical isomorphic $\gamma \rightleftarrows \alpha$ transition, phase equilibrium curve *(Russian)* 80−55397
critical points, catastrophe polynomials 80−8946
critical points and transitions, in phase diagram, geometrical relation *(Japanese)* 80−24568
crystal growth, macroscopic equilib. and transport concepts, book 80−27054
crystal growth and phase diagrams 80−66407
crystal growth from melt, impurity distrib. ratios, kinetic depend. 78−43044
Cu-Mn alloys, thermodynamics, suitability as electrodes 79−66339
cubic crystals, tensile deform. induced transitions 80−59653
cuprous halide-metal halide systems, AC cond. rel. to phase diagram 77−72712
cyclohexane, plastic cryst., NMR determ. of phase diagram 77−12210
determination techniques, review of more sophisticated technique 79−7673
diamond, 'melting' to solid metallic C phase above graphite triple point 80−15236
diamond, P-T diagram, cryst. struct. stability 78−51886
dibenzyl-tolan system, phase diag. 77−63642
dicalcium lead strontium propionate, mixed cryst., phase diagram, dielec. and dilatometric anomalies 77−11689
dielectric materials, amorphous high permittivity *(Japanese)* 79−73876
diemthyl sulphoxide-H_2O-NaCl system, DTA exam. of primary ice phase field 78−48382
dioleoyl-phosphatidylcholine/dipalmitoyl-phosphatidylcholine bilayer membranes, phase transitions 79−39367
dodecane-sodium octylbenzene sulphonate phase diagram *(French)* 79−82339
dodecylamine ($-NH_2$)/H_2O_2 and deuterated cpd., liquid crystal, phase relationships, isotope effects 79−19358
double phase transitions, physical value anomalies *(Russian)* 80−59622
double spin $^1/_2$ lattice gas model, phase diagrams 77−20521
durene-p-dibromobenzene system, phase diagram and X-ray diffr. expts. 78−79774
EBBA-aromatic hydrocarbon systems, solute size and shape effect on nematic-isotropic equilib. 79−23710

phase diagrams continued
electron crystal in strong mag. field, phase diagram, normal mode anal. 80—44287
electron gas, two-dimensional, in strong mag. field, phase diagram properties 79—78024
electron microprobe and STEM determ. exam. of techniques 79—6241
electron system, two-dimensional, melting curve, phase diagram 80—57179
electron-hole paired systems, ferromagnetic ordering phase diagram 80—97097
epoxy resin, cure history effect on dynamic mech. props. 80—54356
ethylene, solid, phase diagram and NMR at high press. 80—11279
eutectic alloy, rim zone formation *(Russian)* 77—85988
eutectic crystal-melt system, interphase boundary struct., Monte Carlo method study 80—1950
excess enthalpy and excess entropy functions derivation by direct method from TX phase diagram, heats of mixing calc. 80—75366
FCC alloys, with multiatom interactions, ground state derivation 79—83173
FCC lattices, ordered superstruct., phase diagrams, cluster variation calc. 80—39256
Fermi liquid, Coulomb, two-component, unusual phase diagrams 79—63137
ferrite (Li-containing)-BiO_2, phase diagrams and sintering conditions 79—52141
ferrofluids, phase diagrams and eqn. of state 80—60280
ferromagnetic fluid, 1D Ising and 3D Heisenberg solns. 77—85478
ferromagnetic fluid, molecule system eqn. of state, exchange interactions, spin independent forces 77—59412
films, polymorphic transforms. and phys. props. 77—43450
first-order transition close to second-order transition 80—59625
flexible polymer chain in nematic solvent, phase diagram *(French)* 80—39253
fluid mixtures, unified mol. theory, statistical thermodynamics 77—31570
2-fluoronaphthalene-2-naphthol system, phase relations, X-ray diffr. and DTA study 80—45287
furan, P-V-T relations, 210 to 260K, up to 1000 MPz 79—95122
Ga_2S_3-Ga_2Te_3 phase diag. *(French)* 78—76635
gas, thermodynamic props. review 80—31694
gas-liquid-solid phase diagram, modified lattice-gas model 80—62591
Gibbs equilibrium thermodynamic pot. second derivatives, discontinuity surfaces rel. to phase boundaries of q-component systems 79—82304
Gibbs phase rule, history and development *(German)* 77—78943
glass, user needs for materials processing 79—11594
glass characteristics, electromagnetic, mechanical and thermal props. 80—106587
glass-forming multicomponent systems, phase behaviour, miscibility, tie lines 80—84294
glycerol protection of slowly frozen human erythrocytes, phys.-chem. basis 78—77020
Heisenberg spin systems, two-dimensional, phase diag., renormalisation group approach to phase diag. 80—4847
p-p′-n-heptyl-cyanobiphenyl-isotropic solute systems, nematic-isotopic phase transformation, volumetric study 80—92653
heterogeneous system, melting, enthalpy and phase relations *(Czech)* 80—45543
hexamethyldisilane, plastic cryst., NMR determ. of phase diagram 77—12210
Hume-Rothery Phases, electronic struct., main features 79—23883
3-hydroxymethyl-2,2,5,5-tetramethylpyrrolidinyl 1-oxyl system; enantiomer solid soln., cryst. struct. and phase diagram 79—86778
ice-water-steam system, two-dimens. triangular lattice model, matrix calc., props. 77—27975
III-V compound crystal growth from solution, computer simulation 77—51332
III-V semiconductor phase diagram and thermodynamic data analysis 78—6913
InAs, gas-phase epitaxy, prep. thermodynamics, use of partial pressure diagrams 79—79279
incommensurate two-dimensional crystal, ground state, spectrum, phase diagram 79—19458
inert gas adsorbed on graphite, phase transitions using Landau model 79—69243
interacting linear Ising spin chain, phase transitions *(Russian)* 80—70920
interstitial compounds, electronic structure and useful phys. props. 77—89683
Invar, Fe-Ni alloy, atomic struct., elastic neutron scatt. obs., phase diagram 79—94964
iodides and mixtures, molten, elec. cond., density, viscosity, surface tension 77—80638
ion beam determination of phase boundaries, exam. of technique 79—8418
ionic mixtures, phase diagrams and phase separation 80—77279
ionic systems, calc. and computer storage 79—10920
Ising antiferromagnet, FCC, nearest neighbour interactions, Monte Carlo method 80—80544
Ising like model, tricritical two-dimensional behaviour, finite size effects, model depend. 79—35641
Ising model, modulated phase with solitons, phasons and devil's staircase 80—95044
Ising model, tricritical two dimensional behaviour, ϵ expansion universal quantities 79—35642
Ising model in 1-D with random transverse field at T=0, real space renormalisation group method 80—4656
Ising model with nearest neighbour ferromagnetic interactions, phase transition theorems 77—22501
isostructural phase transition by Landau phenomenological anal. 79—90757
isoxazolines, thermodynamics charact. of phase diagrams 78—23673
KCl-$BaCl_2$ system, solid solns., phase diagram, enthalpy of soln., vibr. entropy. 78—39751
kinetic exchange interaction, doubly degenerate narrow bands 78—23263
Kondo lattice, phase diagram 80—7077
lamellar liquid cryst. phases, form. at liquid-liquid interface, rheological props. 79—99063
Landau crit. point, mean-field theory, scaling theory and crit. exponents to second order in ϵ^2 79—4395
latex, monodisperse, mechanical props. 78—48701
latex, monodisperse, phase diagram, spectroscopic study 78—85209
phase diagrams continued
latex, monodisperse, reflectivity obs. of phase separation into ordered and disordered phases 77—70345
latex, monodisperse, short-range order, spectroscopic study 78—85208
Lennard-Jones fluid, phase separation by spinodal decomposition, mol. dynamics computer simulation 79—10766
Lennard-Jones system, thermodynamic functions in liq. and vapour region 79—10910
leucite, phase diagram and thermodynamic props. 79—91985
lipid mixtures, phase transitions, theoretical model 80—8032
liquid crystal, lyotropic, phase diagrams and NMR, solubilised mols. effect on struct. 77—84628
liquid crystal, mean-field equations, phase diagrams 78—18751
liquid crystal mixtures, nematic-cholesteric, comp. depend. of helical pitch *(Japanese)* 77—72553
liquid crystal mixtures, nematic-cholesteric, ternary, comp. depend. of helical pitch *(Japanese)* 77—72554
liquid crystal symmetry and thermodynamic states, review 80—10493
liquid crystal-polymer systems 79—23709
liquid crystals, amines and nitriles, binary mixtures, induced phases 79—90765
liquid crystals, phase transitions and pretransition phenomena, book contrib. 79—60491
liquid crystals of amphiphilic compounds 79—1389
liquid metals, lattice model, metal-nonmetal transition, eqn. of state, phase diagrams 77—69220
liquid-vapour, renormalised one-chain approx., square mound reference system 77—11663
lithium n-alkanoates, long-chain, thermal and phase props. 77—62619
lubricant, glass transition, light scattering study 79—29228
2,6-lutidine-H_2O, phase separation, hydrodynamic effects 78—83960
macromolecules, scatt. methods, conf., Prague, Czechoslovakia, (July 1976) 79—1764
magmatic rocks, anchieutectic comp. 80—12381
magnetic order coexistence with charge density waves 80—97096
magnetic systems and mixtures, phase diagrams, Monte Carlo studies, book contrib., review 79—82313
MBBA, electrohydrodynamic instabilities, flow patterns and phase diagrams 77—68915
MBBA nematic liq. cryst. systems, orientational order rel. to solute size, shape 77—4565
melting curve extrema from repulsive step potential, molecular dynamics calc. 77—59102
melting curve maximum phenomenon, computer simulation using two species soft core model 78—6146
mesomorphic mixtures, binary phase diagrams, thermodynamic props., diamag. anisotropy 78—95139
metal oxide-SiO_2 systems, phase diagrams calc. from high press. phases stability study 79—90779
metal silicide growth on Si 78—10230
metal-boron systems, correlation of phase equilibria, with boride crystal chemistry 79—11562
metal-dielectric transition, two-band model, Coulomb interactions, self consistent calcs. *(Russian)* 80—80185
metal-dielectric transition with lattice distortion, two-band model 77—8023
metal-H, phase transitions 80—50631
metal-H system, constitution diagrams and hydride struct. form. 79—24509
metal-H system, elastic interaction and phase transition, book contrib. 79—83178
metal-semimetal alloy, phase diagram computation from thermodynamic functions 80—40329
metallic glasses, stability 80—75184
metallic glasses, structure and formation, thermodynamic props., cluster relaxation approx. 80—54143
metallurgical slags, determ. by hot wire microscopy, exam. of technique 79—8413
metallurgy and ceramics, Conf., Gaithersburg, USA, (Jan. 1977) 79—4946
metals, phase analysis by Mossbauer spectra 80—15922
metals and alloys, use of dilatometric methods *(French)* 79—5100
methane, solid-state phase transitions, 5-80K, PMR spin-lattice relax. up to 3 kbar 77—40137
methane adsorbed submonolayer on graphite, structural transitions between epitaxially ordered phases 80—96740
methanol, solid, phase behaviour up to 3 kbar by DTA 77—76528
microemulsions, phase diagram and homogeneity gap, light scatt. and viscosity meas. 80—16736
microemulsions vs. micellar solns. 77—60131
mixed valence compounds, phase diagrams, lattice props., electron hole symmetry 79—91002
monomer-dimer system with attractive interactions on square lattice, nematic ordering 80—79681
multi-component crystal growth, kinetic equation theory, binary system crystallisation 80—88071
multi-ion system, strong electrolytes, phase diagrams and solubilities calcs. 80—25665
multicomponent alloy, phase diagram calc., computerised data bank 79—1848
multicomponent alloy phase diagrams, calc. methods used at National Physics Laboratory 79—11569
multicomponent alloys, phase diagram calc. program from thermodynamic data 80—3008
multicomponent systems, comput. techniques for thermodynamic data treatment and equil. calc. 78—10172
multicomponent systems, phase diagrams and thermodynamic data, electrochem. determ. 80—71922
multicomponent systems, rel. to electroepitaxy, theoretical model 80—65396
multicomponent systems, use of polynominal representation of excess free energy, in phase diagram calc. 79—10914
multicritical phase transitions, review 79—30385
naphthalene-coumarin solid solution, struct. parameters and phase diagram 77—11532
naphthalene-p-chloronitrobenzene eutectic system, phase diagrams and crystn. 77—47551
Neel ferrimagnets, phase transitions, field-induced spin-orientational 80—75767
nematic binary mixture, smectic phase form. 78—26670

phase diagrams continued
nematic liquid crystal mixtures, binary, induced smectic phases, X-ray diffr. obs. 78−94987
nematic ordering and phase transition, Wulf Rocco model extension 77−84626
nematic-cholesteric binary mixture, EHD instability, phase diagram 78−1980
nematic-isotropic phase equilibria, Flory-Huggins theory appl., heat of transition 77−4187
nematic-smectic A-smectic C Lifshitz point 77−69077
neutron diffraction studies of phase transitions and crit. phenomena, book contrib. 79−60229
non ferrous materials, use in sophisticating pyrometallurgical processes 79−11571
nonionic emulsifier blend-oil-H_2O system, ternary phase diagram 78−20074
nucleation theory and first order phase transition dynamics near critical points 80−84284
nylon II, high-press. X-ray structural study 78−14296
octafluorocyclobutane+n-butane mixtures, 233K, surface tension meas., solid-liq. phase diag. 79−19371
4′-n-octyl-4-cyanobiphenyl, smectic bilayers, press. effects, phase diagrams *(French)* 78−10177
4′-n-octyloxy-4-cyanobiphenyl, smectic bilayers, press. effects, phase diagrams *(French)* 78−10177
Onsager transition in hard plate fluid 77−48696
optimisation by least squares method using simultaneously different types of data 78−6143
optimization by least squares method 79−10915
ordering alloys, effect of press. on phase diagrams and order-disorder transforms. 78−52797
organic compounds, high-press. thermodynamics, review 79−24500
organic eutectic, heat of fusion and excess thermodynamic functions 78−3104
oxide phase equilibria, high temp. appl. 79−8416
oxide systems, quasibinary and quasiternary, data base development for phase diagram calc. 79−96006
oxychalcogenide glasses, phase separation 77−8803
N-pentanol-Na-N-octanoate-water system, partial molar enthalpies 78−75543
perfluorinated mixtures, hydrostatic liquids for obs. of NMR 79−2801
peridotite-CO_2-H_2O and carbonatitic liquids in upper asthenosphere 77−29294
petrological melts and glasses, Fe-containing, Niggli's diagram 80−34170
phase boundaries and multiphase systems, conf., Tokyo, Japan (Sept. 1977) 79−29415
phase diagram interpret. using cryst. chem. formulae 77−81251
phase transitions with two order parameters, Landau theory, mag. reorientation 80−103456
phenylenediamine-dihydroxybenzene mixtures, solid-liquid equilibria, phase diagrams 77−27986
phosphate glasses, non-alkaline, transition states, phys. effects of fluors, phase diagrams and optical effects *(German)* 80−88045
phospholipid mixtures, phase transition anal. by high sensitivity differential scanning calorimetry 77−40637
picric acid-o-bromoaniline binary system, phase diagram and DC elec. resist. 77−15546
planar model electrodynamics, phase diagram, continuum limit, and mass spectrum 79−63426
planar-rotator model with short range interaction 79−80540
poly-γ-benzyl-L-glutamate, soln., liquid crystal transitions anal. 80−65207
polyarylate-polyethylene oxide block-copolymers and mixtures, phase separation, DSC obs. *(Russian)* 79−55895
cis-polybutadiene and butadiene-styrene copolymer mixture, effect of temp. on phase composition 79−96005
polyester-organic solvent mixtures, phase diagrams, eutectic props., devitrification, crystn. *(French)* 80−3015
polyethylene high press. phase, struct., phase diagram and compressibility 78−9961
polyethylene oxide, solns. in toluene and ethyl benzene, phase equilib., struct. and thermodynamic stability *(Russian)* 79−86871
polyethylene oxide trioxane mixtures, eutectic crystallisation 78−56626
polyisocyanates, rigid backbone, ternary phase relationships obs. 80−59371
polymer, multicomponent, homopolymer blends, macroscopic phase separation 80−45289
polymer glass mixture, symm. tricrit. pts. 79−82320
polymer mixtures, thermodynamics, review 79−1506
polymer solns., phase diagrams, pulse-induced critical scatt. 79−1490
polymer-solvent systems with solvent crystn., state diagrams *(Russian)* 79−52185
polymeric macromolecule containing mesogroups, phase diagrams *(Russian)* 80−58433
polystyrene, cyclohexane soln., coil-globule transition 80−54110
polystyrene in tetrachloroxylene and tetrachlorobenzene, morphology of crystallized additives 79−99082
polystyrene-polymethylmethacrylate system, phase relationships and fracture surface morphology 79−61571
polystyrene-tetrachloroxylene(tetrachlorobenzene) glassy solns., additive morphology rel. to mech. props. 79−65007
Potts model, analyticity properties of 3-component models 79−67235
Potts q-state model, variational renormalisation group approach 80−31679
Pourbaix diagrams, calc. using modified linear programming technique 79−10919
propylene, computer generated phase diagrams 78−83928
PVC-vinylchloride system, glass transition, vinylchloride influence *(German)* 80−79917
pyrene central core, discotic mesophase potentiality, isobaric phase diagram method 79−86680
pyroxenes in CaO-MgO-Al_2O_3-SiO_2 system, subsolidus phase relations rel. to geothermometry and geobarometry 79−16440
quantum systems, generalised phase diagram and crit. behaviour 77−31815
quasibinary and quasiternary ceramic oxide systems, calculation of phase diagrams 78−60660
random fields, multicritical points and dimensionality shift 79−40468
random Ising magnet, phase diagrams 80−7065
phase diagrams continued
rare earth compounds, polymorphic phase diagrams, as function of pressure exam. 79−8289
rare earth germanates, R_2O_3-GeO_2 system cpds., physicochem. characts. 80−97469
rare earth hydrides, Mossbauer studies, book contrib. 79−82906
rare earth hydrides, props., book contrib. 80−45291
rare earth metal-B systems, phase equilibria, phase diagrams, book contrib. 78−48389
rare earth metal-O systems, exam. of phase diagrams and crystal structure 79−8291
rare earth oxide containing systems, highly refractive, phase equilib. and metastable phases 80−97467
rare earth oxides, binary, struct. and props., book contrib. 80−45292
rare earth oxides, mixed, phase relations and struct., book contrib. 80−45293
rare earth-cobalt intermetallics, RCo_2, sublattice magnetisation, powder neutron diffr. meas. 79−19725
rare earth-Ga alloys, phase diagrams 79−78932
rare earths, struct. props. rel. to F electrons 78−83951
$(rare\text{-}earth)_2O_3$-H_2O, hydrothermal phase equilibria studies 80−104132
representation of phase equilibria, exam. 79−7675
$(Rochelle\ salt)_{1-x}(ammonium\ Rochelle\ salt)_x$, phase transitions, hydrostatic press. effects 80−93246
rubidium n. alkanoates, long-chain, phase transformations, in melt, DTA obs. 77−76536
sanidine, phase diagram and thermodynamic props. 79−91985
Schiff base liq. crysts., multicomponent, phase diagrams and metathetic reactions 79−56965
semiconductor alloy, pseudobinary, phase diagram calc. 78−52786
semiconductor materials, exam. of compilation activity 79−8288
semiconductor materials, quantitative fitting of experimental phase lines, thermodynamic props. to model parameters 79−11593
semiconductor mixed crysts, calc. from diffuse scatt. of X-rays *(German)* 78−30517
semiconductors, chemical thermodynamics, review 80−55692
shock adiabatics at ultrahigh press. *(Russian)* 77−27941
sine-Gordon chain, $T \neq 0$, commensurability, phase-torque eqn. of state 80−39251
single-phase domain boundary identification by X-ray diffraction line broadening 78−1949
smectic liquid crystals induced phases of liq. cryst. mixtures *(German)* 78−94995
smectic mesophases of binary mixtures, isobaric phase diagrams, non-ideal behaviour *(French)* 79−95141
sodium n-alkanoates, long-chain, thermal and phase props. 77−62619
sodium oleate, frozen soln., NMR study of phase transitions 79−56617
solar cells, use of phase diagrams in material selection 79−10922
solid state reaction, heterogeneous, Avrami parameter calc., modified Kissinger method 78−92239
solid-liquid phase equilib., binary and ternary systems, excess Gibbs free energy 78−30736
specimens at high temp. and under tensile and/or shear stress, theoretical exam. 79−7674
spin glass, random-bond Ising model with continuous distrib. of exchange interactions 77−43837
spinodal decomposition, light scattering, depend. on method of quench 78−18782
spinodals and swallowtails, rel. to phase diagrams 77−7844
staged intercalation compounds, phase diagrams 80−60849
standards for publication of studies 79−10921
standards for single substances and mixtures 78−14481
steel, 12Kh18N9T-TiB_2, eutectic alloy, high temp. props. 78−84931
steel, alloy, thermodynamic aspects of gas-metal heat treating reactions 79−24547
steel, alloy with additions of Mn, Si, Ni, Cr, Mo, Cu, thermodynamic prediction of Ae_3 temp. 78−64524
steel, austenitic and duplex 308 stainless, mech. of intergranular corrosion and pitting corrosion 79−91846
steel, austenitic stainless, AISI 316, irradiation effects on phase stability 79−11566
steel, austenitic stainless, multicomponent phase diagrams at 600 and 650°C 79−78937
steel, C, carbide formation during chromising, exam. in terms of ternary phase diagrams 78−56818
steel, carbide and nitride phases dissolution *(Russian)* 80−20888
steel, Cr (2%), austenite decomp., phase diagrams and struct. form. kinetics 80−76223
steel, Cr-C and C, carbide coating by CVD, interlayer form. 80−11574
steel, Cr-Mn, metastable constitution diagram and phase transforms. *(Russian)* 80−50590
steel, eutectoid and hypoeutectoid, time-temp.-austenization diagram *(Japanese)* 78−6900
steel, eutectoid schematic transform. diagrams 79−56958
steel, hardening, mathematical model including phase changes 79−4950
steel, high-strength, dynamic yield strengths, phase transition press. and Hugoniot parameters 80−75331
steel, low C, austenite transform., TTT diagrams 77−70031
steel, low pearlite, Ti addition effect on transform. behaviour *(German)* 77−90343
steel, low-C-Si, LS1.2, LS1.5, phase transformation 80−45302
steel, Mn-C-O, phase equilibrium, Mn effects at liquidus temp. *(Russian)* 77−66625
steel, sintered Cu, hardenability *(Japanese)* 77−48527
steel, stainless, 12Kh13 and 15Kh11MF, austenite transform. kinetics 79−87612
steel, stainless, Cr-Ni-Mo-N, phase diagrams 80−35161
steel, stainless, type 316, microstruct. changes in creep ductility, SEM, TEM, optical microscopy and X-ray diffr. study 79−38927
steel hardness and ductility variations and micrographs rel. to heat treatment and phase diagram obs. 79−87609
steels 4Kh4VMFSSh and 45Kh3V3MFSSh, grain size, hot deform. and austenitising effects 80−76286
step potential particle systems, 2- and 3-dimens., mol. dynamics 79−28072
structure under press. and phase diagrams, index of substances 79−60484
substitutional solid solutions, new phase nucleation mechanism 80−61135
sulphosalt minerals, exam. of crystal chemistry and morphology 79−10838
superconducting composites, bronze process, metallurgy 80−3004

phase diagrams continued
superconducting ferromagnet, magnetic ordering, spin wave dispersion *(Russian)* 80−54818
superconductors, use of phase diagrams in processing 79−11574
symmetry breaking fields, destruction of first order transitions 79−40517
synthesis of soln. thermodynamics, computer anal. 78−30739
TBBA, liq. cryst., metastable phase, thermodynamic props., differential scanning calorimetry meas. 78−94985
TCNQ anion radical salt, $[(C_6H_5)_3PCH_3]_{1-x}^{+}[(C_6H_5)_3AsCH_3]_x^{+}(TCNA)_2^{-}$, phase transition and phase diagram 77−76555
ternary, examples of clustering and ordering systems 77−32559
ternary, interactive computer program 80−71629
ternary, metals with boron *(Russian)* 77−1833
ternary alloy, metastable miscibility gap determ. by small angle scatt. 77−28780
ternary alloys, AB-AC quasi-binary sections of order-disorder phase diagram 78−88463
ternary BCC alloys, ordering process, effect of short-range order *(Russian)* 80−84908
ternary mixtures, eutectic point localisation, thermodynamic calcs. *(French)* 78−79742
ternary molten mixtures, topology 77−28792
ternary molten salt phase diagrams, computation 79−100118
ternary oxides, coulometric titration method for phase diagram and thermodynamic studies 79−47667
ternary polymer systems, diffusion controlled formation of porous structures 80−7539
ternary system, eutectic-like and peritectic-like reactions at constant pressure 79−99295
ternary systems containing more than three phases, eutectic like and peritectic like reactions 80−29928
ternary systems with two component solid phases, eutectic, peritectic curve eqns. *(Russian)* 80−54344
tetra-n-pentylammonium salts, molten, thermodynamic props., cation struct. 79−55639
tetrebromomethane, thermal resistivity, heat capacity and phase diagram under pressure 80−65316
thermal energy storage technology, application of phase diagrams 79−10923
thermochemical data and calc. of phase diagrams, systems for storage and retrieval 78−31682
thermodynamic analysis of liquidus in ternary system with small content of one component 77−4767
thermodynamic calc., review 79−91620
thermoelectric alloys, phase diagrams, and imperfection chemistry 80−108422
thermophysical property research, metallurgical applications 80−97457
thermosetting materials, formation and props., phase diagram and torsion pendulum anal. 80−55381
thin film alloys, surface magnetism props., Curie temp., Ising model 80−108039
three-component model, global phase diagram 77−37835
TMMC phase behaviour, DTA using Ge-Ag thermocouple 79−65186
toluene, tables of thermodynamic props. 77−24419
transition metal alloys, cluster model for sigma phase occurrence 77−59750
transition metal alloys, group VIII solvent metals, relations involving max. or min. liquidus temps. 79−15651
transition metal alloys, magnetically ordered, effect of magnetic field on P-T diagram 78−52246
transition metal alloys, ternary, phase diagram computed, occurrence of sigma phase 77−48399
transition metal alloys with rare earths or actinides, binary system constitution diagram interrelations *(Russian)* 80−7535
transition metal based solid solutions relationships involving max. or min. liquidus temps. 79−78934
transition metal binary systems, couple phase diagrams and thermochemical data 79−66037
transition metal binary systems, coupled phase diagram and thermochemical data 79−95997
transition metal binary systems, coupled phase diagrams and thermochem. data 78−60647
transition metal binary systems, coupled phase diagrams and thermochem. data 78−60648
transition metal binary-systems, coupled phase diagrams and thermochemical data 79−66036
transition metal carbonitrides, physicochem. props., comp. depend. 80−55370
transition metal hydrides, Mossbauer studies, book contrib. 79−82906
transition metal hydrides, struct. change from metal struct., due to interaction of metal with H 80−49196
transition metal hydrides, synthesis and physicochemical props., conf., Moscow, USSR (Jan. 1978) 80−27032
transition metal solid solutions, max. or min. liquidus temps. 78−39741
transition metal-group III to V p-element binary alloys, correlation between phase diagrams *(Russian)* 79−15649
transition metal-H systems under high H pressure, phase diagrams., electrical cond., mag. props. 80−29923
transition metal-hydrogen systems, eqn. for multiplateau isotherm, lattice expansion role 80−39252
transition metal-nitrogen system, stable phases 79−91622
transition metal-rare earth-B systems, phase diagrams and struct. considerations 80−16286
transition metals, binary systems, coupled phase diagrams and thermochem. data 78−80511
transition metals and alloys, metallurgical props. rel. to electronic struct., energies calc. method 77−20221
triangular and honeycomb lattice gases, order-disorder transitions to 2×2 struct. 80−4674
triangular Ising model, renormalisation group calc., appl. to adsorption 78−10631
1,1,2-trichloroethane, phase diagram, 0-10 kbar 77−72679
1,1,1-trichloroethane, polymorphism under high pressure *(French)* 80−96644
tricritical phenomena, ternary, quaternary fluid mixtures, classical models 78−91416
triphenylene core, discotic mesophase potentiality, isobaric phase diagram method 79−86680
triple point, 180° rule violation criteria, thermodynamic stability 77−7841
phase diagrams continued
triple points, 180° Rule, Butterfly model 80−8945
trivalent metal phosphates, condensed, synthesis in polyphosphoric acid melts, physicochem. equil. considerations 80−97419
two dimensional system, melting and condensation theory 80−57231
type equations for binary equilib. curves, ternary system polythermic sections 80−39250
type II superconductor, phase diagrams, exam. in terms of electronic structure 79−8278
uniaxial antiferromagnetic, phase diagram, spin flop transition *(Russian)* 80−100587
uniaxial ferromagnet, domain struct. in mag. field 80−103853
uniaxial ferromagnet domain struct., phase transition *(Russian)* 80−108044
valence transition, entropy and phase diagram 80−59877
van der Waal's crystal P-V-T diagram, Holmholtz free energy, mean-field model, for teaching 77−33784
water, metastable states diagram *(Russian)* 78−95129
water, spline representation of boundaries, for nuclear reactor programs 77−23207
water-isobutyric acid, crit. mixture 80−24601
Wigner crystal, two dimens., phase diagram in mag. field *(Russian)* 77−62849
YIG, hot spraying to give fine, free flowing, sinterable powder 80−20865
Zircaloy-O_2 phase diagram 80−3003
zircon, dissociated, form. in plasma furnace, comp. and microstruct. 77−36429
Ag-Au-Pd, liquidus and solidus surfaces 78−60649
Ag-Bi, metastable phases *(German)* 77−16543
Ag-Bi-S ternary system, DTA and X-ray diffr. study 80−84917
Ag-Bi-Tl, system calculated from optimised binary boundary systems *(German)* 77−16545
β'-Ag-Cd (45 at.%), growth kinetics of bainite plates and Widmanstatten needles 77−36551
Ag-Cu, metastable solubility lines on Ag side 78−39737
Ag-Cu-Ni, phase diagram determ. 77−63634
Ag-Ge-Te system, chalcogenide, phase equilibria and diagrams *(German)* 80−108418
Ag-Nb-Ga, phase relations, A15 phase diffusion layer formation 78−52764
Ag-Pb-Hg system, DTA of phase diagram 77−12594
Ag-Pb-Te, phase equilibrium *(German)* 79−34018
Ag-Pt, sintering, limited solid solubility, peritectic diagram 77−28754
Ag-Se mixture, activity of Se *(German)* 78−27492
Ag-Sm system, phase diagram, eutectic temps., microstruct. *(German)* 80−104119
Ag-Sn, liquid alloys, thermodynamic props. *(Japanese)* 80−108396
Ag-Sn-Cu-Hg, constitution of quaternary amalgam at 37°C *(German)* 77−81250
Ag-Zn (27-48 wt.%), interphase β'-ζ transform., thermal expansion exam. 77−63630
$AgAsS_2$-$AgSbS_2$ system, thermal, microstructural X-ray phase anal. 77−32565
Ag_7AsS_6, thermal, crystallographic and elec. props. *(French)* 80−40338
Ag_7AsSe_6, thermal, crystallographic and elec. props. *(French)* 80−40338
$Ag_3Au_{1-x}Cu_x$, phase relations, X-ray diffr. and differential thermal anal. 80−108395
AgBr-NaBr, phase diagram, miscibility, binodal curve and demixing kinetics, X-ray meas. 80−96659
$AgGaS_2$-$AgGaSe_2$ system, phase diagram, lattice consts., and IR spectra 80−60841
$AgGa(Se_{1-x}S_x)_2$, crystal growth, phase studies, optical props. 78−48305
$Ag_8GeS_6(Se_6)(Te_6)$, Ag_8SiSe_6, $Ag_8SnS_6(Se_6)$, absorpt. edge investigs. at phase transitions 78−35149
Ag_8GeSe_6, polymorphic transition, absorpt. coeff. meas. 78−2257
AgI, thermal expansion under press. 80−92690
AgI-Ag oxosalt systems, solid electrolytes with glass-like struct., thermodynamic and electrochem. props. 79−10978
AgI-Ag_3AsO_4 system, solid electrolyte stability 77−15619
AgI-AuI, pseudo-binary phase diagram 78−76637
$AgInS_2(Se_2)$-$SnS_2(Se_2)$, degree of solid solubility and phases characts. 78−35377
Ag_8MSe_6, (M=Si, Ge, Sn), forbidden energy gap changes under high press., polymorphic transitions 77−51649
$AgNO_2$, high-pressure phase behaviour, crystal chemistry of univalent nitrites 78−30749
Ag_2S, α- to β-phase transform, phase boundaries effect 79−83179
Ag_2S-(As)(Sb)(Bi), temp.-comp. diagram 78−44105
Ag_2S-Ga_2S system, phase diagram, DTA and X-ray diffr. meas. 77−15544
Ag_2S-In_2S_3-SnS_2 system quaternary and ternary sulphide spinels, solid solubility and struct. 78−35376
Ag_2Se-(As)(Sb)(Bi), temp.-comp. diagram 78−44105
Ag_2Se-Ga_2Se_3, phase diagram in rich Ag_2Se region *(French)* 77−51472
Ag_2Se-Ga_2Se_3, pseudobinary phase diagram determ., DTA, X-ray diffr., cryst. growth investigs. 77−70036
Ag_2Te-(As)(Sb)(Bi), temp.-comp. diagram 78−44105
Ag−S system, phase diagram, 100-600°C *(German)* 80−97471
Al-$Al_{21}Pt_5$ eutectic alloys, unidirectionally solidified, struct. study 80−108394
Al-Al_3Ti, directionally solidified, thermal stability during annealing, 435-660°C 80−108393
Al-B, enthalpies and free energies, effusion and mass spectra, phase diagram 78−23665
Al-B(-C) system, synthesis and struct. of boride phases 80−45282
Al-Cr-Zn (2.5, 1.5 wt%), phase equilibrium, solubility *(Russian)* 78−19723
Al-Cu, superconducting amorphous films of high stability 80−70889
Al-Cu (4 wt.%) alloy, reversion process of Guinier-Preston zones, ^{63}Cu NMR obs. 80−60871
Al-Cu alloys, condensed films, metastable states 79−15046
Al-Cu-Ni, directionally solidified, exam. of struct. of two phase alloys 78−80537
Al-Cu-Zn system, solid-phase reactions, phase diagram 80−50603
Al-Fe (49 at.%) quenched alloy, neutron diffuse scatt., diffuse ω phase obs. 80−84141
Al-Fe-Si(0.5, 0.2 wt.%), cast, phase determ. 77−70032
Al-Ga-Ge, thermodynamic props. of mixing of binary systems, phase diagram 80−45275

phase diagrams continued
Al-Ga-In, liq. alloys, excess Gibbs functions 633 to 1173K 78−60655
Al-Ga-In system, thermodynamic anal. 79−60512
Al-Ga-Sb, ternary phase diagram, appl. to LPE growth 77−59761
Al-Ga-Sb system, ternary phase diagram and appl. to soln. growth 79−74135
Al-Ga-Sb ternary phase diagram, calc., DTA and LPE expts. 80−29931
Al-Ga(-Ge), and Al-Ge, Al activity, EMF study, phase diagrams 79−83175
Al-Ga(In) systems, thermodynamic anal. 79−60512
Al-Ga(In)(Sn), interpretation of metallic phase diagrams, entropy of mixing 79−42274
Al-Ga(Sn), ab initio calcs. of partial enthalpy and result for enthalpy of mixing 79−43197
Al-Ge alloy, effect of high press. on phase equilibrium *(Russian)* 79−1844
Al-Ge-Sn, thermodynamic props. of mixing of binary systems, phase diagram 80−45275
Al-La, thermodynamic interaction in liquid phase *(Russian)* 78−44080
Al-Li-Mg, estimation of isothermal sections of phase diagram 79−11567
Al-Li-Mg system, isothermal sections comput. 78−6896
Al-Mg, thermodynamic props. *(German)* 79−29027
Al-Mg alloys, relationship between props. and nonequilib. phase diagram 79−96000
Al-Mg-Li-Si system, phase diag. *(Russian)* 78−80515
Al-Mg-Si, precipitation of cube-shaped phases, electron diffr. study using TEM *(Japanese)* 79−43251
Al-Mg-Zn alloys, liq./solid phase equilibria determ. *(German)* 80−50601
Al-Mg-Zr, phase diagram *(Russian)* 78−11205
Al-Si-Li alloy system, Al-rich, phase comp., limits of solid solubility *(Russian)* 77−21097
Al-Si-Sr phase diagram *(Russian)* 78−15363
Al-Si-Y alloy, phase equilibria in Al rich region *(Russian)* 80−93537
Al-Sn-U alloy, phase equilib. exam. by metallographic and X-ray anal. 77−21102
Al-Sr-Nd phase diagram *(Russian)* 80−20893
Al-Ti-B alloys, phase comp. and distrib. of components, X-ray obs. *(Russian)* 79−52164
Al-Ti-Fe, ternary phase diagram, computer calculations 80−45274
Al-Ti-Si phase diagram, calc., interpretation of grain refinement results 78−84781
Al-Zn, plastic deform. effect on struct. transform. at elev. temp. *(Czech)* 79−79044
Al-Zn alloy, small-angle neutron scatt. in crit. point regions, 324-435°C *(German)* 77−85993
Al-Zn-Mg, metastable miscibility gap determ. by small angle scatt. 77−28781
Al-Zn-Si, thermodynamic props., meas. by EMF method *(Czech)* 77−59753
Al-Zr (0.8 and 1.5 wt.%), hyperperitectic, non equilibrium solidification 78−3113
Al_4C_3-Be_2C-SiC system, phase equilibria 80−45284
$Al_yGa_{1-y}As_{1-x}Sb_x$ LPE phase diagram 78−11137
$Al_xGa_{1-x-y}In_yAs$, LPE on InP, solid-liq. equilib. calcs. 78−84083
AlN-Si_3N_4-Be_3N_2 system, phase equilibria 80−60844
Al_2O_3-AlN phase diagram and reaction sintering of transparent cubic ALON spinel 80−25669
Al_2O_3-B_2O_3-SiO_2 system, liq. phase calc. for commercial quartzite powders 80−25671
Al_2O_3-BaO system, T-x phase diagram, phase transformation temps. in conc. range 100-65 mole% Al_2O_3 79−24428
Al_2O_3-CaF_2, phase relns. 78−23700
Al_2O_3-Dy_2O_3, phase diagram at high temps. *(Japanese)* 79−38810
Al_2O_3-Dy_2O_3, phase diagram at high temps. *(Japanese)* 80−50619
Al_2O_3-Er_2O_3 system, high temp. phase diagrams 80−40340
Al_2O_3-Eu_2O_3 system, phase diagram at high temp. *(Japanese)* 80−40339
Al_2O_3-Eu_2O_3(Gd_2O_3), phase diagrams at high temps. exam. 78−44114
Al_2O_3-Gd_2O_3 system, high temp. *(Japanese)* 80−45290
β-Al_2O_3-H_3O^+, high press. thermal stability, suggested phase diagram for stability range in Al_2O_3-H_2O system 79−23678
Al_2O_3-Ho_2O_3 system, high temp. phase diagrams 80−40340
Al_2O_3-Nb_2O_5-NiO, isothermal phase sections, 1100, 1250, 1400°C *(Italian)* 79−20032
Al_2O_3-Nd_2O_3, phase diagram at high temps. *(Japanese)* 77−63649
Al_2O_3-Nd_2O_3, phase-diagram at 1100°C *(Japanese)* 78−79747
Al_2O_3-P_2O_5-H_2O system, phase diagram 80−3014
Al_2O_3-Pr_2O_3, phase diagram at high temps. 77−63648
Al_2O_3-Pr_2O_3, phase diagram at high temps. *(Japanese)* 78−88449
Al_2O_3-SiO_2-ZrO_2, liquidus surface, discussion 77−44231
Al_2O_3-Sm_2O_3, phase diagram at high temps. *(Japanese)* 78−19732
Al_2O_3-Sm_2O_3, phase diagram at high temp. *(Japanese)* 78−92253
Al_2O_3-Y_2O_3, melting behaviour and metastability determ. by optical DTA 80−92648
AlSb-CdTe, phase diag. 77−52299
$(Al_xV_{1-x})_2O_3$, heat capacity anomalies, metal-insulator transition, phase diagram 77−11701
Ar-Re, phase diagram between 1866 to 1913K 79−100115
As-S system, glass forming ability and phase diagram 78−59760
As-Te-Ga system, glass-forming region and props. 80−25674
As_2O_5-Rb_2O(Rb_2CO_3) system, phase diagram, polymorphic transform. 79−83181
As_2S_3-$AsBr_3$ and As_2Se_3-$AsBr_3$ systems 77−8804
As_2S_3-HgS, phase diag., IR spectra 77−36479
As_2S_3-Se, glass-forming system, phase diagram 77−16551
As_2S_3-Tl_2S, As_2Se_3-Tl_2Se and As_2Te_3-Tl_2Te systems, vitrification and reaction characts. 77−15560
As_2S_3-Tl_2S glass, phase relns. and crystallisation 78−23675
As_2Se_3-Sb_2Se_3, phase relns. 77−21118
As_2Te_3-Tl_2Te system 77−16559
Au-Cd system, cryst. struct. of $AuCd_3$ and existence of $AuCd_{\sim 5}$ phase *(German)* 77−25020
Au-Co, liquidus line determ. by mag. meas. 80−60250
Au-Cu-Ga, solid soln., phase systems, valence electron density effects *(French)* 78−19724
Au-Cu-Ni, computer characterisation, exam. of phase equilibria and miscibility gap 79−11561
Au-Ge-Te ternary system, solid soln. in vicinity of GeTe, phase diagram *(French)* 77−85994

phase diagrams continued
Au-Mn alloys, equiatomic region of phase diagrams crystallographic and mag. exam. 78−52755
Au-Ni, liquid alloy system, determ. of thermodynamic props. using Knudson effusion method, phase diagram calc. *(German)* 78−51707
Au-Ni-Cu phase diagrams, thermodynamic calc. *(Korean)* 78−68672
Au-Pd-Pt-Ag, composition-property diagrams, mathematical models for diagrams *(Russian)* 79−11554
Au-Pd-Zn system, quasibinary section phases investig. 77−12596
Au-Pt system, phase diagram 79−15646
Au-Si, melt, thermodynamic study of phase diagram *(French)* 78−27482
Au-Tl (29 to 100 at.%), thermal analysis, exam. of phase diagram 78−88445
Au-Zn, (55 to 88 at.%), equilib. diagram, X-ray diffr. obs. 80−25660
AuCu-Al thin film bilayer system, phase formation, backscattering spectra 80−96728
$Au_3Cu_{1-x}Ag_2$, phase relations, X-ray diffr. and differential thermal anal. 80−108395
B-C system, region of existence of B_4C phase 78−76636
B-C(Si) systems, phase diagrams, review, book contrib. 78−48388
B-Mg-N system, precipitation mech. of BN 79−70068
B-Si, (0 to 14.3 at.%), phase charact., regions of existence *(French)* 80−104117
B_4C, melting and phase homogeneity range 80−20911
BN, crystal structure stability, P-T diagrams 78−51886
BN:C, hardening by doping, p-T diagram, cryst. struct. *(Russian)* 77−77491
B_2O_3-BaO, liquid immiscibility region, equilibration and quenching expts. 80−45288
B_2O_3-Nb_2O_5 complexes, high resolution TEM obs. 78−35378
BPO_4-$AlPO_4$, non-equil. phase diagram, electron microscope obs. 79−43225
B_2S_3-Tl_2S system, phase diagram and verification 80−35165
B_2Se_3-Tl_2Se_3 system, phase diagram 80−35165
Ba, phase transitions under high press. 80−96641
Ba-Al-Si, exam. of phase diagram, confirmation of $BaAl_2Si_2$ and $Ba(Al,Si)_2$ *(Russian)* 79−29019
Ba-Al-Si system, phase diagrams construction by simplex designing method 78−6899
Ba-Eu, *(Russian)* 78−80514
Ba-Nd, microstruct., X-ray, chemical and thermal diffusion anal. *(Russian)* 78−52761
Ba-Pb system, intermediate phases, equilib. phase diagram, cryst. struct. 77−44213
Ba-Se(Te) systems, DTA, X-ray and microstruct. analyses 77−36472
Ba-Ti *(Russian)* 78−80513
Ba-Yb *(Russian)* 78−80514
$BaAl_2Si_2O_8$-SiO_2, celsian solid solns., effects on polymorphic transform. kinetics 78−68677
$BaCO_3$-$SrCO_3$-$CaCO_3$, phase inhomogeneity effects on oxide cathode props. 78−52614
$Ba_2Co_{1.65}Fe_{0.35}^{2+}Fe_{28}^{3+}O_{46}$, temp.-mag. field phase diagram, torque method 80−60276
BaF_2-MnF_2-FeF_3 system, X-ray investigation, struct. relations, liquid-solid equilibria diagram, study by DTA *(French)* 79−34017
BaF_2-YF_3 system, phase diagram 78−35363
$BaFe_2O_4$-Fe_2O_3-$ZnFe_2O_2$ system, phase relations at 1200°C 78−72767
$BaMoO_4$-CdO(PbO)(ZnO) and $BaMoO_4$-$CdMoO_4$($PbMoO_4$)($ZnMoO_4$) systems 77−25034
BaO-GeO_2 system, phase equilibrium diagram 79−70047
BaO-In_2O_3 system, stability of synthesized compounds 77−36487
BaO-La_2O_3-GeO_2, exam. of glass forming region, properties and crystallisation 78−88454
BaO-MMO_4, M=Cd,Pb, phase diag. cross sections and reactions 78−27487
BaO-SiO_2, molten, corresponding state principle with KF-BeF_2 and appl. 79−11589
BaO-SiO_2-Fe_2O_3 permanent mag. ceramics, exam. of phase diagram, using X-ray analysis, optical microscopy, electron probe anal., and thermal analysis *(German)* 79−29012
BaO-TiO_2-Al_2O_3 system, subsolidus equilibria, X-ray powder diffr. 80−108413
BaO.$6Fe_2O_3$, solubility of CaO 80−100333
$Ba(PO_3)_2$-$CsPO_3$ system, equilibrium diagram *(French)* 77−28789
$BaPO_3F$-Al_2O_3-B_2O_3 system, liq. phase separation, IR spectra, microstruct. 80−29940
$BaSi_2$, trimorphic, transform. of three-connected Si nets, press.-temp. phase diagram, 40 kbar and 1000°C 80−75198
$BaSiO_3$-$BaGeO_3$, phase diag. 77−48404
Be-Al-Fe system, phase equilibria using high energy ion beams 79−43203
Be-Co (0-50 at.%) alloys, thermal, metallographic and X-ray anal., phase diagram *(Russian)* 78−56611
Be-Co phase diagram *(German)* 77−59759
Be-Co-Ni, phase relations *(German)* 79−43209
Be-Li-V, phase diagram, metallurgical aspects for fusion blanket use 80−32467
Bi, low-temp., using diamond anvil pressure cell and X-ray diffr. 78−1951
Bi-MnBi eutectic region, of Bi-Mn phase diagram 80−81034
Bi-O system, phase equilib., diagram *(German)* 80−55380
Bi-Sb-Sn, Sn and Sb partition coeffs. during crystallisation 77−48394
BiI_3-Bi_2Te_3, p-T-x phase diag. 77−36477
BiI_3-Sb(As)I_3, phase diags. 78−6905
Bi_2O_3-$AlPO_4$, phase equilib. 80−35168
Bi_2O_3-CdO system, thermal and X-ray phase analyses 77−25032
Bi_2O_3-SiO_2(GeO_2), metastable phases form., crystn. conditions, melt viscosity and density effects 80−35167
Bi_2O_3-SrO, solid state phase diagram, thermal and high temp. X-ray anal. *(French)* 79−65190
Bi_2O_3-ZnO, phase diag. 77−40416
$Bi_{1-x}Sb_x$, room temp. press.-comp. diagram, and high press. supercond. crit. temp. 77−8223
BiSeI, sublimation, vapour pressure 77−11686
BiTe-In(Gn,Sn)Te system, physicochemical anal., eutectic type phase diagram with solid soln. region 77−16556
Bi_2Te_3-BiI_3, single phase comp. $Bi_{1.00}Te_{0.98}I_{1.02}$, cryst. struct. of BiTeI 77−28788
Bi_2Te_3-Sb_2Te_3, Bi:Sb=1:2, 2:1, solid soln. deviation from stoichiometric cross section 79−43221

phase diagrams continued
Bi_2Te_3-Sb_2Te_3 solid soln., deviation from stoichiometric cross section 78−35362
BiTeI-SbTeI, solid solns., phase diagrams, photocond., elec. props. 79−38125
$BiVO_4$, ferroelastic phase transition, birefringence meas. at simultaneous high pressure and temp. 80−80743
C, noncrystalline conversion to diamond, diffusion conversion enhanced rate due to shock compression 80−39221
CO, press. depend. of melting and α-β phase transition temp. 77−69075
Ca-Cu system, enthalpy of form. of γ-phase $CaCu_5$ calorimetric determ. *(French)* 80−84915
Ca-Li-Mg, isothermal section calc. 79−29034
Ca-Mn-O system, isobaric phase diagram and subsolidus phase relations 79−24508
Ca-Mn-S-Se system, multicomponent solubilities 80−108416
Ca-Sb, phase diag. 77−52284
$CaAl_2Si_2O_8$-$CaSiO_3$-$CaMgSi_2O_6$, exam. of glass forming regions and properties of glasses 79−4958
$CaCl_2$-$BaCl_2$-H_2O ternary system, 45°C isotherm *(French)* 79−96004
$CaCl_2$-Ca phase diagram, DTA study *(French)* 80−25672
$CaCl_2$-CaF_2-CaO, phase diagram and CaC_2 solubility *(French)* 79−70050
CaF_2, fluorite, phase relations, to 60 kbar and 1800°C 78−84785
CaF_2-$(Y,R)F_3$ (R=any lanthanide except Pm, Eu), phase diagrams 78−84783
CaF_2-$(Y,R)F_3$ systems (R=rare earth), phase diagrams, limiting solubilities and non-stoichiometry 79−47665
CaF_2-AlF_3, phase equilibria, DTA and X-ray diffr. study 78−27493
CaF_2-AlF_3-Na_3AlF_6(-Al_2O_3), phase equilibria, X-ray diffr. and DTA meas. 80−108409
CaF_2-CaC_2, phase diagram and CaC_2 solubility *(French)* 79−70050
CaF_2-CaO-Al_2O_3, phase diagram contribution *(German)* 80−100830
CaF_2-LaF_3, solid soln. with fluorite struct., phase diagram 79−100119
Ca_2GeO_4-$Ca_3(PO_4)_2$ system, X-ray, DTA and cryst. optical analyses 77−36469
$CaMgSi_2O_6$-$Ca_2MgSi_2O_7$-$KAlSi_2O_6$, phase diagram of ternary eutectic system 78−80529
$Ca(NO_3)_2.4H_2O$, high press. phase behaviour, dehydration and congruent melting 79−78947
CaO:$MMoO_4$; M=Cd,Pb, phase diag. cross-sections and reactions 78−27487
CaO-Al_2O_3-P_2O_5, sub-solidus relationships 79−66046
CaO-Ga_2O_3 phase diagram and Czochralski melt growth of $CaGa_2O_4$ 80−29934
CaO-MgO-Al_2O_3-SiO_2, quartz sand-dolomite-magnesia-clay based glasses, crystn. 80−20915
CaO-MgO-CeO_2, fired, phase equilibrium diagram, 1700 to 1200°C 78−92248
CaO-MgO-Cr_2O_3-Al_2O_3-ZrO_2-SiO_2 system, subsolidus region characts. 80−97466
CaO-MgO-$NaPO_3$ system, subsolidus struct. 79−43215
CaO-MgO-ZrO_2-SiO_2, phase study, SiO_2 compatibility relationship 78−95734
CaO-MgO-ZrO_2-SiO_2, phase study, ZrO_2 compatibility relationship 78−95735
CaO-MgO-ZrO_2-SiO_2 refractories, phase diagram 80−11634
CaO-Nd_2O_3-Fe_2O_3-Al_2O_3 system, solid-state reactions 80−35173
CaO-P_2O_5-H_2O system, phase diagram at 200°C 80−45286
CaO-SiO_2-Al_2O_3-MgO, phase equilibria 77−86011
CaO-SrO-Fe_2O_3 system, phase relations, Sr hexaferrite field occurrence 80−93545
CaO-V_2O_5-Fe_2O_3-PbO, crystallisation field of Ca-V ferrogarnet 77−16548
CaO-V_2O_5-SiO_2 system, compatibility triangles 80−81037
$Ca_3(PO_4)_2$-Mg_2SiO_4, partial system, phase diag. 77−86005
$Ca_3(VO_4)_2$-$Mg_3(VO_4)_2$, exam. of phase composition and phase diagrams 79−1851
Cd-As system, $CdAs_4$ struct. 79−74138
Cd-$CdGeP_2$ cross section alloys 77−44139
Cd-Cu-Se, phase diag. 77−52303
Cd-Ge-As system, quenched samples, phase diagram, DTA after annealing 79−69226
Cd-Hg-Te, phase diagram, computer estimation 80−20903
Cd-P, p-T-x phase diagram, thermodynamic props. 80−88300
Cd-Pb, high pressure effects, eutectic temp. 80−55361
Cd-Sb alloys, phase diagram and melts struct., crystn. depend. on heating conditions 79−52155
Cd-Sb system, phase diagram, struct. and stability of phases *(German)* 78−60661
Cd-Sb-Sn ternary system, phase equilib. 80−16266
Cd-Sn binary system, high press. study 80−93539
Cd-Te-Ge system, CdTe-Ge cross section 77−52298
Cd-Tl binary alloy system at high press. 80−97461
Cd-Zn alloys, splat-quenched, X-ray diffr., SEM and TEM study of struct. 79−66077
$CdCr_2Se_4$, ferromag. semicond., P-T phase diagram by annealing expts. between 600 and 964°C 77−63636
$CdCr_2Se_4$, ferromagnetic semiconductor, P_{Se}-T phase diagram, where Se=Se_2, near peritectoid reaction temps. *(Japanese)* 77−52290
$CdCr_2Se_4$-$CdCl_2$, rel. to crystn. of $CdCr_2Se_4$ from high temp. soln. 78−3009
$CdGe(As_{1-x}P_x)_2$, crystal growth, phase studies, optical props. 78−48305
CdI_2-PbI_2-NaI, fusion diag. and thermodynamic calc. *(Russian)* 77−48417
$Cd_{1-x}M_x$ (M=Mg, Ca, Sr), solid soln., phase equilib. diagrams 80−108412
$Cd(NO_3)_2.4H_2O$, high press. phase behaviour, dehydration and congruent melting 79−78947
CdO-TeO_2 system, partial phase diagrams 78−84784
CdO-WO_3, phase rels. and cryst. struct. 80−108410
CdO-WO_3 phase diagram and prep. of $CdWO_4$ single crysts. 80−29933
$Cd(PO_3)_2$-$Sr(PO_3)_2$, physicochemical investigation 78−44102
CdS-CaS, solid soln., rock salt struct., high press. phase equilibrium study 78−52777
CdS-MgS, solid soln., rock salt struct., high press. phase equilibrium study 78−52777
CdS-SrS, solid soln., rock salt struct., high press. phase equilibrium study 78−52777
CdSb, phase diagram, region of homogeneity, elec. cond. 79−43219
CdSb-ZnSb, crystallisation characts., phase diagram 80−55383

phase diagrams continued
$CdSnAs_2$-Sn system, liquidus curve 80−59658
$CdSnP_2$ crystal growth, DTA obs. of Cd-Sn-$CdSnP_2$ phase diagram 80−24394
CdTe, crystal structure stability, P-T diagrams 78−51886
CdTe-Au system, phase diagram rel. to doping 80−16282
CdTe-CdS solid solution phase diagram *(Russian)* 79−100120
CdTe-CdS-CdSe system solid soln. single crysts., forbidden band width determ., comp. depend. 80−55083
CdTe-Co(Mn) systems, reaction of components, DTA, microstruct. and microhardness obs. 79−38804
CdTe-Fe, cross section and solubility of Fe 77−90334
CdTe-In system, equilib. phase diagram and liq. phase epitaxial growth of CdTe from In soln. *(Japanese)* 80−71634
CdTe-Tl, quasibinary cross section 78−3102
CdTe-ZnS system, phase diagram and solid solubility 80−20909
CdTe-ZnS ternary mutual system, phase diagram 80−20904
CdTe-ZnSe pseudobinary system, phase diagram and equil., Bridgman single cryst. growth method 79−43213
Ce, isostructural solid-solid phase transitions, core collapse, cell theory 80−59620
Ce-Ga, phase diagram *(Russian)* 78−27478
Ce-Ga system, phase equilib. and cryst. struct. of phases 80−35159
Ce-In, phase equilibrium and cryst. struct.. 80−66483
Ce-Mn-Ni system, phase diag. 77−52283
Ce-Nd-Si, phase diagram, X-ray anal. *(Ukrainian)* 79−38792
Ce-Tl, phase equilibrium and cryst. struct. 80−66483
$CeAl_2$, resistivity and volumetric meas., phase diagrams, comparison with CeS 80−107789
CeO_n, redox reactions, quasiisothermal thermogravimetric obs. 79−15980
CeS, resistivity and volumetric meas., phase diagrams, comparison with $CeAl_2$ 80−107789
Ce_2S_3-Ga_2S_3 system *(French)* 78−3108
$CeVO_4$, monazite struct., IR and NMR spectra 79−78534
ClF_5-IF_5, determ. of phase diagram, using DTA 79−4955
Co-B, amorphous alloys, phase diagram 79−96002
Co-B-Si ternary system, partial phase diagram, Co rich region 77−52293
Co-Cr system, phase diagram re-determ. from thermodynamic data 78−76631
Co-Cr-W-C, wear-resistant coating alloy, carbide form. and decomp. 77−32711
Co-Cr-Zr, thermodynamically calculated phase diagram 79−91617
Co-Cr-Zr(Ni), phase diagram calc. 79−1848
Co-Fe (2.92 to 30.05 wt.%), determination of phase equilibrium diagram *(Japanese)* 78−48374
Co-Ga alloys, phase diagrams and cryst. struct., DTA, X-ray diffr. and microprobe anal. *(French)* 79−47660
Co-Ga system, exam. of thermodynamics of α and β' phases 78−71870
Co-Ga-B, phase diagram, metallographic, X-ray and electron probe anal. 78−92241
Co-Gd-B, rules of cmpd. form. in related systems 79−34010
Co-Ge binary system, phase diagram rel. to that of Ni-Ge *(French)* 80−97463
Co-Ge-B, Co rich, phase diagram 77−8800
Co-H, system, melting temp., effect of H_2 *(Ukrainian)* 79−52153
Co-Mo, sintering, limited solid solubility, peritectic diagram 77−28754
Co-Ni-Zn, diagram of state, crystalline lattice consts., microhardness *(Russian)* 80−66479
Co-S, thermodynamic anal., phase diagram 79−43226
Co-Sb system, partial phase diagram, rel. to cryst. growth and cryst. chem. of CoSb 78−35286
Co-Sb-Te ternary system, crystn., heat treatment and phase equilib. 79−52156
Co-Se, P-T diagram and structural study 78−56622
Co-Si-Ge system, X-ray diffr. exam., band struct. *(Russian)* 78−56623
Co-Sm-Cu, phase diagram 79−91632
Co-Ti alloys, martensitic transformation depend. on ageing, cryst. struct. 79−91649
Co-V (10 to 23 wt.%) system, phase constitution, X-ray and elec. resist. meas. 80−3007
Co-W-O system, phase relations in dioxide-trioxide region, 1373K 78−11212
Co-X-Co (X=Cr,Mo,W) systems, crystn. temp. and hardness 79−77529
Co-Zn, physical-chemical metallurgy *(German)* 80−108390
Co-Zr, amorphous phase form. in Zr-poor region, hardness and fracture strength *(Japanese)* 80−84914
$CoCl_2$-KCl-NaCl system, melting diagram investigation by thermographic anal. *(Russian)* 78−3111
$Co_{1-x}Fe_{2+x}O_4$, prep. by wet and ceramic methods, struct., mag. and surface props. 78−52307
Co_5Ge_3, phase and struct. characts. 77−36450
CoPr, coercive force variation as function of annealing temp. *(Japanese)* 79−47787
CoS-MnS(ZnS)(CdS), phase study by X-ray obs., lattice const. 79−1854
Co_xS_y, exam. of thermodynamic activity, for several phases, using gas equilibration technique 78−52785
Co_5Sm, coercive force variation as function of annealing temp. *(Japanese)* 79−47787
$CoTe_2$-GeTe, phase diagram, from thermal, X-ray, microstructural analyses 80−55367
Cr-Al-C, ternary system, phase relationships 80−76230
Cr-B system 79−78931
Cr-Co-Ga systems, phase equilibria diagrams at 800 and 600°C *(Ukrainian)* 78−92236
Cr-Co-P, phase diagrams, lattice constants of phosphides 78−44099
Cr-Fe-Ga system, phase obs. at 800 and 820°C *(Russian)* 78−23662
Cr-Fe-Ni, γ-solid soln., thermodynamic activity determ. at 1500K 80−108397
Cr-Fe-Ni, phase diagram calc. 79−1848
Cr-Fe-Ni-Si, ternary phase equilibria for Cr-Fe-Ni rich portion, lattice stabilities 80−71628
Cr-Ge system, phase diagram, thermal anal., X-ray diffr., microhardness, and electron probe anal. *(French)* 80−97462
Cr-Mo-N system, at high-pressure, temp., X-ray anal., phase diagram 80−50607
Cr-N phase diagram, N_2 absorption by molten Cr at high temps. *(Japanese)* 79−43201
Cr-N system, thermodynamic anal. 77−77461

phase diagrams continued
Cr-Nb-Mo alloy system, comp. and temp. depend. alterations in mech. props., phase diagram interpret. *(Russian)* 80−85045
Cr-Ni-Fe, ternary phase diagrams, interactive computer program 80−71629
Cr-Ni-Ga systems, phase equilibria diagrams at 800 and 600°C *(Ukrainian)* 78−92236
Cr-Ni-O, computer-assisted anal. and calcs. of phase diagrams 80−25667
Cr-Os, magnetic transition T-P-C diagram, triple points *(Russian)* 80−54895
Cr-rare earth alloy, calc. of phase diagrams, with immiscibility in liquid state, using thermodynamics *(Russian)* 79−20029
Cr-rare earth alloys, liquid phase, topology in diagrams of state *(Russian)* 80−54121
Cr-rare earth phase diagrams, model of ideal solns. *(Russian)* 77−55946
Cr-Re binary system, isomorphous transition region *(Russian)* 77−55945
Cr-S system, phase diagram exam. between 873 and 1364K 78−3105
Cr-W-O, phase relations, thermodynamic props. of $CrWO_4$ and Cr_2WO_6 80−104120
Cr-X-C (X=Nb, Mo, Ta) alloy system, composition range for amorphous phase formation 79−73133
ε-Cr_2N phase, analysis of expt. results of Mills and Schwerdtfeger to yield partial enthalpy and entropy 78−52783
CrO_2, synthesis and morphology 79−24481
Cr_2O_3-MoO_3, physicochem. investig. of phase struct. 77−8807
Cr_2O_3-TiO_2 system, phase relations 78−80523
Cr_3Si structure, rel. between phase diagrams and superconductivity 80−88330
Cs-O system, phase diagram and O_2 potential 80−3011
CsBr-TlBr, phase diagram and pt. defect parameters 79−96017
CsCl-TlCl solid soln., determ. and computation of phase diagram 80−55379
CsD_2PO_4, pseudo-one-dimensional ferrolec. and antiferroelec. transitions, phase diagram obs., soft modes 80−93245
CsF-EuF_3 system, thermal anal. and X-ray diffr., phase equilibria *(French)* 78−44107
CsH_2PO_4, high press. phase diagram 78−52457
$CsPO_3$-$Sr(PO_3)_2$ system, physicochem. investigation 77−35666
$Cs_3R_2X_9$ (=Sc,Y,Ho-Lu, X=Cl and R=Sc,Sm-Lu, X=Br), prep. and Guinier-Simon X-ray study 80−49204
$Cs_2SO_4.3MoO_3$-In_2O_3, phase diags., chem. reactions 77−86008
$CsSbF_6$, high press. phase relations, vibr. spectra, and cryst. chemistry 80−108200
Cu rich dental amalgams, SEM and energy dispersive X-ray analysis 78−24184
Cu, shock compressed, release isentropes, eqn. of state at high energy density *(Russian)* 80−54340
Cu-Ag-Au, coherent phase diagram, theoretical calc. 80−70373
Cu-Ag-P amorphous alloys, strain gauge factor and elec. props. *(Japanese)* 79−79130
Cu-Ag-S, computation of component activities from ternary miscibility gap data 79−11591
Cu-Ag-X, X=metals, P, S, Se, phase diagrams and thermodynamic props., iso-activity coeff. curves 77−81249
α_2-Cu-Al, antiphase period and tetragonality 78−15374
Cu-Al-Fe-Mn, phase transform. during continuous cooling *(German, English)* 79−70044
Cu-Al-Fe-Mn (10,3,2 wt.%), phase comp. struct., continuous cooling from β-phase effect 79−24499
Cu-Al-Ni, mixed powder compacts, Ni content influence in sintering behaviour *(Japanese)* 80−35130
Cu-Al-Ni, phase diagram associated with stress induced martensitic transform. 79−8272
Cu-Al-Ni alloys, successive stress-induced martensitic transformations and associated transformation pseudoelasticity 79−43245
Cu-Al-Zn, period of periodic antiphases, quant. metallography *(French)* 79−100111
Cu-Au, calc. of coherent phase diagram, using cluster variation method 79−11564
Cu-Au, phase diagram calcs. by means of cluster variation method, meas. of ordering instability 79−38818
Cu-Au off-stoichiometric alloys, long period superlattice 79−55699
Cu-Be (6.2, 9.3, 13.4 at.%), cell growth of discontinuous precipitation *(Japanese)* 79−24525
Cu-Be-Co (2,0.3 wt.%) alloy, heat treatment, influence of tempering on hardness, tensile props. transform diagram *(French)* 78−31384
Cu-Ca-Mg, exam. of phase diagrams and thermodynamics props. 79−8275
Cu-Cd, exam. of diamagnetic susceptibilities *(Russian)* 79−28504
Cu-Cd-Se system, Cu-CdSe cross section and props. of cpds. formed 78−27491
Cu-Co (1.5 and 4 wt.%) alloy, coherent Co-rich separations obs. by positron annihilation *(Russian)* 80−89082
Cu-Co-O, Cu-Fe-O and Cu-Ni-O systems, distrib. of Fe, Co and Ni between Cu and Cu_2O *(Russian)* 77−16540
Cu-Fe phase diagram, 650 to 1050°C *(German)* 78−60658
Cu-Fe-O system, ternary phases, activities in spinel solid soln., phase equilibria and thermodynamic props. 78−6910
Cu-Ge-O, phase diagram and thermodynamics, electrochem. study 80−50617
Cu-Ge-Te system, DTA, crystallographic and metallographic analysis *(French)* 77−25019
Cu-Mn (38 to 58 wt.%), age hardened, exam. of precipitation and strengthing 78−72782
Cu-Mn-P alloys, phase diagram *(Russian)* 80−20891
Cu-Nb-Sn system, phase equilibria and supercond. props. *(Russian)* 80−50589
Cu-Ni-S, molten, thermodynamic props. 80−104122
Cu-Ni-Sn, liq. alloy, calc. and anal. of mixing enthalpies *(German)* 80−44325
Cu-Ni-Ti system, reactions with melt in Cu-rich region *(Japanese)* 79−89202
Cu-Ni-Zn system, tie lines in a two phase region 80−24404
Cu-Ni-Zn-Mn fine grained precipitation-hardenable alloy, high strength and ductility 80−100805
Cu-O system, liq., thermodynamic study *(Japanese)* 78−64529
Cu-Pb (Fe), liq., thermodynamic props. *(Polish)* 80−89199

phase diagrams continued
Cu-Pd alloy, pressure effect on β-phase transition by elec. resist. meas. 79−15660
Cu-Pt alloy, existence regions of FCC superstructs. *(Russian)* 78−52760
Cu-Pt alloy, temp.-press. phase diagram *(Russian)* 78−3100
Cu-Pt type alloys, theory of ordering *(Russian)* 77−1100
Cu-Sb (10-50 wt.%), thermal dilatometric anal. 79−56954
Cu-Sb (24-45 wt.%), phase transform. exam. by thermal expansion 77−63629
Cu-Se mixture, activity of Se *(German)* 78−27492
Cu-Si-Te, DTA and metallographic anal. *(French)* 79−52182
Cu-Sn, self-diffusion of Sn, correl. with other props. *(Russian)* 79−23764
Cu-Sn-Te system, phase diagram exam. *(French)* 77−21107
Cu-Ti, deform. effect on precipitation and recrystallisation, electron microscope study 77−70115
Cu-Ti, liquid phase sintering, metallographic electron beam microanalytical investigation 78−95888
Cu-V alloy, phase equilib. diagram exam. *(French)* 77−21100
Cu-V-Si, partial diag., V_3Si formation by bronze process 77−86032
β'Cu-Zn, martensite to martensite transformations 79−11615
Cu-Zn-Al, TTT diagrams *(German)* 79−43208
Cu-Zr, intermediary phases of equilib. diagram 78−84771
Cu-Zr alloys, isothermal transformation diagram 80−20902
$Cu_3Ag_{1-x}Au_x$, phase relations, X-ray diffr. and differential thermal anal. 80−108395
Cu_3Au-$Cu_3Pd(Pt)$, quasibinary system, order-disorder transform., superlattice form. 80−2159
CuBr-AgI system, ionic cond. and phase diagram 80−2198
CuBr-$PbBr_2$ system, phase diagram, DTA and X-ray diffr. analysis 77−47552
CuCl, ismorphic transitions at high press., 4.2 to 800K *(Russian)* 77−31774
CuCl-TlCl system, phase diagram and high ionic cond. obs. 78−79802
CuCr alloys, supersaturated solid soln. dissociation *(Russian)* 79−52201
$CuCr_2O_4$-$MgCr_2O_4$, X-ray investig. 77−44224
$CuFe_2O_4$-$CuGa_2O_4$, physicochem. props. *(French)* 77−44233
$(CuGaTe_2)_{1-x}$-$(2CdTe)_x$, phase diagram and microstruct. DTA and X-ray diffr. 77−59762
CuI-PbI_2 system, phase diagram, DTA and X-ray diffr. analysis 77−47552
$CuInS_2(Se_2)$-$GeS_2(Se_2)$, degree of solid solubility and phases characts. 78−35377
$(CuInTe_2)_{1-x}$-$(2ZnTe)_x$, phase diagram and cryst. growth of $CuZn_2InTe$ from $ZnCl_2$ flux 80−16287
Cu_xLa_{1-x}, splat-cooled, phase diagram and supercond. props. 80−70881
r-CuMn, annealing ordered phase study by neutron diffr. 80−89265
Cu_2MnAl, Heusler alloy, decomposition at 360°C 80−7536
$Cu_{3-x}Mn_xAl$, and $Cu_2Mn_{2-y}Al_y$, Heusler alloys, order-disorder transitions 80−59619
$Cu_xMo_6S_8$, superconductivity, lattice transforms., electronic instabilities 77−39990
$Cu_xMo_6S_8$, $1.5 \leq x \leq 3.55$, low temp. phase diagram, 1.2-320K 77−85371
$Cu_xMo_6S_8$, constitution diagram, 11-2000K 80−108407
$Cu_xMo_6S_8$ system, low temp. modifications *(French)* 80−50606
CuO-Cu_2O-TiO_2, phase equilibria, thermodynamics of Cu_3TiO_4 phase 80−55374
CuO-MgO-SiO_2 system, phase equilibria 79−70045
CuO-Nb_2O_5, phase anal., density determ. 78−10015
Cu_2O-CuO-MoO_3, subsolidus phase diagram, mag. props. 80−50615
Cu_2O-Nb_2O_5, phase anal., density determ. 78−10015
Cu_2S-Tl_2S system, phase diagram 80−20906
$Cu_2S(Se)$-Ge(Sn)S, phase diagrams 78−44100
Cu_2Se-GeSe quasibinary system, phase diagram and struct. 77−8802
$Cu_{2-x}Te$, $x<0.22$, phase diagram, electronic and ionic cond. meas. 80−6917
Dy, crystal structure, P-T phase diagram 78−84776
Dy-Er, Kaufman approach to calc. of intra-rare earth phase diagrams 80−25657
Dy-Fe-Al, pseudobinary alloy, struct. exam. 77−58979
Dy-Ho, Kaufman approach to calc. of intra-rare earth phase diagrams 80−25657
$DyCo_{5.3}$ noncollinear mag. struct. appearance in mag. fields, magnetostriction meas. *(Russian)* 80−100607
DyF_3-CsF, phase diagrams and ternary fluorides *(French)* 80−81040
DyF_3-KF, phase diagram, cryst. symmetry and lattice constants of phases *(French)* 79−65171
DyF_3-RbF, phase diagrams and ternary fluorides *(French)* 80−81040
Dy_2O_3-ZrO_2 phase diagram and long range ordering 80−93542
Dy_2S_3-Ga_2S_3 system *(French)* 78−3108
$ErFe_2H_n$, pressure-composition-temperature phase diagram 80−3010
$ErOHCO_3$, synthesis of rare earth carbonates under hydrothermal conditions 78−72714
Er_2S_3-Ga_2S_3 system *(French)* 78−3108
Eu selenides, X-ray phase anal. 77−11514
Eu-As system, cryst. struct. of phases formed 78−26493
Eu-As-S, glass forming region, Raman and IR obs. *(French)* 79−99080
Eu-B-C ternary and binary boundary systems, preparation techniques, X-ray analysis 80−60840
Eu-Ce(Pr)-Fe-O system, solid solns. of ferrogarnet and ferroperovskite type 78−27488
Eu-Ga alloys, phase diagrams, struct. and comp. *(Russian)* 79−52163
EuB_6-CrB_2 quasibinary cross section 77−86001
EuO, physical and physicochem. props., review 80−96875
Eu_2O_3-MoO_3, phase diag. 77−48408
Eu_2O_3-R_2O_3-Ta_2O_5, R=La, Gd, Y, quasibinary cross sections 77−90333
Eu_2O_3-Y_2O_3-Ta_2O_5, struct., phase form., luminesc. and X-ray diffr., obs. *(Russian)* 78−6765
Eu_2O_3-ZrO_2, phase decay 77−86002
FE-Zn, prep. and phase diagrams *(French)* 80−76231
Fe, α-, γ-, liq., thermodynamic data *(German)* 80−40328
Fe, cast, alloyed and unalloyed, microsegregation thermodynamics 80−76261
Fe cast, Mg, austenite isothermal transform., Sn addition effect 79−87611
Fe, cast, Mg, high strength bainitic transform. in C-shape diagram *(Russian)* 79−1860
Fe, cast-Ni, 78−44086
Fe, commercially pure, time-temp.-austenization diagram *(Japanese)* 78−6900

phase diagrams continued
Fe corrosion, temp. and Zn aggregates influence *(Dutch)* 78−48571
Fe group transition metal metalloid binary alloys, metallic glass form., eutectic composition 79−74133
Fe, phase diagrams, use in production 79−11572
Fe-Al, equilibria of Fe, Al ordered phase *(Japanese)* 79−70042
Fe-Al, ordering and phase separations *(Japanese)* 80−50595
Fe-Al (25 at.%), double Curie point phenomena 77−73030
Fe-Al alloys with Fe_3Al order, phase separation 77−73258
Fe-Al eutectic alloy, duplex crystals, unit cell parameters, appl. of Weissenberg technique 78−67684
Fe-As, phase equilib. diagram *(German)* 80−16280
Fe-B, amorphous, crystn., metal or metalloid exchange influence 80−75172
Fe-B, amorphous alloys, phase diagram 79−96002
Fe-B-C system, phase composition, morphology after heat treatments, $Fe_{23}B_5C$ struct. 77−28779
α-Fe-Be(P)(Mo)(W)-Co, effect of Co on solubility anomaly due to mag. transition, free energy and phase diagrams *(Japanese)* 79−42257
α-Fe-Be(Ti)(Mo)(P)(Sb), effect of mag. transition on solubility of alloying elements, phase diagrams and free energy curves *(Japanese)* 79−42256
Fe-C, diffusion of Sn, microprobe anal. of intermediate phases *(French)* 80−50596
Fe-C, exam. of phase equilbria, at high temp. and pressure 78−52759
Fe-C phase diagram, thermodynamic anal. 80−60846
Fe-C system, liq.-solid equilib. at high press., influence of graphitising elements *(Russian)* 78−56613
Fe-C system, mixing variables, activities and entropies calc., short range order model *(German)* 80−25655
Fe-C-B, exam. of phase diagram using neutron autoradiography 79−8279
Fe-C-H phase diagram, effect of H on eutectoid equilib. *(Russian)* 79−15648
Fe-Co-Cr, solid state phase equilib., isothermal sections determ. 800-1300°C 79−91623
Fe-Co-Mo, phase relations in system at 1100°C 80−108392
Fe-Co-Mo ternary system, phase diagram *(Russian)* 80−16269
Fe-Co-Ti-Al alloy type YuNDK magnets, metallographic method of distinguishing cracks 80−85096
Fe-Co(Si), determ. of chem. and magnetic interchange energies 77−80925
Fe-Cr, high purity binary alloy, isothermal decomp. of austenite 78−64525
Fe-Cr-C, steel carbide formation during chromising, exam. in terms of ternary phase diagrams 78−56818
Fe-Cr-C system, isothermal sections, 873 to 1373K, computer plotting 78−6894
Fe-Cr-Co alloy, Mossbauer exam. of spinodal decomposition 77−69742
Fe-Cr-Co ductile magnet alloys, phase diagram and mag. props., V or V+Ti addition effects 77−8959
Fe-Cr-Co permanent magnets, phase diagram, miscibility gap 77−89984
Fe-Cr-Co phase diagram, lamination region, resist. meas. *(Russian)* 78−27479
Fe-Cr-Ni, analysis and synthesis of phase diagrams 79−11563
Fe-Cr-Ni system, isothermal diffusion *(Russian)* 79−69300
Fe-Cr-Ni-Mo-V, Mo and V effects on segregation *(German)* 77−55942
Fe-Cr-Ni(Mn)(Ni-Mn)-C alloy, carbide-austenite equilibria, 1173 to 1373K, microscopic and X-ray obs. 78−44085
Fe-Cr-O, computer-assisted anal. and calcs. of phase diagrams 80−25667
Fe-Cr-O system, phase relations at 1200°C using diffusion couple technique 80−89205
Fe-Cr-O-C, stability diagrams, characteristics and calc. 79−10917
Fe-Cu, generation of self-consistent Gibbs energy functions 79−11565
Fe-Cu, thermodynamic analysis of phase relationships 77−73260
Fe-Cu-Zn, high-temperature phase diagrams *(German)* 80−108390
Fe-Ga, constitution between 10 and 50 at.% Ga, heat treatment depend., BCC phases *(German)* 77−90325
Fe-Ga, phase constitution depend. on heat treatment, phase diagram *(German)* 78−39748
Fe-Ga, solid soln., order-disorder transform. *(French)* 78−3121
Fe-Ga (25 at.%), precipitation *(French)* 77−70057
Fe-Ge (10 to 50 at.%), phase diagram rel. to heat treatment, supercooling diagram *(German)* 78−92240
Fe-Ge system, phase diagram 79−61515
Fe-H system, influence of H press. on Fe crit. points and H solubility 78−52758
Fe-lanthanid-O systems, thermodynamic props., composition and lattice constants 78−31390
Fe-M, (M=Cr,W,Mo,V,Ti), morphology and growth kinetics of δ-pearlite formed by carburisation 80−108485
Fe-Mn-C system, isothermal sections, 873 to 1373K, computer plotting 78−6893
Fe-Mn-O, phase equilibrium diagram *(German)* 78−15355
Fe-Mn-Sb, phase comp. 80−16267
Fe-Mn-Zn, high-temperature phase diagram *(German)* 80−108390
Fe-Mo (13-20 at.%) binary alloys, spinodal decomp. on ageing, TEM and X-ray diffr. study 80−97503
Fe-Mo system, thermomech. props. 80−89208
Fe-Mo-C system, isothermal sections, 973 to 1273K, thermodynamic analysis 78−6895
Fe-Mo-Cr(Ni)(Mn)-C, carbide-austenite equilibria, 1173 to 1373K, microscopic and X-ray obs. 78−44085
Fe-MoS_2, exam. of props., using differential thermal analysis, and metallography *(Russian)* 79−15653
Fe-MuS eutectics, unidirectional solidification *(German)* 80−100827
Fe-N phase diagram, thermodynamic anal. 80−60846
Fe-NbC, exam. of phase diagram, and mech. props. *(Russian)* 79−20028
Fe-Ni, liquid and solid, thermochem. props 77−59755
γ-Fe-Ni Invar alloy, phase mixture produced by long annealing 79−5065
Fe-Ni-Al, Curie temp. depend. on ordering, antiferromag. ordering *(Russian)* 79−61101
Fe-Ni-Al alloys, phase diagram, miscibility gap, DTA meas. 78−92237
Fe-Ni-C, Fe rich portion of phase diagram determ. 79−24497
Fe-Ni-C, phase diagram determ. 79−24495
Fe-Ni-C, Redlich-Kister eqns., activity coeffs., phase equilib. 78−23664
Fe-Ni-Co, phase diagram redeterm., Fe-rich portion 77−44219
Fe-Ni-Co-Mo phase diagram and structure *(Russian)* 80−20899
γ-Fe-Ni-Cr, magnetic phase diagram *(Russian)* 78−39292
phase diagrams continued
Fe-Ni-Cr-S, phase relations rel. to sulphidation of austenitic stainless steel 79−38800
Fe-Ni-Mo, phase relations in system at 1100°C 80−108392
Fe-Ni-O, computer-assisted anal. and calcs. of phase diagrams 80−25667
Fe-Ni-Pt system, ordered phase fields of equilibrium diagram 78−48373
Fe-Ni-S, exam. of liquidus surface and tie lines, using electron probe analysis 79−11557
Fe-Ni-(P), phase diagram determ., 700 to 300°C 80−108399
Fe-O system, thermodynamics of viustite-haematite alloy melt *(Russian)* 80−65249
Fe-O-Ca-Al system, inclusion precipitation diagram 80−108415
Fe-P-C, amorphous alloy, crystallisation 79−100112
Fe-Pd Invar, low temp. FCT phase obs. 80−93538
Fe-S phase diagram, thermodynamics 79−56966
Fe-Sb system, α-phase, interdiffusion 79−73349
Fe-Si system, melting equilibria study *(German)* 80−66473
Fe-Sn, thermodynamic assessment, phase diagram 79−91618
Fe-Ti-(Mn)(O), exam. of interrelations between phase diagrams and hydriding props. 79−8277
Fe-TiB_2, eutectic alloy, high temp. props. 78−84931
Fe-VC alloys, struct. and mech. props. 79−52171
Fe-W-Cr-Mo system, mag. and mech. props. rel. to production methods *(Japanese)* 80−71107
Fe-W-O system, phase relations in dioxide-trioxide region, 1373K 78−11212
Fe-X-C (X=Cr, Mo, W), quenched rapidly from melts, nonequilib. phases *(Japanese)* 80−71630
Fe-Zn, crystallographic relations by X-ray diffr. 80−24408
Fe-Zn, δ-phase, X-ray analysis and phase diagram modification 77−59758
Fe-Zn, ferrite-austenite phase boundaries, X-ray diffr. exam. *(German)* 78−80510
Fe-Zn, galvanised coating appl., metallurgy review 79−96199
Fe-Zn, phase diagram, DTA, EDAX, X-ray diffr. study 80−50602
Fe-Zn, physical-chemical metallurgy *(German)* 80−108390
Fe-Zn phase diagram, galvanization study *(French)* 80−66447
Fe-Zr, amorphous phase form. in Zr-poor region, hardness and fracture strength *(Japanese)* 80−84914
$Fe_{0.394}$-$Ti_{0.606}$-O-S subsystem, equil. phase data under reducing conditions rel. to ilmenite upgrading 80−76240
$Fe_{(1-x)}Co_xCl_2.2H_2O$, antiferromag. random mixture, sp. ht. meas., phase diagram 79−65678
$FeGa_2Se_4$, elec. cond., mag. susceptibility 80−88301
$Fe_xNb_yV_{2-2x}O_4$ complex solid solns., synthesis and phase diagram, semicond.-metal transition temp. 79−43214
FeO, wustite, invariant points between stable and metastable phases, T-P-X diagram *(French)* 80−29938
FeO-Fe_2O_3-SiO_2 system, molten, struct. using high temp. X-ray method *(Japanese)* 80−14992
FeO-Fe_2O_3-SiO_2 system, molten, struct. by high temp. X-ray diffr. 80−49084
FeO-FeS, mag. susceptibility, eutectic phase diagram *(Russian)* 80−15682
FeO_x, wustite field, thermodynamic props. and subphases, thermogravimetry, 1100-1300°C 80−76239
$Fe_{1-x}O$-ZnO at 900°C, some peculiarities *(French)* 77−70037
Fe_2O_3-BaO-CoO system, phase comp. and mag. props., Bi_2O_3 additions effect 79−29032
Fe_2O_3-Fe_3O_4-Fe_2SiO_4 system, haematite-magnetite-fayalite nodules, stressed state parameters *(Russian)* 80−40336
Fe_3O_4-Co_3O_4 spinels, phase diagram anal., thermodynamic props. 80−3009
Fe_xO, wustite, subphases in range of stoichiometry, comments and reply 77−47585
Fe_xO_y phase comp. on equilib. heating to 3300K *(Russian)* 80−16285
FeOOH, crystal growth in $FeSO_4$ solution with NaOH or NH_4OH as precipitant, phase diagrams *(Chinese)* 80−44158
$2FeO.SiO_2$-$2MnO.SiO_2$ melt, free energy of mixing 79−61572
$2.33FeO.TiO_2$-$2.33MnO$-TiO_2 melt, free energy of mixing 79−61572
$Fe_xPd_{82-x}Si_{18}$ metallic glass, mag. phase diagram, weak ferromagnet-spin glass transition 80−54893
FeS-MnS system, pseudobinary phase diagram 80−50777
$FeSb_2$, phase structure, X-ray crystallography *(French)* 78−91305
$Fe_{1+x}Sb$, phase structure, X-ray crystallography *(French)* 78−91305
FeSe-MnSe phase relationships in presence of excess Fe 77−52291
Fe_3Se_4, Fe_7Se_8, phase gap, Mossbauer spectra 80−20552
$Fe_{1.2}Te$-MnTe phase relations in presence of excess Fe 77−52292
Fe_xVS_2 ($0.20<x<1.00$), phase diagram and order-disorder transition of vacancies 80−81039
Ga metastable phases, melting curve under atm. and high press. by microcalorimetry *(French)* 77−43314
Ga-Al-As(Sb) solid soln., liquidus surface in ternary phase diagram, simplex lattice method 77−7847
Ga-Al-As(Sb) system, ternary phase diagrams, method for determ. of liquidus surfaces 77−28787
Ga-Al-Sb, liq. phase epitaxy, phase diagram, X-ray microanal. 79−19491
Ga-Al-Si, solubility of Si at 500-800°C liquidus lines *(French)* 77−51498
Ga-AlSb-GaSb, phase diagram, LPE of $(AlSb)_x(GaSb)_{1-x}$ solid soln. 77−40392
Ga-alloys, thermodynamic properties 78−14480
Ga-As-O, equilib. phase diagram, GaAs oxidation 80−104130
Ga-As-P solid soln., liquidus surface in ternary phase diagram, simplex lattice method 77−7847
Ga-As-P system, ternary phase diagrams, method for determ. of liquidus surfaces 77−28787
Ga-As-Sb system, two- and three-phase fields obs. 80−55373
Ga-As-Se, exam. of phase diagram, rel. to LPE of GaAs:Se 79−1849
Ga-Ge-Sn, thermodynamic props. of mixing of binary systems, phase diagram 80−45275
Ga-Ge-Te system, GaGeTe formation, peritectic decomp. and struct. *(French)* 77−85995
Ga-Ge-Zn ternary alloys, thermodynamic props., EMF meas. 80−81033
Ga-In-As solid soln., liquidus surface in ternary phase diagram, simplex lattice method 77−7847
Ga-In-As system, ternary phase diagrams, method for determ. of liquidus surfaces 77−28787

phase diagrams continued
Ga-In-As-Sb quaternary system, phase equilib. and heterojunctions 79−34016
Ga-In-As-Sb system LPE layers, pseudoquaternary phase diagram 78−10293
Ga-In-Sb, solidus isotherms and isoconcentration lines 78−56624
Ga-In-Sb, ternary phase diagram, thermodynamic models of solidus and liquidus isotherms 79−24504
Ga-In-Sb system, phase diagram calcs. in Ga+In rich region 80−60842
Ga-In-Sn, thermal analysis, determination of liquidus and reactions 78−88446
Ga-In(Al) systems, thermodynamic anal. 79−60512
Ga-P-Bi(Sb), liquidus isotherms, GaP solubility in Sb, Bi, rel. to epitaxial growth 78−34721
Ga-rare earth alloys, phase diagram determ. 78−15366
Ga-Se system, phase diagram and cryst. struct. of phases *(French)* 80−93544
Ga-Te system, phase diagram and cryst. structs. *(French)* 79−78946
Ga-transition metal alloys, phase diagrams and cryst. struct. *(French)* 79−47659
GaAlAs, heterostruct. formed by LPE, growth and dissolution kinetics 79−99439
$Ga_{1-x}Al_xAs$ LPE layers, comp. and refr. index, ellipsometry meas. 79−87011
$Ga_{1-x}Al_xAs$:Si, LPE, phase diagram, Hall effect meas., carrier conc., donor ionisation energies 77−72803
$Ga_{1-x}Al_xSb$, LPE growth and phase diagram *(French)* 77−24974
$Ga_{1-x}Al_xSb$, melt growth and elec. props. 79−65999
GaAs, crystal structure stability, P-T diagrams 78−51886
GaAs layers, heteroepitaxy, grown on Si and Ge from multiple component solns. *(Russian)* 78−15319
GaAs:Fe, LPE, phase diagram 77−16509
GaAs-element systems, solidus curves calc. for liq. phase epitaxy technology 77−8768
GaAs-ZnSe system 77−28785
$GaAs_{1-x}Sb_x$, LPE phase diagram meas. 77−20047
$GaAs_{1-x}Sb_x$ ternary phase diagram, LPE, band gap and elec. props. 77−55896
$GaAs_xSb_{1-x}$, lattice-matched LPE growth in InP substrates 79−42402
$GaAs_xSb_{1-y}$, miscibility gap, rel. to LPE 79−33090
GaI_3-$SbCl_3$, total exchange of halogens, Raman spectra and phase equilibrium *(French)* 79−65874
$Ga_xIn_{1-x}As$ on InP, lattice matched LPE film growth and characts. 78−72033
$Ga_xIn_{1-x}As$-InP, lattice matched LPE film growth and characts. 78−15320
Ga_2O_3-TeO_2, phas diag. 77−81252
GaP layers, heteroepitaxy, grown on Si and Ge from multiple component solns. *(Russian)* 78−15319
GaP, n-type, Zn diffusion, p-n junction depth 77−89841
GaP-M, M=Cd, Sn, Pb, polythermal cross sections 77−52300
$(GaP)_x(ZnSe)_{1-x}$, solid solution, reaction of Zn with Se during Czochralski growth and LPE 79−8238
GaS-SmS system, phase diagram 79−78939
GaS-YbS system, phase diagram, reacts., thermal, mag. and elec. meas. 79−11578
Ga_2S_3-PbS system, phase diagram and crystallographic study *(French)* 80−29937
GaSb-Ag, phase diag. 77−90327
GaSb-Zn(Cd)Te, quasibinary system, phase equilibrium, intermol. interaction 77−12601
GaSe-SnSe system, phase diagram and lattice consts. of solid solns. 79−34014
Ga_2Se_3, solid solution, elec. cond. 80−88301
Ga_2Se_3-FeSe, elec. cond., mag. susceptibility 80−88301
Ga_2Se_3-In_2Se_3 solid solution system, X-ray diffr. exam. 77−63639
Ga_2Se_3-MnSe system, crystallographic study, phase diagram, DTA and X-ray diffr. determ. *(French)* 79−24506
Gd, crystal structure, P-T phase diagram 78−84776
Gd-C-N system, isothermal section at 1200°C, X-ray investigation *(German)* 80−93543
Gd-Co intermetallic compounds, magnetocrystalline anisotropy obs. *(Japanese)* 77−80926
Gd-Fe-Si, phase diagram 79−52158
Gd-Y, Kaufman approach to calc. of intra-rare earth phase diagrams 80−25657
GdB_6, crystal preparation, elec. resistance, phase transitions 80−97427
GdF_3-RF_3, R=Tb, Ho, Er, Yb, stabilisation of rhombic β-YF_3 type struct. 78−67700
Gd_2O_3-Ga_2O_3 system, phase diagram relationships of garnet-perovskite transform. 80−97460
$GdOHCO_3$, $Gd_2O_2CO_3$, synthesis of rare earth carbonates under hydrothermal conditions 78−72714
Ge-As, p-T-x diagram 77−11669
Ge-As-Se-Te glasses for 8-12 μm IR optics 80−69475
Ge-GaAs, crystallisation at superhigh cooling rates 80−54349
Ge-GaP system, phase analysis 78−23674
Ge-In-Ga system, microscopic and X-ray phase anal. 77−12606
Ge-In-Te system, region of solid soln. of In in GeTe 77−51499
Ge-InP system, phase analysis 78−23674
Ge-S-Ga(In) system glasses, photoinduced changes 80−24365
Ge-Se-Te glasses, form. region, elec. props. 79−94904
Ge-Si, phase diagrams near melting point, Helmholtz free energy, heat of solution 80−70379
Ge-Si-S system, glass formation, transition temp., crystallisation and melting 80−100178
Ge-Sn-As system alloys, microstruct., X-ray phase and thermal anal. 77−32564
Ge-Te system, microstruct. in phase transform. region 79−52177
Ge-Te system, phase equil. diagram, $GeTe_{1\pm x}$ region analysis by metallography, microhardness and DTA *(French)* 77−70034
Ge-Te-O system, partial pressure diagram 79−83183
GeO_2-CdO system, phase diagram anal. by differential thermal, X-ray anal. 77−8805
GeS-GeSe, limits of solid soln. region, microstructural, X-ray and DTA meas. 78−47530
GeS_2-$GeSe_2$ cross section, $GeSe_2$ single cryst. growth 77−52305
GeS_xSe_{1-x}, IR spectra, differential calorimetry, phase diagram *(Russian)* 78−52513
$GeSe_2$-Te, phase diagram and vitrification region determ. by DTA, SEM, X-ray diffr. *(French)* 77−72565
phase diagrams continued
Ge_xSe_{1-x}, vitrification, liquid-solid phase diagram, viscosity var. *(French)* 77−72680
GeTe, region of homogeneity 77−47582
GeTe-As_2Te_3 system, phase diagram, eutectic comp., thermographic and X-ray anal. *(Russian)* 77−63646
GeTe-Ga_2Te_3, electrophys. props. 77−48403
H-He fluid planets, phase diagram and transport props. 78−28554
H_2, eqn. of state of solid and liq. phases, metallic state *(Russian)* 79−19354
H_2 monolayer, on triangular lattice, orientational phases 78−75934
H_2, solid, metallic, high density, thermodynamic props. 80−88337
p-H_2, solid, phase diagram, HCP-FCC phase transition 79−42340
H_2O-NaCl-sucrose, phase diagram determ., appls. in cryobiology 78−15777
He monolayer, phase diagram, order-disorder transition 80−107604
He^3 liquid, critical fluctuations, Anderson-Morel phase stabilisation *(Russian)* 79−73368
^{3}He, A-phase slab, mag.-field-induced cellular superflow, periodic texture 80−24706
^{3}He fluid-superfluid transition phase diagram, thermodynamic stability, fluctuations *(Russian)* 80−80023
^{3}He, solid, two parameter model of mag. and thermal props., spin exchange 80−49461
^{3}He, superfluid, mag. field-depend. phase diagram below polycrit. point 77−66053
^{3}He-^{4}He mixtures, phase diagram and conc. susceptibility near tricritical pt. 79−56005
^{3}He-^{4}He mixtures, two-dimens., phase diagram of dil. classical X-Y model 79−60593
^{3}He-^{4}He tricritical mixture, universality under press. 80−103533
^{4}He, superfluid, thermo-osmotic convection, at incipient lambda transition, above crit. press. 78−95199
Hf-Al-C, phase diagram and lattice constants, X-ray diffr. method 80−89207
Hf-Be, coupled phase diagrams and thermochemical descriptions 80−25656
Hf-Co, X-ray diffr., thermal anal. and metallography obs. 78−60652
Hf-M-B systems (M=Rh,Ir), phase equilib. and cryst. structs. 80−15072
Hf-Mo, high temp. phase diagrams 77−44217
Hf-Mo-C, isothermal section of phase diagram at 1400°C, X-ray phase analysis determ. 79−34006
Hf-Mo-C, phase diagram, crystallisation patterns of partial system Mo-HfC-Hf 77−12598
Hf-Mo-C, phase diagram and crystallisation of partial system Mo-HfC-C 77−12599
Hf-Mo-C system, isothermal section of phase diag. at 1700°C 78−68674
Hf-Nb-Ga, phase equilibria X-ray study at 800°C *(Ukrainian)* 79−95998
Hf-Ni (65 to 80 at.%), phase diagram and cryst. struct. of intermediate phases 79−52170
Hf-Ni(Cu)-Ge, alloys, phase diagrams and cryst. struct. *(Russian)* 80−25658
Hf-O, phase props. 77−40415
Hf-Zr-Ga, phase equilibria X-ray study at 800°C *(Ukrainian)* 79−95998
HfC-TiC, pseudobinary systems, phase diagrams, computer calcs. 78−44092
$HfCl_4$-CsCl melt, equilib. phase diagram and vapour press., equilib. reaction 77−66764
HfO_2-Al_2O_3, phase diag., 1500-2250°C 77−85998
HfO_2-CeO, solid solutions 77−16549
HfO_2-Eu_2O_3, phase composition in HfO_2-rich region, X-ray anal. 77−12609
HfO_2-Sm_2O_3, X-ray diffr. obs. of phase relations 79−61566
HfO_2-TiO_2, phase relations and thermal expansion 77−21121
Hg-HgTe-CdTe system, liquidus isotherms 78−35359
Hg-Tl, metastable system, prep. by quenching, phase struct. 78−52762
Hg-Tl, phase limits, determ. by enthalpy functions along liquidus *(French)* 80−84911
$Hg_{1-x}Cd_xTe$, p-T diagrams, p=n intrinsic-extrinsic lines 77−36481
Hg_2Cl_2, p-T phase diagram, pressure effect on phase transition 80−107370
$HgGa_2S_4$-HgS, rel. to melt growth of $HgGa_2S_4$ 80−50548
HgSe, point defect model rel. to elec. props. and phase diagram 77−4339
HgSe-CdSe pseudobinary alloy, phase diagram and cryst. growth 78−68620
HgSe-MnSe system, phase exam., solubility limit 77−36488
HgTe, p-T diagrams, p=n intrinsic-extrinsic lines 77−36481
HgTe-CdTe, distrib. ratios of components during crystn. of melt 77−16485
HgTe-CdTe, mixing energy and short-range order, diffuse X-ray scatt. 77−28006
Ho-Tb (50 wt.%) alloy, mag. phase diag. from anomalous US propag. 78−6526
Ho_2O_3-GeO_2-NaOH-H_2O, hydrothermal crystallisation 77−40344
In-As system, p-T-x diagram 77−8801
In-As-P solid soln., liquidus surface in ternary phase diagram, simplex lattice method 77−7847
In-As-P system, ternary phase diagrams, method for determ. of liquidus surfaces 77−28787
In-As-Se-I system, glass form. obs. 77−77466
In-Bi (2-33.3 at.%), phase diagram DTA, X-ray diffr. and supercond. T_c meas. 79−38795
In-Ga-As system, heterophase equilibrium, phase diagram calc. 79−43212
In-Ga-As-P, phase diagram rel. to lattice matched LPE 78−39708
In-Ga-As-Zn, phase diagram, LPE growth conditions for lattice matching on InP 80−70541
In-Ga-P ternary system, low temp. phase diagram rel. to epitaxial growth 80−84916
In-GaP, phase diag. cross section 77−48410
In-Hg amalgam, EMF meas. of In/$InCl_3$/amalgam cell and thermodynamic quantities 79−33999
In-Pb-Sn system, thermal anal. 80−35162
In-Sb-Bi system, solid solns., solubility limits, microhardness, microstruct. investig. 78−35368
In-Sb-Cd system, phase diagrams 79−87617
In-Sb-Te, region of In-Sb-based solid solutions 77−36466

phase diagrams continued
In-Sn system, phase diagram, and superconductivity of In_3Sn 79−38794
In-Te system, IR spectra *(Russian)* 78−84589
InAs-AlAs, phase diagram plotting by DTA and thermodynamic calc. 77−86016
InAs-CdTe quasi-binary system, temp.-comp. diagram, physicochem. and thermodynamic analysis 80−104127
InAs-HgTe, phase diags. 77−52299
$InBr_3$-In_2Te_3 quasibinary system, phase relations 80−100834
$In_{0.53}Ga_{0.47}As$, phase diagram at 650°C and LPE growth of lattice-matched layer 79−96009
$In_{1-x}Ga_xAs_{1-y}P_y$ layers on InP substrate, LPE growth, quaternary phase diagram, and band gaps 79−42403
$In_{1-x}Ga_xP$, epitaxial growth from melt, optimisation of growth conditions 79−52132
$In_uGa_{1-u}P_vAs_{1-v}$-InP, LPE, lattice matching, phase 80−54350
In_2O_3-TeO_2, phase diag. 77−81252
InP-GaP, solid soln. crystallization from stoichiometric melt, solidus construction 77−85927
InSb, crystal structure stability, P-T diagrams 78−51886
InSb, heats of transformation for high pressure, orthorhombic modification, exam. 78−56627
$InSb_{1-x}Bi_x$, metastable epitaxial film, phase diagram 80−76238
InSe-SmSe system, microhardness and electrophys. props. 79−87093
InSe-SnSe system, phase diagram and lattice consts. of solid solns. 79−34014
In_2Se_3-Sb_2Se_3 system, phase diagram 78−44090
In_2Te_3-PbTe system, phase diagram, elec. props. 78−35361
$InVO_4$, synthesis and thermal props. *(French)* 80−97443
K solution, in KBr, conc. fluctuations, neutron small-angle scatt. study in electrolyte-metal transition range 79−14668
K-Cs alloys, elec. resist., minima for K_2Cs, K_7Cs_6 concs. *(German)* 78−14708
$KAlO_2$, phase diagram and thermodynamic props. 79−91985
$KAlSiO_4$, phase diagram and thermodynamic props. 79−91985
$KAsO_3$-K_3AsO_4, phase diag. 78−23681
K_2CO_3Sr-CO_3 phase diagrams, evidence of new compound *(French)* 78−95033
KCl:Pb exam. of simultaneous effect of heat treatment, Pb concentration on state, phase diagram construction 79−96008
KCl-$CaCl_2$-NaCl, ternary phase diagrams, interactive computer program 80−71629
KCl-KF-K_3VF_6, phase diagram 77−21123
KCl-NaCl-$FeCl_3$ system, shape eutectics line calc. *(Russian)* 79−96016
KCl-NaCl-K_2NaVF_6, phase diagram 77−48416
KCl-NaCl-NaF-K_2NaVF_6 system, phase diagram 79−66049
K_2CrO_4-$CaCrO_4$, phase diagram determ., struct. of double salt 77−15543
$K_2CrO_4.MoO_4$-Cr_2O_3 system, phase diag. 77−86007
KD_2PO_4, high press. phase diagram 78−52457
KF-AlF_3 system, compared with NaF-AlF_3, rel. to use of $NaBF_4$ and Na_2TiF_6 in manufacture of Al alloys 78−27453
KF-BeF_2-DyF_3, crystalline and vitreous phases of cross sections 78−44096
KF-BeF_2-DyF_3, phase diagrams, intensification region 78−44097
KF-BeF_2-DyF_3 system, KBe_2F_5-DyF_3 cross section phase diagram, vitreous phases struct. 77−24383
KF-ErF_3, thermal and X-ray phase anal. 80−92645
KF-NaF-K_2NaVF_6, phase diagram 77−48416
KF-YbF_3, KF-LuF_3, phase analysis 78−44101
$KHSO_4$, phase diagram of 3.2 GPa, 450°C 80−76237
KNO_3-$K_2Cr_2O_7$ 77−44232
$(K_xNa_{1-x})NbO_3$ single crystals, growth and phase transitions 79−33915
$KO_{0.5}$-O system, thermodynamic props. 80−29184
K_2O-Al_2O_3 system, high temp. thermodynamics and phase equilibria 78−80521
K_2O-Fe_2O_3-SiO_2, subsolidus sector of phase diagram, X-ray obs. 80−40335
K_2O-Nb_2O_5, revision of phase diagram, $KNbO_3$ single crystal prep. 78−60564
K_2O-SiO_2, vap. press., thermodynamic props. and phase diagram at high temps. 78−83932
KOH-KO_2, phase diagram *(French)* 80−107177
KPO_3-$Pb(PO_3)_2$, phase diagram of binary system 77−21114
K_2SO_4-$CdSO_4$, re-exam., and cryst. growth of $K_2Cd_2(SO_4)_3$ 78−31335
K_2SO_4-Cs_2SO_4-MoO_3 system, fusibility diagram 79−87619
K_2SO_4-$ZnSO_4$ system, glass formation and phase diagram study, physical props. 78−27500
$K_2Si_4O_9$, phase diagram and thermodynamic props. 79−91985
K_3SmF_6, pressure temp. phase diagram to 35 kbar and 900°C 77−15575
K_3YF_6, pressure-temp. phase diagram to 35 kbar and 900°C 77−15575
Kr absorption on graphite, monolayer regime phase diagram 80−49507
Kr, adsorbed on graphite, finite size effect and temp. depend., multicritical phase diagrams 79−42372
La, low temp. P-T diagram 77−47550
La-B, phase and thermodynamic props., vaporisation 78−51660
La-Bi alloy system, phase diagram, struct. of intermetallic compounds 77−44214
La-Cu alloys, cryst. struct. exam. 77−58978
La-Ge-B, X-ray investigation of phase equilibrium 79−99294
La-H, phase equilibria 80−66492
La-In, heat of formation meas. using differential direct isoperibol calorimeter 77−21101
La-Re-B, annealed and quenched, X-ray structural and phase anal. 78−11207
La-S system, phase diagram above 1600°C 79−78938
$LaMnO_3$, phase diagram, mag. moments, neutron diffr. study 80−108414
$La_{10}Mo_2O_{21}$, synthesis and X-ray characterisation of struct. *(French)* 79−99162
La_6MoO_{12}, synthesis and X-ray characterisation of struct. *(French)* 79−99162
$La_6Mo_2O_{15}$, synthesis and X-ray characterisation of struct. *(French)* 79−99162
La_2O_3-Al_2O_3 system, alumina rich phase, X-ray obs. 79−29030
La_2O_3-Y_2O_3, phase diagram at high temps. *(Japanese)* 77−70038
La_2O_3-Y_2O_3 phase, diagram at high temps. *(Japanese)* 77−1218
$LaOHCO_3$, $La_3Cl(CO_3)_4$, synthesis of rare earth carbonates under hydrothermal conditions 78−72714
La_2O_2S-AgS-Ga_2S_3, ionic conducting glasses *(French)* 78−79804
phase diagrams continued
La_2O_2S-Ga_2S_3 system, phase diagram determ. by DTA and X-ray diffr. *(French)* 77−43309
La_2S_3-Ga_2S_3 system *(French)* 78−3108
La_2S_3-LaS_2, p-T-x phase diagram of La-S system 77−21112
La_2Se_3-Ga_2Se_3-$GeSe_2$ ternary system, phase diags., glass formation *(French)* 78−3109
$La_{1-x}Sr_xCrO_3$ system, phase relationships, cryst. struct. 77−69073
$LaVO_4$, monazite struct., IR and NMR spectra 79−78534
$La_2Zr_2O_7$-$La_2Hf_2O_7$ system, cryst. struct., phase diagram 78−83806
(Li,Na,K) (Nb,Ta)O_3, pseudo-binary and ternary systems quenched metastable glassy and cryst. phases 80−29935
Li, martensitic phase transitions, and phase diagrams at moderate press. 78−72775
Li-Al-Cl system, thermodynamic props., phase equilib. 80−89211
Li-B (0-60 at.%), density, elec. resist. and Hall coeff. 78−39089
Li-LiH, evaporation diagram at high liq. phase hydride concs. 77−35681
Li-LiH system, H isotope solubility thermodynamic singularities 80−81356
Li-Mg, liq., elec. transport props. and phase diagram 78−23070
Li-Pd, phase diagram and mag. props. 77−90321
Li-Pd (60 to 75 at.%), phase diagram and cryst. struct. of $LiPd_2$ phase *(German)* 79−51055
Li-Pt, phase diagram for comp. range 0-40 at.% Pt, mag. and elec. props. *(German)* 80−84912
Li-Rh-H system, intermetallic cpds. and phase relationships, cryst. struct. 78−44084
Li-Si alloys eval. as negative electrodes for Li-FeS_2 cells, thermodynamic props. 77−16547
$LiBO_2$-In_2O_3, phase composition, mag. props, elec. cond. 80−55365
Li_2BeF_4-Na(K)BF_4, phase diagram 77−21119
LiCl, frozen soln., NMR study of phase transitions 79−56617
LiCl-$AlCl_3$, phase diagram determ. by DTA and X-ray anal. *(Japanese)* 78−92250
Li_2CrO_4-K_2CrO_4, phase diagram determination by DTA and X-ray diffr. 78−31391
LiF-AlF_3-Na_3AlF_6-Al_2O_3 system, phase equilibrium, X-ray diffr., DTA, quenching, optical microscopy study 80−50610
LiF-MgF_2, high-pressure phase relations rel. to mixed oxide zone of Earth mantle 77−37193
$Li_{0.5}Fe_{2.5}O_4$-$Bi_2O_3(V_2O_5)$ systems, phase diagrams, sintering conditions 78−35366
$Li_{0.5}Fe_{2.5}O_4$-LiNb(Ta)O_3, in situ composite growth, phase diag., melting relns. 77−21132
$Li_{0.5}Ga_{2.5}O_4$-$CuCr_2O_4$ system, phase diagrams, IR spectra, Cu^{2+} electronic spectra *(French)* 78−51461
Li_4GeO_4-Zn_4GeO_4, solid electrolyte system, phase diagram 80−66489
LiH plasma, phase transition 78−42710
LiH, zero temp. phases, high density props. 78−75725
$Li_2K(IO_3)$ in LiIO_3-KIO_3 system, lattice parameter, equilib. and metastable phase diagram *(Chinese)* 80−7538
$LiNH_4SO_4$, P-T phase diagram, phase transitions 78−76399
$LiNH_4SO_4$, press.-temp. phase diagram, NMR and SHG meas. 78−23690
Li_2O-$3SiO_2$ glass, crystallization 79−74141
Li_2O-Al_2O_3-Cr_2O_3 system, subsolidus equilibria 80−60843
Li_2O-BeO-SiO_2, X-ray diffr. exam. of phase equilibrium 78−80522
Li_2O-Cr_2O_3-SiO_2 system, phase equilibria 79−78944
Li_2O-MgO-Al_2O_3 system, subsolidus phase equilibria 80−81036
Li_2O-Nd_2O_3-P_2O_5, phase diagram 79−43124
Li_2O-Nd_2O_3-P_2O_5 phase diagram, $LiNdP_4O_{12}$ single crystal growth 80−25668
Li_2O-NiO-O_2, phase diagram and mag. props. of $Li_xNi_{1-x}O_{1\pm y}$ 78−48380
Li_2O-SiO_2, glass ceramics, phase transformation processes 80−3025
Li_2O-Ta_2O_5 system phase diagram 79−47668
Li_2O-TeO_2 glasses, struct., IR reflection spectra 78−68516
Li_2O-TiO_2, pseudobinary phase rotations, DTA and X-ray anal. 80−108411
Li_2O-TiO_2 liquidus phase relations, Bridgman-Stockbarger crystal growth of $Li_2Ti_3O_7$ 80−25548
Li_2S-Al_2S_3, prep., phase props. and elec. cond. 79−96010
$LiTaO_3$-$CaZrO_3$, struct. and dielec. props. 78−80298
$LiTaO_3$-SiO_2-Al_2O_3, transparency in relation to microstruct. 78−53005
$LiVO_3$-Li(Nb,Ta)O_3 pseudobinary system, phase diagram, rel. to LPE of Li(Nb,Ta)O_3 79−41467
$Li_xV_2O_5$ ($0.1<x<1.0$), phase relationship in ambient temperature system 80−20912
Li_2WO_4-WO_3, phase relns. 77−48407
$Lu_2Si_2O_7$, polymorphism under press., cryst. struct. 77−35692
Mg cast iron, effect of heat treatment on phase comp., microstruct., wear resistance 77−56006
Mg ternary alloys, constitution, review 77−90319
Mg-Ag-Cu, phase comp. in Mg-rich region *(Russian)* 80−40331
Mg-Al-Tl(Pb) systems, phase diags., electrode pots. *(Russian)* 78−80516
Mg-Cu-Pb system, phase equilibria in Mg-rich corner *(French)* 78−76630
Mg-Er (<25%) alloys, struct. and props. 79−96001
Mg-Ga-In(Tl) and Mg-In-Tl, phase diagrams and electrochem. props. *(Russian)* 80−40330
Mg-Ho alloys, phase diagrams and transformations, Ho solubility *(Russian)* 79−52162
Mg-Li-Al, phase diag. *(Russian)* 77−59746
Mg-Li-Ga(Ge)(In)(Tl)(Pb), phase diagram, isothermal cross section *(Russian)* 80−20900
Mg-Li-Sn system in Mg-rich region *(Russian)* 77−52289
Mg-Li-Sn-Al, investigation in Mg rich region *(Russian)* 78−15364
Mg-$MgNi_2$-Zn, diagram of state, Zn solubility, initial phase precipitation *(Russian)* 80−66478
Mg-Nd-Zr, Mg rich region, microscopic anal. and elec. resistivity meas. *(Russian)* 78−56619
Mg-Sm, phase diagram and mech. props. *(Russian)* 80−20892
Mg-Sm, solid soln., phase diagram *(Russian)* 77−25015
Mg-Tb, (up to 45 wt.%), phase diagram, and mech. preps. 80−16277
Mg-Tl liq. systems thermodiffusion of Tl 77−11717
Mg-Tm, phase diagrams in Mg rich region *(Russian)* 77−52286
Mg-Y-Cd, phase equilibria and mech. props. *(Russian)* 80−20894
Mg-Y-Zn (20, 30 wt.%), phase equilibria investigation *(Russian)* 79−74131
Mg-Y-Zn alloys, phase equilib. *(Russian)* 80−16271

phase diagrams continued

$MgGeO_3$-$Ca_{0.5}Fe_{0.5}GeO_3$, solid solns., physicochem. props. 77−44223
Mg_2GeO_4-Mg_2SiO_4 system, struct. similar solid soln. obs. and charact. 80−108403
MgO-Al_2O_3-Cr_2O_3 refractory system, phase conversion and props., X-ray anal. 77−90336
MgO-Al_2O_3-SiO_2, glass ceramics, phase transformation processes 80−3025
MgO-Al_2O_3-SiO_2, metastable liq. phase separation region, electron microscope exam. 78−88451
MgO-Al_2O_3(Cr_2O_3)(Fe_xO_y)-CuO, phase relations and microstruct. 79−74140
MgO-CaMgSiO$_4$-($Al_{0.5}Cr_{0.5}$)$_2O_3$(Al_2O_3)(Cr_2O_3), spinel phase, phase equilibrium relations and spinel bonding 80−55376
MgO-CaO-FeO-Fe_2O_3-SiO_2-Cr_2O_3-Al_2O_3 spinel refractories, physicochem. prod. conditions 80−89185
MgO-CaO-SiO_2-Al_2O_3-$Na_2O.P_2O_5$, effect of $NaPO_3$ on phase composition rel. to basic refractories 78−80528
MgO-KCl, solution under hydrothermal conditions, exam. of phase equilibria 79−8292
MgO-Nb_2O_5-Al_2O_3, solid state equilibria at 1400°C phase diagram *(Italian)* 78−23671
MgO-SiO_2-Si_3N_4-Mg_3N_2, phase relations 77−63614
$MgTi_1O_5$, formation of solid solutions, on chemical reduction, X-ray analysis of phases *(Russian)* 79−33072
Mg_2TiO_4 single crystals, growth by floating zone method 79−78873
Mn metallic perovskite, structural instability *(French)* 79−100123
Mn-Al-C, ferromag. alloy, transform. kinetics 80−76229
Mn-Cu, alloying behaviour and high damping capacity 80−35160
Mn-Cu alloys, spinodal decomp. at 380°C, neutron diffr. anal. *(Russian)* 79−20023
Mn-Fe-C, melts, activities of Mn at 1673K 80−50597
Mn-Fe-C, phase instability 80−11628
Mn-Fe-Si-C, melts, activities of Mn at 1673K 80−50597
Mn-Ga (19 to 30 at.%), phase equilib. diagrams, X-ray diffr., thermal expansion, and mag. meas. *(Japanese)* 78−39743
Mn-N system, γ-Mn and hexagonal ξ-phase equilibrium calcs. 79−61565
Mn-Ni-C system, pressure effect on melting diagram *(Russian)* 77−55943
Mn-Si liquid alloy, vapour-pressure meas. using torsion effusion method 79−42215
Mn-Si-C, melts, activities of Mn at 1673K 80−50597
Mn-Ti-Fe, ternary phase diagram, computer calculations 80−45274
Mn-W-O system, phase relations in dioxide-trioxide region, 1373K 78−11212
$Mn_{0.394}$-$Ti_{0.606}$-O-S system, 1380 and 1485K, phase equilib. study 80−50616
MnAs, generalised P-T phase diagram, mag. and structural phase transition 80−39780
γ-MnAu, antiferromag., phase diagram, X-ray diffr. and Young's modulus meas. 80−71024
$Mn_{1-x}Fe_xAs$, magnetic transition under high press., exchange striction model calcs. *(Russian)* 80−50096
$Mn_3Ga_{1-x}Mn_xN$, perovskite struct., phase transformations *(French)* 80−81048
$Mn_3GaN_{1-x}C_x$, perovskite struct., phase transformations *(French)* 80−81048
$Mn_{1-x}M_xAs$, M=V, Cr, Fe, Co, mag. props., phase diags. 77−66300
MnO-P_2O_6 system, formation of manganese phosphates 77−90331
Mn_3O_4-Co_3O_4 spinels, phase diagram anal., thermodynamic props. 80−3009
MnS-$CuInS_2$, phase relations, 400 to 1300°C, X-ray and microscopic exam. 79−1853
MnSb, cryst. pulling with seed from nonstoichiometric melt 77−16488
$Mn_2Sb_{(1-x)}Bi_x$, mag. phase diagram *(Japanese)* 79−78375
Mo-(Zr+V+C) (1.1 wt.%) alloy, phase composition, carbide phase microhardness *(Russian)* 80−60834
Mo-Al-Ge, X-ray phase and microstructural anal. 80−93536
Mo-Co-Al, phase diagram *(Russian)* 78−19722
Mo-Cr, fusibility diagram *(Russian)* 80−20897
Mo-Ge-B, phase diag., struct. of $Mo_{1.7}Ge_{0.3}B$ 77−52285
Mo-HfC-C, projection of solidus surface, partial system of Hf-Mo-C 77−1834
Mo-N system, phase diagram of solid and liq., high and low press. 78−44083
Mo-Sn-S system, phase relationships, 500-800°C 79−24503
Mo-TiC-Ni phase equilibria, subsolidus temp., metallographic and X-ray anal. 80−16278
Mo-TiC(ZrC)(TiN), phase diagram *(Russian)* 78−27476
Mo-W-S system, phase relationships, 500-800°C 79−24503
Mo-Zr-Nb-C, polythermal sections *(Russian)* 78−15365
Mo-Zr-Nb-C alloys, phase diagram and comp., Zr and Nb influence *(Russian)* 79−52167
MoO_3-MO system, M=alkaline earth metal, eutectic coordinates on phase diag. 77−44227
ND_4Br, neutron diffr. exam. of P-T phase diagram 77−7861
$(ND_4)_3D(SO_4)_2$, press.-temp. phase diagram 78−38834
NH_3-metal, soln., thermophysical props., review 79−77758
NH_4Br, from Raman meas. under high press. 78−52776
NH_4Br, neutron diffr., exam. of P-T phase diagram 77−7861
$NH_4Cl_{1-x}Br_x$ mixed cryst., phase diagram and charact. of phase transitions 77−62637
NH_4HSO_4, ferroelec., press.-temp. phase diagram 77−85663
$(NH_4)_3H(SO_4)_2$, press.-temp. phase diagram, dielec. and DTA meas. 77−81067
NH_4I, from Raman meas. under high press. 78−52776
$(NH_4)_{1-x}M_xX$, and $(ND_4)_{1-x}M_xX$ M=Tl, Rb, Cs, X=Cl, Br, phase diagrams birefringence obs. *(German)* 79−83185
NH_4X, (X=Cl, Br, I), tricritical points, P-T diagrams, theoretical calc. 79−7695
(Na,Cs)(F,Cl,I,) quaternary reciprocal system, calc. of phase diagrams 80−25666
Na, martensitic phase transitions, and phase diagrams at moderate press. 78−72775
Na-C-O, thermodynamic computation of phase equilibria 77−63638
Na-K-Cs alloys, liquid contact material, phase diagram calcs. 78−6145
Na-NaOH-Na_2O-NaH, reciprocal ternary system 77−73263
Na_3AlF_6-LiF-CaF_2-AlF_3-Al_2O_3, electrolyte, exam. of phase equilibria, review 79−11590
$NaBF_4$-$LiBF_4$(KF)(LiF), phase diagram 77−21119
$NaCaPO_4$-Ca_2SiO_4 partial system, phase diagram 78−35364

phase diagrams continued

$NaCaPO_4$-$Ca_3MgSi_2O_8$(CaO) systems, phase diagrams of partial system 78−35369
$NaCaPO_4$-Ca_2SiO_5 partial system, phase diagram 78−35365
$NaCaPO_4$-$CaMgSiO_4$ system, phase diagram 78−35370
$NaCaPO_4$-MgO, $NaCaPO_4$-$NaMgPO_4$, $NaCaPO_4$-Mg_2SiO_4, $Na_2CaMg(PO_4)_2$-MgO, partial systems, phase diag. 77−86005
NaCl, frozen soln., NMR study of phase transitions 79−56617
NaCl-$AlCl_3$, phase diagram determ. by DTA and X-ray anal. *(Japanese)* 78−92250
NaCl-CsCl-$CrCl_3$, thermography *(Russian)* 77−63645
NaCl-CsCl-$CrCl_3$ system, phase struct. anal. by X-ray method *(Russian)* 78−3112
NaCl-KCl-CuCl system diagram investig. *(Russian)* 79−96015
NaCl-KCl-$NiCl_2$ system diagram investig. *(Russian)* 79−96014
NaCl-LiCl mixed crystals, Au decoration study of solid-melt interface, phase separation 80−15026
NaCl-NaBr-TeO_2, condition diagram, thermographic obs. *(Russian)* 80−55377
NaCl-NaF-Na_3VF_6, phase diagram 77−21123
Na_2CrO_4-MoO_3-Cr_2O_3 system, phase diag. 77−86007
NaF-Al_2O_3, β-Al_2O_3 form. *(Japanese)* 78−6912
NaF-AlF_3 system, rel. to use of $NaBF_4$ and Na_2TiF_6 in manufacture of Al alloys 78−27453
NaF-AlF_3 system, thermodynamics, solid soln. in cryolite 79−52183
NaF-YF_3 system, fusibility diagram, quasibinary section of NaF-YF_3-YOF system charcts. 80−55371
NaF-ZnF_2-CrF_3, solid-liquid equilib. diagram *(French)* 77−1216
NaI-LiI, phase diagram 77−21119
$Na_{1-x}Li_xNbO_3$, dielec. const. and X-ray diffr., for Curie temp. and phase diagrams 78−72768
$NaMgPO_4$-MgO, $NaMgPO_4$-$NaCaPO_4$, partial systems, phase diag. 77−86005
Na_2MoO_4-$MMoO_4$, M=Ca, Sr or Ba, phase diagrams 77−36467
Na_2MoO_4-Na_2SO_4, phase diag. and isomorphism 78−27486
$NaNO_3$-$CsNO_3$-$Pb(NO_3)_2$, fusion diag. *(Russian)* 77−48418
$NaNbO_3$-$BaTiO_3$ solid soln. form. and props. *(Russian)* 78−48378
$NaNbO_3$-$SrNb_2O_6$, phase diagram, props. meas. 79−11576
Na_2O-B_2O_3-SiO_2:Yb(Tb), luminesc. cooperative processes, glass struct. and comp. effect 80−16101
Na_2O-Ga_2O_3 system, new superionic conductor *(French)* 78−14504
Na_2O-Ga_2O_3 system β and β″ phases, fast ion cond., prep. and phase comp. 80−59716
Na_2O-SiO_2 glasses and liquids, enthalpy data 79−95183
Na_2O-SiO_2-NaF(NaCl) systems glass, phase relationships and diagrams 79−66048
$NaPF_6$, high press. phase diagram, vibr. spectra 78−60446
$NaPO_3$-$Mn(PO_3)_2$, cpd. formation 77−52307
Na_3PO_4-$Mg_3(PO_4)_2$, phase diag. and $NaMgPO_4$ and $NaMg_4(PO_4)_3$ formation 77−48412
Na_3PO_4-$Ni_3(PO_4)_2$ system, phase equilibrium diagrams, crystallographic study, double orthophosphates *(French)* 80−93546
Na_2S-Al_2S_3, prep., phase props. and elec. cond. 79−96010
$NaVO_3$-BaV_2O_6-SrV_2O_6, phase diagrams, simple eutectic system 78−48379
Na_2WO_4, cationic transport props. and struct. 77−76601
Na_2WO_4-K_2WO_4-WO_3 ternary system, physiochemical anal. methods 77−12608
Na_2XO_4, (X=S, Cr, Mo, W), anal. and calc. of binary and ternary phase diagrams 80−88299
Nb A15 compounds, preferential order-disorder 77−84702
Nb-Al-C, phase diagram and lattice constants, X-ray diffr. method 80−89207
Nb-D system *(Japanese)* 79−78936
Nb-Ga, phase system form. and stability of A15 phase 77−90347
Nb-Ga alloy, A15 type, melt produces specimens, supecond., homogeneity, transition temp. *(German)* 78−2608
Nb-Ga-Cu, metallographic and X-ray study, annealed and as-cast supercond. crit. temp. *(Russian)* 78−56617
Nb-Ga-Fe ternary system, phase equilib. at 1000°C, supercond. transition temp. 80−35158
Nb-Ga-Y, X-ray and microprobe anal., isothermal section and supercond. transition temp. *(Ukrainian)* 79−38793
Nb-Ge, superconductor, phase diagram determ. using various methods up to temp. of 2200°C 79−8414
Nb-Ge system, X-ray diffr., metallography, hardness and DTA expts. 79−38796
Nb-Ge-Cu, phase equilib. and supercond. props. *(Russian)* 80−40332
Nb-Ge-Ni, phase composition and superconducting props., influence of Ni *(Russian)* 80−20898
Nb-H, α+α′ region, precipitation morphology investigation by gamma ray diffr. 77−52333
Nb-H, elastic interaction and phase transition, book contrib. 79−83178
Nb-H interstitial alloy, props. and synthesis 79−69265
Nb-H interstitial alloys, prep. and props. 78−23669
Nb-H system, NMR evidence for low temp. pseudo-cubic phase 78−80526
Nb-H system, phase diagram and transforms., struct. obs. of various phases 80−104125
Nb-H system, phase equilibria studies *(Japanese)* 79−78935
Nb-Ir(Rh) system glasses, form., crystn. and microhardness, resist. obs. 80−89178
Nb-Os, phase diagram exam. 77−21103
Nb-Pd constitution diagram, metallographic and X-ray diffr. anal. 80−89204
Nb-Pt-O system, phase equilibria, diagram, unit cell parameters, supercond. 80−55352
Nb-Rh, radiation disorder model of phase stability 80−16297
Nb-Rh, σ-phase alloy, superconductivity and resistance behaviour 80−70882
Nb-Si diagram of state, melting temp., polymorphic transform. temp. *(Russian)* 80−50594
Nb-Sn, supercond. foils, phase anal. by Mossbauer spectra 78−64305
Nb-Sn-Si(As), ternary A15 phase regions, solubility 77−44215
Nb-Ti-O, isothermal and polythermal cross sections 80−96624
Nb-Ti-Ti_3O system, phase analysis, struct. stabilization 77−90330
Nb-Ti(Zr)(Hf)-N, exam. of phase equilibrium using electron microscopy and X-ray analysis *(Russian)* 79−15654
NbC-NbB_2, phase relns. 78−23677
NbD_x, x=0.55 to 0.88, deuteron and ^{93}Nb mag. resonance, β-α transitions 77−20721

phase diagrams continued
Nb_3Ge film, supercond., electron beam codeposition in O_2, Cl_2 or air, phase diagram 77−28728
$Nb_3Ge_xAl_{1-x}$, ternary supercond. alloys, comp. variations 80−97022
NbH(D), structs. phase diagrams, morphologies, prep. methods, book contrib. 80−25675
$NbH_x(D_x)$, cryst. struct., phase diagrams, order-disorder transition 78−55836
Nb_2O_5-TiO_2-ZrO_2, quasiternary system 77−44229
Nb_2O_5-WO_3, solid-state reactions, electron microscopic obs. 77−16818
Nb_2O_5-ZrO_2 sputtered thin layer structure and optical props. 79−28851
$NbSe_x$, x=1.48-2.0, nonstoichiometric, press.-comp.-temp. rel. determ. by annealing 79−74139
$NbSe_2$(2H), CDW layered cpd., phase diagrams 79−69243
Nb_3Sn, powder metallurgically produced, microstruct. charcts. 80−89233
Nd, crystal structure, P-T phase diagram 78−84776
Nd, magnetoresistance, mag. struct., elec. resistance at low temps. *(Russian)* 80−54936
Nd-Ga, phase diagram *(Russian)* 78−27478
Nd-Ga alloy, phase diagram, DTA, X-ray and metallographic obs. 79−24494
Nd-Gd-Te alloys of R_2Te_3-T_3Te_4 region, physicochem. props. 78−52017
Nd-H, possibility of H ordering, DTA meas. 79−52174
Nd-Pr, Kaufman approach to calc. of intra-rare earth phase diagrams 80−25657
Nd-Sn (0 to 50 at.%), phase equilibria diagram *(Ukrainian)* 79−34001
Nd-Tl system, intermediate phases 78−60653
Nd_2O_3-P_2O_5-H_2O, phase diagram 80−66412
$NdVO_4$, monazite struct., IR and NMR spectra 79−78534
Ni base superalloys, SIGMA-SAFE, phase diagram approach to sigma phase problem 78−64547
Ni complexes, dithiolato complexes, smectic C phase, synthesis, isobaric phase diagrams 78−94970
Ni-Al-Nb ternary system, electron microprobe analysis of nickel-rich region at 1473K 80−71631
Ni-Al-Ta dendritic monocrysts., directionally solidified, coarsening kinetics 80−108425
Ni-Al-Ti-Cr superalloys, estimation of conjugate γ and γ' compositions 79−8282
Ni-Al-Ti-(W) (Cr) (Co) (Mo) (Ta) (Nb), heat resist., solidification range 80−35177
Ni-B, amorphous alloys, phase diagram 79−96002
Ni-C. exam. of metastable phase diagrams, at high temp. and pressure *(Russian)* 79−56955
Ni-Ca-B, Ni-B side of ternary diagram 77−59766
Ni-Co-Mo, phase relations in system at 1100°C 80−108392
Ni-Cr, solubility limit determ., X-ray method 79−43199
Ni-Cr-Al aluminised coating, diffusion paths for formation and degradation of oxidation resistant coatings 78−11431
Ni-Cr-AlPt, exam. of phase diagram 79−8276
Ni-Cr-Mo-Fe-Mn, Kh12M23, intermetallic phases exam. *(Russian)* 78−39740
Ni-Cr-Ta system, phase equilib. of Ni rich region at 1523 and 1273K 80−93541
Ni-Fe-Cu, thermodynamic activities of components in pseudobinary section Ni_3Fe-Cu at 1520K 77−59752
Ni-Fe-Ti-O spinel phase, single-phase region and cryst. chem. characts. 77−52301
Ni-Ga alloys, phase diagrams and cryst. struct., DTA, X-ray diffr. and microprobe anal. *(French)* 79−47660
Ni-Ge binary system, phase diagram rel. to that of Co-Ge *(French)* 80−97463
Ni-H, system, melting temp., effect of H_2 *(Ukrainian)* 79−52153
Ni-H system, phase diagram and thermodynamic properties calcs. 80−66480
Ni-In, thermodynamic props., phase diagram 77−55949
Ni-Mo, sintering limited solid solubility, peritectic diagram 77−28754
Ni-Mo (17.5 at.%), discontinuous precipitation reaction *(German)* 79−87643
Ni-Mo-Al eutectics, unidirectional solidification 77−4769
Ni-Mo-W, diagram of state, W solubility, dispersion hardening *(Russian)* 80−66477
Ni-Pd-Ge, phase relationships and struct. 77−36451
Ni-Pd-Mn ternary alloys, mag. characts., use for thermoseed 80−107995
Ni-Re, sintering, limited solid solubility, peritectic diagrams 77−28754
Ni-S, phase diagram calc. and thermodynamic props. of liq. phase 80−108401
Ni-S, thermodynamics and phase relations 79−47666
Ni-S incongruently subliming system, SEM and TEM obs. of high temp. transitions, temp.-comp. diagrams 80−104136
Ni-S system, Knudsen effusion and thermodynamics 78−79759
Ni-Sb system, partial phase diagram, rel. to cryst. growth and cryst. chem of NiSb 78−35286
Ni-Ta system, phase diagram diffusion relation *(Russian)* 77−52287
Ni-Ta-Al system, phase equilibria and diagram, electron probe, X-ray diffr. anal. 80−29927
Ni-Ta-C, composites of γ+TaC 77−85965
Ni-V system, conc. depend. of interdiffusion coeff., 810-1175°C, rel. to phase diagram *(Russian)* 79−4429
Ni-W-C(Nb) system, γ to (γ+W) phase boundary calcs. using Wigner method *(Russian)* 80−54346
Ni-W-O system, phase relations in dioxide-trioxide region, 1373K 78−11212
Ni-W-O system, phase relns. and Gibbs' free energy of formation of $NiWO_4$ 77−73262
Ni-Zn, physical-chemical metallurgy *(German)* 80−108390
Ni-Zr, amorphous phase form. in Zr-poor region, hardness and fracture strength *(Japanese)* 80−84914
Ni_3Al-Ni_3Nb eutectic alloy, aluminide coating microstruct. exam. 78−15593
Ni_3Fe, order-disorder transition phase diagram, Mossbauer meas. 80−39995
$NiFe_2O_4$-$BuTiO_3$, in situ composite growth, phase diag., melting relns. 77−21132
$(Ni_{1-x}Fe_x)S$, solid solns., electronic props., X-ray, thermal and Mossbauer study 79−78376
Ni_3Ge-Fe_3Ge solid soln., flow stress, transition from positive to negative temp. depend. 80−60906
Ni_3Mn order-disorder transform. and constitution diagram *(Russian)* 77−59776
phase diagrams continued
NiO-CdO-Fe_2O_3 system, phase equilibria 79−11582
NiO-WO_3, phase relns. 78−3106
$NiSi_x$, cryst. struct. of phase *(German)* 79−99119
Ni_3Si, homogeneity region 78−23678
$Ni_{0.685}Zn_{0.177}Fe_{2.138}O_{4+\gamma}$, phase diagram, therm. anal. 79−78945
O_2-O_2 mixture, significant struct. theory appl. to phase separation 77−51503
P-Se, phase diag. 77−52296
P-Se, phase diag. and crystallisation of glasses at high press. 77−52297
P-Se system glasses, magnetochem. investig. 77−51325
PCl_5, phase diagram, PCl_6^- ionising to PCl_4 and $2Cl^-$ under press. 79−82314
PLZT, ferroelectric phase transitions, phase state identification 80−45018
$(Pb,Ba)_5Ge_3O_{11}$ ferroelectric crystals, influence of Pb replacement by Ba on props. 79−87402
Pb, shock compressed, release isentropes, eqn. of state at high energy density *(Russian)* 80−54340
Pb-Bi, supercond. tunnelling, effect of phase composition and press. 79−15261
Pb-Ca-Sn alloys for battery grids, proposed phase diagram, grain struct. development, corrosion phenomena 77−16546
Pb-Fe(Cu), liq., thermodynamic props. *(Polish)* 80−89199
Pb-Pd equilibrium diagram, Pb-rich region 77−48398
Pb-Rb, phase diagram *(Russian)* 78−19720
Pb-Sb, phase transform. at high press., DTA, eta, beta thermodynamic stable phases *(Russian)* 79−66051
Pb-Sn system, soft solder, elec. and thermal cond. at low temps., superconducting transition temp. 80−20150
Pb-Sn-Te system, investigation of liquidus surface by simplex lattice method 79−46784
Pb-Te system, homogeneity region of PbTe investig., equil. consts. of quasichem. reactions 80−108405
Pb-Te-O system, PbTe-$PbTeO_3$ and $PbTeO_4$-PbO cross sections 78−23679
Pb-Zn-Ag, liquid system, 450-750°C, phase boundaries *(French)* 77−69081
$PbFe_{(2/3}W_{1/3)}O_3$-$Pb(Co_{1/2}W_{1/2})O_3$ solid soln., crystallographic, dielectric, magnetic props., Mossbauer spectra 78−43807
$PbHf_{1-x}Ti_xO_3$, phase diagram, influence of poling treatment, ferroelec. antiferroelec. transition *(French)* 77−63374
PbI_2 direct gap polar semicond., electron hole liquid phase diagram *(Russian)* 80−93314
PbI_2, high press. phase diagram to 3.5 GPa 80−104126
PbI_2-$PbBr_2$, optical spectra, solid soln. struct. 78−48247
$Pb_{0.9}K_{0.1}(Zn_{1/3}Nb_{2/3})O_{2.95}$-$PbZrO_3$-$PbTiO_3$, morphotropic tetragonal-rhombohedral phase boundary 78−48129
Pb_xMnO_2, synthesis, chem. stability, use *(French)* 78−80525
$Pb_xMo_6S_{8-y}$, phase relns., stoichiometry, T_c 78−15378
$PbNb_2O_6$-NaNbO$_3$, DTA *(French)* 77−44234
PbNdTiNbO$_7$-PbO-KF-B_2O_3, cross sections rel. to cryst. growth 77−86004
PbO/TeO_2 system, central region of phase diagram, X-ray and thermal anal. 79−70046
PbO-Ga_2O_3 78−80524
PbO-$PbSO_4$ system, thermodynamic study of solid and liq. phases *(French)* 77−35667
4PbO.GeO_2, X-ray phase and thermal anal., new antiferroelectric 79−1744
$Pb_3(PO_4)_2$-$Pb_3(VO_4)_2$ mixed crystal, crit. stress and phase diagram temp. depend. 78−26623
$Pb_3(P_xV_{1-x}O_4)_2$, phase diagram and crystallography *(French)* 78−92252
PbS-$CuS_{1.8}$-ZnS, phase equilib. *(Russian)* 77−28786
PbS-In_2S_3, phase investigation 80−66488
PbS-Sb system alloys, eutectic equilib. 77−25028
Pb_2SiO_4-$PbSiO_3$, Raman and IR spectra of crystalline phases 80−3013
$Pb_{1-x}Sn_xSe(Te)$ epitaxial layers, growth, phase diagram, p-n junctions, optical, elec. props. 78−44029
$Pb_{1-x}Sn_xTe$ layers, LPE, phase diagram rel. to lattice const., distrib. coeffs. 79−37925
$Pb_{1-x}Sn_xTe_{1-y}Se_y$ solid solutions with constant lattice parameter, phase comp. 80−108417
PbTe, solidus line anal., carrier conc. 78−75806
PbTe, thermodynamic props. 77−28023
PbTe-Ga_2Te_3, phase interaction, DTA, XPA and microstructural anal. 80−96625
PbTe-InTe system, phase interactions and solid soln. form., physicochem. and elec. characteris. 80−104129
PbTe-PbS, solid-phase solubility, use of diffusion couple 77−12602
$Pb(Ti,Zr)O_3$ solid solutions, phase coexistence discrepancies 80−96662
$PbTiO_3$, single crysts., lattice parameters and birefringence as function of temp. 79−38517
$PbTiO_3$-$CaFe_{2/3}W_{1/3}O_3$, solid solutions 78−43816
$PbTiO_3$-$PbZrO_3$-based multicomponent ferroelec. solid solns., morphotropic transitions and comp.-temp. phase diagrams 80−55047
$PbTiO_3$-$Pb(Ni_{1/2}W_{1/2})O_3$ system, solid soln. form., struct., dielec. props. and thermal expansion *(Japanese)* 78−27501
$xPbTiO_3+(1-x)PbCd_{1/3}Nb_{2/3}O_3$, phase transition spread, polarisation relaxation, dielectric susceptibility *(Russian)* 80−75922
$Pb(Zr,Ti,Ge)O_3$, antiferro-ferroelectric transition 78−95565
$Pb(Zr,Ti)O_3$, piezoelec., compositional fluctuation and props. 78−18742
$PbZrO_3$ based ferroelec. ceramic, pressure-temp. phase diagrams 79−24273
$PbZrO_3$-$PbCd_{0.5}W_{0.5}O_3$, phase transitions 78−43817
$PbZr_xTi_{1-x}O_3$ ceramics, morphotropic phase boundary 80−81035
Pd-Au-Ag ternary system, isoparametric curves and Wegard's law plots 79−47657
Pd-H, elastic interaction and phase transition, book contrib. 79−83178
Pd-H and Pd alloy-H systems, review of props., book contrib. 80−24605
Pd-H system, phase diagram determ. using Gd^{3+} EPR 79−87608
Pd-H system, phase diagram and thermodynamic properties calcs. 80−66480
Pd-H thin film system, phase diagrams using quartz crystal thickness monitor 80−7537
Pd-H-Gd, dil., ESR exam. of low temp. region of phase diagram, and electronic props. 80−29930
Pd-Pb-Bi supercond. alloy, X-ray, microscopic, thermographic anal. *(Russian)* 77−32106
Pd-S system, and cryst. struct. of $Pd_{16}S_7$ *(German)* 77−11516

phase diagrams continued
Pd-Si, amorphous thin films, laser irrad., metastable phases 80−96622
Pd-Zn system, phase characterisation *(German)* 78−60654
Pd-Zn system, struct. stability of B2 and $L1_0$ phases 78−26495
PdAl-Fe(Ni), phase diagrams, eutectic points and solubility *(Russian)* 80−40333
Pd_2AlCu-PdAl system, interactions and solid-state transforms *(Russian)* 80−16272
PdGdH, diagram of state elec. props., indirect exchange interaction, EPR study *(Russian)* 80−50179
PdH_x, incoherent phase transition, lattice gas model 80−29171
Pr-Cu-Al system, X-ray and microscopic anal. *(Ukrainian)* 78−84774
Pr-Ga (0 to 50 at.%), phase diagram and cryst. structs. of intermetallic cryst. 80−3002
Pr-In system, phase diagram determ. and intermediate phases characterisation 79−91621
Pr-Ni-Al system, Pr (0 to 33.3 at.%), isothermal section at 800°C *(Ukrainian)* 79−34002
$PrVO_4$, monazite struct., IR and NMR spectra 79−78534
Pt complexes, dithiolato complexes, smectic C phase, synthesis, isobaric phase diagrams 78−94970
Pt-Cd, thermodynamic props. 79−43207
Pt-Si, amorphous thin films, laser irrad., metastable phases 80−96622
$Pt_{13}In_9$, exam. of crystal structure, and phase diagrams *(German)* 78−83779
β-PtZn nonstoichiometric Ll_0 phase, thermodynamic activity of Zn 77−90320
Pu alloys, binary, enthalpy of form., atomic model approach, correl. with phase diagrams 77−21415
Pu and other actinides, conf., Baden-Baden, Germany (Sept. 1975) 77−19807
Pu binary alloys, periodical depend. of equilibrium distrib. coeffs. of Pu admixtures on atomic number of admixture 80−18419
Pu-Al-Ga system 77−21108
Pu-O, phase diagram 79−79041
Pu-O system, substoichiometric phase range obs., high temp. thermodynamic parameters 77−21125
Pu-Pt(Rh)(Pt-Rh), exam. of phases and crystal structure 78−80518
Pu-Re-C and Pu-Tc-C systems, phase relationships 77−21127
Pu-Zr alloys, BCC, self-diffusion activation volumes, melting-diffusion correl. validity 77−20122
Rb-Se system, phase equilibria 78−44079
$RbCrI_3$, radiocrystallographic and mag. study *(French)* 79−46632
RbF-EuF_3 system, thermal anal. and X-ray diffr., phase equilibria *(French)* 78−44107
RbF-HoF_3, cpd. formation 77−44226
RbH_2PO_4, high press. phase diagram 78−52457
$RbLiSO_4$, field induced ferroelec. phase 79−78633
$RbPO_3$-$AgPO_3$ system, thermal and X-ray analyses 77−25033
$RbPO_3$-$Mn(PO_3)_2$ system, $Rb_2Mn(PO_3)_4$ and $RbMnP_3O_9$ form. 79−78943
Rb_2SO_4.$3MoO_3$-In_2O_3, phase diags., chem. reactions 77−86008
Re-Al-Si , X-ray determ.of system *(Russian)* 78−19763
Re-Cu-Al phase diagram, X-ray structural and microscopic anal. *(Russian)* 80−20895
Re-Ta-Mo, phase diag. *(Russian)* 77−59747
Re-Zr-V, constitutional diagram *(Russian)* 79−56956
S, melting curves and polymorphism 78−43104
Sb, high-pressure polymorphism, phase diagram 77−43324
Sb-In, electronic work function, contact pot. difference meas. 77−85299
Sb-S, saturated vap. press. 78−43116
Sb-Se-I, phase diagrams of various cross-sections 78−44093
Sb-Se-I system, exam. of glass formation, IR transmission spectra 78−88452
Sb-Sn, electronic work function, contact pot. difference meas. 77−85299
Sb-Zn, electronic work function, contact pot. difference meas. 77−85299
$SbCl_5$, phase diagram to 43 kbar 80−2144
SbI_3-AsI_3, phase diags. 78−6905
$Sb_{0.2(0.4)}MoO_{3.1}$, synthesis, struct. and oxidation state *(French)* 80−64971
Sb_2O_4-$NaSbO_3$($KSbO_3$)-NaF, phase equilibria and crystal growth 77−70035
Sb_2S_3-SbI_3, amorphous phase formation in vacuum condensates, TEM study 79−86712
SbSI-BiSI, solid solns., phase diagrams, photocond., elec. props. 79−38125
$SbSI_xBr_{1-x}$, T-p-x phase diagram *(Russian)* 77−16241
SbSeI, sublimation, vapour pressure 77−11686
Sc-[Co,Ni,Cu]-Ga, phase equilibria, diagrams of state, X-ray, microstructural study *(Russian)* 80−55356
Sc-Co-Si, phase equil. and atomic struct. *(Russian)* 77−77462
Sc-Co(Ni)(Cu), phase diagram determination, using X-ray diffr., metallography and DTA techniques *(Russian)* 79−34004
Sc-Fe system *(Ukrainian)* 78−84773
Sc-Fe-Ga, system alloys, isothermal sections of phase diagram *(Ukrainian)* 78−92235
Sc-Fe-Si system, phase obs. at 800°C *(Russian)* 78−23661
Sc-Ga system, phase diagram from 20-75 at.% Ga, intermetallic compound identification *(Russian)* 77−55944
Sc-H, p-T phase diagram and influence of H pressure, on decomposition temp., DTA exam. 80−29929
Sc-M-B systems (M=Rh,Ir), phase equilib. and cryst. structs. 80−15072
Sc-Mn-Ga system alloys, isothermal sections of phase diagram *(Ukrainian)* 78−92235
Sc-Rh-Si system, partial phase diagram, X-ray diffr. and microprobe anal. 80−25659
$ScCl_3$-NaCl-CsCl ternary system, cpd. form., thermographic investig. *(Russian)* 80−66490
Sc_2O_3-GeO_2-KF-H_2O system, scandium germanates crystallisation in high temp. aq. solns. 77−24942
Sc_2O_3-Ho_2O_3 (Dy_2O_3), solid solution, use of segregation phenomena to exam. solidification phase diagrams *(French)* 79−8293
Sc_2O_3-R_2O_3, regular soln. approx. of solidification diagram *(French)* 79−24505
Sc_2O_3-R_2O_3 (R = rare earth or Y), phases and phase transitions at high temp. *(French)* 79−100126
Sc_2O_3-ScF_3 system, phase ratios at 100 kbar press. 78−19729
$ScRu_4B_4$, superconducting and crystallographic data 80−33968
Se, liquid-glass transition, P-V-T relations 77−24387
Se-Na, and Se, liqs., elec. resistivity and phase separation 79−82573
Si, crystal structure stability, P-T diagrams 78−51886
phase diagrams continued
Si inversion layers, phase diagram in strong mag. fields 80−88492
Si-Al-B-O-N, calc. of phase diagrams from data set 80−55362
Si-Al-Be-C-N system, phase equilibria 80−60839
Si-Al-O-N systems, behavioural diagrams 79−24507
Si-Al-Zr-O-N, calc. of phase diagrams from data set 80−55362
Si-Ge system, phase diagram, lattice const. var. effects 80−97470
Si-Te system, phase diagrams 80−89209
Si-Ti *(Russian)* 78−80513
Si-transition metal systems, Si stabilised C14 Laves phases 78−84777
β-SiC, polytype stability, $\alpha \rightarrow \beta$ phase transformation during growth 78−6028
Si_3N_4, impure, oxidation, phase equilibria 79−70045
Si_3N_4, low pressure CVD, thermochemical calcs. 80−108356
Si_3N_4-Al_2O_3-AlN, isothermal sections, free energy of formation 80−55363
Si_3N_4-Si_2N_2O-Mg_2SiO_4, melting and eutectic studies 80−45285
Si_3N_4-SiO_2-Y_2O_2, subsolidus phase relations 80−60845
Si_3N_4-SiO_2-Y_2O_3 pseudoternary system, phase relations and stability 77−86015
SiO_2, low pressure CVD, thermochemical calcs. 80−108356
SiO_2, melting curves at high press. 77−11672
SiO_2-Al_2O_3, calculated thermodynamic data and metastable immiscibility 78−27495
SiO_2-Al_2O_3 based minerals, phase equilib., struct., comp. *(French)* 78−60659
SiO_2-Al_2O_3-Si_3N_4, isothermal sections, free energy of formation 80−55363
SiO_2-TiO_2 system, true solid soln. existence obs. 77−36475
Si_2ON_2-Y_2O_3-Al_2O_3 phase relations at 1400°C *(Japanese)* 79−38811
Sm, crystal structure, P-T phase diagram 78−84776
Sm-Co-Cu permanent magnets, phase diagram 77−21106
Sm-Cu phase diagram *(Russian)* 78−27477
Sm-Ga, phase diagram *(Russian)* 78−27478
Sm-H, phase equilibria 80−66492
$Sm_{1-x}Gd_xS$ system, equilib. of isomorphous phases and crit. point 78−34772
Sm_2O_3-Ga_2O_3 system, garnet-perovskite transform., phase diagram relationships 80−97460
SmS, high-pressure mixed-valence phase, diagram and electronic entropy, neutron diffr. obs. 79−33267
SmS, physical and physicochem. props., review 80−96875
Sn-Bi-Se, phase diagrams 79−87622
Sn-Cd-Pb system, contacting layer struct. and phase composition *(Russian)* 80−66475
Sn-F system, partial phase diagram construct. in Sn-SnF_4 region *(French)* 80−50605
Sn-Te, molten, elec. cond. and phase diagram 80−84454
SnI_2-SnF_2 system, phase diagram construct. *(French)* 80−50605
SnS-GeS_2, exam. of phase diagram using DTA *(German)* 79−11585
SnS-PbS, phase diag. 77−36476
SnS_2-SnI_4, T-x projection of phase diag. 78−23683
$Sn_5Sb_2S_9$, cryst. struct. *(French)* 80−1991
SnSe, electronic props., region of existence *(French)* 77−35885
SnSe, sublimation growth, deviation from stoichiometry, elec. props. 78−76594
SnSe-Sb_2Se_3 system, differential thermal, microstruct., X-ray phase and microhardness anal. 77−16555
SnSe-Se, p-T projection of phase diag. 78−27485
SnSe-Tl_2Se, phase diagram, DTA and X-ray diffr. peritectic decomposition *(French)* 77−51471
SnSe-TlSe, phase diagram 100-900°C *(French)* 79−83180
$SnSe_2$-$GeSe_2$, phase diag., electrophys. props. of solid solns. 77−52306
SnTe, displacive transform., interband electron-phonon interactions, phase diagram 80−93252
SnTe, polymorphism, high press. and temp., X-ray diffr. study 80−54375
SnTe, press.-temp. phase diagram 77−51497
SnTe, solidus line anal., carrier conc. 78−75806
SnTe, structural phase transition threshold instability in strong EM field 80−103477
SnTe-Bi_2Te_3 system, thermal and microstruct. analysis 77−36474
SnTe-Ga_2Te_3 system, peritectic decomp. at 695°C, $SnGa_6Te_{10}$ struct. *(French)* 79−23580
SnTe-In_2Te_3 system, thermoelec. props., phase diagram, transitions 78−43424
SnTe-Tl_2Te, phase and elec. props. 77−48406
Sr-Al-Nd phase diagrams *(Russian)* 78−27480
Sr-Al-Si system, phase diagrams construction by simplex designing method 78−6899
Sr-Nd, microstruct., X-ray, chemical and thermal diffusion anal. *(Russian)* 78−52761
Sr-Y, phase diag. *(Russian)* 77−59745
Sr_2EuFeO_5-SrO-PbO, quasi-ternary system comp. diagram, rel. to Sr_2RFeO_5, Sr_2RAlO_5 cryst. growth 80−20776
SrF_2-(Y,R)F_3, R=rare earth, phase equilibria, X-ray characts. of phases 79−61570
SrF_2-LaF_3, tentative phase diagram 80−71633
$SrFe_{12}O_{19}$, ferrite, powder effect of SiO_2 during sintering, exam. of grain growth and phase diagram *(German)* 79−24473
$Sr_6Fe_{10}O_{22}$-Fe_2O_3-$ZnFe_2O_4$ system, phase relations at 1100°C 78−68676
$Sr_x(Na_{0.5}Bi_{0.5})_{1-x}$ solid solutions, piezoelec. and ferroelec. props. *(French)* 80−108158
SrO-$MMoO_4$, M=Cd,Pb, phase diag. cross sections and reactions 78−27487
SrO-SiO_2-Fe_2O_3, permanent mag. ceramics, exam. of phase diagram, using X-ray analysis, optical microscopy, electron probe anal., and thermal analysis *(German)* 79−29012
$Sr(PO_3)_2$-$AgPO_3$, phase diag., physicochem. characts. of $SrAg(PO_3)_3$ 77−52302
SrS-SnS_2 system, phase diagram *(French)* 79−34013
$SrSi_2$, phase diagram, 10 to 40 kbar, 600 to 1200°C, polymorphic transform. 80−29165
TTF-TCNQ, high press. structural transitions, neutron scatt. study 80−96647
Ta-Al-C, phase diagram and lattice constants, X-ray diffr. method 80−89207
Ta-D system, thermodynamic stability of Ta_2D, rel. to long-range order parameters *(Japanese)* 78−15376
Ta-D system *(Japanese)* 79−78936
Ta-H, phase diagram revision 77−63641

phase diagrams continued
Ta-H system, phase diagram and transforms., struct. obs. of various phases 80−104125
Ta-H system, phase equilibria studies *(Japanese)* 79−78935
Ta-Ir(Rh) system glasses, form., crystn. and microhardness, resist. obs. 80−89178
Ta-O, steady state O_2 solubility *(German)* 80−44322
Ta-Pd system, phase diagram exam. of composition by X-ray diffr., electron microprobe anal., and metallography 78−76632
Ta-Rh, σ-phase alloy, superconductivity and resistance behaviour 80−70882
TaC-TaB_2, phase diag., solubilities, reactions 77−63643
Ta_2D_{1+x}, phase relations in terms of long-range order 79−38808
$TaH_{0.75}$, calorimetric study of phase transform. 77−48426
TaH_x, phase diagram, mag. susceptibility 78−84778
TaH(D), structs. phase diagrams, morphologies, prep. methods, book contrib. 80−25675
$TaH_x(D_x)$, cryst. struct., phase diagrams, order-disorder transition 78−55836
$TaSe_2$(2H), CDW layered cpd., phase diagrams 79−69243
Tb-Dy-Ho, phase diagram, alloy struct. *(Russian)* 77−25016
Tb-Er, Kaufman approach to calc. of intra-rare earth phase diagrams 80−25657
Tb-Ho, Kaufman approach to calc. of intra-rare earth phase diagrams 80−25657
Tb-Sn-Se system, cross section Tb_2Se_3-$SnSe_2$ phase diagram, physicochem. anal. 79−87621
$Tb(NO_3)_3$-$Fe(NO_3)_3$-$(NH_4)_2CO_3$-H_2O system, cpd. form., comp. and props. 80−100832
Tb_2O_3-H_3PO_4-H_2O system, cpd. form., comp. and props. 80−100832
TbP (As)(Sb)(Bi), mag. transitions, quadrupolar interaction effects 80−80512
Te-Bi-Sb ternary system, Laugier's method 77−27980
Te-In alloys, direct reaction calorimetric study, 737 to 1340K *(French)* 80−49382
Te-Tl, liquid alloy, thermodynamic investigation, enthalpy of form. and phase diagram 77−59756
Te-Tl, thermodynamic investigation, equilibrium diagram calc. 79−34007
Te-Tl liq. systems, thermodiffusion of Tl 77−11717
TeO_2-CoO, phase diag. from thermographic analysis 78−23687
TeO_2-Cr_2O_3 system, phase diagram and vitrification 79−83182
TeO_2-GeO_2 system, X-ray phase analysis, DTA and electron microscopy 77−15545
TeO_2-NiO system, phase diagram and vitrification 79−83182
TeO_2-P_2O_5 system, glass struct., neutron diffr. study 80−70128
$(Th,U)O_2$ fuel conversion to $(Th,U)C_2$ for reprocessing 79−54579
Th-based metal alloy fuels for FBRs, determ. of solidus temperature 80−104124
Th-Mo(Re), high temp. phase diagram, thermodynamic props. of refractory metal solutes in liquid Th 77−25022
Th-Os(Ir) system, phase diagram and thermodynamic props. *(German)* 79−47958
Th-Zr(Nb)(Ru)(Rh)-C, phase diagrams *(German)* 77−48413
ThN-rare earth nitride mixed system, quasibinary existence *(German)* 80−91221
$Th(NO_3)_4$-K_2HPO_3-H_2O, mixed phosphites formation and characterisation 77−52304
$Th_{0.25}NbO_3$-x$NaNbO_3$ solid soln., cryst. struct., perovskite-type phases, X-ray diffr. obs. *(French)* 79−1413
ThO_{2-x} phase, high temp. vaporisation behaviour 79−54508
Ti alloys, metallurgical characterisation using thermoelec. power meas. *(French)* 80−45462
Ti-Ag(Au)(Si), thermodynamics and kinetics of β to α_m transformation 78−84795
Ti-Al, phase diagram in Ti rich region *(Russian)* 77−25013
Ti-Al (30 to 57 wt.%), phase equilibria from mag. susceptibility studies 79−60483
Ti-Al-C, ternary system, phase relationships 80−76230
Ti-Al-V-Cr-Zr-Mo (3, 8, 6, 4, wt.%), phase transforms. 79−100113
Ti-Al-(Mo), phase relations 80−108398
Ti-B-C system, complex carbide phase synthesis by crystallisation from gas phase 77−16526
Ti-B-W(Mo), annealed at 1400°C, exam. of phase diagram, using X-ray phase and metallographic analysis 79−1847
Ti-Be, coupled phase diagrams and thermochemical descriptions 80−25656
Ti-Be, metallic glass form. and props. 80−16219
Ti-Be-Zr, coupled phase diagrams and thermochemical descriptions 80−25656
Ti-Co, radiation disorder model of phase stability 80−16297
Ti-Co(Ni) alloys, absorpt. of H_2, press.-composition-temp. relationships, enthalpy, entropy 80−2267
Ti-Cu-Si alloy system, transforms. in Ti-Ti_3Si_3-TiCu region, 800-1600°C *(Russian)* 77−21099
α-Ti-Fe, solubility, resistivity variation rel. to quenching temp. 79−99324
Ti-Fe-Al(Mn), homogeneity and lattice parameters, Mn and Al effect on hydriding cmpd. FeTi 80−108400
Ti-Fe-H(D) system, struct. phase diagram, thermodynamics and diffusion *(German)* 79−56963
Ti-H, H diffusion and phase consistution, V influence, proton spin-lattice relax. meas. 78−27484
Ti-Hf-O system, ω(0) phase form. 79−11553
Ti-Ir system, high temp. thermodynamic investig. of Ir-rich portion by Knudsen cell mass spectrometry 77−12595
Ti-Mo, phase diagram investigation *(Japanese)* 77−63632
Ti-Mo binary system, solid state phase transform. and miscibility gap, phase diagram 79−8298
Ti-Mo-Zr-Al (15,5,3 wt.%), phase transform. kinetics study by X-ray diffr. 79−56960
Ti-Mo(V), metastable diffusionless equilibria, high press. conditions 80−71627
Ti-Ni, eutectoid decomposition, effect of interphase boundary struct. on mech. 79−4952
Ti-Ni, multiplicity of structural transitions, phase diagrams, elec. cond. meas. 80−71649
Ti-Ni-Co, constitution diagram, isothermal section, interdiffusion coeffs. *(Russian)* 80−89200
Ti-Ni-Cu system, phase relations at 800 and 870°C 78−27481
Ti-Ni-Fe, multiplicity of structural transitions, phase diagrams, elec. cond. meas. 80−71649

phase diagrams continued
Ti-O system, intermediate oxide thermodynamics under equilibrium press. 80−55351
Ti-Ru, phase stability under irradiation, review 79−77722
Ti-Ru, radiation disorder model of phase stability 80−16297
Ti-S, pressure-temp.-comp. phase diagram, TiS_2 growth by chem. vapour transport 77−59764
Ti-Si-C system, complex carbide phase synthesis by crystallisation from gas phase 77−16526
Ti-TiC-TiN system, phases 80−20905
Ti-TiN phase system, diffusion of N_2 77−39699
Ti-V-Mo alloy system, phase equilibria and interstitial effects, TEM and X-ray diffr. study 79−43204
Ti-V-Ru alloy system, metastable phases form. *(Russian)* 77−21098
α-Ti-V(Al)(Sn), Mossbauer spectra, metastable θ- and ω-phases 80−20556
Ti-Zr-W-(Al) alloys, phase struct. and props. *(Russian)* 80−16270
TiC-TiN, physicochem. props., comp. depend. 80−55370
TiC-ZrC, pseudobinary systems, phase diagrams, computer calcs. 78−44092
TiC-Zr(Hf)C, calcs. 77−90329
TiCu-H, construction from absorption isotherms and X-ray data *(Japanese)* 78−23668
TiN_xO_y, phase and structural features 77−48411
TiO_2-Al_2O_3-SiO_2 system, ternary glass-forming region and phys. props. 80−84919
TiO_2-Ga_2O_3 system, phase relations and microstructs. 78−3107
TiO_2-Nb_2O_5 sputtered thin layer structure and optical props. 79−28851
TiO_2-NiO-Sb_2O_3 phase equilibria 78−44098
TiO_2-ZrO_2 sputtered thin layer structure and optical props. 79−28851
TiO_{2-x} reduced, crystallographic shear planes, dislocation struct. 80−107175
$Ti_{1-y}V_yH_x$, electronic props., H alloying effects, book contrib. 79−82522
$(Ti_{1-x}V_x)_4O_7$, elec. cond. and phase diagram near metal-insulator transition 80−11054
$(Tl,NH_4)_2Cd_2(SO_4)_3$, langbeinite type mixed cryst., ferroelec. transitions, dielec. and elastic meas. 78−2810
Tl, phase diagram and high press. phase transforms., DTA study *(Russian)* 80−66474
Tl-B-Se system, vitrification region, primary crystallisation fields 77−15321
Tl-Bi-Hg alloys, phase diagrams and equilib. *(Russian)* 79−52166
Tl-Pb-S system, phase diagram quasibinary Tl_2S-PbS section obs. 80−55372
Tl-Pb-Se system, quasibinary sections 77−86000
Tl-Se phase diagram, 73-100 at.% Se 79−96018
Tl-Sn-Te system equilibria, polythermal and isothermal cross sections obs., ternary cpd. form. 80−104128
$(TlBiS_2)_{1-x}$-$(2PbS)_x$ system 77−36471
Tl_2CO_3, high-pressure phase transforms, phase diagram to 80 kbar 77−15576
TlCl-Tl_2S system, molten, thermodynamic analysis 79−29031
$TlGaS_2$-$TlGaSe_2$, phase and composition-property diagrams 80−55366
TlI-CuI system, phase diagrams, DTA, X-ray diffr. investigs. *(French)* 77−84710
$TlInS_2$-$TlInSe_2$, phase and composition-property diagrams 80−55366
Tl_2O-GeO_2 system, structure of thallium I germanates *(French)* 80−79754
Tl_2O-TeO_2, phase diag. 77−81252
Tl_2S-Tl_2Se(Tl_2Te), exam. of phase equilibria, using DTA, X-ray phase analysis and microhardness 79−4953
$(Tl_2S)_{3x}$-$(Sb_2S_3)_{1-x}$, phase equilibria and struct. of cpds. 77−85996
$(Tl_2Se)_{3x}$-$(Sb_2Se_3)_{1-x}$ system 77−16558
Tl_2Se-SnSe(PbSe) systems, phase equilib. 79−52181
Tl_2Te-HgTe(HgSe) systems, phase diagrams 79−87620
Tl_2Te-Sb_2Te cross section of Tl-Sb-Te system, new $TlSbTe_2$ and Tl_9SbTe_6 cpds. 78−52778
Tl_5Te_3-Tl_4SnTe_3-Tl_4PbTe_3, phase equilib., DTA, SPA and microhardness meas. 80−96628
Tl_3VS_4, growth of inclusion free crystals, for surface wave and bulk wave acoustic devices 80−25549
Tm-Ga, exam. of phase diagram, using differential thermal and X-ray phase anal. *(Russian)* 79−11555
TmSe and its mixed crysts., valence instabilities, phase diagram 80−70651
TmSe, nonstoichiometry, high temp. chem. and valence instability *(German)* 79−23743
$TmSe_{1-x}Te_x$, semicond. with valence instabilities, cryst. chem. considerations 80−100213
$TmSe_{1-x}Te_x$, phase relationships and press. induced transitions 80−19771
$Tm_2Si_2O_7$, polymorphism under press., cryst. struct. 77−35692
U, liq., O_2 solubility and comp. of lower phase boundary of UO_2 at 1950K 80−49366
U-Ba-C FBR nuclear fuels, phase anal., 1400°C 80−66487
U-C system p-T diagram, 1000-2600°C, 0-10^{-16} atm. 77−73265
U-Ce-C system, phase equilibrium exam. *(German)* 78−23670
U-Co(Ce)(Fe)(Mn)(Ni)(V) metallic glasses, glass form. and thermal stability 80−75183
U-Fe(Ni)(Co)-B, isothermal section of phase diagram, X-ray obs. 79−52157
U-H system, thermodynamic parameters 77−21124
U-Hg system, phase relations determ. 79−91624
U-Mo(Re), high temp. phase diagram, thermodynamic props. of refractory metal solutes in liquid U 77−25022
U-Nb-C system, phase equilibrium exam. *(German)* 78−23670
U-Nb-Zr (16.6, 5.6 wt.%), stability of BCC phase 79−66039
U-Pr-C FBR nuclear fuels, phase anal., 1400°C 80−66486
U-Pu-C system, segregation and v.p. obs. 77−28793
U-Pu-C-N system, phase relationships and equil., effects of oxygen, review 77−21126
U-Pu-O system, substoichiometric phase range obs., high temp. thermodynamic parameters 77−21125
U-Re-C and U-Tc-C systems, phase relationships 77−21127
U-Sr-C FBR nuclear fuels, phase anal., 1400°C 80−66487
U-Y-C FBR nuclear fuels, phase anal., 1400°C 80−66485
U-Zr-O system, phase formation, phase equilibrium 80−16667
UC, miscibility with rare earth nitrides *(German)* 80−96654
UC-UN, in equilibrium with UC_2 and/or C, relationship between N_2 pressure and composition, phase relationships 79−43223
$UC_{1-x}N_x$-U-N_2, phase diagram 80−84918

phase diagrams continued
UO_{2+x}-ThO_2-MgO system, in air, phase rel., X-ray diffr., electron probe and metallography anal. 79−74137
V-Al-C, ternary system, phase relationships 80−76230
V-C system, ordering and phase equilibrium processes 79−99311
V-C-O, phase relations 79−96012
V-C(N) system, mutual phase orientation, X-ray diffr. exam. *(Russian)* 77−62498
V-D, exam. of phase diagram, using DTA and calorimetry, isotope effect 78−80527
V-D system *(Japanese)* 79−78936
V-Ga-Cu, phase diagram *(Russian)* 77,−25014
V-Ga-Sc, metallographic and X-ray meas., solubility boundaries *(Russian)* 78−56618
V-H, phase diagram, resistometric contribution 78−15372
V-H system, DTA, phase diagrams, low temp. phase 78−6903
V-H system, phase equilibria studies *(Japanese)* 79−78935
V-H(D), metallographic and thermal differential anal., potential for H energy storage appls. 80−45281
V-H(D), struct. studies, DTA and TEM 80−66491
V-HfV_2-$HfCr_2$-Cr, phase diagram *(Russian)* 77−52288
V-N system, ordering and phase equilibrium processes 79−99311
V-N system, X-ray determ. of phase equilibria *(Russian)* 77−55952
V-Ni-Mo alloy, annealed at 1150°C, isothermal section *(Russian)* 79−52154
V-Os system, equilib. phase fields, X-ray diffr., elec. resist., DTA, and EPMA meas. 79−47661
V-Rh alloy system, intermediate phases 77−44216
V-S system, order-disorder transition of metal vacancies, statistical thermodynamics 78−43012
V-S system, quenched, order-disorder transition of metal vacancies, DTA and X-ray analysis 78−30576
V-Se system, quenched, order-disorder transition of metal vacancies, DTA and X-ray analysis 78−30576
V-W-O system, phase diagram and thermodynamic props. at high temps., in region W-WO_2-VO_2-V_2O_3 80−104133
$V_{0.985}Al_{0.015}O_2$, insulating T-phase cation disproportionation and V-V pairing 77−62825
$V_{1-x}Al_xO_2$, phase diag. 77−52308
$V_{1-x}Al_xO_{2\pm y}$, mag. and struct. props. meas. 78−2658
VC base alloys, ordering processes *(Russian)* 77−36462
VC-Nb(Ta)C, calcs. 77−90329
$V_{3-x}Cr_xSi$, $x=0$ to 3, struct., supercond. and mag. props. 80−1962
$V_{1-x}Fe_xO_{2-x}F_x$, $0<x<0.2$, phase diagrams, ^{57}Fe-Mossbauer spectra, X-ray diffr. studies *(German)* 80−29663
VH_x, positron annihil. lineshape Doppler broadening, H conc. and temp. depend., 20-500K 79−61463
VH(D), structs. phase diagrams, morphologies, prep. methods, book contrib. 80−25675
VN_{1-x}, vacancy ordered structure in cubic mononitride phase, transition entropy determ. 78−43011
VO_2-$CrNbO_4$, solid solns., synthesis and phase diagram 80−35171
VO_2-$VO_{2.5}$-H_2O system, hydrothermal exam. *(French)* 77−52244
V_2O_5-Cr_2O_3, phase diagram 77−70040
V_2O_5-CsV_2O_5 system, phase comp. and phase diagram for conditions of inert atmosphere 77−25030
V_2O_5-P_2O_5-MO system glasses, (M=Ba,Ca,Cu and Mg), phase separation, crystn. and EPR spectra 77−76321
V_2O_5-V_2O_4-$BaZnO_2$ glass, V ion states, mag. and elec. props. 80−88556
V_3O_5, metal-semicond. transition, pressure-temp. phase diagrams anal. 79−87132
V_nO_{2n-1}, V_6O_{13}, V_2O_5, Magneli phases, chem. transport using $TeCl_4$ *(German)* 78−31343
$VaH_x(D_x)$, cryst. struct., phase diagrams, order-disorder transition 78−55836
Ve-Fe-Ga system, phase obs. at 800 and 820°C *(Russian)* 78−23662
W-Ge-B, phase diag. 77−52285
W-Hf-C, phase equilib. 80−55348
W-Nb (0-30 at.%), average thermal expansion coeff., 500-1200K 78−14483
W-Ni-Cr, high-temp. phase diag. *(French)* 77−48393
W-Ni-Fe(Co)(Cr), structural characterisation *(French)* 77−56074
W-Sn-S system, phase relationships, 500-800°C 79−24503
WO_3 in binary oxide systems, exam. of phase relations 79−8290
Xe, adsorbed on graphite, finite size effect and temp. depend., multicritical phase diagrams 79−42372
Xe adsorbed on graphite (0001) surface, monolayer liquid and solid struct. 80−65400
Y-Fe-O, phase equilib. and thermodynamics, solid state high temp. electrochem. obs. 79−56967
Y-Fe-Si alloy, phase diagram 79−52158
Y-Ge-B, X-ray investigation of phase equilibrium 79−99294
Y-Ni-Al ternary system, 800°C isothermal section in range 0 to 33.3 at.% Y *(Russian)* 77−70028
Y-Ni-B, X-ray and microstruct. anal., phase composition 77−16539
Y-Re-B, annealed, and quenched X-ray structural and phase anal. 78−11207
Y-Re-Si system, phase diagram at 800°C 79−38806
$Y_{3-x}Bi_xFe_{5-y}Ga_yO_{12}$-$PbO$-$B_2O_3$-$Bi_2O_3$ system, crystn. fields 78−43996
$Y_{3-x}Gd_xFe_5O_{12}$, mag. phase diagrams, mag. transitions, exchange interaction *(Russian)* 80−54896
$(YGdYbBi)_3(FeAl)_5O_{12}$ epitaxial garnet film, uniaxial ferromagnet domain struct., phase transition *(Russian)* 80−108044
Y_2O_3-Fe_2O_3-Ga_2O_3-PbO-P_2O_5, primary crystallisation regions 77−44222
Y_2O_3-Gd_2O_3-Nd_2O_3 solution *(Russian)* 78−88448
Y_2O_3-Lu_2O_3-Eu_2O_3-CaO-GeO_2-Fe_2O_3-PbO-B_2O_3 system, garnet crystn. fields 78−43995
Y_2O_3-R_2O_3, (R=La,Nd,Sm,Gd and Dy to Yb), cryst. growth by Verneuil method 77−1803
$YOHCO_3$, synthesis of rare earth carbonates under hydrothermal conditions 78−72714
Y_2S_3-Ga_2S_3 system *(French)* 78−3108
Yb-Ga, differential thermal and X-ray analysis *(Russian)* 78−56615
Yb-Ga system, phase diagram, cryst. structs. of phases 79−52169
YbIG, mean field phase diagrams 78−23269
Yb_2O_3-GeO_2-NaOH-H_2O, hydrothermal crystallisation 77−40344
$Yb_2Si_2O_7$, polymorphic transforms. and phase diagram under press. *(French)* 77−15573
$Yb_2Si_2O_7$, polymorphism under press., cryst. struct. 77−35692
Zn-Al, splat quenched and bulk specimens, eutectoid decomposition 77−63628
phase diagrams continued
Zn-Al superalloy, transform. kinetics 79−100114
Zn-Al-Cu-Mg (22, 0.5, 0.01 wt.%), superplastic alloy, strengthening mechanism *(Japanese)* 77−55975
Zn-As system, homogeneity range of $ZnAs_2$ and electrophys. props. 80−60833
Zn-As-Te system, As_2Te_3-ZnTe cross section investig. 77−36473
Zn-Cd-Bi-Sn phase diagram with liquid-liquid immiscibility, computer calc. 77−36463
Zn-Cu-Se system, condensed phase equilibria, 800-1000°C, vapour pressures of Zn, Se_2 77−16553
Zn-Cu-Se system, region of existence of ZnSe phase 77−16554
Zn-Ga liquid soln., thermodynamic props. determ., invariant method appl. 77−59742
Zn-In-Cd, anal. calc. of phase diagram 79−91631
Zn-Sb diffusion couple, ZnSb phase layer growth kinetics, 240-320°C, up to 30 kbar 78−10229
Zn-Sb system, phase diagram, struct. and stability of phases *(German)* 78−60661
Zn-Sb system, phase interactions and phase diagram 79−87607
Zn-Sn-Bi, ternary phase diagrams, interactive computer program 80−71629
Zn-Sn-Hg, diagram of state, melting temp., peritectic and eutectic phases *(Russian)* 80−55350
Zn-Sn-P, phase diag. rel. to $ZnSnP_2$ growth 77−44225
Zn-Ti-Fe-O, spinel solid solns. 77−48409
$ZnAl_2S_4$-$ZnIn_2S_4$, phase relationships, 800 to 1050°C 79−1852
Zn_3As_2-ZnSe(ZnTe) solid solutions, single cryst., phase equilib. and props. 80−16283
$Zn(NO_3)_2.4H_2O$, high press. phase behaviour, dehydration and congruent melting 79−78947
$Zn(NO_3)_2.6H_2O$, high press. phase behaviour, dehydration and congruent melting 79−78947
ZnO-La_2O_3-GeO_2, exam. of glass forming region, properties and crystallisation 78−88454
ZnO-Nb_2O_5 system, Czochralski growth, phase relations and cryst. data 78−9975
ZnO-WO_3, phase rels. and cryst. struct. 80−108410
ZnO.$ZnCl_2.H_2O$ cement, phase equilibrium diagram 77−86013
Zn_3P_2, stoichiometry deviation from phase diagram 80−35164
ZnS-Al_2S_3, phase relationships, 720 to 1110°C 79−1852
ZnS-$CuInS_2$, phase relations, 400 to 1300°C, X-ray and microscopic exam. 79−1853
ZnS-MnS, phase relations, 400 to 1300°C, X-ray and microscopic exam. 79−1853
ZnS-MnS-$CuInS_2$, sobsolidus equilib., phase diagrams 80−3016
ZnSe, P-T diagram, cryst. struct. stability 78−51886
$ZnSiP_2$ crystal growth, DTA obs. of Sn-Zn-$ZnSiP_2$ phase diagram 80−24394
ZnTe, TEM obs. of precipitates, shape of Te solidus line 80−25703
ZnTe-CdSe, solid soln. formation and effects 78−27489
ZnTe-Ga_2Te_3, phase diagram 78−35360
Zr-Al-C, phase diagram and lattice constants, X-ray diffr. method 80−89207
Zr-Be, coupled phase diagrams and thermochemical descriptions 80−25656
Zr-Be, metallic glass form. and props. 80−16219
Zr-C, exam. of metastable phase diagrams, at high temp. and pressure *(Russian)* 79−56955
Zr-Cr-Cu, phase diagram in Zr corner *(Russian)* 78−19721
Zr-H, auto-radiographic and metallographic study of γ-phase *(Russian)* 78−56616
Zr-H_2, exam. of phase diagram, using modified format 79−8280
Zr-M-B systems (M=Rh,Ir), phase equilib. and cryst. structs. 80−15072
Zr-M-H (M=V, Cr, Mn, Fe, Co, Ni), synthesis at high pressure, props 80−29924
Zr-Mo, high temp. phase diagrams 77−44217
Zr-Nb, phase transformation sequences, prediction using free energy composition diagrams 79−4951
Zr-Nb (2.5 wt.%), cold-worked, pressure tubing, metallography and mech. props. 80−89269
Zr-Ni (65 to 80 at.%), phase diagram and cryst. struct. of intermediate phases 79−52170
Zr-O, high temp. phase diagram 78−11211
Zr-W-Cr, Zr-rich corner of phase diag. *(Russian)* 78−80517
ZrC-HfC, pseudobinary systems, phase diagrams, computer calcs. 78−44092
$ZrCl_4$-CsCl melt, equilib. phase diagram and vapour press., equilib. reaction 77−66764
$Zr_3Co_{1-x}M_x$, M=Cu, Ni, Fe, Mn, Ag, and Ru, phase stability and supercond. T_c 78−80519
ZrF_4-BaF_2-MF_n (M=Na, Ca, Ln, Th, n=1, 2, 3, 4), vitreous phases, network formers, modifiers and stabilisers *(French)* 80−64909
ZrO_2, polymorphism rel. to stabilisation *(Rumanian)* 78−59946
ZrO_2-CaO, phase equilibria and ordering 78−27498
ZrO_2-CaO:Mn^{2+}, EPR spectra, impurity substitution behaviour in various phases 77−16160
ZrO_2-Cr_2O_3 system, react., phase diagram 1600-2400°C 79−11580
ZrO_2-$GdO_{1.5}$ (80 mol.%), X-ray diffr. exam. of continuous transition 78−68684
ZrO_2-SiO_2, liquid immiscibility, microstruct. of plasma dissociated $ZrSiO_4$ 80−107429
ZrO_2-ThO_2, high temp. study of phase diagram using X-ray and thermal anal. *(French)* 79−70049
ZrO_2-TiO_2 refractories, TiO_2 effect on props. and phase composition 79−38809
ZrO_{2-x}, high temp. phase diagram, exam. of lower phase boundary 78−76638
ZrO_{2-x}(cubic)-ZrO_{2-x}(cubic+tetragonal), phase boundary 80−81038
Zr_xWO_3, perovskite-type, stability in ZO_2-WO_2-WO_3 phase diagram 77−15582

phase equilibrium
see also phase diagrams; phase transformations; solutions
α-γ interface, struct., thickness, intermediate phase effects 78−71831
A15 superconductors, high press.-high temp. treatment, phase props. 77−28746
acetic acid, PVT props., 448.15-603.15K, press. up to 10 MPa 78−14455
acetone-benzene(cyclohexane), vap.-liq. equilibria 78−30745

phase equilibrium continued
acetone-chloroform-methanol system, multicomponent vapour-liquid equilibrium, direct integration of Gibbs-Duhem eqn. 79−23714
actinide alloys, metastable phases production by splat cooling 77−21134
activities on boundaries of two-phase region in ternary systems 79−34349
alcohol-solvent, associated, excess free energy and enthalpy of mixing 78−31680
alcohol-unassociated active component liquid mixtures, associated soln. theory, thermodynamic parameters 80−7836
alcohols, vapour-liq. equilib. and heats of mixing, simplified group method anal. 80−96637
alcohols in organic solvents, H_2O absorption 80−66788
alkali borate glasses, phase separation 79−41965
alkali metals, liq., soln. chemistry as elucidated from elec. resist. studies 77−52636
alkali nitrates, molten, pVT data, internal energies, eqn. of state 78−43098
alkali nitrates, molten, pVT data, thermal press. coeffs., compressibilities 78−43097
alkanes, ethane-, hexane-polar component binary mixtures, up to 1000 bar, phase separation, critical phenomena 77−35695
alkanes, vapour-liq. equilib. and heats of mixing, simplified group method anal. 80−96637
alkenes, ethene-, 1-hexene-polar component binary mixtures up to 1000 bar, phase separation, critical phenomena 77−35695
alloy, binary, atomic misfit effect on coexistence and spinodal transform. boundary 78−60644
alloy, binary, short range order calc. using equilib. diagram *(Russian)* 79−87610
alloy, binary, stability against conc. fluctuations, pair interaction energy 77−47323
alloy, binary, theory for initial stage of grain growth and unmixing kinetics 78−19714
alloy, coarsening by temp. cycling 79−29111
alloy, Fermi surface and phase stability 77−77459
alloy, splat-quenched, grain size, isothermal transform. 77−77463
alloy phase stability, computer calc. using modified pair potentials 78−35352
alloys, ion-implanted, annealing behaviour and appls. 79−14829
alloys systems, ternary, phase equilibria calc., line compounds 80−10638
aluminosilicate glass, phase separated, phase characterization by STEM and X-ray microanal. 80−50643
aluminosilicate refractories, X-ray struct. determ. of quantitative phase contents 77−52707
anthracene and dianthracene, phase equilib. in photocondensation *(Russian)* 79−7561
azeotropic and two terminal solid solution type binary diagrams, synthesis 80−19901
basalts, terrestrial, lunar and planetary, redox state 78−77217
benzene, free convection heat transfer in tube at supercrit. press. 78−42518
benzene-carbon tetrachloride-cyclohexane system at atmospheric pressure, isobaric-liquid equilib. data 79−46793
benzene-cyclohexane, vap.-liq. equilibria 78−30745
benzene-polybutadiene-cyclohexane system, vapour-liq. equilibria 79−95147
benzol-paraffin, solid-liq. mixtures, phase equilib., Wilson eqn. *(German)* 79−42245
binary alloys, and intermetallic cpds., struct. and stability, ab initio pseudopot. calcs. 78−34460
binary alloys, computer experiments on phase separation 79−43198
binary alloys, region of metastability in normal growth 79−87613
binary heterogeneous vapour-liquid equilibrium, student experiment demonstrating miscibility effects 77−82352
binary liquid mixtures nonidealities, optimal representation 79−42248
binary liquid mixtures trapped in thin pores, binary crit. points *(French)* 77−59117
binary liquid-vapour equilib. data, numerical anal. 78−26675
binary mixture, boiling, liq.-vapour equilib. data, circulation apparatus determ. *(German)* 77−24375
binary mixtures, vapour-liquid critical volume estimation 77−39662
binary phase equilibria, computer program based on Redlich-Kister eqns. 79−10913
binary system, effect of mutual solubility of auxiliary solvent on liq.-liq. equilib. for activity coeff. 77−63945
binary systems, diffusion coeffs., stochastic theory of nonideal behaviour 80−44346
binary vapour-liq. equilib. and heat of mixing data, ternary heat of mixing prediction 79−73312
binary vapour-liquid equilibrium data, determ. and correlation 78−87781
binary vapour-liquid equilibrium experiments, design of experiments 78−14440
binary vapour-liquid equilibrium experiments, parameter estimation and consistency tests 78−14439
block copolymers, microphase separation, thermodynamic treatment *(Chinese)* 80−79947
borosilicate glass, phase separation effect on HF etch rate 78−11208
brass, α and β phases, Hume-Rothery rules for phase stability 79−99292
brass, γ-phase region, X-ray and electron diffr. obs. 79−61562
n-butanol-1,1,2,2-tetrachloroethane, isobaric vapour-liquid equilibria at atmospheric pressure 79−51246
n-butylamine-n-propanol, isothermal vapour-liquid equilib. 80−59639
cell design for use below 300K and to 9 MPa pres. 80−62821
ceramic technology, DTA appl. 80−20913
ceramics, engineering materials, nature and props., book 78−72707
ceramics, high temp. structural, use of equilibria in development 79−11595
charnockite series, form. temp. and press., evidence for geothermal gradients 78−40553
chemically irreversible systems, liquid-vapour equilibrium *(Russian)* 78−3369
chloroalkanes, vapour-liq. equilib. and heats of mixing, simplified group method anal. 80−96637
chloroform-chlorobenzene, isobaric vap.-liq. equilib. 79−73299
chrome-forsterite-periclase refractory constitution and props., phase reactions during firing *(German)* 78−11175
composite, three phase including void phase, phase relationship 77−25036
condensed systems, phase equilibria, 400-1100°C, DTA method 80−218
phase equilibrium continued
cordierite glass ceramics, effect of TiO_2 and ZrO_2 content on phase sequence during heat treatment 78−48381
critical fluctuation pattern, effect of large-scale inhomogeneities, 2nd kind transform. *(Russian)* 78−18741
critical isomorphic $\gamma \rightleftarrows \alpha$ transition, phase equilibrium curve *(Russian)* 80−55397
crystal growth, macroscopic equilib. and transport concepts, book 80−27054
decahydronaphthalene-H_2O, liq.-liq. phase equilib., crit. phenomena 78−18764
diamond, synthesis from graphite, nucleation rate 79−16032
diamond-graphite equilib. line, from synthesis and graphitisation of diamond 78−24811
dilute alloy, equilibrium distrib. coeff. relationship *(Russian)* 79−83186
dilutor method extension to meas. of high activity coeffs. at infinite dilution 79−19372
dimethylsulphoxide-water-0.9 m $NaClO_4$, salt effect on vap.-liq. equilib. 79−51245
1,4-dioxane-1,1,2,2-tetrachloroethane, isobaric vapour-liquid equilibria at atmospheric pressure 79−51246
double exchange reaction, representation of phase equilibria 79−66266
dynamic isomers and spontaneous generation of optical activity, phase rule prediction 79−34421
dynamical equations for system with interface 78−38914
elastic mixtures, stability criteria 78−18514
elastic plastic body, model, and analogy with liquid vapour phase equilib. 77−84155
electrolyte, weak volatile, multicomponent aqueous solns., vapour liquid equilibria 79−51243
electrolytes, binary solns., nonideality, thermodynamics 79−39155
electrolytic ion distribution near phase boundary *(German)* 78−56901
equation of state, perturbed-hard-sphere, applicable to sub- and supercritical temps. 79−19350
equations of state calculation methods *(German)* 78−34588
ethane, coexistence curve diameter singularity, phase boundary position *(Russian)* 79−65179
ethane, liq.-vap. coexistence curve, interferometric meas. 79−99303
ethane+CO_2 system, isothermal vapour-liq. equilibrium data, 10 to 25°C and high press., critical points 78−79754
ethane+N_2, system, vapour-liq. equilib. data 78−83929
ethane-hydrocarbon mixture, phase equilibria and critical phenomena at high press. 78−51648
ethane-n-butane-n-hexane, vap.-liq. equilib. behaviour, visual cell, for 48.3-143.5°C, up to 7619 kPa 79−46790
ethene+N_2 system, vapour-liq. equilib. data 78−83929
ethene-hydrocarbon mixture, phase equilibria and critical phenomena at high press. 78−51648
ethylene glycol-H_2O-lauryl alcohol-nitromethane-nitroethane, liq., multicrit. pts., 37-42°C 79−86868
eutectic binary system, eutectic conc. calc., graphic representation of equations *(Russian)* 77−66622
FBR fuel cladding alloys, phase instabilities and swelling behaviour 79−54500
feldspar electrotechnical porcelain, phase composition calc. 77−21111
ferrite, phase composition in magnetic field, use of DTA-TG-DTG *(Polish)* 78−31393
ferrite systems, thermodynamic stability, dissociation and phase relations *(Japanese)* 80−55378
ferritic weld metal, austenitising and ferritising effects of elements 79−87614
ferromagnetic minerals in basalts, stability region 78−16000
fluid binary mixtures at high press., phase equilibria, critical phenomena calcs. 77−35664
fluid phase equilibrium data, qualities of models for evaluation, representation and prediction 79−14921
fluid-liquid interface, approach of close-packed arrays of drops and spheres 78−84030
fluid-solid coexistence curve of dense coulombic matter 79−97330
fluids with polar, quadrupolar, octupolar mols., thermodynamics, vapour-liq. equilibria 78−95127
fluoride-oxide-SiO_2 system, containing Mg^{2+}, Ca^{2+}, Ba^{2+}, Pb^{2+}, cryoscopy 77−28798
fluoride-oxide-SiO_2 system, containing Na^+, K^+, Li^+, cryoscopy 77−28797
fluorocarbon-water mixture, phase equilibria and critical phenomena at high press. 78−51648
free energy for phase interface, solar-prod. expression, Ising model and cluster approx. 78−34591
Freon, F-13V1 and F-23, thermal cond., −168 to 160°C, up to 6.10^7 Pa 77−47628
garnet lherzolite, high-press. phase equilibria and Mg^{2+}-Fe^{2+} partitioning among constituent minerals 79−66687
gas-gas equilibrium, thermodynamics at high press. 78−18734
gas-liquid surface, penetrable sphere model 78−10261
gas-liquid surface of penetrable sphere model, surface energy and tension 77−4249
gas-liquid system, phase equilib. determ. by gas chromatographic headspace anal. *(German)* 78−18753
gas-mineral equilibria and Earth interior chemical model 77−9411
gas-solid system, phase equilib. determ. by gas chromatographic headspace anal. *(German)* 78−18753
gaseous mixtures at high pressure 77−35291
Gibbs-Duhem eqn. for binary system, direct soln. 77−79041
glass, engineering materials, nature and props., book 78−72707
glass, internal parameters, ordering parameters, history function, rel. to glass transition 78−30738
glass, liquid-phase separated, struct., use of elec. methods 79−66249
glass, ternary oxide systems, metastable two liquid tie line calc. 78−92246
glass, two-phase, struct. and texture, electron microscope 79−64999
glass phase separating, interpretation of temp. dependence of transport process 78−87806
glass workability rel. to melting history, microstruct., apparent liquidus temp., mechanical props. 80−11633
glasses, liq.-phase separated, phase comp., temp. depend. 80−16289
glasses, multicomponent, liquid phase separation, thermodynamics 79−95173
graphite-diamond equilibrium, thermodynamic stability 79−65184
growing phase diffusivity determ. 80−24641

phase equilibrium continued
hard rod system, improved lattice model, nematic and isotropic phases 80−33882
hard-sphere equation of state, vap.-liq. equilib. 77−4181
heat of evaporation and liq.-vapour equilib., appl. to real substances 79−4409
heterogeneous, thermodynamic balance calcs. *(Russian)* 77−59093
high alloys, superalloys *(Chinese)* 78−95728
high pressure phase equilibria and other fluid-phase properties, computational methods 80−75329
high pressure vapour-liquid equilibrium, phenomenological description 78−91415
high pressure vapour-liquid equilibrium, quantitative description 79−1486
high-pressure asymmetric mixture vapour-liquid equilibrium calc. 79−4408
high-pressure phase equilibria in mixtures using partition functions, computational methods 80−75330
Hume-Rothery Phases, electronic struct., main features 79−23883
hydrocarbon+$CO_2(H_2S)$ mixtures, vapour-liq. equilibrium, crit. locus curve, Soave eqn. 78−83913
hydrocarbon-$CO_2(H_2S)(N_2)(CO)$ mixtures, phase equilib. calcs., modified Soave eqn. of state 79−19353
hydrocarbon-CO_2 mixture, phase equilibria and critical phenomena at high press. 78−51648
hydrocarbons, phase equilib. calcs., modified Soave eqn. of state 79−19352
I_2-IV-VI_3 cpds., tetrahedral phase stability 77−48415
II-IV-V_2 semiconductors, equilib. between vapour phase and stoichiometric melt 77−11681
III-V pseudobinary compound, growth and phase equilib. in vertical rotating LPE reactor *(French)* 77−77430
III-VI compound layered materials, prep. and growth, book contrib. 78−19661
ilmenite ore, liquid, behaviour above 1500°C, X-ray obs. *(French)* 79−70100
immiscible liquids, separation kinetics in low gravity environment, computer simulation study 78−34629
inhomogeneous fluid in rigid container, equilib. states stability 80−44392
inorganic emulsions, hydrophile lipophile balance temperature 78−95961
inter-transition metal phase constitution 78−39749
interface structure, in gravit. field, renormalisation calc. in three-dimens. 78−83911
interfacial profile, ϵ-expansion 78−51641
interfacial stability theory, moving symmetric model 78−2230
interfacial stability theory, stationary symmetric model 78−2229
intertransition metal phases, incidence and Fajan's rule 79−29026
Ising model, BCC, spin phase boundaries, struct. and excess free energy 77−59097
isobutyric acid-water binary fluid system, crit. props. 77−76563
isothermal vapour-liquid equilibria, excess Gibbs free energy, general calc. method 77−89552
Kh20N40 alloys, phase composition after quenching, tempering 78−60650
lecithin+cholesterol interaction, equilib., stoichiometry of complexes in bulk systems 78−68985
lecithin+cholesterol interaction, equilib., surface film phase relations and cholesterol condensing effect 78−68986
Lennard-Jones system, molecular dynamics simulation of interfacial and co-existence props. at triple point 78−83916
liquid, superheated, thermal cond. meas. technique using shock heating 77−45834
liquid alloy, dil., partial interfeęence functions of solutes 79−19139
liquid crystal mixture phase equilibria and transition temperatures 78−63845
liquid metals and alloys, book 78−51406
liquid mixture, excess Gibbs free energy, quasilattice local composition model, phase equilib. 78−31681
liquid mixtures, intermol. forces effect on phase diagram and excess props., perturbation theory 80−39287
liquid mixtures, phase separation, umbrella sampling, Monte Carlo calcs. 77−35698
liquid mixtures, showing phase splitting, modified Wilson eqn., phase equilib. prediction 80−96636
liquid phases, non-uniqueness in phase, chem. react. equilib. computations 79−43612
liquid solutions, activity coeffs. at infinite dilution, Wilson and UNIQUAC eqns. correl. 78−64875
liquid state, binary phase equilib. diagrams 79−60473
liquid systems, pure component Gibbs energy using structural group contribution method 79−90797
liquid-gas, hypothesis about integrand of free volume *(Spanish)* 79−90767
liquid-high pressure vapour equilibrium, quantitative description 78−79736
liquid-liquid equilibrium data, correlation 79−51248
liquid-liquid equilibrium data, prediction 80−54367
liquid-liquid equilibrium theory, data and correlation 79−33081
liquid-liquid phase equilibria, theory, chem. models 78−18781
liquid-liquid-ideal vap., isothermal condition, 3-phase equilib. line special point *(Russian)* 80−54345
liquid-solid, expt. methods of determ., review *(Rumanian)* 79−28078
liquid-solid coexistence line, phase instability and direct correl. function integral eqn. 80−65196
liquid-vapour, derivation and extension of UNIQUAC eqn. 79−14933
liquid-vapour co-existence, dipolar hard sphere fluid, Monte Carlo method 79−99293
liquid-vapour coexistence and correlations in interface 80−65212
liquid-vapour equilib., Andiappan-McLean eqns. at infinite dilution 78−43115
liquid-vapour equilib. of systems with and without salts, Wilson eqn. 78−43114
liquid-vapour equilibrium, azeotropic props. meas., differential tensimetrical titration appl. *(Russian)* 80−54363
liquid-vapour equilibrium, thermodynamic props. using modified Redlich-Kwong eqn. of state 77−36775
liquid-vapour equilibrium, Van der Waals' eqn. of state, heat of evaporation 78−51640
liquid-vapour equilibrium data reduction by maximum likelihood 79−51244
phase equilibrium continued
liquid-vapour equilibrium in system with chem. reaction, thermodynamics *(Russian)* 77−63947
liquid-vapour equilibrium theory, data and correlation 79−33081
liquid-vapour phase equilib., modified Redlich-Kwong eqn. of state 78−83908
liquid-vapour system, microheterophase state, characteristic time and size *(Russian)* 78−18740
liquid/vapour, calc. possibilities *(German)* 79−33067
liquids and solutions, group contribution mol. model, thermodynamic props. 77−58932
liquidus boundary meas. by high shear technique 79−61564
Li_2 ordered alloys, positive temp. depend. of strength, phase destabilization 80−81203
macromolecular multicomponent system, phase separation, thermodynamic perturbation theory, calculus 78−18778
magnetic contributions to phase stability calc. 78−6141
martensitic transformations, thermodynamics and morphology, under influence of external stresses *(Russian)* 78−23701
maximum likelihood test in estimation of exptl. inaccuracies, applic. to equilib. data 77−9867
metal, equation of state, isentropic expansion method 78−91414
metal, first transition systems, survey of regular solution parameters 77−44220
metal, simple, phase stability and elastic const. 78−31387
metal, thermodynamic props. of grain and phase boundaries, review *(German)* 79−34012
metal borides and carbides, thermal stability 79−8286
metal interaction with gases and C, conf., Stuttgart, Germany (Sept 1977) *(Russian)* 79−57134
metal refining by crystallisation and reflux, three component Raoultian behaviour 77−28799
metal-H system, hydride formation in high press. range 80−65235
metal-H system, multiplateau absorpt. isotherms, theory 80−103564
metal-H systems, solvus line interpretation, enthalpy change 79−15655
metal-NH_3 solid solutions, phase comp., dissoc. *(Russian)* 77−35665
metallic solution, α-parameter approach to thermodynamics 77−4207
metallic solution, thermodynamics of solutions, α-parameter approach 77−4208
metals, engineering materials, nature and props., book 78−72707
metals, phase formalism in diffusion layers between solid and liquid metals *(Russian)* 79−69257
metals, small-core approx. and structural phase stability 79−99498
metals and alloys, grain and phase boundary model *(German)* 79−99216
metals and alloys, martensitic transitions accompanied by interactions between phases *(Russian)* 80−7568
metastable phases, in metals, ion implantation review 80−49254
methane-ethane liq. mixture, phase equilib., heat of mixing, vol. change, data evaluation 80−15233
methane-trifluoromethane, liq.-liq. phase equilib., crit. phenomena 78−18764
methanol-chlorobenzene, isobaric vap.-liq. equilib. 79−73299
methanol-cyclohexane film, crit. temp. and coexistence-curve determ., optical meas. 77−7952
methanol-ethanol, vapour-liquid equilibrium, transpiration method meas. 79−99305
2-methoxyethanol-1,1,2,2-tetrachloroethane binary system, isobaric vapour-liquid equilib. data 79−46792
2-methoxyethanol-chlorobenzene binary system, isobaric vapour-liquid equilib. data 79−46792
methylcyclohexane-1,1,2,2 tetrachloroethane binary system, isobaric vapour-liquid equilib. data 79−46792
methylcyclohexane-chlorobenzene binary system, isobaric vapour-liquid equilib. data 79−46792
methylethylketone-butanol-water-isobutadiene quaternary system, isobars of liq.-vapour and liq.-liq. equil. *(German)* 79−33079
MHD, need for phase equilibria data in development 79−11551
microclusters, computer simulation of nucleation and thermodynamics, mol. dynamics and Monte Carlo 78−51656
microdrop-gas phase equilib. in small system, mol. dynamics 78−95146
microemulsion phase equilibria, statistical thermodynamics 79−5183
mixture, strongly nonideal, vap.-liq. equilib. data correlation eqn., heat of mixing 78−30763
mixtures, high-press. vap.-liq. equilib., phenomenological description, review 78−30737
mixtures, phase equilibrium, augmented Van der Waals theory 78−79737
mixtures, vapour-liquid equilibria, mixing rules in equations of state 80−19902
mixtures containing polar substances, corresponding states principle use in crit. states calc. 80−39196
modified Soave equation of state for phase equilib. calcs. systems containing hydrogen 79−95118
molecular models of soln. in phase equilib. prediction, study 79−19351
molecular thermodynamics appl. to phase separation and critical phenomena *(German)* 78−14447
molecular thermodynamics calculations, practical appls. *(German)* 78−18733
molten metallic system, contribution to sign inversion of effective charge *(Czech)* 78−60656
mullite, crystallisation from SiO_2-Al_2O_3 melts 78−47243
multicomponent fluids, method of pseudocomponents 77−59094
multicomponent liquid-liquid equilibria, UNIQUAC eqn. appls. 79−19355
multicomponent mixtures, phase envelopes and crit. points calc. 80−54337
multicomponent mixtures, vapour-liquid equilibria predictions, statistical thermodynamic approach 77−55335
multicomponent multiphase equilibria 79−90750
multicomponent systems, comput. techniques for thermodynamic data treatment and equil. calc. 78−10172
multicomponent systems, intensive parameters, thermodynamic props. depend., stability conditions *(Russian)* 80−65186
multicomponent vapour-liquid equilibria, UNIQUAC eqn. appls. 79−23699
multicomponent vapours-condensed phases, equilib., computer modelling 80−44288
mutual alloying behaviour of the elements straddling the line Li-Mg-Cu-Au in the long periodic table 78−84769

phase equilibrium continued
natural gas mixtures, simulated, enthalpy and phase equil., correl. with modified Starling eqn. 80−61127
nematic-isotropic phase equilibria in binary mixtures containing rigid rod solutes 79−86873
nepheline concentrate, low Fe, phase composition 77−21110
nepheline-kalsilite system, subsolidus phase relations at 0.5, 2.0, and 5.0 kbar 79−66041
nitrobenzene-hexane, soln., dielec. permitt. in two phase region 80−2682
nitromethane-isooctane, liq. mixture, coexistence curve, refr. index meas. 80−10655
non-uniform fluids, statistical mechs., spinodal decomposition and crit. interface 79−68998
nonideal behaviour, stochastic theory, microenvironment, chem. pot. and transport 79−82302
nonideal behaviour, stochastic theory, partially miscible ternary systems 79−82303
nonlinear excitations by numerical determination 79−71372
nonuniform fluid state, Van der Waals theory, thermodynamics, struct. and phase stability 79−77475
nonylphenol diethylene glycol ether-water-p-xylene system, liquid crystal stabilization of multiple emulsions 79−16046
nucleation theory, fundamentals *(Spanish)* 78−43101
octafluorocyclobutane+n-butane mixtures, 233K, surface tension meas., vapour-liq. equilib. data 79−19371
opal glasses, phosphate opacified, phase comp. and struct. 80−64919
optoelectronic method for coloured or turbid mixtures, press. and phase equilib. study 78−70152
ordering, high resolution electron microscopy 79−43290
organic compounds, crit. temps. correl. with boiling pts. 78−91421
organic compounds, vapour liquid critical pressures and volumes 79−99306
organic mixtures, liquid-liquid equilibrium data, retrieval 79−46797
oxide phase equilibria, high temp. appl. 79−8416
oxide system, complex, mass-loss Knudsen effusion method for phase equilib. determ. 77−11668
oxide systems, exam. of techniques used to determine phase diagrams and equilibria, and effects on equilibria 79−8415
pentane-benzene solution, vapour-liquid equilibrium study, vaporisation critical state *(Russian)* 80−79931
periclase-spinel refractories, phase conversions up to 1720°C 80−25670
peridotite-H_2O-CO_2 system, phase relationships, rel. to planetary mantles 78−77506
phase boundaries in first-order phase transitions, dynamics stability 80−107403
phenanthrene-d_{10}, oriented in biphenyl, triplet zero-field splittings, conc. depend. 78−2773
pheophytin containing monolayers, phase separation and domain interaction, surface press. and fluoresc. meas. 79−100580
phthalocyanides, thermal stability, DTA *(German)* 80−11945
physiological support medium+NaCl+cryoprotective agent, equilib. and nonequilib. behaviour 77−16561
plasma arc heating, equilib. in gas-melt system *(Russian)* 79−37512
polyatomic fluid mixtures, thermodynamics, phase equilib. calcs. 79−1485
polyethylene, high density, effects of draw rate and temp. on necking stress *(Japanese)* 79−91757
polyethylene, pressure phase transition, function of pressure and temp. 79−77745
polyethylene, stress rel. to draw ratio during ultra draw *(Japanese)* 79−91759
polyethylene-polystyrene blends, crystn. characts. 80−103261
polymer, low conc., complex coacervation occurrence condition 80−79944
polymer crystal and melt, stat. thermodynamics using Midha-Nanda cryst. state theory 79−41979
polymer films, Brillouin scatt. at transitions 80−70312
polymers, engineering materials, nature and props., book 78−72707
polyphenylene terephthalamide in H_2SO_4-H_2O system, phase equilib. 79−73314
polystyrene-cyclohexane, polymer solns., coexistence curve 79−28101
polystyrene-methylcyclohexane, coexistence curve, comparison obs. and free energy calc. 80−88323
polystyrene-methylcyclohexane, coexistence curves, range of simple scaling and critical exponents 80−88322
polyurethanes based on toluene di-isocyanate, struct.-prop. relns. inc. phase mixing and segreg. 78−80509
powder metallurgy superalloy, wrought, phase relations and microstruct., C and Hf conc. effect 77−44218
propane, vapour-liquid and vapour-solid equilib. data, mass spectroscopic tracer pulse chromatography 80−37115
propane+N_2 system, vapour-liq. equilib. data 78−83929
propene+N_2 system, vapour-liq. equilib. data 78−83929
PVC-polyacrylonitrile blends, compatibility determ. 79−4416
pyroxene geotherms, thermodynamics 78−65282
rare earth alloys, config. entropy and stability of intermetallic hydrides 77−84949
rare earth garnets, prep. and props. book contrib. 80−44193
rare earth oxide containing systems, highly refractive, phase equilib. and metastable phases 80−97467
rare earth oxide-ZrO_2 (HfO_2), cubic solid soln., lattice parameters 79−82186
rare earth oxides, phase transition hysteresis, thermodynamic model 77−76570
rare earth systems, RCo_3-H_2 (R=Ce, Pr, Tb, Dy, Er), phase equilibria, from dissociation isotherms 80−50591
rare earth-Au-In, Fe_2P type phases 77−70033
rare earth-Cd double tungstates, with scheelite structure 78−44103
(rare-earth)$_2O_3$-H_2O, hydrothermal phase equilibria studies 80−104132
reactor structural materials, alloy phase thermochemical stability, calc. of radiation effects 79−60406
refractories, castable, X-ray powder diffr. meas. of phase composition, and flexural strength 80−3449
refractory metal pnictides, phase relations and thermodynamics 79−66042
refractory oxide, high temp. props. conf., Odeillo, France (June/July 1977) 79−100125
refractory oxide-metal eutectic system 77−36483
representation of phase equilibria, exam. 79−7675
rod-like molecules in extensional flow field 78−26158
phase equilibrium continued
salt solutions, in liquid alkali metals, phase equilib. and chemistry 78−73040
saturated vapour volume, eqn. 79−95119
semiconductor, binary, estimation of heats of formation from melting temp. 78−27810
separation, competitive statistical and chem. mixing effects *(German)* 77−52665
separation processes simulation in H_2SO_4-Br cycle 79−74413
Si_3N_4-Ce_2O_3-SiO_2 materials: phase relations and strength 80−97465
sigma phase stability and irrad. effect 78−11200
sigma phase structure, ionicity modified pair pot. model anal. 78−51466
Silumin, CsSi phase form. due to Cs diffusion 79−38798
simple solid family of phase states *(Russian)* 80−15216
slag equilibria Flood-Grjotheim treatment 78−39752
slag-metal equilibria involving P and S, effect of fluorspar and other fluxes 77−48414
slag-metal equilibrium, thermodynamics 78−44108
solid soln. form., regions of existence 79−11581
solid solns., phase equilibria, cryst. optical, X-ray struct. characts. 79−11577
solid-liquid coexistence, mol. dynamics simulation 78−67803
solid-liquid equilibrium, UNIFAC group contrib. method 79−42247
solid-phase cell for 40 kbar, 1500°C operation, pressure and temp. distribs. 80−105669
solute interaction parameters, using linear programming technique 77−72678
solutions with closed loop coexistence curves, directionality depend. of lattice models 78−95158
spinel disproportionation reactions, elasticity and phase equilibria 77−78158
spinel solid solutions, $A_xB_{3-x}O_4$ type, quasichemical method of cluster components, electron exchange allowance 79−51475
spinels, oxo and sulpho, boundary conditions for existence 78−23684
spinodal decomposition dynamics, generalised diffusion eqn., numerical soln. 78−10193
β-spodumene-mica glass ceramics, phase evolution and TiO_2, MgF_2 additive effects, exam. 78−44089
stability limit, equilib. between two phases *(French)* 77−13721
stability properties of equilibrium states, free Bose gas 78−8368
standards for publication of studies 79−10921
standards for single substances and mixtures 78−14481
steam-water two phase mixture, relative vel. of vapour phase, determ. of void fraction 78−5791
steel, Al semikilled, $(Fe_xMn_{1-x})O.Al_2O_3$ inclusions, deoxidation, thermodynamic conditions 80−60830
steel, Al-Cr, $FeO.(Al_xCr_{1-x})_2O_3$ inclusions, thermodynamics 80−60831
steel, austenitic, Cr-Mn-B-N, phase composition and struct. transformations 80−104171
steel, austenitic, phase composition of Kh14N16 with Zr, Ti, Nb and N additions after quenching and tempering 77−90378
steel, austenitic stainless, Cu-Mo substituted 18/8 type, austenitic stability 79−91716
steel, austenitic stainless, ferrite volume fraction, high-speed determ. by XDXRD 78−76628
steel, austenitic stainless, Neel temperature and max. susceptibility calcs. 77−43833
steel, austenito-martensitic, struct. changes during plastic deform., mutual influence of phases *(Russian)* 80−30015
steel, C, alloying addition effect on austenite-cementite boundary *(Czech)* 77−85991
steel, carbonitrided 25KhGT, 25 KhGM, exam. of hardenability and phase composition 78−44272
steel, Cr (1 to 5 wt.%), effect on transform. of Cr content and all round press. of 25 kbar *(German)* 78−11219
steel, high V-W-Mo, high speed, phase composition and struct. of atomized powders 77−90323
steel, interfacial tension in phase boundary with MnO-TiO_2-SiO_2(Al_2O_3) *(Czech)* 78−63907
steel, low C, Cr-Ni (25, 25 wt.%), σ phase form., prestrain effects *(Japanese)* 78−92260
steel, low C, dual phase, impact props., microstruct. element influence 80−40525
steel, low C, dual-phase, law of mixtures, applicability 80−89346
steel, low C rimming, effect of addition of Al to Zn on phase composition and morphology *(Polish)* 78−53014
steel, Mn-C-O, phase equilibrium, Mn effects at liquidus temp. *(Russian)* 77−66625
steel, Mn-Cr-V, structural changes during solution annealing *(Czech)* 78−84864
steel, Mn-Si-Cr-Mo, dual phase, as-rolled, continuous cooling transformation diagram to optimize composition 80−100829
steel, molten interfacial tension in phase boundary molten CaO-SiO_2-Al_2O_3-CaF_w2 slag *(Czech)* 78−63908
steel, phase boundary decarburization of pouring jets and droplets *(German)* 77−90318
steel, Rheocast high performance alloy, solid-liquid phase charact. 77−28803
steel, solubility of W and Mo in Ti(C,N)$_x$ 80−16276
steel, stainless, carbide and intermetallic phases, quantitative anal. by X-ray diffr. 80−66514
steel, stainless, Cr-Ni-Mo, phase anal. of carbide phases after isothermal annealing *(Czech)* 80−89224
steel, stainless, Ni-Cr-Mo, two-phase, compositional charge of ferrite and austenite *(Japanese)* 79−4948
steel, stainless, phase instability effect on cladding deform. profile of LMFBR fuel elements 77−74921
steel, stainless, sigma phase stability and irradiation effect 78−11200
steel, stainless, type 316, influence of preirrad. thermal-mechanical treatment on phase stability and swelling 79−55792
steel, U15 and 130 Gz, upper bainite, relation between cementite and ferrite lattice orientations *(Russian)* 78−23663
steels, thermal hardening stress determ. by thermoplasticity theory 79−29076
struct. and form. of metastable phase m-TiBe 78−48375
struct. and props. exam. 78−92245
sulphide ores, phase equilibria in pyrometallurgy 79−11588
surface tension, solid-liq. interphase, thermal meas. procedure *(French)* 77−66072
system, oxyorthophosphates form. 79−78942

phase equilibrium continued
systems far from thermodynamic equilib., dissipative structures, broken symm. equilib. phase transition theory 80−65827
ternary alloy ordering, correlation effects, Kirkwood method calcs. *(Russian)* 79−66038
ternary alloy systems, calc. of phase equilibria using thermodynamic values from different models 78−60646
ternary liquid-liquid equilibria, associated soln. theory capabilities 78−83910
ternary liquid-liquid equilibrium, NRTL equation calcs. 78−34597
ternary liquid-liquid systems, equilib. data correl. 77−4919
ternary system, bubble pt. equilib. compositions determ. from dew pt. meas. 79−77733
ternary system compound formation, comp. and props. w.r.t. component electron struct., computer prediction 80−103444
ternary systems, diffusion coeffs., stochastic theory of nonideal behaviour 80−44346
tetrafluoromethane-trifluoromethane-chlorotrifluoromethane, vapour-liq. equilib. compositions, calc. 80−19925
1,2,3,4-tetrahydronaphthalene-H_2O, liq.-liq. phase equilib., crit. phenomena 78−18764
thermodynamic equation for liquidus line of narrow homogeneity range compound 77−35716
thermodynamic stability criterion for orthobaric volumes *(Russian)* 78−51644
thiophene- or benzene-light alcohol binary system isobaric liquid-vapour equilibrium *(Spanish)* 79−77738
toluene, free convection heat transfer in tube at supercrit. press. 78−42518
transition metal, phase stability, band theory 78−34757
transition metal carbides and nitrides, M_2X, struct. and phase transitions 79−70051
transition metal-hydrogen systems, eqn. for multiplateau isotherm, lattice expansion role 80−39252
transition metalloid atom solubility and electronegativity difference correl. with phase stability and d-electron/atom ratio 78−6914
transition metals and alloys, group IV, electronic basis for ω-phase stability 79−91616
tricritical coexistence in three dimensions, multicomponent limit 80−19907
trine systems, surfaces, isotherms-isobars *(Russian)* 80−65191
triplet phase invariants, formula for acentric case 80−84115
trivalent metal phosphates, condensed, synthesis in polyphosphoric acid melts, physicochem. equil. considerations 80−97419
two order parameter systems, Landau-Ginzburg-Devonshire theory 78−10164
two-phase fluid equilibrium, thermodynamic functions and surface tension 78−2262
type equations for binary equilib. curves, ternary system polythermic sections 80−39250
unstable compounds, free energy of formation calcs., FORTRAN program for ternary phase equilibria. 80−10683
US velocity in crit. region water 80−59582
vapour liquid equilibrium states, thermodynamic properties correl. with pure fluids 78−67819
vapour pressure, between triple and crit. pts., predictive eqn. 78−30744
vapour pressure, rel. to liq. internal press., statistical mech. 79−33094
vapour-liquid, prediction with aid of computer, Wilson and NRTL equations assessment 79−86883
vapour-liquid equilib., component fugacity coeffs. 79−23716
vapour-liquid equilib., perturbation theory of convex end mol. fluids 79−90769
vapour-liquid equilib. meas., automatic gas chromatographic anal., appls. *(German)* 78−88667
vapour-liquid equilibria, algorithm for calcs. 80−19903
vapour-liquid equilibria, and intermol. forces, semi-empirical approach 80−54359
vapour-liquid equilibria, generalised method for calc. and prediction at high press. 78−87780
vapour-liquid equilibria correlation and prediction 80−2141
vapour-liquid equilibria data reduction, vapour phase composition effect, excess Gibb's function 77−59091
vapour-liquid equilibrium, data reduction, extension of Barker's method 78−79735
vapour-liquid equilibrium, ebulliometric determ. 78−18754
vapour-liquid equilibrium, generalised one-parameter Redlich-Kwong eqn., mixtures 78−34589
vapour-liquid equilibrium, high press., quantitative description 79−14923
vapour-liquid equilibrium, high pressure experimental technique 79−42227
vapour-liquid equilibrium, high-pressure, isothermal, meas. and correl. 78−18755
vapour-liquid equilibrium, supercritical components, standard state fugacities 80−15230
vapour-liquid equilibrium, systems with components of very different volatility, total press. static method meas. 79−14922
vapour-liquid equilibrium, T-x meas. by semi-micro method 78−87782
vapour-liquid multicomponent equilib., Gibbs-Duhem eqn. 79−23714
water-ethanol, vapour-liquid equilibrium, transpiration method meas. 79−99305
water-ethylenediamine, liq.-solid equilibrium *(French)* 79−51236
water-methanol-(ethanol), vapour-liquid equilibrium, transpiration method meas. 79−99305
water-propylene 1.3-diamine, liq.-solid equilibrium *(French)* 79−51236
weldable clad metal interlayer growth kinetics model 79−24493
X-ray analysis of minority phases *(German)* 78−26387
X-ray phase analysis, quantitative, optimisation *(German)* 77−84583
$3PbO.GeO_2$, X-ray and electron diffr. exam. *(German)* 80−11632
Ag-Fe, dil., ion implanted, phase comp., Mossbauer study 80−7244
Ag-Ge alloy, liq.-quenched, metastable phase formation and evolution 77−90338
Ag-Ge-Te, phase equilib. from Ag_2Te-GeTe mixture meas. *(German)* 78−84782
Ag-Ge-Te system, chalcogenide, phase equilibria and diagrams *(German)* 80−108418
Ag-Li, solid and liquid alloys, calorimetric investigation of mixing enthalpy *(German)* 78−52773
Ag-rare earth alloys, Ag-rich, phase equilib. 80−45276
Ag-Si-Te, phase equilib. from Ag_2Te-SiTe mixture meas. *(German)* 78−84782
phase equilibrium continued
Ag-Sn-Te, phase equilib. from AgTe-SnTe mixture meas. *(German)* 78−84782
Ag-Sn-Te phase equilib. 79−29033
AgCd-AgMg(AgZn), quasibinary alloys, phase relations 79−8273
Ag_5GaS_4, form. in Ag-Ga-S system 79−87618
AgI-$Ag_2Mo_2O_7$($Ag_2Mo_4O_{13}$), solid, intermediate compounds with fast ion transport 77−43371
AgI-BiI_3, phase equilib. study *(French)* 79−66047
Ag_2S, α-β transform., heterogeneous solid state reactions, role of phase boundaries, dynamic equilib. at interfaces 78−71848
$Ag_2Te_xSe_{1-x}$ system, solid solns. of substitution existence, X-ray phase obs. 79−43217
Ag_2WO_4-$In_2(WO_4)_3$, cpd. formation and polymorphism 77−86009
Ag_2WO_4-$Sc_2(WO_4)_3$, cpd. formation and polymorphism 77−86009
β-$Ag_xW_yV_{2-y}O_5$ bronzes, β-phase existence range, elec. cond. and Ag diffusion 78−35373
AgZn-AgMg quasibinary alloy, phase relation and superlattice form. 78−3097
$AgZr_2(PO_4)_3$ system, phase charact. at different temps. 80−29936
Al, molten, viscous flow, H dissolution temp. depend. X-ray anal. 79−91628
Al-Ag-Si alloys, phase equilibria at 500°C *(Russian)* 78−56612
Al-Au bimetal thin film interdiffusion zone, intermetallic phase form kinetics, 70-160°C 78−75891
Al-Cr-Zr(Nb), calc. of phase equilibria 79−11569
Al-Fe-Si, Fe phase form., solidification condition effects *(French)* 77−70030
Al-Fe-X-Si (X=transition metal), struct. and comp. by electron microscopy 80−88093
Al-Ge (6.8 at.%), quenching from mushy state for production of metastable phases 80−35223
Al-Li-Mg system, isothermal sections comput. 78−6896
Al-Mg, new metastable phase 78−52772
Al-Mg, rapidly solidified, metastable phases *(German)* 79−34011
Al-Mg-Li-Zr alloys, struct., mech. props. 79−24498
Al-Mg-Zn alloys, liq./solid phase equilibria determ. *(German)* 80−50601
Al-Mn, direct chill-cast, struct. changes during heat treating *(German)* 80−40408
Al-Mn(Cr), quenched, thermal stability *(Russian)* 80−20976
Al-Nb-R system, R=rare earth, X-ray diffr. obs. *(Ukrainian)* 77−32560
Al-Ni-Ti, calc. of phase equilibria using thermodynamic values from different models 78−60646
Al-Si (35 wt.%), Cr, Co, Si addition effects on strength of powder 77−24983
Al-Si melts, hypoeutectic, eutectic, hypereutectic structural factors, atomic radial distrib. functions *(Russian)* 79−73091
Al-Si-Cu-Be alloys, phase equilib. *(Russian)* 77−59748
Al-Si-Y alloy, phase equilibria in Al rich region *(Russian)* 80−93537
Al-Ti-B, liquidus surface at Al corner *(Japanese)* 77−55948
Al-Zn, metastable solvus curve, struct. changes 77−55950
Al-Zn, miscibility gap, spinodal region, thermodynamic data transferability *(German)* 79−20027
Al_4C_3-Be_2C-SiC system, phase equilibria 80−45284
Al_4C_3-Be_2C-SiC system, phase analysis and TEM struct. obs. 80−108420
AlN-Si_3N_4-Be_3N_2 system, phase equilibria 80−60844
Al_2O_3, spatial distrib. of β- and β''-phases 79−66045
Al_2O_3-B_2O_3-P_2O_5 glasses, formation and props. 78−83737
Al_2O_3-B_2O_3-SiO_2 system, metastable liq.-liq. phase separation 79−42263
Al_2O_3-B_2O_3-SiO_2 system, liq. phase calc. for commercial quartzite powders 80−25671
β-Al_2O_3-H_2O, stability and dehydration 78−51693
β-Al_2O_3-K2O-MgO, cryst. struct., nonstoichiometry, ion-ion correlations 80−88129
Al_2O_3-Na_2O solid electrolytes phase composition 77−36468
Al_2O_3-SiO_2 system, solid state transform. of andalusite to mullite 80−16281
Al_2O_3-SiO_2-P_2O_5, refractory glasses, exam. of liquid immiscibility and crystallisation 78−55814
Al_2O_3-Ta system, phase comp. of solid products formed in vacuum heating *(Russian)* 77−44185
Al_2O_3-TiO_2 powder, plasma-prepared, morphology and phase constitution 80−100833
Al_2O_3-V_2O_3-VO_2 system, 1273K equil. *(French)* 77−35668
$Al_2O_3.3H_2O$-H_3PO_4-CaO(ZnO), phase equilib., $AlPO_4$ solid soln. 79−11586
$AlPO_4$-Al_2O_3 system, oxyorthophosphates form. 79−78942
$AlPO_4$-Cr_2O_3, system, oxyorthophosphates form. 79−78942
$AlPO_4$-Y_2O_3, system, oxyorthophosphates form. 79−78942
Ar, gas-liquid-solid equilibrium, eqn. of state 80−24563
Ar, liq. nuclei, thermodynamic props. mol. dynamics calc. *(Russian)* 77−47325
Ar, liquid, velocity of second meas. and thermodynamic stability *(Russian)* 79−4374
Ar, phase transition, anharmonic cryst.-gas transition 80−6510
Ar-N_2 gas mixture, vapour-liq. equilib. data *(German)* 77−84915
As-Pb, eutectic, temp. determ. up to 35 kbar 77−85989
As_2O_3, vapour phase equilibria over GaAs 79−66181
As_2Se_3-GeSe$_x$-SnSe$_x$ (x=1,2), exam. of Sn valency and physical props. 79−4753
Au-Fe, dil., ion implanted, phase comp., Mossbauer study 80−7244
Au-In-Pb, $AuIn_2$-In-Pb portion of phase diagram 77−32562
Au-Sn, zeta and AuSn phases, heats of form. and heat contents 80−60837
AuIn-Pb pseudobinary system, DTA 78−23667
B and borides, conference, Varna, Bulgaria (Oct. 1978) 80−12842
BBr_3-PCl_3-H_2, gas phase equilib. comp. 80−35166
BN, hardness rel. to temp., phase compositions 78−60752
BN, phosphided, luminescence spectra of products 77−12418
B_2O_3-NaF-$NaBF_4$, crystalline compounds and glasses 78−11210
B_2O_3-Nb_2O_5 complexes, high resolution TEM obs. 78−35378
B_2O_3-Nb_2O_5 system, phase equil. and phase struct. obs. by high resolution TEM 80−108419
B_2O_3-SiO_2 glass, crack growth, phase separation effects 80−89336
BPO_4-SiO_2 system, new data to prevent B_2O_3 or P_2O_5 loss at elevated temp. 80−20914
$BaAl_2O_4$-Ba_2SiO_4-$BaZrO_3$, fusibility diagram 79−83184

phase equilibrium continued
BaF_2-NiF_2-CrF_3, X-ray crystallography study, phase identification at 700°C, cryst. symm. *(French)* 78−95733
BaF_2-xBaO.ySiO_2, activities rel. to liquidus comp. 77−28798
$BaMoO_4$-CdO(PbO)(ZnO) and $BaMoO_4$-$CdMoO_4$($PbMoO_4$)($ZnMoO_4$) systems 77−25034
BaO-Al_2O_3-SiO_2-H_2O system, phase transitions during hydrothermal treatment 79−43216
BaO-B_2O_3-GeO_2, exam. of glass formation and physicochemical props. 79−4959
BaO-TiO_2-Cr_2O_3, new compound, phase relations *(Japanese)* 78−6911
BaO-TiO_2-GeO_2, subsolidus equilibria 77−86014
BaO-TiO_2-Nd_2O_3, exam. of compositional and dielectric props. 79−33601
$Ba_3(PO_4)_2$ glass, phase equilibrium data 79−27922
$Ba_3(PO_4)_2$ glass, phase equilibrium data 79−27923
$BaTiO_3$-CeO_2 liquid immiscibility region, X-ray diffr. anal. 80−50611
Ba_xVO_2, oxygen vanadium bronze, phase comp., heating in air 77−40417
Be, alloy, metastable phase form. by ion implantation 79−14828
Be-Al-Fe, phase equilibria and diffusion using high energy ion beams 77−16542
Be-Al-Fe system, phase equilibria using high energy ion beams 79−43203
Be-Si-Al-O-N ceramic, phase assemblages, relationships with props. 80−60848
Be-Si-O-N polytypes, X-ray study 78−27496
BeF_2-LiF, thermodynamically predicted miscibility gap 78−11209
Be_3N_2-$BeSiN_2$ system, crystallography and phase relationships, TEM and electron diffr. study 80−92502
Bi-BiI_3($BiBr_3$) liquid binary mixtures, phase separation under press. 80−34183
Bi-Cd-Sb, calc. of phase equilibria using thermodynamic values from different models 78−60646
Bi-MnBi eutectic region, of Bi-Mn phase diagram 80−81034
Bi-Pb-Sn, molten metallic system, contribution to sign inversion of effective charge *(Czech)* 78−60656
Bi_2O_3-TiO_2-Nb_2O_5, subsolidus phase equilibria 77−55954
$Bi_{0.52}Sb_{1.48}Te_3$-Te, phase-equilibrium boundary, Hall coeff. meas. 78−44094
BiTeI-SbTeI solid solns., form., crystn., elec., thermal props. 78−44003
C, high-temp. phase behaviour meas. using laser heating system 77−77699
C, potential in equilibrium with impure high temp. inert gases 80−104135
C, solid-liquid vapour triple point 78−48377
C-O-H-N-Si-Ar, computer calculations of heterogeneous equilib. 79−66044
C_5 hydrocarbons, in binary mixtures, phase equilibria *(German)* 79−37822
CO_2, vapour-liquid and vapour-solid equilib. data, mass spectroscopic tracer pulse chromatography 80−37115
CO_2-2,2-dimethylpropane, liquid, -vapour equili., 220 to 300K and 6.7 MPa 80−62821
CO_2-polar component binary mixtures, up to 1000 bar, phase separation, critical phenomena 77−35695
CO_2+H_2O, pressure-temp. curves under conditions of New Zealand geothermal field 77−51488
CaF_2-ScF_3, phase relationships at 100 kbar and 1200°C 77−43335
CaF_2-SrF_2-BaF_2:Gd^{3+}, luminescence spectrum of Gd^{3+} ion and solid solution region obs. 78−84638
CaF_2-xMgO.ySiO_2, activities rel. to liquidus comp. 77−28798
CaF_2-YF_3, fluorite- and tysonite-related ordered phases *(German)* 79−23725
CaF_2-YbF_3 system, phase relationships *(German)* 79−24501
Ca_2GeO_4-$Ca_3(PO_4)_2$ system, X-ray, DTA and cryst. optical analyses 77−36469
$Ca_{1-x}La_xMgAl_xSi_{2-x}O_6$, crystalline and vitreous phase comp. and props. 77−44221
$Ca_2Nb_2O_7$-$CaTiO_3$ system, mode of formation and stability of $A_nB_nO_{3n+2}$ phases *(French)* 78−3110
$Ca_2Nb_2O_7$-Sm_3NbO_7 system, phase equilib. 80−20907
CaO-Al_2O_3, molten binary slag, dissolved C study *(Japanese)* 78−60662
CaO-Al_2O_3-CaF_2, electroslag remelting slag, solubility of N_2 and C, equilibria 78−44110
CaO-Al_2O_3-Fe_2O_3-SiO_2, phase relations 77−12610
CaO-$CaMnO_{3-x}$-2CaO.Fe_2O_3 pseudoternary system, equilibrium relationships between solid phases at 1300°C *(Italian)* 77−55951
CaO-Fe_2O_3-Al_2O_3 system, solid soln. of $Ca_2Fe_{2(1-x)}Al_{2x}O_5$ *(Russian)* 80−16284
CaO-MgO-Al_2O_3-Cr_2O_3-Fe-O_2-SiO_2 system, exptl. determ. of periclase and spinel comps. 78−6906
CaO-MgO-SiO_2 system, phase equilibria 79−70045
CaO-SiO_2 glass, two phase region, expt. and thermodynamic data 80−16288
CaO-SiO_2/GeO_2-H_2O system, phase relations, influence of Si/Ge isomorphous substitution 79−52180
CaO-ZrO_2 solid soln., thermodynamic investig., by EMF method 77−36485
β-(CaO_2)-SiO_2-H_2O, SEM and X-ray diffr. exam. of structure, crystallisation props. 78−73012
ZCaO.SiO_2-2CaO.$Na_2O.P_2O_5$ system, polymorphism and solid soln. 78−19731
$Ca_{10}(PO_4)_6(OH)_2$, hydroxyapatite, aq. solution system, interfacial props. and equilibria 79−77751
$CaSO_3$.1/2H_2O-$CaSO_4$ solid solution, prepared by coprecipitation from solns., exam. 79−20034
Ca_2SiO_4-$CaMgSiO_4$, T phase, review 80−50612
Ca_2SiO_4-$CaSO_3$-CaO, region of homogeneity of Ca_2SiO_4 77−90332
$CaTiO_3$-$Ca_2Fe_2O_5$, Mossbauer resonance exam. of structure, phase equilibrium 78−76640
Ca_xVO_2, oxygen vanadium bronze, phase comp., heating in air 77−40417
Cd solid-vapour state, quantum statistical mechanics viewpoint *(Croatian)* 79−95154
Cd-As, liq. alloys, thermodynamic props. and cpd. formation 77−1238
Cd-Pb(Sn)(Bi) alloy, molten, EMF meas. of liquid separation 78−39747
Cd-Sn alloy, superconductivity and microstructure 80−107949
$Cd_{1-x}Cu_xCr_2Se_4$ solid solution, spinel struct., X-ray investigation 79−78940

phase equilibrium continued
$Cd_{1-x}M_x$ (M=Mg, Ca, Sr), solid soln., phase equilib. diagrams 80−108412
CdO-B_2O_3-GeO_2 system, phase equilibria at 800°C, X-ray powder diffr. anal. 79−4956
CdO-B_2O_3-SiO_2, phase equilibria at 800°C, photoelectric effects 78−68675
CdS films, chemically deposited, phase comp. and photoelec. props. 77−40394
CdS-CaS, solid soln., rock salt struct., high press. phase equilibrium study 78−52777
CdS-MgS, solid soln., rock salt struct., high press. phase equilibrium study 78−52777
CdS-SrS, solid soln., rock salt struct., high press. phase equilibrium study 78−52777
CdTe-In system, equilib. phase diagram and liq. phase epitaxial growth of CdTe from In soln. *(Japanese)* 80−71634
CdTe-ZnSe pseudobinary system, phase diagram and equil., Bridgman single cryst. growth method 79−43213
Ce-In, phase equilibrium and cryst. struct. 80−66483
Ce-Mn-Co, temp. conc. limits of homogeneous compounds *(Russian)* 78−23666
Ce-Mn-Cu systems, phase equilibria at 600 and 400°C *(Ukrainian)* 80−11625
Ce-Si-Al-O-N ceramic, phase assemblages, relationships with props. 80−60848
Ce-Tl, phase equilibrium and cryst. struct. 80−66483
$CeMg_{11}$V(Cr)(Mn)(Fe)(Co), hydriding and appl. in H_2 storage 80−51009
$CeNbO_{4+x}$, oxidation-reduction reactions 78−39930
CeO_2-PrO_x system, mixed cryst. phase characterisation 79−14936
CeO_{2-x}, 1.5<O/Ce<2, physicochemical equilibria, statistical thermodynamics model *(French)* 78−38688
$CeTaO_{4+x}$, oxidation-reduction reactions, phase equilibrium, thermogravimetry and magnetic susceptibility meas. 78−39930
Cl_2-CO_2 system, vapour-liquid equilib. *(Japanese)* 79−42258
Cm-O system, phase obs. in $CmO_{1.50}$-$CmO_{1.71}$ region 77−36490
Co-Al-Cr(Nb)(Ta), eutectic alloys, charact. by melting, oxidation resistance and composition 78−52768
Co-CoAl eutectic, invariant composition redeterm. 78−3099
Co-Cr-Mo (Zr)(Nb)(Ta), eutectic alloys, charact. by melting, oxidation resistance and composition 78−52768
Co-Cr-Ni superalloy Mar-M509 standard and Mo modified, phase anal. 77−63675
Co-Ge-Te system 80−20908
Co-mischmetall system, phase relations, microstruct., mag. props. 80−104118
β-Co-Mn-Sn Heusler alloy, constitution and magnetic props. *(German)* 79−34009
Co-Sb-Te ternary system, crystn., heat treatment and phase equilib. 79−52156
Co-Si-Nb(Zr), eutectic alloys, charact. by melting, oxidation resistance and composition 78−52768
Co-Ti (22 at.%), amorphous eutectic phase 80−55360
Co-W-C system at 1150°C, phase equilibria, isothermal reactions and thermodynamic study 78−31385
Co-WC hard alloys, rapidly quenched struct. 80−76233
Co_5Ge_3, solid and liquid, physicochemical props. and structure 80−39548
$CoMoO_4$, formation and phase transition in CoO-MoO_3-Al_2O_3 system 79−61569
CoO-SiO_2 systems high press. phases stability and MO-SiO_2 systems phase diagrams code 79−90779
CoO-ZnO-Al_2O_3-Cr_2O_3-TiO_2 system, form. and colour of spinel solid soln. *(Japanese)* 77−25001
CoO.Al_2O_3-Al_2O_3, solid soln. *(Japanese)* 77−32567
B-CoTe phase, thermodynamic study by Galvanic cell meas. 80−29190
Co_2Z ferroxplana form. process peculiarities 80−89368
Cr spinellide, acid extracted, phase transform. on heating in air *(French)* 79−96003
Cr-Fe-V, calc. of phase equilibria using thermodynamic values from different models 78−60646
Cr-Si-Cu, struct. and supercond., Cu influence 80−50592
Cr_2N-CrN, thermogravimetric exam. of equilibrium *(Japanese)* 79−20292
Cr_2O_3-Al_2O_3-$ZrSiO_4$ system, electrosmelted refractories, phase comp., corrosion and glass resist. Cr^{3+} conc. depend. 79−33982
Cr_2O_3-CrO_3-ZrO_2.CrO_3H_2O, exam. of thermal transitions 79−100116
Cr_2O_3-MgO-TiO_2, phase relations in air at 1400°C *(Japanese)* 77−77465
Cr_2O_3-V_2O_3-VO_2, system, 1273K equil. *(French)* 77−35668
Cr_2O_3-WO_3, phase relations 78−92249
$CrPO_4$-Al_2O_3, system, oxyorthophosphates form. 79−78942
$CrPO_4$-Cr_2O_3 system, oxyorthophosphates form. 79−78942
$CrPO_4$-Y_2O_3, system, oxyorthophosphates form. 79−78942
Cs-Cr-O system, phase equilibrium 80−3012
$CsLaF_4$ and $CsCeF_4$, phase equilibria *(French)* 78−44107
Cu, alloy, metastable phase form. by ion implantation 79−14828
Cu alloy solid solution condensed films, influence of alloying components on phase composition and lattice spacing *(Russian)* 80−20047
Cu, equation of state, isentropic expansion method 78−91414
Cu, white metal and SiO_2 saturated slag, under controlled SO_2 press. 77−52294
Cu-Ag, liquid alloy, solubility and activity of O_2 79−29028
α-Cu-Al, short range ordered, struct. and new superlattice phase 78−52756
Cu-Al (In), eutectic systems, specific phase boundary enthalpy, calorimetric study *(German)* 79−29016
Cu-Al-Sn system, coexistence of different and brass like phases 80−89206
Cu-Al-Zn, period of periodic antiphases, quant. metallography *(French)* 79−100111
Cu-Co-S system, phase equilibria determ. by silica tube techniques 79−60482
Cu-Cr system, optimal mutual orientations between FCC and BCC phases *(French)* 78−15371
Cu-Fe, dil., ion implanted, phase comp., Mossbauer study 80−7244
Cu-Fe alloy, cluster form., Fe solubility determ., 450 to 1000°C, Mossbauer spectra obs. *(German)* 79−29021
Cu-Ge-O, phase diagram and thermodynamics, electrochem. study 80−50617
Cu-Nb-Sn(Ge), phase relations and diffusion layer form. 77−36458

phase equilibrium continued
Cu-Ni-O, liquid alloy, thermodynamic study by EME method *(Japanese)* 78−15367
Cu-Ni-Ti system, phase equilibria in Cu rich region and Cu-T quasi-binary constitution *(Japanese)* 80−89203
Cu-Ni-W melt, solubility of W, primary solidification 78−19726
Cu-O system, deposition by chem. transport, thermodynamic anal. *(German)* 78−31344
Cu-Pb-O system, ternary miscibility gap activity determ., thermodynamic method 77−28783
Cu-Sn system, thermodynamic study of gaseous molecules of $CuSn_2$ and Cu_2Sn 79−70360
Cu-Ti system, diffusion obs. *(German)* 78−63881
Cu-Tl-S, phases, semiconductor and metallic behaviour *(French)* 79−96011
Cu-U-O system, equilib. relationships *(German)* 80−35163
$CuInSe_{2-x}S_x$, phase equilibria 77−90328
$Cu_xMo_6S_8(Se_8)$, prep., metallurgical and supercond. props. 77−32102
$CuO-Cu_2O-TiO_2$, phase equilibria, thermodynamics of Cu_3TiO_4 phase 80−55374
$Cu_2O-CuO-(\beta)Ga_2O_3$ system, thermodynamics and phase equilibria, 680-1000°C 77−36489
$Cu_2O-PbO(NiO)-SiO_2$, equilibrated with liquid Cu, Pb and Ni distrib. 77−28790
CuPb, coexistence of ordered and disordered phases, elec. resist. meas. 77−85992
Cu_2S-GeS_2 and Cu_2S-SnS_2 systems dissoc. of ternary congruently melting cpds. 79−87832
$Cu_2Se-GeSe_2$ and $Cu_2Se-SnSe_2$ systems, dissoc. of ternary congruently melting cpds. 79−87832
$Cu_2Te-Ge(Sn)Te_2$, phase equilib., microstructural, DTA investigs. 77−16560
D_2-DT-T_2, three-phase region, temp.-press.-composition correlations 77−84889
Dy_xB_y, prep. and props., DTA study 80−20859
$Dy_3Fe_5O_{12}$, formation mechanism from metallic oxides 77−48376
$DyMnO_3$, thermogravimetric study of phase stability 79−100121
$Dy_2O_3-HfO_2$, kinetics of initial stages of formation of solid soln. 77−48617
$ErMnO_3$, thermogravimetric study of phase stability 79−100121
$Er_2O_3-ZrO_2$, subsolidus phase relations, X-ray diffr. and thermal expansion exam. 78−31382
Fe (100), equilib. surface segregation of dissolved C, N and S 77−62723
Fe, alloy, metastable phase form. by ion implantation 79−14828
Fe base superalloy, PHACOMP appl. to σ-phase estimation of various heats *(Chinese)* 79−100109
Fe, cast, Ce hypoeutectic, new phase formation sequence during crystallisation, X-ray obs. *(Russian)* 78−95731
Fe, cast, high Cr, phase composition, mech. props. rel. to heat treatment 79−29108
Fe, cast, high Mg content (0.33%), exam. of phase composition characts. 78−84780
Fe, cast, Mg-Sb, despheroidising composition and distribution of phases, X-ray obs. *(Russian)* 78−95732
Fe, cast, spheroidal graphite form., role of interphase boundary adsorption 77−63657
Fe, high C, interfacial tension in phase boundary with $MnO-TiO_2-SiO_2(Al_2O_3)$ *(Czech)* 78−63907
Fe oxides, phase equilibrium and microstructure interpretation 80−60847
Fe rich binary alloys, effect of transition impurities on structural stabilisation 77−76552
Fe-Ag-Cu melts, phase interface props., Cu influence *(Russian)* 79−51261
Fe-Al (25 at.%), anomalous magnetic behaviour *(Japanese)* 77−48011
Fe-Al powder cpds., prep. in low-temp. plasma, struct. props. 77−44192
Fe-As-Su-Si (Cr)(Mn) melts, As and Sn distrib., Si, Cr, and Mn influence *(Russian)* 80−16274
Fe-B_4C sintered material, mech. props. and struct. characts. 79−100084
Fe-based oxide film, phase comp., thermal analysis 77−51928
Fe-C (0.8-4.2 wt.%), eutectoid transform., effect of heat treatment in H_2 *(Russian)* 79−4947
Fe-C-Cr, pearlite reaction kinetics 80−3006
Fe-C-Cr, thermodynamics and phase equilibria near eutectoid temp. 80−3005
Fe-C-H phase diagram, effect of H on eutectoid equilib. *(Russian)* 79−15648
Fe-Ce-O-S system, phase equilibrium 79−83498
Fe-Co-Al-Cu-Ti (40, 14, 7.5, 4.5 wt.%), metastable equilibrium, high coercive state *(Russian)* 80−66476
Fe-Co-V (2 wt.%), gamma phase 77−36514
Fe-Cr, thermodynamics of chlorination *(Russian)* 79−52168
Fe-Cr-C alloys, equilibrium partition coeffs. for ferrite/liquid, austenite/liquid 78−39744
Fe-Cr-C system, isothermal sections, 873 to 1373K, computer plotting 78−6894
Fe-Cr-C system at 870°C 77−28782
Fe-Cr-Co-Al(V)-(Nb)(Ti), phase equilib., X-ray diffr. meas. *(Russian)* 79−47658
Fe-Cr-Mo-Ti (13, 1.5, 3.5 wt.%), equilibrium studies on chi-phase strengthening 79−24496
Fe-Cr-N system, distrib. of Er between austenite and ferrite at 1200°C 79−43205
Fe-Cr-Ni, α-particle induced precip. and phase instability 79−1470
Fe-Cr-Ni, Fe-rich, melting equilibria *(German)* 77−52282
Fe-Cr-Ni, thermodynamic prediction in coal gasifier environment 79−43206
Fe-Cr-Ni (12, 15 wt.%) austenitic alloy, Ni^{6+} irradiated, void swelling and phase stability, Si and Ti effects 80−65055
Fe-Cr-Ni alloy, austenitic, Neel temp. and max. susceptibility predictions comp. effects 77−43833
Fe-Cr-Ni alloy, shock loading effect on phase equilib. *(Russian)* 79−29017
Fe-Cr-Ni-Cu-Sn, Cu and Sn effect on Cr and Ni segregation *(German)* 78−72777
Fe-Cr-Ta, eutectic alloy, exam. of eutectic temp., composition, and oxidation resistance 78−52767
Fe-Cr-W-C, carbide/austenite equilibria, expt. and thermodynamic study 77−36459
Fe-Cu, generation of self-consistent Gibbs energy functions 79−11565
Fe-Cu, thermodynamic analysis of phase relationships 77−73260
Fe-Cu-C, phase equilibria, 950 to 1500°C 80−60836
phase equilibrium continued
Fe-Fe_2O_3-$NaFeO_2$, study of Na-containing wustite region *(French)* 77−73264
Fe-Fe_2O_3-SiO_2-Si melt, interacting system, oxidation products *(Russian)* 78−19728
Fe-lanthanid-O systems, thermodynamic props., composition and lattice constants 78−31390
Fe-Mn mag. contributions to $\gamma \rightarrow \varepsilon$ phase transformations 80−25694
Fe-Mn-C, thermodynamic analysis 77−32563
Fe-Mn-C (11.5, 0.2 to 1.6 wt.%), water quenched, effect of C on phase composition, abrasion, plasticity *(Russian)* 78−35445
Fe-Mn-C system, Gibbs energy, high temp. phase relations 78−80779
Fe-Mn-C system, isothermal sections, 873 to 1373K, computer plotting 78−6893
Fe-Mn-S, thermodynamics, solid/liquid phase equilibria, 1100 to 1300°C 79−47663
Fe-Mn-Si-C, cast, Mn effect on struct. during solidification 79−83191
Fe-Mo system, self-diffusion rel. to phase relns. 77−4214
Fe-Mo-C (0 to 4, 1 wt.%), phase equilibria at 1143, 1198 and 1253K 80−60835
Fe-Mo-C system, isothermal sections, 973 to 1273K, thermodynamic analysis 78−6895
Fe-Mo-Cr(Ni)(Mn)-C, carbide-austenite equilibria, 1173 to 1373K, microscopic and X-ray obs. 78−44085
Fe-Nb-V-C-N, equilibrium comp. and solubility in steels, model of ideal solns. *(Russian)* 80−60832
Fe-Ni, FCC, anomalous props. at high temp. and new phase *(Japanese)* 78−80520
Fe-Ni (25 to 50%), FCC, meteorites and thermodynamic equilib., Mossbauer and X-ray diffr. study 80−88087
Fe-Ni heterogeneous alloys, ferrite, martensite and austenite phase distrib., effect on mech. props. 80−45363
Fe-Ni Invar alloy, electron irrad. effects 79−56638
Fe-Ni melt, short-range order, m.p. to 1750°C *(Russian)* 78−94966
Fe-Ni-Al alloy, metastable equilib. in its high-coercivity state *(Russian)* 79−52161
Fe-Ni-Al-Co-Ti base alloys, highly coercive, phase comp., Mossbauer meas. 80−39996
Fe-Ni-C, calc. of activity data, and exam. of phase equilibria 79−10912
Fe-Ni-C, plastic deform. effect on austenite stabilisation *(Korean)* 80−21021
Fe-Ni-C alloys, FCC, effect of two gamma states on C activity 78−6897
Fe-Ni-Co base alloys, composition changes during electron radiation melting *(Russian)* 78−19718
Fe-Ni-Cr-Ti-Al, Ti and Al effect on microstruct. and mech. props. *(Chinese)* 79−74130
Fe-O, exam. of thermodynamic data, using a computer aided strategy 79−11592
Fe-O-V melts *(Russian)* 80−16273
Fe-S-O, equil. cond. *(Rumanian)* 79−29029
Fe-Si system, melting equilibria study *(German)* 80−66473
Fe-Si-Ti(Zr)(V)(Nb), eutectic alloy, exam. of eutectic temp., composition, and oxidation resistance 78−52767
Fe-Ti-S-(C), sulphide phases *(Russian)* 77−25017
Fe-Ti-V-C-N, equilibrium comp. and solubility in steels, model of ideal solns. *(Russian)* 80−60832
Fe-TiB_2, phase composition, secondary ion-ion emission study *(Russian)* 80−20896
Fe-V_2O_3, rel. to deoxidation of Fe by V *(Russian)* 80−16275
Fe-WO_3 system, struct. phase exam. by optical microscopy and X-ray diffr. 78−31389
Fe-X-C (X=Cr, Mo, W), quenched rapidly from melts, nonequilib. phases *(Japanese)* 80−71630
Fe-Zn, homogeneous intermetallic cpd., synthesis and charact., ξ-phase 79−83177
Fe-Zn, homogeneous intermetallic cpd., synthesis and charact., δ_1-phase 79−87616
Fe-Zn, homogeneous phases, Gibbs free energies of form., Knudsen effusion method 80−66481
Fe-Zn intermetallides, initial stages of form. *(Russian)* 80−20889
$Fe_{0.394}-Ti_{0.606}$-O-S subsystem, equil. phase data under reducing conditions rel. to ilmenite upgrading 80−76240
$Fe_4Ca_2S_3O_6$, struct. and phase analysis *(Russian)* 77−58995
$Fe_{10.92}K_{1.55}O_{17}$, ferrite, cryst. struct., nonstoichiometry, ion-ion correlations 80−88130
FeO-Fe_2O_3-SiO_2 -Al_2O_3-$CuO_{0.5}$/Cu slag-metal system, distrib. equilib. of Sn, Se, Te 78−44111
FeO-SiO_2 system, high press. phases stability and MO-SiO_2 systems phase diagrams code 79−90779
$Fe_{1-x}O$, wustite phase, surface elec. props. 78−76133
Fe_2O_3-MgO-NiO, tie-lines between solid solns. of oxide and spinel at 1273K *(French)* 79−100124
Fe_2O_3-WO_3, phase relations 78−92249
FeS-MnS phase relationships in presence of excess Fe 77−4768
Fe_2SiO_4-$KAlSi_2O_6$-SiO_2, phase relations at 1 atm., and low temp. liq. immiscibility 79−47664
FeTi, hydrogen storage, annealing effects *(Japanese)* 79−100542
Ga-As system, phase equilib., Krupkowski model *(German)* 78−95132
Ga-As-O, equilib. phase diagram, GaAs oxidation 80−104130
Ga-Bi liquid binary mixtures, phase separation under press. 80−34183
Ga-Pb, liquid alloy, thermodynamic activity determ. using Knudsen method *(German)* 79−34008
GaAs, annealing rel. to stoichiometry deviation, Hall effect, electron microscope meas. 77−24410
GaAs(Sb), high-temp. thermodynamic data and quantitative fits to liquidus line 77−63637
GaI_3-$SbCl_3$, total exchange of halogens, Raman spectra and phase equilibrium *(French)* 79−65874
GaP(As), liquid interaction parameters determ., 580-670°C 80−65197
Ga_2Se_3-In_2Se_3, semiconducting props. of four stable phases 77−55528
GaTe-SnTe, phase equilib. 77−86006
Gd-Co-B system, phase composition, struct., phase equilibria 78−35355
Gd-Fe-B ternary systems, phase equilibria and cryst. struct. *(Ukrainian)* 80−11626
$Gd_3Al_5O_{12}$ phase obtained by crystallisation of amorphous $Gd_2O_3.5/3Al_2O_3$ by quenching 78−92224
$Gd_{1-x}Ca_xAl_2$, mag. props. and phase relations 80−107991
$GdCrO_3$-$GdAlO_3$ solid solutions 80−20887
$Gd_3Fe_5O_{12}$, formation mechanism from metallic oxides 77−48376
GdP, vapour comp. and dissoc. pressure 77−84916
Ge, liquid, solubility and activity of O_2, 1233 to 1397K 78−44109

phase equilibrium continued
Ge-Cu, liquid, solubility of O_2 at 1373K, in equilibrium with GeO_2 78−44109
Ge-GaSb, metastable continuous solid solutions 79−8284
Ge-I, gas phase equilib. comp. 77−36776
Ge-I_2, equilibrium study 700 to 1300K, vapour transport rate of Ge *(French)* 78−64476
Ge-S glasses, Cu doped, thermal, structural and dielectric props. 79−60283
Ge-S-Cu, phase separation in melt centrifugal quenching 80−25701
Ge-Se-Tl, vitrification region 77−43154
Ge-Si-Sb solid soln., distrib. of components in universal furnace expt. in Soyuz-Apollo programme *(Russian)* 78−31381
Ge-Sn-M, M=Cu, As, Sb, formation of Ge-based solid solns. during crystallisation 77−80625
Ge-Te, exam. of new compound, using light microscopy and X-ray diffr. exam. 78−48383
Ge-transition, metal planar interfaces, first phase to nucleate 77−62764
Ge_xSe_{1-x}, $0<x<0.2$, crystallisation in amorphous bulk and thin films 78−55813
H-He, metallic solid alloys, phase separation and thermodynamic functions calc. 77−43333
H_2-Ar, liq.-vapor equilib. 83 to 141K, to 52 MPa 79−42226
H_2-N_2, liquid-vap. equilib., 63-110K and up to 57 MPa 79−55881
H_2-thianaphthene mixtures, gas-liq. equilib. 79−65177
HF alloys, metatectic reaction prediction 79−29020
H_xMoO_3, $(0<x\leq2.0)$, phase relationships, X-ray diffr. exam. of microstruct. 78−76639
Hf-Co-Ga system, crystal atomic struct. and phase equilibria *(Ukrainian)* 78−84772
Hf-Cr-Ga, X-ray microanalysis of phase equilibria *(Ukrainian)* 78−6898
Hf-Fe-Ga, X-ray microanalysis of phase equilibria *(Ukrainian)* 78−6898
Hf-Ge-B system, phase equilibria 78−35356
HfC-HfB_2, reactions, cpd. formation and props. 78−23685
$HfFe_{2-x}Si_x$, Laves pseudo-binary compound, cubic C15 phase stabilisation 77−39559
HfO_2, obtained by vapo-condensation, exam. of structure and phase props. *(French)* 79−19489
HfO_2-Cr_2O_3 system in Ar medium, phase equilibria, 1600-2500°C *(Russian)* 77−55953
HfO_2-Eu_2O_3, phase equilibrium, 960 to 1900°C, X-ray anal. 78−23688
HfO_2-EuO_2 system, liquidus determ. from thermal anal. *(Ukrainian)* 79−96007
HfO_2-Gd_2O_3, phase relations 78−72769
HfO_2-La_2O_3 system, phase form. and relations, phys. props. 79−43218
HfO_2-MgO system, intermediate phases existence, X-ray diffr. and IR obs. 79−38805
HfO_2-PrO_x, phase equilibria and physicochem. props. in range 1000 to 1800°C 79−100117
HfO_2-TiO_2 system, liquidus determ. from thermal anal. *(Ukrainian)* 79−96007
Hg, liq.-vap. interface, density profile near triple point, X-ray refl. 78−75821
Hg-HgTe-CdTe system, equilib. phases comp. by dew point method 79−78941
Hg-S binary system, phase relations, bulk resist. meas. 79−66040
Hg-U system, thermodynamic props., vap. press. and EMF expts. 79−91625
In, liquid O_2 activity from electrochemical meas. 80−104123
In-As system, exam. of thermodynamic consistence of models, and QCE approx. for activity coeffs. *(German)* 80−24615
In-Bi alloy system at high press. and temp. 78−92238
In-Ga-As system, heterophase equilibrium, phase diagram calc. 79−43212
In-Ga-P system, solvent choice for InP and GaP LPE 79−87589
In-P system, liquid-vapour equil., VP functional depend., 1023 to 1123K 79−42228
In-Pb, liquid alloy, thermodynamic activity determ. using Knudsen method *(German)* 79−34008
In-Pb, thermal anal. solidus determ. 79−20030
In-Te system, thermodynamic props. 77−12821
In-Te-SnTe, phase equilib. 77−86006
In-Tl liquid alloy, thermodynamic props. and struct. *(German)* 77−48400
InAs-CdTe quasi-binary system, temp.-comp. diagram, physicochem. and thermodynamic analysis 80−104127
InAs-InP, phase equilib. and dissoc. 80−35170
InAs(Sb), high temp. thermodynamic data, quantitative fits to liquidus line 77−63637
InP(As), liquid interaction parameters determ., 580-670°C 80−65197
InSb+Ga reaction 78−23682
$(In_2Te_3)x-(Hg_3Te_3)_{1-x}$, $0.15\leq x\leq0.37$, E_g-comp. depend., spectral photo EMF meas. 77−47851
K-La-NH_3 system, cpd. formation, phase analytical and X-ray expts. *(German)* 79−66043
$KAlSi_2O_6$-$Ca_2MgSi_2O_7$-$CaMgSi_2O_6$, phase diagram of ternary eutectic system 78−80529
KF-EuF_3 system, composition of phases determ. by DTA and X-ray crystallography *(French)* 77−68945
KF_2-$3K_2O.2SiO_2$ freezing point depression meas., effect of silica compound additions 77−28797
KH-H_2 crystal-gas system, with D impurity, thermodynamic equilib. 78−59954
K_2O-Al_2O_3-B_2O_3, subsolidus compatibility relations determ. *(Japanese)* 79−4957
K_2O-Al_2O_3-B_2O_3:Fe_2O_3, glasses, liq.-liq. phase separation, Fe^{3+} ions rel. to mag., optical props. 77−15322
K_2O-BaO-B_2O_3 glasses, ESR detection of immiscibility rel. to Cu II ions 80−20916
K_2O-CaO-Al_2O_3-SiO_2 glass, exam. of liquid phase separation phenomena 79−4417
K_2O-CaO-SiO_2 glass, composition-density relationship 77−90326
K_2O-V_2O_3-Al_2O_3 melt, soln. of Al_2O_3 single crystal 80−20910
$K_2O.4TiO_2$, new fibrous phase 80−20917
K_3PO_4-$M_3(PO_4)_2$, M=Ca, Sr, Ba, Zn, Cd, high temp. stabilisation of phases *(French)* 77−44235
Kr-Ar(N_2) gas mixture, vapour-liq. equilib. data *(German)* 77−84915
La-Ge-B, X-ray investigation of phase equilibrium 79−99294
La-H, H equilib. press. 80−66492

phase equilibrium continued
$LaCrO_3$-Cr ceramic, prep., phase comp. and elec. cond. *(Polish)* 80−71621
$LaMnO_3$, O_2 environment, phase stability and nonstoichiometric behaviour, 1200°C 78−43134
LaOF-LaF_3, high pressure phase transitions 80−55368
$La(OH)_2Br$, hydrothermal phase equilib., cryst. struct. 78−35372
$La_7(OH)_{18}Br_3(I_3)$, hydrothermal phase equilib., cryst. struct. 78−35372
$La_2Ti_2O_7$-$CaTiO_3$ system, mode of formation and stability of $A_nB_nO_{3n+2}$ phases *(French)* 78−3110
Li-Al-Cl system, thermodynamic props., phase equilib. 80−89211
Li-LiH liq.-vap. equilib., activity coeff. 80−103468
Li-LiH system, H isotope solubility thermodynamic singularities 80−81356
Li-LiH two-phase equil. system, vaporis. diagram at high temps. 80−19926
Li-LiH(D)(T), decomposition in $(\alpha+\beta)$ field 79−15652
Li-Na alloy, liq., conc. fluctuations and struct. factors 78−30534
Li-Na liquid binary mixtures, phase separation under press. 80−34183
Li-Sn, phase relationships between Li_7Sn_2 and LiSn 79−78933
7LiAl, cryst. growth, Stockbarger method, struct. and homogeneity 80−89137
Li_5B_4 form., thermodynamic considerations 79−56959
$Li_2B_2O_5$ glass, phase separation 79−41965
LiBr-LiF-KBr-KF, fused, miscibility gaps 79−82348
$LiCd_{1-x}Tl_x$, intermetallic, X-ray and Knight shift meas. of ^{205}Tl and ^{113}Cd 79−42851
LiF-AlF_3, mixture at 1293K, thermodynamic function 80−104134
LiF-AlF_3-Na_3AlF_6-Al_2O_3 system, phase equilibrium, X-ray diffr., DTA, quenching, optical microscopy study 80−50610
LiF-$Li_2O.SiO_2$, activities rel. to liquidus comp. 77−28797
Li_2MgSiO_4-Li_2ZnSiO_4, solid soln. formation, phase relns. *(Japanese)* 77−25037
LiO_2-CaO-SiO_2 phase equilibria 78−64528
Li_2O-Al_2O_3-Cr_2O_3 system, subsolidus equilibria 80−60843
Li_2O-BeO-SiO_2, X-ray diffr. exam. of phase equilibrium 78−80522
Li_2O-Cr_2O_3-SiO_2 system, phase equilibria 79−78944
Li_2O-MgO-Al_2O_3 system, subsolidus phase equilibria 80−81036
Li_2O-Na_2O-B_2O_3-SiO_3, exam. of metastable phase separation region 78−88450
Li_2O-V_2O_5-Al_2O_3 melt, soln. of Al_2O_3 single crystal 80−20910
$LiTaO_3$-$NaTaO_3$-$KTaO_3$, quenched metastable glassy and crystalline phases 79−61568
Mg-Ag-Cd, X-ray diff. exam. of phase fields *(Russian)* 79−56957
Mg-Cu(Ni), binary system, nonstoichiometry, of Laves phases, $MgCu_2$ and $MgNi_2$ *(French)* 78−52770
Mg-Ni-W-Co-Al-Cr alloy KhN56VMKYu, Al effect on excess Mg phase 80−29926
Mg-Si-Al-O-N ceramic, phase assemblages, relationships with props. 80−60848
Mg-Y-Al alloys, phase equilib. *(Russian)* 80−20890
Mg-Y-Zn (20, 30 wt.%), phase equilibria investigation *(Russian)* 79−74131
Mg-Y-Zr, phase equilib. and props. *(Russian)* 77−66626
$MgCaH_{3.72}$, synthesis and struct. *(Japanese)* 78−84751
MgF_2-xMgO.ySiO_2, activities rel. to liquidus comp. 77−28798
MgO, Cr bearing basic refractory, prod. from brine MgO 79−83158
MgO-B_2O_3 system, glass and cryst. compd. struct. determ. by ^{11}B NMR 79−94905
MgO-CaO-SiO_2-C, equilibrium partial press. of Mg, SiO, Ca and CO 77−36482
MgO-Ga_2O_3-SiO_2 system, subsolidus phase equilib. 78−44106
MgO-$MgCl_2$-H_2O, cement paste, reaction products, X-ray diffr. study 78−23689
MgO-ZnO-Fe_2O_3 ternary system 77−21116
MgO.nAl_2O_3, nonstoichiometric spinel, DTA 77−28791
Mg_2SiO_4-Fe_2SiO_4-$CaAl_2Si_2O_8$-SiO_2 system phase relations rel. to lunar basalts origin 78−65512
$Mg_yU_{1-y}O_{2+x}$, thermodynamics from EMF meas., high Mg conc. 78−43143
(Mn,Co)O⇌(Mn,Co)Al_2O_4, and (Mn,Co)O⇌(Mn,Co)Cr_2O_4, ion exchange equilib., 1100°C 77−32566
Mn-B system, microhardness and phase analytical studies 79−24502
Mn-Fe-C, phase instability 80−11628
Mn-H, hydride formation in high press. range 80−65235
Mn-N system, γ-Mn and hexagonal ζ-phase equilibrium calcs. 79−61565
Mn-Ni(V)(Fe)(Ti)-Al, phase stability 77−48397
Mn-Si, liq. alloys, equilibria between MnO-SiO_2-CaO-MgO slags 80−10639
Mn-Si-O, phase equilibrium *(Russian)* 77−66630
Mn-Zr-S, phase equilibrium *(German)* 78−72764
$Mn_{0.394}$-$Ti_{0.606}$-O-S system, 1380 and 1485K, phase equilib. study 80−50616
MnO-SiO_2 slag, SiO_2 solubility and MnO activity 79−52184
MnSb-Mn_2Sn alloy system, continuous series of solid solns., homogeneity and ferromagnetic props. 79−52159
Mn_2SnO_4-Mn_3O_4 system, spinel solid soln. form., atm. effects 77−43332
MnZn ferrite, Ti substituted, vacancy contents and phase equilibria 80−29012
MnZn ferrites, spinel use of phase equilibria in manufacture 79−11596
Mo, TEM exam. of Mo_2C precipitates, exam. of crystallographic relationships 78−52811
Mo-Al-Ge, new compounds, structure and props. 80−39003
Mo-Al-Ge, X-ray phase and microstructural anal. 80−93536
Mo-alkali earth oxides, multiple phase system calc. of phase equilibria using thermodynamic analysis *(Russian)* 79−56964
Mo-Cu-Al, phase equilibrium *(Russian)* 78−15361
Mo-Fe-O-H system, thermodynamic equilib. 78−60657
Mo-Hf-C-Ni, electrochemical phase composition anal., precip. of HfC phase *(Russian)* 80−20901
Mo-Ru-V alloys, phase equilib. and corrosion resist. *(Russian)* 79−52165
Mo-Si-Cu, struct. and supercond., Cu influence 80−50592
Mo-Ti(Zr)(Hf)-N, exam. of phase equilibria *(Russian)* 79−29018
Mo-transition metal admixtures, equilib. distrib. coeff., functional dependence *(German)* 77−76566
Mo-W-N system, nitrided annealed samples, W replacement of Mo 80−76227
Mo-Y(La)(Ce)-B, X-ray diffr., reciprocal lattice, crystal struct., phase equilibria 77−21122

phase equilibrium continued
MoO_2-I_2, heterogeneous equilib., vapour transport and cryst. growth 78−27405
MoS_2, homogeneity size estimation, stacking fault conc. effect 80−96661
$MoSi_2$-$CrSi_2$, phase equilib., struct. and props. 80−50608
N_2, dielectric strength, bubble-phase equilib., high press., low temp. *(Russian)* 77−20798
N_2-Ar-O_2, liq. vap. equilib. prediction using cubic eqn. of state 78−18737
N_2-Ar-O_2 system, vapour-liq. equilib., 80−54358
N_2-Kr-Xe, liquefaction, retention of ^{85}Kr from fission exhaust gases, separation technique *(German)* 80−27753
N_2-O_2, vap.-low. equilib., mag. field effect 78−91429
ND_4Br, phase states and transition, from ESR of Cu^{2+} 79−99762
NH_3-ethylene (propylene) mixtures, crit. curves at high-press. 79−23715
NH_3-water system, vapour-liquid equilib., thermodynamics 79−42246
NH_4SCN, polymorphous structural-kinetic transformations, phase orientational relation 79−90590
$N_2O_4 \rightleftharpoons 2NO_2 \rightleftharpoons 2NO+O_2$ dissociating system with NO added, phase equilibria *(Russian)* 79−19363
Na_2-SiO_2 glass, prep. by metallic-organic derived method, phase separation 78−56610
NaF-$3Na_2O.2SiO_2$, freezing point depression meas., effect of silica compound additions 77−28797
NaF-MgF_2-MgO-SiO_2, phase formation 78−27460
Na_2O-Al_2O_3-P_2O_5, exam. of subsolidus structure 79−4954
Na_2O-B_2O_3 glass-forming melts, thermodynamic functions 80−25673
Na_2O-B_2O_3-GeO_2 system glass-forming melts, mass spectrometry obs. of thermodynamic props. 80−97468
Na_2O-B_2O_3-SiO_2 glasses, phase-separated, leaching rate 80−104131
Na_2O-BaO-SiO_2, metastable two liquid tie line calc. 78−92246
Na_2O-Bi_2O_3-TiO_2, subsolidus phase equilibrium at 1000 degrees C 78−48384
Na_2O-CaO-Al_2O_3-SiO_2 glass, exam. of liquid phase separation phenomena 79−4417
Na_2O-CaO-SiO_2-H_2O system gels, metastable nature 80−71952
Na_2O-CaO(Al_2O_3)-SiO_2 glass, composition-density relationship 77−90326
Na_2O-GeO_2-Yb_2O_3, glass struct., Yb^{3+} ion segregation 78−87620
Na_2O-MgO-P_2O_5, subsolidus struct. 77−63640
Na_2O-SiO_2, (5.3, 94.7 wt.%) glass, liq.-phase separated, struct., heat treatment effect 80−16359
Na_2O-SiO_2 glass, stability at high press., X-ray diffraction obs. *(German)* 78−92251
Na_2O-SrO-Nb_2O_5 system, solid state equil., 800°C *(Italian)* 77−47549
Na_2O-TiO_2-SiO_2, phase relations 79−61567
Na_2O-V_2O_5-Al_2O_3 melt, soln. of Al_2O_3 single crystal 80−20910
Na_2O-V_2O_5-$(VO_2)_2$-V_2O_3, phase comp. and equilib. 80−35172
$Na_2O.y(Al_{1-x}Fe_x)_2O_{3-m}$, β''-Al_2O_3 phase stability, lattice constants 80−45283
Na_3PO_4-$M_3(PO_4)_2$, M=Ca, Sr, Ba, Zn, Cd, high temp. stabilisation of phases *(French)* 77−44235
Na_3PO_4-$Ni_3(PO_4)_2$ system, phase equilibrium diagrams, crystallographic study, double orthophosphates *(French)* 80−93546
Na_2SO_4-$CoSO_4$-H_2O, phase equilib., activities, Pitzer eqn. calcs. *(Russian)* 80−65190
Na_2WO_4-$CsWO_4$-WO_3, system form., melting point 79−43222
Na_2XO_4, (X=S, Cr, Mo, W), anal. and calc. of binary and ternary phase diagrams 80−88299
Nb-Al (20 at.%), diffuse scatt. before Nb_3Al phase form., unstable phase *(Russian)* 78−3131
Nb-Al-Ge-Cu, rapidly quenched, comp. and phase equilib. 80−76235
Nb-Al(Ga, Si, Ge, Sn)-Cu, rapidly quenched, comp. and phase equilib. 80−76235
Nb-D system, phase equilibria study *(Japanese)* 79−78936
Nb-D-H, equilib. H/D separation factors 80−59668
Nb-Ga-Ir, phase equilib. at 1000°C, cryst. data for intermediate phases 78−52763
Nb-Ga-Ir system, phase equilib. at 1000°C and supercond., Nb-rich portion 77−36480
Nb-Ge alloys, stoichiometry and phase equilibria, X-ray diffr. study *(French)* 79−70040
Nb-Ge-Si, supercond. state transition temp., influence of Si on alloy constitution *(Russian)* 79−78244
Nb-H, coherent α-α' phase transition, sample shape depend. 79−34005
Nb-H system, phase equilibria studies *(Japanese)* 79−78935
Nb-Ir-O, phase struct., supercond. H-phase 78−39246
Nb-Pt-O system, phase equilibria, diagram, unit cell parameters, supercond. 80−55352
Nb-Re(Ru)-N, α-solid soln., thermodynamics *(German)* 77−12600
Nb-S system, phase relations at high temp., elec. and mag. props. 80−29932
Nb-Si-Cu, struct. and supercond., Cu influence 80−50592
Nb-Sn alloys, stoichiometry and phase equilibria, X-ray diffr. study *(French)* 79−70040
Nb-Sn(Al)(Ga)(Ge)(Si)-C, phase equilib. and supercond. 80−50593
Nb-Ti-O, isothermal and polythermal cross sections 80−96624
Nb-Ti-O system, phase equilib., microstruct., thermal, and X-ray anal. 77−8806
Nb-V system, H_2 absorpt. 80−59808
Nb-Zr-O, corrosion resistance in molten Li *(Russian)* 78−31567
$NbSe_x$, nonstoichiometric, thermodynamic props. and crystal struct. *(Japanese)* 78−11206
$NbSe_x$, x=1.48-2.0, nonstoichiometric, press.-comp.-temp. rel. determ. by annealing 79−74139
Nd-Cr-B system, phase equil. at 800°C, boride lattice parameters *(Russian)* 78−31388
Nd-Fe-B ternary systems, phase equilibria and cryst. struct. *(Ukrainian)* 80−11626
Nd_2O_3-HfO_2, kinetics of initial stages of formation of cpds. 77−48617
Nd_2O_3-HfO_2 system, phase relationships 80−35169
Nd_2O_3-MoO_2-MoO$_3$ system, phase equilibria *(French)* 79−52176
$Nd(OH)_2Br$, hydrothermal phase equilib., cryst. struct. 78−35372
$Nd_7(OH)_{18}Br_3(I_3)$, hydrothermal phase equilib., cryst. struct. 78−35372
$Nd_2Ti_2O_7$-$CaTiO_3$ system, mode of formation and stability of $A_nB_nO_{3n+2}$ phases *(French)* 78−3110
Ne-H_2 liq. mixtures, phase equilib. effects, thermodynamic perturb. theory *(Russian)* 80−92663
Ne-H_2 mixture, liquid vapour phase equilib., sound vel., compressibility, thermodynamic perturbation theory obs. *(Russian)* 80−39306
Ni, alloy, metastable phase form. by ion implantation 79−14828
phase equilibrium continued
Ni alloy, self-fluxing, interaction with oxygen, thermodynamic considerations of slag equilib. 79−61774
Ni base Rheocast high performance superalloy, solid-liquid phase charact. 77−28803
Ni, β-phase form., H enriched, at surface and grain boundaries during H_2 absorption *(Russian)* 78−31410
Ni-Al-Si, β-phase stability *(Russian)* 78−39738
Ni-Al-Ta, solvus surface determ. using precipitation method 79−15674
Ni-Al-Ti, eutectic alloy charact. by melting temp., composition and oxidation resistance 78−52771
Ni-Al-Ti cast superalloy, eutectic transform. on ageing *(Chinese)* 79−100110
Ni-Be bronze, Fe and Si alloying addition effect on phase composition *(Russian)* 78−15360
Ni-Cl boracite, predominance/flux function diagram for phase equilib. and chem. transport rate 79−52091
Ni-Co-Al (1, 35.2 at.%), tempered martensite, new ordered phase 79−11560
Ni-Cr, ordering in the vicinity of Ni_2Cr 79−38819
Ni-Cr alloys, crystallisation anomalies *(Russian)* 78−19719
Ni-Cr-Mo-W-Al-Ti, heat-resist., phase comp. 80−76250
Ni-Cr-Ta system, phase equilib. of Ni rich region at 1523 and 1273K 80−93541
Ni-Cr-Ti(Nb)(Zr), eutectic alloy charact. by melting temp., composition and oxidation resistance 78−52771
Ni-Fe-H and Ni-Co-H, hydride formation in high press. range 80−65235
Ni-Mn-H, hydride phase form. and decomposition in hygh-press. gaseous H_2, magnetisation meas. 79−56953
Ni-Mo (20.8 wt.%), order, heat treatment effects 80−40406
Ni-Pd-Mn ternary alloys, mag. charact., use for thermoseed 80−107995
Ni-Pd-Si, phase composition, isothermal section at 800°C *(German)* 77−16544
Ni-S(Se)(Te) mixtures, binding of phases, two-correl. model 77−80438
Ni-Ta-Al system, phase equilibria and diagram, electron probe, X-ray diffr. anal. 80−29927
Ni-W (20 to 50 at.%), phase distrib. var. with annealing time, metastability of hexagonal phase *(Russian)* 77−8851
Ni-Zn, γ-phase region, X-ray and electron diffr. obs. 79−61562
Ni_5Ge_3, solid and liquid, physicochemical props. and structure 80−39548
NiO-Al_2O_3, Verneuil-grown crysts., phase comp. 77−66586
NiO-CuO, equilibrium relations 80−55375
NiO-$NiAl_2O_4$-Al_2O_3, heterogeneous solid state reactions, role of phase boundaries, dynamic equilib. at interfaces 78−71848
NiSi, dissociation in presence of Ni film 79−47892
$(Ni_{1-y}Y_y)_3Al_{1-x}Sc_x(Ti)_x$, quarternary gamma prime ($L1_2$) pseudobinary props. revealed by ionicity modified pair model 78−19725
Ni_3Zr, cryst. struct. and stability 79−90597
O_2, phase equilibria near 298K, Raman spectral study of solid and fluid 80−19937
O_2, potential in equilibrium with impure high temp. inert gases 80−104135
O_2-^{85}Kr-Xe, liquefaction, retention of ^{85}Kr from fission exhaust gases, separation technique *(German)* 80−27753
O_2-Ar system, low temp. liquid-vapour equilib. 78−83927
Pb, equation of state, isentropic expansion method 78−91414
Pb melts, As and Sn distrib., Si, Cr, and Mn influence *(Russian)* 80−16274
Pb multicomponent glasses, alkali evaporation, mass spectrometry study, thermal anal. 79−74464
Pb, splat-cooled and vapour-deposited, metastable structs. 79−87018
Pb-Ag, high shear technique for liquidus boundary meas. 79−61564
Pb-Bi, peritectic reaction, microstruct. changes 78−52753
Pb-Cr-O system, equil. relationships, stability limits 77−59765
Pb-In-Sn system, liquidus and solidus isotherms 78−44088
Pb-S-O system, phase equilib. *(Rumanian)* 78−19727
Pb-Se-As-Ge, phase separation in melt centrifugal quenching 80−25701
Pb-Sn, melt viscosity rel. to phase equilib. *(Russian)* 79−69272
Pb-Sn-Te, liquidus meas. by DTA 79−95999
Pb-Sn-Te system, solvent choice for PbTe and SnTe LPE 79−87589
Pb-Te-O, thermal stability 78−44104
Pb-Tl-Te, liquidus of ternary system 79−8285
Pb-Zn, liquid phase immiscibility determ., DTA 78−64523
PbF_2-x$PbO.ySiO_2$, activities rel. to liquidus comp. 77−28798
$Pb_xMo_6S_8(Se_8)$, prep., metallurgical and supercond. props. 77−32102
PbO, stoichiometric deviations on heating in vacuum 77−25035
PbO-B_2O_3-Al_2O_3 system melts and glasses, viscosity, phase separation, and supercritical fluctuations effects 79−65235
PbO-Bi_2O_3-GeO_2, exam. of glass forming and liquid phase separation regions, and optical props. 78−88453
PbO-MoO_3-MO and PbO-WO_3-MO systems, M=Ca, Ba, Mg, Sr, perovskite type cpds. detection 80−108404
PbO-MoO_3-P_2O_5, glass phase investigation, density determ. *(Polish)* 77−70039
PbO-$PbSO_4$ system, thermodynamic study of solid and liq. phases *(French)* 77−35667
PbO-SiO_2, molten, activity of PbO, effect of CaO, Al_2O_3, MgO and ZnO 78−60663
PbS-Ni, phase diag., cpd. formation and electrophys. props. 77−85997
$Pb_{1-x}Sn_xTe$, grown by LPE, solid-liquid tie line determ. 78−64526
$Pb_{1-x}Sn_xTe$, solid-liq. phase equilib. above 750°C 79−82316
PbTe homogeneity region investig. in Pb-Te system, equil. consts. of quasi-chem. reactions 80−108405
$Pb(Zr,Ti)O_3$, piezoelec. ceramic, coexistence of tetragonal and rhombohedral phases 77−7845
$Pb(Zr,Ti)O_3$, thermodynamic properties and formation data 80−29939
Pd-Ag, Fermi energy influence on soln. behaviour of H, B and C *(German)* 80−44323
Pd-D-H, equilib. H/D separation factors 80−59668
Pd-Rh-H and Pd-Ni-H, hydride formation in high press. range 80−65235
Pd-S(Se)(Te) mixtures, binding of phases, two-correl. model 77−80438
Pd-Zn, γ-phase region, X-ray and electron diffr. obs. 79−61562
PdD_x, model of instabilities 78−75619
PdGe, dissociation in presence of Pd film 79−47892
PdH_x, model of instabilities 78−75619
PdO, semiconductivity and stability, optical props. 78−43497
Pr-Cr-B system, phase equil. at 800°C, boride lattice parameters *(Russian)* 78−31388
Pr_2NiO_4, elec. props., 300 to 1000°C 78−91694

phase equilibrium continued
$Pr_{1-x}Ca_xAl_2$, mag. props. and phase relations 80−107991
$PrFeO_3$, elec. props., 300 to 1000°C 78−91694
$Pr(OH)_2Br$, hydrothermal phase equilib., cryst. struct. 78−35372
$Pr_7(OH)_{18}Br_3(I_3)$, hydrothermal phase equilib., cryst. struct. 78−35372
PrP-I, heterogeneous equilib. 77−36777
Pt-Au, miscibility gap, thermodynamic anal. *(German)* 79−91629
Pt-S(Se)(Te) mixtures, binding of phases, two-correl. model 77−80438
Pt-Si, constitution 79−29054
Pt-Zr(Hf), high temp. thermodynamic props. 77−63633
PtSi, dissociation in presence of Pt film 79−47892
R-O systems, exam. of phase diagrams and crystal structure 79−8291
rare earth oxide-Nb_2O_5 system, phase formation thermodynamics 77−86348
Rb_2O-Nb_2O_5(Ta_2O_5), phase equilib. relns. and crystal chemistry, structs. useful as ionic conductors 79−20033
$RbRF_4$, R=La, Ce, Pr, Nd, Sm, phase equilib. and cryst. struct. *(French)* 78−44107
Re-Al-Si system, phase equilibria, $ReAl_{1.2}Si_{0.8}$, $ReAl_{1.25}Si_{0.75}$ prod., struct. 78−35357
Re-Fe-Al, physical-chemical investigation *(Russian)* 78−15362
S, new high pressure phase from decomposition of S_4N_4 79−10911
S-benzene systems, liq.-liq. phase separation 80−96658
S-O-C, equilibrium 550 to 1100°C 79−38807
$(SN)_x$ and S_4N_4, high press. study 78−52782
Sb, film, liquid and vapour quenched, metastable struct. 79−56974
Sb, splat-cooled and vapour-deposited, metastable structs. 79−87018
Sb-Te-Bi, computer study of miscibility limits, 273 to 300K 78−52781
$(Sb_{1-x}Bi_x)_2Te_3$, δ phase, equilib. state, electrophysical props. 79−52178
Sb_2O_4-$NaSbO_3$($KSbO_3$)-NaF, phase equilibria and crystal growth 77−70035
Sc-[Co,Ni,Cu]-Ga, phase equilibria, diagrams of state, X-ray, microstructural study *(Russian)* 80−55356
ScN_x, region of homogeneity, physicochem. props. 78−52018
Sc_2O_3, fission and phase transition enthalpies 79−99299
Sc_2O_3-ZrO_2 (HfO_2), cubic solid soln., lattice parameters 79−82186
Sc_2O_3+Sb(V) reaction, phase formation, structs. 77−84712
Se, liq., heat capacity and chem. equilib. 80−103486
Se-Tl(Bi)(Sb), liquid alloys, vapour phase effect on activity determ. *(German)* 79−43210
Si-Al-B-O-N, calc. of phase diagrams from data set 80−55362
Si-Al-Be-C-N system, phase equilibria 80−60839
Si-Al-O-N, mullite like cpd. comp., EPMA, X-ray and chem. anal. obs. *(Japanese)* 80−35175
Si-Al-O-N system, exam. of compounds and properties 78−48387
Si-Al-O-N system, phase analysis and TEM struct. obs. 80−108420
Si-Al-O-N system, stable phase cryst. struct. and microstruct. obs. using TEM 80−108421
Si-Al-Zr-O-N, calc. of phase diagrams from data set 80−55362
Si-N-H gaseous system, deposition ranges of Si_3N_4 and Si *(French)* 77−36405
SiC, polycrystalline, quantitative phase analysis, statistical estimation and mathematical splines *(Bulgarian)* 78−39753
α/β-Si_3N_4, formation during nitridation of Si 80−50609
Si_3N_4, impure, oxidation, phase equilibria 79−70045
Si_3N_4, oxidised, with Y_2O_3 densification aid, temp. and compositional stability of $Y_6Si_6O_{21}$ 78−27664
Si_3N_4, phase content determ., using X-ray diffr. anal. 78−44281
α/β-Si_3N_4, phase yields during form., influencing factors 80−108408
Si_3N_4-AlN-Al_2O_3-SiO_2-Y_2O_3, phase equilibrium study by X-ray diffr. and optical microscopy 80−50614
Si_3N_4-AlN-SiO_2-Al_2O_3 solid-liquid equilibria 78−92247
Si_3N_4-Mg_2SiO_4-Si_2N_2O, compressive creep, composition effect 80−50674
Si_3N_4-SiO_2-MgO, phase relations and interrelation with mech. strength, and oxidation 78−48386
Si_3N_4-SiO_2-Y_2O_3, subsolidus phase relations 80−60845
Si_3N_4-SiO_2-ZrN-ZrO_2, X-ray diffr. phase anal. and reactions Si_3N_4+ZrO_2, SiO_2+ZrN 80−50613
Si_3N_4-Y_2O_3-Al_2O_3-SiO_2, X-ray diffr. exam., phase equilib. at 1400 degrees C *(Japanese)* 78−44113
SiO_2 phase equilibrium and microstructure interpretation 80−60847
SiO_2, sitall coating, control of phase composition, microstruct. and props. 77−32545
SiO_2-Al_2O_3, minerals, phase equilibrium *(German)* 77−73261
SiO_2-Al_2O_3 mixture, depend. of phase comp. on nuclei available 79−11584
SiO_2-Al_2O_3 system, location of metastable immiscibility gap 79−77521
SiO_2-Al_2O_3 system, phase equilibria 79−77724
SiO_2-α-Al_2O_3, metastable phase equilib. diagram without mullite 79−4398
SiO_2-Na_2O-CaO (13, 11 wt.%) glass, phase separation, SiO_2 purity effect 80−44144
SiO_2-Na_2O-CaO glass, phase separation characts., melting atmosphere effect 80−44141
$Si_6O_{15}^{6-}$ double chain anion containing anhydrous silicates, synthesis, cryst. chem. 80−59444
$SiO_2Al_2O_3$-CaO-K_2O system glass, phase separation and crystn., F catalytic effect 79−60280
Sm-Cr-B system, phase equil. at 800°C, boride lattice parameters *(Russian)* 78−31388
Sm-Fe-B ternary systems, phase equilibria and cryst. struct. *(Ukrainian)* 80−11626
Sm-H, H equilib. press. 80−66492
Sm_2Co_7 sintered magnets, coercive force and constitution, annealing temp. depend. *(Russian)* 80−88786
$SmMnO_3$, thermogravimetric study of phase stability 79−100121
Sm_2O_3-HfO_2, kinetics of initial stages of formation of cpds. 77−48617
Sn-Pb, liquid alloy, thermodynamic activity determ. using Knudsen method *(German)* 79−34008
$Sn_xMo_6S_8(Se_8)$, prep., metallurgical and supercond. props. 77−32102
$SnSe_2$, sublimation, temp. depend. of equilib. constants 80−88312
(Sr/Ba)(Fe/Al/Ga)$_{12}O_{19}$ solid soln. crystal for hexaferrite layer substrate *(German)* 78−23672
Sr_2GeO_4-$Sr_3(PO_4)_2$, phase equilibria and struct. 77−85999
$SrNb_2O_6$-$NaNbO_3$-$LiNbO_3$ pseudo-ternary system, DTA, heat treatment and X-ray diffr. obs. *(Chinese)* 79−52175
SrO-Fe_2O_3 system, non-existence of single phase $SrFe_2O_4$, Mossbauer expts. 80−29178
Sr_xVO_2, oxygen vanadium bronze, phase comp., heating in air 77−40417
$Sr_3Zr_2O_7.2H_2O$, cryst. struct. and thermal stability, X-ray characterisation 78−83796

phase equilibrium continued
steel, Si killed, effect of Al addition to Zn on phase composition and morphology of products of Fe-Zn reaction *(Polish)* 78−85021
Ta carbides, changes in phase structure during prolonged heating in vacuum 78−44095
Ta-D system, phase equilibria study *(Japanese)* 79−78936
Ta-Ga phase relationships, X-ray anal. of struct. 77−36453
Ta-H system, phase equilibria studies *(Japanese)* 79−78935
Ta-N, domain configurations of new phase *(French)* 78−56648
Ta-Si-Cu, struct. and supercond., Cu influence 80−50592
TaS_2, decomp. press. and enthalpy of decomposition 79−66042
$TaSi_2$-$CrSi_2$, phase equilib., struct. and props. 80−50608
TeO_2-P_2O_5, electron microscope exam. of phase equilib. and immiscibility 78−52779
TeO_2-V_2O_5-Fe_2O_3 system, phase equilib. and analysis, primary crystn. fields 77−66628
Ti-Al (30 to 57 wt.%), phase equilibria from mag. susceptibility studies 79−60483
Ti-Al-Mo-Cr-Fe, distrib. of Sn, Zr between phases, temp effect. 80−55357
Ti-Al-Zr-Mo alloy 685, phase at α/β interface *(French)* 80−25661
Ti-Al(Fe) microprobe anal. of alloying addition distrib. 80−55358
Ti-B-Mo system, phase equilibria at 1400°C 78−35354
Ti-Mo-Al, determ. of interaction parameters from EPMA data 77−63635
Ti-N system, phase relations, struct. rel. to heat treatment 79−11552
Ti-Nb-W, 20 to 1000°C, isothermal section, X-ray anal., microstruct., hardness, cond., transform. *(Russian)* 77−55947
Ti-O system, intermediate oxide thermodynamics under equilibrium press. 80−55351
Ti-O system, nonstoichiometry between Ti_3O_5 and TiO_2 comps. at high temps. 77−15594
Ti-Ta-Co system, phase stability, X-ray anal. 79−61580
Ti-V-Mo alloy system, phase equilibria and interstitial effects, TEM and X-ray diffr. study 79−43204
Ti-V-Mo-Cr system, β-phase stability 80−55353
Ti-V-Si, equlibrium silicide, X-ray and electron diffr. obs. 78−27483
Ti-ZrO_2(HfO_2), eutectic system metallographic investigation *(Russian)* 77−66629
$Ti_{0.75}Al_{0.25}H_x$, $x<1.5$, metastable hydride form. 78−51682
TiO-ZrO_2, pseudo binary system, effect of Ti addition on struct. and props. of zirconia 79−11583
TiO_2-NiO-Sb_2O_3 phase equilibria 78−44098
TiO_2-Sb_2O_3 system, phase comp. of roasted coprecipitates 78−23651
Ti_2O_3-MgTiO$_3$, phase analysis 78−3103
$TiSi_2$-$CrSi_2$, phase equilib., struct. and props. 80−50608
Ti(Zr,Hf)-Gd-B system, phase equilib. 80−11629
Tl, liquid, O_2 activity from electrochemical meas. 80−104123
Tl-Se, liquid mixtures, press. effect on two-phase region 80−75347
Tl-Se liquid binary mixtures, phase separation under press. 80−34183
Tl-Sn-Te system equilibria, polythermal and isothermal cross sections obs., ternary cpd. form. 80−104128
Tl-Te, phase equilibrium exam., using DTA, X-ray diffraction, and hardness 79−1846
Tl_2S-Ag_2S system, phase equil., DTA, X-ray and microhardness obs. 79−38803
Tl_2S-SnS, phase equilibria exam. 80−55369
Tl_2S-Tl_2Se(Tl_2Te), exam. of phase equilibria, using DTA, X-ray phase analysis and microhardness 79−4953
Tl_5Te_3-Tl_4SnTe_3-Tl_4PbTe_3, DTA, XPA and microhardness meas. 80−96628
U-C-N system, high temp. X-ray diffr. exam. of structure *(French)* 78−72765
U-Nb-Zr (16.6, 5.6 wt.%), stability of BCC phase 79−66039
U-O system, phase equilibrium, thermal, X-ray and cond. meas. 78−35371
U-Pu carbides, advanced LMFBR fuels, equilib. thermodynamics 79−67862
U-Pu-C-N system, phase relationships and equil., effects of oxygen, review 77−21126
U-UNi_2-UCo_2, system, phase equilibria, lattice constants *(German)* 80−50598
U-Zr-O system, phase formation, phase equilibrium 80−16667
UAl_2-UNi_2, phase relationships, thermal, microscopic and X-ray exam. *(German)* 78−88447
UC-UN, in equilibrium with UC_2 and/or C, relationship between N_2 pressure and composition, phase relationships 79−43223
UF_6-MF_x(MF_6), dil. solns., (M=Te, Mo, W, V, Sb, Ta), liq.-vapour equilib. 77−62632
UO_2-Gd_2O_3, interfacial energy meas. 77−59763
US-UC_2, solution studies 77−21120
V-Al(Ga,Si,Ge,Sn)-Cu, rapidly quenched, comp. and phase equilib. 80−76235
V-D system, phase equilibria study *(Japanese)* 79−78936
V-H system, phase equilibria studies *(Japanese)* 79−78935
V-Mn-O system, phase comp. during oxide prep. 78−27447
V-N system, phase formation *(Russian)* 78−39739
V-Ni-Al, phase equilib., elect. cond., hardness *(Russian)* 77−66627
V-Si-Cu, struct. and supercond., Cu influence 80−50592
V-Sn(Al)(Ga)(Ge)(Si)-C, phase equilib. and supercond. 80−50593
V-ZrO_2(HfO_2), eutectic system, metallographic investigation *(Russian)* 77−66629
$V_{3-x}Cr_xSi$, x=0 to 3, struct., supercond. and mag. props. 80−1962
$V_{13}O_{24}$ long-period Magneli phase as product of V_6O_{11}-V_7O_{13} periodic microsyntactic intergrowth 80−50618
V_2O_3-Ti_2O_3-TiO_2, phase equilib. at 1473K 77−16562
V_2O_3-VO_2-GeO_2, phase equilibria as function of O_2 pressure at 1173K *(French)* 79−42216
V_2O_3-VO_2-M_2O_3, (M=Ga, In or Y), phase equilibria as function of O_2 pressure at 1273K *(French)* 79−42216
V_2O_5-P_2O_5-H_2O, formation of $VOPO_4.2H_2O$ 77−44228
VS through V_3S_4, nonstoichiometric, phase relations and thermodynamics 80−29188
V_3S_4-V_5S_8 system, exam. of thermodynamic props. at temp. from 650 to 800°C 78−52784
VSe_2 phase, stability and Se equilib. vapour press., homogeneity range 78−43133
VSi_2, thermodynamic props. determ. using ternary phase equilibria 78−91449
V_3Si, thermodynamic props. determ. using ternary phase equilibria 78−91449

phase equilibrium continued
V_5Si_3, thermodynamic props. determ. using ternary phase equilibria 78−91449
$V_xW_{1-x}O_2$, phase relations, vacuum seal study and DTA obs. 79−100122
W alloys, phase anal., electrochem. separation of carbides 78−60651
W-alkali earth oxides, multiple phase systems, calc. of phase equilibria, using thermodynamic analysis *(Russian)* 79−56964
W-C-(Zr)(Hf)(Nb)(Ta)(Re) alloys, vacuum melted, phase composition, struct. and props. 78−31403
W-O system, surface elect. cond. of oxides in equilib. with gas phase 79−61791
W-Re, neutron irrad. effects on phase stability free energy changes 79−11566
W-Re, sigma phase stability and irradiation effects 78−11200
W-Si-Cu, struct. and supercond., Cu influence 80−50592
W-Y(La)(Ce)-B, phase equilib., struct. of crysts. 77−21122
W-Zr (2.92, 7.42 and 10.02 wt.%), and W_2Zr, thermal expansion, elec. resistance, 100-900°C, crystallisation 78−91455
W-ZrC(-Re) eutectic alloy, Re effect on breaking stress, lattice parameters, electron struct. *(Russian)* 79−1845
W_2As_3, decomp. press. and enthalpy of decomposition 79−66042
Y-Fe-O, phase equilib. and thermodynamics, solid state high temp. electrochem. obs. 79−56967
Y-Ge-B, X-ray investigation of phase equilibrium 79−99294
Y-Ni-Al ternary system, 800°C isothermal section in range 0 to 33.3 at.% Y *(Russian)* 77−70028
Y-Sb compounds, heat of form. meas. 77−36783
Y-Si-Al-O-N ceramic, phase assemblages, relationships with props. 80−60848
Y-Si-Al-O-N solid soln., based on α-Si_3N_4 struct., comp. and struct. 79−74136
Y-Zr-H, phase diag. *(Russian)* 77−59749
YAG, solubility in solvent $PbO-_xPbF_2$, phase form. in system Y_2O_3-Fe_2O_3-PbO-PbF_2-B_2O_3 78−95247
$Y_3Fe_5O_{12}$, formation mechanism from metallic oxides 77−48376
YIG crystals, bulk growth from high temp. solns.; props. 80−66413
$YMnO_3$, thermogravimetric study of phase stability 79−100121
YN, decomp. press.-temp. relations 78−52780
YN-UN, decomp. press.-temp. relations 78−52780
$YO_{1.5}$-PrO_x, phase relns. and electrophys. props. of solid solutions 78−23686
YO_x-ZrO_2, YO_x-rich, phase equilibria 77−21117
Y_2O_3, fission and phase transition enthalpies 79−99299
Y_2O_3-HfO_2(ZrO_2) systems, solid soln. form. mechanisms 79−11579
Y_2O_3-Mn_2O_3, solid-phase reactions 77−48405
Y_2O_3-ZrO_2 (HfO_2), cubic solid soln., lattice parameters 79−82186
YOF-YF_3, high pressure phase transitions 80−55368
$Y(OH)_3$-α-FeOOH, physicochem. props. rel. to growth of $Y_3Fe_5O_{12}$ 77−40418
YPO_4-Cr_2O_3 system, oxyorthophosphates form. 79−78942
YPO_4-Y_2O_3 system, oxyorthophosphates form. 79−78942
$YbCr_{1-x}Al_xO_3$ solid solutions 80−20887
$YbMnO_3$, thermogravimetric study of phase stability 79−100121
Zn-As-Te system, As_2Te_3-ZnTe cross section investig. 77−36473
Zn-Bi, liquid, inconsistent conjugated liquidus 80−76232
Zn-In(Bi) interfacial tension and microstruct. 79−74132
Zn-Pb melt, immiscible component distrib. in crossed EM fields *(Russian)* 77−48396
Zn-Sb system, phase interactions and phase diagram 79−87607
$ZnAl_2S_4$-$ZnCr_2S_4$, nonstoichiometric spinel solid solns., synthesis and cryst. chemistry 77−35526
ZnCaSO, struct. and phase analysis *(Russian)* 77−58995
ZnO-PbO-B_2O_3, exam. of glass formation and its props. 79−8283
ZnO-TiO_2 system, heat treated, X-ray anal. of phase form. sequence 79−1850
ZnSe+CeTe⇄CdSe+ZnTe ternary mutual system, phase equilib. 79−52179
ZnTe-CdSe solid solutions *(Russian)* 79−43224
Zr-Al-O system, diffusion welding, 1000 to 1300°C, Al_2O_3-(Zr-Al) alloy, ZrO_2-(Zr-Al) alloy, Al_2O_3-ZrO_2 couples *(German)* 79−33122
Zr-Fe, Mossbauer spectra parameters of Zr_2Fe particles *(Russian)* 80−29654
Zr-Fe-Cu-W, Mossbauer spectra parameters of Zr_2Fe particles *(Russian)* 80−29654
Zr-Ge-B system, phase equilibria 78−35356
Zr-Mo (3 wt.%), β-phase stability 78−39742
Zr-Mo-Al (3, 1 wt.%), β-phase stability 78−39742
Zr-N system, hydrogenation, phases form. 79−43200
Zr-Nb-Ga, phase equilibria 800°C *(Ukrainian)* 80−35157
Zr-Os quenched alloys, metastable phases *(Ukrainian)* 78−84804
Zr-Sc-Ga, phase equilibria 800°C *(Ukrainian)* 80−35157
Zr-Ti-Be metallic glass, phase separation 80−97464
Zr_3Al base alloy, forming press. tubes 77−8784
ZrC-Ni, refractory-liquid metal, interfacial reactions, C effect, electron microprobe analysis 77−12829
ZrC_x, change in lattice const. in region of homogeneity 77−25029
ZrC_xO_y, C-stabilised low temp. cubic phase 77−36478
$ZrD_{1.82}$, and $ZrD_{1.96}$, struct. and phase equilib., neutron diffr. obs. *(Russian)* 78−92244
ZrF_4-ThF_4-NdF_3(LaF_3), phase equilibrium, vitreous phase struct., charact. temp., optical props. *(French)* 79−11587
(ZrF_4-BaF_2-ThF_4)-EuF_2 system, glass forming region, prep. and props. 79−91633
ZrH_x, two-phase (δ+ε), homogenisation during neutron bombard. *(Russian)* 78−18684
ZrO_2, MgO partially stabilized, microstruct. development during ageing 79−91710
ZrO_2, obtained by vapo-condensation, exam. of structure and phase props. *(French)* 79−19489
ZrO_2, substoichiometric, thermodynamic props. at lower phase boundary 80−29185
ZrO_2-Al_2O_3-SiO_2, subsolidus equilibria and stabilization of tetragonal ZrO_2 78−27497
ZrO_2-La_2O_3 system, phase form. and relations, phys. props. 79−43218
ZrO_2-MgO system, intermediate phases existence, X-ray diffr. and IR obs. 79−38805
ZrO_2-P_2O_5, hydrated, heat treatment and coprecipitation, phase transitions 77−90335
ZrO_2-Sc_2O_3, phase system, X-ray and thermal anal. 78−27494
ZrO_2-TiO_2 system, Z *(Ukrainian)* 79−96007

phase equilibrium continued
ZrO_2-W, eutectic microstruct. 78−27499
ZrO_2-Y_2O_3, phase equilibria and ordering 78−48385
ZrO_2.SiO_2-αAl_2O_3 mixed powders, solid state reactions 80−40337

phase equilibrium diagrams *see phase diagrams*

phase-locked loops
400 Mb/s optical fibre communications, integrating and transimpedance front end performance comparison *(German)* 78−33879
atomic reference frequency stability transfer to quartz crystal oscillator 79−54108
automatic internal friction and modulus meas. apparatus using phase-locked loop 78−13981
automatic NMR field-freq. lock, pulsed phase locked loop approach 78−74041
closed-loop vibration system for measurement of dynamic shear modulus of cylindrical specimens 79−61827
demodulator, ECG-telemetry apparatus appl. *(German)* 78−57097
descriminator for automatic observation of whistlers 78−89014
digital signals, phase measurement using PLL method for low S/N ratio 78−16810
discriminator, five channels, automatic meas. of whistler dispersion *(Japanese)* 80−31143
Doppler US blood velocity meas., phase-locked loop technique 78−61234
EEG automatic sleep staging detectors 78−53551
EEG spindle detection system, human and automatic validation 80−98154
fine frequency analysis device, appl. to biosonar signals of bats 77−56392
flowmeter, implantable Doppler design with phase-locked loop 78−31873
foetal breathing movement electronic anal., phase-lock-loop principles appl. 79−2152
frequency tracker for laser Doppler anemometry 79−72968
frequency-agile phase lock system for mm wave klystrklystron 77−5446
gastroelectric surface signal analysis, phase-lock system design 79−34687
gastroelectric surface signal analysis, phase-lock system performance 79−34688
heart-rate store, PLL circuit, portable *(German)* 78−65139
IC, heart rate measurement system appl. 77−52906
inductive sonde, large bloodvessel movement, transcutaneous meas., design and realisation *(Italian)* 79−70602
Josephson junction analogue to study effects of thermal noise 77−47939
laser intracavity phase lock control system 79−76718
laser printers and scanners, fractional picture element registration clock generation 77−58486
lasers, coherently combined, phase lock control considerations 80−5743
lock indicator and event alarm for multiplexed seismograph telemetry 79−62597
MM-wave klystron for radiospectroscopy phase stabilisation 77−5456
plunger device with PLL distance regulation for nuclear lifetime meas. 79−6806
resonance-bar damping meas. system, phase-locked loop for reson. freq. control 77−2649
RF SQUID magnetometer, synchronous demodulation, amplitude- and phase-sensitive detection 80−105679
SAW delay line and resonator oscillators for phase locking 78−59254
SAW transmitting hydrophone development and performance 79−53586
short range precision navigation and tracking system using PLL 78−53742
sleep spindles, automatic detection device 79−16316
synchrotron beam RF phase lock loops, effect of large delays 79−68046
He-Ne multimode and single-mode lasers, phase locking to very high coherence degree 79−76710

phase measurement
300 MHz oscillators using SAW resonators and delay lines 78−59255
AC polarography, signal components, meas. using multiplier circuitry 78−61119
AC vector diagram, demonstration using CRO 77−37685
AC voltage phase lead-lag and sequence monitor 78−65942
ambiguous correlated measurements, regression problem 79−88903
ATS-6 satellite radio beacon, modulation phase meas. at Ootacamund, India 79−48611
chart recorders, simple test for phase characteristics quantification 79−92409
circuit for selecting signals in specified phase range 78−56863
complex aspheric mirror testing by phase meas. interferometry 80−74467
controlled-current impedance meas. equipment design *(Spanish)* 78−8421
damped and undamped systems, phase relationships *(German)* 80−106746
detector produces unambiguous output 78−4627
digital phase detection used for computing phase angle averages 78−21163
digital phasemeter, tracking, quantisation error reduction *(Russian)* 77−61079
digital signals, measurement using PLL method for low S/N ratio 78−16810
electro-optic spatial phase modulators, resolution meas. techniques 77−79959
electron microscopic diffraction patterns, direct phase determ. *(German)* 77−2713
electronic phase meas. techniques in optical testing 80−106643
expt. error evaluation algorithm *(Russian)* 77−41636
fatigue cracked sample stress meas. by US phase shift detection 77−28971
Fizeau interferometer, spherical-wave, direct phase meas. 80−95126
forced oscillations experiment for students 80−17780
galvanic coating thickness gauges using phase angle meas. 77−79114
Hartmann modified wavefront sensor performance 80−74522
interferometer, single mode optical fibre, small phase shift meas. 80−57366
interferometer with filamentary spatial filter and extended source of polychromatic light 79−71518
ionosphere, radiowave phase and amplitude meas. interpretation *(Russian)* 78−77394
ionosphere reflected signal, sum phase random props. investigation 79−53615
ionospheric EM wave propagation in HF and MF bands, Doppler meas. accuracy 78−77417

phase measurement continued
Kalman filters appl., digital, optimal, synthesis with a priori uncertainty of data 80−98934
laser cavity interferometer, for phase changes $<10^{-5}$Å 77−18087
laser rangefinder operating frequency selection 79−72691
laser sliding reference interferometer for two-dimensional phase meas. 77−19280
lossy waveguide attenuation and phase meas. 77−26343
microwave interference signals from 0 to n.360° for plasma density meas. *(German)* 80−6278
microwave phase shifts, interferometer for high-spatial resolution meas. 77−3994
microwave systems, error anal. due to reflections *(Bulgarian)* 79−88975
optical complex spatial coherence meas. by sinusoidal phase modulation 80−106446
optical fibre material dispersion meas. by baseband modulated envelope detection 78−1368
optical phase measurement in real time using photodetector array, Fourier transform computation 80−9013
phase locked interferometers, phase difference, surface topography measurements, transparent phase object applications 79−58775
phase-angle differences, up to 100 MHz meas. devices classification 80−52269
photoacoustic spectroscopy in solids, phase measurement, appl. to nonradiative transitions, optical absorpt. 80−31885
photoconductor carrier lifetime, nonequilibrium, phase method for determ. 80−65629
plasma density IF phase meas. using three-mirror interferometer 78−75414
precision optical element testing by phase meas. interferometry 80−74520
precision optical evaluation by phase meas. interferometry 80−74533
pulse continuous RF signal amplitude and phase difference measuring device 78−12719
radar interferometry, linear phase detect. *(Italian)* 78−85855
radiointerferometric phase meas. ambiguity detection, recurrence relationship *(Russian)* 79−25513
RF phase bridge, use of piezoelectric resonators 80−4732
spatial phase structure meas. of ionospherically reflected waves using HF array 79−84505
statistical analysis of phase fluctuations, instrument design 77−45861
stellar interferometry, phase effect detect. and appl. to orbit of α Aurigae (Capella) *(French)* 80−36508
straightedge Fresnel diffraction, optical phase distrib. interferometric meas. 79−76579
time-freq. secondary standards, VLF radio station phase reception/processing convertor 77−87739
tissue US attenuation and velocity meas. by direct and phase-contrast imaging 77−64114
transmission acoustic microscopy, meas. using AM carrier 80−74665
two-scale meters, max. likelihood estimate of parameter for error anal. 77−61047
underwater sound, estimation and interpretation of acoustic CW phase fluctuation spectra 77−46850
wavefront distortion sensing for adaptive optics system control 77−19293
Cs stocks, experiments to reduce cavity phase shift errors in the Cs beam tube 80−98893
Ge:Zn^{11} carrier lifetime, nonequilibrium, phase method for determ. 80−65629

phase meters
acoustic wave phase velocity meas. using CW feedback technique 78−83187
cyclic meas. ambiguity elimination *(Russian)* 79−6072
detector produces unambiguous output 78−4627
digital, 2 Hz to 200 kHz range, without freq. tuning *(German)* 78−54409
digital, Dranetz model 314, comparison with analogue techniques and significant advantages *(Italian)* 80−68211
digital, optimal threshold determ., meteorological Doppler radar station appl. *(Russian)* 78−20560
digital, tracking, quantisation error reduction *(Russian)* 77−61079
digital, using delayed pulse train 77−49742
digital, with seven-segment luminescent vacuum display, counter scheme 78−4648
digital phase shift for meter calibration 79−44898
direct-reading phase meter with Schmitt trigger *(Spanish)* 77−37935
expt. error evaluation algorithm *(Russian)* 77−41636
flip-flop type, modulation method automatic testing, digital readout 77−53939
geostationary satellite VHF Faraday rotation mea. for ionospheric electron content 78−61599
heterodyne holographic interferometry, electronic instrumentation employing phase meter 80−87352
intermittent sinusoidal voltage phase difference meas. device 78−77941
IR compensation phasemeter based on Mach-Zehnder interferometer 77−39039
Kalman filters appl., digital, optimal, synthesis with a priori uncertainty of data 80−98934
mechanical vibrations, low freq. and low amplitude, meas. system 78−54359
phase automatic freq. control parameters, optimal values *(Russian)* 80−77814
phase-angle differences meas., up to 100 MHz meas. devices classification 80−52269
pulse-phase, torquemeter, magnetically coupled pulse transducer with electronic phasemeter 80−74819
sensitivity improvement by use of pulse spectra 77−71344
test equipment, based on comparison with angular measure 77−10057
test measuring transducers 78−77894
VHF phase difference meter *(Polish)* 77−87779

phase modulation
see also phase shift keying
acoustic sensor, single multimode fibre, using mode-mode interf. 79−50553
baseline ripple reduction by quasi-optical phase modulation, mm radio spectra 80−56710
bat echolocation system, optimum phase modulation for insensitivity to acceleration 79−53163
beats, interference phenomenon demonstration 79−75307

phase modulation continued
chalcogenide glass films, kinoform optical elements and integrated optics elements prod. 77−75634
chalcogenide glass films, opt. inform. recording uses 77−75633
closed-loop simple system for real-time optical phase meas. 79−63302
continuous deformable mirror multidither coherent optical adaptive system characteristics 77−19297
electro-optic spatial phase modulators, resolution meas. techniques 77−79959
electrooptic radiation modulators utilizing semiconductor ridged waveguides 80−91925
electrooptical waveguide, plamar, thick, mode formalism *(German)* 77−27367
ferroelectric ceramic-photoconductor structure, as optically controlled transparency 80−28343
fibre optic rotation sensor with low drift 80−69530
Fibredyne systems for passive or semipassive fibre-optic sensors 78−71206
high frequency vibr. meas., phase interpolation and modulation principle *(Chinese)* 79−37262
holographic pattern recognition of Korean alphabets, discrimination enhancement using phase modulated matched filters 80−95854
interference pattern electronic heterodyne recording 80−74316
interferometry, combined with object scanning *(French)* 79−2814
interferometry, phase modulation, meas. of phase differences in microscopy *(French)* 77−82593
interferometry, phase-modulation, sine restoration of phase in object field *(French)* 77−79144
laser interferometer, LF, for small vertical vibration meas. 77−37970
laser scanned acoustical imaging systems, demodulation scheme 79−59826
laser speckle reduction by US modulation 79−3638
microwavelength instability meter 77−10054
multimode optical fibre phase modulators and discriminators, theory 78−55446
multimode optical fibre phase modulators and discriminators, expts. 78−55449
optical complex spatial coherence meas. by sinusoidal phase modulation 80−106446
optical fibre data collection highway with piezoelectric phase modulators 77−39098
optical fibres, phase modulation of coherent light using HF sound 78−87142
photoelectronic phase and frequency modulation 78−79131
ruby, phase modulated conjugate wave generation, hologram model 80−83643
ruby laser, ultrashort pulse generation by internal phase and amplitude modulation 80−106551
saturated absorption spectroscopy, optical feedback-effects suppression by phase modulation of refl. light 78−21225
SAW devices based on interaction of SAW with electrons in semicond. 77−80025
signal detection, random process, nonlinear medium *(Russian)* 77−75606
single-mode optical fibre phase modulators, pressure sensitivity meas. 79−7205
speckle elimination using random spatial phase modulation 77−71923
spin-echo Fourier transform NMR spectroscopy, multiple pulse technique 80−37063
two-beam interference pattern monitoring 80−77844
underwater sound, path-length modulation rel. to CW phase fluctuation spectra 77−46850
underwater sound, phase modulation by internal wave vertical vel. 77−46852
underwater sound, simulation of phase modulation by first-mode directional internal wave 77−62089
vibration analysis by wavefront modulated holography 79−3652
CdTe, electro-optic IR phase modulator, phase and freq. characts. 77−54805
GaAlAs LED sources for fibre optic transmission, linearity improvement using phase-shift-modulation technique 77−19403
GaP-AlGaP, stripe-geometry electrooptical modulator 80−23798
He-Ne 3.39 μm laser mode-locking for ultrashort pulse generation 77−83909
$LiNbO_3$ electro-optic phase modulator for unpolarised laser beam 79−50403

phase regulation *see phase control*

phase shift circuits *see phase shifters*

phase shift keying
intermode phase scanning for recovering phase-modulated signals on multimode optical fibres 80−58682
modems, satellite links, high rate data communication 77−49268
multilevel in optical communication channels, carrying capacity 78−78934
turbulent atmosphere, optical DPSK system performance 78−42293
two-phase PSK modulator employing SAW delay line, fundamental performance 80−33398

phase shift microphones *see microphones*

phase shifters
see also phase changing circuits; phase convertors
90° phase shift beam splitter for displacement interferometer 78−87145
94 GHz bulk crystal electro-optical phase shift calc. 80−71382
for amateur radiotelescope 79−21189
analogue-switch, US transducers appl., dynamic focusing 77−52856
commutable circulator, with increased mean-power level 78−4637
controllable electroacoustic phase shifter 79−81640
deterministic phase shifters for hologram memory 77−46787
diffraction grating residual ruling errors, magnetostrictive correction method 79−50454
digital phase-shifter for multiple quantum NMR 80−17974
displacement A/D convertor with multichannel phase shifter 77−5823
electro-optic waveguide deflector performance characteristics 80−33213
electronic phase meas. techniques in optical testing 80−106643
far IR Fresnel prism as quarter-wave plate 77−39067
ferrite, magnetised, nonreciprocal refl. of EM waves, rel. to phase shifter and isolater appls. 78−71006
ferrite rod phase shifter, azimuthally magnetised, soln. of differential eqns. in terms of Bessel and Neumann functions 79−55025
Hall effect transducer, phase-compensating fluorometer appl. 79−8459
holographic memory devices, deterministic phase shifter 77−14676

phase shifters continued
multislit screen induction phase shifter with increased electric reduction coefficient 77−5864
musical appls., digital phase shifter using Bell Labs digital filter module 80−5884
optical for guided-wave signal transformers, synthesis 80−1358
RF charged-particle separator power recovery, for synchrotron 78−66440
rotary, phase meters checking appl. 77−10057
SAW, frequency band broadening of phase shifters 78−55532
SAW devices based on interaction of SAW with electrons in semicond. 77−80025
selfcalibrating AC potentiometer, theory 77−82570
submillimetre wave, multilayer dielec. waveguide struct., theory 77−34003
Tokamak EF coil energy transfer supercond. solenoids and phase-shifting bridge 79−31213
Li ferrite, fine particle, for arc plasma spraying mm-wave phase shifter 78−64469
SbSI single crysts., nonlinear dielec. effects and microelectronic applics. 77−43944

phase space methods
artificial satellite, Vinti problem, extended phase space representation, luni-solar perturbations 79−35101
atom+molecule, collision dynamics, classical trajectory problem Fourier transform method 79−98189
chemical reaction, multistable, separatrices calc. 79−16033
density matrix, semiclassical phase space representation 79−9135
electron storage ring, beam distrib. parameters using transport matrices 79−54725
fluid semiclassical statistical mech., quantum effects nonperturbative incorporation 79−64819
free electron lasers, boundary deform. and Robinson-Liouville theorem 80−48202
gas/solid surface collisions, vel. depend. of ang. distribs., interaction pot. effect 79−11491
granulation due to mode-mode coupling in plasma turbulence simulation 80−38651
heat transfer in linear harmonic chain, nonequilib. steady states, information theoretic approach 80−19214
open chemical reaction systems, arbitrary dynamic behaviour 77−73438
particle growth, mathematical modelling, continuity eqns. for particle distribs. 78−65863
quadrupole ion store, spatial distribution of ions derived by phase space anal. 80−95185
quantum mechanics, Wigner distrib. for ang. coords., for teaching 79−35472
quantum state determinations and phase space distributions, simultaneous meas. 80−90774
semiclassical statistical mech., phase space sampling approach 78−32753
spatial Xe oscillation time-optimal control in PWR 79−628
synchrotron radiation source, X-ray monochromatisation, phase space analysis 78−62276
turbulence kinetic theory, fundamental soln. 80−27137

phase transfer function *see optical transfer function*

phase transformations
see also critical fluctuations; heat of transformation; isothermal transformations; liquid crystal phase transformations; liquid-vapour transformations; phase diagrams; phase equilibrium; solid-liquid transformations; solid-state phase transformations; solid-vapour transformations; spinodal decomposition; vaporisation
α,β-β-trifluoroacetonitrile, liq.-liq. transition rel. to mol. motion, NMR study 80−70383
$\lambda\phi_2^4$, Glimm-Jaffe-Spencer expansion for classical boundary conditions and phase coexistence 79−54245
λ-transition, time development of coherent and superfluid props. 79−4439
σ model, symmetry restoration through finite temp. phase transformation 77−67587
$(\phi^2)_3{}^2$ model with O(N) symmetry, phase transition 77−6007
ϕ^4 theory, three dimens. second order phase transitions, infrared singularities 80−37161
Abelian Higgs model, lattice version, phase transitions and confinement 79−49398
Abelian lattice gauge theories, phase transitions 78−12812
abrupt transformation, data partitioning, cluster anal. optimisation 78−36956
absorbed layer, commensurate-incommensurate transition 80−49494
acoustooptical effects of cooling liquid, absorption of flashlamp radiation with phase transition in medium 80−5868
acrylonitrile, NMR and relax. props., liq.-liq. transition rel. to mol. motion 80−70382
adatoms, elastic interaction between, near distortive phase transition 80−80080
adiabatic and isothermal order-parameter susceptibilities and the thermal diffusion mode 80−36962
adparticle on substrate, pseudopot. near second-order phase transition 80−80065
adsorbate layer, phase transition theory, review 80−44433
adsorbed film on transition refractory metals, phase transitions 77−51606
adsorbed layer, commensurate-incommensurate transition and domain walls 80−107654
adsorbed layers, approx. law of corresponding states 77−59209
adsorbed layers, bitransitions in molecule reorientation processes *(Russian)* 79−99416
adsorbed layers, one-dimensional incommensurate structures at finite temperatures 80−103567
adsorbed layers, two-dimensional phase transitions, review 80−39419
adsorbed layers near λ-transition, thermodynamic relns. of Pippards type for dielectric and mag. props. 78−79881
adsorbed monolayer, phase transitions *(Russian)* 79−95269
aerosol, mixed-salt particle suspension in moist air, phase transform. growth 77−12832
alloy, solid state reactions, effect on microstruct. 79−29015
alloys, low-inertia reverb. furnace for alloy phase transforms. study by mag. method 79−2771
amorphous cation subsystem in binary cpd. by rapid cooling, ionic cond. 77−51322
anisotropic bond percolation in d-dimens. hypercubic lattice 79−75464

phase transformations continued
anisotropic system, random field conjugate to non-crit. variable, effect on phase transition 80−13022
aqueous organic binary mixture, pseudophase transition, heat capacity evidence 78−83937
baryon system, strong interacting, finite temp. many body theory, phase transition 77−65210
baryonic matter, transition to quark matter, appl. to neutron stars 77−5424
BBGKY hierarchy, first eqn. exact linearisation, Ornstein-Zernicke phase instability 79−75461
bicritical point crossover, asymptotic behaviour of a field theory with quadratic symmetry breaking 79−1488
bifurcation and nonequilibrium phase transitions of limit cycles and multiperiodic flows in continuous media 78−81937
bifurcation approach to phase transitions, external field inclusion 78−14446
binary alloy freezing, non-equilibrium thermodynamic processes 80−34167
binary mixtures an and liquid-gas transitions, model for coupling between molecule polarisation and order parameter 78−22823
binodal decomposition near crit. point, scaling hypothesis 80−79912
biochemical model, phase transition induced by external noise 79−17377
biological many-particle systems 79−43803
biological multiparticle systems, stat.-thermodynamic treatment, phase transitions *(German)* 79−16119
biological system with diffusion, noise-induced phase transition 79−100560
biomembrane, phase changes and determination methods *(Czech)* 80−3599
biomembranes, structures and phase transitions *(Japanese)* 77−70423
biopolymers, reversible unfolding, mol. field theory 79−34479
bistable system, catastrophe prediction using externally applied force 78−77823
black hole, thermodynamic theory, phase transition, specific heat, stability criteria 77−33548
black hole thermodynamics, second order phase transitions 80−46897
Bogoliubov transformations for systems of relativistic charged particles 77−45998
Bose gas, with anisotropic dispersion laws, phase transitions, sp. ht. and excitons *(Russian)* 77−4229
Bose superfluid, first and second order phase transform. 79−55977
boson gas, ideal and weakly interacting, phase transition kinetics 77−35775
boson system, phase transition in an exactly solvable nonpolynomial model 79−40455
boundary displacement on pulse heating *(Russian)* 79−68557
brass bicrystals, two-phase (α/β), interphase boundary sliding at high temperature 80−88164
Brownian motion of interacting and noninteracting particles in periodic potential driven by external field, analogy 79−2726
t-butanol aq. soln., heat capacity anomaly, struct. phase transformation 79−10959
2-butoxyethanol, aq. binary mixture, pseudophase transition, heat capacity evidence 78−83937
calorimetry, advantages of spherical samples of low thermal diffusivity materials 79−54134
capillary discharge with evap. walls, phase transitions 78−42839
catastrophe and renormalisation theories, transitions with several order parameters 78−32782
catastrophe indices and fourth checkpoint second-order transitions 80−52147
CDW ordered state in coupled chains of BGD model, props. 80−6756
ceramics, fracture toughness, exam. of methods of enhancing, merits and limitations 78−60771
chain subduction criterion, continuous phase transform, Landau thermodynamic methods 80−62606
chemical fluctuations near nonequilibrium phase transitions to nonuniform states 80−45542
chemical model, Schlogl's, critical fluctuations near non-equilib. critical point 80−85150
chemical system, multiple steady state, phase transform. stochastic theory, nucleation 78−53187
chemical system, nonlinear, open, information, critical fluctuations and phase-transition-like phenomena 79−24720
chemisorbed phases, phase transitions 80−107656
classical lattice gas, surface of separation between phases 79−44868
classical particles in box, continuous system, phase transform. 77−82444
classical spin system with long range interaction, phase transition existence conditions 80−88298
classification scheme, based on group theory, equitranslational transitions 79−17374
clusters of atoms, thermodynamic calcs. 77−59096
collagen, native, PMR study of mol. dynamics 77−25363
colloids, statistical mechanics approach 80−40749
coloured noise induced transitions, results for external dichotomous Markovian noise 79−58638
commensurability in one-dimensional lattices at finite temperature 80−42156
commensurate-incommensurate phase transitions on restricted substrate area 80−49513
computer coupling of phase diagrams and thermochemistry 77−77460
computer experiments and their applications *(Polish)* 78−89420
conference, condensed matter physics, Sarajevo, Yugoslavia (Oct. 1976) 77−51629
conference, statistical physics, Budapest, Hungary (Aug. 1975) 77−49664
conference on dynamical critical phenomena, Geneva (Apr. 1979) 80−27040
conformal-invariant field theory, anomalous dimensions, coupling consts. 80−4870
continuous phase transition, universal combination of critical amplitudes from field theory 80−95051
continuous symmetry breaking in Ising, XY- and Heisenberg model 79−82787
continuum mechanics, discontinuity surface model, balance eqn. and phase transition 78−73850
convection and radiation effects, perturbation solns. 79−76962
Coulomb gas system, correl. with sine-Gordon system 79−54068
Coulomb system, two-dimensional, props. 77−62337
Coulomb systems, thermodynamic functions, phase transitions 79−85108

phase transformations continued
coupled spin $^1/_2$ phonon system, existence of sharp transition 79−69204
critical behaviour of first order transition, mean-field theory, master eqn. and nonlinear Fokker-Planck eqn. 78−8375
critical behaviour of random n≥4 vector models, renormalisation group technique in 4−ϵ dimensions 77−16088
critical dynamics, nuclear relax. 78−75805
critical dynamics in Fokker-Planck formalism 77−22514
critical exponents to order ϵ^3 for ϕ^3 models of critical phenomena in 6-ϵ dimensions 80−86547
critical fluctuations, sound attenuation, caused by inhomogeneity of transition parameter *(Russian)* 79−23698
critical indices, conformally invariant bootstrap method 79−12955
critical phenomena, catastrophe theory appl. 80−8948
critical phenomena, modern theory, graduate level text 77−102
critical point behaviour, probability theory 79−44889
critical points, Ising and other models, review, book contrib. 77−37825
critical scattering theory, book 79−25913
critical thermodynamics, phase transition in transverse field with deform. depend., phonon anomaly separation 80−39258
critical-exponent renormalization and first-order transitions 78−70085
crystal point groups, extended integrity basis 79−69047
crystallographic aspects, conference, International Crystallography Congress, Warsaw, Poland (Aug. 78) 79−23481
cylindrical mould, heat cond. with phase change 79−37108
d-dimensional hypercubical system, phase transition existance 79−97332
degenerate matter, pionisation *(Russian)* 77−91558
dense neutron matter transitions, pion condensation and quark percolation models 80−77277
Dicke maser model, radiation damping, phase transition, presence of phonons 77−19224
Dicke model, generalised, canonical transform theory 77−19216
Dicke model, two-level atoms, phase transition 78−5442
Dicke model for multi-level systems, thermodynamic critical behaviour 77−61038
Dicke model of maser, phase transition, counter rot. and $(A)^2$ terms in Hamiltonian 77−23641
Dicke model phase transition, thermodynamic Green's function method 80−5715
Dicke model with external fields, simple Green function approach, lack of phase transition 78−9353
Dicke-like model structural stability of 2nd order phase transitions 77−26259
Dicke-maser model dynamics, phase transition to the spontaneous coherent state 78−66792
diffusionless first order phase transform. eqns. appl. to liquid crystals and solids 78−30734
dilatometric method for study of dimensional anomalies in metallic materials rel. to crystal struct. *(French)* 79−52563
1,2-dimyristoyl-sn-glycero-3-phosphoserine multilayers, phase transitions, temp. depend., ellipsometric study 80−108846
1,2-dipalmitoyl-sn-glycero-3-phosphocholine multilayers, phase transitions, temp. depend., ellipsometric study 80−108846
dipalmitoylphosphatidylcholine, changes in vol. mag. susceptibility at the phase transition 80−76770
dipole pseudo-spin glasses, collective excitations 80−59617
dipolmitoyl phosphatidylcholine lamellar phases and bilayer phase transitions, structural parameters 78−64948
dispersed flow, heat and mass transfer, phase transition effect 78−67252
distinguishable quantum particles in one-dimens. box, continuous system, dynamics, phase transitions 78−32755
distribution functions, high order reduced, truncation procedure 78−36958
divalent Sr, Ba, Ca, Zn, Cd iodates, complex salts, phase transitions, cryst. struct. *(Chinese)* 80−70171
DNA, helix-coil transition, thermodynamics 79−11883
DNA, phase transition, ψ transition of single coils 80−26200
DNA, phase transitions in water-ethanol solns. *(Japanese)* 80−89709
DNA solution, thermodynamic props., phase transition, one-dimens. Ising model study 79−16125
DTA, thermal curve interpretation 80−45599
dynamical cluster properties in the quantum statistical mechanics of phase transitions 80−77693
Earth core, phase change hypothesis rel. to struct. of terrestrial planets 77−87298
Earth core, phase-change hypothesis rel. to Sun and Moon accels. and mountains origin 79−8592
Earth interior, phase transitions and matter differentiation during formation 77−56610
elastic bars, phase boundary propagation, dynamic elastic bar theory, sound wave interactions 80−69706
elastic continua, modelling, thermodynamic restrictions 78−12568
elastically coupled systems at marginal dimensionalities, crit. dynamics and stability 80−101769
electron-vibration system, nonequilib. first-order type phase transition 80−9633
ellipsoid assembly, solvable model with first order phase transition 77−30101
energy storage unit sizing for air-based solar heating systems 80−7922
even-even deformed nuclei, phase transition in rotational band of excited state *(Russian)* 77−6211
external constraints, critical indices 77−33967
external-noise-induced, chem. model 78−16764
FCC lattice, phase transitions of fully frustrated models 80−29517
fermion system, effect of boson-like excitations on props. just above 2nd order transition 77−61015
Feynman-Wilson gas, KNO scaling, phase transitions 77−30094
finite size scaling theory, static, dynamic, based on renormalisation group approach, critical phenomena exam. 78−16745
finite system, order parameter and sp. ht. for epitaxial ordering renormalisation-group calc. 80−17862
first order, multipurpose eqns. for general laws and p-T curves *(Russian)* 77−1208
first order phase transitions, droplet models, renormalisation, singularities 80−95050
first order transitions, matter transfer formalism *(French)* 79−6065
first-order phase transition, nonlinear relaxation, Ginzburg-Landau theory including fluctuations 79−35658
first-order phase transitions, influence of quenched impurities 79−73289
first-order to continuous phase transition, crossover induced by symmetry-breaking fields 79−82312
first-order transitions, destruction by symmetry-breaking fields 77−67403
fluctuation-induced ordering in system of two interacting fields 79−80556
fluctuations near phase transitions to non-uniform states 79−86870
fluid mixtures, analytic and perturbation theories 78−18516
fluids, low gravity expts. on phase transition and critical phenomena 77−39658
fly's eye intensifier-TV neutron counting camera, appl. to phase transform. studies 79−46519
Fokker Planck equations, quasiadiabatic solutions, time-dependent drift, fluctuation coefficients 80−90785
fourth checkpoint for second-order transitions 80−27248
Frenkel exciton system, phase transition and exciton-photon coupling 78−23024
gauge theories, statistical mechanics of field theories with broken, global, and local SU(3) gauge symmetries 79−58881
gauge theory, spontaneously broken, first-order phase transitions 78−24943
gauge theory phase transition with symmetry restoration 77−5984
Gaussian core classical system, low temp., density limit 77−15538
Gaussian method, attempt to separate long and short range forces 79−63180
generalised lattice correspondence 77−15537
Gibbs ensembles equivalence, phase transitions 80−134
Gibbs phase rule, heuristic theory applied to lattice spin system 77−45811
Gibbs phase rule equivalence to ensembles for classical lattice systems 79−75467
Ginzburg-Landau model, scaling at low temp. 77−30121
glasses, defect reactions, ionicity dependence, negative-U states 80−88510
glassy materials in steep, thermal gradients, apparatus for phase transform. 78−84767
goethite, transformation to maghaemite in CsI discs 79−69259
Goldstone theorem in classical statistical mech., correl. function non-vanishing boundary terms as phase transition origin 80−27253
gradient invariants and incommensurate phase transitions 78−22824
grain boundary migration vacancy generation, and drag force 80−15090
grand canonical ensemble of MIT bags, thermdoynamics 77−79247
group structure for general lattice systems and surface tension 80−4675
group theoretical methods rel. to problems of classical Landau theory 80−73292
growth-disorder model, three-dimensional 78−26462
hadron matter phase transformation at high temps., cosmological consequences *(Russian)* 77−91674
hadronic matter, phase transitions, eqn. of state 79−75889
hadronic matter, Pomeron and critical temp. 80−22566
haemoglobin oxygenation, cooperative phenomena 77−44577
hard disc mixture, eqn. of state, compressibility and phase behaviour, mol. dynamics simulation 77−51291
hard-core lattice gas with tricrit. point, phase transition behaviour 80−8926
hard-sphere lattice gas, Bethe model for phase transitions 79−88884
hard-sphere system, with square well attraction, Percus-Yevick theory 77−43123
heat equation involving moving phase boundaries, analytic soln. 78−90694
heat release on phase boundary motion, self consistent tretment 80−103449
Heisenberg spin 1 system assembly with tunneling, phase transitions, thermodynamic behavior 80−4667
Heisenberg spin systems, phase transitions from strong coupling expansions 79−6058
Helmholtz free energy in Falicov-Kimball model, upper and lower bounds, conditions for phase transitions 79−86906
heterophase fluctuations in two component systems, distrib. function 79−80563
Higgs lattice abelian model, finite temp. behaviour 80−13260
high-temperature phase transformations, investigation via X-ray diffr. unit 77−39503
highly dispersed systems, phase size effect 80−6488
historical and critical remarks of theory 79−44695
hyaluronate solns., cooperative phase transitions, review 80−45850
hybrid cryst., mean energies and probabilities of phase formation 77−65015
hydrodynamic contrib. to two-time correlation functions, using nonequilibrium distrib. function 77−49703
hyperfinite spin system, Markov semigroup, phase transition, nonstandard anal. 79−97302
incommensurate systems, discrete lattice effects 80−107402
incommensurate-commensurate transition in two-dimensional sine-Gordon system 80−90789
incompressible laminar limit layer, heat transfer with phase transition *(French)* 78−94561
inhomogeneous systems, hysteresis of phase transitions, general soln. 78−59926
instability of gradient explosion 78−83917
instantons in a quark plasma, superheavy hadrons and neutron stars *(Russian)* 79−36039
interacting linear Ising spin chain, phase transitions *(Russian)* 80−70920
interaction energy terms quadratic in deformation, influence 77−37836
interface, noncritical, near a crit. end pt., struct. and tension 77−84885
intermediate spherical model 79−30403
interstellar contracting CO clouds, phase transition rel. to fragmentation 80−67838
interstellar ionisation fronts, comparison with phase transitions 77−33594
ionic crystal, sublattice disorder, phenomenological models 77−35663
Ising frustration pots., phase transition 80−52142
Ising lattice, thermal relaxation, nonideal behaviour, stochastic theory 80−22312
Ising model eigenvalue analytic continuation and free energy 77−26236
Ising model for monolayers of coadsorbed atoms, phase transitions 80−19909
Ising model two-dimensional with periodically distributed frustration, rigorous props. 80−46987
Ising O(2), O(3) and O(4) spin systems, Hamiltonian string-coupling expansions 80−20426

phase transformations continued
Ising system, two-state, crit. behaviour, Bragg-Williams approx. calcs. 78−86223
Ising-system, two-state, crit. behaviour, Monte Carlo calcs. 78−86222
isostructural phase transition by Landau phenomenological anal. 79−90757
isostructural phase transitions due to core collapse, one-dimens. model 77−2599
isostructural phase transitions due to core collapse, solid mixtures model 77−84884
isostructural phase transitions due to core collapse, three dimensional model 77−2600
Kellen-Simanzik eqn., correlation function scaling behaviour in phase transitions *(Russian)* 80−57502
kinetic instabilities in 1st order transitions, ageing stage 78−87765
kinetic potential and Maxwell construction in nonequilibrium chemical phase transition 77−87716
kinetics of phase transitions 79−28075
kink dynamics in one-dimens. double-well field theory 80−39247
Kirkwood-Salsburg eqns. for bounded stable Kac pot., instability and phase transitions 78−4553
Korteweg-de Vries equation, higher-order, Backlund transforms. 80−77631
Landau theory, as example of catastrophe theory 79−12750
Landau theory extension, second or first order transition analogy to dye laser 79−953
Landau theory for chem. instabilities 78−16763
Landau theory of phase transitions 77−30120
Landau-type theory of 1st order transition, HF calc. 77−55339
laser system qualitative change in threshold range, analogy with phase transition *(Czech)* 80−32949
lasers and phase transitions, intracavity absorber expt. 78−13676
latent heat storage, physical and chemical processes at low temps. 80−72091
lattice, gas, entropy and phase transitions in partially ordered sets 78−77808
lattice 2-D models with isotropic short range interactions and continuous symmetries 80−36949
lattice gas of big interacting mols., phase transitions *(Russian)* 79−157
lattice gases with linear clusters, phase transitions 80−90787
lattice gauge theories, strong coupling phase large space-time dimension, Ising model 80−27397
lattice gauge theories with fermions, phase transitions and renormalised struct. 78−82105
lattice gauge theory, 4-D Z_2 gauge, verification of first order phase transition 79−58876
lattice gauge theory, phase transitions, recursion relations 78−24953
lattice Higgs models, (non)Abelian, diamag. and crit. props. 79−67465
lattice model with infinite number of phase transitions, equivalent neighbour limit 77−27969
lattice nonlinear $O(2)_3$ model, phase transition between broken/unbroken symmetries 79−9147
lattice systems, phase transition and surface tension 80−77713
lattice systems with short-range and Coulomb interactions, phase transitions and reflection positivity 80−82715
law of mass action, first order phase transition, chemical instability 78−80778
layered spin systems, phase transitions, partition functions and binary correlation functions 80−50133
layered two dimensional Ising lattice, phase transitions, spin glasses *(Russian)* 80−65945
Lennard-Jones type one-dimens. system, Van der Waals type eqn. of state 80−24562
Lifshitz point, critical wavevector 78−36954
light scattering near phase transitions in solids, review 80−29752
limit cycles and multiperiodic flow bifurcation and nonequilibrium phase transitions 78−24759
linear cluster lattice gas, phase transitions, behaviour on Bethe lattice 79−97307
linear cluster lattice gas, phase transitions, interacting dimer models 79−97306
lipid bilayer phase transition, cholesterol effect 80−85361
lipid bilayers, spin-labelled, pure, EPR lineshape evidence of phase transitions 78−69004
lipid mixtures, phase diagrams, theoretical model 80−8032
lipid monolayer phase transitions, model 78−2338
lipid phase transition, cluster model, appl. to bilayer mol. passive permeation and struct. relax. 78−53346
lipids of myocardium mitochondria, composition and phase transitions rel. to depth of hypothermia, rats and dogs 78−53350
liquid physics, book 79−60245
liquid-liquid equilibrium data, retrieval 79−46797
LMFBR hypothetical core disruptive accident, simplified multicomponent phase transition model 79−31016
local critical properties, near isolated impurity 78−6142
long chain molecule, crystals, phase transitions, statistical theory 80−44290
long-range site percolation, crossover from mean-field to crit. behaviour 80−82728
low temperature critical phenomena, review 80−73297
low-temperature series expansions, algebraic techniques 79−17352
2, 6-lutidine-water mixture, phase separation near crit. point, spatial and temporal fluctuations 79−82346
magnetic semiconductors, conference, Montpellier, France (Sept. 79) 80−94916
magnetic systems and mixtures, phase diagrams, Monte Carlo studies, book contrib., review 79−82313
maleic acid-styrene copolymer, aq. soln., conform. transition 78−75526
manifolds of phase coexistence 78−16749
mean field theory, Ginzburg criterion and marginal dimensionality 77−69067
membrane, 2-D transformation rel. to surface tension and deform. 77−1980
metals, eqns. of state between 300-200000K including changes of state *(French)* 77−72672
metastability, spinodal fixed point, renormalisation group anal. 79−40509
metastable state, quantum kinetics of phase transitions *(Russian)* 79−51235
metastable state relaxation, critical point region nucleation in thermodynamic systems *(Russian)* 80−13026
phase transformations continued
metastable states close to instability, phase transition parameter eqn. of motion 80−57230
metastable states in classical continuous model 78−24756
MHD convertor, phase transition in condenser *(Russian)* 79−1350
microemulsions, lattice gas model, surfactant effects 78−23974
microscopic description, transition-active k=0 representations 77−51470
model systems, rigorous existence theorems for phase transitions 79−58649
models for transitions with continuous constant energy surfaces 78−29078
molecular system interacting with radiation field, equilib. mean values 79−27224
molecular thermodynamics appl. to phase separation and critical phenomena *(German)* 78−14447
molecule cluster fluid, phase changes, theory 77−15534
monolayer, anomalous thermal effects, statistical mechanics 80−15367
monolayer, interfacial, thermodynamic treatment, excess quantities, adsorbed and spread layers 80−40732
monolayer, one-dimens., Frank-van der Merwe model, incommensurate-commensurate crossover, transfer integral method 80−88426
monolayer of aliphatic molecules on water surface, phase transition model 79−56041
monolayer on graphite, sp. ht. and u.p., size and steric effects 77−85073
monolayers, bidimens., hydrocarbon chains on aq. substrate, phase transition model 78−51795
monolayers, oriented second order phase transitions *(Russian)* 79−65315
Monte Carlo methods in statistical physics, book 79−80528
Mossbauer radiation inelastic scatt. near phase transition 78−15073
multicomponent, multiphase systems near critical point, phase volume behaviour 80−15212
multicritical phase transitions, review 79−30385
multiplicative renormalisation group, relation to critical phenomena in phase changes *(Hungarian)* 77−54042
negative specific heat paradox, canonical ensemble theory rel. to phase transtions 78−9557
neutron diffraction, book, with emphasis on technical aspects 79−60225
neutron diffraction studies of phase transitions and crit. phenomena, book contrib. 79−60229
neutron star matter, superfluid phase transition 79−59025
noise induced, in parametric oscillator 79−58665
non-conducting chain systems, 3-d Coulomb coupling and charge ordering 78−18980
non-equilibrium phase transitions in cooperative atomic systems 79−80559
nonequilibrium, first-order type, soluble stochastic model 79−12748
nonequilibrium open systems, phase transitions, expt. studies, review 79−75483
nonequilibrium phase transformation theory homogeneous fluctuation effect 80−84277
nonequilibrium phase transition, exact results, stochastic anal. 78−29076
nonequilibrium phase transitions, synergetics study, recent trends and developments 79−75480
nonequilibrium phase transitions in chemical systems 78−54325
nonequilibrium phase transitions in presence of external non-white noise 80−42182
nonequilibrium steady states, distrib. functions and phase transitions 77−61041
nonequilibrium steady states of open systems, 2nd order type transitions and fluctuations 77−49680
nonequilibrium transient behaviour 80−93732
nonequilibrium transitions, dynamical features, appl. to lasers and optical parametric oscillation *(Chinese)* 78−83030
nonisothermal meas. evaluation, non-existence of dynamic correction term 80−107406
nonisothermal transformation kinetics, combined KEKAM eqn. appls. 79−14912
noniterative soln. of phase change problems with temp. dependent thermal conductivity 79−27493
nonlinear dynamics of first order phase transitions 79−11322
nonlinear O(N) σ-model with gauge interactions, two-dimens., phase transitions 77−6029
nonlinear SU(n) a lattice field theory, phase transition 79−252
nontranslationally invariant spherical model, exact soln., phase transition 77−37833
nonuniform nonequilibrium systems, approx. scheme for fluctuations study 79−58637
nuclear matter, described by pseudospin Hamiltonians, phase transition determ. 78−66237
nuclear matter, phase transitions and shock waves 79−49594
nuclear matter, phase transitions at finite temperatures 79−6468
nuclear matter, shock wave matter, shock wave dynamics, phase transition effects 78−21509
nucleation rate, relationship between experimentally determined and true values 80−54343
nucleon matter, phase transitions and eqn. of state at subnuclear densities 80−77278
O(N) σ-model, two-dimens., mag. susceptibility, phase transitions and high temp. expansion 80−47177
O(N) Heisenberg spin systems, N=2,3,4, and Ising model, strong coupling expansions and phase diagrams 79−71378
oil-water microemulsions, US attenuation and structural transitions 79−61917
one dimensional system with phase transform., exact linear renormalisation 78−32769
Onsager transition in hard plate fluid 77−48696
open BSC model, dynamics in weak coupling limit 79−2738
optic mode second sound in distortive phase transitions 79−73366
ordered continuously degenerate systems, props. 79−93040
ordered phases, 1/n expansion method study 77−20043
organic compounds, high-press. thermodynamics, review 79−24500
orientational phase transition in system of flexible mols. 79−82311
oriented bond percolation, threshold probability and correlation length exponent calc. 80−68146
pair correlations, asymptotic decay, Percus-Yevick eqn. solns. 77−47311
particle growth, mathematical modelling, continuity eqns. for particle distribs. 78−65863
partition function of the three-dimensional Ising model 79−71381
Peierls-Frohlich condensate, attracting solitons and discontinuous lock-in transition 80−92840

phase transformations continued
pentadecanoic acid, insoluble monolayer, phase transition, simple lattice model 80−70527
percolation, two dimensions, absence of phase transitions 78−87770
percolation clusters, as teaching aid for Monte Carlo simulation and crit. exponents 78−12477
percolation clusters and lattice animals Monte Carlo method 79−6057
percolation problem, real-space renormalisation group approach 79−93059
percolation theory, review 80−98868
perfect gas/vapour in variable cross-section channel, quasi-one-dimensional flow, numerical investigation 80−79403
permutation representations, epikernels and phase transitions 77−47545
phase diagram classification by catastrophe theory 80−17905
phase transition in elec. discharge plasma between parallel plates, compression by recomb. press. 80−64799
phonon system, local cumulative excitation as transport phase transition 77−74336
phospholipid bilayer, one- and two-component, main phase transition, Landau phenomenological theory 80−97872
phospholipid vesicle phase transition probed by positron annihilation lifetime technique 79−88061
phospholipid vesicles, synthetic, phase transitions, dynamic light scatt. obs. 79−53058
photon-matter system, polariton instability and thermodynamic phase transition 79−86150
photosynthetic systems, discovery of phase transitions 80−81539
physiological support medium+NaCl+cryoprotective agent, equilib. and nonequilib. behaviour 77−16561
planar quantum hamiltonian, continuous kink condensation 79−97329
planar spin model, two-dimens., phase transition 78−59927
planar-rotator model with short range interaction 79−80540
plane rotator model, Monte Carlo simulation 80−73295
plane rotor model, static and dynamic crit. behaviour, Monte Carlo simulation 79−38334
planetary formation as adiabatic phase transition, isoentropic model 80−26763
plasma, three-dimensional rotator and vortex models 78−95266
plastic crystals, phase transition and melting, dynamical model 77−84677
point particle system, grand partition function, zero distrib., logarithmic interaction 77−11296
polyacrylamide, gels and single chains, phase transitions and crit. behaviour 80−40759
polyacrylamide gel and single chain in soln., laser light scatt. obs. near phase transitions 80−93808
polymer, collapsing, self-interacting self-avoiding walk model, phase transition 77−38755
polymer chain, long, in dilute soln. 79−13851
polymer chains, with volume interaction, statistical physics problems, coils and globules, review 78−94347
polymer coil-globule second order phase transition 77−19119
polymer gelation, statistical mech. model, site-band correl. 79−34368
polymer macromolecules, volume interactions, coil-globule transition, statistical physics, review 80−78737
polymer solution, weakly correlated, radial distrib. function 80−84050
polymeric chain with rigid side branches, intramol. phase transition of 1st kind *(Russian)* 80−58432
polymers solns., cooperative phase transitions, review 80−45850
polyorganosiloxane-asbestos composites, high-temp. transitions 79−38802
polystyrene sphere crystals, in aqueous suspensions, solid-like phase transiton 80−50893
polystyrene-cyclohexane, polymer solns., coexistence curve 79−28101
Pomeron and critical temp. 79−12982
porous media, heat and mass transfer during phase and chemical transformations 77−42917
position-space renormalization approach 79−30404
position-space renormalization group transformations, mathematical props. 79−75466
Potts model, 3-dimens. flow problem, calc. of crit. indices *(Russian)* 77−82474
Potts model, crit. behaviour, renormalisation group calcs. *(Russian)* 79−6059
Potts model, discrete, three spin thermodynamic behaviour, Kikuchi cluster variational method anal. 79−35640
Potts model, four state, series studies 79−85088
Potts model, hierarchical, three-state, high temp. susceptibilities 80−77723
Potts model, Monte Carlo simulation in three dimens. 80−163
Potts model, quenched bond disorder, single-bond effective interaction approx. 80−27229
Potts model, three state, lower bound renormalisation transformation 77−28347
Potts model, three-state, effects of symmetry-breaking perturbations 80−105579
Potts model, three-state, high field series expansions and critical props. 79−85090
Potts model, three-state, phase transition continuity 80−22302
Potts model, two dimensional three state, critical exponents 80−105583
Potts model in 2-D, exact results 79−58644
pressure in lattice systems, differentiability props. 80−31677
Prigogine-Defay ratio, macroscopic systems with more than one order parameter 77−20042
Prigogine-Defay ratio, rel. to order parameter theory 78−2232
pseudo-critical dynamics in first-order transitions 79−71391
pseudo-first-order phase transitions in one dimension 80−22270
QCD, dynamical chiral symmetry breaking and explicit breaking due to current quark masses 79−71717
QCD of highly condensed matter 78−70267
QCD phase transitions, chiral symmetry breaking, confinement, as tunnelling through singular barriers 78−82145
quantum field models, Goldstone bosons and topological superselection rules 77−5977
quantum molecular crystal, quantum quadrupolar phase theory *(Russian)* 78−22929
quantum spin systems and classical counterparts 77−57294
quantum-defect theory of heats of formation and struct. transition energies 78−55830
quark-partons, phase transition to baryons rel. to possibility of stable quark stars 77−45471
phase transformations continued
quasi-one-dimensional electron-lattice system, three dimensional CDW ordering temp. 78−23037
quasiaverages, hybrid systems, phase transition description 77−41532
radiation induced phase changes, review 79−77722
radiation induced phase stability, theory 79−77634
random fields, lowering of dimensionality in phase transitions 77−17923
random Ising model on Cayley tree, phase transition 80−42150
random uniaxial systems with dipolar interactions, phase transitions 77−72677
rare earth metals, preparation methods and properties, review 79−69969
reflection positivity and phase transitions, Peierl contour probabilities, long range lattice models 78−89398
Reggeon field theory, critical Pomeron intercept with block-spin methods 79−71615
Reggeon field theory, expanding disc as dynamical vac. instability 77−2774
relativistic heavy-ion collisions, nuclear matter to hot quark matter phase transition 79−3170
relativistic star, curved space-time, vac. stability, polarisation, phase transition 77−49290
relaxation of unstable state obtained by rapid cooling below stratification point 77−76526
relaxation phenomena, Monte Carlo studies, review, book contrib. 79−80531
renormalisation group anal. in 2D Coulomb gas, sine-Gordon theory and XY model 80−36950
renormalisation group approach to crit. phenomena and phase transitions 77−87713
renormalisation group approach to critical phenomena, ferromagnetic example 78−8497
renormalisation group eqns. and thermodynamic anomalies near tricritical point *(Russian)* 80−13027
renormalisation group theory rel. to hamiltonian symm. *(Russian)* 77−11666
renormalization group method in theory of phase transitions 77−80601
representation generating theorems and interaction of improper quantities with order parameter 80−4682
rotational like degrees of freedom system, phase transitions, thermodynamic props. 80−77737
roughness fluctuation in layer between two phases 80−85147
sarcoplasmic reticulum, temp. dependent struct. rearrangements 79−53056
scaling properties of models of nonequilibrium phenomena, 't Hooft renorm. group method 79−26015
second kind, critical fluctuation pattern, effect of large-scale inhomogeneities *(Russian)* 78−18741
second order, in nonlinear extensions of Dicke model 77−34855
second order, modulation struct. form., Lifshitz invariants 80−92644
second order transformations in ideal and disordered systems *(German)* 79−40508
second order transitions, positive definiteness checkpoint, incompatible inequalities 80−105596
second-order phase transitions in crystals, equilibrium configurations, thermoelasticity theory 80−70364
second-order transitions in metals, high-speed dilatometry 77−89951
semiconductors nonequilibrium phase transitions, stability and dissipation, teaching 80−105479
semiinfinite porous media, heat cond., phase transitions effects 78−94523
shock propagation in variable area ducts, with phase changes, extended Chisnell's method 77−68627
shock-wave loading, phase transitions 77−84888
siloxane, temp. transitions, linear dilatometry and X-ray diffr. obs. *(Russian)* 80−59404
simple fluid, correls. near phase transition 78−9928
simulation, using Wien bridge oscillator, threshold instabilities 77−1211
sine-Gordon field theory, two dimens., second order phase transition, lattice model 78−78095
sine-Gordon system, 2-D, renormalization group eqns. 79−12736
sine-Gordon system, two component, phase transition in two-dimens. 80−73279
small cluster formation, fifth state of matter 80−39304
sol-gel transition, theory, polycondensing system, mol. size 79−57303
solid electrolytes, thermodynamic peculiarities 79−33114
Soret-driven convective instability in two-component liq. layer heated from below, phase transition picture 79−77110
sound attenuation in magnetic field at the $2^1/_2$-order phase transition *(Russian)* 80−100487
space environment applications for critical phenomena and condensation, second order phase transformations 79−46783
spatially coherent laser beam form., phase transitions 78−17898
spherical model, phase separation 79−44869
spin systems, far-from-equilib. states, metastability and anomalous fluctuations 79−80561
spin systems, tricritical phase transition, eqn. of state, critical exponents, logarithmic corrections 78−27048
spin systems and lattice theories, phase diagrams and critical points of continuous transitions 80−22528
spin systems in phase transition to superradiant state, dynamics and thermodynamics 79−22925
stability limit, equilib. between two phases *(French)* 77−13721
stability of critical behaviour, critical-exponent renormalization and first-order transitions 79−44895
stars, late-type, gravit. phase transitions 77−49380
statistical mechanical theory of the kinetics of phase transitions, review, book contrib. 80−73270
statistical mechanics 78−71830
Stephan problem, one dimens., direct and inverse solns. 80−14552
stochastic n-vector model below T_c, hydrodynamic excit. spectra 77−74326
strongly random systems, review 79−58647
structural and mag. phase transforms., integral rational basis of invariants *(Russian)* 80−62602
structural phase transition, first order, anharmonic oscillator model in (1+1) dimensions 80−86239
structural stability in physics (conference, Tubingen, Germany, May and Dec. 1978) 80−8739
structural stability in statistical mechanics 80−8932
structural stability theory, phase transition models, mean field theories, Ising model appls. *(German)* 78−77822

phase transformations continued
student laboratory demonstration experiment, using CO_2 79−40325
styrene-butadiene-styrene block copolymer, nature of melt rheological transition 78−75113
subharmonic lasers, quantum theory, first order non-equilib. phase transition 80−83584
super-dense matter, phase transitions in gauge theories and cosmology, review 79−44654
superconductivity and elementary particles theory, review 80−4911
superradiance phase transition problem, applicability of Wang-Hion method 80−31695
superradiant, gauge invariance theory 78−66795
surface film phase transitions, conf., Erice, Sicily, Italy (Jun. 1979) 80−105429
surface polariton scattering by order, parameter fluctuations near crit. pts. 80−92835
surface tension and phase transition in lattice systems 80−27226
symmetry and phase transitions, inverse Landau problem 77−47544
synergetics approach 78−16717
system with chemical reaction, thermodynamic stability, phase transitions 79−5174
systems far from thermodynamic equilib., dissipative structures, broken symm. equilib. phase transition theory 80−65827
teaching, soap film simulation of phase changes, catastrophes 79−62974
temperature wave analysis method 80−15217
tetracritical point phase transitions, Landau theory *(Russian)* 79−17379
theory, electron density of states tail, profile in Gaussian random field 80−6691
thermodielectric electret, Costa Ribeiro effect 80−7272
thermodynamic nonlinear fluctuation-dissipation theory 80−36963
thermodynamic partition function, analytic props. of Lippman-Schwinger variational approx. *(German)* 78−36953
thermodynamics of many identical systems 77−17906
thermoelastic solids, symmetry and stability 79−44743
thermophysical property research, metallurgical applications 80−97457
three state Potts-Kihara model, phase transition 79−85093
three-dimensional model, cubic anisotropy effect 78−10170
threshold phase-transition analogy 79−40471
threshold-phase transition analogy 78−70081
thylakoid membranes of wheat chloroplasts, proton spin-lattice relax. time, −8°C phase transition 80−108853
time-dependent Ising model and Cayley trees 79−75472
transition probability, system size depend., consequences for stochastic eqns. 78−41258
tree like percolation, phase transitions 79−75473
tricritical phase transition, critical exponents, classical N-component spin systems 78−4579
tricriticality and the failure of scaling in the many-component limit 79−6071
tristearin irreversible liq.-liq. phase transition, ^{13}C NMR meas. 78−26681
two level three dimensional system, phase transitions analogy with lasers 78−58965
two state approximation, for sp. ht. anomalies associated with phase transition 79−26013
two-component flow, with phase transitions, thermodynamic processes 77−27584
two-dimensional anisotropic N-vector models 79−85095
two-dimensional classical sine-Gordon system, commensurate-incommensurate transition 80−62605
two-dimensional quantum systems at zero temp., liquid to gas phase transitions 78−77798
two-dimensional system, phase transitions and metal-insulator transitions 80−2143
two-dimensional systems, phase transitions, theory 78−38811
two-level atom, phase transition induced by laser field *(Russian)* 78−29924
two-level system in radiation field, dynamics, temp. depend. props. 78−66793
U(N)-symmetric gauge theory in 1/N expansion, dynamical symmetry breaking 77−6006
unsymmetric disordering system, thermodynamics of single phase transitions and bitransitions *(Russian)* 77−61045
water, in stratified atmosphere, nonadiabatic heat dynamics 79−58004
water, Ising lattice model with directional bonding, renormalisation group study 80−28894
water, lattice gas model, phase transitions 79−80535
water, metastable states diagram and new phase nucleation probability *(Russian)* 78−95129
water, transient heat transfer (0-220°C, 1-10 bars) *(Russian)* 78−38183
Wigner lattice, screeened, solid like phase transitions, statics 80−70370
X-Y model, gauge theory analogue, 4-D self-dual gauge model, phases and transitions 80−27399
Yukawa Bose fluids, Jastrow wave function, Monte Carlo computation 79−73375
zeros distribution, eqns. of state, phase transitions with circular distrib. of singularities 79−58666
π-condensate phase transition at finite temp. *(Russian)* 79−3111
Al-Cr(Mn), struct. form. and phase transform. kinetics *(Russian)* 78−15359
$AlPO_4$, high temp. behaviour up to liq. state, phase relations, X-ray diffr. and therm. anal. study *(French)* 80−10660
Ar film, phase transition phenomena 77−62741
$BaClO_3.H_2O \rightarrow BaClO_3$, dehydration process 78−59932
n-$Bi_{0.924}Sb_{0.076}$, one-ellipsoid to two-ellipsoid fermi surface transition in extended cryst. *(Russian)* 78−14657
CO adsorbed on graphite, fluid-registered solid transition 80−59796
Ca-Sb, phase diag. 77−52284
$CuBr_2(Cl_2)$, aq. soln., structural transition, neutron diffr. study 80−64872
Fe-Co-C(0.8 wt.%), unidirectional transformation, eutectoid reaction kinetics 77−70029
α-FeO_2H, asymmetric line shapes of Mossbauer spectra *(Chinese)* 80−103902
H-He fluid planets, molecular-metallic transition rel. to dynamics He distrib. 78−28555
H-He fluid planets, phase diagram and transport props. 78−28554
HF alloys, metatectic reaction prediction 79−29020
^4He, superfluid, sp. ht. of confined sample, near superfluid transition 79−46859
^3He, A-phase, props. near transition to A_1-phase *(Russian)* 79−7728
^3He, superfluid, B-phase, phase transition to inhomogeneous state induced by elec. field *(Russian)* 77−51566
^3He, superfluid, meas. of A⇄B transition in mag. field near polycritical point 77−11760
^3He, superfluid, phase transitions not controlled by stable fixed points 77−47640
^3He, superfluid, two-dimensional, phase transitions 79−33143
^3He-^4He, liquid, nucleation of superfluid phase transitions at container walls 79−56014
^4He, superfluid, rotating, pressurised, relaxation pheonomena, transition ^4He II 79−99381
^4He, superfluid, slowly rotating, spontaneous acceleration, phase transition in system of macroscopic quantum vortices 79−33131
K adsorbed on W, field emission flicker noise power rel. to phase transition 80−59795
K solution, in KBr, conc. fluctuations, neutron small-angle scatt. study in electrolyte-metal transition range 79−14668
Kr adsorbed on graphite, commensurate-incommensurate transitions, low temp. theory 80−103582
MnZn ferrite single cryst., high temp. phase transform. characts., growth techniques *(Chinese)* 79−33927
N_2, dense monolayer on graphite cleavage face, phase transition 78−56034
$NaAlSi_2O_6$, jadeite, melt, changes in viscosity and struct. at high press. 77−29290
Nb-Sn-Cu, Cu effect on Nb solubility and peritectic transform. temp. in Sn bath *(Czech)* 77−59754
NbO_x, phase comp. on heating 2000-4000K 80−21267
$NiCl_2$, aq. soln., structural transition, neutron diffr. study 80−64872
π phase transition and multiplicity distrib. in Feynman gas model with Bose statistics *(Russian)* 78−89683
Se, liq., ring-chain transition, disordered chain model 78−59943
SiO_2 glass fibres, exam. of phase separation effect on internal friction 78−88455
SiO_2-Al_2O_3-CaO-MgO-TiO_2 system glasses, phase separation and crystn. 77−24384
Th nuclear fuel element reprocessing, avoidance of third phase *(German)* 79−6756
W(110), chemisorption of O, island dissolution phase transition 77−80698
Xe adsorbed on Cu, NaCl, stepped and disordered surfaces, two-dimens. phase transformations 80−103580
$ZnCl_2$, aq. soln., structural transition, neutron diffr. study 80−64872
Zr-Al-Fe (8.9, 0.001 to 0.006 wt.%) Fe partitioning to Zr_2Al during peritectoid transformation 78−39784

phase transitions *see phase transformations*

phased arrays (antenna) *see antenna phased arrays*

phased locked oscillators *see parametric oscillators*

phi mesons
$\pi^+p \rightarrow \pi^+p\phi$, 3.75 GeV/c, ϕ production angular distrib. and derived cross sections 78−58201
ϕ-ω mixing and violation of Okubo-Zweig-Iizuka rule 77−87948
asymptotic SU_5 and a new mass constraint for the ω, ϕ, ψ and Υ mesons 79−36001
Brayshaw and Peierls mechanisms for generating hadron peaks, N*(1470), 0(1020) and charm 79−404
charmed quark content determ. 77−71511
Dalitz arrays from $K^-p \rightarrow \pi^+\pi^-\pi^0\Lambda$ 80−105924
decay of $\rho'(1275)$ vector meson nonet 77−79267
decays, hadronic, asymptotic freedom, one-photon or three-gluon exchange 80−62971
dual unitarisation, renormalisation of trajectories with zero quantum numbers 78−21400
electroproduction with $|t|$ from 0.125 to 1.3 GeV^2 77−79274
estimate of ω, ϕ and baryonium mixing at $t \approx 0$ 79−40814
flavour symmetry breaking and production processes in dual unitarisation, ϕ and ψ prod. 79−45080
inclusive and semi-inclusive prod. in thermodynamic model 77−18238
Klein Gordon equations superposition, meson model, ϕ, f', F, K spectrum 78−58121
Klein paradox and the mass spectra of the neutral vector mesons 79−26299
lepton pair width regularity of vector mesons, ρ, ω, ϕ, ψ and γ 79−63472
mass compilation study 80−52552
mass of radial excitation, quark confinement potential calcs. 78−93860
pion form factor, ω and ϕ effects G-parity violation 79−35963
production in $\bar{p}p$ annihilations, 0.70 to 0.76 GeV, effect on OZI rule 79−22124
QCD and resonance physics, appl. of sum rules to reson. props. of mesons 79−22059
radiative decays anal., ω' meson at 1.2 GeV 77−46045
solar interior, ν-less fusion process, model based on composite neutron model $n=p+\phi$ meson 79−8898
vector meson radiative decay evaluation in spectrum generating SU_4 scheme 79−54342
Zweig suppression and statistical factors 77−46025
$0^- \rightarrow \pi\gamma$ or $\eta\Gamma$, SU_3 symm. breaking schemes, radiative widths 77−6114
e^+e^- annihilations, radial excitations of ρ, ω, ϕ mesons 78−4866
$e^+e^- \rightarrow$hadrons, QCD perturbation theory sum rule, ρ, ω and ϕ mesons 79−85268
$e^+e^- \rightarrow K_S{}^0K_L{}^0$, ϕ meson mass meas., $\omega\phi$ interference obs. *(Russian)* 78−45935
$e^+e^- \rightarrow \phi\pi^0$, OZI rule violation and cryptoexotic mesons 79−71760
$e^+e^- \rightarrow \pi^+\pi^-\pi^0$, 750-1100 MeV, ω and ϕ meson interference 80−105910
$e^+e^- \rightarrow \pi^+\pi^-\pi^+\pi^-$, 890-1100 MeV, cross section, πA_1 prod., ϕ branching ratio 79−36087
$ep \rightarrow ep\phi$, Q^2 depend. of diffractive slope, decay ang. distrib., vector dominance model 79−89169
$\eta\gamma$ decays of ρ^0, ω and ϕ, widths 77−22736
$\gamma N \rightarrow \phi N$, pole-cut nature of Pomeron 77−6136
$\gamma N \rightarrow \phi\pi^0 N$, diffractive photoprod., OZI rule violation and cryptoexotic mesons 79−71760
γp, 30-180 GeV, ρ and ϕ elastic photoprod. cross sections 80−95278
$\gamma p \rightarrow pe^+e^-$, prod. of ρ, ω, ϕ anal. 78−50037
$\gamma p \rightarrow p\phi$, 3.0 to 6.7 GeV, elastic and inelastic ϕ photoprod. 79−9380
$\gamma p \rightarrow \phi p$ photoprod. at CERN SPS and search for charmed mesons 79−26336

phi mesons continued
J/ψ, radiative M1 transitions with charmonium model 79−13132
K^-p, 10 GeV.c, prod. of φ and f' 78−4874
K^-p, 32 GeV/c, vector and tensor meson prod., with quark model anal. 79−80854
$K^-p \rightarrow \rho^- \Sigma^+(1385)$, $\phi\Sigma^0(1385)$, ωA(1520) or 0(1520), cross sections, momentum transfer 77−71531
$K^{\pm}p$, 32 GeV/c, ρ, K*, φ inclusive prod., quark fusion model 80−32135
$\mu^+\mu^-$ pair system, meson reson., leptonic decay *(Russian)* 77−67646
$\nu N \rightarrow e^- N \phi^+$, phi meson as light scalar boson in unified weak and EM interactions 79−17706
ω-φ-baryonium mixing model 80−32072
ω*-φ* interference in multi π prod., origin of Iizuka-Zweig-Okubo rule violation 78−70324
$p+Be \rightarrow \phi + X$, 400 GeV/c, φ decay modes, OZI rule 78−599
$pp \rightarrow e^+e^-X$, 53 and 63 GeV, prod. of high transverse momentum low mass e^-e^+ pairs 79−54365
pp inclusive interactions, narrow vector meson hadroprod., φ, J, ψ charmoniumlike states 77−57573
$pp \rightarrow \phi X$, OZI rule violation 79−58929
φ, photoproduction at high energy, parton model, γ hadronic props. 78−74266
φ(1019) photoproduction on proton, 2.8-4.8 GeV 79−9381
$\phi(1020) \rightarrow 3\pi$, decay amplitudes, OZI rule, dispersion relations, intermediate states contribs. 79−383
$\phi \rightarrow 2\pi$ decay probability *(Russian)* 79−45086
$\phi \rightarrow 3\pi$, decay width for $V \rightarrow 3\pi$ in Bethe Salpeter model 79−58955
$\phi \rightarrow 3\pi$, Zweig forbidden decay 79−17687
$\phi \rightarrow e^+e^-$, decay widths from QCD *(Russian)* 78−45812
$\phi \rightarrow \eta\gamma$, quark loop model, SU(3) splitting of quark masses 80−62990
$\phi \rightarrow \eta\pi\gamma$, three body decay width 79−36083
$\phi \rightarrow K^+K^-$, average mass meas. of $K^{\pm}$ 79−30742
$\phi \rightarrow K\bar{K}\gamma$, three body decay width 79−36083
φ photoproduction, quark multiple scatt. model anal. under vector meson dominance 79−54350
$\phi \rightarrow \pi^0\gamma$, two body photonic decays, SU(4) scheme, ideal mixing angles, amplitudes, quark sectors 78−54630
$\phi \rightarrow \pi^+\pi^-$, π form factor, φ peak, unitarity and gluonic corrections 80−22615
$\phi \rightarrow \pi^+\pi^-$, search in $e^+e^- \rightarrow \pi^+\pi^-$ reaction *(Russian)* 78−45915
$\phi \rightarrow \pi\gamma$, nonet symmetry scheme 79−63480
$\phi \rightarrow \pi\gamma$, SU(3)×SU(3) algebra, appl. to ground state mesons, coupling constraints and decay rate 78−58183
$\phi \rightarrow \pi\gamma$, suppression factors for VMD couplings calc., duality constraints anal. 77−13960
$\phi \rightarrow \rho\pi$, dynamical calc., energy depend. of Zweig-rule violating couplings 78−33063
φ-ω mass mixing sign from gluonic annihilation model, OZI rule violation 79−71722
φ-ω mixing, Okubo-Zweig-Iizuka rule, unitary constraints on resonance mixing 79−22024
$\phi' \rightarrow \phi\pi\pi$, current algebra techniques, pole plus remainder model, chiral symmetry breaking and QCD 80−62972
φφ decay as a parity and signature test 79−17722
φπ prod. in e^+e^- annihilation and diffractive photoprod., 4 quark state signature 79−6324
$\pi^{\pm}N \rightarrow K^-K^+N$, 6 GeV/c, φ-meson prod. 77−26540
π^-p interactions at 19 GeV/c, test of Zweig rule 77−2874
$\pi^-p \rightarrow K^+K^-K^+K^-n$, 22.6 GeV/c, φ prod., Okubo-Zweig-Iizuka rule test 78−89743
$\pi^-p \rightarrow \phi X$, 16 GeV/c, cross-section 77−61330
$\pi^-p \rightarrow \phi n$, 1.6-2.0 GeV/c, total cross-section 77−87998
$\pi^-p \rightarrow \phi n$, OZI rule violation in central region 77−61262
$\pi^-p \rightarrow \phi n$, study of second-order hadronic process 79−22135
$\pi^-p \rightarrow \pi^-\phi p$, 10 GeV/c, prod. cross section meas. 77−65174
$X \rightarrow \phi\phi \rightarrow (K^+K^-)(K^+K^-)$, new spin-0 mesons, Yang's parity test 78−66111
Be+p, high transverse momentum scatt., two particle correlations and φ prod., jet trigger 78−78225
Cu(K^-, φX), *(Russian)* 79−9637
$e^+e^- \rightarrow \pi^+\pi^-\pi^0$, φ meson mass meas., ωφ interference obs. *(Russian)* 78−45935

philosophical aspects
see also humanities
1950s, philosophy and history of science 78−4452
absolute space, soln. 79−58514
ad hoc auxiliary hypotheses and falsificationism 77−33817
age of Universe, impossibility of an infinite past 78−62029
air pollution control philosophy in UK 79−70493
air pollution monitoring philosophy 79−70492
anomalies, science and social intelligence, case of meteorite falls 79−40346
Aristotelian philosophy, J.B. van Helmont's attack 80−31474
asymmetric C atom, case history for independent discovery, inductivist model 79−25821
axioms and theory-independent meanings of physical concepts 79−17185
Boole's search for universal analysis method influence on creation of algebraic logic 77−57144
Boolean systems, atomicity and determinism 79−35518
catastrophe theory, self-immunisation mechanisms of applied mathematics 78−65745
catastrophe theory's role in natural philosophy, definition of science 80−8772
causal influence, at-at theory 77−78949
causal irregularity, a re-examination 79−25818
causal relns., statistical models 77−78948
causality, probabilistic theory, discussion 79−67138
causality laws, violation with tachyon discovery, book contrib. 79−44720
causation analysis refinements rel. to revolutions in modern physics 78−12522
chemical evolution far from equilibrium, concepts *(French)* 80−7761
classical philosophies of science, general systems theories challenge 78−86107
clock synchronisation, distant simultaneity 80−27125
concept acceptance in scientific research phlogiston theory example 80−27102
concept of motion 78−93508
concept of time in physics (considerations on physical time) 79−67139
continental drift theory, scientific growth 79−62992
Copenhagenism, a defence 79−25820

philosophical aspects continued
cosmology, meaningless questions, philosophy 77−13515
cosmology, philosopbical relevance *(German)* 80−90652
deductive nomological explanation definition *(German)* 77−67175
depth perception in terms of hypotheses 78−80878
dimensional analysis 80−27263
dimensionally invariant numerical laws correspond to meaningful qualitative relations 79−12561
duality, fundamental development 78−36788
Eastern mystical philosophy, quantum mechanics and the bootstrap-quark controversy 79−84883
egregious theories, appl. to Tunguska event 79−21229
Einstein's thinking in science 79−75315
Einstein-Podolsky-Rosen paradox, formal statement 79−44769
elementary particle physics, research guiding principles 77−67174
eliminability of masses and forces in Newtonian particle mechanics, Suppes theory 77−57176
EM vector pot., physical interpretation 80−46772
equilibrium and nonequilib. thermodynamics organised and unorganised systems, philosophy 79−40344
essentialism, relative 80−42041
ether as a neutrino sea 77−53728
ether as neutrino sea, materialistic basis for physical explanation 77−53729
evolutionary cosmology and fire in Wright and Kant 79−5764
excitable ether composed of neutrinos, anomalous structural interactions explained 77−53730
explicativity, mathematical theory of explanation with statistical applications 77−45682
Faraday and the concept of force 80−57048
Feyerabend's concept of hidden anomalous fact, nontrivial interpretation appl. to Brownian motion 77−78950
francesco Patrizi da Cherso's concept of space and its later influence 80−31478
frontiers of time 80−12886
gaseous and amorphous states, structure determination by diffraction methods, philosophical aspects 78−50665
general relativity, ideas of Eastern and Western cultures 79−44699
general relativity, initial value formulation, anti-Machian nature 78−8276
general relativity and the conceivability of time travel 80−27192
gravitation, general symmetric structure including attraction and repulsion *(Chinese)* 77−64913
Helmholtz, H. von, evolution of empiricism, study of a universalist 78−8212
high energy physics paradigm analysis 78−20935
human brain functions and foundations of science 80−27103
human brain functions rel. to foundations of physics, science and technology 78−73823
hypothetico-destructive model of scientific theories, significance, new formulation *(Russian)* 79−58516
idealizations and approximations in physics 79−67137
increasing weight of falling bodies, Aristotle's conclusion 80−46770
indeterminism, and epistemic relativisation 77−78947
induction problem interpretation in approximation theory of truth *(German)* 78−12530
inductive statistical explanation, Hempel's conception of inductive interference 77−78945
inductive statistical explanations, Hempel's high probability requirement 77−78946
information uncertainty 79−40506
intrinsic metrics on continuous spatial manifolds 77−41459
Kuhn and philosophical paradigms *(Russian)* 77−26124
Kuhn and scientific revolutions *(Russian)* 77−26123
Lambert, Johann Heinrich, 1728-1777, biography *(German)* 79−17174
laws of nature, ideas on validity *(French)* 77−78944
liberal arts physics, history and philosophy, relevance 77−22348
liquidons and gasons, continuity of state historical controversies 80−12882
logic, quantum, Schrodinger cat paradox 79−97170
Mach, Ernst, autobiographical manuscripts as source material 78−86098
Mach's philosophy, genesis of relativity theory 78−8211
Marxism and German scientific materialism 78−86111
materials conservation ethic 79−44700
mathematical models role in natural sciences *(Afrikaans)* 80−8771
mathematical theories and philosophical insights in cosmology 80−90650
mathematics, renaissance of empiricism 77−1
mathematics nature and foundations, Grassmann's Ausdehnungslehre and Schleiermacher's Dialektik 77−57143
mathesis universalis, philosophers conception from Descartes for Leibniz 80−31479
measurement standards and structure of physical knowledge 77−74347
mechanical interpretation of nature, J.J. Thomson's work 80−57049
microphysics, towards an elemental grounding 78−86106
models in science, philosophical discussion 78−86108
natural disaster fallacies, Sahel drought example 78−57302
natural laws 77−78951
Newton's views about space and time 79−38
Neyman-Pearson theory of testing 78−57728
non-conventional isochrony, establishment 77−57146
non-Euclidean geometry and structures prior to Einstein, speculations *(German)* 80−90651
noncausal world model; can an effect precede its cause? 78−73824
parameterization schemes in solid state physics 79−17183
parton confinement: A different perspective 78−86437
partons, similar concepts in ancient Greek, Hindu and Chinese philosophy, for teaching 78−54143
physical constants, epistemological, historical and general investig. 80−12884
physical theories, formal analysis; inductive inference, physical states, truth and physical states 80−12883
physics, foundation problems 80−12856
physics, philosophical approaches in educational courses 78−81791
physics, role in contemporary world *(Polish)* 79−40345
physics and arms race, physicists participation explored for general education students 80−57023
physics models, nature and purpose 80−42023
Planck's principle, appl. to Darwinian revolution 79−62991
Poincare's conventionalism, origin and significance 78−86109
Poincare's conventionalism of applied geometry 78−86110

philosophical aspects continued
Poincare's retention of Euclid on apparently adverse parallactic findings 79−40429
Poincare's thesis, stellar parallax, compatibility with Euclideanism of astronomical 3-space 79−40428
Polish logic and philosophy of science after Second World War 78−12529
Priestley's mind, synoptic nature, electrical thought 79−84930
principle of identity of indiscernibles, photon violation, discussion 79−25817
probability foundations, modal frequency interpretation 80−12885
probability of laws being zero 77−33820
propensity theory, hidden variables, coin tossing appl. 80−42040
propositional system sublattice representation of physical subsystem with physical interpretation 79−49083
protophysics of time and relativity principle 77−67176
Ptolemy, Galileo, and scientific method 79−25819
quantitative concept formation, distinction between theory of knowledge and science *(German)* 77−67173
quantitative relations between infinite sets 77−57145
quantum interference effects in psychology, Schrodinger's cat, review 80−73158
quantum logic, props. of states 80−12947
quantum logic interpretation of orthocomplemented quasi modular lattice 80−12950
quantum measurement as a communication with nature 79−17253
quantum mech. foundations, conditional probability of a generalised probability theory 80−12949
quantum mechanical observables with continuous spectra, hidden variables problem 78−16690
quantum mechanics, its position in physics 79−44698
quantum mechanics, meas. problem 80−12948
quantum probability in logical space 80−31579
quantum theory, its cognitive repression in contemporary physics 79−97169
quantum theory, philosophically different interpretations and their consequences *(Spanish)* 78−41202
radioactive waste, reprocessing philosophy, German waste management *(German)* 79−54565
radioactivity and quantum mechanics unification, probabilistic conceptions 80−12946
realism and instrumentalism in 19th-century atomism 79−97172
relational theory of physical space 77−74184
relativistic astrophysics, meaningless questions, philosophy 77−13515
relativity, special theory, foundational problems 80−12906
reliability of inductive inference and our innate capacities 79−17186
remote sensing principles, concepts and philosophical problems 77−56772
research project methodology 78−12528
retrocausation and formal assimilation of classical electrodynamics to Newtonian mechanics 79−97175
retrocausation in classical electrodynamics 79−97174
science, new model 77−67177
science and the humanities, The Two Cultures gap, teaching 80−41979
scientific collaboration, professional origins of co-authorship 79−58522
scientific controversies, J phenomenon of Barkla 79−62983
scientific discovery, review of rules appl. to elementary particle physics 79−17184
scientific discovery, roles of dreams and inspiration 79−49007
scientific explanation 79−97171
scientific knowledge, limits, phenomenological anal. 79−21518
scientific laws neither deterministic nor probabilistic 77−33819
scientific progress, competing positions in contemporary philosophy of science *(German)* 79−71217
scientific theories, Planck's principle 79−58515
simultaneity and conventionality in special relativity 77−53778
Solubility Data Project, IUPAC venture 80−19
space, time, geometric style of explanation 80−18
space exploration, concepts and effects 78−81792
spacetime, elementary axiomatisation, particle, signal, transmission, reception concepts 78−70044
special relativity, relative simultaneity, empirical determ. 78−16642
special theory of relativity, relative simultaneity 80−27126
statistic inference, subjective Bayesian approach 78−57729
statistical mechanics, nonequilibrium, review 80−12983
statistical mechanics in classical physics, foundations 78−8334
statistical mechanics of complex systems, linkages from fundamental particles to cosmology 79−25964
stochastic reasoning, history in philosophy 77−82361
subsystem characterisation in physics 79−49082
Ta-You Wu festschrift: science and matter, book 79−44688
Tao of Physics, course in modern physics and Eastern mystical philosophy 80−17730
Taoism, physical phenomena, physics and irrational *(French)* 80−90649
theories as historical entities 77−67172
thermodynamics and natural philosophy, William Thomson's heat theories 77−26122
time's arrow and the structure of spacetime 79−97173
unified theory of reality 77−45722
universality of laws 79−44697
vitalism, nonlinear transforms in Hilbert space 78−73133

phonographs *see gramophones*

phonon bottleneck *see phonons*

phonon-defect interactions
see also lattice localised modes
alloys, binary, lattice thermal cond. at low temps., solute at.-phonon scatt. 77−76512
anharmonic system, generalisation of CPA 78−75783
antiferromagnet with dislocation, phonon relaxation 79−69216
bounded system, influence of size effect and surface roughness on phonon transport 79−46849
brass, lattice thermal cond. component, 30 to 300K, microscopic mechanisms 80−107758
brass, lattice thermal cond. component, 4.2 to 30K, microscopic mechanisms 80−107757
colour-centre-phonon many-mode interaction, absorption band shape, adiabatic approx. 78−2883
complex defects, expt. studies review 79−42190
crystal, subjected to high-energy, particle flux 79−7708

phonon-defect interactions continued
defect tunnelling, phonon assisted, in-band defect-induced phonon reson. modes effect 78−14419
diamond, Jahn-Teller coupling at neutral vacancy 80−71453
diamond, low lying levels of GR 1 centre, satellite line struct. 77−20269
diamond, natural, thermoluminescence, phosphorescence, defects, low temp. 78−11000
diamond, thermal cond. at low temp., correl. with IR absorpt. features 80−49435
diamond, type I_a, phonon scatt. by platelets, N-decorated stacking fault model 77−4173
diamonds, topographically identifiable sources of cathodoluminescence 77−55836
dielectrics, reduced conductivity, effect of boundary and dislocation scattering at low temps. 78−67872
dislocation, coherent motion, lattice dynamics 78−71738
dislocation motion, soliton-like, piecewise linear force model 78−2119
dislocation superradiance collapse *(Russian)* 78−79706
dislocation-phonon interaction in cryst. with anisotropic slip system 80−29137
dislocation-phonon interactions, drag of phonon gas by moving dislocations 80−70218
dislocation-soft mode interaction in displacive transitions *(Russian)* 80−84172
dislocations, influence on low-temperature lattice thermal conductivity of crystals 78−75769
disordered crystal, biphonon spectra, light absorpt. coeff. and density of states, CPA calc. 80−84271
FCC metals, dynamics of multiple interstitials and interstitial impurity complexes 78−75775
ferroelastic, dislocation-phonon interactions, phase transition effects 80−59600
glass, spectral diffusion 78−59914
glass thermal conductivity mechanism at low temps. *(French)* 77−39704
glasses, thermal cond. rel. to diffusion process due to phonon-defect interaction 80−34259
glasses, time-dependent sp. ht. at low temps. 79−60520
insulator, lattice thermal cond., point defect scatt. relax. rate role 80−70478
insulator, low temperature, role of point defect scatt. in lattice thermal cond. 77−76631
insulator, with dislocations, lattice thermal cond. 77−59157
Lamb wave equivalent US mode propagation in thin-walled tubing 79−68459
lattice models of screw dislocation high velocity motion, lattice model effects 79−77600
metal, deformed, microcrack effect on elec. resist. temp. depend. 77−51726
multiphonon effects on dispersion, Faraday rot., associated with point imperfections 78−43839
ordered vacancy compounds, lattice dynamics 78−75770
paraelectric defect relaxation process, quantum interference and multilevel aspects 79−95109
phonon scattering by spherical defect aggregates 80−24552
phonon wind as a nonlinear mechanism of dislocation dragging 79−69215
phonon-assisted defect tunnelling with quadratic defect-lattice coupling, small polaron theory 79−73274
point defect formation in weak shock wave front *(Russian)* 80−6401
pseudocontinuum approach to interaction theory for impurity defects in crystal lattice 79−69214
quartz, lattice attenuation of longitudinal sound 79−86847
resonant phonon scatt. at trigonal Jahn-Teller centres 77−66010
semiconductors, photoionisation cross-sections and phonon coupling 79−51518
thermal conductivity, surface roughness effects, low temp., including defect and boundary scatt. of phonons 77−28057
tunnelling centres, nonadiabatic props. 78−79705
two-level tunnelling system, phonon interaction theory 77−15525
Al, lattice thermal cond. at low temps., Ashcroft pseudopotential method 80−19897
Al, reactor irradiated, neutron inelastic scattering meas. of phonon dispersion curves 78−75758
BaClF, localised vibr. of U-centres 78−75779
BaF_2:Sm^{2+}(Tm^{2+}), vibronic spectra and dynamics of impurity-contaiing lattice 79−1787
Bi, deformed cryst., phonon scatt. by lattice defects, thermal cond. calc. 78−22802
Bi, thermal cond. under plastic deform., phonon scatt. by dislocations and twin boundaries 77−11746
CaF_2:Tm^{2+}, vibronic spectra and dynamics of impurity-contaiing lattice 79−1787
$Ca(WO_4)_x(MoO_4)_{1-x}$, Raman scatt. line shape 78−10898
CdTe, thermal cond. and X-ray topography investig. of cryst. defects 77−39706
CsI, isotope diffusion 78−75875
Cu, defect-phonon perturbations after neutron irrad., neutron scatt. study 80−44278
Cu, vacancy, lattice vibrs., reson. and localised modes 80−39236
Fe, BCC, vib. entropy of $^1/_2\langle 111\rangle\{110\}$ edge dislocations 78−63768
α-Fe, vacancy, lattice vibrs., reson. and localised modes 80−39236
GaAs, dislocation free, phonon-defect interaction 77−69061
GaAs, lattice thermal cond., point defect scatt. relax. rate role 80−70478
GaAs, phonon assisted tunnel emission of electrons from deep levels 80−25532
GaAs:Te, phonon-dislocation interactions, nonstoichiometry effect *(French)* 77−43298
GdS, FCC metallic phase, Raman scatt., phonon density of states 78−19480
Ge, phonon scattering and dislocation effect on low temp. phonon cond. 78−51754
^{3}He, solid, low temp. thermal cond., structural crystalline defects 80−2240
^{4}He, small liq. drop model for vacancy 78−51784
^{4}He, solid, boundary limited thermal cond., Poiseuille phonon flow 80−2241
K, electrical resistivity at low temp., phonon-dislocation scatt. 79−60820
K, low-temp. lattice cond., phonon drag thermopower 79−60789
K, phonon-dislocation scatt. and phonon equilibration at low temp. 79−51561

phonon-defect interactions continued
K, thermomagnetic and thermoelectric properties, phonon scatt. processes 80−29390
KCl, F-centre phonon many-mode interaction, absorption band shape 78−2883
KCl, phonon scattering on small radius colloids 78−38798
KCl:CN^-, phonon-defect interaction, Brillouin scatt. obs. 80−34935
$KMnF_3$, phonon scatt., thermal cond. meas. 77−7916
$K_{1-x}Rb_xCl:HF_2^-$, dynamic inhomogeneous broadening of bands of local vibr. 78−92102
$KTa_{1-x}Nb_xO_3$, paraelectric phase, defect induced fluctuations, Raman meas. 79−15423
$(La,Gd)Al_2$, normal and supercond. state, US attenuation, freq. depend. and mechanisms 80−49992
LiF, γ-irrad. pure and Mg-doped, phonon scatt. and interstitial clusters 80−70254
LiF, thermal phonon scatt. by low angle grain boundaries 78−67795
LiF, thermal phonon-dislocation interaction, thermal cond. and ballistic phonon propag. meas., 0.03-25K 79−95226
MnZn ferrite, thermal cond. of single crystals 77−36079
N_2:N, dynamically induced electronic transitions of matrix isolated atom 78−63825
NaCl, thermal phonon scatt. by low angle grain boundaries 78−67795
NaF, lattice thermal conductivity, point defects effects at low temp. 79−90836
Nb, plastically deformed single crystal, low temp. thermal cond. 79−28336
$Nb_{80}Mo_{20}$, $Nb_{75}Mo_{25}$, supercond., phonon cond. below 1k 78−14881
$Nb_{80}Ta_{20}$, supercond., phonon cond. below 1k 78−14881
$Nd_xLa_{1-x}TaO_4$, polycryst. optical centres, thermodynamic equilib., 1600-1700K *(Russian)* 77−68970
Ni cryst., US wave attenuation, phonon viscosity and dislocation drag coeffs. 80 and 298K 77−76491
Pb, perfect and deformed, phonon mean free path from thermal cond. meas., 0.6 to 7.5K 79−65166
Pb, phonon thermal conductivity of deformed cryst. below 2K *(Russian)* 78−60244
PbTe, TO phonon softening, free carriers and defects effects 78−79720
$RbCaF_3$, phonon scatt., thermal cond. meas. 77−7916
RbCl:Ag^+, off-centre system, quadratic-coupling phonon-assisted defect-tunnelling theory 79−55849
Si, EPR and spin-lattice relax. of dislocation spin chains *(Russian)* 79−91291
Si, phonon scattering at low-angle grain boundary 79−77708
Si:Sn, thermal conductivity, Hall mobility depend. on Sn conc., phonon-defect scatt. 80−29232
SrClF, localised vibr. of U-centres 78−75779
$SrF_2:Sm^{2+}(Tm^{2+})$, vibronic spectra and dynamics of impurity-contaiing lattice 79−1787
TiC, high temp. thermal cond., ambipolar diffusion contrib. 78−26742
V_2O-M_xO, (M=Ni, Co, Mn), solid solutions, exam. of thermal conductivity 78−79827
ZnSe crystals, doped and undoped, optical absorption edge 80−60626

phonon dispersion relations
A15 compounds, coherence length and phonon softening 78−34587
A15 type compound, props. and one-dimensionality 80−2530
acoustic gyrotropic tensor, in crysts., activity rel. to cryst. class 80−107378
actinide compounds, neutron scatt. studies 80−75716
adamantane, lattice dynamics in disordered phase 78−55923
adamantane, plastic phase, librations, phonon branches, neutron scatt. study *(French)* 79−51222
alkali cyanide crystals, lattice dynamics calc. 79−77705
alkali halide, lattice dynamics calc., extended three body force shell model 78−47491
alkali halide, static and dynamic props., appl. to KCl 77−7798
alkali halides, lattice dynamics using breathing shell model 80−88285
alkali metal, Ashcroft pseudopotential, unified study of props. 80−39239
alkali metal, crossing of dispersion curves in (ζ00) direction 78−38795
alkali metal, ideal electrical resistivity, temp. depend. 78−64022
alkali metal, lattice vibr. and Gruneisen parameter 78−59917
alkali metals, axially symmetric model 80−34152
alkali metals, lattice anharmonicity 79−19341
alkali metals, lattice excitation dispersion relations 80−100314
alkali metals, liq., collective excitations and short-range order 78−63665
alkali metals, phonon dispersion, phenomenological model 79−60445
alkali metals, phonon dispersion and electron gas pressure, theory 78−2208
alkali metals, phonon dispersion binding energy, compressibility, elastic consts. electron screening and Ashcroft pot. calcs. 80−65174
alkali metals, phonon dispersion curves using second-order perturbation theory 80−79893
alkali metals, relation between ion-ion pot. and phonon spectra 77−80591
alloys, force-and-mass disordered, average local-information transfer approx. 80−88290
amorphous solid, frozen liquid phonons disorder parameter, Anderson localisation 78−75784
p-azoxyphenetole, single cryst., deuterated, phonon dispersion curves, inelastic neutron scatt. obs. 80−84261
BCC metal, angular force model 77−31735
BCC transition metals, tensor force model, lattice dynamics 80−103428
binary alloy, of simple metals, pseudopotential approach 80−44464
binary alloys, three mode, long wavelength optical vibr., appl. to Ge_xSi_{1-x} 78−6135
binary compound, Kohn anomaly in optical phonon branch 80−92626
charge density distortions and lattice dynamics, appl. to Nb 78−30714
Chevrel-phase superconductors, lattice dynamical calcs. 79−33056
commensurate one-dimens. CDW system, lattice dynamics and elec. props. 79−38057
cooperative Jahn-Teller T-systems dynamics vibronic excitation branches 80−10934
covalent crystals, lattice dynamics, unpaired forces effects 79−95096
covalent crystals, pseudopot. calc. 77−43295
crystal with interstitials, lattice dynamics 80−2128
crystalline films, dispersion law and struct. transition, Fermi line geometry, acoustic spectrum, resist. min. *(Russian)* 79−7764
cubic crystals containing substitutional impurities, slow neutron coherent scatt., phonon mass operator 79−28065
diamond, adiabatic bond charge model 77−69057

phonon dispersion relations continued
diamond, and isomorphic crysts., phonon dispersion relations, Born-von Karman study 79−86855
diamond, lattice dynamical calc. using extended Born-von Karman scheme 78−59889
diatomic lattice, solitary wave solns., ϕ^4 kink, struct. phase transition, phonon dispersion curves 79−80544
dichalcogenide layer compounds, interface plasmon-phonon interactions, transverse cond. 80−49641
p-dichlorobenzene(−d_4), mixed cryst. phases, mol. reorientations and intermol. interactions, Raman obs. 79−28751
dielectric deformed crystal, phonon hydrodynamics 77−20025
dimethylammonium manganese chloride, perovskite type layer struct., lattice dynamics 79−33053
disordered lattice, phonon modes, lattice Green function expansion method 80−79900
elementary excitations in crystals, dielectric theory 78−60076
FCC crystal, small wavenumber behaviour of phonon freq. 77−55330
FCC transition metal, improved Fielek model 79−19335
ferroelectric, ion-ion interaction due to soft phonon modes 79−99838
graphite, intercalation compound, C_8Rb, elastic and inelastic neutron scatt. 78−30597
graphite, new force const. model 77−72643
graphite, phonon dispersion, temp. depend., 4K-1500°C, neutron spectroscopy 78−59906
graphite, phonon dispersion relations calc. 79−90740
graphite intercalation cpds., Raman scatt. and IR refl., review 80−45066
half space layered cryst., vibr. spectrum, Brillouin zone *(Russian)* 80−100313
HCP metals, lattice dynamics, local pseudopotential approach, dielectric functions 80−34151
HCP metals, phonon dispersion 78−59883
HCP metals, phonon dispersion relations, effect of different dielec. functions on model pseudopot. calc. 79−33055
hemicylinder-air-quartz system, semi-infinite crystal, dispersion of surface phonon polaritons 78−71939
II-VI compounds, lattice dynamics, deformable-ion model 78−91396
II-VI compounds, local force variations due to substitution impurities 78−51633
III-V compounds, local force variations due to substitution impurities 78−51633
III-V semiconductors, phonon frequencies, Brout sum rule and trace variable forces 78−59892
inert gas, anomalous terms at small wavenumber 78−2210
inert gas solids, unpaired elastic force model in lattice dynamical study 78−63820
insulators, book, showing curves for over 100 cpds. 80−51970
interface plasmons, longitudinal optical phonons, multilayer struct. 78−19118
ionic crystal, surface vibrational properties, review 78−71928
ionic crystal/degenerate semiconductor interface, localised plasmon-optical phonon coupled modes 77−28071
ionic crystals, dispersion calcs. of cubic nonlinear susceptibility near Raman resonance 79−94292
ionic liquids, collective modes 79−55636
IR reflection bands, complex contours interpretation, dispersional analysis 78−72508
Jahn-Teller cooperative systems, low-freq. dynamics 79−82565
kinetics of phonon system with almost linear dispersion law *(Russian)* 80−29136
lattice dynamical models, phonon dispersion curves 77−89506
linear mixed valence compounds, lattice modes obs. 79−46763
magnetic semiconductor, longitudinal acoustic phonons 77−72893
martensitic transformation, nonlinear mechanical model 78−87789
metal, b.c.c., modified Cheveau model for lattice waves, phonon dispersion and Gruneisen parameter 77−1189
metal, cubic, noncentral force model for lattice dynamics 79−69209
metal, cubic, Sharma-Joshi model, correl. exchange effects 80−10613
metal, in mag. field phonon spectrum, nonadiabatic effects *(Russian)* 78−19106
metal, with d-band, force fields 79−33051
metal carbide, phonon dispersion, three-body-force shell model 77−1191
metal-H alloys, phonon dispersion relation, neutron scatt. studies, review 79−60451
metal-insulator-mseiconductor structure, magnetooptic absorpt. with participation of optical phonons 79−99858
metallic compound, phonon spectrum renormalisation due to electron-phonon interaction 77−66008
metals, BCC, modified tensor force model for lattice dynamics 77−35644
metals, BCC, phenomenological model for lattice dynamics 77−20017
metals, BCC, phonon dispersion, modified de Launay model 78−34573
metals, FCC phonon dispersion relations and Debye-Waller factor calcs. 78−51630
metals, Krebs and Cheveau models, three-body forces inclusion and equilibrium condition 78−47480
metals, lattice dynamics and three body interaction 78−10139
microscopic theory, anomalous terms at small wavenumber 78−2210
molecular rare-gas solids, dispersion relations in central force rigid atom model 80−2131
monoclinic materials, polariton dispersion and cryst. optics 78−79685
MOS structure, two-dimens. Wigner crystallisation induced by strong mag. field 77−28253
naphthalene, lattice dynamics, inelastic neutron scattering 78−79690
naphthalene-d_8, cryst., phonon dispersion curves calcs., low temp. 80−96599
naphthalene-d_8, phonon dispersion meas. and calc. 78−2211
naphthalene-d_8 crystal, dispersion of LF phonons 77−69058
neutron scattering obs. of phonons, book contrib. 77−89504
noble metal, phonon frequency determ. in noninteracting band scheme 78−47483
noble metal, van der Waals forces and their contrib. to vacancy form. energy and phonon dispersion 78−91635
noble metals, electronic properties, form. factors, phonon freq. and elastic consts. 77−4168
noble metals, energy wave number charact., by reson. model 80−10612
noble metals, lattice dynamics, central pair pot. calcs. 77−31736
noble metals, phonon dispersion relation in resonant model potential 80−6473
noncrystalline solid, dispersion relation of phonon-like excitations 78−18727

phonon dispersion relations continued
normal mode calcs. of molecules, crystal phonon dispersion relns. and structure factors for neutron inelast. scatt., computer program 78−91394
one-dimensional conductor, lattice stability, phonon dispersion, Kohn anomaly 80−96603
one-dimensional metal, displacement correlation of classical ions in incommensurate Frohlich model 77−39641
optical activity in crystals, lattice dynamical theory 80−34883
optical characts., bound polaron and phonon states *(Russian)* 78−39556
orbit degenerate electron state localised at point defect, T-term multimode Jahn-Teller effect *(Russian)* 80−15490
Peierls dielectric, one dimensional, selftrapped excitations in Peierls-Frohlich state *(Russian)* 80−54678
pentaerythritol, Bragg reflection, thermal diffuse scatt. meas. *(German)* 78−75509
phonon scattering at multilevel impurities, dispersion, damping, Green's function calc. 79−14892
phonon scattering by spherical defect aggregates 80−24552
piezoelectric surface excitation by far IR laser beam 79−46906
polar semiconductors, phonon-plasmon-polariton mode propag. at interface 79−60731
polariton Fermi resonance, Raman spectra in band of many-particle states 80−25374
polyethylene, H bonding effects on skeletal optical and longitudinal acoustical modes 80−34914
polyethylene, uniaxial, deuterated, interchain forces effects on acoustic phonon branches, neutron scatt. study 79−51228
polysulphur nitride, Kohn anomalies in phonon dispersion 80−24555
polyyne, linear infinite chain, ground-state props., ab initio studies 79−95306
pressure effects on phonon dispersion spectrum and Gruneisen coeff. 77−43287
prevoskite, anisotropically-stressed, Lifshitz-point crit. and transcrit. behaviour 79−33061
quantum crystals, phonon spectrum 77−11766
α-quartz, Γ-A phonon dispersion curves, rel. to $AlPO_4$ lattice dynamics 78−75750
quartz, acoustic activity, inelastic neutron scatt. obs. *(French)* 80−103431
α-quartz, interatomic forces and lattice dynamics 77−7802
Raman spectroscopy, semiconductors *(German)* 79−28729
rare earth intermediate valence systems, neutron scatt., review 80−49674
rare earth metals, HCP, microscopic theory of lattice dynamics 77−43292
rare earth mixed valent compounds, lattice dynamics 79−73268
reststrahlen bands, bulk phonon polariton dispersion 77−35647
rocksalt type ionic crystals, using extensions of shell model 79−77702
Sc, HCP, nonlocal effects in lattice dynamics 78−91397
scheelites, external lattice vibr. modes and elastic wave vels., dispersion relations 79−33050
screw dislocations, inelastic neutron scatt. 78−75774
screw dislocations, phonon dispersion curves of localised modes, inelastic neutron scatt. 77−72661
semiconductor, narrow gap, phonon dispersion and damping 79−7794
semiconductor superlattice, phonon spectrum, effect of strong elec. field, parametric reson. 80−44273
semiconductor with superlattice, phonon spectrum, electron-phonon interaction effects 77−47528
semiconductor-dielectric interface, surface polaritons of LO-phonon-plasmon coupled modes 79−7792
semiconductors, covalent, phonon spectra calc. using dielectric matrix approach 79−4381
semiconductors, covalent, total electronic energy, force consts., and phonon dispersion curves, tight-binding calc. 79−60747
semiconductors, narrow-gap, plasmon-phonon interaction effect on optical phonon dispersion 80−103435
semiconductors, van Hove critical point region, electron-phonon interactions, dispersion law 80−70344
solid, phases I, II, acoustic phonon dispersion curve meas. by neutron inelastic scatt. 78−2212
solid, phonon dispersion effects on nonradiative transitions 78−43926
spectroscopy of high-frequency phonons, transport phenomena, review 80−49325
superconductor, phonon spectrum effect on critical temp. at type 5/2 phase transition 79−28437
superionic conductors, struct. and dynamical props., X-ray and neutron scatt. studies, book contrib. 80−24433
surface, effects of roughness on dynamical props. 78−75923
TBBA, phonon dispersion curves in cryst. and smectic phases 79−86863
Teflon, bond charge model for vib. props. *(German)* 78−75781
thiourea, deuterated, commensurate-incommensurate phase transition, inelastic neutron scatt. 79−28098
thiourea, lattice vibrs. in incommensurate phase 79−28056
thiourea, soft mode and Debye relaxations 78−80347
transition metal, BCC, crystallographic aspects of elastic dispersion 77−20032
transition metal, BCC, phonon dispersion curves and elastic, calc. using cohesive energy 78−59885
transition metal, BCC, phonon dispersion relations, Fielek five-const. model calc. 80−34150
transition metal, cubic, phonon dispersion, Fielek and extended Cheveau models 78−22801
transition metal, FCC, 5-parameter model dispersion relations, appl. to Ni, Pt 78−75748
transition metal, phonon dispersion curves, extended de Launay model 77−4162
transition metal 4d BCC, phonon dispersion 79−95102
transition metal carbides and nitrides, surface energy for brittle fracture from phonon frequencies 78−67790
transition metal dihalides, layer struct., lattice dynamics, calc. 80−65177
transition metal nitrides, lattice sp. ht. and phonon anomalies 78−63867
transition metals, FCC, phonon dispersion curves in highest-symmetric directions 79−51219
transition metals, interatomic forces, phonon spectra, from band structure charge densities 79−7662
transition metals, lattice excitations, classical models 80−29132
transition metals, phonon dispersion using non-central force model 78−91392
s-triazine, transverse elastic mode softening at structural phase transition 79−46777

phonon dispersion relations continued
$(TTF)Br_{0.74-0.79}$, gap in TTF phonon-spectrum 79−55733
TTF-TCNQ, elastic- and inelastic-neutron scatt. study 79−69208
TTF-TCNQ, inelastic neutron scatt., re-examination 78−30721
TTF-TCNQ, Kohn anomalies, phonon dispersion curves 78−10133
TTF-TCNQ, phonon dispersion and Kohn anomaly, inelastic neutron scatt. 77−1196
TTF-TCNQ, phonon dispersion curve meas., Peierls transition exam. 78−10134
TTF-TCNQ, transverse acoustic mode, inelastic neutron scatt. meas. 77−47526
two-parameter dynamical model, appl. to Ag and Al 80−10597
Wigner crystal, two-dimensional, static and dynamic props. 77−43293
zero-gap semiconductor, ferroelec. phase transitions, effect of Coulomb interaction on RPA calc. 79−28691
zinc blende structure, rigid ion second neighbour ionic model, dispersion calc. 77−1194
Ag (111) surface phonon dispersion, He atom scatt. meas. 80−75426
Ag halides, quadrupolar deformability theory by tight binding method 80−10614
Ag, lattice dynamics, ion-ion and ion-electron interactions 80−49321
Ag, lattice dynamics on Kreb's model 80−59594
Ag, lattice vibrations and ideal elec. resistivity 79−46770
Ag, model pseudopotential method for phonon dispersion 79−23685
Ag, modified Bhatia model, phonon dispersion, Debye-Waller factor temp. depend. 77−31729
Ag, modified CGW model calcs., phonon dispersion, sp. ht. and equiv. Debye temp. 78−10135
Ag, phonon dispersion relations and Debye-Waller factor calcs. 78−51630
Ag, pseudopot. optimised form for phonon dispersion study 80−10611
Ag, screened shell model 78−83894
Ag, transverse acoustic phonon branch, temp. depend., neutron scatt. *(German)* 78−71808
AgBr, 4.4K, neutron scatt. expts. 77−39643
AgBr, lattice dynamics, 295K, three-body-force shell model 77−15517
β-AgI, neutron inelastic scatt., phonon dispersion curves 78−67786
Al, lattice vibrations, seven parameter non-central force model 80−44270
Al, liquid, dynamical struct. factor 78−71667
Al, modified Bhatia model, phonon dispersion, Debye-Waller factor temp. depend. 77−31729
Al, neutron irradiated, phonon dispersion curves, neutron scatt. meas. 77−43290
Al, phonon dispersion relations and Debye-Waller factor calcs. 78−51630
Al, reactor irradiated, neutron inelastic scattering meas. of phonon dispersion curves 78−75758
Al, unpaired ion-ion interaction, transverse phonon branch, neutron scatt. expt. *(Russian)* 78−87751
Al-Ag, force-and-mass disordered alloys, vibrs., average local-information transfer approx. 80−88290
Ar, rel. to lattice thermal cond., low temp. 77−35768
Ar, solid, lattice dynamics calc. using energy band theory 80−49320
Ar, solid, phonon dispersion, many body pot. assuming variable at. polarisability, mech. props. 79−55840
Ar, solid, vibr. and thermal props., effect of polarisability 78−71807
Ar, solid, vol. depend. lattice dynamics, pseudo-harmonic approach 79−99260
α-As, neutron scatt. study 79−42178
Au, electron-ion pseudopot., form factor, liquid elec. cond., phonon dispersion 78−34785
Au, lattice dynamics, ion-ion and ion-electron interactions 80−49321
Au, lattice dynamics on Kreb's model 80−59594
Au, lattice vibrations and ideal elec. resistivity 79−46770
Au, model pseudopotential method for phonon dispersion 79−23685
Au, modified Bhatia model, phonon dispersion, Debye-Waller factor temp. depend. 77−31729
Au, modified CGW model calcs., phonon dispersion, sp. ht. and equiv. Debye temp. 78−10135
Au, phonon dispersion, lattice phonons three body interaction model 79−99280
Au, phonon dispersion relations and Debye-Waller factor calcs. 78−51630
Au, screen shell model 78−83894
Au, thermal properties and Gruneisen parameter, Toya's first principle approach 78−38806
B, IR-active phonons, reflectivity and absorption spectra 79−82294
BC_8, IR-active phonons, reflectivity and absorption spectra 79−82294
$Ba(H_2PO_4)_2$, antiferroelectric, phonon spectra 77−62592
$BaMnF_4$, anomalous acoustic phonon dispersion 77−47523
BaO, lattice dynamics calc., three-body force shell model 77−1195
$BaTiO_3$, $A_1(TO)$ phonon spectrum, ferroelectric phase transition, Raman scatt. meas. 78−56478
Be, HCP, electron-phonon interaction, thermal effects 79−33057
Be, HCP metal, lattice dynamical props., unpaired forces, phonon dispersion relations 79−19336
Be, lattice dynamics, phonon dispersion relations and Debye temp. 79−42171
Be, phonon dispersion calc. 79−51218
Be, phonon spectrum from inelastic coherent scatt. of cold neutrons 80−10617
Be, three-body forces in math. model for phonon dispersion branches and expt. degeneracy 77−62593
BeO, valence force fields and lattice dynamics 77−7799
Bi_2Te_3, lattice vibrs. coherent inelastic neutron scatt. meas. 78−34576
$C_8K(Rb)$, graphite intercalated, phonon dispersion relations and Raman spectra 80−44272
CS_2, lattice dynamics of 0K cryst., phonons and lattice energy 79−73269
CaBr(Cl)(I), Gruneisen γ and other thermodynamic props. at zero and elevated press. 78−43142
CaF_2, lattice dynamics in ang. force model, Debye-Waller factors, sp. ht., dispersion relations 77−59081
CaF_2, slab, surface modes of vibr. 78−71935
$CaF_2:Dy^{3+}$, cubic cryst. field effects 80−2368
$CaMg_2$, phonon spectra 77−20031
Cd, anisotropic thermal expansion due to anisotropy of phonon spectra 79−23750
Cd, electron-phonon interactions, inelastic neutron scatt. meas. 79−99285

phonon dispersion relations continued
Cd, HCP, phonon dispersion relations, effect of different dielec. functions in model pseudopot. calc. 79−33055
Cd, HCP anisotropic metal, cryst. dynamics 77−43289
Cd, lattice dynamics 77−15513
Cd, phonon density of states calc. from neutron diffr. data 77−24369
Cd, phonon dispersion, phenomenological model 79−7660
Cd, phonon dispersion relations, specific heat by modified Cheveau model 78−38792
$CdGa_2Se_4$, IR refl. spectra, optical phonon dispersion 80−29746
CdTe, lattice dynamics and phonon parameters bond bending force model 80−59595
γ-Ce, lattice and spin dynamics, inelastic neutron scatt. obs. 79−86859
$CeD_{2.12}$, lattice vibrs., coherent neutron scatt. meas. 77−62598
$CeD_{2.12}$, phonon dispersion relations 78−30716
$CeD_{2.72}$, phonon dispersion relations 80−88287
CeD_x, (x=1.94 to 2.75), phonon dispersion, crystal field splitting, neutron scatt. study 79−60452
CeSb phonon dispersion curves, lattice dynamics of rare-earth monopnictides 79−37780
$CeSn_3$, intermediate valence cpd., search for phonon anomalies, inelastic neutron scatt. 80−100317
Co, FCC, electron response and modified Bhatia model 79−37771
Co, FCC, modified Krebs model, phonon dispersion relations 78−79682
Co, lattice dynamics and compression curves 78−38793
Co, lattice sp. ht. calc. 79−69262
$CoCl_2$, acoustic phonon dispersion determ. from neutron scatt. 77−39645
$CoCl_2$, static displaced shell model 78−79689
$Co_{0.92}Fe_{0.08}$, lattice dynamics by neutron scatt., FCC phase 77−51463
$Co_{0.92}Fe_{0.08}$, phonon dispersion and Debye temp. temp. depend., neutron inelastic scatt. 79−33047
$Co_{0.65}Ni_{0.35}$, precursory phonon obs. of FCC to HCP transition 78−43082
CoO, calc. using extended three-body force shell model 77−27964
Cr, lattice dynamics, and sp. ht., extended de Launay model 79−46762
Cr, lattice dynamics, improved Fielek model 80−59598
Cr, lattice dynamics, phonon dispersion and atomic force constants, phenomenological model 78−26640
Cr, phonon dispersion, Debye temp. and Debye-Waller factors, lattice dynamical model 78−55920
$CrCl_3$, phonon dispersion curves 80−2130
Cs, model pseudopot. for Fermi surface distortion and phonon dispersion calc. 77−15737
Cs-Graphite, interaction ordered and disordered cpd., Raman spectra 80−11393
CsBr, lattice statics and dynamics, deformation shell model 77−20034
CsCN, inelastic neutron scatt. by coupled rotational and translational modes 80−70333
CsCl, phonon dispersion, temp. induced phase transition, deformable shell model calcs. 79−77698
$CsDy(MoO_4)_2$, effect of 38K phase transition on phonon spectrum, IR reflection spectra *(Russian)* 79−10902
CsF, second-order Raman spectra and phonon spectrum 77−90148
CsI, isotope diffusion 78−75875
$CsNiF_3$, one-dimens. ferromag. phonon dispersion surfaces 79−42180
Cs_2SiF_6, lattice dynamics from neutron scatt., Raman and IR absorpt. meas. 79−60449
Cu, interatomic pot., vacancy form., migration energy from phonon dispersion curves 78−42950
Cu, lattice dynamics, ion-ion and ion-electron interactions 80−49321
Cu, lattice specific heat, from two-parameter lattice dynamical model with dispersion 80−10678
Cu, lattice vibrations and ideal elec. resistivity 79−46770
Cu, model pseudopotential method for phonon dispersion 79−23685
Cu, modified Bhatia model, phonon dispersion, Debye-Waller factor temp. depend. 77−31729
Cu, modified CGW model calcs., phonon dispersion, sp. ht. and equiv. Debye temp. 78−10135
Cu, phonon dispersion relations and Debye-Waller factor calcs. 78−51630
Cu, resonant model potential and phonon frequencies 78−30713
Cu-Ga, disordered, phonon dispersion curves, inelastic neutron scatt. study 79−51223
Cu-Ga(Ge), lattice dynamical meas. and anal. *(Russian)* 77−62599
Cu-Ge, disordered, phonon dispersion curves, inelastic neutron scatt. study 79−51223
Cu-Pt system, phonon dispersion relations, force constant disorder effect 80−84263
Cu-Zn alloy, molecular dynamic exam. of perfect and imperfect cryst. 77−39647
Cu_3Au, heterophase fluctuations near order-disorder transform., X-ray and neutron diffr. 77−73272
γ-CuBr, phonon spectra, dispersion curves parameter calc. from zinc blende zone boundary conditions 78−51632
CuBr, specific heat and lattice dynamics 79−37798
CuCl, lattice dynamics at 4.2K 79−19344
CuCl, phonon dispersion curves determined by neutron scatt. at 4.2K 78−6132
CuCl(Br)(I), 9-parameter shell model, compared with expt., and Debye temp. evaluation 78−59891
CuI, parameter calc. from zinc blende zone boundary conditions 77−1194
β-CuI, phonon spectra, model 77−89511
β-CuI, phonon spectra calc. 78−10138
CuI, specific heat and lattice dynamics 79−37798
Cu_2O, theory of lattice dynamics 78−59896
D_2, solid, elastic constants and anisotropic pair correls. 79−33042
D_2, solid, phonon absorption line shape as function of density 80−50329
D_2O_2, lattice dynamics, neutron scatt. study 79−42176
EuO, Raman scatt. and phonon dispersion 77−55786
EuO(S)(Se)(Te), spin-disorder induced phonon Raman scatt. 78−60457
EuS, phonon anomalies and electron-lattice coupling 80−39490
EuS, Raman scatt. and phonon dispersion 77−55786
EuS(Se)(Te), spin-assisted phonon Raman scatt., mag. phase depend. 80−71413
EuSe, first- and second-order Raman scatt. near T_N 79−61374
EuSe, mag. ordered phase, phonon dispersion relations calc. 77−85723
EuSe, mag. phase depend. Raman scatt. 78−10886
EuSe, Raman scatt. and phonon dispersion 77−55786
EuTe, mag. ordered phase, first order Raman scatt. theory, phonon dispersion relations calc. 77−85723
phonon dispersion relations continued
EuTe, Raman scatt. and phonon dispersion 77−55786
EuTe, Raman scatt. exam. 79−61375
$Eu_{1-y}X_yS$ (X=Sr,Gd), spin-disorder-induced Raman scatt. from phonons, theory 80−20636
EuX(X=0,S,Se), spin-disorder-induced Raman scatt. from phonons, theory 80−20636
α-Fe, lattice wave dispersion, lattice consts., elastic consts. 80−24545
α-Fe, vibrational states, phonon dispersion, phonon softening 80−88289
Fe-Rh alloys, ferromag. and antiferromag., spin wave spectrum and phonon dispersion curves 77−63158
$Fe_{65}Ni_{35}$ ferromagnetic alloy, zero sound anomaly, inelastic neutron scatt. 79−46764
FeO, lattice dynamics, coherent inelastic neutron scatt. 78−59899
FeO, phonon dispersion, extended three-body force shell model 79−90743
FeO, wustite, lattice dynamics, inelastic neutron scatt. meas. 77−84867
$Fe_{1-x}O$, wustite, cryst. dynamics, mag. excitations, neutron scatt. study *(French)* 79−51740
Fe_2TiO_4, cooperative Jahn-Teller effect, neutron scatt. study 80−49678
$GaAs_{1-x}Al_xP$, long-wavelength optic phonons, IR reflectance meas. 77−7804
n-GaAs, coupled plasmon-LO phonon modes and Lindhard-Mermin dielec. function 79−82540
GaAs, lattice dynamics, phonon freq., bond bending force model calcs. 80−70335
GaAs-AlGaAs superlattice, selective transmission of HF phonons 80−34154
GaP, lattice dynamics, phonon freq. meas., valence-force-field overlap shell model 80−15205
GaP, lattice dynamics and phonon parameters bond bending force model 80−59595
GaP, polariton dispersion, IR reflection spectroscopy 80−11415
GaP, Raman scattering selection rules for surface polaritons 78−72091
GaP/Te(S), IR lattice band profile, electron spin reversion in mag. field, Nf-R curve 79−28771
GaS, anisotropic phonon dispersion 77−84864
GaS, layer cpd., lattice dynamics 79−95105
GaS_xSe_{1-x} solid solutions, two-mode behaviour of optical phonons, IR reflect spectra 79−78680
GaSb crystal, phonon dispersion curves, valence force field 78−95121
GaSb, lattice dynamics, phonon freq., bond bending force model calcs. 80−70335
GaSe, lattice dynamics, in one-layer approach 79−14900
GaSe, lattice dynamics and elastic props., Born-von Karman model study 80−70337
GaSe, long wavelength IR refl. spectra 80−11401
GaTe, vibr. spectrum 77−89513
Ge, adiabatic bond charge model 77−69057
Ge, extended Born-Von Karman scheme for lattice dynamics 77−27953
Ge, heat capacity and phonon dispersion, using five force schemes *(Russian)* 77−62649
Ge, lattice dynamical calc. using extended Born-von Karman scheme 78−59889
Ge, lattice dynamics under press 80−92627
Ge, lattice dynamics using Born-van Karman model 79−73271
Ge, microscopic screening of ion-ion interaction and phonon dispersion, tight-binding calc. 77−24528
Ge, phonon dispersion and microscopic screening, extreme tight-binding model 80−49324
Ge, phonon dispersion curves, appl. of deformable-ion model 78−59887
GeS, phonon dispersion relations, neutron scatt. study 79−42182
Ge_xSi_{1-x}, long wavelengths optical vibr. 78−6135
H_2, phonon absorption line shape as function of density 80−50329
H_2, solid, elastic constants and anisotropic pair correls. 79−33042
$(HF)_n$, n=1-∞, ab initio hydrogen bond and electronic parameters, phonons 77−14342
He FCC, high press., inelastic neutron scatt. 78−10255
He, liq., rotons and solidons 79−95228
He-4, liquid, phonon-phonon interactions, review 77−55410
^{3}He superfluid, Bose spectrum nonphonon branches *(Russian)* 80−92750
^{4}He, FCC, inelastic neutron scatt., phonon spectra, dispersion curves 78−51785
^{4}He, FCC high-density cryst., lattice dynamics by inelastic neutron scatt. 79−1539
^{4}He, HCP, lattice dynamics, neutron-inelastic-scattering obs. 79−33154
^{4}He, liq., low-momentum phonon dispersion relation, press. depend., US velocity meas. 77−47635
^{4}He, liq., phonon dispersion curve from entropy meas. down to 0.75K 77−7922
^{4}He, liq., sp.ht., 65-850 mK, and phonon dispersion 79−4442
^{4}He, liq., thermal expansion meas. 77−7924
^{4}He, superfluid, anomalous dispersion of zero temp. elementary excitation spectrum, microscopic calc. 79−55976
^{4}He, superfluid, concave energy spectrum of very low wave numbers 79−4438
^{4}He, superfluid, phonon dispersion at long wavelengths and low temps. 77−11752
^{4}He, superfluid, phonon dispersion, neutron scatt. study 79−51336
^{4}He, superfluid, phonon dispersion 80−10722
Hf, HCP, lattice dynamics, thermal and elastic props., model 80−34155
Hf, lattice dynamics, phonon dispersion, mode softening 80−107390
Hg, solid, neutron inelastic scatt. 78−14410
$Hg_{3-\delta}AsF_6$, dynamical props., Hg chain behaviour, neutron scatt. study 79−95103
$Hg_{3-\delta}AsF_6$, one-dimens. phonons and phase-ordering phase transition, neutron scatt. expts. 78−26644
$Hg_{3-x}AsF_6$, energy gap in phonon dispersion of linear Hg chains 79−42172
HgI_2, red, inelastic neutron scatt. obs. 78−75756
HgTe, phonon dispersion relations, neutron study 80−70340
Ho, three-body forces in math. model for phonon dispersion branches and expt. degeneracy 77−62593
Ho, unpaired forces in lattice dynamics of rare-earth HCP metals 77−7805
I_2, lattice dynamics, bond charge model 77−84858
InAs, X-ray thermal diffuse scattering measurements 79−77701
InP, lattice dynamics and phonon parameters bond bending force model 80−59595
InSb, phonon dispersion curves, appl. of deformable-ion model 78−59887

phonon dispersion relations continued
InSe, directional dispersion of extraordinary phonons 79−65154
InSe, layer cryst., Raman and IR refl. spectra meas. 79−95777
InSn, eight-parameter bond-bending forces model 80−70334
Ir, phonon/wave vector dispersion relations, Debye temp., modified axial symmetric model 80−70339
K, alkali metals, electron fluid model 78−75738
K, elastic constants, cryst. equilib. and electronic contrib. 79−73243
K halide solids, lattice dynamics, three body force shell model studies 79−55841
K halides, surface lattice dynamics, by Green's function method 78−71936
K, helicon-phonon interaction for oblique propagation, dispersion relation 80−49315
K, interatomic function from phonon-dispersion curves and Heine-Abarenkov-Shaw optimised model pot. 79−19185
K, model pseudopot. for Fermi surface distortion and phonon dispersion calc. 77−15737
K, phonon spectrum calc., microscopic theory of force constants 78−26647
KBr, mode Gruneisen parameters, acoustic phonon dispersion relations 79−42201
$KBrO_3$, uniaxial cryst., oblique phonon ang. dispersion 77−84861
KCN, lattice dynamics and order-disorder transitions, neutron scatt. expts. 78−14434
KCN, lattice dynamics in disordered cubic phase 78−38794
$(KCN)_{0.25}(KBr)_{0.75}$, rot.-translation interactions, neutron scatt., 0-300K 78−67783
KCl, dispersion curves calc. 77−39648
KCl, TSM study of lattice statics and dynamics 79−82292
$KCl_{1-x}Br_x$, lattice dynamics 78−75761
KCl(Br)(I), lattice dynamics, bond-bending force model 80−54322
KD_2PO_4, acoustic phonon dispersion, elastic stiffness, light scatt. obs. 80−103966
KI, dispersion of phonons calc. 78−26646
KI, relationship between fourth moments in molten state and phonon freq. in solid phase 80−10477
α-KNO_3, lattice dynamics, inelastic neutron scatt. 79−4383
KNO_3, phase II, lattice dynamics, coherent neutron inelastic scatt. 78−59897
$KNbO_3$, ferroelec. phase, phonon dispersion relations and lattice dynamics calcs., comparison with expt. 80−49319
$KNbO_3$, one-dimens., ferroelec., phonon dispersion surfaces 79−42180
$KNbO_3$, one-dimens. ferroelectric, phonon dispersion surfaces 79−42180
$KNbO_3$, orthorhombic, anharmonic effects 78−79721
$KNbO_3$, tetragonal phase, inelastic neutron scatt. 80−19676
$K_2Pt(CN)_4$, quasi-one-dimens. Peierls system, phonon dispersion and neutron scatt., calc. 80−24550
$K_2Pt(CN)_4Br_{0.3}.3.2D_2O$, Kohn anomalies, phonon dispersion curves 78−10133
$K_2Pt(CN)_4Br_{0.3}.3.2D_2O$, dynamic struct. factor, inelastic neutron scatt. study 79−42185
$K_{1-x}Rb_xBr$, lattice dynamics on pseudo-crystal model 78−75762
K_2SnCl_6, elastic consts., inelastic neutron scatt. and US meas. 80−59553
$K_{0.33}WO_3$, hexagonal, neutron scatt. obs. 78−14411
Kr, solid, phonon dispersion, many body pot. assuming variable at. polarisability, mech. props. 79−55840
Kr, solid, phonon freqs., lattice heat capacities, and Debye charact. temps. 79−10905
Kr, solid, vibr. and thermal props., effect of polarisability 78−71807
$LaAg_xIn_{1-x}$, phonon dispersion, elastic consts. and struct. instability, soft mode behaviour 80−103436
$LaNbO_4$, Raman scatt. and fluoresc. spectra 80−20625
LaSb, lattice dynamics 79−37783
Li, alkali metals, electron fluid model 78−75738
Li, anharmonic props., temp. depend. 79−19340
Li, interatomic function from phonon-dispersion curves and Heine-Abarenkov-Shaw optimised model pot. 79−19185
Li, microscopic theory using Bloch wavefunctions 77−35648
Li, phonon cross-over, model 79−60445
Li, phonon dispersion curve crossing in [ζ00] direction 77−59078
Li, phonon frequency, liquid electrical resist. and interionic pair potential 78−10140
Li, phonon limited resistivity struct. depend., Umklapp scatt., elastic consts. 80−88532
LiD, appl. of microscopic and model theories of lattice dynamics of non-metals 78−59871
LiD, deformable-ion model and lattice dynamics 77−47514
LiD, long-range three centre potentials, influence on lattice dynamics 80−96605
LiD, phonon dispersion, microscopic calc. 79−42188
LiH(D), elastic constants, lattice dynamics and phonon dispersion 78−30711
Li_3N, IR and Raman spectra and lattice dynamics 78−48177
$LiNbO_3$, comparative frustrated total refl. and Raman scatt., fundamental mode freq. and phonon dispersion 77−28579
$LiNbO_3$, ferroelec., phonon dispersion relations, neutron inelastic scatt. meas. 78−56435
$LiNbO_3$, ferroelec. phase, phonon dispersion relations and lattice dynamics calcs., comparison with expt. 80−49319
$LiTaO_3$, uniaxial ferroelec., polariton dispersion relations 77−20249
Li, temp. depend., 110-424K, force consts. 77−20033
Lu, lattice dynamics, heat capacity, thermal expsn. 79−86857
Mg, anisotropic thermal expansion due to anisotropy of phonon spectra 79−23750
Mg, HCP, appl. of model for lattice dynamics 78−22795
Mg, HCP metal, lattice dynamical props., unpaired forces, phonon dispersion relations 79−19336
Mg, lattic dynamics and sp. ht. in extended de Launay model 79−51217
Mg, lattice dynamics, phonon dispersion relations and Debye temp. 79−42171
Mg, phonon density of states calc. from neutron diffr. data 77−24369
MgF_2, rutile structure, dielectric props., neutron and Raman scatt. exam. 78−79684
MnF_2, resonant phonon-magnon scatt., phonon spectroscopy obs. 79−65150
MnO, lattice dynamics, coherent inelastic neutron scatt. 78−59899
MnO, lattice dynamics calc. 79−46769
MnO, lattice dynamics using three body force shell model 77−76506
MnO, lattice vibrs., phonon dispersion curves, neutron scatt. study 79−42177

phonon dispersion relations continued
Mo, interatomic pot. from phonon spectra 77−76355
Mo, interatomic pot. from phonon spectrum 78−67784
Mo, lattice dynamics, improved Fielek model 80−59598
Mo, phonon dispersion, anomalous struct., tight-binding calcs. 78−10137
Mo, phonon dispersion, Debye temp. and Debye-Waller factors, lattice dynamical model 78−55920
Mo, phonon dispersion, lattice phonons three body interaction model 79−99280
MoS_2(2H), elastic consts., from dispersion curve and linear compressibility data 77−11618
α-N_2, crystal dynamics at 15K 77−24366
N_2 monolayer on graphite, phonon dispersion curves for postulated four sublattice struct. 78−47667
NB, charge fluctuation model 77−84869
NH_3, phonon dispersion curves, phonon lifetimes, anharmonic effects 80−15202
$NH_4Cl_{1-x}Br_x$, phonon dispersion 78−75760
NH_4I, ND_4I, lattice dynamics calcs. 78−6133
NH_4X, X=halogen, phonon dispersion, cohesive and dielec. props. in three body force shell model 80−79892
Na, interatomic function from phonon-dispersion curves and Heine-Abarenkov-Shaw optimised model pot. 79−19185
Na, lattice dynamics, angular force model 77−31735
Na, lattice dynamics, electron fluid model 77−27954
Na, phonon limited resistivity struct. depend., Umklapp scatt., elastic consts. 80−88532
Na-halide, extended three-body shell-model dynamics 77−7797
NaBr, dispersion of phonons calc. 78−26646
NaCN, lattice dynamics and order-disorder transitions, neutron scatt. expts. 78−14434
NaCN, lattice dynamics in disordered cubic phase 78−38794
NaCl, dispersion curves calc. 77−39648
NaCl, far IR dispersive-reflection meas. at room temp., comparison with calc. 78−35139
NaCl(Br) (F) (I), lattice dynamics and statics, three-body-force shell model 80−49323
$NaClO_3$, acoustic activity, inelastic neutron scatt. obs. *(French)* 80−103431
$NaClO_3$, lattice vibrations and sp. ht., neutron spectroscopic study 80−107388
$NaClO_4$, Brewster type surface mode dispersion, IR refl. meas. 80−11415
$NaD_2PO_4.2D_2O$, Raman spectra, phonon freqs. 79−61370
$NaH_2PO_4.2H_2O$, Raman spectra, phonon freqs. 79−61370
$NaNO_2$, ferroelec., ang. dispersion of internal phonon modes, Raman meas. 79−51211
$NaNO_2$, ferroelectric, second-order vibr. spectra and dispersion of phonon branches 79−69847
Na_2S, phonon dispersion curves, inelastic neutron scatt. obs. *(German)* 78−14414
Nb, and alloys, lattice dynamical models, phonon dispersion curves 77−89506
Nb, charge density distortions and lattice dynamics 78−30714
Nb, modified Sharma-Joshi model 79−51221
Nb, Nb-Mo alloys, phonon dispersion, anomalous struct., tight-binding calcs. 78−10137
Nb, phonon dispersion curves, extended screened-shell model 80−96601
Nb-Zr, acoustic phonon anomalies and superstructure, neutron inelastic scatt. meas. 80−19892
Nb-Zr alloy, BCC-ω phase transition, electronically driven nature 80−103433
NbC, modified 3-body force shell model 77−55332
NbC, nonstoichiometric, simple shell model for phonon dispersion 77−24370
NbC, nonstoichiometric, simple model for phonon dispersion, rel. to C vacancies 78−30718
NbC, supercond., phonon anomalies, microscopic theory 78−14867
NbC_x, phonon density of states and dispersion relations 79−42173
β-$NbD_{0.75}$, phonon dispersion curves 78−67792
$NbD_{0.85}$, phonon dispersion of α' and β phases, neutron scatt. 78−91398
$NbH_{0.15}$, dispersion step in [$\zeta\zeta$0]T_1A branch at ζ=0.03, neutron scatt. study 79−60453
$NbH_{0.82}$, phonon dispersion of α' and β phases, neutron scatt. 78−91398
$NbH_x(D_x)$, acoustic and optic phonons, neutron diffr. obs., book contrib. 79−82296
δ-NbN, phonon dispersion curves, anomalies 79−99284
NbN_x, phonon density of states and dispersion relations 79−42173
$NbSe_2$ (2H), charge density wave transitions, neutron diffr. exam. 77−89515
$NbSe_2$(2H), elastic consts., from dispersion curve and linear compressibility data 77−11618
Nb_3Sn, [111] transverse acoustic phonon softening near martensitic transform. 79−73283
Nb_3Sn, lattice dynamics at 300K 79−65155
Nb_3Sn, phonon softening in [$\zeta\zeta\zeta$] transverse modes, neutron scatt. obs. 79−33062
Nb_3Sn(Al), phonon density of states, temp. depend. 79−42183
NdSb phonon dispersion curves, lattice dynamics of rare-earth monopnictides 79−37780
Ne, phonon dispersion relation, Gruneisen parameters at high press. 79−42179
Ne, solid, lattice dynamics calc. using energy band theory 80−49320
Ne, solid, phonon densities of states and dispersion curves, unpaired elastic force model 79−51220
Ne, solid, phonon dispersion, many body pot. assuming variable at. polarisability, mech. props. 79−55840
Ne, solid, phonon-dispersion, mode Gruneisen parameters and elastic consts. 77−11651
Ni, dispersion curves from deLaunay angular force model 79−33054
Ni, model pseudopotential approach 77−11646
Ni, phonon dispersion curves, θ-T curves 78−26642
Ni, phonon dispersion relations and Debye-Waller factor calcs. 78−51630
Ni, vector dispersion relations along symmetry directions 79−73270
$Ni_{0.89}Cr_{0.11}$, phonons with disorder caused by force consts., neutron diffr. obs. and CPA calc. 80−96602
NiO, calc. using extended three-body force shell model 77−27964
NiO, lattice dynamics, coherent inelastic neutron scatt. 78−59899
NiO, lattice dynamics calc. 79−46769
NiO, lattice dynamics using three body force shell model 77−76506

phonon dispersion relations continued
NiO, phonon dispersion relations, neutron scatt. meas. 79−42181
$Ni_{1-x}Pt_x$, disordered, phonon dispersion relations using neutron inelastic scatt. 79−69212
$Ni_{1-x}Pt_x$, disordered phonon dispersion relations, neutron inelastic scatt. 78−43085
$Ni_{1-x}Pt_x$, disordered system, phonon dispersion relations using pseudo unit cell model 79−28066
$NiTe_2$, acoustic phonon dispersion, inelastic neutron scatt. meas., elastic consts. and sound vels. 79−95098
Pb, calc. by phenomenological method 78−59890
Pb, estimation of stacking fault and twin boundary energies using phonon dispersion curve 78−43031
Pb, model pseudopot. for phonon dispersion calc. 77−15737
Pb, phonon dispersion and cryst. equilib. 78−75752
Pb, phonon dispersion spectra from 5-parameter lattice dynamical model 78−10136
PbF_2, inelastic neutron scatt. study of phonon dispersion relation 78−30712
PbF_2, lattice dynamics 78−79697
PbI_2, 2H polytype, optical mode inversion hear M-critical point, neturon scatt. mass 80−103432
PbI_2 (2H), multi-phonon scatt. near direct absorpt. edge, resonant Raman obs. 79−87448
PbI_2, ionic layer cpd., lattice dynamics, influence of static dipole moments 79−28057
PbI_2, quasi-two-dimens layered struct., phonon dispersion surfaces 79−42180
PbI_2, Raman spectra, phonon dispersion curves, vibrational props., lattice parameters 79−69211
$Pb_3MgNb_2O_9$ diffuse phase transition, Brillouin scatt. and acoustic phonons 78−76401
$Pb_3(PO_4)_2$, ferroelastic phase transition, inelastic neutron scatt. *(French)* 80−24584
$Pb_{1-x}Sn_xSe$, band inversion effect on phonon spectra 78−79699
$Pb_{1-x}Sn_xSe$, gapless state and phonon spectrum *(Russian)* 78−30715
$Pb_{.87}Sn_{.13}Te$, phonon dispersion, mode softening 79−42175
Pd, dielec. screening and phonon frequencies using isotropic noninteracting s-d-band model 79−19343
Pd, FCC, phonon dispersion using non-central force model 78−91392
Pd, Kohn anomalies and phonon dispersion, model including exchange-correl. corrections 78−59886
Pd, phonon dispersion, simplified Frielek model 78−79683
Pd, phonon dispersion curves, freq. spectrum, specific heat calc. 77−15516
Pd, phonon dispersion curves, θ-T curves 78−26642
Pd, phonon dispersion curves in highest-symmetric directions 79−51219
Pd, phonon linewidths, inelastic neutron scatt. meas. 79−95100
Pd, phonon linewidths and electronic mass enhancement, electron-phonon contrib. 79−95099
Pd-D alloys, phonon dispersion relation meas., elastic constants and Debye temp. 78−26639
Pd-Pt, and other substitutional alloys with large mass disorder, phonon modes 78−95122
Pd-Pt, resonant modes, rel. to CPA predictions 78−75757
$Pd_{0.96}Ag_{0.04}$, phonon dispersion curves at 296K 80−24546
$PdD_{0.63}$, inelastic neutron scatt. line shapes, Pd-D, D-D force consts. 78−47481
$PdD_{0.63}$, phonon lineshapes Debye-Waller factors, 80K, inelastic neutron scatt. study 79−42187
$PdH_x(D_x)$, acoustic and optic phonons, neutron diffr. obs., book contrib. 79−82296
$PdH_x(D_x)$, optical mode phonons, nonadiabaticity 78−55916
$Pd_{0.9}Rh_{0.1}$, lattice dynamics, inelastic neutron scatt. meas. at 296K 80−29135
$Pd_{0.95}Rh_{0.05}$, exchange-enhanced, phonon dispersion relations exam. 77−84868
PrSb, lattice dynamics 79−37783
Pt, calc., using transition metal model potential 77−20030
Pt, dielec. screening and phonon frequencies using isotropic noninteracting s-d-band model 79−19343
Pt, phonon dispersion, simplified Frielek model 78−79683
Pt, phonon dispersion, vibr. spectrum, sp. ht., modified ang. force model 77−69054
Pt, phonon dispersion curves, θ-T curves 78−26642
Pt, phonon dispersion spectra from 5-parameter lattice dynamical model 78−10136
Pt, phonon spectrum, Kohn anomaly 79−46766
Pt_3Mn, cryst. dynamics at 80K 79−23688
Rb, alkali metals, electron fluid model 78−75738
Rb, elastic constants, cryst. equilib. and electronic contrib. 79−73243
Rb halide crysts., shell model calc. for dispersion curves 77−55331
Rb halides, role of quantum effects in lattice dynamics, Debye temp., shell model calcs. 80−70336
Rb, interatomic function from phonon-dispersion curves and Heine-Abarenkov-Shaw optimised model pot. 79−19185
Rb, lattice vibr., modified tensor force model 79−86853
Rb, lattice vibrations, seven parameter non-central force model 80−44270
Rb, model pseudopot. for Fermi surface distortion and phonon dispersion calc. 77−15737
$RbAg_4I_5$, single particle excitations, inelastic neutron scatt. obs. 80−59599
RbBr, harmonic and anharmonic props. from phonon dispersion at three temps. 80−39235
RbCN, acoustic and optical phonon dispersion at 300K 80−84266
$RbH_2(SeO_3)_2$, improper ferroelectric phase transformation, neutron scattering study 78−80302
RbI, elastic constants determ. by inelastic neutron scatt. 78−79659
$Rb_{1-c}K_c$, local mode exam. by neutron diffr. 79−37781
$Rb_7I_{K_{29}}$, lattice dynamics, molecular dynamics study 79−37782
Rb_xWO_3, low lying phonon dispersion curves, neutron scatt. study 80−92622
Ru 79−69262
$(SN)_x$, acoustic phonons, inelastic neutron scatt. obs. 78−6136
$(SN)_x$, acoustic phonons 78−79698
$(SN)_x$, phonon spectra, four-parameter valence force model 77−20027
SO_2, lattice dynamics, rigid mol. model 80−44266
SbSI, diffuse X-ray scatt., anisotropy in phonon dispersion relations 77−84866
SbSI, ferroelec. transition, inelastic neutron scatt. 77−40189
SbSI, paraelectric-ferroelectric transition, low freq. phonon branches, neutron scatt. obs. 79−61313
Sc, dielectric screening and lattice dynamics 77−35646
Sc, Kohn anomalies and phonon dispersion, model including exchange-correl. corrections 78−59886
Sc, lattice dynamics, sp.ht. and bulk modulus 78−71814
$ScCl_3$, phonon dispersion curves 80−2130
Sc and Te, homology of phonons, scaling formalism for phonon freqs. 80−54326
Se, trigonal, force field calc. 80−54328
Se, trigonal, low temp. sp. ht. and elastic consts., piezoelec. effect influence on phonons 80−54404
Se, trigonal, model of lattice dynamics using long and short range interactions 78−59893
Se, trigonal, normal mode calcs. 80−84259
Se, trigonal, vitreous and red amorphous, phonon density of states comparison 80−54329
Se, trigonal and vitreous, sp. ht. and thermal cond., 3 to 300K 80−59676
Si, adiabatic bond charge model 77−69057
Si, dielectric screening, microscopic theory, phonon dispersion, moment expansion calcs. 79−55839
Si, lattice dynamical calc. using extended Born-von Karman scheme 78−59889
Si, lattice dynamics under press 80−92627
Si, lattice dynamics using Born-van Karman model 79−73271
Si, phonon dispersion calc., dielectric screening theory, closure approx. 79−77700
Si, pseudopotential calculation of phonon dispersion curves 80−10620
Si-Ge alloy, hot-pressed, rel. to thermal cond. 77−31813
SiC (1 OH), phonon spectrum, dispersion curves energy discontinuity and vibr. modes, IR spectra obs. 80−44274
β-SiC, lattice dynamics, phonon dispersion curves 77−89509
SmS, phonon anomalies and electron-lattice coupling 80−39490
$Sm_{0.25}Y_{0.75}S$, phonon anomalies and electron-lattice coupling 80−39490
$Sm_{0.75}Y_{0.25}S$, intermediate-valence-state system, phonon dispersion meas. 79−19342
$Sm_{0.75}Y_{0.25}S$, intermediate valence compound, phonon investigation by neutron scatt. 80−6476
$Sm_{0.75}Y_{0.25}S$, mixed valence, phonon dispersion theory 80−34153
$Sm_{1-x}Y_xS$, anomalies in phonon dispersion 79−73268
α-Sn, adiabatic bond charge model 77−69057
Sn, Grey, lattice dynamics 77−84865
α-Sn, lattice dynamical calc. using extended Born-von Karman scheme 78−59889
α-Sn, lattice dynamics 80−107389
SnS_2(2H and 4H), Raman scatt. and phonon frequencies 77−48159
SnSe, IR-active optical phonons, vibr. spectra 79−69848
$SnSe_2$ (6Hb), Raman scatt. and phonon frequencies 77−48159
$SnSe_2$, layer struct., acoustic phonon dispersion curves, propag. modes 77−51462
SnTe, displacive transform., interband electron-phonon interactions, phase diagram 80−93252
SnTe, LO phonons affected by dielec. screening 79−77697
$Sr_{1-x}Cd_xF_2$, IR and Raman meas. 78−75763
$SrGa_2$, layered, dispersion of acoustic phonons, inelastic neutron scatt. 78−47484
SrO, 300K, modified three body force shell model 77−20029
$SrTiO_3$ ceramic, electrocaloric effects for refrigeration at cryogenic temp. 80−77789
Ta, internal equilibrium, cryst. dynamics, lattice dynamical theory of BCC metals 78−79688
Ta, phonon dispersion curves compared with Ta-H and Ta-D 77−76504
Ta-H(D), phonon freqs. and dispersion curves 77−76504
TaC, phonon dispersion, deformation dipole model 79−99281
$TaH_x(D_x)$, acoustic and optic phonons, neutron diffr. obs., book contrib. 79−82296
$TaSe_2$ (2H), charge density wave transitions, neutron diffr. exam. 77−89515
Tb, three-body forces in math. model for phonon dispersion branches and expt. degeneracy 77−62593
Tb, unpaired forces in lattice dynamics of rare-earth HCP metals 77−7805
Te and Se, homology of phonons, scaling formalism for phonon freqs. 80−54326
Te, trigonal, model of lattice dynamics using long and short range interactions 78−59893
Th, crystal equilib., lattice dynamics 78−47479
Th, lattice dynamics, unpaired forces 80−15201
Th, lattice dynamics in reson. model pseudopot. theory 79−19334
Th, one parameter model pseudopotential calc. 78−26643
Th phonon dispersion curves, angular force electron gas model 77−7801
Th, phonon dispersion relations, non-central electron fluid model 80−100312
Th, phonon dispersion spectra from 5-parameter lattice dynamical model 78−10136
$ThC_{0.063}$, cryst. struct. and lattice dynamics 80−88088
Ti, HCP, lattice dynamics exam. by inelastic neutron scatt. 79−60447
TiC, lattice dynamics, inelastic neutron scatt. 78−55918
TiC, nonstoichiometric, simple model for phonon dispersion, rel. to C vacancies 78−30718
TiC, Raman scatt., phonon density of states 78−52499
TiC_x, phonon density of states and dispersion relations 79−42173
$TiCl_3$, phase transition, phonon dispersion curves 80−2130
TiN, phonon dispersion curves, soft-mode behaviour, inelastic neutron diffr. 78−43083
TiN, Raman scatt. supercond. transition temp., phonon density of states, Debye temp. 78−52499
TiN_x, phonon density of states and dispersion relations 79−42173
TiO_2, lattice dynamics, unambiguous assignment of fund. absorpt. edge 78−71817
Ti_nO_{2n-1}, long-range strain and localised relax. energies of crystallographic shear structs. 79−94948
$TiO_{1.95}iFe$, quenched near melting point, transverse composition waves 79−99220
$TiSe_2$ (1T), lattice dynamics and phase transitions 78−79727
$TiSe_2$ (1T), phonons and CDWs, inelastic neutron scatt. meas. 79−28059
$TiSe_2$, lattice dynamics, charge density waves transverse phonon dispersion curves, model 80−49322

phonon dispersion relations continued
$TiSe_2$, quasi-two-dimens. layered struct., phonon dispersion surfaces 79−42180
$TiSe_2(S_2)$ (1T), electronic and vibronic struct. 80−44500
Tl, hexagonal lattice equilibrium, electron gas model with noncentral forces, lattice dynamics 78−95123
Tl, phonon spectrum from Krasko-Gurskii pseudopot. calc. 80−96608
Tl_3AsS_4, optical phonons, Raman and refl. spectra 80−11400
TlBr, CsCl and NaCl phases, atomic interactions and lattice statics and dynamics 78−83889
TlCl, phonon dispersion relations, neutron scatt. exam. 78−51628
Tl_3PSe_4, phonon dispersion temp. depend. 80−96600
Tl_3TaS_4 and Tl_3PS_4, optical phonons, Raman spectra study 80−80790
α-U, CDW at 43K 80−80198
α-U, lattice dynamics 79−95101
UAl_2, elastic consts., temp. and mag. field depend. 80−55450
UC, phonon dispersion, three-body-force shell model 77−1191
$UC_{0.60}N_{0.40}$ optical phonon splitting 78−71810
UN, phonon dispersion relation near Neel temp., neutron coherent inelastic scatt. 78−59900
US, phonon anomalies 79−7663
USb, collective elementary magnetic excitation, neutron inelastic scatt. obs. 79−24141
USb, neutron inelastic scatt. meas., phonon spectra, mag. response, anisotropy 80−50065
V, BCC, phonon dispersion using non-central force model 78−91392
V, Debye-Waller exponent, 4.2 to 296K, incoherent elastic neutron scatt. 79−4382
V, dielec. screening and phonon frequencies using isotropic noninteracting s-d-band model 79−19343
V, Kohn anomalies and phonon dispersion, model including exchange-correl. corrections 78−59886
V, lattice dynamics, phonon dispersion and atomic force constants, phenomenological model 78−26640
V, lattice dynamics and cryst. equilib. 78−75753
V, modified Sharma-Joshi model 79−51221
VI_2, lattice dynamics and ionic charge 80−10615
VN, lattice phonons, dispersion and density-of-states 79−99283
V_2O_3:Cr, pure and doped, sound vels. and elastic consts. from phonon dispersion curves 79−55844
V_3Si, (Ge)(Ga), phonon density of states, temp. depend. 79−42183
V_3Si, lattice dynamics, inelastic coherent neutron scatt. 78−26645
W, lattice wave dispersion, lattice consts., elastic consts. 80−24545
W, phonon dispersion, Debye temp. and Debye-Waller factors, lattice dynamical model 78−55920
Xe adsorbed monolayers, thermodynamic props. and lattice const., quasi-harmonic theory 79−42380
Xe, solid, phonon densities of states and dispersion curves, unpaired elastic force model 79−51220
Xe, solid, phonon dispersion, many body pot. assuming variable at. polarisability, mech. props. 79−55840
Y, dielectric screening and lattice dynamics 77−35646
Y, HCP, nonlocal effects in lattice dynamics 78−91397
YIG, resonant phonon-magnon scatt., phonon spectroscopy obs. 79−65150
YS, phonon anomalies and electron-lattice coupling 80−39490
YS, soft-mode behaviour in phonon dispersion, inelastic neutron scatt. meas. 78−38807
YS, supercond., phonon anomalies, inelastic neutron scatt. 78−59901
Zn, anisotropic thermal expansion due to anisotropy of phonon spectra 79−23750
Zn, cyclotron mass and superconducting energy gap calc. as a function of Fermi surface position 79−69625
Zn, hexagonal lattice equilib., electron gas model with noncentral forces, lattice dynamics 78−95123
Zn, lattice dynamics 77−15513
Zn, phonon density of states calc. from neutron diffr. data 77−24369
Zn, phonon dispersion relations, first-principles calc. 79−60448
$Zn_xCd_{1-x}Te$, reson. Brillouin scatt., acoustic domain injection 79−38557
ZnO, polariton dispersion, IR reflection spectroscopy 80−11415
ZnP_2, second-order vibr. spectra and dispersion of phonon branches 80−25376
ZnS, lattice dynamics, phonon freq., bond bending force model calcs. 80−70335
ZnS, phonon dispersion under extreme press. and metallic transform., Raman spectra meas. 78−10895
ZnS(Se)(Te), thermal expansion and lattice dynamics under press. 80−100316
ZnSe, eight-parameter bond-bending forces model 80−70334
ZnSe, phonon dispersion under extreme press. and metallic transform., Raman spectra meas. 78−10895
ZnTe, lattice dynamics and phonon parameters, bond bending force model lattice dynamics and phonon parameters bond bending force model 80−59595
ZnTe, phonon dispersion under extreme press. and metallic transform., Raman spectra meas. 78−10895
ZnTe(S), reson. Brillouin scatt., acoustic domain injection 79−38557
Zr, BCC, lattice dynamics, 1400K, phase transform. 79−19337
Zr, BCC, phonon dispersion relations, d-electron contrib. to Cauchy discrepancy 80−92628
Zr, BCC, phonon vibrs., pseudopot. method 80−15204
Zr, HCP, nonlocal effects in lattice dynamics 78−91397
Zr, HCP, normal vibr. modes, temp. depend. 79−19339
Zr, HCP, temp. depend. of C-axis phonon dispersion curves 78−59884
β-Zr, phonon dispersion, modified Sharma-Joshi model 80−100311
Zr-Nb-Mo, phonon spectra anomalies, lattice dynamics calculations, superconductivity parameters 79−7655
ZrN, phonon dispersion curve anomalies, inelastic neutron scatt. obs. 79−86858
Zr_2Ni, search for soft phonon modes, neutron scatt. 79−23686

phonon drag
acoustic wave in solids, phonon drag 77−27947
acoustoelectric effect, electron drag by coherent Lamb phonons in quantising magnetic field 80−80330
alkali metal, electron-phonon drag effects in elec. cond. and thermoelec. power 77−15824
alkaline earths, cubic, deviations from Wiedemann-Franz law 78−39086
anisotropic normal metal, thermopower calc. 80−24879
dislocation-phonon interactions, drag of phonon gas by moving dislocations 80−70218

phonon drag continued
graphite, carrier mobility, temp. depend. determ. from magnetoresist. expts. 80−11009
graphite, cryst., thermoelec. power, anomalous phonon drag effect 78−19065
graphite, electron-phonon interactions, rel. to elec. transport 80−34156
graphite, neutron irradiation, electron transport, annealing study 80−39165
graphite, thermoelectric power, low temperature, anomaly rel. to phonon drag 80−65610
heavily doped compensated semiconductor, phonon drag effect in disordered media 77−24576
Josephson junction, vortex motion induced by phonon injection 79−4622
metal, acoustic wave drag, acousto-elec.-mag. effects *(Russian)* 79−19638
metal, electron-phonon drag and interaction of first and second sound 77−66009
metal, influence of phonon drag on thermoelec. coeffs. *(German)* 77−80766
metal, magnetothermoelectricity, phonon drag contrib. 79−65432
metal, phonon drag magnetothermoelectricity, semiclassical theory 78−6354
metals, acoustic attenuation in collision regime, variational principle 79−82648
metals, low temp. elec. resist., comparison between first principles form factor and empirical form factor 78−2463
metals, phonon drag direct obs. feasibility *(Russian)* 77−85187
metals, phonon-phonon scatt. role in lattice thermal cond., phonon drag, elec. cond. 80−70483
monovalent metal, resistivity, 1-4K, HF phonons role 77−15828
noble metal alloys, diffusion thermopower, phonon drag 79−65441
quasi one-dimensional conductor, phonon drag conductivity in Frohlich Peierls phase, effect of impurities 78−60114
semiconductor, bounded samples, volt-ampere characts., nonequil. phonons influence on thermal dimensional effects 77−43611
n-semiconductor, electron-phonon drag in longit. quantising mag. field 77−76805
semiconductor, Nernst-Ettingshausen effect, thermopower, strong elec. field 78−23122
semiconductor filament, thermoelectric power 78−19069
semimetal, compensated, hydrodynamic cond., surface scatt. and phonon drag *(Russian)* 77−8088
semimetal, phonon drag, role of surface in thermoEMF *(Russian)* 78−47819
semimetal, two-stage drag of electrons by phonons 77−15843
by sound 79−28062
superconductors, thermoelectric and acoustoelectric effects, influence of mutual drag of excitations and phonons 80−44761
thermal phonon drag by coherent acoustic waves, Umklapp processes 78−14417
wurtzite structure semiconductor, transport in longit. quantizing mag. field 78−26891
zinc blende semiconductors, small-gap, electron scatt. and transport props. 78−95294
zinc blende semiconductors, small-gap, electron scatt. and transport props. 78−95295
Al, band struct. effects on electrical and thermal cond. 78−34820
Al, contrib. to thermopower 77−72854
Al, low temp. thermopower of Frenkel defects 78−19024
Al, Nernst-Ettingshausen coeff., electron-phonon Umklapp scatt. 78−26848
As, electrical and thermal props. 78−14747
As, thermopower and thermal cond. from 8K down to 0.3K 79−19610
As_xSb_{1-x}, semimetal, thermopower, thermomagnetic power, 4.5 to 77K 80−107825
Au-Ag(Cu), dilute, low temp. thermoelec. power, electron diffusion and phonon drag 77−20301
Bi bounded semimetals, phonon two-stage drag of electrons, thermoelectric power, scatt. mechanism 80−92919
Bi, giant negative phonon drag thermopower, pure sample 77−76851
Bi, magnetotransport props. in quantising mag. fields 77−20340
Bi, metallic, thermopower meas., 9K-40 mK 78−91673
Bi, phonon-drag low temperature thermoelectric refrigeration 80−22366
Bi whiskers, thermopower, temp. depend., 77 to 300K phonon drag effect 79−82615
Bi-Sn, thermopower from 50 mK to 25K 80−24880
$Cd_xHg_{1-x}Te$, thermal cond. in mag. field, thermopower, and Nernst-Ettingshausen effect 77−31814
Cu-Al(Ge)(Sn) film, thermoelec. power, 80-350K 78−68096
Cu-Au dilute alloys, thermopower and resistivities, validity of Nordheim-Gorter relation 78−91671
p-GaAs, galvanomagnetic and thermomagnetic effect meas., hole phonon drag effects 77−4367
n-GaAs, piezoelectric semiconductor, influence of acoustic phonon disturbances on conductivity 78−91697
n-Ge, drag effects, heated electron-phonon system 78−23078
Ge, elastic moduli, drag coeffs. and Keating's parameters 79−73238
n-Ge, elastically deformed, anisotropy of thermoelec. effect 78−19066
Ge, electron-hole drops, kinetics of spatial distrib. *(Russian)* 78−43312
Ge magnetoacoustic effects in the drag of electron-hole drops by phonons 78−68057
Ge, phonon drag of electron-hole drops in longit. quantizing mag. field *(Russian)* 78−64070
n-Ge, thermoelec. power in quantising mag. field, phonon-phonon interactions 80−107832
Ge:P, phonon drag thermoelectric power at low temp. 80−107828
$Hg_{2.86}AsF_6$, thermoelectric power 78−34852
$Hg_{3-x}AsF_6$, one-dimens. conductor, thermopower, phonon drag 79−65466
In, magnetothermopower, phonon drag 79−69496
n-InSb, thermoelec. power in longit. quantising field, phonon drag component 78−19064
K, elec. resist., temp. depend., low temp. limit 77−11892
K, low-temp. lattice cond., phonon drag thermopower 79−60789
K, phonon-dislocation scatt. and phonon equilibration at low temp. 79−51561
K, thermomagnetic and thermoelectric properties, phonon scatt. processes 80−29390
$MnAs_{1-x}P_x$ whiskers, thermoelectric power, 5 to 350K, phonon drag effects and mag. transitions 79−28363
Mo-Nb (Re), thermoelec. power, 4.2 to 300K 80−70683

phonon drag continued
$NaNbO_3$, elect. cond. mech., resist., Hall coeff. and thermoelec. power meas. 80−65603
Nb-Zr, thermoelec. power, 4.2 to 300K 80−70683
Ni cryst., US wave attenuation, phonon viscosity and dislocation drag coeffs. 80 and 298K 77−76491
Pd-Co (0.1-45.7 at.%), thermo EMF at 4.2-300K *(Russian)* 80−92881
Pd-Fe (0.54-8.0 at.%), thermo EMF at 4.2-300K *(Russian)* 80−92881
Pd-Ni (15-90 at.%), thermo EMF at 4.2-300K *(Russian)* 80−92881
$(SN)_x$, thermoelec. power, 0.1 to 4.2K, phonon drag contrib. and super-cond. transition 79−56356
$(SN)_x$, thermopower from 0.15 to 4.2K 80−34427
Sb, effective Debye scatt. temp., depend. on phonon drag. 79−73507
n-Si, piezoresist. rel. to piezothermoelec. power, electron-phonon drag region 80−70737
Si:B, piezothermoelec. power 78−56173
p-Si:B, thermoelec. power, 20-300K 78−19067
n-Si:P, piezothermoelec. power in electron-phonon drag region, anisotropy 80−70738
n-SiC (6H), anisotropy, of thermoelec. power and transverse Nernst-Ettingshausen effect 77−69362
SiC (6H), phonon drag and phonon-electron interaction *(Russian)* 78−79701
TTF-TCNQ, irradiated, libron and phonon equilibration, resistivity meas. 79−42530
Ta-W, thermoelec. power, 4.2 to 300K 80−70684
YIG, phonon viscosity effect on dislocation motion 80−24450

phonon-electron interactions *see electron-phonon interactions*

phonon-exciton interactions
alkali halide, polarization dichroism in the optical spectra of Jahn-Teller excitons 79−69435
anisotropic crystal, diffusion of excitons due to scatt. by optical phonons, Stokes line 77−24521
anisotropic crystals, exciton diffusion and relax. time *(Russian)* 77−80742
anthracene, cryst., polariton luminesc. 80−84775
anthracene, luminesc. spectra, exciton-phonon interaction, triplet exciton bands 79−65387
anthracene, molecular crystal, exciton-phonon coupling, absoprt. band profile in first singlet system 78−83888
anthracene, triplet excitons, phosphoresc. and delayed fluoresc. excitation spectra 78−63986
anthracene mol. cryst., exciton-lattice interaction and exciton absorption line shape 78−18968
anthracene-Au interface exciton luminescence Frenkel exciton metallic quenching *(Russian)* 80−50421
anthracene-phenanthrene-tetracyanobenzene, CT-cryst., mini-excitons and lattice dynamics, ESR, optical and Raman spectra 80−60406
anthracene-pyrometallitic dianhydride cryst., refl. and absorpt. spectra of singlet charge transfer excitons 80−71442
anthracene-quartz interface exciton luminescence, Frenkel exciton metallic quenching *(Russian)* 80−50421
anthracene-TCNB charge transfer crystal, EPR spectra of triplet excitons, and Raman spectra 78−26817
anthracene-trinitrobenzene complex, neat and mixed cryst. and glass opt. spectra 77−40274
benzophenone: diphenylmethylene, mixed cryst., emission and absorpt. spectra, 2-30K, excitation-phonon coupling 79−99900
benzophenone, migration of triplet excitons, EPR profiles and phosphoresc. decay data 80−84641
betamethylnaphthalene in $C_{10}D_8$, exciton percolation and coherence 77−59258
charge transfer complexes, doped, excited cryst., fine and hyperfine struct., ESR 77−12188
coupled-mode excitations in cryst., relax. rates, theory 80−59881
9-cyanoanthracene, cryst., excimer emission, spectra, photochem. and multiphonon processes 78−10914
1,4-dibromonaphthalene, substitutionally disordered, energy localisation, optical and ODMR spectra of triplet Frenkel excitons 80−54996
(1,4)-dibromonaphthalene, triplet exciton scatt., absorpt. spectra 78−6696
4,4′-dichlorobenzophenone, cryst., $T_1 \leftarrow S_0$ singlet-triplet absorption profiles, temp. depend., phonon-exciton anal. 78−60436
4, 4′-dichlorobenzophenone, triplet exciton absorpt. band, zero phonon line *(French)* 79−33726
p-dihalobenzene, mixed cryst., Raman spectra, phonons and vibr. excitons, criteria for solid solns. 78−43840
direct semiconductor, exciton luminescence in longitudinal optical photon sideband, formation time 79−61438
electron-hole droplet cloud, role of thermalisation phonons 80−49617
electron-hole drops with vel. close to that of sound, damping of movement *(Russian)* 79−19529
exciton drops, effect of repulsion on formation 78−23029
exciton line shapes and migration with stochastic exciton lattice coupling 79−11070
exciton peak position, temp. depend. *(Russian)* 79−37777
exciton physics, review, book contrib. 80−44517
exciton solitary waves, damping and modification 77−62833
excitonic molecules, population dynamics, collision effects 77−85149
excitonic wave-phonon coupling, struct. transitions 77−15775
excitons, book 80−41951
extrinsic crystals, exciton migration theory 79−87043
ferroelectrics, absorption edge anomalies in phase transitions 80−2718
fluorobenzene crystal, localised excitons 77−31963
Frenkel excitons, high density system, collective excitations 77−43501
frequency dependent optical phonons contrib. to small radius excitons binding energy 77−69236
fusion of Frenkel excitons in exciton-phonon field 77−55484
ground state energy in mag. field 77−11859
hot exciton scattering and decay due to interaction with acoustic phonons 78−47709
hot excitons interacting with acoustic phonons at finite temps., scatt. and decay 78−76005
II-VI semiconductor, resonant secondary emission spectra, relax. of energy and polarisation 80−93331
II-VI semiconductors, photoreflection exciton spectra *(Russian)* 77−20874
inert gas crystal, scatt. and self-localisation phenomena *(Russian)* 77−62831
inert gas crystals, excitons exam. 78−51898
inert gas solid, VUV luminesc. from excitons 79−43020
ionic crystal, anharmonism effect on exciton peak broadening in absorpt. spectra *(Russian)* 80−97317
layer crystals, exciton absorption of light 80−70623
local deformation of EM field due to mol. vibrs. 77−20245
localisation in ionized and excited states, conf. 77−30750
long-wave approximation, exciton-phonon interaction 77−62835
metastable exciton-phonon hybridisation 79−51493
mixed crystal, exciton self-trapping 79−37991
molecular crystal, exciton bandwidth effects on electron-phonon coupling 77−4172
molecular crystal, exciton transport, variational method 78−30870
molecular crystal, exciton transport theory with quadratic exciton-phonon coupling 78−56077
molecular crystal, Hamiltonian for displaced modes 77−15507
molecular crystal, one-dimensional model, exciton-phonon and phonon-impurity interactions 80−24542
molecular crystal, strong and weak coupling 78−51899
molecular crystal trapping processes, exciton-phonon coupling 80−39505
molecular crystal with two sublattices, exciton drop interactions 79−56131
molecular crystals, biexciton and exciton drop formation 77−28125
molecular crystals, charge transfer exciton-phonon interactions 77−84857
molecular crystals, electronic energy transfer, review, book contrib. 77−39789
molecular crystals, electronic excitation energy transfer, external elec. field effect 80−84431
molecular crystals, exciton-lattice interaction and exciton absorption line shape 78−18968
molecular crystals, exciton-phonon coupling and exciton transport 80−84430
molecular crystals, phononless exciton band lineshape, excitation transfer, stochastic models 80−107711
molecular crystals, spectroscopy, bibliography for 1976 78−72585
molecular crystals, two particle exciton-phonon interactions, optical absorpt. line shapes theory 80−55120
molecular crystals of 1-D, linear approx. 78−18717
molecular crystals with several sublattices, exciton-phonon interaction and Bose-Einstein condensation of Frenkel excitons 80−107713
molecular one-dimens. cryst., perturbed Schrodinger eqn., soliton-like soln. 79−7765
molecular one-dimensional systems, electronic collective excitations 77−31959
molecular one-dimensional systems, electronic collective excitons, EPR response 77−31960
molecular organic solid, rigid. lattice calcs. 77−31958
naphthalene, $^1B_{2u}$ supertransfer, exciton percolation, fluoresc. spectra obs. 77−55482
naphthalene, a-exciton temp. depend. scatt., optical absorpt. profile 78−72088
naphthalene, cryst., luminesc., excitons, phase aspects 79−56838
naphthalene, cryst., three-particle complex as impurity-exciton-phonon bound state *(Russian)* 77−62842
naphthalene, cryst., vibronic absorpt. spectrum with totally symm. phonons 79−4817
naphthalene, deformation potential consts. of exciton-phonon interactions *(Russian)* 78−56498
naphthalene, molecular cryst., phonon scatt. and exciton linewidths 78−15185
naphthalene, pure and doped, exciton-phonon luminesc. 80−84773
naphthalene, spectra of directionally deformed crystals and phonon-exciton interaction constants 79−78703
naphthalene, triplet excitons, phosphoresc. and delayed fluoresc. excitation spectra 78−63986
naphthalene in $C_{10}D_8$, exciton percolation and coherence 77−59258
naphthalene-h_8 and d_8, isotopic mixed crystals, exciton spectra in IR region 80−71400
nonequilibrium density matrix method, energy relaxation, coherent props. 77−51673
octafluoronaphthalene crystalline complexes with naphthalene and durene, triplet exciton emissions 80−84760
one-dimensional molecular crystal, rel. to soliton-like solns. of eqns. for excitations 78−84149
one-dimensional solids, energy transfer processes, optically detected electron spin coherence meas. 79−19808
one-dimensional system, coupled exciton and phonon states *(Russian)* 77−69258
optical absorption band shape rel. to exciton-phonon parameters *(Russian)* 77−28533
organic charge transfer crystals, transport props., phase transitions, mol. dynamic *(German)* 80−39507
organic molecular crystals, inelastic neutron scatt., exciton creation 80−70084
organic solid, motion of localised excitations 77−31961
organic solids, cryst. and amorphous, optical spectra, Urbach rule, struct. disorder effect 78−23479
perylene crystal, molecular exciton system, resonance Raman and fluorescence studies, dynamical effects 80−66169
phenanthrene, molecular cryst., phonon scatt. and exciton linewidths 78−15185
phenanthrene, two-photon excitation spectra, exciton-phonon and intramol. vibronic coupling 80−84774
phenazine, substitutionally disordered, energy localisation, optical and ODMR spectra of triplet Frenkel excitons 80−54996
phonon effect on centre of mass or motion, relative motion of particles in exciton 78−6277
phonon wind effect, interaction of electron-hole drops with ballistic phonon in heat pulse 78−6279
photon-exciton-phonon system, coupled, density matrix eqn. solved 77−85156
polar, layered material, quenching of excitonic diamag. shifts 79−19526
polar crystal, Frenkel exciton effective mass temp. depend., lattice displacement interactions *(Chinese)* 80−84429
polar semiconductor, exciton dispersion, influence of optical phonons, effective exciton mass, variational calc. 79−15091
polar semiconductor, hot exciton transitions to excited states, interaction with acoustic phonons 80−96799
polar semiconductor, multiphonon cascade theory of light scatt. 78−19490

phonon-exciton interactions continued
polar semiconductors, effective Hamiltonians and binding energies of Wannier excitons 78−34777
polar semiconductors, exciton-phonon interactions, optical absorpt. spectra, theory 80−49614
polar semiconductors, hot exciton scatt. accompanied by transitions to excited states, phonon interactions 80−44516
polar semiconductors, two-phonon resonance Raman scattering 80−108204
pyromellitic dianhydride-anthracene, cryst., charge transfer exciton transitions, refl. spectra obs. 78−72540
Raman effect in solids, interacting elementary excitations, review 78−43846
resonance light scattering and hot luminesc. of self-trapping excitons 80−93336
resonant Raman scattering via virtual exciton 80−71412
resonant secondary radiation of excitons strongly interacting with phonons 79−60724
resonant secondary radiation of excitons weakly interacting with phonons, theory 78−31241
scattering and decay of hot excitons interacting with longitudinal optical phonons 78−34774
semiconductor, bound exciton recombination, phonon replicas 79−38649
semiconductor, bound excitons, review, book contrib. 80−44519
semiconductor, exciton damping by phonons, appl. to Ge 77−1373
semiconductor, exciton-phonon energy transfer 78−18715
semiconductor, impure, rel. to exciton absorpt. line shape calc. *(Russian)* 78−10934
semiconductor, light absorption, temp. depend., exciton-exciton and -phonon interactions *(Russian)* 77−40265
semiconductor, quasi-one- and quasi-two-dimens., exciton self-localisation *(Russian)* 77−31956
semiconductor, resonant Raman and Brillouin spectroscopy, review, book contrib. 80−49624
semiconductor, thermal cond., exciton-phonon drag 77−15640
semiconductor films, exciton light absorption coefficient *(Russian)* 80−71504
semiconductor thin wires, Wannier-Mott exciton scatt. by phonons *(Russian)* 78−72074
semiconductors, alignment and orientation of hot excitons, secondary radiation polarisation calcs. 79−65392
semiconductors, exciton light absorpt. band formation, linear and quadratic exciton acoustic photon interactions *(Russian)* 80−34368
semiconductors, excitonic polarons, Pollmann-Buttner variational method, donor and exciton binding energies 79−42469
semiconductors, excitons in mag. field, exciton-phonon interaction 80−24806
semiconductors, phonon replicas of bound exciton recombination 79−52008
spectral parameter calculation for exciton-phonon system *(Russian)* 78−43311
trans-stilbene, cryst., triplet excitons, $S_0 \rightarrow T_1$ transition 78−76518
superconductor and normal metal, Raman sound scattering *(Russian)* 78−23199
surface exciton polaritons, book contrib., review 80−49623
tellurophene(-d_4), cryst., struct., phonon spectrum, exciton splittings, assignments 77−81088
tetracene single crystals, exciton refl. spectra, 4.2 to 300K 79−47478
tetrachlorobenzene, pure and doped crysts., triplet exciton trapping, phosphoresc. spectra 77−85766
tetrahedral semiconductors, valence band degeneracy, polar electron-phonon interaction effect, exciton binding energy 79−56140
trap effects on exciton bands, masking by exciton-phonon coupling 80−80186
variational solns. for energy and correl. functions 80−10601
Wannier-Mott exciton decay, on acoustic phonons, in thin semicond. wire *(Russian)* 78−72075
AgBr, exciton relax. by intervalley scatt., reson. Raman meas. 79−33713
AgBr, photoluminesc. study of excitons in high mag. fields 80−80843
AgBr:AgCl, mixed crystals, first order reson. Raman scatt., momentum conservation relax. 79−56790
AgBr:Cl, exciton-phonon interaction, reson. Raman scatt. vs photolum. 80−29798
$Al_xGa_{1-x}As$, indirect, exciton-phonon coupling, photolum. meas. 79−47511
$Al_xGa_{1-x}As$:N, photoluminesc. and optical absorpt. spectra of N impurity bound-excitons 79−47496
Au-Ge Schottky diode, phonon energies, barrier heights, photovoltage spectra 78−64112
BiI_3 film, exciton-phonon interaction, optical consts., Faraday effect, permitt. 80−59884
CaS:Pb^{2+} phosphors, luminesc., refl., emission, and excitation spectra 79−11456
CdS, exciton resonant secondary emission spectrum temporal evolution 79−51499
CdS, exciton-LO phonon interactions under high excitation and temp. conditions 77−69899
CdS, exciton-phonon interaction, interpretation of optical absorpt. data 79−14897
CdS, free-exciton multiphonon luminesc. 78−6741
CdS, LO phonons, size effect reson., first order forbidden light scatt. 77−44002
CdS, laser thresholds and stimulated emission, intrinsic recomb. processes 79−15489
CdS, multiphonon reson. Raman scatt. and exciton-phonon luminesc. 77−16319
CdS, reson. Brillouin scatt. near A exciton 77−69846
CdS, reson. Brillouin scatt., book contrib. 79−42983
CdS, reson. Raman scatt., temp. depend. polarisation, A-exciton 77−12386
CdS, reson. scatt. of exciton-polaritons by acoustic phonons 78−60482
CdS, resonant scatt. of exciton polaritons by LO and acoustic phonons 79−95760
CdSe, exciton-phonon luminesc. 77−16319
CdSe, free-exciton multiphonon luminesc. 78−6741
CdSe, polarisation correl. of resonant Raman scatt. or hot luminesc. 80−25384
CdSe, single cryst., band parameters from optical exciton spectra 79−47021
CdSe:Ag, In, cryst., photocurrent and electroreflection, 77 to 300K *(Russian)* 78−23136
phonon-exciton interactions continued
CdTe, reson. Brillouin scatt., book contrib. 79−42983
$CoBr_2$, paramag. and antiferromag., Raman scatt. from electronic excitations and phonons 79−69826
CuCl, biexciton first excited state, LO phonon assisted two-photon absorption 77−40260
CuCl, phonon interaction of excitonic molecule 80−50316
CuCl, phonon-assisted two-photon absorpt. of excitonic mol., bare-exciton approach 79−78702
CuCl, Urbach rule at excitonic absorpt. edge, theoretical model tests 80−50299
Cu_2O, 1s yellow exciton, lineshape studies by reson. Raman scatt. 78−76465
Cu_2O, exciton-phonon dynamics, reson. Raman scatt. 80−11406
Cu_2O, fine struct. of exciton spectrum 78−18972
Cu_2O, reson. Raman scatt., yellow and green excitonic series 78−72511
Cu_2O, yellow exciton series, 1s paraexciton levels, phonon assisted transitions, optical absorpt. edge 78−79934
EuO(S)(Se), rel. to spin assisted Raman scatt. theory 78−43866
EuS(Se)(Te), spin-assisted phonon Raman scatt., mag. phase depend. 80−71413
$Ga_x In_{1-x}P$, localised exciton-phonon complex as intermediate state in light scatt. 78−39543
GaAs, excitonic polariton reson. interaction with LA phonons 78−60481
GaAs, excitonic spectra broadening, influence of phonons and impurities 77−1711
GaAs, reson. Brillouin scatt., book contrib. 79−42983
GaAs, resonant Brillouin scatt. of excitonic polaritons 77−44010
$GaAs_{1-x}P_x$, bound exciton, luminesc. reson. excitation 79−95840
$GaAs_{1-x}P_x$, localised exciton-phonon complex as intermediate state in light scatt. 78−39543
$GaAs_{1-x}P_x$:N, photoluminesc. and optical absorpt. spectra of N impurity bound-excitons 79−47496
GaP, indirect free exciton ground state, shifted thresholds of absorpt. edge 77−51670
GaP, luminesc. from electron-hole drops, 2 to 77K 79−11454
GaP, MCD of phonon-assisted exciton transitions 78−92053
GaP:N, phonon satellite intensity distrib. in luminesc. spectrum 77−55832
GaP:Zn,O, photodiodes, high temp. emission spectra *(Russian)* 77−66545
p-GaSb, hot exciton luminesc., LO phonon Raman scatt. 80−11474
GaSb, interaction of exciton recombination with LO phonons 79−38647
GaSe, exciton-phonon bound state, photocond. and visible absorpt. spectra obs. 80−50369
GaSe, exciton-phonon quasibound states, photocond. and luminesc. study 80−96800
$GaSe_xS_{1-x}$, layered semicond., electroabsorpt. in fundamental absorpt. edge region 77−52043
GaTe, exciton polariton effect on absorpt. edge, absorpt. and refl. spectra, 4.2 to 300K 80−20664
Ge, acoustic phonon scattering by electron-hole drops, deform. potential 78−10360
Ge, dissociation of hot excitons by long-wavelength acoustic phonons, photocond. spectra 77−4300
Ge, doped, electron-hole drops, low-temp. photolum. spectra obs. 77−69900
Ge, electron-hole drops size effect on far IR absorption and scatt. *(Russian)* 78−10903
Ge, exciton and electron-hole drop entrainment by nonequilib. phonons 80−6751
Ge, exciton energy gap and LA and LO momentum-conserving phonon energies 79−90965
Ge, HF breakdown of excitons effect on kinetic of electron hole droplets *(Russian)* 77−59260
Ge, phonon damping of electron-hole droplet motion 77−85152
Ge, phonon-assisted exciton emission, temp. depend. of relative integrated intensities 77−1375
Ge, piezospectroscopic determ. of electron-phonon to hole-phonon interaction 79−95783
GeS, Urbach's rule, absorption edges 80−97224
HgI_2, phonon struct. in wavelength modulated refl. spectra and mag. circular dichroism 79−8125
HgI_2, red, liminesc. and Raman scatt., biexcitons and exciton-phonon interactions 79−61424
HgI_2, red, resonant Raman scatt. in B-exciton and band to band transition regions 79−61381
$In_{1-x}Ga_xP$, epitaxial film, cathodolum. obs., recomb. mechanisms 78−72613
InSb, interaction of exciton recombination with LO phonons 79−38647
InSe, exciton and polaron anisotropies, reson. Raman scatt. study 80−76033
LiD, cubic cryst., exciton-phonon interaction and exciton anisotropy 78−72083
LiD(H), excitons and exciton-phonon interaction, refl. spectra meas. 4.9 to 5.3 eV 77−44019
LiH, cubic cryst., exciton-phonon interaction and exciton anisotropy 78−72083
LiH, motion and relax. of free excitons, luminesc. spectra 79−43037
LiH, single crysts., refl. photolum., cathodolum., and photocond. meas. 77−52186
MgO, pure and doped, luminesc. of free and relaxed excitons 79−74008
MnO, magnon-sideband lineshape, exciton-phonon interaction effects 80−65846
N_2, solid, exciton-phonon coupling in strong coupling limit, temp. depend. 80−92616
N_2, solid, UV spectra, phonon induced exciton fine struct. 79−15477
NaI, exciton-phonon polarisation interaction *(Russian)* 78−35195
NaI, motion of free excitons and their self-localisation 80−2342
$NaNO_2$, fine struct. in luminesc. spectra in UV region 77−59607
$NaNO_2$, hot luminescence 78−10976
PbI_2, photolum. and reflectivity temp. depend., cryst. anisotropy effect on electron-phonon interaction *(Russian)* 78−15225
PbI_2, visible exciton spectrum, exciton-phonon interactions, dielectric const. and oscill. strengths 80−25405
$PbMoO_4$, near-edge absorpt. band, fluoresc. and photocond. 77−44017
Se, trigonal, cathodolum. at 10K *(German)* 78−2923
Si, amorphous, phonon interaction in luminescence 78−43927
Si, deformed, recomb. radiation from electron-hole drops and free excitons 77−8641

phonon-exciton interactions continued
Si, dissociation of hot excitons by long-wavelength acoustic phonons, photocond. spectra 77−4300
Si, free exciton luminesc. band, resolved splitting 79−73995
Si, free excitons, drift and diffusion, luminesc. obs. 80−84434*
Si, indirect exciton ground state, shifted thresholds of absorpt. edge 77−51670
Si, intrinsic, phonon replicas of electron-hole liq. luminesc. line 79−28831
Si, intrinsic, two-phonon assisted free exciton recomb. radiation 78−2922
Si, LO and TO phonon assisted free exciton luminesc. 79−33833
Si, phonon-assisted exciton emission, temp. depend. of relative integrated intensities 77−1375
Si, piezospectroscopic determ. of electron-phonon to hole-phonon interaction 79−95783
Si:Li, bound-exciton excited states, uniaxial anal. 80−71475
SnO_2 defective crystals, exciton-impurity complex luminescence spectra *(Russian)* 79−65926
SnO_2, exciton luminescence spectra, absorpt. spectra 80−89064
TiO_2, exciton luminescence spectra, absorpt. spectra 80−89064
TlBr, TlCl, ground state energy in mag. field 77−11859
TlBr(Cl), electronic state of excitations and their phonon coupling 79−60719
TlCl, Urbach rule at excitonic absorpt. edge, theoretical model tests 80−50299
$TmAsO_4$, optical side bands, absorpt. spectra in mag. fields 77−52123
Xe, crystalline, polariton effects, reflectivity, absorpt., and resonant luminesc. spectra calcs. 80−20095
Xe, solid, self-trapped exciton emission bands 80−20697
$YCrO_3$, mag. circular dichroism and Faraday rotation in R-lines region 79−28725
YbS, multiphonon processes and exciton-LO phonon interaction 79−95784
YbS, Raman spectra reson., reflectance spectra, multiphonon processes 78−84581
$Zn_xCd_{1-x}S$, resonance Raman scatt. involving exciton complexes 80−16039
$Zn_xCd_{1-x}Te$, reson. Brillouin scatt., acoustic domain injection 79−38557
ZnO, change in exciton-phonon mechanism due to defects 78−71804
ZnO, diffusion of excitons due to scatt. by optical phonons, photoluminesc. 77−24521
ZnO, laser thresholds and stimulated emission, intrinsic recomb. processes 79−15489
ZnO phosphors, origin of UV emission 78−64400
ZnS, temp. coeffs. of charact. reflectivity struct. 77−85745
ZnS(Se), wavelength-modulated refl. spectra, 2.5 to 8 eV, exciton-phonon quasi-bound complex 77−20877
ZnSe, exciton emission, halfwidths, thermal and optical activation energies obs. *(French)* 80−66268
ZnSe, temp. coeffs. of charact. reflectivity struct. 77−85745
ZnTe, laser thresholds and stimulated emission, intrinsic recomb. processes 79−15489
ZnTe, reson. secondary radiation 79−99886
ZnTe, wavelength-modulated reflectance spectrum, electron-phonon and exciton-phonon interactions 79−11434
ZnTe(S), reson. Brillouin scatt., acoustic domain injection 79−38557

phonon-impurity interactions
see also lattice localised modes
absorption and emission spectra, of impurities in solids, bandshapes, moments 80−45122
alkali halide: O^{2-}, photoluminesc. spectra, phonon using struct. *(Russian)* 78−2912
alkali halide:NH_2^-, dipole centre paraelectric alignment, phonon-assisted tunnelling 77−12413
alkali halide=O_2^- soln., phonon wings in luminescence spectra *(Ukrainian)* 79−52001
alkali halide, ReO_4^- doped, saturable absorber at 10.6 μm 80−53384
anharmonic crystal, with isotopic impurities, lattice thermal cond. 77−59158
anthracene-2-methyltetrahydrofuran, glassy solution, site-selective impurity phonon coupling 77−81142
Bethe-lattice dynamics, impurity and localised mode 77−62595
collision operator, linearised phonon 77−27965
crystal impurity librational relax., phonon assisted transitions, direct, Orbach and Raman processes 78−83887
crystal with interstitials, lattice dynamics 80−2128
cubic metals, impurity-host force-constant changes from Mossbauer data, review 78−48097
diamond, natural, thermal cond. with absorpt. at 3.22 μm 79−73353
diffusion of light interstitial impurity, solvent nuclei vibr. anharmonicity effects *(Russian)* 77−24433
dilute alloys, force const. changes due to substitutional impurities 77−24374
disordered crystal, biphonon spectra, light absorpt. coeff. and density of states, CPA calc. 80−84271
disordered systems, time dependent spectral transfer, Monte Carlo calc. 80−11464
electron spin-lattice relaxation, role of soft phonon modes 79−28590
exchange interaction between impurity centres due to phonons *(Russian)* 78−79678
FCC metals, dynamics of multiple interstitials and interstitial impurity complexes 78−75775
ferroelectric phase transition, by impurity carriers, electron-phonon interaction *(Russian)* 78−48134
fluorite and antifluorite structs., (110) surface vibr. modes, dynamics and adiabatic potential 80−6613
fluorite type struct., impurity defect interaction in boundary layer, adiabatic approx. 80−6614
garnet:Fe^{3+}, spin Hamiltonian parameters, g-factors, temp. depend. EPR obs. 77−48038
garnet:Mn^{2+}, spin Hamiltonian parameters, g-factors, temp. depend. EPR obs. 77−48038
impurity pinning, phonon localization, in incommensurate modulated lattices 80−39238
ionic crystals with intermediate polaron coupling, magneto-optical effects in shallow F-centres 80−20615
isotopically disordered ferroelectric cryst., thermal cond. 77−76628
Jahn-Teller multimode effect for E-term with strong vibronic coupling, IR and Raman spectra band shapes 80−20139

phonon-impurity interactions continued
Kramers ions, virtual phonon exchange, field theoretic formalism 80−20137
laminary crystal, phonon spectrum and local vibrations *(Russian)* 80−10623
local vibrations, impurity interactions, effect on spectral distrib. 80−96613
matrix isolation spectra, homogeneous IR line shape, Debye approx., space time phonon correl. functions 79−823
metal, BCC quantum diffusion model of light interstitial atoms 80−2212
metal, diffusion of H(D), slow neutron scatt. obs., review 80−34248
metals, ferromagnetic, nonmagnetic impurity hyperfine field temp. depend. 80−34402
molecular crystal, one-dimensional model, exciton-phonon and phonon-impurity interactions 80−24542
molecular crystal with isotopic impurity molecule, phonon spectrum under Fermi resonance 78−34583
multimode Jahn-Teller effect for E-term with strong vibronic coupling, local and resonant states 80−24858
multiphonon nonradiative transition rates, quadratic impurity-phonon coupling 78−23506
naphthalene, doped, zero-phonon lines and absorpt. spectra, temp. depend. of shift and broadening 79−69866
noble metal dilute alloy, form factors, rel. to residual resist. calc. 77−28156
nonlinear impurity electron-phonon oscillations 80−49327
nonmetal, impurity optical absorption and emission, anharmonic effects 78−56503
nonresonance interaction parameters of rare earth ions, luminescence kinetics obs. *(Russian)* 78−31246
oscillator, highly-excited, decay in cryst. vibr. interaction 80−10600
p-type semiconductors, internal strain on bound hole-phonon interaction 78−91492
paraelectric resonance of nonstationary tunnelling states *(Russian)* 80−34869
paramagnetic ion, reson. phonon scatt. 78−18716
particle dechannelling with phonon scatt., quantum theory 78−18695
phonon scattering at multilevel impurities, dispersion, damping, Green's function calc. 79−14892
phosphate glass:$Nd^{3+}(Yb^{3+})$, nonresonance interaction parameters of rare earth ions, luminescence kinetics obs. *(Russian)* 78−31246
polar crystal with impurity atom, lattice energy change, optical vibrs. freq. shift 77−11652
polar crystals, cryst. surface effect on lattice vibrs. induced by polarisable impurity 79−90737
reson. relax. time for impurity electrons and localised phonons interaction, appl. to thermal cond. 80−59590
semiconductor, zincblende struct., phonon attenuation in presence of internal strains and mag. field 78−76118
semiconductor or insulator, impurity optical spectra, p-phonon processes 80−16061
semiconductors, localised transition metal impurities, lattice relaxation in optical transition *(Polish)* 80−70345
solid solutions, inhomogeneity and site selective impurity-phonon coupling effects 78−84625
soliton-impurity scatt. in Toda lattice, localised modes 78−14420
square lattice isotopic impurity effects, analytic soln. 77−15526
superradiative phonon-type phase transition *(Russian)* 77−27961
TGS, nitroaniline admixture effect on thermal parameters 80−107580
transition metal ions, in solid, nearly degenerate electronic levels, dynamical effects 78−68535
tunnelling, phonon assisted, in-band defect-induced phonon reson. modes effect 78−14419
zero-phonon transitions, spectral characts. 78−2884
$Al_{0.965}Ag_{0.035}$, reson. splitting of phonons 77−59086
$Al_2O_3:Mn^{3+}$, Jahn-Teller Mn^{3+} ions, phonon spectroscopy and thermal cond. meas. 80−88282
$Al_2O_3:Mn^{3+}$ under uniaxial stress, Jahn-Teller model 80−88521
β-$Al_2O_3:NH_4^+(Nd_4^+)$, polarised Raman scatt. 80−103947
$Al_2O_3:Ni^{3+}$, heat transfer at low temperatures 78−91493
$Al_2O_3:V^{3+}$, frequency crossing signals of V^{3+} ions, conc. depend. study using thermal phonons 78−95115
$Al_2O_3:V^{3+}$, phonon scattering, comparison between theory and experiment 78−95116
$Al_{10}V$-Ga, dil., well defined local modes 78−26648
Ar:NO_2, Raman spectra, high press., low temp. effects 78−52479
$BaF_2:Er^{3+}$, fluoresc. spectra of charge compensated cryst., multiphonon and energy transfer relax. 79−87496
$BaF_2:Mn^{2+}$, far IR absorption spectra 78−76507
$CaF_2:Er^{3+}$, fluoresc. spectra of charge compensated cryst., multiphonon and energy transfer relax. 79−87496
$CaWO_4:Nd^{3+}$, thermal behaviour of shape and width of 9145 Å laser line 78−6755
$CdIn_2S_4$:Cr, thermal cond., 1.8 to 200K, phonon scatt. by impurity ions 77−76627
CdS:Ni, nonradiative recomb., photocond. spectra 80−70764
CdTe:Be, impurity modes and IR absorption 78−76506
CdTe:Fe^{2+}, reson. relax. time for impurity electrons and localised phonons interaction, appl. to thermal cond. 80−59590
Cr antiferromagnetic with nonmagnetic impurities, mag. susceptibility using two band model 80−2559
CsBr:Tl^+, perturbed lattice dynamics, breathing shell model calculation 78−75744
Cu, press. depend. of Mossbauer fraction 77−59493
Cu-Al, change in force constant due to volume effects 78−75778
Cu-Al, impurity concentration effects 78−75777
Cu-Be, impurity concentration effects 78−75777
Cu-Si, change in force constant due to volume effects 78−75778
Cu-Si, impurity concentration effects 78−75777
CuBr:Cl(I), lattice-dynamical study of impurity modes 80−29129
CuCl:Br(I), lattice-dynamical study of impurity modes 80−29129
CuI:Br(Cl), lattice-dynamical study of impurity modes 80−29129
GaAs, irradiated with fast neutrons, IR vibrational absorpt. 78−75776
GaAs:Cr, site symmetry of Cr ions, ground-state splitting, ballistic phonon expts. 78−95273
GaAs:Mn, p-type semiconductors, internal strain on bound hole-phonon interaction 78−91492
GaN:Zn, VPE grown, optical cross sections, photoluminesc. and optical absorpt. meas. 80−55160
GaN:Zn, VPE growth, photoluminesc. rel. to doping conditions 80−55159

phonon-impurity interactions continued
GaP:M, M=substitutional impurities, lattice dynamics and local mode freqs. *(French)* 77−66011
GaP:O, optical transitions via deep levels, phonon interaction 78−87939
Ge, hole diffusion 78−6372
n-Ge, magnetothermal cond., 4.2K 80−24688
p-Ge, thermal conductivity meas. down to 50 mK, acceptor state exam. 77−80658
Ge:As(Sb), phonon-bound donor resonance scatt., donor-electron radius mag. field depend. 79−77847
Ge:Ga, resonant scattering of phonons by bound holes in temp. range 1 to 5K 80−75393
Ge:Ga(In), resonant phonon interaction with localised acceptor levels 80−6784
Ge:Si, impurity lattice modes due to single and paired defects 78−75780
Ge:Si, impurity modes and IR absorption 78−76506
Ge-Si, impurity concentration effects 78−75777
^{3}He-^{4}He solid mixture, dil. ^{3}He conc., diffusion coeff. obs. by NMR, impurity-phonon scatt. *(Russian)* 77−62701
^{4}He, diffusion of ^{3}He, pulsed NMR exam. *(Russian)* 78−71902
InP:M, M=substitutional impurities, lattice dynamics and local mode freqs. *(French)* 77−66011
KBr, F-centre spin-lattice relax., theory and MCD meas., phonon-modulated HFS 77−43883
KBr:Au^-, optical absorpt. bands and MCD, electron-lattice interaction 80−108236
KBr:CN^- 80−49316
KBr:$HS^-(HF_2^-)$, anharmonic interaction of impurity intramol. vibrs. with cryst. phonons 77−77217
KBr:MnO_4^-, many-phonon impurity reson. Raman scatt. 80−60603
KCl:CN, reson. scatt. of phonons in thermal cond. 79−14972
KCl:CN^-, phonon-internal mode hybridisation, neutron scatt. 78−2217
KCl:CN^-, coherent admixtures of phonons with impurity libronic excitations, neutron scatt. study 80−49316
KCl:OH^-, paraelec. system, acoustic susceptibility in strong phonon-coupling approx. 78−71801
KCl:OH^- type dipole-phonon system, superradiative phase transition *(Russian)* 78−71806
KCl:Pb, vibr. struct. of absorption band 79−33735
$K(H_{1-x}D_x)_2PO_4$ polarised impurity cluster effects in light scatt. expts. 80−29716
KI:NO_2^-, first-order Raman scatt. meas. 77−52085
KI:NO_2^-, Raman spectra, high press., low temp. effects 78−52479
KM_gF_3:Fe^{2+}, US relax. absorpt., acoustic wave-impurity coupling, spin-orbit splitting 79−4375
K_2SO_4:XO_4^{2-}, X=Cr, Se, Mo, W, lattice-impurity interactions, IR spectra 78−19522
$LaCl_3$:Np^{3+}, phonon-induced relax. in excited optical states, linewidth temp. depend. meas. 80−100688
LiCl:Ni^{2+}, first order induced Raman scatt. from Ni^{2+} and cation vacancies 77−48169
$MgAl_2O_4$:Dy, US attenuation 77−89500
MgO:Cr^{2+}, reson. scatt. of phonons by ions 78−18716
MgO:Fe^{2+}, impurity electron-phonon reson. relax. time, thermal cond. 77−59085
MnF_2, thermal cond., temp. depend., role of reson. scatt. of phonons by OH^- defects 78−38889
MnF_2, thermal cond. mechanism 78−38890
NO ($a^4\Pi$), condensed phase vibr. relax., isotope effect, time resolved obs. 78−94233
NaCl, doped by Ca^{++} and OH^-, thermal conductivity in 5-190K range 78−14520
NaCl-NaBr, elastic wave damping, 300 to 1500 MHz, impurity effects 80−92602
NaI:Cl^-, anharmonic effects on low-frequency impurity phonon resonances 78−75771
Na_2SO_4:XO_4^{2-}, X=Cr, Se, Mo, W, lattice-impurity interactions, IR spectra 78−19522
Nb, thermal cond., 0.3-20K, temp. and impurities effects 78−14883
$NbH_{0.15}$, dispersion step in $[\zeta\zeta O]T_1A$ branch at ζ=0.03, neutron scatt. study 79−60453
Ni film, phonon transport into SrF_2 substrate, diffusive scatt. at impurities 80−49487
$Pb_5(Ge_{1-x}Si_x)_3O_{11}$, ferroelec. soft mode, temp. and Si impurity, effects Raman scatt. 79−1762
PbSe:Tl, scatt. of holes and phonons by impurities 78−19068
$Pd_{0.99}Sn_{0.01}$, lattice dynamics of ^{119}Sn impurities, Mossbauer meas. 77−76507
RbCl:Au^-, optical absorpt. bands and MCD, electron-lattice interaction 80−108236
RbCl:NO_2^-, first-order Raman scatt. meas. 77−52085
RbI:HF_2^-, anharmonic interaction of impurity intramol. vibrs. with cryst. phonons 77−77217
SbSI, ferroelec. semicond., nature of low-temp. phase transition 77−69784
Se, trigonal and vitreous, sp. ht. and thermal cond., 3 to 300K 80−59676
Si, O content determ. by spectral analysis, phonon absorpt. effects *(Russian)* 77−48177
Si, optical absorption by acoustic phonons related to shallow impurity levels 77−4665
Si, resonant interaction of acceptor states with optical phonons 77−1394
Si:B, resonant scattering of phonons by bound holes in temp. range 1 to 5K 80−75393
Si:Sn, thermal conductivity, Hall mobility depend. on Sn conc., phonon-defect scatt. 80−29232
SiO, role of O in phonon conductivity 79−42326
SiO_2:OH^-, vitreous, elec. dipolar echoes 78−52430
SrF_2, doped, far IR absorption spectra 78−76507
SrF_2:Er^{3+}, fluoresc. spectra of charge compensated cryst., multiphonon and energy transfer relax. 79−87496
SrO-Li_2O-Al_2O_3-SiO_2:Tb^{3+} glass, energy transfer, luminesc. efficiency under UV, neutron and charged-particle excitation 79−95822
Ta, thermal cond., 0.3-20K, temp. and impurities effects 78−14883
Ti, press. depend. of Mossbauer fraction 77−59493
V, phonon assisted tunnelling in impurity induced lattice strains 78−47601
V, press. depend. of Mossbauer fraction 77−59493
YAG:Dy(Er)(Tm)(Tb)(Yb), US attenuation 77−89500
YAG:Er, elastic wave damping, 300 to 1500 MHz, impurity effects 80−92602
phonon-impurity interactions continued
YAG:Nd^{3+}, nonradiative multiphonon relaxation of isolated impurity level, transition probability calcs. 79−56853
YAG:rare earth, phonon impurity scatt., lattice thermal cond. and US attenuation meas. 78−87748
Zn-Mn, Kondo-system, ion implantation as method for study 80−70241
ZnS CVD window, IR lattice absorption, phonon assigments and image spoiling 80−33104
ZnS:Be, impurity modes and IR absorption 78−76506
ZnS:Cr(Mn)(Fe)(CoXVi), vibr. modes of transition element impurities 78−76472
ZnS:Cu^{2+}, motional averaging in excited state 77−66137
ZnS:Fe^{2+}, impurity electron-phonon reson. relax. time, thermal cond. 77−59085
ZnS:Fe^{2+}, reson. relax. time for impurity electrons and localised phonons interaction, appl. to thermal cond. 80−59590
ZnS:M, M=substitutional impurities, lattice dynamics and local mode freqs. *(French)* 77−66011
ZrO_2-Y_2O_3, stabilised, light scatt. spectrum 79−73954

phonon-magnon interactions
antiferromagnet, high frequency properties, spin wave spectra corrections magnon interactions *(Russian)* 80−54876
antiferromagnet, low temp., absorption of sound 79−69711
antiferromagnet, magnon damping, influence of magnetoelastic interaction 79−28517
antiferromagnet, mechanism for hard excitation of spin waves *(Russian)* 78−19235
antiferromagnet, phonon-magnon relaxation times, external mag. field depend. 80−44898
antiferromagnet, sound damping by phonon-magnon interaction, high Neel temp. *(Russian)* 78−43626
antiferromagnetic insulators, lattice thermal cond. 80−65319
antiferromagnetic resonance relaxation, multimagnon processes 77−4564
antiferromagnets, easy-plane, nucl. spin wave relax. 80−65850
antiferromagnets, magnon damping due to magnon-phonon interactions *(Russian)* 79−11305
bound state, temp. depend. 79−78349
conference on lattice dynamics, Paris, France (Sept. 1977) 78−59869
continuum approach, general eqns., background soln. 79−95622
continuum approach, hexagonal symmetry, wave propagation 79−95623
dialkylammonium copper chloride, two-dimens. ferromag., energy transport by paramag. magnons 77−80909
dielectric function, theoretical anal. 78−80275
elastic properties of magnetic materials, review 80−7142
ferrodielectric, sound absorption due to interaction with magnons *(Russian)* 77−69663
ferrodielectric, sound wave damping, due to phonon-magnon interactions 77−36107
ferroelectric ferromagnet, soft modes and ferromag. reson. 80−11275
ferromagnet, energy minimum excitation 79−61086
ferromagnet, magnon-phonon interactions, Heisenberg exchange red. 80−80494
ferromagnet, phonon inelastic scatt. by magnons 77−20570
ferromagnet, semi-infinite, surface magnon-phonon interaction processes, scatt. and annihilation *(Russian)* 77−63144
ferromagnet, spin reorientation and magnon-phonon hybridization 78−19233
ferromagnetic resonance in anisotropic Heisenberg model, magnon-magnon, phonon-magnon interactions *(Russian)* 80−11274
ferromagnetic semiconductor, carrier-assisted magnon contrib. to phonon damping 77−20018
ferromagnetic semiconductor, magnon coupling to plasmons and LA phonons, s-d model 80−29536
ferromagnetic semiconductors, mag. excitations, light scatt. 77−63161
kinematic spin-wave levels 78−76231
magnetic Debye crystal, with magnon-phonon coupling, crit. changes in vibr. modes 79−95094
magnetic ferroelectrics, mechanism of phonon relaxation *(Russian)* 79−90742
magnetic insulator, heat transport by magnons, effect of magnon-phonon thermal relax., calc. 77−39705
magnetic semiconductor 77−72893
magnon kinetic eqns. in parametric ultrasonically excited frromagnets 80−44820
metal, ferromag., antiferromag., magnetoelastic coupling effect on magnetoelec. reson. 80−75837
metastable polarised crystals, decay kinetics, exchange magnon-phonon interactions *(Russian)* 80−7060
metastable spin-aligned crysts. decay kinetics 80−34669
rare earth intermetallics, RFe_2 and $R(Co_{0.98}Fe_{0.02})_2$, magnetostrictive material, changes in vibr. modes near mag. phase transition 79−90736
rare earth-Fe_2, magnetomech. coupling and Young's modulus 78−84472
rare earth-Fe alloy, RFe_2 (R=Tb, Dy, Ho and Y) crit. phenomena, Mossbauer exam. 78−52403
semiconductors, magnetic, spin wave electron amplification theory 80−97083
spontaneous symmetry breaking and magnon-phonon spectra 80−65991
system with two singlet levels, phonon coupling to mag. excitations 80−6470
$Au_2(Mn,Z)_2$, Heusler alloy, (Z=Al, Cu, Ga, In or Zn), magnetic order and coupling 79−38303
$BaMnF_4$, antiferromag., dielec. anomalies at low temp. obs. 77−20791
$CdCr_2Se_4$, spin system heating by drifting current carriers, magnon-phonon system energy transfer *(Russian)* 80−29541
$CoBr_2$, paramag. and antiferromag., Raman scatt. from electronic excitations and phonons 79−69826
$CoCl_2$, antiferromag., mag. excitations, mag. neutron inelastic-scatt. meas. 77−85437
$CoCl_2.2H_2O$, antiferromag., light scatt. from phonons and magnons 80−40104
$CoCl_2.2H_2O$, magnon-phonon interactions and two-magnon Raman scatt., magnetoelastic waves and selection rules 80−34917
$CoCl_2.2H_2O$, phonons and electronic transitions, Raman spectra 79−28761
Cr_2O_3, thermal magnetoresist., 0.1 to 100K, magnon-phonon interactions 79−65266
$CsCoCl_3$, Ising like antiferromag., mag. phase transition, ^{133}Cs NMR 80−7184
$CsMnCl_3$, antiferromagnetic resonance, parametric spin wave excitation *(Russian)* 80−93183

phonon-magnon interactions continued
$CsMnCl_3.2H_2O$, thermal cond. in mag. field 80−70481
Eu chalcogenides, spin-dependent Raman scatt. from phonons 80−97274
EuO, spin system heating by drifting current carriers, magnon-phonon system energy transfer *(Russian)* 80−29541
$FeBO_3$, Brillouin scatt. from parametrically excited phonons 79−73956
$FeBO_3$, weak ferromag., FMR instability, parametric excitation of phonons, Brillouin scatt. obs. 79−78529
$FeBr_2$, dynamic Jahn-Teller system, Raman scatt. from electronic excitations and phonons 78−56474
$FeCl_2$, antiferromag., magnon-phonon interactions in thermal cond. 80−65315
$FeCl_2$, dynamic Jahn-Teller system, Raman scatt. from electronic excitations and phonons 78−56474
$FeCl_2$, magnon-phonon hybridisation, inelastic neutron scatt. study 79−47272
$FeCl_2.2D_2O$, magnon-phonon coupling 78−72530
$FeCl_2.2H_2O$, magnon-phonon interactions and two-magnon Raman scatt., magnetoelastic waves and selection rules 80−34917
$FeCl_2.2H_2O$, metamagnetic, resonant magnon-optical phonon coupling 79−28773
$FeCl_2.2H_2O(2D_2O)$, phonons and electronic transitions, Raman spectra 79−28761
FeF_2, magnon-acoustic phonon hybridisation in far IR absorpt. spectra 78−60271
FeF_2, theory of Raman scattering, coupled phonon-magnon excitations 78−72531
FeF_2, theory of Raman scattering and IR obs. 80−71426
$GdVO_4$, antiferromag., US attenuation at 9 GHz 77−24728
$KCoF_3$, antiferromag., with residual orbital moment, nucl. mag. relax. 80−71215
$KCoF_3$, magnon-phonon interaction mechanism 77−20019
$KCoF_3$, NMR, magnon-phonon interaction contribution to nuclear spin-lattice relax. 78−88207
$K_2CoF_4:Mn^{2+}$, impurity induced mag. excitations, magnon gap mode, far IR spectra obs. 80−44821
$MnCl_2.2H_2O$, phonons and electronic transitions, Raman spectra 79−28761
$MnCl_2.4H_2O$, antiferromag., low temp. thermal cond. 80−65320
MnF_2, heat transport by magnons, effect of magnon-phonon thermal relax., calc. 77−39705
MnF_2, resonant phonon-magnon scatt., phonon spectroscopy obs. 79−65150
MnO, cubic antiferromag., magnon-phonon sideband in fine-struct. of optical absorption 77−59590
Ni, phonon assisted magnon transmission at 24 GHz 79−82878
Rb_2MnCl, layer antiferromag., optical absorpt., temp. and mag. field depend. 80−20661
$TlMnCl_3$, antiferromag., absorpt. spectrum, excitation-magnon-phonon process 79−87461
YIG, heat transport by magnons, effect of magnon-phonon thermal relax., calc. 77−39705
YIG, phonon inelastic scatt. by magnons 77−20570
YIG, resonant phonon-magnon scatt., phonon spectroscopy obs. 79−65150
YIG, sound vel., temp. depend., phonon scatt. processes 80−96598
YIG, spinwave dispersion curves 78−19230

phonon-phonon interactions
see also Umklapp process
alkali halide crystals, anharmonic effects, modified Gruneisen relation 79−99290
alkali metals, phonon-phonon scattering relax. times, rel. to elec. resist. 77−39813
antiferromagnet, easy-plane, acoustic wave damping, effective phonon-phonon interactions 79−73797
arsenates, ferroelec. phase, E-mode splitting 78−15163
atom scattering from solid surface, multiphonon theory, tetradic scatt. formalism 79−56905
Boltzmann eqn., phonon and electron transport in bounded systems 80−39545
Bose systems, interacting, sp. ht. at low temps. 77−15651
brass, lattice thermal cond. component, 30 to 300K, microscopic mechanisms 80−107758
2-chloronaphthalene, elastic props. exam. by Brillouin scatt., rel. to polymorphism 79−77669
collision operator, linearised phonon 77−27965
correlation field effect in two-phonon excitations 77−72660
cubic crystal, Klebsch-Gordon coefficients and two-phonon resonance Raman scatt. *(Russian)* 79−1755
degenerate vibration, biphonons in region of overtone 77−69059
desorption, multiphonon processes, quantum-statistical theory 80−107641
diamond, and isomorphic crysts., phonon dispersion relations, Born-von Karman study 79−86855
diamond, two-phonon bound state, Raman freq. 80−65179
p-dibromodiphenylether surface, normal and ultra-Brewster refl. spectra 80−25400
dielectric, complex reflection spectra, dispersional anal. 77−36239
dielectric, kinetic eqn. for thermal phonons with finite mean free time, low-temp. thermal cond. theory *(Russian)* 77−62688
dielectric, thermal cond. at low conc. of phonon scatt. centre, freq. crossing signals 80−2224
dielectric crystal, thermal resist. due to four-phonon processes and optical modes 77−76632
dielectric material, phonon thermal conductivity, Umklapp process, comparison with LiF data 80−39367
dielectric solids, acoustic wave propagation, phonon relax. time 80−44263
disordered crystal, biphonon spectra, light absorpt. coeff. and density of states, CPA calc. 80−84271
disordered crystals, biphonon spectra, CPA calc. 80−70341
dynamic multiphoton processes as criteria for luminesc. of electronically excited centres 80−11463
elastic wave generation comparable to Bain deform., role of multiphonon processes *(Russian)* 80−84246
ferroelectrics, low lying vibrational modes, crit. behaviour of uniaxial materials 78−84539
ferroelectrics, one and two dimensional displacive types, phonon relaxation 78−87761
formic acid, lattice dynamics model to explain neutron scatt. data 79−86856

phonon-phonon interactions continued
formic acid, normal and deuterated, dynamic modes, neutron inelastic scatt. study 79−51214
frequency dependence of TO phonon decay parameter, and phonon-phonon interaction mechanisms 77−59084
frozen media, electron transfer reactions and multiphonon transition theory 80−7812
glass:Nd^{3+}, line narrowed fluorescence spectra and site dependent transition probabilities 79−38640
glycerol(-d_3), single cryst., glassy, and supercooled, polarised Raman spectra, anharmonic multiphonon interactions 79−91419
graphite, finite-size crysts. first- and second-order Raman scatt. 79−95759
graphite, phonon dispersion, temp. depend., 4K-1500°C, neutron spectroscopy 78−59906
graphite, Poco AXM-5Q1, thermal and elec. transport props., 4-3000K 78−6375
Hamiltonian model with scalar displacive transition, crit. dynamics, renormalisation 78−87766
hydrostatic deformation effect, rot. of polarisation vectors of lattice vibrs. calc. 78−18721
ice, Ih, thermal resist. near melting point meas. 80−44375
II-VI semiconductor, resonant secondary emission spectra, relax. of energy and polarisation 80−93331
inhomogeneously broadened systems, spectral-spatial diffusion 77−77280
insulator, low temperature, role of point defect scatt. in lattice thermal cond. 77−76631
insulators, high-intensity US wave vel., phonon-phonon interaction effects 80−70323
insulators, nonlocal hydrodynamic of phonon gas, thermal cond. and second attenuation coeff. 79−65158
interface three-phonon processes, Kapitza conductance and pulse expt. applications 80−2261
interfacial three-phonon processes and anomalous interfacial energy transport 79−46913
ionic crystals, nonradiative multiphonon transitions in impurity centres with extremely weak electron-phonon coupling 80−25436
IR and Raman spectra, morphic effects, appl. of irreducible representations in symmorphic space groups *(Japanese)* 79−77541
kinetics of phonon system with almost linear dispersion law *(Russian)* 80−29136
lattice thermal cond., variational bounds improvement by scaling and Ritz procedures 77−62689
lattice thermal conductivity, contrib. due to correction term, generalised Callaway integral 77−28056
lattice thermal conductivity, contrib. due to correction term in Callaway integral 77−62693
many boson system, excitation modes and interactions 79−71362
many boson systems, excitation modds and interactions 79−71361
metal, Peierls condition and phonon-phonon scatt. 77−62910
metal, struct. factor calc., n-phonon term 77−1206
metal surface, sticking coeff. and transmission problem, quadratic phonon coupling effects 80−39424
metals, FCC, H_2 diffusion, isotope depend. 80−59727
metals, light interstitials diffusion, multiphonon transition modes classification 80−70448
metals, phonon-phonon scatt. role in lattice thermal cond., phonon drag, elec. cond. 80−70483
metals and semimetals, two-phonon sound absorption in quantising mag. field 79−28382
molecular cryst., phonon scatt. times below 10K, optically-detected APR 78−88228
molecular crystal, two-phonon resonances, bound states absorpt. coeff. 78−47486
molecular crystal, two-phonon resonances, bound-states, general theory 78−47485
molecular crystals, dipolar coupling and phonon symm. *(Chinese)* 80−103437
naphthalene crystal, multiphonon i.r. absorption 77−1686
nonradiative transition rate for electrons in semicond. and insulators 78−60503
optic mode-EM mode coupled systems, soliton relation to polaritons 79−77707
n-paraffins, IR spectra, −180°C, two-phonon absorpt. bands 78−72495
Peierls-Frohlich state on many-phonon-coupling model, dynamical props. 78−47773
pentaerythritol, Bragg reflection, thermal diffuse scatt. meas. *(German)* 78−75509
phonon conductivity correction due to three phonon normal processes in presence of dislocations 80−15318
plastic crystal, dipolar autocorrelation function, phonon contrib., IR absorption 78−42928
point defects, optical absorption, Urbach's rule 79−91474
polar semiconductor, secondary emission, multiphonon cascade process *(Russian)* 78−2850
polar semiconductors, anharmonicity influence on cond. in quantising mag. field 80−2406
polar semiconductors, two-phonon resonance Raman scattering 80−108204
polaritons, two-phonon Brillouin scattering 80−20656
polarization dichroism effects in many-phonon optical bands of multiplet-multiplet transitions 79−15125
polyethylene, IR spectra, −180°C, two-phonon absorpt. bands 78−72495
polyethylene, oxidised, paraelectricity, dielec. relax. obs. 77−48123
polyethylene, second order Raman scatt. 78−72504
polyethylene, two phonon Raman spectrum, final state interactions 78−76457
polymer, zigzag chain, second order Raman scatt. 78−72504
quartz, lattice attenuation of longitudinal sound 79−86847
quartz, phonon heat conduction of single crysts. by quantum acoustic method 77−11748
quasi-two dimensional conductor, galvanomagnetic props., optical analogy *(Russian)* 80−60108
quasielastic light scattering near phase transitions 80−93362
Raman scattering, reson., second-order, theory for case of strong excitonic effects 78−76460
rare earth doped cystals, intra- and inter-ionic multiphonon transitions 80−34973
rare earth ions in crystals, nonradiative processes, book contrib. 80−55188

phonon-phonon interactions continued
resonant Brillouin scattering of exciton polaritons 80−11418
ruby, 10^{12} Hz high-freq. acoustic phonons, optical detect. 77−36272
ruby, heat-pulse induced energy transfer, time-resolved optical spectroscopy 77−24456
ruby, inelastic phonon scattering time, inelastic, appl. of time resolved phonon spectroscopy technique 77−31733
ruby, optically induced two-phonon processes connecting ^2E states 80−25443
ruby, phonon heat conduction of single crysts. by quantum acoustic method 77−11748
ruby, spin level population inversion, coherent phonon amplification and generation *(Russian)* 77−24364
semiconductor, absorption of EM and sound waves in strong coupling case, effect of acoustic superlattice 78−26630
semiconductor, Auger transition probability, phonon-assisted 79−15120
semiconductor, magnetophonon resonance due to two-phonon scatt. by acoustic phonons 77−69356
semiconductor, many-phonon impurity absorpt. in external elec. field 77−52144
semiconductor, multiphonon recombination processes 79−38643
semiconductor, non-radiative de-excitation of deep centres 79−38644
semiconductor, nonradiative multiphonon carrier capture props. of deep charged and neutral centres 77−15866
semiconductor, phonon-assisted cyclotron reson., single and two-phonon pinning, review 79−15356
semiconductor, phonon-assisted nonradiative recomb. phenomena, review *(Polish)* 77−69339
semiconductor, resonant Raman scatt., book contrib. 77−36251
semiconductor, statistical theory of multiple-phonon scattering 78−67794
semiconductor, two-phonon Raman scatt. by longitudinal optical phonons, double reson. 77−24852
semiconductors, multiphonon capture rate 79−38022
semiconductors, nonequilib. electron and phonon fluctuations *(Russian)* 77−80770
semiconductors, nonradiative recombination, combination of Auger and many-phonon processes 79−87111
semiconductors, recombination, conference, Southampton, England (Aug.-Sept. 1978) 79−38087
semiconductors, recombination processes, review 79−38088
semiconductors and insulators, phonon cond., three-phonon N- and U-processes 80−65313
semimetal, compensated, hydrodynamic cond., surface scatt. and phonon drag *(Russian)* 77−8088
solid, three-phonon processes 79−55857
solid-state theory, introduction, book 79−33215
spectroscopy of high-frequency phonons, transport phenomena, review 80−49325
spin-state transitions in solids, two-phonon model 79−56170
superconducting properties, effects of anharmonism *(Russian)* 78−39255
superconductors, high temperature, tunnelling spectra, electron pairing anal., appl. to Nb_3Sn 79−87205
1,2,4,5-tetrachlorobenzene, impurity induced states, spin dephasing, spin coherence expts. 78−84498
tetrahedral lattice sites, selection rules for multiphonon transitions 80−92632
tetrebromomethane, thermal resistivity, heat capacity and phase diagram under pressure 80−65316
thermal conductivity, lattice, contrib. due to correction term, generalised Callaway integral 78−2318
thermal conductivity, surface roughness effects, low temp., including defect and boundary scatt. of phonons 77−28057
thermal phonon drag by coherent acoustic waves, Umklapp processes 78−14417
thermomagnetic effects in weak magnetic fields, formulation of theory 77−62953
three-phonon resist. high-temp. comparison of different models 77−4171
transition metal superconductors, specific heat anharmonic components, phonon freq. temp. shift *(Russian)* 79−91183
TTF-TCNQ, anharmonic effects of phonons with Kohn anomalies 77−1197
TTF-TCNQ, pinned charge density wave, far IR bolometric observations, damping 79−60735
uranyl salts, cryst., multiphonon relax. 80−15208
vibrational relaxation, local phonon and roton receiving modes 79−46759
zero-gap semiconductors, reson. two phonon absorpt. 79−55847
Ag, X-ray Debye temp. and isobaric Gruneisen coeff., anharmonicity effects 77−62654
α-Al_2O_3, single crystal transmission and reflectance IR phonon spectra, polariton dispersion 80−66170
Al_2O_3:Ni, heat transfer at low temp. 78−38888
As, amorphous, phonon frequency distrib. 78−30723
As, amorphous, rel. to low temp. thermal cond. and sp. ht. 79−28161
As, electrical and thermal props. 78−14747
AsH_3, plastic cryst., dipolar autocorrelation function, phonon contrib., IR absorption 78−42928
As_2S_3, crystalline, two phonon vibrational spectra 78−35142
As_2S_3, two-phonon vibrational spectra, crystalline and amorphous forms, Raman and IR spectra 78−39537
As_2Se_3, photodarkening and photostructural effects, Raman, IR and NQR studies 80−16036
As_2Se_3-$GeSe_2$ glass, bulk and impurity IR absorpt. 80−71455
$BaMnF_4$, incommensurate transition, Brillouin scatt. investigation 79−87406
BeF_2-KF-CaF_2-AlF_3:Nd^{3+} (Er^{3+}) glass, multiphonon relax., fluoresc. obs. 78−15219
Bi, optical phonon anharmonicity and melting, light scatt. study 80−60621
$BiVO_4$, linear coupling between soft optical and ferroelastic acoustic modes 78−79716
Ca, US attenuation due to phonon-phonon interaction and thermoelastic phenomenon 79−77686
$Ca(WO_4)_x(MoO_4)_{1-x}$, Raman scatt. line shape 78−10898
CdP_2, cryst., tetragonal, 2-phonon IR absorpt. 80−66176
CdS, acoustic wave attenuation, phonon viscosity and dislocation drag 80−70319
CdS, multiphonon reson. Raman scatt. and exciton-phonon luminesc. 77−16319
CdS, Raman shift dispersion near exciton reson., two-phonon cascade processes 80−11405
CdS, reson. Raman scatt., second-order, theory for case of strong excitonic effects 78−76460
CdS, reson. scatt. of exciton-polaritons second emission under monochromatic excitation 77−1717
CdS, two-phonon resonant Brillouin scatt. 78−84597
CdTe, phonon conductivity, 2 to 300K, scatt. mechanisms 79−4436
CsBr, hyper-Raman spectra by single channel method 78−84591
CsI, hyper-Raman spectra by single channel method 78−84591
$Cs_2UO_2Cl_4$, low-lying excited electronic levels, fluoresc. decay meas. 79−47491
Cu, H_2 diffusion, isotope depend. 80−59727
Cu, μ^+ diffusion data anal., theory of incoherent direct and indirect multi-phonon transitions 80−70448
Cu, US attenuation, nonlinearity parameter temp. depend. 79−42152
CuBr, press. depend. of Raman scatt. meas., Gruneisen parameters determ. 77−24845
CuBr, two-phonon optical absorpt. spectra 78−52485
CuCl, anomalous Raman spectrum in transverse optic phonon region 77−24846
CuCl, neutron scatt. of TO phonon at 5K 79−60446
CuCl, phonon interaction of excitonic molecule 80−50316
CuCl, two-phonon optical absorption 77−63406
CuCl, two-phonon optical absorpt. spectra 78−52485
CuCl(Br), multiphonon far IR absorpt., 2-80K 78−60462
CuI, press. depend. of Raman scatt. meas., Gruneisen parameters determ. 77−24845
D_2, solid, phonon absorption line shape as function of density 80−50329
ErP_5O_{14}, single cryst., radiative and non-radiative transitions 79−19920
FeF_2, IR reflectivity spectrum 79−51952
$Ga_{1-x}Al_xP$, two-phonon optical absorpt. 78−88341
GaAs, boundary scattering and phonon conductivity, 2-10K 78−63888
GaAs, highly transparent semicond., multiphonon IR absorpt. 78−60461
GaAs, lattice thermal cond. from three phonon scatt. relax. rate 78−51755
GaAs, lattice thermal cond. at high temp. 79−90838
GaAs, reson. Raman scatt. at indirect gap 79−73931
GaAs, two-phonon Raman scatt. meas. 77−81097
GaAs:B, electron or neutron irradiated, low symmetry interstitial B centre 78−79605
GaAs:Cr, IR absorpt. determ., emissivity meas. 77−63421
GaP, core levels, chem. shift and relaxation energy, temp. dependence 80−39520
GaP, freq. depend. of TO phonon decay parameter, and phonon-phonon interaction mechanisms 77−59084
GaP, obs. of Raman scatt. by Cu vapour laser 78−95586
GaP, Raman spectra, press. depend. optical phonon anharmonicity 77−8586
GaS, infrared optical props., polarisation depend., vibr. modes 80−100658
GaSb, acoustic wave attenuation, phonon viscosity and dislocation drag 80−70319
n-GaSb, coupled LO-phonon-plasmon modes, Raman spectrum 80−11409
GaSe, cascade resonant Raman processes 80−25385
GaSe, multiple-phonon reson. Raman scatt. processes 77−4634
Ge, Akhieser region, nonlinearity parameter and US attenuation coeffs., temp. depend. 79−37762
Ge, contrib. to lattice thermal cond. due to correction term in Callaway integral 77−62693
Ge, elastic moduli, drag coeffs. and Keating's parameters 79−73238
Ge, lattice thermal cond., contrib. due to correction term, generalised Callaway integral 77−28056
Ge, lattice thermal conductivity, contrib. due to correction term, generalised Callaway integral 78−2318
Ge, lattice thermal conductivity three phonon processes 78−34662
Ge, phonon boundary scatt., reduction of lattice thermal cond. 78−55921
p-Ge, phonon thermal cond., 0.1-7K, Ziman model 77−35763
Ge, phonon-phonon scatt. strength, thermal cond. in low- and high-temp. regions 77−43296
n-Ge, thermoelec. power in quantising mag. field, phonon-phonon interactions 80−107832
Ge, two-phonon difference absorption spectra 78−76452
Ge, US attenuation and nonlinearity const., temp. depend. 78−43075
Ge-Si alloy, phonon boundary scatt., reduction of lattice thermal cond. 78−55921
GeO_2 amorphous, phonon frequency distrib. 78−30723
H_2, phonon absorption line shape as function of density 80−50329
HIO_3 crystals, anharmonicity effects in Raman spectra 80−25379
He-4, liquid, phonon-phonon interactions, review 77−55410
^{4}He, FCC, inelastic neutron scatt., phonon spectra, dispersion curves 78−51785
^{4}He, liquid, freq. up-conversion interacting phonon beams 79−55975
^{4}He, solid, thermal cond., 0.4 to 1.8K. *(Russian)* 80−103535
^{4}He, superfluid, elementary excitations, μeV resolution study by neutron spin echo 80−65327
HgSe, two-phonon resonant effect, far-infrared reflectivity 80−108203
InAs, second order Raman scatt., electron-two phonon deform. pots. determ. 78−60473
$In_{1-x}Ga_xP$, two-phonon IR absorpt. 78−52493
n-InSb, anomalous three LO phonon assisted cyclotron resonance 80−108078
InSb, lattice thermal cond. from three phonon scatt. relax. rate 78−51755
InSb, phonon conductivity, temp. depend., 2-300K 77−31812
InSb, phonon conductivity, 2 to 300K, scatt. mechanisms 79−4436
n-InSb, three-phonon assisted cyclotron harmonic transitions in magneto-photoconductivity 80−44652
InSb, US attenuation and Akhieser loss, temp. depend. 79−86842
K, Peierls condition and phonon-phonon scatt. 77−62910
K, phonon-phonon scatt. relax. times, rel. to elec. resist. 77−39813
KBr:MnO_4^-, many-phonon impurity reson. Raman scatt. 80−60603
KBr:MnO_4^-, model system, reson. Raman spectra, general behaviour obs. 80−60592
KCN, order-disorder transition, high-press. Brillouin scatt. exam. 77−44009
KCN, order-disorder transition, press. and temp. depend. of soft elastic const. 78−79769
KCNS, single cryst., IR and Raman multiphonon bands, factor group anal. 77−4644

phonon-phonon interactions continued
KCl, phonon-phonon scatt. strength, thermal cond. in low- and high-temp. regions 77−43296
KCl, TSM study of lattice statics and dynamics 79−82292
KH_2PO_4, damping of transverse acoustic and ferroelec. modes 78−14413
KH_2PO_4, depolarised light scatt., dynamic central peak 78−10858
KH_2PO_4 far IR dispersive reflection obs. with asymmetric polarising interferometer 77−40249
KH_2PO_4 type crysts., evidence of non-linear behaviour of soft modes, Raman spectra 79−33639
KI, far IR, quartic damping, and quasiselection rule for gap compounds 78−31195
$KMgF_3$ residual IR absorption, freq. and temp. dependence obs. 79−15468
$KMnF_3$, phonon scatt., thermal cond. meas. 77−7916
K_2SeO_4, soft modes below incommensurate transition Raman and Brillouin scatt. meas. 79−91387
$KTaO_3$, incipient ferroelectric, mode-mode coupling 78−79717
$LaF_3:Ho^{3+}$ single crysts., multiphonon relax., fluoresc. obs. 79−47495
$LiNbO_3$, freq. depend. of TO phonon decay parameter, and phonon-phonon interaction mechanisms 77−59084
$LiNbO_3$, IR reflectivity temp. depend. 78−27202
MgF_2, transparent, multiphonon IR absorption spectra 80−7348
Mg_2Ge, phonon cond. 4-1000K 78−79826
Mg_2Ge, three-phonon relaxation rate and phonon conductivity 78−14416
Mg_2Si, phonon cond., 3-500K 78−79826
Mg_2Sn, phonon cond., 4-1000K 78−79826
$Mn_xCd_{1-x}Te$, lattice vibrs., Raman and IR spectra meas. 80−93311
MnZn ferrite, thermal cond. of single crystals 77−36079
N_2, luminesc., multiphonon-assisted energy transfer 79−47498
α-N_2, solid, $w^1\Delta_u$-$X^1\Sigma_g^+$ intensity and band shape 79−47427
NH_4Cl, obs. of Raman scatt. by Cu vapour laser 78−95586
Na, dynamical structure factor calc., High temp. 80−15047
NaCN, order-disorder transition, press. and temp. depend. of soft elastic const. 78−79769
NaCl, single cryst., for IR dispersive refl. meas., low temp., rel. to anharmonicity calcs. 80−11371
NaCl(Br) (F) (I), lattice dynamics and statics, three-body-force shell model 80−49323
$NaNO_2$, ferroelectric, second-order vibr. spectra and dispersion of phonon branches 79−69847
$NaNO_2$, vibr. spectrum, interference effects 78−87752
$Na^{15}NO_3$, $Na^{14}NO_3$, multiphonon transitions in microcryst. reflectivity 78−72499
NdP_5O_{14}, ferroelastic, Raman scatt. from soft phonons, 4.2-600K, monoclinic-orthorhombic transition temp. 79−51962
Ne, solid, two-phonon scatt. in inelastic neutron scatt. calc. 78−59910
OCS, third order coupling coeffs. for two phonon absorpt. 80−10621
$O_2(c^1\Sigma_u^-)$, in Ar(Kr)(Ar-Kr) matrices, multiphonon vibr. relax., time-resolved emission obs. 80−18861
$Pb_{1-x}Ge_xTe$, Raman scatt. from soft TO-phonon modes 79−95773
$Pb_{1-x}Ge_xTe$, TO phonon interaction with acoustic phonons near phase transition temp. 79−90776
PbI_2 (2H), multi-phonon scatt. near direct absorpt. edge, resonant Raman obs. 79−87448
$PbMoO_4$, vibr. props. and struct., effect of hydrostatic press. 77−28571
$PrAlO_3$, mechanism of 118.5K phase transition 77−47532
RbBr, rel. to thermal cond. change at press. induced phase transition 77−62694
RbCNS, single cryst. factor group anal. of IR and Raman multiphonon bands 77−4644
$RbCaF_3$, phonon scatt., thermal cond. meas. 77−7916
RbI, hyper-Raman spectra by single channel method 78−84591
SF_6, cryst., IR and Raman spectra at 9 and 97K, cryst. struct. 79−87427
SR, US attenuation due to phonon-phonon interaction and thermoelastic ohenomenon 79−77686
Sb, optical phonon anharmonicity and melting, light scatt. study 80−60621
SbSI-SbSBr system, ferroelec., anharmonic effects in far IR reflectivity spectra 80−76014
Si, core levels, chem. shift and relaxation energy, temp. dependence 80−39520
Si, highly transparent semicond., multiphonon IR absorpt. 78−60461
Si, lattice thermal cond., 2-1400K, phonon scatt. calcs. 78−2311
Si, phonon boundary scatt., reduction of lattice thermal cond. 78−55921
n-Si, phonon-phonon relaxation 80−96609
Si, phonon-phonon relaxation investigation for conventional and neutron doped crystals 80−96927
Si, reson. Raman scatt. at indirect gap 79−73931
SiAs-Au surface barrier diodes, optical props. of SiAs 79−8145
SiF_4, mol. cryst., coupled phonon modes and IR band shapes 78−26641
SiO_2, core levels, chem. shift and relaxation energy, temp. dependence 80−39520
SiO_2, vitreous, multiphonon IR absorpt. 80−25381
$Sn_2P_2S_6$, soft mode, interaction of modes and crit. Rayleigh scatt. 79−99836
SnTe, light scatt. from soft modes, theory above and below displacive transform. temp. 79−95791
SnTe, Raman scatt. from soft TO-phonon modes 79−95773
$SrTiO_3$ film, polycryst., rel. to influence of amplitude of measuring microwave field on dielec. losses 79−99829
$SrTiO_3$, incipient ferroelectric, mode-mode coupling 78−79717
$SrWO_4$, vibr. props. and struct., effect of hydrostatic press. 77−28571
α-Ti, plastic deform., anharmonicity, and Gruneisen parameter 80−88246
TiO_2 anatase, Raman spectrum, temp. depend. 80−76027
TlCl, phonon difference band absorpt., far IR laser spectroscopy 80−93325
UCl_4, single crystal, thermal broadening of IR energy levels 78−35121
UO_2, electronic transitions, crystal field effects and phonons, phase transition 80−97303
YAG:Nd^{3+}, energy transfer between Nd^{3+} ions, laser-excited time-resolved site-selection spectroscopy 79−95839
YAG:Nd^{3+}, many-phonon nonradiative transition probabilities 79−95842
YAG:Nd^{3+}, nonradiative multiphonon relaxation of isolated impurity level, transition probability calcs. 79−56853
$Y_3(Al_{1-x}Ga_x)_5O_{12}:Nd^{3+}$, time-resolved site-selection spectroscopy, energy transfer 80−2814

phonon-phonon interactions continued
$Y_3Ga_5O_{12}:Nd^{3+}$, energy transfer between Nd^{3+} ions, laser-excited time-resolved site-selection spectroscopy 79−95839
YIG, phonon viscosity effect on dislocation motion 80−24450
YIG, sound vel., temp. depend., phonon scatt. processes 80−96598
YbS, multiphonon processes and exciton-LO phonon interaction 79−95784
Zn, optical phonon anharmonicity and melting, light scatt. study 80−60621
ZnO, freq. depend., of TO phonon decay parameter, and phonon-phonon interaction mechanisms 77−59084
ZnO-TeO_2 glass, Ho^{3+} or Er^{3+} doped, visible green emission 79−15523
$Zn_4O(BO_2)_6$, phonon coupling exam. by Raman spectroscopy 78−30719
ZnP_2, cryst., tetragonal, 2-phonon IR absorpt. 80−66176
ZnP_2, second-order vibr. spectra and dispersion of phonon branches 80−25376
Zn_3P_2, multiphonon absorption in IR spectra 78−39554
ZnS, cubic, IR-active phonons obs. 80−55084
ZnS(Se), highly transparent semicond., multiphonon IR absorpt. 78−60461
ZnTe, resonance Raman scatt. of excitonic polaritons by LO and acoustic phonons 79−65879
$ZnTe_xSe_{1-x}$, Raman phonon spectra, resonance interaction effect 80−25375
Zr, two-phonon Raman scatt. at low temps. 79−87433

phonon-plasmon interactions
anomalous EM fluctuations, quantum theory 78−14679
dichalcogenide layer compounds, interface plasmon-phonon interactions, transverse cond. 80−49641
heavily doped semiconductor, magnetoconductivity, effect of resonant phonon-plasmon coupling 80−24954
interface plasmons, longitudinal optical phonons, multilayer struct. 78−19118
ionic crystal/degenerate semiconductor interface, localised plasmon-optical phonon coupled modes 77−28071
ionic solids, surface phonon-plasmon coupling (surface plasmarons) 80−54497
magnetised semiconductor, coupled LO phonon-plasmon modes 79−73459
n-type semiconductors, plasmon-local phonon mode interaction, RPA, CPA theory 78−87932
n-PbTe, dynamical cond. in freq. range of LO-phonon-plasmon excitations 79−19592
piezoelectric semiconductor, longit. phonon-plasmon interaction, density gradient inhomogeneity 79−56156
polar semiconductor, highly excited, optical dielec. function of electron-hole plasma 80−92847
polar semiconductor, optical phonon-magnetoplasmon interface oscills. 78−43467
polar semiconductors, free-carrier absorpt., plasmon generation 79−4578
semiconductor, degenerate, surface optical phonons 80−70520
semiconductor, electron scattering interaction with coupled plasmon-polar-phonon modes 79−42536
semiconductor, ionic, -oxide interface, plasmon-phonon interactions 80−44730
semiconductor, light scatt. spectra, interference effects 79−82977
semiconductor-dielectric interface, surface polaritons of LO-phonon-plasmon coupled modes 79−7792
semiconductors, narrow-gap, plasmon-phonon interaction effect on optical phonon dispersion 80−103435
surface plasmarons, effect of finite thickness of accumulation layer, theory 80−103636
surface plasmon-phonon modes in quantizing mag. field, nonlocal shift 77−72908
CdS crystals, radiative recombination, high excitation rates 80−108269
$Fe_{1-x}O$, IR reflectivity obs. 77−43996
Fe_3O_4, magnetite, optical props. in IR 80−97271
$Ga_{1-x}Al_xAs$:Te, plasmon-LO-phonon coupling, IR refl. obs. 80−50335
GaAs base laminated epitaxial struct., surface plasmon phonon polaritons *(Russian)* 80−59905
n-GaAs, conduction band nonparabolicity and coupled plasmon-phonon modes, IR refl. spectra 80−55110
n-GaAs, coupled plasmon-LO phonon modes and Lindhard-Mermin dielec. function 79−82540
GaAs, effective mass, Raman spectrum determ. 80−24797
p-GaAs IR plasma reflectivity spectra calc., rel. to carrier conc. 78−52511
n-GaAs, implanted, IR refl. meas. of free carrier parameters 77−36244
n-GaAs, magnetised semiconductor, coupled LO phonon-plasmon modes inelastic neutron scatt. 79−73459
GaAs, plasmon-phonon coupling, and IR refl. spectra of impure crysts. 79−56150
n-GaAs, Raman scatt. by coupled phonon-plasmon mode, nonlocal theory 77−36222
n-GaAs, Raman scatt. by wavevector depend. coupled plasmon-LO phonons 77−40232
p-GaAs:Zn, Raman scatt. by LO phonon-plasmon coupled modes, wave vector non-conservation 80−16033
GaP, gain in stimulated Raman scatt. by coupled phonon-plasmon modes from spontaneous Raman spectra 79−68418
GaP, Raman scatt. from plasmon-phonon coupled modes 80−93337
GaSb, accumulation layer localised carriers interaction with LO phonons, Raman interference lineshapes 80−93338
n-$HgCr_2Se_4$, ferromagnetic semiconductor, plasmon refl., 86 to 320K 80−50346
InAs, plasmon-phonon coupling, and IR refl. spectra of impure crysts. 79−56150
InAs(Sb), IR reflectivity, longitudinal optical phonon-plasmon coupling 77−59578
InSb, accumulation layer localised carriers interaction with LO phonons, Raman interference lineshapes 80−93338
InSb, depletion layer, plasma and vibr. plasma type guided polaritons *(Russian)* 80−96933
$Pb_{1-x}Ge_xTe$ magnetoplasma reflectivity and transmission spectra 80−71428
$Pb_{0.8}Sn_{0.2}Te$, single cryst. and epitaxial film, far IR refl. spectra, carrier density, Hall const., and plasma freq. 80−20629
p-PbTe film, for IR magneto-optics, 8-30K 78−23543
Si, non thermal laser induced ordering, plasma life time, phonon interactions 80−84481

phonon-plasmon interactions continued
SnS, coupling of plasma waves with optical phonons 78−31204
$SrTiO_3$, plasmon-phonon reson., IR reflection spectra 78−56093
TiO_2, non-stoichiometric rutile, LO phonon-plasmon coupling, IR refl. spectrum 77−32376
ZnO, surface phonon-plasmon coupling (surface plasmarons) 80−54497
ZnTe, resonance Raman scatt. at high excitation levels *(Russian)* 80−55109

phonon softening *see soft modes*

phonons
see also crystal surface and interface vibrations; electron-phonon interactions; lattice phonons; phonon-defect interactions; phonon dispersion relations; phonon-exciton interactions; phonon-impurity interactions; phonon-magnon interactions; phonon-phonon interactions; phonon-plasmon interactions; spin-phonon interactions; tunnelling spectra; tunnelling spectroscopy; vibrational states in disordered systems
^{4}He, superfluid, one phonon excitation spectrum and interaction pot. 80−54455
A=18 nuclei, negative parity spectra, phonon dynamic interaction propagator approach 78−8739
acoustic superradiance, phonon avalanche, and propagation effects 79−69195
acoustic wave spontaneous birth in early Universe *(Russian)* 80−90593
alkali liquid metals, US absorption due to electrons and phonons 79−28046
alkali metal halide melts, lifetime 77−51527
amorphous film, tunnelling states, at low temps., thermal and acoustical props. 77−24500
biological functions of LF phonons *(Chinese)* 78−24024
biological system, Bose condensation of phonons, Frohlich model 77−16904
biological system, electron and excitation transfer, energy gap and temp. depend. 79−62187
Boltzmann equation, general nonlinear, for electrons and phonons 77−28151
borosilicate glasses, phonon mean-free path *(Japanese)* 77−69124
bose condensation of phonons in biological systems 80−30641
Bose fluid, structure factor determ. 78−34667
Bose gas, weakly interacting in restricted geometries, low-temp. thermodynamics 80−34261
Bose system, Jastrow wavefunction, hypernetted chain method 80−17866
boson system, strongly interacting, excitation spectrum 78−71897
n-butanol, phonon MFP formula, H bond collisions, low temp. 77−35655
cancerous cell culture, phonons, long-range coherence, microwave effects 78−35816
coherent phonons and excitons in biological systems, Bose condensation 80−67042
collagen and muscle elastic moduli, rel. to phonons, Brillouin spectra 77−52824
collective excitations, brief review of expt. and theory 77−1381
Dicke maser model, radiation damping, phase transition, presence of phonons 77−19224
Dicke-type Hamiltonians with hidden variables 78−74874
disordered system, freq. depend. of hopping cond. 77−28174
Einstein phonons renormalisation 77−4159
ethanol, phonon MFP formula, H bond collisions, low temp. 77−35655
even nuclei with A=228 to 240, anharmonicity of vibr. states, quasiparticle+phonon interaction influence 77−61340
Fermi system, Jastrow wavefunction, hypernetted chain method 80−17866
generation and detection expts. with supercond. tunnelling junctions, sources of losses 78−18718
generation and detection of high energy phonons by supercond. junctions 77−4161
glass, backward-wave phonon echoes 77−76513
glasses, acoustic and dielec. props. at low temps., review 78−6128
hyper-Raman scattering, degenerate, quantum statistical props. of photon and phonon fields 79−89873
hyper-Raman scattering, non-degenerate, quantum statistical props. of photon and phonon fields 79−89872
Kapitza conductance, anomalous, absence on freshly cleaved surfaces 79−73391
Kapitza resistance, axiomatic acoustic mismatch theory, with loss 79−33132
Kapitza resistance, metal-liquid He interface, theory of thermal boundary resist. 77−62730
Kapitza resistance and phonon refl. between solids and liq. He 79−86941
liquid metal, mol. motions from NQR, viscosity and sound damping 77−1615
localisation in condensed matter, electrons, phonons and magnons 80−10905
low temperature, effective-medium theory for Goldstone systems with off-diagonal disorder 80−19890
many-particle system, wave eqn. of particle density operator 77−53830
methanol, phonon MFP formula, H bond collisions, low temp. 77−35655
molecule-phonon interaction, radiationless phase relaxation of excited molecular vibrations *(German)* 77−40275
nematic liquid crystal, vibrational IR and Raman spectra 79−73913
neutron star matter, neutrino scatt. by phonons 79−12488
nuclear field theory perturbation expansion for strongly anharmonic systems, convergence, phonons 78−62490
nuclear struct., spherical even-even nuclei, n-quasi-particle collective states 77−10307
one-dimensional ϕ^4 and double quadratic systems, kinks, quantum statistical mechanics 80−47197
paramagnet, dilute, under bottleneck conditions, kinetics 77−77029
Peierls-Boltzmann equations, generalised, for phonons and local excitation kinetics 77−47518
Peierls-Boltzmann nonlinear eqn. for phonons, struct. and stability of solns. 77−84878
plasma, weakly ionised, ion interaction through phonon exchange in neutral gas 79−27775
plasma, weakly ionised, ion interactions through acoustic field, plasmoid existence 79−27776
polyethylene, dielec., cryogenic tunnelling losses at microwave frequencies 77−52016
polymers, thermal conductivity, temp. crystallinity and orientation depends., review 78−10234

phonons continued
PTFE, dielec., cryogenic tunnelling losses at microwave frequencies 77−52016
quadrupole-phonon states, fifth label generating operator, props. and eigenvalues 80−79887
quartz-liquid ^{4}He interface, saturation effects in phonon reflection 80−92736
rare gas clusters, small, structure, thermodynamic properties 80−88341
self consistent iterative method, economic method 77−84859
sine-Gordon ϕ-particles, quantum dynamics and statistical mechanics 79−42475
sine-Gordon chain, evidence for breather excitations 79−63054
smectic liquid crystal, vibrational IR and Raman spectra 79−73913
smectic liquid crystals, structure and dynamics, neutron diffr. studies 78−94972
smectic phases ordered, structural classification, collective modes *(French)* 78−94971
spectrometer, appl. of supercond. Al-PbBi tunnel junction 78−47477
spectroscopy, time resolved, high-energy monoenergetic pulsed source of phonons 77−31733
superconducting film, nonequilibrium energy spectra of emitted phonons 77−27957
superconducting tunnelling junction, quasi-particle recomb. and 2Δ-phonon-trapping 77−8236
superfluid Fermi system, Bose spectrum, hydrodynamic action functional *(Russian)* 78−14534
superfluidity, model Hamiltonian 80−44377
two-dimensional heisenberg ferromagnet, open diffusion effects *(Russian)* 77−32201
AgBr melt, Raman spectra, rel. to sublattice melting in α-AgI 78−10882
AgCl melt, Raman spectra, rel. to sublattice melting in α-AgI 78−10882
p-azoxyanisole, neutron scatt. by collective excitations 77−84651
ClCF, radical in Ar matrix, vibr. relax., multiphonon processes, fluoresc. 77−65430
Ga, liq., Brillouin scatt. obs. 77−24858
Ga_2S_3-La_2S_3-Nd_2S_3:Nd^{3+} chalcogenide glass, Nd^{3+} emission and absorption spectra, nonradiative relax. 77−40268
H-bonded species, in soln., vibr. relax. model 78−84559
He, film, surface backscatt. phonon pulse time delay, heat-sensitive detector obs. 78−22927
He, liq., interface with NaF, freq. of emitted phonons 79−55978
He, liq., multiphonon boundary of excitation spectrum, neutron and inelastic light scatt. 80−92740
He, liq., phonon coupling of two-dimens. Wigner cryst. with second surface sound *(Russian)* 80−92756
He, liq. multiple phonon spectrum boundary and props. *(Russian)* 78−63893
He, liq. surface, electron solid, phonon-ripplon coupling 79−42337
He, liq.-NaF interface, phonon transmission in both directions 79−28164
He, liquid, first and second sound generation by immersed Ge cryst. optical pumping 80−6581
^{4}He superfluid, phonon-roton excitation 80−107586
He-solid interface, freshly cleaved, phonon pulse refl. 79−60573
^{3}He-^{4}He, liq., dilute, phonon absorpt. and scatt. expts. 77−20153
^{3}He-^{4}He, liquid mixture, second sound, quantised vortex creation at constrictions, excitation model 80−44383
^{3}He-^{4}He, superfluid soln., dil., low temp. props., book contrib. 80−15330
^{3}He-^{4}He dil. solns., phonon vel. 79−23803
^{3}He-^{4}He dilute mixture, ballistic phonons, transition to second sound 78−10249
^{3}He-^{4}He mixture, dilute, second sound absorpt. and vel., phonon-^{3}He interactions 77−31835
^{3}He-^{4}He mixtures, dil., ground-state props., variational calc., paired-phonon anal. 79−73372
^{3}He-^{4}He mixtures, excitation spectrum, exptl. studies using neutron inelastic scatt. 77−59170
^{3}He-^{4}He mixtures, excitation spectrum, neutron inelastic scatt. study 79−46877
^{4}He, elementary excitations, Brillouin-Wigner perturbation theory with correlated basis functions 78−2319
^{4}He film, third sound, two-dimens. hydrodynamics and elementary excitations 79−7721
^{4}He, liq., atomic scattering at free surface 78−56003
^{4}He, liq., condensate fraction, low temp. and density calcs. 78−43196
^{4}He, liq., dynamic structure, neutron diffr. determ. 77−11749
^{4}He, liq., excitations produced by impinging ^{4}He atomic beam 78−10241
^{4}He, liq., excited states, variational calcs. 80−80017
^{4}He, liq., ground state, wavefunctions 80−10724
^{4}He, liq., ground state energy and struct. 77−66051
^{4}He, liq., interface with NaF, phonon refl. 79−55979
^{4}He, liq., interface with solid ^{4}He, phonon transmission using heat pulse technique 79−56035
^{4}He, liq., neutron scatt., book contrib. 80−2230
^{4}He, liq., phonon energy spectrum due to thin-film heater 77−76633
^{4}He, liq., phonon temp. depend. above and below T_λ, neutron scatt. meas. 79−55973
^{4}He, liq., two-dimens., excitation spectrum and thermodynamic props. 79−86959
^{4}He, liq., two-dimensional, ground state 80−49438
^{4}He, liquid, condensed phase, long-range order of one- and two-body density matrices 80−10726
^{4}He, liquid, long-wavelength phonon excitation, series expansion 80−88372
^{4}He, liquid, quantum hydrodynamics and two-fluid dynamics 77−69130
^{4}He liquid-solid interface, phonon transmission and Kapitza resist. 79−65271
^{4}He superfluid, acoustic vibration field density of states in piecewise const. parameter media 80−6483
^{4}He, superfluid, evaporation by rotons and phonons, heat-pulse technique 79−33135
^{4}He, superfluid, excitation spectrum, RPA calc. involving simple pseudopot. 80−92738
^{4}He, superfluid, interface with sapphire, 0.25K, ballistic phonon pulse transmission 79−19415
^{4}He, superfluid, multiphonon boundary in excitation spectrum *(Russian)* 79−51324
^{4}He, superfluid, neutron storage 79−86948
^{4}He, superfluid, phonon heat transport and Knudsen's minimum below 0.6K 79−33136
^{4}He, superfluid, phonon relaxation theory 77−85005

phonons continued
^{4}He, superfluid, polarisation pots. and elementary excitations at low temps. 77−15643
^{4}He, superfluid, roton-roton interactions and excitations at large wavevectors 77−28058
^{4}He, superfluid, two-dimens., microscopic theory, excitation spectrum and thermodynamics props. 80−24709
^{4}He, superfluid, viscosity and thermal conductivity *(Russian)* 80−10720
^{4}He, superfluid film, solitons at low temps., Korteweg-de Vries eqn. 80−96717
Hg, liq., Brillouin scatt. obs. 77−24858
KOH, amorphous and aqueous soln., depolarised Rayleigh scatt., phonon-like excitations 77−81109
^{93}Nb, 1 quasiparticle 2 phonon multiplet, microscopic quasiparticle cluster phonon coupling model 77−2908
NiO, bulklike powder, sp. ht., 14-280K 79−69260
PbCu film, amorphous supercond., phonon heat transport, thermal cond. meas. 78−19181
Rb, liq., phonons, collective modes calcs. 78−2218
Si-^{3}He interface, phonon reflection 78−84043
Si-^{4}He boundary, quantitative meas. of phonon energy transmission coeff. 77−66084
Si-liquid He interface, refl. of high frequency phonons, role of phonon focusing 77−80691
^{95}Te, 1 quasiparticle 2 phonon multiplet, microscopic quasiparticle cluster phonon coupling model 77−2908
Tm^{3+}, in oxide glasses, multiphonon relax. rates and fluoresc. lifetimes 77−77266

phosphate glasses
for iron and vanadium phosphate semiconducting glasses see amorphous semiconductors
absorption spectrum of Nd^{3+} ion, chem. composition effects, group IV element effects *(Polish)* 78−10932
alkali, mech. and dielec. relaxs. and interpet. 78−27159
alkali aluminophosphate, ionic cond. mechanism 80−15299
alkali and alkali earth metal metaphosphate glasses exam. of temp. dependence of thermooptical const. 78−88286
alkali and alkaline earth metal metaphosphate glasses exam. of thermooptical and photoelastic props. 78−88287
alkali metal metaphosphate glass:Nd^{3+}, luminesc. and lasing *(Russian)* 77−46724
alkali metal metaphosphate glass, dielec. relax. at medium temp. 79−24257
alkali metal polyphosphates, vitreous IR spectra 80−16043
alkali metaphosphate, M_2O-R_2O_3-P_2O_5 (R=Y or rare earth), glass transition temps. and coeffs. of linear thermal expansion 80−88343
alkali metaphosphate glasses, low frequency Raman scattering and glass transitions 79−95745
alkali phosphate:Nd^{3+}, physicochem., spectral, luminesc. and stimulated emission props. 77−54715
alkali phosphate glasses, colour and absorption spectra of Fe 77−85752
alkali rare earth metaphosphate glasses, $n(M_2O.P_2O_5).(1-x)Y_2O_3.xTb_2O_3.3P_2O_5$, M=Li, Na, K, excitation and emission spectra 80−40150
alkali-alumino-phosphate:U, rontgenoluminesc. and fluoresc., radiative transitions obs. 80−103977
alkaline earth glasses, $45RO.5Al_2O_3.50P_2O_5$, (R=alkali earths), electron beam irrad., exam. of charge accumulation and light-sum kinetics 79−4336
alkaline earth glasses, $45RO.5Al_2O_3.50P_2O_5$, (R=Mg,Ca,Sr,Ba), electron beam irrad., temporal change in electric field produced 79−4760
alkaline earth glasses, $RO-Al_2O_3$ -P_2O_5, R=Mg, Ca, Sr, Ba, exam. of electron beam irradiation effects 79−4253
alkaline earth metaphosphate, MO-R_2O_3-P_2O_5 (R=Y or rare earth), glass transition temps. and coeffs. of linear thermal expansion 80−88343
alkaline earth phosphate ($MO-Al_2O_3-P_2O_5$) irradiated electret glasses, relax. of external field intensity on heating 80−25282
aluminophosphate, alkali free, comp. effect on elec. cond. 78−26725
aluminophosphate, electron irrad., EM pulses during thermoexcitation 79−42107
aluminophosphate, multicomponent, 3.2 micron broad absorption band computer anal., residual H_2O vibr. 78−52478
aluminophosphate, multicomponent, γ-irrad., EPR study 79−91290
aluminophosphate glass:Mn:Mg(Sr), optical props. H_2O effects 77−28600
aluminophosphate melts with V, Cr, Fe and Co oxides, resistivity, 800-1200°C 77−39903
borophosphate glasses, effect of F on props. 78−67657
cation-site interactions, vibrational spectroscopy 80−2744
channel electron multipliers, absolute efficiency for tritium radiation 77−67945
channel multiplier construction, performance channel multiplier made of phosphate glass 77−34522
diffusion of Cu^+ ions, fluoresc. meas. 78−59980
electron detection efficiency of phosphate glass channel multiplier 78−41898
electron irradiated, elec. field distrib. above surface *(Russian)* 77−43763
electron-irradiated, charge accumulation, comp. depend. 78−2159
energy transfer from UO_2^{2+} to Sm^{3+} 79−78732
ESR of VO^{2+} ions 80−100610
fading mechanisms 79−95851
for fission fragment energy meas. 77−67932
fluorescence properties, energy transfer for Sb^{3+}, Dy^{3+} dopants 78−6778
fluorophosphate, magneto-opt. characts. 80−64126
fluorophosphate and fluoroberyllate glass laser damage thresholds and solid inclusions 80−33054
fluorophosphate glass, optical absorpt. comparison with 3d transition elements *(French)* 79−65819
fluorophosphate glass produced in pyrocarbon coated melt vessels, increased light absorpt. 78−71167
fluorophosphate glasses, C determ. by deuteron activation analysis 78−68961
fluorophosphate glasses, rare-earth activated, luminesc., bonding 78−64415
fluorophosphate glasses with silicofluorides, optical props. 77−72040
fluorophosphate laser glass, highly homogeneous, production 80−14411
fluorophosphate laser glasses, low nonlinear refr. index, development 78−50870
phosphate glasses continued
fluorophosphate optical glass development 80−106588
fluorophosphate optical glass melt, disintegration of vitreous C 78−30101
fluorophosphate system glasses alkali free and crystn. products, struct. and IR spectra 79−94913
fluorphosphate glass for SHIVA laser, nuclear fusion reactor appl. 78−37440
formation of glasses in various phosphate systems 80−19708
frequency selection of Nd^{3+} ions under monochromatic laser excitation at reson. transition *(Russian)* 79−78747
gamma dosimetry appl. *(Slovenian)* 80−32521
glass:CuO, band-pass characts. improvement by doping 77−54797
glass formation in phosphate system containing halogens 80−103254
heat treated, thin foil prep. for TEM obs. 78−7154
laser, CW oscillation with Nd dopant 79−50311
laser, statistical props. and stabilisation 80−48266
laser active materials, large laser effect phosphate and fluorophosphate glasses 78−79021
laser amplifiers and optical isolators 78−25885
laser glass, nonradiative energy transfer from Cr to Nd, optical pumping efficiency improvement 80−33001
laser glass cladding composition and design criteria 79−18450
laser glass for improved beam quality and efficiency 77−88774
laser glass inversion density, direct meas. 79−13969
laser glasses, phosphate and fluorophosphate, Nd doped, piezooptic coeffs. meas. 80−99815
laser glasses, review 80−9888
laser oscillator, passively mode-locked, stabilised with acousto-optic modulator *(Japanese)* 79−13999
laser properties under pulse-periodic pumping conditions 79−64236
laser rods, pumped in pseudoelliptic cavities, thermal effects 79−76692
lasers, highly repetitive, development 80−69415
Li^+ motion, ^{7}Li NMR spectra, nucl. relax. 80−34804
luminescence inhomogeneous line profile in Yb^{3+} extcited glasses, excitation migration, energy gap depend. 80−7407
metal oxide metaphosphate glasses, vibr. study of metal cation reduction at surface 78−56797
metaphosphate:Ag, dosimeter, optical absorpt. and radiophotolum., effect of temp. 78−40333
metaphosphate glass: Nd^{3+}, Yb^{3+} luminesc., energy transmission and migration between Nd^{3+} and Yb^{3+} 80−66297
metaphosphate glasses with Ag activator, radiophotoluminesc. 79−38596
metaphosphates, chem. stability in water and acetic acid soln. 80−21144
metaphosphates, vitreous, microhardness 80−25864
mixed alkali glasses, Raman and far IR spectra, vib. at cation site, struct. 78−60435
non-alkaline, transition states, phys. effects of fluors, phase diagrams and optical effects *(German)* 80−88045
nonresonance interaction parameters of rare earth ions, luminescence kinetics obs. *(Russian)* 78−31246
Nova: the laser fusion scientific feasibility experiment 78−59040
nuclear track detector, heavy ions and fission fragments energy meas. 78−17487
opal glasses, phosphate opacified, phase comp. and struct. 80−64919
optical, small thermo-optical characts., stress coeffs. 77−31123
optical and thermooptical properties, calc. from chem. comp. 79−65826
optical breakdown rel. to microscopic inhomogeneous struct. 80−102784
optical fibres, transparent in UV region, manufacturing 78−87113
optical filter glasses with band-pass characts. for red spectral region 78−25936
optical glass, Raman scatt. and nonlinear refr. index 80−2749
optical stress coeff., effect on alkali metal oxides 77−50740
phase separated, EPR rel. to struct., elec. and opt. props. 78−23333
phosphate glass: Ni, absorption spectra, mag. props., coordination behaviour *(German)* 80−40147
phosphate glass:Nd^{3+}, highly conc., electron energy deactivation and transfer *(Russian)* 80−29802
phosphate glass:Nd, comparison of gain with silicate glass:Nd 80−19039
phosphate glass:Tb^{3+}, luminesc. props. 79−33798
phosphate glass:Yb^{3+}, impurity centres, migration of excitations, math. modelling 78−48225
phosphate-tungstate semicond. glass, W (V) complex, EPR and electronic spectra interpretation 77−69682
photochromic glasses, anisotropic recording of optical data *(Russian)* 77−1651
radioactive waste, high-level, evaluation of products for solidification 77−61555
rare earth activated, polarised luminesc. 78−48224
resonant luminescence, migration of excitations of Yb^{3+} ions 77−8642
sealants to Al alloys, elec. and mech. props., glass transition 80−81018
secondary and tertiary coordination number of Co^{2+} and chem. composition *(Polish)* 78−9960
silicate, thermooptical constant, depend. on chem. comp. 79−99861
sodium iron fluorophosphate glasses, EPR and Mossbauer resonance study 80−39968
sodium metaphosphate glasses, γ-irrad., ESR 78−23339
solid state nuclear track detectors, effect of etching conditions on energy resolution of phosphate glass and polycarbonate detectors 80−91390
thermal expansion and chem. durability 77−80636
thermo-optical properties Li_2O and Na_2O effects 78−18029
track detectors, nuclear phys., spectrometric appls., track diameter 78−17466
transition metal phosphate glasses, ohmic contact and dielectric relax. 79−65795
$24BaO.V_2O_5.25P_2O_5$, ESR and absorpt. spectra, V(IV) ions conc. 78−64266
$24CaO.V_2O_5.25P_2O_5$, ESR and absorpt. spectra, V(IV) ions conc. 78−64266
$33K_2O.7Al_2O_3.60P_2O_5$, high expansion glass, chemical durability improvement by ion exchange 79−66180
AgI-Ag_2O-P_2O_5 glassy electrolyte galvanic cells 80−104513
AgI-Ag_2O-P_2O_5 system, glass form. and superionic cond. characts. 78−26722
Ag_2O-P_2O_5 system, electrical conductivity and dielectric relaxation *(Japanese)* 77−66455
$AgPO_3$-AgBr(Cl)(I) system glasses, soln. calorimetry obs., thermodynamic activity correl. with ionic cond. *(French)* 79−33102
$AgPO_3$-AgI glass system, solution calorimetry, enthalpy of formation *(French)* 78−64527

phosphate glasses continued
$AgPO_3$-AgX (X=I, Br), glass-forming regions, struct. model *(French)* 80−100464
$AgPO_3$-CdI_2 glasses, ionic conductivity and structure *(French)* 78−67854
$AgPO_3$-$HgI_2(CdI_2)(PbI_2)$, elec. cond. and Raman. spectra rel. to struct. *(French)* 79−10979
$AgPO_3$-PbI_2 system, elec. conductivity as function of composition and temp. *(French)* 77−69112
Al^{+} ion coordination study by $AlK_{\alpha 1,2}$ X-ray fluorescence spectra *(Japanese)* 78−7308
Al_2O_3-B_2O_3-P_2O_5 glasses, formation and props. 78−83737
Al_2O_3-B_2O_3-P_2O_5 system, glass formation by laser melting 78−44074
Al_2O_3-P_2O_5, electron bombard. induced elec. discharge, electromech. effects *(Russian)* 77−32324
Al_2O_3-P_2O_5:Cr^{3+}, absorpt. spectra, Fano antireson. and vibronic Lamb shift 80−71458
Al_2O_3-P_2O_5:Nd^{3+}, high Nd conc., spectroscopy and lasing obs. 78−46609
Al_2O_3-P_2O_5-Mg(Ca)(Sr)O glasses, Na^{+}, Sr^{2+} diffusion coeffs. rel. to temp. 78−30787
Al_2O_3-SiO_2-P_2O_5, refractory glasses, exam. of liquid immiscibility and crystallisation 78−55814
$Al(PO_3)_3$, vitreous struct. 78−26443
$Al(PO_3)_3$-BaF_2-Al_3 glasses, opt. props., group I-III fluorides effect 80−66143
$Al(PO_3)_3$-LiF system glasses, microhardness and US vel. 79−99274
$Al(PO_3)_3$-NaF system, IR spectra and struct. 79−65882
$Al(PO_3)_3$-NaF system glasses, microhardness and US vel. 79−99274
B_2O_3-V_2O_5-P_2O_5, glass, mech. and elec. props 80−84228
BaO-Al_2O_3-P_2O_5, struct. energetics and charging under irrad. *(Russian)* 77−84791
BaO-BaX_2-P_2O_5 glass, X=F, Cl, Br, conductivity 78−67862
BaO-Nd_2O_3-P_2O_5 ultraphosphate glasses, Nd^{3+} conc. quenching of luminesc. effect 79−19931
BaO-P_2O_5, Nd^{3+} luminesc. quenching by transition metal and rare earth ions 80−25449
BaO-P_2O_5, US velocity rel. to elastic props. 80−103425
BaO-P_2O_5 glasses, Cu^{+} ion electromigration at 400°C, luminesc. meas. 77−76610
BaO-P_2O_5:Mo^{5+} glass, EPR spectra, computer simulation 80−88872
BaO-SiO_2-P_2O_5, effect of thermal history on crystallisation of glasses 77−80424
BaO-WO_3-P_2O_5, struct. and IR spectra 80−64914
$Ba(PO_3)_2$-AlF_2-BaF_2 (SrF_2), elec. cond., density, and IR spectra 79−95215
$Ba(PO_3)_2$-AlF_3-CaF_2, elec. cond. and IR spectra 80−89005
$Ba(PO_3)_2$-AlF_3-MgF_2, elec. cond. and IR spectra 80−89005
$Ba(PO_3)_2$-alkaline earth fluoride and $Ba(PO_3)_2$-YF_3 glasses, pseudobinary, elec. cond. and dielec. losses 77−7890
$Ba(PO_3)_2$-BaF_2-$BaCl_2(BaBr_2)$, elec. cond., mixed anion effect 80−15300
$Ba(PO_3)_2$-fluoride glass, elec. cond., struct. 80−88056
$Ba(PO_3)_2$-MgF_2, vitrification region 77−35676
$Ba(PO_3)_2$-MgF_2=0.4AlF_3.0.6CaF_2 glass system, vsicosity and energy parameters of rheological props. *(Polish)* 79−73331
$Ba(PO_3)_2$-WO_3, electron-absorpt. spectra and structure of W centres 80−88873
$Ba_3(PO_4)_2$ glass, phase equilibrium data 79−27922
$Ba_3(PO_4)_2$ glass, phase equilibrium data 79−27923
$Ba_3(PO_4)_2$ transition metal ion, optical and magnetic props. 78−64196
$BaPO_3F$-Al_2O_3-B_2O_3 glasses, phys. props. 78−63676
$BaPO_3F$-Al_2O_3-B_2O_3 system, liq. phase separation, IR spectra, microstruct. 80−29940
Be metaphosphate glass, crystallization *(Japanese)* 77−72566
BeO-P_2O_5-RO(R_2O) (R=Li,Na,K,Mg,Ca,Sr,Ba) glasses, gamma irrad., cation modifier effect on radiation centre formation 80−40720
BeO(Be_2O)-TiO_2-P_2O_5, electrical resistivity *(Japanese)* 77−12719
Ca aluminophosphate foam glasses, for prosthetic appl., porosity and mech. props. 79−74128
CaO-Al_2O_3-P_2O_5, struct. energetics and charging under irrad. *(Russian)* 77−84791
CaO-CuO-P_2O_5-V_2O_5 glass EPR, Cu impurity effect on elec. props. 79−51849
CaO-P_2O_5, US velocity rel. to elastic props. 80−103425
CaO-P_2O_5 glass, pulsed EPR study of Cu 78−84479
CaO-P_2O_5:Cr^{3+}, absorpt. spectra, Fano antireson. and vibronic Lamb shift 80−71458
CaO-P_2O_5-WO_3 glass, computer simulation of Mn^{2+} EPR spectra 80−34764
CaO(Ca_2O)-TiO_2-P_2O_5, electrical resistivity *(Japanese)* 77−12719
$Ca(PO_3)_2$, crystallisation below T_g 77−20056
$Ca(PO_3)_2$, crystallisation below glass transition temp. *(Japanese)* 77−62480
$Ca(PO_3)_2$ glass, crystallisation below glass transition, stress effect 80−19709
$Ca(PO_3)_2$, rate of crystallisation, SiO_2 additive effects *(Japanese)* 77−68927
$Ca(PO_3)_2$:Eu^{3+}, amorphous, phonon-assisted site-to-site electronic energy transfer, fluoresc. line narrowing obs. 77−81140
$Ca(PO_3)_2$:Eu^{3+}, anomalous spectral props. 79−38614
CdO-Al_2O_3-P_2O_5 glass, γ-irrad., EPR study 80−84639
CdO-P_2O_5 glass, thin film, elec. cond., high and low fields 80−80427
CdO-P_2O_5 glasses, elec. props. at high elec. fields 80−39573
CdO-P_2O_5 glasses, prep., density, elec. and optical props. 79−70033
CdO-ZnO-P_2O_5 glasses prep., density, elec. and optical props. 79−70033
Ce^{3+}→Tm^{3+}, Ce^{3+}→Tb^{3+} energy transfer, temp. depend. 77−24882
Ce_2O_3-P_2O_5, crystallisation 77−51326
Cu^{2+} doped, EPR, optical spectra 78−72399
CuO-CaO-P_2O_5 glass devices, memory switching 78−56192
CuO-CaO-P_2O_5 system glasses, DC cond., hopping transport, 300 to 620K 78−23096
CuO-V_2O_5-P_2O_5 glass, elec. cond. and switching *(Japanese)* 80−34492
$Er(PO_3)_3$ glass, Faraday resonance effect in pulsed mag. field, optical freq. EPR *(Russian)* 80−2734
FeO-P_2O_5 glass, elec. props. effect of high energy γ-radiation 79−11173
FeO-P_2O_5 glasses, electrical and mechanical losses 78−80283
FeO_x-P_2O_5 glass, semicond., dielec. props., thermally stimulated depolarisation meas. 79−95704
Fe_2O_3-P_2O_5 system, vitreous, struct. obs. using neutron scatt. 78−22667
GeO_2-$PO_{5/2}$ glass, struct. and props. *(Japanese)* 77−27837
K_2O-Al_2O_3-P_2O_5 glass, low-temp. viscosity 80−39198

phosphate glasses continued
K_2O-Al_2O_3-P_2O_5-Nb_2O_5 glasses, struct. singularities, IR spectra *(Russian)* 78−2861
K_2O-Al_2O_3-P_2O_5-Nb_2O_5 glasses, struct. role of Nb 78−67653
K_2O-Al_2O_3-P_2O_5-TiO_2, structural role of Ti, kinetic study of chem. destruction 80−88055
K_2O-B_2O_3-P_2O_5 glass struct. studies using NMR 79−24221
K_2O-ZnO-P_2O_5, exam. of chemical durability, glass transformation temp. 79−20221
KO(K_2O)-TiO_2-P_2O_5, electrical resistivity *(Japanese)* 77−12719
KPO_3-Fe_2O_3 glasses, γ-irrad., ESR 80−50182
KPO_3.$Al(PO_3)_3$:U, vibronic excitation, absorption and emission spectra 78−52524
La_2O_3-B_2O_3-P_2O_5, glasses, struct. changes during heat treatment, NMR obs. 77−7672
Li-Al-borophosphate glass, activated with Ag, in-reactor dosimetry *(Russian)* 77−83113
Li-La phosphate glass, Nd, Cr activated, Nd luminesc. quantum efficiency meas., Nd-Cr nonradiative transfer 80−66296
Li-$La_{1-x}Nd_x$ phosphate glasses, stimulated emission spectroscopy of $^4F_{3/2}$ to $^4I_{11/2}$ and $^4F_{3/2}$ to $^4I_{13/2}$ transitions 79−38573
Li-Nd-La phosphate glass, nonradiative losses, pulse periodic stimulated emission and luminesc. 77−83878
Li-Nd-La phosphate glass active elements, laser characts., comparison with Nd:YAG 80−33002
LiCl-Li_2O-P_2O_5 glass system, vitreous domain, struct., elec. cond. *(French)* 80−70135
LiF-$Al(PO_3)_3$ glass, phase decomp., X-ray diffr. and IR spectra study 80−30003
LiF-Li_2O-Al_2O_3-P_2P_5 glass, ionic cond., transport numbers determ. 79−28143
LiF-$NaPO_3$-MeF_x (Me=Mg, Ca, Al) glasses, IR spectroscopy study 80−16042
LiNd phosphate glass, spectral and generation props. 77−1700
$LiNd_{0.3}La_{0.7}$ phosphate glass, stimulated emission characts. 79−18426
Li_2O-Al_2O_3-P_2-O_5:V^{4+}, glass exam. of ESR spectrum of V^{4+}, optical spectra, and structure 78−88180
Li_2O-Al_2O_3-P_2O_5:Cd^{+}, γ-irrad., EPR study 80−84639
Li_2O-B_2O_3-P_2O_5, glass, mech. and elec. props 80−84228
Li_2O-Na_2O-P_2O_5, heat of soln. *(Japanese)* 79−34350
Li_2O-Nd_2O_3-P_2O_5 glass, physicochem., spectral, luminesc. and stimulated emission props. 77−54715
Li_2O-Nd_2O_3-P_2O_5 ultraphosphate glasses, Nd^{3+} conc. quenching of luminesc. effect 79−19931
Li_2O-P_2O_5:Cd^{+} glass, γ-irrad., EPR study 80−84639
Li_2O-ZnO-P_2O_5, exam. of chemical durability, glass transformation temp. 79−20221
$LiPO_3$, crystn. mechanism from melt 80−44139
$LiPO_3$-$Al(PO_3)_3$:Ag glass, ionic motions, thermally stimulated depolarisation study 79−65239
$LiPO_3$-LiX(X=I, Br, Cl) glass, ionic cond. *(French)* 79−99365
$LiPO_3$.$Al(PO_3)_3$:U, vibronic excitation, absorption and emission spectra 78−52524
Li_2S-P_2S_5-LiI, ionic cond. meas. from room temp. to glass transition temp. *(French)* 80−88355
$M_2O(MF_y)$-BeO-P_2O_5 glasses, M=alkali metal, alkaline earth, Cd or Zn, glass-formation 78−67656
MgO-Al_2O_3-P_2O_5, struct. energetics and charging under irrad. *(Russian)* 77−84791
MgO-Al_2O_3-P_2O_5 system glass, heat treatment of aluminium metaphosphate influence on thermolum. 80−108285
MgO-CaO-SiO_2-Al_2O_3-Na_2O.P_2O_5, effect of $NaPO_3$ on phase composition rel. to basic refractories 78−80528
MgO-FeO-P_2O_5 system, ESR spectra, heat treatment conditions effect 79−65722
MgO-P_2O_5, US velocity rel. to elastic props. 80−103425
MgO-P_2O_5:Fe_2O_3 glass, $Fe^{2+(3)}$ impurity ions struct.-chem. state, Mossbauer data 80−40028
MgO-P_2O_5-Al_2O_3-3P_2O_5 glass, absorpt. shift, electron and hole traps, thermolum. meas. 79−65897
$Mg(PO_3)_2$, rate of crystallisation, SiO_2 additive effects *(Japanese)* 77−68927
Mn^{2+} doped, luminesc. colour change 80−7392
MnO-P_2O_6 system, formation of manganese phosphates 77−90331
MoO_3-P_2O_5, varying compositions, DC conductivity, high temp. range, conduction due to polaron hopping 78−6376
MoO_3-P_2O_5 glass, thermoelec. power meas. 78−84242
Na-Fe fluorophosphate glass, EPR and Mossbauer resonance study 80−15838
Na-Fe fluorophosphate glass, Mossbauer study, mag. and optical props. 80−16065
α-$Na_3Fe_2(PO_4)_3$ orthophosphate, cryst. and vitreous, Mossbauer spectroscopy and mag. susceptibility *(French)* 80−80657
Na_2O-Al_2O_3-P_2O_5, used in solidification of radioactive waste *(Russian)* 77−61560
Na_2O-Al_2O_3-P_2O_5, exam. of subsolidus structure 79−4954
Na_2O-Al_2O_3-P_2O_5 glass, low-temp. viscosity 80−39198
Na_2O-Al_2O_3-P_2O_5:Eu glasses, fluorescence line narrowing meas. *(French)* 80−34975
Na_2O-B_2O_3-P_2O_5 glass, mech. and elec. props 80−84228
Na_2O-CaO-P_2O_5:Co glass, bonding, symmetry meas. 79−46572
Na_2O-FeO-P_2O_5 metaphosphate glass, internal friction *(Polish)* 79−96078
Na_2O-P_2O_5, metaphosphate glass, active solute doped, absorpt. spectra of radiation products 78−64865
Na_2O-P_2O_5, numerical optimisation of ESR V^{4+} spectra 79−38370
Na_2O-P_2O_5, XPS quantitative struct. anal. 80−2917
Na_2O-P_2O_5 and Li_2O-Na_2O-P_2O_5 glasses with oxide additions, eval. as membranes for chem. sources of current *(Russian)* 79−96338
Na_2O-P_2O_5 glass, elastic and viscoelastic props. by Brillouin scatt. 79−51972
Na_2O-P_2O_5:Ce (III) and (IV), u.v. absorpt. 77−4658
Na_2O-P_2O_5:Cr^{3+}, absorpt. spectra, Fano antireson. and vibronic Lamb shift 80−71458
Na_2O-P_2O_5:Cu II, glass, O basicity, ESR study 78−80199
Na_2O-P_2O_5-CuO, γ-irrad., CuO effects on EPR 80−84645
Na_2O-P_2O_5-Y_2O_3-Tb_2O_3 glass, conc. quenching of luminesc. in disordered system with dipolar interaction 80−89059
Na_2O-ZnO-P_2O_5, exam. of chemical durability, glass transformation temp. 79−20221

phosphate glasses continued
$Na_2O(K_2O)$-P_2O_5 glasses, P K-band X-ray emission spectra, state anal. 80−40190
$NaPO_3$ glass, Na diffusion 78−63875
$NaPO_3$:Eu^{3+}, luminesc. of Eu^{3+}, transition probabilities 80−80845
$NaPO_3$-AlF_3(-NH_4HF_2) glasses, synthesis, chem. thermal and optical anal. *(French)* 79−100104
$Na_5P_3O_{10}$, γ-irrad., PO_3^{2-} EPR obs. 78−27091
$NaPO_3$.$Al(PO_3)_3$:U, vibronic excitation, absorption and emission spectra 78−52524
Nb_2O_5-V_2O_5-P_2O_5, glasses and glass ceramics, elec. cond., struct. 80−84466
Nd doped (fluoro) phosphate laser glass piezo-optic coeffs. meas. at 0.6328 and 1.15 μm 80−34888
Nd:glass, comparative lasing characts. of silicate and phosphate laser glasses 80−74364
Nd^{3+}:glass, giant laser pulse-induced luminesc., spectral shape temp. depend. *(Russian)* 77−19257
Nd^{3+}:phosphate glass laser, brightness enhancement by spatial filtering in amplifying channel 80−48321
P_2O_5, glassy, high freq. vibr. bands, central force model 80−49330
P_2O_5-Al_2O_3-Na_2O-K_2O-Li_2O-(CaO+MgO) glass system, ion exchange effect on mech. props. 80−30229
P_2O_5-CdO photochromic glasses, Weigert effect *(Russian)* 77−1690
P_2O_5-GO_3-$CaO(Nd_2O_3)$ systems, vitrification regions and physicochem. props. of glasses 77−11673
P_2O_5-GeO_2 glass, absorption spectrum of Nd^{3+} ion, chem. composition effects, group IV element effects *(Polish)* 78−10932
P_2O_5-K_2O-CdO-Na_2O glass:Nd^{3+}, highly doped, spectroscopic props. and CW laser action *(French)* 79−41385
P_2O_5-MO-Al_2O_3, (M=MgO, CaO, SrO, BaO) (45, 5 wt.%) glass, electron irradiation effect on dielec. props. 80−29056
P_2O_5-MoO_3 glasses, EPR study 79−82866
P_2O_5-MoO_3-CaO glasses, EPR study 79−82866
P_2O_5-Na_2O-BaO glass, rare earth doped, nonradiative decay and multiphonon relax. 77−85802
P_2O_5-R_2O_3-M$_2$O(M'O), (M=alkali metal, M'=alkaline earth, R=Y or rare earth), metaphosphate glass phosphors, fluoresc. props., activation conc. effect 80−89058
P_2O_5-WO_3:CuO glass, EPR, Cu impurity effect on elec. props. 79−51849
PbO-MoO_3-P_2O_5, glass phase investigation, density determ. *(Polish)* 77−70039
PtRh5 alloy, phosphate glass addition effect on high temp. strength *(German)* 80−25807
RbO_2-Na_2O-P_2O_5 glasses, Raman and far IR spectra, vib. at cation site, struct. 78−60435
Rb_2O-Li_2O-P_2O_5 glasses, Raman and far IR spectra, vib. at cation site, struct. 78−60435
Sb-containing glasses, ^{121}Sb Mossbauer spectra 77−20764
SiO_2-GeO_2-P_2O_5,optical glass fibre, profile synthesis 77−27333
SiO_2-Li_2O-K_2O-ZnO-P_2O_5, glass ceramic, phase changes and crystn. processes 80−7562
SiO_2-Na_2O-CaO-P_2O_5, BIOGLASS, surface, $Ca_3(PO_4)_2$ film form., bonding to bone 80−85212
spectral behaviour under narrow-line excitation 79−33747
SrO-Al_2O_3-P_2O_5, struct. energetics and charging under irrad. *(Russian)* 77−84791
SrO-P_2O_5, US velocity rel. to elastic props. 80−103425
Tb_2O_3-P_2O_5-MO system glasses, (M=Mg, Ca, Sr, Ba or Pb), photoluminesc. under X-ray excitation 80−89060
TeO_2-P_2O_5, electron microscope exam. of phase equilib. and immiscibility 78−52779
TeO_2-P_2O_5 system, glass struct., neutron diffr. study 80−70128
Ti-containing, MO(M_2O)-TiO_2-P_2O_5, M=K, Ca, Be, elec. resistivity *(Japanese)* 77−12719
TiO_2-Al_2O_3-P_2O_5 glass, ESR of Ti^{3+}, exam. 78−88181
TiO_2-P_2O_5 glasses, reduced, mag. susceptibility, 1 to 400K, mag. exchange between Ti^{3+} ions 79−73691
TiO_2-P_2O_5 reduced glasses, prep., elec. transport, chem. anal., DC, AC cond., seebeck coeff. 78−30924
TiO_2-Ti_2O_3-P_2O_5, glass form., struct. and elec. props. 80−44592
Tm^{3+}, in oxide glasses, multiphonon relax. rates and fluoresc. lifetimes 77−77266
Tm^{3+}-doped, eigenstates and radiative transition probabilities calcs. 77−77265
V phosphate glasses, vibr. spectra 77−52064
V^{4+} doped, EPR, optical spectra 78−72399
V_2O_5-based glasses, amorphous and crystallized electronic cond. and related props. 79−99547
V_2O_5-MoO_3-P_2O_5 glass, semicond., DC cond., dielec. props 79−91044
V_2O_5-P_2O_5, DC conductivity, high temp. range 78−6376
V_2O_5-P_2O_5, EPR investig., samples with varying V^{4+} content and cond. 77−8389
V_2O_5-P_2O_5 (70-30), electrical cond. and thermoelectric meas., Au-glass-Au sandwich 80−29403
V_2O_5-P_2O_5 based glasses, specific heat effect of fast neutron irradiation 77−69096
V_2O_5-P_2O_5 glass, density and O molar volume 78−59759
V_2O_5-P_2O_5 glass, dielec. relax. mechanism, SDRC investigation, Schottky barrier formation in metal-glass-metal systems 78−60388
V_2O_5-P_2O_5 glass, electrical 1/f noise and DC cond. 79−91109
V_2O_5-P_2O_5 glass, in SnO_2/V_2O_5-P_2O_5/Si heterojunction, static optoelectronic characts. 79−87146
V_2O_5-P_2O_5 glass, thermoelec. power meas. 78−84242
V_2O_5-P_2O_5 glasses, anomalous cond. mechanism 77−76832
V_2O_5-P_2O_5 glasses, secondary electron emission 79−87534
V_2O_5-P_2O_5 glasses, threshold and memory switching 77−76887
V_2O_5-P_2O_5-CaO glass with metal electrodes, elec. characts., thermal conditions effect *(Russian)* 78−47884
V_2O_5-P_2O_5-MO system glasses, (M=Ba,Ca,Cu and Mg), phase separation, crystn. and EPR spectra 77−76321
mV_2O_5.(100-m)P_2O_5, (m=100-2), V(IV) complexes conc., absorpt. and ESR spectra 78−64266
$V_{1+x}P_{1-x}O_{5-c/2}$, density and struct. from X-ray scatt. meas. 77−89380
$V_{1+x}P_{1-x}O_{5-c/2}$ glasses, structure, adiabatic hopping conduction model 77−43588
W-glass discs, plasma prod. processes 1.06 μm laser irrad. 78−18431
WO_3-MnO-P_2O_5 system, glass form. and memory effects 77−76888
WO_3-P_2O_5, DC conductivity, high temp. range 78−6376
WO_3-P_2O_5, DC elec. cond., 100-400K 78−39106

phosphate glasses continued
WO_3-P_2O_5 alkali glasses, electrochromic, electron-ion processes 80−25341
WO_3-P_2O_5 glass, AC cond. and dielec. props. 80−92717
WO_3-P_2O_5 glass, thermoelec. power meas. 78−84242
WO_3-P_2O_5 glasses, electrochromic effect 79−95735
W_2O-P_2O_5, glass, 1.06 μm laser radiation interaction 78−91132
Yb^{3+} doped, luminesc. band struct., chronoscopic study at 4.2K 80−60663
Yb^{3+}:phosphate glass, relation between absorption and equilib. luminesc. spectra 77−85754
ZnP glass heavy-ion track detectors 3 to 120 MeV 80−91389

phosphorescence
see also fluorescent screens; MIDP; phosphors
acenaphthene, vibronic spectra, electronic-vibr. interactions 78−1021
acetone, mol., radiative lifetime of phosphoresc. state, influence of high lying triplet states 79−86006
acetone, photochem. and photophysics, 330-250 nm, 0-1000 torr 78−17706
acetophenone, highly purified, luminesc. props. 80−32764
acetophenone, triplet-triplet energy transfer, naphthalene-d_8, in EPA rigid soln., donor phorphoresc. decay 78−10971
acetophenone in toluene glass, quasi-line phosphoresc. spectra 77−69883
3- and 4-acetylamino-N-methylphthalimide, in alcoholic solns., phosphoresc. decay laws 78−17709
acetylene ketones, absorpt. and phosphoresc. spectra 79−54865
adenine film, polycryst., energy conversion processes, quantum yields, 4 to 10 eV 80−88589
alkali halide aq. solns. with O^{2-} anion impurities, luminescence spectra regularities *(Russian)* 77−69876
alkali hexahalogeno compounds: $ReCl_6^{2-}$($ReBr_6^{2-}$), low symm. splittings in vibronic spectrum due to phase transitions 80−55161
alkali metal hexahalogenostannate: $ReBr_6^{2-}$, vibronic transition $\Gamma_7(^2T_{2g})\rightarrow\Gamma_8(^4A_{2g})$, intensity distrib. 80−45142
alkane:toluene, radiolysis at 77K, luminesc., excited singlet toluene form., energy transfer mechanism 77−16846
2-aminopurine, triplet state, electric dipole moments 79−22742
5-aminopyrimidine triplet state, electric dipole moments 79−22742
anilinium ion, $C_6H_5NH_3^+$, fluoresc. and phosphoresc., pKa values 79−13755
anilinonaphthalenesulphonate, room temp. phosphoresc., isomer effects 79−61429
anthracene, triplet excitons, phosphoresc. and delayed fluoresc. excitation spectra 78−63986
anthracene-PMDA crysts., phosphorescence blue shift of charge transfer config. 77−36278
anthracene-TCNB charge transfer cryst., phosphoresc. and delayed fluoresc. detected mag. reson. 79−33565
anthracene/TCNB, charge-transfer cryst., fluoresc., 1.2-300K, mobile triplet excitons 78−43913
anthracenes, long-lived luminesc. in solid state *(German)* 78−23528
β-F-9,10-anthraquinone, internal heavy atom effect, vibronic phosphoresc. spectrum, intermol. spin-orbit coupling 78−82774
9,10anthraquinone, lower triplet states, interactions and position, matrix isolation spectra 80−63634
9,10-anthraquinone, phosphorescence, external heavy atom in mol., 4.2 to 77K, quasiline spectra 78−82773
9,10-anthraquinone, Shpolskii quasi-line phosphoresc. spectra, electronic-vibrational interactions 78−55196
anthraquinone, site selective sublevel phosphoresc. spectra in octane or hectane soln. 79−69878
anthraquinone in pentane solvent, sublevel phosphorescence spectra, molecular distortion 80−74190
arene, photophysics, functionalised micellar assembly, phosphoresc. and triplet Ag^+ enhancement 78−95598
aromatic aldehyde, phosphorescence spectra of mol., intensity and vibronic coupling 79−76461
aromatic amides, intersystem crossing, mol. geom. effects 77−6828
aromatic compounds in benzene polycrystalline host, active N_2 induced chemilum., 77K 80−60691
aromatic esters, in ethanol, luminescence spectra, phosphoresence and fluorescence 79−54899
aromatic esters, phosphoresc. and fluoresc. spectra in organic matrices 80−32756
aromatic hydrocarbons, aqueous micellar soln., triplet state room temp. phosphoresc., hydrophillic quenchers 78−9181
aromatic hydrocarbons, $S_0\rightarrow T_1$ phosphoresc. under Shpolskii effect conditions 77−83643
aromatic hydrocarbons in Shpolskii matrices, $S_0\rightarrow T_1$ absorpt. spectra 79−85995
aromatic molecules, phosphoresc. triplet spins phase coherence, ESR 79−31559
aromatic molecules in clathrates, Raman and phosphoresc. spectra 79−36647
aromatic molecules in cryst. lattice, phosphoresc. intensity and optical nuclear polarisation, level anticrossing effects 78−91992
aromatic rigid soln. phosphoresc. promotion by I^- 80−50387
aromatic-molecules, conformeric fluoresc. and phosphoresc., rotation of chromophoric fragments around single chemical bonds 77−68068
aromatics in stretched PVA films, ESR of phosphorescent triplet state 77−30908
aza-aromatic molecules, intersystem crossing, quantum interference effects 80−53037
benzaldehyde, and deuterated forms, in p-xylene, 4.2K, $n\pi^*$ phosphoresc. assignments 78−9197
benzaldehyde, and substitution products, spectral props. 79−27007
benzaldehyde, electronic spectra, Cl and F substitution effects 80−23456
benzaldehyde gas, nonradiative electronic transition 80−83413
benzaldehyde in methylcyclohexane, $n^3\pi^*$ spectra 80−63627
benzaldehyde in toluene glass, quasi-line phosphoresc. spectra 77−69883
benzaldehyde-biacetyl system, self-quenching and electronic energy transfer obs. 80−5571
benzaldehydes, in mixed cryst., T_1/T_2 interstate interactions, modulation polaris. phosphoresc. spectra, 4.2K 78−9185
1,2-benzanthracene in polystyrene films, delayed luminesc. decay kinetics 80−43088
benzene, deuterated mixed crysts., phonon assisted trap-trap triplet energy migration, 0K limit, phosphoresc. obs. 77−48218
benzene, in inorganic frozen solns., structured phosphoresc. spectra 77−65504

phosphorescence continued
benzene, isotopic mixed crysts., triplet excitation energy transfer theory 77−28611
benzene, lowest triplet state, pulse radiolysis obs. 79−39168
benzene, mixed deuterated crysts., triplet energy transfer mechanism 77−16365
benzene, phosphoresc., radiative and non-radiative decay routes, spin sublevel origin 77−58064
benzene, photoluminesc. at 5K, N_2 and inert gas matrices 77−6838
benzene($-d_6$), in Ar-Kr matrices, phosphorescence decay, external heavy atom effect 79−10132
benzene in 3-methylpentane glass, phosphoresc. polarisation and intensity, 77K 77−46588
benzene in solid rare gas matrix, effect of surface on phosphorescent state 77−88489
benzene-d_0, -d_6, in glass matrix, phosphoresc. lifetime and polarisation, rot. relax. time meas. 77−79648
benzene-d_0,-d_6, phosphoresc., Boltzmann population and spin-lattice relax., decay processes 78−31230
benzene/benzene-d_6, cryst., X-trap phosphoresc., ODMR, 1.3K, triplet state struct. 77−20902
benzil, cryst., phosphoresc. kinetics rel. to spin-lattice relax. 79−87485
benzil, high temp. ODMR obs. of cryst. phases 79−38407
benzil, in PMMA glass, luminesc. temp. depend. matrix controlled photorotamerism 79−22743
benzil triplet-anisole, reversible exciplex form., phosphorescence, photostationary and transient obs., simulation 78−9182
1,2-benzocoronene, phosphoresc. and ODMR meas. 79−18220
1,12-benzoperylene, phosphoresc. in solid matrix, electronic transition multiplets 77−3413
benzophenone, and d_{10}, ODMR and phosphorescence spectra in organic matrix 79−36671
benzophenone, cryst., phosphoresc. spectra and decay time, temp. depend. 79−87479
benzophenone, migration of triplet excitons, EPR profiles and phosphoresc. decay data 80−84641
benzophenone in toluene glass, quasi-line phosphoresc. spectra 77−69883
benzophenone vapour, fluoresc. and phosphoresc., nonradiative transitions between triplet and singlet state obs. 80−99516
benzophenones, in host crysts., triplet state PMDR, phosphoresc. spectra, transitions mechanisms 77−46585
Benzophenones, substituted solvent independence of radiative rate constant 77−30904
benzophenones, triplet state fine struct. parameters and phosphoresc. spectra 79−50065
$^3(n,\pi^*)$benzophenones in 4,4-dibromodiphenylether, oriented triplet state, LAC and cross relax., phosphoresc. 77−81143
p-benzoquinone, mixed crysts., PMDR and thermal modulation spectroscopy, electron-phonon interaction 77−32297
p-benzoquinone($-d_4$), n-π^* excited states, distant intramol. interaction between identical chromophores 78−90203
2,1,3-benzothiadiazole, EPR of phosphorescent state 77−8405
2-benzoylpyridine, mol. cryst. triplet state selective photoexcitation, phosphoresc. spectra and microwave-optical double reson. 79−15507
2-benzoylpyridine, triplet states, phosphoresc. and ODMR 79−38603
2-benzoylpyridine crystals, optical spectra of lowest triplet state 80−16081
1,2-benzpyrene, butyl bromide solid soln., phosphoresc. line struct. obs., vibr. assignments 77−58075
biacetyl, aq. solns., fluoresc., phosphoresc. 77−3395
biacetyl, IR/UV double resonance, fluoresc. and phosphoresc. obs. 77−6810
biacetyl, multiphoton excitation of triplet state, fluoresc. decay 79−31632
biacetyl, SO_2 photosensitised phosphoresc., triplet energy transfer 78−25608
biacetyl in supersonic jet, emission spectra, energy-resolved decay times 79−81224
biaryls, nonplanar, spin-orbit coupling effects, luminesc. quantum yields *(German)* 77−42349
bilirubin, anomalous solvent shift effect and phosphoresc. 77−30899
biological cells, phosphoresc. microscopy 78−3454
biophysical substances, chemical and structural anal. *(Norwegian)* 78−92596
biphenyl:fluoranthene(pyrene)(chrysene), triplet and singlet transport rate ratio 79−56832
biphenyl, in propylene glycol, mol. fluoresc., effect of mol. conformation 78−78736
biphenyl, luminescence spectrum intensity distribution 79−3476
Born-Oppenheimer and true eigenstate prep. by coherent light, large mol. nonradiative relax. 77−88490
9-bromoanthracene, fluoresc. and phosphoresc. spectra 77−14480
p-bromochlorobenzene, T_1 states, zero-field ODMR, MIDP and phosphorescence excitation spectra 80−74191
carbazole, in presence of KI, decay functions of triplet state of fluoresc. and phosphoresc. 78−66590
carbazolyl substituted diacetylene monomer cryst., ODMR and triplet state kinetics 78−76355
cell surface component rotational diffusion, time-resolved phosphoresc. anisotropy 80−97885
charge-transfer crystals, long lived emission 79−33752
1-chloro-9,10-anthraquinone crystal, electronic structure of lowest triplet state *(Japanese)* 79−8158
chlorobenzaldehyde, $a^3A'' \rightarrow X^1A'$ phosphoresc., conformations and ground state fundamentals 80−78642
p-chlorobenzaldehyde, p-dibromobenzene and p-dimethoxybenzene hosts, dipole moments, lowest electronic states 77−18954
p-chlorobenzaldehyde in methylcyclohexane, matrix perdeuteration effects on $^3\pi\pi^* \rightarrow S_0$ phosphoresc. 77−20903
p-chlorobenzene, and deuterated forms, in p-dibromobenzene and p-dimethoxybenzene, 4.2K, $\pi\pi^*$ phosphoresc. assignments 78−9197
chlorophyll a, phosphoresc., triplet state, photochem. reacts. *(Czech)* 78−78842
chlorophyll a and analogues, triplet state, phosphoresc. polaris. 79−39358
chlorophyll a phosphorescence in cellulose triacetate polymer matrix 77−36867
chlorophyll in leaves and algae cells 79−92142
chlorophyll-like molecules, fluoresc. and phosphoresc. polarisation spectra 79−85980
chlorophylls a and b and pheophytins, fluoresc. and phosphoresc. 80−12057
chlorophylls and pheophytins, phosphorescence and fluorescence polarisation spectra 79−70522
chloroquinolines, photophys. behaviour, substituent and solvent effects 80−106342
chromophore emission spectra, exciting wavelength depend., hydroxylated solvent reorientation 78−76514
chrysene, butyl bromide solid soln., phosphoresc. line struct. obs., vibr. assignments 77−58075
copper porphin, Zeeman expt. on phosphoresc. triplet and quartet states 79−33786
coronene, butyl bromide solid soln., phosphoresc. line struct. obs., vibr. assignments 77−58075
coronene, in ethanol soln., external heavy atom effect on triplet state, phosphorescence meas. 79−18231
coronene, luminesc., spin-orbit coupling perturbation by metal chlorides *(German)* 80−1021
coronene, n-alkane matrix, up to 1.8 kbar emission multiplet struct. shift 77−34677
coronene, solution in bromobutane, Zeeman effect in phosphoresc. at laser $T_1 \leftarrow S_0$ excitation 78−37679
decay, apparatus for study at ambient and liquid N_2 temp. 77−82614
1,4-di(triphenyl lead)diacetylene, phosphoresc. spectra, triplet state 79−47490
1,4-di(triphenyl tin)diacetylene, phosphoresc. spectra, triplet state 79−47490
diacetyl, triplet-singlet conversion, by laser spectrosc. technique 79−86002
diacetyl, vap., laser-excited long-lifetime luminesc. 79−54887
diacetyl vapour, fluoresc. and phosphoresc., nonradiative transitions between triplet and singlet state obs. 80−99516
3,6-diacetylamino-N-methylphthalimide, in alcoholic solns., phosphoresc. decay laws 78−17709
diacetylene, luminesc. and ODMR spectra 79−38604
diamond, natural, thermoluminescence, phosphorescence, defects, low temp. 78−11000
diarylalkane, in isooctane soln. triplet excimer form., phosphoresc., delayed fluoresc., triplet-triplet absorption 78−25597
4,10-diazachrysene, absorpt. spectra and luminesc. in cryst. and glassy matrices, 77K 78−37650
p-diazines, polycyclic, $T_1(\pi\pi^*) \rightarrow S_0$ intersystem crossing, isotope effects, ODMR and phosphoresc. obs. 80−91586
1,2,5,6-dibenzocoronene, phosphoresc. and ODMR meas. 79−18220
dibenzofuran, cryst., phosphoresc. spectra and ODMR meas. 80−11470
dibenzofuran, cryst., prompt and delayed spectra, purity *(German)* 77−28622
dibenzofuran-fluorene, mixed cryst., phosphoresc. spectra and ODMR meas. 80−11470
9,10-dibromoanthracene, fluoresc. and phosphoresc. spectra 77−14480
p-dibromobenzene, cryst. electronic and vibr. energy transfer and relax. 78−31229
p-dibromobenzene, T_1 states, zero-field ODMR, MIDP and phosphorescence excitation spectra 80−74191
4,4′-dibromobenzophenone, ODMR and phosphorescence spectra in organic matrix 79−36671
4,4′-dibromodiphenylether:benzophenone-d_{10}, optical decay constants, photoexcited triplet state near level anticrossing field 78−80250
1,4-dibromonaphthalene:octafluoronaphthalene, absorpt. and phosphoresc. spectra, intermol. reson. 79−33764
1,4- dibromonaphthalene, highly disordered quasi-one-dimens., excitation transport 80−34961
1,4-dibromonaphthalene, k-k scatt., exciton dephasing time-resolved phosphoresc. obs. 80−11458
1,4-dibromonaphthalene, proton spin relaxation by optically excited triplet states 79−19810
1,4-dibromonaphthalene, substitutionally disordered, energy localisation, optical and ODMR spectra of triplet Frenkel excitons 80−54996
p-dichlorobenzene-p-dibromobenzene, solid soln., local struct. and triplet energy migration 78−60489
p-dichlorobenzene-p-dibromobenzene mixed crysts., triplet exciton migration, time resolved emission spectroscopy 80−89052
4,4′-dichlorobenzophenone, cryst., X-traps, rel. populations, elec. field effect 77−12414
4,4′-dichlorobenzophenone single crysts., mutual annihilation of triplet excitons, 1.5 and 4.2K, phosphoresc. obs. 80−80850
9,10-dichlorophenanthrene, intramol. heavy atom effect, PMDR obs. 79−13745
2,3-dichloroquinoxaline, in tetramethylbenzene cryst., sublevel phosphoresc. spectra 78−70863
1,1′-diethyl-2,2′-cyanine iodide, neat and mixed crysts., visible absorption and emission spectra assignments 77−1692
diethynylbenzene, radiative and nonradiative processes, triple bond effects 79−3481
difluoromethane, triplet state emission spectra, phosphoresc. and energy transfer 78−53196
dimethylbenzaldehydes in durene matrix, phosphoresc., $^3n\pi^*$ and $^3\pi\pi^*$ states vibronic coupling 79−22746
2,6,dimethylpyrazine, PMMA soln., fluoresc. and phosphoresc. quantum yield and lifetime, 20-120 kbar 79−54902
dinaphtho-(2′.3′:1.2);(2″3″:6.7)-pyrene, triplet state, phosphoresc. and ODMR obs. 79−27013
α,α-dinaphthylalkanes, absorpt. spectra and phosphoresc. in soln., triplet excimers 78−62816
dinucleoside phosphates, polaris. spectra, excimer phosphoresc. and fluoresc. 79−34497
diphenyl:(benzophenone, naphthalene), triplet exciton diffusion, phosphoresc. obs. 78−10964
diphenyl:naphthalene, benzophenone, phosphoresc., triplet diffusion excitons 78−63985
diphenylene, n-paraffin soln., quasiline sensitised phosphoresc. spectra at 4.2K 77−68071
diphenylene sulphide, phosphoresc. vibronic struct., solvent heavy at. effect 78−17710
2,5-diphenyloxazole, phosphoresc., 77K, solvent effect 78−42118
DMSO:Cr^{3+}, Nd^{3+}, energy transfer and migration, donor-acceptor interaction, phosphoresc. quenching conc. depend. 78−64403
DNA, luminescence, excitation wavelength depend. in UV/VUV region 78−31768

phosphorescence continued
durene:fluoranthene(pyrene)(chrysene), triplet and singlet transport rate ratio 79−56832
dyes in rigid matrices, solvent reorientation relax. effect on luminesc. 79−43009
ethylbenzocarbazole, soln., luminesc., effect of electronic excitation energy vibr. 80−55174
N-ethylphthalimide+olefins, photochemical reaction, absorpt., fluoresc., phosphoresc. and triplet-triplet absorpt. spectra 80−85197
ethynylbenzene, radiative and nonradiative processes, triple bond effects 79−3481
flavins, phosphoresc. props., solvent effects 77−12885
fluid film lubrication, velocity profile meas., using ZnS phosphorescent tracer method 78−94866
fluorene:pyrene-d_{10}, exciton-guest, triplet-triplet annihilation, impurity traps effects 80−25433
fluorene, cryst., phosphoresc. spectra and ODMR meas. 80−11470
fluorene, in ethanol soln., external heavy atom effect on triplet state, phosphorescence meas. 79−18231
fluorene, n-paraffin soln., quasiline sensitised phosphoresc. spectra at 4.2K 77−68071
gelatin in nuclear photoemulsion, effect of pulsed elec. field on physical and mech. props. *(Russian)* 78−869
gelatin layers with and without $AgNO_3$, phosphorescence kinetics curves *(Russian)* 80−62776
glyoxal, gas phase emission spectra, mag. quenching 77−18968
glyoxal, intersystem crossing in weak mag. field 78−78743
glyoxal, singlet-triplet coupling, double reson. and level-anticrossing spectroscopy 80−48053
guest/host mixed crystal systems, thermally activated intermolecular effect of deuteration on guest phosphoresc. 79−43010
haloacenaphthenes in n-heptane, quasi-line phosphoresc. spectra, vibronic spin-orbit interaction 80−43096
1-halonaphthalenes, lowest triplet state, spin sublevels decay, internal heavy atom effects 79−95819
α-heptacyclene, in solid matrix, photodissoc. quantum yields, fluoresc. temp. depend., phosphoresc. IR spectra 77−25292
α-(β-)heptacyclene, vibronic spectra, electronic-vibr. interactions 78−1021
heteroaromatic molecules, planar, orientation and phosphoresc. polarisation in stretched film 80−14169
hexahydrohexahelicene, in Shpolskii matrix, absorpt., fluoresc., phosphoresc. spectra 79−76463
hexamethylbenzene charge-transfer complexes, heavy atom effect on radiative and radiationless transitions 78−25607
hexamethylolmelamine, doped, and condensation resin, room temp. phosphoresc., thermal transforms. 80−45132
hexamethylolmelamine, doped, phosphoresc., crystallinity, cross-linking and H-bonding effects 79−73984
hydroxypyridines, phosphoresc. emission, polarisation and lifetimes 78−31232
2-indanone, single cryst., ODMR and phosphoresc. of $^3n\pi^*$ state 79−78570
indeno[2,1-a]indene, in glassy media, phosphoresc., heavy atom effects 80−55153
indole, aq. alkaline soln., charge transfer, luminesc. obs., 77 and 300K 79−69876
indole, in PMMA matrix, high press. luminesc. 78−84629
inert gas crystal, benzene-doped, luminescence excitation investig. 77−77276
intermolecular triplet excitation transfer in diffusive limit 80−28046
1-iodonaphthalene-perfluorated naphthalene solid soln., sensitised phosphoresc., site selection method, Dexter's theory 79−4836
2-isopropoxyphenyl-N-methyl carbamate, fluoresc. and phospheresc. in solns. 79−61426
isoquinoline, fluoresc., phosphoresc. and H bonding 77−79647
ketones, mol. cryst., interband transitions, triplet-triplet absorptions 79−11452
ketones, triplet-triplet absorption carbonyl group role 77−83641
lanthanide porphyrin complexes, intramol. energy migration, mol. luminesc. 77−3412
leucosapphire, phosphorescence, decay obs., impurity effects *(Russian)* 79−15530
luminescence spectrometry, pulsed and continuous wave excitation sources, signal-noise ratios 77−71381
mesitylene, luminesc. excitation spectra in rare gas matrices 78−66575
metalloporphyrin triplet state quenching by Fe II- and Fe III-porphyrins 78−76992
8-methoxypsoralen detection in ocular lens, rel. to psoriasis treatment with photosensitising agent 78−15937
12-methoxypyridine, phosphoresc. emission, polarisation and lifetimes 78−31232
p-methylbenzaldehyde, p-dimethoxybenzene host, dipole moments, lowest electronic states 77−18954
5-methylindole, in PMMA matrix, high press. luminesc. 78−84629
3-methylpentane, γ-irradiated, isothermal luminescence in presence of aromatic solutes at 77K 78−76519
molecular $\pi\pi^*$ and $n\pi^*$ states, rel. positions, single-triplet conversion probability, low temp. 79−816
molecular crystal, coherent 1-dimens. exciton transport and impurity scatt. 78−14666
molecular crystals, spectroscopy, bibliography for 1976 78−72585
molecular crystals, thermal modulation spectroscopy, electron-phonon interaction 77−32392
molecular crystals, triply-excited impurity centres, effect of acoustic wave on phosphorescence 78−27115
molecular nonsteady-state luminesc. behaviour under narrowband laser excitation 80−87159
molecular solid, disordered, exciton migration, dynamical approach 79−65916
molecular solids, substitutionally disordered, Anderson localisation of mol. excitons 77−89733
molecule, complex, Zeeman effect in phosphoresc. at laser T_1←S_0 excitation 78−37679
1,2-naphthacoronene, phosphoresc. and ODMR meas. 79−18220
naphthalene:β-methylnaphthalene, impurity phosphoresc. centres *(Russian)* 77−81151
naphthalene: quinoxaline, anisotropic spin lattice relax. of triplet mols. in high mag. field 77−81141
naphthalene: quinoxaline, isolated triplet mol. direct spin-lattice relax., librational model 79−11444

phosphorescence continued
naphthalene:quinoxaline, spin-lattice relax. of triplet states of high mag. fields 79−19933
naphthalene, chemisorbed on Al_2O_3, radiative and nonradiative processes 79−36686
naphthalene, fluoresc. and phosphoresc., singlet/triplet excimers conform. difference 77−14469
naphthalene, isotopic mixed cryst., phospheresc., photoselection of pure initial triplet states 78−35189
naphthalene, long range exciton percolation, superexchange, energy denominator 77−28609
naphthalene, phosphorescence spectra in rare gas matrices, multiplet struct. and pot. energy functions 80−106341
naphthalene, triplet excimer conformation, σ-π interaction transitions 77−6701
naphthalene, triplet exciton annihilation at high triplet densities 79−37996
naphthalene, triplet excitons, phosphoresc. and delayed fluoresc. excitation spectra 78−63986
naphthalene in Ar matrix, geometry changes and multiplet struct., mol. fluoresc. and phosphoresc. obs. 80−95663
naphthalene in durene matrix, spin-lattice relax. of phosphoresc. triplet state, PMDR study 79−27012
naphthalene mixed crystal, Nh_8/Nd_8, phosphoresc., energy transfer model 79−38600
naphthalene mixed crystal, time resolved excitation migration, triplet and singlet critical concs. 79−78010
naphthalene-betamethylnaphthalene, mixed cryst. ($C_{10}H_8$/$C_{10}D_8$), luminesc., test of excitation transport model 79−65914
naphthalene-h_8, and -d_8 mixed crystals, phosphoresc. excitation spectra of clusters 78−43914
naphthalene-h_8 and -d_8 mixed crystal, two-dimens. lattice, cluster-cluster interactions, model inhomogeneous distribs. 79−23922
naphthalene-O_2 in polystyrene fluff, oxciplex emission 77−23515
naphthalene-TCPA charge transfer triplet states, electron-phonon coupling 79−38601
naphthalene-tetrachlorophthalic anhydride charge-transfer cryst., electronic states 77−32415
2-naphthalensulphonate, fluoresc. and phosphoresc., external heavy atom effect 78−29812
napthhalene-benzophenone mixed crysts., phosphoresc., emitting centres 79−61427
nicotinamide co-enzymes, reduced, phosphorescence obs. at −196°C 79−79471
α-NPO in polystyrene, 77K phosphorescence *(Russian)* 78−27286
octaethylchlorin, metal complexes, polaris. fluoresc. and phosphoresc. spectra 79−54906
octaethylchlorin, phosphoresc. polarisation spectra obs. 77−18963
octaethylisobacteriochlorin metal complexes, polaris. fluoresc. and phosphoresc. spectra 79−54906
octaethylporphin, phosphoresc. polarisation spectra obs. 77−18963
octaethylporphin, radiationless transitions, fluoresc. and phosphoresc., isotope effects 77−65502
octafluoronaphthalene crystalline complexes with naphthalene and durene, triplet exciton emissions 80−84760
open photoreceiver, vacuum ultraviolet 80−52307
organic compound, vap., laser-excited long-lifetime luminesc. 79−54887
organic crystals, kinetic model of triplet exciton dynamics 78−67948
organic donor-acceptor solns., triplet-triplet energy transfer under Shpolskii effect conditions 79−64031
organic molecular crystals, intermolecular interactions, spectroscopic studies, review 80−103958
organic molecular crystals, optical spin alignment, phosphoresc. *(Russian)* 78−84652
organic molecular crystals, phosphoresc., optical spin alignment 79−95827
organic molecules in Shpolskii matrices, phosphoresc. site selection spectrosc., ODMR 79−36687
α-oxalic acid dihydrate, low-lying excited states, ODMR and optical obs. 79−41188
palladium porphin, Zeeman expt. on phosphoresc. triplet and quartet states 79−33786
palladium-octaethylporphyrin, gas phase delayed fluoresc. and phosphoresc., triplet excimer formation 80−18884
[2.2]paracyclophane, delayed luminesc. in cryst. and rigid glass solns. 79−15510
2,2 paracyclophane, dimer vibration influence on emission spectrum 80−69133
[2.2]phanes in glass matrices, transanular π-electron interaction, emission spectra 79−36682
phase resolved phosphorimetry, analytical possibilities 77−90663
phenanthrene, chemisorbed on Al_2O_3, radiative and nonradiative processes 79−36686
phenanthrenequinone, in n-paraffin matrix, electronic-vibr. interaction in phosphoresc. 79−27027
phenanthrolines, in Shpolskii matrices, phosphoresc. spectra 78−94276
phenylacetylene, phosphorescence polarisation, intramolecular heavy atom effect 78−52550
phosphorimetric instrument, automated, for room temp. phosphorimetry with continuous filter paper device 77−90654
phosphorimetry, low-temp., conduction cooling system for sample introduction 80−87158
phthalazine, fluoresc. and phosphoresc., expt. and CNDO/S CI calcs. 79−31585
phthalic anhydride and halogen derivatives, phosphorescence spectra *(Japanese)* 78−48217
phthalimide, soln., triplet state accumulation and deactivation depend. on solvent polarity 79−85982
phthalimide acetyl derivatives in polar solvents, luminesc. kinetics and phosphoresc. quenching 80−18885
platinum phthalocyanine single cryst., triplet state Zeeman effect, phosphoresc. 78−6747
PMA, phosphorescence depolarisation, segmental relax. time 78−95606
PMMA, phosphorescence depolarisation, segmental relax. time 78−95606
poly(N-vinylcarbazole) film, fluoresc. and phosphoresc., energy transfer mechanism 80−16112
poly-N-vinylbenzocarbazole, soln., luminesc., effect of electronic excitation energy vibr. 80−55174
poly-N-vinylcarbazole-biacetyl, triplet exciton quenching, exciton trapping model 80−66267

phosphorescence continued
polyatomic mols., quantum beats 80−37826
polymer solution, rigid, exciton transport 79−69431
polymethyl acrylate, phosphorescence depolarisation studies of relaxation effects 78−56685
polynitramines, solid cyclic, luminesc. meas. 77−32424
polynucleotides, polaris. spectra, excimer phosphoresc. and fluoresc. 79−34497
polypeptide hormones, conformations, ODMR investig. 78−76356
polypeptide hormones, folding, ODMR and phosphoresc. 79−20518
polyvinylbenzocarbazole, weak solution, intramolecular energy transfer by singlet and triplet excitons 80−34971
polyvinylcarbazole, weak solutions, intramolecular energy transfer by singlet and triplet excitons 80−34971
porphin ($-d_2,d_4,d_6,d_8,d_{10},d_{12},d_{14}$), nonradiative transition probabilities, deuteration effects 79−3485
porphinatocopper(II), phosphoresc., appl. to porphyrin 78−11574
porphins orientation in n-alkane Shpolskii hosts, spectra 80−48035
porphyrins, solid solns., phosphoresc. rel. to solvent heavy ats. *(Russian)* 77−40286
proteins, triplet state energy transfer 78−20143
proteins, UV irradiated, luminesc. quenching, EPR and absorpt. spectra 78−15768
pyrazine, electronic energy transfer to metal surface, classical image dipole theory 80−97318
pyrazine, excited and N_{1s} ionised states, ab initio calcs. broken orbital symm. 80−27931
pyrazine, lowest triplet state, phosphoresc., intersystem crossing 78−5269
pyrazine, mol., radiative lifetime of phosphoresc. state, influence of high lying triplet states 79−86006
pyrazine, on Ag surface, time-resolved molecular electronic energy transfer 80−92957
pyrazine, PMMA soln., fluoresc. and phosphoresc. quantum yield and lifetime, 20-120 kbar 79−54902
pyrazine, vibronic bands, MIDP and polarised phosphoresc. in benzene matrix 77−6833
pyrene, triplet state, excitonic energy transfer, phosphoresc. and delayed fluoresc., 2 to 300K 80−84776
pyrene-PMDA complex, electron-phonon interaction, phosphoresc. 78−48208
[2.2](2,7)pyrenophane, emission spectra, transannular interaction 77−489
pyridinium($-d_5$) ion, triplet state obs. by ODMR, rel. to CNDO/2 STO calcs. 77−18951
pyrimidine, vapour, phosphoresc. 80−83408
pyrimidine derivatives, absorpt., luminesc. and polarisation spectra, electronic struct. 79−85993
pyrimidine in cyclohexane at 77K, absorption and phosphorescence spectra 78−61138
quantum beats, in phosphorescence 80−63704
quinazoline, in n-pentane (isooctane) Shpolskii matrices, luminesc. props., vibr. struct. 79−22739
quinoline, fluoresc., phosphoresc. and H bonding 77−79647
quinoline, in binary solvents, luminesc. props. 80−7409
quinoline complexes with proton donors in triplet state, phosphorescence spectra 77−48230
quinoxaline$^+$, (singly protonated), struct. and kinetics of fluoresc. and phosphoresc. states 77−30906
quinoxaline, in naphthalene-d_8, sublevel phosphorescence spectra, radiative mechanisms 77−75203
quinoxaline, in p-dibromobenzene, triplet state NQR, nucl. spin polarisation effects 79−18208
quinoxaline in Shpolskii-type hydrocarbon matrices, vib. struct. of electronic spectra 77−85773
recombination after glow build-up 77−8628
rhodamine, soln., triplet state accumulation and deactivation depend. on solvent polarity 79−85982
rhodamine 6G soln., delayed annihilation fluoresc., external heavy at. effect 79−99931
rhodamine dyes, phosphoresc. quantum yields determs. 79−8179
rhodophorphyrin XV metal complexes, phosphoresc. polarisation 77−23517
ribonuclease T_1 in soln., phosphoresc. at 293K *(Japanese)* 77−44595
ruby, phosphorescence, decay obs., impurity effects *(Russian)* 79−15530
ruby, Raman ^2E and phosphorescence transitions, line widths, time correl. study 80−20621
sapphire, phosphorescence, decay obs., impurity effects *(Russian)* 79−15530
Shpolskii system, 77K, sensitised phosphoresc. spectra 79−815
Shpolskii systems, sensitised phosphoresc., triplet-triplet energy transfer *(Russian)* 78−76527
sodium 4-biphenylcarboxylate, room temp. phosphoresc., student demonstration 77−29
sodium naphthalate, room temp. phosphoresc., student demonstration 77−29
solid, molecular fluoresc., phosphoresc., and ODMR line narrowing 80−43084
spectral line narrowing of triplet state, in laser excited experiments 80−63703
spin-lattice relax. in triplet state of PO_2^- centres, pulsed photoexcitation 79−95644
steady-state molecular luminescence radiance assuming narrowband excitation 79−13747
trans-stilbene, in glassy media, phosphoresc., heavy atom effects 80−55153
trans-stilbenes, triplet energy, substituents effect, singlet-triplet absorpt. and electrochemilum. obs. 79−81225
student experiments using adsorbed dyes 77−26114
substitutionally disordered, energy localisation, optical and ODMR spectra of triplet Frenkel excitons 80−54996
p-terphenyl, cryst., exciton phosphoresc. at 300K 80−108277
tetraalkylammonium tetrahalometalates, opt. lifetimes rel. to thermal transitions 77−28608
tetrabutylammonium tetrahalomanganate, phosphoresc. lifetimes in fused salts and solids 78−72573
1,2,4,5-tetrachlorobenzene, exciton migration and trapping, X-trap phosphoresc. 79−1780
tetrachlorobenzene, in durene, 1.6K, $S_1 \sim\!\!\rightarrow T_1$ relax. mechanism, Zeeman phosphoresc. and PMDR obs. 77−30912
phosphorescence continued
1,2,4,5-tetrachlorobenzene, in durene host, phosphoresc., cross-relax. between spin levels 78−9186
1,2,4,5-tetrachlorobenzene, mol. cryst., coherent 1-dimens. exciton transport and impurity scatt. 78−14666
1,2,4,5-tetrachlorobenzene, mol. solid, heat pulses, phonon-induced delocalisation of trapped excited triplet states 80−89053
1,2,4,5-tetrachlorobenzene, proton spin relaxation by optically excited triplet states 79−19810
tetrachlorobenzene, pure and doped crysts., triplet exciton trapping, phosphoresc. spectra 77−85766
1,2,4,5-tetrachlorobenzene, triplet energy transfer in substitutionally disordered system 79−52000
1,2,4,5 tetrachlorobenzene, triplet excitons, high. mag. field, spin-lattice relax. study 80−20517
1,2,4,5-tetrachlorobenzene, triplet state spin-lattice relax. in cryst. and matrix isolated mol. 79−11449
1,2,3,4-tetrachloronaphthalene, intramol. heavy atom effect, PMDR obs. 79−13745
tetramethyl pyrazine in durene, phosphorescent mols., quantum beats in triplet states 80−58312
tetramethylpyrazine, PMMA soln., fluoresc. and phosphoresc. quantum yield and lifetime, 20-120 kbar 79−54902
tetramethylpyrazine-d_{12}, photoexcited triplet state, in durene, phosphoresc., spin coherence and quantum beats 78−76517
tetramethylpyrazine-d_{12}, photoexcited triplet state, phosphoresc., quantum beats 77−71827
thin layer chromatography, luminesc. meas. methods 78−53305
thin layer chromatography, luminescence quantitation, solvent effects 78−53306
thin-layer phosphorimetry, solvent enhancement effects 78−61082
thionine in sodium lauryl sulphate micellar solns., absorpt. spectra and fluoresc. yield, local dye conc. depend. 80−106343
thiophosgene, laser induced phosphoresc., triplet system 77−61783
thymine film, polycryst., energy conversion processes, quantum yields, 4 to 10 eV 80−88589
time resolved phosphorimetry, phosphoroscope, analogue switch type 78−45725
toluene, luminesc. excitation spectra in rare gas matrices 78−66575
toluidinonaphthalenesulphonate, room temp. phosphoresc., isomer effects 79−61429
tricycloquinazoline, excited states, fluoresc., phosphoresc. 77−61789
1,1,1-trifluoroacetone, photochem. and photophysics, 330-250 nm, 0-1000 torr 78−17706
2,4,5-trimethylbenzaldehyde, durene host, dipole moments in lowest electronic states 77−18954
2,4,5-trimethylbenzaldehyde, in durene, cryst., photochem. and photophys. processes 77−60092
triphenylene, in PMMA matrix, two-photon phosphoresc. spectra 77−42366
triphenylene, triplet state, MIDP and T-S excitation spectrosc. 79−81233
triphenylene-d_{12}, in ethanol soln., external heavy atom effect on triplet state, phosphorescence meas. 79−18231
tryptophan, aq. alkaline soln., charge transfer, luminesc. obs., 77 and 300K 79−69876
tryptophan, aq. soln. charge transfer, luminesc. obs., 77 and 300K 79−69875
tryptophan residue in horse liver alcohol dehydrogenase, room-temp. phosphoresc., temp. and enzymic complex form. effects 80−61512
wheat germ agglutinin, struct. of binding sites, ligands with heavy atoms, phosphoresc. changes 79−24947
xanthene dyes, internal heavy atom effect on radiative and non-radiative rate consts. 80−32765
xanthene dyes, phosphoresc. spectra of T_1 state in ethyl alcohol soln. 79−85981
xanthene dyes, phosphorescence and orbital nature of triplet state *(Russian)* 77−85797
xanthione, large zero-field splitting of lowest triplet state 80−58171
xanthione, solns., triplet state quenching by ground state xanthione 78−42180
xanthone, in n-pentane, heat pulse induced delayed phosphorescence 80−83404
xanthone in host crysts., triplet state PMDR, phosphoresc. spectra, transition mechanisms 77−46585
xanthone in n-hexane, 77 and 4.2K, phosphoresc. spectra, triplet lifetime 78−21957
p-xylene, isotopically mixed cryst., phosphoresc. triplet state, ESR and MIDP obs. 77−58071
zinc octaethylporphin, radiationless transitions, fluoresc. and phosphoresc., isotope effects 77−65502
Ag(II) protoporphyrin IX dimethyl ester, fluoresc. relax. after picosec. excitation 79−45751
β-Al_2O_3:Mn(Co)(Ni), absorpt. and emission spectra, mag. susceptibility 79−87471
β-Al_2O_3-Na_2O:Cr, absorpt. and emission spectra, mag. susceptibility 79−15495
$BaCl_2$, Sn-activated, luminescence studies 80−108246
BaS:Bi phosphors, polycrystalline, effect of grain size on thermolum., phosphorescence obs. 79−61446
BaS:Cu, thermoluminesc. and decay 78−80426
CS, nonexponential decay of $a^3\Pi$-$X^1\Sigma^+$ luminesc., Π sublevel radiative lifetimes, matrix isolated spin-orbit 79−89699
$CaCO_3$, calcite, tunnelling afterglows and retrapping 77−69902
$CaCO_3$, calcite, X-ray irrad., luminesc. and dielec. loss decays 77−12431
CaF_2:Dy(Ho)(Pr)(Tb), V_k-centre recomb. kinetics, phosphoresc. 77−55817
CaO, photoionisation of F-centre, luminesc. and photocond. meas. 80−66270
CaO:Ce,Gd phosphors, trap distrib., phosphoresc. decay characts. obs. 80−29773
CaO:Eu(Tb), phosphor, isothermal decay 80−55156
CaS-Bi, Mn, phosphors, thermoluminesc., phosphoresc. 78−2928
$CaSO_4$:Dy photostimulated luminesc. for radiation dosimetry 77−90910
$CaSO_4$:Sm phosphors, X-ray induced fluorescence and phosphorescence 80−55179
$CaWO_4$, phosphors, energy storage, afterglow decay and thermolum. meas. 77−12422
Cd complex, Cd (II) halide with 8-aminoquinoline, cryst. 77−52152
Cr complex, organic mol. singlet excited state energy transfer to complex quartet levels 77−25291

phosphorescence continued
Cr complex $[Cr(NCS)_{6-n}(DMSO)_n]^{n-3}$, spectra and decay times 78−10970
Cr III complexes phosphoresc. risetime meas. in near IR by photon counting 77−41706
CsBr:Tl, emission bands, press. effect 79−33789
CsI crystals, in scintillation counters, nonstatistical counting rates due to phosphoresc. 78−95597
CsI:Tl, emission bands, press. effect 79−33789
Cu-etioporphyrin I, phosphoresc. polaris. of monomers and dimers 77−34685
Cu(II) protoporphyrin IX dimethyl ester, fluoresc. relax. after picosec. excitation 79−45751
1,6-di-(N-carbazolyl)-2,4 hexadiin, cryst. struct., luminesc., γ-ray polymerisation 78−18629
1,3-diphenylpropane, in isooctane soln., monomer phosphoresc., low binding energy triplet excimer not obs. 78−25597
p-fluorobenzaldehyde, vap., high-resolution electronic emission spectrum assignments 78−78742
KBr:Eu(Yb), electron-irrad., photostimulated luminesc., ionic processes 78−52561
KBr:P, colour centre fine struct., ODMR 78−6604
KBr:PO_2^-, phosphorescence, triplet state sublevels, mixing 80−25446
KCl:Eu^{2+} crystals, photostimulated afterglow investigation at room temp. 80−108259
KCl:P, colour centre fine struct., ODMR 78−6604
KCl:PO_2^-, phosphoresc. and PMDR spectra, electronic and vibr. states 79−65768
KCl:PO_2^-, photo-orientation, spectrosc. and ODMR obs. 80−29772
KCl(Br), triplet state lifetime of F_2 centre, mag. field effect 78−35177
KI:Eu, electron-irrad., photostimulated luminesc., ionic processes 78−52561
KI:$Eu^{2+}(Sr^{2+})(Mn^{2+})$, elec. field effect on mech. of recomb. 78−80397
KI:Tl, emission bands, press. effect 79−33789
$K_2NaAlF_6:Cr^{3+}$, ^2E_g-$^4A_{2g}$ phosphoresc. spectrum, vibr. struct. 79−47494
La_2O_2S:Eu, slow phosphoresc., high press. study 80−80839
LiD, luminesc. of free and localised excitons, UV, X-ray and electron irrad. luminesc. 79−87483
LiH, luminesc. of free and localised excitons, UV, X-ray and electron irrad. luminesc. 79−87483
LiH:LiF, luminesc. of free and localised excitons, UV, X-ray and electron irrad. luminesc. 79−87483
Lu porphyrin complexes, luminesc. 77−18958
Mg porphyrins, additional ligands deuteration effect on luminesc. charact. 79−99932
$MgAl_2O_4$, γ-irradiated crystal, TSC, thermoelec. power, thermolum. and afterglow 80−75583
MgF_2 long-persistence cathode-ray screen, phosphoresc. decay into second-order components 77−20907
Mg_2SiO_4:Tb, TLD material, UV induced thermolum. and phosphoresc. 78−92707
Mn complex, $[Mn(urea)_6](UO_4)_2$, thermal expansion coeff., crystal field parameters, phosphoresc., absorv., excitation spectra 78−43932
Mn complex, $MnCl_2$ with 3,5-lutidine hydrochloride, cryst. 77−52153
$(NH_4)_2Cd_2(SO_4)_3:Mn^{2+}$, UO_2^{2+}, luminesc., vibr. modes 79−38629
NH_4Cl:Tl, phosphoresc. decay rates obs., pretreatment effects 79−4853
Na_2O-SiO_2 glasses, elementary electronic excitations, refl., luminesc., and photoemission meas. 80−84778
P_2-PO, exciplex, chemiluminesc., reduced press. system 77−32795
P_4, vap., oxidation, chemiluminesc., reduced press. system 77−32795
$P_4+H_2O(D_2O)$, vapour, chemiluminesc., transient emitting species 77−1926
$(PO_2)_2$*, excimer, chemiluminesc., reduced press. system 77−32795
RbCl:Eu, electron-irrad., photostimulated luminesc., ionic processes 78−52561
RbI:Tl, emission bands, press. effect 79−33789
$ReCl_6^{2-}$ doped in various host lattices, luminesc. spectra and vibr. struct. 79−43024
rhodamine 6Zh, quantum efficiency of intercombination conversion to triplet state by sensitised phosphoresc. *(Russian)* 77−85798
SO_2 ($^3B_1$), phosphorescent lifetimes, press. saturation effect on quenching by CO_2, CO, N_2 78−1017
SO_2, direct meas. of $^3B_1$ state lifetime in air at atm. press. 77−79653
SO_2, in Xe, Kr, Ar, N_2 matrices, environmental perturbation effects *(French)* 77−3407
SO_2, laser-induced phosphoresc.-excitation spectra of vibr. bands of ($^3B_1$)-($X,^1A_1$) transition 80−18879
SO_2, UV absorpt. spectrum, triplet states, phosphoresc. lifetime 79−50042
$SO_2(^3B_1)$, isolated mol., phosphoresc. decay efficiency 77−75194
$SrCl_2:K^+(Na^+)(Rb^+)$ X-irradiated, recomb. luminesc. between trapped electron and self trapped holes 77−73162
SrF_2:Dy(Ho)(Pr)(Tb), V_k-centre recomb. kinetics, phosphoresc. 77−55817
SrS:Hf^{4+} phosphors, phosphorsc. decay curve 77−63450
SrS:Nd, phosphoresc decay, trapping levels 80−104003
Th porphyrin complexes, luminescence 77−18958
VO-etioporphyrin I, phosphoresc. polaris. of monomers and dimers 77−34685
Y porphyrin complexes, luminesc. 77−18958
Zn complexes, pheophytins a and b, dual phosphorescence molecular splitting 79−89706
Zn-porphin($-d_4,d_8,d_{12}$), nonradiative transition probabilities, deuteration effects 79−3485
$Zn_4B_6O_{13}:Tb^{3+}$, fluoresc. and thermophosphoresc. spectra *(Spanish)* 77−90188
$Zn_4O(BO_2)_6$:Tb, phosphoresc. study *(Spanish)* 80−16105
ZnS:Ag, cryst. struct., electron traps and glow curves 79−61437
ZnS:Cu, polycryst. phosphor, excitation storage, recombination barrier participation 78−27316
ZnS:Cu,Pt phosphors, photoluminesc., thermoluminesc. 78−43915
ZnS:Tb, Cu(Ag) phosphors, luminesc. props. 80−100690
ZnS-CdS:Ag(Cu), cryst. struct., electron traps and glow curves 79−61437
Zn_2SiO_4:Mn, phosphoresc. decay into second-order components 77−20907

phosphorescence microwave double resonance *see PMDR*

phosphorescence microwave photoexcitation spectroscopy *see PMDR*

phosphors
see also fluorescent screens; luminescence
adsorbate phosphor-silica gel substrate, oxygen quenching anomaly of afterglow 77−77275
alkali earth halides, solid soln. spectroscopy, investigs. by F. Klement *(Russian)* 80−8767
alkali halide:Eu^{2+} phosphor, explosive loading method form., spectra, luminesc. charact. *(Russian)* 78−35212
alkali halide:Tl^+-like ions, triplet state lifetime, hyperfine interaction 80−2844
alkali halide, Ag-doped, luminesc. rel. to formation of complex compounds *(Russian)* 80−11454
alkali halide phosphors, Pb^{2+} (Sm^{2+}) doped, luminesc. props., press. effects to 140 kbar 77−40278
alkali halide phosphors, Tl^+ doped, uniaxial stress effects 78−48202
alkali halide phosphors, Tl doped, press. effect on emission spectra at low temps. 77−85771
alkali halides, solid soln. spectroscopy, investigs. by F. Klement *(Russian)* 80−8767
alkali metal complex vanadates, $M^+_3M^{3+}(VO_4)_2$, $M^+_2M^{4+}(VO_4)_2$, M^{3+}=Sc, La, B, Al, Ga, In, M^{4+}=Ti, Zr, Sn, phosphors 77−48217
alkaline earth oxide:Cu phosphors, electroluminesc. 77−32440
alkaline earth oxides, photon multiplication and secondary electron-hole pairs generation *(Russian)* 80−66262
alkaline earth tetraborates, doped, radiothermoluminesc. detectors, dosimetric charcts. 77−61665
alkyl ammonium halide:Tl phosphors, exciton absorpt. spectra 79−28782
aluminate:Ce^{3+}, hexagonal, luminesc. rel. to host lattice structure 78−6776
aluminate phosphors, energy transfer models 79−43019
aluminates:Ce^{3+}, luminesc. exam. 78−56513
aluminates:Mn, Eu, red Mn^{2+}-luminesc. 79−61420
anthracene:2-chloroanthracene, electrolum., voltage- and freq.-brightness charcts., dopant conc. depend. 78−2916
anthracene:9-vinylanthracene, electroluminesc. at room temp. 79−15532
astronomical image-tube systems, effects of phosphor decay on time-modulated meas. 79−88602
carbon tetrachloride-$GaCl_3$-Nd^{3+} nontoxic liquid phosphor system, synthesis 80−55157
cathodluminescence measurement techniques 78−41354
cathodochromic-luminescent sodalite powders, prep. and props. 77−20925
cathodoluminescence phosphor efficiencies, rel. to other material props. 77−81158
cathodoluminophor, nature of ageing 78−10994
2-chloroanthracene:acridine, electrolum. at 300K 79−15531
CRT phosphor types, contrast sensitivity of human eye 79−11933
CRTs appl., observer perception improvements 78−24076
EL-570 M type, electroluminesc. excitation by SAW, nonlinear effects 80−16104
electroceramics, thermoluminescent and dosimetric charcts. 79−8196
Electrochemical Society Meeting, Boston, USA, (May, 1979) 79−91959
electroluminescence intensity of EL-455s commercial phosphor, temp. depend. 80−45146
emission and absorption charcts. for fluorescent lamps *(Japanese)* 80−89067
ethyl substituted ammonium halides, exciton absorpt. spectra 79−28782
film, electrolum. device appl., book contrib. 77−73176
fluorescent lamp phosphors with aluminate host lattices, behaviour 79−11453
fluoride, Mn^{4+} activated, configurational co-ordinate model, predictive use 79−19918
halophosphate, radiation stability, recombination processes effect *(Russian)* 80−7424
II-VI semiconductors, ODMR, defect excited states 78−80254
image intensifiers, phosphor decay and bandwidth meas. 79−37045
light sources, ^{147}Pm sealed sources *(Hungarian)* 80−91348
mammographic X-ray screen sensitivity and resolution 78−7449
model system, thermal quenching, QMSCC calcs. 79−78731
near IR laser beam profile recording using phosphor convertor camera 79−81468
neutron dosimetry, appl. of thermoluminescent materials 79−22497
night vision equipment matching to human observer 77−40937
organic, surface impregnation of Al_2O_3 anodised film, fluoresc. spectrum *(Japanese)* 80−55170
oxide:U^{6+}, struct. sensitivity of luminesc. 77−90187
phosphorescence decay and thermoluminescence, apparatus for study at ambient and liquid N_2 temp. 77−82614
physical chemistry, optimum conditions for producing and examining phosphors 78−10940
polyethersulphone, thin film TLD, skin dosimetry appl. 80−52790
powdered, in host material, solar cells wavelength shifting 80−85286
quantum efficiency meas. for UV, visible, cathode ray and X-ray 77−41699
radiative and nonradiative recomb. at metal ions, core struct. effects, review 79−4834
radiographic intensifying screens, sensitivity to scattered radiation 77−77970
radiographic screen-film system comparisons, fluoresc. X-ray source 78−24132
radioluminescent emitter, continuous action, time and temp. instability 77−10993
rare earth activated, cathodolum., use of internal reference 77−44071
rare earth activated phosphors, chemistry and physics, book contrib. 80−55187
rare earth activated phosphors, for low press. fluoresc. lamps, luminesc. charcts. 78−10960
rare earth compound:$Ho^{3+}(Er^{3+})$ phosphors, active layer effective thickness calc. *(Russian)* 79−43039
rare earth double orthophosphates with alkali metals, conc. depend. of luminesc. props. 80−100673
rare earth double orthophosphates with alkali metals, spectroscopic obs., struct. and chem. nature 80−100674
rare earth germanates, R_2O_3-GeO_2 system cpds., physicochem. charcts. 80−97469
rare earth luminescence from intensity meas. on powdered phosphor screens self-concentration quenching mech. determ. 79−69880

phosphors continued
rare earth oxyhalides and oxysulphides, thermochromic luminescent mats. *(Russian)* 78−48230
rare earth oxysulphides and oxyhalides, Tm^{3+}, Tb^{3+}, Eu^{3+} activated, thermochromatic luminophors, lumines. spectra rel. to temp. 79−56849
rare earth phosphates:Eu^{3+}, vac. UV luminesc.-excitation spectra 77−85774
rare earth phosphor development survey 78−6781
rare earth phosphor intensifying screen speed gain 78−7447
rare-earth-doped, up-conversion and excited state energy transfer, book contrib. 77−36296
review, progress over past 25 yrs. 79−28840
scintillation beta counting of $^{90}Y(^{90}Sr)$, improved method with reusable phosphors 78−9024
scintillators in scanning electron microscopes, prep. and evaluation 79−230
semiconductor, interpretation of thermolum. and TSC, extensions of conventional model 78−27335
sensitised luminescence in crystals, with rare earth activators, computer simulation 78−6723
sodium salicylate, vac. UV scintillators, characteristic props. at 253.7 nm 79−71525
sodium salicylate coated ruby composite phosphor, for Si detector UV sensitization 79−84668
stationary recombinatorial luminesc. without thermal transitions, model 79−8193
stilbene derivatives containing 2-pyrazoline and 1,3,4-oxadiazole groups, spectral-luminescent props. 80−7394
temperature meas. appl. using fibre optics 80−73360
p-terphenyl, vac. UV scintillators, characteristic props. at 253.7 nm 79−71525
thermoluminescence, minimum entropy prod. 79−28845
thermoluminescence, UV dosimetry 80−853
thermoluminescent, for radiation dosimetry and dating 78−11004
thermoluminescent phosphors, thermolum. induced by 254 nm UV photons 80−55204
thermostimulated luminesc., mech. milling effects *(Russian)* 78−76537
TLD, γ-induced sensitisation and residual thermolum. 79−28844
TLD phosphors, use for high-level gamma-ray dosimetry 80−13934
2-(2-tosylaminophenyl)-4H-3,1-benzoxazine-4-one, cryst. and mol. struct. 80−84167
trypaflavine, on silica gel, luminesc. quenching, activator location effects 77−52172
tungstate phosphors, thermoluminesc. and afterglows 79−38681
vanadates, Dy^{3+} activated, photoluminesc. meas. 77−77277
X-ray image intensifier output screens 78−4755
X-ray luminesc. energy yield *(Russian)* 77−48280
X-ray phosphors and screens based on compounds activated with rare-earth elements 79−8169
zeolite, new crystal phosphors *(Russian)* 78−2903
ZnS:Mn,Cu, thin-film phosphors, LV DC electroluminescence 79−11472
Al_2O_3 and double oxides, photon multiplication and secondary electron-hole pairs generation *(Russian)* 80−66262
Al_2O_3:Si, Ti, pure and doped, luminescence, optical absorpt. and colour centres 79−87501
Al_2O_3:Si thermoluminescent phosphor, annealing characts. and nature of traps 77−85817
Al_2O_3:Si(Ti), sensitised TLD phosphor, photon energy dependence 80−78498
BN, phosphided, luminescence spectra of products 77−12418
Ba luminate:Eu, effect of non-stoichiometry on luminesc. 78−68550
$BaAl_{12}O_{19}$:Mn, vac. UV excitation spectra, appl. to gas discharge display 80−2816
$BaCl_2$, Sn-activated, luminescence studies 80−108246
$BaCl_2$:Pb crystal phosphor, emission spectra 80−66298
BaFCl:Eu X-ray intensifying screen 78−11735
$BaMgAl_{14}O_{23}:Eu^{2+}$, vac. UV excitation spectra, appl. to gas discharge display 80−2816
$Ba_{1-x}Mg_xSO_4:Eu^{3+}$ phosphor, thermolum. characts. 77−90203
$Ba_3(PO_4)_2$, ionisation of capture centres, thermolum. spectra 80−11487
$Ba_3(PO_4)_2$:Eu, X-ray phosphor, study of emission and trapping centres 79−8197
BaS:Bi phosphors, polycrystalline, effect of grain size on thermolum. 79−61446
BaS:Cu, thermoluminesc. and decay 78−80426
BaS:Cu phosphor, photo- and electro-luminescence 79−43030
$Ba_5SiO_4Cl_6$:Eu, blue-emitting phosphor high quenching temp. 80−16076
Ba_2ZnS_3:Mn, luminescent props. 77−77292
BeO ceramic TLD, gamma ray response 80−23153
Bi^{3+} activated phosphors, luminesc. characts. 80−2849
$Bi_2Al(Ga)_4O_9$, fluoresc. and X-ray data 78−80403
Ca halophosphate luminophors, grinding influence on thermolum. 79−95854
CaF_2, kinetics of thermoluminesc. buildup 79−65936
CaF_2:Ce,Mn, heavily-doped phosphor, cathode-ray irrad., energy transfer 79−87509
CaF_2:Dy, TLD-200, thermolum. phosphor, photolum. and absorpt. spectra, thermolum. mechanisms 80−97321
CaF_2:Eu, thermolum. in presence of lanthanide impurities 80−2870
$CaF_2:Eu^{2+}$, energy transfer to luminesc. centres, pulsed excitation obs. 77−85781
$CaF_2:Gd^{3+}$ evaporated film, struct. of impurity centres, substrate temp. effects 79−99943
$CaF_2:Mn^{2+},Yb^{3+}$, efficient luminesc. energy transfer from Mn^{2+} to Yb^{3+} 78−19536
$CaF_2:Mn^{2+},Yb^{3+}$, luminescent energy transfer efficiency obs. 78−6777
$CaF_2:Yb^{3+}$, Er^{3+}, and CdF_2-$CaF_2:Yb^{3+}$, Er^{3+}, IR to visible upconverting system 77−44035
$CaLaGaO_4:Eu^{3+}(Bi^{3+})$, luminesc. of α- and β-phases 77−90186
$CaMoO_4$, luminesc. efficiency, temp. and high-press. 78−23507
$CaMoO_4$, scheelite struct., intrinsic hole centres, EPR study 78−64274
CaO:Ag (Au), electroluminesc. meas. 80−40162
CaO:Ce,Gd phosphors, trap distrib., phosphoresc. decay characts. obs. 80−29773
$CaO:Ce^{3+}$, Gd^{3+}, sensitization of Ce^{3+} luminesc. by Gd^{3+} 80−97326
CaO:Cu(Ag)(Au), thermoluminesc., following UV excitation, 290-500K 77−40292
CaO:Eu,Tb phosphor emission under X-ray excitation 79−52011
$CaO:Eu^{3+}$, influence of crystal field on luminesc. *(Russian)* 80−80834
CaO:Eu(Tb), phosphor, isothermal decay 80−55156

phosphors continued
CaO:F(Cl)(Al), phosphon, luminesc., electron-hole recombination processes 79−65919
CaO:Y phosphor, chemical instability, thermoluminescence study 79−38682
$Ca_2P_2O_7$:Sb, (Sb,Mn), luminesc., activation, colour centres *(Russian)* 78−92123
$Ca_3(PO_4)_2$:Sb,(Sb,Mn), luminesc., activation, colour centres *(Russian)* 78−92123
$Ca_5(PO_4)_3F:Nd^{3+}$ site symmetries, EPR and spectral obs. 78−6571
$Ca_{10}(PO_4)_6X_2$, halophosphate luminophor, forming during annealing of briquetted mixture 78−11173
$Ca_{10}(PO_4)_6X_2$:Sb, halophosphate luminophor, causes of Sb loss during synthesis 78−11172
CaS, atomic and mol. centres of O; ESR and luminesc. methods *(Russian)* 80−84764
CaS, colour centres and photoluminesc., flash stimulation bands *(Russian)* 77−20923
CaS optical flash stimulation, optical absorption, MCD, thermally stimulated luminescence expts. 78−10951
CaS, phosphors, hole recombination luminescence *(Russian)* 78−72576
CaS, polycryst., point defects, EPR obs. 79−61214
CaS, tunnel luminescence *(Russian)* 78−72577
CaS:Bi, Tm, phosphor sensitisation mechanism, energy transfer 78−60507
CaS:Bi,Dy phosphors, thermoluminesc. 77−69921
CaS:Bi phosphors, UV dosimetry by thermolum. 80−55199
$CaS:Bi^{3+}$, Pd^{2+}, phosphor, electroluminesc., brightness and mechanism 77−48248
$CaS:Bi^{3+},Na^+(Li^+)$, luminescence of associated centres *(French)* 80−40155
CaS:Ce, Na, photon sidebands in emission and excitation spectra, pseudolocalised vibrs. 79−28800
CaS:Ce, Na phosphor, photoluminescence and excitation spectra 80−89049
CaS:Cu, colour centres, optical and thermal depths determ. 80−66275
CaS:Cu, colour centres and photoluminesc., flash stimulation bands *(Russian)* 77−20923
CaS:Mn,Ce, phosphor, fluoresc. spectrum, fine struct., $^4T_{1g}(^4G) \rightarrow {}^6A_1(^6S)$ transition 80−45130
CaS:Nd, Cu, phosphor, electroluminesc., spectral characts. 79−19936
CaS:Nd, X-ray powder diffr. anal. 80−100204
CaS:Pd phosphor, thermally stimulated elec. cond., kinetics, 300-413K 78−76088
CaS:Pd phosphors, trap and luminescent centre location, photo-, thermo- and electroluminescence studies 80−71482
CaS:Tb,Eu, fluoresc. spectra under X-ray excitation 80−16083
CaS:Zn phosphor, photoluminesc. meas. 77−20913
CaS:Zr, Gd phosphors, thermoluminesc., trap distrib., activator effects 78−2929
CaS:Zr phosphors, photoluminesc. 79−28806
CaS:Zr phospors, photoluminesc. 79−28805
CaS-BaS:Cu phosphors, X-ray diffr. and fluoresc. spectra 80−40148
CaS-Bi, Mn, phosphors, thermoluminesc., phosphoresc. 78−2928
CaS-Pb,Mn, phosphors, thermoluminesc. and fluoresc. spectra 78−64396
$CaSO_4$ with rare-earth and Y dopants, ESR, thermolum. correlation studies following gamma irradiation 77−59628
$CaSO_4$:Ce(Eu) phosphors, fluorescence spectra, thermolum. glow curve 80−2879
$CaSO_4$:Dy, α and γ thermoluminescence response comparison 79−85814
$CaSO_4$:Dy, competing deep trap model for thermoluminescence 79−83039
$CaSO_4$:Dy, dosimetric appls. 79−76154
$CaSO_4$:Dy, high exposure UV response and sensitisation 79−91506
$CaSO_4$:Dy, phosphor, X-irrad., thermoluminesc., role of Na_2SO_4 as charge compensator 79−78764
$CaSO_4$:Dy, thermolum. origin, test of model on $CaSO_4$:Eu 77−85813
$CaSO_4$:Dy, thermolum., studies for dosimetry 79−29634
$CaSO_4$:Dy embedded Teflon TLD phosphor photon energy dependence obs. 79−26761
$CaSO_4$:Dy phosphor, effect of Dy conc. on TL characteristics 79−93881
$CaSO_4$:Dy phosphors, photomag. susceptibility 78−2724
$CaSO_4$:Dy TLD phosphor, γ radiation changes in glow curve 80−60688
$CaSO_4$:Dy thermoluminescence sensitivity and glow curves, 700° to 1300°C 79−85815
$CaSO_4$:Dy-KBr thermolum. phosphor, thermal neutron detect. by activation 80−32581
$CaSO_4$:Dy(Tm), thermolum. thermolum. phosphor, photolum. and absorpt. spectra, thermolum. mechanisms 80−97321
$CaSO_4$:Mn, phosphor, thermoluminesc., low energy ion excitation 77−55838
$CaSO_4$:Sm phosphors, mag. susceptibility temp. depend. 300-453K 78−52196
$CaSO_4$:Sm phosphors, X-ray induced fluorescence and phosphorescence 80−55179
$CaSO_4$:Sm phosphors, X-irrad., thermoluminesc., charge compensation effects 80−97351
$CaSO_4$:Tm, sensitised TLD phosphor, photon energy dependence 80−78498
$CaSO_4$:Tm intrinsic thermoluminescence stability for UV dosimetry 80−12262
$CaS(Se):Eu^{2+}$, emission and excitation spectra obs. 80−55162
$CaSe:Sn^{2+}$, dimer centre, emission and excitation spectra, temperature quenching *(French)* 79−99937
$CaSe:Pb^{2+}$, luminesc., refl., emission, and excitation spectra 79−11456
$CaWO_4$, energy storage, afterglow decay and thermolum. meas. 77−12422
$CaWO_4$, luminesc. efficiency, temp. and high-press. 78−23507
$CaWO_4$ phosphor, interaction between intrinsic and impurity emission 79−8198
$CaWO_4$, type selfactivated luminophors, nature of optically active centres 77−69880
$CdMoO_4$, luminesc. efficiency, temp. and high-press. 78−23507
$CdNd_4(SiO_4)_3O$, synthesis, cryst. struct. 78−87653
CdS, effect of halide (NaCl, $CdCl_2$, $CdBr_2$, CdI_2) and polysulphide (Na_2S_x, K_2S_x) on recrystn. 78−11171
CdS, single cryst., surface treatment effects on photoluminesc., struct. and optical props. *(Russian)* 78−15224
CdS:Ag, Ni thermographic phosphor luminesc. screen, for IR laser pulse recording 79−64342

phosphors continued
CdS:Ag phosphor, mechanism of trap ionisation by elec. field, Gudden-Pohl flashes 79−74007
CdS-based, microstruct. and luminesc. efficiency 78−10959
CdSe, effect of halide ($NaCl$, $CdCl_2$, $CdBr_2$, CdI_2) and polysulphide (Na_2S_x, K_2S_x) on recrystn. 78−11171
$CdWO_4$, luminesc. efficiency, temp. and high-press. 78−23507
$CeBO_3$:Tb^{3+}, vacuum UV excitation spectra and quantum efficiencies 79−28811
CsCl:Ag phosphor, spectral characts., optical range 77−1724
CsI based powdered phosphors and screens possible appl. in X-ray radiography and fluorography 79−6245
CsI evaporated coating, photodetector sensitivity enhancement in VUV 79−85180
CsI:Na phosphor screen, absolute efficiency under fluoroscopy conditions 78−82084
CsI:Tl, crystallophosphor, luminesc. characts., temp. and conc. depend. 80−55175
CsI:Tl, gamma-scintillation growth front, external elec. field effect 80−34984
CsI:Tl powdered phosphor screen for X-ray image intensifier 79−6246
CsI:Tl X-ray phosphor, spectral characts. 79−8172
Cs(Br):Mn phosphors, luminesc. spectra 77−59610
Er^{3+} doped phosphors, IR excitation and absorpt. and emission spectra *(Russian)* 79−52021
Eu double metaphosphates with alkali metals or H, luminesc. props. 80−100675
Eu ion based, liq., using aprotonic solvents 80−20686
Eu^{2+} activated phosphors, luminesc. efficiency, temp. and high pressure 78−23508
Eu^{3+} doped, rel. band intensities in luminesc. spectra *(Russian)* 77−48238
GaN:Zn epitaxial films, luminesc. spectra separation into individual bands by impurity absorpt. region excitation 79−74002
GaP luminophor powders, SAW nonlinear acoustoelectro-luminescence 80−45143
Gd neutron radiographic amplifying screen sensitivity 78−7448
$GdBO_3$:Eu^{3+}(Tb^{3+}) and $GdBO_3$:Bi^{3+},Eu^{3+}, vacuum UV excitation spectra and quantum efficiencies 79−28811
GdB_3O_6:Bi^{3+}, Tb^{3+}, energy transfer from sensitiser to activator, intermediate role of Gd^{3+} 80−50389
$GdNbTiO_6$:Eu^{3+} emission under UV excitation 78−6770
Gd_2O_2S, compact specimen prep. 77−85951
Gd_2O_2S:Yb^{3+},Ho^{3+}, anti-Stokes emission band assignments, energy transfer mechanism 77−40277
$GdPO_4$:Dy^{3+}, Bi^{3+}(Sb^{3+}), energy transfer from sensitiser to activator, intermediate role of Gd^{3+} 80−50389
$(Gd_{1-x}Tb_x)_2O_2S$ phosphor, concentration quenching of Tb^{3+} luminesc. 80−29785
$HgMoO_4$, luminesc. efficiency, temp. and high-press. 78−23507
$InTa_{1-x}Nb_xO_4$ system, structural and luminescent props. 80−84769
KBr:Tl, 480K thermal glow peak, Tl^+ centres 80−108284
KBr:Tl, Jahn-Teller system, negative mag. circular polarisation in emission spectrum 80−20694
$K_{2(1-x)}Ca_xSO_4$:Tl^+ phosphor, thermolum. characts. 77−90203
KCl:Ag,Tl, cryst. high-press. energy transfer, sensitised luminesc. 77−36281
KCl:Tl, mixed phosphor, dimer absorption bands, 200-300 nm 79−73976
KCl:Tl phosphors, heavily doped, luminesc. obs. 77−32427
KCl-KBr:Mn mixed cryst. system for thermoluminescence dosimetry, glow curves, dose response 78−24150
KCl-Tl, Jahn-Teller system, negative mag. circular polarisation in emission spectrum 80−20694
KI evaporated coating, photodetector sensitivity enhancement in VUV 79−85180
KI:Tl, emission and excitation spectra, press. effects 79−83028
KI:Tl, Jahn-Teller system, negative mag. circular polarisation in emission spectrum 80−20694
KI:Tl, phosphor, press. effect on emission spectra at low temps. 77−85771
KI:Tl, X-ray phosphor, influence of different factors on emission intensity 79−8171
KI:Tl^+, anomalous stress-induced dichroism 79−4828
KI:Tl^+ type, press. effects on triplet relaxed excited states, quadratic Jahn-Teller interaction 78−23510
$(K_{1-x}Na_x)_2SO_4$:Tl^+ phosphor, thermolum. characts. 77−90203
$LaAlO_3$:Tb^{3+}, cathodo- and photoluminesc. 77−12448
$LaGaS_3$:Ce^{3+}, luminesc. props. 80−103979
La_2O_3:Eu(Tb)(Tm), powder layer, electrolum., comparison with Y_2O_3 and Y_2O_2S 77−20927
LaOBr:Tb phosphor X-ray mottle reduction by multilayer screen construction 78−4756
LaOBr:Tm X-ray emission spectra and screen-film system design 78−11024
LaOCl:Sm^{3+}, conc. quenching of X-ray and UV-excited luminescence *(Russian)* 77−55829
La_2O_2S, compact specimen prep. 77−85951
La_2O_2S penetration phosphor, penetration and cathodoluminescent props. 80−20718
La_2O_2S:Eu, high press. effect on luminesc. efficiency and lifetime, charge transfer absorpt. 80−66266
La_2O_2S:Eu, slow phosphoresc., high press. study 80−80839
La_2O_2S:Tb, cathodoluminesc. efficiency changes due to processing, XPS meas. of surface changes 79−99951
La_2O_2S:Tb based barrier layer phosphors, prep. and cathodum. props. in penetration phosphors 77−1738
La_2O_2S:Yb^{3+},Er^{3+}, IR excited visible luminesc. of Er^{3+} 78−2910
La_2O_2S:Yb^{3+},Ho^{3+}, anti-Stokes emission band assignments, energy transfer mechanism 77−40277
$LaSiO_3F(Cl)(Br)$, phosphor host, luminesc. and struct. props. 78−48212
$La_{1-x}Tb_xOBr$ phosphor, concentration quenching of Tb^{3+} luminesc. 80−29785
$Li_2B_4O_7$:MN bulb dosimeters, nonuniversality of TL linear energy transfer response 79−97948
$Li_2B_4O_7$:Mn, gamma ray response 80−23153
$Li_2B_4O_7$:Mn TLD phosphor, additivity of α and γ response 79−9891
$LiBaAlF_6$:Eu^{2+}, luminesc., band emission and line emission 79−28810
LiF, high sensitivity, for low dose meas. 79−13538
LiF, prep. and dosimetric props. of new highly sensitive form 79−22483
LiF, sensitised TLD phosphor, photon energy dependence 80−78498
LiF, TLD 100, thermolum. peaks anal. 77−44073
phosphors continued
LiF, TLD phosphor, Z_3 centre, thermolum. and optical absorption spectra 79−24374
LiF TLD-100 phosphor, sensitisation mechanism study, thermolum. glow peak intensity obs. 80−55202
LiF:Mg, role of impurity-vacancy pairs in thermolum. 79−8195
LiF:Mg, TLD-100, thermolum. phosphor, photolum. and absorpt. spectra, thermolum. mechanisms 80−97321
$LiGaO_2$:Fe, phosphor, luminesc. 78−92108
$LiGaO_2$:Fe IR emitting phosphor preparation and props. 78−6789
$LiNbO_3$:phosphor, piezoelec., interaction with SAW, excitation of electrolum. 79−60615
$LiY_{1-x}Tb_xP_4O_{12}$, and $LiY_{1-x}Eu_xP_4O_{12}$, prep. and fluoresc. 77−48219
$Li_{14}ZnTa_4O_{18}$:Eu, fluorescence and cryst. symm. 77−24886
MgB_4O_7:Dy, TLD phosphor development 79−79661
MgO doped powder phosphors, photo- and thermostimulated luminesc. obs. *(Russian)* 80−66263
MgO, electronic excitations and luminescence, review *(Russian)* 78−72575
MgO-NH_4F-GeO_2:Mn phosphor, luminance. spectra due to UV irrad., 26-294°C 79−83005
MgS:Ce^{3+}, emission and excitation spectra *(French)* 80−93380
MgS:Eu^{2+}, emission and excitation spectra obs. 80−55162
MgS:Eu^{2+} phosphors, anal. of absorption spectra $4f^{N+1}\rightarrow 4f^N5d$-6s 80−7383
Mg_2SiO_4:Tb, sensitised TLD phosphor, photon energy dependence 80−78498
Mg_2SiO_4:Tb, thermolum. phosphor, photolum. and absorpt. spectra, thermolum. mechanisms 80−97321
Mg_2SiO_4:Tb TLD, response to X-ray and electron irrad. 79−3285
Mg_2SiO_4:Tb thermoluminescence phosphor, response to high energy electrons *(Japanese)* 78−78502
$MgWO_4$, luminesc. efficiency, temp. and high-press. 78−23507
NH_4Cl-TlCl, mixed phosphors, diffuse absorption spectrum 79−24342
NH_4NO_3, intrinsic electroluminescence obs. 78−80420
$(NH_4)_2SO_4$, intrinsic electroluminescence obs. 78−80420
NaBr:Ho^{3+},Eu^{2+}, single cryst. synthesis, rel. to purification methods 77−8744
$Na_3Ce_{1-x}Tb_x(PO_4)_2$, UV excitation, emission spectra 79−38595
NaCl:Tl, deformed phosphors, thermoluminesc., impurity conc. effects 77−63473
$Na_3La_{1-x}Gd_x(PO_4)_2$, UV excitation, nonradiative transfer 79−38595
$NaYF_4$:Ho, Yb, two photon anti-Stokes effect, excited by 2 μm radiation 78−50852
Na_2ZrSiO_5, scintillation props., excited by α particles 80−29809
Nd ion based, liq., using aprotonic solvents 80−20686
O containing, cathodoluminescence, photoluminescence, afterglow excitation spectra 78−10952
P_2O_5-R_2O_3-M_2O(M′O), (M=alkali metal, M′=alkaline earth, R=Y or rare earth), metaphosphate glass phosphors, fluoresc. props., activation conc. effect 80−89058
$POCl_3$-$SnCl_4$:Nd^{3+}; laser parameters and physiochem. props. 77−14709
RbCl:Ag, phosphor, luminesc., absorpt. and excitation spectra 77−12424
RbI:Tl, emission and excitation spectra, press. effects 79−83028
$ScBO_3$:Tb^{3+}, vacuum UV excitation spectra and quantum efficiencies 79−28811
Sc_2O_3 and double oxides, photon multiplication and secondary electron-hole pairs generation *(Russian)* 80−66262
Si:P, Au, neutron irradiated, distrib. of P and Au determ. 78−79627
SiC luminophor powders, SAW nonlinear acoustoelectro-luminescence 80−45143
Sm^{3+}-doped, rel. band intensities in luminesc. spectra *(Russian)* 77−48238
SnO_2 red-orange emitting luminescent material for low voltage excitation, props. *(Japanese)* 77−73169
SnO_2:Eu powder phosphor, prep., low energy electron excitation 78−39608
$SrCl_2$, in-activated, luminescence studies at 77 and 300K 80−108247
SrS:Cu, phosphor, photolum. meas. 78−80393
SrS:Cu, phosphor electroluminescence characts. 79−33838
SrS:Hf, phosphor fluoresc. spectra, host lattice defect 77−12416
SrS:Hf phosphor, activation energy and freq. factor calcs. from glow curves 77−12451
SrS:Hf^{4+} phosphors, phosphorsc. decay curve 77−63450
SrS:Ho phosphor, prep. methods, X-ray diffr. appraisal 77−51350
SrS:Mn, Zr phosphor, photodielectric effect 80−107848
SrS:Zr(Zr,Mn), yellow and red fluoresc. mechanism 77−32419
$Tb_xLa(Y,Gd)_{1-x}$.DAM.Sal_3, DAM=diantipyrylmethane, luminesc. *(Russian)* 77−55830
Tb_2O_3-P_2O_5-MO system glasses, (M=Mg, Ca, Sr, Ba or Pb), photoluminesc. under X-ray excitation 80−89060
$Tb_xY_{1-x}PO_4$, H_2 VUV laser excitation, fluoresc. decay characts. 78−60510
(Y,Gd)BO_3:Eu^{3+}, vac. UV excitation spectra, appl. to gas discharge display 80−2816
YAG, undoped and Ce^{3+}-doped, cathodolum. intensity and decay time, 10-480K 79−99952
YAG:Ce phosphors, luminesc. efficiency, prep. and dopant effects 80−45151
YAG:Ce^{3+}, photoluminescence excitation energy, crystal field and temp. effects 80−11460
YAG:Ce^{3+}(Eu^{3+})(Gd^{3+})(Tb^{3+}), cathodoluminesc. efficiency rel. to activator conc. 80−11479
YAG:Ce^{3+}(Tb^{3+}), recomb. processes, spectral, kinetic and relative quantum intensity meas. 79−61443
YAG:R^{3+}, CRT and X-ray phosphor lattice-activator energy transfer model 78−6792
YAG-Ce^{3+}(Eu^{3+})(Tb^{3+})(Gd^{3+}), cathodolum. intensity, temp. depend., comparative study 79−99953
$YAlO_3$:Ce, fast decay UV phosphor 80−71471
YBO_3:Bi^{3+},Eu^{3+}, vacuum UV excitation spectra and quantum efficiencies 79−28811
YF_3:Yb,Er, IR to visible light conversion, effect of temperature on efficiency *(Russian)* 77−28628
YF_3:Yb,Er, limit efficiency of transformation of IR to visible radiation 80−29784
YF_3:Yb^{3+}, Tm^{3+}, IR to blue up-converting phosphor 79−83004
$Y_3Ga_5O_{12}$:Tb^{3+}, luminesc. 77−48251
$YNbTiO_6$:Eu^{3+} emission under UV excitation 78−6770
Y_2O_3 and double oxides, photon multiplication and secondary electron-hole pairs generation *(Russian)* 80−66262

phosphors continued
Y_2O_3, rare earth activated, cathodolum., use of internal reference 77−44071
Y_2O_3:Eu, cathodoluminesc. investig., appl. to cathode ray tube screening 80−108282
Y_2O_3:Eu_2O_3 based sputtered ternary metal oxides, DC electrolum. obs. 77−77300
Y_2O_3:Eu^{3+}, absorpt. spectra, fluoresc., electron beam excitation 78−92093
Y_2O_3:Eu^{3+}, quantum yield in candoluminescence process by low energy H^+ ion bombard. 79−65930
Y_2O_3:Eu(Tb)(Tm), powder layer, electrolum., comparison with La_2O_3 and Y_2O_2S 77−20927
Y_2O_3:Tb^{3+}(Dy^{3+}), conc. quenching of X-ray and UV-excited luminesc. *(Russian)* 77−55829
YOF:Tb^{3+}, conc. quenching of X-ray and UV-excited luminesc. *(Russian)* 77−55829
Y_2O_2S, compact specimen prep. 77−85951
Y_2O_2S:Eu, high press. effect on luminesc. efficiency and lifetime, charge transfer absorpt. 80−66266
Y_2O_2S:Eu, temp. meas. by line shift method 77−13750
Y_2O_2S:Eu particles of different sizes, prep. by flux method 77−44140
Y_2O_2S:Eu phosphor, luminescence saturation effects due to N_2 laser and cathode-ray excitation 80−40151
Y_2O_2S:Eu(Tb)(Tm), powder layer, electrolum., comparison with La_2O_3 and Y_2O_3 77−20927
Y_2O_2S:Ho, Yb, two photon anti-Stokes effect excited by 2 μm radiation 78−50852
Y_2O_2S:Tb, cathodoluminesc. efficiency at low electron energy 78−6790
Y_2O_2S:Tb, cathodoluminesc., nonlinear depend. on activator concs. 79−8190
Y_2O_2S:Tb, cathodoluminesc. efficiency changes due to processing, XPS meas. of surface changes 79−99951
Y_2O_2S:Tb^{3+}(Eu^{3+}) temp. and viscosity depend. of colour coords. 80−40149
Y_2O_2S:Yb^{3+},Ho^{3+}, anti-Stokes emission band assignments, energy transfer mechanism 77−40277
YPO_4, ionisation of capture centres, thermolum. spectra 80−11487
$YSiO_3F(Cl)(Br)$, phosphor host, luminesc. and struct. props. 78−48212
$Y_{1-x}Tb_xAl_3B_4O_{12}$ phosphors, cathodoluminesc. 77−73177
$Y_{1-x}Tb_xP_3O_9$, and $Y_{1-x}Eu_xP_3O_9$, prep. and fluoresc. 77−48219
YVO_4, ionisation of capture centres, thermolum. spectra 80−11487
YVO_4:Eu, cathodoluminesc. investig., appl. to cathode ray tube screening 80−108282
YVO_4:Eu^{3+}, absorpt. spectra, fluoresc., electron beam excitation 78−92093
YVO_4:Eu^{3+} phosphor, cathodoluminesc. and photon statistics 77−59621
$(Y_{0.80}Yb_{0.19}Er_{0.01})F_3$ phosphors, IR to visible conversion 78−48210
$(Y_{0.80}Yb_{0.19}Ho_{0.01})F_3$, IR to visible conversion 78−48210
Yb^{3+} doped phosphors, IR excitation and absorpt. and emission spectra *(Russian)* 79−52021
(Zn, Cd, Hg)S:Cu,In, electroluminesc. temp. depend. 77−1732
(Zn,Cd)S:Cu,Al, luminesc. efficiency deterioration due to surface oxidation by $(NH_4)_2Cr_2O_7$ thermal decomp. 80−29810
(Zn, Hg)S:Cu, Cl, effect of superposition of two sinusoidal fields and freq. on electroluminesc. 78−39606
Zn-CdS:Mg, electroluminescent storage screens for X-ray flaw detection, expt. 77−77722
$Zn_3(BO_3)_2$:Sm^{3+}, photoluminescence obs. *(Spanish)* 79−73986
ZnCdS:Ag, phosphor screen, electron beam excited, light ang. distrib., modulation transfer function 80−45150
(ZnCd)S:Ag phosphor, absolute efficiency under fluoroscopy conditions 78−73203
$Zn_xCd_{1-x}S$:Cl, Cu^+(Ag^+), high pressure luminesc. 78−19533
$Zn_xCd_{1-x}S$:Cu crystallophosphors, spectra of IR electrophotographic sensitivity *(Russian)* 80−50423
ZnO, green luminesc. band, UV irrad. photocond. and quantum yield 77−36284
ZnO phosphor fired with Zn, luminesc. in green and red region 80−66265
ZnO, phosphors, emission spectra, impurity effects 77−32420
ZnO phosphors, origin of UV emission 78−64400
ZnO powders, UV luminesc. spectral distrib., comparison with single crysts., excitons role 80−55167
ZnO, self-activated phosphor, band width and shift, temp. depend. 77−8623
ZnO:Ce(Sm) phosphors, electrolum. 79−99946
ZnO:Ce(Tb), electrolum. brightness, voltage and freq. depend. 80−60681
ZnO:Dy(Nd)(Sm), phosphor, electroluminesc., photoluminesc. spectra 78−80421
ZnO:Er, phosphors, photo- and electroluminesc. 77−12428
ZnO:Er,Ag, photoluminescence and electroluminescence 78−27327
ZnO:La, electrolum. brightness waves, −168 to +85°C 78−52580
ZnO:Pr(Gd)(Er), photoluminesc. and electroluminesc. spectra 79−11457
ZnO-GeO_2-MnO-B_2O_3 wideband cathodoluminescent phosphor 80−55196
ZnO-PbO electroluminesc. phosphors, AC field excitation green and yellow emission 77−59617
ZnO-SiO_2 system, struct. and phase comp. of luminescent Zn orthosilicate 80−19951
ZnS, electrolum. phosphors, surface phenomena occurring during ageing *(Russian)* 79−33842
ZnS electroluminophors, ageing effects *(Russian)* 78−15231
ZnS, excited phosphor, IR stimulation and quenching of luminesc., review *(Russian)* 80−11455
ZnS, exciton struct. in luminesc. excitation spectra 77−52176
ZnS film production, for luminophors, method and apparatus *(Bulgarian)* 80−7499
ZnS, Gudden-Pohl effect, temp. depend. and decay rate 77−44070
ZnS, Gudden-Pohl effect, field ionis. of trapping centres 77−73170
ZnS, heteroepitaxial growth on GaP by closed space technique 79−28939
ZnS, IR stimulation and quenching of luminesc., review *(Russian)* 80−11455
ZnS, interimpurity high press. luminesc. 78−19532
ZnS, optical flash stimulation, optical absorption, MCD, thermally stimulated luminescence expts. 78−10951
ZnS powder phosphors electroluminescent cells, AC electrolum. characts. *(Japanese)* 80−71489
ZnS, rare earth activated phosphor, scintillation mechanism *(Russian)* 78−48231
phosphors continued
ZnS, synthesis under unidirectional pressure and roasting in vacuum 77−32547
ZnS, VPE on GaP in open tube system 79−28938
ZnS, voltage and temp. dependence of pre-breakdown electroluminescence 80−45147
ZnS, voltage depend. of electrolum. brightness 80−45148
ZnS:^{90}Sr, continuously acting luminous solid for photoelec. meas. over 300-800 nm range 79−3757
ZnS:Ag, electroluminesc., surface barriers *(Russian)* 78−2919
ZnS:Ag, luminesc. efficiency deterioration due to surface oxidation by $(NH_4)_2Cr_2O_7$ thermal decomp. 80−29810
ZnS:Ag, luminesc. of surface glow centres 80−29782
ZnS:Ag, nature of fluorescent centres and traps 79−91484
ZnS:Ag, Ni thermographic phosphor luminesc. screen, for IR laser pulse recording 79−64342
ZnS:Ag, ZnS-CdS:Ag(Cu), cathodoluminesc. investig., appl. to cathode ray tube screening 80−108282
ZnS:Ag,Cl, embedded in HBO_3-glass matrix, blue electrolum. 80−55195
ZnS:Ag,Sm, recomb. centre interaction, luminesc. quenching 78−10946
ZnS:Ag phosphor prep., physicochemical investigation of processes 78−11170
ZnS:Ag phosphors, luminesc. of glow surface centres *(Russian)* 79−28836
ZnS:Al,Cu(Ag)(Au) phosphors, luminesc. excitation spectra and exciton struct. 80−55164
ZnS:Al(Te) phosphors, luminesc. excitation spectra and exciton struct. 80−55165
ZnS:Au, phosphor, 'blue' and 'green' centre form. *(German)* 79−38665
ZnS:Cl^-, Cu^+(Ag^+), high press. effect on thermoluminesc. 78−64419
ZnS:Cu, Al phosphors, mechanism of IR stimulated and quenching 77−69881
ZnS:Cu, Cl, I, anisotropy of blue Cu luminesc. centres 77−81137
ZnS:Cu, Cl luminophor, photoluminesc. and struct. props. 77−32414
ZnS:Cu, Er, Na, mechanism of sensitisation effect of Cu and Na ions 77−16369
ZnS:Cu, Gudden-Pohl effect, flash kinetics 79−24367
ZnS:Cu, H, double band phosphor, electrolum., −100 to +100°C 78−10987
ZnS:Cu, Mn DC electroluminescent powder panels, bulk and junction effects 80−89068
ZnS:Cu, Pb, phosphors, ruby laser stimulated time delayed emission spectra 77−69874
ZnS:Cu, polycryst. phosphor, excitation storage, recombination barrier participation 78−27316
ZnS:Cu, spectral distrib., rise and decay behaviour *(German)* 80−60625
ZnS:Cu,Al phosphor, shallow hole traps 78−31237
ZnS:Cu,Cl, exciton refl. spectra, hexagonal struct. 77−44021
ZnS:Cu,Cl phosphor, effect of charged imperfections on electrolum. 77−32443
ZnS:Cu,Co, phosphor luminesc. screen, spectral characts. determ. of IR pulsed lasers 79−10341
ZnS:Cu,Pt phosphors, photoluminesc., thermoluminesc. 78−43915
ZnS:Cu 79−24350
ZnS:Cu crystallophosphors, spectra of IR electrophotographic sensitivity *(Russian)* 80−50423
ZnS:Cu phosphor, electric field quenching of photoluminesc. and flashlike rise in luminesc. 78−2911
ZnS:Cu(Pb), photocapacitive effect, Gudden-Pohl effect 79−65520
ZnS:Mn, electrolum. film, direct impact excitation of Mn centres 77−24900
ZnS:Mn, phosphor, surface changes following interaction with H *(Russian)* 78−72602
ZnS:Mn films, surface struct., microrelief rel. to morphology of SnO_2 transparent cond. support 79−56092
ZnS:Mn on SnO_2/glass transparent conductive base, surface morphology effects on electroluminesc. *(Russian)* 78−48238
ZnS:Mn-H atom systems, surface physiochem. changes, radical recombination luminesc. investig. 79−56863
ZnS:Mn^{2+} phosphors, luminesc. excitation spectra and exciton struct. 80−55164
ZnS:Ne, implanted single crysts., photolum. and bombardment effect, thermolum. curve obs. 80−55166
ZnS:Pb, ionisation mechanism of field trapping centres 80−45156
ZnS:Pb phosphor, electrolum. brightness, temp. depend. 77−48249
ZnS:Pb phosphor mech. of elec. field liberation of electrons from traps 78−72616
ZnS:Pb^{2+}(Mn^{2+}), high press. luminesc., localised excitations 78−19534
ZnS:Tb, Cu(Ag) phosphors, luminesc. props. 80−100690
ZnS-based, microstruct. and luminesc. efficiency 78−10959
ZnS-CdS phosphor coating for large-screen IR visualiser 78−18070
ZnS-CdS system, solid soln. form. mechanism 79−43177
ZnS-CdS:Ag, Ni, Co, thermoluminesc. glow curves 78−95611
ZnS-CdS:Ag, Ni, Co phosphor, thermoluminesc. 77−66547
ZnS-CdS:Ag, Ni, temp. sensitive, biological effects of microwaves determ. appl. 80−36186
ZnS-CdS:Ag(Cu), nature of fluorescent centres and traps 79−91484
ZnS-CdS:Ag(Ni)(Co), electron-irradiated phosphors, void formation mechanism 79−55780
ZnS-CdS:Tm,Ni, recomb. centre interaction, luminesc. quenching 78−10946
ZnS-Mn sublimated phosphor films, annealing effects *(Russian)* 78−43949
ZnS.CdS, flux growth, processes accompanying roasting of CdS+NaCl 78−23590
ZnSe, Gudden-Pohl effect, release of electrons from traps 80−45149
ZnSe, LPE from Zn-Ga soln., characts. 79−28965
ZnSe:Cu, Cl, high press. luminesc. 78−19532
Zn_2SiO_4:As,Mn, enhanced luminesc. stimulation, 20-320K *(German)* 77−20900
Zn_2SiO_4:Mn, energy storage effect and retrieval 80−100684
Zn_2SiO_4:Mn, luminesc. saturation under intense vac. UV irrad. 79−56841
Zn_2SiO_4:Mn phosphor, efficiency enhancement by $AlPO_4$ substitution 80−11452
Zn_2SiO_4:Mn^{2+}, quantum yield in candoluminescence process by low energy H^+ ion bombard. 79−65930
ZnTe high-purity single cryst. growth by sublimation travelling heater method 79−28901
$ZnWO_4$, scintillation characts. 80−66256

phosphorus
see also nuclei with .....
addition to Fe-Ni-B amorphous alloy, effect on crystn. and elec. cond. 80−75179
addition to high Mn austenitic steel, effect on creep rupture *(Korean)* 80−93646
adsorption on GaAs (110), UPS and EELS study, tight-binding calcs. 80−49496
adsorption on Ni, coadsorbed Pb or Sn, AES study 80−54521
adsorption on Ni (100), effects on secondary electron spectra 80−50480
aerosol, deposition velocity over southern Lake Huron 79−83666
allotropic modifications, muonic X-ray intensities, computer analysis 80−23577
amorphous, NMR studies 79−69740
amorphous, prepared by chem. transport in low-press. H_2 plasma, radial distrib. function 80−64899
amorphous, red, far IR absorpt. spectra 80−34923
amorphous, red, photolum. props. and band gap 80−50403
amorphous, stability in air, XPS study, comparison with cryst. polymorphs 80−25517
amorphous, struct. by electron microscopy 80−84065
amorphous, US attenuation and sound vel. meas., 4.2 to 300K; 80−49308
amorphous, vibrational excitations of defect sites 80−49332
amorphous, XPS anal. of stability, form. of oxidised layer *(German)* 79−11496
amorphous high resolution imaging by electron microscopy 79−99039
amorphous red, bulk, Raman scatt. and IR absorption 79−24323
amorphous red P, Raman scattering 80−11416
amorphous semiconductor, defect states 79−87057
amorphous thin film, prepared by chemical transport in glow discharge, electronic props. 79−24011
atom, ab initio effective valence shell Hamiltonian for neutral and ionic valence states 80−74117
atom, and ions, two and three-electron Auger transition, with vacancies in 2p-shell 79−63972
atom, excited config., Hulthen and Slater type 2d functions 78−41972
atom, ground state $3p^3(^4S_{3/2})$, time-resolved reson. fluoresc. obs. 79−34333
atom, highly ionised, beam foil radiative lifetimes and EUV spectrum 80−32671
atom, MINDO parameters 78−86786
atom, neutral, IR spectra and HFS 80−91478
atom, neutral, spectra and term anal. 80−91481
atom, $np^2(n+1)s$ excited-state config. quadrupole moments, Sternheimer shielding factor 80−37755
atom, s-shell spin polarisation calcs. 77−75318
atom, SCF electron-gas local-spin-density model including correlation 80−9488
atom, spin magnetic moment densities, spin density functional method calcs. 77−67969
atom, Stark widths and shifts, visible and UV 77−57927
black, pseudopotential crystal-struct. stability calcs. as function of press. 79−60503
black allotrope, orthorhombic bonding, up to 26.6 kbar, neutron diffr. obs. 79−99106
bone, sheep, transportable system for neutron activation anal. determ. of P 80−109066
chemisorbed on Ni(100), LEED and angle-resolved AES obs. 79−95258
chemisorption on Cu, Auger spectra 78−43248
contaminated Ni surface, coadsorption of Sn, AES study 80−88437
content in Elbe, Trave, Eider, Schwentine river sediments, bonding form *(German)* 79−34868
crystalline to amorphous transition, thermodynamic functions 80−54354
deep diffusion into Si, expt. results 80−54437
depth profiles in Si-SiO_2-Si structs., ion microanal. *(Japanese)* 78−85251
determination, in natural waters, in presence of As, Si and $HgCl_2$ 79−44277
determination, in organic media, using at. absorption with graphite atomiser, sample prep. 78−31729
determination, in phosphosilicate glass passivation layer, SEM analysis and interpretation 78−35759
determination, in Si(SiO_2), by AES *(Japanese)* 78−91356
determination by activation anal. (α,n), (α,p) reacts. investig. 80−61206
determination in Lake Ontario tributary waters 79−79418
determination in optical waveguide glass by DC plasma emission spectroscopy 80−87446
determination in ores of reduced heteropoly acids, photometric method 78−61103
determination in Si by ion microanal. *(Japanese)* 78−85250
determination in small bone biopsies by neutron activation 79−88154
dietary intake, effect on ^{90}Sr balance in man 78−15911
diffusion in Cu single- and polycrystals, 548 to 1046°C 77−1265
diffusion in liq. In, coeff. determ., capillary reservoir method 79−23754
diffusion in Si, dislocations, creation conditions 79−95039
diffusion in Si, effect of dislocation struct. on migration rate 77−51551
diffusion in Si, elastic deform. relax. and dislocation generation 80−79997
diffusion in Si, excess vacancy generation by E-centre dissociation 77−72720
diffusion in Si, implantation damage effects 78−55988
diffusion in Si, impurity distrib. in surface layer with porous oxide film 77−39944
diffusion in Si, influence of dislocations 78−18840
diffusion in Si, open-tube diffusion kinetics 79−33117
diffusion in Si, oxidation effects 79−51309
diffusion in Si, proton enhanced diffusion and vacancy migration 78−67747
diffusion in Si, radn. enhanced 80−29216
diffusion in W, 1880-2180°C *(Russian)* 78−43182
diffusion into Si, 900-1150°C, controlled surface conc. condition 77−7746
diffusion into Si from spin-on SiO_2:P film 80−2050
diffusion into SnO_2 films *(Japanese)* 79−95218
diffusion mechanism in Si, migration channels along vacancies and interstices 80−79996
diffusional doping of Si, solid planar source with SiP_2O_7 active component 77−1139
distribution control in estuary water 77−21823
doping of amorphous tetrahedrally bonded semicond., mechanism, gap density of states 79−19545
elemental abundances of S, K and P in aerosols from S.American rain forests 79−100910
Ge:P, radiation-accelerated diffusion 80−6559
implantation in GaAs, influence of damage on diffusion 78−6082
impurities in low alloy steels, effect on neutron irrad. embrittlement 80−85055
impurity in Al-Si eutectic and hypoeutectic alloys, effect on mech. props. and thermal cond. 79−83271
impurity in Cr-Mo-V low-alloy steel, effect on high-temp. ductility and crack growth 80−66652
impurity in Ni, dissolution and passivation in acid environment, effect of P *(French)* 80−45440
impurity migration from doped Si sources in epitaxial layers *(Russian)* 80−107570
interstellar abundance towards 20 stars, Copernicus obs. 78−36646
intestinal absorption of Ca and P in rat, simultaneous in vivo determ. using ^{47}Ca and ^{32}P 78−48882
ion implantation, in amorphous Si, asymmetrical profiles 79−46693
ion implantation in laminar Si-SiO_2 systems struct. change investig. by MSSI *(Russian)* 80−107918
ion implantation in Si, processing parameters for diffusion redistribution 79−10871
ion implantation of Ni, amorphous Ni-P prod. 80−75257
ions, charge distrib., 72-123 MeV 80−27849
Jupiter Great Red Spot, red P form and depend. on solar activity 79−101110
K-shell X-ray production, by 0.4 to 2.4 MeV ^4He and ^1H ions 79−47550
Lake Carl Blackwell, Oklahoma, atmospheric contrib. of P to aquatic system 79−100545
Lake McIlwaine, Rhodesia, distrib. in sediments 77−33114
lake P budget, snow and ice effects 79−62540
lake P input, uncertainty analysis 78−81262
laser and thermal annealing, elec. cond. and Hall effect meas. 79−69145
lattice and grain boundary diffusion in Cu, exam. of diffusion rates by tracer sectioning technique 78−79817
life on primitive Earth, P availability 78−20518
Lithuanian lake catchment area soil N and P distrib. *(Russian)* 79−96780
molecule, geometry optimisation, ab initio MO calcs. 77−42232
molecule, valence electron photoionisation, ionisation pot. and spectral intensities 78−70883
molecule, vibr. struct. calcs. from photoelectron spectra 77−18973
muonic allotropes, muonic Roentgen intensities *(German)* 80−53168
muonic K-shell X-ray transitions, nuclear charge radius 78−66195
in natural waters, automated procedure for P determ. 80−81517
neutron activation anal. of urine samples *(French)* 78−61254
nuclear thin red target preparation 78−46196
phosphor bronze, beam, cylindrical, flexurally vibrating, Timoshenko's shear coeff. 78−83866
phosphor bronzes, surface Cs^+ impact, 5.5 keV negative secondary ion emission obs., rel. to Cu *(French)* 77−66562
phosphosilicate glass, CVD, P conc. meas. 77−80533
plasma, dense, nondegenerate, electron transport, thermal cond. *(Russian)* 79−98865
pollution of stream draining agricultural watershed 77−33116
α-quartz:P, dynamic interchange among 3 states of P^{4+}, EPR obs. 80−66010
quench-deposited Al-type films, superconducting props. 79−15264
radioactive ion implantation using Lublin separator 79−82251
Raman vibr. spectra and bonding 80−11411
reaction with Ti, at high temp. 78−44260
red, atmospheric aerosol absorption to extinction coeff. ratio meas. 80−90217
red to black conversion in quasiisentropic compression 79−33036
reduction in sewage effluent by electrochemical process 80−104445
River Main, County Antrim, N and P loads meas. by discrete and intensive sampling 79−44213
segregation to free surface in ferritic Fe-Ni-Cr-C, 723 to 823K 78−48411
Si:P^+, ion-implanted, annealing characts., X-ray diffr. exam. 78−14372
solubility in solid Fe, alloying element effects *(Russian)* 79−69248
steel, Cr-Mo (2.25, 1 wt.%), SCC and temper brittleness, P grain boundary segregation effect 80−55571
steel, grain boundary segregation, effect on brittle fracture after quenching and tempering *(Russian)* 80−81145
steel, hardenability, role of B and P segregation 80−97486
surface runoff, New Zealand, P transport, effect of fertiliser and grazing cattle 77−53094
Texas impoundments, critical levels of P and N_2 78−11929
transport in sandy soils, expt. and simulation 77−66940
vapour pressure above solution of GaAs and GaP in Sn 77−51485
water pollution, P conc. streams draining from agricultural watershed 80−61474
water pollution, removal process modelling and control by multivariate time series method 79−74561
water pollution control, phosphorus removal system, automation 80−76669
wet and dry deposition into Lake Huron 79−57991
white, dendritic solidification, fluid flow effect 78−11215
white, high purity, cryst. growth morphology 77−15330
Si:P, sheet resistance of Gaussian n-type ion-implanted layers 79−87103
$^{32, 33}P$ incorporated in DNA, transmutation effects 80−26283
Al-Si, hypereutectic silumins, P and Na modification 78−84792
Al-Si:P, neutron activation anal. of phosphorus content *(Russian)* 77−40614
BN:P film, effect of CVD parameters on props. 80−25571
$BaWO_4$:Mo, P, thermoluminesc. traps, EPR meas. 77−90032
Be_2SiO_4:P, EPR and ENDOR 78−76295
C:H,P film, amorphous elec. props., chem. modifications by doping with P 80−84523
$CaSO_4$:Dy, phototransferred TL studies 80−80875
$CaWO_4$:Mo, P, thermoluminesc. traps, EPR meas. 77−90032
$Cd_{1-x}Mg_xTe$:P, luminescence centres, photoluminesc. meas. 78−31236
CdS:N, P, As, Sb, Bi photoluminescence obs. 78−10965
CdS:P, implanted, photoluminesc. and electroreflection spectra *(Russian)* 78−52544
CdSe:P, effect of P on edge luminesc. 78−64399

phosphorus continued
CdSe:P, implanted, electroreflection obs. 80−40089
CdSe:P, single crystals, luminesc. 79−87493
CdTe:P, annealing induced lattice defects, TEM obs. 80−2010
CdTe:p, defect model, from Hall effect meas. 77−43620
CdTe:P, ion implanted, elec. props. 80−65021
Co-P, metallic glass, phonon propagation at low temp. 78−87756
Cr-SiO, P^+ implantation effects on elec. props. of film 79−11239
Fe, P determination by at. emission spectroscopy using steeloscope 79−57330
Fe, single cryst., segregation behaviour of S, O and P at (100) surface 80−100841
Fe-Ni (3 wt.%), grain boundary segregation of Sn and P embrittling additions, STEM microanal. 78−76654
α-Fe-P, grain boundary adsorption of P, internal friction *(Russian)* 77−32609
Fe-P-Cu-SiO_2-$FeAl_3$-asbestos composite, thermal and elec. conds., temp. and composition depends. 77−66609
(FeNi)PB amorphous wires, surface oxidation and annealing influence on induced anisotropy 80−100957
$Fe_{100-x}P_x$, structural analysis of models for amorphous metallic alloys 80−103249
GaAs:P, form. of $GaAs_{1-n}P_n$ by diffusion 80−54389
GaAs:P films, epitaxial growth from melt with components introduced by ion bombardment 77−21044
GaAs:P^+, defect form. on P^+ implantation at various temp., He^+ backscatt. obs. 78−59828
GaAs:P^+, implantation profiles, backscatt. meas. 80−70238
GaAs:P^+, ion-implanted, refr. index, IR reflection and transmission meas. 77−1671
GaN:P, implanted single cryst. film, cathodolum. 78−60523
GaN:P, photoluminesc. 79−78730
GdTe:P and CdTe:P,In(Ga)(Al), IR absorpt. investig. of localised vibr. modes of impurity centres 77−52136
Ge, high-purity, with Al, B and P, residual impurities, photothermal cond. 80−24965
Ge:Be, P, absorption of radiation, 0.6-2.8 mm, 4.2 to 20K 80−66332
Ge:P, amorphous, electronic transport and photocond. 79−60834
Ge:P, bound-exciton luminesc. and absorpt. 79−87469
Ge:P, charact. temp. and lattice thermal cond. 80−59743
Ge:P, conc. depend. of diffusion coeff. at P diffusion 78−95185
Ge:P, doping of epitaxial layers, in chloride and hydride processes 78−43036
n-Ge:P, electric dipole excitation of spin resonance 77−4551
Ge:P, growth atm. effect on struct. microdefect form. 80−20779
Ge:P, γ-irrad., carrier trapping and recomb. at point radiation defects 80−107810
Ge:P, implantation doping, annealing and doping profile determ. 77−19972
Ge:P, impurity ground state levels from photo-thermal cond. in mag. field 77−51699
Ge:P, impurity photocond. spectra under uniaxial compression 80−44656
Ge:P, ion implanted, laser-induced regrowth 79−69130
Ge:P, lattice thermal cond., role of electron-phonon interactions and peripheral phonons 78−79702
Ge:P, peripheral phonons and phonon cond. 79−14973
Ge:P, phonon drag thermoelectric power at low temp. 80−107828
n-Ge:P, uniaxial compression, 0.6-2.9 mm radn. absorpt. 79−82629
n-Ge:P,Ga, compensated, uniaxially compressed, anisotropy of mm. and submm. wave absorpt. 78−19074
(In+InP) melt, critical undercooling determ. and P content change after annealing *(Slovak)* 80−55430
In_2O_3-SnO_2-CdTe:P, p-n homojunction solar cell, elec., photovoltaic props., photoluminescence 80−81463
Ir-W (0.3 wt.%), P segregation to grain boundaries, effect on high temp. ductility 78−95754
KBr:P, colour centre fine struct., ODMR 78−6604
KCl:P, colour centre fine struct., ODMR 78−6604
$Mg_xCd_{1-x}Te$:P, vibr. modes of defects, IR absorpt. expts. 77−62601
Ni-P undercoat, effect on struct. form. in sintered electrophoretic Cr_3C_2 alloy coatings 80−61027
P II, CI calcs. of oscillator strengths, L-S framework 80−14089
P II, reson. transitions, radiative lifetimes, astrophys. appls. 78−62767
P II homologous ions series, Stark broadening trends 80−105157
P III, UV and vis. spectrum, ionisation limit calcs. 78−936
P IV, 200-9800 Å, spectral line classification and term system 77−79564
P in upper atmosphere 79−40130
P V, beam foil excited, alignment effects 77−34605
P VI, UV spectrum, anal. 78−17595
P XII, beam-foil obs. of oscillator strengths for E1 transitions 80−14112
P XIV, intercomb. line obs., in laser-produced plasma 78−9106
P XV, H-like ion, anal. of satellites to reson. lines in X-ray region 77−88421
P^-, contracted Gaussian basis sets for mol. calcs. 80−83264
P^-, metastable, electron affinity calcs. 79−31439
P^-, photodetachment cross-section meas., crossed beam expt. 77−61723
P^+, beam-foil excitation; absolute Auger yield meas. 79−45685
P^+, ionisation pot., periodic regularities, relativistic corrections calcs. 79−49950
P^+, reson. line regularities in plasma Stark widths and shifts 80−43881
P^{2-}, parameters for analytical radial orbitals, total and binding energies 77−6668
P^{3+}, static dipole quadrupole polarisabilities and shielding factors calc. using HF scheme 80−99450
P^{5+}, ionic size rel. to Koopmans' ionisation pot. 79−85892
P-C, one-bond couplings, orbital and spin dipolar contribs., INDO approx. 79−31552
P-SiO_2, film, quantitative anal. by DC arc optical emission spectroscopy 78−68940
P^+-ion penetration tails in SiO_2-Si two-layer system, expt. and computer anal. 80−75249
P_2, ($A^1\Pi_g \rightarrow A'^1\Sigma_u^-$), IR emission spectra, Fourier spectroscopy, mol. parameter determ. 78−42056
P_2, $b^3\Pi_g$-$w^3\Delta_u$ and $A^1\Pi_g$-$W^1\Delta_u$ systems, IR emission spectrum 78−94244
P_2, electron affinity, vibr. struct. in radiative electron attachment spectra 77−88592
P_2, intersystem transition obs. in absorpt. spectrum 80−48008
P_2, perturbations in $b^3\Pi_g$ state, existence of $^5\Sigma_g^+$ state, visible and IR systems *(French)* 77−68035
P_2 radical, $A^1\Pi_g$-$X^1\Sigma_g^+$ transition, vibr. consts. *(French)* 77−75176
phosphorus continued
P_2 radical, $b^3\Pi_g$-$a^3\Sigma_u^+$ transition, perturbed by $1^5\Sigma_g^+$ state *(French)* 80−18855
P_2 radical, emission spectrum, perturbations in $c^3\Pi_u$ and $C^1\Sigma_u^+$ states *(French)* 77−23484
P_2, vertical valence ionis. pot., many-body Green's functions 78−22051
P_2^-, photodetachment cross section, 0.5 to 3.0 eV photon energy *(German)* 77−65518
P_2^+, electronic states pot. energy curves, dissoc. energy, ionisation pot., curve fitting 80−32796
P_4, allowed multiplets, coordinate wavefunctions 78−33444
P_4, closed-shell SCF calcs., mol. symmetry 78−41930
P_4, core and mol. orbital XPS spectra, binding energies 77−65508
P_4 normal coordinates, allowable representations 79−2595
P_4, photoionisation, mass spectra 77−30935
P_4, vap., oxidation, chemiluminesc., reduced press. system 77−32795
P_4+$H_2O(D_2O)$, vapour, chemiluminesc., transient emitting species 77−1926
PO, Rydberg states, UV absorption spectrum 78−90184
$P^-(^3P_{2,1,0})+h\nu$, P electron affinity, P^- fine struct. interval 77−79590
$P(P^+)(P^{2+})$, static quadrupole polarisability and shielding factor, Hartree-Fock calc. 78−41950
$P_2(X^1\Sigma_g^+)$, He I photoelectron spectrum, ab initio and semiempirical calcs. 77−34691
^{30}P, short lived positron emitter, cyclotron production 79−76236
^{31}P, mechanism of spin transfer to next neighbours in complexes 78−86892
^{31}P, muonic, 3d-2p X-ray transition 80−9764
^{31}P NMR applications to cells 80−46110
^{31}P, NMR obs. of lipid bilayer head group, orientational order and rotational diffusion 80−21451
^{31}P NMR of DNA in nucleosome core particles of chromatin 78−40112
^{31}P NMR of the perfused heart 80−77534
^{31}P, nucl. mag. screening in PH_3, pseudopot. calcs. 79−6879
^{31}P, obs. of DNMR using RYa-2308 radiospectrometer with attachment 80−98957
^{31}P-NMR spectra of chicken erythrocyte nucleosomes, temp. dependence 80−94280
^{31}P-NMR study, crayfish perfused ventral nerve cords 79−79475
^{32}P and ^{45}Ca determination in biological samples by Cherenkov and liq. scintillation counting 80−98183
^{32}P, comparison with ^{47}Ca in profile scanning of skeletal disease 80−51218
^{32}P, radioactive interference with neutron activation anal. of biosamples 79−12059
^{32}P, whole-body counting of retention in man 79−62378
^{33}P transmutation lethal effect on bacteriophage A13 mech. of DNA double helix rupture *(French)* 80−98018
α-quartz:P, X- and γ-irradiated, EPR studies of phosphoric ion 77−63263
S:P, ion implanted, defect annealing 450-800°C, deep-level transient spectroscopy 79−47042
Se:P, vitreous, crystn. kinetics study by elec. cond. meas. 79−64998
Si diffusion profiles, P and B diffusion determ. *(Rumanian)* 79−77615
Si epitaxial layers, grown in vac. at low temps. P and Sb doping 80−88189
Si, floatzone, P doping by thermal-neutron irradiation 78−22750
Si, neutron transmutation doping, ^{31}P conc. meas. 80−19833
Si, P diffused sample, stacking faults and dislocations formation from interstitials 78−95059
Si, P^+ implantation, induced disorders. 80−6422
Si:$^{31}P^+$, implanted layers, characterisation by ellipsometry 79−90683
Si:Al, P-diffused, recomb. centres, thermally stimulated capacitance meas. 77−72834
Si:Au, P-induced point defects influence on Au gettering mechanism 80−65030
Si:B, P, first and second order Raman scatt. by pair modes 79−65869
Si:B, P, high temp. diffusion, effects of laser irrad. on diffused layer 79−14834
Si:B, P, long range enhancement of B diffusivity by P diffusion 80−103386
Si:B,P, anomalous diffusion 80−29229
Si:B,P, diffusion patterns obs., for SiO_2 deposited by means of centrifuge *(Bulgarian)* 77−76429
Si:B,P, double implanted layer, n-p-n struct., single pulse laser annealing 80−49247
Si:B,P, high conc. diffusion without disloc. generation 78−10072
n-Si:B,P, radiative recombination at thermal defects, luminescence centre electron struct. 79−91496
Si:B,P, simultaneous diffusion, radioactivation techniques 77−76622
Si:Ga,P(As), sequential diffusions, comparison of interactions 77−80655
Si:H,P, amorphous, heavily hydrogenated, high gap state densities 80−49803
Si:H,P, amorphous, in MOS tunnel junction, electron tunnelling charact. 79−73592
Si:H,P amorphous film, elec. cond., thickness and temp. depend. 80−65559
Si:In,P, photoinduced IR absorpt. and luminesc. 79−33828
Si:I, obs. of donor exciton in far IR transmission meas. 79−91477
Si:Os, P, photoelec. props., depend. on P conc. 79−91099
Si:P, absorpt. due to creation of bound excitons 78−23025
Si:P, acceptor bound multiexciton complex recomb., shell model, luminesc. line splitting 78−6275
Si:P, amorphised by Ne^+ implantation, high fluence P implants, plasma region obs. 79−86807
Si:P, amorphous, CVD, defect compensation 80−54644
Si:P, amorphous, CVD, substitutional doping, electronic props. 79−23923
Si:P, amorphous, elec. cond. and thermoelectric power 77−89783
Si:P, amorphous, laser effects 79−69921
Si:P, amorphous, negative magnetoresist., localised mag. states 80−70731
Si:P, amorphous, photo- and dark conductivity 77−28216
Si:P, amorphous, substitutionally doped CVD, electrical props. 79−99566
Si:P, amorphous, thermoelectric power and conductivity 77−89782
Si:P, and of P diffused layers 78−38736
Si:P, and Si:P,Gd, depth of energy levels of As from impurity photocond. 79−90996
Si:P, annealing after ion implantation, ellipsometric study 80−65018
p-Si:P, annealing behaviour, recovery, surface carrier density and Hall mobility meas. 77−32012

phosphorus continued
Si:P, annealing characteristics at low temp., elec. props. 78−63781
Si:P, anomalous doping profiles, numerical anal. 79−73206
Si:P, appl. of ion implantation systems, high throughput 80−34029
Si:P, BF_2^+ ion implantation, anomalous carrier profiles 80−2048
Si:P, bound exciton and multiexciton complex struct., luminesc. obs. 77−81138
Si:P, bound excitons and bound multiexciton complexes for shallow donors, luminesc. meas. 79−24363
Si:P, bound multiexciton complexes, work function thermodynamic determ. 78−72078
Si:P, carrier lifetime depth distrib. due to Ar ion implantation 80−70232
Si:P, carrier mobility and distrib. rel. to annealing, 400-910°C 78−79995
Si:P, characterisation by IR reflectivity 78−56501
n-Si:P, charact. of piezoresist. 77−51750
Si:P, conc. profiles of ions and recoiled N after implantation through Si_3N_4 films 79−55764
Si:P, conc. profiles of P and recoiled O atoms after ion implantation into SiO_2-Si, SIMS obs. 79−51138
p-Si:P, Cu, influence of Cu on diffusion of P meas. 77−1267
Si:P, Cu(Au) radiation-doped, influence of growth defects on elec. props. 79−69144
Si:P, Czochralski growth, dopant evaporation coeffs., resistivity distrib. 77−16487
Si:P, defect annealing, ionisation effects, DLTS meas. 80−24483
p-Si:P, defect energy levels, ion implantation effects, Hall coeff., sheet resist. meas. 77−85173
Si:P, defects, SEM in EBIC mode vs. HVEM images 78−9923
Si:P, depth of melting produced by pulsed-laser irrad. 79−55756
Si:P, depth profiling using Cs^+ bombardment and negative SIMS in UH vac. 79−99232
Si:P, determ. of P content in high-purity Si using meas. of Mo in 12-molybdophosphoric acid by NAA and AAS 80−15148
Si:P, dielec. susceptibility meas., polarisation catastrophe at metal-insulator transition 80−59873
Si:P, diffusion eqn. numerical soln. 79−51311
Si:P, diffusion for gettering of Au in Si 78−91346
Si:P, diffusion from ethylene glycol grown anodic oxide 77−76440
Si:P, diffusion induced imperfections, laser annealing, rel. to junction characts. 78−75678
Si:P, diffusion of P, 900-1100°C, distrib. of excess vacancies 77−72631
Si:P, diffusion of P impurities stimulated by gas discharge Ar plasma, low temp. 80−6560
Si:P, diffusion-doped laser irradiation effects, electrical reactivation of P 80−39124
Si:P, diffusional doping, diffusion-induced strain and dislocation effects 79−42084
Si:P, diffusivity, strain-induced band gap narrowing, E-centres 80−29228
Si:P, dislocated crystals, DC conductivity, Hall effect, energy spectrum 78−10400
Si:P, dislocated crysts., microwave cond., localised electron energy spectrum 78−14694
Si:P, dislocation dissoc. mode obs. by weak-beam TEM 80−107259
Si:P, dislocations under high stress, stacking fault energies, TEM study 80−70202
Si:P, distrib. of implanted impurity after laser annealing, e.s.r. and neutron activation analysis 77−4122
Si:P, donor excited state lifetime, delayed avalanche breakdown 77−85231
Si:P, donor-polarizability enhancement as the insulator-metal transition is approached from the insulating side 80−80184
Si:P, dopant profile changes induced by laser irrad. using SIM and backscatt. meas. 79−69148
Si:P, doped by neutron transmutation, electron traps 78−84164
Si:P, doped by neutron transmutation, lattice defects 80−34018
n-Si:P, doping, by zone melting using solid dopant source 78−43035
Si:P, doping, new paint-on diffusion source 77−4118
Si:P, doping by diffusion from phosphosilicate glass sheets *(German)* 77−39604
Si:P, doping by neutron transmutation, residual radioactivity 79−33009
Si:P, doping during growth from gas phase, thermodynamic analysis 80−59489
Si:P, E-centre formation mechanism 77−72614
Si:P, EPR line shift, 0.56 to 4.2K, investig. of interacting donor clusters 77−77084
Si:P, EPR of interacting donor centres, Overhauser effect and ENDOR 77−77085
Si:P, ESR-induced changes in DC resistance 78−35037
n-Si:P, edge dislocation energy level, differential capacitance meas. 79−23927
Si:P, effect of annealing on charge carrier conc. on floating zoned crystals 78−47805
Si:P, effect of impurities on solar cell performance 80−55848
n-Si:P, elec. cond. oscills., electron instability effects due to dislocations 80−103704
Si:P, electrical conductivity oscillation, effect of dislocations 78−6388
n-Si:P, electron mobility and resist., dopant density and temp. depend. 77−76816
Si:P, electron-nucl. interaction under optical pumping, ^{29}Si optical polarisation meas. 79−95680
Si:P, electronic states, NMR of metallic and intermediate samples 79−4511
Si:P, electrostatic field on impurity atoms, heavy doping effects 78−51570
Si:P, emitter-misfit dislocation formation during P diffusion 78−91338
Si:P, epitaxial layer, vapour phase grown, temp. dependence of dopant inclusion, differential molar solution enthalpy *(German)* 79−52128
Si:P, excess vacancy generation by P diffusion *(Japanese)* 77−89460
Si:P, excitation density depend. of cathodoluminesc. from bound multiexciton complexes 78−72609
Si:P, excitation spectrum of P donors introduced by neutron transmutation, high resolution study 79−47460
Si:P, exciton two-electron luminesc., temp. and impurity-conc. depend. 78−39585
Si:P, expt. evidence against shell model of bound multiexciton complexes 78−10368
n-Si:P, fast neutron irrad., defect clusters and defect build-up kinetics 79−33019
Si:p, film, polycrystalline, low press. CVD, resist. meas. 80−2494
phosphorus continued
Si:P, float-zone cryst. growth, shape of melt interfaces and radial P distrib. 77−24952
Si:P, Gd, optical orientation of ^{29}Si nucleus, effect of donor level implantation depth *(Russian)* 77−8452
Si:P, Ge, simultaneous diffusion processes, elastic stress influence 77−89591
Si:P, Ge(B), impurity-pair diffusion, influence of elastic stresses 78−87824
Si:P, glow discharge deposited amorphous film, UV absorpt. spectra 80−25420
Si:P, Hall effect 78−72176
a-Si:P, Hall effect and impurity cond. 77−72871
n-Si:P, heavily depend., spin-lattice relax. at high temp. 78−39403
Si:P, heavily diffusion-doped layers, Co diffusion 78−59982
Si:P, heavily doped, 100 GHz ESR of impurity band 79−95631
n-Si:P, heavily doped, carrier conc., Hall coeff. and elec. cond. meas. 77−8094
Si:P, heavily doped, degenerate electron gas, Friedman effect, review 77−20242
Si:P, heavily doped, diffusion of Au 77−51550
Si:P, heavily doped, EPR spectra of electron irradiation induced defects 77−81008
n-Si:P, heavily doped, elec. cond. and Hall effect meas., impurity effects 78−19032
Si:P, heavily doped, electron-hole droplets, photolum. obs. 1.5 to 80K 77−36289
Si:P, heavily doped, electronic sp. ht. meas., rel. to metal-nonmetal transition 78−6162
Si:P, heavily doped, electron mobility carrier conc. relationship 79−65470
Si:P, heavily doped, glow-discharge-produced, elec. and optical props 80−2497
Si:P, heavily doped, IR bound-exciton luminesc. spectra 78−15211
Si:P, heavily doped, influence of impurities and crystalline defects on electron mobility 79−78095
Si:P, heavily doped, mag.-field depend. of sp. ht. 80−29183
Si:P, heavily doped, metallic region, resist. decrease due to ESR 77−16178
Si:P, heavily doped, origin of photoluminesc. 79−56856
Si:P, heavily doped, paramagnetic spin susceptibility 79−78306
Si:P, heavily doped, sp. ht. near metal-nonmetal transition, generalized Matsubara-Toyozawa theory 79−73321
Si:P, heavily doped, sp. ht., calc. using AMO-MT scheme for impurity bands 79−95182
Si:P, heavily doped, thermal oxidation 78−56793
Si:P, heavily doped semicond., scatt. mechanism, resist, and Hall coeff. maxima 80−75586
Si:P, heavily doped wafer, anomalous bending obs. 78−10074
Si:P, heavily ion implanted, polycrystalline, grain growth 79−19477
Si:P, high dose implantation, outside dislocation generation 78−87672
Si:P, high fluence ion implantation, layer thickness and refr. indices, IR refl. meas. 79−82248
Si:P, high resolution study of group V impurities absorption 80−7388
Si:P, homogeneous epitaxial layers, production, appl. of neutron transmutation doping 78−38737
Si:P, homogeneous nuclear transmutation technique, thyristors appl. 80−70236
Si:P, IR absorpt. and D^--band 78−52533
Si:P, impact excitation of P at low temps. 78−23098
Si:P, implantation damage of channelled P ions, elec. activity recovery stages 77−59034
Si:P, implantation damage removal by laser irrad. and its thermal stability, TEM study 79−74024
Si:P, implantation depth distrib. meas. by neutron activation anal., SIMS, junction depth method 77−31693
Si:P, implanted, dislocations obs. by backscatt. spectrometry and TEM 79−4308
Si:P, implanted, pulsed electron beam annealing, Hall effect and sheet resist. meas. 80−34467
Si:P, implanted, SiO_2-film-covered, laser annealing behaviour 79−86808
Si:P, implanted, two-stage laser annealing of lattice disorder 79−1452
Si:P, implanted layers, ionisation-enhanced crystallisation 79−51151
Si:P, implanted low temp. annealed, elec. activation, damage depend. 80−88182
Si:P, impurity band states calc. and photoluminesc. meas. 77−8046
Si:P, impurity conc. from photoluminesc. anal. 78−63785
Si:P, impurity conductivities 78−91691
Si:P, impurity content characterisation, exciton luminesc. 80−60653
Si:P, impurity diffusion from implanted layer, influence of radiation damage 77−76621
Si:P, impurity doped, electron lifetime and transport in upper Hubbard band 79−95452
Si:P, impurity redistrib. by Ar ion hot implantation 77−72633
Si:P, impurity-peak form. during proton-enhanced diffusion 79−55772
Si:P, incoherent light flash annealing, elec. props., backscattering spectra 80−97504
Si:P, interstitial supersaturation near P-diffused emitter zones 79−65541
Si:P, ion implantation, 20-2800 keV, obs. of X-rays produced 78−14367
Si:P, ion implantation, channelled, through metal silicide film 80−70231
Si:P, ion implantation, effects of high dose rate 78−83835
Si:P, ion implantation defect annealing investig. by CESR 77−8404
Si:P, ion implantation doped, positron annihilation meas. 78−14380
Si:P, ion implanted, damage layer props. obs. using ellipsometric parameters *(Russian)* 77−43234
Si:P, ion implanted, doping profile, pulsed laser annealing effects 80−88197
Si:P, ion implanted, IR transmission and rel. spectra study 80−108244
Si:P, ion implanted, ionisation enhanced annealing, resist. changes meas. 78−30667
Si:P, ion implanted, irrad. by laser of different wavelengths, annealing behaviour 79−69132
Si:P, ion implanted, laser annealed, elec. characterization 79−69137
Si:P, ion implanted, lattice damage and electrical activation correlation 78−67726
Si:P, ion implanted, polycryst., annealing charact. 77−24324
Si:P, ion implanted, redistrib. of dopants by pulsed laser annealing 79−7620
Si:P, ion implanted, regrowth of damage structs. by laser annealing 80−107289
Si:P, ion implanted, resist. changes induced by ESR 78−68377

phosphorus continued
Si:P, ion implanted, selective annealing of amorphous layers by Nd^{3+}:YAG laser irrad. 79−14823
Si:P, ion implanted, sheet resistance variations at elevated temps. 78−43041
Si:P, ion implanted, subsurface damage, TEM and channelled Rutherford backscatt. study 80−107337
Si:P, ion implanted, TEM study after laser and furnace annealing 80−70234
Si:P, ion implanted crystalline and amorphous, laser annealing 80−97509
Si:P, ion implanted film, elec. prop. impurity depend. 80−24467
Si:P, ion implanted layers, carrier distrib. meas. precision 77−43603
Si:P, ion implanted low temp. elec. cond. 79−56225
Si:P, ion implanted with small doses, defect annealing by nanosecond laser pulses 80−107297
Si:P, ion-implanted, carrier conc. reduction caused by wet O_2 oxidation 80−10565
Si:P, ion-implanted, damage-dependent elec. activation 79−55793
Si:P, ion-implanted, optical refl. obs. of damage 78−55883
Si:P, ion-implanted layers, CESR meas., impurity distrib. inhomogeneity 78−2738
Si:P, ion-implanted polycrystalline films, laser annealing 79−73181
Si:P, laser annealing, photoluminesc. study 80−2049
Si:P, low energy and high dose ion implantation, through SiO_2 film 77−15435
n-Si:P, low-compensated, Hall factor, electron-phonon interactions 79−4570
Si:P, luminesc., stress effects on donor exciton satellites 77−85786
Si:P, luminesc. lines, multiexciton complexes and unaixial stress 78−92114
Si:P, luminescence associated with transitions from bound exciton excited states 78−23534
Si:P, luminescence circular polarisation, emission by many exciton complexes 80−93398
Si:P, many-valley semicond., donor binding energies, variational calc. 78−23041
Si:P, measurement techniques for determining P densities 80−75262
Si:P, mechanism of diffusion of P 77−7906
Si:P, metal-nonmetal transition, Anderson localisation 79−95335
Si:P, metallic, heat treatment effects, EPR and photoluminesc. 77−77262
Si:P, microdefect formation depend. on doping, Cu decoration, X-ray transmission topography, preferential etching 79−69120
Si:P, minority carrier diffusion coeffs. 79−99559
Si:P, model for exciton bound to donor pair, photolum. data anal. 79−51498
Si:P, multiparticle impurity complexes *(Russian)* 78−72601
Si:P, multiple-particle exciton-impurity complex form. *(Russian)* 78−43925
Si:P, N implantation through Si_3N_4 film, depth distrib. of knock-on N, SIMS meas. 78−10066
Si:P, neutron irrad. crysts., qualitative distrib. of P using autoradiography 80−24486
Si:P, neutron irradiated, influence of growth defects on change in cond. 78−39117
Si:P, neutron transmutation doping distrib. by emitted β-radiation meas. 77−19977
Si:P, neutron transmutation doped, electron trap annealing, deep level transient spectra 78−14368
Si:P, neutron transmutation doped, radiation damage exam., elec. props. 78−95080
Si:P, neutron transmutation doped, EPR obs. of annealing behaviour 79−1453
Si:P, neutron transmutation doped, EPR, electron trapping 79−73179
Si:P, neutron transmutation doping, elec. props. rel. to neutron fluence 80−96555
Si:P, neutron transmutation doping, resist. homogeneity rel. to compensation ratio 80−96556
Si:P, nonequilibrium solid solutions obtained by heavy ion implantation and laser annealing 80−92544
Si:P, optical excess charging $D^0 \rightarrow D^-$, photoelectron spin relaxation *(Russian)* 79−78572
n-Si:P, optical orientation of ^{29}Si and its depend. on pumping light intensity *(Russian)* 77−4581
Si:P, optically induced divacancy reorientation, EPR spectra 78−80216
Si:P, Orbach spin-lattice relax. rate, uniaxial stress depend. 78−72391
Si:P, oxidation-enhanced diffusion of impurities 79−46840
Si:P, phonon cond., electron-phonon relax. rate 79−46771
Si:P, photocond. spectra of H^--H^+-type complexes 79−95451
Si:P, photodielectric effect associated with impurity excitation 79−82630
Si:P, photolum. obs. of donor pairs 79−52014
Si:P, photoluminesc. associated with impurity clusters 79−38656
n-Si:P, piezoresist. under strong uniaxial elastic deform. 77−15858
Si:P, piezospectroscopic studies of bound multiexciton complexes 80−16006
n-Si:P, piezothermoelec. power in electron-phonon drag region, anisotropy 80−70738
Si:P, polarisation of recombination radiation from multiparticle exciton-impurity complexes, induced by uniaxial deform. *(Russian)* 79−78754
Si:P, polycryst., CVD, elec. activation of impurities, EPR obs. 80−34774
Si:P, polycryst., channelling of implanted P during MOS device processing 80−65017
Si:P, polycryst., growth in epitaxial reactor at 800°C, using PH_3 doping 77−1815
Si:P, polycryst., neutron transmutation doped, elec. props. 78−34836
Si:P, polycryst. etching characts. in CF_4 plasma 78−76777
Si:P, polycryst. films, elec. props., EPR, defect states, doping effects 80−75660
Si:P, polycrystalline, thermal oxidation in wet O_2 78−92376
Si:P, polycrystalline laser recrystallised film on Si substrate, cryst. struct., thermal oxidation 80−65391
Si:P, positron annihilation in 100 and 111 orientation 77−44083
Si:P, proton enhanced diffusion, vacancies diffusion length 80−29226
Si:P, proton-irrad., impurity uphill diffusion, vacancy mechanism 80−92719
Si:P, quantitative model for diffusion of P and emitter dip effect 77−76611
p-Si:P, random and aligned implants, Rutherford backscatt. and TEM exam. 78−47454

phosphorus continued
Si:P, recombination spectra of bound multiexciton complexes, Zeeman splitting *(Russian)* 79−38526
Si:P, satellite of bound excitons, transient decay 80−11466
n-Si:P, Sb, reson. four wave mixing, valley orbit splitting 79−89960
Si:P, secondary defect generation suppression and diffusivity restraint by HCl oxidation 79−70191
n-Si:P, secondary defects produced by high-temp. electron irrad. 79−33017
Si:P, shallow donor electrons, hyperfine interactions, reply to Onffroy's calcs. 78−51934
Si:P, shallow donor states with strong central cell perturbation theory 78−51933
Si:P, shallow strain distrib. near cryst. surface, asymmetric X-ray Bragg reflexion 77−76252
Si:P, SiP precipitation concomitant with P predeposition 77−24326
n-Si:P, single cryst., ion implantation, positron annihilation meas. 79−15555
Si:P, single cryst., transmission characts. for IR optical components 77−27325
Si:P, single crysts., oxidation investigations, 780°-1150°C 79−5068
Si:P, spin relax. time of electrons determ., dynamic polarisation of ^{29}Si nuclei 77−55730
Si:P, spin-on borosilica diffusion source, doping uniformity factors 77−76442
Si:P, sputter-deposited polycryst. films, resist. meas. 78−14842
Si:P, stacking fault and dislocation growth induced by P predeposition 77−59023
Si:P, strain-induced band-gap narrowing effect on P diffusion 79−55935
Si:P, strongly compensated, temp. depend. cond. meas. down to 1K 77−72865
Si:P, submillimetre wave study of metal-insulator transition 79−95336
Si:P, temp. depend. of anomalous struct. in wavelength-derivative absorption spectra 77−52143
Si:P, thermal cond., electron-phonon interaction at low temps. 80−92730
Si:P, thermally annealed, high dose, ion-implanted, dislocation array prevention by prior laser annealing 79−73187
Si:P, through-oxide implanted samples, anomalous residual defects after annealing 77−76432
Si:P, uniaxially deformed, multiparticle impurity complexes, luminesc. spectra *(Russian)* 79−4854
Si:P, uniaxially stressed, impurity-assisted intervalley scatt., photoluminesc. obs. 80−34979
Si:P, variable range hopping conduction, in lowest temp. region 79−73511
Si:P, variable range hopping at very low temp. 80−49736
Si:P,B, amorphous, localised level density 79−56168
Si:P,B, wafer, long range enhancement of B diffusivity induced by high surface conc. P diffusion 79−46687
Si:P,Sb(Te), impurity implantation effect on CESR, spin-orbit interactions 77−36133
n-Si:P,V, degeneracy ratios and impurity levels of V, resist. and Hall effect meas. 77−20260
Si:P amorphous films, doping and annealing effects on localized states, ESR meas. 79−38380
Si:P bipolar transistors, interstitial supersaturation and misfit dislocation climb, TEM study 80−70203
Si:P bound multiexciton complexes, expt. evidence for shell model 78−39036
Si:P CVD films, ion-implanted, doping effect on elec. props. 80−2495
Si:P Czochralski crystal donor homogenisation by thermal neutron irradiation 78−6108
Si:P diffused solar cells, laser treatment to dissolve diffused P precipitates 80−45667
Si:P dislocation p-n junctions, capacitive props. 80−20300
Si:P epitaxial layer, incorporation conc. depend. of P from silane-phosphine-H_2 mixture 80−2053
Si:P epitaxial layer, strain distrib. at interface with substrate, obs. by X-ray double cryst. method 79−99461
Si:P film, amorphous, unusual temp. depend. of thermoelec. power 77−59343
Si:P film, CVD polycrystalline, low press. and atmos. press., oxidation 80−3214
Si:P film, doping and transport props. *(French)* 78−47403
Si:P film, electronic props. 78−84330
Si:P film, implanted, elec. cond., sheet resist. as function of ion dose and temp. 79−78235
Si:P film, polycryst., heavily doped, mobility and carrier conc., optical determ. 80−66314
Si:P film, polycryst. pulsed electron beam annealing 80−10566
Si:P heavily-doped, photoluminescence 78−72572
Si:P high temp. impurity diffusion via vacancies and self-interstitials 80−24667
Si:P implantation profiles, neutron activation anal. 78−7284
Si:P implanted, low temp. annealing characts. 77−11576
Si:P implanted, multiscanning electron beam annealing 80−75242
p-Si:P implanted films, piezoresist. stress tensors, ion dose depend., −80 to 120°C 80−100538
Si:P implanted layers as strain sensors 77−35098
Si:P impurity conc. profile determ. by anodic oxidation 79−28010
Si:P mean square dynamic displacement of atoms, effect of electron-phonon interactions *(Russian)* 78−10145
Si:P non-Fickian diffusion, parameter depend. on doping level and impurity gradient *(German)* 80−54440
p-Si:P p-n junctions, dislocations investig. rel. to P diffusion, SEM, X-ray topography techniques 77−76433
Si:P photochronic detector, IR detect. using delayed breakdown 79−58786
Si:P polycrystalline layer, role in lattice defect reduction assoc. with P predeposition 80−70229
Si:P polycrystalline thin film, plasma annealing, effect on elec. props. 80−7005
Si:P solar cell, minority carrier lifetime degradation during ion implanted processing, surface photovoltage 79−39305
Si:P solar cells, improved P diffusion using laser treatment 80−55850
Si:P wafer, stacking faults, preoxidation gettering by reverse side P diffusion-induced misfit dislocations 80−60988
$Si:P^+$, highly implanted, two step annealing effect on crystallinity 77−31683
$Si:P^+$, ions implanted through SiO_2 mask window, lateral spread 79−77627

phosphorus continued
Si:P^+, misfit dislocation formation mechanism, effect of implantation temp. 78−38708
Si:P^+, misfit dislocation net propagation due to osmotic forces 79−65108
Si:P^+, Zeeman energy transfer at surface layer 80−11247
Si:P^+ ion implanted single crysts., secondary defects development during annealing 80−44228
Si:P(O) p^+-n-n^+ solar cells, comparison rel. to resistance to 1.5 MeV electron irrad., majority carrier trapping 80−94087
p-Si:P(P^+) photolytic props. in HF 80−89504
Si:Sb,P, double implants, residual defect reduction after damage anneal 80−88170
n-Si:Sm,P, carrier conc. and mobility, electron irrad. effects *(Russian)* 77−66168
n-Si:Zn,P, local deform. of cryst. lattice, charact. parameters or recomb. waves 77−4386
Si-Au-P system, partition coeff. of P, temp. depend. 79−43158
Si-B, P diffusion and activity after Ar ion bombardment 78−95192
Si-F-H:P, film, dark cond., struct., Raman scatt. 80−88588
Si-Ge:As,P, heavily doped, electron scatt., Hall coeff., Seebeck coeff. and resist. meas., 4-300K 77−4379
Si-Ge:P, hot-pressed alloy, thermoelec. props. 78−91711
Si-H,P, in situ prepared amorphous film, photoemission studies 80−35060
Si-H:P amorphous film, dark cond., struct., Raman scatt. 80−88588
Si-P, dislocation networks due to ion implantation, TEM exam. 77−35563
Si-P, excess carrier recomb., photocond. 79−65495
Si-P dust, electrification and cond. 79−82662
Si-P film, polycryst., laser annealed, resistivity changes during thermal annealing 79−91163
Si-P MOS devices, time dependence of depletion region formation at cryogenic temp. 80−34522
$Si_{1-x}H_x$:P film, amorphous, RF sputtered, optical consts. 79−95866
Si_3N_4:P film, penetration of P ions, 50 to 500 eV 77−76444
SiO_2, P-doped amorphous, porous and hydrophilic, water adsorpt. and IR spectra obs. 80−80061
SiO_2:P, diffusion from spin-on source 80−44367
SiO_2:P film, high temp. deposition and evaluation 79−69989
SiO_2:P film, penetration of P ions, 50 to 500 eV 77−76444
SiO_2:P films, P content determ. by IR absorpt. and activation anal. 79−51139
SiO_2:P optical fibre, single-polarisation single-mode, exposed cladding fabrication 80−58725
SiO_2:P thin films, plasma deposition in prod. planar reactor and P doping 80−2966
SiO_2-Si structure P^+ bombardment damage, exoelectron emission obs. 78−95383
SiO_2-Si:P, P pile-up at interface 78−84303
SiO_2:B, P films doped by pyrolisis and ion implantation, IR absorpt. obs. of impurity conc. 77−72802
SiO_2:Ge, B, P, optical fibre, radiation induced optical absorpt. spectra, 0.4 to 1.7 μm region 80−58761
Si;P, neutron transmutation doping, detect. and identification of potential impurities activated 79−42090
SmS:P, neutron irrad., semiconductor-metal transition 80−24975
SnO_2:P, CVD films, elec. props., cryst. to amorphous transition effects 80−107933
SnO_2:P, CVD growth and etching charact., doping effects 80−107667
^{99m}Tc radiopharmaceuticals, As for P substitution, bone-seeking agent analogues 80−51250
Te:P, impurity spectroscopy 80−65499
$Ti_{(s)}+P_{(v)} \rightarrow TiP$, direct two-temp. synthesis 77−81237
VO_2, thin films, doping by ions of Ar, B, P 77−84781
WC-Co alloys, P additions, effect on hot pressing, hardness and wear resist. 78−11162
Zn+P reaction mechanism and kinetics, effect of Ag and Mn impurities 77−21416
$Zn_xCd_{1-x}Te$-P, vibr. modes of defects, IR absorpt. expts. 77−62601
ZnO:$^{31}P^+$ implanted nonlinear resistor production and characteristics *(Russian)* 80−49252
ZnSe:Ga, P, optically detected mag. reson. of P_{Se}-centre 79−33566
ZnSe:P, 1.91 eV red emission, optically detected mag. reson. study 79−69750
p-ZnSe:P, LPE layers, photocapacitance and photocond. meas. 79−99572
ZnTe:P, binding energy of shallow acceptors from photoluminesc. excitation spectra for donor-acceptor pairs 79−95809
ZnTe:P, electronic Raman scatt. and IR absorpt. spectra of shallow acceptors 79−73978
ZnTe:P, excitations spectra of donor-acceptor pair photoluminesc. 78−23522
ZnTe:P, g-values, spin temp., determ. from Raman spectra 78−43856
ZnTe:P, ion implanted, cathodoluminescence emission spectrum 80−108281
ZnTe:P, pure and doped, electron and exciton excited states of neutral donor 80−34393
p-ZnTe:P, semicond. selective pair luminesc., excited impurity state investigation 79−61439
ZnTe:P, shallow-acceptor, donor, free-exciton, and bound-exciton states 80−60667
ZnTe:P, spin flip scatt., shallow acceptor states 77−8587

phosphorus compounds
air pollutants, conc. meas. with flame photometric apparatus 80−16883
alkali halide, PO_4^{3-}-Al^{3+}(Sb^{3+}) anion-cation impurity mol. complex, IR absorpt. obs. *(Russian)* 77−16317
binary, with non-transition elements, at. vol. and semicond. props. 77−20089
α-$Ca_3(PO_4)_2$, wet-process formation of nonstoichiometric $Ca_x(PO_4)_y(OH)_z$ *(Japanese)* 78−84752
chemisorption on Cu, Auger spectra 78−43248
crystal chemistry of inorganic compounds with O 79−1406
doping of Si epitaxial layers, process parameters effect on electrophys. charact. 78−38734
electron attachment, compound form. in K-seeded flame 79−11794
ESCA shifts and effective charges 80−78648
fertilizers, nitrogenous and phosphate, pollution problems from manufacture 79−34450
globular compounds, struct. criteria for plastic behaviour 78−51454

phosphorus compounds continued
metabolites, ^{31}P spectroscopic zeugmatography 80−76872
NMR of ^{31}P in inorganic solids, chem. shift 78−52369
orthophosphate transport in sandy soils, expt. and simulation 77−66940
P_2O_5, U removal in Spain *(Spanish)* 79−30927
pentaphenylphosphorus cyclohexane, cryst. packing 78−9994
phosphate, potentiometric determ., solid-state ion-selective electrodes prep. 79−92044
phosphate and alkaline phosphate activity determ. by dual microcomputer-controlled stopped-flow spectrometer 80−57379
phosphate binder based chamotte concretes, strength props. 80−89305
phosphate binder based corrosion protective coating, for steel 79−79151
phosphate bonded refractory plastics, hot modulus of rupture, 1500 to 2500°F 78−19855
phosphate containing materials, technological prod. processes, review 80−97452
phosphate fertilizers, leaching from agricultural soils to groundwater 79−20901
phosphate fertilizers, occupational dose from natural radionuclides 79−100751
phosphate working in direct flow plasma reactor *(Russian)* 80−55663
phosphates, chem. determ. of Ca 78−23976
phosphates, condensed, crystal chemistry, survey 79−86745
phosphates, in oceans, accumulation rates in metalliferous sediments on E.Pacific Rise 77−60364
phosphates, vib. calcs. 77−51457
phosphates in Atlantic and Mediterranean near Gibraltar *(Russian)* 78−16058
phosphates rel. to seawater transparency at 30 m depth in tropical Atlantic *(Russian)* 77−64307
phosphoric acid melt reactions with transition metal oxides, form. and analysis of phosphates 77−12517
phosphoric acids, glass transition temps. 77−4050
phosphosilicate glass film, vapour-deposited, structural model, IR spectra meas. 77−1084
phosphosilicate glass passivation layer P content, SEM analysis and interpretation 78−35759
polyacetylene:PF_6, metallic, band theory 80−49570
solid, ^{31}P NMR and π bond 79−4732
trivalent metal phosphates, condensed, synthesis in polyphosphoric acid melts, physicochem. equil. considerations 80−97419
$_2$, photoluminesc. spectrum, ^{31}P Fermi interaction, hyperfine struct. 78−33536
$AgX-Ag_2O-P_2O_5$ (X=I, Br, Cl), glass formation and ionic conductivity 80−65290
$Al_2O_3-B_2O_3-P_2O_5$ system, glass formation by laser melting 78−44074
$Al_2O_3-P_2O_5-H_2O$ system, phase diagram 80−3014
Ar+PCl_3 reaction PCl emission spectra 78−21938
BBr_3-PCl_3-H_2, gas phase equilib. comp. 80−35166
25 Bi_2O_3,P_2O_5, hydrothermal growth, vib. spectrum 77−63555
CCl_3PCl_4, cryst., libration freqs., temp. depend., combination light scatt. and NQR obs. *(Russian)* 77−66436
$CaO-Al_2O_3-P_2O_5$, sub-solidus relationships 79−66046
$CaO-P_2O_5-H_2O$ system, phase diagram at 200°C 80−45286
$Ca_x(PO_4)_y(OH)_z$, nonstoichiometric, wet-process formation from α-$Ca_3(PO_4)_2$ *(Japanese)* 78−84752
$Ca_{10}(PO_4)_6X_2$ (where X is F, Cl, OH or Co), influence of mech. treatment on struct. and reactivity *(German)* 79−43272
$CdGe(P_xAs_{1-x})_2$, glass, static current-voltage characteristics *(Russian)* 77−15925
$CdO-P_2O_5$ glasses, elec. props. at high elec. fields 80−39573
Co-P alloys, geometric struct. models and diffraction exam. techniques 80−79700
Co-P metallic glasses, crystn. kinetics by differential scanning calorimetry 78−91257
Cu-P-Se system, glasses, semicond., density, microhardness, softening point rel. to conc. 77−7674
$FeO-P_2O_5$ glass, elec. props. effect of high energy γ-radiation 79−11173
$Fe_{80}P_{13}C_7$, amorphous and crystalline, electrochemical and semicond. behaviour *(Russian)* 80−101021
$(Ge,Si)_{1-x}P_x$, amorphous struct., kinetically determined topological model 79−55666
Ge-P-S glass system, EPR of intrinsic and Mn^{2+} impurity centres 80−88870
Ge-P-Se system, glasses, semicond., density, microhardness, softening point rel. to conc. 77−7674
Ge-P-Se system glasses, penetration by indentor, activation parameters, microhardness 79−43419
$GeO_2-P_2O_5-SiO_2$ graded index optical fibres optimised for 1.3 μm wavelength region, fabrication techniques *(Japanese)* 80−99888
H+PH_3, abstraction rate consts., 209-495K, time-resolved fluoresc. 77−16807
HCP, force fields and force consts. of electronically excited states 80−69116
H_2PNH_2, inversion-rot. mechanism, basis set and geometry optimisation effects 80−83273
HPO_3, overlapping Raman lines resolution by coherent ellipsometry 79−98110
H_3PO_2, H_3PO_3, H_3PO_4, polarisable acid-acid and acid-water hydrogen bonds 79−76423
H_3PO_4 acid, etching of MgO {100} 78−67714
H_3PO_4, inhibitory additives, for anatase-rutile transition *(Japanese)* 78−95744
$H(UO_2PO_4)4H_2O$, H motion, PMR obs. 78−80239
$KBr(Cl)PO_2^-$, spin-lattice relax. in triplet state of PO_2^- centres, pulsed photoexcitation 79−95644
$KCl:PO_2^-$, ODMR spectra at 2K, HFS tensor of P 79−87333
$KCl:PO_2^-$, phosphoresc. and PMDR spectra, electronic and vibr. states 79−65768
$KCl:PO_2^-$, photo-orientation, spectrosc. and ODMR obs. 80−29772
$KCl:PO_2^-$, triplet state pseudonuclear Zeeman effect, optical detections *(Russian)* 79−78571
$KCl:PO_2^-$, triplet state, level anticrossing and pseudonuclear Zeeman effect, microwave ODIMR 80−39896
$KCl(Br)(I):PO_2^-$, vibr. spectra and struct. of PO_2^- impurity ions 77−16354
KH_2PO_4, press. and deuteration effects on static ferroelec. props., four-particle cluster approx. 80−34861
$K_2O-Al_2O_3-P_2O_5$ glass, low-temp. viscosity 80−39198
$K_2O-Ga_2O_3-P_2O_5-H_2O$, reactions, 150-500°C 80−35514

phosphorus compounds continued
La_2O_3-P_2O_5-H_2O, solubility, regions of crystallisation, 100-500°C 77−16483
Li+$SnCl_4(PCl_3)(SF_6)$, product mag. deflection slotted disc vel. anal. mol. beam kinetics 77−25250
Li_2O-Nd_2O_3-P_2O_5 phase diagram, $LiNdP_4O_{12}$ single crystal growth 80−25668
$100(Li_2O.2SiO_2).3P_2O_5$, directionally solidified, thermal and mech. props. *(Japanese)* 80−16295
$N_3P_3Br_6$, ^{81}Br NQR, conformation investig. 80−63665
Na_2O-Al_2O_3-P_2O_5 glass, low-temp. viscosity 80−39198
$Na_2O(K_2O)$-P_2O_5 glasses, P K-band X-ray emission spectra, state anal. 80−40190
Na_2S-P_2S_5, glass forming region, struct. and ionic cond. 80−88358
Na_2S-P_2S_5, synthesis, structure and ionic conduction *(French)* 80−65291
$NbCl_5OPCl_3$, vibr. amplitude and normal coord. anal. *(German)* 78−66536
$NdCl_3$-$SnCl_4$-$POCl_3$, complex formation, struct. and comp. 77−89413
Ni-P metallic glasses, crystn. kinetics by differential scanning calorimetry 78−91257
$Ni_{1-x}P_x$, electrodeposited, amorphous, mag. and transport props. 78−52106
OPF_3, distortion moment microwave obs., rot. consts., mol. config. 77−50426
OPF_3, forbidden transitions, mol. beam elec. reson. obs. using avoided crossings 78−29775
$^{16}OPF_3$, microwave centrifugal distortion moment spectrum 78−78684
$(P_xAs)_2O_7^{4-}$, vibr. calc. by method of normal coordinates 78−22796
P-As-Se glasses, mag. susceptibility, dielec. const., opt. props. 78−64184
P-O bond parachors 80−14247
P-O cpds., bond lengths rel. to force consts. 77−46653
P-S, amorphous, glass transition and specific heat, intermolecular bond saturation 80−15011
P-Se, amorphous, glass transition and specific heat, intermolecular bond saturation 80−15011
P-Se, phase diag. 77−52296
P-Se, phase diag. and crystallisation of glasses at high press. 77−52297
P-Se glass, effect of Ag electrodiffusion on volt-ampere characteristics 79−7869
P-Se glass system, IR spectra 78−64365
P-Se glasses, solubility, photostimulated changes 80−24602
P-Se system, glass form. props., effect of P concentration *(Russian)* 78−2019
P-Se system glasses, magnetochem. investig. 77−51325
P-Se-Te system glasses, mag. susceptibility and opt. props. 80−25079
P-Se-Te system glasses, vitrification region 78−51425
P-Se-Tl glasses, NMR of ^{31}P and ^{205}Tl 80−15812
P-Se-Tl system glasses, polarisation, refr. index and dielec. const. meas. 80−20608
P_2-PO_2 exciplex, chemiluminesc., reduced press. system 77−32795
PBr_3, ^{31}P scalar relax. using off-reson. RF field 79−93193
PBr_3, low temp. struct. study *(French)* 79−32968
PBr_3, Raman scatt. spectrum, intermol. interaction and dimeric assoc. *(Russian)* 77−54562
PBr_3, Raman scatt. spectra in gas, liq. and solid states, mol. dynamics *(Russian)* 77−55779
PBr_3, X-ray cryst. struct. determ. at 193K *(French)* 79−37667
PCH, nucl. spin-spin coupling consts. to H, INDO calcs. 77−83621
PCl, visible and near IR emission, $A^3\Pi \rightarrow X^3\Sigma^-$ and $b^1\Sigma^+ \rightarrow X^3\Sigma^-$ systems vibr. anal. 78−21938
PCl_3, bond polarisability and force constants 80−69260
PCl_3, low temp. struct. study *(French)* 79−32968
PCl_3, mol. orbital calcs. core-valence approx. scheme 80−42927
PCl_3, structural study at 123K *(French)* 80−88111
$P^{35}Cl_3$, microwave, rotational spectra, excited vibrational states 79−98080
PCl_3+$Xe(6s,^3P_2)$, vibr. energy disposal from XCl* spectrum 79−100345
PCl_5, ^{31}P NMR of three solid phases, ionis. of PCl_6^- at high-press. 79−82882
PCl_5 III, Raman spectra of phase formed by high-press., PCl_6^- ionising dissoc. 79−82968
PCl_5, phase diagram, PCl_6^- ionising to PCl_4 and $2Cl^-$ under press. 79−82314
PCl_5, sublimed phase studied by ^{31}P NMR, Raman spectra and X-ray diffr. 80−100209
PCl_5-$HgCl_2$, Raman spectra, solid and melt, species identification *(German)* 80−45083
PCl_5-$SnCl_4$, mixtures, liq. and solid, Raman spectra study *(German)* 79−91451
PCl_5-$TiCl_4$, gas, melt, and solid, dimer-monomer conversion, Raman spectra obs. *(German)* 79−70320
PD^+, IR emission spectra, rot. anal. and mol. parameters 80−69134
PD_3, forbidden rot. spectra, spectal consts., bond lengths and angles 77−83581
PD_3, liq. and plastic cryst. states, vibr. dephasing and correl. functions 79−69036
PD_3, $n\nu_2$ vibrational levels, prediction of inversion splittings 78−90146
PF, (PF^{++}), pot. energy curves and dissoc. energy, Hulbert-Hirschfelder calc. 80−30210
PF_3, anharmonic force field from mm wave spectra of vibr. excited states 79−13701
PF_3 bond charge parameters from integrated IR absorption intensities 77−6853
PF_3, chemisorption on Fe (110), UV photoelectron obs. 78−19629
PF_3, cryst., mol. motion, ^{19}F NMR investig. 77−73093
PF_3, in smectic solvent, ^{31}P NMR, ^{19}F and ^{31}P mag. shielding 77−18942
PF_3 ligands, interactions with transition metal atoms, MO calcs., bounding props. of adsorption systems 79−85896
PF_3, microwave l-type reson. transitions in $v_4=1$ state 77−57988
PF_3, mol. geometry calcs. using centrifugal distortion const. 80−18841
PF_3, mol. vibr., G-intensity sum rule 78−74632
PF_3, nuclear resonance, effects of intermolecular interactions and intramolecular dynamics 80−63658
PF_3 pyramidal mols., intramol. forces, fundamental vibr. freqs., centrifugal distortion consts. 78−5202
PF_4, MS Xα calcs., pot. energy surface, electronic struct. 77−57877
PF_5 dopant for polyacetylene 80−88171
PF_5, ESCA chemical shift, energy levels, SCC-MO calcs. 79−64045
PF_5, normal coord. anal., generalised valence force field calcs. 77−58195
phosphorus compounds continued
PF_5, nuclear resonance, effects of intermolecular interactions and intramolecular dynamics 80−63658
PF_5, second virial coeff. meas., Lennard-Jones pot. determ. *(German)* 77−19658
PF_5, total nuclear spin in rovibronic state, three calc. methods for hyperfine mag. struct 78−58658
PF_5-graphite intercalation cpds., prep. and props. 80−40686
PF_6^-, bond order and Raman intensity, delta function eqn. 77−61693
PF_6^-, octahedral complex, ionis. energy, SCF-Xα study 78−70967
PF_3Br_2, spin systems under multiple pulse NMR conditions, chem. shift relax. 80−34808
$PF_2H(D)$, vibr. spectra and normal coordinate anal., Raman and IR spectra 80−14147
$(PF_2)_2O$, IR and Raman spectra, vibr. assignment 78−50544
$PF_5.BrF_3$ complex, F NMR 78−37658
γ-$PH_{3-x}D_x$, Raman and IR spectra, phase transition, internal and external modes 77−77191
PH, ($b^1\Sigma^+$) state, radiative lifetime, time resolved spectra 78−78750
PH, $b^1\Sigma^+$ band emission visible and UV regions 78−46357
PH, far IR laser mag. reson. of $X^3\Sigma^1$ and at $^1\Delta$ states 79−54869
PH, fine struct. in $X^3\Sigma^-$ and $A^3\pi$ states, GTO and STO calcs. 77−6679
PH, nucl. spin-spin coupling consts. to H, INDO calcs. 77−83621
PH^+, IR emission spectra, rot. anal. and mol. parameters 80−69134
PH^+, PNO-CI and CEPA calcs. of electron correl. effects 77−34561
PH+He, collisional deactivation of PH($b^1\Sigma^+$), time resolved quenching 79−54948
PH+$N_2(CO)(NO)(H_2)$, collisional deactivation of PH($b^1\Sigma^+$), time resolved quenching 79−54948
PH_2, laser mag. reson. spectra. 9-9.6 μm, ν_2 band 79−89694
PH_2 radial, pot. energy curves. config., ab initio SCF-MO calcs. 77−50419
PH_2 radical, laser-induced fluoresc. 78−94277
PH_2, X^2B_1-state, rot. laser mag. reson. spectrosc. 80−28038
PH_3, ^{31}P NMR chem. shift, virial coeff. determ. 78−58721
PH_3, $3\nu_2$ and $4\nu_2$ states, K=3n A_1-A_2 centrifugal splitting 79−59484
PH_3, absorpt. lines in far IR spectrum of Saturn 78−12147
PH_3, and d_3, ^{31}P NMR of liq. and gas, isotope effect on coupling consts. 79−76451
PH_3, bonding by electron impact coincidence expt. 77−65536
PH_3, conc. meas. by vacuum UV absorpt. spectra 80−71972
PH_3 conversion to P crysts. in Jupiter Great Red Spot, depend. on solar activity 79−101110
PH_3, core-excited states, valence-Rydberg mixing and term values, XUV spectra and CI calc. 79−76444
PH_3, dipole moment derivatives, polar tensors, effective charges, CNDO calcs. 77−38613
PH_3, dipole moment in ground and excited states, submm. spectrum obs. 80−28056
PH_3, Doppler-free optical double reson. Stark spectra 77−58051
PH_3, Doppler-free optical double reson. spectroscopy using single-freq. laser and modulation sidebands 80−68274
PH_3, electron binding energies, one-centre expansion method 77−6677
PH_3, electron impact dissoc. ionisation, mass spectrometric obs. 78−9264
PH_3, equilibrium structure and harmonic force field, ab initio calc. 80−9502
PH_3, excitation energy, one-centre approx. calcs 78−70737
PH_3, forbidden rot. spectra, spectal consts., bond lengths and angles 77−83581
PH_3 formation in Jupiter's upper atmosphere 79−40130
PH_3 gas, use in control of thermal degradation in InP LPE growth 79−33949
PH_3, IR intensity anal. 77−58081
PH_3, IR intensity formulations 77−58004
PH_3, IR spectrum rel. to absorpt. in Jupiter 5 μm window 80−31243
PH_3, inner valence electron ionisation calcs., photoelectron spectra obs. 78−82619
PH_3, Jupiter atmos. comp., IR spectral obs., 800-1000 cm^{-1} 78−16336
PH_3, laser emission 83 to 223 μm region, laser line assignments 78−71084
PH_3, laser photolysis, PH and PH_2 radical excited states 79−16023
PH_3, liq. and solid, Raman spectra., vibr. correl. functions, rot. motions 80−55087
PH_3, millimeter spectra, $\nu_2=1$, $\nu_4=1$ excited vibr. states, J=0→1 rot. transition 79−6936
PH_3, mol., XPS and KLL Auger effect, line shifts 79−31602
PH_3, mol. vibr., G-intensity sum rule 78−74632
PH_3, monitoring using Fourier IR technique 79−16106
PH_3, NMR shielding consts. and mag. susceptibilities, coupled HF with extended GTO basis 80−5480
PH_3, $n\nu_2$ vibrational levels, prediction of inversion splittings 78−90146
PH_3, nucl. spin-spin coupling consts., ab initio calcs. 80−95647
PH_3, nuclear mag. shielding of ^{31}P, pseudopot. calcs. 79−6879
PH_3 on Saturn, abundance, IR obs. 80−82278
PH_3, photolysis and abstraction reactions, rel. to Jovian atmosphere 79−66327
PH_3, second order mag. props., coupled Hartree-Fock perturbation theory 80−87042
PH_3, UV photolysis, scavenging reactions of acetylene and ethylene in Jovian atmosphere 78−81582
PH_3, vac. UV photolysis, emission spectra 78−46357
PH_3, X-ray K-fluoresc. obs. of electronic struct. 80−37818
PH_3+PH^*, collisional deactivation of PH ($b^1\Sigma^+$) state, time resolved spectra 78−78750
PH_3+radical ion, thermal energy charge transfer, reaction mechanism 77−16796
PH_4^++Ca, proton transfer reaction cross sections, 1-6 eV 78−20003
PH_5, equilibrium structure and harmonic force field, ab initio calc. 80−9502
PH_5, rearrangements, CI calcs. in large at. orbital basis 79−94106
P_2H_4, conformation, ab initio, HF, PNO-CI and CEPA calcs. 77−46495
P_2H_4, nucl. spin-spin coupling, scanning MO HF LCAO calc. 79−50045
PHD_2, vibr. dephasing in liq. and solid PD_3, calcs. 80−19884
$PH_3(D_3)$, ^{31}P NMR, chemical shielding, centrifugal distortion, anharmonic vibr., cubic force consts. 78−82752
PH_2F, total energy, MOs nonempirical minimum STO-4LGF calcs. 78−9074
PH_xF_{3-x}, geometry changes during inversion, ab initio calcs. 78−5154
$PH_2(F_2)(Cl_2)$, SCF-MO-HF calc., struct. and one-electron props., population anal. indices 79−76338
$P_xH_yH_z$, synthesis and struct. 80−54201

phosphorus compounds continued
$PH_3(PD_3)(PT_3)$, harmonic force fields, equal coord. method calcs. 77−30845
PH(PF), effective spin-spin parameter and singlet-triplet transition intensities, ab initio calc. 78−9067
$PH_2(PH_2^+)(PH_2^-)$, electronic structure, ab initio LCAO MO SCF calcs. 79−10027
$(PMo_{11}O_{39})_n^{7}$ decomp., in aq. soln., Raman spectra obs. 79−13719
$PMo_{12}O_{40}$, vibr. anal., symmetry coords. and force field anal., IR and Raman spectra 77−15522
$PMo_{12}O_{40}^{3-}$, vibr. force const. for spectroscopically active freqs. 77−57976
PMo_9O_{34} model vibr. freqs. 80−23408
PMu_3, (Mu=muonium), $n\nu_2$ vibrational levels, prediction of inversion splittings 78−90146
PN, absorpt. and emission spectra, electronic transition and vibr. obs. 80−91573
PN, matrix IR spectra, aggregation to P_3N_3 77−83599
PN, photoelectron spectra, ionisation pot., vibr. struct., Green's function method 77−61799
PN, valence electron photoionisation, ionisation pot. and spectral intensities 78−70883
PN, valence state interactions, ab initio and semiempirical estimates 78−74567
PN, vibr. struct. calcs. from photoelectron spectra 77−18973
P_3N_3, matrix isolated, IR isotope freq. and intensity patterns 78−46338
P_3N_5, appl. in P doping of Si by zone melting method 78−43035
$PN(X^1\Sigma^+)$, VUV photoelectron spectrum 78−1024
PO, $B^2\Sigma^+$ state perturbations 77−30849
PO, $C^2\Sigma^-$-$X^2\pi_r$ state, Franck-Condon factors and r-centroids 77−65512
PO, in Ar matrix, IR and UV absorpt. spectra 80−47985
PO, rot. struct. of absorpt. bands 1850-1600 Å, valence $^2\Pi$ state 79−13739
PO, $SiCl_2$ band system reassignment to PO and P_2 radicals 77−23505
^{18}PO, spectral intensity of $E^2\Sigma$-$X^2\Pi$ transition 79−50084
$P^{18}O$, UV absorpt. spectra, valence and Rydberg states, rot., vibr., anal., predissoc. 79−41184
PO_2^-, in K halides, ODMR in zero and weak mag. fields 80−88894
PO_4, distortion from T_d symm. 78−63706
PO_4 electron structure rel. to synthesis and utilisation of ATP 80−40955
PO_4 groups in biomembrane models, quantum-chemical investigation of cation motion mech. 80−30678
PO_4 ions, promotion of fusion of human erythrocyte ghosts, with Ca^{2+} ions 77−4987
PO_4^{2-} anion radicals + organic compounds, reaction rate consts. 78−15669
PO_4^{3-} adsorption equilibria in lake sediments 79−66354
PO_4^{3-}, ionisation energies, SCF-Xα transition state calcs. 80−74115
PO_4^{3-}, NO_3^-, $Si(OH)_4$, ratios in Moroccan upwelling region 80−4045
PO_4^{3-}, O isotope effect in ^{31}P NMR spectra 78−42100
PO_4^{3-}, removal kinetics in small alkaline lakes, natural and artificial processes 79−79417
PO_4^{3-}, synchrotron radiation excited fluoresc., O K-emission spectrum, electronic struct. 77−42335
P_2O_5 gas, for glazing ceramics 80−108609
P_2O_5, glass, refractive index, effects of alkali oxide comp. changes *(Russian)* 78−22182
P_2O_5, marine pollution determ. in Jordan Gulf of Aqaba 79−12142
P_2O_5, marine sediment content, India, W. continential shelf 80−8288
P_2O_5, pure vitreous, Raman spectra and struct. 79−69838
P_2O_5 type water vapour sensor 80−98907
P_2O_5, vitreous, Raman cross sections, rel. to appl. in fibre Raman lasers 78−31176
P_2O_5-CdO photochromic glasses, Weigert effect *(Russian)* 77−1690
P_2O_5-FeO glass, electrical cond., nonadiabatic hopping of small polaron 77−1417
P_2O_5-glass, diffusion of Cu^+, fluoresc. meas. 78−59980
P_2O_5-SiO_2 clad low-loss monomode fibres for 1.2 to 1.6 μm, modified CVD prep. 80−48479
$(P_2O_5)_x$-$(SiO_2)_{1-x}$, spontaneous Raman scattering *(French)* 79−78674
P_4O_6, IR and Raman spectra vibr. spectra, valence force field calc., pot. function *(French)* 78−50549
$POCl_3$ emitter diffusion effect on Si minority carrier lifetime degradation 77−76917
$POCl_3$, He I(II) XPS spectra comparison, ion states assignments, pseudopot. calcs. 77−61794
$POCl_3$ reaction with $ZrCl_4$ in O_2, for ZrP_2O_7 prep. 80−21272
$POCl_3^+$, ion states assignments, from He I(II) XPS spectra comparison, pseudopot. calcs. 77−61794
$POCl_3$:Pr^{3+} fluoresc. and lifetimes of excited states 80−71466
$POCl_3$:$ZrCl_4$:Nd^{3+}(Er^{3+}), radiative transition probabilities within 4f configs. 77−8617
$POCl_3$-$SnCl_4$, Sm^{3+} fluoresc. quenching temp. depend., near reson. interaction 79−65915
$POCl_3$-$SnCl_4$: Tb^{3+}, Sm^{3+}, lifetime and quantum yield of fluoresc. emission 77−20909
$POCl_3$-$SnCl_4$:Nd^{3+} laser, relaxation oscillations with high power spikes obs. 78−42331
$POCl_3$-$SnCl_4$:Nd^{3+}, liquid laser material, luminesc. centres conc., temp. depend. 79−50287
$POCl_3$-$SnCl_4$:Nd^{3+}, liquid laser material, luminesc. centres changes, crystn. process effects 79−50288
$POCl_3$-$SnCl_4$($ZrCl_4$)($TiCl_4$), splitting of Sm^{3+} near IR absorpt. bands 80−2750
$POCl_3$-$ZrCl_4$:Nd^{3+} free-running liquid laser, design and performance 77−14706
$POCl_3$-$ZrCl_4$:Yb^{3+}, Er^{3+}, energy transfer from Yb^{3+} to Er^{3+}, agglomeration formation 78−64405
$POCl_3$+N,N-dimethylformamide or N,N-dimethylbenzamide, reaction products 78−7199
$POCl_3$.$SnCl_4$:Nd^{3+}, phosphor, laser parameters and physiochem. props. 77−14709
POF_3, IR rot.-vibr. spectrum, mol. consts., laser Stark spectroscopy obs. 78−33508
POF_3, level anticrossing effects, vibr., laser Stark spectra obs. 80−32771
POF_3, nuclear resonance, effects of intermolecular interactions and intramolecular dynamics 80−63658
PON, synthesis and struct. 80−54201
$PO(SCN)_3$:Nd^{3+} solns., spectroluminesc. props. 77−16362
$(PO_2)_2$*, excimer, chemiluminesc., reduced press. system 77−32795

phosphorus compounds continued
PS, electronic transition $B^2\Pi$-$X^2\Pi$, vibr. and rot. anal. *(French)* 78−78716
PS, UV bands, rotational anal. 79−76443
P_2S_5-Ag_2S glass, Ag diffusion, 50-120°C 78−18828
P_4S_{10}, ^{31}P multiple pulse NMR, chem. shift anisotropy 78−52369
P_4S_{10}, gas, vaporisation and thermal dissoc. obs. *(French)* 78−47511
P_4S_3, ^{31}P NMR spectrum and spin-lattice relax. time, 77 to 500K and 7 to 25 MHz 79−8064
P_4S_3, gas, vaporisation and thermal dissoc. obs. *(French)* 78−47511
P_4S_3, UV photoelectron spectra, mol. orbital symm. 77−14494
P_4S_3, XPS spectra, binding energies, differential photoelec. cross sections ratios 77−65508
α-P_4S_4, cryst. struct. 78−51486
P_4S_7, gas, vaporisation and thermal dissoc. obs. *(French)* 78−47511
P_4S_9, P_4S_{10}, ^{31}P NMR spectra, cf. related cpds. 77−8427
P_4Se_3, UV photoelectron spectra, mol. orbital symm. 77−14494
$P_2Se_xS_y$ glass, thermophysical props., 303-413K, struct. interpretation 78−47615
P_2Se_xSy glass, vitrification temp., elec. props. and hardness meas. *(Russian)* 77−28177
$P(SiH_3)_3$, vibr. force fields and amplitudes, zero-point struct. 77−54551
α-$PVW_{17}O_{40}^{5-}$, α_2-$P_2VW_{17}O_{12}^{8-}$, aq. soln., hydrodynamic radii from ESR line width 79−78504
PbFCl+Gd^{3+}(Eu^{2+}), crystal field splifting, parametrisation of temperature dependence 78−91652
SPF_3, electronic struct. of valence shell, UV photoelectron spectroscopy 78−82781
$SbCl_5OPCl_3$, vibr. amplitude and normal coord. anal. *(German)* 78−66536
SiC filament reinforced phosphate foam ceramics, bending strength 80−11716
SiO_2:P_2O_5, GeO_2 fibre, anomalous conc. profile of P_2O_5 and GeO_2 77−79943
SiO_2:P_2O_5 optical fibres intrinsic attenuation 78−30067
SiO_2-Al_2O_3-CaO-BaO-SrO-ZnO-Na_2O-K_2O-B_2O_3, glaze effect of P_2O_5 additions 80−60824
SiO_2-CaO-Na_2O-P_2O_5 system, water, alkali, acid resist., chem. durability 79−34162
SiO_2-Li_2O-K_2O-ZnO-P_2O_5, glass ceramic, phase changes and crystn. processes 80−7562
$Si_{10}Te_{40}As_{30}P_{20}$, amorphous films, optically assisted mono-stable switching 77−11968
$Sn_2P_2S_6$, illumination effect on soft mode and dielectric props., luminesc. study *(Russian)* 80−50420
$Sn_2P_2S_6$, investigation of p-T diagram near a singular point *(Russian)* 80−88937
$Sn_2P_2(Se_xS_{1-x})_6$, ferroelec. tricrit. phase transform., light transmission study 80−71355
$TaCl_5OPCl_3$, vibr. amplitude and normal coord. anal. *(German)* 78−66536
TeO_2-P_2O_5, electron microscope exam. of phase equilib. and immiscibility 78−52779
$Te(OH)_6.Na_2HPO_4.H_2O$, X-ray cryst. struct. determ. *(French)* 79−69077
$Te(OH)_6.2(NH_4)_2HPO_4$, X-ray cryst. struct. determ. *(French)* 79−69077
U assay of phosphate materials 78−82589
U content, α-ray autoradiography, fluorimetry, comparison of results 78−20414
V_2O_5-P_2O_5 glass, EPR investig., samples with varying V^{4+} content and cond. 77−8389
V_2O_5-P_2O_5 glasses containing metallic particles, elec. props. 79−42547
V_2O_5-P_2O_5-H_2O, formation of $VOPO_4.2H_2O$ 77−44228
V_2O_5-P_2O_5-Nb_2O_5 glasses, switching 80−88604
ZrO_2-P_2O_5, hydrated, heat treatment and coprecipitation, phase transitions 77−90335

phosphosilicate glasses
AES quantitative anal., electron irrad. induced surface comp. changes 77−48709
binary, fibre fusion temp. rel. to composition 78−95131
bridge structure across V-groove formed by etching in Si 80−104312
coatings in semicond. devices, corrosion in high temp. water and moisture 77−48564
cored fibre CVD production 77−39120
CVD, flow for integrated optical cct. fabrication 80−79005
CVD, P. conc. meas. 77−80533
CVD coatings, P content meas. using SEM and energy-dispersive X-ray anal. 80−76588
deposited, P conc. meas. 79−69014
deposition on contaminated Si wafer, Au redistrib. during growth 77−4121
etching characts. by plasma reactive sputter etching 78−27661
film, CVD, P conc. profile by etch rate technique 80−96450
film, passivation of MOS struct., flat-band voltage, effect of growth conditions 80−107913
film, props., rel. to deposition conditions, appl. in semicond. devices 78−23612
film, SiO_2 rich, prepared by modified CVD, refr. index behaviour 78−60526
film, thickness and IR spectrum changes on heat treatment in H_2 80−70549
film, vapour-deposited, structural model IR spectra meas. 77−1084
film , for IC protection, X-ray fluoresc. method for rapid P determ. 77−40612
graded-index fibre material dispersion evaluation using nanosecond pulse radiator 79−81520
multimode fibres, cladding influence on light attenuation 79−76855
optical fibre waveguide, possibility of near IR operation 78−50935
optical fibres, refr. index and comp. data 77−79950
optical single-mode fibre with low attenuation, MCVD fabrication 80−53461
passivation films, advances in deposition processes, review 78−23620
passivation layer P content, SEM analysis and interpretation 78−35759
phosphosilicate glass flow mechanism, and appl. in MOS devices 77−77393
refractive index behaviour, optical fibre appl. 77−46777
selective etching rel. to Si by plasma reactive sputter etching 80−81221
silicophosphate melts, diffusion 79−46824
single-mode fibre birefringence and optical activity obs. 78−1394

phosphosilicate glasses continued
$BaO-P_2O_5-SiO_2$, photoelastic consts. and polarisability 79−65839
$BeO-P_2O_5-SiO_2$ glasses, photoelastic consts. and polarisability 79−65839
$CaO-P_2O_5-SiO_2$, photoelastic consts. and polarisability 79−65839
$CdO-P_2O_5-SiO_2$ glasses, photoelastic consts. and polarisability 79−65839
$GeO_2-P_2O_5-SiO_2$ glass fibre, incorporation of OH in modified CVD process 80−50560
$GeO_2-P_2O_5-SiO_2$ graded-index fibres, effect of deposition rate on spectral loss 80−87485
$GeO_2-P_2O_5-SiO_2$ long spliced graded-index fibre transmission charact. at 1.27 μm 79−81536
$Li_2O-SiO_2-P_2O_5$ glass ceramic fibres, heat treatment, crystn., tensile strength 80−84995
$MgO-P_2O_5-SiO_2$, photoelastic consts. and polarisability 79−65839
$Na_2O-P_2O_5-SiO_2$ glass, metastable liquid immiscibility 80−100331
$Na_2O-P_2O_5-SiO_2$ glass, substitution of Li^+, Mg^{2+}, Sr^{2+}, Ba^{2+}, Zn^{2+} for Na^+ 80−100332
P content determ. by Rutherford backscatt., PIXE, and activation anal. *(Hungarian)* 80−85233
$P_2O_5-SiO_2-GeO_2$ graded-index optical fibre, UV induced losses 80−87518
$P_2O_4(OH)_4^{2-}$ group, electronic struct. calcs. 78−67971
$PbO-P_2O_5-SiO_2$ glasses, photoelastic consts. and polarisability 79−65839
SiO_2:$GeO_2-P_2O_5$ graded-index fibre, spectral loss charcts. in long wavelength band 79−59811
$SiO_2-CaO-Na_2O-P_2O_5$ system, water, alkali, acid resist., chem. durability 79−34162
$SiO_2-GeO_2-B_2O_5-P_2O_5$, optical waveguide glass, comp. determ., plasma emission spectra 80−87446
$SiO_2-P_2O_5$, optical attenuation in IR region 77−75665
$SiO_2-P_2O_5$, optical fibre, wavelength dispersive props. and comp. 78−33793
$SiO_2-P_2O_5$ cladding vapour-phase axial deposition fibres at 1.3 μm and 1.6 μm 80−9996
$SiO_2-P_2O_5-GeO_2$, optical fibres, UV radiation-induced losses 80−87517
$SiO_2-P_2O_5-GeO_2$ optical fibres, CVD, losses, reactant impurity effects 80−87522
$SiO_2-PO_{5/2}$ glass, props. and struct. *(Japanese)* 77−27837
SiO_2-PSG-Si_3N_4 composite layer, on Si, crack occurrence, PSG film thickness and comp. effects 77−72806
$SrO-P_2O_5-SiO_2$, photoelastic consts. and polarisability 79−65839
$ZnO-P_2O_5-SiO_2$, photoelastic consts. and polarisability 79−65839

photoacoustic effect
acoustic microscope modification for microscopic scale photoacoustic obs. 79−18637
acoustically nonresonant optoacoustic signal depend. on pressure, buffer gases and microphone response 79−59862
aerodynamic effects of supersonic flow past laser beam 78−38366
alkali halide thin films, photoacoustic determ. of optical absorptance of highly transparent solids 79−40632
atmospheric propagation of modulated laser beam, acoustic pulse generation, thermal defocusing 79−92597
benzene, liquid, C-H stretch, seventh harmonic, absorption profile 79−56806
carbon tetrachloride, laser generated acoustic wave press. saturation, absorptivity at higher laser power 79−60435
ceramics, piezoelectric, photoacoustic effect 80−84252
chiral compound, circular dichroism, polarisation modulated photoacoustic spectroscopy 80−18018
Doppler thermooptical source of US waves 80−58852
dye solns., single and two-photon spectroscopy, using pulsed acousto-optical effect 77−68087
excitation of sound by a moving opticoacoustic source which emits pulses of arbitrary shape 80−79041
far IR optoacoustic material probing and imaging 80−83559
ferromagnetic resonance detection 80−20463
FIR laser, optically pumped, nearly transparent power monitors 80−5773
first order phase transitions at increasing and decreasing temp. studied 80−70320
floating optoacoustic antenna, statistical characteristics 79−27485
fluid half-space, sound generation by modulated laser absorpt. 78−9526
gas, acoustical theory 80−1729
generalised theory 78−63232
imaging with the optoacoustic effect 80−106473
IR detector, optoacoustic, micromodular version 79−49291
laser beam energy monitoring, photoacoustic detector, construction and calib. *(Czech)* 78−29156
laser beam moving over fluid surface, sound radiation from thermal sources 80−38161
laser beam sound generation in liquid, effect of harmonic variation of modulation freq. 79−19321
laser generation of sound in fluid half-space with 2 types of boundary roughness 80−15194
laser pulse absorption for thermal generation of sound, theory and expt. 79−64393
laser radiation interaction with liquids and solids, sound generation 78−1485
laser thermooptical sound source in liquid, anal. of wave zone 80−87631
laser-generated stress waves in liquids 79−14887
laser-generated US waves, freq. spectrum 80−53537
liquid, absorbing intense IR radiation, behaviour of pressure 80−102749
liquid, acoustic field of moving optoacoustic antenna 79−14193
liquid, laser breakdown, photoacoustic and photohydrodynamic parameters 78−52597
liquid, laser-induced acoustic waves, CO_2 laser transverse mode struct. influence 79−77683
liquid, pulse phenomena 78−1486
liquid acoustical theory 80−1729
liquid film, thermal interf.-optical excitation of US waves 78−71794
liquid half-space, sound generation by FM modulated laser beam 78−38781
liquid half-space bounded by solid layer, optical generation of sound 80−38158
liquid layer floating on liquid half-space, acoustic field generated by laser beam 78−51615
liquid surface scanned by laser beam, acoustic field of moving optoacoustic antenna 79−90108
liquid waveguide, sound generation by modulated laser beam 78−1539
liquids, acoustic perturbations caused by laser radiation 79−4373

photoacoustic effect continued
liquids, photoacoustic and photorefractive detect. of small absorpts., electrostrictive limits 80−108171
metal, EM generated ultrasound, position dependent amplitude 79−37763
metal-liquid interface, laser generated MHz elastic waves 79−73387
methane, 6190 Å spectral line, press. broadening detected by photoacoustic 79−94033
methane, liquid, opto-acoustic study of weak optical absorpt. 80−93278
methane-d + methane-d_4 (inert gas), vibr. relax. time meas. by photoacoustic effect 77−88541
microscope using, with resolution of several microns 79−64456
microscopy, principle and appl. to semiconductor industry 80−14525
moving inhomogeneous fluid, optical generation of sound 78−34568
moving pulsed optoacoustic sources for sound generation 80−87634
one dimensional theory for solids 80−65168
optical fibre, optoacoustic effect obs. using piezoceramic transducer 80−48423
opto-acoustic antenna, floating, acoustic field statistical charcts., surface waviness depend. *(Russian)* 78−1536
optoacoustic exciter, nonlinear limit on efficiency 80−28406
pentacene doped p-terphenyl mol. cryst., laser induced photoacoustic grating effects 79−55215
physical and technical acoustics, conf., Parnu, USSR (Apr. 1976) 78−1451
polymer film, thickness effect on magnitude of optoacoustic signals 80−11969
polymethine dye solution, optoacoustic response 80−6465
pulsed thermoacoustic array, near field waveforms 79−95083
review, appl. to telephone receiver, optical links development *(Czech)* 78−77994
review 79−41786
SAW generation using CW laser, NDT appl. 80−87683
semiconductor, determ. of bulk and surface absorption coeffs. 80−4781
semiconductor surface, depth profiling, optoacoustic technique 80−65337
solid, photoacoustic effect, three-dimensional 80−107379
solid, photoacoustic signal, heat loss influence 80−100308
solid, signal production accounting for surface thermal resist 79−64473
solid flaw remote sensing, laser system prod. acoustic waves, interferometric detect. 78−60975
solids, review *(Japanese)* 80−31887
sound generation by laser, nonlinear theory of thermal mechanism 80−38147
sound generation by long laser pulses incident on liquid surface 80−5900
sound generation in a liquid by laser pulses of arbitrary shape 79−33669
sound generation of absorpt. of laser radiation in fluid half space 78−18089
sound wave generation in liquids by laser pulse 78−83882
sound with finite tracks, generation by laser beam 79−90731
Stark modulation of absorbed laser radiation in optoacoustic detector 79−94325
steel, C, EM excitation of US at high temps. 80−33412
stroboscopic method for study of optoacoustic interactions 78−94498
subsurface structure detection by scanning photoacoustic microscopy 80−6323
supersonic optoacoustic antenna, acoustic field 78−1540
teaching approach, rel. to wave physics 80−42003
temperature nonlinearity in thermal generation of sound by laser radiation 79−99271
thermal wave microscopy, physical processes 80−74652
thermal-wave microscopy, high-resolution studies 80−74647
thermally thin solids, photoacoustic effect 80−75304
thermooptical generation of nonsteady acoustic fields 80−15193
three- and four-dimensional photoacoustic store readout 80−48413
three-dimensional heat flow 80−48840
transonic gas flow, optical excitation of intense acoustic waves 80−74564
water, photoacoustic effect, nsec. and psec. laser pulse induced 78−38777
water, thermal excitation of acoustic waves by periodic sequence of nanosecond laser pulses 79−95084
Al, subsurface flaw detection by photoacoustic microscopy 80−66725
$BaTiO_3Fe_2O_3$, photoacoustic effect, first order phase transitions at increasing and decreasing temp. 80−70320
CdS crystals, orientational depend. of photoacoustic effect *(Russian)* 80−65167
CuCl, mech. vibrs. in piezoelec. solid, excitation by light pulses 80−75305
$CuSO_4$ solution, thermooptical excitation of sound by ns. laser pulses 80−79884
Fe films, ferromagnetic reson., photoacoustic detection 80−80613
Fe, foil, ferromagnetic resonance detection by photoacoustic effect 80−20463
Ga, photoacoustic detection of phase transitions 78−75810
Ga, solid-liq. transition, photoacoustic effect study 80−70320
Ge crystals, orientational depend. of photoacoustic effect *(Russian)* 80−65167
H_2O, photoacoustic detection of phase transitions 78−75810
I_2, vibr.-translational relax., collisional predissoc., opto-acoustic effect obs. 80−43157
KCl:Eu^{2+}, radiationless processes 78−80391
K_2SnCl_6, photoacoustic detection of phase transitions 78−75810
N_2, liq., photoacoustic and photorefractive detect. of small absorpts., electrostrictive limits 80−108171
Ni films, ferromagnetic reson., photoacoustic detection 80−80613
Si, photoacoustic signal changes assoc. with crystallinity, recrystallisation after laser annealing 80−16127
SiC-ceramic, nondestructive evaluation, scanning photoacoustic microscopy 80−85115
Si_3N_4-ceramic, nondestructive evaluation, scanning photoacoustic microscopy 80−85115
SmS, film, laser generation of US using metal-insulator transition 79−90734
VO_2, photoacoustic effect at first order phase transitions at increasing and decreasing temp. 80−70320

photoacoustic spectroscopy
absorption coefficient, optical, absolute meas., photoacoustic spectroscopy 80−82828
absorption coefficients meas., photoacoustic calorimetry technique 78−24839
absorption coefficients meas. technique 78−24864

photoacoustic spectroscopy continued
acetic acid, photocatalytic oxidation, photoacoustic spectroscopic obs. 79−16010
acetylene smoke, optoacoustic meas. of absorpt. at 0.5145, 10.6 μm 80−43060
acetylene smoke particles, optoacoustic meas. 80−50895
acoustically nonresonant optoacoustic signal depend. on pressure, buffer gases and microphone response 79−59862
air containing carbohydrates, methane, ethylene, ethane IR spectra, optical acoustic method *(Russian)* 78−74663
air pollution monitoring, spectrophone measurement of absorpt. coeffs. at CO_2 laser wavelengths 80−26193
air pollution photoacoustic detector charact. at CO_2 laser freqs. 79−100554
analytical applications, direct exam. of solid and liq. samples 80−7886
atmospheric aerosol, in situ absorption meas. using reson. CW laser spectrophone 77−73860
atmospheric aerosol absorption of visible light, spectrophone meas. 78−4000
background signal in optoacoustic detector 80−31913
benzene, $^1B_{2u}$ and $^3B_{1u}$ states nonradiative decay, collisional deactivation 77−6819
benzene, liq., C-H stretch vibr. overtones, optoacoustic spectrosc. obs. 79−93982
benzene, optoacoustic spectroscopy, weak visible absorpt. spectra, pollution monitoring in liquid phase 79−58797
benzene+$O_2(^1\Sigma_u^-)$, photo-oxidation mechanism, optoacoustic determ. 77−12808
benzene and deuterates, highly vibr. excited intramolecular V-V transfer, visible and photoacoustic spectra 80−32729
benzene in CCl_4, weak 607nm absorpt. band obs. by optoacoustic spectroscopy 79−35855
benzene liquid, two-photon absorption spectra and cross-section meas. 79−82993
biological and medical appls., book contrib. 80−109078
bridge type receiving system for acoustic detector of photoacoustic spectrometer *(Russian)* 77−61128
buffer gases, role in optoacoustic-spectroscopy 78−62228
cartenoprotein, lobster shell, organisation studied by photoacoustic spectroscopy 79−62192
cell, high-performance, small vol. 78−8451
cell design, reson. enhancement, background signals 78−4700
cell design and characteristics for photoacoustic spectroscopy of condensed matter 80−52326
cell for liquids and solids, one-dimens. model generalisation 80−82827
cell for mirror scan Michelson interferometer 80−68277
cell resonances from standard ultrahigh vacuum components 79−12862
cell size considerations, pulsed excitation response, time depend. 78−65977
cell size considerations, rel. to gas thermal diffusion length 77−45894
cell with improved performance for NO detect. 77−66987
ceramics, piezoelectric, photoacoustic effect 80−84252
chain reactions, photochem., opto-acoustic detect. method 80−90913
chemical analysis by acoustic emission following laser irradiation of actively absorbing impurities *(Russian)* 77−21451
chlorodifluoromethane, photoacoustic spectra meas. at CO_2 laser wavelengths 80−18849
chrysotile asbestos, photoacoustic spectrum using CW HF laser 80−7980
circular differential photoacoustic spectroscopy 80−47114
coal, cleaved surface, photoacoustic IR spectra 80−87104
condensed samples, spectrometer and sample cell 77−5921
corrosion resistant optoacoustic cell for spectrosc. of liquids 80−42269
crystalline material optical absorption meas. 80−105718
dermatological applications, water content meas. and drug detect. 78−31883
dermatology research appls. 79−57823
diacetylenes, photopolymerisation, solid-state reaction, photoacoustic photocalorimetric obs. 80−61089
dichlorofluoromethane, photoacoustic spectra meas. at CO_2 laser wavelengths 80−18849
dichroism measurements 78−62227
dielectric coatings, for laser mirrors, surface optoacoustic spectrometry 78−87085
diesel smoke particles, optoacoustic meas. 80−50895
differential spectrophone meas. of IR laser absorpt. by atm. dust 77−9513
dye solution, fluoresc. yield, photoacoustic determ. method 78−42117
dye solution, luminesc. quenching, pulsed photoacoustic detection technique 77−85780
dyes, spectra and quantum yields *(French)* 80−101845
eosin, photoacoustic spectra in soln. 80−9606
ethyl acetate, photoacoustic spectra meas. at CO_2 laser wavelengths 80−18849
ethylene, IR multiphoton excitation, optoacoustic meas. 80−1038
ethylene in exhaust gas, optoacoustic detect. using line-selectable CO_2 laser 78−56947
ethylene in gas mixtures, optoacoustic detect. in urban areas and fruit storage chambers 79−87886
excited state vibrational energy transfer, for optoacoustic spectroscopy 78−37724
experimental apparatus *(Japanese)* 80−31903
explosive vapours, laser optoacoustic absorpt. spectra 78−76941
far IR gas laser pump line, optoacoustic determ. 79−31872
fluorescent solutions, quantum yields, optoacoustic determ. 77−12415
fluoromethane, optically pumped laser, IR-FIR transferred Lamb dip spectra 80−1193
fluoromethane, vibrational-translational transfer rate, optoacoustic meas. using short pulse CO_2 laser 80−74258
Fourier rapid scan spectroscopy 78−78004
Fourier transform IR spectroscopy of liquid and solid samples 80−90911
frequency dependence, surface and bulk absorpt. coeffs. 77−53981
furan, photoacoustic spectra meas. at CO_2 laser wavelengths 80−18849
gas cell, surface and bulk absorption coeffs. meas. of transparent media 77−5920
gas trace conc. meas., spectroscopy, and photochem. appls. of photoacoustic detect. 79−74474
glass, transition metal and rare-earth doped, photoacoustic spectrosc. 80−92611
glucose powder and aqueous soln., photoacoustic spectra in middle IR 77−81101
glyoxal, $S_0 \rightarrow S_1$ band, opto-acoustic phase angle meas. 80−68256

photoacoustic spectroscopy continued
graphitic C, optically absorbing component of urban aerosol particles, photoacoustic meas. 79−96493
haemoglobin macroporous particle study, photoacoustic spectrometry 80−85543
Helmholtz resonance cells for dye laser excited spectra 80−9048
Helmholtz resonance effect in photoacoustic cells 79−75602
Helmholtz resonator as optoacoustic detector 80−31896
high-resolution photoacoustic spectroscopy for dopant depth profiling 80−77883
hydrazine rocket fuel in ambient air, CO_2 laser absorption spectra and photoacoustic detection 80−104540
imaging and image processing 80−95143
impurity microconcentrations in liquids analysis using opto-acoustic effect 80−50916
industrial application possibilities 80−106692
insulator, mag. transition sp. ht. anomaly, photoacoustic meas. 80−4773
IR optoacoustic spectroscopy of atmospheric gases 77−41243
IR photoacoustic Fourier transformed spectroscopy of solids 80−86465
IR photoacoustic spectra of solids 80−73484
IR spectroscopy of solids and liquids 80−13163
laser optoacoustic detection spectroscopy, appl. to mol. measurements 77−54629
laser optoacoustic spectroscopy for gas chromatographic detection 78−92521
laser photoacoustic detector spectroscopy, calibration using HD 5-0 transitions 80−77877
laser radiation action on condensed medium, hydrodynamic effects 80−93439
laser radiation detector, IR, spatial resolution 79−17493
laser radiation optoacoustic power monitors 79−41404
laser window materials, surface and bulk absorpt., photoacoustic meas. 78−25912
light scattering effects, diffusion processes 80−95144
linear base spectroscopy opto-acoustic technique, review 78−29170
liquid, laser induced acoustic pulses, photoacoustic cell arrangement 78−21222
liquid, photoacoustic Raman gain spectroscopy 79−75606
liquid film, micron thick, optoacoustic spectroscopy using pulsed dye laser 80−42265
liquids, linear and nonlinear absorpt., photoacoustic determ. *(German)* 80−37090
liquids, trace anal., freq. modulated laser optoacoustic technique 77−70349
liquids, weak absorption spectra meas. by pulsed dye laser optoacoustic spectroscopy technique 79−58797
liquids acoustic relaxation mechanism, using coherent optoacoustic spectroscopy scheme 80−5890
luminescence quantum field meas. of solns. 77−86335
luminescent solid, nonradiative processes obs., theoretical assessment and expt. 77−90185
magnetospectrophone for Zeeman spectroscopy of NO 77−83647
metal, optoacoustic phase angle meas. for subsurface struct. 80−28388
methane, (methane-Xe)(methane-NH_3), mol. relax., optoacoustic reson. meas. 80−27351
methane, liquid, opto-acoustic study of weak optical absorpt. 80−93278
methane, photoacoustic Raman spectroscopy under pulsed laser excitation 80−82825
methane, photoacoustic Raman spectroscopy using CW laser sources 79−44947
methane+methane and methane+monatomic collisions, photoacoustic study of vibr. relaxation *(French)* 77−30969
methanol, optically pumped laser, IR-FIR transferred Lamb dip spectra 80−1193
methanol excited by CO_2 laser, sub-Doppler optoacoustic spectrum 80−5545
methyl alcohol, photoacoustic spectra meas. at CO_2 laser wavelengths 80−18849
methyl halide-inert gas mixtures, vibr. energy relax., opto-acoustic obs. 80−95711
methyl halides, vibr. energy relax., opto-acoustic obs. 80−95711
methyl sulphoxide, photoacoustic spectra meas. at CO_2 laser wavelengths 80−18849
microscope development which gives map of thermal properties of sample surface 80−73479
molecular excited vibr. states, optoacoustic laser spectroscopy 77−19106
molecular fluorescence quantum yield meas., appl. to benzene vap. 77−88595
molecular gases, optically pumped, use of optoacoustic effect to discover CW far IR laser lines 77−79803
molecular solid, intermolecular interactions, laser induced phonon probe 80−79891
molecular vibrational-translational transfer rate, optoacoustic meas. using short pulse CO_2 laser 80−74258
multiphoton molecular absorption in strong i.r. field 77−507
nonlinear signal, appl. to nsec. time resolution 77−74511
open membrane spectrophone, spectral meas. on liq., powder and anodic films 79−225
optical absorption coefficients, absolute, photoacoustic determ. 77−38019
optical coatings and materials, photoacoustic spectroscopy study 80−64124
optical communications appl. *(French)* 78−48143
optoacoustic detection of absorption, sensitivity to laser geometry 80−73473
organic liquids, pulsed opto-acoustic spectroscopy 80−62743
organic molecules, far IR laser active, optoacoustic spectra 79−59448
pentacene in p-terphenyl, intermolecular interactions, laser induced phonon probe 80−79891
perylene, intermolecular interactions, laser induced phonon probe 80−79891
phase measurement, appl. to nonradiative transitions, optical absorpt., in solids 80−31885
phosgene, spectrophone meas. at selected CO, CO_2 laser wavelengths 78−57310
photoacoustic double-beam spectrometer, for use in UV, visible and near IR regions 79−79320
photoacoustic Raman spectroscopy using CW laser sources 79−44947
photoinduced gas consumption system, photoacoustic spectroscopic obs. 79−16010
photoinduced gas evolution system, photoacoustic spectroscopic obs. 79−16010

photoacoustic spectroscopy continued
photothermophone, device for absolute calibration of photoacoustic spectrometers 78−16854
piezoelectric detection of photoacoustic signals 78−54467
piezoelectric photoacoustic detection, theory and expt. 80−90904
polarization modulated, for measurement of circular dichroism 80−18018
polymer film, thickness effect on magnitude of optoacoustic signals 80−11969
polystyrene film, Fourier-transformed IR photoacoustic spectra 80−34993
powder samples, signal enhancement technique 78−65976
powder solids, spectrometer and performance characts. *(Korean)* 79−9247
powdered sample, expt. system 77−87846
powders, analysis by photoacoustic and photothermal spectroscopy 79−61929
principles and applications, PAS market 80−68258
propynal, rovibronic populations, collisionless IR multiphoton spectra, energy deposition, photoacoustic determ. 80−83354
pulsed dye laser technique for small absorpts. meas. in liquids 79−35855
pulsed photoacoustic Raman spectrosc., gaseous trace anal. 80−40769
pulsed source spectrophone, DF laser wavelengths, appl. to methane 77−23494
quantitative absorption spectra, by phase angle meas. 79−17502
quartz optoacoustic apparatus for highly corrosive gases 79−35843
quinine bisulphate, aq. soln., abs. fluoresc. quantum efficiency, optoacoustic determ. 78−16849
rapid-scan Fourier spectroscopy and methyl alcohol interferograms 79−30585
rare earth ions in aq. solns., optoacoustic spectroscopy using pulsed dye laser for micron thick film 80−42265
reflection-absorpt. spectroscopy for IR anal. of surface species 80−105723
relaxation time measurements in frequency and time-domain photoacoustic spectroscopy in condensed phases 80−82826
resonant cell design optimisation, for photoacoustic gas spectroscopy 78−56924
resonant optoacoustic cells for trace gas analysis 79−11840
response of optoacoustic cell, data taken with fixed-freq. lasers 78−37077
review, appl. to telephone receiver, optical links development *(Czech)* 78−77994
review, theory, operation of instruments and test results 78−4705
review *(Japanese)* 78−89554
rhodamine 6G, photoacoustic spectra in soln. 80−9606
Rosencwaig-Gersho theory, extension to include sample coating effects 80−52319
rubrene, photooxidation, photoacoustic spectroscopic obs. 79−16010
ruby, nonradiative processes obs. 77−90185
ruby, quantum efficiency, photoacoustic meas. 80−73472
sample cell, for photoacoustic spectrometer, appl. to solids, liqs. 77−74520
scattered light effects 77−18099
semiconducting powders, band-gap energies, photoacoustic meas. 80−70579
semiconductor, determ. of bulk and surface absorption coeffs. 80−4781
semiconductors, electron-phonon interaction, photoacoustic cell appl. 78−68027
signal production in solid, theory accounting for surface thermal resist. 79−64473
Signal/noise ratio in opto-acoustic channels of gas analysers for the case of an electrometric microphone circuit *(Russian)* 77−82616
simple cell for single and differential meas. 78−86349
single beam spectrometer, for near IR region 79−14167
small optical absorption coefficients, photoacoustic meas., extended theory 79−71533
smoke aerosols, optical absorption to extinction ratio, photoacoustic determ. 80−58459
solar selective coatings, photoacoustic determination of absorptance and emittance 80−77876
solid, heat flow effects 79−89007
solid, optical absorption coeff. meas. technique 77−26402
solid, phase transitions 80−69615
solid, photoacoustic measurement of absolute quantum efficiencies 79−19924
solid, semi-solid and liquid samples, photoacoustic spectroscopy review 79−89013
solid materials, anal. using microcomputer assisted single beam photoacoustic spectrometer 78−58044
solid spatially varying absorpt., theory of photoacoustic meas. 77−32341
solid-state reaction, photoacoustic photocalorimetric obs. 80−61089
solids, criteria for light sources, sample chambers and data acquisition systems 78−4709
solids, optical absorption spectra determ. of CdS, $KMnO_4$ and rare-earth elements 80−13160
solids, review *(Japanese)* 80−31887
solids and surface species, IR photoacoustic spectroscopy 80−90909
solids immersed in transparent liquids 80−22452
spectrometer design considerations for spectroscopy of solids 77−41687
spectrophone, contamination source removal 77−18110
spectrophone, resonant, transversely excited 79−23153
spectrophone resonant cavities, theoretical model 80−92001
subsurface imaging 80−74648
surface analysis techniques and appls., symposium, Dayton, USA (Jun. 1979) 80−62363
surface species, IR photoacoustic spectra in 4000 to 2000 cm^{-1} region using broadband source 79−26149
technique and applications to solids 79−44953
techniques, general description 80−31884
theoretical aspects 78−65975
theory, techniques and appls., book contrib. 80−9050
thermally available vibrational energy levels, energy transfer, photoacoustic and IR emission obs. 79−72402
thermally thick samples, quantitative spectroscopy 80−68257
thermoacoustic coupling effects 79−44954
thin film, laser damage, photoacoustic study 80−80098
time resolved, applications 78−89550
time-domain, nonradiative lifetime meas. of condensed phases 80−55232
time-domain photoacoustic spectroscopy of solids, one-dimens. model 79−89010
photoacoustic spectroscopy continued
toxic gas monitor based on laser photoacoustic spectrometer *(German)* 80−12046
trace gas analyser with CO_2 laser 79−5245
trace gas analysis, with reson. optoacoustic cell operating inside CO_2 laser cavity 78−27836
trace-gas remote analysis, optoacoustic radiometry limitations 80−108759
water, optical absorption coeff. 79−82992
water vapour, attenuation of HF/CO_2 laser beam 80−61905
water vapour, i.r. CO laser beam absorpt., optoacoustic meas. 77−2241
water vapour absorption of CO_2 laser beam, optoacoustic detector meas. 77−9512
water vapour submillimetric-wave absorption obs. 80−61901
Al_2O_3, films on Al, photoacoustic refl.-absorption spectroscopy 78−31264
$Al_2O_3:Cr^{3+}$, crystal, radiationless relaxation processes exam. 78−27264
As_2S_3, appl. of expt. system for powdered samples 77−87846
$BaTiO_3:Cr^{3+}$ crystal, radiationless relaxation processes exam. 78−27264
BiI_3, photoacoustic spectroscopy 79−42992
C particulate, airborne, photacoustic and absorption spectrum using tunable dye laser 80−4102
CO, sensitive optoacoustic detection by reson. absorpt. 78−44981
CO_2, collision relax. 180-400K, spectrophone method 77−61832
CO_2, excited by CO_2 laser, sub-Doppler optoacoustic spectrum 80−5545
CO_2, photoacoustic Raman spectroscopy under pulsed laser excitation 80−82825
CO_2, pure rotational stimulated Raman photoacoustic spectroscopy 80−32724
$CO_2+CO(N_2)$, vibr. relax., optoacoustic obs. *(French)* 78−42178
CO_2+inert gas, intramol. energy transfer, 153-393K, photoacoustic obs. 79−54943
$CO_2+N_2(CO)$, CO_2 1st vibr. levels collisional deactivation, photoacoustic study 79−98187
$CO_2(01^10)+N_2(CO)(O_2)$, collisional deactivation rate const., 160-375K, photoacoustic obs. 79−10179
CdS, phonon-coupled photoacoustic spectroscopy 80−54317
CdS-$NiCl_2$ interface, elec. props. using SAW techniques 79−56302
D_2O, pulsed opto-acoustic spectroscopy 80−62743
Dy_2O_3, powdered cryst., high resolution optoacoustic spectroscopy 80−31898
Er_2O_3, powdered cryst., high resolution optoacoustic spectroscopy 80−31898
GaAs, ion implanted and laser-annealed, photoacoustic meas. 80−47117
Ge, laser irradiation, photoacoustic detection 80−2901
HCl, overtone vibr.-rot. bands, intracavity dye laser techniques meas. 80−91532
HD, 5-0 transition, intracavity photoacoustic detector spectrosc. obs. 80−77877
HD, $\nu=0$ to $\nu=5$ rot.-vibr. band, photoacoustic spectrosc. obs. 80−9589
H_2O, D_2O, visible absorpt. meas., pulsed dye laser optoacoustic spectroscopy 80−11426
H_2O isotopes, spectrophone meas. at selected CO, CO_2 laser wavelengths 78−57310
H_2O, pulsed opto-acoustic spectroscopy 80−62743
Ho_2O_3, photoacoustic spectra using Helmholtz reson. cells 80−9048
Ho_2O_3, powdered cryst., high resolution optoacoustic spectroscopy 80−31898
I_2, Doppler-free optoacoustic spectra 80−995
$^{127}I_2$, Doppler-free optoacoustic spectroscopy 80−57396
KCl crystals with NaF surface absorpt. regions, photoacoustic detect. 79−87466
KCl:Eu^{2+}, radiationless transitions, photoacoustic spectra 77−32405
Li, seeded flames, excitation, laser radiation absorpt., sound vel., optoacoustic effects obs. 80−43345
Li seeded in acetylene-air flame, optoacoustic pulses, energy transfer from laser excited atoms 78−25490
MgO:Cr^{3+} crystal, radiationless relaxation processes exam. 78−27264
NH_3, photoacoustic spectroscopy at 9 μm, 10 μm $^{12}C^{16}O_2$ laser wavelengths 79−21014
$(NH_4)_2SO_4$ powder and aqueous soln., photoacoustic spectra in middle IR 77−81101
NO, $^2\Pi_{1/2}$ and $^2\Pi_{3/2}$ band centre freqs., opto-acoustic detection 77−58108
NO excited state vibrational energy transfer, for optoacoustic spectroscopy 78−37724
NO isotopes, spectrophone meas. at selected CO, CO_2 laser wavelengths 78−57310
^{15}NO, vibr.-rot. transitions, Λ-doubling, optoacoustic spectroscopy meas. 78−42062
NO_2, optoacoustic detect. using pulsed dye laser 78−27835
N_2O, pure rotational stimulated Raman photoacoustic spectroscopy 80−32724
Na seeded flames, excitation, laser radiation absorpt., sound vel., optoacoustic effects obs. 80−43345
Na seeded in acetylene-air flame, optoacoustic pulses, energy transfer from laser excited atoms 78−25490
$Na_2NdPb_6(PO_4)_6Cl_2$, self-activated mini-laser material, quantum yield determ. 79−33773
Nd^{3+} ions, in solids, radiationless decay processes, laser photoacoustic spectroscopy meas. 80−84766
Nd:glass, Fourier-transform photoacoustic spectroscopy 79−9246
Nd:glass laser rod, piezoelectric detection of photoacoustic signals 78−54467
$NdAl_3B_4O_{12}$, self-activated mini-laser material, quantum yield determ. 79−33773
$NdMoO_4$, photoacoustic spectroscopy, dichroism meas. 78−62227
Nd_2O_3 powder, piezoelectric detection of photoacoustic signals 78−54467
NdP_5O_{14}, fluoresc. lifetime meas., IR and photoacoustic spectroscopy 80−60652
NdP_5O_{14}, self-activated mini-laser material, quantum yield determ. 79−33773
$Nd_xY_{1-x}P_5O_{14}$, conc. quenching 79−61435
PbF_2-TlI graded coatings on KCl laser windows 80−33052
S compounds, unstable, forbidden transitions, laser optoacoustic spectroscopic obs. 77−61756
SF_6, CO_2 laser excited, optoacoustic meas. of energy absorpt. 77−83667
SF_6, CW CO_2 laser spectroscopy 80−83367
SF_6, collisionless multiphoton dissoc. rate, statistical thermodynamic process 77−50482

photoacoustic spectroscopy continued
SF_6 detection in air, photoacoustic spectroscopy, resonant cell design optimisation 78−56924
SF_6, multiple-photon two-freq. IR laser pumping, optoacoustic spectroscopy 79−36717
SF_6Ar, multiple photon excitation, saturation and linear absorpt., pulsed optoacoustic detect. 78−42148
SO_2, optoacoustic detect. in air-pollution control below parts per billion level 78−41355
SO_2, vibr. relax., phase spectrophone method obs. 80−87059
Si, electron-phonon interaction anal. using photoacoustic cell 78−68027
Si solar cells, photovoltaic energy conversion efficiency, photoacoustic spectra 79−15178
Si_3N_4 ceramic, surface and subsurface struct. by photoacoustic spectroscopy 78−68481
$SrTiO_3:Cr^{3+}$ crystal, radiationless relaxation processes exam. 78−27264
TlI coatings on KCl laser windows 80−33052
TlI powders, photoacoustic spectroscopy obs. 79−12855
UF_4, quantitative determ. of amorphous deposits from plasma 78−53303
UF_6, CW CO_2 laser spectroscopy 80−83367
VO_2:Al, photoacoustic effect study of phase transitions 80−69615
WF_6, CW CO_2 laser spectroscopy 80−83367
ZnSe laser windows, AR coated, photoacoustic chopping freq. studies using CO_2 laser 80−83629
ZnSe laser windows, photoacoustic signal var. with chopping freq. 80−75309
ZnSe laser windows and coatings on CaF_2 80−33052

photobleaching *see optical saturable absorption*

photocapacitance
see also photodielectric effect
diamond Schottky barriers, photocapacity meas. 78−52057
Franz-Keldysh effect, optically enhanced for n^+-p-n^+ phototransistor struct. 78−60423
III-V semiconductors, deep level defects, review 80−24841
magnesium phthalocyanine, film, depletion layer studies, temp. depend. of LF capacitance 80−65617
MIS struct., photocapacitance-current investigation of fundamental absorpt. edge 77−4397
MIS structures, surface recomb. and photoeffect, statistics *(Russian)* 78−39221
MOS interface states density, photoemission obs. using photocurrent and photocapacitance meas. 80−92990
MOS system photocapacitance, influence of surface charge fluctuations *(Russian)* 78−43480
photo-deep level transient spectroscopy, capacitance transient spectra with lock-in method *(German)* 79−65512
semiconductor, remanent deep impurities, capacitative spectrosc. 79−82628
semiconductor, surface photoelectric effects, influence of excitation rates 79−69547
semiconductor devices, remanent deep impurities, capacitative spectrosc. 79−82628
semiconductors, defect characterisation by capacitance methods 77−51692
tetracene, film, depletion layer studies, temp. depend. of LF capacitance 80−65617
Al-amorphous Se-Al struct., capacitance variation with illumination 79−87165
Al-Si_3N_4-Si struct., surface energy bands under step function illumination 80−49840
$Al_xGa_{1-x}As$, DX photocond. centres, photocapacitance and DLTS meas. 80−11044
$Al_xGa_{1-x}As$, LPE layer, deep levels, photocapacitance obs. 77−15790
$Al_xGa_{1-x}As$:Cr, deep level props. 79−69465
$Al_xGa_{1-x}As$:Te, persistent photocond. trapping centre, donor complex model, photocapacitance meas. 79−65517
$Ba_xSr_{1-x}Nb_2O_6$, nonequilibrium processes 78−48124
$CdIn_2S_4$, impurity centres, photoluminesc. and photocapacitance data on config.-coordinate diagrams 78−10938
CdS Schottky barrier solar cells, spectral distrib. and photocapacitance 80−55864
CdS:Cu film, dynamic quenching of photocapacitance, deep levels obs. 77−85175
CdS:Cu films IR quenching of photocapacitance, deep level detection 79−56258
CdS/Cu_2S thin film heterojunctions, photocapacitance meas. of solar cell parameters 80−93897
CdS-Cu_2S heterojunction, energy-band struct., capacitance-voltage charcts., illumination effects 80−96982
CdSe, polycryst. film, photocapacitance, inductive effect and US oscills. *(Russian)* 77−8142
$CdSeTl_x$-As_2Se_3Tl, thin layer system, charge transport 77−76985
CdTe:Cl, capacitance meas. and trapping, mol. centre model *(French)* 77−39872
CdTe:Cl, description of anomalous centres by non-purely electronic model 78−30886
CdTe-CdS heterojunction, photocapacitance and photocond. 80−96978
$Ga_{1-x}Al_xAs$-$Ga_{1-y}Al_yAs$ p-n heterojunction, minority carrier lifetime, elec. charcts. and electrolum. meas. 78−2554
GaAs, deep levels, photocapacitance meas. under hydrostatic press. 77−85259
GaAs, deep trap charcts. by photocapacitance spectroscopy 78−6398
GaAs epitaxial film, deep centre reson. charging, photocapacitance meas. on Schottky barrier 78−26908
GaAs grown by VPE using organometallic method, deep trap levels 80−10923
GaAs, LPE layer, deep levels, photocapacitance obs. 77−15790
GaAs LPE layers, deep levels by photocapacitance and related techniques 78−6334
GaAs microcharacterisation for device appls. 80−10922
GaAs, optical cross sections associated with deep levels, O centre obs. 80−6777
GaAs, photocapacitive MIS IR detector, spectral response, noise charcts. 80−75644
n-GaAs Schottky barrier, boat-grown, deep levels *(Japanese)* 79−47043
GaAs Schottky barrier, Auger de-excitation of metastable state 79−65410
n-GaAs, Schottky barriers, minority carrier trap meas. 78−26951
GaAs:Cr, acceptor levels, photocapacitance meas. 79−95443

photocapacitance continued
GaAs:Cr, deep levels, wavelength-modulated photocapacitance spectroscopy 80−76055
GaAs:Cr, Schottky barrier, trapping processes effect on photocapacitance 77−76866
GaAs:Cr(O), photocapacitance of deep levels obs. 79−38021
n-GaAs:Cu, electron-phonon interaction in optical transitions between deep impurity level and allowed bands 79−42591
GaAs:Fe epitaxial diode, photocapacitance meas. 77−43708
GaAs:O, deep traps, photocapacitance meas., complementary transition energy threshold determ. 79−19550
GaAs:O, evidence for metastable state of O centre, Schottky barrier photocapacitance meas. *(French)* 78−10556
GaAs:O, photocapacitance quenching effect 78−91727
GaAs:O epitaxial film, impurity states, photocapacitance spectra 80−65625
GaAs-Si heterojunction, IR quenching of photocapacitance 80−92968
$GaAs_{0.65}P_{0.35}$, gamma irradiated, deep level study using DLTS and photocapacitance methods *(Japanese)* 80−49665
GaN:Zn, cathodoluminesc., photocapacitance 79−38679
n-GaP, deep state controlled minority carrier lifetime 80−20211
GaP green-emitting lamps, deep level photocapacitance spectra 77−69409
GaP LED, red, efficiency degradation and deep level change, photo-and thermally stimulated capacitance obs. 77−81155
GaP:Cr, local level near valence band, photocapacitance 79−11080
GaP:N VPE LED, deep level centres, DLTS studies 79−42493
Ge MIS photocapacitative IR detector 80−47106
Ge, spectrum of photocapacitance current near fundamental absorpt. edge 77−28217
InP, deep trap charcts. by photocapacitance spectroscopy 78−6398
n-InP Schottky barriers, photocapacitance effects of deep traps 78−43325
InSb inversion layer, spectroscopy of electron subband levels 78−10569
Si, deep level transient spectroscopy *(French)* 79−11079
Si, diffusion of Os, diffusion parameters using photocapacitance and four-probe methods 79−51314
p-Si, fast electron irrad., energy levels determ. by photocapacitance meas. 79−51531
Si, MIS photocapacitive IR detector 78−62223
Si, photocapacitive MIS IR detector, spectral response, noise charcts. 80−75644
Si, positively charged divacancy photoionisation cross section by photocapacitance meas. 80−6901
Si:Au diodes, γ-irrad. effects, photocapacitance meas. 77−66199
-Si:Fe, effect of γ-irradiation, photocapacitance meas., impurity centre conc. 78−18993
Si:Ir, precipitation of solid soln., photocapacitance, electrical resistivity meas. 78−47833
Si:Os, P, photoelec. props., depend. on P conc. 79−91099
Si:Os, photocapacitance meas. of impurity levels 77−55579
n-Si:Pd Schottky diodes photocapacitance meas., photon and carrier capture cross sections 80−20309
Si:Pt, photoionisation cross-sections, photocurrent and photocapacitance meas. 78−10497
Si:Re, diode, barrier capacitance and photocapacitance, uniaxial press. effect 77−20416
Si:Re, photocond. and photocapacitance 77−15902
n-Si:Re, photon capture cross sections of Re levels, spectral depend. 77−89726
Si:Re diode, photocapacitance and induced photocapacitance spectra 77−4404
n-Si:Re diode photocapacitance spectra, Re centre dissociation 79−90997
Si:Ru, photon- and carrier-capture cross sections of Ru levels 79−90995
Si:S, two-electron donor centre, photoionisation cross-section meas. 77−8044
Si:S diode, ionisation energies of S levels, photocapacitance meas. 77−4432
Si:Sc, photocapacitance and photoconductivity 80−107859
Si:Y, photoelectric props. 80−107860
Si-SiO_2-Si_3N_4, internal photoemission 80−7475
ZnS:Ag film, evaporated, IR quenching of photocapacitance, deep levels obs. 78−56180
ZnS:Ag film, photocapacitance IR quenching, hole photoionisation energy and spectral distrib. 79−87127
ZnS:Cu(Pb), phosphor, photocapacitive effect, Gudden-Pohl effect 79−65520
ZnSe, deep centres, photolum., photocapacitance and photocurrent expts. 78−39053
ZnSe:Cu, deep energy levels 80−6774
p-ZnSe:Li(Na)(N)(P), LPE layers, photocapacitance and photocond. meas. 79−99572
ZnSe:Ni, impurity level meas. 77−69372
ZnSe-Si heterojunctions, IR quenching of photocapacitance 80−92968
ZnTe, electronic and optical parameters of O-related centre 77−24534
ZnTe:Cu, red centre, electric and optical props. 80−20239
ZnTe:O, deep centres, photocapacitance detection 79−95362
ZnTe:O, electronic and optical parameters of O related centre, photocapacitance obs. 78−6399
ZnTe-In Schottky diodes, photocapacitance determ. of electron-hole recomb. *(French)* 79−47119

photocatalysis *see catalysis*

photocathodes
see also photoemission
alkali antimode, prep. and props. 78−84693
alkali metal multilayers, high field enhancement of photoemission 78−19639
astronomical ultralow light level imaging by intensified CCD 77−41287
biplanar image converter, photocathode switching 80−19105
dissector operation, advantage of one-electron mode 78−58039
electron gun with photocathode for electron beam controlled laser 77−50678
extra-fast shutter, for soft X-ray photography *(French)* 78−41397
GaP/$In_xGa_{1-x}P$/GaAs:(Cs-O) high sensitivity transmission photocathodes, photosensitivity, electron diffusion length 79−78832
high resolution imaging X-ray detector, for astronomical meas. 78−49333
image, dissector tubes, echelle spectrographs, design considerations 80−91918

photocathodes continued
light spot location photocathode of quantum detect. accuracy estimation 78−77832
metal photocathodes, for absolute intensity meas. in soft X-ray and vac. UV region 77−71412
multialkali antimonide photocathodes, emission and work functions 79−78836
multialkali photocathodes, secondary emission characts. 78−84687
multialkaline antimonides, (Sb, Na, K, Cs) type, photoemission rel. to chem. struct. *(French)* 78−39655
negative electron affinity devices *(Japanese)* 79−38710
negative electron affinity III-V photocathodes for soft X-ray detection 78−93110
negative electron affinity model and photoemission quantum efficiency, with GaAs expt. *(French)* 77−8724
one-electron dissector, LI-604, exponential branch of output pulse amplitude distrib. 77−30203
optical communication, atmospheric UV propagation 77−79770
Photicon, new imaging optical detector 77−67499
photocathode polarisation sensitivity, two-beam interferometer expts. 80−4772
photoemission review, book contrib. 77−32506
photomultiplier amplitude-time characteristics 79−12850
photomultiplier nonlinear mode of operation of photocathode with focused laser beam 79−85183
photomultipliers for BBQ applications 80−27896
prebreakdown ionisation current spatial growth expts., initial photoelec. current changes 78−67566
reradiation effects in negative electron affinity photocathodes 80−55274
scintillation counter, large, light collection uniformity improvement 78−78569
semiconducting photocathodes, carrier transport simulation, Monte Carlo method 80−71575
semiconductor photofield emission cathode, potential distrib. and model 78−2977
semitransparent multialkali photocathodes, UV response, efficiency 77−167
sensitivity uniformity over surface, distortion of zone charact. by interference in substrate 80−58709
transmission, III-V semiconductor materials, charcts., and epitaxial growth *(French, English)* 78−52616
X-ray camera, photocathodes, charcts., for X-ray diagnostics of laser-induced plasmas 77−54031
X-ray ionization chamber, high-pass photocathode, for surface EXAFS 79−68164
Ag, photoemission-into-electrolyte 79−74390
Ag/p-$In_{0.77}Ga_{0.23}As$ photocathode, field assisted photoemission to 2.1 microns 80−76130
Ag-Cs_2O photocathode, light absorption and photoemission 80−50510
Ag-Cs-O photocathode, operation mechanism involving Cs_2O_2 80−66384
Ag-O-Cs, Ag granules and colloidal particles on Cs_2O film *(Chinese)* 80−2279
Ag-O-Cs, for image convertor tube, temporal resolution 78−33908
Ag-O-Cs, photoemission investig. 77−16461
Ag-O-Cs cathode, photoemission mechanism *(Chinese)* 79−19966
Ag-O-Cs photocathode, Ag colloidal particles and long wavelength response *(Chinese)* 80−45195
Ag-O-Cs photocathode, role of Ag colloidal particles in photoemission *(Chinese)* 80−40215
Ag-O-Cs photocathode structure 78−95661
Ag-O-Cs photocathodes, time resolution, contrast-time charcts., calcs. 77−7208
Ag-O-Cs surface, oxidation, role of Cs suboxides in low work function surface layers, XPS 80−76131
Al, photocathode in X-ray detector photoelec. diode, calibration 77−54033
$Al_xGa_{1-x}As$ semitransparent photocathode, LPE, quantum efficiency spectrum 80−76153
Al_2O_3, anodised film, arc cathode root initiation, electron emission, UV radn. effects 78−2985
Al_2O_3, anodised film, charge storage, UV radn. effect on electron emission arc roots 78−6827
Al_2O_3, for windowless XIV photodiode, photoefficiency 20 to 250 eV 78−65963
Al_2O_3, optical absorption and external photoeffect, 6-40 eV 77−55802
Au, photoemission-into-electrolyte 79−74390
Au, X-ray cathode, secondary electron energy distrib. excited at 277 and 1487eV 77−8716
CdTe, photochemical production of H_2, characteristics 77−70311
CsI photocathodes, efficiency evaluation for soft X-ray diagnostics 80−57442
Cs_3Sb photocathode, wavelength-modulated photoemission spectra 80−29857
Cs_2Te, photocathode for proximity focused image convertor, field enhancement of photoemission 78−72677
Cs_2Te photocathode middle UV low light level imaging devices 77−41319
CuI photocathodes, efficiency evaluation for soft X-ray diagnostics 80−57442
$Ga_{1-x}Al_xAs$ based layer structures, optimum growth conditions, comp. and struct. perfection 80−104069
GaAs (111) epitaxial film, adsorption of Cs, Cs+O, ellipsometric study, photocathode sensitivity 80−29282
GaAs epitaxial multilayer photocathode structures, TEM obs. of dislocations generated 80−100241
GaAs, high performance refl. NEA photocathode 77−48303
GaAs negative electron affinity cold cathode 79−87558
GaAs, photo-field cathode, ageing and surface state effects *(Russian)* 77−28703
GaAs photocathode, emitted electron transverse energy 77−12489
GaAs photocathode and aspheric lenses for filter-tilting type nightglow photometer 77−73889
GaAs, photocathodes, photoelectron emission, energy levels, influence of dimens. quantisation *(Russian)* 78−64447
GaAs photoemission characteristics, parameters of emitters with negative electron affinity 79−4898
GaAs, produced by pyrolytic synthesis 79−43100
GaAs, spin polarised electron source for LEED 78−83693
GaAs, surface segregation of implanted alkali metals, photoemitter prep. and charcts. *(French)* 78−60544
photocathodes continued
GaAs, with Cs-O adlayer, negative electron affinity, core level photoemission of adlayer 79−19965
GaAs-$Al_xGa_{1-x}As$-GaP, minority carrier diffusion length determ. by photoluminesc. 80−103992
GaAs-Cs-O, negative electron affinity, fabrication and charcts. 78−2979
GaAsP, negative electron affinity process obs. by laser beam scanning *(Japanese)* 80−55262
$GaAs_{1-x}P_x$, high quantum efficiency photoemission 77−44115
GaInAs, photocathode with negative electron affinity, photoemission, influence of strong elec. field 79−8227
$Ga_{1-x}In_xAs$, negative electron affinity, photoelectron scatt. in Cs-O film 79−28899
$Ga_{1-x}In_xAs$, photocathode, work function depend. of photoelectric emission 78−68071
GaP, Cs(Cs-O) activated, with negative electron affinity, thermalised electron emission 78−11073
GaP, Cs(Cs-O) activated, with negative electron affinity, near UV photoemission and secondary emission 78−11074
p-GaP electrode, spectral response extension by metal adatoms 78−34895
p-GaP photocathode, charge transfer via surface states, water photoelectrolysis anal. 80−75636
gaAs photocathodes for low light level imaging 79−37043
Ge, photo-field cathode, ageing and surface state effects *(Russian)* 77−28703
Ge photocathodes, Au absorbed photofield emission current spectral investigation 80−29856
$In_{0.53}Ga_{0.47}As$, LPE growth on (100) InP, for field assisted photocathode appl. 78−15318
InGaAsP heterojunction cathode, transferred electron photoemission 78−48272
InGaAsP photocathodes for astronomical detectors, UV response 77−57387
InGaP/InGaAs struct. for transferred electron photocathodes, VPE growth and characterisation 80−76193
p-InP field-assisted photocathodes, quantum efficiency 80−84831
InP/InGaAs/InP field assisted photocathode, minority carrier electron transport across p-p heterojunction 78−95651
InP-$In_xGa_{1-x}As$ alloys, semiconductor photoemitters, field-assisted, 1-2 μm range 80−97396
InP-InGaAsP bias assisted photocathodes, photoemission in 1-2 μm range 78−48289
K_3Sb, and Na_2KSb, band struct., empirical pseudopotential calc. 78−10346
K_3Sb, photocathode material, optical and dielec. props., energy spectra, density of states calc. 80−20083
Na_2KSb(Cs), photocathode, optical props. 79−78827
Na_3Sb, and Na_2KSb, band struct., empirical pseudopotential calc. 78−10346
Rb_2Te film electron affinity and photoelectron work function obs. 79−69959
p-Si, achievement of negative electron affinity 78−2980
Si field emission photocathodes, emission current noise charcts. 80−100746
Si multiple tip field emission photocathode, photokinetics 80−100480
Si, negative electron affinity surface activation, laser beam scanning obs. 79−4890
Si, negative electron affinity process obs. by laser beam scanning *(Japanese)* 80−55262
Si, photo-field cathode, ageing and surface state effects *(Russian)* 77−28703
Si photofield cathode, BaO adsorbed layer, work function and emission props. *(Russian)* 78−68608
Si, single-tip and multitip cathodes, fabrication, and photofield emission charcts. 78−2976
Si:Cs-O photocathodes negative electron affinity electron emitting devices, reson. transmission 77−90240
Si_xGe_{1-x} multitip photofield emission cathode, fabricated by crystn. from vapour, emission charcts. 78−2975
SiO_2, optical absorption an external photoeffect, 6-40 eV 77−55802
W (100), Cs and O_2 coadsorbed, high photoemission efficiency 77−55862
W, for windowless XUV photodiode, photoefficiency 20 to 250 eV 78−65963
ZnO electrode surface, dye sensitisation mechanism, from reson. Raman spectrum obs. 78−42066
ZnO-Cs, fabrication, UPS meas. 78−15279
ZnTe electrodes for photochemical production of H_2, a comparison 77−70311

photocells *see photoelectric cells*

photochemistry
see also photochromism; photodissociation; photoelectrochemical cells; photolysis; photosynthesis
E,E-1,4-diphenylbutadiene-(1,3), isomerisation, reaction quantum yields, exciting light bandwidth influence study *(German)* 80−21310
abietic acid in polymer matrix, photosensitised oxidation, singlet O_2 diffusion *(Russian)* 79−52655
acetic acid, photocatalytic oxidation, photoacoustic spectroscopic obs. 79−16010
acetone-d_6, multiphoton dissoc., recomb. to ethane 80−3371
acetylcholine receptor response to rapid photochem. prod. increases in agonist conc. 77−36909
acetylene, multiphoton UV photodissoc. 78−50602
acetylene, photolytic polymerisation rel. to presence in Jupiter stratosphere 80−31244
acetylene+ICl, isotopically selective photoaddition, ^{37}Cl enrichment 77−60084
acrylamide, laser-initiated polymerisation kinetics, holographic obs. 79−29383
adatom laser stimulated migration and multiphoton excitation, relax. and reaction enhancement 79−39200
aerosol, photochem. prod. of submicron particles of very narrow size distrib. 79−29491
aging of nonsilver photographic materials in different gas media *(Russian)* 79−44972
air pollutants from N oxides 78−36271
air pollution, photochemical, potential form. in United Kingdom, numerical estimation method. 80−76682

photochemistry continued
air pollution, weekend-weekday differences 78−3921
air pollution in NE.United States 79−83677
L-alanine:Cr^{3+}, X-irrad., thermoluminesc., ESR, UV photobleaching 77−9104
albumin, human serum, kinetics of eosin-sensitised photochemilum. of solns. 78−68991
aldehydes, formation, anal. *(Japanese)* 78−88648
alicyclic ketones, triplet state behaviour, non-RRKM photochemical decay, vibr. relax. 78−61030
alkaline ice, trapped electrons, photostimulated decay, time-depend. rate const. 79−52692
allyl isocyanide, state-selected, visible absorption spectra and photoisomerisation kinetics 80−11879
amino acid photodegradation in presence of TiO_2 78−11531
6-amino-7-hydroxy-4-methylcoumarin solutions, additions effect on fluoresc. 80−2833
3-aminophthalimide-ethanol soln., luminesc. quantum yield, photoacoustic method, reaction energy 77−86335
anthracene:2-hydroxyanthracene, site-selective photochem., fluoresc. spectra at 3K 78−80756
anthracene:2-hydroxyanthracene cryst., site selective photochem. change, fluoresc. obs. 77−40273
anthracene:rhodamine, triplet exciton density, isotope substitution effect, in weak mag. field 77−90184
anthracene, and related derivatives, fluoresc. and photoreactivity 77−48668
anthracene, in atmosphere, photooxidation on particulate matter 80−61487
anthracene, single cryst. with photoinduced local centres, luminesc. 79−61433
anthracene, singlet and triplet excitons as probes for photochem. reactivity 79−74406
anthracene, spectral evidence for green incipient dimers after photooxidation and photodimerisation 78−15687
anthracene and dianthracene, phase equilib. in photocondensation *(Russian)* 79−7561
anthracene cryst., mol. orientational disorder calc. vacancies, dislocations, photodimerisation 77−4915
anthracene in polychlorinated alkanes photochemical study by rapid scanning fluoresc. spectroscopy 80−86440
anthracene-aliphatic amine, photochemically induced H isotope exchange 79−11771
anthracenes, bridged, photochemistry and spectra 77−77793
anthraquinone dyes, phototropic transformations, fibre-forming polymer substrates effects *(Russian)* 77−66762
bis(9-anthryloxy)polyoxaalkanes,, intramolecular excimer form. and photodimerisation, kinetic anal., rate constants determ. 80−66800
antiStokes photosensitisation, red light to blue light transmission 79−20391
aqueous glasses, mixed solute, luminesc. following laser excitation of trapped electrons 78−31666
1-arylbutadienes, lowest excited singlet states, photochemical implications 77−30795
atmosphere, annual var. of effects of diffuse solar radiation on O_3 photodissoc. 80−109210
atmosphere, gas-to-particle conversion in photochem. smog, organic aerosol growth rates 77−73826
atmosphere, hydrocarbon concentrations meas., photochemical reaction appl. *(Dutch)* 78−36300
atmosphere, O_2 and O_3 photodissoc. in stratosphere and mesosphere through solar UV radiation absorpt. 80−109248
atmosphere, O_3 budget, zonal mean circulation model and linearized photochem. 77−70780
atmosphere, O_3 layer, photochemical-diffusive model, chlorocarbon industry impact 78−40648
atmosphere, O_3 photochem. prod., W.Europe, rel. to meteorology 77−78292
atmosphere, one-dimensional photochemical model rel. to instantaneous global O_3 balance 80−109211
atmosphere, one-dimensional photochemical model rel. to O_3 evolution over geological time 79−96788
atmosphere, perturbed, photochemical radiative convective model for thermal struct. and relaxation rates 80−8408
atmosphere, photochem. smog enhancement by N,N′-diethylhydroxylamine in polluted ambient air 77−91262
atmosphere, photochemical air pollution initiation by HONO (nitrous acid) in urban air 80−76677
atmosphere, photochemical form. of natural organic aerosols of terrestrial origin 80−36381
atmosphere O_3 production transport and distribution, numerical simulations with global general circulation model 80−56544
atmosphere photooxidation reactions, rates, reactivity and mechanism for organic compounds reaction with OH radicals 80−72104
atmosphere pollution, photochemical numerical model 80−40943
atmospheric chemistry, reaction rates and photochemical data 78−77312
atomic collisions with energy conservation by photons 77−60098
axially irradiated cylindrical photoreactor, plug flow model 79−47942
7-azaindole dimers, photoautomerisation by double proton transfer, fluoresc. kinetics 80−11880
azastilbenes, trans-cis photoisomerisation, theory 77−50466
azides, in polymer matrices, photooxidation, rel. to crosslinking 80−66832
azoethane, in hydrocarbon glass, 77K, photoisomerisation, matrix memory effect, quantum yield 78−7213
azomethines, photochromic, intramol. proton phototransfer sensitisation, organic cation energy transfer 78−53230
bacteria, photosynthesis, primary electron acceptor, EPR, ENDOR investigs. 78−77004
bacterial photosynthesis, light collection and harvesting processes investig. on psec. time scale 77−90743
bacteriochlorophyll, photochem. oxidised, kinetics of dark reduction, R. rubrum chromatophores 77−25390
bacteriochlorophyll, photooxidation, picosecond absorption spectroscopy investig. 78−82053
bacteriochlorophyll, R. rubrum reaction centres, selective ps laser excitation in condensed phases 79−48217
bacteriochlorophyll P870, photo-oxidised, dark reduction kinetics, temp. depend. 77−36888
bacteriorhodopsin, 13-cis and trans isomers, photochem. and dark equilib. 77−90798
photochemistry continued
bacteriorhodopsin, excited state energy surface to explain photochemistry 79−48218
bacteriorhodopsin, kinetic isotope effects in photochem. cycle 77−44592
bacteriorhodopsin, new intermediates in photochem. conversions 78−96010
bacteriorhodopsin, photoreactions, purple membrane light energy transduction 77−90726
bacteriorhodopsin, photosynthetic cycle, time-resolved Raman spectra 78−85294
bacteriorhodopsin, primary intermediates in photochem. cycle 78−96011
bacteriorhodopsin, selective ps laser excitation in condensed phases 79−48217
bacteriorhodopsin, subpicosecond spectroscopy, photochemical formation of bathobacteriorhodopsin 79−16156
bacteriorhodopsin, time-resolved resonance Raman spectroscopy 77−29103
bacteriorhodopsin 580 nm ultrafast transient, psec kinetics 78−44455
bacteriorhodopsin chromophore, light-induced isomerisation 80−108956
bacteriorhodopsin in purple membrane, chromophore mobility 77−25366
bacteriorhodopsin isomers, dark equilib. and photochem. 78−15771
bacteriorhodopsin of purple membrane, quantum efficiency for photochem. conversion 77−29099
bacteriorhodopsin photoconversion products, EPR and low temp. spectrophotometry 78−15769
bacteriorhodopsin photocycle quantum efficiency 77−29098
bacterioviridin, photochem. oxidation mechanism 77−25370
bacterioviridine photo-oxidation in monomer and aggregated states, free radical form., EPR 78−76994
beam-addressable optical display using supersaturated vapour photonucleation 80−4691
benzene, fluoresc., triplet state and isomerisation yields, photochem. 77−1942
benzene+$O_2(^1\Sigma_u^-)$, photo-oxidation mechanism, optoacoustic determ. 77−12808
benzophenone, sensitised crosslinking, polymerisation, UV curing, IR investig. 78−35709
benzyl radical, in solid Ar, absorption and photodissociation spectra 80−69156
2-benzyl-5-benzylidenecyclopentanone, and substituted form, topochem. single-cryst.-to-single-cryst. photodimerisation 80−66819
biimidazole+leuco dye photochem. reaction, modulation by photopolymerisation 80−40714
bimolecular mixed-valence metal complex, intramol. intervalence charge transfer 79−76405
binaphthyl anion radicals, photoisomerisation, local heating effects 78−85179
biological objects, reactions, excitation by pulsed LED *(German)* 79−16250
biological photochemical and photophys. processes, conf., New Delhi, India, (Jan.' 72) 78−11694
biomolecules, laser irradiated, selective photochemical mechanisms 79−66450
biphenyl gluterate diacetylene, monomer, single cryst., stable and metastable UV photoexcited states, EPR obs. 79−78522
bleaching-wave front, stability 77−42574
brass photocorrosion in $CuCl_2$ and $FeCl_3$ aq. solns. 79−57145
s-cis-butadiene, natural orbitals, photochem. cyclisation 79−85900
trans-2-butene, Ar matrix, TEA CO_2 laser irrad. photoisomerisation study 80−21303
calorimetric techniques for excited states detection 78−32847
carbocyanine dye solns., photoisomerisation and internal conversion rates, time-resolved spectra 77−75201
β-carotene in PVC matrix, photo-oxidation *(French)* 79−34327
cationic dyes, adsorbed ionisation energy, local environment effects 79−34337
CdTe thin polycrystalline film for photoelectrochemical cell 78−23162
cells, electrochemical, photovoltaic phenomena and mechanisms 78−8198
cellulose acetate fibre and film, stabilisation, post UV-irrad. mech. strength *(Russian)* 79−24778
chain reactions, opto-acoustic detect. method 80−90913
charge exchange, photon-assisted nonresonant, mol. model 77−16803
chemical reaction wave, propag. of coherent probe light pulse 80−61190
chirping laser for photochemical applics. 77−38902
chlorin, free-base, in n-alkane matrices, photochem. hole burning, optical dephasing 80−21305
chlorin in n-alkane host, photoautomerisation and hole-burning 79−47954
chloroform, production from polyelectrolytes, enhancement by UV irrad. 77−78252
chlorophyll, photooxidation, triplet state mechanism 78−27791
chlorophyll, photosynthesis mechanism, upconversion, EPR and O_2 evolution data anal. 78−35811
chlorophyll a, phosphoresc., triplet state, photochem. reacts. *(Czech)* 78−78842
chlorophyll a, photo-oxidation by p-benzoquinone, nature of electron-excited state 78−76991
chlorophyll a, photo-oxidation obs. using pulse photoconductivity 79−79447
chlorophyll a-n-chloranil lamellar system, heat stimulated conductivity 79−53043
chlorophyll analogues, mechanism of activation of photosensitising action 79−57583
chlorophyll excited stated, redox pots. 77−25372
chlorophyll in marine dinoflagellates, photosynthetic characts. and organisation 79−5260
chlorophyll monolayer electrodes, light energy conversion, photosynthesis electrochem. simulation 79−43833
chlorophyll photo-oxidation, role of singlet-excited and triplet states 80−51156
chlorophyll photo-oxidation by quinones, cation-radical yield 77−86442
chlorophyll photochemical activity, rel. to microviscosity of detergent micelles 77−21478
chlorophyll photoexcited aggregates, pigment-pigment electron transfer and charge separation 77−81468
chlorophyll pigments of photosynthetising organisms redox pots. rel. to evolutionary development 77−56337
chlorophyll-a, photoinduced electron transfer to duroquinone in micellar soln., charge separation 78−23955
chlorophyll-duroquinone photochemical interaction, photopot. 77−16903
chlorophylls a and b, photo-oxidation primary processes 79−79468

photochemistry continued
chloroplast fragments, fine struct. of fluoresc. spectra, derivative spectroscopy method *(Russian)* 79−34502
chloroplast fragments, paramagnetic centres and photochemical reactions 79−53061
cholecalciferol, UV dependent synthesis in a green plant 80−35860
cholesteryl cimmanate, photoreaction in solid, mesomorphic, and isotropic phases 79−87863
circular dichroism of phototransients, meas. apparatus using modulation excitation 77−46656
closed illuminated system, oscillatory and runaway states 79−47950
collisional processes, nonreson. laser field effects 77−60093
collisionless processes, nonreson. laser field effects 77−60093
colloidal photochromic dyes, quasi-crystals produced in applied electric field 80−85225
comet comae, gas-phase chemistry in one dimension 78−93154
comets, CO-rich, photochemistry and struct. of ionospheres 77−29723
conference, Gaithersburg, MD, USA (June 1976) 79−52709
conference, Heverlee, Belgium (July 1978) 80−3378
cryogenic solutions, spectrosc. and photochem. 80−16713
curing, UV, photochem., liq. ink appl. 78−35709
cyanine dye sensitisers, J-aggregate formation, spectral changes of UV bands 77−70318
cyanine dye sensitisers, J-aggregates, circular dichroism and induced Cotton effect 77−70319
cyanine dye sensitisers, J-aggregates, meso substituents effect on mol. assoc. 77−70320
9-cyanoanthracene, cryst., excimer emission, spectra, photochem. and multiphonon processes 78−10914
9-cyanoanthracene, quenching of solid state photodimerisation reaction by cryst. doping 78−68547
cycloheptatriene, and substituted forms, vibr. highly excited, steady-state photoisomerisation 80−16704
cycloheptatrienes, substituted, photoisomerisation, rate consts. 78−35708
cyclohexane-NO_2-air mixtures, photochem. particulate form. 78−11529
cytosine derivatives, photosensitised induction by H-addition radicals in frozen aqueous soln. 78−20146
11-cis-13-demethylretinal, photoisomerisation, high quantum yield 79−57253
di-tert-butylazodicarboxylate, photochem. generated alkali cationic triple ions, ESR 78−80758
diacetylene, low temp. photochemical polymenisation, decay kinetics, ESR spectra obs. 80−100616
diacetylene, photopolymerisation, optical absorpt. spectra, time depend., reaction kinetics 80−85174
diacetylene, single cryst., EPR of low-temp. photoproducts, photopolymerisation 78−85175
diacetylene, single cryst., photopolymerisation, intermediate states, struct. changes 80−30235
diacetylene (TSHD), low temp. photopolymerisation, short chain intermediates obs. 80−93754
diacetylene monocarboxylic acids, multilayers, struct. phase transitions and polymerisability 80−80129
diacetylene single crystals, photopolymerisation, optical transmission spectroscopic exam. 78−27757
diacetylene-d_2, excited quintet states during photopolymerisation, ESR obs. 80−84635
diacetylenes, photopolymerisation, solid-state reaction, photoacoustic photocalorimetric obs. 80−61089
diacetylenes, solid state photopolymerisation, reaction products, electron spin resonance anal. 80−81338
p-diazoquinone, photodecomp. 80−7827
dibenzoyl peroxide, UV irrad., radical pairs EPR 79−73813
dibromodifluoromethane, isotopically specific TE laser induced chem. reactions 77−90622
dicarbocyanine solns., photoisomerisation, fluoresc. and absorpt. spectra of photoisomer 78−85181
1,8-dichloro-9-methylanthracene, structural changes, photodimerisation and stacking fault energy 77−62548
dichlorodifluoromethane, isotopically specific TE laser induced chem. reactions 77−90622
trans-1,2-dichloroethylene, Ar matrix, TEA CO_2 laser irrad. photoisomerisation study 80−21303
trans-dichloroethylene, isomerisation by laser multiphoton vibr. and electron excitation radiation *(Russian)* 78−73041
dichromated photoresist, photochem. reactions 80−7830
dicyclopentadiene, liq., CO_2 laser pulse induced chem. reactions 80−66821
3,3′-diethyl-2,2′-thiatricarbocyanine iodide, solns., photoisomerisation and internal conversion rates, time-resolved spectra 77−75201
N,N-diethylaniline-pyrene, photochem. polarisation transfer, scalar paramagnetic exchange mechanism 78−25557
3,3′-diethyloxadicarbocyanine iodide, kinetic model and expt. results of picosecond photobleaching 78−53226
difluorocarbene, $\tilde{A}^1B_1$-$\tilde{X}^1A_1$ system spectrosc. and photophysics 80−5577
difluoromethane, IR laser-induced reactions 77−77792
dihydroporphin free base, in n-octane cryst., zero-field optically detected mag. reson., triplet state kinetics 78−42103
dihydroxyanthraquinone, light-induced proton transfer, photochem. hole-burning obs. 80−76535
3,3′-dimethyl-1′-phenyl-6-nitro-spiro [(3H-7,8-benzochromen)-3,2′-indoline] (II), photochromic transform., temp. depend. 80−104456
3,3′-dimethyl-1′-phenylspiro [(3H-7,8-benzochromen)-3,2′-indoline] (I), photochromic transform., temp. depend. 80−104456
dimethyl-N-nitrosamine in urban air, concs. and chemistry 78−81378
dimethyl-s-tetrazine, vapour, mol. fluoresc., photodissoc. product 80−81352
dimethylether-HCl(I)(Br) mixture in N_2 matrix, IR induced proton transfer isotope effects, bond strengths 79−29335
6,6′-dimethyloxyindigo, picosec. kinetics, and photostability, spectrosc. obs. 79−45748
2-(2,4-dinitrobenzyl)pyridine, powdered sample, kinetic photochromic charcts. 78−23957
diodes, using p-n heterojunction or Schottky barrier immersed in electrolyte 77−66201
diolefins, substituted, topochemically controlled solid-state polymerization 80−35532
2,5-diphenyl-1,3,4-oxadiazole, vapour, spectral, fluoresc., photochem. and laser props. 80−106344
2,5-diphenyl-1,3-oxazole vapour, spectral, fluoresc., photochem. and laser props. 80−106344
photochemistry continued
2,5-diphenylfuran vapour, spectral, fluoresc., photochem. and laser props. 80−106344
4-diphenylphosphenylstilbenes, fluoresc., photodimerisation 80−1015
dipropionyl peroxide, photochemical production of ethyl radical 80−3373
DNA bases, selective ps laser excitation in condensed phases 79−48217
dye chemistry for new instant film 80−81342
dye laser induced photochemistry 79−39182
dye solutions, high power UV irrad., bleaching and diffusion 77−42533
EDA complex, photoinduced ionic dissociation, radical-anion formation 77−40556
electron pulse radiolysis, appl. 79−52698
electron transfer in monolayer assemblies 80−3383
electronic phototransition CW chemical laser with thermal initiation by shock wave 80−53283
electronic processes and energy transfer, conf., Tallahassee, Fla., USA (Jan. 1976) 77−27042
endothermic reaction rate enhancement in EM field 80−66852
energy requirements vibr. and translational energy depends. 79−57206
energy transfer dye lasers and laser induced intermol. and intramol. energy transfer processes 80−9647
1,2-epoxypropane, photopolymerisation by arenediazonium salts, obs. 79−24747
etching, of Si monocryst., by Br, Ar laser beam initiation *(Russian)* 77−73358
ethanol, multiphoton UV photodissoc. 78−50602
ethanol glasses containing anion radicals of fluorene and isologs, γ-irrad., optical absorpt. and EPR obs. after photobleaching 77−44491
ethyl acetate, CW laser induced reactions, activation energies, temps. and rate consts. 80−40710
ethyl radical, photochemical studies 80−3373
ethylacetate, CW laser induced reactions, activation energies, temps. and rate consts. 80−40710
ethylene, CW CO_2-laser irrad., low-press., chem. relax. 79−74404
ethylene, multiphoton UV photodissoc. 78−50602
N-ethylphthalimide+olefins, photochemical reaction, absorpt., fluoresc., phosphoresc. and triplet-triplet absorpt. spectra 80−85197
excimer formation in micellar surfactant solns., distributional effects 78−64855
excited electronic state, photoelectrochemistry 78−76872
F_1-layer, mid-latitude, mean diurnal var. of O^+, NO^+, O_2^+ and N_2^+ ions 79−96856
F-region, Atmosphere Explorer photochemistry rel. to airglow obs. 80−98496
fast electron transfer processes, investigation by magnetic fields 79−8479
fast reactions, pulsed selective photoexcitation, rate determ., spectral method 77−86336
ferricytochrome, photoreduction in presence and absence of electron donor 78−53337
flame, laser excitation, rate eqns. 77−86327
fluorene: acridene, radical pair form. from excited states, optical nucl. polarisation obs. 80−14155
fluorene crystal, doped, photochemical hydrogen abstraction, proton hyperfine structure via optical nuclear polarisation 80−63659
fluorescence quantum yield measurements, real, observed and mol. parameters, ref. soln. standards 78−32898
fluorescent tagged reagents, time integrated emission, photochem. bleaching 77−21440
fluorobromomethanes, matrix photoionisation and radiolysis, IR spectra of free radicals 79−24765
fluorocarbon solutions, dye-sensitized, spectroscopic obs. of 1.27 μm and 1.58 μm emission of single ($^1\Delta_g$) mol. O_2 80−85178
fluoromethane+$Br(^2P_{3/2})(^2P_{1/2})$, photobromination 78−11535
formaldehyde, α-cleavage, feasible forbidden photochem. reaction 77−9092
formaldehyde, intramol. energy transfer, photodecomp., radiationless decay 77−29027
formaldehyde, rearrangement to hydroxycarbene, pot. energy surface 79−79271
formaldehyde in New Jersey air, statistical anal. 77−73833
free-base porphin, S_2-S_0 transition vibronic bands, photochem. hole-burning 79−36631
frequency-domain nonvolatile optical storage scheme 80−43282
fuel production, by photochemical conversion and chemical storage 79−66413
furil, photochem. generated alkali cationic triple ions, ESR 78−80758
furil, photochem. reduction by pentachlorophenol, zero-field CIDNP study 77−90625
n-GaAs, stabilisation against photodecomposition, surface damage influence 80−76390
gas cell, suitable for chromatographic sampling after photolysis 77−70375
gas phase chemical reactions in atmosphere, evaluated kinetic and photochemical data 80−101671
gases, nonmonochromatic photochemical waves, stationary propag. 77−31421
glass, light-sensitive, photochem. method for Ag particle precipitation *(German)* 79−27350
glycerol monooleate bilayers, photoinitiated mediated transport of OH^- and H_3O^+ 79−88059
greening bean leaf low-temp. fluorescence induction obs. 79−39354
halides, F-centre form., review 78−63763
Halobacterium halofium, photo-products spectral conversions, purple membrane formation 79−57605
heterogeneous catalysis, photoinduced, review 78−40080
heterogeneous reactions, mech. of activation by laser radiation *(Russian)* 78−53233
hexafluorobutadiene, electronic ground state photochem., isotope separation by IR multiphoton isomerisation 79−79264
hexafluorocyclobutene, electronic ground state photochem., isotope separation by IR multiphoton isomerisation 79−79264
hexafluoroethane, photochem. prod., ^{13}C enrichment *(French)* 80−91615
hexafluoroethane+H_2(hexane), multiphoton induced chemistry 79−20382
hexamethyl indatricarbocyanine iodide-ethanol soln., luminesc. quantum yield, photoacoustic method, reaction energy 77−86335
hexamethyl-2,2′-indotricarbocyanine iodide, solns., photoisomerisation and internal conversion rate, time-resolved spectra 77−75201
highly excited molecular systems, high energy photochem. 80−66831
hole burning, photophysical and photochemical theories 80−58322

photochemistry continued
hole-burning memory magnetic and electric field addressing 79−81371
hologram recording on semiconductor, photochem. etching control 80−28179
hydrocarbon+N oxide mixtures in air, photochemistry 79−53427
hydrocarbon mixtures, photochemical reactivities 78−61533
β-hydroxy acrolein, lower excited states, electronic struct. and H-bonding, ab initio SCF and CI calcs., photochemical mechanism 80−83278
hydroxyquinones, H-bonded, zero-phonon photochem., hole burning obs. 79−11802
hypsorhodopsin, squid, form., picosec. spectrosc. obs. 79−39183
ice, aqua-acid, UV-radiation illuminated, nuclear-electron effects in EPR, of atomic protium and deuterium *(Russian)* 79−20388
ice nucleation threshold on Cu_2S, Ag_2S, MoS_2 and CdS photosensitive surfaces 77−55343
indigo, picosec. kinetics, and photostability, spectrosc. obs. 79−45748
indoline spiropyrane, photocolouring process, spectral depend. 79−66315
indoline spiropyrans, methoxysubstituted, activated solns., photochromism, laser nanosecond spectroscopy 77−70317
inert gas halide lasers, operation and use in photochem. 80−9860
inorganic photochemistry, review 80−3382
interface of two phases or liquids, selective processes induced by resonance laser radiation 78−64867
interstellar medium, mol. form, from grain mantles UV photolysis, laboratory analogue expts. 80−26944
intramolecular energy transfer theory 77−29027
ionosphere, lower, photodetachment as source of reflecting layer below classical D-region 80−98508
IR emulsions, chemical hypersensitization 77−2706
IR laser applications in chemistry 80−16710
IR laser applications in vibrational photochemistry *(Russian)* 79−5169
IR laser chemistry research using mol. beam *(German)* 80−55683
IR laser induced chem. reacts., review *(Japanese)* 79−39176
IR laser induced chemical reactions 77−90621
IR laser isotope separation appls. 79−64113
IR source using four wave mixing in Ge 77−88852
IR spin flip laser, matrix isolated photochemistry, isotopic, stereochemical and lattice site selectivity 78−92492
isomerisation, complexing, proton transfer, initiation of internal conversion processes 80−40713
isorhodopsin, physiological activity in rat rods 77−60204
isotope separation, laser photochemical method using relativistic electron beam microwave source 77−38750
isotope separation, microwave reson., triplet state photochem. technique 77−32818
isotope separation by laser photochemistry in nozzle flows with heterogeneous condensation 80−50862
Jupiter, NH_3 and PH_3 photochemistry in stratosphere 77−53463
Jupiter atmosphere, hydrocarbon and H I photochemistry rel. to Lyman alpha albedo 80−105194
Jupiter atmosphere, organic compounds hot-atom synthesis 79−101109
Jupiter simulated atmosphere, synthesis of UV photoprod. organic solids, mol. anal. 78−69740
Jupiter upper atmosphere, photochemical models 80−36567
Jupiter upper atmosphere, photochemistry rel. to CO extraplenatary source 78−93144
ketone, H abstraction, feasible forbidden photochem. reaction 77−9092
labile species, electron photoejection, reaction kinetics characterisation 80−26089
laser applications, review 80−45535
laser beam appl., LASL developments 79−31719
laser chemistry, conf., Pasadena, USA, (March 1978) 79−39181
laser chemistry 79−100415
laser dye mixtures, photodegradation 80−9880
laser dyes, fluoresc. efficiency and standards 78−35205
laser dyes, inert gas halide laser pumped, photochem. stability 78−33733
laser dyes, photochemical quantum yield determ. using fluorescence data 80−55685
laser engineering and appls., conf., Washington, USA (May-June 1979) 80−1216
laser field interaction, Floquet theory, HF appl. 80−63716
laser induced isotope separation and selective photochem. reactions 77−77800
laser induced photochem. of vibr. excited mols., review 80−71925
laser induced reactions, activation energies, temps. and rate consts. 80−40710
laser interactions, conf. Tsakhkadzor, USSR (Jan. 1976) 77−23706
laser isotope separation, appl. of on-line computer controlled dye laser 78−70948
laser photochemical reaction kinetics, holography use 79−29383
laser properties, survey of existing lasers *(German)* 78−13744
laser radiation, selective action on matter, review 80−7832
laser radiation controlled reactions 77−25293
laser selective photophysics and photochemistry, book contrib. 79−79273
laser specific and thermal reactions classifications 80−11919
laser spectroscopy, conf., San Diego, USA (Aug. 1978) 80−13153
laser stimulation of surface reactions by excitation of adsorbed molecules 77−56242
laser studies of relaxation and reaction of species in defined quantum states 80−11918
laser-controlled unimolecular and bimolecular processes, field-depend. rate const. 80−11906
laser-induced chemical processes, optical selection of reagent orientation 80−11914
laser-induced photochem. reactions, excitation model 77−60090
laser-induced photoelectrochem., photoemission related currents depend. on laser characts. 79−20390
laser-induced predissociation, diatomic and polyatomic mols., photocatalytic effect 80−11907
laser-induced processes in molecules, conf., Edinburgh, Scotland (Sept. 1978) 80−9577
laser-induced radiative collisions, review 79−10196
laser-initiated chain reactions, rates, mechanisms, chemiluminesc. obs. 80−55651
lasers, excimer, applications in photochemistry 79−98379
leaves of African crop plants, optical props. rel. to photosynthesis 77−25629
light intensity meas. instruments 79−49295
light source, immersion type, radiation utilisation factor calc. aspects *(Russian)* 80−48374
photochemistry continued
lipid peroxide oxidation fluorescing products, effect of UV on formation 79−57585
liquid phase, nonthermal laser excitation, reaction control *(Russian)* 77−9106
lysozyme, light-induced riboflavin binding 78−27899
macromolecules, nonlinear laser photomodification, radiation damage 80−61120
maleic anhydride, and its photochem. transform. products, IR spectra *(Russian)* 77−66761
marine atmosphere diurnal kinetic photochemistry 79−48549
Mars, photochemistry of CO_2-H_2O-N_2 atmosphere 77−29692
Mars atmosphere, photochemistry 77−91458
Martian atmosphere, O_3 photochemistry and global distrib. 77−78710
matrix-isolated molecules, IR laser photochem. 79−34329
MB^+-Fe^{2+} system, solar energy utilisation *(German)* 80−45713
medium-induced relaxation, laser pulse meas. 79−38667
membranes, artificial, light-driven carrier-mediated electron transfer 77−29110
membranes, carrier-mediated photodiffusion 78−23965
merocyanine dyes, non-photochromic, for autoprocessor reprography system 80−35555
mesosphere, chemical response to changes in UV solar flux 77−33167
mesosphere, O-H atmospheric model rel. to OH emission problem 77−60503
mesosphere diffusion-photochemical model, turbulent diffusion coeff. seasonal vars. 79−53424
metal combustion under CW CO_2 laser radiation action 80−30241
metalloporphyrins, photoelectrochemical props. 80−50991
methacrylate polymer, carbazolyl substituted, excimer and charge transfer complex trapping of excitons 80−34367
methane, $1B_1(1T_2)$ state, photodissoc., extended basis calcs. 78−9093
methane, atmospheric circulation, destruction through photochemical oxidation *(German)* 79−84424
methane, D enrichment by CW CO_2 laser induced reaction 79−18300
methane isotopic mixtures, enrichment of D using vibrationally sensitized reaction 80−76532
methane-BCl_3, single-photon absorption reaction chemistry in solid state 77−73454
methane-O_2 mixture, laser initiated combustion 80−55661
methane-SF_6, single-photon absorption reaction chemistry in solid state 77−73454
methanol, multiphoton UV photodissoc. 78−50602
3-methoxybenzanthrone in ethanol, photoprotolytic reactions, spectra, rate consts. and lasing thresholds 80−43327
methyl isocyanide, intracavity CW dye laser state-selective activation of isomerisation 78−11533
methyl isocyanide, laser initiated thermal isomerisation, thermal explosion 78−80725
methyl isocyanide photoisomerisation, laser isotope separation, C-isotope enrichment by one-photon vibr. photochemistry 80−81336
methyl viologen, chlorophyll a sensitised reduction in non-ionic micelles 79−1962
3-methyl-pentane glass, trapped electrons, model 77−48661
methylcyclohexane glass, trapped electrons, model 77−48661
methylenimine, photoisomerisation, SCF MO pot. surfaces 79−11772
11-cis-14-methylretinal, photoisomerisation, high quantum yield 79−57253
α-methylstyrene, photoinduced ionic polymerisation 80−7828
1,4-Bis(2-methylstyryl)benzene, laser dye, picosec. laser obs. 79−36891
1,4-bis(2-methylstyryl)benzene, picosec. gain kinetics 79−45940
micellar system, photoinduced redox processes kinetics, intramicellar electron transfer 78−92603
molecular collisions in intense laser field, quantum mechanical model 78−62876
molecular crystals, mixed, laser-induced photochemistry 78−85185
molecular excitation, laser induced, effect of chem. reactions 78−21979
molecule+molecule, enhancement by collision induced absorpt. of IR laser radiation 80−66798
multiphoton absorption induced reactions, appl. of effective photon concept 78−88651
multiphoton processes, chemisorbed species on solid surfaces, desorption dynamics, quantum-stochastic approach 80−66864
multiple photon photochemistry in low temp. matrices 80−76533
N-allyloxymethyl-poly(ε-caprolactam), electron crosslinkable, electron and photosensitivity *(Japanese)* 79−91951
naphthalene, adsorbed on silica gel surface, biphasic photochemistry, time-resolved spectra 80−30252
naphthol complexes, H-bonded, form. of ion pairs in presence of crown ethers, proton-transfer photoreactions 80−85199
naphthylalanine polypeptides, fluoresc. quenching and energy transfer 79−34332
β-naphthylamine, soln., fluoresc., photochem. quenching, excitation wavelength depend. 77−50470
β-naphthylamine-cyclohexane soln., luminesc. quantum yield, photoacoustic method reaction energy 77−86335
nitromethane+H_2 reaction, CO_2 laser initiated, mechanism and yield 80−11912
3-nitropyrene, triplet state, absorption spectra in soln. 78−33440
non-Ag photography with physical development *(Russian)* 79−44970
nonmethane hydrocarbons, photochemical effects in atmosphere 78−49090
nuclear fuel reprocessing, photochemical modification of purex process, commercial benefits 77−79453
nuclear isomers, photochem. separation 79−50153
nucleic acid, multiphoton photoreactions of aq. soln., picosec. UV pulse 79−34487
optical image phase recording using sensitised photooxidation reactions 80−87350
optically active molecules and polarised bremsstrahlung 77−63938
organic compounds, photochem. produced, abundance in outer planets atmospheres, lab. simulation 79−75142
organic crystal, appl. of TEM 80−24327
organic dyes, stimulated fluorescence, energy level scheme, photoisomerisation effect 77−70310
organic dyes, two-band stimulated fluorescence, laser action and bleaching effect 79−41190
organic glass, photochem. of trapped electrons 79−52722
organic reactions in solid state 80−21309
organic solids, one- and two-photon laser photochem., hole burning appls. 80−21304

photochemistry continued
organometallics, with applications to imaging systems 77—4914
origin of life, form. of self-sustaining coacervates 78—11611
oscillating chemical reaction, entrainment by periodic light pulses of variable freq. *(French)* 80—35551
oscillations and runaway states in closed illuminated system 78—7188
ozonosphere, photochemical-dynamical model rel. to maintenance of zonal mean O_3 distrib. in N.Hemisphere 80—109220
ozonosphere, radiative-photochemical model for temp. coupling effects on O_3 depletion 78—57246
paraaminophenol and paraphenylenediamine analogue molecular complex, free radicals of developers, EPR obs. *(Russian)* 80—7814
s-trans-1,3-pentadiene, photoisomerisation, excited state pot. energy curves, CIPSI calc. CNDO/2 parametrisation 78—11505
phenoxy radicals, electronically excited states, photochem., flash photolysis obs. 77—77797
phenoxyacetic acid, photoinduced selective isomerisation in comparison with X-ray induced decomp., aq. soln., 25°C *(German)* 77—63931
m-phenylene diacrylic acid, four-centre-type photopolymerisation in cryst. state, holographic appl. 78—37832
phenyloxazolyl pyridinium salt dye lasers, flashlamp pumped, blue-greenlasing 80—95886
pheophytin a, photo-oxidation primary processes 79—79468
pheophytin reduction obs. in higher plant photosystem II 79—43817
pheophytin-a, photochem. generation of cation-radical, spectral-kinetic characts. 78—96008
phospholipid lateral diffusion in membranes, photochem. method 79—100583
phospholipid vesicle walls, photosensitised electron transport 78—80787
photoactive catalyst used in light induced photocuring of coating systems 80—7820
photobleaching of large mols., kinetic model 78—53226
photochemical reaction, avoided crossings in excited states potential energy surfaces 78—76881
photochemical smog, transferred contaminant air pollution model *(Japanese)* 78—32217
photochromic powder, with photochem. reaction and/or thermal reverse reaction, kinetics 78—23957
photocondensation, molecular compounds behaviour in strong light beams *(Russian)* 77—49798
photodecomposition, by MW IR laser, nonstatistical behaviour 77—73455
photoelectrochemical investigation of the influence of gelatine and polyvinyl alcohol on the formation and lifetime of a latent image in photographic layers on a ZnO base *(Russian)* 80—3389
photofragment distrib. in two-photon photochem., isotope separation appl. 80—81344
photogalvanic solar energy conversion, photochem. determ. of efficiency 80—89654
photographic emulsions, increase in sensitization by stabilizers and antifoggants 79—24781
photographic information recording, new techniques, review *(German)* 77—26411
photographic stabiliser reactions with colloidal Ag, decoloration reaction kinetics *(German)* 77—40563
photographic unconventional systems, amplification processes 79—61882
photography, physical development using a single-solution treatment *(Russian)* 79—44965
photoimaging system based on photopolymerisation in cryst. coatings 80—40716
photoinduced gas consumption system, photoacoustic spectroscopic obs. 79—16010
photoinduced gas evolution system, photoacoustic spectroscopic obs. 79—16010
photoinduced recombination of atoms and radicals 79—5170
photoinitiated cationic polymerization by photosensitization of onium salts 80—7822
photolabile species, picosec. meas. method, appl. to emission lifetime of bacteriorhodopsin 77—17009
photopolymer systems, conf., Washington, USA (Nov. 1978) 80—4799
photopolymerisation, 0_2 inhibition elimination 80—7821
photopolymerisation, dye-sensitized, activation by trialkylbenzylstannanes 80—7824
photorecombination reactions initiated by shock wave, light amplification *(Russian)* 80—38011
photoresist, negative, Kodak microresist 747, Spectral sensitivity improvement 79—66304
photoresist, positive, photochem. props., Wolff rearrangement teaching appl. 78—89284
photoresists, photochemical reaction rates, intensity depend., kinetic model 80—104452
photosensitised reacts. in continuous chem. processes, scatt. effects 78—73057
photosensitive glass, full-colour polychromatic, subcolloidal Ag precipitation 79—47953
photosensitive layers with chromic acid salts, photochemistry *(Russian)* 80—50869
photostimulated solid-state reactions 78—53222
photosynthesis, carbon fixation cycle, model, teaching appl. 78—73806
photosynthesis, in vitro appls. 78—95941
photosynthesis, in vitro models 78—77023
photosynthesis of green plants, tripartite model for photochem. apparatus 78—44474
photosynthesizers, contrived, biosystems and photoelectrochem. conversion 79—52953
photosynthetic reaction centres, primary electron transfer rate 79—8481
phototropy, kinetic investig. *(German)* 78—64868
phthoralocyanin porous films, Becquerel photovoltaic effect 77—16907
phytochrome, role of light in regulating plant growth and development, review 78—11695
picosecond absorption spectroscopy, photochem. and photobiol. appls. 78—82053
picosecond spectroscopy, appl. to chem. and biological reactions 79—80697
pigment reversible changes due to illumination of leaves 79—43818
pigments, ionisation reactions in soln., automatic conductimetric instrument for kinetic studies 77—4971
PMMA, laser initiated polymerisation kinetics, mol. wt. distrib. of resultant polymer 78—15673
PMMA, photodielectric media for holographic recording, photochem. response 78—7219
photochemistry continued
PMMA-spirobenzopyran mixed monolayers, photoresponsive effects 79—66316
PMMA-spiropyran Langmuir monolayers, reversible photochemical strain 80—50867
polyatomic molecules, primary photochem. processes *(French)* 77—90620
polyatomic mols., multiple photon IR processes, reviews 80—43125
1,4-polybutadiene, oxidation stabilisation by singlet O_2 quencher 4-(1-imidazolyl)-phenol 80—16677
polycarbonate films, effect of UV and visible mono- and polychromatic radiation, stability *(Russian)* 79—57268
polyenes, photoisomerisation, triplet pot. energy surfaces and normal mode anal. 80—108700
polyesters, photoreactive, synthesis and struct.-prop. relations 80—7826
polyethylene, laser irrad. chem. and struct. modifications *(Russian)* 79—27931
polyethylene, with various antioxidant, stabilized and TiO_2 pigment additions, photo-yellowing and oxidation 79—16015
polymer, crosslinking with X-ray irrad., active group and heavy atom effects 80—7829
polymer, degradation, mol. mechanisms *(German)* 78—76860
polymer, photo-oxidation 80—3380
polymer, photochromic, thermal effect in photomech. conversion 80—16706
polymer, photoradiative processes in free radical form. *(Russian)* 79—57269
polymer ageing through exposure to light, device *(French)* 80—30126
polymer fibre, lifetime under load, in presence of UV radiation stress depend. 78—48534
polymer fibre, lifetime under load, in presence of UV radiation, stress depend. 78—48535
polymer film, photoreticulation by UV irradiation 80—40717
polymer materials, photodegradation tests, problems *(Japanese)* 77—55245
polymer media 80—3381
polymer solutions, automatic recording capillary viscometer meas. 77—27631
polymer spectral sensitivity and photochem. stability using Xe high press. lamp *(German)* 80—61119
polymer-bisazide photoresist. layer, effect of thickness on photosensitivity *(Russian)* 77—70324
polymerisation, laser initiated, mol. wt. distrib. 78—15673
polymers, photochemical probes 77—90626
polymethine, IR-140 laser dye, photoisomerisation processes 78—27800
polymethine dye behaviour in lasers, efficiency and photoisomer generation 80—14335
polymethine dye unstable photoisomers, superluminesc. and stimulated emission 79—31896
polymethine dyes, excited mols., photoisomeric transformations 79—87854
polymethine dyes, laser action and photoisomeric transforms. 79—89905
polymethyl isopropenyl ketons, spectrally sensitized decomposition and Deep UV resists 80—40715
polymethyl-α-cyanoacrylate, photodielectric media for holographic recording, photochem. response 78—7219
polypeptide copolymer, trans-cis photoisomerisation 78—3331
polystyrene, laser irrad. chem. and struct. modifications *(Russian)* 79—27931
polystyrene films, UV irrad., struct. changes, gel permeation chromatogram computer manipulation, substraction 79—96387
polystyrene photophysical behaviour, solvent effect obs. *(Spanish)* 79—57267
polyvinyl alcohol, laser irrad. chem. and struct. modifications *(Russian)* 79—27931
polyvinylbenzocarbazole, weak solution, intramolecular energy transfer by singlet and triplet excitons 80—34971
polyvinylcarbazole, fluoresc., photooxide quenching, exciton migration effects 79—56830
polyvinylcarbazole, weak solutions, intramolecular energy transfer by singlet and triplet excitons 80—34971
polyvinylcinnamate, crosslink form. by photoreaction 80—7823
POPOP vapour, spectral, fluoresc., photochem. and laser props. 80—106344
porous Vycor glass, quenching by O_2 and NH_3, photoluminescence obs. 80—93773
porphin, free base, in n-octane crystal, S_1 from S_0 transition, freq. shift and dephasing temp. depend. 78—25584
porphin, free-base, in n-octane cryst., photochem. hole-burning, vibronic relax. 79—31587
porphin in host n-alkane crystals, phototautomerism, IR spectral obs. 80—34963
porphin in n-alkane host, photoautomerisation and hole-burning 79—47954
porphyrin, free-base, in n-alkane matrices, photochem. hole burning, optical dephasing 80—21305
porphyrin, reduced, photoregeneration mechanism in the presence of O_2 79—57582
porphyrin free base in n-octane, $S_1 \leftarrow S_0$ transition homogeneous linewidth, photochemical hole burning 78—7217
porphyrin free base in n-octane crystal at 4.2K, laser-induced photochem. isomerisation 77—12815
porphyrin-pyridine complex, 4.2K, visible absorption spectrum gap burning-out 78—53232
porphyrin-water interface, photoinduced charge separation 77—81408
powder, conc. and radiation intensity reaction time and depth depend. 77—29023
preassociation, laser induced, in presence of natural predissociation 78—85174
prebiotic model atmospheres, far UV irradiation effects 78—40668
Precambrian solution photochemistry, inverse segregation, and banded iron formations 79—20863
prelumirhodopsin, psec. kinetics, primary photochem. event in vision, proton translocation 78—44508
prereaction effects on laser-initiated reaction rate meas. by chemilum. obs. 78—44386
protein aggregates exposed to UV radiation, limiting conc. of paramag. centres 78—24029
protein crosslinking and affinity labeling, use of photoreagents 79—96517
proton transfer photoreaction kinetics, in singlet excited state 78—48671
pure and applied chemistry, conf., Tokyo, Japan (Sept. 1977) 78—95906

photochemistry continued
purification of materials with overlapping absorpt. spectra 80−78452
purple membrane of Halobacterium halobium, energy transfer 78−44467
purple membrane of Halobacterium holobium, review 77−86457
purple membrane of H.halobium, effect of 560⇄570 transition and blue light on photochem. 80−30673
purple membrane protein chromophore, fluoresc. 78−44454
purple membrane protein retinal chromophore, role of protein in photochem. 78−15772
purple membranes from Halobacterium halobium, spectral transitions 80−12056
PVA, photooxidation, kinetic eval. for carbonyl form. *(Japanese)* 79−39007
PVC surfaces, natural and stabilised, composition, ageing, oxidation and weathering, ESCA obs. *(French)* 80−61139
pyrene adsorbed on silica gel surface, biphasic photochemistry, time-resolved spectra 80−30252
pyrene excimer formation in micellar surfactant solns., distributional effects 78−64855
quantum mechanical interpretations of photoreactions, review *(German)* 78−61034
quantum-chemical π-electron system, molecules-in-molecule model *(German)* 80−5490
quinzarin in alcohol glasses, electron-phonon coupling, photochemical hole burning 80−97265
radial light intensity profile in cylindrical photoreactors 78−68901
radiative preassociation, in presence of natural predissociation 78−85174
radical ion reactions, photo-initiated, CIDNP 78−13526
radiometry appls. 79−49294
rare earth purification, laser induced photochem. separation methods, review 79−61883
rare earths, purification, laser methods 80−16712
reaction, instability, mol. dynamics model, computer soln. 77−4892
reaction control using chemical lasers 77−70312
reaction kinetics, in absence of diffusion, small conversion approx. 77−36768
reaction kinetics measurement and control using laser technology, free electron laser appl. 80−81349
resonance picosecond spectroscopy of physical stages of photosynthesis using returnable generators *(Russian)* 78−15688
resonant electronic-vibrational energy transfer and use in pumping IR mol. lasers 80−9700
retinal, highly polar excited electronic states, electron transfer 78−48757
retinal, proton donor-acceptor isomerisation coupling, bacteriorhodopsin as light driven proton pump 79−79473
retinal chemical processes, reprint of 1879 paper 78−20933
retinal isomers, dark equilib. and photochem. 78−15771
11-cis-retinal prep. by irrad. of all-trans-retinal and high press. liq. chromatography 78−40453
retinal Schiff-base, photochem. step of vision, H-bonds, intermol. associations 78−31812
retinal-entrapped membrane, photo-induced potential 78−20148
reversible excited-state electron-transfer reactions, kinetics 78−76885
reversible photoredox system, thionine type and I_2 type, chem. equilibria *(German)* 77−90630
rhodamine 101, quenching of emission in methanol and latex particle suspensions 80−3374
rhodamine 6G, aqueous soln., absorpt. spectra, ground and triplet state photoprotonation pH depend. 80−42961
rhodamine 6G, photoreaction mechanisms, effect of pumping spectral composition *(Russian)* 77−70323
rhodamine 6G in soln., photochem. stability 78−37878
rhodamine 6G-isopropyl or ethyl alcohol solution, flashlamp pumped laser, photochem. effects 80−53287
rhodamine B, adsorption on ZnO single crystal, photooxidation, electrochem. meas. 78−31645
rhodamine B-ethanol soln., luminesc. quantum yield, photoacoustic method 77−86335
rhodamine R derivatives, water (heavy water) detergent solns., luminesc., lasing 79−56836
rhodamine-B solutions, thermochromic and hyperchromic effects 79−91977
rhodopsin, bovine, photochem. cis-trans isomerisation at liq. He temps. 78−64939
rhodopsin, cis-trans isomerisation on psec time scale 77−86498
rhodopsin, conformeric states, spectrophotometry 77−90725
rhodopsin, excited state energy surface to explain photochemistry 79−48218
rhodopsin, isorhodopsin, photochem. on picosecond time scale, bathorhodopsin form. 79−83706
rhodopsin, isorhodopsin and bacteriorhodopsin, and photoproducts, temp. and wavelength effects on photochem. 78−11612
rhodopsin, primary photophys. and photochem. processes in visual excitation 78−15773
rhodopsin, relevance of Halobacterium photosensory mechanism to visual photoreception 77−90738
rhodopsin and intermediates, absorpt. spectra and orientational change of chromophore 78−7321
rhodopsin kinetics at room temp. meas. by picosec. spectroscopy 77−64036
rhodopsin visual pigment, photochemical transformations 79−66472
rose bengal, electron transfer to TiO_2 electrodes, photoelectrochem. meas. 77−66758
rubrene, photooxidation, photoacoustic spectroscopic obs. 79−16010
rubrene film, photooxidation in solid, UPS obs. 79−52693
scalable tunable IR laser operating characteristics and limitations 77−54713
selection rules for spectra and photochemical reactions *(Chinese)* 80−21308
selective dissociation, ionis., and chem. reaction stimulation, by ultra-short pulses, isotope separation *(Russian)* 78−29825
selective interactions of laser radiation, photoionisation [-] elementary processes 77−27034
selective laser photophysics and photochemistry, applications 77−56243
semiclassical theory for near adiabatic photon assisted mol. collisions 79−5141
semiconductor, anodic etching, physicochemical parameters for maximum resolution 79−74276
semiconductor electrodes, photoelectrode kinetics of H_2 evolution reaction 78−44388
photochemistry continued
semiconductor-electrolyte interface, photoelectrochem. processes, hologram recording utilisation 77−88667
semiconductor-electrolyte interfaces, prediction of flatband pots. from atomic electronegativities 78−40068
semiconductor-metal system, photochemical transformations rate rel. to light-stimulated diffusion coeff. 77−76626
semiconductor-metal system, photosensitivity, theory *(Russian)* 78−3357
semitransparent rotating disc electrode, photochem. and electrochem. surface reactions 78−40056
separation of metals in aq. soln. 77−60082
shock-wave-initiated photorecombination kinetics and lower mode waveguide amplification *(Russian)* 79−96313
silica spectrometer cell and photochemical assembly 77−67512
silicate glasses:Cu^+, effect of UV irrad., absorption bands 78−31222
smog, effect of latit. on form. pot. 77−2227
smog, rate parameters and computer simulation 78−48677
solar chemistry research and developments *(French)* 80−11999
solar energy, photochemical conversion and storage 77−86330
solar energy chemical conversion and storage using norbornadiene-quadricyclene photoisomeric interconversion 80−89664
solar energy chemical storage, effect of micellar phase on photo-induced reactions 80−89678
solar energy chemical storage, photosensitization mechanisms for energy storing isomerizations 80−89679
solar energy chemical storage using novel photocyclization reactions of 1-alkenyl-2-pyridones 80−89680
solar energy conversion, photo-induced electron transfer reactions in solution, organised assemblies and at interfaces 80−89677
solar energy conversion, photoelectrochemical cells, chlorophyll sensitised reactions 80−7948
solar energy conversion, photoredox reactions of metal ions 77−86334
solar energy conversion and storage using artificial photosynthetic systems 80−89662
solar energy symposium, Phoenix, Az., USA (Nov. 76) 77−86329
solar energy utilisation, photoelectrochemical systems *(German)* 80−45713
solar photochemical energy conversion, nonbiological 77−86331
solid state, IR lasers appl. 80−11929
solid-gas interfaces, laser induced reactions 77−25308
solutions, easily ionised emitters, photoelectron emission theory 77−21403
solvent effects, energy differences calc. methods 78−61031
spiropyrane, triplet-triplet absorpt. by laser photoexcitation 77−10685
spiropyrans, photochromic, thermophotodegradation for autoprocessor reprography system 80−35555
stilbene, cis→trans photoisomerisation rate const., direct meas. 80−30250
stilbene, direct photoisomerisation theory, from fluoresc. and absorption spectra 79−79262
trans-stilbene, fluoresc. decay, picosecond anal. 79−31569
stilbene, ps photoisomerisation, time-resolved spectra obs. 79−57252
trans-stilbene, two-photon excitation, phantom photochemical singlet, assignment 77−75247
stilbene anion radicals, photoinduced isomerisation, 77K 80−66818
trans-stilbene photoisomerisation, ps dynamics under collision-free conditions 79−91975
stratosphere, at. Cl and ClO radical in situ obs., rel. to O_3 depletion 78−36241
stratosphere, chlorofluorocarbon effects, O_3 photochemistry 77−41160
stratosphere, Cl-ClO-Cl cycle, possible roles of ClO*, $ClNO_3$ and HOCl 77−17185
stratosphere, concise chem. model 78−85634
stratosphere, halocarbon sinks, photooxidation, $O(^1D)$ atom and OH radical reactions 77−17165
stratosphere, laser photochemistry of O_3 and distant spectroscopy *(Russian)* 78−28314
stratosphere, laser spectroscopy relevant to photochem. 78−88951
stratosphere, model, Monte Carlo anal. of imprecisions due to reaction rates 78−85635
stratosphere, NO and ClO at twilight rel. to interpretation of conc. meas. via solar occultation 80−85756
stratosphere, O_3 destruction by fluorocarbons 77−9459
stratosphere, O_3 reduction by natural NO_x and man-made pollution, model 77−60461
stratosphere, orbital simulator using superpress. balloon 79−29966
stratosphere, photochemical-radiative damping and instability in the stratosphere 78−28259
stratosphere O_3, natural depletion mechanism, energetic radiation belt electron precip. 77−41134
stratosphere photochemical-radiative damping and instability, numerical results 78−81286
stratosphere photochemistry model, O_3 calcs. uncertainty 79−16567
stratospheric photochemistry, computer simulation 79−21481
sudden polarisation effect 79−34328
supersaturated vapour nucleation on photoexcited mols. 77−76540
surface photochemistry and photodesorption, isotope separation aspects 78−64863
synchrotron radiation obs. appls. 80−66830
TCNB-MTHF EDA complex, sensitized biphotonic radical anion formation 77−40556
TEM, appl. to organic solid-sate chemistry, review 79−60235
terbium salicylate, fast reactions, pulsed selective photoexcitations, rate determ., spectral method 77−86336
p-terphenyl anion radicals, photoisomerisation, local heating effects 78−85179
p-terphenyl vapour, spectral, fluoresc., photochem. and laser props. 80−106344
terrestrial atmosphere, H escape at low O_2 levels, photochem. model 77−56784
2,3,4,4-tetrachloro-1-keto-1,4-dihydronaphthalene, photochromic single cryst., triplet photochem. 79−39164
1,2,4,5-tetrachlorobenzene, in durene host, phosphoresc., cross-relax. between spin levels 78−9186
tetrachloroethylene, trimerisation, IR laser action and BCl_3 sensitiser effects 77−12809
s-tetracyanobenzene+p-xylene, photoassoc., exciplex form., excitation energy and isotope depend., vibr. effects 80−55634
tetrazine-Ar, van der Waals bond, nonstatistical vibr. energy distrib., photochemical reaction effects 80−30255

photochemistry continued
s-tetrazine-benzene, mixed cryst., 2K, lifetime limited photochem. hole burning 78−9183
s-tetrazines, mol. crysts., laser-induced photochem., isotope separation and hole burning 78−85185
thermal chemistry as an exercise in photochem. 80−3379
thermosphere, ion photochemistry from Atmosphere Explorer C meas. 78−32261
thermosphere, lower, diffusion-photochemical model, turbulent diffusion coeff. seasonal vars. 79−53424
thermosphere, lower, one-dimensional diffusion-photochemical model for O and O_2 distrib. simulation 80−4159
thermosphere, O^{++} photochemistry 77−45226
thermosphere, photochemistry rel. to N and NO diurnal variability 77−78549
thermosphere O and O_2 densities, photochemical deviations from diffusive equilib. 77−37470
thioindigo, in nonpolar solvent, photoisomerisation mechanism, fluoresc. obs. 77−63933
thioindigo adsorbed on Al_2O_3, photoisomerisation 80−89503
time-correlated picosecond laser pulses generation, rapid sampling of optical relax. phenomena 80−9969
Titan atmosphere, photochemistry rel. to N_2 atmosphere evolution 79−30005
TMPD, nonpolar photoionised soln., geminate pair quantum field, recombination fluoresc. elec. field quenching 79−20389
toluene cation in solid Ar, absorption and photodissociation spectra 80−69156
tolusafranine-EDTA, photoredox reaction, photopot. and photocurrent generation 77−81420
transition metal foil-electrolyte interface, optical and elec. expts. 78−88644
transition-metal coordination compounds, electronic energy transfer processes 78−56907
transparent polymers, laser-induced optical breakdown, chem. reactions effects *(Russian)* 78−35676
tricarbocyanine solns., photoisomerisation, fluoresc. and absorpt. spectra of photoisomer 78−85181
2,4,5-trimethylbenzaldehyde, in durene, cryst., photochem. and photophys. processes 77−60092
triphenylantimony, single crystal, irrad. by UV, diphenylantimony radical prod., ESR 78−31662
troposphere, evidence for significant in situ photochemical O_3 source 80−72619
troposphere, halocarbon sinks, photooxidation, $O(^1D)$ atom and OH radical reactions 77−17165
troposphere, methane variations, transport and photochemistry 77−53138
troposphere, nonurban, oxidation of NH_3, H_2S and methane 78−32183
troposphere, O_3 budget, one-dimens. photochem. model 78−32180
troposphere, O_3 photochemical prod. and influence on climate 80−36365
troposphere, O_3 photochemistry 77−81968
troposphere, O_3 transport and photochemistry 77−53137
troposphere, photochemical and physical transformations, obs. by tunable lasers 77−60460
troposphere, photochemical mechanisms, computational methods 78−49084
troposphere, urban photochemistry, computer simulation 78−49085
TTF, origin of Raman spectrum instability 79−15456
TTF-TCNQ, origin of Raman spectrum instability 79−15456
tunable lasers and applications, conference, Loen (1976) 77−54720
tunable-diode-laser IR spectroscopy applics. 80−40798
unimolecular decay, nonadiabatic interactions, transition probability as function of Massey parameter 80−35503
unimolecular IR multiphoton decomp., energy grained master eqn., approx. model and exact soln. 80−66829
unimolecular reactions, induced by monochromatic IR radiation 78−88645
upper atmosphere, Mg and Mg^+ photochemistry 77−21954
uracil derivatives, effects of UV radiation, IR spectra obs. 78−27801
uracil derivatives, photosensitised induction by H-addition radicals in frozen aqueous soln. 78−20146
Uranus upper atmosphere, photochemistry rel. to mean temp. and temp. vars. 80−46477
urban atmospheric photochemistry, O group anal. and O_3 prod., theory 78−48626
urban troposphere, photochemistry, kinetic study 77−45058
UV radiation meas. using ferrioxalate actinometer 80−41731
UV radiometric standards 79−49193
UV/visible gas lasers, appls. in commercial photochemical processes, review 79−55123
Venus atmosphere, photochemical ractions rel. to UV absorbers identification 78−20665
vibrationally excited molecules, reactive behaviour 77−60097
vinyl fluoride based polymer stabilisers, thermal degradation, post UV-irrad. mech. strength *(Russian)* 79−24778
vision, initial photochem. process, evidence against proton transfer 77−1999
visual phosphenes, X-ray induced, mech. of formation, photochem. investigations 80−108877
visual pigment chromophores, models, spectroscopic and photochemical studies 80−30723
visual pigment long-lived photoproducts, in frog green rod 77−25433
visual pigment model systems, spectroscopy and photochem. 77−32871
visual pigment retinal chromophore, role of protein in photochem. 78−15772
visual pigments, reson. Raman studies, review 77−90729
VUV, the early years 79−49006
water, photo-oxidation at $BaTiO_3$ electrodes 77−12000
water, photoassisted electrolysis using Fe_2O_3 semicond. electrolyte 77−77771
water, photoassisted oxidation at TiO_2:Be electrodes 80−30502
water, photoelectrolysis, appl. of semiconductor interface system *(French)* 80−6935
water, photoelectrolysis, suitability of $FeTiO_3$, Fe_2TiO_4 and Fe_2TiO_5 anodes 77−63920
water, photoelectrolysis, WO_3 electrode behaviour 77−66757
water, photoelectrolysis using $YFeO_3$ photoanode 77−81409
water, photoelectrolytic decomposition by visible irrad. of p-GaP electrode 77−77778
water photo-oxidation in phospholipid bilayers containing chlorophyll a 77−16917
photochemistry continued
water photo-oxidation in presence of porphyrins adsorbed on octane-water interface 78−64933
water-acid ices, UV irrad., EPR of H and D, nucl. electron effects 79−83488
zinc etioporphyrin I anion radical, photoreduction obs. *(Russian)* 78−23958
zinc octaethyl porphin, soln., photochem. ionogenesis 80−61116
Ag films, UV photostimulated oxidation, electron microscopic study *(Russian)* 78−95850
Ag halide, photographic image form., defect and impurity states, LCAO calc. 78−16876
Ag halide diffusion transfer development chemistry 79−96340
Ag solvation, in ice matrix, ESR and irrad. at 4.2 and 77K 79−8444
Ag solvation, in ice matrix 79−5166
AgBr, Ag speck formation, ionic and electronic effects in photographic process 77−4917
AgBr, electron-hole kinetics 79−24005
AgBr evaporated layer chemical sensitisation 79−24766
AgBr, form. of mixed AgBr(J) phase during two-jet photographic emulsification *(Russian)* 79−44968
AgBr photographic emulsions, sensitivity, fog rel. to treatment in redox-buffered solns. 78−32906
AgBr:Pt, photochemistry and role of Pt impurity ions 79−24783
AgCl:Pt, photochemistry and role of Pt impurity ions 79−24783
AgCl:Pt^{2+}(Pt^{4+}), single crystal EPR, substitution effects on photochemistry 79−15348
Al-As_2Se_3-Al, photographic process based on electrochem. reactions *(Russian)* 79−6213
AlH_3, photoelectric effect spectra and kinetics, photochem. mechanism colour centres 78−56506
AlH_3, photographic processes, thermo- and electrochemical transformations 78−89576
AlH_3, synchronous photochem. processes in lattice 80−101029
Ar:Xe:Cl_2, photochem. XeCl prod., ESR 77−18947
As-Ge-S(Se), glass films, photostruct. changes 77−85822
As_2S_3, amorphous film, light enhanced vaporisation, photolithographic process, photographic appls. 77−5949
As_2S_3, amorphous film, photooxidation, substrate depend. 78−64866
As_2S_3 films, kinetics of light-enhanced vaporisation rel. to photocond. 77−84919
As_2S_3-Ag, light sensitivity for high exposure densities *(Russian)* 79−6212
As_2S_3-Ag system, activation energy for photochem. conversion, 80-340K, radiation intensity depend. *(Russian)* 78−3356
B, laser photochemical isotope separation using Ti catalyst 77−61612
BCl_3-$COCl_2$, impurity removal by laser irrad., IR spectra meas. 78−15686
BCl_3-H_2, photochem. with Ti, Pb catalysts, isotopic excitation by laser 78−64882
BCl_3+H_2 laser induced chemistry, theory 78−76884
BCl_3+methane reaction, laser-induced, vibr. excitation influence on reactivity, isotope selectivity 80−11921
Ba+SO_2→BaO+SO reaction, laser-induced fluoresc. obs., vibronic distrib. of BaO, collisional energy depend. 80−11917
Br+Br+Ar, photoinduced recombination, numerical simulation 79−16018
Br+H_2, laser field interacting with collision dynamics, model system 78−62876
Br+HCl(DCl), relax. rates, vibr. photochem. 79−66290
Br_2, (B-X) band spectrum in laser induced fluorescence 79−47931
Br_2, absorpt. spectrum, rel. to laser isotope separation 77−10683
Br_2+acetylene, laser-induced photochemistry 80−45498
C_2N_2, multiphoton UV photodissoc. 78−50602
CO-Ar(-N_2), C_2 and CN form. by optical pumping, room temp. 80−16701
CO-SF_6, single-photon absorption reaction chemistry in solid state 77−73454
CO_2, aqueous solution, photoelectrochemical reduction on p-type GaP in liq. junction solar cells 78−88649
CO_2 lasers for selective interactions with matter 77−27296
CO_2 photochem. reduction to organic fuels using photoelectrochem. solar cells 80−55880
CO_2 photofixation to formic acid in water, photosynthesis mimicking 78−88650
CS_2, aerosol form. by laser, kinetics study and photoreaction products chem. nature study 80−21324
Ca+CCl_4→CaCl+CCl_3 reaction, laser-induced fluoresc. obs. 80−11916
n-CdS electrode, photoelectrochemical behaviour in acetonitrile solns. 78−31644
n-CdS in DMF solns., electrochem., photoelectrochem., redox. pot. determ. 79−96322
CdS, photoanodes in sulphide-polysulphide electrolytes, instability 78−80755
n-CdS, photoanodic behaviour in acetonitrile-iodide solns. 78−47868
CdS:Li, donor-acceptor interactions, photochem. reactions *(Russian)* 77−40285
n-CdS-CdSe mixed polycryst. electrode for photoelectrochem. cell 78−47867
CdSe, photoanodes in sulphide-polysulphide electrolytes, instability 78−80755
Ce, photochemical separation from rare earth mixtures in aq. soln. 79−39165
Cl atoms, photorecombination, rate constants determ., identification of spectral distribution of recombinative emission intensity 80−85195
Cl+fluoromethane, photochlorination electron and oscill. energy 80−81320
Cl+H_2S→HCl+HS, laser-initiated chain reactions, rate consts., product energy distrib. 78−85144
Cl+methane-methane-d_2, free radical chain reaction, D isotope photochem. enrichment 79−36790
Cl_2, photochemical reaction using Ar ion laser, Cl isotope enrichment 78−74780
Cl_2^-, vibrationally excited, reactions and photodestruction 77−60048
Cl_2-O_3 system rel. to stratospheric composition 77−16849
Cl_2+H_2(H_2S)(methanethiol), laser-initiated chain reactions, rates, mechanisms, chemiluminesc. obs. 80−55651
$ClCO_3NO_2$, synthesis by UV irrad. of Cl_2, NO_2, CO in air, decomp. kinetics 78−76880
ClF+SF_4 (perfluoroethane)(Xe), thermal and photochem. reactions investig. 80−61117

photochemistry continued
ClONO, prod. via Cl+NO_2 react., FT IR obs. 79−8427
ClOO, stratospheric chem., formation and loss reactions 78−16138
$Co(CN)_6^{3-}$, electronic struct., photochem. props., MS Xα calcs. 79−22600
trans-Cr (III)$(NH_3)_4XY$ complexes, d-d irradiation preferential labilisation, Adamson's rules, ang. method overlap 77−40557
Cs-D_2, vap., oscill. production of particulates, by CW laser beam 77−77794
Cs-H_2 vapour, resonant character of laser induced formation of particles 80−89481
CsH, crystallisation in Cs+H_2 gas mixture, laser snow effect 80−40712
$CsSn_2I_5$, surface props., Auger study, elec. cond. meas., photochem. study 80−66339
Cu electrode, photopotentials, rel. to corrosion 79−24648
Cu, photo-assisted corrosion in anaerobic acidic medium 79−43466
Cu photocorrosion in $CuCl_2$ and $FeCl_3$ aq. solns. 79−57145
Cu, photosensitive film formation 77−9105
Cu phthalocyanine thin film electrodes, near IR photoelectrochemical responses 80−93766
Cu-Al(Ni) alloy electrode, photopotentials, rel. to corrosion 79−24648
Cu(II) complexes, reversible excited-state electron transfer reactions for solar energy conversion 80−89655
D enrichment by CW vibr. photochem. of methane, economic aspects 80−11920
D_2 isotope enrichment by CW CO_2 laser-induced vibr. photochem. 79−36790
Eu complex, fast reactions, pulsed selective photoexcitation, rate determ., spectral method 77−86336
Eu*+Sr, light-induced collisional energy transfer 78−50614
F+$CH_3I(CF_3I)$(ICl) reactions, product state analysis using laser-induced fluoresc. 80−11915
Fe complex, tris (1,10-phenanthroline) iron(II), transient bleaching, excitation wavelength absorpt. 78−73060
Fe organometallics, interaction of naked Fe atoms with small mols., Mossbauer study of bonding in products 80−43080
Fe-I system, photochemical conversion efficiency 80−71923
Fe-thionine, photogalvanic cell, photostationary state comp., current depend. 77−90629
Fe+$N_2(NH_3)$ interaction, chemical species formed studied by Mossbauer effect 80−43080
$FeBr_3$ aqueous soln. photogalvanic effect 79−24902
$Fe(CO)_4$, IR laser induced isomerisation, non-Berry pseudorotation 78−31658
$Fe(CO)_4$, IR spectra and laser photochem., matrix isolated at 20K 78−74651
$Fe(CO)_4$, in N_2, Ar low temp. matrix, IR laser photochemistry, orientational and site selectivity 78−23954
α-Fe_2O_3, photochem. props. of sintered and doped samples for solar photoelectrochem. cell appls. 80−89651
α-Fe_2O_3, pure and TiO_2 doped, electrode, photooxidation of H_2O appl. 78−76886
n-Fe_2O_3, sintered and flame-oxidised, photoelectrochemical props. 79−70355
n-GaAs, preferential photoelectrochemical dissolution in Fe(III) based etches 78−7066
p-GaAs/heptyl viologen system, photoreduction, appl. in photoelectrochemical cells and photoelectrochromic displays 80−76640
n-GaAs(P) in DMF solns., electrochem., photoelectrochem., redox. pot. determ. 79−96322
$Ga_xIn_{1-x}P$, flat band pot., impedance meas. and photoelectrochemistry *(French)* 80−49894
p-GaP, cathode of photoelectrochemical cell 78−10552
n-GaP electrode, photoelectrochemical behaviour in acetonitrile solns. 78−31644
p-GaP electrode, photoelectrochemical effect 80−55673
GaP photoelectrode, role of Au overlayers 78−14812
Ge-S-Ga(In) system glasses, photoinduced changes 80−24365
Ge+Br_2, heterogeneous photochem. reaction kinetics, laser radiation intensity effect 79−66326
Ge+Br_2, surface reaction, rate-limiting step, ellipsometric and photochem. meas. 80−16730
H, photochem. reactions in HCl frozen aq. soln. at 77K 77−9093
H photoelectrochemical prod., solar beam-assisted electrolyser applied to Yokohama marks 5 and 6 [system for hydrogen production] systems 80−45768
H+NO+M→HNO+M, HgH+NO→HNO+Hg, rate consts. of photosensitised reactions 77−36757
H_2, photocatalytic prod., TiO_2 electrodes, solar energy conversion 77−1932
H_2 photocatalytic production by carbohydrate conversion using RuO_2/TiO_2/Pt photocatalyst powder 80−94120
H_2 photoelectrochem., prod., ZnTe and CdTe photocathodes, characteristics 77−70311
H_2, production by solar energy, homogeneous photoredox system 80−3387
H_2 production by solar photochemical decomposition of H_2O 80−16822
H_2+H(F)(Cl), collision induced IR laser absorpt., rate enhancement, theory 79−66275
H_4, excited potential energy hypersurfaces, trapezoidal geometry, rel. to photochem. 2s+2s processes 77−30797
H_4, excited potential energy hypersurfaces, rel. to photochem. 'cross-bonding' processes 77−83501
HCl+Br, IR fluoresc. studies of state-selected energy transfer, photochemistry 77−77768
HO_2+NO_2, UV irradiated, kinetics and mechanism, peroxynitric acid form., smog 77−63885
H_2O, electrochem. splitting, solar energy assisted, on MoS_2 layer cryst. surface 77−90612
H_2O, multiphoton UV photodissoc. 78−50602
H_2O, photooxidation by α-Fe_2O_3 electrodes 78−76886
H_2O+CO_2, photoassisted reaction on $SrTiO_3$ (111) face, methane form. 78−76878
HOCl, stratospheric chem., formation and loss reactions 78−16138
HONO+NO+NO_2+CO+air, UV irradiated, computer simulation, peroxynitric acid form., smog 77−63885
HO_2NO_2, in stratosphere, photochemistry and abundance 78−20467
HO_2NO_2, photochemistry and significance in atmospheric NO_x chemistry 78−11971

photochemistry continued
H_2SO_4, secondary particles form. and growth, kinetic aerosol model 79−29492
He H^+, formation and destruction in gaseous nebulae, assoc. IR emission line spectrum 79−44589
Hg, determ., in fresh and saline waters, automated UV digestion-AAS method 78−44414
Hg+2NH_3→$HgNH_3$+NH_3, photosensitised, $HgNH_3$ complex lifetime 78−53193
Hg_2 excimers, photoassoc., spectroscopy and kinetic processes of high-lying vibronic states, laser applics. 80−9649
Hg(6^3P)+O_2, photosensitised reaction, excited intermediates, energy transfer detect. 78−73030
I_2+acetylene, laser-induced 1,2-diiodoethylene form., isomerisation 80−85157
ICl selective photoaddition to acetylene, isotope enrichment, influence of press., buffer and wavelength 80−11927
InP electrodes, photo-induced electrogenerated chemilum. and up-conversion 79−91510
InSe film, photochem. production of holograms on surface *(Russian)* 79−7101
K+$HgBr_2$, laser irrad., HgBr* form., chemiluminescence 80−55658
KBr, additively coloured, self-enhancement of amplitude hologram *(Russian)* 80−9828
KBr, S centres, luminesc. and photochemistry *(German)* 77−44055
KBr(I): $O^{2-}(S^{2-})(Se^{2-})(Te^{2-})$, low temperature photochemistry on chalcogen vacancy centres 78−18641
KCl, S centres, luminesc. and photochemistry *(German)* 77−44055
KI:S^{2-}, impurity-vacancy dipole UV absorpt. and ionic thermocurrent, F-centre form. 77−36271
KI:S^{2-}, photochemical reaction, F-centre production 78−64861
$^{83}Kr_2F$ radical, in UV-irrad. Kr/CF_3OF, 10K, ^{83}Kr hyperfine EPR spectrum, struct. 78−42101
$^6Li^*$+$^7Li^*$, laser-induced Penning and associative ionis., $^{13}Li_2^+$ enrichment 78−58796
Li($2^2P_{1/2,3/2}$), laser induced flame chemistry, saturated mode fluoresc. meas. 80−89491
$MgSi_2$, laser irrad. induced form., cryst. microstruct. 80−35011
Mn^{2+} and $P700^+$, light-dependent reactions in pulsed illuminated chloroplasts 79−53062
N^+ in thermosphere 79−96847
N_2, photoreduction, to NH_3, by desert sand 79−83483
NH_2^-, photodetachment energy calcs. 77−27123
NH_3, laser photochemistry 79−43604
NH_3 photochem. in Jupiter's atm. 77−45354
NH_3 sensitiser, excitation in MW region using CO_2 laser, pumping models 80−11911
NH_3 synthesis, industrial, using N_2 reducing solar cells 80−89632
NO in Earth's thermosphere, solar activity depend. 80−77178
NO/NO_2/O_3, atmospheric, photostationary state relationship rel. to monitors intercalibration 78−69529
NO-SF_6, single-photon absorption reaction chemistry in solid state 77−73454
NO+O_3, (001), laser enhanced reaction, temp. depend., reactive and non-reactive channels 78−48642
NO+O_3(001), laser-enhanced reaction, rates, temp. depend. 78−48675
NO+O_3(001)→$NO_2(^2B_{1,2})$+O_2, laser enhanced reaction, temp. depend. 77−81397
NO_2, laser-induced fluoresc. quenching rate const. and lifetimes 80−11930
NO_2+SO_2 aerosol, form. kinetics, irrad. by 488 nm light 78−40067
N_2O, atmospheric, instantaneous global photochemical reaction rates 80−17335
N_2O-SF_6, single-photon absorption reaction chemistry in solid state 77−73454
$NO^+(NO)$+SO_2, cluster form., equilib. const. and rate coeffs., UV irrad. effects 77−60060
NO(N_2O)-SF_6, single-photon absorption reaction chemistry in solid state 77−73454
NO(N_2O_3)-SF_6, single-photon absorption reaction chemistry in solid state 77−73454
Na+O_3→NaO*+O_2, in upper atm., rel. to Na I nightglow intensity vars. 79−70905
Na_2+Ar(Ne)(He), collision induced dissoc. rate, vibr. distrib. depend. 79−22791
$NaClO_4$ glass, radiation induced trapped electrons, photobleaching, H form. 77−44494
NaOH glass, radiation induced trapped electrons, photobleaching, H form. 77−44494
Na($3^2P_{1/2,3/2}$), laser induced flame chemistry, saturated mode fluoresc. meas. 80−89491
Ni complex, bis-4-dimethylaminodithiabenzyl nickel, tetrachlorethane soln., photochem. and thermal stabiljty 80−16708
O, photochem. enrichment of ^{17}O and ^{18}O using ArF laser 77−16834
O, singlet, photosensitised luminesc. in soln. 77−70309
O+ethylene, (OCS), reaction dynamics, IR laser excitation effects 79−66288
O+methane, photochem. reaction, high temp., rate coeff. meas. 80−16699
O+saturated hydrocarbon, chem. reaction dynamics. OH prod. investig. 80−101016
O_2, laser photochemistry 79−43604
O_2 singlet in natural waters 77−56659
O_2, singlet product. detect. by EPR 79−66597
O_3 column, increase rel. to NO_x emission from SST and subsonic aircraft 78−11979
O_3 layer, photochemistry rel. to possible O_3 reductions and Earth surface UV radiation 80−94577
O_3, photochemical generation, sources, air sampling programme 79−66430
O_3+NO, laser enhanced reaction, fluoresc. obs. 79−66285
O_3+NO(v=1), IR laser enhanced reactions 79−66286
OClNO, form. in matrix reaction, IR absorpt. obs., photoisomerisation 78−15667
$O_2{}^1\Delta_g$, singlet and triplet precursors of photosensitised addition to organic acceptor 79−52714
OH+alkanes (alkenes), photooxidation, 305K, absolute and rel. rate consts. 77−16782
OH+RH→H_2O+R_x, radical substitution reaction 80−81321
P, ground state $3p^3(^4S_{3/2})$, time-resolved reson. fluoresc. obs. 79−34333
PbI_2, cryst., photochem. phenomena investig. *(Russian)* 78−35204

photochemistry continued
PbI_2-Ag light sensitive system, photochem. conversion process under continuous laser radiation, nonreciprocity *(Russian)* 77−79179
PbI_2-Ag system, effect of bound and free exciton states on light sensitivity *(Russian)* 78−71169
PbI_2-Ag(Au)(Cu), light sensitive, internal photoelectric emission 80−107910
Rb-tetrahydrofuran solution, polarised photoelectron and loose ion pair (Rb^+, e) obs., optical-ESR study 80−85196
$RbAg_4I_5$-metal interface, photocurrents, photoelectrochem. effects 78−34897
Rh complexes, Rh(III) halopentaammines, solns., luminesc. and excited state lifetimes, photoaquation 79−8175
Rh(III) complexes, luminesc. rise time meas. by wavelength shifter 80−50390
Ru complex, $[Ru(bpy)_3]^{2+}$-Ti (III), photochem. H_2 prod. from aq. soln. 80−85192
Ru complex, photooxygenation, actinometric laser intensity meas. appls. 77−30193
Ru complex, ruthenium(II) tris(2,2′-bipyridine), absorption spectrum and quantum yield of formation *(French)* 80−5554
Ru complex, tris-(2.2′-bipyridyl)-Ru(II) complex, photoelectrochemical systems, solar energy utilisation *(German)* 80−45713
Ru complexes, $[Ru(bipy)_n(pq)_{3-n}]^{2+}$ mixed-ligand, electronic absorpt. and emission spectra meas. 80−71441
S chemistry and thermodynamics on Venus 79−44391
SF_6 mixtures, laser initiated explosions, chemilum. in near UV, visible and IR 78−48674
SF_6, multiphoton isotope selective dissoc., pulse shape, energy, press. and geometry effects 78−25733
SF_6, photon-enhanced dissociative electron attachment, isotope selectivity 80−18939
SF_6, unimolecular reaction model 78−7189
SF_6+NO+O_3, laser sensitised reaction, time-resolved NO_2* emission obs. 78−20017
$SF_6+SiH_4 \rightarrow S_2$*$+SiF_4+HF+H_2$, laser augmented reaction, isotopic selectivity retention during detonation 78−48673
SF_6+Si(surface), IR laser induced reaction, mol. vibr. and mol. dissoc. obs. 80−93798
S_2F_{10}, IR laser irrad., absorpt., reaction parameters 78−94241
SO_2, atmospheric, photochem. oxidation 79−70873
SO_2, NO_2, atm. pollutants, UV radiation effect on photochem. reactions 77−21894
SO_2, oxidation, precursor effects, rel. to air pollution 79−1960
SO_2 photochem. effects on nitrate conc. in aerosols 77−49103
SO_2, photooxidation, gas phase, in cloud chamber 79−47951
SO_2, photooxidation in gas phase, nucleation appls. 79−83479
$SO_2+CO(C_2H_2)$, photochem. reactions, rate consts. 78−23956
SSF_2, FSSF, and ^{34}S isotropic forms, matrix IR and Raman spectra *(German)* 79−89674
Se-Ge amorphous films, obliquely deposited, photoinduced chem. changes 80−76385
Si, laser induced formation of metal silicides 79−70366
Si, laser induced reactions with metal films, silicide formation 79−70365
Si n-p planar diode, Al layer covered, laser beam produced alloy areas, characterisation 79−69594
n-Si, passivation, photoactivation kinetics in conc. alkali, ellipsometric investig. 77−1885
Si surface electron beam deposited silicide formation using scanning CW laser beam 80−66862
Si-metal thin film reactions, laser annealing 79−70364
Si-SiC chemical interaction in rarefied O_2 under pulsed action of concentrated solar radiation 80−71930
SiH_4, vertical excited states, CI calcs. 79−18127
SiH_4+UF_6, IR laser single photon absorption reaction chemistry, solid state 79−66308
Sr_2 dimer, photoassoc., photoluminesc., collisional dissoc. 80−58303
$SrTiO_3$ electrode, surface comp. changes during photoelectrolysis, XPS obs. 79−7894
Ti, passive oxide layer form. in H_2SO_4, ageing with and without photoexcitation *(French)* 80−45432
TiO_2 (100), chemisorption of H_2, O_2, and H_2O, electron spectroscopy, evidence for Ti^{3+} photogeneration 78−38940
TiO_2 electrode, illuminated, Hg deposit from Hg(II) solns. *(French)* 79−52696
n-TiO_2 electrode, photo-oxidation of acetate and iodide 80−81331
TiO_2, nonstoichiometric anodic films, O incorporation kinetics 80−97733
TiO_2, photodesorption of H_2O, pulsed-laser-dynamic-mass-spectrometer study 80−35568
TiO_2 electrodes, effect of processing variables on photoelectrochem. props 80−6975
TiO_2 electrodes, room temp. diffusions, capacitance, spectral response and volt-ampere characts. 80−15294
U enrichment by photochemical laser, two-phase flow with condensation, mathematical model *(French)* 80−74029
UF_6, laser chemistry 80−69198
UF_6+SiH_4, photoinduced reaction in low temp. SiH_4 matrix 80−30256
UO_2^{2+}, excited, in liq. and glassy media, luminesc. decay processes, temp. activation 79−91978
UO_2^{2+} in aq. solns., luminescence quenching by metal ions 78−39588
UO_2^{2+} in aq. solns., luminescence quenching by H_2O mols. 78−39589
$UO_2^{2+}{}_{(aq)}+UO_2NO_3^{+}{}_{(aq)}$, ground and excited state interaction, struct., thermodynamic functions, photochemistry obs. 80−32779
V (III) complex, alcoholic VCl_3 soln., fluoresc. and photoreduction 78−85177
$Xe+F_2$, collision induced photoabsorpt. indicating $Xe+F_2+h\nu \rightarrow XeF$*$+F$ 78−27786
n-ZnO electrode, photoelectrochemical behaviour in acetonitrile solns. 78−31644
ZnO electrode, role of triplet states in xanthene dye sensitisation 78−76869
ZnO, photodesorption of CO_2, pulsed-laser-dynamic-mass-spectrometer study 80−35568

photochromism
Alexandrite effect in solids *(German)* 79−51924
alkali silicate glass, photochromism 77−43955
alkaline earth fluorides, radiation damage and photochromism in doped and undoped crysts. 79−51148
aluminoborosilicate glass, holography using photoinduced anisotropic media 79−41354

photochromism continued
anils, cryst., high-press. optical effects 78−31170
anils, polystyrene soln., high-press. optical effects 78−31171
azomethines, photochromic, intramol. proton phototransfer sensitisation, organic cation energy transfer 78−53230
bilevel absorber, partial differential rate eqns. 78−37950
borosilicate photochromic glasses, photosensitivity rel. to AgCl particle shape 78−31223
N-5′-chlorosalicylideneaniline, photochromism and thermochromism, NQR spectra, temp. and UV irrad. depend. 80−54968
colloidal photochromic dyes, quasi-crystals produced in applied electric field 80−85225
cuprous halide photochromic glasses, spectral props., shell model *(Russian)* 79−27354
diamond, electron irradiated, photochromism 80−71454
3,3′-dimethyl-1′-phenyl-6-nitro-spiro [(3H-7,8-benzochromen)-3,2′-indoline] (II), photochromic transform., temp. depend. 80−104456
3,3′-dimethyl-1′-phenylspiro [(3H-7,8-benzochromen)-3,2′-indoline] (I), photochromic transform., temp. depend. 80−104456
4-(2′,4′-dinitrobenzyl)-pyridine, photochromism, nanosec. laser absorpt. spectrosc. obs. 80−85193
2-(2′,4′-dinitrobenzyl)-pyridine, photochromism, ns laser absorption spectra 78−48138
2-(2,4-dinitrobenzyl)pyridine, powdered sample, kinetic photochromic characts. 78−23957
2,2′-dinitrodiphenylmethane, nanosecond laser flash photolysis and absorpt. spectra, photochromism, solvent polarity 78−61029
electrolyte, solid film, size-selective photochromism 79−99968
fluorescence solvatochromism kinetics 77−30898
fulgimide planar photochromic structures for optical waveguide components 80−64196
glass, γ-ray effects on sensitivity *(Japanese)* 79−38583
glass, Ag halide type, photobrown, transmittance meas. at environmental extremes 79−46020
glass, coloration kinetics, isothermal relax., and spectral sensitivity using spectrosensitometer 80−27358
glass, holographic data recording optimisation, diffr. efficiency 78−25829
glass, light effects, history of development of photosensitive and polychromatic glasses 80−40080
glass, light sensitive, review of types 80−91870
glass, parameter standardisation 80−69476
glass, photochromic, thermo-optic transitions 80−50307
glass, photochromic, types FkhS-3, S-4, S-4a and FkhPP, exam. of magnetooptical rotation 78−88284
glass, phototropic, kinetic investig. *(German)* 78−64868
glass, spectral characts. control 80−16073
glass, thermochemical effects on photochromic props. 80−87448
glass darkening and bleaching kinetics, pulse photometry 79−46021
glasses, electron-hole separation, influence on recombination probability 80−11445
halide photochromic centres, isothermal relaxation kinetics 80−16072
hologram recording medium, characteristic transfer curve description, using heuristic exponential model 80−78796
hologram storage in inorganic photochromic materials, book contrib. 78−25835
holographic information storage material 79−50265
holographic storage capacity, photochromic and photorefractive media 79−27203
indoline spiropyrans, methoxysubstituted, activated solns., photochromism, laser nanosecond spectroscopy 77−70317
integrated programmable planar waveguide components formed by optically writing Bragg diffraction gratings into photochromic structs. 80−79011
ionic crystals, review, optical information storage appl. 78−82926
maleic anhydride-styrene copolymer, photochromic, recording material for holograph 79−72537
membranes, carrier-mediated photodiffusion 78−23965
modulation photolysis as alternative method for photochromic soln. obs. 77−90613
optical data storage material requirements and possibilities *(German)* 78−25937
optical recording media, review 78−71172
organic material, for real-time coherent optical processing 78−50876
organic photochromic materials, holographic recording *(Russian)* 80−1161
2′-oxaindan (dihydroisobenzofuran) spiropyrans, photochromic transforms, spectrokinetic study 80−30259
pentamethinemerocyanine dye, electronic spectrum and struct., solvatochromism, microstructural model 77−61817
phenanthridinic spiropyran photocoloration mechanism 79−83487
6-phenoxy-5,11-napthacenequinones, photochromism, molar extinction coeffs. meas. 80−66220
photochromic glasses, anisotropic recording of optical data *(Russian)* 77−1651
photochromic tracer film, measurements using POLLY, film reading computer system 78−42696
photochromic tracer technique, for nondisturbing flow measurement 78−38435
polarised photochromism in solid solutions 78−64859
polymer, photochromism 80−5805
polymer, thermal effect in photomech. conversion 80−16706
polymer films, electronic cond., electro-, photoresponsive effects, review 79−56261
positional coding optical correlator, tabular coordinate search method *(Russian)* 79−98292
powdered sample, with photochem. reaction and/or thermal reverse reaction, kinetics 78−23957
PTA-ZnCdS, electrochromic material mixed with photosensitive powder, photoinduced coloration and electrochemical bleaching 77−81082
PVC, Cu evaporated film, electron-induced metallochromic reaction for metal image formation 80−86476
quartz, fused, photochromic LITMO, optical props. 80−1287
retinal-entrapped membrane, photo-induced potential 78−20148
salicylidene-2-chloroaniline, photochromism and thermochromism, NQR spectra, temp. and UV irrad. depend. 80−54968
salicylideneaniline, photochromic, optically induced changes in refr. index 79−81497
α_1-salicylideneaniline, photochromic props., appl. as holographic recording 77−68183

photochromism continued
N-salicylideneanilines, photo- and thermo-chromic, ^{14}N quadrupole resonance temp. depend. 78−48077
N-salicylideneanilines, thermochromic and photochromic, ^{14}N quadrupole coupling, NQR meas. 77−28480
silicate glass, CeO_2 activated, surface treatment effect on absorpt. 78−71168
sodium-alumoborosilicate photochromic glasses, Weigert effect *(Russian)* 77−68250
solvatochromism, microstructural model 77−61817
Spacelab optical techniques for liquid flow and temp. meas. 79−82007
spectrosensitometer for spectral-kinetic characts. meas. of photochromic materials 80−27358
spirobenzopyran copolymer photochromic soln., photoviscosity effect 80−6536
spiropyrane, triplet-triplet absorpt. by laser photoexcitation 77−10685
spiropyrans, photochromic, thermophotodegradation for autoprocessor reprography system 80−35555
spiropyrans, photochromic transform., dipolar cryst. form. 79−20386
spiropyrans, photochromic transformation by electro-optical chronography 79−57264
spiropyrans, polymer matrix effect 80−76537
spiropyron solutions, nitro-substituted, electronic state participation in photochromy 80−81347
surface polariton use in optical storage 80−48414
2,3,4,4-tetrachloro-1-keto-1,4-dihydronaphthalene, photochromic single cryst., triplet photochem. 79−39164
transient characteristics of photochromic process 77−34920
waveguide, gradient photochromic film, acousto-optical props., integrated optics appl. 80−33207
Ag formation on Ag-halide surface, flash photolysis expts. on Ag halide photochromic glasses 79−94310
Ag halide, glass, kinetics of photochromic processes 80−103930
Ag halide, photochromic glass, optically induced anisotropy 80−1282
Ag halide, photochromic glasses, optical properties, effect of Cu ions 80−93364
Ag halide doped photochromic glass absorption spectra *(Russian)* 78−60490
Ag halide glasses, optical absorp. of Ag, optically induced dichroism 80−108177
Ag halide photochromic glass:Cu^{2+}, characterisation of Cu ions 78−5530
Ag halide photochromic glass, darkening mechanisms under pulsed laser excitation 78−25938
Ag halide photochromic glasses, props., effect of temp. 78−83057
Ag halide photochromic glasses, colour centres struct. 80−66254
Ag halide photochromic glass, darkening mech., temp. depend. 80−87449
Ag halide:Cu^{2+} photochromic glasses, darkening mechanisms, from flash photolysis and EPR studies 77−16156
Ag halides, formation of metallic Ag on surface, optical absorpt. calcs. 79−24791
Ag halides:Cu in photochromic glass, formation and theoretical models, review 80−43418
Ag-containing glasses, colour adaptation, photoinduced optical anisotropy 79−61331
AgBr(Cl)-CuBr(Cl), photochromic film for hologram recording 79−64184
AgCl photochromic glass, additional absorpt. spectrum, ellipsoidal model of colour centres 80−40142
$Ag_xHg_ySI_2$, prep. of mixed sulphide iodides, photochromism 77−36385
$Ag_2S.HgI_2$ and $Ag_2Se.HgI_2$ thin films, transmission spectra and photochromism 79−52032
As-S glassy film, photobrightening effect 80−11498
As-Se system, chalcogenide vitreous semiconductors, darkened films, thermal and optical bleaching, light transmission obs. 80−50447
$Bi_{12}GeO_{20}$:Mn, Cr, reversible photochromic effects, absorpt. spectra before and after illum. 79−91471
$Bi_{12}SiO_{20}$, optical quality, Czochralski growth 78−31324
$Bi_{12}SiO_{20}$:Mn, Cr, reversible photochromic effects, absorpt. spectra before and after illum. 79−91471
CaF_2, additively coloured, photothermal bleaching of Ca colloids 79−15500
CaF_2:Ce^{3+}, ENDOR meas. on Ce^{3+} photochromic centre 78−19372
CaF_2:La, pulse hologram recording 79−55091
CaF_2:Tb, EPR in new photoexcited centre 78−19319
CdO-GeO_2:Tl_2O photochromic glass for optical information retention media 80−33108
CdO-SiO_2 glasses, photochromism *(Japanese)* 78−15140
Cu halide based photochromic glasses, spectral props. 80−29708
Cu-Cd-Cl stretched photochromic glass, polorisation effects 79−95729
Er_2O_3-TiO_2-WO_3-PbO, glass form., refr. indices and density meas. 77−90312
H_xWO_y film, effect of struct. on optical and electrical props. 78−84671
KBr, additively coloured crystal, amplitude-phase holograms *(Russian)* 79−59654
KBr F→M transform., electrostatic field control of optical information recording *(Russian)* 80−48370
KCl, additively coloured photochromic crystals, spectral sensitivity *(Russian)* 80−91871
KCl, amplitude-phase holograms, optical parameter dispersion 80−58481
$Li_2B_4O_7$, ferroelectric glass, phase transition, permittivity, electrochromism, photochromism 80−80719
Li_2O-B_2O_3-WO_3 glass, photochromic and electrochromic props. 79−28787
$Na_8(Al_6Si_6O_{24})Cl_2$, sodalite, ESR and optical spectra obs. 77−32407
NaCl, additively coloured, sensitised with O, photochromic props. 79−28792
NaCl, hologram recording, F-centre bleaching by 633 nm light 79−22922
NaCl:O, photographic recording in far-UV, colour-centre formation 79−23035
Na_2O-Al_2O_3-B_2O_3-SiO_2:Ag, photochromic glass, EPR of Ag^0 and Ag_2^+ centres 77−24741
Na_2O-Al_2O_3-B_2O_3-SiO_2 photochromic glass, $AgCl_{1-x}Br_x$ activated, comp. optimisation by Box-Wilson method 77−50741
Na_2O-Al_2O_3-B_2O_3-SiO_2-AgBr(Cl), photochromic glass, exam. of role of O and Cu ions, using luminescence spectra 79−4849
Na_2O-Al_2O_3-B_2O_3-SiO_2, CuCl crystal activated photochromic glasses, absorpt. spectra 79−27353

photochromism continued
Na_2O-Al_2O_3-B_2O_3-SiO_2-AgCl(Br), photochromic glass, kinetics of thermal decolorisation 80−103931
Na_2O-SiO_2:Ce photochromic glass absorption centres 79−27352
Na_2O-SiO_2:CeO_2, photochromic glass, form. and decay kinetics of absorpt. centres 78−13774
PLZT, Fe doped, photochromic effect 77−16347
PLZT:Fe, enhancement of photochromic effect by multi-reflection scatt. 77−75632
P_2O_5-CdO glasses, Weigert effect *(Russian)* 77−1690
Se, vitreous, darkened films, thermal and optical bleaching, light transmission obs. 80−50447
$SrTiO_3$:Fe, photochromic Fe^{5+} in non-cubic local fields, EPR spectra of $S=^3/_2$ centre obs. 77−40127
$SrTiO_3$:Fe^{4+}, opt. absorpt. 77−16349
$SrTiO_3$:Ni, photochromism, optical absorption spectra and EPR meas. 77−1708
TeO_2, ferroelectric glass, phase transition, permittivity, electrochromism, photochromism 80−80719
V_2O_5 amorphous film, photochromism and thermochromism 80−93254
WO_3, amorphous coloured film, charge transfer, XPS 77−12491

photoconducting devices
see also photoconductive cells; photodiodes; phototransistors
astronomical far IR bolometric and photoconductive detectors 77−41305
compact real-time matched-filter optical processor 78−74869
elastomer storage device evaluation for optical signal processing 80−48444
electric signal pulse shaping using laser-excited solid-state plasmas in Si, expt. 77−19397
electro-optic light valve, photoconductor controlled 77−7214
electroluminescent, photoconductive image intensifier parameters *(Russian)* 78−42421
electrophotographic and electroradiographic image convertors with electronic readout 79−71554
electrophotographic copier photoconductor drum cooling methods 78−62245
electrophotographic properties of plate with polyvinylcarbazole overlayer and CdS-resin layer 77−61146
ferroelectric ceramic-photoconductor structure, as optically controlled transparency 80−28343
holographic recording materials and devices, book contrib. 78−25838
hybrid field-effect liquid crystal light valve, sensitometry control 80−23788
image processing, digital, parallel logic device and half-adder circuit 80−10027
imaging systems, limitations on sensitivity 80−6907
IR detectors, astronomical, low-noise preamplifier 77−61124
IR detectors, microwave-biased, noise performance 80−9037
IR detectors, microwave-biased extrinsic photoconductors, equivalent circuit model 78−49898
IR imaging appl., development trends *(Czech)* 79−97383
IR photodetector, microwave biased, module construction 80−9038
light valve, fast photoconductor coupled liq. crysts. 79−59805
magneto-optical photoconductor sandwich 77−40213
opto-acoustic transducer structs., recent investigations 80−74688
optoelectronic devices and optical imaging techniques, book 80−27059
photoconductor thermoplastic devices for high density optical storage, expt. 77−3546
photodetector, very-fast-response uncooled, based on intraband μ-photocond. 79−30562
photodetector with integrated waveguide struct. 80−48456
photoplethysmographic vaginal transducer, blood vol. change monitoring 78−92733
photothermoplastic devices, conventional and self-developing, sensitivity and development 79−44958
photothermoplastic devices, single layer, sensitization of N-vinylcarbazole containing polymers to Ar laser 80−83651
Photititus, image intensifier and convertor for electron microscope 77−45918
Photititus spatial-temporal light modulators, image formation kinetics 79−50397
Pockels readout optical modulator, current status and appls. 77−72085
Ruticon, image storage and optical processing appls. 77−72086
Ruticon optical processing capabilities 78−79140
semiconductor switch, light controlled, with picosecond precision, appl. to Kerr cell 78−1327
space-time light modulator sensitivity enhancement *(Russian)* 77−58427
spatial light modulator, using KD_2PO_4 and Se photoconductor, optical processing appl. 80−9988
switch, laser-activated, high-power switching with ps. precision 80−2416
thermoplastic-photoconductor image transducer, input to coherent optical processor 78−83098
UHF biased semicond., cylindrical resonator for photoconductivity investig. 78−21117
UV radiation source output monitoring detector for psoriasis photochemotherapy 78−53473
$Bi_{22}SiO_{20}$, Pockels readout modulation struct., information registration *(Russian)* 77−10990
(Cd,Hg)Te, photoconductive detector, uncooled, for 8-14 μm region 80−31868
CdHgTe detectors for CO_2 laser appls. 79−40615
(CdHg)Te photoconductive detector, thermal figure of merit limit 78−89540
CdS-$LiNbO_3$ monolithic two-dimensional Fourier transformer 79−72516
$CdS_{0.5}Se_{0.5}$, picosecond optoelectronic switching 80−54734
CdSe image convertor, liquid-crystal, hybrid optical processors appl. 80−33166
GaAs, extrinsic, DC- and microwave-biased, performance 80−70750
GaAs extrinsic photoconductor detectors, DC and microwave bias comparison 77−37998
GaAs switch, laser-activated, high-power switching with ps. precision 80−2416
GaAs:Cr, IR spectral detectivity 78−70184
n-GaSb:S-metal surface barrier struct., elec. and photoelec. props. 78−56229
Ge far IR photoconductive detector speed, limitation 79−30550
Ge:Au, IR detector, impurity photoconductivity *(German)* 78−82036
Ge:Cu, IR detector, impurity photoconductivity *(German)* 78−82036
Ge:Ga photoconductor detector performance in low optical background 77−37999

photoconducting devices continued
Ge:Hg photoconductive detector, laser damage thresholds calc. 78−90443
$Hg_{1-x}Cd_xTe$ photoconductive IR detector, optimum bias attainment with batteries 79−58789
In-GaAs:Cu-In structure, phototrigger effect 78−56238
InP, far IR LPE photodetector performance 79−30546
InSb fast response submm. detector 78−89541
InSb laser detector, dynamic range increase 78−49899
$MoSe_2$-I^-, photoelectrode, time resolved photocurrent, nanosecond excitation 80−45708
$Pb_xSn_{1-x}Te$, RF sputtered film IR detector, photocond. response speed improvement by annealing 79−58790
$Pb_xSn_{1-x}Te$-PbTe p-n junction, epitaxial, elec. props. and photoresponse 78−56225
Si disc semiconductor-insulator structure, for liq. cryst. incoherent-coherent image convertor 80−28342
Si extrinsic photoconductive IR detector, counterdoping scheme 78−49896
Si extrinsic photoconductive IR detectors, VLF behaviour 78−81542
Si light-controlled switch, appl. to high speed Kerr and Pockels cells 78−26925
Si:As photoconductive detector for IR astronomy, responsivity and system noise 80−51665
Si:H, amorphous, image pickup devices 80−100481
Si-electrolyte interface, incident radiation image form. *(Russian)* 77−7199
Si-GaAs heterojunction photothyristor, spectral charact. 78−10546
Zn-tetraphenylporphine/metal electrode, photocurrent generation mechanism 78−76868

photoconducting materials
see also photoconductivity
anthracene, off-diagonal electron mobility and lateral space charge drift 78−72192
bisphenol-A-polycarbonate:N-isopropylcarbazole, hole photogeneration efficiency 79−56243
bisphenol-A-polycarbonate, hole transport meas. in solid soln. 78−43438
bisphenol-A-polycarbonate polymer, triphenylamine doped, photoinjection of holes from amorphous Se 78−72191
carrier lifetime, nonequilibrium, phase method for determ. 80−65629
charge transfer electroradiography, physical processes 79−17594
charge transport random fluctuations, influence on electroradiographic image quality 78−66015
copper organoacetylenides, photoconductivity sensitisation using dyes *(Russian)* 79−58824
p-diiodobenzene, phase transition obs. using interferometry 78−34616
electrophotographic image form. by long-term memory ion modulator imaging process 79−26158
electrophotographic KC film, solid state camera speed 78−70211
electrophotographic layer, electrostatic force calc. *(German)* 80−42285
electrophotographic processes using insulator overcoated photoreceptors 79−2858
electrophotographic receptor, near IR sensitive 80−48369
electrophotographic recording media, high resolution, expt. charact. 78−70208
electrophotographic system solid area imaging response, math. model 79−2856
electrophotography, charge transfer, desirable photocond. props. 78−65989
electrophotography, conf., Washington, USA (Nov. 1977) 79−2849
electrophotography, history, present status and future potential 79−2854
electrophotography, process configuration, architectures, review 78−29188
electrophotography developments in Western Europe (1974-77) 79−71556
electrophotography systems, xerographic and insulator-photoconductor, comparison 79−17520
electrostatic readout, use of powder or liquid toners 78−70212
film for rapid access instrumentation recording 80−62755
image charge transfer to electrographic film 80−101864
Kuehnle-Coulter inorganic crystalline photoconductive film 79−71553
molecular crystals, electronic props. *(German)* 78−23089
noise theory and measurements for modelling electronic processes and transport phenomena 79−56264
optical data storage material requirements and possibilities *(German)* 78−25937
optical recording media, review 78−71172
optical storage materials and methods, conf., San Diego, USA (Aug. 1977) 78−71171
organic double-layer electrophotographic system, photoconduction mechanism 79−26161
organic photoconductor, electric field-induced fluoresc. quenching 80−34967
organic photoconductor memory effect, use for electrostatic duplication master 79−17521
organic semiconductor photoelectrode processes and effects *(German)* 80−26145
pentamethinium cyanine dye, single cryst., photocond. meas. 79−51626
photo-copiers, organic photoconductors, charge acceptance calc. 78−80020
photothermoplastic recording with rapid switching 80−32941
phthalocyanine films, metal-free, adsorbed o-chloranil effect on surface photovoltage 80−34485
pigmented organic photoreceptors for plain paper copying 80−49824
poly(N-vinyl carbazole) sensitisation with Se, purification effect on electrophotographic charact. 80−49825
poly-1,6-di-N-carbazolyl-2,4-hexadiyne, synthesis, thermal expansion, photocond., optical transition 78−76858
poly-N-vinyl carbazole by melt extrusion, orientation 78−67665
poly-N-vinylcarbazole, polymerisation, struct., props., elec. charact., review 79−41972
polycarbonate:triphenylamine, field-depend. UV photogeneration of holes, polymer composition depend. 78−76104
polymer, molecularly doped, photosensitisation processes 79−2857
polymer films, electronic cond., electro-, photoresponsive effects, review 79−56261
polymeric double layer system, high field cond., xerographic charact. 79−95448
polystyrene:triphenylamine, field-depend. UV photogeneration of holes, polymer composition depend. 78−76104

photoconducting materials continued
polyvinyl butyral:triphenylamine, field-depend. UV photogeneration of holes, polymer composition depend. 78−76104
polyvinylcarbazole-trinitrofluorenone, organic photoconductor, photoinduced paramag. centres 80−25188
PVK/PVK-TNF/TNF.PMG system, electrophotographic charact. 80−62759
pyrazoline-based carrier transport layers use in layered photocond. systems for electrophotography 77−69375
recording film demonstrator/processor 79−17551
relief plate preparation by subtractive development 79−21831
semiconductor, amorphous, photoelectric properties in ionic contact regime 77−76873
semiconductors, exhibiting negative photocond., photovoltaic effects 80−96943
semiconductors with deep impurities, resist. inhomogeneity effects on photoelec. props. 77−8151
squarylium and cyanine-TCNQ dye Schottky-barrier sandwich cells 79−29468
surface charges produced in photoconductor-air gap-semicond. system, calc. 80−6905
thermoplastic, hologram recording appl. 79−31837
thermoplastic film, photoconducting, double exposure holographic interferometry using memory effect *(Chinese)* 80−37967
thermoplastic photoconductor media, review *(Japanese)* 78−78956
thermoplastic photoconductor tape development for holographic recording 77−88671
thermoplastic photoconductor tape performance for optical recording 80−43305
thermoplastic photoconductor technology for optical recording and storage 78−71175
thermoplastic recording with homogeneous mixture of thermoplastic and organic photoconductors 78−63161
thermoplastic-photocond. device for holographic recording, diffr. efficiencies 80−5707
thermoplastic-photoconductor, holographic recording technique 78−9346
thermoplastic-photoconductor films for optical data processing 78−50875
thermoplastic-photoconductor hologram recording media, frost suppression 78−17869
thermoplastic-photoconductor media, charge carrier behaviour, microscopic response 79−28370
thermoplastic-photoconductor plate, exam. of microsocpic response in holographic recording 78−58947
thermoplastic-photoconductor tape for holographic recording, spatial filter prod. 78−90391
TNF-carbazolyl compound charge transfer complexes, equilib. consts. 78−64877
transparent electrophotographic films, information recording 78−70210
1,3,5-triaryl-2-pyrazolines, glass-forming props. 77−11677
TTF derivatives, smectic and nematic, for liq. cryst. device appl. 80−54124
vacuum deposition, from strip source, onto arbitrarily oriented rotating cylinder, for xerography appl. 78−95696
N-vinylcarbazole containing polymers, cryst. violet doped, for single layer photothermoplastic devices, photo and dark cond. 77−69374
N-vinylcarbazole containing polymers, sensitization to Ar laser for single laser photothermoplastic devices 80−83651
xerographic discharge in binder layers 80−47140
xerographic photoconductor, bimol. recomb., reciprocity 77−51775
xerography, amorphous Se and chalcogenide glasses electronic props. and defects 79−97454
AgBr(I), sensitization mechanism of a tetraazaindene stabilizer 79−20415
AlH_3, synchronous photochem. processes in lattice 80−101029
$Al_2In_{12}Se_{21}$, cryst. growth from melt, elec. props. 79−56922
As_2Se_3, amorphous, photocond. and photoinduced optical absorpt. 79−82645
As_2Se_3, film, amorphous, fatigue and recovery of electrophotographic props. 78−21253
As_2Se_3-HgSe double-layer system detector for temp. meas. 79−88952
$Ba_{0.25}Sr_{0.75}Nb_2O_6$, inhomogeneous ferroelec., photorefractive effect 79−42935
$Bi_{12}GeO_{20}$, high sensitivity read write vol. holographic storage 77−7026
$Bi_{12}GeO_{20}$, single cryst., electro-optical and photocond. props., image recording *(Russian)* 77−73129
$Bi_{12}GeO_{20}$, vol. hologram recording, charge transfer process 78−5437
$Bi_{12}SiO_{20}$ crystal, real-time holographic recording 79−72540
$Bi_{12}SiO_{20}$, high sensitivity read write vol. holographic storage 77−7026
$Bi_{12}SiO_{20}$ photoconductive electrooptic crysts. for time average holographic interferometry 78−25813
$Bi_{12}SiO_{20}$ photoelectret, in optical processing and X, γ ray imaging 80−23764
$Bi_{12}SiO_{20}$, vol. hologram recording, charge transfer process 78−5437
(CdHg)Te photoconductive IR detectors, ultimate detectivity 79−58788
$Cd_{0.2}Hg_{0.8}Te$, annealing in saturated Hg vapour *(German)* 79−43447
$Cd_xHg_{1-x}Te$, carrier lifetime, effect of comp. fluctuations and second-phase inclusions 80−80294
n-$Cd_xHg_{1-x}Te$ crystals, carrier recomb. in extrinsic conduction range 80−70722
$Cd_xHg_{1-x}Te$, high-speed quenching of melt *(German)* 79−65997
$Cd_xHg_{1-x}Te$, long term stability at 300K, rel. to device appl. 80−59978
$CdIn_2S_4$, photoconducting semiconductors, fundamental absorption edge 80−40130
CdO-B_2O_3-SiO_2, phase equilibria at 800°C, photoelectric effects 78−68675
CdS, convolution voltage enhancement due to carrier transverse drift in SAW convolver 80−1381
CdS film, double-layered polycrystalline on $LiNbO_3$ substrate, fabrication and props., rel. to SAW appl. 78−64480
CdS, film with high photocond. and good reproducibility, prep. by chemical deposition 79−66019
CdS films, growth, residual cond., inclusions 78−43492
CdS films, photosensitive, growth by reactive RF sputtering, props. *(French)* 78−35308
CdS, films, photovoltaic effect in wedge shaped film 79−56331
CdS films, precip. from soln., phase comp. change during annealing in air at 200-600°C 80−15393
CdS layers from CdS+Cr_2O_3 system, effect of heat treatment on spectral distrib. of photosensitivity 78−80017
CdS, photocond., acoustoelec. fluctuations 79−24022

photoconducting materials continued
CdS, photocond. cryst., stationary and non-stationary temperature-electric instabilities 79−7833
CdS, photocond. cryst. characterisation of electron-trap responsible for acoustic holographic echoes *(French)* 79−19544
n-CdS, photocond. film, phase memory effect and deep levels 79−82556
CdS, photoconducting, surface acoustic noise amplification by carrier drift 78−72208
CdS, photoconductive, obs. of high intensity sound self-defocusing 80−24972
CdS photoconductor, penetration depth of Bleustein-Gulyaev waves 79−28186
CdS, polycryst., photoelec. props., pressure time influence *(Russian)* 79−19615
CdS powder layers, surface pot. dark decay, moisture sorption and heat treatment effects 80−18038
CdS, spatial homogeneities exam. using DC and microwave techniques 80−93895
CdS, spectral sensitisation, role of local centres *(Russian)* 80−90924
CdS, surface photovoltage, characterisation 80−60033
CdS, thin film, dark- and photo-currents, annealing time effect 79−38199
CdS, transverse acoustoelec. effect, for SAW optical image scanning 77−11001
CdS:Cd(In), Cu- or defect-compensated, optical ageing rel. to storage cond. 78−84247
CdS:Cu,Cl film, applied voltage freq. effect on props. 80−39635
CdS:Cu,Cl film, use in laser-addressed electrolum. display screen 77−51777
CdS:Cu binder layer, photoactive, AC impedance meas. 80−25299
CdS:Na, thin film, dark- and photo-currents, annealing time effect 79−38199
CdS-HgI_2 binder layers, surface charge characts. for electrophotography 77−10123
CdS-In, photosensitive granular superconductor 79−78246
CdS-$LiNbO_3$ separated medium convolver, illumination effects 77−72766
$CdS_{1-x}Se_x$-Cu, electrophotographic props. 77−45910
CdS_xSe_{1-x} photosensitive films, prep., props., and use for photodetectors 80−55298
CdS_xSe_{1-x} triode cathode sputtered films, electrophysical props. *(Russian)* 79−42642
CdSe evaporated films, photoconductivity and effect of deposition conditions 79−95442
CdSe, photocond. film, plasma reson., IR refl. obs. 80−11037
CdSe, photosensitivity of elastic properties 78−92049
CdSe:Cu surface layer of CdSe, microstruct., photoelec. props. 78−43221
$CdSe_yTe_{1-y}$ triode cathode sputtered films, electrophysical props. *(Russian)* 79−42642
CdTe, electrodes for photochemical production of H_2, a comparison 77−70311
CdTe, suitability for solar photocells, photovoltaic conversion props., band gap 77−43652
$Cd_{1-x}Zn_xS$, electro-optical multilayer film, for data storage and display 78−71176
$Cd_{1-x}Zn_xS$, RF sputtered electro-optical film for data storage and display 78−83047
$Cd_{1-x}Zn_xS$ reactively sputtered photoconductive films for high field applications *(German)* 78−39154
GaAs, minority carrier diffusion length, photon absorption reemission 79−87109
GaAs:Cr plane-parallel photocond. plate, oscills. in current and light intensity in laser irradiation 80−49819
GaAs:Cr plate, illuminated, oscills. in V-I charact. 80−11038
Ge:Au, IR detector, impurity photoconductivity *(German)* 78−82036
Ge:Cu, IR detector, impurity photoconductivity *(German)* 78−82036
Ge:Hg, anomalous photocond. with 10.6 μm laser light *(Russian)* 77−47861
Ge:Zn^{II} carrier lifetime, nonequilibrium, phase method for determ. 80−65629
$Hg_{0.6}Cd_{0.4}Te$ LPE layer growth from Te-, Hg-, and HgTe-rich solns., comparison 80−76199
n-$Hg_{0.61}Cd_{0.39}Te$ single crystals, flicker noise due to grain boundaries, meas. 79−1611
n-$Hg_{1-x}Cd_xTe$, photoconductor, contact noise at 77K 78−88028
$Hg_{1-x}Cd_xTe$ photoconductors, gamma ray effects on surface props. and detector props. 79−17489
HgI_2:CdS, photodielectric effect 77−11955
HgI_2:CdS binder layer photoreceptor, surface charge characts. thickness depend. 80−57409
HgI_2-CdS binder layers, surface charge decay characts. 77−43642
HgS film, deposition from colloidal solns. 78−92209
In_2O_3-SnO_2, magnetron RF sputtered electro-optical film for data storage and display 78−83047
In_2O_3-SnO_2 electro-optical film, for data storage and display 78−71176
InSb, surface analysis, X-ray photoelectron spectra, surface oxidation-etchant correlation 78−56029
$In_{2-x}Sn_xO_{3-y}[SnO_2]$-CdSe-CdS:Cd,Cl sandwich photoconductor injection obs. *(Russian)* 80−54773
$KNbO_3$:Fe photorefraction and photocurrent effects *(Russian)* 79−7091
PLZT ceramics, photoinduced charge transfer process 79−50362
PbI_2, defect levels, TSC meas., photoconductor models, trap level capture cross section 79−69463
PbI_2 single crysts., photo-induced AC impedance meas., photodielec. effect 78−52034
PbO, disordered photoconductor, dielec. props., temp. depend. anomalies 78−43765
PbO, ion plating, X-ray sensitive photoconductor 77−44174
PbO layer vapour deposition, structure, and props. 80−65408
PbO, reactively evaporated, photocond., H_2O induced phase transform. 80−60122
PbO_x, phase transitions, occurrence of ferroelectricity, pyrocurrent obs. 79−11395
PbS-base photodetectors, struct. invest. by proton irrad. 80−104388
PbS-Si, photosensitive p-n heterojunction, energy band diagram 79−95489
$Pb_{1-x}Sn_xTe$ film, sputtered, for IR detector appl. elec. and optical props. 80−35084
Se, amorphous, evap. layers, electrophotographic props. depend. on thermal treatment of initial material 77−76978
photoconducting materials continued
Se amorphous layer structure, influence of vacuum deposition conditions *(German)* 78−63957
Se, appl. to xerography 80−57415
Se electrophotographic film current density/voltage characteristic rel. to substrate temp. *(German)* 77−55629
Se, evaporation kinetics from temp. programmed large area source 77−69996
Se layers, impedance-freq. charcts. meas. *(Japanese)* 79−38120
p-Se photocond. film, phase memory effect and deep levels 79−82556
Se, photoconductive film, field instability, Ar^+ ion irrad.-induced defects 78−87997
Se, single crystals, fast neutron irradiated, annealing expts., dark conductance, reflectivity spectra 77−85266
Se-As alloys, appl. to xerography 80−57415
Se-As film, evaporated, thickness, substrate temp. effects 79−15610
Se-Bi-I, amorphous, high sensitivity visible-near IR photoconductor development and characterisation 78−39153
Se-binding agent electrophotographic film characteristics and sensitivity *(German)* 80−4789
SeTe/Se multilayer photoreceptor, transient photoconductivity *(Japanese)* 80−75596
Si, amorphous, as photo-receptor for electrophotography 80−47126
Si, amorphous, undoped, photocond., continuous illum. effect 80−84486
Si, amorphous glow discharge films, H_2 content, elec. props., and photostability 80−25577
Si photoconducting films, amorphous, undoped, I-V charcts. of vacuum deposited films 80−60049
Si:H, amorphous, radiative recomb. by diffusion and tunnelling, photocond. quantum efficiency 80−50394
Si:H amorphous semiconductors, prep. from SiH_4 and charcts. 78−48326
WO_3 layers, semiconductor electrodes, electrochromism and photoelectrochemistry 80−35544
ZnCdS:Cu, binders effect on electrophotographic charcts. 79−80712
$Zn_{0.35}Cd_{0.65}S$ binder layers, doped and undoped, xerographic charcts. 79−56288
ZnO, adsorbing p- and n-type dyes, surfaces pot., UV light illum. effect 80−75624
ZnO electrode, reson. Raman spectra of adsorbed rose bengal 78−76446
ZnO pellets, and ZnO:Li single crysts., photo-induced AC impedance meas., photodielec. effect 78−52034
ZnO, photodielectric effect, improved model including effect of traps 77−1445
ZnO, photodielectric effect, space-charge polaris. 79−60872
ZnO powder, Hall effect, O_2 partial press. and illumination effects 79−51607
ZnO, spectral sensitisation mechanism 77−43651
ZnO:Cu, O, Fe(Co)(Ni) photocond., electron escape probabilities and trap depths 77−32041
ZnO-binder system, reciprocity failure, photoconductivity 78−39151
ZnO-polystyrene photoreceptors sensitised by β-Cu phthalocyanine 79−17552
ZnO-resin electrophotographic photosensitive layers, dark decay mechanism of corona charge *(Japanese)* 79−24002
ZnO-resin layers, impedance-freq. charcts. meas. *(Japanese)* 79−38120
ZnO-ZnS powder mixtures, Hall effect and elec. cond. 79−51607
ZnS, spectral sensitisation, role of local centres *(Russian)* 80−90924
ZnS:Cu, O(Fe,Co,Ni) photoconductors, killer impurities effect on electron escape probabilities and trap depths 77−4392
ZnTe electrodes for photochemical production of H_2, a comparison 77−70311
ZnTe single crystal, power depend. of photocurrent on excitation intensity, sublinear behaviour 78−43442

photoconductive cells
exposure measurement, fundamental aspects 77−30197
nephelometer, photoelectric, for liquids 80−101812
photoelectrochemical, H_2 generation at p-semiconds. photocurrent-pot. relations 77−89844
photoelectrolytic, water decomp. with semicond. materials 78−2562
pulse time resolution when optical pulse shorter than photoelectron transit time, theory *(German)* 80−9035
radiometer/photometer appl., commercial devices survey and classification 78−16830
richardson-Schottky type photoinjection current from photoconductor into insulating liquid 80−15608
surface-channel insulator-semicond. photocell, photoelec. charcts. 78−26909
transparent electrode photo-galvano-voltaic cell, using Mg-meso-tetraphenylporphine-coated glass *(Chinese)* 80−40865
two-photon photoconductivity detector for measurement of picosecond light pulses from Nd-glass laser 80−77872
$BaTiO_3$ electrodes, photocurrent efficiency, photo-oxidation of water 77−12000
CdTe-$SnCl_2$ electrolyte heterojunction photoelec. props., feasibility as solar energy convertors 77−76918
$Cu_{2-x}S$-CdS heterojunctions, nature of longwave photo EMF 78−84284
$FeTiO_3$, Fe_2TiO_4, and Fe_2TiO_5 anodes, appl. to photoelectrolysis of water 77−63920
WO_3 anode, props. and appl. to photoelectrolysis of water 77−66757

photoconductivity
see also photoconducting devices; photoconducting materials
adenine film, polycryst., energy conversion processes, quantum yields, 4 to 10 eV 80−88589
aggregate organic photoconductor, composition prep., struct. and optical props. 79−24006
aggregate organic photoconductor, photoconduction props. 79−24007
n-$Al_xGa_{1-x}As$, large-lattice relax. model for persistent impurity photocond. 77−85261
alkali halide, dislocation photocond. spectrum, F-centres in neighbourhood of charged dislocations 79−56256
alkali halide crystal, activator centres, excited state transitions, bleaching dynamics 79−4527
alkali halide thin films, high-field electron injection, ionic cond., photocond. 80−75665
alkali halides, F-centre trapping of conduction electrons, photocond. study 78−56179
alkaline earth fluorides, rare earth doped, photoionis. thresholds 79−78132

photoconductivity continued
alkaline frozen solutions, polycryst. and glassy, photocond. and radiometric obs. 80−45531
alloxazine, photoconduction *(German)* 79−78129
ambipolar photoconductivity and its optical quenching, possible obs. in photoconductors 78−14764
amorphous, photogeneration, thermalisation model calcs., band gap *(French)* 80−75595
amorphous material, carrier recomb. and trapping, exponential trap distrib. case 78−14760
amorphous semiconductor, cond. mechanism and localised states *(Japanese)* 80−84467
amorphous semiconductor, electronic properties and localised states, review 77−62871
amorphous semiconductor, modulated photoconductivity anal. 80−44650
amorphous semiconductor, substantially doped, electronic props., review 79−87175
amorphous semiconductor, trapping, photo-stimulated and thermally-stimulated current obs. 77−28192
amorphous semiconductor film, density of localised band tail states, transient photoconductivity 77−15898
amorphous semiconductors, doped, electronic props. 78−19030
amorphous semiconductors, modulated photocurrent, trap limited case *(Japanese)* 80−60030
amorphous semiconductors, photostimulated processes in inorganic materials and optical information storage, review 78−82926
amorphous semiconductors props., principles and appl., w.r.t. electronic band state *(Japanese)* 79−23979
amorphous solid, photoconduction, model involving capture and escape from multiple traps 77−76863
anthracene, charge carrier photoexcitation quantum yield 79−99581
anthracene, charge-carrier generation by singlet-singlet collision-ionisation process, singlet photoionisation process 78−72195
anthracene, cryst., photocurrent induced by detrapping of charge carriers trapped by radicals 79−82643
anthracene, cryst., with electrolytic contacts, photocurrent anomalous behaviour, current-volt. characts. 77−39933
anthracene, drift mobility expts., arrival-time detection 79−33308
anthracene, electron drift mobility, temp. depend., transient photocond. 77−66164
anthracene, excited by laser pulse, photocond. meas. 79−69437
anthracene, field depend. of photocond. 79−99578
anthracene, laser-induced photocond., excited charge carriers 77−28211
anthracene, photocond. spectrum induced by excitons *(Japanese)* 80−29440
anthracene, photoconduction *(German)* 79−78129
anthracene, photogeneration of charge carriers through two photon excitation 80−11033
anthracene, pulsed electron excitation, triplet excitons, spectral and electrical investigations 80−92828
anthracene, single cryst., photocond. threshold, excitation spectrum 80−44639
anthracene, single crystal, disperse photocurrent transients rel. to multiple trapping 79−99564
anthracene, single crystal, photoconductivity quantum yield, experimental validation of fund. theory 80−6909
anthracene, surface states and persistent internal polarisation via photocurrent transients 77−89825
anthracene, time-resolved transient photocond. obs. 80−6892
anthracene crystal, sensitised injection from surface oxidation products 78−76143
anthracene crystal, triplet exciton absorpt., high resolution photoconductivity spectroscopy 78−10504
anthracene crystals, carrier trapping in deformed surface region 78−47806
anthracene crystals, photocond. by polaritons 77−69373
anthracene crystals, superficial trapping levels, pulsed photocurrent transients 78−76021
anthracene ion in liqs., photoelectron emission and photocond. 80−75600
anthracene-dimethylpyromellitimide charge-transfer complex, photoconductivity mechanism 77−47860
anthracene-pyromellitic dianhydride complex, optical and photoelectric props. *(Russian)* 80−15570
anthracene-tetracyanbenzene, charge transfer, magnetic resonant modulation of photoconductivity 78−64062
anthracene/aq. electrolyte contact, illuminated, space charge behaviour 78−84290
anthroquinone, temp. depend. and anisotropy of electron drift mobilities 78−19089
auramine crystal, photocond. and intermol. electron interaction, tight binding approx. 77−15765
auramine single crystal, lifetime and mobility of photogenerated charge carriers 78−2516
azulene, drift mobility expts., arrival-time detection 79−33308
benzophenone, charge carrier generation and mobility 78−84231
bimolecular recombination effects on photocurrent discharge 78−60156
biphenyl, electron mobility and photogeneration temp. depend., polaron hopping 78−19033
black-body radiation field interaction with photoconductor, noise, Langevin method 78−30950
cadmium arachidate mixed with cyanine dyes, mol. layers, photoelec. props. 80−80401
capture probabilities of two deep impurity levels, photoconductivity decay analysis 77−89808
β-carotene, hole mobility meas. by transient photocond., Poole-Frenkel effect 77−11957
β-carotene glass, photoconductivity mechanism 79−28368
carrier lifetime measurements from transient elect. photoresponses in solar cells 80−61346
carrier photogeneration efficiency, Onsager theory of geminate recomb. 79−56242
chalcogenide glass, charged dangling bond model reassessment 77−72813
chalcogenide glass, mech. for electron-hole recomb. 78−72196
chalcogenide glasses, photoconductiyity dependences applied elec. field 80−107857
chalcogenide glasses, trap controlled transient photocond. 80−44641
chalcogenide semiconductors, amorphous, analysis 78−72197
chalcogenide vitreous semiconductors, reversible photoinduced changes in optical, physicochem. and contact props. 79−24378
Chlorella microwave photocond., rise/fall kinetics, depend. on physiological state 78−15793
photoconductivity continued
chlorophyll-a, crystalline film, energy levels and carrier generation by photocond. and fluoresc. 77−16909
chlorophyll-acceptor and chlorophyll+protein-acceptor lamellar systems, steady photocond. 78−53328
Chorella cell microwave photocond., long wave illum. and Emerson effect 78−15794
Compton currents, historical aspects and recollections 78−80018
crystal without symmetry centre, photogalvanic effect *(Russian)* 78−91731
cyanine dye monolayer assemblies with Al and Ba electrodes, photovolt., dark cond. and photocond. 80−80400
cyanine dye monolayer/p-chloranil crystal, charge carrier injection rate const. determ., energy transfer vs. charge transfer method 79−83031
cytosine monohydrate, cryst. growth from aq. soln., elec. props. 78−3007
dark current relaxation, barrier cond. mech. 80−6904
dark relaxation of anomalous photocond., photofield model 77−51776
diamond: Li, ion implantation doped, IR photocond. 80−20249
diamond:B, photoconductivity and electroabsorpt. spectra 77−4647
diamond:N, photocond. in N2 absorpt. band 79−91102
diamond, electroluminescence, thermoluminesc., photocurrents 79−38675
diamond, electron irradiated, photocurrent and Hall current, 290 and 4.2K 79−87129
diamond, N9 and ND1 energy levels, electron irrad. photocond. obs., thermolum. 78−6324
diamond, natural, dislocation-N_2 impurity interaction, photoconductivity spectra, resistivity 79−91097
diamond, natural semicond. motor photocond. and internal photoemission 79−69546
diamond, semicond., energy band struct., elec. and optical props., review 77−35862
p-diamond, synthetic, semicond., photoconductivity spectra 79−69550
diamond, type Ia, electron irrad. effect on photocond., acceptor centre form. 77−47853
9,10-dichloroanthracence, monoclinic, photocond. carrier mobility 80−39630
β-9,10 dichloroanthracene, hole mobility anisotropy and cryst. struct., transient photocond. 78−95310
dielectric, trap-controlled transient photocond., numerical study 80−50285
dielectrics, transient photocurrent theory 77−8136
diffusion length and surface recomb. vel. determ., light excitation 78−91725
2,3-dimethylnaphthalene, transient photocurrents, hole trapping *(German)* 77−59303
diphenanthra[4,5,6-abcd, 4,5,6-jklm]perylene, high photoresponse, O_2, N_2 and SF_6 effects 77−32036
N,N′-diphenyl-p-phenylenediamine, current carrier traps, space-charge-limited currents 78−47799
diphenylanthracene in benzene soln., extrinsic photocond. kinetics 80−92691
5,10-diphenylphenazine, photoconduction *(German)* 79−78129
disordered semiconductor, DC hopping cond., photon- and US-induced, microscopic theory 77−76872
disordered semiconductor, photon-phonon-assisted hopping, theory 80−44642
disordered semiconductor with random field, new photocond. type *(Russian)* 77−11961
donors with excited states, kinetics of electron transitions 80−39600
donors with excited states, non-equilibrium phenomena, theory of kinetics of electron transitions 78−79961
drift mobility meas., arrival time detection using interdigital electrode 77−11954
durene, photoconductivity, charge carrier mobility 77−47852
durene, transient photocond. and charge carrier mobility anisotropy, temp. depend. 77−80805
dye pair, chromophorically degenerate, adsorbed on AgBr, supersensitised photoconductance 79−61887
electrets and dielectrics, conf., Sao Carlos, Brazil, Sept. (1975) 80−7251
electro-optic crystals, photo-induced electron and hole transport holographic method for determ. 79−28375
electrode and volume controlled photocurrents 80−6908
electron trapping, donor state generation, photo I-V study 80−20210
electrophotographic films, surface charge meter using electrostatic induction *(Japanese)* 80−77886
ESCA expt., photoconducting effect on charging 78−21971
ethanol glass, 4K γ-irradiated, presolvated electron photoconductivity 78−47827
ethylene glycol-water glass, γ-irrad., temp. depend. photobleaching of trapped electrons 79−66320
EuSe, photocond. and photodiffusive voltage spectra 80−96940
extrinsic semiconductor, photocurrents anal. 79−42588
fatty acid-cyanine dye mixed monolayer, on metal electrodes, photocond. 78−68050
ferroelectrics, photogalvanic current 80−70748
fluorene, photoconductive props., sample purity depend. 78−10508
fluorenone derivatives as electron transport materials, electron affinity and electrochemistry, rel. to photocond. 79−38127
Franz-Keldysh, optically enhanced for n^+-p-n^+ phototransistor struct. 78−60423
Frenkel exciton-charge transfer state mixing near charged defect model of photocond. 77−51663
frozen-in conductivity, nature of recomb. barriers 79−56245
n-GaAs, persistent photocurrents, Hall effect anal. 79−87130
p-GaAs, spin relaxation of photoelectrons 77−85207
p-GaSe, relaxational oscillations of photoconductivity and dark conductivity 77−69379
glass, alcoholic and aq., 4.2K, trapped electron photocond. and optical spectra following radiolysis 79−29378
heat treatment effects on elec. props. 78−43411
heavily doped semiconductor, compensated, hopping photoconductivity 79−38130
heterojunction, model of anomalous photocond. 77−76914
hexamethyltriaminotriphenylcarbenium chloride, cryst. violet, photoconductive characts. 78−39163
n-hexane, liq. trapped electron photoionis., photocond. 80−2418
high resistivity material, deep level spectroscopy 78−72165
homogeneous semiconductor, imperfections and photocond., electronic nonequilibrium behaviour 80−44667
hopping conduction in presence of strong EM wave 78−76107

photoconductivity continued
II-IV-V_2-Cu, pseudo-straight-zone semiconductor, Schottky barriers, IR photosensitivity and photocond. *(Russian)* 77−8195
II-VI compounds with three deep trapping levels, theory of transient photocond. processes 77−76865
III-V semiconductor based layered multielectronic systems, electronic process investig. survey *(Russian)* 80−107891
III-V semiconductors, optical heating of electrons at 78K 79−15185
imaging systems, limitations on sensitivity 80−6907
impurity, monopolar injection *(Russian)* 79−24004
impurity centres, photocond. due to optical transitions between excited states 79−73545
impurity photoconductivity and autoionisation calc. 80−44648
inert gases, solid, V_0-values, photoelectric determ. 80−92938
inhomogeneous semiconductor, impurity opt. absorpt. and photocond. spectral line profile variation 77−16352
inhomogeneous semiconductor, negative photocond. and IR quenching of residual cond. 77−24587
inhomogeneous semiconductor, spurious effects 77−55583
inhomogeneous semiconductor structure with p-n junction, nonlinear current-voltage characts. 77−11929
n-InSb, photoconductivity relax. temp. depend., carrier recomb. processes 77−4363
p-InSb-Au, surface barrier, structure, photosensitivity spectrum 79−51674
insulated crystal, primary photocurrent kinetics for simultaneous trapping and recomb. 80−6899
insulator with uniform distrib. of traps, nonequilib. photocond. *(French)* 78−43433
iron phthalocyanine, annealed, elec. cond., daylight exposure and thickness effect *(French)* 80−84484
Langmuir films, dye-sensitized, anisotropic photocond. 80−80327
Langmuir multilayer films with and without dye-sensitisers, elec. props. 80−97006
laser measurement, of semiconductor materials and devices *(Rumanian)* 78−52035
lead phthalocyanine:O_2, photocond., impurity-induced 79−47120
leucosapphire, electronic band struct., optical props. 79−95329
Lexan:triphenylamine, photosensitisation using rhodamine B or thiapyrylium 78−34856
lifetime measurement technique, using linearly increasing intensity light source 77−35960
low-conductivity fluids, dark currents, forced diffusion model 79−15182
lumichrome, photoconduction *(German)* 79−78129
many-valley semiconductor, two-photon transitions from deep neutral impurity centres, light absorpt. and drag effect 79−91478
merocyanine dye monolayer on p-chloranil cryst. in sandwich cell, electrochromic detection of internal charges 78−11549
metal, without symmetry centre, photogalvanic effect for free carriers *(Russian)* 78−87999
metal electrode, in liq. NH_3, photoelectron emission 79−60868
metal-$RbAg_4I_5$ solid electrolyte interface, photocurrent obs. on illumination 80−34513
metal-semiconductor contact, frequency relationships of photocurrent and photo-EMF *(Russian)* 80−107908
metal-semiconductor junction photoelec. phenomena, effect of dielectric gap and surface states *(Russian)* 78−84299
metal-semiconductor transition, i.r. detection model 77−1442
3-methylpentane, glassy insulator, γ-irrad., IR enhancement of carrier radiation yield 77−76870
3-methylpentane glass, electron-ion pair polarisation, γ-irrad. induced current and IR photocurrent 77−69768
MIMIM structure, photostimulated tunnelling 77−8204
MIMIM triodes, photoresponse 77−39963
minority carrier diffusion length, spectrometric determ. *(Russian)* 78−84230
minority carrier lifetime, eval, from photocurrent 78−10515
minority carrier lifetime determ. by relative amplitude method 77−72869
MIS capacitor, light induced electron-hole pair generation 79−38167
MIS flat-band volt. determ., photoelec. method 79−38168
MIS solar cell, photocurrent depend. on thickness of Schottky barrier metals 79−34437
MIS structure, photocurrent flow mechanism, carrier tunnelling 77−28258
MIS structures, surface recombination and photoeffect, statistics *(Russian)* 78−39221
MIS transistor threshold range under illumination 79−69599
MIS tunnel diodes, photoionisation of states 80−11099
MISIM, photoresponse in alternating elec. field 79−38189
MISM structure, photoresponse of residual conductivity 77−15968
mobility anisotropy determ. by photoelectromag. effect and photocond., method and appl. to HgI_2 79−38126
molecular crystals, spectroscopy, bibliography (1977) 80−7317
molecular crystals, spectroscopy, bibliography for 1976 78−72585
MOS diodes, minority carrier lifetime determ. from photocurrent spectra 80−49920
MOS insulator, energy and spatial distrib. of electron traps, photocurrent response 77−39947
MOS interface states density, photoemission obs. using photocurrent and photocapacitance meas. 80−92990
MOS structure, insulator bulk trapped charge densities and centroids, photocurrent-voltage characts. meas. 77−1489
MOST, photocurrent spectral response, bias depend. 77−69422
multistable self-wave media 80−86094
naphthalene, cryst., photocurrent induced by detrapping of charge carriers trapped by radicals 79−82643
naphthalene, electron band hopping transition 78−39155
naphthalene, hole mobility, anomalous current transients 78−76091
naphthalene, photoconductivity elec. field depend. 77−32035
naphthalene, pure and deuterated, band-hopping mobility transition 80−6833
narrow band gap semiconductor multilayers with p-n junctions, relaxation and photocurrent analysis 79−7883
narrow gap semiconductors, recombination mechanisms, review 80−96905
narrow-band semiconductor, nonlinear anisotropic photoresistive effects 78−72202
noncentrosymmetric crystal, influence of electron spin on photogalvanic effect 79−69558
noncentrosymmetric crystals, photogalvanic effect 79−69554

photoconductivity continued
noncrystalline materials, optical props., lecture 78−27263
nonlinear interference of EM fields, contrib. to transport coeffs. 80−80324
nonstationary current transfer by light pulse injection of carriers *(Russian)* 77−8134
nucleic acid bases, charge carrier photoexcitation quantum yield 79−99581
one-dimensional, semiconducting polymer, demonstration of high mobility 80−20212
optical amplification, laser-produced layer system *(Russian)* 77−24585
organic xerographic photoconductors, bimolecular recomb., reciprocity failure 80−49798
p-n heterojunction solar cell, general formulation of current-voltage characts. 80−80361
p-n junction, CdTe-based, photoeffect quantum efficiency depend. on photon energy *(Russian)* 79−78168
p-n junction with hot carriers, thermophotoelectric effects 79−73576
p-n tunnel junctions, photoinduced transitions, theory 80−65669
pentacene layers, photogeneration, charge carrier transport *(Russian)* 78−56181
pentamethinium cyanine dye, single cryst., photocond. meas. 79−51626
perovskite oxides, single cryst., photocond. and TSC meas. 78−43436
perylene, energy structure, photocond., photoemission and absorpt. spectra meas. 77−39895
PET, pyroelectric effects and depolarisation currents, illumination effects 80−34859
photocathode polarisation sensitivity, two-beam interferometer expts. 80−4772
photoconduction decays, fast, measurement, DC-10 MHz low noise amplifier system 80−57326
photoconductor-insulator interface, carrier injection 80−24970
photocurrent spectral distribution 79−56259
photodielectric, stationary recombination equations, analytical solutions in source limiting cases 80−44662
photoexcitation effects during laser trimming on thin film resistors on Si 80−64093
photoexcitation phenomena, low density 78−27319
photoexcited hot electrons in high mag. field, mean energy 78−30955
photogeneration and fluoresc. quenching theory, appl. to x-metal-free phthalocyanine 79−65513
photographic emulsion latent image formation, photoemf method 79−17545
photographic emulsion photocharge decay kinetics correl. with efficiency 79−19634
photoinjection in chalcogenide semicond.-PVK systems 79−19633
photon fluctuations and interaction with solids 77−748
photorefractive memory materials, elec. field and photocurrent meas. 78−71066
photorefractive process sensitivity *(French)* 77−31124
photovoltaic devices, dark current and photocurrent superposition 79−43769
phthalocyanine, X-metal-free in polyvinylacetate, elec. field induced fluoresc. quenching, carrier photogeneration 78−48207
phthalocyanine thin films, transient photocond. obs. technique, freq. depend. 77−76860
phthalocyanine-alkane interface, charge transfer, rel. to photoelectrophoretic image form. 80−65616
phthalocyanine-dodecane interface, photostimulated charge transfer flash expt., trapping model 77−66182
phthalocynanine, doped photovoltaic cell, photoconductivity, elec. field induced flouresc. quenching, charge carrier photogeneration 80−84485
piezoelectric semiconductor, influence of thermal quenching of photocond. on US amplification 77−4410
piezoelectric semiconductor, photocurrent in quantising magnetic field in presence of nonequilibrium photoelectrons, spectral oscill. and energy relax. by interaction with acoustic phonons 79−91100
plant leaves, microwave photoconductivity obs. 80−104637
point defect electrons and vibrations, dislocation field effect, dislocation photoconduction spectrum *(Hungarian)* 80−51977
polar crystals, relaxation currents; point defects *(Russian)* 80−100486
polar glasses, aq. and alcoholic systems, trapped electrons, photocond., optical spectra 77−85742
poly(5,7-dodecadiyne-1, 12-diol-bis phenylurethane), visible refl. spectra, photocond., excitons 77−81117
poly(n-vinylcarbazole)-trinitrofluorenone films, charge carrier trapping 78−14846
poly(N-vinylcarbazone), charge transport and struct., bromination effect 78−11516
poly (N-vinylcarbazole), hole photoinjection from Au 78−76144
poly-2-chloro-p-xylylene, photoinjection of holes from metal electrodes, barrier height 78−76145
poly-2-chloro-p-xylylene, photoinjection of holes using Au, Ag, Cu, Sn, Pb and Al electrodes 79−47161
poly-γ-ethyl-D-glutamate, pulsed photoconduction 80−24969
poly-(bisphenol) carbonate, photocond., of double layer polymer systems doped with charge transfer complexes 79−87124
poly-aryl-vinyl, photon generated radical ions, photocond. *(German)* 79−52708
poly-n-epoxypropilcarbazole electrophotographic layers, photogeneration and drift mobility 79−19631
poly-N-epoxypropylcarbazole layers, optical and photoelec. props. 77−39896
poly-N-vinyl carbazole containing cation radicals, photocond. 78−68052
poly-N-vinylcarbazole, synthesis and photocond. props. 77−55563
poly-N-vinylcarbazole−metal electrode, photoemission of electrons, photocond. meas. 79−91142
poly-N-vinylcarbazole films, drift mobility of photocarriers, polymerisation method influence 77−76986
poly-N-vinylcarbazole-polycarbonate mixture, hole drift mobility and photosensitivity 77−85260
polyacetylene, phototransport effects 80−44653
polyacetylene films, AsF_5 doped, photocond. and junction props. 80−70770
polyacrylonitrile, pyrolized, pulsed photoconduction 80−24969
polycarbonate, photoconductivity, UV-IR light, absorpt. and photoluminescence. spectra *(Japanese)* 78−34857
polycrystalline film, photocond. probe studies 80−80326
polydiacetylene, photoconduction in multilayer structs. and single cryst. 78−80024

photoconductivity continued
polydiacetylene bis-(toluenesulphonate), single cryst., charge carrier mobility and recomb. 77−8132
polydiacetylene-bis(toluenesulphonate), transient photocond. meas. 78−30951
polydiacetylene-p-(toluenesulfonate), photocurrent transients, intensity depend. 78−52027
polydiacetylene-toluenesulphonate, photocond. meas., 0.62-3.1 eV 80−70757
polydiacetylenes, photocond. action spectrum of single crysts., charge transport obs. 80−15557
polyenes, semicond., compensation temp. 80−39625
polyethylene, γ-irradiated, investigation of traps by photostimulated detrapping current analysis 77−15894
polyethylene, carrier traps, photostimulated detrapping currents and TSC meas. 78−10458
polyethylene, intrinsic photocond. under vacuum UV irrad. 80−70759
polyethylene films, surface pot. decay, appl. of Scher-Montroll method 79−7851
polyethylene naphthalate, photoconductivity, UV-IR light, absorpt. and photoluminescence. spectra *(Japanese)* 78−34857
polyethylene terephtalate, carrier generation mechanism at UV and IR light region 77−80803
polyethylene terephthalate, insulating material, photoinjection 77−47849
polyethylene terephthalate, mechanism of photocarrier generation 77−89798
polyethylene terephthalate, photocarrier transport mechanism 78−10499
polyethylene terephthalate, photoconductivity, UV-IR light, absorpt. and photoluminescence. spectra *(Japanese)* 78−34857
polyethylene terephthalate photoelectret, TSC and photostimulated detrapping current obs. 78−10459
polyethylene-2,6-naphthalate, pulsed photoconduction 80−24969
polyethylene-terephthalate, field-controlled photogeneration and carrier trapping 80−25285
polyhexamethylene adipamide, photocond. 80−103718
polyhexamethylene adipamide, photocond. and dielectric props. 80−84489
polymalononitrile, plasma polymerized film, photoelec. props. 78−39158
polymer, photoelectric effects and relation to cond. processes 77−43640
polymer UV photoconduction expts. and electronic props. 80−15572
polymer-bisazide system, photoresistive films, photosensitivity *(Russian)* 77−48641
polymers, electrical phenomena, nature and appl., book contrib. 80−50254
polymonochloro-p-xylylene, γ-ray-induced cond., hole injection effects 80−34452
polynaphthalene films, plasma polymerised, photovoltaic and photocond. props. 80−34479
polyolefins, elec. cond., review 78−26867
polyparaxylyrene, photoconductivity, UV-IR light, absorpt. and photoluminescence. spectra *(Japanese)* 78−34857
polystyrene, γ-ray-induced cond., hole injection effects 80−34452
polystyrene, photoconductivity, UV-IR light, absorpt. and photoluminescence. spectra *(Japanese)* 78−34857
polystyrene, pure and doped, metal contact effect on persistent internal polarisation 79−78617
polystyrene atactic carrier transport and photogeneration 80−80318
polystyrene film, in MIM struct., elec. conduction and free radicals 80−20340
polystyrene thin film, glow discharge formed, dark current and photocurrent obs. *(Japanese)* 80−15633
polythiourea, plasma polymerized film, photoelec. props. 78−39158
polyvinyl alcohol film containing Cu^{2+} complexes, photoconductivity 80−107849
polyvinyl carbazole in UV range, organic thin film appls. in electronics *(German)* 78−44011
polyvinylcarbazole, fast hole transport 79−51628
polyvinylcarbazole, photocond., of double layer polymer systems doped with charge transfer complexes 79−87124
positive photoresists, photocond. factor rel. to composition *(Russian)* 80−42289
PVC thin films, pure and I doped, photoconductivity study 80−44646
pyrazoline-based carrier transport layers use in layered photocond. systems for electrophotography 77−69375
pyrene-TCNE, vapour-grown cryst., transit-time meas. of photocarriers 78−39149
quantum statistics of photocurrent in optimal light detector, atm. 'seeing' conditions 80−53244
quartz, photocond., X-ray and other irrad. effects 78−76103
quartz, photoelectric and photoluminescent props. in fundamental absorpt. region 78−39596
rate and continuity equations solution, for time region before excited carriers recomb. *(Japanese)* 79−4584
recording at UHF, simple method 77−41642
relaxation semiconductor, anal. of intrinsic photocond. spectrum 79−73541
relaxations of photoelectric conductance meas., submicrosecond *(Czech)* 80−31804
rubrene, in benzene soln., extrinsic photocond. kinetics 80−92691
rubrene, orthorhombic cryst. photogenerated carriers, transit time meas. 80−49811
rubrene-in-benzene, excited state migration and charge transfer 77−55559
S-diode, influence of light on semiconductor compensated in upper half of forbidden gap *(Russian)* 77−85303
sapphire, Czochralski-grown, excess charge carriers, generation, transport and trapping 79−82646
scanning background-limited IR sensor with adaptive threshold signal processing logic, performance 80−37082
Schiff's base, thin layer samples, mechanism of change carrier photogeneration *(Russian)* 77−32045
Schottky barrier, real and ideal, photosensitivity losses 80−2452
Schottky barriers, photocurrent, recomb. losses *(Russian)* 80−2470
screening charge formation time at illuminated spot boundaries 80−29438
self-oscillatory semiconductor medium, coupled temp. and carrier density self-oscills., photoelectron heating, microwave field 79−11166
semi-infinite direct-gap semiconductor effect of reabsorbed recombination radiation 78−95312
semiconducting electrodes, defect doped, ageing effects, photocurrent meas. 79−69592
photoconductivity continued
semiconducting polycrystalline films, cond., photocond. mechanisms 78−47891
semiconductor, adiabatic approx. in transient donor recomb. 80−49761
semiconductor, amorphous, photoelectric properties in ionic contact regime 77−76873
semiconductor, anomalous photoconductivity model 79−7860
semiconductor, apparent ageing, caused by defect migration, dark and photocond. 79−11169
semiconductor, capture probabilities of two deep impurity levels by photocond. decay 80−49799
semiconductor, carrier relax. time and effective masses determ. by microwave photocond. meas. *(Russian)* 78−19071
semiconductor, complex energy band under optical excitation, high-frequency negative cond. and population inversion 80−107858
semiconductor, deep impurities, exptl. techniques *(Japanese)* 80−15476
semiconductor, doped, metal-insulator transition, anal. 80−88478
semiconductor, due to phonon scatt. and emission 78−10514
semiconductor, energy relaxation of photoexcited hot electrons in near-surface region 80−92928
semiconductor, exciton condensation, microwave cond., book contrib. 80−11043
semiconductor, high intensity photoexcitation, hot electrons and phonons 78−26905
semiconductor, hole drag current in two-photon transitions due to EM wave momentum 79−15187
semiconductor, impurity photocond., temp., elec. field and impurity centre conc. effects 78−56190
semiconductor, impurity photoconductivity for nonuniform impurity distrib. 79−82632
semiconductor, inhomogeneous elec. fields in oscillatory photocond. 80−2421
semiconductor, irradiated, Hall mobility, dark and photo-conductivity calc. 78−47835
semiconductor, kinetics of photoinjection currents 78−47834
semiconductor, layered, direct and indirect two photon processes 77−40261
semiconductor, lifetime meas. by photoconductivity null apparatus 78−56184
semiconductor, low-temp. photocond., effect of electron phonon interactions 77−66186
semiconductor, nonequilibrium processes exam. by method of transient holograms 78−23105
semiconductor, one-dimensional with deep levels, ambipolar transport of carriers 77−4356
semiconductor, optical absorpt. coeff. and minority-carrier diffusion length, differential photocurrent method of meas. 80−96896
semiconductor, optical generation of carriers under Franz-Keldysh effect conditions, instability 79−24017
semiconductor, optically anisotropic, orientation, use of polarisation depend. of photo-EMF and photoconductivity 77−89807
semiconductor, optically stimulated negative conductivity 77−4357
semiconductor, photocurrent spectra investig. of fund. absorption edge 77−4397
semiconductor, photoelectret state form. by IR light quenching photoelec. current *(Russian)* 79−91345
semiconductor, photoinjection characts. 77−43654
semiconductor, photoionisation of deep impurity centres, drag of electrons 78−51938
semiconductor, photostimulated transport effects 79−11182
semiconductor, photothermal cond., low temp. depend. 80−70756
semiconductor, polarisation effects in photoconductivity, exptl. method for study 79−4581
semiconductor, recomb. centre distrib., scanning photocurrent microscopy 79−35822
semiconductor, spin-depend. recomb. effect 78−34841
semiconductor, spin-dependent recomb. and scatt. in presence of optical orientation of electrons 80−96908
semiconductor, stationary recombination equations, analytical solutions in source limiting cases 80−44662
semiconductor, strong electron-lattice interaction, review *(Japanese)* 80−49664
semiconductor, surface electronic props., optical spectroscopic techniques, review 80−11070
semiconductor, surface photoelectric effects, influence of excitation rates 79−69547
semiconductor, surface space charge layer spectroscopy 77−20386
semiconductor, theory, allowance for long-range fields of charged impurities 79−24013
semiconductor, thermomagnetic photoeffect 79−23991
semiconductor, transport equation and photocurrent of electrons, in EM field 78−26913
semiconductor, two-photon absorpt., free carrier storage by deep centres *(Russian)* 78−23131
semiconductor, two-photon interband transitions, carrier drag 79−7858
semiconductor, unipolar high-resistivity, directionality of longitudinal photocurrent 79−11177
semiconductor, wafer characterisation by photonic injection+microwave meas., appl. to Si *(French)* 78−23106
semiconductor, weakly inhomogeneous, impurity absorpt. and impurity photocond. line profiles 78−19098
semiconductor, with superlattice, heating photocond. 79−19622
semiconductor, without symmetry centre, photogalvanic effect for free carriers *(Russian)* 78−87999
semiconductor anomalous props. and appearance mechanism 78−95313
semiconductor bicrystal, charge carrier interface recomb., photocond. meas. method 79−99431
semiconductor electrode, photogenerated free carriers and photocurrent relax., simulation 77−15951
semiconductor film, carrier temperature and density self-oscills. near instability threshold 80−11118
semiconductor film, photoconductor, thermal-density hysteresis 79−51631
semiconductor in highly excited state, thermodynamic theory 77−47742
semiconductor non-equilibrium periodic stratification by diffusion 77−55544
semiconductor submillimetric-wave spectroscopy 79−33221
semiconductor thin film electrode, photosensitization by cyanine dye in lipid bilayer 80−75639
semiconductor thin films, degenerate one-valley and many-valley, photogalvanic effect calcs. 80−34487

photoconductivity continued
semiconductor under illumination, simple model of generation and recombination processes 79−69523
semiconductor with anisotropic conductivity, elec. and photoelec. props., review 78−10447
semiconductor with elliptical isoenergetic surface, photon drag theory 77−1443
semiconductor with superlattice, optoelectric effect, theory 80−70768
semiconductor with traps, ambipolar photoelec. current 79−91101
semiconductor with uniform distrib. of traps, nonequilib. photocond. *(French)* 78−43433
semiconductor-dielectric structure, photoresponse on electron beam scanning, video signal enhancement *(Russian)* 77−47863
semiconductor-electrolyte functions, photocharacts. 78−91764
semiconductors, amorphous, doped, electronic props. 80−80283
semiconductors, amorphous, electronic transport mechanisms and coeffs. 80−80282
semiconductors, book contrib. 80−84488
semiconductors, compensated, spectral depend. of photoresponse 80−15562
semiconductors, cpd., large-lattice-relax. model for presistent impurity photocond. 77−85261
semiconductors, cyclotron resonance, high frequency differential cond., needle shaped distribution model 79−65509
semiconductors, even dynamic photoelectric Hall effect 78−91708
semiconductors, influence of surface space-charge layer 80−15563
semiconductors, optical saturation for high carrier recomb. freq. *(Russian)* 80−88585
semiconductors, photoconductivity measurement at UHF and at high excitation levels 80−65627
semiconductors, photoconductivity study using SAW convolver 79−42587
semiconductors, photoelectric spectra, conf., Moscow, USSH, (May 1977) 79−82622
semiconductors, photoelectric spectra of impurities 79−82623
semiconductors, photosensitive area localisation, expt. apparatus 80−75599
semiconductors, two-photon conductivity calc., nano-pico sec. pulse excitation 78−72188
semiconductors, weakly doped compensated, hopping photoconductivity in disordered systems *(Russian)* 80−65573
semiconductors with deep impurities, resist. inhomogeneity effects on photoelec. props. 77−8151
semiconductors with layer and defect structures, characts. of photocond. in strong absorption region 77−66184
semiconductors with UHF biasing, investig. using cylindrical resonator 78−21117
sensitised photocurrents, temp. depend., electrochem. meas. 78−72205
short-pulse, transit time effects 80−70754
Si:B, isolated A^+ states under high compressive stress, long wavelength photocond. spectra 79−60765
Si, ion implanted by high energy C ions structural and optical props. 80−107292
solar cell, polycrystalline, photocurrent loss in depletion region anal. 79−39309
solar cells, electrochem. liquid-junction, Schottky barrier height, photovoltage and photocurrent 80−26162
solar cells, polycryst., scanning optical microscopy examination of grain boundaries 78−79618
solar EM radiation measurement using CdS photoresistor 80−31092
solid, one-carrier photoconductive process associated with broadened trap distributions 77−72881
solid discs and flakes, cond. meas. cells with variety of contacts 78−24816
space charge limitation, under bulk generation conditions 77−8137
space-oscillating photocurrent in crystals without symmetry centres 78−64060
spectral sensitization of copper organoacetylenides photoconduction by means of dyes *(Russian)* 79−58824
statistics of photoelectrons, influence of statistics of fluctuations on EM field 77−20360
stilbene, pulsed electron excitation, triplet excitons, spectral and electrical investigations 80−92828
stilbene, single cryst. triplet excitons, delayed fluorescence 78−63988
stilbene, single cryst. under pulsed electron excitation, elec. and spectral characts. 79−7838
strong inhomogeneous magnetic field meas. using n-type Si photoconductance 78−45661
styrene film, plasma polymerised, in vacuo photocurrent meas. 77−89799
superlattice semiconductor, odd photomagnetoresistance effect 79−95425
superlattice semiconductor impurity photoconductivity electron spectrum reconstruction 80−24966
surface charges produced in photoconductor-air gap-semicond. system, calc. 80−6905
surface recombination velocity and diffusion length, meas. method, solar cell appl. 80−93965
suspension of absorbing particles, simultaneous meas. of dichroism and birefringence in elec. field., photocurrent signal obs. 80−82801
TCNB complexes, hole mobility, photocurrent meas., 260-300K 78−60161
TCNE, hole drift mobility, temp. depend. and anisotropy, photocond. meas. 80−80314
TCNE electron donor/acceptor complexes, photoionic dissoc., photocurrents 77−14502
TCNQ, electron mobilities from 210 to 350K using transverse photocond. meas. 79−19618
TCNQ, single cryst., photocond., electron donor gas effects 77−20357
TCNQ-pyrene complex, evaporated layers and single crysts. *(Russian)* 78−6416
temp. depend. of conductivity and photocond. at 632.8 nm *(Russian)* 80−44666
teracene, photoionisation of triplet excitons 77−62837
p-terphenyl, carrier generation and transport, temp. depend. around phase transition at 180K 78−47783
p-terphenyl, cryst., DC photocond. in near UV, carrier generation 79−82644
tetrabenzo-[a,cd,j,lm]perylene thin films, high photoresponse, O_2, N_2 and SF_6 effects 77−32036
tetracene, cryst., hole drift mobility, photoexcitation 77−1444
tetracene, layers, photogeneration, charge carrier transport *(Russian)* 78−56181
tetracene, organic insulator action spectra of photocurrent 80−34482
photoconductivity continued
tetracene surface states, electric field effects, exciton-charge carrier interactions *(Russian)* 80−24989
tetracene/aq. electrolyte contact, illuminated, space charge behaviour 78−84290
N,N,N'N'-tetramethyl-p-phenylenediamine, alkane soln., charge carrier generation, elec. field depend. 80−107846
tetramethylsilane, liq., photocond., ionis. threshold 79−15191
tetrathiotetracene, charge transfer state parameters, evaluation by mag. field effect *(Russian)* 80−10924
thymine film, polycryst., energy conversion processes, quantum yields, 4 to 10 eV 80−88589
TMPD, nonpolar photoionised soln., geminate pair quantum field, recombination fluoresc. elec. field quenching 79−20389
tolusafranine-EDTA, photoredox reaction, photopot. and photocurrent generation 77−81420
transition metals, BCC, films, vac. evaporated, optical cond. 80−76100
transport equation for electrons in nonmonochromatic EM field 80−10937
trap-controlled transient photoconduction 78−10507
trapping kinetics of electrons at broadened levels, transient behaviour 77−47826
trinitrofluorenone-polyvinylcarbazole, freq. depend. 77−8141
1,3,5-trithiane, single cryst., photocond. meas. 77−11959
TTF-TCNQ, energy gaps, far IR photocond. meas. 77−32004
TTF-TCNQ, Peierls transition, photocond. meas., absorption coeffs. above gap 78−72198
TTT, dark cond. and photocond. effect of strong mag. field, at charge carrier injection *(Russian)* 79−69607
UV transparent material, multiphoton-induced cond. and free carrier lifetime 79−19629
N-vinylcarbazole containing polymers, cryst. violet doped, for single layer photothermoplastic devices, photo and dark cond. 77−69374
N-vinylcarbazole-1-vinylnaphthalene copolymer, triplet-triplet annihilation carrier photocurrent, delay fluoresc. 78−2513
wave hierarchy interpretation of multiple trapping model 80−6894
wide-gap semiconductor, recomb.-trap barriers 77−8119
zinc etioporphyrin I anion radical, photoreduction obs. *(Russian)* 78−23958
Ag halide, Dember effect, photographic emulsion grain parameter depend. 78−16870
Ag halide microcrystal, photoconductivity meas. by microwave technique 80−103719
Ag-Al_2O_3-Al junction, internal photoemission 79−82683
Ag-Al_2O_3-Al structure, photoinduced currents, UV detection characts., 325 nm 77−53979
Ag_3AsS_3, proustite, light effects on dielec. props., elec. resist. 80−49816
Ag_3AsS_3, proustite, nonequilibrium carrier exam. 77−15912
Ag_3AsS_3, proustite, residual conductivity and low-temp. phase transitions 78−91729
AgBr, electron-hole kinetics 79−24005
AgBr emulsion, cubic, supersensitisation of microwave photocond. 77−41713
AgBr evaporated layer response in ionisation semiconductor photographic system *(German)* 80−101859
AgBr microcrystals, sintered, photocurrent-inversion effect at room temp. 78−62246
AgBr, photolysis, diffusion and recombination processes 79−24789
AgBr:I emulsion, photocond. and luminesc. at −186°C, rel. to incident light intensity 78−64063
AgBr(I) microcrystals, photohole motion 78−26903
AgBr(I) microcrystals, photocond. and luminesc. 78−26904
AgCl, photoconductivity and photoluminesc., 6.8 to 80K, exciton and valence band states 77−43644
AgCl(Br), crossed elec. and mag. fields, hot electrons, streaming motion, population inversion 80−44649
AgCl(Br), hot electron population inversion, in crossed elec.-mag. fields, 4.2K 79−38128
$AgGaSe_2$ single crysts., opt. quenching of photocond., temp. depend., slow centres activation energy *(Russian)* 77−69370
n-Ag_8GeSe_6, elec. cond. and photoelec. props. 77−69380
AgI, growth, elec. and optical props. 79−77805
β-AgI:Cu, pure and doped, photoconductivity, band struct., trap nature 79−95449
Ag_2O, film, photocond., annealing and time effects *(French)* 78−23135
Ag_2O, photoconductivity of crystals grown under hydrothermal conditions 78−14765
Ag_2S layers, quenching of photocond. by UV radiation 78−68047
α-$AgSbS_2$ crystals, photoelectric props. 80−107861
Ag_3SbS_3, pyrargyrite, US absorption, influence of illumination, photocond. and photoabsorption of sound 79−42153
Al/SiO_x/pSi MIS solar cells, stability 80−85287
Al-Al_2O_3-Al MIM struct., photocond. anal. *(French)* 77−72921
Al-amorphous Ge-nSi, photoelectric props. 80−70822
Al-As_2Se_3-Al layers, photoelectrochem. process 77−76953
Al-GaAs-$Al_xGa_{1-x}As$ Schottky barrier diodes, prep., characts. 80−6948
Al-gelatin-GaAs, capacitance-voltage characts. after and before incorporation of $AgNO_3$ 79−51684
Al-Si_3N_4-SiO_2-Ge structure, small signal HF photo EMF meas. 78−52097
Al-SiO_2-Si structure, photocurrents, 1.4 to 3.1 eV 79−65514
Al-SiO_2-Si structure, small signal HF photo EMF meas. 78−52097
Al-SiO_2-Si-Pb, MIS system, photocurrent, effect of supercond. to normal transition in Pb 78−72271
$Al_xGa_{1-x}As$ DH laser material, Ar laser induced catastrophic damage 79−86178
p-$Al_xGa_{1-x}As$, DH under optical orientation conditions, diffusion of spin labelled electrons 77−8189
$Al_xGa_{1-x}As$, DX photocond. centres, photocapacitance and DLTS meas. 80−11044
$Al_xGa_{1-x}As$, electron mobility illumination, compensation, space charge regions, carrier scatt. 80−70691
$Al_xGa_{1-x}As$ p-n junction, photolum. and current, interface recomb. effects 78−95346
$Al_xGa_{1-x}As$: Sn(Te), persistent photocond., due to donor-related centres, symmetry 80−15558
$Al_xGa_{1-x}As$:Cr, deep level props. 79−69465
$Al_xGa_{1-x}As$:Cr, high resist. film, photolum. and photocond. meas. 78−72596
$Al_xGa_{1-x}As$:Te, persistent photocond. trapping centre, donor complex model, photocapacitance meas. 79−65517

photoconductivity continued
$Al_xGa_{1-x}As$-GaAs heterostructure, effect of photon recycling on diffusion length and internal quantum efficiency 77−39929
AlGaAsSb, photodiode, lattice-matched to GaSb 79−71527
$Al_xGa_{1-x}Sb$-Pd contacts, band gap depend. of barrier height 80−65685
AlH_3, dark electrical cond., exam. 80−39624
AlH_3, I-V and relax. characts. in dark cond. 77−85235
AlH_3, localised states spectrum, photosensitivity 79−78135
AlH_3, photocond., photocurrent carrier-type 78−34855
AlH_3, photocond., reversible processes 79−65516
AlH_3, photoelectric effect spectra and kinetics, photochem. mechanism colour centres 78−56506
AlH_3, polycrystalline, photoconductivity and photochemical decomp. 80−44638
AlH_3, spectral distrib. of photoconductivity and condensed photoeffect before and after illumination *(Russian)* 77−72889
$Al_2In_{12}S_{21}$, preparation, struct. and elec. props. 77−59685
$Al_2In_{12}Se_{21}$, cryst. growth from melt, elec. props. 79−56922
AlN, photocond., 6-12 eV, prior UV illum. effect, mechanism 77−89796
α-Al_2O_3, defects in unirradiated cryst., optical absorpt. spectra 79−61409
Al_2O_3 film, MOS gate insulator, photoconductive processes 77−8216
Al_2O_3, high purity, pot. for electrophotography in radiographic imaging 78−35936
As, amorphous, AC cond. and photo-induced states 79−87128
As chalcogenides, deep levels, photoluminesc. and photocond. 80−70641
a-As, opt. and elec. props. 77−39894
As-Ge-Se system, synthesis and phys. props. of amorphous layers 77−52252
As-S amorphous chalcogenide thin film, transient photoinduced phenomena 80−80884
As-S chalcogenide glass holographic recording efficiency, photocond. and annealing effects *(Russian)* 80−15556
As-S-Te, vitreous semiconductor, photoconductivity *(Russian)* 79−11172
As-Se, glassy, surface phenomena, gas adsorption effects on elec. props. 79−42621
As-Se amorphous system, photocond. props. 80−88587
As-Se glasses, low temp. photocond. 80−49808
As-Se-Cu system glass films, elec. and photoelec. props. variation with photostruct. transforms. 77−76980
As_2Se_3-Bi_x amorphous system, elec. and photocond. props. 79−51574
As_2S_3 (Se_3), electron irradiated, effects on elec., photoelec. and optical props. 80−49806
As_2S_3, amorphous, elec. cond. mech. obs., in bulk material and evaporated thin films *(Japanese)* 80−11028
As_2S_3, amorphous, kinetics of photoconductivity, near fundamental absorption edge, energy gap determ. *(Russian)* 79−56263
As_2S_3 and As_2S_3-Sb_2S_3 system glasses, long-term photocond. relax. 77−76874
As_2S_3, As_2Se_3, optical props., electronic struct., photocond., book contrib. 77−44024
As_2S_3, crystalline and vitreous, nonlinear absorption of ruby laser radiation *(Russian)* 78−22165
As_2S_3, drift mobility, along molecular direction, 207-465K 77−43643
As_2S_3, electron drift mobility temp. depend., transient photocond. obs. 77−66164
As_2S_3 films, kinetics of light-enhanced vaporisation rel. to photocond. 77−84919
As_2S_3 high-resist. vitreous, photopolarisation and photoelectret effects 77−76876
As_2S_3 vitreous, Ag, Cu, Sn and Ge impurities infleunce on electrophys. props. 77−76826
As_2S_3-HgSe structure, anomalous photocond., relax. curves 77−55567
As_2S_3-PbS glass, DC elec. cond. and photocond. 78−39107
As_2S_3(Se_3):Ag glassy films, doped by photodiffusion and thermodiffusion, photocond. 80−29441
As_2Se_3, amorphous, hole mobility expt., transient photocurrent shape 79−99582
As_2Se_3, amorphous, modulated photocurrent 78−10500
As_2Se_3, amorphous, modulated photoconductivity anal. 80−44650
As_2Se_3, amorphous, nonradiative recombination of photocarriers 80−11046
As_2Se_3, amorphous, photoconductivity exam. 78−30953
As_2Se_3, amorphous, time resolved meas. of photoinduced optical absorpt. and photocond. 80−49807
As_2Se_3, amorphous AC cond. and photo-induced states 79−87128
As_2Se_3 amorphous thin films, illumination-induced change in contact pot. 80−20251
As_2Se_3, AsSe and As_3Se_2 films, photostimulated changes in opt. and elec. props. 77−76979
As_2Se_3, crystalline, photocurrent spectral distribution 79−56259
As_2Se_3, glassy, with adsorbed $H_2O(NH_3)(NO_2)(O_2)(CO_2)(CO)$, surface cond., photocond. 78−80038
As_2Se_3, modulated photocurrent, analysed for trap-limited case *(Japanese)* 80−60030
As_2Se_3, photosensitive layer, in metal-photosemiconductor-insulator multilayered struct., optical image recording 80−42286
As_2Se_3, vitreous, elec. and opt. prop. changes on densification 77−11958
As_2Se_3 vitreous films, crystn. stimulated by org. subst. and electrophotographic parameters 77−76319
As_2Se_3-Ge glassy thin films, flash photoresponse 80−107863
As_3Se_2 amorphous film, photocond., TSC, light-induced changes 80−49810
As_3Se_2, electron irradiated, effects on elec., photoelec. and optical props. 80−49806
$As_{60}Se_{40}$, amorphous films, spectral characts. of photodarkening 78−76494
As_2Se_3Ag, glassy semicond. film, prep. by photodiffusion of Ag, negative photocond. 80−92934
$AsSeI_x$, glasses, cond. and photocond. 80−20253
Au/oxide/n-GaAs struct., photocurrent relax. 80−92978
Au-As_2Se_3 sandwich cell, origin of dark currents 77−76920
Au-$CdIn_2S_4$ surface-barrier diodes, mech. of current flow 78−56228
Au-dye-amorphous SiO_2-Au struct., dye-sensitised steady-state photocond. 80−107924
Au-GaAs, photosensitivity losses, field and spectral depend. 80−2452
Au-GaAs Schottky barrier, photocurrent, recomb. losses *(Russian)* 80−2470
Au-n-Si-p-Si structure with wavelength depend. photocurrent sign, photodetector 79−12849
photoconductivity continued
Au-oxide-GaAs struct., steady-state and transient photocurrents 80−6994
Au-oxide-n-GaAs MIS structures, reverse bias influence on photocurrent 80−107921
Au-oxide-n-GaAs structs., reverse-bias depend. photocurrent, photoionisation of surface states 80−20323
Au-tetrathiotetracene-Al systems, dark cond., photocond. mechanisms rel. to contact phenomena *(Russian)* 78−52103
Au-ZnSe:Ga(Al), Schottky diode, wavelength modulated photoresponse spectra 78−6714
B multidionate acceptors for electrophotography 79−19632
B, residual photoconductivity in single crysts. 80−20241
β-B, rhombohedral, localised states charact., review, book contrib. 78−47728
β-B, rhombohedral, photo-EPR, book contrib. 78−48041
$B_{14}Si$, β rhombohedral, conduction mechanism, thermoelectric props. 80−24932
$B_{14}Si$ elec. props., medium range disorder model 80−15522
$Ba_2NaNb_5O_{15}$, ferroelec. conversion to single domain, elec. and photoelec. props. 78−88271
$Ba_{2.09}Na_{0.72}Nb_{5.02}O_{15}$, cryst. growth, monodomenisation, detwinning, optical homogeneity, composition, dielec., spectral props. 77−44151
$Ba_{2.09}Na_{0.72}O_{15}$, ferroelec., photocond. and optical absorpt. spectra. 77−8149
$Ba_{0.25}Sr_{0.75}Nb_2O_6$, anomalous photovoltaic effect and photocond. 79−38122
$Ba_{0.25}Sr_{0.75}Nb_2O_6$, ferroelec., photocond. and optical absorpt. spectra 77−8149
$Ba_{0.25}Sr_{0.75}Nb_2O_6$, photoresponse in transition region 77−1451
$Ba_{0.25}Sr_{0.75}Nb_2O_6$, thermal and spectral variations in the photovoltaic current in ferroelectrics 78−91719
$Ba_{0.5}Sr_{0.5}Nb_2O_6$, electronic props. and photoresponses 80−92925
$(Ba_{1-x}Sr_x)_{1-y}(Nb_2O_6)_y$:$CeO_2$ crystals, photoelectric and photorefractive props., hologram recording 80−53239
$Ba_xSr_{1-x}Nb_2O_6$, anomalous photovoltaic effect and photocond. 78−52449
$Ba_xSr_{1-x}Nb_2O_6$, nonequilibrium processes 78−48124
$Ba_xSr_{1-x}Nb_2O_6$:Ce, pure and doped, photoelec. props. and photorefraction 80−60538
$Ba(Ti,Sn)O_3$, thin film elec. and photoconductivity 79−33366
$BaTiO_3$, anomalous photovoltaic effect and photocond. 78−52449
$BaTiO_3$, anomalous photovoltaic effect and photocond. 79−38122
$BaTiO_3$, doped single cryst., photoexcitable levels 77−4391
$BaTiO_3$, ferroelectric semicond. anomalous photovoltaic effect due to ionising radiation 80−29437
$BaTiO_3$, photorefractive effects and light-induced charge migration 80−69447
$BaTiO_3$, pure and doped, photocurrent kinetics 79−42576
$BaTiO_3$, thin film elec. and photoconductivity 79−33366
$BaTiO_3$:Co, trap recomb. consts., photocurrents 78−43435
$Bi_{40}Ga_2O_{63}$ electro-optic and electrogyratory coefficient meas. 77−43974
$BiGeO_{20}$, photocurrent oscills. in pulsed illumination rel. to piezoelec. props. 80−80325
$Bi_{12}GeO_{20}$ crystals, principal carriers obs., in dark and under laser illumination *(Russian)* 80−80312
$Bi_{12}GeO_{20}$, electrophys., props. determ. *(Russian)* 78−51987
$Bi_{12}GeO_{20}$, photocond. spectra, current-voltage charact., photoelectret effect 79−69552
$Bi_{12}GeO_{20}$, photoelectret state 80−11315
$Bi_{12}GeO_{20}$, pulse photocond., V-I charcts., 0.35-0.55 μm *(Russian)* 78−68048
$Bi_{12}GeO_{20}$, single cryst., electro-optical and photocond. props., image recording *(Russian)* 77−73129
$Bi_{12}GeO_{20}$ vacuum-deposited film elec. and photoelec. props. *(Russian)* 78−60237
$Bi_{12}GeO_{20}$ wide-zone dielectric injection contact characteristics *(Russian)* 78−60236
$Bi_{12}GeO_{20}$:Ga,Ca, photocond. suppression by simultaneous Ga and Ca doping, and appl. to electro-optic light valve 79−78134
Bi_2O_3 anodic films, struct. and electronic props., photoeffects 80−44749
Bi_2S_3-$CuPbBi_5S_9$, solid solution, semiconductor and dielectric props. 79−69511
$Bi_{1-x}Sb_x$ narrow band gap semicond., photocond. and photomagnetic effect 79−51630
$Bi_{1-x}Sb_x$ narrow band gap semiconductors, galvanomagnetic, optical and photoelectric props. 80−15544
$Bi_{1-x}Sb_x$, semicond., photoconductivity *(Russian)* 79−7857
$Bi_{12}SiO_{20}$ film, RF-sputtered, UV illumination effects obs. *(Russian)* 80−80313
$Bi_{12}SiO_{20}$ in insulator-semicond.-insulator struct., induced birefr., influence of kinetics of transient processes 79−24294
$Bi_{12}SiO_{20}$, stationary current obs. on polarised light illum., photogalvanic effects *(Russian)* 79−91095
Bi_2Te_3-Sb_2Te_3 film, residual cond. 78−52110
BiTeI-SbTeI, solid solns., phase diagrams, photocond., elec. props. 79−38125
BiTeI-SbTeI solid solns., form., crystn., elec., thermal props. 78−44003
$Bi_{12}TiO_{20}$ electro-optic and electrogyratory coefficient meas. 77−43974
CaO, electron irradiated, photocond. and luminesc. meas., F-centre electronic struct. determ. 78−6409
CaO, photoionisation of F-centre, luminesc. and photocond. meas. 80−66270
Cd_x-$Hg_{1-x}Te$, cyclotron magneto-optical resons., photoconductivity meas. *(Russian)* 78−23133
$CdCr_2S_4$ ferromag. semicond. film, props. 78−76175
$CdCr_2S_4$:Cu, magnetic microregions caused by s-d exchange 77−77050
$CdCr_2S_4(Se_4)$, thermoreflectance, photoconductance, Raman scatt. near mag. phase transition 80−97298
$CdCr_2Se_4$, photoferromag. effect quenching, photocond. 78−68488
$CdCr_2Se_4$ single cryst., photocond. in air, vacuum, mechanism 77−8138
$CdCr_2Se_4$:Ga(Ag), and pure, photocond. and photomagnetoresist. spectra 77−80809
$CdCr_2Se_4$:Ga(In), photoconductivity, photomagnetoresistance near Curie point *(Russian)* 80−100485
$CdCr_2Se_4$:In , impurity band, photocond. spectral depend. 78−19088
$CdCr_2Se_4$:In(Ga)(Cu), magnetic microregions caused by s-d exchange 77−77050
CdF_2, colour centres, IR absorpt. and photocond. after UV irrad. 80−79784

photoconductivity continued
CdF_2: $YF_3(YbF_3)$, photoconversion from insulating to semicond. state, IR absorption and elec. cond. 78−14759
CdF_2:NaF(AgF), colour centres, IR absorpt. and photocond. after UV irrad. 80−79784
CdF_2-Au metal-semiconductor contact, capacitance and photocurrent, barrier height 77−85321
$CdGaS_2$, single crysts., peculiarities of photocond. in strong elec. field 80−54736
$CdGa_2S_4$, photoluminesc. and photocond. meas. 78−60159
$CdGa_2S_4$:Ag(In), photoluminesc. and photocond. meas. 78−60159
$CdGa_2Se_4$, electron traps, energy spectrum, photocurrent decay, TSC temp. depend. *(Russian)* 78−64057
$CdGa_2Se_4$, struct. of valence band, photocond. and reflection spectra meas. 80−6719
$CdGa_2Te_4$ film, effect of thermal annealing on struct., optical absorpt. and photocond. 79−65342
$CdGeAs_2$, photosensitivity to linearly polarised radiation 77−55569
$Cd_xHg_{1-x}Te$, photodetectors, recomb. processes, photoconductive decay obs. 79−38129
$Cd_{1-x}Hg_xCr_2Se_4$, photoferromag. effect and photocond. obs. 79−28376
n-$Cd_{0.3}Hg_{0.7}Te$, photoelec. props. at 78K, relax. time, minority carrier extraction 80−107864
n-$Cd_{0.3}Hg_{0.7}Te$, recomb. levels 79−91076
n-$Cd_xHg_{1-x}Te$, action of laser pulses, elec. charcts. 79−11212
n-$Cd_xHg_{1-x}Te$ alloys, x=0.19 to 0.21, electron optical heating influence on photoelec. effects 79−11183
$Cd_xHg_{1-x}Te$ films, epitaxial growth, optical, elec., and photoelec. props. 79−11512
$Cd_xHg_{1-x}Te$ graded-gap epitaxial layers, photocond. meas. 0.5 to 6 μm, detector appl. 79−60869
$Cd_xHg_{1-x}Te$, IR detector appls., prep., elec. props. *(German)* 78−86332
n-$Cd_xHg_{1-x}Te$, in strong mag. field, photoresponse to 29.97 μ wavelength 78−87980
$Cd_xHg_{1-x}Te$, inhomogeneous composition effect on carrier lifetime and photosensitivity *(Russian)* 79−73526
$Cd_xHg_{1-x}Te$, photoconductivity under uniaxial compression, band gap 77−43657
$Cd_xHg_{1-x}Te$, photoelectric props. at high temp. 77−4403
$Cd_xHg_{1-x}Te$, photothermomag. effect and photocond. in millimetre wavelength range 80−44657
n-$Cd_xHg_{1-x}Te$, quantum oscills. of transverse photocond., fields up to 30 kOe, 1.5-4.2K *(Russian)* 77−72885
n-$Cd_xHg_{1-x}Te$, recombination due to surface excitation, photoconductivity, impurity states *(Russian)* 80−60042
n-$Cd_xHg_{1-x}Te$, semicond. current carrier recombination heating in photoelectric effects *(Russian)* 79−78138
$Cd_xHg_{1-x}Te$ single crystal, photoconductivity spectral distrib. rel. to surface condition 79−78136
$Cd_xHg_{1-x}Te$, variable-gap struct., additional p-n junction in epitaxial film, photosensitivity 77−24588
$CdIn_2$:Cr, photocond. and photoluminesc. spectra 77−28214
$Cd_{1-x}In_xCr_2Se_4$, electric, photoelectric and mag. props., metal-semicond. transition *(Russian)* 80−54738
$CdInGaS_4$ plate in elec. field, photostimulated ocills. 79−65799
$CdIn_2S_4$ film, vac. deposited, growth, struct., optical and photoelectronic props. 80−10831
$CdIn_2S_4$, photocond. and trap. distrib. 78−39164
$CdIn_2S_4$, photocond. and electron trap distrib. 79−28373
$CdIn_2S_4$, single cryst., oscill. behaviour of photocurrent and luminesc. 78−10501
$CdIn_2Se_4$, cryst. growth, photoresponse and optical props. 78−39165
$Cd_{1-x}M_xS$ (M=Sr, Ca, Mg, Pb, Sn), solid soln., prep. and semicond. props. 80−2383
CdO-B_2O_3-GeO_2 system, phase equilibria at 800°C, X-ray powder diffr. anal. 79−4956
CdP_2:Bi,Zn, photolum. and photocurrent stationary charcts. 78−27317
CdP_2:Cu, photoluminescence and photocond. charcts., interimpurity recomb. of carriers 77−8637
$Cd_4P_2Cl_3(Br_3)(I_3)$, elec. and photoelec. props. 80−34480
CdS, Auger excitation mech. of 1.6-2.0 micron luminesc. band and photocurrent and photo EMF spectra 79−8184
CdS, charged impurity centres, drift during passage of photocurrent 80−70767
CdS, compensated, charcts. of Auger excitation spectra of photoluminesc. and photocurrent 77−90194
CdS, electron and hole trapped centres, EPR, photoluminescence, photoconductivity study 80−108071
CdS epitaxial layers on sapphire, exciton struct. of absorpt., photoluminesc. and photocond. spectra 80−89027
CdS, evaporated film, effects of heat treatment on photosensitivity *(Japanese)* 78−39237
CdS film, anomalous noise rel. to photomemory effect 77−20374
CdS film, chemically sprayed, elec. and photocond. props. 78−34913
CdS film, dark cond., negative temp. depend. 78−47892
CdS film, doping and recrystn. effect on photocurrent relax. time. 77−4409
CdS film, growth by chem. bath deposition, photocond. props. 77−59703
CdS film, influence of nonstoichiometric surface layer on props. 78−64148
CdS film, on Si, structural and transport props. 78−6463
CdS film, strain-induced modulation of photoconductivity 79−24009
CdS film, temp. depend. of dark and residual cond. 77−55625
n-CdS film, transient photoconductivity effects *(French)* 78−87994
CdS, film electrolytically deposited, surface and bulk photocond. props. 78−60154
CdS, film with high photocond. and good reproducibility, prep. by chemical deposition 79−66019
CdS films, photosensitive, growth by reactive RF sputtering, props. *(French)* 78−35308
CdS, films, photovoltaic effect in wedge shaped film 79−56331
CdS films, pure and Na doped, chemical bath deposited, photothermoelectric effect 80−6906
CdS films, vac. evaporation from CdS.Cr_2O_3 system, photoelec. props. 78−80074
n-CdS, growth from Te soln., photocond. and cryst. perfection 79−99579
CdS, hole-capture coeff. of deep charged centres, temp. depend., photocurrent meas. 79−7804
CdS, impact ionisation of excitons, photocond. and photolum. meas. 79−56266
CdS, impurity cond., temp. depend. *(Russian)* 78−47829

photoconductivity continued
CdS laser irrad. native defect formation, influence on photoelectric props., IR luminescence *(Russian)* 80−11039
CdS, neutron irradiated, photoelectric props. 77−35962
n-CdS, new type photoconduction due to magneto-phonon reson. 77−55565
CdS, obtained from CdS-Cr_2O_3 system, α-Cr_2O_3 effect on props. *(Russian)* 79−65469
CdS, optical quenching of noise photooscillations, connection with photoconduction *(Russian)* 77−20363
CdS, photocond., spectral depend. at high excitation intensity, exciton effects 80−65619
CdS, photocond. meas. using surface wave acoustoelec. current 77−8131
CdS, photocond. on supplementary X-irrad. *(Russian)* 77−28212
CdS, photoconductive, transverse electric current effect on SAW propagation 79−47127
CdS, photoconductivity, luminescence, radiative and radiationless transition mechanisms 78−10948
CdS, photoinduced sensitisation process, thermal activity *(Russian)* 80−34477
CdS, photoplasticity and photocond., excitation energy conc. near dislocations, hardening 77−24346
CdS, photosensitivity degradation mechanism due to photocurrent, phtotcarrier lifetime 80−6903
CdS, polycryst. films, microstruct. and X-ray cond. 79−56336
CdS polycrystalline layers, electron trapping depend. on preparation conditions 79−78232
CdS precipitates from acetate solns., crystal structure and photocond. obs. *(Japanese)* 78−10502
CdS, props. of shallow acceptors, photocurrent meas. 79−7805
CdS, pure and Al doped, vacuum deposited film, photoelectric props., optical absorption 78−60162
CdS, recombination electric domains, production mechanism 80−29433
n-CdS, reson. obs. in far IR transverse magnetophotoconductivity 78−30949
CdS Schottky contact, photovoltage 78−95337
CdS, semicond. film, contoured anodic photodissolution 79−74277
CdS, single cryst., effects of annealing in Cd or S vapour on photoelectric props. 77−16370
CdS single crystal growth by sublimation *(Japanese)* 78−11093
CdS sintered film, photolum. and recomb. photocurrent noise spectra 78−6743
CdS, spectroscopic study of local centre interaction, change with external illumination 80−80323
CdS sputtered film, photocond. props. 78−10586
CdS, stress-induced photolum. bands, photocond., rel. to dislocation electron states 80−25447
CdS surface spectroscopy using acoustic surface waves, spectral response 77−69402
CdS, thin film, dark- and photo-currents, annealing time effect 79−38199
CdS thin layers, recryst. from CdS-Cr_2O_3 mixtures, phys. and photoelec. props. 80−96935
CdS type semiconductors, bulk laser damage mechanism, photocond. meas. 80−15567
CdS vacuum evaporated film photoconductivity and In doping effects *(Japanese)* 79−87174
CdS:Ag, induced impurity photocond. spectrum obs. 77−1447
CdS:Ag, orange luminesc. at 77K and induced impurity photoconductivity 79−43035
CdS:Ag crystals, spectral shifts of induced impurity photocond. bands 80−39633
CdS:Bi film, implantation and post annealing, superlinearity 78−52028
CdS:Bi film, spectral response charcts. 78−2512
CdS:Cd, Cu, single crysts., IR restoration after optical degradation of photosensitivity 79−60867
CdS:Cl, Cu^+(Cu^{2+}), photoconductive sensitivity 77−43648
CdS:Cu, Cl films, photocond. growth and decay time 80−60041
CdS:Cu, dye-sensitised, photocond. and photocurrent decay time obs. 80−6893
CdS:Cu, fast electron irradiated, isochronous annealing of IR photocond. quenching spectra 77−1450
CdS:Cu, Fermi level position, luminesc., and photosensitivity, electron irrad. effects *(Russian)* 78−14652
CdS:Cu, photocond. under high excitation intensity 78−52033
CdS:Cu, photocurrent, elec. field effect on recombination processes *(Russian)* 80−100484
CdS:Cu, photosensitivity degradation mechanism 80−107851
n-CdS:Cu, Si, photocond., carrier lifetime, X-ray effects 77−59300
CdS:Cu, spectral sensitisation by cyanine dyes 78−64064
CdS:Cu, US absorpt. in heavily doped piezoelec. semicond. 79−11189
CdS:Cu sintered layers, relaxation photocurrent kinetics *(Russian)* 80−107852
CdS:$CuCl_2$($CdCl_2$) sintered layer, distrib. of energy levels of local centres 80−15568
CdS:Cu(Cl) polycrystalline films with residual conduction, kinetic phenomena *(Russian)* 77−15981
CdS:Cu(Cl) thin films, surface and bulk photoconc. 80−88653
CdS:Li, electron and hole traps obs. 77−8140
CdS:Li, luminescence bands, photocurrent spectra *(Russian)* 80−60677
CdS:Li, nature of recombination centres responsible for 0.95 μm luminesc. band 77−69908
CdS:Li, TSC and optical photocurrent quenching spectra, Auger excitation of recomb. centres 79−33294
CdS:Li, thermochemical changes in microstructure of anisotropic centres, polarisation modulation method meas. 79−38027
CdS:Li chemically deposited filter, elec. props. 80−11113
CdS:Li film, chemical bath deposited, photocond. and optical props. 80−2426
CdS:Li film, photocond., effects of annealing, S vacancies, and O_2 adsorption 78−34854
CdS:N photoluminescence, resistivity and photoconduction obs. 78−10965
CdS:Na, thin film, dark- and photo-currents, annealing time effect 79−38199
CdS:Na thin film, photoconducting props. 80−39623
CdS:Ni, dark cond. and photoconductivity 78−76110
CdS:Ni, elec., photoelec. and luminesc. props. *(Russian)* 78−84259
CdS:Ni, elec., photoelec. and luminesc. props. 79−95828
CdS:Ni, impurity to band electronic transitions, photocond. and dark cond. obs. *(Russian)* 77−8150

photoconductivity continued
CdS:Ni, nonradiative recomb., photocond. spectra 80−70764
CdS:Ni, recomb. parameters, photocond. spectra meas. *(Russian)* 80−49820
CdS/$LiNbO_3$ system SAW convolution signal photoenhancement obs. 77−27431
CdS-CdSe, unactivated film, calc. of induced impurity photocond. due to donor-acceptor pairs 77−43749
CdS-CdTe sintered film, prep. and photocond. props. 77−28220
CdS-CdTe thin film photoresistors, optimum photoelec. performance *(German)* 79−60941
CdS-Cu_2S heterojunction, slow relax. of photocurrent 78−26943
CdS-Li, hexagonal crystl., orientation degeneracy of anisotropic centres, dichroism of impurity photocond. 79−73981
CdS-$LiNbO_3$ structure, acoustoelectric interaction of surface waves with inhomogeneously distributed free carriers 77−43668
CdS-PbS heterojunctions, photoresistive props. 80−6970
CdS-resin layer on electrophotographic plate with polyvinylcarbazole overlayer 77−61146
CdS-Te-Ge heterojunction, prep. photosensitivity, and negative cond., 77K *(German)* 77−20413
n-CdS(Se), bipolar photocond. and acoustoelectric current 79−19636
$CdS_{1-x}Se_x$ single crysts., photocond. and excitonic luminesc. under high laser excitation 78−23127
CdS_xSe_{1-x}, photosensitive layer, in metal-photosemiconductor-insulator multilayered struct., charge pattern form. 80−47129
CdS_xSe_{1-x} photosensitive films, prep., props., and use for photodetectors 80−55298
n-CdS(Se)(Te) semicond. liq. junction solar cells, photocurrent spectra, carrier recombination 78−76142
CdS_xTe_{1-x}, recryst. from CdS_xTe_{1-x}-Cr_2O_3 mixtures, photocond. props. 80−96936
p-CdSb, photoconductivity and absorpt. in submm region, electroluminesc. 77−32046
CdSb:Al, p-n junction formation by laser emission, photoelectric effects *(Russian)* 80−70815
CdSb:Te, photoconductivity charact. 77−43653
CdSe crystals, photocurrent and electrorefl. spectra, stoichiometry defects revealed by annealing *(Russian)* 77−52134
CdSe, dark current relaxation 80−44613
CdSe, effect of heat treatment in Se vapour, photocond. acoustoelec. effect and surface morphology 78−39152
CdSe, electrorefl. and photocurrent of ground state excitons 79−99905
CdSe evaporated films, photoconductivity and effect of deposition conditions 79−95442
CdSe film, electrophys. props. rel. to evap. rates and comp. of initial cryst. 77−85940
CdSe film, stimulated recrystn. influence 77−43754
CdSe, IR quenching and photocond., photon trapping energy depend. 79−56267
n-CdSe, partially illuminated single crystal, current-voltage characteristic and potential distrib. 79−65519
CdSe, photoconductivity, recomb. charact. 77−8118
CdSe, photodetector, limiting sensitivity 79−63309
CdSe, photoionization cross-section temp. depend., deep local levels 79−65408
CdSe, pulsed Hall photoeffect, transient processes in scattering of carriers 80−15546
CdSe, reson. absorpt. of coherent IR radn. by acceptors, photocurrent and emission spectra 79−73974
CdSe, saturation of optical absorpt. and photocond. 79−18487
CdSe, Se-annealed and Cu-diffused, photocond. props. 79−99580
CdSe, single crystal, low-frequency current noise, effect of temperature quenching of photoconductivity 78−34874
CdSe single crystals, effects of impurities on photocond. *(Japanese)* 77−28221
n-CdSe, with single deep electron trap, negative photocond. 77−15905
CdSe:Ag, In, cryst., photocurrent and electroreflection, 77 to 300K *(Russian)* 78−23136
CdSe:Au impurity light absorpt. for current control in negative resistance region 80−11052
CdSe:Cd, Cu, photo-induced changes in absorpt. spectra 78−80382
CdSe:Cu, doping profile rel. to photoelec. props. in alloyed surface layers *(Russian)* 77−85268
CdSe:Cu, impurity photocurrent, kinetics and oscills. 80−65624
CdSe:Cu,Cl film, induced impurity photocond., 0.6 to 1.2 eV 79−24012
CdSe:Ti, optical and elec. investig. of shallow donor levels, reson. states 77−63437
CdSe-Sb_2Se_3 heterojunction, photoelec. props. 80−70816
$CdSe_xTe_{1-x}$ film, polycrystalline, deposition and physical props. 77−4741
$CdSeTl_3$-$As_2Se_3Tl_3$ thin layer system, charge transport 77−76985
$CdSiP_2$:Na(Bi), single crystal, under laser excitation 80−44661
p-$CdSnP_2$, photocond. meas., polarisation depend. 78−39157
CdTe, amorphous, photocond., effective density of localised states 77−28210
p-CdTe, bipolar photocond. and acoustoelectric current 79−19636
CdTe, bipolar photoconductivity exam. 78−6410
n-CdTe, deep trapping levels in high resistivity films 77−72930
CdTe detectors, photoscanning, determ. of crystal quality and contact behaviour 77−61664
CdTe, elec. and photoelec. props. due to double injection, quenching spectra 80−70765
CdTe, film, theoretical models of impurity levels 79−82557
n-CdTe films, uniform trap distrib., transient photocond. effects 79−28423
CdTe, hot electron and exciton effects in oscill. excitation spectra of photocond. and photolum. 79−38645
CdTe, IR quenching of photocurrent and switch in type of photoconductivity 77−47862
CdTe, minority carrier diffusion length from photocurrent meas. in semicond.-electrolyte boundary 80−65584
CdTe optical applications, review 77−42580
p-CdTe, photocond., photoluminesc., spectral studies 80−88593
CdTe, photoconductivity, extrinsic, contrib. by hopping through excited states of donors 78−6411
CdTe, semiinsulating, anomalous photocond. and dark cond. 77−62959
CdTe, shallow donors, excited state transitions 78−6710
CdTe sputtered films, struct., photocond., and trap distrib. 80−29489
p-CdTe, surface barrier struct., internal photoelec. emission 77−15958
photoconductivity continued
p-CdTe, surface photovoltage spectroscopy in IR and visible range 80−39632
p-CdTe:Cl, deep level characterisation, gamma-ray detector parameters 77−39802
p-CdTe:Cl, mech. of electron recomb. 79−11176
CdTe:Cl, semi-insulating, impurity photocond. spectra, local state distrib. in band gap 80−107865
CdTe:Fe, annealed, magnetically ordered, Hall effect and photocond. 78−19060
CdTe:Ge, negative thermally stimulated cond. 79−19621
CdTe:In, photoconductivity exam. and IR quenching 79−11181
CdTe-CdS heterojunction, photocapacitance and photocond. 80−96978
CdTe-$SnCl_2$ electrolyte heterojunction photoelec. props., feasibility as solar energy convertors 77−76918
$CdTe_{1-x}Se_x$ solid solution films, prep., struct., and photocond. 80−54541
$Cd_{1-x}Zn_xCr_2Se_4$, synthesis Curie pt., photomag. effect 77−51937
CdZnS-CdS bifilm solar photocells, feasibility, study 78−76113
$Cd_{1-x}Zn_xS$ films, thermal evaporation prep., phys. props. 80−84410
$Cd_xZn_{1-x}S$ films, chem. sprayed, carrier density and mobility 80−60121
Cr island film photoconductivity obs. 78−95392
Cr_2O_3 addition to CdS_xSe_{1-x} photoresistors, extension of cutoff freq. *(Russian)* 78−84248
Cs-Sr(He) mixtures, photocond. at atm. press. 80−87844
Cu anode, passivating behaviour and illum. effects in alkaline soln. 80−104449
Cu, anodic oxidation, photoelectrochemical effects *(French)* 80−93701
$Cu_{10}As_{31}Se_{38}O_{21}$, chalcogenide glass, exam. of electron mechanism of photo induced changes 78−87998
$CuGaS_2$, photoelectronic props., 77 to 300K 78−34865
$CuGaS_2$, single cryst., photocond. spectra 78−84252
$CuInS_2$ film, photoconductivity effects 77−43662
$CuInS_2$, minority carriers lifetime, photoelectromag. effect meas. 79−47125
$CuInSe_2$ film, photoconductivity effects 77−43662
$CuInSe_2$, influence of impurities and free carriers on optical props. 80−108225
p-$CuInSe_2$, minority carrier lifetime and surface recomb. velocity, photoelectromag. meas. 78−19085
$CuInTe_2$ film, photoconductivity effects 77−43662
Cu_2O, excitons and structural defects at low temp. 78−84255
Cu_2O, growth by melting, photocond. spectra 78−52029
Cu_2O, photoconductivity in 1S excitonic line 80−34366
Cu_2O, photoconductivity of crystals grown under hydrothermal conditions 78−14765
Cu_2O, photomemory effect, EPR expts. 78−52353
Cu_2O, positive and negative photomemory, IR luminesc. spectra, illum. effect 79−69557
Cu_2O, residual conductivity, role of vacancies, photoluminesc. and photocond. 77−15901
Cu_2O single crystals, photomemory effect, kinetics of excitation and deexcitation processes 77−85262
Cu_2O solar cells, electrical and optical props., photocurrent anal. 80−101116
Cu_2O:Mn, photomemory mobility components, charged centre conc. 80−103725
CuPbBiS, ferroelec. semicond., elec. cond., photocond. permittivity, phase transitions 77−47822
Cu_2S-CdS, solar cell, photocurrent, spectral depend. 79−7853
Cu_2S-CdS heterojunction characteristics and CdS polarity *(Japanese)* 78−23154
Cu_2S-CdS heterojunction, elec. and photoelec. charact., effect of etching of CdS 78−80048
Cu_2S-CdS p-i-n structure diode, photoelec. charact. 78−2557
$Cu_{2-x}S$ in chem. formed $Cu_{2-x}S$-CdS heterojunction, photosensitivity charact. 78−72199
$Cu_{2-x}S$-CdS heterojunctions, nature of longwave photo EMF 78−84284
$Cu_{2-x}S$-CdS p-n heterojunction, optical energy convertor, struct. and recomb. props. 80−72065
Cu_xS, photon and electron excitation phenomena 79−7865
$CuSbS_2$ crystals, growth and characterisation 80−60770
p-Cu_2Sn-n-ZnS heterojunction, I-V charact., photocond. and electrolum. 78−72251
9,10-dichloroanthracene, mag. field effect on exciton processes and photodetrapping 77−4668
Eu, film, optical cond. meas. 78−76112
EuO, photoelectron anomalous transport phenomena 78−23114
EuO:Gd, pure and doped, elec., mag., and optical props. rel. to electronic conc. 80−96880
Fe oxide films, semicond. electrode props. 79−91093
$Fe_{2-x}Cr_xO_3$, elec., optical and photocond. props. 79−56262
FeO-P_2O_5 glass, elec. props. effect of high energy γ-radiation 79−11173
α-Fe_2O_3 electrode, carrier density determ. by optical absorpt. and photoelectrolysis spectra 80−71462
α-Fe_2O_3, photochem. props. of sintered and doped samples for solar photoelectrochem. cell appls. 80−89651
α-Fe_2O_3, polycryst., pure and TiO_2 doped, flatband potentials, donor densities, photocurrent meas. 78−76089
Fe_2O_3 semiconductor electrode, photocurrent response 77−77771
Fe_3O_4, 70-130K, temp. range including metal-semicond. transition *(Russian)* 78−56178
Fe_3O_4, metallic phase, photocond. and mag. permeab., photoinduced changes 80−15566
$FePS_3$, layered semiconductors, optical and electronic props. 80−70761
$FePb_4Sb_6S_{14}$, photosensitive semiconductor, with high permittivity, elec. props. 79−65518
FeS_2, natural pyrite, photocond. spectra 80−70758
n-GaAlAs:Sn LED DH donor-level analysis, DLTS obs. 79−47040
GaAlAs/GaAs solar cells, efficiency optimisation at high and low current levels *(French)* 80−61348
p-$Ga_{1-x}Al_xAs$ crystals, spectral charact. of photosensitivity, mechanism 80−44735
$Ga_{1-x}Al_xSb$ variable-gap p-n struct., selective photoelec. effect 77−76912
$Ga_{1-x}Al_xSb$ variable-gap p-n structures, wide-band photoelec. effect 79−42635
GaAs, deep trapped impurities, photocond. spectra, interpretation 78−52030
GaAs, donor energy spectrum, mag. field effect, submm. photocond. meas. *(Russian)* 77−43666
GaAs, electrical and optical props. at low temps. 80−39636

photoconductivity continued
n-GaAs, electron irradiated, defect energy levels, influence of irrad. temp., photocond. meas. 78−2446
GaAs, electron mobility illumination, compensation, space charge regions, carrier scatt. 80−70691
GaAs, electron-exciton collision influence on luminescence line profile due to bound excitons and photocond. meas. 80−29800
n-GaAs, epitaxial, ionised donor pair spectrum 77−63477
GaAs, epitaxial, residual donor identification by far IR photocond. 80−60047
GaAs, epitaxial, residual donor identification by far IR photoconductivity meas. 80−103717
n-GaAs epitaxial film, undoped, correl. incorporation of donors, photocond. meas. at 4.2K 80−6898
GaAs epitaxial film recombination props. *(Russian)* 80−49812
GaAs epitaxial films, deep levels, impurity photocond. 80−20247
n-GaAs epitaxial films, residual cond. meas., struct. perfection rel. to photomemory 80−7010
GaAs epitaxial layer, laser mag. photoelec. spectra 79−82635
GaAs epitaxial layers, photocond. high field effects on carrier capture and recomb. 77−43646
GaAs epitaxial layers, undoped, recomb. of non-equilib. carriers, steady-state photocond. 77−85357
GaAs, epitaxial struct., nonuniform electroconductivity *(Russian)* 80−70753
GaAs, exciton effects in photocond., photoluminesc. 80−96797
GaAs, extrinsic, DC- and microwave-biased, performance 80−70750
GaAs, far IR photoconductivity 77−15893
p-GaAs, Fe-compensated, photocond. under strong excitation 77−15904
GaAs film, photovoltage anomaly investig., p-n-p microjunction model 77−4398
GaAs, γ- and electron irradiation, influence on recomb. characts. 80−71478
n-GaAs, H-like impurities photocond., mag. field effect 79−82634
GaAs, high-purity, residual donors, ionisation energies determ. 78−6333
GaAs, illuminated, carrier lifetime profile, depth depend. 78−68036
GaAs, impact ionisation rates for electrons and holes, photocarrier multiplication obs. 78−87995
n-GaAs, LPE, deep trapping centre characterisation by Hall and photo-Hall meas. 80−88578
GaAs, laser-induced bulk breakdown and free carrier generation, photocond. meas. 80−35018
GaAs layers, photocond. spectra 79−65340
GaAs, lightly doped, p-n structure, parameters of nonequilib. carriers, transient photoeffect method 79−11143
GaAs MOS solar cells by anodisation in active region 80−101107
n-GaAs, magneto-impurity effect, review 79−91081
GaAs n-i-n junction, photoelec. props. investig., 77 to 300K 77−28248
GaAs, n-i-n junctions, simulation of long-term relax. of nonequilib. conductivity 79−38156
GaAs, neutron transmutation doping, shallow donors magneto-optical effects 80−20255
GaAs p^+-n^0 junction, photocurrent, hole diffusion length in lightly doped n-type region 77−28246
GaAs, p-n junction, Zn^+ implanted, residual radiation defect influence on characts. *(Russian)* 78−84287
GaAs, photoconductive carrier lifetime meas. by optoelectronic gating technique 77−47857
GaAs, photoconductivity, impurity induced, low energy edge spectral shift 80−65630
GaAs, photoconductivity and photomagnetic effect spectra 79−11178
GaAs, photoconductivity meas. of cyclotron resonance 79−82638
GaAs, photoelectric memory effect, effect of metallic island struct. on surface 77−55570
GaAs, photoemission modulation by IR illumination, saturation photocurrents 80−108318
GaAs, photoexcitation phenomena, low density 78−27319
GaAs, photoexcited, carrier relaxation determ. from time resolved transmission spectrum changes 79−99583
GaAs, plastically deform., photocond., spectral response and decay process 80−29435
GaAs, proton irradiated, low energy, deep level defects and hole diffusion length meas. 80−60000
n-GaAs, real epitaxial surface, photoelec. spectroscopy, mechanisms 78−34858
GaAs, relaxation of photoexcited carriers 78−19080
GaAs, semi-insulating, conduction model 80−10986
GaAs, semi-insulating, magnetophotoconductivity as function of etching time 79−56265
n-GaAs semicond. liq. junction solar cells, photocurrent spectra, carrier recombination 78−76142
GaAs, shallow donors, excited state transitions 78−6710
GaAs, struct., elec. props., effects of illumination, O_2 absorpt., electron bombard. *(French)* 78−34690
GaAs, surface photogalvanic effect, polarisation depend. photocurrents *(Russian)* 80−80322
n-GaAs, surface recomb. vel. meas., diffr. from transient optical grating 79−1604
GaAs, transmutation doped, shallow donors, magneto-optical study, photocond. meas. 78−87996
GaAs, VPE, high purity, residual donors, photocond. expts. 77−85174
GaAs VPE layers, elec. props., semi-insulating substrates effect 80−11123
GaAs:B, deep levels, optically stimulated transient current method *(French)* 80−59919
GaAs:Cr, current voltage characterisation, deep levels and Fermi level determ. 79−7823
GaAs:Cr, photoconductivity and photo Hall spectra 78−19091
GaAs:Cr, photoluminescence in strong electric fields 80−108270
GaAs:Cr, plane-parallel plate subjected to laser illumination, photocond. meas., photodetector for far IR 79−93221
GaAs:Cr, semi-insulating, i.r. induced modulation of cathodoluminescence, and specimen current 77−1737
p-GaAs:Cr, semi-insulating photoelectronic analysis 77−80804
GaAs:Cr, semi-insulating, characterisation by photoelectronic data 78−68051
GaAs:Cr, semi-insulating, I-V characts. and photocond. spectra dependencies on Fermi level 79−99576
GaAs:Cr, semiinsulating, hole recomb. domains, Hall mobility and photocond. 77−15867

photoconductivity continued
GaAs:Cr, semiinsulating, I-V characts., photocond., Fermi level, and deep levels 78−39118
GaAs:Cr, single cryst., optical quenching spectrum, disappearance of stationary high-field domain 78−47830
GaAs:Cr,O, semi-insulating, photocond. anal. of levels 80−20243
GaAs:Cr (Cr-Te), and undoped, transverse-acoustoelec.-voltage spectroscopy 79−99586
GaAs:Cr photoconductivity, large scale fluctuations of impurity electostatic potential 77−8145
GaAs:Cr plane-parallel photocond. plate, oscills. in current and light intensity in laser irradiation 80−49819
GaAs:Cr plate, illuminated, oscills. in V-I charact. 80−11038
GaAs:Cr(O), deep impurity levels, AC photocond. meas. 78−19082
GaAs:Cr(O), mechanism of thermal quenching of luminesc. and photocurrent stimulation 77−55821
n-GaAs:Cr(Si), deep-level extrinsic photocond. response, decay at 4.2K 80−2420
GaAs:Cu, diffused layers, photocond. spectra, hole conc. and mobility *(Russian)* 78−14758
p-GaAs:Cu, impurity photocond. and absorpt. coeff., Hall meas. 80−6770
GaAs:Cu, LPE, photoelec. meas. of electron density for different Cu introduction methods 78−43437
GaAs:Cu, sensitivity of impurity photocond., ordered surface irregularities 79−24018
GaAs:Cu(Cr) S-type diodes, thermal quenching of injection currents and current-voltage characts. 78−26942
GaAs:Fe, p-π-ν-n struct., photoelec. props. 80−107862
GaAs:Fe, photoionisation cross section meas. of deep levels 77−8042
GaAs:Ge,Se transmutation shallow donor transition obs. 80−59925
GaAs:Ni, behaviour of Ni impurity in $3d^8$ state, optical absorption and photocond. meas. 78−47737
n-GaAs:Ni, negative photocond. at low temps., impurity levels 80−6900
GaAs:O, deep level, Franck-Condon shift, photocond. and Hall effect study 80−70642
GaAs:O, high-resist., extrinsic photocond. meas. 77−85255
GaAs:O, impurity photocond. in high elec. field, 90K 78−19095
GaAs:O, oxygen-compensated single GaAs cryst., photoelec. memory 79−11184
GaAs:O, photocond., electron traps, level-broadening, 90 to 150K 78−60158
n-GaAs:O, photocond. associated with deep level at 0.4 eV 80−44640
GaAs:O p-ν-n structs., injection current and negative photocond., saturation mechanism 80−92967
n-GaAs:S, Zn VPE film, LF current oscill., negative photocond. 77−80858
GaAs:Si epitaxial films, elec. and photoelec. props., impurity distrib. 80−7006
GaAs:Te, recombination barrier, dark cond., photocond., and Hall mobility meas. 80−15559
p-GaAs:Zn, optical absorpt. spectra and photocond. after 2 MeV electron irrad. *(Russian)* 77−69859
GaAs-$Al_xGa_{1-x}As$ heterojunctions, MBE grown, photocollection efficiency and interface charges 79−11199
GaAs-$Al_xGa_{1-x}As$ superlattice, electronic props. 80−11080
GaAs-AlGaAs DH laser, degradation rate rel. to photocurrent 80−28233
GaAs-AlGaAs:Si heterojunction interface, two-dimens. electron gas, Hall effect and cyclotron reson. meas. 79−65530
n-GaAs-electrolyte interface, surface pretreatment rel. to photocurrent, spectral response 80−3204
GaAs-$Ga_{1-x}Al_xAs$ variable gap p-n junction, variable gap and photo EMFs 80−15596
GaAs-$Ga_xAl_{1-x}As$ superlattice, with high sensitivity and reduced dark current 79−7881
GaAs-$Ge_{1-x}(GaAs)_X$ n-p heterojunctions, hydrostatic press. effect on elect. and photoelectric props. 80−20304
GaAs-metal diode, surface-barrier, excitons effect on photocurrent 79−82670
GaAs-metal struct., photoresponse spectra, electron thermalisation *(Russian)* 79−15221
GaAs-ZnSe, X-ray cond. 5.4 to 17.5 keV, spectral and dosimetric characts. *(Russian)* 77−35964
$GaAs_{1-x}P_x$:S, deep level, photoconductivity, carrier nonradiative recombination 80−20112
$Ga_{1-x}In_xSe$, layered, luminescence and photocond. obs., two-photon excitation 78−76521
$Ga_xIn_{1-x}Se$, fabrication, struct., elec. and optical props. 80−44180
GaN:Al, VPE grown, luminesc. and elec. props. depend. on doping conc., bound excitons 80−20688
GaN:Zn, heavily doped, photocond. spectra 77−72887
β-Ga_2O_3, low temp. meas. in the region of UV emission 78−80396
GaP, anomalous photoeffect on connected excitons *(Russian)* 80−92929
GaP complex band semicond. photogalvanic effect mechanism 80−11036
GaP, electrical and optical props. at low temps. 80−39636
n-GaP electrode, photoanodic dissolution rate, effect on surface electronic band energies 80−103748
GaP, epitaxial layer, thickness and diffusion length, photocurrent meas. 77−32096
n-GaP, optical rectification and photon drag 77−36224
GaP, p-i-n LED, I-V characts., electrolum., and photocond. meas. 77−20930
GaP photoelectrode, stability 77−20422
n-GaP, shallow trapping centres, electron lifetime from photocond. meas. 79−99563
GaP, vac. deposited film, structural, elec. and photoelectric props. 79−82698
GaP:Cu, elec. and optical props., rel. to doping and heat treatment 80−16056
GaP:Cu, LPE, photoconductive props. obs. 78−47836
GaP:Cu, thermally and optical excited cond., deep level centres 78−72190
GaP:Fe n-i-n epitaxial struct., photoconductivity, recombination scheme *(Russian)* 80−15569
n-GaP:Ge, photomemory effect and thermal field impurity breakdown 77−20362
GaP:O, multicharged state of O, TSC and photoinduced currents 79−7808
GaP:S(Se)(Te)(Si)(C)(Zn), IR photocond. response spectra 79−56257
n-GaS, Bridgman crysts., hole traps, photocond. and thermal quenching study 80−75580

photoconductivity continued
GaS two-photon absorpt., cond. and luminesc. meas. 77−52166
GaS:Bi_2S_3, photocond. and optical absorpt. 79−51634
GaSb, p-type, effects of accumulation layer on photocond. *(French)* 77−24582
n-GaSb:S, thermal quenching of residual cond. 78−56188
GaSe, exciton-phonon bound state, photocond. and visible absorpt. spectra obs. 80−50369
GaSe, exciton-phonon quasibound states, photocond. and luminesc. study 80−96800
GaSe, impurity photocond., induced illumination corresponding to fundamental absorption region 80−92933
GaSe, interlayer interaction and exciton spectra study 77−52165
GaSe, layered, photoelectromag. effect meas. of transport parameters 77−59301
p-GaSe, negative residual photoconductivity 79−51632
GaSe, photocond., influence of stacking disorder 80−2422
GaSe, photocond. at high excitation rates 78−52036
n-GaSe, photoconductivity and TSC investig. of trapping centres 77−20359
n-GaSe, photomagnetoelec. and photocond. current spectral distrib. 79−42585
n-GaSe, photomagnetoelectric effect, photocond., in presence of traps 80−39631
GaSe, photosensitivity anisotropy in polarised light, pleochroism coeff., suitability as photoelec. analysers 79−60873
GaSe plate in elec. field, photostimulated ocills. 79−65799
p-GaSe, single cryst., negative photocond. induced by elec. field 79−19623
GaSe, thin film, photoelectrical props. at high electric field *(Russian)* 79−11247
GaSe, two-photon absorpt., cond. and luminesc. meas. 77−52166
GaSe:Sn, single crystal, transient photoconductivity *(Russian)* 79−11171
Gap-Ge, compensated, photosensitivity 79−19624
$Gd_2(MoO_4)_3$, ferroelec.-ferroelastic, photolum. and photocond. meas. 80−84768
$Gd_2(MoO_4)_3$, one-dimensional ferroelectric image sensor with polymer photoconductor 80−80729
Ge, acceptors, transitions from second excited state, photocond. meas. 79−11082
Ge, amorphous, elec. and opt. props., review 78−23094
Ge, amorphous film, persistent photoconductivity, dangling bonds 80−84487
Ge amorphous films, self-ion bombard., electronic props. 79−28422
Ge and Ge:O(Li), shallow defects, PTIS meas. 80−24971
p-Ge, carrier drag by photons, comparison with p-GaAs 79−11185
n-Ge, compensated, impurity photoconductivity 78−10512
Ge, compensated, impurity photocond. relax times 80−88592
n-Ge, D^- state struct. rel. to photocond. expts. 80−59924
Ge, determ. of nonradiative decay rate in electron-hole drops at 1.6K 77−8143
n-Ge, dislocated pressure influence, 130 to 260K 78−76109
Ge, dislocation electron states, from press. depend. of photocond. 80−96819
Ge, dissociation of hot excitons by long-wavelength acoustic phonons, photocond. spectra 77−4300
Ge, donor energy spectrum, mag. field effect, submm. photocond. meas. *(Russian)* 77−43666
Ge, donor-acceptor electron transfer at low temps., photocond. tail 78−84249
Ge, electrical and optical props. at low temps. 80−39636
Ge, electron irrad., light-sensitive defects 80−24498
Ge, electron-hole drop ejection from continuously generated electron hole liquid 79−78017
Ge, electron-hole drop motion at low exciton densities 77−47865
Ge, electron-hole drop net negative charge, giant fluctuating photocurrent obs. 77−35963
Ge, electron-hole drops, IR absorpt. spectra 79−87423
Ge, electron-hole drops at high mag. fields 79−60721
Ge, electron-hole fluid drift in crossed electric and mag. fields, photocurrent dynamics *(Russian)* 79−99487
Ge, electron-hole liquid, MHD effects 80−80190
Ge, electron-hole luminesc. and transport props. 77−48241
Ge, electronic states of isolated negative donor ion, binding energy 79−65404
Ge, exciton condensation, microwave cond. below 1K, book contrib. 80−8997
Ge, exciton condensation, microwave cond., book contrib. 80−11040
Ge, exciton condensation, microwave breakdown, luminesc., book contrib. 80−11471
Ge, exciton contrib. to oscillatory magnetophotocond. 79−15180
Ge, exciton microwave breakdown, electron-hole drops, book contrib. 80−11041
p-Ge, free-carrier reson., photoconductivity spectra in submillimetre wavelength 79−15353
n-Ge, γ-irrad. and subjected to arbitrary excitation and rate, recombination 79−38101
Ge, high-purity, with Al, B and P, residual impurities, photothermal cond. 80−24965
Ge, IR detector based on carrier photon drag 77−74507
Ge, impurity determ. in very pure sample by photoelec. spectroscopy 77−39888
Ge, impurity photoconductivity 79−82631
Ge, inversion of magneto-impurity oscills. 77−15913
Ge, irradiation by 3.5 MeV electrons at high temp., carrier density and lifetime changes 77−4128
Ge, laser-induced bulk breakdown and free carrier generation, photocond. meas. 80−35018
Ge, microwave absorption by nonequilibrium carriers, carrier density determ. method 77−8148
Ge, microwave absorption by nonequilib. current carriers, book contrib. 80−11042
Ge, microwave exciton breakdown and luminesc., under one- and two-photon excitation 77−31955
Ge, n- and p-type, magneto-impurity effect, review 79−91081
n-Ge, nonlinear absorption of CO_2 laser radiation by nonequilib. carriers 79−32000
p-Ge, optical cooling and carrier heating, intraband photocond. meas. 79−11174
Ge, optical excitation of dislocation states 77−85265
photoconductivity continued
p-Ge, p-n junction with hot carriers in charge accumulation regime, influence of light on operation 79−51661
n-Ge, photocond., excited by CO_2 laser pulses, depend. on intensity 79−69548
Ge, photoconductivity, carrier lifetimes in excited states of impurities *(Russian)* 77−76864
Ge, photoconductivity, magnetoimpurity oscills. 79−82626
Ge, photoconductivity spectra of shallow impurities 79−82625
Ge, photocurrent magneto-oscillations 80−6911
Ge, photocurrent oscillations in mag. field, intense excitation *(Russian)* 78−26915
Ge, photoelectric spectra of shallow impurities, mag. field effect 79−82624
Ge, photoelectric spectra of impurity groups 79−82627
Ge, photoelectric spectra of remanent impurities 79−87125
p-Ge, photoexcited charge carrier capture by shallow impurity centres *(Russian)* 80−15571
p-Ge, photon drag spectrum 77−32044
Ge, photothermal cond., low temp. depend. 80−70756
n-Ge, plastically deform., dislocation state spectrum, photocond., elec. cond., and Hall const. meas. *(Russian)* 80−2362
Ge, plastically deformed, photocond. and absorpt. spectra, dislocation levels 77−28219
Ge, plastically deformed, photocond. produced by polarised light 79−82641
Ge, pure and doped, electron-hole drops net charge, photocond. and photoluminesc. 79−38589
Ge, recombination at dislocations 79−38023
p-Ge, relaxation dynamics and photoconductivity 79−51636
Ge shallow hydrogenic centres, ground states, isotope shifts, photoelectric spectrosc. 78−39055
Ge shallow impurity bound states, IR spectroscopic obs. 77−39806
p-Ge, spectral depend. of drag of electrons by photons 79−42590
Ge, sputtered hydrogenated amorphous, steady-state and transient photocond. meas. 78−10506
n-Ge surface, chemical channel of recombination 80−39656
Ge surface, X-irradiated, slow relaxation of surface states 77−62980
Ge surface during X-irradiation, oxide hydration degree determ. 77−24605
Ge, transport props. of high density electron-hole plasma at low temp. 77−47864
p-Ge, uniaxially deformed, magneto-impurity oscills. of photocond. 78−34862
n-Ge: Ga(P), uniaxial compression, 0.6-2.9 mm radn. absorpt. 79−82629
Ge:Al, acceptor levels, Zeeman splitting, far IR photoconductivity spectrum 78−43444
Ge:Al, Zeeman effect in excitation spectra, photoelectric spectroscopy 79−82633
Ge:Al(B), uniaxially stressed, photoionisation of acceptors, impurity photocond. meas. 78−10509
Ge:As(Ga), photoconductivity oscillation with respect to applied mag. field *(Russian)* 78−80026
Ge:As(P)(Sb), impurity photocond. spectra under uniaxial compression 80−44656
Ge:As(Sb), D^- states in mag. fields, photocond. spectra, and far IR absorption spectra 79−95370
Ge:As(Sb), D^- states investigated by long wavelength photoconductivity 78−6323
Ge:Au, IR detector, impurity photoconductivity *(German)* 78−82036
n-Ge:Au, negative photocond., field and temp. depend. 77−43660
n-Ge:Au, negative photoconductivity 78−34863
Ge:Au, p-n junction, injection amplification of photocurrent 79−51663
Ge:Au, recomb. at repulsive centres, photocond. lifetime meas. 77−43617
Ge:Au,Sb, electron irradiated, Hall effect, photocond., and photomagnetic effect meas. 77−4369
Ge:Au under laser illumination, non-equilibrium conduction 80−6896
Ge:Cd, compensated, complex oscillatory impurity photocond. spectrum 77−43656
Ge:Cu, IR detector, impurity photoconductivity *(German)* 78−82036
Ge:Cu short wavelength quenching of photoconductivity 78−26907
Ge:Ga, uniaxially stressed, far IR photocond. meas. 78−10496
p-Ge:Ga far IR absorption and photoconductivity obs. 77−39899
Ge:Ga photoconductors in low IR backgrounds 79−63305
Ge:H, photoelec. spectra, acceptor and donor behaviour 80−29443
Ge:Hg, anomalous photocond. with 10.6 μm laser light *(Russian)* 77−47861
Ge:Hg, anomalous room-temp. impurity photocond. 78−39159
Ge:Li, Cu p-n junctions, current stimulated LiCu complex formation, photocurrents 80−107897
Ge:Li, long wavelength photoconductivity spectrum 77−43641
Ge:Li-O, donor complex EPR and photoelectron piezoelectric spectra, dynamic tunnelling 79−1711
n-Ge:Ni, quasi-surface conduction effects on photocond. spectrum and IR quenching 77−1452
n-Ge:Ni, recombination of hot electrons on Ni impurity centres 80−44612
n-Ge:Ni,Sb, transient response at 4K, nonequilib. carrier recomb. 77−43659
Ge:P, amorphous, electronic transport and photocond. 79−60834
Ge:Pd and pure, photoelectric props., surface states *(Russian)* 80−60043
n-Ge:Sb, electron irrad., impurity photoconductivity 77−15900
n-Ge:Sb, γ-irradiated, trapping and recomb. coeffs. 77−43616
Ge:Sb, Zn(Hg), photoelec. props., 70 to 300K 80−65621
Ge:Sb,Au, photoelectronoc exam. of multilevel gold structure 77−69272
Ge:Sb,Cu, exactly compensated, impurity absorpt. and photocond. spectra 78−56189
n-Ge:Sb,Cu, exactly compensated, static photocurrent-voltage characts. 79−38131
n-Ge:Sb,Cu, exactly compensated, unipolar injection influence on photoconductivity 79−42592
Ge:Sb,Cu, high resist. compensated, impurity of photocond., pulsed unipolar injection carriers 80−92935
Ge:Sb,Cu, photoelec. props., fast electron irrad. effects 80−60036
Ge:Sb (As), isolated D^- states and D^- complexes in mag. fields 80−15473
Ge:Sb(Ga), fast electron radiation defects, 0.52 eV absorpt. band, impurity photocond. and Hall effect meas. 78−27273

photoconductivity continued
Ge:Zn photoresistor, current responsivity rel. to nonequilib. hole lifetime 80−60035
Ge-GeO_2, optical charging memory, influence of doping GeO_2 with metal ions *(Russian)* 79−24077
n-Ge-metal Schottky barrier contacts, IR optoelectronic props., quantum detector appls. 80−75640
Ge-S, amorphous, photocond., photo-induced ESR, optical edge shift 80−49809
Ge-Sb, D^- complexes and band form., photocond. 78−84251
Ge-Si, single crysts., photocond. 79−87126
Ge-Si_3N_4 system, potential barriers determ. from photoinjection carriers trapping 80−103756
Ge-ZnSe p-n heterojunctions, effect of interfacial condition on optoelectronic props. 79−24061
n-$Ge_{1-x}Al_xAs$:Te, long-lifetime photocond. effect obs., Hall effect meas. 77−89795
p-GeS, crystalline, photoelectric props. 80−70769
GeS film, photocond. kinetics 77−39897
GeS, interband transitions, intrinsic photocond., anisotropy 80−20244
Ge_2S_3, electron irradiated, effects on elec., photoelec. and optical props. 80−49806
Ge_2S_3-Ag contact, photoinduced diffusion of Ag in amorphous semicond. film 80−49418
GeS_xSe_{1-x}, form. of solid soln. and phys. props. *(Russian)* 77−1232
GeSe, amorphous film, photocond. meas. 77−43647
GeSe amorphous films, recombination model 78−64061
$GeSe_2$, amorphous film, photocond., photo-induced ESR, optical edge shift 80−49809
$GeSe_2$ amorphous layers, photoconductance meas. 80−65632
$GeSe_2$, drift mobilities of electrons and holes, photocurrent decay meas. 80−2424
Ge_xSe_{1-x} amorphous film, photocrystallisation, elec. cond. meas. 79−32911
Ge_xSe_{1-x} amorphous film, photocrystn., elec. cond. and optical microscopy obs. 79−87024
Ge_xSe_{1-x} chalcogenide glasses, drift mobility of optically injected carriers 79−19627
$Ge_{1-x}Si_x$, with Si implanted ions, optical and photoelec. props. 79−24014
Ge_xSi_{1-x}, solid solution, single crystal, photoconductivity *(Russian)* 79−11170
Ge_xSi_{1-x}:Cu, solid soln., single cryst., photocond. spectra 79−24015
n-HgCdTe, photocond., Hall mobility and resist. 80−34478
HgCdTe, radiation effects on low-temp. carrier recombination lifetimes, photocond. meas. 78−6400
HgCdTe, recomb. effects, mag. quantum oscills. in Auger transition rate 79−82610
$Hg_{1-x}Cd_xTe$, carrier conc., Hall effect, photocond., IR spectra meas. 80−49771
$Hg_{1-x}Cd_xTe$ hot-electron photoconductive detection of near mm wave radiation 80−57377
$Hg_{1-x}Cd_xTe$, recombination processes using impact ionization capture cross sections 80−75577
n$Hg_{1-x}Cd_xTe$, single-phonon and plasmon recomb. lifetime effect, with magnetically tuned bandgap 79−38098
$Hg_{a-x}Cd_xTe$, single-LO-phonon and -plasmon recombination channels narrow-bandgaps 78−91728
$HgCr_2Se_4$, thermoreflectance, photoconductance, Raman scatt. near mag. phase transition 80−97298
$HgGa_2Se_4$, anisotropic photocond., pleochroism, and band struct. 78−19094
HgI_2, and photomagnetoelectric and photocond. meas., carrier lifetimes 77−55562
HgI_2, layered, photoelectromag. effect meas. of transport parameters 77−59301
HgI_2, mobility anisotropy determ. by photoelectromag. effect and photocond. 79−38126
HgI_2, photo-EM effect and photocond., trapping effects 77−32042
HgI_2, photoelectronic props. 78−41897
HgI_2, photomagnetoelectric effect anisotropy, photocond. 77−15897
HgI_2:Ag, trapping effects, TSC, photocond. and photolum. meas. 77−32023
HgI_2-CdS mixed system, photocond. depend. on composition and binder content 79−51625
α-HgS films, sputter-deposited in Hg vapour, growth and props. 80−75467
$HgSb_4S_8$, photosensitive semiconductors with high permittivity, elec. props. 79−65518
HgSe film, anomalous photocond., electron microscope study 80−65623
HgSe, film form. in amorphous Se:Hg, photocond. anomaly 77−66183
HgSe film on Se, dark relax. of anomalous photocond., photofield model 77−51776
HgTe, photocond. and magnetoabsorption, 1.4-20K 78−34859
p-In-Sb, effect of static mag. fields on transverse photocurrent spectrum 78−14766
InAs, intrinsic point defects, nature and influence on electrophys. props. 78−79609
InAs, laser excitation, photocond., optical absorpt., electron-hole scatt. 77−43661
n-InAs, negative photocond. and photomemory due to pot. barrier on surface 79−19620
n-InAs, oscillations in photocond. and photomag. effects 77−4405
n-InAs, photoelectric props., inhomogeneous impurity distrib. 80−107867
n-InAs:Cd, p-n junction, photosensitivity spectra depend. on mag. field 79−91137
InAs:S(Mg), ion implanted, photocond., photo-EMF, and optical absorpt. spectra 80−70763
InAs/$LiNbO_3$ structure, SAW generated transverse acoustoelectric voltage, image scanning and signal processing appl. 80−49826
p-InAs-Au contacts, influence of free surface on elec. behaviour 78−95362
InAs-GaSb heterojunction, photoelec. props. 77−28245
$InAs_{1-x}Sb_x$ p-n junctions, avalanche multiplication 80−6965
In_2O_3-SnO_2-Si SIS solar cells, reverse current-voltage characts. under illumination 80−89622
InP, electrical and optical props. at low temps. 80−39636
n-InP, magneto-impurity effect, review 79−91081
InP, n- and p-type, surface recomb. vel. meas., diffr. from transient optical grating 79−1604
n-InP, oscill. intrinsic photocond. 79−60871
photoconductivity continued
InP:Fe, deep acceptor levels, photocond. meas. 80−20116
InP:Fe, photocond., Fe^{2+} intracentre excitation model 80−29436
InP:Fe, resonance photocond. 80−44651
InP:Fe shallow trap thermally stimulated cond. spectroscopy, photocond. spectrum under DC conditions 80−65585
InP-InGaAsP p-n junction avalanche photodiodes, surface passivation techniques 80−100508
In_2S_3, film struct. and props. 77−80706
InSb, absorpt. processes near bandgap, laser-induced hot electron and photocond. meas. 79−42584
n-InSb, absorption of millimetre radiation in mag. field 79−11083
n-InSb, compensated, LF current instabilities 79−7859
InSb, covered with thin oxide protective film, intrinsic photocond. 77−55578
p-InSb, cyclotron reson. of nonequilib. photoelectrons, distrib. function and line profile 78−60336
p-InSb, deformed, Landau levels, photocurrent spectra obs. 78−19097
n-InSb, deformed, spectral oscills. of absorption in quantising mag. field 80−34486
InSb, donor excitation spectra in high mag. field 78−80027
InSb, donor spectrum, effect of strong mag. field 79−7806
InSb, doping depend. of high-field donor spectra 77−90175
n-InSb, H-like impurities photocond., mag. field effect 79−82634
InSb, high-resistivity p-type or crystals of n-type, recombination processes, photocond. and photomag. effect meas. *(Russian)* 80−88567
n-InSb, hopping photoconductivity *(Russian)* 77−89801
InSb, intraband photocond. in mag. fields 79−47123
InSb, intrinsic, photoinjected electron hole pairs, Auger lifetime, photoconductive decay obs. 80−39629
n-InSb, laser induced magneto-photoconductivity, conduction band transitions 77−55566
InSb MOS structs., energy spectrum of traps in oxide layer 80−107922
n-InSb, magneto-optical transitions from deep levels, photocond. obs. 80−55069
n-InSb, magneto-photoconductivity, phonon assisted combined reson. magneto-optical absorpt. reson. 78−47831
InSb n^+-p junctions, photocurrent spectrum near long wavelength edge of fundamental absorption band 80−100483
n-InSb, n-type, photoconductivity with different surface treatment 78−2517
p-InSb, negative photocond. in strong mag. fields 79−82636
InSb, optical mixing by mobile carriers 78−25920
n-InSb, optical phonon emission in intraband magneto-optical transitions, photocond. meas. 80−34481
p-InSb, oscills. of microwave photocond. and cyclotron reson. of photoelectrons 79−28377
InSb, oxidised surface, photocond. meas. *(Russian)* 77−43664
InSb p-n junctions, diffused, avalanche multiplication and impact ionisation 80−15595
p-InSb, phonon assisted cyclotron harmonic transitions 78−48046
n-InSb, phonon-assisted cyclotron reson. strongly depend. on surface condition 80−70755
n-InSb, photo-induced magnetophonon reson., 4.2K, peak shifts 78−84250
InSb, photocond. under uniaxial deform. 79−82637
InSb, photoconductive and photoelectromag. effect spectral distrib., sample thickness depend. 77−4394
n-InSb, photoconductive lifetime, surface pot. effects 80−11029
n-InSb, photoconductivity, 1.8K, hot-carrier and free-carrier absorption. effects 78−84254
n-InSb, photoconductivity, recombination processes 80−11030
n-InSb, photoconductivity meas. in crossed fields 79−7852
n-InSb, photoconductivity of laser excited hot electrons 80−11045
n-InSb, photoconductivity mechanism, 4.2 to 77K 80−70766
InSb, photoresistor in mag. field, increased responsivity 78−39162
n-InSb photoresistors of Carbino disc shape in mag. field, enhancement of responsivity 78−56186
p-InSb, quantum oscills. of photocurrent due to relax. of photoelectron energies via acoustic phonons 79−73546
n-InSb, recomb. of hot electrons, photoelectromag. and dynamic photocond. meas. 79−38081
InSb, recombination processes using impact ionization capture cross sections 80−75577
n-InSb, sub mm photocond. *(Russian)* 79−38134
p-InSb, uniaxially stressed, elec. cond., Hall coeff. and photocond. at 15K 77−47828
n-InSb, weakly compensated, sub MM photocond. 80−15565
InSb:Cr, electron and hole lifetimes, recomb. at trapping and acceptor levels 77−51760
p-InSb:Ge, photocond. in quantising mag. field, uniaxial press. influence 77−15907
InSb:Ge annealing effect on electrical parameters, absorption spectra and photocond. 77−11939
InSb-NiSb plate, transverse EMF due to modulated illumination 77−55572
InSe, anomalous photocond. obs. 77−76869
InSe, characts. of photocond. in strong absorption region 77−66184
InSe, current induced by impurity-absorbed IR radiation 78−10511
InSe, direct gap exciton exam. by magneto-optics and photoconductivity 79−19527
InSe films, residual photocond., field quenching 80−60037
n-InSe, influence of elec. fields on anomalous photocond. 77−8147
InSe, LF oscills. of current 78−56187
n-InSe, negative photocond. and photocurrent quenching under impurity excitation conditions 77−4399
n-InSe, optical spectra, photocond. and resistivity 78−88321
InSe, photoconductivity anisotropy at high optical excitation levels *(Russian)* 80−103721
InSe, photoelec. props. 79−73543
InSe, photosensitivity anisotropy in polarised light, pleochroism coeff., suitability as photoelec. analysers 79−60873
In_2Te_3 defect semicond., photoconductivity kinetics 80−11035
In_2Te_3, photosensitivity on γ- and neutron-irrad., γ-ray dosimeter mat. applic. 77−85258
α-In_2Te_3 single crysts., elec. and photocond., temp. depend., linear thermal expansion coeff. 79−42541
In_2Te_5, photocond. and absorption spectra, polarisation dependences 80−20642
$(In_2Te_3)_x(Hg_3Te_3)_{1-x}$, characts. of photocond. in strong absorption region 77−66184

photoconductivity continued
$(In_2Te_3)x$-$(Hg_3Te_3)_{1-x}$, $0.15 \leq x \leq 0.37$, E_g-comp. depend., spectral photo EMF meas. 77−47851
KCl, coloured, trap-controlled photoelectron mobility, transit-time expts. 77−72880
KCl, ion processes in F→Z_1 transition, photocond. meas. 77−15412
KCl, photoconductivity during F→X transition *(Russian)* 77−43663
KH_2PO_4(KD_2PO_4), photoelectric phenomena, nonlinear optical rectification *(Russian)* 79−19628
KH_2PO_4, KD_2PO_4, crystals, photoresponse under laser irrad., impurity photocond. 80−100479
$KNbO_3$, photoconductivity and TSC 78−2520
$KNbO_3$, photoferroelectric effects 78−92029
$KNbO_3$, photovoltaic effect lux ampere characts., photoconductivity 80−15561
$KNbO_3$, reduced, phase hologram recording, energy transfer and sensitivity 80−69338
$KNbO_3$:Fe, ferroelec., anomalous photovoltaic effect and photocond. 78−52449
$KNbO_3$:Fe, photorefr. effects and photocurrents 78−43434
$KNbO_3$:Fe, photovoltages, photocurrents and photorefractive effects 79−42580
$KNbO_3$:Fe, thermal and spectral variations in the photovoltaic current in ferroelectrics 78−91719
$KTaO_3$, photoconducting, negative differential conductivity 79−65515
$KTaO_3$, photoconduction in ferroelectrics 78−91720
$La_2Ti_2O_7$, ferroelecs., nonlinear optical props. 80−33086
LiCl aqueous glass, X-irradiated, localised electron optical, IR and photoconductivity spectra 78−73064
LiH (D), single crystals, electronic excitations, review *(Russian)* 78−72574
LiH, excitons, reflection, cathodolum. and photocond.-excitation spectra 78−10989
LiH, ionic cond., thermocurrent and photocond., defect and electronic props. 77−15621
LiH, single crysts., refl. photolum., cathodolum., and photocond. meas. 77−52186
$LiNbO_3$, anomalous photovoltaic effect and photocond. 78−52449
$LiNbO_3$, anomalous photovoltaic effect and photocond. 79−38122
$LiNbO_3$, doped, photorefr. and photovoltaic effects 77−38835
$LiNbO_3$, laser induced optical inhomogeneity in external electric field 79−95730
$LiNbO_3$, photocond. induced by N_2 laser *(Japanese)* 78−2521
$LiNbO_3$, photorefractive effect sensitivity 78−43833
$LiNbO_3$ pure and Fe doped, IR induced acousto-photorefractive memory effect 80−80746
$LiNbO_3$, thermal and spectral variations in the photovoltaic current in ferroelectrics 78−91719
$LiNbO_3$:Cu(Fe), light induced charge transport, photovoltaic effects, impurity states 80−80317
$LiNbO_3$:Fe, anomalous photovoltaic effect in polarised light *(Russian)* 80−34484
$LiNbO_3$:Fe, electro-optic cryst., light induced charge transport, holographic obs. 80−70747
$LiNbO_3$:Fe, induced optical inhomogeneity, refr. index and short-circuit photocurrent meas. 79−69806
$LiNbO_3$:Fe, optical damage induced by laser light, X-ray irrad., carrier mobility effects 79−33657
$LiNbO_3$:Fe, origin of photoelectrons and conc. of point defects 77−43645
$LiNbO_3$:Fe, photocond. and photorefractive effects 79−38124
$LiNbO_3$:Fe, photovoltaic effect and charge transport mechanism 79−38123
$LiNbO_3$:Fe, pure and doped, photocond. and dark cond. 80−29439
$LiNbO_3$:Mn, photorefractive sensitivity, holographic and photocurrent investig. 77−24581
$LiNbO_3$:transition metal, photorefr. effect, 1.5-4.0 eV 77−28213
$LiNbO_3$-CdS, layered structure, transverse acousto-electric current 80−44669
$LiTaO_3$, characterisation as holographic storage materials 78−29909
$LiTaO_3$, photorefractive sensitivity, holographic and photocurrent investig. 77−24581
$LiTaO_3$:Cu(Fe), light induced charge transport, photovoltaic effects, impurity states 80−80317
$LiTaO_3$:Fe, electro-optic cryst., light induced charge transport, holographic obs. 80−70747
MOS capacitor, photoionisation cross section and interface state density 80−92974
MOS, photocurrent-voltage characts., insulator bulk trapped charge 78−30991
MgF_2, X-irradiated, radiation conductivity 79−69555
$MgSiP_2$, elec. props. and diode struct. exam. 79−51665
NH_3 electrolyte-semiconductor interface, photo-assisted electron injection 79−87152
NaCl crystal with aggregate colour centres, photocond. kinetics 78−19100
$NaNbO_3$, elec. and photoelec. props. near ferroelec.-antiferroelec. phase transition 80−15989
$NaNbO_3$, photoconductivity and TSC 78−2520
$NaSbSe_2$ films, struct., photoelec. and opt. props. 78−51834
Nb_2O_5, electron energy spectrum by optical and thermal methods 79−69418
Ni-Cr, interband absorpt. and refractive index, photoconductivity dispersion function 77−36263
Ni-Nichrome, MOM diode, breakdown effect in visible and near-IR regions 80−6999
$NiBr_2$, photoconductivity spectrum meas. using rate of charge method, transport props. 78−60160
NiO, transient photocond. 78−60163
$NiPS_3$, layered semiconductors, optical and electronic props. 80−70761
P, amorphous thin film, photocond., spectral depend. 79−24011
PLZT ceramics, optical recording *(French)* 77−31078
PLZT ceramics, transparent ferroelec., photorefraction and photocond. study 79−42581
PLZT ceramics photosensitivity enhancement by H- and He-ion implantation 80−96934
PLZT, photorefractive effect and photoconductivity 78−92046
Pb chalcogenides, spectral depend. of internal quantum efficiency 77−4402
$Pb_9As_4S_{15}$, gratonite, single crystal, photoelectric props. 80−49822
photoconductivity continued
$Pb_5Ge_3O_{11}$, pulsed polarisation switching process depend. on illumination 80−93253
$Pb_{1-x}Ge_xTe$:Ga, Fermi level stabilization, transport props. meas., 77-400K 78−56065
PbI_2 (2H), electronic transport and cyclotron reson. 79−28369
PbI_2, cryst., photocond., energy gap localised level obs. 78−43443
PbI_2 film, photolyzed, refr. index change 78−11010
PbI_2, layered, photoelectromag. effect meas. of transport parameters 77−59301
PbI_2, photocond. induced by polaritons at band-edge 79−95450
PbI_2, photoelectromagnetic investigation, expt. 79−24010
PbI_2, single cryst., luminesc., photocond. and absorpt. after thermal treatment 79−56855
PbI_2 two-photon absorpt. cond. and luminesc. meas. 77−52166
PbI_2-Ag(Au)(Cu), light sensitive, internal photoelectric emission 80−107910
$PbMg_{1/3}Nb_{2/3}O_3$, electro-opt., elasto-opt., opt. and photo-induced props. 78−95560
$PbMg_{1/3}Nb_{2/3}O_3$, photocond., 20-150°C; and photoelectret state 77−24590
$PbMg_{1/3}Nb_{2/3}O_3$, photoinduced phenomena at diffuse phase transition 78−43814
$PbMoO_4$, near-edge absorpt. band, fluoresc. and photocond. 77−44017
$PbMoO_4$, photoconductivity spectral depend. 79−7856
PbO powder layers, adsorbed rhodamine B dye, charge storage and photocond. 78−64056
PbO, reactively evaporated photoconductive film, phase transform. induced by water vapour 79−78233
PbO single crystals, current-voltage characts., electrolum. *(Russian)* 80−2863
PbS, chem. deposited thin film, effect of morphological struct. on photosensitivity 80−70760
PbS, chemically deposited film, photosensitivity, effect of morphological struct. 79−82647
PbS film, form. by chem. spraying, elec. and optical props. 78−2588
PbS film, photosensitivity, role of surface oxide and ion bombardment 77−24631
PbS, thin film, photoconductivity expts. 79−78130
PbS-base photodetectors, struct. invest. by proton irrad. 80−104388
PbS-Ge heterojunction, influence of conduction band discontinuity on lux-ampere characts. 78−39200
PbS-PbO vacuum evaporated films, elec. cond. and photocond. 80−75656
PbS-Sb_2S_3 semicond., optical and photoelec. behaviour 80−96938
PbS-Si, photosensitive p-n heterojunction, energy band diagram 79−95489
$Pb_6Sb_{14}S_{27}$, zinkenite, electrophysical properties 78−34834
PbSe, film, photoconductivity, temp. depend. 79−38200
PbSe, polycryst. film, low temp. illumination, residual cond. 77−43756
$Pb_{1-x}Sn_xSe$, displacive transition, temp. and press. depend., elec. meas. 80−10672
$Pb_{1-x}Sn_xSe(Te)$:I epitaxial layers, photoelectric props., doping donor impurity behaviour 77−80810
$Pb_{0.78}Sn_{0.22}Te$:In, transport phenomena, below 20K *(Russian)* 79−38074
$Pb_{0.78}Sn_{0.22}Te$:In epitaxial layers, dislocation density, Hall effect, conductivity, photoeffects 80−25024
$Pb_{0.8}Sn_{0.2}Te$-PbTe p-n heterojunction, prep., elec. and photoelec. props. 79−51664
$Pb_{0.83}Sn_{0.17}Te$, recomb. at high levels of optical excitation 78−10503
$Pb_{1-x}Sn_xTe$, Cd-In diffusion, changes in elec. props. 78−91348
$Pb_{1-x}Sn_xTe$, charact. of photocond., 12-130K 78−26914
p-$Pb_{1-x}Sn_xTe$, electron irrad., photosensitivity at 10.6 μ, increase after electron bombardment 79−56227
$Pb_{1-x}Sn_xTe$, epitaxial layers, carrier lifetime meas. 79−42559
$Pb_{1-x}Sn_xTe$ film, Burstein-Moss effect, absorpt. and photocond. spectra 78−18961
$Pb_{1-x}Sn_xTe$, inter- and intraband magneto-optical transitions 80−25346
$Pb_{1-x}Sn_xTe$, photoconduct., photoelectromag. effect, laser intensity depend., carrier lifetimes 77−15896
$Pb_{1-x}Sn_xTe$, single cryst. grown from vapour, photocond. meas. 79−24016
$Pb_{1-x}Sn_xTe$, small-gap, recomb. mech. 79−38099
$Pb_{1-x}Sn_xTe$:Cd, impurity photocond. spectra 80−6902
$Pb_{1-x}Sn_xTe$:Cd, long-wavelength photosensitivity shift on annealing, Cd influence 78−26912
$Pb_{1-x}Sn_xTe$:Cd, photocond., photomag. effect, carrier lifetimes 80−44658
$Pb_{1-x}Sn_xTe$:Cd, photoelec. props., surface recomb. effect 80−44659
$Pb_{1-x}Sn_xTe$:In, Hall effect and photoconductivity *(Russian)* 80−103720
$Pb_{1-x}Sn_xTe$:In(Cd), photoconductivity 78−23129
$Pb_{1-x}Sn_xY$, Y=Te, Se, S, photocond. anisotropy rel. to lifetimes 78−52032
PbTe, Auger recomb., photocond. decay time expts. 77−72879
PbTe epitaxial films, carrier recomb. and deep levels, photocond., Hall effect, and luminesc. meas. 79−38024
PbTe, epitaxial layers, carrier lifetime meas. 79−42559
PbTe film, characts. of photocond. spectra and reflectivity 77−55624
PbTe film, residual conductivity 78−2595
PbTe film, struct. anal. and sensitisation 78−22982
PbTe, polycryst. film, RF sputtered, time stability 77−43758
PbTe, resonant scattering, photocond. 80−6910
PbTe:Bi-PbSmTe-PbTe, epitaxial laser struct., growth, p-n junction position and lasing region 79−89908
$PbTiO_3$, anomalies in elec., photoelectric and mechanical props. 80−55051
$PbTiO_3$, ferroelec. phase, photocond. and photovoltaic effect, temp. depend. 78−95309
$PbTiO_3$, photocond. and TSC meas. 77−15911
$PbTi_3O_7$, photocond. and optical transmission 78−64058
PbX_2, PbFX, X=Cl, Br, photoconductivity obs. 77−43650
$PbZn_{1/3}Nb_{2/3}O_3$, electro-opt., elasto-opt., opt. and photo-induced props. 78−95560
PdO, semiconductivity and stability, optical props. 78−43497
Pt electrode, in liq. NH_3, photoelectron emission 79−60868
Pt island film photoconductivity obs. 78−95392
$RbAg_4I_5$-metal interface, photocurrents, photoelectrochem. effects 78−34897
Rb_2ZnBr_4, ferroelec., photovoltaic and photorefractive phenomena 80−75598

photoconductivity continued
Ru complex, Ru(2,2′-bipyridine)$_3$Cl$_2$-6H$_2$O, photocond., optical absorpt. and fluoresc. 77−80807
S, orthorhombic, photogeneration of charge carriers 80−107844
S, polycryst., photoelectret state following X-irrad. 80−60485
Sb-S-I system crystals and glasses, adhesion levels, TCE spectra 77−24529
$SbNbO_4$, anomalous photovoltaic effect and photocond. 79−38122
$SbNbO_4$, ferroelec. anomalous photovoltaic effect and photocond. 78−52449
Sb_2O_3 anodic layers on Sb, semicond. props. 79−56303
Sb_5O_7I, polytypes 2MC and 2MA, photoferroelastic phenomena 79−95447
Sb_2S_3, amorphous layer, scattering of visible light, rel. to substrate temp. during deposition 79−65950
Sb_2S_3, defect drift in elec. fields and bistable switching 80−92947
Sb_2S_3, phase transitions and improper photoconductivity, effect of growth conditions *(German)* 78−39515
Sb_2S_3, vacuum deposited films, struct. and photoelec. props. 77−85092
SbSI, ferroelec. semicond. near phase transition, anomalies of photocond. 79−42579
SbSI, ferroelectric, dark current and spontaneous polarisation, ferro-paraelectric transitions obs. 80−60521
SbSI, photoelectric current, modulated due to light intensity 79−19626
SbSI-BiSI, solid solns., phase diagrams, photocond., elec. props. 79−38125
Sb_2Se_3, energy gap, light absorpt., elec. cond., photocond. meas. 78−47826
Sb_2Se_3 film, struct. and photoelec. props. 77−85257
Sb_2Se_3, photocond., photo-EMF and photodielectric effect, expts. 80−20245
$(Sb_2Se_3)_x$-$(Bi_2S_3)_{1-x}$ single crystals, elec. and photoelec. props., stoichiometry deviations influence 79−60870
$(Sb_2Se_3)_{0.7}(Bi_2Se_3)_{0.3}$, solid soln., prep. and elec. properties of layered crystals 80−70762
Se, amorphous, photoconductivity quantum yield, experimental validation of fund. theory 80−6909
Se, amorphous, thermal quenching of photocond. 78−23137
Se, amorphous film, dark and photoconductivities 79−87173
Se, amorphous film, influence of wavelength on optical quenching of photoconductivity 80−60046
Se, amorphous film, photocond., dark cond., rel. to crystn. 80−88596
Se amorphous film, stabilisation by thermal treatment *(French)* 79−47176
Se, amorphous layer, localised states in band gap 80−59928
Se film, amorphous *(French)* 77−72886
p-Se film, photocond., phase-memory effect 78−91723
Se, Hg activated amorphous film, anomalous photocond. 77−43658
Se layers, amorphous, steady-state photocond. meas. 77−35961
Se, modulated photocurrent, analysed for trap-limited case *(Japanese)* 80−60030
α-Se, multiple-trapping model and time-dependent random walk 78−34842
α-Se, multiple-trapping model of anomalous transit time dispersion, transient photocurrent data 78−34860
Se, photoelectronic behaviour, in glass transition region 80−60045
Se, photosensitive particle migration, electrophotographic film structure and process 80−101863
Se, polycryst., low-frequency coupled photocurrent and temp. oscillation 80−60044
Se, polycrystalline trigonal layer, freq. depend. elec. behaviour and its relationship to xerographic performance of Se particle contact photoreceptors 79−82640
Se, single crystals, fast neutron irradiated, annealing expts., dark conductance, reflectivity spectra 77−85266
Se, trigonal, transverse magnetoresistance meas., influence of illumination 80−65607
Se, trigonal single crystal, dark current relax., barrier cond. mech. 80−6904
Se, trigonal single crystal, peak in temp. dependence of elec. cond. 80−44663
Se, X-ray sensitivity, induced photocurrents, xeroradiographic meas., pair creation energy 80−22490
Se:Hg amorphous film, anomaly due to HgSe layer form. 77−66183
Se:Hg film, amorphous, anomalous photocond. and residual interelectrode photo-EMF 77−69376
Se:O, amorphous, photocond. spectrum impurity effect 77−76862
Se:Tl, hole drift mobility meas. by light pulse technique 78−19086
Se-As, photoelectronic behaviour, in glass transition region 80−60045
Se-Bi-I, amorphous, high sensitivity visible-near IR photoconductor development and characterisation 78−39153
Se-polystyrene hexylmethacrylate, interface photocurrent studies, charge transfer mechanism 79−99627
a-$Se_{97.5}As_{2.5}$, trapping, photo-stimulated and thermally-stimulated current obs. 77−28192
SeTe/Se multilayer photoreceptor, transient photoconductivity *(Japanese)* 80−75596
$Se_{1-x1}Te_{x1}$-$Se_{1-x2}Te_{x2}$ heterostructure, amorphous, rectification phenomena and photovoltaic effects 79−99610
p-Si (100) inversion layers, intersubband spectroscopy by photocond. and absorpt. 78−10566
Si, adsorbed Pd impurity, effect on surface electronic props. *(Russian)* 79−91124
Si, amorphous, control of dihydride bond density using RF sputtering, dark anal. and photocond. 80−34327
Si, amorphous, discharge produced, reversible cond. changes 77−85256
Si, amorphous, discharge produced, optical and photocond. props. 78−39147
Si, amorphous, doped, drift and Hall mobility, photocond. 79−65477
Si, amorphous, doped, photoconductivity and recomb. meas. 77−89800
Si, amorphous, elec. and opt. props., review 78−23094
Si, amorphous, elec. props., ion implantation effects 80−79828
Si, amorphous, electrical transport and photocond. 77−85355
Si, amorphous, electron-hole recombination, mech. 78−72196
Si, amorphous, photo-induced changes in elec. props., defect states 79−82553
Si, amorphous, photoconductivity, mag. field depend. 78−80023
Si, amorphous, photovoltaic diodes, influence of mag. field on charge transport 80−49891
Si, amorphous, prep. by RF sputtering, photoconductivity determ. 77−73231

photoconductivity continued
Si, amorphous, solar cells, and photovoltaic devices *(Japanese)* 80−50965
Si, amorphous, spin-depend. photocond. 77−59302
Si, amorphous, substantially doped, electronic props., review 79−87175
Si, amorphous, transport results interpretation 80−44590
Si, amorphous, transport results, interpretation 80−80260
Si, amorphous, undoped, photocond., continuous illum. effect 80−84486
Si, amorphous co-sputtered doped, photovoltaic material appl. 80−93488
Si, amorphous evaporated, picosecond optoelectronic detect., sampling and correlation meas. 80−100478
Si, amorphous film, drift mobility and photocond. 79−15143
Si amorphous film, sputter-deposited, elec., optical, and photoelectronic props. 79−24433
Si, amorphous films, halogenated and hydrogenated, elec. and optical props. 80−97016
Si, amorphous films, ion implanted, elec. and photocond. props. 80−49717
Si amorphous films, self-ion bombard., electronic props. 79−28422
Si, amorphous glow discharge films, H_2 content, elec. props., and photostability 80−25577
Si, amorphous hydrogenated solar cells, field depend. quantum efficiency, electron-hole recombination 80−66971
Si, amorphous sputtered film, elec. cond. and photocond. 79−87097
Si based alloys, amorphous, photovoltaic behaviour, solar cell appl. 80−94051
Si based MIS structure, photoelectric characts. carrier injection levels *(Russian)* 80−96946
Si, CVD films, polycryst., elec. and optical props., electronic density of states model 79−56332
Si, carrier lifetime, comparison of meas. by photocond. decay and surface photovoltage 78−68038
p-Si, compensated by radiation defect centres, photoresistors 77−62961
P-Si, conductivity and carrier lifetime, high injection effects 80−70719
Si DC sputtered, amorphous, dark conductivity and photocond. obs. *(French)* 78−64155
Si, deep level transient spectroscopy *(French)* 79−11079
Si, dislocation energy spectrum, appl. of EPR and elec. meas. 79−82547
Si, dissociation of hot excitons by long-wavelength acoustic phonons, photocond. spectra 77−4300
Si, divacancy charge states, photoconductivity spectra 77−15899
Si, elec. props., plastic deform. and annealing temp. depend., dislocation effects *(Russian)* 77−89765
Si, electronic states of isolated negative donor ion, binding energy 79−65404
p-Si, energy spectrum and thermal stability of radiation defects, impurity photocond. spectra 77−4406
Si, epitaxial layers, minority carrier lifetime and diffusion length meas., photocurrent technique 78−95302
Si, exciton-plasma transitions, dense electron-hole system portrait composition *(Russian)* 80−49622
Si, heat treated, spin-depend. recomb. at dislocations 79−47122
Si, heteroepitaxial films, photomagnetoelectric effect 77−85264
Si, high level photogeneration, absorpt. and free carrier distrib. 79−33309
Si, homogeneous plates, theory of arising longitudinal photoeffect *(Russian)* 79−19614
Si, hydrogenated amorphous, gap states, comparison of photoemission and photocond. results 80−103724
Si, IR photoresponse at 1.15 microns 79−7864
n-Si, IR spectra of surface photocond. and photo-EMF 77−76868
Si, impurity determ. in very pure sample by photoelec. spectroscopy 77−39888
n-Si, influence of deform. on capture of electrons by divacancies 77−1449
Si, influence of surface recombination rate and carrier diffusion on photocond. 80−44660
Si inversion layer, far IR photoresponse 77−38002
Si inversion layer, photoconductivity meas. 78−10498
Si inversion layers, discrepancies between absorption and photocond. meas. 78−6451
Si, inversion layers, intervalley transitions and subband splitting 77−20455
n-Si, irradiated with large neutron doses, defect annealing 80−19849
Si, kinetics, effect of exciting illumination *(Russian)* 80−11032
Si, laser annealed, elec. props. 79−69609
Si, laser annealing at 1.06 μm, free carrier absorpt. role 80−24964
Si, laser-induced bulk breakdown and free carrier generation, photocond. meas. 80−35018
Si, local electron irrad., Frankel pair separation, influence on photo EMF 80−44203
Si MOSFET inversion layers, IR photocond. and absorption 78−64123
Si MOSFET structures, photocond. rel. to intersubband transitions 78−64127
n-Si, meas. of recomb. rates of non-equilib. carriers, absorption modulation method 77−55575
p-Si, millimetric and far-IR cond., freq.-depend. carrier relax time 80−34460
Si, neutron and electron bombard., radiation defect recomb., photoelec. props. meas. 80−60039
n-Si neutron and electron irrad., isochronous annealing influence on edge absorpt. 80−11449
n-Si, neutron or γ-irrad., elec. props., in strong elec. fields 79−95416
Si, nonequilib. carriers generated by Nd laser, relax. rate temp. depend. 78−26911
Si, nonideal, lifetime and diffusion length rel. to solar cell appl. 79−15192
Si, optically stimulated ESR, dielec. effects 77−73080
Si p-n heterojunction, DC sputtering growth, photocond. and photovoltaic effects 79−33337
Si p-n junction in surface region obtained by evaporation in UHV 78−39198
Si p-n junctions, high-voltage, elec. props. by optical scanning 80−6969
n-Si, photocond. of negative donor ion states, for far IR detect. 77−59299
Si, photoconductivity, extrinsic, contrib. by hopping through excited states of donors 78−6411
Si, photoelectric spectra of remanent impurities 79−87125
p-Si, piezo-spectroscopic study of influence of defects *(Russian)* 77−28607
Si, plastically deformed, spin-depend. charge transport 80−6895

photoconductivity continued
Si, polycrystalline, Hall mobility 80−60006
p-Si radiation defects due to 30 MeV proton irrad., rel. to solar energy convertors 78−71776
n-Si, Re-compensated, deep levels, electron traps, photocond. 77−15902
Si, recomb. centre study by spin-depend. photocond. 80−49805
Si, recombination at dislocations 79−38023
a-Si, resonant and non-resonant photoconductivity changes 80−49814
a-Si, resonant and non-resonant luminesc. changes theory 80−50410
Si shallow impurity bound states, IR spectroscopic obs. 77−39806
n-Si shallow impurity states for far IR heterodyne detection 77−38005
Si solar cells, light-enhanced diffusion length obs. by DC photocurrent meas. 79−39301
Si solar cells, polycrystalline n^+/p, computer model of spectral response and photocurrent 80−55853
Si, spin dependent recomb. at dislocations, EPR and photocond. 79−38095
Si, spin dependent recombination and photoconductive resonance 78−43439
Si, spin effects in electron transitions via dislocation states 79−82642
Si, spin-depend. recomb. at exchange-coupled dislocation centres 77−89725
Si, sputtered amorphous film, photocond. and electronic props., effects of annealing in plasma gas 80−44644
Si, surface, spin-depend. carrier recomb., photocond. expt. 78−19096
n-Si, surface photocond. and photo-emf spectra 79−73544
Si, temp. dependence, excitation with laser pulses *(Russian)* 80−11031
Si, temporary trap characteristic after heat treatment *(German)* 80−34459
Si, two-step photoconductivity by dislocations 78−14761
Si with thermal defects, photocond., effect of annealing on elec. resist. 80−6837
Si, X-irrad., photocond. spectrum 77−15903
p-Si, X-irrad., subthreshold defect prod., Hall meas. of carrier conc. and photocond. spectra 77−89470
Si:Ag, photoexcitation of electrons from ionised AG acceptors 78−2519
Si:As, neutron damage mechs. in IR detectors 78−30668
Si:As detector, high-low junction contact at low temp. 77−39925
Si:Au, impurity photocond., for IR electrophotographic system 77−24589
Si:Au, nonequilib. population of electron states and photomemory of surface pot. 78−56206
Si:B, irrad. with fast neutrons true profiles of impurity photocond. bands from piezodichroisms 79−91103
Si:B, photoconductivity, impact neutralisation of H^--like centres 77−69377
Si:B photodiode front region collection efficiency models 80−96899
Si:B(P), amorphous, photo- and dark conductivity 77−28216
Si:B(P), photocond. spectra of H^--H^+-type complexes 79−95451
Si:Cd n^+-n-n^+ structs., photoresist. props. under exclusion conditions 80−39666
Si:Cd(Zn), n^+-n-n^+ structure, photocond. lifetimes, deep level occupancy in exclusion region 78−72253
Si:Cr, photoconductivity exam. 77−20361
Si:Cu, photocond. spectra and IR quenching 77−55568
Si:F, H amorphous films, optical props., photoconductivity, photostructural changes 80−11034
Si:F,H, amorphous, elec. and optical props. 80−60031
Si:F,H, amorphous, glow discharge deposited elec. props. and device aspects 80−44744
Si:Fe, photoconductivity and Hall effect 79−4579
Si:Fe(Au)(Pt)(Ag)(Ti), photoionisation cross-sections and energy levels 79−87060
p-Si:Ga, neutron transmutation counterdoped, shallow defect levels, Hall effect and photocond. obs. 79−87055
Si:Ga, possibility of use in fabrication of fast response photodetectors 79−15184
Si:Ga (Al)(In) extrinsic detector material props. 77−89797
n-Si:Gd, depth of energy levels of As and P from impurity photocond. 79−90996
Si:Gd(Pr), photoconductivity anomalies due to mag. impurities *(Russian)* 80−103722
Si:H, amorphous, band tail absorpt., photocurrent meas. for Schottky barrier solar cell 80−60032
Si:H, amorphous, discharge prod., optically induced cond. changes 80−96937
Si:H, amorphous, effect of gap state density on photocond. and photolum. 79−91096
Si:H, amorphous, excess carrier thermalisation and recomb., luminesc. decay and photocond. 80−50397
Si:H, amorphous, HV photovoltaic cells, design parameters 80−101105
n-Si:H, amorphous, photoelectromagnetic effect 80−107845
Si:H, amorphous, plasma-deposited, effect of DC elec. field superimposed during deposition 80−44643
Si:H, amorphous, prod. by high temp. thermal decomp. of SiH_4, and photocond. 79−87585
Si:H, amorphous, RF sputtered, suitability as solar cell material 80−40864
Si:H, amorphous, Schottky diodes, elec. props., light-induced effects 80−103741
Si:H, amorphous, solar cell struct., photocurrent meas., absorpt. coeff. 80−50960
Si:H, amorphous, sputtered on $Gd_2(MoO_4)_3$, ferroelec. domain wall motion, image scanning 80−83663
Si:H, amorphous field induced and quenched-in excess cond. 80−24968
Si:H, amorphous film, anal. of intrinsic photocond. spectrum 79−73541
Si:H, amorphous film, prep. by plasma decomp. of SiH_4 under mag. field, and characterisation 80−45239
Si:H, amorphous thin film solar cells 80−81478
Si:H, amorphouse film, optical and elec. props. 79−82694
Si:H, Cl(F), amorphous, photocond., dark cond. and photoluminesc. 80−49802
Si:H, evaporated amorphous film, prep. elec. cond. and photocond. 79−38201
a-Si:H, spin defect and recombination influence on electronic transport 80−50409
Si:H,P, amorphous, heavily hydrogenated, high gap state densities 80−49803
Si:H amorphous, solar cell structure, optical absorption by gap states 80−94052
photoconductivity continued
Si:H amorphous films, optoelectronic behaviour depend. on impurity incorporation during plasma deposition 80−49804
Si:H amorphous films, photovoltaic and photocond. spectra, photoluminesc. 80−44645
Si:H amorphous films, photoinduced optical absorpt. and photocond. 80−50361
Si:H amorphous films, role of Ar in deposition process, IR absorpt. and photocond. meas. 80−50321
Si:H amorphous films for solar cells, optical and elec. props. of RF glow discharge deposited films 80−54576
Si:H amorphous sputtered film, photoluminesc., photocond. 80−20729
Si:H film, amorphous, elec. cond., effect of adsorbed gases and illumination 78−88048
Si:H film, amorphous, photocond. imaging 80−1300
Si:H film, amorphous, reactively sputtered, H content effect on props. 80−49714
a-Si:H MIS junction, electronic struct. study by tunnelling 80−44729
a-Si:H solar cells, photoexcited carrier collection efficiency 79−100526
Si:In, neutron irrad. to compensate for residual B, photocond., iR focal plane array 78−67727
Si:In, new acceptor level 77−66136
Si:In, p-n junction, spin-dependent recomb. at dislocations, revealed at reverse current 79−24062
Si:In extrinsic detectors, compensation of residual B by neutron transmutation 78−281
Si:In extrinsic IR detector material with high responsivity compensated by neutron transmutation, float-zone growth 80−75597
Si:Mn, characts. of residual cond. 79−15188
p-Si:Mn, giant residual cond. 80−20250
Si:Mn, negative photoconductivity 79−38132
Si:Mn, photosensitivity, residual cond. effects 78−19099
p-Si:Mn, temp.-elec. instability, photocond. meas. 77−1448
Si:N, amorphous, DC sputtered, enhanced, photocond. 78−56183
Si:N, amorphous, prep. by RF sputtering and props. 80−44229
Si:Ni, capture probabilities of two deep impurity levels by photocond. decay 80−49799
Si:Ni,Co,Mn, γ-irrad., interaction of deep-level impurity atoms with radiation defects 77−76457
Si:Ni deep impurity levels, electron capture probabilities rel. to temp. 78−2523
Si:O, heat treated, excess carrier recomb. rate, defect levels 80−75579
Si:Os, P, photoelec. props., depend. on P conc. 79−91099
Si:P, amorphous, CVD, defect compensation 80−54644
Si:P, amorphous, CVD, substitutional doping, electronic props. 79−23923
Si:P, amorphous, substitutionally doped CVD, electrical props. 79−99566
Si:P, impurity doped, electron lifetime and transport in upper Hubbard band 79−95452
Si:P, polycryst. films, elec. props., EPR, defect states, doping effects 80−75660
n-Si:Pd, surface, photocond. and photo-emf spectra 79−73544
Si:Pt, photoionisation cross-sections, photocurrent and photocapacitance meas. 78−10497
Si:S IR detectors, performance and elec. transport props. 78−45702
Si:S p^+-n junction, optical props., photocurrent meas. 77−4425
Si:S(Se), IR absorption and photocond., donor levels 77−55809
Si:Sc, photocapacitance and photoconductivity 80−107859
Si:Se,B(Ga)(Al)(In), diffusion of Se, solubility and ionization levels, Hall effect and photocond. meas. 79−42486
Si:Y, photoelectric props. 80−107860
Si:Zn, resist. inhomogeneity effects on photoelec. props. 77−8151
Si/Si-Ge junction, elec. and photoelec. props. 78−10545
n-Si-Ag(Au) evaporated contact photoelectric props. *(Russian)* 78−43473
Si-$As_2Se_3Ge_4$ heterojunction, elec. props. 78−6434
Si-Au amorphous system, optical absorpt., IR photocond. 79−42582
n-Si-Au surface barrier diode, photosensitivity in spectral range, 1-6 eV 77−89850
Si-F-H amorphous alloy for electronic appls. 79−15627
Si-F-H amorphous solar cells, DC glow discharge fabrication 80−72041
Si-F-H:P, film, dark cond., struct., Raman scatt. 80−88588
Si-GaP, heterojunction, photosensitivity spectrum, characts. 79−24071
Si-Ge solid solns., p-n junctions, photoelec. props. obs. 77−1471
Si-H, RF sputtered amorphous alloy, influence of Ar press. on elec. props. and photoluminesc. 79−91585
Si-H amorphous film, reactively sputtered, prep. and props. 79−78889
Si-H:P amorphous film, dark cond., struct., Raman scatt. 80−88588
Si-P, excess carrier recomb., photocond. 79−65495
Si-SiO_2, SiO_2 layer charging in UV irrad. of MISS struct., photoinjection currents *(Russian)* 80−39680
Si-SiO_2 interface, electrically active paramag. centres detect., photocond. reson. obs. 80−50185
Si-SiO_2 interface, light induced reson. centres, photocond. reson., EPR obs. 80−50184
Si-SiO_2 systems, spectral characts. *(Russian)* 79−42657
Si-SiO_2-Al, interface barrier energies for tunnel oxides, internal photoemission meas. 80−84512
Si-SiO_2-Al with thick dielec. layer, photoelec. props. 80−92979
Si-SiO_2-Si_3N_4, internal photoemission 80−7475
Si-SiO_2-Si_3N_4 system, internal photoelec. emission and residual photoelec. effects 79−73599
Si-SiO_2-metal structures, tunnelling probabilities for electrons and holes in ultrathin SiO_2 from photocurrent meas. 79−99631
Si-TiO_x-Ni, MIS amorphous solar cell, increase in open-circuit voltage and short-circuit current on addition of TiO_x layer 79−57425
Si-V_2O_5 p-n heterostructure, photocond. *(Russian)* 79−42622
SiC, negative photoconductivity and photoconductivity quenching 78−6414
β-SiC, residual photocond. meas. 77−4408
α-SiC, short-wavelength photocond. and capacitance photo-EMF meas. 78−26906
$Si_{12}Ge_{10}As_{30}Te_{48}$, dark cond. and thermoelec. power, thermal activation energies interpret. 78−23123
$SiH_{0.16}$ amorphous films, optical props. and photocond. near optical gap 80−50443
SiH_x amorphous films, internal photoemission, metal contacts 80−96964
SiH_x discharge produced amorphous film, gap state role in carrier transport 79−73608
a-$Si_{1-x}H_x$, oxygenated thin film, sputtered, elec. cond. and optical props. 79−15239

photoconductivity continued
Si_3N_4 CVD films on Si, dark currents 79−78240
Si_3N_4 film, in MNS structures, dark conduction and photoconduction phenomena 78−30989
Si_3N_4 film, on W-coated Si, photocond., 1.31-3.10 eV, mechanism 79−19679
Si_3N_4 films on Si, photocurrents study 79−24092
$Si_xN_yO_z$ film, band diagram, optical props. and elec. cond. meas. 78−84333
SiO_2, As-implanted, electron trapping and detrapping characts. 80−65692
SiO_2 CVD layer, high current injection from Si rich SiO_2 film 80−80430
SiO_2 film, localised states, low-temp. photocurrent spectroscopy 78−19090
SiO_2, film, transmission, photocond. and band gap meas. 79−73540
SiO_2 film electron beam induced conductivity theory and expts. 80−15640
SiO_2 implantation with Al, trapped charge location obs., MOS struct. 79−15227
SiO_2, in MIM struct., dye sensitisation of photocond., steady state and pulse photoelectric props. 78−6408
SiO_2 in MOS struct., room temp. cond., mobile Na^+ location 78−39217
SiO_2 layers on Si, ionis. thresholds of electron traps 80−92983
SiO_2, thermally grown film, optical absorption and photocond. 78−64421
a-SiO_2, transient photocond. simulations using multiple-trap model 80−49801
SiO_2 tunnelling barrier asymmetry to electrons and holes in MOS struct., photocurrent 80−75645
SiO_2, vitreous, photoelectric and photoluminescent props. in fundamental absorpt. region 78−39596
SiO_2:As^+ implanted layers in MOS struct., electron trapping and detrapping characts. 80−92982
p-Si_2Te_3, photoelectric props., luminesc., hole lifetime and trapping 77−39892
Si_2Te_3, photoconductivity of cryst. with clean surface 77−4395
$Si_{10}Te_{40}As_{30}P_{20}$, amorphous films, optically assisted mono-stable switching 77−11968
SmS, semicond., photocond. meas. 78−60164
SnO_2 electrodes, dye-modified, erythrosin, attachment, X-ray photoelectron, photocond. investigs. 79−43600
SnO_2 far IR photoconductivity response obs. 77−38000
n-SnO_2, high resist., photoelectronic processes 78−60157
SnO_2, optical props. and photocond., review 77−1673
SnO_2, temp. and light flux dependence 78−80395
SnO_2-Si, heterojunction solar cells, anomalous photocurrent 80−3515
SnO_2-Si, solar cell, max. theoretical efficiency 79−83598
SnO_2-Si solar cells, electron-beam deposited, struct., photovolt. props. 80−50956
$Sn_2P_2S_6$, ferroelec., IR and Raman spectra, photocond., edge absorpt. spectra, spontaneous polarisation, forbidden gap 78−68514
$Sn_2P_2S_6$, illumination effect on soft mode and dielectric props., luminesc. study *(Russian)* 80−50420
p-SnS, IR photocond., direct and indirect gaps 78−2514
SnS, photoconductivity 77−72888
SnS_2, cryst. growth, photoconductivity 77−85912
$Sr_{0.65}Ba_{0.35}Nb_2O_6$, internal field distrib. and photorefraction 79−99843
$Sr_2Nb_2O_7$, electronic props. and photoresponses 80−92925
$Sr_2Nb_2O_7$, ferroelecs., nonlinear optical props. 80−33086
SrO, irradiated, low temp. photocond. 77−39891
SrO, luminesc. band edge, 4-6.5 eV, optical absorpt., photoluminesc., cathodoluminescence, photocond. obs. 80−50411
$SrTiO_3$ semicond. electrode, electrochem., photoelectrochem. props. 80−3352
$SrTiO_3$-Si junction, photoresponse 78−72254
p-Te, 1.6-4.2K, spectral features 77−24591
Te, carrier recombination at high optical excitation 77−72884
Te, energy gap meas. under press., photocond. and transmission spectra 77−85267
Te, impurity spectroscopy 80−65499
Te in MIS structure, impurity photocond. 78−72203
Te, interband photocond. at up to 10 kbar, 1.6-200K 77−47850
p-Te, magneto-impurity effect, review 79−91081
Te, negative photoconductivity, intraband absorpt. *(Russian)* 80−107854
Te, opt. props. under high press., band struct. transform. 80−55112
p-Te, photocond. and lifetime, surface trapping, spectral distrib. 78−34840
Te, photoconductivity in strong mag. fields, doping effects, impurity levels 80−75602
Te, photoconductivity under pulse excitation conditions 80−2425
Te, photon drag effect 77−1443
Te, spectrum in 1.6-4.2K band, nonequilibrium electron mobility *(Russian)* 77−11960
a-$Te_{40}As_{35}Ge_7Si_{18}$, trapping, photo-stimulated and thermally-stimulated current obs. 77−28192
Ti-oxide film electrode, photocurrents induced by subbandgap illumination 79−91094
TiO_2, crystalline, photocurrent spectral distribution 79−56259
TiO_2 electrode, carrier density determ. by optical absorpt. and photoelectrolysis spectra 80−71462
TiO_2 electrode, silanisation effects on semicond. props. 79−96364
n-TiO_2 electrode in $AlCl_3$-NaCl melt, electrochem. and photoelec. props. 80−81328
TiO_2 electrodes, chemically modified, nature of surface states 80−107905
TiO_2 electrodes in photoelectrochem. cell, photothermal effect 80−7947
TiO_2 photoelectrode, stability 77−20422
TiO_2 sputtered film, photocond. and TSC meas. 80−15560
TiO_2:V(Cr)(Mn)(Fe), impurity levels, photocurrent and ESR meas. 80−29346
TiO_2:Zn^{2+}, reduced by H_2, photoconductive props. 77−55558
TiO_{2-x}, comparison of photoelec. props. with system $TiO_{2-x}F_x$ 79−28371
$TiO_{2-x}F_x$, comparison of photoelec. props. with system TiO_{2-x} 79−28371
$TlGaS_2$, optical and photoelec. props. 77−55571
$TlGaS_2$, optical and photoelectric exam. 79−11180
$TlGaS_2$-$TlGaSe_2$, phase and composition-property diagrams 80−55366
$TlGaS_2(Se_2)$ film, elec. and photoelec. props. *(Russian)* 78−52109

photoconductivity continued
$TlGaS_xSe_{2-x}$, optical and photoelectric props., composition depend. 79−15183
$TlGaSe_2$, impurity conductivity and TSC 78−23128
$TlGaSe_2$, monocrystal, processes of recombination and trapping levels, photocond. meas. *(Russian)* 80−70751
$TlInS_2$-$TlInSe_2$, phase and composition-property diagrams 80−55366
$TlInS_2(Se_2)$, electrical cond. of single crysts. with symm. and asymm. Ag-In contacts 80−6835
$TlInS_xSe_{2-x}$ solid solution, optical and photoelectric props. 79−11179
$TlInSe_2$, single cryst., elec. cond., photocond. and IR spectra absorpt. spectrum 79−47097
$TlSbS_2$, photocond. characts. 77−4407
Tm, polycryst., optical props., temp. depend., photocond., relaxation parameters 78−84603
to film, vacuum-deposited, gas adsorpt. effects on photoelec. props. 78−15298
V_2O_5 crystal, photoinduced threshold switching in VO_2 channel 80−29450
V_2O_5, ferroelec. semicond., dielec. and elec. meas. 80−60516
V_2O_5 layer, amorphous, photocond. investig. using V_2O_5-n-Si system 77−76875
V_2O_5-Si, sandwich system, 380-1000 nm 77−32034
W-Ni, MOM diode, breakdown effect in visible and near-IR regions 80−6999
Zn silicates:Mn, sintered *(German)* 79−51627
ZnCdS:Cu, high field photoconduction in binder layer 79−47121
$Zn_xCd_{1-x}S$ film, prep. by soln. spray method, and struct., optical and elec. props. 78−52666
p-$Zn_xCd_{1-x}Te$, negative photocond. excited by fundamental absorpt. region light 77−15905
$ZnGeP_2$, single cryst., polarised light photocond., optical transparency anisotropy *(Russian)* 78−2518
$ZnIn_2S_4$ (I) film, one-packed polytype, resist., photocond. and luminesc. 79−1608
$ZnIn_2S_4$ film, photoluminesc. and photocond. 78−52677
$ZnIn_2S_4$-Ni diode, electric and photoelectric characts. 77−12005
$Zn_xIn_2S_{3+x}$, residual cond. 78−56185
ZnO crystal, adsorption of merocyanine dye, spectral sensitisation of photocond. 77−47854
ZnO crystals, adsorbed dye laser, charge transfer, field effect and spectrally sensitised photocond. meas. 80−49815
ZnO, electric field dependence of photoconductivity *(Russian)* 80−49821
ZnO electrode, role of triplet states in xanthene dye sensitisation 78−76869
ZnO, green luminesc. band, UV irrad. photocond. and quantum yield 77−36284
ZnO, negative photocond. by excitation of exciton-impurity complexes, recomb. mechanism *(Russian)* 79−28379
ZnO, powder layers, conductivity, O_2 chemisorpt. and photodesorpt. effects 78−43441
ZnO, red, electronic and opt. props., electrophotographic props. 77−57419
ZnO, single cryst. and film, in visible and near infrared range *(Russian)* 77−52133
ZnO, single crysts., photocond. lifetimes, Zn^+ hole traps 80−75581
ZnO, spectral sensitisation mechanism 77−43651
ZnO, surface phenomena, interpretation by compensation model 78−95323
ZnO, with chemisorbed neutral red, photocond. meas. *(Japanese)* 79−42572
ZnO-electrolyte interface, electron transfer sensitisation by salt additions 78−34894
ZnP_2, α-β heterojunction, I-V characts. and photoresponse 78−64105
α-ZnP_2, local centre parameters, photoelectron transition scheme, recomb. process anal. 80−44654
ZnP_2 tetragonal crystals, polarisation study of photocond. 80−96942
p-ZnP_2:S(Se)(Te), photocond., carrier generation and recomb. at high excitation levels *(Russian)* 78−64059
Zn_3P_2, photocond. and Dember effect meas., 0.5 to 1.2 μm, possible detector appl. 78−91721
Zn_3P_2-Al(Mg)(Be), diode, spectra response meas. of minority carrier diffusion length 79−78131
Zn_3P_2-Au Schottky diodes, influence of additional laser illumination on photoresponse spectra 77−89852
Zn_3P_2-Au surface barrier diode, wavelength-modulated photoresponse spectra 77−12004
n-ZnS based heterojunctions, epitaxial, elec. props. *(Russian)* 78−88023
ZnS, high-level photocurrent excitation and carrier recombination expt. *(Russian)* 79−95446
ZnS, photocond. excited with laser radiation near fundamental absorpt. edge 77−76867
ZnS, S annealed, IR enhancement and quenching of photocond. 78−14763
ZnS, self-activated, trap distrib. and photoelectronic effect due to UV, IR and visible excitation 77−36282
ZnS sputtered film, interband photocond. edge *(French)* 77−8212
ZnS, zinc blende-wurtzite-zinc blende, optical quenching of photocond. *(Russian)* 77−28240
ZnS:Ag, TSC and induced impurity photoconductivity, existence of two electron trapping centres 80−44655
ZnS:Ag,Al, computer calc. of band model for luminesc. and photocond. *(Russian)* 78−52542
ZnS:Cl, single cryst., deep centre study by impurity electroabsorpt., photocond. meas. 77−12411
ZnS:Cl, spectral distrib. of photocond., effect of powerful UV illumination 78−14767
ZnS:Cr^+, Fe^{3+}, luminesc., cond. and paramag. centre conc. parameters 78−6724
ZnS:Cu, Al phosphors, mechanism of IR stimulation and quenching, IR induced photocond. meas. 77−69881
ZnS:Cu, O(Fe,Co,Ni) photoconductors, killer impurities effect on electron escape probabilities and trap depths 77−4392
ZnS:Cu,O, photocurrent spectral distrib., Fe, Co and Ni impurity effects 77−8135
ZnS:Ga(Cl), deep traps, impurity electroabsorpt. and photocond. meas. 78−6707
ZnS:Pb current pulses due to elec. field liberation of electrons from trapping centres by tunnel processes 79−28378

photoconductivity continued
ZnS:S, photoconductivity and negative differential photo-effect 78−39156
ZnS-metal interface in MIM struct., photoexcitation level assignment *(French)* 80−15622
$(ZnS)_{0.2}(CdS)_{0.8}$, elec. props. effect of wurtzite-sphalerite boundary 77−55531
ZnS(Se):Ni, optical absorpt., impurity ionisation, optical phonon coupling 80−88505
ZnS_xSe_{1-x}, VPE, characterisation of defect centres by photoelectronic meas. 80−10914
ZnSe and ZnSe:Sb, photoconduction under Nd laser irrad., local level distrib. 77−55580
ZnSe, cryst., elec. cond., dislocation motion effects 80−54710
ZnSe, deep centres, photolum., photocapacitance and photocurrent expts. 78−39053
ZnSe, dislocation motion, influence on cond. and photocurrent 79−15149
a-ZnSe, elec. and optical meas., Mott-type model for amorphous semicond. 78−2414
ZnSe, elec. props. efect of wurtzite-sphalerite boundary 77−55531
ZnSe in insulator-semicond.-insulator struct., induced birefr., influence of kinetics of transient processes 79−24294
n-ZnSe, long persistent cond. relax. and frozen cond. 80−54735
a-ZnSe, low temp. photocond., increase of activation energy as temp. decreases 78−26902
ZnSe, photoplasticity and photocond., excitation energy conc. near dislocations, hardening 77−24346
ZnSe, residual cond., recomb. of photoexcited carriers, Hall coeff. 80−75605
ZnSe, reson. absorpt. of coherent IR radn. by acceptors, photocurrent and emission spectra 79−73974
ZnSe, temp. depend. and extinction, elec. inhomogeneity effects *(Russian)* 77−32037
ZnSe, with wurtzite-sphalerite boundaries, LF photofluctuations 79−69560
ZnSe, X-ray cond. 5.4 to 17.5 keV, spectral and dosimetric charact. *(Russian)* 77−35964
ZnSe:B(F), ion implantation, photocond. and cathodoluminesc. meas. 78−26586
ZnSe:Co, effect of in-band position of states on photoelec. props. 78−23132
ZnSe:Cr^{+}, Fe^{3+}, luminesc. cond. and paramag. centre conc. parameters 78−6724
ZnSe:I/aqueous electrolyte junction, electrochem. behaviour in dark and under illum. 80−25003
p-ZnSe:Li(Na)(N)(P), LPE layers, photocapacitance and photocond. meas. 79−99572
ZnSe:Mn^{2+} Schottky barrier diodes, spin depend. cond. and photovoltage 79−91141
ZnSe:Pb, luminescence photocond. 79−38634
ZnSe-electrolyte junction, current photoresponse 79−82669
ZnSe-GaAs heterojunction, LF noise, I-V and C-V charact., illumination effects *(Russian)* 77−66200
ZnSe-ZnTe heterojunction, prep. and props. 79−95483
ZnSe(:Ga)(Al), effect of thermal treatment and doping on elec. props. 77−85223
$ZnSiP_2$, photocond. and photolum. spectra, optical anisotropy 78−72200
$ZnSiP_2$, photocond. under laser excitation *(Russian)* 78−84258
ZnTe based metal-semicond. struct., spectral photosensitivity obs. 79−95492
p-ZnTe, doped and pure, photoluminesc. and photocond. spectra 77−55826
ZnTe film, LF oscills. of dark current obs. 78−19093
ZnTe films, residual conductivity, Kikuchi lines of electron diffr. pattern 79−91173
ZnTe, photoinduced dielec. loss and capacitance changes, rel. to space charge polarisation 80−2417
ZnTe single crystal, power depend. of photocurrent on excitation intensity, sublinear behaviour 78−43442
ZnTe-CdSe single cryst. film heterojunctions, prep. and props. 79−19652

photoconductors *see photoconducting materials*

photocopying
see also electrophotography
colour correction requirements, dependence on original 78−21239
contact-copying process resolution improvement 79−12876
copier techniques, gamma reproduction, DIN and ASA sensitivity scales and sensimetry *(German)* 79−26155
electrophotography for improvement of information content 79−21837
exposure modulation during photoprinting of highly-contrasting negatives by electronic copier *(Russian)* 80−292
fibre-optic light source for curved platen illumination 78−63163
gradient index fibre array for photocopying machine 80−14482
gradient index lens array fabrication for office photocopier 80−13178
grain struct. for facsimile reproduction, screenless lithography 79−35872
holographic reader-copier development and speckle suppression 79−81395
lens array design, Wood lens and gradient index fibre comparison 80−14479
low contrast negative photoprinting on elec. copier, time modulation of exposure, contrast enhancement *(Russian)* 77−67526
microprocessor control system, semiconductor mask manufacture appl. *(Spanish)* 79−17529
mismatch moire grating reproduction, critical aperture openings 78−78014
monochrome photographic process, subjective optimum reproduction cycle 79−49318
photochemistry of organometallics, with applications to imaging systems 77−4914
pigmented organic photoreceptors for plain paper copying 80−49824
radiograph diazotype duplicating system with appl. as diagnostic aid 78−69249

photocurrent *see photoconductivity; photoemission*

photodetectors
1-2 micron wavelength range *(Japanese)* 79−63307
absolute luminous intensity meas., apparatus *(Danish)* 78−62217
acousto-optical tunable filter, for optical coherent detect. 77−88932
aerosol, photoelectric analyser, theoretical anal. of optical detector 79−67455
aerosols examination, mixed phase 80−86404
photodetectors continued
amplitude-frequency charact., meas. using interferometer with US modulation 77−10112
angle meas., freq. doubler nonlinear distortions effect on errors 78−36968
angular displacement meas. by photoelec. amplitude-phase modulation method 78−16774
array, in system for automatic tracking of white blood cells 77−78064
aspect sensor, for small geophysical vehicles 77−45279
astronomy, optical multi-element detectors charact. 78−53830
atomic emission spectroscopy, spark source, linear Si photodiode array detector *(German)* 79−87926
attitude and orbit control systems, conference, Noordwijk (1977) 78−65480
automatic centring system for bubble chamber film measuring and premeasuring tables 77−83455
avalanche, electron and hole impact ionisation coeffs., influence on performance 78−6389
avalanche photodiode, for fibre optical communication lines 78−46793
avalanche photodiode, n^{+}-p-π-p^{+}, epitaxial Si diode for optical fibre communication at 800 to 900 nm 77−79961
avalanche photodiode, operating conditions in phase optical rangefinding 77−13799
avalanche photodiode receiver sensitivity, specification and testing *(German)* 78−38015
beat signal amplitude, influence of photoreceiver diaphragm diameter and interf. fringe width during interf. 79−7071
bioluminescence sensor, moving linear, for ocean light field meas. 79−20732
birefringence small area change real-time detection *(Japanese)* 78−15938
book, optical and IR radiation detection 79−2821
book, photoelectron statistics 78−25842
bulk extrinsic photoconductive detector with partially illum. sensitive areas, charact. 77−79151
calibration for radiant flux meas. of arbitrary source 77−34022
calibration method for distorted optical short pulse 77−71373
channelled, with charge storage, S/N ratio *(Russian)* 77−53978
charge-coupling photodetector for optical information processing 80−91753
coherent detection of partially coherent sources 80−47109
coherent differential reception *(Russian)* 77−87835
coherent laser detection system, radiation effects analysis 78−30056
coincidence detection fo optical pulse streams, high resolution heterodyne system 77−690
colorimeter, to determine moisture content of gases, exam. 78−56936
colour film densitometer with Si photodetector 80−4791
communication, conference, Amsterdam, Netherlands (Sep. 1979) 80−46733
compensation densitometer servosystem using integrated operational amplifiers 78−89525
conversion factor meas., kinetics of laser radiation appl. 79−2820
cooling element for radiation detector, shape effect on heat removal efficiency 78−12691
cooling system for photoreceivers 79−93218
coordinate-sensitive photodetector test illuminator 79−72643
correction filter selection for Si photodiodes 77−50767
detection process, basic theory and modern appl., book contrib. 78−37067
detective quantum efficiency and granularity rel. to quantum noise 79−21829
diamond, radiation detector for light and charged particles 78−49900
differential light detector using two antiparallel Si photovoltaic diodes 79−35837
digital energy meter for laser pulse meas. 77−71375
digital optical communication receiver amplifier design *(German)* 78−33878
direct detection optical communication systems, photoelectron counter dead time effect 77−54796
displacement meas. of violin G-string under sinusoidal EM force 80−53540
dissector operation, advantage of one-electron mode 78−58039
dissectors operating in one-electron and DC modes, illumination characteristic coupling 78−58034
distance meas. methods fundamentals, using twin diode technique *(German)* 80−13064
Doppler signal simulator for optical heterodyne receiver parameter meas. 79−80684
double-junction Si photodiode, high UV responsivity 77−74504
dual-grating direct-reading spectrograph mirror system design and performance 80−81397
dynamic range loss with modulated or pulsed laser beams 78−74057
electron-optical streak camera for picosecond pulse detect., book contrib. 77−61138
elementary cells, of photodetector matrices and scanistors, switching transients 78−45703
epitaxial graded gap semiconductor layer appl. 78−74060
ferroelectric thin film, pyroelectric radn. detector development *(Russian)* 79−47394
fibre fault detection using optimal time domain reflectometer 79−54173
fibre optic communication sources, detectors and circuits 77−27374
fibre optics, photoelectric detection improvements 80−91919
fibre optics communications, 1979 status and development trends 80−53408
fibre optics systems, technology and components *(Hungarian)* 78−66900
fibre pigtail incorporation 79−36998
fibre-optic communication receiver designs 77−68281
fibre-optic communications source and detector props. and performance 78−22212
fibre-optic delay line signal processing devices 80−48443
fibre-optic LED and laser source and Si photodetector development 78−42430
fibre-optic transmission system components *(Spanish)* 79−94348
field of view shaper for background illumination protection 77−74506
field of view shaping with interf. filters 77−58456
film photopot detector characteristics for adaptive optical systems 79−59741
flat image focussing spherical lens, used for Si light detector 80−91880
fluctuating pulsed signal detect., effect of unstable quantisation level 77−10113

photodetectors continued
fluorescence lifetime measuring system with picosecond resolution CW laser and AM radio 78−41357
focal plane design and optimal processing for scattered optical fields 78−78935
Fourier spectrometer reflector displacement precision meas., photoelectric method 77−18107
Fourier transform spectroscopy, photon and detector noise quantitative limit, definition *(German)* 80−9049
frequency response meas. using laser mode beating 78−8442
frequency shift laser meas. of water and wind velocities 77−39385
GaAs photo-FET high speed photoconductive integrated optical receiver 80−58816
gas discharge detector miniaturisation, rise time spectral depend. 78−86318
gauging by remote image tracking used in production 79−86264
guided-wave optical signal processing, diode laser sources and photodetectors 80−48465
guided-wave optical systems and devices, seminar, Washington, USA (April 1979) 80−31418
half-duplex optical transmission link using LED source-detector scheme 78−71214
Heliotrop, sensory aid for blind *(Polish)* 78−81074
heterodyne charcts. meas., modulation method 77−34029
heterodyne detection, optimum conditions 77−2694
heterodyne detection of random gaussian signals, pulse duration optimisation 79−12848
heterodyne detectors, evaluation at 5145 Å 77−71370
heterostructures for integrated optics 77−39112
high concurrency data bus using arrays of optical emitters and detectors 79−76805
highspeed, performance testing, optical communication appl. 79−26129
holographic recording of 1-D data 78−1195
holographic system path length difference controller *(Russian)* 79−22916
hybrid-type integrated photodetector using partially metal-clad dielectric-slab waveguide struct. 77−11050
III-V semiconductor emitters and detectors for 1.0-1.6 μ fibre-optic communications 80−10007
III-V semiconductor heterostructure avalanche photodiodes, high speed response, high quantum efficiency 79−80682
III-V semiconductors, p-n heterostructures, epitaxial growth techniques, appl. to optoelectronics, review 80−54770
image Fourier transform correlator using US light modulator *(Russian)* 77−58264
image intensifier tube with self-scanned photodiode array, photoelectron counting 77−18090
imaging photon detector for geophysical and astrophysical research 80−86405
impulse characteristics of irregular surface for oblique irrad. and incoherent reception 77−31069
incoherent image processing by multiple aperture scanning 79−76627
InSb detector system in Fourier spectrometer, use of improved preamplifier circuit, with integrator in feedback loop 80−73474
integral error, matching to weighting function *(German)* 80−31876
integrated light-sensor device with broad operating range and enhanced-blue spectral response 80−13140
integrated MOM device, detect. expts. at 10.6, 3.39, 1.15 and 0.6328 μm 77−89878
integrated optical detector array, waveguide, and modulator, based on Si technology 77−11049
integrated optical RF spectral analyser acousto-optical readout scheme 79−50446
integrated optical waveguide and CCD image array 77−34962
integrated optics appl., detectors development with and without optical coupler *(Czech)* 80−33227
integrated optics high quantum efficiency waveguide coupled photodetectors on Si substrate 80−58805
integrated photoductive detector and waveguide struct. 80−48456
integrating rod as grating detector 79−94334
integration over cylindrical luminous volumes, using calibrated piston source 77−5923
interference fringe position determ. accuracy improvement by photodetector signal conversion 78−58015
interference measuring devices, parameter optimisation 78−16844
ion beam synthesis, of Si_xC_{1-x}, Si_xGe_{1-x}, $GaAl_xAs_{1-x}$ and GaP_xAs_{1-x} 79−46688
IR, technology evolution 77−5934
IR focal planes in intrinsic semiconductors 78−37994
IR imaging, doped Si detector photoresponse measurement problem 78−37000
IR reflectance detection for haemoglobin conc. meas. in whole blood 77−52860
irradiation timer for shutter of ^{60}Co teletherapy head 77−66836
lag correction network ccts. 78−288
laser, pulse detector, using SAW generation 77−57392
laser beam, spectral analysis, photomixing method 78−46698
laser beam position sensor, using single photodetector 78−46705
laser characteristics measuring device based on intraband heating photoconductivity 79−44930
laser detection by coherence discrimination, angle-scanned interferometer as coherent energy modulator 79−58777
laser detection using tunable acoustooptic filters 78−29159
laser flash absorption change kinetics spectroscopy at 820 nm, photosynthesis study appl. 78−92769
laser meas. appl., metrological certification, using acoustooptical modulators 80−23727
laser pulse detection using receivers with photoresistors 78−45705
laser pulse energy digital indicator *(Russian)* 79−22995
laser pulse monitor, 50 psec detector 77−3600
laser pulse tracking position-sensitive photodetector characteristics 77−18098
laser radiation energy photoelectric meter, digital output 78−58040
laser radiation fluctuation-spectrum recording for USSR state standard 78−45696
laser radiation recording using semicond. films with anomalous photovoltages 77−37989
laser radiation wavelength meas., 3.39 μm and 0.63 μm 79−30555
laterally illuminated p-n junction, spectral response calc. 77−8180
lecture on optoelectronic devices 78−25990
LED pulsed light signal receiver 79−93216
photodetectors continued
light flash envelope isolation from fluctuating background 77−37993
light-activated switch, photo-gate, pulse method of switching, circuit 80−42021
linearity meas. of photometric devices using two LEDs 80−17996
linearity testing procedure *(Hungarian)* 79−89001
logarithmic transfer characteristic photosensor 79−93215
low level light detectors for astronomy 78−28525
low-contrast optoelectronic primary information processing system, energy efficiency 79−76617
low-noise multistage avalanche photodetector using heterojunctions 79−88999
m-distributed optical signals, statistical props. and photoelectron counting distrib. 77−38809
magnetic tape linear velocity meas. scanistor 79−71425
manometer, differential pressure meas., interference system 78−86323
matrix pyroelectric detector for laser oscills. investigation 77−74502
metal film, laser induced transverse voltages, detector appl. 0.33 to 10.6 μm 77−39824
metal-oxide-metal photodetector, noise, ultimate sensitivity 77−5915
microcirculation flow dynamics meas. using video microscope 77−78009
microwave thermophotoindicators, based on cholesteric liquid crystals, analysis of diffuse light spectra 80−73457
MIM discontinuous metal film, fast detector for MM-wave through optical freq. range 77−18092
MIS avalanche photodetector linear array 79−63308
MIS Schottky barriers, photocurrent suppression and interface state recomb. 78−39222
MIS structure based pulsed avalanche photodetector with stable internal amplification, feasibility 79−58794
MIS tunnelling Schottky barrier, reverse biased, appl. to photodetection 79−7904
modulation spectroscopy using solid-state and gas lasers 79−30572
MTF evaluation by photoresist 79−3636
multianode microchannel array photon-counting detectors 80−77869
multichannel photoelectric systems, immersion optics 80−53405
multichannel plate, detectors, operation, struct., performance charcts. 78−12758
multichannel radiometer, programmable, for Earth remote sensing 80−77253
multicolour semiconductor detectors, principle and developments *(Czech)* 79−26126
multidetector scanner image striping abatement 80−102660
multiphoton detectors of laser radiation, statistical charcts. 80−86408
multispectral linear array, pushbroom scan mode, satellite earth resources survey sensor appl. 80−56693
near IR (1 to 2 μm) optical communications, colloquium, London, England (May 1980) 80−86040
noise power spectrum density meas. using null radiometer scheme 78−21197
noiselike optical signals, photoelectron counting statistics and error rate characteristics 78−1178
non-contact rotational speed measurement and integrated spatial filter detector *(Japanese)* 79−93107
noncontact optical gauging by remote image tracking in production environment 80−8961
nonlinear photoelectric or photographic receiver signal value calc. *(German)* 80−31866
nonlinear tunnelling devices, photon detection, theory 79−6177
nonlinearity determ. by relative differential sensitivity meas. 79−71530
nonlinearity of low noise Si detectors, radiant flux ratio meas. 80−47089
object dimension meas. by computer-controlled laser beam scanning 79−98431
oil thickness on wavy water surface, light sensitive gauge 79−8720
one-electron dissector, LI-604, exponential branch of output pulse amplitude distrib. 77−30203
one-electron dissector, S/N ratio rel. to image contrast 79−50407
open photoreceiver, vacuum ultraviolet 80−52307
optical antennas focused at finite distances, angle-distance pattern 78−33842
optical binary discrete deflector with deflection angle degeneracy 79−55239
optical communication channel and photodetector array, computer simulation 77−71944
optical communications systems, components, review 80−87539
for optical fibre communication *(Japanese)* 80−78977
optical fibre systems receiver design, review 78−30077
optical heterodyne receiver output signal dependence on angle of incidence 79−45910
optical heterodyning, additive noise component reduction 79−50239
optical memory readout by superluminescent diode with integrated photodetector 80−32922
optical multichannel analyser, nanosecond gating, performance 79−17462
optical noncontacting transducer, for machined surface profile meas. 79−58765
optical PCM with envelope modulation, pulse detection characteristics 77−11010
optical phase measurement in real time using photodetector array, Fourier transform computation 80−9013
optical radar, logarithmic fast-response photodetector for atm. sounding, photometric properties 80−51585
optical radar pulsed systems using photodetectors with lag, charcts. 79−13918
optical receiver system, narrow-field, spherical aberration effect on radiation power losses 80−28299
optical sensor array systems for astronomic longitude determ. 77−82023
optical sensor system simulation and evaluation 80−96030
optical storage focus error detection, skew beam and Foucault knife-edge techniques 80−102649
optical transmission evolution and development trends 79−23065
optical/digital pattern recognition automated system 80−48175
optimisation for radiation environments 78−29158
optoelectronic devices and optical imaging techniques, book 80−27059
optoelectronic system for detect. and tracking, optimisation in search operation mode 77−50765
optoelectronic system threshold sensitivity calc., background spatial charact. determ. errors 79−26134
optoelectronic vibration transducer based on coordinate photodetector 79−75495
optogalvanic, for photoexcited high-lying levels of Ba 79−98055

photodetectors continued
oscillating beam spectrometer for organic thin film transmission 80−18022
p-i-n, Au-diffused, for freq. multiplexing optical fibre system 77−88914
p-i-n laser detector, Si, wavelength and temp. depend. charact. 80−13134
p-i-n photodetector under transient conditions, simulation and expts. 79−58793
p-i-n photodetector unit characterisation, baseband fast modulation of GaAlAs laser diode 77−11025
p-i-n photodiode photometer 79−32
p-i-n photodiode with internal reflection 78−37059
p-n junction, anomalous hot carrier-voltaic effect, electron emitter and light detector appls. 77−76861
p-n junction, direct integration with $Ga_{1-x}Al_xAs$ LOC DBR laser 78−38066
p-n-n^+ structures, Zn doped Si, use as light sensitive devices 77−8178
packaging approaches, review 77−10108
parameters measurement, via optomechanical/electronic unit 78−284
partial tracking optical heterodyne receiver arrays, operating in turbulent atm. 79−41345
partially coherent radiation, optical heterodyne detection 80−77871
phase meas. receivers, closed loop direct detection 77−88661
phase transformation interference reversible light reflector material, visualisation of CW EM radiation 79−71531
phase-sensitive detection, representation of observable signals in Chebyshev polynomials 79−89857
Photicon, new imaging optical detector 77−67499
photoamplifier circuit, dynamic compensation of photodetector DC component temp. drift 80−73460
photocathode polarisation sensitivity, two-beam interferometer expts. 80−4772
photodiode array, self-scanned, for high dispersion astronomical spectrophotometry 78−45230
photodiode array for single-particle light scatt. meas. 78−28146
photodiode array sampled light distrib. profile reconstruction *(French)* 79−30557
photodiode arrays, charact. and appl. 79−89002
photodiode detector calibration using synchrotron radiation 80−90810
photodiode detector for optical cable, optimal filter struct. and charact. 78−18067
photodiode detector for optical fibre communication *(German)* 78−33874
photodiode with IC amplifier, camera shutter control appl. *(German)* 80−52341
photodiodes, gas-filled, improved detectivity for UV radn., μs-order rise-time 78−37062
photoelectric convertors, one-coordinate, signal processing algorithm 80−33199
photoelectric scanning microscope output linearisation 77−5905
photoelectron statistics, joint moment method, phase radiation 80−23647
photoemissive detector, picosec., using metal-oxide-metal junctions 79−44932
photoemissive detectors, classical and modern device study, book contrib. 78−37070
photographic flash light meas. instruments development *(Hungarian)* 80−57411
photoionisation detectors, coupling to gas scintillation proportional counter 78−82581
photomixer with spatially periodic photodetectors, charact., appls. 79−12852
photomulitplier meas. of threshold optical radiation fluxes, errors 78−12760
photomultiplier linearisation and system stabilisation, for photometric ellipsometers and polarimeters 78−54441
photomultipliers as quantum receivers in red region *(Bulgarian)* 78−45704
photon bunching in thermal radiation, temp. depend., photodetector thermal fluctuation 78−24748
photon correlator, near ideal, with SAW device 80−68252
photon count statistics, detector temp. and field effect 80−74325
photon counter, statistical deviation due to dead time, calc. *(Japanese)* 77−10105
photon detectors for optical communications *(Czech)* 79−50396
photon pulse delay estimation, nonregularity 78−29157
photoplethysmographic vaginal transdcuer, blood vol. change monitoring 78−92733
photoreceiver charact. meas. using CO_2 freq.-tunable laser 77−14728
photoreceiver sensitivity nonlinearity determ. by high-speed raster device 77−79150
photoreceiver system, photodiode-FET, achievable threshold limit calc. 79−49292
photosensitivity charact. in pulsed operation, meas. 79−30556
photosensor array aliasing and MTF effects 77−39086
photosensor array XY addressing and organisation schemes 77−39076
photosensor spectral responsivity calibration microprocessor system 80−86409
photovoltaic operation of nonuniformly doped intrinsic photoconductors 79−224
pickup, of photoelectric analyser, optical method of forming counting vel. 79−93270
picosecond, using Schottky barrier switching diode, for 257 nm to 1 μm laser pulses 79−67388
piezoceramic bimorph element for photoelec. autocollimator detector 77−7206
piezoelectric crystal, appl. to ultraweak EM signal meas. 78−82032
pin- and avalanche diodes, charact. *(Swedish)* 78−89545
plasma position detector, using segmented photodiode 78−1901
polariscope quartet for induced birefringence meas. 78−21204
position sensitive light detectors with high linearity 78−89538
position sensitive photodetectors with high linearity 77−79057
position sensor, light sensitive head and elec. circuit 77−54806
position-sensitive, for focusing on variable luminous mark 79−75598
position-sensitive, for meas. of lateral displacement of laser beams, selection of parameters 79−17490
pulse detection, atm. scintillation effect 77−7004
pulse gas calorimeter, for vacuum UV radiation meas. *(Russian)* 78−93688
pulse rate meter for heart monitoring 78−31915
pulse receivers for distance meas., basic params. determ. 78−33843
pulsed-light detector for checking optical cables 78−54455

photodetectors continued
pyranometer for total hourly horizontal solar radiation data, USA 77−25765
pyroelectric detector, 40-1100 nm range 77−87834
pyroelectric radiation detectors, review 77−45889
pyromagnetic detector for wideband laser radiation *(Russian)* 79−93220
quadrant detector for STEM, appls. 80−77914
Quadrant Photosil Autoguider for Cambridge Schmidt telescope 77−60612
quantum detectors for astronomical spectrometry 77−25950
quantum radiation from a point source, angular coords. determ. 77−65050
quantum statistics of photocurrent in optimal light detector, atm. 'seeing' conditions 80−53244
radiation detection in turbulent atmosphere, photodetector current fluctuation statistics *(Russian)* 79−92591
radiation standards for source spectral emission and detector spectral sensitivity 77−39007
receiving optical antenna, angle-distance sensitivity variation anal. 78−33841
rectilinear scanning, optimal meas. of optical signal parameters 78−17865
refractometer laser detector for anal. of liquids 80−101830
relative spectral sensitivity meas. method using two tandem monochromators *(Japanese)* 80−101840
repetitive photoelec. scanning system for high resolution optical spectra accumulation 78−54456
rocket attitude control, solar sensor system pointing accuracy *(Japanese)* 78−24420
rotary incremental transducer, design problems *(French)* 78−21121
S/N ratio with optimal filtering, noise stability for pulsed signals 77−31072
SAW spectrum analysers in photon-counting mode, statistical props. 80−105712
scanning optoelectronic device with multielement photodetector, error probabilities 77−58455
scanning optoelectronic system, S/N ratio, effect of objective lens quality 77−10111
scanning optoelectronic systems, optical and electrical filter simultaneous optimisation 79−72696
scattered radiation reception by optical quantum amplifier 78−17946
selection criteria for weak signals *(German)* 77−82601
selection w.r.t. operating parameters 79−30542
selective receivers for 0.2 to 0.3 μ spectral region 79−30560
self-scanned photodiode array, image detect. from Fabry-Perot spectrograph *(French)* 80−73465
self-scanned photodiode array as multichannel spectrometric detector 80−73466
semiconductor, determ. of theoretical threshold 78−37065
semiconductor, for optical fibre communications, state of art *(Czech)* 78−5575
semiconductor, narrow band gap, charact. *(German)* 77−20356
semiconductor, with superlattice, heating photocond. 79−19622
semiconductor diodes, appl. to long wave laser radiation detect. 79−26135
semiconductor heterostructures, elec. and optical phenomena, discrete devices, review 78−72250
semiconductor IR photodetectors, comparison of extrinsic and intrinsic devices, temp. limitations 80−73456
semiconductor junction transceiver, for fibre optic communication 78−42410
semiconductor light-sensitive diode acoustic airgap convolver, theory 79−49288
seminar, optical radiation meas., San Diego, CA, USA (Aug. 1979) 80−86036
sensitivity, informational threshold, rel. to human vision 77−87838
sensor, digital meas. of rotational speed, applications to automatic testing of electric machines *(Czech)* 79−71419
short-pulse photodiode receiver quasioptimal filtering 79−26132
Si detector array for AlGaAs laser array 80−58817
signal levels number in presence of additive noise 77−58458
single-element matrix and mosaic photodetectors, comparison for point source signals 78−70186
solar cells, Si_xGe_{1-x} diffused p-n junction, electric and photoelectric props. 80−101095
solar cells for use as optical detectors, background illum. effects 78−70182
solar flux mapping sensor, Si p-n junction, for high intensity appl. 78−40720
solid-state imaging, conference, Louvain-la-Neuve (Sept. 1975) 77−39073
solid-state photosensor array for electronic imaging 79−21836
source location, comparison of pulsed and continuous modulation and pseudorandom coding 77−71374
Space Telescope spectrograph Digicons 80−85858
spatial noise reduction in detector arrays, controlled lateral shifts 80−53436
spatially periodic photodetector, photomixing of coherent radiation 79−12851
spectral characteristics of MIS struct. with variable-gap semicond. 80−44735
spectral response determ. using calibrated lamp and interference filters 79−71528
spectral response measurement 79−21812
spectral sensitivity distribution meas. systems 77−26398
spectral sensitivity meas. using two tandem monochromators *(Japanese)* 80−47107
spectral slit width correction for precision energy measurements 80−96020
spectrally selective, for broadband radiometry 80−68255
spectrofluorometer components, state of the art *(Slovak)* 78−56940
spectrograph photoelectric detector for photographic plate holder replacement *(French)* 79−75623
spectrophotometer, Hewlett-Packard 8450A UV/Vis model 80−68270
spectrophotometer, photoelectronic, using p-n junction photovoltaic cells and inherent compensation 79−54200
spectrophotometry, solid state image sensor, photodiode appl. *(Japanese)* 78−4677
spectroscopic cooled and intensified array detectors 78−65983
stabilised photoreceiver unit 77−39038

photodetectors continued
star transit instants, automatic recording 77−91435
statistics of photoelectrons, influence of statistics of fluctuations on EM field 77−20360
stratospheric O_3 and aerosol monitoring using orbiting photodetectors 77−78445
submillimeter radiation field, transverse distribution, scanning device for visualisation 78−4693
subnanosecond optical detector developments 80−77870
subnanosecond source studies from UV to beyond 1 μm, simple inexpensive design 80−86433
Sun position sensors using fibre optic selector 77−49262
sunlight polarisation detection, ships compass adjustment appl. in fog 78−24831
surface-barrier, GaP and GaAs with Au film deposition 77−77423
surface-barrier semiconductor, registration of pulsed radiation 80−91373
switching process and plasma effects in photodiode, theory 80−65667
technology and technical anal., book 78−37066
telecentric imaging system focus detector 80−53397
temperature dependence of dark current and quantum efficiency 80−90896
temperature dependent response of optical radiation meas. instrumentation 78−24857
ternary semiconductors, pot. practical appl., review 79−10344
test installation for elec. contact transducer testing 78−12683
thermal detectors and photondetectors, operating conditions and applications, review 80−47110
thermal imaging system resolution and S/N ratio, optical aberration effect 79−81552
thin film detector for integrated optical systems, description and exam. 78−38080
threshold level adjustable photodetector, design considerations 80−62724
threshold sensitivity, effect of transmission sector of mech. chopper 79−7222
threshold sensitivity for semiconductor photography 80−18017
time characts. meas. using meter with programmed strobing of anal. zone 78−283
time position accuracy determ. of optical pulsed signals for correlated noise types 78−12761
time resolution capabilities of microchannel plate and static crossed field photomultipliers 78−37061
time resolution meas. of photoreceivers using gas-discharge lamps 80−73461
time response determ. at 1.06 μm, LED source 79−89004
time-domain reflectometer with gated photomultiplier receiver, optical fibre break detection appl. 77−65620
transient process anal. in photoreceiver 78−29162
transparency of metal films on semicond. substrates 77−16411
two-photon photoconductivity detector for measurement of picosecond light pulses from Nd-glass laser 80−77872
UL-DN3 sonic laser radiation detector *(Polish)* 79−85113
ultrahigh-speed photodetector design 80−47108
ultrashort time resolved photodetection theory 79−89003
urine glucose analyser with audible output 77−52909
UV photocell, 0.22-0.36 μm 77−71376
vacuum detector array, for broadband UV radiation from plasma using photoelectric effect 79−90464
velocity measurement for moving surface using sensing arrays 79−58677
very-fast-response uncooled photodetector based on intraband μ-photoconductivity 79−30562
vibration meas., non-contact and non-reactive, at 60 kHz *(German)* 78−32805
video disc information retrieval by optical readout 80−43284
Viking Lander camera design 77−41285
Viking Lander camera performance and data reduction 77−41286
visible/UV radiation meas. of high-power lamps *(Polish)* 79−26130
vision systems, active and passive, 0.35-14 μm, atm. effects *(German)* 77−9500
wavefront sensing systems compared 79−58766
wavelength selection for transhorizon optical communication 79−7088
wavelength specific photon detector for the VUV 80−91380
weak light fluxes with slowly varying intensity detector 79−2806
weak optical signal meas. in strong interference *(German)* 77−65623
wideband photoelectric detector for daytime lightning 78−57336
X-ray detector, self-scanning photodiode array, direct X-ray response 77−54032
X-ray fluorescence spectra, energy-dispersive, least-squares anal., detector response function approach 80−3457
X-rays, photoelec. diode with Al photocathode, calibration 77−54033
Zn_3P_2, UV photoconductive detectors 80−4766
$Al_xGa_{1-x}As$-GaAs, DH, optical power conversion at 8500 Å and I-V characts. 77−87833
As_2S_3 thin films for integrated optics, photodetector elements, relief-type diffraction gratings 79−32094
As_2Se_3-HgSe double-layer system detector for temp. meas. 79−88952
Au-n-$Ga_{1-x}Al_xAs$-n-GaP narrow-band variable-gap surface-barrier photoedetector 80−96944
Au-n-Si-p-Si structure with wavelength depend. photocurrent sign, photodetector 79−12849
Bi film fast-response photodetector, employing charge carrier photon entrainment 80−73462
CO_2 laser pulse meas., single sweep 5 GHz oscilloscope detector system 77−88817
Cd_xHg_{1-x} Te, photodetectors, recomb. processes, photoconductive decay obs. 79−38129
$Cd_xHg_{1-x}Te$ graded-gap epitaxial layers, photocond. meas. 0.5 to 6 μm, detector appl. 79−60869
CdS detector, Voyager Sun sensor, evaluation of radiation interference, simulation 79−23644
CdS, for integrated optical half adder circuit 79−76877
CdS photoresistor, errors in exposure meter accuracy calc. 77−49773
CdS_xSe_{1-x} photosensitive films, prep., props., and use for photodetectors 80−55298
CdSe, photodetector, limiting sensitivity 79−63309
$CdSiAs_2$ diode, photoelec. props., potential photodetector and solar cell appl. 77−43655
$CdSnP_2$-InP, n-n heterojunctions, growth, elec. characts. 77−11992
$CuInSe_2$, photovoltaic props. and p-n junction form. 77−69371
Cu_2Se-$AgInSe_2$ heterojunction, photodetection props. 78−39195
GaAlAs DH photovoltaic detectors, high efficiency 79−11198
n-$Ga_{1-x}Al_xAs$, variable gap photodetector, quantum efficiency 79−7903
$Ga_xAl_{1-x}As_x$, photodetector diode on GaAs substrate dark currents, tunnelling, energy gaps, effective masses 80−70805
GaAs, and its alloys, as integrated optics materials, book contrib. 79−64362
GaAs, electroabsorpt. avalanche photodiode waveguide detector, freq. demultiplexing 79−17486
GaAs high speed avalanche photodiode design 78−8446
GaAs integrated multijunction photodetector with high output voltage 79−6178
GaAs MESFET, optical detector appl., sensitive high-speed device 80−13143
GaAs, p-i-n avalanche photodiode, temp. depend. characts. 79−35835
GaAs photoconductors, extrinsic, DC- and microwave-biased, performance 80−70750
GaAs, planar ion-implanted avalanche photodiodes 80−22431
GaAs, reach-through avalanche photodiode, temp. depend. characts. 79−95482
GaAs Schottky barrier charge-accumulation detector, photosensitivity spectrum 77−55582
GaAs Schottky barrier diode, beat freq. generation between visible lasers 80−1253
GaAs-$Al_xGa_{1-x}As$ integrated injection lasers and detectors with etched reflectors 77−62074
GaAs-$Al_xGa_{1-x}As$ integrated lasers and detectors fabricated by wet chemical etching 77−88961
$GaAs_{0.6}P_{0.4}$, low dark-current MOS photodiodes 77−32083
$GaAs_{1-x}P_x$, photodiode used for camera 79−89019
$GaAs_{1-x}P_x$-Au, surface-barrier struct., photodetectors of visible and UV radiation 77−20437
$Ga_{0.47}In_{0.53}As$, photodetector applications 80−95140
$Ga_{1-x}In_xAs$ photodetectors for 1.3 micron PIN-FET receiver 80−13145
$Ga_xIn_{1-x}As$, review of fibre optical communication devices 77−58446
GaP:Te, photon drag, optical rectification response meas., anomalous polarisation depend. 78−33769
GaSe, photoelec. analysers of polarised light, suitability from photosensitivity and pleochroism meas. 79−60873
Ge IR photon drag detector, photosensitivity spectrum 79−12853
Ge, p-i-n avalanche photodiode, temp. depend. characts. 79−35835
Ge, reach-through avalanche photodiode, temp. depend. characts. 79−95482
Ge:Cu, I-V characts. 78−19141
Ge:Ga photoconductors in low IR backgrounds 79−63305
He-Ne laser, competitive oscillation mode frequency stabilisation *(Russian)* 79−22962
(Hg,Cd)Te photodiode IR detectors, planar technology 80−9043
(Hg,Cd)Te photodiodes, wide-bandwidth 10.6 μm IR heterodyne detect. 80−9042
HgCdTe, 0.1 eV photodetector performance background dependence 77−32038
HgCdTe, 0.1 eV photodetector performance 77−32039
HgCdTe, 0.1 eV photodetector performance, geometrical enhancement 77−32040
HgCdTe, incoherent heterodyne detect. for atm. pollution remote sensing 77−87130
HgCdTe varactor photodiode, heterodyne detection for CO_2 isotope laser freq. calibration 77−19230
HgCdTe-, IR heat camera component, night vision appl. *(German)* 79−49287
HgCdTe-CdTe IR detector arrays, 3 to 11 μm, fabrication techniques 80−9041
$Hg_{0.74}Cd_{0.25}Te$ thin film deposition on Si substrates by RF triode-sputtering, large-area photodetector arrays 80−80965
$Hg_{1-x}Cd_xTe$, multicolour photovoltaic detectors *(Czech)* 79−26126
$Hg_{1-x}Cd_xTe$ photoconductors, gamma ray effects on surface props. and detector props. 79−17489
$Hg_{1-x}Cd_xTe$, props. and appls., book contrib. 77−39834
$Hg_{1-x}Cd_xTe$ Schottky barrier photodiodes, for IR detection 80−13144
$Hg_xCd_{1-x}Te$, photodiode, anomalous noise behaviour in heterodyne and background limited operation 79−69568
InAs, photovoltaic detector, photoelectric evaluation, for Gaussian incident pulse 79−63306
InAsSb/GaSb broad-spectral-band IR detector, backside-illum. heterostructure approach 80−73450
$InAs_{1-x}Sb_x$-InAs backside-illum. narrow band photodetectors 77−61118
InGaAs-InP heterojunction detector for 1.0-1.7 μm wavelength range 78−49895
InGaAs-InP punch-through type photodetector fabricated by VPE 80−68253
$In_{0.53}Ga_{0.47}As$ p-i-n photodiode-FET photoreceiver for 1.0 to 1.7 μm wavelength optical fibre communications systems 80−58794
$In_{0.53}Ga_{0.47}As$/InP avalanche photodetector 80−4764
InGaAsP avalanche photodiodes, leakage current; shot noise, quantum efficiency, gain saturation 79−67381
InGaAsP, improved two wavelength demultiplexing 80−58795
InGaAsP:Be, avalanche photodetectors annealing temp. effect on photolum. spectra 79−69872
InGaAsP/InP phototransistors, fabrication by LPE, photodetectors 80−95139
InGaAsP-InP high-gain heterojunction phototransistor 80−103745
$In_{1-x}Ga_xAs_yP_{1-y}$-InP photodetectors, high-efficiency with selective wavelength response, 0.9-1.7 μm 79−21810
$In_xGa_{1-x}As_xP_{1-x}$-InP photodetectors, construction and performance 78−65966
$In_xGa_{1-x}As_yP_{1-y}$ photodetector diode on InP substrate dark currents, tunnelling, energy gaps, effective masses 80−70805
InSb laser detector, dynamic range increase 78−49899
InSb n^+-p and p^+-n photodectors fabrication by S and Be ion implantation 78−49906
InSb-, IR heat camera component, night vision appl. *(German)* 79−49287
InSe, photoelec. analysers, suitability from photosensitivity and pleochroism meas. 79−60873
LaF_3 superionic conductor insulating layer, used for photocapacitive detectors 80−92976
Ni-NiO-Ni, integrated MOM junctions, characts. at DC and optical freqs. 78−41349
PbS, contactless thermometer appl., for 600 to 1200°C *(Slovak)* 78−54366
PbS-base photodetectors, struct. invest. by proton irrad. 80−104388

photodetectors continued
PbSe photocells, multicolour detectors in combination with Si photodiodes *(Czech)* 79−26126
PbSnTe-, IR heat camera component, night vision appl. *(German)* 79−49287
PbTe:In, diffused planar detector arrays 78−41348
n-PbTe/p-$Pb_{0.8}Sn_{0.2}Te$, multicolour photodetectors *(Czech)* 79−26126
PbTe-$Pb_{0.82}Sn_{0.18}Te$, p-n heterojunctions, electrical and photoelectrical properties 78−39193
PbTe-$Pb_{1-x}Sn_xTe$ n-p^+ heterojunction photodetector, hot wall evaporation technique 80−65673
$PbySn_{1-x}Se$ epitaxial film narrow band photovoltaic detectors, detection at long wavelengths 78−8443
Pt-Pd discontinuous film MIM point-contact diode detector 77−5917
Se, laser beam detection appl. expt. *(Czech)* 78−62225
Se, linearity, stability, fatigue and light memory effects meas. *(Spanish)* 77−87837
Se photocell optical vibration transducer 80−77768
Si, amorphous CVD film photodetector for picosecond pulses 80−47101
Si, amorphous evaporated, picosecond optoelectronic detect., sampling and correlation meas. 80−100478
Si crystal production and perfection for photodetectors 78−11107
Si detector for IR charge transfer devices 77−83991
Si detectors, vac. UV performance, 500-2000 Å 77−26397
Si diffused junction photodiode performance characteristics 80−80367
Si digital Sun sensor electrical and optical props. *(Japanese)* 78−32313
Si film double-mesa reach-through avalanche photodiode with large gain-bandwidth product 79−12845
Si, for improved short-wavelength quantum efficiency 80−31874
Si, free carrier absorption 78−37060
Si high-resistivity structure, photoelec. props. 78−91730
n-Si high-temp. vacuum etching, p-n junction photodetectivity 78−95355
Si, linearity, stability, fatigue and light memory effects meas. *(Spanish)* 77−87837
Si, p-i-n avalanche photodiode, temp. depend. characts. 79−35835
Si, p-n junction, quantum efficiency as absolute radiometric standard 79−49284
Si photodetector, surface-barrier 80−4771
Si photodetector storage-mode operation 77−39075
Si photodetectors with increased blue sensitivity *(Rumanian)* 80−62720
Si photodiode, light detection in dielec. waveguide through direct evanescent field coupling 78−30094
Si photodiode, multidecade linearity meas. 79−75592
Si photodiode, refl. and external quantum efficiency change after surface cleaning 79−93212
Si, photodiode, shallow junction n^+-p, spectral response limitation mechanisms 78−37058
Si, photodiode, UV enhanced responsivity 77−74499
Si, photodiode, violet and near UV sensitive, prep. and expt. study *(Chinese)* 79−49285
Si photodiode absolute spectral response self-calibration 80−73448
Si photodiode array for integrated optical spectrum analyser 80−33241
Si photodiode for optical channel waveguides 80−102805
Si photodiode saturation at high modulation freq. 78−54453
Si photovoltaic detector, radiometric meas. description 78−29140
Si photovoltaic detector, quantum efficiency rel. to position and wavelength 79−75593
Si, position-sensitive photodiode, for angular displacement recording 77−49712
Si, reach-through avalanche photodiode, temp. depend. characts. 79−95482
Si, review of fibre optical communication devices 77−58446
Si, shallow junction type, internal quantum efficiency meas. model fits, visible quantum yield 80−267
Si, solar irradiance meas. using optical fibres and Si detectors 79−100960
Si vidicon, performance at low signal levels, astronomical spectroscopy appl. 77−22085
Si vidicon optical detector, laser data acquisition/analysis system 78−58041
Si waveguide photodetector matrix, appl. in integrated-optics demultiplexer 79−32095
Si:Ga, possibility of use in fabrication of fast response photodetectors 79−15184
n-Si-Au surface barrier diode, photosensitivity in spectral range, 1-6 eV 77−89850
Si-CdS p-n heterojunction photodetector fabrication and characts. 78−52068
Si-p-i-n photodiode as detector in optical power meter for fibre-optic appls. 78−93746
SiC p-n junction photodetector, spectral characts. 77−41685
SnO_2, time-resolving high-intensity laser-light detectors 78−77982
Ti-TiO_2 gated MOS diode light sensor, scan freq. improvement 78−58037
n-ZnSe−p-GaAs heterojunction high-detectivity threshold photodetectors 79−6181

photodielectric effect
cholesterol, dielectric props. under UV excitation 80−6912
cholic acid, dielectric props. under UV excitation 80−6912
ferroelectrics, optically induced internal fields 80−107855
haemoglobin, dielectric props. under UV excitation 80−6912
photoferroelectric image storage in antiferroelectric-phase PLZT ceramics 80−71353
photoferroelectric phenomena, physical models derivation 79−15407
polyhexamethylene adipamide, photocond. and dielectric props. 80−84489
polymer films, electronic cond., electro-, photoresponsive effects, review 79−56261
semiconductor, disordered, theory of photodielec. effect 78−6413
semiconductor, photodielectric effect associated with impurity excitation 79−82630
stationary recombination equations, analytical solutions in source limiting cases 80−44662
testosteron, dielectric props. under UV excitation 80−6912
AgBr, photodielectric effect at low temp. *(Russian)* 80−96947
HgI_2-CdS system, photodielec. effect in freq. range 50 Hz to 20 MHz 77−11955
$KtaO_3$, photocond. props. meas. 78−91720
PLZT ceramic;, visible light scatt. depend. on photoferroelectric space charge fields 80−80806

photodielectric effect continued
PLZT ceramics photosensitivity enhancement by H- and He-ion implantation 80−96934
PbI_2, single cryst., photo-induced AC impedance meas. 78−52034
Sb_2Se_3, photocond., photo-EMF and photodielectric effect, expts. 80−20245
SrS:Mn, Zr phosphor, photodielectric effect 80−107848
ZnO pellets and ZnO:Li single cryst., photo-induced AC impedance meas. 78−52034
ZnO, photoconducting, improved model 77−1445
ZnO, photodielectric effect, space-charge polaris. 79−60872
ZnTe, photoinduced dielec. loss and capacitance changes, rel. to space charge polarisation 80−2417

photodiffusion effects *see Dember effect*

photodiodes
see also avalanche photodiodes
2 km 20 Mb/s optical fibre transmission system 78−42437
16 and 32 Mb/s optical data links 77−68275
array, plasmascope for vel. meas. in thermal plasmas 77−39462
array, thermal behaviour *(French)* 80−37083
array for single-particle light scatt. meas. 78−28146
array for use in student demonstration of diffraction patterns 78−86069
array integration with optical power spectral analysis 80−99645
astronomical image degradation, contrib. of lower atmospheric layers, use of photodiode array 79−21019
automatic focusing of cameras using self-contained IC 78−82069
avalanche, double epitaxial, for optical fibre communications 77−54782
avalanche, model, fibre optic receiver optimisation 77−792
avalanche, n^+-p-π-p^+, epitaxial Si diode for optical fibre communication at 800 to 900 nm 77−79961
avalanche, operating conditions in phase optical rangefinding 77−13799
avalanche photodiode receiver sensitivity, specification and testing *(German)* 78−38015
avalanche photodiodes for 400 MHz optical fibre communication systems, construction and characts. 77−11011
avalanche receiver in optical fibre communication system 77−27382
avalanche semiplanar mesa-type passivation by slightly conductive chalcogenide film 78−2556
avalanche Si photodiode receiver, for fibre-optic transmission systems 77−19455
book, optical and IR radiation detection 79−2821
calibration using synchrotron radiation 80−90810
calibration using synchrotron UV radiation, 5 nm wavelength 78−77959
camera shading correction cct. used in chromosome anal. 80−56325
coeff. and surface conc. 80−39122
coherent image processing photodiode array 79−55076
current conversion during pulsed illumination *(Russian)* 78−49905
cursor, aided-track, with rotatable linear photodiode array, for graphic materials digitisation 79−29899
detection of light in dielec. waveguide by photodiode through direct evanescent field coupling 78−30094
detector arrays, characts. and appl. 79−89002
differential light detector using two antiparallel Si photovoltaic diodes 79−35837
differential optical polarisation device for angular velocity meas., expt. *(Russian)* 78−29093
Doppler velocimeter with differential photodiode array 79−76743
double-junction Si photodiode, high UV responsivity 77−74504
electron beam depth profiling, using carrier collection models 80−70723
electronic speckle pattern interferometry apparatus with linear photodiode array 79−80671
enlarger exposure meter, using photodiode and multimeter 80−101857
EUV photodiodes for high accuracy location of orbital plane in storage ring 80−91335
exposure meter appl., enlarging, digital, for black-and-white photography 79−85190
fast solid-state camera for high-speed event diagnostics 80−78985
fibre communication devices, directional couplers, atennuators, switches development 79−3782
fibre communication lines, use of semicond. lasers and avalanche photodiodes 78−46793
fibre optic communication systems, utilisation of optoelectronic devices 80−1328
gas scintillation counters, use of vacuum photodiode as light sensing element 79−13601
gas scintillation proportional counters, large vacuum photodiode imaging appl. 80−58050
gas-filled, improved detectivity for UV radn. μs-order risetime 78−37062
glass fibre communication: introductory review, status and development *(German)* 79−89997
heterodyne detectors, evaluation at 5145 Å 77−71370
HgCdTe/CdTe, limited diffusion volume photodiode, characterisation 80−75627
holographic memory photodiode matrix readout system *(Russian)* 77−58266
hybrid p-i-n photodiode-FET preamplifier design for digital optical receivers *(German)* 78−33878
III-V DH photodiodes, diffusion limited transient response 80−70809
image scanning for nuclear fuel cladding tube deformation monitoring 79−30938
impuse response, optoelectronic sampling in picosecond range 77−58451
InSb detector system in Fourier spectrometer, use of improved preamplifier circuit, with integrator in feedback loop 80−73474
integrated light-sensor device with broad operating range and enhanced-blue spectral response 80−13140
integrated optical, influence of characts. on optical fibre system performance 77−83984
integrated optical detector array, waveguide, and modulator, based on Si technology 77−11049
integrating photodiode detectors, thermal background subtraction 80−90342
IR, optimisation for higher temp. operation by excess volume reduction 79−2824
IV-Vi semiconductor film, quantum efficiency 79−75596
IV-VI semiconductor lateral-collection photodiodes, for 3-5 μm region 78−32871
laser beam profile monitor system using photodiode or pyroelec. array 77−58364
laser low-level pulse meas. system at 1.064, transfer standards 80−86253
laser power radiation instability meas., of CW gas lasers 80−23704

photodiodes continued
laser pulse monitor, 50 psec detector 77—3600
light distribution profile sampled by photodiode array, reconstruction *(French)* 79—30557
lightwave pulse regenerator for triggerable semiconductor lasers 80—69408
linearity meas. of photometric devices using two LEDs 80—17996
long wave laser radiation detect. appls. 79—26135
metal-dielectric-semiconductor structures, with sub-micron channels, photosensitivity *(Russian)* 77—89876
n^+-p diffused diode, optical lifetime meas. in heavily doped diffused regions 77—80829
narrow band gap semiconductor IR devices, advances 80—48464
neutron spectra meas. with photodiodes as recoil particle detectors 79—97927
optical communication appl. *(Dutch)* 77—11036
optical fibre, communication link between computer units, using LED-photodiode pair 78—71224
optical fibre communication system device, review 79—76858
optical fibre sources and detectors *(Italian)* 80—69390
optical fibre-photodiode alignment by etched Si structure 80—53430
optical information transmission *(German)* 79—41449
optical power meters for laser photometry 78—65953
optical receivers, transmission error investigation *(Italian)* 77—54775
optical sound track reproduction using photodiode as current source 79—10439
optical vibration analyser, meas. principle 79—6119
optimisation for radiation environments 78—29158
optoacoustic IR detector, micromodularisation 79—49291
optoelectronic devices and optical imaging techniques, book 80—27059
p-i-n, Au-diffused, for freq. multiplexing optical fibre system 77—88914
p-i-n, for optical fibre communication *(Japanese)* 80—78977
p-i-n, wideband nuclear radiation monitor appl., cct. 78—78591
p-i-n detector, for rocket-borne photometry of near IR airglow 77—13128
p-i-n diode with $Ga_{1-x}Al_xAs$-GaAs-GaAs heterojunction 78—26938
p-i-n laser detector, Si, wavelength and temp. depend. characts. 80—13134
p-i-n photodetector under transient conditions, simulation and expts. 79—58793
p-i-n photodetector unit characterisation, baseband fast modulation of GaAlAs laser diode 77—11025
p-i-n photodiode, time resolution in electron detection 79—14608
p-i-n photodiode photometer 79—32
p-i-n photodiodes as low-energy photon spectrometer, resolution, efficiency, for ~22 keV X-rays 78—17471
p-i-n thin film with internal reflection 78—37059
p-n junction photodiode terminology 80—70800
p-n junction photodiodes, dark currents *(Russian)* 77—24612
p-n junction photovoltaic diode, appl. as IR detector 78—86330
photochemical diode using p-n heterojunction or Schottky barrier immersed in electrolyte 77—66201
photodetector for optical cable, optimal filter struct. and characts. 78—18067
photodetectors in 1-2 μm wavelength region *(Japanese)* 79—63307
photodiode array spectrometer, for ICP emission spectroscopy, correl. readout system 78—31726
photometer using Si photodiodes as light detectors 78—20651
photometric working standard establishment using photoreceptors *(Japanese)* 80—98964
photon detectors for optical communications *(Czech)* 79—50396
photoreceiver system, photodiode-FET, achievable threshold limit calc. 79—49292
photosensor spectral responsivity calibration microprocessor system 80—86409
photosensor with IC amplifier, camera shutter control appl. *(German)* 80—52341
photosensor with logarithmic transfer characteristic photosensor 79—93215
PIN photodiode for high-sensitivity optical power meter with tuning fork optical chopper 79—80661
pin- and avalanche diodes as photodetectors, characts. *(Swedish)* 78—89545
PIN-diode for optical fibre analogue/digital communication system with 5 MHz bandwidth *(German)* 78—30062
PIN-photodiodes, comparison for X-ray spectrom. 78—74531
pulsed light signal receiver 79—93216
pyrometers for domestic oven temp. meas. *(Russian)* 78—70128
quantum efficieny definition and determ. 77—38009
radio antenna arrays, incoherent optical 1-bit cross-correlators, radioastron. appls. 80—98555
radiometry, far UV standards comparison 77—5912
reach-through photodiodes, Si, avalanche buildup time 77—15892
reliability tests on devices for optical fibre transmission systems 80—43464
Reticon photodiode array for spectral source profiling 77—63999
Schottky barrier, quantitative meas. of body motion using laser beam 80—12207
Schottky barrier IR detector, nomographs for parameter evaluation, 77K 80—31870
Schottky-barrier diode wavelength-modulated photoresponse spectra *(Russian)* 78—84300
scintillation spectrometers, with LED and PIN photodiode, stabilising system 80—47821
scintillator photodiode detector, for intense pulsed ion beams diagnostics 77—61160
segmented photodiode, for plasma column position detect. 78—1901
selection criteria for weak signals *(German)* 77—82601
self scanned linear array for direct display of TEM energy loss spectra 78—45753
self-scanned array, with image intensifier, for photoelectron counting 77—18090
self-scanned photodiode array, evaluation for integrated optics spectrum analyser 80—58806
self-scanned photodiode array, for high dispersion astronomical spectrophotometry 78—45230
self-scanned photodiode array, image detect. from Fabry-Perot spectrograph *(French)* 80—73465
self-scanned photodiode array as multichannel spectrometric detector 80—73466
self-scanning linear array, emission spatial profile meas. appls. 78—16850
self-scanning photodiode array for fast ion detection 80—87018
self-scanning Si diode array, X-ray appls. 77—41739
self-scanning silicon photodiode array with microcomputer control 80—35612
semiconductor light-sensitive diode acoustic airgap convolver, theory 79—49288
sensor arrays, circuits and performance 77—39077
shallow junction n^+-p, spectral response limitation mechanisms 78—37058
solar power measurement, microcomputer-controlled photodiode light meter and thermistors 80—50946
solid-state image sensor resolution evaluation by aperture sampling response 78—50939
solid-state image sensors for electro-optical systems 77—39104
solid-state imaging application 77—37707
spectral response of laterally illuminated p-n junction, anal. 77—8180
spectrophotometry, solid state image sensor, appl. *(Japanese)* 78—4677
sphere photometer using photodiodes 77—71359
storage matrix control system *(Russian)* 77—58263
submillimeter radiation field, transverse distribution, scanning device for visualisation 78—4693
switching process and plasma effects in photodiode, theory 80—65667
telecentric system condenser alignment 80—33115
TEM image and electron energy loss spectrum display by self-scanned linear Si photodiode arrays 80—68330
temperature dependent response of optical radiation meas. instrumentation 78—24857
three-terminal charge-injection device image sensor 77—39084
transient process anal. in photoreceiver 78—29162
transmission system, semiconductor device reliability tests 80—58573
transparent, photodiode detector for optical fibre communication *(German)* 78—33874
ultrahigh-speed photodetector design 80—47108
vacuum detector array, for broadband UV radiation from plasma using photoelectric effect 79—90464
velocity meter, appl. of photodiodes, for internal combustion engine 77—57303
weak optical signal meas. in strong interference *(German)* 77—65623
wide-bandwidth, in heterodyne and background-limited operation, anomalous noise behaviour 79—69568
wide-gap diode detectors of IR radiation, positive feedback 78—24863
wideband 1064 nm laser communications detector evaluation 77—18097
wideband subcarrier PFM analogue optical communications channel 77—27378
windowless XUV photodiodes with Al_2O_3, W photocathodes, photoefficiency 20 to 250 eV 78—65963
X-ray analysis, appls., conf., Denver, USA (Aug 1975) 77—56307
X-ray detector, photoelec. diode with Al photocathode, calibration 77—54033
X-ray detector, self-scanning photodiode array, direct X-ray response 77—54032
X-ray generators, meas. of peak voltage with PIN-photodiodes 80—105754
X-ray imaging, MOS solid-state detector arrays 78—47180
Al-GaAs-$Al_xGa_{1-x}As$ Schottky barrier diodes, prep., characts. 80—6948
Al-SiO_x-Si, experimental verification of theoretical predictions 80—29485
Al-SiO_x-Si minority-carrier MIS photodiodes, elec. characts. 79—51676
$Al_xGa_{1-x}As$-GaAs heterojunction photodiodes, high-efficiency fast-response 78—52073
AlGaAsSb, photodiode, lattice-matched to GaSb 79—71527
AlGaSb, growth and characts. for 1.0-1.8 μm heterojunction devices 78—6870
Au-GaAs, photosensitivity losses, field and spectral depend. 80—2452
AuSi ionizing radiation detector, photosensitivity variation 79—36464
$CdGeAs_2$, photosensitivity to linearly polarised radiation 77—55569
$CdGeP_2$:In based surface barrier diode, photosensitivity 79—33330
Cd_xHg_{1-x} Te Ir detectors, props. and manufacture *(German)* 77—2693
CdHgTe detectors for CO_2 laser appls. 79—40615
(CdHg)Te, ion implanted graded gap photodiodes 78—39192
$Cd_xHg_{1-x}Te$, high efficiency, energy level diagram 77—15891
$Cd_xHg_{1-x}Te$, IR responsivity and detectivity 78—19139
$Cd_xHg_{1-x}Te$, tunnelling effect in p-n junctions 80—75630
CdSb:Al, p-n junction formation by laser emission, photoelectric effects *(Russian)* 80—70815
$CdSiAs_2$, photoelec. props., potential photodetector and solar cell appl. 77—43655
$CdSnP_2$-InP, n-n heterojunctions, growth, elec. characts. 77—11992
$CuInS_2$, p-n junction photovoltaic props. and detectors 79—99574
Cu_2S-CdS heterojunction diodes, barrier model estimated from photovoltage and cathodoluminesc. spectra 79—78165
Cu_2S-CdS p-i-n structure diode, photoelec. characts. 78—2557
$Ga_xAl_{1-x}As_x$ photodetector diode on GaAs substrate dark currents, tunnelling, energy gaps, effective masses 80—70805
GaAs, electroabsorpt. avalanche photodiode, waveguide detector for 1.06 μm 78—16842
GaAs high speed avalanche photodiode design 78—8446
GaAs injection photodiode IR radiometer 79—75597
GaAs:Fe epitaxial diode, photocapacitance meas. 77—43708
GaAs-$Al_xGa_{1-x}As_x$, heterojunction photodiode, electric and photoelectric characts. 77—55604
GaAs-metal diode, surface-barrier, excitons effect on photocurrent 79—82670
$GaAs_{0.6}P_{0.4}$, low dark-current MOS photodiodes 77—32083
$GaAs_{1-x}P_x$, light detector for camera 79—89019
$GaAs_{1-x}Sb_x$, photodiode structures, current-voltage characts., photo-EMF spectra 80—29472
$GaAs_{1-x}Sb_x$ photodiode, speed and sensitivity meas. 80—92937
GaInAs, efficient photodiode for near IR detection 78—16848
GaInAs p-i-n/FET hybrid optical receiver for communication systems 80—33158
$Ga_{0.47}In_{0.53}As$, homojunction avalanche photodiode, exam. of props. 78—37072
$Ga_{0.47}In_{0.53}As$, photodetector applications 80—95140
$Ga_{0.7}In_{0.3}As$ photodiodes, fibre optic appls. 79—40613
$Ga_{1-x}In_xAs$ photodetectors for 1.3 micron PIN-FET receiver 80—13145
GaInAsP on InP substrate, epitaxially grown, fabrication of avalanche photodiode 78—37071
$Ga_xIn_{1-x}Sb$ p-n junction photodiode fabrication, sensitivity as 1 to 2.5 μm detectors *(Japanese)* 80—52311

photodiodes continued
GaP:Zn,O, photodiodes, high temp. emission spectra *(Russian)* 77−66545
n-GaP-Au, Au overlayer potential on photoelectrodes, I-V curves 77−89848
GaSb mesa photodetectors with very high quantum efficiency between 1.3 and 1.6 μm 80−47102
p-GaSb−n-$Ga_{1-x}Al_xSb$, photodiode, LPE, spectral response, quantum efficiency 78−47850
Ge, intrinsic photodiode as IR detector, fabrication and performance 77−57388
n-Ge p^+-n photodiodes, electron irradiated, energy levels 79−28316
Ge, S-type diode, photoelec. props. 77−24614
Ge, spectral response and responsivity 78−29160
Ge:Hg S-type diodes, photoelec. props. 80−6964
(Hg,Cd)Te, for 2 μm IR detection 77−82603
(Hg,Cd)Te n^+-p photodiodes, 8 to 12 μm IR imaging appls. 80−9044
(Hg,Cd)Te photodiode IR detectors, planar technology 80−9043
(Hg,Cd)Te photodiodes, wide-bandwidth 10.6 μm IR heterodyne detect. 80−9042
(Hg,Cd)Te photovoltaic detector, 5 μm, direct coupling with CCD multiplexer 77−83987
HgCdTe, imperfections and surface conditions using electron induced current technique 79−67385
HgCdTe photodiode IR detector, selection 79−58791
HgCdTe photodiodes formed by double-layer LPE 80−104078
HgCdTe reverse-biased photodiodes for wideband appls., excess noise 80−107876
HgCdTe Schottky barrier diode and n-p diffused junction IR detectors, comparison 80−9039
HgCdTe solid solution photodiode for CO_2 laser active medium study 80−95868
HgCdTe varactor, heterodyne detection for CO_2 isotope laser freq. calibration 77−19230
HgCdTe wide bandwidth photomixers 77−3682
HgCdTe-CdTe IR detector arrays, 3 to 11 μm, fabrication techniques 80−9041
HgCdTe-CdTe photodiode, 1.33 μm, grown by LPE, phys. props. 80−107892
$Hg_{0.68}Cd_{0.32}Te$ photodiode, minority carrier lifetime determ. 79−38084
$Hg_{1-x}Cd_xTe$ IR detector technology 78−77989
$Hg_{1-x}Cd_xTe$ IR focal plane status and performance 78−77987
$Hg_{1-x}Cd_xTe$ implanted detector 8 to 14 μm, performance, p-n junction characts. 77−15941
$Hg_{1-x}Cd_xTe$, material capabilities for 1 to 1.3 μm room temp. photodiodes 78−24859
$Hg_{1-x}Cd_xTe$ photodiodes, implanted n^+-p, improved performance using insulated field plates 80−52309
$Hg_{1-x}Cd_xTe$ photodiodes, long cutoff wavelength, effect of trap tunnelling on IR detector performance 80−73451
$Hg_{1-x}Cd_xTe$ Schottky barrier photodiodes, for IR detection 80−13144
$Hg_{1-x}Cd_xTe$-CdTe, backside-illum., LPE growth and thermal noise characts. 79−40610
$Hg_xCd_{1-x}Te$, anomalous noise behaviour in heterodyne and background limited operation 79−69568
InAsSb, for hybrid IR focal plane modules construction 77−87825
$InAs_{1-x}Sb_x$, epitaxial heterojunction photodiodes, IR detector appls. 77−79155
$InAs_{1-x}Sb_x$-InAs backside-illum. narrow band photodetectors 77−61118
InGaAs, lattice-matched VPE on (100) InP, photodiode appl. 80−35102
InGaAs, VPE on (100) InP substrate, photodiodes fabricated 80−40267
InGaAs/InP p-i-n small area photodiodes, fabrication, characts. and performance in 274 Mb/s receivers at 1.31 microns 80−53415
InGaAs-InP punch-through type photodetector fabricated by VPE 80−68253
$In_{0.53}Ga_{0.47}As$ p-i-n photodiodes, for long-wavelength fibre-optic systems 80−5826
$In_{0.53}Ga_{0.47}As$ photodiodes with dark current limited by generation-recombination and tunneling 80−107893
$In_{0.53}Ga_{0.47}As$-InP, 1.7 μm heterojunction lasers and photodiodes fabrication 78−25880
InGaAsP, dual-wavelength demultiplexing photodiode 79−63304
InGaAsP IR heterojunction photodiode detector 79−21813
InGaAsP, lattice-matched, LPE growth on (100) InP, heterojunction photodiodes fabricated 78−64483
p-InGaAsP, on InP surface, diffusion coeff. and surface recombination velocity 80−39598
InGaAsP quaternary alloy IR heterojunction detectors, props. 79−2823
InGaAsP-InP photodiodes antireflectively coated with InP native oxide 80−13137
$In_{1-x}Ga_xAs_yP_{1-y}$-InP photodetectors, high-efficiency with selective wavelength response, 0.9-1.7 μm 79−21810
$In_xGa_{1-x}As_xP_{1-x}$-InP photodetectors, construction and performance 78−65966
$In_xGa_{1-x}As_yP_{1-y}$ photodetector diode on InP substrate dark currents, tunnelling, energy gaps, effective masses 80−70805
$In_xGa_{1-x}As_yP_{1-y}$-InP n-p heterojunction, characts. 78−14800
In_2O_3-Si highly photosensitive diodes, and their appl. 78−23152
InP photodiodes, dark current and breakdown characts. 80−70806
InP-$In_{1-x}Ga_xP_{1-y}As_y$, LPE for optoelectronic devices *(German)* 79−95280
$InSb/Pb_{0.79}Sn_{0.21}Te$ photodiodes, two-colour sandwich detector 77−82602
MoO_3-Si, fabrication as function of O_2 partial press. 80−29464
(Pb,Sn)Te, (Pb,Sn)Se IR detector diodes, junction resist. comparison, minority carrier lifetimes 78−24858
PbS_xSe_{1-x}, multispectral photovoltaic IR detectors 80−105710
PbS_xSe_{1-x}, Schottky-barrier IR detector, comp. tuning 78−12752
$Pb_xSn_{1-x}Se$, multispectral photovoltaic IR detectors 80−105710
PbSnTe, for hybrid IR focal plane modules construction 77−87825
PbSnTe/PbTe inverted heterostructure mosaics, long wavelength, energy gap-Fermi level temp. depend. 79−85182
$Pb_{0.8}Sn_{0.2}Te$, film photodiodes, quantum efficiency 79−75596
$Pb_{1-x}Sn_xTe$, impurity defused IR detector, spectral response depend. on impurity conc. *(Japanese)* 78−58036
PbSnTe(Se) Schottky barrier diode and n-p diffused junction IR detectors, comparison 80−9039
PbTe, film photodiodes, quantum efficiency 79−75596
PbTe IR diode, epitaxially grown and ion implanted, minority carrier lifetimes, efficiency 77−20411
Si, 1.06 μm range, neutron and γ-irrad. effects 79−97433
photodiodes continued
Si, amorphous, photovoltaic diodes, influence of mag. field on charge transport 80−49891
Si, amorphous vacuum deposited p/undoped photodiode and diode-voltage variable resistor combination 80−61380
Si array detector for at. emission spectroscopy *(German)* 79−87926
Si, as position sensing detectors for precision measurement and control 79−86273
Si avalanche photodiode, microplasma sites in n^+-p junction SEM and TEM characterisation 77−43702
Si, correction filter selection 77−50767
Si crystal whiskers for use as photoconvertors 79−67386
Si detectors, vac. UV performance, 500-2000 Å 77−26397
Si diffused junction photodiode performance characteristics 80−80367
Si, for position-sensitive X-ray detector 80−52831
n-Si high-temp. vacuum etching, p-n junction photodetectivity 78−95355
Si, laser beam detection appl. expt. *(Czech)* 78−62225
Si, linear arrays, use for high-energy electrons detection, SEM assessment 78−32951
Si, n-type, thermally oxidised, natural inversion layer, UV photodiode construction 79−30559
Si p-i-n photodiode meas. of X-ray tube kVp *(German)* 79−232
Si, p-n junction, quantum efficiency as absolute radiometric standard 79−49284
Si p-n junction diodes and solar cells, minority carrier diffusion length 80−107894
Si, p-n junction photodiode growth by ionised-cluster beam deposition, sensitivity 77−32527
Si, PIN photodiode, appl. in photon irradiance sensor 78−32843
Si photodetector storage-mode operation 77−39075
Si photodetector UV enhanced responsivity 77−74499
Si photodiode, correcting absorber selection for flash photometry 79−72699
Si photodiode, in combination with PbS and PbSe photocells, multicolour detectors *(Czech)* 79−26126
Si photodiode, multidecade linearity meas. 79−75592
Si photodiode, refl. and external quantum efficiency change after surface cleaning 79−93212
Si, photodiode, violet and near UV sensitive, prep. and expt. study *(Chinese)* 79−49285
Si photodiode absolute spectral response self-calibration 80−73448
Si photodiode array, position-sensitive photon detector for the UV or X-ray range 80−90970
Si photodiode array for integrated optical spectrum analyser 80−33241
Si, photodiode array for radiation detection in AES and analytical appl. *(German)* 80−11992
Si photodiode for optical channel waveguides 80−102805
Si photodiode imaging array design factors 77−39085
Si photodiode internal quantum efficiency basis for absolute radiometric standard 80−86410
Si photodiode saturation at high modulation freq. 78−54453
Si, position-sensitive photodiode, for angular displacement recording 77−49712
Si, radiometer/photometer appl., commercial devices survey and classification 78−16830
Si ring photodiode reflectometer for cavity reflectance 80−86376
Si, Schottky diodes on sputtered amorphous Si:H, light induced ageing effects, interpretation of photovoltaic stability 80−54780
Si, solar irradiance meas. using optical fibres and Si detectors 79−100960
Si:B photodiode front region collection efficiency models 80−96899
Si:H, amorphous, Schottky diode, spectral response and hole drift mobility 80−39673
Si:Re, barrier capacitance and photocapacitance, uniaxial press. effect 77−20416
Si:Re diode, photocapacitance and induced photocapacitance spectra 77−4404
Si:Rh, p^+-n-n^+, n^+-n-n^+, p^+-n-p^+, structs., S- and N-type I-V characts. 77−43706
n-Si-Au surface barrier diode, photosensitivity in spectral range, 1-6 eV 77−89850
Si-CdS p-n heterojunction photodetector fabrication and characts. 78−52068
Si-p-i-n photodiode as detector in optical power meter for fibre-optic appls. 78−93746
Si-SnO_2 highly photosensitive diodes, and their appl. 78−23152
SnO_2-Si n-n photodiode, 5.4 MeV electron irrad. effects 77−80806
W-Ni point contact diode fast acting detector for modulated CO_2 laser beams 79−3730
$ZnGeP_2$ p-n homodiode, polarisation photosensitivity and photopleochroism spectra 80−107866
$ZnIn_2S_4$ diode struct., photoelec. props. *(Russian)* 77−43720
Zn_3P_2-Al(Mg)(Be), diode, spectra response meas. of minority carrier diffusion length 79−78131
n-$ZnSiAs_2$ photodiode, fabrication and photoelec. props. 77−8146

photodisintegration
see also deuteron photodisintegration; photofission
few body systems and EM interactions, conference, Frascati, Italy (March 1978) 79−71804
high energy photon absorption cross section for matter, review *(Japanese)* 78−74506
photospallation systematics, complementary study 78−17179
three-nucleon systems, EM processes 79−71806
three-nucleon systems, props. and interactions 79−71805
two-step processes in photonuclear reactions 77−54205
virtual photon theory, validity 77−2977
$^9Be(\gamma,\alpha_0)^5He$, 18 to 26 MeV, integrated cross section 78−37327
$^9Be(\gamma,n)^8Be$, 18 to 26 MeV, integrated cross section 78−37327
Be(γ,p)X, 180-420 MeV, quasifree NN system photodisintegration, p spectrum 80−106049
^{12}C, photodisintegration induced by 40 MeV γ-rays, correl. spectroscopy 77−6345
$^{12}C+\gamma\rightarrow 3\alpha$, photodisintegration theory using 3α model and hyperspherical functions *(Russian)* 78−78365
$^{12}C(\gamma,n)^{11}C$, relativistic heavy ions, Coulomb disintegration, photodisintegration cross section *(Russian)* 78−89851
^{13}C, decay props. of giant dipole reson. photoreactions anal. in continuum shell model 77−26665
^{14}C, photodisintegration induced by 40 MeV γ-rays, correl. spectroscopy 77−6345

photodisintegration continued
^{59}Co, spallation by 0.3-1.0 GeV photons, cross-sections 78−41691
Fe, spallation by 0.3-1.0 GeV photons, cross-sections 78−41691
^{2}H, integrated cross section for trinucleon photoeffect 78−82334
^{3}H, quadrupole contribution to cross-section, isospin sum rules 77−30550
^{3}H, three-particle photodisintegration, hyperspherical functions method *(Russian)* 78−589
^{3}H, total photodisintegration cross-section calc. using coupled hyperspherical harmonics 77−18525
^{3}H(γ,X) two- and three-body photodisintegration cross sections 80−32263
^{3}He, integrated cross section for trinucleon photoeffect 78−82334
^{3}He, isospin 1/2 three body photodisintegration suppression 79−40902
^{3}He photoeffect to isospin 3/2, coupled hyperspherical harmonics 78−41696
^{3}He, quadrupole contrib. to cross section, isospin sum rules 77−30550
^{3}He, three-particle photodisintegration, hyperspherical functions method *(Russian)* 78−589
^{3}He(γ,2p)n, 80-120 MeV, proton energy distribs., diffr. cross sections, direct breakup 80−86897
^{4}He, clustering effects 79−36227
^{4}He, in giant resonance region 77−41944
^{4}He photodisintegration, 9-dimens. space hyperspherical harmonics 79−75975
^{4}He photodisintegration, pair correlation study *(Russian)* 80−86899
^{4}He photodisintegration, total, dipole, and quadrupole cross sections, sum rules *(Russian)* 80−83094
^{4}He, photodisintegration down to meson prod. threshold *(Russian)* 79−13282
^{4}He, quadrupole contrib. to cross section, isospin sum rules 77−30550
^{4}He, soft-core radial wave function, photo-disintegration calculation 80−18209
^{4}He(γ, pnd), ^{4}He(γ,p), ^{4}He(γ,n), 60-170 MeV, quasideuteron mechanism calcs. 77−2978
^{4}He(γ,P)^{3}H, 20 to 50 MeV, 2^{+} resonances *(Russian)* 79−59052
^{4}He(γ,X), X=p,n, 50-150 MeV, total cross sections, quasiparticle formalism calcs. 80−78277
^{4}He(γ,2n)2p, final state interaction effects, 2 nucleon photoabsorption mechanism 79−36228
^{4}He(γ,d)d, total cross-section calc. 77−18526
^{4}He(γ,n)^{3}He, 20 to 50 MeV, 2^{+} resonances *(Russian)* 79−59052
^{4}He(γ,pn), clustering effects 79−6562
^{4}He(γ,pn)^{2}H, three particle photodisintegration, pole mechanism contrib. *(Russian)* 80−91176
^{6}Li, quasi α-particle photodisintegration at 35-55 MeV *(Russian)* 78−46046
^{6}Li(γ,d)^{4}He cross-sections extracted from ^{6}Li(e,d)e′ ^{4}He meas. 77−6355
^{7}Li, quasi α-particle photodisintegration at 35-55 MeV *(Russian)* 78−46046
^{A}Li, A=6, 7, photodisintegration, particle ang. distribs., (γ,t) cross section 79−75974
^{55}Mn, spallation by 0.3-1.0 GeV photons, cross-sections 78−41691
^{16}O(γ,n)^{15}O, relativistic heavy ions, Coulomb disintegration, photodisintegration cross section *(Russian)* 78−89851
^{32}S(γ,n), (γ,p), cross sections, ^{31}S, ^{31}P excited residual states 78−8795
Ta photodisintegration yields, 600 to 1300 MeV, cross sections *(Russian)* 77−50112
^{51}V, spallation by 0.3-1.0 GeV photons, cross-sections 78−41691
W photodisintegration yields, 600 to 1300 MeV, cross sections, photo- to electro-yield ratio *(Russian)* 77−50112

photodissociation
see also molecular photodissociation
acetaldehyde, HCO form., wavelength depend. 79−83490
alkali metal reson. line lasers based on photodissoc. 79−72560
allylmethylether, thermal and IR laser induced unimol. decompositions 78−20012
atmosphere, diurnal average photodissoc. rates determ. 77−78311
atmospheric photodissociation wave in open channel, transparency channel form. 78−79407
bleaching-wave front, stability 77−42574
copper oxalate hemihydrate, photographic props. eval. for use as high-speed photographic materials 77−44497
cryptopleurine derivatives, absorpt. and fluoresc. obs. of photodecomp. processes, dye laser relevance 80−55686
diacyl peroxides, for matrix isolation study of IR spectra of alkyl radicals 78−33510
dibromodifluoromethane, vac. ultraviolet photodissociation, CF_2 emission 79−47955
dichlorodifluoromethane, UV absorpt. cross sections temp. depend., stratospheric appls. 77−64423
ethylacetate, thermal and IR laser induced unimol. decompositions 78−20012
halomethanes, multiphoton dissoc., energy deposition 78−82800
8-hydroxy, 1,3,6-pyrene trisulphonate, picosec. proton ejection, ultrafast pH jump 79−83475
ortho-hydroxybenzophenone, soln., intramol. proton transfer and energy relax. photostability, transient absorption obs. 80−28032
ion photofragment spectroscopy, via laser-ion coaxial beams spectrometer 78−12775
ionosphere D-region, sunrise variations of negative ions and electron conc. 80−31157
IR multiphoton dissoc., quantal and classical calcs. 80−83431
isopropylbromide, thermal and IR laser induced unimol. decompositions 78−20012
ketene, multiphoton laser-induced decomp. chemilum. and collision-assisted dissoc., rephotolysis 79−83491
multiphoton dissociation, collisionless, laser pulse shape effect on product yield 80−78667
2-naphthol-3,6-disulphonate, picosec. proton ejection, ultrafast pH jump 79−83475
nickel oxalate dihydrate, photographic props. eval. for use as high-speed photographic materials 77−44497
oxazine dyes, comparative photostability 80−3376
planetary atmospheres, diurnal average photodissoc. rates determ. 77−78311
poly-1-vinylnaphthalene solution, time-resolved fluoresc. spectroscopy, excimer form. and dissoc. 79−38637
polyatomic molecules, primary photochem. processes *(French)* 77−90620

photodissociation continued
polymers, synthetic, radiative degradation, chem., phys., environmental, technological effects, review 80−40948
polystyrene solution, time-resolved fluoresc. spectroscopy, excimer form. and dissoc. 79−38637
saturation effect in stimulated transitions between states of discrete and continuous spectra 77−42295
selective interactions of laser radiation, photoionisation [-] elementary processes 77−27034
semiconductor-electrolyte contact, electrolytic decomposition and photodecomposition 78−95357
trichlorofluoromethane, UV absorpt. cross sections temp. depend. stratospheric 77−64423
trifluoroethene, dissociation from 2,2-dichloro-1,1,1-trifluoroethane, fluence threshold 79−64112
water, photosensitised decomposition, electron transport across phospholipid vesicle walls 78−80787
$As_2S_3(Se_3)$ films, vitreous, photodecomp. and photostruct. changes 77−76318
$CCl_2FO_2NO_2$, thermal dissoc., rel. to photodissoc. and stratospheric Cl budget 79−74931
$C_7H_8^+$ ion, dye laser-induced photodissoc. in gaseous toluene 77−25286
CO-haemoprotein photolysis, transient Raman study, quantum yield origin 80−67155
$ClONO_2$, form., photolysis in stratosphere, photochem. absorpt. cross sections, UV spectra 77−33154
D_2, D(2p) dissoc. products detection 78−50605
HN_3 in ethane or propane solution, photodecomp., NH reactions 79−83471
HN_3, photodissoc., NH photofragment energy distrib. and reaction rates 77−90618
H_2O, photodissociation, semiclassical approach to abnormal rotation of $OH(A^2\Sigma^+)$ 78−40069
I photodissociation laser, high-power, pulse amplification 80−48234
I_2, flashlamp excited photodissociation laser 79−72558
ICN, rotational distribs. in photodissociation 77−9097
KBr, X-irrad. crysts., halogen aggregation, absorpt. spectra obs. *(Russian)* 80−66234
KCl and KCl:NO_2, X-irrad. crysts., Cl_3^- centres photodissoc., optical anisotropy and creation mechanisms *(Russian)* 80−66235
N_2 in high press. air plasma, photodissoc. 80−64691
NH_3, appl. to solar energy conversion 80−30513
SF_6, laser-induced isotope separation, threshold intensity 77−4898
SF_6, multiphoton dissoc., energy deposition 78−82800
SF_6, multiphoton IR dissoc., quantum or classical approach 78−82801
n-Si:Re diode photocapacitance spectra, Re centre dissociation 79−90997
TlI, UV photodissoc., time of flight spectra and ang. distrib., excited state assignment 79−64061
UF_6, ^{235}U enrichment by laser isotope separation 77−19113
W, multiphoton ionisation and absorpt. 80−95575
XeF_2(C) state lifetime, quenching rate consts., photolysis in inert gas atmospheres 80−66816

photodissociation of molecules *see molecular photodissociation*

photoelasticity
see also mechanical birefringence
acoustic electronic signal processing devices, photoelastic materials, nonlinear elastic interactions *(French)* 79−41525
alkali and alkaline earth metal metaphosphate glasses exam. of thermooptical and photoelastic props. 78−88287
alkali halide, strain polarisability parameter, evaluation 77−35617
alkali halides, photoelastic constants effect of many body forces 78−47464
alkali halides, photoelastic consts., short range polarisability effect 80−80748
alkali halides, piezo-optical properties, temperature dependence 78−92050
alkali halides, three-body interactions, effect on electronic polarisabilities and photoelastic behaviour 79−47382
alkaline earth fluorides, vol. depend. of refr. index 78−88275
alkaline earth oxides, photoelastic consts. 78−71781
Araldite CT200/Hardener HT907 cylinder, thermal stresses and photoelastic fringe order 77−62219
axisymmetric bodies, integrated photoelasticity, nondestructive anal. 79−18842
axisymmetric problem, simplification 80−38272
basic concepts 80−14637
beam, stress distrib. around slender notch, two-dimens. photoelastic investig. 78−34069
beams, rectangular with abrupt changes of section, flexural rigidity 77−35035
biaxial testing machine, for flat specimens, photoelastic model *(Japanese)* 77−70268
birefringence measurement using photoelastic modulator 80−31838
birefringent, rotating, and achromatic quarter wave plates, appl. to ellipsometry and photoelasticimetry *(French)* 80−14278
birefringent material stress determ. in single hologram exposure 80−106770
birefringent materials, meas. of time-depend. principal strain directions 77−2647
bridge plate of pin joints, elastic-plastic anal., photoelasticity method *(Polish)* 79−64608
Brillouin scattering process kinematic dispersion relation, wave vector surfaces representation *(German)* 78−19492
bulk forces modelling, increasing effectiveness of centrifuging *(Russian)* 78−87314
ceramic turbine disc, subjected to centrifugal stresses, failure probability, photoelastic model 79−18816
chalcogenide glasses, optimum glasses for acoustic delay lines and deflectors 78−55420
characteristic parameters, fast iterative determ. procedure 79−27530
characteristic parameters three dimens. case, approx. mathematical determ. procedure 79−1112
circular ring, inner boundary shapes, optimised, diametral compression 80−38369
coating, photoelastic tests, construction of polariscope *(Polish)* 77−5887
complex part stress anal., photoelasticity and finite element methods 78−71279
composite, constrained zones at singular pts. of inclusion contours, method of caustics 77−51003

photoelasticity continued
composite cylinder, mechanical loading, photoelastic stress anal. 78−26031
composite material, sintered, microstrained state, opt. polarisation investig. 78−11476
composite prism under partial compression, photoelastic anal. 79−18852
composites, appl. of exptl. methods to fracture 80−11869
compound optical polarisation materials for stress meas. *(Russian)* 78−87313
computer simulation of stress field, use in photoelasticity technique 79−41637
concrete, joints glued with reaction resinous mortar, photoelastic exam. *(German)* 78−76825
concrete, stress determ. by holographic and speckle techniques *(French)* 79−27603
concrete, stress distribs. under splitting loads *(Japanese)* 78−35495
constitutive relations in photomechanics 80−43251
countersunk hole in flat bar in tension and transverse bending, stress concentration factors 79−46274
couple stress effect on stress conc. near inhomogeneity, photoelasticity meas. 77−89076
crack, stress concentration near apex, elasticity theory and photoelastic expts. 80−23959
crack growth, 3-D geometric effects, implications for composite material structures 80−10204
crack in pressure vessel nozzles, stress intensity factors, photoelastic meas. 77−44360
crack propag. angle prediction under tensile stress 80−87748
crack tip mixed mode isochromatic fringe patterns 80−28464
cracks in press. vessel nozzles, stress intensity factors, photoelastic anal. 77−80125
crystalline optical material props., symmetries and tensorial relationships 80−108174
cubic crystal, application of integrated photoelasticity *(Russian)* 78−47465
cubic crystal, elastooptic consts., theory 77−65998
cubic ionic crystal, photoelastic shear consts. 79−86833
cubic single crystal, integrated photoelasticity 79−33671
curvilinear cracks in bonded dissimilar materials, expt. soln. based on caustics 77−58622
cyclic stress amplitude meas. by time-averaged photoelasticity 78−18261
cylinder, circular, thermal stress conc. determ. by integrated photoelasticity *(Russian)* 77−46925
cylindrical punch, three-dimensional stress field, photoelastic studies 80−93272
cylindrical shell, stress concentration near inclined holes 80−33460
demonstration, colour image of stress pattern 77−13548
diatomic crystal, exchange charge polaris. effect 77−81046
dielectric bodies, stress determ. using EM waves 80−38370
dielectric permeability sound wave induced nonlinear modulation *(Russian)* 80−16008
dielectric tensor field determ. in weakly inhomogeneous anisotropic media 79−72492
disc specimens, photoelastic study of fracture process under superimposed static and dynamic loading *(German)* 79−34267
discs, impact stresses, photoelastic investigation 79−37182
discs, static and dynamic contact conditions obs. *(Japanese)* 80−23970
duralumin, elastic-plastic stress anal. by photoelasto-plastic method and X-ray method *(Japanese)* 78−13978
dynamic photoelastic constant meas., time averaged holography technique *(Japanese)* 79−64610
elastic wave excitation by laser beam, through thermoelastic effect 80−103503
elastic-plastic boundary, photoelastic determ. 79−81739
elasto-optical detection of gravitational waves 80−126
elasto-optical effect estimation for differing mats. 77−48145
elastodynamic stress states rel. to photoviscoelastic model *(Russian)* 78−75080
elastooptical constants and refractive index, thermo-optical method for meas. 80−7327
elastoplastic medium with cylindrical cavity, stress distrib., photoelastic investigations, successive elastic solns. *(Polish)* 80−64391
electric polarisation effects on piezoelec. and photoelastic interactions *(German)* 78−35091
electronic dielectric const. of cryst. under hydrostatic press., volume depend. 79−42887
elliptic retarder, expt. method for optical parameters determ. 77−88941
ellipticity, azimuth and system parameters linking eqns., 3-dimens. model propag. 78−50695
Epon 828, simple procedure for casting plates for 2D photoelastic models 79−39061
Epon 828 epoxy, composite three dimensional model for photoelasticity 78−52871
epoxies and polyurethane rubbers, material and optical props. in complete photoelastic analysis 77−42734
epoxy, three-component modified, development for dynamic photoelastic obs. of fracture 78−35474
epoxy resin, crack propagation, photoelasticity investig. 79−8341
epoxy resin, exam. of stress conc. around conical cutouts, using photoelastic method 79−41639
epoxy resin, stresses arising during high-speed droplet impact 80−71764
epoxy resin (Araldite B), photothermoelasticity meas. by heating method 80−6000
epoxy resin reinforced by multilayer systems, exam. of stress states, using photoelastic method 79−41638
equidensiometric applications 77−27495
equidensity fringe pattern lines on special film, calibration 77−18118
error assessment using equidensity fringes 80−28475
ethylene-propylene copolymers, mech., photoelastic props. rel. to chain microstruct. 77−48468
experimental technique, shrinkage stress semicircular inclusion in semi infinite plane *(Japanese)* 77−65672
fibre reinforced composite, unidirectional, representative volume, elastic moduli, calcs. by photoelasticity *(Russian)* 79−34094
fibrous composite models, photoelastic analysis of interlaminar matrix stresses 77−3799
film, fluctuations of acoustic Love waves and light scattering *(Russian)* 77−28543
force meas. exerted by moving organisms; photoelastic substrate technique 79−39621
fracture mech. techniques, review 79−41635
fracture of compact tensile test pieces with starting notches *(German)* 77−58619
fracture studies 80−38358
fringe pattern analyser, computer aided 80−38359
fringe photography, improved photograph quality 80−27364
frozen stress fields, study of crack-tip nonlinearities in photoelastic materials 79−37239
frozen stress model repeated use 77−7309
frozen stress slices, fractional fringe order lines obtained by controlled density techniques, self-calibration 77−51001
GaAs epitaxial layer photoelastic channel optical waveguides 80−48457
girder webs, epoxy resin models, flange thickness, stress effects, photoelasticity study 79−41640
glass, float, surface stress meas. by optical waveguide effect 80−43681
glass, ion-exchanged, anomalous stress profile, photoelastic meas. 78−90803
glass, photoelastic const. for chem. strenthening, circular plate compression method *(Japanese)* 80−93279
glass, stroboscopic photoelasticity appl. in US wave visualisation for NDT teaching 77−57136
glass fibre reinforced epoxy, exam. of interlaminar shear stress distribution 79−43308
glass fibre reinforced epoxy composite, mech. and photoelastic props. at high temps. 78−19799
glass fibre reinforced polyester, photoelasticity, optical charact. 79−18709
glass-metal seal, finite element anal. of stresses, photoelastic meas. 79−29197
gravitational radiation detection method, elastooptical antenna, photoelastic effect 80−46947
half-planes, distributed load end values by optical caustics technique 79−18851
Holmalite-100, dynamic photoelastic and dynamic finite-element analyses of dynamic-tear-test specimens 79−55348
holographic, investigation of 2-D models *(Polish)* 78−18263
holographic determination of absolute retardation fringes by vectorial reconstruction 78−87315
holographic measurement, separation of constraints, frozen deform. *(French)* 77−68187
holographic photoelasticity, Faradays effect appl. *(Chinese)* 80−5998
holographic photoelasticity, using dual-hologram method 77−19198
holographic technique for calibration of isochromatic and isopachic fringe pattern *(Rumanian)* 79−86388
holography, sandwich technique, theory of images and fringes *(French)* 78−17872
holography *(Chinese)* 79−81828
Homalite, specimen geometry effect on crack propag. and arrest 79−34148
Homalite 100, dynamic fracture specimens, dynamic photoelastic analysis 77−44364
Homalite-100 plate, fracturing, dynamic energy release rates 77−7340
Homalite-100 plates, modified compact-tension specimens, dynamic anal. 80−97561
Homalite-epoxy duplex specimens, crack arrest study via dynamic photoelasticity 78−31515
hydrostatic stress and deformation meas., photoelasticimetry appl. 79−7353
II-VI partially covalent crysts., vol. depend. of refr. index 78−88275
imaging using IR polariscope 79−94567
impacted pretensioned plate, dynamic finite element and photoelastic analyses 78−67111
inert gas crystal, dielec. const., Brillouin scatt., short-range at. interaction effect 78−43881
inert gas solids, Brillouin scatt. intensity, elastooptical coefficients 78−10907
integrated retardation technique, rotationally symmetrical bodies, thermal stress 80−38362
interferometer, Moire method appl. 78−51138
interferometer for precise photoelastic consts. meas. 77−26384
interferometric and holographic fringe patterns, unified interpretation 79−18844
inversion method for study of two-dimens. photoelastic model *(Polish)* 78−22266
ionic crystal, analysis based on Claussius-Mossotti theory of dielec. const. 77−12358
ionic crystal, electronic dielec. const. strain derivative, photoelasticity 77−4620
ionic crystals, effect of Lundqvist's many body potential on phototelastic behaviour 77−63391
ionic crystals, evaluation of photoelastic consts. 80−50297
IR region meas. 79−30443
IR window materials, optical phenomena, book contrib. 78−9420
isochromatic crack tip fringe patterns, dynamic 3-parameter method for stress intensity factors 80−38365
isochromatic fringes, comparison of stress intensity factor determ. methods 77−84197
isoclinic and isochromatic lines, simultaneous determ. by holographic recording using CW TEM laser 80−63946
isoclinic indicator for photoelastic studies 77−19577
isoclinics, photographic recording and sharpening 77−51002
isodynes, new type of stress modulated light intensity distrib. 78−26092
joints, stress concentrations, Modeltech method, full scale models and photoelastic coatings *(Polish)* 80−64369
laser light diffraction, appl. to meas. of acoustic and acousto-optic props. of crystals *(Polish)* 78−76425
laser window materials, temp. and stress effects on refr. index 77−46771
laser-Raman spectroscopy with AC differential analysis 77−38031
Lexan, optical and phys. parameters 79−32004
Liebmann formula appl. to photoelastic meas. *(Polish)* 78−13979
light diffraction by sound in impurity containing crystals 79−8119
light wave propagation in photoelastic materials and crystals 79−898
linear stress detection at point in three dimensional photoelasticimeter *(French)* 79−34268
liquid, crit. evaluation of eqns. of state 79−78650
liquid, photoelastic, EM wave-excited, radiation from uniformly moving charge 79−13882
liquid, under high press., refr. index vs. density 79−28712
liquid, under high press., refr. index vs. press. and strain 79−33668
load carrying flat bar with hole, Poisson ratio influence on stress distrib. *(Polish)* 77−9032

photoelasticity continued
load meas. and testing *(German)* 80−19297
loaded projection, photoelastic anal. of stresses 78−87275
matrix method for determining 3-d photoelasticity 79−41636
matrix theory of photoelasticity, book 79−64612
microelectronic component thermal stresses, photoelastic anal. 77−62217
mixed-mode stress intensity factors, photoelastic determ. method 79−18841
mode I, stress intensity factors, determination 78−90781
mode I stress intensity factors, method of caustics 80−38364
mode II fracture test specimen, boundary-collocation anal. and photoelastic expt. 77−50982
modelling, suitability of materials under γ-irradiation *(German)* 79−33666
Moire strip attainment at specified pt. on contour of stress concentrator 77−52573
molecular crystal, Brillouin scatt. intensity 79−73958
negative selection, for production of uniform intensity of light 77−2685
nematic liquid crystal, flexural elasticity meas. *(Dutch)* 80−34112
non-destructive photoelasticity, whole field method, visualisation of isochromatics and isoclinics *(French)* 80−64502
nonlinear photoelasticity in impure crystals, theory 80−108179
nonlinear photomechanics, birefringence in polymers, stress anal. appl. 80−33545
nozzle corners, cracked, determination of flaw shapes, stress intensity distributions, using frozen photoelastic stress method 79−43547
opaque crystal, Brillouin scatt., photoelastic and surface corrugation contribs. 79−42980
optical fibre hydrophone sensitivity, strain configs. 80−23771
optical fibre preforms, nondestructive struct. meas. with photoelastic effect 79−86255
optical fibre refractive index change due to external forces 78−74971
optical fibre waveguide transmission, mechanical stresses effect 80−10032
optical glass, thermally tempered, surface stress meas. by crit. ray method 80−106766
optical glass under stress, refr. index based upon polarisation charact. *(Japanese)* 79−4781
optical material, photoelastic investigation of freezing and defreezing of temperature stresses 77−66733
optical materials, elasto-optic coefficient determ. under static loading, by acousto-optic and Brillouin scatt. techniques 79−4787
optical retardation determ. by colour photography 79−72865
optical slicing method for 3-D photoelasticity 78−26093
optically isotropic mats., stress intensity factor determ. by dynamic method of caustics 80−33546
optically-sensitive materials with disc-shaped macrosplits, determination of tension distrib. using photoelastic method *(German)* 79−37267
optimisation of photoelastic stress separation procedures 79−32402
orthotropic, appl. of shear difference method 77−23924
orthotropic composite model materials, photoelastic calibration 80−87715
phosphosilicate glasses, photoelastic consts. and polarisability 79−65839
photoelastic material, holographic method for matching and measuring refractive index 79−17466
photoelastic method, automated system for treating expt. data 79−15929
photoelastic strain gauge, concrete structure boundary stress meas. appls. *(Chinese)* 79−72867
photomechanical information, acquisition and processing 79−32403
photothermoelastic technique, appraisal for transient 2D thermal stress analysis 80−79244
photoviscoelastic data, two procedures for recording and analysing on a μs time scale 79−37188
piezoelectric semiconductors, photoelasticity and acousto-optic diffr. 80−29715
plane isotropic elastic medium, photoelastic determ. of complex stress intensity factors 80−43664
plane slice optically isolated in three dimens. photoelasticity, plane and circular anal. 77−68540
plate, photoelastic test evaluation *(German)* 80−92098
plate, square with inset circular discs, elastic consts. effect on interference fit *(Russian)* 79−77031
plate stability under uniaxial compression, moire fringe technique *(Russian)* 79−27609
plates, uniaxially loaded, minimising stress concentrations around circular holes 79−18806
Plexiglas 55, optical and phys. parameters 79−32004
PMMA, fracture toughness for moving crack 77−44365
PMMA, glassy, photoelasticity 80−45034
PMMA, modified with dibutyl phthalate, mech. and optical props. *(Polish)* 77−52423
PMMA, pulsed dielectric breakdown, mech. stress photoelasticity obs. *(Russian)* 78−2800
PMMA, shear-wave Brillouin scatt. intensity from photoelastic consts. 79−91454
point loaded beam, stress distrib., analysis using symmetric/antisymmetric loading 79−41641
polarisation scrambling using photoelastic modulator, appl. to linear dichroism meas. 78−4683
polybutadienes, use of high modulus inclusion gauge, in stress analysis 80−21254
polycarbonate, shear-wave Brillouin scatt. intensity from photoelastic consts. 79−91454
polycarbonate plates, modified compact-tension specimens, dynamic anal. 80−97561
polymer, birefringent, stress intensity factor determ. 80−14633
polymer, brittle photoelastic, use of gelatin gels in prep. for optical polarization stress study 80−40325
polymer, principal stress distrib. meas. at running crack tip *(Japanese)* 77−42784
polymer, viscoelastic-plastic, birefr. relation 77−31266
polymer films, ultrathin, photochemical props., transducer appl. 80−37020
polymer foil, optical props. study by photoelasticity in const. and oscillating mech. fields *(German)* 78−31168
polymer granules, compression, stress state by photoelasticity method 80−10218
polymer solution, short-range solvent orientational order, IR dichroism and photoelasticity obs. *(Russian)* 78−26415
polymers, composite three dimensional model for photoelasticity 78−52871
photoelasticity continued
polymethacrylic acid, swollen networks, viscoelastic photoelastic behaviour 80−59366
polystyrene, shear-wave Brillouin scatt. intensity from photoelastic consts. 79−91454
polyurethane rubber, photoelastic, behaviour at elevated temps. 77−25094
polyvinylidene fluoride, thermodynamic model and appl. 80−75955
pressed powder bed, determ. of side pressure distrib. 78−84734
pressure vessel, stress concentrations around multiple windows photoelastic anal., strain gauge tests 77−72254
principal stress separation using a computer 79−94496
punch indenting elastic half-plane, stress distrib. 79−64606
PVC, commercial tubes, photoviscoelastic investigation 79−34095
quartz, Dauphine twinning, stress-induced, acoustic emissions and photoelastic. effect obs. 80−6414
quartz, fused, photoelastic light scatt. from surface Rayleigh waves 80−97235
quartz, stress buildup due to UV irrad. *(Japanese)* 79−19278
reactor pressure vessel, stress intensities for nozzle cracks 78−70583
refractive index meas. of photoelastic specimen by immersion technique 77−41671
ribbed plate, stress distrib. modelling using combined photoelastic-moire method *(German)* 79−32280
rock, discontinuous, photoelastic anal. *(German)* 79−34811
sandwich composite beam, four point bending stress, multilayer built-up theory anal. *(Japanese)* 79−8322
sandwich composite beams, stress distrib. meas. under four-point bonding, multilayer builtup theory 80−96190
scattered light, for meas. of stress distrib. in cubic single cyrstals *(Russian)* 80−7326
scattered light photoelasticity, appl. to determ. bottom pressure distrib. in pressed powder bed *(Japanese)* 79−75543
scattered light photoelasticity for stress and strain determ. in axisymm. problems 77−72168
semiconductor, IR radiation ultra-fast switching by laser-produced carriers 79−98417
semiconductor, population-inverted, resonant Brillouin scatt., photoelastic consts. 80−89016
semiconductors, doped, light diffr. by sound, photoelasticity consts. 79−11404
semiconductors, population inverted, resonant Brillouin scatt., photoelastic consts. 80−89015
SF-14 flint glass, acoustic vel., absorpt. coeff. and photoelastic consts. rel. to acoustooptical parameters 79−56762
shell subjected to centrifugal force, stress anal. *(German)* 80−23900
shock-front loading method for dynamic studies 77−7349
shrink-fit stress analysis by photoelastic stress-freezing method *(Chinese)* 79−37256
sliding contact, stress conc. on rough surfaces determ. by polarisation-optical method *(Russian)* 78−30244
solids of revolution, stressed state 77−14910
speckle pattern props., appl. to three-dimensional photoelasticity *(French)* 77−23920
speckle technique for 3D nondestructive photoelasticimetry 77−58623
Spherical shell, shallow, on elastic subgrade, under ring load along the edge 79−41644
split birefringent coating on birefringent material, determ. of dynamic stress intensity factors 79−50684
steel, C, elastoplastic stress anal. by photoelasto-plastic method and X-ray method *(Japanese)* 78−13978
steel, C (0.1-1.15 wt.%), fatigue under reversed tension-compression stresses, photoelasticity investig. *(German)* 78−31493
steel, herringbone specimen weld stresses rel. to heat-affected zone rigidity 79−29130
steel, joints glued with reaction resinous mortar, photoelastic exam. *(German)* 78−76825
steel, mild, plastic flow, photoelastic investigation of temp. and strain rate effects 77−86238
steel pressure vessel, multilayer, without longitudinal seam, model investigation *(German)* 79−34276
stimulated acoustooptical effects due to nonlinear photoelasticity 80−103941
strain measurement, in-plane component, combined moire fringes and photoelastic coating technique *(Japanese)* 79−32400
stress anal. appl. *(Polish)* 77−12768
stress anal. of solids, shadow and interference methods *(Russian)* 79−7352
stress analysis, expt., conf., Munich, Germany (Sept. 1978) 79−34256
stress analysis, relationship between optical theories 78−63302
stress analysis in elasto-plastic media using birefringent coatings *(French)* 79−18846
stress analysis method, automatic, of photoelastic fringes 80−14639
stress analysis technique using photoelectric coatings 77−84201
stress analysis under hydrostatic press. up to 700 MPa 78−18260
stress and strain measurement methods, monograph 78−19988
stress distribution, 3D, scatt. light meas. method using depolarised incident light 79−37254
stress field components measurement, integrated plane photoelastic isodynes method 80−14638
stress gradient effect in photoelastic specimens upon the light propagation direction 79−45903
stress intensity factor, simplified three parameter method 79−1138
stress intensity factor determ. by photoelast. stress freezing model *(Chinese)* 79−32395
stress intensity factor determ. from isochromatic fringe loops 78−34097
stress intensity factor K_{III}, photoelastic determ. method *(Chinese)* 79−64602
stress intensity factors, mixed mode, photoelastic determ., notch effects 80−14632
stress intensity factors, photoelastic meas. correlation, for various specimen and defect geometries *(German)* 80−53727
stress intensity factors determ. from isochromatic fringe loops, three-parameter method 79−18843
stress meas., absolute retardation patterns, laser diametrically compressed photoelastic disc 77−27496
stress meas., complete photoelastic param. from scatt. light meas. 79−18848
stress meas. by photoelastic sensor *(Russian)* 77−11150
stress measurement method for crysts., appl. to Si 80−48656

photoelasticity continued
stress obs. in thin webs, under partial edge loading, influence of longitudinal stiffening determ. 80−79857
stress-concentration factors, intersecting and closely approaching orthogonal coplanar holes 77−50892
structural components, photoelastic methods of stress distrib. anal. *(Polish)* 77−9031
Super Phenix nuclear reactor containment vessel, stress anal. *(French)* 79−41023
superposition of data 79−59952
superposition principle, appl. to rod under diametral loads and pure bending 77−51000
surface strain field meas. on rubber structures, optical method 77−34017
tensile specimen preparation, stress distrib., for TEM 78−73973
TGS, photoelastic const. behaviour new ferroelectric transition 78−19441
thermal stress determ. circumferentially grooved cylinder 80−38363
thermal stress fields due to travelling heat source *(Japanese)* 77−42747
thermal stresses in photoelastic cylinder, fringe order due to integrated relative retardation 77−62219
thermoplastic rectangular parallelepiped pressure vessel, photoelastic coating anal. 79−59950
thick plate, with elliptical hole, subjected to simple out of plane bending, photoelastic anal. to determ. stress distrib. 79−37187
thick plate with oblique hole, stress conc. determ. by photoelasticity 77−84149
thick walled cylinder subject to torsion, stresses at offset oblique holes 79−32404
thiourea, room temp. photoelastic consts., Brillouin scatt. obs. *(French)* 78−15182
three dimensional, non-destructive method for stress-state determ. using scattered light 78−90805
three dimensional stress analysis holophotoelastic method appl. *(Chinese)* 79−72866
transition metal dichalcogenides, layered, surface Brillouin scatt. obs., surface ripple and elasto-optic mechanisms 80−16048
transparent materials, low-modulus, mech. props. determ. method 78−5704
transparent materials, use of photoelastic modulator in radiation damage meas. 78−87724
transparent solid plates, evaluation of stress-optical coeffs. using interferometry 79−97418
transparent-solid US transducer field visualisation 79−55285
turbine-engine component, photoelastic and holographic anal. 79−37257
two-layer plane elastic system on rigid base, stress distrib. 77−39263
tyre, photoelastic modelling of stresses 79−34274
urethane rubber, viscoelastic disc, contact problem, photoviscoelasticity obs. *(Japanese)* 78−30202
US propagation in solids, visualisation using Schlieren photoelastic apparatus *(Italian)* 80−88274
US transducers, variable-angle, qualitative evaluation by photoelastic visualisation method 78−18143
US wave visualisation, evaluation of US probes 78−80688
US waves in liquids, photoelastic visualisation 80−28374
UV high-power laser material, refractive props. and optical constants 80−106555
viscoelastic plastic components, stress/strain meas. from Moire fringes *(German)* 78−22309
webs, stress state under uniform partial edge loading 79−77028
Ag-halides, photoelastic const. calc. 77−76484
AgCl, ratio of photoelastic constants 77−84828
Al, isoaxial bicrystal, deformation behaviour, study by photoelastic coating and moire methods *(Japanese)* 78−11294
Al, joints glued with reaction resinous mortar, photoelastic exam. *(German)* 78−76825
BaF_2, CaF_2 and SrF_2, dielectric const. and polarisability strain derivatives 77−73125
BaF_2, electronic polarizability and dielectric const., strain derivatives 78−19406
BaF_2, strain induced splitting and oscillator strength anisotropy of IR transverse optic phonon 80−92625
$Bi_{12}GeO_{20}$, acoustic vel., absorpt. coeff. and photoelastic consts. rel. to acoustooptical parameters 79−56762
$Bi_{12}SiO_{20}$, acoustic vel., absorpt. coeff. and photoelastic consts. rel. to acoustooptical parameters 79−56762
CaF_2, electronic polarizability and dielectric const., strain derivatives 78−19406
CaF_2, strain induced splitting and oscillator strength anisotropy of IR transverse optic phonon 80−92625
$CdIn_2S_4$, Brillouin scatt., elastic and photoelastic consts. determ. 80−60619
CdS, characts. of interaction of light with dislocations 78−2137
CdS, population-inverted, resonant Brillouin scattering and photoelastic consts. 80−76042
CdS, resonant Brillouin scatt., photoelastic const., imag. part contrib. 80−108218
CdS, theory of photoelastic effect 77−55769
$CsCuCl_3$, phys. props. 77−62511
CsH_2AsO_4 and $Cs(H_xD_{1-x})_2AsO_4$, acoustooptical and photoelastic props. 78−27181
CsH_2AsO_4, elastic props., photoelasticity near ferroelectric phase transition 80−29107
$Cs_2NaBiCl_6$, optical, photoelastic, acoustooptic props. 80−55064
$CsPbCl_3$, refr. index and birefr., struct. transition effects 77−90126
$CsSrCl_3$, refr. index and birefr., struct. transition effects 77−90126
Cu halides, photoelastic consts. 79−65837
CuBr, photoelastic tensor, acousto-optical meas. 77−12359
CuBr, theory of photoelectric consts. 79−61335
CuCl, photoelastic tensor, acousto-optical meas. 77−12359
CuCl, theory of photoelectric consts. 79−61335
CuCl(Br)(I), photoelasticity theory 78−10868
CuI, photoelastic tensor, acousto-optical meas. 77−12359
CuI, theory of photoelectric consts. 79−61335
α-Fe_2O_3, haematite, birefr. under uniaxial stress in mag. field *(Russian)* 78−88285
GaAs, birefringence, photoelastic consts. dispersion 80−11361
GaAs, phonon surface density, Brillouin elasto-optic cross section 78−72536
GaAs, population-inverted, resonant Brillouin scattering and photoelastic consts. 80−76042
GaAs, resonant Brillouin scattering 79−78695
GaAs, surface Brillouin scattering from acoustic phonons 80−55113

photoelasticity continued
GaAs-$Ga_{1-x}Al_xAs$ stripe geometry lasers 79−94245
GaP, birefringence, photoelastic consts. dispersion 80−11361
$Gd_2(MoO_4)_3$, photoelastic tensor components 77−48146
Ge, photoelastic consts. determ. 78−68474
Ge-Pb-Bi-O glass, photoelasticity, glass transition limits 79−33670
HgO_2-Y_2O_3, solid soln., elastic and photoelastic props., Mendelstam-Brillouin scatt. 78−6693
KBr-KCl, birefringence, annealing effects, photoelasticity 78−72483
KCl birefringence, annealing effects, photoelasticity 78−72483
KCl, stress distrib., meas. by scattered light photoelasticity *(Russian)* 80−7326
KCl, TSM study of lattice statics and dynamics 79−82292
$KH_{2(1-x)}D_{2x}PO_4$, photoelasticity and electrooptic effects at forbidden deform. *(Russian)* 78−35117
KH_2PO_4 and $K(H_xD_{1-x})_2PO_4$, acoustooptical and photoelastic props. 78−27181
KH_2PO_4, photoelastic const. behaviour new ferroelectric transition 78−19441
$K_2Mn_2(SO_4)_3$, optical and dielectric props. 79−11403
LiF, pulsed dielectric breakdown, mech. stress photoelasticity obs. *(Russian)* 78−2800
$LiNbO_3$, collinear light diffr. by transverse acoustic waves 77−52040
$LiNbO_3$, photoelasticity tensor, including piezoelectrooptic interaction correction, Brillouin scatt. 77−24820
$LiTaO_3$, near ferroelec. transition, elasticity, photoelasticity 78−88268
$LiTaO_3$, photoelastic consts., Brillouin scatt. 77−28546
MnF_2, magnetic, thermal, elastic refraction of light, mag. order influence on refractive index *(Russian)* 80−34880
$NH_4H_2PO_4$, acoustooptical and photoelastic props. 78−27181
$NaBi(MoO_4)_2$, photoelastic props., acousto-optical figure of merit meas. 78−60420
NaCl, pulsed dielectric breakdown, mech. stress photoelasticity obs. *(Russian)* 78−2800
NaCl(Br) (F) (I), lattice dynamics and statics, three-body-force shell model 80−49323
$PbCl_2$ crystals, acousto-optical props. and photoelasticity 80−40085
$PbMoO_4$, Brillouin spectra, photoelastic consts. and optical purity 78−60480
$PbMoO_4$, photoelastic constant determ., molecular light scattering obs. 78−72537
Rb halides, photo-elastic constants and pressure derivatives of shear moduli 80−75284
RbBr(Cl)(I), evaluation of photoelastic consts. 80−50297
RbH_2AsO_4, acoustooptical and photoelastic props. 78−27181
RbH_2PO_4, acoustooptical and photoelastic props. 78−27181
S, orthorhombic, dielectric theory of strained mol. cryst. 79−65836
Sb_5O_7I, polytypes 2MC and 2MA, photoferroelastic phenomena 79−95447
Sc_2O_3, Mandelshtam-Brillouin spectra, transverse phonon contrib., elastic and photoelastic consts. 77−81115
Si, appl. of photoelastic stress. meas. technique 80−48656
Si film, optical characterisation from guided wave optics 78−48245
Si, optical spectroscopy, absorpt. coeff., lattice vibrs. modes, band gap, acoustic approach 77−69822
p-Si, photosensitivity of elastic moduli and surface tension 78−83864
Si, process stress analysis by IR photoelastic meas. 78−11488
Si, surface Brillouin scatt. from acoustic phonons 80−55113
SiO_2, fused, photoelastic coeffs., freq. depend. 77−4619
SiO_2, fused, shear-wave Brillouin scatt. intensity from photoelastic consts. 79−91454
SrF_2, electronic polarizability and dielectric const., strain derivatives 78−19406
SrF_2, strain induced splitting and oscillator strength anisotropy of IR transverse optic phonon 80−92625
Te, acousto-optic props. at 10.6 μm, independent photoelastic tensor components 79−91401
TiO_2, acoustic vel., absorpt. coeff. and photoelastic consts. rel. to acoustooptical parameters 79−56762
TiO_2, dispersive asymmetry of elasto-optical tensor 78−35112
TiO_2, rutile, vol. depend. of refr. indices under hydrostatic press. 77−52036
Tl-halides, photoelastic const. calc. 77−76484
TlBr-TlCl, photoelastic consts. dispersion 79−65136
TlBr-TlI(Cl) crystals, photoelastic moduli 80−97230
TlCl-TlBr solid solution, photoelastic constants obs. *(Russian)* 78−39526
$TlMnCl_3$, refr. index and birefr., struct. transition effects 77−90126
Y_2O_3, Mandelshtam-Brillouin spectra, transverse phonon contrib., elastic and photoelastic consts. 77−81115
ZnO, photoelastic consts., absolute sign determ. by Biegelsen method 79−1749
ZnO, theory of photoelastic effect 77−55769
ZnP_2, Brillouin scattering and optical props. meas. 80−76041
ZnS, theory of photoelastic effect 77−55769
ZnSe, photoelastic and elastic constants determ. using thermal Brillouin scatt. *(Japanese)* 79−51974
ZnSe, reson. Brillouin scatt., dispersion curves, piezobirefringence anal., electronic state lifetime broadening effects 79−61390
ZnSe, resonant Brillouin scatt. by injected acoustic waves 77−12394
ZnTe, Brillouin scatt. spectra, elastic and photoelastic consts. 77−59585
ZrO_2-Y_2O_3, solid soln., elastic and photoelastic props., Mendelstam-Brillouin scatt. 78−6693

photoelectrets
chalcogenide glass optronic receiver with simultaneous direct and memory effect 77−75706
dielectric-photosemiconductor two component systems, photoelectret state 80−25287
ferroelectric semiconductors, props., book 80−82590
ferroelectrics, photoelectretic states in real time spatial light modulators, photorefractive effect 80−80676
internal counter-EMF determ. by pot. meas 80−45003
narrow band gap semiconductor electrophotographic processes 80−13169
perovskite oxides, single cryst., photocond. and TSC meas. 78−43436
photoferroelectric phenomena, physical models derivation for photo-thermoelectret, photoferroelectret states 79−15407
photoresist, KTFR, thermally stimulated discharge current studies 80−75924
poly(vinylcarbazole), photoelectret state 77−55745

photoelectrets continued
polyethylene terephthalate photoelectret, TSC and photostimulated detrapping current obs. 78−10459
polystyrene, pure and doped, metal contact effect on persistent internal polarisation 79−78617
semiconductor, photoelectret state form. by IR light quenching photoelec. current *(Russian)* 79−91345
tetramethyldiaminodiphenyl ketone, binder layer, photoinduced polarisation and voltage 80−75923
trap parameters, calc. method from TSC under monomolecular recomb. conditions 77−8495
AsI_3, photopolarisation, photoelectret state, electron-hole transitions 77−12300
As_2S_3 high-resist. vitreous, photopolarisation and photoelectret effects 77−76876
$Ba_xSr_{1-x}Nb_2O_6$, ferroelectric with diffused phase transition, photoelectret states 80−20583
$Bi_{12}GeO_{20}$, mechanism of creation of internal fields and photoelectret effect 80−25290
$Bi_{12}GeO_{20}$, photocond. spectra, current-voltage charact., photoelectret effect 79−69552
$Bi_{12}GeO_{20}$, photoelectret state 80−11315
BiI_3, photopolarisation, photoelectret state, electron-hole transitions 77−12300
$Bi_{12}SiO_{20}$, mechanism of creation of internal fields and photoelectret effect 80−25290
$Bi_{12}SiO_{20}$ photoelectret, in optical processing and X, γ ray imaging 80−23764
CdTe film, photopolarisation 80−25286
CdTe:Ag, with microscopic p-n junction, photopolarisation in anomalous photovoltage 79−11175
CdTe:Ag film, photoelectret effect *(Russian)* 79−28676
$GeSe_2$ amorphous layers, photoconductance meas. 80−65632
$KNbO_3$, photoconductivity and TSC 78−2520
$KNbO_3$, photoferroelectric effects 78−92029
$NaNbO_3$, photoconductivity and TSC 78−2520
$NaNbO_3$, photoferroelectric effect 78−35108
$PbMg_{1/3}Nb_{2/3}O_3$, electro-opt., elasto-opt., opt. and photo-induced props. 78−95560
$PbMg_{1/3}Nb_{2/3}O_3$, ferroelectric with diffused phase transition, photoelectret states 80−20583
$PbMg_{1/3}Nb_{2/3}O_3$, photocond., 20-150°C, and photoelectret state 77−24590
$PbZn_{1/3}Nb_{2/3}O_3$, electro-opt., elasto-opt., opt. and photo-induced props. 78−95560
S, polycryst., photoelectret state following X-irrad. 80−60485
S, polycryst., X-ray irrad. in elec. field 78−31147
Sb-S-I system crystals and glasses, adhesion levels, TCE spectra 77−24529
SbI_3, photopolarisation, photoelectret state, electron-hole transitions 77−12300
Si, high dislocation density crystals, photoelectret state investigation 80−97191
Si, photoelectret effect, plastic strain induced dislocation relax. time enhancement *(Russian)* 79−15397
ZnO, photoelectret, nonisothermal relax. 77−12306
ZnO photoelectret, recomb. and trapping kinetics determ. 79−38083
ZnO, TSC reversals 77−8493

photoelectric cells
see also photoconductive cells; photovoltaic cells
analogue output device for Rotameter flow rate measurements 78−75237
angular meas. by Fraunhofer diffraction pattern, appls. *(Japanese)* 80−52159
antimonic caesium vacuum photocell, test instrument for contactless circuits *(Russian)* 79−58676
barrier-layer photocells with Au films, spectral distrib. of transmission coeffs. of films determ. 77−1744
colorimeter reconditioning methods 79−39618
continuous exposure mode, discharge model, surface generation of pairs *(Russian)* 77−72890
covalently-bound dyes on semiconductor surfaces 77−69414
elementary cells, of photodetector matrices and scanistors, switching transients 78−45703
fast-response photocell time characteristics meas. 77−5913
FP and FPU electron-trap photocells, for laser flux intensity meas. 78−286
hole position measurement, optoelectronic alignment technique 78−93650
Kerr cell, spark source of light, construction and operation *(Russian)* 77−72042
laser radiation pulse width meas., integral method with direct reading 77−72019
mechanical component features comparative metrology, misalignment meas. using photocell 80−31716
microcooler, threestage, with cascade thermocouples 79−2765
MIM, sandwich sputtered film, interfacial effects characterisation 79−82685
monochromatic pyrometer with silicon photocell as a detector *(Japanese)* 79−93145
photochemical diode using p-n heterojunction or Schottky barrier immersed in electrolyte 77−66201
photoelectric convertors, p-n mesa structure for investigating optical and energy characts. of solar and radiant energy concentrators 80−97783
photomotogram evaluation Achilles tendon reflex, biomedical measurement appl. *(German)* 78−7465
probe design for fluidised bed meas. 79−82000
proximity pick-ups, optical detection of light source and photoelectric cell *(Dutch)* 79−36985
quantum efficiency yields, automatic recording system 77−67489
review, Russian devices 80−57371
selective receivers for 0.2 to 0.3 μ spectral region 79−30560
sensing devices recording movement of small animals in enclosure, chart recording 77−81765
solar photoelectric conversion cost reduction *(Italian)* 80−30479
specifications, for USSR state standards of radiation sources 78−45695
teaching experiments using photocells and oscilloscope 78−36778
two-cell mesopic photometer 77−37966
UV photocell, 0.22-0.36 μm 77−71376
$Al_xGa_{1-x}As$-GaAs linear-gradient heterostruct., photoelec. props. 79−11205

photoelectric cells continued
n-$CdGeP_2$-p-$CdGeAs_2$ heterojunction photocells, polarisation-sensitive 80−11075
CdS-Cu_2S heterojunction, slow relax. of photocurrent 78−26943
CdS-CuI film heterojunction photocells, prep., photoelec. props. 78−80044
Cu_2S-CdS heterojunction, thin film structure, props., manufacture 77−51806
Fe-thiazine photogalvanic cell, blue sensitization, photoredox reaction, insolation spectrum match 77−90628
Fe-thionine, photogalvanic cell, photostationary state comp., current depend. 77−90629
n-GaAs photoanodes for water photoelectrolysis 77−77789
GaAs, photoconvertor, short-circuit current and load current depend. on angular sensitivity 79−83594
GaAs, photovoltaic conversion charact. *(Czech)* 77−76903
GaP, minority carrier quasi-Fermi level meas. in illuminated photoelectrolysis cell 77−85308
Se photocells, temp. coeff. of sensitivity 78−82033
Si epitaxial p-i-n photoconvertor characteristic deterioration at high illumination 78−89536
p-Si inversion-channel photoelectric cell characteristic *(Russian)* 80−49941
Si, photoconvertor, short-circuit current and load current depend. on angular sensitivity 79−83594
Si preparation by electrolysis of fluorosilicate solns. in molten alkali halide mixtures *(French)* 78−64491
SnO_2/V_2O_5-P_2O_5/Si heterojunction, static optoelectronic charact. 79−87146
n-TiO_2, rutile anode, water photolysis 78−2563
ZnS photocells, thickness depend. of interband transition photovoltaic voltage and short circuit photocurrent 77−76871

photoelectric devices
see also image sensors; photocathodes; photoconducting devices; phototubes
aerosol counter, use of laser light sources *(Russian)* 79−100969
aerosol counters, calibration by sedimentation method 80−99031
angular displacement transducer, accuracy 80−8977
angular velocity meters, using ring lighting devices *(Russian)* 77−37863
annular photoelectric goniometer sensitivity calc. 78−41327
astronomical, for stellar transit times recording *(Russian)* 78−73635
astronomical, on Dresden Univ. transit instrument, obs. results *(Russian)* 78−73634
astronomical, phase device for time service transit instrument *(Russian)* 78−73632
astronomical, with high time resolution, obs. results *(Russian)* 78−73633
astronomical circle reading recording meas. appl. *(Russian)* 78−20644
astronomical laser ranging equipment, photoelectric circuit *(Japanese)* 78−89075
autocollimator, polyhedral prisms checking instrument 77−7221
automatic photoelectric analyser of aerosol dispersity, 0.3-40 μm size range 80−57251
chalcogenide glass optronic receiver with simultaneous direct and memory effect 77−75706
comparator, for temp. scale representation in 1337-58-2200K range *(German)* 78−4621
concentration meter, acceptable error determ. for automatic biochemical anal. 79−92435
condensation nucleus counter with digital recording 80−8448
contactless photoelectric fibre-optic vibration transducers 77−57319
correlative data processing system using semiconductor injection laser 80−74307
direct display of gas-gun projectile velocity 78−177
direct view type night vision aids 79−72711
displacement transmitter, LED appl. *(Hungarian)* 78−4606
Elektroftalm, optoelectronic instrum. with tactile display for blind people *(Polish)* 78−81073
error monitor for photoelectric tracking systems 79−97373
fibre optic sensor for photoelectric recording, design 80−28338
film camera construction impact of electronics *(German)* 77−79170
haemoglobinometer type GF-3 79−92438
inclinometer, sensitivity stabilization by negative feedback *(Russian)* 78−4012
inclinometers with photoresistors in transducers *(Russian)* 78−4013
line standard meas. using He-Ne laser photoelectric microscope 77−82599
logarithmic photoelectric receiver for spectral ratio pyrometers *(Russian)* 80−57302
low light level device applications, conference, Reston, USA (1976) 77−39091
luxmeter design using linear ICs *(Rumanian)* 80−17993
meridian instrum., performance characts., sensitivity *(German)* 77−17374
micropyrometer for rapid temp. var. meas. 77−41618
microscope with oscillating slit 78−82030
microscopes, scale graduation reading method *(Russian)* 77−26395
multichannel photoelectric systems, immersion optics 80−53405
multichannel spectrometer, quantometer, design trends for computerised control 79−80694
opacity measurement of smoke and suspensions under ambient lighting conditions 77−26382
photo-optical polarising optical system as elec. signal generator 79−1000
photographic plate spectral line setting photoelectronic arrangement 78−78015
photometer, high speed, computerised, for 60 cm astronomical reflector *(Japanese)* 78−32345
physiological light-emitting diode photocell monitor 79−92444
pick-ups for induction motor freq. and speed meas. *(Russian)* 78−65911
picosecond switch for optoelectronic sampling, oscilloscope and photodiode testing appl. 77−58451
piezoceramic bimorph element for photoelec. autocollimator detector 77−7206
plethysmography system for brain blood flow meas. in the cat 79−83887
polarimeter, effect on accuracy of light interference in biquartz modulator 80−62713
powder particle size distrib. anal., photoelectric device 77−74379
pulse shaper for optoelectronic aerosol classifier 79−16049
radiation flux density meas. technique 78−89521

photoelectric devices continued
recorder, for kinematics obs. of artificial heart valve closing elements 79−48370
refractometer based on semiconductor scanistor, operational amplifier 77−53971
rotation speed control attachment for rotary viscometer with weight-driven rotor 79−50822
scanner for spectrometer, vacuum UV molecular photoabsorpt. cross-section meas. 80−37096
screw photoelectric measuring machine for circle reading photographs *(Russian)* 78−24463
shadow methods for studying turbulence using reflection from a mirror in the medium 80−95801
snowfall detectors and automatic depth recorder *(Japanese)* 79−8700
spectral comparator, automatic testing standard temperature-calibrated lamps appl. 77−53907
synchrotron radiation instrumentation utilising surface photoelect. effect 80−92927
Talcott photoelectric micrometer for Bamberg zenith telescope latitude obs. *(Russian)* 78−4113
tilt meters with negative feedback, block diagrams anal. *(Russian)* 78−88948
transducer for linear displacement meas. 79−50404
transducers with astatic characts., statistical errors 78−93760
turbidimeter *(Polish)* 80−31840
vernier sine-cosine angle convertors, output signal eqn. 80−10031
vibrometers, analogue, systematic errors determ. 80−79246
$Ga_{1-x}Al_xAs$ p-i-n structure photoelectric props. 78−95353
GaAs MIS dynamic optically controlled transparencies 78−90523
GaAs:Cr, IR spectral detectivity 78−70184
PLZT ceramic photoferroelectric image storage device, characts. 77−55756
PLZT ceramic photoferroelectric image storage and display systems 77−72084
Si epitaxial photoconvertors, p-n and p-i-n structures, props. 77−51807
Si, IR photoresponse at 1.15 microns 79−7864
Si, slice double-sided free polishing 78−11380

photoelectric effects *see photoelectricity*

photoelectric electron emission *see photoemission*

photoelectric emission *see photoemission*

photoelectric tubes *see phototubes*

photoelectricity
see also Dember effect; photocapacitance; photoconductivity; photodielectric effect; photoelectrets; photoelectromagnetic effects; photoemission; photoionisation; photorefractive effect; photovoltaic effects
amorphous and liquid semiconductors, conference, Cambridge, MA, USA (Aug. 1979) 80−41933
amorphous semiconductor, light irradiation, nonequilib. electron distrib. function in forbidden gap *(Russian)* 78−75988
anodic oxide film, photodepolarisation *(Russian)* 77−32316
bacteriorhodopsin, elec. response of a back photoreaction 80−98008
bacteriorhodopsin, photoelec. conversion in charged synthetic membranes 80−108954
bacteriorhodopsin generated photocurrents on planar bilayer membranes 80−51050
bacteriorhodopsin proton pump, elec. demonstration of rapid light-induced conform. changes 77−44597
chlorophyll a-n-chloranil lamellar system, heat stimulated conductivity 79−53043
compensated semiconductor, theory of transient processes 80−24930
counting photon correls. and stimulated emission, comment 77−23639
counting photon correls. and stimulated emission, reply 77−23640
crystal with polar axis, photogalvanic effect *(Russian)* 77−80811
differential photoelectric charging of nonconducting surfaces in space 79−25439
Einstein's nonrelativistic work *(Czech)* 80−27095
Einstein and the quantum theory, review 80−22237
energy relaxation of photoexcited hot electrons at very low temperatures 78−91724
ferromagnet, photoelectric effect rel. to saturation magnetisation 80−65618
ferromagnetic semiconductor, magnon instability, under intense EM field 77−40048
gamma photon detection processes, statistics of radiation 77−65010
hologram writing by photorefractive effect, Gaussian beam at const. voltage 77−3552
interstellar dust grains, photoelectric effect rel. to gas heating by galactic UV radiation 80−67839
Langmuir film, dark and photo-stimulated relaxation similarity 78−92021
Langmuir-Blodgett films, elec. and photoelec. transport props., device appl. 80−80431
latex, laser spectrometer for submicronic aerosols, photoelec. determ. of conc. acid dispersity 79−54244
lipid bilayer membrane voltage transients from photo-isomerising azo dye 79−92166
lunar surface, intense local photoelectric charging in sunset terminator region 77−45330
lunar terminator, localised photoelectric supercharging with progression of sunset 77−45331
magnetic semiconductor, photomagnetisation, photoinduced heterojunctions 77−63259
maximum midsection area, determ. for large coarse particles by photoelec. method 79−70240
metal-barrier-metal junction, nonlinear optical response 77−28259
metal-semiconductor barrier heights, photoelectric meas., correction diagram 79−33343
metal-semiconductor interface, photoelectron injection, quantum mech. transmission and optical phonon scatt. 80−84511
metal-semiconductor structure, variable-gap, differential optospectrometric effect 77−62994
metals, inner photoeffect and photon absorpt. *(Hungarian)* 79−51624
MIS insulator charge centroid determ. by photoinjection or photodepopulation 77−85323
MISS, potential barrier height determ. using photoelectric methods *(Polish)* 80−20317
MNOS memory device, trapped charge behaviour, UV light effects 77−12014
MNOS structure photoelectric writing operation 78−95382

photoelectricity continued
MOS structure, photon-assisted tunnelling at Al/SiO_2 and Si/SiO_2 interfaces 77−89865
new theory of photon and energy based on two primitive particles 79−67145
optical information, two-dimensional, correlation reduction in course of photoelectric registration 80−19000
organic semiconductor photoelectrode processes and effects *(German)* 80−26145
orofacial posture and movement, photo-elec. recording method 80−108995
p-n junction, electrical parameters, optical derivative meas. 80−2455
photo-induced polarisation, model 79−56714
photodetection, temp. effects 79−26131
photoelectrolysis cell for solar energy conversion 77−20423
photoelectrolysis irreversibilities 78−23161
photoelectron spectra, Auger electron spectra of atomic Fano resonances 80−93454
photoexcited semiconductor electrode, I-V curve 78−14811
photoferroelectrics, book 80−2702
photogalvanic effect under electron-hole interaction conditions 80−88591
phthalocyanine, metal-free, singlet-triplet fusion rel. to carrier photogeneration 77−36276
PMMA, large deforms. at tip of running crack, opt. interference obs. 80−85062
poly(N-vinylcarbazole), hole photogeneration 78−80021
polyethylene, anomalous photodepolarisation, trapping 78−10838
polyethylene terephthalate, anomalous photodepolarisation, trapping 78−10838
quantum utilizing solar energy convertor efficiency in absence of intraband thermalisation 80−26144
Schottky barrier, optically biased tunnelling MIS device 77−85334
Schottky barrier height approaching semicond. band gap, minority carrier injection effect 77−20434
Schottky diodes, quantum photoelectric yield, theoretical anal. 77−39939
semiconducting oxide anode in water, photoassisted electrolysis 77−69413
semiconductor, graded-gap, internal photo-effects, excess carrier distribs. 80−107847
semiconductor, hot electrons, photoexcited in quantizing mag. field, energy distrib. calcs. 79−42586
semiconductor, inhomogeneity effects on thermoelec. and photothermoelec. power meas. 80−54728
semiconductor, n-type, nonequilibrium photoelectron distribs. and absolute negative cond. in quantising mag. fields 80−65622
semiconductor, odd magnetophotoresist. effect 77−15908
semiconductor, parametric reson. of acoustic and optical phonons in laser field 77−51779
semiconductor, photochemical etching mechanism 77−16709
semiconductor, photoelectric fatigue 78−10513
semiconductor, photoexcitation, electron lifetime and capture by trapping centres *(Russian)* 77−32047
semiconductor, photostimulated impurity absorpt. of US 77−62962
semiconductor, photostimulated odd magnetoresist. 77−15910
semiconductor, unipolar, acoustophotoelectric effect theory 77−55577
semiconductor impurity anal. by photoelectric spectroscopy, review 77−24584
semiconductor photosensitive element, discharge process, capture of carriers *(Russian)* 77−69343
semiconductor photosensitive etching for hologram recording, attainable spatial freqs. 80−69343
semiconductor-metal interface photoelectron injection, theory and expt. 77−85314
semiconductor-metal surface-barrier structs., photoelec. effect, theoretical anal. 80−15564
semiconductors, disordered, light induced stationary non-equilibrium distribution of electrons, balance equation 80−39528
semiconductors, electron drag by photons during intraband absorption of light 79−51633
semiconductors, photoelectric fatigue 77−80808
semiconductors, polycryst., opto-electronic processes at grain boundaries 77−43667
shock compression of solids, review 80−24534
solar energy conversion, photoelectric response of photosensitive liquid membranes and chloroplast discs 80−81482
solar photoelectrolysis with semiconductor electrodes for solar energy conversion and storage, review 79−74533
stearic acid, laser spectrometer for submicronic aerosols, photoelec. determ. of conc. acid dispersity 79−54244
stearic acid multilayer films, dark and photo-generated dielec. response 77−72882
synchrotron radiation instrumentation utilising surface photoelect. effect 80−92927
temperature effects 79−26131
transition metal compounds, valence band struct., X-ray spectroscopic study 80−29319
triphenylamine-bisphenol-A-polycarbonate, binary solid soln., hole photogeneration, Onsager theory and expt. 78−39148
variable-gap surface barrier structures, photoelec. effect 79−7903
Vespa orientalis, photoelec. props. of 'yellow strips' on cuticle, math. model 80−104638
volume phase holography, crystal two light wave interaction, photoexcited, photogalvanic effects 79−27214
AgBr, doped, neutralisation of trapped photoholes 78−76108
AgBr, photoexcited electrons and holes in latest image form., review 80−73496
α-$AgSbS_2$ crystals, photoelectric props. 80−107861
$Al_xGa_{1-x}As$-GaAs linear-gradient heterostruct., photoelec. props. 79−11205
AlH_3, photoelectric effect spectra and kinetics, photochem. mechanism colour centres 78−56506
AlH_3, spectral distrib. of photoconductivity and condensed photoeffect before and after illumination *(Russian)* 77−72889
As_2S_3, glassy, interface with metal, photoelec. props. 79−73589
As_2S_3-Ag system, photosensitivity depend. on As_2S_3 thickness *(Russian)* 80−54784
As_2S_3-Ag system, photosensitivity depend. on metallic layer thickness *(Russian)* 80−54785
a-As_2Se_3-Au contact sandwich, response to voltage step in dark and with illum. 77−69431

photoelectricity continued
Au-$Ga_{1-x}Al_xAs$ variable-gap surface-barrier struct., photoelectric effect 80−39634
$BaTiO_3$ and $BaTi_{1-x}Fe_xO_{3-x}F_x$, electrical, optical and mag. props., photoelectrolysis 77−47856
$BaTiO_3$, domain struct. characts. of unipolar ferroelec., photocarrier effects 78−19435
$BaTiO_3$, electron exoemission unipolarity associated with phase transitions 80−97415
$BaTiO_3$, photo-ferroelectric noise effect *(Russian)* 78−52450
$BaTiO_3$:Cu, photoferroelec. props., Jahn-Teller effect, laser irrad. effect on pyroelec. props. 78−60400
Bi, photon drag of carriers, longit. EMF, 77.3-300K *(Russian)* 77−32048
$CdGeAs_2$, p-n junction form. by heat treatment, photosensitivity 77−28247
Cd_2GeO_4, n-type, prep. and photoelectronic props. 80−39628
$CdIn_2S_4$ films, vac. deposited, struct. and photoelec. props. 79−87006
$CdO-B_2O_3-SiO_2$, phase equilibria at 800°C, photoelectric effects 78−68675
CdS, and CdS_xSe_{1-x}, thermoelec. and photothermoelec. power meas., inhomogeneity effects 80−54728
CdS, defects formed by laser radiation of subthreshold intensity, bulk photo-EMF investigation 79−91098
CdS film, chemically sprayed, carrier conc. and mobility, thermoelec. and photothermoelectric meas. 80−2503
CdS films, chemically deposited, phase comp. and photoelec. props. 77−40394
CdS, low resist. single cryst., photodeform. mechanism 77−89806
CdS, phase memory effect and vel. of trap-controlled high-field domains 77−47855
CdS photosensitive film production from chelated metallo-organic compounds *(Russian)* 80−49813
CdS, surface photovoltage in exciton absorpt. range 78−19119
CdS:Cu, Cd, data storage, optical and photoelec. reading 78−1193
CdS:Li(Cu), pure and doped, electrodiffusion of shallow donors, photocurrent, TSC, and exciton luminesc. meas. 80−79992
CdS-Cu_2S heterojunction, influence of surface recomb. on photoelec. props. 77−43711
CdS_xSe_{1-x}, triode sputtered films, photoelec. props. *(Russian)* 79−15179
CdSb heterojunction, formation by laser irradiation, photoelec. meas. *(Russian)* 77−76915
CdSe (1120), surface electronic struct. and chem. struct. 78−14788
CdSe, phase gratings in semiconductors with one- and two-photon excitation 77−8546
CdSe photosensitive film production from chelated metallo-organic compounds *(Russian)* 80−49813
CdSe:Au impurity light absorpt. for current control in negative resistance region 80−11052
$CdSe_xTe_{1-x}$, triode sputtered films, photoelec. props. *(Russian)* 79−15179
p-CdTe, barrier heights of metals on etched surface 80−80378
p-CdTe single crysts., photoreversal of Hall effect 77−43631
CdTe:Cl(In), photoelectronic investig. of trap depths, TSC and SCL cond. 77−39893
CdTe-Ag diode, Schottky type, elec. and photoelec. props. 77−43719
CdTe-Au Schottky diodes, quantum photoelectric yield, theoretical anal. 77−39939
CdTe-CdS p-n heterojunction, coordinate sensitive photoelements, longitudinal photovoltage 79−95440
CdTe-Ge heterojunction, photoelec. props., sensitivity in near IR region *(Russian)* 77−69405
Cu-$CdSiP_2$ surface-barrier -diode, photoelec. props. 77−4442
$CuInSe_2$-$CuInS_2$, solid soln., photo-EMF spectra 80−20248
Cu_2S-CdS heterojunction, photoelectric props. 80−29467
Cu_2S-CdS thin film heterojunctions, base doping effect on elec. and photoelec. props. 78−80043
EuO, light-induced metal-insulator transition, mol. mag. polarons 77−4396
$FeTiO_3$, Fe_2TiO_4, influence of cryst. struct. on photoresponse of electrodes 78−43471
$Ga_{1-x}Al_xAs$-GaAs p-n structures, variable-gap front layer, photoelec. props. 79−7884
$Ga_{1-x}Al_xSb$ p-n structure, variable-gap, elec., photoelec. and electrolum. props. 77−11996
GaAs based MOS capacitors, scanning photovoltage investigation 80−80396
GaAs, IR field induced Gunn oscills. 78−30956
GaAs, surface photovoltage due to photo-thermo-ionization of surface states 78−14787
GaAs:Cu, Te, photoelec. props. 80−92936
n-GaAs-metal Schottky barrier, ultrathin native oxide, thickness determ. from C-V and photoresponse meas. 80−70821
n-GaP, CO_2 laser induced photon drag effect 79−42589
GaP, surface sensitivity, low energy electron transmission optical modulation 78−76567
GaP, transverse acoustoelec. voltage spectroscopy and photoenhanced acoustoelec. effect 80−49828
Ge (111), electron struct., photoelec. props. 80−100493
Ge, amorphous, doping, Schottky barrier and p-n junction form. by RF sputtering 77−8187
Ge, far IR photon drag and radiation pressure in refractive media 80−60048
Ge, homopolar semiconductor, quantum efficiency 80−20254
Ge, IR absorption by laser-excited nonequilibrium holes *(Russian)* 79−95752
Ge, internal photoelectric effect, spectral depend. of quantum efficiency 78−39150
Ge, nonequilibrium carrier excitation by CO_2 laser radiation 77−89803
Ge p-n junctions, impurity photoelec. effect 79−56300
Ge, periodic explosions of electron-hole drops 77−11950
Ge, photoacoustic effect, free flexural vibrs. damping 77−89813
Ge single crystals, photopiezoelectric effect under elastic deform. 80−107856
Ge surface, optical charging meas., 120-300K 80−49817
Ge, surface recomb. before and after laser annealing, 10-μm transmission meas. 80−1247
n-Ge:Au, current oscill. damping in weak transverse mag. field 77−4365
Ge:Cu, hot photoexcited holes at low temp. 78−30954
Ge:Hg S-type diodes, photoelec. props. 80−6964

photoelectricity continued
GeS, gas-phase single-cryst. growth, photoelec. props. 77−36381
HgI_2, photoexcited, Hall effect, magnetocond., and cyclotron reson., carrier mobility and effective mass 77−59294
HgSe-Se, photo-field model, rel. to anomalous photocond. in Se:Hg 77−43658
InAs, transverse acoustoelec. voltage spectroscopy and photoenhanced acoustoelec. effect 80−49828
InAs-$Al_xGa_{1-x}Sb$ heterojunctions, elec. and photoelec. props. 79−11206
p-InGaAsP-Au, Schottky barrier height comp. depend., photoelec. meas. 77−20433
InP p^+-n abrupt junctions, ionisation coeffs., photomultiplication meas. 80−65655
n-InSb, cond. electron cooling induced by CO laser and non-ohmic DC field 80−96941
InSb, MIS struct., background radiation effect on photoelec. processes 80−25015
n- InSb, Shubnikov-de Haas effect, CO_2 laser induced hot electron effects 78−30957
InSb:Zn p-n junctions, ion implantation and diffusion spreading, elec. and photoelec. props. 79−73573
InSe, photoelec. props., generation of elec. pulses 77−55574
In_2Se with p-n junctions produced by laser radiation, photoelec. characts. *(Russian)* 78−56226
In_2Te_3, photoelectric props. 77−8144
$(In_2Te_3)_x$-$(Hg_3Te_3)_{1-x}$, photoelec. and luminesc. props. 77−39889
KCl, photoelec. effect produced by far UV light, memory effect 79−24008
KH_2PO_4, KD_2PO_4 crystals, photoresponse under laser irrad. 80−100479
$LiNbO_3$, photorefractive medium, hologram form. theory 77−68185
PLZT ceramic, proton implanted, photoferroelectric effect for image storage and display devices 80−80315
PbS film surface with oxysulphate layer, photoelec. memory effect 77−55584
PbS heterojunctions nonideal, photoelec. props. and elec. characts. 79−15215
$Pb_{0.92}Sn_{0.08}Te$, photoelec. props. 78−6415
$Pb_{1-x}Sn_xTe$, photoelec. props. 30 to 4.2K, temp. depend. of electron density 80−20246
$Pb_{1-x}Sn_xTe$, x=0.2, monocrystal, photoelectric props. of p-n structures *(Russian)* 80−70808
PbTe film, on NaCl and TGS substrates, photo-EMF investig. of induced elec. inhomogeneity 77−15909
PtSi-n-Si, photoelec. barrier height and elec. props. 79−33344
Sb_2S_3, glassy, interface with metal, photoelec. props. 79−73589
Se electrophotographic films, ageing effects on structure and properties 77−47699
Se, electroradiographic layer, radiographic contrast 80−12241
Se:As, amorphous, pure and doped, photoelectronic preps. in glass transition region 79−4583
Si, amorphous, doping, Schottky barrier and p-n junction form. by RF sputtering 77−8187
Si based MOS capacitors, scanning photovoltage investigation 80−80396
Si, clean cleaved, surface photovoltage, effects of atomic steps 78−19120
Si coated with copper phthalocyanine dye, optical modulation of low energy electron transmission 79−69939
Si, far IR photon drag and radiation pressure in refractive media 80−60048
Si high-resistivity structure, photoelec. props. 78−91730
Si, homopolar semiconductor, quantum efficiency 80−20254
Si, internal photoelectric effect, spectral depend. of quantum efficiency 78−39150
Si MIS phototransistors, photoelec. props. at high illum. intensities 80−60101
Si, nonequilib. carrier excitation by CO_2 laser radiation 77−89803
Si, p-n junction, alpha-particle effects, photoelec. parameters determ. *(Russian)* 77−31702
Si, phase gratings in semiconductors with one- and two-photon excitation 77−8546
Si, photoacoustic effect, free flexural vibrs. damping 77−89813
p-Si, photopassivation kinetics in alkali soln., spectral depend. 77−1886
n- Si, surface electron states, props. determ. at 77K 77−55598
Si surface layers, impurities, elec. and photoelec. props. 80−2298
Si, surface space charge layer, electron subbands, mag. field effect 77−20393
Si:In, photoelec. props. meas 77−89804
Si-GaAs heterojunction photothyristor, spectral characts. 78−10546
n-Si-Re(Os) Schottky contact barrier height meas. 80−65675
Si-Si_3N_4-Al, photoexcitation of emission currents, I-V characts. *(Russian)* 77−72917
Si-SiO_2 interface in MIS struct., B^+ ion implanted, elec. props. due to laser irrad. 78−72272
n-SiC-n-CdS heterojunctions, photoelec. props. 78−80042
SiC-Si struct. formation on ^{12}C ion implantation in Si, optical and photoelectric props. 79−91136
SiO_2 in MOS struct., exciton transport rel. to surface states 78−34901
SnO_2-GaTe(GaSe)(InSe) heterojunctions, photoelec. props. 80−96945
SnO_2-InSe n-n heterostructures, photoelec. props., 80 to 300K 80−20297
SnO_2-Si, heterojunction, elec. and photoelec. props. 77−1477
Te, carrier recombination at high optical excitation, photomagnetoelectric effect 77−72884
Te detector for CO_2 pulsed laser radiation, using photon drag and optical rectification 78−21216
Te, laser induced EMF, photon drag, optical rectification and spurious signals 78−19083
Te, MIS structure, photosensitivity spectrum 78−14834
Te, photon drag effect theory 78−19084
Ti-TiO_2-Au diode, spectral photoresponse and I-V characts. 80−15617
n-TiO_2 electrode in photoelectrochem. cell, anomalous photoresponse 77−11998
TiO_2, plasma growth, photoelectronic props. 78−52662
$TlInSe_2$, monocrystal, photoelec. props. *(Russian)* 80−70752
W-Ni point contact diode, rectifying props. in CO_2 laser radiation 77−76942
$ZnIn_2S_4$ diode struct., photoelec. props. *(Russian)* 77−43720
ZnO:Li_2O single crystal, triboelectric charge and photodischarge obs. 79−82663
ZnSe surface barrier diode, hot charge carriers, elec., photoelec., and electroluminesc. props. *(Russian)* 79−33841
ZnSe-CdTi, epitaxial film, cond. transition, laser switched memory *(Russian)* 77−8182

photoelectricity continued
ZnSe-Ge(GaAs)(GaP) heterojunctions, elec. and photoelec. props. *(Russian)* 77−32070
ZnSe-ZnTe heterojunction, epitaxial, photosensitive, photoelec. props. 79−11203
p-$ZnSiP_2$, single cryst., recomb. processes, photoelec. props. *(Russian)* 78−68053
ZnTe-metal structures, photosensitivity spectrum *(Russian)* 78−76147
ZnTe-ZnSe(CdSe), LPE growth, elec., photoelec. and luminesc. meas. 77−4745

photoelectrochemical cells
see also solar cells
biological solar cells, photosynthetic bacterial reaction centres on sputtered C and SnO_2 electrodes 80−66981
chlorophyll a dihydrate photoelectrochemical cell 80−61387
developments, conversion efficiency estimates for different cells 80−50993
electrochemistry, power sources and energy science 80−101023
electrode materials, for photoelectrolysis of water 79−29478
energy conversion, review 79−52941
energy conversion system, principles and appl. 80−89652
energy conversion system modelled by photosynthesis 79−48139
excited electronic state, photoelectrochemistry 78−76872
flatband potentials, temp. depend. at semiconductor-electrolyte interfaces 78−60201
hydride concentration cells for solar conversion 80−35698
interface phenomena rel. to solar cell *(Japanese)* 78−53220
laser applications in photoelectrochemistry for solar energy conversion 80−40873
liquid-junction solar cells, Schottky barrier height, photovoltage and photocurrent 80−26162
low cost solar cells 80−50972
material aspects of solar conversion systems, charge transport, energy output 80−12022
MB^{+}-Fe^{2+} system, solar energy utilisation *(German)* 80−45713
metal electrodes in contact with fluorescent dye solns., photovoltage generation, comprehensive model 80−40871
metalloporphyrins, photoelectrochemical props. 80−50991
model energy conversion systems, evaluation 79−43777
n-type semiconductor anode, illum., charge transfer modes, digital simulation 80−2464
organic semiconductor photoelectrode processes and effects *(German)* 80−26145
photoelectrolysis cells, props. of oxide-based heterostruct. photoelectrodes 80−12023
photogalvanic cell based on photolysis of Rb anions in THF 80−85294
photogalvanic solar energy conversion, photochem. determ. of efficiency 80−89654
photogalvanovoltaic cell, features 79−29479
photogalvanovoltaic cells and photovoltaic cells using glassy carbon electrodes 80−89630
photosynthesizers, contrived, biosystems and photoelectrochem. conversion 79−52953
photosynthetic reaction centre from bacteria working on SnO_2 electrode 80−94092
polyacetylene photoelectrochemical solar cell, fabrication and efficiency 80−50954
reversible solar galvanic cell 79−62016
secondary cells, Pb/acid, design and performance characteristics for remote photovoltaic applications 80−55833
semiconductor, quantum efficiency and energy efficiency determ. by photothermal spectroscopy 80−72072
semiconductor based, interaction of light and transport control 80−12020
semiconductor electrodes for photoelectrolysis of water, appl. to solar energy conversion 79−29477
semiconductor photoanodes, corrosion stability 80−21130
semiconductors for photoelectrolysis, book contrib. 79−65547
solar, function and construction of regenerative cell 80−26147
solar cell *(Dutch)* 80−85295
solar cells, design and operation, underlying theoretical principles 80−40872
solar cells, power conversion efficiency monitoring 80−50989
solar cells, semiconductor/redox electrolyte junctions, functions examples and problems 80−45714
solar cells review of cell types and electrode props. 80−61385
solar energy conversion, chlorophyll sensitised reactions 80−7948
solar energy conversion, photo-electrochemical production of C-C bonds from carbon dioxide 80−21407
solar energy conversion, photoelectrochem. processes 80−72068
solar energy conversion, use of oxide semiconductors as anodes 80−101120
solar energy conversion and storage appl., EDTA-methylene blue cells props. obs. 80−21406
solar energy conversion and storage using PEC regenerative and storage cells *(French)* 80−61386
solar energy conversion principles, review 80−35695
solar energy direct conversion to H_2 fuel by water photoelectrolysis 79−62014
solar energy direct photoelectrochem. conversion and storage 79−62015
solar energy utilisation *(German)* 80−45713
solar H_2O photoelectrolysis, H_2/hydrocarbon fuel prod. via biomass conversion wastes 80−89653
surface aspects 80−12021
thiazine dye-Fe photoelectrochem. cells for H_2 production, cell instabilities 80−16814
thionine-coated electrode for photogalvanic cells, electrochem. and XPS anal. 80−72071
TTF polymer thin film batteries 80−45709
Ag/AgCl photogalvanic cells for solar energy conversion, basic electrochemistry 80−45715
AgCl crystal plate supersensitisation, photoelectrochemical obs. 79−83486
AgI-Ag_2O-P_2O_5(MoO_3) glassy electrolyte galvanic cells 80−104513
Cd-S-Fe regenerative cell for photoelectrolytic H prod. 80−51016
CdS electrode, photoexcited, charge transfer in electrolyte with Na_2S additive 79−99618
CdS film, chemical bath deposited, solar energy conversion by photoelectrochem. cells 80−108804

photoelectrochemical cells continued
CdS, photoanode, flat band pot., depend. on surface ion effects 79−62013
CdS polycrystalline thin-film liq. junction photovolt. cell 80−50988
CdS:Te-based photoelectrochem. cell, luminesc., thermal manipulation of deactivation processes 80−81479
CdS(Se) photoanodes, effect of S(Se) substitution, photoelectron spectroscopy obs. 80−2463
CdSe, chemically sprayed thin films as photoanode in photoelectrochem. cells, power charact. meas. 80−85293
CdSe electrochem. photovoltaic cells, effect of thin film electrode prep. and conc. on efficiency 80−55847
CdSe film, electrodeposited, for photoelectrochemical cell for solar energy conversion 80−94093
CdSe film photoanodes for electrochem. photovoltaic cells, fabrication and evaluation 80−76641
CdSe photoanode improved efficiency by photoelectrochem. etching 80−104512
CdSe photoelectrode, immersed in polysulphide soln., S/Se substitution, XPS obs. 79−19656
$CdSe_{0.65}Te_{0.35}$, polysulphide photoelectrochem. solar cell 80−72073
$CdSnO_3$, single crysts., elec. props. 80−6978
Cd_2SnO_4, single crysts., elec. props. 80−6978
Cu(II) complexes, reversible excited-state electron transfer reactions for solar energy conversion 80−89655
Fe-thionine cell, performance 79−52691
Fe-thionine cells 80−50993
Fe-thionine homo/heterogeneous cells, power output enhancement 80−45711
Fe-thionine homogeneous cells, power output enhancement 80−45710
Fe-thionine photogalvanic, cells 80−35696
Fe-thionine photogalvanic cell, thin layer, totally illuminated, electrodic phenomena at anode 79−20374
$FeBr_3$ aqueous soln. photogalvanic effect 79−24902
α-Fe_2O_3 electrode, carrier density determ. by optical absorpt. and photoelectrolysis spectra 80−71462
n-Fe_2O_3 electrodes, enhanced photoeffects by electrocatalysis and peroxide effects 80−16815
α-Fe_2O_3, photochem. props. of sintered and doped samples for solar photoelectrochem. cell appls. 80−89651
Fe_2O_3, sintered semicond. electrode, photoeffects 79−51669
n-GaAs electrodes in acetonitrile solns., liq. junction photovolt. cell 79−99617
n-GaAs, metal filmed photoelectrochemical cell, energy conversion charcts. 80−101118
GaAs photoanode, using n/n^{+} struct., power conversion efficiency 80−50990
p-GaAs/heptyl viologen system, appl. in photoelectrochemical cells and photoelectrochromic displays 80−76640
n-GaAs/K_2Se-K_2Se_2-KOH/C solar cell, Ru (III) chemisorption on photoanode, effect on performance 80−3516
n-GaAs/K_2Se-K_2Se_2-KOH/C liq. junction cell, effect of Ru ion chemisorption on grain boundaries 80−55879
n-$Ga_xIn_{1-x}P$ photoelectrochemical cells, bandgap energy, electronic transition mode, and diffusion length 80−72070
p-GaP electrode, for solar cell, differential capacitance meas. for flatband potential determ. 78−72256
p-GaP semiconducting photoelectrode 80−101119
p-GaP semiconductor-electrolyte solar cells for photochemical reduction of CO_2 to organic fuel 80−55880
p-GaP-NaOH-Pt cell, H_2 evolution quantum efficiency potential charcts. 80−55673
H photoelectrolytic production by H_2O decomposition using sunlight, cell energetics 80−45774
H_2 prod., semiconductor-liquid junction systems, review 80−61453
H_2 production using solar energy and Zn(Mg)(Cr)(Ni) phthalocyanine dyes *(French)* 80−55936
InP, N- and p-type electrodes in acetonitrile solns., photoelectrochemical behaviour 79−99616
$LaCrO_3$-TiO_2 photoactive anode, for photoelectrolytic production of H_2 and electricity 80−12024
$LuRhO_3$, elec., mag. and photoelectrochemical props. 80−96925
$MoSe_2$ layer-type electrochem. solar cells, electrode material performance, doping effect 79−74532
$MoSe_2$, layered dichalcogenide, hole reactions, electrochem. solar energy conversion appl. 79−7893
n-$MoSe_2$, synthetic, performance in electrochemical solar cells 79−66412
$MoSe_2$-I^-, photoelectrode, time resolved photocurrent, nanosecond excitation 80−45708
n-Si, Fe_xO_y-coated, heterostruct. photoanode for photoelectrolysis of water 80−61384
Ru complex, tris-(2.2′-bipyridyl)-Ru(II) complex, photoelectrochemical systems, solar energy utilisation *(German)* 80−45713
Si:H, amorphous, photoelectrochem. behaviour 80−81480
n-SnO_2 pigmented solar cell for electrolysis of water, two-photon process 80−93932
$SrTiO_3$ (111), surface struct., electronic props., LEED, AES, UPS study, photoelectrochem. cell anode appl. 78−84035
$SrTiO_3$, electrode, surface photovoltage expts. 78−72227
$SrTiO_3$, transition metal doped anodes for water photoelectrolysis, response to visible and UV 79−74531
TiO_2, doping processes, influence on photoelectrochem behaviour 80−79822
TiO_2 electrode, carrier density determ. by optical absorpt. and photoelectrolysis spectra 80−71462
TiO_2 electrode, doping density dependent attachment of rhodamine B 80−54777
TiO_2 electrodes, in aq. electrolytes, surface states, photocurrent obs. 80−49895
TiO_2 electrodes in photoelectrochem. cell, photothermal effect 80−7947
TiO_2 films as solar photocatalysts, preparation 79−74530
n-TiO_2 photoanode, band bending at surface used to dissociate water under solar illumination 78−91765
n-TiO_2 photoanodes, corrosion suppression mechanism 80−2462
n-TiO_2 photoelectrochemical electrodes, effect of Nb doping on quantum efficiency 80−101121
TiO_2 semicond. films for water photoelectrolysis 80−26146
TiO_2, solar energy utilisation *(German)* 80−45713
TiO_2, sputtering defects, associated surface electron states, UPS, XPS and AES obs. 80−60755

photoelectrochemical cells continued
TiO_2, transition metal doped anodes for water photoelectrolysis, response to visible and UV 79−74531
TiO_2:Al(Y), polycrystalline photoanode, improved solar efficiency 79−96479
n-TiO_2:Be electrodes, photoassisted oxidation of water 80−30502
TiO_2:H photoanodes, diffusion and surface chemistry 80−35546
n-TiO_2-electrolyte interface, electrolum. obs. 79−47520
n-TiO_2-electrolyte interface, charge-transfer-controlled photocurrent 80−50992
TiO_2-$LaCrO_3$-GaP photoelectrochem. reactor for materials synthesis using solar energy 80−45712
TiO_2-O_2/OH^- photoelectrochemical cell, temp. effects on performance 79−92084
TiO_2-Si solar cell hybrid electrodes for photoelectrochem. H prod. 80−45775
n-WSe_2 electrode in aq. iodide medium, high efficiency photoelectrochemical solar cell 80−72069
ZnO cell, enhancement of photoelec. effect by organic additives 79−57437
ZnO sintered electrode, for dye-sensitised solar photocell 80−16816
$ZrSe_2$, photo-intercalation: possible application in solar energy devices 80−108803

photoelectromagnetic effects
contactless measurement apparatus, operation analysis using equiv. cct. 77−41655
current research status, review 79−69559
diamond, electron irradiated, photocurrent and Hall current, 290 and 4.2K 79−87129
ferroelectric crystal without centre of symmetry, photo-Hall effect *(Russian)* 78−60152
ferromagnetic film in mag. field, pulsed laser beam induced EMF *(Russian)* 77−55564
heat treatment effects on elec. props. 78−43411
inhomogeneous semiconductor, nonequilibrium carrier mobility 77−15879
mobility anisotropy determ. by photoelectromag. effect and photocond., method and appl. to HgI_2 79−38126
p-n junction, photomagnetic current generated by front illum. 79−51666
photoexcited hot electrons in high mag. field, mean energy 78−30955
photomagnetoelectric effect, current vs. load curve 79−51629
piezoelectric semiconductor, n-type, heavily doped, laser beam modulational instability 79−99570
piezoelectric semiconductor, photocurrent in quantising magnetic field in presence of nonequilibrium photoelectrons, spectral oscill. and energy relax. by interaction with acoustic phonons 79−91100
plasma, laser prod., photon drag of electrons *(Russian)* 78−18433
semiconductor, graded-gap, photoelectromagnetic effect 78−43445
semiconductor, heterogeneous, Dember and photomagnetic effect, spectral characts. *(Russian)* 77−89809
semiconductor, highly excited, photomagnetoelectric effect under Auger recombination 80−44664
semiconductor, photomagnetoelectric effect, injection-level dependent lifetime 80−80319
semiconductor, variable gap, photomagnetic EMF exam. 78−10510
semiconductors, photocarrier distrib. and photomagnetoelectric effect near stimulated emission threshold 80−80320
semiconductors, photomagnetoelectric effect, expt. parameters rel. to material props. 79−99584
semimetal, photo-magneto-electric effect 79−56260
Shubnikov de Haas type of photomag. effect, monotonic component of quantum oscills. 80−49818
Al-Al_2O_3-InSb MIS structures, recomb. processes and carrier lifetimes 79−38177
Bi, quantum photomagnetoelectric effect 77−72883
$CdCr_2Se_4$:Ga(Ag), and pure, photocond. and photomagnetoresist. spectra 77−80809
Cd_xHg_{1-x}, x=0.2 and 0.26, photomagnetoelectric effect in strongly excited samples 79−47124
CdHgTe photoelectromagnetic detector for 10.6 μm radiation, non-cooled, performance 80−82818
n-$Cd_xHg_{1-x}Te$ alloys, x=0.19 to 0.21, electron optical heating influence on photoelec. effects 79−11183
$Cd_xHg_{1-x}Te$, characts. of low temp. transport props. 78−39160
$Cd_xHg_{1-x}Te$, effects of electron heating at low temps. 80−49823
$Cd_xHg_{1-x}Te$ films, epitaxial growth, optical, elec., and photoelec. props. 79−11512
$Cd_xHg_{1-x}Te$, graded gap epitaxial layers, spectral characts. of photoelectromagnetic effect 80−60022
$Cd_xHg_{1-x}Te$ layers, photoelectromagnetic effect 78−43445
$Cd_xHg_{1-x}Te$, photomag. and photothermomag. effects *(Russian)* 79−78137
n-$Cd_xHg_{1-x}Te$, photomagnetic effect in the quantum limit under electron heating conditions 79−69553
$Cd_xHg_{1-x}Te$, photomagnetic and galvanomagnetic effects in quantising mag. fields 80−20223
n-$Cd_xHg_{1-x}Te$, quantum oscills. of transverse photocond., fields up to 30 kOe, 1.5-4.2K *(Russian)* 77−72885
n-$Cd_xHg_{1-x}Te$, semicond. current carrier recombination heating in photoelectric effects *(Russian)* 79−78138
p-CdSb, photomagnetic and transverse Dember effects, 90 to 300K 77−4400
CdTe film, photogenerated carrier transport props. 80−88590
CdTe, influence of heat treatment on carrier lifetime, photoelectromagnetic effect meas. 77−55576
CdTe:Ge, negative thermally stimulated cond. 79−19621
$CuInS_2$, minority carriers lifetime, photoelectromag. effect meas. 79−47125
p-$CuInSe_2$, minority carrier lifetime and surface recomb. velocity, photoelectromag. meas. 78−19085
Cu_2O, odd photomag. effect. meas. 77−89805
GaAs epitaxial layer, laser mag. photoelec. spectra 79−82635
n-GaAs, H-like impurities photocond., mag. field effect 79−82634
GaAs, illuminated, carrier lifetime profile, depth depend. 78−68036
n-GaAs, photo-Hall effect meas. of ionised impurity scatt. 78−56182
GaAs, photoconductivity meas. of cyclotron resonance 79−82638
GaAs, photomag. effect anomalies and state of surface layer 80−100482
p-GaAs:Cr, semi-insulating, illumination effect on mobilities 77−32043
GaAs:Cr, semi-insulating impurity photomagnetoelectric effect 78−34861

photoelectromagnetic effects continued
GaAs:Cr, semi-insulating, characterisation by photoelectronic data 78−68051
p-GaAs:Cr, semi-insulating, mobilities and carrier concentrations, temp. depend. 80−70702
n-GaAs:Si, optically enhanced Hall mobility meas. 77−39884
GaSe, layered, photoelectromag. effect meas. of transport parameters 77−59301
n-GaSe, photomagnetoelec. and photocond. current spectral distrib. 79−42585
n-GaSe, photomagnetoelectric effect, photocond., in presence of traps 80−39631
Ge, before and after alpha-particle irrad. radiative electromagnetic effect 78−10434
Ge, exciton contrib. to oscillatory magnetophotocond. 79−15180
Ge, irradiation by 3.5 MeV electrons at high temp., carrier density and lifetime changes 77−4128
Ge, photoconductivity, magnetoimpurity oscills. 79−82626
Ge, photomag. EMF, reson. struct., energy relax. mechanisms 78−2515
Ge:Al, Zeeman effect in excitation spectra, photoelectric spectroscopy 79−82633
Ge:Au,Sb, electron irradiated, Hall effect, photocond., and photomagnetic effect meas. 77−4369
p-Ge:Ga(Sb), proton irradiated, kinetics of accumulation of radiation defects, minority carrier lifetime 79−10885
Ge:Sb,Au, photoelectronoc exam. of multilevel gold structure 77−69272
n-$Hg_{0.785}Cd_{0.215}Te$, slightly compensated, transport props. of photo-excited carriers 78−47832
HgI_2, and photomagnetoelectric and photocond. meas., carrier lifetimes 77−55562
HgI_2, layered, photoelectromag. effect meas. of transport parameters 77−59301
HgI_2, mobility anisotropy determ. by photoelectromag. effect and photocond. 79−38126
HgI_2, photo-EM effect and photocond., trapping effects 77−32042
HgI_2, photomagnetoelectric effect anisotropy, photocond. 77−15897
InAs, intense photoexcitation, photoelectromagnetic effect, sign inversion 77−85263
n-InAs, oscillations in photocond. and photomag. effects 77−4405
InSb, donor excitation spectra in high mag. field 78−80027
n-InSb, H-like impurities photocond., mag. field effect 79−82634
InSb, high-resistivity p-type or crystals of n-type, recombination processes, photocond. and photomag. effect meas. *(Russian)* 80−88567
n-InSb, hole mobility temp. depend. after electron bombardment 79−33290
n-InSb, laser induced magneto-photoconductivity, conduction band transitions 77−55566
n-InSb, magneto-photoconductivity, phonon assisted combined reson. magneto-optical absorpt. reson. 78−47831
n-InSb, magnetophonon oscillations by photomag. effect *(Russian)* 77−43665
p-InSb, negative photocond. in strong mag. fields 79−82636
n-InSb, optical phonon emission in intraband magneto-optical transitions, photocond. meas. 80−34481
InSb, photoconductive and photoelectromag. effect spectral distrib., sample thickness depend. 77−4394
n-InSb, photomagnetic effect anomalies, 90 to 300K *(Russian)* 78−84257
n-InSb, recomb. of hot electrons, photoelectromag. and dynamic photocond. meas. 79−38081
n-InSb, surface recomb. velocity, temp. and α-bombardment dose effects 77−8173
n-InSb, surface recomb. vel., repeated cyclic surface treatment effects 77−32065
InSb thin layers, melt grown, mag. field depend. of PEM effect 79−95445
n-InSb, three-phonon assisted cyclotron harmonic transitions in magneto-photoconductivity 80−44652
InSb-NiSb plate, nature of transverse photo-EMF 79−15186
InSb-NiSb two-phase system, photomag. effect, orientational depend., 90-300K *(Russian)* 78−2524
$LiNbO_3$, reduced, electron Hall mobility, photo-Hall meas. 77−8121
MnO, Hall mobility of photoelectrons 77−69352
PbI_2, layered, photoelectromag. effect meas. of transport parameters 77−59301
PbI_2, photoelectromagnetic investigation, expt. 79−24010
$Pb_{0.83}Sn_{0.17}Te$, recomb. at high levels of optical excitation 78−10503
$Pb_{1-x}Sn_xTe$, photoconduct., photoelectromag. effect, laser intensity depend., carrier lifetimes 77−15896
$Pb_{1-x}Sn_xTe$, photomagnetic effect at low temps. 77−62960
Si, heteroepitaxial films, photomagnetoelectric effect 77−85264
Si:Au(Hg), photomag. effect 77−4401
n-Si:H, amorphous, photoelectromagnetic effect 80−107845
Si-SiO_2-Si_3N_4 system, internal photoelec. emission and residual photoelec. effects 79−73599
ZnO powder, Hall effect, O_2 partial press. and illumination effects 79−51607

photoelectron multipliers *see photomultipliers*

photoelectron spectra
see also Auger effect; photoemission; X-ray photoelectron spectra
π-systems interpretation using linear combinations of fragment orbitals 79−18119
acetaldoxime, photoelectron and far UV absorpt. spectra 78−17712
acetic acid, monomer and dimer, photoelectron spectrosc. 80−87172
acetone oxime, photoelectron and far UV absorpt. spectra 78−17712
acetones, halogen substituted, photoelectron spectra 77−14490
acetylene, and $C_2H_2^+$, ionis. pots., photoelectron spectra, ab initio VB calcs. 77−88396
acetylene, angular dependent photoelectron spectral meas. 80−28060
acetylene, chemisorbed on α-Fe, struct., bonding, dissoc., UPS obs., MO calcs. 78−84050
acetylene, chemisorbed on metal surfaces, geometric and electronic struct., UPS obs. and HF LCAO calc. 79−86988
acetylene, chemisorbed on Pt and Pd (111), surface complex form., UPS spectra 77−12826
acetylene, chemisorbed on W(100), geometry distortion 77−30919
acetylene, electron propagator theory for mol. electron binding energies and photoionis. intensities 80−47848
acetylene, photoelectron spectrum, satellite line intensity, photon energy depend. 80−53042

photoelectron spectra continued
acetylene, valence level photoelectron spectra, excitation sources effects 78−78749
acetylene cation, UPS by threshold photoelectron spectrosc. by electron attachment method 79−89708
acetylene molecular geometry determ., adsorbed on Cu, Ni, Pd and Pt surfaces 79−19454
acetylene photoelectron spectroscopy, review 78−50578
acrolein, excitation, ionisation and electron affinity, expts., HAM/3 calcs. 80−18790
adatom binding site, UV photoemission intensity modulation, angle-resolved 79−47589
adatoms on metal surface, photoelectron angular distrib. from cryst. field split levels 77−63533
adenine, UV photoelectron spectra, valence electronic struct. 77−16905
adsorbate, photoelectron core level spectra calc. 77−85896
adsorbate bond geometry, determ. using photoemission 78−71951
adsorbates, core level spectra, exactly soluble limits of model 78−80459
adsorbates, photoexcitation theory rel. to angle-resolved UPS and surface EXAFS 80−39426
adsorbates, valence photoemission book contrib. 78−95672
adsorbates deep level spectroscopy, many body effects 80−39441
adsorbed atom on solid surface, photoemission from valence band, surface plasmon emission, model Hamiltonian calcs. 80−50525
adsorbed atoms, electronic struct. and UPS, appl. to O on Ni 78−15281
adsorbed atoms and molecules, photoelectron spectra, review 78−27372
adsorbed layers, photoelectron diffr. aximuthal patterns, struct. sensitivity 80−107644
adsorbed layers, photoelectron spectra, review 79−52072
adsorbed molecules, photoelectron line shapes, vibr. excitation and hole delocalisation effects 79−95905
adsorbed Xe layers, on Pd-Pt, Ir, and Ru, 5p photoemission, local surface struct. influence 80−2920
adsorption layers, core level photoemission, book contrib. 78−95673
air pollution, particulate matter, analysis 77−41150
aldehydes, conjugated, ethylenic, UV photoelectron spectra *(French)* 78−90215
aliphatic anhydrides, photoelectron spectra, orbital energies 79−10151
aliphatic compounds, alkyl substitution effects on photoionisation, photoelectron spectrosc. obs. 79−31604
alkali graphite intercalation compound, evidence for alkalilike cond. bands 80−45201
alkali graphite intercalation compounds, evidence for alkali-like conduction band, UPS study 80−45208
alkali halides, photoelectric yield spectra, 10 to 40 eV photon energy 79−28887
alkali halides, photoelectron spectra of ionic mols. using mol. beam technique 78−50576
alkali metal atom, outer-shell photoelectron ang. distrib. 80−37797
alkali metal atom, polarised, spin-deposited photoelectrons from two-photon ionisation 79−63971
alkali metal atom, two-photon ionis. with two light beams, photoelectron polaris. 80−43011
alkali metal atoms, ground state correl., photoelectron spectra, multiconfig. Hartree-Fock calcs. 77−50471
alkali metal atoms, near-resonant two-photon ionis., non-Coulomb phase shifts of photoelectron partial waves 80−106302
alkali metal atoms, two-photon ionisation, polarisation effects 78−1039
alkali metal cyanides, He I photoelectron spectra 79−64046
alkali metal salts with aromatic hydrocarbons, photoelectron emission and optical absorption *(Russian)* 78−80456
alkali metal suboxides, thermal and struct. anal., elec. and optical props., photoelectron spectra 79−47587
alkali metals, outer p shells multiplet and satellite struct., photoelectron spectra 80−87039
alkali perrhenates, UV photoelectron spectra 78−50575
alkaline earth chlorides and iodides, photoelectron spectra, geometry 78−29816
alkaline earth compounds, valence shell electronic struct., ab initio SCF calc., photoelectron spectra 79−31383
alkanes, band struct. evolution and electronic relax. in photoemission *(French)* 77−36358
n-alkanes, conduction band struct., LEED, secondary electron emission and UPS study 80−70601
alkanes, linear, elec. struct., evolution of electronic level towards band struct. *(French)* 78−5282
alkanes, linear, electronic struct., electronic relax. during photoemission *(French)* 78−5283
n-alkanes, methane to n-tridecane, ESCA of core electron relax. and valance bands 77−18978
n-alkenes, photoelectron spectra, MINDO/1, MINDO/3 and Fenske-Hall calcs. 78−5285
alkyl cadmium, valence and core electron energies, photoelectron spectra, ab initio calc. 78−25613
alkyl silanes, far UV and He I photoelectron spectra 79−18204
alkyl substituted diacetylene radical cations, optical emission and photoelectron spectra, fragmentation decay 80−53004
alkylbenzenes, electronic struct., photoelectron spectra rel. to semiempirical CNDO/S CI calcs. 79−54770
allene, ionis. pots., Green's function method 77−14608
allene, non-degenerate vibr. mode induced Jahn-Teller effect, photoelectron spectra calc. 79−817
allene, photoionisation and threshold photoelectron photoion coincidence obs. 78−21981
1H-alloxazine, and derivatives electronic struct., photoelectron spectrosc. and ab initio study 80−106261
amino acid methyl esters, photoelectron spectrosc. 79−24954
amino acids, He(I) photoelectron spectra 79−34499
amorphous pyramidally bonded solid, electronic density of states, photoemission interpretation 77−8001
analyser brightness determ. of electrostatic photoelectron spectrometer 77−25331
analyzer for low energy photoelectron spectra 78−22052
angle resolved photoemission, multiple scatt. approach 78−72693
angle resolved photoemission spectroscopy, importance of thermal disorder 77−90243
angle resolved UPS and XPS disorder effects 78−15287
angle-resolved, final-state symm. and polarisation effects 77−40332
angle-resolved, from localised orbitals at solid surfaces, theory 78−15292
angle-resolved photoelectron spectroscopy, miniature plant mirror analyser 77−63539

photoelectron spectra continued
angular dependence from arbitrary oriented surface 77−21005
angular distributions, nonrelativistic dipole approx. calcs., validity limitations 77−42291
angular distributions, relativistic, higher multipole corrections 77−18864
angular distributions, relativistic, multipole and screening effects 78−58635
angular photoemission using synchrotron rad. *(French)* 78−19640
angular resolved UV spectra, CEM addition to Varian movable Faraday cup assembly 77−44130
anthracene, intermol. relax. energies, UPS 78−31304
anthracene, single crystal, contact charging and photoemission 79−47586
anthracene surface, Ar impact, Penning ionisation electron spectra and photoelectron spectra 80−66352
aromatic higher perfluoro compounds, He(Iα) photoelectron spectra 79−31610
aromatic hydrocarbons, catacondensed, photoelectron spectra, correlations with UV absorpt. spectra 77−34690
aromatic hydrocarbons, UV photoelectron spectra 77−88498
atom, np^6 subshells, interaction effect on ang. distribs. 79−10076
atom, photoelectron peak size rel. to photoionis. cross section 77−88508
atom, photoionization cross-section, ground state inversion pot. method 79−31484
atom, UV photoelectron spectra at high temp., interpretation 78−17718
atom-ion core level shifts, ΔSCF calcs. 80−87176
atomic and electronic struct. 80−54746
atomic inner shell ionisation phenomena, conf., Freiburg, West Germany (Mar.-Apr. '76) 77−27040
atomic $np^5(n+1)s^2$ state, atomic resonant autoionisation, photoelectron spectra 77−18980
atomic photoeffect, K-shell, radiative corrections and HF end of bremsstrahlung spectrum 77−23477
in atomic physics, review *(French)* 77−34599
atoms, open-shell, s electrons ang. distrib. 77−65445
atoms, power broadened two-photon ionisation, reson. linesshape and photoelectron spectra 80−58229
atoms, two-photon photoelectron energy spectra, AC Stark splitting 78−86834
Auger electron spectra of atomic Fano resonances 80−93454
Auger emission from solids, photon-induced, deep-hole interferences 79−95900
Auger processes and photoelectron spectra formation 79−2403
cis-azo group, ab initio calc. 79−72236
azobenzene, derivatives, photoelectron spectra, ionisation pot., electronic struct. determ. 80−1024
azomethine compounds, nonaromatic, photoelectron and far UV absorpt. spectra 77−58079
benzene, appl. of valence electron spectroscopy using polarised He I radiation 77−492
benzene, photoelectron and optical spectra, occupied virtual orbital energies and eigenvalue ordering, CNDO/S calc. 77−61796
benzene, photoelectron ang. distrib. with linearly polarised HeI radiation 78−50580
benzene, photoelectron spectra, HAM/3 MO calcs. 78−13414
benzene, photoelectron spectra ang. distrib., π- and σ-orbital assignments 79−818
benzene, Rydberg series, second ionis. process assignment, vibronic coupling 77−42333
benzene, UV photoelectron spectra, valence electron shake up approx. methods 80−18788
benzene, valence electron spectra, vibr. band struct. 77−23520
benzene in rare gas matrices, photoelectron energy distrib. 79−10147
benzene molecules adsorbed on Ni and Pd surfaces, ang. distrib. of photoemitted electrons 77−69968
benzenes, monosubstituted and related cpds., He(I) photoelectron ang. distrib. 79−18236
benzenes, substituted, dihydroxy, electronic structure, photoelectron spectra and ab initio MO calculations 79−49937
benzenes, substituted, electronic struct., ab initio calcs., photoelectron spectra 80−58314
benzenes, substituted, fluoro-derivatives, electronic structure, photoelectron spectra and ab initio MO calculations 79−49937
benzenes, substituted, methyl-derivatives, electronic structure, photoelectron spectra and ab initio MO calculations 79−49937
benzenes, substituted, phenol, electronic structure, photoelectron spectra and ab initio MO calculations 79−49937
benzothiazole, and homologues electronic struct., photoelectron spectra and MO calcs. *(French)* 79−31598
benzoyl chloride, HeI/He photoelectron spectra, band intensity anal. 79−31601
binding energy in solids, sudden approx. approach *(French)* 77−36355
biological applications of photoelectron spectroscopy, review 77−56558
biological molecules, UPS, ionisation energy, assignments and electron donation 78−77005
biological xanthines, (theophylline, theobromine, caffeine) UV PES, constitutive subunits, methylatron effects 78−29798
biologically active molecules, photoelectron spectrosc. 79−24954
biphenyl, photoelectron spectroscopy obs. of heterocycles 78−94286
bromobenzene, photoelectron spectra ang. distrib., π- and σ-orbital assignments 79−818
bromobenzene ion fragmentation, photoelectron-photoion coincidence spectra 80−95682
1,2-bromochloroethane, photoelectron spectra, trans- and gauche-conformers 79−27034
bromofluorobenzens, He(Iα) and He(IIα) photoelectron spectra, assignments, ionis. energies 80−78651
bromopropyne, mol., He(I) photoelectron spectra 79−27033
N-bromosuccinimide lone-pair struct., photodetection spectra 78−37684
bromotrifluoromethane, photoelectron spectra, spin-orbit splitting, vibr. fine struct. 78−21974
bulk bands of solids, electron-phonon interaction effects 80−20767
but-3-yn-2-ol, mol., He(I) photoelectron spectra 79−27033
butadiene, photoelectron spectra, HAM/3 MO calcs. 78−13414
butadiene, UV and photoelectron spectra, first Rydberg states, vibr. components 77−46573
butatriene, ionis. pots., Green's function method 77−14608
trans-2-butene, charge transfer mass spectra and photoelectron spectra 80−40778
t-butyl radical, VUV photoelectron spectrum, geometry, vibr. struct. and ionisation pots. 78−50577
n-butyraldoxime, photoelectron and far UV absorpt. spectra 78−17712

photoelectron spectra continued
carbazole, CNDO/S and CI calcs., photoelectron spectrum assignment 77−67982
carbazole, photoelectron spectroscopy obs. of heterocycles 78−94286
carbonyl-containing biological molecules, UV photoelectron spectra 77−88498
β-carotene, electronic struct., classical and double beam photoemission obs. 78−9285
catalysis studies, review *(French)* 77−29045
chalcogens, photoionisation cross sections and ang. distribs., outer p subshell 80−9572
chemisorbed atoms, atomic and extra-atomic relax. and IR catastrophe in core spectra 77−48304
chemisorbed layers, photoelectron spectra, line shapes and relaxation effects 79−69956
chemisorption site determ., by angle-resolved UPS 78−71970
chemisorption study, ethylene and halogen-substituted alkenes on Pt (100), Pt (111) substrates, dissociation model 77−43429
chloramine, HOCl, isoelectronic mols., vap. phase UV photoelectron spectra, struct. 78−66600
chlorin, UV absorption and photoelectron spectra, CNDO/S3 calcs. 77−75210
chlorobenzene, photoelectron spectra ang. distrib., π- and σ-orbital assignments 79−818
chlorobenzene ion fragmentation, kinetic shift and phenyl ion heat at formation, photoelectron-photoion coincidence meas. 80−25998
chlorofluorobenzene cations in gaseous phase, emission spectra and lifetimes in B(0°) states 80−63711
chlorofluorobenzenes, He(Iα) and He(IIα) photoelectron spectra, assignments, ionis. energies 80−78651
chlorofluoromethanes, valence photoelectron spectra, electronic and vibr. bands 78−50582
chloropropyne, mol., He(I) photoelectron spectra 79−27033
N-chlorosuccinimide, lone-pair struct., photodetection spectra 78−37684
chlorotrifloуromethane, UV photoelectron spectra, vibr. fine struct. 78−9196
closed shell atoms, photoelectron ang. distrib. and spin polarisation, theory 80−91618
coating characterisation 77−31919
coincidence device for meas. of photons and photoelectrons 77−27205
collective effects, relax. and localisation of hole levels 80−52950
condensed phase photoelectron asymmetry 80−80930
conference, Lyons, France (Apr. 1976) *(French)* 77−36354
core ionisation in 3d, 4f and 5f series, rearrangement effects 80−53065
coronene, polycrystal, photoemission 78−27367
crystalline solids numerical spectral integration within linear analytic approx. 78−60545
cyanoacetylene, photoelectron spectra, electronic states of radical cations 79−22756
cyanodiacetylene cation, gas phase, UV emission spectra of $\tilde{A}(\pi^{-1})\rightarrow\tilde{X}(\pi^{-1})$ band system 80−95636
cyanogen adsorbed in Pt (100), UPS 77−36351
cyclic hydrocarbons, chemisorpt. on W(100) surface, decomp., UPS and thermal desorpt. obs. 80−59782
cyclobutenedione derivatives, photoelectron spectra, 2p lone pair delocalisation 78−46392
1,3,5,7-cyclooctatetraene, photoelectron ang. distrib. meas. 79−50082
cyclopentadienone, photoelectron spectra, ionisation pot., PERTCI method and obs. *(German)* 78−42130
cyclopentadienyl ion, electron affinity and Jahn-Teller effect, laser photoelectron spectra 77−88499
cyclopenta[h]cycl[4.2.2]azine, photoelectron and visible, and UV spectra 78−5286
cyclopropanone, electronic struct., UV photoelectron spectrum 78−33428
cyclopropene, photoionisation and threshold photoelectron-photoion coincidence study 80−53062
cyclopropyl ketones, photoelectron spectra, MO calcs. 77−27115
d^6-complexes and oxides, spin-state transitions, PES study 79−100014
data acquisition system for EXAFS and photo-electron spectroscopy expts. 78−62676
decamethylferrocene, vac. UV photoemission 77−85883
decamethylferrocene-bis(TCNQ), vac. UV photoemission 77−85883
diacetylene polymers, photoelectron valence band spectra 78−43979
diamond, semiconducting, (111) surface, quantum photoyield and secondary-electron distribs., stable negative-affinity emitter 79−100023
diamond, valence electrons, energy-depend. photoionisation probability calc. 77−16462
diamond ratio of photoionisation cross-sections of valence s- and p-electrons *(Ukrainian)* 77−73211
diatomic molecules, dipole moments, electronegativity and photoemission chem. shifts 79−13655
diatomic molecules, inner-shell ionisation, relax. effects calcs. 77−42351
diatomic photoelectron spectra, vibr. struct. calcs., cost-effective program 77−18973
dibenzofuran, photoelectron spectroscopy obs. of heterocycles 78−94286
dibenzothiophene, photoelectron spectroscopy obs. of heterocycles 78−94286
dibenztetrathiafulvalene, absorbed on Au, Al, ionisation and polarisation energies of mol., UPS meas. 78−79886
1,2-dibromoethane, gauche and trans conformers, photoelectron spectra 78−50574
trans-dibromoethylene, VUV and photoelectron spectra, Rydberg series, vibr. fine struct. 77−6799
1,3- and 1,4-dichlorobenzene radical cation, emission and photoelectron spectra, lifetimes meas. 78−86905
dichlorodifluoromethane, UV photoelectron spectra, vibr. fine struct. 78−9196
dicyanodiacetylene radical cation, photoelectron and emission spectra 80−5558
diene-iron tricarbonyl complexes, π-orbital perturbation energies, ionisation energies; UV photoelectron spectra 80−32775
diethyl cadmium, core d-level high resolution photoelectron spectra, spin-orbit splitting 78−50579
p-difluorobenzene, electronic struct., many-body calc., photoelectron spectrum assignment 77−23421
difluorobenzenes, X-ray and UV photoelectron spectra, ionis. pots., ab initio GO calcs. 77−61795
difluoroethene, cis- and trans-, photoelectron-photoion coincidence study, fluoresc. obs. 80−95678
dimethyl cadmium, core d-level high resolution photoelectron spectra, spin-orbit splitting 78−50579
photoelectron spectra continued
dimethyl cadmium, core level ligand field splitting, PES, model for covalent mols. 78−37681
dimethyl cadmium, photoelectron spectra, 4d spin-orbit splitting, crystal field and band-broadening effects, CNDO calcs. 78−76577
dimethyl mercury, high resolution photoelectron spectra, 5d orbital energy ordering reassignment 78−74700
dimethyl zinc, core level ligand field splitting, PES, model for covalent mols. 78−37681
dimethyl zinc, core level photoelectron spectra, electric field gradient splittings 77−88494
dimethyl zinc, valence band and Zn 3d levels, electric field gradients 77−88495
3,6-diphenyl-pyridazine, valence electronic structure 79−72360
3,6-diphenyl-s-tetrazine, valence electronic structure 79−72360
diphenylethers, 1st ionisation energy, substituent effects, photoelectron spectra 77−42354
diphenylsulphides, 1st ionisation energy, substituent effects, photoelectron spectra 77−42354
p,p'-diphenylsulphines, (He I) photoelectron spectra, assigned by perturbational mol. orbital and CNDO/2 calcs. 78−46396
dipyridylethylenes, photoelectron spectra, conformation, SCF LCAO calcs. 77−79651
diynes, acyclic, non-conjugated, UPS comparison, obs. and calc. 80−32772
Drude energy absorption, photoemission theory from electron gas 77−63534
dynamic symmetry breaking, mol. photoelectron ang. distrib. 79−829
Earth ionosphere and plasmasphere, fluxes and spectra of Auger electrons and photoelectrons 78−45094
effective hamiltonian matrix parameter optimisation, least squares method 79−26874
electrode-electrolyte interface, solid film props., review of expt. techniques 77−77780
electron binding energies reference level problem in photoelectron spectra of solids and adsorbates 78−63936
electron spectroscopic quantitative surface analysis 78−92552
electron spectroscopy, book 78−16896
electron spectroscopy, coincidence experiments, two-parameter 78−20135
electronic elementary excitations in far UV, core level exciton and core hole polarisation 78−39032
energy analysis of trapped ions, strong mag. field, elastic scatt. effects 78−62950
ESCA, principles and appls. 78−27375
ESCA apparatus, calibration and use as soft X-ray spectrometer *(French)* 77−13832
ethane, ab initio MRD-CI calc., 14-25 eV PES region, Rydberg states 78−41962
ethane, photoelectron spectrum below 14 eV, ab initio calc. 77−54575
ethyl radical, photoelectron spectra, first ionis. pot. 77−58078
ethylcyanodiacetylene cation, gas phase, UV emission spectra of $\tilde{A}(\pi^{-1})\rightarrow\tilde{X}(\pi^{-1})$ band system 80−95636
ethylene, $^2B_{3u}+e\leftarrow{}^1A_g$ transition, appl. of photoelectron spectroscopy using supersonic mol. beam source 79−68264
ethylene, -d_{0-4}, UPS using 584Å line, adiabatic ionis. pot. of excited states 79−76467
ethylene, autoionisation and photoemitted electron ang. distrib., cylindrical mirror analyser study 80−18049
ethylene, benzene, and fluorinated derivatives, photoelectron ang. distribs. of C-C π electrons 79−10146
ethylene, chemisorbed on α-Fe, struct., bonding, dissoc., UPS obs.; MO calcs. 78−84050
ethylene, chemisorbed on metal surfaces, geometric and electronic struct., UPS obs. and HF LCAO calc. 79−86988
ethylene, chemisorbed on W(100), geometry distortion 77−30919
ethylene, electronic struct., CNDO/S2 calc., photoelectron and UV absorpt. spectra 77−30783
ethylene, ionis. pots., Green's function method 77−14608
ethylene, photoelectron spectra, HAM/3 MO calcs. 78−13414
ethylene, photoelectron spectrosc., ang. depend. 80−9641
ethylene, photoelectron spectrum, vibronic coupling effects 79−10090
ethylene, UV photoelectron spectra, valence electron shake up approx. methods 80−18788
ethylene(-d_1,d_2), high-resolution UPS, mol. ion vibr. assignments, symmetry 79−27032
ethylene glycol, conformational anal., photoelectron spect. 80−43107
ethylene glycol, UV photoelectron spectra, up to 21.2 eV 77−71831
ethylene molecular geometry determ., adsorbed on Cu, Ni, Pd and Pt surfaces 79−19454
ethylene to acetylene conversion on Ni (111), UPS 78−88657
ethylenes, substituted, He I and He II photoelectron spectra, CNDO/S calcs. 78−55201
excitation process theory, book contrib. 78−95664
exploding wire photon sources induced electron emission spectra, yield and energy meas. 78−31299
F-region, photoelectron energy loss and spectral features deduced by plasma line technique 77−45227
ferricytochrome c and c_3, ionis. pot. from VUV photoelectron spectra 79−43821
ferrocene, vac. UV photoemission 77−85883
ferrocytochrome c, ionis. pot. from VUV photoelectron spectra 79−43821
fixed molecule, spectral variations of photoelectron ang. distribs. 77−14489
fixed molecule high energy photoelectron ang. distribs. 78−39667
float glass, Sn penetration depth meas. 77−76614
fluorene, photoelectron spectroscopy obs. of heterocycles 78−94286
fluoroacetylene, He(II) photoelectron spectra 80−91601
fluorobenzene, photoelectron spectra ang. distrib., π- and σ-orbital assignments 79−818
fluorobenzenes, electronic struct., CNDO/S2 calc., photoelectron and UV absorpt. spectra 77−30783
fluorodiacetylene, He(II) photoelectron spectra 80−91601
fluoroethylenes, variable angle photoelectron spectra, ionisation pot. asymmetry parameter 80−28064
fluorophenol cations, emission and photoelectron spectra in gaseous phase 80−58316
fluorosilanes, far UV and He I photoelectron spectra 79−18204
formaldehyde, adsorbed on Ru(110), UPS study, 80K 78−73080
formaldoxime, photoelectron and far UV absorpt. spectra 78−17712

photoelectron spectra continued
formamide, photoelectron spectrum, Green's function calcs., satellite lines 80−28061
formamide, UV photoelectron spectra, up to 21.2 eV 77−71831
formamide, valence ionisation energy and electron affinity, HAM/3 calc. and photoelectron, UV spectra 79−50081
formic acid, dimer, UPS, expt. and MO theory 79−86005
formic acid, ionis. and photoelectron spectra, inner valence electrons 78−82784
formic acid ions, fragmentation, energy selected, photoelectron-photoion spectra 80−95676
formic anhydride, He(I) and He(II) photoelectron spectra 79−54910
formyl chloride, photoelectron spectrum, vibr. struct., ionis. pots., assignments 78−9195
formyl radical, -d_0, (-d_1), first ionis. pot., photoelectron spectrosc. determ. 80−48039
free metal atoms photoelectron and Auger spectra, core level energies 78−50522
furan, photoelectron ang. distrib. from mol. 79−31596
[2,2](2,5)furanophane, through bond and through space interactions, UPS obs. 78−82786
furnace, inductively heated, high temp., construction and operation 77−82521
gas, external photoionisation energies, comparison with liq. phase 77−90237
GaSb surface, Au overlayer, adatom interactions, photoemission obs. 79−33898
gaseous compounds, He I spectra, vac. UV photoelectron intensity meas. 79−31604
graphite, band struct. determ. by angle-resolved photoemission 80−45203
graphite, layered, electronic band struct., direct evaluation by angle resolved photoemission 77−51652
graphite, photoemission, C 1s core-electron line shape, excitonic effects, Fermi energy and hole density of states 80−29848
graphite, surface alteration by interaction with Ar^+ and Xe^+ beams 78−91347
graphite monofluoride, surface alteration by interaction with Ar^+ and Xe^+ beams 78−91347
graphite-alkali metal intercalation cpds., electronic props. 80−45202
Group IV-VI diatomic molecules, He(I) photoelectron spectra, calcs. 80−1023
haloacetylenes, photoelectron spectra, electronic states of radical cations 79−22756
halogens, photoionisation cross sections and ang. distribs., outer p subshell 80−9572
halomethanes, valence photoelectron spectra, vibr. and vibronic struct. 78−50581
HAM/3 semiempirical MO theory, photoelectron spectra calcs. 78−13414
heavily doped semicond., photoemission lineshapes of impurity levels, p-wave resonance 80−76154
heterocyclic aromatic molecules, Penning election spectra and photoelection spectra, rel. intensities 80−95725
hexafluoro ethyl cation fragmentation, mass spectrometry 80−53070
high temp. vapours 80−52238
high-temperature chemical processes, review, book contrib. 77−40545
high-Z elements subshells, photoelectron angular distribution 80−99487
hole recoil, vibrational shake-up and photoelectron lineshapes, in mols. and solids 80−55265
hole states of free atoms, SCF theory 77−10610
Hubbard model, photoemission spectrum, effect of electron correlation 79−78828
hydrocarbons, 30.4 nm He(II) photoelectron spectra 80−82589
hydrocarbons, unsaturated, ang. distrib. He I, Ne I and Au I photoelectron spectra 79−31605
hydrocarbons, unsaturated, Penning electron and photoelectron spectra, relative intensities comparison 79−81237
ice, amorphous, vac. UV photoelectric threshold 78−48273
ice, electronic structure investig. by XPS, UPS and UV absorpt. spectra 77−16452
ice, UPS, valence band struct. 79−33890
ice, UPS study 79−43101
III-V semiconductor, d core levels, electron-hole interaction 77−11880
III-V semiconductor Schottky barrier formation, Fermi-level pinning, defect mech. 78−95358
III-V semiconductor surfaces, adatom interactions, photoemission obs. 79−33898
III-V semiconductor-oxide interface states, photoemission obs. of energy levels induced by adsorpt. 80−93000
III-V semiconductors, oxide film growth, optical props. *(German)* 78−34730
imidazole, photoelectron spectra and electronic struct. 79−22758
indium(I) cyclopentadienide, He I and He II photoelectron spectra 79−13767
inelastic mean free paths of solids, data tables 78−84686
inert gas, atomic photoionisation, Dirac-Fock calcs., branching ratios and angular distrib. in p shells 80−63601
inert gas atom photoelectron ang. distribs., theoretical calcs. comparison 79−59412
inert gas matrices, photoelectron energy distrib. meas. 78−48271
inorganic molecules, UV photoelectron spectroscopy, spectral assignment criteria, bonding 78−17717
interface, internal photoemission, phonon scatt. effects 77−85315
iodobenzene, photoelectron spectra ang. distrib., π- and σ-orbital assignments 79−818
iodotrifluoromethane, photoelectron spectra, spin-orbit splitting, vibr. fine struct. 78−21974
ion+molecule reactions, state selected, threshold electron-secondary ion coincidence method obs. 79−5190
ion fragmentation mechanisms and photoelectron spectroscopy, book contrib. 80−14179
ionic and partially ionic solids, electron-lattice interaction 77−20274
ionic molecule photoelectron spectra using mol. beam technique 78−50576
ionosphere, comparison between calculated and measured photoelectron fluxes from Atmosphere Explorer C and E 78−28400
ionosphere, photoelectron flux calcs. 79−21103
ionosphere midlatitude, photoelectrons ang. and energy distribs. model 77−67009
10H-isoalloxazine, and derivatives electronic struct., photoelectron spectrosc. and ab initio study 80−106261

photoelectron spectra continued
isobutylene, photoelectron spectrosc., ang. depend. 80−9641
isocyanates, nonbonding and π-orbital interactions, photoelectron spectra 80−32774
isopropyl benzene, mol. solid, temp. depend. UPS linewidths 80−89115
isothiothiocyanates, nonbonding and π-orbital interactions, photoelectron spectra 80−32774
ketene(-d_2), radical cations, doublet electronic states, photoelectron spectra 77−88496
ketones, conjugated, ethylenic, UV photoelectron spectra *(French)* 78−90215
labile species, electron photoejection, reaction kinetics characterisation 80−26089
lanthanoid ions, 4f photoelectron spectral intensity, relativistic calc. 79−54816
large molecule, electronic struct., photoemission and optical absorpt. spectrum, CNDO/S3 model 80−53172
layered compounds, book contrib. 77−44133
lead phthalocyanine, photoemission, outer core levels, cross-section depend. 79−50079
liquid, external photoionisation energies, comparison with gas phase 77−90237
liquid metals and alloys, electronic structure 77−48321
liquids, UV photoelectron spectra, up to 21.2 eV 77−71831
localised and delocalised calcs. 80−63709
malonic acid, and α-alkyl derivatives, photoelectron spectra, lone-pair interactions 80−58315
many electron and final state effects, book contrib. 79−61498
many-electron theory, in electron spectroscopy book 78−17714
Mars ionosphere 79−53751
metal, jellium model, H chemisorption, relax. energies in UPS 78−91544
metal, multiplication photoemission in strong field 77−85891
metal, narrow d-band, with adsorbate, semiempirical theory 78−75927
metal, photoelectron emission processes at high laser intensities, multiphoton phenomena 78−60550
metal, refraction effects in angle resolved photoemission from surface states 79−38720
metal, screening energies in photoelectron spectroscopy of localised electron levels 77−1781
metal, surface photoeffect, energy and angular energy distribs. 77−63535
metal, symmetry props. of energy bands determ. by UPS with unpolarised radiation 78−48275
metal conduction electron photoemission spectrum, effect of recoil on shake-up spectra, infinite summation method 80−50526
metal foils, naturally passivated, ESCA, sputter etching 77−70218
metal molecular clusters, UPS 80−80940
metal oxide, molecular adsorption, UPS studies, review 80−84374
metal oxides, ESCA, Madelung pot. effects 80−104036
metal phthalocyanine, vap., photoelectron spectra 79−64043
metal simple, CDW detection by angle-resolved photoemission 78−95658
metal surface, chemisorption, vac. UV photoelectron spectrometer for study *(Japanese)* 78−62264
metal surface, chemisorptive bonding anal. using PES 80−10791
metal surface, clean and adsorbate, covered, exptl. aspects of angle-resolved photoemission 78−15294
metal surface, reactivity, review of electron spectra 77−62748
metal surface photoemission, spatially-varying photon field effects 80−2921
metal surface photoemission spectra selection rules, clean and adsorbate covered single crystals 79−33896
metal with incomplete shell, core photoelectron spectra, spin-depend. final-state interactions 77−69965
metal-InP contacts, intermediate adsorbed layer effect on electronic props. 80−39674
metallic superhigh-vacuum apparatus for 10 eV photoelec. meas. 78−21145
metallocenes, photoelectron spectra, band assignment 80−91604
metals, chemisorption of gases, book 79−69370
metals, photoelectron spectroscopy of surface states 79−56909
methane, high resolution photoelectron spectra, vibr. progression 78−74700
methane, photoabsorpt. cross section, 10 to 50 nm 77−61797
methane, photoelectron ang. distrib., near threshold to 30 eV, photon energy depend. 80−53045
methane, photoelectron spectra, 21.2-151.4 eV and soft X-ray, ionis. cross-section 78−37683
methanol, and -d_1, -d_4, photoelectron spectra, internal rot. in ground ionic state 77−65509
methanol, ionic dissoc., photoelectron-photoion coincidence spectroscopy 80−66774
methanol, processes of photoionisation studied using ion-electron coincidence method 80−74204
methanol, valence photoelectron spectra, vibr. and vibronic struct. 78−50581
methanol-d_4, dissoc. following photoionis., using coincidence spectrometer 79−54998
methoxide surface complexes on Li, He(I) photoelectron spectra, MO calcs. 80−83417
methoxide-d_0(−d_3) anion, electron affinity, vibr. struct., photodetachment electron spectra 78−94282
methoxy species on Ni (111), photoelectron spectra, electronic struct. and orientation 80−83420
methyl ethyl ketone, processes of photoionisation studied using ion-electron coincidence method 80−74204
methyl halide ions, unimol. dissoc. and internal conversions, coincidence meas. 77−6869
methyl radical, HeI photoelectron spectrum, Franck-Condon factors 77−34692
methyl vinyl sulphide, rotational isomerism, variable temp. photoelectron spectroscopy appl. 77−6846
2-methyl-but-3-yn-2-ol, mol., He(I) photoelectron spectra 79−27033
N-methylaniline, UV photoelectron spectra, up to 21.2 eV 77−71831
methylchloramines, CH_3NHCl, CH_3NCl_2, $(CH_3)_2NCl$, UV photoelectron spectra, assignments 78−86911
methylcyanodiacetylene cation, gas phase, UV emission spectra of $\tilde{A}(\pi^{-1}) \rightarrow \tilde{X}(\pi^{-1})$ band system 80−95636
methylene, photoelectron spectra, singlet and triplet state calcs. 78−42127
3-methyleneoxetane, electron structure, orbital-O interaction, MO calcs., UV photoelectron spectra 80−28058

photoelectron spectra continued
o-methylhydroxylamine, ionisation energies, He I photoelectron spectra, orbital calcs. 77−88497
methylimidazoles, photoelectron spectra and electronic struct. 79−22758
3-methylpent-4-yn-3-ol, mol., He(I) photoelectron spectra 79−27033
mineral, rel. to bond lengths *(French)* 77−36364
mixtures, quantitative analysis using PES and XES 77−90678
molecular adsorbed on surfaces, atomic dipole theory of photoemission 78−84695
molecular negative ion, photoelectron ejection ang. distrib. theory 77−491
molecular photoelectron spectroscopy, review 78−94283
molecular structure determ., review 78−1026
molecule, oriented or rot. resolved unoriented, ang. distribs., dynamic and struct. data 78−37682
molecule, photoelectron peak size rel. to photoionis. cross section 77−88508
molecule, photoionization cross-section, ground state inversion pot. method 79−31484
molecule core 1s and 1b, photoelectron bands, vibr. excitations, ab initio calc. 80−63543
molecules, condensed, vibr. excitation in photoemission spectra, appl. to CO 77−28689
molecules, diatomic, photoelectron ang. distrib. and intensity, vibr.-rot. struct. 78−42128
naphthacene film, electron escape depth, energy depend. 79−38709
Nb_2O_5 *(French)* 77−44541
near UV photoelectron energy and ang. distribs. *(French)* 77−36359
negative ions, autodetachment, spectroscopy 80−23385
negative ions, sputtered, characteristic electronic and vibrational temp., laser photoelectron spectral meas. 80−66346
nickel phthalocyanine, resonant photoemission at 3p-core threshold from quasiatomic Ni 79−78847
p-nitroaniline, adsorbed layer, core ionisation, negative shake-up energy 79−56913
p-nitroaniline, core ionisation negative shake up energy, ab initio SCF CI calc. 79−64041
nitronaphthylamines, ESCA and UV photoelectron spectra, assignments 78−50588
nomenclature and spectral presentation for photoelectron spectroscopy, IUPAC recommendations 77−68075
noncrystalline materials, optical props., lecture 78−31219
nonlinear photoelectric emission from metals by high power layer radiation review 78−48288
nucleic acids and related compounds, photoemission rel. to absorpt. and luminesc., 120 to 250 nm 77−81466
octachlorofulvalene, electronic structs., semi-empirical MIEHM calcs. 77−75057
optical Be filter in He discharge lamp for photoelectron spectroscopy 78−79115
optically active molecule, photoelectron ejection ang. distrib. theory 77−491
organic compounds, HeI photoelectron spectra *(Japanese)* 80−16150
organic compounds, photoelectron spectroscopy, ionis. pots., MO models 78−17716
organic ion, excited electronic state correlation with mass-spectral fragmentation pattern 80−45482
organic molecular crystals, photoemission, book contrib. 80−16158
organic molecules, photoelectron ang. distrib., for band assignment rule 79−13768
organic molecules, UV photoelectron spectroscopy, systematic review 80−28057
organic samples on metal supports, origin of photo-electron-microscope pictures 80−26431
overlayer covered systems, contribs. of substrate multiple scatt. to angle-resolved UPS 78−84694
3- oxetanone, electron structure, orbital-O interaction, MO calcs., UV photoelectron spectra 80−28058
pentacene, polycrystal, photoemission 78−27367
pentatetraene, non-degenerate vibr. mode induced Jahn-Teller effect, photoelectron spectra calc. 79−817
perovskites, d-band, concepts of surface states and chemisorption, book contrib. 80−107651
perylene, energy structure, photocond., photoemission and absorpt. spectra meas. 77−39895
perylene film, electron escape depth, energy depend. 79−38709
perylene polycrystal, photoelectron spectroscopy 77−59670
phenanthrene, photoelectron spectroscopy obs. of heterocycles 78−94286
1-phenyl-2-(4-pyridyl) cyclopropanes, UPS of cis- and trans-forms 79−36699
phlorin, UV adsorption and photoelectron spectra, CNDO/S3 calcs. 77−75210
photoelectron ang. distrib. and spin polarisation, theory 80−91618
photoelectron injection in gases from thin metal films on quartz 79−68899
photoelectron-photoion coincidence spectroscopy, fixed-wavelength, improved resolution 79−18318
photoion-photoelectron spectroscopy, ion internal energy and reaction 79−30616
photoionisation, atoms and molecules review, expt. techniques, processes, theory 77−14402
photoionisation branching ratios, photoelectron spectrometric meas. technique 79−31607
photoionisation mass spectrometer for threshold photoelectron spectroscopy 77−87868
photoionisation of atoms and molecules, UV photoelectron spectrosc. obs. 79−31603
photoionisation theory, atomic photoelectron spectroscopy, book contrib. 77−79591
phthalocyanine, vap., photoelectron spectra 79−64043
phthalocyanine compounds, valence band studies, UPS meas. 77−52221
phthalocyanines, UV photoemission, valence band struct. 77−85884
piperazine-2,5-diones, and N-chloro derivatives, UV photoelectron spectra and geom. struct. 79−18235
plasmon effects in electron spectroscopies and chemisorption 79−33190
platinum phthalocyanine, photoemission, outer core levels, cross-section depend. 79−50079
polyacetylene:AsF_5, AES, XPS, UPS, and X-ray induced 80−66400
polyacetylene:I, electronic structure, XPS and UPS meas. 80−66385
polyacetylene, electronic struct., spectra interpretation, CNDO/S2 calcs. 79−6870
photoelectron spectra continued
polyatomic mol. photoelectron ang. asymmetry parameter vibr. state depend., vibronic coupling 79−36698
polyatomic molecule, multiphoton absorpt. resons., dynamic Stark splitting 80−9670
polyatomic system, multiple scattering method for photoelectron and absorpt. spectra 77−88501
polyethylene, conduction band struct., LEED, secondary electron emission and UPS study 80−70601
polyethylene-metal contact charging, electron transfer mechanism, PES characts. 80−35055
polymer, degradation products, chem. anal. by UV photoelectron spectroscopy 78−53300
polymer film, electron inelastic mean free paths 79−33369
polymer film, electron inelastic mean free paths 79−33370
polymers, vacuum-UV irrad. photoelec. emission and contact charging 79−52075
polypyridines, photoelectron spectra, SCF LCAO calcs. 78−33551
porphins, UV absorption and photoelectron spectra, CNDO/S3 calcs. 77−75210
prop-2-yn-1-ol, mol., He(I) photoelectron spectra 79−27033
propane and deuteropropane, fragmentation, threshold photoelectron photoion coincidence mass spectra 77−14505
β-propiolactone, electron structure, orbital-O interaction, MO calcs., UV photoelectron spectra 80−28058
purines, biological, UV photoelectron spectra, valence electronic struct. 77−16905
pyridine, photoelectron spectra, HAM/3 MO calcs. 78−13414
pyridine adsorbed on Cu (110) surface, photoemission selection rules 80−100751
pyridine-N-oxide, electronic struct. assignment, He I/He II intensities *(German)* 80−83423
pyrrole, photoelectron ang. distrib. from mol. 79−31596
quartz, photoelectric and photoluminescent props. in fundamental absorpt. region 78−39596
α-quartz electron states, self-consistent pseudopot. calc. 77−62823
rare earth atoms at surface, photoionisation of 4f electrons 78−11077
rare earth films, Auger emission from excited atoms 77−20967
rare earth metals, 5s electron excitation energies 78−10408
rare earth pnictides, prep. and props., book contrib. 80−54212
rare earths, and their alloys and cpds., book contrib. 80−16157
rare earths cpds., Fano-resonances, surface and bulk effects in photoemission 80−97405
rare gas crystal, pure and benzene-doped, photoelectron emission, exciton states 77−44116
relaxation energies, non-relativistic ΔSCF-optimised HFS calcs. *(French)* 77−36357
resonance, monochromatized synchrotron radiation examination, difluoroethylene 79−59514
resonant multiphoton ionisation, line profile as Fano profile with background struct. 79−72290
review, electron spectroscopy appls. *(Japanese)* 79−40645
review, on photoemission spectroscopy, book contrib. 77−63546
t-RNA, rot. relax. time, 10^{-9}s range Fabry-Perot and photoelectron time of arrival method 80−21437
rubrene film, photooxidation in solid, UPS obs. 79−52693
satellite struct., at. and mol. electron-correls. using initial-state-CI 77−18980
saturated organic molecule, photolysis, primary step prediction using Rydberg and valence-shell transitions 77−21404
second-row atom, photoemission energy, rel. to homonuclear diatomics 78−86832
second-row homonuclear diatomics, photoemission energy, rel. to atoms 78−86832
semiconductor, core-level photoyield exam. of empty surface states 77−55593
semiconductor, laser-modulated photoemission, technique for band struct. determ. 77−28686
semiconductor, multiplication photoemission in strong field 77−85891
semiconductor, surface electronic props., optical spectroscopic techniques, review 80−11070
semiconductor surface, atomic and electronic struct. 78−72223
semiconductor surface electron states, optical methods of detection 77−66191
semiconductor with s-like valence band and p-like cond. band, photoemission characts. *(Russian)* 77−81195
semiconductor-oxide interface and Schottky barriers, photoemission and Auger spectroscopy 80−50536
semiconductors, optical props. above band edge, book contrib. 80−84425
semiconductors, photoelectron spectra and band struct., book contrib. 80−16155
simple metals, photoemission theory, book contrib. 80−16159
small molecules, angular distribution He I (Ne I) photoelectron spectra 79−31606
sodium ethanoate, solid, low energy photoelectron spectra 78−95656
solid, photoemission spectra calc. using wave mech. scatt. techniques, book contrib. 78−95666
solid, photoionisation cross section of free atoms, book contrib. 79−61497
solid-state, with synchrotron radiation, review 80−71570
solids, angular dependent photoemission, book contrib. 79−61500
solids, band struct., angle resolved photoemission obs. 79−33899
solids, book 80−12860
solids, electronic states determ. using synchrotron radiation 77−20882
solids, general principles, book 79−61494
solids, independent particle model, book contrib. 79−61496
solids, photoemission, book contrib. 79−61495
solution, external photoionisation energies, comparison with gas phase 77−90237
spectrometer, design for teaching lab. 78−86078
spectrometer, variable angle, for meas. electrons photoejected by rare gas reson. light 78−1110
spectrometer construction 78−27874
spectrometer for surface studies, including angle-resolved photoemission meas. 79−58849
spectroscopy in strong mag. field, trapped ions, with ion cyclotron reson. 78−50666
spin polarisation of photoelectrons, ang. depend. 80−78652
steel, Fe-Mo-C low-alloy, photoelectron microscopy of diffusional transformations 77−44242

photoelectron spectra continued
substrate-split localised adsorbate levels, spin polarisation effects in photoemission 79−19971
surface anal., deconvolution of exptl. curves *(French)* 80−16153
surface analysis, expt. and one-step model calcs. *(French)* 77−36366
surface analysis, system, modular combined ESCA, UPS, AES, and SIMS 78−73107
surface analysis techniques, AES, ESCA, and photoelectron spectroscopy 79−95252
surface characterisation, multiple technique instrument, ESCA, scanning Auger, UPS and SIMS 78−73108
surface chemical analysis, direct comparison of AES and ESCA 77−1969
surface chemical bonding, electron spectroscopy, book contrib. 80−24992
surface electron states, electron emission spectroscopy probe 77−51798
surface electronic struct. and UV photoemission 77−62975
surface physics, conf., Eindhoven, Netherlands (June 1976) 77−62708
surface science, conf., York, England (March 1977) 78−14540
surface state spectroscopy, theories for expt. data anal. 77−63541
surface studies using polarised source of He I radiation 78−74959
surfaces, electron spectroscopy, review 78−92169
TCNQ, anions, screened INDO model, appl. to photoelectron, optical, Raman spectra 79−765
TCNQ, charge transfer complexes, changes in valence electronic structure 80−7477
TCNQ, elect. struct. determ., CNDO parametrisation and UPS data 77−1350
Teflon, surface alteration by interaction with Ar^+ and Xe^+ beams 78−91347
temperature measurement by photoemission method, systematic error 79−93140
ternary semiconductor, $A^{II}B_2^{III}C_4^{VI}$, crystal structure effects in electronic states 80−20085
p-terphenyl, valence electronic structure 79−72360
tetrachloromethane, He(II) photoelectron spectra, spectral intensity patterns 79−98152
tetraethyl lead, core d-level high resolution photoelectron spectra, spin-orbit splitting 78−50579
tetraethyl lead, core level photoelectron spectra, electric field gradient splittings 77−88494
tetrafluoroethylene, electronic struct., CNDO/S2 calcs., photoelectron and UV absorpt. spectra 77−30783
3,3,4,4-tetramethyldiazetine, photoelectron spectra, ring size effects on azo group ionis. pots. 77−61793
tetramethyldiphosphine, UV photoelectron spectra trans/gauche isomer equilib. 79−31600
tetramethylethylene, photoelectron spectrosc., ang. depend. 80−9641
tetraselenafulvalene, monomer and dimer electronic struct. scattered wave calc. comparison with photoelectron spectra 78−50465
thallium(I) cyclopentadienide, He I and He II photoelectron spectra 79−13767
theory, techniques, and appl., book 80−8748
thermal light with orthogonally polarised multiple-peak spectrum, intensity fluctuations 80−87303
thermosphere, photoelectron energy spectra, rocket born meas. in 2-100 eV range 78−77379
thin surface layers, depth and composition determ. by depth-selective photoelectron spectroscopy 79−43090
thioacetamides, CNDO calcs., internal rot., ionisation pots., photoelectron spectra 78−5143
p,p′-thiobenzophenones, (He I) photoelectron spectra, assigned by perturbational mol. orbital and CNDO/2 calcs. 78−46396
thiocyanates, nonbonding and π-orbital interactions, photoelectron spectra 80−32774
thioformamide($-d_2$), photoelectron and absorption spectra, vibr. struct., excited state configs. 77−6847
thiomethoxide anion, electron affinity, vibr. struct., photodetachment electron spectra 78−94282
thiophene, photoelectron ang. distrib. from mol. 79−31596
[2,2](2,5)thiophenophane, through bond and through space interactions, UPS obs. 78−82786
thiophosphoryl compounds, bond ionisation energies, mol. struct. from UV photoelectron spectra 78−82782
threshold photoelectron spectrometer, and applic. 77−14491
threshold photoelectron spectroscopy by electron attachment, high-resoln. 77−27202
threshold photoion-photoelectron coincidences method for ion state selection 80−63718
transient species, vacuum UPS, book contrib. 80−14178
transient species formation methods 79−31739
transition metal, dihalide, high temp. vapour photoelectron spectra 79−36697
transition metal, group VIII, O_2 chemisorption, UPS 79−7752
transition metal, group VIII, O_2 chemisorption, UPS 79−7751
transition metal, inner shell photoelectron and photoabsorpt. spectra 79−43091
transition metal carbonyl complexes, UV and X-ray photoelectron spectra, effect of adsorbed CO 79−4897
transition metal carbonyls, photoelectron spectra, time depend. relax. effects 77−71829
transition metal dihalides, MS potential from a set of overlapping densities 80−52850
transition metal glasses and amorphous films, supercond. and electronic props. 79−73612
transition metal ion system, multiplet and cryst. field split photoemission spectra 77−66577
transition metal monosulphides of first-row, XPES and UV PES 80−20760
transition metal oxides, UPS, LEED and AES studies of mol. adsorption 79−4480
transition metal pentachlorides, photoelectron spectra 79−821
transition metal surface (adsorbate), intermediate UPS/XPS synchrotron radiation study 78−52633
transition metals, and their alloys and cpds., book contrib. 80−16156
transition metals, chemisorption of H, O and CO, interpretation of photoemission spectra 78−2378
transition metals, gas phase, He I photoelectron spectra, photoionisation cross section meas. 79−98051
transition metals, photoemission spectra, core-level satellite struct. 80−29855

photoelectron spectra continued
transition-metal perovskitelike compounds, covalency effects, partial densities of p- and d-states photoelectron spectra 79−38718
transiton metal oxide perovskites, UPS, XPS, X-ray absorpt. spectra, band struct. study 79−56885
triallyl orthoformate, photoelectron spectra, ionisation pot. bands, conformation, SPINDO calc. 78−9194
triatomic mols., Renner-Teller effect, orbital angular momentum 80−78513
triazastilbenes, photoelectron spectrosc. 80−106353
1,2,4-triazine, and methyl derivs., photoelectron spectra 77−30922
1,3,5-triazine, photoelectron ang. distrib. meas. 79−50082
1,3,5-trichlorobenzene radical cation, emission and photoelectron spectra, lifetimes meas. 78−86905
trichlorofluoromethane, UV photoelectron spectra, vibr. fine struct. 78−9196
triethylamine-perfluoro-T-butanol, photoelectron and Rydberg bands, UV spectra study 80−18865
trifluoroacetic acid, monomer and dimer, photoelectron spectrosc. 80−87172
trimethyl gallium, core level photoelectron spectra, electric field gradient splittings 77−88494
trimethyl indium, core d-level high resolution photoelectron spectra, spin-orbit splitting 78−50579
trimethyl orthoformate, photoelectron spectra, ionisation pot. bands, conformation SPINDO calc. 78−9194
trimethylethylene, photoelectron spectrosc., ang. depend. 80−9641
triphenylamine cation radical, condensed and vapour phase geometry, photoelectron spectra 79−31597
l-tryptophan, gas, UV photoelectron spectrum, photoionisation threshold 79−86004
TSeF salts, mol. props., one-dimens. cond. salts form. 78−6363
unimolecular decay, photoion-photoelectron spectroscopic obs. 79−30616
unpolarised atoms, spin polarisation of ejected photoelectrons 79−45682
upper atmosphere, photoelectron energy spectra 78−49190
upper atmosphere, photoelectron spectra allowing for Auger effect 78−69557
UPS, angle-resolved, in modified LEED system 78−15293
UPS, angle-resolved, initial state symmetries from polarisation effects 80−40227
UPS, high resolution, fast pumping for study of transients and unstable species 77−83764
UPS, rel. to band struct., appl. to Cu 79−52080
UPS ultrahigh vacuum apparatus, appl. to clean and gas covered Si(III) surfaces *(Japanese)* 80−37125
UV, surface analysis, spectroscopic methods, review *(Chinese)* 79−34414
UV and X-ray, review of literature, 1975-1977 78−85225
UV angle-resolved photoemission spectroscopy, using high intensity discharge lamp 79−12870
UV photoelectron spectra at high temp., interpretation 78−17718
UV photoelectron spectrometer, gas and vap. phase operation 78−82865
UV photoelectron spectroscopy, basic concepts, spectra 78−17715
UV-valence electron spectroscopy, multichannel detector system 77−23520
vacuum UV line source, He lamp, for photoelectron spectroscopy 78−94419
vacuum UV photoelectron spectrometer for metal chemisorption studies *(Japanese)* 78−78044
valence bands in solids, photoelectron spectroscopy, review 78−39668
valence shell electrons ang. distrib. meas. by fully automated spectrometer 77−58202
vapours, oven heated inorganic solids, charact. technique 80−52239
vibrational state depend. of asymmetry parameter of ang. distrib. 77−75218
vibrationally-excited ions form. in Franck-Condon gaps, threshold photoelectron spectra obs. 79−68262
vinyl isocyanate, microwave and photoelectron study of cis- and trans-forms 78−70819
water irradiated by photons up to 2 MeV, initial energies of Compton electrons and photoelectrons 80−108320
X-ray intensity due to photoelectrons, calc. for fluorescence anal. 80−26075
xanthine, and biological methyl derivatives, electronic struct. from UV photoelectron spectra 79−24949
yield, high-resolution, information on semiconductor surface states 77−69392
yield from monocrystrals under X-ray diffr. conditions, meas. method 80−50521
YIG, energy location of mag. Fe levels, spin polarised photoemission 79−24413
zinc phthalocyanine, resonant two hole bound state at 3p core threshold 80−60750
Ag, 4d bandwidth influence on $M_{4,5}N_{4,5}N_{4,5}$ Auger spectra 79−100017
Ag, 4d level He II photoelectron spectra, energies and intensities 80−5511
Ag (001), Cl adatom bonding effects from coverage-depend. angle-resolved photoemission 79−82436
Ag (100), (110), (111), high resolution photoelectron energy distrib. curves 77−28693
Ag (100) and (111) epitaxial films, ang. depend. UPS 80−55270
Ag (110), adsorption of O_2 and coadsorpt. of Na and O_2, XPS and UPS obs. 77−69183
Ag (110) surface, photoelectron spectroscopy and surface order, UPS and XPS obs. 78−56568
Ag (111), adsorbed layers of $O_2(N_2)(S)$, electronic props., XPS and UPS 78−10279
Ag (111), angle resolved photoemission free electron final state model 78−72694
Ag (111) surface, ethylene adsorption, XPS and UPS investigation 80−103573
Ag, (111) surface, failure of plane wave, OPW and APW final states 78−11080
Ag, adsorption and surface reaction of formic acid 80−40741
Ag, angular resolved photoemission from low index faces 78−48282
Ag clusters, chemisorption of I, UPS obs. 80−84830
Ag, electronic density of states, cluster approx., compared with photoemission spectra 79−60675
Ag faces, single cryst., low-energy photoemission 78−60548
Ag film, angular depend. UPS, surface electronic struct. 79−83095

photoelectron spectra continued
Ag, film, electron inelastic scatt. mean free paths, synchrotron radiation photoelectron spectra meas. 78−76587
Ag film, enhancement of electron photoemission by excitation of surface plasmons *(French)* 77−63524
Ag film, initial stages of growth on Si (111) 7×7, LEED, AES and UPS expts. 78−38988
Ag halides, tetrahedrally coordinated, semiempirical band struct. model 77−51655
Ag halides, valence and cond. states, UPS, temp. depend. 77−20997
Ag, intrinsic surface states, UV photoemission meas. 77−20983
Ag, K-shell photoelectric cross section 79−22676
Ag monolayer on (111)Si surface, Schottky barrier, interface electronic nature and epitaxy 79−77934
Ag photocathode work function, decrease due to adsorption of alkali halides 79−78824
Ag, photoelectric cross section, derived from total absorpt. cross sections 77−10646
Ag, photoelectric cross sections for 323 keV gamma rays 77−88432
Ag, photoelectric cross sections, from total absorption cross sections, 5 to 130 keV 79−26947
Ag, photoelectric cross section in region 187 to 662 keV 79−69952
Ag, photoelectron spectra 77−73218
Ag, photoionisation, photoelectron spectra 80−87086
Ag, polarised photoelectron yields in VUV region 80−106307
Ag surface, (111) and (100), crystallographic anisotropy in surface plasmon decay to photoelectrons 79−24052
Ag surface, clean and oxidised, $M_{4,5}VV$ Auger spectra, anal. based on self-convolution of measured UPS 77−77332
Ag surface, optical photoemission, high index faces, angle of incidence variation 79−100024
Ag, UPS, expt. methodology aspects 77−90245
Ag-O-Cs photocathode, Ag colloidal particles and long wavelength response *(Chinese)* 80−45195
Ag-Sn alloys, UV photoelectron spectroscopy of valence bands 77−24924
$AgAsS_2$, cryst. and amorphous, band struct., photoemission and refl. spectra obs. 77−66581
AgBr, vapour, photoelectron spectrosc., interpretation 80−95679
$(AgBr)_3$, gas, He(I) photoelectron spectra 80−43103
AgCl, vapour, photoelectron spectrosc., interpretation 80−95679
$(AgCl)_3$, gas, He(I) photoelectron spectra 80−43103
$(AgCl)_3$, photoelectron spectrum and valence shell struct. 78−62843
AgI, superionic conductor, density of valence states, photoelectron spectra meas. 80−25523
AgI, vapour, photoelectron spectrosc., interpretation 80−95679
$(AgI)_3$, gas, He(I) photoelectron spectra 80−43103
AgN_3, optical absorpt. spectra, and photoemission, electron band scheme 79−100015
Ag(111), valence band struct. along Λ, angle resolved photoemission spectra 79−95316
Al (001), enhanced photoexcitation 80−80937
Al (100), chemisorbed O, photoemission ang. depend., MO cluster model calc. 78−76576
Al (111), adsorption and condensation of O_2 at 30K, UPS obs. 79−60635
Al (111), angle-resolved UPS obs. of 2-dimens. band structs. of S, Se and Te 80−60059
Al (111), bonding of O, electronic struct. calcs., rel. to UPS data 80−59801
Al (111), chemisorbed ordered O overlayer, angular resolved photoemission 79−82462
Al (111), O-induced band dispersion and symmetry, photoelectron spectrosc. obs. 79−61490
Al (111), ordered O overlayer, angle-resolved photoemission, band struct. 80−40229
Al, ARPES using synchrotron radiation 78−72682
Al, adsorption and decomp. of methanol., UPS, XPS and thermal desorption obs. 79−82441
Al, atom, photoelectron ang. distrib. of 3s subshell 79−76397
Al caesiated thin film, surface plasma wave excitation by polarised light, photoemission obs. 80−50518
Al clean films, O_2 interaction study using synchrotron-radiation-induced-photoemission 80−55709
Al film, caesiated, photoelectron escape length, 1.5-4 eV *(French)* 79−47585
Al film, polycryst., chemisorpt. of O_2, synchrotron radiation photoemission expts., 70-150 eV 78−95228
Al film, two photon photoelectron effect in surface plasma reson. 77−69962
Al, multiple oxidation states, obs. by photoelectron spectra of core level shifts 77−8720
Al, photoelectric cross section, derived from total absorpt. cross sections 77−10646
Al, photoelectric cross sections, from total absorption cross sections, 5 to 130 keV 79−26947
Al, photoemission study of energy depend. of bulk plasmon loss intensity 79−47035
Al, plasmon sideband exam. by synchrotron radiation tuning of electron escape depths, UPS 77−47755
Al, secondary-electron energy distribution in high-energy photoemission 77−48305
Al, single cryst., surface reson. and oxidation 78−72225
Al surface, oxidation, synchrotron radiation photoelectron obs. 78−52634
Al, surface broadening of 2p core level photoemission spectra 80−25524
Al, surface photoelec. effect, surface photoemission spectroscopy on jellium 79−4900
Al, surface photoelectric effect, optical excitation using synchrotron radiation 79−4892
Al, XPS theory, valence band spectra band struct. 78−72702
Al-SiO_2, surface reactions and interdiffusion, photoemission study 80−49532
$Al_xGa_{1-x}As$, valence and core level photoemission spectra 79−19973
α-Al_2O_3, chemisorbed water, electron binding energies, UPS, SCF-Xα-SW calcs. 77−69169
Al_2O_3, optical absorpt. and external photoeffect, 6 to 40 eV 77−55802
Al(100), angular resolved photoemission from intrinsic surface states 78−39665
Ar, 0-10 eV photoelectron spectra obs., new differential retarding field analyser characts. 77−41735
Ar 3s, photoelectron ang. distrib., relativistic Dirac-Fock calc. 79−59411
Ar film, electron MFP, vacuum UV photoemission data 77−28690

photoelectron spectra continued
Ar II, (e,2e), photoelectron and conventional spectroscopies 78−90298
Ar, impurity lines in He resonance source 77−14787
Ar, ns→εp photoelectrons, spin polarisation 80−37792
Ar, outer shell photoelectron spectrum, correl. satellites 78−78671
Ar, photoelectron emission, polarisation depend. on incident unpolarised VUV radiation wavelength 80−52952
Ar, photoelectron spectra, 21.2-151.4 eV and soft X-ray, ionis. cross-section 78−37683
Ar, photoelectron spectrum ang. distrib. abnormality in strong mag. field 78−50666
Ar, plane polarised VUV irrad., emitted photoelectron polarisation, ang. depend. 80−47952
Ar, shake-up energies, Slater transition-state calcs. 79−89651
Ar, spin-polarised photoelectrons by circularly polarised synchrotron radiation 80−91516
Ar, threshold photoelectron spectra by electron attachment 77−75211
Ar, valence shell photoelectron spectrum, CI calcs. 79−31419
Ar:Xe film, solid, competition between electronic energy transfer and relax., photoelectron spectra 77−24929
Ar_2, photoelectron spectra 78−78748
As film, sputtered, density of valence states by XPS and UPS 77−24926
As-Se amorphous film, density of upper valence band states, annealing effects, UPS obs. 80−29845
As_2O_3, density of valence states, photoemission meas. 77−72808
As_2O_3, electronic struct., X-ray emission, XPS, UPS obs., CNDO cluster calc. 78−52638
As_4O_6, UV photoelectron spectra, mol. orbital symm. 77−14494
As_2S_3, amorphous, density of valence states, XPS and UPS obs. 77−48308
As_2S_3 and As_4S_4 vapour-deposited films, valence states, thermal and photo-induced changes UPS study 80−93459
As_2S_3, cryst. and vitreous, struct. determ. 79−65979
As_2S_3, electronic struct., X-ray emission, XPS, UPS obs. 78−52638
As_2S_5, amorphous, struct., vibr. and electronic spectra 80−64908
As_4S_3, UV photoelectron spectra, mol. orbital symm. 77−14494
AsSI, cryst. and vitreous, struct. determ. 79−65979
As_2Se_3, cryst. and vitreous, struct. determ. 79−65979
AsSeI, cryst. and vitreous, struct. determ. 79−65979
As_2Te_3, cryst. and vitreous, struct. determ. 79−65979
$As_4Te_5I_2$, cryst. and vitreous, struct. determ. 79−65979
Au, 4f-subshell photoionisation cross section, energy depend. from Auger and photoelectron spectra 80−35057
Au (100), normal and reconstructed, electronic struct. changes, ang. resolved photoemission obs. 80−25520
Au (111), interfacial photoemission into electrolyte, 3.4-5.0 eV, vectorial volume effect 77−36375
Au alloys, surface electron states, photoelectron spectra meas., rel. to Au 78−14781
Au, CO physisorption and chemisorption, high resolution UPS 78−39666
Au, electron inelastic scatt. MFP, 60-140 eV 77−62909
Au, electronic density of states, cluster approx., compared with photoemission spectra 79−60675
Au film, angular depend. UPS, surface electronic struct. 79−83095
Au, film, electron inelastic scatt. mean free paths, synchrotron radiation photoelectron spectra meas. 78−76587
Au film, photoelectron emission, intershell interaction influence on 3d and 5d branching ratio 80−104038
Au, intrinsic surface states, UV photoemission meas. 77−20983
Au, low energy photoemission from indirect optical excitations 79−43103
Au, multiphoton photoeffect, new effect due to ps laser pulses 78−80452
Au, photoelectric cross section, derived from total absorpt. cross sections 77−10646
Au, photoelectric cross sections for 323 keV gamma rays 77−88432
Au, photoelectric cross sections of low energy photons 78−46309
Au, photoelectric cross sections, from total absorption cross sections, 5 to 130 keV 79−26947
Au, photoelectric cross section in region 187 to 662 keV 79−69952
Au, photoelectron count rates, using VUV He reson. line radiation source in UHV apparatus 78−89602
Au, photoelectron spectra, occupied surface-state bands in sp gap 79−43094
Au, photoelectron spectra, bulk and surface, rel. to band struct. 80−20770
Au, photoelectron spectra 77−73218
Au, photoemission, location of transitions in k space along lines of high symmetry 79−47594
Au, photoemission, polarisation and ang. dependencies 77−12495
Au, polycryst., UPES, in appl. of spectroscopic monochromated UV discharge lamp 78−89601
Au subshell photoelectron branching ratio meas. using synchrotron radiation 80−66397
Au, surface electron states, photoelectron spectra meas., rel. to Au alloys 78−14781
Au, surface state on (111), $E(k_\parallel)$ relation, ang. resolved photoemission 78−76582
Au, UPS, band struct. 77−16455
Au, UPS, expt. methodology aspects 77−90245
Au, UPS examination, temp. effects 78−68604
Au, ultrathin island films, band struct. formation 77−85893
Au, valence bands, angle-resolved photoemission meas. using synchrotron radiation 77−24930
Au-3d transition metal alloys, UPS study, localised states 80−93449
Au-Cd(Ga)(In) alloy, UPS exam. of valence bands 79−19511
Au-Ge Schottky diode, phonon energies, barrier heights, photovoltage spectra 78−64112
Au-Pd alloy, He(I) photoelectron spectra, 5d band 79−33892
Au-Si interface, valence band and core levels, Si diffusion, alloy form., photoelectron spectra obs. 80−45205
Au(111), Λ-line valence bands, angle-resolved photoemission determ. 80−108323
BF_3, threshold photoelectron, photoionisation and coincidence ion-threshold photoelectron spectra 79−820
BP-BAs, quasi-binary system, X-ray emission and electron spectra of solid soln. *(Russian)* 77−1764
Ba, $5p_{3/2}$ level broadening, ligand field splitting, photoelectron spectra 80−47950
Ba, He IIα photoelectron spectra, 20-25 eV, 5p ionis. 79−81188
Ba, UV photoelectron spectra, config. interaction effects 77−50413

photoelectron spectra continued
$BaBr_2$, mol., He(II) photoelectron 79−59509
$BaCl_2$ film, UPS exam. 79−38716
$BaCl_2$, mol., He(II) photoelectron 79−59509
BaF_2 film, UPS exam. 79−38716
BaI_2, mol., He(II) photoelectron 79−59509
$BaTiO_3$ (001), LEED and UPS studies 80−100747
$BaTiO_3$, band struct. calc., interpretation of XPS and UPS spectra 80−70597
$BaTiO_3$, photoelectron and optical spectra derived from self-consistent charge MO and band calcs. 80−96785
$BaTiO_3$, valence band UPS and partial p and d density of states 80−71560
$BaTiO_3$, XPS and UPS from surface defects 80−76136
Be (0001) surface, work function and purity, AES, LEED and photoelectron spectra meas. 78−68606
Be, XPS theory, valence band spectra band struct. 78−72702
BeO, free film and Au substrate, transmission spectra and photoemission characts. 77−24925
Bi (0001) surface, angle resolved UV photoemission spectra 77−66578
Bi film, on Sb_2Te_3, mean scatt. length of low energy electrons meas. 77−36370
Bi, film, oxidation, UPS, valence band, cond. band and 5d core states 77−20995
Bi, liquid and solid, UPS, optical densities of states 80−2924
Bi, oxidation, charge transfer obs. from final state changes 77−51703
Bi phosphates, X-ray electron spectra 77−36352
BiI_3, excitonic shifts of quasiatomic optical core to cond. band transitions, UPS obs. 78−11079
BiI_3, layered semicond., valence bands UPS and XPS obs. 78−11078
BiI_3, octahedrally coordinated, layer cpd., electronic struct. using synchrotron-radiation photoemission spectroscopy 79−74058
Bi_2O_3, electronic struct., X-ray emission, XPS, UPS obs. 78−52638
$Bi_xSb_{2-x}Te_3$, 2-dimens. cryst. interface props. of Bi overlayer UPS obs. 78−34881
Bi_2Te_3, layered semiconductor, angle resolved photoemission 79−28893
Br, He (I) PES 78−37609
Br, photoelectron spectra, photoionisation cross-sections 78−90131
BrCl, photoelectron spectrum, assignments 78−5284
BrF, He(I) photoelectron spectra, interpretation 79−13766
BrF_3, electronic struct. and ionisation pot., SCF DV Xalpha method 80−69057
BrF_5, electronic struct. and ionisation pot., SCF DV Xalpha method 80−69057
BrN_3, VPS obs., comparison with ab initio and semi-empirical calcs. 80−53043
BrNCO, VPS obs., comparison with ab initio and semi-empirical calcs. 80−53043
$BrO(X^2\Pi_i)$ radical, ionisation potential, photoelectron spectroscopic determ. 78−25612
C foil, extreme UV induced forward photoemission 80−76137
C, photoelectric cross sections, from total absorption cross sections, 5 to 130 keV 79−26947
C_2N_2, and $C_2N_2^+$, electronic struct. UV and PE spectra 80−23304
C_2N_2, satellite struct. of electron spectra, CI and vibronic coupling, dynamical calc. 80−53044
C_2N_2, valence excitation and UV spectra by HAM/3, expt. photoelectron spectra 78−25454
CO adsorbed layers on Ni (001), angle-resolved polarisation-dependent photoemission, adsorbate orientation 77−4716
CO adsorbed on Ni, valence band photoemission, SCF MO CNDO calc. 80−100754
CO adsorbed on Pd clusters, binding energy, d-electron emission particle-size depend. 79−4888
CO adsorbed on W, electron-stimulated desorption, photoemission, relax. energy 80−100401
CO asymmetry parameter, angle resolved photoelectron spectra, multiple scatt. method 80−63708
CO, chemisorpted on Ni, UV PES *(German)* 78−29751
CO, chemisorption on Pt (111) and Ni (100), (111), C-O bond lengths, electronic struct. 78−6210
CO, condensed film, UPS linewidths 78−31294
CO, core ionisation and single orbital relax. calcs. 78−5133
CO, fixed molecule, spectral variations of photoelectron ang. distribs. 77−14489
CO, inner-shell ionisation, relax. effects calcs. 77−42351
CO, inner-valence ionisation, correl effects calcs. 78−9198
CO molecular adsorbed on Mo (110) surface, electronic states, photoemission spectra 80−65363
CO, oriented molecule, photoelectron ang. distrib., energy depend. 80−76152
CO oxidation by NO on Ir surface XPS and UPS 78−15702
CO, photoabsorpt. cross section, 10 to 50 nm 77−61797
CO, photoelectron ang. distrib., energy depend. 79−22760
CO, photoelectron ang. distrib., multiple scatt. calc. 79−81238
CO, photoelectron ang. distrib., photon energy depend., 16-25 eV 80−53046
CO, photoelectron ang. distributions, wavelength and vibr. state depend., reson. effects, asymmetry parameters 80−91602
CO, Photoelectron angular distrib. of C and O K-shell ionisation 78−52628
CO, photoelectron spectra, 21.2-151.4 eV and soft X-ray, ionis. cross-section 78−37683
CO, photoelectron spectra ang. distrib., vibr. transitions, autoionis. state 79−31609
CO, photoelectron spectra, fourth band system assignment 79−72361
CO, valence X-ray photoelectron spectrum, satellite struct. 77−61800
CO, vibr. intensity meas. in photoelectron spectra for ionic ground states 77−18972
CO, $X^2\Sigma^+$, vibr. levels, UPS electron attachment obs. 80−95683
CO, Xe matrix-isolated and solid, UPES obs. 79−45762
CO^+, UPS by threshold photoelectron spectrosc. by electron attachment method 79−89708
CO^+, vibr. intensity distribs. for electronic states prod. by photoionis. 78−25614
CO_2, asymmetry parameter, angle resolved photoelectron spectra, multiple scatt. method 80−63708
CO_2, high resolution UV photoelectron spectra 80−91603
CO_2, photoabsorpt. cross section, 10 to 50 nm 77−61797
CO_2, photoelectron ang. distrib. asymmetry parameter for 30.4 nm photons 79−98151
photoelectron spectra continued
CO_2, photoelectron spectra, 21.2-151.4 eV and soft X-ray, ionis. cross-section 78−37683
CO_2, spin polarised photoelectrons, synchrotron excited 80−43101
CO_2, threshold photoelectron and photoionisation spectra 77−14491
CO_2^+, photoelectron and ion emission quantum yields, interelectronic state effects 79−6967
$CO_2(CS_2)(COS)$, Penning ionisation and photoelectron spectra 77−83653
$CO_2^+(C^2\Sigma_g^+)$, formation and predissoc., photoelectron spectra 78−5300
COS, asymmetry parameter, angle resolved photoelectron spectra, multiple scatt. method 80−63708
COS, high resolution UV photoelectron spectra 80−91603
CS molecule, calc. of HeI photoelectron spectrum, ionisation pot., vibr. struct. 77−3415
CS, vibr. struct. calcs. from photoelectron spectra 77−18973
CS_2, asymmetry parameter, angle resolved photoelectron spectra, multiple scatt. method 80−63708
CS_2, electronic autoionisation branching 80−91614
CS_2, high resolution UV photoelectron spectra 80−91603
CS_2, photoelectron ang. distrib. asymmetry parameter for 30.4 nm photons 79−98151
CS_2, photoelectron spectra (He II), Green's function anal. 79−27031
CS_2, photoelectron spectrum, spin-orbit splitting, excited state form. 80−43102
C_3S_2, electronic struct., optical and photoelectron spectra 78−70745
C_3S_2, electronic struct., optical and photoelectron spectra 78−70982
Ca film, vac. deposited, photoionisation coeff. from photoemission meas. 79−91569
Cd, atomic UV photoelectron spectra, wavelength depend. of satellite struct. 77−34597
Cd, ground state correl., photoelectron spectra, multiconfig. Hartree-Fock calcs. 77−50471
Cd I, $4d^{10}$ subshell photoelectron ang. distrib. 80−14123
Cd, K-shell photoelectric cross section 79−22676
Cd, oxidation, chemisorption and oxide regimes, UPS and EELS study 80−81236
Cd, partial photoionis. cross section 78−42022
Cd, photoelectron spectra, 4d spin-orbit splitting, crystal field and band-broadening effects, CNDO calcs. 78−76577
CdF_2, electronic structure of outermost levels, UPS study 80−7468
CdF_2, UPS and XPS spectra, rel. to optical props. 80−66386
CdF_2, valence band struct. determ. 79−47591
CdI_2, band struct., tight binding calcs. and photoemission spectra 78−23018
$CdIn_2S_4$, electronic states, sensitivity to cryst. struct., UPS study 80−45209
$CdIn_2Se_4$, defect zincblende semicond., valence band, cryst. struct. effects 78−48278
CdP_4, λ-modulated photoemission spectra 79−87565
CdS-Au contacts, electronic states, vacuum UV photoelectron spectra 80−70827
CdS-metal interface, chemical reactions and local charge redistrib. 79−19661
CdS(Se) photoanodes, effect of S(Se) substitution, photoelectron spectroscopy obs. 80−2463
CdSe (11$\bar{2}$0), surface electronic struct. and chem. struct. 78−14788
CdSe-$As_2S_3(AsSbS_3)$ heterostructure, energy bands and interface props., photoelectron spectroscopy 78−2551
CdSe-Au contacts, electronic states, vacuum UV photoelectron spectra 80−70827
CdSe-metal interface, chemical reactions and local charge redistrib. 79−19661
CdTe, bulk and surface states anal. using synchrotron radiation 77−66574
CdTe-Au contacts, electronic states, vacuum UV photoelectron spectra 80−70827
Ce, oxidation, ESCA and UPS meas., core levels 77−63542
γ-Ce, photoelectron spectra, 4f level position 80−25519
γ-Ce, valence band exam. by XPS and UPS 79−37977
α-Ce, valence band photoemission intensity, giant enhancement 79−19972
Ce-pnictides, XPS exam. 79−38717
CeF_3, CeF_3+, MS Xα electronic struct. calc., inner shell photoelectron spectra 77−10594
CeF_3, ionisation energies, satellite struct., photoelectron spectra, MS Xα calcs. 78−13425
CeP_5O_{14}, photoemission spectra, 4f, 5p and 5s giant reson. enhancement 78−95660
Cl, 3s subshell photoelectron ang. distrib. 77−65445
Cl, photoelectron spectra, photoionisation cross-sections 78−90131
Cl_2, chemisorpt. on Ag (110), XPS and UPS meas. 78−31293
Cl_4, He(II) photoelectron spectra, spectral intensity patterns 79−98152
ClBS, form., photoelectron and microwave spectra 78−90214
ClN_3, VPS obs., comparison with ab initio and semi-empirical calcs. 80−53043
ClNCO, VPS obs., comparison with ab initio and semi-empirical calcs. 80−53043
$ClO(X^2\Pi_i)$ radical, first ionis. pot., photoelectron spectrosc., vibr. struct., bond length 77−14495
$ClO(X^2\Pi_i)$, radical, He(I) photoelectron spectrum, ΔSCF calcs. 79−72359
Co (0001), adsorption of O_2 and CO, XPS and UPS study 79−74050
Co (0001) surface state, photoemission and synchrotron radiation obs., symmetry determ. 80−20771
Co, energy band dispersion and mag. exchange splitting, angle-resolved photoemission meas. 80−71567
Co, energy band dispersions and mag. exchange splitting 80−76146
Co, polycryst. surface interaction with O_2, CO and CO_2 *(French)* 77−73219
Co, spin polarised photoemission, surface magnetism 79−52083
Co, UPS, single cryst. and polycryst. film, electronic struct. 78−11081
Co, UPS of adsorption of O_2, CO and CO_2 *(French)* 77−36362
Co^-, photoelectron spectra, electron affinity and fine-struct. interval 79−68212
Co^{3+} d^6-complexes and oxides, spin-state transitions, PES study 79−100014
Co_3B, crystalline, photoemission and electronic struct. 80−2926
$Co_{0.32}NbS_2$, intercalation compound, struct. and photoemission meas. 77−16453
CoO, electronic struct., XPS and UPS expts. *(French)* 79−38711

photoelectron spectra continued
CoO, valence band struct., cryst. field anal., photoelectron data 79−47007
CoO, valence photoelectron spectrum, relative intensities, limited CI calcs. 79−63918
Co_3O_4, electronic struct., XPS and UPS expts. *(French)* 79−38711
$Co_{78}P_{14}B_8$, amorphous, photoemission and electronic struct. 80−2926
$CoS_2(Se_2)$, electronic struct., UPS and XPS study 80−80935
Cr (100), adsorption of O_2 and initial oxidation at room temp. 80−20034
Cr, adsorption of O, photoemission exam. 79−19976
Cr film, 3p-3d intershell interaction, photoemission 80−80934
Cr^{3+} compounds, 3p photoelectron spectra, light-inuced changed in multiplet satellites 80−80946
$CrOCl_3$, electronic structure and valence ionisation energies, obs. by ab initio and SW-Xα methods 80−69073
Cs, 6s, photoelectron ang. distrib., anisotropic effects 78−50514
Cs and CsCl, comparison of photoelectron spectra of Cs 5p levels 80−83419
Cs, He IIα $5p^{-1}$ photoelectron spectrum, config. interaction effects 80−5510
Cs, oxidation, adsorbate-induced structs., UPS obs. 79−47828
Cs, photoelectron energy distrib. curves, depend. on light polarization 79−15591
Cs, photoionis. of 6s electron, spin-orbit interaction, ab initio calc. 79−81191
Cs, two-photon ionis. via $6^2P_{3/2}$ state, photoelectron spin polarisation 77−3328
Cs^-, in tetrahydrofuran soln., transient photoelectron nutation 79−3418
Cs-Au alloy, cryst., UV photoemission investig. of band struct. 77−24923
Cs-O film, metallic, on Ag substrate, photoemission, surface plasmon excitation 77−16461
CsAu, photoelectron spectroscopy and energy bands calc. 78−76581
CsCl(Br)(I), electron-phonon interaction effects, Monte-Carlo calc. and expt. 78−11071
CsCl(Br)(I), He II photoelectron spectra, ionisation energy 77−18977
$CsPO_3$, He(I) photoelectron spectra, UTARC calc., assignments 79−72357
$CsPbCl_3(Br_3)$, optical and photoelectronic spectra 79−24410
Cu (001), M-point surface state, high-resolution angle resolved photoemission study 80−108322
Cu (001), O_2 chemisorption, Cu3d-O2p interaction study by angular-resolved photoemission using synchrotron radiation 80−84836
Cu (001) surface, angle-resolved photoemission spectra calc. 77−40323
Cu (100), adsorbed layers of N, O and S, electronic props., UPS, XPS and Auger spectra 77−66088
Cu (100), adsorpt. of CO, UV and X-ray photoelectron spectra, LEED 78−56037
Cu (100), ordered Cl overlayer, adatom bonding effects, photoemission study 80−104044
Cu (100), photon angle depend. 77−59674
Cu, (100) and (111), surface states, d-band, angle-resolved photoemission spectra obs. 80−20768
Cu (100) and (111) surfaces, high resolution normal and near-normal UPS 80−80933
Cu (100) surface, adsorption of O_2, angularly resolved UPS meas. 78−71956
Cu (100) surface, angle-resolved PES study 80−55273
Cu, (100) surface, d-like surface state band, angle-resolved photoemission obs. 79−78840
Cu, (100) surface, UPS, two-electron reson. at 3p threshold, rel. to Ni 80−25522
Cu (110), adsorption of pyridine, angle-resolved photoemission, selection rules 80−40231
Cu (110), surface angle resolved photoemission 79−83097
Cu (110), valence bands, angle-resolved photoemission spectra meas. 79−74056
Cu, (110) surface, photoemission obs. of new surface state band 79−91121
Cu (111), angle-resolved UPS, free electron final state model calcs. 78−31302
Cu (111), chemisorption of CO, coverage depend. photoelectron spectra, adsorption sites 78−95647
Cu (111), interfacial photoemission into electrolyte, 3.4-5.0 eV, vectorial volume effect 77−36375
Cu (111), partially Cs covered, oxidation effect on UPS 79−78826
Cu (111), photoelectron angle resolved spectra, perpendicular momentum conservation oxidation induced breakdown 79−24412
Cu (111), photoelectron spectra, angle averaging, Cs adsorbate effects 79−83100
Cu (111) face, surface state band, photoemission cross section 77−90252
Cu (111) surface, high resolution photoemission spectra 79−52082
Cu (111) surface, PES and band struct. calcs. 80−89118
Cu (111) surface, polarisation depend. of angle resolved photoemission spectra 78−56557
Cu (111) surface band energy shift upon adsorption of Cs and O, angle-resolved UPS study 80−40228
Cu (111)/Cs, adsorption-induced changes of photoemission spectra and surface electronic struct. 80−55260
Cu (111)/Na interface, UPS study of surface electronic struct. 80−80350
Cu, adsorption and surface reaction of formic acid 80−40741
Cu, adsorption of CO, angle-resolved UPS and adsorbate induced struct. 78−71983
Cu, adsorption of NO, NH_3 and N_2H_4 78−6830
Cu, ang. distrib., final state effects 77−66580
Cu, angle resolved photoemission, thermally induced breakdown of direct-transition model 77−77346
Cu, angle resolved photoemission spectra 78−43986
Cu, angle-resolved photoemission, prediction of spectra peak intensities 78−72695
Cu, angle-resolved photoemission, energy band symmetries 79−43104
Cu, Auger-photoelectron coincidence measurements 79−19968
Cu, band structure and high-resolution normal emission UPS 80−6712
Cu, Bloch states, photoelectron spectra, angle resolved 78−92175
Cu, bulk and (001) film, extended tight-binding calcs. 80−70592
Cu, CO physisorption and chemisorption, high resolution UPS 78−39666
Cu, chemisorption on low-index and stepped surfaces, LEED, AES and UPS obs. 80−84391
Cu, cluster and bulk, struct. and electronic props. 78−95592
photoelectron spectra continued
Cu clusters, valence band and core binding energies, UPS meas. 79−38721
Cu, electronic density of states, cluster approx., compared with photoemission spectra 79−60675
Cu, energy band dispersions, absolute determ. using ang.-resolved photoelectron spectrosc., symmetry method 79−15590
Cu, energy band dispersions and lifetimes using angle-resolved photoemission 79−77998
Cu film, angular depend. UPS, surface electronic struct. 79−83095
Cu, film, growth on amorphous C, electronic props., UPS and XPS obs. 79−82476
Cu film, photoelectron emission, intershell interaction influence on 3d and 5d branching ratio 80−104038
Cu, film growth on graphite and amorphous C, electronic struct. by photoemission and Auger obs. 79−77947
Cu, final energy bands, high energy, angle resolved photoemission 80−2327
Cu halides, tetrahedrally coordinated, semiempirical band struct. model 77−51655
Cu, intrinsic surface states, UV photoemission meas. 77−20983
Cu, liq., 3d bandwidths 77−4286
Cu, low energy photoemission from indirect optical excitations 79−43103
Cu, ordered monolayer on Zn (0001), electronic struct., photoelectron spectra 78−39660
Cu, photoelectric cross section, derived from total absorpt. cross sections 77−10646
Cu, photoelectric cross sections for 323 keV gamma rays 77−88432
Cu, photoelectric cross sections of low energy photons 78−46309
Cu, photoelectric cross section in region 187 to 662 keV 79−69952
Cu, photoelectric interaction around the K edge 78−5183
Cu, photoelectron spectra 77−73218
Cu, photoelectrons, energy-angle depend. for UV light *(German)* 79−11495
Cu, photoemission, temp. and photon-energy induced breakdown of direct transition model 78−95681
Cu, photoemission from valence bands 77−20996
Cu, photoemission spectra, interpretation in terms of surface density of states 79−52081
Cu, photoemission spectra and band struct., extensions of combined interpolation scheme 79−78844
Cu, photoemission with polarised light, cryst. symm. effects 78−23581
Cu surface, (001) and (111), angular resolved photoelectron spectroscopy 78−95652
Cu surface, (100), O chemisorption, angle-resolved UPS study 80−84384
Cu surface, (110), methanol adsorption, XPS, UPS and thermal desorpt. study 80−84388
Cu, surface, photoelectron spectra, electron refraction and light polarisation effects 78−72700
Cu surface, photoemission 78−52619
Cu surface, with chemisorbed CO, UPS peaks interpretation, SCF-Xα-scatt. wave calcs. 77−62742
Cu, surface electron states, (111) terrace of stepped (211) face, photoemission meas. 78−84697
Cu, surface energy band calc., significance for photoemission 78−95330
Cu, surface states, (100) and (111), polarisation depend. photoemission 80−100495
Cu, two photon photoelectric emission, photocurrent vectorial depend. 79−95906
Cu, UPS, 14-45 eV, density of states function 77−90244
Cu, UPS, rel. to band struct. 79−52080
Cu, valence bands, angle-resolved photoemission meas. using synchrotron radiation 77−24930
Cu-Ni, adsorption of H_2+CO on (110) surface, TDS and UPS obs. 80−80052
Cu-Ni, evaporation limited segregation 80−70513
Cu-Ni, oscills. in composition depth profile, UPS meas. 78−71919
Cu-Ni, UPS, surface and bulk density of states, comp. depend. 77−44125
Cu-Ni (100), UPS spectra, direct transition and matrix element effects 80−55268
Cu-Ni (110), adsorption of CO and H_2, UPS, thermal desorption, AES,and LEED study 80−80087
Cu-phthalocyanine, photoemission multielectron effects from quasi atomic Cu 80−93458
Cu-Zn, α-phase, photoelectron meas. 78−35247
Cu-Zr, metallic glasses, valence band struct. investigation 80−11533
CuBr, UPS, temp. depend., dynamic hybridisation 77−20998
$(CuBr)_3$, gas, He(I) photoelectron spectra 80−43103
$(CuBr)_3$, photoelectron spectrum and valence shell struct. 78−62843
CuCl (100), obs. of p- and d-like surface states, angle resolved UPS study 80−104045
CuCl, UPS meas., electronic struct. 80−50529
$(CuCl)_3$, gas, He(I) photoelectron spectra 80−43103
$(CuCl)_3$, photoelectron spectrum and valence shell struct. 78−62843
$CuCl_4^{2-}$, core ionisation in 3d, 4f and 5f series, rearrangement effects 80−53065
$Cu_{0.83}Ga_{0.17}$, α-phase, photoelectron meas., impurity level 78−35247
$Cu_{0.87}Ge_{0.13}$, α-phase, photoelectron meas., impurity level 78−35247
$(CuI)_3$, photoelectron spectrum and valence shell struct. 78−62843
$Cu_{0.85}Ni_{0.15}$, liq., 3d bandwidths 77−4286
Cu_xNi_{1-x} random alloy, angle-resolved photoemission 78−95683
CuO, on Cu, identification by electron spectroscopic methods 80−60747
Cu_2O, on Cu, identification by electron spectroscopic methods 80−60747
CuPd, chemical shift effects and origin of Pd 3d core level satellite 80−104039
Cu_2S, threshold photoelectric emission *(French)* 78−60549
$CuS_2(Se_2)$, electronic struct., UPS and XPS study 80−80935
$Cu_{60}Zr_{40}$ glassy metal, photoemission and mag. susceptibility 79−28896
Cu(100), chemisorption of CO, angle resolved UV photoemission spectroscopy exam. 78−10284
Cu(100), photoemission via Bloch states and evanescent band gap states, polarised synchrotron irradiation 79−61492
Cu(100) surface, oxidation studied by angle-dispersive photoemission spectra 78−15585
Cu(110), photoemission, bulk versus surface effects 78−52626
Cu(111), bulk s orbital bands, sensitivity to oxidation, photoelectron spectra 79−47597
Cu(111) surface, UPS at const. wavevector component 80−16151
D_2, threshold photoelectron spectra, 15-20 eV 79−54912

photoelectron spectra continued
DF, threshold photoelectron spectra, photoionis. threshold, resonant autoionis. 77−499
D_2O, effect of phase density on ionisation process and electron localisation 77−89731
N,N'-dimethyl-p-toluidene, UV photoelectron spectra, up to 21.2 eV 77−71831
$ErFe_2$ surface, effect of H and O adsorption, spin polarised photoemission study 80−29854
Eu, UV photoelectron spectra, config. interaction effects 77−50413
EuO:Gd, 4f-photoelectron spin polarization, temp. depend. 79−78842
EuO:Gd, surface depolarisation of photoelectrons 78−15286
EuO:Gd, surface mag. props. 80−71566
EuO:La, photothreshold reduction by mag. induced space charge layer 78−72692
EuO:La(Gd), photoelectron spin polarisation, temp. depend. 77−69966
F, He (I) PES 78−37609
F_2, threshold photoelectron spectra, photoionis. threshold, resonant autoionis. 77−499
FCN, and assignment 77−30920
$FO(X^2\Pi_i)$ radical from $F+O_3$ reaction, VUV photoelectron spectra 80−104455
Fe (11O), coadsorption of K and 0_2, XPS, UPS, AES, and LEED study 80−80084
Fe (110), adsorption and decomposition of ammonia, LEED, AES, UPS, work function and desorption meas. 79−69345
Fe (110), adsorption of C, N, O, S, CO, NO and C_2H_2, UPS and LEED/Auger meas. 77−72773
Fe (110), adsorption of K, LEED, AES, UPS and XPS meas. 79−77919
Fe (110), complexes with PF_3, CO and cyanomethane, UV photoelectron obs. 78−19629
Fe (110), K promoted, adsorption of CO, UPS, XPS, AES, and flash desorption obs. 79−82463
Fe, (111), (100) and (110) surfaces, UPS obs. 79−38712
Fe, adsorption and surface reaction of formic acid 80−40741
Fe, adsorption of N_2 and NH_3, 80-290K, XPS and UPS obs. 77−31901
Fe, adsorption of O_2, oxide formation, XPS/UPS obs. 77−85074
α-Fe, chemisorption of CO, surface deactivation effects 77−76669
Fe, density of states, photoemission expts. above and below T_c, rel. to magnetism model 77−20536
Fe, energy band dispersion and mag. exchange splitting, angle-resolved photoemission meas. 80−71567
Fe, ferromag., evidence for itinerant electron model, angle resolved photoemission from surface 79−24414
Fe, ferromagnetic, chemisorption of H, spin-spin interactions, UPS spectra calc. 80−6630
Fe, NO adsorbed layer, anal. at low press., XPS, UPS 77−7970
Fe, photoelectron spin polarisation and itinerant magnetism 78−68602
Fe, photoemission and electronic spectra, exchange splitting 77−4717
Fe, photoemission study of (100), (110) and (111) surfaces, ferromag. band struct. 79−38714
Fe, spin polarised photoemission, surface magnetism 79−52083
Fe surface, (111) and (100), adsorpt. and decomp. of NH_3 78−40077
Fe surface, H_2 chemisorption LEED, UPS, thermal desorption spectroscopy, work function meas. 78−14566
Fe surface, purposeful modification by gas adsorption, charact. by photoemission 78−71955
Fe, UPS, density of states determ. 78−52623
Fe^-, electron affinity, nonstatistical fine-struct. detachment intensities at 488 nm, laser electron spectra 79−41144
Fe^{2+} d^6-complexes and oxides, spin-state transitions, PES study 79−100014
Fe-W(Co)(Ni)(Mo)(NB)(Cr)(V), dil. system, high freq. induction melting and centrifugal casting, working curve sample prep. photoemission anal. *(Japanese)* 78−53050
$Fe_{84}B_{16}$, metallic glass, ion implanted, UPS meas. 80−97411
$FeBr_2$, transient species, He(I) photoelectron spectrosc. calcs., relativistic corrections 80−95677
$Fe_{0.33}NbS_2$, intercalation compound, struct. and photoemission meas. 77−16453
$Fe_{0.65}Ni_{0.35}$, UPS, density of states determ. 78−52623
FeO, electron affinity, ground state vibr., new assignment 77−75212
FeO, valence band XPS and UPS, LCAO-MO calcs. 80−45197
FeO, XPS and UPS 79−91565
Fe_2O, for UPS, rel. to 3d photoelectron spectrum of Fe_3O_4 77−1785
Fe_2O_3, XPS and UPS 79−91565
Fe_3O_4, 3d-photoelectron spectrum, final state effects, compared with Fe_2O 77−69964
Fe_3O_4, magnetite, final-state effects in 3d photoelectron spectra 77−1785
Fe_3O_4, single cryst., surface magnetism, spin polarized photoemission 78−52622
Fe_3O_4, spin polarised photoemission, surface magnetism 79−52083
Fe_3O_4, XPS and UPS 79−91565
Fe_xO, antiferromag., surface magnetism probe by photoelec. currents 77−73214
$Fe_{1-x}(P,B)_x$, amorphous and crystalline, photoemission and band structure 80−60754
Fe(110) surface covered with C, O, N, S, CO adsorption, photoemission spectroscopy study 80−54527
Fe(111), single cryst. surface, chemisorption of N_2, NH_3 and H_2, photoelectron spectra and LEED meas. 77−66087
α-Fe(111) single crystal surface, chemisorption of ethylene, halogeno-substituted alkenes, photoelectron spectroscopy study 77−62740
α-Fe(111) surface, chemisorbed CO, 300K, photoelectron spectroscopy study 77−62739
Fe(111) surface, interaction with hydrazine, UPS and XPS 79−46956
Ga I, absorption spectrum 320-1000 Å, intersubshell correls., simultaneous ejection of two photoelectrons 77−50391
Ga, liq. optical density of states, low-energy photoemission meas. 77−77341
Ga, reson. photoemission shake-up and Auger processes at 3p photothreshold 80−100748
Ga, transition from ordered solid to disordered liquid, viewed by photoemission 80−45217
GaAS, O_2 chemisorption on (110) surface, bonding sites 78−38938
$Ga_{1-x}Al_xAs$, varizone layer photoelectron yield depth estimation 80−100745
GaAs, 5-450 eV, surface states, oxidation behaviour 77−66579
GaAs (100), angle-resolved photoemission spectra 80−50516
GaAs (100) and (110), photoelectrons spin polarisation 80−11530
GaAs (100) surface struct. determ. by LEED, UPS, and EPR 80−49475
photoelectron spectra continued
GaAs, (100) surfaces, reconstructed, ang. resolved photoemission from surface states, adsorption and annealing effects 80−16143
GaAs (110), adsorption of In, N, P, and As, UPS and EELS study, tight-binding calcs. 80−49496
GaAs (110), adsorption of O_2, oxide form., XPS/UPS study 80−49497
GaAs (110), chemisorption of Cl, photoemission spectra and tight-binding calcs. 80−6629
GaAs (110), chemisorption site geometry and interface electronic struct. of Al and Ga, photoelectron spectra 80−49843
GaAs (110), low O_2 exposure effects on electronic surface props. 79−47146
GaAs (110), surface core-level binding-energy shifts 80−103737
GaAs (110), surface electronic struct., ang. resolved photoemission expts. and tight binding calcs. 78−91743
GaAs (110), surface states and matrix elements in angle-resolved photoemission 78−91741
GaAs (110), surface states symmetry determ. using polarisation-depend. ang. resolved photoemission 78−91742
GaAs (110), with Al or Ga overlayers, interfacial electron states, UPS and LEED obs. 80−80377
GaAs (110) surface, chemisorption of O_2, electronic struct. theory, oxidation, electron spectra interpretation 79−42376
GaAs (110) surface, exposed to O and O_2 photoemission spectra meas., Space Shuttle expt. 78−35246
GaAs (110) surface, O_2 interaction, order-disorder effects, LEED, UPS anal. 80−6634
GaAs, (110) surface, oxidation, photoemission spectra obs. 77−16460
GaAs (110) surface, surface states, angle-resolved photoemission meas. 77−20984
GaAs (110)-Al(Ga) interface, interface states, photoemission study 78−95359
GaAs (110)-Au Schottky barriers on ordered and disordered GaAs surfaces, props. 78−95360
GaAs ($\bar{1}\bar{1}\bar{1}$), MBE prep., angular resolved UPS of surface states 79−47598
GaAs, adsorbed O, (110), surface electronic struct., synchrotron irradiated photoemission 78−43453
GaAs, adsorption of O_2, adsorption states and Ga depletion, UPS, AES, and thermal desorption meas. 79−46952
GaAs, angle-resolved photoemission and valence band dispersions 80−7469
GaAs, conduction band mapping by angle-resolved photoemission 79−83105
GaAs epitaxial thin films with neg. electron affinity, photoelectron energy distrib. 80−100755
GaAs, epitaxially grown (001), (111) and ($\bar{1}\bar{1}\bar{1}$) surfaces, LEED, AES, photoemission 78−38924
GaAs, heavily oxidised photoemission escape depth for electrons, energy depend. 77−69969
GaAs, lower conduction band minima, ordering and props. 77−28114
GaAs photocathode with Cs-O adlayer, negative electron affinity, core-level photoemission of adlayer 79−19965
GaAs, photocathodes, photoelectron emission, energy levels, influence of dimens. quantisation *(Russian)* 78−64447
n-GaAs, photoemission and work function of (111A) and (111B) surfaces, energy states 77−20980
GaAs, surface, (110), ang.-resolved photoelectron spectra 78−43984
GaAs, surface, electron struct. and Fermi level pinning by O_2 and metals 80−11066
GaAs surface, electronic props., interaction with Au and O adsorbate layers 77−20385
GaAs surface, O_2 sorption and excitonic effects, photoemission expts. 77−85055
GaAs, surface chemistry and electronic struct., adsorption of O_2, photoemission meas. 77−20985
GaAs, surface electron states, (110), photoemission 80−25529
n-GaAs, surface states, photoemission yield obs. 77−16459
GaAs, surface studies during MBE growth 79−90899
GaAs surfaces (110) and (111)As, UPS and LEED 78−91514
GaAs, UV photoemission, polarisation-depend., angle-resolved spectroscopy 77−66573
n-GaAs, valence band studies of clean and O_2 exposed surfaces 78−43298
GaAs, valence-band dispersions, electron and hole lifetimes, angle-resolved photoemission 80−80947
p-GaAs:Cd, (110) cleaved surface, defect-induced surface states 80−6925
GaAs:Cs, oxidation process, UPS obs. 80−50511
GaAs/III-V solid soln. heterostructure composition profile by photoemission microanalysis 80−44717
GaAs-Al(Ga)(Ge), surface reactions and interdiffusion, photoemission study 80−49532
GaAs-Au Schottky barriers, PES and depth profiling obs. 79−42641
GaAs-Cs-O photoemitter, negative electron affinity, fabrication and characts. 78−2979
GaAs-Ge heterojunction, band discontinuities, angle-resolved UPS obs. 79−7878
GaAs-Ge interface, photoemission 80−25530
GaAs(110), high resolution photoemission yield, surface states 77−69392
GaAs(110) surface, adsorption of water and methanol, UPS study 80−6632
GaAs(110), surface states, photoemission spectroscopy and tight binding calcs. 77−85888
GaAs($\bar{1}\bar{1}\bar{1}$)As surface, 3 states, comp., struct., surface states and O_2 sticking coeffs. 77−66080
GaP, (001), adsorpt. of Cs, photoemission meas. 78−87874
GaP (110), electronic surface states, initial steps of O_2 chemisorption 80−49844
GaP (110), surface bands in relaxed cleavage surface, tight binding model, compared with photoemission data 78−91744
GaP, cleaved (110) surface, electron surface props. 80−11067
GaP, Cs(Cs-O) activated, with negative electron affinity, thermalised electron emission 78−11073
GaP, Cs(Cs-O) activated, with negative electron affinity, near UV photoemission and secondary emission 78−11074
GaP, reson. photoemission shake-up and Auger processes at 3p photothreshold 80−100748
GaP, surface states, UPS meas. 78−14780
GaP(As)(Sb), electronic surface props., contact potential difference and photoemission expts. 77−47884

photoelectron spectra continued
GaP(As)(Sb), surface states, contact pot. difference, photoemission, and low energy loss spectra expts. 77−85285
GaS, layered, conduction band photoelectron spectroscopy 77−52217
GaS, photoemission props. of III-VI layer compounds 79−65976
GaS, polarisation selection rules for photoemission spectra, test of band struct. calcs. 77−52216
GaS, two-photon photoemission 79−28890
GaS, UPS, polarisation effects 77−12494
GaS, valence and conduction bands, synchrotron radiation photoemission spectra 77−63536
GaS_xGe_{1-x}, valence band states, composition depend., photoemission spectra study 80−100434
GaS(Se), $GaS_{0.6}Se_{0.4}$, angle resolved UPS, energy band dispersion curves determ. 79−100022
GaS_xSe_{1-x}, wavefunction symm. and binding energies, synchrotron radiation photoemission spectroscopy 80−50532
GaSb, 5-450 eV, surface states, oxidation behaviour 77−66579
GaSb (110), chemisorption of Cl, photoemission spectra and tight-binding calcs. 80−6629
GaSb (110), oxidation, initial stages, photoemission study 80−16529
GaSb (110), surface core-level binding-energy shifts 80−103737
GaSb, photoemission investig. of surface states, effects of O_2 and alkali metals 77−48312
GaSb, surface, electron struct. and Fermi level pinning by O_2 and metals 80−11066
GaSb, surface chemistry and electronic struct., adsorption of O_2, photoemission meas. 77−20985
GaSb-Au Schottky barriers, PES and depth profiling obs. 79−42641
GaSe, ARPES using synchrotron radiation 78−72682
GaSe, band struct. from ang. resolved photoemission 77−59673
GaSe, core level excitation effects, synchrotron radiation UPS study 80−40234
GaSe, core-level photoemission anisotropy 78−11076
GaSe, layered, conduction band, photoelectron spectroscopy 77−52217
GaSe, layered, electronic band struct., direct evaluation by angle resolved photoemission 77−51652
GaSe, photoemission props. of III-VI layer compounds 79−65976
GaSe, photoyield reson. enhancement near Se 3d core threshold, photoelectron spectra obs. 80−45207
GaSe, polarisation selection rules for photoemission spectra, test of band struct. calcs. 77−52216
GaSe, two and three dimensionality of electron states, normal photoemission obs. 77−32503
GaSe, UPS, polarisation effects 77−12494
GaSe, valence and conduction bands, synchrotron radiation photoemission spectra 77−63536
GaSe, valence band struct., angle-resolved photoemission spectroscopy 77−1360
GaSe, wave function symmetries of valence band states revealed by polarisation effects in angle-integrated photoemission spectroscopy 79−67395
GaSe(Te), optical spectra in 2 to 50 eV range 78−10915
Gd, resonance recomb. lines in AES and photoelectron spectra 80−97390
Gd-Co, amorphous film, RF sputtering, DC bias role 77−16494
Gd-Fe, mag. moment of Fe, multiplet splitting in photoemission 79−78846
$Gd_{0.67}La_{0.33}P_5O_{14}$, photoemission spectra, 4f, 5p and 5s giant reson. enhancement 78−95660
Ge (100), chemisorption of H_2, expt. results compared with pairing model calcs. for Si (100) 78−34719
Ge (100), dimer reconstruction, photoemission obs. 80−80939
Ge (100), surface structure and chemical state 77−15670
Ge (111), chemisorption of Cl, chemisorpt.-site geometry from polarised photoemission 77−15684
Ge, (111) surface, clean and O_2 adsorbed photoemission yield spectroscopy of electronic surface states 79−91122
Ge (111) surface, clean and CO-covered, UPS and ion-neutralisation spectroscopy 80−10785
Ge, chemisorption of Cl_2, photoemission polarisation effects with synchrotron radiation 78−14580
Ge, chemisorptive bonding of CO(Cl), photoemission investig. using synchrotron radiation 78−73079
Ge, film, electronic struct. charge on ordering, double beam photoemission 78−19634
Ge photocathodes, Au absorbed photofield emission current spectral investigation 80−29856
Ge, photoemission spectroscopy of surface states and oxidation 77−55863
Ge, ratio of photoionisation cross-sections of valence s- and p-electrons *(Ukrainian)* 77−73211
Ge, ultra pure, method to determ. composition and struct. of non-elemental acceptor and donor centres 78−39658
Ge:H amorphous films, photoemission spectra 80−50517
Ge:inert gas, ion implantation, UV photoemission exam. 78−80457
Ge-GaAs (110), heterojunction chemistry, photoemission expts. 78−95244
GeO, mol., VUV photoelectron spectra, $X^2\Sigma^+$ state 79−72358
GeO_2, electronic struct., photoemission spectra calc. 77−35865
GeO_2, photoemission and X-ray emission spectra calc. 77−89866
GeS (001), density of empty states, core-level EELS and photoemission spectra meas. 79−78145
GeS, amorphous, UPS and XPS, valence band struct. 77−90247
GeS, angular resolved UV photoemission and band structs. 77−85144
GeS, electron-hole interaction in d-electron excitations, photoelectron and optical spectra 78−34776
GeS, photoelectron spectra, rel. to ionicities and phase transitions 77−69960
GeS, valence level photoelectron spectra 77−27114
GeS_2, amorphous film, reversible and irreversible photostructural changes 79−74061
$GeS(S_2)$ amorphous films, photostructural changes, UPS study 80−49550
GeSe (001), density of empty states, core-level EELS and photoemission spectra meas. 79−78145
GeSe, amorphous, film, thermally induced effects, UPS study 80−104042
GeSe, amorphous, UPS and XPS, valence band struct. 77−90247
GeSe, photoelectron spectra, rel. to ionicities and phase transitions 77−69960
photoelectron spectra continued
GeSe, valence level photoelectron spectra 77−27114
$GeSe_2$, amorphous, film, thermally induced effects, UPS study 80−104042
$GeSe(Se_2)$ amorphous films, photostructural changes, UPS study 80−49550
GeTe, amorphous, UPS and XPS, valence band struct. 77−90247
Ge(111), high resolution photoemission yield, surface states 77−69392
Ge(111), surface electronic struct., atomic geometry effects 77−85283
H_2, ang. distrib., 304 Å line, vibr. state depend. 79−45764
H_2, angular distribution He I (Ne I) photoelectron spectra 79−31606
H_2, D_2, photoionisation, body-frame Hund's case b description 78−94295
H_2 discharge products, investigation using photoelectron spectroscopy 79−36455
H_2, photoelectron ang. distrib., rot. states anal. 78−33550
H_2, photoelectron ang. distrib. for He II 79−59511
H_2, photoelectron angular distrib. and intensity, vibr.-rot. struct. 78−46393
H_2 photoelectron spectra, rot. intensity distrib. 80−91605
H_2, photoionisation, ang. distrib. of photoelectrons 80−37834
H_2, photoionisation, dissociative, at 304 Å, photoion ang. distribs. photoelectron channels 78−82792
H_2, photoionisation cross-sections, ang. distrib. and intensity, vibr.-rot. struct. 79−50091
H_2, threshold photoelectron spectra, 15-20 eV 79−54912
H_3, photoelectron spectra, ang. distrib. asymmetry parameter, vibr. state depend. 77−75218
HBr, photoelectron angular distrib. 80−58318
HBr+He(2^3S), Penning ionis. electron spectra, 584Å photoelectron spectra 77−79687
HCN, ionis. and photoelectron spectra, inner valence electrons 78−82784
HCN^+, photoelectron spectra of third electronic state, ab initio calc. of pot. energy surface 78−70871
HCl+He(2^3S), Penning ionis. electron spectra, 584Å photoelectron spectra 77−79687
HF, ab initio valence band calcs. 79−6869
HF, Auger transition energy calcs. 77−34704
HF, threshold photoelectron spectra, photoionis. threshold, resonant autoionis. 77−499
HF+He(2^3S), Penning ionis. electron spectra, 584Å photoelectron spectra 77−79687
HI, photoelectron angular distrib. 80−58318
HI+He(2^3S), Penning ionis. electron spectra, 584Å photoelectron spectra 77−79687
HNF_2 and DNF_2, photoelectron spectra, vibr. struct. obs, ionisation pot. determ., ab initio calcs. of ionic geometry 80−83418
H_2O, 1s shake-up spectrum, ab initio equiv. cores, improved virtual orbital and CI calcs. 77−46597
H_2O, $(D_2O)(HDO)$, photoelectron spectrum, Franck-Condon, factor calc., geometry and vibrs. *(French)* 77−83652
H_2O, ESCA peak intensity, sudden approx. calc. 79−54911
H_2O, electron propagator theory for mol. electron binding energies and photoionis. intensities 80−47848
H_2O, photoabsorpt. cross section, 10 to 50 nm 77−61797
H_2O, photoelectron ang. distrib. asymmetry parameter for 30.4 nm photons 79−98151
H_2O, photoelectron spectra, 21.2-151.4 eV and soft X-ray, ionis. cross-section 78−37683
H_2O threshold PES, OH^+ fragment obs. 80−78647
H_2O^+, vibr. and rot. struct., intensity factors and orbital angular momentum 80−83246
HOCl, chloramine, isoelectronic mols., vap. phase UV photoelectron spectra, struct. 78−66600
H_2S, gas-phase, states in valence photoelectron spectrum 78−94284
H_2S, inner valence electron ionisation calcs., photoelectron spectra obs. 78−82619
H_2S, Penning ionisation and photoelectron spectra 77−83653
He, photoabsorption, modified RPA calcs. with exchange 78−13477
He, two-electron photoionis., threshold law and photoelectron spectra 78−29767
HfX_4, (X=Cl,Br,I), He I and He II photoelectron spectra, ionis. energy, chem. bonding 78−46394
Hg, 5d level open shell interactions, 304 Å photoelectron spectrum 80−87087
Hg, atomic UV photoelectron spectra, wavelength depend. of satellite struct. 77−34597
Hg, ground state correl., photoelectron spectra, multiconfig. Hartree-Fock calcs. 77−50471
Hg, partial photoionis. cross section 78−42022
Hg, photoelectron angular distrib. resonance 79−13687
Hg, transition from ordered solid to disordered liquid, viewed by photoemission 80−45217
Hg, two photon photoelectric emission, photocurrent vectorial depend. 79−95906
Hg-Cd, behaviour of Cd d-bands, comparison with Au and Ag alloys 79−37972
$HgCl_2$, intensity changes between He(I) and He(III) photoelectron spectra 78−21969
HgF_2, electronic structure of outermost levels, UPS study 80−7468
HgI_2, relativistic effects, photoelectron spectra, Hartree-Fock-Slater method, perturbation theory approach 80−27962
α-HgS, gas-phase and solid-state Hg 5d photoionisation processes, direct comparison 80−76149
I, He (I) photoelectron spectrum by I_2 photodissoc. 80−83325
I, partial photoionis. cross sections, rel. intensities, irreducible tensor anal. 79−98048
I_2, relativistic effects, photoelectron spectra, Hartree-Fock-Slater method, perturbation theory approach 80−27962
I_2^+, fragmentation ang. distrib., energy disposal, branching, photoelectron-photoion coincidence spectra 79−68263
IBr^+, fragmentation ang. distrib., energy disposal, branching, photoelectron-photoion coincidence spectra 79−68263
ICl^+, fragmentation ang. distrib., energy disposal, branching, photoelectron-photoion coincidence spectra 79−68263
IF, He(I) photoelectron spectra, interpretation 79−13766
INCO, VPS obs., comparison with ab initio and semi-empirical calcs. 80−53043
In inorganic and organometallic cpds., photoelectron spectra, valence bands, ligand field broadening 77−63525

photoelectron spectra continued
In, transition from ordered solid to disordered liquid, viewed by photoemission 80−45217
In, VUV photoelectron spectra, pseudo-atomic beam technique 80−58225
In-GaAs(Ge)(Si) Schottky barrier interface, covalent bonding of metal atoms 77−20429
InAs, electron surface props., contact potential difference and photoemission expts. 77−47884
InAs, oriented single crysts., photoemissive props., photoelec. thresholds 77−59666
InCl, InBr, InI, UV photoelectron spectra of valence d shells, gas-phase 78−62845
InGaAs, transferred electron photoemission to 1.65μm 78−68600
InP (110), oxidation, initial stages, photoemission study 80−16529
InP, cleaved surface, angle resolved photoelectron spectroscopy 80−55258
InP, photoemission and LEED meas., minority carrier diffusion length 77−69959
InP, surface, electron struct. and Fermi level pinning by O_2 and metals 80−11066
InP surface, interaction with Cl, electron spectroscopic obs. 78−56036
InP, surface chemistry and electronic struct., adsorption of O_2, photoemission meas. 77−20985
InP-Au Schottky barriers, PES and depth profiling obs. 79−42641
InP(As), surface states, contact pot. difference, photoemission, and low energy loss spectra expts. 77−85285
InSb (110), chemisorption of Cl, photoemission spectra and tight-binding calcs. 80−6629
InSb, (110) surface, core level photoionisation spin-orbit branching ratio, initial and final state effects 79−83094
InSb (110) surface struct. determ. by LEED, UPS, and EPR 80−49475
InSb, external photoelec. effect 78−27366
InSe, ang. depend. of core level photoemission 79−43099
InSe, angle resolved photoemission, 15-29 eV, valence band struct. 77−48319
InSe, band structure, XPS, UPS and tight-binding calc. 77−47727
InSe, core-level photoemission anisotropy 78−11076
InSe, energy band structure, chem. bond polarity, photoemission, semiempirical tight binding method 80−44504
InSe, photoemission props. of III-VI layer compounds 79−65976
InSe, polarisation selection rules for photoemission spectra, test of band struct. calcs. 77−52216
InSe, two and three dimensionality of electron states, normal photoemission obs. 77−32503
InSe, valence and conduction bands, synchrotron radiation photoemission spectra 77−63536
Ir (100), adsorption of Xe, local surface struct., UPS study 80−39429
Ir (100), chemisorption of acetylene, benzene and ethylene, geometric and electronic effects 77−55457
Ir (100), chemisorptive bonding of CO, photoemission investig. using synchrotron radiation 77−12498
Ir, (100) and (111) surfaces, chemisorptive bonding and reaction of NO, UPS obs. 77−72786
Ir (100)-1×1 surface struct. and reconstruction kinetics, LEED, UPS and work function meas. 79−90851
Ir (111), chemisorbed NH_3, mol. adsorbate structs. from angular-resolved photoemission 80−76141
Ir (111), chemisorption of CO, UPS and XPS obs., comparison with Pt 78−38942
Ir (111), oxidation, combined LEED/UPS obs. 78−19955
Ir, (111) surface, flash desorption spectra of NO, recombined mol. identification 79−86996
Ir, (111) surface states, surface Umklapp effects, photoelectron spectra 80−93457
Ir, chemisorbed CO, XPS and UPS 77−16450
Ir, chemisorption, clean normal and reconstructed (100) surfaces, multiplets role 77−15694
Ir, chemisorption of H_2, adsorption and desorption kinetics, struct. of overlayer 80−84367
Ir, chemisorption of NO, chemisorptive bonding and reaction 77−51596
Ir, electronic struct., double beam photoemission 79−83098
Ir(111), CO chemisorption, coverage dependent interaction, UPS 77−85897
K adsorbed on Fe(110), UPS and XPS meas. 80−95675
K adsorbed on Pt(111), UPS and XPS meas. 80−95675
K, oxidation, adsorbate-induced structs., UPS obs. 79−47828
K surface, clean and O_2-exposed, X-ray and UV photoelectron spectra 78−52636
K, valence p-shell HeIIα photoelectron spectra, final state CI effects 80−14121
KCN, He I photoelectron spectra 79−64046
K_2CO_3, solid, low energy photoelectron spectra 78−95656
KCl surface states, detection by photocharging spectroscopy 77−66193
KCl:Eu crystallophosphores, aggregation of $Eu^{2+}v_c^-$ centres *(Russian)* 78−43909
KCl(Br)(I), He II photoelectron spectra, ionisation energy 77−18977
K_2CsSb, evaluation as photocathode material 78−11072
$KMnF_3$ film, photoelec. yield spectra, rel. to band struct. 78−43980
KPO_3, He(I) photoelectron spectra, UTARC calc., assignments 79−72357
$KZnF_3$ film, photoelec. yield spectra, rel. to band struct. 78−43980
Kr, 3p core hole spectrum, many electron description 78−50517
Kr, 4p asymmetry parameter and cross section photoelectron energy depend. pseudopot. method 78−9130
Kr 4s, photoelectron ang. distrib., relativistic Dirac-Fock calc. 79−59411
Kr, appl. of valence electron spectroscpy using polarised He I radiation 77−492
Kr film, electron MFP, vacuum UV photoemission data 77−28690
Kr, ns→εp photoelectrons, spin polarisation 80−37792
Kr, photoelectron emission, polarisation depend. on incident unpolarised VUV radiation wavelength 80−52952
Kr, shake-up energies, Slater transition-state calcs. 79−89651
Kr, spin-polarised photoelectrons by circularly polarised synchrotron radiation 80−91516
Kr_2, photoelectron spectra 78−78748
LaB_6 (001), surface state exam. by angular resolved UPS 78−19114
LaB_6 (001) surface, struct., initial oxidation, XPS, UPS, LEED, AES, work function meas. 79−99403
LaB_6 (100), (110), and (111), surface structs. and work functions 80−70512
photoelectron spectra continued
LaB_6 (100) surface, O_2 adsorption, UPS and LEED study 80−49519
LaB_6 (210) surface, work function, struct. and chemisorpt. stability, XPS, UPS and LEED 80−65344
LaB_6, direct recomb. and Auger deexcitation channels of La 4d to 4f reson. excitations, photoemission spectra 80−66395
LaB_6 surfaces, (100), (110) and (111), electron states, UPS study 80−100752
LaB_6, UPS and XPS of valence band 78−84703
LaB_6, valence band dispersions, angle-resolved photoemission 80−11536
LaB_6(001) surface, struct. and initial oxidation, UPS, XPS and work functions meas. 77−86195
$LaBr_3$, ionisation energies, satellite struct., photoelectron spectra, MS Xα calcs. 78−13425
LaF_3, ionisation energies, satellite struct., photoelectron spectra, MS Xα calcs. 78−13425
LaF_3, MS Xα electronic struct. calc., inner shell photoelectron spectra 77−10594
LaF_3, quantum yield, photoelectron spectra, density of states struct. 78−68601
$LaFe_{1-x}Co_xO_3$, UPS, XPS, X-ray absorpt. spectra, band struct. study 79−56885
$LaNi_{1-x}Fe_xO_3$, UPS, XPS, X-ray absorpt. spectra, band struct. study 79−56885
$LaNi_5$, self restoring of active surface, photoemission, mag. susceptibility study 78−48280
$LaNi_{1-x}Co_xO_3$, UPS, XPS, X-ray absorpt. spectra, band struct. study 79−56885
LaO_4^{5-}, ionisation energies, satellite struct., photoelectron spectra, MS Xα calcs. 78−13425
$La_{1-x}Pb_xMnO_3$, spin polarised XPS and UPS, elec. struct. 77−8717
Li, K-edge photoabsorpt. cross section 79−10080
Li, two-photon ionis., many-body perturbation theory 79−22679
Li/H_2O, surface complex form., obs. using photoelectron spectra 79−69359
Li_2Br_2, UPS of dimeric mol., expt. and Xα calc. 80−9640
LiC_6, intercalated, charge-transfer and non-rigid-band effects 80−44496
LiC_6, intercalated graphite, band struct. determ. by angle-resolved photoemission 80−45203
Li_2Cl_2, UPS of dimeric mol., expt. and Xα calc. 80−9640
LiF, evaporated film, UPS, valence and cond. band struct. 77−63528
LiF, Li 1s ionisation pot. calc., Li 1s XUV absorpt. spectrum 77−23443
Li_2F_2, UPS of dimeric mol., expt. and Xα calc. 80−9640
Li_2I_2, UPS of dimeric mol., expt. and Xα calc. 80−9640
$LiNbO_3$, influence of spontaneous polarisation on photoelec. emission 79−28898
$LiNbO_3$, valence band UPS and partial p and d density of states 80−71560
$LiNbO_3$, XPS and UPS from surface defects 80−76136
Li_2SO_4, solid, low energy photoelectron spectra 78−95656
Li_2SO_4, UPS, expt. methodology aspects 77−90245
LiX,(X=F,Cl,Br,I), UPS, expt. methodology aspects 77−90245
LuH_2, electronic struct., photoelectron spectra study 80−50527
Mg clean films, O_2 interaction study using synchrotron-radiation-induced-photoemission 80−55709
Mg, film, electron inelastic scatt. mean free paths, synchrotron radiation photoelectron spectra meas. 78−76587
Mg film, polycryst., chemisorpt. of O_2, synchrotron radiation photoemission expts., 70-150 eV 78−95228
Mg film, synchrotron radiation photoemission, plasmon loss struct. 79−28897
Mg, polycryst., adsorpt. of O_2 at 100 and 300K, XPS, UPS, XAES 78−18906
Mg, X-ray excited L Auger spectra, double ionisation satellites 77−32497
Mg, XPS theory, valence band spectra band struct. 78−72702
MgAg, 4d bandwidth influence on $M_{4,5}N_{4,5}N_{4,5}$ Auger spectra 79−100017
Mg_2Ge, valence band, XPS meas. 77−8018
MgO, film, low energy electron absorpt., struct. and absorpt. centres 79−7763
MgO, free film and Au substrate, transmission spectra and photoemission characts. 77−24925
Mg_2Si, valence band, XPS meas. 77−8018
Mg_2Sn, valence band, XPS meas. 77−8018
$MnF_2(I_2)$, SCF-Xα MO calcs. of core photoelectron shake-up satellites 77−20991
$Mn_{0.26}NbS_2$, intercalation compound, struct. and photoemission meas. 77−16453
$MnO_3F(Cl)$, He (I) photoelectron spectra, metal-ligand bonding, EHMO calc. 78−9193
Mo (001) surface, surface states and photoemission 79−60887
Mo (100), CO chemisorbed, surface kinetics, photoemission study method 80−80941
Mo (100), sharp peak in UPS near Fermi level 77−52220
Mo (100) and (110) surface, directional UPS obs. 77−8722
Mo (100) face, surface reson. 78−72226
Mo, ARPES using synchrotron radiation 78−72682
Mo, adsorption of CO, O_2, metastable He de-excitation spectroscopy and UPS study 80−34314
Mo complex, hexadimethylamino molybdenum, electronic description of triple bonds and verification by photoelectron spectroscopy 78−41949
Mo complexs. bis(η-cyclopentadienyl) Mo halides, electronic struct., photoelectron spectra 77−75214
Mo cpds, chemistry and uses, conf., Oxford, Eng., Sep (1976) 77−77749
Mo, K-shell photoelectric cross section 79−22676
Mo, $N_2N_3N_{45}$ super Coster Kronig processes 80−106303
Mo, photoelectric cross sections of low energy photons 78−46309
Mo polycrystalline surface, CO chemisorption, substrate mediated C-O interaction, photoelectron spectra 79−34353
Mo, quenched sample, UV photoelectron spectra, exoelectron-like emission 79−15587
Mo superconducting film, amorphous and crystalline, transition temp. exam. by UPS 79−28433
Mo, surface resonances on (100) plane, angle-integrated photoemission spectra 77−85894
Mo, surface sensitive structure in angular resolved photoemission *(French)* 77−40326
Mo, two-photon photoemission induced by picosecond laser pulses 77−77347
Mo, UPS, angle-resolved, surface resonances on (100) face 78−2987

photoelectron spectra continued
Mo-Ca, ion implanted, range distrib. of Ca^+ ions, work function and AES obs. 78−27365
MoF_6, valence electron spectra, vibr. band struct. 77−23520
$Mo_2(NH_2)_6$, electronic description of triple bonds and verification by photoelectron spectroscopy 78−41949
MoO_2, photoelectron spectra, X-ray and UV polycrystalline 79−28889
$Mo_2(OH)_6$, electronic description of triple bonds and verification by photoelectron spectroscopy 78−41949
MoS_2, electronic struct. by photoelectron spectroscopy using line and synchrotron sources 79−87560
MoS_2, UPS meas. band struct. determ. 78−35250
α-$MoTe_2$, band struct. photoelectron spectroscopy 77−51653
α-$MoTe_2$, electronic struct. by photoelectron spectroscopy using line and synchrotron sources 79−87560
Mo(100), adsorbed H_2, photoemission rel. to surface resonances and surface reconstruction 80−44417
Mo(110), surface densities of states for normal photoemission 78−35251
N_2, 0-10 eV photoelectron spectra obs., new differential retarding field analyser characts. 77−41735
N_2 adsorbed on Ni, valence band photoemission, SCF MO CNDO calc. 80−100754
N_2 airglow solar activity effect on (0,0) second positive band 77−70902
N_2, angular distribution He I (Ne I) photoelectron spectra 79−31606
N_2 asymmetry parameter, angle resolved photoelectron spectra, multiple scatt. method 80−63708
N_2, condensed film, UPS linewidths 78−31294
N_2, differential photoelectron cross sections, energy depend. 79−10149
N_2, fixed molecule, spectral variations of photoelectron ang. distribs. 77−14489
N_2, inner-shell ionisation, relax. effects calcs. 77−42351
N_2 inner-valence ionisation, correl effects calcs. 78−9198
N_2, K-shell photoabsorption spectrum, mol. effects 77−27124
N_2, partial cross sections depend. on photon energy, 16 to 40 eV 78−1025
N_2, photoabsorpt. cross section, 10 to 50 nm 77−61797
N_2, photoelectron ang. distrib., energy depend. 79−22760
N_2, photoelectron ang. distrib., multiple scatt. calc. 79−81238
N_2, photoelectron ang. distrib. asymmetry parameter for 30.4 nm photons 79−98151
N_2, photoelectron ang. distrib., photon energy depend. , 16-25 eV 80−53046
N_2, photoelectron spectra, ang. distrib. asymmetry parameter, vibr. state depend. 77−75218
N_2, photoelectron spectra, 21.2-151.4 eV and soft X-ray, ionis. cross-section 78−37683
N_2, photoelectron spectra, valence region strong shake-up bands, Koopman's theorem breakdown 79−72354
N_2, photoionis., transition probabilities at threshold, to $X(^2\Sigma_g^+)$, $A(^2\Pi_u)$ and $B(^2\Sigma_u^+)$ vibr. levels 78−94294
N_2, threshold photoelectron spectra by electron attachment 77−75211
N_2, threshold photoelectron spectra, 15-20 eV 79−54912
N_2, total and partial photoionis. cross sections, threshold to 100 Å 77−58092
N_2, vibr. intensity meas. in photoelectron spectra for ionic ground states 77−18972
N_2, Xe matrix-isolated and solid, UPES obs. 79−45762
N_2^+, partial photoionisation cross section and photoelectron angular distribution for $X^2\Sigma_g^+$ state determ. 80−83429
N_2^+, vibr. intensity distribs. for electronic states prod. by photoionis. 78−25614
N_2^+ $X^2\Sigma_g^+$-state, vibr. states asymmetry parameter and photoelectron spectrum 80−95591
N_2^++Group IV elements and oxides, XPS and UPS prod. determ. 78−73084
ND_3, effect of phase density on ionisation process and electron localisation 77−89731
N_2F_2, trans- and cis-isomers, photoelectron spectra, Green's function calc. 77−83650
NH^-, photoelectron spectra, NH electron affinity and intercombination separation 77−18970
NH_3, photoabsorpt. cross section, 10 to 50 nm 77−61797
NH_3, photoelectron spectra, 21.2-151.4 eV and soft X-ray, ionis. cross-section 78−37683
NH_3, solid, UPS, valence band struct. 79−33890
NH_3^+, ionisation pot. of ^2E state, Jahn-Teller effect 78−62948
N_2H_2, isomers, photoelectron spectra, vibr. struct., ionisation pots., Green's function calcs. 77−75213
$NHBr_2$, He(I) photoelectron spectra of NH_3+Br_2 gas phase reaction 79−31599
NH_2Br, He(I) photoelectron spectrum 78−25615
NH_2Cl, $NHCl_2$, NCl_3, UV photoelectron spectra, assignments 78−86911
NH_2OH, ionisation energies, He I photoelectron spectra, orbital calcs. 77−88497
$NH_2(X^2B_1)$ radical, and ND_2, ionisation pot., vibr. anal., ab initio calcs. and vacuum UPS obs. 80−53047
NO, adsorbed on Cu, species identification, struct., dissoc. chemisorption, desorption, UV photoelectron spectroscopy 78−52635
NO, ang. distrib. valance photoelectron spectra, vibr. depend., autoionisation and Franck-Condon factors 79−72356
NO, ionic ground state, vibr. intensity, Frank-Condon factors 77−79650
NO, N 1s photoelectron spectrum, correl. effects 77−10702
NO, photoabsorpt. cross section, 10 to 50 nm 77−61797
NO, UV irrad. photoionisation, NO^+ high vibr. excitation, photoelectron spectra 77−71830
NO, UV photoelectron spectrum, autoionisation from Rydberg state, vibr. progressions, Franck-Condon factors 78−50583
NO $X^2\Pi(v''=0)$, ionis. energies to NO^+ $X^1\Sigma^+(v=0\text{-}34)$, NO^+ mol. consts., UPS obs. 80−14177
NO^+, fragmentation ang. distrib., energy disposal, branching, photoelectron-photojon coincidence spectra 79−68263
NO^+, $X^1\Sigma^+$ state, UV irrad., high vibr. excitation, photoelectron spectra 77−71830
N_2O, electronic autoionisation branching 80−91614
N_2O, impurity lines in He resonance source 77−14787
N_2O, non-Franck-Condon transitions in resonant autoionization 79−50092
N_2O, photoabsorpt. cross section, 10 to 50 nm 77−61797
N_2O, spin polarised photoelectrons, synchrotron excited 80−43101
N_2O, $X_2\Pi$ state, Ne I photoelectron spectra 77−30924

photoelectron spectra continued
N_2O^+, dissoc., threshold photoelectron-photoion coincidence obs. 80−87189
N_2O_4, He I photoelectron spectrum 77−6845
N_2O_4, He I photoelectron spectrum, new interpretation 78−17713
N_2O_4, photoelectron spectrum interpretation 79−22761
N_2O_4, photoelectron spectra, 304 Å 79−59510
N_2O_4, UV photoelectron spectrum, variable temp./fast pumping technique, ionis. pots. 77−30926
$N_2O(NO_2)$, Penning ionisation and photoelectron spectra 77−83653
$N_3P_3Cl_6$, ionisation energy and electronic struct., UV photoelectron spectra and Xα calcs. 78−94281
NS, ground ionic state, photoelectron spectra determ. 77−46596
Na adsorbed on Ni, photoemission, directional memory effects 80−100753
Na, reson. two-photon ionis., photoelectron ang. distrib. and polaris., nucl. spin influence 79−10083
Na, reson. two-photon ionisation via $3p^2P_{3/2}$ state, photoelectron ang. distrib. 80−43016
Na, Rydberg states, high resolution spectroscopy 80−52901
Na, XPS theory, valence band spectra band struct. 78−72702
$Na_3B_3O_6$, solid, low energy photoelectron spectra 78−95656
NaCN, He I photoelectron spectra 79−64046
NaCl (100) face, angle-resolved photoemission 78−56567
NaCl film, UPS linewidth, phonon broadening of core levels 77−36371
NaCl, photoemission exam. of Na^+-2p core excitons 78−43982
NaCl, surface states, detection by photocharging spectroscopy 77−66193
NaCl, UPS, expt. methodology aspects 77−90245
NaF, UPS, expt. methodology aspects 77−90245
Na_2KSb, evaluation as photocathode material 78−11072
$Na_2KSb(Cs)$, photocathode, optical props. 79−78827
NaOH, UPS, expt. methodology aspects 77−90245
$NaPO_3$, He(I) photoelectron spectra, UTARC calc., assignments 79−72357
Na_xWO_3, core level photoelectron spectra, final state effects 80−50509
Na_xWO_3, vacuum UPS exam. 78−84700
Nb binding energies and ESCA chemical shift *(French)* 77−44541
Nb, H chemisorption, photoemission studies 80−76145
Nb, $N_2N_3N_{45}$ super Coster Kronig processes 80−106303
Nb, oxidation, ESCA *(French)* 77−36361
Nb, oxidation at high temp. and low O_2 pressure, ESCA study *(French)* 77−25179
Nb surface, clean and oxidised, electronic struct., UPS meas. 78−95682
Nb-Ni glass, photoemission spectra meas. 77−55867
Nb-Ti alloys, oxidation, ESCA *(French)* 77−36361
NbC, electronic structure, PES study 80−70594
NbO binding energies and ESCA chemical shift *(French)* 77−44541
NbO, electronic struct. from photoelec.- and X-ray emission spectra and X_α calcs. of NbO_6^{-10} cluster 79−23892
NbO_2 *(French)* 77−44541
NbO_2, photoelectron spectra, X-ray and UV polycrystalline 79−28889
$NbSe_2$ (2H), metallic layer cpd., angle-resolved photoemission spectra 79−47593
$NbSe_2$(2H) intensity vars. of angle-resolved photoemission spectra 79−83104
NdF_3, ionisation energies, satellite struct., photoelectron spectra, MS Xα calcs. 78−13425
Ne 2s, photoelectron ang. distrib., relativistic Dirac-Fock calc. 79−59411
Ne, photoelectron spectra, 21.2-151.4 eV and soft X-ray, ionis. cross-section 78−37683
Ne, shake-up energies, Slater transition-state calcs. 79−89651
Ne, solid, pure and Xe, Kr, Ar doped, photoemission yields and reflectance spectra, exciton dynamics 77−28123
Ne, total and differential photoemission cross sections, final state approxs. comparison 77−50414
Ne:Xe film, solid, competition between electronic energy transfer and relax., photoelectron spectra 77−24929
Ni (001), adsorbed c(2×2) Na overlayer, core level excitation effects, synchrotron radiation UPS study 80−40234
Ni (001), adsorbed Se and Te, photoelectron diffr. obs. 80−40223
Ni (001), adsorpt. of S, multiple binding sites and diffusion, photoelectron spectra and LEED struct. 77−66569
Ni (001), chemisorption of CO, back donation in chemisorption bond, UPS study 80−107642
Ni (001), chemisorption site determ. for S and CO, angle-resolved UPS 78−71970
Ni (001) surface, c(2×2) Se overlayer, angular resolved UPS 78−76584
Ni (001) surface, electronic struct. of ordered S overlayers 80−84835
Ni (001) surface, O monolayer, angle-resolved UV photoemission calc. 77−24927
Ni, (001) surface, Se adsorbed, resonancelike peaks in angle-resolved UPS 79−69955
Ni (001) surface with adsorbed Se, angle resolved UPS, resonancelike peaks 79−87562
Ni (100), adsorbed c(2×2) CO, photoemission orientation determ. 79−19974
Ni (100), adsorbed chalcogen, structure, force consts., binding energies and photoemission, importance of final state multiplet splitting 78−71966
Ni (100), adsorption of chalcogens, orbital identification in INS and UPS spectra 77−43427
Ni (100), angle resolved photoemission, final-state effects 78−56565
Ni (100), bonding of chalcogen overlayers, expt. 77−35819
Ni (100), catalysis of $CO+H_2$, reaction rate, AES and UPS obs. 79−79290
Ni (100), chemisorption of H_2 and O_2 and their interaction, UPS investig. 77−51600
Ni (100), chemisorption of acetylene and ethylene, angular resolved UPS exam. 78−72685
Ni (100), chemisorption of NO, LEED, AES, UPS, and thermal desorption study 80−39449
Ni (100), electronic struct. of c(2×2) and p(2×2) O overlayers 79−47144
Ni (100), reson. behaviour of interband excitations in photoelectron spectra 80−104043
Ni (100), resonant photoemission exam. 78−27371
Ni (100), with chemisorbed c(2×2)O, c(2×2)S and CO, photoemission angle-of-incidence depend. 77−32502
Ni (100) and (110), reaction of acetylene, room temp., UPS expts. 80−61151
Ni (100) and (110) surfaces, S saturated, UPS 77−32500

photoelectron spectra continued
Ni (100) surface, adsorption of CO, UPS study 79−76473
Ni (100) surface, bonded Se, electronic orbitals 78−72224
Ni (100) surface, c(2×2)O overlayer, angle-resolved photoemission study 79−33903
Ni (100) surface, chemisorbed ordered overlayers of O and S, angle-resolved photoemission 77−59671
Ni (100) surface, electron binding energies of core levels in adsorbed Cs 78−18896
Ni (110) and (111), two-photon photoemission 80−76150
Ni (111), adsorption of chalcogens, angle-resolved photoemission 80−40230
Ni (111), band struct. and temp.-depend. mag. exchange splitting, angle resolved photoemission obs. 78−60546
Ni (111), chemisorbed CO, orientation of CO from angle resolved photoemission 77−8721
Ni (111), chemisorption and reaction of NH_3, LEED, desorption and photoemission expts. 80−59799
Ni (111), chemisorption of methanol, UPS and flash-desorption exam. 77−55455
Ni (111), chemisorption of H, electronic struct. of H using angle-resolved photoemission 79−69573
Ni (111), electron spin polarised photoemission spectrum 80−25525
Ni (111), H_2 adsorption, u.v. photoelectron UPS obs. 77−1786
Ni (111), isothermal desorption of CO, UPS study, time-resolved approach 80−39440
Ni (111) and (110), laser-induced charge transfer to adsorbed CO, photoemission expts. 80−59798
Ni (111) chemisorption bonding of H, UPS obs. 77−76671
Ni (111) surface, clean and with CO absorbed layer, angle-resolved photoemission meas. 77−16463
Ni, (111) surface, Λ_1-symmetry surface state, angle resolved photoelectron spectra 78−80034
Ni (111) surface, with O_2, Se, S and Te adsorbed layers, bonding geometry and electronic struct. 79−77909
Ni, adsorbed CO, core level spectrum, satellite struct., ab initio HF-LCAO calc. 80−40233
Ni, adsorbed O, electronic struct. and UPS 78−15281
Ni, adsorbed S(Se) surface bonding mechanism for ang. resolved photoemission 79−69360
Ni, adsorption of N_2, photoemission and electronic struct., cluster calcs. 80−97403
Ni, angle resolved photoemission from 0 superstructure on (001) surface 77−85898
Ni, angle resolved photoemission spectra 78−43986
Ni atoms, Xe matrix isolation, photoemission 80−27987
Ni, band struct., angle-resolved photoemission meas. 80−71569
Ni, band struct. and multielectron excitations, angle-resolved photoemission determ. 80−76147
Ni, chemisorbed H_2 photoemission spectrum, Anderson model parameterisation 77−40334
Ni, chemisorption of H, model, comparison with UPS data 79−46932
Ni, chemisorptive binding of O, CNDO calc. of potential energy curves *(German)* 80−44431
Ni clusters, valence band and core binding energies, UPS meas. 79−38721
Ni, core level excitation effects, synchrotron radiation UPS study 80−40234
Ni, d-band width, angle-resolved UPS meas., 77−20234
Ni, density of states, photoemission expts. above and below T_c, rel. to magnetism model 77−20536
Ni, electronic and magnetic props., spin split energy band dispersions 79−78829
Ni, electronic structure, photoelectron spectra, theory 80−80168
Ni, energy band dispersion and mag. exchange splitting, angle-resolved photoemission meas. 80−71567
Ni, energy-band dispersions and exchange splitting, angle-resolved photoelectron spectroscopy 79−69402
Ni, exchange splitting of 3d bands, angle-resolved photoemission meas. 80−71568
Ni, ferro- to paramag. transition, angular resolved photoemission 78−68603
Ni, ferromag., exchange splitting, angle-resolved photoemission meas. 78−43985
Ni, ferromagnetic, chemisorption of H, spin-spin interactions, UPS spectra calc. 80−6630
Ni, ferromagnetic, photoemission spectra and band struct., spin polarisation of bulk photoemission 79−78843
Ni film, surface properties and photoelectron spin polarisation 78−14782
Ni, film growth on graphite and amorphous C, electronic struct. by photoemission and Auger obs. 79−77947
Ni, growth on amorphous C, electronic props., UPS and XPS obs. 79−82476
Ni, hydrocarbon chemisorption, C 2s levels, initial state shift 78−34703
Ni monolayer and submonolayer films, on ZnO, UPS study 80−7472
Ni, near-Fermi part of energy band struct. from PES 80−2328
Ni, photoelectron spectra, threshold Auger emission 80−29849
Ni, photoemission near Curie temp. 79−78841
Ni, photoemission spectra, valence band and core level satellite due to excitation of d electron 80−97408
Ni, photoemission spectra of d-band, bound hole pairs 79−47590
Ni, polarisation-dependent angle-resolved photoemission for band structure studies 78−95678
Ni, quasiatomic excitation, causing energy loss peak, UPS 78−72691
Ni, S and CO chemisorption, surface struct. from ang. resolved UPS 78−31303
Ni, spin polarisation of reson. two-hole bound state 79−83099
Ni, spin polarised photoemission, surface magnetism 79−52083
Ni surface, adsorbed CO, N_2, valence band photoemission, SCF MO CNDO calc. 80−100754
Ni surface, adsorbed Se layers, photoelectron intensity for binding site 79−47589
Ni surface, clean and with adsorbed Na, photoemission, directional memory effects 80−100753
Ni surface, photoemission 78−52619
Ni surface (111), photoyield near theshold negative-positive spin polaris. crossover 80−2922
Ni surfaces, clean and S-saturated, directional UV photoemission 78−15295
Ni, surfaces (100), (110), and (111), interaction with O_2, 295 and 485K, photoemission obs. 77−72784
photoelectron spectra continued
Ni, UPS, density of states determ. 78−52623
Ni, UPS, two-electron reson. at 3p threshold, rel. to Cu (100) expt. 80−25522
Ni, valence-band photoemission spectra, self-energy corrections effect 80−11534
Ni^-, photoelectron spectra, electron affinity and fine-struct. interval 79−68212
Ni^{2+} compounds, 3p photoelectron spectra, light-inuced changed in multiplet satellites 80−80946
Ni-Al, Raney nickel catalyst, surface texture studied by N_2 adsorption and ESCA *(French)* 79−69348
Ni-Au alloy, electronegativity and core electron binding energy shifts of Au 77−15346
Ni-Se interface, reactive diffusion, electronic struct., UPS study 78−51748
$Ni(CO)_4$, bonding, shakeup energies, and shakeup intensities for photoelectron spectra 80−50528
$Ni_{1-x}Cu_x$ (x=0.03, 0.16, 0.24), photoemission study, surface, bulk electronic struct. 78−48281
$Ni_{23}Cu_{77}$ random substitutional alloy, (001) surface, angle resolved photoemission 77−85895
$Ni_{0.34}NbS_2$, intercalation compound, struct. and photoemission meas. 77−16453
NiO, bulk props., initial state MO Ni_4O_4 and $Ni_{13}O_{14}$, cluster model, lattice and force consts., photoemission and CT absorpt. spectra 80−84828
NiS, semiconductor-metal transition, UPS and XPS 79−23896
$NiS_2(Se_2)$, electronic struct., UPS and XPS study 80−80935
Ni_3Ti, electronic struct., Xα calc., photoelectron and AES spectra 80−20769
Ni(001), adsorbed Na(Te), core-level photoelectron diffraction 78−95659
Ni(001) surface, p(2×2) and c(2×2) O superstructure, angle resolved photoemission from adsorbates 78−23585
Ni(100) magnetic surface states, photoelectron spectra, surface Brillouin zones 80−6928
Ni(100), oxidation, UPS obs. 80−6648
Ni(100) surface, CO ordered overlayers, angle resolved, UV photoemission 78−56570
Ni(111), adsorption of acetylene, chemisorbed O_2 effects, CH formation 78−18902
O, photoelectron ang. distrib. meas. 77−61721
O, photoelectron ang. distrib. anal. branching ratios determ. 78−5181
O^-, photodetachment, fine struct. transitions, photoelectron spectra 78−55151
O_2, 0-10 eV photoelectron spectra obs., new differential retarding field analyser characts. 77−41735
O_2, ab initio CI STO calc., photoelectron spectra 78−74585
O_2 adsorbed layer on Ni (001) surface, angle-resolved UPS 77−40333
O_2 chemisorbed on TiO_2 and $SrTiO_3$, phase investig. by UPS 78−72684
O_2, electron attachment threshold photoelectron spectra, vibr. excitation 80−83422
O_2, I and I′ resonance series, vibr. level populations in autoionisation, photoelectron spectra, bond length determ. 80−91612
O_2, multiphoton ionisation, electron energy spectra 77−6865
O_2, photoabsorpt., photoionis, and photodissoc., dipole oscill. strengths in UV 79−76468
O_2, photoabsorpt. cross section, 10 to 50 nm 77−61797
O_2, photoelectron ang. distrib. asymmetry parameter for 30.4 nm photons 79−98151
O_2, photoelectron ang. distrib., photon energy depend., 16-25 eV 80−53046
O_2, photoelectron spectroscopy using supersonic mol. beam source 79−68264
O_2, photoexcitation and photoionisation cross sections, HF Gaussian method 80−53064
O_2, photoionisation, partial channel cross-sections calcs. 80−53061
O_2, RH-GTO-MCSCF calc., 1s photoelectron spectra, multiplet intensity ratio 78−5134
O_2^+, fragmentation ang. distrib., energy disposal, branching, photoelectron-photoion coincidence spectra 79−68263
O_2^+, photoelectron spectra, vibronic transition ionisation energies, ground state mol. consts. 79−89710
O_2^+, predissociation of $b^4\Sigma_g^-$, $c^4\Sigma_u^-$ states, threshold photoelectron-photoion coincidence 78−42144
O_2^+, vibr. energy levels, dissoc. energy, photoelectron spectra 77−83651
O_2^+, vibr. intensity distribs. for electronic states prod. by photoionis. 78−25614
O_2^+, $X^2\Pi_g$ photoelectron spectra, vibr. intensity, Franck-Condon factors 77−42352
O_3, photoelectron spectra, HAM/3 MO calcs. 78−13414
O_3, photoelectron spectrum, vibr. struct., ionos. pot. 77−75217
O_3^-, photoelectron, photodetachment and photodestruction spectra 79−64042
OH(OD) radical, photoelectron spectra 77−27113
O_2*, vibrationally excited, study by variable temp. photoelectron spectroscopy 78−21972
P_2, vibr. struct. calcs. from photoelectron spectra 77−18973
PH_3, inner valence electron ionisation calcs., photoelectron spectra obs. 78−82619
PN, photoelectron spectra, ionisation pot., vibr. struct., Green's function method 77−61799
PN, vibr. struct. calcs. from photoelectron spectra 77−18973
$PN(X^1\Sigma^+)$, VUV photoelectron spectrum 78−1024
$POCl_3$, He I(II) XPS spectra comparison, ion states assignments, pseudopot. calcs. 77−61794
P_4S_3, UV photoelectron spectra, mol. orbital symm. 77−14494
P_4Se_3, UV photoelectron spectra, mol. orbital symm. 77−14494
$P_2(X^2\Sigma_g^+)$, He I photoelectron spectrum, ab initio and semiempirical calcs. 77−34691
Pb, 5d level open shell interactions, 304 Å photoelectron spectrum 80−87087
Pb, inorganic and organometallic cpds., photoelectron spectra, valence bands, ligand field broadening 77−63525
Pb, liquid and solid, UPS, optical densities of states 80−2924
Pb, photoelectric cross section, derived from total absorpt. cross sections 77−10646
Pb, photoelectric cross sections for 323 keV gamma rays 77−88432
Pb, photoelectric cross sections of low energy photons 78−46309

photoelectron spectra continued
Pb, photoelectric cross sections, from total absorption cross sections, 5 to 130 keV 79−26947
Pb, photoelectric interaction around the K edge 78−5183
Pb, photoelectron spectra, electron correlations and spin-orbit interaction influence 80−102495
Pb, photoionisation cross section of atomic and final state effects on 5d core levels 78−84699
Pb subshell photoelectron branching ratio meas., using synchrotron radiation 80−66397
Pb, two photon photoelectric emission, photocurrent vectorial depend. 79−95906
Pb, VUV photoelectron spectra, spin polarisation autoionis. reson. 78−33483
$PbCl_2$, $PbBr_2$, PbI_2, UV photoelectron spectra of valence d shells, gas-phase 78−62845
$PbCl_2$, photoionisation cross section of atomic and final state effects on 5d core levels 78−84699
$PbCl_2$, valence band electronic struct., XPS and UPS obs. 78−6826
$PbCl_2(Br_2)(I_2)$, valence band electronic struct., XPS and UPS obs. 78−6826
PbF_2 optical props. 77−32394
$Pb_5Ge_3O_{11}$, single crysts., photoemission anamoly during ferroelectric phase transitions 79−47599
PbI_2, electronic struct. and exciton problem, photoelectron spectra meas. 77−63540
PbI_2, excitonic shifts of quasiatomic optical core to cond. band transitions, UPS obs. 78−11079
PbI_2, layered, electronic band struct., direct evaluation by angle resolved photoemission 77−51652
PbI_2, layered semicond., valence bands UPS and XPS obs. 78−11078
PbI_2, octahedrally coordinated, layer cpd., electronic struct. using synchrotron-radiation photoemission spectroscopy 79−74058
PbI_2, optical props. 77−32394
PbI_2, semicond., band struct., angle resolved photoemission meas. 78−15296
PbI_2, two-photon photoemission 79−28890
PbN_6, electronic transitions and energy band struct. 79−74053
PbS, (100), angular resolved UV photoemission 78−2989
PbS (100) surface, electronic struct., O_2 adsorption effects, UPS study 80−54756
PbS, band struct., angle resolved photoemission obs. 79−33899
PbS, temp. effects on valence bands, UPS study 80−11537
PbS, valence band struct., angle-resolved photoemission spectra obs. 77−48310
PbS(Se), photoionisation cross section of atomic and final state effects on 5d core levels 78−84699
PbS(Se)(Te), angle resolved UPS and electronic band struct. 79−37981
PbS(Se)(Te), chemisorption of O_2, room temp., UPS and XPS obs. 78−91529
PbS(Se)(Te), photoemission interpretation 80−25531
PbSe, band struct. angle resolved photoemission obs. 79−33899
PbSe, spin-orbit splitting in valence bands, angle-resolved UV photoemission 78−2991
PbSe surface, clean and O_2-exposed, XPS (UPS) obs., electronic struct. 78−52637
PbSe, temp. effects on valence bands, UPS study 80−11537
PbSe, valence band structure from angular resolved photoemission spectra 78−84143
$Pb_{1-x}Sn_xTe$, MBE, O_2 uptake, AES, XPS and UPS expts. 78−95227
PbTe (111), adsorption of O_2, UPS and XPS exam. 78−71962
PbTe, band struct., angle resolved photoemission obs. 79−33899
PbTe, valence level photoelectron spectra 77−27114
Pd (100), $(\sqrt{2}\times\sqrt{2})R45°$ s layer, adsorbate induced surface reson. obs. in photoemission 80−7470
Pd (100), adsorption of Xe and CO, lateral interactions, effect on work function, UPS, and IR spectra 79−77904
Pd (100), chemisorption of CO, adsorbate band formation, UPS expts. compared with calcs. 79−77916
Pd (100), with CO adlayer, band formation, calcs. and photoemission expts. 79−95463
Pd, (100) surface, benzene chemisorbed, angle-resolved photoemission symm. anal., polarisation depend. and lateral interactions 79−91568
Pd (100) surface, chemisorbed acetylene influence of substrate struct. on bonding, photoelectron spectra 78−63933
Pd (111), adsorpt. of NO, LEED, UPS, and thermal desorpt. expts. 77−69179
Pd (111), adsorpt. of O_2 and NO, LEED, photoelectron spectra and thermal desorpt. expts. 77−69180
Pd (111), adsorption of O_2, UPS and thermal desorption spectra meas. 79−78833
Pd (111), electronic states calc. and adsorbate-induced photoemission struct. interpretation 78−60179
Pd (111), energy dispersions for valence and conduction bands 79−38719
Pd (111), H_2 adsorption, UPS obs. 77−1786
Pd (111) chemisorption bonding of H, UPS obs. 77−76671
Pd (111) surface, adsorbed O_2, UPS and thermal desorpt. charcts. 80−54754
Pd (111) surface, angular-resolved UPS meas. 79−95902
Pd, adsorbed CO, photoelectron spectra, 40-180 eV, adsorbate sensitivity enhancement 78−80453
Pd, adsorbed CO investig. by UPS, comparison with $Rh_6(CO)_{16}$ 77−51598
Pd, chemisorption and decomp. reactions of O containing organic mols., UPS 77−63953
Pd, chemisorption of H, model, comparison with UPS data 79−46932
Pd clusters, valence band and core binding energies, UPS meas. 79−38721
Pd, electronic band struct. and photoemission 80−97410
Pd, electronic struct., double beam photoemission 79−83098
Pd, electronic struct. determ. by relativistic APW method, rel. to UV spectroscopy 77−4289
Pd, film, growth on amorphous C, electronic props., UPS and XPS obs. 79−82476
Pd, film, on ZnO, struct., elec. props., AES, UPS study 78−76168
Pd, film growth on graphite and amorphous C, electronic struct. by photoemission and Auger obs. 79−77947
Pd particle array, on amorphous SIO_2 substrate, model catalyst, electron microscopy and UPS expts. 79−4899
Pd particle arrays on C film, UPS, Pd valence band width 78−88403

photoelectron spectra continued
Pd, photoemission spectra, valence band and core level satellite due to excitation of d electron 80−97408
Pd, single cryst., ang. resolved photoemission at 21.2 and 16.8 eV 77−63543
Pd surface, segregated S state, AES, EELS, UPS and XPS study 80−93452
Pd-Ag alloys, photoelectron spectra of core electrons 79−100021
Pd-Au alloy, electronegativity and core electron binding energy shifts of Au 77−15346
Pd-Si, metallic glasses, XPS and UPS studies 79−74062
Pd-Si (111) interface, microscopic Pd_2Si form., UPS obs. 80−24743
Pd-Si glasses, changes in density of states with alloys comp., UPS obs. 80−50531
Pd-Zr, metallic glasses, valence band struct. investigation 80−11533
Pd_2, ab initio relativistic core pot. studies of metal-metal bonding 80−106257
PdH, ab initio relativistic core pot. studies of metal-H bonding 80−106257
PdO, electronic struct., XPS and UPS study 80−35061
$Pd_{0.81}Si_{0.19}$, amorphous, partial densities of states, XPS, UPS and AES meas. 79−95315
$Pd_{18}Si_{14}Cu_6$, glass, changes in density of states with alloys comp. UPS obs. 80−50531
$Pd_{80}Si_{17}Cu_3$, glass, changes in density of states with alloys comp., UPS obs. 80−50531
Pd(110) surface, adsorption of Xe, UPS study 80−6633
Pd(111) chemisorption of H, photoemission spectra, SCF electrical struct. 79−33320
PrF_3, ionisation energies, satellite struct., photoelectron spectra, MS $X\alpha$ calcs. 78−13425
Pt 6(111)×(100), clean and O_2-covered, UPS studies 80−76151
Pt (100), adsorption of NO, 40-400°C LEED, AES, XPS and UPS obs. 77−35820
Pt (100) chemisorption of acetylene and benzene, LEED, AES, HPS and temp. programmed dehydrogenation exam. 77−55456
Pt (100) surface, chemisorption of acetylene and benzene, AES, UPS, LEED and flash dehydrogenation 77−59216
Pt (111), adsorption of CO using XPS, UPS, TDS and dynamic meas. of work function 79−65322
Pt (111), adsorption of CO, XPS, UPS, thermal desorption, and work function meas. 79−77905
Pt (111), chemisorbed CO, orientation of CO from angle resolved photoemission 77−8721
Pt (111), chemisorption bonding of H, UPS obs. 77−76671
Pt (111), chemisorption of mol. O_2, XPS, UPS, EELS, and work function meas. 80−76139
Pt (111), interaction with water, thermal desorption, UPS, and XPS study 80−80088
Pt, adsorption of CO, O_2, H_2, UV photoemission spectra 78−14608
Pt and Pt-Au (100), chemisorption of H_2 and O_2 and their interaction, UPS investig. 77−51600
Pt band-structure determ., angle-resolved photoemission 80−66398
Pt, chemisorbed CO photoemission meas. 77−63531
Pt, chemisorption of H, model, comparison with UPS data 79−46932
Pt, core level excitation effects, synchrotron radiation UPS study 80−40234
Pt, electronic struct., double beam photoemission 79−83098
Pt subshell photoelectron branching ratio meas. using synchrotron radiation 80−66397
Pt, surface, (111), O_2 interactions, UPS, EELS and thermal desorption study 80−100409
Pt, UV photoemission, from (111) and [6(111)×(100)] surfaces 79−91566
Pt-Au alloy, electronegativity and core electron binding energy shifts of Au 77−15346
Pt-$SrTiO_3$ (100) interface, struct. and electronic props., AES, LEED, EELS, and UPS study 80−24986
Pt-$SrTiO_3$ (100) interface, Auger and photoemission studies, relax. and chem. shift effects 80−54749
Pt_2, ab initio relativistic core pot. studies of metal-metal bonding 80−106257
PtH, ab initio relativistic core pot. studies of metal-H bonding 80−106257
PtO_x films, electronic struct., reduction processes, photoemission, optical absorpt. and resist. meas. 80−80931
Pt(100), adsorpt. of ethylene 78−18905
Pt(111), chemisorption of acetylene, reaction at room temp., form. of vinyl-like species 79−46939
Pt(111), chemisorption of ethylene, reaction at room temp., form. of vinyl-like species 79−46939
Pt(111), Λ-line valence bands, angle-resolved photoemission determ. 80−108323
Pt(111) surface, adsorption of acetylene and ethylene, UPS meas. 77−52223
Rb, 4p level He II photoelectron spectra, energies and intensities 80−5511
Rb, oxidation, adsorbate-induced structs., UPS obs. 79−47828
Rb, π-photoionisation spectra in DC field, Fano profile 79−59410
Rb, valence p-shell HeIIα photoelectron spectra, final state CI effects 80−14121
Rb^-, in tetrahydrofuran soln., transient photoelectron nutation 79−3418
Rb-halide, UPS exam., band struct. determ. 77−40330
RbAu, photoelectron spectroscopy and energy bands calc. 78−76581
RbC_8, intercalated graphite, band struct. determ. by angle-resolved photoemission 80−45203
RbCl, electron bombard., colour centre photoemission, surface contamination and escape depth 80−66392
RbCl(Br)(I), He II photoelectron spectra, ionisation energy 77−18977
Rb_2CsSb, evaluation as photocathode material 78−11072
$RbPO_3$, He(I) photoelectron spectra, UTARC calc., assignments 79−72357
Re (0001), chemisorption of CO, role of d-orbitals, angular resolved UPS and thermal desorption meas. 80−40232
Re, (0001) surface, nonuniform attenuation of d-bond photoemission, CO chemisorption 79−74060
Re, electronic struct. and CO adsorption charcts., XPS, UPS, and thermal desorption study 80−71571
Re_3Br_9, atomic clusters, electronic struct. and photoelectron spectra 80−69287

photoelectron spectra continued
$(Re_3Cl_{12})^{3-}$, atomic clusters, electronic struct. and photoelectron spectra 80−69287
Re_3Cl_9, atomic cluster, electronic struct. and photoelectron spectra 80−69287
Re_3Cl_9 metal cluster complexes, He(I) photoelectron spectrum, SCC DV Xα calcs., $Re_2Cl_8^{2-}$ comparison 80−28063
Re(0001), adsorption of O_2, CO, NO, and H_2O, XPS, UPS and temp. programmed desorption 80−71574
Rh (110), chemisorption of CO and NO, LEED, AES, XPS, UPS, and desorption obs. 79−77899
Rh (111) surface, UPS meas. of chemisorbed and condensed CO using synchrotron radiation 79−33902
Rh, band structure and photoemission from low index surfaces 80−24790
Rh, electronic struct., double beam photoemission 79−83098
Rh, $N_2N_3N_{45}$ super Coster Kronig processes 80−106303
$Rh_6(CO)_{16}$, UPS investig., comparison with metal/adsorbate system 77−51598
Ru (0001) surface, chemisorbed acetylene influence of substrate struct. on bonding, photoelectron spectra 78−63933
Ru (001), adsorption of H_2S and S, LEED, UPS, AES, and thermal desorption meas. 79−99420
Ru (001), adsorption of NO, KPS, UPS, and X-ray AES meas. 80−6655
Ru (001), dissociation of adsorbed H_2S, chemisorption and electronic struct. of S layer 79−79292
Ru (001) surface, adsorbed layer of CO, electron induced dissociation, XPS and UPS 77−59215
Ru (110), adsorption of H_2S, H_2, and S, UPS and work function change meas. 79−78834
Ru, $N_2N_3N_{45}$ super Coster Kronig processes 80−106303
RuO_2, photoelectron spectra, X-ray and UV polycrystalline 79−28889
Ru(110), adsorption of H_2S, H_2, and S, UPS and work function meas. 79−99424
S, (^3P) atom, UPS in VUV region 79−98153
S, photoelectric cross sections, from total absorption cross sections, 5 to 130 keV 79−26947
S^-, photodetachment, fine struct. transitions, photoelectron spectra 78−55151
S-N system, inorganic, electronic struct. obs. by photoemission XPS and UPS, CNDO calcs. 80−78653
SB_2 photoelectron spectra, visual assessment stripping program anal. 80−28062
SBr_2, transient species, He(I) photoelectron spectroscopy, discrete variational HFS calc. 79−31594
$(SCN)_2$, prep., UV photoelectron spectrum and structure 80−28059
SF_2, He I photoelectron spectra 79−10148
SF_6, ab initio electronic struct., and photoelectron spectral assignment 79−54764
SF_6, partial photoionis. cross-sections, 20-54 eV, photoelectron spectrum 79−13769
SF_6, photoelectron ang. distrib., orbital assignments 79−819
SF_6, valence electron spectra, vibr. band struct. 77−23520
SH, ($X^2\Pi_i$) radical, UPS in VUV region showing vibr. struct. 79−98153
$(SN)_x$, electronic struct., X-ray and UV photoemission obs., OPW and pseudopot. calcs. 78−6832
$(SN)_x$, polycryst. films, single crysts., UPS, valence band struct. 77−69967
S_2N_2, photoelectron spectrum, interpretation, Green's function calcs. 80−87175
SO_2, Penning ionisation and photoelectron spectra 77−83653
SO_2, photoelectron spectrum, vibr. struct., ionos. pot. 77−75217
SO_2^+, state selected vibr. levels, fragmentation, photoelectron-photon coincidence spectroscopy 79−89707
SO_3, photoelectron spectrum assignment, ionisation pot. and electron affinity, Green's function method 77−54576
SPF_3, electronic struct. of valence shell, UV photoelectron spectroscopy 78−82781
Sb inorganic and organometallic cpds., photoelectron spectra, valence bands, ligand field broadening 77−63525
Sb thin film, pH sensitivity and electrode potential *(Japanese)* 79−39159
Sb trihalides, non-empirical valence electron MO calcs., ion states spin-orbit splitting 77−34544
SbI_3, valence band, UPS meas. with synchrotron radiation 79−56914
Sb_2O_3, density of valence states, photoemission meas. 77−72808
Sb_2O_3, electronic struct., X-ray emission, XPS, UPS obs., CNDO cluster calc. 78−52638
Sb_2S_3, amorphous, density of valence states, XPS and UPS obs. 77−48308
Sb_2S_3, electronic struct., X-ray emission, XPS, UPS obs. 78−52638
ScAg(Pd)(Ir)(Ru), UPS exam. 78−48276
ScH_2, electronic struct., photoelectron spectra study 80−50527
Se, amorphous film, highly disordered, UPS study 80−76148
Se overlayers on Ni(100), normal photoelectron diffr. of Se 3d level 79−11501
$SeBr_2$, He I photoelectron spectra, ionis. pots. calcs. 79−50080
$SeBr_2$, photoelectron spectra, visual assessment stripping program anal. 80−28062
$SeCl_2$, He I photoelectron spectra, ionis. pots. calcs. 79−50080
$SeCl_2$, photoelectron spectra 80−69186
Se_2Cl_2, photoelectron spectra 80−69186
SeF_2, He I photoelectron spectra, ionis. pots. calcs. 79−50080
SeO_2, HeI and II photoelectron spectrum, valence electronic struct. 77−61798
Si, (001) and (111), geometrical and electronic struct., review 80−80039
Si (100), chemisorption of H, pairing model calcs., compared with expt. 78−34719
Si (100), dimer reconstruction, photoemission obs. 80−80939
Si (100), intrinsic surface states, photoemission study 80−50514
Si (110), adsorption of H, kinetics of H generation and adsorption, UPS 77−55450
Si (110) surface, chemisorption of H, UPS spectra meas. 77−20186
Si, (111), 7×7 and 1×1, chemisorption of Cl_2, UPS obs. 78−34704
Si (111), chemisorption of Cl, chemisorpt.-site geometry from polarised photoemission 77−15684
Si (111), Cl_2 chemisorption, ang. resolved UPS and LEED meas. using Vidicon intensity processor 78−71972
Si, (111), struct. depend. oxidation, high resolution photoemission yield spectroscopy 77−1305

photoelectron spectra continued
Si (111), surface reproducibility and impurity segregation ion neutralisation spectra and UPS obs. 78−34688
Si (111), surface states and surface struct., angle-resolved PES 79−28390
Si (111) 1×1, chemisorption of Cl in surface vacancies 79−77910
Si (111) 7×7 surface, chemisorption of H_2O, AES, EELS and UPS 80−10792
Si (111) 7×7 surface, Schottky barrier formation, photoemission, exam. of filled surface states and band bending 77−28250
Si (111) 7×7 surface electronic struct., angle-resolved UPS study 80−50513
Si (111) face, surface states and photoemission 77−72900
Si, (111) surface, ang.-resolved photoemission, matrix element effects 79−69957
Si (111) surface, oxidised, energy depend. of photoelectron attenuation length 78−52643
Si (111) surfaces, cleaved, electronic structure following Al adsorption 80−75610
Si (111)-Au interface, chemically driven intermixing, UPS study 80−50533
Si (111)7×7 surface electronic struct., angle-resolved UPS study 80−40226
Si, amorphous, hydrogenated bonding 78−19636
Si, amorphous, position of Fermi level, spectroscopic and transport determ. 80−6706
Si, amorphous and crystalline, ion implanted, UPS meas. 80−97411
Si, amorphous film, Fermi energy shift with substitutional doping 79−46998
Si, bonding states of adsorbed O_2, photoemission obs. 78−92170
Si, chemisorption of Cl_2, photoemission polarisation effects with synchrotron radiation 78−14580
Si, chemisorptive bonding of CO(Cl), photoemission investig. using synchrotron radiation 78−73079
Si, hydrogenated amorphous, gap states, comparison of photoemission and photocond. results 80−103724
Si in 3d transition metal silicides, yield spectrum, complete energy diagrams 77−28680
Si, O_2 adsorption, UPS, new adsorption state 78−34702
Si, oxidation, AES photoelectron spectra exam. of early stages 79−74272
Si p-n junctions, electron emission from depletion layers 80−100509
Si, photoemission spectroscopy of surface states and oxidation 77−55863
Si, photoemission study of energy depend. of bulk plasmon loss intensity 79−47035
Si phthalocyanine, monomer and dimer, UV photoelectron spectra, valence level splitting 77−38695
Si, plasmon sideband exam. by synchrotron radiation tuning of electron escape depths, UPS 77−47755
Si, pure and heavily doped, 2p core levels and core exction binding energy, photoemission obs. 78−76583
Si, ratio of photoionisation cross-section of valence s- and p-electrons *(Ukrainian)* 77−73211
Si surface, UPS before and after N_2^+ bombardment, 500 eV, chem. reactions 78−48265
Si, valence electrons, energy-depend. photoionisation probability calc. 77−16462
Si:B, detection of atomic plane displacement in near-surface layers, ang. depend. of photoemission during X-ray Bragg diffr. 78−47207
Si:H, amorphous, doped, Fermi level position, photoelectron spectra 79−47592
Si:H, amorphous, electronic struct. calc., rel. to UPS data 80−39527
Si:H, amorphous, surface activated, photoemission spectra, minority carrier diffusion length 80−40235
Si-SiO_2 interface, Auger sputter profiling and photoelectron spectroscopy obs. 78−10287
Si-SiO_2 interface, barrier height in MOS tunnelling structures 80−88644
$SiCl_4$, He(II) photoelectron spectra, spectral intensity patterns 79−98152
SiF_4, photoelectron spectra, bonding, MS Xα calcs. 79−18116
SiF_4, valence electron spectrum, vibr. struct. 77−75209
Si_xGe_{1-x} multitip photofield emission cathode, fabricated by crystn. from vapour, emission characts. 78−2975
$Si_{0.5}Ge_{0.5}O_2$, band struct., photoemission spectra calc. and meas. 77−35865
$Si_xGe_{1-x}O_2$, $0 \leq x \leq 1$, XPS and UPS, electronic struct. 77−48318
SiH_4, photoelectron spectra, bonding, MS Xα calcs. 79−18116
SiH_x amorphous films, internal photoemission, metal contacts 80−96964
Si_2H_6, bond lengths, photoelectron spectrum, mol. orbitals calcs. 78−5132
$SiH_{4-n}F_n$ (n=1 to 3), photoelectron spectra, bonding, MS Xα calcs. 79−18116
SiO, condensed amorphous, valence states, photoelectron spectra meas. 77−36353
SiO film and powder, effect of heat treatment on chemical and electronic struct., electron spectroscopy 77−48320
SiO surface, UPS before and after N_2^+ bombardment, 500 eV, chem. reactions 78−48265
SiO_2 vibr. struct. calcs. from photoelectron spectra 77−18973
SiO^+, vac. UV photoelectron spectra, ab initio mol. orbital and Xα calcs., ($X^1\Sigma^+$) state 78−46395
SiO_2, amorphous and α-cristobalite cryst., band struct., photoelectron and X-ray spectra interpret. 80−24787
SiO_2, electronic struct., photoemission spectra calc. 77−35865
SiO_2, electronic struct., review of spectroscopic and theoretical data 77−76749
SiO_2, optical absorpt. and external photoeffect, 6 to 40 eV 77−55802
SiO_2, photoemission and X-ray emission spectra calc. 77−89866
SiO_2 surface, UPS before and after N_2^+ bombardment, 500 eV, chem. reactions 78−48265
SiO_2, vitreous, photoelectric and photoluminescent props. in fundamental absorpt. region 78−39596
SiO_x semi-insulating polycryst. films, AES and PES studies 80−107939
SiX_4 (X=Cl,H,F), chemical shifts, relax., X-ray spectra, SCF Xalpha calcs. 80−27928
Si(111), high resolution photoemission yield, surface states 77−69392
Si(111), partial monolayers of H, UV photoemission, disordering effect 77−1308
Si(111), surface electronic struct., atomic geometry effects 77−85283
Si(111) surfaces, H atoms chemisorption, monohydride and trihydride phases formation 79−15004

photoelectron spectra continued
Si(111)-(7×7), and impurity stabilised Si(111)-(1×1) surface, photoemission studies 80−104041
Sm, divalent surface states, photoemission meas. 78−47841
Sm, UV photoelectron spectra, config. interaction effects 77−50413
SmS (100), resonant photoemission 79−28895
$SmS_{1-x}P_x$, valence changes, XPS and UPS study 80−97402
Sn inorganic and organometallic cpds., photoelectron spectra, valence bands, ligand field broadening 77−63525
Sn, K-shell photoelectric cross section 79−22676
Sn, photoelectric cross section, derived from total absorpt. cross sections 77−10646
Sn, photoelectric cross sections for 323 keV gamma rays 77−88432
Sn, photoelectric cross sections of low energy photons 78−46309
Sn, photoelectric cross sections, from total absorption cross sections, 5 to 130 keV 79−26947
Sn, photoelectric interaction around the K edge 78−5183
Sn tetrahalides, non-empirical valence electron MO calcs., ion states spin-orbit splitting 77−34544
Sn, UPS, electron distrib. curve 78−15282
$SnBr_2$, UPS, 40.81 eV, valence band struct. 79−33891
$SnCl_2$, $SnBr_2$, UV photoelectron spectra of valence d shells, gas-phase 78−62845
$SnCl_2$, UPS, 40.81 eV, valence band struct. 79−33891
$SnCl_2$, valence band electronic struct., XPS and UPS obs. 78−6826
$SnCl_4$, He(II) photoelectron spectra, spectral intensity patterns 79−98152
SnF_2, valence bands, electronic struct., UPS 78−39656
SnS, electron-hole interaction in d-electron excitations, photoelectron and optical spectra 78−34776
SnS photoelectron spectra, rel. to ionicities and phase transitions 77−69960
SnS, valence level photoelectron spectra 77−27114
SnS_2, conduction and valence band density of states 77−62817
SnS_2, octahedrally coordinated, layer cpd., electronic struct. using synchrotron-radiation photoemission spectroscopy 79−74058
$Sn(S_xSe_{1-x})_2$, valence band states, composition depend., photoemission spectra study 80−100434
SnSe, electron states, UPS data anal. 77−66115
SnSe, photoelectron spectra, rel. to ionicities and phase transitions 77−69960
$SnSe_2$, band struct., angle resolved photoelectron spectra meas. 78−72680
$SnSe_2$ intercalated with cyclopropylamine, electronic struct. 78−84698
$SnSe_2$, single crystal, reflectivity, XPS, UPS, and band struct. 78−6701
SnTe, valence level photoelectron spectra 77−27114
Sr film, photoemission, action of elec. field 77−48317
SrF_2, UPS and XPS spectra, rel. to optical props. 80−66386
$SrTiO_3$, (100), LEED and UPS studies 80−100747
$SrTiO_3$ (100) surface, struct. and electronic props., AES, LEED, EELS, and UPS study 80−24986
$SrTiO_3$ (111), O_2, H_2 and H_2O chemisorption, UPS and XPS studies, illum. effects 80−71572
$SrTiO_3$ (111), surface struct., electronic props., LEED, AES, UPS study, photoelectrochem. cell anode appl. 78−84035
$SrTiO_3$, chemisorbed phases of water, UPS meas. 78−10285
$SrTiO_3$ photoelectrolytic electrodes, defect surface states obs. 78−14815
$SrTiO_3$, surface defects, electronic struct., LEED, AES, UPS study 78−84273
$SrTiO_3$, valence band UPS and partial p and d density of states 80−71560
T 79−45757
Ta film, photoemiss. from conduction band and core levels 77−16464
Ta, photoelectric cross sections, derived from total absorpt. cross sections 77−10646
Ta, photoelectric cross sections for 323 keV gamma rays 77−88432
Ta, photoelectric cross sections of low energy photons 78−46309
Ta, photoelectric cross sections, from total absorption cross sections, 5 to 130 keV 79−26947
Ta two-photon photoemisson induced by picosecond laser pulses 77−77347
TaS_2 (1T), angular resolved photoemission at low energy and high atomic number 77−36373
Te (10$\bar{1}$0) and (0001), direction effects in double beam photoemission 79−74059
Te, band struct., laser-modulated photoemission expts. 77−28686
Te double-beam photoemission, electronic structure 77−66576
Te, film, electronic struct. charge on ordering, double beam photoemission 78−19634
Te overlayer, c(2×2), on Ni surface, 4d levels, angle resolved photoemission cross section, atomic and solid-state effects 80−29853
$TeCl_2$, transient species, He(I) photoelectron spectrosc. calcs., relativistic corrections 80−95677
Th, photoelectric cross sections of low energy photons 78−46309
Th, photoelectron spectra study, core and valence levels 80−66394
$ThF_4(Cl_4)$, electronic struct., MS-SCF-Xα calcs. and VUV photoelectron spectra 80−63710
ThH_2, electronic struct., photoelectron spectra meas. 77−85143
Th_4H_{15}, electronic struct., photoelectron spectra meas. 77−85143
ThN, photoelectron spectra study, core and valence levels 80−66394
Ti (0001), with adsorbed N (1×1) layer, underlayer geometry, electronic struct. calcs. and UPS meas. 80−54751
Ti (10$\bar{1}$1), of CO, XPS, UPS, flash desorption mass spectra, and active ion bombard. obs. 79−11822
Ti (10$\bar{1}$1) surface, HCP→BCC transition He II UPS study 79−42345
Ti, oxidation, ESCA *(French)* 77−36361
Ti, oxidation, ESCA and UPS meas., core levels 77−63542
Ti, polycryst., adsorpt. of O at room temp. 77−89645
Ti-Cu dissolution mechanisms, photoelectron spectra study *(French)* 80−45198
TiC (001) surface, change in work function with chemisorption of O_2 and H_2O 80−29461
TiC, electronic structure, PES study 80−70594
TiC, valence band electron distrib. 77−44120
$TiCl_4$, intensity changes between He(I) and He(III) photoelectron spectra 78−21969
$TiCl_4$, optical and Ti 2p core photoemission spectra, SCF Xα anal. 79−94032
$TiCl_4$, photoelectron and UV spectra, SINDO theory 77−50360
TiO_2 (100), chemisorption of H_2, O_2, and H_2O, electron spectroscopy, evidence for Ti^{3+} photogeneration 78−38940

photoelectron spectra continued
TiO_2, (110) and (100) surfaces, LEED and electron spectra 77−72757
TiO_2 (rutile), (001) and (110) faces, UPS and LEED obs. 80−45206
TiO_2, chemisorbed phases of water, UPS meas. 78−10285
TiO_2, sputtering defects, associated surface electron states, UPS, XPS and AES obs. 80−60755
TiO_2, UV photon induced secondary electron emission 79−52079
TiO_2, UV photon induced secondary electron emission 79−78835
TiO_2:V, localisation and migration of V^+ ions, ESR and ESCA study *(French)* 79−33529
TiO_2-Ni (100) interface, electronic props., struct., comp., chemical bonding 80−84499
TiO_x, UPS meas. of band struct., energy gap 78−72698
Ti_2O_3, semiconductor-metal transitions, photoelectron spectra meas. 78−84144
Ti_3O_5, semiconductor-metal transitions, photoelectron spectra meas. 78−84144
TiS_2, band struct., angle-resolved photoemission studies 80−70610
$TiSe_2$, band struct., angle-resolved photoemission studies 80−70610
$TiSe_2$, UPS, excitonic instability indicated from study of band struct. 78−56069
$TiSe_2(S_2)$ (1T), electronic and vibronic struct. 80−44500
TiX_4, (X=Cl,Br,I), He I and He II photoelectron spectra, ionis. energy, chem. bonding 78−46394
Tl, 5d level open shell interactions, 304 Å photoelectron spectrum 80−87087
Tl, core level binding energies, UPS obs. 80−66388
Tl, liquid and solid, UPS, optical densities of states 80−2924
Tl, polycryst. film, UV incident 78−2986
Tl, transition from ordered solid to disordered liquid, viewed by photoemission 80−45217
Tl, VUV photoelectron spectra, pseudo-atomic beam technique 80−58225
$TlBO_2$, $TlNO_2$, Tl_2SO_4, $TlReO_4$, gaseous species, mol. orbital assignment of photoelectron peaks 77−18974
TlBr, He II photoelectron spectra 78−94285
TlCl, He II photoelectron spectra 78−94285
TlCl, TlBr, TlI, UV photoelectron spectra of valence d shells, gas-phase 78−62845
TlCl, UPS, valence band struct., dynamic hybridisation 77−20999
TlCl, valence band electronic struct., XPS and UPS obs. 78−6826
TlI, He II photoelectron spectra 78−94285
TlI, XPS and UPS study of phase transforms. 80−45210
TmSe, electron energy loss spectroscopy and UV photoemission meas. 78−31305
U, He (I) PES 78−37609
U, photoelectric interaction around the K edge 78−5183
U, photoelectron spectra study, core and valence levels 80−66394
$UAl_2(Co_2)$, surface comp. and electronic struct., photoemission study 80−66382
UC, electronic struct., comparison with photoemission spectra 80−91450
UCl_6, electronic struct., photoelectron spectra and SW Xα calcs. 79−72355
UF_6, valence electron spectra, vibr. band struct. 77−23520
$UF_4(Cl_4)$, electronic struct., MS-SCF-Xα calcs. and VUV photoelectron spectra 80−63710
UN, band struct. and density and states, PES meas. 79−42454
UN, electronic struct., comparison with photoemission spectra 80−91450
UN, photoelectron spectra study, core and valence levels 80−66394
UO_2, photoelectron spectra study, core and valence levels 80−66394
UO_2, valence electronic configuration determ. by photoelectron spectroscopy 78−15284
US, band struct. and density and states, PES meas. 79−42454
US(Se)(Te), photoelectron energy distrib. and spin polarisation, electronic and mag. props. 80−16146
US(Se)(Te), spin polarisation and magnetism, photoelectron study 80−40219
USb, UPS and XPS, surface oxidation 80−7465
UTe, electronic and spin struct. negative spin polarisation of photoelectrons 79−19514
UTe, ferromag., negative electron spin polarisation in photoemission 79−19967
UTe, photoemission energy distrib. curve and electron spin polarisation 79−52074
UTe_xSb_{1-x}, photoemission energy distrib. curve and density of states 79−52074
UTe_xSb_{1-x}, photoemission, densities of states 80−16147
V, photoelectric cross sections of low energy photons 78−46309
VCl_4, photoelectron and UV spectra, SINDO theory 77−50360
VO_2, semiconductor-metal transitions, photoelectron spectra meas. 78−84144
V_2O_3, semiconductor-metal transitions, photoelectron spectra meas. 78−84144
VRu, soft X-ray emission, photoelectron spectra and electron structure 79−37978
VSe_2, angle-resolved UPS, Fermi surface determ. 80−55257
VSe_2, k-dependent photohole scatt. in photoemission 79−56912
VU_4, intensity changes between He(I) and He(III) photoelectron spectra 78−21969
W (001), clean and H_2 chemisorbed, angle resolved photoemission, symmetry-related polarisation effects 78−56566
W (001) surface, angle-resolved photoemission spectroscopy, polarisation expt. anal. 77−40332
W (001) surface with adsorbed Cs, core-level photoemission anisotropy 78−11076
W (100), coadsorption of H and CO, photoemission and thermal desorpt. investig. 77−28079
W, (100), with ordered C overlayer, adsorption of O_2 and CO, UPS meas. 79−77907
W (100) face, surface reson. 78−72226
W (100) surface, chemisorption of CO_2, NO, UPS studies 79−23841
W (110), adsorpt. of N_2, N_2O, and NO_2/N_2O_4, 300K and 100K, XPS, UPS, and XAES 79−28203
W (110), adsorpt. of NO, 300K and 100K, XPS, UPS and XAES 79−28204
W {110}, chemisorption of β-N_2, underlayer mechanism 80−39432
W, angled resolved UPS exam. 77−55865
W, chemisorption of H, angled resolved UPS exam. 77−55865
W, chemisorption of H_2, HFS model cluster calcs., compared with UPS data 77−51795

photoelectron spectra continued
W, chemisorption of halogens, UV photoelectron spectrosc. study 80−7854
W, photo field emission spectra of optical transitions, band struct. 77−16467
W, polarisation-dependent angle-resolved photoemission for band structure studies 78−95678
W, secondary emission and photoemission props., effect of one-electron density of states 80−16152
W, surface state transferability, UPS meas. for (011) states 80−39650
W, two-photon photoemission induced by picosecond laser pulses 77−77347
W, UPS, angle-resolved, surface resonances on (100) face 78−2987
WCl_5, intensity changes between He(I) and He(III) photoelectron spectra 78−21969
WF_6, valence electron spectra, vibr. band struct. 77−23520
WO_3, electron spectroscopic exam. of reduction 77−4714
W(100) surface, angle-resolved photoemission from surface states, refraction effects 78−48279
W(110), adsorbed CO, adsorbate characterisation by UPS, XPS and X-ray AES 77−15683
W(111), surface densities of states for normal photoemission 78−35251
Xe, 4d ionis, photoelectron spectrum, post-collision interaction 77−30837
Xe, 5p shell photoelectron branching ratio, energy depend. 77−88435
Xe, 5p subshell photoelectron branching ratio, Dirac-Fock calcs. 78−42021
Xe, 5s, 5p ESCA spectrum, photoionisation many electron description 78−50516
Xe 5s, photoelectron ang. distrib., relativistic Dirac-Fock calc. 79−59411
Xe, 5s photoelectron ang. distrib. 78−33482
Xe, 5s photoelectron satellite spectrum 79−13690
Xe, 5s→εp photoelectrons, ang. distrib. and spin polarisation 78−58634
Xe, absolute photoionis. cross sections of spin-orbit components of 4d electron 77−38646
Xe, adsorbed on Ni (100) or Fe (110), UPS obs. 79−33897
Xe, adsorbed on Pd (110), anomalous 5p photoemission 80−7471
Xe adsorbed on W, $P_{3/2}$ level splitting mechanism 77−31880
Xe crystal, photoelectron spectroscopy, hole-electron valence bound state 77−36369
Xe film, electron MFP, vacuum UV photoemission data 77−28690
Xe, K-shell fluoresc. yield determ. by proportional counter method 77−27023
Xe, many-electron interactions from 4s and 4p core levels 77−18861
Xe, N-shell Coster-Kronig transitions 79−13691
Xe, ns→εp photoelectrons, spin polarisation 80−37792
Xe, photoelectron spectra, intershell correl. effects 77−18863
Xe photoelectron spectrum ang. distrib. abnormality in strong mag. field 78−50666
Xe, photoelectron studies of 5p branching ratio 80−37793
Xe, photoelectron-Auger electron post collision interaction, Auger peak shift obs. 77−27039
Xe photoionisation, spin-polarised photoelectrons angular distrib. 80−106306
Xe, physisorbed layer, UPS spectra, lateral interaction 78−92174
Xe, physisorbed on Pd (100), angular-resolved photoemission 79−43102
Xe, plane polarised VUV irrad., emitted photoelectron polarisation, ang. depend. 80−47952
Xe, polarised photoelectron ejection by unpolarised light 79−72289
Xe, resonantly enhanced multiphoton ionis., photoelectron energy anal. 80−63597
Xe, satellite lines in 5s-5p photoelectron spectrum 78−25493
Xe, single crystal, photoemission exam. 79−78845
Xe, six-photon ionis., electron energy spectra 79−54824
Xe subshell photoionisation, multichannel k-matrix calc., spin orbit interactions 80−63600
Xe^+, UPS by threshold photoelectron spectrosc. by electron attachment method 79−89708
Xe_2, photoelectron spectra, $X^1\Sigma^+_{(1/2)g}$ ground state pot. 78−5280
Xe_2, van der Waals mol., photoelectron spectra 78−66599
Y, K-shell photoelectric cross section 79−22676
YH_2, electronic struct., photoelectron spectra study 80−50527
YIG, epitaxial layer, n and p-type, UPS, elec. struct. 77−4710
Yb III compounds, 4f photoelectron spectral intensity, relativistic calc. 79−54816
Yb, UV photoelectron spectra, config. interaction effects 77−50413
Yb, valence-charge-induced Fano reson. 80−55267
Yb-Al, valence changes during autoionisation and Auger electron emission 80−50475
YbF_3, MS Xα electronic struct. calc., inner shell photoelectron spectra 77−10594
Zn, 3p-3d² super Coster-Kronig and 3p-3d4s Coster Kronig transitions 78−50522
Zn (0001), adsorption of Te, UPS investigation 79−91563
Zn (0001) surface, interaction with water, UPS meas. 78−76585
Zn, atomic UV photoelectron spectra, wavelength depend. of satellite struct. 77−34597
Zn, ground state correl., photoelectron spectra, multiconfig. Hartree-Fock calcs. 77−50471
Zn halides and chalcogenides, extra-atomic photoemission relax. energies, ionicity depend. *(French)* 77−36357
Zn, interaction with O_2, evolution of O-derived struct., UPS study 79−100296
Zn, resonant two hole bound state at 3p core threshold 80−60750
Zn/Cu film system, UPS during atomic diffusion 79−43097
Zn-Cu system, sputtering during atomic diffusion, UPS meas. 78−92159
Zn-tetraphenylporphine/metal electrode, photocurrent generation mechanism 78−76868
$ZnAs_2$, λ-modulated photoemission spectra 79−87565
$ZnCl_2$, UPS, cryst. field splitting 79−83103
ZnF_2, electronic structure of outermost levels, UPS study 80−7468
ZnF_2, UPS, cryst. field splitting 79−83103
$ZnGeAs_2$, photoelectron spin polarisations, electron level struct. 79−87557
$ZnIn_2S_4$, cond. and valence band states, photoemission study 80−35054
$ZnIn_2S_4$, valence band photoemission spectroscopy 78−56569
ZnO (0001), (000$\bar{1}$) and (10$\bar{1}$0), UPS rel. to elec. struct. 78−15288
ZnO, chemisorpt. of pyridine, acetone, dimethyl sulphoxide, UPS, mol. orbitals effect on bonding 78−72699
ZnO, electronic surface and bulk transitions exam. by electron energy loss spectra 78−30964
ZnO, powder, adsorption of methanol, electron spectrosc. obs. 79−52076
ZnO-Cs, fabrication, UPS meas. 78−15279
ZnS bulk and surface states anal. using synchrotron radiation 77−66574
ZnSe, bulk and surface states anal. using synchrotron radiation 77−66574
ZnSe, undoped and doped, pair spectra, edge emission and shallow acceptors 77−28617
$ZnSiAs_2$, photoelectron spin polarisations, electron level struct. 79−87557
ZnTe (110) surface struct. determ. by LEED, UPS, and EPR 80−49475
ZnTe, bulk and surface states anal. using synchrotron radiation 77−66574
ZnTe clean and adsorbed O_2 (110) surfaces, UV photoemission spectra *(Japanese)* 80−93456
Zr, K-shell photoelectric cross section 79−22676
Zr, photoelectric cross section, derived from total absorpt. cross sections 77−10646
Zr, photoelectric cross sections for 323 keV gamma rays 77−88432
Zr, photoelectric cross sections, from total absorption cross sections, 5 to 130 keV 79−26947
Zr, UPS constant final state energy spectra, direct emission and Auger decay from multiplet final states 77−44131
ZrX_4, (X=Cl,Br,I), He I and He II photoelectron spectra, ionis. energy, chem. bonding 78−46394

photoelectron spectroscopy
30-800 eV, using synchrotron radiation 79−31608
adhesion measurement, locus of failure, bond failure in adhesive joints 80−50801
adsorbate on single crystal, anal. of electronic state by angle-resolved photoelectron spectroscopy 80−11541
adsorbed atoms, relax. shifts, satellites and sum rules 80−11539
aerosol sampling, chemical heterogeneity revealed by X-ray photoelectron spectroscopy 80−55970
angle resolved photoelectron spectrometer for atoms and molecules using synchrotron radiation 80−90932
angle-resolved photoelectron spectroscopy, miniature plant mirror analyser 77−63539
angle-resolved photoemission, expt., Adelaide Univ., 1908 79−30187
angle-resolved spectroscopy with cylindrical mirror analyzer, use of position-sensitive detector system 80−57426
atom, UV photoelectron spectra at high temp., interpretation 78−17718
charged particle oscillator He II photon source 79−58845
1-chloropropyne cation, internal energy decay studied by photoelectron-photoion coincidence spectroscopy 80−69185
controllable photomultiplier for optical spectra meas. 79−89009
cylindrical mirror analyser, design and use with synchrotron radiation, autoionisation obs. 80−18049
ellipsoidal mirror display analyzer system for electron energy and angular measurements 80−90908
energy analysis of trapped ions, strong mag. field, elastic scatt. effects 78−62950
energy band dispersions, absolute determ. using ang.-resolved photoelectron spectrosc., symmetry method 79−15590
ESCA appl. to thin film production, surface analysis *(Hungarian)* 80−54537
ESCA spectrometer, sample probe microcomputer automation 79−58846
ferrocytochrome c_3, anhydrous, ionisation pot., UV photoelectron spectrosc. obs. 80−85328
film, thickness distrib. determ. by XPS 77−39743
fixed energy photoelectron spectroscopy, technique 80−62797
gas-phase time-of-flight photoelectron spectrometer using synchrotron radiation 80−4818
halides, UV photoelectron spectra at high temp., interpretation 78−17718
heated vacuum monochromator for 40-280 nm spectroscopy 80−33176
high resolution, iterative deconvolution algorithm 79−97472
high temp. vapours 80−52238
high temperature, charact. of vapours oven heated inorganic solids 80−52239
industrial research 79−39232
inorganic compounds, XPS chem. anal., chem. shift, core binding energy 78−20134
inorganic molecules, UV photoelectron spectroscopy, spectral assignment criteria, bonding 78−17717
ion fragmentation mechanisms and photoelectron spectroscopy, book contrib. 80−14179
lunar soil grains, surface comp. from Auger and X-ray photoelectron (ESCA) spectroscopy 78−32366
magnetic order and spin depend. of electron scatt. meas technique using photoemission 80−60748
metal catalysts, structural exam. of monometallic and bimetallic systems 79−95264
metallurgical applications of XPS, AES, and SIMS *(French)* 80−81253
molecular beams supersonic, appl. to ethylene and O_2 79−68264
molecules and atoms, UPS by threshold photoelectron spectrosc. by electron attachment method 79−89708
organic compounds, photoelectron spectroscopy, ionis. pots., MO models 78−17716
phase-sensitive vidicon detector for angle-resolved electron spectroscopy 80−90933
photoelectron counting statistics, theory, fully quantum, review 80−52312
photoelectron spectroscopy, biological appls., review 77−56558
photoelectron spectroscopy, nomenclature and spectral presentation IUPAC recommendations 77−68075
photoelectron-photoion coincidence spectrometer, with double field TOF mass anal. 79−54998
photoelectron-photoion coincidence spectroscopy, fixed-wavelength, improved resolution 79−18318
photoemission spectroscopy, book contrib. 77−63546
photoion-photoelectron spectroscopy, ion internal energy and reaction 79−30616
photoionisation, absolute cross-sections, expt. meas. techniques 80−63598
photoionisation branching ratios, photoelectron spectrometric meas. technique 79−31607
physical problems *(Chinese)* 79−80730
rotating triple-reflection polariser 78−94443
semiconductor, electron spectroscopy techniques, review *(Japanese)* 80−49061

photoelectron spectroscopy continued
semiconductor surface, instrument for angle-resolved UV photoemission spectroscopy *(Japanese)* 80−93455
semiconductor-metal contact investigation by photoelectron spectroscopy 80−100517
soft X-ray spectra, meas. by photoelectron anal. 80−73557
solid state spectroscopy using synchrotron radiation, book contrib. 80−7375
solids, review 80−55263
spectrometer, calibration using binding energy scale 80−90930
strong mag. field, trapped ions, with ion cyclotron reson. 78−50666
surface analysis, in space exploration, analytical appls. of Auger and XPS 78−35756
surface analysis techniques and appls., symposium, Dayton, USA (Jun. 1979) 80−62363
surface and thin film, chemical analysis, comparative survey of methods, book contrib. 79−66393
surface atomic and electronic struct. studied with synchrotron radiation 80−80945
surface structure, by angle-resolved UPS 79−91567
surface studies, gas press. up to 1 Torr, photoelectron spectrometer 80−4822
surface study of clean and adsorbate covered surfaces *(French)* 80−50519
synchrotron radiation, application to EXAFS and angle resolved photoemission spectros. *(Korean)* 80−74453
synchrotron radiation appls., book contrib. 80−14035
theory, techniques, and appl., book 80−8748
threshold photoelectron spectroscopy by electron attachment, high-resoln. 77−27202
transient species, vacuum UPS, book contrib. 80−14178
transient species generation methods 79−31739
UPS, high resolution, fast pumping for study of transients and unstable species 77−83764
UV angle-resolved photoemission spectroscopy, using high intensity discharge lamp 79−12870
UV photoelectron chemical anal., appl. to conjugated carbonyl cpds. *(French)* 78−90215
UV photoelectron spectrometer, gas and vap. phase operation 78−82865
UV photoelectron spectroscopy, basic concepts, spectra 78−17715
UV-valence electron spectroscopy, multichannel detector system 77−23520
vacuum UV, for study of chemisorption on metal surfaces *(Japanese)* 78−62264
vacuum UV line source, He lamp, for photoelectron spectroscopy 78−94419
valence electron, using polarized He I radiation 77−492
VUV He reson. line radiation source, for UHV photoelectron spectroscopy 78−89602
X-ray photoelectron, charge corrections, comparison of use of different spectrometers 77−20989
X-ray photoelectron microanalysis and microscopy applics. *(French)* 77−36835
X-ray photoelectron spectroscopy, factors affecting quantitative determ. 78−7249
X-ray photoelectron spectroscopy, hydrocarbon contamination reduction 77−44542
XPS, prediction model for ang. distrib. intensity and lineshape 77−41734
XPS azimuthal angular-depend. studies, using electron spectrometer 80−57428
XPS binding energy determ. without retarding pot., relativistic mass increase 78−41377
XPS charge effects on insulator sample current *(French)* 78−41376
XPS technique for studying quick frozen solutions *(German)* 77−44119
Ag, adsorption of pyridine, UPS, AES and flash desorption meas. 80−92776
An alloys, bonding investig. 80−55263
$CO_2(CS_2)(COS)$, Penning ionisation and photoelectron spectra 77−83653
H_2S, Penning ionisation and photoelectron spectra 77−83653
He II resonance discharge lamp, for UV photoelectron spectroscopy 79−58847
He II resonance lamp for UV photoelectron spectroscopy 79−93232
Mg, Kα radiation, X-ray photoelectron spectroscopy resolution 80−18888
$N_2O(NO_2)$, Penning ionisation and photoelectron spectra 77−83653
Ni, one-electron energy investig. 80−55263
SO_2, Penning ionisation and photoelectron spectra 77−83653
ZrS_3, paired-anion ligand effects in valence band, photoemission spectrosc. obs. 80−87173
$ZrSe_3$, paired-anion ligand effects in valence band, photoemission spectrosc. obs. 80−87173

photoemission
see also photoelectron spectra; photoemissive devices
actinide compounds, spectroscopic techniques for electronic props. meas. 80−11427
adsorbate induced electronic states, rel. to photoemission, book contrib. 78−95326
adsorbate induced photoemission, book contrib. 78−95668
adsorbates, angle-resolved photoemission, book contrib. 78−95669
adsorbed molecules, ang.-resolved photoemission, independent atomic centre approx. 78−84701
adsorption effects, theory 78−2996
AES, internal photoemission peaks 78−52621
alkali halide, photo- and thermostimulated electron emission under ultrahigh vac. conditions *(Russian)* 80−66383
alkali halides, heterogeneous adsorption, photoelec. work function changes 77−69175
alkali halides, photoemission, energies and lineshapes 80−89119
alkali metal atom, heavy, polarised, circ. dichroism of ang. distrib. of photoelectrons 80−37789
alkali metal atom, spin polarisation of photoelectrons, one-quantum photoeffect 80−37790
alkali metal multilayers, high field enhancement of photoemission 78−19639
amorphous film, anomalous scatt. of photoinjected electrons *(Russian)* 78−52642
angle-integrated, experimental geometry for studying polarisation effects 79−67395

photoemission continued
angle-resolved photoemission, expt., Adelaide Univ., 1908 79−30187
angle-resolved photoemission, review 80−45214
angle-resolved photoemission from bulk bands of solids 79−4895
angular distribution, cosine law theory 78−35233
aniline, photoemission for mol., polarised photoelectrons 78−66607
annealing twins density, photoemission microscopy 80−35208
anthracene crystal, sensitised injection from surface oxidation products 78−76143
atom, unpolarised, spin polarisation of ejected electrons 78−78765
Auger emission, photon-induced, deep-hole interferences 79−43098
bone-tissue interface, dose distrib. due to anisotropic electron emission 80−36144
book, photoelectron statistics 78−25842
cathode spot shape and kinetics, cathode photoeffect from discharge UV irradiation 80−38836
cell, surface photoelectron micrographs and quantum yields 78−61148
chain method appl. to electron emission 78−43983
cholesteryl caprinate, liq. cryst. mesophase electron emission 79−55664
clean surfaces, electron states, photoemission data anal., book contrib. 78−95325
coronene, electron escape depths and absorpt. coeffs. 78−23580
diamond, natural semicond. motor photocond. and internal photoemission 79−69546
dielectric surface, conductor-like behaviour 79−101046
dielectric-metal bounds, derivations of Fresnel eqns., use in theory of angle-resolved photoemission 78−39659
dimethylanilines, photoemission for mol., polarised photoelectrons 78−66607
Einstein theory of stimulated emission of radiation *(Hungarian)* 79−89880
electron energy, distrib. calc. 80−40237
electron microscopes, photoemissive, electrostatic retarding-field energy analyzer 79−12890
electron microscopy, principles and appls. 80−89424
electron microscopy in high vacuum region, influence of residual atm. and other parameters on image brightness and contrast 78−55791
electron source for measurement of channel electron multiplier efficiency 79−100016
electron-black body radiation strong coupling at high temps. 78−52624
escape depths of X-ray induced photoelectrons and relative photoionisation cross section for 3p subshell 77−73212
ferromagnet, itinerant electron, temp. depend. of angle-resolved photoemission 80−76142
ferromagnet, polarised photoelectron emission, review 77−32505
ferromagnet, spin polarisation of emitted photoelectrons 80−45215
field emission, photo-induced, total energy distrib. meas. 79−74068
final states in photoemission and field emission 78−15299
fixed-orientation atomic orbitals, rel. to plane-wave final state approx., angle-resolved photoemission 79−28891
flavins, photoemission of electrons in polar media 79−29507
fluorescence anisotropy decay determ. by single photoelectron counting 78−84635
fractional spin polarisation in model of photoemission from localised shells 78−92172
p-GaAs, photoemission into electrolyte soln., energy diagrams, Volta pots., voltage drop 77−62990
hardness, elec. cond., photo emission, and mag. props. *(Norwegian)* 79−32909
heavy elements, photoemission characts. *(Dutch)* 79−1811
inert gas solids, benzene doped, energy transfer processes, excitons, photoemission, luminescence spectra 77−69886
3-iodoaniline, photoemission for mol., polarised photoelectrons 78−66607
ionic crystals, exposed to ultrasoft X-rays, thermal luminesc. and electron emission 79−8192
ionic crystals, photostimulated electron emission after photoexcitation, diffusion approach 78−52641
ionosphere, general photoelectron current, meas. technique 80−12636
K-shell photoelectric cross section meas., by coincidence method 78−86754
laser- or black-body radiation, strong electron coupling, limitation of Fermi-Dirac statistics 80−29843
lattices, FCC and BCC, optical transitions, dipole selection rules 80−97409
light intensity fluctuations, higher-order correls. and photoelectron time-interval distrib. 77−61932
light intensity probability density determ., from photoelectron statistical distrib. 78−24840
local and integral emission meas., electron emission microscope adaptation 79−93258
magnetic materials, spin polarised electron emission, review 77−73215
magnetic semiconductors, conference, Montpellier, France (Sept. 79) 80−94916
many-body aspects, external photoemission, Green's functions 78−72703
many-body effects, book contrib. 78−95667
matrix elements and cross-section calcs. with wave functions with definite ang. mom. 77−30839
metal, creep-electron emission relation 78−6994
metal, electrodynamics at boundary, including plasma waves 77−59317
metal, laser irradiated, optical and electronic emissions *(French)* 80−2919
metal, negative ion emission during microsecond laser pulse irrad. 78−2981
metal, nonlinear surface photoemission, picosecond lightpulse, electron heating effects *(Russian)* 77−40331
metal, photofield emission, vol. effect 77−32494
metal, volume photoemission, theory 78−2978
metal surface, expts. on photoelectric effect, apparatus 78−81745
metal surface, nonlinear photoelectric effect, laser-induced electron emission 78−19638
metal surface cleanness control by photoemission recording *(Russian)* 80−49839
metal-electrolyte boundary, elec. refl. and photoemission relationship 80−45211
metal-electrolyte boundary, photoemission effect on elec. refl. 80−45212
metal-electrolyte contacts, interfacial photoemission, book contrib. 78−95676
metal-electrolyte surface, physical struct. details 78−80798
metal-insulator contacts, interfacial photoemission, book contrib. 78−95676

photoemission continued
metal-semiconductor surface barrier structures, two-photon photoelec. effect 80−88594
metallic surface state, influence of refr. of p-polarised light on photoemission 80−20772
metallic surface states, effect of refraction of p-polarised light on photoemission 78−72686
metals, influence of oxide films *(Russian)* 77−81194
metals, laser and nuclear radiation induced emission anomalies, current sources *(Russian)* 80−25536
metals, multiphoton phenomena in photoelectron emission at high laser intensities 79−28886
metals, nonlinear vol. photoelectric effect, anal. 79−15593
metals, photoemission, theory, book contrib. 78−95670
metals, resonant photoemission, mech. 80−50524
metals, volume nonlinear photoeffect, involving stepwise radiation absorpt. *(Russian)* 77−44129
2-methylaniline, photoemission for mol., polarised photoelectrons 78−66607
microscopy, bacteriochlorophyll monolayer quantum yield and image contrast 78−44453
MIM, internal photoemission and quantum mech. transmission coeff. 77−1494
MIS structure, internal electron photoemission phenomenon in MISS *(Polish)* 79−91144
MIS structure charge distrib., optoelectric determ. methods *(Polish)* 80−39675
MNOS structure, non-biased, charge storage by irradiation with UV light 77−43735
model amorphous semiconductor struct., electronic props. 79−65974
molecular crystal, band structure, excitonic processes, trap distrib. 80−6720
molecular crystal, photoemission theory 78−39662
molecular solid, electronic struct., polarisation fluctuations effect 77−72833
MOS insulator trapped electron release by UV photoinjection 78−6453
MOS interface states density, photoemission obs. using photocurrent and photocapacitance meas. 80−92990
MOS structure, photon-assisted tunnelling at Al/SiO_2 and Si/SiO_2 interfaces 77−89865
multialkali antimonide photocathodes, emission and work functions 79−78836
multialkaline antimonides, (Sb, Na, K, Cs) type, photoemission rel. to chem. struct. *(French)* 78−39655
naphthacene, electron escape depths and absorpt. coeffs. 78−23580
nonlinear photoelectric emission from metals by high power layer radiation review 78−48288
nuclear explosions EMP, system generated by photoelectron emission current, anal. 78−21772
nuclear reactor pressure vessel/cladding interface, residual gas analysis *(German)* 77−40603
nylon 6, evidence of electron transfer as mechanism of static charge generation, contact with Hg 79−47153
one-quantum photoeffect, ang. photoelectron distrib. due to elliptically polarized light 79−6920
optical communication with two-photon coherent states, quantum meas. realisable with photoemissive detectors 80−53220
organic solids, photoemission and photoionisation in three stage model 80−100744
orientation, detector integrated angular distrib., photoexcitation depend. on target orientation, anal. 78−56564
oriented orbitals, photoemission cross-sections, surface Green function formalism 80−93453
p-n junction, anomalous hot carrier-voltaic effect, electron emitter and light detector appls. 77−76861
pentacene, electron escape depths and absorpt. coeffs. 78−23580
perylene, electron escape depths and absorpt. coeffs. 78−23580
photocathodes exhibiting negative electron affinity, model and GaAs expt. *(French)* 77−8724
photoelectric work function, depend. on light freq. *(Russian)* 77−32066
photoelectrochemistry, laser sources use for solar energy conversion 80−40873
photoelectron spectroscopy, 30-800 eV, using synchrotron radiation 79−31608
photoionisation theory, atomic photoelectron spectroscopy, book contrib. 77−79591
photostimulated field emission, triangular barrier pot. model 80−100759
Planck's constant experiments, for teachers 79−28
poly-N-vinylcarbazole−metal electrode, photoemission of electrons, photocond. meas. 79−91142
polyalkali photocathode films, photoelectron emission depth rel. to thickness 79−83106
polymer, photoelectric effects and relation to cond. processes 77−43640
polymer films, photoelectric emission and contact charging, surface states 79−33885
polyvinylcarbazole-Hg interface, contact electrification, internal photoemission study 78−60191
positive ion photoemission, vacuum UV quantum yield limit 78−79896
prebreakdown ionisation current spatial growth expts., initial photoelec. current changes 78−67566
pulsed laser light stimulated desorption and local vaporization 77−16432
pyrene, band structure, excitonic processes, trap distrib. 80−6720
qualitative results of theory *(French)* 77−36368
quantum absorber theory, direct-action, photoelectron antibunching effect 80−57535
quantum efficiency yields, automatic recording system 77−67489
random alloy, optical absorption and photoemission spectra 80−45216
reradiation effects in negative electron affinity photocathodes 80−55274
review, photoelectron origin, book contrib. 77−32506
rhodamine B adsorbed on NaCl, photoelectric meas. and contact charging 79−19643
sample manipulation and rotation using ultra high vacuum angle resolving photoemission chamber 80−57317
sapphire-Al interface barrier, transport and trapping obs. 77−76921
scaling props. of laser light, photoelectron and photon statistics 77−14729
scanned internal photoemission characterisation of MOS structs. and contact barriers 80−49915
semiconductor, doped, calc. of escape probability of electrons *(Russian)* 79−24408
semiconductor, photoemission meas. of surface and bulk states 80−25527
photoemission continued
semiconductor physics, conf., Edinburgh, Scotland (Sept. 1978) 79−95303
semiconductor surface, instrument for angle-resolved UV photoemission spectroscopy *(Japanese)* 80−93455
semiconductor surface, photoemission, book contrib. 78−95671
semiconductor with p-n junction, X-ray diffr., photoelec. EMF produced *(Russian)* 79−8225
semiconductor-metal system, long wavelength photosensitivity edge 80−6984
soft X-ray induced electron emission, yield and energy spectrum prediction 78−31297
soft X-ray photoemission, electron transport method development 78−31296
solid state physics, conf. Munster, Germany (March 1979) 80−41941
solution, optical methods of studying solid-liquid interface *(French)* 80−7318
solutions, easily ionised emitters, photoelectron emission theory 77−21403
spectra calculation program 80−55256
spectrometer, variable angle, for meas. electrons photoejected by rare gas reson. light 78−1110
spin and energy analysed photoemission, feasibility anal. 80−55271
spin polarised electrons, expt. techniques and apparatus, book contrib. 77−81198
spin polarised photoelectron emission, book contrib. 78−95675
spin-polarization measurements by Mott scattering, use of 90° spherical deflector 80−31951
streak photography, electron optical, photoemission limit of time resolution 77−18103
student laboratory experiment and apparatus design, Planck's const. determ. 78−41109
surface electronic properties and photoemission, book 78−95662
surface electronic properties and photoemission, book contrib. 78−95663
surface photoexcitation of model system, book contrib. 78−95665
synchrotron radiation appls., including angle-resolved photoemission 78−32963
synchrotron radiation source, book contrib. 78−95677
teaching demonstration, using electroscope 77−2505
tetracene, double quantum external photoelec. effect 79−87564
tetracene, monocrystal, photoelectron emission, quantum yield spectral dependence, in near-threshold region *(Russian)* 79−69954
theoretical aspects, review 80−45213
time interval photoelectron statistics, nongaussian scattered light 77−19177
transition metal, extraatomic relaxation energies *(Russian)* 78−31295
transition metal surface, photoemission theory 78−95679
two-dimensional systems, directional photoemission, book contrib. 78−95674
ultrafine particles in gas, information on size, surface props. from photoelectron emission 78−68598
ultrahigh vacuum setup for photo- and thermostimulated electron emission and luminesc. obs. *(Russian)* 80−66383
ultrathin films, on nonphotosensitive cond. substrate 77−40325
violanthrene-A, electron escape depths and absorpt. coeffs. 78−23580
work function fast variation meas., photoelectric method 79−91561
yield of photoelectrons, single cryst., X-ray diffr. conditions *(Japanese)* 80−16144
Ag (001) surface, photoemission, electron escape effect 79−1814
Ag (111), angle-resolved photoemission, free-electron final state model 79−4896
Ag (111), angular distrib., effects of transmission factors and matrix elements 77−44128
Ag, multiphoton photoemission, expt. at 5° incidence of laser beam *(Hungarian)* 77−52214
Ag, photoemission yield anomalies, quantitative analysis, dielec. response nonlocality *(French)* 79−61489
Ag, photoemission-into-electrolyte 79−74390
Ag-Al_2O_3-Al junction, internal photoemission 79−82683
Ag-O-Cs cathode, photoemission mechanism *(Chinese)* 79−19966
Ag-O-Cs photocathode, Ag colloidal particles and long wavelength response *(Chinese)* 80−45195
Ag-O-Cs photocathode, role of Ag colloidal particles in photoemission *(Chinese)* 80−40215
Ag_3SbS_3, pyrargyrite, thermoelec. and photoelec. work functions, Fermi level and electron affinity *(Russian)* 77−15939
Al (100) model surface, ang. terms in optical pot. 80−55269
Al alloys, contamination, automated nondestructive inspection 80−16629
Al, anodised, photostimulated exoelectron emission, effect of oxide thickness 78−80461
Al, autoionisation reson. determ. from photoelectron polarisation meas. 80−58221
Al, influence of oxide films on photoemission *(Russian)* 77−81194
Al, photoemission cross-sections for 2s and 2p levels 80−93453
Al, photoemission from (100), (110), and (111) cryst. faces, surface states 79−4893
Al/III-V interfaces, photoemission 80−25526
Al-SiO_2 interface, internal photoemission and photon-assisted tunnelling 80−6982
Al-SiO_2-Si, photoelectron-grain boundary scatt. in Al film 78−64120
$Al_xGa_{1-x}As$ epitaxial films, microanal. in photoemissive electron microscope 79−16068
AlGaSb, growth and characts. for 1.0-1.8 μm heterojunction devices 78−6870
Ar, electron ionisation and excitation coeffs. in low E/N region 80−48090
$Ar^{6+}+H_2$ collisions, ionisation and excitation resulting from electron capture 80−78683
As, 3d subshell, photoionisation partial cross-section, energy depend. meas. 80−29850
Au, 5d and 4f subshells, photoionisation partial cross-section, energy depend. meas. 80−29850
Au, foil, X-ray induced electron emission 77−4713
Au in electrolyte, photoemission-into-electrolyte 79−74390
Au, multiphoton photoeffect, induced by single selected ultrashort laser pulses, anomalies 77−28692
Au, photoemission study of bulk and surface electronic struct. 79−4894
Au-Si, spatial origin of electrons in internal photoemission struct. *(French)* 78−91770
Au-Si (polyethylene) interfaces, algorithm for energy deposition of X-rays 77−28648

photoemission continued
Au-Si internal photoemission struct., spatial distrib. of excited electrons *(French)* 78−23166
β-B, rhombohedral, photon energy depend. of work function 78−19637
Ba film, structure effects on work function, electron micrographs and photoemission meas. 79−83107
Ba film, work function and struct. 78−80040
Ba, resonant photoemission, time-depend. density-functional technique 80−89114
Bi_2O_3 anodic films, struct. and electronic props., photoeffects 80−44749
C foils, forward photoemission and transmittance meas. 80−25516
CN violet ($B^2\Sigma$-$X^2\Sigma$) band system, photoelec. intensity meas., transition probabilities 78−37649
CO on Ni, adsorbed mol. bond config. and orientation, ang. resolved photoemission 77−44506
CO_2 TEA laser, UV preionised, characts. 80−69414
Ca film, structure effects on work function, electron micrographs and photoemission meas. 79−83107
Ca films, thin and ultrathin, vac. deposited, struct. and photoemission meas. 80−11538
CaO with adsorbed metal, photoexcited ions and electron emission *(Russian)* 77−40324
Cd, photon interactions, energy role 77−36305
$CdCr_2S_4$, photothreshold changes below mag. ordering temp. 80−97406
CdF_2-metal Schottky diode, photoemission, capacitance and I-V meas. barrier heights 78−26950
CdS, due to direct transition near L- and M-points in Brillouin zone 77−16451
CdS:Cu sintered layers, relaxation photocurrent kinetics *(Russian)* 80−107852
p-CdTe, surface barrier struct., internal photoelec. emission 77−15958
Ce, resonant photoemission, time-depend. density-functional technique 80−89114
Co (0001), photoemission, exchange-split energy-band dispersions 80−35059
Cs-O, low work function surface, prod. by Cs_2CO_3 decomp. and emission characts. 77−85882
CsI photocathodes, efficiency evaluation for soft X-ray diagnostics 80−57442
Cs_3Sb photocathode, wavelength-modulated photoemission spectra 80−29857
Cs_3Sb vacuum deposited photoemitter, XPS study 80−89122
Cs_2Te, photocathode for proximity focused image convertor, field enhancement of photoemission 78−72677
Cu (001) and (110), electronic wave functions by spherical wave method, vel. to photo-induced field emission 79−42604
Cu (100) and (111), angle-resolved photoemission and band struct. 79−95904
Cu, angle-resolved photoemission, band struct. 78−95680
Cu film, pure and CO covered, work functions 79−91570
Cu, single cryst., two-photon photoemission near single-photon photoelec. effect threshold 80−89121
Cu-Al (3 wt.%), annealing twins density, photoemission microscopy 80−35208
Cu-CdS, Schottky barrier, Cu diffusion and photovolt. mechanism 80−6980
Cu-Ni, optical absorption and photoemission spectra 80−45216
Cu-phthalocyanine, electron escape depths and absorpt. coeffs. 78−23580
CuI photocathodes, efficiency evaluation for soft X-ray diagnostics 80−57442
Cu_2O films arc cathode emission study 78−23583
Cu_xS, photon and electron excitation phenomena 79−7865
EuO:La, metallic, photothreshold, correl. and exchange energy of electron gas 77−62852
EuO:La(Gd), photothreshold changes below mag. ordering temp. 80−97406
Fe (111), photoemission, exchange-split energy-band dispersions 80−35059
Fe (111), spin polarised photoemission 80−45221
$Fe_{80}B_{20}$, hardness, elec. cond., photo emission, and mag. props. *(Norwegian)* 79−32909
$Fe_{0.91}O$, photothreshold changes below mag. ordering temp. 80−97406
n-Fe_2O_3, sintered and flame-oxidised, photoelectrochemical props. 79−70355
Ga, 3d subshell, photoionisation partial cross-section, energy depend. meas. 80−29850
Ga, liquid and solid, photoemission, conduction electrons 79−87566
GaAs (111) epitaxial film, adsorption of Cs, Cs+O, ellipsometric study, photocathode sensitivity 80−29282
GaAs, chemisorpt. of O_2 and thin oxide layer form., reviews of synchrotron radiation meas. 79−60637
GaAs, doped, calc. of escape probability of electrons *(Russian)* 79−24408
p-GaAs, electrode, photoemission into electrolyte solns. 77−24616
GaAs, modulation by IR illumination, saturation photocurrents 80−108318
GaAs, negative electron affinity, face depend. 77−32496
GaAs, negative electron affinity, optically pumped, depolarization of emitted photoelectrons 79−8223
GaAs photocathode, emitted electron transverse energy 77−12489
GaAs, photocathodes exhibiting negative electron affinity *(French)* 77−8724
GaAs photoemission characteristics, parameters of emitters with negative electron affinity 79−4898
GaAs, produced by pyrolytic synthesis 79−43100
n-GaAs, real epitaxial surface, photoelec. spectroscopy, mechanisms 78−34858
GaAs:Zn (110), spin polarised electron production by photoemission from Cs-O overlayer 79−95903
GaAs-Ge structure, electronic struct., ang.-resolved photoemission obs. 80−49881
GaAs-metal interface form., chem. and electronic struct. 80−25009
GaAsP cathode, negative electron affinity process obs. by laser beam scanning *(Japanese)* 80−55262
GaAsP, negative-electron-affinity, photoemission transmission coeff. 78−56560
$GaAs_{0.62}P_{0.38}$, negative electron affinity, photoemission of spin polarised electrons 80−2916
$GaAs_{1-x}P_x$, high quantum efficiency photoemission 77−44115
GaInAs, photocathode with negative electron affinity, photoemission, influence of strong elec. field 79−8227
photoemission continued
$Ga_{1-x}In_xAs$, photocathode, work function depend. of photoelectric emission 78−68071
GaP (III) B surface, negative-electron-affinity, photoemission transmission coeff., comparison with GaAsP 78−56560
GaP (100), prep. of negative electron affinity surface by Cs adsorption 80−10768
GaP, adsorption and desorption of Cs, LEED, AES, and photoemission meas. 80−70532
GaP-In LPE layers, carrier diffusion lengths and escape probabilities optical absorpt. and photoemission meas. 79−87559
GaSb, adsorption and desorption of Cs, LEED, AES, and photoemission meas. 80−70532
Ge, amorphous layer on Ge bulk, photoemission during X-ray Bragg diffr. 78−47209
Ge, electrodes, photoemission into electrolyte solns. 77−24616
Ge, n- and p-type, photoemission into electrolyte soln., energy diagrams, Volta pots., voltage drop 77−62990
Ge photocathodes, Au absorbed photofield emission current spectral investigation 80−29856
Ge-metal interface, internal photoemission mechanisms 80−60077
H-like atom in super-strong mag. field, photoeffect and relativistic positron annihilation *(Russian)* 77−75112
He+OCS, emission spectra in He afterglow 80−87139
Hg dropping electrode, photoemission into electrolyte solns. 77−24620
Hg, photoemission, into electrolyte soln., five-halves law 77−44132
p-InP field-assisted photocathodes, quantum efficiency 80−84831
InP-$In_xGa_{1-x}As$ alloy photocathodes, semiconductor photoemitters, field-assisted, 1-2 μm range 80−97396
InP-InGaAsP bias assisted photocathodes, photoemission in 1-2 μm range 78−48289
InSb-anodic oxide-Ni, energy band diagram, internal photoemission meas. 79−33356
KCl crystal, use of photoelectrons to investigate surface charges 80−2444
KCl, photoelectric emission in photon energy region 1.0 to 6.0 eV 80−108321
KCl with adsorbed metal, photoexcited ions and electron emission *(Russian)* 77−40324
Kr, electron ionisation and excitation coeffs. in low E/N region 80−48090
LaB_6, Shockley surface states, angle-resolved photoemission 79−56278
LiF, cryst., laser irrad., electron emission 80−80948
$LiNbO_3$:Fe, intrinsic field effect, photoelectric emission study 79−69961
$LiNbO_3$:Fe, lattice-strains induced by light, X-ray topography 77−76458
Mg, influence of oxide films on photoemission *(Russian)* 77−81194
MgO, photostimulated electron emission, manifestation of Auger processes 77−52225
MgO:Al(Li)(F)(Sn), hole processes in photostimulated luminesc., electron emission, X-ray irrad., ESR relaxation 79−69889
Mo (100), surface resonances, photoemission and field emission meas. 79−4593
N_2 3371 Å dayglow emission, excitation by photoelectron impact 77−33236
Na c(2×2) overlayer on Ni (001), surface struct. effects via photoexcited core electron diffr. 79−74063
NaCl, cryst., laser irrad., electron emission 80−80948
NaCl, laser irradiated, electron emission, surface layer electric discharge effects 79−74032
Na_2O-SiO_2 glasses, elementary electronic excitations, refl., luminesc., and photoemission meas. 80−84778
NbO, photoemission and X-ray emission spectra 78−64442
Ni (001), chemisorption of O and S, dynamical calc. of angle-resolved UV photoemission 77−85890
Ni, (001) surface, spin polarised photoemission theory 79−15584
Ni (100), spin polarised photoemission 80−45221
Ni (111), photoemission, exchange-split energy-band dispersions 80−35059
Ni (111), single crystal, spin polarisation of emitted photoelectrons 80−45215
Ni, (111) surface, VUV photoyield, electron spin polaris. enhancement 79−74054
Ni, (99 wt.%), annealing twins density, photoemission microscopy 80−35208
Ni, angle-resolved photoemission, band struct. 78−95680
Ni atoms, Xe matrix isolation, photoemission 80−27987
Ni d-band photoemission, resonance enhancement by coupling to 3p excitation 80−20766
Ni, photoelectric effect in paramag. and ferromag. states, Auger spectra 78−95649
Ni, photoelectron spin polarisation 77−32501
Ni, spin polarisation of reson. two-hole bound state 79−83099
O, adsorbed on Ni, photoemission intensities from core states 78−95654
Pb, 5d subshell, photoionisation partial cross-section, energy depend. meas. 80−29850
$Pb_5Ge_3O_{11}$, single crysts., photoemission anamoly during ferroelectric phase transitions 79−47599
Pd overlayers, on Nb, form. of Pd (111) surface states and reson. d-levels, photoemission obs. 80−50523
Pd-SiO_2 interface, H induced interfacial polarisation, internal photoemission meas. 77−1490
Pt (100), adsorption of S, obs. 78−14606
Pt, photodesorption of acetone, photoion emission, quantum yield limit 78−79896
Pt-electrolyte interface, electron states, photoemission studies 78−85171
Rb_2Te film electron affinity and photoelectron work function obs. 79−69959
Rh foil, work function determ. rel. to heat treatment temp., extrinsic photoeffect meas. 77−39918
S absorbed on Ni, photoelectron diffr. data 80−29851
Sb, 4d subshell, photoionisation partial cross-section, energy depend. meas. 80−29850
Se adsorbed on Ni, photoelectron diffr. data 80−29851
Se, adsorbed on Ni, photoemission intensities from core states 78−95654
Si cathode, negative electron affinity process obs. by laser beam scanning *(Japanese)* 80−55262
Si, clean-cleaved, Schottky barrier height meas. accuracy 78−52081
Si field emission photocathodes, emission current noise characts. 80−100746
Si, negative electron affinity (100) surface, electron emission 77−52215

photoemission continued
Si, negative electron affinity surface activation, laser beam scanning obs. 79−4890
Si, photoelectron emission due to Bragg diffr. of X-rays 79−69960
Si, shallow p-n junction, energy loss and escape depth of hot electrons 79−78159
Si:Cs-O photocathodes negative electron affinity electron emitting devices, reson. transmission 77−90240
Si-SiO_2, electron photoemission from Si, band struct. effects 79−19977
Si-SiO_2 interface, electronic struct., field depend. internal photoemission probe 77−20450
Si-SiO_2 interface, props. 78−23170
Si-SiO_2-Al, internal photoemission, pot. barrier height determ. 80−65699
Si-SiO_2-Si_3N_4, internal photoemission 80−7475
SiO_2 film, in Al-SiO_2-Si struct., positive trapped charge location by internal photoemission 77−51820
SnS_2, Sn4d photoionisation, second threshold 80−40222
Sr film, structure effects on work function, electron micrographs and photoemission meas. 79−83107
Ta, photo field emission characteristics, band struct. influence 78−27373
Ta, photo field emission spectroscopy of band structure by He-Ne laser irrad. 80−55276
Ta, photofield emission spectroscopy of band struct. 78−35261
Te, adsorbed on Ni, photoemission intensities from core states 78−95654
Te, polarographic prewave, photo-effect 77−36833
Tl, autoionisation reson. determ. from photoelectron polarisation meas. 80−58221
to film, vacuum-deposited, gas adsorpt. effects on photoelec. props. 78−15298
US, electron spin polarisation 79−65978
USe, ferromag., spin polarisation of photoelectrons 79−78831
W (001) adsorbate system, directional photoemission of polarised electrons 77−36374
W (100), optical magnetisation from spin polarised photoemission 79−78830
W (100), surface resonances, photoemission and field emission meas. 79−4593
W (110) surface states, characterisation and transferability obs. 79−33319
W field emitter, periodic field-dependent photocurrent 78−35260
W field emitter, strong polarisation effect in photoinduced field emission 78−95684
W, four-photon photoemission, incident angle and polarisation depend. 80−40221
W, optically polarised conduction-band electrons, spin-polarised photoemission obs. 79−74055
W, photo field-emission, periodic current deviation, wavelength depend. *(German)* 78−23579
W, photoemission of spin polarised electrons 78−35248
W, pure and Ba covered, photo-stimulated field emission, effect of light polarisation *(French)* 80−7480
W, surface pot. barrier effect on photofield emission 78−60551
W tip, pure and Ba coated, photoemission in electric field *(French)* 78−80458
W(001), surface density of states for directional photoemission spectroscopy 77−20396
Xe adsorbed on Pd (110), anomalous 5p photoemission, electron binding energies 80−100750
Xe, electron ionisation and excitation coeffs. in low E/N region 80−48090
$ZnAs_2$ Schottky diodes, elec. and photoelec. props., excitons 80−65653
ZnO, photodesorption of $H_2O(NH_3)(NO)$(acetone), photoion emission, quantum yield limit 78−79896
ZnO, with adsorbed metal, photoexcited ions and electron emission *(Russian)* 77−40324
ZnP_2 Schottky diodes, elec. and photoelec. props., excitons 80−65653
ZnS, laser radiation initiated electron emission, evidence for photoelec. mechanism 77−69970

photoemission spectra *see photoelectron spectra*

photoemissive devices
see also photocathodes; photoemission
image convertors, time resolution, contrast-time characts., calcs. 77−7208
photoemissive detector, picosec., using metal-oxide-metal junctions 79−44932
solar-cells, efficiency calc., use of negative affinity photoemitters 80−55876

photoemissivity *see photoemission*

photofission
actinide nuclei, photo- and electro-fission cross sections and yields, giant resonances 80−5187
actinide nuclei, subthreshold photofission yields, data anal. 78−82400
Catania 13.5 MeV microtron facility, photofission experiments 79−41050
detector assembly for photofission and photoneutron studies using BF_3 detector 80−63484
fissionability, target mass depend. for π, γ, α, p, cascade-evaporation and liquid drop calcs. *(Russian)* 80−106089
heavy isotope photofussion, delayed neutrons kinetic functions 79−63709
heavy nuclei, fine structure of yields of Xe isotopes, A=131-135 78−86560
laser induced fission, Monte Carlo anal., critical mass and radius for bare spheres 78−62583
laser induced photonuclear and fusion-fission reactions 77−61599
light elements, photofission by massive neutrinos radiative decay rel. to cosmic abundances 79−92668
(γ,f), linear polarised photon on even-even nuclei 80−543
(γ,f), non-destructive testing of fissile and fertile material 77−74917
^{227}Ac, 7 to 16 MeV photofission, giant resonance and nuclear deformation *(Russian)* 78−41795
Ag(γ,f), max. energy 580 MeV, track detector anal. 77−18640
^{A}Am, A=241, 243, relative probabilities of photofission by bremmstrahlung γ *(Russian)* 79−9646
^{A}Am(γ,δ) 7-26 MeV, A=241,243, photofission cross section in E1 giant resonance region *(Russian)* 80−5182
^{A}Am(γ,n), 10-80 MeV, A=241, 243, delayed/prompt fission yield ratio, cross section, isomer prod. 79−80924
^{241}Am, 15 to 1300 MeV, cross sections meas. *(Russian)* 77−6473
^{243}Am, 15 to 1300 MeV, cross sections meas. *(Russian)* 77−6473
Au, photofission induced by 220-500 MeV coherent beam 77−3056

photofission continued
Au(γ,f), 140 to 1000 MeV, energy depend. of nuclear fissility 77−82971
Au(γ,f), max. energy 580 MeV, track detector anal. 77−18640
Bi (γ,f), 140 to 1000 MeV, energy depend. of nuclear fissility 77−82971
Bi, photofission induced by 220-500 MeV coherent beam 77−3056
^{209}Bi(γ,f), 40-65 MeV, absolute total photofission cross section, compound nucleus form. 80−86934
^{209}Bi(γ,f), bremsstrahlung of 600 MeV max. energy, fragment energy correl. meas. 77−71630
Cr(γ,f), max energy 580 MeV, track detector anal. 77−18640
Cu(γ,f), max. energy 580 MeV, track detector anal. 77−18640
^{4}He(γ,2np)p, total photofission theory in hyperspherical basis *(Russian)* 79−22347
^{24}Mg, photofission cross sections deduced from electrofission data 78−54744
^{24}Na yield from light and intermediate nuclie in 2-5 GeV photonuclear reactions *(Russian)* 77−2980
^{237}Np, relative yields of Xe isotopes 77−54265
Pb, photofission induced by 220-500 MeV coherent beam 77−3056
Pb(γ,f), 140 to 1000 MeV, energy depend. of nuclear fissility 77−82971
Pt, photofission induced by 220-500 MeV coherent beam 77−3056
Pt(γ,f), 140 to 1000 MeV, energy depend. of nuclear fissility 77−82971
^{239}Pu(γ,f), 15-55 MeV, photofission symmetric and asymmetric yields 80−83135
^{239}Pu(γ,f), asymmetry depend. on bremsstrahlung energy maxima 77−23117
Re, photofission cross section, 220-550 MeV, coherent electron bremsstrahlung beam 79−13353
Se(γ,f), max. energy 580 MeV, track detector anal. 77−18640
Ta, photofission cross section, 220-550 MeV, coherent electron bremsstrahlung beam 79−13353
Te(γ,f), max. energy 580 MeV, track detector anal. 77−18640
^{232}Th (γ, f), deep subbarrier photofission ang. anisotropy from fragment ang. distrib. *(Russian)* 79−97739
^{232}Th, determ. of neutron multiplicities 80−32311
^{232}Th, effect of isomer shelf in photofission cross sections *(Russian)* 79−9648
^{232}Th, photofission yields of bremsstrahlung γ *(Russian)* 79−9647
^{232}Th, quadrupole photofission and role of nucl. symm. *(Russian)* 78−17258
^{232}Th subthreshold photofission 78−66323
^{232}Th three hump fission barrier. photofission cross section and half life 79−67788
^{232}Th(γ,X) 5-18.3 MeV, photoneutron and photofission cross sections, giant resonance and deformations 80−68712
^{232}Th(γ,f), 15-55 MeV, photofission symmetric and asymmetric yields 80−83135
^{232}Th(γ,f), 9, 15, 38 MeV peak bremsstrahlung 78−33229
^{232}Th(γ,f), BF_3 detector assembly for photofission and photoneutron studies 80−63484
^{232}Th(γ,f), bremsstrahlung of 600 MeV max. energy, fragment energy correl. meas. 77−71630
^{232}Th(γ,f), deep subthreshold photofission, double humped fission barrier anal., shape isomer 80−5179
^{232}Th(γ,f), fission-neutron and fragment ang. distrib. 77−65239
^{232}Th(γ,f), sub-barrier photofission, triple humped fission barrier profile 78−58311
^{A}U, A=235, 236, 238, determ. of neutron multiplicities 80−32311
^{A}U(γ, f), A=236, 238, deep subbarrier photofission ang. anisotropy from fragment ang. distrib. *(Russian)* 79−97739
^{A}U(γ,X), A=235, 236, 238, 5-18.3 MeV, photoneutron and photofission cross sections, giant resonance and deformations 80−68712
^{A}U(γ,f), A=235, 236, 238, deep subthreshold photofission, double humped fission barrier anal., shape isomer 80−5179
^{A}U(γ,f), A=235,238, 15-55 MeV, photofission symmetric and asymmetric yields 80−83135
^{233}U(γ,f) asymmetry depend. on bremsstrahlung energy maxima 77−23117
^{234}U under barrier photofission, 4-5.7 MeV, fragment ang. distribs. *(Russian)* 80−106090
^{235}U, fission product mass. distrib. from 25 MeV bremsstrahlung irradiation 78−13175
^{235}U, relative yields of Xe isotopes 77−54265
^{235}U, subthreshold photofission 78−66323
^{235}U(γ, f), 12-70 MeV bremsstrahlung, product yields and γ-spectra 80−42716
^{235}U(γ,f), 20 MeV, long range α-particle spectrum 80−47516
^{235}U(γ,f), 25 MeV bremsstrahlung, neutron emission curve 77−10457
^{235}U(γ,f), ang. distrib. of fragments *(Russian)* 78−54808
^{236}U, 5.2-6.4 MeV, ang. distrib. and yields of fission fragments 77−3059
^{236}U, giant E2 isoscalar resonance determ. 80−27607
^{236}U, photofission, deep sub-barrier anomalies 77−65241
^{238}U, 15 to 1300 MeV, cross sections meas. *(Russian)* 77−6473
^{238}U, 20-60 MeV, relative E1 contrib. 77−6471
^{238}U, deep subthreshold photofission using 3.8 to 5.7 MeV γ-rays 78−41787
^{238}U, delayed neutron energy spectrum 77−23155
^{238}U, fission product mass. distrib. from 25 MeV bremsstrahlung irradiation 78−13175
^{238}U, photofission, deep sub-barrier anomalies 77−65241
^{238}U, photofission products, ang. distrib., isomeric shelf region *(Russian)* 77−6475
^{238}U, photofission with bremsstrahlung, charge distrib., fractional independent yields 79−36283
^{238}U, subbarrier photofission, differential cross section 78−41796
^{238}U subbarrier photofission, cross section and half-life, double hump model 80−102217
^{238}U(α,f), 100-1000 MeV, resonance production 80−52658
^{238}U(e,e'f), 5.5-28.3 MeV, E2 isoscalar giant resonance in photofission cross section 79−512
^{238}U(γ,f), ^{135}Xe, direct meas. of absolute and fractional independ. yields 80−78341
^{238}U(γ,f), 12-70 MeV bremsstrahlung, cumulative and fractional product yields for A=128-136 79−36288
^{238}U(γ,f), 12-70 MeV bremsstrahlung, fragment mass and energy distribs. 80−27680
^{238}U(γ,f), 20 MeV, fission product yields, charge distrib. 80−42533
^{238}U(γ,f), 25 MeV bremsstrahlung neutron emission curve 77−10457
^{238}U(γ,f), BF_3 detector assembly for photofission and photoneutron studies 80−63484

photofission continued
^{238}U(γ,f), bremsstrahlung of 600 MeV fragment energy correl. meas. max. energy 77−71630
^{238}U(γ,f), neutron capture γ-rays, Γ_n/Γ_f meas. 80−57813
^{238}U(γ,f), neutron capture γ-rays, ^{134}I fractional independ. yield 80−57814
^{238}U(γ,f) 20 MeV, computer program for yield determ. of short-lived products 80−102215
^{238}U(γ,f) fission-neutron and fragment ang. distrib. 77−65239
U(γ,f), 5.2-6.4 MeV, A=234, 236, 238, doubly even isotopes, ang. distribs., fragment yields 78−50219
U(γ,f) A=235,238, 25 MeV bremsstrahlung, prod. yields, mass chains, charge distribs. 77−6470
U(γ,f), max. energy 580 MeV, track detector anal. 77−18640
W, photofission cross section, 220-550 MeV, coherent electron bremsstrahlung beam 79−13353

photoflash lamps *see flash lamps*

photoglow tubes *see phototubes*

photogrammetry
aerial lenses and their technology *(Japanese)* 79−35868
aerial photography for densification of urban geodetic nets 77−78462
aerial photography lenses and their production technology *(German)* 78−4717
aided-track cursor for improved digitizing accuracy 79−29899
American Society of Photogrammetry Annual Convention, Washington, USA (March 1978) 80−4149
American society of photogrammetry usage of the international system of units 79−21692
analytical bridging, solving problems encountered 80−105080
analytical plotter-its future 78−40708
analytical plotters, software aspects 78−40709
analytical plotters 78−40710
analytical stereoplotting system, C-100 planicomp 78−40711
atmosphere refraction compensation for long photographic distances 80−56339
automatic image processing Zenit photogrammetric system, technical implementation *(Russian)* 78−24466
automatic reseau meas. with simple optical correlator 78−69496
biomechanical properties estimation of three body types using photogrammetric method 79−43947
body joint instantaneous centre and angle of rotation, minimum error optimisation 79−96605
cameras, multi-, planar control in photogrammetric calibration for 3-D gait studies 80−67194
cancer diagnosis appl., cytographs automatic analysis *(Russian)* 78−24161
cartography, point transfer error determ. 80−17227
close range X-ray and cold neutron techniques at Rolls-Royce 79−75637
close-range photogrammetry problems solved by analytical plotter 77−71397
coastal mapping, problems due to water effects 80−104960
coherent correlator operation in image segment identification, aerial photograph anal. 80−102654
colour maps produced from B & W negatives exposed to visible and IR 80−109270
contouring from digital terrain models, accuracy 79−84085
contrast enhancement of Landsat imagery 79−29896
coordinate system for aerial frame photography 79−2179
data analysis by collocation method 80−77130
Death Valley, geological interpretation from composited radar and Landsat imagery 80−56647
digital orthophoto production using scanning microdensitometers 80−41571
digital stereo mapping, flexible algorithm 79−84543
digital terrain data appl. to meteorological and air quality modelling 79−84440
digital terrain model appls. to Forest Service 79−84086
digital terrain modelling, symposium (St. Louis, Missouri, 1978, May 9-11) 79−84083
digital terrain models, review 79−84084
distortion calibration, lateral chromatic aberration effects, operational data reduction 79−35881
edge operator evaluation test procedure 79−75646
electron microscope calibration by photogrammetric technique 78−336
Geosat geological industry recommendations on remote sensing from space 78−69495
graphical data automatic processing algorithms using photogrammetric automation Zenit *(Russian)* 78−21106
hard copy imagery from remote sensing systems, laser beam recorder appl. 79−80715
high intensity dot grids, for accurate area determ. 80−17225
hologrammetric plotter 79−7103
human motion 3-dimens. monitoring by optoelectronic means 78−31913
hydrographic chart preparation using Landsat 79−29894
iceberg volume meas. using photogrammetric techniques 77−82048
image interpretation and remote sensing, book 79−100985
image quality specification and anal. 77−87125
image scanner technology for digital mapping systems 80−85773
images with convex boundaries, read-out procedure design *(Russian)* 78−21105
inertial systems appl. *(French)* 79−62603
inland wetland photointerpretation evaluation, cell analytical method 79−29898
instant photogrammetry with a grid 79−21834
interference coordinate meas. system of photogrammetric automation Zenit, control module 78−21103
International Orthophoto Expt. 1972-76 results 77−44903
land-use/land-cover mapping from aerial photographs 80−41569
Landsat imagery, planimetric restitution using Zeiss Stereotop 80−56648
Large Format Camera for Space Shuttle 79−101043
lineament and joint densities, rapid determination 78−32255
linear features enhancement by rotational exposure 79−35874
low Sun-angle photography, flight planning, interpretive techniques 77−78465
lunar far-side radii determ. from Apollo photography, topographic map 79−66934
Mapsat (Automated Mapping Satellite System), proposed parameters 80−17468
Mars, topography, photogrammetric portrayal 80−67609
Mars synthetic topographic mapping 78−45253

photogrammetry continued
model deformation, interactive demonstration program 77−74183
moire fringe biostereometry using parallel light beam 79−100701
moire fringe electronic processing, comparison of moire topography and photogrammetry 79−40601
multispectral photography appl. using MKF-6 camera and MSP-4 projector 80−56633
network densification and land register surveying *(German)* 79−92633
numerical photogrammetry, orientation, triangulation and digitisation 78−36312
offshore shoal positioning using LANDSAT imagery 77−73883
online processing, general sequential algorithm 77−78463
optic disc changes meas. using retinal stereophotogrammetry, glaucoma detect. appl. 80−3757
orientation and calibration method for nontopographic appls. 79−35875
OTF/MTF standards 77−78471
perimeter survey by photogrammetric methods 79−25185
photographic investigation of earth, RADUGA 1 experiment, results *(German)* 80−36224
photointerpretation and photogrammetry teaching in natural resources field 77−74175
photomapping data collection, storage and retrieval system 79−71549
plotting instrument for close-range photogrammetry 78−77137
precision comparator, Zeiss PK-1, accuracy, appls. *(German)* 79−97359
prism correlator, application to stereo photogrammetry 78−86368
production mapping with orthophoto digital terrain models 79−84545
radiation therapy, topography of patient's body surface by photogrammetric technique 77−77972
real-time, instrumentation for analytical video stereoscopy of extended images 78−88926
reflexive prediction and digital terrain modelling 79−2175
remote sensing *(Russian)* 79−29897
remote sensing/photogrammetry education in USA and Canada 77−74174
rotated image correlation by gradient vector sum histograms 79−75647
saline seep detection and mapping, IR remote sensing techniques 80−4154
satellite image macrophotography 79−29895
satellite photogrammetry, dynamical constraints 78−15943
SEM photography, simplified numerical transformation *(German)* 79−17572
SEM stereo data 78−21297
slippage in crystals, photogrammetric obs. method 80−100975
spherical blast wave, high-speed photogrammetry of real and ideal reflections 78−42694
stereo electron micrograph restitution, approx. soln. 79−26189
stereo X-ray, use in absorbed dose determ. in radiation therapy 80−12222
stereometric measurement of streambank erosion 80−17421
stereophotogrammetry, automatic, using structural pattern recognition techniques 78−61632
stereophotogrammetry, digital profile to contour convertor, display 77−9501
stereophotogrammetry, meas. of deforms. in human body *(Croatian)* 80−108997
stereophotogrammetry of objects at close range, integral photography method 77−61148
stereoscope for viewing aerial photographs, interpretoskop optics, modifications 80−105081
steroscopic SEM pictures by eucentric rot. in tilted specimen plane 79−12908
stress corrosion fractures, determ. of orientation by photogrammmetric technique 79−79163
Tampa Bay bottom configuration and environmental studies, photogrammetric method 77−87124
techniques and appls. 80−31927
W.Tennessee, wetland mapping and classification, high altitude photography 80−8340
terrestrial integration and photogrammetric measurements *(German)* 78−92776
topographic mapping, digital terrain model appls. 79−84544
TOPOMAT all-automatic photogrammetric system for aerial photography 77−66993
Traster 77' matra analytical stereoplotter 78−40712
video stereophotogrammetry, interactive computerised, for Mars Viking 1975 Lander data 78−81557
Viking lander camera data processing 78−20649
Viking lander cameras calibration and performance 78−20639

photographic applications
see also photogrammetry; photolithography; remote sensing
acetone, condensation in presence of instabilities, photographic study 78−10180
active faults, aerial photographs interpretation *(Japanese)* 78−96124
aerial data processing, automatic, for agricultural resources inventory and survey expt. 77−78505
aerial film rapid processing using low gamma photographic developer 77−54001
aerial landscape photography, haziness factor in image contrast *(Russian)* 77−37449
aerial photographic analysis and stereographic mapping with electro-optical pattern recognition 77−19186
aerial photographic equipment developments, aerial survey camera and navigation telescope 77−66997
aerial photography, high altitude, aspects and results 78−36309
aerial photography, multispectral, soil survey in New Zealand 78−85728
aerial photography for densification of urban geodetic nets 77−78462
aerial reconnaissance film screening using optical matched-filter image-correlator technology 78−94371
aero-acoustic effects in CO_2 laser discharge fast photography and interferometry obs. 79−36875
aerodynamics, parachute opening flowfield computation, using He bubble technique 78−30374
aerophotographic system, synthesis and applications *(Russian)* 79−58836
aerotriangulation by Skylab Earth terrain camera photography 77−33209
alphanumeric/graphic print photo-embossing for tactile reading 79−80710
aspectrogram filtering, multiplying mask prod., photographic method 79−27196

photographic applications continued
astrometric reduction of photographs and calibration of wide-angle cameras *(Russian)* 78−28532
astrometry, photography against stellar background, iterative trajectory search algorithm *(Russian)* 77−17376
astrometry, sky photography programme with wide-angle astrographs *(Russian)* 80−72747
astronomical negative information processing using thick-film holograms 79−48690
astronomical observations, photographic method optimisation, review *(Russian)* 79−35144
astronomical photography, controlling contrast by special development techniques 77−67046
astronomical photometry using twin refractor 77−17382
astronomical telescope, large, photographic detection optimisation 78−24468
astronomy, cooled emulsion photography for amateurs 80−56714
astronomy, faint images photographic amplification 79−16839
astronomy, galaxy image picture processing system for colour 77−49303
astronomy, limiting stellar magnitudes *(Russian)* 79−92680
astronomy, negatives superposition method for galaxies *(Russian)* 77−13251
astronomy, plates meas. via automatic microdensitometer 79−80230
astronomy, semi-automated blink comparator for large photographic plates *(Japanese)* 78−89081
astronomy, stellar position, magnitude and colour index meas. from photographs, automated technique 79−21194
astronomy, unsharp masking technique 79−88603
atomisation units for powder metallurgy, gasdynamic and acoustic props. 80−66451
audio visual slide preparation 78−54139
ballistics, high-speed and other photographic methods 80−9068
biological objects, elec. discharges, electrographic investigation methods 80−46118
biological photography, future development 79−71551
bolides topocentric coordinates determination, use of photography 78−61818
borosilicate glass, microparticle impact, high speed photography obs. 78−44223
bubble chamber, automatic measurements of reference crosses on photographs in a spiral-meter system 79−67403
bubble chamber film exposure for meas. by HPD 78−58553
bubble condensation, in subcooled liquid, high-speed photographic study 78−42654
bubble motion and bubble-droplets in immiscible liq., photographic obs. method *(German)* 79−72931
cavitation emulsification mechanism employing high-speed photography *(Chinese)* 78−14049
cavitation shock wave, investigation by coherent optical methods 78−38431
cellulose nitrate film ion data, dark-field illum. image recording photographic method 80−70031
Cherenkov photographic detector appl. to search for Dirac monopole 78−70700
circular surface trueness testing by laser speckle photography 79−86266
citrus orchards, diseased, automatic interpretation of IR aerial colour photographs 77−56749
cloud analysis via space-derived pictures, appl. of photographic equidensity curve method *(Russian)* 77−53155
coastal zone development pressure monitoring by remote sensing 78−78013
colour astrophotography, slide and print developing 79−29996
colour holography, determining exact characts. of photographic recording materials 77−634
colour image recording on monochrome film by carrier frequency photography *(Japanese)* 77−41711
colour IR film for mapping and multispectral photointerpretation 79−25356
combustion phenomena deflection mapping, speckle superposition techniques 78−44379
composite insulation breakdown under AC and impulse voltages 78−23398
computerised tomographic image display by TV and photography 80−8129
cosmic ray expts. on ocean floor 80−36509
CRO photographic recording status 79−93247
crop canopy complex aerial photographic images, analysis and electronic area meas. 79−26159
CRT display documentation 79−21827
CRT photography, self developing film utilisation, applications 79−58811
CRT recording, fibre optic face-plate for high-efficiency photographic recording *(German)* 77−54801
CRT thermal image recording, scale and luminance distortion elimination 79−50398
cryogenic liquid, bubble population density meas. on immersed heated surface 77−30169
cylinder, heated, melting around it, photographic appl. 79−23195
cytogenetics, applications of photomicrography 80−21577
demonstrations, audio-visual presentations for physicians, photography of medical X-ray plates 80−37103
depth contours determ., double photography in coherent light *(French)* 77−87733
diamond, identification from reflection pattern photographs 78−54481
dielectric liquids, breakdown mechanism obs. using high speed photography 79−91367
diesel engine transient fuel jet droplet photography using light pipes 80−23784
diffusing object axial displacement meas. in speckle photography 77−57301
diffusing object surface state study by double speckle photography 79−85120
diffusing surface determ. by speckle photography 79−85117
diffusing surface inclination determ. rel. to viewing direction, speckle photography 79−2815
digital crop identification, high-altitude versus Landsat imagery 79−25357
dilatometry, photography appl. 79−15622
discs, impact stresses, photoelastic investigation 79−37182
dust trajectory photography for compressible flow velocity meas. 79−82008

photographic applications continued
Earth's atmosphere, optical parameters determ. by aerial photography at sunset 80−90219
Earth exploration from satellite Soyuz 22, Raduga expt. *(German)* 77−56765
Earth resource thermal imaging by airborne system, possible LED use 78−93010
Earth resources surveying, multispectral photography from space *(Russian)* 78−16197
Earth surface multispectral photography from space *(Russian)* 78−16198
ecosystem succession detection by aerial IR photography 78−81459
electric discharge through sheet of paper, printed letters transcription onto plate 79−75634
electrical phenomena, observation using high-speed photography 79−17515
electrode effects, in aq. solns., high-speed camera obs. *(French)* 79−24751
electron diffraction, kinematic photographing of static patterns 77−18113
electron diffraction patterns of mols., photometry via IFO-451 microphotometer 77−27201
electron microscopy photographic exposure timer 77−41730
electron photomicrography of marine microorganisms on submerged surfaces 78−85454
emission spectrum recording of single-pulse CO_2 laser, using parametric conversion 79−10357
energy resource development role of Sandia Laboratories' photometrics division 78−58077
engineering struct. surface deform. meas. by laser speckle photography 79−40534
environmental change detection in digitally registered aerial photographs 80−106477
equidensiometric applications to photoelasticity 77−27495
exploding wire cylindrical blast wave high-speed photography for material impact testing 79−79189
explosive cratering phenomena, small scale, in geologic materials, photographic study 78−37093
eye, operations, photographic documentation using model 310 surgical microscope 80−56161
eye fundus photographs, automatic assembly using blood vessel structure 79−83991
filament velocity measurement, during spinning, streak photography 78−41367
fireball networks, review of 12 years of operation 77−33427
flame size determination over flat terrain 77−67516
floor mapping, Light-Behind Camera photography 77−5359
flow visualisation techniques eval. for liquids 77−58817
fluid flow in tube bundle beds, reaction kinetics appl. 77−84315
fluid section flow pattern speckle photography 80−103096
fluid velocity distribution meas. by speckle photography, expt. 79−86543
fluid velocity measurement by speckle photography and interferometry 78−26221
fluorescein angiography of the ocular fundus 80−67185
fluorescence angiography, colour and black and white, use of interference filters 78−48856
fluorescence photomacrography, bone growth and remodelling exam. 78−31982
fracture, recognition from stereo photographs 78−54140
Fresnel zone plate imaging, of solar active regions 78−49342
frost blisters, growth meas. using long-term automatic time-lapse photography 80−12437
fundus photography in optometric practice 80−67183
gamma scintillation camera, GSG-2 twin-transducer, colour shading, grey-scale photographic recording 79−34631
gamma-camera used in nuclear medical examinations, developments in photographic recording *(German)* 78−88733
gas bubble boundary surfaces in turbulent liq. flow, equivalence of photographic, chem. determs. *(German)* 79−32630
gas laser medium, large-bore CW high-energy, holographic interferometry during power extraction 80−28172
general object deformation decomposition by speckle displacement 80−106486
geological joints, mapping via photogrammetry and EDP appl. 80−56470
geometric correction for LANDSAT MSS data 79−58120
goniophotography in optometry 80−67182
gross surgical specimen photography, centimetre rule/elevator rod technique 78−61287
n-hexane, tank flame, turbulence, holographic interferometric synchronous photography *(German)* 78−51255
high detective quantum efficiency image detectors, review 77−71010
high speed bubble domain motion, high resolved obs. system 77−40096
high speed cine photography, in industrial engineering environment 78−37099
high-speed cineradiography, of projectiles 78−41395
high-velocity gas jets, interaction, photographic study 78−42695
holographic interferometry and speckle photography, scatt. geometry, topology vector fields theory 80−87347
holographic recording of digital colour TV signals on photographic film *(German)* 78−22101
holographic summation using thermoplastic photographic plate *(Russian)* 79−22911
hot gas plasma, building up compression rings by dielectric spark discharge in layers of liquid 78−38493
human chromosomes, fluorescent, improved photography method and system 77−60318
hybrid image processing 78−25810
hypersonic ballistics experiment, application of laser light source 78−38433
idiopathic scoliosis, adolescent, monitoring with Moire fringe photography 80−17047
image difference detection using the Weigert effect 79−81376
image transmission by modulation spectroscopy *(French)* 77−14663
immunogram recording apparatus, self-contained, modified version using Polaroid film 80−17209
in-plane vibrational analysis, time-averaged moire method 79−68665
interferometric gratings, three beam interf. images, sinusoidal complex object with phase modulation 80−53208
interferometry, double-exposure, with instant Polaroid film 79−221
ion detector, electro-optical, for spark source mass spectrometry 80−42246

photographic applications continued
IR photography, principles and appls., book 78−82068
IR time-resolved spectral photography, transient broadband absorption spectra 80−18024
knee joint movement during walking, meas. method using photographic records 80−17048
Lagrangian turbulence characteristics meas. using photographic techniques 77−58811
land-use photo classification using optical spectrum anal. 78−12023
landform photograph three-dimensional projection system 77−74181
LANDSAT image photointerpretation/classification using negative spectral bands 77−78498
LANDSAT imagery, photographic data extraction 77−33212
Landsat satellite programme for remote sensing of the Earth *(French)* 79−40058
large-spot laser damage meas., multibeam apparatus 77−19286
laryngeal cinematography, high speed, optical/lighting system 80−17055
laser energy meas. of Q-switched ruby laser, photographic film calibration 78−5517
laser fusion, shadowgraph and interferometry experiments, with ten-picosecond light source 78−42824
laser intensity distrib., hot spot detect. using Ag halide film 78−82945
laser IR pulse recording, semicond. ionisation-type photographic system 78−49903
laser light energy distribution analysis, film calibration method 77−79875
laser produced plasma, ultraviolet probing with picosecond pulses 78−42827
laser recorder of video signals, on dry-developed photosensitive paper *(French)* 78−92998
laser speckle, transient Benard convection, vel. meas. 79−32508
laser speckle photography, double-exposure, magnification change effect 79−40607
laser speckle photography, for nondestructive testing 77−67515
laser speckle photography for fluid flow vel. meas. 78−14112
laser speckle photography for in-plane displacement sign detect. 77−79140
laser stereometry using range-dependent time delay in reflected light 77−10127
laser-matter interactions, automatic treatment of data *(French)* 78−42830
LEED, photographic-vidicon camera method for intensity meas. 79−37596
LEED beam intensity measurement by photographic method, use of Vidicon camera 77−7638
light sectioning, three-dimensional measurement system in medicine 78−24113
lightning, return stroke rise-speed meas. method *(French)* 80−51493
lightning, rotating camera obs. in Northern Poland 77−91185
lightning, stationary camera photographic obs. 77−91184
logarithmic filtering using inherent film nonlinearity 77−88646
low Sun-angle photography, flight planning, interpretive techniques 77−78465
lunar photography for amateur astronomers 78−45238
macrophotography, simple flash equipment 79−17513
manufacturing processes, industrial visual testing, photographic methods as technical aid *(German)* 80−31923
map intensification from small format camera photography 79−25354
maps extraction from satellite images 80−76899
marine photography and side-scan sonar image processing 77−5357
marine profiling images, recording, signal amplitude preservation 78−36326
marksmanship training, moving target screen system with laser beam firing 78−54488
mass spectra, automatic recording microphotometer modification 77−12845
mechanical impulse testing techniques, computer evaluation, high-speed film recording 78−44343
medical, organization of photographic department at large hospital 79−17514
medical photomicrography, elimination of dust 77−70576
medical treatment and litigation 80−36189
medicine, diagnostic radiology, radiation therapy, nuclear medicine, sensitometry, review 78−20260
medicine, problems encountered in hospitals 79−12875
metal erosion by solid particles, high-speed photography 78−39919
metal granules, form. mechanism study during centrifugal atomisation of rotating blank 80−100798
metal pipe, thermal strain recording at elevated temp., photographic technique 77−66731
meteor camera network on Canada 78−65563
meteor observation, effective field of view for line sources 78−36535
meteor wind radar, semiautomatic display and photographic recording system 79−8712
micrographic information storage and image retrieval, perforated film, mag. striped film, pocket microfilm reader 78−16779
microstructure observation apparatus, observation during heating, stressing, under vacuum, photography facility 77−73403
mineralogy, goniometry, from photographs or angle-true sketches 79−55619
miniature exploding foil, pulsed laser stereophotography 78−41364
monocomparator use of digitised stereoscopic plotter 77−26420
multiband photography for geomorphology, soils and land use study, feasibility 78−12025
multispectral camera, use on Soyuz 22 spacecraft 78−40794
multispectral photography, using MKF-6 camera and MSP-4 projector 80−56633
multiuser particle track photograph meas. computer programs *(Russian)* 77−38591
natural convection patterns in inclined box, three-dimensional photography 77−19600
neural unit activity rel. to movement, photographic technique for anal. 80−67310
noctilucent clouds, cine and television high-resolution obs. 79−39891
North Sea pollution detection by remote sensing *(Dutch)* 78−36202
nova searching, projection blink comparison method 79−12407
ocean wave imaging and wavelength meas. by aerial photography 80−46323
ocean wave slope determ. from surface photographs 79−16680
oceanography, bubble populations in coastal waters, analysis 79−100849
ocular cinema photography 80−67186

photographic applications continued
ocular photodocumentation, conf., Birmingham, USA (Dec. 1977) 80−62362
ocular photography, accessory fill-in flash for the Nikon photo-slit lamp 80−36056
ocular photography, new instrumentation and techniques 80−67187
one-dimensional coded apertures, applications 78−45746
one-dimensional kinoform preparation using photographic template *(Russian)* 79−22914
ophthalmic photography, external 80−67180
ophthalmic photography instrumentation, survey of clinical impressions 80−67188
optical diffraction slits, production, photographic method 79−71191
optical image quality data derivation from edge sharpness, simple math. methods 78−50722
optical system aberration testing using speckle shearing interferometer *(French)* 77−65616
orthomapping review 78−88777
orthophoto mapping, accuracy prediction 77−40970
orthophotography, history, advantages and uses 77−66995
orthophotography, system errors of differential rectifiers with optical projection 77−40971
oscilloscope cameras, new fast oscilloscope makes special photographic techniques redundant 80−27287
Palomer Schmidt plates, astrometric accuracy 78−57455
paraffin, solid-liq. interface motion during melting, convection effects, photographic obs. 79−18890
particle analysis in sedimentation, semiautomatic device for photograph analysis 77−44515
particle camera, aircraft-borne, for in situ photography of cloud particles 78−85750
particle motion in gas stream, motion parameters determ. with photographic system 78−5837
particle sizing using laser photography 78−81946
particle track recording in nuclear emulsion, using microscope nonachromatic objective 77−400
particle tracking, association with laser fringe anemometry 80−38512
patient diagnosis on thermal burns 78−3648
patient topology, optical process for three dimensional assessment 79−20692
pendant drops, surface area meas. 78−30813
periphotography for irradiation specimens 79−17512
personnel exposure during cardiac catheterisation, calc. technique using time-lapse photography 79−39504
photochromic tracer film, measurements using POLLY, film reading computer system 78−42696
photochromic tracer technique, for nondisturbing flow measurement 78−38435
photographic recording feed mechanism 78−78564
photointerpretation and photogrammetry teaching in natural resources field 77−74175
photokeratoscopic technique for corneal image study 77−1993
photomapping using earth terrain camera, Skylab photographs quality evaluation 77−2283
photomicrometry with moire 78−4690
picosecond laser meas. of ultrafast mol. processes 77−79709
pin bowing in AGR fuel elements, meas. by camera device 80−106146
pinched electron beam prod. expanding gas bubbles, fast photography obs. 80−79564
pipe-exit flow visualisation using high-speed photography 80−106863
planetary surfaces brightness characts. calc. method 79−62754
plasma spatial temp. distrib. meas., interference filter photographic method 78−67332
polyethylene terephthalate, joint prosthesis fragment dispersal meas. *(German)* 79−8566
polymer, loaded, mech. of macrocrack generation and propag., photometric and X-ray meas. 77−4886
polypropylene, transparent film, strain anal. by scattered-light speckle photography 79−32399
portal film duplication using instant photography 79−30591
posture and spinal disease documentation by moire topography *(German)* 79−16264
precision circular scale manufacture by contact photographic printing 79−75638
pressure vessel, defect detection, strain evaluation laser holographic and speckle photography methods 77−81365
principle surface strain determ. of arbitrarily deformed objects using tandem speckle photography 79−32408
projectile rotation meas., Brenneke slugs 78−45744
pyrometry, optical, accuracy improvement using photography 80−62673
pyrometry technique and external calibration 79−93144
radiographic image analogue processing by photographic spatial filtering 78−57070
radioisotope rectilinear scanning, direct recording of images on 4×5 in. film 77−5066
rain impact and erosion recording, laser techniques 79−62610
rapid events, photographic study by picosecond techniques 78−42826
Rayleigh-Benard flow, equal velocity fringes by speckle photography 80−75005
real time laser recording, plastic versus metal coatings 77−74536
remote sensing, introductory review 77−2286
remote sensing, spectral reflectance, scene composition, instrument for simultaneous recording 78−81443
remote sensing imagery, spatial filtering 78−90385
remote sensing in visible spectrum 77−56773
remote sensing of forests, two-camera intervalometer appl. 78−77367
remote sensing of natural resources, pattern classification techniques 77−64454
remote sensing of ocean surface currents, recent progress 77−87114
remote sensing/photogrammetry education in USA and Canada 77−74174
roll film back for photographic spectral detection 79−12857
rotating object, vibration anal., image detector in hologram interferometry and speckle photography 78−59351
rotation measurement, in-plane, speckle photography appl. 80−31714
Salyut-6, photographic investigation of ionospheric D- and F-regions *(French)* 79−40059
satellite, using electron beam film recording equipment 77−10120
SAW grating, Ag film on piezoelectric quartz *(Russian)* 78−18134
scanning laser beam direct picture printers on photographic paper, appl. in life sciences *(French)* 80−72119

photographic applications continued
scintigrams recorded on X-ray films, simple method for copying and photographic data processing 79−16283
SEM, instant imaging systems appl. 78−21300
SEM, photographic densitometry, appl. to chromosomes 78−77168
SEM positive print photography of CRT image 78−82082
semiautomatic device for analysing photographs of tracks of settling particles 77−44515
sensitometry, use of photographic film in radiometric meas. 78−269
shock wave instability determ. by high-speed photography *(Russian)* 77−75940
shutter system, digitally controlled, for spectroscopic appls. 77−82609
silhouette photography, high-speed, of small biological subjects 78−44743
sky image coherent-optical processor for moving object location 78−78944
Skylab imagery, method to differentiate saline from non-saline rangelands 77−91322
Skylab photographic X-ray images, analysis 78−49341
slides and overhead transparencies 79−80405
slit alignment in X-ray tubes, rapid photographic procedure 77−26448
slit lamp photodocumentation of ocular structure 80−67181
smoke flow visualisation combined with hot-wire anemometry, technique, appl. to turbulent boundary layer 78−91044
soda lime glass, microparticle impact, high speed photography obs. 78−44223
soil surface moisture determination, photographic method for polarised visible light recording 79−53557
soil survey, lowland England, moisture content and soil discrimination from air photos 79−88504
solar aureole almucantar radiance meas., comparison between photographic and photoelec. methods 78−77321
solar aureole meas., validity of aerosol single scatt. 77−5448
solar aureole rel. atm. aerosol props., photogrammetry 78−57315
sound triggered electronic photo flash unit, using variable time delay 80−57407
Spacelab optical techniques for liquid flow and temp. meas. 79−82007
spatial inverse filters, simplified holographic fabrication 79−23077
spatial recording of radiation intensity in caustic, photographic recorder 78−58007
speckle, meas. of longit. rot. and lateral motion of diffuse surfaces 78−21235
speckle applications, review 77−83820
speckle averaging, imaging step, subchannel holography 79−22918
speckle interferometric analysis of transient phenomena 80−105701
speckle interferometry, displacement meas. errors rel. to camera displacements during exposure 79−17479
speckle patterns, photographic recordings, fringes generated in Fresnel plane 78−66763
speckle photography, flow velocity distrib. meas. 78−67288
speckle size variation with film density, example of Babinet's principle 79−76592
spectral reflectance photography of the ocular fundus 80−67184
spectroscopy, time-resolved, IR, using freq. upconversion, methyl isocyanide isomerisation obs. 80−57400
spectrum analyser photographs improved using double-exposure technique 78−12714
sports activities, velocity meas., stroboscopic photography, teaching appl. 79−44679
square-field scanned image construction time optimisation *(Russian)* 80−63933
steam generator inspection by photographic and visual methods 79−54557
stellar photographic photometry, PDS microdensitometer technique 79−88600
stellar spectra recordings 79−16956
stereo-ophthalmoscope 110, stereophotography of fundus 78−48906
stereo-orthophotography, method and accuracy 77−44904
stereo-orthophotography in cadastral and general mapping 77−40972
stereo-photogrammetry for determ. of patient surface geometry 79−62330
STEREOMETROGRAPH model G with fast motor drive 77−66996
stereophotography, using camera slit lamp, ophthalmic applications 78−48904
stereoscopic instrumentation, kinematic and kinetic analysis of human wrist 80−16999
strain meas. by speckle photography technique, accuracy assessment 79−86389
strain meas. speckle photography with hybrid optical/electronic image processing 80−106768
strain measurement by speckle photography, hybrid optical and electronic image processing 80−99976
stress analysis using holographic interferometry and speckle photography 78−70095
stress measurement by sandwich speckle photography *(German)* 80−10216
striascopic imaging of profiles with laser light, surface tension measurement 79−2845
subspeckle size changes meas. by laser-speckle photography 80−31853
sulphate residues of fresh waters, elemental, anal., spectrographic technique *(Russian)* 77−12868
surface of engineering structures, defocused speckle photography, tilt topology technique 77−26419
surface rapid motion under dynamic loading, high speed photography of Moire fringes 78−32789
surface roughness meas., speckle correlation of diffuse surface image *(French)* 77−61115
sweeping slit camera, characterisation of 1060 nm picosecond laser impulse *(French)* 78−42366
swimming parameters of aqueous organisms, determination by cine recording and computer processing *(Russian)* 77−32921
synchrotron, electron beam spot, photographic obs. 77−71709
terrain classification using colour imagery, algorithms 77−78466
thermal spectrozonal aerial photography, capabilities and future prospects 80−18036
thermoplastic moulding quality assurance using holography and speckle photography 78−27720
three dimensional deformation measurement, Moire and light slicing methods 78−8382
three-dimensional trajectory of luminous pointlike object, recording method 78−12671
photographic applications continued
thunderstorm photography and lightning recording with modified cine sound camera 79−21058
time-resolved coded aperture imaging system, for nuclear fuel motion HCDA conditions 78−45764
TOPOCART-ORTHOPHOT C system for prod. of stereo orthophotos 77−66994
topographical mapping of the human face by Moire photography 80−85462
transient cavitation, on marine propellers, high-speed photography 78−38432
transient jet experiment, multiple-laser light source 78−14114
turbulent shear flow, coherent structure, stereoscopic camera obs. 79−32485
TV teaching demonstration 77−49538
underwater photography 79−58812
US intensity pattern characterisation, thermographic-photographic technique 80−106689
vegetation resources interpretability for various space acquired image types 79−26160
velocity contour generation by speckle photography 77−2638
vibrating object speckle photography, contrast of time-averaged pattern 78−50703
Viking Orbiter rectified photography, planimetric Martian triangulation 77−87276
virgin land resources, remote sensing, appl. of aerial and satellite photography *(Chinese)* 79−53551
visual behaviour monitoring system, EMG triggered photographic technique 78−31919
visual task prediction from image quality data 78−53415
vortex-excited vibration mechanism of cylindrical struct., photographic evidence 79−46406
water jet, penetration through water surface, high-speed photography 78−42693
welded joint inspection by X-ray TV intrascope, photographic recording of images 80−86485
welds obs. at high temperature, by moire photography 79−74336
wrist, human, kinematic and kinetic analysis by stereoscopic instrumentation 79−92274
X-ray diffraction patterns, recording on photographic film 78−41130
X-ray imaging, conf., Reston, USA (Apr. 1977) 78−45762
X-ray photographic method for determ. of stable I in tissue 77−70540
X-ray tomography, transaxial 79−93242
AgCl emulsion, spatial differentiation, of intensity distrib., using Weigert effect 79−81377
Al plastic flow visualisation in plain strain extrusion 80−7626
As_2S_3 chalcogenide glass films, photographic Ag photodoping to produce negative relief image 80−59490
CO_2 pin-bar TEA laser, internal arcing, ultra high speed photography 78−9357
CO_2 pulsed laser output, spatial distrib. meas. by photographic device 79−14008
Fe-B amorphous ribbons formation, high-speed photography investigation 80−76216
^{4}He, superfluid, turbulence, electron photography *(French)* 80−54456
^{4}He, superfluid, vortex photography progress report 79−55968
I laser energy profile meas. using hypersensitised photographic plates 78−5518
$LiNbO_3$, low freq. Raman scatt. spectra of polaritons, photographic recording 79−73952
$LiTaO_3$, low freq. Raman scatt. spectra of polaritons, photographic recording 79−73952
OH emissive layer, waves, atmospheric dynamical process study 80−51545
Xe discharge lamps, large, electrode temp. meas. *(Russian)* 80−47057
Xe, high power pulse gas dischargees development, photographic obs. 80−14954
$(YLuSmCa)_3(GeFe)_5O_{12}$ garnet films, bubble expansion saturation vel., sampling optical photography 80−75820

photographic developers *see photographic materials*

photographic development *see photographic process*

photographic emulsions
adenine, restraining effect on photographic emulsion *(German)* 79−39175
aerochrome IR film var. and high-altitude photographic appls. 79−2180
astronomical photography, emulsion shifts and astrometric accuracy of the photographic plate 77−71006
astronomical photography, hypersensitisation, state of the art review 77−2344
autoradiographic emulsions, effect of antimasking substances on Ag grain size and structure in developed image *(Russian)* 77−49799
blackness-exposure curves for low energy X-rays 79−21842
cellulose base, extraordinary reflection halo *(German)* 80−42282
characteristic curve, projective approximation *(Russian)* 80−95180
characteristic curves of photographic material used in emulsion chambers 79−49905
chemical ripening in presence of aurous complexes, role of gelatine, pH, pBr and thiosulphate 79−20422
chemical sensitization, modification by stabilizers and antifoggants 79−24781
chlorobromide halide-exchange emulsion, mass and distrib. of photolytic Ag in solarisation region 78−29185
coated on birefringent substrate, construction of multicapacity matched filters 80−74478
coating evenness in raw films, test results *(Hungarian)* 80−57410
coded-aperture image deconvolution, single-emulsion-layer holographic inverse filters 79−76647
colour cine film emulsion, math. model of charact. curve, developing effects *(Russian)* 78−16888
colour holography, emulsion VRE-52, determining charact. 77−634
colour imaging technology for instant photography, high speed emulsions 78−62247
colour negative film Gevacolour type 682, 35 mm, 16 mm professional film making appl. 80−82838
colour photographic paper, minimum surface conc. of Ag and colour components *(Russian)* 79−67409
colour reproduction of objects by speckle interferometry in white light 80−47094
colour reversal films, colorimetrical investigations *(German)* 79−44961
conference, Rochester, USA, 1978, Aug. 79−20394

photographic emulsions continued
contrast, effect of light incident angle 79−67400
cooled emulsion photography for amateurs, astronomical appls. 80−56714
couplers-gelatin (hydrophilic synthetic polymer), viscometric behaviour 78−16866
CRT film exposure device, gamma correction method 77−10125
cyanine dyes, low dimensional aggregate models from crystal struct. anal. 79−19241
Dancer microphotographic emulsion identification 79−17177
desensitization by spectral sensitizing dyes in liquid sensitometry 79−20429
detection threshold and photometry, influence of granularity and light diffr. 79−21839
developed photographic emulsion, relation between exposure and optical density and charact. curve parameters *(German)* 80−105742
developers, ID2 and ID11, development rate parameters 78−16868
development probability, AgBr grain diameter depend. 80−9056
diazo film, dark image stability 78−16882
diazo salt sensitised gelatin for holographic recording, grating form. 80−78798
dichromated gelatin as holographic material, book contrib. 78−25833
dielectric loss 79−19836
diethylimidacarbocyanines, relation between photographic desensitising action and alkalinity *(Russian)* 79−67418
direct positive emulsions, reduction and S sensitization for core and shell 79−20411
displays, colloquium, London (1978) 79−50258
dry silver recording materials, 3M and Kodak, for laser imagery transmision appl. 78−70209
dye clouds, random-sphere model 78−4722
dyed Ag halide powders and emulsions, light induced ESR signals 79−24211
Ektachrome-X, thin layer chromatographic anal. of dyes formed by development *(Japanese)* 77−26418
electric field effects on photographic emulsion layers, sensitivity *(Russian)* 77−67524
electron diffraction studies of high-temp. vapours, photographic plate 77−39516
electron image plates, response in gas-phase electron diffraction expts. 78−54482
electron microscopy, HV, design features of photographic film 78−8478
EM, electron exposure-dependent contrast transfer 80−104837
energy transfer in spectral sensitization 79−20427
EPR signals, nature of paramag. centres *(Russian)* 77−36112
equidensity film, calibration of lines 77−18118
evanescent wave holography using Gaussian beam, recording geometry and colour sensitivity 80−58473
exposure fluctuations, grain shielding effects on the characteristic curve 79−30594
film grain size and transmittance influence on fluctuation and diffraction spectra *(German)* 80−4788
film response to 25 MV X-rays, sensitometric curves, relative dosimetry 80−52376
film-grain noise degraded image estimation 78−54479
film-grain noise in holography 79−55082
fine-grained bleached emulsion scatt. model and expt. 80−102670
finite-width line axial optical density prediction 79−27193
fixing process, developing agent influence *(Russian)* 77−41721
fogging by metals, peroxide/exoelectron controversy 77−63939
frequency-contrast characteristic, effects of optical parameters and boundary conditions *(Russian)* 79−5168
gelatin, effect of air humidity on photolayer thickness, holographic characteristics *(Russian)* 80−105736
gelatin coating swelling meas. by real-time holographic interferometry 79−98316
gelatin enzymic hydrolysis expts. 79−79311
gelatin hardened layer structuralisation, kinetic anal. using swelling 78−62255
gelatin-Pd II complex formation, circular dichroism and absorpt. spectra meas. 79−61881
gels, coloured component addition, struct. form., dynamic shear modulus, viscosity meas. *(Russian)* 80−7871
gradation characteristics, effect of absorbing layer on photosensitivity *(Russian)* 80−62778
grain interaction effects, Markov random field model 77−54002
grain sensitivity, γ/κ ratio 79−44963
grain size, uniform, sensitivity spread contributory factors 78−16864
grey tone rapid process films for US imaging 78−96081
Herschel effect as a rehalogenation process 80−26034
high diffraction efficiency film preparation methods, holography appl. *(Italian)* 78−50730
high shear rate viscosity and dynamic surface tension 79−19495
high-resolution film, facile image evaluation 77−74533
hologram grating on Kodak 649F plate, diffr. efficiency with modulation depth var. 77−3553
hologram interference fringe bending due to pre-stress in photographic emulsion 79−98318
hologram recording, effects of photographic emulsion speed and contrast nonlinearity 80−106497
holograms, 3-dimens., emulsion thickness change effects 78−78968
holographic display, large scale, in photographic emulsion, image reconstruction 78−78974
holographic emulsion monobath and reversal processing techniques 80−102668
holographic emulsions for stellar spectra recording by interferometric method 78−73651
holographic requirements 79−50262
holography, diffraction efficiency, depend. on size of developed Ag particles 78−78965
holography, three-beam polarisation, influence of photographic material nonlinearity 78−58952
holography with chromogen developed photography emulsions 78−55319
hypersensitisation by heating *(Russian)* 79−58823
hypersensitisation for astronomy *(Swedish)* 78−85853
hypersensitised astronomical plates, detective quantum efficiency gains and speed 77−64660
hypersensitization techniques for astrophotography 77−33356
image restitution quality of layers, effective MTF concept *(Russian)* 77−38044
image sharpness, influence of emulsion layer parameters 79−21847

photographic emulsions continued
image weak modulation detection in film grain noise with partially coherent illumination 80−77897
instant film development, interdisciplinary and international approach 80−81342
IR chemical hypersensitization 77−2706
IR emulsions, sensitisation and use in vacuum-cold camera 80−90341
IR film, colour compensating filters for remote sensing 77−33210
IR film, density shifts with colour compensating filters 78−62256
Kodak IIIaJ hypersensitized plates, low intensity reciprocity failure elimination 77−9667
Kodak spectroscopic plates type 103a long term storage in dry N 77−71391
Kodirex film, use in high resolution TEM 77−54025
laser damage to photographic emulsions used in optical correlators 79−27303
laser imaging dry process development film *(German)* 79−9253
latent image distrib., etching and recrystn. effects of solns. 80−77890
latent image form, grain diameter depend. 78−62244
latent image formation, concentration theory 79−34334
latent image formation, influence of recombination 77−5945
latent image formation, photoemf method 79−17545
latent images rel. to wavelength, photometric obs. *(Russian)* 78−49927
latent photographic images, erasion by electric field *(Russian)* 79−97462
layer, scattering indication in forward hemisphere *(Russian)* 78−37091
light sensitivity, effect of applied electric field *(Russian)* 80−296
luminescence rel. to latent image 80−73498
luminescence spectra of emulsion microcrysts., effect of adsorbed Ag ions *(Russian)* 77−69912
mammography film/screen combination, reciprocity law failure 78−65103
medical image lesion contrast and photon count density rel. to D-log E curve 78−69195
medical imaging, sensitometry 78−69193
medical X-ray film/screen system noise 79−21841
microdensitometers, props. effect on photographic emulsion charact. curve 79−43673
modulation transfer function, interference-diffraction method 79−21844
monochrome photographic film densitometry errors and standards *(German)* 80−37102
monodisperse Ag halide photographic emulsion production methods, review of patents 1955-75 *(Russian)* 78−58084
monodispersive emulsions, frequency-contrast responses, resolution magnitude, sensitisation effects *(Russian)* 80−295
monomeric dye spectral sensitising efficiencies, conc. depend. 79−20426
mountain aerial photography, colour film types compared 77−29500
noise diffraction spectra 80−27368
nonoptimally exposed holograms, reprocessing techniques 80−58474
nuclear medicine images, minimum detectable grey-scale differences 78−61249
optical emission spectroscopy, emulsion calibration curve 79−43650
Orwo ZU 2 plate with improved props., astron. appl. *(German)* 78−89571
p+emulsion, 200 GeV, star event containing single electron, charmed particle generation, anal. 77−61414
partially coherent perpendicularly polarized vibrs., anisotropic photographic recording, interferograms 80−57364
penetration rate of developer components through gelatin and photoemulsion layers 79−20436
photocharge decay kinetics correl. with photographic efficiency 79−19634
photolysis of ultra-fine grained emulsions, nature of produced colour centres *(Russian)* 80−73517
photon noise rel. to granularity 77−2708
photosensitivity, H_2 hypersensitisation with Au sensitiser *(Russian)* 80−73511
plate making, relationship between Ag halide emulsion and non-Ag halide sensitive materials 79−17541
Polaroid film, developed, use as recording medium for pulsed laser radiation 79−94270
preparation, explosion hazard of ammoniated silver salt solns. 78−4727
production, effect of mixing on diffusion rate *(Russian)* 80−3388
proton detection, fluorescent intensification screen+photographic film combination, response, radiography appl. 78−20268
radioactive uniform sources of extended area using radiotoned photographic 78−78537
radiography, integral formulation of total unsharpness 77−16978
radiography screen-film combination selection 80−46047
redox potential evolution during development, potentiometric anal. 78−16865
reduction sensitised emulsion by dyes, redox potentials, quantitative correlations 79−34298
removal from cinefilm waste using Protosubtylin 13x-I *(Russian)* 80−105734
response relationship for holography 80−1148
response to temporally coherent radiation *(Spanish)* 77−87860
scale-up factors in the batch precipitation of silver halide photographic emulsions 79−20410
scattering, Callier effect, influence on image contrast 78−63017
scattering characts. of emulsion layers into rear hemisphere *(Russian)* 79−44967
SEM autoradiography for location and study of microscopic β-active particles 77−57425
semiconductor mask, emulsion processing chemical and plastic factors 78−16872
sensitisation of photographic film in elevated temp. H_2 gas, development 79−61885
sensitivity, effect of mech. loads, changes in optical density *(Russian)* 79−67410
sensitivity, empirical density function anal. of gradient curves 78−32909
sensitivity, latent image formation *(Italian)* 79−80709
sensitivity, long wave, rel. to impurity centres *(Russian)* 78−49925
sensitivity centre variation with AgBr grain diameter 80−9055
sensitivity of films used in high-voltage electron microscopy 80−22474
sensitizing dyes, efficiency and physicochemical props. 79−20424
signal-dependent film-grain noise, optimal image estimation 80−102659
Skylab environmental effects on photographic film 77−60620
small-grain development of emulsion monofilms for electron-microscope autoradiography *(Russian)* 80−297

photographic emulsions continued
soft X-ray film, Ilford Special Industrial-G, sensitometry 2.1 to 21.6 Å *(German)* 77−10126
solarization, elimination of adding halogen acceptors, electron microscopy investigation 79−24790
speckle pattern evaluation, emulsion swelling due to wet processing 78−49922
spectral, colorimetric characteristics colour positive cine film dyes *(Russian)* 79−49323
spectral sensitisation theory, review *(German)* 79−39172
spectral sensitization theory, review *(German)* 79−39174
spectral sensitizing dye design, use of molecular orbitals calcs. 79−20425
spectrochemical analysis, photographic emulsion calibration technique 79−79321
speed-granularity relations for X-ray and γ-ray exposures 79−21828
spreading and coating, electrical drive system description *(Russian)* 77−79172
stabiliser reactions with colloidal Ag, decoloration reaction kinetics *(German)* 77−40563
stabilization mechanisms 79−20416
step-wedge exposed emulsion, dependence of activation energy for development on size of latent image 77−5944
sulphide sensitisation of cubic and octahedral emulsion microcrystals, effect on photographic ageing *(Russian)* 80−95181
sulphide sensitisation of negative emulsions, quality composition of photosensitivity and fogging centres *(Russian)* 80−62781
supersensitisation by hydroxy-tetraazaindenes 80−3384
supersensitization by Dember effect, ESR meas. 79−20423
supralinear emulsions, radiobiological aspects of X-ray exposure 79−8549
surface microstructure of photographic emulsion layers *(Russian)* 79−58819
swollen gel layer, solute penetration times 78−16867
thermoplastic film for holographic display and recording 79−50263
thickness variation effects on photographic density *(Spanish)* 79−67401
thin layer chromatographic anal. of dyes formed by development *(Japanese)* 77−26418
thiolic antifoggants sensitizing emulsions, latent image form. enhancement 79−17519
two-jet emulsification kinetics of form. of mixed AgBr(J) phase *(Russian)* 79−44968
ultracontrasting film, Schwarzschild const. determ. *(Russian)* 78−37092
unconventional films, for satellite images macrophotography 79−29895
undeveloped emulsion layer, determ. of 3-D light scatt. function *(Russian)* 79−97460
undeveloped emulsion layer, MTF calc. 79−21840
undeveloped photographic film, MTF meas., target base dimension influence 80−102653
video photography in computed tomography and US imaging, film selection 80−41224
volume-phase reflection hologram, recording medium thickness effect on image luminance 80−58479
VR-M fine grained photographic films for holography with opposing beams *(Russian)* 79−68370
X-ray, for industrial radiography *(French)* 77−38069
X-ray film characts., heuristic model 77−195
X-ray films sensitive to green light, reciprocity law failure 78−69199
X-ray screen-film processing sensitometry standard developed by ANSI 78−69196
XUV Schumann-type films, experience on Skylab 77−60599
Ag halide, crystals and photographic emulsions, luminescence parameters at 77K 79−24787
Ag halide, Dember effect, photographic emulsion grain parameter depend. 78−16870
Ag halide, effect of Rh and other polyvalent ions on photographic props. 79−24785
Ag halide, fine grain, colloidal stability 79−20443
Ag halide, for holography, book contrib. 78−25832
Ag halide, grains, breakdown of $Na_2S_2O_3$, electron microscopy 78−21237
Ag halide, mechanism of development 79−39169
Ag halide, photomoment investigations of ionic and electronic props. 79−24782
Ag halide, SEM investig. of grain props., specimen prep. technique 77−41715
Ag halide, sensitivity and struct. characts., review *(Russian)* 79−2868
Ag halide, unsensitized, quantitative interpretation of latent image distrib. data 79−20403
Ag halide, visible luminescence obs. at or below 77K 80−108263
Ag halide crystals, relative dissolution rates meas. by flow calorimetry 80−85220
Ag halide crystn. during double-jet emulsification *(Russian)* 79−58826
Ag halide diffusion transfer development chemistry 79−96340
Ag halide dyed powders and emulsions, nature of light induced ESR signal 79−2852
Ag halide emulsion colouring, k-value and sensitivity relationship *(German)* 80−7815
Ag halide emulsion crystal growth, complex solubility computation 79−83516
Ag halide emulsion grains, photographic effects of electron and positive hole traps 77−82635
Ag halide emulsion props., Tl^+ ion influence 79−100413
Ag halide emulsions, hot carriers multiplication and latent image formation 79−20408
Ag halide emulsions, induced sensitized photodichroism 80−9061
Ag halide emulsions, positive, formation of microcrystals *(Russian)* 78−49930
Ag halide emulsions, primitive and $AgNO_3$-digested, IR luminescence obs. at 77K 80−103983
Ag halide emulsions, spectral sensitisation, review 78−4719
Ag halide emulsions, ultra-fine-grain, spectral absorption 79−24793
Ag halide film for nanosecond photography, 10.6 μm CO_2 laser pulse spatial distrib. recording 79−89016
Ag halide film physical props., effect of gelatin structure 80−97715
Ag halide films, DQE and ratio of gradient to granularity 79−21838
Ag halide gelatin emulsions, fixation and washing aspects 77−79176
Ag halide grains, latent image form. 77−5939
Ag halide grains, photographic sensitivity and response to charged particles, interstitial generation 77−10124
Ag halide hydrosol models 79−20470

photographic emulsions continued
Ag halide microcrystal, photoconductivity meas. by microwave technique 80−103719
Ag halide microcrystal, sensitised and stabilised, concentration speck and development centre growth 79−83484
Ag halide microcrystals, electron acceptoring props., chronovoltammetry 79−20441
Ag halide microcrystals, mechanism of reduction by electrode 79−20404
Ag halide microcrystals, pulsed luminescence expts. 79−24786
Ag halide monodisperse emulsions, granularity prediction in processed coatings 79−26163
Ag halide photographic layers, 3D holograms recorded with short exposures, diffr. efficiency 79−55087
Ag halide photography and xerography compared *(Japanese)* 78−24876
Ag halide system, high speed, for producing direct positives 79−20435
Ag halides, effects of ZnO, dyed ZnO and cyanine dyes on spectral sensitivity 79−20432
Ag halides, Ostwald ripening in non-ionic surface active agent environment 79−20412
Ag halides, sensitivity calc. 79−21843
Ag halides, spectral sensitivity of Herschel effect, photo- and thermostimulation photographic effects *(Russian)* 78−58082
Ag halides, spectral sensitisation, estimation of rate constant 78−89575
Ag, halides sensitivity to multiply charged ionising particles, temp. depend. 79−80714
Ag in developed emulsion, X-ray emission microanal. for β-ray quantitative microautoradiography 78−20545
Ag iodobromides, spectral absorpt. curves, density, wavelength and temp. depend. 78−16871
Ag layer reflectance and absorbance, influence on amplitude reflective holograms *(Russian)* 77−54683
Ag-AgCl emulsion, anisotropy induced by two coherent perpendicular light vibrs. 79−55196
Ag-AgI island granular film, Weigert effect, anomalous dichroism 77−12455
Ag-Br-I emulsion, high illumination, departure from reciprocity, intermittence effects, charact. curves *(French)* 78−79085
Ag-Cl-Br emulsion, high illumination, departure from reciprocity, intermittence effects, charact. curves *(French)* 78−79085
Ag-halide microcryst., space charge characts. 78−15097
AgBr (100) microcryst., dielectric loss meas., ionic conductivity 77−43931
AgBr and $AgBr:PbBr_2$, emulsion grains, dielec. loss, ionic cond. and surface space charge 77−28038
AgBr, and $AgBr_{1-x}I_x$, photolum. and X-ray luminesc. spectra *(Russian)* 79−2867
AgBr cryst. growth mechanism in gelatin solns. 77−54004
AgBr crystal face influence on aggregation of sensitizing dyes 79−20428
AgBr, crystal growth behaviour, influence of Gibbs-Thomson effect 78−24883
AgBr, cubic, supersensitisation of microwave photocond. 77−41713
AgBr developed layer, light scattering and absorption *(Russian)* 78−37090
AgBr, distrib. of Ag_2S on sensitised emulsion grains 78−62248
AgBr, dye sensitized photo-process 79−20433
AgBr, effect on photographic characts. of subbing glass substrate *(Bulgarian)* 78−78016
AgBr, electron simulation, luminescence and hidden image formation *(Russian)* 79−47515
AgBr emulsion, desensitizing action of a secondary iodide *(Russian)* 79−58820
AgBr emulsion, influence of iodide content on ripening behaviour 79−24794
AgBr emulsion, latent image speck size, characteristic curve anal. 79−34338
AgBr emulsion, latent image fading 79−34335
AgBr emulsion, model system, Ostwald ripening obs. 77−2707
AgBr emulsion crystal habit transitions 79−100447
AgBr emulsion grains, adsorbed dyes, light-induced ESR spectra 80−88862
AgBr emulsion grains, edge length dependence of ionic conductivity, space charge characteristics 80−88360
AgBr emulsion layer with gelatin, IR absorpt. spectra before and after laser exposure *(Russian)* 80−62776
AgBr emulsions, apparatus for studying reciprocity variations and intermittent effects *(French)* 77−71392
AgBr, epitaxial layer, ionic field effect 78−10588
AgBr evaporated layer chemical sensitisation 79−24766
AgBr evaporated layer response in ionisation semiconductor photographic system *(German)* 80−101859
AgBr film coatings, luminesc. props. for H_2 and other reduction sensitisation 79−61886
AgBr, grain disorder and its influence on emulsion response 77−5940
AgBr, Herschel effect, latent image centre struct. changes under laser irrad. 80−77900
AgBr homogeneous emulsions, iodide influence on photographic props. 79−44959
AgBr, hydrosol, latent-image stability, chem. sensitisation 78−21236
AgBr, influence of Cd ions on crystal shape 79−19235
AgBr, ionic thermocurrents 79−19399
AgBr, large grain emulsions, reciprocity errors and disturbance effects in high illuminations *(French)* 79−97452
AgBr, latent pre-image specks, investigations on temp. dependence of lifetimes by 'two-flash' method 79−20406
AgBr, low-intensity reciprocity failure *(French)* 78−37085
AgBr, luminescence of photographic emulsions sensitised by 1,1′-diethyl-2,2′-cyanine with Ag_2S clusters *(Russian)* 80−73513
AgBr melts, surface energy and surface tension coeffs., effect on photographic emulsion microcryst. growth rate *(Russian)* 80−47132
AgBr microcryst., ionic cond., dielec. loss meas. 79−23768
AgBr microcrystals, Herschel effect, $Na_2S_2O_3$ etching soln. effects *(Russian)* 79−5167
AgBr microcrystals, S sensitization effects on ionic conductivity 79−19398
AgBr microcrystals, spectrally sensitised, luminesc., effect of hydrophobic organic compounds 80−97331
AgBr monocrystals, dimensioning rel. to light scatt. of highly dispersive photographic emulsions *(Russian)* 79−49327
AgBr, monodisperse emulsion, cubic or octahedral, Ag sub-specks due to chem. reduction 78−16875
AgBr monosize emulsion growth 79−79312

photographic emulsions continued
AgBr octahedral emulsion, reduction sensitization 79−20420
AgBr, photographic emulsions, dye spectral sensitization, latent image form., subcond. band events 78−32905
AgBr photographic emulsions, sensitivity, fog rel. to treatment in redox-buffered solns. 78−32906
AgBr photographic emulsions, adsorpt. of thiolic antifoggants, chem. struct., ESCA investig. 78−32907
AgBr, photographic gelatin dispersion, cryst. habit. rel. to Br^-, cyanine absorpt. 78−32908
AgBr, photolysis, diffusion and recombination processes 79−24789
AgBr polydispersed particles in unsensitised holographic emulsion, bulk attenuation and absorpt. *(Russian)* 79−2865
AgBr, Se sensitized, high intensity reciprocity failure 79−20421
AgBr, sensitisation by hydroxy-tetraazaindenes 77−54006
AgBr single crystals, adsorption and orientation of cyanine dyes 79−20431
AgBr, sol, electrophoresis of spectral sensitising dyes, dye layering obs. 77−56240
AgBr, sub-image and latent image specks form. and props. 78−21245
AgBr surface, vibr. freq. of adsorbed Ag atom, LCAO-MO calc. *(Russian)* 79−2866
AgBr, thin layers, evaporation conditions, photoresponse *(Bulgarian)* 78−78017
AgBr, very fine grained emulsions, effect of hole and electron acceptors on photosensitivity *(Russian)* 80−73515
AgBr:I, photocond. and luminesc. at −186°C, rel. to incident light intensity 78−64063
AgBr:I single jet precipitation, grain growth kinetics 79−20414
AgBr:Pb^{2+}, cubic microcryst., ion influence on ionic cond. and space charge characts. 79−55928
AgBr-AgI emulsion sensitivity improved by AgCl shell crystallisation *(German)* 80−104453
AgBr(Cl)(I) ultra fine grained photog. emulsions, impurity obs. spectra *(Russian)* 79−69871
AgBrI, development, processing and DQE 79−24801
AgBr(I), emulsion coating, H hypersensitisation to diminish recomb. and increase quantum efficiency 77−5942
AgBrI, fine grain emulsion, spectral and reduction sensitization interaction 79−20430
AgBrI grains, TEM investig. of morphology and crystallography 77−57418
AgBr(I) microcrystal dispersed in gelatin, effect of I^- on interstitial Ag ions 78−26726
AgBr(I) microcrystals, photohole motion 78−26903
AgBr(I) microcrystals, photocond. and luminesc. 78−26904
AgBrI microcrystals, luminescence spectra 79−19935
AgBrI microcrystals, growth mechanisms 79−19171
AgBrI negative emulsions, sensitivity and fog centres with S sensitization 79−20418
AgBrI preparation, double-jet nucleation turbidimetry 79−100446
AgBr(I), sensitization mechanism of a tetraazaindene stabilizer 79−20415
AgCl, AgBr and AgI emulsions, kinetics of fixation by thiosulphate and Ag ion 77−82634
AgCl, anisotropy induced by two incoherent and perpendicular light vibrs. 79−41428
AgCl, crystal growth modification in aq. gelatin by incorporation of Br^- and I^- ions 77−5946
AgCl, electron simulation, luminescence and hidden image formation *(Russian)* 79−47515
AgCl emulsion, spatial differentiation, of intensity distrib., using Weigert effect 79−81377
AgCl melts, surface energy and surface tension coeffs., effect on photographic emulsion microcryst. growth rate *(Russian)* 80−47132
AgCl microcrystals in sol., cryst. growth, optical absorpt. 77−12835
AgCl monosized emulsions, S sensitization 79−20417
AgCl nucleation from aqueous solns., stopped-flow UV absorption spectrophotometry 79−20413
AgCl, photolum. and X-ray luminesc. spectra *(Russian)* 79−2867
AgCl, Weigert effect appl. to contrast reversal of black and white transparency 79−26165
AgI-Ag thin granular film, Herschel effect 78−82063
AgI-AgBr, low-intensity reciprocity failure *(French)* 78−37085
AgX, selectivity of development of small aggregates of microcrystals in photographic layer *(Russian)* 79−58832
Au sensitization mechanisms 79−20419
$Na_2S_2O_3$ digested AgX emulsions, red-IR photoluminescence obs. at 77K 80−103982
$PbCl_2$ emulsion layer, effect of elec. field on microcrystal sensitivity *(Russian)* 79−58831
PbI_2 suspension, chem. sensitization 80−73492
S and Au sensitisation, internal image speed 78−16869

photographic filters *see optical filters*

photographic lenses
see also aberrations
16 mm cine projection lens 79−72646
35 mm cinematography, effects of aspheric surfaces on optical performance and appl. to lenses 79−89021
aerial lenses, for multispectral photographs from high altitudes 79−35868
amateur camera light scatt. coefficient factors 79−71559
amateur camera objective lens production quality, MTF test freq. selection 79−81581
antireflection coating, multilayer, for camera objectives, practical effectiveness 78−58081
apochromat planar lens 133 mm f/6.3, astigmatism and longit. chromatic aberration meas. *(German)* 79−75636
apochromatic pancratic objective component chromatic aberration formulae 79−76795
Arriflex 35BP-II motion picture camera mounted with 350PF-1A zoom lens for wide-screen filming *(Russian)* 80−95176
Asahi Pentax 110, review 79−71544
aspheric optics production costs, instrumental and photographic applications 80−28308
astronomical camera lens, focal length determ. *(Spanish)* 77−64663
automatic focusing systems 80−18028
axial ray bundles achromatisation and Staeble-Ligotsky isoplanasie condition *(Russian)* 78−65988

photographic lenses continued
camera objectives, quality testing by semiautomatic modulation transfer coeff. meas. 79−14124
catadioptric lens system, possible appl. for satellite and astronomical photography *(German)* 79−76793
chromaticity of camera lenses, spectral transmission curves analysis 80−31925
cine camera, spectral characteristics measuring techniques, zoom lenses appl. *(Russian)* 79−49322
cine objectives quality evaluation, frequency transfer function *(Russian)* 77−41718
cinematographic, photo-pattern producing by optical method *(Russian)* 78−37959
cinematographic image quality improvement, dependence of resolving power on lenses *(Russian)* 80−27371
cinematographic lenses with fixed and variable focal length, comparison of types *(Russian)* 80−27370
cinematography, OMNIMAX system using Leitz wide-angle lens, domed roof in planetarium appl. 80−276
colour photography, lens transmittance 78−62250
colour TV camera lens testing, meas. of spectral transmission and modulation transfer function 78−94456
complex photographic lenses for low cost high production, design example 79−85193
Cooke triplet, air-spaced anastigmatic quadruplet design 80−1291
Cooke triplet derivative of five-element config., design 80−33111
$cosine^4$ losses in photographic lens example demonstrating 79−97456
design, new developments and trends at Zeiss 80−62746
design of lenses with long overall length and large diameter for movie cameras 79−30597
design parameters, 35 mm format enlarging lenses, survey 80−13168
development and trends at Zeiss 80−62745
EKTRAMAX camera lens design and performance 80−77894
electron micrographs of metal shadowed objects, low cost internegative prod. 78−74109
enlarger, Czechoslovak Opemus Standard (2) *(Czech)* 80−18034
equipment and services, 1979 video yearbook 79−14197
five-component wide-angle pancratic objective design 78−71190
focusing, close-up, new optical solns., macro mirror lenses 79−93240
focusing, close-up, new optical solns., spherical aberrations 79−97453
four-colour thin apochromat design 79−27364
four-element lens systems of Cooke-triplet family design considerations 80−57404
gradient index lens array fabrication for office photocopier 80−13178
gradient singlet, design techniques based on total aberrations 80−69479
gradient singlet, total aberrations 80−13177
gynaecological endoscopic photography, increased mobility using articulated lens 77−48928
image contrast theory of electronic focus 79−13914
image detection and recognition visual factors, optimal viewing conditions 78−4724
image formation, lenslet array with periodic sampling structure 78−37964
image quality, MTF meas. for lens testing 77−45912
image quality improvement 80−47123
image quality rel. to MTF for 48-inch camera 78−49938
imaging system assessment, conference, London, England (Nov. 1976) 78−50718
integral photography, lenslet-array system parameter selection 79−49317
interchangeable lens evaluation for 35 mm cameras, MTF based test method 78−41363
IR telephoto lens design, Ge 8-14 μm region 77−39011
kinoform lens production and optical testing *(Russian)* 79−98310
lens polariscope, non uniform illumination, remedies 77−87858
lens-array photographic system, depth of sharp focusing, resolution 80−62763
lens-array photography, longitudinal distortion compensation, integral image reconstruction 80−52345
lens-spectral filter combination, off-axis illum. distrib. determ. 79−26152
long focal length aerial reconnaissance system response to thermal shock 80−78939
long focal length reconnaissance lenses, reponse to thermal shock 80−77892
mass-produced camera objectives, effects of cosmetic defects 80−47135
mechanical compensation zoom objective, general Gaussian theory *(German)* 79−58810
modular optical design, control of fifth-order aberrations 79−55199
modulation transfer functions for lenses used with liquid crystal cells *(Russian)* 79−89025
motion-picture and TV camera objective lenses, testing by projection 80−9060
movie projector objective lenses, standardisation of optotechnical parameters and testing methods 80−28301
MTF based simplified test method, for 35 mm camera interchangeable lenses 78−49937
MTF measurement in France, ACOFAM and ACOMAT instruments 78−50727
MTF measurement of standard lenses in Japan, interlaboratory comparison 78−50720
multilens system image field curvature and residual spherical aberration mutual correction *(Russian)* 77−87857
objective colour correcting coatings 79−75631
objective decentring modulus, probability density distrib. calc. 79−76798
objective for deep underwater photography *(Russian)* 79−226
objective matching with film channel in serial prod., tolerances 78−16885
objectives in large scale production, testing 78−18035
optical glasses, development and manufacturing processes 80−53393
OTF, numerical calc. from lens design data *(Korean)* 80−19085
OTF standardisation in Japan 78−50726
OTF testing, USA standards 78−50725
pancratic telephoto lens, design and optical characts. 79−6207
performance meas. system, routine checking film, TV cameras appl. 80−277
photocopier lens array design, Wood lens and gradient index fibre comparison 80−14479
photogrammetry, distortion calibration, lateral chromatic aberration effects, operational data reduction 79−35881
Pinatar 4/125, aerial multispectral-photography appl. *(German)* 78−4717

photographic lenses continued
plastic optics for optoelectronics, moulding techniques for single, multi-element systems 78−63210
polishing and shaping techniques *(German)* 80−33114
PRAKTICAR, for B 35 mm reflex cameras 80−82839
reflex cameras, lens-array focusing system tests 80−86479
reflex cine camera Bolex H16, conditions for using ordinary lenses 79−26154
resolution of lens film system, computation from numerical MTF data 79−44960
retrofocus lens system designs for film cameras *(German)* 77−54768
retrofocus type, for motion-picture cameras 78−37963
rotating lens system for cine projection with continuous film transport 80−62766
rotating prism camera lens, 100 mm focal length, White Sands Missile Range, testing methods 79−86249
serial testing, resolving power limits 79−35870
spherical aberration measurement using solid-state image sensor 80−23812
surface quality testing at Zeiss factory *(German)* 80−33113
teleconcentric system for underwater use *(Russian)* 78−305
teleobjective types, image sharpness adjustment *(Hungarian)* 78−12780
telephoto apochromat lenses, design 80−31924
telephoto lens design, two-component, with positive Petzval coefficient 79−71557
testing using m.t.f., mass production 77−181
tomofluorographic camera with lens objective and angular tube 79−57750
TV 300 m lenses, modular construction method, Gaussian optics, Seidel aberrations 78−311
TV zoom lenses, MTF meas., distortion influence, normal and inverse conjugate techniques 78−78008
ultrashort pulse operations using flat lenses 78−66883
underwater lens system, metrical fundamentals 77−78457
variable focus objectives with mech. compensation 77−74539
veiling glare, simulation method to correct photometric meas. 78−58085
wide angle correcting lens for underwater colour TV 80−91883
wide angle lens family design 79−85194
wide-angle, fish-eye, lenses, optical constructions 80−18037
wide-angle lens, Flektogon F/2.8-20 mm 79−35869
Wood lens, third order aberrations 77−26413
zoom, for TV cameras, review *(Russian)* 78−90493
zoom lens, aperture diagram *(German)* 77−39016
zoom lens, Delano diagram *(German)* 77−18117
zoom lens design by pocket calculator 78−55423
zoom lens focusing system *(Japanese)* 80−31922
zoom lens system design and manufacture 80−68288
zoom lens systems for 8 mm and super-8 cameras *(German)* 78−93771
zoom lens vignetting analysis using Delano diagram *(German)* 77−61147
zoom lenses, aberrations analysis using Delano and aperture diagrams *(German)* 77−88888
zoom objective, displacement of individual lenses from ideal positions *(German)* 78−71186
zoom projection lens, optical level system, paraxial charact. 80−53399
zoom systems, varifocal eqns. *(Chinese)* 77−67517

photographic light sources *see light sources; photography*

photographic material sensitivity
adsorbed dyes, ionization energies rel. to spectral sensitization 79−19553
aging of nonsilver photographic materials in different gas media *(Russian)* 79−44972
amplitude hologram efficiencies, photographic film model 78−9345
astronomical plates, hypersensitisation, testing, for threshold imagery 78−32351
average film transmission function synthesis 79−2843
cardiac catheterization laboratory sensitometric system application and clinical evaluation 78−20263
cellulose complexes with pyredene and its derivatives, photosensitivity *(Russian)* 80−73506
cellulose triacetate films, local loss of stability, expt. anal. using high speed cinefilming *(Russian)* 79−58822
chemical sensitization, modification by stabilizers and antifoggents 79−24781
cholesteric liquid crystal panel, energetic sensitivity, as IR registrator *(Russian)* 79−89995
cholesteric liquid crystal photographic plate, for images in IR, extreme charact. *(Russian)* 79−89994
cine, automatic densitometer analyser *(Russian)* 77−41720
colour, copier technology appl. *(German)* 79−26156
colour film densitometer with Si photodetector 80−4791
colour film spectral sensitivity meas. by Hadamard spectrosensitometry 77−26414
colour negative film, rapid access processing 78−21240
colour sensitometry characteristic curves corresponding to visual impression 80−82803
colour sensitometry system based on spectral densitometer 80−82804
conference, Rochester, USA, 1978, Aug. 79−20394
copper oxalate hemihydrate, photographic props. eval. for use as high-speed photographic materials 77−44497
cyanine dye sensitisers, J-aggregate formation, spectral changes of UV bands 77−70318
cyanine dye sensitisers, J-aggregates, circular dichroism and induced Cotton effect 77−70319
cyanine dye sensitisers, J-aggregates, meso substituents effect on mol. assoc. 77−70320
cyclorubber with bisazides, effect of photoresist layer thickness on photosensitivity *(Russian)* 80−73510
desensitising dye polarographic half-wave potential meas. 80−7802
desensitization by spectral sensitizing dyes in liquid sensitometry 79−20429
detection threshold and photometry, influence of granularity and light diffr. 79−21839
developed photographic emulsion, relation between exposure and optical density and charact. curve parameters *(German)* 80−105742
developer activity, rel. to difference of electrochem. and redox potentials *(Russian)* 78−62243
developer redox pot., influence on sensitivity and quantity of developed silver *(Russian)* 79−44966
development and materials sensitometry *(Italian)* 79−93241
diazo materials, system aspects of spectral sensitization 79−20434

photographic material sensitivity continued
diethylimidacarbocyanines, relation between photographic desensitising action and alkalinity *(Russian)* 79−67418
diffraction, transmission, sensitivity at 442, 633 nm for holographic appls. *(Russian)* 80−43301
dry silver recording materials, 3M and Kodak, for laser imagery transmission appl. 78−70209
edge response curve, midpoint location, development microeffects effect 78−29196
electric field effects on light sensitivity of films *(Russian)* 80−290
electric field effects on photographic emulsion layers, sensitivity *(Russian)* 77−67524
electron microscopy, high-voltage, film sensitivity 80−22474
electrophotographic molecular recording media, photosensitivity during nanosecond exposure *(Russian)* 80−73516
electrophotography, deterioration of coloured images due to illum. in diaprojector *(Russian)* 80−62782
emulsion gradient curves, empirical density function anal. 78−32909
emulsion requirements for holography 79−50262
emulsion response to electrons in gas-phase electron diffraction expts. 78−54482
emulsion sensitivity, effect of mech. loads, changes in optical density *(Russian)* 79−67410
emulsion supersensitisation by hydroxy-tetraazaindenes 80−3384
emulsions, contrast, effect of light incident angle 79−67400
emulsions, effect of applied electric field on light sensitivity *(Russian)* 80−296
emulsions, H_2 hypersensitisation with Au sensitiser *(Russian)* 80−73511
emulsions, latent image formation *(Italian)* 79−80709
energy transfer in spectral sensitization 79−20427
film characteristics control by modulating intensity and space 79−2844
film grain noise, spectral density estimation, in electron microscopy *(French)* 80−9075
film material measurement, film copying appl. *(German)* 79−35867
film response to 25 MV X-rays, sensitometric curves, relative dosimetry 80−52376
fog and sensitivity centre form. kinetics and activation energies during chem. sensitisation 77−44495
fogging effect of an electric field on a photographic film *(Russian)* 80−62783
fogging effects diagnosis, use of granularity meas. 79−47952
frequency-contrast characteristic, effects of optical parameters and boundary conditions *(Russian)* 79−5168
gamma measurement, algorithms 77−34042
gelatine films containing AgBr, effect of AgBr comp., aging, UV exposure *(Russian)* 79−67408
grain size, uniform, sensitivity spread contributory factors 78−16864
Herschel effect in sensitive photographic materials, depend. on exposure and development conditions *(Italian)* 78−82062
high-speed cassette film fogging and shielding 78−8460
hologram recording using photolithography, photog. props. of photoresists *(Russian)* 79−98324
holographic interferometry, highly sensitive plates for short exposure times *(Russian)* 80−1164
hypersensitisation by forming gas baking and $AgNO_3$ bathing, astron. appl. *(Japanese)* 79−101084
hypersensitisation of photographic emulsion for astronomy *(Swedish)* 78−85853
hypersensitisation of photographic layers of heating *(Russian)* 79−58823
IAE films for pulse holography, effect of wavelength on photosensitivity *(Russian)* 79−68372
image resolution in single-stage photographic process *(Russian)* 79−44969
impurity centres in emulsions rel. to long wave sensitivity *(Russian)* 78−49925
ion-sensitive photographic plate evaluation using optical wedge microdensitometer *(German)* 80−42298
Judd's phase simulation for daylight and W illum. in Xe sensitometers 78−29192
Kodak 649F plates, intermittent characteristic curves at 514.5 nm 80−23637
Kodak 649F plates, specular multiplexed hologram recording, diffr. efficiency 80−23638
Kodak IIIaJ hypersensitized plates, low intensity reciprocity failure elimination 77−9667
Kodak SO-143 film sensitivity, comparison with CCD for streamer chamber appl. 78−21820
Kuehnle-Coulter inorganic crystalline photoconductive film 79−71553
laser unconventional recording materials for He-Ne laser 80−18040
latent image formation, influence of recombination 77−5945
limiting sensitivity of photographic materials in process of direct blackening *(Russian)* 80−90920
lithographic coated polyester panchromatic plate system 80−13172
medical X-ray and fluorographic film sensitometry 77−48858
monodispersive emulsions, frequency-contrast responses, resolution magnitude, sensitisation effects *(Russian)* 80−295
monomeric dye spectral sensitising efficiencies, conc. depend. 79−20426
negative photoresists, photosensitivity *(Russian)* 80−50872
negative polymer-bisazide photoresistors, influence of O_2 on resolution *(Russian)* 79−44974
nickel oxalate dihydrate, photographic props. eval. for use as high-speed photographic materials 77−44497
non-Ag photography with physical development *(Russian)* 79−44970
optical density, depend. on exposure for photographic action by high energy electrons, 250 to 1000 kV *(Russian)* 80−90923
optical dispersion, effects of dispersion indicatrix on obs. of radiant energy *(Russian)* 79−58821
optical reticle and scale fabrication, cyclohexadiene-1,3 pleinomer photoresist 79−27452
organic dyes, spectral sensitization and electronic struct. 79−19551
organic imaging systems, overcoming thermal instability and fog problems 79−2851
organic media, photosensitivity anal., holographic grating appl. *(Russian)* 77−179
papers, spectral sensitivity, meas. of optical density in reflected light *(Russian)* 80−300
Permalloy films, energy charact. expt. determ. *(Russian)* 79−67417
photochromic layers based on spiroindoline, effect of thickness on photosensitivity, optical density *(Russian)* 79−67416

photographic material sensitivity continued
photodetector, threshold sensitivity for semiconductor photography 80−18017
photographic development, nucleation and growth phenomena 80−101858
photographic grain in coherent optical system, signal dependence 79−30598
photoimaging system based on photopolymerisation in cryst. coatings 80−40716
photoresist, negative, math. model for expt. behaviour 77−38043
photoresist films, effect of drying temp. on photosensitivity *(Russian)* 79−58828
photoresists, cross-linking, photographic characteristic curve, sensitivity 77−10128
photosensitive layers with chromic acid salts, photochemistry *(Russian)* 80−50869
photothermoplastic film, high resolution, meas. of sensitivity and transmissivity *(Russian)* 79−46022
photothermoplastic materials, electrophotog. sensitivity, diffr. efficiency *(Russian)* 80−47130
picture sharpness, influence of transfer components, parametric eval. *(Czech)* 79−71552
polymer-bisazide system, light sensitivity of photoresisting films *(Russian)* 79−6214
polymethine dyes, investigation of chemical transformations 79−20445
polymethyl isopropenyl ketons, spectrally sensitized decomposition and Deep UV resists 80−40715
polyvinyl alcohol, dichromated, sensitisation to visible laser wavelengths 78−4716
polyvinylcarbazole xerographic film, discharge kinetics 77−13810
polyvinylcinnamate light-sensitised, reciprocity law in 240 to 436 nm range *(Russian)* 77−34052
positive photoresist film, reson. absorption charact. 77−38046
prediction of maximum attainable sensitivity for photographic systems *(Russian)* 80−298
programming of sensitometric problems on microcalculator Electronica B3-21 *(Russian)* 80−77901
pyrylium dye J-aggregate species, circular dichroism spectropolarimetric charact. 79−3456
reduction sensitised emulsion by dyes, redox potentials, quantitative correlations 79−34298
review of process physics, silver halide phys. props. and sensitivity *(Japanese)* 77−54007
safelight for Agfa 10E75 and 8E75 plates 78−74087
safelight for Agfa 10E75 and 8E75 plates 79−63318
scattering charact. of emulsion layers into rear hemisphere *(Russian)* 79−44967
sensitizing dyes, efficiency and physicochemical props. 79−20424
sensitometer for exposures 100 to 10^{-7} sec 78−29189
sensitometric sources, photometric and radiometric calibration, tutorial 77−34044
sensitometry, black and white, photographic testing procedures, film evaluation 78−29191
sensitometry measurements used in printing *(German)* 79−6201
silver salts of organic acids, photolysis investig. for use as photosensitive material for PC forming 77−44496
silverless photographic materials, non-equivalence of artificial and natural ageing *(Russian)* 79−58829
silverless photographic processes, quantum yield and photosensitivity formulae *(Russian)* 78−49934
Skylab environmental effects on photographic film 77−60620
soft X-ray film, Ilford Special Industrial-G, sensitometry 2.1 to 21.6 Å *(German)* 77−10126
solid state diode model for spectral sensitivity 77−41716
spectral sensitisation, physical basis for models 77−5941
spectral sensitisation theory, review *(German)* 79−39172
spectral sensitivity meas., automated densitometer system 78−29190
spectral sensitization of copper organoacetylenides photoconduction by means of dyes *(Russian)* 79−58824
spectral sensitization pathways, influence of dye energy levels, structure and environment 79−19554
spectral sensitization theory, review *(German)* 79−39174
spectral sensitizing dye design, use of molecular orbitals calcs. 79−20425
spectral sensitizing dyes, energy levels 79−19552
speed determ., methods used to relate sensitometry and exposure 79−89020
supersensitization by Dember effect, ESR meas. 79−20423
supralinear photographic emulsions, radiobiological aspects 80−26290
thermal photographic image receivers, freq.-contrast charact. *(Russian)* 79−44971
thermophotographic paper, UV and visible energy sensitivity 77−71399
thiolic antifoggants sensitizing emulsions, latent image form. enhancement 79−17519
UF-VR film, exposed to soft X-rays, quantum discrimination efficiency and sensitivity 80−22499
undeveloped emulsion layer, determ. of 3-D light scatt. function *(Russian)* 79−97460
UV-4 film, microphotometric granularity for registering vacuum UV spectral region *(Russian)* 79−58833
vesicular film sensitometry, review 78−16878
wholebody autoradiography, B-radioluminescence method for tritium detection 77−52945
X-ray calibration of Kodak RAR 2490 film, appl. to laser plasma expts. 77−35383
X-ray films sensitivity increase, for X-ray defectoscopy 77−90552
X-ray images, influence of visible light of development and intensity *(Russian)* 79−97463
XUV Schumann-type films, fogging in proximity to metals 77−60599
Ag halide, sensitivity and struct. charact., review *(Russian)* 79−2868
Ag halide bleached photographic plate, uniaxial medium generation 79−2848
Ag halide crystals, effect of redox potential on photosensitivity *(Russian)* 80−73507
Ag halide crystals, investigation of sensitizing and desensitizing action of cyanine dyes 79−20446
Ag halide dry materials for laser printing appls. 80−13179
Ag halide emulsion colouring, k-value and sensitivity relationship *(German)* 80−7815
Ag halide emulsions, sensitivity calc. 79−21843
Ag halide emulsions, spectral sensitisation, review 78−4719
photographic material sensitivity continued
Ag halide film for nanosecond photography, 10.6 μm CO_2 laser pulse spatial distrib. recording 79−89016
Ag halide films, DQE and ratio of gradient to granularity 79−21838
Ag halide grains, photographic sensitivity and response to charged particles, interstitial generation 77−10124
Ag halide high resolution materials, 3-D hologram recording, exposure charact. 78−17880
Ag halide layers, ultimate sensitivity and resolving power 79−17546
Ag halide microcrystal, sensitised and stabilised, concentration speck and development centre growth 79−83484
Ag halide photography and xerography compared *(Japanese)* 78−24876
Ag halide photography in middle IR using laser sources 77−53997
Ag halides, effects of ZnO, dyed ZnO and cyanine dyes on spectral sensitivity 79−20432
Ag halides, latent image centres, determ. of stability and dimens. *(Russian)* 80−90922
Ag halides, spectral sensitisation, estimation of rate constant 78−89575
Ag halides, theory of supersensitisation, review *(Russian)* 80−62786
Ag, halides sensitivity to multiply charged ionising particles, temp. depend. 79−80714
Ag iodobromides, spectral absorpt. curves, density, wavelength and temp. depend. 78−16871
AgBr, (100) and (111) face, influence on aggregation of sensitising dyes 79−39202
AgBr crystal face influence on aggregation of sensitizing dyes 79−20428
AgBr, decoration of sensitivity specks 79−24784
AgBr, distrib. of Ag_2S on sensitised emulsion grains 78−62248
AgBr, dye sensitized photo-process 79−20433
AgBr emulsion, cubic, supersensitisation of microwave photocond. 77−41713
AgBr emulsion, desensitizing action of a secondary iodide *(Russian)* 79−58820
AgBr, emulsion, grain disorder and its influence on emulsion response 77−5940
AgBr, emulsion, sensitisation by hydroxy-tetraazaindenes 77−54006
AgBr emulsion grains, adsorbed dyes, light-induced ESR spectra 80−88862
AgBr emulsions, effect of gelatin replacement with polyvinyl alcohol 79−20440
AgBr, evaporated layer, influence of sublayer on stability and photographic characteristics *(Bulgarian)* 80−42281
AgBr evaporated layer chemical sensitisation 79−24766
AgBr evaporated layer response in ionisation semiconductor photographic system *(German)* 80−101859
AgBr evaporated layers, spectral sensitization using cyanine dyes 80−26035
AgBr, evaporated layers, use as registrating system *(Bulgarian)* 80−52344
AgBr, free holes in spectral sensitisation 78−4720
AgBr grains, photographic emulsion, sensitivity centre variation with grain size 80−9055
AgBr, hydrosol, latent-image stability, chem. sensitisation 78−21236
AgBr, large grain emulsions, reciprocity errors and disturbance effects in high illuminations *(French)* 79−97452
AgBr, localisation of polarons on (100) surface, rel. to photographic sensitivity *(Russian)* 77−35983
AgBr, luminescence of photographic emulsions sensitised by 1,1′-diethyl-2,2′-cyanine with Ag_2S clusters *(Russian)* 80−73513
AgBr monocrystals, dimensioning rel. to light scatt. of highly dispersive photographic emulsions *(Russian)* 79−49327
AgBr octahedral emulsion, reduction sensitization 79−20420
AgBr, photographic emulsions, dye spectral sensitization, latent image form., subcond. band events 78−32905
AgBr photographic emulsions, sensitivity, fog rel. to treatment in redox-buffered solns. 78−32906
AgBr photographic emulsions, adsorpt. of thiolic antifoggants, chem. struct., ESCA investig. 78−32907
AgBr, sol, electrophoresis of spectral sensitising dyes, dye layering obs. 77−56240
AgBr vacuum evaporated thin films, sensitometric obs. 78−78010
AgBr, very fine grained emulsions, effect of hole and electron acceptors on photosensitivity *(Russian)* 80−73515
AgBr-Ag light sensitive system, diffusion of excited states *(Russian)* 78−59101
AgBr-AgI emulsion sensitivity improved by AgCl shell crystallisation *(German)* 80−104453
AgBr(I), emulsion coating, H hypersensitisation to diminish recomb. and increase quantum efficiency 77−5942
AgBrI, fine grain emulsion, spectral and reduction sensitization interaction 79−20430
AgBrI negative emulsions, sensitivity and fog centres with S sensitization 79−20418
AgCl crystal plate supersensitisation, photoelectrochemical obs. 79−83486
AgCl monosized emulsions, S sensitization 79−20417
AgCl:Hg^{2+}, effect of Hg^{2+} addition of photosensitivity *(Russian)* 79−67412
AgI large single crysts., gel and soln. growth and props. 80−35071
AgX (X=halide) structure and stability of photographic sensitivity centres *(French)* 77−41708
AgX, selectivity of development of small aggregates of microcrystals in photographic layer *(Russian)* 79−58832
AlH_3, synchronous photochem. processes in lattice 80−101029
As_2S_3-Ag, light sensitivity for high exposure densities *(Russian)* 79−6212
As_2Se_3, film, amorphous, fatigue and recovery of electrophotographic props. 78−21253
As_2Se_3 layers for electrophotographic use *(German)* 80−42283
As_2Se_3, photosensitive layer, in metal-photosemiconductor-insulator multilayered struct., optical image recording 80−42286
Au, sensitivity speck, formation during ripening, role and nature 79−39171
Au sensitization mechanisms 79−20419
BiI_3 photosensitive layers, optical and thermal development *(Russian)* 80−73512
CdS_xSe_{1-x}, photosensitive layer, in metal-photosemiconductor-insulator multilayered struct., charge pattern form. 80−47129
β-Cu phthalocyanine electrophotographic props. rel. to particle size *(Japanese)* 80−13171

photographic material sensitivity continued
2,5-diphenyloxazole enhanced emulsion, effectiveness of light microscope autoradiography 80−47100
KCl, additively coloured photochromic crystals, spectral sensitivity *(Russian)* 80−91871
Mn salts in developing solution to improve image sensitivity *(Russian)* 77−34050
NaF crystal M-centre storage element, photosensitive characteristics 79−14067
$Na_2S_2O_3$, breakdown on Ag halide grains, electron microscopy 78−21237
$Ni(N_2H_4)B_xH_y$ development, effect on photosensitivity of paper *(Russian)* 80−73509
Pb halide based photodevelopable materials 79−21830
$PbCl_2$ emulsion layer, effect of elec. field on microcrystal sensitivity *(Russian)* 79−58831
PbI_2 layers, fogged with metals, spectral sensitivity and optical absorpt. *(Russian)* 77−30209
PbI_2 suspension, chem. sensitization 80−73492
PbS photosensitive deposit precipitation, alkali and acetate conc. effects 79−76781
S and Au sensitisation, internal image speed 78−16869
Se xeroradiography films, photosensitivity recovery from X-ray induced fatigue 77−2709
Se-Bi-I, amorphous, high sensitivity visible-near IR photoconductor development and characterisation 78−39153
TiO_2 photographic layers, sensitivity enhancement by addition of Ag^+ during cuprous development *(Russian)* 80−62780
TlI layers, fogged with metals, spectral sensitivity and optical absorpt. *(Russian)* 77−30209
ZnCdS-Ag binder layers, electrophotographic charact. eval. for use in charge transfer electrophotography 77−41714
$Zn_xCd_{1-x}S$:Cu crystallophosphors, spectra of IR electrophotographic sensitivity *(Russian)* 80−50423
ZnO binder layers, regeneration of sensitising dyes 78−21241
ZnO dye sensitisation in electrostatic photography 79−67404
ZnO particulates, Dember effect 79−20380
ZnO, photocond., spectral sensitisation mechanism 77−43651
ZnO-polystyrene photoreceptors sensitised by β-Cu phthalocyanine 79−17552
ZnS:Cu crystallophosphors, spectra of IR electrophotographic sensitivity *(Russian)* 80−50423

photographic materials
see also photographic emulsions
AgBr, thin layers, struct. and photographic charact. 78−49919
aging behaviour in non-Ag materials 79−24780
aging of nonsilver photographic materials in different gas media *(Russian)* 79−44972
AHU microfilm Kodak 5460 Recordak, 35 mm, black/white microphotography appl. 79−6204
albumen paper, manufacture and use 79−35515
alpha naphtol, developer, use in nuclear photography 78−17490
aluminoborosilicate glass, holography using photoinduced anisotropic media 79−41354
ambiguity processing by joint Fourier transform holography 80−58468
aminohydroquinone as developer 77−5947
aminophenols, photographic development, comparison with 1-phenyl-3-pyrazolidone 78−64825
4-aminopyrazolone-5 and 5-aminobarbituric acid mixtures, developing charact. *(Russian)* 78−49931
ascorbic acid developer, lith development mechanism 80−77889
automatic inspection by IR laser beam 79−30593
benzenediazonium compounds, structure-property relationships, quantum chemical calcs. 79−22605
benzoin containing system, photosensitized free radical polymerisation 80−7825
benzophenone containing system, photosensitized free radical polymerisation 80−7825
benzothiazoline products, bicondensed, for thermographic recording 79−24767
benzotriazole developer additives, effect on photographic development mechanism 80−77891
biazide-polymer based photoresist. films, positive image production *(Russian)* 78−16887
bleach system for colour positive and negative film for waste treatment 78−49923
bleaches, organically accelerated, role in holographic image form. 77−14672
camera films, automatic exposure, theoretical anal. 78−86363
camera speed diffusion transfer offset master on filmbase 80−37108
camera speed negative working diffusion transfer material 80−37107
cellulose triacetate films, local loss of stability, expt. anal. using high speed cinefilming *(Russian)* 79−58822
cellulose triacetate soln. plastification *(Russian)* 78−49929
chalcogenide film, effectiveness for optical holographic recording *(Russian)* 77−71960
chalcogenide glass-metal light sensitive systems with barrier layer 77−75635
characteristic curves, for holographic grid production modelling *(Russian)* 77−631
chemical-photographical processing influence on physical-mechanical props. of motion picture materials *(Russian)* 78−93778
chromate gelatin props. for holographic recording 79−18381
cine film processing wastes, environmental pollution control of industrial plants *(Russian)* 79−44964
cine-film, slitting in the laboratory 78−93770
cleaning solvents survey, w.r.t. safety 77−10130
color developer recovery, ion-exchange method 79−49319
colour astrophotography, slide and print developing 79−29996
colour component triads, colorimetric determ. for positive materials *(Russian)* 80−95178
colour developer recovery, ion exchange method practical application 79−49320
colour developing agents in processing solns., polarographic determ. 78−4726
colour film archival storage, white light processing technique 80−99637
colour mixing and colour films *(German)* 78−93774
colour motion picture using diffractive surface-relief structures 78−37089
colour negative cinefilm LN-8, properties *(Russian)* 79−2861

photographic materials continued
colour negative film, rapid access processing 78−21240
colour photographic paper, minimum surface conc. of Ag and colour components *(Russian)* 79−67409
colour positive cinefilm standardisation on sensiometric tests *(Russian)* 80−287
colour positive developer comsumption, bromine ion extraction from overflow using ion exchange resins *(Russian)* 80−105733
colour processing monobath with high pH 77−41712
colour reversal film, method for increasing resolution during processing *(Russian)* 79−75644
colour reversal film, strip film for microfilm retrieval systems appl. *(Japanese)* 79−97455
colour reversal films for 3200K *(German)* 79−54207
colour slides preparation, using heat shrinkable material 79−6202
composite film with high loading factor, extension of Maxwell-Garnett dielectric loss theory 79−19835
computerised tomography, picture documentation and filing 79−66554
conference, Rochester, USA, 1978, Aug. 79−20394
connection between the topography of luminescence centres and the latent image *(Russian)* 80−62785
contact copying process, film material gap meas. 79−26166
copper oxalate hemihydrate, photographic props. eval. for use as high-speed photographic materials 77−44497
daguerreotypes, plates and process obs., by electron microprobe analysis 80−68286
detective quantum efficiency and granularity rel. to quantum noise 79−21829
developer redox pot., influence on sensitivity and quantity of developed silver *(Russian)* 79−44966
developers reuse for motion pictures, replenishers formulae *(Russian)* 78−54487
developing agents, oxidized, diffusion and sharpness of colour image 79−20449
developing solutions, temperature control *(Russian)* 78−29202
developing-fixing solution concentration analysis, using autopotentiometric method *(Russian)* 77−54009
diazo compounds, continuous tone diazotype imaging films, model 78−32911
o-diazonaphthoquinones, thermal decomposition of light sensitive materials *(Russian)* 80−73504
p-diazoquinone, photodecomp. 80−7827
1,1′-diethyl-2,2′-cyanine iodide, sensitising dye 77−72602
3,3′-diethylthiatricarbocyanine iodide, cryst. and molecular struct. 78−26554
diffusion transfer based negative and positive working camera speed overlay color system 80−37109
disulfides as antisilvering compounds in fixing developers 79−24795
dye, colour coupling in soln., kinetic anal., appl. of flash-light photolysis *(German)* 79−39173
electrographic toner, recycled in xerographic development system, cycle distrib. 80−62760
electrophoretic developers for pictorial electrophotography 79−17523
electrophotographic developer, size distrib., particle charge and toner-carrier force *(German)* 80−73493
electrophotographic film evaluation apparatus 79−93244
electrophotographic KC film digital recording performance 78−78024
electrophotographic liquid developer, permittivity and conductivity meas. *(German)* 78−62257
electrophotographic properties of plate with polyvinylcarbazole overlayer and CdS-resin layer 77−61146
electrophotographic two-component developer discharge and contact interaction *(German)* 78−62258
electrophotography, liquid developer, standardisation of props., manuf. process *(Czech)* 79−30592
emulsion, for spectrographic anal., calibration curve computer calcs. 78−4706
estar base reconnaissance film, in optical correlator, birefr. effects 77−74538
exponential transformation using film nonlinearity for optical homomorphic filtering 80−58467
ferricyanide bleach regeneration, simplified electrolytic method 78−74090
film, exposure while immersed in seawater, effects on photographic props. *(Russian)* 77−79180
film, for medical diagnostic imaging 77−78023
film, for SEM, electron beam photographic recording system 80−101903
film, Fujicolour colour negative and positive, for cinematographic production 79−85191
film, problems of slitting in printing laboratory *(German)* 79−6199
film, props. of latent image formed by X-ray exposure 79−20407
film, versatile X-ray detector 78−45763
film cleaning by ultrasonic liquid cavitation and acceptable solvents 80−62769
film grain noise in partially coherent imaging 80−101860
film movement nonuniformity study in film-advance channel 80−68285
film positive, reproduction of subject, relationship between objective and subjective phases 79−30596
films, 16 mm Fujicolor reversal film RT 500 and RT125 80−106585
films, high speed, colorimetric testing of Boots 400 and Agfa CNS 400 80−18026
films, new Gevacolor negative film type 682 80−106586
films and processes, non-standard, for feature-film production *(Russian)* 79−49326
films used in subtraction radiography, charact. and limitations 77−2046
fixing solutions, Ag extraction using sulphide-containing cellulose fibres *(Russian)* 79−58835
frequency contrast charact., effect of Ag content and Ni image intensification processing *(Russian)* 80−95183
frequency-contrast characteristics, determ. by interference-diffraction method *(Russian)* 80−73501
gelatin, fine struct., IR spectroscopic study of effects of impurities and other actions *(Russian)* 78−58083
gelatin, gel-sol transition, gel charact. 78−35724
gelatin classification problem 79−100448
gelatin films with Fe,Cu,Ag and S containing compounds, IR spectra *(Russian)* 78−49928
gelatin layer, in MIS struct., C-V charact. and gelatin-semiconductor interaction rel. to photographic process *(Russian)* 80−49944
gelatin layers in photog. developers, effect of diffusion on swelling *(Russian)* 79−97461

photographic materials continued
gelatin layers with and without $AgNO_3$, phosphorescence kinetics curves *(Russian)* 80−62776
gelatine layer with Ag salts, characteristic curve struct. 79−24800
gelatine-polyvinyl alcohol films, effect of pH on transparency *(Russian)* 79−58830
gelatins, anal. of nucleic acid bases by liquid chromatography 79−20501
granularity noise, effect on meas. of quality characts. of aerial photogrammetric systems *(Russian)* 77−67525
graphic arts imaging material and laser source cost tradeoffs 80−14383
hexacyanoferrate removal from photographic process effluents by ion exchange 79−54211
high resolvance interference spectrometry, visible spectrum 79−26145
holographic interferometry, selection of working point on amplitude-exposure curve for uniform illumination *(Russian)* 80−1162
holographic methods developments use of photothermoplastic instant film *(German)* 78−39975
holographic photomaterials with mirror layer for newly developed holographic process *(Russian)* 78−55325
holographic transmission characts. determ. from amplitude coeff. for hologram recording *(Russian)* 80−91760
holography, determ. of freq.-contrast charact. by multibeam method *(Russian)* 79−27219
holography, diffraction efficiency, depend. on size of developed Ag particles 78−78965
homogeneous solid layer, diffusion, one-dimensional case *(German)* 80−73495
hydroquinone, oxidation of centre of photographic development, electrochem. kinetics *(Russian)* 80−3367
hydroquinone developer, lith development mechanism 80−77889
instant colour-discrimination shadowgraphic technique and film 80−9057
IR photographic films, highly-sensitive 77−49794
Kalvar film, damage threshold variation with spot size at 10.6 μm 79−36945
Kodak 649-F plate 5-min. processing monobath 77−633
laser printing, seminar, Los Angeles, USA (Jan. 1979) 80−12852
laser unconventional recording materials for He-Ne laser 80−18040
laser-compatible materials for graphic arts 80−13180
latent-image bleaches, enhancement of latent-image and fog 78−24879
light sensitive layers with chromate salts, photochemistry 79−20439
liquid photopolymer materials, mathematical modelling of hardening, layer thickness and exposure parameters *(Russian)* 80−62784
magenta pyrozolone azomethine dye, electrochemistry of fading mechanism 79−24761
mammographic dose reduction, Kodak Definix Medical rel. to Kodak Min R film *(German)* 80−12243
manufacture, polyester film compared with nitrocellulose film *(German)* 78−86366
merocyanine dyes, non-photochromic, for autoprocessor reprography system 80−35555
metal carbonyl film exposure and development *(Russian)* 78−58075
α-methylstyrene, photoinduced ionic polymerisation 80−7828
MTF automatic evaluation 80−95170
nickel oxalate dihydrate, photographic props. eval. for use as high-speed photographic materials 77−44497
5-nitrobenzimidazole in photographic processing solns., AC polarography determ. 79−24861
non-Ag photography with physical development *(Russian)* 79−44970
optical density measurement accuracy by means of optical wedge 80−73416
optical image phase recording using sensitised photooxidation reactions 80−87350
optical recording materials *(Japanese)* 80−105730
optical resolving power, determ. *(Russian)* 80−42292
optical storage materials and methods, conf., San Diego, USA (Aug. 1977) 78−71171
organometallics, photochemistry with applications to imaging systems 77−4914
organotellurium compounds, thermally developable light sensitive systems 79−2850
paper, resin-coated and polyethylene 80−86474
paper print residual thiosulphate, methylene-blue and Ag densitometric meas. correlation 79−74472
papers, polarised light refl. 80−64127
permalloy films, thermoelastic stresses and magnetostriction effects during light recording *(Russian)* 79−97465
phase relief in photographic layers, determ. using optical methods *(Russian)* 79−98518
photo-doping of Ag into amorphous chalcogenides modified with foreign elements 79−20438
photoactive catalyst used in light induced photocuring of coating systems 80−7820
photoanisotropy in yellow mordant azo dyes *(Russian)* 80−42290
photocatalytic diazosystem, light-sensitive, possibility of creation 79−20451
photoconducting film for rapid access instrumentation recording 80−62755
photoconductive recording film demonstrator/processor 79−17551
photoflash units, chemical and electronic, temporal spectral characts., meas. method 80−95171
photographic stabilisers, reaction with yellow colloidal Ag, semiconductor props. *(German)* 78−86369
photoinitiated cationic polymerization by photosensitization of onium salts 80−7822
photometric calibrator appl., inverse fourth power, NBS development 80−73412
photopolymer, biaxial stress-strain test 80−40417
photopolymer in holographic real-time fluid flow measurement 80−6176
photopolymer industry in Japan 80−4800
photopolymer laser recording materials development 77−54678
photopolymer printing surfaces for gravure 79−35871
photopolymer systems, conf., Washington, USA (Nov. 1978) 80−4799
photopolymerisation, O_2 inhibition elimination 80−7821
photopolymerisation, dye-sensitized, activation by trialkylbenzylstannanes 80−7824
photostating techniques *(German)* 78−89572
photothermoplastic film in holography *(German)* 78−22097
photothermoplastic film on flexible terylene backing, heating to record optical information *(Russian)* 77−71959
photothermoplastic films, effect of latent image formation on band-pass transfer charact. 79−18382

photographic materials continued
photothermoplastic recording material for holographic interferometry 77−7038
pinakryptol yellow, photographic dye desensitization mechanism *(French)* 79−9250
plastic versus metal coatings, real time laser recording 77−74536
pneumoelectric automatic device for passing splices in cinefilm, still photography film *(Russian)* 79−2864
Polaroid film, damage threshold variation with spot size at 10.6 μm 79−36945
Polaroid print coaters, comment 79−35864
Polavision, first instant colour movie system 78−24882
poly-n-epoxypropilcarbazole electrophotographic layers, photogeneration and drift mobility 79−19631
poly-N-vinylcarbazole, electrophotographic film, dark discharge 78−34864
polyester filmbase experience in motion picture industry, review 80−42278
polyesters, photoreactive, synthesis and struct.-prop. relations 80−7826
polyethylene resin coated paper formulation 80−4794
polymer, crosslinking with X-ray irrad., active group and heavy atom effects 80−7829
polymer, photochromism 80−5805
polymer film, photoreticulation by UV irradiation 80−40717
polymeric electrophotographic developer, triboelec. two-step decay scheme 79−80711
polyvinylcinnamate, crosslink form. by photoreaction 80−7823
positive film density, depend. on conc. of stabilizers and antifoggants added to developer *(German)* 80−73497
processing solns., anal. by AC polarography 77−12861
pseudocolour density encoding of photographic materials, white light processing system 79−18360
pulp quality control using He-Ne laser scanning system *(German)* 80−3272
PVC, Cu evaporated film, electron-induced metallochromic reaction for metal image formation 80−86476
pyrazoline-based carrier transport layers use in layered photocond. systems for electrophotography 77−69375
pyrocatechol, oxidation pots., correl. of V-I characts. and photographic developing power *(Russian)* 80−45534
pyrocatechol derivatives, developing ability and structural data, correlation analysis 79−20448
quality improvement, colour spots detection using laser-operated device *(German)* 80−57412
radiological film, cassettes, automatic handling 77−45907
reciprocity failure model, asymptotic behaviour at low and high intensities 78−89573
recording media, review 78−71172
reflection holograms, reduction of resolving power requirements of photographic materials *(Russian)* 79−59658
review of process physics, silver halide phys. props. and sensitivity *(Japanese)* 77−54007
α_1-salicylideneaniline, photochromic props., appl. as holographic recording 77−68183
self-developing materials available professionally 77−67519
semiconductor, amorphous, photoelectric properties in ionic contact regime 77−76873
semiconductor sensitised photolysis and latent image structure 79−24768
sensitometry, black and white, photographic testing procedures, film evaluation 78−29191
short time exposure, expt. technique 80−86477
silicate glass, nonactivated, far UV image recording, colour centre formation *(Russian)* 77−5950
silver thioamides, precip., electron microscope and potentiometric studies, growth of photosensitive crysts. 80−33107
silverless photographic materials, non-equivalence of artificial and natural ageing *(Russian)* 79−58829
solution management for ferricyanide bleach and fix, Rotex system, high speed film processing appl. 79−54206
spiropyrans, photochromic, thermophotodegradation for autoprocessor reprography system 80−35555
stabiliser, reaction with colloidal Ag, equilib. conditions *(German)* 78−61067
sucrose benzoate host for recording volume phase holograms 77−632
ternary chalcogenide sensors, imaging by photo- and thermal doping 78−1342
thermal photographic image receivers, freq.-contrast characts. *(Russian)* 79−44971
thermophotographic paper for recording long-wavelength IR laser radiation 79−40636
thermoplastic layers with fast heating, discharge process 78−49920
thermoplastic recording, amplitude characts. *(Russian)* 79−44973
thermoplastic recording material, latent image and surface deformation *(German)* 80−42284
thin film magnetic recorders of optical images, sensitometry using glass Nd laser *(Russian)* 77−79178
thin film thermomagnetic strip-domain type recorders, frequency-energy charact. *(Russian)* 77−67521
thiocarbocyanine dye, adsorpt. on AgBr photographic gelatin dispersion 78−32908
thiolic antifoggants, chem. struct., adsorpt. on AgBr emulsions, ESCA investig. 78−32907
UF-VR film, exposed to soft X-rays, quantum discrimination efficiency and sensitivity 80−22499
UK 1.2 m Schmidt telescope plates, electronographic calibration for photometric transfer props. 79−88703
UV-4 film, microphotometric granularity for registering vacuum UV spectral region *(Russian)* 79−58833
UV-cured inks for edge numbering on all motion picture films 79−9254
vesicular film, contact printing density determ. by densitometer meas. 77−53995
vesicular film sensitometry, review 78−16878
video disc master recording, high density, replication by contact printing 80−62761
X-ray film/intensifying screen system, MTF and Wiener spectrum, film and screen quality effect *(German)* 80−73560
xerographic developer, collisional dynamics of charge exchange 77−10122
Ag complexes in fixing baths, math. model 77−34043
Ag diffusion transfer systems, graphic arts appl. 80−37106
Ag film, photodissolution in amorphous As_2S_3 78−26737

photographic materials continued
Ag formation on Ag-halide surface, flash photolysis expts. on Ag halide photochromic glasses 79−94310
Ag, granular film, anomalous light absorpt., oblique incidence 79−6205
Ag, granular films, optical props., depend. on refractive index of surrounding medium 78−84672
Ag halide bonding LCAO-MO treatment 79−23561
Ag halide microcrystals, low-temp triboluminescence 77−87861
Ag halide microcrystals, topography of latent image centres and ionic conductivity 79−20442
Ag halides, defect sites and impurities, latent image formation, LCAO calc. 78−16876
Ag halides, fundamental absorpt., nature and function of A-centres determ. the extra band at the long wave edge *(Russian)* 80−76060
Ag halogenide, grain form. and growth in metastable soln. *(Russian)* 77−34048
Ag latent image particles, electronic effects 80−82840
Ag, vacuum deposition, on evaporated AgBr layers, growth mechanism 80−35095
Ag-AgX films, (X=Br,Cl,I), Weigert effect 79−64298
Ag-complexes, stability increase during simultaneous photographic development and fixing *(Russian)* 80−95179
AgBr absorption of gelatine *(Russian)* 79−100420
AgBr, adsorption of gelatin on single crystals, ellipsometric investigations 79−24779
AgBr, Ag speck formation, ionic and electronic effects in photographic process 77−4917
AgBr, connection between the topography of luminescence centres and the latent image *(Russian)* 80−62785
AgBr crystal produced by action of free radicals, developability 80−66838
AgBr crystals, electrical potential distrib. near interface, recording using automatic device 79−24759
AgBr, electron-hole kinetics 79−24005
AgBr, evaporated layer, vacuum deposition of Ag at room temp. 79−20409
AgBr, film and microcrystal, interstitials and surface conductance 79−23776
AgBr, high-temp. ionic transport processes 79−23777
AgBr layer, sensitised, topography of developed centres 80−73491
AgBr layers, solubility and transport of Ag 79−23742
AgBr microcrystals, influence of Pb^{2+} ions on ionic conductivity and space charge characts. 79−23778
AgBr microcrystals, sintered, photocurrent-inversion effect at room temp. 78−62246
AgBr, neutralisation of trapped photoholes 79−24788
AgBr, photo-EMF relaxation, temp. depend. 230 to 316K *(Russian)* 80−73508
AgBr, photodielectric effect at low temp. *(Russian)* 80−96947
AgBr, photoexcited, dye sensitized bleaching of surface silver specks 78−308
AgBr, photoexcited electrons and holes in latest image form., review 80−73496
AgBr sensitized photolayer, overall spectra of local electronic levels 79−23933
AgBr sols, kinetic exam. of halide conversion 77−82636
AgBr, thin epitaxial layer, surface ionic cond., lattice disorder, space charge region 77−11730
AgBr thin film interstitials, Frenkel and space-charge contributions 79−18494
AgBr thin films, influence of bromine vapour on spectral props. 77−71393
AgBr:Pt, photochemistry and role of Pt impurity ions 79−24783
AgBr(I) crystals, luminesc. of individual monocrystals *(Russian)* 80−301
AgCl crystal growth in gelatin soln. 80−64942
AgCl crystals, optically detected magnetic resonance 79−24233
AgCl, epitaxial overgrowth on AgBr sheet crystals 79−19988
AgCl, high-temp. ionic transport processes 79−23777
AgCl, luminesc. excited by UV radiation at 80K *(Russian)* 78−31256
AgCl sols, kinetic exam. of halide conversion 77−82636
AgCl:Pt, photochemistry and role of Pt impurity ions 79−24783
AgCl-AgBr, microcryst., halide comp. profiles, XPS 77−12850
AgI nascent hydrosol absorption spectra and microcrystal growth 79−100449
AgI precipitations, effects of pAg on crystal growth 79−19172
$Ag_2S_2O_3$ solubility limit below 0°C 79−19376
AlH_3, photo-and thermochem. reactions, 200-350K, UV Induced local states 78−31667
As_2S_3, amorphous film, light enhanced vaporisation, photolithographic process, photographic appls. 77−5949
a-As_2S_3, photodesactivation, direct positive imaging 79−17544
As_2S_3-Ag light sensitive material, development of non-interchangeability under continuous laser radiation *(Russian)* 80−50870
As_2S_3-Ag photosensitive film systems, hologram recording 78−1194
As_2Se_3 vitreous films, crystn. stimulated by org. subst. and electrophotographic parameters 77−76319
As_2Se_3-Ag photosensitive semiconductor-metal systems, effect of AsS_3 barrier layer *(Russian)* 80−62777
$CdGa_2Se_4$, electrophotographic props. *(Russian)* 78−59100
CdS, spectral sensitisation, role of local centres *(Russian)* 80−90924
CdS-HgI_2 binder layers, surface charge characts. for electrophotography 77−10123
$CdS_{1-x}Se_x$-Cu, electrophotographic props. 77−45910
Cu-PbI_2 photosystems, null-refl., cermet and Fabry-Perot types 78−46738
$Cu_{15}(AsSe)_{85}$ photographic layers, temp. depend. of reverse optical recording *(Russian)* 79−67415
HgI_2-CdS photoconducting binder layers, surface charge decay characts. 77−43642
$Hg_3Se_2I_2$ film, holographic characts. *(Russian)* 77−79786
InCl powder, effect of thermal treatment on photographic props. *(Russian)* 80−291
KBr, change of state of F-centres due to electrostatic field *(Russian)* 79−58827
KCl and KCl:S, change of state of F-centres due to electrostatic field *(Russian)* 79−58827
$LiNbO_3$:Fe, photorefractive recording of vol. holograms 77−637
MnBi, problems for holographic recording *(Russian)* 80−91761
NaCl:O, photographic recording in far-UV, colour-centre formation 79−23035

photographic materials continued
$Ni(NH_3)_6^{++}$, photographic developer, potentiodynamic polarisation curves for Ag-less development *(Russian)* 80−90921
$NiSO_4$, photographic developer, potentiodynamic polarisation curves for Ag-less development *(Russian)* 80−90921
$PbBr_2$, determ. of sign and drift mobility of majority carriers *(Russian)* 79−69512
$PbCl_2$, determ. of sign and drift mobility of majority carriers *(Russian)* 79−69512
PbI_2, determ. of sign and drift mobility of majority carriers *(Russian)* 79−69512
PbI_2-Ag, photolysis, effect of PbI_2 photo-EMF effect *(Russian)* 80−92939
PbI_2-Ag light sensitive system, photochem. conversion process under continuous laser radiation, nonreciprocity *(Russian)* 77−79179
Sb_2S_3 layers, sensitised photolysis, determ. of iso-opaque contours *(Russian)* 79−100418
Se, amorphous, interface with poly-N-vinyl carbazole, photoinsulator-air gas-dielectric system, charges on surfaces 79−67407
Se amorphous layer structure, influence of vacuum deposition conditions *(German)* 78−63957
Se, appl. to xerography 80−57415
Se, electrophotographic characts. of films rel. to viscosity of bulk specimens *(Russian)* 80−73505
Se, vacuum evaporated film, photoinduced amorphous-crystalline transition obs. *(German)* 79−82156
Se-As alloys, appl. to xerography 80−57415
Se-poly(N-vinylcarbazole), double layer polymeric photoreceptor, potential discharge kinetics 78−72194
Se-Te film, evaporated, drift mobility of holes, elec. field and comp. depend. 77−39977
TiO_2 transparent film photographic layers, props. *(Russian)* 80−43420
ZnCdS:Cu, binders effect on electrophotographic characts. 79−80712
ZnO based films, photographic props. *(Russian)* 77−71401
ZnO, electrophotographic layer, fatigue recovery 79−63321
ZnO, fatigue of electrophotographic layers 79−63320
ZnO, red, electronic and opt. props., electrographic props. 77−57419
ZnO sensitized photolayer, overall spectra of local electronic levels 79−23933
ZnO-resin electrophotographic photosensitive layers, dark decay mechanism of corona charge *(Japanese)* 79−24002
ZnS, spectral sensitisation, role of local centres *(Russian)* 80−90924

photographic process
see also photochemistry
3D image, longitudinal definition of details and information density *(Russian)* 80−40721
accuracy for chemical photographic processing of colour positive motion picture films *(Russian)* 80−93780
adenine, restraining effect on photographic emulsion *(German)* 79−39175
adjacency effects prediction and removal from images 77−54003
adsorbed dyes, ionization energies rel. to spectral sensitization 79−19553
aerial film rapid processing using low gamma photographic developer 77−54001
AgBr, monodisperse emulsion, cubic or octahedral, Ag sub-specks due to chem. reduction 78−16875
aging of nonsilver photographic materials in different gas media *(Russian)* 79−44972
amines, aromatic, photochem. reactions with carbon tetrachloride, initiation mechanism 79−61888
p-aminophenol, oxidation in aq. soln., chem. equilib. of free radicals, review 79−43573
aminophenols, photographic development, comparison with 1-phenyl-3-pyrazolidone 78−64825
arenediazonium salts, photolysis, quantum efficiencies, reactive intermediaries, EPR 78−64860
astronomical photography, controlling contrast by special development techniques 77−67046
astronomical photography, hypersensitisation, state of the art review 77−2344
astronomy, faint images photographic amplification 79−16839
autoradiographic emulsions, effect of antimasking substances on Ag grain size and structure in developed image *(Russian)* 77−49799
benzotriazole developer additives, effect on photographic development mechanism 80−77891
biimidazole+leuco dye photochem. reaction, modulation by photopolymerisation 80−40714
bleaches, accel. by organic dyes, role in holographic image form. 77−14672
chemical-photographical processing influence on physical-mechanical props. of motion picture materials *(Russian)* 78−93778
cinefilm copying equipment using interference light filters, additive printing appl. *(Russian)* 80−62774
cinefilm processing, effect of antifogging substances on Ag grain size *(Russian)* 79−67414
cinematographic, analysis of contamination product in main drainage systems *(Russian)* 79−89023
cinematographic, image information properties, highspeed vs. standard processing techniques *(Russian)* 79−58817
colour, distortions due to inaccurate modelling of process, cinematography appl. *(Russian)* 79−17533
colour and density table, cinematography appl. *(German)* 79−49309
colour film washing by cascade-counterflow water supply *(Russian)* 79−17535
colour image amplification by redox couple reaction 79−24802
colour mixing and colour films *(German)* 78−93774
colour negative film, rapid access processing 78−21240
colour negative motion picture film, latensification representation *(Russian)* 78−86373
colour negatives, commercial processing technique *(German)* 80−13173
colour print film process efficiency improvement for motion pictures 78−78023
colour processing monobath with high pH 77−41712
colour reproduction of halftone prints, effects of fluorescent brightening agents *(Japanese)* 77−26417
colour reversal cinefilm, rapid processing technique for TV studios *(Russian)* 80−3385
colour reversal film, method for increasing resolution during processing *(Russian)* 79−75644

photographic process continued
colour reversal films, accelerated development process, activating substances *(Russian)* 77−34047
colour slide processing service at Univ. of Calif. at Davis 79−71550
concentration theory 79−34334
conference, Rochester, USA, 1978, Aug. 79−20394
contact copying process, film material gap meas. 79−26166
continuous film copying equipment *(German)* 80−68281
contrast enhancement in developers containing glutaraldehyde 79−17542
contrast reversal, appl. to reversal of photographic transparencies 80−57406
copier techniques, gamma reproduction, DIN and ASA sensitivity scales and sensimetry *(German)* 79−26155
copying process for colour reversal films *(German)* 80−30254
cyanine dye, sensitizing and desensitizing action depending on AgHal crystals structure 79−20446
daguerreotypes, plates and process obs., by electron microprobe analysis 80−68286
darkroom exposure control circuit *(German)* 79−6198
developed photographic emulsion, relation between exposure and optical density and charact. curve parameters *(German)* 80−105742
developer activity, rel. to difference of electrochem. and redox potentials *(Russian)* 78−62243
developer redox pot., influence on sensitivity and quantity of developed silver *(Russian)* 79−44966
developer reuse technology and environmental protection *(Japanese)* 80−22457
developers, ID2 and ID11, development rate parameters 78−16868
developers reuse for motion pictures, replenishers formulae *(Russian)* 78−54487
developing agents, oxidized, diffusion and sharpness of colour image 79−20449
developing and colour balancing, description of Thomson-CSF flying-spot twin format telecine *(French)* 80−37110
developing and fixing, simultaneous, research works review *(Russian)* 78−86372
developing charact. of 4-aminopyrazolone-5 and 5-aminobarbituric acid mixtures *(Russian)* 78−49931
developing of colour cine film emulsion, math. model of charact. curve *(Russian)* 78−16888
development, electrochem. models 79−52697
development, nucleation and growth phenomena 80−101858
development and fixation (simultaneous), effect of $Na_2S_2O_2$ on image microgranularity *(Russian)* 79−100419
development and materials sensitometry *(Italian)* 79−93241
development by aminophenols, rate/conc. relationship 78−21244
development course plotting 78−24880
development of spectral plates, use of gaseous-lowest agitation technique 77−67520
development probability, AgBr grain diameter depend. 80−9056
development process, electrocatalysis 79−20400
development rate, effect of developer ion charge 79−24753
3,5-diamino-1,2,4-dithiazolium salts as development accelerators, evaluation 79−34336
diazo salt sensitised gelatin for holographic recording, grating form. 80−78798
diazonium, amplifying material, kinetic and sensitometric props. *(German)* 79−43607
diazotype imaging film, continuous tone, for duplicating of radiographs 78−32911
diffusion transfer based negative and positive working camera speed overlay color system 80−37109
direct imaging system using photoelectrophoretic behaviour of TiO_2 77−54005
direct positive emulsions, reduction and S sensitization for core and shell 79−20411
discrimination in development 79−20398
disulfides as antisilvering compounds in fixing developers 79−24795
dye, colour coupling in soln., kinetic anal., appl. of flash-light photolysis *(German)* 79−39173
dye chemistry for new instant film 80−81342
dye clouds, random-sphere model 78−4722
dye pair, chromophorically degenerate, adsorbed on AgBr, supersensitised photoconductance 79−61887
edge response curve, midpoint location, development microeffects effect 78−29196
electron microscope film, image reversal process 79−2892
electrophotographic edge effect in large area imaging with ZnO binding agent layers and development electrode *(German)* 77−38045
electrostatic image development, high speed 78−62249
emulsion layers, α-irradiated, processing by iron oxalate developer *(Russian)* 78−50443
emulsion stabilization mechanisms 79−20416
emulsion supersensitisation by hydroxy-tetraazaindenes 80−3384
emulsions, exposure fluctuations, grain shielding effects on the characteristic curve 79−30594
emulsions thickness variation effects on photographic density *(Spanish)* 79−67401
enzyme systems, immobilized, appls. 79−20450
evaporated layers for the study of the primary processes of photography 79−17540
exponential transformation using film nonlinearity for optical homomorphic filtering 80−58467
feature-film production, non-standard films and processes *(Russian)* 79−49326
ferricyanide bleach regeneration, simplified electrolytic method 78−74090
film copying, control mechanism to reduce waste quota *(German)* 78−93772
film copying, control of completeness, objective evaluation criteria *(Russian)* 77−54010
film copying for TV projection *(German)* 79−49311
film development and the environment *(German)* 80−7806
film development kinetics of viscous solutions *(German)* 79−83482
film positive, reproduction of subject, relationship between objective and subjective phases 79−30596
film printing, processing, automatic control system structure *(Russian)* 77−61149
film processor, Russian 9P-55, with intensive solns. feed for cine-film negatives *(Russian)* 79−49324

photographic process continued
film response to 25 MV X-rays, sensitometric curves, relative dosimetry 80−52376
fixation and washing, of Ag halide gelatin emulsions 77−79176
fixing process, developing agent influence *(Russian)* 77−41721
fluctuation problems, computer simulation 77−3218
fog and sensitivity centre form. kinetics and activation energies during chem. sensitisation 77−44495
fogging effects diagnosis, use of granularity meas. 79−47952
formazan dye, physical development, high gain amplification process 79−39170
gelatin, layers, swollen, electrolyte diffusion 78−32910
gelatin layers in photog. developers, effect of diffusion on swelling *(Russian)* 79−97461
gelatin-Pd II complex formation, circular dichroism and absorpt. spectra meas. 79−61881
grain interaction effects in emulsion, Markov random field model 77−54002
granularity theory approximations 78−4721
halide-insulator interface, interfacial polarisation, dielec. loss meas. 77−2705
halides, unsensitized photographic emulsion, quantitative interpretation of latent image distrib. data 79−20403
Herschel effect as a rehalogenation process 80−26034
high acuity development of evaporated AgBr layers 79−24798
high speed direct positive Ag halide system 79−20435
high-speed machine for film processing using helix-eliminating angle drive system 79−2860
holograms, diffraction efficiency of recordings on high resolution photographic plates *(Rumanian)* 80−48188
holograms, recorded with backward and accompanying beams, transmission and reflection props. *(Russian)* 77−68194
holographic emulsion monobath and reversal processing techniques 80−102668
holography, white light refl., developer compositions compared 80−102669
Hough-Powell digitizer for processing film from bubble chamber Mirabelle in K^+p expt. at 32 GeV/c 80−69040
Hurter and Driffield, photographic research, biography 80−22181
hydroquinone, oxidation of centre of photographic development, electrochem. kinetics *(Russian)* 80−3367
hydroquinone development, effect of oxidation products 79−24796
hypersensitisation in astrophotography, review 78−32348
IAE films for pulse holography, effect of wavelength on photosensitivity *(Russian)* 79−68372
image enhancement using fluorescent light emission techniques 80−31928
image formation and development *(German)* 78−86366
image intensification by autoradiography 77−5937
image intensification processing, effect on paper freq. contrast charact. for varying Ag content *(Russian)* 80−95183
image resolution in single-stage photographic process *(Russian)* 79−44969
image sensitivity, improvement using Mn salts in developing soln. *(Russian)* 77−34050
images with irregular screen struct., investigation 79−17547
induction period, additives on physical development, const. pAg 78−16873
induction period of development 77−5948
information recording, new techniques, review *(German)* 77−26411
information recording and retrieval techniques, review *(German)* 77−26410
instant cine film development and projection 78−78012
interior scenes, optimum photographic representaton of brightness 80−31921
ion-exchange wash water recycling system, pair exchange tanks, solar panels for tempering, processing laboratory appl. 80−42277
kinoform lens production and optical testing *(Russian)* 79−98310
Kodak 649-F plate 5-min. processing monobath 77−633
latent and developed electrophotographic images, stat. correl. 77−71400
latent and sublatent images, alternation of electrochemical props. 79−20405
latent image, formed by X-ray exposure, props. 79−20407
latent image centre, model form. 78−62253
latent image distrib., etching and recrystn. effects of solns. 80−77890
latent image formation, Ag_6 cluster as quantum chemical model 79−24792
latent image formation, in photographic emulsion, grain diameter depend. 78−62244
latent image formation, influence of recombination 77−5945
latent image formation *(Italian)* 79−80709
latent image formation in Ag halides, nucleation, growth and developability 79−20395
latent image in photothermoplastic process *(Russian)* 78−49935
latent image latensification, mathematical interpretation *(French)* 77−41707
latent image size, dependence of activation energy for development 77−5944
latent images, effect of longwave radiation *(Russian)* 77−49801
latent images rel. to wavelength, photometric obs. *(Russian)* 78−49927
latent-image bleaches, enhancement of latent-image and fog 78−24879
latent-image centres, validity of Gibbs-Thomson equation 77−5943
latent-image formation: the contribution of the Research Division, Kodak Limited, Harrow, review 80−22458
liquid-developed migration image fixing and abrasion resistance 80−4792
lith development mechanism, developing agents 80−77889
luminescence rel. to latent image 80−73498
magnetic brush development characteristics for xerography 80−4798
magnetic field effects in monochrome cinefilm development *(Russian)* 79−17534
masked antifoggants, hydrolysis stability, photographic process depend. *(German)* 80−45530
mass spectrometric photoplate processing, microcomputer based system 80−62787
mathematical modelling of growth of spherical metallic particles at slow diffusion stage *(Russian)* 80−50871
metal carbonyl film exposure and development *(Russian)* 78−58075
metal-photosemiconductor-insulator multilayered structure, charge pattern formation during recharging 80−47129
metal-photosemiconductor-insulator multilayered structure, optical image recording, As_2Se_3 photosensitive element 80−42286

photographic process continued
modular contact printer for high speed automatic additive colour cinefilm printing 80−42276
monochrome cinefilm prints using two silent 16 mm projectors as contact printers, medical research lab. appl. 79−35865
monochrome photographic print exposure control cct. *(Danish)* 80−62748
monochrome photographic process, subjective optimum reproduction cycle 79−49318
motion picture, single-frame, automation *(Russian)* 78−86374
motion picture IR travelling matte system with electronic masking 79−75642
motion picture printing using new colour attenuation system 79−2859
narrow band gap semiconductor electrophotographic processes 80−13169
non-Ag photography with physical development *(Russian)* 79−44970
non-Ag process based on polyvinyl spirit-transition metal halide system *(Russian)* 80−73502
non-mechanical dispergation of color couplers 79−24799
nuclear emulsions, regression of latent image under action of pulsed electric field *(Russian)* 77−49802
optical density, depend. on exposure for photographic action by high energy electrons, 250 to 1000 kV *(Russian)* 80−90923
organic dyes, spectral sensitization and electronic struct. 79−19551
organic imaging systems, overcoming thermal instability and fog problems 79−2851
organotellurium compounds, thermally developable light sensitive systems 79−2850
orthophotoquad processing using photodensity control system 78−7807
oxiphenol developers, free radicals *(Russian)* 79−39138
paper print residual thiosulphate, methylene-blue and Ag densitometric meas. correlation 79−74472
paraaminophenol and paraphenylenediamine analogue molecular complex, free radicals of developers, EPR obs. *(Russian)* 80−7814
penetration of developing agents into gelatine films, approx. modelling using diffusion theory *(Russian)* 79−67411
penetration rate of developer components through gelatin and photoemulsion layers 79−20436
permeation of photographic developer into a gelatin layer, potentiometric exam. *(Russian)* 80−73500
phenanthridinic spiropyran photocoloration mechanism 79−83487
1-phenylpyrazolidin-3-one adsorption on metal electrodes, obs. 79−100391
photoactive pigment electrophotographic imaging system, dark charge exchange process 80−62758
photocatalytic diazosystem, light-sensitive, possibility of creation 79−20451
photochemical unconventional systems, amplification processes 79−61882
photocondensation, molecular compounds behaviour in strong light beams *(Russian)* 77−49798
photoconducting film for rapid access instrumentation recording 80−62755
photodelamination imaging, new dry processing approach 79−2853
photoelectrochemical investigation of the influence of gelatine and polyvinyl alcohol on the formation and lifetime of a latent image in photographic layers on a ZnO base *(Russian)* 80−3389
photoimaging system based on photopolymerisation in cryst. coatings 80−40716
photopolymer latent imaging system, for vol. phase hologram recording 78−42298
photoresist, positive, simultaneous exposure and development model 78−4715
photoresist, positive simultaneous exposure and development model 77−74532
photoresists, cross-linking, photographic characteristic curve, sensitivity 77−10128
photosensitive glass, full-colour polychromatic, subcolloidal Ag precipitation 79−47953
photostating techniques *(German)* 78−89572
photostimulated solid-state reactions 78−53222
physical development using a single-solution treatment *(Russian)* 79−44965
Polaroid negative, salvaging data 78−78020
Polaroid print coaters, comment 79−35864
Polavision, first instant colour movie system 78−24882
polyethylene glycol, effect on photographic film during fast development *(Russian)* 80−45533
polymethine dyes, investigation of chemical transformations 79−20445
positive film density, depend. on conc. of stabilizers and antifoggants added to developer *(German)* 80−73497
positive photoresist film exposure, formal kinetics *(German)* 80−104454
print timer, using ring of LEDs 80−77899
printing and processing conditions for dye transfer process materials, choice using automatic systems *(Russian)* 79−75643
printing methods, photometry and sensitometry measurements *(German)* 79−6201
PVC, Cu evaporated film, electron-induced metallochromic reaction for metal image formation 80−86476
pyrocatechol derivatives, developing ability and structural data, correlation analysis 79−20448
quantum chemical models and computational methods *(German)* 78−53229
radiographs timer for processing 79−5125
reaction tensor analytical treatment *(German)* 79−83481
reciprocity law failure, effects on exposure time and contrast 80−47124
recycling of colour processing solutions 79−20437
redox potential evolution during development, potentiometric anal. 78−16865
reflection holograms of diffusely reflecting objects, improved efficiency 80−32939
release prints, increasing quality of sound tracks, direct positive recording process *(Russian)* 79−9255
relief plate preparation by subtractive development 79−21831
reversal cinefilm development, effect of temperature, concentration factors on speed of process *(Russian)* 80−105735
review of process physics, silver halide phys. props. and sensitivity *(Japanese)* 77−54007
rotary tube photographic processor design 80−4795
scattering characts. of emulsion layers into rear hemisphere *(Russian)* 79−44967
sensitisation of photographic film in elevated temp. H_2 gas, development 79−61885
photographic process continued
sensitometric and thermodynamic properties of developable and subdevelopable silver specks 79−20396
silver halides, photographic information recording and retrieval techniques *(German)* 77−26410
silverless photographic processes, quantum yield and photosensitivity formulae *(Russian)* 78−49934
small-grain development of emulsion monofilms for electron-microscope autoradiography *(Russian)* 80−297
solarization, elimination of adding halogen acceptors, electron microscopy investigation 79−24790
sound track stripe applicator, control system, colour release prints for both positive, reversal stocks appl. 80−42275
spectral anal., optimisation of photographic registration *(Bulgarian)* 79−44956
spectral photographic plates blackening intensification *(Bulgarian)* 79−30590
spectral sensitization pathways, influence of dye energy levels, structure and environment 79−19554
spectral sensitizing dyes, energy levels 79−19552
stabilisation of photographic image, introduction of $N(CH_2PO(ONa)_2)_3.6H_2O$ in thiocarbamide *(Russian)* 80−302
stable latent image form. 78−62252
stationary potential and oxidation current density of developing substances *(Russian)* 79−100417
sub-image and latent image Ag specks, thermodynamics of formation 78−16874
sulphide sensitisation of negative emulsions, quality composition of photosensitivity and fogging centres *(Russian)* 80−62781
SX-70 system of instant photography, history of design 79−97457
synergism of PQ developers 79−24732
tanning developer rel. to formation of gelatin relief images 77−82638
thermal photographic image receivers, freq.-contrast characts. *(Russian)* 79−44971
thermoplastic recorder development, interaction of regular and chaotic deformation *(Russian)* 80−42291
thermoplastic recording, amplitude characts. *(Russian)* 79−44973
thermoplastic recording, theoretical problems 79−24803
thermoplastic recording development, electrocapillary effect, nonlinear distortions *(Russian)* 80−294
thermoplastic recording material, latent image and surface deformation *(German)* 80−42284
thermostatic control device for developing bath *(Spanish)* 80−77898
thin layer chromatographic anal. of dyes formed by development *(Japanese)* 77−26418
thiolic antifoggants sensitizing emulsions, latent image form. enhancement 79−17519
thiosulphate processing technique, cinefilms appl. *(Russian)* 80−3386
toner deposition by cascade development with developing electrode *(German)* 80−73494
treatment processes, diffusion kinetics 79−20447
two-jet emulsification kinetics of form. of mixed AgBr(J) phase *(Russian)* 79−44968
using Cu-ascorbic acid *(Russian)* 79−67413
UV-4 film, microphotometric granularity for registering vacuum UV spectral region *(Russian)* 79−58833
volume holograms, mode theory allowing for photographic process nonlinearity 80−102673
wetprinting, historical review 80−283
X-ray film characts., heuristic model 77−195
X-ray films, automatic development *(German)* 80−280
X-ray films, reciprocity law failure in reversal processing 79−97483
xerographic image, measurability of structure fluctuations 77−18119
xerographic process, role of photoreceptors *(Japanese)* 80−82842
Ag cluster growth on AgBr microcrystals after X-ray and low-temp. light exposure 79−83485
Ag clusters, open-shell CNDO-MO calcs. 79−20397
Ag deposition on AgBr evaporated layers at room temp. 79−20409
Ag diffusion transfer systems, graphic arts appl. 80−37106
Ag formation on Ag-halide surface, flash photolysis expts. on Ag halide photochromic glasses 79−94310
Ag, graining, comparison with colour image *(German)* 79−29380
Ag halide, absorpt. and vac. photolysis 78−8458
Ag halide, exposed and unexposed grains, discrimination in photographic development 79−83447
Ag halide chemical development 79−20399
Ag halide diffusion transfer development chemistry 79−96340
Ag halide dry materials for laser printing appls. 80−13179
Ag halide emulsion, mechanism of development 79−39169
Ag halide emulsion grains, photographic effects of electron and positive hole traps 77−82635
Ag halide emulsion props., Tl^+ ion influence 79−100413
Ag halide emulsions, hot carriers multiplication and latent image formation 79−20408
Ag halide emulsions, positive, formation of microcrystals *(Russian)* 78−49930
Ag halide emulsions, ultra-fine-grain, spectral absorption 79−24793
Ag halide microcrystal, sensitised and stabilised, concentration speck and development centre growth 79−83484
Ag halide microcrystals, low-temp triboluminescence 77−87861
Ag halide microcrystals, topography of latent image centres and ionic conductivity 79−20442
Ag halide monodisperse emulsions, granularity prediction in processed coatings 79−26163
Ag halide photography, semiconducting models 79−19630
Ag halide photography in middle IR using laser sources 77−53997
Ag halide sensitised gelatin processing, phase volume hologram form. 80−78797
Ag halide solvation, effect of restrainers in reversal first developer 79−24797
Ag halides, defect sites and impurities, latent image formation, LCAO calc. 78−16876
Ag halides, formation of metallic Ag on surface, optical absorpt. calcs. 79−24791
Ag halides, photoinduced phase transition 79−20402
Ag halides, physical props. rel. to photographic processes 79−19555
Ag halides, spectral sensitivity of Herschel effect, photo- and thermostimulation photographic effects *(Russian)* 78−58082
Ag latent image particles, electronic effects 80−82840
Ag particles, charge sign determ. during development *(Russian)* 79−100417

photographic process continued
Ag photographic films, thermal development *(Russian)* 80−303
Ag, photolytic, mass and distribution in the solarisation region 78−29185
Ag speck nucleation and phase formation in latent image 80−97716
Ag specks, latent pre-image, investigations on temp. dependence of life-times by 'two-flash' method 79−20406
Ag, vacuum deposition, on evaporated AgBr layers, growth mechanism 80−35095
Ag-complexes, stability increase during simultaneous photographic development and fixing *(Russian)* 80−95179
AgBr, connection between the topography of luminescence centres and the latent image *(Russian)* 80−62785
AgBr crystal produced by action of free radicals, developability 80−66838
AgBr, decoration of sensitivity specks 79−24784
AgBr dispersion in gelatin, adsorbed S and Au, transient absorpt. spectra, latent image form. and decay 80−66837
AgBr, emulsion, grain disorder and its influence on emulsion response 77−5940
AgBr emulsion, influence of iodide content on ripening behaviour 79−24794
AgBr emulsion, latent image fading 79−34335
AgBr emulsion, latent image speck size, characteristic curve anal. 79−34338
AgBr emulsion, sub-image and latent image specks form. and props. 78−21245
AgBr evaporated layer chemical sensitisation 79−24766
AgBr film coatings, luminesc. props. for H_2 and other reduction sensitisation 79−61886
AgBr homogeneous emulsions, iodide influence on photographic props. 79−44959
AgBr, hydrosol, latent-image stability, chem. sensitisation 78−21236
AgBr layer, sensitised, topography of developed centres 80−73491
AgBr microcrystals, Herschel effect, $Na_2S_2O_3$ etching soln. effects *(Russian)* 79−5167
AgBr, neutralisation of trapped photoholes 79−24788
AgBr, nucl. emulsion, latent image form., grain diameter depend. 80−9453
AgBr, photoexcited, dye sensitized bleaching of surface silver specks 78−308
AgBr, photoexcited electrons and holes in latest image form., review 80−73496
AgBr, photographic emulsions, dye spectral sensitization, latent image form., subcond. band events 78−32905
AgBr photographic emulsions, sensitivity, fog rel. to treatment in redox-buffered solns. 78−32906
AgBr:I, refilling of recombination centres during thermal stimulation 78−10464
AgBr:I single jet precipitation, grain growth kinetics 79−20414
AgBr:Pb^{2++}, cubic microcryst., ion influence on ionic cond. and space charge charact. 79−55928
AgBr-$Na_2S_2O_3$-H_2O system, thermodynamic and kinetic investigations 79−20444
AgBr(Cl) vapour-deposited epitaxial film, surface structure 80−59814
AgBrI emulsions development, processing and DQE 79−24801
AgBr(I) microcrystal dispersed in gelatin, effect of I^- on interstitial Ag ions 78−26726
AgBr(I) microcrystals, photohole motion 78−26903
AgBr(I) microcrystals, photocond. and luminesc. 78−26904
AgCl, AgBr and AgI emulsions, kinetics of fixation by thiosulphate and Ag ion 77−82634
AgCl electrode, electrochem. dye spectral sensitization, gelatin addition *(Japanese)* 79−57262
AgCl, luminescence fatigue, adsorbed Ag atoms 80−66281
AgCl nucleation from aqueous solns., stopped-flow UV absorption spectrophotometry 79−20413
AgCl single cryst. foil, photographic elementary process 78−17519
AgI, connection between the topography of luminescence centres and the latent image *(Russian)* 80−62785
AgI-Ag thin granular film, Herschel effect 78−82063
AgX, selectivity of development of small aggregates of microcrystals in photographic layer *(Russian)* 79−58832
AgX, XX *(Russian)* 80−293
AgX, X=halide, form. and migration of catalytic nuclei *(Russian)* 79−70378
Al-As_2Se_3-Al, photographic process based on electrochem. reactions *(Russian)* 79−6213
Al-gelatin-GaAs, capacitance-voltage charact. after and before incorporation of $AgNO_3$ 79−51684
AlH_3, thermo- and electrochemical transformations 78−89576
a-As_2S_3, photodesactivation, direct positive imaging 79−17544
As_2S_3-Ag, light sensitivity for high exposure densities *(Russian)* 79−6212
$As_{15}S_{40}Ag_{45}$ glass, photosurface deposition of metallic Ag discs 77−76650
Au, function in latent image formation 79−39171
Au sensitisation during latent image formation, nature of sensitivity specks 77−82637
BiI_3 photosensitive layers, optical and thermal development *(Russian)* 80−73512
Cu SCN-based photographic system, charact. of development process *(Russian)* 79−58834
$Cu_{15}(AsSe)_{85}$ photographic layers, temp. depend. of reverse optical recording *(Russian)* 79−67415
GaAs:Cu electrode photographic device, CO_2 pulsed laser output high-speed meas. 79−14008
NH_4ClO_4, photothermochemical process 79−24769
NH_4ClO_4, photothermochemical process, influence of phase transition 79−24770
NaCl:O, photographic recording in far-UV, colour-centre formation 79−23035
$Na_2S_2O_3$, breakdown on Ag halide grains, electron microscopy 78−21237
Ni-hypophosphite developer, physical development as function of pH 79−24760
$Ni(N_2H_4)B_xH_y$ development, effect on photosensitivity of paper *(Russian)* 80−73509
$Ni(NH_3)_6^{++}$, photographic developer, potentiodynamic polarisation curves for Ag-less development *(Russian)* 80−90921
$NiSO_4$, photographic developer, potentiodynamic polarisation curves for Ag-less development *(Russian)* 80−90921
S and Au sensitisation, internal image speed 78−16869
Sb_2S_3:Ag, sensitised photolysis and structure of latent photographic image 78−89574
Se, appl. to xerography 80−57415
Se layers, latent electrophotographic image, formation mechanism *(Russian)* 79−26157
Se-As alloys, appl. to xerography 80−57415
TiO_2 photographic layers, sensitivity enhancement by addition of Ag^+ during cuprous development *(Russian)* 80−62780
ZnO binder electrophotography, tone reproduction and copy quality *(German)* 78−62259

photographic recording media *see photographic materials*

photographic techniques *see photography*

photography
see also cinematography; colour photography; electrophotography; microphotography; photographic applications; photographic lenses; photographic materials; photographic process; radiography; streak photography
accurate fan-beam reconstruction 78−78931
additive photographic film printers, programmed control of light metering valves *(Russian)* 80−95174
aerial, reseau mensuration with sensing arrays 77−26412
aerial frame photography, coord. system 79−2179
aerial photogrammetric systems, granularity noise, effect on meas. of quality charact. *(Russian)* 77−67525
aerial photograph statistical spatial filtering 79−13908
aerial photography, pattern recognition, Mellin transform method 78−63021
aerial photography rapid screening by optical power spectrum analysis 78−63033
aerophotographic system, synthesis and applications *(Russian)* 79−58836
anaglyphs, printed, use of fluorescent green ink 78−4714
aspectogram, spectral props., image multiplication appls. 79−55090
aspectrograms, produced with hexagonal lens raster, props. 78−46528
astronomical, development and history, review *(Italian)* 77−56839
astronomical, hypersensitisation, testing of emulsions for threshold imagery 78−32351
astronomical photographs, reduction via intensity microphotometer with step-drives *(Russian)* 78−57457
astronomical photography, gain of quality by plates superposition 79−75114
astronomy, near IR photography with vacuum-cold camera 80−90341
astrophotography, exptl. summer course 77−64902
automated comparator-microphotometer for spectral line position meas. 78−77962
automatic cameras, exposure error compensation 80−52346
automatic control of photographic analysis precision using minicomputer and meas. engine 77−41710
automatic enlarger timer 79−67406
automatic time-lapse photography, long term, for frost blisters meas. 80−12437
biomedical, plotting instrument for close-range photogrammetry 78−77137
black and white picture grey-differentiation displayed, using computer generated arbitrary colours *(French)* 79−81370
brightness two-dimensional field simulation 77−79778
Bruce telescope photographic plates, computer readable mag. disc catalogue 79−88605
calotypist-photographer correspondence (1841-7) 79−21515
camera, 35 mm compact, with fully automatic exposure control 80−90916
camera automatic focusing system, Visitronic, description *(German)* 79−6200
camera automation developments 80−18027
camera shutter control, use of photosensor with IC amplifier *(German)* 80−52341
cassette, 10×10 cm, for photographic recording from oscilloscope screen 77−25574
charged particle detection by photographic recording systems, appls. 78−17527
chromaticity analysis for automated TV complex 3 zonal objects registration process *(Russian)* 79−89026
coherent image deblurring using computer generated holographic filters 77−14669
coherent multiplicative photometric analysis, photorecorder meas. system sensitivity threshold *(Russian)* 79−67373
coherent optical processing cervical cytological samples 78−36007
coherent optical processing equipment cervical cytological samples screening 78−36006
composite photographic-human visual system, spatial-freq. filtering effects in performance 78−4725
confidential picture taking technology laser holography for picture scrambling 77−19208
contrast enhancement viewer for film 78−16879
copier techniques, gamma reproduction, DIN and ASA sensitivity scales and sensimetry *(German)* 79−26155
corona discharge photography, image modulation 77−5952
coronagraph, white-light, on Skylab, radiance calibration 77−60606
course for fine arts students 77−33731
CRO attachment, electron-optical converter for increased recording speed 79−21732
dark photography laser as flash-lamp+image intensifier *(Russian)* 77−79177
dark room timer, logarithmic calibrated 78−8457
darkroom timer, IC, DIY *(German)* 78−82065
data extraction and classification from film, conf., San Diego, USA (Aug. 1977) 78−63023
data processing by coherent light, photographic noise *(Italian)* 78−22088
deep space, large area CCD imaging systems charact. 77−57426
defocused grainy photographs, digital restoration by noise cheating and Fourier techniques 77−50626
defocused speckle photography, topological information extraction technique 77−41676
deformation measurement, out-of-plane, using holographic interferometry and speckle photography, comparative accuracy 80−78804

photography continued
densitometer measurement transformation into spectral density distrib. and colour coordinates *(Russian)* 80−77902
digital illumination timer, TTL, darkroom appl. *(German)* 79−49315
digital photometric system for photographic image computer input 77−18112
display system using computer generated integral photograph 78−87021
double exposure for controlled density eval., replacement of quarter wave plates 77−87859
education, perspective distortion in photography, eye as simple lens 80−17734
electric exposure meters, appl. *(German)* 77−87856
electrographical imaging of objects, in electric discharge *(Czech)* 80−37104
electron micrographs of metal shadowed objects, low cost internegative prod. 78−74109
electron microscopy freeze-fracture image enhancement by reversal processing of sheet film 78−62267
electron-optical photography in pico-femto-second range, conf., USSR Acad. of Science, (June 1977) 79−18062
electron-optical photography in pico/femto-second range 79−18342
electronic flash unit, synchronised or free running, cct. details *(German)* 78−21250
EM, external photographic system 80−101902
enlarger, Czechoslovak Opemus Standard (2) *(Czech)* 80−18034
enlarger analyser using Si-blue photoamplifier IC 80−42288
enlarger digital timer, 0.1 second steps or 0.1 minute steps 80−77893
enlarger exposure meter, using photodiode and multimeter 80−101857
enlarger exposure meter 79−89018
enlarger timer cct. without transformer 78−49924
enzyme systems, immobilized, appls. 79−20450
exposure meter, enlarging, digital, using photodiode, for black-and-white photography 79−85190
exposure meter and development timer, used for photographic enlarger 80−101856
exposure meter for electron microscopy 77−26435
exposure meter for electronic flash 80−77835
exposure meter for flash lamp photography 80−9058
exposure prediction techniques, still, motion-picture photography appl. 80−66817
external occulting disc as radially-graded neutral density filter, for solar coronal obs. during eclipses 79−80233
fault identification in badly taken photographs *(French)* 77−71390
film, large format, for use with laser scanning system 78−62260
film colorimetry 80−22461
film copying, control mechanism to reduce waste quota *(German)* 78−93772
film movement nonuniformity study in film-advance channel 80−68285
film processing machine, high speed, using helix-eliminating angle drive system 79−2860
film-grain noise, low-contrast image detection 78−94370
film-grain noise degraded images, nonlinear detection and estimation 77−50627
fixing solution, Ag^+ ion electrochem. removal using porous flow-through electrode 77−60076
flash light meas. instruments development *(Hungarian)* 80−57411
flash sequencer, using thyristor control 80−62749
flash trigger, multimode 78−21248
flash trigger, sound operated 77−41717
flash unit triggered by acoustic shock wave, cct. details objections in rapid motion photography appl. 80−101862
flash units, basic types 79−71548
flashgun slave trigger, using Si solar cell 80−47125
flashlamp trigger circuit 80−62750
fogged photograph restoration by optical spatial filtering 78−74857
forest aerial photograph spectral investigation *(Russian)* 77−34041
gonioscopy, foot-operated camera trip for Nikon photo slit lamp 78−80986
grainless focusing screen for light scatter reduction 80−101836
granularity measuring system 78−21200
halftone images, detail reprod. and spurious signals generation 77−53996
halftone images produced by random quasiperiodic process 77−622
halftone or line printing, Yule-Nielsen curve fitting parameter 79−13906
hand-held and film-plane photographic exposure meters 78−58078
Herschel-Talbot photographic pioneering correspondence 79−97168
high speed, in aeroballistic range, track facilities of von Karman gas dynamics facility 78−37094
high speed, stroboscopes appl. 78−55453
high speed photography framing of fast processes, using OLZ-7 optical delay line 79−23080
high speed photography of water jet turbulence fine struct. 78−26178
high speed raster cameras, image dissection and mech. scanning for photographic recording *(Russian)* 80−95182
high speed silhouette photography 78−37088
high-speed, conf., Toronto, Canada (Aug.1976) 78−32912
high-speed, using inorganic liquid laser 77−30211
high-speed cine schlieren photography for meas. of V-gutter stabilised flame 77−35263
high-speed mirror photochronograph 78−37098
high-speed photography combined with real-time holographic interferometry 78−37839
history, contribution of W.H. Fox Talbot 78−17
hologram production for cylindrical surfaces, shape meas. 79−7095
holographic method for hypervelocity particle meas. 78−36978
holography appl., commercial methods development *(Czech)* 78−37838
Hurter and Driffield, photographic research, biography 80−22181
illumination timer for hobby photography *(German)* 80−98992
image coloration psychophysics 78−65025
image detail enhancement system 78−58086
image detection and recognition visual factors, optimal viewing conditions 78−4724
image enhancement using fluorescent light emission techniques 80−31928
image evaluation, coherent and incoherent optical spectrum analysis 78−63031
image evaluation by single bar and disc. anal. (aerial photographic system) 77−2704
image motion velocity compensation, in oblique panoramic photography 79−6209
image noise, intragrain transmittance distrib. in random dot model theory 77−45911
photography continued
image quality, scattered light effect 78−16884
image quality criteria 77−79171
image reproduction system, information losses 79−71558
images autoradiographic intensification using Thiourea-^{35}S, quantitative anal. 80−90343
imaging of moving object, in high-speed photography, anticausal behaviour 79−81381
instant, lab. appl. 80−90915
instant imaging of electric, radio and acoustic fields 78−58079
intaglio imaging with nuclear particles 78−65993
integral photography, transform of 3-D image produced by lens raster 78−82921
integral photography method, limiting achievable parameter values of various subjects 80−101866
intensification of underexposed photographs of prebreakdown luminescence in dielectrics 77−24793
interference fringe localisation, by double exposure speckle photography 78−37803
invariant photographic system, matrix model, nonlinearity *(Russian)* 77−34049
IR aerial photography for agriculture, potato blight detection 80−13174
IR photographic methods 79−93243
IR photography, principles and appls., book 78−82068
IR photography at 5 and 10 μm 79−49328
IR photography on wax films at 10 μm 80−4784
IR sky survey telescope, wide field photography 80−105167
Japanese photographic education history and status 79−92910
Kirlian, moisture detection using charged Al plate *(Italian)* 78−49916
Kirlian photography, 'camera' construction 78−12779
LANDSAT imagery, photographic contrast enhancement 79−29896
laser application to high-speed photography of fast processes 77−68236
laser gas breakdown, shock and ionisation waves, photographic absorpt. obs. 80−87967
laser high-speed framing photography *(Japanese)* 79−2847
laser speckle photographic technique, strain, small displacement measurement appl. *(German)* 78−1616
laser speckle photography, review *(Chinese)* 79−35880
latent photographic images, erasion by electric field *(Russian)* 79−97462
LEED intensity measurement by photographic method with digital image processing appl. to Si (111) surface 79−60234
lens-array photography, longitudinal distortion compensation, integral image reconstruction 80−52345
level slicing performance using film nonlinearity *(Chinese)* 80−102628
light control unit using logarithmic A/D convertor *(German)* 79−93117
light distribution pattern math. calc. for camera copyboard illumination 79−21800
light sources, guide number formulae for pulsed illumination systems *(Russian)* 80−73503
liquid crystal indicator of variable light-reading angle 78−57932
low light security and projectile photography using channel-plate image intensifier cameras 79−40639
macrophotographic techniques 79−49312
medical, problems encountered in hospitals 79−12875
metal cluster growth and props., appl. to photographic processes, conf., Villeurbanne, France (Sep. '79) 80−105431
meteor spectra photography using TV apparatus 77−67047
microdensitometric evaluation *(Czech)* 79−30524
mineral particles settling in liq., X-ray photography 79−20469
Moire photography, appls. of slotted apertures 77−65053
multicolour frames, method for checking quality 80−105728
multicoloured photothermoplasticity process, coding and decoding indices *(Russian)* 77−67523
multiframe shadow photography using optical delay like 77−764
multispectral projector, colour synthesis instrument for evaluating multispectral photographs 78−40688
Mylar, shells, conical and cylindrical, high speed photographic exam. of buckling 78−44184
nanosecond photography with Ag halide film, 10.6 μm CO_2 laser pulse spatial distrib. recording 79−89016
negative print production, electron micrographs of metal shadowed materials 80−18051
nonlinear photoelectric or photographic receiver signal value calc. *(German)* 80−31866
nuclear, use of alpha naphtol, developer 78−17490
nuclear track sensitive target expts., automatic film meas. 78−55105
nucleonics history, record of lost opportunities 78−65986
oblique panoramic aerial photographs, geometrical characts. 80−47128
oblique transmitted light techniques for photomacrography and photomicrography 78−58026
ophthalmic photography to prevent diabetic blindness 80−16920
optical flashes from double wire explosion, photographic appl. 80−1865
optical images of plasma objects, synchronisation with electrical parameters 80−31919
phasometric method of measuring the thicknesses of transparent recording carriers and substrates *(Russian)* 80−73514
photo flood dimming, thyristor circuit, to reduce heating and extend life of lamps *(German)* 78−29193
photodetector, threshold sensitivity for semiconductor photography 80−18017
photoelastic fringe photography, improved photograph quality 80−27364
photoelastic frozen stress slices, fractional fringe order lines obtained by controlled density techniques, self-calibration 77−51001
photoelasticity, photographic recording and sharpening of isoclinics 77−51002
photogrammetric instrum. applic. of incremental and parallel computing 77−10121
photographic image threshold luminance detail value, effect of target and photographic parameters 78−56989
photographic images, information content 79−17548
photographic images with irregular screen struct., investigation 79−17547
photographic plate spectral line setting photoelectronic arrangement 78−78015
photolamps, thermal interference reduction using Therm-O-lux 85 film 78−41302
photomacrography, high resolution, zoom instrument with automatic exposure 80−62756
photomacrography, the appl. of photographic techniques to image scales in the range 1:1 to 60:1 78−78009

photography continued
photomacrography and photomicrography, oblique transmitted light techniques 78−306
photomapping data collection, storage and retrieval system 79−71549
photomicrographs, high quality image prod. 78−24881
photomicrography, exposure control 80−90888
photomicrography, instrumentation, vibr. problems, films, illum. and magnification 77−57417
photomicrography of submicrometer birefringent contaminants in C black dispersions in polymer particles 80−62757
photomicroscopy, universal microscope 77−57384
picosecond light pulse techniques, historical overview of rapid phenomena meas., book contrib. 77−65026
pneumoelectric automatic device for passing splices in cinefilm, still photography film *(Russian)* 79−2864
polarised light for high fidelity reproduction 79−44957
Polaroid film artifacts in nuclear medicine laboratories 77−18115
Polaroid negative, salvaging data 78−78020
Polaroid print spray lacquer coating 78−54478
post-development image intensification by autoradiography, technique, astron. appls. 80−26752
printing with electronic dodging, background effect 77−71398
prism correlator, appl. to stereo photogrammetry 78−86368
prism-scanning panoramic camera for reconnaissance aircraft 77−79181
pseudo-colour encoding using halftone screens and coherent filtering 77−71939
pseudocolour density encoding, white-light, using contrast reversal 80−83560
psychophysical model of positive evaluation 79−21846
reciprocity law failure, effects on exposure time and contrast 80−47124
recording of fast processes, extension of meas. parameter ranges 80−57413
regulator of light quantity utilisation, centrifugal, streaks in mine shafts meas. appl. 77−79173
reliefographic process during signal recording *(Russian)* 80−47131
review of photographic science state, 1928 to 1978 79−58513
rotating prism compensator, high speed filming techniques 77−75700
satellite imagery, linear features enhancement by rotational exposure 79−35874
satellite images macrophotography, technique 79−29895
satellite photograph production using laser beam recorder *(German)* 80−5777
Sayce test chart, modified design 78−16877
Schade detail S/N ratio derived from decision theory 78−63022
schlieren image colorisation using electro-optical technique 78−33904
schlieren system, aberration and diffr. effects on resolution 77−34040
sector device for electron diffraction studies on liquids 78−55788
SEM, photographic recording system 80−101903
SEM, real-time stereo, used in microdissection of biological tissues, methods for photographing video recordings 79−80724
semiconductor-photoemulsion photographic system, charact. 77−87863
semiconductors and ICs used in cameras, review *(German)* 79−58813
sensitometer, Xe flash, for daylight, W illum. simulation 78−29192
sensitometry, conference, Binghamton, N.Y., USA (Sep. 1976) 77−30214
shutter, drum or sector wheel, accuracy, specification 77−30210
shutters, efficiency rel. to picture quality 77−74531
simple darkroom timer design and construction 78−89577
single-exposure, with channel-plate intensifiers 78−38036
sky photographs, star position meas. error reduction by Gaussian freq. distribution curves *(German)* 77−17384
slave triggers for photographic flash 80−95168
slide scanner with P-CCD line sensors *(German)* 79−49308
slides and overhead transparencies 79−80405
small subjects, basic lighting 77−41709
solar faculae and sunspots, direct photographs with balloon-borne 10 cm telescope *(Japanese)* 79−80292
solar observations using Hα filters 78−40833
sound recording, computer simulation 78−78022
sound triggered flash cct., using variable time delay 80−57414
sound-controlled flashlamp trigger circuit *(Spanish)* 80−13175
spatial high pass filtering using photochem. adjacency effect 77−71929
speckle, double-exposure, analysis using electro-optical readout system 80−62708
speckle noise and object contrast, detection thresholds eval. technique 78−5434
speckle patterns, contrast 77−604
speckle photography, defocusing problem, rel. to holographic interferometry 77−18083
speckle photography, double exposure, anal. technique 80−62718
speckle photography, effect of lens aberrations 78−32866
speckle photography, fringe shifting technique appl. 79−54210
spray, photomicrographic anal., droplet size and vel. spectra determ. by Dimant's rotating mirror microscope 77−36800
stereo image digitiser for automatic feature extraction 80−106614
stereography, principles, technique, and equipment 79−6206
stereoscope for viewing aerial photographs, interpretoskop optics, modifications 80−105081
streamer chamber, rapid-cycling cameras, stereo images 78−37484
superimposition of alphanumeric data at time of exposure 78−58080
SX-70 system of instant photography, history of design 79−97457
system for recording the activation times of pulsed light sources 80−73488
temperature control using electronic thermostat, with 0.1°C accuracy and economical operation 80−77774
terrestrial atmosphere photographic obs. from Skylab 77−60505
thermography of fast processes, appl. to photographic recording of combustion processes *(Russian)* 80−62779
thermoplastic record and electrocapillary effect, frost deform. anal. *(Russian)* 78−16889
thermoplastic recording, amplitude charact. *(Russian)* 79−44973
thin film, Kirlian-type images and transport in high-voltage corona discharges 79−55590
three dimensional photography system using lenticular screen 79−80706
three-dimensional image production, Nimslo system 79−89017
time resolution improvement in high-speed holography 78−37840
timer, touch controlled, photography appls. *(Spanish)* 80−86478
total exposure error, digital instrum. for cameras with or without built in exposure meter 79−6208
transfer functions due to complex linear motions in photographic imagery 79−18355
photography continued
transients, shutter mechanism for oscilloscope photography *(Danish)* 78−234
triggered light pulse generator for recording fast processes 80−105727
triple frame camera, with beam-splitting prism 78−37097
UK 1.2 m Schmidt telescope plates, electronographic calibration 79−88703
ultrafast, using optical Kerr shutter, book contrib. 77−31140
ultrafast photography, with 10.6 μm radiation, fast IR switches 78−38035
underwater luminaires, technical requirements *(Russian)* 80−9064
unsharp masking technique for astronomy 79−88603
UV channel photographic photometer, for stellar obs. from Skylab 77−60608
UV photography and fluoresc. photography techniques 80−18033
velocity measurement technique, error estimation *(German)* 78−304
visual perception of noisy photographic images, threshold contrast, parametric model of observer *(Russian)* 77−52794
volume holographic multiple recording on photographic plates *(German)* 80−43288
wedge-sensitometer for photographic photometry *(Japanese)* 79−44373
wide-angle integral photography, Integram system 78−78025
X-ray intensifying screens for pulsed X-ray sources, calibration in 15-70 keV energy range 77−26446
X-ray photographic exam. of paintings, method for optimal contrast *(Russian)* 79−97459
X-ray photographic system, dispersive, for recording X-ray spectrum in 0.1-1.9 nm range 79−35904
X-ray photography, using Polaroid film 77−67161
X-ray pinhole photography of the target pellet in laser fusion *(Chinese)* 79−97458
Ag^+ ion automatic sensor-analyser for photographic fixing bath regeneration systems *(Russian)* 80−95172
AgBr, adsorption of cyanine, pH depend. 78−62254
I_2, high-dispersion polarisation-labelled spectrum 80−990
Li cells appl., 1979 state of art *(Spanish)* 79−96432
$ZnCl_2$-oil system, simulation of steel-slag, macrophotographic method of diagnosing disperse system 80−25952

photoionisation
($\hbar\omega$,2e) reactions, Green's function method and correlated electron motion 77−88431
absolute cross-sections, exptl. meas. techniques 80−63598
absorbing boundary method, Golden Rule generalisation 79−97226
acetaldehyde, lowest Rydberg state, multiphoton ionisation spectra 80−83435
acetaldehyde, multiphoton ionisation mass spectra 80−83436
acetaldehyde, primary and secondary photoionis. processes, ion-mol. reactions 79−36709
acetaldehyde-d_1(-d_3), fragmentation processes, H scrambling, photoionis. mass spectra 78−42139
acetic acid vapours, clustering, effect of supersonic mol. beam sampling, mass spectrometric study 80−104481
acetone and acetone-d_6, molecular beam photoionisation 79−3504
acetophenone, enolate anion, electron photodetachment cross-section resons. 78−5298
acetylene, photoionisation cross section at distance from threshold, chemical bond influence 80−69196
acetylene, vibr. fine struct. accompanying core ionis., STO calcs. 78−62844
acridine, aqueous soln., laser induced two-photon ionisation investig. 80−32780
aliphatic compounds, alkyl substitution effects on photoionisation, photoelectron spectrosc. obs. 79−31604
alkali atom, two-photon ionis. using elliptically polarised light 79−98052
alkali atoms, excited state, laser photoionisation theory, hyperfine coupling effect 80−102493
alkali halides, F-centre photoionisation, semicontinuum model 79−99509
alkali halides, XPS, trapped electrons at F-centres and anion defects, photoionis. cross sections 77−90249
alkali metal, quantum beats in photoionis. by fine struct. levels coherent superposition 79−6922
alkali metal, two-photon ionis. by unpolarised light, depolaris. effects 79−59409
alkali metal, two-photon ionis. via reson. intermediate state 78−42023
alkali metal atom, near-resonant two-photon ionis., non-Coulomb phase shifts of photoelectron partial waves 80−106302
alkali metal atom, polarised, spin-deposited photoelectrons from two-photon ionisation 79−63971
alkali metal atom, resonant multiphoton ionis. *(Russian)* 79−3401
alkali metal atom, transition oscillator strengths in discontinuous and continuous spectra, review 80−52937
alkali metal atoms, cross sections, scaled Thomas-Fermi method, absorpt. coeffs. 77−46549
alkali metal atoms, laser three-photon absorpt., ionisation cross-sections *(French)* 78−5182
alkali metal atoms, spin-polarised, near-reson. two-photon ionis., light polarisation effects 80−106308
alkali metal atoms, two-photon ionisation, polarisation effects 78−1039
alkali metals, two-photon ionisation with two light beams, polarisation effects 79−81190
alkaline earth atoms, multiphoton ionisation spectroscopy 78−82703
alkaline earth metal atoms, cross sections, absorpt. coeffs., scaled Thomas-Fermi method 77−46549
alkanes, polycyclic, three-photon ionisation spectra, 3s Rydberg orbital 79−68282
alkyl iodides, two-photon reson. ionis. spectra 80−28071
allene, photoionisation and threshold photoelectron photoion coincidence obs. 78−21981
amines, caged, multiphoton ionisation, two-photon transition resons. 78−33558
aniline, laser two-photon ionisation in mol. beam and bulk gas phase 80−18891
aniline, photoemission for mol., polarised photoelectrons 78−66607
1,8-anilinonaphthalene sulphonate, aq. and ethanolic solns., excited singlet state decay pathway 78−17703
anthracene ion in liqs., photoelectron emission and photocond. 80−75600
aromatic compounds, two-stage photoionisation in solns., UV laser irrad. effects *(Russian)* 78−13556
aromatic higher perfluoro compounds, He(1α) photoelectron spectra 79−31610

photoionisation continued
aromatics, biphotonic reactions at 77K, quantum efficiency 78−80763
atom, absorption spectra of 3d subshell in Kr I, Cd I, Rb I, Sr I, Cs I 77−10648
atom, AC Stark splitting in doubly reson, three-photon ionisation, nonmonochromatic field 78−94220
atom, Auger effect, post-collision interactions, near-threshold inner-shell photoionisation 77−68021
atom, collision-induced three-photon ionization 80−23384
atom, correlation effects 78−58842
atom, correlation effects in photoabsorpt. 77−42299
atom, double photoionisation, two-step autoionis. 77−50415
atom, doubly resonant multiphoton ionisation 78−42024
atom, electron polarisation produced by reson. ionisation by intense EM field *(Russian)* 78−50518
atom, excitation and ionisation by strong EM field, threshold features *(Russian)* 79−85940
atom, gamma-ray photoionisation cross sections, low, medium and high Z 77−54544
atom, inner-shell ionisation, fluoresc. X-ray ang. depend. 77−10649
atom, inner-shell photoionis., anisotropy of X-rays and Auger electrons 78−58633
atom, ion alignment, many electron correl. effect 78−74622
atom, ionis. by pulse of coherent radn. 77−38647
atom, microwave ionisation of highly excited states, and excitation 79−31482
atom, multiphoton ionis., intense field, via complex dressed states 78−17629
atom, multiphoton ionis., laser temporal coherence and high laser intensity effects 78−66524
atom, multiphoton ionis., probability rates 79−13686
atom, multiphoton ionis., r-photon reson., theory 79−49998
atom, multiphoton ionisation, effects of self-induced reson. 80−91519
atom, multiphoton ionisation, resonant, in strong EM wave field 79−10079
atom, multiphoton ionisation, short-time behaviour 79−59418
atom, multiphoton ionisation from excited states 77−88433
atom, multiphoton resonant ionis. in incoherent field 79−26952
atom, multiphoton transition amplitudes, exact summation of higher-order terms 77−18878
atom, multiphoton transitions, continuum level shift effects 79−26956
atom, one-electron excitations, local pots., many-electron effects 79−54817
atom, photoelectron peak size rel. to photoionis. cross section 77−88508
atom, photoionis. from excited states 79−10078
atom, photoionisation cross section calc. by model pot. method 79−26951
atom, photoionisation cross-section, intershell interactions 79−26948
atom, photoionisation from low or high excited states, radial transition integrals 80−18832
atom, photoionization cross-section, ground state inversion pot. method 79−31484
atom, photon ionisation, incident light polaris. effects 78−62772
atom, polarised electron prod., Fano effect *(Russian)* 79−26954
atom, post collision interactions in at. excitation processes 78−58803
atom, R-matrix method 78−58833
atom, R-matrix theory 78−58761
atom, radiative collision-induced 78−62858
atom, relativistic RPA calcs. 77−61719
atom, reson. interaction of intense EM waves *(Russian)* 78−33480
atom, reson. region, partial cross-sections, branching ratios 77−83555
atom, resonance multiphoton processes of laser radiation interaction 80−37800
atom, resonant ionisation by intense EM field 77−71784
atom, resonant ionisation under adiabatic level inversion conditions *(Russian)* 80−32691
atom, resonant multiphoton ionisation, influence of excitation pulse charcts. 77−34598
atom, resonant multiphoton ionisation, model calc. 78−62773
atom, resonant multiphoton ionisation *(Russian)* 79−3421
atom, resonant multiphoton ionization by finite-bandwidth chaotic fields 79−54819
atom, resonant photoionisation, nuclear polaris. *(Russian)* 79−49997
atom, resonant two photon ionisation, polarisation effects *(Dutch)* 78−5185
atom, resonant two-photon ionisation, saturation and Rabi oscills. 77−79589
atom, single photon, AC Stark splitting of bound-continuum decay 80−5502
atom, spectral broadening, resonance ionisation under action of intense pumping wave *(Russian)* 77−42283
atom, three-photon ionisation, reson. and non-reson., theory 79−36590
atom, two step reson. photoionisation, multimode and level degeneracy effects 80−78583
atom, two-photon ionis., sturmian expns. 79−98053
atom, two-photon ionis., time depend. model, finite bandwidth light 79−81193
atom, two-photon reson. ionis. with sub-ns laser pulses 78−9131
atom, two-photon resonant ionis. 78−58631
atom+atom, two photon ionisation, radiative collision effect 80−106388
atom ionisation, polarisation of photoelectrons, review 80−78584
atom models, ionisation time depend. under intense EM fields 80−32683
atom two-electron multiphoton ionisation *(Russian)* 79−54822
atomic, photoionisation, fluoresc. radiation polarisation 80−87076
atomic and molecular processes, developments in ab initio methods 80−63550
atomic continuum processes, R-matrix method, program 78−74558
atomic cross sections, calc. using effective Feynman diagrams, in plasma 80−38566
atomic inner shell ionisation phenomena, conf., Freiburg, West Germany (Mar.-Apr. 1976) 77−27040
atomic inner-shell ionisation, post-collision photoelectron-Auger electron interactions 77−18870
atomic ionis., reson. and direct 77−83553
atomic ionisation by strong coherent EM field, nonperturbative calc. methods 80−5512
atomic ionisation pots. in EM field, Kramers-Henneberger transformation, QED and semiclassical 77−23481
atomic ions, highly stripped, photoionisation, relativistic calcs. 79−26953
atomic ions, photoeffect, theory 78−94219
photoionisation continued
atomic multiphoton ionisation probability, Green's function model pot. 78−25498
atomic non-Rydberg spectroscopy, review 78−90127
atomic photoionisation, in intense radiation and magnetic fields, quasienergy formalism 79−72284
atomic photoionisation, selective, use in laser isotope separation and spectros., review 80−83332
atomic photoionisation anal. using relativistic random phase approximation and multichannel quantum defect theory 80−63602
atomic photoionisation spectroscopy, book 77−78906
atomic resonant photoionis., coherence versus incoherence 77−18859
atomic systems, book contrib. 77−27125
atoms, highly selective multistep ionisation by laser radiation 79−59408
atoms, in gas-filled photodiodes, improved detectivity for UV radn. 78−37062
atoms, laser isotope separation, review 77−34784
atoms, multichannel relativistic RPA calcs. 80−9570
atoms, multiphoton ionisation, Green's function method calcs. 79−89650
atoms, multiphoton ionisation, reson. cross-section, very-narrow-bandwidth source 78−55150
atoms, multiphoton ionisation, reson. effects, light coherence effects 80−58232
atoms, multiphoton ionisation dynamics 80−91517
atoms, multiphoton ionisation probability, laser pulse 78−86835
atoms, near threshold struct. in K-shell spectra, photoionisation or fast charged particle ionisation 80−87064
atoms, one-photon decay of two-hole states *(Russian)* 77−79592
atoms, photoionisation, electron spectrosc. obs. using synchrotron radiation 79−31485
atoms, photoionisation cross sections, electron correl. reson. struct., relax. effects many body perturbation calcs. 80−47852
atoms, polarisation of electrons and nuclei in resonant multiphoton ionisation 80−99486
atoms, power broadened two-photon ionisation, reson. lineshape and photoelectron spectra 80−58229
atoms, resonance ionization spectroscopy with amplification 79−54996
atoms, two-photon photoelectron energy spectra, AC Stark splitting 78−86834
atoms, two-step laser selective method 80−23473
atoms, X-ray Compton and photo-effect in laser field 79−13688
atoms and molecules, UV photoelectron spectrosc. obs. 79−31603
cis-azo group, ionisation and excitation energies depend. on bond angle, ab initio MO calc. 79−72236
1-azo-bicyclo-2,2,2-octane, multiphoton ionis. spectra polaris. characts., two-photon symmetry assignment 78−74718
azulene, multiphoton ionisation, mass spectra 80−63717
benzaldehyde molecules, photoionisation mass-spectrometry with excimer KrF laser 80−95691
benzene, ^{13}C substituted, mass selective two-photon ionis., mass spectroscopy obs. 80−9651
benzene, mol. beam, fragmentation by reson. enhanced multiphoton ionisation 79−54213
benzene, multiphoton ionis. spectra polaris. characts., two-photon symmetry assignment 78−74718
benzene, multiphoton ionisation fragmentation patterns, statistical theory 80−95693
benzene, multiphoton ionisation mass spectra 80−57420
benzene, resonance-enhanced multiphoton ionis. and fragmentation of mol. beam 79−100411
benzene, S_0-S_1 transitions, two-photon absorpt. spectra by nozzle beam-multiphoton ionisation method 80−63728
benzene, two-photon ionis. of mol. beam, mass spectrometer ion source 79−27118
benzene, UV photoelectron spectra, valence electron shake up approx. methods 80−18788
benzene, visible and UV photoionisation and fragmentation 80−69195
benzene liquid multiphoton ionisation polarisation experiments, molecular symmetry 79−98162
benzene molecules, photoionisation mass-spectrometry with excimer KrF laser 80−95691
benzophenone, laser spectroscopy by cascade photoionisation method in mass spectrometer 80−99496
Born-Oppenheimer electronic wave function, density matrices, electronic and nucl. motions separation 79−59332
bound electron photon scatt., atomic ionisation, field theoretic anal. 80−23380
branching ratios, photoelectron spectrometric meas. technique 79−31607
bromobenzene ion fragmentation, photoelectron-photoion coincidence spectra 80−95682
bromofluoromethane cations in solid Ar, absorpt. spectra and photochem. 79−96339
bromoform and Cl substitutes, VUV photoionis. during condensation with Ar, IR spectra of $(CHX_2^+)X$ and X^--HCX_2 ions 79−13773
trans-1,3-butadiene, multiphoton ionis. spectra polaris. characts., two-photon symmetry assignment 78−74718
butadiene, resonance-enhanced multiphoton ionis. and fragmentation of mol. beam 79−100411
butene, isomers, ion-mol. reactions, photoionisation mass spectra 80−81298
2-butene ion, fragmentation, angular momentum in ion-mol. reacts., RRKM calc. 80−66773
carbon tetrahalides, matrix photodissoc. and photoionisation by inert gas reson. radiation 77−83587
chalcogens, photoionisation cross sections and ang. distribs., outer p subshell 80−9572
chemisorptive bonding on metal surface, PES 80−10791
chlorobenzene, S_0-S_1 transitions, two-photon absorpt. spectra by nozzle beam-multiphoton ionisation method 80−63728
chlorofluoromethane cations in solid Ar, absorpt. spectra and photochem. 79−96339
1-chloropropyne cation, internal energy decay studied by photoelectron-photoion coincidence spectroscopy 80−69185
chlorotrifluoromethane, matrix radiolysis, photoionis., IR spectra of CF_2Cl^+ and parent cations 78−80767
closed shell atoms, photoelectron ang. distrib. and spin polarisation, theory 80−91618
colliding atoms, two-photon ionisation 78−13482
collision radiation spectrometer, for absolute intensity distrib. meas. of light sources 79−93233

photoionisation continued
collisional ionisation in intense laser field, quasimol. state reson., quantum mechanical anal. 78−33589
collisional photoionisation emission spectroscopy and apparatus 79−55001
complex atoms, multiphoton ionisation cross-section calcs. 78−21888
Compton bound electron state scatt., binding and off-mass shell effects, relativistic anal. 78−17637
computer controlled photoionisation mass spectrometer 80−77905
conference, electronic and atomic collisions, Paris (July 1977) 78−58758
cooperative multiphoton ionisation, bistability effects, Bonifacio-Lugiato model 80−19010
core ionisation in 3d, 4f and 5f series, rearrangement effects 80−53065
cosmic dust, photoelectric yield of insulating dust grains 80−90507
cross sections, positive integer spectral power moments in moment-trace calcs. 78−17729
cyclopropane-d_0, -d_6, multiphoton ionisation spectra, electronic struct. 78−82803
cyclopropene, photoionisation and threshold photoelectron-photoion coincidence study 80−53062
deep impurities, charged, photoionisation allowing for Coulomb interaction 77−15793
HR Delphini (Nova 1967), models of envelope ionization 77−87439
dense metal vapour, radiation trapping, multiphoton ionisation and reson. fluoresc. 80−32654
detector, application in gas chromatography 78−92561
detector, appls. in gas chromatography 77−21441
detector, gas chromatograph, appl. 80−71963
diatomic molecule, resonance multiphoton processes of laser radiation interaction 80−37800
diatomic mols., photoabsorpt. cross-section, photoionis. continuum 77−68029
dichlorodifluoromethane, matrix radiolysis, photoionis., IR spectra of CF_2Cl^+ and parent cations 78−80767
dimethylanilines, photoemission for mol., polarised photoelectrons 78−66607
diphenylmercury, mol. photoionisation, up to 13.5 eV, formation of $HgPh^+$. 78−25633
dipole operators in calcs. 77−58091
Dirac-Slater potential, hole and exchange terms, influence on photoionisation cross-sections 80−952
distributed spark discharge for volume photoionization laser appls. 79−14634
doubly charged ion formation, 2-electron multiphoton ionisation of atoms, mechanism *(Russian)* 80−5514
dye proflavine bound to synthetic polynucleotides, selective laser photodamage 80−99525
dynamic symmetry breaking, mol. photoelectron ang. distrib. 79−829
electron propagator theory for mol. electron binding energies and photoionis. intensities 80−47848
electron wave function pair Fourier transforms, at., mol. and solids, by (γ,2e) and (e,3e) *(Russian)* 77−71878
electron wavefunctions for (γ,2e) and (e,3e) processes at high energy, double Fourier transform 78−17628
electronic and at. collisions, conf., Kyoto, Japan (Aug.-Sept. 1979) 80−57011
electronic and at. collisions, conference, Kyoto, Japan (Aug.-Sept. 1979) 80−62394
ESCA photoionisation cross section, relative intensities calcs., comparisons 78−50464
escape depths of X-ray induced photoelectrons and relative photoionisation cross section for 3p subshell 77−73212
ethane, photoionisation cross section at distance from threshold, chemical bond influence 80−69196
ethane, photoionisation spectra, cond. hole model 80−58326
ethanol, H-bonding investigated with supersonic mol. beam using photoionisation quadrupole mass spectrometer 80−102543
ethyl chloride-NH_3, positive ion molecule reactions 79−24729
N-ethylcarbazole, soln., laser induced ionic photodissoc., transient polyelectrolyte form. 80−53068
ethylene, π-electron system photoionisation cross-section, 2nd Born approx. calcs. 77−3424
ethylene, dimer and trimer, dissoc. following photoionis. of mol. beam 79−57212
ethylene, photoionisation cross section at distance from threshold, chemical bond influence 80−69196
ethylene, UV photoelectron spectra, valence electron shake up approx. methods 80−18788
ethylene oxide-d_0, -d_4, ion chemistry, photoionisation and ion cyclotron reson. obs. 77−21373
ethylenimine, multiphoton ionisation spectra, electronic struct. 78−82803
excimer laser charcts. 80−102712
excited atom photoionisation by low intensity light, effective cross section 79−26946
excited atoms, in DC gas discharges by low intensity light rel. to high-intensity laser gas-breakdown 79−50904
excited state photoionisation, at. and mol. photoabsorpt. cross sections determ. 80−32783
fast photoionisation processes, Dyson orbital theory 77−27122
ferrocene, multiphoton dissoc. and ionisation by tuneable dye lasers 80−99524
ferrocene, multiphoton ionis. spectra, at. Fe transitions 80−106361
fluorobenzene, multiphoton ionisation spectrum in one-photon wavelength region 80−63727
fluorobenzene, multiphoton reson, ionis. spectrum, 51000 cm^{-1} assignment 79−86021
fluorobenzene, S_0-S_1 transitions, two-photon absorpt. spectra by nozzle beam-multiphoton ionisation method 80−63728
fluorobenzene ions, fluoresc. quantum yields and lifetimes, meas. method ion form. 77−6815
fluorobromomethanes, matrix photoionisation and radiolysis, IR spectra of free radicals 79−24765
formaldehyde, photoabsorpt. and ionis., intensities, assignments, ST, IVO calc. 79−31614
formaldehyde, two-step photoionisation, $^1A_2$ state lifetime 77−10711
formaldehyde, vertical photoexcitation and photoionisation spectra, CI calc. 78−918
formic acid ions, fragmentation, energy selected, photoelectron-photoion spectra 80−95676
Freon, matrix radiolysis, photoionis., IR spectra of CF_2Cl^+ and parent cations 78−80767
photoionisation continued
fumaronitrile exciplexes, photoisomeris. and photoionis, dissolved O_2 effect 78−27789
furan, resonantly enhanced multiphoton ionisation 80−106362
galaxies, photoionisation model for Seyfert 2 and narrow-line radio galaxies spectra 78−93391
galaxies active nuclei, photoionisation model for emission line spectra 79−88730
gas, external photoionisation energies, comparison with liq. phase 77−90237
gas, self-sustained discharge form. condition, atm. press., photoionis. process 77−27770
gas atom, photoionisation cross-section, multiconfig. Hartree-Fock calc. 78−17630
gas chromatography with photoionis. detection for chlorobenzenes determ. in air and biological samples 80−35809
gas discharge, photoionis. at low illumination intensity, nonlinearities, effective cross section 78−87517
gas mixture, self sustained volume photoionisation discharge existence conditions 80−79610
gases, single photon counting in multiwire proportional chambers, Cherenkov ring imaging 77−54448
globular star clusters, gas outflow models including photoionisation 78−93338
group VI atoms, $(np)^4\ ^1S_0$-level photoionisation via autoionising levels 79−76398
Group VIA photolytic laser systems, for fusion research 78−59002
halide anions, in gas, photodetachment cross-sections, OPW and APW calcs. 77−38607
halogens, photoionisation cross sections and ang. distribs., outer p subshell 80−9572
heteroaromatic compounds, two-stage photoionisation in solns., UV laser irrad. effects *(Russian)* 78−13556
n-hexane, liq. trapped electron photoionis., photocond. 80−2418
trans-hexatriene, multiphoton ionization spectrum in 6.2 eV region 77−27133
1,3,5-hexatriene radical cation, in Ne matrix, laser induced fluoresc. and emission spectra 80−87163
high energy electron spectroscopy techniques 80−62740
highly excited atoms, acted on by EM radiation, oscillator stochastic instability theory *(Russian)* 79−31487
hydrocarbons, aromatic, ultrasensitive detection by two-photon photoionisation 80−104473
hydrocarbons, saturated and unsaturated, ionisation spectral intensities, correlation effects 78−90234
hydrogen atoms, threshold behaviour of multiphoton ionisation 80−954
inert gas, atomic photoionisation, Dirac-Fock calcs., branching ratios and angular distrib. in p shells 80−63601
inert gas atom, photoionis. cross sections of excited levels, quantum defect method calcs. 80−37795
inert gas atom $+H^+$, electron capture, charge-state distrib. 80−32814
inert gas isoelectronic sequences, positive ion p-subhsell photoionisation cross-sections calcs. 77−50374
inert gas metastable atoms, photoionisation rel. to laser development 78−13476
inert gas mixture, electrophotoionization discharge, laser pumping 80−91781
inert gas plasma, free-bound continuum determ. using photoionis. cross sections calc. 80−43878
inert gas-halogen bearing molecule three-component mixture, self-sustained electric photoionization discharge 80−54073
inert gases, initial state wave functions for photoionisation cross-sections, multiconfigurational HF calcs. 80−47908
inert gases, inner-shell optical photon excitation, Auger, autoionisation, photoionisation processes 77−18867
inert gases, multiphoton ionisation, by ultrashort laser pulses from tunable Nd:glass laser 77−58095
inert gases, multiple photoionisation, threshold to 280 eV, time of flight meas. 79−85939
inert gases, outer shell photoionisation, relativistic RPA calcs. 80−9571
inert gases, photoabsorption to bound state and photoabsorption to continuum state (ionisation), comparison, HF calcs. 80−47910
inert gases, photoelectron spin polarisation, ab initio calcs. 80−18833
inert gases, photoionisation cross sections of excited atoms and dimers 78−66523
inert gases, photoionisation cross-sections, multiconfig. Hartree-Fock calcs. 77−50373
inert gases, quantum defects, photoionisation cross-sections, central pot. model calcs. 77−54510
inert gases, self-sustained discharge possibility with bulk photoionisation impurities 80−75113
inner-shell vacancy filling detector, scintillation counter 77−18749
inorganic anions, solns. in aromatic solutes photochem. hydrated electron decay kinetics 77−52656
interference in two-channel two photon ionization 80−23381
3-iodoaniline, photoemission for mol., polarised photoelectrons 78−66607
ion fragmentation mechanisms and photoelectron spectroscopy, book contrib. 80−14179
ionosphere, kinetic theory of photoelectrons and secondary electrons 77−13148
ionosphere, photoelectron flux near photoionization peak energies 79−16738
ionospheres, ionic reactions in lab. and planetary atmospheres 80−59168
ions, photoelectric cross-section, scaled from neutral atom 78−13479
K-shell photoionization of multielectron atomic systems 80−47949
ketene, photoionis., ion fragmentation kinetic energy 78−9206
ketene-d_0,-d_2, mol. ion reactivity, vibr. energy effects, mass spectrometric obs. 77−44470
labile species, electron photoejection, reaction kinetics characterisation 80−26089
lanthanides, Rydberg spectra and ionisation thresholds, time resolved resonant multistep technique 78−82701
laser detection, of individual atoms 79−26950
laser ionisation, modelling 78−90133
laser ionisation mass spectroscopy, appl. to fragmentation obs. via. multiphoton ionisation 79−54213
laser pumping using self-sustained electron-photoionization discharge 80−33013
laser radiation, selective action on matter, review 80−7832
laser radiation-matter interactions, dissertation 79−86555
laser selective detection of ultralow concentrations of atoms 78−3407

photoionisation continued
laser selective detection of ultralow concentrations of molecules 77−90669
laser selective photophysics and photochemistry, book contrib. 79−79273
laser-enhanced ionisation, appl. to anal. flame spectrometry 78−92528
laser-induced selective multistep processes: impact on nuclear physics, chemistry and biology 80−61122
Li, multiphoton ionis. at ruby laser wavelength 80−9566
liquid, electron-hole interactions and double proton transfer, picosec. laser obs. 79−45773
liquid, external photoionisation energies, comparison with gas phase 77−90237
malachite green leucocyanide, photoionization in polar solvents, mechanism 77−25295
many body perturbation calculations of photoionization 79−59406
many-photon ionization, resonance scattering on a nonstationary potential, and complex poles of the S-matrix 79−22677
mass spectrometer, balloon-borne for stratospheric gas meas. 78−85732
mass spectrometry, applic. of vacuum UV lasers 77−87865
mass spectrometry, of high temp. vapours 80−52238
mass spectroscopy, ion registration, stepwise selective photoionisation technique *(Russian)* 78−21262
matrix elements and cross-section calcs. with wave functions with definite ang. mom. 77−30839
metal vapour coherent two photon reson. third and fifth harmonic VUV generation 79−72627
metal vapours, at. inner-shell optical photon excitations, Auger, autoionisation, photoionisation processes 77−18867
metastable atomic or molecular species, multiphoton transition detection 80−58231
methane, photodissoc. ionis., 16-41 eV 77−18995
methane, photoionis., ion fragmentation kinetic energy 78−9206
methanol, and deuterates, dissoc. ionisation mechanisms, photoionisation mass spectra, ionic struct., interstellar formation 79−3503
methanol, processes of photoionisation studied using ion-electron coincidence method 80−74204
methanol (-d), H-bonding investigated with supersonic mol. beam using photoionisation quadrupole mass spectrometer 80−102543
methanol-d_4, dissoc. following photoionis., using coincidence spectrometer 79−54998
methanol-methyltetrahydrofuran glass:β-naphtholate, electron solvation, laser flash photoionis. compared with pulse radiolysis 79−74405
methyl chloride-NH_3, positive ion molecule reactions 79−24729
methyl ethyl ketone, processes of photoionisation studied using ion-electron coincidence method 80−74204
N-methyl pyrrole, resonantly enhanced multiphoton ionisation 80−106362
2-methylaniline, photoemission for mol., polarised photoelectrons 78−66607
methylbenzenes, 3p Rydberg transitions, multiphoton ionis. spectrosc. obs. 80−95644
molecular electron scatt. and photoionisation shape-resonance enhanced nuclear motion effects 80−63603
molecular gas, vol. discharge with UV preionisation by capillary discharge, ionis. pots. depend. 80−44065
molecular inner-shell photoabsorpt., shape resonances, extended X-ray absorpt. fine struct. 77−18979
molecular multiphoton ionisation dynamics, rate eqn. modelling 80−48046
molecular photoionisation, selection rule, parity unfavoured transitions 77−83662
molecular photoionisation cross sections, at. extrapolation, ground state inversion method appl. 80−18787
molecular photoionisation mass spectroscopy, reson. peak shapes 80−42295
molecule, cross section by complex basis function calcs. of resolvent matrix elements 80−78662
molecule, ground and selectively excited states, by vac. UV laser *(Russian)* 78−9205
molecule, inner-shell spectra anal., rel. to electron impact vibr. excitation 80−5629
molecule, multiphoton ionisation and fragmentation, UV laser induced, time of flight mass spectra 79−31625
molecule, multiphoton ionisation by spontaneous emission absorpt. 78−74721
molecule, oriented or rot. resolved unoriented, ang. distribs., dynamic and struct. data 78−37682
molecule, orthogonalised-plane-wave approx., cross-section 79−41202
molecule, photoelectron peak size rel. to photoionis. cross section 77−88508
molecule, photoionisation ang. distrib. asymmetry, parity favouredness 78−50600
molecule, photoionization cross-section, ground state inversion pot. method 79−31484
molecule, shape-reson. enhanced nucl. motion effects 80−1031
molecule, UV cross section, modified plane wave model 77−88509
molecule in mass spectrometer, using H_2 vac. UV laser 77−88606
molecules, cross-section calc., absorbing boundary method 79−31623
molecules, diatomic, photoelectron ang. distrib. and intensity, vibr.-rot. struct. 78−42128
molecules, techniques and discussion 80−17721
molecules, valence and core photoionisation, spectral lines, many body effects 80−47853
monohalobenzenes, inner shell excitation and ionis., electron energy loss spectra, XPS, assignments 78−62934
multiphoton absorption above ionisation threshold 80−58224
multiphoton ionisation, resonance peaks strengths 77−42293
multiphoton ionisation, short time behaviour, theory appl. 80−47951
multiphoton ionisation, simple model, transition rates 80−953
multiphoton ionisation, theory of two strongly interacting resons. 80−52955
multiphoton ionisation, using pulsed output, from mode-locked laser, quantised field representation 78−79054
multiphoton ionisation in gaussian beam focal space, ion generation *(French)* 77−6740
multiphoton near-reson. ionisation, chaotic versus coherent light 78−33489
multiphoton transitions, perturbation theory, atomic ionisation and intermediate reson., dissoc. review 79−41145
multiple, infrared laser 80−69194
multiplet ratios for photoionisation and electron attachment, shell model, LS coupling and correl. 78−17636
Na, fluoresc. study, reson. radiation illum. 80−83314
naphthalene, multiphoton ionisation, mass spectra 80−63717
naphthalene, photoionis., negative ions role in photoionis. plasma 79−27048
naphthalene, stepwise photoionisation process 78−82791
naphthalene-He photoionis. plasma, CO_2 additive effect 80−10359
nebulae, gaseous, photoionisation models for third period elements 80−46640
negative ions, photodetachment cross-sections, crossed beam meas. *(German)* 77−42298
NGC 7662, planetary nebula, photoionisation model with charge transfer reactions rel. to emission-line spectrum 80−62233
nickelocene, multiphoton dissoc. and ionisation by tuneable dye lasers 80−99524
nitromethane, IR laser mutliple photon ionis. 79−74403
non-methane hydrocarbons in atmosphere, photoionisation monitoring technique 78−73549
nonlinear photoionisation, testable Noyes-like interpretation of Panarella's effective-phonons theory 77−61929
nonresonant multiphoton atomic ionisation in stochastic EM field *(Russian)* 80−99490
nuclear reactor pressure vessel/cladding interface, residual gas analysis *(German)* 77−40603
one-atom detection by reson. photoionisation spectroscopy, demonstration 77−38742
one-atom detection by reson. photoionisation spectroscopy 77−79706
one-atom detection in individual ionisation tracks, heavy ion stopping in buffer gas 78−70802
organic molecules, multiphoton ionisation mass spectra by ArF excimer laser 80−81381
organic seedants for UV preionised lasers, photoionisation and photoabsorpt. characts. 78−13688
organic solids, photoemission and photoionisation in three stage model 80−100744
organic vapours, air pollution detection by variable selectivity photoionisation analyser 80−81511
paraterphenyl, dye vapour, intense multistep photoionisation 79−10298
parity violating neutral currents in two-photon and autoionisation atomic transitions 80−32034
Penning ionis., radiative, photoionis. cross section depend. of continuum radiation 77−19034
phenol, aq. soln., electron ejection, picosec. obs. 80−87187
phenolate, aq. soln., electron ejection, picosec. obs. 80−87187
photoabsorpt. spectra, band struct., at. ionisation mechanisms, electron energy loss spectra 77−24909
photodetachment cross-sections, OPW and APW calcs. comparison 77−38607
photoelectric cross section, total to K-shell ratios in Zr, AG, Ta, Th 78−5188
photoelectron ang. distrib. and spin polarisation, theory 80−91618
photoelectron angular distribution, theory 78−17730
photofragment spectroscopy of mol. ions using fast ion beams 80−9755
photoion-photoelectron spectroscopy, ion internal energy and reaction 79−30616
pigments, ionisation reactions in soln., automatic conductimetric instrument for kinetic studies 77−4971
pinacyanol dye, adsorbed on CdS substrate, aggregation effect on mol. electronic states 80−37757
planetary nebulae, photoionisation models for He I 584 Å transfer problem 80−67550
planetary nebulae, photoionisation models for permitted lines excitation 80−109527
planetary nebulae of galactic halo, photoionisation models and chemical abundances of K 648, 49+88.1° and (108−76.1°) 80−109507
polar glass, UV and γ-prod. electrons geminate recombination, radical yield 77−9094
poly N-vinylcarbazole, soln., laser induced ionic photodissoc., transient polyelectrolyte form. 80−53068
polyatomic molecule, multiphoton absorpt. resons., dynamic Stark splitting 80−9670
polyatomic molecules, multiphoton ionisation spectroscopy 79−41203
polyatomic molecules, new method, laser photoionisation in a mass spectrometer 78−78840
polyatomic molecules, photoionisation cross section and efficiency, double ion chamber meas. 80−91613
polyatomic molecules, visible and UV photoionisation and fragmentation 80−69195
polydiacetylene-p-(toluenesulfonate), photocurrent transients, intensity depend. 78−52027
positive atomic ions with $Z \leq 30$, photoabsorpt. cross sections 80−26727
positive ions, photoionisation and Auger effect 78−90135
propyl halides, photoionisation mass spectrometry 80−40779
propynyl cation+propyne, reactant structure effects 80−89469
protein, radical limiting conc. on UV irrad. at 77K, effect of luminesc. quenchers 80−30662
pyrazine, multiphoton ionisation spectra, circular to linear polarisation ratios, lowest ionisation pot. 78−74716
pyrazine, multiphoton ionisation spectra, of three-photon ionisation region 78−37689
pyrene, in alcohol solns., polar fluid electrons optical absorption coeffs., ns laser ionis. obs. 78−84600
pyrene, laser-induced two-photon photoionisation, simulation, double pulse investig. 78−37690
pyrene, mol. ionisation pot., two photon ionisation, micellar interface effects on ionisation threshold 80−91609
pyrene, photoionisation in alkane liqs., laser induced fluoresc. 78−61038
pyrene in n-heptane solution, laser two-photon ionisation spectroscopy, photoionisation threshold determ. 80−78668
pyridine, multiphoton ionisation spectra, circular to linear polarisation ratios, lowest ionisation pot. 78−74716
pyridine, multiphoton ionisation spectra, of three-photon ionisation region 78−37689
pyrrole, multiphoton ionisation, photoionisation threshold meas. 79−27047
pyrrole, resonantly enhanced multiphoton ionisation 80−106362
QSO emission-line region clouds, photoionisation model for absorpt. spectrum 80−62308

photoionisation continued
QSOs, high-redshift, emission-line regions photoionisation model 79−21458
quantum beats, origin 80−52954
quantum beats in light absorption from atoms, expression for photoioisation of Rydberg states 78−25499
quasar clouds, photoionisation models for He I 584 Å transfer problem 80−67550
quasar emission lines, photoionisation models 80−27009
quasar spectra, photoionisation theory for H line emission from dense plasmas 80−51900
quasars, emission spectra, photoionisation anal. 78−16560
quasars photoionised clouds model, Mg II and Fe II lines excitation 80−67896
quasienergy formalism, for multiphoton ionisation induced by circularly polarised radiation 78−37610
radiative capture of an electron of a target atom by multiply charged ions 80−5617
rare earth atoms at surface, photoionisation of 4f electrons 78−11077
rare earth elements, laser isotope separation by two-step photoionisation 78−46461
rare earth metals, photoionisation thresholds and Rydberg spectra 78−66522
recoil atoms meas. by laser spectroscopy neutron detect. possibility 79−22864
relative cross-section meas. by X-ray detection 78−33369
relativistic multichannel RPA, appls. 80−47925
relativistic R-matrix theory 78−5184
resonance interaction of intense light with atoms, reviews 79−68216
resonance ionization spectroscopy and one-atom detection 80−22441
resonant, ground-state electron simultaneous vs. sequential two-photon absorption 80−23383
resonant ionisation spectroscopy, chem.-physics appls. 80−68259
resonant multiphoton ionisation, line profile as Fano profile with background struct. 79−72290
resonant multiphoton ionisation, photon correl. effects, near reson. levels 80−43020
resonant multiphoton ionisation, pulse area effects 80−91514
resonant multiphoton ionisation by pulsed excitation, Beers-Armstrong model 78−17645
resonant phenomena, complex stabilisation method 80−78515
resonant two-photon ionisation, time-independent rates, coherence vs. incoherence 79−54820
resonant two-photon ionisation in partially coherent radiation field 78−66525
review, expt. techniques, processes, theory 77−14402
rotated coordinate method use, rel. to stabilisation method 80−37845
rotated-coordinate method, rel. to stabilisation method 80−74097
Rydberg atoms, expts., metastable states, multiphoton ionisation, spectroscopy, Stark struct., collisions, polarisability *(Dutch)* 78−5160
Rydberg atoms, microwave ionisation and excitation 78−94217
Rydberg states, fine struct. splitting, quantum beat and double reson. spectroscopy 78−86979
saturation effect in stimulated transitions between states of discrete and continuous spectra 77−42295
selective dissociation, ionis., and chem. reaction stimulation, by ultra-short pulses, isotope separation *(Russian)* 78−29825
selective photoionisation of atoms by laser radiation, appls. 78−5189
semiconductor, deep impurity centre photoionisation cross-section, freq. depend. 77−55494
semiconductor, photoionisation of deep impurity levels 80−34386
semiconductor impurities, photoionisation cross section calcs. 78−2450
semiconductor with superlattice, optical phonon excitation by light absorpt., impurity photoionisation 80−44275
semiconductors, deep level impurity photoionisation cross-section 80−65485
semiconductors, impurity photoionisation, quantum-defect, billiard-ball model comparison 80−65486
semiconductors, photoionisation cross-sections and phonon coupling 79−51518
Seyfert galaxies photoionised clouds model, Mg II and Fe II lines excitation 80−67896
solar chromospheric flares, H Lyman α excitation by photoelectrons rel. to profile and polarisation 80−41780
solid, avalanche ionis., multiphonon ionis. *(Russian)* 79−51906
solid, photoionisation cross section of free atoms, book contrib. 79−61497
solution, external photoionisation energies, comparison with gas phase 77−90237
surface anal. by photon-induced field ionisation mass spectroscopy 80−40780
surface layers, photon induced ion desorption, surface atom core ionisation, Auger decay 80−59809
synchrotron radiation source for atomic photoionisation studies in extreme UV and X-ray regions 80−43017
synchrotron radiation techniques for studying atomic physics 80−63583
tertiary amines, lasing action feasibility, excited state absorpt., two step photoionisation 80−23682
N,N,N′,N′-tetramethyl-p-phenylenediamine, TMPD, glassy soln., photoionisation, recombination isothermal luminesc. *(French)* 77−16404
tetramethylsilane, liq., photocond., ionis. threshold 79−15191
theory, concept and expt. techniques, atomic photoelectron spectroscopy, book contrib. 77−79591
three-level atom, multiphoton ionisation, rate eqns., Bloch eqns. calcs. 77−83557
threshold photoion-photoelectron coincidences method for ion state selection 80−63718
Titan, upper ionosphere 77−60720
TMPD, nonpolar photoionised soln., geminate pair quantum field, recombination fluoresc. elec. field quenching 79−20389
Tokamak impurity problems, atomic and mol. struct. and collision data, review 80−43959
toluene, two-photon ionisation spectrum, of ^1L_b←S_0 transition 80−14180
trans-hexatriene, 6.2 eV Rydberg state symmetry, multiphoton ionis. spectrum polaris. assignment 78−70759
transition metal oxides, XPS, trapped electrons at F-centres and anion defects, photoionis. cross sections 77−90249
transition metals, gas phase, photoelectron spectra, photoionisation cross section 79−98051
transition probabilities, extended statistical law, photoionisation and fast electron ionisation or attachment 77−54613
photoionisation continued
transparent dielectric, laser damage, appl. of gas breakdown model 77−63496
transparent dielectrics, laser damage, electron avalanche and multiphoton ionisation roles 80−35016
triatomic ions, fluoresc. quantum yields and lifetimes, meas. method, ion form. 77−6815
trichlorofluoromethane, ion pair formation by photoionisation 79−89718
trichlorofluoromethane, matrix radiolysis and photoionis. at 15K,IR spectrochem. anal. 78−76893
triethylamine, for imaging Cherenkov detector using gas-filled MWPC 80−91400
triethylenediamine, multiphoton ionis. and two-photon fluoresc. excitation spectra 79−98164
trifluoroethanol, H-bonding investigated with supersonic mol. beam using photoionisation quadrupole mass spectrometer 80−102543
trifluoromethyl halides, matrix photoionis., IR spectra of CF_3^+, CF_2X^+ and CF_3X^+ cations 78−74710
tryphoton, aqueous, one and two photon ionisation by Na laser harmonics 80−69193
l-tryptophan, gas, UV photoelectron spectrum, photoionisation threshold 79−86004
tryptophanyltryptophan, laser flash photolysis, photoionis. mechanism 77−90619
tryptophanyltyrosine, laser flash photolysis, photoionis. mechanism 77−90619
two-electron Fourier amplitudes of atomic and mol. wavefunctions using the (γ,2e) and (e,3e) processes 79−3419
two-level atom, multiphoton ionisation, rate eqns., Bloch eqns. calcs. 77−83557
two-level atom, reson. pulse excitation, ionisation 78−42029
two-photon resonant three-photon ionisation with ultrashort pulses, optical nutation effect 79−89654
two-valence electron systems, cross sections 77−3259
tyrosine, UV absorpt. in aq. soln. of trypsin, photoluminescence after UV irradiation *(German)* 79−92137
unimolecular decomposition, photon catalysed, first-order rate constant 80−99528
unpolarised atoms, spin polarisation of ejected photoelectrons 79−45682
upper atmosphere, photoelectron spectra allowing for Auger effect 78−69557
vacuum UV radiation, circularly polarised, for spin-polarised photoelectrons prod. 78−1310
vibrationally-excited ions form. in Franck-Condon gaps, threshold photoelectron spectra obs. 79−68262
vinyl fluoride, vibr. excitation effects on ion-molecule reaction pathways, photoionisation mass spectra 77−16804
volume high-pressure discharge with photoionization for laser pumping 80−54058
water, laser-induced ionisation, quantum yield, temp. and wavelength depend. 80−11924
X-ray photoionisation cross section calcs., at. and mol. levels, HF rel. to OPW method 77−42353
XPS, quantitative, rel. to subshell photoionis. cross-sections and electron mean free path 80−81389
zinc blende structured semiconductor surface analysis by X-ray photoelectron spectroscopy *(Japanese)* 78−88672
zinc octaethyl porphin, soln., photochem. ionogenesis 80−61116
(γ, e) reaction, determ. of atomic wave function, electron energy levels *(Russian)* 78−957
AR, population inversion, intershell transitions, photoionisation, from UV irradiation *(Russian)* 78−70803
acetaldehyde, multiphoton ionisation meas., two-photon polarisation ratio of n→3s transition 80−91610
Ag, photoionisation, photoelectron spectra 80−87086
Ag, photoionisation cross sections, electron-impact inverse mean free paths, and stopping powers for each subshell 80−69113
Ag, photon absorption and photoelectric cross-sections calcs. 79−31486
Ag, polarised photoelectron yields in VUV region 80−106307
Ag, VUV absorption spectrum, autoionised level Fano parameters, photoionis. 79−49973
Al, photionisation and electron impact ionisation relationship, mean free paths 79−22672
Al, photon absorption and photoelectric cross-sections calcs. 79−31486
$Al_xGa_{1-x}As$:Te, persistent photocond. trapping centre, donor complex model, electron photoionisation cross section 79−65517
Ar, $2p^6$ shell, oscillator strength, photoionisation cross sections, electron shell alterations determ. *(Russian)* 80−58144
Ar 3s, photoelectron ang. distrib., relativistic Dirac-Fock calc. 79−59411
Ar, 3s electron partial photoionis. cross section, branching ratios 78−29765
Ar, absolute photoionis. cross sections for VUV regions 77−46547
Ar, collision processes, photoionisation mass spectra obs. 79−31479
Ar discharge, optogalvanic and excited state photoionisation signals, space charge effects 80−14947
Ar, double photoionis. cross section, calc. 77−14397
Ar, double photoionisation, many-body perturbation approach 78−17634
Ar, excited atom photoionisation, for sensitive UV detector 77−61122
Ar, isoelectronic sequence, many-body photoionization calcs. 78−17631
Ar, M-shell photoionis., many-body interactions 79−10081
Ar, multiphoton ionisation, EM field gradient forces 78−66608
Ar, optical gas breakdown, reduced threshold in two-freq. field 80−64819
Ar, outer $p_{1/2}$ subshell photoionisation, polarised electrons, relativistic RPA calcs. 80−83331
Ar, photoelectron angular-distribution β parameters, resonance parameters 78−21886
Ar, photoexcited LMM Auger processes, post-collision interaction 80−32682
Ar, photoionis. cross section ratio, energies 0 to 0.05 eV above $^2P^0_{3/3,1/2}$ thresholds 78−25492
Ar, photoionisation, Auger processes, decay lifetime, line shift, profile, X-ray photoelectron spectra 80−37798
Ar, photoionisation, many-body atomic transition theory 77−75111
Ar, photoionisation cross sections for excited states, rel. to KrF laser 77−75110
Ar, photoionisation cross-sections, ground state inversion pot. method 78−33481
Ar, polarisation effects in photoionisation *(Russian)* 79−3420
Ar, preionised, CO_2 laser induced breakdown press. and pre-ionisation depend., cascade model 80−54010

photoionisation continued
Ar, radiative level lifetime, photoionisation and photoexcitation rates, in shock tube 77−34594
Ar, UV photoion density meas. using high press. Langmuir probe 78−51340
Ar-Xe-tetrachloromethane, self-sustained electrophotoionised discharge in compressed gas 80−38003
Ar_2 $^1\Sigma_u^+$ excimer state, photoionis. cross section 78−70882
Ar_2, photoionisation 77−54578
As, 3d subshell, photoionisation partial cross-section, energy depend. meas. 80−29850
Au, 4f-subshell photoionisation cross section, energy depend. from Auger and photoelectron spectra 80−35057
Au, 5d and 4f subshell, photoionisation partial cross-section, energy depend. meas. 80−29850
Au, K-shell photoionisation, cross section meas. K X-ray-photoelectron coincidence method 79−72285
Au L-subshell, relative cross-section meas. by X-ray detection 78−33369
Au, photionisation and electron impact ionisation relationship, mean free paths 79−22672
Au subshell photoelectron branching ratio meas. using synchrotron radiation 80−66397
Au, total L-shell photoelec. cross section ratio 77−30836
Au, VUV absorption spectrum, photoionis. cross section, Fano parameters 79−93947
B, X-ray laser, inner-shell photoionis. pumped, practicability 77−58319
BF_3, threshold photoelectron, photoionisation and coincidence ion-threshold photoelectron spectra 79−820
Ba, 4d subshell spectra, strong interaction regime 79−18165
Ba, $4d^{10}$ shell, photoionisation cross sections, electron shell alterations determ. *(Russian)* 80−58144
Ba, $4d^{10}$ subshell photoionisation cross section, electron shell rearrangement 77−14400
Ba atom, laser excited, ionisation studies 80−83330
Ba, diamag. quasi-Landau spectrum near ionis. threshold, two-photon ionis. spectra obs. 78−58642
Ba, double ionisation, 20-25 eV photoionisation cross-sections 80−83328
Ba, efficient ionis. by reson. laser pumping 80−32685
Ba I, 5p spectra collective excitation, rel. to double photoionis. 77−50387
Ba, multiphoton ionis. spectroscopy of even- and odd-parity states 78−86973
Ba, multiphoton ionisation spectra of msnp^{3}P^0 states 77−83554
Ba+HCl, beam-gas reaction, multiphoton ionisation, product identification 78−23946
Be atoms, double-photoionisation cross section, core polarisation effects 78−17626
Be, inner-shell photoionis., fluoresc. yield 77−57945
Be isoelectronic series, inner-shell cross sections 78−74623
Be-like ions, photoionisation, 2-channel relativistic random phase approx. calcs. 79−59407
Bi, photoionisation cross section of d-core level synchrotron radiation study of spin-orbit branching ratio 79−74057
Br, photoelectron spectra, photoionisation cross-sections 78−90131
C, electron impact calcs. using R-matrix and linear algebraic methods 79−59579
C I photoionisation by sunlight, C II line excitation 80−58223
C III, photoionization cross sections calc. 78−17625
C, photoionisation cross section, CI calcs. 79−98050
C, photoionisation of 2s shell, photoelectron ang. distrib. 78−86833
CH, photoionis. and photodissoc. near ionis. threshold, SCF MO CI and Stieltjes imaging 78−58749
CO adsorbed on W(100), electron and photon-stimulated desorption 79−99414
CO, partial photoionisation cross-section determ. using synchrotron radiation 77−75243
CO, photoabsorption, photoionisation cross section, separated channel static exchange Stieltjes-Tchebycheff calc. 79−3502
CO, photoabsorption and photionisation, UV region meas. 78−42087
CO photodissoc. ionis., 16-41 eV 77−18995
CO, photoelectric cross section and angular distribution calcs. 80−58323
CO, photoelectron ang. distributions, wavelength and vibr. state depend., reson. effects, asymmetry parameters 80−91602
CO, photoionis., vibr. intensity distrib., shape reson. effects 79−98167
CO, $X^2\Sigma^+$, vibr. levels, UPS electron attachment obs. 80−95683
CO^+, fluoresc. and production cross-sections by photoionis. of CO 78−9204
$CO^+ + D_2$, state selected reaction cross-sections, coincidence technique obs. 80−66797
CO_2 dimer, photoionisation efficiency curve, supersonic mol. beam expt. 78−46406
CO_2, double ionis. by photon impact 77−88506
CO_2 laser, atmospheric pulsed photoionisation, active medium optical homogeneity 80−58508
CO_2 laser, photoionis. TEA type, output pulse characts. calc. 80−32953
CO_2 laser, spark photoionisation, tripropylamine additive 78−13679
CO_2 laser gas mixture, vol. photo-preionisation by VUV radiation 80−87966
CO_2 laser gas mixture seeded with tripropylamine, photoionisation meas. 80−78829
CO_2 laser waveguide, photoionisation stabilisation using Blumlein-type pulser 77−54734
CO_2, partial photoionisation cross-sections, branching ratios, synchrotron radiation meas. 78−42141
CO_2, partial photoionisation cross-sections meas. 20 to 60 eV 79−31624
CO_2, photodissoc. ionis., 16-41 eV 77−18995
CO_2, photoionisation, nuclear motion effects 80−58324
CO_2, photoionisation efficiency curve, supersonic mol. beam expt. 78−46406
CO_2 photoionisation laser with 300 J output energy 79−31939
CO_2, pulse laser, UV photoionisation, impurities effect 78−1206
CO_2, pulsed laser characts., UV preionisation 77−7059
CO_2 pulsed laser with continuously tunable radiation frequency 80−48292
CO_2 sealed photoionisation TEA laser, limiting processes 78−82946
CO_2, seeded laser mixture, photoabsorption and ionisation cross sections 77−23645
CO_2 TEA laser, UV preionisation, parametric studies 80−64040
CO_2 TEA lasers, one-step photoionisation, preionisation discharge effect on electron density 80−53256
CO_2, threshold photoelectron and photoionisation spectra 77−14491

photoionisation continued
CO_2, valence shell ionic photofragmentation, oscill. strengths, EELS and electron-ion coincidence meas. 80−37879
CO_2 waveguide lasers, high-power, high-press., photoionisation-stabilised 78−46641
CO_2^+, photoionisation reson. spectra and threshold electron-ion coincidence meas. of fragmentation 77−38700
CO_2-Ar(He), stepwise pulsed photoionisation 77−50479
CO_2-N_2-He volume discharge, self-sustained, with UV preionis. 79−60211
CO_2^+ ($C^2\Sigma_g^+$), formation and predissoc., photoelectron spectra 78−5300
COS, dissoc. photoionisation, mass spectrometric obs. 79−72366
COS^+, photoionis. reson. study of ($^2\Pi$) and ($^2\Sigma^+$) states, vibr. freqs., ionis. pot. 78−29821
CS molecule, calc. of HeI photoelectron spectrum, ionisation pot., vibr. struct. 77−3415
CS, valence electron photoionisation, ionisation pot. and spectral intensities 78−70883
CS_2, dissoc. photoionisation, mass spectrometric obs. 79−72366
CS_2, photoionisation and dissociative ionisation due to 60-129 nm light, mass spectra study 79−94044
CS_2^+, and $(CS_2)_2^+$, photoionis. in supersonic mol. beam 79−98165
CS_2^+, photoionis. reson. study of ($^2\Pi$) and ($^2\Sigma^+$) states, vibr. freqs., ionis. pot. 78−29821
$CS_2^* + CS_2 \rightarrow CS_3^+ + CS + e^-$, chemiionisation, mol. beam photoionisation 80−76495
CSe_2, photoionis. mass spectrum, Rydberg states props., heat of form., CSe dissoc. energy and ionis. pot. 77−46604
Ca atom, laser excited, ionisation studies 80−83330
Ca, bound-even parity spectra, multichannel quantum defect theory anal. 77−34600
Ca, efficient ionis. by reson. laser pumping 80−32685
Ca, multiphoton ionis. spectroscopy of even- and odd-parity states 78−86973
Ca, multiphoton ionisation spectra of msnp^{3}P^0 states 77−83554
Ca, multiphoton ionisation by Nd laser radiation *(Russian)* 78−21889
CaF_2:Dy crystal with M centre, antiresonance line, mag. field effect 80−55138
CaO, photoionisation of F-centre, luminesc. and photocond. meas. 80−66270
Cd, partial photoionis. cross section 78−42022
Cd, photoionisation, alignment, linear polarisation 77−83556
Cd, photoionisation cross section, many-body perturbation theory, dipole length and vel. calc. 78−78674
Cd UV subshell photoionisation cross section, expt. and GIPM theory 78−21887
Cd^+, polarised emission of light following photoionis, Cooper-Zare model 79−81179
CdTe:Cr_2 impurity photoionisation transitions, EPR meas. 80−39857
CdTe:Ti^{2+}, Jahn-Teller effect on $^3T_1(^3F)$ state, resonance on $^3T_1(^3P)$ state 78−27271
Cl I, photoionisation cross section, calc. by many-body perturbation theory 78−62771
Cl, initial state wave functions for photoionisation cross-sections, multiconfigurational HF calcs. 80−47908
Cl, photoelectron spectra, photoionisation cross-sections 78−90131
Cl, photoionis. cross sections, RPA with exchange method generalisation 79−10077
Cl, photoionis. cross section of open 3p subshell 79−68213
Cl, photoionisation cross section, RPA with exchange 77−30838
Cl, photoionisation cross section and reson. theory, many body perturbation theory, 3p and 3s subshells 80−69114
Cr, $K\alpha^h$ hypersatellite spectra and K-shell double photoionisation cross-section 78−21874
Cr, $K\alpha^h$ hypersatellite spectra and double photoionisation cross-section 79−85922
Cr, multiphoton ionisation and absorpt. 80−95575
$Cr(CO)_5$, multiphoton ionisation, mol. cooling in pulsed supersonic beam 80−28070
$Cr(CO)_6$, photoionisation reson., 30 to 100 eV 79−76473
Cs, 16^2P states, reson., 3-photon ionisation, DC Stark effect 78−42026
Cs, 2-photon and 4-photon ionisation cross-sections, absolute determ. 80−83326
Cs, $4d^{10}$ shell, photoionisation cross sections, electron shell alterations determ. *(Russian)* 80−58144
Cs, $4d^{10}$ subshell photoionisation cross section, electron shell rearrangement 77−14400
Cs, 6s-electron photoionisation, ab initio calcs. 80−91523
Cs, 7^2P excited states, photoionisation cross section meas. 77−18858
Cs, atom, excited state, two-photon ionisation by ruby laser light 78−74621
Cs atom, resonant multiphoton ionisation *(Russian)* 79−3421
Cs atoms, exp. multiphoton ionisation through $9D_{3/2}$ resonant level 77−34602
Cs, cross-section meas. for four-photon ionisation 77−42297
Cs, elec. dipole approx. and elec. quadrupole resons. allowed in multiphoton absorpt. *(French)* 78−5190
Cs, excited state, laser photoionisation theory, hyperfine coupling effect 80−102493
Cs, excited states photoionis. cross-section, quantum defect method 78−25494
Cs, four-photon ionis., strongly interacting resons. theory 80−52955
Cs, four-photon ionisation, new resonances 78−5187
Cs, four-photon ionisation, reson. effects 79−45689
Cs, four-photon resonant ionisation calculations 78−37613
Cs, ground state, photoionisation cross-section meas. 77−57949
Cs, He IIα $5p^{-1}$ photoelectron spectrum, config. interaction effects 80−5510
Cs I, pulsed 4-photon 6f-reson. ionis. 80−18831
Cs I, three-photon 16p reson. ionis. and DC Stark effect 80−14124
Cs, multiphoton ionis. cross sections, absolute meas. evaluation 80−14122
Cs, multiphoton ionisation, reson. shift obs. 77−445
Cs, multiphoton ionisation, reson. peak amplitude, temporal effects 78−78760
Cs, multiphoton ionisation, rel. to light statistics 79−72287
Cs, multiphoton ionisation spectroscopy, molecular satellites of 6^2S-7^2P doublet 78−17632
Cs, one-atom detection by reson. photoionisation spectroscopy 77−38742
Cs, one-atom detection by reson. photoionisation spectroscopy 77−79706

photoionisation continued
Cs, oscillator strengths in principal series, Rozhdestvenskii hook obs. 80−37760
Cs, photoionis. of 6s electron, spin-orbit interaction, ab initio calc. 79−81191
Cs, photoionisation cross sections determ. in vacuum UV using Xe excimer laser 80−102494
Cs, polarised photoelectrons produced by circ. polarised synchrotron radiation 80−18830
Cs, reson. multiphoton ionisation by pulsed excitation, Beers-Armstrong model 78−17645
Cs, reson. multiphoton ionisation by ultrashort laser pulses, 1.06 μm 78−58630
Cs, resonant multiphoton ionis. 79−36589
Cs, resonant multiphoton ionisation, spatio-temporal effects 80−37794
Cs, three-photon ionisation, reson. and AC Stark effects 77−68020
Cs, two photon ionisation, destructive interference effect 80−74153
Cs, two-photon ionis., profiles of $6^2S_{1/2}$-$7^2P_{1/2,3/2}$ lines 80−958
Cs, two-photon ionis. rates for linear and circular polaris. 77−50416
Cs, two-photon ionis. via $6^2P_{3/2}$ state, photoelectron spin polarisation 77−3328
Cs, two-photon ionis. via $7^2P_{1/2,3/2}$ intermediate states 77−57946
Cs, two-photon ionisation, 6s-6d quadrupole resons., ion asymmetry and spin polarisation 79−72286
Cs two-photon ionisation, effective order nonlinearity var. 80−106304
Cs, two-photon ionisation rate, time depend. 79−31622
Cs, two-photon photoionisation theory 77−6741
Cs, two-photon two-channel ionisation, laser bandwidth effect 79−59516
Cs^+ ion source, CW monoenergetic, by photoionisation 80−63910
Cs-Sr(He) mixtures, photocond. at atm. press. 80−87844
Cs+Ar, laser two-photon ionisation, collisional line broadening, atomic forces 77−83543
Cs+Ar, two-photon ionisation spectra, satellites, absorption line shape 78−82668
Cs_2, $\tilde{a}^3A_2$-state detect. by reson. enhanced multiphoton ionis. spectrosc. 80−95551
Cs_2, ion-pair form. in two-photon absorpt. 77−88507
CsI, four-photon ionisation near 6f resonance 78−70801
Cu, γ-ray absorption cross-sections, 10-160 MeV 78−90136
$CuCl_4^{2-}$, core ionisation in 3d, 4f and 5f series, rearrangement effects 80−53065
D detection by resonant three photon ionisation 78−74624
DF, threshold photoelectron spectra, photoionis. threshold, resonant autoionis. 77−499
D_2O, collisionless multiphoton ionis. energy depend. by TEA-CO_2 laser 78−46405
Dy atom K-shell ionisation and X-rays from $^{158}Gd(\alpha,xn)$ 79−93960
Dy, hyperfine structure of odd isotopes, two step photoionisation, mass filtration *(Russian)* 77−46550
Er, hyperfine structure of odd isotopes, two step photoionisation, mass filtration *(Russian)* 77−46550
Eu I, 5p spectra collective excitation, rel. to double photoionis. 77−50387
Eu, laser isotope separation by two step photoionisation 77−61720
^{151}Eu (^{153}Eu) excitation transfer, effect on selective photoionisation 80−99538
^{151}Eu, ^{153}Eu, two-step laser photoionisation *(Russian)* 77−6952
F^-, photodetachment cross section, Stieltjes imaging method 78−55149
F_2, photoexcitation and ionisation cross sections, Stieltjes -Chebyshev static exchange calc. 80−53060
Fe, inner-shell vacancies, cascade decay, multiple ionisation and X-ray emission calcs. 80−87072
Fe, $K\alpha^h$ hypersatellite spectra and K-shell double photoionisation cross-section 78−21874
Fe, $K\alpha^h$ hypersatellite spectra and double photoionisation cross-section 79−85922
Fe, photoionis. cross section meas. 79−22674
Fe, photon absorption and photoelectric cross-sections calcs. 79−31486
Fe, UV photoionisation cross-section, resons. 77−14398
Fe^{n+}, photoionis. cross sections, Hartree-Slater central pot. model calcs. 79−22673
$Fe(CO)_5$, multiphoton ionisation, mol. cooling in pulsed supersonic beam 80−28070
$Fe(CO)_5$, multiphoton ionis. spectra, at. Fe transitions 80−106361
Ga, 3d subshell, photoionisation partial cross-section, energy depend. meas. 80−29850
GaAs, photoionisation of impurities with deep levels 80−65484
GaAs, surface photovoltage due to photo-thermo-ionization of surface states 78−14787
GaAs:Cr, photoionisation transition $Cr^{3+}\rightarrow Cr^{2+}$, EPR studies 80−60638
GaAs:Cu, photoionisation spectrum of deep impurities in presence of weak electron-phonon interactions 79−51529
GaP, deep level profiles at substrate-epitaxial interfaces, photoionisation meas. 79−38025
GaP:O, photoionisation of deep impurity levels 80−34386
GaP:Si(s)(O)(Ta), donor centre struct. and conduction band nonparabolicity 78−14695
Gd atom, long-lived autoionisation state *(Russian)* 78−94216
Gd, laser isotope separation by two step photoionisation 77−61720
Ge shallow impurity bound states, IR spectroscopic obs. 77−39806
H detection by resonant three photon ionisation 78−74624
H, highly excited, multiphoton ionisation rates, perturb. theory calcs. 77−54542
H I, ionisation pot. photoionisation mass spectra 78−25632
H in quasars, photoionisation rel. to line and continuum emission 80−27003
H, ionisation, by EM wave field, Reiss approx. calcs. 77−10647
H, ionisation, by microwave-stimulated multiphoton excitation, resons. obs. 77−68019
H like atoms, multiphoton ionisation Pade-Sturmian approach 80−87089
H like atoms, photoionisation in homogeneous elec. field *(Russian)* 80−106309
H, metastable quenching, subsequent photoionis., polarised proton prod. *(Russian)* 78−46202
H, multiphoton ionis., intense field, via complex dressed states 78−17629
H, multiphoton ionis., use of Coulomb Green's function 77−57907
H, multiphoton ionis. pot. in intense circ. polarised laser beam 80−43010
H, multiphoton ionisation, Pade approx. calcs. 79−98049
H, multiphoton ionisation potential, circularly polarized light 79−27101
photoionisation continued
H, photoionisation, two- and three-photon, calc. methods comparison 78−956
H, photoionisation cross sections elec. field-induced oscills. 80−955
H plasma hemispheric layer total radiation calc. *(Russian)* 78−34278
H, resonant ionisation by laser radiation, as polarised proton source 78−78541
H, three-photon reson. photoionis. in plasma 80−58640
H, two photon ionisation in presence of one photon ionisation, cross section calc. 80−83327
H, two-photon ionis. simultaneously with one-photon ionis. 78−33484
H, two-photon ionisation, Laplace transform method 79−10084
H^-, bound-free photodetachment cross section, rel. to opacity in cool stellar atms. 79−49996
H^-, bound-free photodetachment cross-section calcs. 80−9567
H^- photodetachment, Feshbach resonances 80−37753
H^-, photodetachment cross sections, one and two electrons, multichannel J-matrix calc. 77−18860
H^-, photodetachment cross section, dynamic polarisability calc., sum rules, basis set depend. 78−17635
H^-, two-electon photodetachment threshold, blackbody radiation effects 80−91524
H-like atoms in intense long wave EM field, multiphoton photoionisation cross sections 79−89652
H+H collisions in laser field, excitation, charge exchange and ionis. *(Russian)* 79−94078
H_2, Born-Oppenheimer Hamiltonian, resolvent matrix elements complex coord. calc. 80−52878
H_2, D_2, photoionisation, body-frame Hund's case b description 78−94295
H_2, diabatic and reson. states, dissociative photoionisation calcs. 80−47883
H_2, dissociative photoionis. at 26.9 eV 77−3423
H_2, dissociative photoionisation, 19.8-40.8 eV, proton kinetic energy spectra 79−68273
H_2, photoabsorption, photoionisation, predissoc., high resolution obs. 77−477
H_2, photoelectron ang. distribs., oriented or rot. resolved unoriented mol., dynamic and struct. data 78−37682
H_2, photoelectron ang. distrib., 304 Å line, vibr. state depend. 79−45764
H_2, photoelectron angular distrib. and intensity, vibr.-rot. struct. 78−46393
H_2, photoionisation, ang. distrib. of photoelectrons 80−37834
H_2, photoionisation, dissociative, at 304 Å, photoion ang. distribs. photoelectron channels 78−82792
H_2, photoionisation, resonant, dissociative 79−68272
H_2, photoionisation cross sections, photoelectron ang. distribs. 78−5299
H_2, photoionisation cross-section, calc. for vibr. excited mol. 78−17732
H_2, photoionisation cross-sections, involving vibr. states, data tables 79−18242
H_2, photoionisation cross-sections, ang. distrib. and intensity, vibr.-rot. struct. 79−50091
H_2, photoionised continuum states, electron scatt. eqns. convergence 78−66663
H_2^+, photoionisation calcs., role of dipole operators 77−58091
H_2^+, photoionisation effective cross sections 80−43121
$H_2^+ + H_2$, state selected reaction cross sections, coincidence technique obs. 80−66797
HBr, proton affinity, mol. beam photoionisation method determ. 79−89622
HCN, transversely excited waveguide laser with UV preionisation 77−54730
HCN, vibr. fine struct. accompanying core ionis., STO calcs. 78−62844
HCl, proton affinity, mol. beam photoionisation method determ. 79−89622
HD, ionisation, Franck-Condon factors calcs. 77−58102
HF, proton affinity, mol. beam photoionisation method determ. 79−89622
HF, threshold photoelectron spectra, photoionis. threshold, resonant autoionis. 77−499
$(HF)_2$, photoionis., HF proton affinity 78−17731
HN_3, photodissoc. ionis., 16-41 eV 77−18995
H_2O, collisionless multiphonon ionis. 77−65517
H_2O, D_2O, fragment ion formation on photoionisation, energetics and mechanism 77−501
H_2O, dipole oscillator strengths, 10-60 eV, for photoabsorpt., photoionis. and fragmentation 78−42133
H_2O, photodissoc. ionis., 16-41 eV 77−18995
H_2O, photoionis. cross section by atomic extrapolation method 79−81242
$(H_2O)_2$, photoionis., H_2O proton affinity 78−17731
H_2S, valence shell binding energy spectrum, 8-34 eV, electron scatt. simulation of photoionis. 79−10213
He, 2^1S state, two-photon ionisation, multipole interference 79−22675
He, 2^3S and 2^1S states, two-photon ionization 80−37791
He 2S metastable state, three-photon ionis. 79−18167
He, 2S metastable states, singlet and triplet; two and three photon ionisation cross section, absolute determ. 80−83329
He, absolute photoionis. cross sections for VUV region 77−46547
He, absolute photoionisation cross section curve 78−37612
He, double photoionisation calcs., variational method 80−37734
He, elastic electron scatt. phaseshifts, 2s2p ^3P autoionisation, 1s2s $^3S\rightarrow$1sep ^3P triplet continuum photoionisation 79−31480
He excited atom photoionization, for UV photopreionisation CO_2 laser 78−17902
He, ionisation by UV radiation from CO_2 laser produced Cu plasma 78−17624
He, laser-induced breakdown 80−96339
He, many electron system, photoionisation and photoexcitation, at. transition strong config. interaction effect 80−47909
He, metastable, multiphoton transition detection, n^3S-n^3D splitting meas. 80−58231
He, metastable, two-photon ionisation calc. for linearly and circularly polarised laser light 79−797
He, metastable, two-photon ionisation, multipole interference effects 80−23466
He, metastable $1s2s^1S$ state, photoionisation, perturbation theory calcs. 78−78759
He metastable state, two- and three-photon ionisation 80−91518
He, multiphoton ionis. pot. in intense circ. polarised laser beam 80−43010

photoionisation continued
He, multiphoton ionisation potential, circularly polarized light 79−27101
He, photoabsorption, modified RPA calcs. with exchange 78−13477
He, photoionis. and photoabsorpt. cross sections for aeronomic calcs., data tables 80−41599
He, photoionis. cross-section, hyperspherical coord. method calcs. 80−102496
He, photoionisation, frozen-core HF perturbation theory, oscillator strength, dipole length and vel. calc. 78−78672
He, photoionisation above n=2 photoionis. threshold 80−102497
He, photoionisation cross section from excited state $^4p^1P_1$ *(Russian)* 77−61722
He, photoionisation cross sections up to n=2 excited state, evidence of autoionisation 80−91520
He, photoionisation cross-sections, ground state inversion pot. method 78−33481
He, photoionisation cross-section, using UV laser plasma light source 79−19096
He, three-photon ionisation from metastable states, cross-sections 77−42296
He, two-electron photoionis., threshold law and photoelectron spectra 78−29767
He, two-photon ionisation cross-section calcs. 78−21888
He, two-step photoionisation via $4p\ ^1P_1$ state *(Russian)* 79−59413
He^+, ion+electron scatt., static exchange approx. Schwinger variational principle, photoionisation cross section 80−43192
He-like ions, multiple charged, reson. photoionis. 79−54818
He-like ions, photoionisation, 2-channel relativistic random phase approx. calcs. 79−59407
$He+H^+$, determ. of He excited state populations by two-photon reson. ionisation spectroscopy 78−82707
He+NO, multiphoton ionisation spectra in supersonic expansion, laser entranced collisional effects 80−83459
He(I), XPS relative intensity and photoionisation cross-section 80−63599
He(II), 80−63599
He*+Ar, Penning ionisation, laser modified collisional effects in electron energy spectrum 78−90278
Hg, four-photon resonance ionis. 77−42289
Hg, partial photoionis. cross section 78−42022
Hg, photoionisation cross sections, Hartree-Slater and Hartree-Fock calc. 79−89653
HgPh, photoionisation effectiveness curves 78−25633
α-HgS, gas-phase and solid-state Hg 5d photoionisation processes, direct comparison 80−76149
I, partial photoionis. cross sections, rel. intensities, irreducible tensor anal. 79−98048
I, reson. UV fluoresc. and photoionis. obs., in nonlinear I_2 photodissoc. 78−37692
I_2, coherent multiphoton transitions, nonlinear resonant photoionis. 77−61814
I_2, multiphoton ionis. and dissoc. vibronic/mass spectra method 79−3507
I_2, multiphoton reson. ionis. bands, 360-600 nm 78−90233
I_2, resonance-enhanced multiphoton ionis. and fragmentation of mol. beam 79−100411
I_2^+, fragmentation ang. distrib., energy disposal, branching, photoelectron-photoion coincidence spectra 79−68263
IBr^+, fragmentation ang. distrib., energy disposal, branching, photoelectron-photoion coincidence spectra 79−68263
ICl^+, fragmentation ang. distrib., energy disposal, branching, photoelectron-photoion coincidence spectra 79−68263
In I, absorption spectra, 320 to 1000 Å, intersubshell correls. 4d spectrum two-electron detachment 77−10617
In, photoionisation cross section calc. for $4d^{10}$ subshell in RPA with exchange 77−23479
In, photoionisation cross section of d-core level synchrotron radiation study of spin-orbit branching ratio 79−74057
K, cross section depend. of many-photon ionisation on light polarisation 77−42294
K II, isoelectronic series, photoionisation, multichannel CI calcs. 79−93931
K, multiphoton excitation, Rydberg transitions, ionisation detection 77−42304
K, photosensitised assoc. ionisation, excited from reson. levels 77−83710
K, reson. three photon ionisation, saturation effects 78−90137
K_2, two-step photoionisation, triple crossed beam obs. 78−66616
K_2^{2+}, photoionisation cross sections calc., R-matrix theory 77−18865
K^{2+}, R-matrix theory for photoionisation cross-section 78−82702
K_2, beam, multiphoton ionisation mass selective laser spectroscopy, vibronic, gyrovibronic states, clusters 78−21985
K_2, supersonic mol. beam, isotope selective two-step photoionisation study 80−74203
K_x, $(KNa)_x$, prep. and photoionisation pots. 78−55268
KF:Pd^{++}, pure and doped, two-step photoionisation, laser-active F_2^+ centre form. 79−963
KX, (X=F, Cl, Br), photoelectron spectra using Zr Mζ, Al Kα and other X-ray lines, photoionis. cross sections ratios 77−90246
Kr 4s, photoelectron ang. distrib., relativistic Dirac-Fock calc. 79−59411
Kr, 6p levels, two-photon excitation, time resolved fluoresc., quenching, lifetimes and photoionisation cross section 80−78587
Kr, absolute photoionis. cross sections for VUV region 77−46547
Kr, electron energy loss spectra, energy-depend. multichannel quantum defect theory anal. 77−61860
Kr, outer $p_{1/2}$ subshell photoionisation, polarised electrons, relativistic RPA calcs. 80−83331
Kr, photoionisation cross sections for excited states, rel. to KrF laser 77−75110
Kr, photoionisation cross-sections, ground state inversion pot. method 78−33481
Kr, population inversion, intershell transitions, photoionisation, from UV irradiation *(Russian)* 78−70803
Kr, twelve-photon ionis. at 10^{13} W cm^{-2} laser field 80−32687
Kr_2, photoionisation 77−54578
KrAr, photoionisation spectra of ground and excited states 78−5297
KrF, electric discharge pumped laser, model for UV preionisation 77−23658
KrF X-ray-preionized high-pressure laser 79−18403
KrF_2, mass spectrometric study 79−45772
La, 4d subshell spectra, strong interaction regime 79−18165
Li, and isoelectronic series, photoionisation resons. characts., Z depend. 77−50412

photoionisation continued
Li atoms, photoexcitation and ionisation cross sections, Stieltjes-Tchebycheff procedure 78−17633
Li, isoelectronic sequence, photoionisation cross section, core polarisability effects 77−57944
Li, laser excitation and ionisation, autoionising states obs. 77−61699
Li, photoionis., one-electron pseudopotential calc. 79−18166
Li, photoionisation, depolarisation effects 77−83663
Li, photoionisation, two- and three-photon, calc. methods comparison 78−956
Li, photoionisation cross section meas. at 2P level 78−58637
Li, saturated three-step resonance ionisation spectroscopy 79−81189
Li, selective two-step photoionisation and isotope separation 77−71783
Li, two photon ionisation in presence of one photon ionisation, cross section calc. 80−83327
Li, two-photon ionis., many-body perturbation theory 79−22679
Li, two-photon ionization spectra 80−23382
Li, vap., multiphoton absorption, space-charge ion detect. 79−54827
Li vapour, by laser beam, cross-section obs. by absorpt. spectroscopy 77−71782
Li^+, doubly excited autoionis. resons., laser prod. plasma absorption spectra obs. 77−50392
Li-like ions, partial photoionization cross sections and radiative recomb. rate coeffs. 79−49994
Li-like ions, partial photoionis. cross-sections and radiative recomb. rate coeffs. 80−52951
Li_2, isotope separation, by two-photon ionisation, ionisation pot. determ. 78−70950
Li_2, isotopes fractionation in two step photoionization, due to Ar laser beam 78−25631
LiCl, photoelectron spectra using Zr Mζ, Al Kα and other X-ray lines, photoionis. cross sections ratios 77−90246
LiF, photoelectron spectra using Zr Mζ, Al Kα and other X-ray lines, photoionis. cross sections ratios 77−90246
LiH_2 and LiH_2^+ binding energies, LiH_2 ionis. pot. and form. heat 79−94042
Mg, $K\alpha^h$ hypersatellite spectra and K-shell double photoionisation cross-section 78−21874
Mg, photoabsorpt. and photoionisation, RPA with exchange calcs. 77−54543
Mn, $K\alpha^h$ hypersatellite spectra and K-shell double photoionisation cross-section 78−21874
Mo, photon absorption and photoelectric cross-sections calcs. 79−31486
Mo^{29+} to $^{39+}$, photoionis. cross sections, radiative recomb. rate coeffs., rel. to plasma diagnostics 80−52953
$Mo^{30,\ 12+}$, photoionis., relativistic RPA calc. 80−47913
Mo^{n+}, photoionisation and Auger effect 78−90135
$Mo(CO)_6$, multiphoton ionisation, mol. cooling in pulsed supersonic beam 80−28070
N, $^4S^0$ ground state, photoionisation calcs. 79−85909
N, photoionis. cross section, many-channel quantum defect method 78−17638
N_2, $3\sigma_g$ photionis., shape-reson.-induced non-Franck-Condon vibr. intensities 80−43120
N_2, cross sections, K-shell photoabsorpt. spectra using synchrotron radiation 78−74711
N_2, electric breakdown, vol. discharge with external photoionisation, plasma focus spark channel *(Russian)* 80−38738
N_2, gas breakdown threshold using laser radiation 79−1283
N_2, ionisation by UV radiation from CO_2 laser produced Cu plasma 78−17624
N_2, K-shell photoionis. cross section 77−88505
N_2, K-shell photoionisation, symmetry breaking hole localisation 79−829
N_2, multiphoton ionisation, EM field gradient forces 78−66608
N_2, partial photoionisation cross-section determ. using synchrotron radiation 77−75243
N_2, photoabsorption, moment anal. 78−46321
N_2, photoabsorption and photionisation, UV region meas. 78−42087
N_2 photodissoc. ionis., 16-41 eV 77−18995
N_2, photoionis., shape-reson. enhanced nucl. motion effects 80−1031
N_2, photoionis., transition probabilities at threshold, to $X(^2\Sigma_g^+)$, $A(^2\Pi_u)$ and $B(^2\Sigma_u^+)$ vibr. levels 78−94294
N_2, photoionis. and photoabsorpt. cross sections for aeronomic calcs., data tables 80−41599
N_2, photoionisation of π-shell, π-π* transition, modified static-exchange calcs. 79−98163
N_2, total and partial photoionis. cross sections, threshold to 100 Å 77−58092
N_2^+, fluoresc. and production cross-sections by photoionis. of N_2 78−9204
N_2^+, fluoresc. quantum yields and lifetimes, meas. method, ion form. 77−6815
N_2^+, partial photoionisation cross section and photoelectron angular distribution for $X^2\Sigma_g^+$ state determ. 80−83429
NH_3, and ND_3, new electronic state, multiphoton ionis. obs. 78−74717
NH_3, $\tilde{C}$-state, 3-photon gas phase spectroscopy obs. 79−89715
NH_3, expansion cooled, mol. photoionisation, rot. struct., rot. predissoc. of excited states 80−91611
NH_3, gas phase proton solvation energetics, mol. beam-photoionis. obs. 79−29345
NH_3, photoionisation branching ratios and partial oscill. strengths 78−5303
$(NH_3)_nH^+$, n=1-9, detected in photoionisation of supersonic mol. beam mass spectra, H-bonding 79−74356
NO, 4-photon ionis. spectrum 2- and 3-photon resons., low temp. assignments 78−70887
NO, autoionisation struct. at first ionisation limit, photoionis. data 78−58748
NO, multiphoton ionis. spectrum 79−10157
NO, photoabsorption and photionisation, UV region meas. 78−42087
NO, photodissoc. ionis., 16-41 eV 77−18995
NO, photoionis. resonant processes, preionis. and predissoc. 77−65516
NO, photoionisation and ionisation pot., mol. beam meas. 77−10709
NO, resonance-enhanced multiphoton ionis. and fragmentation of mol. beam 79−100411
NO, selectively excited rovibrational states, multiphoton ionisation spectra 80−69202
NO, state selective step-wise photoionis. with mass spectroscopic ion detect. 80−43119
NO, UV irrad. photoionisation, NO^+ high vibr. excitation, photoelectron spectra 77−71830

photoionisation continued
NO^+, fragmentation ang. distrib., energy disposal, branching, photoelectron-photoion coincidence spectra 79−68263
NO_2, laser spectroscopy by cascade photoionisation method in mass spectrometer 80−99496
$(NO)_2$, photoionisation efficiency curve, bound vibr. states 77−61811
N_2O, cross sections, K-shell photoabsorpt. spectra using synchrotron radiation 78−74711
N_2O, non-Franck-Condon transitions in resonant autoionization 79−50092
N_2O, partial photoionisation cross-sections meas. 20 to 60 eV 79−31624
N_2O, photoabsorption and photionisation, UV region meas. 78−42087
N_2O, photoionisation, partial oscill. strengths 79−6973
N_2O, photoionisation and ion dissoc., isotope effects, mass spectra 78−9203
N_2O, valence shell ionic photofragmentation, oscill. strengths, EELS and electron-ion coincidence meas. 80−37879
N_2O^+, dissoc., threshold photoelectron-photoion coincidence obs. 80−87189
N_2O^+, fluoresc. and production cross-sections by photoionis. of N_2O 78−9204
Na (3p state), partial photoionis., cross sections $\sigma_{3p,s}$ and $\sigma_{3p,d}$, expt. separation and study 78−42020
Na, absolute photoabsorpt. cross section, 45-250 eV 77−88434
Na arc lamp, light-induced ignition method 80−77599
Na, core polarisation effects, influence on photoionisation cross sections, ground and excited states 78−46308
Na, cross section depend. of many-photon ionisation on light polarisation 77−42294
Na, cross-section meas. for five-photon ionisation 77−42297
Na, detection of nF Rydberg levels by photoionisation *(French)* 77−71785
Na, efficiency laser ionisation via superelastic collisions and reduced ionisation pot. 77−79588
Na, excited 4D and 5S state, absolute photoionisation cross-section 80−99488
Na, high-lying Rydberg states, field ionisation 79−45683
Na, ionisation of high-lying states by pulsed laser field *(Russian)* 77−75113
Na, laser temporal coherence effects in two-photon resonant three-photon ionisation 80−32686
Na, multiphoton ionis., AC Stark effect 77−57948
Na, multiphoton ionisation in third harmonic generation by mode locked Nd:YAG laser 78−94413
Na, one and two-photon ionis. of 3s and 3p states 78−50512
Na, photoabsorpt. and photoionisation, RPA with exchange calcs. 77−54543
Na, photoionis., one-electron pseudopotential calc. 79−18166
Na, photoionis. cross section resons., time-dependent HF theory 80−32684
Na, photoionisation cross-section, electron correls. Brueckner-Goldstone calcs. 77−6742
Na, photosensitised assoc. ionisation, excited from reson. levels 77−83710
Na, quantum beats of hyperfine levels observed in photoionisation 80−32690
Na, reson. multiphoton ionisation, broadband laser AC Stark splitting 78−70808
Na, reson. two-photon ionis., photoelectron ang. distrib. and polaris., nucl. spin influence 79−10083
Na, reson. two-photon ionisation via $3p^2P_{3/2}$ state, photoelectron ang. distrib. 80−43016
Na, resonant three-photon ionis., saturation effects 78−58632
Na, Rydberg atoms, photoionisation, 300K background radiation effects 79−68271
Na, single atom detection by laser photoionisation *(Russian)* 78−33487
Na, spontaneous field induced optical SHG, multiphoton ionisation 80−14395
Na, Stark effect for selective stepwise ionisation by laser radiation 79−13669
Na, three-photon ionisation, laser bandwidth and intensity effects 80−52956
Na, vap. associatively ionised by CW IR laser beam *(Japanese)* 80−5515
Na vapour, by laser beam, cross-section obs. by absorpt. spectroscopy 77−71782
Na_2, 2-photon ionisation by Ar laser 78−55204
Na_2, beam, multiphoton ionisation mass selective laser spectroscopy, vibronic, gyrovibronic states, clusters 78−21985
Na_2, supersonic mol. beam, characterisation by multiphoton ionisation 78−23946
Na_2^+, photodissoc. and photoionisation in Na_2 multiphoton absorpt. 79−31628
$Na_x(NaK)_x$, prep. and photoionisation pots. 78−55268
NaF:Mn^{2+}, two-step photoionisation, laser-active F_2^+ centre form. 79−963
NaX, (X=F, Cl, Br), photoelectron spectra using Zr $M\zeta$, Al Kα and other X-ray lines, photoionis. cross sections ratios 77−90246
Ne, 1s and 2s photoionis. cross sections, L^2 calc. 80−951
Ne 2s, photoelectron ang. distrib., relativistic Dirac-Fock calc. 79−59411
Ne, absolute photoionis. cross sections for VUV region 77−46547
Ne, atomic deexcitation effects of X-rays, X-ray preionisation in TEA lasers 79−793
Ne, double photoionisation, many-body perturbation approach 78−17634
Ne, electron or photoionisation, electron shake-off, continuum states interaction 78−29766
Ne, electron shake-off following electron or photon bombardment, continuum states interaction 77−14403
Ne II, III, and IV ground state, photoionis. cross sections, close coupling calcs. 80−5513
Ne II, III, IV, photoionisation cross sections calc. 80−43014
Ne, isoelectronic sequence, many-body photoionization calcs. 78−17631
Ne, metastable, photoionis. cross section calc. 78−33485
Ne, photoelectron angular-distribution β parameters, resonance parameters 78−21886
Ne, photoionis. cross-sections, L-subshells, 30-300 eV 79−31483
Ne, photoionisation, complex amplitudes at low energy singly and doubly excited resons. 78−78673
Ne, photoionisation, many-body atomic transition theory 77−75111
Ne, photoionisation, relativistic R-matrix theory 78−5184
photoionisation continued
Ne, photoionization mass spectroscopy using synchrotron radiation, reson. width meas. 79−31478
Ne, total and differential photoemission cross sections, final state approxs. comparison 77−50414
Ni, Kα^h hypersatellite spectra and double photoionisation cross-section 79−85922
Ni, $M_{II,III}$ spectrum, ab initio calculation 80−83276
Ni V spectrum, 990 to 1400 Å, ionisation pot. 77−30811
^{237}Np electron transition excitation following K-shell photoionisation, deexcitation γ-rays 80−78196
O and O_2, photoionis. and photoabsorpt. cross sections for aeronomic calcs., data tables 80−41599
O, autoionis., radiative emission, competition in excited state decay 77−75109
O, dipole transition oscill. strengths, photoionis. cross section 78−9120
O, electron impact calcs. using R-matrix and linear algebraic methods 79−59579
O I, photoionis. cross section 79−13685
O IV bound states, oscillator strengths and photoionisation cross sections 80−106293
O, photoelectron ang. distrib. meas. 77−61721
O, photoionisation absolute cross section 78−94218
O, UV photoionisation cross-section calc., 304 and 584 Å 80−43015
O^-, photodissoc. and photodetachment in $O_2/CH_4/H_2O$ mixtures, 3500-8600 Å 79−45776
O^{6+} to O, photoionis. cross sections, from ground states, Hartree-Slater model 77−57947
O_2, angular distribution of photoelectrons 78−90235
O_2, gas breakdown threshold using laser radiation 79−1283
O_2 molecule, soft X-ray photoionisation cross-sections, 6 to 22 Å 77−14499
O_2, multiphoton ionisation, electron energy spectra 77−6865
O_2, photoabsorpt., photoionis, and photodissoc., dipole oscill. strengths in UV 79−76468
O_2, photoabsorption and photionisation, UV region meas. 78−42087
O_2, photodissoc. ionis., 16-41 eV 77−18995
O_2, photoexcitation and photoionisation cross sections, HF Gaussian method 80−53064
O_2, photoionisation, partial channel cross-sections calcs. 80−53061
O_2, photoionisation, producing $O_2^+(A^2\Pi_\mu \rightarrow X^2\Pi_g)$ and $O_2^+(b^4\Sigma_g^- \rightarrow a^4\Pi_u)$ emissions 79−94041
O_2, photoionisation cross section and asymmetry parameters calc. in UV region using static pot. 80−95692
O_2, photoionisation cross-sections, 100-800 Å 78−5302
O_2^-, photodissoc. and photodetachment in $O_2/CH_4/H_2O$ mixtures, 3500-8600 Å 79−45776
O_2^+, fragmentation ang. distrib., energy disposal, branching, photoelectron-photoion coincidence spectra 79−68263
O_2^+, symmetric charge transfer reactions, selected states, photo-ion, electron coincidence 78−73028
$O_2^+ + NO \rightarrow NO_2^+ + O$, photoionis. mass spectra, photoionis. efficiency 77−40537
O_3, photoionisation, O_4^+ and O_5^+ form., mass spectra 77−50477
O_3^-, photodissoc. and photodetachment in $O_2/CH_4/H_2O$ mixtures, 3500-8600 Å 79−45776
O_3^-, photoelectron, photodetachment and photodestruction spectra 79−64042
O_4^-, photodissoc. and photodetachment in $O_2/CH_4/H_2O$ mixtures, 3500-8600 Å 79−45776
OCS, high-intensity laser photolysis at 157 nm, S(^1S) prod., photoionisation, and loss, laser appl. 80−21306
OH^-, and OD^-, photodissoc. and photodetachment in $O_2/CH_4/H_2O$ mixtures, 3500-8600 Å 79−45776
$O^+(^2P)$ ionisation freq. determ. using satellite airglow and neutral comp. data 77−5384
$O_{2-3}^-.H_2O$, photodissoc. and photodetachment in $O_2/CH_4/H_2O$ mixtures, 3500-8600 Å 79−45776
P_2, valence electron photoionisation, ionisation pot. and spectral intensities 78−70883
P_4, photoionisation, mass spectra 77−30935
PN, valence electron photoionisation, ionisation pot. and spectral intensities 78−70883
Pb, 5d subshell, photoionisation partial cross-section, energy depend. meas. 80−29850
Pb, γ-ray absorption cross-sections, 10-160 MeV 78−90136
Pb, K-shell photoionisation, cross section meas. K X-ray-photoelectron coincidence method 79−72285
Pb, photoelectron spectra, electron correlations and spin-orbit interaction influence 80−102495
Pb, photoionisation cross section of d-core level synchrotron radiation study of spin-orbit branching ratio 79−74057
Pb subshell photoelectron branching ratio meas., using synchrotron radiation 80−66397
Pb, total L-shell photoelec. cross section ratio 77−30836
$Pb_{1-x}Sn_xTe$, epitaxial layers, carrier lifetime meas. 79−42559
PbTe, epitaxial layers, carrier lifetime meas. 79−42559
photoionisation cross section and asymmetry parameters calc. in UV region using static pot. 80−95692
Pt, photon absorption and photoelectric cross-sections calcs. 79−31486
Pt subshell photoelectron branching ratio meas. using synchrotron radiation 80−66397
Rb, high lying Rydberg states, atomic beam laser spectra 79−94101
Rb, isotopically selective ionisation through Rydberg states 78−5186
Rb, multiphoton ionis. processes, fine struct., hybrid reson. 77−18877
Rb, photoionis. cross section, elec. field depend. 80−37796
Rb, photoionisation from ground state in DC elec. field, narrow resonances *(French)* 77−61718
Rb, photoionization cross-section, reson. induced by elec. field 79−13689
Rb, π-photoionisation spectra in DC field, Fano profile 79−59410
S^-, photodetachment in mag. field 79−41143
SF_6, absorpt. structs. in VUV region, ionis. efficiencies 79−3458
SF_6, multiphoton-excited in mol. beam, photoionsation probe of vibr. energy distrib. 79−76476
SF_6, partial photoionis. cross-sections, 20-54 eV, photoelectron spectrum 79−13769
SF_6, photoabsorption and ionic fragmentation, 5-63 eV, absolute oscill. strengths 79−72367
SF_6, photoionisation spectra in XUV region 80−37837
SF_6, valence levels, photoionisation cross-sections, MS Xα calcs. 79−54923

photoionisation continued
SF_6-hydrocarbon mixtures, IR laser induced ionis., mechanism 77−81415
$(SN)_x$, XPS calc. using photoionisation cross sections 78−72697
S_2O, photoionis. mass spectrum, heat of form., dissoc. energy 77−46605
Sb, 4d subshell, photoionisation partial cross-section, energy depend. meas. 80−29850
Sc and Sc_2O_3, photoabsorpt. spectra, at. ionisation, band struct. mechanisms, electron energy loss investig. 77−24909
Se, $L_2M_{4,5}M_{4,5}$ Auger spectrum following photoionisation, post collision interaction, chemical shifts 79−22678
n-Si, carrier recomb. and photoionisation via E-centre resonance state 79−60847
n-Si, photoionisation of doubly charged divacancies 79−51526
Si shallow impurity bound states, IR spectroscopic obs. 77−39806
Si:Zn, photoionisation of deep impurity levels 80−34386
SiO_2 layers on Si, ionis. thresholds of electron traps 80−92983
^{29}Si, nuclear dynamic polarisation, impurity centre photoionisation, extrinsic light absorpt. *(Russian)* 79−15378
Sm, isotope separation by two step photoionisation method 77−58205
Sm, laser isotope separation by two step photoionisation 77−61720
Sm, multiphoton ionisation by laser beam, Sm^+ and Sm^{2+} form. 77−58093
Sn, electron inelsatic MFP from photoionisation cross sections and ang. var. studies 77−66572
Sn, γ-ray absorption cross-sections, 10-160 MeV 78−90136
Sn, K-shell photoionisation, cross section meas. K X-ray-photoelectron coincidence method 79−72285
Sn, photoionisation cross section of d-core level synchrotron radiation study of spin-orbit branching ratio 79−74057
SnS_2, Sn4d photoionisation, second threshold 80−40222
Sr, autoionisation reson. states elec. field depend., three-photon ionisation 78−33478
Sr, bound even-parity J=0 and J=2 states, multiphoton ionisation spectra 77−71789
Sr, diamag. quasi-Landau spectrum near ionis. threshold, two-photon ionis. spectra obs. 78−58642
Sr, double multi-photon ionisation *(Russian)* 77−71786
Sr, efficient ionis. by reson. laser pumping 80−32685
Sr, multiphoton ionis. spectroscopy of even- and odd-parity states 78−86973
Sr, multiphoton ionisation spectra of msnp $^3P^0$ states 77−83554
Sr, Zeeman effect of J=2 states, g-factor, interacting Rydberg series 78−17609
Sr-Cs mixture, laser induced collisional two-photon ionisation, fluoresc. monitoring 80−91515
Ta, γ-ray absorption cross-sections, 10-160 MeV 78−90136
Ta, K-shell photoionisation, cross section meas. K X-ray-photoelectron coincidence method 79−72285
Ta, total to L-shell photoelec. cross section ratio 77−30836
Te, relax. energies for photoionisation 77−20988
Th, K-shell photoionisation, cross section meas. K X-ray-photoelectron coincidence method 79−72285
Ti, $K\alpha^h$ hypersatellite spectra and double photoionisation cross-section 79−85922
Tl atom, two-photon laser spectroscopy and ionisation 78−55153
Tl, ionisation limit and oscill. strength in VUV absorpt. spectra 80−74152
Tl, photoionis. cross section, spin polaris. and ang. distrib. of photoelectrons, RPA calc. 78−13478
Tl, photoionis. cross section and spin polarisation of photoelectrons 78−46307
U atom, by Ar ion laser radiation, appl. to U laser isotope separation 78−42233
U, enrichment by two step photoionisation, laser isotope separation *(Japanese)* 79−49865
U, L-shell photoionis., transition radn. ang. distrib. 78−33486
U, laser isotope separation, atomic spectroscopy requirements 78−33638
U, Rydberg levels, time-resolved stepwise laser photoionisation obs. 77−27038
UF_6, strong UV-visible emission and weak ionisation induced by focused KrF laser 79−64034
^{235}U, hyperfine struct. and isotope shift meas., laser separation by two-step photoionisation 78−78822
^{235}U isotope separation enhancement with RF hyperfine transitions 79−41249
^{235}U, photoionisation, isotope separation and enrichment by Ar ion laser *(Japanese)* 79−81192
V, $K\alpha^h$ hypersatellite spectra and K-shell double photoionisation cross-section 78−21874
W, photon absorption and photoelectric cross-sections calcs. 79−31486
Xe, 11 photon ionisation probability in 1 μm beam 77−46548
Xe, $4d^{10}$ and $3d^{10}$ shell, photoionisation cross sections, electron shell alterations determ. *(Russian)* 80−58144
Xe, $4d^{10}$ subshell photoionisation cross section, electron shell rearrangement 77−14400
Xe, 5p shell photoelectron branching ratio, energy depend. 77−88435
Xe, 5p subshell photoelectron branching ratio, Dirac-Fock calcs. 78−42021
Xe, $5p^6$ subshell, photoelectron ang. distrib., ionisation cross section 77−14401
Xe, 5s, 5p ESCA spectrum, photoionisation many electron description 78−50516
Xe 5s, photoelectron ang. distrib., relativistic Dirac-Fock calc. 79−59411
Xe, 5s electron photoionisation cross section with synchrotron radiation 78−5180
Xe, 5s→εp photoelectron ang. distrib. near Cooper minimum 80−18834
Xe, absolute photoionis. cross sections of spin-orbit components of 4d electron 77−38646
Xe, atom, photoionis., collective level existence RPA with exchange calc. 78−42025
Xe, electron energy loss spectra, energy-depend. multichannel quantum defect theory anal. 77−61860
Xe, intershell correlation, double electron ejection from outer shell 78−42019
Xe, low-energy 5s-εp photoionization, relativistic effects 78−50515
Xe, multiphoton ionisation spectrum, interatomic effects in multiphoton transitions 78−29764
Xe, outer $p_{1/2}$ subshell photoionisation, polarised electrons, relativistic RPA calcs. 80−83331
Xe, photoelectron branching ratio in 4d subshell 79−18164

photoionisation continued
Xe, photoelectron-Auger electron post collision interaction, Auger peak shift obs. 77−27039
Xe, photoionis., $\sigma 3/2{:}\sigma 1/2$ branching ratio in $5s5p^6p(^1P_1)$ resonance 77−42292
Xe photoionisation, spin-polarised photoelectrons angular distrib. 80−106306
Xe, polarisation effects in photoionisation *(Russian)* 79−3420
Xe, population inversion, intershell transitions, photoionisation, from UV irradiation *(Russian)* 78−70803
Xe precursors, associative ionisation and photoionisation, relative contrib., electron density prediction 80−43858
Xe, recently enhanced multiphoton ionisation and third harmonic generation 80−91526
Xe, six-photon ionis., electron energy spectra 79−54824
Xe subshell photoionisation, multichannel k-matrix calc., spin orbit interactions 80−63600
$Xe^+ + O_2 \rightarrow O_2^+ + Xe$, $O_2^+ + Xe \rightarrow Xe^+ + O_2$, charge transfer, photoionisation mass spectra 77−16793
Xe_2, van der Waals mol., photoionisation 77−18991
XeAr(XeKr) photoionisation spectra of ground and excited states 78−5297
XeF, electric discharge pumped laser, model for UV preionisation 77−23658
Y, and Y_2O_3, photoabsorpt. spectra, at. ionisation, band struct. mechanisms, electron energy loss investig. 77−24909
Y, XPS relative intensity and photoionisation cross-section 80−63599
Yb I, high Rydberg levels of $4f^{14}$ 6snd configs., very high resolution obs. 80−106300
Yb, photoionisation cross-section of $^3P_1$ excited state, laser isotope separation *(Russian)* 78−25496
Zn, UV subshell photoionisation cross section, expt. and GIPM theory 78−21887
Zr, XPS relative intensity and photoionisation cross-section 80−63599

photolithography
see also masks; photoresists
cell type optical circuitry fabrication using photopolymer 77−42633
conference on electron, ion and proton beam technology, conf., Boston, MA, USA (29 May-1 June, 1979) 80−67927
diffraction grating generation for integrated optics, interference method 80−48460
guided-wave optical components, electron-beam and photolithographic fabrication 78−13818
holographic grating ruling with stepped profile 79−76898
holographic interference lithography for integrated optics 79−14116
integrated optics, functional components, fabrication of microstructs. in micrometre/submicrometre range, microlithographic techniques *(German)* 80−106637
integrated optics techniques 78−46844
interdigital transducer and 1.1 GHz SAW oscillator, photolithographic contact printing *(Japanese)* 78−33981
Josephson junctions fabrication, tunnelling through edge-grown barriers 80−100567
Josephson microbridges, submicron, fabrication using optical projection lithography and liftoff techniques 79−28458
Josephson microbridges, ultrasmall, step-edge fabrication 80−49997
laser lithographic system, integrated optical device fabrication appl. 78−55477
lenses for projection photolithography 77−58423
lithographic coated polyester panchromatic plate system 80−13172
LSI, lithographic manufacturing techniques *(German)* 79−71547
microminiature cryogenic refrigerators, design, construction 79−26059
microstructure fabrication, using STEM and X-ray lithography and reactive ion etching, appl. 79−15844
MTF evaluation for optical and electron-beam lithography 80−4801
multiple optical fibre connector fabrication 77−3669
offset, four-colour reproduction, colorimetric anal. by photomechanical means 79−75635
optical channel waveguide arrays coupled to integrated CCD 80−33244
optical MTF for photolithographic technology *(Japanese)* 78−90387
optical multimode strip-waveguides made by thick film technology, loss meas. 79−59846
optical transfer measure, system relations, appl. wide field microscopy and microelectronic photolithography *(German)* 80−9815
optical waveguide taper couplers, photolithographic fabrication processing sequence 79−41464
photopolymer printing surfaces for gravure 79−35871
photosensitive materials which change their adhesion to a substrate due to the action of light *(Russian)* 79−97464
projection printing, partial coherence 79−31834
pulsed X-ray lithography, laser-plasma source 79−30636
SAW device fabrication, book contrib. 79−50523
screenless lithography rel. to plate grain struct. 79−35872
soft X-ray microscopy and lithography using synchrotron radiation 78−66018
spatial period division, submicrometre linewidth grating prod. 80−69556
steel, mild, photoetched profiles 80−25907
steel, stainless, photoetched profiles, quantitative examination 79−20268
surface relief gratings, 3200 Å period fabrication, effect on film growth 78−84089
surface relief gratings with linewidths below 2000 Å, fabrication 78−42478
synchrotron radiation appls., characts. and sources 78−74960
thick film optical waveguide integration with fibre-optic connectors 80−33246
thin-film waveguide, on Si substrated, optical power losses calc. and obs. 80−106640
three layer optical waveguide for photolithographic fabrication of film lenses 77−39113
tonal reproduction via unscreened positive printing plates 79−17517
UV, high resolution aplanetic holographic objectives 79−32031
UV irradiated electroless selective plating, improvement 80−84848
UV lithography, 150 to 260 nm *(Japanese)* 78−78018
UV objectives, for submicron photolithography 79−32032
wafer exposure camera, optical, step-and-repeat, with dark field automatic alignment 80−68283
waterless planographic plate development 80−105729
X-ray, fabrication of submicrometer period gratings with precisely defined profiles for integrated optics applications 80−58814
X-ray, laboratory apparatus *(Polish)* 79−89050

photolithography continued
X-ray, using synchrotron radiation 77−22628
X-ray high resolution lithography, diamond as X-ray source 79−21884
X-ray lithography fabrication of microcircuits 77−34059
X-ray lithography using synchrotron radiation, resist sensitivity 80−62820
X-ray lithography with thin polymer resists, high energy irrad. and selective dissolution *(German)* 80−13167
X-ray microfabrication for guided-wave optical devices 80−58812
X-ray microsource, scanning 79−9266
x-ray zone plates fabricated using electron-beam and X-ray lithography 80−68335
Al-Cu alloy layer, photolithographically patterned, separation from substrate using plasma etching *(Slovak)* 80−45405
$Al_xGa_{1-x}As$ heterojunction LED, fabrication by negative profiling of substrate and characts. 78−56523
As_2S_3, amorphous film, light enhanced vaporisation, photolithographic process, photographic appls. 77−5949
As_2S_3 thin film, diffr. grating production, using laser photolithographic process, image evaluation 78−42479
Bi_2WO_6 film, RF sputtering, possible piezoelec., pyroelec. and photolithography appl. 77−15705
GaAs wafer, double-etching technique for submicron channel fabrication, laser fabrication appl. 80−74387
$LiNbO_3$:Ti in-diffused optical waveguide fabrication 79−76892
Pb-Sn Josephson junctions, small area high current density normal resistance, RC times 80−34555
Si alignment chips for optical fibre cable connector 78−1411
Si chip manufacture for fibre alignment in lightguide cable connectors 80−64188
Si, optical waveguides along both sides of groove 80−96006
Ti line fabrication, shadow deposition method using optical lithography for 0.15-0.3 μm widths 79−43148

photoluminescence
see also fluorescence; phosphorescence
absolute luminescence quantum yields, actinometric meas. 77−41691
acetone, γ-irrad., isothermal luminesc. decay, temp. depend. 79−66322
activated crystal, electron excitation energy transfer, collective coherent phenomena 77−90189
activated crystal, electronic excitation energy migration efficiency, inverse transfer influence 78−19546
activated crystals, electronic excitation energy transfer efficiency, inverse transfer effects 78−2897
adamantane, plastic cryst., radio- and photothermoluminesc. *(Russian)* 79−11477
alkali aluminometaphosphate glass, $MPO_3.Al(PO_3)_3$:U (M=Li,Na,K), vibronic excitation, absorption and emission spectra 78−52524
alkali chloride:Mn^{2+} luminesc. spectra and decay *(German)* 77−48234
alkali cyanides, mol. excitons, X-ray excited emission spectra obs. 80−66287
alkali disulphide species, $M^+S_2^-$, laser photoluminescence spectra in solid Ar at 12K 79−5148
alkali halide: monovalent cation, recomb. luminesc. $(V_K+e)_A$-type emission 77−28615
alkali halide: O^{2-}, photoluminesc. spectra, phonon using struct. *(Russian)* 78−2912
alkali halide:$Cu^+(Ag^+)$, luminesc. spectra and lifetime, high-press. effects 78−35194
alkali halide:O_2^-, frozen soln., impurity luminesc., zero-phonon lines interpretation 79−87488
alkali halide:Tl^+-like ions, triplet state lifetime, hyperfine interaction 80−2844
alkali halide=O_2^- soln., phonon wings in luminescence spectra *(Ukrainian)* 79−52001
alkali halide, rel. between thermoluminescence and X-ray induced luminesc. 79−28830
alkali halide aq. solns. with O^{2-} anion impurities, luminescence spectra regularities *(Russian)* 77−69876
alkali halide crystals, activated, physical phenomena and optical data processing appl. *(Russian)* 80−80819
alkali halide crystals, deformation spectroscopy, dislocation interactions with electron and hole centres 78−10983
alkali halide F-centres, cation vacancy model, rot. mechanism 77−76393
alkali halide phosphors, Tl doped, press. effect on emission spectra at low temps. 77−85771
alkali halide surface light emission, 10.6 μm laser pulse irradiation *(Russian)* 78−27352
alkali halides, aq. solns. with extrinsic O_2^- ions, spectral props. *(Russian)* 78−6766
alkali halides, coloured, light amplification at activator centres 80−2795
alkali halides, luminesc. polarisation and low-temp. photoinduced orientation change in O_2 and S_2 mol. centres 78−6735
alkali halides, luminescence excited by vacuum UV lasers 78−10941
alkali halides, luminescence of Tl^+-like centres, Ga^+-centre polaris. effect 79−33806
alkali halides, rare earth ion doped, optical props., review 79−15492
alkali iodides, free exciton reson. luminesc. lines 77−77272
alkali phosphate glass:Nd^{3+}, laser material evaluation 77−54715
alkaline earth fluorides, luminescence excited by vacuum UV lasers 78−10941
alkaline earth halides, rare earth ion doped, optical props., review 79−15492
alkaline earth oxides, luminescence excited by vacuum UV lasers 78−10941
alkaline earth oxides, reversible quenching, surface state spectra 79−47505
alkaline glass: tryptophan (tyrosine), γ-irrad., electron traps, stimulated luminesc. 78−11536
aluminate:Ce^{3+}, hexagonal, luminesc. rel. to host lattice structure 78−6776
aluminate:Eu^{2+}, Mn^{2+}, efficiency of $Eu^{2+}\rightarrow Mn^{2+}$ energy transfer, struct. effects 77−8629
aluminates:Ce^{3+}, luminesc. exam. 78−56513
aluminates:Mn, Eu, red Mn^{2+}-luminesc. 79−61420
4-amino-N-methylphthalimide-decalin-n-propanol, translational relax. kinetics, luminesc. obs. 79−8180
amorphous semiconductor, defect chemistry and states in gap, models 79−38030
amorphous semiconductors, doped, electronic props. 78−19030

photoluminescence continued
amorphous semiconductors, photogeneration of charge carriers and recomb. 77−81147
amorphous semiconductors, photoluminesc. props. 79−56862
anisotropic media, multipole emission, energy transfer, classical theory 77−8625
anodic oxide films on Al, heat treatment effect on photoluminesc. props. 77−28610
anodic oxide films on Al, photoluminesc. obs. 77−1729
anthracene:tetracene, singlet exciton fission, fluoresc. in mag. field 79−69877
anthracene, γ-irradiated, temp. depend. of photolum. *(Russian)* 78−56511
anthracene, γ-irradiation influence on defects, luminesc. study *(Russian)* 80−55185
anthracene, aromatic solvents, two-photon absorption cross section meas. by energy migration 77−58204
anthracene, cryst., polariton luminesc. 80−84775
anthracene, excimer form. in soln. and cryst., fluoresc. study 79−45759
anthracene, excitation and propagation of phonons, luminesc. meas. *(Russian)* 78−35202
anthracene, film substruct., vacuum deposited, low temp. luminesc. *(Russian)* 78−15226
anthracene, in cyclohexane soln., triplet state decay consts. by sampling flash apparatus 79−51998
anthracene, lifetimes of exciton-polariton luminesc. 79−33761
anthracene, luminesc. spectra, exciton-phonon interaction, triplet exciton bands 79−65387
anthracene, photon-emitting singlet excitons spatial distrib. 79−83009
anthracene, reson. Raman emission and hot luminesc. *(Russian)* 79−61377
anthracene, single cryst. triplet excitation form. 79−69437
anthracene, singlet exciton annihilation kinetics 79−19926
anthracene, singlet exciton fission, fluoresc. in mag. field 79−69877
anthracene, structural defect, photolum., γ-irrad. and temp. depend. *(Russian)* 79−28797
anthracene, thin surface layer, delayed fluoresc. obs., surface trap influence 77−77291
anthracene, with pentracene and tetracene impurities, laser-pulse-excited luminesc. 80−7408
anthracene crystal, resonance secondary emission, Raman scatt. in exciton absorpt. region *(Russian)* 80−40120
anthracene crystals, local biexciton formation, luminesc. spectra *(Russian)* 78−2428
anthracene isotopic mixed crystals, exciton spectra 79−38602
anthracene Langmuir film, lightly substituted, electrolum., photolum. and electroabsorption 80−20726
anthracene single crystals, effect of γ-irrad. on photolum. *(Russian)* 80−2852
anthracene-Au interface exciton luminescence Frenkel exciton metallic quenching *(Russian)* 80−50421
anthracene-pyromellitic dianhydride complex, optical and photoelectric props. *(Russian)* 80−15570
anthracene-quartz interface exciton luminescence, Frenkel exciton metallic quenching *(Russian)* 80−50421
antibunching phenomena on single-scatterer fluorescence in weak-field limit 80−63580
aqueous glasses, mixed solute, luminesc. following laser excitation of trapped electrons 78−31666
aromatic compounds, in n-paraffin cryst., luminesc. characts. 79−3480
automated luminescent topographic system 78−74081
azulene, soln., laser-excited $S_2\rightarrow S_1$, $S_1\rightarrow S_0$ emission and $S_2\rightarrow S_n$ absorption 79−10131
bacteria, effect of mag. field on recomb. fluoresc. 80−35856
1,2-benzanthracene, secondary reson. radiation and hot energy transfer, soln. luminesc. 80−87167
1,2-benzanthracene in soln., luminesc. and vibr. relax. 79−52007
benzene phenol crystal, asymmetry of phonon side bands, absorption, luminesc. and specular spectra 77−1730
1,12-benzoperylene in n-alkane, zero-phonon lines in luminesc. spectra 78−56512
biacetyl, multiphoton excitation of triplet state, fluoresc. decay 79−31632
biexciton luminescence, influence of free excitons on profile 77−4684
binary inorganic crystal, activation conditions 78−10394
bisphenol-A-diglycidyl epoxy, light emission under high elec. field, compared with photolum. 80−25465
borate glass:Er^{3+}, $^4I_{13/2}$ level relax. 79−87476
caesium uranyl propionate, low temp. absorpt., luminesc. spectra, intermol. interactions 80−2830
calcite, luminescence spectral anal. of polycyclic aromatic hydrocarbon impurities 80−71483
calibo glass:Eu^{3+}, Ho^{3+}, energy transfer 78−76510
carbazoles, luminescence, $AgNO_3$ heavy atom effect, donor-acceptor interaction *(German)* 78−84651
CdS:Cu, V, photoluminescence spectra 79−83027
CdS, green edge luminescence spectrum, temp. depend. 80−108274
cellulose-PAN copolymer, luminesc., ageing effect 78−64401
chalcogenide glass, charged dangling bond model reassessment 77−72813
chalcogenide glass, mech. for electron-hole recomb. 78−72196
chalcogenide glasses, Luminescence, temp. depend. rel. to nonradiative transitions 80−71485
chalcogenide glasses, neutrality of luminescence centres 78−88356
chalcogenide glasses, optical versus transport processes. 80−84449
chalcogenide semiconductors, optical and elec. props., comparison with SiO_2 78−6721
chalcopyrites, for electrolum. device appl., props. and technology, book contrib. 77−73175
chlorophyll, in maple leaf, −196-18°C, red shift explanation 78−61144
chlorophyll, singlet-triplet optical resonance in solid soln. 77−52741
chlorophyll pigments, aggregated forms in soln., spectral-luminesc. characts. *(Russian)* 78−23529
chlorophyll solutions, photolum. of singlet O_2 78−80831
chromone, solns., pH dependent fluorescence spectra, pK_a and tautomerism 79−59506
concentration depolarisation, by excitation transfer, selfquenching considerations 77−32413
concentrational depolarisation by excitation energy transfer 80−2821
conference, Szeged, Hungary (Aug. 1976) 78−27279
coumarin 1, multiphoton cross-section determination by means of luminescence experiments 80−93377

photoluminescence continued
crystal, radiationless relax. of excitation energy *(Russian)* 77−32418
crystal luminescence, polariton mechanism, reabsorption, spatial dispersion effects, boundaries *(Russian)* 80−55186
9-cyanoanthracene, luminesc., excimeric species 78−84637
9-cyanoanthracene, metastable crystal, red excimer emission 78−6757
cyclohexane crystals, luminesc. emitted at 55 cm^{-1} near phase transition point 77−52180
decane: pyrene (coronene), quasiline spectra, multiplet struct., freezing conditions and solvent effects 79−1786
decay curve simulation, finite breadth light pulse excited *(Hungarian)* 80−11473
deconvolution of expt. data 78−5369
deuteronaphthalene:β-deuteromethylnaphthalene crystal, asymmetry of phonon side bands, absorption, luminesc. and specular spectra 77−1730
di-isobutyl kitone, γ-irrad., isothermal luminesc. decay, temp. depend. 79−66322
diamond, GR1 and UV band, fine struct. 80−20678
diamond, GR1 band, E to T state transitions coupled to e vibrs. 77−12430
diamond, GR defect, high resolution optical spectra after electron irrad. 78−56515
diamond, impurity centres, vibronic spectra, Van Hove singularities, quasi-local vibrs. 77−85782
diamond, irradiated, optical study of TR12 and 3H defects 77−85772
diamond, Jahn-Teller coupling at neutral vacancy 80−71453
diamond, natural, N3 luminesc. decay time 78−76520
diamond, optical absorption and luminesc. spectra, review 80−2848
diamond, vibronic bands at 2.498 eV (H4), 2.417 eV and 2.536 eV, absorpt. and luminesc. under stress 77−85758
dibenzene-naphthalene, relax. time of vibr. levels of ground state *(Russian)* 77−44054
p-dichlorobenzene-p-dibromobenzene, mol. cryst., intermol. mixing of electronic states 77−85768
diethylammonium manganese chloride, antiferromag., low temp. luminesc. spectra, magnetoelastic effect 80−2810
Diffusion of excitons and energy transfer to impurity molecules *(Russian)* 78−27282
diffusion recombination theory in case of particle generation 78−52553
dimethyl POPOP, multiphoton cross-section determination by means of luminescence experiments 80−93377
p-dimethylaminoacetophenone, ps reversible isomerisation kinetics, O_2 quenching obs. 79−5133
dimethylammonium manganese chloride, antiferromag., low temp. luminesc. spectra, magnetoelastic effect 80−2810
diphenyl:pyrene, self induced transparency under nonreson. excitation, luminesc. and stimulated emission 80−11436
diphenyl:pyrene, stimulated emission at 0-0 transition, 4.2K 80−11437
disordered systems, electronic energy transfer, generalized master eqn. 80−57221
disordered systems, time dependent spectral transfer, Monte Carlo calc. 80−11464
donor-acceptor pair luminesc. band maximum position 77−52177
dosimeter glass, radiophotoluminescence intensity change by intense laser light 80−89050
dosimeter radiophotoluminescent, with miniature detectors, for clinical use 79−8543
dyes, S_2-S_0 luminesc. for picosec. excitation 79−87506
electron+phonon system, weakly coupled, reson. light scatt. and luminesc. 77−12374
electron excitation energy transfer between molecules, theory, including reabsorpt. *(Russian)* 78−10981
electron recombination kinetics, Debye-Edwards law 79−87495
electron-hole drop radiation in far IR spectrum *(Russian)* 78−72600
electron-hole plasma condensation, in supersaturated gas of free excitons 77−69242
electronic states determ. using synchrotron radiation 77−20882
energy transfer and two-centre optical transitions in OH^- and rare earth double-doped solid 80−7398
energy transfer between 5d electronic states 80−2808
ethylene, dye laser probing of C_2 radicals, IR intense field photolysis 77−16851
excitation spectra, automatic analysis 77−52154
excitation spectroscopy, time-resolved photoluminescence emission and lifetime meas., synchrotron radiation use 78−66687
exciton luminescence, RF coherence and polarisation 78−10937
excitonic molecules, reson. Raman scatt. and luminesc. 79−95763
excitonic molecules, theory, luminescence spectra of crysts., biexcitonic states classification 77−69238
excitons and related states, conf., Tomakomai, Japan (Sept. 1975) 77−43510
extrinsic molecular crystal, luminesc. spectra, relax. of vibr. levels 79−87484
F-centres, relaxed excited state, spin polarisation, saturated optical pumping 79−15522
fatty acids, anisotropic layers, multipole emission, energy transfer, classical theory 77−8625
filter, luminescent, efficiency for Nd:glass lasers 80−1213
fluoride:Pr^{3+}(Tm^{3+}), photon-cascade emission quantum yield calc. 77−4669
fluorophosphate glasses, rare-earth activated, luminesc., bonding 78−64415
formylstyrene copolymers, luminesc. *(Russian)* 79−56861
Frenkel excitons, optical resonance 78−91621
p-GaAs:Zn, diffusional doping, photoluminesc. in mag. field 77−16384
GaAs-$Ga_{1-x}Al_xAs$ DH crystals, <110> oriented dark line defects 77−80510
n-GaP, quasidirect radiative recombination of free holes at neutral shallow donors 78−64410
GG GaS, indirect exciton exam. 78−39029
glass:Nd^{3+}, $^4I_{11/2}$ level population, absorpt. and relax. rate meas. 77−36290
glass:Nd^{3+},Cr^{3+}, nonradiative energy transfer from Cr to Nd, optical pumping efficiency improvement 80−33001
glass:Nd, for lasers, luminesc. absolute quantum efficiency 77−34893
glass:Nd, laser material, population inversion depend. on pump pulses 77−23679
glass:Nd laser materials, intensities of optical transitions 77−689
glass, conduction and valence bands props., review 77−66106
glass, electron migration and spectral relax., random-walk model 80−80280
photoluminescence continued
glass, rare-earth activated, polarised luminesc. 78−48224
glass with nonequivalent optical centres, decay rate averaging 79−8178
glasses:Nd^{3+}, energy transfer processes, radiative transitions *(Chinese)* 79−61431
glasses, non-radiative recombination at valence-alternation pairs 80−89048
heterolasers, active layer, photoluminesc., temp. depend. *(Russian)* 79−10310
heterostructures, multipass, external quantum efficiency of luminescence 77−20419
hexane:pyrene (coronene), quasiline spectra, multiplet struct., freezing conditions and solvent effects 79−1786
highly anisotropic scatt. medium, luminesc. of layer 80−100685
highly photoexcited semiconductors, picosec. luminesc. spectrosc. 79−47517
hot electron distribution functions, expts., review 78−27231
hot luminescence and relaxation 78−6722
hot luminescence in F centres, nonradiative quenching 80−11467
hot photoluminescence polarisation spectrum, photoelectron momentum distrib. function anisotropy relax. 80−7404
7-hydroxy-2-methylchromone, solns., pH dependent fluorescence spectra, pK_a and tautomerism 79−59506
II-VI compounds, electron energy radiation damage threshold meas., EPR and luminesc. 77−84799
II-VI semiconductors, highly excited blend type involving free particle scatt. 79−38648
II-VI semiconductors, impurity and defect centre energy states, luminesc. meas., review 80−55150
II-VI semiconductors, radiation effects, optoelectric props. control 80−25458
III-V semiconductor, acceptor levels, anisotropy of Zeeman splitting and polarization of luminesc. in mag. field 79−24365
III-V semiconductor epitaxial structures as wide-gap substrates, minority carrier diffusion length determ. by photoluminesc. 80−103992
III-V semiconductors, optical transitions, effect of perturbed k-selection and gap shrinkage 80−66257
III-V semiconductors, radiative recomb., optical evaluation review 80−60647
4,5-iminophenanthrene, polymorphism, X-ray diffr. and photoluminesc. obs., 77 to 300K 77−63449
implantation temperature meas. using impurity luminesc., for insulating materials 79−52012
impurities in solids, absorption and emission spectra, bandshapes, moments 80−45122
impurity centres, theory of time depend. of resonant secondary emission specta 78−92082
impurity luminescence quantum efficiency, temp. depend. 78−35198
impurity molecules, population kinetics *(Russian)* 78−56519
inelastic biexciton-biexciton collision, effect on radiative recombination of biexcitons 79−15529
inert gas:Eu(Sm), absorpt. and emission spectra, phonon sidebands 79−43021
inert gas crystals, excitons exam. 78−51898
inert gas solid, VUV luminesc. from excitons 79−43020
intermolecular energy transfer and high energy excitations, in condensed phase 80−66269
ionic crystal, fundamental luminescence at high ionisation levels *(Russian)* 80−103985
ionic crystals, exposed to ultrasoft X-rays, thermal luminesc. and electron emission 79−8192
ionic crystals incorporating S-state ions, expt. exam. 79−28326
kinetic equations for parameters of quantum subsystems *(Russian)* 79−1789
lanthanide porphyrin complexes, intramol. energy migration, mol. luminesc. 77−3412
lattice relaxation and time resolved polarization of emission from localized electron with level crossing 79−4840
lifetime measurements using AlGaAs DH pump laser 78−74085
LiH, cubic, vibronic struct. and anisotropy of excitons, refl. and edge luminesc. spectra 78−23523
liquid, migration mechanism of approaching particles, energy transfer, luminesc. quenching study 80−100343
lone-pair semiconductor, defects, valence-alternation model and new directions 80−54646
Long-range energy transfer in systems of different dimensions 78−27283
luminescence, $AgNO_3$ heavy atom effect, donor-acceptor interaction *(German)* 78−84651
luminescence spectroscopy, VUV time and energy resolved, system using synchrotron radiation excitation 78−65982
malachite green, luminesc. decay kinetics on ps time scale 79−19916
manganese minerals, photoluminesc., cryst. field theory *(Russian)* 78−84654
metal, laser irradiated, optical and electronic emissions *(French)* 80−2919
metal oxide:U^{6+}, luminesc. sensitivity to vibrational fine structure 78−6772
metal oxides, mixed, luminesc., of U^{6+} 79−33765
metaphosphate glass: Ag dosimeter, optical absorpt. and radiophotolum., effect of temp. 78−40333
metaphosphate glass: Nd^{3+}, Yb^{3+}, luminesc., energy transmission and migration between Nd^{3+} and Yb^{3+} 80−66297
metaphosphate glasses with Ag activator, radiophotoluminesc. 79−38596
2-methylchromone, solns., pH dependent fluorescence spectra, pK_a and tautomerism 79−59506
methylcyclohexane, γ-irrad., isothermal luminesc. decay, temp. depend. 79−66322
methylcyclohexane glasses, γ-irradiated in presence of naphthalene, isothermal luminesc. 80−93388
3-methylpentane glasses, γ-irradiated in presence of naphthalene, isothermal luminesc. 80−93388
micellar aggregate, solubilisation parameters and dynamics, photoluminescence obs. 79−79297
micelle-confined molecules reaction, diffusion-controlled, luminesc. quenching, excimer form. 80−50890
microspecimens obs., with size ≥0.8 mm, installation for 300 to 1100 mm range 80−57381
Migration of the excitation energy in luminescent media 78−27280
minority carrier recombination at surfaces, dislocations and microdefects, luminesc. evaluation 78−6769

photoluminescence continued
molecular crystal, coherent pairing of excitons in reson. EM field, biexciton spectra 77−47736
molecular crystal, sensitised luminesc. calc. for trapping models using momentum-space theory of exciton transport 80−11447
molecular crystal, surface exciton levels, radiation corrections 80−34962
molecular crystal with impurities, nonequilib. phonon excitation by laser pumping *(Russian)* 79−38664
molecular excited state relaxation processes, oscillatory versus dissipative limits, education appl. 80−31468
3-monomethylamino-N-methylphthalimide solns., fluoresc. and excitation spectra 79−61425
multilayer epitaxial heterostructures, use of two-photon absorption in study 79−8185
naphthalene:β-naphthyl-n-biphenyl-ethylene, relax. time of vibr. levels of ground state *(Russian)* 77−44054
naphthalene:anthracene, cryst. energy transport and luminesc. at room temp. and 4.2K 79−56828
naphthalene:benzofuran, luminescence spectra and intensity, 1.6-77K 79−87477
naphthalene:indole, luminescence spectra and intensity, 1.6-77K 79−87477
naphthalene:thionaphthalene, luminescence spectra and intensity, 1.6-77K 79−87477
naphthalene, microcryst. and evaporated film, excimer emission 80−2823
naphthalene, pure and doped, exciton-phonon luminesc. 80−84773
naphthalene anthracene doped, decay times and diffusion coeffs. of singlet excitons, under press. 77−20911
naphthalene-d_4(d_8) crystal, with isotopic impurities, Rashba effect, luminescence spectra, impurity states 80−29768
naphthalene-triethylamine exciplex, effect of dipolar molecules on quenching curves 78−52551
naphthalenes, phonon satellite narrowing in local exciton luminesc. *(Russian)* 79−47507
1,8-naphthoilene-1′,2′-benzimidazole-phenylimide of 4-aminonaphthalic acid luminophor mixture *(Russian)* 79−47514
nitrate glass: Eu^{3+} struct. reorganisation in glass transition interval, polarised luminesc. obs. 80−45141
NMR under optical pumping conditions 80−25253
noncrystalline materials, optical spectroscopic anal. *(French)* 77−77284
nonequilibrium free carrier distrib. in EM wave field, luminesc. intensity and IR scatt. cross section 79−69888
nonequilibrium thermodynamics of luminescent processes in solids 80−50435
nonresonance interaction parameters of rare earth ions, luminescence kinetics obs. *(Russian)* 78−31246
nonresonant transfer of energy between impurities in solids 78−23520
nucleic acids and related compounds, photoemission rel. to absorpt. and luminesc., 120 to 250 nm 77−81466
1,3,5,7-octatetraene, UV, visible, and fluoresc. spectra and assignments, evidence for ^1A_g state 78−33518
OEBBA, polarised luminesc. 77−24897
one-dimensional systems, luminesc. props., nonradiative excitation energy transfer effects 79−19915
open photoreceiver, vacuum ultraviolet 80−52307
optical fibre, neutron and gamma induced transient absorpt. and luminesc. 80−58763
organic glass, electron-cation recombination; charge distrib. simulation and luminesc. kinetics 80−2855
organic luminophores, luminesc. under action of atomic H *(Russian)* 79−8177
orientation factor in conc. effects due to nonradiative energy transfer 80−25425
orthovanadates, rare earth activated, spectroscopic props. 77−16363
oxide:U^{6+}, struct. sensitivity of luminesc. 77−90187
oxide glass:Cr^{3+} absorption and emission 78−6774
oxide semiconductor crystals, with forbidden energy gap, review of spectroscopic props. 78−2876
p-n junction, luminesc. due to photoinduced injection 78−10939
p-type epitaxial layer, thermalisation of electron-hole plasma, photolum. meas. 78−80408
partially oriented molecules, uniaxial, two-photon processes, polarised spectrosc. 80−74209
pentacene, laser fluoresc. of mol., excitation bandwidth and optical dephasing 79−36679
pentacene films, luminesc., struct. 80−11461
perfect crystals, low-temp. exciton luminesc. 79−56826
perylene in n-alkane, zero-phonon lines in luminesc. spectra 78−56512
perylene-N,N-dimethylaniline exciplex, effect of dipolar molecules on quenching curves 78−52551
phenyl methacrylate copolymers, photoluminescent behaviour 80−25432
pheophytin solutions, photolum. of singlet O_2 78−80831
phonon spectroscopy, phonon pulse spatial, spectral and temporal evolution 78−34580
phonon spectroscopy, phonon pulse spectral distrib. 78−34579
phonon spectroscopy, spectral, spatial and temporal 78−83892
phonon-assisted radiative transfer 77−90192
phosphate glass: Nd^{3+}, miniature laser with high ion conc., luminesc. charcts. 80−19038
phosphate glass:Ce^{3+},Tm^{3+}(Tb^{3+}), temp. depend. of energy transfer $Ce^{3+}\rightarrow Tm^{3+}$, $Ce^{3+}\rightarrow Tb^{3+}$ 77−24882
phosphate glass:Nd^{3+}, giant laser pulse-induced luminesc., spectral shape temp. depend. *(Russian)* 77−19257
phosphate glass:Nd^{3+}, highly conc., electron energy deactivation and transfer *(Russian)* 80−29802
phosphate glass:Nd^{3+}(Yb^{3+}), nonresonance interaction parameters of rare earth ions, luminescence kinetics obs. *(Russian)* 78−31246
phosphate glass:Yb^{3+}, excitation migration in inhomogeneous line profile, energy gap depend. 80−7407
phosphate glass:Yb^{3+}, luminesc. band struct., chronoscopic study at 4.2K 80−60663
phosphate glass:Yb^{3+}, migration of electronic excitations, manifestation in reson. luminesc. 77−8642
phosphate glass, Nd^{3+} frequency selection by monochromatic laser excitation at resonant transition *(Russian)* 79−78747
phosphate glass Mn^{2+}, luminesc. colour change 80−7392
phosphate laser glasses, review 80−9888
phosphors, containing O, intensity relation between synchronous and delayed luminesc. 78−10952
phosphors, quantum efficiency meas. 77−41699
photographic emulsion, luminescence rel. to latent image 80−73498
photoluminescence continued
picosecond interactions, book contrib. 77−65057
pigment associations, conc. effects, luminesc., absorpt. spectra and dichroism obs. 80−1007
plagioclase:Mn^{2+}(Fe^{3+}), ligand field bands of impurity luminesc. centres and their site occupancy 78−88350
plastic scintillators, radioluminesc. absolute output following ^{60}Co γ-ray irrad. *(Russian)* 78−92124
poly-N-vinyl carbazole, pulsed laser excitation, time resolved fluoresc., 80−89041
polybutylene terephthalate film, photoluminesc. exam. 78−48213
polyethylene terephthalate film, photoluminesc. exam. 78−48213
polymer chains with rigid bonds, local relax. times, mol. dynamics study *(Russian)* 80−59373
polymer network systems, intramol. mobility, polarised luminesc. obs. *(Russian)* 77−42455
polymer orientation measurement, in solid, by spectroscopic techniques, mech. anisotropy 78−75558
polymethacrylic acid network systems, intramol. mobility, polarised luminesc. obs. *(Russian)* 77−42455
polymethine dye solutions, photochem. transformations and short-wavelength luminesc. 80−100686
polymethine dyes, mol. struct., lasing props. 79−3693
polymethine dyes, secondary luminesc. 79−99934
polymonochloroparaxylylene film, photoluminesc. exam. 78−48213
polynuclear aromatic hydrocarbons, analysis by X-ray excited optical luminescence technique 80−66891
polyparaxylylene film, photoluminesc. exam. 78−48213
polyvinylcarbazole, exciton migration, luminesc. and quenching *(Russian)* 77−36275
porous Vycor glass, quenching by O_2 and NH_3, photoluminescence obs. 80−93773
ps reversible isomerisation kinetics, O_2 quenching obs. 79−5133
pulsed proton radioluminescence in binary liquid scintillators 79−52731
pyrene, in cyclohexane soln., triplet state decay consts. by sampling flash apparatus 79−51998
pyrene, luminescence of free and self-trapped excitons 80−108250
pyrene, perylene doped, decay times and diffusion coeffs. of singlet excitons, under press. 77−20911
pyrene in diphenyl cryst., luminesc. polaris. to induce radn. at O-O transition freq. *(Russian)* 79−38663
pyrene-triethylamine exciplex, effect of dipolar molecules on quenching curves 78−52551
pyridinium tetrachloromanganate II, luminesc. spectra, expt. and calcs. *(French)* 78−10967
quantum and radiant efficiency meas. methods, standard materials 78−32899
quartz:Cu, glassy and cryst., luminesc. centres 77−4679
quartz:Mn, X-ray and thermally stimulated luminesc. *(Russian)* 78−84626
quartz, luminescence centres at 396 and 280 nm 80−103996
quartz, photoelectric and photoluminescent props. in fundamental absorpt. region 78−39596
radiative electronic transitions of impurities, effects of hydrostatic press. 80−11446
radiophotoluminescence detector reading device, glasses for fluoresc. standards 77−67944
Raman scattering, luminesc., electron-phonon interaction effects on polarisation 80−55088
Raman spectroscopy, luminesc. rejection 77−18100
Raman-luminescence problem, interference analogy and expt. discrimination by polarisation correl. 79−95764
rare earth double orthophosphates with alkali metals, conc. depend. of luminesc. props. 80−100673
rare earth double orthophosphates with alkali metals, spectroscopic obs., struct. and chem. nature 80−100674
rare earth germanates, R_2O_3-GeO_2 system cpds., physicochem. charcts. 80−97469
rare earth laser materials, linear conc. quenching of luminesc. 79−31908
rare earth luminescence, relaxation phenomena, book contrib. 77−32439
rare earth luminescence from intensity meas. on powdered phosphor screens self-concentration quenching mech. determ. 79−69880
rare earth niobates, with fergusonite struct., model of energy transfer processes 77−4670
rare earth oxyhalides and oxysulphides, thermochromic luminescent mats. *(Russian)* 78−48230
rare earth oxysulphides and oxyhalides, Tm^{3+}, Tb^{3+}, Eu^{3+} activated, thermochromatic luminophors, lumines. spectra rel. to temp. 79−56849
rare earth phosphates:Eu, electronic-vibr. spectra rel. to struct. 79−56850
rare earth stoichiometric cpds., reson. energy transfer 79−99930
rare earth tetracyanoplatinates, energy transfer from linear stacks of donors 78−68546
rare earth vitreous dielectric, electronic energy transfer to impurity OH^-, luminesc. kinetics *(Russian)* 79−47509
rare earths, trivalent, 5d states charge transfer and intershell spectra, separation and overlap 78−10966
recombination interactions, unimolecular processes, diffusion-limited kinetics 78−6794
recombination kinetics, subject to allowance for correl. between particles 80−80858
relaxation between systems with equidistant levels *(Russian)* 78−23526
resonance Raman scattering and luminescence of excitons in self-trapping process 80−20689
resonant optical excitation, luminesc. rel. to light scattering *(Japanese)* 80−84781
resonant scattering of light by slowly fluctuating localized electrons 80−7365
retinals, prod. and quenching of singlet oxidation 80−35840
rhodamine 6 Zh solution, radiant transport effect on luminesc. duration 80−103995
rhodamine 6G molecules in solution, photoluminescence study, fluorescence decay time 80−80832
rhodamine 6G, blue and UV luminesc., obs. and mechanism 79−3486
rhodamine 6G, in glycerine-water solns., anti-Stokes fluoresc., conc. quenching 79−24349
rhodamine 6G, in organic solvent, hot luminesc. 79−4842
rhodamine 6G and rhodamine B adsorbed on AlH_3, luminesc. spectra during AlH_3 photolysis 80−55171
rhodamine 6G soln. in ethanol, luminesc. liq., pump radiation conversions to enhance laser efficiency 80−48293

photoluminescence continued
rhodamine B, in glycerine-water mixtures mol. agglomeration effect on fluoresc. polaris. spectrum 78−25595
rhodamine dye polar frozen solns., luminesc. broadening 80−2834
rhodamine G solutions, LiCl and $NaClO_4$ electrolyte influence on its lasing props. 80−91788
rhodamine solns., short-wavelength luminesc. 79−78738
rubidium uranyl propionate, low temp. absorpt., luminesc. spectra, intermol. interactions 80−2830
ruby:Cr^{3+}, diffusion of localised optical excitations and trap emission 77−24887
ruby, cryst., lasing action, spectrum, luminesc. spectrum effects *(Russian)* 78−13716
ruby, energy transfer time const. between single Cr^{3+} and Cr^{3+} pairs 79−38627
ruby, excited state spin-phonon interaction, time resolved spectroscopic exam. 78−19549
ruby, ground state of Cr(III) pair 79−33782
ruby, high energy phonon spectroscopy 78−83893
ruby, luminescence, red emission intensity at various temps., mag. field depend. 77−32423
ruby, nonequilibrium luminesc. of hot electrons, nonradiative transition probability 77−32436
ruby, resonance radiation transfer and nonequilibrium phonons *(Russian)* 78−80418
ruby, resonantly trapped 29 cm^{-1} phonons, spectral diffusion 78−92113
sapphire, luminesc. of F centre 79−73990
sapphire, neutron bombard., F-centre fluorescence, photoluminescence 80−100676
sapphire, pure and doped, luminesc. centres 79−33791
scintillator systems, liq., organic, energy transfer, fluoresc. intensity-max. solvent depend. 78−21966
semi-infinite direct-gap semiconductor effect of reabsorbed recombination radiation 78−95312
semiconductor, biexcitons, one-photon radiative recomb. 80−70621
semiconductor, bound excitons, review, book contrib. 80−44519
semiconductor, broad-band, meas. setup with GDM 1000 grating double monochromator 78−21226
semiconductor, donor-acceptor pair luminesc. polarisation with optical orientation 77−24895
semiconductor, excited by strong EM wave, self-polarisation of nonequilib. electrons 77−69910
semiconductor, high intensity photoexcitation, hot electrons and phonons 78−26905
semiconductor, highly excited states, ps spectroscopy 77−48245
semiconductor, luminescence in presence of intense laser field 79−38621
semiconductor, optical and IR characterisation 79−95846
semiconductor, optical parameters in strong EM field, effects of finite wavelength of light 77−44050
semiconductor, optical props. under intense laser field 79−43040
semiconductor, optical props. under intense laser fields 78−72513
semiconductor, photo-excited electron momentum distrib., hot luminesc. polarisation 77−16396
semiconductor, photoexcitation phenomena, low density 78−27319
semiconductor, photoluminescence, deep level recombination temp. depend. 79−47497
semiconductor, photoluminescence, temp. modulated 79−38623
semiconductor, polariton dispersion change by virtual biexciton form. under laser irrad. 79−38607
semiconductor, radiative spectra from hot photocarriers 78−31249
semiconductor, recomb.-enhanced defect reactions 77−51377
semiconductor, resonance secondary radiation emission, theory 78−60452
semiconductor, temp. modulated photolum. induced by photoexcitation 78−95605
semiconductor, variable band, recomb. radiation polarisation oscills. in mag. field *(Russian)* 77−77283
semiconductor, variable-gap, photoluminesc. 78−48222
semiconductor, variable-gap, with high band-gap gradient, charact. of radiative recomb. 79−56858
semiconductor, wurtzite-type, emission lineshape of excitonic mols., polariton states 77−20918
semiconductor alloys, reson. light scatt., luminesc. and Raman spectra 79−38615
semiconductor crystals, with high quantum efficiency, minority carrier lifetime meas. *(Japanese)* 80−54711
semiconductor electron-hole pair creation and migration 77−77304
semiconductor epitaxial layers, varizonal, parameter determ. by photoluminescence method *(Russian)* 80−108291
semiconductor film, electron spin orientation in quantum size effect conditions 78−68575
semiconductor heterostructure, multipass, effective lifetime of nonequilibrium carriers 78−6435
semiconductor layer structure, laser-induced photolum. and collective effects *(Russian)* 79−95830
semiconductor layers, direct gap, optical compensation profiling 77−76450
semiconductor optical characterization 80−50352
semiconductor-metal structure, luminesc. due to photoinduced injection 78−10939
semiconductors, amorphous, luminescence 80−80862
semiconductors, exciton and domain luminesc., book 80−82588
semiconductors, heavily doped, compensated, long wavelength recomb. radiation 80−7403
semiconductors, intervalley electron-electron scattering effect on optical transitions 80−108267
semiconductors, luminesc. parameters, absorpt. parameter effects *(Russian)* 78−80419
semiconductors, p-type, mag. oscills. of momentum distribution of hot photoexcited electrons *(Russian)* 80−2854
semiconductors, PH luminescence band profile 80−20702
semiconductors, phonon replicas of bound exciton recombination 79−52008
semiconductors, photoluminescence in crossed electric and magnetic fields 79−11464
semiconductors, quasi-equilib. approx. 80−84779
semiconductors, radiative recomb., book contrib. 80−84784
semiconductors, radiative two-electron transitions 79−43026
semiconductors, spin-depend. luminescence of donor-acceptor pairs 77−48223
semiconductors, variable gap thin structs., radiative recomb. photoluminesc. spectra 79−43036
photoluminescence continued
semiconductors, variable-gap, photoluminesc. under transient excitation conditions 80−20698
sensitised anti-Stokes luminesc., theory 77−66537
serum albumin, human, mechanism of eosin-sensitised photochemiluminescence 79−53044
β-SiC, optical quenching of luminesc., acceptor ionisation energy 80−55178
silica glass:Nd^{3+}, laser-spectroscopic method, for studying solids with nonuniform spectral broadening *(Russian)* 79−40630
silicate galss:Eu^{3+}, fluoresc. linewidth variation, electron-phonon coupling 78−19531
silicate glass: Cr^{3+}, optical props., 88-273K, energy levels in crossing region 78−6709
silicate glass: Er^{3+}, $^4I_{13/2}$ level relax. 79−87476
silicate glass:Tb^{3+}, photoluminesc. and optical absorption spectra 79−19919
single crysts. and thin films, absorpt. edge temp. depend., gap energy changes 79−42991
small-polaronic glass, dynamics of optically induced props. 80−49630
sodium uranyl acetate (deuteroacetate) 80−2830
solid, hot luminescence and relaxation processes in resonant secondary emission 78−52549
solution, photolum. quantum yield of primary light absorbers and nearest neighbours 77−52148
solution, photoluminesc., decay and self depolarisation 79−24351
solution, rigid, luminesc. exchange promotion kinetics 80−50387
solutions, photoluminesc. decay time, donor conc. effect 80−66299
spectroscopy using Weierstrass sphere geometry 77−49777
steel, trace element UV emission, spectrochem. anal. *(French)* 80−71997
stilbene, single cryst. under pulsed electron excitation, triplet exciton luminescence and opt. absorpt. 79−7838
strain-confined electron-hole liquid, lifetime and radiative efficiency vs density 79−38000
superionic conductors, transitions, structures, dynamics and spectra, review 79−60549
tetracene, excimer luminesc. spectra, 4.2-300K 79−87478
tetracene, optical obs. of charge transfer 78−35199
tetracene, photoluminescence spectra, 4.2-300K, phase transition and excitons 79−4847
tetracene, spatial distrib. of electrolum. and recomb. process 79−19938
tetracene surface states, electric field effects, exciton-charge carrier interactions *(Russian)* 80−24989
1,2,4,5-tetrachlorobenzene, localised excitations thermal promotion to exciton band, impurity states effect 78−52539
tetraethylammonia iodide:Pb, spectra of diffuse reflection and photoluminesc. *(Russian)* 79−11447
3,6-tetramethyldiamino-N-methyphthalimide, in organic solvent, hot luminesc. 79−4842
1,1,4,4-tetraphenyl-1,3-butadiene, photoluminesc., degree of polarisation 79−21803
three component system, nonradiative energy transfer parameters 78−27292
time-dependent resonant secondary radiation spectra *(Russian)* 78−48228
transient resonant secondary emission spectra, theory 79−56827
transition metal complexes, excited states geometrical parameters, Franck-Condon anal. 77−27047
transition quasilinear spectra of resonant secondary emission *(Russian)* 80−16102
trap depths, appl. of thermodynamics of single particle *(French)* 77−77264
trap dynamics rel. to minimum entropy prod. *(French)* 77−77263
trialkylammonium, iodides, absorpt. and luminesc. spectra of self-localized excitons 80−97340
triboinduced luminescence 78−19581
trypsin, photoluminescence after UV irradiation *(German)* 79−92137
tungstates:Eu, electronic-vibr. spectra rel. to struct. 79−56850
ultrahigh vacuum setup for photo- and thermostimulated electron emission and luminesc. obs. *(Russian)* 80−66383
uniaxial crystal, macroscopic exciton luminesc. charact., high reabsorption conditions 78−19545
uniaxially compressed crystal, exciton molecule radiation *(Russian)* 80−108264
up-conversion and excited state energy transfer in rare earth doped materials, book contrib. 77−36296
uranates, luminesc. 79−33765
vacuum UV laser possibility for crystals pumped by X-ray synchrotron radiation 79−41387
variable gap semiconductor, photolum. emission and excitation spectra 78−76526
variable-gap semiconductors, anal. of drift of recombination radiation 80−16096
X-ray phosphors and screens based on compounds activated with rare-earth elements 79−8169
zircon, natural and synthetic crysts. Hf and Tb activated, capture centres and luminescence mechanism *(Russian)* 77−28626
$_2$, photoluminesc. spectrum, ^{31}P Fermi interaction, hyperfine struct. 78−33536
Ag halide, visible luminescence obs. at or below 77K 80−108263
Ag halide emulsions, primitive and $AgNO_3$-digested, IR luminescence obs. at 77K 80−103983
AgBr, and $AgBr_{1-x}I_x$, photolum. and X-ray luminesc. spectra *(Russian)* 79−2867
AgBr, Bose-Einstein condensation of triplet excitons 77−44057
AgBr, decay of proposed Bose-Einstein condensed excitons 78−15221
AgBr, EPR of excitons, detected in X-ray excited luminesc. spectra at 4K 77−55732
AgBr, electron-hole liq. and biexciton pocket, luminesc. obs. 78−15216
AgBr, evidence for excitonic mol. 77−8633
AgBr excitonic mols., time-resolved luminesc. line obs. 77−69888
AgBr film coatings, luminesc. props. for H_2 and other reduction sensitisation 79−61886
AgBr, highly excited, time resolved luminesc., recomb. of excitonic mols. 77−69889
AgBr, indirect near edge emission, 1.5-50K 77−16380
AgBr, luminescence of photographic emulsions sensitised by 1,1'-diethyl-2,2'-cyanine with Ag_2S clusters *(Russian)* 80−73513
AgBr microcrystals, spectrally sensitised, luminesc., effect of hydrophobic organic compounds 80−97331

photoluminescence continued
AgBr, new shoulder in luminesc. spectra, triplet excitons 80−20706
AgBr, one-phonon sidebands, rel. to anal. of 4.4K neutron scatt. data 77−39643
AgBr, photoluminesc. study of excitons in high mag. fields 80−80843
AgBr, shoulder in luminesc. spectra due to triplet excitons 79−15525
AgBr, time resolved luminesc. spectra at high excitation density 79−78751
AgBr:Cl, exciton-phonon interaction, reson. Raman scatt. vs photolum. 80−29798
AgBr:Cu^{+}(Cu^{2+}), luminesc., ion interactions 77−66534
AgBr:I, activator luminesc., energy model 79−28808
AgBr:I, isoelectronic trap 79−43016
AgBr:I emulsion, photocond. and luminesc. at −186°C, rel. to incident light intensity 78−64063
AgBr:I^{-}, emission spectra at 4.2K 79−4841
AgCl, and Br doped, EPR of excitons, detected in X-ray excited luminesc. spectra at 4K 77−55732
AgCl, cryst. luminesc. and photovoltaic effect kinetics 78−64391
AgCl, luminesc. excited by UV radiation at 80K *(Russian)* 78−31256
AgCl, optically detected EPR of excited states rel. to luminesc. 77−12256
AgCl, photoconductivity and photoluminesc., 6.8 to 80K, exciton and valence band states 77−43644
AgCl, photolum. and X-ray luminesc. spectra *(Russian)* 79−2867
AgCl:Cu^{+}(Cu^{2+}), luminesc., ion interactions 77−66534
AgCl:Ni, optically detected double resonance, radiative recombination electron traps 80−20518
AgGaSe, direct gap semicond., exciton energy at 300K from reabsorption of luminesc. 79−78728
$AgGaSe_2$, two-photon absorpt. and short pulse stimulated recombination 80−89054
Ag_2HgI_4, preparation, optical and luminescence spectra 80−104064
β-AgI, exciton luminesc. of 2H and 4H polytypes 77−85783
AgI large single crysts., gel and soln. growth and props. 80−35071
β-AgI, luminesc. of 2H- and 4H-polytypes 80−2843
$AgNO_3$, soln., visible luminescence obs. at or below 77K 80−108263
$AgNO_3$-Ag_2S system, visible luminescence obs. at or below 77K 80−108263
Ag_2O, exciton luminesc. spectra, mag. field influence 80−80860
Ag_2S sols, red-IR photoluminescence obs. at 77K 80−103982
Al, anodic oxide layers, meas. of growth by photoluminescence, description of equipment 79−52511
Al anodisation, 'flaw-free' film growth and luminesc. characterisation 78−15605
Al, anodisation, intensity of luminesc. and film thickness 78−80413
Al-Mn, anodisation, intensity of luminesc. and film thickness 78−80413
AlAs-GaAs, heterostructure electroluminesc. characts., active region electron density depend. 77−12446
AlAs-GaAs double heterostructure, effective lifetime of nonequilibrium carriers 78−6435
AlAs-GaAs monolayer crystal, two-photon absorpt. spectrum 78−52589
AlAs-GaAs multipass heterostructure, spectral and ang. charact. of luminesc. 77−20418
AlAs-GaAs multipass heterostructure 77−20419
AlAs-GaAs:Ge double heterojunctions, efficiency of radiative recombination 77−77286
(AlGa)As DH, proton-striped, proton-induced defects, photoluminesc. study 80−48251
AlGaAs DH, temp. depend. of intensities and times of radiative transitions 79−38660
AlGaAs heterojunctions, nonradiative recomb. vel. estimate from edge luminesc. props. 80−65668
(AlGa)As heterostruct., proton irrad., photoluminesc. 80−29808
AlGaAs layer, epitaxial, grown from pre-heated Ga soln., photolum. study 78−39591
p- (AlGa)As:Zn, MBE grown, elec. props., shallow junction solar cell use 79−91175
AlGaAs-GaAs heteroepitaxial wafers, Mg doping, surface morphology and photoluminesc. props. laser applics. 77−3591
AlGaAs-GaAs heterostructures, luminescent characts., efficiency and radiative lifetime conc. depend. 80−55151
$Al_xGa_{1-x}As$ DH, origin of $n \simeq 2$ injection current, photolum. expts. 78−14799
$Al_xGa_{1-x}As$ DH lasers, deep-level luminesc. 79−65913
$Al_xGa_{1-x}As$ DH p-n junction, surface recomb. effects on current, luminesc. expts. 78−72246
p-$Al_xGa_{1-x}As$, DH under optical orientation conditions, diffusion of spin labelled electrons 77−8189
n-$Al_xGa_{1-x}As$, epitaxial, photolum. emission and excitation spectra 78−76526
$Al_xGa_{1-x}As$ film, hot photoluminescence spectrum, polarisation depend. 78−31254
$Al_xGa_{1-x}As$ grown by organometallic VPE, luminesc. efficiency 79−78892
$Al_xGa_{1-x}As$, indirect, exciton-phonon coupling, photolum. meas. 79−47511
n-$Al_xGa_{1-x}As$, ion implanted films, optical and luminesc. props. 80−60699
$Al_xGa_{1-x}As$ MBE layers, ionized beam doping, elec. and optical characts. 79−37721
$Al_xGa_{1-x}As$, optically magnetised, luminescence polarisation anisotropy, hysteresis effect symmetry props. 80−34982
$Al_xGa_{1-x}As$, organometallic VPE growth, and characterisation 79−78899
$Al_xGa_{1-x}As$ p-n junction, photolum. and current, interface recomb. effects 78−95346
$Al_xGa_{1-x}As$, p-n junction solar cells, effect of interface recombination on photoluminescence and current 80−93893
$Al_xGa_{1-x}As$, pure and Ge doped, shallow acceptor photoluminescence 80−76064
$Al_xGa_{1-x}As$, VPE growth and characterisation 78−35315
$Al_xGa_{1-x}As$ variable gap thin structs., radiative recomb. photoluminesc. spectra 79−43036
n-$Al_xGa_{1-x}As$, variable-gap solid solns., diffusion length, photolum. meas. 79−38659
p-$Al_xGa_{1-x}As$:Be layer, MBE growth, Be doping and diffusion, elec. and optical props. 77−51397
$Al_xGa_{1-x}As$:Cr, deep level props. 79−69465
$Al_xGa_{1-x}As$:Cr, exptl. verification of Cr^{2+} models of photoluminescent transitions 78−27320
photoluminescence continued
$Al_xGa_{1-x}As$:Cr, high resist. film, photolum. and photocond. meas. 78−72596
$Al_xGa_{1-x}As$:Cu, variable-gap semicond., impurity props., carrier recomb. 80−96907
$Al_xGa_{1-x}As$:Ge(Te)(Zn), photo- and cathodolum., comp. depend. *(Russian)* 77−48215
$Al_xGa_{1-x}As$:N, ion implantation, in situ annealing photoluminesc. obs. 80−10567
$Al_xGa_{1-x}As$:N, photolum. excitation spectra 77−63451
$Al_xGa_{1-x}As$:N, photoluminesc. and optical absorpt. spectra of N impurity bound-excitons 79−47496
$Al_xGa_{1-x}As$:N^{+}, (x=0.58), laser annealing of optically active impurities, photolum. charact. 80−20682
$Al_xGa_{1-x}As$:O-n-GaAs heterojunction for MIS device, capacitance voltage meas. 79−87157
$Al_xGa_{1-x}As$:Sn(Te)(Ge), anneal-induced defects, photoluminesc. obs. 79−61422
$Al_xGa_{1-x}As$-GaAs, quantum-well MO-CVD heterostructure lasers, band-filling props., photolum. spectra 79−22954
$Al_xGa_{1-x}As$-GaAs heterostructure, effect of photon recycling on diffusion length and internal quantum efficiency 77−39929
$Al_xGa_{1-x}As$-GaAs heterostructure photoluminesc., origin of large dark spots 77−85763
$Al_xGa_{1-x}As$-GaAs heterostructures, nonradiative large dark spots exam. 78−23149
$Al_xGa_{1-x}As$-GaAs quantum-well heterostruct., exciton in recomb. 80−103990
p-$Al_xGa_{1-x}As$-n-GaAs heterojunction solar cells, optical characts. study 77−24609
$Al_xGa_{1-x}N$ epitaxial layers, growth and props. 79−11522
$Al_{2x}Ga_{2(1-x)}O_3:Cr^{3+}$, luminesc., lifetimes 79−33784
$Al_xGa_{1-x}P$, photoluminescence excitation spectra, bound excitons, Al conc. depend. 80−20687
AlGaSb, growth and characts. for 1.0-1.8 μm heterojunction devices 78−6870
$Al_xGa_{1-x}Sb$, photolum. intensity increase due to composition variation 79−15528
$Al_xGa_{1-x}Sb$, solid soln., depend. of forbidden-band width on composition 78−39602
$Al_xGa_{1-x}Sb$, soln.-grown, photolum. 80−71476
$Al_xGe_{1-x}Sb$, photolum. spectra 78−95602
AlN, luminesc. excitation spectrum and band struct. 80−84783
AlN:Mn, vol. and surface excited luminesc. 79−38630
AlN:Mn(Eu), luminescence at high excitation levels with and without doping 77−1721
AlN:O, influence of O on luminesc. excitation spectrum in interband transition range 77−8644
AlN:O, UV spectra of deep impurity centres, radiative recombination 79−87490
$AlNbO_4$, diffuse refl. and luminesc. spectra 78−56516
Al_2O_3, anodic oxide films, luminesc., breakdown and colouring 78−19528
α-Al_2O_3, crystal defects from X-ray irradiation, F-centres, X-ray luminesc. obs. 80−55176
α-Al_2O_3, defects in unirradiated cryst., optical absorpt. spectra 79−61409
Al_2O_3, optical props. of F-centre 79−43003
α-Al_2O_3, polarised luminescence in neutron- and proton-irradiated single crystals 80−66271
α-Al_2O_3 recombination luminescence excitation by synchrotron radiation 79−95841
α-Al_2O_3, recombination luminescence mechanism 80−71477
Al_2O_3:Eu, surface luminesc. centres excitation charcts. 78−52560
Al_2O_3:Mg, pure and doped, recombination luminesc. spectra 79−83021
Al_2O_3:Si, Ti, pure and doped, luminescence, optical absorpt. and colour centres 79−87501
α-Al_2O_3:V^{3+}, near IR spectra, line lifetime, 2, 10, 77K 78−10972
β-Al_2O_3-Na_2O:Fe, coordination site, oxidation state, Mossbauer, absorpt., emission spectra, mag. susceptibility meas. 78−68431
$AlPO_4$:Fe^{3+}, luminesc. emission and excitation spectra 79−69873
Al_2TeO_6:U^{6+}, luminesc. spectrum 79−56845
$AlVO_4$, luminesc. spectrum 79−56846
$Al_2(WO_4)_3$:Cr(Eu), and undoped crystals, luminesc. obs. 80−89047
Ar, cryst., luminesc., absorpt. spectra, free, self-localised excitons coexistence *(Russian)* 78−31231
Ar, optical absorpt. and luminesc. spectra, obs. of relaxed exciton states 77−52082
Ar:Eu, matrix isolated, obs. of Stokes and anti-Stokes vibrational sidebands in emission spectra 77−73164
Ar:N_2O, O(^{1}S) photodissociative prod., photoluminesc. excitation spectra, exciton energy transfer 80−89508
Ar:O_2(N_2), long-wave UV luminesc. *(Russian)* 78−88347
Ar:OCS, O(^{1}S) and S(^{1}S) photodissociative prod., photoluminesc. excitation spectra, exciton energy transfer 80−89508
ArO, in doped inert gas matrix, photoluminesc. 79−31579
ArS, photoluminesc. in rare gas matrices 80−5568
As, amorphous, bulk and sputtered thin films 80−25457
As chalcogenides, deep levels, photoluminesc. and photocond. 80−70641
As-Se glasses, low temp. photocond., complementary nature of photocond. and photolum. 80−49808
As_2S_3, amorphous, band to band radiative recomb. 80−25435
As_2S_3, amorphous, charged defect pair photolum. meas. 80−16078
As_2S_3, amorphous, luminesc. and optically detected ESR, photoinduced struct. change 80−50399
As_2S_3, amorphous, quantum efficiency and fatiguing behaviour of luminesc. processes 80−7402
As_2S_3, amorphous, time resolved spectroscopy of valence alternation pair luminesc. 80−50400
As_2S_3, amorphous, time resolved luminesc. 80−66288
As_2S_3, amorphous, time-resolved photolum., spectrosc. 79−24360
a-As_2S_3, time-resolved photoluminescence study 80−89057
As_2S_3:Ag, vitreous, doping influence on photolum. at 77K 77−77293
As_2S_3:B glass, impurity effect on photoluminesc. and optically induced EPR 79−65918
As_2S_3:Fe glass, photolum. and ESR, Fe impurities as non-radiative recomb. centres 80−29788
As_2Se_3, amorphous, defect states, exptl. study. 80−54645
As_2Se_3, amorphous radiative interband recombination 80−66286
a-As_2Se_3, doped film, photoluminescence intensity and lineshape study 80−50448

photoluminescence continued
As_2Se_3 glasses, impurity effect on photoluminesc. and optically induced EPR 79−65918
As_2Se_3, neutrality of luminescence centres 78−88356
As_2Se_3:In, amorphous, photoluminesc. fatigue, metallic additive effect 79−61434
As_2Se_3:Tl, hole transport, photoluminesc. and photoinduced ESR 79−8183
$As_{50}Se_{50}$ and $As_{20}Se_{80}$ semicond. glasses, densified, photoluminesc., inelastic deform. effect 80−66293
AuBr, spectra and luminesc., 100 to 200K *(Russian)* 77−69911
$AuBr_3$, spectra and luminesc., 100 to 300K *(Russian)* 77−69911
AuCl, luminesc., excitons 80−2839
BH_x, photoluminesc. spectra 80−2815
BN, phosphided, spectra of products 77−12418
B_2O_3-SiO_2:Ce glasses, radiation resistance mechanism, optical absorpt. and luminesc. obs. *(Polish)* 79−86825
BP, cryst. growth from Cu-fluxed melt, and characterisation 77−85920
$BaAl_{12}O_{19}$:Mn, phosphor, vac. UV excitation spectra, appl. to gas discharge display 80−2816
$Ba_2CaTe_{1-x}W_xO_6$, tungstate luminescence 77−69904
Ba_2CaUO_6, luminescence and energy migration 79−4837
$BaCl_2$:Pb, absorption and emission spectra *(Russian)* 78−23527
$BaCl_2$:Pb crystal phosphor, emission spectra 80−66298
BaF_2:Gd^{3+} film, Gd^{3+} luminesc. spectrum and kinetics 78−6763
BaF_2:Tb^{3+}, cubic Tb^{3+} centres, energy level and cryst. field parameters 77−52181
BaFCl, luminesc. and ionic conduction 79−28829
$BaGd_4Si_5O_{17}$, cell consts., luminesc. of various rare-earth activators 80−93376
$BaMnF_4$, luminesc., emission from localised traps 79−33777
BaO, ground state vibr. pop. distribs. from photoluminesc. in Ba+O_2 and Ba+N_2O 77−34731
BaO, lowest triplet state, photoluminesc. optical-optical double reson. obs. 79−68254
BaO-Nd_2O_3-P_2O_5 ultraphosphate glasses, Nd^{3+} conc. quenching of luminesc. effect 79−19931
BaO-P_2O_5 glasses, Cu^+ ion electromigration at 400°C, luminesc. meas. 77−76610
$Ba_3(PO_4)_2$:Eu, X-ray phosphor, study of emission and trapping centres 79−8197
BaR_2O_4, luminesc. on activation by Eu^{3+}, Nd^{3+}, Eu^{3+}-Tb^{3+} 77−52156
BaS:Cu phosphor, photo- and electro-luminescence 79−43030
$Ba_5SiO_4Br_6$:Eu, blue emitting X-ray luminescent material for intensifying screens *(French)* 80−66260
$BaTiO_3$, intrinsic luminesc. 80−71467
$BaTiO_3$, pure and Fe doped, X-ray induced luminesc. 79−69885
$BaTi(PO_4)_2$, cryst., luminesc., struct. interpretation 79−47489
BaY_2F_8, energy transfer from Eu^{2+} to trivalent rare earth ion 79−91490
$BaY_4Si_5O_{17}$, cell consts., luminesc. of various rare-earth activators 80−93376
Ba_2ZnS_3:Mn, luminescent props. 77−77292
$Ba[Pt(CN)_4].4H_2O$, polarised time-resolved emission spectra 79−33811
BeF_2:Eu^{3+} glass, luminesc. of Eu^{3+}, transition probabilities 80−80845
Bi complex, $BiCl_7^{4-}$ in HCl aq. soln., photolum. excitation spectral charcts. by stroking method *(Russian)* 79−78753
Bi^{3+}, in soln., luminesc., halide ion effects 78−35187
$Bi_{12}GeO_{20}$:Dy(Ho)(Er), luminesc., emission and excitation spectra 80−103975
BiI_3, charcts. of low-temp. photoluminesc. 77−8646
BiI_3, doped, IR photolum. and EPR spectra 78−19558
BiI_3 single crystals, refl., absorpt. and photoluminesc. spectra, exciton transitions 77−52164
$Bi_{12}SiO_{20}$:Nd, light absorpt. and transmission spectra, photoluminescence spectrum, optical absorpt. coeff. 79−74001
$Bi_{12}SiO_{20}$:Nd, single cryst., photoluminesc. meas. *(Russian)* 78−23519
$Bi_2W_2O_9$, energy transfer and luminesc. props. 80−55177
$Bi_2W_2O_9$:Mo(Eu), energy transfer and luminesc. props. 80−55177
CC GaP, improvements in synthesis, solute diffusion (SSD) growth and characterisation 79−65992
CN, from IR photolysis of cyanomethane, photoluminesc. spectroscopy 77−73452
CO, cryst. at 5K, absorpt. and emission spectra, exciton interpretation 79−87481
CO^+, fluoresc. spectra of ion beam, laser and electron excitation 79−45743
CO-Ar, cryst. at 5K, absorpt. and emission spectra, exciton interpretation 79−87481
CO-Ne, cryst. at 5K, absorpt. and emission spectra, exciton interpretation 79−87481
C_3PbCl_3, single crysts., X-ray and photoluminesc., and reflection spectra 77−69896
Ca, flame luminesc., laser irrad. effects 77−77766
Ca_2, new ground state, photolum. obs. vibr. consts., dissoc. energy 80−5576
CaF_2, EXAFS, intrinsic UV luminesc. excitation spectra 78−52567
CaF_2:Co, X-irrad., luminesc. spectra 79−28801
CaF_2:Dy, TLD-200, thermolum. phosphor, photolum. and absorpt. spectra, thermolum. mechanisms 80−97321
CaF_2:Er, γ-irrad., photostimulated luminesc. meas. 77−66538
CaF_2:Eu_2, X-ray luminesc. 79−99933
CaF_2:Eu^{2+}, circular polarisation in luminesc. and optical orientation 78−6740
CaF_2:Eu^{2+}, energy transfer to luminesc. centres, pulsed excitation obs. 77−85781
CaF_2:Eu^{2+}, photoluminesc. mag. circ. polaris. 80−89056
CaF_2:Eu^{2+}, short high-energy pulse induced X-ray luminesc., anomalous kinetics 77−59608
CaF_2:Eu^{2+}, X-ray excited luminesc., $^5D_0$-$^7F_1$ transition 80−2842
CaF_2:Eu^{2+}, X-ray induced luminesc. kinetics, energy transfer processes 79−8181
CaF_2:Gd^{3+}, Mn^{2+}, photo- and radioluminesc. investig. of intracentric energy transfer 77−16378
CaF_2:Gd^{3+} film, Gd^{3+} luminesc. spectrum and kinetics 78−6763
CaF_2:Mn, low temp. X-irrad., Mn centres, optical absorpt. and emission props. 80−60635
CaF_2:Mn^{2+},Yb^{3+}, efficient luminesc. energy transfer from Mn^{2+} to Yb^{3+} 78−19536
CaF_2:Mn^{2+},Yb^{3+}, luminescent energy transfer efficiency obs. 78−6777
CaF_2:Na, tunable room temp. laser action of M-centres, luminesc. and absorpt. spectra 79−31907
photoluminescence continued
CaF_2:Pr^{3+}, laser selective excitation and energy transfer 79−38612
CaF_2:Sm^{2+}, luminesc. spectra, vibronic wing, 2K 79−8182
CaF_2:Sm^{2+}, pseudo-Jahn-Teller effect 79−69476
CaF_2:Sm^{2+}(Eu^{2+}), cubic crysts., vibronic spectra, induced dichroism method 77−81131
CaF_2:Tb^{3+}, cubic Tb^{3+} centres, energy level and cryst. field parameters 77−52181
CaF_2:Tb^{3+}(Eu^{3+}), one- and two-photon luminesc. excitation spectra 79−83023
CaF_2:Tm^{2+}, vibronic spectra and dynamics of impurity-contaiing lattice 79−1787
CaF_2:U, γ-irrad., EPR and luminesc. studies of U^{5+} and U^{6+} centres 79−51854
CaF_2:Yb^{2+}, cryst., stress polarisation of luminesc. and emitting states struct. 77−69897
CaF_2:Yb^{2+}, divalent ion radiative state, magneto-optical obs. 77−69893
CaF_2:Yb^{2+}, spectra, kinetics and polarisation of luminesc. 77−69892
CaF_2-YF_3:Nd^{3+}, selective excitation of activator centres, time resolved luminesc. 78−15223
CaF_2-YF_3:Nd^{3+}, spectral migration of electronic excitation, selective laser excitation *(Russian)* 78−80417
CaI_2:Pb(Mn), recomb. processes, luminesc. charcts. *(Russian)* 80−25450
$CaLaBO_4$, crystallographic and Pb^{2+} luminesc. data 79−32971
$CaLaGaO_4$:Eu^{3+},Bi^{3+}, luminesc. influenced by struct. transition 78−6773
$CaLaGaO_4$:Eu^{3+}(Bi^{3+}), luminesc. of α- and β-phases 77−90186
$CaLa_{1-x}Gd_xGaO_4$, ($0 \leq x \leq 1$), Gd^{3+} luminescence and cationic distrib. *(French)* 79−78734
$CaMoO_4$, luminesc. efficiency, temp. and high-press. 78−23507
$CaMoO_4$:Na(Y), pure and doped, luminesc. props., emission decay time 79−95835
CaO, electron irradiated, photocond. and luminesc. meas., F-centre electronic struct. determ. 78−6409
CaO, Eu, Eu^{2+} to Eu^{3+} charge transformation *(Russian)* 78−72403
CaO, undoped and Cl-, F- or Al-doped, X-ray and UV luminesc., electron-hole recombination processes *(Russian)* 78−76528
CaO:Bi^{3+}(Pb^{2+}), impurity centres vibronic spectra, lattice dynamics and electron-phonon interactions 80−7396
CaO:Eu,Tb phosphor emission under X-ray excitation 79−52011
CaO:F(Cl)(Al), phosphon, luminesc., electron-hole recombination processes 79−65919
CaO(S):Pb^{2+}(Bi^{3+}), SrO(S):Pb^{2+}(Bi^{3+}) 77−73166
$Ca(PO_3)_2$:Eu^{3+}, anomalous spectral props. 79−38614
$Ca_2P_2O_7$:Sb(,Mn), luminesc., colouration 80−2828
β-$Ca_3(PO_4)_2$:Sb(,Mn), luminesc., colouration 80−2828
$Ca_5(PO_4)_3F$:Nd^{3+}, luminesc. and absorpt. spectra, line shift and broadening 77−4678
$Ca(Pt(CN)_4)5H_2O$, transition energy tuning from 3.3 to 1.4 eV 79−61436
CaS, colour centres and photoluminesc., flash stimulation bands *(Russian)* 77−20923
CaS:Bi, Tm, phosphor sensitisation mechanism, energy transfer 78−60507
CaS:Bi^{3+},Na^+(Li^+) phosphors, luminescence of associated centres *(French)* 80−40155
CaS:Ce, Na phosphor, photoluminescence and excitation spectra 80−89049
CaS:Cu, colour centres, optical and thermal depths determ. 80−66275
CaS:Cu, colour centres and photoluminesc., flash stimulation bands *(Russian)* 77−20923
CaS:Eu, Eu^{2+} → Eu^{3+} charge transformation *(Russian)* 78−72403
CaS:Pb^{2+} phosphors, luminesc., refl., emission, and excitation spectra 79−11456
CaS:Pd phosphors, trap and luminescent centre location, photo-, thermo- and electroluminescence studies 80−71482
CaS:Zn phosphor, photoluminesc. meas. 77−20913
CaS:Zr phosphors, photoluminesc. 79−28806
CaS:Zr phospors, photoluminesc. 79−28805
$CaSO_4$ phosphors:Ce(Eu)(Dy)(Tm), gamma-irradiated valency conversions in rare-earth ions 80−55198
$CaSO_4$:Bi, cryst. growth, luminesc. props. 77−58993
$CaSO_4$:Dy, photo-stimulated thermolum., for high-exposure dosimetry 77−9262
$CaSO_4$:Dy photostimulated luminesc. for radiation dosimetry 77−90910
$CaSO_4$:Dy(Tm), thermolum. thermolum. phosphor, photolum. and absorpt. spectra, thermolum. mechanisms 80−97321
$CaSO_4$:Sm phosphors, X-ray induced fluorescence and phosphorescence 80−55179
CaS(Se):Eu^{2+}, emission and excitation spectra obs. 80−55162
CaSe: Sn^{2+}, dimer centre, emission and excitation spectra, temperature quenching *(French)* 79−99937
CaSe:Pb, luminesc. and EPR props. of Pb centres 80−55168
$CaTaRO_6$, (R=La, Nd, Gd, Sm, Er, Lu), synthesis and physicochem. props. 79−52139
$CaWO_4$, luminesc. efficiency, temp. and high-press. 78−23507
$CaWO_4$ phosphor, interaction between intrinsic and impurity emission 79−8198
$CaWO_4$:Eu^{3+}(Sm^{3+}), energy transfer after red edge excitation 78−52552
$CaWO_4$:Na(Y), pure and doped, luminesc. props. 79−95835
$CaYAlO_4$:Nd^{3+}(Er^{3+}), absorpt. and luminesc. spectra 77−69901
$Ca_3Y_2Ge_3O_{12}$:Eu^{3+}, garnets, prep., struct., luminesc., absorpt. spectra, Eu^{3+} localisation 77−69884
$CaZrO_3$:Pb^{2+}, UV luminescence temp. depend., three-level model 77−4683
$CaZrO_3$:Pb^{2+} (Bi^{3+}) and related Pb^{2+}(Bi^{3+})-actuated hosts, cryst. struct. effects on luminesc. 77−16376
Cd complex, Cd (II) halide with 8-aminoquinoline, cryst. 77−52152
$CdCl_2$:Cu, optical props. 78−43918
$CdCl_2$-$CdBr_2$, solid soln., luminesc., optical absorpt. 78−19538
CdF_2:Eu(Gd)(Nd), semicond., symmetry of optical centres, optical and elec. props. 77−59592
CdF_2:Mn,Y, in MIS struct., blue-green electrolum. 79−52025
$CdGa_2S_4$, photoluminesc. and photocond. meas. 78−60159
$CdGa_2S_4$:Ag(In), photoluminesc. and photocond. meas. 78−60159
$CdGeP_2$, direct gap crystal, polarisation of recombination radiation 78−19562
$CdGeP_2$, polarisation of luminescence emitted 77−69909
$CdGeP_2$:In, photolum. spectra and kinetic coeffs. 79−19927

photoluminescence continued
$CdGeP_2$:In, polarisation of recombination radiation 78−19562
n-$Cd_{0.3}Hg_{0.7}Te$, recomb. levels 79−91076
CdI_2, layered cryst., photoluminesc., and reflection spectra obs. 78−6726
CdI_2, luminesc., relaxed excitonic states 79−33758
$(CdI_2)_x(PbI_2)_{1-x}$, layered cryst., photoluminesc., and reflection spectra obs. 78−6726
$(CdI_2)_x(PbI_2)_{1-x}$, reflection and luminesc. spectra obs. 77−8648
$CdIn_2$:Cr, photocond. and photoluminesc. spectra 77−28214
$CdIn_2S_4$, impurity centres, photoluminesc. and photocapacitance data on config.-coordinate diagrams 78−10938
$CdIn_2S_4$, photoluminesc. spectra anal. by method of moments 77−12433
$CdIn_2S_4$, photoluminesc., reson. Raman scatt. 78−48179
$CdIn_2S_4$, photoluminesc., thermal quenching and recomb. centres 79−24362
$CdIn_2S_4$, single cryst., oscill. behaviour of photocurrent and luminesc. 78−10501
$CdIn_2S_4$ single crystals, recombination process and localised levels 80−93383
$CdIn_2S_4$:CO^{2+}, site symmetry, spectral meas. 79−78729
$CdIn_2S_4$:Cr, absorpt. and photoluminesc. spectra, Cr conc. depend. 79−78712
$Cd_{1-x}Mg_xTe$:Al, donor-acceptor pair and self-activated luminesc. 77−52161
$Cd_{1-x}Mn_xTe$, exchange induced ionization of bound excitons, luminesc. meas. 80−97328
$CdMoO_4$, luminesc. efficiency, temp. and high-press. 78−23507
$Cd_2Nb_2O_7$, photolum. and carrier drift mobility at ferroelec. transition 80−71469
CdP_2:Bi,Zn, photolum. and photocurrent stationary charact. 78−27317
CdP_2:Cu, photoluminescence and photocond. charact., interimpurity recomb. of carriers 77−8637
$Cd_xPb_{1-x}I_2$, photoluminescence comp. and energy depend., band gap 77−44045
CdS, Auger excitation mech. of 1.6-2.0 micron luminesc. band 79−8184
CdS, Auger interaction between luminescence centres and donor-acceptor pairs 77−63458
CdS, biexciton levels, luminescence-assisted two-photon spectra 80−29795
CdS, biexcitonic luminesc. for allowed and forbidden polarisation 77−44040
CdS, compensated, charact. of Auger excitation spectra of photoluminesc. and photocurrent 77−90194
CdS, condensation of optically excited carriers, electron-hole-liquid phase diagram 77−31950
CdS crystals, doped with groups III and VII elements, self-activated emission, modelling *(Japanese)* 78−31247
CdS crystals, electron-hole plasma, carrier optical orientation 80−100689
CdS crystals, radiative recombination, high excitation rates 80−108269
CdS, deep level IR luminescence, origin 80−20704
CdS, deform. effects on exciton excitation spectra 78−35191
CdS, dislocation effects on radiative recombination processes 79−8186
CdS, dislocation emission, photoluminesc. spectra 80−16084
CdS, dislocation structural optical absorpt., plastic deformation *(Russian)* 80−34959
CdS, doped laser mechanism and output study 80−43340
CdS, edge emission spectra alteration by uniaxial stress *(Russian)* 78−72486
CdS, electron and hole trapped centres, EPR, photoluminescence, photoconductivity study 80−108071
CdS, electron-hole condensate, luminesc. obs. *(Russian)* 78−19552
CdS, emission and transmission spectra, excitonic mols. effect 77−44062
CdS, emission lineshape of excitonic mols., polariton states 77−20918
CdS epitaxial layers on sapphire, exciton struct. of absorpt., photoluminesc. and photocond. spectra 80−89027
CdS, excitation spectroscopy, relation between I_2 bound exciton line and CdS excitonic molecule line 80−40153
CdS, exciton condensation, photoluminesc. spectra 80−25448
CdS, exciton optical and luminescence spectra charact. near dislocation slip bands 80−45111
CdS, exciton resonant secondary emission spectrum temporal evolution 79−51499
CdS, exciton-LO phonon interactions under high excitation and temp. conditions 77−69899
CdS, excitonic mol. emission, strain induced splitting 77−44060
CdS, fine struct. of two-photon absorption, luminesc. meas. 77−24893
CdS, free-exciton multiphonon luminesc. 78−6741
CdS, group velocity of light and polaritons, refl. and luminesc. spectra 77−24863
CdS, high intensity excited, exciton reflection spectra, reflection struct. 80−20692
CdS, high-energy electron irrad., photoluminescence spectra, course of annealing 77−90198
CdS, highly excited cryst., biexciton, impurity transition and electron-hole plasma 79−15092
CdS, highly photoexcited, picosec. luminesc. spectrosc. 79−47517
CdS, IR stimulated edge emission 77−59613
CdS, impact ionisation of excitons, photocond. and photolum. meas. 79−56266
CdS, ion implantation effect on luminesc. and cryst. damage 78−6758
CdS, kinetics of recomb. radiation 78−31243
CdS laser irrad. native defect formation, influence on photoelectric props., IR luminescence *(Russian)* 80−11039
CdS, low temp. IR-induced flash of green edge luminescence 77−63457
CdS, luminesc. and gain spectra of two-photon excited excitons 79−33815
CdS, luminesc. of I_2 bound exciton and excitonic mol. 79−91492
CdS, magnetoreflectance and magnetoluminesc. of A exciton 78−39597
CdS, multiphonon reson. Raman scatt. and exciton-phonon luminesc. 77−16319
CdS, multiphoton cross-section determination by means of luminescence experiments 80−93377
CdS, neutron and fast electron irrad., local centre form., TSC and photoluminesc. meas. 78−87719
CdS, nonequilibrium electron-hole plasma, optical orientation of carriers *(Russian)* 78−2904
CdS, ps decay kinetics of luminesc., streak camera obs. 79−78752
CdS, psec time resolved spectroscopy, electron-hole plasma 79−47500
CdS, pure and Cl doped, stimulated emission due to indirect band-band transitions 80−7376

photoluminescence continued
CdS, reflectance, transmittance and luminesc. spectra, light group vel. near exciton reson. *(Russian)* 77−69857
CdS, reson. scatt. of exciton-polaritons second emission under monochromatic excitation 77−1717
CdS, resonant scatt. of exciton polaritons by LO and acoustic phonons 79−95760
CdS, reversible threshold modification of luminesc. spectrum by uniaxial compression 79−38662
CdS, single cryst., bound excitons in surface layers, luminesc. obs. 79−28294
CdS, single cryst., effects of annealing in Cd or S vapour on photoelectric props. 77−16370
CdS, single cryst., laser emission following single-photon excitation *(Russian)* 78−37889
CdS, single cryst., surface treatment effects on photoluminesc., struct. and optical props. *(Russian)* 78−15224
CdS, single crystal, subnanosecond light pulse generation by laser radiation pumping 79−64234
CdS single crystal growth by sublimation *(Japanese)* 78−11093
CdS single crystal laser screen, photolum., determ. of layer depth disturbed by polishing 78−17977
CdS single crystals, depend. of radiative props. on equilib. carrier density 79−19932
CdS single crystals, Roentgenoluminescence, exciton interactions *(Russian)* 80−2853
CdS sintered film, photolum. and recomb. photocurrent noise spectra 78−6743
CdS, size effect of dense electron hole systems 80−7413
CdS, spatial diffusion of excitons under intense excitation 77−44061
CdS, spectroscopic study of local centre interaction, change with external illumination 80−80323
CdS, spontaneous and stimulated emission from electron-hole plasmas 77−69241
CdS, streamer luminescence 78−6762
CdS, stress-induced photolum. bands, photocond., rel. to dislocation electron states 80−25447
CdS thin films, growth and evaluation for fabrication of high performance photovoltaic solar cells 80−93501
CdS, three-photon absorpt. coeff. determ. by nonlinear luminesc. expt. 80−14384
CdS, time-resolved spectra of spontaneous luminesc. from high density electron-hole plasma 80−40156
CdS, two-photon-excitation, tunable laser emission, luminesc. processes 80−55127
CdS, up-conversion and optical storage, spatially modulated band struct. 78−64397
CdS:Ag, orange luminesc. at 77K and induced impurity photoconductivity 79−43035
CdS:Cu, diffusion doping, photolum. 79−91493
CdS:Cu, IR photolum. at 10K 79−28824
CdS:Cu, photocurrent, elec. field effect on recombination processes *(Russian)* 80−100484
CdS:Er^{3+}, spectra of different emission centres *(Russian)* 77−16356
CdS:In(Cl) concentration quenching mechanism of luminescence 80−97336
CdS:Li, complex luminescence centres, recombination-stimulated conversion 80−108268
CdS:Li, donor-acceptor interactions, photochem. reactions *(Russian)* 77−40285
CdS:Li, luminescence bands, photocurrent spectra *(Russian)* 80−60677
CdS:Li, nature of recombination centres responsible for 0.95 μm luminesc. band 77−69908
CdS:Li, pure and doped, green edge luminesc., complex nature of centres 80−60671
CdS:Li, TSC and optical photocurrent quenching spectra, Auger excitation of recomb. centres 79−33294
CdS:$Li^+(N^+)(Ne^+)(P^+)$, ion-implanted, edge emissions 77−77274
CdS:Li(Cu), pure and doped, electrodiffusion of shallow donors, photocurrent, TSC, and exciton luminesc. meas. 80−79992
CdS:N, P, As, Sb, Bi photoluminescence obs. 78−10965
CdS:Na, Hagemark theory, green edge emission line intensity 80−75517
CdS:Ni, elec., photoelec. and luminesc. props. *(Russian)* 78−84259
CdS:Ni, elec., photoelec. and luminesc. props. 79−95828
CdS:P, implanted, photoluminesc. and electroreflection spectra *(Russian)* 78−52544
CdS:Te-based photoelectrochem. cell, luminesc., thermal manipulation of deactivation processes 80−81479
CdS-based phosphor, microstruct. and luminesc. efficiency 78−10959
CdS-Co^{2+}, IR spectrum, 4.2K, electron-phonon interaction effect on emission spectrum 78−27270
CdS(Se), magnetooptic study of P line at high excitations, biexciton binding energy values 78−48220
CdS(Se), with dislocations, optical props. 79−83001
$CdS_{1-x}Se_x$, chem. comp. and luminescence obs. 80−80869
$CdS_{1-x}Se_x$ mixed crystals, free excitons, disorder effects 80−34365
$CdS_{1-x}Se_x$, mixed crystals, deformation effects on free excitons 80−76073
$CdS_{1-x}Se_x$ single crysts., photocond. and excitonic luminesc. under high laser excitation 78−23127
CdS(Se)(Te):Co^{2+}, IR luminesc. quenching, Co^{2+} level position, ionisation energy 80−16079
CdS_xTe_{1-x}, emission spectra at high excitation levels *(Russian)* 79−74004
CdS_xTe_{1-x}, low temp. photoluminesc. *(Russian)* 78−43931
CdSe, electron irrad., edge emission 80−25461
CdSe, exciton-phonon luminesc. 77−16319
CdSe, free-exciton multiphonon luminesc. 78−6741
CdSe, high intensity excited, exciton reflection spectra, reflection struct. 80−20692
CdSe, highly photo-excited, time-resolved luminesc. spectra, 1.8K 78−35197
CdSe, kinetics of recomb. radiation 78−31243
CdSe, low resist., mech. for nonradiative recombination of carriers, photoluminesc. and photocurrent charact. 78−19092
CdSe, luminesc. of high density electron-hole plasma at elevated temps. 80−20696
CdSe, magnetoreflectance and magnetoluminesc. of A exciton 78−39597
CdSe, optical gain spectra, exciton collision processes and electron-hole plasma 79−28814

photoluminescence continued
CdSe, oriented single-crystal films, edge luminescence at high excitation levels 77−1720
CdSe, pico-second time depend. of luminesc. line due to exciton-exciton collision 78−39587
CdSe, picosecond time-resolved luminesc. spectra 79−93890
CdSe, plastically deformed, luminescence line 0.96 eV 78−10950
CdSe, polar semiconductor, collisions between hot excitons and hot electrons 80−7415
CdSe, psec time resolved spectroscopy, electron-hole plasma 79−47500
CdSe, pure and In-doped epitaxial growth on ZnTe (111), and characterisation 78−14631
CdSe, radiative recomb. process, P-band, 2-psec time resolution 79−24346
CdSe, recombination mechanism at dislocations, photoluminescence 80−103993
CdSe, reson. absorpt. of coherent IR radn. by acceptors, photocurrent and emission spectra 79−73974
CdSe single crysts., exciton luminesc. and polarisation spectra under one- and two-photon excitation 79−65391
CdSe, single crysts., luminesc. of electron-hole plasma 80−60675
CdSe:Cl(In), photoluminesc. props. near fund. absorpt. edge, impurity conc. effects 79−52003
CdSe:P, effect of P on edge luminesc. 78−64399
CdSe:P(Zn), single crystals, luminesc. 79−87493
$CdSiAs_2$, polarisation of photoluminesc. 77−16389
$CdSnP_2$, luminescent props. *(Russian)* 78−35201
$CdSnP_2$:Cu, deep centres, emission transitions, polarisation *(Russian)* 78−84650
CdTe, average number of phonons emitted in optical transition 77−8614
CdTe crystals, exciton luminescence spectra rel. to shallow impurity conc. 80−97335
CdTe, electron-hole liquid formation in pure and doped crystals, luminesc. study *(Russian)* 80−55184
CdTe, excitation spectra, resonant Raman scatt. versus hot electron effects 79−38645
CdTe, growth from Te-rich soln. by travelling heater method, cond. and luminesc. 77−40351
CdTe, high-resistivity, irradiation effects on carrier transport and trapping process 78−2164
CdTe, low temp. luminesc. *(Russian)* 79−91497
CdTe, luminescence and reflect. investig. of excitons, stress and Zeeman splitting 77−40281
p-CdTe, nondoped, heat treatment in vacuum, dissoc. obs. effects on struct. and props. *(Japanese)* 80−60662
p-CdTe, photocond., photoluminesc., spectral studies 80−88593
n-CdTe, plastic deform. effects 79−15509
CdTe, recombination radiation due to high-density excitons 80−93392
CdTe:Cl, electron irrad., defects 80−25460
CdTe:Cl, heavily doped, elec. and photoluminesc. investig. of defect interactions 77−39603
CdTe:Cl, interaction of impurities and lattice defects, changes in elec. props. and photoluminesc. 77−4685
CdTe:Cr^{2+}, absorpt. and luminesc. of $Cr^{2+}(d^4)$, cryst. field theory interpretation 79−83000
CdTe:Fe(Ni), luminesc. and refl. spectra, high temp. annealing effects 80−24472
CdTe:In, pure and heavily doped, electron-hole liq. form., luminesc. spectra 80−10884
CdTe:Li(Cl), acceptor states study by donar acceptor pair excitation luminesc. 80−100683
CdTe:Mn^{2+}, luminesc. and magnetooptic reson., mag. field effect 80−93390
CdTe:Mn(Fe)(Ni), exciton refl., photoluminesc., and mag. suscept. meas., influence of impurities 77−39787
CdTe:V,Cr, optical props. meas. 79−73969
CdTe(Se):Co, impurity luminescence no phonon line depend. on temp., Debye temp. 80−66273
$CdWO_4$, luminesc. efficiency, temp. and high-press. 78−23507
CdZnS thin films, growth and evaluation for fabrication of high performance photovoltaic solar cells 80−93501
$Cd_{1-x}Zn_xS$ heteroepitaxial single-cryst. layers, photoluminesc. props. 80−100692
$CeBO_3$:Tb^{3+}, vacuum UV excitation spectra and quantum efficiencies 79−28811
$Ce_xLn_{1-x}P_5O_{14}$, UV luminescence lifetimes obs. 78−6775
CeP_5O_{14}:Gd^{3+}, EPR and emission spectra *(French)* 77−69686
CeP_5O_{15}, IR absorpt. and luminesc. spectra 80−55079
Cs-He, new absorption/emission bands perturbed Cs transitions assignment, pot. energy curves 78−66486
CsBr, luminesc. polarisation for free and bound excitons 78−10942
CsBr, self-trapped excitons, magneto-optical props., 1.3-50K 80−49606
CsBr:Cl(F), luminescence investig. of F_H-centre lifetime 77−20917
CsBr:Cu, polarisation study of tetragonal Cu^{++} aggregate centres 78−39590
CsBr:Cu^+, excitation and absorpt. spectra 80−108255
CsBr:NO_2^-, luminesc. centre polarisation and reorientation *(Russian)* 78−76529
CsBr:O_2^- centres, luminesc., polarisation temp. depend. 78−87943
CsBr:Pr, absorpt. and fluoresc. spectra, crystal field 78−2885
$CsCaCl_3$:Pb, and undoped crystals, photolum. and thermolum. meas. *(Russian)* 77−85767
$CsCa_{0.95-x}Mg_xEu_{0.05}F_3$, blue luminesc. obs. 77−32428
CsCl, luminesc. in vac. UV range above and below phase transition temp. 80−93399
CsCl(Br)(I):NO_2^-, vibronic and reson. Raman spectra of BCC cryst. 79−87468
Cs_2GeF_6:Mn^{4+}, magnetically circularly polarised emission and MCD of vibronic lines 77−16377
CsI based powdered phosphors and screens possible appl. in X-ray radiography and fluorography 79−6245
CsI, correl. between UV emission band at 300 nm and self-trapped excitons, 4.2K 78−75998
CsI, F- and F_H-centres, luminesc. meas. 78−10397
CsI, pure, influence of strain on photolum. 79−15527
CsI, pure and Na(Tl)-doped, luminesc. from bound excitons, UV absorpt. and EPR 77−77282
CsI, self-trapped excitons, magneto-optical props., 1.3-50K 80−49606
CsI:NO_2^-, luminesc. centre polarisation and reorientation *(Russian)* 78−76529
CsI:Na, electronic struct. and luminesc. 80−16080

photoluminescence continued
CsI:Na, localised excitons, absorption and emission 77−32425
CsI:Na, photoluminescence spectra and lineshapes anal., exciton energies 77−77281
CsI:Na, self-trapped exciton emission polarisation 80−49607
CsI:$Na^+(K^+)$, luminesc. processes 80−103989
CsI:Tl single crystal gamma-optical converting screens, factors influencing relative afterglow intensity 79−8173
CsI:Tl X-ray phosphor, spectral characts. 79−8172
CsI(Br):Mn phosphors, luminesc. spectra 77−59610
Cs_2MX_6(M=Se, Te, X=Cl, Br), $\Gamma_4^-(^3T_{1u})$ state, Jahn-Teller effect, luminesc. obs. 80−60650
$CsMnBr_3$:Nd^{3+}, nearly 1-dimens. cryst., emission spectrum, extensive energy transfer 79−15516
$CsMnCl_3.2H_2O$, luminesc., electronic excitations localisation *(Russian)* 79−87492
$CsMnCl_3.2H_2O$, nonequilibrium magnon population obtained by optical pumping *(Russian)* 80−11457
$CsMnF_3$, exciton migration, excitation and luminesc. study *(Russian)* 80−66264
$CsMnF_3$, magnon absorption and luminesc. 80−7400
$Cs_2NaTbCl_6$, emission spectra, mag. dipole transitions assignments 78−23505
$Cs_2NaTbCl_6$, mag. circ. polarised emission, MCD, $^7F_J \rightleftarrows {}^5D_4$ transitions 77−77242
$Cs_2NaTbCl_6$, Tb^{3+} $^5D_4 \rightarrow {}^7F_J$ transitions, mag. and elec. dipole intensities 78−76033
Cs_2NaYCl_6:Bi^{3+}, luminesc., cryst. growth, Stockberger method 79−8174
Cs_2NaYCl_6:Bi^{3+}, luminescence props., emission and excitation spectra 80−108262
Cs_2NaYCl_6:Tb^{3+}, emission spectra, mag. dipole transitions assignments 78−23505
α-$CsNd(PO_3)_4$, single cryst. struct. and spectral-luminescent props. 80−96490
$CsPbBr_3$, $CsPbCl_3$, ionic semiconductors, electronic and optical props. 79−38594
$CsPbBr_3$, electronic and optical props. 80−25414
$CsPbCl_3$, electronic and optical props. 80−25414
$CsPbCl_3$, electronic struct. and optical props. in fundamental absorpt. region 80−93367
$CsSrCl_3$:Pb, luminesc. spectral distrib., transitions identification *(Russian)* 77−40276
$CsSrCl_3$:Tl, absorpt. and luminesc. spectra 78−72586
Cs_2TeCl_6:Re^{4+}, vibronic transitions progressions, intensity distrib. 79−78735
Cs_2TiF_6:MnF_6^{2-}, $^4A_g \rightleftarrows {}^2E_g$ transition of Mn^{4+}, absorpt., emission, linear and MCD, MCE 78−10929
$Cs_2UO_2Cl_4$, luminesc. spectra of cryst., polarised, vibr. anal. 79−73983
Cs_2ZrCl_6:Os^{4+}, multiple state luminesc. 78−72584
Cs_2ZrCl_6:Re^{4+}, cryst., mag. circularly polarised emission 77−28613
$Cs_2[Pt(CN)_4].H_2O$, polarised emission, correlation to cryst. struct. 79−19917
CuBr, biexciton luminesc. 77−44056
CuBr, emission spectra after two-photon excitation, Raman scatt. 79−47518
CuBr, excitonic mols., two photon generation 77−43511
CuCl, biexciton luminesc. 77−44056
CuCl, biexciton luminesc., subnanosecond time resolved spectroscopy 77−73167
CuCl, biexciton luminescence and two photon Raman emission, polarisation props. 78−80406
CuCl, biexcitons, two-photon absorption and luminesc. 77−43513
CuCl, decay time mas. of biexcitonic photoluminesc. 78−10935
CuCl, direct creation of high biexciton density at K=0, two-photon absorpt. and emission spectra 79−33727
CuCl, donor-acceptor recomb. spectra 80−45131
CuCl, emission spectra after two-photon excitation, Raman scatt. 79−47518
CuCl, excitonic mol. luminesc. spectra, picosecond time anal. 78−52548
CuCl, excitonic molecules, secondary emission under two-photon reson. excitation 80−11468
CuCl, excitonic mols., ps time resolved luminesc. spectra 77−16383
CuCl, excitonic mols., two photon generation 77−43511
CuCl, luminesc. and Raman processes under reson. two-photon excitation 79−33796
CuCl, luminesc. and reson. Raman scatt. of excitonic mols. 79−33814
CuCl, luminesc. from Bose-condensed state of biexcitons 79−23905
CuCl, luminesc. of excitonic mols. 80−2817
CuCl, picosecond spectroscopy of secondary radiation from resonantly excited excitonic molecules 79−15461
CuCl, polariton effects in resonant Raman scatt. 78−10881
CuCl, psec time resolved spectroscopy, excitonic mols. 79−47500
CuCl, Raman and luminesc. processes under reson. two-photon excitation of excitonic mol. 79−8143
CuCl, relaxation of excitonic molecules generated by two-photon excitation, forward Raman scatt. 78−2838
CuCl, reson. Raman scatt. and luminesc. of biexcitons 79−38618
CuCl, reson. Raman scatt. and luminesc. due to excitonic mols. 79−91425
CuCl, reson. Raman scatt. and luminesc. under two-photon excitation 79−95765
CuCl, resonantly excited excitonic molecules, time resolved spectroscopy 78−92109
CuCl, time resolved exciton-biexciton transitions, UV excitation, luminescence spectra 79−69883
CuCl, time-resolved study of induced absorption due to exciton-biexciton transitions 79−38658
CuCl, two-photon absorpt. and luminesc., biexcitons 80−11434
CuCl, two-photon reson. Raman scatt. and luminesc. of excitonic mols. 79−28819
CuF, from gas phase reaction, photon yields, chemi- and photo-luminesc., excitation spectra 79−5157
$CuGaS_2$, crystal growth and luminesc. *(Japanese)* 78−23515
$CuGaS_2$, direct gap semicond., exciton energy at 300K from reabsorption of luminesc. 79−78728
$CuGaS_{2-2x}Se_{2x}$, mixed crysts., luminesc. spectra 77−63454
$CuGaSe_2$ crystals, I_2 vapour transport grown, luminesc. spectra 78−88349
$CuGaSe_2$, photoluminesc. spectra at 76K 79−38655
$CuGaSe_2$ single crystals, elect. and optical props. for solar cell appl. 80−10981

photoluminescence continued
$CuGaSe_2$ thin films, on GaAs substrates, structural and elec. props., photoluminesc. meas. 79−65564
CuI, effect of heat treatment temp. 77−52151
CuI, single crysts., growth and optical props. 80−93470
Cu_2O, evidence of competitive phenomenon between 0.72 μm and 0.93 μm luminesc. 78−27310
Cu_2O, exciton luminesc. spectra, mag. field influence 80−80860
Cu_2O, positive and negative photomemory, IR luminesc. spectra, illum. effect 79−69557
Cu_2O, residual conductivity, role of vacancies, photoluminesc. and photocond. 77−15901
Dy complex, acetoacetic ether, luminesc. spectral band intensities, solvent effects *(Russian)* 78−84653
Dy^{3+} activated vanadates, photoluminesc. meas. 77−77277
DyP_5O_{14}, luminesc. spectra 77−52155
Er^{3+} doped phosphors, IR excitation and absorpt. and emission spectra *(Russian)* 79−52021
Er^{3+}:Yb^{3+} in liq. media, luminesc. cooperative sensitisation 80−2827
Eu complex, $(Et_4N)_3$ $[Eu(NCS)_6]$, Eu^{3+} ion site symm. 78−84656
Eu complex, benzoylacetonate, energy transfer at high pressures 78−52541
Eu complex, with benzoylacetone, isotropic solns., Eu^{3+} luminesc. excitation spectra and polaris. spectra 79−87487
Eu complexes, luminesc. spectra, electronic-vibr. transitions 77−52171
Eu double metaphosphates with alkali metals or H, luminesc. props. 80−100675
Eu monochalcogenides, anti-Stokes luminesc. 78−60515
Eu, monochalcogenides, multiphonon inelastic light scatt. 77−90144
Eu piperidinium salts, emission spectra, ligand field symmetries 79−61413
Eu^{2+} activated phosphors, luminesc. efficiency, temp. and high pressure 78−23508
Eu^{2+}, broadband luminesc. in fluorite struct. crysts. 79−65923
Eu^{2+} doped microcrystals, unusual optical emission 79−73992
Eu^{2+} impurities in cubic crystals, 5d→4f radiative transition probability calc. 80−71474
Eu^{3+} soln., luminesc. quantum yield spectral depend. 80−2838
$EuGa_3(BO_3)_4$, luminesc. spectra, local symmetry of rare earth ion determ. 80−16095
$Eu_xLa_{1-x}Ta_7O_{10}$, polycryst., luminesc. and excitation spectra 80−60659
$Eu(NO_3)_3.6H_2O$, isotropic solns., Eu^{3+} luminesc. excitation spectra and polaris. spectra 79−87487
$EuNa_2Mg_2(VO_4)_3$, disordered, thermal quenching of luminesc. 80−71472
EuO, anti-Stokes luminesc., magnon assisted 78−31252
Eu_2O_3-Y_2O_3-Ta_2O_5, struct., phase form., luminesc. and X-ray diffr., obs. *(Russian)* 78−6765
$Eu_3O_4(S_4)$, mixed valence system, inelastic light scatt., photoluminesc. 77−90145
EuP_5O_{14}, luminesc. of Eu^{3+}, transition probabilities 80−80845
EuP_5O_{14}, luminesc. spectra 77−52155
Eu_3S_4, inelastic light scatt., photoluminesc., anomalous vibr. 77−48229
$Eu_xSr_{1-x}O$, ferromag. ordering and photoluminesc. 77−66313
$Eu_xSr_{1-x}S$, ferromag. ordering and photoluminesc. 77−66313
$Eu_xSr_{1-x}S$, magneto-optical redshift in absorpt. and photoluminesc., mag. short-range order 80−71388
Ga complex, photoluminesc. spectra, $\pi\rightarrow\pi^*$ and charge transfer L→M transitions, Stokes shift 78−64407
n-GaAS epitaxial film, radiative recomb. under influence of mech. stresses 80−66291
GaAS, photoluminescence in polycrystalline samples at 5K, possible solar cell material 79−99929
GaAS, semiinsulating, heat treatment effects 78−6382
GaAlAs DH laser, optimum p-n junction depth, photoluminesc. method 79−4598
GaAlAs DH laser diodes, catastrophic degradation 79−50290
(GaAl)As DH laser wafer, photoluminesc. improvement with buffer layer 80−64014
(GaAl)As, DH lasers, degradation mechanisms, temp. depend. 78−66825
GaAlAs DH lasers, proton-bombard., nonradiative recomb., luminesc. time-response meas. 79−98371
GaAlAs, luminescence circular polarisation, electron optical orientation resonant variation *(Russian)* 80−84782
GaAlAs:Zn recombination radiation drift, charge carrier photon induced drift in varigap semicond. 80−50418
GaAlAs-GaAs double heterostructure, interfacial recomb. velocity, photolum. meas. 78−68075
$Ga_{0.5}Al_{0.5}As$-GaAs, DH, interfacial recomb., photolum. time decay meas. 78−95347
$Ga_{0.5}Al_{0.5}As$-GaAs(:Ge) DH structure, minority carrier lifetime and internal quantum efficiency of surface-free GaAs 79−43013
$Ga_{1-x}Al_xAs$ DH catastrophically degraded laser, TEM obs. of defects 80−32989
$Ga_{1-x}Al_xAs$, epitaxial, radiative deep states 80−76061
$Ga_{1-x}Al_xAs$, hot electron distrib. meas. and calc. 78−27318
$Ga_{1-x}Al_xAs$ LPE layer photoluminescence obs. *(Polish)* 77−77268
$Ga_{1-x}Al_xAs$, photoluminescence, deep level trap emission capture 80−29805
$Ga_{1-x}Al_xAs$:Si, Si determ., spectrochem. method, photoluminesc. spectra, Hall effect meas. *(German)* 77−77851
$Ga_{1-x}Al_xAs$:Si p-n junction, reemission effects 78−15230
$Ga_{1-x}Al_xAs$-GaAs heterojunctions grown by metallorganic CVD 80−15599
$Ga_{1-x}Al_xAs$-GaAs solar cells, photoluminesc. characterisation 80−3512
$Ga_xAl_{1-x}As$-GaAs double heterostructure laser diode, temp. depend. of photolum. 80−5734
GaAlAsP-GaAs T-Q DH laser, light induced misfit dislocation motion 77−75518
$Ga_{1-x}Al_xAs_{1-y}P_y$-GaAs heterojunctions, light-induced misfit dislocation motion, photoluminesc. and X-ray diffr. meas. 79−11200
$Ga_{1-x}Al_xN$ heteroepitaxial films, photoluminesc., cathodoluminesc. 80−66292
Ga(As,P):N, isoelectronic impurity states, long-range, short-range model 80−75524
GaAs, ambient-enhanced photoluminesc. props., mol. adsorption and gas-flow effect 79−99925
GaAs, Auger recombination, luminesc. meas. 77−85850
n-GaAs, Auger transitions, nonlinear extrinsic luminesc. study sublinear emission 79−95833
p-GaAs, circular polarisation of hot luminesc. 78−52572
GaAs, complex luminesc. centres at 1.20 and 1.30 eV 77−16386
photoluminescence continued
GaAs, degraded layer form. by annealing, photolum. obs. of defects 78−10968
GaAs diode, with Schottky barrier, photoluminesc. *(Russian)* 79−28410
GaAs, donor and acceptor concs. determ. by optical method 78−19525
GaAs, donor-acceptor type complex, mag. field splitting of photolum. line 79−15512
GaAs, electrical and optical props. at low temps. 80−39636
GaAs, electron gas coding influence in ion-bombarded layers 80−108272
p-GaAs, electron minority carrier diffusion lengths 80−29807
GaAs, electron-exciton collision influence on luminescence line profile due to bound excitons 80−29800
GaAs, electron-hole liquid form., luminesc. 79−33804
GaAs, electron-spin relaxation and recomb. kinetics, time-resolved luminesc. study 80−108074
GaAs epilayers, high-quality, sharp-line transitions due to donor-acceptor recomb. 78−6768
GaAs, epitaxial, nonequilibrium carrier relax., recombination radn. 80−7416
GaAs, epitaxial film, photon transfer of excitation of nonequilibrium carriers, radiative recomb. 77−8639
GaAs epitaxial layer, comparison of compensation ratios determ. by photolum. and elec. methods 79−28818
GaAs epitaxial layer, photoluminesc. defect complex 80−29804
GaAs epitaxial layers, electronic surface props., photoluminesc. exam. 77−20901
GaAs, epitaxial layers, high density electron-hole plasma luminesc. 78−19537
p-GaAs epitaxial layers, electron-hole plasma, quantum effects in magnetoluminesc. 78−72591
GaAs, epitaxial layers, multiexciton complex bound to neutral acceptors, photoluminesc. obs. 79−87503
GaAs, excited luminescence, influence of IR illumination 80−76072
GaAs, exciton effects in photocond., photoluminesc. 80−96797
n-GaAs, exciton luminescence, excitation intensity depend. 78−52554
GaAs FET structure, sharp line photolum. spectra 78−72248
GaAs, gamma and electron irrad. defect formation depend. on interface, luminescence study 80−34057
GaAs, γ- and electron irradiation, influence on recomb. charcts. near surface 80−71478
n-GaAs, heat treated, origin of 1.41 eV emission band, photolum. expt. 78−72579
n-GaAs, heavily doped, non-linear extrinsic luminesc., role of Auger recombination 79−52010
GaAs, highly deformed samples, absence of dislocation-induced luminescence 79−4835
GaAs, holes optical orientation, luminesc. 80−25452
GaAs homoepitaxial interface, thermal degradation 77−11988
n-GaAs, hot electron distrib. function with LO phonon kink, photoluminesc. 79−19925
GaAs, hot electrons and exciton-electron collision under external elec. field 78−43928
GaAs, hot photoluminescence spectrum, polarisation depend. 78−31254
GaAs, hot photoluminescence depolarisation in mag. field, 0.4 eV energy state electron lifetime *(Russian)* 80−16086
GaAs, hot photoluminescence spectrum on pumping across the L-valley *(Russian)* 80−103984
n-GaAs, IR luminescence from acoustoelectric domains 77−55822
GaAs, impact ionisation of excitons 79−38079
GaAs, impurity anal. by photoluminescence *(Japanese)* 77−24888
GaAs, indirect band edge, determ. by quantum-well bandfilling 78−92120
GaAs injection lasers, amplified luminesc. 80−2824
n-GaAs, intrinsic emission intensity, role of local centres in determ. of conc. depend. 78−39599
n-GaAs, intrinsic luminescence intensity, effect of 0.94, 1.0, 1.2 and 1.3 eV radiative centres 78−23517
GaAs, ion bombarded, defect distrib., photolum. meas. 77−20920
GaAs, ion etching, effects on optical props. and lattice disorder 78−83122
n-GaAs, ion implanted films, optical and luminesc. props. 80−60699
GaAs, LED, absolute internal quantum efficiencies determ. 77−63461
GaAs LED, optimum p-n junction depth, photoluminesc. method 79−4598
n-GaAs, LPE, impurity compensation photolum. and free carrier conc. meas. 77−62558
GaAs LPE buffer layers for MESFET appls. 80−29887
GaAs, LPE layers, ambient O_2 effect on defects and elec. props. 77−76683
GaAs LPE layers, dopant tracing of terrace growth 78−75948
GaAs laser material, secondary dislocation climb during optical excitation 78−75672
p-GaAs, linear polarisation of hot photoluminescence 79−38661
n-GaAs, low energy photolum., 77K, deep centre obs. 77−69877
GaAs, luminesc. emitted by deep centres, illumination-induced change in internal quantum efficiency 79−91495
GaAs, luminescence by laser excitation, photocarrier thermalisation and polariton kinetics 77−66533
GaAs, luminescence due to deep centres, annealing effect on quantum efficiency 77−55825
n-GaAs, luminescence emitted from deep centres, γ-irrad. induced changes in internal quantum efficiency 80−20701
GaAs, luminescence emitted from deep centres, plastic deform. effect on internal quantum efficiency 80−60672
GaAs, MBE, growth temp. depend. and charcts. 79−28946
GaAs, MBE, undoped, growth and characterisation 80−10836
GaAs MBE epilayers, photoluminesc. and elec. characterisation 80−11500
p-GaAs, MBE grown, As_2 and As_4 effects on photolum. 80−103974
GaAs MOS and Schottky systems, electromodulated reabsorption of luminesc. 79−15524
p-GaAs, magnetoluminesc. of cond. band to acceptor transition 77−1716
GaAs, melt grown, improve elec. and luminesc. props. after short time heat treatment 77−63452
n-GaAs, melt-grown, stoichiometry, photolum. obs. 78−72583
GaAs, minority carrier diffusion length, reabsorbed radiation effect 77−28191
n-GaAs, non-Maxwellian electron distribution function, from electric field-depend. photolum. spectrum 79−11450
GaAs, nonlinear extrinsic luminescence 78−84645
GaAs, nonlinear light absorpt., photoluminesc. meas. 77−66528

photoluminescence continued
GaAs, O^+ implantation, energy levels, photoluminesc. 80−24838
GaAs p^+-n diode, radiative hot carrier recomb., photoluminesc. and electroluminesc. meas. 79−38676
GaAs, photocarrier thermalisation by laser excitation spectroscopy 78−31250
GaAs, photoexcitation phenomena, low density 78−27319
n-GaAs, photolum., rel. to n-InP 77−40272
GaAs, photolum. intensity degradation caused by excitation-enhanced oxidation 78−15205
GaAs, photoluminescence, deep level trap emission capture 80−29805
GaAs, photoluminescence, electron-acceptor, from non-Maxwellian distrib. of photo-excited electrons 80−45138
GaAs, photoluminescence at low temp., free exciton recomb. mechanisms *(Russian)* 77−32438
GaAs, photoluminescence and resonant Raman spectra, press. depend. 78−31251
GaAs, photoluminescence intensity rel. to heat treatment in S vapour *(Russian)* 78−48216
GaAs, photoluminescence intensity of cleaved surface, ambient gas influence 78−88345
GaAs, photon transfer of excitation of nonequilib. carriers, conc. profile and relax. time 77−69907
GaAs, polar semiconductor, collisions between hot excitons and hot electrons 80−7415
GaAs, polarisation anisotropy of hot photolum. *(Russian)* 77−90195
GaAs, prep. of thin films by ionised-cluster beam deposition, photolum. meas. *(Japanese)* 80−25576
GaAs, psec time resolved spectroscopy, electron-hole plasma 79−47500
GaAs pure and Se-doped, photoluminescence at dislocations, band gap electronic levels 79−99926
GaAs, radiative yield improvement by laser annealing 80−45128
GaAs, recombination radiation, anomalous temp. depend. 80−2847
n-GaAs, recombination scheme for $\hbar\nu_m \approx 1.0$, 1.2 and 1.3 eV luminesc. bands 77−69906
n-GaAs Schottky diode 80−29781
GaAs, semi-insulating, thermal conversion, Hall effect and luminesc. meas. 78−6405
GaAs solar cell structs., photolum. props. 80−50958
GaAs, spin-depend. recomb., photoluminesc. obs. 80−60666
GaAs, spontaneous luminesc. due to high density electron-hole plasma under nano- and picosecond pulse excitation 80−40157
n-GaAs substrates, ion implanted, compensation 78−75680
GaAs thin layers, MBE, growth conditions and phys. props. *(German)* 80−55307
GaAs, two-photon 1.06 μm absorption coeff., absolute meas. 78−19527
GaAs, two-photon absorpt. spectrum, band gap luminesc. 78−10888
n-GaAs VPE layers, Hall mobility, effect of Cu contamination, photolum. expts. 80−54810
GaAs, VPE on Ge substrate, and characterisation 78−72736
n-GaAs vapour phase epitaxial film electrophysical props. rel. to growth temp. *(Russian)* 80−49961
GaAs, weakly excited, luminesc. from exciton polaritons, based on exciton-electron collisions 79−83020
GaAs: Si(Te), radiative recomb. *(Russian)* 79−91499
GaAs:Be, ion implanted, elec. profiling and optical activation expts. 77−89457
GaAs:Be, ion-implanted, photolum. spectra, effects of implantant depth distrib. 78−27293
GaAs:Be,Se VPE layers, ion implanted, donor-acceptor pair radiative recomb. 79−91489
p-GaAs:Be layer, MBE growth, Be doping and diffusion, elec. and optical props. 77−51397
GaAs:Be(C)(Ge)(Sn), MBE layers, photoluminesc. 80−29803
GaAs:C, Zeeman effect of effective mass acceptor, polarised luminesc. 79−4541
GaAs:Co VPE layers, bound-exciton luminesc., Zeeman anal. 79−95818
GaAs:Cr, 0.84 eV no-phonon luminesc., fine struct. and origin 80−103980
GaAs:Cr, exptl. verification of Cr^{2+} models of photoluminescent transitions 78−27320
GaAs:Cr, intracenter radiative transition in Cr^{2+} ions 79−11463
GaAs:Cr, luminesc. stress splitting, 4.2K 78−84627
GaAs:Cr, Mg, ion implanted, elec. meas. and optical activation studies 79−86806
GaAs:Cr, O, effect of O in photoluminesc. meas. 80−29799
GaAs:Cr, photoluminescence, YAG laser or krypton laser 80−60668
GaAs:Cr, photoluminescence in strong electric fields 80−108270
GaAs:Cr, semi-insulating, Zeeman studies of 0.839 eV emission 80−103987
GaAs:Cr, Si, deep centre photoluminescence spectra 78−95601
GaAs:Cr, surface and bulk recombination parameter determ. from photoluminesc. spectra 77−55820
GaAs:Cr, VPE growth, carrier conc. profiles, photoluminescence spectra 79−74099
GaAs:Cr photoluminesc. meas. 78−6761
GaAs:Cr semi-insulating substrate, photoluminescence obs. of surface degradation during LPE growth 78−6865
GaAs:Cr semi-insulating wafer, heat treatment technique for no thermal conversion 80−100857
GaAs:Cr(O), mechanism of thermal quenching of luminesc. and photocurrent stimulation 77−55821
GaAs:Cr(W), deep trapping centre exam. by thermally stimulated capacitor discharge method and luminesc. 77−55495
n-GaAs:Cu, contaminated single cryst., deep level photoluminesc. model 78−68554
n-GaAs:Ge, film, substrate temp. depend. of Ge incorporation during MBE 80−76196
GaAs:Ge, ion-implanted, photoluminesc., deep emission centres 80−34965
GaAs:Ge, LPE, on semi-insulating GaAs, film-substrate interface characterisation 78−72017
GaAs:Ge, vap. grown, diatomic complex donor and acceptor model 78−80003
GaAs:Mg, photoluminesc. temp. depend., 4.2-293K 77−69878
GaAs:Mg ion implanted, photoluminesc. and annealing characts. 77−16361
GaAs:Mg(Be)(Cd)(Zn), implanted, low temp. photolum. spectra 78−39583
GaAs:Mn, LPE layer, near band edge photoluminescence, 2K, low excitation intensities 78−48218
photoluminescence continued
GaAs:Mn, photoluminesc., emission props. and radiative mechanism 79−56842
GaAs:O, electrolum., photolum., negative differential resist. rel. to recomb. processes 80−66304
GaAs:O, field depend. of radiative recomb. 80−20700
GaAs:O, optical characterisation of deep O implants 77−55294
GaAs:S, LPE growth, photoluminescence spectra at liquid N_2 temps. 79−33948
GaAs:Si, accelerated growth rate effect on MBE, Hall mobility and photolum. meas. 80−104067
GaAs:Si, epitaxial layers, photo- and cathodoluminesc. 77−77285
GaAs:Si, influence of stoichiometry on recomb. processes 80−93396
GaAs:Si, ion implanted, photoluminesc. 79−69887
n-GaAs:Si, ion implanted and/or annealed, As vacancy form., photolum. line 77−27875
n-GaAs:Si, thermally treated, photolum., acceptor levels obs. 79−38587
GaAs:Si, thick LPE layer growth and characterization 77−12511
GaAs:Si encapsulated with AlN, Si_3N_4 layers, photolum., annealing effects 80−20681
GaAs:Si layers, MBE growth, elec. and optical props., doping characts. 80−10819
GaAs:Si p-n structure, radiative recombination region 78−52071
GaAs:Si(Ge) LPE layers, luminesc. props. rel. to substrate quality 78−52583
n-GaAs:Si(Te), radiative transitions induced by modest annealing, photoluminesc. spectra 80−55158
GaAs:Si(Te)(S), vapour phase epitaxial grown layers, photoluminesc. and emission spectra 80−29774
GaAs:Sn, 1.39 eV luminescence, injection level depend., freq. response and thermal quenching 78−19529
n-GaAs:Sn, photoluminesc. spectra 79−43031
GaAs:Sn, selective LPE, orientation dependent growth, luminesc. 77−12551
GaAs:Sn, Te, luminescence props. 79−52017
GaAs:Sn epitaxial layer, electronic props. and epilayer-substrate interface props. 77−89886
GaAs:V, ion implanted, luminesc., level splitting 80−97338
GaAs:W^{2+}, radiative transitions, photoluminesc. obs. 80−108271
GaAs:Zn, diffused, depth profile meas., LED applic. 78−72587
GaAs:Zn, distribution of radiative recombination efficiency 79−78725
GaAs:Zn, heavily doped, photolum. obs., above gap 80−29796
p-GaAs:Zn, luminescent, ion doped MBE growth 80−44436
GaAs:Zn films, VPE growth and photoluminesc. props. 79−38642
GaAs:Zn MBE layers, ionized beam doping, elec. and optical characts. 79−37721
GaAs-(GaAl)As epitaxial layers and DH lasers, deep centre 1.02 eV luminesc. 78−80387
GaAs-$Al_xGa_{1-x}As$ DH laser structures, high-resolution composition profiling with photolum. 78−71101
GaAs-$Al_xGa_{1-x}As$ DH lasers, MBE grown, substrate temp. effect on current threshold 80−48243
GaAs-$Al_xGa_{1-x}As$ heterostruct., photon recycling, diffusion length and lifetime determ. 79−47499
GaAs-$Al_xGa_{1-x}As$ multilayer, photoluminesc., electron spin orientation 80−25453
GaAs-AlAs, epitaxial struct. with alternate layer comp. modulation, fabrication and characterisation 77−1322
GaAs-AlAs layered films, MBE prep., struct., rel. to optical props. 79−77950
GaAs-AlAs multilayer heterostructure laser, power and photoelectroluminescence characts. 80−53297
GaAs-AlGaAs photoelectroluminescent diodes, characts., radiant power 80−6972
GaAs-Au, quenching of exciton luminesc. by surface elec. field 80−29801
GaAs-disperse metal film, photoluminesc. at interface 78−26953
GaAs-$Ga_{1-x}Al_xAs$, DH, dark line defects induced by mech. bending 77−683
GaAs-$Ga_xAl_{1-x}As$ heterostructure, depend. of efficiency of radiative transitions on composition 78−2909
GaAs-$Ga_xIn_{1-x}P$ heterostruct., MBE layers, photolum. props., assessment as laser struct. 80−20705
GaAs-GaAlAs, DH laser material, LPE grown, obs. of melt carryover 78−91553
GaAs-GaAlAs DH lasers, optical studies of defects and degradation 78−18654
GaAs-GaAlAs DH lasers, strain-enhanced luminesc. degradation, photoluminesc. obs. 80−69392
GaAs-GaP heterostructure, radiative recomb. under influence of mech. stresses 80−66291
GaAs-insulator film interface, evidence for growth-induced damage from photolum. expts. 78−75953
GaAs-Si_3N_4 system, photoluminesc. edge line *(Russian)* 79−4852
GaAs-ZnS p-n heterojunction, struct., multibeam electron microscopy obs. 79−11031
GaAs-ZnSe system, heterovalent solid solns. of substitution, prep. and investig. 77−24553
$GaAs_{1-x}P_x$, hot photoluminescence spectrum, polarisation depend. 78−31254
$GaAs_{0.6}P_{0.4}$:N, isoelectronic tape by ion implantation and CO_2 laser annealing 80−24464
$GaAs_{0.6}P_{0.4}$:$Zn^+(Ar^+)$, ion-implanted, thermal degradation of mechanical surface perfection and surface photolum. 77−77271
$GaAs_{1-x}P_x$, bound exciton, luminesc. reson. excitation 79−95840
$GaAs_{1-x}P_x$ epitaxial films, VPE grown, photolum. spectra 79−73997
$GaAs_{1-x}P_x$ epitaxial layers, prep. *(Czech)* 78−48233
$GaAs_{1-x}P_x$, indirect-gap, evidence for exciton localization by alloy fluctuations, photolum. 80−66276
$GaAs_{1-x}P_x$, mol. beam epitaxial growth, cryst. quality, composition investig. *(Japanese)* 77−55895
$GaAs_{1-x}P_x$, N implantation, characterisation by photolum. and channelling 80−54262
$GaAs_{1-x}P_x$, N^+ implantation photoluminesc. props. 77−68987
$GaAs_{1-x}P_x$, N^+ implantation, annealing props. 77−68988
$GaAs_{1-x}P_x$, structural defects, optical props. effect 80−55208
$GaAs_{1-x}P_x$:N, $0.6<x<1$, photoluminesc., comp. depend. 78−52546
$GaAs_{1-x}P_x$:N, doping using inonised beam in MBE, photolum. meas. 78−47400
$GaAs_{1-x}P_x$:N, film, optical absorpt. from photoluminesc. meas. 78−92134

photoluminescence continued
$GaAs_{1-x}P_x$:N, Koster-Slater model and N-states 78−47732
$GaAs_{1-x}P_x$:N, N isoelectronic trap, model calc. of N_Γ and N_X electronic states 78−10398
$GaAs_{1-x}P_x$:N, photoluminesc. and optical absorpt. spectra of N impurity bound-excitons 79−47496
$GaAs_{1-x}P_x$:N, photolum. and electrolum. study of N isoelectronic traps 80−89061
$GaAs_{1-x}P_x$:N, upper branch of N isoelectronic trap., photo- and electrolum. expts. 77−63462
$GaAs_{1-x}P_x$:N epitaxial layers, absorption and photolum. spectra meas. 77−24894
$GaAs_xP_{1-x}$ epitaxial film nonlinear light absorpt., photoluminesc. meas. 77−66528
$GaAs_xP_{1-x}$, liquid phase epitaxial growth on GaP, growth and properties 79−47641
$GaAs_{1-x}P_x$(Te), bound exciton stress depend., piezoluminescence, photoluminescence 80−80206
$GaAs_{1-x}Sb_x$, ($x \leq 0.05$), band gap, temp. depend., from edge photolum. meas. 80−71486
$GaAs_{1-x}Sb_x$ undoped epitaxial layers, photoluminesc. meas. 80−20703
GaInAs-InP, growth by low-pressure metalorganic CVD 80−71595
p-$Ga_xIn_{1-x}As$, Auger recomb., theory and luminesc. expts. 78−56518
$Ga_xIn_{1-x}As$, prep. and props. 79−100047
$Ga_xIn_{1-x}As_{1-x}P_x$ film, energy band struct., photolum. meas. 79−7784
n-$Ga_xIn_{1-x}As_{1-y}P_y$, photoluminesc. of epitaxial films, isovalent substitution 80−16097
$Ga_xIn_{1-x}As_yP_{1-y}$, LPE layers, growth and characterisation 78−38983
$Ga_xIn_{1-x}As_ySb_{1-y}$, epitaxial film and DH, efficiency 77−686
$Ga_xIn_{1-x}P$, undoped liquid epitaxial layers, effect of heat treatment on photoluminescence 78−60512
$Ga_xIn_{1-x}P$:N layers, LPE growth, luminesc. and direct exptl. obs. of band struct. effects 77−52157
$Ga_xIn_{4-x}PyAs_{1-y}$, In rich bulk single crysts. growth from melt via gradient freeze method, and characterisation 78−68618
$Ga_{1-x}In_xSb$:Zn(Te), photolum. and stimulated emission obs. 78−72595
$Ga_{1-x}In_xSe$, energy bands near absorpt. edge, transmission and photoluminesc. spectra 79−83022
$Ga_{1-x}In_xSe$, layered, luminescence and photocond. obs., two-photon excitation 78−76521
GaN, epitaxial growth on sapphire substrates, elec. props., X-ray diffr. anal., photoluminescence spectra 79−4919
GaN, photoluminesc. characts. for 35 implanted elements 77−24884
GaN, photoluminesc. spectra, energy distrib. 80−97339
GaN, pure and Zn-doped epitaxial layers 78−10955
GaN:Al, VPE grown, luminesc. and elec. props. depend. on doping conc., bound excitons 80−20688
GaN:P, photoluminesc. 79−78730
GaN:Zn, LED, blue, yellow and green emission, temp. depend. 77−8658
GaN:Zn, n-i struct., anomalous luminesc. 80−80865
GaN:Zn, polarised electroluminescence, mag. field intensity depend. *(Russian)* 79−91502
GaN:Zn, VPE grown, optical cross sections, photoluminesc. and optical absorpt. meas. 80−55160
GaN:Zn, VPE growth, photoluminesc. rel. to doping conditions 80−55159
GaN:Zn epitaxial films, luminesc. spectra separation into individual bands by impurity absorpt. region excitation 79−74002
$GaNbO_4$, diffuse refl. and luminesc. spectra 78−56516
β-Ga_2O_3, doped, photolum., emission centres struct. 78−52557
β-Ga_2O_3, pure and doped samples, UV luminesc. obs., 5 to 300K 78−80396
β-Ga_2O_3:Cr, temp. depend. of luminesc. characts. *(Russian)* 77−28621
GaP, donor-acceptor pair spectra, electron-phonon interactions 79−38631
GaP, donor-acceptor pair luminesc., excitation spectroscopy 80−25440
GaP, electrical and optical props. at low temps. 80−39636
GaP, electron-hole drop, luminesc. 79−33812
GaP, electron-hole liquid obs. by luminesc. spectra 77−51668
GaP, electron-hole liquid props., luminescence at high excitation intensity 79−69882
GaP, electron-hole plasma photolum. obs. 78−52559
GaP, GPE layers, nonradiative dark regions along surface ripples 77−59600
GaP, growth and props. of LPE layers on Si substrates 78−6864
GaP, impurity interaction on excited acceptor states, luminesc. excitation spectra 79−15517
n-GaP, ion implanted films, optical and luminesc. props. 80−60699
GaP, LEC crystal, cathodolum. and photolum. around dislocations 78−84663
n-GaP, LPE, minority carrier bulk lifetime and diffusion coeff. meas. 77−11932
GaP, LPE layer for LED, photoluminesc. distrib. meas. *(Czech)* 78−48209
GaP, luminesc. emission band, electron-hole liquid 77−69245
GaP, luminesc. from electron-hole drops, 2 to 77K 79−11454
GaP, mol. beam epitaxial growth, cryst. quality composition investig. *(Japanese)* 77−55895
GaP, rare earth doped, photolum. and elec. props. *(Russian)* 78−52545
GaP, spectral depend. of O photoneutralisation cross-section near threshold, and band gap 79−1788
GaP:Bi,N, photoluminesc., electroluminesc., 4.2 to 300K, excitons and hole traps 80−108275
GaP:Bi(N), luminesc. decay kinetics 79−38646
GaP:C(Mg)(Zn), excited acceptor state investig. by photoluminesc. 77−8632
GaP:Ce(Dy)(Pr) epitaxial films, photoluminesc. spectra 80−66294
GaP:Co, deep levels, IR photoluminesc., stress effects 80−55163
GaP:Co, optical spectra and Zeeman anal. of Co 3d^7 state 80−66247
GaP:Co(Ni), photolum. excitation spectroscopy 80−80841
GaP:Cr, ESR of doubly ionised Cr acceptor and IR luminesc. 78−56374
GaP:Cu, deep levels, photoluminesc. and optical cross sections 79−38653
GaP:Dy_2, photolumines. spectra 79−52015
GaP:Fe^{2+}, absorpt. and luminesc. spectra 77−16388
GaP:N, appl. of temp. modulated photolum. induced by photoexcitation technique 78−95605
GaP:N, bound excitons, low temp. photoluminesc. thermal quenching 77−48228
GaP:N, Cd(Zn),(C), interimpurity recomb., acceptor binding energies 78−34796
GaP:N, electron-hole liq., luminesc. obs. 80−25438
GaP:N, luminesc. from electron-hole drop 79−33813
photoluminescence continued
GaP:N, photoluminesc., temp. depend., exciton recombination mechanism 78−88355
GaP:N, photoluminescence, temp. modulated 79−38623
GaP:N, radiative recomb. from electron-hole drops, impurity induced transition 78−19547
GaP:N, radiative recomb. of electron-hole liq. 79−73442
GaP:N, spin dependent exciton recombination at N_2 isoelectronic traps 77−69734
GaP:N, temp. modulated photoluminesc. 77−55818
GaP:N, temp.-modulated photoluminesc., phonon assisted tunnelling process 78−23511
n-GaP:N,O,S,C end, dielec. const. from S-C donor acceptor pair spectra 79−65788
GaP:N(N,O) epitaxial struct., luminesc. study of degradation during heat treatment 80−45139
GaP:Ni, absorpt. and luminesc. spectra 79−42996
GaP:Ni, deep traps, near IR luminesc., polarised spectra meas. 80−16077
GaP:Ni, optical and EPR study of two-electron-trap state 79−73806
GaP:Ni, VPE GaP, Ni detection 78−15212
GaP:O, optical transitions via deep levels, phonon interaction 78−87939
GaP:O, optical transitions via deep levels, cross section temp. depend. 78−87940
GaP:S, effects of uniaxial stress on luminesc. 79−78739
GaP:S(Se), donor bound exciton excited states 80−66284
GaP:S(Se)(Te), pot.-depend. g-values and quenched diamag., props. of donor states 77−62861
GaP:S(Se)(Te), pot.-depend. g-values and quenched diamag., pseudoacceptors D^0, X 77−62862
GaP:Zn, luminesc., acceptor-bound multiple excitons 80−11476
GaP:Zn, O, influence of impurity-absorbed illumination on luminesc. 80−93395
GaP:Zn,O, Auger coeff. from luminesc. decay and Hall effect 77−48226
GaP:Zn,O, Auger coeff. from luminesc. efficiency and Hall effect 77−48227
GaP:Zn,O, degradation of bulk luminesc. induced by laser excitation 77−1715
p-GaP:Zn,S, spin polarisation of donors and acceptors in mag. field, optical and microwave study 80−93393
GaP:Zn(Mg)(Cd), multiple bound excitons, photoluminesc. obs. 79−95837
GaP-GaAlP-GaP LPE layers, lattice matched and mismatched, photoluminesc. spectra 79−51445
GaP-ZnSe solid solutions, spectral studies *(Russian)* 79−91498
GaP_xAs_{1-x}, N doped, alloying induced shift between excitation and luminesc. of N bound exciton 79−52013
GaP_xAs_{1-x}:N, luminesc. of N bound state excitons, local-environment effects 80−100691
$(GaP)_x(ZnS)_{1-x}$ solid solutions, X-ray fluorescence spectra, photoluminescence *(Russian)* 79−74003
GaS, anti-Stokes photon replica emission under two photon excitation 77−52175
GaS, luminescence excited by high-intensity two-photon pumping 77−44038
GaS two-photon absorpt., cond. and luminesc. meas. 77−52166
Ga_2S_3-La_2S_3-Nd_2S_3:Nd^{3+} chalcogenide glass, Nd^{3+} emission and absorption spectra, nonradiative relax. 77−40268
GaS_xSe_{1-x}, recomb. radiation intensity, temp. depend. *(Russian)* 79−33830
GaSb and alloys, struct. defect, photoluminesc. 80−25459
GaSb, Auger recombination, luminesc. meas. 77−85850
GaSb, bound excitons at doubly ionisable acceptors 79−42459
GaSb high-purity and doped layers grown by LPE and VPE methods 78−6863
p-GaSb, hot exciton luminesc., LO phonon Raman scatt. 80−11474
GaSb, interaction of exciton recombination with LO phonons 79−38647
p-GaSb, interband optical pumping, optical detection of EPR 77−28483
GaSb, inversion of Γ and L conduction bands under uniaxial stress, photoluminescence meas. 79−33229
GaSb, photolum., electrolum. meas. in p-n junction, temp. influence 78−72594
GaSb, photolum. spectra under hydrostatic press. 79−19930
GaSb:Sn, p-n junction, electroluminesc. and photoluminesc. 80−66306
p-GaSb:Te, effective radiative recombination centre nature, photoluminescence spectra 79−90998
n-GaSb:Te, heavily doped, electron-hole recomb. photolum. 78−84644
n-GaSb:Te, heavily doped, spontaneous radiative recomb. vel., photoluminesc. spectra 79−11458
GaSb:Te, indirect gap photolum. 80−29797
p-GaSb:Zn film, epitaxial, lifetime of nonequilib. carriers, determ. from circular polarisation of luminesc. 77−24898
$GaSb_{1-x}As_x$, disorder-enhanced Auger recomb. 79−43014
GaSe, 4.2 to 40K 78−10974
GaSe, deep free and constrained excitons and biexcitons, collective interactions *(Russian)* 80−66282
GaSe, direct exciton excited state hot luminescence, band struct. props. 80−55183
GaSe, exciton, excitation-induced absorption and luminesc. 78−60516
GaSe, exciton luminesc. kinetics, intermediate electron-hole states 80−93389
GaSe, exciton spectra at 4.2K rel. to layer struct. 77−16336
GaSe, highly excited, exciton-exciton and exciton-carrier scatt. 77−48244
GaSe, highly excited, polarisation of luminesc. spectra and electron-hole plasma radiation 77−52169
GaSe, interlayer interaction and exciton spectra study 77−52165
GaSe, luminesc. emitted by electron-hole plasma 77−85795
GaSe, luminesc. from exciton-electron and exciton-exciton collisions 77−52168
GaSe, luminescence and absorpt. spectrum in region of high-energy resonance 77−44044
GaSe, luminescence excited by high-intensity two-photon pumping 77−44038
GaSe, magnetoluminesc. at 4.2K 79−61345
GaSe, optical excitation, excitonic spectra, stimulated luminesc. 80−40132
GaSe, optical orientation and alignment of free excitons, on resonant excitation *(Russian)* 77−90196
GaSe, photolum. decay 79−15518
GaSe, photolum. under strong optical excitation 79−24364

photoluminescence continued
GaSe, polarized exciton luminesc. 78−6734
GaSe, population dynamics and spin relax. of excitons 77−66122
GaSe, radiative decay of direct and indirect excitons 78−10975
GaSe, reson. light scatt., luminesc. and Raman spectra 79−38615
GaSe, triplet indirect bound exciton, level anticrossing effect on magnetolum. 79−47513
GaSe, two-photon absorpt., cond. and luminesc. meas. 77−52166
$GaSe_{1-x}S_x$, polytypes, exciton gap energies, luminesc. study 80−54611
$GaSe_{0.9}Te_{0.1}$, undulation spectra associated with acceptor complexes 78−80392
$GaSe_{1-x}Te_x$, energy bands near absorpt. edge, transmission and photoluminesc. spectra 79−83022
$GaSe_{1-x}Te_x$ layered crystal, photoluminesc. meas. 77−1725
Gd complex, benzoylacetonate, energy transfer at high pressures 78−52541
Gd^{3+} in host lattices, energy transfer from sensitizer to activator 79−38628
$GdAlO_3:Er^{3+}$, $^4S_{3/2}$ to $^4I_{9/2}$ transition laser action, optical and luminescence spectra 80−16082
$GdBO_3:Eu^{3+}(Tb^{3+})$ and $GdBO_3:Bi^{3+},Eu^{3+}$, vacuum UV excitation spectra and quantum efficiencies 79−28811
$GdB_3O_6:Bi^{3+}$, Tb^{3+}, energy transfer from sensitiser to activator, intermediate role of Gd^{3+} 80−50389
$Gd_3Ga_5O_{12}:Nd^{3+}$, growth, stimulated emission, spectral props. 78−95593
$Gd_2Gi_2O_7:Nd^{3+}$, spectroscopic props. 77−69866
$Gd_2(MoO_4)_3$, ferroelec.-ferroelastic, photolum. and photocond. meas. 80−84768
$GdNbTiO_6:Eu^{3+}$ emission under UV excitation 78−6770
$Gd_2O_2S:Tb$, recomb. processes and emission spectra *(Russian)* 78−6797
$GdPO_4:Dy^{3+}$, $Bi^{3+}(Sb^{3+})$, energy transfer from sensitiser to activator, intermediate role of Gd^{3+} 80−50389
Gd_2S_3, resonance excitation of Nd^{3+}, luminescence, absorption spectra *(Russian)* 80−50381
β-$Gd_2S_3:Nd^{3+}$, spectroscopic props. from absorpt., photoluminesc. and excitation spectra 80−34968
$(Gd_{1-x}Tb_x)_2O_2S$ phosphor, concentration quenching of Tb^{3+} luminesc. 80−29785
Ge, amorphous, elec. and opt. props., review 78−23094
Ge, biexciton and trion existence, photolum. *(Russian)* 80−16088
Ge, compressed electron hole plasma, luminesc. 78−72592
Ge, cyclotron resonance and radiative recomb. with laser excitation, book contrib. 80−11472
Ge, direct gap recombination, at high excitation level and low temp. 79−38650
Ge, doped, electron-hole drops, low-temp. photolum. spectra obs. 77−69900
Ge, electrical and optical props. at low temps. 80−39636
Ge, electron hole drop diffusion const., hysteresis effect determ. 79−23902
Ge, electron hole drop recombination spectrum, low energy tail 77−59612
Ge, electron-hole drop binding energy, optical threshold studies 79−38652
Ge, electron-hole drop emission kinetics, effect of nonequilib. phonons, 4.2K 78−14674
Ge, electron-hole drop luminescence at high mag. fields 79−65390
Ge, electron-hole drop luminesc., phonon wind induced anomalous depend. at low mag. fields 80−34980
Ge, electron-hole drop motion 80−6744
Ge, electron-hole drop recombination radiation due to heat pulse action *(Russian)* 80−16087
Ge, electron-hole droplets, transient photoluminesc. intensities 78−88353
Ge, electron-hole droplets in high stress limit 78−10369
Ge, electron-hole drops, Auger recomb. 77−48240
Ge, electron-hole drops, motion in low mag. fields 79−23904
Ge, electron-hole drops, photoluminesc. kinetics 78−23524
Ge, electron-hole drops, US absorpt. and recomb. radiation, 1.8 to 3.5K 77−31954
Ge, electron-hole drops at high mag. fields 79−60721
Ge, electron-hole gas and liq. coexistence 78−14668
Ge, electron-hole liquid, luminesc. under infinite uniaxial compression 78−87915
Ge, electron-hole liquid, strain-confined 78−10355
Ge, electron-hole liquid, strain-confined 80−6745
Ge, electron-hole luminesc. and transport props. 77−48241
Ge, electron-hole-droplet cloud, photoluminesc. of laser excited surface, phonon wind 78−84146
Ge, electron-hole-liquid, de Haas-van Alphen-like oscills. in luminesc. line shape 79−60720
Ge, exciton condensation, light scatt. by electron-hole drops 80−84435
Ge, exciton condensation, microwave breakdown, luminesc., book contrib. 80−11471
Ge, exciton energy gap and LA and LO momentum-conserving phonon energies 79−90965
Ge, exciton gas, entropy ionisation, luminesc. meas. 78−35196
Ge, exciton luminesc. polarisation in mag. field *(Russian)* 77−12436
Ge, exciton recombination with emission of single phonon, luminesc. replicas, detect. and anal. 79−60728
Ge, heavily doped and compensated, photoluminesc. exam. 78−2902
Ge, high excitation intensities, direct and indirect gap transitions 77−12429
p-Ge, hot-hole relax. rates by saturation spectroscopy 77−65611
Ge, indirect excitons, photoexcitation spectra, 2.0-2.6 meV 77−44051
Ge, influence of dislocations on free-exciton lifetime 78−60064
Ge, luminescence circular polarisation in mag. field, Landau levels paramag. splitting 77−32435
Ge, luminescence kinetics and electron-hole drop motion 77−77288
Ge, luminescence line shape of free exciton, electron-hole droplet binding energy 77−44041
Ge, luminescence meas., presence of trions, molecules and excitons above Mott density 77−80737
Ge, mag. field luminesc. lifetime, quantum oscills., phonon wind effects 80−93385
Ge, magnetoluminescence of electron-hole liq. 80−29790
Ge, magnetostriction of electron-hole drop 77−85540
Ge, microwave exciton breakdown and luminesc., under one- and two-photon excitation 77−31955
Ge, Mott distortion of the electron-hole fluid phase diagram, luminesc. meas. 79−42457
photoluminescence continued
Ge, nonequilibrium charge carrier-mag. field interaction electron-hole drops, recombination *(Russian)* 80−75511
Ge, nonuniformly deformed, electron-hole drop density depend. on size *(Russian)* 80−20092
Ge, nucleation anal. of electron-hole drops 77−69243
Ge, optically stimulated, electron-hole drops and appearance of dense plasma *(Russian)* 77−4688
Ge, phase diagram of electron-hole fluid in low temp. photoexcited semicond. 77−69237
Ge, phonon-assisted exciton emission, temp. depend. of relative integrated intensities 77−1375
Ge, photoluminesc. decay from electron-hole drops 77−66532
Ge, plasma excitation, ultrafast optical props. 78−31248
Ge, pure, magnetic phase transition between electron-hole drops and free-excitons 78−6278
Ge, pure and doped, electron-hole drops net charge, photocond. and photoluminesc. 79−38589
Ge, recombination luminesc. spectra from hot and cold carriers in electron-hole drops 79−38608
Ge, size distrib. of electron-hole drops, kinetics of recomb. 79−28292
Ge, strain-confined electron-hole liq. 77−47738
Ge, strain-narrowing of luminesc. line from excitons 79−24356
Ge, stressed, α_1 and α_3 electron-hole droplet luminesc. 79−28820
Ge, stressed, metal-insulator transition, luminesc. 80−20695
Ge, stressed cryst., props. of strain-confined electron-hole liquid 79−7787
Ge, strong microwave field effect on electron-hole drops, luminescence kinetics 79−87047
Ge, surface energy effect on electon-hole drop luminesc. 77−48239
Ge, ultra high vac. cleaved, photolum., role of intrinsic surface states 78−52571
Ge, ultra-pure electron-hole drop condensation nucleation phenomena 77−47744
Ge, uniaxially deform., electron-hole drop flight, photolum. max. press. depend. 78−10977
Ge, uniformly stressed, density and binding energy of electron-hole droplets, photolum. meas. 78−60062
n-Ge:As, heavily doped, luminesc. from electron-hole drops 77−81144
Ge:As, recomb. of donor bound excitons, luminesc. intensity decay 80−25441
n-Ge:As closely compensated, photolum. of charge carriers localised in trails of density of states 77−77294
Ge:As(Bi), donor bound exciton luminesc. and absorpt. 80−29777
n-Ge:As(Sb), moderately heavily doped, electron-hole drops photoluminesc. 80−7417
Ge:B(Al)(Ga), shallow acceptor spectral line intensities 80−88517
Ge:B(Al)(Ga)(In)(Tl), binding energy, excited state spectra, photolum., semi-empirical short range pot. 80−44534
Ge:In (Sb) and pure cryst., kinetics of strain-confined large electron-hole drop and its clinging exciton system 80−75508
Ge:P, bound-exciton luminesc. and absorpt. 79−87469
Ge-Se, glassy, photoinduced photolum. fatigue *(Russian)* 78−60520
Ge-Se glass system, effect of changes in local surrounding of atoms on optical props. *(Russian)* 78−80414
Ge-Se glasses, radiative localised centres, photoluminesc. 79−83025
GeO_2 based glasses, absorpt. and emission of Ho^{3+} 79−11439
GeS, exciton luminescence 78−52555
GeS, low temp. photoluminesc. 77−77287
GeS orthorhombic layer crystals, photolum. spectra 80−2851
GeS_x glass, chem. struct. effects 77−63460
Ge_2S_3-Ge_2Se_3, glass, photoluminesc. spectra, solid soln. form. *(Russian)* 78−23525
GeSe, low temp. photoluminescence 77−77287
$GeSe_2$ glass, photoluminesc. spectrum, rel. to cryst. forms 77−55819
$GeSe_2$, glassy, powdered and bulk, fatigue of photolum. 80−80855
$GeSe_2$, glassy and single-cryst., photoluminesc. at 77K 77−63456
$GeSe_2$, glassy photoinduced photoluminescence fatigue 79−28827
$GeSe_2$ powdered crystalline, photoluminescence intensity under continuous excitation 80−71480
$GeSe_2$, single crysts., 3 polymorphic forms, DTA, photolum., IR and Raman sepctroscopy 80−33923
$Ge_{1-x}Se_x$, photolum. and optical props. meas. 77−20908
Ge_xSe_{1-x}, amorphous, excitation spectra of photolum. fatigue and creation of paramag. centres 80−50402
Ge_xSe_{1-x} glasses, defect states, photoluminesc. and ESR obs. 79−61418
α-Ge_ySe_{1-y}, fatigue effects in glasses 78−84648
$Ge_{1-x}Si_x:Ga,As$, interimpurity radiative recombination; composition depend. 79−11465
$glass:Nd^{3+}$, kinetic description of excitation spectra 78−68557
H-bond complex formation, enthalpy change due to electronic excitation, spectroscopic determ. 78−92496
$HCl:Bi^{3+}$ solution, characts. of luminesc. spectra, 82 to 130K *(Russian)* 79−28835
$HCl:Bi^{3+}$ solution, kinetics and struct. of luminesc. spectra *(Russian)* 77−77290
$Hg_{0.7}Cd_{0.3}Te$, 17 to 77K, photo- and cathodoluminesc. 78−52569
$Hg_{1-x}Cd_xTe$, near band-gap photoluminesc., bound exciton luminesc. obs. 80−103973
$Hg_{1-x}Cd_xTe$, photolum. and optical pumping 80−50424
Hg_2Cl_2, single cryst., luminesc. 397 nm band props. 77−66529
HgI_2, emission spectra in highly excited state 77−52167
HgI_2, low temp. luminesc. spectra by holographic spectroscopy 79−33820
HgI_2, phonon-assisted recomb. of free electron-hole pair 78−23521
HgI_2, red, liminesc. and Raman scatt., biexcitons and exciton-phonon interactions 79−61424
HgI_2, red, luminesc., excitation spectra on M-band 79−28822
HgI_2, red, reson. Raman scatt. and luminesc. 78−84579
HgI_2 X-ray luminesc., emission band characts., use as X-ray detectors 77−55815
$HgI_2:Ag$, trapping effects, TSC, photocond. and photolum. meas. 77−32023
$HgMoO_4$, luminesc. efficiency, temp. and high-press. 78−23507
α-HgS, cinnabar, photolum. meas. 79−19929
α-HgS, cinnabar, reson. Raman effect and luminesc. meas. 80−50338
I_2, matrix samples, laser spectroscopy, evidence for $(I_2)_2$ species 78−58735
III-V alloys, disorder-enhanced Auger recomb. 79−43014
In complex, photoluminesc. spectra, $\pi \rightarrow \pi^*$ and charge transfer L→M transitions, Stokes shift 78−64407

photoluminescence continued
In-ZnO-Al metal-semicond. diode, electrolum. and photoluminesc. spectra 79−99948
$In_{1-x}Al_xP$:Bi(N)(Zn,O) radiative recombination at isoelectronic centres 79−52027
InAs and solid solutions, recombination mechanisms of excess carriers, luminesc. obs. 80−97337
p-InAs, Auger recomb., theory and luminesc. expts. 78−56518
n-InAs, edge luminescence band, shape depend. on degree of doping, band gap 80−7405
InAs, photoluminescence exam. 79−28809
n-InAs, recomb. of nonequil. charge carriers at high photoexcitation levels 77−44053
$InAs_{1-x}Sb$, disorder-enhanced Auger recomb. 79−43014
$InAs_{1-x}Sb_x$, epitaxial film, carrier recomb., elec. and optical props. 79−15164
p-$In_{0.53}Ga_{0.47}As$:Zn on InP, elec. and optical props. 80−75662
$In_{1-x}Ga_xAs$, LPE growth on InP substrate, quasi grown layers, photoluminescence meas. 79−23862
$In_{1-x}Ga_xAs$, LPE layer on InP substrate, phys., elec. and optical props. 78−39235
$In_xGa_{1-x}As$, heteroepitaxial, MBE grown, props. 78−84328
$In_xGa_{1-x}As$, MBE layers on InP substrates, elec. props., photoluminesc., X-ray and Auger obs. 79−51450
$In_xGa_{1-x}As$ multilayer struct., photoluminesc. and X-ray spectroscopic microprobe analysis 77−4687
InGaAsP, bandgap energy by electroreflectance and photoluminesc. spectra 80−107700
InGaAsP DH, luminesc., quantum efficiency determ. 80−108273
InGaAsP, quaternary alloy, physical props. *(Japanese)* 80−15449
InGaAsP, with and without InP cladding layers, low photolum. regions 79−33754
InGaAsP:Be, avalanche photodetectors annealing temp. effect on photolum. spectra 79−69872
InGaAsP-InP, anomalous luminesc., near heterojunction interface 79−65932
InGaAsP-InP DH laser, optical gain meas., low-intensity luminesc. and absorpt. spectra 79−98356
InGaAsP-InP DH lasers, perturbed InP growth, photoluminesc. study 80−106518
$In_{1-x}Ga_xAs_{1-y}P_y$ layers on InP substrate, LPE growth, quaternary phase diagram, and band gaps 79−42403
$In_{1-x}Ga_xAs_yP_{1-y}$, DH laser material, spatially resolved photolum. characterisation and optically induced degradation 79−47486
$In_{1-x}Ga_xAs_yP_{1-y}$ DH laser, low threshold current density, near equilibrium LPE growth 80−19040
$In_xGa_{1-x}As_yP_{1-y}$ layers on InP, LPE and opt. props. characteris. 79−28849
InGaP-GaAs junction, effect of elastic strain on energy band gap and lattice parameters 79−24057
$In_{0.3}Ga_{0.7}P$, N free and implanted, photoluminescence study 80−97322
$In_{1-x}Ga_xP$, LPE, on $GaAs_{1-y}P_y$, photo- and cathodolum. 78−19559
$In_{1-x}Ga_xP$, solid soln. film, photoluminesc. meas. 78−27321
$In_{1-x}Ga_xP$, temp. depend. of forbidden band width, photoluminesc. meas. 78−19556
$In_{1-x}Ga_xP$:Bi(N)(Zn,O) radiative recombination at isoelectronic centres 79−52027
$In_{1-x}Ga_xP$:N_2, N-trap bound states, photoluminesc. and absorption data 77−1719
$In_{1-x}Ga_xP$:N(Te), composition depend. of bound state luminesc. transitions 78−39595
$In_{1-x}Ga_xP$:Te,Zn, photolum. and electrolum., direct transition region 77−8659
$In_{1-y}Ga_yP$-GaAs heterojunction, VPE, energy band gap and lattice parameter, lattice mismatch effects 78−95345
InGaPAs LPE layers, compositional inhomogeneity, photoluminesc. obs. 80−75451
$In_{1-x}Ga_xP_{1-y}As_y$ lattice-matched epitaxial layers, LPE growth on GaAs(100), characterisation 80−75465
$In_{1-x}Ga_xP_{1-z}As_z$ single thin active layer visible spectrum heterostruct. lasers 78−63120
InI, photoluminesc., Raman scatt. 79−38593
In_2O_3-SnO_2-CdTe:P, p-n homojunction solar cell, elec., photovoltaic props., photoluminescence 80−81463
In_2O_3-SnO_2-InP solar cell junctions, efficiency, InP surface props. 80−85288
n-InP, (110) surfaces, photolum. intensities in vac. and gas ambients 79−61412
InP, acceptor excited states, luminesc. spectra 80−16091
InP, ambient-enhanced photoluminesc. props., mol. adsorption and gas-flow effect 79−99925
InP, bulk grown, selective spectroscopy, acceptor level studies 80−29778
InP, deep level electron traps, emission and capture props. 80−29806
InP, electrical and optical props. at low temps. 80−39636
InP, exciton localisation at impurity pairs 79−37999
InP, excitons bound to neutral donors in VPE layers, luminesc. and absorpt. obs. 79−42460
InP films, organometallic VPE grown, props. 80−96753
InP, growth and props. 79−1822
InP growth from soln. and LEC, photolum. and elec. meas. 79−87575
InP, luminescence, hot electron effects 80−66277
InP, model for ∼1.10 eV emission band 80−66289
n-InP, photolum., evidence for low surface recomb. vel. rel. to n-GaAs 77−40272
InP, photolum. depend on surface treatment 79−78727
InP, photoluminesc. of epitaxial films, isovalent substitution 80−16097
InP, photoluminescence at dislocations, band gap electronic levels 79−99926
InP, photoluminescence intensity of cleaved surface, ambient gas influence 78−88345
InP, photoluminescence meas. using diamond-anvil press. cell 80−108256
InP, polar semiconductor, collisions between hot excitons and hot electrons 80−7415
p-InP, single cryst. and epilayers, photoluminesc. 77−81211
InP, synthesis solute diffusion grown, elec. props., photoluminesc., etch pit profiles 79−4914
InP, VPE growth for MESFET's 80−103602
InP:Bi, isoelectronic impurity states, emission and absorpt. obs. 79−42491
InP:Fe, deep levels 79−56166
InP:Fe, Fe acceptor charge states, photolum., absorpt. and ESR meas. 77−36123
p-InP:Zn, vapour grown, prep. and props. 80−54268
InP-electrolyte struct., field effect of photoluminesc. 79−99928
InP-$In_{1-x}Ga_xP_{1-z}As_z$ laser, phonon-assisted recombination 79−89906
InP-$In_{1-x}Ga_xP_{1-z}As_z$, valence band discontinuity, quantum well luminesc. 79−91483
InP-$In_{1-x}Ga_xP_{1-z}As_z$ heterostructure laser, single and multiple quantum-well, liquid-phase epitaxial growth 80−38031
InP(100) undoped homoepitaxial films grown by MBE, photoluminesc. props. 80−2809
InSb, absorpt. saturation by nonequilib. electron-hole plasma, luminesc. 78−9418
InSb, electron spin levels resonant excitation, photolum. 80−25454
InSb, interaction of exciton recombination with LO phonons 79−38647
InSb p-n junction, minority carrier injection in mag. field, recomb. radiation obs. 80−11078
n-InSb, photoluminesc. in crossed EM fields *(Russian)* 77−24892
n-InSb, photoluminescence exam. 79−28809
InSb, prep. of thin films by ionised-cluster beam deposition, photolum. meas. *(Japanese)* 80−25576
InSb, reabsorbed radiative recomb. and photon recycling 80−76076
InSe, excitonic absorpt. edge 78−88352
InSe luminescent film, production and characterisation *(Russian)* 78−39581
InSe, optical props. near fundamental absorption edge 77−12434
$(In_2Te_3)_x$-$(Hg_3Te_3)_{1-x}$, photoelec. and luminesc. props. 77−39889
Ir(III) complex, cis-dichlorobis(1,10-phenanthroline) iridium chloride, luminesc. excited states, solvent effects 80−97319
K halide, Yb^{2+} activated, X-ray and intracentre luminesc. 78−6737
$K_5Bi_{1-x}Nd_x(MoO_4)_4$ solid soln., growth, spectroscopic and laser props. 78−2901
KBr, F-centre lifetime, perturbation effects, luminesc. meas. 80−108252
KBr, F-centre luminesc., MCD effects 78−39598
KBr, F-centre radiative lifetime meas. near 65K 80−25439
KBr, interaction between F- and α-centres, luminesc. meas. 79−73988
KBr, optical conversion, luminesc. and colour centre formation 79−24354
KBr, photoluminescence under pulsed UV laser excitation 77−77289
KBr, S centres, luminesc. and photochemistry *(German)* 77−44055
KBr, spectral distrib. of triplet to singlet luminesc. of F_2 centre 77−59601
KBr:Ag, mag. field effect on luminesc. of paired Ag^- ions 78−27313
KBr:Br_2^-, triplet luminesc. kinetics, 0.4-4.2K 79−87482
KBr:I, energy transfer due to excitons and holes under host sensitization 79−15526
KBr:I, luminesc., exciton and hole migration to I^- sites 79−38626
KBr:In^+, emission lifetimes, temperature dependence 79−78745
KBr:$Li^+(Na^+)$, electronic struct. of $(V_K e)_A$ 78−95269
KBr:Pb, luminesc. spectra obs. 78−95604
KBr:Pb; A-luminesc ., 8-80K 80−2836
KBr:Tl, A-emission, line shapes and relative efficiencies 79−83011
KBr:Tl, Jahn-Teller system, negative mag. circular polarisation in emission spectrum 80−20694
KBr:Tl, luminesc., decay model for A_T and A_X emissions 80−93379
KBr(Cl):Tl, visible emission, temp. depend. 78−60511
KBr(Cl)(I), electron-spin memory and magnetic-circular-dichroic effects in F-centre luminesc. 80−29794
KBr(Cl)(I):O_2^- centres, luminesc., polarisation temp. depend. 78−87943
KBr(I), photostimulated recomb., electron spin polarisation 80−60673
KCN, F-centre emission spectrum 77−12420
KCN, F-centres, optical props. 78−2892
KCN, optical F centres and phase transitions 78−56504
KCl, absence of energy transfer between F- and M-centres 79−99935
KCl, F_3-centre quartet state, IR emission spectra 78−43930
KCl, F-center pairs, light excitation, mag. field and resonance effects on absorption bands 78−92094
KCl, F-centre luminesc., MCD effects 78−39598
KCl, γ-irradiated, photo- and thermoluminesc., F-centre interstitial recomb. 77−44036
KCl, luminesc. excitation spectra of F-aggregate centres, 400-900 nm. *(Russian)* 78−10980
KCl, luminesc. under 10.6 μm laser pulse irrad. *(Russian)* 77−16381
KCl, M-centres, F-centre sensitised luminesc. 77−4681
KCl, S centres, luminesc. and photochemistry *(German)* 77−44055
KCl, self-trapped exciton luminesc. 77−48225
KCl, spectral distrib. of triplet to singlet luminesc. of F_2 centre 77−59601
KCl, X-irrad. induced deform. effects, glow curves *(Russian)* 79−52022
KCl:Ag, hole capture radius, scintillation luminesc. obs. *(Russian)* 78−39582
KCl:AgCl, tunnelling-recombination luminesc. 78−88354
KCl:Ag(Cu), strong IR luminescence obs. of Ag_F^0 centres 78−6736
KCl:Ag(In)(Tl), excitation in fund. absorpt. region, luminesc. and thermolum. 80−50433
KCl:Ba(Sr), Z-centre, luminesc. and absorpt. spectra obs. 80−49221
KCl:Cu, EPR, optical absorpt. and luminesc. investig. of anisotropic Cu_F^0 centres 77−20893
KCl:Cu,Tl, plastic deform., charge exchange of hole centres *(Russian)* 77−11876
KCl:Cu^- excitation and absorpt. spectra 80−108255
KCl:Eu, luminescence and absorption of color centres in RbCl:Cu and KCl:Eu crystals 78−92118
KCl:Eu^{2+} crystals, photostimulated afterglow investigation at room temp. 80−108259
KCl:I, luminesc. at low temp. 80−2818
KCl:Li(Na), M_A-centre, decay 77−77278
KCl:Pb, 420 nm A-emission band *(Russian)* 79−56852
KCl:Pb, luminesc. spectra obs. 78−95604
KCl:Pb, photolum. in A band region, spectral and time decay anal. 79−33823
KCl:Pb, photoluminesc. induced by Suzuki-like occlusions, ionic thermocond. 79−33808
KCl:Pb^{2+}, decay of luminescence emission 78−39593
KCl:Pb^{2+}, highly doped, state of dispersion of Pb^{2+} 77−1144
KCl:Pb^{2+}, origin of 420 nm emission band 77−40279
KCl:Sn, pure and doped, thermoluminesc. and luminesc. decay 79−83041
KCl:$SnCl_2$, photostimulated hole recombination luminesc. *(Russian)* 80−80833

photoluminescence continued
KCl:$SnCl_2$, Sn^+ centres, polarised luminesc. and EPR 79−65076
KCl:$SnCl_2$, X-ray irrad., polarised luminesc. and EPR study of Sn^{3+} centres 80−39868
KCl:Sr, M-centre photoluminesc. *(Russian)* 78−84649
KCl:Sr crystal, Z_4 colour centre, luminesc. study 80−64993
KCl:Tl, effective cross sections ratio of charged and neutral centres for holes and electrons *(Russian)* 79−28319
KCl:Tl, low-temp. ionisation of activator, photoexcitation, in region of interzone transitions *(Russian)* 79−28320
KCl:Tl^+, decay modes of 3000 Å emission band 77−73168
KCl-CuCl solid solution supersaturated, precipitation, impurity aggregation 80−29174
KCl-KBr:Tl^+, cryst., luminesc. and excitation spectra 77−66535
KCl-$SrCl_2$, photoluminescence of Z_4-centre and associated Z type colour centre *(Russian)* 79−4851
KCl-Tl, Jahn-Teller system, negative mag. circular polarisation in emission spectrum 80−20694
KCl(Br), F-centre emission, mag. circular polarisation 80−108251
KCl(Br)(I):Ga^+, polarisation of Ga^+ centre A_T emission, temp. depend. 80−80842
KCl(Br)(I):Tl, emission spectra, press. effects 78−23509
KClIn, absolute quantum output of low-inertial energy transmission *(Russian)* 77−32429
$K_2Cr_2O_7$, luminesc., vibr. anal. 79−38620
KF(Cl)(Br), mag. props. of relaxed excited state of F-centre, vibronic theory 78−60502
KH_2PO_4, electrophotoluminescence obs. 79−47521
KI, edge emission of excitons 77−59606
KI, edge luminesc. under UV excitation 77−77273
KI, exciton diffusion, luminesc. quenching, meas. 4 to 77K 77−32433
KI, F-centre luminesc., MCD effects 78−39598
KI, free exciton-F^- centres interaction, electron excited emission 79−83036
KI, growth time of π emission in picosecond range 80−76067
KI, intrinsic luminesc. quenching, by X-ray induced coloration 78−19539
KI, luminesc. due to free excitons, line shapes 79−33803
KI, luminesc. lines due to n=2 free exciton state of Wannier series 80−29776
KI, luminesc. polarisation for free and bound excitons 78−10942
KI, mag. circular dichroism in luminesc. of F-centres 77−20919
KI, quenched, absorpt. and emission spectra, α-centres 80−11442
KI, spectral distrib. of triplet to singlet luminesc. of F_2 centre 77−59601
KI, surface, 420 nm band laser-stimulated emission, V_2 centres 78−84633
KI, zero phonon and LO phonon assisted luminesc. of free excitons 79−28799
KI:Eu^{2+}(Sr^{2+})(Mn^{2+}), elec. field effect on mech. of recomb. 78−80397
KI:I_2^-, triplet luminesc. kinetics, 0.4-4.2K 79−87482
KI:In^+ luminesc. decay, excited state symm. and g-value 79−99922
KI:Pb^{2+}, absorpt., excitation and luminesc. spectra 78−19519
KI:S_2^- centres, luminesc., polarisation temp. depend. 78−87943
KI:Se_2^-, reson. secondary emission, total spectrum *(Russian)* 78−19551
KI:Sn^{2+}, luminesc. 79−33817
KI:Sn^{2+}, red emission, mag. field effect on radiative decay time 79−33818
KI:Sn^{2+} luminesc. decay, excited state symm and g-value 79−99922
KI:Tl, activated crystal, induced recombination emission *(Russian)* 78−48214
KI:Tl, $(Tl^+)_2$ centre luminesc. 78−84632
KI:Tl, cryst., induced recomb. emission 79−4845
KI:Tl, emission and excitation spectra, press. effects 79−83028
KI:Tl, Jahn-Teller system, negative mag. circular polarisation in emission spectrum 80−20694
KI:Tl, phosphor, press. effect on emission spectra at low temps. 77−85771
KI:Tl, polarised luminesc. of $(Tl^+)_2$ centres 80−71473
KI:Tl, X-ray phosphor, influence of different factors on emission intensity 79−8171
KI:Tl^+ type phosphor, press. effects on triplet relaxed excited states, quadratic Jahn-Teller interaction 78−23510
KI:Tl(In) and KBr:In, A-luminescence spectra and polarisation, Jahn-Teller minima 77−20914
$KLi(Pt(CN)_4).2H_2O$, cryst. struct., polarised emission obs. 78−52538
$KMgF_3$:Ni, Co, emission from Ni-Ni and Ni-Co pairs, exchange coupling const. 79−33788
$KMgF_3$:Ni^{2+}, absorpt., MCD and emission spectra 79−51953
$KMgF_3$:Sm^{2+}, luminesc. spectra 4.2, 77 and 295K and Zeeman spectra, 4.2K 77−81146
$KMnF_3$, antiferromag., multi-magnon luminesc. sidebands 78−76525
$KMnF_3$, antiferromag. cryst., luminesc. enhancement in mag. field, exciton model *(Russian)* 77−48214
$KMnF_3$, exciton and exciton-magnon emission 79−33779
$KMnF_3$, luminesc., emission from localised traps 79−33777
$KMnF_3$, stress-induced phase transition, optical props. meas. 77−20067
K_2MnF_4, quadratic layer antiferromag., intrinsic emission obs. 77−20906
$K_6Nb_6Si_4O_{26}$, luminesc. bands, Stokes shift, rel. to crystal struct., stacking faults 80−34974
$K_8Nb_{14}Si_4O_{47}$, luminesc. bands, Stokes shift, rel. to crystal struct., stacking faults 80−34974
$K_5NdLi_2F_{10}$ (KNLF), spectroscopy and lasing 80−5737
$K_5Nd(MoO_4)_4$, spectral and struct. props. *(Russian)* 79−52020
K_2O-B_2O_3 glass, PbO-activated, luminesc. and excitation spectra *(Russian)* 78−10979
K_2O-BaO-GeO_2:Bi^{3+}, Nd^{3+}, absorpt. and excitation spectra, fluoresc. 77−90183
K_2O-GeO_2:tb^{3+}, Yb^{3+} glass, luminesc, cooperative sensitization correlated with Rayleigh scatt. intensity 78−52573
$K_5PrLi_2F_{10}$:Pr^{3+}, emission spectroscopy, ionic interaction 79−83015
$K_{1.75}Pt(CN)_4.1.5H_2O$, Raman scatt. and luminesc. studies 80−25394
K_2PtCl_6:Os^{4+}, multiple state luminesc. 78−72584
$K_3(UO_2)F_5$, optical spectra, vibr. freqs, calcs. *(Russian)* 78−31205
KYF_4, KY_2F_7, KY_3F_{10}, Er^{3+} and Yb^{3+} doped, IR excitation curves for visible luminesc. 79−33795
KY_3F_{10}:Eu^{2+}, luminescence 79−78746
$KZnF_3$, Cu^{2+} and Mn^{2+} exchange interactions, luminesc. line temp. depend. 79−69480
$KZnF_3$:Mn^{2+}, Cu^{2+}, exchange coupled, luminesc. props. 79−33781
$KZnF_3$:Ni^{2+}, absorpt., MCD and emission spectra 79−51953

photoluminescence continued
Kl:Tl, excitation in fund. absorpt. region, luminesc. and thermolum. 80−50433
Kr:N_2O, cryodeposited film, exciton-enhanced KrO excimer luminescence 77−36288
Kr:N_2O, photoluminesc. from KrO (^1S) excimers 78−68544
Kr:OCS, O(^1S) and S(^1S) photodissociative prod., photoluminesc. excitation spectra, exciton energy transfer 80−89508
KrO, in doped inert gas matrix, photoluminesc. 79−31579
KrS, photoluminesc. in rare gas matrices 80−5568
$LaAlO_3$:Tb^{2+}, cathodo- and photoluminesc. 77−12448
$La_2Be_2O_5$:Nd^{3+}(Pr^{3+}), cryst. growth, spectral and laser properties in $^4F_{3/2}\rightarrow{}^4I_{11/2}$ and $^4F_{3/2}\rightarrow{}^4I_{13/2}$ transitions 80−80853
$LaBr_3$:Pr, continuous wave and pulsed laser pumped Pr IR quantum counters 79−93219
LaCl-Pr(Dy)(Sm), mech. for X-ray luminesc. and thermolum. 79−8170
$LaCl_3$:Nd^{3+} radiation upconversion, 1.06 to 0.873 μm 78−19530
$LaCl_3$:Pr, continuous wave and pulsed laser pumped Pr IR quantum counters 79−93219
$LaCl_3$:Pr^{3+}, Nd^{3+}, single cryst., optical double reson. excitation, energy transfer and transform. 77−69891
LaF_3:Er^{3+}, spin-lattice relax. meas. in excited $^4S_{3/2}$ state by purely optical method 79−19923
LaF_3:Nd^{3+} vacuum UV luminesc. *(Russian)* 78−64414
$LaGaS_3$:Ce^{3+}, phosphor, luminesc. props. 80−103979
$La_2MgSn_{1-x}Ti_xO_6$, luminescence and energy transfer 77−28619
$LaNbO_4$:Eu^{3+}, single cryst., photoluminesc. obs., vibronic transition dichroism 77−69890
$La_{2-x}Nd_xTi_2O_7$, luminesc. and absorpt. props. 79−65928
La_2O_3-Al_2O_3-SiO_2:Sm^{3+}, luminesc. selective laser excitation line narrowing 80−25434
LaOCl:Sm^{3+}, conc. quenching of X-ray and UV-excited luminescence *(Russian)* 77−55829
La_2O_2S:Eu, high press. effect on luminesc. efficiency and lifetime, charge transfer absorpt. 80−66266
La_2O_2S:Eu^{3+}, luminesc., excitation spectra, cooperative phonon sidebands 79−33771
La_2O_2S:Tb, recomb. processes and emission spectra *(Russian)* 78−6797
La_2O_2S:Yb^{3+},Er^{3+}, IR excited visible luminesc. of Er^{3+} 78−2910
$La_{1-x}Tb_xOBr$ phosphor, concentration quenching of Tb^{3+} luminesc. 80−29785
Li, photoexcitation of high levels, reson. radiation at 670.7 nm 79−783
Li-La phosphate glass, Nd, Cr activated, Nd luminesc. quantum efficiency meas., Nd-Cr nonradiative transfer 80−66296
Li-Nd-La phosphate glass, nonradiative losses, pulse periodic stimulated emission and luminesc. 77−83878
$LiBaAlF_6$:Eu^{2+}, band emission and line emission 79−28810
LiBr, aqueous soln., NO_2^- impurity anions, temp. quenching of luminesc. *(Russian)* 77−1714
$LiCdVO_4$, luminesc. spectra in visible region, vanadate group 78−43921
LiCl, aqueous soln., NO_2^- impurity anions, temp. quenching of luminesc. *(Russian)* 77−1714
LiCl, electron irrad., F-centre emission 78−60501
LiCl, radiation effects on decay time of F-centre emission 80−93381
LiCl:Ag, luminesc. anal. using synchrotron radiation 79−38639
LiD, luminesc. of free and localised excitons, UV, X-ray and electron irrad. luminesc. 79−87483
LiF, coherent radiation generation in F_2-centres 78−50782
LiF, effect of impurity traces on physical props. 77−12450
LiF with stable F_2 centres, F_2^+ colour centre generation accumulation, tunable laser production *(Russian)* 80−28238
LiF:Mg, TLD-100, thermolum. phosphor, photolum. and absorpt. spectra, thermolum. mechanisms 80−97321
LiF:Mg, Ti, luminesc. increase by O implantation 78−64412
LiF-Li_2O, F-aggregate centres *(Russian)* 78−64394
$LiGaO_2$:Fe, phosphor, luminesc. 78−92108
LiH (D), single crystals, electronic excitations, review *(Russian)* 78−72574
LiH, effect of surface hydrolysis to LiOH on IR absorption, X-ray luminesc. and EPR spectra 80−60660
LiH, LiD, single cryst., reson. zero-phonon exciton luminesc., polariton emission 78−52564
LiH, luminesc. of free and localised excitons, UV, X-ray and electron irrad. luminesc. 79−87483
LiH, motion and relax. of free excitons, luminesc. spectra 79−43037
LiH, single crysts., refl. photolum., cathodolum., and photocond. meas. 77−52186
LiH, UV induced luminescence 77−85784
LiH:LiF, luminesc. of free and localised excitons, UV, X-ray and electron irrad. luminesc. 79−87483
LiH(D), resonant Raman scattering in crystals with self-trapping excitons 80−7344
LiI crystal, emission spectra under UV-light excitation at 77K 78−92110
$LiIO_3$, crystal, parametric superluminescence in ps band 80−11469
$LiInS_2$, blue-band emission 80−76062
$LiInS_2$, single cryst. growth by directional solidification, photoluminescence meas. 79−61514
$LiMgP_{1-x}V_xO_4$, luminesc. spectra in visible region, vanadate group 78−43921
$LiMgVO_4$, luminesc. spectra in visible region, vanadate group 78−43921
Li_3N, photoluminesc. props. 80−50414
Li_3N, superionic conductor, cryst. growth and struct., phys. props., book contrib. 79−42308
$LiNbO_3$, spontaneous parametric light scatt. characts. meas., 1000-4000 cm^{-1} 77−8640
$LiNbO_3$:Cr^{3+} glass, roller quenched, crystn. kinetics 80−44143
LiNd phosphate glass, spectral and generation props. 77−1700
Li_2O-Fe_2O_3-siO_2 glass, struct. and crystallisation behaviour 78−83738
Li_2O-Nd_2O_3-P_2O_5 ultraphosphate glasses, Nd^{3+} conc. quenching of luminesc. effect 79−19931
$LiScO_2$:Bi^{3+}, luminesc., vibr. struct. 79−33790
Li_3WO_4:U^{6+}, luminescence meas. 77−32432
Li_4WO_5, IR, Raman, luminesc. spectra meas., cryst. struct. investig. 77−52074
Li_4WO_5:U^{6+}, vib. fine struct. in luminesc. spectra 77−8620
$LiYF_4$ UV reflectance, transmission and photoluminescence obs. 79−15488
$LiYF_4$:Yb^{3+}, Ho^{3+}, sensitised anti-Stokes luminesc., theory 77−66537
$LiYFd_4$:Er^{3+}, optical spectra and multifreq. stimulated emission 79−56818

photoluminescence continued
$LiYO_2:Nd^{3+}$, absorption and luminesc. spectra, energy level diagram 77−63441
$LiZnVO_4$, luminesc. spectra in visible region, vanadate group, and high-press. phase 78−43921
$Lisd4UO_5$, energy transfer, cryst. struct. and chemical composition effect 80−108248
$LuAlO_3:Er^{3+}$, $^4S_{3/2}$ to $^4I_{9/2}$ transition laser action, optical and luminescence spectra 80−16082
$LuAlO_3:Nd^{3+}$, spectral-generation characts., expt. and theory *(Russian)* 77−7090
$Lu_2O_2S:Eu^{3+}$, luminesc., excitation spectra, cooperative phonon sidebands 79−33771
$LuPO_4:Yb^{3+}$, charge transfer type luminesc. 78−64392
$Lu_2(WO_4)_3:Cr(Eu)$, and undoped crystals, luminesc. obs. 80−89047
Mg, flame luminesc., laser irrad. effects 77−77766
Mg_2, Ar matrix isolated laser photoluminescence spectra, electronic absorpt., emission, vibronic and vibr. relax. 78−82744
$Mg_{(S)}+Ne^+$, O-dependent photon emission 79−1810
$MgAlO_4:Cr^{3+}$, exchange parameters of Cr^{3+} pairs, optical and EPR meas. 77−69282
$MgAl_2O_4:Cr^{3+}$, exchange parameters determ. from emission and luminesc. excitation spectra 77−52160
$MgAl_2O_4:Cr^{3+}$, luminesc. spectrum, N-lines *(German)* 77−16382
$MgAl_2O_4:Cr^{3+}$, N-lines and Cr^{3+} pairs 78−2896
MgF_2, cryst., Roentgenoluminesc., exciton emission *(Russian)* 78−95609
MgF_2 crystal, $M(D_{2h})$ centre absorption and emission spectra obs. 79−19910
MgF_2, nonactivated, X-ray luminesc., 80−2832
MgF_2, X-ray luminesc. polarisation 80−11462
MgF_2:Mn, X-ray luminesc. yield temp. depend. 77−4680
MgF_2:Mn(Co), photoluminesc. due to X-rays, colour centre thermal breakdown 79−24359
MgO, cryst. short-wave luminesc. V-centre electron recomb., impurity effects *(Russian)* 77−20921
MgO doped powder phosphors, photo- and thermostimulated luminesc. obs. *(Russian)* 80−66263
MgO, electronic excitations and luminescence, review *(Russian)* 78−72575
MgO, F centre luminesc., effects of uniaxial stress and ODMR 80−20690
MgO, laser induced photoluminesc. spectra 78−82757
MgO, photoluminesc. during mechanical deform. 80−60665
MgO, pure and doped crysts., X-ray stimulated luminesc. 79−28802
MgO:Al(Li)(F)(Sn), hole processes in photostimulated luminesc., electron emission, X-ray irrad., ESR relaxation 79−69889
$MgO:Cr^{2+}$ (V^{2+}), coupling of T_{1u} and T_{2u} vibr. to $^2E_g \rightarrow {}^4A_{2g}$ transition 77−63453
$MgO:Cr^{3+}$, $^4T_{2g}$ excited level of Cr^{3+} 78−43920
$MgO:Cr^{3+}$, broad band luminesc., relaxed level and emission processes 78−31234
$MgO:Cr^{3+}$, emission and excitation spectra 80−93387
$MgO:Cr^{3+}$, no-phonon lines associated with broad band emission *(French)* 77−52163
$MgO:Cr^{4+}$, optical excitation transfer 80−97325
$MgO:Cr^{3+}$, site symmetry of Cr^{3+}, polarised luminesc. meas. 77−12426
$MgO:Li_x$ oxidation and reduction up to 1700K, defect prod. 79−39013
$MgO:Ni^{2+}$, near IR luminesc. from isolated and exchange-coupled Ni^{2+} ion pairs, temp. depend. 80−93382
$MgO-Al_2O_3-SiO_2:Ce^{3+}$ glass scintillator, energy transfer, luminesc. efficiency under UV and charged-particle excitation 79−95821
$Mg(Pt(CN)_4)7H_2O$, transition energy tuning from 3.3 to 1.4 eV 79−61436
$MgS:Ce^{3+}$ phosphors, emission and excitation spectra *(French)* 80−93380
$MgS:Eu^{2+}$, emission and excitation spectra obs. 80−55162
Mg_2SiO_4:Tb, thermolum. phosphor, photolum. and absorpt. spectra, thermolum. mechanisms 80−97321
$Mg_4Ta_{2-x}Nb_xO_9$, luminescence, model of niobate and tantalate centres 77−16373
$MgUO_4$, energy transfer, cryst. struct. and chemical composition effect 80−108248
$MgUO_4$, luminesc. props. 79−83012
$Mg_3(VO_4)_2$, luminesc. spectra in visible region, vanadate group 78−43921
$MgWO_4$, luminesc. efficiency, temp. and high-press. 78−23507
Mn complex, Mn amine, luminesc. spectra *(French)* 79−51997
Mn complex, $MnCl_2$ with 3,5-lutidine hydrochloride, cryst. 77−52153
Mn complex, $MnCl_2$.3,5-lutidene hydrochloride complex, photoluminesc. and photoexcitation 78−92106
Mn complex, papaverine hydrochloride with $MnCl_2$, cryst. 77−55812
Mn complex, with 4-benzylpyridine hydrochloride, photoluminesc. props. 80−89044
Mn complexes, with pyridine, excitation luminesc., ligand field effect 77−48213
Mn minerals, photoluminesc. 79−95829
Mn^{2+} in crystals with different site symmetries, luminesc. spectra 78−80400
$Mn_xCd_{1-x}Se$ single crysts., photoluminesc., composition depend. 80−80854
$MnCl_2$ in soln., luminesc., strong vibronic coupling 79−65922
$MnCl_2$-lutidine HCl complex, photoexcitation, photoluminesc. 78−27301
MnF_2, antiferromag., multi-magnon luminesc. sidebands 78−76525
MnF_2, fluorescence props. 79−73994
MnF_2, one-magnon luminesc. sidebands of excitonic transition 78−60517
MnF_2, two-exciton light absorption, with four-photon excitation *(Russian)* 78−35186
$MnF_2:Eu^{3+}(Er^{3+})$, fluorescence props. 79−73994
MnP_2, nonequilibrium luminesc. and relaxation processes, 25 to 300K *(Russian)* 78−80415
MnX_2 solns., (X=Cl, Br, I), heavy at. effect on rate consts. of radiative and non-radiative transitions 79−78736
N_2, luminesc., multiphonon-assisted energy transfer 79−47498
N_2, solid, vacuum UV luminesc., 8K 78−10958
N_2, solid and matrix isolated mol., triplet state spectra *(Russian)* 80−5574
$NH_4Br:Cu^+$, luminesc., orientation phase transition 80−100687
Na-fluorescein, glycerol-alcohol soln., luminesc. decay time, conc. depend. 80−34960
$Na_{56}(AlO_2)_{56}.(SiO_2)_{136}:Eu^{3+}$, Y-type zeolite, luminesc. props. 79−83017

photoluminescence continued
$Na_6Al_6Si_6O_{24}$, zeolite, luminescence and coloration *(Russian)* 78−72578
$Na_4Al_3Si_3O_{12}Cl:Br,Ge$, sodalite, reflectance and luminescence obs. 79−4839
$Na_8Al_6Si_6O_{24}F_2(Cl)(Br)(I)$, sodalite, luminescence and coloration *(Russian)* 78−72578
$Na_3Al_6Si_6O_{24}X_2$, optically erasable colouring and luminesc. *(Russian)* 77−85801
$Na_8Al_6Si_6O_{24}.Cl(Br)(I)$, cathodochromic sodalites, coloured crysts., tunnel and recomb. luminesc., temp. depend. *(Russian)* 80−66261
NaBr, lifetime of colour centres 78−92115
$NaBr:Cu^+$, luminesc. and lifetimes, press. depend. 79−33809
$NaBr:Eu^{2+},Ho^{3+}$, single cryst., cluster luminesc. centres *(Russian)* 77−20922
NaBr:Pb, absorpt. and emission spectra of Pb centres 79−78717
$NaBr:Tl^+$, emission spectra, excitation in A-band 78−15218
NaBr(:I), exciton ionisation and decay, photoluminesc. in elec. field 77−44046
$NaCaVO_4$, luminesc. spectra in visible region, vanadate group 78−43921
$Na_3Ce_{1-x}Tb_x(PO_4)_2$, UV excitation, emission spectra 79−38595
NaCl, F_3-centre quartet state, IR emission spectra 78−43930
NaCl, luminesc. singlet from triplet self-trapped excitons 79−99936
NaCl, luminesc. under 10.6 μm laser pulse irrad. *(Russian)* 77−16381
NaCl, migration of nonrelaxed holes, self-trapping, ESR and luminesc. obs. *(Russian)* 80−66033
NaCl, optical conversion, luminesc. and colour centre formation 79−24354
NaCl particle, luminesc. duration rel. to time in CO_2 laser beam focal zone 80−34983
NaCl, photoluminescence under pulsed UV laser excitation 77−77289
NaCl, pure, indoped, luminesc. obs. 77−32412
NaCl:Ag, excitation in fund. absorpt. region, luminesc. and thermolum. 80−50433
NaCl:Br, host-sensitized luminesc., energy transfer due to excitons and holes 79−38590
NaCl:Cu, UV absorpt., emission, excitation spectra, Cu^- centres 77−81127
$NaCl:Cu^+$, luminesc. and lifetimes, press. depend. 79−33809
$NaCl:Ga^+$, polarisation of Ga^+ centre A_T emission, temp. depend. 80−80842
$NaCl:O_2^-$, excitation and absorpt. spectra at 2K, O_2^- excited state field 79−56843
NaCl:Pb, luminesc. spectra obs. 78−95604
$NaCl:Pb^{2+}$, decay of luminescence emission 78−39593
$NaCl:Pb^{2+}$, emission spectra obs., and luminesc. centre model 77−36286
NaCl(Br):Tl, emission spectra, press. effects 78−23509
NaF, F_3^+-centre decay by optical free induction 78−68555
NaF, gamma irrad., colour centre stimulated emission, threshold pump power, tuning range 79−73971
NaF, two-photon absorpt. cross sections of N_1 and F_3^+ centres 79−73991
NaF:U, luminesc. spectra, Vibr. struct. 80−80840
$NaGdO_2:Tb^{3+}$, obs. of efficient luminesc., UV excitation 78−43922
NaI and NaI:Tl^+, intrinsic and impurity induced luminesc., exciton diffusion 77−16367
NaI, exciton luminesc., characteristics near absorption edge 78−88363
NaI, exciton-phonon polarisation interaction *(Russian)* 78−35195
NaI, luminesc. polarisation for free and bound excitons 78−10942
NaI, motion of free excitons and their self-localisation 80−2342
NaI, resonant Raman scattering in crystals with self-trapping excitons 80−7344
NaI, single cryst., reson. zero-phonon exciton luminesc., polariton emission 78−52564
NaI, thermal dissoc. of photoproduced excitons at UV band edge, recomb. luminesc. obs. 80−50412
NaI:Cu^+, luminesc. of iolated V_K-centres 78−84641
NaI:Tl^+, luminescence spectrum, excited states of monomer centre 77−66536
$Na_3La_{0.98}Eu_{0.02}(VO_4)_2$, luminesc. spectrum 77−4673
$NaLaO_2:Pr^{3+}$, obs. of efficient luminesc., UV excitation 78−43922
$Na_3La(PO_4)_{1.9}(VO_4)_{0.1}$, luminesc. spectrum 77−4673
$Na_3La(VO_4)_2$, luminesc. spectrum 77−4673
$NaLnO_2:Bi^{3+}$, (Ln=La, Gd, Sc), luminesc., vibr. struct. 79−33790
$NaMgF_3$, defects induced by X- and vacuum UV irrad., optical and elec. study 80−107319
$NaMgF_3:Sm^{2+}$, luminesc. spectra 4.2, 77 and 295K and Zeeman spectra, 4.2K 77−81146
$NaMnCl_3$, antiferromagnet, exciton self-localisation luminesc. and excitation spectra *(Russian)* 80−11456
$NaNO_2$, hot luminesc. 78−6722
$NaNO_2$, hot luminescence 78−10976
$(NaNO_3-Mg(NO_3)_2):Nd^{3+}$, glass, cryst., absorpt. luminesc. spectra, term struct. of Nd^{3+}, bonding 77−8624
$Na_2NdPb_6(PO_4)_6Cl_2$, self-activated mini-laser material, quantum yield determ. 79−33773
$Na_2O-B_2O_3-SiO_2:Yb(Tb)$, luminesc. cooperative processes, glass struct. and comp. effect 80−16101
$Na_2O-P_2O_5-Y_2O_3-Tb_2O_3$ glass, conc. quenching of luminesc. in disordered system with dipolar interaction 80−89059
Na_2O-SiO_2 glasses, elementary electronic excitations, refl., luminesc., and photoemission meas. 80−84778
$NaPO_3:Eu^{3+}$ glass, luminesc. of Eu^{3+}, transition probabilities 80−80845
$Na_2(Pt(CN)_4)3H_2O$, transition energy tuning from 3.3 to 1.4 eV 79−61436
$Na_2S:Mn^{2+}$, polycrystalline, EPR and luminesc. of Mn^{2+} 78−27082
$Na_2S_2O_3$ digested AgX emulsions, red-IR photoluminescence obs. at 77K 80−103982
$NaY_{1-x}Sm_xF_4$, luminesc. expt. suggesting Sm^{3+} ion pairing 80−76065
Nd glasses, luminesc. obs. by chronospectroscopic technique 79−11467
Nd^{3+} activated laser matrices, luminesc. quantum efficiency, conc. depend. 79−27263
Nd^{3+} in $Nd(NO_3)_3$(tributylphosphate-d_{27})$_3$, soln. luminesc., stimulated emission *(Russian)* 78−33734
Nd^{3+} ions in solids, anti-Stokes effects 78−80405
Nd:glass, luminesc. quantum yield meas., relative method *(Russian)* 78−35203
Nd:silicate glass, resonance laser excitation, inhomogeneously broadended emission spectra 80−66295
Nd^{3+}:glass, kinetic description of excitation spectra 78−68557
Nd^{3+}:glass, laser props., uncorrelated inhomogeneous broadening of 1.06 μm band induced luminesc. quenching 79−31914

photoluminescence continued
Nd^{3+}:glass, multitype opt. centres 78−68558
Nd^{3+}:glass luminesc. band profile deform. under free-oscillation conditions 80−71487
Nd^{3+}-Yb^{3+}:glass, excitation transfer, selective filling of levels in inhomogeneous contour 77−69898
$NdAl_3B_4O_{12}$, self-activated mini-laser material, quantum yield determ. 79−33773
$NdAl_3[BO_3]_4$, luminescence and lasing charact., solubility 79−31910
$Nd_xLa_{1-x}P_5O_{14}$, Nd^{3+} stoichiometric materials, luminesc., conc. quenching 78−27315
Nd_2O_3, transmission and luminesc. spectra 79−65929
Nd_2O_3-Al_2O_3-SiO_2 glass, exam. of spectroscopic and luminescent props. 78−88364
Nd_2O_3-SiO_2 glass, exam. of spectroscopic and luminescent props. 78−88364
NdP_5O_{14}, laser materials, linear conc. quenching of luminesc. 79−31908
NdP_5O_{14}, luminesc. excited by LED radiation 79−24366
NdP_5O_{14}, self-activated mini-laser material, quantum yield determ. 79−33773
$Nd_2Ti_2O_7$, transmission and luminesc. spectra 79−65929
Ne, solid, quasi-line emission in transitions between excited states *(Russian)* 79−91494
Ne:Ar(Kr)(Xe), luminesc. in vacuum-UV excitation of guest atoms by free and relaxed excitons 79−15519
Ne:H, exciton states and L_α,L_β emission 80−93372
Ne:O_2 (N_2), long-wave UV luminesc. *(Russian)* 78−88347
Ne:Xe(Ar), electronic relax. cascades in Wannier and Frenkel type exciton states 79−33759
O, singlet, photosensitised luminesc. in soln. 77−70309
O_2, liq., photoluminesc., dimer effects 78−31233
P, amorphous, red, photolum. props. and band gap 80−50403
PLZT, opt. spectra and luminesc. 78−76508
$POCl_3$-$SnCl_4$:Nd^{3+}, liquid laser material, luminesc. centres conc., temp. depend. 79−50287
$POCl_3$-$SnCl_4$:Nd^{3+}, liquid laser material, luminesc. centres changes, crystn. process effects 79−50288
$PO(SCN)_3$:Nd^{3+} solns., spectroluminesc. props. 77−16362
Pb^{2+}, in soln., luminesc., halide ion effects 78−35187
$PbBr_2$, cryst., red luminesc. at low temps. *(Russian)* 78−92125
$PbBr_2$, red luminesc., absorpt. spectra 80−2831
$PbBr_2$, single cryst., photolum. meas. 77−69882
$PbBr_2(Cl_2)$, light sensitive material, regularities in exciton states 77−20885
$PbCl_2$, blue emission 78−23518
$PbCl_2$, single cryst., photolum. meas. 77−69882
β-PbF_2, single cryst., photolum. meas. 77−69882
PbF_2:Tb^{3+}, cubic Tb^{3+} centres, energy level and cryst. field parameters 77−52181
PbFBr, single cryst., photoluminesc. 77−16375
PbFCl, single cryst., photoluminesc. 77−16375
PbI_2 (2H), angular depend. magnetoluminesc. 79−43029
PbI_2 (2H), layer cpd., band parameter determ. 79−95332
PbI_2 (2H), photolum. spectrum, in strong photoexciton mixing region 78−48223
PbI_2, cryst., photochem. phenomena investig. *(Russian)* 78−35204
PbI_2 crystals, exciton condensation, excitation and luminesc. study 80−55182
PbI_2 direct gap semiconductor, exciton lifetime and condensation threshold, luminescence spectra 80−34981
PbI_2, emission spectra, 80K, high excitation intensity effects at different pump wave lengths 77−52170
PbI_2, exciton spectra depend. on strong excitation, crystal transmission 79−69433
PbI_2 film, highly excited, oscillator strength of excitons, absorpt. and emission spectra 78−76001
PbI_2, first-order 2H-4H polytype transition, exciton spectroscopic study 80−59647
PbI_2, layered cryst., photoluminesc., and reflection spectra obs. 78−6726
PbI_2, luminescence excited by high-intensity two photon pumping 77−44038
PbI_2, multiphoton cross-section determination by means of luminescence experiments 80−93377
PbI_2, photoexciton interaction, luminescence spectra, polariton dispersion diagram 80−93397
PbI_2, photolum. and reflectivity temp. depend., cryst. anisotropy effect on electron-phonon interaction *(Russian)* 78−15225
PbI_2, photoluminesc. spectra, generation of stimulated radiation 77−8647
PbI_2, single cryst., luminesc., photocond. and absorpt. after thermal treatment 79−56855
PbI_2, temp. depend. of electron-hole drop emission *(Russian)* 77−16394
PbI_2, three-photon absorpt. coeff. determ. by nonlinear luminesc. expt. 80−14384
PbI_2 two-photon absorpt. cond. and luminesc. meas. 77−52166
$PbMg_{1/3}Nb_{2/3}O_3$, carrier mobility and photoluminesc. near ferroelec. transition *(Russian)* 78−2813
$PbMg_{1/3}Nb_{2/3}O_3$, photolum. near ferroelec.-paraelec. phase transition 80−16100
$PbMg_{1/3}Nb_{2/3}O_3$, photolum. and carrier drift mobility at ferroelec. transition 80−71469
$PbMoO_4$, doped and undoped single crysts., polarisation of luminesc. and assignments 80−76069
PbO, laser excitation IR spectra, photoluminescence obs., rot. anal., rot. const. determ. 80−95619
PbO, single crysts., exciton and impurity luminesc. 80−60674
PbO, vapour, photoluminescent decay, a(1) state 78−58745
$PbS_{1-x}Se_x$ thin film, stimulated emission, temp. depend. 80−66232
PbSe film, stimulated photoluminesc. charact. meas., room temp. 77−90193
PbSe, photoluminesc. spectra and stimulated emission, effect of temp. 77−8638
PbSe, X-ray diffr. exam. of struct., and luminescence props. 80−55209
$Pb_{1-x}Sn_xSe$ epitaxial layers, radiative and nonradiative recomb. processes 80−60670
$Pb_{1-x}Sn_xSe$ solid solns., photoluminesc. spectra, energy band parameter determ. 80−71484
$Pb_{1-x}Sn_xSe(Te)$ epitaxial layers, growth, phase diagram, p-n junctions, optical, elec. props. 78−44029
$Pb_{1-x}Sn_xSe_{1-y}Te_y$ optically pumped heterojunction laser with matched gratings, photolum. obs. 79−89909
photoluminescence continued
$Pb_{0.78}Sn_{0.22}Te$, $Pb_{0.91}Sn_{0.09}Se$, radiative and nonradiative recombination 80−80849
$Pb_{0.4}Sn_{0.1}Te$, situated in quantizing magnetic field, photolum. spectra 79−71461
$Pb_{1-x}Sn_xTe$, energy band parameter determ. from photoluminescence. spectra in mag. field 79−11066
$Pb_{1-x}Sn_xTe$, epitaxial layers, photolum. in mag. field 79−83033
$Pb_{1-x}Sn_xTe$ films, size quantisation, optical orientation of free carriers, polarisation props. of luminesc. 80−20725
$Pb_{1-x}Sn_xTe$ solid solution, radiative recombination 79−52016
$Pb_{1-x}Sn_xTe$:Cd(In), solid solutions, impurity states in photoluminescence spectra *(Russian)* 80−97333
$Pb_{1-x}Sn_xTe$:In, impurity influence on photoluminescence at large excitation levels *(Russian)* 80−93384
$Pb_{1-x}Sn_xTe$:In epitaxial layers, growth, elec. props., and luminesc. 80−54542
PbTe epitaxial film, stimulated emission, absorption spectra and recombination 78−80409
PbTe, recombination radiation polarisation direction, two-photon selective energy valley occupation *(Russian)* 77−20924
PbTe, spin orientation under two-photon pumping 79−74000
$PbTiO_3$, photolum. and carrier drift mobility at ferroelec. transition 80−71469
$PbWO_4$, doped and undoped single crysts., polarisation of luminesc. and assignments 80−76069
RbBr:O_2^- centres, luminesc. polarisation temp. depend. 78−87943
RbBr-Ag, mag. field effect on luminesc. of paired Ag^- ions 78−27313
$RbCa_{0.95-x}Mg_xEu_{0.05}F_3$, green luminesc. obs. 77−32428
RbCl:Ag(Cu), strong IR luminesc. obs. of Ag_F^0 centres 78−6736
RbCl:Eu, luminescence and absorption of color centres in RbCl:Cu and KCl:Eu crystals 78−92118
RbCl(Br), F-centre emission, mag. circular polarisation 80−108251
RbI, edge emission of excitons 77−59606
RbI, edge luminesc. under UV excitation 77−77273
RbI, intrinsic luminesc. quenching, by X-ray induced coloration 78−19539
RbI, luminesc. spectra induced by pulsed Ne^+ and electron beams and X-rays 80−80851
RbI, photostimulated recomb., electron spin polarisation 80−60673
RbI, zero phonon and LO phonon assisted luminesc. of free excitons 79−28799
RbI:Pb^{2+}, luminescence under B-band excitation 78−35192
RbI:Tl, emission and excitation spectra, press. effects 79−83028
$RbMnCl_4$, quadratic layer antiferromag., intrinsic emission obs. 77−20906
$RbMnF_3$, antiferromag., multi-magnon luminesc. sidebands 78−76525
$RbMnF_3$, antiferromagnetic resonance, optical detection, luminescence 80−7174
$RbMnF_3$, exciton and exciton-magnon emission 79−33779
$RbMnF_3$:Er^{3+}, absorption, emission, excitation and lifetime meas. 80−71460
$RbMnF_3$:Fr, pure and doped, unirradiated and electron irrad., energy transfer 80−108254
Rb_2TeCl_6:Re^{4+}, vibronic transitions progressions, intensity distrib. 79−78735
$ReBr_6^{2-}$, in cubic crysts., luminesc. spectra and relax. processes 78−68552
Ru complex, Ru(II)-polypyridine, excited charge transfer states, multiple emissions 79−3468
S_2 mol. $B^3\Sigma_u^- \rightarrow X^3\Sigma_g^-$ fluorescence induced by N_2 laser *(Japanese)* 80−14175
SbSI, photolum. spectra in ferroelec. phase, 600-800 nm., 14-100K 80−71468
$ScBO_3$:Tb^{3+}, vacuum UV excitation spectra and quantum efficiencies 79−28811
$Sc_2(WO_4)_3$:Cr(Eu), and undoped crystals, luminesc. obs. 80−89047
Se, exciton luminesc. in trigonal form 79−33802
Se, glassy, localised electronic states, photoluminesc. and ESR studies 80−65501
Se, glassy, pure and K-doped, photolum. and optically induced ESR 80−50398
Se, trigonal, indirect exciton ground states, photoluminescence 79−24361
Si, amorphous, elec. and opt. props., review 78−23094
Si, amorphous, electron-hole recombination, mech. 78−72196
Si, amorphous, glow discharge deposited 78−72590
Si, amorphous, glow discharge, fatigue effect in luminesc., recovery by annealing 80−50416
Si, amorphous, glow discharge produced, defect creation, high optical excitation 80−97327
Si, amorphous, hydrogenated, heating effects 78−15204
Si, amorphous, hydrogenated, spin depend. photoluminesc. 78−72589
Si, amorphous, luminesc. of diode structures 77−8656
Si, amorphous, mag. field depend. of luminesc. 79−43034
Si, amorphous, phonon interaction in luminescence 78−43927
Si, amorphous, photoluminesc. spectra from 77K to room temp. 77−20916
Si, amorphous, photoluminesc. and radiative lifetimes 79−61419
Si, amorphous, photoluminescence, fast radiationless recombination 79−99939
Si, amorphous, radiative and non-radiative tunnelling, photoluminesc. decay meas. 79−83026
Si, amorphous, spin depend. recomb., luminesc. and light induced ESR 80−50393
Si, amorphous, time resolved photoluminesc. near band gap 80−25445
Si, amorphous, time-resolved ODMR and luminesc. 80−25254
Si amorphous film, optical props., electronic states 80−25475
Si, amorphous film, plasma-deposited, photoluminesc. and EPR meas. 79−4864
Si, annealed, photoluminesc. anal. of defects 80−80836
Si, Auger recomb. coeff. meas. using laser excitation 79−38654
Si, biexcitons, photoluminesc. spectrum exam. 78−47705
Si, bound exciton lifetimes for acceptors 77−80738
Si, bound exciton-dopant Auger lifetimes 78−18970
n-Si, bound excitons and bound multiexciton complexes, excitation spectra 80−96792
Si, bound multiexciton complexes, luminesc. 80−10888
Si, CW laser annealed, defect luminesc. 80−50388
Si, characterisation by photoluminescence method *(Japanese)* 78−80404
Si, characterisation by photolum. method *(Japanese)* 79−38638
Si, correl. between photolum. spectra and impurity conc. 78−23513

photoluminescence continued
Si, deformed, recomb. radiation from electron-hole drops and free excitons 77−8641
Si, diamagnetism of excitons and biexcitons, recomb. spectra *(Russian)* 80−7412
Si, dislocation luminesc. obs. 78−15217
Si, dislocations, luminesc. spectra *(Russian)* 77−90197
Si, donor bound excitons and bound multiexciton complexes 77−40282
Si, electron irradiated, photolum. due to interstitial complex 77−44048
Si, electron-hole drop luminescence, hysteresis effect and surface energy 78−2907
Si, electron-hole droplet luminesc., laser excitation threshold meas. 79−33821
Si, electron-hole droplet spatial distrib., luminesc. obs. 80−49615
Si, electron-hole droplets nucleation at swirl defects 79−15095
Si, electron-hole drops, Auger recomb. 77−48240
Si, electron-hole drops, near and far IR emission spectra 77−48242
Si, electron-hole drops, nonequilib. paramagnetism 80−6749
Si, electron-hole drops, nucleation, time resolved luminesc. spectroscopy 78−6280
Si, electron-hole drops, nucleation, luminesc. threshold obs. 79−33822
Si, electron-hole drops, thermodynamical parameter determ. from luminescence data 80−2845
Si, electron-hole drops radius, luminesc. meas. 80−50415
Si, electron-hole liquid, free excitons, biexciton gas, luminesc. 80−6750
Si, electron-hole liquid, spatial condensation of strain-confined excitons and excitonic mols. 78−39592
Si, exciton-impurity complexes, emission spectra, Zeeman splitting *(Russian)* 78−64413
Si, exciton-plasma Mott transition, luminescence spectra 77−62836
Si, excitons and electron-hole drops, phonon assisted luminescence lineshape 79−99942
Si, excitons and electron-hole liquid, luminesc. 80−6746
Si, fast electron irradiated, models of luminescence centres, role of interstitials 77−81153
Si, fast neutron and ion irradiation, radiative recombination centres 77−81152
Si, free exciton luminesc. band, resolved splitting 79−73995
Si, free excitons, drift and diffusion, luminesc. obs. 80−84434
Si, H_2^+ irrad., annihilation of free excitons, inelastic scatt. by SiH_4 mols., photolum. obs. 78−19561
Si, high purity, exciton lifetime, temp. depend., photoluminesc. meas. 80−44508
Si, highly doped and highly exerted, Auger coeffs., radiative band to band recomb. lifetime meas. 77−85764
Si, hydrogenated amorphous, laser annealing, photolum. spectra 80−100713
Si, impurity content characterisation, exciton luminesc. 80−60653
Si, intrinsic, phonon replicas of electron-hole liq. luminesc. line 79−28831
Si, ion implanted films, optical and luminesc. props. 80−60699
Si, irradiated, nature of 0.97 eV A band luminesc. 77−44049
Si, LO and TO phonon assisted free exciton luminesc. 79−33833
Si, luminesc., simultaneous kinetics of drops and excitons during drop formation 77−48222
Si, luminescence of multiparticle exciton-impurity groups 79−83003
Si, neutron transmutation doping, photoluminesc. characterisation 80−11453
Si, phonon-assisted exciton emission, temp. depend. of relative integrated intensities 77−1375
Si, photoluminescence of annealed cryst., defect anal. 79−87500
Si, photoluminescence of electron-hole drops under uniaxial stress 79−91491
Si, photoluminescence of thermal donors after annealing 79−87499
Si, piezospectroscopic effect on zero phonon luminescence lines 80−50406
Si, plastically deformed, hot-exciton luminesc. as function of strain 78−88361
Si, proton irradiated and annealed, hydrogen-containing radiative recomb. centres 77−24896
Si, pure and doped amorphous photolum. meas. 77−36285
Si, radiative recomb. centre accumulation due to high temp. electron irrad. 80−93394
Si, radiative recombination involving silane mols. 79−73998
Si, recombination luminescence, electron-hole drop, excitons orientation in mag. field 78−88362
a-Si, resonant and non-resonant luminesc. changes theory 80−50410
Si, shallow impurities, photolum. anal. 78−23512
Si, swirl defects, gettering effects, obs. by photoluminesc. meas. 78−84623
Si, uniaxial stress effects and excited states for multiple bound excitons 78−6281
Si, uniaxially deformed, biexcitons *(Russian)* 77−59611
Si, uniaxially stressed, excitonic molecule emission spectra, electron valley degeneracy effects 80−60669
Si wafers, Czochralski grown, crystal defects, photoluminesc. topographic obs. 79−1432
Si:Al, bound exciton and bound multiexciton complexes, electronic structure, luminesc. obs. 79−56139
Si:Al, localised exciton bound to isoelectronic trap 80−66283
Si:As(Li)(P), luminesc., stress effects on donor exciton satellites 77−85786
Si:B, bound many-exciton complexes, luminescence spectra, mag. props. 80−103994
Si:B, bound multiexciton luminesc., recomb. kinetics 79−38591
Si:B, impurity conc. from photoluminesc. anal. 78−63785
Si:B, many-body exciton-impurity complexes, stress depend. of photolum. meas. 79−28833
Si:B, photolum. of heavily doped p- and n-type 80−20708
Si:B,In, sharp line series in near-band-edge photolum. 80−16092
n-Si:B,P, radiative recombination at thermal defects, luminescence centre electron struct. 79−91496
Si:B recombination emission polarisation of bonded multiple-exciton complexes in mag. field *(Russian)* 78−2905
Si:B(Al)(Ga)(In)(Tl), binding energy, excited state spectra, photolum., semi-empirical short range pot. 80−44534
Si:B(Ga), even-parity acceptor excited states, bound exciton two hole transitions 77−85793
Si:B(P), uniaxially stressed, impurity-assisted intervalley scatt., photoluminesc. obs. 80−34979
Si:B(P)(Sb), multiparticle impurity complexes *(Russian)* 78−72601

photoluminescence continued
Si:C(O), photoluminescence spectra, radiation damage investig. 77−28620
Si:Ga, luminescence fine struct. from bound exciton and multiexciton complexes 77−32430
Si:Ga(Al), edge luminesc. spectra of acceptors, multiexciton complexes 78−56517
Si:H, amorphous, defect creation and H evolution 80−50392
Si:H, amorphous, defect photoluminesc. meas. 80−97334
Si:H, amorphous, defect states, luminesc. and ESR obs. 80−76075
Si:H, amorphous, effect of gap state density on photocond. and photolum. 79−91096
Si:H, amorphous, excess carrier thermalisation and recomb., luminesc. decay and photocond. 80−50397
Si:H, amorphous, geminate recombination model for photoluminescence decay 80−71481
Si:H, amorphous, glow discharge deposited, laser annealing 80−49104
Si:H, amorphous, light-induced ESR and photoluminesc., dangling bonds with positive correl. energy 80−50161
Si:H, amorphous, luminesc., band tail states and thermalization 80−25455
Si:H, amorphous, radiative recomb. by diffusion and tunnelling, photocond. quantum efficiency 80−50394
Si:H, amorphous, radiative recomb. and luminescent processes 80−55152
Si:H, amorphous, rehydrogenation, photoluminesc. recovery 78−72571
Si:H, amorphous, temp. depend. of photolum. 80−89063
Si:H, amorphous and crystalline, hydrogenation and dehydrogenation, luminesc. spectra 80−11477
Si:H, amorphous sputtered, excitation spectra and photoluminesc. 80−50396
Si:H, Cl(F), amorphous, photocond., dark cond. and photoluminesc. 80−49802
Si:H, ion-implanted, photoluminesc. spectrum 80−45129
a-Si:H, spin defect and recombination influence on electronic transport 80−50409
Si:H,F,O amorphous, plasma deposited, comp. and optical props. 80−50441
Si:H,Li, amorphous, photoluminescence obs. 80−66280
Si:H,P, amorphous, heavily hydrogenated, high gap state densities 80−49803
Si:H amorphous, plasma-deposited, luminesc. decay 79−73989
Si:H amorphous film, sputtered IR vibr. spectra and photolum., effects of partial evolution of H 80−44413
Si:H amorphous films, optoelectronic behaviour depend. on impurity incorporation during plasma deposition 80−49804
Si:H amorphous films for solar cells, optical and elec. props. of RF glow discharge deposited films 80−54576
Si:H amorphous sputtered film, photoluminesc., photocond. 80−20729
Si:H sputtered amorphous film, luminesc. and non-radiative decay 80−50395
Si:In, bound exciton photolum. obs. 78−95607
Si:In, capture cross section of excitons on neutral In impurities, photoluminesc. decay 78−6760
Si:In, obs. of long lifetime lines in photolum. 79−47512
Si:In, photoluminesc., In acceptor excited level 79−47506
Si:In,P, photoinduced IR absorpt. and luminesc. 79−33828
Si:K, bound exciton luminescence in mag. field *(Russian)* 80−108278
Si:Li, bound exciton complexes associated with Li, photolum. meas. 79−28823
Si:Li, bound-exciton excited states, uniaxial anal. 80−71475
Si:Li, luminesc. of bound exciton and bound multiexciton complexes 79−28821
Si:Li, photolum. of bound exciton and bound multiexciton complex, Zeeman effect 80−108265
Si:O,H amorphous, plasma-deposited, electronic and struct. props. 80−50391
Si:O,H amorphous, time resolved luminesc. 80−66288
Si:P, amorphous, CVD, defect compensation 80−54644
Si:P, bound exciton and multiexciton complex struct., luminesc. obs. 77−81138
Si:P, exciton two-electron luminesc., temp. and impurity-conc. depend. 78−39585
Si:P, heavily doped, electron-hole droplets, photolum. obs. 1.5 to 80K 77−36289
Si:P, heavily doped, IR bound-exciton luminesc. spectra 78−15211
Si:P, heavily doped, origin of photoluminesc. 79−56856
Si:P, impurity band states calc. and photoluminesc. meas. 77−8046
Si:P, impurity conc. from photoluminesc. anal. 78−63785
Si:P, ion-implanted and unimplanted, laser annealing, photoluminesc. study 80−2049
Si:P, luminescence circular polarisation, emission by many exciton complexes 80−93398
Si:P, metallic, heat treatment effects, EPR and photoluminesc. 77−77262
Si:P, model for exciton bound to donor pair, photolum. data anal. 79−51498
Si:P, photolum. obs. of donor pairs 79−52014
Si:P, photoluminesc. associated with impurity clusters 79−38656
Si:P, satellite of bound excitons, transient decay 80−11466
Si:P heavily-doped 78−72572
Si:P(B), multiple-particle exciton-impurity complex form. *(Russian)* 78−43925
Si:Sb(As)(P), bound excitons and bound multiexciton complexes for shallow donors, luminesc. meas. 79−24363
Si:Tl, optical absorption and photolum. of bound exciton 78−88359
Si-H, amorphous, plasma-deposited, H evolution and defect creation 80−44914
Si-H, amorphous, sputtered, photolum. obs. 80−80856
Si-H, RF sputtered amorphous alloy, influence of Ar press. on elec. props. and photoluminesc. 79−91585
Si-H amorphous film, reactively sputtered, prep. and props. 79−78889
Si-type, semiconductor, interimpurity radiative recomb. with phonon cooperation 77−16385
α-SiC, 6H, excited states, photoluminesc. efficiency 78−39604
SiC (15 R), polytype, many valleyed polar semicond., electron-hole-liquid, obs. from excitation and time delayed spectra 79−28289
SiC, (6H), radiation damaged, luminesc. 80−25462
α-SiC, afterglow stimulated by IR radiation *(Russian)* 80−89066
SiC, cubic, electron-hole liq., luminesc. obs. 78−31239
α-SiC, deep centre levels, IR photoluminescence 77−16387
SiC, donor exciton satellites, multiple bound excitons 77−11857

photoluminescence continued
SiC epitaxial layers, energy distrib. in photolum. spectra, influence of synthesis conditions 79−52009
p-SiC, inequivalent sites of IR luminescence centres *(Russian)* 77−1722
SiC, influence of plastic deform. on struct. of photoluminesc. spectra 77−55824
SiC LED, defect luminesc. 80−89069
SiC, laser Raman spin-flip scatt. from excitons, luminesc. 80−80786
SiC, luminesc., electron-hole drop 79−38606
SiC, phys. props. and crystal growth, rel. to appl. in electrolum. devices, book contrib. 77−77299
SiC polytypes, free exciton luminesc. meas., phonon energies 80−80852
SiC, spin-flip scatt. of laser light from photoexcited excitons 80−93330
SiC:Al(B)(Ga), 4H-, 6H- and 3C-polytypes, melt growth and photoluminesc. 77−24885
SiC:Al(Ga)(B) (6H) LEDs, fabrication by rotation dipping technique, electrolum. mechanisms 80−50426
4H-SiC:B, very slow decays of luminesc., 2-300K 77−1718
β-SiC:Ga, donor-acceptor pair emission 77−4682
4H-SiC:Ga(Al), photoluminesc. spectra 77−66530
SiC:N(Al)(Ga) (6H), photoluminesc., site-depend. donor and acceptor levels 79−61421
α-SiC:Sc, quasiline luminesc. spectrum 77−4686
SiC:Tb(Sc), various polytypes photolum. meas., identification of 4H and 6H polytypes 77−63459
Si_xC_{1-x}, amorphous, comp. depend. 78−68541
a-$Si_{1-x}H_x$, oxygenated thin film, sputtered, elec. cond. and optical props. 79−15239
Si_3N_4, encapsulant for annealing of GaAs, photolum. and AES evaluation 78−27657
Si_3N_4 layers, on GaAs, encapsulation, low-energy ion beam sputtering 79−78882
Si_3N_4-GaAs, layer struct., near-edge surface luminesc., temp. depend. 79−69434
Si_3N_4-GaAs structure, photoluminesc. and collective effects 78−6727
SiO_2, amorphous, intrinsic defects, photoluminesc. 79−78740
SiO_2, amorphous, optical and elec. props., comparison with chalcogenide semiconds. 78−6721
SiO_2, amorphous and cryst., neutron irrad. and unirrad., intrinsic defect photolum. 80−50401
SiO_2, encapsulant for annealing of GaAs, photolum. and AES evaluation 78−27657
SiO_2, exciton study, luminescent centres as exciton detectors 80−66278
SiO_2, film, diode expt. for detecting photoluminescence and excitons 79−73540
SiO_2, intrinsic luminescence 80−16098
SiO_2, vitreous, luminesc. centres, decay time and polarization props. 79−33829
SiO_2, vitreous, neutron irrad., luminescence nature and ESR signals correl. 79−43038
SiO_2, vitreous, photoelectric and photoluminescent props. in fundamental absorpt. region 78−39596
SiO_2, vitreous, pure and Ge doped, luminescence centres at 396 and 280 nm 80−103996
SiO_2:Ag, cryst. and glassy, X-ray induced EPR and luminesc. centre 80−65043
SiO_2:Ag, crystalline, fused, colour centres 78−10954
SiO_2-LiO_2-Al_2O_3 glass, luminesc., polarisation degree distrib. 80−108257
p-Si_2Te_3, photoelectric props., luminesc., hole lifetime and trapping 77−39892
Sm_3S_4, mixed valence system, inelastic light scatt., photoluminesc. 77−90145
SnI_2, layered cryst., photoluminesc., and reflection spectra obs. 78−6726
SnI_2, single crysts. and film, optical props. 77−32437
SnO_2, emission spectra, 77 to 185K 78−80395
SnO_2, exciton luminescence spectra, absorpt. spectra 80−89064
SnO_2, rare earth ion doped, luminesc. and charge compensation 78−76532
SnO_2, semiconductor, photoluminescence, depend. on lattice temp. and excitation intensity 80−45137
SnO_2:Eu^{3+}, luminesc. and charge compensation 77−28618
$Sn_2P_2S_6$, illumination effect on soft mode and dielectric props., luminesc. study *(Russian)* 80−50420
Sr_2 dimer, photoassoc., photoluminesc., collisional dissoc. 80−58303
SrB_2O_4:Eu^{2+}, luminesc. of high-press. phases 80−100680
$SrCl_2$:Pb^{2+}, intracentre luminesc. *(Russian)* 77−16395
$Sr_{1-x}Eu_xB_2O_4$, luminesc. props. 80−34972
$Sr_{1-x}Eu_xB_4O_7$, luminesc. props. 80−34972
$Sr_{1-x}Eu_xB_6O_{10}$, luminesc. props. 80−34972
SrF_2:Eu^{2+}, circular polarisation in luminesc. and optical orientation 78−6740
SrF_2:Eu^{2+}, phonon spectroscopy, phonon pulse spatial, spectral and temporal evolution 78−34580
SrF_2:Eu^{2+}, spectral, spatial and temporal phonon spectroscopy, new spectrometer 78−83892
SrF_2:Gd^{3+} film, Gd^{3+} luminesc. spectrum and kinetics 78−6763
SrF_2:Na, γ-irrad. cryst., spontaneous and induced colour centre emission 79−7131
SrF_2:Na, tunable room temp. laser action of M-centres, luminesc. and absorpt. spectra 79−31907
SrF_2:Sm^{2+}, interconfig. luminesc., spectral and kinetic characts., appls. 77−4677
SrF_2:Sm^{2+}, pseudo-Jahn-Teller effect 79−69476
SrF_2:Sm^{2+}(Tm^{2+}), vibronic spectra and dynamics of impurity-contaiing lattice 79−1787
SrF_2:Tb^{3+}, cubic Tb^{3+} centres, energy level and cryst. field parameters 77−52181
$Sr_2Gd_{1-x}Tb_xGaO_5$, Gd^{3+}→Tb^{3+} energy transfer, emission and excitation spectra *(French)* 80−84770
$SrLaBO_4$, crystallographic and Pb^{2+} luminesc. data 79−32971
SrO, luminesc. band edge, 4-6.5 eV, optical absorpt., photoluminesc., cathodoluminescence, photocond. obs. 80−50411
SrO:Pb^{2+}(Bi^{3+}), impurity centres vibronic spectra, lattice dynamics and electron-phonon interactions 80−7396
SrO-Li_2O-Al_2O_3-SiO_2:Tb^{3+} glass, energy transfer, luminesc. efficiency under UV, neutron and charged-particle excitation 79−95822
$Sr_2R_2O_4$ luminesc. on activation by Eu^{3+}, Nd^{3+}, Eu^{3+}-Tb^{3+} 77−52156
SrS:Cu, phosphor, photolum. meas. 78−80393
$SrTiO_3$, photolum. and carrier drift mobility at ferroelec. transition 80−71469
photoluminescence continued
$SrTiO_3$, photoluminesc., thermoluminesc. and thermally stimulated currents 78−92121
Sr_2TiO_4:Eu, synthesis, luminesc. of materials 79−11534
Tb complex, acetoacetic ether, luminesc. spectral band intensities, solvent effects *(Russian)* 78−84653
Tb complexes, intermol. energy transfer to Eu complexes in aq. soln. 80−25426
Tb complexes, intermol. energy transfer to Eu complexes in aq. soln. 80−25427
Tb^{3+}, bound to benzene-carboxylic acid derivatives, emission intensity 79−18230
Tb^{3+} in rare earth ion cryst. field in YF_3 struct., spectra 78−19563
Tb^{3+} soln., luminesc. quantum yield spectral depend. 80−2838
Tb^{3+}:Yb^{3+} in liq. media, luminesc. cooperative sensitisation 80−2827
$TbAlO_3$:Nd^{3+}, absorpt. and luminesc. spectra 79−91470
TbF_3:Sm^{3+}, induced visible emission of Sm^{3+} 80−97330
$TbGa_3(BO_3)_4$, luminesc. spectra, local symmetry of rare earth ion determ. 80−16095
$Tb_xLa(Y,Gd)_{1-x}$.DAM.Sal_3, DAM=diantipyrylmethane, luminesc. *(Russian)* 77−55830
Tb_2O_3-P_2O_5-MO system glasses, (M=Mg, Ca, Sr, Ba or Pb), photoluminesc. under X-ray excitation 80−89060
$Tb(OH)_3$, exciton dynamics within an inhomogeneously broadened line, luminesc. spectra 80−50407
$Tb(OH)_3$, sign of energy dispersion of one dimens. excitons, time resolved spectroscopy 77−1377
TbP_5O_{14}, IR absorpt. and luminesc. spectra 80−55079
TbP_5O_{14}, luminesc. spectra 77−52155
$Tb_{0.8}Yb_{0.2}(PO_3)_3$, cooperative sensitisation of luminesc., order-disorder transition effect 77−36283
$ThBr_4$:U^{4+}, IR luminesc., zero phonon lines 79−33769
ThO_2, pure and Tb^{3+} doped, impurities effect in absorboluminesc. and photoluminesc. 79−38597
ThO_2, temp. programmed desorpt. and photoluminesc. of surface states 79−73399
ThO_2:Pr^{3+}, luminesc., calcination temp. and excitation process depend. 79−33749
$ThOF_2$:Ce,Tb, photolum. obs. 77−77270
TiO, photoluminesc. of $\alpha(C^3\Delta$-$X^3\Delta)$ system in chemiluminesc. flames 77−38690
TiO_2, exciton luminescence spectra, absorpt. spectra 80−89064
TiO_2 pigments in commercial polyethylene, luminesc. props. and photoactivity 79−83008
Tl^+, in soln., luminesc., halide ion effects 78−35187
TlBr, hot-exciton effects, luminesc. excitation spectra 77−32434
TlBr, two indirect excitons decay to direct and indirect excitons 77−44058
TlBr:I, isoelectronic donor, broad-band photoluminesc. meas. 77−8636
TlBr(Cl), light sensitive material, regularities in exciton states 77−20885
TlCl, hot-exciton effects, luminesc. excitation spectra 77−32434
TlCl, two indirect excitons decay to direct and indirect excitons 77−44058
$TlGaS_2$, optical and photoelec. props. 77−55571
$TlR(MO_4)_2$, R=Eu, Dy, Er; M=Mo, W, luminesc. *(Russian)* 78−48229
U containing minerals, luminescence spectra, chemical bond effect 78−72597
UO_2^{2+} in aq. solns., luminescence quenching by metal ions 78−39588
UO_2^{2+} in aq. solns., luminescence quenching by H_2O mols. 78−39589
UO_2^{2+} in aqueous solution, time resolved luminesc. for lifetime, $U_2O_4H^{4+}$ exciplex 79−61417
UO_2^{2+}, in $HClO_4$ soln., photoluminesc. intensity, conc. depends. of uranyl and H^+ 77−68069
UO_6^{6-} group, in perovskite type hosts, luminesc. var. with chem. environment 77−16374
UO_6^{6-} in oxides, excitation and emission transitions involved in green luminesc. obs. 77−16372
UO_6^{6-}, octahedral uranate group, charge transfer transition and luminesc. 80−97324
UO_n^{6-2n} ion in cryst. matrices, luminesc. 78−84640
$UO_2.HCONH_2.0.5H_2O$, prep., cryst. struct. and charact 80−29010
V (d^3) in II-VI semiconductors, absorption and luminesc. spectra 78−15203
WO_6^{6-}, in lattice electronic struct., luminesc. ab initio calcs. 78−6337
Xe, cryst., X-ray and photoluminesc. 79−87480
Xe, crystal, edge hot emission, free exciton luminesc. *(Russian)* 79−15520
Xe, crystalline, photoluminesc. lifetime meas. 78−19548
Xe, crystalline, polariton effects, reflectivity, absorpt., and resonant luminesc. spectra calcs. 80−20095
Xe, solid, luminesc. from self trapped excitons (excimers) 79−1785
Xe, solid, self-trapped exciton emission bands 80−20697
Xe, solid, synchrotron irradiation pulse excitation photoluminesc. decay, exciton generation 78−6746
Xe:N_2O, photoluminesc. from XeO (^1D) excimers 78−68544
XeF fragment luminescence, during XeF_2 photodissoc. in solid Xe and Kr 80−3372
XeS, photoluminesc. in rare gas matrices 80−5568
(Y,Gd)BO_3:Eu^{3+}, phosphor, vac. UV excitation spectra, appl. to gas discharge display 80−2816
YA-O_3:Er^{3+}, pulsed laser action, $^4S_{3/2}$ to $^4I_{9/2}$ transition laser action, optical and luminescence spectra 80−16082
YAG:Ce^{3+}, photoluminescence excitation energy, crystal field and temp. effects 80−11460
YAG:Cr, optical detection of phonons 80−92630
YAG:Cr^{3+}, absorption and luminesc., spectra, Cr conc. depend. 77−12435
YAG:Eu^{3+}, reson. fluoresc. spectra, showing multiple Eu^{3+} sites 80−2812
YAG:Ho^{3+}, spectroscopy, stimulated emission 80−93374
YAG:Nd^{3+}, Ce^{3+}, sensitisation, luminesc., absorpt. and emission spectra *(Russian)* 78−10982
YAG:R^{3+}, CRT and X-ray phosphor lattice-activator energy transfer model 78−6792
YAG:R^{3+}, R=Nd, Er, (Er, Ga), LPE and luminesc. 78−64408
YAG-Ti, polarised luminescence 79−95843
$YAl_3B_4O_{12}$:Bi^{3+}, luminesc., vibr. struct., energy transfer 79−38584
YBO_3:Bi^{3+},Eu^{3+}, vacuum UV excitation spectra and quantum efficiencies 79−28811

photoluminescence continued
YE+AG:Er^{3+}, laser material, radiative and nonradiative transitions, conc. quenching 77−16391
YErAG:Er^{3+}, $^4I_{11/2}$ to $^4I_{13/2}$ laser transition cross section, luminesc. energy 77−79833
YF_3:Er^{3+}, Yb^{3+}, IR excitation curves for visible luminesc. 79−33795
YF_3:Nd, Ce, energy transfer between 5d electronic states 80−2808
YF_3:Tm, Nd, energy transfer between 5d electronic states 80−2808
YF_3:Yb,Er, IR to visible radiation transform., limit yield *(Russian)* 79−28838
YF_3:Yb,Er, limit efficiency of transformation of IR to visible radiation 80−29784
$Y_3Ga_5O_{12}$:Nd^{3+}, $YGaO_3$:Nd^{3+}, spectroscopic characts. 77−12427
$(Y_{0.8}Gd_{0.2})AlO_3$:Er^{3+}, spectroscopic props. 77−85791
$YNbTiO_6$:Eu^{3+} emission under UV excitation 78−6770
YO, $A^2\Pi$-$X^2\Sigma^+$ photoluminesc. 78−55195
Y_2O_3, autolocalised excitons *(Russian)* 79−19523
Y_2O_3, electron and hole migration distances determ. 78−19526
Y_2O_3, vacuum UV luminesc., excitation by X-ray synchrotron radiation 79−8168
Y_2O_3:Eu, surface luminesc. centres excitation characts. 78−52560
Y_2O_3:Tb^{3+}(Dy^{3+}), conc. quenching of X-ray and UV-excited luminesc. *(Russian)* 77−55829
YOCl:Yb,Er, anti-Stokes luminesc., temp. depend. *(Russian)* 78−6764
YOCl:Yb^{3+}, Er^{3+}, anti-Stokes luminesc., 4.2 to 293K 77−59609
YOF:Tb^{3+}, conc. quenching of X-ray and UV-excited luminesc. *(Russian)* 77−55829
$Y(OH)_3$:Tb^{3+}, excited state relax., ns time resolved spectroscopy 77−61140
Y_2O_2S:Eu, high press. effect on luminesc. efficiency and lifetime, charge transfer absorpt. 80−66266
Y_2O_2S:Eu phosphor, luminescence saturation effects due to N_2 laser and cathode-ray excitation 80−40151
Y_2O_2S:Eu^{3+}, luminesc., excitation spectra, cooperative phonon sidebands 79−33771
Y_2O_2S:Tb, recomb. processes and emission spectra *(Russian)* 78−6797
YPO_4:Ce(Tb), luminesc. and optical spectra 79−65921
YPO_4:Yb^{3+}, charge transfer type luminesc. 78−64392
$YP_{0.99}V_{0.01}O_4$, luminesc. spectra in visible region, vanadate group 78−43921
δ-Y_2S_3:Nd^{3+}, spectroscopic props. from absorpt., photoluminesc. and excitation spectra 80−34968
$Y_2Ti_2O_7$:Nd^{3+}, spectroscopic props. 77−69866
Y_6UO_{12}, energy transfer, cryst. struct. and chemical composition effect 80−108248
YVO_4, luminesc. spectra in visible region, vanadate group 78−43921
YVO_4:Er^{3+}, Yb^{3+}, IR excitation curves for visible luminesc. 79−33795
Y_2WO_6:U^{6+}, luminesc. 77−55816
$Y_2[Pt(CN)_4]_3.21H_2O$, first order phase transform., spectroscopic and thermodynamic anal. 78−38829
Yb monochalcogenides, multiphonon inelastic light scatt. 77−90144
Yb^{2+}, broadband luminesc. in fluorite struct. crysts. 79−65923
Yb^{3+} doped phosphors, IR excitation and absorpt. and emission spectra *(Russian)* 79−52021
Yb^{3+}, in dessicated (nondessicated) and protonated (deuterated) solvents, photoluminesc. energy degredation 78−19544
Yb:glass, luminesc., low temp. energy transfer 80−2837
Yb^{3+}:phosphate glass, relation between absorption and equilib. luminesc. spectra 77−85754
YbP_5O_{14} and $Yb_{0.9}Tb_{0.1}P_5O_4$, IR absorpt. and luminesc. spectra 80−55079
Zn-tetraphenylporphine/metal electrode, photocurrent generation mechanism 78−76868
$ZnAl_2O_4$:Cr^{3+}, N-lines and Cr^{3+} pairs 78−2896
$Zn_3(BO_3)_2$:Sm^{3+}, photoluminescence obs. *(Spanish)* 79−73986
$Zn_xCd_{1-x}S$ epitaxial layers, elec. resist. and luminescence obs. 78−19540
$Zn_xCd_{1-x}S$, forbidden band width, exciton refl. and luminesc. meas. 78−10947
$Zn_xCd_{1-x}S$, graded single crysts., laser or electron beam excited, luminesc. 77−85792
$Zn_xCd_{1-x}S$:Cl, Cu^+(Ag^+), high pressure luminesc. 78−19533
$Zn_xCd_{1-x}S$:Cu, local centres responsible for photoluminescence 80−29783
$Zn_xCd_{1-x}S$:Cu, photoluminesc., Birman effect *(Russian)* 79−28837
$Zn_xCd_{1-x}Te$, absorpt. edge luminesc. on high-intensity excitation 78−6745
$Zn_xCd_{1-x}Te$, relaxation processes, emission spectra *(Russian)* 78−72598
$ZnCr_2O_4$, antiferromag. spinel, absorpt. and luminesc. spectra 80−66225
p-$ZnGeP_2$, photoluminescence of crystals with varying comp. and dopants 77−32431
$ZnGeP_2$, pseudodirect gap crystal, polarisation of recombination radiation 78−19562
$ZnIn_2S_4$ (I) film, one-packed polytype, resist., photocond. and luminesc. 79−1608
$ZnIn_2S_4$ film, photoluminesc. and photocond. 78−52677
$ZnIn_2S_4$, photoluminesc., reson. Raman scatt. 78−48179
$ZnIn_2S_4$, recomb. process of photoexcited carriers 77−44042
$ZnIn_2Se_4$, luminescence spectra, recomb. processes and energy level scheme 77−1726
$Zn_{1-x}Mg_xTe$, cryst. growth conditions and luminesc. *(French)* 77−21019
$Zn_{1-x}Mg_xTe$, P doped alloys, elec. props. 80−2813
ZnO, band gap depend. on energy of zero-point vibrs., luminesc. obs. 79−73436
ZnO, biexciton levels, luminescence-assisted two-photon spectra 80−29795
ZnO, change in exciton-phonon mechanism due to defects 78−71804
ZnO, diffusion of excitons due to scatt. by optical phonons, photoluminesc. 77−24521
ZnO epitaxial film, UV luminesc. due to one-, two-photon excitation, laser possibility 79−11468
ZnO epitaxial film on Al_2O_3 substrate, recombination radiation in intense single photon excitation 80−7410
ZnO, epitaxial layers, influence of deposition conditions on luminescence, electrical props. 79−99924
ZnO epitaxial layers, rel. between elec. and photoluminesc. props. and their deposition conditions 79−95530
ZnO, excited states of bound excitons, photoluminesc. obs. 80−44513
ZnO, exciton luminesc., 16 to 77K 80−97329
ZnO, excitonic mol. emission, strain induced splitting 77−44060

photoluminescence continued
ZnO, excitonic molecule transitions, M-band emission 79−78742
ZnO, ion implantation effect on luminesc. and cryst. damage 78−6758
ZnO, luminescent, phonon detection by shallow electronic trap states 79−14902
ZnO, multiparticle exciton complexes, luminesc. spectra *(Russian)* 80−16090
ZnO, phosphors, emission spectra, impurity effects 77−32420
ZnO phosphors, origin of UV emission 78−64400
ZnO powders, UV luminesc. spectral distrib., comparison with single crysts., excitons role 80−55167
ZnO, pure and rare earth doped, photo- and electroluminesc. 79−28803
ZnO, self-activated phosphor, band width and shift, temp. depend. 77−8623
ZnO, single cryst., photo- and thermoluminescence 80−66311
ZnO, single cryst. and film, visible and near IR spectra *(Russian)* 77−52133
ZnO, single cryst. growth in ZnO-H_2-H_2O-O_2 vapour, morphology, electrophys. and opt. props. 78−52649
ZnO, stimulated two-photon emission from excitonic molecules 79−28815
ZnO, two-photon-excitation, tunable laser emission, luminesc. processes 80−55127
ZnO, Zeeman splitting of A1-exciton emission lines, k-linear term effects 78−52563
ZnO:Dy(Nd)(Sm), phosphor, electroluminesc., photoluminesc. spectra 78−80421
ZnO:Er, phosphors, photo- and electroluminesc. 77−12428
ZnO:Er(Ag), photoluminescence and electroluminescence 78−27327
ZnO:Li, effect of LiOH mineraliser on struct. and optical props. 77−8737
ZnO:Li, luminesc. donor-acceptor pairs, exchange broadened optically detected EPR spectra 78−23373
ZnO:Li(Na), band-edge emission obs. 77−20933
ZnO:Pr(Gd)(Er), phosphors, photoluminesc. and electroluminesc. spectra 79−11457
ZnO:Yb(Nd)(Pr)(Sm), electro- and photoluminesc. 79−83024
ZnO-GeO_2-MnO-B_2O_3 wideband cathodoluminescent phosphor 80−55196
ZnO-TeO_2 glass, Ho^{3+} or Er^{3+} doped, visible green emission 79−15523
α-ZnP_2, local centre parameters, photoelectron transition scheme, recomb. process anal. 80−44654
Zn_3P_2, photoluminesc. spectra 79−87502
ZnS, additively coloured or neutron irradiated, near IR emission 77−90199
ZnS crystals, luminescence kinetics, centre discrimination exam. 78−15215
ZnS, electroluminesc. and photoluminesc. spectra, fine struct. *(Russian)* 78−84661
ZnS, epitaxial film, CVD growth, photolum. spectra *(French)* 77−36403
ZnS, excited phosphor, IR stimulation and quenching of luminesc., review *(Russian)* 80−11455
ZnS, high temp. annealing effects on photoluminescence 78−19564
ZnS, interimpurity high press. luminesc. 78−19532
ZnS ion beam etching, topographic changes, amorphisation, luminescence study 80−76078
ZnS, ion implantation effects on luminesc., thermo-EMF 80−88178
ZnS, luminescence of M-centre 80−29779
ZnS, photoluminesc. quenching by weak alternating field 77−85778
ZnS, polarisation of self-activated luminesc. 77−73159
ZnS, powder phosphor, IR-induced changes in emission spectra 78−80389
ZnS, self-activated, IR sensitivity 78−6742
ZnS, self-activated, trap distrib. and photoelectronic effect due to UV, IR and visible excitation 77−36282
ZnS, single cryst., radiation emission, stimulation by IR light *(Russian)* 77−66542
ZnS, single crysts. excited by laser beam and elec. field, streamer luminesc. and photolum. obs. 80−34986
ZnS:Ag, phosphor, luminesc. of surface glow centres 80−29782
ZnS:Ag,Sm, recomb. centre interaction, luminesc. quenching 78−10946
ZnS:Ag phosphors, luminesc. of glow surface centres *(Russian)* 79−28836
ZnS:Al,Cu(Ag)(Au) phosphors, luminesc. excitation spectra and exciton struct. 80−55164
ZnS:Al(Te) phosphors, luminesc. excitation spectra and exciton struct. 80−55165
ZnS:B, new luminesc. centre 79−38635
ZnS:Cl, self-activated, blue emission band 79−38633
ZnS:Cr^{2+}, excitation spectrum of IR emission 77−12421
ZnS:Cu, Al phosphors, mechanism of IR stimulated and quenching 77−69881
ZnS:Cu, Cl, I, anisotropy of blue Cu luminesc. centres 77−81137
ZnS:Cu, Cl luminophor, photoluminesc. and struct. props. 77−32414
ZnS:Cu, effect of elec. field on photoluminescence, model of luminogen centre 78−76522
ZnS:Cu, Er, Na, phosphor, mechanism of sensitisation effect of Cu and Na ions 77−16369
ZnS:Cu, Pb, phosphors, ruby laser stimulated time-delayed emission spectra 77−69874
ZnS:Cu,Al, anisotropy of blue-Cu luminescence centres 78−64390
ZnS:Cu,Al phosphor, shallow hole traps 78−31237
ZnS:Cu,Cl(Br)(I), green luminesc., interimpurity phototransitions investig. *(Russian)* 77−66541
ZnS:Cu crystal, powder, epitaxial film, luminescence anomalous thermal 80−76077
ZnS:Cu phosphor, electric field quenching of photoluminesc. and flashlike rise in luminesc. 78−2911
ZnS:Cu^{2+}, Jahn-Teller effect, stacking faults and formation of polytypes, absorption and emission spectra 77−4660
ZnS:Cu(Cl), electroluminesc. and photoluminesc. spectra, fine struct. *(Russian)* 78−84661
ZnS:Er^{3+}, luminesc. centres with cubic symmetry 79−38636
ZnS:Fe, luminesc. and ESR investigations 80−2822
ZnS:In, polarisation of deep centre electroabsorpt., effect of random electric fields 77−48148
ZnS:In, recombination emission by optically detected magnetic resonance 80−66272
ZnS:Mn, electrolum. film, direct impact excitation of Mn centres 77−24900

photoluminescence continued
ZnS:Mn, self-activated and Mn^{2+} emission, high press. action 80−16093
ZnS:Mn, spectral distribution and decay times of the luminescence of Mn^{2+} on different lattice sites 79−78743
ZnS:Mn film, luminesc. of highly efficient DC diodes 77−8630
ZnS:Mn films, photoluminesc. and electroluminesc., excitation mechanism of luminesc. centres 79−11459
ZnS:Mn^{2+} phosphors, luminesc. excitation spectra and exciton struct. 80−55164
ZnS:Mn(Al)(Te), luminesc., exciton struct. 79−33801
ZnS:Ne, implanted single crysts., photolum. and bombardment effect, thermolum. curve obs. 80−55166
ZnS:Ni, IR luminesc. and absorpt. spectroscopy 80−108261
ZnS:Pb_x luminescence, polaris. emission 79−38634
ZnS:Pb^{2+}(Mn^{2+}), high press. luminesc., localised excitations 78−19534
ZnS:Tb_x Cu(Ag) phosphors, luminesc. props. 80−100690
ZnS:Tb^{3+}, sputtered film, DC electroluminesc. and host-excited photoluminesc., Tb^{3+} content depend. 77−85807
ZnS:TbF_3, photoelectroluminescence, effect of electron-hole pairs 78−27328
ZnS:Te, single crysts. grown from Te soln., photolum. props. 79−52005
ZnS:Tl(Al)(Zn), UV spectra of donor-doped single crysts. 77−12404
ZnS-based phosphor, microstruct. and luminesc. efficiency 78−10959
ZnS-CdS system, IR luminesc. and absorpt. centres, donor-acceptor pair model 77−44043
ZnS-CdS:Tm,Ni, recomb. centre interaction, luminesc. quenching 78−10946
ZnS-Mn crystal, polarisation meas., luminesc. and Raman spectra 79−8138
ZnS-ZnO, solid solns., edge emission and exciton spectra *(Russian)* 77−24899
ZnS-ZnSe mixed powders, hot-pressed polycrystalline, photolum. and electrolum. 77−32426
ZnS_xSe_{1-x}:Fe, photolum. meas. 79−19921
ZnS(Se)(Te):Co, impurity luminescence no phonon line depend. on temp., Debye temp. 80−66273
ZnS(Se)(Te):Co^{2+}, IR luminesc. quenching, Co^{2+} level position, ionisation energy 80−16079
ZnS(Se)(Te):Cr^{2+}, absorpt. and luminesc. of $Cr^{2+}(d^4)$, cryst. field theory interpretation 79−83000
ZnSe, band-edge photoluminesc., far-below band-gap excitation 80−76063
ZnSe, blende type struct., luminesc. under high excitation 79−19928
ZnSe, blue photoluminesc. excited with strong laser radiation 80−93391
ZnSe, direct gap semicond., exciton energy at 300K from reabsorption of luminesc. 79−78728
ZnSe, donor-acceptor pair emissions charact. *(French)* 80−108249
ZnSe, epitaxial, organometallic CVD, on GaAs, and photolum. 79−8249
ZnSe, epitaxial layers, close-spaced technique, preparation and optical props. 79−47637
ZnSe epitaxial layers, organometallic CVD prop., growth kinetics and luminescent props. 79−51458
ZnSe, exciton emission, halfwidths, thermal and optical activation energies obs. *(French)* 80−66268
ZnSe film, MBE and resistivity 79−100059
ZnSe, grown from Ga soln., near band-edge luminesc. 79−69881
ZnSe, hot-pressed powder LED fabrication and charact. 78−23639
ZnSe layers, LPE growth from Zn-Ga soln., photoluminesc. 79−56840
ZnSe, low resist. single crysts., radiative recomb. mechanism, photolum. and electrolum. 78−6744
ZnSe, luminesc., hot electron effects 80−66277
ZnSe, luminesc., reson. Raman scatt. due to excitonic mols. 79−33816
ZnSe, MBE growth, elec. and optical props. 80−75462
ZnSe, near band edge photoluminescence, electron-hole recombination 80−80835
ZnSe, optically pumped stimulated emission at 4580 Å, near band edge luminesc. 78−71105
ZnSe, photoexcited hot electrons at 2K, photolum. meas. 79−78741
ZnSe, photolum. and blue electrolum. in MIS structs. 77−20928
ZnSe, reabsorpt. of excitonic luminesc. in direct band gap semiconds. 77−63469
ZnSe, reson. absorpt. of coherent IR radn. by acceptors, photocurrent and emission spectra 79−73974
ZnSe, resonance Raman scatt., exciton-polariton luminescence *(Russian)* 80−97287
ZnSe, single cryst. film, MBE, quality obs. using photoluminesc. 77−77419
ZnSe single crystal, exciton photolum. and refl. spectra, 4-90K *(Russian)* 77−66540
ZnSe, thermally treated crystals 80−60661
ZnSe, undoped and doped, pair spectra, edge emission and shallow acceptors 77−28617
ZnSe:Ag, low-temp. photolum. meas. 77−20912
ZnSe:Al single crysts., photoluminescence spectra *(Russian)* 77−28627
ZnSe:Al(Ga)(In), single cryst., doping, blue luminesc. 78−39584
ZnSe:Al(Mn), elec. and luminesc. props. 77−39844
ZnSe:Co, optical props. in near IR 78−43924
ZnSe:Cr^{2+}, excitation spectrum of IR emission 77−12421
ZnSe:Cu, Cl, high press. luminesc. 78−19532
ZnSe:Cu, luminescence and diffusion behaviour of Cu impurities 78−35188
ZnSe:Ga(As), edge luminesc. 80−20699
ZnSe:I, I vapour transport prep., conductive and photolum. cryst. 79−100035
ZnSe:In, single crysts., new vapour phase growth method, elec. cond. props. and photoluminesc. spectra 79−19982
ZnSe:In films, MBE growth, doping effect on photoluminesc. 80−10818
n-ZnSe:Li, semicond. selective pair luminesc., excited impurity state investigation 79−61439
ZnSe:Li(Na), shallow acceptor excited states, luminescence spectra, Rydberg energy 79−78750
ZnSe:Li(Na)(Ga) doped and pure cryst., donor-acceptor bands 80−11465
ZnSe:N, ion implanted cond. type conversion on annealing *(Korean)* 78−18668
ZnSe:Na, characterisation of edge emission 78−27312
ZnSe:Ni, evidence for exciton binding at Ni impurity sites, photolum. excitation spectrum 80−45135
ZnSe:Ni, photolum. excitation spectroscopy 80−80841
ZnSe:Pb, luminescence photocond. 79−38634
$(ZnSe)_x(CdTe)_{1-x}$, low temp. photoluminesc. *(Russian)* 78−43931

photoluminescence continued
$(ZnSe)_{1-x}(GaAs)_x$ solid solns., photoluminescence spectra 80−40159
$ZnSe_{1-x}S_x$, luminescence, polaris. emission 79−38634
$ZnSe_xS_{1-x}$, melt grown, 10K, band edge photoluminesc. 78−84628
ZnSe(Te), photolum. excitation spectra of tightly bound holes, valence band contrib. 80−60658
ZnSe(Te), Raman-luminescence problem, interference analogy and expt. discrimination by polarisation correl. 79−95764
p-$ZnSiAs_2$:Au(Tl)(S), photoluminesc., radiative recombination 77−24883
Zn_2SiO_4:As,Mn, enhanced luminesc. stimulation, 20-320K *(German)* 77−20900
Zn_2SiO_4:Mn, energy storage effect and retrieval 80−100684
Zn_2SiO_4:Mn phosphor, luminesc. saturation under intense vac. UV irrad. 79−56841
Zn_2SiO_4:Mn phosphor, efficiency enhancement by $AlPO_4$ substitution 80−11452
$ZnSiP_2$ monocryst., impurity induced photoluminescence *(Russian)* 79−4850
$ZnSiP_2$, photocond. and photolum. spectra, optical anisotropy 78−72200
p-ZnSnAs, LPE, electronic struct. obs. by laser excited photolum. 80−60654
p-$ZnSnP_2$, photolum. anisotropy, 77K 78−19557
ZnTE, MBE growth, elec. and optical props. 80−75462
p-ZnTe 79−43028
ZnTe, band parameters from bound exciton, donor-acceptor pair excitation luminescence 78−92111
ZnTe, blende type struct., luminesc. under high excitation 79−19928
ZnTe crystals, polariton effects in luminesc. 80−103988
ZnTe crystals, secondary radiation polarization and relaxation of optical excitation 80−11399
ZnTe, dominant acceptors, annealing and quenching 80−24463
ZnTe, donor acceptance pairs, photoluminesc. excitation spectra *(Japanese)* 78−64409
p-ZnTe, doped and pure, photoluminesc. and photocond. spectra 77−55826
ZnTe, elec., SEM and TEM studies of impurity segregation during long annealing 80−30001
ZnTe, electron-phonon coupling, donor-acceptor pairs selective excitation 80−11475
ZnTe, excited acceptor, donor states, luminesc. 78−72604
ZnTe, exciton localisation at impurity pairs 79−37999
ZnTe, excitonic complexes, stress splitting of luminesc. lines 77−4672
ZnTe, free-exciton emission band under high-intensity photoexcitation 79−73993
ZnTe, high purity acceptor bound and free exciton states 79−99941
ZnTe, high quality p-type cryst., predominant acceptors 78−60504
ZnTe, irradiation induced radiative centers obs. 80−66290
ZnTe, low voltage green LED, struct. double diffusion procedure 80−100697
ZnTe, luminesc., donor-acceptor-pair excitation spectroscopy 80−25456
ZnTe, luminescence spectra struct. surface and volume polaritons *(Russian)* 80−16089
ZnTe, magneto-optical effect, I_2 bound exciton 77−12432
ZnTe, optical identification of substitutional acceptors by low temp. photoluminescence 79−99940
ZnTe, photoluminesc., donor and acceptor excited states 79−38622
ZnTe, pure and P(As) doped, shallow-acceptor, donor, free-exciton, and bound-exciton states 80−60667
ZnTe, radiative recombination involving free particle scatt. 79−38648
ZnTe, Raman scatt. and exciton luminesc. under reson. excitation 79−38617
ZnTe, real structure effect on luminescence and absorption spectra, dislocations 80−16085
ZnTe, refined, undoped, Cu acceptor, optical absorption and photoluminesc. meas. 80−34970
ZnTe, relax. processes at high excitation levels, Bose-Einstein condensation of excitons 78−48219
ZnTe, relax. times of secondary radiations, circular polarisation correlation 79−28816
ZnTe, relaxation processes, emission spectra *(Russian)* 78−72598
ZnTe, reson. secondary radiation 79−99886
ZnTe, SEM and luminesc. study of Li segregation 79−38657
ZnTe, secondary emission, transient behaviour under band-to-band excitation 80−108266
ZnTe, single cryst., electron-hole drop conc. *(Russian)* 79−11460
ZnTe, temp. depend. of Raman scatt. and exciton luminesc. spectra 78−39586
ZnTe, unalloyed, mechanism of radiative transitions 80−50405
ZnTe:Ag, real structure effect on luminescence and absorption spectra, dislocations 80−16085
ZnTe:Al,Cl, photolum., complex acceptor, ionization energy 80−20693
ZnTe:As(Li), donor-acceptor pair excitation and recomb., photoluminesc. obs. 80−20691
ZnTe:As(P)(Li), binding energy of shallow acceptors from photoluminesc. excitation spectra for donor-acceptor pairs 79−95809
ZnTe:Au, impurity identification and characterisation, capacitance, luminescence and IR absorption 80−60639
ZnTe:Cu, doping behaviour, SEM in cathodoluminesc. and photoluminesc. exam. 79−65927
ZnTe:Cu, elec. and optical identification of persistent acceptor 79−60764
ZnTe:Li, diffusion investigation by SEM and TEM 80−10706
ZnTe:Li, Zeeman splitting of ground and excited acceptor states, selective pair luminesc. 80−84780
ZnTe:Li(Cl)(Al)(In), ion implanted and annealed, photoluminesc. meas. 78−15208
ZnTe:Li(Na)(K)(Cs), fluorescence spectra meas. 78−10949
ZnTe:O,Zn, dual ion implantation, luminesc. spectra obs. 78−87697
ZnTe:P, excitations spectra of donor-acceptor pair photoluminesc. 78−23522
ZnTe:P, pure and doped, electron and exciton excited states of neutral donor 80−34393
p-ZnTe:P, semicond. selective pair luminesc., excited impurity state investigation 79−61439
ZnTe:P(Li), luminesc. transitions, quantum efficiency 79−1783
ZnTe(:In), single cryst. film, MBE, quality obs. using photoluminesc. 77−77419
$Zn_3(VO_4)_2$, luminesc. spectra in visible region, vanadate group 78−43921
$ZnWO_4$, scintillation charact. 80−66256
$ZnWO_4$:Ni^{2+}, luminescence rel. to Ni concn. 79−24352

photoluminescence continued
ZrF_4:Eu^{3+} glass, luminesc. of Eu^{3+}, transition probabilities 80−80845
ZrO, in Ne matrix, laser photoluminesc. 77−14481
ZrS_3, photolum. from excitons 80−66274

photolysis
see also photodissociation
acetaldehyde, first triplet state geometry, fragmentation into free radicals 80−47915
acetaldehyde, UV photolysis, transient species IR spectra 80−86464
acetaldehyde photolysis, HCO product microwave spectra 79−5163
acetone, photochem. and photophysics, 330-250 nm, 0-1000 torr 78−17706
acetonitrile, low press. IR multiple photon photolysis 79−16022
acetyl radical, absorpt. spectrum obtained by flash photolysis and kinetic spectroscopy 79−13731
N-acetyl-DL-valine, single cryst., paramag. centre form. by UV photolysis, room temp. 77−21480
9-acetylanthracene subpicosecond laser photolysis and time resolved absorpt. spectra *(Japanese)* 79−79272
acetylene, excited state, photochem. and spectrosc. investig. 80−95553
acetylene, in Ar matrix, irrad., C_2^- form. 77−75172
acetylene ($-d_2$), fluoresc., in matrix-isolated acetylene and ethylene photolysis 79−59505
acid amide+H_2O_2, aq. solns., photolysis, EPR study of spin-trapped radicals formed during photolysis 78−68996
acrolein, vap., visible luminesc. excited by pulsed CO_2 laser 79−54894
albumin, human serum, assoc. solns., excited state deactivation, flash photolysis obs. 79−54895
aliphatic amino acids, N-acetyl substituted, photolytic production of methyl radicals 79−96622
alkali halides, F^--centres, thermal and photolytic decay processes 78−95053
alkyl aryl ketones, in homogeneous n-heptane solns., quasi-isoenergetic triplet energy migration, photolysis obs. 79−61878
alkyl bromides, and perfluorinated mols., Br branching ratios, broadband flash photolysis 78−27787
alkyl halide photolysis by pulsed CO_2 TEA laser, mechanism 77−12807
alkyl iodide-$I_{(atom)}$ complex, multiple charge-transfer bands in liquid-phase 77−32776
allene, IR multiphoton photolytic C_3 prod., C_3 vibr. relax., chem. kinetics 80−66820
amides, substituted, aqueous solns., UV-irradiated, EPR and spin-trapping study of free radicals 79−16154
amines, aromatic, photochem. reactions with carbon tetrachloride, initiation mechanism 79−61888
amino acid photoresolution, rel. to origin of optical activity in life 77−40634
anthracene single crystals, hole trapping by photo-oxidation products, injection currents *(Russian)* 80−92904
anthracene/trans, trans-2,4-hexadiene-exciplex, fluoresc. rel. to photodimerization 77−3401
aqueous glass, γ-radiolysis, photolysis of trapped electrons, quasi-free electron IR absorpt., luminesc. 77−21401
aqueous glass, laser excitation, bleaching of trapped electron absorpt. bands 79−43606
arenediazonium salts, photolysis, quantum efficiencies, reactive intermediaries, EPR 78−64860
aromatic ethers, comparative study of X-ray and γ-induced photolysis and radiolysis *(German)* 78−64854
aromatic hydrocarbon, quenched with Ag^+ in ethanol, triplet state form. 79−11801
aromatic hydrocarbons, oxygen quenching of triplet states, charge-transfer interactions 77−23516
aromatics, biphotonic reactions at 77K, quantum efficiency 78−80763
atmosphere, daily average solar heating or photolysis, exponential approx. 77−5285
atmosphere, daylight or diurnally averaged photolytic rate coeffs. 79−53458
atmosphere, diurnal average photodissoc. rates determ. 77−78311
atmospheric photochemical smog formation, solar spectral distrib. 79−52983
atom+molecule reaction rate meas. 80−16676
autonitrile, photolysis in solid Ar, CCN radical spectra 78−70868
azo dyes, cis-trans photochem. isomerisation 78−27785
bacteriorhodopsin, dark-adapted, photocycle and light adaptation 77−73508
bacteriorhodopsin, ps flash-photolysis obs., room and low temps. 79−57581
bacteriorhodopsin in purple membrane fragments, proteolysis and flash photolysis obs. 79−62185
bacteriorhodopsin photocycle hydration effects, in thin purple membrane layers 78−7320
bacteriorhodopsin phototransients, circular dichroism meas., comment 78−21954
Bengal pink-anthracene, mixed annihilation delayed fluoresc. 80−74193
benzene, nanosecond laser photolysis 80−66825
benzene, resonance-enhanced multiphoton ionis. and fragmentation of mol. beam 79−100411
benzene, UV laser photolysis, electronic 3-wave mixing spectra of transient fragments 79−68223
benzene excimer, nanosecond laser photolysis 80−66825
benzoin containing system, photosensitized free radical polymerisation 80−7825
benzophenone betyl radical, photochem. yield mag. field effect on spin rephasing, double-pulse technique 77−90615
benzophenone containing system, photosensitized free radical polymerisation 80−7825
benzophenone in isopropanol, submicrosecond time resolved EPR, lser photolysis, CIDEP polarisation mech. 78−80764
benzophenone ketyl radical, in micelle, decay rate in mag. field, photolysis meas. 80−85154
benzophenone-N,N-dimethylaniline, intramolecular exciplex systems, laser photolysis obs. 80−35550
p-benzosemiquinone monoprotonated radical, submicrosecond time resolved EPR, lser photolysis, CIDEP polarisation mech. 78−80764
9-benzoylanthracene, subpicosecond laser photolysis and time resolved absorpt. spectra *(Japanese)* 79−79272
benzyl halides, in matrix, UV-, γ-irrad., benzyl radical-halide ion form., charge transfer bands 77−16854
photolysis continued
benzyl radicals, monomtheyl- and dimethyl-substituted, electronic spectra and electron affinity 80−63618
biologically important molecules, nanosec. flash photolysis 78−68905
biradical, photogenerated in Norrish type II reaction, solvent effects on lifetime 79−11804
bromofluoromethane cations in solid Ar, absorpt. spectra and photochem. 79−96339
bromomethane, VUV laser multiphoton dissoc., CH excited state branching ratio, chemiluminesc. 78−70884
bromomethyl radical+alkane, rate constants 77−25248
bromotrichloromethane, ^{13}C isotope selectivity press. depend., multiphoton IR photolysis 80−45523
butadiene, resonance-enhanced multiphoton ionis. and fragmentation of mol. beam 79−100411
carbazole in diethyl ether, carbazole cation radical, otpical absorpt. spectra 77−40564
carbocyanine dyes, sterically hindered short-lived isomers, laser photolysis study 78−40063
carbonyl to oxacarbene rearrangement, conformation, ab initio SCF MO calcs. 77−32780
carboxyhaemoglobin, aq. soln., photolysis using nanosec. pulse, transient effects 79−79453
carboxylic esters, γ-irrad. glass, trapped radical photolysis, ESR 78−85178
chlorodifluoromethane, heat absorbed when laser irrad., laser calorimetry 79−16012
chlorodifluoromethane, IR multiphoton dissoc., CF_2 form., time-resolved optical absorption obs. 80−16702
chlorofluorocarbons, photodecomposition under simulated tropospheric conditions *(German)* 79−53408
chlorofluoromethane cations in solid Ar, absorpt. spectra and photochem. 79−96339
chlorofluoromethane in stratosphere, effect on O_3 conc. 80−109197
chlorofluoromethanes, laser photolysis, product vibr. relax. rates and diffusion coeffs. 80−55680
chlorophyll a: Cu^{2+}, in pyridine fluoresc. quenching mechanism 79−56837
chlorophyll a and b, assoc. solns., excited state deactivation, flash photolysis obs. 79−54895
chlorophyll photo-oxidation, spectral detect. of exciplex in triplet state 77−25368
chlorophyll photo-oxidation mechanism, effect of spectral composition of light 77−25369
chlorotrifluoroethylene, multiphoton dissoc., fragment energy partitioning 80−55681
chlorotrifluoromethane, photolysis, transient species, matrix isolation spectra 78−48635
$ClONO_2$, form., photolysis in stratosphere, photochem. absorpt. cross sections, UV spectra 77−33154
closed illuminated system, oscillatory and runaway states 79−47950
cofacial diporphyrins, electron transfer reactions following picosecond excitation, CT state lifetimes, optical difference spectra 80−25995
complex molecules, laser induced dissoc., thermal energy effects 80−53071
copper oxalate hemihydrate, photographic props. eval. for use as high-speed photographic materials 77−44497
cyanine dyes, trans-cis isomerisation, ps kinetics 79−87853
cyanoethylene, photofragment recoil, state selective time of flight- fluoresc. method 79−11809
cyanomethane, IR photolysis, CN radical photoluminesc. 77−73452
cyanomethane, matrix-isolated, VUV photolysis, CNC radical vibr. and electronic spectra 78−85180
9-cycanoanthracene, subpicosecond laser photolysis and time resolved absorpt. spectra *(Japanese)* 79−79272
cyclobutane+diazomethane (ketene) photolysis, methylcyclobutane form., decomp., CH_2 vibr. energy distrib. 78−61032
cyclobutanone, IR laser photolysis sensitised by NH_3, and reaction temp. 79−47944
cyclododecanone, photolytic biradical anomalous CIDNP enhancement, pulse spin echo NMR obs. 78−46369
cycloheptanone, photolysis, CIDNP effects 80−18869
cyclopropane, IR laser photolysis, decomposition, flame reaction 77−66760
cyclopropane, multiphoton IR laser-induced reactions 79−66312
L-cysteine HCl, free radical formation by two photon absorpt. at 3371 Å 77−32815
data acquisition, Biomation 8100 recorder interfaced to remote computer 78−21107
diazo compounds, continuous tone diazotype imaging films, model 78−32911
diazonium, amplifying material, kinetic and sensitometric props. *(German)* 79−43607
dibenzoylperoxide, triplet sensitized photolysis, mag. isotope effect 77−60081
dibenzylketone, photolysis in micellar soln., quantum yield and ^{13}C enrichment 80−97711
dibromodifluoromethane, excimer laser photolysis, luminesc. from Br_2, Br, C_2, and CF_2 79−39184
dibromodifluoromethane, UV laser fluoresc. and photochem., CF_2, CF and Br_2 fluoresc. obs. 80−16703
dibromodifluoromethane, vac. ultraviolet photodissociation, CF_2 emission 79−47955
dibromofluoromethane, photolysis, IR matrix isolation spectra of CF_2Br free radical 78−27788
p-dichlorobenzene, collision induced photodecomposition with ethane, CO_2 and SF_6, quantum yields 79−79270
dichlorodifluoromethane, IR photolysis, isotopic selectivity factors 79−47946
dichlorodifluoromethane, laser photolysis for Cl isotope enrichment 78−58859
dichlorodifluoromethane, UV absorpt. cross sections temp. depend., stratospheric appls. 77−64423
dichlorodifluoromethane, UV photolysis, free radical emission 80−30263
dicyanoacetylene, at 160 nm, production of CN(X) free radicals 77−9107
6,6′-diethoxy-thioindigo, cis⇌trans isomerisation, nanosecond flash photolysis and steady state methods, triplet state 78−35648
3,3′-diethyloxadicarbocyanine iodide, lasing and photoisomerisation, conc. and temp. effects 77−7081

photolysis continued
1,1-difluoroethane, unimol. decomposition, direct meas. via IR laser photolysis, collision effects 79−57254
difluoroiodomethane, vacuum UV photolysis, IF in solid Ar visible spectra 80−87137
dimethylaminophenyl-(methylene)$_n$-(1-pyrenyl), intramolecular charge transfer, heteroexcimer formation processes 78−27783
4-(2′,4′-dinitrobenzyl)-pyridine, photochromism, nanosec. laser absorpt. spectrosc. obs. 80−85193
2-(2′,4′-dinitrobenzyl)-pyridine, photochromism, ns laser absorption spectra 78−48138
2,2′-dinitrodiphenylmethane, nanosecond laser flash photolysis and absorpt. spectra, photochromism, solvent polarity 78−61029
dipeptides, aliphatic, EPR studies of direct photolysis 78−48678
2,6-diphenyl-1,4-benzoquinone+aromatic amine, triplet exciplex quenching, H-transfer mechanism 79−79228
1,3-diphenylisobenzofuran solns., rubrene sensitised photooxidation, S_1 excited state O_2 quenching 80−45529
all-trans-diphenyltetradecaheptaene, oriented, photochem. reaction production and monitoring, reson. Raman spectroscopy 77−29020
dissolved pollutants photolysis rates, suspended sediments effects 79−100546
DNA bromodeoxyuridine substituted, photolysis using UV light source 78−22185
DTTC, subpicosecond laser photolysis and time resolved absorpt. spectra *(Japanese)* 79−79272
durene, aldehyde doped cryst., photolysis 10 to 20K, physical and chem. defects 79−52721
duro-semiquinone monoprotonated radical, submicrosecond time resolved EPR, lser photolysis, CIDEP polarisation mech. 78−80764
dye solutions, picosecond flash photolysis and very fast processes 80−30249
Earth atmosphere, translationally hot O(^{3}P) atoms energy distrib. function 80−21811
electrocyclic isomerisation of ground state induced by IR laser multiphoton absorpt. 77−32811
ethyl acetate, heat absorbed when laser irrad., laser calorimetry 79−16012
ethyl acetate, multiphoton dissoc. by CO_2 laser beam 80−7811
ethyl acetate-isopropyl bromide, IR laser induced decomposition 79−16011
N-ethylcarbazole, soln., laser induced ionic photodissoc., transient polyelectrolyte form. 80−53068
ethylene, dye laser probing of C_2 radicals, IR intense field photolysis 77−16851
ethylene, photoassisted decomposition at room temp. over Pt/TiO_2 80−55703
ethylene(−d_4), matrix-isolated, photolysis, acetylene fluoresc. 79−59505
ethylene episulphide, form. at S surface by laser irrad. in presence of ethylene 79−57258
ethylenimine, gas phase photolysis and mass spectra of products 77−29022
ethylperoxy radicals+NO reaction, flash photolysis and kinetic spectroscopy obs. of rate consts. 79−83470
excited charge transfer systems, in polar solvents, dynamic behaviour obs. 78−58772
field ion (emission) microscope tip prep. from sheet and block metal 78−7155
flash, in time and frequency domains, atmosphere chemical behaviour obs. appl. 79−39874
flash photolysis, appl. to biological systems, review 78−11530
flash photolysis, optical grating method 78−27785
fluorenone photoreduction by DABCO, ion-radical yield enhanced by mag. field, cage recomb. region 79−79268
fluoride photodissociation, F atom quantum yield meas. in chem. laser 78−58753
fluorinated organic iodides, absorpt. spectra and primary photolysis processes, near and vac. UV 79−20393
fluorobenzenes, matrix laser fluoresc. spectra of radical cations 80−1009
fluorobenzenes in Ne matrices, molecular cation electronic absorption spectra, new photolytic technique 80−58415
fluorocarbon-11, estimated future atmos. concs. for various tropospheric removal rates 77−21892
fluorodiiodomethane, vacuum UV photolysis, IF in solid Ar visible spectra 80−87137
formaldehyde, low-temp. matrix photolysis, hydroxymethylene intermediacy, IR obs. 78−76877
formaldehyde, multiphoton dissoc. using focused DF laser, H-isotope separation 79−94094
formaldehyde, normal and deuterated solid films, UV dissociation at 77K 77−29021
formaldehyde, photochem., ab initio calcs. rel. to hydroxycarbene intermediate 79−61880
formaldehyde, photochemistry, past and present 79−52711
formaldehyde, photolysis, HCO prod., vibr. relax., chem. kinetics and spectra 79−11808
formaldehyde, photolysis in Ar matrix, role of cage dimer 79−91973
formaldehyde, photooxidation products, HO_2CH_2OH observed in IR spectra 79−93994
formaldehyde, selective laser photolysis for ^{14}C enrichment 80−108720
formaldehyde, selective photolysis in single line to ^{14}C enrichment 79−10220
formaldehyde, UV photolytic separation of D from H in cryogenic solns. 78−95937
formaldehyde(-d_2), photolysis quantum yields, radical production, NO reactions, freq. depend. 78−44387
formaldehyde ($\tilde{A}\,^1A_2$) single vibronic level photolysis, H atom prod., HNO chemiluminescence 77−9108
formaldehyde in air, photodecomposition, CO and H_2 quantum yields 79−66311
formyl radical, form., vibr. relax., spectrosc. 79−36746
free radical reactions, photolytically initiated, high temp. kinetics meas. technique 80−61085
free radicals, photolysis, excimer laser UV obs. 80−16711
fumaronitrile exciplexes, photoisomeris. and photoionis, dissolved O_2 effect 78−27789
furil + pentachlorophenol, photochem. reduction, cross-relax. and CIDNP, PMR relax. obs. 79−52694
glyoxal, selected state photodissoc., vibronic effects, CO quantum yield, 1-10 torr 78−37691
photolysis continued
glyoxal-photoreduction-product-radicals, kinetics and intramol. dynamics 77−32808
Group IV photolytic laser expts., for fusion research 78−63101
Group VIA photolytic laser systems, for fusion research 78−59002
haemoglobin-CO reaction kinetics, relax. meas. on photolytic illum. 77−70405
heptafluoroiodopropane light amplifier, wave-front distortion due to photolysis-gas dynamic effects 79−18412
1,5-hexadiene, D-labelled, IR laser induced isomerization via electronic ground state 77−25289
hexafluoroacetone, 147 nm photolysis, quantum yield press. depend. 78−68903
hexafluorocyclobutene, ground state, electrocyclic isomerisation of ground state induced by IR laser multiphoton absorpt. 77−32811
hot-atom reactions, photolytically-driven, kinetic theory, appl. to DI 79−74408
hydrocarbons, photochem. in atm. of Titan 79−53766
hydrocarbons, reactions, rate consts., temp. depend., photolysis, high temp. fast flow reactor technique 80−42231
hydroxyanthraquinones, lightfastness and flash photolysis 79−96341
I_2He, I_2He_3, and I_2He_3, photodissoc. products energy distrib. 79−100410
imidazoles, reaction with photochemically generated α-hydroxyalkyl radicals, EPR study 80−35558
indole, aq. solns., flash photolysis, transient absorpts., 600 to 800 nm 78−53228
indoles, laser flash spectroscopy in presence of nitroxide radicals, protein-membrane interaction probing 79−87855
inorganic anions, solns. in aromatic solutes photochem. hydrated electron decay kinetics 77−52656
interstellar grain mantles, UV photolysis rel. to mol. form., laboratory analague expts. 80−26944
iodoheptafluoropropane, photolysis, reaction rate consts. meas., photodissociation I laser characts. 79−52671
iodomethane, photofragmentation in vap. phase, photoacoustic meas. 78−95943
iodomethane laser, photolysis wavelength, repetitive operation 79−3689
iodomethyl radical, vibr. excited, photofragmentation IR emission obs. 80−87162
n-iodopropane, UV photolysis, metastable I radiative lifetime reson. fluoresc. obs. 79−11799
iodotrifluoromethane, photolysis, reaction rate consts. meas., photodissociation I laser characts. 79−52671
IR laser induced reactions for IR inactive species 78−80761
IR laser photolysis of polyat. mols. photochem. appls. 80−66835
IR multiple-photon photolysis, fluence-depend. dissociation probabilities calc. 80−32786
iso-butene, flash photolysis, β-methallyl radical extinction coeffs. 77−1938
isopropyl radical, Ar matrix isolated, IR spectra and UV photolysis 80−66827
ketene, CH_2 photoprod., wavelength depend. 80−11936
ketene, near UV photolysis, bimol. mechanism, products quantum yield, press. depend. 77−77799
ketene-cyclobutane-O_2, UV photolysis producing chem. activated methylcyclobutane, S/D ratio 79−87856
kinetic data acquisition, and anal., by computer based system 79−39180
kinetic IR spectroscopy IR, appl. to biochem. systems 80−98178
lanthanide mixtures in aq. solns., photochemical separation of Eu 78−31660
laser collision induced chemical reactions, collinear exchange model 79−66313
laser dye, photodecomposition of rhodamine dye *(Russian)* 77−29017
laser photolysis installation for investigation of phototransformations of substances in nanosecond time interval 80−33006
laser-assisted excitive Penning ionisation 79−41232
laser-induced, effective manifold reduction, criteria 80−43123
luminol, chemiluminesc., quantum and excited state yields, pulse radiolysis 79−47930
mammalian cells, replicon sizes estimated by X-ray plus bromodeoxyuridine photolysis method 79−16353
Mars, lower atm., O_3 distrib. and photochemistry 79−35169
matrix photolysis, in vac. UV region, using windowless Ar discharge 77−71798
metarhodopsin I-II transition obs. by absorpt. changes of eriochromblack T 77−44593
methanethiol+OH radical, reaction rate const., 299-426K 77−40525
methanol, IR laser photolysis of vap., product distrib. 79−39160
methanol, IR multiphoton photolysis, OH and CH form., rovibronic relax. 78−68902
methanol, multiphoton decomposition with laser, isotope separation 79−66306
methanol, photolysis, IR multiphoton decomposition processes 78−3358
methanol (dimethyl ether)+Cl, absolute rate consts., 200-500K, stratospheric chem. appl. 79−66271
methoxy prod. from methyl nitrite photolysis 80−85200
methyl isocyanide photodissoc., cyanide radical energy partitioning chemical laser determ. 78−73063
methyl radical, vibr. excited, photofragmentation IR emission obs. 80−87162
γ-methyl valerophenone, photolysis, biradical form., lifetime, interaction with O 77−60086
methyl viologen, chlorophyll a sensitised reduction in non-ionic micelles 79−1962
N-methyl-2-N-phenylamino-6-naphthalene sulphonates, triplet excitation, multiple fluoresc. 77−71826
3-methyl-3-buten-2-one copolymers with styrene and methyl methacrylate, photodegradation *(Japanese)* 80−108725
o-methylacetophenone, laser flash photolysis, temp. depend. 80−93770
methylamine, photochemical conversion to HCN with ArF laser, mol. fluoresc. obs. 80−97710
methylamine+OH radical, reaction rate const. 299-426K 77−40525
2-methylbut-1-ene, flash photolysis, β-methallyl radical extinction coeffs. 77−1938
3-methylpentane, glassy soln., Hg sensitised UV photolysis, radical production 79−52720
methylviologen, photoreduction to H_2, adsorbed on cellulose, hydrogen economy 80−81491
micellar system, photoinduced redox processes kinetics, intramicellar electron transfer 78−92603

photolysis continued
modeling of elementary step of chemical transform. of crysts., appl. to decomp. 79−15985
modulation photolysis as alternative method for photochromic soln. obs. 77−90613
monomer gas photopolymerisation, polymer film form. on semicond. 78−10561
multiphoton excitation, molecular dynamics 77−29019
myoglobin, O_2 and CO bonds, flash light photolysis *(Hungarian)* 79−29501
myoglobin+CO, recombination after flash photolysis, kinetics meas. using minicomputer 78−7200
β-naphthol, aq., solvated electron prod. using laser excitation 77−60087
nickel oxalate dihydrate, photographic props. eval. for use as high-speed photographic materials 77−44497
9-nitroanthracene, subpicosecond laser photolysis and time resolved absorpt. spectra *(Japanese)* 79−79272
nitromethyluracil, radiation-induced oxidation and reduction 77−32816
1-nitropropane, gaseous, primary processes, study at 22°C and 100°C 80−89507
2-norbornyl radical, photolysis prod. and EPR, hyperfine splitting 77−56237
Norrish type II reaction biradicals, spectra, extinction coeffs., solvent effect on lifetime 77−90617
nuclear fuel reprocessing, U(IV) photochem. prod. for use as reductant for Pu(IV) 79−36383
olefin triplet lifetime measurement by electron transfer interception 79−79269
pentafluoroacetone, IR laser induced decomp., free radical mechanism 80−71924
perfluoroalkyl halides, at. I form., quantum yields 78−3355
perfluoroalkyl iodides, laser photolysis, quantum yields 79−29382
perfluoroalkyliodide, pyrolysis of vapour due UV irrad. 78−73070
perfluoroiodoethyl perfluoromethanoate, absolute quantum yields of $I(^2P_{1/2})$ and $I(^2P_{3/2})$ 79−34339
perfluoropropyl iodides, absolute quantum yields of $I(^2P_{1/2})$ and $I(^2P_{3/2})$ 79−34339
peroxidase, photo-induced reduction, reaction with indole acetic acid 79−79452
phenanthrene, subpicosecond laser photolysis and time resolved absorpt. spectra *(Japanese)* 79−79272
phenol derivatives, neutral aq. solns., flash photolysis, N_2O and alcohol effects 78−40065
phenoxy radicals, electronically excited states, photochem., flash photolysis obs. 77−77797
2-phenylcycloalkane, photolysis products studied by ^{13}C CIDNP and intersystem crossing 79−79275
pheophytin a and b, assoc. solns., excited state deactivation, flash photolysis obs. 79−54895
photobiological conversion of solar energy *(German)* 79−2013
photoelectrochemical cells, metal, electrodes in contact with fluoresent dye solns., photovoltage generation, comprehensive model 80−40871
photoelectrochemistry, laser sources use for solar energy conversion 80−40873
photoelectrolysis, basic electrode processes and appls. to H prod. from H_2O 80−51016
photoelectrolysis, semiconductor electrodes properties influence 78−14816
photoelectrolysis irreversibilities 78−23161
photoelectrolysis of water using semiconductor electrode, surface state charge transfer 79−28405
photoelectrolysis of water with semicond. surface, review *(Japanese)* 78−6440
photographic dye, colour coupling in soln., kinetic anal., appl. of flash-light photolysis *(German)* 79−39173
photographic emulsions, ultra-fine grained, nature of produced colour centres *(Russian)* 80−73517
photoinduced radical pair recombination in high mag. field, Monte Carlo method 79−87861
photoreceptor membrane viscosity and component dynamics, recombination kinetics method 79−39366
photosynthetic pigment, intersystem crossing 77−58057
photosynthetic systems, reaction centre struct., triplet state ODMR 77−29093
photosynthetic systems, temperature dependence of excitation transfer 78−92598
picosecond flash, in biology, biophysics, book contrib. 79−5328
pivalophenone, organic soln., triplet reactivity solvent depend., flash photolysis study 80−11902
planetary atmospheres, diurnal average photodissoc. rates determ. 77−78311
polar glass, UV and γ-prod. electrons geminate recombination, radical yield 77−9094
poly N-vinylcarbazole, soln., laser induced ionic photodissoc., transient polyelectrolyte form. 80−53068
poly-2-vinylnaphthalene, soln., lowest triplet props., flash photolysis and radiolysis obs. 80−32861
poly-aryl-vinyl, photon generated radical ions, photocond. *(German)* 79−52708
poly-N-vinylcarbazole and N-isopropylcarbazole with p-dicyanobenzene in dimethylformide soln., laser photolysis 79−100360
polyethylene, photodegradation study by Fourier transform IR spectroscopy *(Japanese)* 79−24772
polyethylene with rutile pigment-antioxidant, photo-oxidation 77−63816
polymer solution, disentanglement of fractions 79−66314
polymethine dye solutions, photochem. transformations and short-wavelength luminesc. 80−100686
polypropylene, photooxidation, initiation process nature 77−52523
propyl compounds, photolysis, photofragment free radicals, mass spectra *(Japanese)* 78−7220
protohaeme-CO binding dynamics, flash photolysis, activation energy, entropy 77−21472
protoporphyrin: Cu^{2+}, in pyridine fluoresc. quenching mechanism 79−56837
protoporphyrin IX, triplet states, flash photolysis, obs. 80−95555
protoporphyrin IX dimethyl ester, triplet states, flash photolysis, obs. 80−95555
pulsed laser spectroscopy, review 79−26140
pulsed photolysis of gas, radial oscills. in a cylindrical cell 78−56908
PVC+$Br_2(I_2)$, reaction in surface-modified film subject to thermal-radiative and photochem. action *(Russian)* 77−21385

photolysis continued
pyrene-diethyl aniline in acetonitrile-toluene, triplet exciplex state in pulsed laser photolysis 77−16836
pyrene-N,N-diethylaniline exciplex, visible spectra obs., picosec. laser photolysis, solvent polarity depend. 77−38677
pyrene-N,N-dimethylaniline heteroexcimer systems, micellar solns., fluoresc., photoinduced electron transfer 78−25590
pyrimidines, substituted, UV irrad. in aq. solns., EPR of free radicals 78−40115
quinacrine mustard, 2-step laser-induced photodamage 80−85198
quinoline, photooxidation on rutile, ESR and effects of surface states 79−66352
quinones, triplet quenching by organometal cpds., time resolved CIDEP and ESR obs. 80−95654
quinones-Zn porphyrin, quinones sensitised reduction in vesicle systems 80−71897
radical generation for EPR 80−11271
radical pair generation, diffusion, spin motion, recombination in soln. nanosecond scale 77−77798
radicals prod. by flash photolysis, CIDEP 78−13535
11-cis-retinal, donor energy effects on triplet-sensitized isomerization 78−3353
retinal, isomeric triplets, low temp. spectrosc. and kinetic flash photolysis obs. 79−85972
retinal rod external segment mag. anisotropy decrease after total photolysis 77−52838
reverse pinch effect cavity pulsed light source 78−87114
rhodamine 6G, dye soln., laser flash photolysis 77−21402
rhodamine 6G, solns., delayed fluoresc. of simple associates 79−56847
rhodamine 6G in ethanol, photobleaching mechanism *(Russian)* 78−48680
rhodamine 6G in ethanol dye soln., lasing props. recovery after photolysis 77−34888
rhodamine dyes, triplet state, role in intermediate prod. 77−29018
rhodopsin, bathorhodopsin and isorhodopsin, mech. of photoconversion 78−53336
rhodopsin, bovine, kinetics of intermediate photolysis processes 79−43608
rhodopsin, photo- and thermo-bleaching rel. to heterogeneity problem 80−41114
rhodopsin, transient light-induced conform. changes 78−15774
rhodopsin flash photolysis, rabbit retina 78−76996
rhodopsin visual pigment, photochemical transformations, laser flash photolysis 79−66472
saturated organic molecule, photolysis, primary step prediction using Rydberg and valence-shell transitions 77−21404
selenophene, flash photolysis, transient absorpt. spectra 80−14153
semiconductor, photochemical etching mechanism 77−16709
semiconductor sensitised photolysis and latent image structure 79−24768
silver salts of organic acids, photolysis investig. for use as photosensitive material for PC forming 77−44496
simple molecules, two-photon dissoc., spectrosc. obs. 80−32787
solar energy conversion, materials used in water photolysis technique 77−20423
spiropyrans, photochromic transformation by electro-optical chronography 79−57264
stilbene, cis- and trans-, picosecond flash photolysis, intramol. charge-reson. transition obs. 80−7810
trans-stilbene dianion, photolysis, intermediate struct., time-resolved reson. Raman spectra obs. 79−52695
stratosphere, NO_x catalytic O_3 destruction, sensitivity to rate coeffs. 77−37472
styrene, polymerisation, photoinitiation by aliphatic azo cpds., EPR obs. 78−80746
sulphononaphthols, rapid pH and $\Delta\mu H^+$ jump by short laser pulse 80−16709
synchronized flash photolysis and pulse deposition in matrix isolation experiments 78−73120
temperature jump and photochem. studies, fast flashlight appl. 78−22588
p-terphenyl solns., mag. field effects on scintillation pulse shape, ion pair recomb. 77−16835
tetrabromomethane, excimer laser photolysis, luminesc. from Br_2, Br, and C_2 79−39184
tetrachloromethane, UV laser photolysis 80−66826
1,2,4,5-tetracyanobenzene, CT complex in micellar soln., fluoresc. and photolysis study 79−61911
tetrafluorodilhietane, IR photolysis, multiphoton dissoc. models 80−30253
tetrafluoroethylene, photolysis, CF_2, form., excitation by Hg 253.7 nm line, reson. fluoresc. spectra 80−63694
tetramethyldioxetane, IR laser dissociation, chemilum. spectrum 79−5171
tetramethyldioxetane, photolysis, unimolecular decay probed by picosec. spectroscopy 77−60083
thioindigo, cis⇌trans isomerisation, nanosecond flash photolysis and steady state methods, triplet state 78−35648
thiophene, flash photolysis, new transient absorption spectrum, C_4H_3 radical, assignments 78−46354
transient species, form., quantitative anal. by extrapolation method 78−15685
transition metal complex anions, ligand-bridged, binucl., reson. Raman spectra 78−42067
transparent dielectric, mechanism of destruction 79−39177
triatomic linear molecule, photodissoc., products rot. distrib. 79−66309
trichlorofluoreomethane, UV laser photolysis 80−66826
trichlorofluoromethane, IR multiple-photon laser-induced decomposition, Cl and Cl_2 form. 78−40066
trichlorofluoromethane, UV absorpt. cross sections temp. depend. stratospheric 77−64423
1,1,1-trifluoroacetone, photochem. and photophysics, 330-250 nm, 0-1000 torr 78−17706
trifluoroacetyl iodide, UV photodissoc. into three fragments, expt. and trajectory calc. 79−70356
trifluorobromomethane, multiphoton laser induced chemistry 79−91974
trifluoroiodomethane, IR multiphoton dissoc. yields, new technique, non-linear pumping effects 79−100406
trifluoroiodomethane, laser photolysis, I* form., quenching obs. 77−3299
trifluoroiodomethane, UV absorption induced by excitation of ν_1 vibrational mode photolytic production of I 78−50552
trifluoroiodomethane, vap. phase photolysis, UV irrad. 78−73070

photolysis continued
trifluoromethane, D ultrahigh single-step enrichment by CO_2 laser photolysis 80−45527
trifluoromethyl halides, matrix photoionis., IR spectra of CF_3^+, CF_2X^+ and CF_3X^+ cations 78−74710
trimethylgallium-AsH_3-H_2, GaAs VPE UV stimulated 78−35313
triphenylmethane dye soln., electronic relax., viscosity-depend., using picosec. flash photolysis 80−66258
troposphere, solar UV flux meas., $O(^1D)$ photoprod. rate determ. 79−12197
tryptophan, laser flash spectroscopy in presence of nitroxide radicals, protein-membrane interaction probing 79−87855
tryptophanyltryptophan, laser flash photolysis, photoionis. mechanism 77−90619
tryptophanyltyrosine, laser flash photolysis, photoionis. mechanism 77−90619
unimolecular reaction kinetics, monochromatic IR radiation 79−47949
unimolecular reactions, monochromatic IR radiation induced, rate const. intensity depend. 79−87857
uranyl hexafluoroacetylacetonate tetrahydrofuran, IR laser photodissoc., O and U isotope selective 80−50868
vinyl chloride, IR laser induced photoreactions, product identification 79−57257
vinyl chloride, IR multiphoton energy deposition and reaction yield, press. and intensity 78−95936
vinyl cyanide, electronically excited species production via collisionless, IR laser photolysis 79−57255
vinyl polymers quenched with electron donor (acceptor) in soln., ionic photodissoc. 79−11800
visual pigment solutions, flash photolysis, time resolved difference spectra, temp. var. 77−25434
visual pigments, slow flash photolysis using conventional spectrophotometer 78−68904
visual pigments in solution, flash photolysis kinetics, effect of prep. 77−32892
water, biophotolysis, living electrode of algae as long-lived photoconvertor 80−104510
water, CW and flash photoelectrolysis using ferroelectric photoanodes 80−81339
water, photoassisted electrolysis, Fe_xO_y electrode prep. and charact. 78−15683
water, photoelectrolysis, using Fe_xO_y-coated n-Si heterostruct. photoanode 80−61384
water, photoelectrolysis by irradiation of platinized n-type semicond. $SrTiO_3$ and $KTaO_3$ 77−86332
water, photoelectrolysis in sunlight, using sensitised TiO_2 electrodes 78−19143
water, photoelectrolysis with TiO_2 catalyst 80−60755
water, photooxidation at α-Fe_2O_3:TiO_2 electrodes 78−15684
water in n-TiO_2-KOH-Pt cell, H_2 partial press. 78−64858
water photoelectrolysis, rel. to charge transfer via surface states of semicond. 80−75636
water photoelectrolysis with transition metal doped TiO_2, $SrTiO_3$ anodes 79−74531
xanthione, solns., triplet state quenching by ground state xanthione 78−42180
Ag, cluster and microcrystal, matrix isolated, optical absorpt. spectra, photolysis and plasmon absorpt. 79−89820
Ag complexes, Ag(II) porphyrins, picosec. flash photolysis, transient absorpt. 80−52976
Ag formation on Ag-halide surface, flash photolysis expts. on Ag halide photochromic glasses 79−94310
Ag halide, absorpt. and vac. photolysis 78−8458
Ag halide photochromic glass:Cu^{2+}, characterisation of Cu ions 78−5530
Ag halide photochromic glass, darkening mechanisms under pulsed laser excitation 78−25938
Ag halide photochromic glasses, flash photolysis expts. 79−20401
Ag halide:Cu^{2+} photochromic glasses, darkening mechanisms, from flash photolysis and EPR studies 77−16156
Ag salts of carboxylic acids, Ag mirror formation 77−75720
AgBr, diffusion and recombination processes 79−24789
AgBr dispersion in gelatin, adsorbed S and Au, transient absorpt. spectra, latent image form. and decay 80−66837
AgBr:Pd(II), photolysis-induced trapping behaviour, EPR study 80−54949
AgCl, defects induced by energetic ion implantation 78−17518
AgCl, light scatt. during photolysis 77−40565
AgCl, luminescence fatigue, adsorbed Ag atoms 80−66281
AlH_3, effect of 1 MeV Co^{60} γ-irrad. on isothermal decomp. 78−92472
AlH_3, I-V and relax. characts. in dark cond. 77−85235
AlH_3, photo-and thermochem. reactions, 200-350K, UV Induced local states 78−31667
AlH_3, photolysis, luminesc. spectra of adsorbed rhodamine dyes 80−55171
AlH_3, polycrystalline, photoconductivity and photochemical decomp. 80−44638
Ar:N_2O(CO)(CO_2), fluoresc. and thermoluminesc. after photolysis 79−89700
Ar:PH_3:N_2O, photolysis, HPO and PO form., IR(UV) matrix isolation spectra 80−47985
As_2Se_3, amorphous, electrophotographic props., photodecomp. effect 78−49918
Bi, UV absorption spectrum, flash photolysis method 78−90105
BiI_3 photographic film, photochem. decomposition kinetics *(Russian)* 80−93782
Br+NOBr, primary and secondary photochemistry, vibrationally excited NO, IR fluoresc. obs. 80−48030
Br_2, laser-induced photodissoc. spectroscopy 77−90614
Br_2, photodissoc., $Br^*(4^2P_{1/2})$ yield, wavelength depend., collisional release 78−64857
Br_2-CO_2 IR laser with $Br^* \rightarrow CO_2$ electronic-vibr. energy transfer as pump mechanism 80−53260
Br_2-Xe, UV transient absorption following flash photolysis 79−61879
BrCN photolysis, IR stimulated emission from CN 79−31888
$BrONO_2$, stratospheric photolysis, UV and IR spectra 78−53227
C_2 radical kinetics prod. by IR photolysis of acrylonitrile 80−95668
C_2+NO, laser-induced chemilum. reaction 80−61101
CCl_3O_2+NO+NO_3, photolysis, $CCl_3O_2NO_2$ thermal decomposition in stratosphere 79−57256
C_2F_4 VUV photolysis, $CF_2(^1B_1)$ energy distrib. 80−50861
photolysis continued
CF_2Cl^+, and parent cations, IR spectra in matrix radiolysis and photoionis, of Freons 78−80767
$CF_2Cl_2^+$, CF_3Cl^+, IR spectra, in matrix radiolysis and photoionis. of Freons 78−80767
CF_3I, I laser medium, UV absorption profile modification by vibr. excitation, for fusion ignition 78−58717
$CF_3NO \rightarrow CF_3NO$, photodissociation dynamics, two-photon laser-induced fluorescence study 80−43122
$CH_{2(triplet)}$+CO_2, reaction rate constant determ. 77−36727
CH_3O_2+NO, rate const., flash photolysis and kinetic spectroscopy 79−70305
CN radical, photofragment spectroscopy of A-X transition 79−52726
CN+O$\rightarrow$CO+N, flash photolysis, absorption spectrosc. obs. 79−66289
C_2N_2, photolysis, predissoc. to $CN(A^2\Pi_i)$ and $CN(X^2\Sigma^+)$, energy partitioning 77−48667
CO, ^{13}C isotope enrichment by 123.58 nm Kr reson. radiation photolysis 78−33624
CO, multiphoton UV photolysis, isotope effects obs. 80−55679
CO photodesorption from metal, forming CO_2 79−52777
CO_2, photoelectrocatalytic reduction in aq. suspensions of semicond. powders 79−39141
CO_2, photolysis, 1470 and 1302-1306 Å, absolute O atom yield 78−48681
CO_2, photolysis, $O(^1S)$ absolute quantum yield spectral depend. meas. using XeO luminesc. 80−35561
CS_2 photolysis, $S(3^1D_2)$ electronically excited state prod. 80−99476
CS_2, VUV photolysis in Ar matrix, thermoluminesc. 77−52659
CS_2, VUV photolysis in inert gas matrix, CS radical radiative lifetimes 79−89699
CS_2-NO_2, flash photolysis of CO laser medium, laser mode 79−86172
$C_2(a^3\Pi_u)$, prod., reactions 79−74355
$C_2(a^3\Pi_u)$+NO(vinyl cyanide)(ethylene), laser-generated radical kinetics 79−100352
Cd_2GeO_4 anode for H_2O photoelectrolysis 80−108716
CdI_2 crystals, photolysis obs. *(Russian)* 80−7833
$CdIn_2O_4$ anode for H_2O photoelectrolysis 80−108716
CdS, aq. dispersion, O_2^- generation by photolysis, spin trapping detect. 78−11538
CdS(Se)-based photoelectrochem. cells, charact. 77−25287
Cd_2SnO_4 anode for H_2O photoelectrolysis 80−108716
Cl+formaldehyde, photolysis, Fourier transform IR studies, metastable species detection 80−81293
Cl+methane$\rightarrow$HCl+CH_3, absolute reaction rate, flash photolysis-reson. fluoresc. obs. 77−56222
Cl+NOCl, primary and secondary photochemistry, vibrationally excited NO, IR fluoresc. obs. 80−48030
Cl_2-Kr(Xe), UV transient absorption following flash photolysis 79−61879
Cl_2-O_3-H_2 dilute mixtures, photolysis products, Fourier Transform IR kinetic obs. 80−26033
ClF-H_2 chemical laser, HF rot. laser emission 79−98349
ClO_2-O_3 mixtures, photolysis quantum yields, atmos. chem. 79−52724
$ClONO_2$, chem. degradation in stratosphere 77−33134
$ClONO_2$, gaseous, UV photolysis mechanism at 302.5 nm, stratosphere appls. 78−20031
$ClONO_2$, photolysis products, very-low press. meas. 79−29376
$ClONO_2$+$O(^3P)$, photolytic gas phase kinetics at 245K 79−52719
$ClONO_2$+$O(^3P)$, rate consts., flash photolysis-reson. fluoresc. obs. 77−77796
$Cl(^2P)$+$CH_4 \rightarrow CH_3$+HCl, reaction rate const., laser flash photolysis-resonance fluoresc. kinetic study 80−45485
$Cl(^2P)$+$ClONO_2$, rate consts., flash photolysis resonance fluoresc. meas. 77−60038
$Cr(CO)_6$, electronic spectra following flash photolysis, intracavity laser technique 79−31538
CrMo molecule, electronic absorpt. spectrum from flash photolysis 77−6796
CrO_2Cl_2, collisionless IR multiphoton production of electronically excited parent mols. 79−41211
Cs_2, two-photon dissoc., spectrosc. obs. 80−32787
Eu^{2+} solutions, cyclic photoredox quantum yields, solar energy conversion 77−90627
F+H_2+$\hbar\omega$, reactive scatt. and inelastic collision in laser field, semiclassical calc. 79−47948
F+O_2+M$\rightarrow FO_2$+M, flash photolysis IR chemiluminesc., rate const. 78−3311
Fe-thiazine photogalvanic cell, blue sensitization, improved match to insolation spectrum 77−90628
$Fe(CO)_5$, solns. with dissolved NO, photolysis, $Fe(NO)_3CO$ form. 80−53024
formaldehyde+Cl_2 mixtures, Cl+CH_2O rate const. 78−85136
n-GaP, Au-coated semicond. electrode, photoelectrochem. behaviour in water 77−21399
Ge(3^3P_0)+O_2(Cl_2)(COS)(N_2O)(NO_2)(NO+Ar) oxidation reacts., gas phase, kinetics 78−92468
H+$H_2 \rightarrow H_2$+H, IR laser induced reaction 78−80761
H+NO+M$\rightarrow$HNO+M, HgH+NO$\rightarrow$HNO+Hg, rate consts. of photosensitised reactions 77−36757
H+PH_3, abstraction rate consts., 209-495K, time-resolved fluoresc. 77−16807
H_2 generation by water solar photolysis, large-scale impracticability 80−26172
H_2 photochemical dissociation utilising solar energy for H_2 prod., review 80−61452
H_2, photoelectrochemical generation at p-semiconds. 77−89844
H_2, production of exciton states and L_α,L_β emission of H atoms in Ne matrix 80−93372
H_2-F_2 cooled mixture photolysis, possibility of short laser pulse generation in HF 79−22946
H_2-O_2-N_2 flame, photochem. reactions involving Na*, laser saturated conditions 78−80762
H_3BPF_3 and D_3BPF_3, laser augmented decomposition 79−52713
HBr+OH$\rightarrow H_2O$+Br, absolute rate const., 249-416K 79−70303
HCN(DCN), photodissoc. dynamics, rot. (vibr.) energy disposal 78−48672
HCl flash initiated chemical laser, Cl_2-HI reaction pumped 79−94224
HCl-Br_2-Ar, flash photolytically produced Br* to HCl electronic to vibr. and rot. energy transfer 80−48069
HI photolysis, ESR spectrum of ^{127}I atoms in Xe matrices 80−1005
HN_3, flash photolysis leading to NH pure rot. lasing 79−86175

photolysis continued
HN_3, photodissoc., NH photofragment energy distrib. and reaction rates 77−90618
HN_3, UV photolysis 80−101027
HO, detection by laser excited fluoresc., press. depend. of fluoresc. and photolytic interferences 80−95666
H_2O and activated C, photoassisted decomposition at room temp. over Pt/TiO_2 80−55703
H_2O, biophotolysis for H prod. using solar energy 80−61457
H_2O, for H fuel prod. *(French)* 80−55776
H_2O, for H_2 prod. using chlorophyll photocatalysts 80−61458
H_2O, for photoelectrochem. H_2 production using solar energy and Zn(Mg)(Cr)(Ni) phthalocyanine dyes *(French)* 80−55936
H_2O, H_2 and O_2 determ. by gas chromatography 78−61089
H_2O, photochem. prod. of H using sunlight 80−45776
H_2O photoelectrolysis, H_2/hydrocarbon fuel prod. via biomass conversion wastes 80−89653
H_2O photoelectrolysis, stable cells prod. 77−44484
H_2O photoelectrolysis at high current density, using TiO_2 and $SrTiO_3$ photoanodes 78−15679
H_2O, photoelectrolysis using TiO_2 and $SrTiO_3$ electrodes, solar energy conversion 79−52959
H_2O photoelectrolysis with semicond. materials 78−2562
H_2O photolysis using biological and artificial catalysts for H prod. 80−61444
H_2O photolysis using fission pumped gas lasers for H prod. 80−45810
H_2O photolysis using Pt/(chlorophyll a.$2H_2O$) reaction for H_2 production 80−89663
H_2O, photolysis with n-TiO_2 anode 78−2563
H_2O solar photolysis for O_2, H_2 prod. by engineering methods using biological materials *(Japanese)* 80−45765
H_2O, using solar energy for H_2 prod., feasibility of large scale generation 80−72095
H_2S, valence and Rydberg excited states, SCF-Xα-SW mol. oribtal study 79−36550
H_2SO_4, frozen soln., EPR of trapped H-atoms produced by UV and X-irrad. 80−3369
H_2SO_4:Fe^{2+}, frozen aq. soln., photolysis, H form., distrib. and diffusion 78−20044
H_2SO_4:Fe^{2+}, frozen soln., photo- and radiation-produced H-atoms obs. 79−39162
Hg-Cl_2-Ar, producing $HgCl(B^2\Sigma^+)$, chemiluminesc. study 79−39154
Hg_2 and Hg_3 metastable states in flash photolysis of Hg vapour, electronic absorpt. spectra 79−76438
HgBr, laser photolysis prep., laser induced fluoresc., collisional quenching processes 80−38014
$HgBr_2$ photolysing, HgBr* fluorescence, steady state meas. 80−42986
$HgCl_2$ photolysing, HgCl* fluorescence, steady state meas. 80−42986
HgI_2, photolysis, HgI B-state radiative lifetime determ. 79−10130
I laser, photolytically pumped, chem. kinetics 80−48235
I^- in aq. soln., anthracene sulphonate sensitised photooxidation via singlet $^1O_2$ 77−32812
$I+I+O_2 \rightarrow I_2+O_2$, photolysis, rate const. obs., mechanism 77−63883
I_2, collisional release and photocomp. kinetics, I* prod. 78−66819
I_2, gas phase flash photolysis, in ethane and propane, cage effect temp. depend. 78−80770
I_2, photolytic cage effect in gas phase 80−81345
I_2, resonance-enhanced multiphoton ionis. and fragmentation of mol. beam 79−100411
I_2-Xe, UV transient absorption following flash photolysis 79−61879
$I_2+O_2 \rightarrow IO$, flash photolysis reaction mechanism 77−32813
$I_2+O_2 \rightarrow 2IO$, flash photolysis, emission in 3400 Å band 77−3398
IBr, photodissoc., $Br^*(4^2P_{1/2})$ yield, wavelength depend., collisional release 78−64857
IBr-CO_2 IR laser with $Br^* \rightarrow CO_2$ electronic-vibr. energy transfer as pump mechanism 80−53260
ICN, A-state photolysis, $I(^5P_{1/2,3/2})$ branching ratio wavelength depend. 80−81335
ICN, laser photolysis, CN radical form. and energy partitioning 77−16853
ICN, photodissoc., product rot. distribs. 79−66310
ICN, photodissoc. and predissoc., cyanide radical fluoresc. excitation spectrum and laser emission 78−76892
n-InP photoelectrode, stabilisation to photoanodic dissolution, in aqueous solutions of Te^{2-}/Te_2^{2-} 78−14814
n-InP photoelectrode, stabilisation to photoanodic dissolution in solns. containing Te^{2-} and Te_2^{2-} 78−19144
p-InP-Cd(Zn), ohmic contact formation on InP by laser photochemical doping 80−80369
$KBrO_4$, UV- and X-irrad., ESR spectra of trapped O_2 78−84474
$K_3Zr_2(O_2)_2F_7.2H_2O$, photodecomp. 80−108724
KrF* radiative lifetime, pulsed photolysis obs. 78−29819
KrF(B), excimer, collisional quenching rates, photolysis meas. 78−63066
Li, cluster and microcrystal, matrix isolated, optical absorpt. spectra, photolysis and plasmon absorpt. 79−89820
methyl nitrite, 266 nm photolysis, methoxy radical prod. 80−76534
$Mo(CO)_6$, electronic spectra following flash photolysis, intracavity laser technique 79−31538
$Mo(CO)_6$, flash photolysis, Mo_2 form. and electronic spectra 79−36622
MoF_6, in Ar matrix, photolysis, MoF_5 form., IR spectrum 80−87115
N_2 dye laser flash photolysis system, 5 μJ with 3 ns time resolution 80−1211
NH_2+NO_2, reaction rate const. meas. 80−7772
NH_2+O_3, reaction mechanism, flash photolysis obs. 80−104425
NH_2+propylene, reaction kinetics, laser reson. absorpt. obs. 77−9096
NH_3, ($\tilde{A}^1A_2''$) predissoc., vac. UV photolysis, NH_2 form. 78−13547
NH_3, photodissociation in A←X absorption region, D isotope effects 77−77790
NH_3, photodissociation in A←X absorption region, translational excitation of H atoms and predissociation mechanism 77−77791
NH_3, photolysis, $NH(X^3\Sigma^-)$ radical form., detect. and reactions 79−64036
NH_3 photolysis and greenhouse effect in primordial atmosphere 79−39864
NH_3, photooxidation mechanism, computer simulation 77−32810
NH_3, UV laser photodissoc., NH_2 internal energy distribs., NH states 80−11901
NH_3-^{57}Fe, solid, Mossbauer study of iron bonding to solid ammonia and its photofragments 80−15833
NH_3+O_2, flash photolysis, NH_2+HO_2 rate const. 79−47943
$(NH_4)_2Ce(NO_3)_6$, acid soln. photolysis, NO_3 radical study 79−52717

photolysis continued
NH_4ClO_4, photothermochemical process 79−24769
$(NH_3)_nH^+$, n=1-9, detected in photoionisation of supersonic mol. beam mass spectra, H-bonding 79−74356
$NH_3(ND_3)$, photolysis, excited NH(ND) prod., collisional quenching 77−19018
NH_2O_2, long-lived radical prod. by photolysis of ammoniacal KO_3 soln. 77−16838
NO, in Ar and N_2 matrices, 6K, vac. UV photolysis, β and M band emissions 78−73069
NO in stratosphere, effects on NO_y mixing ratios 77−29399
NO, resonance-enhanced multiphoton ionis. and fragmentation of mol. beam 79−100411
NO, stratospheric growth before sunrise by photolysis 77−29356
NO+BrO, temp. depend. kinetic study, stratospheric Br photochemistry implication 80−50866
NO+N ^{4}(S) state reaction rate, discharge flow and photolysis reson. fluoresc. method 79−5142
NO_2 in nonane, supersaturated gas, photoinduced nucleation 78−80760
NO_2^-, photolysis as source of free radicals in productive surface seawater 79−62522
N_2O in troposphere, absence of photolysis 79−53493
N_2O, photolysis, $O(^1S)$ absolute quantum yield spectral depend. meas. using XeO luminesc. 80−35561
N_2O, relative rate consts. of $O(^1D_2)$+olefin reactions 79−83472
N_2O_4, UV photodissoc., NO_2* form. and emission, quantum yield 79−66298
Na, cluster and microcrystal, matrix isolated, optical absorpt. spectra, photolysis and plasmon absorpt. 79−89820
$NaClO_4$, frozen soln., EPR of trapped H-atoms produced by UV and X-irrad. 80−3369
$NaClO_4$:Fe^{2+}, frozen soln., photo- and radiation-produced H-atoms obs. 79−39162
NaN_3, solid, CO_2 laser radiation decomposition, for high-press. chem. laser 79−34326
NaOH, frozen soln., EPR of trapped H-atoms produced by UV and X-irrad. 80−3369
Ni complexes, Ni(II) porphyrins, picosec. flash photolysis, transient absorpt. 80−52976
NiO electrode for photolysis 80−40696
O+acetylene reaction, kinetics, flash photolysis-reson. fluoresc. meas. 77−73439
O+chloroethylene reaction, kinetics, flash photolysis-reson. fluoresc. meas. 77−73439
O+H_2S, ^{3}P-state, absolute reaction rate, flash photolysis reson. fluoresc. obs. 79−66283
O+H_2S, matrix reactions, IR spectra of products, chemiluminesc. 77−60057
O+methane→OH+methyl reaction, photolytically initiated, high temp. kinetics meas. technique 80−61085
O+OCS (ethylene), reaction dynamics, IR laser excitation, vibr. effects 77−12788
O_2^-, in nonpolar liqs., laser photodetachment, elec. cond. obs. 79−64057
$O_2+CH_3 \rightarrow OH+H_2CO$, 368K, rate const. upper limit 80−7771
O_3, high energy pulsed O_2 laser feasibility at 1.27 μm 78−63117
O_3, laser flash photolysis, $O(^1D)$ quantum yield 78−20033
O_3, laser flash photolysis, $O(^1D)$ quantum yields in fall-off region 80−45524
O_3, laser photolysis, $O(^1D)$ quantum yield 79−53492
O_3, laser-induced photolysis, reactions of $O(^3P)$, $O(^1D)$ and $O_2(^1\Delta)$ 80−11928
O_3, multiphoton dissociation by IR laser 79−36710
O_3, photolysis, near UV, temp. depend. of $O(^1D)$ formation 78−15689
O_3 photolysis, $O(^1D)$ quantum yields as function of temp. (230-320K) and wavelength (295-320 nm) 78−56903
O_3 photolysis, $O(^3P)$ quantum yield at 266 nm 80−78568
O_3, photolysis, $O(2^1D_2)$ prod. and deactivation 79−20384
O_3, photolysis, rel. quantum yield of $O(^1D)$, in 250-300 nm region 79−20383
O_3 photolysis at 248 nm, $O(^3P_J)$ direct obs. 80−101028
O_3 photolysis by sunlight, rate constants at ground level 80−61836
O_3, primary products electronic and vibr. state distrib. 80−50865
O_3, UV photodissoc. rate, expt. and theory 80−40722
$O_3+O_2(^1\Delta_g)(O_2^*)$, UV photolysis, $O(^3P)$ prod., rate consts. determ. 80−55636
$O_3+O(^1D)$, UV photolysis, $O(^3P)$ prod., rate consts. determ. 80−55636
OCS, high-intensity laser photolysis at 157 nm, $S(^1S)$ prod., photoionisation, and loss, laser appl. 80−21306
OCS in Ar matrix, photolysis, S_2 and S_3 absorpt. spectra 79−5149
OCS laser, two-quantum excitation, photolysis, energy transfer, for fusion expts. 78−59003
OCS, multiphoton dissociation by IR laser 79−36710
OCS, two photon and vibr. depend. photolytic prod. of $S(^1S)$ atoms 79−13775
OCS, VUV photolysis in Ar matrix, thermoluminescence 77−52659
OCSe, flash photolysis, $Se(4^1D_2)$ direct obs. 78−25461
OCSe, laser action from $Se(^1S_0)$ 79−31889
OCSe, laser photolysis using ArF laser, $Se(^1S)$ quantum yield rel. to OCSe vibr. excitation 79−83478
OCSe, photolysis, $Se(^1S)$ prod., quenching of high concs. 79−6904
OCSe photolysis producing Se, using high efficiency ArF laser source 80−33032
OCSe, quantum yields for Se, $^1S_0$, $^1D_2$, and $^3P_{0,1,2}$ atoms determ. in photolysis, lifetime and quenching rate meas. 80−97741
$O(^1D_2)+NH_3 \rightarrow OH(v,N)+NH_2$, bimodal OH rot. distrib. obs. and energy disposal 80−76501
OH, prod. by photolysis, Λ-doublets, population, rot. states, hyperfine struct., microwave spectra 80−32694
OH+alkene, absolute rate consts., 297K 79−100353
OH+dimethyl sulphide, flash photolysis reson. fluoresc. rate consts. determ., pollution aspects 78−95913
OH+formaldehyde (acetaldehyde), rate consts., 299-426K, UV flash photolysis, reson. fluoresc. obs. 78−68873
$OH+H_2O_2$, reaction rate const., 298K, flash photolysis-reson. fluoresc. obs. 79−57215
OH+methane+M, absolute rate consts., 296K, flash-photolysis reson. absorpt. technique 77−86290
OH+n-propyl acetate (sec-butyl acetate) (tetrahydrofuran) (peroxyacetyl nitrate), raction rate consts., in irrad. NO_x mixture 78−7171
$OH+OCS(CS_2)$, flash photolysis reson. fluoresc. rate consts. determ., global S cycle 78−95914

photolysis continued
OH+CO(N_2O), rate consts. 77−16781
$^{18}OH+CO_2(CO)$, evidence for at. exchange 79−47910
$O(^3P)$+alkenes, absolute reaction rate consts., 298-439K, photolysis-chemiluminesc. determ. 77−77747
$O(^3P)$+benzene (toluene), absolute reaction rate consts., 299-440K 79−70304
$O(^3P)+CH_3CN(CF_3CN)$, reaction mechanisms and kinetics 77−36728
$O(^3P)+H_2S(D_2S)$, reaction rate, flash photolysis-reson. fluoresc. obs. 77−4918
$O(^3P)$+n-butane (NO(M=Ar)), reaction rate constants using flash photolysis-NO_2 chemiluminesc, method 77−44458
$O(^3P)$+vinyl halides, reaction rate consts. 298-442K flash photolysis obs. 78−7195
$O(2^1D_2)+N_2(O_2)(N_2O)(CO_2)(H_2O)$(methane), collisional deactivation meas., 295K, rel. to atmospheric processes 80−16663
$O_2(b^1\Sigma_g^+)$, temp. dependent quenching, photochemical study by H_2-VUV laser 80−63702
PH_3, laser photolysis, PH and PH_2 radical excited states 79−16023
PH_3, photolysis and abstraction reactions, rel. to Jovian atmosphere 79−66327
PH_3, scavenging reactions of acetylene and ethylene in Jovian atmosphere 78−81582
PH_3, vac. UV photolysis, emission spectra 78−46357
PbI_2 film, photolyzed, refr. index change 78−11010
PbI_2, thin films, photolysis kinetics 77−36769
PbI_2-Ag, photographic mat., photolysis, effect of PbI_2 photo-EMF effect *(Russian)* 80−92939
Rb anions, THF soln., photolysis, appl. to photogalvanic cell 80−85294
Rb-tetrahydrofuran soln., photolysis, photoelectron emissive EPR signal, scavenger electron affinity reactivity 78−53224
S_2Cl_2 UV photolysis in matrices, $SSCl_2$ IR spectra 78−61033
SCl(Br), unstable radicals, matrix-isolated, IR spectra force const. *(German)* 80−43053
SF_6, collisionless dissociation in intense IR field 79−87858
SF_6, collisionless multiphoton energy deposition and dissoc. 79−61884
SF_6, film, IR laser induced processes at low temp. and under ultrahigh vac. 79−69914
SF_6, IR multiphoton photolysis, master eqn. anal. 79−47945
SF_6, matrix photolysis, vac. UV, using windowless discharge, IR spectra 77−71798
SF_6, pure and H_2 mixture photolysis, S atom nucleation particulate formation 78−76836
SF_5Cl, laser induced reactions, yields, product distrib. and isotropic selectivity 78−53225
SF_5NF_2, multiphoton excitation, absorption and dissoc., isotope selection 79−100408
SF_5X, (X=Cl, Br, Sf_5), VUV photolysis, SF_5 radical form. in Ar matrix, IR spectrum 78−981
SO_2, chemiluminescence at ($c^1\Sigma^- \rightarrow a^1\Delta$) in Ar matrix, photolysis prod. and thermoluminesc. 79−5158
SO_2, gas, photooxidation, cloud chamber obs. 79−1961
SO_2, IR photolysis, associated visible luminesc., 2-25 torr 79−29384
SO_2, photooxidation, aerosol evolution, rel. to air pollution 78−81392
SO_2-alkane-H_2O gaseous mixture, photoinduced nucleation and quantum yields 79−96348
SO_2-gas mixtures, flash photolysis, H_2SO_4 aerosol form. 79−66307
Sb_2S_3 layers, sensitised photolysis, determ. of iso-opaque contours *(Russian)* 79−100418
Sb_2S_3:Ag, sensitised photolysis and structure of latent photographic image 78−89574
Se_2, photolysis by UV lasers, appl. to kinetics of group VI laser systems 80−7807
SeF_6, IR photolysis, $NH_3^-+CO_2^-$ laser isotope separation and dissoc. enhancement 79−29377
SeH, isotope effects, Rydberg levels-ground state transitions, rot. const., VUV spectra obs. 80−58279
$Se(^3P_1)$+inert gas, gas phase flash photolytic deexcitation obs., 1000K *(Russian)* 78−50626
o-semiquinone, form. by photolysis, isomerisation, ESR 77−16840
p-Si:$P(P^+)$ photolytic props. in HF 80−89504
SiF_4, CO_2 laser-irrad., dissoc. product fluoresc., wavelength depend. 80−11900
SiH_4, IR photochemistry 79−39185
SiH_4 purification by selective photolysis using UV laser 78−31657
SiO+F_2, matrix reaction, $OSiF_2$ prod., IR spectra and force consts. calcs. *(German)* 80−97718
$Sn(4^3P_0)+O_2(Cl_2)(COS)(N_2O)(NO_2)(NO+Ar)$ oxidation reacts., gas phase, kinetics 78−92468
$Te(^3P_1)$+inert gas, gas phase flash photolytic deexcitation obs., 1000K *(Russian)* 78−50626
U complex, bis-hexafluorocetylacetonate uranyl tetrahydrofuran, laser-induced dissoc. 80−53071
UF_5, transient mol., IR absorption spectrum, 580-630 cm^{-1}, assignments, mol. struct. 79−68227
UF_6, laser flash photolysis, transient UF_5 IR spectrum 79−45715
UO_2F_2, methanol soln., O isotope photochem. enrichment 79−36786
V_2O_5-water, EPR of VO_{aq}^{2+} formed by solar light photoreduction, electrolysis appl. 78−11540
$W(CO)_6$, electronic spectra following flash photolysis, intracavity laser technique 79−31538
WO_3 electrodes, electrochem. and photoelectrochem. behaviour 78−26949
^{186}WO, electronic spectra following flash photolysis, intracavity laser technique, rot. consts. 79−31538
XeF, B-X transition vibr. anal., flash photolysis UV absorpt. spectroscopy 78−42088
XeF, transfer and quenching rate constants for (III, 1/2) and (II, 3/2) states 79−16003
XeF_2, lifetime and collisional quenching meas. of XeF*(B) 78−33545
XeF_2, photodissoc. yield in solid Xe and Kr, time-resolved photolum. excitation obs. 80−3372
XeF_2 photodissociation for XeF laser 80−32976
XeF_2 photolysis with VUV radiation, XeF (B,C) state prod. and kinetics 80−32975
$XeF_2 \rightarrow XeF^*$, vac.-UV photolysis, B→X fluoresc. and quenching 77−58061
XeO, Ar-matrix-isolated, UV absorpt. spectra 77−3375
ZnO electrode, in aq. soln., phototransition at 380 nm, anodic photocurrent obs. 78−19145

photolysis continued
ZnO, surface phenomena, interpretation by compensation model 78−95323
ZnO, thin Zn or O rich layers, thermolysis, photolysis, SEM, XPS 77−11821

photomagnetic effect
coronene, triplet state, photomagnetism 80−97125
ferrites, EM wave effects on mag. and optical props., lecture 78−27031
ferromagnetic semiconductor, optical transparency, photoferromag. effect, Curie temp. shift *(Russian)* 78−72387
III-V semiconductors, optical heating of electrons at 78K 79−15185
magnetic semiconductor, photomagnetisation, photoinduced heterojunctions 77−63259
paramagnetic crystal, magnetisation change by light pulse 80−70932
ruby, optically induced magnetisation 78−76292
SQUID magnetometer, optomagnetic meas. appl. 80−98950
$Bi_{1-x}Sb_x$, narrow band gap semicond., photocond. and photomagnetic effect 79−51630
$CaSO_4$:Dy phosphors, photomag. susceptibility 78−2724
$CdCr_2Se_3$:Ga, synthesis and photoferromag. effect 77−51936
$CdCr_2Se_4$, ferromag. semicond., photoinduced mag. anisotropy 80−50086
$CdCr_2Se_4$ magnetic semiconductor, photoinduced centre kinetics 80−71110
$CdCr_2Se_4$, magnetisation, study of photoindduced charges 80−80567
$Cd_{0.15}Hg_{0.85}Te$, photothermomagnetic effect in mm range 80−92932
$Cd_xHg_{1-x}Te$, photothermomag. effect and photocond. in millimetre wavelength range 80−44657
$Cd_{1-x}Zn_xCr_2Se_4$, synthesis Curie pt., photomag. effect 77−51937
EuS, ferromagnetic film, optically induced magnetisation amplification, Curie temp. increase *(Russian)* 77−24719
Fe garnet, optical radiation interaction with magnetostatic waves 80−76009
Fe_3O_4, metallic phase, photocond. and mag. permeab., photoinduced changes 80−15566
GaAs, photoconductivity and photomagnetic effect spectra 79−11178
Ge, photomagnetic effect, space inhomogeneous nonequilibrium carrier lifetimes *(Russian)* 80−71152
n-Ge, proton and γ irrad., minority carrier recombination 80−65591
InSb-NiSb, photovolt. effects rel. to theory of semicond. with internal elec. short circuits 80−65620
K vapour, mag. props. changes under laser irrad., induced EMF obs. 80−100059
Mn ferrite, magnetic permeability, photoinduced reduction *(Rumanian)* 80−75794
NiZnCo ferrite, model of photomagnetic effect 77−43853
$Pb_{1-x}Sn_xTe$:Cd, photocond., photomag. effect, carrier lifetimes 80−44658
Rb vapour, mag. props. changes under laser irrad., induced EMF obs. 80−100059
Si, photovoltaic and photomagnetic effects, rel. to intervalley electron transfer 80−60034
Si-SiO_2-Si_3N_4, internal photoemission 80−7475
Te, carrier recombination at high optical excitation, photomagnetoelectric effect 77−72884
$YFeO_3$, influence of photomagnetic effects on ^{57}Fe NMR 78−52365
$YFeO_3$, mag. domain walls, photomagnetic effects, ^{57}Fe NMR obs. 78−95464
$Y_3Fe_{5-x}Si_xO_{12}$, charact. of photoinduced mag. effects in weak magnetising field 78−27071
$Y_3Fe_{5-x}Si_xO_{12}$, photoinduced change of mag. permeability *(Russian)* 77−1560
YIG ceramic, transient flash effect on permeability 78−27024
YIG, electron and γ-irrad., photomagnetic effect 80−103877
YIG:Co^{2+}, mag. permeability, illumination and impurity depend. *(Russian)* 78−64220
YIG:Si, photo-induced low freq. mag. permeab. *(Russian)* 78−39368
YIG:Si^{4+}, mag. permeability, illumination and impurity depend. *(Russian)* 78−64220
YIG:$Si^{4+}(Ti^{4+})(Zr^{4+})$, X-ray induced change in initial permeability 78−19280
$(Y_{1-x}R_x)_3Fe_5O_{12}$, photoinduced decrease in permeability, 77K 77−85497

photometers
see also photometry; spectrophotometers
additive photographic film printers, programmed control of light metering valves *(Russian)* 80−95174
annular scanning photometer, detect. of optical halo around spiral galaxy (NGC 4565) 78−12364
Ascoris photometer, description and use 80−4256
astronomical, LED field stop boundary and reticle illumination control circuit 80−37070
astronomical, URSULA, twin-beam multiband computer-controlled photometer 78−49334
astronomical IR instrumentation on NASA airborne observatories 78−45224
astronomical monitor photometer for Dodaira 91 cm telescope *(Japanese)* 79−101071
astronomical photoelectric photometer, appl. to occultations obs. *(Chinese)* 80−105172
astronomical photoelectric photometer, multifunction, system design 77−73949
astronomical photometer, using Si diodes as light detectors 78−20651
astronomical photometer calibration for extended sources 77−9669
astronomical photometers, thermal stability rel. to Balmer-index photometry 78−96404
astronomical reflective telephotometer, distant contrast meas. of atm. extinction coeff. 78−61730
astronomical semi-automated iris photometer for large photographic plates *(Japanese)* 78−89070
astronomical UBV photoelectric photometer for amateur use 78−65502
astronomical variable iris photometer as automation example *(French)* 79−62748
atmospheric tracking of Li release, upper atm. daytime neutral winds obs. 79−39871
atomic absorption photometer for human serum anal. 79−34417
auroral photometer, 2972 Å, for rocket studies of aurora 79−25334
automated comparator-microphotometer for photographic plate spectral line position meas. 78−77962
automated isophotometer for large photographic plates *(Japanese)* 78−89069
automatic, new concepts for luminaire studies 80−4752

photometers continued
automatic cameras, exposure error compensation 80−52346
automatic fluorescence microphotometer 79−97413
automatic rotary diaphragm for microphotometer 80−22415
biomedical catheterisable sensors, PO_2 probes, press. transducer and photometers 80−46080
calorimeter, pulse gas, for vacuum UV rad. meas. 80−251
chopper wheel in photometer, third harmonic freq. suppression in modulated radiation 77−50754
classroom photometer with artificial star 77−74180
compensation densitometer servosystem using integrated operational amplifiers 78−89525
computer-controlled, for quantitative anal. of thin layer chromatograms 77−60326
computerized differential photometer for Geneva seven colour system 79−48682
contrast telephotometer, multiwavelength, instrument design, data interpretation, atm. visibility determ. 79−66842
conversion to scanning microphotometer 80−86374
coronal photometer, automatic, 5303 Å emission line photoelectric meas. 79−12454
Coude spectrograph of 188 cm reflector, integrating exposure meter *(Japanese)* 77−73961
crystal, semi-empirical method for photofraction determ. 79−54168
cytophotometer, automatic 2-wave, with a calculator 80−104820
detector type, commercial devices survey and classification 78−16830
device for arterial thrombosis investigations 78−85456
differential light scattering photometer, for rapid analysis of particles in flow, appl. to biological cells 80−77834
differential photometer, 6800 microprocessor control, astronomical appl. *(French)* 79−58253
digital, laser Raman and spectrofluorometer systems appl. 77−5881
digital integrating microphotometer 77−71360
digital multipurpose integrating microphotometer, type TsIMF-2 80−4753
digital radiometer/photometer (Tektronix) optical transmission charact. meas. *(French)* 79−89000
direct-reading photometry system with automatic instability correction 79−26099
discrete photoelectric tracking system of variable precision *(Russian)* 78−57458
double-beam, for meas. small changes in optical absorption 80−62709
drift errors due to ageing and preheating evaluation method *(German)* 77−10087
dual flame photometric detector, operation and charact. *(Chinese)* 79−71506
electric exposure meters, photography appl. *(German)* 77−87856
electronic exposure sensor, Agfa Optima 535 and 1035, features *(German)* 77−82633
ElrephoMat DFC 5, a new reflectance photometer 79−30528
emission photometer for human serum anal. 79−34417
enlarger exposure meter, using photodiode and multimeter 80−101857
enlarger exposure meter, with digital display *(Dutch)* 80−101865
equivalent sphere illumination meas., new instrument features 79−9243
exposure meter accuracy calc., CdS photoresistor errors 77−49773
exposure meter and development timer, used for photographic enlarger 80−101856
exposure meter errors during colour photographic printing 80−101818
exposure meter for flash lamp photography 80−9058
exposure meter for KSR-1M film camera *(Russian)* 78−93779
exposure meter with photoresistor, semi-automatic, bridge circuit error calc. *(Russian)* 77−54008
exposure meters for colour positive process, review 78−12781
Fabry ten-colour photometer on Skylab for gegenschein and zodiacal light obs. 77−60610
far IR photometer, for Kuiper Airborne Observatory 79−66926
filter-tilting type nightglow photometer 77−73889
flame photometer, for S containing aerosols continuous meas. and speciation 78−95974
flame photometers with automatic dilutor 78−49878
fluorescence polarisation meas., T-format photon-counting polarisation photometer 78−54423
fluorophotometer, slit lamp type, for tear measurements 77−2064
FM-89 conversion to measuring instrument, reflection coefficient meas. 79−71507
focal grating photometer for magnitude difference determ. of double stars 80−67567
four-filter, for total atm. O_3 meas. 78−61597
Fourier photoellipsometers and photopolarimeters based on modulated optical rot. 78−54439
gas chromatography detectors, single- and dual-flame, quenching effects 78−61072
general-purpose objective photometer, FOU 79−49268
goniophotometer, total luminous flux meas. on radiometric base 80−42250
granularity measuring system 78−21200
grid-gated photomultiplier photometer with subnanosecond time response, for fluorescence photobleaching recovery expts. 80−37071
hand-held and film-plane photographic exposure meters 78−58078
high speed photometer of Asiago Observatory 79−25505
high-resolution photometer, for upper atmosphere daytime Li releases obs. 78−45023
hybrid null-photometric ellipsometer using sinusoidal optical rotation 77−61110
hygrometer, automatic IR, humidity determ. by water vapour absorpt. 78−12707
IKA-65 UV stellar photometric equipment on Cosmos 215 satellite *(Russian)* 77−64642
illuminance, scalar and cylindrical illuminance meas., instrument quality *(German)* 77−10088
illuminance at reflex-reflector, photometer for performance meas. 78−45668
illuminance meter error sources *(Hungarian)* 79−88995
illuminance meters accuracy test *(Hungarian)* 79−88996
illumination control of cine projectors, foreign equipment *(Russian)* 80−105741
illumination meters, metrological requirements *(Hungarian)* 80−17997
instruments and appl. techniques for microscopy, Zeiss equipment 77−74497
integrating, method of indirect comparison of luminous fluxes, fluorescent lamp testing appl. *(Polish)* 79−93200
integrating, spherical, optimum screen determination *(Polish)* 78−37043
integrating wide-field IR photometer for globular clusters study 80−62029
intensified CCD photon counting array photometer 77−37964
intensity microphotometer with step-drives, for negatives transparency conversion *(Russian)* 78−57457
inverse-fourth, for optical transmittance calibration 78−82021
IR and mm wave techniques, for Cosmic Background Explorer Satellite 78−49344
IR and sub-MM spectroscopy, conf., Bonn, Germany (Mar. 1977) 78−12778
IR instrumentation of Calar Alto telescopes 78−16295
IR photometer, astronomical, with vibrating dichroic filter, southern stars obs. 77−26017
IR photometer, wide field for extended stellar sources 77−82582
IR pinhole photometer for solar intensity obs. in 1.5-2.4 μm range 79−101069
laser beam detection, Se photoelement and Si photodiode suitability obs. *(Czech)* 78−62225
laser photometer based on boxcar integrator principle *(Chinese)* 80−31842
laser power meter, calibration, Si solar cell 80−46780
light filter optical density monitoring *(Russian)* 78−86317
light flux recording system, multichannel 79−35809
light meter system with submersible sensing element 77−41666
light meters and their appl. *(German)* 78−8434
light scattering, meas. of structural change dynamics in biological particles 79−39615
linearity meas. of photometric devices using two LEDs 80−17996
liquid crystal indicator of variable light-reading angle 78−57932
logarithmic convertors and amplifiers appl. *(German)* 79−9233
loss of contrast in visual tasks using a visual and physical photometer, study 79−9234
luminous flux meas. error equation permits correct choice of auxiliary lamp *(Polish)* 78−70175
luxmeters with large measuring ranges, method for calibration 80−13123
mass spectra, automatic recording microphotometer modification 77−12845
meridian-scanning photometer for airglow and aurora studies 77−70903
MEX2, concentration and turbidity meas. *(Dutch)* 78−21203
microphotometer, automated, SAMB, for morphometric and densitometric analysis *(French)* 77−10085
microphotometer, MF-2 type, scatt. light effects on optical densities of electron-photon cascade tracks 77−61655
microphotometry, compensation for fluctuations in illumination 80−73413
microscope photometer/semiautomatic image anal. instrument system for morphometric and photometric value meas. 80−82815
mirror reflection coefficient meas. instrument 78−18036
movie projection brightness meter, 2Y aKP, using CdS photoresistor, optical system 77−10090
multipurpose photometer for measuring colour absorption, transmission, turbidity 77−153
night natural illumination measurement in 0.4 to 1.2 μm spectral region 78−57367
nondispersive IR photometer selectivity improvement *(German)* 80−90880
oceanographic photometer for deep-sea work, using acoustic telemetering 80−98460
ophthalmic fluorophotometry, improved slit-lamp fluorophotometer 79−92326
optical feedback stabilised photometer, compensation for thermal drift 77−2695
optical power meter for fibre-optic appls. 78−93746
optomechanical scanner, noise analysis 80−47090
p-i-n photodiode photometer 79−32
particle size meas., laser flowthrough microphotometer, double-beam technique, internal calibrated 79−17391
photoelectric, high speed, computerised, for 60 cm astronomical reflector *(Japanese)* 78−32345
photoelectric concentration meter, acceptable error determ. for automatic biochemical anal. 79−92435
photoelectric luxmeter using linear ICs *(Rumanian)* 80−17993
photoelectric photometer for point spread function energy conc. meas. 78−30099
photoelectronic precision logarithmic light meter, cct. details, theory and performance 78−32844
photographic colour printing, correcting light filter selection 80−62764
photographic enlarger exposure meter 79−89018
photographic exposure meter for electron microscopy 77−26435
photographic exposure meter for electronic flash 80−77835
photometer-bichromator, elec. ratio system with phase separation of signals 78−270
photomultiplier linearisation and system stabilisation, for photometric ellipsometers and polarimeters 78−54441
photon counting photometer with 60 cm reflector, at Kagoshima rocket launching centre *(Japanese)* 78−32344
photon scalar irradiance meter, rel. to energy evaluation for photosynthesis in sea 79−79436
photosensor time charact. meas. meter 78−283
Photozavr modulation photometer for artificial aurorae/airglow 79−21076
Pioneer Venus Orbiter cloud photopolarimeter 78−57429
polarising No photometer, for meas. of airglow NO 2150 Å (1,0) γ-band intensity 78−45076
polymer impregnating soln. concentration meas. by transmission photometer *(Russian)* 77−73484
programmable PRP 8 computer photometer, design, uses 77−74483
pulsed electrostatic precipitator and flame photometer for total S aerosol conc. meas. 78−95975
ratiometric photometer using photoelectronic divider system 79−12834
reading error anal. 78−12742
relative spectral detector response meas., 350 to 1200 nm using monochromator based spectral comparator 79−67374
repetitive filter cycle photometer, with sky background compensation 80−62025
retroreflectometer, NBS reference 80−73410
return path ellipsometer, for isotropic and anisotropic surfaces 78−58009
rocket borne resonant absorption spectrometer and photometer for geocoronal and interplanetary He obs. 80−4155

photometers continued
scanning microphotometer with on-line reduction of Schmidt plate data 78−7884
scanning telephotometer, spatial transfer characts. 80−73415
seawater attenuation matrix photometer *(Russian)* 77−78453
SEC Vidicon photometer, appl. to photometry of ω Centauri main sequence 80−90491
selective receivers for 0.2 to 0.3 μ spectral region 79−30560
single lens reflex through-the-lens camera, error in stopped-down metering *(Japanese)* 77−26416
snowfall intensity photometer theory *(Japanese)* 78−85736
solar luxmeter, calibration 77−9661
solar MUV photometer, rocket borne, stratospheric ozone concentration measurement 80−52292
solar power measurement, microcomputer-controlled photodiode light meter and thermistors 80−50946
solar simulator calibration photometer 79−26103
solarimeter, autonomous with permanent readout *(French)* 79−24893
space telescope, design features 78−45229
spectral reflectance and transmittance measuring apparatus for variable angle of incidence 80−250
spectrum microphotometer connection to PDP 11 digital processor for astronomical photographic plate meas. *(Italian)* 80−8550
sphere photometer using photodiodes 77−71359
spherical integrating photometers, luminous flux meas. accuracy, expt. anal. of group discharge lamps *(Polish)* 80−73407
stellar chopping photometer to eliminate auroral sky background 80−72776
stellar photometry of rapid fluctuations, microprocessor controlled instrument *(Spanish)* 80−82222
sub-mm, for astronomical obs., optical components 78−16297
sub-mm, for ESO 3.6 m telescope 78−16296
submarine quantum irradiance and photoperiod meter, with digital recording 80−98474
sunphotometer aperture effects on atmospheric turbidity meas. 79−84483
superposition photometer for material absorptivity meas. 78−89522
tachistoscope lamp luminance meas. 80−42248
telephotometer for aerosol scattering function determ. 80−105055
Terskol Peak telescope and electrophotometer, apparatus function and atmosphere monochromatic extinction coeffs. *(Russian)* 79−44246
toxic gas microconcentration determ. by automatic belt photometer *(Russian)* 78−28347
TTL spot exposure meter for colour photography, with three light sensitive elements 78−12782
two channel rocket photometer, for O I 5577 Å nightglow meas. 78−45078
two-cell mesopic photometer 77−37966
two-star photoelectric photometer at Wise Observatory, performance assessment 78−73657
universal stellar photometer *(German)* 77−17379
UV channel photographic photometer, for stellar obs. from Skylab 77−60608
UV double-beam, for atm. O_3 calibration 78−69505
UV photometer for atmospheric ozone monitors calibration 78−77960
UV photometric standards for atmospheric O_3 concs. meas., interagency comparison 79−35000
UV radiation, semiconductor ratemeter 78−285
UV two-channel photometer 79−2805
X-ray, proportional counter design and characts. *(Polish)* 78−41388
Zeeman photometer for Na I dayglow meas. 78−69558
CdS photo resistance, light density meters *(Hungarian)* 80−27366
NO photometric process analyser using resonance absorption method 80−57360
Se photocell, high-gain amplifier cct. 78−4679

photometric light sources
colour measurement using D65 light source 79−32018
D65 source, reproduction accuracy 79−32016
finite planar source, radiant intensity and spatial coherence 77−50743
integrating photometer screen error minimisation using linear numerical model 80−95117
lamp radiator for uniform heating of substrates rotating in circle, photometric calc. 77−54765
luminous flux meas. error equation permits correct choice of auxiliary lamp *(Polish)* 78−70175
optical parametric amplifier as absolute radiometer 78−13759
optical-null spectrophotometers, photometric scale nonlinearity 80−101816
pulsed laser, for photometer based on boxcar integrator principle *(Chinese)* 80−31842
pulsed Xe light source, programmed command unit 77−79163
radiant energy source, highly stable, circuit design and evaluation 79−7190
radiation standards for source spectral emission and detector spectral sensitivity 77−39007
radioluminescent emitter, continuous action, reference source for stellar simulator 77−10993
radioluminescent sources, basic characts., reference emitter appl. 77−58410
spherical integrating photometers, luminous flux meas. accuracy, expt. anal. of group discharge lamps *(Polish)* 80−73407
stabilisation by negative feedback *(Russian)* 77−49762
UV radiometric standards, gas discharges, plasma diagnostics appls. 80−47088
UV range assessment of artificial sources, for best fit to D65 standard 77−58407
vacuum UV Cherenkov source as radiation standard *(Russian)* 78−63164
vacuum UV radiation scales 77−30124
VUV light source, transfer standard, low-current AR arc with MgF_2 window 79−35856
working standard establishment using photoreceptors *(Japanese)* 80−98964
Ar mini-arc as spectral radiance secondary standard 77−34921
D lamp, calibration, operating time variation of spectral radiance 77−10992
D_2 lamp, spectral irradiance standard for UV, calibration 78−42397
H high-power arc as continuum radiation standard source, 53 to 92 nm, VUV radiometry 79−94311

photometric light sources continued
Hg high pressure sources, spectral distribution of irradiance, 240 to 600 nm *(German)* 77−79910
ZnS:^{90}Sr, continuously acting luminous solid for photoelec. meas. over 300-800 nm range 79−3757

photometry
see also brightness; colorimetry; densitometry; spectrophotometry; stellar photometry
0957+561A, B, double quasar, IR obs. of quasar and intervening galaxy 80−73065
absolute luminous intensity meas., apparatus *(Danish)* 78−62217
aerosol, solar radiation absorpt., visual photometric meas. technique 80−85750
agarose-water gels, stability, conc. and isotope effects, photometric obs. 79−66362
alkaline earth flame chemistry, photometric meas. of $H_2+O_2+N_2$ flames with/without Ca, Sr, Ba additions 79−8439
amino acid chromatographic instrument analysis and synthesis *(Hungarian)* 79−92030
amplifier, phase-sensitive, appl. to interference suppression and light detection *(Czech)* 78−86331
analogue system for fast light curve registration, lunar occultations appl. 79−53725
antimalarial drugs, lifetime meas. via reiterative convolution using fluorescence decay curves 80−57380
AO 0235+164, BL Lacertae object, photometric obs. of optical outburst 80−56924
387 Aquitania, slow spinning asteroid with rot. period of nearly one day, photometric evidence 80−17529
asteroid 186 Celuta, slowly spinning asteroid, photometry rel. to rot. period and comp. type 78−61782
asteroid 194 Prokne, photoelectric photometry and rot. period 79−84727
asteroid 216 Kleopatra, photometry rel. to comp., diameter, elongated shape and possible stellar occultations 80−94743
asteroid 26 Proserpina, photoelectric photometry and rot. period 79−84727
asteroid 287 Nephthys, photoelectric photometry and rot. period 79−84727
asteroid 337 Devosa, unusual object with triple extrema in photoelectric light curve, rot. period 79−40116
asteroid 52 Europa, photometry and rot. period 78−12133
asteroid 554 Peraga, photoelectric photometry and rot. period 79−84727
asteroids, IR (JHK), photometry 79−2531
asteroids, photoelectric photometry of seven objects 79−35175
asteroids, photographic photometry with Schmidt telescope during 1977 and 1978 80−72844
asteroids, photometric method for shape and spin axis orientation determ. *(Russian)* 80−8581
asteroids, photometric obs. and physical props. *(Polish)* 78−16330
astronomical, development and history, review *(Italian)* 77−56839
astronomical diffuse objects, strip photometry appl. to globular clusters multicolour obs. 78−89229
astronomical IR photometry, atmospheric extinction meas. above Mauna Kea 80−12546
astronomical occultations photometry, photoelectric photometer appl. *(Chinese)* 80−105172
astronomical photoelectric photometry, data recording system for KSC 60 cm reflecting telescope *(Japanese)* 80−94717
astronomical photographic photometry, direct sensitometer *(French)* 77−13246
astronomical photographic photometry using twin refractor telescope 77−17382
astronomical photometry, appl. of general image anal. system 78−53834
astronomical photometry, investigation of double astrograph system *(Russian)* 80−72771
astronomical time-modulated measurements with image-tube systems, effects of phosphor decay 79−88602
astronomy, appl. of SIT vidicon detector system for Palomar 1.5 metre telescope 79−92674
astronomy, thermal background subtraction in photodiode detectors 80−90342
astrophotometric scale definition by N.R. Pogson 77−49306
automated high-speed photometer for beam type incandescent lamp tests 77−26379
automated light-scattering apparatus, for polymer film study 77−53969
automatic exposure of photographic camera films 78−65992
automatic LEED spot tracing method 80−10467
automatic reactive analysers, H_2O composition checking 80−27330
autoradiography in radioisotope work, appl. to metabolic studies 78−3576
B2 1652+39, BL Lacertae-type object, photoelectric intraday photometric obs. 78−36681
balloon-borne IR telescope for absolute surface photometry of night sky 78−36453
beam incidence angle determ. from refl. meas. *(French)* 80−37072
776 Berbericia, slow spinning asteroid with rot. period of nearly one day, photometric evidence 80−17529
bipolar nebulae, photometry and spectra rel. to evolutionary status 78−41026
BL Lacertae-type objects, variable, IR and visible polarimetry and photometry 78−16528
black body sources, in band flux density calcs. 79−37135
blinds with internal diaphragms, light-blocking effectiveness 79−50405
blood clotting time measurement, digital display *(Danish)* 77−90826
blood erythrocyte count and haemoglobin determ. by mobile minipho-tometer *(German)* 79−5416
blue objects in Tautenburg catalogue, UBV photometry rel. to number suspected as quasistellar objects (QSO) 79−80365
bright galaxies, UBVRI photoelectric photometry 78−32578
burner, for emission flame photometry 80−17988
3C 120, Seyfert galaxy, IUE and visual spectrophotometry 79−92856
3C 273, UBV obs., (1975 to 1979) 80−62309
3C 279, variable quasi-stellar source, IR and visible polarimetry and photometry 78−16528
3C 295 galaxy cluster, two-colour ISIT photometry rel. to galaxies evolution 78−24557
3C 371, BL Lacertae-type object, photoelectric intraday photometric obs. 78−36681
3C 66 A, BL Lacertae-type object, photoelectric intraday photometric obs. 78−36681

photometry continued
C-CD camera description performance and calibration 80−73499
CA 0340-538 (3U 0328−52?), southern cluster of galaxies, photometry and spectra 78−36705
calibrator, inverse fourth power, NBS optical density standards development and appl. 80−73412
calligraphic projection display resolution and contrast photometer and X-Y plotter 80−86373
camera lens veiling glare, simulation method to correct photometric meas. 78−58085
Candela, radiometric definition appraisal *(German)* 78−32845
carbonized bitumen, refractive index and absorpt. coeff. as measures of structural organization 79−35811
cD galaxies in poor clusters, photometry, spectra and redshifts 79−48907
cell average size and shape meas. light scatt. photometry compared with microscopy 79−84030
cell image analysis on PDP-12, software system for information from scanning microphotometer *(German)* 78−20333
Charon (1978 P 1), stellar occultation obs., 1980 April 6, rel. to satellite dia. and struct. 80−94754
chemical analysis methods, review 79−43660
chemical analysis of solution components, automatic photometric method for determining and controlling concs. 79−79350
chromatic replacement of matched luminance, chromatic stimuli, duration thresholds 79−57657
chromatin structure of cell nuclei using scanning microphotometry and TV image anal. 79−34720
cine projection brightness meter *(Russian)* 77−49797
cinematographic film eval., microprocessor control 79−21801
circumferential field, spectrum charact. *(Polish)* 78−29136
city plume aerosol size distrib. and turbidity meas. 77−37408
Cl 0024, galaxy cluster, two-colour ISIT photometry rel. to galaxies evolution 78−24557
cloud identification against snow background, aircraft obs. *(Russian)* 77−29392
clusters of E and S0 galaxies, colour distribution rel. to redshift 80−105361
coherent multiplicative photometric analysis, photorecorder meas. system sensitivity threshold *(Russian)* 79−67373
colour and density table, photographic parameters for film processing appl. *(German)* 79−49309
Coma Cluster galaxies, photometry 78−12381
Comet Meier (1978 XXI), photoelectric BV photometry rel. to opposition effect 80−31258
cometary nuclei, brightness meas. technique 79−84745
comets, isophotometric atlas, pt. II 80−109377
comets, recent, periodic, photometry rel. to gas and dust props. 79−70997
composite stellar systems, CO and JHK obs. of E and S0 galaxies 78−36684
conversion factor for radiometric to photometric data, international standard 78−86315
correcting absorber selection for Si photodiodes, luminous meas. in flash photometry 79−72699
correlated colour temp. determ. *(Hungarian)* 78−93749
cylindrical volumes, calibrated piston source and light path computation techniques 78−4676
cytophotometric and autoradiographic simultaneous anal. device 78−77172
cytophotometric histogram, computer aided analysis of cell-cycle phase 78−92759
cytophotometry, multiparametric pulse technique for cell and radiation research *(German)* 77−78060
D and cD galaxies in poor clusters, struct. and photometry 78−32580
dark filter, integrated transmission coeff. meas., zonal method 77−34953
Deimos, photometry from Viking orbiter images 80−72838
349 Dembowska, rot. period and phase curve 79−35174
designations of photometric and radiometric equipment *(German)* 79−75570
diffuse quadratic surface light scatt., photometric representation 79−81365
digicons, image detection with semicond. array for multichannel photon counting 77−83989
digital compensation system, high speed 77−18112
digital integrator for chemiluminesc. light flux meas. 78−21196
digital meter for photometric meas., cct. and operation *(Polish)* 78−65943
discs, impact stresses, photoelastic investigation 79−37182
distant cluster of galaxies, photometry and red shift 78−12377
electrical instruments in photometric laboratory, selection, care, and use 80−86283
electron diffraction patterns of mols., photometry via IFO-451 microphotometer 77−27201
electronographic photometry, narrow-band high spatial resolution, astron. appls. *(French)* 80−46408
354 Eleonora, rot. period and phase curve 79−35174
ellipsometers and polarimeters, drift stabilization and photomultiplier linearization 78−54436
elliptical galaxies, isophotes struct. 78−41058
emission spectrographic analysis system, minicomputer based, using scanning microphotometry 80−22436
Enceladus, IR photometry rel. to presence of water frost 78−12146
energy irradiance from pulsed source, curve fitting problems 77−71377
energy photometry and spectral measurements of radiation detectors 80−252
equivalent sphere illumination, maximum contrast sensitivity publication proposal, advantages 79−9235
equivalent sphere illumination meas., new instrument features 79−9243
ESO 012-G21, Seyfert 1 galaxy, spectrum, redshift, UBV photometry and X-ray identification 80−8695
ESO 113-IG45, galaxy and/or quasar, spectrum, photometry and struct. 78−28782
ESO 113-IG 45 (= Fairall 9), Seyfert galaxy, spectroscopic and multiaperture photometric obs. 80−31362
45 Eugenia, rot. period and photoelec. light curve determ. 80−72846
exposure measurement, fundamental aspects 77−30197
extragalactic optically variable objects, calibration of photoelec. comparison sequences 77−87537
facilities at National Measurement Laboratory, Australia 78−82019

photometry continued
Fairall-9 (ESO 113-IG 45), extreme Seyfert galaxy, IR and visible photometry 79−25720
flame photometry, for continuous in situ meas. of particulate S pollution 78−96296
flames, premixed, structure investig. by light intensity distrib. meas. 80−16680
fluorescence measurements of opaque samples, proposed indices of degree of fluoresc. 78−54425
fluorophotometric measurement, supplementary unit for hand ophthalmoscope 78−48907
force-flow chromatography, alkaline earth ions detected by photometric method 80−71965
Fourier transform spectrometer performance, instrumentation for assessment 80−95165
galactic nuclei, variable, photometric techniques, finding charts and comparison stars 78−81691
galaxies, bright, in Virgo cluster area, standard total magnitudes and mean errors 78−65685
galaxies, bright, southern, photoelectric photometry 79−21436
galaxies, BV photometry rel. to galactic extinction coeff. amplitude 80−17664
galaxies, early-type, photometric determ. of twists in three objects 79−25703
galaxies, early-type, UBV photometry rel. to relative distance moduli 80−22080
galaxies, elliptical and S0, ten-colour photometry rel. to absorpt. line strengths 80−4430
galaxies, interacting, with compact components, UBV photometry 78−20888
galaxies, multiply observed, revised standard total magnitudes and colours catalogue 78−8116
galaxies, photometry of remote clusters 80−105364
galaxies, southern, UBV photometry of 262 objects 79−35364
galaxies, spectroscopy and photometry rel. to evolution of faint objects 80−105353
galaxies, surface photometry, computerized analysis method 78−12100
galaxies, UBV photoelectric photometry and photometric parameters 80−67855
galaxies, V−K colours and IR Hubble diagram for giant ellipticals 80−105359
galaxies in rich cluster at 00^h47^m, −29°46′, static props. using COSMOS meas. 79−40279
galaxies in righ Abell clusters, photometry and luminosity functions 79−88752
galaxies in Virgo area, reduction of magnitudes to standard B_T system 79−92852
galaxies near late-type spiral NGC 4945, radial vels. and BV photometry 80−109547
galaxies of Virgo cluster, photographic surface photometry 77−78870
galaxy clusters, photographic photometry *(German)* 80−46681
galaxy NGC 3379, surface photometry, computerised analysis 78−12101
Galilean satellites, eclipse spectrophotometry 79−96949
Galilean satellites, photometry of Io, Europa and Callisto, 1976 to 1979, possible solar variability detect. 80−98623
gas analyser calibration and accuracy 78−49877
gaussian-lorentzian light, photoelec. pulses, two-fold time interval distrib. 77−41683
GL 915, 618, 2688, IR sources assoc. with double-lobed refl. nebulae, far IR obs. 78−54009
glass fibre reinforced plastic, fatigue fracture kinetics studied by diffusion scatt. of luminous fluxes 80−76446
glass filter, simulating CIE spectral tristimulus value $\bar{z}(\lambda)$ 78−30037
globular clusters, photoelectric photometry rel. to structural parameters and integrated magnitudes 80−46623
globular clusters, UV energy distribs. from Orbiting Astronomical Observatory photometry 80−73009
globular clusters (M3, M5, M13, M15), equidensity curve meas. *(Russian)* 79−97041
globular clusters in Virgo cluster of galaxies, photometry, and luminosity distrib. 78−12308
globular clusters near galactic centre, IR studies 80−82434
gloss measurements, polarisation effects 79−80662
grazing incidence spectrometry, photometric calibration of 1.0 m spectrometer 80−92386
He 1-3, planetary nebula, Hα photometry and misidentification correction 79−62895
high-conductivity channel electron multipliers, performance charact. 78−86334
high-energy, IR laser component optical characterisation techniques 80−14347
high-temperature black-body model for energy photometry 77−26300
HPLC detection systems, review 78−48733
Hurter and Driffield, photographic research, biography 80−22181
IC 4329A, Seyfert galaxy, photographic photometry and optical spectrum 80−36706
illumination engineering, contributions of luminous surfaces *(Rumanian)* 80−4750
illumination engineering measurements using photometry and spectroradiometry 80−22416
illumination measurement using photoresistors, digital linearisation using microprocessors *(German)* 78−77961
illuminators light distribution indication method for computerised illumination projecting *(Hungarian)* 80−27333
image space, illumination and light flux determ. by optical system eikonal 79−26102
instrument for determining the difference between light fluxes 79−97415
integrating cavity for small optical absorption meas. 79−12838
integrating photometer screen error minimisation using linear numerical model 80−95117
integrating photometric rotating analyser ellipsometer, precision estimation 78−12744
integrating sphere arrangement for reflectance and transmittance accurate meas. *(German)* 80−31844
integrating sphere window, illum. distrib. uniformity *(Chinese)* 80−86368
integrating spheres for absolute refl. meas., goniophotometric corrections 78−21202
intensity probability density determ., from photoelectron statistical distrib. 78−24840

photometry continued
interference coating deposition by Balzers BA-710 vac. system, photometric monitoring 78−46850
interference patterns, noise elimination 79−97414
interpretation process for colour film 80−42251
Io, M-band photometry and 5 micron variability 80−46463
IR, technology evolution 77−5934
IR flash, metrological support 79−75569
iris diaphragm photometry, nonuniform background correction 80−12680
isophotometric photorecording method for optical system image quality meas. 77−34967
Jupiter, IR images at 5 microns wavelength during Voyager 1 encounter 80−26799
Jupiter tropical and temperate belts, 0.6 to 1.1 μm spectrophotometry, brightness distrib. and atmosphere optical parameters 79−92715
22 Kalliope, pole coordinates from photoelectric photometry 80−31230
BL Lacertae, optical monitoring by three-colour photographic photometry 78−16525
BL Lacertae, photoelectric intraday photometric obs. 78−36681
BL Lacertae type objects, southern, optical monitoring 80−56969
lactate concentration meas., enzymatic and electrochem. methods *(German)* 79−2169
laser microphotometry with laminar hydrodynamic focusing 77−37965
laser particle size analyser, using diffraction of light by particles 79−6090
laser radiation, pulsed and steady-state, metrological provision for parameter meas. 79−14007
LED luminance meas. *(Japanese)* 77−82584
LED luminous intensity and flux meas. appl. *(Japanese)* 77−57378
LEED intensity measurement by photographic method with digital image processing appl. to Si (111) surface 79−60234
light attenuation systems, comparative analysis 79−12839
light beam energy indirect meas. accuracy *(Russian)* 78−74046
light distribution pattern math. calc. for camera copyboard illumination 79−21800
light emitting diode, light flux meas. by photometric sphere 80−253
light flash intensity meas. for neurophysiological research 79−49270
light flux brightness meas., EM vacuum fluctuations, quantum noise 80−57361
light meters and their appl. *(German)* 78−8434
light source brightness measurement, standard photometric system errors 78−58005
light sources, psychophysical luminous efficiency *(Polish)* 80−33110
light sources props. meas., laboratory equipment requirements and standards *(Slovak)* 80−17990
lock-in amplifier, for measurements when signal-to-noise ratio is less than unity 78−29134
long fibre, mirror and hollow dielec. lightguides, photometric characts. 80−33201
low-alloy steel, photometric anal. by time resolution of radiation *(Russian)* 78−23995
luminaire photometry, new concepts using automatic photometer 80−4752
luminous flux meas., automatic null method *(French)* 80−27331
M13, globular cluster, Calculated and observed integral magnitudes comparison 79−97043
in M31, colour excesses rel. to galaxy gas-to-dust, ratio 78−8120
M31, isophotometry of nuclear region and position angle of major axis 77−53682
M31, M51, nuclei, isophotometry 79−71114
M51 system, photometric study 79−30125
M87, evidence for supermassive object in galaxy nucleus from SIT and CCD area photometry 78−49528
M87 halo globular clusters, energy distribs. and metallicity 78−89244
Magellanic Cloud supernova remnants, Hα photometry rel. to optical emission from shocks 79−92831
Markarian 185, 186, UBV surface photometry *(Russian)* 77−91614
Markarian 298 (=IC 1182-4), multicolour photometry *(Russian)* 78−57641
Markarian 79, Seyfert galaxy, IUE and visual spectrophotometry 79−92856
Markarian galaxies, nature from photometry and classification 78−28781
Mars, integral photometry 78−61780
Mars, phase function, July to November 1976, Viking orbiter photometric obs. 78−20677
Mars, UV spectra and photometry by TD1A and OAO-2 satellites 77−91459
Mars surface topography, photometric study method 79−25537
Mercury, optical photometry interpretation rel. to surface material props. 78−12130
Merope nebula, uvby photometry and dust grains phase function in UV 78−32553
metal halide lamps, photometric charact. 79−9236
metallic mirror as complex rough surface, light scatt. 80−1293
metameric white samples for testing relative UV content of light sources and daylight 79−58767
meteorites, IR (JHK), photometry 79−2531
meteors, television photographs photometry 78−96441
9 Metis, pole coordinates from photoelectric photometry 80−31230
Michelson interferometer, double-passed, influence of surface roughness on photometric setting-accuracy 78−12746
micro-light guide photometry of biological tissues 80−46005
micro-optics testing, width meas. of slit test objects 80−64223
microcomputer appl. *(German)* 77−74480
microcomputer controlled, chemical analysis 79−49267
microphotometer, MF-2 type, scatt. light effects on optical densities of electron-photon cascade tracks 77−61655
microphotometry of biological materials, digital picture analysis 80−17991
microscope, appls. in materials science 80−21236
microscope photometry, on-line data collection and processing for solids, fossils and organic matter *(German)* 79−26101
microscope photometry in studies of molecular struct. of carbonized bitumens and pyrobitumens 80−18011
microscopic image anal. system, cell cycle, cancerous blood and bone marrow cells appls. 79−88223
mine large particle size photometric sorting machine, DATAC system 78−32853
Moon, optical photometry interpretation rel. to surface material props. 78−12130
photometry continued
Moon, photometric and polarimetric obs., 1976 April to 1977 December 80−51677
Moon, photometric function and new three-dimensional scatt. indicatrix 80−101538
multichannel photon counting image detector arrays 78−65970
NAB 0137−01, quasar, UBV photometry and brightness vars. 80−56967
NDIR, partially layered detector, function and properties 80−105696
Neptune, effective temp. from IR photometry 78−32394
NGC 1068, Seyfert galaxy, IR photometry and polarimetry 78−54035
NGC 1084, NGC 7331, spiral galaxies, surface photometry and mass distrib. 79−40265
NGC 1275, photometric and spectrum vars. 80−22075
NGC 1313 barred spiral galaxy, photographic photometry rel. to asymmetric rot. *(French)* 79−97082
NGC 157, spiral galaxy, surface photometry and mass distrib. 79−40264
NGC 253, barred spiral galaxy, detailed surface photometric study 80−105327
NGC 253, Sc-type galaxy, two-micron spectrophotometry 80−4442
NGC 2768, galaxy, optical and IR photometric study 78−36683
NGC 3115, galaxy, optical and IR photometric study 78−36683
NGC 3115, lenticular galaxy, photometry and struct. 80−36707
NGC 3227, Seyfert galaxy, photoelectric and spectroscopic study and comparison with galaxy chain (VV 150) 80−98724
NGC 3686 galaxy quartet, surface photometry, mass distribs. and group stability 80−62297
NGC 4314, barred spiral galaxy, UBV surface photometry of central region 80−77482
NGC 4378, anaemic Sa galaxy, spectrum, photometry and extended rot. curve 79−8990
NGC 604, H II region in M 33, Hβ photometry and Fabry-Perot interferometry rel. to core-halo struct. 80−85984
NGC 6251, radio galaxy, CCD photometry rel. to central supermassive object 80−26966
NGC 6440, globular cluster, surface photometry of cluster core 80−82436
NGC 6902, H I rich southern supergiant spiral galaxy, opticals studies 80−8680
NGC 7000/IC 5070 (North American/Pelican) nebular complex, photometry rel. to obscuration and excitation 78−36667
NGC 7027, planetary nebula, near IR line fluxes 78−73748
nonlinearity measurements on photometric devices 79−71505
nuclear emulsion, photometric meas. of thin CNO particle tracks 79−76281
44 Nysa, pole coordinates from photoelectric photometry 80−31230
opaque surface, roughness determ., photometric method 80−95072
optical coating deposition by high freq. cathodic method, photometric monitoring 79−76900
optical element contamination modelling, photometric characts. estimation 80−48429
optical power meters for laser photometry 78−65953
optical radar, logarithmic fast-response photodetector for atm. sounding, photometric properties 80−51585
optical radiation composition and effects and usage in plant experiments *(Hungarian)* 80−109076
optical radiation power photometry, USSR system of standards 77−30194
optoelectronics, physical fundamentals *(German)* 77−37981
oxazine dyes, orientation of $S_1 \rightarrow S_n$ transition moments, continuous ps photometry 79−10152
Palermo four-colour far IR astronomy program *(Italian)* 79−48688
panoramic, background subtraction problem *(Italian)* 80−98570
panoramic photometry reduction, search algorithms 78−32354
peculiar extragalactic sources, multiaperture UBV photometry 78−28772
Periodic Comet Ashbrook-Jackson (1978 XIV) 80−31258
Periodic Comet d'Arrest (1976 XI), tail photometry rel. to meteoroids characts. 78−53876
Periodic Comet Encke, photometry rel. to large dust grains emission 78−85908
Periodic Comet Tempel 2 (1977d), BV photometry, (1979, January 28 and 31) 79−30012
petrographic characterization of coal using automatic image analysis 80−18002
Phobos, photometry from Viking orbiter images 80−72838
Phoenix group of galaxies, example of plate processing via two-dimensional digital filtering 79−16835
phospholipid membranes, artificial, lamellarity determ. by photometric phase-contrast microscopy 79−39368
photochromic glass darkening and bleaching kinetics, pulse photometry 79−46021
photodiode calibration down to 5 nm wavelength, synchrotron UV radiation appl. 78−77959
photoelectric photometry, circuit for astronomical laser ranging equipment *(Japanese)* 78−89075
photographic printing, photometry and sensitometry measurements *(German)* 79−6201
photographically recorded spectral lines, of nonuniform half-width, microphotometric errors 78−86337
photometric etalons, scatt. matrix and brightness coeffs. of MS-20, MS-14 reflectors 78−82020
photometric studies of low-absortion optical media, apparatus *(Russian)* 80−98965
photon irradiance sensor, Si PIN photodiode and rhodamine B dye quantum counter, construction and expt. tests 78−32843
PKS 1144−379 BL Lacertae object, optical and IR photometry and optical spectrum 80−4451
PKS 2126−15, QSO (z=3.27), JHK photometric obs. 80−94888
planar object photometric characts. recognition *(German)* 79−17463
planetary nebulae in M31 (Andromeda galaxy), identifications and photometry 78−28737
planetary photometry, theory 80−67601
planetary satellites of outer solar system, IR photometry and identification of new class 78−12146
point source lighting computation using point-by-point method *(Rumanian)* 80−17987
polarised light definitions and nomenclature 78−29897
polymer lightguide attenuation coeffs. meas., data anal., accuracy 79−1005
polymer relaxation props. determ. using photometric transducer method of meas. 80−3268

photometry continued
power illuminance unit, USSR state standard for continuous spectral radiation in range 0.2 to 4.5 micron 78−89524
power luminescence spectral density unit of continuous spectral radiations, 0.25 to 2.5 micron, USSR state standard 78−93752
power spectrum determination of random pattern, comparison between numerical and analogic processing methods *(French)* 78−58922
precision increase in photometric measurements using indirect refractometric techniques *(Russian)* 77−79136
primary mirror of large azimuthal telescope, isophotometric recording 77−73953
proton flux measurements using photometric calorimeter 80−4718
ps light pulse length determ. by parametric amplification in nonlinear crysts. 78−1306
PVC soln., mol. wt. meas. by light scatt. photometry 79−7045
Q 0420−388, QSO (z=3.13), JHK photometric obs. 80−94888
quantitative microscope for clinical appls. 77−60273
quantitative photometric scanning of thin layer chromatograms, analysis of organic substances appl. 78−92558
quartz in metamorphic rocks, photometric method for c-axis fabrics anal. 80−101456
quasar, strong emission line, with redshift z=0.189, spectrum and photometry 80−8710
quasars, southern, optical monitoring 80−56969
quasi-stellar objects, variable, photometry and completeness of faint blue objects in Sandage-Luyten field 78−54069
quasi-stellar objects, variable, photometry and completeness of faint blue objects 78−93446
quasi-stellar radio sources from 4C and Parkes catalogues, spectra and photometry 78−65714
radiant flux ratio meas., nonlinearity of low noise Si detectors 80−47089
radiation energy units reproduction, error anal. 78−45670
radiation equivalent and meas. units *(German)* 79−54166
Raman spectra, on photographic plates, meas. by computer-controlled photometer 77−65051
ray optics, theory of light field, statistical optics, light meas., photometry, polarimetry 77−79748
reflectance map calc., surface bidirectional refl.-distrib. function 79−75568
reflectance measurement at diffuse incidence *(German)* 78−21201
reflectance microscopy of coal, considerations involved in automation 80−18001
retroflectors and retroflective material luminous intensity coeffs. meas. 77−74479
retrorefelctance measurement of photometric standards and coatings 78−25940
retroreflectance measurements, unified coordinate system 80−73408
retroreflecting material metrology, errors in luminous refl., chromaticity meas. 80−68235
retroreflector photometric and goniometric accuracy 80−86375
retroreflector photometry, meas. error rel. to aperture size 80−73409
retroreflectors and retroreflective materials meas., accuracy assessment *(Dutch)* 79−85159
Rhea, planetary, 1976 to 1979, rel. to possible solar variability detect. 80−98623
RMB 56 (1216+141), compact blueshifted galaxy, photometry and spectrum 78−16527
rocks, photometric analyser for crystallographic orientations in thin sections 80−41560
rough surface reflection, empirical representation of goniophotometric data 80−87314
S0 galaxies, luminosity distrib. perpendicular to plane of discs rel. to struct. and origin 80−36705
satellite auroral photometry, spectral albedo corrections 77−49208
Saturn, atmosphere upper layers props. from polarimetry photometry and spectrophotometry *(Russian)* 78−40867
Saturn, UV spectra and photometry by TD1A and OAO-2 satellites 77−91459
Saturn ring system, low tilt angle photometry and thickness 79−35186
Saturn rings, photometric determ. of thickness 79−66959
Saturn spatially resolved IR obs., 10 and 20 μm disc scans at (B′=−11°.8) 79−84741
scanning microscope photometric image analysis, appl. to chromatin packings *(German)* 79−5409
scattering media optical meas. for biomedical applications 79−83890
semi-transparent film, optical cond., complex index and thickness, photometric meas. *(French)* 77−52193
seminar, optical radiation meas., San Diego, CA, USA (Aug. 1979) 80−86036
sensitometric sources, photometric and radiometric calibration, tutorial 77−34044
Seyfert galaxies nuclei, optical variability from U, B, V and Hα photometry 78−96543
Seyfert galaxies with large z, electronographic survey 77−91624
shadow photometry of high vel. gas flow, complex diaphragm shape 77−35270
shell, internally exploded, displacement meas. by photometric method 80−14642
SI unit proposition 78−93644
signal processing unit based on hybrid fast instrumentation amplifier 78−41342
sky background estimation on starfield plate 80−67577
sky noise at telescope focus, photometry of atmospheric IR emission, statistical props. *(French)* 78−53731
sky noise correl. for IR telescope focal plane *(French)* 78−53725
SMC, photometric study of wing and eastern halo 78−86011
solar energy meas., photometric and bolometric methods 78−12470
solar MUV photometer, rocket borne, stratospheric ozone concentration measurement 80−52292
spatial recording of radiation intensity in caustic, photographic recorder 78−58007
speckle patterns in polychromatic light, short detector integration times 77−14660
spectral adaptation for receivers and light sources *(German)* 80−77837
spectral energy distribution characterisation *(German)* 77−34011
spectral irradiance scale, 1973 NBS standard 77−83942
spectral irradiance scales, international comparison 77−106
spectral luminous efficacy maximum, definition *(German)* 78−54333
spectral sensitivity distribution meas. systems 77−26398
spiral galaxies, early-type, multiaperture UBV photometric props. 80−98706
spiral galaxies, optical surface photometry rel. to local mass-to-light ratio 80−31361
spiral galaxies studied at Westerbork, optical surface photometry 80−17655
stainless steel determination of 0.001 to 0.01% by extraction and photometry 77−56275
standard lamp gas flow visualisation using holographic interferometry 79−12835
standardized density scale for photographic photometry *(Japanese)* 79−101075
standards, colour matching and adaptation exam., using Japanese observers *(Japanese)* 79−6163
standards development, calibration 79−6161
starch gelatinisation investigation using small-angle light scatt. photometer with solid-state photodetector 77−86382
stellar Balmer-index photometry, quantitative anal. of influencing factors 78−96404
stellar colour photometry through clouds, appl. of single repetitive filter cycle photometer 80−62025
stellar multicolour photometric systems, early-type stars synthetic UBV colours and temp. scale 79−16933
stellar photoelectric photometry, efficiency as function of image quality 80−62034
stellar photometry, appl. of focal reducer using Fresnel lens 80−67568
stopped-flow apparatus for rapid mixing and study of two fluids under high hydrostatic pressures 80−98929
subtractive colour photographic printing, exposure parameter calc. 79−26167
subwavelength focused light beam, knife edge scanning meas. 77−75641
supergiant elliptical galaxies nuclei, CCD photometry rel. to supermassive object in (NGC 6251) 80−26966
surface orientation determ. from multiple images, photometric method 80−52163
surface roughness meas. appl. 78−4682
synchronous observations of periodical optical sources, optimum meas. time estimation 77−73965
terminology and units 77−61108
terminology for refl., transmission, scatt. and emission 77−74477
terminology of transmission, refl., scatt., and emission 78−37044
thickness measurement of Al coating on polyethylene terephthalate 80−62626
thin film, optical characterisation *(French)* 79−11402
Titan, JHK photometry and suspected near IR variability 80−46469
Tololo emission-line galaxies, nature from photometric and spectroscopic obs. 78−49531
total luminous flux meas. on radiometric base, goniophotometer 80−42250
transition metal disilicides, powdered, determ. of free metals, oxides, photometric method 78−61101
TTL spot exposure meter, applications, for incident and reflected light measurement 78−12782
units, new candela and lumen definitions 79−6162
units and terminology used in light meas. rel. to photometry and displays 79−21691
vacuum UV, detect. efficiency of ceramic channel electron multiplier 78−12759
value definitions and commentary *(French)* 78−268
visibility measurement, photometric contrast *(German)* 80−95118
vision, extinction photometry, entoptical scatter, model 80−51087
VV 150, galaxy chain, photoelectric and spectroscopic study 80−98724
VV 8, galaxy, BV photometry rel. to rot., mass and surface brightness obs. *(Russian)* 79−48937
wave optics, partially coherent fields of illumination, pencils of rays 79−98275
wavelength calculation, selected coord. method using Chebyshev integration formulae, tristimulus values *(German)* 77−82586
weak optical laser radiation in random-pulse sequence, recording 77−37988
whiteness formulae 79−58768
X-ray astronomy, spectroscopic and photometric facilities of 80 cm X-ray telescope *(German)* 80−109358
X-ray source fields from Einstein Observatory, RI photometry with CCD camera 80−62315
zodiacal light UV observation from D2B-Aura satellite, extraneous light evaluation 79−58299
As determ. in ores of reduced heteropoly acids, photometric method 78−61103
B determination in nuclear power station waters, flame photometer method 78−45672
Ba, forced-flow chromatography, detection by photometric method 80−71965
$BaSO_4$, pressed powder Eastman White reflectance standard, absolute refl. meas. 78−25939
$BaSO_4$ white reflectance standard, Kubelka-Munk optical props. 77−42581
$BaSO_4$ white reflectance standard, Kubelka-Munk optical props. 78−4675
Ca, forced-flow chromatography, detection by photometric method 80−71965
Co film, optical props. by self-consistent photometric technique 80−55217
Cu-Sn alloy components, photometric determ. *(Russian)* 79−11842
Ge IR photon drag detector, photosensitivity spectrum 79−12853
Ge, surface structure, LEED and spot photometric meas. 79−23811
H II regions, compact, in galaxy NGC 6822, new discoveries and photoelectric magnitudes 80−51854
I_2, heat of sublimation, laser photometric meas. 79−5942
Mg, forced-flow chromatography, detection by photometric method 80−71965
NH_3 actinometry, appl. to ground level meas. of solar 1950-2150 Å radiation 79−2345
O I airglow emission rate, midlatitude maximum characts. obs. 79−84561
OH 0739-14, IR source assoc. with double-lobed refl. nebulae, far IR obs. 78−54009
P determ. in ores of reduced heteropoly acids, photometric method 78−61103
Si multielement photoelectric convertors, p-n mesa structure for investigating optical and energy characts. of solar and radiant energy concentrators 80−97783

photometry continued
Si, surface structure, LEED and spot photometric meas. 79−23811
Si:P, measurement techniques for determining P densities 80−75262
Sr, forced-flow chromatography, detection by photometric method 80−71965
Ti (III), (IV), simultaneous photometric determ. 78−61102
WO_x, powders, coarseness meas. using powder surface reflectance 79−96246

photomultiplier tubes *see photomultipliers*

photomultipliers
56 AVP tube, gain stability meas. 77−14306
absolute spectral sensitivity in photon-counting mode 79−67383
active bias chain, cct. 79−71481
after-pulse suppression in RCA 8850 series 77−26940
afterpulses, time distrib. 78−54459
afterpulses effect in coincidence systems 77−82583
alignment procedure for large photomultiplier arrays efficient method using standard dynode resistor chain 77−3229
alkali halides, secondary electron emission statistics, photomultiplier appl. 79−47564
amplitude-time characteristics 79−12850
Anger scintillation cameras, state-of-the-art in suitable photomultiplier tubes 78−40304
arc quasistationary plasma, scatt. diagnostics using periodically pulsed UV lasers 78−67481
astronomical applications, weak light flux recording in pulsed mode 77−13242
astronomical UBV photoelectric photometer for amateur use 78−65502
automatic compensator for background and dark current in output 77−87851
autoradiography, track density determ. in solid-state particle detector 79−85859
base, for high-rate appl. 77−54469
base cct. for high pulsed anode currents 77−54472
bias effects in photomultiplier used in laser Doppler anemometry 80−59140
binary encoded position-sensitive scintillation hodoscope with reduced photomultiplier, pion detection 78−17506
channel plate multipliers, operation in strong mag. field 77−79510
channeltrons and channel plates, influence of radiations, review 77−26933
Cherenkov aerogel counter, increased photoelectron collection efficiency of photomultiplier 79−45568
Cherenkov counter appl. of photomultiplier and small size phototube performance 78−37511
Cherenkov counter photomultiplier, sensitivity to gamma quanta 78−9032
Cherenkov counter spectrometric channels, optimum supply conditions of 58AVP photomultipliers 78−9031
Cherenkov light photomultipliers, improved yield 79−22549
chevron microchannel plate photomultiplier tube with 400 anodes for high energy appl. 79−45545
conference on nuclear power systems, Washington, USA (1978) 79−41045
conical adaptors between light guides and phototubes, optimisation 78−70690
control unit construction for high-performance dichrograph 78−21122
controllable, for optical spectra meas. 79−89009
controlled photomultiplier tube with subnanosecond input gate 77−87830
cooling by semiconductor microrefrigerators 78−57942
cosmic ray induced noise from Cherenkov radiation 77−33308
cosmic ray induced noise in photomultipliers, Cherenkov radiation 77−18735
curved microchannel plate photomultipliers, impulse response 78−12743
direct detection optical communication systems, photoelectron counter dead time effect 77−54796
dissector pickup tube operating as a counter 80−95153
dissectors operating in one-electron and DC modes, illumination characteristic coupling 78−58034
EHT supply automatic cut-out unit 77−82544
electrokymographic pick-up, external device 77−21606
environmental γ flux meas. method using NaI(Tl) scintillation counter and photomultiplier 78−21786
fast, influence of incident light wavelength on time jitter 77−38557
FEU-106, one-electron response 77−87827
FEU-114 with Venetian-blind dynodes for photon counting 77−87829
FEU-118 in operation with NaI(Tl), CsI(Tl) dets., params. in γ spectrometry 79−3284
FEU-17, phase characts. in radioheterodyne regime 79−93214
FEU-49, time resolution improvement for Cherenkov spectrometer 77−87831
FEU-49 photomultiplier, gain stability study 77−41663
fluorimeters, weak fluoresc. detect., analogue method 77−40581
focon raster lightguide for transmission onto photomultiplier photocathode, optimisation 78−13805
gain short term instability meas. 79−59305
gain stabilisation system for high counting rates scintillation and Cherenkov counters 79−76277
gain stabilisation with high counting rate, feedback resistor series effect appl. 80−106232
gain-changing protection circuit, scintillation neutron detector 80−74074
gas concentration meas. using Raman intensity depend. on giant pulse laser polarization 80−98986
gas scintillation proportional counter using a photomultiplier tube array 79−76294
Gaussian light, photocount statistics, finite aperture corrections 77−34012
GFEU-30 hodoscopic photomultiplier 79−93869
grid-gated photomultiplier photometer with subnanosecond time response, for fluorescence photobleaching recovery expts. 80−37071
heterodyne detectors, evaluation at 5145 Å 77−71370
high energy physics large counter expts., photomultiplier assemblies and associated electronics 77−83469
high resolution imaging X-ray detector, for astronomical meas. 78−49333
high-current photomultiplier with disc electrode leads 78−58032
high-gain microchannel plate photomultipliers, characteristics and performance 79−45551
hodoscope containing scintillation counters, and small FEU-87 photomultipliers, charged particle meas. 78−78562

photomultipliers continued
hodoscopes, scintillation, with hodoscope photomultipliers 80−47817
hodoscopes for high intensity muon beam, high-rate photomultiplier-base and precise timing calibration 79−22544
HV amplifier, 50 MHz passband, stellar electrophotometer appl. 77−74434
HV readout system 77−54492
hysteresis effect of gain, anomalous results in liquid scintillation counting 79−22554
hysteresis effect on rate-dependent gain variation mechanism 78−89543
image intensifiers for nocturnal remote sensing, recent developments 77−23752
impulse response improvement by external compensation networks *(German)* 77−41682
intrinsic amplitude resolution for photomultipliers with large photocathodes 77−41664
ionisation coefficient of gases, meas. using photomultiplier 78−1786
ionospheric rocket expt. high-power electron gun *(Japanese)* 78−61566
ITT FW-130 photomultiplier, linearity test 79−58255
ITT FW-130 photomultiplier, nonlinearities 78−85852
laser beam registration sensitivity to incidence angle obs. 80−31843
laser heated surface colour temp. meas. pyrometer 78−57956
laser pulse recording using photomulitiplier with capacitive load 79−37542
light pipes with smooth and mosaic ends for photomultiplier 78−1328
light scattering in aqueous polymer solutions meas., apparatus 78−74058
linearity, meas. in pulsed mode using GaAs injection laser 77−37961
logarithmic scale using AGC *(Czech)* 77−5884
low light level photomultipliers, recent advances 79−45547
low-level imaging, optical signal detection and meas. 79−94350
luminescence spectroscopy, image devices and photomultiplier detectors, signal-noise calcs. 77−81433
magnetic shielding for photomultiplier array in strong external field 80−32573
magneto-electrostatic electron multipliers, long-term efficiency changes *(German)* 80−5448
microchannel, with subnanosec. characts. for time meas. 80−37001
microchannel plate, applications, development status 77−54437
microchannel plate, improved perform. with resistive anode encoder 78−5104
microchannel plate dark current meas. 79−81555
microchannel plate detector for far UV spectrograph, rocket-borne astronomy appl. 77−22086
microchannel plate image intensifier, quantum detection efficiency 77−83462
microchannel plate life tests 77−61117
microchannel plate multiplier for self-scanned anode array UV detector 77−78632
microchannel plate photomultiplier, appl. to subnanosec. lifetime meas. 78−37520
microchannel plate photomultipliers, performance studies of prototypes 77−54442
microchannel plate photomultipliers for plasma diagnostics 79−41077
microchannel plate surface finishing using liquid 78−90544
microchannel plate system image contrast rel. to object size 79−27421
microchannel plate technology and applications 79−23075
microchannel plates, geometry effect on characts. 77−58460
microchannel spatial light modulator, for real-time optical data processing 79−18534
microchannel spatial light modulator development, for real-time optical data processing 79−72714
modulating cct. with spurious signal compensation 78−58033
NDT flaw detector with analogue data processing, param. optimisation 77−81374
neutron counter, scintillation, photomultiplier noise characteristics 80−74077
noise figure, secondary electron emission model 78−86336
nonlinear mode of operation of photocathode with focused laser beam 79−85183
nuclear event simulation, green LED, trigger circuit, wavelength matched to photomultiplier 77−3238
nuclear medicine, photomultiplier tube balance assessment 80−41196
nuclear medicine appl., equipment improvements 77−44787
one-electron characteristics for photon counting 78−58038
opto-coupled system for photomultiplier blanking 79−81137
peak detection of current pulses, recording of 10^{-12} lm fluxes 80−73471
photocathode sensitivity uniformity over surface, distortion of zone charact. by interference in substrate 80−58709
photocathodes for BBO applications 80−27896
photometric ellipsometers and polarimeters, drift stabilization and photomultiplier linearization 78−54436
photometric ellipsometers and polarimeters, photomultiplier linearisation and system stabilisation 78−54441
photomixer with spatially periodic photodetectors, characts., appls. 79−12852
photon correlation in nanosecond range using programmable digital counter, photomultiplier evaluation 78−54464
photon counter design for low light detection systems, spectroscopy, cathodolum. materials appl. 80−105711
photon counting, vacuum UV region, 120-200 nm, detection limit of apparatus *(German)* 78−45691
photon counting appl., system components evaluation 78−21215
photon counting meas. of small light flux, accuracy and reliability 77−74481
photon detectors for optical communications *(Czech)* 79−50396
photoreceiver sensitivity nonlinearity determ. by high-speed raster device 77−79150
photosensor with logarithmic transfer characteristic photosensor 79−93215
power supply using HF transmission 77−41651
protection against optical overloads, electromagnetic shutter control 80−23255
pulse processing automatic gain control circuit for photomultiplier tube 79−97955
quadrant position sensitive photomultiplier with high detection efficiency 79−45546
quantum receiver appl. peculiarities *(Bulgarian)* 78−45704
radiometer/photometer appl., commercial devices survey and classification 78−16830
Raman spectroscopy, pulsed, using Nd:YAG laser, photon counting compression effects 78−74086

photomultipliers continued
rate dependent photomultiplier gain, time depend. 80−87020
rate-dependent gain variations, obs. of hysteresis effect 77−54451
review, Russian devices 80−57371
scintillation camera, photomultiplier tube imbalance, field nonuniformity, effects on cold lesion detectability 79−5352
scintillation camera, with 2 mm intrinsic resolution, biomedical appl. 77−70525
scintillation counters, time-of-flight, electronics system for Mark II Detector 80−58093
scintillation counting PM tubes, anomalous gain changes 78−54458
scintillation detector, in SEM 80−52819
scintillation spectrometer, photomultiplier gain stabilization, computer control software 78−13369
scintillation spectrometers, with LED and PIN photodiode, stabilising system 80−47821
scintillator, sampling grid, calibrated intensity monitor for intense high energy charged particle beams 80−69034
selection for time and one-electron operation 77−87828
selective receivers for 0.2 to 0.3 μ spectral region 79−30560
SEM adaptation for transmission mode 79−71579
sequential linear scanning systems for mol. fluorescence meas. in soln. 77−79638
signal controller for photomultiplier output in magnetic circular dichroism 77−67511
single-photon counter, with 9789 QB photomultiplier *(Chinese)* 80−27332
SIT image detector, for anal. fluoresc. spectrometry 77−61134
solid-state, for improved gamma counting techniques 79−54748
spectral sensitivity of RCA 4522 photomultiplier tube 78−21818
spectrometer light detector, cooling system 78−45718
squirrel-cage photomultiplier base design, for nanosec. fluoresc. decay meas. 77−30204
stability behaviour of photomultiplier using Pb glass channel type secondary electron multiplier *(German)* 78−852
subnanosecond optical detector developments 80−77870
Sun-blind photomultipliers for near UV 77−41665
thermoluminescence low level detection 77−61132
threshold optical radiation flux meas. errors 78−12760
time resolution capabilities of microchannel plate and static crossed field photomultipliers 78−37061
time resolution studies of fast photomultipliers 80−99415
time response variation with wavelength, ratio correction rel. to fluoresc. lifetime meas. 77−18065
time-domain reflectometer with gated photomultiplier receiver, optical fibre break detection appl. 77−65620
timing props. of plastic scintillation detectors 79−22540
transient characteristics and intercascade time-of-flight dispersion 78−86333
tube instability, consequences for radioactivity meas. accuracy 79−76272
ultra-fast detectors for laser fusion diagnostics, quenched plastic scintillator with microchannel plate photomultiplier 80−74084
UV plasma spectroscopy, broadband stable detector 78−87495
voltage dividers to stable photomultiplier running *(German)* 79−68172
voltage-frequency convertor for astronomical photometry with photomultipliers 78−45233
wavelength dependent errors in decay time meas., correction method 79−30558
wavelength shifter, coating technique 80−18760
wavelength specific photon detector for the VUV 80−91380
weak light flow, analysis of measurement methods *(Russian)* 78−45694
XP 2020, wavelength depend. of timing props. 79−18083
GaAs single-cell radiometer for artificial satellite measurement system 80−13147
^{3}H calibration of photomultipliers on liquid scintillator *(Czech)* 79−31324
InGaAsP photocathodes for astronomical detectors, UV response 77−57387
Kr, ^{85}Kr diffusion meas., precision apparatus 78−54520
Pb-glass total absorption counters, photomultiplier size at high energy 80−74085
Si intensified target image detector for inductively coupled plasma emission spectrometer 80−86439

photon counting
60 cm reflector, at Kagoshima rocket launching centre *(Japanese)* 78−32344
1024 channel apparatus for time interval distrib. meas. 78−81950
acridine orange, fluoresc. decay meas. by high repetition rate gated photon counting 80−86402
antibunching in resonance fluorescence in presence of atomic number fluctuations 80−91764
astronomical photoelectric photometer, multifunction, system design 77−73949
astronomical proportional control autoguidance system using photosil detector 77−49296
astronomical speckle interferometry, stellar image recovery, photon noise limitations 77−49309
astronomy, parameter estimation via appl. of likelihood ratio 79−44374
atmospheric optical communication line operating under photon counting conditions, adaptation to turbulence 80−9930
atomic vapour quantum counter, Stark tuning 80−53242
atomic vapour quantum counter for upconversion of narrowband IR radiation in 1.5-20 μm region, expt. results 80−73455
ATP content meas. in single red blood cell, using firefly bioluminescent reaction with optical instrument 79−79695
basic research tool, antibunching and hidden variables 79−7105
book, optical and IR radiation detection 79−2821
book, photoelectron statistics 78−25842
Brownian motion, photon correlation study 78−25798
cathodoluminescence radiation, photon statistics theory 77−59620
ceramic channel electron multiplier, detect. efficiency in vacuum UV 78−12759
chaotic light with Lorentzian spectrum, two joint time interval distrib. 79−50269
Charlier approximation in photocount statistics 80−74328
chevron microchannel plate photomultiplier tube with 400 anodes for high energy appl. 79−45545
clip-level crossing rates in photon correl. and analogue signal processing 77−88650
photon counting continued
coherent-incoherent light, polarised superposition, photon counting statistics 77−42513
correlator, Malvern, based on photon correlation and laser scattering spectroscopy, development and appl. 80−5741
correlator for meas. transient waveforms of very weak fluorescence 80−87250
count cct. using high-speed comparator in discriminator 78−77979
counting distribution, quantum mech. derivation 77−58302
cross-beam rate correlation, advances 80−58621
dead time correction for bright star photometry 77−22106
dead time modified Poisson processes, rate variation effects on counting statistics 78−65968
dead time study, error optimization, in photon counting spectroscopy system *(Spanish)* 79−80693
dead-time effects in photon counting statistics 79−3665
dead-time-modified photocounting distrib. obs., for modulated laser radiation 79−12846
deadtime perturbed doubly stochastic Poisson counting system, information, error and imaging 79−22901
design for low light detection systems, spectroscopy, cathodoluminescent materials appl. 80−105711
detector for subMM wavelengths using Rydberg atoms 80−77867
digicons, image detection with semicond. array for multichannel photon counting 77−83989
digital lock-in, fast low cost design 77−62036
digital photometer, laser Raman and spectrofluorometer systems appl. 77−5881
dissector operation, advantage of one-electron mode 78−58039
Doppler spectrum, radiation energy cumulants 80−1172
dye laser, photon statistics 77−727
dye laser amplifiers, exam. of photonic efficiency *(French)* 78−59004
electric field light scattering by photon counting and signal averaging 80−95794
exponentially decaying sources, exact photocounting distribs. 79−64192
far IR to visible conversion in ruby, for tunable quantum counter 77−5909
fast light phenomena, detection and analysis *(French)* 80−13133
FEU-114 photomultipliers with Venetian-blind dynodes for photon counting 77−87829
flames, local temperature measurement, by two-line at. fluoresc. and photon counting method 79−71447
fluid dynamics, sinusoidally perturbed flow meas., photon correlation technique 77−42945
fluorescence, polarisation anisotropy meas. via single-photon counting 77−18072
fluorescence, subns., decays, meas. by sampled single-photon detect. 78−21219
fluorescence correlation, clip-correlator *(Russian)* 80−42270
fluorescence decay signal analysis by photon time-correlated counting 78−49910
fluorescence intensity correlation, photon counting using clip-correlator *(Russian)* 80−42271
fluorescence life time decay curve meas. and anal. 78−54465
fluorescence polarisation meas., T-format photon-counting polarisation photometer 78−54423
fluorometric system, nanosec. time-resolved spectrometry with tunable dye laser and pulse-gated photon counter 80−11968
Fokker-Planck equation, for parametric processes, photocounting statistics 79−3664
gaussian light, approx. two-fold generating function of photocounts 78−58963
Gaussian light, photocount statistics, finite aperture corrections 77−34012
gaussian light, with triangle-shaped correl. function, photocount statistics 77−34859
Gaussian-Lorentzian light, clipping level depend. of photon count autocorrel. amplitude 77−79168
gaussian-lorentzian light, photoelec. pulses, two-fold time interval distrib. 77−41683
Gaussian-Lorentzian light, photon counting distrib. factorial moment, spatial coherence 80−83571
Geiger coordinate counters for UV and X-ray photons 80−69026
Glauber-Sudarshan representation of density matrix 79−31844
high detective quantum efficiency image detectors, review 77−71010
high-gain microchannel plate photomultipliers, characteristics and performance 79−45551
high-speed dual-lag photon-correlation signal processor development 77−18095
higher order coherence functions for photon counting distrib. 79−13934
image intensifier tube with self-scanned photodiode array, photoelectron counting 77−18090
impurity atoms in solids, photon antibunching in reson. fluorescence 79−43025
inert gas photoelectron counter, XUV intensity meas. 78−32842
intensified CCD photon counting array photometer 77−37964
intensified CCD test results 77−41318
intensity fluctuation linewidth, Jakeman-Pike approx., black-body and laser models 78−58960
intensity fluctuation spectrum, theory of registration *(Russian)* 78−1199
inverse source problems in optics, book 79−31821
inverse source problems in optics, book contrib. 79−31822
inversion problem in photon counting with dead time 80−99682
irradiance sensor, consisting of Si PIN photodiode and rhodamine B dye quantum counter, construction and expts. tests 78−32843
laser anemometry, flow statistics retrieval via photon correl. 77−3896
laser anemometry and other photon correlation data, stabilized model-fitting approach 80−58622
laser Doppler anemometry in internal combustion engine cylinder 79−77296
laser light signal through turbulent atm., photoelectron counting distrib. *(Japanese)* 77−50711
laser radiation scattered by atmosphere, photocount distrib. 80−9921
laser spectroscopy uses and applics. 77−57397
laser velocimetry, photon correlation signal processor 77−62035
lecture on introduction to quantum optics 78−25843
level crossing detection through photon counting distrib. second factorial moment meas. 80−99485
light scattered from microscopic regions, photon correlation spectroscopy 79−44933

photon counting continued
low-level imaging, optical signal detection and meas. 79−94350
low-noise photon counting system using photosil detector 77−45890
lyoluminescence meas. by photon counting system 79−97441
m-distributed optical signals, statistical props. and photoelectron counting distrib. 77−38809
magnetograph and polarimeter for stellar circular polarisation meas. *(Russian)* 78−65500
maximum photon antibunching in generalized coherent states 79−41358
microchannel plate, improved performance with resistive anode encoder 78−5104
microchannel plate as VUV photon and metastable atom detector, 1-0.1 Pa region 77−82618
microchannel plate image intensifier, quantum detection efficiency 77−83462
microchannel plate photomultipliers for plasma diagnostics 79−41077
microphotometer, automatic fluoresc., using image dissector tube, quantitative cytochem. appl. 79−97413
microprocessor-controlled counter, ODMR appl. 79−88992
microspectrophotometer for study of single vertebrate photoreceptor cells 80−12323
modified-triggered photocounting and its application to optical superheterodyne spectrum analysis 80−31865
modulation effects on counting distrib. 80−43307
multianode microchannel array photon-counting detectors 80−77869
multichannel photon counting image detector arrays 78−65970
multichannel spectrometer for optical spectroscopy of faint astronomical objects 77−22079
multidetector photon statistics 78−32873
nanosecond emission spectroscopy, developments 77−34037
noise immunity of digital optical communication lines receiving wholly coded messages *(Russian)* 78−87020
noiselike optical signals, photoelectron counting statistics and error rate characteristics 78−1178
non-classical effects in the statistical properties of light, review 80−99686
non-gaussian field, clipped time autocorrelation function of intensity fluctuations 80−106472
nonlinear detector effects on statistics of fluctuating signal 78−24735
nonlinear intensity conversion, photocount statistics 77−3636
nonlinear optical amplifier, coherent radiation statistical props. 80−99691
observatory scanning spectrophotometer *(French)* 78−20638
open system theory of photodetection 77−79790
optical communication, signal amplification, practical limits of photon counting 79−50234
optical heterodyning at single-photon level 79−26127
optical radiation source with rectangular intensity profile, estimate of coordinates 79−31819
optical time domain reflectometry by photon counting 80−95122
optically pumped ruby far IR quantum counter 77−38001
optimal light detector photocurrent analysis, quantum statistics, atmospheric 'seeing' conditions 80−53244
optimum photon detection with simple counting processor 78−27956
parametric frequency up-conversion with stochastic pumping, canonical model 80−53368
parametric generation, from quantum noise effect of photon statistics 78−25921
parametric processes, photon statistics of fields generated by correlated mode interf. 80−106500
phase screen statistical features from scatt. data, book contrib. 79−36851
phosphoroscope nanosecond IR detector, time-selection technique 79−49293
photicon, 2D array imaging detector for visible light, review of imaging characts. 79−45554
Photicon, new imaging optical detector 77−67499
photocounting distributions statistical props. for intensity modulated sources 79−72541
photodetection, open system theory, dynamics of field and atomic moments 78−70185
photoelectric counting as test of existence of photon 78−5440
photoelectric counting photon correls. and stimulated emission, comment 77−23639
photoelectric counting photon correls. and stimulated emission, reply 77−23640
photoelectric pulse statistics for Gaussian-Lorentzian light 78−54452
photoelectron counting statistics, theory, fully quantum, review 80−52312
photoelectron statistics, joint moment method, phase radiation 80−23647
photometer, high-speed, computerised, for 60 cm astronomical reflector *(Japanese)* 78−32345
photomulitplier meas. of threshold optical radiation fluxes, errors 78−12760
photomultiplier, FEU-106, one-electron response 77−87827
photomultiplier absolute spectral sensitivity in photon-counting mode 79−67383
photomultiplier afterpulses effect in coincidence systems 77−82583
photomultiplier one-electron characts. 78−58038
photomultiplier selection for time and one-electron operation 77−87828
photomultipliers for low light level appl. 79−45547
photon bunching in thermal radiation, temp. depend., photodetector thermal fluctuation 78−24748
photon correlation in nanosecond range using programmable digital counter, photomultiplier evaluation 78−54464
photon counting and fluctuation of molecular movement 79−29686
photon existence testing by photoelectric counting and nonexistence of photons 80−9842
photon fluctuations and interaction with solids 77−748
photon pulse delay estimation, non-regularity anal. 79−3334
polarisation meas. of low-intensity fluxes by photon counting 77−13795
polydisperse suspension, two-parameter size distribs. eval. using photon correl. data 79−92011
polymer solutions, random coil, intramol. fluctuations by photon correl. spectroscopy 77−48184
printing scalar, single channel, for photon counting 77−5919
proportional response photon counter, meas. of energy albedo of backscattered photons 80−99408
proportional response photon counter 80−87021
pulse counter, high-speed DC coupled, sensitivity and performance 79−89524
photon counting continued
pulse counting measurement systems, optimum parameters determ. 79−89523
pulse delay estimation, nonregularity 78−29157
pulse fluorimetry, mol. rot. correl. times determ., statistical accuracy 77−61777
pulsed reference source, for photon counting systems 77−3640
pyrometer, 1400K to above 2200K within 0.5K and 1.0K 80−52232
quadrant position sensitive photomultiplier with high detection efficiency 79−45546
quantum efficiency yields, automatic recording system 77−67489
radiation in phase space, statistical props. 79−64190
radiographic $CaWO_4$ intensifying screen, meas. of X-ray induced light photons emitted 80−41218
Raman scattering investig. of polaritons in solids 77−40238
Raman spectroscopy, pulsed, using Nd:YAG laser, photon counting compression effects 78−74086
Rayleigh spectrometer, minicomputer system using autocorrelation or FFT 78−41351
reflected-beam laser anemometry using photon correlator 80−106861
resonance light scattering, spectral props. and photon correls. 80−91510
resonant Raman scattering in laser fields of arbitrary strength, antibunching effects 80−23653
ring dye laser, optical bistability and first order phase transition 80−95918
ring laser, two-mode, intensity fluctuations meas. near threshold 78−55388
rocket exhaust anemometry, Doppler difference and two focus methods, correlator and photon counting 79−60084
ruby, optical pumped, tunable quantum counter for far IR radiation 77−53977
sampled photon counting with multilevel discrimination 79−6188
satellite solid-state imaging for meteorology and astronomy 77−39074
scaling props. of laser light, photoelectron and photon statistics 77−14729
scattered light spectroscopy, signal processing by add-subtract digital correlator 77−61053
scintillation delay curves meas., single photon counting *(Japanese)* 78−78555
scintillation detectors, improvement of light collection 79−45548
scintillation pulse shape meas. by single photon technique 79−35810
second-order coherence effects due to the superposition of two independent thermal light beams 80−23618
SEM, cathodoluminescence, detector system 80−101898
SEM measurements of minority carrier lifetimes at dislocations in GaP, employing photon counting 78−23109
short fluorescence lifetime meas. by single photon counting 77−5883
single-photon counter, with 9789 QB photomultiplier *(Chinese)* 80−27332
single-photon counting fluorescnece decay-time spectrometer 77−82620
single-photon counting system for measuring laser parameters 79−89915
small light flux, accuracy and reliability 77−74481
solid-state array and camera tube imagers compared 77−39090
speckle imaging, photon by photon, diffr. limited performance for large telescopes 79−53729
speckle interferometry S/N ratio, photon counting autocorrelation mode at low light levels 79−76613
spectroscopy of high power resolution by means of photon statistics *(Spanish)* 79−21818
spermatozoa mobility, photon correlation study 80−12063
statistical deviation of counted quanta due to dead time, calc. *(Japanese)* 77−10105
statistical deviations analysis, due to counter dead time *(Japanese)* 77−10104
statistical properties, appl. to scatt. problems 77−34864
statistics of photon count, detector temp. and field effect 80−74325
stellar electrophotometer, 50 MHz passband amplifier for photomultiplier 77−74434
stellar objects monitoring, using TV type photon counter, minicomputer-controlled *(Russian)* 80−31212
stellar speckle pattern statistics, photon counting techniques 79−25324
stimulated versus spontaneous emission as cause of photon correlation 77−34862
subnanosecond fluorescence lifetime meas., photon counting system 77−2699
subnanosecond single photon counting fluorescence spectroscopy using tunable dye laser excitation 78−86355
subnanosecond time-correlated photon counting with tunable lasers 78−45701
superconducting tunnelling devices as mm wave photon detectors 79−30554
superheterodyne spectrum analyzer with triggered photon counting method 79−80691
superposed coherent and chaotic radiation, computer simulation 80−58485
synchronous, automatic stipulation of precise measurement intervals circuit 77−18093
synchrotron radiation with single photon counting or phase shift techniques, for fluoresc. lifetime meas. 79−13841
system components evaluation 78−21215
T-density for speckle and photocounting statistics 78−50700
television systems, photon counting and analogue, with digital real time image processing 78−96402
thermal light with orthogonally polarised multiple-peak spectrum, intensity fluctuations 80−87303
thermal particles, multimode laser light scatt., photon statistics 80−99631
three-level quantum counters for far IR radiation 77−53977
threshold detection equivalence with and without dead time 80−32580
time interval photoelectron statistics, nongaussian scattered light 77−19177
time-resolved fluorescence spectroscopy using pulsed lasers 80−57393
transient emission spectra, observability in theory 78−55199
transient resonance Raman scatt., quantum theory, appl. to strongly coupled localised electron-phonon system 78−94412
tris(bipyridine)ruthenium(II)dichloride, fluoresc. decay meas. by high repetition rate gated photon counting 80−86402
tunnel junction mixers, quantum limited detection 80−18015
two photon coherent states in degenerate four wave mixing 80−5717
unclipped digital correlator constr. for photon correlation spectroscopy 80−57387

photon counting continued
vacuum UV fluorescence lifetime meas. instrument 77−49785
vacuum UV region, 120-200 nm, detection limit of apparatus *(German)* 78−45691
weak light flow, analysis of measurement methods *(Russian)* 78−45694
weak light signal detection by single photon counting *(Chinese)* 80−77873
weak optical laser radiation in random-pulse sequence, recording 77−37988
Cr III complexes phosphoresc. risetime meas. in near IR 77−41706
He-Ne laser photon statistics variation with cavity length 80−53265
Hg 6^3P_1 states, detection impact excitation cross section meas., using self calibrating apparatus 79−50135
K_2, $B^1\pi_u$ state radiative lifetime, quenching cross section, fluoresc., single photon counting 77−75202
$LaBr_3$:Pr, continuous wave and pulsed laser pumped Pr IR quantum counters 79−93219
$LaCl_3$:Nd^{3+}, cryst., appl. to phosphoroscope IR detector 79−49293
$LaCl_3$:Pr, continuous wave and pulsed laser pumped Pr IR quantum counters 79−93219
Na vapour, quantum counter, IR detection 78−30016
Pr^{3+}-based IR quantum counters, photon avalanche 79−97431
UF_6 admixture effect on N_2 and Ar excited state lifetimes 79−10281
YVO_4:Eu^{3+} phosphor, cathodoluminesc. and photon statistics 77−59621
ZnS:Ag, photon counting statistics of cathodoluminesc. light emission 79−24371

photon-deuteron interactions
see also photon-deuteron scattering
Coherent Tube Model for very high energy inelastic interactions of deuterons 77−18347
disintegration amplitudes with arbitrary number of EM multipoles 79−93437
$d(\gamma,\pi^0)d$ differential cross section, investigation of ΔN interaction in the deuteron 79−67597
$\delta d \rightarrow \pi^0_s$ multiple scatt. contrib. to threshold photoprod. 80−73718
$\delta d \rightarrow \pi^+ nn$, final state interaction effects *(Russian)* 78−41558
$\gamma \rightarrow \eta d$, differential cross-section calc. using resonance model 79−93432
$\gamma d \rightarrow d\omega$ or $pn\omega$, 3.9 GeV, cross sections, A_2 exchange amplitude 77−34168
$\gamma d \rightarrow \eta d$, coherent photoproduction impulse approximation 77−82749
$\gamma d \rightarrow K^+ \Delta n$, differential cross section, influence of Δn interaction *(Russian)* 79−394
$\gamma d \rightarrow nn\pi^+$, cross-section and asymmetry ratios in region of first resonance *(Russian)* 78−78196
$\gamma d \rightarrow np$, 300 MeV, dibaryon resonance manifestation, pseudoindependent amplitude elimination *(Russian)* 80−57612
$\gamma d \rightarrow np$, 400-700 MeV, p polarisation *(Russian)* 80−106046
$\gamma d \rightarrow pn$, 250 to 800 MeV, differential cross-section and proton polarisation, theoretical models 80−78081
$\gamma d \rightarrow pn$, 400 to 650 MeV, ang. depend. of proton polarisation and partial wave anal. of possible dibaryon resonances 79−58967
$\gamma d \rightarrow pn$, EM properties of πNN system, virtual π reabsorption 79−22109
$\gamma d \rightarrow pn$, proton polarisation energy depend., 400-700 MeV *(Russian)* 80−63000
$\gamma d \rightarrow pp\pi^-$, cross section, double pion photoprod. on one nucleon 78−70378
$\gamma D \rightarrow pp\pi^-$, π rescatt. through Δ(1236) for nucleon high momentum 77−57547
$\gamma d \rightarrow \pi^0 d$, 1 to 10 MeV above threshold 79−85454
$\gamma d \rightarrow \pi^0 d$, 450 MeV cross section asymmetry *(Russian)* 79−89171
$\gamma d \rightarrow \pi^0 d$, meson-exchange currents in photomesic reactions, relativistic many-body theory 80−422
$\gamma d \rightarrow \pi^0 d$, photoproduction amplitudes, cross-sections, asymmetry relations review *(Russian)* 78−54636
$\gamma d \rightarrow \pi^0 d$, recoil deuteron polarisation statistical tensors anal. 78−74348
$\gamma d \rightarrow \pi^+ nn$, photoproduction amplitudes, cross-sections, asymmetry relations review *(Russian)* 78−54636
$\gamma d \rightarrow \pi^- NN$, off-energy shell photoprod. amplitudes for reactions on bound neutrons 80−421
$\gamma d \rightarrow \rho d$, double scatt. at high energy, unstable particle scatt. amplitude 78−45929
ω, photoproduction at high energy, parton model, γ hadronic props. 78−74266
φ, photoproduction at high energy, parton model, γ hadronic props. 78−74266
ρ, photoproduction at high energy, parton model, γ hadronic props. 78−74266
$\pi d \rightarrow \pi^0 d$, 350-500 MeV, differential cross section asymm., impulse approx. with pion rescatt. terms 77−30389

photon-deuteron scattering
see also photon-deuteron interactions
Compton small-angle scatt. of 5 and 6 GeV photons on ^1H and ^2H 77−46052

photon echo
advance and retardation effects, ruby crystal expts. *(Russian)* 78−71158
anomalous time shape, induced by two successive light pulses 78−18021
atom, coherent transients, spherical tensor treatment 79−26940
atom, Stark effect, modulation light wave vibrs. *(Russian)* 79−98027
atomic collisions, feasibility of investigation by photon-echo technique *(Russian)* 77−79673
atomic resonance interaction, photon echo meas. 79−27061
atomic system, photon echoes in standing-wave fields: time separation of spatial harmonics 80−9759
atomic system, transient four-wave mixing and real time holography 79−55171
atomic vapour, obs. of optical echoes generated by standing-wave fields 80−23755
coherent optical spectroscopy 78−1112
coherent optical transients, atom, mol. and solid spectroscopy using lasers 77−53986
coherent transients by laser freq. switching 78−66873
collisional optical coherence transfer, laser spectroscopy 77−42360
crystals with paraelectric impurities, superradiative transitions, acoustic and EM excitation 78−66872
depolarising collisions effect in mag. field *(Russian)* 79−59776
double-quantum photon echo, adiabatic vector model 77−23719
excited molecular ensemble, photon echoes, optical coherence in electronic transitions 77−58392

photon echo continued
fluoromethane, rotary photon echoes 78−25929
gas, photon echo in a magnetic field at small areas of the exciting pulses 80−95961
gas, small-area exciting pulses *(Russian)* 79−76766
gaseous media, rephasing phenomena, generalised theory 80−23757
grating echoes, in Na gas, the temporally recurrent spatial ordering of at. population 79−98447
high resolution light echo angular spectroscopy, inhomogeneously broadened lines 80−43406
inert gas plasma, weakly ionised, photon echo relax. obs. in RF discharge 80−43986
irreversible relaxation, effect on light echo type signals on multipulse excitation *(Russian)* 77−68245
irreversible relaxation time contribution to photon echo decay 80−58646
localised electron-phonon system, strongly coupled, photon echo phenomenon 80−64118
many-level system, spontaneous coherent responses, from states involving super-radiative phase transitions *(Russian)* 78−71069
mixing collisions and quantum beats, spectral line shifts 77−34914
modulation echo spectroscopy in double reson. mode 80−1284
molecular crystals, spectroscopy appl. *(Dutch)* 78−71156
molecular optical spectroscopy, by 90° photon echo, during reson. scatt. and radiationless transitions 78−86978
molecules, large optical free induction decay, photon echoes 78−37945
molecules, luminesc., photon echoes and coherence 79−31586
naphthalene: pentacene, intermol. interaction dynamics and optical dephasing 80−64112
naphthalene, in durene and perdeutero-naphthalene mixed crystals, photon-echo decay 78−42388
napthalene:pentacene, zero-phonon transition bottlenecks, photon echo detect. 80−33092
nutational photon echo 80−28283
Optical nutation and phonon echo by phase shift of a light wave 80−78914
optical spectroscopy of crysts., review 80−83648
optical wave front, time reversed, generation by backward wave photon echoes 78−87105
organic mixed crystals, transverse relax. and freq. shifts of optical transitions 78−84599
paraelectric induction theory, strong inhomogeneous broadening 80−108168
particle motion effect on transient optical phenomena 80−1283
pentacene, in naphthalene (p-terphenyl), picosec. coherent transients obs. 79−46013
pentacene−p-terphenyl, optical dephasing, optical mixing-detected ps photon echoes obs. 78−71155
pentacene in naphthalene (p-terphenyl), mol. mixed crysts., optical dephasing and vibronic relax. 80−95957
pentacene in naphthalene crystal, relax. of vibronic states, photon-echo and ab absorpt. relax. expts. 79−95807
pentacene-d_0, -d_{14}, in p-terphenyl-d_0, mixed cryst., photon-echo relax. 77−72034
phase-conjugate wave front generation using photon echoes 80−58650
picosecond, stimulated from accumulated grating 80−33092
polarisation properties, for small exciting pulse areas *(Russian)* 79−23030
polyethylene, microwave photon echo 80−66330
pulse formation theory *(Russian)* 79−55192
resonant gaseous media, photon echo meas. of population, orientation, alignment relaxation times *(Russian)* 80−91863
review *(Japanese)* 77−745
RF superradiance generated to optical pulses under photon-echo conditions 80−95858
ruby, echo intensity depend on mag. field, Cr^{3+} and ^{27}Al nuclei superhyperfine interaction 79−68419
ruby, light echo signal correlation with exciting pulse shape *(Russian)* 80−106576
ruby, modulation in μs pulse separation regime 78−30029
ruby, optical nutation echoes, Stark switching obs. 80−69467
ruby, photon echoes, optical free induction decay, Stark switching technique 79−7182
ruby, primary and stimulated photon echo generation 79−10364
ruby, reversed light echo due to two pulse laser resonance excitation *(Russian)* 80−87439
ruby, Stark induced optical transients, photon echo 78−33785
ruby, stimulated photon echo modulation 80−38074
ruby crystal, photon echo generation, control method 80−87440
smectic A liquid crystals, thermooptical recording, echo images 80−91928
space-time coherence reestablishment of laser radiation 77−34915
spatial synchronism for exciting pulses with spherical wavefront 79−64288
stimulated optically induced nucl. spin polaris., optical coherence storage 80−58649
stimulated photon echo under two-quantum resonance 80−28284
three frequency stimulated photon echoes 79−81493
three level system, photon echo with relax. 80−43405
three-level system, photon echo modulation 79−18486
three-level system with adjacent optically allowed transitions *(Russian)* 80−33093
transitions, identification by photon-echo technique 80−78915
tri-level echo, multilevel systems inhomogeneously Doppler broadened 78−17774
triphenylmethyl, in triphenylamine, photon-echo decay, in lowest doublet-doublet electronic transition 77−79903
triphenylmethyl in triphenylamine, photon echo stimulated from optically induced nucl. spin polarisation 79−76460
two-level degenerate system, superradiance 78−46553
two-level system, backward photon echo and free induction decay generation 80−99805
two-level system, optical coherent transients 77−19222
two-level system, optical echo signal form. in single-pulse and stimulated excitation regimes 80−58647
two-photon optical echo effect, appl. in nonlinear echo spectroscopy 80−48357
two-pulse photon-echo decay due to weak velocity-changing collisions 79−55190
ultrahigh resolution spectroscopy using light echo effect *(Russian)* 78−70774
vacuum, memory effect *(Russian)* 77−14782

photon echo continued
wavefront correction 78−9417
Cs, $6S_{1/2}$-$7P_{1/2}$ transition, photon echo polarisation rotation in mag. field 78−22180
Cs, $7P_{3/2}$-$6S_{1/2}$ transition, photon-echo quantum beats obs. 80−23373
Cs vapour, photon echoes on 6S-7P transitions 77−19369
Cu_2O, self-induced transmission and radiation echo for intraseries and interseries exciton transitions 78−5528
He plasma, photon echoes obs., collisional relax. on $2^3S_1-3^3P_{012}$ 79−19089
I_2+I_2, optical coherent transients detected by frequency-switched tunable laser 77−54762
$LaF_3:Pr^{3+}$, nuclear hyperfine interactions, photon echo relax. obs. 79−59771
$LaF_3:Pr^{3+}$, optical line narrowing by nuclear spin decoupling, photon echo meas. 80−48353
$LaF_3:Pr^{3+}$, photon echo lifetimes, conc. independ. 78−74951
$LaF_3:Pr^{3+}$, photon echo decay as modulation process 78−79078
$LaF_3:Pr^{3+}$, photon-echo quantum beats in $^3P_0$-$^3H_4$ transition 79−86219
$LaF_3:Pr^{3+}$, spectroscopic and relaxation character of $^3P_0$-$^3H_4$ transition, photon echo 80−39897
$LaF_3:Pr^{3+}$, ultrahigh resolution photon echo spectroscopy 80−28285
$LiAl_5O_8:Cr^{3+}$, self-induced transparency and light echo *(Russian)* 77−62016
Na, backward-wave three-pulse echo in two-level system, Ar collisions effects 79−64289
Na, D-lines, inert gas broadening, photon echo meas. 80−91475
Na, excited state photon echo relax. 78−37606
Na, vap., picosec. photon echo and self-induced transparency 79−46015
Na, vap., two-photon echo, quantum beats, superposition relax. 78−83041
Na vapour, focusing and phase conjugation of photon echoes 79−23028
Na vapour, laser induced population grating 80−69466
Na vapour thin cell forward phase conjugation obs. 80−78917
Na+CO velocity-changing collisions, stimulated photon echo obs. 79−81258
Na+He, Na ($3S_{1/2}$-$3P_{1/2}$) photon echo, collision vel. changes and dissimilar electronic states superposition 80−32803
Na($3S_{1/2}$,$3P_{1/2}$)+He, total cross section, stimulated photon echo obs. 79−76503
Rb_2, vapour, laser radiation absorpt. superradiance 78−46553
SF_6 10.5 μm spectrum, high-J assignments, identification of levels pumped by CO_2 P(12) and P(22) 78−70837
SF_6, photon echoes, polarisation and amplitude decay meas. 77−88872
SiF_4, photon echoes, polarisation and amplitude decay meas. 77−88872
YAG:Nd^{3+}, formation of photon echo using dye laser 77−23720
$YAlO_3:Pr^{3+}$, ultrahigh resolution photon echo spectroscopy 80−28285

photon-hadron interactions
see also photon-hadron scattering; photon-nucleon interactions
charm photoprod. with linearly pol. photons, QCD calcs., gluons 80−68464
generalized vector dominance, photon-hadron interaction anal., review, book contrib. 80−47265
hadronic props. of photons, book contrib 78−82217
hadronics props. of photons, effect of large intermediate masses in hadron-mediated photon-nucleus interaction 80−27625
heavy quark prod. in photoproduction, QCD model, possible large p_T process connection 78−78137
heavy vector meson photoprod., vector meson dominance model anal., Regge trajectories 78−78195
high energy photon absorption cross section for matter, review *(Japanese)* 78−74506
high energy photons, particle prod., review *(German)* 79−40779
high-energy, hadronic struct. of photon 77−10254
high-energy interactions, hydrodynamical model *(Russian)* 77−229
lepton pair production, perturbative QCD, twist-2 photon operator, parton subprocesses 80−73716
multibody channels, review, book contrib. 80−47303
multiperipheral parton model, deep inelastic processes 80−82961
pulsars, hadronic photoabsorpt. and pair production 78−12261
pulsars, photohadronic absorpt. reactions rel. to pair prod. in magnetosphere 79−44515
QCD, charm photoprod., ψ, D, F etc. prod., sum rules, cross sections 78−58169
QCD Compton effects, quark and gluon jets 80−32101
quark fragmentation distribs., meson, baryon and photon reactions 77−74655
$SU(4)_W$ symmetry, dibaryon coupling constants for γ, π and baryon interactions *(Russian)* 80−13329
$SU(6)_W$ structure of baryonic reson. photocouplings duality constraint 79−71649
sum rules, semiclassical method, bound state energy relations 78−70308
γg, Higgs boson photoproduction 80−78068
$\gamma\pi$, hadron photoprod. and saturation of sum rules *(Russian)* 79−49529
$\gamma\pi\to\pi\pi$, obs. in $A(\pi^\pm,\pi^\pm\pi^0)A$ *(Russian)* 79−9639
$\gamma_{virtual}$ hadron$\to\pi^\pm$ anything, sum rules using PCAC 77−34161

photon-hadron scattering
see also photon-hadron interactions
Compton scattering amplitude constraints, below photoprod. threshold 80−32102
multipole polarisabilities of hadrons from Compton scatt. amplitudes 80−13311
$\gamma\pi$ high multipole polarisabilities from Compton scatt. amplitudes 79−85301

photon interactions *see photon-deuteron interactions; photon-hadron interactions; photon-lepton interactions; photon-nucleus reactions; photon-photon interactions*

photon-lepton interactions
see also photon-lepton scattering
hydrodynamic theory of high energy interactions *(German)* 80−406
J particle discovery, review *(Hungarian)* 79−17778
three-photon coalescence at electron 80−91026
X-ray generation distribution formulae *(Danish)* 80−47269
e^+e^- photoprod., book contrib. 79−21889
$\gamma\to\nu\bar{\nu}$ in strong mag. field, absorpt. coeff. and energy loss rate 77−22728
γe collisions, jet production, QCD study 79−89142
$\gamma e\to\gamma\gamma e$, polarised photon splitting on unpolarised electron *(Russian)* 79−371

photon-lepton interactions continued
$\gamma e\to\gamma\mu$, muonic number nonconservation, pole model anal., total and differential cross sections *(Russian)* 79−80817
$\gamma e^-\to e^-\nu\bar{\nu}$, energy spectra of recoil fermions, Weinberg-Salem model 78−12895
$\gamma e^-\to e^-\nu\bar{\nu}$, weak current anomalous interaction with EM field *(Russian)* 77−6104
$\gamma e^-\to\nu\bar{\nu}e^-$ in mag. field *(Russian)* 77−26506
$\gamma_1 e^-\to\gamma_2\gamma e^-$, plane quantized EM wave, differential and total cross sections *(Russian)* 77−74665
$\gamma\gamma e$, fusion of polarised photons at unpolarised electron *(Russian)* 77−79260
$\gamma\nu$ weak interaction, spontaneous breakdown of γ and gauge symm. at finite temp. 78−70299
e^-e^+ pair photoproduction in crystals by circularly polarised γ-quanta 78−17005

photon-lepton scattering
see also photon-lepton interactions
Compton scattering of laser photons on relativistic electrons, energy spectrum *(Japanese)* 77−13908
electron-laser photon elastic scatt., Coulomb background 77−74666
electron-photon scattering, symmetrical formulation in relativistic quantum mech. 77−67599
laser-electron scattering, monochromatic photon beam generation by high energy electron beam *(Japanese)* 78−74821
photon-electron scattering, opacity due to electron correls. 77−64634
quasars and active galactic nuclei, magnetic flare model, magnetised accretion disc around massive black hole 80−22113
$e\gamma$ scatt., coherent states and quantum nonperturbing measurements 79−315
γe Compton and Thomson scatt. in strong magnetic fields, differential cross sections, neutron star appl. 79−67530

photon-nucleon interactions
see also photon-nucleon scattering; photon-proton interactions
contact EM terms and nuclear shadowing of high energy photons, absorpt. by nucleons and nuclei 77−49980
EM probes of nucleons, photo- and electro-excitation, quark model anal. of nucleon struct. 79−49520
equivalent photon spectra, hydrogen or complex nuclear target 77−6129
hadron photoproduction nondiffractive processes, review, book contrib. 80−47313
high p_T hadronic jet photoprod., QCD anal., quark and gluon jets 80−42474
inclusive γN collisions, charmed meson pair prod., semileptonic decay spectra 77−49952
lepton pair photoproduction in thick target, Monte Carlo simulation 78−21432
neutral current effects in Berthe-Heitler pair prod. 78−33022
nuclear shadowing of electromagnetic processes, vector dominance model anal., review, book contrib. 80−47266
photon shadowing in nuclei, vector meson dominance model 79−89162
photon-nucleus scattering, photon shadowing, two component model, GVMD model 77−46159
physical pion low energy electro- and photoprod., Ward identity, chiral symmetry breaking struct. 80−5003
physical pion low energy photo- and electroprod., photoprod. phenomenology, quark mass 80−5004
pion production, multipole amplitudes, dispersion relations, Δ(1232) production 80−5002
polarisation, lepton and photon nuclear interactions, bremsstrahlung, pair production *(Russian)* 77−88104
resonance photoproduction, Melosh transformation 77−46059
s-channel helicity conservation at $\gamma V,\gamma\gamma$ and NN vertices, vanishing of spin-zero covariant coupling 79−40691
t-flavoured meson production in photonuclear and pp collision 80−22623
total cross sections by vector meson dominance model, contrib. of $q\bar{q}$ and $c\bar{c}$ 78−58192
two gluon mechanisms, quarkonia, glueballs and Higgs scalars 80−78077
vertices in reactions involving higher spin particles, gauge invariance 77−41844
virtual photon-nucleon scatt. anal. for spin 1/2 parton in covariant parton model 80−4966
D^0 prod. and decay in high energy photon interaction, mass and decay time 80−42478
$\gamma\to\pi n$, threshold-450 MeV, energy dependent multipole anal. 80−78082
$\gamma+d\to p+n+\pi^0$, interactions of nucleons in final state 78−37220
$\gamma+N\to N+\pi$, spatial parity nonconservation in π-meson photoproduction *(Russian)* 77−61301
$\gamma^*N\to\psi N$, gluon momentum, spin, parity and coupling 80−42395
$\gamma d\to\pi^-NN$, off-energy shell photoprod. amplitudes for reactions on bound neutrons 80−421
$\gamma^3He\to\pi^+\pi^-{}^3He$, E<800 MeV, gauge invariant one-pion-exchange model 77−18298
γN, exclusive photoprod. reactions, Okubo-Zweig-Iizuka rule 80−95277
γN, inclusive pion production due to $\gamma q\to\pi q'$ process, quark-parton model *(Russian)* 80−78073
γN, jet cross sections and quark current-photon pointlike coupling, sum rules 80−32104
γn, n electric polarisability, from photoabsorption cross-section 80−57597
$\gamma N\to\pi^\pm$+anything, 9-18 GeV, forward hemisphere 77−6134
$\gamma N\to DC_1$, charm particle photoproduction near threshold *(Russian)* 78−8675
$\gamma N\to\Delta$ magnetic dipole photoexcitation, singular integral equations 78−50040
$\gamma N\to\Delta\pi$, mag. dipole photoexcitation, singular integral eqns., polynomial ambiguity 80−57608
$\gamma N\to e^+e^-$, total cross-section near threshold determ. *(French)* 78−455
$\gamma N\to$jet+X, QCD cross sections 80−73715
$\gamma N\to K^+\Sigma$, meas. of asymmetries and cross sections using 16 GeV linearly polarised photons 80−13318
$\gamma N\to K^\pm$+anything, 9-18 GeV, forward hemisphere 77−6134
$\gamma N\to l^+l^-X$, pol. γ, neutral current effect, Weinberg Salam model calcs., p violation 80−5000
$\gamma N\to l^+l^-X$, polarisation effects on P-violating asymmetry in Weinberg-Salam model 80−32055
$\gamma N\to$large p_T jets, QCD predictions for processes involving real photons 79−6330
$\gamma N\to$lepton pairs, weak neutral currents anal. 78−8670
$\gamma N\to\mu^+\mu^-N'$, E_γ=20-400 GeV, equivalent photon spectra 77−6129

photon-nucleon interactions continued
$\gamma N \rightarrow \mu\bar{\mu}X$, QCD cross sections 80−73715
$\gamma N \rightarrow NX(2.8)$ as possible means of $X \rightarrow 2\gamma$ width determ. *(Chinese)* 77−57541
$\gamma N \rightarrow N\pi$, P-odd effects, weak interaction *(Russian)* 78−54638
$\gamma N \rightarrow N\pi$, P-odd multipole amplitude, dispersion relations *(Russian)* 79−93435
$\gamma n \rightarrow n\pi^+\pi^-$, threshold to 1 GeV, Δ production 77−26532
$\gamma N \rightarrow \omega\Delta$, pion exchange mechanism anal. 77−82750
$\gamma N \rightarrow p$+anything, 9-18 GeV, forward hemisphere 77−6134
$\gamma n \rightarrow p\pi^-$, to 500 MeV, multipole anal. near P_{33} reson. *(Russian)* 77−74695
$\gamma n \rightarrow p\pi^-\pi^0$, threshold to 1 GeV, Δ production 77−26532
$\gamma N \rightarrow \phi N$, pole-cut nature of Pomeron 77−6136
$\gamma N \rightarrow \phi N$, suitability of reaction for revealing pomerons pole-cut nature 79−13091
$\gamma N \rightarrow \phi\pi^0 N$, diffractive photoprod., OZI rule violation and cryptoexotic mesons 79−71760
$\gamma n \rightarrow \pi^- p$, 0.9-1.65 GeV, pol. γ, cross section asymmetry *(Russian)* 80−86728
$\gamma n \rightarrow \pi^- p$, 250 to 500 MeV, multipole anal. *(Russian)* 77−10266
$\gamma n \rightarrow \pi^- p$, 250 to 790 MeV, cross section features 77−46053
$\gamma n \rightarrow \pi^- p$, 700 MeV, polarised neutrons, target asymmetry meas. 77−13967
$\gamma n \rightarrow \pi^- p$, 700 to 1200 MeV, recoil proton polarisation 80−78075
$\gamma n \rightarrow \pi^- p$, 850 MeV, target asymmetry meas. 78−21438
$\gamma n \rightarrow \pi^- p$, proton polarisation in $^2H(\gamma,np)$ *(Russian)* 78−41700
$\gamma n \rightarrow \pi^- p$ reaction cross-section asymmetry in photon energy range 0.9 to 1.65 GeV *(Russian)* 80−32108
$\gamma n \rightarrow \pi^-\pi^0 p$, Chew-Low amplitude correction 77−2844
$\gamma N \rightarrow \pi^+ X$, QCD cross sections 80−73715
$\gamma N \rightarrow \pi^+ n$, meas. of asymmetries and cross sections using 16 GeV linearly polarised photons 80−13318
$\gamma N \rightarrow \pi^+\pi^- \Delta$, EM mixing effects, dynamics of vector meson prod. *(Russian)* 78−58191
$\gamma N \rightarrow \pi\Delta$, Δ-isobar density matrix *(Russian)* 78−45932
$\gamma N \rightarrow \pi\Delta$, low energy prod. and Δ-N axial transition vertex 77−49981
$\gamma N \rightarrow \pi\Delta$, meas. of asymmetries and cross sections using 16 GeV linearly polarised photons 80−13318
$\gamma N \rightarrow \pi\Delta$ reaction amplitude, equivalence theorems *(Russian)* 80−52522
$\gamma N \rightarrow \pi N$, backward π prod., effective pole model phenomenological study 79−3030
$\gamma N \rightarrow \pi N$, dispersion rels. by method of Pade approx. 77−34166
$\gamma N \rightarrow \pi N$, fixed Regge singularities 77−74694
$\gamma N \rightarrow \pi N$, P-odd partial amplitudes, dispersion relns. *(Russian)* 79−85304
$\gamma N \rightarrow \pi N$, resonance region photoprod., dispersion model, M1 and E2 photoexcit. $N \rightarrow \Delta(1236)$ 78−70377
$\gamma N \rightarrow \psi N$, spin and mass depend. of constituent and phenomenological models 77−61304
$\gamma N \rightarrow \psi(3.1)$+anything, cross section and N charmed quark composition 80−423
$\gamma n \rightarrow \rho^- p$, ρ-meson as dormant Goldstone boson 80−368
$\gamma n \rightarrow \rho^0(p\pi^-)$, 7.5 GeV, cross channel isospin amplitude meas. and anal. 77−18299
γn to 5.3 GeV, multipion and strange particle prod., reson. 77−10261
$\gamma_v N \rightarrow \pi^\pm X$, current fragmentation region, quark cascade model of deep inelastic lepton-nucleon scatt. 78−25052
$\Gamma_{pol} N \rightarrow \pi^\pm N$, weak neutral interactions, QCD renormalisation 79−93433
$\gamma p \rightarrow p\nu\bar{\nu}$, energy loss from stellar bodies through ν-prod. by second class weak neutral current 79−35997
$\gamma p \rightarrow \pi^0 p$, recoil polarisation meas. using C plate and liq. H_2 polarimeters 79−93898
$\lambda n\gamma(Z)$ vertex in vector-like model of weak and EM processes, appl. to K decay 77−6071
$\nu N \rightarrow \pi^\pm \Delta$, dynamical model 79−401
ω, inelastic photoprod., 7.5-10.5 GeV, with Δ(1236) and higher masses 78−45930
π photoproduction, multichannel N/D model fit, Δ^+ pole parameters 77−10265
$\pi^\pm$ photoprod., low energy, emission ang. depend. *(Russian)* 80−57769
ψ photoproduction by nucleons and nuclei, soliton model *(Russian)* 77−46071
$\rho^\pm$ inelastic photoprod., 7.5-10.5 GeV, with Δ(1236) and higher masses 78−45930
$\gamma N \rightarrow \eta X$, 9.7 GeV, inclusive η photoprod. on H- and ^2H-targets, ρ^0-dominance model anal. 79−63486
$\gamma N \rightarrow \eta\pi^\pm$, 9.7 GeV, one-pion-exchange model 78−25054
$\gamma n \rightarrow \pi^- p$, photoproduction amplitudes, cross-sections, asymmetry relations review *(Russian)* 78−54636

photon-nucleon scattering
see also photon-nucleon interactions; photon-proton scattering
Compton amplitudes, $\pi^0 \rightarrow 2\gamma$, $\eta^0 \rightarrow 2\gamma$ and N EM polarisabilities 77−18289
cross sections in dispersion-relation anal., geometrical scaling 78−74260
$\gamma^* N$ scattering amplitude, nonreson. part, dispersion sum rule with derivative *(Russian)* 78−66121
γN, inelastic virtual Compton scatt., quark struct. 79−89164
$\gamma NN \rightarrow \gamma NN$ forward scatt. amplitude and generalised optical theorem, dispersion relations 79−93446

photon-nucleus reactions
for inelastic photon-nucleus scattering, see "photon-nucleus scattering"
see also photodisintegration; photon-deuteron interactions; photon-nucleon interactions
(γ, p) reactions at intermediate energies, Δ(1232) contrib. 77−18522
A=2, 4, 16, photonuclear sum rule enhancement factor, Hartree Fock, Bethe-Goldstone eqns. 79−3137
A=63 to 238, photoprod. of ^{24}Na, mean cross sections, 400 to 1000 MeV 77−41952
A dependence of photoabsorpt. processes, from inelastic electron and muon scatt. studies 77−82911
activation yield curves of photonuclear reactions for multielement photon activation analysis 79−20490
baryonic inclusive spectra in hadron-, photon- and HI-nucleus collisions, fireball model 80−86892
bremsstrahlung spatial distribution in water and water-iron by 22 MeV electron bombardment, meas. with activation detectors 77−57754
bremsstrahlung-induced reactions in nuclei with A=27-238, 450 MeV to 2.2 GeV *(German)* 78−33164

photon-nucleus reactions continued
cascade model, space-time model, tests and predictions 80−68633
Compton excitation of nuclear levels, cross section estimation *(Russian)* 79−49620
conference on nuclear interactions, Canberra, Australia (Aug.-Sep. 1978) 80−4476
conference on nuclear physics with EM interactions, Mainz, Germany (June 1979) 80−22145
contact EM terms and nuclear shadowing of high energy photons, absorpt. by nucleons and nuclei 77−49980
continuum shell model calcs. of particle emission threshold effects, cross section, line shape of resonances 78−46014
Coulomb correction to electron pair prod. by intermediate energy photons 78−13060
cross sections, use of method of ordered risk minimisation 77−41951
cross-section determ. in near-threshold region by iteration method modification *(Russian)* 77−18523
cross-sections, 5 to 500 MeV and nuclear research bibliography 78−29338
crystal nuclei, e^+e^- and e^- bremsstrahlung photoprod. cross sections, longitudinal polarisations 79−75969
deep inelast. electron scatt., nucleon polarisabilities 77−82919
deformed nuclei, photoreactions as struct. probe 77−2975
differential polarisation coefficients for $(\gamma,\vec{X})$ reactions 80−73838
differential polarisation coeffs. 78−4926
dipole sum rule, relation to photoabsorption of nuclei 78−17111
E1 giant resonance of deformed nuclei in the region $150<A\leq186$ *(Russian)* 78−78348
E1 giant resonances, features 77−79350
e^+e^- angular distribution of e^+e^- pairs produced by linearly polarized photons *(Russian)* 79−40904
electric dipole sum rule in correlated nuclear matter 80−83056
electro- and photonuclear EM sum rules 80−22810
electron pair production, 1-10 GeV, total cross section meas. 80−78280
electron pair production, cross section calc. on nuclei in range $1\leq Z\leq92$ 80−503
electron pair production, screening corrections for intermediate, high energies, using relativistic form factors 78−93986
electron-positron pair, and photon, formation from photon in nuclear field *(Russian)* 79−22267
electronuclear sum rules 77−82906
emulsions, cross section for ^8Be production for $E_\gamma=1.5$ to 4.5 GeV *(Russian)* 77−74834
equivalent photon spectra, hydrogen or complex nuclear target 77−6129
explosive r process cooling process 78−69791
few nucleon systems, intermediate energies 77−79363
few-nucleon systems studied with electromagnetic probes, future prospects 79−71809
fission products, photoneutron spectra, fission of U, Pu 77−23127
gamma beam facility from Frascati linac positron beam 79−72034
gamma-rays, half-life vs. energy map, photon activation anal. appl. 77−16883
giant analogue resonances in medium and heavy nuclei, intermediate struct. 78−62517
giant dipole resonance, isospin shift of energy 77−50111
giant dipole resonance, role of compound nucleus levels *(Russian)* 78−25164
giant dipole resonance intermediate struct. using (n,γ) and (γ, n), Brink hypothesis test 80−63150
giant E1 resonance, Galilean invariant pairing 77−88094
giant multipole reson. fragmentation over two-phonon states in spherical nuclei 78−575
Glauber screening eqns. in fast backward particle prod. in high energy processes, role of short range nucleus struct. 79−63670
hadron photoproduction on targets H-U, nuclear shadowing, VMD model comparison 77−82748
hadron-mediated, effect of large intermediate masses 80−27625
heavy isotope photofussion, delayed neutrons kinetic functions 79−63709
heavy lepton pairs photoprod. and decay, energy and ang. distribs. of decay leptons 77−41836
high energy photon absorption cross section for matter, review *(Japanese)* 78−74506
high energy photons, particle prod., review *(German)* 79−40779
high-energy interactions, hydrodynamical model *(Russian)* 77−229
hydrodynamical model for high-energy interactions *(Russian)* 77−229
inclusive proton production, A-dependence, momentum spectra, max. bremsstrahlung energy 2.0 to 4.5 GeV *(Russian)* 77−34287
intermediate energies, work at Saclay, facilities and expts. 77−61636
intermediate energy reactions as struct. probes with p,πK,γ,e projectiles 77−88107
isobar propagation and collective effects, pion-nucleus and photonuclear investigation 80−22676
isoscalar giatn resonances, sum-rule approacH 77−82898
Jastrow correlations and nuclear photoeffect 78−4927
laser-induced resonant absorption of γ radiation 80−18290
level lifetime determ. by reson. fluoresc. under bremsstrahlung bombardment *(French)* 77−54179
light nuclei, total photonuclear cross sections 79−71841
light nuclei photonuclear reactions on ^{27}Al, ^{28}Si, ^{31}P, ^{32}S, ^{40}Ca targets, residual nuclei yields *(Russian)* 77−61399
mass yield formula for intermediate energy photospallation of medium weight nuclei 78−29445
medium energy, above giant dipole resonance, survey 77−79358
medium nuclei, photoproton spectra and preequilib. decay, microscopic theory 80−47464
meson exchange current theories 79−71798
mesonic and relativistic effects in the nuclear electromagnetic interaction 80−22818
mesonic effects in photonuclear sum rules, book contrib. 80−476
neutrino pair photoprod. in strong mag. field, pulsar neutrino luminosity *(Russian)* 80−68648
neutron dosimetry, photointerference corrections for reactor pressure vessel lifetime studies 80−99345
neutron focus in radiation field of relativistic channelled particles 79−85852
neutron production by electron linear accelerator beam, bremsstrahlung and (γ,n) processes *(Japanese)* 78−78532
neutron resonances, partial E1 radiative strength functions, shell and optical model interpretation *(Russian)* 77−82895
nucleon form factors, Lorentz invariance and nuclear photoabsorpt. 77−88110

photon-nucleus reactions continued
one-particle formalism in continuum approach for photonuclear cross-section calcs. 80−37355
optical model description, photon shadowing suppression 77−46158
p-nuclei, low-temp. photonuclear nucleosynthesis in degenerate H burning zones rel. to novae 78−57540
photo-nucleon spectra, shell and pre-equilibrium decay model of giant reson. decay *(Russian)* 78−579
photoabsorption, σ_{-2} sum rule, gauge invariance and locality 77−34286
photoabsorption, exchange current effects on orbital g-factor and E1 sum rule 77−41950
photodisintegration and π photoprod. coincidence expts. at Bonn 500 MeV synchrotron 80−22815
photoeffect, simple model, various cross-sections 77−30553
photon shadowing in nuclei, vector meson dominance model 79−89162
photon splitting cross sections in nucleus Coulomb field 80−32041
photoneutron reaction cross sections for 1d-2s shell nuclei, isospin fission of GDR *(Russian)* 77−14020
photoneutron reactions near threshold, optical model, review *(Russian)* 77−82904
photonuclear data index 1973-1977 79−6568
photonuclear energy integrated cross-sections, calcs., A=2-40 77−50110
photonuclear reaction cross section, one particle in continuum approach 79−93604
photonuclear reactions review, giant dipole resonances and cross sections 80−5125
photonuclear reacts., conf., International school, Erice, Italy, 1976 77−88111
photonuclear reacts., coupled channels method *(Russian)* 78−50153
photonuclear resonances, energy correction for unfolded cross-section data 77−10387
photonuclear sum rule, spin current contribs., strong violations 80−18291
photonuclear sum rules from continuum calcs., dependence on residual interactions 80−22807
photoprocesses in few-nucleon systems, exchange meson currents role *(Russian)* 79−22269
photoproduction of negative pions, 510 to 750 MeV 78−74347
photoproduction reactions, energy depend. determ. by quasimonochromatic photon beam *(Russian)* 79−75970
pion photoprod. near threshold 77−14101
pion photoproduction on nuclei in Δ(1236) region, nonrelativistic operator 77−41949
pion production thresholds, pseudoscalar and pseudovector Lagrangian densities 78−29449
pre-equilibrium particle decay in photonuclear reactions 78−25173
reaction mechanisms, 40 to 140 MeV, shell model based description 77−79360
real and virtual photons, Weizsacker-Williams method, Moller potential 77−79361
real photon expts. from continuous wave accelerator 80−42635
review of photonuclear research at Lund and future accelerator plans 77−82907
S-matrix element transformation, particle polarisation in photonuclear reactions 79−89293
Saclay linac, photon beam prod., 10-100 MeV, giant dipole resonance *(French)* 79−523
semileptonic weak and EM interactions, multipole operators, HO single particle matrix elements 80−73840
shadowing in electroproduction, geometrical origin, virtual photon generation 77−82913
shadowing in hadronic photoproduction cross section in C, Cu, Pb, 20 to 185 GeV 79−30823
shadowing in photoabsorpt., generalised vector dominance model 77−2976
shadowing in photon-nucleus scatt., two component model, GVMD model 77−46159
shell model continuum calcs., centre of mass problems 77−82909
spallation, A=23 to 127 targets, mass yield distrib. 80−73835
spallation reaction and its appls. *(Japanese)* 78−74345
spallation reactions, intermediate energies, isomeric cross-section ratios 77−41954
spin-orbit interaction, independent particle model of nuclear Fano effect 80−519
sum rules 77−79362
three-nucleon systems, EM processes, total photoabsorption cross sections 79−71806
total photoabsorpt. cross section meas. and results 77−82908
total photoprod. cross sections for E>4 GeV, review, shadowing in heavy nuclei 78−78186
two-nucleon system EM processes, baryon resonances 77−79364
vector dominance model, book contrib 78−82335
vector mesons, photoprod., book contrib. 79−21889
yield function anal. by modified least struct. method 77−79521
$d(\gamma,\pi^0)d$ differential cross section, investigation of ΔN interaction in the deuteron 79−67597
e^+e^- production, intermediate energy, Coulomb correction to total cross section 78−21540
(γ,d), odd-Z light nuclei, from (e,e'd), cross section, E2 transistors giant resonance and clusters 80−63169
(γ,n), 45-160 MeV, cross sections in quasi-deuteron model for direct reactions 80−63170
(γ,N), ang. distribs. from direct-semidirect model 79−71852
(γ,N), fine structure in ang. distrib. in giant resonance region 77−6342
(γ,N), intermediate energies, nucleon current interactions, direct knock out mechanism 80−27624
(γ,n), nuclear spectroscopy, unbound excited level, spin, parity and width of resonance level 80−18287
(γ,n), preequilibrium exciton model with evaporative component, photoneutron spectra, giant resonances 80−57762
(γ,n), valency mechanism near threshold, optical nuclear model *(Russian)* 77−6351
(γ,n) intermediate-energy reactions in complex nuclei, analysis of expt. data 79−526
(γ,p), >100 MeV, using monochromatic photons, leading to final nuclear states 80−22814
(γ,p), ineffectiveness of quasi-deuteron interaction mechanism in yielding (γ,nucleon) reactions in complex nuclei 79−9546
(γ,p), wave function orthogonality, bound state to continuum transitions 78−78335

photon-nucleus reactions continued
(γ,p) 60-100 MeV, single particle knock-out using shell model wavefunctions, mass depend. 79−13273
$(\gamma,p\pi^-)$ reaction on nuclei, investigation using 2-arm spectrometric arrangement 79−711
(γ,π), few body pion photoprod. in Δ-resonance, region 80−42636
(γ,π), improved surface prod. model including π-nucleus effects 79−85455
(γ,π), light nuclei near threshold, π mass difference effects, nuclear K-matrix 80−27674
(γ,π), photopion reaction sensitivity to optical pot. 80−78278
(γ,π), π electromag. processes, theoretical aspects 80−22822
(γ,Π) in nuclear matter, optical pot. and Fermi gas model, Li, Be appl. 79−36230
(γ,π^0), near threshold photoprod. on ^1H and ^2H, cross section calcs. 78−25174
$(\gamma,\pi^\pm)$, low energy photoprod., emission ang. depend. *(Russian)* 80−57769
$(\gamma,\pi^\pm)$, threshold production 79−85452
(γ,π^-p), detector system and ccts. 78−877
(γ,ρ^-), forward photoprod. on Al, Be, C, Cu up to 4.5 GeV *(Russian)* 77−50113
(γ,X), A=14 nuclei, isospin T=2, 1 and 0 collective resonances, shell model 80−510
(γ,X), A=154-209, 7-20 MeV, total photoabsorption cross section 80−57766
(γ,X), A=2, 3, 4, photonuclear and EM interactions 80−22816
γ+A→p+X, effect of short range pairing correl. in cumulative nucleon prod. *(Russian)* 79−30794
γN→Nπ, instability of anal. results near Nπ reson. region *(Russian)* 79−9385
γp→X, strong interaction model anal., review, book contrib. 80−47310
$^2H(\gamma,\pi^0)$, near threshold, total and differential cross-sections 77−14106
$^6Li(\gamma,\pi^+)^6He$, cross-section determ. 77−14100
ω, photoproduction at high energy, parton model, γ hadronic props. 78−74266
ω meson photoproduction on D, Be, C, Al, Cu, Ag, Au, cross sections 78−58261
φ, photoproduction at high energy, parton model, γ hadronic props. 78−74266
π photoproduction, current algebra model with hard pions *(Russian)* 77−74890
ψ photoproduction by nucleons and nuclei, soliton model *(Russian)* 77−46071
ρ, photoproduction at high energy, parton model, γ hadronic props. 78−74266
$^{18}O(\gamma,\sigma_0)$, 19-32 MeV, E1 and E2 cross section, E1-E2 phase difference 80−63172
$^{16}(\gamma,X)$, bremsstrahlung weighted cross section, two-body correlations effects, linked cluster expansion 80−106047
Ag, recoil energies of photoproduced ^{24}Na, 800 MeV bremsstrahlung 77−41953
^{107}Ag, comparison of absolute cross sections for electron and photon induced reactions, DWBA calc. test 77−41958
Ag(γ,X), X=p,d,t,^{3}He,^{4}He, cascade-evaporation 80−57770
^{27}Al, inclusive proton photoprod., momentum spectra, max. bremsstrahlung energy 2.0 to 4.5 GeV *(Russian)* 77−34287
$^{27}Al(\gamma,X)$, 3-30 MeV, photoabsorption cross section, giant dipole resonances 80−78254
$^{27}Al(\gamma,p)$, cross sections and proton energy spectra from (e,e'p) 80−13461
$^{27}Al(\gamma,p)^{26}Mg$, energy and angular distribution *(Korean)* 80−18289
$^{27}Al(\gamma,\pi^+)$, 130 to 580 MeV, cross sections, impulse approx., multipole decomp. 77−54206
Al(γ,X) photoabsorption cross-section, Levinger's factor, mass number dependence 80−63165
^{A}Am(γ,δ) 7-26 MeV, A=241,243, photofission cross section in E1 giant resonance region *(Russian)* 80−5182
^{A}Am(γ,n), 10-80 MeV, A=241, 243, delayed/prompt fission yield ratio, cross section, isomer prod. 79−80924
$^{40}Ar(\gamma, xp\ yn)$, 9-29 MeV, cross sections in giant resonance region, particle decay modes 80−13462
$^{40}Ar(\gamma,2p)^{38}S$ production on recirculatory, Ar gas target 79−88185
$^{40}Ar(\gamma\text{-}p)^{39}Cl$ production on recirculatory, Ar gas target 79−88185
Au, photonuclear cross-sections in giant reson. region 78−17178
Au, recoil energies of photoproduced ^{24}Na, 800 MeV bremsstrahlung 77−41953
$^{197}Au(\gamma,n)^{196}Au$ energy levels and Q-value 80−37329
$^{197}Au(\gamma,\pi^-)$, cross sections for $^{197}Hg^{g,m}$ states 79−9548
$^{197}Au(\gamma,\pi^-xn)$, threshold to 750 MeV, activation method determ. of yields, and expt. mean cross sections 79−54430
Au(γ,X), X=p,d,t,^{3}He,^{4}He, cascade-evaporation 80−57770
Au(γ,n), photoneutron Q-value determinations using monochromatic photons 79−22271
$^{11}B(\gamma,n\gamma^1)$ 30 MeV giant dipole resonance decay, ^{10}B transitions *(Russian)* 80−13433
$^{11}B(\gamma,p)^{10}Be$, 18 to 31 MeV, photoproton spectra and ang. distrib., excited state transitions 78−13056
$^{11}B(\gamma,\pi^-)^{11}C$, 142.0-169 MeV, cross-section near threshold 77−6348
$^{138}Ba(\gamma,n)$, E1 and M1 radiative strength functions 77−22999
$^{138}Ba(\gamma,\pi^-xn)La$, 150-300 MeV, pion production cross sections calc. 80−9287
Be, meas. of mass no. depend of ψ photoprod. 77−26668
^7Be, photoprod. from target with masses <40, cross-sections 79−22268
^9Be, photoabsorption total cross sections 30-100 MeV *(Russian)* 78−89850
$^9Be(\gamma,X)$, charged particle emission in (e,e'x) reaction, virtual phonon theory 80−13460
$^9Be(\gamma,n_0)^8Be$, 18 to 26 MeV, ang. distrib. and cross section 77−26662
$^9Be(\gamma,n)$, cross section, strong coupling model 80−22682
$^9Be(\gamma,\pi^+)$, 100-800 MeV, cross section, surface prod. model anal. 80−47466
$^9Be(\gamma,\pi^+)$, threshold to 175 MeV, total cross sections, DWIA anal. 80−13459
$^9Be(\gamma,\pi)$, photoabsorption and sum rules, structure, RMS radius, polarisability and exchange parameters 80−22686
Be(γ,X) photoabsorption cross-section, Levinger's factor, mass number dependence 80−63165
Be(γ,p), intermediate energy bremsstrahlung, cross sections 78−13061
Be(γ,p)X, 180-420 MeV, quasifree NN system photodisintegration, p spectrum 80−106049

photon-nucleus reactions continued
^{209}Bi(γ,X), 3-30 MeV, photoabsorption cross section, giant dipole resonances 80−78254
^{209}Bi(γ,3n)^{206}Bi, photon activation anal. 78−85273
^{209}Bi(γ,xn), x=2,3 or 4, cross sections at intermediate energies 78−8793
Bi(γ,n) cross section discrepancies, NBS P-2 chamber calibration 77−26671
Bi(γ,n), photoneutron Q-value determinations using monochromatic photons 79−22271
C, photonuclear cross sections in giant reson. region 78−17178
C, total hadronic photoprod. cross sections, 12-30 GeV 79−9379
^{11}C, photoprod. from target with masses <40, cross-sections 79−22268
^{12}C, comparison of absolute cross sections for electron and photon induced reactions, DWBA calc. test 77−41958
^{12}C, inclusive proton photoprod., momentumm spectra, max. bremsstrahlung energy 2.0 to 4.5 GeV *(Russian)* 77−34287
^{12}C(γ,π$^-$)^{12}N$_{gs}$, threshold prod., 15.11 MeV M1 form factor 78−62519
^{12}C(γ,π$^-$p), final state interaction, plane and distorted wave momentum distrib. 80−18286
^{12}C(γ,π^{0}p), 0.7-1.65 GeV, cross section asymmetry of π^0 photoprod. *(Russian)* 80−63164
^{12}C(γ,π^{0}p), 450 MeV, pion^0 photoproduction with proton ejection 79−80921
^{12}C(γ,π), ^{12}N ground state electric quadrupole moment *(Russian)* 80−42538
^{12}C(γ,P), up to 4.5 GeV, ang. depend. of normalised invariant cross section parameters *(Russian)* 78−17180
^{12}C(γ,2n)^{10}C, 100 to 800 MeV, yields, cross sections 77−34285
^{12}C(γ,γ) scatt. study of electron prod. high energy synchrotron radiation spectrum struct. 78−13062
^{12}C(γ,nα)^{7}Be, electric quadrupole transition cross-sections, behind giant resonance *(Russian)* 80−78281
^{12}C(γ,nα)^{7}Be, threshold-120 MeV, ^{11}C intermediate resonance and electric quadrupole transition contribution *(Russian)* 79−40896
^{12}C(γ,p), p-shell nucleon momentum distrib. determ. 78−17182
^{12}C(γ,p), up to 0.25 GeV, from bremsstrahlung γ-quanta *(Russian)* 80−5123
^{12}C(γ,p)^{11}B, 40-120 MeV, reaction mechanism *(Russian)* 77−65221
^{12}C(γ,p)^{11}B, electric quadrupole transition cross-sections, behind giant resonance *(Russian)* 80−78281
^{12}C(γ,p)^{11}B, threshold to 120 MeV, cross section meas. *(Russian)* 78−41699
^{12}C(γ,pα)^{7}Li, electric quadrupole transition cross-sections, behind giant resonance *(Russian)* 80−78281
^{12}C(γ,pα)^{7}Li, threshold-120 MeV, ^{11}B intermediate resonance of electric quadrupole transition contribution *(Russian)* 79−40896
^{12}C(γ,π$^-$), 160-250 MeV, total cross section from elementary Hamiltonian model 80−18292
^{12}C(γ,π$^-$), (γ,π$^-$p), knockout p interaction, optical model and quasifree π photoprod. mechanism *(Russian)* 80−42638
^{12}C(γ,π$^-$), at 44.2°, inclusive reaction, pion momentum spectra 77−50109
^{12}C(γ,π$^-$), model yield calc. 77−14107
^{12}C(γ,π$^-$), near (3,3) resonance, differential cross-section meas. 77−10385
^{12}C(γ,π$^-$), threshold to 360 MeV, total cross sections in Δ region 80−13457
^{12}C(γ,π$^-$), total cross section calc. in impulse approx. 80−13458
^{12}C(γ,π$^-$)^{12}N, near threshold, total cross section 77−14104
^{12}C(γ,π$^-$)^{12}N, threshold to reson., total and differential cross sections 79−85456
^{12}C(γ,π$^-$)^{12}N, total cross-section anal. 77−14102
^{12}C(γ,π$^-$)^{12}N, total cross section calc., Δ(1232) contrib. 80−91175
^{12}C(γ,π$^-$)^{12}N$_{g.s.}$, near threshold, total cross section calc. 78−50152
^{12}C(γ,π$^-$p), 340-380 MeV, quasi-free photoprod., impulse and shell model anal. *(Russian)* 80−5124
^{12}C(γ,π$^-$p), final state interaction, distorted and plane wave momentum distribs. 80−78275
^{12}C(γ,π^0), pionic and EM A* resonance excitation 80−91160
^{12}C(γ,π^0)^{12}C, 220-360 MeV, phenomenological isobar doorway model calcs., total cross section 79−525
^{12}C(γ,π^{0}p), 0-600 MeV residual nucleus impulse *(Russian)* 79−59050
^{12}C(γ,π$^+$)^{12}B, nuclear critical opalescence study 80−105988
^{12}C(γ,π$^+$)^{12}B, spin flip transition strength 77−14103
^{12}C(γ,π$^+$)^{12}B$_{g.s.}$, 0-4 MeV, pion photoprod. cross section 80−42637
^{12}C(γ,π$^+$)^{12}C, up to 175 MeV, total cross sections, DWIA anal. 79−59049
^{12}C(γ,π$^\pm$), 300 to 850 MeV, charged pion momentum spectra 78−93987
^{12}C(γ,π$^\pm$), PWIA anal. 77−14108
^{12}C(π$^-$p) in Δ(1232) region, differential yield, impulse and shell model anal. *(Russian)* 79−67744
^{13}C, photoexcited giant dipole resonace, continuum shell model anal. 80−18266
^{13}C(γ,n$_{0,1}$)^{12}C, 98° diffr. cross-sections, reson. due to ^{13}C level struct. 78−586
^{13}C(γ,n), 6.5-9.3 MeV, ang. distribs., E1, M1 and E2 excitations, resonance radiative widths 80−68581
^{13}C(γ,n), 7.6-24 MeV, photoneutron ang. distribs., level scheme and J$^\pi$ assignments 80−466
^{13}C(γ,n), threshold to 25 MeV, photoneutron cross-section 77−14113
^{13}C(γ,n) 7.6 to 41.8 MeV, photoneutron cross section meas., giant resonance isospin splitting 79−63657
^{13}C(γ,n)^{12}C, 24-26 MeV, photoneutron energy and ang. distribs. 77−30554
^{A}Ca(γ,X), A=42, 44, 48, photoneutron and photoproton cross section systematics 80−13463
^{40}Ca, photoneutron cross-section above giant dipole resonance region, quasi-monochromatic photon beam *(French)* 80−78276
^{40}Ca photonuclear reactions, differential cross section calcs., direct-semidirect model 78−33166
^{40}Ca(γ,n), 100-750 MeV, yields and cross sections 77−41948
^{40}Ca(γ,p), 100-750 MeV, yields and cross sections 77−41948
^{44}Ca(γ,p) cross-sections calc. from (e,e'p) meas. 77−26666
Ca(γ,X) photoabsorption cross-section, Levinger's factor, mass number dependence 80−63165
Cd(γ,n), photoneutron Q-value determinations using monochromatic photons 79−22271
Ce, photoneutron cross-section above giant dipole resonance region, quasi-monochromatic photon beam *(French)* 80−78276
^{140}Ce(γ,n) E1 and M1 radiative strength functions 77−22999

photon-nucleus reactions continued
Ce(γ,n), 30 to 140 MeV, partial photoneutron cross section, total cross section approx. 80−22809
C(γ,X) photoabsorption cross-section, Levinger's factor, mass number dependence 80−63165
^{59}Co(γ,p), isospin effects in GDR region 78−78344
^{59}Co(γ,xn), 10-36.5 MeV, photoneutron cross sections, integrated cross sections, giant dipole resonance 79−89289
^{59}Co(γ,xn) reactions in complex nuclei, cross sections at intermediate energies 78−8793
^{52}Cr, total photoneutron cross section, high resolution meas., isospin effects 78−8792
^{52}Cr(α,p$_0$(p$_1$)) differential cross section in giant dipole resonance region from (e,p$_0$(p$_1$)) 79−63655
^{52}Cr(γ,X), photoneutron and photoproton cross section systematics 80−13463
^{53}Cr(γ,p)^{52}V, cross-section, 14.4-27 MeV, isospin splitting 80−520
Cu (γ,X), 2-5 GeV, spallation 77−71604
Cu, recoil energies of photoproduced fragments, 800 MeV bremsstrahlung 77−41953
^{63}Cu, comparison of absolute cross sections for electron and photon induced reactions, DWBA calc. test 77−41958
^{63}Cu, inclusive proton photoprod., momentum spectra, max. bremsstrahlung energy 2.0 to 4.5 GeV *(Russian)* 77−34287
^{63}Cu(γ,n), cross-section determ., 12-25 MeV *(Russian)* 79−89295
^{63}Cu(γ,p), up to 0.25 GeV, from bremsstrahlung γ-quanta *(Russian)* 80−5123
^{63}Cu(γ,p), up to 4.5 GeV, ang. depend. of normalised invariant cross section parameters *(Russian)* 78−17180
Cu(γ,X), X=p,d,t,^{3}He,^{4}He, cascade-evaporation 80−57770
Cu(γ,n) cross section discrepancies, NBS P-2 chamber calibration 77−26671
Cu(γ,π$^+$), quasifree photoprod. cross sections 79−75972
D(γ,n), photoneutron energy spectra meas. *(Dutch)* 79−3281
^{19}F(γ,X), 14-30 MeV, X=p,n,α, integrated cross sections to excited residual states 80−18200
Fe, photonuclear cross sections in giant reson. region 78−17178
Fe photonuclear process and Fe(μ,μ') cosmic ray scatt. >200 GeV 77−23001
Fe+cosmic ray photon, prod. of 300-1000 GeV muons, cross section, shadowing 77−64580
^{54}Fe(γ,X), photoneutron and photoproton cross section systematics 80−13463
^{54}Fe(γ,n), cross section meas., E1 giant dipole isospin splitting 79−17892
^{56}Fe(γ,n), 13.3 MeV bremsstrahlung, resonance spectrum and cross-section meas. *(Russian)* 77−6349
^{58}Fe(γ,n), near threshold, cross sections 78−13055
Fe(γ,n), A=54, 56, GDR intermediate struct. in 5-26.3 MeV range 77−74824
Ge, photon induced electron pair prod. cross section *(French)* 79−524
Ge(γ,e$^+$e$^-$), cross section near threshold, atomic electron screening effects 80−78279
Ge(γ,e$^+$e$^-$), near threshold, variable energy source, total cross section *(French)* 80−37367
^{1}H(γ,π^0), 1 to 10 MeV above threshold 79−85454
^{1}H(γ,π^0), 290 to 360 MeV, differential cross sections in Δ(1232) region *(Russian)* 78−89852
^{1}H(γ,π^0), polarised γ, 0.76-1.3 GeV, asymmetry meas. in photoprod. cross section *(Russian)* 79−59051
^{1}H(γ,π$^+$), 3.4-18 GeV, πNN form factor and differential cross sections, one pion exchange 80−68526
^{2}H (γ,π), theoretical and expt. results. 80−42698
^{2}H, dynamic and static polarisability from Rayleigh scatt., two-photon disintegration 79−75867
^{2}H, photonuclear sum rules and interaction effects, integrated cross-section determ. from double commutator 78−21542
^{2}H(δ,π^0), multiple scatt. contrib. to threshold photoprod. 80−73718
^{2}H(γ, pp)π$^-$, high momenta of emitted nucleons 78−70512
^{2}H(γ, π$^-$)2p, target asymmetry and effective neutron polarisation, polarised d 80−9286
^{2}H(γ,η)^{2}H, impulse approx. calc. of elastic η photoproduction 77−14110
^{2}H(γ,nnπ$^+$), threshold form factors 79−85453
^{2}H(γ,np), cross-sections from 74 to 241 MeV 77−30552
^{2}H(γ,p), recent developments in lepton scattering 79−80929
^{2}H(γ,p)n, tensor NN force effects 77−57649
^{2}H(γ,pπ) photoexcitation in Δ(1236) region 80−22813
^{2}H(γ,π$^-$p)^{1}H, π$^-$-p coincidence obs., mechanism and rescatt. effects *(French)* 79−3133
^{2}H(γ,π^0), 1 to 10 MeV above threshold 79−85454
^{2}H(γ,π^0), 1-7 MeV, yield meas. 78−82333
^{2}H(γ,π^0), 300 to 700 MeV, differential cross sections, partial wave analysis *(Japanese)* 78−17177
^{2}H(γ,π^0), 450 MeV cross section asymmetry *(Russian)* 79−89171
^{2}H(γ,π^0), coherent photoprod., binding effects and threshold amplitude calc. 80−32264
^{2}H(γ,π^0), cross section and threshold effects using dynamical γN→Nπ^0 model 80−27627
^{2}H(γ,π^0), impulse approx. calc. of differential cross-section 77−18524
^{2}H(γ,π^0)^{2}H, recoil deuteron polarisation statistical tensors anal. 78−74348
^{2}H(γ,π$^+$), 1-4 MeV, cross-section meas. 78−21544
^{2}H(γ,π$^+$), threshold prod., excitation function 77−14105
^{2}H(γ,π$^+$)2n, π$^+$ energy spectra and emission angle *(Russian)* 79−40903
^{2}H(γ,π$^+$)2n, threshold to 22 MeV, bremsstrahlung yield and total cross section 80−9288
^{2}H(γ,π$^+$)2n cross section, threshold charged photopion prod. operator props. 79−89292
^{2}H(γ,π$^+$)nn, n-n final state interaction effects 80−102181
^{2}H(γ,π$^+$)nn, photoprod. near threshold, nucleus axial props. rel. to nucleon spin-flip *(French)* 79−522
^{2}H(γ,π$^\pm$), photprod. on neutrons effect of Fermi motion 78−74349
^{2}H(γ,π), 210-700 MeV, total and differential cross sections from impulse approx. 80−68647
^{2}H(γ,π), impulse approx. and π rescattering effects 77−6346
^{2}H(γ,π), threshold photoprod. cross sections, elementary nucleonic amplitudes 80−22812
^{3}H, enhancement factor calc. in photonuclear electric dipole sum rule 78−37288
^{3}H photoeffect, electric dipole sum rules 79−36231

photon-nucleus reactions continued
^{3}H photoeffect, hyperspherical harmonics and elec. dipole sum rules 77−57650
^{3}H, photonucl. sum rules 79−6427
^{3}H(γ,π^{0}), 0-8 MeV, cross sections, taking π rescatt. amplitudes into account 78−78364
^{3}H(γ,π^{0}), polarisation effects 180 to 700 MeV, impulse approx. calcs. *(Russian)* 80−37368
^{3}H(γ,π^{0})^{3}H, polarisation effects 180 to 700 MeV, impulse approx. calcs. *(Russian)* 80−37368
^{3}H(γ,xπ), x=1 or 2, photodisintegration cross sections 80−22817
^{A}H(γ,π^{0}), A=1, 2, 1-10 MeV, photoprod. yields, DWIA anal., dipole photoprod. amplitudes 80−68645
^{3}He, enhancement factor calc. in photonuclear electric dipole sum rule 78−37288
^{3}He, threshold pion photoproduction and radiative capture, π-^{3}He-^{3}H coupling constant 79−40962
^{3}He trinucleon photoeffect, electric dipole transitions to isospin 1/2 trinucleon states 79−45246
^{3}He(γ,2p)n, 15-50 MeV, three-body calc. with spin-depend. separable pot. 77−38257
^{3}He(γ,n), photodisintegration cross sections 80−22817
^{3}He(γ,p)^{2}H, 165 to 330 MeV, EM and pion exchange contribs. to unpolarised differential cross section 77−18521
^{3}He(γ,p)^{2}H, intermediate energy, ang. distribs., reaction amplitude and ^{3}He vertices 80−22835
^{3}He(γ,pd) and ^{2}H(p,γ) anal. using Reid soft-core pots. 77−26664
^{3}He(γ,π^{0}), 0-8 MeV, cross sections, taking π rescatt. amplitudes into account 78−78364
^{3}He(γ,π^{0}), 1 to 10 MeV above threshold 79−85454
^{3}He(γ,π^{0}), cross section and threshold effects using dynamical $\gamma N \rightarrow N\pi^{0}$ model 80−27627
^{3}He(γ,π^{0}), polarisation effects 180 to 700 MeV, impulse approx. calcs. *(Russian)* 80−37368
^{3}He(γ,π^{0})^{3}He, polarisation effects 180 to 700 MeV, impulse approx. calcs. *(Russian)* 80−37368
^{3}He(γ,π^{-}) near threshold, photoprod. yield and transition matrix element 79−89291
^{3}He(γ,π^{+})^{3}H, exchange current effects, two body processes 79−71839
^{3}He(γ,π^{+})^{3}H, Fermi motion and off-shell effects, impulse approx. 80−27626
^{3}He(γ,π^{-})^{3}H, threshold π prod., and axial vector form factor 79−574
^{3}He(γ,π^{+})^{3}H, threshold form factors 79−85453
^{3}He(γ,π^{+})^{3}H cross section near threshold , 80−83093
^{3}He($\gamma,\pi^{+}\pi^{-}$)^{3}He, gauge-invariant one-pion-exchange model 77−18298
^{3}He($\gamma,\pi^{\pm}$), (3,3) resonance region, nuclear wave functions, kinematics 78−78361
^{3}He(γ,π), threshold photoprod. cross sections, elementary nucleonic amplitudes 80−22812
^{4}He, (γ,^{2}H)/(γ,^{3}He) cross section ratio for 31-51 MeV, deduced $\sigma(\gamma,p)/(\gamma,n)$ ratio 79−67743
^{4}He harmonic oscillator sum rules for photonuclear reactions, shell model, perturbative corrections 78−41692
^{4}He, photoabsorption total cross sections 30-100 MeV *(Russian)* 78−89850
^{4}He photodisintegration, electric dipole transitions, photoeffect cross section 79−67742
^{4}He, photonuclear reaction cross-section continuum calcs. 77−71603
^{4}He, π^{0} coherent photoprod., screening corrections and rescatt. *(Russian)* 78−41697
^{4}He(γ,P)^{3}H, 20 to 50 MeV, 2^{+} resonances *(Russian)* 79−59052
^{4}He(γ,2d), 30-35 MeV, 2^{+} state search *(Russian)* 80−42553
^{4}He(γ,2np)p, total photofission theory in hyperspherical basis *(Russian)* 79−22347
^{4}He(γ,d)^{2}H, ^{4}He elec. quadrupole reson., multipole expansion *(Russian)* 78−66264
^{4}He(γ,n), 30-35 MeV, 2^{+} state search *(Russian)* 80−42553
^{4}He(γ,n), cross section and asymmetry shell model calcs. 79−17824
^{4}He(γ,n) shell model continuum calcs., centre of mass problems 77−82909
^{4}He(γ,n)^{3}He, 20 to 50 MeV, 2^{+} resonances *(Russian)* 79−59052
^{4}He(γ,n)^{3}He, electric dipole and quadrupole cross section *(Russian)* 77−6352
^{4}He(γ,p), 200-450 MeV, ang. distribs., differential and total cross sections 79−75971
^{4}He(γ,p), cross section and asymmetry shell model calcs. 79−17824
^{4}He(γ,p), shell model continuum calcs., centre of mass problems 77−82909
^{4}He(γ,p)^{3}H, 165 to 330 MeV, EM and pion exchange contribs. to unpolarised differential cross section 77−18521
^{4}He(γ,pn)^{2}H reaction, distribution along Treiman-Yang angle *(Russian)* 80−27628
^{4}He(γ,pπ^{-}), π^{-}-p coincidence obs., mechanism and rescatt. effects *(French)* 79−3133
^{4}He(γ,π^{0}), 1 to 10 MeV above threshold 79−85454
^{4}He(γ,π^{0}), cross-sections determ., selection rules calc. 77−82905
^{4}He(γ,π^{0}), differential cross section, complex momenta theory for nondiffractive processes *(Russian)* 80−32266
^{4}He(γ,π^{0}), impulse approx. for differential cross sections in resonance region *(Russian)* 78−41698
^{4}He(γ,π^{0}), P-odd effects, Regge and boson pole interference *(Russian)* 79−6564
^{4}He(γ,π^{0}), polarisation effects 180 to 700 MeV, impulse approx. calcs. *(Russian)* 80−37368
^{4}He(γ,π^{0}), reaction cross section meas. equipment 78−29694
^{4}He(γ,p^{0})^{4}He, eikonal and quasi-eikonal models in complex ang. momentum plane *(Russian)* 77−50160
^{A}He(γ,π^{0}), A=3, 4, 1-10 MeV, photoprod. yields, DWIA anal., dipole photoprod. amplitudes 80−68645
He($\gamma,p\pi$), photoexcitation in Δ(1236) region 80−22813
Hf(γ,xπ), x=1, 2; A=176, 178, 180, 8-21 MeV, GDR, neutron yields and multiplicities *(Russian)* 77−82894
H(γ,π^{0}) prod. at 320 MeV 77−22742
H(ϕ,π^{0}), 350 MeV, differential cross sections 78−86527
In, photonuclear cross sections in giant reson. region 78−17178
^{115}In^{m}, nuclear excitation by e^{+} annihilation with K-shell electrons 79−22230
In(γ,n), photoneutron Q-value determinations using monochromatic photons 79−22271
Ir, A=191, 193, shape of stable transition nuclei, photoabsorpt. cross-sections *(Russian)* 77−79307

photon-nucleus reactions continued
^{A}Ir, A=191,193 photoneutron yield curves, nuclear shape and giant dipole resonances, 8-21 MeV *(Russian)* 79−13268
^{138}La, low temp. photonuclear nucleosynthesis in stellar H-CNO burning zones 77−13319
^{6}Li(α,π^{+})^{6}He, threshold prod. in α-d cluster model 77−79356
^{6}Li(γ,X), X=n,p, 10.2-15.4 MeV bremsstrahlung, photoreaction mechanisms 80−68644
^{6}Li(γ,d)^{4}He, cross section calc. by cluster model *(Japanese)* 77−67733
^{6}Li(γ,η), partial photoprod. cross-section calc. 77−14111
^{6}Li(γ,η)^{6}Li, E_{γ}=3.56 MeV, partial photoproduction cross-section calc. *(Russian)* 79−9547
^{6}Li(γ,η)^{6}Li partial cross section for photoproduction of η mesons 77−65220
^{6}Li(γ,η)^{6}Li*(3.56 MeV), partial photoproduction reactions, large momentum transfer anal., form factor choice 80−22808
^{6}Li(γ,π^{0}), cross-sections determ., selection rules calc. 77−82905
^{6}Li(γ,π^{0}p), 0-600 MeV residual nucleus impulse *(Russian)* 79−59050
^{6}Li(γ,π^{+}), cross-section calc. 78−17248
^{6}Li(γ,π^{+})^{6}He, analysis using current algebra model with rigid π-mesons *(Russian)* 77−14112
^{6}Li(γ,π^{+})^{6}He, photoprod. near threshold, nucleus axial props. rel. to nucleon spin-flip *(French)* 79−522
^{6}Li(γ,π^{+})^{6}He, threshold to 7 MeV, cross sections rel. to proton target 77−54207
^{6}Li(γ,π^{o})^{6}Li*(3.56 MeV), partial photoproduction reactions, large momentum transfer anal., form factor choice 80−22808
^{7}Li, photoabsorption total cross sections 30-100 MeV *(Russian)* 78−89850
^{7}Li, photodisintegration, cluster model wave function, bremsstrahlung weighted cross section 80−63163
^{7}Li(γ, n)^{6}Li* (3.56 MeV), integral reaction cross section *(Russian)* 78−46048
^{7}Li(γ,π^{-}), threshold to 360 MeV, total cross sections in Δ region 80−13457
^{7}Li(γ,π^{-}), total cross section calc. in impulse approx. 80−13458
^{7}Li(γ,t), <50 MeV, total and differential cross sections, levels, cluster model calcs. 80−32265
^{7}Li(γ,t)^{4}He, N-fold coincidences, on-line acquisition 77−79527
^{A}Li(γ,π), A=6, 7 80−22686
Li(γ,X) photoabsorption cross-section, Levinger's factor, mass number dependence 80−63165
^{7}Li(γ,n), photo neutron cross sections, branching ratios 77−41943
^{24}Mg (γ,p), 17-30 MeV, giant dipole resonances and transitions, shell effects *(Russian)* 80−13434
^{24}Mg(γ,p), cross sections and proton energy spectra from (e,e'p) 80−13461
^{24}Mg(γ,p), up to 0.25 GeV, from bremsstrahlung γ-quanta *(Russian)* 80−5123
^{26}Mg(γ,n)^{25}Na, 19.5 to 27.0 MeV, giant dipole resonance decay channel determ., isospin component 79−26423
^{26}Mg(γ,p), 16-23 MeV, proton ang. distrib. meas. 77−41946
Mn photonuclear cross sections in giant reson. region 78−17178
^{52}Mn, 2-5 GeV photospallation, ratios of isomeric yields *(Russian)* 78−46047
^{55}Mn(γ,X), 2-5 GeV, spallation 77−71604
^{55}Mn(γ,xn), 10-36.5 MeV, photoneutron cross sections, integrated cross sections, giant dipole resonance 79−89289
Mo+γ, obs. in TFR Tokamak 77−34441
^{100}Mo(γ,n)^{99}Mo^{m1,m2,g}, isomeric cross section ratios 78−29448
^{14}N(γ,n_{0})^{13}N, 17 to 26 MeV, angular distrib., giant dipole resonance, single-particle nuclear model 80−52659
^{14}N(γ,pn)^{12}C, cross-section and ^{12}C distrib., quasi-deuteron mechanism 80−63166
^{14}N(γ,π^{-}), DWIA anal., wave function and π optical pot. effects on cross section 80−63168
^{14}N(γ,π^{-})^{14}C, threshold, impulse approx. anal. 77−14109
^{14}N(γ,π^{-})^{14}O, 145-325 MeV, Gamow-Teller suppression and M1 radiative widths 80−52609
^{14}N(γ,π^{+}), anomalous $^{14}N_{gs} \rightarrow {}^{14}C_{gs}$ transition, Kroll Ruderman terms 80−63167
^{15}N, photoabsorption, shell-model anal. of giant dipole state 78−29447
^{15}N(e,t_{0}), 20-25 MeV, photodisintegration and electrodisintegration 79−80922
^{15}N(γ,d)^{13}C, ^{15}N giant resonance and cross sections 79−93587
^{24}Na yield from light and intermediate nuclie in 2-5 GeV photonuclear reactions *(Russian)* 77−2980
^{24}Na(γ,n), 42 MeV, photoneutron flux determ. from induced activity meas. in water 78−20112
Nb(γ,n), photoneutron Q-value determinations using monochromatic photons 79−22271
^{20}Ne(γ,α), EM induced α emission, α spectroscopic amplitudes, anal. solvable model 80−32267
^{20}Ne(γ,n) cross sections and giant resonance struct. 80−13441
^{A}Ni(γ,α) A=58, 60, 62, 50 MeV electroproduction and decay of giant resonances 79−26413
^{62}Ni(γ,X), 19.2-26.2 MeV, photoneutron and photoproton spectra, giant dipole resonance-decay, isospin conservation 80−13443
Ni(γ,p), 17.5-32.0 MeV, isospin effects in decay of highly excited ^{58,60}Ni states 77−61398
^{16}O, photoneutron cross-section above giant dipole resonance region, quasi-monochromatic photon beam *(French)* 80−78276
^{16}O(e,e), T=1 level form factors, Helm model, pion photoprod. and muon capture appls. 80−52553
^{16}O(γ, p), 300 to 900 MeV/c, p-shell momentum distrib. calc. 78−50151
^{16}O(γ, p)^{15}N and ^{16}O(γ, n)^{15}O, 60-300 MeV, absorpt. mech., residual nucleus form factor 78−70511
^{16}O(γ,N), giant resonance region, features in energy depend. of ang. distrib. 77−6343
^{16}O(γ,N), shell model calcs. with and without continuous spectrum *(Russian)* 77−2979
^{16}O(γ,2n)^{14}O, 100 to 800 MeV, yields, cross sections 77−34285
^{16}O(γ,n_{0}), 21.6-25.7 MeV, ground state photoneutron polarisation ang. distrib. 80−57765
^{16}O(γ,n), 25-45 MeV, isovector giant quadrupole resonance evidence, E2 cross section 80−18268
^{16}O(γ,n), photoneutron energy spectra meas. *(Dutch)* 79−3281
^{16}O(γ,n) total photoneutron cross sections 80−42619
^{16}O(γ,n)^{15}O, ang. distrib. asymmetry anal. 78−25172

photon-nucleus reactions continued
$^{16}O(\gamma,n)^{15}O$, two-step charge exchange contrib., corrections to direct photonuclear process 78−62518
$^{16}O(\gamma,p_0)$ 100-300 MeV, short-range, high-momentum effects 77−26667
$^{16}O(\gamma,p)$, 40-105 MeV bremsstrahlung, ang. distribs. meas. 77−41945
$^{16}O(\gamma,p)$, role of Δ(1232) isobar 79−85451
$^{16}O(\gamma,p)^{15}N$, 50 to 350 MeV, evaluation of isobar photoprod. contrib. to (γ,p) reaction 79−45245
$^{16}O(\gamma,p)^{15}N$, electric quadrupole transition cross-sections, behind giant resonance *(Russian)* 80−78281
$^{16}O(\gamma,p)^{15}N$ up to 120 MeV, cross-sections, energy levels *(Russian)* 80−47465
$^{16}O(\gamma,\pi^0)$ coherent photoprod. in isobar-hole formalism, DWIA comparison 79−89290
$^{16}O(\gamma,\pi^0p)$, 0-600 MeV residual nucleus impulse *(Russian)* 79−59050
$^{16}O(\gamma,\pi^+)$, 200-350 MeV, cross sections, DWIA anal. 80−106048
$^{16}O(\gamma,\pi^+)$, differential cross section from elementary Hamiltonian model 80−18292
$^{16}O(\gamma,\pi^+)$, threshold to 175 MeV, total cross sections, DWIA anal. 80−13459
$^{16}O(\gamma,\pi)$, total cross section, Δ-hole states damping, π^0,ρ exchange, Δ isobar hole model 80−91174
$^{17}O(\gamma,n_0)^{16}O$, 4.3-7 MeV, resonance radiation width, channel and pot. radiative capture, R-matrix anal. 79−6567
$^{17}O(\gamma,n)$, 5-33 MeV, ground state differential cross section at 98° resonances 79−89288
$^{17}O(\gamma,n)$, 8.5-39.7 MeV, cross section, giant dipole and pygmy resonance decays 80−42619
$^{17}O(\gamma,n)$, cross section, Lane-Lynn radiative capture mechanisms 80−52660
$^{18}O(\gamma,n)$ 8.0 to 41.8 MeV, photonuclear cross section meas., resonance decay branching 79−63656
$^{18}O(\gamma,xn)$ 8-33 MeV, integrated cross sections 77−10386
$O(\gamma,X)$ photoabsorption cross-section, Levinger's factor, mass number dependence 80−63165
$^{A}Os(\gamma,xn)$, 7-30 MeV, A=186,188-190,192, photoneutron cross section and giant resonances 79−54422
$Os(\gamma,xn)$, photoneutron cross section, bremsstrahlung yield curves 78−17176
$^{31}P(\gamma,n)^{30}P$, primary first-order interference in γ-activation anal. 79−16088
$^{31}P(\gamma,x)$, (x=2p,2pn,3p,3pn), 75 to 640 MeV, yields and cross sections 78−37328
Pb, 35 to 106 MeV, data fit using modified quasi-deuteron model with 60 MeV damping factor 79−49619
Pb, photoneutron cross-section above giant dipole resonance region, quasi-monochromatic photon beam *(French)* 80−78276
Pb, total photonucl. absorpt. cross sections, 25-106 MeV 79−6565
$^{A}Pb(\gamma,n)$, A=206, 208, levels using tagged photons 80−23245
$^{A}Pb(\gamma,n)$, A=206,207,208, photoneutron Q-value determinations using monochromatic photons 79−22271
$^{206}Pb(\gamma,n)$, 8.5-11.4 MeV, ^{205}Pb multipole resonance E1-E2 and E1-M1 interference 80−32251
$^{207}Pb(\gamma,n)$, 7632 keV level photoexcitation, cross section and J^π 80−37330
$^{207}Pb(\gamma,n)$, new 86 keV neutron source 79−704
^{208}Pb γ absorpt., cross section near threshold, E1, E2, M1 resonances, finite Fermi-system theory 77−50055
^{208}Pb, inclusive proton photoprod., momentum spectra, max. bremsstrahlung energy 2.0 to 4.5 GeV *(Russian)* 77−34287
^{208}Pb, photonuclear induced high multipole giant reson., Australian nuclear physics review 77−88021
$^{208}Pb(\gamma,\gamma)$, 6.92, 7.12 MeV, reson. fluoresc. meas. 78−8797
$^{208}Pb(\gamma,n_0)$, 170-320 keV, search for collective M1 resonance 77−46103
$^{208}Pb(\gamma,n_{pol})$, evidence for M1 collective strength at 8-10 MeV 77−38255
$^{208}Pb(\gamma,n)$, 7.4-8.4 MeV, cross section, E1 and M1 transitions, collective and giant M1 resonance 79−89267
$^{208}Pb(\gamma,n)$, 8 to 13 MeV, total cross section, resonance struct. 78−4928
$^{208}Pb(\gamma,n)$, 9.5-12 MeV, photoneutron ang. distribs., struct. below giant resonance 80−13444
$^{208}Pb(\gamma,n)$, polarimeter for threshold photoneutron spectroscopy 77−30739
$^{208}Pb(\gamma,n)$, s-d wave admixture in $^{207}Pb+n$ system 77−30555
$^{208}Pb(\gamma,n)$ giant mag. dipole resonance location, photoneutron polarisation method 80−37357
$^{208}Pb(\gamma,p)$, up to 0.25 GeV, from bremsstrahlung γ-quanta *(Russian)* 80−5123
$^{208}Pb(\gamma,p)$, up to 4.5 GeV, ang. depend. of normalised invariant cross section parameters *(Russian)* 78−17180
$^{209}Pb(\gamma,\pi^+)^{209}Pb$, photoprod. to single particle states 77−22998
Pb(γ, n), 30 to 140 MeV, partial photoneutron cross section, total cross section approx. 80−22809
Pb(γ,n) cross section discrepancies, NBS P-2 chamber calibration 77−26671
$Pb(\gamma,\pi^\pm)$, quasifree photoprod. cross sections 79−75972
Pr(γ,n) cross section discrepancies, NBS P-2 chamber calibration 77−26671
Pt, A=194, 195, 196, 198, shape of stable transition nuclei, photoabsorpt. cross-sections *(Russian)* 77−79307
^{A}Pt, A=194-8 photoneutron yield curves, nuclear shape and giant dipole resonances, 8-21 MeV *(Russian)* 79−13268
^{239}Pu, giant resonance in total photoabsorpt. cross section 77−6347
^{239}Pu, transition effects in total photoabsorpt. cross section 77−46160
$^{239}Pu(\gamma,2n)$, ^{237}Pu fission single particle isomers, half lives and isomeric ratio 80−18181
$^{239}Pu(\gamma,2n)$, 45 MeV, ^{237}Pu fission isomers, half lives and yield ratio, statistical model anal. 79−40885
^{240}Pu, 42.9 keV γ transition, Mossbauer reson. obs. 79−36229
$^{85}Rb(\alpha,n)$, CC Rb cross sections and decay props. 79−49600
Re, photofission cross section, 220-550 MeV, coherent electron bremsstrahlung beam 79−13353
$^{102}Ru(\gamma,p)^{101}Tc^{m,g}$, isomeric cross section ratios 78−29448
^{32}S, photoneutron cross-section above giant dipole resonance region, quasi-monochromatic photon beam *(French)* 80−78276
$^{32}S(\gamma,p_0)$, giant dipole resonance decay model, cross section and p spectrum 79−6563
$^{32}S(\gamma,p)$, 17-30 MeV, giant resonance p decay channel, state transition distrib. *(Russian)* 78−89840
$^{32}S(\gamma,pn)^{30}P$ primary first-order interference in γ-activation anal. 79−16088
photon-nucleus reactions continued
Sb(γ,n), photoneutron Q-value determinations using monochromatic photons 79−22271
^{44}Sc, 2-5 GeV photospallation, ratios of isomeric yields *(Russian)* 78−46047
$^{45}Sc(\gamma,p)$, cross-sections calc. from (e,e'p) meas. 77−26666
$^{28}Si(\gamma,p)$, 18.1-29 MeV, giant dipole resonance, contrib. from various configs. 80−18264
$^{28}Si(\gamma,\alpha)^{24}Mg$, 28 MeV, cross-sections to residual excited states 77−74832
$^{28}Si(\gamma,n)^{27}Si$, 28 MeV, cross-sections to residual excited states 77−74832
$^{28}Si(\gamma,p)$, 18.1-29 MeV, photoproton energy spectra, contribs. to giant dipole resonance 80−78242
$^{28}Si(\gamma,p)^{27}Al$, 28 MeV, cross-sections to residual excited states 77−74832
$^{30}Si(\gamma,2p)$, 75 to 640 MeV, yields and cross sections 78−37328
$^{30}Si(\gamma,p)$, 75-800 MeV, yield meas. by activation method 77−71605
Sn, photoactivation by 42 MeV bremsstrahlung, gamma transition energies and line intensities 78−13057
Sn, photoneutron cross-section above giant dipole resonance region, quasi-monochromatic photon beam *(French)* 80−78276
^{117}Sn, substructure in radiative strength function using quasiparticle-phonon nucl. model 79−40901
^{118}Sn, inclusive proton photoprod., momentum spectra, max. bremsstrahlung energy 2.0 to 4.5 GeV *(Russian)* 77−34287
$^{118}Sn(\gamma,p)$, up to 0.25 GeV, from bremsstrahlung γ-quanta *(Russian)* 80−5123
$^{118}Sn(\gamma,p)^{117}In$, 150 to 750 MeV, reaction cross section 78−37329
^{119}Sn, substructure in radiative strength function using quasiparticle-phonon nucl. model 79−40901
$^{119}Sn(\gamma,n)$, giant mag. dipole resonance location, photoneutron polarisation method 80−37357
^{120}Sn, γ absorpt., cross section near threshold, E1, E2, M1 resonances, finite Fermi-system theory 77−50055
Sn(γ, n), 30 to 140 MeV, partial photoneutron cross section, total cross section approx. 80−22809
$^{88}Sr(\gamma,\gamma)$, reson. fluoresc. yield meas. width of 1.836 MeV level determ. 77−79357
Ta, meas. of mass no. depend. of ψ photoprod. 77−26668
Ta, photofission cross section, 220-550 MeV, coherent electron bremsstrahlung beam 79−13353
^{180}Ta, low temp. photonuclear nucleosynthesis in stellar H-CNO burning zones 77−13319
^{181}Ta, photoneutron cross-section above giant dipole resonance region, quasi-monochromatic photon beam *(French)* 80−78276
$^{181}Ta(\gamma,X)$, 3-30 MeV, photoabsorption cross section, giant dipole resonances 80−78254
$^{181}Ta(\gamma,n)$ photoneutron absorpt. cross section meas. 20.9 to 837.8 keV *(German)* 80−5122
$Ta(\gamma,n)$, 30 to 140 MeV, partial photoneutron cross section, total cross section approx. 80−22809
$Ta(\gamma,n)$, photoneutron Q-value determinations using monochromatic photons 79−22271
$^{130}Te(\gamma,p)$, 75-800 MeV, yield meas. by activation method 77−71605
^{232}Th, grant resonance in total photoabsorpt. cross section 77−6347
^{232}Th, transition effects in total photoabsorpt. cross section 77−46160
$^{232}Th(\gamma,X)$ 5-18.3 MeV, photoneutron and photofission cross sections, giant resonance and deformations 80−68712
$^{A}Ti(\Gamma,X)$, A=46, 48, 50, photoneutron and photoproton cross section systematics 80−13463
^{46}Ti (γ,N), 12-25 MeV, isospin splitting in giant dipole resonance 79−45152
$^{46}Ti(\gamma,p)$ cross-sections calc. from (e,e'p) meas. 77−26666
$^{48}Ti(\gamma,n)$, 15-27.5 MeV, giant dipole resonance splitting, dynamic collective model 80−57755
$^{48}Ti(\gamma,p)$, prep. of carrier-free ^{47}Sc for radiopharmaceutical appl. 77−90892
^{50}Ti (γ,n), ^{49}Ti nuclear levels from n-capture γ-rays 80−37327
$^{50}Ti(\gamma,X)$, photoneutron and photoproton cross sections, giant dipole resonance isospin splitting 80−13442
$^{50}Ti(\gamma,n_0)$, cross sections in giant dipole reson. energy range 79−89286
$^{50}Ti(\gamma,n)$, cross sections in giant dipole reson. energy range 79−89286
Tl(γ,n), photoneutron Q-value determinations using monochromatic photons 79−22271
U, photoneutron cross-section above giant dipole resonance region, quasi-monochromatic photon beam *(French)* 80−78276
^{A}U, A=237,238, nuclear excitation rate for low lying states, e and γ induced transitions 79−17856
$^{A}U(\gamma,X)$, A=235, 236, 238, 5-18.3 MeV, photoneutron and photofission cross sections, giant resonance and deformations 80−68712
^{235}U, giant resonance in total photoabsorpt. cross section 77−6347
^{235}U, transition effects in total photoabsorpt. cross section 77−46160
^{238}U, giant resonance in total photoabsorpt. cross section 77−6347
^{238}U, transition effects in total photoabsorpt. cross section 77−46160
$^{238}U(\Gamma,2n\gamma')$ 45 MeV, ^{237}U shape isomer, γ-decay search, branching ratio 78−93961
$^{238}U(\gamma,2n)$, ^{236}U fission isomer, cross section, half life 78−46045
$^{238}U(\gamma,2n)$, 4.5 MeV, ^{236}U fission shape isomer, γ-decay 80−18230
$^{238}U(\gamma,\alpha)$, 15.5 MeV, cross section upper limit 79−85457
$^{238}U(\gamma,\alpha)$, 9 MeV, cross section upper limit 79−85458
$^{238}U(\gamma,f)$, 12-70 MeV bremsstrahlung, cumulative and fractional product yields for A=128-136 79−36288
U(γ,n), 30 to 140 MeV, partial photoneutron cross section, total cross section approx. 80−22809
^{50}V, low temp. photonuclear nucleosynthesis in stellar H-CNO burning zones 77−13319
$^{51}V(\alpha,p_0)$, differential cross section in giant dipole resonance region from (e,p_0) 79−63655
$^{51}V(\gamma,X)$, 2-5 GeV, spallation 2-5 GeV, spallation yields 77−71604
$^{51}V(\gamma,3n)$, cross sections at intermediate energies 78−8793
$^{51}V(\gamma,p)$, isospin effects in GDR region 78−78344
$^{51}V(\gamma,\pi^\pm)$, 130 to 580 MeV, cross sections, impulse approx., multipole decomp. 77−54206
W, photofission cross section, 220-550 MeV, coherent electron bremsstrahlung beam 79−13353
$^{64}Zn(\gamma,n)^{63}Zn$, giant dipole reson. isospin splitting, reaction cross section *(Russian)* 78−46040
$^{64}Zn(\gamma,n)$, photoneutron energy spectra and intermediate struct. of the giant dipole reson. *(Russian)* 79−22270
$^{68}Zn(\gamma,p)$, 75-800 MeV, yield meas. by activation method 77−71605

photon-nucleus reactions continued
^{90}Zr, γ absorpt., cross section near threshold, E1, E2, M1 resonances, finite Fermi-system theory 77−50055
^{90}Zr(γ, α), above GDR region, cross sections, DWBA anal. 80−63173
^{90}Zr(γ,α) statistical and pre-equilibrium cross sections and multipolarities from (e,α) 80−68646

photon-nucleus scattering
see also photon-deuteron scattering; photon-nucleon scattering
5 to 30 MeV energy range, angular distribs., polarisations, electric quadrupole scatt. in continuum 77−79359
backscattering of γ-rays, atomic number depend., Monte Carlo calcs. 77−67734
Compton scattering, diffractive behaviour, meson exchange effects 78−33165
Compton small-angle scatt. of 5 and 6 GeV photons on ^{1}H and ^{2}H 77−46052
conference on nuclear physics with EM interactions, Mainz, Germany (June 1979) 80−22145
Delbruck and Rayleigh scattering below 5 MeV 80−13456
Delbruck scattering, elastic scatt. of photons by Coulomb field 78−21541
Delbruck scattering amplitudes, numerical calcs. 77−88108
diffraction small-angle scatt. on complex nuclei at 3 and 5 GeV 77−46157
EM interactions, high duty cycle accelerators and experimental possibilities 80−23187
EM sum rules for (γ,γ), (e,e), transitions and giant resonances 80−5090
exchange effects, scatt. amplitude and integrated photoabsorpt. cross section 77−82910
few-nucleon systems studied with electromagnetic probes, future prospects 79−71809
geophysical prospecting, allowance for scattered gamma radiation *(Russian)* 80−105067
giant resonances in deformed nuclei, cross section determ. by semimicroscopic approach 79−9545
light nuclei, total photonuclear cross sections 79−71841
Mossbauer polarimetric resonance electron spectroscopy, theory 79−99808
nuclear resonance excitation by synchrotron radiation 78−78363
photonuclear reacts., conf., International school, Erice, Italy, 1976 77−88111
Rayleigh and Compton contribs. to nuclear resonance scattering of gamma rays, line inversion 80−39919
real photon expts. from continuous wave accelerator 80−42635
two-nucleon system EM processes, baryon resonances 77−79364
virtual photon-nucleus scatt., VMD model alternative space-time view 77−54090
(γ,γ), 2.5-3.5 MeV, level photoexcitation 80−78193
(γ,γ), 412, 468, 662 keV, elastic scatt. cross sections, Rayleigh scattering anal. 80−86898
(γ, γ), low energy computing of photon scattering amplitude 80−68643
(γ,γ) processes using (n,γ) photons 80−18288
(γ, γ'), reaction activation anal. of elements using ^{16}N γ-rays 78−88689
(γ,γ'), resonance scatt., bound or unbound excited level, spin, parity and width of resonance level 80−18287
(γ,γ') scattering at 7.28, 7.63 MeV on Cd, Cd, Ba, ^{239}La, ^{141}Pr, ^{209}Bi, levels of La, Bi anal. 78−13058
γ-ray absorption, enhancement using radiation field of high-power laser, cross section determ. 79−59033
Tl(γ,γ), 4.5 MeV to neutron emission threshold, strengths in energy levels 79−36164
^{11}B, radiative widths meas., 2.125 to 8.92 MeV levels, intensity calibration of photon spectrum 79−13242
^{11}B(γ,γ), resonance scatt., molecular orientation effects 80−78252
^{A}Ba(γ,γ) A=136-8, 1.68-5.0 MeV, nuclear resonance fluorescence, levels transitions and spins 79−6543
^{138}Ba(γ,γ), E<MeV, E(1) and E(2) transitions 77−74797
^{9}Be(γ,γ'), 32 MeV, energy spectra, d prod. process *(Russian)* 80−91177
^{209}Bi(γ, γ), reson. fluoresc. meas., levels, ground state widths 77−74799
^{209}Bi(γ,γ), 4.5 MeV to neutron emission threshold, strengths in energy levels 79−36164
^{209}Bi(γ,γ) 2.754 MeV photons, Delbruck scatt., differential cross section meas. 79−26422
^{12}C(γ,γ), 15.11 MeV energy level excitation, branching ratio 77−30548
^{12}C(γ,γ), 23.5-39 MeV, cross sections and giant resonances, E2 strength 80−63122
^{12}C(γ,γ), 5.5-7.2 MeV, elastic differential scatt. cross section, Thomson scatt. obs. 77−74833
^{12}C(γ,γ), total photoabsorption and elastic cross sections, spectroscopic information *(Russian)* 80−83095
^{13}C, giant reson. isospin splitting, photonuclear and e-scatt. cross-sections 78−577
^{40}Ca(γ,γ), 6.95, 7.12 MeV, strengths of isospin forbidden E1 transitions 78−13059
^{111}Cd(γ,γ), isomeric states excitation, integral cross sections 80−27528
Cd(γ,γ) differential cross sections, 244 to 1408 keV 79−49618
Ce(γ,γ), 2754 keV photon Delbruck scatt. 79−67741
Cl(γ,γ), neutron capture γ-ray Rayleigh scatt. 80−52661
^{52}Cr(γ,γ'), 35 MeV, 2^{+} state deexcitation γ-rays, differential cross sections, deformation *(Russian)* 80−13406
^{52}Cr(γ,γ), up to 12 MeV, highly excited spin-1 resonances, γ-transitions 80−13427
Cu(γ,γ), differential cross sections, 244 to 1408 keV 79−49618
Cu(γ,γ), neutron capture γ-ray Rayleigh scatt. 80−52661
^{166}Er(γ,γ'), 14.4-16.6 MeV, γ-vibr. band head transitions, dynamic collective model 80−57662
^{166}Er(γ,γ), 15 MeV, elastic and nuclear Raman scatt. 80−22811
^{56}Fe(γ,γ), up to 12 MeV, highly excited spin-1 resonances, γ-transitions 80−13427
^{57}Fe, 14 keV state excitation by synchrotron radiation 78−25147
^{2}H, dynamic and static polarisability from Rayleigh scatt., two-photon disintegration 79−75867
Hg(γ,γ), 4.5 MeV to neutron emission threshold, strengths in energy levels 79−36164
^{165}Ho(γ,γ') 8.5-11.4 MeV, elastic and Raman scatt., giant reson. struct. 77−34284
I(γ,γ), 2754 keV photon Delbruck scatt. 79−67741
^{115}In(γ,γ')^{115m}In, appearance energies of In complex cpds. determ. 78−8794

photon-nucleus scattering continued
^{115}In(γ,γ), isomeric states excitation, integral cross sections 80−27528
In(γ,γ), neutron capture γ-ray Rayleigh scatt. 80−52661
^{7}Li(γ,γ'), 32 MeV, energy spectra, d prod. process *(Russian)* 80−91177
^{175}Lu(γ,γ'), elastic and Raman scatt. at 8.5-11.4 MeV, GDR parameters 78−587
^{24}Mg(γ,γ), 5.5-7.2 MeV, elastic differential scatt. cross section, Thomson scatt. obs. 77−74833
^{55}Mn(γ,γ), 5.5-11.4 MeV, interference between reson. and Thomson scatt. 78−33167
^{92}Mo(γ,γ), to 5.1 MeV, excited state lifetimes 77−30512
Mo(γ,γ), 2754 keV photon Delbruck scatt. 79−67741
Mo(ν,γ), 1.17 and 1.33 MeV, cross-sections 79−75973
^{14}N(γ,γ'), 32 MeV, energy spectra, d prod. process *(Russian)* 80−91177
^{15}N(γ,γ), 6.324 MeV, resonance scatt. cross section temp. depend. in BN, NH_4Cl 80−57767
^{15}N(γ,γ), zero point vibr. energy in BN and NH_4Cl 80−59593
^{93}Nb(γ,γ'), energy levels, spin and parity, 6465 KeV resonance total width 78−93940
^{142}Nd(γ,γ), 1.85-5.0 MeV, resonance fluorescence, level radiative widths, spin assignments 79−9538
^{146}Nd(γ,γ'), reson. fluoresc., J$^{\pi}$, M2/E1 and Γ meas. 77−26663
Nd(γ,γ), 2754 keV photon Delbruck scatt. 79−67741
^{22}Ne(γ,γ), up to 18 MeV, nuclear resonance fluorescence, states, transitions and lifetimes 79−45234
Ni giant resonances using virtual and real photons 80−22791
^{58}Ni(γ,γ), M1 strength isospin splitting for dipole ang. distrib. states 80−13412
^{60}Ni, photon scatt., direct obs. by giant dipole reson. 78−93988
^{237}Np(γ,γ') 8.5-11.4 MeV, elastic and Raman scatt., giant reson. struct. 77−34284
^{16}O(γ,γ), 6.95, 7.12 MeV, strengths of isospin forbidden E1 transitions 78−13059
^{16}O(γ,γ), total photoabsorption and elastic cross sections, spectroscopic information *(Russian)* 80−83095
^{17}O, giant reson. isospin splitting, photonuclear cross-sections 78−577
^{206,207,208}Pb(γ, γ), reson. fluoresc. meas., levels, ground state widths 77−74799
Pb (γ,γ), 344-1408 keV ^{152}Eu γ rays, differential cross sections 80−99170
Pb, elastic scatt. cross section for 279 keV γ-rays 79−26421
Pb isotopes, gamma radn. reson. scatt. 4.7-8.3 MeV 78−78362
Pb, Rayleigh and Delbruck scatt., 6.8-11.4 MeV 77−26669
^{A}Pb(γ,γ), A=206-8, 4.5 MeV to neutron emission threshold, strengths in energy levels 79−36164
^{208}Pb(γ,γ), mean polarisation meas. of 4843 keV 78−29446
^{208}Pb(γ,γ), parity of bound J=1 levels 79−22188
Pb(γ,γ) 1.17 and 1.33 MeV, cross-sections 79−75973
Pb(γ,γ), differential cross sections, 244 to 1408 keV 79−49618
Pu(γ,γ) 12.754 MeV, Delbruck scatt., Coulomb correction terms, differential cross sections 80−27629
^{34}S(γ,γ), E<18 MeV, state lifetimes, excitation energies and level cross sections 78−93966
^{123}Sb(γ,γ'), energy levels, spin and parity, strong M1 transitions 78−93940
^{144}Sm(γ,γ), resonance fluorescence up to 5 MeV 78−66263
^{154}Sm(γ,γ'), reson. fluoresc., J$^{\pi}$, M2/E1 and Γ meas. 77−26663
Sn, elastic scatt. cross section for 279 keV γ-rays 79−26421
^{117}Sn(γ,γ'), excitation of 6517 keV level, resonant scatt. 79−3135
^{120}Sn(γ,γ'), excitation by 7310 keV level, resonant scatt. 79−3135
^{120}Sn(γ,γ') nuclear resonant scatt. from 6730 keV level 79−3134
Sn(γ,γ), 2754 keV photon Delbruck scatt. 79−67741
^{88}Sr(γ,γ), 14 MeV, highly excited spin-1 resonances, spin and radiative widths 80−86876
Ta (γ,γ), 2.754 MeV, elastic scatt. diffr. cross section, Rayleigh, Thomson, Delbruck scatt. interference 79−528
Ta, elastic scatt. cross section for 279 keV γ-rays 79−26421
^{181}Ta(γ,γ')^{181}Ta, elastic and Raman scatt. at 8.5-11.4 MeV, GDR parameters 78−587
^{181}Ta(γ,γ), 9 MeV, Delbruck amplitude contrib. determ. 77−41947
Ta(γ,γ), 1.17 and 1.33 MeV, cross-sections 79−75973
Ta(γ,γ), differential cross sections, 244 to 1408 keV 79−49618
Ta(γ,γ), neutron capture γ-ray Rayleigh scatt. 80−52661
^{159}Tb(γ,γ') 8.5-11.4 MeV, elastic and Raman scatt., giant reson. struct. 77−34284
^{232}Th(γ,γ) 2.754 MeV photons, Delbruck scatt., differential cross section meas. 79−26422
^{49}Ti(γ,γ'), nuclear levels from n-capture γ-rays 80−37327
U linear polarisation of elastically scatt. γ-rays of 279 and 662 keV 77−6344
U, Rayleigh and Delbruck scatt., 6.8-11.4 MeV 77−26669
^{238}U(γ,γ), 15 MeV, elastic and nuclear Raman scatt. 80−22811
^{238}U(γ,γ), 6.84-11.39 MeV, Rayleigh and Delbruck scatt. destructive interference, cross sections 79−6566
^{238}U(γ,γ) 7.9, 9.0 MeV, differential cross section, Delbruck scatt., Coulomb correction effect 79−3136
U(γ,γ), 0.1-1.5 MeV, Delbruck and Rayleigh scatt., differential cross sections 80−102180
U(γ,γ), 2.75 MeV, Delbruck theory, multiphoton exchange 78−8796
U(γ,γ), neutron capture γ-ray Rayleigh scatt. 80−52661
Zn(γ,γ), 2754 keV photon Delbruck scatt. 79−67741
Zr, elastic scatt. cross section for 279 keV γ-rays 79−26421
^{91}Zr, nuclear reson. fluoresc., γ-ray spectra 78−588

photon-phonon excitations *see polaritons*

photon-photon interactions
see also photon-photon scattering
charged scalar meson pair prod. by two virtual photons *(Russian)* 77−6069
cosmological red shifts, critical anal. of explanation by photon interaction field 77−9828
electron pair photoproduction, in field of bichromatic plane EM wave *(Russian)* 77−30291
electron-positron pair form. in nuclear field *(Russian)* 77−30290
experimental aspects 79−97627
Fusion of two photons into one on a moving electron *(Russian)* 78−62471
gauge theory, anomalous cross-sections, deep inelastic structure functions 77−38169

photon-photon interactions continued
heavy lepton bound state pair photoprod. in nuclear Coulomb field 77−6103
helicity method, back factorisation procedure, deep inelastic config. 80−22606
jet and single particle prod. at large p_T 79−49565
jet production, QCD study 79−89151
jet struct. at large transverse momentum 78−82225
manifestation strength of colour below and above colour threshold 80−381
polarised positron, electron production by colliding photon beams in storage ring 80−5426
Pomeranchuk singularity in QCD *(Russian)* 79−22078
QCD, two-photon scatt. amplitudes, leading order behaviour 80−52458
QCD tests in γ-γ collisions and high p_T photon production 79−89129
Regge poles, fixed and moving, $\gamma\gamma$ scatt. 78−21406
s-channel helicity conservation at $\gamma V,\gamma\gamma$ and NN vertices, vanishing of spin-zero covariant coupling 79−40691
single tagged event interpretation in $\gamma\gamma$ events, helicity formalism 80−52551
sum rules for charmonium and charmed mesons in QCD 77−30327
tensor meson production in photon-photon collisions 79−93414
theoretical aspects 79−97626
three-photon vertex, weak interaction contributions 77−2787
ultrahigh energy photons traversing cosmic blackbody photon gas, effective penetration distance 79−5742
$ee\rightarrow ee\mu^+\mu^-$, virtual photon-photon collisions, equivalent photon approx. validity 80−5033
e^+e^- calorimetric experiments, $\gamma\gamma$ processes, tests of QCD 80−22628
e^+e^- collisions, jet prod. and two-photon annihilation, hadron spectra 80−91121
$e^+e^-\rightarrow e^+e^-X$, virtual 2 photon processes, luminosity functions, rapidity distrib., QED factors 80−86734
$e^+e^-\rightarrow e^+e^-X$, $X=e^+e^-$, $\mu^+\mu^-$, $\pi^+\pi^-$, η', photon-photon interactions, QED test 79−93425
$e^+e^-\rightarrow e^+e^-$+2 gluon jets from $\gamma\gamma$ interactions cross section, gluon role in QCD 80−4976
$e^+e^-\rightarrow e^+e^-$+2 jets, $\gamma\gamma\rightarrow q\bar{q}$ contrib. to cross section, QCD corrections 80−78106
$e^+e^-\rightarrow e^+e^-e^+e^-$, $\gamma\gamma$ interactions, partial width upper limit 79−40825
$e^+e^-\rightarrow e^+e^-qq(\bar{q}\bar{q})$+ jet, $\gamma\gamma$ initiated 3 jet events in QCD 80−102057
e^+e^- initiated $\gamma\gamma$ processes, charged pair prod., $f^0\rightarrow\gamma\gamma$ width 80−91123
$\gamma^*\gamma^*\rightarrow$2 jets in e^+e^-, parton model QCD corrections for doubly deep processes 80−73758
$\gamma\gamma$, jet cross sections and quark current-photon pointlike coupling, sum rules 80−32104
$\gamma\gamma$ collision radiative corrections from $e^\pm e^\pm$ processes 79−40777
$\gamma\gamma\rightarrow$hadrons, 1-5 GeV, hadron prod. cross sections 80−37315
$\gamma\gamma\rightarrow$hadrons, double equivalent-photon approx. *(Russian)* 79−403
$\gamma\gamma\rightarrow$hadrons, energy pattern for two and three jets, colour corrections, calorimetric expts. 79−71774
$\gamma\gamma\rightarrow$hadrons, sum rules and non-Regge terms 78−25093
$\gamma\gamma$ in electron storage rings, Dalitz-Yennie type equivalent photon spectrum 80−86774
$\gamma\gamma\rightarrow K\bar{K}$ amplitude, coupled channel calc. of final state interactions 77−2809
$\gamma\gamma\rightarrow$large p_T jets, QCD predictions for processes involving real photons 79−6330
$\gamma\gamma\rightarrow\nu\bar{\nu}$, nonzero neutrino mass, early Universe process 78−21483
$\gamma\gamma\rightarrow\pi\pi$, inelasticity effects for real photons in e^+e^- collisions 77−67667
$\gamma\gamma\rightarrow\pi\pi$ amplitude, coupled channel calc. of final state interactions 77−2809
$\gamma\gamma\rightarrow\pi\pi$ scalar-isoscalar amplitude and p EM polarisability 77−82743
$\gamma\gamma\rightarrow$X, equivalent-photon approx. for two-photon processes, role of dynamical cut-off 80−47314
$\gamma\gamma e$, fusion of polarised photons at unpolarised electron *(Russian)* 77−79260
$\gamma p\rightarrow K^+K^-p$, 20-36 GeV, $\Phi(1019)$ prod., cross sections 80−105907
$\gamma p\rightarrow K^+K^-p$, 7 GeV, S-P wave interference near K^+K^- threshold, $S^*\rightarrow K^+K^-$ cross section 79−6343
$\gamma p\rightarrow\mu^+\mu^-$, cross sections, γ struct. function determ. 80−42473
$\gamma p\rightarrow pe^+e^-$, 900 to 1500 MeV, 1100 MeV struct. confirmation, $\rho'(1250)$ leptonic decay obs. 79−30738
$\gamma p\rightarrow\pi^+\pi^-\pi^-p$, $\rho'(1.2)$ production 80−102056
$\gamma p\rightarrow\pi\Delta(1236)$, 744 to 1044 MeV, momentum spectra, differential cross sections *(Japanese)* 78−17032
$\gamma p\rightarrow\rho$+anything, 2.8, 4.7, 9.3 GeV, cross section, multiplicity, energy depend. 77−61303
$\gamma vp\rightarrow\omega p$, ω prod. by virtual photon, ep quasi-elastic scatt. study 77−61302

photon-photon scattering
see also photon-photon interactions
charm production, mass scales, in deep inelastic processes, parton model, generalised VDM 77−13930
dimensional scatt. amplitude and gauge invariance in lowest order 77−71471
effective photon scattering cross section, high intensity laser radiation+-matter interactions 78−74872
laser experiment for possible photon-photon scatt. obs. in vac. 77−74741
mass correction in intense field, pair and photon photoproduction *(Russian)* 77−22673
n-vertex loop diagrams in superstrong calc. field, calc. method 77−71472
pair creation in strong mag. field 78−4816
pair production on photon scattering by intense EM wave in homogeneous mag. field *(Russian)* 80−47227
QCD higher-order asymptotic freedom, corrections, γ struct. function calc. 79−89130
QED tests of electron propagator, vacuum polarisation 80−77994
S-matrix one loop divergences, cancellation in extended supergravity 77−5730
sum rules, meson couplings to two photons 77−6128
supergravity, SO(3) and SO(4), finiteness and renormalisability of scalar multiplet coupling 78−4821
e anomalous mag. moment, γ-γ scatt. contrib. 79−433
$e^+e^-\rightarrow e^+e^-gg$, gluon jet polarisation in photon-photon scatt., QCD test 80−52550
e^+e^- production, high order interactions with relatively low thresholds 77−87962
μ, anomalous mag. moment, sixth order, photon-photon contrib. 78−16958

photon polarisation
atom, outer shell ionisation, ang. distribs. and polaris. of charact. X-rays and Auger electrons 79−10205
beam production, 100 GeV energy range 77−38522
Cherenkov radiation polarisation 77−79241
circularly polarised EM evanescent wave, helicity, reversion by Lorentz transform 78−32696
circularly polarised photon beam prod. by imperfection resonance methods in electron synchrotrons 77−38512
Compton scattering cross sections for circularly polarised photons on polarised electrons 77−18260
deflection of polarized microwave radiation, relative phase delay technique 78−53818
double helix struct., 2 intertwined neutrinos, polarisation, helicity props. of photon 78−37255
e^+e^- angular distribution of e^+e^- pairs produced by linearly polarized photons *(Russian)* 79−40904
Einstein paradox, time symm., photon polarisation in cascade transitions 78−21008
Einstein-Podolsky-Rosen paradox, experimental evidence, quantum theory predictions 77−57225
gravitational effects on polarised radiation from vicinity of black hole 77−82440
linear polarisation following positron annihilation, quantum mech. test 77−69932
monochromatic polarised photon source from Compton backscattered laser light on electrons 80−52800
muon capture, $^{12}C(\mu^-,\nu_\mu\gamma)^{12}B$, impulse approx. calc., photon polarisation 78−37315
neutral current effect in bremsstrahlung and pair production 80−73655
photoemission spectroscopy, angle-integrated, experimental geometry for studying polarisaion effects 79−67395
positronium, triplet, asymmetrical decay, two- and threefold polarisation correlation of photons 80−57536
positronium annihilation, correl. function 78−78158
template modulated coherent light for X- and γ-ray production, energy spectra, freq., polarisation 77−13833
γ source generation and properties, review 80−14029
$\gamma e\rightarrow\gamma\gamma e$, polarised photon splitting on unpolarised electron *(Russian)* 79−371
$\gamma\gamma e$, fusion of polarised photons at unpolarised electron *(Russian)* 77−79260
$np\rightarrow d\gamma$, d relativistic effect on photon circular polarisation 78−93900
$np\rightarrow d\gamma$, γ-polarisation, NN weak pot. in simple gauge model 78−54644
$np\rightarrow d\gamma$, parity nonconservation effects due to $\rho^\pm\rightarrow\pi^\pm\gamma$, short dist. contrib. to γ circular polarisation 77−41855
$np\rightarrow d\gamma$, photon circular polarisation, d P-state, Dirac spinor 78−70390
$np\rightarrow d\gamma$ radiative capture, relativistic effects, parity violation, Weinberg-Salam model *(Russian)* 80−32120
$np\rightarrow\gamma d$, gamma polarisation due to weak parity violating effects 77−41851
$np\rightarrow\gamma d$, photon circ. polarisation calc. using relativistic d wave function 79−67582
$\pi N\rightarrow\mu^+\mu^-X$, longitudinal photon polarisation from helicity ang. distrib. 80−5025
$qg\rightarrow1^\gamma$, high P_T photon polarisation as QCD test 80−4934
Ar+K, photon emission polarisation anal., coincidence studies 80−5614
K+He, photon emission polarisation anal., coincidence studies 80−5614
K+Kr, photon emission polarisation anal., coincidence studies 80−5614
K+Ne, photon emission polarisation anal., coincidence studies 80−5614
K+Xe, photon emission polarisation anal., coincidence studies 80−5614

photon-proton interactions
see also photon-proton scattering
baryoniums coupled directly to photon 79−17694
charm particle prod. by photon-gluon fusion 78−45923
charm photoproduction, threshold bump 78−70379
contact EM terms in inclusive photo- and electroprod., γp total cross sections, generalised VMD 78−70348
core valence quark model, vector meson dominance total photoproduction cross section 79−49497
dispersion relations, Thomson limit calc. using rising total cross sections 79−22103
jets as source for observed increase in γp cross-section 80−22620
proton Compton scattering, dispersion relation anal. 79−36084
total cross sections, 18 to 185 GeV, vector meson dominance model calc. 78−54635
total cross sections, VDM anal. of ψ family 79−22083
total photoprod. cross sections for E>4 GeV, review 78−78186
$\gamma n\rightarrow\pi^+p$, π^+n, π^-p, $K^+\Lambda$, $K^+\Sigma^0$ final state comparisons above resonance region 80−105906
γp, 30-180 GeV, ρ and ϕ elastic photoprod. cross sections 80−95278
γp, 40-70 GeV, inclusive $\bar{D}^0$ photoprod. cross sections, pair and associated prod. 80−91097
γp, 46-180 GeV, ω-meson photoprod. cross section, $\omega\gamma$ coupling constant 80−13319
γp, heavy quark particle photoprod., QCD model, vector dominance implications 80−86730
γp, π multiplicity and asymmetric fireballs 79−93474
$\gamma p\rightarrow$ lepton pair, P violating asymmetry 80−105901
$\gamma p\rightarrow(p\bar{p})p$, inclusive and exclusive $p\bar{p}$ photoprod. S(1936) prod. 80−86729
$\gamma p\rightarrow cX$, c=hadron, photon fragmentation region, Regge pole expansion 77−54108
$\gamma p\rightarrow e^+e^-p$, reson. struct. obs. background process *(Russian)* 78−89722
$\gamma p\rightarrow\eta^0p$, phtotproduction cross-section asymm. for 1.39 to 1.78 GeV polarised photons *(Russian)* 77−79273
$\gamma p\rightarrow\gamma$+jet+X, perturbative QCD predictions large p_T real photon in final state 79−89165
$\gamma p\rightarrow h^\pm X$, large p_T photoprod., perturbative QCD test 80−37276
$\gamma p\rightarrow hX$, quark jet model and total cross section 79−13133
$\gamma p\rightarrow hX$, SU(3)×SU(3) invariant interaction of quarks, large p_T, gluon bremsstrahlung 78−33072
$\gamma p\rightarrow K^+K^-\pi^+\pi^-p$, 20-70 GeV, $K^+K\pi$ threshold enhancment 80−78076
$\gamma p\rightarrow K^+\Lambda$, meas. of asymmetries and cross sections using 16 GeV linearly polarised photons 80−13318
$\gamma p\rightarrow K^+\Lambda^0$, 1.1 to 1.3 GeV, polarised proton target 78−66125
$\gamma p\rightarrow K^+\Lambda^0$, resonance region, Λ^0 polarisation 78−66131
$\gamma p\rightarrow N\pi$, 250-500 MeV, multipole anal. *(Russian)* 77−246
$\gamma p\rightarrow N\pi$, Δ^+ isobar mass and total width, $M^{3/2}{}_{1+}$ amplitude pole position *(Russian)* 78−86453

photon-proton interactions continued
$\gamma p \rightarrow N\pi$, position and residue of the pole in the $M_{1+}^{(3/2)}$ amplitude *(Russian)* 79−22112
$\gamma p \rightarrow n\pi^+$, cross-section and asymmetry ratios in region of first resonance *(Russian)* 78−78196
$\gamma p \rightarrow n\pi^+$, multipole anal. by regularisation method *(Russian)* 77−82753
$\gamma p \rightarrow n\pi^+$, multipole anal. in region of first reson. 80−22622
$\gamma p \rightarrow n\pi^+$, photoprod. of π^+ by unpolarised and linearly polarised photons 77−46055
$\gamma p \rightarrow n\pi^+$, pion photoprod. using coherent bremsstrahlung beam and polarised proton target *(Russian)* 79−80830
$\gamma p \rightarrow n\pi^+$ 340 MeV, cross section asymmetry *(Russian)* 79−63487
$\gamma p \rightarrow n\pi^+$ reaction, with polarised protons and photons at 340 MeV *(Russian)* 79−89170
$\gamma p \rightarrow n\pi^+$ section asymmetry, pion-proton twin birth contribution *(Russian)* 80−47308
$\gamma p \rightarrow n\pi^*$, 340 MeV, pol. p, first resonance region, π^+ photoprod., T-asymmetry *(Russian)* 80−62997
$\gamma p \rightarrow pX$, 710 to 950 MeV, momentum spectrum of recoil protons 79−22108
$\gamma p \rightarrow p$+vector meson, total cross section *(Russian)* 78−8674
$\gamma p \rightarrow pe^+e^-$, 7.2 GeV, new vector meson search in 0.9-2.2 GeV 77−54110
$\gamma p \rightarrow pe^+e^-$, prod. of ρ, ω, ϕ anal. 78−50037
$\gamma p \rightarrow p\omega$, backward prod., baryon exchange dip and parton effects 78−17030
$\gamma p \rightarrow \bar{p}pp$, threshold −4.8 GeV, elastic photoprod. cross section 80−52521
$\gamma p \rightarrow p\phi$, 3.0 to 6.7 GeV, elastic and inelastic ϕ photoprod. 79−9380
$\gamma p \rightarrow p\pi^0$, 500 MeV, double polarisation expt. *(Russian)* 77−74696
$\gamma p \rightarrow p\pi^0$, multipole anal. in region of first reson. 80−22622
$\gamma p \rightarrow p\pi^0$, photoproduction, in low-energy region, complex multipole amplitudes 80−68463
$\gamma p \rightarrow p\pi^0$, pion photoprod. using coherent bremsstrahlung beam and polarised proton target *(Russian)* 79−80830
$\gamma p \rightarrow p\pi^0$, quantum chromodynamics and P-odd effects *(Russian)* 79−89172
$\gamma p \rightarrow p\pi^0(n\pi^+)$, to 500 MeV, multipole anal. near P_{33} reson. *(Russian)* 77−74695
$\gamma p \rightarrow p\pi^0\pi^0$, 710 to 950 MeV, cross section determ. from momentum spectrum of recoil protons 79−22108
$\gamma p \rightarrow p\pi^+\pi^-$, 710 to 950 MeV, cross section determ. from momentum spectrum of recoil protons 79−22108
$\gamma p \rightarrow \pi^0 X$, invariant cross section at large p_T, hard scatt. model 80−22621
$\gamma p \rightarrow \pi^0$+jet+X, perturbative QCD predictions 79−89165
$\gamma p \rightarrow \pi^0(p^+)p$, energy independ. multipole anal. through second resonance region 78−62410
$\gamma p \rightarrow \pi^0 p$, 0.6 to 1.8 GeV, backward angles, η-cusp 80−57609
$\gamma p \rightarrow \pi^0 p$, 0.9 to 1.2 GeV, ang. distribs. of differential cross section 77−87982
$\gamma p \rightarrow \pi^0 p$, 1 to 10 MeV above threshold 79−85454
$\gamma p \rightarrow \pi^0 p$, 1.0 and 1.1 GeV, forward prod. on polarised protons 77−74692
$\gamma p \rightarrow \pi^0 p$, 1.4 GeV, differential cross section meas. 80−42476
$\gamma p \rightarrow \pi^0 p$, 2 to 6 GeV, differential cross section meas., parton model anal. of energy depend. 79−63485
$\gamma p \rightarrow \pi^0 p$, 250 to 500 MeV, multipole anal. *(Russian)* 77−10266
$\gamma p \rightarrow \pi^0 p$, 290 to 360 MeV, differential cross sections in $\Delta(1232)$ region *(Russian)* 78−89852
$\gamma p \rightarrow \pi^0 p$, 360-500 MeV, secondary proton polarisation meas. *(Russian)* 78−54637
$\gamma p \rightarrow \pi^0 p$, 390-975 MeV, differential cross section 80−86725
$\gamma p \rightarrow \pi^0 p$, 400 to 1142 MeV, recoil proton polarisation 80−82981
$\gamma p \rightarrow \pi^0 p$, 450 to 800 MeV, proton polarisation, Walker-type anal., $P_{11}(1470)$, $D_{13}(1470)$, $S_{11}(1535)$ resonances 80−73721
$\gamma p \rightarrow \pi^0 p$, 480-800 MeV, proton polarisation at second πN resonance *(Russian)* 78−78192
$\gamma p \rightarrow \pi^0 p$, below 1 GeV, polarised target asymmetry meas., comparison with phenomenological anal. 78−62409
$\gamma p \rightarrow \pi^0 p$, differential cross sections at large angles, 2-6 GeV 78−37214
$\gamma p \rightarrow \pi^0 p$, E_γ=1.3 to 2.1 GeV polarisation parameter meas. 79−80829
$\gamma p \rightarrow \pi^0 p$, high energies, semiempirical amplitude anal. dispersion relations and Regge poles 80−86726
$\gamma p \rightarrow \pi^0 p$, photoproduction amplitudes, cross-sections, asymmetry relations review *(Russian)* 78−54636
$\gamma p \rightarrow \pi^0 p$, proton polarisation vector components *(Russian)* 79−85305
$\gamma p \rightarrow \pi^+ n$, low energies, complex amplitudes in s- and p-wave approx. 80−102053
$\gamma p \rightarrow \pi^+ n$, 0.5-0.8 GeV, ang. distrib. of polarised target asymmetry 77−34165
$\gamma p \rightarrow \pi^+ n$, 1.35-1.65 GeV, pol. γ, resonance energy region, cross section asymmetry *(Russian)* 80−86727
$\gamma p \rightarrow \pi^+ n$, 250 to 500 MeV, multipole anal. *(Russian)* 77−10266
$\gamma p \rightarrow \pi^+ n$, 250 to 790 MeV, cross section features 77−46053
$\gamma p \rightarrow \pi^+ n$, 520 to 2250 MeV, meas. of Σ, T, and P polarisation parameters 79−75778
$\gamma p \rightarrow \pi^+ n$, 600-1875 MeV, pol.p and γ, G and H polarisation parameters 80−99105
$\gamma p \rightarrow \pi^+ n$, 850 MeV, target asymmetry meas. 78−21438
$\gamma p \rightarrow \pi^+ n$, photoproduction amplitudes, cross-sections, asymmetry relations review *(Russian)* 78−54636
$\gamma p \rightarrow \pi^+ n$, π^+ form. asymm. near first πn resonance *(Russian)* 78−66124
$\gamma p \rightarrow \pi^+ n$, $\pi^+ n$, $\pi^- p$, $K^+\Lambda$, $K^+\Sigma^0$ final state comparisons above resonance region 80−105906
$\gamma p \rightarrow \pi^+ n$ below 1.02 GeV, polarized target asymm. meas. 78−17029
$\gamma p \rightarrow \pi^+\pi^- p$, Chew-Low amplitude correction 77−2844
$\gamma p \rightarrow \pi^+\pi^- p$, Lagrangian model, polarised and unpolarised photons 78−17028
$\gamma p \rightarrow \pi^+\pi^-\pi^0\pi^0 p$, 20-70 GeV, $\omega\pi^0$ state enhancement at 1.25 GeV 80−78078
$\gamma p \rightarrow \pi^+\pi^-\pi^0\pi^0 p$, $\rho_3^+(1.6)$ production 80−102056
$\gamma p \rightarrow \pi^-\pi^-\pi^+\pi^+\pi^- p$, diffractive production, jet-like structure 80−57606
$\gamma p \rightarrow \pi^\pm X$, comparison with $\bar{p}p \rightarrow p\pi^\pm X$, quark parton model anal. 79−63512
$\gamma p \rightarrow \pi^\circ X$, duality and finite energy sum rules 80−42477
$\gamma p \rightarrow \pi N$, universal function for large angle cross sections of exclusive hadronic reactions 77−50010
photon-proton interactions continued
$\gamma p \rightarrow \pi N$ multipole isotopic anal., soln. irregular behaviour near P_{33} resonance *(Russian)* 80−5005
$\gamma p \rightarrow \pi X$, large p_T, perturbative QCD 80−86723
$\gamma p \rightarrow \pi\pi N$, 710-950 MeV 79−63484
$\gamma p \rightarrow q\bar{q}p$, quark-antiquark jet diffractive photoprod. in perturbative QCD 80−73714
$\gamma p \rightarrow \rho^- \Delta^{++}$, 2.8 to 4.8 GeV, cross-sections, ρ spin density matrices 80−62999
$\gamma p \rightarrow \rho^- \Delta^{++}$, 9.7 GeV, pion exchange mechanism anal. 77−82750
$\gamma p \rightarrow \rho^+ n$, 2.8 to 4.8 GeV, cross-sections, ρ spin density matrices 80−62999
$\gamma p \rightarrow \rho^+ n$, 9.7 GeV, pion exchange mechanism anal. 77−82750
$\gamma p \rightarrow V^0 p$, one-pion exchange contrib., vertex corrections 78−50039
$\gamma p \rightarrow$ vector meson+p, elastic and total cross section using Reggeon-photon coupling analogy 78−78193
$\gamma p \rightarrow W^+(Z^0)+X$, inclusive cross sections, quark-parton model calcs. 79−71755
$\gamma p \rightarrow W^+ n$, current algebra and sum rules high energy W^+ prod. 80−102039
$\gamma_v p \rightarrow K^+ X^0$, $K^+\Lambda$, or $K^+\Sigma^0$, K^+ electroprod. along virtual photon direction, cross sections 77−41848
$\gamma\gamma \rightarrow \pi^0 p$, phase shift anal., shrinking photon, geometrical duality 77−87983
$\gamma_v p \rightarrow \pi^+\Delta^0$, Δ^0 prod. characts. 79−9383
$\gamma p \rightarrow \pi^+\pi^- p$, 20-70 GeV, dipion enhancemment, $\rho'(1600)$ observation 80−78079
K^+K^- high mass pairs, 1.4 to 2.4 GeV mass range, in H 79−22110
$\nu p \rightarrow \pi$, threshold to 450 MeV, energy depend. multipole anal. 80−32110
p electric polarisability, from photoabsorption cross-section 80−57597
π^0 inclusive photoprod. and quark-parton model 78−78189
π^0 photoproduction from protons, 0.7-1.45 GeV, polarised target asymmetry 77−46054
π^0 prod., 1300-2300 MeV, meas. of double polarisation parameters 80−13317
π^0 production in γp interactions, resonance region, asymm. *(Russian)* 78−17031
$\pi p \rightarrow p\pi^0\pi^0$, medium energy, cross section *(Japanese)* 77−41847
$\pi p \rightarrow \pi^0 p$, 650 and 700 MeV, angular depend. of secondary p polarisation *(Russian)* 78−78191
$\gamma p \rightarrow K^+\lambda(\Sigma^0)$, $\pi^+ n$, $\pi^- p$, $K^+\Lambda$, $K^+\Sigma^0$ final state comparisons above resonance region 80−105906

photon-proton scattering
see also photon-proton interactions
Compton differential cross sections, 450 to 950 MeV 78−93885
Compton effect, <450 MeV, dispersive anal. 79−396
Compton scattering, 375 to 1150 MeV, differential cross section 80−57604
Compton scattering of protons, simple Regge pole model 78−93884
Compton small-angle scatt. of 5 and 6 GeV photons on ^1H and ^2H 77−46052
dispersion relation anal. of Compton scatt. at low energies 77−82744
elastic scatt. <400 MeV, proton polarisability coeff. *(Russian)* 77−49973
low energy, one-particle-exchange model 78−457
low energy proton Compton scattering, p polarisabilities 78−93886
quark loop contrib. to photon total cross sections 80−4999
γp, low energy scatt., one-particle exchange model 80−22617
γp, proton polarisability determ. 78−17025
$\gamma p \rightarrow \gamma p$, 2 to 6 GeV, differential cross section meas., parton model anal. of energy depend. 79−63485
$\gamma p \rightarrow \gamma p$, differential cross sections in 240 to 440 MeV range, $\Delta(1232)$ region 77−10255
$\gamma p \rightarrow \gamma p$, differential cross sections at large angles, 2-6 GeV 78−37214
γp high multipole polarisabilities from Compton scatt. amplitudes 79−85301
γp low energy scatt., one particle exchange model 78−33070
$\phi(1019)$ photoproduction on proton, 2.8-4.8 GeV 79−9381
γp scatt. in $\Delta(1236)$ resonance region, dispersion relation anal. 80−18140

photon scattering *see photon-deuteron scattering; photon-hadron scattering; photon-lepton scattering; photon-nucleus scattering; photon-photon scattering*

photon transport theory
absorption, k-photon, unsaturated, exact soln. of master eqn. 80−37984
adjoint photon transport, Monte Carlo biasing scheme, Compton scatt. and absorpt. 78−77819
air-over-ground calcs. for various cross sections, weapon effect studies 77−23164
Ambartsumian's function derivatives w.r.t. single scatt albedo *(Russian)* 77−49698
anisotropic dispersive media, generalisation of Planck's law 78−18153
annihilation radiation from point isotropic photon sources, numerical calc. 79−85096
antibunching in two-photon absorption 78−78980
asymptotic solution of γ-ray transport eqn. 77−45810
atmosphere photon transport problems, modified Monte Carlo procedure 78−61560
attenuation and energy absorpt. coeffs. for ICRP Reference Man organs and tissues 77−73582
attenuation coeffs. in heterogeneous media, nuclear geophysics methods 79−39708
biological materials, extrapolation of linear attenuation coefficients from diagnostic energies to megavolt range 78−24145
bremsstrahlung in bulk media, shielding study, Monte Carlo anal. of thick target spectra 78−59839
bunching in thermal radiation, temp. depend., photodetector thermal fluctuation 78−24748
complex particle transport problem soln., general-purpose Monte Carlo codes 79−583
Compton effect, multiple scattering, energy profiles, anal. and numerical calcs. 77−93
Compton effect, multiple scattering, Monte Carlo calcs. 77−94
Compton scattering, Monte Carlo simulation including γ-ray polarisation 77−34476
concrete Eisenhauer-Simmons γ-ray build-up factors, Taylor coeffs. 77−34394
data covariance estimation methods for sensitivity-based data assessment 78−13400
deep-penetration radiation transport, event and point value in Monte Carlo importance sampling 78−8869

photon transport theory continued
direct coupled-ray method for design oriented 3-D anal. 77−83111
Doppler broadening, photon kinetic eqn. 77−74334
dose and LET distributions due to neutron and photons from stopped pion 77−52878
dual gauging using penetrating and scattered photon fluxes 77−41551
early universe, photon and neutrino diffusion rel. to nonlinear primordial fluctuations 79−25773
earth, radiation transport for neutron and γ-ray point sources above air-ground interface 80−32526
electron beam fusion of D-T pellets, neutronics and photonics 80−52781
electron-photon cascade production and transport is externally applied EM field, appls. 77−68157
EM cascade showers, electron/photon energy flow 77−22027
emission power spectra described by solns. of Kompanyets' kinetic eqn. *(Russian)* 78−152
ENDF/B-V nuclear data for shielding appls., energy balance anal. 80−47745
entropy estimation by weight functions 78−408
finite moments algorithm for particle transport problems 79−67237
fusion reactor materials, nuclear response functions library, MACKLIB-IV 79−67950
fusion reactor shielding experiment, cross-section sensitivity calcs., one- and two-dimensional models 80−27799
fusion reactors, TFTR test cell, calc. dose rates from induced activity, Monte Carlo methods 80−57967
gamma buildup factors for photons in air, water, iron, moments method code 80−27828
gamma photon detection processes, statistics of radiation 77−65010
gamma ray coherent scatt., semiempirical formulation 77−55846
gamma-ray albedo data, removal of negative albedo terms 80−5347
gamma-ray heating in 300 MW(e) GCFR 77−61486
gamma-ray intensity from an activated cylinder 78−16761
gamma-ray natural flux spectral distribution, analytical approx. 78−815
gamma-ray penetration in heterogeneous systems 79−18050
gamma-rays, anisotropic computations selection of angular quadrature 77−37828
gastrointestinal tract, specific absorbed fractions for photons emitted in walls 77−90903
heating, nuclear, approx. method, direct energy balance calc., γ transport, accuracy 77−6495
impulse of photon in medium with negative group velocity *(Russian)* 79−3670
integral equation methods 77−53843
laser driven fusion reactor, Monte Carlo study of asymmetric effects of LiO_2 blanket 78−74464
laser fusion blanket, neutronics and photonics 78−5025
LMFBR, heterogeneous core design, neutron and γ-transport effects 78−8893
low-energy photon attenuation within human thorax 79−5373
LWR lattices, Monte Carlo radiation transport program for reactor bundle gamma transport and energy deposition analysis 80−22915
mass energy-absorption coeff. air/medium ratios for ionometric dosimetry, 0.1 keV to 20 MeV 77−40784
matrix methods for radiation transport 78−13198
Monte Carlo biased transport calcs. optimisation, prediction of statistical error 79−58654
Monte Carlo calculation of γ-ray backscatt., atomic number depend. 77−67734
Monte Carlo deep penetration calcs., appl. of fictitious scatt. transport model 78−29526
Monte Carlo energy sampling method, adjoint transport processes 77−22503
Monte Carlo shielding calcs., biased selection of particle flight directions as variance resolution technique 78−29653
Monte Carlo track rotation estimator, calc. of total flux at point 79−71385
multigroup Monte Carlo photon cross section technique 78−4570
neutron-photon multigroup cross sections for neutron energies ≤60 MeV 79−30880
nonlinear radiation transport, soln. by renormalisation group method 80−67555
photon-photon scattering, effective-photon theory for cross-section 78−58962
probability table method extension 79−584
pulsed source, distrib. of scattered γ-radiation, unsteady transport 80−27830
PWR, shielding against neutron and gamma streaming, computational methods 78−21783
radiation dose deposition calcs. in human marrow 80−26365
radiation field in flat parallelepiped, ideal photon gas eigenvalue spectrum 78−8344
radiation protection studies expt. and theoretic results comparison 80−47750
radiation shielding, cross section sensitivity analysis 78−21778
radiation streaming, shield design problems 78−21780
radiation transport calc., Monte Carlo approach for engineers 79−585
radiative transfer calculations, appln. of multiband method 80−95333
radiography, contrast in computerised transverse axial tomography of brain 77−86608
radiography, photon path visualisation by Monte Carlo simulation 77−66848
RCP01 Monte Carlo program, neutron capture and photon heating rates 79−71912
reactor core and shield calc., radiation transport program benchmark tests 78−78440
reactor shielding, current status and future prospects 78−25328
reactor shielding methods, development in USA 78−21776
reactor shielding methods, evolution, data 78−21775
relativistic Maxwellian electrons, moment generated radiative transfer functions 78−24747
resonance fluorescence, photon antibunching, quantisation of light 78−66791
S_N methods, exponential supplementary eqns., one-dimens. case 77−50189
scattering angles selection in MORSE, rejection technique 78−4571
shielding, in 3-D direct-coupled-ray method 78−21785
slowing down in highly anisotropic scatt., statistical fluctuations of collision energy losses 77−62572
terrestrial γ radiation transport in plane semi-infinite geometry 80−73284

photon transport theory continued
TFTR, isodose contour map construction using DOT 3.5 computer code 79−67949
TIGERP, 1-D multilayer electron/photon Monte Carlo transport code 79−54079
tissue, 4th order polynomial coeffs. for photon interaction data of 69 ICRP reference man tissues 78−28077
tissue substitute material formulation using basic interaction data 77−86640
Tokamak, expt. power reactor, neutronic and photonic calcs., blanket and shield design 78−29644
Tokamak fusion test reactor, dose rates from induced activity in test cell 80−23144
transport-equation, with anisotropic scatt. in finite slab geometry 79−17364
turbulent medium, photon interactions *(Russian)* 79−88
unsteady γ-ray transport, small angle scatt. approx. 78−16760
water/air mass stopping power ratios for megavolt. photon and electron beams 78−28082
weapon physics, appl. of space angle synthesis to 2-D transport 77−83107
X-ray spectral composition following backscatt. from semi-infinite reflectors 77−54028
Z-depend. of gamma-ray elastic scatt., power law 78−45578
γ 6 MeV scalar leakage flux spectra through Pb-Al and Fe-Al shields 79−85871
γ-ray build-up factors for finite media 77−61623
^{60} γ-ray scatt. in air, anal. by discrete ordinates transport codes 80−32525
D-D fusion reactor blanket, nucl. characts., summary 78−89973
Li, T breeding performance eval., multigroup neutron and photon transport calc. 80−13831
LiO_2, T breeding performance eval., multigroup neutron and photon transport calc. 80−13831
Li_7Pb_2, T breeding performance eval., multigroup neutron and photon transport calc. 80−13831
N, neutron scatt. and gamma-ray prod., Monte Carlo anal. 77−26682
$^{14}N(n,\gamma)$, gamma-field from monodirectional neutron source in air 77−67785
Pb/H_2O stratified radiation shields, calc. of gamma-ray buildup factors using BIGGI 4T code 80−86994
U well logging, gamma-ray spectra calc. using discrete ordinates transport code 79−53572

photons
see also cosmic ray photons; gamma-rays; light; photon transport theory; X-rays
ballistic theory of light based on EM force laws and Newtonian mechanics 80−50
behaviour in high intensity coherent laser beams 80−28185
black hole geometry, photon orbit charts for teaching 77−33783
charged photons of magnitude αe (α=fine structure constant) 79−97551
creation, Planck's const. and fine struct. calcs. 78−82135
curved space-time, propag. of photons and neutrinos 77−79011
Dirac-like equation, transform. props. 79−58914
discharge, impulse-type cathode streamer, emitted photons estimation *(Japanese)* 79−32845
distribution functions, QCD predictions using Altarelli-Parisi eqns. 80−78019
dosimetry standardisation in Germany 80−5353
double helix struct., 2 intertwined neutrinos, polarisation, helicity props. 78−37255
Einstein and the quantum theory, review 80−22237
emission from biological systems *(German)* 79−96527
emission from blackbody, thermodynamic laws, teaching 80−105451
fine-structure constant, coupled Maxwell and Dirac eqns., QED 80−62894
fission in intense laser fields and nuclear Coulomb field, QED test 80−4895
form factor, asymptotic behaviour in QED 80−18096
fuzzy ball model, motion in free space 77−74622
gravitational interaction, QED corrections 77−65131
hadronic props., effect of large intermediate masses in hadron-mediated photon-nucleus interaction 80−27625
hadronic props. of photons, book contrib 78−82217
hadroproduction, QCD test 79−17745
heavy guided photon in gravit. field 80−67949
invariant struct., wave function 77−71475
mass of photon, fermion radiative decay 78−41456
mass upper limit and effect on static planetary mag. fields 77−33477
massive, and tachyon monopoles 78−20986
massive photons, rel. to hot gas stability in clusters of galaxies *(Russian)* 79−44614
matter formation, photon condensation, treatment using Bose-Einstein statistics 78−12435
multiphoton events in p-nucleus interactions, 300 GeV/c 77−10283
new theory of photon and energy based on two primitive particles 79−67145
nonlocal form factors, extended extremal approach 77−61227
pair prod. in strong mag. field 78−407
para-fermion composites, limitations 79−40704
position operator, Galilean components 77−33906
positronium hyperfine struct., $m\alpha^6$ contribs. from two photon virtual annihilation 78−89642
production, hadronic, AB→γγX, scaling and quark mass dependence, quark parton model 80−73749
QCD quark-gluon plasma, hadronic prod. of leptons, photons and ψ *(Russian)* 78−89672
QCD quark-gluon plasma, hadronic prod. of leptons, photons charm and ψ 78−89669
QED treatment of scalar and longitudinal photons, EM field quantisation, Lorentz gauge 77−34111
quantum absorber theory, direct-action, photoelectron antibunching effect 80−57535
quantum mechanical theory 77−13519
relativistic transformations, Newtonian force and EM field, for teaching 78−49601
rest frames for tachyons and photons 77−60928
rest mass, as cosmic test of Maxwell's eqns. 77−45708
rest mass upper limits from astrophysical data 77−34200

photons continued
scalar boson scatt., impact on Planck's radiation law and Hubble effect 78−54212
scalar mode rel. to Hubble effect *(German)* 77−45305
scattering by bosons, appl. to anomalous astron. redshifts, effects on spectral line profiles 77−13458
spin, relation to isospin, strangeness and charm 80−37183
spin dependent photon structure functions from Drell-Yan and e^+e^- reactions 80−82973
splitting into 3, cosomological limits, spectral broadening, frequency-dependent and multiple red-shifts 80−77284
stochastic phase space kinematics 79−2649
structure function determ. in $\gamma p \rightarrow \mu^+\mu^- X$ expts. 80−42473
structure functions, anomalous components, using Altarelli-Parisi eqns. for QCD scale breaking 79−63479
structure functions, QCD predictions in asymptotically free gauge theory 79−30736
structure functions parametrisation 80−37267
tensor mesons, EM decay possible source of photons and leptons 79−13130
unpolarised lepton-lepton collisions, photon 3rd struct. function, QCD implications 80−73708
variable mass across anisotropic medium *(French)* 77−13624
visual perception of dim light, seen as uniform light not isolated flashes due to photons 78−96052
$\gamma \rightarrow \nu\bar{\nu}$, in strong mag. field, rel. to pulsars and neutron stars *(Russian)* 77−17360
$\gamma \rightarrow \pi^+\pi^-$ decays in nuclear matter 77−65209
pp, 31-63 GeV, direct photon prod. at large p_T, π^0/γ prod. ratio 80−63038
pp, 62.4 GeV/c, direct single photon prod. at large p_T 80−91113
pp, ISR energies, high p_T π^0 and single photon events, associated charged particle multiplicity 80−63039
$p\bar{p} \rightarrow e^+e^-X$, large p_T, reference to $\Upsilon(9.5)$, $\xi(3.5)$ and direct γ-prod. 78−89749

photonuclear reactions *see photon-nucleus reactions*

photophoresis
action spectrum of photophoretic force 79−50841
aerosol, large particles, photophoresis in optical radiation field 77−12836
aerosol, low Knudsen number spherical particles 77−63965
aerosol, photophoretic motion, particles ≪ light wavelength, gas collisional effect 77−90646
aerosol, photophoretic motion of nonvolatile particles, thermal diffusion effect 78−79364
aerosol particles, volatile, large-size, theory of photophoretic motion 77−9132
brick dust in air, aerosol, photophoresis in optical radiation field 77−12836
droplet motion in optical radiation field for small Knudsen number values 78−35730
film, ultrathin, effort of optical radiation on growth and struct. 78−72045
irradiated sphere absorption centres, temperature distribution theory, source function 79−50221
particle orbits in focused light beam *(German)* 79−61908
perylene crystallite, photophoretic force, action spectrum determ. 79−50841
phthalocyanine-alkane interface, charge transfer, rel. to photoelectrophoretic image form. 80−65616
rarefied gas, thermophoresis, photophoresis *(Russian)* 77−27560
spectrometer for spectral dependence meas. of radiometric force on micron sized particle 80−105719
spectroscopy, broadband photophoretic 80−86469
spherical particle in slightly rarefied gas, forces calcs. 79−94672
stable orbits, circular, cycloidal and oscillating *(German)* 79−80545
Se, amorphous film, photodeposition by Selor process, kinetics 78−75963
Se, amorphous film, photodeposition by Selor process, struct. and kinetics 78−75964
Se, amouphous film, photodeposition by Selor process struct. 78−75962
TiO_2, suspended in highly insulated liq., photoelectrophoretic phenomenon, direct imaging system 77−54005

photoplasticity
discs, doubly-connected, noncircular, full yielding at collapse, photoplastic verification 80−74756
II-VI semiconductor, charged dislocation motion during plastic deform. 79−82233
polyester, stress-optic law, photoplasticity, RPE transition temp. 78−10120
polyester model material, optical response and yield behaviour 78−31453
review of photoplastic effects *(Japanese)* 78−6121
CdS, photoplastic effect due to α, β dislocations, spectral depend. 77−90180
CdS, photoplasticity and photocond., excitation energy conc. near dislocations, hardening 77−24346
CdS, surface layer, photomechanical and photoplastic effects 79−99264
CdS(Se)(Te), charged dislocations, flow of charge with plastic deform. 80−85010
CdTe, crystal size depend. of photoplastic effect 80−92592
CdTe, crysts., mech. behaviour, yield stress function of temp., stress relaxation 79−60427
CdTe, negative and positive photoplastic effect 79−51192
CdTe, photoplastic effect, influence of plastic deform., heat treatment and doping 79−82277
GaP, mech. props. and photomechanical effect 77−84833
KCl, γ-irrad., photoplastic effect and internal friction aftereffect 80−24529
KCl:Ba, negative photoplastic effect, photodestruction of Z-centres 77−43272
NaCl, γ-irrad., photoplastic effect and internal friction aftereffect 80−24529
NaCl, photoplastic effect *(Japanese)* 79−82279
ZnO(S)(Se)(Te), charged dislocations, flow of charge with plastic deform. 80−85010
ZnSe, cryst., elec. cond., dislocation motion effects 80−54710
ZnSe, photoplasticity and photocond., excitation energy conc. near dislocations, hardening 77−24346

photorefractive effect
acousto-optic memory correlator, long duration, using acousto-photorefractive effect 78−79124
acousto-optic memory correlator using acousto-photorefractive effect 78−71248
acousto-optic real-time radar and sonar signal processing 79−72515
acousto-optical devices for real- and near-real-time signal processing 80−10024
application to optical memories, holographic interferometry, and integrated optics 79−3756
Bragg deflector, using photorefract. effect in $As_{40}Se_{15}S_{35}Ge_{10}$ film loaded on $LiNbO_3$ waveguide 80−58673
edge enhancement, real-time, using photorefr. effect 80−99642
electro-optic crystals, hologram formation arbitrary transport length anal., photovoltaic effects 80−78802
ferroelectric, photoinduced changes in refractive index and spontaneous polarisation 78−43804
ferroelectric materials, mechanisms 78−92045
ferroelectrics, photoelectretic states in real time spatial light modulators, photorefractive effect 80−80676
hologram recording, dispersion photorefraction due to triplet state processes 79−27210
hologram recording sensitivity in photorefractive medium 78−5438
holographic grating form. in photorefractive cryst. with arbitrary electron transport lengths 80−1151
holographic grating recording, pyroelectric mechanism 78−42300
holographic memory materials, elec. field and photocurrent meas. 78−71066
holographic storage capacity, photochromic and photorefractive media 79−27203
$LiNbO_3$:Fe(Cu), photorefractive recording of volume holograms 78−37849
liquids, photoacoustic and photorefractive detect. of small absorpts., electrostrictive limits 80−108171
materials for optical data storage 78−79086
optical fibre, nonlinear effects, appl. to active and passive device fabrication 80−58638
optical storage materials and methods, conf., San Diego, USA (Aug. 1977) 78−71171
PLZT, optically induced birefr. change 78−43832
salicylideneaniline, photochromic, optically induced changes in refr. index 79−81497
SAW delay line acousto-optic signal processing devices 79−94328
volume holograms in electrooptic birefr. crysts., light diffr. 79−55084
$Ba_{0.25}Sr_{0.75}Nb_2O_6$, inhomogeneous ferroelec., photorefractive effect 79−42935
$Ba_2NaNb_5O_{15}$, ferroelec. conversion to single domain, elec. and photoelec. props. 78−88271
$Ba_2NaNb_5O_{15}$:Fe,Mo, photorefraction mechanism and photoelec. props. 80−71381
$Ba_{0.25}Sr_{0.75}Nb_2O_6$, thermal and spectral variations in the photovoltaic current in ferroelectrics 78−91719
$(Ba_{1-x}Sr_x)_{1-y}(Nb_2O_6)_y$:$CeO_2$ crystals, photoelectric and photorefractive props., hologram recording 80−53239
$Ba_xSr_{1-x}Nb_2O_6$:Ce, pure and doped, photoelec. props. and photorefraction 80−60538
$BaTiO_3$, holographic storage props. 80−87354
$BaTiO_3$, photorefractive effects and light-induced charge migration 80−69447
$Bi_{12}GeO_{20}$, holographic recording and photoinduced refractive index change exam. 78−37851
$Bi_{12}GeO_{20}$, vol. hologram recording, charge transfer process 78−5437
$Bi_{12}RO_{20}$, R=Ge, Si, photoinduced birefringence, dynamic transparency prod. 78−90472
$Bi_{12}SiO_{20}$, electrooptic photorefractive crysts. for optical information processing 80−74313
$Bi_{12}SiO_{20}$, holographic recording and photoinduced refractive index change exam. 78−37851
$Bi_{12}SiO_{20}$, optically active photorefractive cryst., light diffr. by vol. holograms 79−64185
$Bi_{12}SiO_{20}$, photorefractive, vibr. struct. mode pattern visualisation, phase conjugation and dynamic holography 80−95938
$Bi_{12}SiO_{20}$, photorefractive medium, real-time image processing via four-wave mixing 80−95944
$Bi_{12}SiO_{20}$, vol. hologram recording, charge transfer process 78−5437
GeO film, optical props., rel. to possible appl. in holography 80−29816
$K(D_xH_{1-x})PO_4$, ferroelectric, photovoltaic and photorefractive effects 78−72187
KD_2PO_4-type crysts., photorefractive and photovolt. effects 79−15189
KH_2PO_4, ferroelectric, photovoltaic and photorefractive effects 78−72187
KH_2PO_4-type crysts., photorefractive and photovolt. effects 79−15189
$KNbO_3$ crystals, reduced, hologram recording and erasure sensitivity *(Russian)* 80−78795
$KNbO_3$, reduced, diffr. efficiency and energy transfer during hologram form. 79−72528
$KNbO_3$, reduced, phase hologram recording, energy transfer and sensitivity 80−69338
$KNbO_3$:Fe, photorefr. effects and photocurrents 78−43434
$KNbO_3$:Fe, photovoltages, photocurrents and photorefractive effects 79−42580
$KNbO_3$:Fe, thermal and spectral variations in the photovoltaic current in ferroelectrics 78−91719
$KNbO_3$:Fe photorefraction and photocurrent effects *(Russian)* 79−7091
$KTa_{1-x}Nb_xO_3$, holographic storage using photorefractive effect, dielectric const. 80−78800
$La_2Ti_2O_7$, ferroelecs., nonlinear optical props. 80−33086
$LiNbO_3$, acoustophotorefractive effect, appl. at acousto-optic memory correlator 78−15145
$LiNbO_3$ acoustophotorefractive memory correlator enhancement 79−55080
$LiNbO_3$, acoustophotorefractive effect, phenomenological theory 79−78649
$LiNbO_3$, electrooptic photorefractive crysts. for optical information processing 80−74313
$LiNbO_3$, hologram storage depend. on envelope field, space charge field 80−78801
$LiNbO_3$, holograms stored by photorefractive effect, reading and optical erasure 78−90390
$LiNbO_3$, imaging of photorefractive effects by double cryst. X-ray refl. topography 78−39521
$LiNbO_3$, $LiNbO_3$-Fe, photorefraction in ferroelectrics rel. to electro-opt. effects 78−92048

photorefractive effect continued
$LiNbO_3$, light diffraction from volume phase holograms 79−36860
$LiNbO_3$, optical damage in doped and undoped ferroelectric, mechanism 78−95570
$LiNbO_3$, photoinduced surface storage of SAW patterns 80−74309
$LiNbO_3$, photorefractive, optical information storage 78−33708
$LiNbO_3$, photorefractive effect sensitivity 78−43833
$LiNbO_3$ photorefractive reversible optical memory *(Russian)* 78−58943
$LiNbO_3$, photorefractive sensitivity, dependence on impurity Fe^{2+}/Fe^{3+} ratio, EPR and APR data 79−73893
$LiNbO_3$ photorefractive crystals for computer interfaced optical memory system, hologram characterisation 80−58475
$LiNbO_3$, pure, two-photon photorefractive recording 78−31220
$LiNbO_3$, pure and Fe doped, photorefraction kinetics under irradiation and heating 79−42934
$LiNbO_3$, pure and Fe doped, photorefraction, effect of external elec. field and light intensity *(Russian)* 79−56766
$LiNbO_3$, pure and Fe doped, photorefraction, temp. and light intensity depend. 80−50288
$LiNbO_3$ pure and Fe doped, IR induced acousto-photorefractive memory effect 80−80746
$LiNbO_3$, pure and Fe doped, two-photon photorefractivity 80−80753
$LiNbO_3$, Raman scatt. intensities, photorefractive index change effects 78−84590
$LiNbO_3$, thermal and spectral variations in the photovoltaic current in ferroelectrics 78−91719
$LiNbO_3$, two-photon and X-ray induced Nb^{4+} and O^- small polarons, ESR and optical absorpt. 78−76306
$LiNbO_3$, vol. hologram recording and reconstruction 78−9349
$LiNbO_3$:Fe, anomalous photovoltaic effect in polarised light *(Russian)* 80−34484
$LiNbO_3$:Fe, calc. of photorefraction *(Russian)* 78−90474
$LiNbO_3$:Fe, dynamic optical storage 78−33706
$LiNbO_3$:Fe, efficient hologram recording using Nd:YAG laser pulses 79−55081
$LiNbO_3$:Fe, electron irrad., photoinduced charge transfer and hologram recording 79−36859
$LiNbO_3$:Fe, holographic recording and thermal fixing, invest. of mechanisms 80−78810
$LiNbO_3$:Fe, intensity enhanced bulk photovoltaic effects 79−19616
$LiNbO_3$:Fe, laser induced optical damage 78−95572
$LiNbO_3$:Fe, local photodeformation 79−42932
$LiNbO_3$:Fe, local photodeform. and photorefraction 80−16003
$LiNbO_3$:Fe, optical damage induced by laser light, X-ray irrad., carrier mobility effects 79−33657
$LiNbO_3$:Fe, optical damage, Fe ion conc., EPR and optical spectra evaluation 79−42933
$LiNbO_3$:Fe, optical damage depend. on temp., press., and applied elec. field *(Japanese)* 79−81498
$LiNbO_3$:Fe, photocond. and photorefractive effects 79−38124
$LiNbO_3$:Fe, photoinduced refractive index discontinuities at surface 80−75999
$LiNbO_3$:Fe, photorefractive effect in a ferroelectric 78−92047
$LiNbO_3$:Fe, photorefr., surface recombination 79−56759
$LiNbO_3$:Fe, photorefraction, γ-irrad. influence, polarisation-optic and holographic obs. 80−11359
$LiNbO_3$:Fe, pulsed photorefr. process for hologram recording 80−53235
$LiNbO_3$:Fe, spontaneous polarisation reversal and photorefractive effect 78−31163
$LiNbO_3$:Fe, white-light image processing 80−87321
$LiNbO_3$:Fe crystal conductivity and photoinduced birefringence obs. *(Russian)* 78−60151
$LiNbO_3$:Fe; photorefraction for holographic recording, thin hologram diffr. efficiency 79−55086
$LiNbO_3$:Fe(Cu)(Co), pure and doped, nonlinear excitation, multiphoton photorefractive process 79−36950
$LiNbO_3$:Ti waveguide and cryst., absorpt. loss and photorefractive index changes 80−48368
$LiNbO_3$:Ti waveguide directional coupler switches, optically-induced crosstalk 80−48417
$LiTaO_3$, characterisation as holographic storage materials 78−29909
$LiTaO_3$:Fe crystal, holographic storage process 80−32942
$LiTaO_3$:M, optical damage of transition-metal-doped ferroelectric 78−95571
N_2, liq., photoacoustic and photorefractive detect. of small absorpts., electrostrictive limits 80−108171
PLZT ceramics, photoinduced charge transfer process 79−50362
PLZT ceramics, transparent ferroelec., photorefraction and photocond. study 79−42581
PLZT, photorefractive effect and photoconductivity 78−92046
$PbMg_{1/3}Nb_{2/3}O_3$, ferroelec., crit. electron-phonon phenomena and diffuse phase transition in elec. field 79−38497
$PbMg_{1/3}Nb_{2/3}O_3$, photoinduced phenomena at diffuse phase transition 78−43814
$PbMg_{1/3}Nb_{2/3}O_3$, photoinduced birefr., reversible optical information recording 78−50874
Rb_2ZnBr_4, ferroelec., photovoltaic and photorefractive phenomena 80−75598
Sb_7O_7I, polytypes 2MC and 2MA, photoferroelastic phenomena 79−95447
$Sr_{0.65}Ba_{0.35}Nb_2O_6$, internal field distrib. and photorefraction 79−99843
$Sr_{1-x}Ba_xNb_2O_6$, photorefraction in space charge field, phase transitions 80−97229
$Sr_{0.75}Ba_{0.25}O_6$, photorefractive effect, spectral characts. 78−43829
$Sr_2Nb_2O_7$, ferroelecs., nonlinear optical props. 80−33086

photoresistors
3-channel far IR detector based on coded Si;B, Ge:B, n-GaAs photoresistors 80−101839
contactless temperature indicator *(Russian)* 77−10023
detecting medium-energy electron-streams, cathodoluminescence/photoresistor composite detect. characts. *(Russian)* 79−41080
dilatometer appl., with high stability and sensitivity, for polymers testing 80−81251
functional photopotentiometers, synthesizing method, calc. examples and expt. test results 79−6151
illumination measurement appl., digital linearisation using microprocessors *(German)* 78−77961
impurity photoresistor in interferometer, threshold charact. 80−31856
instrument for determining the difference between light fluxes 79−97415
IR detectors for optical investigation at high pressures 78−21217

photoresistors continued
kinoform lens production and optical testing *(Russian)* 79−98310
laser pulse detection using receivers with photoresistors 78−45705
linearity testing, I laser attenuation by variable water filters 78−55397
noise measurement, determ. of drift mobility of semiconductors 77−4414
optoelectronic ps switch using pulsed lasers and photoresistive semiconductor *(German)* 77−72066
temperature profile recorder using InSb photoresistor 80−105642
$Cd_{0.2}Hg_{0.8}Te$ IR photoresistors/detectors, lateral geometry requirements *(German)* 79−93213
$Cd_xHg_{1-x}Te$, performance at large bias currents *(Russian)* 78−76105
CdS, errors in exposure meter accuracy calc. 77−49773
CdS, for 2Y aKP brightness meter 77−10090
CdS layers from $CdS+Cr_2O_3$ system, effect of heat treatment on spectral distrib. of photosensitivity 78−80017
CdS photoresistor for measuring solar EM radiation 80−31092
CdS-CdTe thin film photoresistors, optimum photoelec. performance *(German)* 79−60941
CdS(Se) II-VI semiconductors in optoelectronics *(German)* 77−7745
CdS_xSe_{1-x} photosensitive films, prep., props., and use for photodetectors 80−55298
CdS_xSe_{1-x} thin-film position-sensitive photoresistor prod. and props. *(Russian)* 78−43503
CdSe linear photopotentiometers, output characts. 77−1453
Cr_2O_3 addition to CdS_xSe_{1-x} photoresistors, extension of cutoff freq. *(Russian)* 78−84248
Ge, Cu doped, liquid N_2 cooled, detectability 78−80019
Ge:Zn photoresistor, current responsivity rel. to nonequilib. hole lifetime 80−60035
InSb, photoresistor in mag. field, increased responsivity 78−39162
n-InSb photoresistors of Carbino disc shape in mag. field, enhancement of responsivity 78−56186
PbSe base, infrared detector with thermal stability over range 0°C to 60°C 80−73458
p-Si, compensated by radiation defect centres 77−62961
p-Si, compensated with radiation centres, current responsivity and detectivity 79−17492

photoresists
see also electron resists
antireflection coatings on metal layers for photolithographic purposes 79−76837
antireflective coating, semiconductor laser, transverse modes, mirror reflectivity dependence 79−68404
biazide-polymer based photoresist. films, positive image production *(Russian)* 78−16887
conference on electron, ion and proton beam technology, conf., Boston, MA, USA (29 May-1 June, 1979) 80−67927
contact printing method utilising heated photoresist adhesive prop. for hologram copying 80−5704
crosslinking, photographic characteristic curve, sensitivity 77−10128
crosslinking efficiency, exptl.-determ. 77−87862
cyclorubber with bisazides, effect of photoresist layer thickness on photosensitivity *(Russian)* 80−73510
o-diazonaphthoquinones, thermal decomposition during drying and storing of photoresist layers *(Russian)* 80−73504
dichromated photoresist, photochem. reactions 80−7830
diffraction grating, interferometric piecewise generation 77−42590
diffraction grating form. on optical waveguide surface, ion-beam etching through photoresist mask 80−14492
diffraction gratings, photoresist and GaAs, exposure and etching time optimalisation 80−23816
dry etched inorganic resist. for lithographic appl. 79−24633
etching by plasma stream transport method 78−52684
grating fabrication, linearity and enhanced sensitivity of Shipley AZ-1350B photoresist 77−72090
grating profile evolution under ion beam erosion 79−94374
grating structure fabrication with variable period 77−19460
hologram recording, book contrib. 78−25837
hologram recording using photolithography, photog. props. of photoresists *(Russian)* 79−98324
holographic grating, fine, made of positive photoresist AZ2400, anal. of two-dimensional etching effect on profile 78−82928
holographic grating production by laser irradiation of photoresist *(German)* 80−33254
holographic recording material, beamsplitter choice for minimum exposure time 79−59655
image formation in photosensitive layers on highly conductive substrates 80−43419
integrated optics photoresist testing and phase filter synthesis 77−39116
ion-bombardment-induced improved mask props. for RF sputter-etching 77−77601
layer partially covering Au electrode, ferricyanide reduction 78−85236
metal foil photoetching profile, quantitative obs. 78−39943
metallo-organic photoresists for inorganic lithography 80−79024
microlens production for semiconductor lasers 78−9398
MTF evaluation by photoresist 79−3636
negative, as phase profile material for near IR, IR spectrophotometric meas. 78−37953
negative, Kodak microresist 747, spectral sensitivity improvement 79−66304
negative, math. model for expt. behaviour 77−38043
negative, RF O_2 plasma stripping, optical detect. systems 77−40585
negative, RF O_2 plasma stripping, visible spectra 77−40591
negative, spin-coating technique for producing multilayer IR optical medium 80−74451
negative film, index and surface simultaneous modulation 78−37951
negative photoresist, KMR-747, transmission and refr. index 2 to 10 μm, interferometric meas. *(French)* 79−76780
negative photoresist behaviour, simple math. model 78−37952
negative polymer-bisazide photoresistors, influence of O_2 on resolution *(Russian)* 79−44974
nonlinear optical processing with Fabry-Perot interferometers containing phase recording media 80−48158
optical diffuser form. of simple known statistical props. 78−90539
optical lens system, for photolithographic purposes 79−36976
optical recording media, review 78−71172
optical reticle and scale fabrication, cyclohexadiene-1,3 pleinomer photoresist 79−27452
optical system MTF measurement using positive photoresists, cross sectional features 78−9337

photoresists continued
optical waveguide, grating coupler fabrication *(Czech)* 80−28354
periodic surface corrugation generation by holography 78−55469
photochemical reaction rates, intensity depend., kinetic model 80−104452
photofabricated profile quantitative exam., etch factor meas. 79−61779
photopolymer industry in Japan 80−4800
photosensitivity, effect of drying temp. of photoresist. films *(Russian)* 79−58828
photosensitivity of negative photoresists *(Russian)* 80−50872
plasma etching charact., effect of dark space in RF glow discharge, ashing charact. 79−15830
plasma etching methods for semicond. struct. and devices *(Slovak)* 80−40564
PMMA, exposure for C K X-rays, diamond soft X-ray source for high-resolution lithography 79−21884
poly [2-(p-azidobenzoyloxy)ethyl methacrylate], MW distrib. effects on photosensitivity *(Japanese)* 78−94418
polyimides, appl. of thin film thickness meas. technique 79−58672
polymer, thin, high energy irrad. and selective dissolution, X-ray lithography *(German)* 80−13167
polymer photoresist, KTFR, thermally stimulated discharge current studies 80−75924
polymer-bisazide layer, effect of thickness on photosensitivity *(Russian)* 77−70324
polymer-bisazide system, light sensitivity of photoresisting films *(Russian)* 79−6214
polymethacrylates degradation obs., for PMMA, PBMA, PMA and PMA AN 78−27795
polymethyl isopropenyl ketons, spectrally sensitized decomposition and Deep UV resists 80−40715
polymethyl methacrylate, use of synchrotron radiation in X-ray lithography 80−62820
polyvinyl alcohol, dichromated, sensitisation to visible laser wavelengths 78−4716
positive, formulation, photochem. props., chem. teaching appls. 78−89284
positive, simultaneous exposure and development model 77−74532
positive, simultaneous exposure and development model 78−4715
positive photoresist., computer simulation of exposure and development 79−54208
positive photoresist film, reson. absorption charact. 77−38046
positive photoresist film exposure, formal kinetics *(German)* 80−104454
positive photoresists, FP-383, prod. of holograms *(Russian)* 80−74323
positive photoresists, photocond. factor rel. to composition *(Russian)* 80−42289
positive resist, plasma etching durability, additive effects 80−66683
precision circular scale manufacture by contact photographic printing 79−75638
residual film on thermally oxidised Si, ellipsometric meas. 77−48266
SAW devices, standing waves and other interference elimination 80−69614
Shipley AZ-1375, sensitivity and nonlinearity at 441.6 and 457.9 nm 78−90475
soft X-ray microscopy, high resolution, appl. to biological materials 77−87889
stainless steel, photoetching, props. of liq. photoresists 78−39942
surface grating relief pattern pofile altering, oblique shadow deposition technique 79−68451
zone plate production by laser irradiation of photoresist. *(German)* 80−23782
AsGe amorphous semiconductor layers for recording information *(German)* 78−42395
As_2S_3, inorganic resist, optical monitoring of etching 79−52412
$As2S_3$ amorphous chalcogenide film inorganic photoresists, holographic resolution evaluation 79−76629
Cr films, photoresist film on reverse gas plasma etching 80−97634
Nb thick layer vapour deposition by photoresist stripping 79−83135
Nb-NbO_x-PbIn, window type tunnel junctions photoresist coated, mag. field enhancement 79−65607
Se-Ge amorphous films, obliquely deposited, photoinduced chem. changes 80−76385
SiO_2, etching charact. in trifluoromethane gas plasma 80−76392

photosphere
absorption lines formation in inhomogeneous medium, rel. to waves and convective motions *(Russian)* 80−72901
abundances of elements Na to Ca 78−49411
active region, mag. and vel. fields config. and changes 77−17486
active region, mag. field correl. with circularly polarised 6 cm emission 80−62096
active region, Mg I, Mg II, reson. lines obs. 79−40163
active region oscills., standing Alfven wave driven by photospheric vel. field 80−98639
active regions, elec. currents as solar wind energy source 80−94768
active regions, photosphere mag. field strength rel. to submillimetre emission 78−12177
active regions and X-ray bright points, birthplaces 80−12739
active regions gross energy balance 78−28633
activity centres during descending branch of 20th cycle, catalogue and peculiarities *(Russian)* 79−96926
axisymmetric convection, stability, solar granulation appl 79−77093
axisymmetric convection with a magnetic field 78−89165
background magnetic field, contrib. to solar mean field compared with fields of active regions and spots *(Russian)* 78−57530
boundary magnetic field effects on cylindrical prominences 80−90396
brightness field near disc centre, two dimens. spatial spectrum 78−7964
brightness fluctuations, two-dimensional spectral anal. of disc centre granulation 77−53520
brightness oscillations obs. at solar limb 79−62798
brightness temp. and continuous absorption coeff. 79−96986
buoyant magnetic flux tubes in supergranules 79−75170
continuum intensities and limb darkening coeffs., synthetic and meas. 78−65590
convection, correction to spectral lines measured wavelengths 78−93181
convection, effect on spectral lines and appl. to stellar convection parameters meas: 79−21273
convection, rel. to small-scale mag. fields 78−53906
convection zone, angular vel. gradients 79−53787
convection zone, momentum and energy transport using rotation model 79−25586

photosphere continued
convection zone mass rel. to diffusion time scales and accretion 77−33454
convective instability in intense magnetic flux tube 79−30038
convective motion scales, ensemble-averaged eqns. 80−67698
convective motions, rel. to vertical struct. of quiescent prominences vel. field 77−53522
convective overshooting, model granular vel. field 78−89166
convective vels. from granule contrast profiles in Fe I 6569.2 A line 77−17507
convective zone dynamics 79−58316
cooling with increased sunspot activity 78−40896
cophasal regions model of convection zone, appl. to sunspot groups kinematics 78−96469
damping constant and microturbulent velocities determ., study of errors *(Russian)* 80−72899
diameter meas. rel. to variation of solar constant 79−84767
differential rotation of magnetic fields, solar cycle variations 78−20781
differential rotation rel. to Ca II chromosphere network 79−25585
dipole-like progressive wave and magnetic field analysis 77−56905
disc centre visible continuum emission, absolute meas. *(French)* 78−96453
distortion rotating with period of 12.2 days 77−17502
downdraught development at sunspot origin, hydrodynamic anal. 80−72908
downflow motion in mag. tubes 78−77530
electric currents, rel. to flares energy source 77−17483
electric currents, subphotospheric Joule dissipation rel. to quiescent prominences downward motion 78−20779
electric fields generated by motion of mag. features 78−12194
emerging flux regions and evolving mag. features, rel. to flares 77−82202
ephemeral region flares and supergranulation network diffusion 79−21265
Evershed flow in chromosphere-photosphere transition region 78−65593
evolving force-free magnetic fields, preflare stage development 77−29739
evolving force-free magnetic fields, variational formulation 78−93182
excitation temperature from Ni I lines, effect of parity of spectral terms 77−53539
exploding granules, evolution pattern 78−89164
extreme limb spectrograms, 4545-4579 Å, during 1970, March 7 eclipse 77−17472
facula models, CH, CH^+ lines equivalent widths 79−66972
faculae, 1972-7 white light obs. 79−16920
faculae, 5000 Å continuum diagnostics 80−4315
faculae, contrasts at solar disc centre using filigree pictures 78−12181
faculae, direct photographs with balloon-borne 10 cm telescope *(Japanese)* 79−80292
faculae, effects on solar constant 78−4163
faculae, inhomogeneous model 80−109415
faculae, line profile families rel. to total mag. flux 78−49408
faculae, line profiles and models 77−45375
faculae, mag., vel. and brightness struct. 79−25557
faculae, models, Ca II K line wings and magnetic fields 78−16392
faculae, models 80−12716
faculae, oblateness and rot. period 77−9735
faculae, photographic obs. model, lifetime calc. 79−48761
faculae and pores, line profiles 78−16391
faculae and sunspots, mag. field effects on solar luminosity 80−46515
faculae excess brightness, wavelength depend., rel. to solar oblateness 78−7955
faculae heating mechanism, convective motion interaction with mag. field 77−82193
faculae intensity, centre to limb var. 80−21967
faculae rel. to sunspot cycle 80−90390
facular and photospheric granules, interpretation *(Russian)* 79−40158
facular granules, morphological props. and origin 77−78744
facular K line profiles, partial redistrib. 77−78748
facular motions and surface Reynolds stresses, rel. to differential rot. 77−2379
fine structure, no correlation between brightness and radial obs. *(Russian)* 80−17564
finite-sized eddies, effect on spectral line widths, Fourier anal. appl. 77−17500
five minute oscillation, power spectra 77−87357
five-minute oscillation, IR continuum obs. 77−78745
five-minute oscillations, observational search for large-scale organisation 78−65589
flare model based upon photospheric dynamo action 80−62102
flare models, current interruption and impulsive flux transfer 79−12438
flares, temp. min. region struct. and significance for flare heating 79−12458
flares flash phase and current sheets thermal evolution 77−17485
flows in magnetic flux tubes 78−16393
flux tubes and coronal magnetic fields 79−16922
force-free magnetic field bifurcation 78−40901
Fourier transforms appl. to contrast profile method of vector mag. field meas. 78−53839
Fraunhofer line profiles interpretation 78−7976
Fraunhofer line shifts in spectrum *(Russian)* 77−71072
Fraunhofer lines, east-west asymmetry of central residual intensities and other parameters 78−53916
Fraunhofer lines, effective form. depths calculated by various methods 79−12447
Fraunhofer lines, progressive sound waves effect on profiles *(Russian)* 78−73689
Fraunhofer lines, weak, effective depths of form. *(Russian)* 79−44438
Fraunhofer lines asymmetry, centre-to-limb var. *(Russian)* 78−40892
Fraunhofer lines asymmetry, rel. to photospheric macromotions 78−4175
Fredholm integral equation, free-knot spline inversion using nonlinear least squares method 79−2486
gas entry into non-spot magnetic tubes 77−78749
gas motions in single sunspot *(Russian)* 78−65582
global magnetic field, changes rel. to equatorial K-corona temporal evolution 78−28618
global oscillations, long-period, observational evidence 79−2539
global oscillations, obs. as oscills. in apparent limb darkening function 79−35226
granular and oscillatory velocities height var. 77−29775
granular brightness fluctuations, centre to limb var. 79−66971
granular buffeting, resonant response and spicules 79−44444

photosphere continued
granular cells charact. scales and convection zone struct. 78−7981
RMS granular contrast, new meas. of centre to limb var. 78−4176
granular convection, effects in response of C I 5380 Å response to solar luminosity vars. 80−85910
granular motions, influence on spectral lines limb shift 79−12448
granular velocities around sunspots 77−29776
granular velocity vertical component, height depend., spectral obs. 79−66980
granulation, 2-dimens. power spectrum analysis, data processing 80−101570
granulation, convection models, book contrib. 80−4329
granulation, dark dot form. in cell 80−31274
granulation, discovery and history 77−2382
granulation, dynamical model 77−60736
granulation, lifetime from balloon-borne imagery 78−28601
granulation, mean vertical vel. 80−62094
granulation, one-dimensional speckle interferometry 78−45299
granulation, photometric props. from balloon-borne imagery and digital image enhancement 78−7956
granulation, physical model 79−30026
granulation, power spectrum calibration by Michelson stellar interferometry 77−17464
granulation, speckle interferometric obs. *(French)* 80−46523
granulation, spectral props. of random arrays 80−12727
granulation, wavelength depend. in 0.38-2.4 μm region 78−12188
granulation brightness fluctuations, low-wavenumber power 77−82201
granulation morphology and granule spatial distrib. 80−26830
granulation scale, physical model 78−57521
granulation scales, penetrative instabilities theory for convective modes in solar atmosphere 80−109406
granulation seeing at Chinese solar observatory testing sites *(Chinese)* 77−67032
granulation spatial power spectrum, morphological interpretation 78−65581
granulation statistical properties and seeing, speckle interferometry obs. 79−88634
granulation structure, vertical motion models 80−90375
granulation structure, vertical motions spatial and temporal behaviour obs. 80−85912
granule diameters near penumbra 80−8607
granule fragmentation, morphological study in Ca II K-line 80−56799
granule/intergranule brightness contrast, new determ. 78−20797
granules, dimension variation in vicinity of sunspots *(French)* 78−89145
Hale solar sector boundary definition 77−17517
hard X-rays backscatter, effects on anisotropy and polarisation 78−28594
hard X-rays photoelectric absorpt., approx. formula 77−22187
impulsive X-ray bursts, polarisation, directivity and spectrum of bremsstrahlung radiation 78−4160
incompressible fluid flow along mag. flux tubes, stability 77−53488
intense magnetic fields formation near solar surface 77−49359
intense magnetic flux tube, vertical motions inside 78−40900
intensity, rel. and temp. fluctuations in upper regions 77−56886
IR atomic lines identification, 3.3-8 μ spectral region 77−45383
K faculae as tracers of solar differential rotation 77−53501
large scale magnetic dipole and multipole progressive waves 77−17505
large-scale magnetic field, harmonic anal. rel. to coronal holes 77−64713
large-scale magnetic field, Stanford obs. compared with Hα synoptic charts 78−28612
large-scale magnetic fields spatial distrib. rel. to interplanetary mag. field 79−84772
latitudinal angular momentum transport estimation from Doppler vels. 77−64712
light absorption in photospheric layers, eclipse limb darkening obs. *(French)* 80−8612
limb darkening function at 5012 Å, possible vars. 80−67677
limb darkening in 1-4 μ range *(French)* 77−74023
limb darkening meas., 1945-3245 Å, Skylab data 79−12439
limb darkening of quiet Sun in continuum 78−7975
limb emission lines near Ca II H and K, spatial intensity vars. obs. 80−51720
limb region, UV light polarisation 78−45302
limiting optical depth for valid LTE conditions *(Russian)* 78−20785
linear hydrodynamical eqns. coupled with radiative transfer, Mg I 5172 Å line interpretation 78−77529
linear hydrodynamical equations coupling with radiative transfer in non-isothermal atmosphere, method 78−20794
long-lived supergranules 77−17504
magnetic activity, role of mag. buoyancy in Sun 79−21256
magnetic features visibility on filtergrams and spectroheliograms 77−29781
magnetic field, importance for coronal energy storage, solar flare model 80−72906
magnetic field intensity and Hα line behaviour 78−57522
magnetic field patterns, evolution during Skylab 78−20798
magnetic field polarity rel. to circular polarisation of moving type IV bursts 78−53915
magnetic field rearrangement, rel. to disparitions brusques of solar filaments *(Russian)* 80−51726
magnetic field var. during class 2b flare, meas. and anal. 78−89160
magnetic fields, hydraulic concentration near equipartition 77−13293
magnetic fields, influence on accelerated particles escape into interplanetary space 79−62807
magnetic fields, meas. from saturated and blended lines via Fourier transform techniques 77−22165
magnetic fields, possible explanation for fine struct. 80−98646
magnetic fields, pots. rel. to active regions fields zero points 78−96465
magnetic fields, rel. to coronal holes 79−58312
magnetic fields, rel. to coronal mag. fields and solar flares 77−17474
magnetic fields, rel. to quiescent prominences mag. field orientations and classification 78−45305
magnetic fields, source regions of interplanetary mag. field and solar wind 77−45275
magnetic fields, weak and strong, magnetogram obs. 79−44432
magnetic fields and convection dynamic interaction 78−24458
magnetic fields and motions, granulation and sunspots *(Russian)* 78−16376
magnetic fields assoc. with coronal holes, differential rot. 77−22167
magnetic fields beneath large coronal holes, nature 78−28613

photosphere continued
magnetic fields hydraulic concentration, adiabatic cooling and conc. in downdraughts 78−45300
magnetic fields hydraulic concentration, dynamical effects in stratified atmosphere 77−13294
magnetic flux, appearance 79−40161
magnetic flux element in horizontally stratified compressible plasma, stability 78−28610
magnetic flux emergence, form. of current sheets 77−22176
magnetic flux tubes, props. rel. to solar activity theories 77−5513
magnetic flux-tubes emergence, interchange instability and coronal field reconnection 77−56894
magnetic fluxes and field strengths meas. in active region network cell 77−71083
magnetic fluxtubes, multidimens. non-LTE radiative transfer 77−60741
magnetic fluxtubes, polarised radiation multi-dimensional non-LTE transfer 78−69673
magnetic fluxtubes press. equilib. and energy balance 77−29780
magnetic structures, correl. with radio noise storms 78−4185
magnetic structures, models *(Italian)* 78−81603
magnetised expanding plasma gaskinetic press. 77−45394
magnetoatmospheric waves conical propag. and spicule motions 77−49351
magnetograph data, appl. to constant α force-free mag. fields determ. 79−12445
magnetograph measurements, appl. to mapping of coronal mag. field 77−56892
McMath region 13043, opposite polarity sunspots collision rel. to centimetre-wave sources rapid var. 80−67688
mean magnetic field, 1968-74 period, obs. method, rel. to interplanetary field 77−71082
mean magnetic field, obs. at Stanford 78−20800
metallic line profiles var. with heliographic latit. 78−61837
MHD wave propagation in mag. flux sheath in presence of vel. field 79−62735
micro- and macroturbulence, spectrophotometric determ. *(Russian)* 77−56896
micro-turbulence model test on flux spectrum 78−16365
'microturbulent' velocity and damping const., introductory review *(Russian)* 80−12719
microturbulent and macroturbulent filter functions, improved values 78−20796
microturbulent motions 79−75189
model atmosphere, rel. to solar Fe abundance and Fe II lines oscillator strengths 80−56791
modelling, hydrodynamic and mag. features *(Italian)* 78−81599
models, survey of last 30 years' research 78−69764
models and rotational temps. of C_2 and MgH 80−62099
motions, large-scale structures, research programme 77−71101
network, dark component, Ca I 6103 line scan 77−29759
network model 79−48747
network properties, link with sunspot plage fragment characts. 80−98634
network structure from Mn I lines obs. 79−30039
nonadiabatic radial wave equation, rel. to solar oscills. detect. 79−5800
nonthermal vels. in six giants and the Sun 78−4219
north-south brightness asymmetry, obs. 78−45303
open magnetic structures evolution, Skylab obs. 78−16362
oscillations, Doppler meas., atmospheric differential extinction 79−101131
oscillations, PEPSIOS spectrometer obs. 78−93203
oscillations, power spectra, phase spectra and coherence spectra 79−8897
oscillations, search for long period modes 77−41370
oscillations depth depend. 80−31275
oscillations in mag. tubes, spectral line obs. 79−25564
oscillations of 160-min. period, no terrestrial atmospheric extinction effects 80−105216
oscillations producing, coronal arcades mag. instability, two ribbon flares origin 80−72911
oscillations with 160 min. period, terrestrial origin refuted *(Russian)* 80−98629
photosphere-chromosphere transition region, spectra during eclipse June 30 1973 80−8614
plage region magnetic points, vertical vel. fluctuations 77−71084
polar magnetic features rot. rate 79−30037
polar magnetic fields strength, obs. 79−12446
polar vortex, spectroscopic search 79−5801
poloidal and toroidal mag. field components near solar min. 79−66978
pores, line profile families rel. to total mag. flux 78−49408
potential magnetic fields, comparison of meas. and calc. 78−77532
proton flux influenced by photosphere mag. field 80−41672
pulsations, radial vel. meas., atmospheric transparency effects 79−101130
radial velocity, meas. via reson.-scatt. solar spectrometer 78−96393
radiative equilibrium, rel. to upper bound on energy transport by solar global oscills. 78−32430
resonance line spectrum, polarisation in line cores 77−29744
rotation, determ. using sunspot spectra 79−92745
rotation, obs. methods 79−75179
rotation rate, variation with activity cycle 77−13304
seiches in supergranules rel. to solar radius oscillations 77−13310
small scale structures correl. depend. on resolution 79−84769
small-scale photospheric magnetic fields 78−12196
small-scale solar magnetic field, size, struct. and strength 77−78738
solar rotation from Doppler obs. 80−105219
solar surface oscillations, geophysical effects 79−8777
spectral line profiles, acoustic wave effects 80−46517
spectral line profiles for Na I and O I, acoustic wave effects 80−17558
spectral line wavelengths and limb effect 77−49357
spectral lines, response functions and contrib. functions 77−17462
spectroscopic Doppler rotation rates, 1966-1978 period 79−66977
spectrum intensities, centre to limb vars., statistical anal. 77−53537
structure, magnetograms and spectroheliograms from Kitt Peak 60 cm vacuum telescope *(Norwegian)* 77−60613
structure and dynamics, rel. to Sun as variable star *(French)* 79−2540
structure compared with chromosphere 77−29777
subphotospheric activity assoc. with large flares, X-ray data 79−35225
sunspot formation mechanism 77−45395
sunspot light bridges fine structure 79−66984
sunspot magnetic field and vel. quasiperiodic oscills. *(Russian)* 78−12186

photosphere continued
sunspot magnetic fields higher rot. rate at photosphere, Doppler meas. 80−46516
sunspot moats, lifetimes from magnetograph obs. 80−21966
sunspot model, radiation transfer theory 80−21964
sunspot penumbrae, fine struct. of mag. field and brightness 77−22179
sunspot research, past and present, review *(Norwegian)* 79−75312
sunspot structure, vars. correl. with Earth climate 80−31272
sunspot umbrae, material motions obs. 77−45374
sunspots, characts. of penumbral bright grains displacement 77−22177
sunspots, CO fluoresc. obs. in EUV spectrum 78−93184
sunspots, cooling by Alfven waves refl., theory 79−5799
sunspots, darkening rel. to heat flow near obstacles in convection zone 78−28609
sunspots, direct photographs with balloon-borne 10 cm telescope *(Japanese)* 79−80292
sunspots, distrib. between N and S solar hemispheres and var. with solar cycle 77−56881
sunspots, gases rot. motion *(Russian)* 77−64716
sunspots, macroscopic motions rel. to origin of broad-band circular polarisation 78−45301
sunspots, magneto-optical effects rel. to linearly polarised intensity distribs. obs. with vector magnetograph 80−21965
sunspots, MHD wave damping and heat transport 77−5514
sunspots, morphology of form. during solar cycles (19 and 20) 77−78763
sunspots, photoheliographic results, (1968 to 1971) 79−2487
sunspots, running penumbral waves origin 78−93188
sunspots, stability of axisymmetric mag. flux tube 77−64734
sunspots, steady-force-free dynamos theory 78−20777
sunspots, struct. and dynamic props. of large group of 1972 August 78−49409
sunspots, thermal struct. 77−5517
sunspots, thermal struct. 77−64735
sunspots and mag. flux tube physics, connective overstability in mag. field in downdraft 80−21960
sunspots and magnetic flux tubes physics, umbral dots and longitudinal overstability 80−26825
sunspots and physics of mag. flux tubes, aerodynamic drag 79−71012
sunspots and physics of mag. flux tubes, aerodynamic lift on thin cylinder in convective flows 79−101126
sunspots and physics of mag. flux tubes, general nature of sunspots 79−75168
sunspots and physics of mag. flux tubes 79−101127
sunspots cooling mechanism, overstability and Alfven wave prod. 77−78733
sunspots umbras, outward wave propag. and motions in mag. tubes 79−16927
sunspots Wolf numbers, rhythmic struct. amplitude-phase disturbances anal. 79−62806
sunspotsand physics of mag. flux tubes, aerodynamic lift 79−101125
supergranular vels. from UV obs., height var. 79−30025
supergranulation, appl. of finite-amplitude convection theory in compressible media 79−88637
supergranulation, dynamics of gas and mag. field below photosphere 78−16366
supergranulation, mag. field effect on thermal convection onset under const. flux boundary conditions 78−69676
supergranulation and giant cells origin in convective zone 79−66979
supergranulation as solar rip currents 79−48749
supergranulation cells, equatorial rotation rate 80−90388
supergranulation study with diode array magnetograph 77−2384
supergranule boundary, chromosphere hydromagnetic struct. 77−13298
supergranule cells, lifetime determ. 77−2385
supergranules, vel. and magnetic field evolution 77−53555
surface (capillary) waves, props. *(Russian)* 80−12726
surface oscillations and pulsations, rotation speeds 80−67676
temperature at chromosphere photosphere boundary, from emission spectrum in far infrared *(German)* 80−51721
temperature fluctuations and vel. height var. 79−8891
temperature from C I 5380 Å line, rel. to solar luminosity vars. and global oscills. 77−53487
temperature in low photosphere, horizontal var. 77−22163
temperature minimum, absolute brightness temp. meas. in far IR with balloon-borne interferometer 80−62095
temperature variations, line profile vars. with heliographic latit. 77−2383
temperature variations, rel. to solar radius vars. due to mag. buoyancy 79−92749
thermal models of sunspots 79−84773
total velocity field, determ. using weak absorpt. lines *(Russian)* 78−40894
transition region emission, spectral obs. in Hα region 79−35233
turbulence, review 79−30056
turbulence *(French)* 80−31270
twisted flux tube theory, stability 77−60737
two-dimensional stochastic motions, theory rel. to differential rot. problem 77−53518
umbral fine struct. and granulation, statistical anal. 77−74032
upper photo sphere models, re-examination rel. to Ca abundance and empirical damping parameters 77−33445
UV continuum high resolution photographic obs. 80−17565
u.v. radiation, absolute intensities in 1750-2100 Å range, vars. with solar activity 77−2405
velocity field, spatially averaged props. 79−16912
velocity field and Hα filaments spatial correl. 77−2401
velocity field assoc. with sunspot formation 77−2396
velocity field peculiarities in active regions *(Russian)* 77−64720
velocity fields, large-scale, from Doppler line shift obs. 80−12730
velocity fields, observations *(Italian)* 78−81601
velocity fields, theory *(Italian)* 78−81600
velocity fields and spectral line shift obs. interpretation 80−51714
velocity gradients retrieval from photospheric line asymmetries, linearised approach 80−62093
velocity oscillations meas. via high-resolution spectroscopy, solar rot. effects 78−96403
velocity research, effects of apparent yearly precession of Sun 78−20809
vertical motion in intense mag. flux tube, slender tube approx. 80−31278
wave propagation, spectral lines fluctuations obs. 77−22162
wave propagation in nonisothermal atmosphere, rel. to solar five minute oscills. 80−31276
waves, vertical propag., phase delay obs. 79−96981

photosphere continued
weak absorpt. features in Ca II H and K wings rel. to nonthermal broadening in photosphere 77−60735
weak Fraunhofer lines, effective form. depths tables *(Russian)* 79−44439
Ba II spectrum, partial freq. redistrib. 79−101128
C I 5380 Å line sensitivity to temp. changes in static and oscill. systems 77−60743
C III 1909 Å and Si III 1892 Å emission lines, echelle obs. 80−31277
C, N, O, abundances 78−24497
C_2, rotational temperatures, centre to limb behaviour 79−84758
CH photospheric lines and $^{12}C/^{13}C$ atmospheric ratio determ. 77−5518
CO first overtone line centre-to-limb vars. and average facula models 79−80291
CO spectrum, centre to limb behaviour of first overtone vibr.-rot. transitions 79−8889
Ca I 6573 Å and Ca II 7324 Å forbidden line, centre-to-limb behaviour 79−25572
Co photospheric abundance 77−58206
Cr I in photospheric spectra, solar abundance and oscillator strengths 78−69757
Fe abundance, curve of growth and fine anal. 77−56883
Fe abundance, determ. from weak Fe I Fraunhofer lines with microturbulence and damping *(Russian)* 80−12720
Fe group elements abundances from singly-ionised lines 78−93189
Fe I even-odd and odd-even transitions, difference in curves of growth 77−25996
Fe I Kα fluorescence in solar flares, photospheric Fe abundance probe 79−75192
Fe I line profiles and magnetic field in quiet network regions 78−69758
Fe I lines, damping const. determ. preliminary results *(Russian)* 80−72900
Fe I lines, equivalent widths and microturbulent vels. determ. *(Russian)* 80−51719
Fe I lines, line broadening, Smirnov Roueff pot. calcs. 80−98632
Fe I lines, statistical anal., mag. line broadening 77−74028
Fe I spectrum, 300 to 900 nm, microturbulence, Fe abundance, damping, oscillator strengths 77−5516
Fe-group elements, oscillator strengths for V I and Co I 78−40905
H_2, detect. in sunspots EUV spectra 78−12184
Hf abundance from Hf II spectral lines obs. 77−17518
La, abundance, new lifetime meas. of La^+ 78−17618
La abundance from exptl. lifetime determ. 77−30827
Li production during white light flares 77−71092
Mg I 2852 Å line sensitivity to partial redistrib. effects 78−7951
Mg I and II, line profiles calc., comparison with expt. results 80−82320
Mg II h and k lines in active regions and network, wings rel. to photosphere models 78−57518
Mn abundance, Mn^+ oscillator strengths 78−17619
Nd II, branching ratios and transition probabilities, photospheric abundance 78−9104
Ni I abundance from oscillator strength obs. 80−98625
O I 7774.177 Å line asymmetry rel. to O isotope abundance 77−17530
OH, continuum opacity in solar atmospheric model 79−40162
Pr lines in photospheric spectrum, Pr abundance 79−44443
Sm II, photospheric abundance, spectral transition probability, 3000-7000 Å 79−31453
Ti I lines, rel. to photosphere vel. field, non-LTE effects and solar Ti abundance 78−45306
TiO, rot. temp. in sunspots, rel. to photospheric and sunspot models 78−69766
Zn abundance, discrepancy with meteorite abundance 80−72897

photosynthesis
algae in cylindrical photoreactor, radiation intensity and absorption profiles *(German)* 80−3610
antenna chlorophyll A and P700, exciton transitions in chlorophyll A arrays 78−35802
antenna system, exciton collection into accessible traps, photosynthesis model 79−62018
apparatus for meas. of small absorption change kinetics at 820 nm 78−92769
bacteria, effect of mag. field on recomb. fluoresc. 80−35856
bacteria, mechanism of mag. field effects 79−83810
bacteria, mechs. of charge separation 80−30684
bacteria, photosynthetic, triplet-state spin polarisation 78−44469
bacterial photosynthesis, low-temp. electron transfer 78−44470
bacterial photosynthesis, optical and paramagnetic identification of a primary electron acceptor 78−77004
bacterial photosynthesis, picosecond studies of some ultrafast events 79−39375
bacterial photosynthesis primary steps, wide-band multichannel picosecond absorpt. spectroscopy 79−66462
bacterial photosynthetic reaction centres, light induced electron spin polarisation 80−63681
bacteriochlorophyll, temp. dependence of dark reduction kinetics 77−36888
bacteriochlorophyll a, triplet state energy and lifetime 80−30682
bacteriopheophytin a, triplet state energy and lifetime 80−30682
bacteriorhodopsin Br570, bathochromic shift of absorpt. band in external elec. field 80−35838
bacterium Chromatium minutissimum, linear dichroism of oriented chromatophores and pigment-protein complexes 80−35841
bimolecular quenching of excitons and fluorescence in the photosynthetic unit 77−16908
bioconversion of solar energy, review 80−45720
bioenergetics 80−61521
biomass, review of possible energy conversion processes *(French)* 80−93843
biomass energy conversion, energy sources for rural development 80−30509
biomass energy production and the photosynthetic pathway 80−61393
biomembranes, electron and proton transport 80−67052
Blinks effect and its explanation 79−57590
blue-green algae, absorpt. spectrum, struct. resolution 80−76715
British coastal waters, possible influence of Zn pollution on photosynthesis 79−24921
Calvin photosynthesis cycle parameter identification 79−92186
carboxylation reactions and delta ^{13}C-valves of plant material, ^{13}C-kinetic isotope effects 79−57566

photosynthesis continued
chemical reactions in condensed media, theory and appls. to biological processes 80—3575
Chlamydomonas mutants, chlorophyll spectral forms and chloroplast struct. 80—81556
Chlamydonomonas mutants with inactive photosystem 2, electron transport chain disturbance 80—94179
Chlorella, primary processes of photoinduced H_2 evolution, flashing light expts. 77—25398
Chlorella biomass growth, efficiency rel. to solar energy utilisation 80—67049
Chlorella synchronous culture, quantum productivity in different spectral regions 77—25392
chlorophyll, photosystem 2, activation energy and lifetime of fluoresc. 80—35842
chlorophyll a, absorpt. and fluoresc. spectra, observance of Stepanov relation 80—81554
chlorophyll A, delayed fluoresc. course in absence of electron transport, photosystem 2 77—70428
chlorophyll A, determ. of triplet and excited singlet absorpt. with a tunable dye laser 79—59477
chlorophyll A, fluoresc. duration dependence obs. 77—25393
chlorophyll A, low-intensity 2-step absorpt. in vivo 78—35801
chlorophyll A, thin films, charge injection and storage 78—53317
chlorophyll A adsorbed on aerosil, absorpt. spectra 78—53327
chlorophyll A fluorescence and absorpt. spectra, resolution into components 79—57584
chlorophyll A in photosynthetic material, luminesc., effects of temp. and preillumination 79—34498
chlorophyll A-N-chloranil lamellar system, heat-stimulated conductivity 79—53043
chlorophyll and its analogues, mixed associates, intermolecular interaction and energy transfer 78—64924
chlorophyll and related compounds, molecular triplet states study 79—36691
chlorophyll C in the cell at −196°C, spectral obs. 78—53329
chlorophyll complex, reaction centre struct. obs. 79—20517
chlorophyll derivatives molecular transitions, effect of molecular struct. 79—92138
chlorophyll excited states, redox pots. 77—25372
chlorophyll fluorescence in bilayer lipid vesicles and liposomes, conc. quenching 77—4985
chlorophyll function in the photosynthetic reaction center 79—5251
chlorophyll native forms at 77K, variable fluoresc. obs. 77—70417
chlorophyll oxidation reaction mechanism, effect of light spectral composition 77—25369
chlorophyll photooxidation, role of the triplet state 78—27791
chlorophyll precursor, energy migration in photoactive complexes 77—36889
chlorophyll special pair models, reaction centres 80—3574
chlorophyll spectral forms, Chlamydomonas mutants with inactive photosynthesis 80—51054
chlorophyll under intense laser excitation, enhancement of fluorescent mag. resonance detect. *(Russian)* 78—91995
chlorophyll-a, conc. quenching rel. to functional charge transfer 80—30666
chlorophyll-a, hydration, field desorpt. mass spectral obs. 80—71936
chlorophyll-A, nonlinear absorpt. *(English, Russian)* 78—25522
chlorophyll-A in liquid crystals, spectral props. *(English, Russian)* 78—27291
chlorophyll-a radical cation lifetime in water-acetonitrile soln. 80—72136
chlorophyllide fluorescence quantum yield during photochlorophyllide reduction in etiolated leaves 80—81542
chlorophylls, triplet states, luminescent ananl. *(Russian)* 78—27288
chlorophylls A and B, solvent effects on the lowest singlet-singlet transition 79—24952
chlorophylls orientation within chloroplasto, optical and electrochtomic props. obs. of the photosynthetic membrane 77—48763
chloroplants, bean, effect of salts on EPR II signal 78—64952
chloroplast, mag. relax. of water protons and state of water photodissociation system 80—51133
chloroplast EPR signal props., effect of ferricyanide, dark adaption, ageing 79—57607
chloroplast fluorescence, investigated using laser spectrofluorimetry 80—81558
chloroplast fragments, fine struct. of fluoresc. spectra *(Russian)* 79—34502
chloroplast thylakoids, struct. rel. to light-induced slow absorbancy and scatt. changes 78—69019
chloroplasts, isolated, effect of temp. on photo-induced pH gradient 80—81566
chloroplasts, millisecond afterglow, activation and suppression 78—96025
chloroplasts and subchloroplast particles, optical absorpt. at 700 NM and EPR spectra 77—25394
chloroplasts responding to illumination sequence of 4 flashes, EPR signals 78—7325
chromatophores of R. rubrum, induction of elec. pot. diff. by laser flash 80—81560
concentration effects in mixed asspciations of pigments 80—1007
crops, leaf discs and chloroplast preps., effects of 298 nm radiation on photosynthetic reactions 78—61220
cytochrome C, immobilised, investigs. using magnetic micromixer attachment for SPECORD UV VIS spectrophotometer 80—56302
cytochrome f function in photosynthetic electron transport 79—62206
delayed light in photosynthesis 77—86466
donor-acceptor energy transfer of higher plant photosystem I, model *(Ukrainian)* 77—70435
dye-detergent model systems, degree of polarisation *(English, Russian)* 78—27287
dye/detergent system, model for energy transfer in photosynthetic unit 80—20685
early reactions in green-plant photosystem. I 80—104567
efficiency in the green region of the spectrum 78—69010
electrochemical simulation of photosynthetic primary processes, in vitro expts. 79—43833
electron conformation interactions in fast photosynthetic processes 80—94183
electron flow, photosynthetic and respiratory, in dual functional bacterial membrane 80—16914
electron spin echo studies of complex biological systems, appl. to 'signal Ii' of plant photosynthesis 78—96118
photosynthesis continued
electron spin polarisation in photosynthetic electron transfer, development by the radical pair mechanism 79—34471
electron spin polarisation rel. to electron transfer mechanism in photosystem I, expt. obs. 78—40122
electron transfer in bacterial photosynthesis and in mode systems, picosecond studies 79—48214
electron transfer processes, fast, exploration by mag. fields 79—8479
electron transfer reactions in carrier mol. complexes, kinetics and thermodynamics 80—108859
electron transport and energy migration in higher plants 80—40976
electron transport in higher plant photosynthesis, adaptional phenomena at different light intensities 78—64953
electron transport in higher plant photosynthetic systems, EPR investigations of P700 78—77014
electron transport in higher plant photosynthetic systems, EPR investigations of bean membranes 78—77015
electron tunnelling, thermal and photoassisted, theory, fast charge separation in photosynthesis 80—89730
electronic excitation energy, transfer from monomeric to dimeric chlorophylls *(Russian)* 78—27289
electronic structural props. of mols. relevant to photosynthesis 80—16902
electronic transitions of chlorophyll A, rrotochlorophyll A, location 79—43825
electrons, path in photosynthesis 77—44607
energy and electron transfer speed, time resolution meas. *(Russian)* 80—94161
energy conversion, quantum efficiency 78—44473
energy conversion radiation enhancement using surface polaritons 80—7941
energy migration between native forms of chlorophyll at 77K, sensitised fluorescence obs. 77—70429
energy transfer and fluorescence quenching in chlorophyll containing vesicles 79—39349
energy transfer in photosynthetic organisms, expt. obs. 77—81479
energy trapping dynamics in 2D model of photosynthetic unit, theoretical investigation 78—88697
energy upconversion and the minimum quantum requirement in photosynthesis 77—29115
enhancement and chromatic transitions, modelling 80—104565
entropy balance in photosynthesis 79—92181
entropy changes in energy bioconversion 80—3609
entropy of radiation and its role during photosynthesis 80—108858
ESR, appl. in photosynthesis, review 79—92450
excitation transfer in photosynthetic systems, temp. dependence 78—92598
exciton annihilation in the 2 photosystems in chloroplasts at 100K 77—25371
exciton dynamics in photosynthetic membranes, picosecond pulse train study 79—8483
exciton percolation in molecular alloys and aggregates inc. model for photosynthesis 77—36297
fluorescence and energy transfer in photosynthesis 79—48216
fluorescence and fluorescence quenching in chlorophyll A and bacteriochlorophyll A, stimulated 78—27895
fluorescence changes in isolated broken chloroplasts and involvement of elec. double layer 78—44464
fluorescence induction phenomena in photosynthesis, elec. diagram for modelling 79—57589
fluorescence phenomena in photosynthetic membranes, picosecond laser-induced, anal. 79—39350
fluorescence picosec. kinetics in chromatophores and reaction centres from R.sphaeroides, 295 to 80K 80—35857
fluorescence polarisation in magnetically oriented photosynthetic systems, theory 79—16165
gastopod photosynthesis with incorporated algal chloroplast, Placobranchus sp. 80—61522
green alga, Haematococcus pluvialis, induction of fluoresc. of single chloroplast 78—24037
greening bean leaves, low-temp. induction of fluoresc. 79—39354
higher plant leaves, $P700^+$ reaction centres, reduction processes 78—64954
higher plant photosynthesis, energy migration and electron transport, theoretical study 78—64957
higher plant photosynthetic systems, electron transport investigation, EPR obs. 77—21495
higher plants, energy migration and electron transport, fundamental eqns. and their soln. 78—20150
hydrocarbons production for chemical feedstock 80—89661
hyperfine coupling in chlorophyll radical cations, NMR approach 79—8482
in vitro models for photosynthesis 78—77023
intersystem crossing in photosynthetic pigments 77—58057
IR analyzer and Geiger-Muller counter meas. of photosynthesis *(German)* 77—70436
kinetics of luminescence and electron transport in photosystem 78—7324
kinetics under saturating light 80—35858
laser remote probing of photosynthesising organisms, fluoresc. technique 79—66434
laser spectroscopy of primary energy conversion in photosynthesis 79—66461
life support system with autonomous control employing plant photosynthesis 77—25563
light absorption by leaves and pigment containing cells 77—75416
light collection and exciton dynamics in photosynthetic membranes 79—48215
light collection and harvesting processes, bacteria, pirosecond time scale obs. 77—90743
light non-additiveness in green plant photosynthesis 78—40123
lipids of isolated chloroplasts, photoperoxidation reactions 78—77016
marine dinoflagellates, photosynthetic characts. and organisation of chlorophyll 79—5260
membrane, photosynthesising, near photosystem II, hydrophobic pocket 80—55999
membranes, functional processes, polarisation effects 80—67045
non-additiveness principle in action of light and 2 photosystems concept in green plant photosynthesis 78—80842
oceanic photosynthesis, in situ quantum efficiency 79—39760
optical properties of the leaves of some African crop plants 77—25629
P700, photo-induced redox conversions kinetics, EPR obs. 77—21494

photosynthesis continued
pea chloroplants, photosynthetic electron transport rel. to light-induced fluoresc. quenching of atebrin 77−56351
pea leaf cells, microwave photolosses, electrophysical process obs. 79−70535
phase transitions discovery in photosynthetic systems 80−81539
pheophytin pigments, triplet state obs. 78−27896
phospholipid bilayer membranes containing chlorophyll A, photo oxidation of water 77−16917
photo-induced charge transfer, critical test of mechanism and range of biological electron transfer processes 77−60182
photo-oxidation of chlorophyll A by p-benzoquinone 79−79447
photo-oxidation of chlorophylls A and B and pheophytin A 79−79468
photobiological conversion of solar energy *(German)* 79−2013
photobiological processes in different lights, method for investigating relative quantum yield 78−65154
photochemical apparatus of green plant photosynthesis, tripartite model 78−44474
photoconductivity, steady, in lamellar systems of chlorophyll-acceptor and chlorophyll+protein-acceptor 78−53328
photoelectrochemical conversion, using bacteria reaction centre working on SnO_2 electrode 80−94092
photoinduced dielectric constant shift in chloroplasts, first kinetical anal. *(French)* 78−61147
photoinduced electron transport across phospholipid wall of liposome using methylene blue, photosynthesis model 79−74614
photon irradiance sensor for underwater meas. of energy available for photosynthesis 78−32843
photon scalar irradiance meter, rel. to energy evaluation for photosynthesis in sea 79−79436
photooxidation of chlorophyll A by p-benzoquinone 78−76991
photophosphorylation in chloroplasts in a pulsed regime of illumination 78−64958
photosystem I, of green plants and algae, CIDEP obs. 80−63679
photosystem I of Chlorella, electron phototransfer in reaction centres, hole-burning spectroscopy 80−81561
photosystem II activity rel. to photoinduced changes in chloroplast suspension oxidation-reduction pot. 77−25399
photosystem II of chloroplasts, photoinduced paramagnetic centres 79−39372
photosystem II of higher plants, reduction of pheophytin in photoreaction 79−43817
photosystem-2 in sub-chloroplast fragments, paramagnetic centres and photochemical reactions 79−53061
phycobilin pigments, role in photosynthesis 78−48752
picosecond flash photolysis in biology and biophysics 79−5328
picosecond lasers, use in studying photosynthesis 77−81480
picosecond spectroscopy, appl. to photosynthesis research 78−68964
picosecond spectroscopy applied to the study of chemical and biological reactions 79−8069
pigment lowest triplet state, phosphorescence polarisation and electronic struct. 79−39358
pigment molecule organisation and interaction in reaction centres of Rhodopseudomonas viridis 80−35843
pigment redox photoreactions, excited complexes 77−25368
pigment spectral forms of Rhodospirillum rubrum, picosecond energy transfer 79−92182
pigment state, reversible changes due to illumination of leaves 79−43818
pigment-pigment electron transfer and charge separation in photoexcited chlorophyl aggregates 77−81468
plant biophysics, review 77−60180
plant growth and development regulation, role of light 78−11695
Porphyridium cruentum, efficiency of energy transfer from photosystem II to photosystem I 77−40641
primary electron-transfer processes in bacterial photosynthesis, picosecond dynamics 78−80841
primary events, picosecond fluorometry 79−8476
primary photosynthesis selectively excited by tunable picosecond parametric oscillator 79−48163
primary processes kinetics, influence of certain back reactions 79−79491
primary processes of photosynthesis, picosecond spectroscopy *(Russian)* 79−39362
primary step, analogue reaction in a porphyrin-quinone linked mol. 80−89720
productivity engineering review 79−62209
purple photosynthetic bacteria, in vitro duplication of the primary light-induced charge separation 79−39361
quantitative cartographic analysis, SYMAP auxiliary programs, geoenvironmental appls. 79−70469
R. sphaeroides, polarisation of photosynthetic membranes and reaction-centres in elec. field 80−94277
reaction centre, struct. investigation, optical detect. of triplet state mag. resonance 77−29093
reaction centre chromophore organisation, high-resolution magnetophotoselection 80−97880
reaction centre functional reconstitution in planar lipid bilayers 80−97881
reaction centre spectroscopy by tunable picosec. parametric oscillators 80−61513
reaction centres, modulation of the primary electron transfer rate 79−8481
reaction centres, triplet population, mag. field and g-factor differences effect 80−97879
reactions of Ma^{2+} and $P700^{+}$ in chloroplasts, pulsed illumination 79−53062
redox conversion kinetics in the electron transport chain 80−40950
redox conversions, electron transport, EPR obs. 79−92179
redox potentials of chlorophyll pigments of photonsynthesising organisms at different evolutionary levels 77−56337
repression b 2-deoxy-D-glucose, low-temp. fluoresc. spectra of intact Chlorella cells 80−81559
review of biophysics of photosynthesis 78−92605
Rhodopseudomonas spheroides, growth yield in light-anaerobic and dark-aerobic cultures 80−3608
Rhodospirillum rubrum, chromatophores electron transport chain, functional organisation 80−81555
solar energy conversion, biomimetic approach 79−52914
solar energy conversion, microbial production of energy sources from biomass 80−61392
solar energy conversion, photoelectric response of photosensitive liquid membranes and chloroplast discs 80−81482
photosynthesis continued
solar energy conversion and storage using artificial photosynthetic systems 80−89662
solar energy conversion by plant photosynthesis 79−43781
solar energy conversion utilising biomass 80−61391
solar energy utilisation via plant photosynthesis 80−3491
soybean plants, radiation-stressed, photosynthesis and photophosphorylation rel. to photoassimilate export 80−56140
spectra of chlorophyll A and B molecules and complexes in PMMA and MTHF 79−3433
spectral red shift in plant leaf chlorophyll 78−61144
spectrophotometry, scanning and kinetic, computer-assisted, in study of photosynthetic systems 78−68963
spinach chloroplasts, laser photoinduced changes in high freq. dielectric constant 80−85449
stereoelectronic properties of photosynthetic and related systems 79−16139
supramolecular organisation of photosynthetic membranes, interpretation 77−29106
technoeconomic analysis of an photosynthesis energy factory as an integrated bioconversion system 80−30510
thylakoid membrane, in plant cell, electron microscopy 80−26210
thylakoid membrane of green plants, simulation model of electron transport *(German)* 77−86468
thylakoid membranes and govindjee pulsed NMR 78−80839
time-resolved raman spectroscopy, appl. to photosynthetic cycle of bacteriorhodopsin 78−85294
triplet states in photosystem I of spinach chloroplasts and subchloroplast particles, EPR obs. 80−85344
triplet-state electron spin resonance of chlorophyll molecules and complexes, expt. obs. 78−25574
triplet-state electron spin resonance of chlorophyll molecules and complexes, interpretation of expt. results 78−25575
upconversion considerations in green plant photosynthesis 78−35811
vegetation canopies, solar radiation absorpt. simulation 80−104635
C fixation cycle, semi-dynamic model 78−73806
^{11}C, continuously produced, high specific activity for studies of photosynthesis, transport and metabolism 79−39502
H biological photoprod. using sunlight, review 80−45777
H biological prod. by solar energy conversion, coupling of hydrogenase and chloroplast photosystems 80−45778
H prod. by H_2O solar photolysis methods based on photosynthesis *(Japanese)* 80−45765
H production by photobiological energy conversion 79−70456
H synthetic chloroplasts 80−30508
H_2 evolution, the photosynthetic unit 77−77875
H_2 gas, photosynthesis prod. by green algae, turnover times and pool sizes 80−16821
H_2, photobiological prod., key enzymes and biochem. systems, tech. problems of H_2 prod., review 80−61446
H_2 production by biological and biochemical solar energy conversion, review 80−61454
H_2O, photoelectrochemical evolution of O_2 using manganese chlorophyll electrode 79−83719
O_2 formation rate on pulsed illumination of Scendesmus obliquus 79−57606

phototelegraphy *see facsimile*

photothermal conversion
see also solar absorber-convertors
amorphous semiconductor role in photovoltaic and solar thermal conversion 79−61981
concentrator/photovoltaic system design for electricity and heat generation 79−61997
concentrator/photovoltaic/Rankine cycle steam turbogenerator system efficiency 79−62002
domestic space heating using low-temp. solar thermal systems *(Czech)* 79−83566
efficiency, meas. method 79−79399
greenhouse solar distillation and cultivation materials 79−74496
heat generation for multipurpose utilization systems by heat of dilution converted from solar energy 80−55915
hot water supply systems using solar collectors, technical problems *(German)* 80−94106
insolator, copper belt type tube structure, design, construction and testing *(Czech)* 79−83626
mobile field dormitory, solar energy space and hot water heating 79−83623
passive solar heating systems, calc. of heat-transport-medium flow rate in heat receivers 80−99913
photovoltaic-solar thermal system role of high performance solar cells 79−61978
R and D by US DoE 80−89674
solar desaliniation unit with evaporation chamber, test results 80−96178
solar energy closed loop systems, general design method 79−74542
solar energy collector design for low capital costs and least steady-state heat losses 80−104517
solar energy cooling, operating systems and current developments, review 80−85265
solar energy storage area design coefficients for consumer demand and solar radiation *(Rumanian)* 80−89670
solar furnace, materials melting process dynamics rel. to automatic control 79−39317
solar heating system for dwellings, temp. regime investigations 80−97802
solar house heating system, possibilities of integrating heat pump *(Rumanian)* 80−97804
solar installation for refrigeration and water heating, energy characts. 80−101124
solar power, direct conversion and storage, review of developments, review 79−43741
solar power generation, system developments and research aims *(German)* 80−108799
solar still, industrial, stepped oblique type, annual operating data 79−39318
solar systems installation for domestic heating *(German)* 80−94103
solar thermal power system, 10 MWe pilot central receiver design concept 80−16792
solar thermoelectric generators, metallic thermo-electric materials utilisation, economic characts. 80−101122
solar water heating systems, economic assessment based on measured performance 80−97807

photothermal conversion continued
space heating, solar installations for utilisation of solar radiation and heat from outside air *(German)* 80−94104
space heating, water heating system using solar collectors *(German)* 80−94105
spectrally selective surfaces for photothermal conversion of solar energy 80−101125
sun-mill, version of dunking-bird, solar-powered, gravity-assisted heat engine 80−89672
thin film technology, appls. in energy, optics, and electronics, review 80−78932
water thermolysis, solar furnace, thermodynamic analysis 79−83625
Al_2O_3-Au, cermet coatings, solar energy photothermal conversion, Bruggeman effective medium theory 79−83627
H_2 production, by thermolysis of water in solar reactor, thermal calculations 79−39319
MGO-Au, cermet coatings, solar energy photothermal conversion, Bruggeman effective medium theory 79−83627
MgF_2-Au, cermet coatings, solar energy photothermal conversion, Bruggeman effective medium theory 79−83627
Ni cermet selective absorbers, photothermal conversion appls. 80−21413

phototransistors
camera shutter mechanism control, photography of transients on oscilloscope appl. *(Danish)* 78−234
double, sensitive to coordinate of light spot 79−93217
Franz-Keldysh, optically enhanced for n^+-p-n^+ phototransistor struct. 78−60423
GaAs photo-FET high speed photoconductive integrated optical receiver 80−58816
graded composition semiconductor, minority carrier transport, rel. to transistor 78−80022
IC phototransistor static characteristics, effect of insulating p-n junction *(Russian)* 78−52069
image sensing array performance 77−39078
injection laser transistor, heavily doped semiconductor devices, review 79−47039
MOS, current-illumination and spectral characts., 0.22 to 2.5 μm *(Russian)* 77−35996
MOS with Si-SiO_2 systems, spectral characts. *(Russian)* 79−42657
MOST, photocurrent spectral response, bias depend. 77−69422
optical communication appl. *(Dutch)* 77−11036
optoelectronic devices and optical imaging techniques, book 80−27059
photoelectric convertor for automated spectral measurements 80−22449
solid-state imaging application 77−37707
$Al_{0.5}Ga_{0.5}As$-GaAs heterojunction phototransistors, growth by metalorganic vapour deposition 79−67380
GaAs MESFET, optical detector appl., sensitive high-speed device 80−13143
GaAs-$Al_xGa_{1-x}As$ heterojunction, avalanche phototransistors, detectivity and noise 78−2558
InGaAsP/InP phototransistors, fabrication by LPE, photodetectors 80−95139
InGaAsP-InP high-gain heterojunction phototransistor 80−103745
InP/InGaAs heterojunction phototransistor, high-sensitivity 80−100505
Si detectors, vac. UV performance, 500-2000 Å 77−26397
Si MIS phototransistors, photoelec. props. at high illum. intensities 80−60101
Si phototransistors, slow contamination and fast surface state effects, SEM study 80−107896

phototubes
see also photocathodes; photomultipliers
gas discharge detector miniaturisation, rise time spectral depend. 78−86318
gas filled phototubes as sensitive UV detectors, excited atom photoionisation mechanism 77−61122
image tube lens, MTF 78−9428
Kron camera, single electron counting by self-scanning diode array 78−9429
light flux fluctuations, limiting factors in photoelectric meas. 80−13136
microphotometer, automatic fluoresc., using image dissector tube, quantitative cytochem. appl. 79−97413
multichannel photon counting image detector arrays 78−65970
Photicon, new imaging optical detector 77−67499
photocell, FEK-37, for HV pulse shaping and electrooptic switch control in lasers 79−64340
picosecond streak camera for pulse detect., book contrib. 77−61138
proximity focused image tubes, image transfer props. 77−83950
streak camera tubes with picosecond time resolution, dynamic range measurements 80−73490
streak tube technology 77−79184
thermionic emission student expt. 77−24919
UV detection by gas filled phototube photoionisation of excited atoms 77−87823
X-ray detector, suitable for X-ray lasers, interchangeable cathode, Fe, Al *(German)* 77−10107
Ti tritide collector for ion beam profile imaging 78−78032

photovoltaic cells
see also solar cells
5 kW photovoltaic generator system, analysis, design and realisation 80−45704
25 kW plant, irrigation and grain drying appl., US expt. 79−70442
100 kW peak photovoltaic power system, design, construction and capabilities 80−45705
aerospace photovoltaic generators, symposium, Noordwijk (1978) 79−96449
aggregating cells in series and parallel, technique 80−93954
$Al_{1-x}Ga_xAs$-GaAs heterophotoconvertors, HV, investigations 80−101097
$AlSiO_x$-Si photodiode, experimental verification of theoretical predictions 80−29485
amorphous semiconductor role in photovoltaic and solar thermal conversion 79−61981
antireflection coatings applied from metal-organic derived liquid precursors 80−5847
array, for meas. of random water surface waves 77−29503
array modules and systems, circuit design considerations 80−93955
back surface field effect on photocurrent in semicond. junction 78−91762
chlorophyll-a, microcryst., trapped-electron doping in photovoltaic sandwich cells 78−53334

photovoltaic cells continued
combined photovoltaic/thermal flat plate collectors, analysis using Hottel-Whillier-Bliss model 77−39106
comparative evaluation *(Italian)* 80−60023
compound parabolic concentrator photovoltaic solar collector design 79−61998
concentrator array technology, status report 80−94024
concentrator/photovoltaic system design for electricity and heat generation 79−61997
concentrator/photovoltaic/Rankine cycle steam turbogenerator system efficiency 79−62002
conductor-insulator-semicond. (CIS) solar cells, noncrystalline (poly and amorphous), interface importance 80−81466
conference, photovoltaic technology, Washington, DC, USA, (June 1978) 79−7863
cost minimisation, of self-contained power supplies 79−48098
current production and future prospects *(French)* 79−100531
dark current and photocurrent superposition 79−43769
desalination plant coupling to solar conversion system, technical and economic evaluation 80−55804
diffusion, chemical reactions, contamination, AES and SIMS 80−72066
distributed photovoltaic systems for electricity generation, economic and technologic feasibility 80−55906
distributed series resistance effects in photovoltaic devices 80−93968
economic power generation, photovoltaic modules fabrication cost analysis 80−45674
electric power sources, applications overview *(Italian)* 80−72044
electrical load feeding prospects *(Italian)* 80−60028
electrochemical, using covalently-bound dyes on semiconductor surfaces 77−4393
electron beam induced currents appl., topotaxiality and dead region determ. 80−3518
encapsulation of photovoltaic cells using silicone materials 80−94019
energy conversion radiation enhancement using surface polaritons 80−7941
epitaxial polySi and amorphous Si photovoltaic thin film developments 79−74524
fission product detectors 79−93873
flat plate module design evolution, influence of module requirements 80−94065
French solar energy collection, research programme, outline *(French)* 79−74498
front surface field solar cell, spectral response, theory 80−76633
G. Donegani Institute activity *(Italian)* 80−60027
GaAs, polycrystalline, grain boundary resistance meas. effect on solar cell performance 80−93891
Galileo works activities *(Italian)* 80−60029
generator operation and cost simulation 79−61975
glassy C electrodes for photogalvanovoltaic and photovoltaic cells 80−89630
grid lines, optimal design to reduce conductive losses 80−7945
homojunction solar cells, conversion efficiency, maximum theoretical efficiency as a function of temp. 80−81469
ionized cluster beam deposition and epitaxy, cell characts. 77−77416
IR detector, absolute detectivity determ. 77−13535
LAMEL activities *(Italian)* 80−60026
lifecycle cost minimisation, sizing anal. 80−94039
line-focus parabolic-trough photovoltaic arrays, active and passive cooling 80−93988
logarithmic light meter using Si junction photovoltaic cells 78−32844
low-temperature collector and thermal or photovoltaic concentrator development 79−62009
material selection for solar photovoltaic cells 79−57434
materials, fabrication and research for low cost photovoltaic solar cells 80−55838
MIS, influence of interface states, efficiency improvements 78−39227
MIS solar cell, effects of pinholes, oxide traps and surface states 78−80055
MIS solar cells with diffused back surface field (BSF), and diffused junction solar cells with MIS BSF 80−94074
monolithic solar cell panel of amorphous Si 80−45666
Moss relation between refr. index and energy gap of semiconductors rel. to photovoltaic solar cells 80−11357
multi-bandgap concentrator cells, Si and $Al_xGa_{1-x}As$ systems, operation with spectrum splitting filter 80−45698
NASA space power technology program 79−96883
operation using solar simulator lamp 80−42004
organic photovoltaic solar cells, solid state chem. effect on performance 79−48129
p-n junction photodiode terminology 80−70800
parabolic concentrator arrays, collector end shadowing effects minimisation 80−93987
photoconverter, bilateral sensitivity, n^+-p-p^+ structure, volt-ampere characts. under illumination 80−40855
photoelectric conversion, MIS structures utilisation, and manufacture, photoelectric parameters *(Czech)* 79−83595
photon detector, nonuniformly doped intrinsic photoconductor, photovoltaic operation 79−224
photovoltaic concentrator cells development project, developments, performances and future trends 80−45699
photovoltaic power systems, equipment performance and manufacturing techniques improvements and system design problems for telecommunication applications 80−55843
photovoltaic solar energy conversion [conf. Berlin, West Germany, April 79] 80−30482
photovoltaic technology, conf., San Diego, CA, USA (Jan. 1980) 80−86041
photovoltaic-solar thermal system role of high performance solar cells 79−61978
phthalocynanine, doped photovoltaic cell, photoconductivity, elec. field induced flouresc. quenching, charge carrier photogeneration 80−84485
point-focus Fresnel lens photovoltaic arrays, active and passive cooling 80−93988
polyacetylene photoelectrochemical solar cell, fabrication and efficiency 80−50954
power generation, reviews *(Japanese)* 79−39304
power loss in photovoltaic arrays due to mismatch in cell characteristics 80−16802
power system elements, efficiency and terminology summary 80−97790
power system reliability assurance methods 80−61315
principles and solar power appls. *(Portuguese)* 79−70452

photovoltaic cells continued
pyrometer for ultrahigh vac. systems, using Si photovoltaic cell 77−5908
radioisotope-powered photovoltaic generator, using radioactive waste for electricity prod. 79−57432
radioisotope-powered photovoltaic generator 79−22495
review of US DOE R and D program 80−55874
satellite generators, low-orbit, D2B and Signe 3, performances comparison 80−3524
Schottky barrier solar cell, comparison of thin film and bulk single cryst. 78−80053
Schottky barrier solar cells, back-illuminated, theoretical performance 80−61345
semiconductor heterostructures, elec. and optical phenomena, discrete devices, review 78−72250
semiconductor-electrolyte junction photovoltaic cells, interface charge transfer, recombination rate, C-V characts. 80−70818
semiconductors, direct gap 79−92075
sensitisation, appl. of ion-pair effects involving OH^- and rare earth ions 79−38624
sheet edge-defined film-fed Si growth 79−61982
solar array for Halley's comet rendezvous mission, ultralow-mass designs 79−53702
solar arrays and DC motors, direct coupling theory 80−3523
solar cell, efficiency, bandgap and temp. parameters relations 79−52935
solar cell arrays, DC to AC power conversion and utility interfacing, technqiues, requirements and components used 80−45703
solar cell arrays, parametric cost analysis 79−100535
solar cell developments and new appls., cost effectiveness 80−16800
solar cell efficiency calc., using irradiance-transmittance solar spectrum 80−26137
solar cell electricity, cost reduction possibilities 80−97793
solar cell electricity, future development prospects, research projects and new appls. 80−16798
solar cell panels and systems, US DOE photovoltaic program 80−93879
solar cell spectral response characterisation, 400 to 1000 nm 80−35675
solar cell trends using Si 79−61974
solar cells, for satellite solar power systems, developments and future trends 80−45694
solar cells, photovoltage source in photocond. materials due to comp. and doping var. 80−7938
solar cells, polycryst., influence of grain boundaries electronic structure on diode characts. 80−94068
solar cells, polycryst., recomb. at grain boundaries, effect on photoresponse 80−108796
solar cells, SnO_2-SiO_2-n-Si heterojunction, cheap solar elements for ground-based appls. 80−40860
solar cells, thin film, performance analysis employing loss minimisation of essential characteristics 80−45682
solar cells for use as optical detectors, background illum. effects 78−70182
solar cells in undersea environment, performance 80−93900
solar devices, modular system *(German)* 80−89629
solar energy, conference, Luxembourg (1977) 78−64106
solar energy, review using rational units 80−30389
solar energy conversion, concentrated, feasibility assessment 79−57436
solar energy conversion, materials science aspects, lecture 78−25989
solar energy plant electricity storage, battery appls. potential 80−72067
solar energy powered deep well irrigation system 79−92082
solar flat panel procurement, qualification test results 80−94064
solar generators, ampere-hour efficiency, charging and discharge power 80−29434
solar heating and electricity generation, retrofitting of existing residence, expt. results and economic assessment 79−61952
solar photovoltaic cells for remote islands telecommunication repeater stations power supply 80−61382
solar photovoltaic cells production technology, future systems efficiency and cost effectiveness 80−16799
solar photovoltaic electricity generation in India 80−21381
solar photovoltaic energy conversion, review 79−100530
solar photovoltaic energy system, 25 kWp, for agricultural appl., performance anal. 80−30491
solar photovoltaic generators using optical concentration, current status and development trends review 80−45697
solar photovoltaic modules, physical and electrical degradation in terrestrial environment 80−30492
solar photovoltaic power stations, nominal costs and performance goals 79−34438
solar photovoltaic power systems for rural areas of developing countries 80−50967
solar photovoltaic system feeding unusual length radio link, characteristics and design data 80−61383
solar photovoltaic systems, design for intermediate-sized appls. 80−30490
solar power satellites using microwave link, developments 79−24891
solar powered electrodialysis, water desalination appl. 80−55805
solar space power generators, past developments and future trends 80−45693
Solarex two-axis tracking linear concentrating collector system, design and operation 80−93989
solid-dielectric compound parabolic concentrator with Si solar cells, prototype 77−39107
space heating, photovoltaic and thermal collector system design and testing 80−45675
spectral response, pulsed measurement, test set-up and apparatus, shortcomings and planned improvements 80−45695
squarylium and cyanine-TCNQ dye Schottky-barrier sandwich cells 79−29468
static photovoltaic concentration improvement, two-sided Transcell 79−61999
table top pulsed solar simulator, design and construction, for testing solar cell arrays powering artificial satellites 80−45696
tandem solar cell system efficiency, solar energy conc. ratio and temp. depend. 79−74516
technological and economic barriers to be overcome for competitive power production 80−72049
ternary semiconductors, use in thin film heterojunction and homojunction photovoltaic devices 78−39208
terrestrial flat plate photovoltaic modules, environmental testing 80−30560
terrestrial solar generators, design, fabrication, testing and economic power generation 80−45672
photovoltaic cells continued
terrestrial solar modules, sandwich type glass encapsulation, climatic parameters effect, economic anal. 80−45673
thermal/photovoltaic system powers Texas house, performance data and power conditioning equipment 80−94036
thermophotovoltaic energy convertor, development of new Si cells 80−12016
thin film prep. for solar energy utilisation 80−84847
transparent electrode photo-galvano-voltaic cell, using Mg-meso-tetraphenylporphine-coated glass *(Chinese)* 80−40865
tunnel MIS solar cells, grain boundary effect on performance 79−79394
tunnelling MIS structures photovoltaic energy conversion, band struct. 80−92995
USA photovoltaic industry development programme 79−61976
Al/copper phthalocyanine/Au cell, photoexcitation, doping, energy loss mechanisms 79−99573
Al/magnesium phthalocyanine/Nesatron, depletion layer studies, temp. depend. of LF capacitance 80−65617
Al/metal-free phthalocyanine Schottky barrier solar cells, photovoltaic props. 79−100527
Al/tetracene/Nesatron, depletion layer studies, temp. depend. of LF capacitance 80−65617
Al-Ge photovoltaic cell, charact. 79−40612
Al-Si-Al(Mo), sputtered Si film, photovoltaic props. 77−24623
AlGaAs heterojunction photocell with luminesc. wavelength converter 80−108800
AlGaAs-GaAs proton irradiated solar cells, deep level defects and recombination parameters 80−94032
Al_2O_3 MIS Schottky structures, photovoltaic response 80−101115
Al|chlorophyll-a|Hg/In, sandwich cell, photovoltaic, rectifying and tunnelling effects 79−1628
Au/(Zn-)phthalocyanine/Al(In), photovoltaic effects, dark elec. props. of rectifying cells 79−4604
Au/(Zn-)phthalocyanine/Al(In), photovoltaic effects, illuminated thin-film cell props. 79−4605
CdO, aqueous-deposited films, struct. and electronic props. for solar cell appls. 80−100797
CdS, aqueous-deposited films, struct. and electronic props. for solar cell appls. 80−100797
CdS heterojunction solar cells by CVD method 80−45685
CdS photoanode appl., thin film, prep. and characts. 78−14818
CdS solar cells, construction, solar photovoltaic systems for remote communications power supply 80−66980
CdS solar photovoltaic panels, deposited by spray pyrolysis, film and junction structure studies 80−45689
CdS:Cu(Cl) thin films, surface and bulk photoconc. 80−88653
CdS/Cu_2S heterojunction solar cells, optimal material props. theory and experimental verification 80−45686
CdS/Cu_2S solar cell, design and fabrication 80−30481
n-CdS/p-$ZnIn_2Se_4$ thin film solar cell, photovoltaic props. 80−89628
CdS-CdTe p-n junction screen printed thin film solar cells 80−72055
CdS-Cu_2S photovoltaic cell, effects of O_2 on efficiency 78−14807
CdS-Cu_xS solar cells, screen printed, prep. and photovoltaic props. 80−40863
CdSe MIS thin film solar cell 80−45688
CdSe(Te)-electrolyte photovoltaic cells, solar cell appls. 77−35990
CdTe thin film polycrystalline solar cells prepared by electrodeposition 80−93948
CdTe thin films, oriented, VPE growth, infrared transmission, photovoltaic cells 80−59825
CdTe-CdS p-n heterojunction, coordinate sensitive photoelements, longitudinal photovoltage 79−95440
$Cd_{1-x}Zn_xS/Cu_2S$ thin film heterojunction solar cells, operational charact. 80−45687
$Cd_zZn_{1-z}S$-Cu_2S, heterojunction interface double layer, dislocation field, charge compensation 79−7855
$Cu_{1-y}Ag_yInS_{2-x}Se_{2x}$, for solar photovoltaic cells 80−10982
$CuCl_2$-brass, chemically deposited photosensitive cells, photovoltaic characts. 79−39303
$CuIn_{1-y}Ga_ySe_{2(1-x)}Te_{2x}$ pentenary alloy compounds for photovoltaic solar energy conversion 80−93971
$CuInS_2(Se_2)(Te_2)$, thin films and photovoltaic devices, AES evaluation 78−67928
Cu_2S/CdS, developments, appls., and economics of solar photovoltaic conversion *(German)* 80−26132
Cu_2S-CdS, characteristics, for various solar radiation incidence angles 79−83593
Cu_2S-CdS back illuminated high efficiency thin film solar cells 79−74515
Cu_2S-CdS solar cells with interdigitated grid, current-voltage analysis 80−93981
$Cu_{2-x}S$/CdS heterostructures, heat treated, capacitance voltage meas. anal. 80−20292
$Cu_{2-x}S$-CdS, chem. formed heterojunction, photosensitivity characts. of $Cu_{2-x}S$ 78−72199
$Cu_{2-x}S$-CdS, collection coefficient theoretical anal. at conjunction 80−101094
Cu_xS-CdS thin film solar cell using chem. sprayed CdS film 78−43465
p-Cu_2Sn-n-ZnS heterojunction, I-V characts., photocond. and electrolum. 78−72251
$Ga_{1-x}Al_xAs$:Si photoelectric convertors, broadband varizone creation 80−40856
$Ga_{1-x}Al_xAs$-GaAs p-n solar cell, with thin variable gap layer, high efficiency 79−24064
GaAs antireflecting MOS solar cells, epitaxial and polycryst. using OM-CVD techniques 80−94072
GaAs crystals appl. with nipi superstructures *(German)* 78−95064
GaAs, developments, appls., and economics of solar photovoltaic conversion *(German)* 80−26132
GaAs photovoltaic solar system, appl. in electric utility system 80−55875
GaAs polycryst. solar cell diagnostics using IR electroluminesc. 80−93885
GaAs prospects *(Italian)* 80−60025
GaAs solar cells, photoreactance of p-n junction diodes 80−81464
GaAs thin film polycrystalline Schottky barrier solar cells, grain boundary chemistry 80−94067
GaAs-GaAlAs LPE grown, parameters dependence upon impurity concentration and temp. performances for series resistance reduction 80−45692
H_2O photoelectrolysis, stable cells prod. 77−44484

photovoltaic cells continued
In_2O_3:Sn/n-Si heterojunction solar cell, fabrication and charact. 78−15314
In_2O_3-SnO_2 film on Si, heterojunction, photovoltaic effect, sunlight induced 77−1470
In_2O_3-SnO_2/SiO_x/Si diode solar cells, loss mechanisms, charact., band struct. 80−26135
In_2O_3-SnO_2-InP solar cell junctions, efficiency, InP surface props. 80−85288
InP homojunction solar cell, antirefl. coated, high-efficiency 80−104505
n-InP, MOS solar cells, electrical and photovoltaic characteristics 80−85276
InP thin films for photovoltaic devices 80−93972
p-InSb IR detector, photovoltaic operation, theoretical anal. 79−224
$In_{2-x}Sn_xO_{3-y}$-CdTe(InP) photovoltaic heterojunctions, surface and interface studies, efficiency 80−45691
$PbySn_{1-x}Se$ epitaxial film narrow band photovoltaic detectors, detection at long wavelengths 78−8443
Se photocell, high-gain amplifier cct. 78−4679
Si, 100 kW generation, costs and efficiency *(German)* 79−79398
Si, amorphous and solar cells *(Japanese)* 80−50965
Si amorphous cell generating more than 2.0 V 79−100518
Si, as-grown Czochralski crystal, multiple p-n junction structure obtained by heat treatment, appl. to solar cells 80−101099
Si, characteristics, for various solar radiation incidence angles 79−83593
Si concentrator solar cells, effects of nonuniform illumination 80−93942
Si, developments, appls., and economics of solar photovoltaic conversion *(German)* 80−26132
Si, film, polycryst., for photovoltaic appl., grain size effects 78−72034
Si, fixed-base, flat panels, possible developments for more competitive power production 80−72050
Si, for tristimulus colorimeter *(German)* 80−17994
Si, grain boundary defects in thin semicrystalline material 80−93889
a-Si ITO/p-i-n solar cells 80−101113
Si, ionising radiation detector appl. *(Czech)* 77−18748
Si, low series resistance photovoltaic concentrator 80−93940
Si n^+-p solar cell, forward and reverse bias tunnelling 80−85274
Si n-p junction vertical solar cells, Al-plated, photovoltaic effect variation with impurity conc. 79−100522
Si p^+-n-n^+ back surface field concentrator solar cells 80−93939
Si photoconvertors, p-i-n structure, high resistivity, operational parameters theoretical and experimental analysis 79−96441
Si photoelectric convertors, photoelectric parameters under illumination 80−40857
Si photoelectric convertors, bilateral sensitivity, optical charact. anal. 80−40858
Si, polycryst. solar cells, production problems *(Rumanian)* 80−21398
Si, polycrystalline, solar cells, grain-boundary hydrogenation technique for improvement 80−85273
Si, polycrystalline Czochralski-grown, MIS solar cell characterisation using scanned laser response exam. 80−93884
Si polycrystalline film, effect of defects/grain boundaries on photovoltaic mech. 80−93883
Si, prospects *(Italian)* 80−60024
Si, radiation damage effects on charact. *(Korean)* 79−60402
Si ribbon growth by laser zone melting 80−93482
Si ribbon solar cell, EFG, diffusion length enhancement under illum. 78−14756
Si Schottky barrier solar cell, V-I charact. and efficiency 78−14828
Si solar cell array with concentration, design and development 80−45700
Si solar cell parameters, grain size dependence 80−94049
Si solar cells, developments *(French)* 80−55845
Si solar cells, photoreactance of p-n junction diodes 80−81464
Si solar cells, review of physics underlying recent improvements 80−93974
Si solar cells for cathode protection of submerged marine structures 80−40859
Si solar cells with concentrating collectors and integrated heat use system 80−45701
Si solar concentration cells, concentrated sunlight effects, experimental results, interpretation 80−35690
Si solar concentrator cell, effects of nonuniform illumination and temp. profiles under concentrated sunlight 80−93941
Si terrestrial photovoltaic systems, historical developments and current research and development trends 80−45702
Si:F,H, amorphous efficient carrier generation for solar photovoltaic energy conversion 80−92906
Si:H, amorphous, HV photovoltaic cells, design parameters 80−101105
Si:H, amorphous, horizontal cascade type integrated photovoltaic cell module 80−94091
Si:H, amorphous, p^+-i-n^+ struct. solar cells, material parameters and deposition condition optimisation study for higher efficiencies 80−45676
Si:H, amorphous, RF sputtered, Schottky barrier solar cells, photovoltaic props. and capacitance-voltage charact. 80−45678
Si:H, amorphous, Schottky barrier solar cell, degradation mechanisms affecting stability and operation 80−45680
Si:H, amorphous, solar-cells, charge collection and spectral response 80−85275
Si:H, amorphous thin film solar cells 80−81478
Si/Si-Ge alloy, amorphous, solar cell, multijunction structure, increased conversion efficiencies, low cost 80−45677
Si-ion-ceramic, short-circuit current density meas. using light-beam-induced-current tech. 80−93887
Si-SiO_2-CdS solar cell, I-V characteristics 80−89621
Si-SnO_2, p-n heterojunction, prep., elec. and optical props., expt. *(Korean)* 77−4427
Si_xGe_{1-x} diffused p-n junction, electric and photoelectric props. 80−101095
SiH_x, amorphous, solar cells, short circuit-currents and collection efficiencies 80−94028
SnO_2/n-Si solar cells subjected to different weathering conditions, stability 79−52936
SnO_2-GaSe heterojunction photocell, fine struct. of photo-EMF spectra 80−6967
SnO_2-Si, solar cell, max. theoretical efficiency 79−83598
SnO_2-Si heterojunctions, elec. and photovoltaic props. 80−26141
SnO_2-Si solar cells, electron-beam deposited, struct., photovolt. props. 80−50956
SnS, photovoltaic energy conversion efficiencies 79−7854
$Zn_xCd_{1-x}S/Cu_2S$ heterojunction solar cells, junction anal. 79−92080

photovoltaic cells continued
ZnO, aqueous-deposited films, struct. and electronic props. for solar cell appls. 80−100797
Zn_3P_2 thin polycrystalline films for solar photovoltaic cells 80−97797
ZnS, photocell, transient photoelec. phenomena 79−82687

photovoltaic effects
see also Dember effect
$A_{1-x}B_xC$, rapid localised non-destructive optical charact. of ternary layer *(French)* 77−62725
amorphous semiconductor *(Japanese)* 80−54737
anisotropic semiconductors, bulk photovoltaic effect and transverse Dember effect 77−55573
anomalous photovoltaic effect of ferroelectrics, review 80−65628
anthracene, surface photovoltage 80−2419
back surface field effect on photocurrent in semicond. junction 78−91762
back surface field semiconductor junction, temp. depend. of open circuit photovoltage 80−15593
p-CdTe, surface photovoltage spectroscopy in IR and visible range 80−39632
cells, electrochemical, photovoltaic phenomena and mechanisms 78−8198
chromophore phospholipid Langmuir films, photoeffects 80−80409
circular photogalvanic effect optically active crystal 79−73542
conference, photovoltaic technology, Washington, DC, USA, (June 1978) 79−7863
copper phthalocyanine film, electron acceptor surface states due to O_2 adsorption 80−88586
copper phthalocyanine film, photocelectrochem. behaviour on SnO_2 electrodes 80−15626
crystal without inversion centre, current quadratic in field and photogalvanic effect 78−10505
cyanine dye monolayer assemblies with Al and Ba electrodes, photovolt., dark cond. and photocond. 80−80400
degenerate semiconductor, surface photo-EMF 79−69580
detector, photoelectric evaluation, for Gaussian incident pulse 79−63306
1,1′-diethyl-2,2′-quinocyanine-$[TCNQ]_2$ anion radical salt single crystals *(Japanese)* 78−2522
dynamic lateral photovoltaic effect, appl. to junction capacitance meas. 77−85304
dynamic lateral two co-ordinate photoeffect with flying light spot 79−28401
electro-optic crystals, hologram formation arbitrary transport length anal., photovoltaic effects 80−78802
electrooptic crystals, holographic recording, photogalvanic effect mechanism of nonlinear wave interaction 80−102672
EuSe, photocond. and photodiffusive voltage spectra 80−96940
ferroelectric, anomalous bulk photovolt. effect, quantum-mechanical theory of electron transport 79−69545
ferroelectric, existence of bulk photocurrents, model calc. 78−84256
ferroelectric, large-gap type, vibronic theory and opt. props., anomalous bulk photovoltaic effect 80−103939
ferroelectric, photovoltaic current, general formula *(Russian)* 80−39627
ferroelectric semiconductors, anomalously high photovoltage 77−69378
ferroelectric semiconductors, props., book 80−82590
ferroelectric-photosemiconductor two component systems, photoelectret state 80−25287
ferroelectrics, bulk photovoltaic effect response coeff. 80−65631
ferroelectrics, optically induced internal fields 80−107855
ferroelectrics, photovoltaic and photorefractive effects, fluctuation model interpretation 77−69369
ferroelectrics, theory of photogalvanic effect 79−42575
film, vacuum-deposited, struct. and props., basic relationship 78−6236
film solar cells 78−72204
Fokker-Planck eqn., kinetic effects due to detailed equilibrium violation, elastic scatt. *(Russian)* 80−31687
heterogeneous semiconductor systems, elec. cond. and EMF relax., pulsed radiation effects 77−89842
heterojunction solar cell, relation between efficiency and heterojunction parameters, review 79−74523
heterojunctions, growth and charact. 77−39931
homogeneous ferroelectrics; bulk photovoltaic effect 79−42578
II-VI heterojunction, photovoltaic props. 77−55600
II-VI heterojunctions, photovoltaic effects and solar efficiency 78−52076
impurity centre models *(Russian)* 78−60153
IR detector, antenna coupled 77−87824
laser measurement, of semiconductor materials and devices *(Rumanian)* 78−52035
merocyanine organic solar cells, photovoltaic props. in terms of exciton transport 79−43763
metalloporphyrins, photoelectrochemical props. 80−50991
MIS, and amorphous materials *(Japanese)* 80−54737
MIS, pulse effect 78−2577
MIS capacitor, light induced electron-hole pair generation 79−38167
MIS solar cell open-circuit photovoltage rel. to oxide thickness 79−61985
MIS structure, fast surface states density, photoelectric methods of determ. 80−70835
MIS structure, photovoltaic efficiency, effect of insulating film and interface states *(French)* 77−1488
MIS structure, photovoltaic efficiency, interface states effect 77−80844
MIS structure, surface state density, determ. from surface saturation photo-EMF meas. 80−75652
MIS-Schottky barrier solar cells, photovoltaic props. anal. 78−6448
MIS-Schottky barriers, photovoltaic props. anal. 78−26966
MOS capacitor photovoltage characterisation 78−10573
multilayer p-n systems, nonstationary photoelectric effect *(Russian)* 77−76908
nickel phthalocyanine film, electron acceptor surface states due to O_2 adsorption 80−88586
niobates, ferroelectric, anomalous bulk photovoltage effect, Jahn-Teller mechanism 77−28218
ohmic contact, hot minority carrier effects on thermoEMF and photovoltage 77−15956
p-n junction, anomalous hot carrier-voltaic effect, electron emitter and light detector appls. 77−76861
p-n junction solar cell response to concentrated sunlight and partial illum. 79−61996
p-n junction with hot carriers, thermophotoelectric effects 79−73576
p-n junctions, photoeffect, quantity effective diffusion length *(Russian)* 78−56212

photovoltaic effects continued
pentacene, surface photovoltage 80−2419
phthalocyanine film, surface photovoltage, central ligand effect 79−78231
phthalocyanine films, metal-free, adsorbed o-chloranil effect on surface photovoltage 80−34485
phthalocyanine-metal interfaces, surface photovoltage 80−20308
phthoralocyanin porous films, Becquerel photovoltaic effect 77−16907
physical model 78−95311
piezoelectric ceramics, photovoltaic effect application to information storage 80−80316
piezoelectric material, phonon mechanism 79−7862
PLZT ferroelectric ceramic, anomalous bulk photovoltaic effect and cond. *(Russian)* 80−54733
polar crystal, bulk photovoltaic effect due to electron-phonon coupling 77−20358
polar crystal, bulk photovoltaic effect due to electron-phonon coupling 78−14757
polyacetylene, phototransport effects 80−44653
polyacetylene films, AsF_5 doped, photocond. and junction props. 80−70770
polymalononitrile, plasma polymerized film, photoelec. props. 78−39158
polymer films, photovoltaic props., solar cell appls. 80−60040
polymer p-n junction, rectification effects in dark and photocurrents 77−69407
polymeric double layer system, high field cond., xerographic characts. 79−95448
polymethine semiconducting films, surface photovoltage 80−70857
polynaphthalene films, plasma polymerised, photovoltaic and photocond. props. 80−34479
polythiourea, plasma polymerized film, photoelec. props. 78−39158
porphyrin films, methine bridge substituted, surface photovolt. depend. on fabrication method 80−60119
pyroelectric materials, photovoltaic effect, photoelectron transport 79−4582
rhodamine B surface state hole traps, surface photovoltage meas. 80−39654
$Se_{1-x1}Te_{x1}$-$Se_{1-x2}Te_{x2}$ heterostructure, amorphous, rectification phenomena 79−99610
semiconduct-electrolyte interface, phenomenological theory and expt. confirmation 80−15601
semiconductor, bulk photovoltaic effect, solar energy convertor theory with p-n junction 78−72201
semiconductor, diffusion length, meas. by surface photovoltage method effects of optical beam size 80−60002
semiconductor, doping factor, mobility ratio and excess conc. determ. extreme band bendings 78−91726
semiconductor, optically anisotropic, orientation, use of polarisation depend. of photo-EMF and photoconductivity 77−89807
semiconductor, photo-EMF during charge carrier trapping *(Russian)* 79−42574
semiconductor, surface photoelectric effects, influence of excitation rates 79−69547
semiconductor, surface properties, investigation by laser and photovoltages *(Russian)* 78−23130
semiconductor electrode, open-circuit photopotential, simulation 77−15950
semiconductor electrode, sensitised photocurrent by energy and electron transfer in dye monolayers 79−38119
semiconductor film, photovoltaic and photodiffusion mechanisms responsible for anomalously high photovoltages 78−26910
semiconductor films with anomalous photovoltages for radiation recording 77−37989
semiconductor surface electron states, appl. of surface photovoltage spectroscopy 77−69391
semiconductor surface probing using scanned photovoltage techniques 80−49915
semiconductor with bipolar diffusion intervalley overpopulation *(Russian)* 78−23092
semiconductor with internal elec. short circuits, bulk photovolt. effects, calc. 80−65620
semiconductor-metal contact, absorption coefficient of semicond. detem., photo-EMF meas. 79−11224
semiconductors, exhibiting negative photocond., photovoltaic effects 80−96943
semiconductors, intravalley carrier transfer, transverse photo-EMF for various absorpt. coeffs. 79−69551
semiconductors, photocond., photoelec. effects, book contrib. 80−84488
shallow junction devices, minority carrier diffusion lengths 78−72168
solar cell, diffusion equation, surface boundary condition 80−66975
solar cell, photovoltaic effects in p-n junctions, Schottky barriers, review *(Czech)* 77−24583
solar cell fabrication, photovoltaic process based on thick film technique 80−94016
solar cells, photovoltaic mechanism, emitter-junction boundary conditions 79−100523
solar-powered solid-state heat transfer device based on photovolt. and Peltier effects 80−217
solid discs and flakes, photovoltaism meas. cells with variety of contacts 78−24816
squarylium dye films, surface photovolt. 80−75594
surface photovoltage transients, surface state parameters determ. 77−72905
ternary semiconductor device applications, review 78−39207
tetracene, surface photovoltage 80−2419
thin film solar cells, unified anal. of potential 80−81436
thin sandwich film photovoltaic analyzer for wavelength meas. in 2000-7000 Å range *(French)* 79−95441
thin solar cell photovoltaic and thermal props. 79−96452
vibron ferroelectric, intrinsic anomalous photovoltaic effect *(Russian)* 80−44665
water, CW and flash photoelectrolysis using ferroelectric photoanodes 80−81339
a-Si:H, effect of H conc. on photovoltaic props. 79−99577
AgBr, photo-EMF relaxation, temp. depend. 230 to 316K *(Russian)* 80−73508
AgCl, cryst. luminesc. and photovoltaic effect kinetics 78−64391
Al/metal-free phthalocyanine Schottky barrier solar cells, photovoltaic props. 79−100527
Al-Si-Al(Mo), sputtered Si film, photovoltaic props. 77−24623
Al-SiO_2-Si, MOS struct., lateral photovoltaic effect 79−4601

photovoltaic effects continued
Al-tetracene-Au cell, depletion layer, LF capacitance meas. 79−56328
Al-ZnS-Au structure, coulombic centres, thermal ageing, cond. and photovoltaic characts. *(French)* 77−43741
p-$Al_xGa_{1-x}As$ film, variable-gap photo-EMF 80−65626
$Al_xGa_{1-x}As$, graded band-gap heterostruct., photo-EMF 79−24072
$Al_xGa_{1-x}As$ variable gap junction, photosensitivity 78−39204
Al_2O_3 MIS Schottky structures, photovoltaic response 80−101115
AlSb Schottky barrier solar cells, characteristics and efficiency of Czochralski-grown crystals 80−61366
AlSb solar cell material, epitaxy, ionicity and bond struct. 80−61367
As-Se(Te)-Ge, fabrication of amorphous semicond. thin films with graded band struct. *(Japanese)* 77−55623
As_2Se_3, glassy, photostimulated changes in contact props. 78−19162
$AsSeI_{0.1}$, glassy, photostimulated changes in contact props. 78−19162
Au/(Zn-)phthalocyanine/Al(In), photovoltaic effects, illuminated thin-film cell props. 79−4605
Au/(Zn-)phthalocyanine/Al(In), photovoltaic effects, dark elec. props. of rectifying cells 79−4604
Au-CdS, Schottky junction, surface defects, photovoltaic, piezoelectric and V-I characteristics *(French)* 80−49898
Au-Ge Schottky diode, phonon energies, barrier heights, photovoltage spectra 78−64112
Au-InSb Schottky-barrier, photovoltage, temp. effects 77−69415
Au-p-n-Si Schottky barrier solar cell, photovoltaic characts., barrier heights, carrier mobility 79−83601
$Ba_{0.25}Sr_{0.75}Nb_2O_6$, inhomogeneous ferroelec., photorefractive effect 79−42935
$Ba_2NaNb_5O_{15}$:Fe,Mo, photorefraction mechanism and photoelec. props. 80−71381
$Ba_{0.25}Sr_{0.75}Nb_2O_6$, anomalous photovoltaic effect and photocond. 79−38122
$Ba_{0.25}Sr_{0.75}Nb_2O_6$, photovoltaic current, temp. and spectral depend. 78−47828
$Ba_{0.25}Sr_{0.75}Nb_2O_6$, thermal and spectral variations in the photovoltaic current in ferroelectrics 78−91719
$Ba_xSr_{1-x}Nb_2O_6$, anomalous photovoltaic effect and photocond. 78−52449
$BaTiO_3$, anomalous photovoltaic effect and photocond. 78−52449
$BaTiO_3$, anomalous photovoltaic effect and photocond. 79−38122
$BaTiO_3$, bulk photovoltaic effect in ferroelecs. 79−15181
$BaTiO_3$, dynamic Rayleigh light scatt. in region of ferroelectric-paraelectric transition 78−64371
$BaTiO_3$, ferroelectric semicond. anomalous photovoltaic effect due to ionising radiation 80−29437
$BaTiO_3$:Fe, photoinduced Rayleigh scatt. and bulk photovoltaic effect 79−38554
$BaTiO_3$:Fe, short circuit photocurrent, depend. on polarization 79−38121
$BaTiO_3$:Fe^{3+} bulk photovoltaic effect and photoinduced Rayleigh scatt. 77−77226
Bi film fast-response photodetector, employing charge carrier photon entrainment 80−73462
$Bi_{12}SiO_{20}$, stationary current obs. on polarised light illum., photogalvanic effects *(Russian)* 79−91095
Bi_2WO_6 layered ferroelectric, anomalous photovoltaic effect, photovoltaic current 80−75603
(CdHg)Te, ion implanted graded gap photodiodes 78−39192
$Cd_{0.175}Hg_{0.825}Te$-Au(In) contacts, photo-effect in the 77-300K range, barrier height estimation 80−107850
$Cd_{0.24}Hg_{0.76}Te$, mag. quantum oscills. in photovoltaic effect 79−19619
$Cd_xHg_{1-x}Te$, epitaxial layer p-n junction, current-voltage characteristics of photovoltaic detectors, 1 to 15 μm 80−86407
$Cd_xHg_{1-x}Te$, graded gap epitaxial layers, elec. and photoelec. props. 77−85362
$Cd_xHg_{1-x}Te$ photodiode, high efficiency, energy level diagram 77−15891
$CdIn_2S_4$, band edge study by photovoltaic effect 79−95444
n-$CdIn_2S_4$/p-$CuInSe_2$ heterostructure, form. and photovolt. meas. 80−10831
CdS, Auger excitation mech. of 1.6-2.0 micron luminesc. band and photocurrent and photo EMF spectra 79−8184
CdS film, surface states, surface photovoltage spectroscopy meas. 77−1504
CdS, films, photovoltaic effect in wedge shaped film 79−56331
CdS, photon drag effects 78−23134
CdS, photopotential changes due to Ar ion bombardment 77−8174
CdS, plastically deformed, photo-EMF rel. to cryst. polarity 77−55581
CdS, surface photovoltage, characterisation 80−60033
CdS, thermal desorption of O_2, photopot. and surface pot. changes 77−11795
CdS vacuum evaporated film photoconductivity and In doping effects *(Japanese)* 79−87174
CdS, XPS, secondary illumination effects, band bending, level shifts 80−108324
CdS/Cu_2S, polycryst. thin film photovoltaic materials, photon loss anal., expt. determ. 80−93888
CdS-Cu_2S heterojunctions, photovoltaic mechanism, model 77−43715
CdS-Cu_2S solar cell photovoltaic effects, self-consistent model 79−61989
CdS-InP(CdTe)(GaAs)(Ge), solar cell heterojunctions, CVD fabrication, photovoltaic response 80−93878
CdS-metal interface, chemical reactions and local charge redistrib. 79−19661
n-CdS-p-CdTe heterojunctions, photovoltaic energy conversion, solar efficiency 77−43700
CdSb:Al, p-n junction formation by laser emission, photoelectric effects *(Russian)* 80−70815
CdSb:Al(In)(Ga)(Te); p-n junction formation by laser radiation 80−96983
CdSe, photovoltage transients, expt. and model 77−89802
CdSe-metal interface, chemical reactions and local charge redistrib. 79−19661
CdSe-Si n-p heterojunction, vacuum deposition, photovoltaic effects *(Korean)* 77−28243
$CdSiAs_2$ chalcopyrite photovoltaic material 79−74526
$CdSiAs_2$ diode, photoelec. props., potential photodetector and solar cell appl. 77−43655
$CdSnP_2$-InP, n-n heterojunctions, growth, elec. characts. 77−11992
CdTe, film, anomalous-photovoltage, current-voltage characts. 79−69549
CdTe film, photopolarisation 80−25286
CdTe, MSM detectors, charge collection 77−61660

photovoltaic effects continued
CdTe, obliquely deposited layers with reduced resist., photovoltaic props. and Cd doping effects 77−43755
CdTe, optical absorpt. coefficient, photovoltaic determ. 77−39890
CdTe p-n homojunction, elec. and photovoltaic props. rel. to solar energy conversion 79−51668
CdTe, photoelectron spectra at Schottky barrier *(Korean)* 79−11220
CdTe sputtered films, struct., photocond., and trap distrib. 80−29489
CdTe, surface photovoltage 78−2540
CdTe:Ag film, photoelectret effect *(Russian)* 79−28676
CdTe:As^{2+}, photovol. props. of p-n junction prod. by ion implantation 78−43038
CdTe-Au(In) contacts, photo-effect in the 77-300K range, barrier height estimation 80−107850
Cr-SiO_x-Si MIS solar cells, photovoltaic performance and interface states, nucl. radiation effects 80−94004
Cu/$CuGaSe_2$ Schottky-barrier cells, photovoltaic effect 79−96440
Cu-CdS, Schottky barrier, Cu diffusion and photovolt. mechanism 80−6980
$CuGa_{0.5}In_{0.5}Se_2/Zn_{0.29}Cd_{0.71}S$ heterojunction solar cell, preparation and props. 80−101110
$CuGaSe_2$ single crystals, electrical and photovoltaic props. 80−92940
$CuInS_2$, minority carriers lifetime, photoelectromag. effect meas. 79−47125
$CuInS_2$, p-n junction photovoltaic props. and detectors 79−99574
$CuInSe_2$, photovoltaic props. and p-n junction form. 77−69371
$CuInSe_2$ polycrystalline thin film anomalous photovoltaic effect *(German)* 78−68102
$CuInSe_2$-CdS heterojunction, rel. to optimum conditions for solar cell fabrication 77−51810
Cu_2O film, reactively sputtered, for solar cell applic. 79−7914
Cu_2O-Cu diode junction, Schottky barrier, electronic structure and minority carrier diffusion length *(French)* 80−65682
Cu_2S-CdS heterojunction, elec. and photoelec. characts., effect of etching of CdS 78−80048
Cu_2S-CdS heterojunction diodes, barrier model estimated from photovoltage and cathodoluminesc. spectra 79−78165
Cu_2S-CdS heterojunctions, role of deep levels in controlling photovoltaic props. 80−92941
Cu_2S-CdS solar cells in backwall configuration, model of photovoltaic effect 80−55861
$Cu_{2-x}S$-CdS, solns. cell, photo-emf, depend. on degree of doping of CdS 79−52934
$Cu_{2-x}S$-CdS heterojunction V-I characteristic and max. photovoltage, long-term changes *(Russian)* 78−43468
$Cu_{2-x}S$-CdS p-n heterojunction solar cells, props., Burstein-Moss effects 80−21404
Fe-thiomine solution, modified, photogalvanic effect 78−91722
GaAlAs DH photovoltaic detectors, high efficiency 79−11198
GaAlAs/GaAs solar cells, efficiency optimisation at high and low current levels *(French)* 80−61348
$Ga_{1-x}Al_xAs$-SnO_2, rapid localised non-destructive optical charact. of ternary layer *(French)* 77−62725
$Ga_{1-x}Al_xSb$ p-n homojunction LPE and photovoltaic effect obs. *(French)* 78−64108
GaAs (110), adsorption of O_2, H_2, H_2O and H_2S, surface photovolt. spectroscopy 80−49499
n-GaAs, absorption tails in surface depletion layer and bulk 78−64379
GaAs conducting MIS structures and metal-semicond. structures, effects of ultrathin oxides 79−1626
GaAs, deep level photoionisation, absorpt. by derivative surface photovoltage spectroscopy 79−99575
GaAs, electrodes in acetonitrile soln., photovoltaic effect due to surface films 79−70341
GaAs epitaxial film, photo-EMF echo at 4.2K 80−60038
GaAs MOS system, surface and interface exam. by derivative surface spectroscopy 79−82674
GaAs microcharacterisation for device appls. 80−10922
GaAs, photon drag effects 78−23134
GaAs, photovoltage transients, expt. and model 77−89802
GaAs, primary radiation defect separation by elec. field 80−92522
GaAs Schottky barrier charge-accumulation detector, photosensitivity spectrum 77−55582
GaAs surface, clean and O_2 covered, work function and photovoltage meas. 77−1446
GaAs, XPS, secondary illumination effects, band bending, level shifts 80−108324
GaAs:Zn, sign inversion of the linear photogalvanic effect *(Russian)* 80−80321
n-GaAs-Al surface barrier diodes, influence of exciton effects on photo-EMF spectrum 78−10557
p-GaAs-$Cd_{1-x}Zn_xS$ heterojunctions, elec. and photovolt. props. rel. to growth technique 80−29466
GaAs-$Ga_{1-x}Al_xAs$, variable band gap, photo-EMF 80−20296
GaAs-$Ga_{1-x}Al_xAs$ variable gap p-n junction, variable gap and photo EMFs 80−15596
n-GaAs-GaAs:Cr, interface elec. props., substrate effects 78−6438
$GaAs_{1-x}Sb_x$ photodiode structures, current-voltage characts., photo-EMF spectra 80−29472
n-GaP, Au-coated semicond. electrode, photoelectrochem. behaviour in water 77−21399
GaP LED, N content by photovoltage meas. 77−11993
GaP, photovoltage transients, intensity and chopping freq. depend. 77−47859
GaP-Si, heteroepitaxial growth, electronic and optical props. 80−104075
GaSb, real surface elec. props., light effects *(French)* 77−72906
p-GaSe, back wall Schottky barrier cells, diffusion length, RT spectral response meas. 80−107806
GaSe, layered, photoelectromag. effect meas. of transport parameters 77−59301
GaSe, photovoltaic spectra 80−20240
GaSe, semiconductor-metal contact, photovoltaic props. 77−59330
GaSe:Cu(Cd, Sb), photovoltaic spectra 80−20240
Ga_xSe_{1-x}-SnO_2 heterostruct., amorphous, photovoltaic effect 78−14803
GaSe(Te)-SnO_2 spray heterojunction, electro-optical props. 78−64102
GaTe, Schottky barrier, photovoltaic props. 79−7854
p-Ge, laser radiation excited, gradient EMF anisotropy 80−75604
Ge, p-n junction, hot photocarrier and hot electron effects 78−30980
Ge p-n junction, photo-EMF generation in saturation region 80−75635
p-Ge, photon-drag voltage nonlinearity at high laser intensity 78−19081

photovoltaic effects continued
Ge, semiconductors, intravalley carrier transfer, transverse photo-EMF for various absorpt. coeffs. 79−69551
Ge surface with p-n junction, photovoltaic effect under conditions of surface recomb. of H atoms 77−66185
p-Ge, theory of photon-drag effect, parabolic and anisotropic band-struct. approx. 78−47825
Ge-Si n-n heterojunctions, response 78−14804
p-GeS, crystalline, photoelectric props. 80−70769
Ge_2S_3, photoenhanced diffusion of Ag 79−65257
GeSe amorphous films, blocking metal contacts characteris. and photo/EMF obs. 77−76924
$GeSe_2$ amorphous layers, photoconductance meas. 80−65632
Ge_xSe_{1-x}, thin film Schottky diode, photovoltaic effect 77−15895
$Ge_{20}Te_2Se_{80-x}Si$, amorphous-cryst. heterojunctions 79−65546
$HgCr_2Se_4$-$CdIn_2S_4$ heterojunction, prep. and photovoltaic prop. *(Japanese)* 78−34889
$HgCr_2Se_4$-$CdIn_2S_4$ heterojunctions, prep. and photovoltaic prop. 78−34892
HgI_2, excitons, spectral obs. 78−23492
HgI_2, layered, photoelectromag. effect meas. of transport parameters 77−59301
HgI_2, photoelectronic props. 78−41897
HgS, photo-stable semicond. in electrolyte soln., photo-EMF and photocurrent obs. 79−42637
II-VI semiconductor-electrolyte boundaries, electrolyte boundaries, photo e.m.f. meas., semicond. energy bands 77−1481
InAs:S(Mg), ion implanted, photocond., photo-EMF, and optical absorpt. spectra 80−70763
$In_{1-x}Ga_xSb$ alloy system, interband magnetooptical study using Schottky barrier 79−8124
$In_{1-x}Ga_xSb$, energy gap, temp. depend. and photovoltaic effect 80−70746
$In_{1-x}Ga_xSb$-Au, photovoltaic effect and Schottky barriers 80−49897
In_2O_3-Si(Ge)(GaAs)(InP) heterostructure solar cells, photovoltaic and rectifying props., electron affinity determ. 79−1618
In_2O_3-SnO_2 film on Si, heterojunction, photovoltaic effect, sunlight induced 77−1470
In_2O_3-SnO_2-CdTe:P, p-n homojunction solar cell, elec., photovoltaic props., photoluminescence 80−81463
In_2O_3-SnO_2-Si heterojunctions, elec. and photovoltaic characts. 78−52070
n-InP (100), photovoltage transients by retarding pot. electron beam techniques 77−24586
InP, photovoltage transients, expt. and model 77−89802
n-InSb, conduction band effective mass anisotropy and nonsphericity 79−69414
InSb, degenerate semicond., surface photo-EMF depend. on bulk consts. 79−69580
n-InSb, MIS diode, time-dependent photovoltaic effect 80−75601
InSb-Au Schottky barrier, photovoltaic spectra and magneto-optical transitions, Landau levels and excitons 77−47858
InSb-NiSb, photovolt. effects rel. to theory of semicond. with internal elec. short circuits 80−65620
InSb-NiSb plate, nature of transverse photo-EMF 79−15186
InSe, metal-semiconductor structs. diffused on InSe substrates 77−55882
InSe, semiconductor-metal contact, photovoltaic props. 77−59330
InSe solar cells, photovoltaic conversion efficiency 80−61356
In_xSe_{1-x}, amorphous film, in metal-In_xSe_{1-x}-SnO_2 system, photovoltages 77−28215
In_xSe_{1-x}-SnO_2 amorphous film-SnO_2 system, photovoltic spectra, annealing effect *(Japanese)* 80−92926
In_xSe_{1-x}-SnO_2 heterostructure, anomalous temp. depend. obs. on photovoltage 78−56209
$In_{2-x}Sn_xO_{3-y}$-insulator-poly-Si solar cells, photovoltaic conversion parameters 80−101093
$In_{2-x}Sn_xO_{3-y}$-n-Si, electron deposited solar cell, photovoltaic props. 79−96446
In_2Te_3, photosensitivity on γ- and neutron-irrad., γ-ray dosimeter mat. applic. 77−85258
KD_2PO_4-type crysts., photorefractive and photovolt. effects 79−15189
KH_2PO_4, ferroelectric, photovoltaic and photorefractive effects 78−72187
KH_2PO_4-type crysts., photorefractive and photovolt. effects 79−15189
$KNbO_3$, photovoltaic current, temp. and spectral depend. 78−47828
$KNbO_3$, photovoltaic effect lux ampere characts., photoconductivity 80−15561
$KNbO_3$ reduced, phase hologram recording sensitivity, energy transfer, photovoltaic effects 80−78799
$KNbO_3$:Fe, ferroelec. semiconductor, anomalously high photovoltage 77−69378
$KNbO_3$:Fe, ferroelec., anomalous photovoltaic effect and photocond. 78−52449
$KNbO_3$:Fe, photovoltages, photocurrents and photorefractive effects 79−42580
$KNbO_3$:Fe, thermal and spectral variations in the photovoltaic current in ferroelectrics 78−91719
$La_2Ti_2O_7$, layered ferroelectric anomalous photovoltaic effect, photovoltaic current 80−75603
$LiNbO_3$, anomalous photovoltaic effect and photocond. 78−52449
$LiNbO_3$, anomalous photovoltaic effect and photocond. 79−38122
$LiNbO_3$, anomalous photovoltaic effect obs., Anderson method 80−88595
$LiNbO_3$, doped, photorefr. and photovoltaic effects 77−38835
$LiNbO_3$, $LiTaO_3$ transition metal doped, photovoltaic and photorefractive effects, origin 77−20364
$LiNbO_3$, optical damage induced by X-irradiation 77−20814
$LiNbO_3$, photovoltaic current, temp. and spectral depend. 78−47828
$LiNbO_3$, photovoltaic effect, latent-image formation kinetics, electrophotography appl. 78−84246
$LiNbO_3$, reduced, photovoltaic effect and holographic recording mechanisms 79−69556
$LiNbO_3$, reduced cryst., photovoltaic effect, appl. to holographic recording *(Russian)* 79−51635
$LiNbO_3$, rel. to hologram recording by photorefr. effect 77−83830
$LiNbO_3$, thermal and spectral variations in the photovoltaic current in ferroelectrics 78−91719
$LiNbO_3$, transition metal doped, photovoltaic effects, spectroscopic investigation 77−20365
$LiNbO_3$, transition metal doped, photoferroelectric phenomena and optical storage 79−42577

photovoltaic effects continued
$LiNbO_3$:Cu(Fe), light induced charge transport, photovoltaic effects, impurity states 80−80317
$LiNbO_3$:Fe, anomalous photovoltaic effect in polarised light *(Russian)* 80−34484
$LiNbO_3$:Fe, bulk photovoltaic effect in ferroelecs. 79−15181
$LiNbO_3$:Fe, ferroelec. semiconductors, anomalously high photovoltage 77−69378
$LiNbO_3$:Fe, hologram writing, beam coupling and transport length in bulk photovoltaic effect 79−94190
$LiNbO_3$:Fe, holographic recording and thermal fixing; invest. of mechanisms 80−78810
$LiNbO_3$:Fe, influence of anomalous photovoltaic effect on exoelectron emission 79−28374
$LiNbO_3$:Fe, intensity enhanced bulk photovoltaic effects 79−19616
$LiNbO_3$:Fe, optical damage induced by laser light, X-ray irrad., carrier mobility effects 79−33657
$LiNbO_3$:Fe, optical damage depend. on temp., press., and applied elec. field *(Japanese)* 79−81498
$LiNbO_3$:Fe, photoinduced Rayleigh scatt. and bulk photovoltaic effect 79−38554
$LiNbO_3$:Fe, photorefractive recording of vol. holograms 77−637
$LiNbO_3$:Fe, photovoltaic effect and charge transport mechanism 79−38123
$LiNbO_3$:Fe, recording dynamical holograms in crystals with photovoltaic effect, nonstationary energy exchange *(Russian)* 79−31842
$LiNbO_3$:Fe crystal conductivity and photoinduced birefringence obs. *(Russian)* 78−60151
$LiNbO_3$:Fe(Cu), pyroelectric, photorefractive props., optical absorption, EPR and Mossbauer spectra meas. 77−32403
$LiNbO_3$:transition metal, photorefr. effect, 1.5-4.0 eV 77−28213
$LiNbO_3$:Fe, anomalous photovoltaic effect and diffraction efficiency *(Russian)* 79−15190
$LiTaO_3$, characterisation as holographic storage materials 78−29909
$LiTaO_3$:Cu(Fe), light induced charge transport, photovoltaic effects, impurity states 80−80317
Mn ferrites, photogalvanomagnetic effects 80−34483
$Na_2SO_4.10H_2O$, solid-liq. transform., solar energy conversion applicability 78−60155
$Na_2S_2O_3.5H_2O$, solid-liq. transform., solar energy conversion applicability 78−60155
$Nd_2Ti_2O_7$, layered ferroelectric, anomalous photovoltaic effect, photovoltaic current 80−75603
PLZT ceramics, short circuit photocurrent, depend. on polarization 79−38121
PLZT ferroelectric ceramic 79−99585
Pb-SnTe semiconductor, spectral response calcs. 77−87826
$Pb_{1-x}Ge_xTe$, ferroelectric phase transition effect on forbidden band width 80−24794
$Pb_{0.97}Hg_{0.03}Te$ photovoltaic detector produced by Sb^+ ion implantation 80−82821
PbI_2, layered, photoelectromag. effect meas. of transport parameters 77−59301
PbI_2, photo-EMF, effect on photolysis of PbI_2-Ag *(Russian)* 80−92939
$Pb_{1-x}Mn_xTe$, photovoltaic effect, p-n junction, energy gap determ. 80−92931
$PbSe_{1-x}Te_x$, p-n junction, inversion of conduction level 78−47856
$PbSe_{1-x}Te_x$, symmetry change in cond. levels, photovoltaic effect and reflectivity obs. 78−34766
$Pb_{1-x}Sn_xSe(Te)$ epitaxial layers, growth, phase diagram, p-n junctions, optical, elec. props. 78−44029
$Pb_{1-x}Sn_xTe$, surface photo-EMF under laser excitation conditions 80−6897
$Pb_{1-x}Sn_xTe$-PbTe heterojunction, Sn diffusion and elec. effects of dislocations, elec. and metallurgical expts. 77−89839
PbTe film, of uniformly varying thickness 77−51774
PbTe photovoltaic detector, detectivity limits 80−105709
PbTe, wedge shaped film, photovoltaic effect 77−1454
$PbTe$-$Pb_{0.82}Sn_{0.18}Te$, p-n heterojunctions, electrical and photoelectrical properties 78−39193
$PbTiO_3$, ferroelec. phase, photocond. and photovoltaic effect, temp. depend. 78−95309
$Pb(Zr,Ti)O_3$ photovoltaic ferroelectric as optical memory storage medium 78−50877
$Pb(Zr,Ti)O_3$, thin film evaporated on stainless steel, photovoltaic effect 79−4580
$Pb(Zr_xTi_{1-x})O_3$, anomalous photovoltaic effect 79−19625
$Pr_2Ti_2O_7$, layered ferroelectric, anomalous photovoltaic effect, photovoltaic current 80−75603
Rb_2ZnBr_4, ferroelec., photovoltaic and photorefractive phenomena 80−75598
S, single crystal, photoinduced discharge 400 to 580 nm 77−8139
$SbNbO_4$, anomalous photovoltaic effect and photocond. 79−38122
$SbNbO_4$, ferroelec. anomalous photovoltaic effect and photocond. 78−52449
$SbNbO_4$, ferroelec. semiconductor, anomalously high photovoltage 77−69378
$SbNbO_4$, ferroelectric, anomalous photovoltaic effect 79−7861
Sb_2O_3 anodic layers on Sb, semicond. props. 79−56303
SbSI, anomalous photovoltaic effect 79−38133
SbSI, anomalous photovoltaic effect 80−70749
$SbSI_{0.3}Br_{0.7}$, anomalous photovoltaic effect 80−70749
Sb_2Se_3, photocond., photo-EMF and photodielectric effect, expts. 80−20245
Se, activated film, interelectrode residual photo-EMF 77−69376
Se, amorphous film-metal system, contact pot. distrib. and photo-EMF; work function 77−76925
Se:As(Cl), trigonal, defect and impurity electron levels, surface photovoltage spectra 78−72108
$Se_{1-x}Te_x$-$Se_{1-y}Te_y$ junctions, photovoltaic effects and rectification phenomena 80−84506
Si, (111) surface, Cu phthalocyanine dye deposition, low energy electron optically modulated transmission increase 79−78133
Si, amorphous, p-n junction devices, barrier profile effect on elec. props. 80−49890
Si, amorphous, photovoltaic characts., rel. to appl. in solar cells 78−84253
Si, amorphous, photovoltaic diodes, influence of mag. field on charge transport 80−49891
Si based alloys, amorphous, photovoltaic behaviour, solar cell appl. 80−94051

photovoltaic effects continued
Si, carrier lifetime, comparison of meas. by photocond. decay and surface photovoltage 78−68038
Si, cast, growth structure and photovolt. props. of solar cells 80−94008
Si, defects, electrically active, correl. of electrolytic etch and surface photovoltage methods 79−77929
Si, diffused p-n junction, computer calcs. of photoresponse using Gummel-de-Mari algorithm 78−56221
Si dip-coated on graphite substrate, Si-SiC p-n heterojunctions 80−29442
Si, electron irrad. induced defects, bulk photo-EMF meas. 80−39160
Si, float zone, meas. of deep levels by photovoltage spectroscopy 80−103723
p-Si, high-resistivity, TSC and photo-EMF in p-n junction, deep levels 77−72913
n-Si, IR spectra of surface photocond. and photo-EMF 77−76868
Si, ion implantation with Li^+, characts. for thin film solar cell use *(Korean)* 77−51812
Si, ion implanted, photovoltaic effect related to annealing 78−76111
Si n-p junction vertical solar cells, Al-plated, photovoltaic effect variation with impurity conc. 79−100522
Si p^+-n junction, defect free, very shallow, rel. to solar cell appl. 79−15218
Si p-n heterojunction, DC sputtering growth, photocond. and photovoltaic effects 79−33337
p-Si, photon drag detection 78−43440
Si phototransistors, slow contamination and fast surface state effects, SEM study 80−107896
Si, photovoltaic and photomagnetic effects, rel. to intervalley electron transfer 80−60034
Si, polycryst., elec. and photovolt. props., grain size effects 80−49800
p-Si polycrystalline films on graphite substrates *(French)* 78−64154
Si polycrystalline-metal Schottky barrier solar cells, elec. and photovoltaic contact props. 80−93936
Si, RTR ribbon, impact of defects on photovoltaic potential 79−11186
Si, Schottky diodes on sputtered amorphous Si:H, light induced ageing effects, interpretation of photovoltaic stability 80−54780
Si slice, minority carrier diffusion lengths, surface photovoltage meas. 78−72168
Si solar cells, photoelectric effect and principles of operation and efficiency 80−50983
Si surface, electron states, surface photovoltage spectroscopy study, doping effects 80−49860
Si, surface, optical modulation of low energy electron reflection and transmission 78−88388
n-Si, surface photocond. and photo-emf spectra 79−73544
Si, surface potential, influence of metal impurities, surface photo-EMF obs. 78−19122
Si, surface state distrib. after treatment with HF and H_2O using photovoltage pulses 79−60888
Si, wafer, photovoltaic technique for meas. resistivity variations 79−21783
Si wafers, Czochralski grown, minority carrier transport props., laser beam scan for homogeneity anal., photovoltaic cell appls. 80−92905
Si:Au surface, electronic props. 77−66194
Si:B, N-implanted junction capacitance meas., appl. of dynamic lateral photovoltaic effect 77−85304
Si:F,H, amorphous, elec. and optical props. 80−60031
Si:H, amorphous, Schottky diode, spectral response and hole drift mobility 80−39673
Si:H amorphous films, photovoltaic and photocond. spectra, photoluminesc. 80−44645
p-Si:N_2^+ implanted, anneal behaviours of lateral photovoltaic method 79−14825
Si:P solar cell, minority carrier lifetime degradation during ion implanted processing, surface photovoltage 79−39305
n-Si:Pd, surface, photocond. and photo-emf spectra 79−73544
Si:Re, diode, barrier capacitance and photocapacitance, uniaxial press. effect 77−20416
n-Si-Au Schottky barrier, role of surface states in appearance of photo EMF 79−11222
Si-Au Schottky-barrier, formation process anal., V-I characts. *(French)* 78−91768
Si-CdSe n-n heterojunction, photovoltage sign reversal, energy band profile *(Korean)* 80−29469
p-Si-In Schottky barrier structure, optical quenching of photovoltaic effect 77−55608
Si-SiO_2-Si_3N_4 system, internal photoelec. emission and residual photoelec. effects 79−73599
Si-ZnSe n-n heterojunction frequency meter in visible wavelength *(Korean)* 79−60915
SiC, cubic, photo EMF on microtwinning lamella *(Russian)* 78−60165
α-SiC, short-wavelength photocond. and capacitance photo-EMF meas. 78−26906
SiH_x amorphous reactively sputtered films, in Pd Schottky barrier devices, photovoltaic props. 80−49910
SiH_x discharge produced amorphous film, gap state role in carrier transport 79−73608
SiO_2-InP MOS struct., capacitance-voltage and surface photovoltage meas. 79−60931
SnO_2-GaAs heterojunctions, elec. and optical props., photovoltaic appls. 77−43714
SnO_2-GaSe heterojunction photocell, fine struct. of photo-EMF spectra 80−6967
SnO_2-InP heterojunctions, elec. and photovoltaic characts. 80−75628
SnO_2-$Sb_xSi_{1-x}Sn$ structures, photovoltaic effects *(Korean)* 80−44647
$Sr_2Nb_2O_7$, layered ferroelectric, anomalous photovoltaic effect, photovoltaic current 80−75603
$SrTiO_3$, electrode, surface photovoltage expts. 78−72227
T-metal, thin film contact, time evolution of photovoltaic effect 80−65687
Te, circular photogalvanic effect in optically active crystal 79−73542
Te crystal, photo-EMF obs., depend. on sign of circular polarisation of light *(Russian)* 78−80025
Te, optically active crystals, circular photogalvanic effect 80−54739
Te, photocurrent generated by polarised light, direction depend. on polarisation *(Russian)* 78−64065
Te, photovoltaic effect in thin films, 10.6 μ, prep. methods 80−20252
Te-Se-CdO struct., fabrication and characts. 78−76106
Tl_2Se-As_2Te_3 and Tl_2Te-As_2Te_3, vitreous, photo-EMF kinetics 77−76877

photovoltaic effects continued
WSe_2, refl. spectra and photovoltaic effect, 1.5-3.2 eV, 4.1-300K 79−47470
$Zn_{0.1}Cd_{0.9}S$-CdTe p-n junction, prep. by spray pyrolysis, photovoltaic props. 78−60196
ZnO cell, enhancement of photoelec. effect by organic additives 79−57437
ZnO, chemisorption of O_2, charge transfer obs. by surface photovoltage 77−89824
ZnO dye sensitisation in electrostatic photography 79−67404
ZnO, low-energy-electron transmission, optical modulation 79−83070
ZnO powder layers, dyed, dependence on adsorbed dye amount *(Japanese)* 79−24003
ZnO, surface charge transfer in presence of photosensitising dyes 78−68049
ZnO, surfaces, charge transfer in prescence of photosensitising dyes, photovoltage spectra 78−72193
ZnO-CdSe thin film n-n heterojunctions, prep. elec. and optical props. *(Korean)* 77−28244
Zn_3P_2 bulk and thin film, UV reflectivity spectra, photovoltaic effects, optical consts. 80−25472
Zn_3P_2, direct and indirect optical transitions, metal-Zn_3P_2 contact photovoltage response 80−25402
Zn_3P_2 photovoltaic material and Schottky diode characteristics 78−64066
Zn_3P_2, polycryst. thin film photovoltaic materials, photon loss anal., expt. determ. 80−93888
Zn_3P_2-metal contacts, photoelectric props. 80−92930
ZnS film, photovoltaic effects under illum. from above and below 78−52031
ZnS, high-voltage photovoltaic effect in polycryst. layers 79−42573
ZnS photocells, thickness depend. of interband transition photovoltaic voltage and short circuit photocurrent 77−76871
ZnS, single cryst. plate, photovoltaic spectra, intensity depend. 78−14762
ZnS:S, photoconductivity and negative differential photo-effect 78−39156
ZnS-metal interface in MIM struct., photoexcitation level assignment *(French)* 80−15622
ZnSe, cubic, anomalous photovolt. effect in absorpt. tail 79−42583
ZnSe, minority carriers diffusion length by surface photovoltage method 80−60003
ZnSe surface states, electron interaction characterisation, by low energy electron transmission photovoltaic modulation 79−60896
ZnSe:Mn^{2+} Schottky barrier diodes, spin depend. cond. and photovoltage 79−91141
ZnSe:N, ion implanted cond. type conversion on annealing *(Korean)* 78−18668
n-$ZnSiAs_2$ photodiode, fabrication and photoelec. props. 77−8146
$ZnSiP_2$-In Schottky diode, photovoltaic spectra 80−2423
p-ZnTe surface barrier structures, photo-EMF 77−89851
photovoltaic generators, solar *see photovoltaic cells; solar cells*
phthalocyanines *see organic compounds*
physical chemistry
see also chemical analysis; chemical equilibrium; chemical reactions; chemical structure; crystal chemistry; electrochemistry; nuclear chemistry; pH; photochemistry; radiation chemistry; radiochemistry; solvated electrons; surface chemistry; thermochemistry
annual review, vol.27 (book) 77−40519
annual review, vol.28 (book) 78−40019
educational course, integration of macromol. soln. studies 78−77642
high-temperature chemical processes, review, book contrib. 77−40545
ion-ion, ion-dipole, and dipole-dipole interactions, teaching 78−10
laser spectroscopy applications, conf., Anaheim, USA (Mar. 1978) 80−36781
lipid films, at fluid interfaces, phys. chem., review, book contrib. 77−39725
liquid metals, conf., Konigstein, Germany (Mar. 1976) 77−1059
phase change derivation, phys. chem. textbook assumption removal 80−17772
pyrometallurgy, industrial methods and research, review, book contrib. 77−40407
rare earths, physics and chemistry (book) 79−69384
superacids, props. and appls. *(French)* 79−74482
teaching, macromol. principles 78−77643
teaching method of successive approx. 78−89281
$ClSO_2OH$, superacid, props. and appls. *(French)* 79−74482
physical data, collections of *see collections of physical data*
physical instrumentation control
absolute thermodynamic manometer for ultralow pressure control 79−35766
AC calorimetry technique *(Japanese)* 80−27306
aerosol electrical analyser, microcomputer-modified, for particle size anal. 80−40756
aerosol filter sampler, automatic time sequence, for proton induced X-ray emission anal. 77−60171
AGS, microprocessor based beam loss monitor system 79−72070
alignment system for large high-power pulsed CO_2 laser fusion system 78−59075
analyser automatic, for melting point of paraffin wax determ. 79−14223
Anglo-Australian 3.9 m telescope, computer-controlled slewing, setting and tracking 77−17371
Anglo-Australian Telescope, computer control system 77−91434
application node system image manager subsystem within distributed function laboratory computer system 79−45606
astronomical laser ranging equipment, system controller *(Japanese)* 78−89079
astronomical laser ranging equipment, telescope drive *(Japanese)* 78−89078
astronomical mirror horizontal control, deforms. calc. 80−17494
astronomical photoelectric photometer, multifunction, system design 77−73949
astronomical telescope, space, low-cost, pointing control system 77−5430
astronomical telescopes, computer appls. 78−4111
Atmospheric Cloud Physics Laboratory on Shuttle/Spacelab, droplets optical motion control appl. 80−12634
atom probe time-of-flight field-ion microscope, for metal defects study 77−82645
atomic absorption spectroscopy with nonflame sample atomisation, thyristor thermostabiliser use 79−96388
physical instrumentation control continued
atomic emission spectroscopy, quantometric meas. of spectra of controlled arc, spark generators, correls. 79−66382
Auger microprobe, scanning, computerised image processing 80−68304
Auger scanning electron microprobe, analytical techniques, and computer control 79−79359
Auger SEM incorporating concentric hemispherical energy analyser 77−79199
Auger spectrometer, digital methods for film anal. 77−56268
autocollimator, photo-electric, calibration with laser interferometer system and microcomputer 80−1304
autodensitometer, flatbed, for biophys. appl., error analysis 77−52937
autoguiders for optical telescopes 79−75109
automated, qualitative anal. 80−22497
automated calorimeter and scanning Doppler interferometer 78−45680
automated Fourier-Stokes analyser ellipsometer system for in situ investigations 78−49886
automatic digital magnetic recording system in Tihany Observatory 79−39989
automatic heat flow calorimeter for heats of reaction meas. 78−54373
automatic internal friction and modulus apparatus, phase-locked loop control module 78−13981
automatic power-spectrum density meter for pulsed laser beam 78−45698
automatic rotary diaphragm for microphotometer 80−22415
balance, precision, read-off automation using Michelson interferometer 77−5809
beam scanning system, automatic computer-controlled, for merged beams expts. 77−13818
beam-foil spectroscopy facility at University of Liege, computer controlled system 79−45866
biological, sampling of aerosol inhaled, exhaled, for dust deposition investigs. 79−96719
Bonn isochronous cyclotron, beam stabilisation and automatic energy variation 79−54705
boxcar integrator instruments, automatic baseline correction, appl. to plasma chromatography 77−52717
Bragg crystal spectrometer, on line, step scan control and data accumulation system *(Japanese)* 78−5088
broadband time relay for automatic activation 79−88940
bubble chamber film analysis, semiautomatic measuring system 80−58105
bubble chamber photographic recording feed mechanism 78−78564
Burrow permeameter with automatic compensation 77−10067
calorimeter, low temperature investigations, simple off-line arrangement 80−90850
calorimetric system, 3-300K, with on-line computer, adiabatic shield temp. control 78−4620
CAMAC, 2-D anal. of spectroscopic data, electronics 80−5460
CAMAC based high-resolution repetitive waveform generator 79−76214
CAMAC based mobile automated high speed transient data recording and transmission system 77−54488
CAMAC control of π^- biomedical beam line 77−90886
CAMAC I/O module based on Signetics 8X300 microcontroller 80−47835
CAMAC instrumentation in European labs. 77−54482
CAMAC spectroscopic data anal., programming techniques 80−5461
CAMAC system and microprocessors in physical instrum. 79−26041
capillary viscometer, automatic recording, for study of polymeric reactions 77−27631
Cary 14 spectrophotometer, remote control via digital interface 77−2697
cation-exchange sorption microcalorimetry, automatic micro-injection system 78−24777
CERN, Intel 8080 microprocessor development system 77−83314
CERN ISR, control system, addition of local intelligence to CAMAC 79−72212
CERN ISR control scheme for acceleration by phase displacement 79−72213
CERN proton synchrotron, automatic procedures 79−72074
CERN proton synchrotron, improvement project for computer assisted controls 79−72209
CERN PS, computer controlled beam local radial perturbation and rotation 79−72072
CERN PS booster, microprocessors in control and beam obs. 77−88302
CERN SPS, control systems operating experience, suggested principles for future accelerators 79−72211
CESR computer control system, description 79−72210
CESR control system, distributed microprocessors appls. 79−72217
CESR control system, interface hardware 79−72069
CESR magnet power supply system 79−76210
chart recorder timer control, pen overload protection systems, at. absorpt. appl. 77−73481
chemical laser flameout using fluidic switching 78−29943
Cherenkov counters, spectrometric channel control using blocks 78−866
chromatograph, gas, high-precision, process control appl. 78−53283
chromatograph, microcomputer controlled GC with data processor and printer-plotter *(Japanese)* 80−50921
chromatography, automatic liquid sample injector for GC, syringe-type *(Japanese)* 80−50923
chromatography, nonlinear detector response quantification with lab. automation system 80−40775
circular dichroism spectrophotometer, near IR, microprocessor controlled 80−22454
cloud chamber adaptive closed-loop expansion control system 79−93889
co-evaporation prep. of two component alloys, control system 79−24457
coercivity meter with automatic current setting and recording for heat treatment monitoring 77−87795
communication network within hierarchical control system, appl. to Fermilab beam line 79−45610
computer controlled gain stabilizing system for scintillation spectrometer using LED, processor in feedback 78−17473
computerised pulse radiolysis system using Biomation recorder and PDP 11/40 computer 77−40560
computerized GCMS solid state magnet control 79−12879
conference on cyclotrons and their appl., Bloomington, USA (Sept. 1978) 79−54626
Cornell electron ring, high resolution digital time base 79−76215
COSMOS plate-measuring machine, online control software 77−64652
coulometer, controlled-pot., design, operation, anal. appls. 77−25335
coulometric analysers with controlled potential, review 79−39244

physical instrumentation control continued
coulopotentiograph system, automatically controlled, for trace analysis of metal ions 79−92026
crack length automatic recording in sheet samples 78−60907
Cs beam freq. standard, servo-control system anal. 80−42201
CW dye laser spectrometer with computer control 79−75618
cyclotron at MSU, computer control 79−54704
cyclotron beam automatic centring and matching 79−54708
cyclotron corporation bus-oriented computer control system 79−54703
D-T generator, neutron yield control *(German)* 77−23336
delay unit for automatic variable-path-length US meas. 77−11095
densitometer, automated for radiograph interpretation, ^{252}Cf wire anal. appl. 77−61643
densitometer system for photographic spectral sensitivity meas. 78−29190
Dewar flask, self-opening valve for N_2 decanting siphon 80−57310
dichrograph, control unit construction 78−21122
dielectric properties of solid and liquid dielectrics meas., vs. temperature, automatic meas. set *(Polish)* 78−32836
dielectric spectrometer for 20 Hz to 80 kHz range, automatic 77−13768
differential pulse voltammetry, stationary electrodes, computer based instrum. appls. 77−36809
differential rectifiers, digitally controlled, for photogrammetry *(German)* 77−60495
digital modulator and synchronous demodulator system: an alternative to the analog phase detector 78−70107
digital stepping motor control system for repetitive scanning of a monochromator 78−54355
Digitron fast multichannel time recorder 77−67949
Dobson O_3 spectrophotometer, automation *(Dutch)* 77−70867
double NMR spectrometer, wide line CW 78−45667
doubler tevatron microprocessor quench protection system 79−72088
drawing instruments for surveying, appl. of electronic control *(German)* 78−20348
drift chambers, CAMAC/NIM for data acquisition and monitoring 77−88338
duoPIGatron ion source, optical telemetry and data transfer system 78−66443
electric resistance high precision meas. and control in He II environment 78−54403
electrochemical rotating disc-ring electrode equipment, automated, appls. 78−95933
electrodic potentiometry system, automated, for chem. anal. 78−35735
electron injector in HV terminal, control and protection system 80−27836
electron microprobe, automation using microcomputer system, anal. appl. 79−43703
electron microprobe analysis, computer controlled beam-scanning and camera cct. 79−43706
electron microscope, UHV, const.-load tensile device and appls. to materials science 78−11462
electron microscope-microprobe systems, automated, for quantitative metallography 78−35631
electron microscopy, scanning, high voltage, computerised, particulate charact. 79−48036
electron probe anal., energy dispersive/wavelength dispersive combined X-ray system, automated control 79−43705
electron probe analysis, electron beam positioning, computer automated 79−43704
electrostatic accelerator, foil strippers, remote control system 78−29670
electrothermograph, compensation-type with pulse-width control 77−41612
ellipsometer, high speed with servosystem 77−2682
ellipsometer, null-setting type, design and performance 77−45884
EM analyser control, automatic registration of the back-scattered ions 80−18042
emission current regulator for ion cyclotron resonance spectrometers using optical coupler 78−45749
Enraf-Nonius CAD-4 diffractometer, mechanical design, computer control and system performance 80−24318
EOSCOR: A light weight, microprocessor controlled solar neutron detector 79−101063
EPMA, computer-controlled, CAMEBAX system, operating experience 78−35779
EPR, block for electronic digital sweep of mag. field 77−26371
EPR spectrometer, simple temp. controller, 85-400K *(German)* 78−45663
ESCA spectrometer, sample probe microcomputer automation 79−58846
ESR and NMR spectrometers inexpensive temp. controller 79−35803
Fabry-Perot air-spaced piezoelectric etalon, stabilisation technique 77−82591
Fabry-Perot etalon, piezoelectrically controlled, linear scanning cct. 78−4704
Fabry-Perot interferometer digital electronic system 78−12748
far IR laser stabilisation servo electronics 77−38928
Faraday balance susceptometer, computer controlled 78−65946
Faraday double transmitting cup, ion optical control device 78−82556
fast beam scraper, stepping motor control 79−71562
fast digital two channel pulse generator, for controlling time resolved expts. 78−93670
fatigue testing machine, EM resonance, two-frequency and programmed tests 79−96232
fatigue testing machine 77−1906
feedback controlled particle suspension system for laser initiated target expt. mag. mirror fusion facility 78−1864
FEM field emitter thermocopule temp. controller 78−24898
Fermilab, multi-user control and data acquisition systems 77−54480
Fermilab booster, low level RF system 79−76205
Fermilab booster beam damper, logic and control module 77−83313
Fermilab master slave servo-manipulator, control system 77−83309
file management for experiment control parameters in distributed function computer network 77−57306
flexible multi-scaler system with micro-processor control 78−90037
float glass, heat transfer and temp. control in annealing, computer appl. 78−27543
flowmeter, gas, low speed, constant gas flow production *(Hungarian)* 80−1702
flowmeter calibration, microcomputer-controlled flow rigs 80−10320
flowmeters and level meters, commercial instruments survey *(French)* 80−83871
physical instrumentation control continued
flux pump power supply using inductive current transfer, primary current waveform control 78−12704
frequency stabilization of laser using single-photon detection, D/A lock-in circuit 79−50334
fusion reactor, 2XIIB, neutral beam injector system, automated control 78−62620
fusion reactor, pulsed expts., computer-based control systems 78−62624
fusion reactor laser, Shiva pulse power, isolation and control system 78−54935
fusion reactor visible monochromator scanning drive 78−54940
gamma spectroscopy on-line system, automatic sequencing using microprocessor controller 77−54393
gamma-ray irrad. time control for dosimeter calibration *(Japanese)* 78−66452
gamma-resonance spectrometer, electronic control block for moving system 77−38075
gas anal. of ^{14}C-labelled compounds using piston-type counter tube, automated 77−56281
gas chromatograph development, temp. control system *(Japanese)* 80−50922
gas chromatography, advantages of pressure balancing 79−70408
gas chromatography, programmed temp., retention index calcs. by linear interpolation 78−27844
gas chromatography-mass spectrometry, computerised, data-blocking cross-correlation peak detection 80−62725
gas chromatography-mass spectrometry data system, research-oriented, principles and applics. 80−40770
gas chromatography-mass spectrometry integrated anal. systems, review 79−1972
gas phase electron diffraction, primary electron beam centring via rot. sector 77−55214
graphite furnace anal., autosampling system, timing circuit for baseline absorbance monitoring 77−73482
gyrowave interaction experiment, pulsing and timing circuits 77−45191
hardness meas. device, attachment for automatic appl. of indentations 77−1907
HEAO-B X-ray telescope, gas control system 78−40827
heavy ion beam buncher control system 79−72148
Heidelburg postaccelerator, computer control system 79−72214
high-pressure laser system, electron beam control 78−5496
high-speed cine camera control desk type PIK-73M 79−2758
HPLC, two-pump gradient, accuracy and reproducibility 80−16742
HV generator for accelerator beam control 79−26797
hydrophones, towed, location system, shipboard microcomputer controller 79−2401
image analysing computer, Quantimet, device for automatic scanning of irregular areas 77−5906
image sharpening telescope, atm. distortion compensation 77−49294
indicator-setting operator terminal 78−32804
INDOR, pseudo, heteronuclear selective decoupling, automatic, using Fourier transform NMR spectrometer appl. 79−93185
inductive sensors for coating thickness meas., correction for thermally produced errors *(Russian)* 77−13740
instrumentation and control technology, decentralisation, past developments and future trends 80−4701
intensity regulator for 5 to 50 keV electron guns *(French)* 78−54499
interferometer superposition fringe pattern, automated central achromatic fringe setting 78−24852
internal friction apparatus for freqs. up to 200 Hz, automated control 78−22308
internal friction meas. servo system 77−39265
ion beam prod. for implantation appl. 78−66004
ion source electron beam modulator automatic control system 79−72173
ion-selective electrode, flowing systems meas. 78−92527
ionisation chamber, electrical sensitivity control 78−865
ISABELLE half-cell control system 77−88303
ISABELLE ISR, computer based control and monitoring system 78−46191
isochronous cyclotron, energy variation, microcomputer control 79−13565
IUCF control system 79−54702
Joyce-Loebl microdensitometer, computer control for objective-prism spectra meas. 80−105173
Karlsruhe cyclotron, computerised diagnostics, control and extended beam optimization 79−54709
KEK, minicomputer assisted function generator for the dynamic control of chromaticity correction sextupoles 79−68009
KEK beam line magnets control by CAMAC serial highway 79−68007
KEK proton synchrotron, closed orbit control system for main ring 79−68008
KEK proton synchrotron, control computer system 77−88301
KIM-9-75 light source, controllable luminous flux regulator 77−39010
laboratory data acquisition and control system based on Commodore PET microcomputer 80−204
Lang topography, automatic Bragg angle correction, extremum control *(German)* 78−59718
Langmuir probe, control system for maintaining prone at plasma potential 78−5943
large azimuthal telescope, axes coords. determ. system 77−60615
large azimuthal telescope photoelectric automatic control system 78−16301
Large Space Telescope, optimal manoeuvring and fine pointing control with annular momentum storage device 77−22078
laser, radiation pulses formation and stabilisation 80−23735
laser Doppler anemometer-computer system, for flow rate meas. 79−68881
laser frequency stabiliser using electronic servocontrol system 78−1240
laser giant pulses, time of appearance control with KS-19 glass passive switch 77−38959
laser gyrometer, accuracy increase by automatic output signal correction *(Russian)* 80−215
laser mirror, simple high-resolution mount 77−3618
laser system, He-Ne, automatic frequency trimming circuit *(Russian)* 80−1217
laser systems, Faraday rotator isolator with solid state switching 77−88734
lasers, coherently combined, phase lock control considerations 80−5743
light beam control system, for ang. displacement control via fast error-signal transducer 78−186

physical instrumentation control continued
liquid, self-diffusion meas., automated technique, using NMR spin echo 78−27114
LLL, microprocessors appl. 77−54481
load cell, automatically controlled using capacitive and US sensors *(German)* 79−35715
lunar occultations observations, microprocessor-controlled data acquisition system 77−49311
magnet winding supply, current regulator based on industrial thyristor convertors, 77−37921
magnetic circular dichroism spectrophotometr, signal controller for photomultiplier output 77−67511
magnetic field distr. control in pulsed eight-solenoid system 77−87793
magnetometer system, automatic field-tracking, 0.1 to 3.2 T, for use with ESR/NMR spectrometers 79−63279
Marx's composite oscillator method, automated, for internal friction and Young's modulus meas. 80−37151
mass spectrometer, digital recording system for automated isotopic analysis 78−12783
mass spectrometer, ion-cyclotron reson. type, optically-coupled feedback emission current regulator 77−61150
mass spectrometer, isotope ratio, automatic inlet system with pneumatic changeover valves 79−49333
mass spectrometer, microcomputer-based controller for temp. programming direct inlet probe 78−16893
mass spectrometer, spectrum sweep using HF pickup control 77−13812
mass spectrometer mag. field stability control, solid-state device 77−26423
measuring projector for bubble chamber film, minicomputer on-line system 80−27878
MEIRA isotope separator, HV power supply and automatic ion source control system 77−13778
meter for photosensors time characts., using programmed strobing of anal. zone 78−283
microcomputer crate controller for CAMAC 77−54491
microcomputer interfaced spectrophotometer for kinetic studies 80−62726
microcomputer-controlled visual stimulator for eye movement and visual evoked pots. study 80−41350
microdensitometer for X-ray crystallography use in molecular biology lab. 77−35438
microdensitometer with minicomputer connecting facilities 78−21198
microdensitometer with minicomputer for semiautomatic interpret. of spectral plates 78−21199
microphotometer with programmable microprocessor control unit *(French)* 77−10085
microprocessor based interface/controller for desktop programmable calculator 79−35690
microprocessor based timed reading and time plot CAMAC modules 77−54484
microprocessor controlled dual parameter ADC system with CAMAC interface 79−3337
microprocessor controlled long lived alpha emitter monitor 80−58069
microprocessor controlled multipoint recorder with graphical video output for reactor core temperatures 80−57873
microprocessor-controlled gas chromatograph, low temp. range extension 78−3395
microprocessor-minicomputer combination for instrumental flexibility 77−54483
microscope, computerised focusing technique 77−22596
microscope, system for automatic tracking of white blood cells 77−78064
microscope for automatic metaphase spread finding 77−56550
microwave spectrometer, RE1301, wide-range magnetic current regulator 79−21779
MIRABELLE hydrogen bubble chamber, control by minicomputer *(French)* 77−3225
molecular beam epitaxy apparatus, controlled by quadrupole mass spectrometer *(French)* 78−15315
molecular flow measurement, precision, and control for single and multi-gas systems 78−70135
monochromator, minicomputer controlled, with repetitive optical scanner 78−27843
monochromator, programmable, for ICP emission spectrometry, intensity meas. 80−62728
monochromator scanning control system using microprocessor, spectral line shift correction *(Japanese)* 80−57384
MORPHOQUANT automatic microscope image analyser, universal program system 80−56160
Mossbauer const. velocity spectrometer, control circuits 79−93866
Mossbauer microprocessor controlled spectrom. 79−97931
Mossbauer spectrometer, absolute vel. control via laser interferometer 77−71715
MP-Tandem at Munich, diagnostic and control system 78−29667
multichannel analyser, built from microcomputer 79−58490
multichannel analyser, versatile programmable power supply 77−42218
multichannel analyser buffer store, 4096 channel sequential memory, control circuitry 77−57829
multichannel spectrometer, quantometer, design trends for computerised control 79−80694
multiple detector data acquisition system, microcomputer based 78−90049
multiple electron spectroscopy instrument, computer control 78−73108
neutral beam system, 120 keV, for fusion reactor ignition 78−66377
neutral beam test stand, 120 keV, computer based diagnostic and control system 78−66389
neutron activation anal. of soils, computerised 77−44546
neutron depolarisation meas., exptl. set up and process program 80−18771
neutron diffractometer, four-circle, single cryst., automatic control using FORTRAN software 80−38876
neutron diffractometer operation by computer-controlled CAMAC system *(German, English)* 77−19843
neutron spectrometer control using microprocessors *(German)* 79−49363
NIM-controlled rabbit system 80−18731
NMR, pulse type, programmable pulse sequence generator 80−17979
NMR magnetometer, large-scale automation 80−57343
NMR spectrometer, for quantitative analysis, microprocessor-controlled digital integrator 80−11971
NMR spectrometer, programming device for control of frequency synthesizers 80−22400

physical instrumentation control continued
NMR spectrometer, pulse, controlled by programmable digital unit *(Czech)* 78−77952
NMR spectrometer automatic magnetic field control, 0.1 to 2 T *(French)* 79−30450
NMR spectrometers, time-sharing control by minicomputer 79−93192
nondispersive IR analysers, programmable switching device for semiautomated multichannel gas analysers 77−77830
nonlinear optics, digital data acquisition and on-line processing at Moscow State University 78−46709
NQR, panoramic pulsed spectrometer programmer 77−61100
NQR scanning spectrometer, improved super-regenerative oscillator and quench generator 78−8429
NQR signal seeking method 77−13786
NQR spectrometer, digitally programmed bidirectional square-wave freq. mdoulation 78−21189
NQR spectrometer, programming device for a spin-echo installation 80−17972
NQR spectrometer, weak signal relax. meas. with Sigma type digital storage device, pulse-train program blocks 80−17970
NQR temperature meas. and regulation system 77−10020
NQR thermometer, capture effect 77−10018
nuclear reactor fuel consumption determ., automated techniques *(German)* 77−14236
ocean-bottom seismometer capsule, operationally optimized 79−39911
oceanographic monitoring stations in Arabian Gulf, computer control and data acquisition 79−8728
odour analyser, automatic, for atmospheric sulphide anal. *(Japanese)* 80−50924
on-line display aid for bubble chamber film automatic meas. 78−5098
optical fibre automatic refr. index profiling 78−46836
optical image restoration using computer-controlled microdensitometer 77−23628
optical shutter, electronic control system 77−3678
particle beam phase space meas. at 2 MHz particle rate 77−54383
particle physics expts., on-line data acquisition system using PDP-11 computers 80−27913
particle size distrib., on-line measurement techniques, instruments *(German)* 78−60895
PEP storage ring, computer control systems, design and performance 79−72208
personnel thermoluminescence dosimetry reader, microprocessor controlled 79−45428
PETRA storage ring, control system 77−83315
pH titration system, computer controlled, for complex equilibria in soln. anal., appl. 79−87892
phosphate and alkaline phosphate activity determ. by dual microcomputer-controlled stopped-flow spectrometer 80−57379
photogrammetric instrum. applic. of incremental and parallel computing 77−10121
photographic zenith tube obs., automatic control using minicomputer *(Japanese)* 79−101083
photometer for quantitative chromatogram analysis, computer controlled 77−60326
photometric eval. of high speed cinematographic films, microprocessor control 79−21801
photomultiplier protection against optical overloads, electromagnetic shutter control 80−23255
plasma diagnostics, automatic system for addition at. conc. meas. in MHD generator 79−50892
plasma disruptive instability in TO-1 Tokamak, feedback stabilisation *(Russian)* 79−55546
plasma position detection and control, in Tokamaks, interferometric method 80−1850
plastic extension control during fatigue tests 77−25220
polariscope interactive control system to evaluate stresses 80−19299
polarograph, microprocessor controlled 77−12844
pollution measurement, automated systems 77−21885
portable microprocessor controlled neutron spectrometer, NE213 organic scintillator 80−58022
potentiometric analyser, automated, with selective electrodes, microcomputer control 80−40773
potentiometric analysis with ion-selective electrodes, computer automation 80−3424
potentiometric system, nanovolt, self-balancing for thermometry and calorimetry 77−53903
potentiometric titrations with ion-selective electrodes, automated, equivalence pt. determ. method 78−3391
potentiostat, electrochemical, with automatic resist. polarisation compensator 77−21393
prismatic astrolabe, improved drive and instrumental characts. *(Russian)* 78−89066
probes, electro-optical, for liquids refraction index sensing *(German)* 77−5889
process chromatograph system, minicomputer-based, computer controlled 79−16102
process gas chromatograph, microcomputer based 79−16101
programmable PRP 8 computer photometer, design, uses 77−74483
programmed controlled temperature microscope stage 79−35821
proton storage ring, NAP-M, supervising system 77−65365
proton synchrotron, CERN, online function generation optimisation 78−834
proton synchrotron slow extraction beam parameter monitoring and control system in CAMAC standard online with ES 1010 computer 78−29674
pulse generator for pumping semiconductor lasers, amplitude control 77−27299
pulse height anal. system, CAMAC based 77−87749
pulsed ion cyclotron resonance spectrometer, integrated control system 79−71560
Quadmagnova, GC/MS system, computer scanning and control 78−76946
quadrupole gas analyser with integral microprocessor 78−73109
quantum magnetometer using optical pumping, broadband freq. multiplier 77−37951
radio telescope system, fully automatic, for interplanetary scintillation obs. 79−101064
λ 8-cm radioheliograph at Toyokawa, control for new local oscillator system phase stability 79−101073
λ 8-cm radioheliograph at Toyokawa, sensitivity and phase stability improvement project 79−101066

physical instrumentation control continued
radioheliograph control system, 8 cm instrument at Toyokawa, Japan 80−98549
radiometers, multichannel, AGC using digital control *(Russian)* 77−26399
radiopolarimeters, fully automatic, for solar patrol at microwave freqs. 79−101065
radiospectrometer, automatic thermostatic control, using Diapazon variator 80−47160
radiotelescope RT-22, automatic obs. by computer 80−109359
Raman spectrometer, digital control system, appl. to soft mode spectroscopy 78−86345
real time distrib. computer systems 77−54486
reciprocating pumps, control system, high performance liquid chromatographic detectors appl. 78−92559
reflecting telescopes with zero expansion material mirrors, temp. control rel. to defocusing *(Russian)* 79−96912
reflectometer, UV, automatic concentric shaft with stepping motor drive 77−2684
repetitive photoelec. scanning system for high resolution optical spectra accumulation 78−54456
resonance bar damping meas., reson. freq. control 77−2649
RF linac cavities, microprocessor based control 79−71996
Rheovibron viscoelastometer, dynamic, direct reading, automation, appls. to polymer films, fibres 79−3980
ring specimens, computer controlled mag. meas. system 80−86346
Rutherford backscattering analysis, automatic ang. distrib. measuring system 77−20975
sample changer, automatic, for semi-automatic photometric anal. systems 77−48705
sample heater, high vacuum, using Zener diode 78−12690
Saturne II, beam liner computerised control system, organisation, function, hardware 77−83400
scanning electron microscope, stroboscopic microcomputer controlled, for measuring signal waveforms on MHz IC 79−21871
scanning microprobe, digitally controlled, for tube element anal. 79−52801
Schmidt telescope, 105 cm, software *(Japanese)* 79−101067
Schmidt telescope at Campo Imperatore, automatic control using PDP 11 processor *(Italian)* 80−8541
scintillation counter arrays, testing with computer controlled LED flashing system 77−57802
scintillation probe containing long plastic scintillator, AGC circuit 77−57833
Scylla IV-P, computer-based control and data acquisition system for CTR 78−62621
sedimentation anal., automatic recording system 78−60897
seismic instrumentation and data analysis, conf., Durham, England (Aug. 1977) 79−39905
seismic recording equipment, digital automatic amplitude control unit parameters choice *(Russian)* 79−39964
seismographs, feedback-controlled wide-band, design, rel. to undesired side effects 79−39909
seismometer digital automatic amplitude controller with preliminary smoothing, parameter selection *(Russian)* 79−74985
seismometers, EM and hybrid instruments, developments 79−39906
seismometers, wide-band feedback instrument 79−39907
SEM, automatic focusing and stigmating system 79−12893
SEM, focusing and stigmating system using minicomputer 78−37113
SEM, on-line stereo processing technique using minicomputer 78−37114
SEM, voltage meas. via new electron energy analyser using feedback loop 77−54019
SEM multisample stage, viewing via rotary control 78−4738
SEM system, computer controlled for quantitative three-dimens. characters. of particulate materials 77−2714
servo force-balance instrum. for wall shear stress meas. 79−1273
servocontrolled Fabry-Perot interferometer, 3 in 10^{11} laser wavelength meas. 78−89452
Shiva alignment systems 78−59033
Shiva laser beam diagnostics 78−59037
Shiva laser computer control system 78−59034
SIMS, computerised system for energy spectra determ. 80−3423
SIN meson factory, computer control strategies 79−54701
single crate CAMAC control system for negative ion source test facility 79−72216
single-beam spectrophotometer, EPROM for automatic baseline control 79−35691
SLAC, control and monitoring system, use of microprocessors, cost 77−83177
SLAC accelerator, automatic phasing using microprocessor controller 77−88305
SLAC beam, feedback system for steering and energy correction in beam switchyard 79−93852
solar flat-plate collector loops with on-off control, anal. of dynamic behaviour *(French)* 80−55901
Soviet 6 metre reflecting telescope, position control via computer *(Norwegian)* 78−36456
Space Telescope pointing control fine guidance subsystem design 80−82201
spark source, electronically controlled, adjustable waveform, spectrometric obs. 78−45727
spark source, electronically controlled, for anal. emission spectroscopy 78−16857
specific heat meas. at low temps. via adiabatic calorimeter 77−41614
spectral slit, digitally controlled 77−34035
spectrometer, for surface barrier detectors study 77−83443
spectrometer, grazing-incidence, automatic scanning system 80−14250
spectrometer, semiconductor mosaic type, amplification-conversion tract meas./monitoring automation 78−78547
spectrometer for nuclear quadrupole double resonance with programmable calculator control 79−12830
spectrometer shutter system, digitally controlled 77−82609
spectrophotometer, controlled rapid-scan, for turbidity meas. 77−41700
spectrophotometer, near IR, SPECORD 61 recording-type grating spectrophotometer with LT1 air drier 77−45906
spectrophotometer, single beam, enlarged and thermostatted cuvette chamber 77−5925
spectrophotometer for multielement atomic spectrum anal. under computer control 80−27357
spectrophotometers, microprocessor based data acquisition and control system 80−22335

physical instrumentation control continued
spectrophotometric measurement, dual wavelength, precision optimisation 79−92019
spring-piston differential manometer 77−67456
SPS computer control system, operational experience 77−83292
static plate flow meter, for pulsating flow meas., automatically controlled 79−68870
stereo image processing, control system 78−4728
stopped-flow systems, automated, for fast react. rate anal. methods, review 78−95971
storage rings, magnetic beam position detector 77−88307
storage rings, single feedback systems for simultaneous damping of horizontal and longitudinal coherent oscillations 79−72075
stratosphere balloons, buoyancy control expts. 77−87113
superconducting heavy-ion resonator, microprocessor based feedback system 77−88292
synchrotron radiation facility expts., distributed computing system for data acquisition and control 77−38513
telescope control, zenithal blind spot of altazimuth-mounted equipment 78−53823
TEM, high resolution, electronic control systems 78−32939
temperature regulator for liquid ^{4}He bath near 4.2K 78−41319
thermal desorption mass spectroscopy, computer control, data acquisition, appls. 80−61181
thermal diffusivity meas. system using microprocessor *(French)* 80−14559
thermogravimetric apparatus, automatic device with digital output 78−7281
thin film thickness monitor shutter 78−56583
thyristor temp. regulator for pulsed NMR spectrometer 80−105687
tide-recording equipment, phototransducers emission source light output ratio stabilisation *(Russian)* 78−88949
tilt meters, photoelectric, with negative feedback, block diagrams anal. *(Russian)* 78−88948
time sharing method in high modulation NMR of fluids *(German)* 78−16822
TOPOCART-ORTHOPHOT C system for prod. of stereo orthophotos 77−66994
TOPOMAT all-automatic photogrammetric system for aerial photography 77−66993
torque magnetometer, automatic rotating-head, microcomputer control 78−21183
transient phenomena recording, microcomputer controlled, student experiment 79−84919
TRIUMF 100 μA beam, achievement and control 79−54699
TRIUMF biomedical pion beam automated dose mapping system 78−73254
TRIUMF cyclotron, meas. and corrections to beam props. 79−54710
TRIUMF data interface 77−88304
UK 3.8 m IR telescope electronic control mechanism and computer interfacing 78−16300
ultrasonic open channel flowmeter with microprocessor 79−68877
underwater robot/manipulator, development and remote control 78−77356
UTR-2 radiotelescope northern sky survey, expt. techniques and data processing 78−57461
UV spectrometers, on OSO-8, computer-controlled, mission operations 80−41723
vacuometers, ionisation, with cold or hot cathodes *(Czech)* 80−73376
vacuum apparatus *(Czech)* 80−52256
vacuum chamber target, two-axes sample positioning mechanism 77−61076
vacuum system backing pressure automatic regulation device 79−49241
vapour-liquid equilib. meas. *(German)* 78−88667
VICKSI accelerator, computer aided control system 79−54697
VICKSI computer control system, operating experience 79−72215
VICKSI cyclotron, automatic isochronisation and computer aided centering 79−54706
viscometer, capillary type with a feedback system, stabilization of press. difference 79−14502
voltammetric analysis, automatic controller, design 80−71968
voltammetry, cyclic differential pulse, computerised instrumentation 78−85235
volume gauge, gas-dynamic, with pressure pulsations stabilisation 77−5806
weak X-ray scatt. interpretation by automated diffractometer 79−68977
Wyoming Infrared Telescope (Jelm Mountain), computer control 78−85848
X-ray anal., conf., Denver, USA (Aug. 1976) 77−70382
X-ray diffr. anal., single cryst. automated technique, comparison with powder method 77−70386
X-ray diffraction chem. anal., historical review 77−70383
X-ray diffraction expts., SPADE software package 79−63195
X-ray diffractometer, HAG 4/A universal instrument, applic. versatility of basic software 80−52375
X-ray fluoresc. anal. system for small medical samples, computerised target changer 77−60249
X-ray fluoresc. spectrograph, automatic computerised, for rock trace elemnt anal. 77−56320
X-ray fluoresc. spectrometer system, automated, for chem. shift meas. 78−4750
X-ray fluoresc. spectrometry using pulsed X-ray excitation, for environmental anal. 77−56319
X-ray fluorescence analyser, computer-controlled 78−23982
X-ray image processing with SEM, automated data acquisition *(French)* 78−41379
X-ray residual stress anal., computer controlled, software, precision 78−5712
X-ray small-angle scattering expts., temp. stabilisation of sample cell 77−13830
X-ray spectrometer, computer controlled, for steel alloying element determs. 77−56318
X-ray spectrometer, full automation of Philips 1220 model 77−196
X-ray spectrometer control, interactive program for data collection, manipulation chem. anal. appl. 78−7312
X-ray studies of phase transitions at low temp., automatic system 77−15281
X-ray survey instruments, automated calibration and recordkeeping system 77−37876
X-ray telescope, balloon-borne, attitude control system for telescope pointing *(Japanese)* 79−80220

physical instrumentation control continued
X-ray topography camera, high speed, semiconductor lattice defects exam. appl. 77−11443
ZGS, low level beam diagnostics for polarised proton operation 77−83311
ZGS, mini-computer based digital RF control system 77−83310
ZGS 500 MeV booster synchrotron, data acquisition and control, sequential logic and minicomputer 77−83304
H masers, with automatically tuned resonators 80−95859
H_2 bubble chamber, temp. and press. control 79−85860
H_2 target, liquid, microprocessor-based cryogenic refrigerator controller 79−45491
H_2SO_4 mist monitor, semicontinuous 80−61495
He refrigerator system for Fermilab switchyard, microprocessor based control facility 79−68006
Pu, determ. by automated coulometric method, apparatus 79−16114
U, determ. by computer-controlled titration system, evaluation 79−16113

physical metallurgy *see metallurgy*

physical optics
acousto-optic modulator temporal response, physical optics model in low scatt. efficiency limit 78−66897
astronomical telescope resolution explanation *(Spanish)* 79−40075
chemical laser, power spectral performance, coupled fluid dynamic, kinetic and physical optics model 78−79040
coherence and radiation laws, review 77−23612
coherence theory rel. to theory of radiative transfer 77−65568
contemporary optics, book 79−81353
critical angle scattering of light by air bubble in water, approx. 80−9797
diffraction catastrophes, optical caustics 80−9801
Dirac-spinor form of Maxwell's eqns., polarised light beams in gravitational fields 78−50696
education, lateral-angular magnification relationship for simple magnifier 80−57031
energy flow lines, Maxwell eqns., interpretation of diffr. and interf. 77−34806
Fresnel's classical papers, history and present appls. *(French)* 78−37800
Gaussian beam, plane-wave-type expansion, errors incurred 80−48312
Gaussian beam modes by multipoles with complex source points 77−68171
gradient index imaging system theory 80−14294
gravitational lenses, high-intensification regions 79−25463
Herschel's condition as wave optics theorem 80−87301
holography, two-dimensional volume, coupled wave differential eqns. derivation 78−55317
holography and coherent optics, information theory, book 80−98764
Huygens' principle on emission from moving bodies *(Spanish)* 79−31795
immersed object EM signature determ., modified physical optics technique 77−5372
incoherent backscatter from rough surfaces, polarisation coeffs. for two-scale model 78−71013
information content of image, physical limitations 78−33697
inverse problem, evanescent waves, finite source area 77−10831
inverse problem, source reconstruction from far-field intensity data 77−10830
inverse scattering methods for EM fields 77−31048
laser interaction with matter, nature of light, nonlinear spectroscopy 77−50712
models of optical systems 80−9821
moving object imaging, anticausal behaviour 79−81381
polarised light impulse response matrix formalism, appl. to holography 78−63045
principles for electronic engineers *(Japanese)* 80−9799
quasi-monochromatic incoherent optical image processing 79−76626
radiation sources for USSR state standards, 0.4-10.6 μ range 78−46739
spatial and temporal variables 77−3531
stellar occultations by planets, wave optics of central spot 77−67053
surface waveguide electrooptical deflector, high-resolution, prism model 80−48454
three-dimensional radiation and scatt., surface-type integral eqn. approach 77−38782
wave and particle descriptions of light, equivalence, rel. to radar freq. shift 80−101692
wave optics, partially coherent fields of illumination, pencils of rays 79−98275

physics
see also physics computing
advanced placement examination, multiple choice component validity obs. 78−16596
American contemporary fiction, world view, influence of physics 79−58517
in archaeology, nonscience undergraduate course 77−26104
Australian Institute of Physics conf., 1979 80−4477
book, physics for applied biologists 78−53310
book, secondary school general physics course 78−57725
career opportunities for physicists, changes, role of American Physics Society 78−62046
career opportunities for physicists, discussion 78−61966
citation patterns in scientific revolutions 79−75318
citation study of Argentina, Brazil and Norway 79−97180
computer-aided teaching, hinted finding scheme, simulation appls. *(French)* 80−98777
conference, physics in industry, Dublin, Ireland (9-13 March 1976) 77−60887
contemporary frontiers in physics 79−40310
contemporary needs, conf., Nathiagali, Pakistan (June 1978) 80−62387
current developments review (book) 80−77600
David Ausubel learning theory as reference system for content organisation in physics 80−22172
education, in developing-country universities 79−35458
education, joint honours degree course at Manchester University 79−35456
education, physical sciences at Lanchester Polytechnic 79−44658
education, physical sciences in medicine diploma 80−31444
education, physics, engineering and teacher training at Loughborough University of Technology 79−35455
education, university science course for talented secondary-school students 78−89282
education and employment, situation and prospects 78−61963
education versus job training 78−61965
electronics technology development, teaching 80−31470
engineering as source of scientific ideas 78−8213
European physics bibliography 79−40341
European physics publication output, by country 79−88776
frontiers, role in society 79−49008
gas breakdown in homogeneous elec. field, physical aspects *(German)* 79−82108
human resources and career opportunities 78−61962
interdisciplinary course, physical theory in biology 79−58462
International Centre for Theoretical Physics, objectives and scope 80−12839
mathematical physics, personalised system of instruction course, problems in developing country 79−5930
medical applications of physical methods *(Polish)* 80−12048
medical education, premed requirements, in physics 79−58458
metrology, scope and relationship with physics 80−52153
MHD generators 78−83623
models, nature and purpose 80−42023
nature, unity of, as an incentive to research *(German)* 80−77533
patent information time distrib. 79−97181
perspective of physics, vol.I, book 78−54105
physical acoustics, history and future, review 77−49548
physical acoustics, International School of Physics, Course 63 (Varenna, Italy, 1974 Aug. 5-17) 77−50785
problem-solving, teaching and understanding 80−8752
research bureaucracy 79−97179
research project methodology 78−12528
role in contemporary world *(Polish)* 79−40345
school physics syllabuses, review 79−62952
scientific career migration, bibliography 79−71220
scientific collaboration, professionalization and co-authorship 79−97178
solid state parameterisation schemes 79−17183
solid-state, conf., Munster, Germany (Mar. 1977) 78−2401
solid-state research at Bell Laboratories 77−41449
Soviet physics, review articles, book 80−46742
Soviet physics publication output, 1910-79 79−88777
student attitudes to physics as a subject 77−9833
students in electronics and physics, examination, reliability 77−26103
superconductivity and very low temp. generation *(German)* 77−55650
superfluidity and very low temp. generation *(German)* 77−55650
Ta-You Wu festschrift: science and matter, book 79−44688
teaching, 'talk and chalk' method 79−44660
teaching a course based on the fundamental principles of hi-fidelity sound reproduction 77−33733
teaching and research on universities, vocational aspects 79−62951
teaching curriculum development, systems approach *(French)* 77−9834
teaching methods, of Joseph Henry, biographical review 79−44692
teaching physics for related sciences and professions 77−22339
undergraduate courses, role of nomograms 77−49519
undergraduate engineering education, physics requirements 79−44656
university physics curricula, review 79−62953
welding arc 78−55771
world physics publication output, by country 79−88778

physics computing
see also computerised instrumentation; spectroscopy computing
3-D computer program for nonlinear EM fields, TOSCA 80−95765
3j and 6j coeffs., recursive computation 77−5687
^{252}Cf based nondestructive assay system for fissile material, Monte Carlo anal. 78−73119
ab initio LCAO-HF-concentrated GO crystal-orbital program 77−55471
ab initio orbitals calculations, using minicomputer 79−31375
ablating boundaries, algorithm for automatic tracking 79−32240
absolute, standardisation of radioactive sources and solns., 4π β-γ coincidence, program 77−18760
absolute neutron spectrum determination, by S and II code from reaction rates in $\Sigma\Sigma$-ITN facility *(Rumanian)* 79−63862
absolute retardation patterns, laser diametrically compressed photoelastic disc 77−27496
absorbed energy distrib. in γ-irradiated layered target, Monte Carlo program 79−19279
absorbing film-nonabsorbing substrate system optical parameters, FORTRAN code *(Rumanian)* 77−69923
absorptance, reflectance and transmittance of number of parallel surfaces 78−42273
absorption correction, optimisation *(French)* 79−68973
acetone-chloroform-methyl isobutyl ketone, ternary phase diagrams, interactive computer program 80−71629
achromatic antireflection coatings, thin-layer, layer thickness calcs. 80−87468
achromatic metal-dielectric mirror coating, computer synthesis 78−46750
acoustic field in finite cuboidal spaces, computer-aided geometrical field analysis of directional props. 80−19157
acoustic filters, arbitrary profile, circular cross section, finite element simulation 77−11059
acoustic noise characts. comp. using PL/1 program 78−59192
acoustic source holographic detection, computer reconstruction 78−38153
acoustic wave reflection on free surface, reflection coeffs. 77−31152
acoustical holography, digital reconstruction and computer graphics display 80−23842
activation detector ave. cross sections in ^{252}Cf benchmark field 78−82598
activity data for three component systems, mathematical representation, exam. of Fe-Ni-C system 79−10912
ADDES quasi dynamical code, comparison of many bodied and binary collision cascade models up to 1 keV 78−29051
Adler-Adler cross section formalism, improved resonance formula for fissile elements 78−74358
adsorbed chain structure, Monte-Carlo simulation *(Russian)* 77−19122
adsorption, computer simulation 79−65308
adsorption, density functional theory, computer simulation 80−24735
adsorption isotherms for heterogeneous substrates, improved CAEDMON program 79−77895
adsorption of macromolecules at plane surface, computer rel. to real expts. *(Russian)* 79−56077
advanced continuous fluid Eulerian comput. scheme for flows with large density gradients 77−46236
advection eqn., anal. of local second moment conserving quasi-Lagrangian scheme 79−72871

physics computing continued
advection-diffusion simulations, finite-element and finite-difference methods comparison 77−22424
aerodynamic tube, nonsteady heat transfer method 79−37147
aeroelasticity, flutter testing, modal parameter identification 79−3938
aerofoil in unsteady viscous flow, numerical soln. procedures 78−75165
ageing metals, new particle phase spatial distributions, computer calcs. *(Russian)* 79−83202
air coils, magnetostatic field FFT calcs., linear system theory 80−32868
air showers for 10^4 to 10^6 particles, lateral distrib. of EM component, detection, data handling 80−17459
air-based solar heating systems with phase-change energy storage, performance anal. using computer simulation 80−35762
airborne noise, personal calculator program for A-weighted sound pressure level and noise ratings 80−23828
airborne plume dispersion, 2-D computer hydrodynamic simulations 80−45837
aircraft design technology, fluid dynamics computer program assessment data base 80−1637
airfoil, conformal mapping, including multiply connected regions 77−23981
Airy pattern calculation by simple program run on HP 25 pocket calculator 79−72481
Alfven-ion cyclotron instability, physical mechanism, computer simulation 77−72437
algorithm for computing the coordinates of an acoustic-emission source 79−94432
algorithm for high order polynomial extrapolation 79−88798
algorithms, fast least squares, on-line data fitting, for physics teaching 77−33787
algorithms, mol. fragment recognition in E maps and electron density maps 78−55772
alkali chlorides, thin film, crystal-vacuum (100) surface, mol. dynamics computer simulation 80−34288
alkali halides, thin films, crystal-vacuum (110) interfaces, mol. dynamics computer simulation 80−34289
alkali metal, bulk properties, computer simulation 78−30729
alkaline earth halides, thermodynamic and structural props., computer simulation 78−75849
n-alkane, polymer, liq., mol. arrangement, computer model 80−92446
n-alkane liquids, molecular orientational correlations 79−19131
alloy, AB type, equilib. props. by Markovian simulation 78−91302
alloy, binary, conc., with short and long range order, computer simulation of diffusion 78−30778
alloy, binary, quenched, computer simulation of cluster dynamics of two dimensional model systems 78−31434
alloy, cubic, computer simulation of formation of tweed and modulated structs. 79−96029
alloy, FCC, Monte Carlo simulation of surface segregation 78−31413
alloy, quenched, binary, time evolution, computer simulation of three-dimensional model system 78−31433
alloy phase stability, computer calc. using modified pair potentials 78−35352
alloy random, binary, diffusion correlation factors calc., comparison of matrix inversion, Monte Carlo and diffusion of probability techniques 78−30779
alloys, binary, constitution diagrams, computer calc. *(Russian)* 80−84909
alloys, binary substitutional, determ. of local atomic configurations 79−86739
alloys, ion-implanted, integral Gaussian profile determ. method 80−107313
alloys, segregating phases identification, single crysts., radiographs computer calc. 80−84934
alloys systems, ternary, phase equilibria calc., line compounds 80−10638
alumina reduction cells electrolytic, instabilities of metal surface, computer simulation 78−39720
ambient gas, computer expts. on ionic recombination, coeff., binary recombination 78−22028
amorphous Ising system, computer simulation 80−60299
amorphous materials, dispersive transport, computer simulation, time of flight signals 80−70696
amorphous metal, struct., simple computer modelling 79−19154
amorphous metals, computer simulations of tensile deformation and radiation damage *(Japanese)* 79−42137
amorphous semiconductors, hopping conductivity in 3-D disordered systems 77−4336
amorphous semiconductors, simulation of elec. conductivity in one-dimens., temp. depend. 77−4334
amorphous semiconductors, simulation of elec. conductivity in two-dimens., temp. depend. 77−4335
amorphous solid, structural defects, computer simulation study 80−88040
amorphous state simulation using parallel computers in University research 79−54114
amorphous structure, computer simulation 78−30541
amorphous thin film on crystalline substrate, computer simulation 79−15045
amplitude transformation procedure, for fatigue life prediction 78−68796
anadalusite, thermal expansion and cell parameters 79−90801
ANALYT, analytic extrapolations towards interior points from a cut, applic. to elementary particle scatt. theory 80−12952
angular momentum coefficients in relativistic atomic struct., Fortran program MCP75 77−10605
angular momentum expressions reduction by matrix arithmetic, computer method, perturbation calcs. 77−26126
ANISN code for calc. of neutron bomb rad. penetration in air 80−47743
anisotropic axisymmetric solids, asymmetric stress anal. 78−26033
anisotropic system, computer simulation, energy and specific heat temp. depend. 78−9947
annular plate, algorithm for numerical soln. of critical buckling 78−83275
anodic film, automated interpretation of ellipsometer obs. 78−56902
anthracene, single cryst., fluoresc. decay, Monte-Carlo simulation *(German)* 79−61440
antireflection coating, multilayer achromatic, extended region of low reflection coeff. values 80−95982
aperture shaping, diffracted energy spatial distrib. control, computer analysis 78−59152

physics computing continued
arbitrarily defined differential equations, automated soln. using FORSIM VI program package 79−63007
architectural acoustics, image method for simulating impulse response between two points in small room, using digital computer 79−68487
associated Legendre polynomial $P_L^M(x)$, Chebyshev expansion 80−8774
atmospheric air simulation, temporal evolution of negative ions *(French)* 77−21869
atmospheric sound absorpt., personal computer program 80−96065
atom, Breit interaction between electrons, calc. angular coeffs., computer program 80−18779
atom, first-order wave functions, computer calcs. using Green's functions 78−41934
atom packing projections, along real or reciprocal lattice directions, computer program 79−14707
ATOM programme package for atomic calculations 79−10010
atom surface scatt., hard corrugated surface model, calc. methods 77−16447
atom-atom collision cascades localisation, impurity and thermal vibr. influence, computer simulation method 80−88227
atomic, molecular, and solid-state theory, collisions, quantum statistics, symposium, Florida, USA (March 1979) 80−51946
atomic collisions, multistate mol. treatment, impact parameter approx. 77−38705
atomic collisions, multistate mol. treatment, impact parameter approx., differential cross sections from transition amplitudes 77−61820
atomic continuum processes, R-matrix method, program 78−74558
atomic dislocation modelling, flexible boundary conditions and nonlinear geometric effects 78−75667
atomic electron elastic scatt., perturbation theory calc., computer program 78−50637
atomic electron scatt., intermediate coupling strengths from LS coupled R-matrix elements 79−18292
atomic excited terms generator program 79−54759
atomic multiconfigurational eqns., numerical soln., computer program 77−42226
atomic orbitals, hydrogen-like, shape, teaching appl. 78−93496
atomic scale computer simulation of lattice defects, stress tensor determ. 78−30602
atomic shells, internal conversion coefficients, numerical solution of Dirac equation 80−47434
atomic struct., numerical HF radial function during SCF iteration, convergence 78−58574
atomic terms for equivalent electrons, combinatorial computation 78−17549
atomistic computer experiments of point and extended defects 78−30610
audiometry, threshold, optimum crossings and time-window validation 80−19187
Auger and line optical data acquisition, synchrotron radiation source 78−63019
austenite, computer simulation of C diffusivity 79−77803
Auto-Resonant acceleration, computer simulation of linear and nonlinear wave growth phenomena 80−9439
auto-resonant ion acceleration concept, computer simulation 77−24208
autoepitaxial growth of Ge films, computer model 79−95927
automated method for fission-fragment track density determ. in solid state track detection using MAGMO-1 system 80−42891
automated ship routing appl., meteorological surveillance 79−84390
automatic piecewise linear approximation of yield function in ideal plasticity 77−46929
automatic subdivision of 2-d region into finite elements, use of computer algorithm 78−81819
autoresonant acceleration, numerical simulation of cyclotron waves 79−72022
axial channelling, in monatomic and diatomic cryst., multistring model computer simulation, foreign atom location appl. 79−42128
axisymmetric confined flame, aerodynamic and heat transfer, finite difference scheme, program 78−94689
axisymmetric plasma, ideal MHD spectrum, finite hybrid elements method 78−42734
axisymmetric transducers, with various boundary conditions, single integral computer method for Green's function 80−87591
azimuthal scanning method, allowance for X-ray absorpt. in single-crystal diffractometry 80−38874
back sputtering and ion penetration into polycryst. target, computer simulation 78−60537
backscattering of low energy noble gas ions from single cryst. surface, computer simulation of ang. depend. 79−19961
ballistics, max. range at elevated launch height, expt. and BASIC program 79−97156
bar magnet field, analogue simulation by electrostatic field, boundary conditions 77−61892
bar undergoing bending oscillations, shape optimisation *(Russian)* 79−37210
barytes concrete, gamma ray buildup factors, PIPE code 80−27823
BASIC overlay for CAMAC data and command handling 80−18772
Bayesian deconvolution, appl. and algorithm implementation 78−70103
BCC lattice, probability of visiting new site in random walk 79−88891
BCC metals, plastic deform., computer simulation 80−40456
BCC metals, stressed, computer simulation of vacancy and divacancy migration 78−47573
BCC structures, simulation of vacancy-thermotransport 78−47570
beam line magnet misalignment effects 77−30688
beam vibration frequencies by Schelkunoff iteration with HP-65 calculator 78−1592
beam-beam simulation for modest Fermilab proton colliding beam expt. 77−83337
beams, finite element soln. using element averaging technique 78−26079
beams, nonlinear bending, finite element anal. 78−26068
bending, of plate, powerful finite element method for computing 78−1583
Benjamin detector unfolding, MATXUF improved on-line uncertainty calc. 79−85876
Benjamin detectors, on-line, real-time neutron spectrum unfolding 79−59297
Berkeley 88 inch cyclotron, systematics in the control settings, beam parameter prediction 78−78526
Bernstein's polynomials, differentiation and integration 78−40
Bernstein modes, two dimens. electrostatic particle simulation 78−71531
Bessel functions, $J_n(z)$, $Y_n(z)$, $H_n^{(2)}$ and $H_n^{(2)}(z)$ calc., of integer order and complex argument 79−63004

physics computing continued
Bessel functions, $Y_\nu(x)$ and $J_\nu(x)$, of real order and argument, calc. prog. 80−8776
Bessel functions $J_0(z)$ and $J_1(z)$ of complex argument, code for calc. 77−64923
best fit strain tensors method for stress computation in two material elastic media 77−46910
betatron, electron beam rapid extraction by parametric reson., analogue computer anal. 77−18731
bimetallic tube, residual stress after thermal cycling 77−90465
binary alloy, model quenched computer simulation of time evolution in nucleation region 79−82344
binary alloy, quenched, time evolution, computer-simulation of three-dimensional model system 77−48422
binary alloys, computer experiments on phase separation 79−43198
binary alloys, diagrams of state, component interaction parameters, computer calcs. *(Russian)* 80−55355
binary alloys, short range order, program for study 77−62444
binary crystal growth, computer simulation 78−9979
binary phase equilibria, computer program based on Redlich-Kister eqns. 79−10913
binary system, thermodynamic props., comparison Bale-Pelton and Redlich-Kister representations 77−47598
BIODOSE, chronic radioactive release assessment 80−13710
biostereochemical modelling, interactive computer graphics, appl. to DNA-protein interaction 78−88693
BIOT2, heat conduction, three-dimens. code *(Hungarian)* 80−43593
BKWAVE, program, calculation of 1-dimensional shock wave propagation 80−38448
black body sources, in band flux density calcs. 79−37135
black hole MHD 78−12281
Blasius profile, eigenvalues determ. using Riccati transform. method 77−65731
blunt-body boundary layers, three dimensional, surface curvature effects 80−1520
boiling curve, water in cylindrical cavity in copper block, quenching data and heat loss 77−84119
Boltzmann equation, time independent, gas mixture in elec. field, soln. using Fortran program BOLTZ 77−11304
Bonner sphere spectrometer, least-squares technique for extracting neutron spectra 78−33366
Borel-type sums in scatt. theory, computation method 78−57823
borides, lightweight ceramic armour appls., ballistic tests, computer simulation, book contrib. 78−48556
boundary integral equations, numerical treatment, three-dimens. elastostatic anal., fracture mechs. appls. 77−46909
boundary layer flows, finite difference method 78−51155
boundary layer flows in tilted square cavity, finite difference method 77−7385
boundary layer turbulence, differential methods and finite-difference methods comparison 78−18279
boundary-layer flow over blunt bodies 78−79296
Bragg reflection multiplicities for any space group, computer program 77−55213
Bragg reflections, ang. positions calcs. by computer program 80−38863
brass, stress corrosion cracking constitution of Pourbaix diagrams for ternary systems by digital computer 78−35595
bremsstrahlung, ang. distrib. of nonrelativistic intensity calcs., program 78−87001
bremsstrahlung in bulk media, shielding study, Monte Carlo anal. of thick target spectra 78−59839
bremsstrahlung intensity distrib. at origin in thick W target by attenuation anal., 60 to 140 kV 77−34060
bright- and dark-field, microscopy, iterative algorithms in single side band holography 77−7640
brittle fibre reinforced composite, failure, mathematical simulation 78−3221
brittle material, fast crack propagation, computer simulation 80−38331
bubble and spark chamber photographs analysis with PA-BESM-4 system, exchange apparatus 78−9045
bubble chamber film, on-line measuring system with manual digitiser 77−18736
bubble chamber film, track rescue system 78−70728
bubble chamber film meas. automisation in Spiral reader system 80−14045
bubble chamber photographs, online analysis system *(French)* 77−42223
bubble motion in rotating liquid, computer study, Runge Kutta Nystrom method 77−47063
buckling, finite element analysis by ASKA program system 79−18753
burnup codes for calc. of fuel depletion and fission product poisoning 77−67800
BWR fuel assembly, radiant heat transfer 78−17287
BWR in-core neutron detector sensitivity to control rod vibr. using neutron noise anal. 80−57910
CAI, student response to comput. phys. teaching lab. project at Surrey Univ. 77−53724
CAL packages at Univ. of Surrey 78−81756
calorimeter, low temperature investigations, simple off-line arrangement 80−90850
calorimeter for temp. range 4-380K 80−98915
calorimetry, differential scanning, computer-interfaced, heat capacity meas. 78−65935
CAMAC diagnostic module for on-line monitoring of CAMAC integrity 80−5459
CAMAC high rate data acquisition system 80−23281
CAMAC hodoscopic recording system, coding and reading data unit 78−13397
CAMAC Q signal as device-ready indicator 79−6809
carburizing in glow discharge methane plasma 79−11724
casting, continuous, heat transfer anal. by finite element anal. 78−30167
cathode lens having a quasispherical field 80−95782
Cauchy integral-equation method, steady water wave problem numerical soln. 79−10574
cavitation failure, incorporating cavity nucleation with strain, computer program 80−16451
central pairwise potential alternative in computer simulation in materials science 78−30585
CEPADAS, real-time computer program for off-site radiological impact assessment of nuclear facilities 80−95475

physics computing continued
ceramic, laser drilling and cutting, anal. of results using computer model 79−70180
cermet film, as solar selective absorbers, production, struct. and optical props. 79−29485
CERN, software standardisation 79−89553
CERN computing school, La Grande Motte, France (1976) 77−65414
CERN ISR, control system, addition of local intelligence to CAMAC 79−72212
CERN ISR clearing current monitoring system 77−83249
CERN ISR control scheme for acceleration by phase displacement 79−72213
CERN Omega spectrum., data monitoring system 77−18768
CESR control system, distributed microprocessors appls. 79−72217
chain molecule in solutions, finite concentrations, different solvent conditions, simulation 79−45872
chain molecules in soln., thermodynamic props. related to chem. pot. 80−3394
channelling in sdlids, computer simulation of ion trajectories 77−80563
channels with single- or two-phase heat transfer fluid, computer simulation of transients 78−90969
charge bunch radiation losses in pill-box resonator, time domain numerical computations of EM fields 79−31781
charge carrier conc., temp. depend., computer data anal., effect of band parameter errors *(Russian)* 78−52006
charged particle transport in one-dimensional finite system 77−61035
chemical kinetics models, partial and differential eqn. parameters, estimation using Galerkin's method 79−66258
chemical laser nozzle, TRW CL XV, fluid mechanical and optical analysis, LAMP and BLAZER code calcs. 79−98350
chemical laser resonator modelling, LAMP and BLAZER code calcs. comparison with CL XV meas. 79−36890
Cherenkov counter optical system evaluation 77−34523
Cherenkov radiation from large cosmic-ray showers, computer simulations 79−66899
chromatography, nonlinear, nonideal, computer simulation models 80−62639
circular electron accelerators, beam stability calc. 79−72099
classical and special relativistic physics arithmetic models formulation 78−86130
Clebsch-Gordan coeffs. for S_n, generation programs 78−86172
Clebsch-Gordan coeffs. program for finding functions on tableaux and frames of the symmetric group S_n 78−86173
cluster identification, computer expts. on systems of particles 78−59725
cluster systems, program for calc. electronic struct. with double self-consistency-Bersuker's method 80−69289
CNDO calcs. with config. interaction 77−50372
COBRA-IV, multi-dimens. simulation of flow nonuniformities in fissured porous media 80−28559
coincidence matrix, fast, programmable 79−97961
COL, Laue patterns, cylindrical, flat transmission or flat back-reflection Laue photographs, calc. of crystal orientation 80−19670
cold rolling, non-circular arc roll force model 78−48423
collective modes in solids, computer simulation 80−54325
collinear asymmetric model reaction probabilities quantum and quasiclassical calcs. 80−85145
collision probability integrals, props. in annular geometry-11 evaluation 79−67812
collocation method, appl. to boundary-value problems in applied mechanics 77−68434
n-colour complex kinoform, distortions in reconstructed image *(Russian)* 78−66790
command language based data acquisition and anal. system for low energy nuclear physics 77−57846
complete structures, appl. of phase refinement, use of statistical information in tangent-formula refinement 79−7511
composite, unidirectional, percolation in thin ply 79−42511
composite flat belt drive material, tension relaxation under simulated drive conditions 78−56688
composite fracture with bonding strength defects between components, computer simulation 80−11771
composite superconductors, stability anal. by thermal analyser digital computer program 78−54995
composite systems, cracked, finite element microscopic stress anal. 78−34083
compressed magnetic field power supplies, characts. of helically wound generators, using a 2-d MHD computational model 78−17838
compressible flow, conservative difference scheme, second order sequel to Godunov's method 79−72907
compressible flow around an aerofoil or a cascade, up to shockfree transonic range 78−22365
compressible flow fields, two-dimensional, computation by modified local stability scheme 78−1681
compression struts, of nonlinear viscoelastic materal time dependent load bearing capability *(German)* 78−48474
Compton scattering, γ-rays off bound electrons, nonrelativistic form factors, Fortran program 77−10252
computational atomic and molecular physics, conf., Nottingham, England, (Sept. 1978) 79−59567
computational fluid mechanics, book 80−1517
computed electron micrographs, use in defect identification 79−69101
computer, unconventional electron lens calcs. 77−67542
computer aided indexing, of transmission electron diffr. patterns 78−38595
computer experiments and their applications *(Polish)* 78−89420
computer in the nuclear science laboratory 79−72220
computer method for analysing TEM diffr. patterns 77−47309
computer models of magnetically confined plasmas, review 77−11388
CONAN code, effects of evaporation and condensation on LMFBR post-accident containment response 80−47637
concrete, reinforced cross-section, reponse to short-term and sustained loads 79−52358
concrete slab, reinforcement optimisation by linear programming 77−89022
condenser efficiency and performance enhancement, evaporative cooling *(German)* 79−72781
conductometric probe, field disturbances in conducting fluid modelling *(Russian)* 78−231
configuration interaction, perturbation theory, partial transformation 78−37562
confined plasma column, soft X-ray lasing action conditions 80−74346

physics computing continued
conformal representation of arbitrary multiconnected airfoil sections 78−30308
conformations of rotational isomers, interactive access data program 78−62786
conical flow of non-Newtonian elastic power law fluid with injection/suction, similarity solns. 79−14439
contact stress anal. involving fretting fatigue loadings, computer soln. 78−34096
contact stress problems, counterformal, improved numerical method and program 79−41632
continuation method, adaptive step size selection 78−45476
continuous flow pinch, model and computer simulation 77−80343
Controlled Fusion Atomic Data Center 78−17432
convective coupled heat transfer, Nusselt no. computation, laminar fluid film 78−59398
convective heat transfer anal. by finite element method 78−18148
conversion from two to three functional modes of logical address space 78−36981
COREF-1 nuclear fuel behaviour code, appl. to LMFBR during overpower transient 80−57853
corner, three-dimens., Navier-Stokes eqn. soln., numerical code 78−30314
corona discharge, electrons and ions distribution determ. 79−4204
correlation time calc. from nuclear mag. relax. data, computer program 78−88210
cosmic rays, velocity diffusion, turbulent mag. field, Monte Carlo calc. 78−53777
Coulomb coeffs. for complex ionic crystals, computer program 77−39656
Coulomb functions with complex angular momenta, calculation subroutine 79−85245
coupled channel Born approximation code, OUKID, finite range heavy ion direct reactions, appls. 78−89832
coupled finite element-finite difference anal. of hydrodynamic and elastoplastic problems 77−71200
coupled large linear damped structures, eigenvalue anal. 78−1561
coupled multiconfiguration SCF perturbation theory, analytic techniques 78−17550
coupled radiative and conductive transfer thermokinetics *(French)* 79−1095
crack initiation notches, pure strain rate role, finite element computer program 77−70166
crack propagation, computer simulation 80−59573
crack stress intensity factor calc. *(Japanese)* 78−9603
creep data, 3- and 4-element response curve fitting 77−90395
creep prediction during random changes in load, ambient temp. and humidity, computer calc. 77−70121
CRETA 74, improvement of PAL 11 A assembler for IML syntax implementation 78−33406
critical heat flux in boiling channels, BURN-2 computer program 77−54863
critical two-phase flow, nonequilibrium vapour production model, K-FIX 80−52719
cross-spring hinge problem, 2-D, use of minimization methods in solving 78−18163
crystal, point defects, anisotropic cubic elastic Green's tensor function, elastic energy coeff., Algol 60 program 77−11537
crystal atomic structure refinement, least squares programs 78−26375
crystal atomic structures, computer-aided graphical representation of projections onto planes 79−60217
crystal defects and disorders, computer simulation of electron dynamical diffuse scattering 79−23505
crystal growth, dynamic computer models 80−103284
crystal growth, from soln., implication for industrial crystn. 80−49147
crystal growth disorder, 3D model, rel. between Ising models 79−51025
crystal growth from vapour, simulation 78−31312
crystal habits, graphical presentation, programmable method 79−32935
crystal orientation determ. by Laue method, computer calc. *(Chinese)* 79−32853
crystal setting, and data reduction, on a PW 1100 diffractometer, program using simple method based on real space 80−59342
crystal step motion, in the presence of a mobile impurity computer model 79−14713
crystal structural fragment, automatic construction, taking account of attainable chem. bond lengths 80−92419
crystal structure, cavity location, computer program 78−18481
crystal structure determination with DAR-UM+BESM-6 automatic system 77−76386
crystal structure image computation for high-resolution TEM 78−71653
crystal structure least squares refinement technique based on fast Fourier transform algorithm 78−91197
crystal surface, (1n0), stepped relief machine model 80−34283
crystal surface, ion bombardment, equilib. at. struct. 79−56051
crystal surface structures, Monte Carlo simulations, appl. of statistical tests, cryst. growth 77−4060
crystal vacancy migration induced by subthreshold collisions, computer simulation exam. 78−47365
crystal wave functions, symm. transformation, computer programs, symmetrisation procedure 78−10315
crystal-melt interface, computer built random model 77−20165
crystalline solutions, binary isostructural, thermodynamic mixing parameters computation, FORTRAN IV subroutines 77−86344
crystallisation course in condensed eutectic systems, computer calc. 77−86018
crystallite deformation in rolling, computer simulation *(French)* 78−31421
crystallographic computing correlation with artificial intelligence research 77−17960
crystallographic data, molecular geometry, computer retrieval and anal., general principles and methods 78−83643
crystallographic data, molecular geometry, computer retrieval and anal., variance and interpretation 78−83644
crystallographic data, molecular geometry, computer retrieval and anal., geometry of β-1′-aminofuranoside fragment 78−83645
crystallographic molecular packing plotter program 77−15272
crystallographic orientations distribution function, computer calc. for cubic metals 80−64827
crystallography, conference, International Crystallography Congress, Warsaw, Poland (Aug. 78) 79−23481
crystallography, coords. calc. from distance information 78−38581
crystallography, determ. of periodic bond chains *(French)* 78−26474

physics computing continued
crystallography, DSC-1 and DSC-2 lattices, coincident and near coincident cells for two lattices 77−84746
crystallography, electron diffr., background correction, automated procedure 77−27782
crystallography, electronic stationary picture method 78−38582
crystallography, layered structure, spherical voids determ., APL program 77−27872
crystallography, least squares refinement for powder film profile anal. 77−27778
crystallography, linked-atom least-squares reciprocal-space refinement system, LALS, incorporating stereochemical restraints 78−26377
crystallography, low angle X-ray diffr., pore or particle size distrib. calc. 77−39512
crystallography, modelling of FCC solid solutions 78−26475
crystallography, modern techniques and apparatus survey 77−4019
crystallography, monoclinic substances, trial and error indexing program for powder patterns 78−34390
crystallography, phase relationships, appl. to complex struct., use of magic integers in phase determ. 78−26379
crystallography, phase relationships, appl. to complex struct., choice of reflexions 78−26380
crystallography, phase relationships applic. to complex structures, MAGLIN, successor to MULTAN 77−19816
crystallography, powder photograph indexing program for orthorhombic crysts. 77−31563
crystallography, sphere tangent to four spheres, APL soln. 77−27773
crystallography, structural fragments located on basis of interatomic vector functions, automatic anal. 78−1947
crystallography, transmission factor calc. 77−84574
crystallography, X-ray, neutron diffr., charge deformation density refinement, computer program 78−71639
crystallography, X-ray or neutron, program for determining multiplicities of powder reflections 77−39509
crystallography, X-ray struct. amplitudes, data averaging 78−47211
crystallography electron diffraction pattern indexing, Fortran program *(Chinese)* 78−67625
crystallography powder patterns, LAZY PULVERIX computer program 77−27784
CTR, model blanket expt., neutron spectra sensitivity analysis 78−29648
CTR, spherical implosions, instability growth and saturation simulation 77−79480
cubic bell spline sum function in least squares sense 79−12583
cubic crystal electronic energy band calc. by LCGO method, FORTRAN IV program 78−75977
cubic harmonics computation, using point groups and an algorithm 78−20994
cubic spline interpolation of unequally spaced data points 79−30210
curve fitting to data with low statistics 80−9471
CW optically-pumped submm laser performance prediction using computer model 78−87041
cyclic voltammetry, data treatment 78−61076
cyclopentane, pseudorot., effect of 10 fold barrier 78−74792
cyclotron, emittance measuring instrumentation, program for phase ellipse area *(German)* 78−58512
cyclotron kaon factory, radial betatron oscillations, simulation of integral resonance motion *(Russian)* 77−10506
cyclotrons, superconducting, spiral electric gap effects on ion orbits, computer program calc. 80−52795
cylinder in incompressible flow, finite element anal., wake development and stability 79−14364
cylindrical demagnetisation matrix computation, FORTRAN IV program 78−76274
damage function anal., computer simulation 78−87721
dark-field imaging, computer simulation 80−100151
data acquisition system for EXAFS and photo-electron spectroscopy expts. 78−62676
data acquisition system on-line, for particle physics expts. using PDP-11 computers 80−27913
data communications 79−89576
data handling and standard practices 80−58009
data processing of TSC/thermoluminescence ratio 78−10463
data sets with jump discontinuities, interpolation method 79−30211
deconvolution of experimental outcomes, program DEO 78−70729
deconvolution of experimental spectra using moments method 78−29094
defect clusters, nucleation and growth due to energetic particle radiation, chemical rate reaction theory, computer program 80−49263
defect contrast numerical calc. in X-ray transverse topographs 77−84572
defect coordinate determ. by calibration of AE method 80−35473
defect displacement field construction from angular dislocation segments, electron microscope image simulation 80−6325
defect images produced by piezobirefringence, simulation 78−30521
defect prod. and annealing, radiation-induced, computer expts. 78−87710
defect superlattices, hardening influence, computer simulation *(Russian)* 79−83206
deflection of cables, cylindrical suspended roofs with complex loading, incremental algorithm 78−9558
deformation of bar elements, derivatives of deformation parameters, appl. to buckling and post buckling anal. 77−89047
deformed nuclei calc. by HF method with Skyrme's interaction *(Russian)* 79−456
dendritic crystal growth computer simulation, impurity trapping 78−38992
dendritic particle characterisation of automatic methods 80−25590
dense fluids, relative motion of atomic pairs investigated in short-time regime 80−96426
dense liquids and their mixtures, mol. dynamics, numerical algorithm 80−28890
densities of states, computational algorithm 80−44466
density wave instability in once-through boiling flow system, distrib. parameter model 79−67815
diagrammatic many-body perturbation expansion, computer program 78−50454
diagrammatic many-body perturbation expansion, ladder energies, computer program 78−50455
diagrammatic many-body perturbation expansion, ring energies, computer program 78−50456
diamagnetic susceptibility calculation using Pascal's consts., BASIC program 80−37717
diatomic bonding energy, changes due to Van der Waals interactions with other atoms 78−95012

physics computing continued
diatomic gas, molecular dissociation, recombination reactions simulation 78−23934
diatomic one-electron mols., wavefunction calc., collision matrix elements, computer program 78−50457
diatomic photoelectron spectra, vibr. struct. calcs., cost-effective program 77−18973
diatomic polar molecule in electric field, energy levels 79−18136
dielectric, freq. crossing signals in thermal cond., extension to high conc. of phonon scatt. centres using computer anal. 80−2224
dielectric, solid, energetic struct. of traps, from SCL currents 80−24941
dielectric fluid, electro-dielectrophoretic forces acting on spherical impurity particles, analytical evaluation 78−88641
dielectric inhomogeneous medium, refractive index profile determ. from inverse scattering 78−58914
dielectric liquid, DC cond. due to impurity particles, computer simulation and comparison with expt. 79−91060
dielectric multilayer systems for optical appls., computer program synthesis *(German)* 78−46788
dielectric thin film refractive index and thickness, algorithm for determ. on basis of ellipsometric meas. 80−34881
dielectrics, thermally stimulated dipolar processes, simulation 78−35080
differential interference contrast microscopy, computer simulation 77−53973
differential neutron spectra estimation using foil activation data and IUNFLD code 78−29690
diffr. studies using minicomputer *(Chinese)* 77−72528
diffraction, generation of ordered unique reflection sets 78−18485
diffraction data unique reflection sets generation, in FORTRAN IV 78−18501
diffusion, chemical, highly defective solids, steady-state computer simulation method for lattice gas 80−49401
diffusion, nonlinear problem, integral soln. 78−36945
diffusion eqn. analogue simulation *(French)* 77−5653
diffusion in low-beta devices, finite element analysis 77−80277
diffusion of impurities, computation of diffusion profile *(Russian)* 77−47621
diffusion process, by means of electric analogies *(Hungarian)* 79−17361
diffusion time scale Tokamak code, G2M, two dimens. 78−42795
diffusion via vacancies, correl. factors calc. using Monte Carlo computer simulation 77−15615
diffusion-convection const. coeff. eqn., centred differencing, box scheme, mesh size, errors 77−7386
digital radiation monitoring system, signal processing by distributed microcomputer data modules 79−59279
dilute frustrated lattice, spin-glass ordering, triangle and FCC lattices, Monte Carlo simulation 80−15746
dilute linear Heisenberg chain, partition function and irreducible representation of permutation groups by HLISP 78−34945
dilute solutions, Monte Carlo algorithm for preferential sampling near solutes 77−51287
directional integration method for 2-D fluid transients 78−683
disc with regular system of holes, stress concentration, computer computation 77−3723
discharges between plane parallel electrodes, axial and radial development computation with SPARK2 program 78−91173
discrete Poisson eqn. soln. with complicated boundaries, appl. to KEMP-II machine 77−15225
discrete vortex method for flow representation including separated regions 77−80172
dislocation, straight line, motion in conc. solid soln. computer simulation 77−81268
dislocation, two-dimensional model system, computer calc. 78−30621
dislocation array, equilibrium configuration by computer simulation 78−30616
dislocation array problems 78−30617
dislocation image in X-ray plane wave topography 80−54234
dislocation motion, lattice resist., effect of impurity interstitials 80−84170
dislocation motion, straight line, in concentrated solid soln., computer simulation 77−15413
dislocation motion through random array of point obstacles, thermally activated, computer simulation 78−30636
dislocation motion through random array of short range barriers, digital simulation 78−30634
dislocation motion through random array of weak obstacles of finite width, digital computer simulation 78−30633
dislocation segment oscillations, internal props., point obstacle collisions, glide plane motion *(Russian)* 80−39088
dislocation unzipping, low temp., computer simulation *(Russian)* 79−86792
dislocations, straight edge, nonlinear computation of anisotropic elastic fields 77−7718
disordered structures, two-dimensional, computer program for modelling *(French)* 80−59337
disordered systems, Coulomb gap computer simulation 79−51465
dispersion of equal spheres, random, average nearest-neighbour spacing 79−58639
dispersion strengthening, dislocation interaction treatment, digital simulation models 78−31419
displacement spike annealing, Mont Carlo method computer expteriments 78−30672
display-assisted automation in data processing *(Bulgarian)* 79−85131
distributed processing data acquisition system at Brookhaven National Laboratory 79−89532
dither signals for binary display of images, computer-aided design 79−94161
divergent beam diffr. phenomena, computer generation of identification 78−30520
dose-rate conversion factors for external exposure to photons and electrons, modifications to DOSFACTER code 80−104775
DOSFACTER code, dose-rate conversion factors for external exposure to photons and electrons 80−104775
dosimetry, programs for internal absorbed dose determ. 78−15895
DOT-III, anal. of ^{60}Co γ-ray scatt. in air 80−32525
double cantilever beam, dynamic stress intensity factors computation and crack arrest stress intensity factors 78−34088
drift chambers, track reconstruction decay electron trajectory meas., MSR at CERN 78−82593
drift-diffusion problem with special boundary conditions, numerical soln. by integral eqns. 77−76591
physics computing continued
drift-flux model of LMFBR Na boiling transient 80−47636
DSA recoil distance lifetimes, comprehensive anal. formalism, computer code 77−6653
ducted and exhaust plume flow fields, computer anal. 79−7397
dye laser wavelength scanning with microcomputer control 79−94248
dynamic buckling of shells 78−18210
dynamic destinations, removal of redundant operations in front algorithm 78−62064
dynamic electric and magnetic field evolutions, visualisation using computer graphics display 80−46776
dynamic fatigue tests, statistical reproducibility of crack propag. parameter 80−25842
dynamic heat transfer meas. at Mach 8, digital Fourier anal., boundary layer transition 80−14682
dynamic plasticity, implicit and explicit computational schemes 78−34038
dynamic stability of dislocation sub-boundaries during straining, computer simulation 78−30635
dynamical thermoplasticity, appl. of mathematical system theory 78−83271
earthquakes, records, optimal digitisation 77−91044
EAS, electron-photon and muon components, simulation 77−49255
EAS array, at Durham, data anal. 77−91392
EAS data relation to high-energy particle prod. models, simulation 77−70962
easy glide, computers modelling, range of permissible parameters *(Russian)* 78−47375
ECSIMPACT, version of IMPACT for CDC machines with ex-core memory, electron impact 80−18924
eddy current through type transducer, operating condition simulation when inspecting ferromagnetic rods 78−53077
edge dislocation thermally activated motion, appl. to KCl-KBr solid soln., computer simulation 79−19249
EHT calcs. on large mols., computer method 77−26982
Eindhoven AVG cyclotron, on-line determ. of acceptances and emittances of beam guiding system 77−38515
Einstein-Petrov eqns., type I complete integrability conditions 77−71249
elastic coefficients, independent 4th-order for all cryst. classes, numerical methods anal. 79−69219
elastic coefficients of fourth order, independent, for 32 cryst. classes *(French)* 80−34117
elastic contact problems, in fracture mech., friction effects 78−67142
elastic contact stress minimisation by contour design 78−63396
elastic continuum penetrated by elastic tube, biaxial stress field, appl. to concrete pressure vessel 77−46921
elastic crack problem, soln. by superposition of finite elements and singular fields 78−38249
elastic interaction energy calcs., for Guinier-Preston zones in Al-Cu, Cu-Be 79−11617
elastic long thin profiled strips, numerical soln. *(French)* 77−72182
elastic scattering cross sections with coupled channels, optical model fitting code 79−13264
elastic structures, computer automated synthesis for minimum struct. weight 78−34015
elastic-plastic deformation stress-strain anal., parametric linear programming method 79−37194
elastic-plastic incremental finite element anal. 78−34034
elastic-plastic-creep response of high-temp. nucl. components 77−3112
elastic-viscoplastic analysis of plates by finite element method 78−34031
elasticity, pot.-type singular integral approx. algorithm 80−27132
elasticity theory, dynamic problem soln., curvilinear co-ord. computer evol. 77−46961
elasto-plastic buckling of curved webs, Gauss-Seidel iterative procedure 78−34043
elasto-plastic flow in computer simulated, A533 steel 78−56720
elasto-plastic material, crack tip stress and strain fields and fracture behaviour, work hardening 78−22304
elasto/visco-plastic finite element analysis, unconditionally stable algorithms 78−34030
elastomeric bearings, high-capacity, laminated, finite-element anal. 80−96197
elastomers, tackiness, fracture mechanics theory *(French)* 80−38344
elastoplastic anal. using ASKA program system, bending, isotropic/kinematic hardening 78−63312
elastoplastic fracture mechanics for reactor piping 78−68777
electrical and magnetic fields, using ELMAG program system *(German)* 77−3516
electro-optical phenomena of disperse systems, computer calc. method 78−50699
electrochemical impedance meas. method, automatic, computerised data anal. 77−70307
electrocrystallisation, chess board type computer simulation 80−54157
electromagnet GFUN program with interactive graphics 77−18053
electron accelerators, elimination of electron multipacting in supercond. structs. 78−9004
electron beam X-ray source, X-ray spectral distribs. FLASH code 79−22524
electron beam-whistler wave nonlinear interaction, computer simulation 77−3938
electron collision theory, asymptotic soln. calc. program 80−53129
electron density mapping in mols., cyrsts., conf., Rehovot, Israel, (Apr. 1977) 78−71622
electron diffraction computer simulation for one-dimens. studies *(French)* 80−1902
electron diffraction pattern interpretation, case of small Au particles on NaCl surface *(French)* 77−76700
electron diffraction patterns, computer anal. 77−1049
electron diffraction patterns, computer assisted indexing 78−9918
electron diffraction patterns, extinction problem, automatic indexing program *(Chinese)* 78−91204
electron diffraction patterns, point, computer indexing 80−100136
electron diffraction spots, computer indexing, appl. to bicryst. *(French)* 78−75507
electron dosimetry in tissue equiv. phantoms 78−7454
electron elastic scattering by gases, computer anal. of differential cross section 77−58160
electron impact calcs. using R-matrix and linear algebraic methods 79−59579
electron lens aberration coeffs., computer calc. using CAMAL 77−38798

physics computing continued
electron micrograph, 500 kV, atomic resolution, computer image processing 80−100149
electron micrograph, computer simulation for crystal defect identification 78−30525
electron micrographs, computer-aided anal. 80−4813
electron micrographs, noisy, phase retrieval algorithms for semi-weak objects 78−78047
electron microscope image contrast of small dislocation loops and stacking fault tetrahedra 80−6326
electron microscope W support film, phase contrast simulation 78−334
electron microscopy, bright field images, signal-to-noise enhancement in incoherent superposition 80−101906
electron microscopy, electron object interaction, multislice approach 78−26394
electron microscopy, high resolution, digital processing use for image assessment and restoration 78−37116
electron microscopy, many-beam structure images, optimal comput. techniques 80−95203
electron microscopy, phase contrast simulation, of Au cluster atoms on W support film 80−100150
electron microscopy, simulation of digital image restoration 77−57431
electron microscopy, structure image high-speed calc. methods 79−55622
electron microscopy of biological objects, 3-dimens. image, computer simulation 77−13046
electron motion in elec. and mag. fields, student lab and computing studies 80−27076
electron optics, mag. field with min. spherical aberration 78−9313
electron optics, potential in system of rotational symm., integral method 77−587
electron optics, potential in system of rotational symm. 77−586
electron optics aberrations, algorithm computation using Chebyshev polynomials 79−27156
electron repulsion integrals, computation involving Gaussian basis functions 78−58572
electron ring and accelerator lattices, linear and nonlinear, interactive computer program 77−83332
electron solid, two-dimens., shear modulus and melting, temp. depends. 80−158
electron spectroscopy programs 78−86390
electron storage ring, horizontal wiggler, modelling of effect on beam parameters 79−68029
electron trajectories in multi-element electrostatic cylinder lenses, program for calculation 80−87283
electron transport, discrete ordinates calc. using standard S_n neutron transport codes 80−46998
electron-diatomic molecule static interaction potl. calc. 77−3255
electron-image calculation system, interactive, for use in electron microscopy 80−24325
electron-photon cascade simulation by Monte Carlo programs 79−54330
electronic energy loss of ions in solids, 10-10^4 keV nucleon^{-1} 79−23666
electronic excitation energy transfer in activated crysts., math. modelling 79−38028
electrophysical information collection, recording and processing system 78−8388
electrostatic and magnetostatic particle simulation models in three dimensions 79−64903
elemental sensitivity data modeling for in situ neutron capture gamma-ray experiments 79−61928
elementary particle physics, use of database management systems 80−899
ellipsometer, polarisation-modulation, Fortran simulation program ELLIPS 78−271
EM particle simulation codes, initial noise, quiet start 78−1883
EM pulse propagation, in weakly nonlinear plasma, numerical calc. 77−58863
EM scatt. from surfaces, nonrectangular patch model, program availability and appls. 79−81332
EM wave scattering, by complex shaped bodies, effective scattering area *(Russian)* 78−13647
empirical relationships for random self-avoiding walks on lattices 79−9190
emulsion chamber C-jets, computer simulation using conventional particle physics 79−58990
enthalpy, using pocket calculator data-base library formation 77−67391
entropy calculation with computer simulation 77−22504
environmental radiation dose assessment of a growing nuclear industry 80−3553
environmental radioactive releases from nuclear installations, computer simulation of effects 80−3550
EPIQUANT structure analysis, appl. to GaAs *(German)* 77−72619
epitaxic derivatives, program (AIDED) for automatic indexing, appl. to graphite lamellar compounds 79−50927
EPR of Mn^{2+}, in polycrysts. of low symmetry, computer simulation *(French)* 79−95635
EPR spin Hamiltonian parameters for paramagnetic ions in tetragonal symmetry, optimal computation 77−4550
equation of state variables calculation using TI-59 80−77738
equations of state, search procedure, based on step-wise least-squares technique 80−19900
equilibrium and elastic stability problems, appl. of triangular facet shell element method, TRUMP 77−46946
ERATO code, plasma MHD stability, convergence of solns. 80−83906
ESP-TIMOC modular code for neutron transport problems, in FORTRAN IV 78−50236
ETA gun, beam dynamics calc. with EBQ code 79−72023
ethane, ionis. efficiency curves by electron impact, fragment appearance pots. 77−61863
evaluated nuclear data, estimated uncertainties 77−23169
Evaluated Nuclear Structure Data File for basic and applied research 78−17544
evaporated dielectrics, ion drift and diffusion numerical calc. 77−4215
event analysis program using EVAL language 79−89561
Event Handler II CAMAC coupled event handler interface 79−89542
Ewald method, convergence of reciprocal lattice sums 77−11834
exact finite range DWBA form factor for heavy-ion induced nuclear reactions, calc. program adaption 80−9271
exact Slater integrals determ. for H wave functions, computer method 78−90074
experiment design 79−89577
physics computing continued
experiment planning, optimum plans calc. on convex polyhedrals 80−57084
experimental data processing method based on piecewise-linear dependences 80−62640
experimental heat transfer data processing, automatic unit 79−93110
explicit finite difference method, anal. of dynamic crack and fracture 77−75860
explosive heating due to projectile impact, numerical anal. 77−72142
exponential distrib. parameter estimates under poor statistics, computer program 78−57863
exponential integrals, general method for accurate numerical evaluation 78−36
extended plane fluid sheet, swelling finite element anal. 79−37277
externally cracked cylinder, elastoplastic response anal. by method of lines, computer program 80−28435
fast breeder reactor benchmark calcs., effects of recent changes in ENDF/B 77−23177
fast ion Fokker-Planck code FIFPC 78−34342
fast neutron facility in CP-5 reactor, neutron flux, energy spectrum, primary recoil distribution 79−41056
fast neutron spectra, activation technique determ., fusion reactor blanket model appl., unfolding program 77−79500
fast neutron spectrum unfolding code MATXUF 78−5091
fast power reactor, material distrib. optimisation by nonlinear programming method 77−14210
fast reactor, plate lattice heterogeneity effect with course group consts. 77−3075
fast reactor adjoint neutron spectrum calc. using bilinear weighted cross sections 77−83003
fast reactor benchmark anal., appl. of FORSS sensitivity and uncertainty methodology 77−46276
fast reactor finite difference diffusion theory codes, optimised iteration strategies and data management 77−83005
fast reactor transfer functions determ. 77−3082
FASTBUS, high speed nucl. data acquisition 78−46251
FASTBUS, project evaluation 79−89555
FASTBUS−details of addressing and bus mastership 79−89554
fatigue, cumulative damage, under random loads algorithm of hysteresis loop counting 80−21064
fatigue, low cycle, charact. determ. using digital computers 79−100263
fatigue crack, computer simulation of propag., model based on Elber's eqn. *(Japanese)* 78−7030
fatigue crack, dynamic treatment of growth *(Japanese)* 78−34084
fatigue crack closure, computer model, based on surface roughness and residual strain 77−73347
fatigue crack growth, mechanisms 78−64703
fatigue crack growth rate data, effect of meas. precision and data processing procedures on variability 79−61817
fatigue cracks, computer simulation of propag. based on BCS model *(Japanese)* 78−7029
fatigue life prediction, computer based 80−21251
fatigue life prediction techniques, appl. of computer for materials substitution 79−61820
fatigue life predictions using computer modelling, cyclic stress/strain curves 80−19290
fatigue limit, in bi-freq. loading 80−104289
FBR, multigroup 1-D diffusion program MED 78−78456
FBR analysis, general multigroup nodal procedure based on response matrix principles [for FBR analysis] 80−57827
FBR fuel, accuracy and computational time of hierarchy of growth rate definitions 79−80979
FBR radial blanket, comparison of economic perform. for LMFBR and GCFR 79−49654
FBR safety related slowing down problems 78−678
FCC lattice, computer simulation of low energy displacement cascade 78−47367
FCC metal, polycrystalline, computer simulation of rolling texture *(Japanese)* 77−63686
FCC metals and alloys texture transitions, computer simulation 79−90666
FCC/BCC partial coherent, boundaries, computer modelling 79−46669
feed through eddy current transducer, numerical anal. or operating mode during ferromagnetic rod inspection 80−108670
FERDOR, neutron spectrum unfolding, optimised smoothing 80−27860
Fermi liquids, computation of second order energies using reference spectrum Euler eqn. 79−71359
Fermilab, beam intensity and efficiency display system 79−72218
Fermilab booster tunes, control system 77−83382
fermion expectation values, using program SCHOONSCHIP 78−74555
ferroelectric hysteresis cycle computing from a statistical model *(French)* 79−11393
ferromagnetic crystal, domain wall pinning effect and intrinsic coercivity, computer simulation 78−64217
ferromagnetic linear chains of spin 1/2 particles, one-magnon states 78−14946
fibre reinforced composites, fracture processes modelling, digital computer appl. 80−65147
fibrous material failure kinetics, internal stresses, computer simulation *(Russian)* 80−40479
field electron source geometry determination by computer assisted shadowgraph technique 77−87882
field evaporation of W in FIM, computer simulation 77−69973
field line computation for diverse configurations, program 77−22401
film, amorphous, of hard spheres, computer simulation 78−22984
film growth, island growth and coalesc. stage, computer model 79−11034
film growth modelling, condensation coeff. influence evaluation *(Czech)* 79−77935
finite difference scheme, appl. of second and third degree methods 77−5651
finite element anal., data struct. 78−16633
finite element anal., hierarchical approx. 77−71197
finite element analysis of elastodynamic fields near running cracks 78−34066
finite element determ., operational stress-state of field ion microscope specimen 78−32933
finite element method, reduced integration, appl. to elastostatics 78−75066
finite element stiffness matrices, incompletely integrated shape functions, numerical stability 78−1567

physics computing continued
finite elements method, iterative algorithm for continuous stress field anal. 77−72179
finite moments algorithm for particle transport problems 79−67237
fins, extended surface array, heat flow evaluation, efficient algorithm 78−90635
fissile isotopes, thermal parameters, proposed reevaluation 77−23135
fission fragment deexcitation, statistical model anal. of spin influence 79−17941
fission fragments, kinetic energies and fly-off angles, ionisation method of meas., online numerical processing *(Russian)* 80−52838
fission product nuclear data evaluation, cross sections up to 15 MeV, resonance parameters 77−23044
fission products, neutron cross-sections data for ENDF/B-IV library 78−25290
fission products gamma-ray and photoneutron spectra 77−23127
fission reactor, ^{235}U, Pu fission fragment conc., fragment capture cross section, heat production 78−17296
fission reactor, VVR-S, Bucharest, IRT-M expt. bundle power distrib., obs. and computer anal. 77−18655
fission reactor and plasma nonlinear optimisation algorithms 80−18623
fission reactor materials, ion penetration distance calculations with multi-group transport computer codes 80−102246
fission reactor materials damage by heavy ion bombardment, comparison of analytical and Monte Carlo computer codes 80−102245
fission reactor poisoning by Xe and Sa, transient anal. using XESAMO code *(Spanish)* 80−52749
fission-gas-induced swelling in UC, porosity effects study by UCSWELL code 78−8959
fixed mirror solar concentrator, optical-thermal performance anal. 80−30392
flame, mutual ion neutralisation 80−35537
flames, ignition and propagation, self-consistent 2-dimens. hydrocode 78−47066
flames, premixed, laminar, time-depend. soln. determ. 78−67282
flames, unsteady, propagation, numerical modelling 79−64794
flow, annular, turbulent, with rot. core tube, numerical predictions 77−55010
flow, boundary-layer, laminar to turbulent transitions, numerical simulation 78−38286
flow, gas-liq., hot-film anemometer signal anal. method 79−32639
flow, inviscid, hyperbolic, computational algorithms tests 80−27140
flow, new viscous-inviscid interaction method 79−1154
flow, rot., between rot. and static discs, with radial flow, numerical method 78−59403
flow about arbitrary 2-dimens. boundary, implicit finite difference simulation 78−94628
flow calcs., three-dimens., low Reynolds no. 77−49600
flow curve correction by FORTRAN program *(German)* 78−79394
flow field, multiply connected, curvilinear coords. and macro-elements 80−19318
flow field meas., near nozzle outlet using laser Doppler anemometer 80−28582
flow meas., thin orifice plate, turbulent flow numerical modelling 78−34229
flow prediction, Monte Carlo and Bayesian probability techniques 78−30256
flow probe output digital processing, appl. to cylinder wake charects. 80−19541
flow reversal and separation at unsteady boundary layers 78−75163
flow splitting tee junction, three dimens. turbulent flow field, coarse field computations 78−63494
flowmeter standard orifice plate calc., for meas. flowrate of liquids, gases and vapours 80−1714
flowmeters, variable area, calculator algorithm *(German)* 78−30377
fluence limit analysis of nuclear reactor component, damage function methods, computer simulation 77−18668
FLUID, Galerkin method program, viscoelastic fluid flow in fixed geometry 80−14750
fluid, Monte Carlo calculations, optimisation of sampling algorithms 80−54099
fluid and structural dynamics, transient 3-D potential flow problems, SING-S 80−48668
fluid computations using infinitesimal functionals, variational approach 79−14365
fluid dynamics, coarse mesh methods appl. *(German)* 77−88197
fluid dynamics, Navier-Stokes equations, finite element soln., applied to blood flow 80−94269
fluid dynamics, pseudo-spectral FFT technique, non-periodic problems 78−59359
fluid dynamics, transient 3-D potential flow problems and dynamic response of surrounding structures, singularity method, SING 80−48667
fluid dynamics eqns., asymmetric weighted residual method 77−79421
fluid dynamics random choice soln. of nonlinear hyperbolic systems of conservation laws 77−7362
fluid flow, marker and cell technique 79−9121
fluid flow prlblems, incompressible, free surfaces 80−106774
fluid flows with large density gradients, Eulerian finite difference technique 77−79424
fluid mechanics, book contrib. 78−59366
fluid structure, ionic, boundary conditions distorting effects in simulation 79−50968
fluid structure and dynamical props., computer simulation, using Monte Carlo and mol. dynamic methods *(German)* 80−69757
fluid velocity vector and temp. fields reconstruction, three-dimens., from acoustic transmission meas. 78−51261
fluid wave theories, Stokes, cnoidal, higher order solns. *(Japanese)* 78−42625
fluid-struct. interaction, added mass computation by boundary integral method 78−38228
fluid-structure coupling method in dynamic analysis of structs. 79−7322
fluids, crit. pt., scaling and extended scaling eqns. of state implementation, program 79−46780
fluids, multidimensional flux-corrected transport algorithms 79−68672
fluorescence decay, nontrandom errors, moment index displacement calcs. 77−6835
flutter eqn., continuation and direct soln. 78−34047
flux-corrected transport algorithm, rezoning technique 80−31516
foil bearing, deflection due to finite width bump, iterative methods 78−77691

physics computing continued
force const. adjuster program for least squares fit to observed frequencies of molecules and crystals 78−91395
forced convective film boiling, math. model 79−18686
FORMAC73, use in general relativity 77−41522
FORTRAN program for Fourier coeffs. of assoc. generalised Legendre polynomials of generalised spherical harmonics in texture analysis *(French)* 77−15279
FOURGEN, fast Fourier transform program generator 77−41466
fourier analysis with splines, a FORTRAN program 79−12582
Fourier hologram optimisation, computational method 77−50639
Fourier transform holography system, lensless, at 14 and 34 kHz *(Japanese)* 78−30133
Fourier transform IR spectrometer software package for phase correction 80−95162
Fourier transform of 2-D curves by 1-D integral, appl. to X-ray imaging 77−40851
Fourier-transformed neutron slowing-down kernel moments, MAGGIE code 78−29540
fractional parentage coeffs., nucl. shell model, reduced SU(3), computer program 78−50097
fracture analysis, 2D linear, elastic, finite element anal. vs. the edge function method 80−99963
fracture initiation site prediction, idealized polycrystalline materials, stress and strain fields 78−34092
fracture mechanics, conformal mappings to delete singularities, finite element anal. 77−72251
fracture mechanics, influence function method computer program 77−75859
fracture mechanics of reactor primary system under operating and accident conditions 78−66342
fracture toughness testing, elastoplastic range, computer simulation 80−21217
fragile lattice packings of spheres in 4D space 80−100194
frameworks calc., composed of thin-walled open sections 78−51059
Franck-Condon factors 77−50341
free convection mass transfer from downward facing horizontal plates, analog soln. 80−43706
free electron laser simulations using relativistic EM plasma simulation codes 79−68376
free electron lasers, energy transfer, computer simulation 80−83578
free energy differences between canonical ensembles, Monte Carlo calc. 77−2632
FREINT, an integration routine calculating Fresnel diffraction 79−30612
Frenkel pair formation in solids, due to passage of relativistic electrons, computer simulation *(Russian)* 80−6402
Fresnel integrals, computer evaluation, for teaching 77−33795
Frevel ZRD-SEARCH-MATCH program, for powder diffr. anal., generalisation 80−59341
frontal method for structural mechanics, algorithm for excluding unknowns 80−79157
frontal solution algorithm for finite element frequency analysis 79−3942
frozen core Hartree-Fock program for atomic discrete and continuous states 80−9509
full unsymmetric matrices, out of core eqn. solver 78−45477
furnace heat transfer, 3-dimens, computer model predictions test 78−59504
fusion driven symbiotic energy systems, neutronic and economic anal. of CTR blanket using XSDRNPM code 80−57955
fusion plasma reaction rates, velocity-space methods 77−79475
fusion power plant simulation model 80−13865
fusion reactor, effects of suprathermal alpha particles, phase-space grouping techniques 77−79479
fusion reactor, MFTF, end loss region high energy plasma gettering 80−102343
fusion reactor, mFTF plasma diagnostics Data Acquisition System 80−99319
fusion reactor, microscopic behaviour and neutral beam heating of Tokamak 77−79476
fusion reactor, TEXTOR, mag. diagnostics and monitoring systems data acquisition 80−99320
fusion reactor, toroidal field ripple effects, computer simulation 78−54892
fusion reactor magnetic coil systems, EM field, force and inductance calc. by EFFI code 78−62648
fusion reactor materials, appl. of dynamical computer models to high energy cascades 80−34046
fusion reactor radioactivity calc. code and decay chain data library, DKR 78−786
fusion reactors, PLT and PDX data acquisition systems, networking and distrib. processing improvements 80−99318
fusion test reactor, cross section requirements 77−23294
G1M/HYBRID quasi-equilib. MHD code for plasma simulation 80−64689
Galerkin-finite element formulation in viscous flow 79−14367
gamma spectra of fission products, estimation using nucl. systematics 78−70587
gamma-gamma directional correlations and anal. of ang. distrib. data, program 78−86503
gamma-ray detection, scintillator response, pulse height spectra unscrambling, computer program 78−55092
gamma-ray multiplicity meas., fast converging bootstrap method for data anal. 78−70730
gamma-ray spectra, rapid reduction via desk-top calculator 77−53870
gas, Lennard-Jones mols., self-diffusion coeffs. at moderate densities, mol. dynamic simulation 78−38440
gas, rapidly rotating, spin-up problem, perturbation calcs. 78−75147
gas (mixture), compressibility, virial coeffs., Burnett data reduction, fast least-squares method 78−47082
gas bubbles, on liq. surface, bursting, jet and droplet form., math. model *(German)* 77−24012
gas centrifuge, fluid flow anal., numerical integration of Navier-Stokes eqns. 77−75924
gas cooled fast breeder reactor thermohydraulic design codes, expt. verification 77−14221
gas discharges, electron swarm motion, computer simulation 77−89339
gas dynamic flow fields with discontinuities, computational method checking test 80−36864
gas dynamics, partial ionis. computation method 78−38447
gas dynamics, self-adapted algorithms 80−38432

physics computing continued
gas flow in catalytic convertor, numerical soln. 78−67281
gas lasers, computer modelling, at. and mol. processes 80−23661
gas lasers, computer modelling, book 79−41364
gas mixture, binary, condensation in boundary layer flow, numerical method 79−1236
gas mixtures, viscosities estimation, new simplified methods 77−80261
gas phase electron diffraction analysis, use of spline functions, program description 79−89810
gas-filled microballoons, radiation effects MEDUSA code calcs. 80−83220
gas-liquid surface of mol. fluids, mol. dynamics computer simulations 80−39387
gas/solid surface collisions, vel. depend. of ang. distribs., interaction pot. effect 79−11491
Gaussian optics parameters, HP-67 calculator program 80−106439
GAUSSIAN-70, integral labelling technique 77−10583
Gaussian-70 MO program, LCAO-SCF eqn. soln., population anal., appl. 78−70742
GCFR, 1000 MW, calc. of depressurisation and flow coast down accidents 78−50274
GCFR, Argonne, calc. of void streaming in critical expts. 77−83007
GCFR, Pu fuelled, fission products and secondary gamma-ray spectra 78−676
GEC Elliott CAMAC interface on PDP-11 computer running RSX-11M executive, software driver module 77−38590
general inverse problem, appl. of dynamic programming 78−45475
general relativity, slowly pulsating axisymmetric systems 77−5715
general-purpose molecular mechanics program construction principles 78−13411
generalised harmonic oscillator bracket calculation program 79−53996
generalised routine for defect image simulation in TEM obs. 78−29220
generalized sampling theorem with application to computer-generated transparencies 79−41343
German nuclear data library KEDAK-3, evaluation 77−23042
Giessen polarisation facility, multi-detector analysing system 77−65373
glass, refractive index freq. depend., dispersion enq. calc. 80−40083
glass surface, ellipsometric study of zone of optical contact 80−4754
glass viscosity, as function of temp., computer calc. 79−29100
Glen body, viscous nonlinear fluid flow around smooth sphere, stresses and strain rates *(French)* 79−7387
glide, interacting dislocation motion, resisted by point-like barriers, computer simulation 78−71742
graded-index fibre transmission characteristic computation 80−1321
grain boundaries, molecular dynamics studies, use of coincidence lattice theoretical model 78−30645
grain boundaries computer simulation, effects of rigid body translations 79−60386
grain boundary dislocation structure, atomistic computer simulation 79−60383
grain boundary entropy computation in computer simulation 78−30647
grain boundary segregation, computer simulation using Mie type interatomic pot. 80−54259
grain boundary sliding and migration, computer modeling 78−87687
grain density, determ. in space filling geometries from measurable 2D parameters, computer simulated model verification 79−38838
grain growth, chem. driven, during liq. phase sintering, computer simulation 80−55427
grain growth, steady-state and dynamic, computer simulation 79−38836
graphite, interaction with Cs, study of surface diffusion, computer simulation 78−30837
gravitation, gauge theory, vacuum field eqn. generation by MACSYMA system 78−36919
gravitational collapse, finite-particle scheme for three-dimens. gas dynamics 78−67218
gravitational fields, Bel-Petrov classification 78−93566
grid generation, automatic mesh-point clustering elliptic partial differential eqns, grid generation, automatic mesh-point clustering 80−31487
GROCS, underground heat flow model for solar source heat pump system 80−66987
growing bubbles on heated plate, meas. using computerised image anal. system 80−22322
guided light propagation mode computing, in fibres with non-circular cross sections 79−76874
Guinier-type focusing cameras, powder diffr. line profiles, simulation 79−58856
haemoglobin, sickling deer type III, macromol. struct. refinement by restrained least-squares and interactive graphics 80−28870
hard rod system, initially ordered, one-dimens., mol. dynamics computer simulations 78−71658
hard-sphere liquid, glass transition, computer mol. dynamics simulation 77−11674
Hartree-Fock wave functions, convergence in Roothaan's SCF eqns., 'level-shifting' method 78−41920
Hauser-Feshbach two step code for nuclear cross-sections evaluation 77−23045
HEAP, heat energy anal. of cavity-type solar receivers 80−30548
heat, conduction, finite element explicit algorithm 77−46885
heat and mass transfer systems, modelling of eigenvalues and eigenfunctions 77−14872
heat conduction, combination of Lagrange and Euler methods 79−76941
heat conduction, interior algorithm for optimisation of forms *(French)* 77−72130
heat conduction, inverse nonlinear problems, simulation methods 78−94513
heat conduction, inverse problems using analogue computer 79−37121
heat exchange modelling of marine two stroke compression ignition engines 80−30529
heat exchange tube thickness meas. by eddy current for corrosion testing, computer study 78−68852
heat exchanger, dynamic analysis, digital algorithm for initial value problem 77−42727
heat exchanger, thermal modelling for computer simulation 77−46904
heat of transport in solids, computer simulation of a vacancy in FCC cryst. 79−14955
heat transfer calc., programming 77−7289
heat transfer calc., programming 77−7292
heat transfer calcs., finite element anal., HEATRAN, diffusion eqn. soln. 77−3710
heat transfer finite difference computer programs 79−14221
physics computing continued
heat transfer model, sequential estimation of thermal parameters 77−80047
heat transfer parabolic partial differential equatn. TEDDY2 program package 79−2613
heat treatment, prediction of large component response 78−31435
heating, nuclear, approx. method, direct energy balance calc., γ transport, accuracy 77−6495
heavy atom location in struct. from Patterson function, computer aided 77−11439
heavy ion deep inelastic processes fragments, element identification in ΔE-E telescope, computerised method 77−57839
heavy ion induced two nucleon transfer, exact finite range microscopic DWBA, FORTRAN program SATTNT 77−61449
heavy ion irradiated target, number of point defects in displacement cascade, computational code *(French)* 79−19300
heavy ion radiation transport computer codes for thick targets 80−39180
heavy ion scattering, optical model code A-THREE 78−89837
heavy ion track reconstruction program 79−31348
heavy lepton pairs produced in e^+e^- annihilation leptonic decay, computer calcs. 78−21409
heavy water production, Girdler-sulphide process phys. props., computer program 78−25300
heavy-ion transfer reactions, DWBA program 78−50145
heavy ion lateral range calc., adaption of energy/depth distrib. program E-DEP-1 77−62571
Heidelburg postaccelerator, computer control system 79−72214
Heisenberg dilute systems, computer simulation, mag. conc. of clusters, linearised eqns. of motion 79−78409
helical turbulence, diffusion of passive-scalar and mag. fields, computer simulation 77−11272
HEPROP, programs for the caclulation of thermophysical and thermodynamic props. of He 80−6529
Hertz indentation test and Auerbach's law, computer simulation 78−19967
heterogeneous plasma discharge, spatial information modelling and processing algorithms 78−14229
n-hexane, impurity particle motion, under DC and AC conditions, expt. results and computer simulation 78−88642
HGTR core, multiregional coupled conduction-convection model 78−94083
high energy physics, optical computing introduction 79−89581
high energy physics and microcircuits 79−89572
high energy physics computing, CERN conf. Jadwisin, Poland (June 1978) 79−89570
high energy physics data acquisition packages 79−89535
high energy physics expts., computer technology effects 79−89536
high pressure phase equilibria and other fluid-phase properties, computational methods 80−75329
high spin state population, compound nucleus reaction, computer code CARLA 78−89843
high-pressure phase equilibria in mixtures using partition functions, computational methods 80−75330
high-speed shaping of free-flowing materials 80−25591
high-temperature media, thermodynamic and thermophys. props. calcs. 79−47964
higher-order monotonic convective difference schemes 77−13597
histogram manipulation program 79−54115
histogram plotting, FORTRAN program 'HIST' 78−77876
hologram, computer generated, 3D reconstructed images, characts. 80−43297
hologram, computer generated, as space-variant optical elements 78−37856
hologram, computer-generated, displayed by line printer, phase coding effects 78−25819
hologram generation, expt. using NaF 77−61923
hologram generation for 3-D display, stereoscopic approach 77−7025
hologram spatial filter, computer-generated, for large object formats, interpolation 78−22099
holograms, binary Fourier, wavefront coding by Lee method 77−75441
holograms, computer-generated, three-dimensional, image reconstruction using line printer 77−42506
holographic aberration compensation of optical system, computer modelling 77−50640
holographic filter generation for large objects 77−23753
holographic interferograms, computer anal. for nondestructive testing 80−9836
holographic interferograms evaluation, of thermal boundary layers *(Czech)* 78−62220
holographic optical element design using analogous lens model 78−58955
holographic reconstruction, near region, fast algorithm based on fast convolution *(Chinese)* 79−18368
holography, Fourier transform computer-generated, generalisation *(Japanese)* 77−34847
holonomic formulation of boundary layer eqns., use of tensors 79−1153
homogeneous nucleation and growth processes, computer simulation 78−30764
hopping conduction, random one-dimens. system, Monte Carlo computer simulation 80−80278
HPD-SHP-IBM 360/44 system for anal. of meson diffraction dissoc. experiments 79−22573
HTGR fuel particle, computer code for anal. of transient behaviour 78−8964
Hubbard model, one-dimensional $2k_F$ and $4k_F$ correl. functions, computer renormalisation-group calcs. 79−78029
HWAGR, 1800 MWt, cylindrical geometry, CECAS modeling code 78−41811
HWR, multidimens. space time kinetics studies 78−29547
hybrid thermal energy storage system, transient simulation 80−30588
hybrid thermal energy storage with water systems, eval. using analytical models 80−30589
hydration, hydrophobic, of nonpolar mols. in dilute aq. soln., Monte Carlo simulation 80−3314
hydraulic fracturing operations, material and structural simulations 78−31540
hydrocarbon crystal, calc. of internal friction resulting from molecular defects 78−31448
hydrocarbon crystal structure calc. by molecular packing analysis 78−14303
hydrocode convergence 78−36834
hydrodynamic stability computation, algorithm construction 80−19329

physics computing continued
hydrodynamic stability problems, computer program for testing linear stability of vel. profiles 77−54975
hydrodynamics codes, Eulerian and Lagrangian, pressure iteration, multigrid method 80−53738
hydrodynamics computer codes, limited compressibility 80−53803
hydrogen-bonded liquids, HF, H_2O, NH_3, computer simulation, intermolecular potentials 80−38890
hyperfine splitting factors of ^{157}Gd, determ. by interferometer with digital data processing 79−31723
hypersonic gas flow past thin triangular wings, difference method anal. *(Ukrainian)* 78−1686
IBMOL-5 service program 78−86765
ice, dislocation form. kinetics, computer simulation 78−30622
ice, hexagonal, lattice struct., computer simulation 78−14324
ideal strength of solids, computer calc. 78−30697
III-V compound crystal growth from solution, computer simulation 77−51332
image contrast loss in presence of chromatic magnification difference, numerical estimate 80−95823
image reconstruction, iterative computer method 80−102634
image reconstruction, projection completions methods, computational examples 78−46524
image reconstruction formulae, computer implementation 80−52179
image reconstruction from projections 80−52178
image restoration, constrained least squares, improved computational scheme 78−82915
image speckle pattern rel. to object surface profile, simulation 77−19175
image speckle patterns rel. to object surface profile, computer simulation 78−13660
imbedded neutron flux calc., reconstruction of original material struct. of fuel bundle 77−88196
immiscible liquids, separation kinetics in low gravity environment, computer simulation study 78−34629
IMPACT, FORTRAN program for electron-atom collision theory, soln. of coupled integro-differential eqns. 78−86948
implanted ions, energy deposition profiles from range data, simple method for calc. 77−39619
implanted-ion range, computing moments of energy distrib. 77−4120
implicit-explicit finite elements in transient analysis: implementation and numerical examples 79−17216
impurity diffusion, correl. factor, computer simulation 79−19404
inclusive backward proton cross sections, calc. program adaptation 80−9185
incompatible quadrilateral basis functions 78−41146
incremental compiler for data acquisition 79−89550
incremental formulation in nonlinear mechanics, large strain elasto-plasticity 78−77692
indeterminate beams, variable cross section, stress anal. using repeated integration 79−64510
indicial tensor manipulation on MACSYMA 78−12547
inelastic structural behaviour, finite element computational aspects 78−42546
infrasound signals, dynamic spectral anal. by FFT *(Chinese)* 78−1453
initially stressed Mindlin plates, finite strip method, buckling anal. 78−26067
inter-electron repulsion integrals for three open shell configurations in cubic symmetry 78−90061
interactive computer terminal as 'lab. assistant' in introductory physics expt. 78−36761
interface problems, computational techniques, conference, San Francisco, CA, USA (Dec. 1978) 79−41655
interference fringes, algorithm for fast digital analysis 80−73426
interferogram aberration evaluation program 80−13130
interferometry, Fabry-Perot, program for TI-59 calculator 79−35816
intermittent gaseous release from nuclear plant, probability distrib. of atm. dispersion factor 78−11994
internal conversion data anal., nuclear parameter determ. 80−52626
internal friction curves, numerical anal., program in ALGOL-1900 *(Polish)* 79−95079
internal stress determ. by Sachs method, digital computer use 77−54894
interstitial loop finite, modelling of growth under irrad. 79−23607
intramolecular potentials, quantum chemical calc. 78−13436
inverse heat conduction problems, numerical solns. 77−39193
inverse pole figures, calc. method on digital computer 80−20950
inviscid fluid conservation law eqns., coeff. matrices for implicit finite difference soln. 78−42580
ion autoresonant acceleration, numerical simulation 78−21789
ion backscattering and implantation, H and He ions, computer simulation, comparison of MARLOWE and TRIM codes 80−66350
ion beam focusing for low energy heavy ion accelerator 77−14654
ion beam trajectory focusing effects on toral reflection coeff., computer studies 80−89102
ion beams, transport, space charge effects, computer simulation 78−50328
ion bombardment collision cascades, computer simulation, Monte Carlo code 78−67756
ion extractor electrode CAD *(Japanese)* 78−86680
ion implantation, in crystals of diamond struct., computer modelling 77−43235
ion optics, high current beam extracted from plasma, iteration scheme 78−50693
ion scattering by atomic chains on solid surface 79−52065
ion scattering by single cryst., orientational effects in charge state 79−52064
ion scattering from single crystals, computer simulation 80−2911
ion source, accelerator system computer solns. 77−88309
ion source trajectory computation, computer simulation 78−71510
ion trajectories in any sector field in third order approx. 77−79741
ion-acoustic waves, nonlinear freq. shift and modulation, computer simulation 77−68789
ion-lattice interactions, modelling displacement correls. in computer simulations 78−2179
ion-metal atom processes, charge exchange cross sections, calcs. and computer program 78−55236
ion-solid interactions ion motion computer simulation 79−43088
ion-surface impact, interatomic pot. screening function correction factor for computer simulation 78−23574
ionic and plasma cluster equilibrium and kinetic props., computer simulation 78−71533
ionic crystal, stacking fault computer simulation 78−30652
physics computing continued
ionic crystals, defects, computer modelling, review 80−107205
ionic motion, 3-D quadrupole electric field, charge exchange collisions 78−9315
ionographic detectors, identification of nuclear reactions 77−3243
ionospheric ray-tracing calc. through Bradley/Dudeney ionospheric model 78−7826
IPNS time of flight neutron scattering instruments system 79−89558
IR reflection spectra computed for inhomogeneously doped semiconds. 78−27205
Ising ferromagnets, correlation decay, zero-field susceptibility, mass gap 80−50116
Ising finite amorphous systems, exact ground state 79−12725
isobar nuclei, separation of alkali and alkaline earth elements using surface ion source 80−37688
isochoric const. strain finite elements, modification of TRIM 3, TET 4, and TRIAX 3 elements 78−41144
effective neutron isolation thickness values from reflector savings data 78−669
isomers, structural formulae, graphs generation by computer *(Russian)* 79−49967
isoparametric finite elements 78−45479
isoparametric surface contouring algorithm 79−30215
isoparametric surfaces contouring 78−20948
isopermalloy, permeability stability calc. rel. to texture *(Chinese)* 80−65959
isotope separation, nonstationary processes in multistage cascades 78−5370
isotropic thin shells with circular hole, stress state, numerical investigation 80−48586
iterative algorithm for continuous stress and displacement solns. 79−1109
iterative Newton-Raphson method, stability anal. of nonlinear dynamical systems 77−72150
JET, CODAS, control and data acquisition 78−36982
jet noise, geometric acoustics model, computer prediction program 78−34118
jj-coupling, one-particle matrix element calculation program 79−13624
Johnson-Mehl and cellular microstructure, comparative analysis, computer simulation 80−54392
Josephson junction, computer simulation of vortex motion, induced by phonon injection 79−73636
Josephson junction, frequency-agile, biasing for precise freq., analogue computer study 79−28455
K-FIX, critical two-phase flow, nonequilibrium vapour production model 80−52719
K-shell hole production by light ions, hydrogenic and Hartree-Fock model of target 77−83715
Kabsch's procedure, program BMFIT for matching of rigid bodies 79−50930
KEKNET, a high speed on-line network for high energy physics 79−36493
kinetic Ising model of ferromagnetism, simulation of equilib. critical props. 78−89410
Kramers-Kronig transforms, Fourier method numerical soln. by computer 78−2825
laboratory experiments, graphic computer simulations 80−105470
Lagrangian hydrodynamics meshes, discrete rezoning algorithm, hot interacting bubbles calcs. 78−42628
laminar boundary layer, optimal control by wall suction or blowing 79−1242
laminar flow in toroidal pipe 78−51242
laminar swirling impinging jet, heat transfer, numerical calc. 79−1228
laminate, time and temp. effects, mech. response, computer simulation 78−35466
laminated anisotropic shells, transverse shear stiffness calc. 78−42526
laminated plate, moderately-thick, biaxial buckling 77−58573
laminates analysis, desktop calculator library module appl. 80−77764
LAMPF beam dynamics, PARMILA computer model 77−38504
LAMPF standard data-acquisition system 79−89534
Laplacian mag. field component computation from boundary obs. only 77−3513
large computer systems and new architectures 79−89578
large molecules, rotational dynamics program package 79−59609
large real symmetric matrices, generalised eigenvalue problem, group coord. relax. method 78−16622
laser, free electron, relativistic, rippled static mag. field, simulation, waves and instability 77−54686
laser, multiple-beam pellet irradiance, diffraction analysis 78−50845
laser amplifier gain, program for programmable calculator 79−18442
laser anemometry, high Reynolds number flow, review, data anal. for photon correl. method, simulation 79−60082
laser anemometry and other photon correlation data, stabilized model-fitting approach 80−58622
laser focused gaussian beam optical parameters, SR-52 calculator programme for calc. 78−79056
laser fusion microspheres, computer modelling, image analysis of X-ray radiographs 78−50311
laser fusion targets, X-ray meas. using least squares fitting 80−32425
laser imploded glass microspheres, numerical modelling 77−24115
laser plasma simulation code, PHD-IV 78−59640
laser produced plasma, gas target, hydrodynamic expansion simulation 79−55524
laser produced plasma, spontaneous mag. field generation, simulation and expt. 79−46472
laser pump system, analytical theory 80−106540
laser resonator standing wave simultaneous forward and backward integration 79−94258
laser system, interferometric optical anal. 80−87401
laser target behaviour, anal. in CASTOR 2 code 79−86594
lattice disorientations 80−28936
lattice dynamics of group IV semiconductors using an adiabatic bond charge model 80−10599
lattice images of crystal defects, computer simulation 80−107208
lattice parameter program, least squares method 79−64958
Laue method, rapid indexing of spot pattern, computation method *(French)* 79−37575
Laue patterns, indexing back-reflections by computer 79−14644
Laue photograph indexing and monocrystal orientation determination by computer, new approach *(Chinese)* 80−79636

physics computing continued
LEED, surface potential barrier, reflection and transmission coeffs., Schrodinger eqn. 80−87998
LEED intensity measurement by photographic method with digital image processing appl. to Si (111) surface 79−60234
LEED surface struct. determ., multiple scatt. theory based FORTRAN computer programs, book 79−86971
Lennard-Jones 12-6 system, triple pt. props., mol. dynamics simulation 78−2231
Lennard-Jones fluid, phase separation by spinodal decomposition, mol. dynamics computer simulation 79−10766
Lennard-Jones fluid in contact with Lennard-Jones wall, interfacial density profile 78−67901
lens CAD, three-lens zoom system 80−43424
lens design, aspheric, stigmatic, for ruby or He-Ne laser *(Czech)* 78−55427
lens design optimisation, Version 14 program 78−90488
lens film system resolution computation from numerical MTF data 79−44960
lens system design with extended depth of focus, Version 14 optimisation program 78−90489
lens testing, MTF-based optical sensitivity and tolerancing computer programs 80−83686
ligand field calculations for arbitrary point groups in strong field coupling, energy diagrams, plotter routines 77−76778
light, polarized, radiative transfer eqns., adjoint Monte Carlo treatment 78−37799
light interferometry, 3D orthographic projection plotting program 79−85172
light pulse excited decay curve simulation, finite breadth *(Hungarian)* 80−11473
light scattering by dielectric particles, statistical theory 80−32913
light wave diffr. by complex spectral composition US 80−95939
linac injection system beam dynamics 80−13989
linac particle tracing simulations 79−71999
linear accelerator, RF cylindrical cavity, evaluation by computer code SUPERFISH 77−38463
linear accelerator cavity anal., evaluation of LACC program 78−90000
linear accelerator cavity code, based on finite element method 78−33307
linear accelerator EM field in cavity, by MESSYMESH computer program 77−38462
linear accelerator simulation, code PARMILA, longitudinal tuning of LAMPF 77−83159
linear elliptic and parabolic partial differential eqns. with boundary singularities, numerical soln. 78−41142
linear magnetic solenoid reactor plasmas, dynamic behaviour 80−64751
linear systems, generalised backward substitution method of soln. 79−63008
linear time dependent partial differential eqns., solns. by Laplace transform and FFT 78−57763
liquid, polar, computer simulation, thermodynamic props., diffusion coeffs. 79−90507
liquid cavitation and droplet impact erosion, predictability of prototype machine from lab. tests 78−64723
liquid crystal, X-ray structural analysis, computer program for analysing expt. data 78−1956
liquid flow, incompressible, electro-hydrodynamic analogy, design 77−27627
liquid flow in tube with frozen layer, crust profile method 78−30359
liquid metals, viscosity calc. using microinhomogeneous struct. model *(Russian)* 80−15284
liquid mixture, excess thermodynamic function prediction, program description 78−27818
liquid phase crater profile calc., formed by conc. heat source *(Russian)* 77−72131
liquid phase epitaxy, two-dimensional computer anal. 79−95286
liquid radial distribution functions, method of reducing termination errors 80−24332
liquid scintillation counting, single and double labels, absolute activity analyser vs. on-line computer 77−83470
liquid scintillation counting, single and double labels, quench correction with on-line computer 77−79520
liquid-liquid solubility, critical phenomena in binary mixtures 80−54376
liquid-vapour interface, fluid phase coexistence, Monte Carlo computer simulation 80−49349
liquids, computer simulation techniques, review 77−7653
liquids, long-range dipolar interactions in computer simulations of polar liquids, Monte Carlo method 78−87603
liquids, non-mol., individual and collective atomic motion, inelastic neutron scatt. and computer simulation 77−55226
LISP programming language appl. *(Polish)* 78−61749
LMFBR, comparison of neutron diffusion computer codes 77−88188
LMFBR, in-reactor irrad. creep expt., thermal anal. 79−67854
LMFBR, intermediate Na activation, Monte Carlo anal. 78−4997
LMFBR, unified model for fission gas release and Na boiling in reactor coolant channel 78−8921
LMFBR benchmark calcs. by 2 and 3 dimens. diffusion methods 78−74432
LMFBR cores, performance of advanced alloys 77−42092
LMFBR coupled fluid-struct. problems, advanced Eulerian method 78−682
LMFBR critical assembly, neutron diffusion calc., DB^2 transverse leaking predictions 80−13529
LMFBR fuel, fission gas behaviour during overpower transient, calcs. using COREF-1 code 80−57853
LMFBR interlaboratory reaction rate program, evaluated decay scheme data 77−22928
LMFBR plant, modelling thermal hydraulic transients 77−88207
LMFBR safety, review of computer code packages 77−83053
LMFBR subassembly, central blockage wake anal. 78−29556
local Green's function method for heat conduction and fluid flow problems 77−79420
locally modified structs., derivatives of eigenvectors 78−5651
long rod penetration of targets at hypervelocity impact, HELP computer code 78−26061
LORA−an accurate four node stress plate bending element 79−27527
Lorentz gas, two-dimens., collision-induced absorption, simulation 78−46424
Lorentzian broadened K-series X-ray peaks of heavy elements, fitting algorithm 77−57799
physics computing continued
low field magnet, computer controlled, for optical and magnetic resonance studies 80−95113
luminescence decay time evaluation, computer programs, student expts. 77−26115
LWR, ENDF/B-IV eigenvalue calcs. for UO_2 and mixed oxide critical lattice expts. 78−25272
LWR, molten fuel coolant interaction during HCDA 77−3136
LWR anal., CASMO fast transport theory assembly depletion code 78−25278
LWR cell depletion code EPRI-CELL 77−50225
macromolecular dynamics, constraint dynamics, computer simulation 78−9932
macromolecular structure, interactive model building program 77−52738
macromolecular structure factor, FFT calc. 77−51268
macromolecular structures, struct. factor least squares refinement procedure 77−84573
macromolecule, branched, particle scatt. factor, light, computer simulation 79−64128
macromolecules, computer simulation techniques for mol. theory verification 78−13633
macromolecules in solution, US degradation simulation program 79−14148
Madelung constants, first derivatives with respect to cell lengths, calc. 78−34459
MAGIC, multisoln. direct methods procedure 79−73062
magic integer phase representation for complex structs., MULTAN program soln. 77−84571
magnet shimming, using computer routine 80−245
magnetic bubble domain Bloch lines motion, computer simulation 80−54916
magnetic bubble materials, BUBMAT program for domain parameters 77−12173
magnetic bubble motion, computer simulation 77−85526
magnetic domain wall pinning simulation, coercive force, susceptibility, defect depend. 77−16103
magnetic field, three dimensional finite element program 77−38769
magnetic field anal., THESEUS distributed processing system 79−41293
magnetic field analysis, AC, three-dimensional, using finite element method, Tokamak device appl. 79−50191
magnetic field and force eqns., solns. using programmable calculator 80−91721
magnetic field calc., saturable, by finite element method, using scalar magnetic potential 77−38773
magnetic field computation, conference, Grenoble (1978) 79−41262
magnetic field parallel computation array-processor structure 79−41277
magnetic fields, boundary-value problems, finite element and finite difference anal. 78−94353
magnetic first order instability in finite model system 80−65932
magnetic hysteresis, vector model, based on interacting dipoles 78−76271
magnetic materials search, appl. of cybernetic prediction systems 80−108048
magnetic MG field generation by EM flux-compression, computer simulation 79−50189
magnetic model systems 80−65924
magnetic susceptibility data analysis program SUSCEPT2 78−91847
magnetically confined plasma, numerical computation of MHD flow in Scyllac 77−80282
magnetometer freq. optimisation, computer anal. and expt. 77−18057
magnetosonic wave propag., computer simulation and theoretical anal. 78−5861
magnetostatic computer program GFUN3D, user guide 77−31044
magnetostatic problems, soln. by MAGGY2 problem package 80−28134
magnetostatic problems, two-dimens., numerical soln. by augmented Lagrangian methods 78−1119
magnetron ion sputtering, thin film layers depositon uniformity investigation *(Russian)* 80−20787
magnox fuel cladding, surface struct. data acquisition and processing system 80−898
many-bodied displacement cascade simulation up to 1 keV 78−87711
many-electron atoms, one-electron operators, Z-expansion of matrix elements 80−9489
mass spectrometer, quadrupole mass filter with flat electrodes, computer simulation 78−54492
mass spectroscopy computer acquisition and analysis of metastable transition data using electric sector voltage variation 78−70102
material phase diagrams calc. using thermodynamic data 79−7672
materials testing appl. of microcomputer, comparison of automatic and conventionally obtained data *(German)* 77−73398
mathematical physics equation soln. by variable-structure environment simulation 77−41470
matrix eqn. soln. 78−45478
matrix Pade approximants, Fortran IV calc. subroutine 77−9877
matter modelling conf. Anaheim, USA (Mar. 1978) 80−51954
MBNIM, modular approach to fast trigger logic for high energy physics expts. 79−49920
measuring projector for bubble chamber film, minicomputer on-line system 80−27878
mechanics, computational methods of treating nonlinear and special linear problems 77−74226
mechanics conservation law derivation using digital computers 78−12552
medical X-ray diagnostics, NDT impetus, novel techniques *(German)* 78−7146
melt flow during Czochralski growth, computational simulation 78−48306
melting and freezing, computer simulation of simple systems using array processor 80−54353
melting curve maximum phenomenon, computer simulation using two species soft core model 78−6146
meson mass formula broken SU_N 77−6043
metal, BCC, computer simulation of stacking faults 78−30653
metal, BCC, computer simulation of twin boundary and twinning dislocation struct. 78−30644
metal, BCC, struct. of twinning dislocations, computer simulation 78−2140
metal, BCC, twin boundary and stacking fault structs., computer simulation 80−59485
metal, computer prediction of long term strength by generalised diagram method 77−70133

physics computing continued
metal, FCC, anisotropy of surface free energy, computer simulation *(Russian)* 78−87858
metal, FCC, structure and dynamics of multiple interstitials 78−47330
metal, FCC and BCC, self-diffusion along edge dislocations by vacancy mech. *(Russian)* 78−87810
metal, FCC and BCC, vacancy diffusion along single edge dislocations, computer modelling *(Russian)* 77−47612
metal, He deposition and promotion of void nucleation during accelerator expts. computer simul. 79−23658
metal, plastic flow, during extrusion, computer simulation 78−31491
metal, plastic flow, finite element approach to axisymmetric problems, METFLO 78−31490
metal, strength, long-term charact. interpolation calc. using generalized curves and computer 77−86121
metal, void growth in irrad. sample, fully dynamic rate theory 79−73212
metal BCC, divacancy binding energy, appl. stress effect, computer simulation 77−15408
metal crystal, lattice defects, relax. studies 78−79604
metal foils, electron irrad., loss of pt. defects 79−73215
metal hydride, computer simulation of H reflection and scattering 79−1806
metal surface, self consistent electronic struct. effect on atomic positions, computer simulation 78−30969
metal working by pressure, full scale adaptive simulation applied to computer aided management 79−79055
metallic system, compound formation rel. to heat of mixing 80−55689
metallurgy, cellular microstructure, 3-dimens. anal. by computer simulation 78−87640
metals, FCC, twist boundaries, high-angle (001) CSL, struct. by computer simulation 79−46677
metals, FCC, twist boundaries, struct. invest. using computer simulation technique 80−84185
metals, FCC and BCC, grain boundary struct., and segregated impurity sites, computer simulation 79−73173
metals, FCC and CC, role of latent slip, computer simulation *(French)* 79−32998
metals, grain struct. form. during two-dimensional recrystallisation, simulation on electronic calc. machine *(Russian)* 79−87666
metals, heating by concentrated energy sources, simple analytical expressions *(Russian)* 80−38215
metals, interstitial loop growth, pulsed irrad. effects 80−88210
methane, liq., mol. dynamics simulation using singularity-free algorithm 80−54116
MHD channel flow eqns. between electrode walls, fast parabolic module 77−72423
MHD codes, linear and nonlinear, plasma instabilities, PL1 program 77−76040
MHD convertor, U-25, diagnostics system data processing 78−26339
MHD spectrum of straight plasma column with arbitrary cross section, finite element calc. 77−11327
MHD topping generator system, closed-cycle, nonequilib. ionisation 77−72508
microcomputer controlled UV ozone calibrator 80−13149
microcut, stable, in hexagonal 2-dimens. cryst., computer modelling 78−18704
micromagnetism, numerical calcs. 80−11222
micromechanical constants of statistical model interpetation of anisotropic work hardening *(Bulgarian)* 79−100169
microphysics to macrochemistry, discrete simulations, review 80−54102
microprocessor applications in deformation processes *(German)* 80−40627
microprocessor-assisted high-precision viscometry 79−50816
microscopic depletion in UO_2 and mixed oxide fuel rods, MICBURN code 78−25276
microstructure alterations and texture form. in normal grain growth, computer simulation 79−90679
microstructures simulation, based on optical electron and field-ion microscopy 80−19679
microtron, cathode focusing and drift apertures, hybrid computer calc. 78−21796
microtron electromagnet optimum shape, computer numerical anal. 77−18718
microwave EPR self-induced transparency in free radical powder, waveguide propag. 77−24747
Micu-type invariants of simple Lie algebras 80−12934
Mie scattering by sphere, numerical methods 79−50225
Mie theory calculations, particle sizing appl. 80−14282
minicomputer, high speed, economical 79−36496
minicomputer appl. to electron diffr. study of indexing patterns of single crystals unknown lattices *(Chinese)* 78−14249
minicomputer data acquisition system for Princeton cyclotron facility 78−90048
minicomputer open ended configuration interaction program, BERKELEY 78−37563
minicomputer software for high-energy physics experiments 79−89575
minicomputer-based gamma spectrum analysis system SAMPO78 80−14043
mirror, dielectric, Rayleigh scatt. at 441.6 nm 80−97367
mirror field ion-electron convertor, particle trajectories, IBM 360/91 computer calcs. 77−6626
misaligned beam transport elements, ion beam optics, IONBEAM program 77−65564
mixing of multicomponent solids, mixing index and contact number estimation by spot sampling 80−16214
modal anal., formulations for numerical calcs. 78−57767
modeling of a thermal wall panel using phase change materials 80−35758
modular trigger processing system for high energy physics experiments 79−49919
moire, computer generated, for profile testing 80−105689
molecular crystals, group theory anal. of lattice vibrs. 77−80590
molecular crystals, optimum packing in atom-atom approx., algorithm and computer program 80−1960
molecular crystals, thermal motion computer simulation 79−46577
molecular dynamics, dilute gas simulation, pattern recognition algorithm for mol. formation 77−75249
molecular dynamics, high speed computation of correl. functions 77−7648
molecular dynamics computer simulation, multiple time-step methods 78−47220

physics computing continued
molecular dynamics data 77−7647
molecular dynamics simulation of dense gases, test particle motion 78−9930
molecular electronic states, open-shell, general CI program 79−36539
molecular electronic structure, semiempirical CNDO method, calc. progam 78−86782
molecular energy gradient, ab initio HF program 79−89606
molecular fluid, computer simulation of liquid-vapour surface 80−54478
molecular fluid, hard-core triatomic, Monte Carlo simulations 80−38880
molecular force fields and molecular unit definitions database 77−23575
molecular fragments, oriented, use of struct. factors to find origin 77−51266
molecular Hartree-Fock calcs., symmetry adapted Fock matrices construction algorithm 77−23424
molecular inelastic collision cross-sections, exponential distorted wave and effective Hamiltonian 78−37709
molecular internal energy levels, exact counting, backtracking algorithm 78−25407
molecular mechanics computer program MOLMEC, design and performance 78−13410
molecular model building, computer program MMB 80 *(Japanese)* 79−36793
molecular orbital and energy level calc., program of SCF-Xα scattered wave method 78−50453
molecular packing arrangement drawings, plot of packing program POP1 79−94839
molecular rotational spectra, assignment by double reson. technique, computer program 80−32751
molecular spatial structure, spectra interpretation, computer method 79−49962
molecular structure, functional group discovery using central atoms concept 77−34537
molecular structure determination, computer applications 79−50158
molecular systems, electron density, spatial, rel. to conform. props., computer simulation 78−70763
molecular systems including up to 232 orbitals, CNDO calcs., computer program 78−86788
molecular vibration, non-rigid mol., FORTRAN FORMAC products of non-numerical matrices 78−50540
molecule, double min. vibr. potential, FORMAC program 77−23444
molecule electron density distrib. maps, graphical construction from MO LCAO calculated wave functions 77−83480
molecules containing heavy atoms, program for calc. electronic struct. by quasirelativistic method 80−69088
monatomic liquids, short wavelength collective density excitations, computer simulation 79−46540
Monte Carlo anal. of multiple scatt. in fast neutron polarisation expts. 78−13052
Monte Carlo analysis of backscattering and sputtering in vacuum systems 80−235
Monte Carlo computer simulations, of cryst. surfaces and cryst. growth 79−14710
Monte Carlo iterative scheme for adaptive multidimensional integration 78−57762
Monte Carlo radiation transport program for reactor bundle gamma transport and energy deposition analysis 80−22915
Monte Carlo shielding calcs., biased selection of particle flight directions as variance resolution technique 78−29653
Monte Carlo simulation diffusion and evaporation on (100) surface of FCC crystal 78−30836
Monte Carlo study of sputtering 78−95627
MORSE code, neutral particle transport in toroidal plasma 80−33750
Mossbauer effect, computer program 79−56631
moving dislocations, low-temperature statistical charcts. *(Russian)* 79−90654
moving interfacial cracks, dynamic stresses, finite difference approx., iterative process 77−46966
MTF calculation, modified FORTRAN program 78−25807
muffin tin cavity, computer calc. of EM fields 79−9923
multi-configuration Hartree-Fock program 78−50471
multi-layer optical system, reflection and transmission coeffs. calcs., computer program 80−66316
multichannel analyzer data processing by minicomputer systems 79−36497
multichannel focusing collimator, computation of efficiency distrib. functions 77−10519
multichannel spectra, discrimination of counting fluctuations 79−36494
multicomponent alloy, phase diagram calc., computerised data bank 79−1848
multicomponent alloy phase diagrams, calc. methods used at National Physics Laboratory 79−11569
multicomponent alloys, phase diagram calc. program from thermodynamic data 80−3008
multicomponent vapours-condensed phases, equilib., computer modelling 80−44288
multiconfiguration Hartree Fock problem, finite-difference Newton-Raphson soln., He $1s2s\,^1S$ state appl. 77−6663
multiconfigurational Hartree-Fock calcs., radial orbitals anal. approxs. 79−54760
multidimensional body, radiative-convective heating, unsteady temp. calc. method 78−90640
multidimensional neutron transport computation 77−82980
multidipole plasma, probable errors assoc. with minicomputer anal. of Langmuir probe charcts. 77−24193
multifluid Tokamak transport code, two dimens., time evolution 77−58880
multigrid iteration strategy appl. to neutron diffusion eqn. 79−85577
multigroup Monte Carlo computer codes, bounded flux-at-a-point estimators 79−40499
multigroup neutron data production from ENDF/B-IV, survey of codes 77−23170
multigroup neutron slowing down codes, resonance treatment modification 78−82412
multigroup time-dependent delayed γ-spectra from fission and activation of U and Pu 78−13184
multilayer nonabsorbent coating reflectivity computation program 80−28293
multilayer part, discontinuity type defect revealability, comparison of thermal inspection methods, computer simulation 79−79207

physics computing continued
multilayer shells, stress-strain state and stability at high temps. 77−54903
multilayer stack reflectance derivatives, fast computation method 78−46508
multilayer structure devices, nonideal, computation of optical props. 80−5684
multiparameter data acquisition and display program 79−89547
multiphase materials, finite element anal. 77−3717
multiplane hodoscope, D/A system for charged particle track analysis 77−14325
multiple data streams, dynamically configured software system 79−89548
multiplicity measurements, statistical algorithm 78−29721
multiprocessor based data acquisition system, design 79−89556
multislice method for high-energy electron scatt., computing technique 77−84594
multistage multicomponent separation, calc. using thermodynamic props. from SRK/PR eqn. of state 79−34346
multiuser facility, experimental data processing 79−88922
muonic atom energy levels, computer calc. codes 79−31743
mutual diffusion coeffs., calc. by computer for Fe-Mn diffusion pair 79−69299
MWPC, programmable track selector 79−3316
MWPC positron camera, 3-D iterative reconstruction method 78−40302
n-particle relativistic phase space integral, invariant variables, Monte Carlo calc. algorithm 79−9312
n-space dimensions, approx. integration formulae 78−16659
Nairi-K use in multichannel installation for activation meas. 80−23271
NATOF-2D for Na flow transient anal. in LMFBR 80−47633
natural convection heat transfer from horizontal ice cylinder, anal. and obs. 77−27521
Navier Stokes eqns., block iterative finite element algorithms 78−20971
Navier-Stokes eqns., central difference algorithm for high mesh Reynolds nos. 78−46920
Navier-Stokes equation soln. method, finite element anal., 2D unsteady viscous flow 77−89088
Navier-Stokes equations, implicit-explicit soln. method 78−83354
Navier-Stokes equations, laminar flow through cylinder array, finite difference method 78−42585
Navier-Stokes equations for turbulent and transition flows, num. soln. methods 77−54979
Navier-Stokes flow with suspended particles, mathematical modelling, numerical simulation 77−72348
near-field jet entrainment, overlaid viscous/inviscid model, BOAT computational model 80−19457
neutral gas transport in infinite cylindrical plasma, Tokamak model, Monte Carlo algorithm 78−79459
neutron 2-D integral transport eqn. approx. soln. by collision probability methods 77−82984
neutron activation anal., self attenuation of neutrons and gammas, Monte Carlo determ. 79−1980
neutron and gamma transport, direct coupled-ray method for design oriented 3-D anal. 77−83111
neutron balance and flux distrib. calc. for Oklo natural fission reactor *(French)* 80−21767
neutron bomb radiation protection, calc. of rad. penetration in air using ANISN code 80−47743
neutron cross section requirements of CTR program model calcs. 77−23292
neutron cross sections, U and Pu isotopes, ENDF/B-IV library, integral data 77−23200
neutron data for ^{233}U, ^{235}U, ^{239}Pu, and ^{241}Pu, 2200 m/s and 20°C 77−23136
neutron detector efficiency calc. using Monte Carlo computer program 79−63874
neutron differential cross section data generation, appl. to resonances and neutron transport *(German)* 78−82414
neutron diffraction, multiple scatt. correction, Monte Carlo simulation 78−9913
neutron diffraction, pulsed source expts., optimized Monte Carlo simulation 78−9914
neutron diffraction crystallography, constrained refinement of powder data, program EDINP 77−19839
neutron diffractometer, 4-circle, intensities meas. method and computer program for use with twinned and clustered crysts. 78−14247
neutron diffractometer, computer-controlled CAMAC system *(German, English)* 77−19843
neutron diffusion, Galerkin-type spectral synthesis of asymptotic error estimates and convergence 77−82989
neutron diffusion 3-D coarse mesh code, ROCS 77−46252
neutron diffusion eqns., finite difference method approx. by coarse mesh method 77−88185
neutron diffusion eqns., param. adjustment with DELILAH correlation code 79−13413
neutron diffusion equation, three dimens., MULTIPOL code for coarse mesh approx. *(German)* 77−88186
neutron diffusion flux calc., use of Aitken extrapolation method 79−13379
neutron diffusion in 2-D, finite element energy depend. method 77−82987
neutron diffusion multigroup three dimensional calcs. with finite element method *(German)* 77−88189
neutron diffusion scheme, new brief three-dimens. calcs., BWR core 77−42014
neutron diffusion synthetic acceleration methods for diamond differenced discrete ordinates eqns. 77−82983
neutron dose determ. using calculated neutron spectra 77−60263
neutron experiments, Braunschweig accelerator facility, data acquisition and anal. 80−47806
neutron field charact. calc., beyond Fe barrier, effect of scatt. indicatrix approx. and consts. representation 78−17272
neutron flux peaking anal., nuclear fuel bundle ends, program PEAKAN 78−82493
neutron flux spatial approximation using coarse mesh methods QUABOX and CUBBOX, and higher order polynomials *(German)* 77−88192
neutron flux spectral uncertainties in ENDF/B dosimetry cross section file benchmark spectra 77−23306
neutron flux synthesis program KASY, consideration and appl. to reactor design problems 77−88184
physics computing continued
neutron Fourier time-of-flight diffractometer, computer control 77−26918
neutron induced displacement damage anal., program DISPKAN 79−14854
neutron induced gamma-ray production cross sections for reactor materials 77−23067
neutron information at National Neutron Cross-Section Center 78−13403
neutron Monte Carlo elastic angular data, equal probability steps 78−668
neutron multigroup diffusion program EWA-II-30, two dimens., flux distrib. *(Russian)* 77−38318
neutron multigroup discrete ordinates transport eqns., computational efficiency of numerical methods 79−80970
neutron physics continuous energy Monte Carlo code VIM, cross section preparation 77−23166
neutron scatt., automatic data processing *(Russian)* 80−54079
neutron slowing-down problem, comparison of VIM and MC^2-2 codes 77−23167
neutron source, 14 MeV, skyshine anal., Monte-Carlo computer code 78−66429
neutron spectra analysis, informational-computer system *(Russian)* 79−89514
neutron spectra calcs., transmitted, reflected fractions from homogeneous slab shields 77−3067
neutron spectrometer system, data acquisition and anal. 77−26930
neutron spectrum unfolding, optimised smoothing, FERDOR method 80−27860
neutron TOF expts., control and data processing system 78−25385
neutron TOF spectra, multiple scatt. corrections and neutron attenuation 77−26928
neutron transport, 2-D, diffusion synthetic acceleration method 79−22357
neutron transport, anisotropic scattering treatment using improved comput. code *(Japanese)* 80−13526
neutron transport, compatible product ang. quadrature in x-y geom. 77−82981
neutron transport, multi-group two-dimensional eqn., cylindrical geometry, finite element method appl. 78−29522
neutron transport, state-space splitting in Monte Carlo calcs. 77−65264
neutron transport, transverse buckling effects in 2-D calcs. 80−32318
neutron transport, two-dimensional, appl. of constrained finite elements 79−22360
neutron transport, ZEPHYR code for general two-dimensional geoms. 77−65249
neutron transport calcs., user's guide to MARC, PN computer codes 77−3068
neutron transport codes, linear continuous triangular-mesh difference scheme 79−59134
neutron transport eqn., response matrix finite element soln. 80−13527
neutron transport eqn. cylindrical and spherical geometrics, characteristics formulation in CHART program 80−5197
neutron transport in non-multiplying homogeneous slab assembly, time depend. multigroup P1 eqn. soln. 78−17267
neutron transport Monte Carlo simulation for design studies and integral expt. anal. 77−26828
neutron transport one-group criticality in infinite rectangular prism, S_N-method 77−14205
nonuniform neutron transport problems, perturbations estimate, Monte Carlo method 78−17271
neutron transport problems, toroidal geometry 78−22538
neutron transport theory, S_N calcs. using ANL DIF3D diffusion code 80−47526
neutron two-group diffusion calc. by spatial synthesis algorithm 78−13200
neutronic data base generation for transient reactor calcs. 77−83004
Niels Bohr Institute on line data acquisition system 79−89557
NISUS facility, sensitivity anal. for secondary intermediate energy standard neutron field 79−36451
NMR spectra of symmetric spin system, SYMTRY computer program 77−85587
NN interaction with separable pots., two body problem soln., models, computer calcs. *(German)* 77−54156
nodal codes, efficient coarse mesh rebalancing method 77−14211
nodal methods for solving time depend. group diffusion eqns. 77−82988
nodal reactor simulation code, response matrix approach 77−83000
non-crystalline materials, hole struct. of computer models 80−49109
non-ferrous, recycling, system study, computer simulation 78−35278
non-Newtonian fluid, steady flow, numerical modelling 78−51205
non-Newtonian pulsatile laminar pipe flows, multiviscous approx. 77−3871
noncrystalline semiconductors, threshold switching simulation 78−88002
nondestructive materials assay system for LASL's U recovery plant 77−42167
noniterative method for fitting Gaussian to peaks from Ge(Li) and Si detectors 77−57840
nonlinear elastic half-space, dynamic contact stresses due to axisymmetrical projectile impact 78−42573
nonlinear estuarine response to tidal action for potential hydroelectric power generation 77−70692
nonlinear finite element analysis, review of soln. techniques 79−3914
nonlinear hyperbolic conservation laws, finite difference methods 78−49649
nonlinear material and structural behaviors, soln. procedure, theoretical basis for program composite−III 78−30204
nonlinear mechanics, problem oriented software for asymptotic methods *(Ukrainian)* 79−49028
nonlinear modified difference eqns., ALTRAN computer programs 79−9092
nonlinear optics, digital data acquisition and on-line processing at Moscow State University 78−46709
nonlinear shell analysis via mixed isoparametric elements 78−1566
nonlinear wave propagation, spectral and pseudospectral methods, turbulent sound wave appl. 77−5672
nonlinear wave-particle interaction in magnetosonic mode, pure sinusoidal wave model 78−26320
nonperiodic objects, reconstruction from electron micrographs using correlation methods 80−86527
nonrelativistic ϕ^3 field theory in two spatial dimens., automation, FORTRAN system 78−8502

physics computing continued
nonrelativistic atomic orbital calc. program using Slater functions 79−49930
nonrelativistic atomic states matrix element generator program 79−54758
nonrelativistic bremsstrahlung, program determ. of ang. distrib., extension to high freq. 79−64162
nonsteady heat conduction in solid cylinder, analogue computer soln. *(Rumanian)* 77−68362
normal coordinate calcs., computer program for Z-matrix determ. 80−23388
normal mode calcs. of crystals and molecules, coordinates and force matrices generation 78−91393
normal mode calcs. of molecules, crystal phonon dispersion relns. and structure factors for neutron inelast. scatt. 78−91394
nozzle, heat flux determ. 77−42894
nozzle flow, steady state arcs 78−32664
NRU, NRX reactors, homogeneous cell parameters for 2-D reactor codes by axial averaging of 3rd parameter 79−54577
Nuclear Code Centre, Japan, history, activities *(Japanese)* 79−13618
nuclear code ISOBAR-EVA modification for prompt-γ $^{32}S+\pi^-$ reaction 77−18616
nuclear criticality safety, misleading assumption in array analysis 79−63772
nuclear criticality safety, uncertainties in K-effective calcs. 79−63771
nuclear cross section tabular file generation, utilisation techniques 77−23397
nuclear data anal. algorithm, NICC program, appl. to ^{139}La internal conversion 77−46137
nuclear data files of UK Chemical Committee, summary of data, available in ENDF/B format 78−82425
Nuclear Data Sheets, computer-readable form 77−22828
nuclear decay data, ENDF/B file, applications 77−22978
nuclear decay scheme construction from gamma transitions and coincidences, SMUDLA 80−83063
nuclear elastic scatt. with optical potential, complex angular momentum methods, poles and zeros of S-matrix, REGGE 80−47445
nuclear energy level lifetime measurement using on-line computer and registration time shift compensation 80−68577
nuclear facilities, off-site radiological impact assessment real-time computer program CEPADAS 80−95475
nuclear fast reactor integral expt. anal., appl. of uncertainty and sensitivity theory 78−50239
nuclear fuel, quantitative metallographic anal., computer program, QMA 79−15951
nuclear fuel burnup computer codes, physical simplifications 77−6483
nuclear fuel sheath deform. following fuel power transients, simulation 78−33258
nuclear interactions around 20 TeV, characts., comparison with Monte Carlo simulation 79−58991
nuclear K-X-ray satellites, Z=50-83 cascade anal. algorithm 80−42984
nuclear lab. computing facilities 79−89527
nuclear liquid drop model deformation energy calculation program 79−13197
nuclear materials safeguarding, statistical anal. of materials accountability, computer simulation 80−73933
nuclear optical model parameter searches, minimisation procedures, use of derivatives 77−10379
nuclear physics, impact of changing computer technology 79−89538
nuclear physics, impact of changing computer technology 79−89539
nuclear physics course, computer simulation techniques 80−36823
nuclear physics experiments, displays for data output 78−9046
nuclear physics expts., versatile data handling system based on PDP 11/03 microcomputers 79−76319
nuclear physics GSI data acquisition system 79−89533
nuclear physics high-performance data-acquisition and data-analysis computer system 79−93899
nuclear plant airborne effluent variable-trajectory puff advection model modifications 78−94149
nuclear preequilibrium decay, microscopic exciton model 77−41935
nuclear radiation detection lab., desk top calculators 80−36821
nuclear reactor, fluid-structure system dynamics, reactor safety anal., computational algorithms 77−71669
nuclear reactor, PWR, KWU 1300 MWe facility, neutron flux computer calcs., radiation damage 77−34370
nuclear reactor, transient overpower, comparison of EPIC and PLUTO fuel-coolant interaction codes 78−8920
nuclear reactor bare charge expts., parametric REXCO H calcs. 77−3190
nuclear reactor calcs., multidimensional, interface current techniques 77−88193
nuclear reactor core pin power distribution det. based on nodal coarse mesh calcs. 77−88195
nuclear reactor experiments, control and data processing by Siemens-301 computer *(German)* 77−83032
nuclear reactor fluid dynamics, prospects for accurate computer simulation 77−79422
nuclear reactor fuel pin behaviour, computer code FRUMP, stress, strain, temp. distribs., displacements 77−14235
nuclear reactor kinetics, computational methods and computer codes for space-dependent transient analysis 80−52716
nuclear reactor kinetics eqns., piecewise polynomial approx. 78−4981
nuclear reactor oxide fuel transient gas release and swelling, generalised parametric model 77−83039
nuclear reactor thermal-hydraulic anal., COBRA IIIP/MIT code 77−79423
nuclear reactor thermal-hydraulic calcs., effect of variable thermal conductivity 77−3084
nuclear reactor with dissociating coolant, transient process dynamics *(Russian)* 77−42050
nuclear reactors, computer program for T balancing *(German)* 79−3204
nuclear rotational levels, Coriolis effect 77−61341
nuclear standard cross sections, uncertainties and correls. in evaluated data sets 77−23196
nuclear structure calcs., convergent algorithm, gradient method appl. 78−12987
nucleation in finite systems, theory and computer simulation 80−26038
nucleation models, 2D, computer simulation of cryst. growth 79−73116
nucleation of incoherent precipitates, irrad. effects 79−8303
nucleation processes, computer simulation, single spin flip kinetic Ising model 77−62613
physics computing continued
null event method in simulation, ion collision appl. 78−90262
numerical analysis and computational methods in physics, computer appls. 80−62456
numerical Bessel transformation calc. program 79−49016
numerical generation of boundary fitted curvilinear coord. systems on fields containing 2-D bodies, TOMCAT code 77−64941
numerical modelling of fatigue, crack, creep and corrosion test results, review 78−30243
on-line calculation of experimental neutron spectra uncertainties 79−59298
one-dimensional chain, thermal fluctuation induced rupture, computer simulation 78−91378
one-dimensional crystal subjected to deform., static and dynamic equilib. 79−28037
one-dimensional polycrystalline structure, computer simulation *(German)* 77−68935
online filtering 79−89574
open electron optical system with rotational symmetry, Fourier-Bessel series soln. for pot. and field intensity 79−76570
open flow cross sections, local velocity variations *(Bulgarian)* 78−18268
optical axisymmetric aspheric figuring, computationally directed 79−23105
optical coatings, absorptive, at normal incidence, program for TI-59 calculator 80−84793
optical coatings, algorithms for determ. of reflectance and transmittance 79−98271
optical constants and thickness of films, automatic evaluation *(French)* 77−13808
optical crystallography computer anal. of spindle stage data 78−85702
optical design techniques, for desk and pocket calculators 78−71181
optical dielectric perturbed waveguide approximate analysis *(Japanese)* 78−42423
optical fibre, graded-core, numerical description of propag. characts. 77−23758
optical fibre preform, refractive index profile and cross-sectional geometry meas. method 80−91893
optical filters, multilayer, thin films, automatic design method 77−58449
optical image quality evaluation from aspheric replica master data, using ACCOS V SPLINE program 78−66964
optical interference coatings, synthesis, nonlocal computer method 77−50761
optical interference fringe location by digital scanning methods 80−13128
optical multilayer filters, non normal incidence, optical monitoring, allowable tolerances *(French)* 80−87526
optical multilayer synthesis program, Fourier transform model 79−7196
optical recording, ablative 80−91752
optical resonator, annular, adaptive mirror effects on performance 80−58596
optical signal receivers, optimal and nonoptimal, logical structs. efficiency comparison, simulation *(Russian)* 78−71041
optical system, computer optimisation program 77−54766
optical system design, k-stage objectives corrected to infinity *(Hungarian)* 79−81502
optical system design 79−94322
optical system stray light suppression, optical design, computer analysis 78−59113
optical system stray radiation analysis using first-order deterministic APART program 78−59116
optical system stray radiation rejection capabilities, GUERAP II program analysis 78−59115
optical thin film, Smith chart and charact. matrix for reflectance computation 79−45904
optical transform masks, manufacture, model drawing programs 79−40334
optics, saturable slab, steady state theory 77−68242
optimal design of dynamically loaded continuous structs. 78−38185
optimal nodal point distribution for improved accuracy in computational fluid dynamics 80−48670
orbital pairs, transformation into localised pairs, use of FORTRAN for angle selection 80−27922
organic π-radicals, open shell systems, spin density calc., program for semiempirical calc. *(Rumanian)* 79−72241
organic compound structural elucidation, CHEMICS-F 79−18310
organic scintillator efficiency using Monte Carlo code 80−889
orientation distribution determ. from incomplete pole figures, computer program 78−64804
ORIGEN2 point-depletion and decay computer code 80−99248
oscillation diffraction data, processing, for very large unit cells with automatic convolution technique and profile fitting 79−50929
Ostwald ripening, effect of precipitate vol. fraction 80−40356
OTF calculation using gaussian quadrature, rel. to lens system design 78−90383
oxidation kinetics, C by CO_2 in Fe-C melts *(Russian)* 80−40680
oxides, fluorite and ReO_3, n-beam struct. images, expt. observations and computer calc. 78−38593
oxides, spinel struct., impurity ion pairs, local struct. characts. 78−2146
p-convergent finite element approx. in fracture mechanics 78−38252
pair distribution functions, non-cryst. material, neutron diffr. data parameter calc. program 79−14652
pair distribution functions, non-cryst. materials, neutron diffr. data calc. program 79−14653
PALLAS discrete ordinates transport code, improvement 79−76052
PALLAS-2DCY, anal. of ^{60}Co γ-ray scatt. in air 80−32525
parabolic partial differential eqns., sensitivity anal., appl. to reaction and diffusion processes 79−49178
parametric biostimulation, mag. field calcs. 80−36054
partial vapour pressure calculation, phase comp. of Nb oxides on heating 2000-4000K 80−21267
partial-wave Schrodinger differential and integral eqns., comparison of numerical solns. 78−16671
particle and nuclear physics, conference, Santa Fe, NM, USA (1979) 79−88779
particle and pore size distrib. curves quantitative evaluation, Fortran program *(Czech)* 78−80795
particle beam-plasma interaction, ion-acoustic turbulence effects 78−91121
particle counting by size, optical-digital training method 77−71305
particle detectors, combinatorial logic trigger system 77−54465
particle dispersion coarsening, computer simulations 80−30289

physics computing continued
particle dynamics computer modelling, alternating phase focusing LINAC *(Russian)* 80−23234
particle profile charact. rel. to profile Fourier coeff. 78−11142
particle scattering amplitude, analytic extrapolations, EMZERO 80−47221
particle simulation models, three dimens., for cylindrical and toroidal plasmas 78−1884
particle solids, computer generation 78−26026
particle tracks, time digitiser in CAMAC format 80−14062
particle tracks momentum determ. by iterative tracking 78−70723
particle-particle correlation experiment, on-line four parameter anal. system *(Chinese)* 80−42910
Patterson functions, identification of double peaks, P$\bar{1}$ space group 79−32859
Patterson maxima shape calc., program in AKIT 78−5987
PBLG solns., dielec. meas., using pseudorandom noise dielectric spectrometer 78−15084
PBR, fast power excursions, DYN and COSTANZA programs 78−50241
PDQ-8 neutron diffusion-depletion program 79−71876
PEP storage ring vac. system, synchrotron-radiation-induced heating effects, Monte Carlo based computer code 79−81107
percolation and cluster distrib., cluster multiple labelling technique and crit. conc. algorithm 77−2622
percolation phenomena, simple cubic lattice, Monte Carlo study, cluster shapes and sizes 77−17919
percolation threshold, computer generated pictures of infinite clusters 78−56117
perturbation stable cell comparison technique 80−49133
PEST, plasma instability, axisymmetric, in non-circular Tokamak 80−87877
phase diagram, of metal-semimetal alloy, from thermodynamic functions 80−40329
phase diagrams, computer generated for ethylene and propylene 78−83928
phase diagrams, Conf., Gaithersburg, USA, (Jan. 1977) 79−4946
phase diagrams and synthesis of soln. thermodynamics, computer anal. 78−30739
phase diagrams of Fe-Cu-Mn(Ni), Fe-Cr-Ni, computer calc. synthesis 79−11563
phase diagrams of ionic systems, calc. and computer storage 79−10920
phase equilibria and characterisation, of Au-Cu-Ni system, using computer methods 79−11561
phase space integral, n-particle, relativistic, Monte Carlo integration program 78−33001
phosphor, rare earth activators, sensitized luminesc., computer simulation 78−6723
photo-Compton deposition profiles, anal. approach, QUICKE4 code 77−20948
photoelastic fringe pattern analyzer, computer aided 80−38359
photoelectron spectra of cryst. solids, numerical integration within linear analytic approx. 78−60545
photoemission spectra calculation program 80−55256
photographic gamma measurement, algorithms 77−34042
photographic materials, MTF automatic evaluation 80−95170
photoionisation TEA CO_2 laser *(Russian)* 80−83589
photon correl. laser anemometry, on-line data reduction system 79−60080
photon scattering angles selection in MORSE, rejection technique 78−4571
photonuclear reactions, on-line acquisition of N-fold coincidences 77−79527
physical optics farfield inverse scatt., mathematical inversion technique for nondestructive eval. 80−69580
piezoelectric thickness vibrator, digital computer simulation 77−88998
PIGMI, accelerator control system 79−45475
pion-nucleus scatt. momentum space optical potl. code, PIPIT 77−6442
PIPE, barytes concrete, gamma ray buildup factors 80−27823
PIXE data handling, statistical techniques 77−52715
planar channelling effects for relativistic protons and π^- mesons, deflection effects 79−77656
planar positron cameras, 3-D reconstruction using Fourier deconvolution of generalised tomograms 78−40295
plane coalescence, at grain boundaries 80−70221
plane triangular element, stress-strain finite dynamic element, FORTRAN IV program 80−53
plane wave diffraction by circular transmission grating: finite-difference approach 79−68352
plasma, chemical reactions, rate coeffs., database creation, DATSTOR 80−48846
plasma, chemical species, number density variation with time, numerical model, PLASKEM 80−48845
plasma, collisionless drift modes, graphical method for finding complex roots of nonlinear eqn. 80−33762
plasma, computer simulation, statistical mechs., for teachers 78−62014
plasma, cross-field electron heat transport due to high frequency electrostatic waves, simulation 80−53932
plasma, laser produced, ionisation process computer simulation code, atomic transition processes 80−28764
plasma, local spectroscopy methods, rational algorithm selection to treat expt. data 78−51346
plasma, neutral atom transport, computer code SPUDNUT 80−48962
plasma, neutral beam injection heating, computer simulation, Monte Carlo method 77−68859
plasma, one-dimensional, electrostatic simulation code 77−58888
plasma, population densities of excited states of H-like ions 77−39402
plasma, rapidly changing, numerical integration of ionisation rate eqns. 78−55734
plasma, simulation anomalous transport processes, G1M/HYBRID quasi-equilib. MHD code 80−64689
plasma, submillimetre diagnostics, active, of Ar arc, data numerical anal. 80−48979
plasma afterglows, simulation by computer code GLOWCODE 77−39480
plasma and astrophysics computing conference 77−29639
plasma confinement, boundary condition for computational MHD 78−1811
plasma confinement mag. field, computer simulation of finite linear multipole with closed ends 77−35382
physics computing continued
plasma containment vessels, backscatt. and sputtering from pocket and finned structs. 79−14558
plasma diagnostics, Abel inversion program for emissivity, in FORTRAN, book contrib. 77−51242
plasma diffusion rates, automatic computation, stellar interiors appl. 78−57434
plasma diodes, relativistic, time depend. ion and pinched electron flow 77−89330
plasma drifting, cold or hot, radiation potential of immersed point antenna, DRFT computation 80−14906
plasma equilibrium in toroid, computational method, book 79−14601
plasma flow calcs. 77−76045
plasma hybrid simulations of quasineutral phenomena 78−67403
plasma instability, axisymmetric, in non-circular Tokamak 80−87877
plasma ionisation and recombination processes simulation 79−14604
plasma MHD, nonlinear time-dependent hydromagnetic model, spatial and temporal finite-difference techniques 80−59192
plasma MHD, stability code, ERATO, convergence of solns. 80−83906
plasma MHD, toroidal axisymmetric config., vacuum potential energy change, spectral codes 80−87869
plasma microinstabilities, low frequency, simulation model 78−38525
plasma mirror machines, computer simulation of field reversal 78−26316
plasma nonlinear wave interactions, symbolic computation code MACSYMA 77−27660
plasma of given chemical content, chemical reactions, computer generation, REACS 80−48844
plasma probe, spherical, slightly ionised continuum, current-pot. curves 77−72494
plasma recycling at surfaces using self-consistent model 77−35355
plasma RF confinement near critical density, computer simulation 77−72492
plasma RF confinement simulation near critical density 77−24178
plasma simulation, GUIDON computer code 77−27713
plasma simulation, magnetostatic code, current penetration and microinstabilities 78−38526
plasma simulation, magnetostatic particle code 77−27714
plasma simulation, splines and higher order interpolations 79−64902
plasma simulation spatial grid effects reduction using higher order multipoles and splines 78−91148
plasma transport, anomalous, electron temp. gradient instability 80−75034
plasma turbulence development and decay mechanisms, wave interactions, analogue simulation *(Russian)* 79−7462
plasma turbulence simulation, phase space granulation due to mode-mode coupling 80−38651
plasma waves, phase, ray and group vel. surfaces 77−65852
plasma-pinch configurations, one-dimens. equilibrium-diffusion code 78−75401
PLASTEF code, numerical simulation of thermoelastoplastic behaviour using finite element method 78−90731
plastic buckling of structures 78−63342
plastic flash chambers, particle identification 79−59301
plastic instability during tensile deform., numerical calc. 78−30203
plastic props. of ferrous and nonferrous materials, stress-strain relations, use of computer program 77−1865
plastic scintillator, neutral radiation incident spectrum determ. 77−54398
plastic zone ahead of crack, development under creep conditions, computer simulation 78−34091
plate, rectangular, variable thickness, stability and vibr. anal., finite element method 77−54918
plate structures, two-dimensional, stress intensity factors calc. *(Japanese)* 78−51123
plates on elastic foundation, simplified finite element soln. 78−26041
PLOMAC, plot program for 80−19669
point defect, elastic strain energy, stable configuration determ., computer calc. 78−30663
point defects short term annealing, simulation, in α-Fe 80−54282
point group symmetry, derivation and recognition schemes, computer assisted learning programmes 77−29973
point to line data reduction, computer links and hardware processor test 79−45613
Poisson's eqn. in 3-d, direct solns. using algorithms 78−20954
Poisson's equation for isolated source distribs., computer soln. using finite mesh, Green's function 78−35
Poisson equation, accurate soln. by expansion in Chebyshev polynomials 79−49023
POL, data analysing interactive system 79−31347
polar semiconductors, hot exciton scatt. accompanied by transitions to excited states, phonon interactions 80−44516
polarisation meas. with high press. He scintillation counter 80−14061
polarised laser beam propag., numerical soln. of spinor Helmholtz eqn. 79−72479
pole pieces with cavities, correction effect modelling *(Czech)* 79−45879
pollutant release assessment, JEREMIAH computational system environmental transport and dose calcs. 78−94150
pollutants releases in shallow sea, numerical simulation 77−78234
polyamide resin, computer approx. of families of curves of physically nonlinear creep 77−66684
polycrystal cold neutron incoherent inelastic scatt., computation of phonon spectrum 78−34572
polycrystalline film couples, diffusion during recrystn., numerical simulation 79−77844
polyethylene, crystalline, twist disclination formation and longitudinal motion of defects 80−19810
polyethylene, high density, creep, computer program calc. *(German)* 78−60715
polyethylene, hot-stretched, small angle X-ray scatt., computer anal. 79−14699
polyethylene crystal, computer simulation of {110} twin boundary 78−30646
polymer, dielectric relaxation time distrib. function determ. 77−73111
polymer chain, of bistable oscillators, Brownian dynamics of transitions 78−86983
polymer chain dynamics, in soln., computer simulation 78−83718
polymer crystal, conformational energy calcs., appl. to defect props. 80−54154
polymer dynamics simulation, general theory 78−91210
polymer dynamics simulation, relax. rates and dynamic viscosity 78−91211

physics computing continued
polymer films, vertical development, from gas phase, computer simulation *(German)* 77−27839
polymer foil, electron irradiated, charge dynamics, computer simulation 79−82915
polymer impregnated concrete, computer simulation 78−31375
polymer melt, viscoelastic, 2-dimens. nonisothermal processing between calender rolls, mathematical model 79−68670
polymer melts, crystallisation models, Avrami eqn. extension 80−19723
polymer relaxation, computer used to calculate mech. charact. 77−52388
polymer solns., phase diagrams, pulse-induced critical scatt. 79−1490
polymer solution, concentrated, computer-aided simulation of individual chain conforms. *(Russian)* 77−42454
polymer solution, configurational props. of model lattice chains under varying solvent conditions 77−89364
polymer solution, simulation of macromol. dynamics, Monte-Carlo method, conc. depend. *(Polish)* 78−51404
polymeric networks, macromol. chain conforms., computer simulation, network form. process *(Russian)* 78−70994
polymers, adsorbed molecules, configurational behaviour, computerised dynamic display 79−874
polymers, breaking down of anharmonic chain, computer calc. 80−106410
polymers, glassy, craze surface displacements, model 80−93651
polymers, linear and ring, intrinsic viscosities, perturbation calc. 79−55914
polynuclear clusters, programs for calc. electronic struct. by Mulliken-Wolfsberg-Helmholtz method 80−69288
positive and negative ion beams nonlinear interaction, math. simulation and expt. 77−595
POSITRON, evaluating system for positron annihilation R-40 computer meas. 79−78787
positron annihilation ang. correl. curves anal. using ANNIH program 80−37709
positron annihilation decay consts., temp., elec., and mag. field depend., computer anal. 78−78809
positron lifetime spectra, anal. using DBLCON version of POSITRONFIT with nonGaussian prompt 78−33359
positron lifetime spectra, analysis of the computer program 78−88379
positron scattering by atoms, computer simulations, review 77−79692
potential flow about bodies of revolution, general analytic method 78−1629
potential flow problems, partition technique integral eqn. method 78−49652
potential-pH diagram, improved algorithms for computer generation, max. constriction method 80−26019
Pourbaix diagrams, calc. using modified linear programming technique 79−10919
powder, fine particle shape characterisation by decision matrix design and cybernetic mode operation 78−11143
powder, particle size analysis by chord method, digital computer calc. 77−4890
powder least-squares program, POWLS 80−1892
powder reflections, computer program for determining multiplicities, correction for $\bar{3}$1m Laue symmetry 79−10759
powder X-ray diffraction data, cubic lattice parameter, Fortran program 77−11440
powders, semiconducting, exam. of freeze drying rate in cryochemical prep. 78−52706
power plant effluents, gaseous, AEOLUS code for dispersion during normal, sea-breeze, and accident conditions 78−11993
power series expansions by computer 79−84679
preequilibrium spectrum analysis, computer code ASPIS 79−68174
press. by Monte Carlo computer simulation 78−4564
Preston-Prausnitz method and program for solubility calc. of solidified hydrocarbons in liq. N_2 78−26686
Princeton cyclotron data acquisition system 79−89528
principal stress separation using a computer 79−94496
prism design, Fresnel rhomb, TI 58/59 program 79−32040
prism dimensional design, rhombic *(Czech)* 80−53431
prismatic plate assemblies, buckling and vibr. anal. with compact computer program 78−90737
probe data reduction in axially symmetric expts. 78−89464
product operators, closed basic diagram generation program 80−8817
programmable calculators appls. in scientific calcs. 77−64940
programs for high-school expts. 78−86094
projection of angular momentum 77−5689
prompt fission neutron logging technique, computer modelling 79−53566
proportional counter data acquisition system 80−42913
protein molecule, simulation of single mol. images combining computer and electron micrograph analysis 78−37781
proton beam, intense, space charge neutral, trapping in mag. mirror, simulation 78−9825
proton channelling simulation, for diamond 80−79849
proton recoil data, frequency filtering 78−46240
proton rings, mag. compression, computer simulation 78−22548
proton rings in mag. mirrors, computer simulation 78−67405
protostar formation, physical and numerical problems 77−29800
prototype autoresonant, accelerator, computer system, data acquisition and processing 80−99433
pulse height analysis programs for high event rates, organisation 77−407
pulse pile-up, role of waveform 77−88358
pulse pile-up in detection systems with rapidly varying counting rates 77−88359
pulsed field-gradient spin echo diffusion data, interpretation using FORTRAN program 79−65758
pulsed neutron source on multiplying media, anal. and interpretation of experimental data *(Rumanian)* 78−46203
pulseless corona, space-charge limited current flow, computer solutions of Poisson and current continuity equations 79−86627
PVC, amorphous, orientation study by creep thermomechanical method, computer anal. 78−75561
PVC, creep meas., use of computer in rational determination of material values *(German)* 78−31474
PWR, improved water density feedback model for neutron diffusion calc. 79−67890
PWR, Xe-induced spatial flux transient, anal. and control, parameter identification 80−18441
pyridine, proton-coupled ^{13}C J NMR, strong coupling 78−17691
pyrometry, photoelec., radiance temp. direct calc. 80−73367
Q data acquisition system for PDP 11 79−89545
physics computing continued
Q system: an experiment in software standardization for data acquisition 79−89549
QAL: a language for nuclear physics data acquisition 79−89552
QAL, data acquisition language 79−89551
QCD jets, algorithm for parton spectra 78−89680
QCD jets, algorithm to determ. multiparton distribs. 79−45064
QCD jets, resolution algorithm 79−63455
QED, automatic generation of Feynman graphs 77−6065
quadrilateral shell element utilising isoparametric principles 78−34012
quadrupole distorted NMR powder patterns, simulation, Fortran program 77−77105
quantal Coulomb excitation calcs., error anal. of code AROSA 77−2550
quantitative image analysis, appls. using sequential transforms. 80−23627
quantum correlation calculation programs 79−30275
quantum liquids and crystals, computer modelling 80−54472
quantum measurements, interactive computer program, for teaching 78−41113
quantum mechanical measurements, simulation using programmable pocket calculator 80−41982
quantum mechanics CAI via graphics 77−67164
quantum mechanics in films and graphical representations *(German)* 77−49534
quartz, surface structural modification by high temp. gases, computer simulation of RHEED patterns *(German)* 79−95251
quartz filter resonators with energy trapping, optimum design 78−32663
quasibound state wavefunctions for particles inside Coulomb barrier 77−2914
quenching, temp. field, exact calc. in large pieces, computer use 77−70086
R-matrix anal. of light element standards 77−23041
Racah and Clebsch-Gordan coefficient calculation program ANGMOM 78−89359
radial coupled equation solution, fast numerical method, applic. to collision processes 77−14545
radial wave equation, particle in asymptotically Coulomb pot., eigenvalues and eigenfunctions calcs. 77−57214
radiation damage computer simulation system, WINERY 78−30675
radiation damage in crystals, computer modelling methods 77−7760
radiation damage in fusion reactors, computer expts. on Nb 80−13839
radiation damage produced by energetic heavy particles, computer simulation *(Japanese)* 80−29094
radiation damage simulation in amorphous Fe 80−34045
radiation detector fluctuations, computer simulation 77−3218
radiation dosimetry, standardised radioactive decay data sets 80−13945
radiation induced defect migration, computer simulation by mol. dynamics technique 77−19982
radiation induced low-energy collision cascades in Cu, computer simulation 78−87705
radiation induced solute segregation, kinetic model, GEAR package of subroutines 78−30673
radiation monitoring, digital data collection and display 79−59278
radiation monitoring, distributed processor-based system for large scale power plant monitoring 79−59280
radiation shielding, in 3-D direct-coupled-ray method 78−21785
radiation shielding, Monte Carlo calcs., event-value path-length biasing 77−38421
radiation shielding benchmark experiments and sensitivity studies, neutron plus gamma library 77−26947
Radiation Shielding Information Centre, available computer codes and data 77−65343
Radiation Shielding Information Centre, data activities 77−23307
radiation spectra unfolding code COOLC 78−5090
radiation transport, ang. biasing of collision process in multigroup calcs. using Monte Carlo method 78−4975
radiation transport in Earth for neutron and gamma-ray point sources above an air-ground interface 80−32526
radiative, diffusive MHD eqns., ALFVEN two-dimens. code based on SHASTA 79−32684
radiative decay curve anal., computer applications *(Hungarian)* 79−45617
radiative heat exchange, calculation methods, for inhomogeneous absorbing and dispersive media 79−81698
radioactive atoms, counting small samples 78−17535
radioactive decay, Bateman equations solution using transition matrix approach 77−57632
radioactive isotopes, probability determ. of number of atoms at end of production 79−63637
radioactive material release to atmosphere, calc. of consequences with TIRION-4 code 79−29494
radioactive nuclide decay data for reactor calcs., activation products and related isotopes 78−82426
radioactive plume in atmosphere, depletion calc., and exposure from deposited activity 79−66561
radioactive waste disposal safety criteria, ORIGEN2 point-depletion and decay computer code 80−99248
radioactive waste geologic repositories, computer anal. of long-term radiation hazards 80−18483
radioactivity, decay product radioactive accumulation, FORTRAN program 80−68611
radioactivity meas., statistical distribs. accumulation in real time 78−94178
radiographs processing 80−3259
radioisotope transport in terrestrial food chains, dynamic modelling using RAGTIME code 80−104776
radionuclide decay, computer simulation, levels, transitions, internal conversion 80−63136
radionuclide disposal, GARD computer program for geochemical assessment 79−31068
RAGTIME code for dynamic modelling of radioisotope transport in terrestrial food chains 80−104776
Ramsauer chamber, positron scatt., optimisation study using Monte Carlo method 78−70706
random distrib. of voids, computer simulation 79−90723
random packing of spheres, computer simulation 80−77705
random sampling of scattering angle in neutron transport 79−85574
rare earth chalcogenides, compositions, props., computer prediction 79−42429
rare earth compounds, binary, regression eqns., for calc. props. from electron struct. 80−39498

physics computing continued
ray trace program for TI-59 calculator with PC100A printer 79−89985
ray tracing program, CUPID, for continuously varying refracting media 80−18990
ray tracing through tilted and decentred optical surfaces, computer program 80−33120
RCPL1 program, calc. of Doppler broadened neutron resonance cross-sections 79−67810
reactance matrices, fine struct. cross sections, JAJOMPRE program 78−90312
reactant distribution functions in fusion reactors, fast computing method using Legendre polynomials expansion 78−78491
reactor analysis, 3-D integral transport code SHETAN 80−63238
reactor analysis neutron thermalisation, THERMOS spectrum code, accurate reduced mesh model 80−57829
reactor core design, utility use and requirements 78−17299
reactor criticality calculations, Monte Carlo MONK code 77−14226
reactor depletion chain eqns., FORTRAN program for solns. using analytical methods 78−74423
reactor dynamics, finite element analysis for two dimensional eqn. *(German)* 77−88190
reactor fuel element modelling, LMFBR, LWR 78−86617
reactor fuel pin imagery, computer enhancement and mensuration 78−37395
reactor fuel pin performance anal., COMETHE III-K code 80−13605
reactor hypothetical core disruptive accident anal., hydrodynamic/neutronic coupled code FX2-POOL 77−23219
reactor kinetics, smoothing and extrapolation techniques 77−83002
reactor real time offsite dose calc. 79−45429
real-time prediction of calorimeter equilibrium 79−75532
reciprocal lattice plane fundamental data, extinction problems in automatic calc. *(Chinese)* 79−73072
rectangular laminated plate, free vibrs., freq. and shape determ., complex boundary conditions 80−79203
rectangular orthotropic plates with nonlinear stress-strain relns., large deflections 78−26040
recurrence formulas for phases and amplitudes of free wave spherical functions 78−56
recursive method for partition function calc., average energy calc., APL program 79−9050
REDUCE, Feynman diagrams, dimensionally regularised, symbolic evaluation, quantum gravity application 80−13259
reduced SU(3) matrix element calculation program 78−89627
refractive index, Hartmann interpolation equation solves using TI-59 calculator 79−98451
refractive index data interpretation, collection of program library 80−55056
refractories, strength and thermal properties, automated test system 80−100986
reinforced concrete structs., initial stress approach to nonlinear dynamic anal. 77−83036
relativistic electron beam accelerator, FX-75, 1-D coaxial transmission line model, FXPULSE program 78−58506
relativistic electron beams simulation 79−26789
relaxation data anal., superimposed exponentially decaying signals, computer technique 78−23360
resistive MHD instabilities, diffuse pinch configs., numerical study 77−58853
resonance analysis of neutron transmission data, least square fitting program REFIT 80−22840
resonance integral calc. in reactor cell lattice, Monte Carlo code, RISO 77−3088
resonant particle effects in Langmuir and whistler waves, long-time-scale plasma simulation 78−42796
reversed field pinch, burn stability 78−58467
reversed-field pinch burn dynamics, global computer code 78−63579
RFIT, data evaluation program, theoretical background 78−29562
rheological props., rotational viscometer use in calc., programme *(German)* 77−60026
Rietveld neutron profile refinement, interactive computer system, POWDER 80−1900
rod impact, numerical soln. using Volterra integral eqns. 77−68437
rolling, torque calc., mechanical model 79−20078
rolling coin, computer anal. of motion *(Hungarian)* 78−73837
rolling contact with dry friction, Duvorol computer code 79−90194
rolling of complex metal sections, unified anal. function of surface of strain focus *(Russian)* 80−21017
rolling texture formation, computer simulation in HCP and orthorhombic metals 80−3095
room resonance, computer-aided anal. 78−87205
rotated remelted ingots, macrosegregation 79−52196
rotating disc problem, Taylor coefficients, computational methods 80−106802
rotating two-ring electrode, constant current effects, digital simulation *(French)* 78−7212
rough sphere fluid, computer simulations 79−99041
rough surfaces computer simulation of contact 79−19470
round notch tension test, computer simulation 79−24705
Runge-Kutta method for track fitting in mag. field 79−31782
SAS-3D analysis of natural-convection boiling behavior in the sodium boiling test facility 80−47635
SAS-3D evaluation of LMFBR boiling of decay-heat levels in FFTF 80−47634
satellite photogrammetry, dynamical constraints 78−15943
scalar interactions, microscopic, histogram collection by FORTRAN program 78−34958
SCAM, Stirling cycle anal. model of compressible flow 80−35717
scattering amplitudes, unitarity condition homogeneous linear inequalities, calc. program 79−85013
scattering cross sections and transport props. 78−78767
Schmid equal factor, automatic curve plotting *(French)* 79−46507
Schrodinger eqn., linear plus Coulomb pot., energy levels 78−4521
Schrodinger eqn. eigenvalue and eigenfunction computation by stepwise potential function approximation 77−17853
Schrodinger eqn. with double-minimum potential, numerical integration 78−58573
Schrodinger equation, nonlinear time-depend., one dimens. wave packet soln., Fortran prog. 77−9897
Schrodinger equation, solution by hand-held calculator 80−52052
Schrodinger equation, two dimens., finite element package MANFEP 78−36870
physics computing continued
Schrodinger integral equation, soln. using El-Gendi approx. method 78−77749
scintillation counter optical system evaluation 77−34523
scintillation quenching curves, solns. by second-order polynomial regression 77−3220
screw dislocation motion in BCC metal, under shear and uniaxial stress, computer simulation 77−4102
sea surface waves diffraction and refraction, using finite and infinite elements, structures loading at sea calc. 77−81910
secondary electron emission characts. calc. by Monte Carlo methods 79−28868
segment description, of unique set of reflections to data collection and data reduction 80−1881
segmented calorimeter, high energy performance, Monte Carlo simulation 80−58029
selective solar absorbers, reflectance calcs. for inhomogeneous surfaces 80−12029
self-avoiding random walks, exact enumeration method and Monte Carlo sampling 79−67228
self-diffusion, correlated, via randomly migrating vacancies, in cubic crysts., computer simulation 78−2283
self-diffusion, flux of vacancies and atoms, computer simulation 79−73332
self-diffusion in cubic crystals, random motion of vacancies, correl. factor and NMR diffusion parameters 78−2284
self-replicating macromolecules, Monte Carlo computer models 78−46473
semi-empirical SCF-LCAO calc. including energy minimisation 77−23428
semiconductor, deep levels, review 80−103640
semiconductor, deep-level centre discrimination from capacitance versus time transients 78−10395
semiconductor, inductively heated, computer simulation of temperature and EM fields 78−55961
semiconductor crystal growth, Czochralski bulk flow, digital simulation 78−31320
semiconductor second breakdown electro-thermal model, computer program 77−24561
sensitivity analysis, nonlinear, of multiparameter model systems 78−28931
shale oil, in situ retorts, computer simulation of ignition with hot inert gas 80−30356
shallow shells, force loading and temp. field effects, algorithm construction *(Ukrainian)* 78−89338
shells, nonlinear geometrical anal. 78−77709
shells, paraboloid, elliptic, stress analysis 78−59294
shells of arbitrary geometry, finite element anal. 78−34044
shells of revolution, rigid perfectly plastic, limit anal. program, plasticity criterion *(French)* 79−37155
SHETAN−a three-dimensional integral transport code for reactor analysis 80−63238
shielded cables, nonlinearities and multiple exposure anomalies at CASINO, MCCABE code verification 78−58502
Shiva laser fusion facility, target diagnostic system, data acquisition and anal. 78−51366
shock wave propagation in inhomogeneous medium using finite differences 77−7414
shock wave reflection, regular to Mach transition, Monte Carlo simulation 77−75936
shock waves, converging, stability calcs. by computer 79−41715
shock waves in bubbly liquids *(French)* 78−26183
short range local interactions, radial wave functions and scatt. phase shift calc. program 79−84976
Shubnikov-de Haas quasi-periodic oscill. curves, harmonic analysis, computer method *(Russian)* 78−39132
SIMON, FORTRAN Monte Carlo program for time-of-flight neutron diffractometer simulation 79−50955
SIMULATE, general multigroup nodal procedure based on response matrix principles [for FBR analysis] for FBR anal. 80−57827
simulated laboratory exercises, validity of graphic approach 78−81780
simulation appl. to materials, conf., Gaithersburg, USA (April 1976) 78−27387
simulation of dark field electron micrographs, of metal point defects 78−47219
simulation of dislocation glide through fields of point obstacles 78−34521
simulation of inter/cross modulation levels for GaAlAs diode laser 78−55455
simulation of spherical powder sintering, by surface diffusion 78−48344
simulation of sputter broadening in impurity depth profiling 80−2908
simulation of vacancy annealing kinetics, for deformed Au 78−47353
simulation plasma, boundary conditions in magnetic field 80−10392
SINDA heat transfer modelling for thermionic converter array 80−40886
single channel Schrodinger eqn. for e-scatt. off static pot., de Vogelaere's method 79−63062
single crate CAMAC control system for negative ion source test facility 79−72216
single crystals, growth simulation 80−88069
single particle energies of neutrons and protons, stepwise multiple laser regression technique 78−78235
single particle inclusive prod. reactions, ONCPLT Fortran program for observables calcs. 77−57845
sintering, computer simulation 79−61526
sintering mechanism diagrams, computer program 79−28978
SIR program, use of negative quartets 80−24304
skew ray tracing with the TI-59, programmable calculator 80−48141
slag and metal flow in ESR process, mathematic model 77−73249
Slater-transform-Preuss functions, one centre integral calculation program 79−13626
slip band, action of dislocation sources in irregular stress field *(Russian)* 77−15426
slurry flow, confined, mean vel. field skewness computation 78−63481
small angle X-ray scatt., slit height smearing correction prog. 80−10456
small angle X-ray scatt., slit height smearing correction prog. 80−10457
small angle X-ray scatt., slit height smearing intensity correction program 79−86644
small angle X-ray scatt., slit height smearing intensity correction factor program 79−86645
small-angle scattering, data evaluation method 77−84580

physics computing continued
SMUDLA, nuclear decay scheme construction from gamma transitions and coincidences 80−83063
SNM safeguards, LASL DYMAC accountability system, software development 80−99212
soil, moist, dielectric relaxation model suitable at microwave frequencies 77−43930
soil mechanics, optimal lower bounds 77−72262
solar buildings, climatological design assessment interactive CAD techniques 80−61289
solar collector, focused, slightly curved, reflected light pattern anal. 77−23728
solar collectors, tubular, computerised performance simulation 80−55903
solar energy concentrators, segmented parabolic mirrors, optical performance anal. by THEK computer code *(French)* 80−61294
solar ground coupled heat transfer, expt. and GROCS computer model of heat pump system 80−66987
solar heating of buildings, numerical simulation of thermal performance 80−66942
solar ponds, salt gradient, computer simulation of thermal behaviour 80−101126
solar radiation levels on tilted surfaces, computer model validification 80−35641
solar receivers, cavity-type, HEAP computer simulation program for heat energy anal. 80−30548
solid, zone structure in tight binding calc., program 79−42430
solid laser, CW, actively mode locked, picosecond pulse form., computer model 79−36939
solid mixture charact. discrete fourier transform, spectroscopy, computer simulation 78−63859
solid soln. strengthening, conc., computer simulation 78−31420
solid solution hardening, statistical behaviour analysis *(Japanese)* 80−11658
solid state detection spectra, fast analysis, LIZA program 80−37706
solid-state reactions at elevated temps., X-ray diffr. study, computer control 77−47303
solidifying melt, two phase zone formation, convection *(Russian)* 80−93547
soliton inelastic interaction, examples and Boussinesq. eqn., computer investigation 78−51
solitons, computer calcs. 80−46832
sonic boom, nonlinear propag., including asymm. effects, numerical soln. program 77−72326
space filling molecular models 79−18309
space group symmetry operations, program for deducing from symbolic notation 79−94942
space time curvature tensor, Newman Penrose formalism, CAMAL program calcs. 78−24701
spark chamber photographs, automatic and semiautomatic handling, comparison 77−23371
speckle, non-Gaussian, correlated weak scatterers, computer simulation 80−28159
spectrophotometer (UR-20), data handling attachment 77−26409
spherical Bessel function $j_l(r)$, Chebyshev series 80−8775
spherical X-ray wave, dynamic diffr. theory, numerical results 80−38867
spin 1/2 particles, config. representation, bit patterns appl. 77−43804
spin glass, and mictomagnet, computer simulation 77−66365
spin glass, computer simulation 77−66370
spin glass, computer simulation 80−60299
spin glass, metallic, computer simulation 77−32203
spin glasses, 2-dimens., computer expts. 77−80945
spin Hamiltonian consts., computation from EPR single cryst. data 77−90013
spin-glass, two-dimensional Ising model, low temp. dynamic props. 80−20425
SPODE, Monte Carlo radiation transport code, comparison of electron transport models 80−23030
sprays, drop trajectories, aerodynamic drag effects, computing methods 77−72347
SPS, real-time control system, operating system principles 80−875
SPS control system, modifications since instalment 79−26866
sputtering, collision cascades and disturbed zone, computational model 79−74037
sputtering mechanism for light ions, computer simulation 79−56901
sputtering processes, due to Ar^+ bombardment, computer modelling 79−19957
square duct, developing turbulent flow and heat transfer, computational procedure 80−69926
stainless steel, type 316, neutron induced charged particle spectra 78−5024
static condensation stress recovery algorithms, cost comparison 78−41145
static structure factor, non-cryst. material, neutron diffr. data, normalisation, instrument correction program 79−14651
steel, alloy with additions of Mn, Si, Ni, Cr, Mo, Cu, thermodynamic prediction of Ae_3 temp. 78−64524
steel, Charpy V-notch toughness test, computer simulation 79−70138
steel, high strength sheets, finite element anal. of crack propag. expts. 80−40498
steel, mild, corrosion rate meas. in H_2SO_4 using microprocessor controlled potentiostat 80−71798
steel, parts, stress calcs. during cooling, program system THEPLA *(German)* 80−35237
steel, quenching, computer anal. of thermal processes 77−70085
steel, stainless, ferritic, 430, precipitate study using ion microprobe mass analyser 79−15678
steel, stainless, stress distribution effect on chipping of blanking punch *(Japanese)* 78−31543
steel for nuclear pressure vessels, transient finite element crack propag. model 77−3106
steel production, heat treatment, computer based interpretation of heat and cooling *(German)* 79−78995
Stefan problem, two dimens., space-time finite element computation of free boundary 78−1556
Stefan problems, particle model 78−32779
STEM, image formation, 2-D computer simulation of heavy atom model compounds 80−75135
stereographic projections, standard, computer generated 79−37579
stereoprojections for crystals of all syngonies computer program Mir-1 *(Ukrainian)* 80−24299
physics computing continued
stereoregular polymers, electronic density of states, new algorithm 78−18939
stereoscopic diagrams prepared by desk calculator and plotter 77−37692
stereoviews and morphological data on microcrystals 78−18510
stiff differential eqns. of chemical kinetics 79−15960
stiffened plate struct., nonlinear anal. by combined Rayleigh-Ritz-finite element method 77−72162
stiffened plates, constraint method anal. 78−26066
Stirling Laboratory Research Engine, preliminary test results 80−35717
strain gauge meas. in cyclic elastoplastic tests, automatic processing on portable computer 77−5829
strain hardening curve computation 77−90363
strain hardening structures under repeated loading, deflection analysis 78−63313
stray light phenomena, GUERAP III Monte Carlo simulation 78−58907
stray light simulation with advanced Monte Carlo techniques 78−58906
streaming, of vel. and temp., in oscill. boundary layers 78−83358
stress analysis, energy methods, book 78−1571
stress analysis, three dimensional finite element code 77−49586
stress intensity factors, UNCLE finite element system calcs., appls. in fracture mechanics 78−67098
stress intensity factors for reactor vessel nozzle cracks 79−15796
stress relieving notches, expt. and computer aided study, and optimisation 79−59926
stress state and temperature distrib. in prismatic body for nonstationary thermal action *(Russian)* 78−13905
stress-cycle asymmetry degree, determ. problem 79−90187
struck string, discrete model 79−3838
structural analysis, dynamic, soln. of quadratic eigenproblems 77−89017
structural phase transition, intrinsic and extrinsic central peak properties, review 80−34168
structural stiffness matrix eqn., algorithms for direct access Gaussian soln. 78−57766
structure imaging, direct, in electron microscopy 79−68990
structure model, photograph to digital convertor 79−60213
structured programming in physical applications 77−2529
structures, dynamic instability region, computation by finite element method 80−23927
STRUKTURA, program system for cryst. struct. investigations 80−44071
student computer aided laboratory instruction Karlsruhe Univ. 79−12556
subcritical reactor, neutron joint factorial moments and count bivariate distribs. 79−59120
suction effects on shock wave-boundary layer interaction, numerical Navier-Stokes soln. 79−1243
SUNSPOT, sensitivity anal. of direct gain passive solar space heating systems 80−35647
superposed coherent and chaotic radiation, computer simulation 80−58485
supersonic flow, finite difference method calcs. *(French)* 78−34157
supersonic flow, two-dimens., finite-difference calc. 77−51081
supersonic three-dimens. flow, finite difference method 78−51190
surface acoustic wave modes in solids, computer program 78−2352
surface diffusion, influence on surface anal., model calc. 79−15016
surface roughness meas., effect of stylus radius meas., digital simulation 77−67413
surface semichannelling effects on spatial distrib. of reflected ions, computer simulation for Cu 80−35030
surface tension in molecular dynamics experiments 78−30815
suspension, random behaviour simulation, interval of quiescence method 78−31708
swirling particle fluids, computer studies, evolution of planetary-type bodies 79−35121
symbolic algebraic computation, appl., review 79−58535
symmetric double diode, time depend. theory and computer simulation of electron and ion flow 77−24065
symmetric SOR and SIP methods, numerical soln. of multigroup diffusion eqn. 78−74431
symmetric top on horizontal surface, computer program for initial value problem 79−44714
synchrotron spectral tip calc. refinement, transition rates for mag. bremsstrahlung, computing techniques 79−49430
system performance optimization 79−89579
tandem lab. data acquisition system 79−89529
Taylor vortex flow, finite difference transient implicit method, stability 79−14404
teaching, Newtonian motion anal. using micro-computer simulations *(Japanese)* 80−31462
teaching, two-dimens. Brownian motion simulation on micro-computer *(Japanese)* 80−31461
teaching using SWTP 6800 system in BASIC 80−98776
TEM, high resolution, surface struct. of (001) Au film 80−100383
TEM imaging of W(111) split crowdion interstitial, computer simulation 78−71723
TEM micrograph image restoration, of weak-phase object using computer *(Japanese)* 79−71571
terminal velocity, analogue technique 79−97163
ternary molten salt phase diagrams, computation 79−100118
ternary phase diagrams, interactive computer program 80−71629
ternary solution phases, empirical methods of predicting and representing thermodynamic props. 80−70423
ternary system compound formation, comp. and props. w.r.t. component electron struct., computer prediction 80−103444
texture, calc., library program, in FORTRAN IV 78−22598
texture anal., pole figure calc. by computer 77−71303
texture anal., three dimensional, computer simulation of errors 78−64805
texture analysis, numerical calc. of generalised spherical harmonic function *(French)* 78−18484
texture development in grain growth, computer simulation 79−96036
texture of materials, data acquisition and processing 80−64828
textures, deformation, eulerian simulation 80−3096
THEK analysis of optical perform. of segmented parabolic mirrors *(French)* 80−61294
thermal analysis, nonlinear temp.-time program *(German)* 78−8406
thermal blooming: round beam vs square beam, computer study 80−38076
thermal conduction of solids, temperature stochastic field in cylinder digital simulation algorithm *(Polish)* 79−71370

physics computing continued
thermal conduction of solids, temperature stochastic field in cylinder, digital simulation algorithm *(Polish)* 80−17879
thermal conductivity prediction of heterogeneous mixture, digital simulation technique 78−87247
thermal contacts fluxes modelling, electrolytic *(Italian)* 77−24504
thermal diffusivity meas. by laser-pulse technique, instrumental recording and data processing 77−45846
thermal pressure in solid and eqn. of state, computer simulation 78−34593
thermal problems, one-dimens., with phase change, efficient numerical technique 78−59270
thermal regenerator, with variable mass flow rate, computer model 78−75047
thermal stress simulation in continuous casting, finite element method 78−30170
thermal stresses rel. to uncoupled thermoelasticity, finite element method appl. *(Italian)* 79−18719
thermally expandable fluid transients, finite difference method 77−79418
thermally stimulated currents, computer simulation 78−39609
thermochemical water splitting cycles for H prod., thermodynamic anal. and optimisation 80−45766
thermodynamic activity of C in austenite, computer simulation 79−37852
thermodynamic computation data bank, appl. to inorganic and metallurgical systems 77−59100
thermodynamic data treatment centre, facility for chem. thermodynamics anal. 79−10918
thermodynamic functions of gases, liquids by computer simulation 79−86866
thermodynamic properties, of interacting particle ensemble, by simulation of stochastic disordering 77−87697
thermodynamic props. of water and steam, numerical calc. program *(French)* 77−69101
thermoelasticity anisotropic 3-D problems, numerical projective method 77−68436
thermogenesis in flow calorimeters, efficiency of harmonic analysis 79−88956
thermokinetics, linear system output deconvolution for detn. of input 78−12699
thermoluminescence, computer simulation 78−39609
thermonuclear react. rates, computation with STEEP code 78−18375
thermonuclear reaction wave in high density plasma, computer simulation 78−742
thermophysical properties, computer based determ. system *(German)* 78−18795
thermophysical properties of ethane from 90 to 600 at press. up to 700 bar, in FORTRAN 77−84940
THERMOS spectrum code, accurate reduced mesh model for neutron thermalisation 80−57829
theta-pinch machines, computer modelling 79−10703
theta-pinch machines, linear, computer model of plasma 77−89296
thick cylinder under non-axisymmetric loads, computer stress analysis 77−54880
thin film condensates coalescence, influence on morphological changes, modelling 80−107676
thin film deposition process, line-edge profile simulation appl. 80−104068
thin shells, algebraic constraints for weak C^1 continuity 78−4458
three body break up reaction energy spectra, computer program 80−27593
three dimensional structures, system of mathematical calc. 79−98623
three-dimensional field modelling, finite-element interactive computer methods *(French)* 79−41294
three-dimensional permeable solid, magnetisation distrib., computer calc. 78−72366
three-dimensional texture analysis, data processing, subroutines 77−25240
three-dimensional topographic mensuration, laser electro-optic system 80−99784
three-nucleon system, bound state calc. program PERFECT 80−13390
threshold foil meas. of reactor neutron spectra, radiation damage appl. 78−29691
TIGERP, 1-D multilayer electron/photon Monte Carlo transport code 79−54079
TiO, single cryst., short range ordering of vacancies, X-ray anal., computer simulation 79−73163
TLD, safety and reliability of decentralised reading in Sweden 77−40780
TNS conceptual design, parametric anal. 78−54991
Toda lattice, undamping of strongly nonlinear surface impurity localised mode, computer simulation 79−97315
Tokamak, 2-D neutronics model for major penetrations 78−5027
Tokamak, neutral beam injection, low density ignition scenarios 80−48937
Tokamak, plasma simulation using nonuniform spatial mesh technique 77−79478
Tokamak, start-up phase, plasma impurities effects 77−14265
Tokamak data processing, no. of computers required 80−59252
Tokamak fusion reactor, effects of blanket-shield penetration on performance 78−21765
Tokamak fusion reactor, energy balance, computing method 78−54982
Tokamak fusion reactors, mathematical simulation of plasma equibilbrium and power supply operating conditions 79−76125
Tokamak fusion reactors, pulsed electrical power systems, computer design and simulation 80−13827
Tokamak magnets, EM forces, TORMAC computer program 78−62647
Tokamak plasma, neutral atom transport by multigroup methods, time reduction techniques 78−18385
Tokamak reactor first walls, thermal response during cyclic operation 78−62651
Tokamak test reactor, neutron activation code REBATE 79−49852
Tokamak transport simulation models 77−79474
Tokamaks, neutral beam heated, radial transport/Fokker-Planck model 77−15224
toroidal pinch discharge, preionisation phase, numerical computation 80−64696
toroidal pinch equil. config., nonlinear operator eqn., optimisation soln. 78−59649
toroidal plasma, 2-D neutral H transport 78−59661
physics computing continued
toroidal plasma compression, computer model, appl. to topolotron 77−15233
torsional vibrators, design by computer optimisation *(Japanese)* 80−33405
track chamber slide processing, calibration programming problems *(Russian)* 80−73305
train noise, prediction of equivalent mean energy level from relatively short parts of railway lines 80−38172
transactinide elements, atomic and chemical props. by gas chromatography and aqueous chemistry, book contrib. 78−85121
transient data systems, state of the art and trends 79−89546
transient flow, split band Cholesky eqn., strategy for finite element anal. 78−46923
transient neutral gas interactions with plasmas and walls 78−94134
transient thermal hydraulic analysis, RELAP4 transform. into fully implicit iterative code 77−65257
transonic airfoil problem, variational principles 78−42626
transonic axisymmetric pot. flow around inlets, Cartesian mesh soln. 77−72323
transonic flow, two- and three-dimens., perturbation soln. method 79−1208
transonic flow, unsteady, implicit shock-fitting computational scheme 78−94763
transonic flow around airfoil, finite-difference calc., computer code 78−26147
transonic flow solution method using acceleration technique based on Wynn's ε-algorithm 77−58724
transonic potential floW, axisymmetric inlets and bodies at angle of attack 78−9648
transplutonium multigroup neutron cross-sections 77−26754
TRANSPORT, design program for charged particle beam transport systems 80−106220
transport code, H atoms in cylindrical hydrogenic plasma 78−51284
transport properties of dilute gas mixtures, calc. prog. 80−10342
tritiated water intake, calc. of committed dose equiv. 79−16311
TRNSYS, transient simulation of hybrid thermal energy storage system 80−30588
TRNSYS optimization formulation for solar heating systems 80−61414
Trombe-Michel wall using phase change materials, solar energy collection and thermal storage, computer anal. 80−55909
trypsin inhibitor, mol. dynamics, computer simulation 78−9932
TSC data handling by on-line use of computers 78−10832
tube, vertical, steam generating annular flow, dry-out position prediction, computer model 78−59447
tubes flow with periodic step changes in diameter, numerical soln. 78−22423
turbulence, heat and mass transfer, TURF computer schemes 79−4014
turbulence, numerical modelling 77−80144
turbulence breakdown coefficient determ., influence of data treatment technique *(Russian)* 78−7690
turbulent boundary layer on a moving surface, integral and numerical methods 78−63421
turbulent boundary layer-transonic shock wave interaction, integral computation method 79−1213
turbulent diffusion, nonlinear integrodifferential eqn., numerical soln. 78−38306
turbulent electron beam plasma interactions, PN calc., numerical anal. 79−14560
turbulent flow, computational modelling by finite elements 79−1163
turbulent flow, press. fluctuation spectrum, elastic boundary compliance effect 78−63422
turbulent flow fields, evaluation of stereoscopic trace particle records 78−1648
turbulent flow in pipes, numerical anal. by finite element method 78−18341
turbulent liquid, coherent struct.-caused mass transfer at wall, numerical computation 78−59379
turbulent shear flows, pattern-recognised coherent structures, computer analysis 78−22334
turbulent transport eqns. soln. by accurate numerical method 80−28498
turbulent vertical gas flow, steady-state dispersed particles radial distrib. 78−55680
turbulent vortex flow, vel.-derivative data bispectral analysis 77−920
two dimensional electrostatic field shape investigation *(Czech)* 79−27126
two dimensional recirculating flow, finite difference grid for non-rectangular flow fields 79−14374
two- and three-dimensional magnetostatic problem program packages 79−41276
two-dimensional shear flow, viscosity effects, microscopic model 77−89085
two-electron integral four-index transformation algorithm 79−9996
two-fluid thermohydraulics computer program, RELAP/SLIP 78−94092
two-phase anisotropic medium, interfacial dislocation, stresses, displacements and energy calc. 80−79786
two-phase cryst. structures, orientational electron microdiffr. anal. with aid of OMEGA program 80−103218
two-phase flow, horizontal stratified, 1-D two-fluid eqns. for LWR LOCA 80−91226
two-phase flow through porous media, starting algorithm for numerical simulation 78−38388
two-phase fluid dynamics, semi-implicit differencing method calcs. 78−42649
two-phase nonstationary velocity tracking by adaptive cross-correl. algorithm 78−14074
type II superconductor, elastic vortex lattice, pinning by lattice defects, computer simulation 79−56465
U-tube steam generator transient simulation using extend implicit continuous-fluid Eulerian method 79−89356
ultracold neutrons (UCN) transmission through moving goffered foils 79−17955
underwater sound, model for determining significance of beam pattern side lobes in fluid flow measurement 80−19136
underwater turbulent jets, velocity field calcs. for expansion region *(Russian)* 77−31351
unified field theories, relativistic, computer field interaction simulation system 80−68412
unimolecular reactions, master eqn. for rate coeff. Nesbet's algorithm 78−48612

physics computing continued
unstable compounds, free energy of formation calcs., FORTRAN program for ternary phase equilibria. 80−10683
unsteady boundary layer over an impulsively started flat plate using finite elements 79−14366
unsteady flow in radial channel, incident shock wave 78−1744
urethane prosthetic compound, dynamic mode determ. 79−48376
US propagation in solids, visualisation using Schlieren photoelastic apparatus *(Italian)* 80−88274
US testing sensitivity selection based on probabilistic techniques 79−91871
VAC4, fourth order vacuum polarisation accurate computation subroutine 78−89639
vapour pressure, constrained fitting of limited data 78−34615
vapour pressure measurement, torsion-effusion method, automatic data acquisition 80−52188
Vavilov energy straggling calc., validity limits 78−33405
VEGA 1 interpreter language for meas. evaluation in nuclear physics 77−65413
very high current beams, transport calcs. computer program 79−76226
vibrating beam min. wt. design, optimal control approach 77−80059
VICKSI computer control system, operating experience 79−72215
virtual crack extension method, nonlinear material behaviour 78−18230
virtual photon spectra calc. by matrix differential eqn. 77−88115
viscoelastic material, stress-strain behaviour, mathematical simulation *(German)* 80−1442
viscometric data from Brookfield RVT viscometer, conversion to shear stress-shear rate relationship 80−1495
viscous flow, 3D, finite difference method 79−32447
viscous supersonic flow over external axial corners, shock and bubble generation computation 80−14734
viscous transonic cascade flows around airfoil, coord. system for numerical calcs. 78−42627
Vlasov eqn., two-dimens., splitting schemes for numerical soln. 78−67310
Vlasov eqn. integration in configuration space 77−7512
Vlasov equation, two dimens., numerical soln., multistep technique 78−1795
void sink strength depend. on mutual recombination, point defect loss to fixed sinks 80−33995
void size distribution during irradiation and annealing, time depend. computation 78−30674
Voronoi polyhedra, construction procedure 79−71236
waiting time calc. of dislocation motion for computer simulation 78−30638
waste air at nuclear plants, dose conversion factors for radiation exposure estimation *(German)* 77−70558
water, liq., Monte Carlo studies of struct., review 80−54101
water, long range forces in mol. dynamics calcs. 78−79517
water, thermodynamic props., computer programme calcs. *(French)* 80−54409
water phase diagrams, spline representation, for PWR programs 77−23207
water pollution by radioactive waste, computer anal. of relative potential hazards 80−21422
wave beam self focusing with plateau-like intensity distributions *(Russian)* 79−89976
wave diffraction theory appl. to free floating and moored rigid structs. 79−7321
wave equation, finite element Laplace transform. soln. 78−4488
wave functions, Serber-type spin-adapted, and time reversal 78−5117
wave-plasma interaction, boundary conditions, refl. coeffs. 77−24094
waxicon design and fabrication, computer algorithm 78−5543
weight multiplicity for unitary groups, program 78−74166
weldbonded joint deform., finite element simulation 78−35636
welded component fatigue life and crack propag. analysis with internal stresses 77−77576
welding, thermal stresses and metal movement, computer simulation 78−34002
wind-wave interaction, two-layer flow, numerical simulation 78−92823
X-ray, neutron, and electron diffr., radial distrib. anal., computer program 80−28875
X-ray absorption corrections in single cryst. diffractometry, FORTRAN program 77−11438
X-ray crystallographic computations for students using programmable calculator 80−36811
X-ray crystallography, difference Fourier refinement using minicomputer 77−58924
X-ray crystallography, holographic computing step for image display 78−91199
X-ray crystallography, SHAPE and GAUSAB programs 78−67622
X-ray crystallography computer simulation of back reflection Laue patterns 77−55199
X-ray diffr. line profile analysis, on-line computer routine 78−79498
X-ray diffraction, time-resolved, using position sensitive counter 77−13831
X-ray diffraction 79−50947
X-ray diffraction apparatus, classification of methods 77−51282
X-ray diffraction data collection on macromolecules, FORTRAN program 77−51279
X-ray diffraction energy dispersive diagrams, eval. using small computer on-line techniques 80−92423
X-ray diffraction powder pattern indexing, crysts. of orthogonal symmetry 77−47298
X-ray diffractometer, HAG 4/A universal instrument, applic. versatility of basic software 80−52375
X-ray diffractometer controlled by laboratory automation module 80−317
X-ray diffractometer data, automatic attachment for punching to tape 78−34385
X-ray diffractometer data, profile anal. using computer program 79−37580
X-ray diffractometry, of superimposed twins and clusters, establishing UB matrices of single cryst. individuals 79−37586
X-ray diffractometry of single cryst., absorption corrections, cryst. shape and size determ. 78−1954
X-ray equivalent reflections averaging, using small computers 80−79634
X-ray image reconstruction, iterative scheme 78−66014
X-ray integration method, extension of $\sin^2\psi$ method *(German)* 80−92420
X-ray phase analysis, information retrieval system 78−79501
physics computing continued
X-ray phase analysis data, algorithmic processing 78−1953
X-ray powder diffraction, computer automation 80−1899
X-ray powder diffraction, research and quality assurance appl. 80−73556
X-ray powder diffraction anal., Guinier camera, film densitometry and search match procedures 80−3454
X-ray powder diffraction data, cryst. materials identification with semi-automated system 77−15276
X-ray powder diffraction data, search-match system 80−28874
X-ray powder diffraction data, unit cell volumes estimation for triclinic case 77−15277
X-ray powder diffraction patterns of heterogeneous materials, program for separating high-symmetry component 78−1955
X-ray powder diffraction system, computer-controlled, with automatic sample changer 77−84577
X-ray powder patterns, composite, computer program for generation 79−50931
X-ray powder reflections positions calc., FORTRAN program FIREBIRD 77−62443
X-ray projection topograms for crystal with dislocations, calc. 79−86647
X-ray reconstruction by finite field transforms 77−67549
X-ray scattering curve desmearing, FORTRAN program 77−84587
X-ray scattering data, calc. from variety of models, computer program using fast Fourier transform algorithm 77−76256
X-ray small angle scatt. curves, comparison of two smoothing methods *(German)* 77−89346
X-ray small angle scattering, curve anal., by triaxial body models using graphic display model 80−28873
X-ray spectrometer, matrix correction coeff. derivation by Siemens P88/MAR 320 programs 77−65412
X-ray spectroscopy, equivalent wavelength representation and secondary fluoresc. calcs., minicomputer program 80−321
X-ray streak camera electrode design using a plasma simulation code 79−30632
X-ray stress meas., computer-aided system *(Japanese)* 80−104366
X-ray topographs of stacking faults 78−30513
X-ray topography, computer simulation methods 79−23484
X-ray traverse topographs, computer simulation on basis of Green function method 80−49044
X-Y model, classical one-dimens., computer simulations 79−78396
XESAMO code for Xe and Sa poisoning transient anal. in fission reactors *(Spanish)* 80−52749
Yunan big cloud chamber set; momentum selector program *(Chinese)* 79−59308
YZARC, multisoln. direct methods procedure 79−73062
ZAF corrections, quantitative X-ray anal. programs 79−21878
ZGS, low level beam diagnostics for polarised proton operation 77−83311
zincblende structure compounds, lattice dynamics, calc. program 79−33048
zincblende structure compounds, lattice dynamics calc. program 79−86854
Zircaloy-Z, thermal diffusion of H, numerical soln. with computer *(Korean)* 80−19989
zone plate, profiled, chromatic props. 80−43451
zone refining-cascade purification, theoretical solute redistrib. computational results 79−74083
zoom lens design by pocket calculator 78−55423
K^-p quasi two body processes extraction from three body final states: program EXTRA 78−82238
(π,π) differential cross sections, calculation program modification for differing p and n radii 79−54456
(π,π') differential cross section calculation program modification 79−54457
π-nucleus elastic scatt., momentum space optical pot. code PIPIT 77−38298
π^-p inelastic interactions at 205 GeV/c, three-fireball model, computer simulation 78−474
^{60} γ-ray scatt. in air, anal. by discrete ordinates transport codes 80−32525
Ag solder strip continuity, US inspection 79−52605
AgCl:Na^+, Frenkel defect formation energy, impurity diffusion and migration 79−99179
Al alloys, fatigue crack initiation, computer simulation 80−100893
Al and Al alloys, solidification of castings, electrical modelling study *(Rumanian)* 79−74142
Al, computer simulation of tilt grain boundaries 78−30642
Al, elastic grain boundary responses, thermodynamic props., computer calc. 77−39593
Al, ion-induced Auger electron emission, depend. on ion energy 79−78814
Al, periodic grain boundaries struct., computer simulation 77−89448
Al, phonon anharmonic response, neutron-scatt. test of computer calcs. 80−44281
Al, plane stress calc. with two dimensional elastic-plastic computer program 78−35465
Al, rapid melting and solidification of surface layer, exam. using computer heat flow model 78−83228
Al, tilt boundaries ⟨110⟩, computer simulation, struct. and symmetry 79−37713
Al, tilt boundary, $\Sigma=5$, struct. and atomic vibr., computer simulation 80−70223
Al-Al_3Ni eutectic, cryst. struct., orientation, electron microscopy, computer calcs. *(German)* 77−72582
Al-$CuAl_2$ lamellar eutectic, computer simulation of two dimensional Zn diffusion 78−30799
Al-Ga-Ge, thermodynamic props. of mixing of binary systems, phase diagram 80−45275
Al-Ga(Ag), dil, Hall coeff. by OPW Fermi surface model 80−6816
Al-Ge-Sn, thermodynamic props. of mixing of binary systems, phase diagram 80−45275
Al-Ti-Fe, ternary phase diagram, computer calculations 80−45274
Al_2O_3, Czochralski bulk flow, in microgravity, digital simulation 80−28934
Al_2O_3, sintering of single phase and multiphase components *(German)* 78−80494
Ar, positron vel. distrib. at equilib. elec. and mag. fields 77−71870
Ar-Ne, positron vel. distrib. at equilib. elec. and mag. fields 77−71870
Au, atomic struct. of large angle [001] twist boundary, determ. by computer modelling and X-ray diffr. study 80−70162

physics computing continued
Au, curved cryst., planar and axial channelling of protons, numerical simulation 79−65132
Au film (001) surface, computer modelling of high resolution TEM images 80−6330
Au, polycrystn., deformed, computer simulation of vacancy annihilation to dislocations *(Japanese)* 80−88205
B fibre reinforced W double coaxial composition rod, waveguide, normal mode US propag. 79−100317
BaF_2, ionic conductivity meas., computer anal. point defect parameters 80−54429
Be-Cu dynode, depth profiling anal. of surface layer 80−2253
C graphitic, imperfectly ordered, high resolution electron microscopy imaging, computer simulation calcs. 79−77463
C-O-H-N-Si-Ar, computer calculations of heterogeneous equilib. 79−66044
CO, emissivity, computer calcs. 77−84386
CO_2 laser light pulse amplification calc. Fortran program PULSAMP 77−58312
CO_2 laser pulse, nonlinear propag. characts., computer simulation 80−106575
CaF_2, mol. dynamics studies of superionic conductors 80−107547
CaO, (100) surface struct. using LEED meas. and rumpled ionic models 80−20019
Cd-Hg-Te, phase diagram, computer estimation 80−20903
$Cd_xHg_{1-x}Te$, flameless atomic absorpt. anal. using interactive computer processing 79−66380
CdS, electron traps, admittance spectra on hetero- and Schottky junctions 79−56159
Cl_2, liquid-vapour surface, computer simulation 80−54478
CoO, pressure sintering densification model, computer program 78−44040
$^{59}Co+n$, calc. using pre-equil. statistical model code GNASH 78−4946
Cr, paramagnetic, Hartree band struct., Fermi surface, nesting wave vector 80−49583
Cr-Fe-Ni-Si, ternary phase equilibria for Cr-Fe-Ni rich portion, lattice stabilities 80−71628
Cr-Ni-Fe, ternary phase diagrams, interactive computer program 80−71629
Cr-Ni-O, computer-assisted anal. and calcs. of phase diagrams 80−25667
CsCl(Br)(I), molten, structural props., computer simulation 77−84616
Cu, amorphous, sputtering, computer simulation in binary collision approx. 79−56900
Cu, continuum representation of computer simulated dislocations 78−30623
Cu, elastic grain boundary responses, thermodynamic props., computer calc. 77−39593
Cu, electron radiated, formation of Frenkel pairs 79−23598
Cu halides reflection spectra, minicomputer based data acquisition system 79−61402
Cu, He-vacancy clusters, computer simulation 77−39583
Cu matte converting, thermodynamics of process, Noranda process, exam. using computer model 78−80492
Cu, neutron irrad., replacement sequences, calcs. using ADDES and COMENT codes 79−46714
Cu, point and planar defects, computer simulation 80−59455
Cu vapour laser, rate processes, computer simulation 80−69371
Cu_3Mn, atomic short-range order, TOF neutron diffraction 79−10831
$Cu_{57}Zr_{43}$, amorphous alloy, computer simulation of atomic structure 80−70125
DF-HF CW lasers, performance, computer modelling 78−71094
D_2O, neutron scatt. cross section determ. by DEUKER computer code 79−54468
DT laser compression, computer simulation, shock and thermal waves *(Chinese)* 79−90428
α-Fe, a/2 ⟨111⟩ {110} edge dislocation, at. simulation 77−89435
Fe, amorphous, realistic structural model, search for Bernal holes 78−83734
Fe, amorphous, tensile deform., three-dimens. computer simulation 79−43350
Fe, BCC, computer simulation of entropy of $^1/_2\langle 111\rangle\{110\}$ edge dislocation 78−67716
α-Fe, BCC metals, stressed, computer simulation of vacancy and divacancy migration 78−47573
Fe, cast, quantitative metallography, study by image anal. 78−31492
Fe, FCC, grain boundary struct. and energy, computer expt. 78−30643
Fe fast neutron spectra, an assessment of ENDF/B-IV based on integral meas. 77−50194
Fe polycrystals, grain misalignment, electron microscope determ. *(Russian)* 80−103358
Fe, rapid melting and solidification of surface layer, exam. using computer heat flow model 78−83228
Fe-Al, Mossbauer study of ordering *(Japanese)* 79−19822
Fe-C, exam. of phase equilbria, at high temp. and pressure 78−52759
Fe-Cr-O, computer-assisted anal. and calcs. of phase diagrams 80−25667
Fe-Ni-C (0.15, 0.05 wt.%) pore formation kinetics during crystallisation, FORTRAN study *(Russian)* 80−54158
Fe-Ni-O, computer-assisted anal. and calcs. of phase diagrams 80−25667
Fe-O, exam. of thermodynamic data, using a computer aided strategy 79−11592
Fe-Si, grain oriented sheet, grain struct. by computer mapping 80−88168
Fe-Si-C, austenitic, C diffusivity *(German)* 80−92705
Fe_3Al, computer simulation of energy dissipation from near threshold knock-ons 78−30666
Fe_3Al, ordered binary alloy, computer simulation of radiation effects 78−87709
FeF_3, amorphous, struct. and mag. props., computer model 80−96446
$Fe_{75}P_{25}$ amorphous alloy, atomic struct., computer simulation 80−88043
Ga-Ge-Sn, thermodynamic props. of mixing of binary systems, phase diagram 80−45275
n-GaAs, and Te doped, homogeneity, IR introscopy investig. 79−15446
GaP, temp. depend. of Fermi Level, calc. 80−39491
Ge(Li), calc. of finite angle correction coeffs. and linear polarisation sensitivity 79−736
Ge(Li) detector, calc. of gamma-ray efficiency 80−37693
Ge(Li) γ-ray spectra, effect of base line shape on peak unfolding 78−851

physics computing continued
H, low energy ion scattering from polycrystalline solids, computer study 77−36338
$H+H^+$, classical 3 body collision, cross section, energy transfer, computer calcs. 78−17783
H_2 plasma, nonequilib., radiative props., computer program 79−90388
H_2, vibr. relax. in H_2-Ar mixtures, mechanism, computer simulation 78−46434
HCl liq., time correlation function, computer simulation 80−79670
H_2O, free energy of liq. water, ab initio Monte Carlo calc. 78−83975
HX, chemical laser performance isotope effects, computer simulation 78−29944
$He-H_2^+$, classical trajectories, on 3D cardinal spline fitted surfaces 77−90584
Hf-Be, coupled phase diagrams and thermochemical descriptions 80−25656
HfC-TiC, pseudobinary systems, phase diagrams, computer calcs. 78−44092
I_2, $(B^3\pi_{0+u})$, dissoc. reaction, computer simulation 78−48639
$^{127}I(p,5n)^{123}Xe \rightarrow {}^{123}I$ statistical model based computation 79−26416
$^{127}I(p,n)^{127}Xe$ statistical model based computation 79−26416
InP, temp. depend. of Fermi Level, calc. 80−39491
KCN, liq., mol. dynamics computer simulation 78−38609
KCl, (100) face, mol. dynamics computer simulation of surface props. 78−18880
KCl microcrystal, computer simulation of melting and glass form. 79−65173
$KCl-CaCl_2-NaCl$, ternary phase diagrams, interactive computer program 80−71629
$KNbO_3$ powder synthesis, unit cell determ. 78−11168
KrF^*, electron beam pumped laser, pulse shape and laser-energy extraction, model and expt. comparison 79−98345
Li, liq. cooled pulsed fusion reactor blanket heat transfer, numerical calc. 78−94141
metal, BCC, multi-layer faults on (112) planes and interatomic pots. 78−51563
Mg, HCP, vacancy clusters and interstitials, computer simulation study 80−64992
Mg, ion-induced Auger electron emission, depend. on ion energy 79−78814
MgF_2-Ag (Al)(Cu)(Au) film substrate tunable external-reflector retarder, computer based anal. 80−53407
MgO, HADES program to calc. defect structure, shell model 79−99180
MgO solution in UO_{2+x}, shell model calcs. of enthalpy, computer program for formation energies 79−42251
Mn^{2+} EPR spectra in glasses with $g_{ef}=4.29$ computer simulation 80−34764
Mn-Ti-Fe, ternary phase diagram, computer calculations 80−45274
Mo polycrystals, grain misalignment, electron microscope determ. *(Russian)* 80−103358
Mo(d,d), A=92, 94, 96, 98, 100, inelastic scatt., anal., automatic parameter search code 78−94017
N gas discharges, electron swarm motion, computer simulation 77−89339
N_2, dense gas near metallic target, laser spark *(Russian)* 80−38682
N_2 high intensity arc anode region, temp., current density, flow field, numerical anal. 78−9827
N_2, liquid-vapour surface, computer simulation 80−54478
α-N_2 simulation of dynamical props. of molecular solids 78−30710
NH_3, double min. vibr. pot., FORMAC program 77−23444
$(NH_4)_2BeF_4$, γ-irrad. cryst., F_2^- ions, ESR meas. 80−34770
$(NH_4)H_2PO_4$, single cryst., X-ray diffr. contrast at twin boundaries, computer simulation 79−33000
Na, neutron cross sections, ENDF/B-IV assessment and evaluation 78−25291
Na-K liquid alloys, struct., X-ray and neutron diffr. meas. 80−107041
NaCl aqueous soln., mol. dynamics simulation, central force model 80−49077
NaCl, edge dislocation dissoc., computer simulation of core struct. 79−37703
NaI:Tl, right-circular cylindrical detector, Monte Carlo calc. of efficiency 79−734
NaI(Tl) detectors, response functions to terrestrial γ-radiation, computer program 80−83233
$Na_2O.5Al_2O_3$, diffusion of Na, computer simulation based on Monte Carlo method 77−24431
Na_2XO_4, (X=S, Cr, Mo, W), anal. and calc. of binary and ternary phase diagrams 80−88299
Nb, (001) surface, low energy H^+ and He^{++} ion refl., computer simulation 80−11524
Nb, neutron bombarded, defect size distrib. influence on hardening *(Russian)* 80−10580
Nb, relaxation from room temp. to 114°C, computer optimisation of elastic aftereffect curves 77−90390
Nb_3Sn fatigue effects in unidirectional composites, computer simulated model 80−35289
Nd complex, Nd^{3+}:ATP, electron spin echo decay envelope anal. 79−54871
Ne, positron vel. distrib. at equilib., elec. and mag. fields 77−71870
Ni (110) surface, Ar^+ refl. at grazing angles, computer simulation 79−87549
Ni based superalloys, sigma phase prediction techniques 80−7567
Ni, cyclically deformed, polarisation stress field, dislocation shuttling, computer calcs. 79−96095
Ni, deuteron range profiles in 100 to 400 keV region, expt. and computer simulation 77−51422
Ni, pure, heavy ion irradiated, dendritic void growth 78−14386
Ni, rapid melting and solidification of surface layer, exam. using computer heat flow model 78−83228
Ni single crystal, depth distrib. of self-ion damage, TEM 77−51419
O, isoelectronic sequences, energy spectra inc. relativistic corrections 78−924
$O_2+La(Y)(Sc)$, crossed beam chemiluminescence reaction, spectral simulation, hyperthermal energy meas. 78−80732
Pd sponge powder, sintering shrinkage kinetics 80−29900
Pd-Cu-Si, metallic glass, miscibility limits, computer study 79−65198
$(Pu,U)O_2$, <5 wt.% PuO_2, criticality data generated by SU-HAMMER 79−3198
^{239}Pu neutron data evaluation for ENDF/B-V 78−25288
^{222}Rn daughter conc., meas. sensitivity computer optimisation 78−49126

physics computing continued
SF_6, compressed in space-charge stabilised nonuniform fields, corona threshold computation 79−19118
SO_2, emissivity, computer calcs. 77−84386
Sb-Te-Bi, computer study of miscibility limits, 273 to 300K 78−52781
Sb-Te-Bi, miscibility limits, computer study 78−79773
Si, (111) surface, low energy H^+ and He^{++} ion refl., computer simulation 80−11524
Si, dendritic web growth processes for solar cells, computer modelling 79−11508
Si epitaxial wafer, impurity profile meas. by multilayer spreading resist. anal. 77−76449
Si, ion penetration, computer program 80−88185
Si, ion-implanted, laser annealing at 1.06 μm, computer simulation 79−47556
Si, ion-induced Auger electron emission, depend. on ion energy 79−78814
Si, n-type inverted MOSFET (100) surfaces, quantitative determ. of valley splitting 79−51678
Si, perfect cryst., X-ray acoustic reson. 79−27873
Si solar cells, polycrystalline n^+/p, computer model of spectral response and photocurrent 80−55853
Si surface, (111), energy states, computer renormalisation-group calc. 80−75617
Si:H, amorphous, density of states determ. using field effect 80−49937
p-Si-Al, ohmic contacts, Si dissoln. and recrystn. effects, computer calc. 80−103749
Si-Al-B-O-N, calc. of phase diagrams from data set 80−55362
Si-Al-Zr-O-N, calc. of phase diagrams from data set 80−55362
Si-SiO_2, two layer system, P^+-ion penetration tails, expt. and computer anal. 80−75249
Si+n, binary and tertiary reactions, ENDF/B-IV calcs. of energy distribs. of secondaries 77−23043
Si_3N_4-Al_2O_3-AlN, isothermal sections, free energy of formation 80−55363
a-SiO_2, transient photocond. simulations using multiple-trap model 80−49801
SiO_2-Al_2O_3-Si_3N_4, isothermal sections, free energy of formation 80−55363
T, release from CTR, radiological dose calc. 78−78511
$Tb(OH)_3$, powder and single crystal, mag. props. 80−2558
$^{124}Te(p,2n)^{123}I$ statistical model based computation 79−26416
ThO_2-^{233}U exponential expts. anal., cross section library sets, resonance integral correls. 77−23215
ThO_2-UO_2 in PWR fuel rod, LIFE-THERMAL computer code anal. 78−86623
Ti-Be, coupled phase diagrams and thermochemical descriptions 80−25656
Ti-Be-Zr, coupled phase diagrams and thermochemical descriptions 80−25656
Ti-Mo-Al, determ. of interaction parameters from EPMA data 77−63635
Ti-Mo(V), metastable diffusionless equilibria, high press. conditions 80−71627
TiB_2, CVD from $TiCl_4$, BCl_3 and H_2, equilib. thermodynamic anal. 77−59694
TiC-ZrC, pseudobinary systems, phase diagrams, computer calcs. 78−44092
TiS, vaporisation chemistry and thermodynamics, computer-automated simultaneous Knudsen-torsion effusion 80−48837
U enriching gas centrifuge cascade, computer program for performance anal. 79−85805
U neutron criticality, solid angle computations using computer code 80−13726
UC_x, computer simulation of C activity and transport 78−86618
UIG, Ga-substituted, computer simulation of temp. and field depend. of sublattice magnetisation and spin-flip transition 79−11300
UO_2, computer model of Young's modulus 78−31450
UO_2, modified Ashby's computer method for constructing sintering diagrams 79−43165
UO_2, thermal cond. meas. under simulated in-reactor conditions 78−94079
$^{235}U(n,f)$, time correlated associated particle method, CAMAC experiment 80−52702
^{236}U, fission induced by $^{235}U(d,p)$, subthreshold cross section meas., 2-centre shell model calc. 79−6719
^{238}U, evaluation for ENDF/B-V 78−25289
^{238}U, single charged, numerical anal. of longitudinal motion of 9.5 GeV 79−54737
^{238}U total neutron cross section, ENDF/B-IV representation 77−2983
$^{238}U(\gamma,f)$ 20 MeV, computer program for yield determ. of short-lived products 80−102215
V, diffusion of O and N, least squares computer technique 78−38881
V_3Si, single cryst., computer simulation of channelling meas. 79−51180
W, self-interstitial diffusion, fully dynamic computer simulation 77−39687
W/Cu powders, liq. phase sintering, particle rearrangement 80−45253
Xe, solid, elastic consts., thermodynamic props., Monte Carlo simulation 77−62575
^{135}Xe-induced core instabilities, extended λ-mode linear anal., CANDU appl. 78−82494
YIG, vitreous electric-field-gradient distrib., Mossbauer quadrupole splitting meas. 80−75901
Zn-Cd-Bi-Sn phase diagram with liquid-liquid immiscibility, computer calc. 77−36463
Zn-Sn-Bi, ternary phase diagrams, interactive computer program 80−71629
Zr-Be, coupled phase diagrams and thermochemical descriptions 80−25656
ZrC-HfC, pseudobinary systems, phase diagrams, computer calcs. 78−44092
ZrC-NbC-MoC_{1-x} alloys, physicomech. props., comp. depend. 79−66097
$Zr(Ca,Y)O_{2-x}$, local ionic arrangement, X-ray diffr. study 80−100203

physics fundamentals
see also classical field theory; complementarity; cosmology; elementary particles; fundamental law tests; mechanics; quantum field theory; quantum theory; relativity; thermodynamics; units (measurement)
$\alpha^{-1}=137.0324$, physical interpretation 79−25891
absolute temperature, a definition combining the classical method and Caratheodory's 79−49186

physics fundamentals continued
acceleration due to gravity, absolute determ. *(Chinese)* 79−71426
Ampere's theorem appl. to magnetic effect of finite length line current 77−71905
atomic scale in a self-similar hierarchical cosmology 79−101230
axiomatic formulation of six dimens. phys., 3+3 dimens. spacetime 78−81834
Bogolyubov axiomatic approach to nonlocal QFT microcausality and broken microcausality *(Russian)* 79−12972
Bohr's correspondence principle *(Russian)* 79−17627
causal independence in local relativistic free quantum fields 79−21894
causal interpretation of quantum mech., superluminal propag. of quantum pot. 79−40400
causal irregularity, a re-examination 79−25818
causal logic of Minkowski space, states defined by conserved currents 79−54282
causal nature of the motion of wavelets 79−67176
causal paradoxes implied by hypothetical coexistence of positive- and negative-mass matter 80−82685
causal struct. of space-time, covariant representation of Galilean logic 77−5619
causal structure and four-momenta conservation law *(Rumanian)* 80−46887
causal theory, removal of Einstein's objections to quantum theory, unification 80−31572
causal universe, cosmological matter creation 79−53945
causality, generalized integral condition for S-matrix, reln. to algebraic approach 78−37150
causality, localisation and spreading of wave packets 80−90715
causality, probabilistic theory, discussion 79−67138
causality, problems in theory of tachyons 78−28945
causality and fixed points in the renormalization group 79−71597
causality and possible faster than light processes 77−54061
causality and proton-neutron mass difference 77−61286
causality and relativity 78−81901
causality for tachyons in macrophysics, extended relativity 77−22411
causality for tachyons in macroscopic processes 77−2542
causality laws, violation with tachyon discovery, book contrib. 79−44720
causality principle rel. to light diffr. 78−55295
causality problems in special relativity, tachyons in an expanding universe 79−67155
causality recovery in special relativity for tachyons 78−73843
causality structure, relativistic, representations by operator density current 77−45767
causality violation by controlled creation and absorption of tachyons 77−45693
causality violation by controlled creation and absorption of tachyons, answer 77−45694
causality violation by tachyons 77−22412
causality violation in controlled creation and absorpt. of tachyons 77−22413
causality violation region, positive- and negative-energy states 78−29024
causally connected events, obs., means of perception 78−28944
causation analysis refinements rel. to revolutions in modern physics 78−12522
charge and action polarity and their order props. 77−37771
charge quantum determination, computer programs for high-school expts. 78−86094
charged particle spin, theory using fluid basis for matter and energy 79−97542
chronon, fundamental time interval, in quantum theory 77−41500
chronon in quantum theory of electron, existence of heavy leptons, neutrino spectrum 78−70008
classical mechanics, new variational approach 77−71206
classical relativistic dynamics fundamentals revisited *(French)* 78−62074
clock synchronisation rules and transitivity 77−29982
Compton electron wavelength, determ. by cryogenic metrological technique 78−37165
concept of time in physics (considerations on physical time) 79−67139
conformal invariance in elementary particle physics, review *(Russian)* 79−21964
cosmological changes in atomic and nuclear constants 77−49286
cosmological constant and supergravity 77−74171
cosmology, physics and biology in an open universe 79−97119
cosmology, traditional assumptions, critical comments 77−13511
covariance principles, Einstein study, 1912 to 1916 79−40343
dielectric const., space-time dispersion, causality principle *(Russian)* 78−56418
dimensional analysis 80−27263
dimensionality of physical space, assumption of three-dimensionality 78−93515
dimensionless numbers and possibility of life, historical data in cosmic cycle 79−80245
dimensionless numbers and possibility of life, Machian variational cosmology 79−80246
Dirac's large-number hypothesis, angular momentum for Regge trajectory with n=2 80−18091
Diracs hypothesis on time depend. of fundamental consts. 80−90772
Einstein correlation, S-matrix and Feynman zigzag 78−77761
Einstein-Maxwell equations, solns., causality violation in rotating universe 79−44828
electric fractional charge, $^1/_3e$, expt. determ. on Nb sphere 79−21694
electric neutrality of matter, meas. 77−57579
electromagnetic vacuum, isotropy, testing 77−87254
electron charge and velocity, independence limit, atomic neutrality 79−97549
electron modelling by phase-locked cavity 79−63089
elemental abundance, symmetry theory of unit cubes in a cube of side three 79−97541
energy conservation and the principle of equivalence 79−54018
energy in a highly ordered universe, new theory of photon and energy based on two primitive particles 79−67145
equivalence principle, gravitational collapse, and the classical particle problem 79−25927
equivalence principle, or formal mathematical statement, for teachers 79−71200
equivalence principle according to Mach 79−44823
equivalence principle test for spin-$^1/_2$ particles 79−12707
equivalence principle test using space-borne clock 79−49152
expanding universe model with continuous mass creation 79−44647

physics fundamentals continued
Feynman path integral and quantum mech. as $\hbar \to 0$ 77−2557
fine-struct.-const. calculated value, gravit. charge quantisation 77−26524
finite-struct. and gravit. const. in unified theories 77−41802
force concept in classical mech. and field theories 77−49
formalisation of physical theories 80−12883
fractional charge on matter, obs. by mag. levitation of Nb spheres 77−49709
fractional electric charges and mag. monopoles, existence in matter, model 79−13238
fractionally charged ions, search in He gas 80−8954
fundamental constants, calcs. in various theories 77−30354
fundamental constants, self-consistent values *(German)* 79−12758
fundamental length hypothesis, concept in gauge vector field theory 78−93836
fundamental physical constants and their development in time *(Hungarian)* 79−25922
gas constant. determ., low freq. acoustic thermometry, 4.2 to 20K 79−30477
gedanken expt., observation without interaction, effects 78−89362
generalized macro-causality in relativity theory 79−85021
geometric objects with fractional dimension, seacoasts, galaxy clusters, turbulence and soap, book contrib. 77−87640
Grassmann variables, possible interpretation of theories 77−79001
gravitational constant, impossibility of var. in Newtonian physics 78−69675
gravitational constant meas. using evacuated torsion balance 77−49707
gravitational constant value, constraints from obs. of white dwarfs 79−25464
gravitational constant variation, Dirac's Large Numbers Hypothesis 79−16819
gravitational redshift and principle of equivalence 77−9944
gravitational time dilation according to absolute space-time theory 77−43
gravity as gauge theory of de Sitter group, fundamental length parameter 77−64990
hadronic bremsstrahlung models, ordinary and charge conserving, causality and unitarity breakdown 77−57486
high energy physics, experimental basis *(Danish)* 79−9357
high-energy physics, progress and prospects 78−45989
human brain functions rel. to foundations of physics, science and technology 78−73823
idealizations and approximations in physics 79−67137
inertia, origin, experimental approach to understanding 77−17799
infinite diffusion velocity and causality in special relativity 79−63027
inversion problems, information theoretical approach 80−27210
irreversibility, time and anisotropies, cosmological origin 77−13510
Kerr metric, causality violation 79−80479
Kerr metric, vortical type geodesics, causality non-violation 78−54251
large-scale uniformity of physical laws, evidence from QSO absorpt. redshifts 80−73079
laws, physicist's role 80−105523
laws of nature, ideas on validity *(French)* 77−78944
light and neutron vels., relative anisotropy *(Russian)* 79−49194
light deflection by Sun, principle of equivalence calcs. 78−81729
light propagation in Earth rotating frame, time discontinuity obs. in clock synchronisation 77−60333
light velocity meas., current status *(Chinese)* 79−97342
local causality and quantum mech. state vector 77−22438
local commutativity, possible expt. test 77−74266
localisation concept of relativistic particles, consistency with causality 77−33883
locality concepts, Bell's theorem, quantum theory predictions and interpretations 78−93550
long range interactions, range definition 79−54001
Mach's Principle, relative motion and fundamental numbers 77−9943
Mach's principle equivalence principle, violation, for teachers 78−61998
mathematical physics, success and failure viz. Kolmogorov-Arnold-Moser theorem, gravit. collapse, singularities, matter stability *(German)* 78−65744
measurement standards and structure of physical knowledge 77−74347
microcausality principle in QFT *(Chinese)* 78−86195
microphysics, stochastic basis for quantum mechanics 79−53997
microphysics foundations, use of Bell inequalities in expt. test 79−102
microscopic causality for quantised solitary wave theories 78−82095
Minkowski space, causal logic 78−16739
molecular computer, biophys. rel. to phys. of real world 80−30630
negative energies, teaching approach 77−13553
neutron charge determination, expt. using ultraslow neutrons 79−9370
Newton's first law of motion, formulation and interpretation in various languages *(Czech)* 78−45481
noncausal wave propagation in spin-0 theories with external field interactions 77−41770
noncausal world model; can an effect precede its cause? 78−73824
nonintegral dimens. spaces, axioms, measures, topology, physical implications 77−64929
nonrelativistic algebraic models, gauge invariance, causality props. 78−62319
nuclear constants, direct test of constancy 77−2889
particle detection and creation for scalar quantum field in curved space-times 77−67597
particles and fields in simple model of physical system, unified view 79−25951
photon bunching in thermal radiation, temp. depend., photodetector thermal fluctuation 78−24748
physical constants, conceptual nature 77−67167
physical constants variation, limits from 21 cm absorpt. detect. at $Z \approx 1.8$ in QSO 1331+170 79−75292
physical operations, diagram operations 80−46846
physical systems, principle of stability of invariance 77−26164
Planck's constant, Lorentz invariance interpretation 79−6006
Planck's constant, meas. in 3rd yr undergrad. expt. on Josephson effect 78−54126
Planck's constant, numerical value, dynamic mechanism, classical/quantum physics borderline 79−21573
Planck's constant determ., photoelectric experiment and apparatus design 78−41109
Planck's constant to neutron mass ratio *(German)* 79−6077
Planck constant, upper limit determ. to freq. dispersion by nonlinear spectroscopy 77−79050

physics fundamentals continued
Poincare cycle, general relativity, cosmology and thermodynamics 79−80378
precise measurement, significance in physical science and metrology *(Chinese)* 79−75487
principle of equivalence, red-shift, Eotvos expts., EM system free-fall 77−64982
principle of identity of indiscernibles, photon violation, discussion 79−25817
proton half life, Dirac approach to large number coincidences 80−27501
proton/electron mass ratio, limits to past variability from quasar absorpt. line redshifts 77−61338
protophysics of time and relativity principle 77−67176
QED, nonlocal, relativistically invariant, bubble electron model, fundamental length and causality 79−30687
quantum and relativistic unitary interpretation 77−87641
quantum field theory, microcausality, lack of consistency with exponential growth in momentum representation 78−16931
quantum logic and Jauch-Piron states 77−33887
quantum logics, extended characterisation theorem 77−87658
quantum measurement, consciousness and environment 77−61
quantum measurement as a communication with nature 79−17253
quantum measurement problem, collapse of wave function 77−62
quantum mech. commutator acting on finite space with discrete spectrum 77−64
quantum mech. reformulation, modification and EPR paradox 77−22441
quantum mechanics, consequences of more general theory of symmetries, isolated system 78−49718
quantum mechanics, EPR paradox, reduced density matrix method, review 78−77766
quantum mechanics and nonlocal models comparison 78−4510
quantum mechanics as stochastic process in phase space 77−64964
quantum mechanics expectation values as averages on fuzzy phase space 77−33888
quantum mechanics quantisation postulate 78−72
quantum nonlocal interactions and Bell's inequality 77−22442
quantum numbers, uncertainty, min. entropy and discrete spacetime 77−87659
quantum objects, point defects as possible model 77−22433
quantum of time, relation between proton mass and ρ-meson lifetime 77−22716
quantum proper and improper mixtures, observable differences 77−67325
quantum single system and ensemble interpretation of pure quantum states 77−33878
quantum states and preparation procedures 77−67321
quantum theory, causal interpretation 78−54241
quantum theory, compatibility of sets of propositions 78−54239
quantum theory, hidden variables and locality 77−58
quantum theory, implication of quantum theory 78−54241
quantum theory, new approach 78−54240
quantum theory, paradoxes, interpretation and time symmetry 77−59
quantum theory, single system measurement and description 77−22440
quantum theory, superluminal connections of events, a theorem 77−67324
quantum theory multivalued observables, new tests 77−57226
quantum theory propensity microrealistic interpretation 77−9899
quantum theory realist interpretation, indeterminancy and measuring process 77−9898
quantum thermodynamics and mech. unified theory, irreducible dispersions 77−60
quarks, fractional charge search using a Millikan type apparatus 78−54334
quarks, unbound, attempts to reconcile recent evidence for existence in stable matter 78−58160
quaternion physical quantities 77−45671
reciprocity and conservation theorems, for fields with general time dependence 79−80452
reference frames and the velocity of light, book contrib. 79−58542
relational theory of physical space 77−74184
relativistic causality in QED 79−71670
relativity, extended projective and conformal 79−21547
retrocausation in electrodynamics 77−19150
reversed causality illustration, Kac ring, expt. searches 77−49704
Rydberg const., direct freq. determ. by two-photon mm spectroscopy 80−43018
Rydberg constant, determ. from Hα line fine struct. meas. 79−54093
scaling, classical and quantum 79−35626
segmented structures, space-time point segment 78−32
simultaneity and conventionality in special relativity 77−53778
simultaneous verifiability of yes-no measurements 79−44768
space-time models causal foundations *(Russian)* 77−37759
space-time primordial continuum, principle of least action 77−60921
space-time structure operational anal. in quantum-relativistic theory 77−67322
spacetime, elementary axiomatisation, particle, signal, transmission, reception concepts 78−70044
spatially dispersive media, generalised Kramers-Kronig formula, vac. polarisation tensor 77−17798
special relativity, arithmetic basis 77−74220
special relativity, consistency of postulates, comment on recent paper 77−9883
special relativity, postulate consistency, reply to recent paper 77−9900
special-relativistic theory of locally anisotropic space-time 77−67278
statistical concepts, for teaching 79−35501
stochastic physics, quark bag model 79−54000
supergravity, unified theory of basic forces 78−50001
superluminal and subluminal causal transformations through transformations of metrics 78−28943
superluminal wave propagation, causality criteria 78−73861
symmetry and conservation, for teachers 79−26
symmetry breaking, and nature of weak interactions 80−27428
symmetry principles, historical review *(Hungarian)* 78−73818
symmetry related to conservation law, Noether theorem 79−45034
tabulation of 1973 CODATA-recommended values 77−57298
tachyon quasi-catastrophe theory, tachyon existence, imaginaries, and causality, book contrib. 79−44815
tachyon theory, information flow, causality 78−82261
tachyon theory, information flow, causality 79−9429
tachyons, causality, recovery in macrophysics 77−26172

physics fundamentals continued
tachyons, causality in macrophysics, paradoxes, extended relativity theory 77−22406
thermodynamics, first law from microphysics, suggestion 77−87714
thermodynamics, second law rel. to time, structure, and fluctuations 79−30398
thermodynamics with nonconservative forces and internal degrees of freedom, exterior calculus 77−2631
thermoelasticity, dynamic theory, based on causality principle 80−69657
time, the concept in physics 78−28946
time analysis, universal and relativistic time 79−30299
time asymmetry for mixing system 78−12663
time reversal logic 79−30677
time without clocks 79−71272
transformations of physical systems, decay, molecular rearrangement, causality 77−2551
unified theory of reality 77−45722
unified thoery of matter, derivation of fundamental physical law 78−20982
units of space and time, difficulty in microscopic definition *(French)* 77−54060
universality of laws 79−44697
Universe isotropy and homogeneity, origin 80−22125
variation of constants, summary of obs. evidence 79−12759
vitalism, nonlinear transforms in Hilbert space 78−73133
wave function, inclusion of observer, geometrodynamics 78−54234
wave processes description, by ordinary differential equations *(Russian)* 78−81850
Weisskopf-Wigner theories, causality 77−67598
$e^+e^- \rightarrow l^+l^-$, l=3, μ, τ, charged lepton universality test 80−32091
$\gamma \rightarrow e^-e^+$ generalised conservation laws of physics, electron energy spectra theory 79−85246
$\gamma \rightarrow e^-e^+$ generalised conservation laws of physics, electron energy spectra theory 79−85247
W ions, fractionally charged, search 78−29083

physiological models
see also brain models; neurophysiology; physiology
Acetabularia cell electrical parameters and equiv. cct. 77−56350
acoustic biotope neural representation, stimulus event relations for sensory neurons 79−66475
acoustic fluctuation strength models comparison 78−65033
acoustic reflex adaptation to combined steady-state and repeated pulse stimuli 78−44555
active transport and energy transformation, quantum mechanism 78−53364
acupuncture, transient impedance between stimulation points 79−43977
adaption model evaluation for vestibulo ocular reflex 79−11931
adenylate cyclase regulation, depend. on sugar transport system, review 78−69031
adrenocortical steady-state characts., blood flow and ACTH conc. 77−81517
alpha-rhythm, neural vet model 80−76719
ambulatory neuromuscular activation control model 79−57638
anaesthetised human subject temperature change model 79−92160
aneurysm, pulsatile pressure and flow distrib. using latex fusiform models 77−21547
antagonistic muscles, functional elec. stimulation optimisation, math. modelling, joint motion 80−61730
aorta, canine, finite element soln. of Navier-Stokes eqn. 79−29550
aorta, dog, simulation via adaptive model 79−11964
aorta, stroke volume calc. from transthoracic impedance plethysmogram 78−7381
aorta model, two chambered, viscoelastic, press. estimation in ascending and descending aorta 78−77076
aortic coarctation distal flow profiles 78−44528
aortic dynamics in man, analogue simulation model 78−80903
aortic stenoses modelling 79−79581
aortic valve, vortex motion and induced pressures 79−62288
aortic valve model time-depend. laminar incompressible flow through spherical cavity 77−9217
arm and forearm exercise joint force musculoskeletal model 79−92272
arm movement control, central integration function model 79−83757
arm movements controlled by peripheral feedback, in humans, simulation 78−80891
arm posture control, spring model and equivalent neural network 80−101196
arm swing in human locomotion, mathematical model, electromyographic recordings 79−39434
arterial bifurcation, steady convective diffusion model 77−21546
arterial bifurcations, glass models, pressure meas. 79−25021
arterial blood flow, shock wave formation, math. model 79−5305
arterial dynamics, model of multilayered shell with fluid flow 77−29171
arterial dynamics in mammals, similarity principle 78−44532
arterial elasticity, transcutaneous assessment by US Doppler flowmeter 77−77948
arterial flow lipid transport model 78−44552
arterial impedance estimation, systemic, from cardiac catheterisation data 78−11691
arterial models, preparation method for flow studies *(German)* 79−53166
arterial segment loading-unloading simulation and analysis 79−83844
arterial stenosis, math. model 80−72202
arterial stenosis model, pulsatile flowfield downstream 80−17001
arterial stenosis models, initiation of turbulence, steady and pulsatile flow 79−79577
arterial system and cardiac activity, optimum tuning model *(German)* 79−16225
arterial system characterisation in time domain 78−40213
arterial system least energy regulation 78−53434
arterial system math. model, press.-flow relationships 78−53435
arterial system model validity, quantitative evaluation 80−61599
arterial system nonlinear model validation 79−96600
arterial systolic blood pressure monitoring, circulation model 77−60224
arterial velocity flow system, transmission-line model 77−44715
arteries with nonlinear elastic modulus, press. pulse propag. 78−44550
arteriosclerotic flow models, velocity fluctuation and shear stress obs. *(German)* 79−16226
artery pressure-radius relationships, comparison of elastic tube models 77−64077
articular cartilage, function of collagen fibril ultrastruct. 79−34597

physiological models continued
articular cartilage, load-displacement-time characts., rel. to fluid flow in matrix 77−48820
articular cartilage biphasic rheological model 79−92264
articular cartilage single layer model, flow fields created by a sliding load 80−104630
articular surfaces, math. representation of positron 80−3685
articulation development, possible nonlinear time varying control in feedback path 78−35870
artificial head for head-related stereophonic recording, design *(German)* 78−40199
artificial heart, simulation of fluid dynamics *(Japanese)* 79−43954
artificial kidney dialysis exchange model reliability tests *(German)* 79−2165
artificial knee simulator requirements and prototype trials *(German)* 79−8578
artificial liver support, protein-bound substance removal kinetics 79−20710
artificial ventricle, pneumatically driven, sac-type 78−15925
atherogenesis at branching sites, steady laminar flow field 77−21553
atherosclerosis, simulated, US assess., in-vitro and in-vivo comparisons 79−96639
atrial contraction, model anal. of contrib. to ventricular filling 80−85424
audition coordinating cerebral activity model 80−85404
auditory and visual impairment simulator development project 79−83982
auditory detection of intensity increments of narrowband noise signals, amplitude model 80−61591
auditory frequency measurement based on neural timing 77−5011
auditory function, linear system model 80−51127
auditory models and signal processing, conf., Munster, Germany (Sep. 1978) 80−90610
auditory nerve, effect of response suppression on exposure to 2-tone stimuli 80−51115
auditory nerve data appl. to binaural interaction theory, tone detect. in noise 77−36950
auditory nerve discharge rate, two-tone suppression, phenomenological model 77−16936
auditory nerve fibre model 80−94227
auditory nerve firing rates, patterns for spoken digits 79−83802
auditory neuron, characts. of digital model 78−3516
auditory perception nonlinear model with autocorrel. feedback 80−81615
auditory peripheral feedback qualitative model 79−39422
auditory selectivity, two-stage lateral inhibition 77−56382
auditory system from middle ear to primary auditory nerve, analogue and computer model 77−29158
auditory system of crickets, acoustical analysis 79−92226
auditory system pitch detection mechanism model 77−90811
auditory transmission from mech. part of nerve endings 79−57667
auto-immunity, math. model of cell dynamics 77−16900
autonomic neuron development 78−77033
autoregressive model order selection applied to physiological signals 80−104780
axon, motor, reflexes following intranervous regeneration 79−34541
axon, squid giant, exponentiated exponential model g Na^+ and K^+ cond. changes 78−44493
axon membrane, squid, null space in Hodgkin-Huxley eqns., critical test 79−83747
axon membrane freq. domain currents 79−62222
axon membrane white noise, stimulation, strength-freq. relationship, squid 78−3466
axon Na conductance and Ca transport, squid, mol. model 78−85305
axonal K^+ transport, single-file model for squid giant axon 77−73517
axonal membrane transport, elec. field distrib., ionic selectivity and permeability 79−34532
bacteria, attachment to solid surface, influence of substratum critical surface tension 79−79493
bacterial chemoreception, response regulator model in simple sensory system 77−73534
bacterial migrating chemotactic bands, quasi-elastic light scatt., E. coli 78−77018
ballistic walking, math. model of swing phase 80−67131
barnacle photoreceptors, lateral vs. median, elec. props. and early receptor pots. 77−44651
basilar membrane, electrical model giving displacement 77−90810
basilar membrane, nonlinear electric circuit model, distortion 77−25459
basilar membrane, nonlinear model rel. to two-tone suppression 77−48811
basilar membrane displacement, electronic model 77−29159
basilar membrane electronic model for evaluation of speech disorders 78−40206
basilar membrane model, nonlinear, meas. apparatus and circuits *(Japanese)* 78−35868
basilar membrane motion linear and nonlinear models 77−90800
basilar membrane nonlinear model assessment, spatial differentiation as auditory second filter 77−36949
basilar membrane using digital filter for voice features extraction 78−77069
bat echo-locator, phenomenological model of system of precise determ. of direction to target 77−36962
BEIR relative risk and absolute risk models for estimating effects of low level radiation 80−26263
bilayer membranes, ion transfer parameter calcs. 79−53053
bile acid hepatobilary kinetics, compartmental model validity 80−30971
bilipid vesicles, theoretical shapes under conditions of increasing membrane area 79−24960
binaural hearing, monaural information processing on short sounds, neuronal model 78−65031
binaural hearing digital model, stimulus-response characts. 78−20192
binaural signal analysis by cross correl. 78−27958
binocular depth perception, model suggested by neurophysiological evidence 77−21527
binocular vision, fusional vergence eye movements rel. to fixation disparity 80−56031
biochemical activity computer simulation 77−40629
bioelectric rhythms represented by coupled synthesized relax. oscillators 80−26218
bioengineering advances conference, San Francisco, USA (Dec. 1978) 79−92416
bioengineering and medical instrumentation, symposium, Laramie, USA, (May '76) 77−25571

physiological models continued
biological multiparticle systems, stat.-thermodynamic treatment, phase transitions *(German)* 79−16119
biological n-compartment model, identification by filtering techniques 79−34507
biological rhythm research, second-order correlation functions and bi-spectra 78−3441
biological two compartment model parameter estimation, computer expt. study 77−70402
biomaterial growth phenomena and behaviour, math. theory 77−81458
biomechanical properties estimation for three body types using photogrammetric method 79−43947
biomembrane, quantum-chemical investigation of cation motion mech. 80−30678
biomembrane electronic cct. model utilising time variant negative res. 78−88696
biomembrane ionic channels, dipole cooperative model 79−53054
biosystems under stress, prerupture behaviour 79−39437
biped locomotion control, digital simulation 78−80904
bipedal locomotion, inverted pendulums stabilisation algorithm *(Japanese)* 80−81630
bladder and urethral function during micturation 79−88110
bladder distensibility and contractility characterisation indices 79−92265
bladder smooth muscle impulse propag., math. anal. *(Japanese)* 78−53359
blood, effect of flow channel thickness on surface-induced damage 79−39439
blood, rheological behaviour, viscoelastic model *(French)* 80−76779
blood, unsteady viscous flow in non-uniform channels, numerical anal. 77−52830
blood cell banding in US standing wave field 79−62291
blood circulation simulation development 77−66825
blood damage by artificial part-hearts and pumps, dwell minimisation model *(German)* 79−16345
blood flow, laminar-turbulent transition, in pulsatile flow *(French)* 77−5022
blood flow, post-stenotic turbulent wall pressure fluctuations 80−16994
blood flow, US Doppler signal LF spectral analysis 79−62312
blood flow in artery, math. model 78−31831
blood flow in collapsible tubes 79−25020
blood flow model, hydrodynamic study with simulant fluid 79−25023
blood flow simulation using a hydrodynamic generator 79−79706
blood flow through small diameter tubes, two-fluid model 80−3667
blood glucose regulation parameter estimation, optimal inputs 78−64920
blood in vessel with actively deforming wall, numerical simulation of movement 80−72205
blood mass flow distrib., aortic arch atherosclerotic formations effect 80−16995
blood motion in large vessel partly replaced by prosthesis 77−64082
blood perfusion rate determ. from temp. perturbation, unbiased minimum variance linear estimator 79−92283
blood pressure control model 77−21557
blood streaming in channel with diverging walls 77−52828
blood unsteady flow curved elastic tube model 80−16998
blood vessel simulation, ideal fluid small oscillations, mass forces in elastic shell 79−77253
blood vessels, effects of laser surgery 79−66505
body fluid distribution, flowing-mixing compartmental hybrid model 77−44582
bone, anisotropy of Young's modulus, fibre-reinforced composite model 80−35944
bone, distrib. of piezoelec. effects in bent long bone, anal. model 77−36983
bone, human cortical, local piezoelec. polarisation as function of stress freq. 77−32933
bone, stress generated potentials rel. to collagen piezoelectricity 77−32932
bone, stress generated pots., linear piezoelec. model 80−3688
bone, transport mechanism between blood supply and osteocytes in long bones 77−86472
bone imaging radiopharmaceutical local accumulation model 78−24127
bone mechanical model with appl. to human upper tibia, porous material, deform. *(Japanese)* 78−88724
bone tissue, dry, piezoelectric model 79−25015
bones, long, struct. anal., appl. to human tibia 77−21551
brain, planning and problem solving mechanisms 80−45877
brain cortices large-scale simulation via BOSS system 79−2039
breast cancers, microwave irradiation, EM energy and temp. distrib., numerical calculations 79−100697
breathing control hierarchical goal-seeking model description 78−80899
breathing control hierarchical goal-seeking model performance 78−80900
breathing process analogue model *(German)* 79−16228
brightness perception and retinal rivalry in binocular vision, integrated model 80−101180
bronchial branches, time-dependent flow model 77−44701
bronchial elasticity and ventilation mechanism inequalities, theoretical anal. *(French)* 79−48281
bronchial tree, non-symmetrical, flow study, asynchronous ventilation appl. 79−70573
burnt skin heat and water losses, thermal modelling 78−31790
bursting pacemaker neurons, Ca^{2+} effects modelling 78−44484
calf, human, impedance plethysmographic sampling field 79−57740
caloric nystagmus, air and water, mathematical model 79−24983
capillary blood flow and transcapillary fluid exchange, methematical model 77−29173
capillary counter-current system hydrodynamic effects 77−40695
capillary tracer exchange, 4-phase model 80−101152
capillary-tissue diffusion in multicapillary system, anal. 79−2095
carbohydrate and lipometabolism systems interaction, control appl. 78−31758
carbohydrate membrane, potassium p-nitrophenoxide transport, ionic equilibria perturbation by cyclodextrin 79−96523
carcinogenesis, time and dose factors 79−70590
cardiac acoustic model for computer-aided surface acceleration mapping 78−35791
cardiac adaptation and hypertrophy, ventricle model *(Japanese)* 78−31828
cardiac and torso models for ECG forward and inverse problems 77−40837
cardiac arrhythmia simulation device 78−44636

physiological models continued
cardiac assistance, in-series, by intra-aortic balloon pumping, haemodynamic responses, computer model 79−96711
cardiac chemical power, appl. of power, work and efficiency eqns. to left ventricular energetics in man 80−16912
cardiac chemical power, derivation of chem. power eqn. and determ. of eqn. consts. 80−16911
cardiac conduction and propag., equiv. cct. 78−31791
cardiac contractile filament and series elastic work and power, mathematical model 80−16981
cardiac dipole moment variation with body size, double-layer model 77−56358
cardiac electric field probabilistic model 79−39387
cardiac electromechanical field model and computation, inverse problems 79−39400
cardiac injury potentials, inadequacy of solid angle formulation 77−44633
cardiac left ventricle, contractile filament stress rel. to wall stress 80−56096
cardiac muscle, mathematical contractile model *(Japanese)* 79−57632
cardiac muscle force-velocity relation, anal. in time domain 80−35943
cardiac muscle model activation parameter behaviour, numerical study 78−11686
cardiac output control mechanism modelling *(Japanese)* 78−69133
cardiac output estimation from aortic pressure curves, simulation model 79−53177
cardiac output flow wave calculator *(Japanese)* 77−70489
cardiac potential function represented by chains of maps, analysis 77−37062
cardiac Purkinje fibre, Na current model 79−43861
cardiac Purkinje fibres, sheep, intercellular clefts effect on elec. props. 79−34522
cardiac R-R interval prediction models, comparison of 79−39549
cardiac rhythm disturbances, Markov process model *(German)* 79−2019
cardiac slowing, respiratory gating mechanism 77−12902
cardio-pulmonary system, thermal indicator heat and mass transfer, pulsatile flow 79−25017
cardio-pulmonary system, thermal indicator heat and mass transfer, pulsatile flow 79−25018
cardiovascular computerised modelling, pressure regulation in hypertension 79−88098
cardiovascular control dynamic test method evaluation, model considerations *(German)* 77−52813
cardiovascular dynamics simulation, with all-pneumatic artificial ventricle system 78−81082
cardiovascular modelling of pressure regulation effects, hypertension 77−73539
cardiovascular modelling to study effects of pressure regulation: hypertension 79−25027
cardiovascular simulation of infants with transposition of great arteries after surgical correction 77−44713
cardiovascular system, analogue circuit and compartmental model, normal and defective states 79−57700
cardiovascular system, nonlinear math. model, computer anal. of external counterpulsation 77−2069
cardiovascular system as fluid cct., elec. network analogue 80−30759
cardiovascular system simulation by elec. compartmental model 79−5388
carotid artery Na kinetics 3-compartment model, incorporation of diffusion effects 78−27996
carotid body, model for chemoreceptive process *(German)* 77−29162
cartilage, model for surface flow 80−85431
category detecting nerve cells formation, mathematical theory 78−80859
cell, interference effects on observation 79−84055
cell clone growth computer model 77−40643
cell division, model relating cell deformation to elastic props. of cell membrane 80−3606
cell electric circuit model, alternating signal interaction 78−77011
cell electric circuit model, alternating signal interaction 78−77012
cell energy metabolism, ATP effect on initiator stage enzyme activity and conc. 78−64950
cell external elec. fields, Fourier transform anal. 79−62223
cell kinetics stochastic model using DNA microfluorometric data 79−83723
cell lethality model for radiation therapy population kinetic parameter derivation 79−43965
cell population auto-activation, math. model 78−77017
cell population auto-oscillations, influence of delay 77−36892
cell representation by an elec. circuit, voltage gain 80−40977
cell survival curves, biological variability model 80−108978
cell survival dependence on radiation quality, models and exptl. data analysis 80−26287
cells, volumetric changes during freezing and thawing, thermodynamic model 80−108863
cells laser Doppler meas., scattering characts. of intersecting beams *(Russian)* 80−3874
cells without highly permeable cell contacts, elec. connection 77−70440
central venous pressure and blood volume distrib., abdominal pressure model 79−92282
cerebellar cortex associative memory model 77−21506
cerebellar cortex model, temporal behaviour study 77−86482
cerebral blood flow, linear computer model 79−92288
cerebral blood flow control in hypercapnia, model 79−100641
cerebral blood flow dynamics, computer model 79−83837
cerebral collateral circulation, simulated on computer model 77−36995
cerebral dynamics model, information sources *(Spanish)* 79−29520
cerebroside-lipid mixed films, surface viscosity 79−74601
cerebrospinal fluid system models for rat, dog, man, intracranial pressure regulation 79−88111
charge transfer in thin membranes, steady state, discrete models 77−16913
chelonian muscle spindles motor stimulation model 77−44636
chemical reactions, perturbation spread in active media with auto-oscillatory props. 79−57562
chemical synapse, feedback mechanism model through elec. current 78−96043
chemically reacting system, temporal oscillations 77−25359
chemoreflex responses to hypercapnic stimuli models 79−34578
chemotactic bacteria travelling bands 78−44516
chlorophyll special pair models, reaction centres 80−3574
choroidal blood flow meas., theoretical basis using radioactive inert gas 79−92349

physiological models continued
chronic obstructive pulmonary disease detection, airway resistance model 79−96603
circadian clocks, mathematical models 79−34470
circadian oscillators, two-dimensional limit model for constant light 79−92255
circadian rhythm related to human body temp. 79−70525
circulation models, numerical integration method for improving soln. stability 78−69118
circulatory, heart valves, insufficiency and pressure loss in mitral position 79−20717
circulatory clinical model matching techniques 79−53176
circulatory system polynomial model *(Japanese)* 77−70488
claw hand optimal surgical correction, finger biomechanical model 79−92268
clonus, simplistic model rel. to diagnosis and therapy 77−48786
cochlea, hydroelastic modes 77−77915
cochlea, mammalian, fluid flow permeability through hair cell cilia 79−53157
cochlea, one-dimensional model illustrating resonance 80−61581
cochlea 2-D model, heuristic approach and numerical results 77−16937
cochlea freq. selectivity sharpening models comparison 78−53418
cochlea model, for signal anal. 77−26281
cochlear fluid mechanics, kinetic theory 78−53440
cochlear hydrodynamics model, digital simulation 78−31821
cochlear LF variable geometry model for morphological disorder compensation 78−40182
cochlear micromechanics, mechanism for transforming mech. to neural tuning within cochlea 78−11666
cochlear model, three-dimens., comparison of WKB calcs. and experimental results 79−70556
cochlear model, two-dimens., comparison of WKB and finite difference calcs. 79−70555
cochlear models−1978 80−94221
cochlear nucleus neurone response, model of phase struct. of bitonal stimulus 78−80887
collagen, hydration and intramolecular fusion, NMR and calorimetry obs., dynamic model 79−79451
colonic electrical control activity, human, computer model 80−61537
colour prediction model for multispectral imagery 77−71395
colour sensing optoelectronic device, neural mechanism modelling 80−12128
colour vision, human, 3-D homomorphic model and digital colour image processing 79−88077
colour vision, line elements 80−97910
colour vision models, vector magnitude operation, derivation from signal detect. theory 80−101174
colour vision opponent processes, psychophysical and electrophysiological studies 78−53402
compartment tracer flow modelling and digital imaging 80−101257
compartmental models, identification of exchange parameters, biomedical appls. *(French)* 80−42044
compartmental models with delays, phys. realisability 78−53313
compartmental models with delays, physical realisability 80−7998
compartmental systems, multi-input and multi-output, controllability, observability and structural identifiability 78−76978
compound action potentials, volume conductor study, forward problem 79−88067
cone, computer-driven hardware model, response obs. 80−72402
cone cell of tiger salamander, hardware model 78−44505
cone saturation in humans, rel. to cone signal eqn. 77−44663
cone specific c-wave in turtle retina 78−69060
control system simulation and modelling 77−90848
cornea formation, human 78−35840
corneal hydration endothelial control theory 78−35841
coronary artery bypass fluid mechanics, for introductory physics course 77−78911
coronary flow model, of horse, method of characts. calc. 77−86524
coronary haemodynamic parameter estimation using elec. analogue 77−37092
coronary regional intravascular resist. determ. 78−31853
cortex ensemble distribution patterns in different functional states 77−48774
cortical event-related potential waveform, effect of stimulus sequence 77−2011
cortical evoked potentials, math. model for source localisation, somatosensory stimulation 80−89774
counter-current system with capillary-size vessels, fluid movements due to hydrodynamic forces 77−5024
counterpulsation dynamics simulation, rel. to heart assist. blood pump 80−16996
cranial structure exposed to RF radiation, thermal response model 80−94285
crayfish antenna mechanoreceptor unit sine-wave stimulus response obs. and model 79−57640
crustacean cardiac pacemaker control system, model analysis 77−52766
crustacean cardiac pacemaker control system, simple model 77−52765
crystalline lens accommodative efficiency rel. to anterior chamber depths 79−83765
crystalline physiology, model for non-chemical form of life 77−90978
curve crossing problem for Gaussian stochastic processes, neural modelling appl. 78−85299
cyprinid retina, model of function at outer plexiform layer 80−12103
cytoplasm spherical drop with effective surface tension influenced by oscillating enzymatic reactions 80−108862
decompression model for deep sea diving 77−44709
decompression sickness, bubble form. in gelatin 77−13051
dendritic membranes, active vs. passive effects on simulated neuron transfer properties 79−24976
dialysis therapy, single compartment model appl. to urea and creatinine kinetics 78−48931
diastolic semilunar valve vibrations, heart sounds, one-dimensional model 79−79580
diffusion neuron model, parameter estimation 77−40654
digestive tract electrical rhythms simulation 78−64970
directed cell locomotion model, turning-angle and run-length distributions 77−21502
direction sensitivity in visual cortex, neural net model 79−48248
disabled human operator, new approaches to modelling 79−92253
disease prognosis, appl. to haemorrhagic shock, nonlinear dynamical model 79−83838

physiological models continued
distributed type associative memory model with quantised Hadamard transform 80−108867
disturbed cell renewal systems, simulation by microprocessor system 80−35859
diuresis, medullary Na depletion, digital computer simulation 77−60226
DNA, UV irrad. of mammalian cells, postreplication repair model 78−80918
dorsal hippocampus curvature effect on elec. field generated by it 79−57619
drug elimination interactions, physiological flow model in rat 80−81628
drugs and tracers distribution determ. by biological system simulation 77−40956
duodenal slow waves, human, anal. and modelling. 80−72146
dynamic phantom for radionuclide cardiology 80−12232
dynamic receptor pattern generation model 79−62207
ear, use of larger replica for KEMAR manikin 79−70557
ear level dependent freq. selectivity model *(German)* 77−64038
ECG, electrical generator, integral characts. meas. by automatic cylindrical coordinator 79−29646
ECG, models solving direct and inverse problems, systems approach 78−28121
ECG activity models for computer simulation *(Spanish)* 78−11758
ECG digital simulator, for test appl. *(Spanish)* 78−40359
ECG eccentric spheres model for geometry and inhomogeneities study 79−70540
ECG signals, homomorphic anal. and modeling 79−74768
ECG sources in a 2D anisotropic activation model 80−40994
ECG theory computer application programs *(Spanish)* 78−20165
echo-locating animal, neurocorrelometer model 78−96059
EEG, power spectral density estimates of subcortical spiking frequency 79−24972
EEG analysis by all-pole model 80−41287
EEG potential, theory, model with thin meninges 80−51283
EEG potentials in model of thin membranes of brain, multilayered spherical cable model 77−25408
egg cell membranes, starfish, inward rectification blocking model 80−61523
elbow flexion-extension and forearm pronation-supination for elbow endoprosthesis design 80−3682
electrical impulse spread in medium with non-monotonic function 79−92201
electrically excitable membrane, phys. model, voltage-current characts. 77−25382
electrocardiological diagnostic efficiency improvement by cardiovascular system model dynamic optimisation 79−39569
electrocardiology 4th International Congress, Balatonfured, Hungary (Sept. 1977) 79−39384
electrokinetic phenomena in biology, book contrib. 80−12326
electrolyte-membrane-electrolyte, freq. depend. of capacitance and cond., model 77−21488
electromechanical model for human articular cartilage 80−104631
electron transfer kinetics models 79−39339
electronic neuron model incorporating both active and passive responses 80−8040
electrophysiological research animal model, chronically instrumented 80−26323
electroreceptor-electric organ system, electronic circuit simulation *(Japanese)* 78−40132
electroretinogram, adaptation-overlap model, response to laser stimuli 79−74650
electroretinogram, E- and b-wave analogue model, retinal expression of inductive reactance 77−48797
electroretinogram P III component model, luminance variations 77−81495
electrosurgical dispersive electrode site temp. and current density distrib. model 79−92424
EM dosimetry for human and animal models, numerical techniques review 80−36142
EM energy deposition for realistic model of man, numerical calc. 80−12180
embryo in utero, human, injurious effects of microwaves 79−83850
EMG, surface, digital simulation, spectral anal. 78−80863
EMG, surface, model for digital simulation 78−80862
EMG of biceps brachii muscle, single motor unit action pot. model 78−53386
EMG power spectra linking to recruitment and rate coding 80−3616
EMG rel. to muscle force 78−40231
EMG signal generation, quantification using automata theory 77−29132
EMG signal nonstationary model 77−86481
EMG spectra, factors affecting interpretation, stochastic process model 77−44825
end plate current quantitative description and reconstruction 77−52770
endocrine and metabolic systems simulation 77−86434
enzymatic active transport model 80−51049
enzyme mechanisms, multiple pathway, computer-aided analysis and modelling 77−81388
epicardial excitation pattern spherical double layer model, using human multipole data 78−27928
epileptic activity modelled as chain reaction within system of interconnecting cells 77−48787
epileptic seizure spatiotemporal patterns, neuronal network model 77−64019
epithelium, tight, impedance anal. using distributed resistance model 79−62201
ERG, effects of conducting media inhomogeneities 80−51078
ERG, oscillatory pots., analogue circuit model and frog obs. 80−89750
erythrocyte, human, chloride distrib. and transport, cell membrane struct. 77−1983
erythrocyte, human, steady rate of glycolysis rel. to ATP conc., quantitative model 78−53354
erythrocyte aging, model for pharmacological effects on erythrocyte flexibility *(German)* 79−79583
erythrocyte haemolysis, human, thermodynamic and kinetic model 79−92191
erythrocyte tank-treading motion in a shear flow 80−104568
erythrocytes, frozen human cells, conc. polarisation effect 78−3460
erythrocytes, human, effect of hydration on water content 77−16921
erythropoietic activity clinical assess., distrib. model of Fe kinetics 79−100587
excitable elements, approx. methods of theroy of networks 77−86479

physiological models continued
excitable medium, 1-dimens., non-steady processes, division of arrested excitation front 77−70401
excitable medium diffusion discrete models and spatial patterns 78−93629
excitable medium model with existence of several stable pulses of different duration 78−77036
excitable medium self-sustained activity, role of inhomogeneity 78−64968
excitable medium wave vel. calc. 77−56366
excitable membranes, nonstationary ion fluxes 77−44599
excitation properties of the squid axon membrane and model systems with current stimulation 80−67054
excitation spread equation boundary conditions for undistorted impulse movement pattern 77−56365
exhalation in lung model, effect of ventilation and diffusion nonuniformity 80−104603
expiratory flow, expt. test of wave-speed theory of flow limitation in elastic tubes 78−27981
expiratory flow, wave-speed limitation model 78−27980
external counterpulsation, optimal phase shift determ. model 79−29557
external geniculate body receptive fields, neuronal network model 78−64990
extracellular potentials generated by curved fibres in a vol. conductor, modelling 80−97889
extraocular muscle system mechs. model for clinical ophthalmology 78−40155
eye, accommodation and vergence static behaviour, computer simulation of interactive dual-feedback system 80−94205
eye, aqueous temperature stabilisation, laser induced temp. changes and model 77−40713
eye, cone saturation, human, function of ambient intensity 79−2049
eye, direction-selective cells formation modelling in developing retina 80−30721
eye, human, adaptive model using accommodation index 80−51073
eye, hydrodynamic model of aqueous flow in posterior chamber 78−69122
eye, of horseshoe crab, anal. of adapting bump model 78−73160
eye, retinal photoreceptor model, FET cct. realisation 80−56027
eye, retinal receptor model, input intensity adaptive 77−90786
eye, schematic, for the opossum 79−62243
eye, schematic for the rat 79−74647
eye, vergence movements, heuristic feedback system model 77−21517
eye lens formation models, human 77−25423
eye long-term growth and shortsightedness model 79−83768
eye movement, gaze-evoked nystagmus, analogue model 78−27938
eye movement hierarchical control model 77−25429
eye movements, caloric nystagmus, mathematical model 77−73525
eye movements, vergence and version, reciprocal innervation model 77−48798
eye non-ionising radiation absorption, hot spots study, stochastic model 78−35884
eye readaptation after dazzle, multidimensional functional model *(German)* 79−16208
eye tapered parabolic-index fibre waveguide model 79−76803
eye tracking movements of acoustic targets, mathematical model 78−80870
femoral components, probability model for fracture taking into account patient's age 80−41070
femoro-popliteal by-pass graft, flow in idealised models 79−39429
femur, human, finite-element plane stress model 79−79590
femur, three-dimensional finite element analysis 78−7379
fetal head moulding, finite element model investigation 80−57129
fibrin molecule formation, thermodynamic model 79−70527
finger tapping by both hands, coordinated, two coupled oscillators as model 80−101163
flagella bend propagation, derivation of eqns. of motion and simulation 78−77074
flow absorption system, reaction vel. parameters rel. to absorbed solutes conc. profile *(Japanese)* 79−74710
flow in lung and vascular tree structs., optimisation of diameters and bifurcation angles 78−11683
fluorescein tracer model, determination of flow rate of aqueous humor in eye 79−43943
fluoresceindiacetate conversion to fluorescein, in living cells and in vitro, kinetics 77−56332
foetal membrane rupture, human, mechanics, superempirical mathematical model 79−83843
forearm musculature, quantitative anal. 77−36981
foveal colour thresholds, quantum fluctuation model 77−44669
free walking insect leg movement coordination model 77−64073
frequency response charact. meas. using swept sine wave 78−28133
gallbladder epithelial cells, compartmental anal. of osmotically induced permeability changes 78−3455
gas exchange across membrane 77−12870
gas transport in human lungs, revised model 79−100643
gas trapping mechanism model in excised lungs 79−96604
gastro-intestinal electrical activity model, frequency entrainment of oscillators 77−81489
gastro-intestinal electrical rhythms, freq. estimation using auto-correlation and auto-regressive modelling 77−44875
gastro-intestinal tract, physiological signals, spectral analysis, autoregressive technique appl. 80−41269
gastrointestinal electrical activity, Hodgkin-Huxley type electronic modelling 78−61165
gastrointestinal electrical rhythm freq. estimation using autoregressive modelling 78−80855
gastrointestinal electrical rhythm frequency estimation by autoregressive modelling 78−56948
gastrointestinal electrical rhythm simulation, differential quadrature method 77−44634
genetic and physiological process control by magnetic methods *(Russian)* 79−2088
gramicidin A channel cation permeation interactions and anion binding 78−53370
gramicidin A ion channel kinetic behaviour, electrostatic calcs. 78−53368
gramicidin ion pore, potential variation 79−34506
granulocytes, human, spatial trajectories in isotropic medium 79−34523
growth, self-reproduction and autoregulation model, anal. of reactions with stretchable semi-perm. walls 77−81460
physiological models continued
haemodialyser, lumped-parameter model, simulation of artificial kidney-patient system 80−56281
haemodialysis treatment model for metabolic waste conc. dynamics and cerebrospinal fluid pressure 77−60305
haemodynamic model for phasic press. and flow in large arteries 80−94254
haemodynamics, coronary, analysis by circulation model, use of hybrid simulator *(Japanese)* 77−5021
haemoglobin, O_2 linked Cl^- binding sites, pH dependence 79−62174
haemoglobin cooperativity, simple tension-displacement model 79−34472
haemoperfusion through fixed-bed adsorber 78−31976
haemopoietic stem cell population and proliferation model 77−44610
haemopoietic stem cells, functioning kinetics study 79−53063
hand prosthesis, electromyograph controlled aid development *(Spanish)* 78−15924
hand-arm system, distributed-parameter dynamic model 78−92663
head heating by EM waves, human and infrahuman models 80−56125
head-neck system mechanics, for visually triggered head movements 77−36977
hearing, binaural processing of information on short sounds, neuronal model 78−80885
hearing, freq. discrimination as function of freq. and sensation level 77−32910
hearing, intensity discrimination as function of freq. and sensation level 77−36944
hearing, pedestal experiments, formulae for predicting effect of signal on duration, pedestal level and quadrature addition 79−68524
hearing model, cellular approach 78−44515
hearing nonlinearities model described by active processes with saturation at 40 dB 80−56058
hearing sensation induced by pulsed microwave radiation 77−60229
heart, cross-sectional shape change during beats, simulation 77−44714
heart, ellipsoidal model, appl. to left ventricular contractions study 80−104608
heart, long-term adaptation modelling, oscillatory phenomena *(Russian)* 78−40212
heart, mech. model, role of pericardium 80−35938
heart, minimal O_2 consumption and optimal contractility, theoretical approach 79−74694
heart, source impedance and internal reactive power in infarcted left ventricle 77−37007
heart adaptation to large loads structural changes simulation 79−5258
heart conduction system modelling 79−83741
heart congenital defect evaluation from dynamic tracer meas. 78−40378
heart contraction mechanism, modelling 80−72204
heart ejection process, stroke volume calc. appl. *(German)* 78−3631
heart left ventricle, finite element stress analysis, computerised procedure 77−86518
heart multipole moments rel. to activated parts of epicardium and endocardium 79−100588
heart muscle, excitation contraction coupling, mathematical model 79−96542
heart muscle contractility modelling of atria and ventricles 79−53079
heart muscle contraction force, rhythm influence modelling, intracellular pool Ca 79−79568
heart muscle contraction simulation 77−12954
heart muscle preparations, isolated, viscoelastic props., math. model *(German)* 79−53167
heart natural pacemaker, modelling as pulse-freq. modulator 78−40135
heart polyphase harmonic generator model and application to ECG 77−60278
heart rate and blood pressure biofeedback theoretical models review 80−16974
heat and H_2O migration through normal skin, unsteady state 79−92155
heat transfer, transient, analytical solns. for living tissue 79−62197
heat transfer equations, model of clothed man 79−24958
heat transfer in tissue, Pennes model vs. Wulff model 77−40635
Henle's short loop, microperfused, of rates, computer simulation of flow-depend. absorpt. 79−83820
hind-limb reflex movements, chelonian, simulation 79−74642
hip joint, maximum force analytical determ. by biomechanical model *(German)* 79−88099
Hodgkin-Huxley equations for nerve membrane elec. activity, crit. topological test 78−35826
Hodgkin-Huxley model of electrical excitability novel molecular interpretation 79−2024
Hodgkin-Huxley reduced model, speed of spread of excitation, integral differential eqn. 77−21509
Hodgkin-Huxley standard model, squid axons in reduced external Ca^{2+} 80−94188
holographic brain model for associative memory chains 77−90753
homologous displacement resulting from simultaneously applied rostral-caudal tactile stimuli, physiological mechanism 78−20198
human body model, health, disease and treatment use 79−48205
human head EM induced field and power absorption, ellipsoidal model 80−3724
human model, multilayered, EM wave absorpt. 79−70580
human model near a ground plane, approx. calc. of SAR for planewave irradation 79−100660
human motion and force sensory mechanism model 80−8094
human retinal image processing, two-channel model 80−94215
human skull, experimental analysis of vibrational characts. 79−81780
human visual system model for electro-optical imagery display efficiency study 77−73531
human visual system models for image enhancement and display design 77−58279
hypertension in end-stage renal failure, math. model 78−31829
identification of biological systems, survey 78−31753
IEEE 7th Northeast Bioengineering Conference, Troy (1979) 79−79672
iliac arterial bed of unanaesthetised baboon, LF dynamics 79−83816
image number perception in neuron structure, multilayer determined neuron network appl. 77−44674
image size perception in neuron structure, neuron matrices apparatus appl. 77−44673
immobilised enzyme membrane oscillations and pH fronts 77−25387
immobilised enzyme systems, hysteresis, oscillations and pattern formation 79−62173
impulse circulation in excitable medium, critical size of closed circuit 79−92200

physiological models continued
impulse spread through smooth inhomogeneity in an excitable medium 79−79445
inert gas dynamics in subcutaneous gas pockets 77−44707
inert gas transport in the microcirculation, isobaric supersaturation risk 80−45939
inert-tracer technique for myocardial blood perfusion and transport 77−5121
inferior vena cava hydrodynamics, passive mechanical model, negative resistance effects 77−81521
insect flight muscle, rigor cross-bridge pattern modelling 79−20508
insulin secretion neural control, math. model 78−31796
intensive care, instrumentation and control, conf., London, England (May 1979) 79−70702
intestinal electrical rhythms model, stability of entrainment conditions for RLC coupled Van der Pol oscillators 77−56361
intestinal modelling, method of harmonic balance 79−96530
intestinal modelling, spectral anal. of coupled non-linear oscillators under modulation conditions 78−44754
intestinal motor activity mathematical model 77−90847
intestinal myoelectrical activity model 79−70537
intestinal myoelectrical models, pulse synchronisation expts. 80−67061
intestinal tissue, electronic modelling of slow-waves and spike-activity 80−89737
intra-aortic balloon pumping efficacy evaluated by nonlinear cardiovascular system model 78−44732
intracranial pressure dynamics modelling 79−25026
intracranial pressure regulation, nonlinear parametric feedback model 79−96599
intrathoracic airway models, impedance during low-freq. periodic flow 80−41077
intravascular radioactive tracers, calc. of residence time distribs. in fields of external registration 80−72291
involuntary human-voice tremor, anal. 79−5301
ion transport model, intracellular osmoregulation mechanism 77−25400
ionic channels in excitable membranes, current problems and biophysical approaches 78−53369
ionophoretic model for Na-Ca counter transport 79−2017
IPFM neural model, input-output anal., spike regularity and record length effects 80−56016
ischaemic and infarctive ECG simulation during ventricular activation and recovery 78−36018
joint differential mobility meas., periodontal ligament and temporomandibular joint 80−8093
joint lubrication model, nonporous compliant bearing, effects of cartilage stiffness and lubricant viscosity 80−3692
kidney, rat, functional model 79−62282
kidney, six-tube vasa recta model as test problem 80−104610
kidney counter current mass transport spatially discrete models 79−39442
kidney model, numerical soln. by multiple shooting 80−104609
kidney model transient behaviour 78−65065
kidney modelling, numerical continuation method 79−43944
kidney preservation, analogue model of perfusion dynamic changes 79−83724
kidney process modelling 78−44524
kidney solute concentration, control core model, input-output studies 77−56405
kidney solute concentration, renal medulla model and limit cases 77−52821
kinetic schemes theory, integral method 79−53064
knee, human, nonlinear coupled stiffness characts. 77−36974
knee joint, anatomy, menisci load carrying capacity, expts. using four-spring model 80−41067
knee joint, menisci load carrying capacity 80−41068
knee joint replacement, lubrication mechanism model 79−74790
Korotkoff sounds, model expt. on generation 80−98207
larger head-neck motion analysis 79−79579
laryngeal control for pitch change in Japanese word accentuation, neuromuscular model *(Japanese)* 78−40205
lateral geniculate body, types of receptive fields and freq. characts. 77−25424
lateral-inhibition type neural fields, pattern formation dynamics 77−90761
leaf CO_2 absorption and diffusion, sun vs. shade leaves 78−80850
leaf radiation stochastic model 77−32880
Leaky-Integrator Neuron Model, input-output relationship 80−72152
left heart and systemic circulation, 2-stage identification scheme 80−41071
left ventricle, effects of external pressures on pressure-volume relation 79−11954
left ventricle, math. model of mechs. 80−101195
left ventricle, model study of isovolumic and non-isovolumic contracts 80−85428
left ventricle active model deform., nonlinear finite element anal. 78−35877
left ventricle and systemic vascular bed model parameter estimation 77−21548
left ventricle model, diastolic pressure-vol. relations and wall pressure distrib., fibre extension 80−8079
left ventricle model parameter estimation, global search algorithms *(French)* 78−3529
left ventricle stress and power, computer simulation 77−56406
left ventricle time-varying capacitance model, driving energy and cardiac O_2 consumption *(Japanese)* 80−21486
left ventricular flow pattern index of pumping efficiency 79−96601
left ventricular hypertrophy, model based on myocardial infarction simulation 77−37005
left ventricular mech. behaviour, orthotropic elastic moduli 79−57695
left ventricular pressure/volume relation, large-deformation model *(Japanese)* 79−2091
left ventricular wall force, comparison of models used in calc. 80−56093
left-heart haemodynamics, mathematical model 78−65074
leg, human dynamic nonlinear finite element model 80−35949
leg muscle forces, normal human walking, optimisation methods 79−16240
light adaption model and Weber's law 79−8508
light response and kinetics in Aplysia giant neuron 78−53381
lipid mixtures, phase transitions, phase diagrams, theoretical model 80−8032
lipid transport through water, exchange mechanism 79−62203
physiological models continued
liver, distributed model for transcapillary exchange and solute removal 79−34524
living cell volumetric changes in freezing and thawing, thermodynamic model and expt. 79−92192
locomotion, human, dynamic modelling 80−8095
locomotion, human, multi-link chain model anal. 79−8518
locomotion dynamics, human, math. model 80−97981
locomotion motor coordination and neuromuscular activities study, humans 77−44635
long-latency reflex pathway dynamics, monkey 80−30706
lower leg reflex asynchronous control via spinal motor neutron pool 78−27935
lumbar spine, human, dynamic 3D modelling, computer code 80−108948
lumbar spine, human 79−83840
lumbar spine curvature in sagittal plane, meas. and modelling 79−96607
lung, aerosol particle regional deposition 77−44579
lung, amplitude-frequency response of pulmonary air tract 79−20574
lung, analytic model, Green's function for convection-diffusion eqn. 78−11684
lung, apical and basal regions, asynchronism in non-sequential ventilation 78−48820
lung, deposition of inhaled particles, airway generations of normal subjects 80−67125
lung, deposition of particles in model airways 80−72192
lung, duck, O_2 and CO_2 exchange and cardiopulmonary control interaction model 80−3600
lung, effects of body position and respiration on regional differences 79−25073
lung, effects of smoking on regional differences 79−25075
lung, finite element model for macroscopic deform. 80−108945
lung, functional residual capacity and ventilation interaction with occlusion press. 77−86521
lung, human, with uneven ventilation, gas transport *(Japanese)* 80−3700
lung, inert gas a-A differences, direct reflection of dV/dQ distrib. 79−20567
lung, inert gas elimination characts., computer model 79−20566
lung, intrapulmonary haematocrit maldistrib., effect on O_2, CO_2, inert gas exchange 80−8033
lung, macroscopic deformation, finite element model 80−89781
lung, math. model, for regional ventilation meas. using ^{81m}Kr 77−86611
lung, mechanical response at high frequencies, input impedance computation method 79−16239
lung, nonlinear mathematical model, parameter tracking adaptive algorithm 77−60227
lung, static mech. behaviour 77−36993
lung, US tissue characterisation 77−40717
lung, ventilation-perfusion inequality, susceptibility of different gases 80−8089
lung airway flow patterns during mech. ventilation of infants 79−57685
lung airway smooth muscle mech. alterations in canine asthmatic model 79−100648
lung airways aerosol deposition, two-component theory 79−34582
lung alveolus, air mixing 79−62287
lung compartmental models, steady state inert gas exchange 80−26249
lung compartmental models, transient inert gas exchange 80−26251
lung gas concentrations during air breathing, influence of gas exchange 77−12942
lung gas transport model, derived from human anatomical data 77−5020
lung mathematical models, effect of common dead space on inert gas exchange 80−67126
lung model, human, velocity distrib. and pressure drop, expt. 79−96602
lung models, inert gas elimination studies without mixed venous partial pressures 80−26250
lung numerical modelling, human 78−80911
lung parenchyma, math. model 80−108940
lung phantom, dynamic, use as educational tool 80−8757
lung regional differences, effects of left heart failure 79−25076
lung simulation model, simultaneous He and N_2 single-breath washout 79−16233
lung structure and elasticity, 3-dimens. modelling 77−36992
lung tissue elasticity, constitutive eqn. 79−96595
lung tissue volume and blood flow, rebreathing methods for determ. 79−20569
lung transport and metabolic processes, indicator-dilution study 77−44711
lung ventilation model, radioactive tracer tidal breathing 80−56095
lung washout, multibreath, modelling and moments 79−43940
macromolecular transport in living cells, fluid mechanical hypothesis 79−62219
mammal thermoregulation, based on balance-control 77−40648
mammalian tendon stress/strain relations obs. and structural model 79−29554
martingale model for estimation in nonlinear stochastic physiological systems 77−77865
maternal-placental blood flow model with vel.-depend. permeability 78−40224
mathematical, muscle commands from nervous system in normal walking *(French)* 80−51071
mathematically exact soln. by Laplace transform *(German)* 79−1991
McCollough effect, synaptic modification associative learning model 77−21531
mechanism of production of summating potential, hair cell functional differences, elec. cct. model 80−72176
mechanoreception, Millipore-DOPH model membrane showing excitation with press. stimulus *(Japanese)* 78−3526
mechanoreceptor hair motion in fluid environments, mathematical model 79−88092
mechanosensitive ionic channel, model of reception and macromolecular rearrangement, effect of deform. 79−79564
membrane, elec. excitable, phys. model, excitation mechanism 77−36902
membrane, electrogenic ion transport along oligomer channels capable of conformational transitions 80−108854
membrane, thin, ionic transport, jump vs. electrodiffusion description, for steady transfer 77−36895
membrane, thin, ionic transport, jump vs. electrodiffusion description, volt. clamp 77−36896
membrane, thin non-uniform, jump vs. electrodiffusion description, volt. clamp 77−36897
membrane bilayers, quasitwo dimens., theoretical models 80−76713

physiological models continued
membrane dynamic equation solving, practical algorithm 78−77038
membrane excitability mechanisms, book contrib. 80−12062
membrane excitability models, electrostriction and/or cooperativity 79−79487
membrane fluid flux, Kedem-Katchalsky eqns., flow limits 77−1979
membrane Na-channel gating current carriers, electronic model 79−70542
membrane regulation of cell cycle 79−92180
membrane-moderated controlled release, dynamics 79−2016
membranes, artificial, permeab. to pluridisperse soln. of ^{125}I-polyvinylpyrrolidone 77−12890
membranes, excitable, bursting phemomena 79−66455
membranes, excitable, ionic channels dipole cooperative model 79−79480
membranes, excitable, statistical theory nonlinear force-flux reln. and fluctuation 77−9179
memory of temporal sequences, model, simulation studies 77−9181
meninges, US propag., influence of subarachnoid struct., rel. to brain lesion prod. 77−16952
mesenteric artery Na distrib. in early salt-induced hypertension 78−27999
mesenteric artery Na kinetics, digital simulation of 3 compartment model 77−44616
mesh generation-optimisation, for partitioning of intricate biological struct. for 3-D finite element anal. 77−40630
mesomorphic monolayers, quasitwo dimens., theoretical models 80−76713
metabolic model for Po, dosimetry appls. 79−79657
metabolic regulation and math. models, review 77−90714
metabolism, energy conservation 77−81459
metacarpophalangeal joint, human, kinematic investigation 79−8519
metacarpus-phalangeal joint movement modelling 79−88112
methotrexate effects, cellular response simulation 77−40647
microcirculation autoregulation mechanistic theories, computer simulation 78−27995
microcirculation mathematical modelling 79−2094
micropolar fluid model for blood flow through narrow tubes 80−67109
micturition hydrodynamic model and test results *(Slovene)* 78−44520
middle ear systems simulation from physiological data 78−44514
Millipore-dioleylphosphate model membrane potential oscillation mechanism 79−57603
minicomputerized automatic radiocardiogram analysis *(Japanese)* 79−29614
mitochondrial membrane charging by cytochrome oxidase, role of protons 79−43807
mitral valve prostheses, hydromechanical simulation facility 79−20708
morphogenesis and biological differentiation, computer simulation 80−30691
motoneuron firing rates with strong random synaptic excitation 77−9184
motoneuron optimal control model 77−86486
motoneurone model with early inactivation, after hyperpolarisation conductance time-course and repetitive firing 80−40987
motor control, muscle representation 78−24057
motor response of hemiparetic patients, biocybernetic model of hypnosis influence *(Slovenian)* 79−2037
motor unit action potential study using computer simulation 79−11914
motor unit recruitment and rate coding for isometric contractions production 77−73523
movement detection, model investigations of lateral inhibition 79−53127
movements of humans, computer modelling 77−21544
mucociliary flow mechanics, channel model obs. 80−97957
multicompartment system simulation 80−55976
multicompartment systems, analytical techniques 79−83689
multipath neural systems, statistical anal. 80−101162
multiple dipole heart generator location optimisation in simple torso model 80−41277
multiple indicator-dilution study of saturable uptake of metabolised substance in dispersing organ 78−27998
muscle, anatomical model, internal pressure effects 80−67103
muscle, contractile element behaviour as force and shortening generator, Hill's model 80−3681
muscle, elastic and viscous props. of resting frog skeletal muscle 77−44700
muscle, frog skeletal fibres, mesh model of tubular system, elec. props. 77−25395
muscle, kinetic model of single contraction 79−57629
muscle, linear systems model, EMG recordings of muscular contract., estimations of active-state 80−3623
muscle, multifibre preparation, intercellular clefts influence on pot. and current distrib. 80−72145
muscle, skeletal, bond graph simulation of glucose metabolism 77−36894
muscle, skeletal, dynamic behaviour modelled as unidimens. viscoelastic medium 77−25484
muscle, skeletal, exptl. results and modelling of biomech. props. 77−25486
muscle, skeletal, quantitative model of actin-myosin interaction 77−52753
muscle, striated, analytical soln. to isometric mechanogram of Hill's model 78−73168
muscle, striated, mol. basis of force development 78−40126
muscle, three-element model with viscoelastic passive elements 77−32930
muscle actions, model for semi-quantitative studies 80−61605
muscle activity prediction, optimisation method adaptation 79−92273
muscle and nerve fibre electric field resolution for EMG analysis 79−57627
muscle contraction, math. model with account of excitability 77−25417
muscle contraction, simulation of thermophysical processes 78−96063
muscle contraction cross-bridge model 78−44475
muscle contraction kinetics, 3-state model 78−48769
muscle coordination in cat hindlimb during maximal vertical jump, computer model 77−40662
muscle fibres, computed extracellular pots. 79−43843
muscle fibres, computed extracellular pots. 79−74620
muscle force prediction, use of optimisation techniques 79−16242
muscle length reflex control, servosystem simulation 79−57639
muscle mechanics in isometric contraction, linear approx. 77−73535
muscle mechanics thermodynamic model 78−80908
muscle power flows, bond graph model 79−92260
muscle preparations, viscoelastic props. anal., meas. and model *(German)* 79−83817
physiological models continued
muscle spindle, mammalian, position and velocity sensitivities *(Japanese)* 77−44638
muscle stretch reflex system, math. model *(Japanese)* 80−67067
muscle tissue, math. models 77−25358
muscular fatigue, EMG meas. and analogue model *(Japanese)* 79−8498
musculoskeletal joint systems, graphical interpretation of redundant problem solution 79−29561
musculoskeletal system modelling, interactive computing and graphical display techniques 77−40685
muslce mass potential, stochastic model, NMV activity *(Japanese)* 78−24056
myelinated axon impulse cond. simulation, sensitivity to nodal and internodal parameters 78−35831
myelinated nerve fibre steady-state/dynamic model, threshold comparison 78−27917
myocardial cell transmembrane potential QRS-T wave simulation *(Japanese)* 77−90740
myocardial electrical activity modelling, dialogue mode *(Russian)* 79−2021
myocardial fibre shortening velocity dependence on inotropic and haemodynamic conditions 78−31833
myocardial infarction dimension model and FORTRAN program *(Russian)* 79−2038
myocardium, frog, model of excitation-contraction coupling 79−70541
myoelectric signal variance parameter 77−29130
myoelectric signals, physiology and mathematics 79−74621
myoelectric signals, power spectra interpretation, model and appls. 77−44641
myoelectric single motor unit potential generation model 77−29131
myofibrils, contracting, tension fluctuations and their interpretation 80−41065
myotonia, Ca induced, computer simulation 79−57633
myotonia and Ca permeab., math. model 78−11620
nematode oesophagus pumping mechanism 78−69121
nephron functioning model *(French)* 80−36218
nephron operating model 79−48283
nerve, temporal stability of solitary impulse solns. of nerve eqn. 78−35830
nerve action potential model 80−30697
nerve and muscle elliptical fibres, physico-math. anal. 78−11639
nerve axon, leading edge approx. 77−12903
nerve axon, phys. model, ionic distrib., pot. profile and resting pot. 77−12901
nerve axon, two-factor two-mode model, travelling waves *(Japanese)* 78−20173
nerve axon adsorption model, action pot. and excitation currents, volt. clamp test 80−56018
nerve bundle conduction velocity distrib. meas. and transfer function anal. 77−44867
nerve conduction in squid axon, Hodgkin-Huxley equations, large amplitude periodic solns. 78−20166
nerve conduction model, FitzHugh-Nagumo, repetitive activity and Hopf bifurcation under point-simulation 79−11915
nerve conduction velocity distribution based on compound nerve action pot. 78−40138
nerve fibre, active, in finite volume conductor, surface action potentials 79−24980
nerve fibre conduction vel. distribs., estimation from action pots. 80−3633
nerve fibre membrane analogue-code conversion, ionic mechanisms 80−81575
nerve fibre regeneration passing through nerve suture, stochastic model 79−83740
nerve impulse conduction along a myelinized fibre, math. model 80−94195
nerve impulse electro-diffusion model 79−53078
nerve impulse equation, dynamic responses of impulse 78−64972
nerve impulses, phase locking of pulse encoders 79−34546
nerve membrane, excitable, charge density due to optical irrad. 79−8526
nerve membrane, steady-state finite cable model, complementary variational principles 79−34545
nerve membrane flicker noise model 77−29125
nervous system, optical system for investigating bioholographic models *(Russian)* 77−40650
network analysis of biological systems, review 80−30635
network thermodynamic two-port element, representation of salt, current coupled flow 79−34505
neural and cellular control systems, stability props. 77−40640
neural coding schemes, integrate-to-threshold anal. 80−35868
neural communication system model, single signed integral PFM and PPM comparison 79−5268
neural encoder, adaptive model 80−97897
neural encoding model test, phase-locking meas. significance 79−2036
neural inhibitory network, probabilistic and stochastic anal. *(Japanese)* 79−39410
neural membrane two-factor two-mode model 78−7330
neural modelling and identification, state variable approach 78−35825
neural net coherent electrochemical emission model *(Russian)* 78−27879
neural nets, dynamic charact. of encoders in receptors and neurons *(German)* 77−36914
neural network, aggregation simplifying simulation 79−8497
neural network memory storage capacity analytic study 79−2023
neural network model, self-organising multilayered 77−40661
neural network modelling by computer simulation, spatial firing patterns 79−74686
neural network models, excitation and inhibition structures 79−2044
neural network simulation using fast Fourier transform 77−1986
neural populations, simplified model eqns. and envelope eqns. 78−31798
neural repetitive firing, Hodgkin-Huxley axon modification suggested by crustacean axon results 77−48776
neural signal space entropy, neurodynamic basis of Weber's and Steven's laws 77−73516
neural transmitter kinetics model anal. 78−3465
neuromuscular junction endplate current simulation 79−62230
neuromuscular oscillations, interaction between those centrally and peripherally generated 79−62232
neuromuscular reflex excitability curve assess. using cubic spline function 79−79510

physiological models continued
neuromuscular response to ankle rotation, human, simulation with segmental reflex model 79−8500
neuromuscular system deterministic neuron models 79−29523
neuromuscular system energy-optimal controls, mammals 77−73522
neuromuscular system model for small isometric tensions, human 77−52771
neuromuscular system output response, effect of correlated adjacent interspike interval sequences of input, computer simulation 78−80858
neuromuscular unit discharge during muscle fatigue, structural model anal. 80−67066
neuron, digital model *(Russian)* 78−27924
neuron, digital simulation model *(Polish)* 79−16189
neuron, spatially distributed, response to white noise current injection 79−83728
neuron, stochastic electronic model 77−48775
neuron adaptation model allowing for Ca influence on membrane K permeability 79−79508
neuron electric potential field evaluation, with time-dependent surface potential, using hybrid computer 77−86478
neuron electronic model *(Spanish)* 80−104580
neuron extracellular electric field model 79−62233
neuron firing threshold model, empirical examination 80−56014
neuron inhibition simulation in electrochemiluminescence cell *(Russian)* 78−27925
neuron mathematical model, freq. characts. *(Japanese)* 80−35866
neuron model, ICs, teaching aid 78−85301
neuron model, response for density modulated Poisson pulse trains *(Japanese)* 78−35829
neuron model, two-terminal electronic circuit 80−61526
neuron model as component of neural network, hardware realisation 80−61534
neuron model of burst generation, FET analogue 77−44630
neuron model using stochastic syncoder 78−15822
neuron models Volterra-like polynomial representation 77−90754
neuron multi-input model diffusion approx. 77−29135
neuron population, local, model performance 79−20531
neuron soma model with high reliability and low power consumption 80−72392
neuron with shunting inhibition, stochastic modelling 77−9183
neuronal activity firing pattern evoked by monosynaptic inputs, stochastic model 77−29134
neuronal circuit with recurrent inhibition two-component model *(Japanese)* 77−48784
neuronal ensembles, spike transfer 79−57631
neuronal firing stochastic model, non-renewal point process properties 77−70447
neuronal impulse generation, modulation of point processes 80−30698
neuronal interspike time histograms for random input model 78−40134
neuronal mechanism modelling in electrochemiluminesc. cell, adaptation *(Russian)* 77−40653
neuronal mechanism modelling in electrochemiluminesc. cell *(Russian)* 77−40651
neuronal nets, randomly connected layered, pattern separation considerations 77−44644
neuronal response in rat hippocampus, dynamic model 79−34547
neuronal spike trains, simulation, multiple Markov sequences 77−25413
neuronal synapses, information processing, electrical neuronal model design *(Korean)* 80−35865
neuronal template-matching mechanism for sensory search with olfactory bulb, anal. 80−56069
neurone compartmental chain model membrane voltage changes 77−29124
neurone impulse activity, limiting behaviour of a model 79−57630
neurone stochastic activity models, book 77−44632
neurone susceptibility to changes in synaptic inflow, evaluation using stochastic model 78−24059
neurons, excitatory and inhibitory impulse sequence interactions in math. models *(Japanese)* 78−27919
neurons, synergism and antagonism caused by electrical synapse 80−30696
neurotransmitter release statistics: moment estimates for inhomogeneous Bernoulli trials 79−62228
NMR intensity of ^{23}Na in rat liver homogenate, effects of alkali cations 77−12893
NMR relaxation decay in living and ischaemically damaged tissue 77−12895
node of Ranvier, crit. pot. of repeat responses 79−70538
nonhomogeneous ventilatory mechanics, analogue computer model 79−79575
nonlinear coupled dynamic physiological systems, network thermodynamic simulation 79−96504
nonlinear system Volterra kernels representation determ. 79−2034
normal and tumour-like cell growth model 77−12894
ocular contusion injury from propelled objects, evaluation model 79−43955
olfactory pattern recognition modelling by adaptive spatial filter 78−24080
one-dimensional excitable medium, non-steady processes, excitation front division 77−86475
ophthalmological instruments and eye models in teaching, training and education 80−51993
optical mechanism of image formation in Limulus eye 79−83767
optimal control, breathing model example 80−41058
optimization concepts in models of phsyiological systems 79−74591
orientation sensitivity of visual movement detection system activating landing response of blowflies 80−101176
oscillatory biochemical model, spatial differentiation 78−44476
oscillatory neural networks in the rabbit hippocampus 80−89743
otolith membrane, finite element model, computer soln. of differential eqns. 77−40636
oviductal egg transport, stochastic model 80−51059
papillary muscle in rat, dynamic behaviour stochastic model 78−35821
papillary muscle Na kinetics, diffusional and compartmental models 77−44617
Paramecium excitation, model anal. 80−61524
Parkinson tremor generation, linear modelling of possible mechanisms 80−3615
particle flow behaviour in branching vessels models, vortices in 90° T-junctions 80−16971
patellofemoral joint, anal. model 80−104625
physiological models continued
pattern generation in lobster stomatogastric ganglion, pyloric network simulation 80−12076
pattern induced flicker colours, sensory process sensitivity to short time delays 78−96048
pattern separability and the effect of the number of connections in a random neural net with inhibitory connections 79−20532
Penrose tube, water filled, fluid velocity/wavespeed ratio, supercritical-subcritical transition 79−81975
perception of uniform rhythm in sound impulse sequences, functional model 78−65032
perfusion pulse attenuation in dog autoregulation 78−44545
pericardial potential simulation and mapping in dog 79−39399
peripheral auditory system, anal., noise appls. 78−80888
peripheral polymorphonuclear leucocyte system model, humans 78−56956
peristaltic reflex dynamics model 80−56080
permeable tube mass transport simulation using perfectly mixed compartments 77−40696
phantom model techniques, biological effects of EM radiation appl. 80−8239
phantom models of man, head resonance, numerical solns. and expt. results 80−12181
phase-locked responses in Limulus lateral eye 77−86491
pheophytin containing monolayers, phase separation and domain interaction, surface press. and fluoresc. meas. 79−100580
phosphatidylcholine bilayers, artificial, interaction with C-reactive protein 80−3579
phospholipid bilayer, hydrated, monoclinic (ripple) phase, thermodynamic model 79−70532
photoreception, transmitter-medicated, diffusion and reaction modelling system 79−70547
photoreceptor electric response, in invertebrates and vertebrates, quantitative model 77−44656
photoreceptor models, vertebrate, response waveforms 79−43894
photoreceptor rod cells, vertebrate, visual transduction, book contrib. 79−96561
photosynthesis, modelling of enhancement and chromatic transitions 80−104565
photosynthetic productivity engineering 79−62209
photosystem I of higher plants, model of donor-acceptor energy transfer *(Ukrainian)* 77−70435
physical fitness test evaluation, bioenergetic model *(German)* 79−1992
physiopathological mechanisms study by computer 77−70562
pigmented biomembranes, photoelec. and magneto-orientation effects, review 77−48766
pituitary thyrotropic responsiveness to protirelin, CUSP catastrophe model 78−81095
placenta, human, rational modelling 79−11962
placenta models, heat, O_2 and CO_2 transport, construct. and usefulness of models 80−3604
plant biophysics, book 77−60180
plant sieve tube sucrose loading, role of pH gradient and membrane ATPase 77−52757
polymer chain, uniform, elastic, possible conformational states 80−37913
posthaemorrhage blood volume control model for intravenous fluid therapy 77−40697
postsynaptic conductance charge, quantal event at nicotine synapses, numerical reconstruction 79−83748
presynaptic Ca^{2+} current rel. to synaptic transmission, in squid giant synapse 77−16926
primary visual cortex, orientation selectivity development models, normally and dark reared kittens 80−41007
prokaryote epigenetic control mechanisms, distributed model 77−77879
prolate spheroidal mammalian models, EM near-field irrad., long wavelenth anal. 80−41115
prolate spheroidal models of humans and animals of EM waves for specific absorpt. rate 79−100658
prolate spheroidal models of humans in near field of short electric dipole, irrad. 80−104639
prosthesis simulator, use of electrohydraulic knee-torque controller 78−11779
prosthetic aortic valve mechanics, apparatus for in vitro study 79−44054
prosthetic cardiac valve, concave-convex pivoting disc two-dimensional model 79−84028
prosthetic heart valve design flow evaluation using finite difference transforms 78−44733
protein nucleic acid recognition, role of unspecific complexing 79−79449
protein transport across endothelial membrane 80−3601
proton transport across charged membrane and pH oscillations 80−61516
pulmonary air emboli, effect of ventilation with different gas mixtures 78−27991
pulmonary and recirculation parameter identifiability following sequential bolus inputs of ^{133}Xe 78−44605
pulmonary arterial blood flow dynamics, nonlinear anal. 78−44527
pulmonary arterial circulation process nonlinearity 77−12944
pulmonary arterial compliance effect on pulmonary blood flow distrib., analogue simulation 78−44553
pulmonary diffusing capactiy, anatomic dead space meas. 77−25502
pulmonary function analysis, parameter estimation, lumped-parameter model 77−44815
pulmonary gas exchange function model *(Russian)* 79−2092
pulmonary model for ventilation automatic control 77−21556
pulmonary oedema fluid transport, hybrid computer simulation 78−27915
pulmonary parameter identification adaptive analogue tracker 77−48911
pulmonary radiograph interpretation, review of models used 80−36089
pulmonary regional electroaerosol deposition model 79−83842
pulmonary vascular disease, resist. model of arterial morphology and mechanics 77−36997
pulsatile flow in arteries simulation, utilitarian approach 80−3669
pupil, human, normal and diseased, model for computer simulation 77−77895
pupil light reflex simulation model 77−70462
pupillary escape, positive off-diagonal kernels as correlates of dynamic process 80−26229
pupillary light reflex system, modelling and identification 80−61554
Purkinje fibers, delay, block, oneway conduction model 80−21462
radiation science, role of models 80−67144

physiological models continued
radiation therapy, equivalence of quantitative models for tumour response 80−30770
radiobiological simulation by supralinear photographic emulsions 80−26290
radioisotope imaging, digital images, math. models and physiological parameters 80−98107
radioisotope uptake of bone-seeking radioisotopes in normal bone rel. to blood flow 80−94320
radiolysis of heterogeneous inanimate systems, radiobiology appl. 80−66824
random neural nets, experimental studies 80−12077
random pulse generators 78−24189
random walk model for cell mixture sorting 77−44606
receptive field types in lateral geniculate body and functional model 78−69046
recurrent inhibition and afterhyperpolarisation, neuronal discharge effects 79−2035
reliability range of model parameters 79−96500
renal arteries model, human, qualitative and quantitative flow studies *(German)* 80−21483
renal autoregulation, math. model of transient adjustments 77−90842
renal countercurrent mechanism, transient and steady state simulation 77−36967
renal countercurrent model eqns., numerical soln. 77−40698
renal counterflow system transient soln. computation 77−40699
renal counterflow systems, differential eqns. numerical soln. using sparse matrix techniques 77−21545
renal counterflow systems differential equation, soln. by numerical method 78−24082
renal dialysis, improved patient management by computer simulation 79−70703
renal functions, mathematical modelling 79−83841
renal medulla, human, math. model 78−24081
renal medulla, multinephron models, canonical mass balance eqn. 77−12941
renal medulla, osmotic equilibration by descending limbs of Henle's loop 77−40701
renal medulla single loop solute cycling model, transient behaviour 78−73167
renal medulla solute cycling model soln. by Laplace transforms 77−40694
renal network flow eqns. anal. 79−11961
renal network flows, a priori bounds 77−40693
renal solute and water movement models and soln. 77−40692
renal tubule model injection transient response calc. 77−40700
Renshaw spinal interneuron repetitive firing, model 77−90760
repetitive firing computer models nonlinear systems anal. 78−80854
respiration, computer-assisted PaO_2 management during veno-arterial bypass and mech. ventilation 77−44838
respiration, density depend. of max. expiratory flow 78−27993
respiration, human, managment of artificially ventilated patients 79−70576
respiration, optimal control of long-term forced ventilation of lungs 77−60296
respiration, two-stage ladder network model for detect. of small airway disease 78−31846
respiration dynamic model eqns., explicit solns, and periodic functions *(French)* 79−79574
respiration effects model, left ventricular performance 80−3670
respiration model analytical soln. 79−48282
respiration model eqns. soln. *(French)* 79−62283
respiration rhythmogenesis model, Lotka-Volterra equations *(German)* 77−48772
respiratory airflow pattern modelling by optimisation criteria 78−80898
respiratory control, human, input stimulus design for model discrimination 79−53183
respiratory control system, time series cluster anal. 78−56959
respiratory control system simulation, state-of-the-art 78−53441
respiratory controller model 77−44697
respiratory gas exchange by avian embryo 77−44708
respiratory mechanical behaviour lumped parameter models evaluation using simplex algorithm 80−89783
respiratory mechanics and body plethysmography 77−90846
respiratory period prediction, men exercising while wearing masks, comparative model study 80−94253
respiratory plant dynamics under open control loop conditions 77−44705
respiratory resistance, central and peripheral, estimation using elec. analogue model 80−81636
respiratory resistance freq. depend. in normal dogs 78−44542
respiratory rhythm generation, mathematical model, respiratory neuron classification 80−35873
respiratory rhythm generator, neural network model 77−86485
respiratory rhythm influence on fluid flow *(French)* 77−40702
respiratory system, forced perturbation, continuum mechs. anal. 79−100640
respiratory system, human, mechanics of regulation 80−41102
respiratory system, human, modelling and parameter estimation 80−12169
respiratory system, human, modelling and parameter identification 79−39444
respiratory system, role of the Van der Pol oscillator 78−65073
respiratory system forced perturbation, traditional model 79−83815
respiratory system model, identification via mathematical pattern recognition 79−2096
respiratory tract, heat exchange during inspiration analysis, under environmental conditions of deep diving 78−15856
respiratory tract, human, model, aerosol particle deposition meas. 78−24086
respiratory tract, human, polydisperse aerosol deposition models 78−24085
respiratory ventilator model and design optimisation 79−20713
retina, rat, rod elec. model, early receptor pot. generation 79−57647
retina early receptor potential, quantum mechanical model 79−57644
retina of cat, neural path real time simulation *(Spanish)* 78−96046
retinal cells of cat, spatio-temporal model 78−92621
retinal ganglion cell firing patterns, implications for separate ON and OFF processes goldfish 77−70458
retinal ganglion cell of cat, refractoriness in maintained discharge 78−64991
retinal horizontal cell reaction to non-uniform illum. 77−56375
physiological models continued
retinal horizontal cell receptive field centre/surround interaction model 77−86497
retinal horizontal cells, nonlinear characts. of spatial summation in receptive field, model 80−26232
retinal hue signal generation, optoelectronic robot model 80−3647
retinal image disparity, fusional response central and motor components 77−25457
retinal information processing, computer model 77−66814
retinal model, layered visual processing 80−16925
retinal models, experimentation, program framework 79−53108
retinal neuron, variability of interspike intervals during sustained firing 77−86492
retinal neuron interspike intervals variability, model dynamics 79−24984
retinal neurons, catfish, spatiotemporal testing and modelling 80−41005
retinal processing, nonlinear, generalised model 79−53107
retinal responsivity compression, V-log I functions and increment thresholds 78−61181
retinal single-photon impulse coding mechanisms *(Russian)* 78−27941
retinal spectral-response characteristics model, light propag. through human eye 79−92215
retinal synaptic transmission effectiveness, neurone regulator model 79−57645
retinotectal projection development, Gierer-Meinhardt eqns. appl. 80−56022
retinotectal projection development, mathematical model *(Japanese)* 80−21467
reverberation cycles of a single neural equation 79−2022
RF EM plane wave incident on a man model, energy absorpt. by and fields in calcs. 80−56115
RF higher-frequency energy absorpt. by biological models, geometrical optics calcs. 80−56116
rhodopsin orientation in photoreceptor membrane, model 77−90775
rhythmic heart-cell clusters, fluctuations in interbeat interval, membrane voltage noise role 80−30705
rod outer segment adaptation anal. based on a simple equiv. cct. 78−73157
rod outer segment birefringence gradient, struct. interpretation, 3-dielectric layer model 79−83771
rod photoreceptor model sensitivity, depend. on level of background light intensity 78−20179
running, influence of track compliance 80−61602
saccadic and vergence eye movements, reciprocal innervation model 78−31811
saccadic eye movement control system, digital analogue simulation 77−44654
saccadic ocular dysmetria simulation using sampled-data model 77−56373
Schroeder-Hall hair-cell model, further investigations 79−70554
Schwann cell layer of squid axon, diffusion models 80−40985
sekeletal muscle dynamics, isometric and isotonic contraction model 78−31807
self-propelled uniflagellated micro-organism, hydromechanical model 79−92199
semicircular canals, unsteady fluid dynamic response, math. model 77−9216
sensorimotor control and learning model 78−69033
sensory coding, distributed, applied to iconic storage and metacontrast simulations 79−34531
sensory information coding, adaptation and differential sensitivity in system of detectors 77−56367
sensory processes, information received by receptors 77−73521
serial section models of human lung endothelial cell nuclei, estimation of mean caliper diameter 79−29679
serial section models of rat lung cell nuclei, estimation of mean caliper diameter 79−25165
shoulder complex in arm elevation, mechanism approach 79−29547
sickle cell blood in capillaries, flow resistance, O_2 consumption effect model 78−48821
signal conditioning for system identification 77−44578
single ligand binding constant computation, regulatory enzyme exponential model 79−79454
single myocardial fibre model, source-field relationships 79−39385
sinus node and AV junction, automaticity model based on weakly coupled relax. oscillators 78−24017
skeletal blood flow, implications for bone-scan interpretation 80−72199
skeletal muscle, lumped and population stochastic models, implications and predictions 80−76724
skeletal muscle fibre with helicoidal T system, linear elec. props. 78−80852
skeletal muscle general myocybernetic control model 78−53385
skeletal muscle myocybernetic control model 77−12906
skeletal muscle O_2 and lactic acid transport, effet of reactive hyperaemia 78−35817
skeletal muscle rhythmic contractions, temp. distrib. study 79−11901
skeletal muscle rhythmic oscillation simulation and analysis 78−31806
skeletal muscles, contracting, simulation studies of mech. stretch 80−94263
skin, cumulative radiation effect, cell survival description 80−30771
skin, human, impedance meas. circuit 79−20607
skin, thermal recovery after cooling 79−53050
skin, transport of radioactive substances, diffusion model 77−81483
skin blood flow, human, modelling of thermal effects 79−24959
skin burns, elec., due to defibrillator ground-loop current, computer simulation 77−78039
skin electric field intensity distribution due to external pot. 77−73553
skin impedance, Laplace plane anal. 79−39458
skin impedance change, equivalent cct. 77−81773
skin impedance simulation w.r.t. Cole-Cole circular arc law 77−5101
skin model of photoacoustic effect 79−57823
skin of frog, radioactive Na washout rate anal., numerical simulation 78−3456
skin reflectance rel. to serum bilirubin conc., neonatal jaundice screening 79−92328
skin resistance during square-wave elec. pulses of 1 to 10 mA, rel. to nerve stimulation 78−31929
skin rheological behaviour, expt. results and struct. model 80−16968
skin stress-strain relation, model calcs. 79−74705
skin temperature during sweating, estimation by graphical method and thermal cct. model 77−48757

physiological models continued
slow motor nerve cond. meas. by blocking technique, computer simulation 78−36027
soft tissues, elastic stress/strain relation based on a struct. model 80−101205
solid tumour growth model, apoptosis as volume loss mechanism 78−96027
spacecraft trace contaminant concentration, toxokinetic/toxodynamic model 79−83952
spatial movement of man, biodynamic characts. model 77−16944
spectral sensitivity of human eye, colour coordinates number triple *(Russian)* 80−76741
spectral sensitivity of human eye, deductive derivation of mathematical model *(Russian)* 80−76740
speech, normalisation and adaptation *(Japanese)* 77−90815
speech discrimination scores, binomial variable model 79−53161
speech perception model used to evaluate speech recognisers 77−32905
speech production, physiology and acoustical props. of vocal system *(Japanese)* 80−26242
sperm, human, flagellar propulsion in cervical mucus, interaction hydrodynamics model 80−97878
spike transfer in statistical neuronal ensembles, neurone as nonlinear source of spikes 78−15819
spinal cord electrical stimulation, 2D finite element anal. 80−98054
spinal motoneurones refractoriness accumulation and secondary range firing model 77−1985
spine, human, finite element model for in vivo freq. response anal. 80−104623
statistical mechanics 79−66456
statistical mechanics of biophysical systems, ensemble theory 79−96502
stenoses model disorder distal, steady and pulsatile flow 79−57688
stenosis model, pulsatile flow downstream 79−92279
stenotic flow, vascular anal. model 79−79593
stick insect leg movement sensory control 77−12904
stick insect leg position control, feedback, open loop anal. 77−36907
stochastic anal. and control, cancer detection and therapy 77−90713
stochastic automaton models for interaction of excitatory and inhibitory impulse sequences in neurons 78−20168
stochastic compartmental models, parameter estimation 78−40109
stochastic neuron models, multi-input-output information transmission 80−30707
stretch receptor array reflex inhibition enhanced contrast 77−2016
stretch receptor neuron excitation and inhibition summation, crayfish 77−2015
stretch reflex system in human forearm, adaptive control characts. 79−83758
striate cortex functional architecture quantitative model 80−89747
stutterers' disfluency rate effects of verbal stimuli 79−57677
stuttering model, movement disorder 80−94241
substance diffusion in tissue with nonlinear consumption, math. model 80−67326
substrate exchange between vascular and extravascular compartments, saturation kinetics 80−104571
synaptic conductance changes, nonlinear effects 79−2045
synaptic transmission modulation and information processing model 77−29142
syncytia, cylindrical, and muscle fibres, elec. pots. induced by current point source 79−74610
syncytial tissues, elec. pot. induced by current point source 79−74609
syncytium, passive three-dimens. and anisotropic, modelled as continuous medium 77−16898
synovial fluid boundary lubrication model, structuring of boundary water 80−35950
synovial fluids and models, rheological exam. *(German)* 79−79584
synovial joints, three layer model, incompressible fluid+linear elastic solid, natural lubrication 77−70490
systemic arterial bed, quantitative evaluation by parameter estimation of a simple model 80−56094
systemic vasculature, importance of non-linear contribs. 78−44549
temperature distrib. in microwave-irradiated cylinders simulating living tissues 80−3760
temperature increase model for exposure to nonionising radiation 79−57706
temperature measurement, human body-temp. sensor-environment system, analogue model of interaction 80−104783
temperature regulation in man, control theory model 78−35805
temperature response of tissue and heated thermocouple probe, in perfusion meas. 77−5110
tendon mechanics, discrete nonlinear viscoelastic model *(German)* 78−44525
thalamic ventrobasal neurone discharges during sleep and wakefulness, computer simulation 79−20533
thermodynamic network analysis of biosystems, book 77−86435
thermographic system model parameter calc. 79−79477
thermoregulation, math. model 80−94173
thermoregulation mechanism model, human 80−8028
thermoregulatory system, human, engineering models, review 77−81471
thermoregulatory system structure and function maths. treatment 77−12888
thoracic electrical impedance, cardiac-associated changes in man 79−25128
throat-wall, human, modelling and vocal tract study from input/output meas. 79−34577
thylakoid membrane of green plants, simulation of electron transport in primary photosynthesis reaction, in PL/1 *(German)* 77−86468
thyroid cells in culture as radiobiological model, sheep, culturing method 80−41327
thyroid hormone nuclear receptor, protein-hormone and protein-DNA interactions in prealbumin 77−66793
thyroid junction assay digital simulation 77−44778
timbre differences, functional model *(German)* 80−30733
tissue induced EM power distribution in closed environment 80−3725
tissue microwave heating models, surface cooling and blood flow effects 78−7388
tissue model, two-layer, theoretical anal. of diffuse reflectance 80−35956
tissue pulse-echo US absorption estimation model 79−48304
tissue reflectance oximetry, exptl. and theoretical models 79−79624
tissue response to retraction during open-heart surgery 80−26254
tissue simulation, acoustic attenuation CW meas. in oil-polymer mixture 80−35961
tissue spherical model near-zone microwave exposure 78−7387

physiological models continued
tooth support, model of periodontal vasculature 80−85434
tooth-jaw system, mech. anal. 77−40703
torso model for potential distrib. from VCG data 79−39401
torso surface isopotential simulation using simple conduction-elec. field model with Neumann boundary 80−89706
tracer transport in blood, model accounting for recirculation, rel. to cardiac output meas. 77−36978
tracheal direct phase velocity meas., distal branch reflection artifact model 79−92280
tracheobronchial clearance of inhaled particles in man 80−8080
transcapillary water movement resulting from non-oncotic osmotic forces 78−44548
transfer function synthesis given magnitude or phase response 77−77864
transfer function synthesis given magnitude or phase response 78−64919
transistor current gain characteristic as model for living structure 79−74590
transmembrane channel, synthetic volt.-depend. cation-selective channel characterisation 78−77009
transmitter kinetics model computer simulation results 78−92617
trap action model 79−16176
3,3′,5′-triiodothyronine plasma to tissue transport rate estimation from 3-compartment model 78−31792
tumour growth simulation, in vitro, with aid of computer 77−86464
tumour model, potentiation of radiation lethality by hyperthermia 79−25037
two-body and massless leg model for human level walking 79−83839
upper airway, aerodynamic forced oscill. method for meas. of velopharyngeal orifice area 77−5017
urinary bladder passive props., collection phase model 79−34596
US tissue characterisation model selection nomogram 79−62321
US tissue model, liq. mixture component selection aid 77−78066
uterine deformation during labour, thin shell model and kinematic analysis 79−2090
valvular regurgitant fraction meas. by radionuclide angiocardiography, iterative estimation 79−34668
vascular bed modelling, optimal dialysis appl. 80−30758
vascular beds, optimum modelling using indicator-dilution measurements 77−40686
vascular murmurs, model studies of origin and character 77−56398
vascular stenoses, steady flow through 79−70563
vascular tonus model 77−25482
vectorcardiogram, human, computer dialog modelling 79−39389
veins, simulation of collapse 78−44535
venoarterial indicator-dilution curves, improved correction of distortion 79−25013
ventilation, human, twin exponential model fitting process development 79−48284
ventilation inhomogeneity identification using minicomputer data processing 77−44816
ventilation-perfusion ratio intraregional maldistribution simulation 78−31834
ventilation-perfusion ratio obtained by noninvasive freq. response technique 77−12952
ventricle, artificial sac-type, in mock circulation, digital simulation 78−11780
ventricle, left, human, geometric modelling, using biplane cineangiograms 80−35955
ventricle dynamic model, using optimisation concept of systolic elastance 77−16951
ventricular action potential, mammalian, analysis 79−62227
ventricular aneurysms, mechanical behaviour, mathematical model 79−11953
ventricular arrhythmia model 80−89893
ventricular excitation, digital simulation, computer model evaluation 78−85302
ventricular volume determ. from indicator dilution curves, dog expts. 79−57696
ventricular wall dynamics and obs. on blood flow 78−80896
vertebra, dynamical response analysis 80−3684
vertebra, use of mesh-generation-optimisation method 77−40630
vertebral response to laminectomy, finite element model 80−41090
vertebrate retina modelling and simulation, extended networks 80−108884
vertebrate retina neuronal activities modelling and simulation 80−85386
vertebrate retinal horizontal cells, spatial integration, computer analysis 77−36920
vesicular transport and endothelial membrane interaction, theoretical models 80−45869
Vespa orientalis, photoelec. props. of 'yellow strips' on cuticle, math. model 80−104638
vestibular apparatus, transform. of angular accels. by system of semicircular canals 77−16943
vestibular nuclei neurons in goldfish, model with ocular proprioception 78−40142
vestibular system, model of influence on blood press. during sleep 77−25410
vestibulooocular reflex of cat, quick phase generation model 78−56971
virus self-assembly by collisions 77−77867
virus-cell interactions, early molecular events, kinetic study 79−100562
visceral function voluntary control, electrophysiological concept 78−35827
vision, apparent brightness rel. to contrast threshold on photopic background 77−9200
vision, associative learning model, voltage-dependent Ca^{2+} and K^+ conductances 80−72166
vision, binocular grating perception, contrast effects 77−70473
vision, Broca-Sulzer effect, combined temporal and spatial unified model 80−35893
vision, chromatic adaptation effect anal. by linkage model 77−70467
vision, gloss perception, model using binocular cells in lateral geniculate body 80−72167
vision, horizontal cell response in carp to monochromatic light, dynamic model, pattern recognition appl. 78−44507
vision, inductive colour contrast, expt. investigation of model *(Russian)* 80−76739
vision, lateral inhibition as mechanism of movement detect., forward inhibition 78−20176
vision, matched filter model of brightness change detect. 78−65001
vision, neural light intensity analyser model 79−57648
vision, opponent-colour channel spectral sensitivity 78−7359

physiological models continued
vision, threshold spatial, four mechanism model 79−43897
vision lateral inhibition process, semi-group theory appl. 78−65010
vision model using optical engineering theory concepts 79−96555
vision threshold model incorporating visual field inhomogeneity 77−44660
visual activity lateral impedance theory, Markov processes appl. 79−2046
visual anal., Lie group representation, computational results 78−27939
visual behaviour modelling using catastrophe theory 79−83784
visual cortex development model for mammals 77−44672
visual cortex neurons, cat, mechanisms underlying receptive field props. 79−74662
visual difference thresholds modelling, appl. of ordered topological vector spaces 80−104587
visual excitation, light-induced transmembrane channel form. in membranes 77−52784
visual excitation, molecular mechanism for initial process 79−100598
visual image contrast and its dependence on luminosity, physical model *(Italian)* 79−62261
visual images, model of local spectral description 79−79545
visual nervous system, human, temporal props. 78−7353
visual path neuron simulation using analogue and digital electronic circuit *(Spanish)* 78−27942
visual pattern recognition *(Japanese)* 80−97920
visual perception, spatial Fourier transform model 79−11940
visual perception of noisy photographic images, threshold contrast, parametric model of observer *(Russian)* 77−52794
visual perception of relative motion extraction, neural mechanism model *(Japanese)* 78−56987
visual pigment chromophores, models, spectroscopic and photochemical studies 80−30723
visual processing, nonlinear, in cat's retina 80−85385
visual response function models, psychophysical tests 79−79557
visual system, human, colour differences 77−21525
visual system, hyperacuity decision model 79−5294
visual system, inference upon the neural network finding binocular correspondence 79−34557
visual system, inhomogeneous model predictions, detect. of local, extended spatial stimuli 80−45894
visual system, intensity and struct. of evoked neural activity 77−25426
visual system, nonlinear receptive field model 78−27951
visual system, quantum fluctuations and adaptive spatial interactions 79−16206
visual system, sensitivity variations, contrast resolution and eye movements 79−53088
visual system brightness generation, chromatic signals contribution 77−90795
visual system movement processing model 79−66473
visual system simulator, human *(Russian)* 80−76877
visual task subjective performance, noise and quality influence 78−53416
visual-vestibular interactions, model of cerebellar influence 78−40156
vocal cord vibration, computer simulation of pathological conditions 77−16940
vocal cord vibration, continuous model 80−85418
vocal cords vibratory behaviour in tension and mass imbalance 79−83803
voice production, analysis synthesis, computer appl. *(Dutch)* 77−12938
volume conductor electrical source information from elec. and mag. surface data 79−83727
walking, connections between different legs, quantitative model 80−101161
walking, individual leg control, model 80−101160
walking, nervous command study 79−53184
water exchange dynamics of body in normal and pathological conditions 78−64914
water excretion control by antidiuretic hormone, modelling 78−31830
water vapour circulation in human organism *(Russian)* 79−2093
whale biothermal mathematical model 80−12059
work-effort ratio of a large muscle group, theoretical model 80−108949
wrist kinematics investigation 79−70570
wrist motion, human, muscular activity model and expt. 79−92285
Ba treated nerve cells, generation of long potential waves 80−56002
Ba-treated nerve cells, reduced systems, qualitative anal. of model generating long potential waves 80−26213
CO_2 circulation in human organism *(Russian)* 79−2093
Ca^{2+} concentration in extracellular fluids in body, digital simulation of short term regulation 79−83725
Cu, metabolic model and dosimetric data 78−65130
^{18}F, skeletal tracer kinetics in rats, evaluation of model 80−56188
^{59}Fe migration, as citrate, in irrad. rats, math. model 77−32942
I metabolism, gonadal dose and genetic significance of ^{131}I therapy of hyperthyroidism 77−5082
N_2 circulation in human organism *(Russian)* 79−2093
N_2 storage in man, dynamic model 78−27997
Na channel, fully coupled excited state model, conductance in volt. clamped case 78−85297
Na channel, fully coupled transient excited state model, action potential generation, threshold, accommodation and repetitive firing 79−57634
Na channel, graph of states 77−25383
Na channel fluctuations, phys. nature, microscopic model 80−35869
Na current in cardiac and nervous tissues, validity of dV_{max}/dt as meas. 78−77037
Na exchange in tissue, incorporating diffusion effects into multicompartment models using digital simulation 80−3611
Na pump, electrogenesis in model of boundary transfer 77−25401
Na^+ saturation kinetics in frog skin, compartmental aspects 80−67050
O_2, circulation in human organism *(Russian)* 79−2093
O_2 diffusion and reaction in biological tissue, Michaelis-Menten kinetic model 78−31793
O_2, facilitated diffusion in muscle tissues 80−56327
O_2 mass transport and regulation, microelectrode and math. modelling study 78−44534
O_2 supply to porous implants in bone analysis 79−70707
O_2 transmural transport to retina, mathematical model 79−34583
O_2 transport system, functional state, math. model 80−104548
O_2 transport system, multivariate anal. of blood and air flow data from dogs 77−44706
O_2-CO_2 transport real-time and interactive control in mechanically ventilated patients in ICU 79−62404

physiological models continued
Pu body burden estimation from urine data influenced by DTPA therapy 78−73259
PuO_2 aerosol, acute inhalation, predictive model of early mortality 80−36028
^{239}Pu, bone model for calc. of annual limits of intake in man 79−53252
THO, prediction of flux from air to plant leaves 80−26381
^{133}Xe washout curve discriminant analysis for lower extremity vascular impairment 78−35949

physiological optics *see vision*

physiology
see also blood; haemodynamics; hearing; neurophysiology; physiological models; speech; vision
ambulatory noninvasive monitoring of physiological data, recording systolic time intervals 79−66574
biofeedback diagnosis system, physiological parameter meas. considering psychic effects 79−100774
biotelemetry, conf., Garmisch-Partenkirchen, W.Germany (May, June 1978) 79−43980
blink reflex studies in stroke patients, role of dynamic sensory perception 80−3641
blood, US Doppler-shift waveforms, physiological interpretation 80−89814
blood pressure control, racial differences 80−30757
blood pressure waves, physiological interpretation of spectra, heart rate, respiration waves 79−29540
bone, X-irrad., histopathological and physiological changes, rabbit expts. 80−51171
cardiovascular response to acute aquatic and treadmill exercise in the untrained rat 80−8085
chest radiology, introduction to physiological aspects 79−25071
circulation control study *(Japanese)* 77−36969
control systems, oscills. and chaos 77−90715
corneal sensitivity and thickness after wearing PMMA and gas-permeable contact lenses 80−61544
corona discharge, image modulation in Kirlian photography 77−5952
deltoid muscle, myoelectric signal rel. to physiological props. 79−70539
diving physiology research facility 80−82106
dolphin, lung collapse and intramuscular circulation during diving 80−81643
ear barotrauma, new aspects in oto-rhino-laryngology 79−11946
educational simulation involvement indices based on physiological responses 78−31760
efficiency in physiological systems, conf., Lodz, Poland (Sept. 1978) 79−100559
Electrophysiological Data Interface 79−79677
electrophysiology, fast-recovery electrode amplifier 79−70654
EMG curves peak detection algorithm 78−96107
exercise physiology in teenagers and asthmatic children 80−12170
eye, abnormal movements control method using audio feedback 80−41156
eye, jerk nystagmus, some new findings 80−67074
eye, pursuit after-nystagmus obs. 80−41018
eye, rapid action and movements during the jump, theoretical anal. 79−79521
eye, saccadic latency predictability in a novel voluntary oculomotor task 80−72157
eye, smooth pursuit movements, role of perceived motion 79−100618
eye, smooth pursuit movements rel. to perceived motion 80−3649
eye and retina development in kittens 80−12113
eye blink rate, human, long-term trends 80−35879
eye convergence and divergence, large and sustained improvement after short isometric exercise 80−8049
eye convergence insufficiency rel. to school achievement 80−8048
eye corrective saccadic movements, for refixation amplitudes of 10° or less 79−43886
eye divergence excess, prevalence and management 80−35877
eye divergence paralysis, association with papillar oedema *(Italian)* 79−79520
eye movement meas. using ocular mag. search coil 79−74798
eye movements, additivity of fusional vergence and pursuit eye movements 80−35884
eye movements, smooth, oculomotor and perceptual localisation 79−74680
eye movements, vel. precision in smooth pursuit 79−57656
eye movements in paralysed cats induced by drugs and sympathetic stimulation 80−51083
eye saccades, counting accuracy obs. 79−43889
eye torsion in response to tilted visual stimulus 80−45891
flow problem, one tube 80−89703
hand-arm energy dissipation in using vibratory tools and accel. levels 78−96116
hand-arm vibration, subjective response characts. to hand-induced vibr. 77−64062
hearing loss, ageing, statistical study of urban population not subjected to occupational noise *(French)* 80−81623
heart physiology, ^{31}P NMR investigations of metabolism, pH and contractile performance 78−69018
hip joints, human, study of synovial fluid, friction and lubrication 79−11956
history of physiological acoustics, Ohm-Seebeck dispute and work of Helmholtz 77−57141
human respiratory airways, diffusional deposition of airborne particles in curved tract 77−81519
industrial noise onset effects on physiological and psychological functions 80−91959
ionising radiation induced behavioural and physiological changes in rats, hormonal radioprotection 80−98026
IR recording retinoscope for accommodation monitoring 80−36055
isobaric gas counterdiffusion in rabbit eye 80−30718
jaw action of lizard, mechanical significance of streptostyly 80−51143
kidney physiopathology concepts from ^{197}Hg fixation test *(French)* 77−70518
leaf temp. meas., infrared thermometer method in connection with plant physiology *(Japanese)* 78−31993
lighting, physiology response of human eye *(German)* 78−8434
living and lifeless matter, complementarity 79−66436
lung, radioisotopes and radiography 79−25072
lung, regional distrib. of (dV/dt)A/(dQ/dt) in man, at rest and with exercise, meas. with ^{81m}Kr 79−16232

physiology continued
macromolecualr thermodynamics and its possible relevance in physiology 80−53176
mechano-receptors, model for stimulus processing 79−74633
microwave chronic exposure, physiological and behavioural effects, rat obs. 80−67152
multiplexing system for measuring physiological responses 80−56292
nasal mucous velocity and airflow resistance, effect of exercise in normal subjects 80−8088
NIGMS evaluation workshop recommendations for research, inc. biomedical engineering 79−12018
NMR imaging, physiological effect threshold for RF and mag. fields 79−66484
noise, physiological defensive activation 79−5318
nuclear physics appl. to life sciences 78−15882
occupational physiology and psychology laboratory 77−48885
ocular accommodation dynamics, range nonlinearity 79−83770
ocular peripheral saccades, latency obs. 80−12089
ocular physiology review 80−56023
oculomotor deficiencies, association of symptoms with meas. 79−96556
oculomotor performance in smooth pursuit of targets, effect of luminance 79−48268
oculomotor slow control, effect of expectations, periodic target steps 79−100604
oculomotor slow control, effect of expectations, single target displacements 79−100605
odour perception, Cu (I) as olfactory binding site 78−96060
optokinetic reactions, rabbit, rel. to visual streak 79−43884
optokinetic reactions in man elicited by localised retinal motion stimuli 80−45889
patient physiologic profiling, automated, in acute ill patients 80−30914
pCM telemetry for physiological data 80−36059
perimetric examination in visual physiology *(Italian)* 79−62244
peristaltic transport, influence of wave form *(German)* 79−79570
plant leaves, spectra of nonlinear optical effects *(Russian)* 78−48829
plant tissues, herbicidal activity of N_1-aryl-N_2-alkyl thioureas, structure relationships 79−62176
polymeric cryoprotectants in preservation of biological ultrastructure, physiological effects 78−65158
porta hepatis irradiation, anatomic and physiological considerations 79−20661
psychophysiological function of the human eye *(Czech)* 80−21472
psychophysiological techniques applied to aircraft design and other operational problems 80−26384
pupil responses, human, instrumentation for automated study 80−36164
renal perfusion dynamics during preservation 79−25006
retinal image stabilisation 80−12088
saccadic eye movements, small, perceptual function 80−61577
saccadic system, anal. by double step stimuli 80−41014
skin burn thermal conditions, review of exptl. results for man and animals 77−48758
space research, biology and medicine 80−41265
spatial localisation during pursuit eye movements 80−51081
speech, voice quality registration 77−21539
stereoscope vergence, convergence and divergence independence obs. 80−30714
subcutaneous tissue gas space pressure during superficial isobaric counter-diffusion 80−30968
support medium +NaCl+cryoprotective agent, equilib. and nonequilib. behaviour 77−16561
telemetry system, implantable, multichannel, for physiological research 80−67292
telemetry system, totally implantable, for dimensions meas., animal physiological research 80−67294
temperature regulation, thermography in environmental physiology 78−58043
thermal insulation of animal coats and human clothing, review 78−73139
thermoregulatory behaviour of rats subjected to microwave irrad. 80−81547
thermoregulatory responses of unanaesthetised rats, acceleration effects 77−48882
thoracotomy, calves, physiological variables obs. 79−53280
tissue surrounding single capillaries, substrate concs. 80−97853
vagina, rats, delay of constant light-induced persistent oestrus by 24-hour time cues 80−12182
vestibulo-ocular reflex, horizontal, linear system anal. appl. to alert rhesus monkey 79−100600
vision, compensatory eye movements to miniature rotations, rabbit, retinal image stability implications 80−45890
vision fixation disparity rel. to rapid prism adaption 80−16929
visual accommodation, reaction and response times obs. 80−67073
visual accommodation in infants, photorefractive study 80−56028
visual patterns having the same coordinates pre- and post-saccades, interaction 80−61551
visual saccades, small, lack of useful purpose considerations 80−61553
visual-motor development in the cat, eye movement obs. 79−83774
vocal-tract length, control during speech 78−11680
wind speed limits to work under hot environments for clothed men 80−8030
Ag-Sn alloys and amalgams, electrochem. considerations, corrosion in physiological soln. 80−93760
CO_2 responses of conscious rabbits at ambient temps. of 5, 20 and 35°C 80−56085

PI control *see two-term control*

pi mesons *see pions*

pick-up reactions
A=16-40, α-spectroscopic factors between ground states, shell model prediction 79−13204
differential cross sections meas. by SPES I 79−75983
even-even nuclei in 2p1f shell, HF calcs. using velocity depend. effective interaction 79−71792
heavy ion induced deep inelastic transfer, decay of binary nuclear system 80−22848
heavy ion inelastic scatt., stripping-pick-up mechanism, coupled channel theory 78−54784
heavy ion stripping and pickup reactions on closed shell nuclei, level shifts, DWBA 80−91168
light nuclei, m-particle n-hole struct. from few nucleon transfer reactions, review 78−50062

pick-up reactions continued
multi-nucleon transfer and direct reactions, nuclear struct., review 78−50060
neutron pickup reactions to $(i_{13/2})^2$ bands, theoretical rot. signatures, backbending 80−52558
(p,t) reactions, ang. momentum selection rules in DWBA theory 77−46154
unbound ejectile pickup reactions, finite range DWBA calcs. 79−85439
(α,^{12}C), 90.3 MeV, multi-α-cluster transfer and direct pickup cross sections 80−57760
α-particle pickup on Ba, Ce, Nd, Sm, Er isotopes with (d,^{6}Li) reaction, 35 MeV 77−18571
(d,α) reactions, ang. momentum transfers, determ. using polarized beams 78−37354
(d, ^{6}Li), 54.25 MeV, α-cluster spectroscopic factors, DWBA anal. 80−52571
(d,^{6}Li), A=144-238, alpha-cluster transfer from alpha-decaying nuclei 80−91166
(N,α), microscopic finite-range anal. 80−63181
(p,d), 52 MeV, deeply bound hole state transition strength giant resonance, DWBA anal. 80−47426
(p,d), pol. p, 65 MeV, A=12-94, differential cross sections and anal. powers, pickup 80−91172
(p,d) backward pick-up react. for inclusive deuteron spectra at 180° 78−17203
(p,X), 400 GeV/c, deuteron prod. mechanism, pick up reactions 80−83096
p+nucleus, n pickup reaction, intermediate and high energies, review 78−94010
90 MeV, α-n coincidence ^{5}He breakup kinematics 77−6419
Ag+p, role of pick-up processes in prod. of fast t and ^{3}He 80−27632
^{27}Al(n,d), 56.3 MeV, spectroscopic factors, ^{26}Mg levels 78−4935
^{36}Ar(n,d), 14.1 MeV, absolute ang. distrib. meas. 78−595
Br+p, role of pick-up processes in prod. of fast t and ^{3}He 80−27632
^{12}C(^{3}He,α)^{11}C, 11 MeV, multistep mechanism, CCBA calcs. 78−41734
^{12}C(α,^{5}He), 90 MeV, α-n coincidence, ^{5}He breakup kinematics 77−6419
^{12}C(α,Li*), unbound Li, relative energy distrib. of correlated decay products 79−13274
^{12}C(p,^{6}Li)^{7}Be, 51.9 MeV, direct ^{5}He pick-up process 78−46058
^{12}C(p,d)^{11}C, 185 MeV, one- and two-step processes 77−38282
^{12}C(p,d)^{11}C, 700 MeV, transitions confirm multistep processes 78−46110
^{12}C(π^+,p)^{11}C, 49.3 MeV, transitions confirm multistep processes 78−46110
^{13}C(d, ^{3}He), isospin violating direct reaction, Coulomb interaction role 80−102170
^{13}C(d, t), isospin violating direct reaction, Coulomb interaction role 80−102170
^{13}C(p,d), 200, 500 MeV, differential cross section scaling, reaction mechanism 80−42625
^{13}C(p,d), 800 MeV, cross sections, DWBA anal. 80−42667
^{40}Ca(^{11}B,^{12}C), 32, 68 MeV, single proton pickup, DWBA anal., optical pot. 80−106037
^{40}Ca(^{11}B,^{12}C), 51.5 MeV, p pickup, DWBA anal. with Woods-Saxon and double folding optical pots. 80−102171
^{40}Ca(^{13}C,^{14}N), 40, 68 MeV, single proton pickup, DWBA anal., optical pot. 80−106037
^{40}Ca(^{13}C,^{14}N), 50 MeV, L=1 proton pickup, ^{39}K $s_{1/2}$ and $d_{3/2}$ states, DWBA anal. 79−67734
^{40}Ca(^{14,15}N,^{15,16}O), 70 MeV, L=1 proton pickup, ^{39}K $s_{1/2}$ and $d_{3/2}$ states, DWBA anal. 79−67734
^{40}Ca(^{7}Li,^{8}Be), 34 MeV, ^{39}K states and spectroscopic strengths DWBA anal. 80−5069
^{40}Ca(α,αp), 96.8 MeV proton pickup by α-particles to unbound states DWBA anal. 79−22305
^{40}Ca(d,^{6}Li), 80 MeV, DWBA calcs. spectroscopic factors 79−6623
^{40}Ca(d,^{6}Li), DWBA anal., angular distrib., spectroscopic factors 79−6625
^{42}Ca(p,t) form factor, hole and continuum contribs. for pick-up reactions 80−78256
^{106}Cd(p,t)^{104}Cd, 42 MeV, hole states at high excitation 78−50158
Cd(p,t), 11-15 MeV, ^{A}Cd, A=104-116, low lying level scheme, mass excess 80−73807
^{142}Ce(^{3}He,α), 24 MeV, ^{141}Ce levels, single neutron holes, spectroscopic factors, DWBA anal. 79−85353
^{142}Ce(d,t), 17 MeV, ^{141}Ce levels, single neutron holes, spectroscopic factors, DWBA anal. 79−85353
^{35}Cl(n,d), 14.1 MeV, absolute ang. distrib. meas. 78−595
^{37}Cl(n,d), 14.1 MeV, absolute ang. distrib. meas. 78−595
Cr(^{14}C,^{16}O), 51 MeV, pickup reaction, ^{48,50}Ti excited states and transition ang. distribs. 80−95308
^{151}Eu narrow band and pickup strength, shape coexistence from (d,t) 80−86799
^{54}Fe(p,d)^{53}Fe, 40 MeV spectroscopic factors, ang. distrib., DWBA anal. 79−22287
^{54}Fe(ρ,α)^{51}Mn, 35 MeV, nuclear struct. study 79−75980
^{56}Fe(^{3}He,α), 18 MeV, ^{55}Fe levels, J$^\pi$, spectroscopic factors, DWBA anal. 80−99127
^{56}Fe(ρ,α)^{53}Mn, 35 MeV, nuclear struct. study 79−75980
Gd(p,α), 17 MeV, ^{153,155}Eu single proton hole states in pickup reactions 80−78128
Gd(p,α)^{153,155}Eu, 17 MeV, direct and sequential reaction mechs., (t,α) comparison 79−540
(^{3}He,^{8}He), microscopic optical pots. to overcome DWBA difficulties 77−54198
(^{3}He,α), 217 (205) MeV, reaction mechanism *(French)* 78−41735
(^{4}He,^{8}Be), A=9-16, 65-72.5 MeV, α-cluster pickup DWBA anal. 77−6418
^{4}He(p,d) pickup reaction, isobar configurations and short range correlations 80−22798
^{4}He(p,d)^{3}He, 770 MeV, differential cross section meas., DWBA anal. 77−46166
^{4}He(p,d)^{3}He, 770 MeV, multiple-scattering approach 80−27636
Ir(t,α), 15 MeV, ^{A}Os, A=190,192, two-quasiproton states, level struct., DWBA anal. 79−89237
^{6}Li(^{3}He,pα)α, 36 MeV, ^{5}Li breakup meas. 77−18590
^{6}Li(n, d)^{5}He, 6.77, 6.57 MeV, two body breakup, ang. distrib., DWBA, optical model anal. 77−18539
^{6}Li(n, t)^{4}He, 7.25-4.71 MeV, ang. distrib., excitation function, DWBA optical model anal. 77−18539
^{6}Li(n,α)^{3}H, low energy, deuteron exchange mechanism, S-matrix theory 79−30840

pick-up reactions continued
^{7}Li(p,d), 800 MeV, cross sections, DWBA anal. 80−42667
^{24}Mg (α,Li*), unbound Li, relative energy distrib. of correlated decay products 79−13274
^{24}Mg(α,^{12}C)^{16}O, E_α=90 MeV, reaction mechanism 79−6646
^{24}Mg(d,^{6}Li)^{20}Ne, 28 MeV, α pick up, angular distribs. and spectroscopic factors 78−78352
^{24}Mg(p,p'), 40 MeV, two step pickup-stripping process, negative parity states 80−32256
^{53}Mn(ρ,α)^{52}Cr, 35 MeV, nuclear struct. study 79−75980
Mo(^{6}Li,^{8}B), 90 MeV, ^{92,96}Zr first excited 0^+ state transition strength 80−78260
^{14}N(n,α)^{11}B, 12-18 MeV, pickup of three nucleons, distorted wave approx. 80−22793
^{93}Nb(^{3}He,α), 19.5 MeV, ^{92}Nb levels determ. 77−88154
Nd(^{3}He,α), 24 MeV, ^{A}Nd, A=145, 147, 149, single neutron hole states spectroscopic factors, DWBA anal. 80−78109
Nd(d,t), 17 MeV, ^{A}Nd, A=145, 147, 149, single neutron hole states spectroscopic factors, DWBA anal. 80−78109
Nd(t,α), ^{A}Pm, A=143-153, odd-A, spectroscopic factors, shell model anal. 80−78137
^{22}Ne(^{3}He,α), 15 MeV, ang. distrib. meas. for levels <10 MeV in ^{21}Ne 79−63684
Ni(^{18}O,^{20}Ne), even Ni isotopes, 63 MeV, energy spectra, ang. distribs., spectroscopic strengths 77−335
^{58}Ni(^{3}He,α), 130 MeV, selected transition, DWBA anal., cross sections 80−83086
^{58}Ni(d,$\alpha\gamma$), 7 MeV, mean lifetimes of ^{56}Co levels 78−4950
^{60}Ni(^{18}O,^{18}O'), stripping-pick-up mechanism, coupled channel theory 78−54784
^{61}Ni(d,^{3}He), ^{60}Co low lying states, DWBA anal. 78−29478
^{64}Ni(d,^{3}He)^{63}Co, proton pickup strength determ. in ^{63}Co 79−22163
^{16}O(d,^{6}Li)^{12}C, 54.25 MeV, residual nuclei excited states angular distribs. 79−6624
^{16}O(d,^{7}Li)^{11}C, angular distribs., direct five nucleon transfer E_d=80 MeV 79−6627
^{17}O(d,t) and (d,τ) pick-up reactions, particle-hole spectra of ^{16}O, ^{16}N, spectroscopic strengths 78−58288
^{192}Os(d,3nγ) 19 to 28 MeV, ^{191}Ir levels, Coriolis coupling model and asymmetric rigid rotor model 79−22164
^{192}Os(p,2nγ) 12 to 24 MeV, ^{191}Ir levels, Coriolis coupling model and asymmetric rigid rotor model 79−22164
^{208}Pb(α,αp) 96.8 MeV, proton pickup by α-particles to unbound states DWBA anal. 79−22305
^{208}Pb(p,α), 20 MeV, ^{3}H pick-up, $^{205}\pi$ transition strengths and ang. distribs. 79−13271
^{104}Pd(p,t)^{102}Pd, 42 MeV, hole states at high excitation 78−50158
^{210}Po(d,t), 17 MeV, ^{209}Po deduced levels, J^π assignments, spectroscopic factors 79−22197
^{210}Po(p,d), 17.8 MeV, ^{209}Po deduced levels, J^π assignments, spectroscopic factors 79−22197
^{A}Pt(d,t), A=192-198, even, 26 MeV, levels obs. 78−50089
^{A}Pt(p,d), A192-198, even, 26 MeV, levels obs. 78−50089
Pt(p,d)^{193,195,197}Pt, l-assignments, spectroscopic factors 78−8810
^{85}Rb(p,d), level location, spin and parity determ. in ^{84}Rb 78−82338
Rh(α,^{3}He), 90 MeV, α-n coincidence, ^{5}He breakup kinematics 77−6419
^{32}S(^{3}He,α), 15 MeV, ^{32}S levels and spectroscopic factors from pickup DWBA anal. 80−9235
^{A}Sc, A=45, 47, 49 positive parity states from Ti(d,^{3}He)Sc reactions 79−97656
^{45}Sc, n transfer, spectroscopic sum spin dependence for stripping and pickup 79−36219
^{45}Sc(d,t), (^{3}He,α), absolute normalisations from spin depend. sum rule anal. 78−8828
^{28}Si(^{15}N,^{16}O), 44 MeV, p pickup, DWBA and coupled channel anal., two step processes 79−6552
^{28}Si(^{15}N,^{16}O), 44 MeV, modified optical pot. from backward elastic scatt. 80−32255
^{28}Si(d,^{3}He)^{27}Al, multistep processes, CCBA anal., SU(3) model 77−30609
^{30}Si(p,α)^{27}Al, 40.75 MeV, differential and relative cross sections, distorted wave direct pickup calcs. 78−94009
^{150}Sm(^{12}C,^{14}C)^{148}Sm, 2_1^+ ang. distributions, shape difference between pickup and stripping reaction 78−33209
^{150}Sm(^{16}O,^{18}O)^{148}Sm, 2_1^+ ang. distributions, shape difference between pickup and stripping reaction 78−33209
Sm(p,α), 17 MeV ^{147,149,151}Pm single proton hole states in pickup reactions 80−78128
Sm(p,α)^{147,149,151}Pm, 17 MeV, direct and sequential reaction mechs., (t,α)-comparison 79−540
Sn(^{3}He,α), 81 MeV, deeply bound hole states, isobaric analogue states in ^{113,117,119,123}Sn 77−30570
^{A}Sn(d,^{6}Li)^{108}Cd, even A=112 to 124 spectra for E_d=33 MeV 79−6626
^{116}Sn(^{3}He, α), 39 MeV, ^{115}Sn weak coupling neutron hole states 80−73786
Sn(d, ^{6}Li)Cd, alpha-cluster pickup reactions, spectroscopic factors and reduced widths 80−534
Sn(p,d), 52 MeV, deeply bound hole states, isobaric analogue states in ^{113,117,119,123}Sn 77−30570
Sn(p,t), A=116, 118, 120, 122 and 124, 42 MeV, hole states at high excitation 78−50158
Sr isotopes, $1g_{9/2}$ nucleon-transfer reactions, nucleon radial distrib. 78−50068
^{88}Sr(p,d), two step processes, excitation of core coupled states, in ^{87}Sr 77−88150
Te(^{3}He,α), 20 MeV, A=122, 124, 126, ang. distrib. anal. 77−88153
^{124}Te(^{12}C,^{14}C)^{122}Te, 70 MeV, optical model parameters, CCBA anal. 77−18591
^{124}Te(d,t), 10 MeV, ang. distrib. anal. 77−88153
Te(d, ^{6}Li)Sn, alpha-cluster pickup reactions, spectroscopic factors and reduced widths 80−534
Ti(^{14}C,^{16}O), 51 MeV, pickup reaction, ^{44,46}Ca excited states and transition ang. distribs. 80−95308
^{A}Ti(d,^{3}He)$^{A-1}$Sc, A=46, 48, 50, 52 MeV, Sc positive parity states, spectroscopic factors, ang. distrib. 79−97656
^{49}Ti, p transfer, spectroscopic sum spin dependence for stripping and pickup 79−36219
Ti(p,d), A=46,48,50, DWBA calcs., rms radius pick-up reaction cross sections 79−541
U(α,^{5}He), 90 MeV, α-n coincidence, ^{5}He breakup kinematics 77−6419
^{51}V(p,d)^{50} V, 51.9 MeV, symm. pot. anal. 78−33182

pick-up reactions continued
^{A}Zn(d,^{3}He), 23.3 MeV, A=64-70, p pickup spectroscopic factors, ang. distribs. 79−6422
^{64}Zn(d,^{3}He)^{63}Cu, proton pickup strength determ. in ^{63}Cu 79−22163
^{70}Zn(^{3}He,^{8}B)^{65}Co, mass excess of ^{65}Co 78−93931
^{70}Zn(^{4}He,^{7}Be) pick-up reaction, ^{67}Ni mass excess 79−9452
^{90}Zr(α,αp) 96.8 MeV proton pickup by α-particles to unbound states DWBA anal. 79−22305
^{92}Zr(β,α)^{89}Y, 35 MeV, analysing power study *(French)* 79−75981

pick-up tubes, television *see television camera tubes*

pick-ups
acceleration pick-ups, miniature vibrator for mechanical calibration *(German)* 80−95095
beam-position pickup, for relativistic electron beams 77−65392
contactless for displacement meas., operational description *(Russian)* 77−65020
corona discharge, positive, sound effects 80−28858
magnetic, for gravitational wave antennas 79−85052
magnetoinductive, for Barkhausen noise spectra meas. *(Russian)* 78−65945
mass spectrometer, spectrum sweep using HF pickup voltage supply control 77−13812
NMR double-tuned pickup for cryogenic flow meas. 77−13756
piezoelectric, for pulsed pressures meas. 80−31778
piezoelectric, using high polymer film *(German)* 77−62128
piezoelectric for induction motor freq. and speed meas. *(Russian)* 78−65911
pressure pick-up with Si column strain-gauge convertor 80−31732
read head for magnetic tape recorders using magneto-resistance principle 80−87688
rotation-angle pickup, for goniometer, using precision variable resistor 80−47047
S/N ratio improvement in magnetostrictive wire readout system for spark chamber 77−79518
speed meas., contactless, of running strips or bands, transit time determ. *(German)* 80−14862
superconducting resonators, coaxial type, mech. vibration meas. appl. 77−74383
two coil pickup, for meas. of electron beam parameters in adherer during compression 77−65393

pickups *see pick-ups*

pictorial bandwidth compression *see bandwidth compression*

picture processing
see also computerised picture processing; pattern recognition
2-D image processing applications of acoustooptical devices 80−53231
3D, biomedical appls. 79−100736
acoustic image reconstruction in parallel processing analog electronic systems, secondary images 79−81638
acoustic imaging, analogue fast Fresnel transform methods 79−46116
acoustic imaging signal processing, review 79−64403
acousto-optic heterodyning image processor, OTF 80−5833
active wavefront compensation device image degradation and post-processing 77−58283
additive-obtained moire patterns *(German)* 80−47017
aerial data processing, automatic, for agricultural resources inventory and survey expt. 77−78505
aerial photograph statistical spatial filtering 79−13908
aerial reconnaissance film interrogation by optical matched filtering 77−78484
aerial survey image interactive hybrid optical/video processing system 77−53254
air gap diode acoustic imaging and scanning 79−50524
airborne, reconnaissance, data collection, conf., Washington, DC, USA, March 1978 79−32078
Algebraic Reconstruction Techniques, modifications 80−3774
altimetric data file acquisition automatic digital correlation method 78−61633
analogue and digital optical image processing, feedback, review 80−102639
analogue image processing, Japanese achievements 77−50634
annular coded-aperture images, decoding techniques 78−37818
Arizona University optical signal processing activities 78−78946
aspectrogram filtering, multiplying mask prod., photographic method 79−27196
astronomical image processing, atmospheric turbulence effects, interferometer data technique 80−12679
astronomical images, coherent optical processing expts. *(Russian)* 80−12675
astronomical images iterative reconstruction, non-negativity constraint 79−101081
astronomical images optimal classification into stars or galaxies, Bayesian approach 80−21920
astronomical negative information processing using thick-film holograms 79−48690
astronomical photography, gain of quality by plates superposition 79−75114
astronomical plates, meas. via automatic microdensitometer 79−80230
astronomical plates for iris diaphragm photometry, nonuniform background correction 80−12680
astronomical speckle imaging for diffr. limited image recovery 77−45318
astronomy, faint images photographic amplification 79−16839
automatic target screener for tactical thermal imaging system 79−32083
autostereoscopic 3-D image synthesis from binocular stereoscopic images, computer simulation, 3-D displays appl. *(Japanese)* 79−31812
autostereoscopic 3D image synthesis from binocular stereoscopic images 79−36842
back projection speed improvement for 3-D reconstruction, tomographic machines 78−4742
bandpass filters, multiple, appl. 80−109002
BEBC pictures, automatic anal. using flygin spot digitiser 77−88342
bilinearly distorted image linear restoration using Wiener filters 80−83557
binary image correlator in absence of geometric distortion, statistical analysis 79−22907
binary image statistical modelling, enhancement and recognition *(Russian)* 80−63929
biomedical, activities in Japan, survey 79−62400
biomedical image processing, state of art *(Japanese)* 80−56251
biomedical image processing and understanding 79−100737

picture processing continued
biomedical pictures, digital processing and enchancement techniques 77−40815
bionic image analysis using lines and edges 77−36931
bipolar spatial filtering, incoherent, review 80−102822
blind deconvolution, zero phase blurring function estimation 80−106482
blurring due to object movement, image reconstruction from projections 80−78784
brain computer tomograms, shape anal. in isodence lesion characterisation 80−8152
bubble chamber track extraction using single vidicon tube 78−82580
C-CD imager, edge enhancement using 3×3 pixel neighbourhood operator functions 80−102644
C-CD imagers, evaluation techniques 77−83990
cartography stereomapping processes 78−61631
cellular image segmentation using multispectral information 79−88224
ceramics, porosity, exam. using image analyser and optical microscopy *(French)* 79−15880
chest radiograph texture anal. model 78−40323
chromosome analysis, problems and progress in automation 80−94436
closed orthogonal functions, digital coding, X-ray pictures appl. 77−77965
coded and transmitted images, optimum restoration technique 77−58278
coded grating method for measuring three dimensional objects 78−86240
coded-aperture image deconvolution, single-emulsion-layer holographic inverse filters 79−76647
coded-aperture images, pre-folded Fourier filter reconstruction 80−53222
coherent and incoherent optical spectrum analysis techniques in image evaluation 78−78928
coherent coded imaging without side lobes 79−25079
coherent image processing photodiode array 79−55076
coherent optical image processing, halftone screen techniques 77−75434
coherent optical power spectrum analysis for image evaluation, contrast effect 79−81367
coherent optical processing for multisensor image processing 79−31830
coherent-optics image recognition by hybrid series-parallel processing *(Russian)* 77−58265
coherent-optics image recognition using contour transparencies *(Russian)* 77−58260
colour component detection in SAW scanning 78−59149
colour edge detection, choice of coordinates 77−79775
colour encoded aperture masks used for incoherent filtering of images 79−41348
colour images, rate distortion coding simulation for colour images 78−7361
colour prediction model for multispectral imagery 77−71395
colour reproduction of objects by speckle interferometry in white light 80−47094
compact real-time matched-filter optical processor 78−74869
complex controllable nonholographic image filter production and implementation *(Russian)* 78−46516
computed axial tomography and nuclear medicine, scatter reduction 79−5368
constrained least squares image restoration, improved computational scheme 78−82915
context-dependent automatic image screening system 80−95820
continuous tone picture reproduction, image quality and information capacity 79−59644
degraded picture restoration by scanning multiple-aperture *(Japanese)* 79−45908
detector array spatial noise reduction, controlled lateral shifts 80−53436
diagnostic imaging systems, non-silver halide, recent developments and pot. 80−41223
difference detection by digitised moire pattern processing 80−52156
differential operator processor, filter fabrication feasibility studies 78−58925
diffraction limited image from obs. through irregular atmosphere *(Ukrainian)* 80−9814
diffraction pattern sampling for optical power spectrum meas., error sources 78−63030
digital colour recording system for digital-analogue hybrid image processing 78−16880
digital filtering for image processing *(Italian)* 80−98573
digital image change detection 80−102637
digital image coding techniques, performance analysis 77−58277
digital image processing by smoothing spline functions 77−50628
digital processing aerial images, conf., Huntsville, Alabama, USA (May 1979) 80−48165
digital processing techniques applied to astronomical images 77−60626
digitising cursor, aided-track, with rotatable linear photodiode array, for graphic materials 79−29899
digitizer and image analyzer, microcomputer-controlled 80−86270
direct picture transmission in single optical fibre, restoration with holographic filters 79−89871
direct transmission via single optical fibre 80−106628
discrete image tone gradation scale transform. on grid coding basis 79−10266
Earth resource image, numerical filtering and data compression *(Italian)* 77−82063
ECG, isopotential surface map data reduction 79−39557
echocardiography, 2D, transducer beam profile effects on tissue aperture detection 78−73185
edge detection, numerical, optical and hybrid methods compared 80−102662
edge detection and coding using directional masks 77−79774
edge detection for meteorological data 79−100989
edge point linking by thresholding 80−99665
electron micrograph images, determ. of structs. relative orientation 79−70714
electron micrographs taken at different defocus, image synthesis 79−54234
electron microscope image analysis 80−31947
electron microscope image contrast and localized signal selection techniques 80−37126
electron microscopy, image processing, optical diffraction and filtering, fast Fourier transforms 80−30956
electron microscopy, image processing by linear integration technique, periodic structures obs. *(Japanese)* 80−52363
electron microscopy, image processing system for micrographs based on minicomputer 80−73549
electron microscopy image restoration of weak phase objects 78−58098
picture processing continued
electronic, for X-ray astronomy appls. *(Italian)* 79−16826
electronic image data processing using incoherent light 80−78793
electronic imaging techniques in EUV spectral region 79−30564
electronic speckle pattern interferometry, fringe contrast analysis 79−72506
enhancement using two-dimensional digital filters *(Italian)* 78−53539
entropy expression for max. entropy image restoration 78−42283
eye movement research, data collection using on-line computers 80−41329
fault identification in badly taken photographs *(French)* 77−71390
feedback systems for analogue and digital optical image processing 80−102650
film grain multiplicative noise anal. 78−58932
film-grain noise degraded image estimation 78−54479
film-grain noise degraded images, nonlinear detection and estimation 77−50627
fogged photograph restoration by optical spatial filtering 78−74857
gamma-ray camera using Compton effect 78−10087
gammagraphy, 3-dimens. image processing appl. to coded aperture imaging *(French)* 78−57067
geological IR multispectral aircraft scanner data, image processing 80−98454
geometric correction for LANDSAT MSS data 79−58120
halftone image coding rel. to visual performance characteristics 77−58280
halftone screen techniques for photographic film response shaping, medical X-ray image processing 79−83895
heart radiographic images, automatic extraction of location of surgically implanted markers 79−88175
high-speed photography and photonic recording 78−86367
holographic interferograms, interference anal. by analogue/digital video technique 79−86139
holographic optical sectioning for three-dimensional image information reduction 77−88679
holographic picture scrambling for confidential picture taking technology, method 77−19208
holographic summation using thermoplastic photographic plate *(Russian)* 79−22911
human motion 3-dimens. monitoring by optoelectronic means, calibration and meas. 78−31913
human retinal image processing, two-channel model 80−94215
human visual system models for image enhancement and display design 77−58279
hybrid image processing, potential of optical methods 79−27185
hybrid image processing based on coherent/incoherent lights 78−33689
hybrid image processing for feature extraction and constant variance enhancement 80−53224
hybrid image processing system, space and time picture oscillation, by active incoherent feedback 78−58924
hybrid optical and electronic image processing 78−33690
hybrid optical-digital image processing, appl. to handwriting and aerial photos 77−68178
hybrid processors, liquid-crystal convertor appl., incoherent-to-coherent 80−33166
image alignment errors due to aliasing 80−106480
image analyser FAS II, interactive terminal 78−89597
image bandwidth compression, scene analysis algorithms and rule-based controller 80−95819
image coding with far-field holograms 78−90389
image compensation and restoration principles 79−58260
image correlation based on extracted edges 80−99658
image correlation of geometric distortion, optimal window functions 79−45907
image correlation with geometric distortion acquisition performance 78−71039
image correlation with geometric distortion effect on local accuracy 78−71040
image degradation identification 78−58941
image digitiser system design 80−48441
image edge enhancement 80−43273
image enhancement and restoration concept 78−58931
image formation using fan-beam scanning and noncircular source motion 80−101913
image Fourier transform correlator using US light modulator *(Russian)* 77−58264
image multiplication using duplex spatial sampling filtering 79−7090
image processing, conference, Pacific Grove (1976) 77−50625
image reconstruction, Fourier techniques evaluation in relation to number of X-ray sums 78−77112
image reconstruction from divergent ray, 3D 79−98299
image reconstruction from partial Fourier transform 78−33691
image reconstruction using polar sampling theorems 79−81366
image registration, similarity measures and preprocessing techniques 78−32240
image registration and differencing by coherent optical pattern recognition 80−99648
image registration using material information 80−99664
image restoration, 2D coded Poisson process, appl. to nuclear imaging *(French)* 79−57767
image restoration, algebraic methods comparison 78−58930
image restoration, optimum filter *(Ukrainian)* 78−55308
image restoration, surface area or arc length constraints 77−38812
image restoration algorithm 77−14666
image restoration and enhancement, conf., London, England (Dec. 1978) 79−25101
image restoration by Gauss LU decomposition 79−76600
image restoration methods compared 79−13907
image restoration of space variant blurs by sectioned methods 78−66780
image restoration using a norm of maximum information 80−102633
image restoration using maximum information norm 80−106476
image restoration using volume diffraction gratings 78−94378
image sampling/scanning, two-dimensional Fourier transform props. 78−58929
image segmentation algorithms, development trends 78−58938
image segmentation and texture unit cell size determ. 80−95817
image segmentation based on second-order grey level statistics 80−99663
image segmentation using prototype similarity 79−31832
image spectrograms of three-dimensional objects, thickness meas. appl. 79−7228

picture processing continued
image structure anal. using light optical diffraction *(German)* 79−72501
image transformations, human factors, algorithm 78−58939
image transmission through monomode fibres, restoration using grating 80−69512
Image Understanding Program philosophy and results 80−95818
image understanding systems, seminar, San Diego, CA, USA (Aug. 79) 80−94918
image visual capabilities of animals and man 78−61190
images with linear spatially-varying degradations, singular value decomputation and projection iterative restorations 77−58274
imaging system fundamental limits and degrees of freedom 77−50630
improvement of cross-correlation peaks by image filtering 79−76610
incoherent 78−46519
incoherent complex signal detection, spatial filtering technique 79−3639
incoherent image processing by multiple aperture scanning 79−76627
incoherent image two-dimensional Fourier transform by optoacoustic transducer 79−50243
incoherent processor for restoring images degraded by linear smear 78−78921
integral photography, lenslet-array system parameter selection 79−49317
integral photography, transform of 3-D image produced by lens raster 78−82921
intensified-Si intensity target vidicon application to IR astronomy 78−81544
interactive user-oriented digital image processing system 77−38813
land use change monitoring system based on LANDSAT 77−78542
LANDSAT image principal component technique for studying structural basin, Spain 77−78521
LANDSAT image registration performance, spatial distortion effects 77−78492
Landsat imagery, planimetric restitution using Zeiss Stereotop 80−56648
LANDSAT imagery and synthetic aperture radar combination 79−5650
LANDSAT multispectral sensor image adaptive coding techniques 78−45060
LANDSAT pictures, DIBIAS, digital images 77−82062
LANDSAT spectral data classifications, atmospheric correction 78−69548
laser image storage mass memory 80−102752
laser line art optical processor, optimal enhancement filter 79−59648
least squares image restoration 80−37961
left ventricular parameter meas., noninvasive radioisotope images with digital prefiltering and boundary detection 78−48887
leukocytes automatic anal., nuclear texture parameters appl. 78−77136
linear line screen for image reproduction, analysis 80−32925
linear motion blurred picture, motion estimate, spectrum anal. 77−3547
linear restoration of partially coherent images, minimum mean square error 79−3637
local image restoration by a least-squares method 80−14289
lunar synthetic-aperture mapping from Earth-orbiting telescope 79−75119
M87 jet, optical photograph deconvolution by maximum entropy 80−62032
mammography, optimum radiographic image conditions 77−90879
maps extraction from satellite images 80−76899
matched filter correlator memory techniques and storage capacity 80−102643
maximum likelihood spatial filtering examples 78−63038
maximum-entropy image processing in gamma-ray astronomy 79−48684
medical 2D images, 3D enhancement scheme 80−101255
medical diagnostic techniques, picture-display systems, developments and limitations *(German)* 79−100705
medical image processing, in nuclear medicine, measure of quality 77−86626
medical image processing, introduction *(Japanese)* 80−81699
medical imaging appls. 80−17038
medical radioisotope images, nonlinear digital filtering *(Japanese)* 78−35930
medical tomography, convolution algorithms for arbitrary projection angles 79−66509
medical tomography, convolutional reconstruction from cone-beam projection data 79−66512
medical tomography, image reconstruction of non-scalar parameters 79−66510
medical X-ray video images, enhancement 80−94353
meteorological satellite data, IR, automatic segmentation and classification 79−5638
Meteosat image processing 78−36297
microphotometry of biological materials, digital picture analysis 80−17991
microscopic image anal. system, cell cycle, cancerous blood and bone marrow cells appls. 79−88223
microwave holography, 3D image-construction technique and appl. to microwave diagnostics 80−83565
microwave scattering parameter imagery of isolated canine kidney 80−3755
monochrome picture signal, digitally coded, level reassignment technique 78−55307
mosaic IR image differencing for track assembly 80−86420
multi-image regeneration by white light processing 80−95814
multiband image spatial domain filtering by Karhunen-Loeve transform 78−78952
multidetector scanner image striping abatement 80−102660
multidimensional convolution, efficient transforms 79−36846
multifrequency hologram matrix, appl. to two-dimens. imaging, computer simulation 79−22921
multigradation image, representation in Boolean algebra 77−31071
multigradation image decomposition by iso-image technique 77−56834
Multiple Mirror Telescope guide alignment system 79−75107
multisensor image pattern recognition, statistical and deterministic aspects 80−99647
multispectral digital images, intensity variations and false colour display correlation 77−78514
multispectral image visual interpretation aided by colouring 79−58281
multispectral images, region extraction and classification by entropy index 79−58130
multispectral images, vectoral representations, arithmetic processing *(Japanese)* 79−35532
multispectral scanner data principal-axis transformation to colour composite picture 79−29879

picture processing continued
multitarget association problem, image reconstruction approach 79−72522
natural terrain scenes, segmentation-based boundary-modelling processor 80−99661
neural net properties rel. to image processing algorithm 80−40993
NGC 5128 (Centaurus A) optical struct., picture processing anal. 79−53907
nonlinear halftone screen preprocessing, analysis and synthesis 77−58267
nonlinear image processing, binary pulse position encoding 78−29906
nonlinear image processing with optical feedback *(Russian)* 77−58258
nonlinear nonmonotonic function synthesis 77−50633
nonlinear operator realisation, coherent optics method *(Russian)* 79−94157
nuclear imaging of tumour, optimum detector spatial resolution performance study 78−73223
nuclear medical images, digital technique for accurate change detect. 79−48326
nuclear medicine, image processing review 80−81694
nuclear medicine, image processing system 80−41174
nuclear medicine, sigma scan, method for enhancement of statistically significant differences 80−36096
numerical holography application 78−33692
object reconstruction from projections, influence of detector arrays fixed errors 78−4743
object spatial location, TV meas. system accuracy 79−49200
ocean surface radar imaging, synthetic aperture technique 78−77334
ocean wave image data from synthetic aperture radar, processing 78−77335
octagonal distance transformation of digitised binary pictures appl. to rib image recognition in chest radiograms 80−89842
offshore shoal positioning using LANDSAT imagery 77−73883
on-axis coherent optical feedback system 77−50631
one-electron dissector, S/N ratio rel. to image contrast 79−50407
optical A/D conversion using single halftone photograph 78−78919
optical fibre laser plate for digital image processing, all-optical parallel logic operation 80−106463
optical hybrid image processing trends and prospects 80−32927
optical image and signal processing, United States Air Force programmes 78−74854
optical image charact. processing methods 77−625
optical image processing by spatial filtering, noise problems 78−37817
optical image processing using dynamic spatial filters to remove multiplicative noise 79−59650
optical image subtraction, real time grid coding and interlacing 78−33694
optical instruments, image evaluation using target detection 79−94378
optical matched filter correlator memory techniques and capacity 80−43280
optical parallel logic device and half-adder cct. for digital optical processing 79−94364
optical pseudocolouring through contrast reversal filtering 79−81378
optical signal and image processing, conference, San Diego (1977) 78−74853
optimal estimation in signal-dependent noise 79−41344
optimal restoration filter for Poisson noise impaired and linearly blurred images 80−106481
orthogonal transforms program for medical scintigrams 80−72365
orthogonalization, Bernstein polynomials, and image restoration 79−36841
partial spatial coherence blur correction by postdetection image processing 80−78792
pattern recognition by hybrid image processing 78−58942
pattern recognition theory and application, book 78−64927
perfect image correction by unsharp masking 78−33693
phase problems, image recovery from Fourier transform modulus 78−82918
phase-inverting grating construction, use in deblurring filters 80−48398
phased array US imaging with multiscan processing 79−57736
photoelectrophoretic imaging, mechanisms 79−24758
photogrammetric system 'Zenit', automatic image processing *(Russian)* 78−24466
photogrammetry, least squares prediction by multiquadric and covariance functions 77−78464
photogrammetry, SEM appls., simplfied numerical transform. for distortion correction *(German)* 79−17572
photograph simulations, on storage display, appls. to X-ray topography and TEM 79−14637
photographic image optical power spectra anal., S/N concepts 78−63028
photographic images, quantitative anal. of autoradiographic image intensification using Thiourea-^{35}S 80−90343
polychromatic processing technique for colour image transparencies 80−86473
power spectrum determination of random pattern, comparison between numerical and analogic processing methods *(French)* 78−58922
practical techniques, astronomy, medical radiography, remote sensing appl. 78−87022
protein supramolecular structure, ordered, electron micrographs, image processing 80−89923
pseudo colour equidensitometry, analogue optical method 78−32903
pseudocolour encoding of spatial frequency information 78−87018
qualitative and quantitative image analyses compared 77−56779
quantitative microscopy, object delineation program 80−41338
quasi-monochromatic incoherent optical image processing 79−76626
radioastronomy, Clean and Restore technique appl. to WSRT and Northern Cross radiotelescope obs. *(Italian)* 80−98563
radiograph digital tomogrpahic restoration 78−40322
radiographic inspection algorithm speedup by array processor 80−108659
radiographic pictures, digital encoding, redundancy reduction 77−40850
radiographs, industrial, discontinuous registration using profile analysis and piecewise correlation techniques 80−102645
radiographs, signal to noise ratio improvement *(German)* 79−39078
radiography, contour extraction *(Japanese)* 80−81702
radiography, tomographic image quality evaluation 77−86607
radioisotope angiocardiographic image, left ventricular contour extraction and vol. computation *(Japanese)* 80−3798
radioisotope imaging, source dependent imaging system 77−77983
radiological imaging systems, unified view using Schade aperture theory, noisy images 77−73563
radionuclide mean clearance time transverse section imaging 78−73222

picture processing continued
radionuclide tomographic image reconstruction, optical processing 77—73572
random checkerboard process, two-dimens., generalisation 79—81374
random halftone contact screens, transmittance control of tone reproduction 78—66775
random spatial phase modulation for speckle elimination 78—58920
raster scanned images, matched filter processing 77—7018
raylography, acoustic medium characterisation and imaging, non-biological model expt. 77—25528
raylography, freq. domain deconvolution technique for pulse echo ultrasonography 77—25527
real time optical correlation of 3-D scenes 77—27262
real-time Hadamard transform coding quantiser design 77—27263
real-time image optical subtraction scheme 78—74856
real-time incoherent subtraction of irradiance 80—74301
real-time one-step in incoherent level slicing of optical images 78—82919
reconstruction, three-dimensional, from planar projections 80—99639
reconstruction algorithms, 2-dimens. 77—82379
reconstruction of images distorted by smearing 79—76614
rectilinear bone scanning techniques 77—56460
recursive filtering, two-dimensional, system theory concept 78—58934
remote sensing image data processing/acquisition techniques 78—61627
remote sensing imagery, optical and electronic enhancement 77—53253
remote sensing imagery, spatial filtering 78—90385
remotely sensed Earth imagery, atmospheric blurring removal 79—88517
review of optical and electronic aspects 77—38814
robust feature matching through maximal cliques 80—99671
Ruticon optical processing capabilities 78—79140
SAR/LANDSAT data set assembly and anal. 77—78493
satellite acquired image geometric distortion correction 79—74588
satellite image sensing and multiplexing system tradeoffs 77—60498
satellite imagery, linear features enhancement by rotational exposure 79—35874
satellite on-board processing for Earth resources data 78—61626
scanning acoustic microscope, image enhancement using analogue filters 78—18131
scanning microscope photometric image analysis, appl. to chromatin packings *(German)* 79—5409
scene matching methods 80—48167
scene matching with feature detection 80—48166
scintigraphy of human organs, digital image anal. 78—20251
scintillation images, from biomedical systems, nonlinear filtering methods 77—81559
sea surface temp. meas. from meteorological satellite images 79—100990
segmentation and texture anal. 80—98167
segmentation by preprocessing and averaging 77—58272
segmentation using material information 80—102642
SEM colour images, electronic adding-up and storing 79—21879
SEM image enhancement and digital reproduction 77—38060
sequential scene matching using edge features 78—32239
serum-electrophoresis, quantitative, by digital picture processing *(German)* 80—94306
sky image coherent-optical processor for moving object location 78—78944
Skylab spectral channel evaluation for classification and thematic mapping 77—78500
small-area ultrasonotomogram magnification and smoothing 77—86572
smeared photographic image restoration by white light processing 79—18352
sonoprobe survey, automatic recognition of submarine sediments *(Japanese)* 79—39985
space-frequency conversions for image transmission and processing 78—71046
space-variant optical pattern recognition by coordinate transformations 78—78945
spatial filtering of Fourier transform of half-tone picture using photographic replica 79—27184
spatial image filter with noncoherent incandescent source, model and expt. *(Russian)* 79—7083
spatial light modulators, near real-time reusable for coherent optical processors 77—11035
speckle image digital processing 78—71053
spectrum analysis techniques, coherent and incoherent, in image evaluation 78—63031
spiral tomography, optimum blurring 78—69181
stereo electron micrographs restitution, approximate soln. 79—26189
stereo-pair images, correlation error prediction 80—102636
strain evaluation by specimen-grating photograph electro-optical processing 77—39266
subwavelength spaced scatterer resolution, by superdirective data processing simulating evanescent wave illum. 79—36847
super-resolution derivation by analytical continuation methods 78—29915
system design considerations in optical power spectrum analysis 78—63029
TEM, specimen prep. methods, review 79—17405
temporal frequency spectrum, optical filtering 78—33695
thermal imager pictures delining, using digital processing technique 80—106466
thermal imaging system static performance model 77—65636
thermal viewing system, image integral scanning effectiveness 79—50402
thermogram enhancement by tissue-condition correction 79—39460
thermographic meas., three-dimensional signal detection, expt. 78—3662
thoracic X-ray image comparison automation *(Japanese)* 79—29615
three colour channel hybrid system to synthesize complex point spread functions 79—41347
three dimensional video images formed by parallax panoramagrams, real-time transmission 79—31807
threshold vision aspects of picture encoding 77—81509
thyroid I measurement by X-ray fluoresc. scanning, effect of background radiation change 78—73216
time-varying images, object displacement estimation adaptive algorithm 80—99668
tomograph noise filtering, lung boundaries determ. using neuristic search 78—73240
tomographic machines generalised $|\omega|$ filter for 3-D reconstruction 78—4741
tomographic scanner appl. 79—100738
tone reproduction analysis with square, circular and concentric-ring patterned screens 80—53229
picture processing continued
transaxial tomography, optical improvement for data treatment 79—34666
transmit/receive 2D ceramic piezoelectric arrays, construction and performance, medical, NDT appls. 78—87223
transverse analogue tomography, cross-sectional imaging of X-rays 80—56201
tunable spatial filtering with a Fabry-Perot etalon 80—58668
turbulence-degraded image a posteriori restoration using multiframe imagery 77—60469
TV techniques in image processing, remote sensing imagery appl. 78—93005
two dimensional unitary transforms appl. 78—58928
two-dimensional acoustic processor 79—72514
two-dimensional photoacoustic image processing with longitudinal waves 79—50244
two-dimensional velocity measurement by automatic analysis of trace particle motion 79—64810
Two-stage holographic rejector filter *(Russian)* 77—75675
two-tone image analysis using one-dimensional autocorrelation function *(Russian)* 80—63931
ultrasound B-mode scans, speckle reduction 78—22233
ultrasound image coding, mammograms appl. 77—81544
US dynamic imaging, high resolution 80—17042
US grey scale sonoarterographic imaging 77—25532
US image processing, appl. to film recorded images 77—25531
US image processing device status and prospects 80—48446
US image reconstruction processing limitations 78—73184
US imaging annular array design and logarithmic processing 79—34615
US medical image digital processing methods *(Chinese)* 80—30805
US tissue analysis, comprehensive system 80—51189
US tomography based on perturbation solns. of wave eqn. 79—70593
vegetation canopy modelling for signature correction/anal. 77—78515
Venera 9 televised pictures of Venus cloud layer, geometrical correl. methods 80—67604
ventricle, left, contour extraction from radioisotope angiocardiograms, and wall motion classification 79—88180
vibration measuring system using interf. fringes TV detect. and electronic image processing 80—103004
video-electronic hologram interferometry for in-plane displacement measurement 80—106488
vision, problems in matching images to the eye—effects of pictorial noise 80—51113
visual prosthesis, processing and tactile stimulation of images *(French)* 79—100788
visual prosthesis design, human factors and electrophysiological considerations 78—53583
visually optimised image restoring filter 79—3644
volume holograms for image restoration 80—83566
water penetration imagery, surface/depth data separation by multispectral scanning 78—69539
wavefront registration and volume object image reconstruction by stimulated Raman scatt. *(German)* 80—53367
weak modulation detection in film grain noise with partially coherent illumination 80—77897
weather satellite picture processor for TIROS-N series, visible and IR pictures 80—67439
Weigert effect appl. to contrast reversal of black and white transparency 79—26165
weighted-filter imaging technique appl. to lunar surface chem. 78—12124
white light optical processor for edge enhancement and spectral filtering 79—76599
Wiener image filtering, object fast restoration after PSF degradation 78—90379
X-ray absorption-edge fluoroscopy, spectral considerations 77—21618
X-ray computerised tomography, system resolution recovery by motion blur recovery technique 80—105756
X-ray images, electronic recording 80—62815
X-ray imaging collimator, for Sun hard X-ray spectroscopy 77—5437
X-ray picture examination TV equipment 77—21607
X-ray picture source coding for compact storage or fast transmission 78—40310
X-ray quantum statistics limited electrostatic imaging 78—7451
X-ray scanners, picture reconstruction 77—40849
CdS film SAW two-dimensional image processor 77—39164
CdS-$LiNbO_3$ monolithic two-dimensional Fourier transformer 79—72516
KD_2PO_4 photo-spatial light modulator, optical data processing 80—102839
$LiNbO_3$:Fe, nonlinear image processing in 3-dimens. hologram 80—14303

picture transmission *see facsimile*

picture tubes, television *see television picture tubes*

PID control *see three-term control*

piecewise-linear techniques
adaptive model for flood warning system, on-line, use of desk-top computer 79—34977
agricultural land urbanisation hydrologic impact, distributed watershed model 77—37277
approximated ECG waveform recognition 78—57119
curvilinear multimode optical waveguide statistical tolerance calc. 78—1361
dynamic system, piecewise-linear non-linear, several degrees of freedom, forced oscillations 78—54173
first-order linear differential eqns., optimum integration operators 77—78962
graded-index slab waveguide TE modes, exact soln. 79—81568
Lorenz attractors, topological classification 78—77720
nerve axon, leading edge approx. 77—12903
radioimmunoassay data processing, semiautomated polylinear system 79—70614
Steiner surface, piecewise surface approx., finite element calcs., isoparametric method 80—12881
Stokes problem with conforming Lagrangian finite elements, soln. error estimates *(French)* 78—62085
temperature meas. by compensated thermocouples *(German)* 78—41304
vowel identification using piecewise separation technique 79—46123

piezo-magneto-optical effects *see magneto-optical effects; piezo-optical effects*

piezo-optical effects
see also piezoreflectance
adamantane, plastic cryst. lattice vibr. study of phase transition 80−7355
2-adamantanone, absorption and fluoresc., high-press. 77−52113
alkali halide:$Cu^+(Ag^+)$, high press. studies of luminesc. phenomena 79−43017
alkali halide:In, high press. studies of luminesc. phenomena 79−43017
alkali halide:$O_2^-(NO_2^-)$, effect of press. on vibronic spectra 78−52532
alkali halide crystal, piezooptical coeffs. temp. depend. 77−4622
alkali halide crystals, deformation spectroscopy, dislocation interactions with electron and hole centres 78−10983
alkali halide high-pressure submillimetric-wave spectra 79−33694
alkali halide phosphors, $Pb^{2+}(Sm^{++})$ doped, luminesc. props., press. effects to 140 kbar 77−40278
alkali halide phosphors, Tl^+ doped, uniaxial stress effects 78−48202
alkali halide phosphors, Tl doped, press. effect on emission spectra at low temps. 77−85771
alkali halides, emission spectra of O_2^- and NO_2^- centres at high hydrostatic press. 78−10943
alkali halides, linear dichroism spectra, stress-induced, reorientation of O_2^- and NO_2^- impurity ions *(Russian)* 80−45127
alkali halides, off to on centre defect transitions under hydrostatic press. 78−15199
alkali halides, temp. and press. depend. of transverse-optic modes and anharmonic self-energies 77−11649
alkali halides, temperature dependence 78−92050
anils, cryst., high-press. optical effects 78−31170
anils, polystyrene soln., high-press. optical effects 78−31171
anthracene, cryst., fluoresc. spectra, press. tuning 77−28612
anthracene, Davydov splitting of lowest singlet exciton under high press. 77−72823
benzene liqs., refractive index, pressure effect 80−71375
Brillouin scattering in reflection and transmission modes, rel. to intense acoustic flux, relation linearity test 80−45098
cholesteric liquid crysts., light reflection by crysts. with tilted molecular struct. 80−29713
cholesteryl nonanoate, polymorphism of blue phase, circular dichroism at high-press. 79−37821
COOB, sheared liq. crystal, near T_{A-N}, optical response 79−94895
coronene, n-alkane matrix, up to 1.8 kbar emission multiplet struct. shift 77−34677
crystal inhomogeneous in optical anisotropy due to stress distrib., light propag. eqns. 79−13897
cubic crystal, elastooptic consts., theory 77−65998
diamond, elasto-optical constants, determ. from piezobirefringence 79−73899
diamond, GR 2-3 absorpt. line, uniaxial stress effects 78−72563
diamond, Jahn-Teller coupling at neutral vacancy 80−71453
diamond, optical absorption lines, GR4 and GR8, effect of uniaxial stress 80−34956
diamond, pseudo-Jahn-Teller effects in H3 vibronic spectrum 77−90182
diamond, refr. index, temp. and press. var. 78−27174
diamond, type Ia, secondary absorpt. edge, optical study 79−19912
diamond, uniaxial stress splitting of E to E transitions at trigonal centres in cubic crystals 80−97312
diamond, vacancy, mol. orbital theory of transitions 77−85757
diamond, vibronic bands at 2.498 eV (H4), 2.417 eV and 2.536 eV, absorpt. and luminesc. under stress 77−85758
dielectrics, electric, optical and acoustic interactions from Lagrangian representation, book 80−2715
diethylammonium manganese chloride, antiferromag., magnon sideband exam. by absorpt. spectra 77−12108
diethylammonium manganese tetrachloride, quasi two-dimensional antiferromag., magnon sideband in absorption spectra 78−43895
n-dodecane liqs., refractive index, pressure effect 80−71375
dye DFB laser, single-freq., 10 Å continuous pressure tuning 79−76705
elasto-optic coefficients, signs 78−64346
elasto-optical birefringence modulator construction method *(Japanese)* 77−54809
ellipticity, azimuth and system parameters linking eqns., 3-dimens. model propag. 78−50695
F centre luminescence polarisation, stress induced, temp. dependence 79−56857
ferroelectric semiconductors, appl. to optical storage *(Russian)* 80−80749
fibre optic waveguide transmission, mechanical stresses effect 80−10032
fibre pressure sensitivity meas. and limitation 80−106605
fibre reinforced composite, imperfections, piezo- and elasto-optical effects under longitudinal shear *(Russian)* 78−56457
fibres, single-mode, subjected to tensile stress, polarisation performance 79−59808
fluorophosphate laser glasses, Nd doped, piezooptic coeffs. meas. 80−99815
gel rods, elastic dilatational mode, light beam positional modulation 80−64167
glass, laser, elastic, elasto-optic consts. and extinction coeffs., Brillouin scatt. meas. 79−11429
glass, plate 79−28713
glass, small thermo-optical characts., stress coeffs. 77−31123
graphite, reflectivity in near IR and hydrostatic press. 79−91423
graphite, reflectivity in near IR under hydrostatic press., lineshape anal. 79−91424
heavy water, piezo- and elasto-optic props. under high press. 80−50296
n-heptane liqs., refractive index, pressure effect 80−71375
n-hexane liqs., refractive index, pressure effect 80−71375
hologram interference fringe bending analysis and expt. 80−106494
ice, hexagonal, Raman spectrum of translational lattice vibrs., press. effects 79−24304
ice VI, OH stretching peak freq. press. depend., Raman spectra using diamond anvil cell 80−16023
impurity radiative transitions, hydrostatic press. effects 79−38632
indole, in PMMA matrix, high press. luminesc. 78−84629
integrated optical elastomeric modulators 77−75715
interferometer for precise photoelastic consts. meas. 77−26384
inversion of Γ and L conduction bands under uniaxial stress, photoluminescence meas. 79−33229
ionic equilibria in water and mol. dynamics of pure liqs. using high-press. Raman spectroscopy 79−24301

piezo-optical effects continued
isoquinoline luminesc. in polymeric media at high press. 79−13756
Jahn-Teller impurity centres, piezo-optics and magneto-optics 78−39579
laser wave propagation in piezoelectric crystal, lax's estimates appl. to critical crystal thickness 79−98440
laser window materials, temp. and stress effects on refr. index 77−46771
laser with electro-opt. shutter, piezo-opt. effect on dynamics and spectral characts. *(Russian)* 77−83912
light wave propagation in photoelastic materials and crystals 79−898
liquid, crit. evaluation of eqns. of state 79−78650
liquid, under high press., refr. index vs. density 79−28712
liquid, under high press., refr. index vs. press. and strain 79−33668
methylammonium aluminium sulphate, third order elastic consts. from stress shifted reson. freqs. 78−55905
5-methylindole, in PMMA matrix, high press. luminesc. 78−84629
mixed crystals, of equimol. conc. with NaCl struct., piezo-optic birefringence theory 80−100643
modulator/chopper for modulating polarization of light beam *(German)* 79−27395
modulators, photoelastic radiation polarisation, review 80−102846
naphthalene, cryst., fluoresc. spectra, press. tuning 77−28612
naphthalene-d_8:naphthalene, symmetry reduction obs. of deformed crysts. by absorbt. spectrum method 79−15504
nonlinear processes in crysts., power stabilisation by electro-, piezo-optical tuning 77−88856
nonlinear second-order crystal processes, electro-optic, piezo-optic tuning 78−46718
n-octane liqs., refractive index, pressure effect 80−71375
optical fibre, refractive index profile distortion, stress-induced 80−91889
optical fibre data collection highway with piezoelectric phase modulators 77−39098
optical fibre hydrophone, high-linearity multimode optical fibre sensor 79−68429
optical fibre refractive index profile distortion due to thermal stresses 80−58726
optical fibres, acoustic modulation of light propagation 80−33209
optical fibres, phase modulation of coherent light using HF sound 78−87142
optical fibres, piezo-optical effects due to thermal stresses 80−87519
optical fibres, single mode, polarisation and magnetooptic props., expt. meas. 78−33830
optical materials, piezo-optic coeff. determ. under static loading, interferometric and polarimetric techniques 79−4787
optically isotropic and anisotropic materials, rapid optical method for stress-optical const. determ. 77−5899
optically transparent materials, evaluation of elastic ratio by interferometry 78−90804
optomechanical properties determ., polarisation device application, by compensation method 80−40643
organic solids under pressure, IR spectra and phase transitions 79−95743
oscillating quartz crystal stress distribution meas. by laser probe 77−20803
oxide semiconductor crystals, with forbidden energy gap, review of spectroscopic props. 78−2876
perovskite-type crystals, nonlinear optical phenomena, expt. *(Japanese)* 77−38990
PET, IR, spectra of prefractured state 77−69032
PET film interatomic bond determ. by IR transmission and reflection spectroscopy 77−65958
PET films, one-way drawn, constant strain effects, IR meas. 80−60584
phonon-assisted radiative electronic transitions 79−24348
phosphate glass, optical-stress coeff., effect of alkali metal oxides 77−50740
phosphate glasses, depend. on chem. comp. 79−99861
phosphate laser glass, Nd doped, piezooptic coeffs. meas. 80−99815
piezochemiluminescent, piezochemomagnetic and piezochemovoltaic effects *(Russian)* 77−85820
PMMA, oriented by extrusion 78−47248
PMMA, piezobirefringence, optical and mech. relaxations, temp. depend. 80−34885
polarised light in chemistry, electro-optic and photoelastic modulators 77−45896
polarised light in materials research, birefr., electro-, magneto-, elasto- and acousto-optics 77−48143
polydiacetylene, monocrystal, vibr. freq. stress depend., Raman obs. 77−50574
polydiacetylene, single cryst. piezomodulated and specular refl. spectra 77−20869
polydiacetylene-bis(toluenesulphonate), refl. spectra, 0-15 kbar, doublet press. shift 78−43891
polyethylene terephthalate, simultaneous mech. loading, UV rad. effects on overstrained chem. bonds 79−52706
polymer, amorphous, segmental distrib., light-, neutron- and X-ray scatt., piezooptical and dielec. meas., review 78−51444
polymer, amorphous, stress-optical investig. of short-range order 78−22672
polymer film, pressed, light-scattering, effect of birefringence *(Russian)* 77−44007
trans-1,5-polypentenamer, stress-opt. behaviour 77−90128
polypropylene drawn film, rheo-optical studies 78−15440
polyurethanes under tension loads, spectral exam. *(Ukrainian)* 78−92058
polyvinylidene fluoride, electro-optic and elasto- optic effects 80−80754
α- quartz, ferrobielastic hysteresis 80−19869
quartz, natural, gamma-irradiated, stress effect on thermolum. sensitivity 80−11482
α- quartz, Raman spectrum, piezospectroscopic behaviour 78−35138
α-quartz, Raman spectrum of optical phonon mode, stress splitting and wave-vector depend. 77−77214
α-quartz, secondary Dauphine twinning, visualisation method 79−51121
quartz, thermoluminescence sensitivity change due to stress 77−59627
rare earth formate, IR spectra and phase transitions, under pressure 78−31179
reflected caustics method for stress-optical consts. determ. 79−51931
ruby, optical spectra freq. shifts press. depend., nonperturbative theory 78−23499
ruby, piezo-spectroscopy of exchange coupled Cr^{3+} pairs 79−33783
ruby, press. effects on fluoresc. R-lines, appl. to press. calibration 77−18106
semiconductors, optical props. under press., book contrib. 80−84715

piezo-optical effects continued
silicate glass, optical stress coeff., effect of alkali metal oxides 77—50740
silicate glasses, depend. on chem. comp. 79—99861
single crystal, Pockel coeffs. and short-range-interaction parameters 79—73962
single-mode fibre lightguide, phase of coherent signal, temp. and stress effects 80—33208
smectic liquid crystal, homeotropic to confocal texture transformation *(Russian)* 78—18548
stress measurement at surfaces, elasto-optical technique 79—7347
stress measurement method for crysts., appl. to Si 80—48656
stress-induced Raman tensors and effective charges for 32 point groups 79—33667
styrene-butadiene triblock copolymer films, mech. props., effect of casting solvent 79—11651
swollen rubber network, stress-optical coeff. and amorphous order 77—77169
TCDU, polydiacetylene cryst., elec. struct. change, stress induced 78—70990
TCNQ-TSef, Drude optical edge, press. depend. 79—19882
tetrachloromethane liqs., refractive index, pressure effect 80—71375
toluene sulphonate diacetylene, strain dependence of dominant electronic excitation 78—80373
toluene sulphonate diacetylene polymer, vibr. modes, strain depend. using Raman spectra 80—20626
TTF-chloranil visual pressure or temperature indicator 80—87443
TTF-TCNQ, Drude optical edge, press. depend. 79—19882
twisted single-mode fibres, polarisation optics 79—81524
uniaxial noncentrosymmetric crysts. with intersecting dispersion curves, external actions effect 78—84552
wave packet self focusing in medium with striction nonlinearity, numerical simulation 78—83042
wurtzite-type crystals, deform. effects on biexcitons 77—52038
Ag halides, temp. and press. depend. of transverse-optic modes and anharmonic self-energies 77—11649
AgCl, piezo- and elasto-optic consts., temp. depend., 20-350°C 77—63392
$AgGaS_2(Se_2)$, press. depend. of energy gap, absorption edge obs. 77—12401
$AgInSe_2$, press. depend. of energy gap, absorption edge obs. 77—12401
p-$Al_xGa_{1-x}As$-n-$Al_yGa_{1-y}As$ junction, electrolum. spectra at high press. 77—48246
Al_2O_3, sintered, residual stress meas., piezospectroscopic technique 78—52704
$Al_2O_3:Cr^{3+}$, shock compression, absorpt. spectra 80—20675
α-$Al_2O_3:Cr^{3+}$, stress-induced linear dichroism in $^3A_2(^3T_1)\rightarrow{}^3T_2$ transition, Jahn-Teller effect 80—34884
$Al_2O_3:Mn^{3+}$, electronic and vibronic Raman scatt. 78—2839
α-$Al_2O_3:V^{3+}$, near IR spectra, line lifetime, 2, 10, 77K 78—10972
α-$Al_2O_3:V^{3+}$, stress-induced linear dichroism in $^3A_2(^3T_1)\rightarrow{}^3T_2$ transition, Jahn-Teller effect 80—34884
Ar, single crystal, Pockel coeffs. and short-range-interaction parameters 79—73962
As_2S_3 glass, press. effect on optical props. 80—50363
As_4S_4, effects of pressure and temp. on phonons, Raman scattering study 80—7360
$As_2S_3(Se_3)$, film on KCl, strain-induced refractivity anisotropy, 10.6 μ ellipsometric obs. 79—14064
Au-GaS, Schottky-barrier electroreflectance spectra under uniaxial stress 79—56767
Ba hexafluorometallates, $BaMF_6$, (M=Si,Ge,Sn,Ti), Raman spectra at press. up to 25 kbar 78—6670
BaF_2, CaF_2 and SrF_2, dielectric const. and polarisability strain derivatives 77—73125
BaF_2, piezo-optical coeffs. meas. at 0.6328, 1.15 and 3.39 μm 80—34888
BaF_2, strain induced splitting and oscillator strength anisotropy of IR transverse optic phonon 80—92625
$Ba_2NaNb_5O_{15}$, high press. phase transitions, Raman scatt. studies 80—71402
$BaTiO_3$, elastooptic effect near ferroelec. transition, temp. depend. 80—97233
$Bi_{12}GeO_{20}$, optical phonon freq. in vicinity of Brillouin zone, linear wave-vector depend. 79—19892
$Bi_{12}GeO_{20}$, piezo- and thermo-optical props., dispersion theories and models 79—56764
BiI_3 film, exciton peaks, temp. depend. 90-270K, and press. depend. up to 3500 atm. 77—36265
CaF_2 piezo-optical coeffs. meas. at 0.6328, 1.15 and 3.39 μm 80—34888
CaF_2, strain induced splitting and oscillator strength anisotropy of IR transverse optic phonon 80—92625
CaF_2:Dy, colour centres, antiresonance-type phenomenon in external fields 78—68529
$CaF_2:Eu^{2+}$, tunable optical detection and generation of THz phonons 79—65149
$CaF_2:Sm^{2+}(Eu^{2+})$, cubic crysts., piezodichroism absorpt. curves 77—81131
$CaF_2:Yb^{2+}$, cryst., stress polarisation of luminesc. and emitting states struct. 77—69897
$CaF_2:Yb^{2+}$, luminesc. polarisation, elastic uniaxial compression effect, radiative state model 78—6739
CaO, electron irradiated, symmetry assignment of new point defect 78—31261
$CdBr_2(I_2)$, exciton spectra, temp. and press. effects 77—20881
$CdCr_2Sr_4$, press. depend. optical aborption edge shift and compressibility 79—28714
CdS, calc. deform. effects on biexcitons, compared to piezoemission meas. 77—52038
CdS, deform. effects on exciton excitation spectra 78—35191
CdS, edge emission spectra alteration by uniaxial stress *(Russian)* 78—72486
CdS, excitonic mol. emission, strain induced splitting 77—44060
CdS, plastically deformed, optical and electronic transport anisotropies 77—8611
CdS, reversible threshold modification of luminesc. spectrum by uniaxial compression 79—38662
CdS, strain- and electro-gyration, polarised light dispersion curve pseudocrossing 77—36196
CdS, stress-induced photolum. bands, photocond., rel. to dislocation electron states 80—25447
CdS, thermal equilib. phonon populations, acoustic intensity meas. by Brillouin scatt. intensity obs. 80—45098

piezo-optical effects continued
$CdS_{1-x}Se_x$, mixed crystals, deformation effects on free excitons 80—76073
CdSe, optical parametric devices, freq. tuning possibility by uniaxial press. 78—59084
CdSe, thin films, exciton piezotransmission 79—24380
CdTe film, exciton spectra, press. and temp. depend. 80—80886
CdTe, transmission spectrum under uniaxial compression 80—29714
Cds, reson. Brillouin scatt. by piezoelectrically inactive TA phonon domains 78—84593
$CeF_3:Pr^{3+}$, absorpt. spectrum, 400-700 nm, 78K, 22 kbar press. effects 77—81133
$CsAl(SO_4)_2.12H_2O$, third order elastic consts. from stress shifted reson. freqs. 78—55905
CsBr, F-centre absorpt., uniaxial stress effects 80—60634
CsBr:Tl, emission bands, press. effect 79—33789
Cs_3CoBr_5, optical anisotropies of mechanism of vibronic transitions in spectra 77—12372
Cs_3CoCl_5, optical anisotropies of mechanism of vibronic transitions in spectra 77—12372
CsD_2AsO_4, SHG, electro-optic and piezo-optic tuning 78—46718
CsH_2AsO_4, Mandelstam-Brillouin spectra and US vel. meas. near ferroelec. Curie point 79—38553
CsI, and Na doped sample, elastically loaded, effect of annealing on optical absorption 77—44034
CsI, pure, influence of strain on photolum. 79—15527
CsI:Tl, emission bands, press. effect 79—33789
$CsI:Tl^+$, Jahn-Teller split luminesc., high press. study 78—52565
CuBr, press. depend. of Raman scatt. meas., Gruneisen parameters determ. 77—24845
CuCl, anomalous Raman spectrum in transverse optic phonon region 77—24846
CuCl, press. depend. of Raman scatt. meas., Gruneisen parameters determ. 77—24845
CuCl, zincblende struct., high press. Raman scatt., 77K 78—60463
$CuGaS_2$, press. depend. of energy gap, absorption edge obs. 77—12401
CuI, press. depend. of Raman scatt. meas., Gruneisen parameters determ. 77—24845
Cu_2O, reson. Raman scatt. from stress-split forbidden excitons 80—93332
Cu_2O, uniaxial stress effects on excitons 80—60589
Cu_3VS_4, Raman linewidth of A_1 mode under high press., reson. effects 80—108210
p-D_2, far IR absorpt. in ordered state 79—91430
D_2, solid, compressed, anomalons double peaked one-phonon for IR absorption 79—56788
D_2, solid, press. depend. of phonon lineshape in ordered state, far IR spectra 79—56023
Eu complex, benzoylacetonate, energy transfer at high pressures 78—52541
EuO, ferromagnetic, mag. field effect on optical absorpt. edge, piezotransmission spectra 78—95578
EuO, ferromagnetic piezotransmission behaviour in magnetic field 80—97272
EuO, stoichiometric, crit. behaviour of piezotransmission at Curie temp. 77—85688
EuO, transmission and resistivity, stress modulation effect near Curie temperature 80—96874
n-GaAS epitaxial film, radiative recomb. under influence of mech. stresses 80—66291
GaAs, conduction band effective mass, influence of high uniaxial stress 80—80162
GaAs, luminescence emitted from deep centres, plastic deform. effect on internal quantum efficiency 80—60672
GaAs, manifestation of local vibrs. of dislocations in IR spectra 78—88339
GaAs p-n junctions, electron irrad. induced defect levels, hydrostatic press. effect 80—92858
GaAs, photoluminescence and resonant Raman spectra, press. depend. 78—31251
n-GaAs, piezo-absorpt. meas. 79—87455
GaAs, resonant Brillouin scattering 79—78695
GaAs, Schottky barrier electrorefl. under uniaxial stress, band struct. 77—48193
GaAs, thermal equilib. phonon populations, acoustic intensity meas. by Brillouin scatt. intensity obs. 80—45098
GaAs, transmission spectrum under uniaxial compression 80—29714
$GaAs:Co^{2+}$, piezoabsorption meas. tunnel splitting and Jahn Teller effect in $^4T_1(P)$ state 79—15494
GaAs:Cr, luminesc. stress splitting, 4.2K 78—84627
GaAs:Ge, stress depend. of donor-acceptor recomb. energy 79—15113
GaAs-$Ga_{1-x}Al_xAs$ stripe geometry lasers 79—94245
GaAs-GaP heterostructure, radiative recomb. under influence of mech. stresses 80—66291
$GaAs_{1-x}P_x$, epitaxial layer, modulation of direct and indirect gaps, piezotransmission meas. 77—24819
$GaAs_{1-x}P_x$, piezomodulation spectra of indirect gap, zero-phonon and phonon-assisted transitions 77—48192
$GaAs_{1-x}P_x$:N heterojunction, N_x and $N\Gamma$ bound states, high-press. effects on electroluminesc. meas. 77—11870
$GaAs_{1-x}P_x$(Te), bound exciton stress depend., piezoluminescence, photoluminescence 80—80206
$Ga_xIn_{1-x}P$, piezomodulation spectra of cond. band struct. 77—48191
GaP, deformation potentials of direct and indirect absorpt. edges 79—69854
GaP, excited 1s-level of S-bound excitons 79—82996
GaP, indirect exciton fine struct. in absorpt. spectrum, stress effects 79—42986
GaP, indirect exciton fine struct. and effect of uniaxial stress 79—95805
GaP, manifestation of local vibrs. of dislocations in IR spectra 78—88339
n-GaP, many-valley semiconductor, relative displacement of D_1 and D_2', bands under shear deform. influence 79—15080
GaP, piezo-modulated spectroscopic investigation of N and N-N pairs, bound exciton 77—66474
GaP, Raman spectra, press. depend. optical phonon anharmonicity 77—8586
GaP, S-bound exciton stress depend. 80—29333
$GaP:Fe^{2+}$, absorpt. and luminesc. spectra 77—16388
GaP:S, effects of uniaxial stress on luminesc. 79—78739

piezo-optical effects continued
GaP:S, ground and excited states of bound exciton complex, stress effects 80−65463
GaP:Zn, Raman spectra of Zn acceptor 77−77187
GaP-GaAsP planar heterostructure strip ridged waveguide under mech. load, polarisation modulation 80−96038
GaS, optical absorption edge under hydrostatic press. 78−23487
GaS(Se), absorpt. edge, exciton levels and Raman scatt., press. effects above 40 kbar 77−48187
GaSb, bound excitons at doubly ionisable acceptors 79−42459
GaSb, cond. band L-states, i.r. absorption, uniaxial stress 77−1674
GaSb crystals, uniaxial deform., effect on polarised luminesc. 78−10957
GaSb, manifestation of local vibrs. of dislocations in IR spectra 78−88339
GaSb, photolum. spectra under hydrostatic press. 79−19930
ε-GaSe, Raman scatt., hydrostatic press. effect 80−84745
Gd complex, benzoylacetonate, energy transfer at high pressures 78−52541
$Gd_2(MoO_4)_3$, ferroelec., anomalous damping of phonons, Raman spectra, stress and temp. effects 79−38503
$Gd_2(MoO_4)_3$, spontaneous birefringence, pulsed field switching, compression effect, domain movement 78−27187
Ge, biexciton and trion existence, photolum. *(Russian)* 80−16088
Ge, electron-hole correlation density depend., in electron-hole liq., under uniaxial stress 79−15090
Ge, electron-hole liquid, luminesc. under infinite uniaxial compression 78−87915
Ge, piezospectroscopic determ. of electron-phonon to hole-phonon interaction 79−95783
Ge, piezospectroscopy of group V impurities 79−99915
Ge, polycrystalline thermal-imaging lens, optical requirements 80−69495
Ge, pressure tuning of picosecond pulse transmission, enhanced transparency 77−88871
Ge, reson. Raman scatt. under uniaxial stress near E_1 gaps 79−42960
Ge, Schottky barrier electrorefl. under uniaxial stress, band struct. 77−48193
Ge, strain-confined electron-hole liq. 77−47738
Ge, strain-confined electron-hole liquid, lifetime and radiative efficiency vs density 79−38000
Ge, strain-narrowing of luminesc. line from excitons 79−24356
Ge, stressed, metal-insulator transition, luminesc. 80−20695
Ge, stressed, recombination luminescence from hot carriers in electron-hole droplets 78−6754
Ge, uniaxially deform., electron-hole drop flight, photolum. max. press. depend. 78−10977
Ge, uniformly stressed, density and binding energy of electron-hole droplets, photolum. meas. 78−60062
Ge:As, uniaxially stressed, electronic Raman scatt. from valley-orbit transitions 78−15166
n-Ge:As(Sb), far IR absorpt. spectra 79−91469
n-Ge:Ga(P), uniaxial compression, 0.6-2.9 mm radn. absorpt. 79−82629
Ge:Li_2O, EPR and piezospectroscopy 80−25338
n-Ge:P,Ga, compensated, uniaxially compressed, anisotropy of mm. and submm. wave absorpt. 78−19074
Ge:Zn^-, G and D lines, stress induced components 80−71447
GeS(Se), layer cpds., Raman spectra, press. coeffs. and mode Gruneisen parameters 78−10891
O-H_2, far IR absorpt. in ordered state 79−91430
H_2, solid, compressed, vibr. Raman spectrum 79−47422
Hg_2Br_2, powder, Raman spectra, press. effects 78−2837
$Hg(CN)_2$, phonon freq. anomalous press. depend., mol. struct. distortion 80−88981
Hg_2Cl_2, powder, Raman spectra, press. effects 78−2837
HgTe, uniaxial stress effect on magneto-optical props. 77−59558
InP, depend. of phonon spectrum on hydrostatic press., Raman spectra 80−93315
InP, manifestation of local vibrs. of dislocations in IR spectra 78−88339
InP, photolum. meas. using diamond-anvil press. cell 80−108256
InP, press. depend. of direct absorption edge 80−93365
InP:Bi, uniaxial stress effect on free and Bi-bound excitons 79−56854
n-InSb, deformed, spectral oscills. of absorption in quantising mag. field 80−34486
InSb, reson. Raman scatt. under uniaxial stress near E_1 gaps 79−42960
InSe, optical props. near fundamental absorption edge 77−12434
$KAl(SO_4)_2.12H_2O$, third order elastic consts. from stress shifted reson. freqs. 78−55905
KBr, residual birefr., 3000-7000 Å, rel. to intrinsic piezooptical behaviour 78−60416
KBr:H^-, U-centre absorpt. band shape, piezodichroism dispersion curve and electron-phonon interaction 77−24873
KBr:Tl^+, Jahn-Teller split luminesc., high press. study 78−52565
KCN, cryst. phases at press. up to 55 kbar, Raman spectra obs. 79−82975
KCN, Raman spectra, at very high press. 79−1759
KCl, photoelastic consts. at 10.6 μm, interferometric and polarimetric meas. 78−25934
KCl single crystals, piezobirefringence and plastic deform., stress-strain curves 77−69798
KCl:Au^-, fluorescence, stress and mag. field depend., Jahn-Teller effect and relax. processes 77−48220
KCl:Li^+, defect induced tunnelling states, depend. on strain, pot. model calcs. 79−69865
KCl-KBr, with equimol. conc., piezo-optic birefringence theory 80−100643
KCl-KBr mixed crystals, sign reversal of piezo-optic birefringence 79−99849
KCl(Br)(I):In^+, Jahn-Teller split luminescence, high press. study 78−52565
KCl(Br)(I):Tl, emission spectra, press. effects 78−23509
$KD_3(SeO_3)_2$, optical and dielec. props. near ferroelastic phase transition 79−38518
KH_2PO_4, and isomorphs, IC spectra and phase transitions, under pressure 78−31180
KH_2PO_4, optical props., plastic deform. effect 77−59552
$KH_3(SeO_3)_2$, $KD_3(SeO_3)_2$, second-order ferroelastic phase transitions, piezo-opt. props. obs. 78−95558
$KH_3(SeO_3)_2$, optical and dielec. props. near ferroelastic phase transition 79−38518
KI:OH^-, HF phonon studies under uniaxial stress 79−83002
KI:Tl, emission and excitation spectra, press. effects 79−83028
KI:Tl, emission bands, press. effect 79−33789
piezo-optical effects continued
KI:Tl, phosphor, press. effect on emission spectra at low temps. 77−85771
KI:Tl^+, phosphor, anomalous stress-induced dichroism 79−4828
KI:Tl^+ type phosphor, press. effects on triplet relaxed excited states, quadratic Jahn-Teller interaction 78−23510
KI-KCl:Cu^+ mixed cryst., off-centre Cu^+ 79−65112
$KMnF_3$, stress-induced phase transition, optical props. meas. 77−20067
$KNiF_3$ and K_2NiF_4, MCD and stress linear dichroism on double excitonic transitions 77−52051
K_2SeO_4, Raman spectra, effects of temp., substitutional cations, and stress 80−71405
$KniF_3$, K_2NiF_4, antiferromag., two-exciton transition, stress-induced linear dichroic spectrum 77−32398
Kr, single crystal, Pockel coeffs. and short-range-interaction parameters 79−73962
$(La,Nd)P_5O_{14}$, optical props., ferroelastic phase transition induced 79−95731
LaF_3, zone centre optical phonon stress dependence, point group symm., Raman spectra meas. 79−78686
La_2O_2S:Eu, high press. effect on luminesc. efficiency and lifetime, charge transfer absorpt. 80−66266
La_2O_2S:Eu, slow phosphoresc., high press. study 80−80839
LiF, manifestation of local vibrs. of dislocations in IR spectra 78−88339
LiH, optical parameters of localised centres at high hydrostatic press. 78−10943
α-$LiIO_3$, piezoelec. mat. for acoustooptic cells, piezoelectric transducers 78−95575
$LiNH_4SO_4$, $LiNH_4SeO_4$, nonlinear opt. props. including SHG 78−76396
$LiNbO_3$ optical waveguide, Bragg interaction of leaky and Rayleigh waves 77−23783
$LiNbO_3$, planar lightguide, optical mode interaction with standing elastic surface waves 80−99836
$LiNbO_3$:Fe, optical damage depend. on temp., press., and applied elec. field *(Japanese)* 79−81498
$LiNbO_3$:Ti optical waveguide, surface wave mode conversion, static strain-optic effect 80−87561
$(Mg,Fe)_2SiO_4$, olivine, fayalite rich, single cryst., UV absorpt. spectra at high press. 78−85545
MgO, electron irrad., V^--centres, stress-induced optical dichroism, absorpt. spectra 79−61406
MgO, photoluminesc. during mechanical deform. 80−60665
MgO, stresses on hot pressing 77−36425
MgO:Cr^{3+}, no-phonon lines associated with broad band emission *(French)* 77−52163
MgO:Fe, cathodolum. after plastic deform. 79−95849
MgO:Li, $[Li]^0$ defect, stress induced optical dichroism 78−35179
$Mg[Pt(CN)_4].7H_2O$, high press. tuning of optical transitions 79−28813
MnF_2, birefringence variation on uniaxial compression *(Russian)* 80−34887
$MoS_2(Se_2)$, effect of uniaxial stress on excitonic optical spectra 78−84606
N_2, solid, Raman spectroscopy up to 374 kbar 80−7353
ND_4I, Raman spectrum, press. effects 80−97261
$NH_4Al(SO_4)_2.12H_2O$, third order elastic consts. from stress shifted reson. freqs. 78−55905
NH_4Br and NH_4I, Raman scatt., 1 bar-7 kbar, 86-295 K 80−34909
NH_4Br, phase diagrams, from Raman meas. under high press. 78−52776
NH_4Cl Raman spectra, pressure effects 80−97268
NH_4I, phase diagrams, from Raman meas. under high press. 78−52776
NH_4I, Raman spectrum, press. effects 80−97261
NaCN, cryst. phases at press. up to 55 kbar, Raman spectra obs. 79−82975
NaCN, Raman spectra at very high press. 79−1759
NaCN, Raman spectrum, hydrostatic press. effects 78−6663
NaCN, single cryst., orientationally disordered, Brillouin scatt., elastic consts. 77−85732
NaCl, uniform deformation and birefringence in nonuniform elec. field *(Russian)* 79−87396
NaCl:$^{63}Cu^+$, resonant bandmode, stress spectroscopy with far IR laser 78−2847
NaCl:H^-, U-centre absorpt. band shape, piezodichroism dispersion curve and electron-phonon interaction 77−24873
NaCl(Br):Tl, emission spectra, press. effects 78−23509
$NaClO_3$, electrogyration and piezogyration meas. 79−28716
NaF, piezooptical coeffs., 200-600 mμ 77−69800
$NaNH_4SO_4.2H_2O$, $NaNH_4SeO_4.2H_2O$, nonlinear opt. props. including SHG 78−76396
Nd doped (fluoro) phosphate laser glass piezo-optic coeffs. meas. at 0.6328 and 1.15 μm 80−34888
NdP_5O_{14}, fluoresc. lifetime meas., IR and photoacoustic spectroscopy 80−60652
PLZT ceramics, elastooptic effect, stress induced birefr. 80−60543
$PbBr_2(Cl_2)$, exciton spectra, temp. and press. effects 77−20881
$Pb_5Ge_3O_{11}$, ferroelec. transition, US and elasto-optic props. 80−60527
PbI_2, press. depend. of band-gap excitons, 77K, optical absorpt. spectra 79−8157
$PbMg_{1/3}Nb_{2/3}O_3$, electro-opt., elasto-opt., opt. and photo-induced props. 78−95560
$PbZn_{1/3}Nb_{2/3}O_3$, electro-opt., elasto-opt., opt. and photo-induced props. 78−95560
$RbCoF_3$, single oriented antiferromag. domain, polarised Raman scatt. under uniaxial stress 78−23463
RbI:Tl, emission and excitation spectra, press. effects 79−83028
RbI:Tl, emission bands, press. effect 79−33789
$RbMnF_3$, triplet states, piezospectroscopy 79−38562
$RbNiF_3$ and Rb_2NiF_4, MCD and stress linear dichroism on double excitonic transitions 77−52051
S_4N_4, effects of pressure and temp. on phonons, Raman scattering study 80−7360
S_4N_4, Raman scatt., press. and temp. depend., 0-10 kbar, 10-295K 78−15160
S_4N_4, Raman scatt. and opt. absorpt., press. and temp. depend. 77−36227
SbI_3 film, exciton peaks, temp. depend., 90-270K, and press. depend., up to 3500 atm. 77−36265
Sb_5O_7I, polytypes 2MC and 2MA, photoferroelastic phenomena 79−95447
Se amorphous Au clad waveguides piezoelastic modulator for 10.6 μm radiation 78−66956

piezo-optical effects continued
Se, trigonal, behaviour of optical gap under press. 80−80171
Se, trigonal, Raman scatt. at very high press. 80−60566
Si, appl. of photoelastic stress. meas. technique 80−48656
Si, deformed, recomb. radiation from electron-hole drops and free excitons 77−8641
Si, diamagnetism of excitons and biexcitons, recomb. spectra *(Russian)* 80−7412
Si, dislocation luminesc. obs. 78−15217
Si, divacancy charge states, photoconductivity spectra 77−15899
Si, elasto-optic constants, real and imaginary, direct absorpt. and Raman scatt. meas. 80−97234
Si, exciton and deformation pot. fine struct. 78−88301
Si exciton luminescence in mag. field or under uniaxial stress 78−27322
Si, far IR impurity spectra, effects of high uniaxial stress 78−56508
Si, film, amorphous, optical absorption at high press. 78−35216
Si, heavily disordered, fast neutron irrad., IR absorption following heat treatment 78−2448
p-Si, heavily doped, intra- and interband Raman scatt. 79−95788
p-Si, heavily doped, intra- and interband Raman scatt. by free carriers 80−108208
n-Si, heavily doped, intraband Raman scatt. by free carriers 78−19483
n-Si, heavily doped, self energy of phonons interacting with free electrons, Raman scatt. 78−64366
n-Si, many-valley semicond., relative displacement of D_1 and D_2' bands under shear deform. influence 79−15080
Si, mass-anisotropy exciton splitting determ. 78−6685
Si, photoluminescence of electron-hole drops under uniaxial stress 79−91491
Si, piezo-optical consts., Raman meas. 78−65951
p-Si, piezo-spectroscopic study of defects *(Russian)* 77−28607
Si, piezo−spectroscopic study of ratio of electron−TO phonon to hole−TO phonon interaction 79−24289
Si, piezospectroscopic determ. of electron-phonon to hole-phonon interaction 79−95783
Si, piezospectroscopic effect on zero phonon luminescence lines 80−50406
Si, plastically deformed, hot-exciton luminesc. as function of strain 78−88361
Si, polarisation of recombination radiation from multiparticle exciton-impurity complexes, induced by uniaxial deform. *(Russian)* 79−78754
Si, Raman cross section and its press. depend., theoretical study 79−91448
Si, Raman spectrum, two-dimens. tensile stress effects 78−48173
Si rubber as electro-optic material for optical hydrophones 80−43412
Si, stretched, lattice vibr. anharmonicity, influence of stress on elastic moduli, Raman spectra 80−80791
Si, uniaxial stress effects and excited states for multiple bound excitons 78−6281
Si, uniaxially deformed, photoluminesc., biexcitons *(Russian)* 77−59611
Si:Al, absorpt. line broadening 78−95594
Si:Al, bound exciton and bound multiexciton complexes, electronic structure, luminesc. obs. 79−56139
Si:As(Li)(P), luminesc., stress effects on donor exciton satellites 77−85786
Si:B, irrad. with fast neutrons true profiles of impurity photocond. bands from piezodichroisms 79−91103
Si:B, many-body exciton-impurity complexes, stress depend. of photolum. meas. 79−28833
Si:B(Li)(P), piezospectroscopic studies of bound multiexciton complexes 80−16006
Si:B(P), uniaxially stressed, impurity-assisted intervalley scatt., photoluminesc. obs. 80−34979
Si:Li, bound-exciton excited states, uniaxial anal. 80−71475
Si:P, acceptor bound multiexciton complex recomb., shell model, luminesc. line splitting 78−6275
Si:P, expt. evidence against shell model of bound multiexciton complexes 78−10368
Si:P, luminesc. lines, multiexciton complexes and unaixial stress 78−92114
Si:P, uniaxially deformed, multiparticle impurity complexes, luminesc. spectra *(Russian)* 79−4854
Si:P, Zeeman and stress-induced spectra, shell model for bound multiexciton complexes 77−31953
Si:P bound multiexciton complexes, expt. evidence for shell model 78−39036
Si:P(B), multiple-particle exciton-impurity complex form. *(Russian)* 78−43925
SiC, influence of plastic deform. on struct. of photoluminesc. spectra 77−55824
SiO_2, fused, stress optical coeff. 79−28713
SiO_2 thin film grating for $LiNbO_3$:Ti waveguide mode convertor and reflector 80−64216
SiO_2, vitreous, electron irrad., vol., refr. index and stress changes 77−47482
SiO_2-LiO_2-Al_2O_3 glass, luminesc., polarisation degree distrib. 80−108257
SmS, press. effect on lattice parameter, mag. susceptibility, and reflectivity 79−56272
SmSe, pressure-induced reflectivity changes and semiconductor-metal transition 79−56763
SnI_4, Raman spectra, temp. and press. meas. and lattice dynamical calcs. 78−56472
SnS_2, 2H and 4H, effect of press. on optical absorpt. edge 77−77238
SnS_2, optical props., modulation spectroscopy 77−52117
SnS_2 press. effects on optical absorpt. edge 77−52119
$SnSe_2$, optical props., modulation spectroscopy 77−52117
$SnSe_2$, press. effects on optical absorpt. edge 77−52119
$Sr_xBa_{1-x}Nb_2O_6$, high press. phase transitions, Raman scatt. studies 80−71402
SrF_2 piezo-optical coeffs. meas. at 0.6328, 1.15 and 3.39 μm 80−34888
SrF_2, strain induced splitting and oscillator strength anisotropy of IR transverse optic phonon 80−92625
SrF_2:Eu^{2+}, tunable optical detection and generation of THz phonons 79−65149
$Sr_2Nb_2O_7$, high press. phase transitions, Raman scatt. studies 80−71402
$Sr_2Nb_2O_7$, optical mode softening in incommensurate phase 80−7352
Te, intervalence band absorption, press. and defects influence 80−55149
Te, opt. props. under high press., band struct. transform. 80−55112
Te, trigonal, Raman scatt. at very high press. 80−60566
Te, uniaxially stressed, cyclotron resonance 79−87319

piezo-optical effects continued
TeO_2, elastic wave parametric instability kinetics in dielectrics *(Russian)* 80−45035
TeO_2, paratellurite, phase transition at high-press., Raman and far IR spectra 78−80328
TeO_2, paratellurite, stress induced changes in Raman spectrum 78−39540
TiO_2, anatase, effect of hydrostatic press. on Raman spectrum 79−61384
TiO_2, deform. pot. meas. of direct forbidden transition 79−95806
TiO_2, energy band struct., uniaxial stress depend. 80−2334
TiO_2, rutile, first order Raman spectrum, uniaxial stress effects 80−66196
TiO_2, rutile, first-order Raman spectrum, uniaxial-stress depend. 80−60586
TiO_2, subsidiary valence band extrema, piezospectroscopic exam. 79−19516
TiO_2, uniaxial stress depend. of direct-forbidden and indirect-allowed transitions, absorpt. edge obs. 79−42990
Tl halides, temp. and press. depend. of transverse-optic modes and anharmonic self-energies 77−11649
TlBr-TlI(Cl) crystals, photoelastic moduli 80−97230
$TlSbF_6$, Raman spectra at press. up to 25 kbar 78−6670
$WS_2(Se_2)$, effect of uniaxial stress on excitonic optical spectra 78−84606
Y_2O_2S:Eu, high press. effect on luminesc. efficiency and lifetime, charge transfer absorpt. 80−66266
$ZnIn_2S_4$, Raman scatt., hydrostatic press. effect 80−84745
ZnO, excitonic mol. emission, strain induced splitting 77−44060
ZnS, plastically deformed, anisotropic cond. 78−56143
ZnS, reson. Brillouin scatt. and piezobirefringence 80−93348
ZnS:Cl^-, $Cu^+(Ag^+)$, phosphor, high press. effect on thermoluminesc. 78−64419
ZnS:Co, Jahn-Teller interaction energy determ., piezospectroscopic expt. *(Russian)* 77−4623
ZnS:Cu 79−24350
ZnS:Fe, piezospectroscopic effect on electron-vibr. lines of Fe^{2+} 78−27269
ZnS:Mn, self-activated and Mn^{2+} emission, high press. action 80−16093
ZnSe, dielec. const. strain depend., spectral behaviour by acousto-optic method 77−48147
ZnSe, reson. Brillouin scatt., dispersion curves, piezobirefringence anal., electronic state lifetime broadening effects 79−61390
ZnSe:Cr, piezodichroism due to reorientation of Jahn-Teller centres 80−11363
ZnSe:Cr^{2+}, stress-induced alignment of Jahn-Teller centres 79−78651
ZnTe, excitonic complexes, stress splitting of luminesc. lines 77−4672
ZnTe film, exciton spectra, press. and temp. depend. 80−80886

piezoelectric devices
see also crystal filters; crystal resonators; piezoelectric transducers
acceleration sensors, lower limiting frequency and indication threshold *(German)* 80−95093
accelerometer, magnetic fastening using new magnetic material $SmCo_5$ 79−77035
accelerometer/velocimeter, range of 10^5 g to 10^{10} g and time resolution of few nanoseconds 77−45826
accelerometers, effect of strain sensitivity on accel. meas. of flexural vibrations 80−58991
accelerometers *(German)* 80−22334
acoustic signal storage device, DIAM, appl. to adaptive correl. *(French)* 77−7272
acoustic waveguide, Young sound wave propagation 78−38112
acoustical holographic piezoelectric integrated acoustic array, system anal. 80−79067
artificial acoustic anisotropy of a controlled piezoelectric element 77−50848
atmospheric aerosol automatic mass conc. meas. techniques 77−64459
bimorph piezoelectric flexible mirror constructed from glass plates and $Pb(Zr,Ti)O_3$ ceramic 79−59787
bimorph plate, adaptive optical element analysis 79−50389
biodynamic subminiature piezoresistive accelerometer performance evaluation 78−20340
bistable piezoelectric Fabry-Perot interferometer 79−97420
Bleustein-Gulyaev waveguides with gratings, anal. Bleustein-Gulyaev waveguides with gratings, anal. 80−1391
cascade particle analyser for aerosol size distrib. and mass conc. 79−71583
ceramic radiators, defects visualisation using holographic interferometry *(Russian)* 78−1530
ceramics, photovoltaic effect application to information storage 80−80316
conductor-dielectric conductor system, electric signal rel. to plane load wave parameter 77−90105
continuous deformable mirror multidither coherent optical adaptive system operation 77−19296
convolution by membrane waves, using transversal piezoelectric effect of PVF_2 film 79−3859
cylindrical thin shell, appl. of one-dimensional finite elements to normal mode anal. 77−31163
deformable mirror figure sensor control 77−19384
deformable mirrors for wavefront error correction, piezoelectric material requirements 80−78928
deformable mirrors with bimorph actuators 80−33135
detector for photoacoustic microscopy, principle and appl. to semiconductor industry 80−14525
dielectric/piezoelectric layered waveguide, surface acoustic wave amplification *(Russian)* 78−23138
differential integrated pressure sensor, using microprocessor cct. given *(French)* 79−54149
discrete actuator deformable mirror 80−33133
displacement device, inchworm operation in vac., SEM X-Y stage driving appl. 79−21729
displacement generator, annular, mathematical theory 78−62185
doubly rotated crystal frequency and temp. coeff. angular dependence 77−39142
drive, implantable, for left ventricular assist device, invertor improvement 78−15927
dynamometer for dynamic force meas. *(Hungarian)* 78−65918
earphone, piezoelectric plastic film transducer theory 80−43582
earphones, usefulness in recording brain stem auditory evoked pots. 80−94389

piezoelectric devices continued
electronically controlled insulin pump and valves for diabetes patients 78−53565
electrostatic voltage sensor *(Japanese)* 80−105632
EM radiation detector, for ultraweak signals 78−82032
equivalent cct. parameters calc. for radially polarised piezoceramic sphere 80−14538
Fabry-Perot etalon, piezoelectrically controlled, linear scanning cct. 78−4704
Fabry-Perot scanning interferometer with piezoelec. spacers, appl. to solar UV spectrum 80−12678
glass microelectrode, piezoelectric drive appl., for cell membrane penetration 79−5420
gravitational antenna for use at 3 mK 78−58103
grouped receiver array, seismic signals distortion *(Russian)* 79−39948
high dynamic pressure measurements in solids 80−47070
IC pressure transducer for barometer and blood-pressure meter 79−35709
impact accelerometer, effect of damping on dynamic error 79−30435
laser beam control by piezoelec. stack 77−72012
laser beam deflector, basic charcts., multielement 77−54808
laser beam deflector, bimorph, theory and expt. 77−54807
laser intracavity phase lock control system 79−76718
laser pulse shaping on multiple rot. lines, using piezoelec. length tuner 80−78879
light beam control appl. *(Czech)* 80−19090
light shutter array, large area electronically controllable, using polyvinylidene fluoride bimorph vanes 80−58696
memory-correlator cells employing acoustically induced charge hologram in piezoelectric semiconductors 78−86290
microscope objective, piezoelec. and electrodynamic automatic focusing servo mechanisms 80−73445
mirror translator, piezoelec., stabilisation of narrow-bandwidth CW dye laser 80−33036
monolithic deformable mirror/heat exchanger unit evaluation 80−33139
monolithic layered piezoelectric-semicond. structures, acoustoelectric coupling 77−32050
Mossbauer spectrometer, piezoelec., with fast channel advance rates 78−24904
multiactuator deformable mirror evaluations 80−14416
multielectrode composite piezoceramic bar, equivalent elec. cct. 77−46877
multielectrode piezoelectric bar, flexurally vibr., derivation of equiv. electric circuit 78−94481
noise cancelling microphone with piezoelectric plastic diaphragm, coupled oscillator theory 80−43581
optical beam scanners, piezoelec. bimorph, analysis and construction 79−36992
photoacoustic thermal-wave microscopy, high resolution studies 80−74647
photoelectric autocollimator detector using piezoceramic bimorph element 77−7206
pick-up, for pulsed pressures meas. 80−31778
plunger device with piezoelec. fine adjustment for nuclear lifetime meas. 79−6806
polyvinylidene fluoride piezoelec. film for adaptive deformable mirror system 80−74455
position transducer three-axis coordinate convertor for optical scanners 79−63199
quartz crystal microbalance for sorption studies under dynamic conditions 80−73323
quartz piezoelectric crystal, electron-acoustic signal processing *(Russian)* 77−62111
quartz thickness monitor, low temp. film thickness meas. 77−79052
quartz thickness monitor, low temp. film thickness meas. 78−41275
reactor diagnosis by acoustic meas. methods, magnetostrictive and piezoelec. high-temp.-resistant sensors 80−32411
relays, multilayer plates bending, anal. 80−40064
resonator, disturbances characterised by dissipative mech. parameters 79−28682
respirable aerosol mass conc. meas., using piezoelec. microbalance 78−69518
RF sputtering systems, discharge suppression within piezoelectric gas admission valves 80−100110
SAW convolver, efficiency 78−18124
SAW IDT filter with thre inclined tapered transducers 79−81637
sensor element for press. meas. in soil pores *(Polish)* 79−25363
shutter control, for He^{+} microbeam facility with scanning system, for two dimensional backscatt. images 79−2879
spectrometer, Fabry-Perot, piezoelectric scanning nonlinearities 79−6183
spherical mirror with piezoelectrically controlled curvature 78−33796
storage convolution, correlation, signal processing appl. *(French)* 79−32146
strain gauges, biaxial gauge factors 80−52185
tactile hearing aid, portable with microprocessor control 79−84029
tensile device, const.-load, for UHV electron microscope, appls. to materials science 78−11462
three- and four-dimensional photoacoustic store readout 80−48413
three-actuator deformable water-cooled mirror 80−33134
two-laser frequency difference stabilisation electronic system 79−68401
two-layer systems with an air gap, interaction of Rayleigh waves with electrons 77−39901
US defectoscope, theory of operation, fundamental equations of electroacoustic channel 78−53123
US focusing device with IDT on thin piezoelectric plate 80−1398
US imaging systems, piezoelec. face plate response anal. 79−14169
vibration-producing, reduce solid body friction *(German)* 77−35101
vibrator, flexural, split-electrode, suppression of spurious responses *(Japanese)* 78−83204
vibrators, elec. steered line array, US probe charcts. 80−35486
xerographic cascade flow, carrier bead velocity distribution meas. probe 80−47136
C piezoresistive gauges, shock loading and unloading behaviour up to 5 GPa 80−87750
Hg vapour monitor, personal dosimeter 77−21672
$LiNbO_3$ TE-TEM light mode convertor using acousto-optic interaction, expt. 78−46794
$Pb(Zn,Ti)O_3$ piezoelectric electrically deformable diffraction grating 80−78963

piezoelectric effects *see piezoelectricity*

piezoelectric filters *see crystal filters*

piezoelectric materials
see also piezoelectric semiconductors; piezoelectric thin films; piezoelectricity
absolute configurations, bibliography 77−48129
acoustic surface wave velocity measurement, pulse technique 78−5618
acoustic transverse wave polarisation and energy flow in external static fields 80−19123
acoustic wave mixing in piezoelectric crystals 78−83155
acoustic wave resonant transmission across piezoelectric gap 78−87855
acousto-optical properties, light scatt. by thermal acoustic phonons 78−48144
asbestos, piezoelec. and ferroelec. rel. to asbestosis and model of carcinogenesis 77−78075
atomic displacements, in pyroelec. and piezoelec. crysts., temp. and stress depend. conds. 79−24265
ceramic, bend and compressive strength, stressing rate effect 77−52409
ceramic, meas. using autocorrel. anal., stress charcts. 77−1639
ceramic, phase method of microwave flaw detection 78−72968
ceramic, piezoelectric, US instrument for determ. charcts. 80−66752
ceramic, reflection and transmission of elastic waves at boundary with water 80−87588
ceramic, reviews appl. and recent developments 79−78628
ceramic, SAW nonsynchronous interaction *(Russian)* 78−26002
ceramic, statically compressed layer, electrical energy of instantaneous discharges *(Russian)* 78−39503
ceramic, TsTBS-3, mech. strength, effect of glass powder additions 78−31370
ceramic, TsTS-19, dynamic peizoelec. modulus *(Russian)* 79−28681
ceramic blocks, TsTS-23, TBk-3, TsTSNV-1, longit. piezoelec. effect and moduli 78−56430
ceramic complex composites near morphotropic phase boundary, dielec. and electromech. anomalies *(German)* 77−20800
ceramic cylinders, finite axially polarised, vibr. anal. 77−11081
ceramic materials, piezoelec. props., review *(Japanese)* 77−73115
ceramic platelets, geometry effect, effect on props. of flexural oscillator *(German)* 79−32168
ceramic resonators, eigencoupling state space vector representation 80−2697
ceramics, bimorph element for loudspeakers props. and manufacture *(Japanese)* 80−53597
ceramics, electromechanical energy conversion in nonuniformly deformed bodies *(Russian)* 78−19418
ceramics, photovoltaic effect application to information storage 80−80316
connectivity and piezoelectric-pyroelectric composites 78−80290
coupling of elastic surface waves in piezoelectric crystals 77−85045
crystal bridge for equivalent electrical parameters meas. 78−54404
crystals, elastic surface waves 80−103558
crystals, of classes 422 and 622, transverse-transverse elastic polarisation waves 79−95077
cubic crystals, stimulated Raman effect 79−73927
deformable mirrors for wavefront error correction, piezoelectric material requirements 80−78928
dicalcium lead propionate, ferroelec., piezoelec. and elastic props. 78−84528
disilicate, piezoelectric glass ceramic, recrystallisation, pyroelectric response, permittivity 80−80703
electro-optical and nonlinear-optical materials, review 80−74450
electroacoustic echo 78−95549
electroacoustic interaction, parametric interaction of 550 MHz elastic wave with 1100 MHz elec. pump field 77−11966
electrostatic voltage sensor *(Japanese)* 80−105632
epoxy resin-ferroelectric $Pb(Zr,Ti)O_3$ composite, dielec., elastic and piezoelec. consts. 77−8515
fatigue fracture of piezoelec. materials, fractographic features 79−52374
finite amplitude SAW distorted rippling profiles, optical probing obs. 80−34287
fracture mechanics, deform. anal., crack development 77−24349
glass, US detector applications 78−33974
Griffiths cracks in a piezoelectric medium, critical load calcs. *(Russian)* 79−46264
hexagonal crystal, acoustoelectric wave excitation 77−76880
high temp. US generation, piezoelectric material and adhesive props. 80−43586
hilgardite and parahilgardite, piezoelectric zeolite type structures and composition 78−16003
hydrazinium iron tri(hydrazoformate) monohydrate single cryst., effective EFG tensor, Mossbauer spectra obs. 79−56628
length changes in subnano-meter range meas., by laser interferometry *(Slovak)* 78−77861
lithium ammonium tartrate, ferroelectric and ferroelastic transitions, Brillouin scatt. meas. 79−33716
lithium ammonium tartrate, piezoelec., proper ferroelastic transition 78−2812
lithium ammonium tartrate monohydrate, spontaneous shear strain, X-ray obs. 78−56433
lithium ammonium tartrate monohydrate elastic props., piezoelec. reson. method meas. 77−63370
magnetoelastic/piezoelectric composite media, SH-type guided elastic waves, transmission line model 78−27069
nonuniform polarisation, microwave Kerr effect obs. 78−72969
nylon 11, pyroelectricity and piezoelectricity 77−69780
oscillatory systems, piezoelectric materials and cells, method of measuring parameters 78−72989
piezoceramic, industrial, nondestructive testing using radiodefectoscopy 77−90555
piezoceramic, polarisation method effect on mech. strength 78−39879
piezoceramic elastic compliance and mechanical Q-factor at high drive levels 78−60395
piezoceramic planar Poisson ratio variation with poling conditions 79−11391
piezoceramic Poisson ratio rel. to electromech. coupling and energy trapping 78−43796
piezoceramic SAW propagation loss reduction by hot pressing 78−2356
piezoceramics, energy dissipation in high-freq. cyclic loading 80−15779
piezoelectric-semiconductor interface, periodically irregular, electron absorp. and acoustic wave amplification 79−42361

piezoelectric materials continued
piezoelectric-semiconductor struct., nonlinear acoustoelectric effects for large amplitude SAW 80−92942
plasmon transformation into SAW in piezoelec. cryst. 80−59903
polar materials, appl. to SAW and other devices 80−66114
polarisation echo in piezoelec. crystals 77−90104
poly-vinylidene fluoride-co-tetrafluoroethylene, dipolar theory applications to piezoelectric props. 79−78627
polydomain ferroelec. crysts., phys. consts., self consistent calcs. 80−88942
polymer, props. and appls. 78−80289
polymer films, electronic cond., electro-, photoresponsive effects, review 79−56261
polymeric, transducers appls. 79−32169
polymers, and their applics. *(Japanese)* 78−19416
polypropylene, electron bombarded, radical formation, piezoelectric and pyroelectric effects, ESR study 80−7169
polyvinylidene fluoride, bimorph vanes, use in large area electronically controllable light shutter array 80−58696
polyvinylidene fluoride, corona-charged, surface effects 80−66102
polyvinylidene fluoride, film, piezoelec., pyroelec., thermal expansion, elastic consts. 78−84529
polyvinylidene fluoride, film, piezoelec. relax. 79−87394
polyvinylidene fluoride, hysteresis phenomena under high elec. field 80−66134
polyvinylidene fluoride, piezoelec., pyroelec., and improper ferroelec. 80−7301
polyvinylidene fluoride, piezoelec. and pyroelec., rigid dipolar model *(French)* 79−8090
polyvinylidene fluoride, piezoelec. parameters versus bias field strength 79−91376
polyvinylidene fluoride, poling process, kink propag. model 80−80679
polyvinylidene fluoride, poling process, solitary wave propagation model 79−87398
polyvinylidene fluoride, poling process effect on fine struct. 80−7285
polyvinylidene fluoride, polycryst. ferroelec., microstruct., piezoelec. and pyroelec. props. 80−7303
polyvinylidene fluoride, props., polarisation and appls. 80−75947
polyvinylidene fluoride, struct. study, piezoelec. and pyroelec. props. 80−7300
polyvinylidene fluoride, suitability as underwater transducer material 78−1531
polyvinylidene fluoride acoustic transducer arrays, fabrication on Si wafer 80−74683
polyvinylidene fluoride film, anisotropy and temp. depend. of piezoelec. consts. 77−1640
polyvinylidene fluoride film, biaxially oriented, charact. for transducer appl. 80−88931
polyvinylidene fluoride film, piezoelec., appl. in confocal pair of concave transducers 78−22241
polyvinylidene fluoride film, piezoelec. coupling factor meas. servo system 78−60397
polyvinylidene fluoride film, piezoelectricity, importance of metal-polymer interface 78−76391
polyvinylidene fluoride film polymer transducer, with US appl., durable lead attachment techniques 80−79094
polyvinylidene fluoride films, corona-charged, struct. changes, piezo- and pyroelec. props. 79−11389
polyvinylidene fluoride films, corona-poled, piezoelectricity *(Japanese)* 80−55040
polyvinylidene fluoride films, SH and Lamb waves propag. 80−75948
potassium iron tri(hydrazoformate), Debye-Waller factor, Mossbauer spectra obs. 79−56627
powder, electroacoustic echo 77−8517
powder, polarisation echo and surface props. theory *(Russian)* 77−48122
powders, dynamic electroacoustic echo and recording *(Russian)* 79−87397
PVDF dielectric, piezoelec. and pyroelectric props. rel. to crystalline forms 80−15982
PVF_2, plastic film sensors 79−99826
PZT/polymer composites, simplified fabrication 80−40323
Q-factor determ. method 77−87788
quartz:Ge, optical and piezoelectric props., ang. distrib. *(Russian)* 78−23404
quartz, AC and BC crysts., rotated elastic consts., coupling factors and conversion efficiencies 79−19838
quartz, complex piezoelec. const. meas. by interferometric method, at freqs. up to 50 kHz 79−63270
quartz, crystal growth in fluoride environment, growth features and props. 80−6373
α-quartz, doubly-rotated-cut, numerical anal. of props. of SAWs 80−74616
quartz, effects of the He ion implantation on SAW propag. 80−75421
quartz, elastic constants and piezoelec. props. 80−92590
α- quartz, ferrobielastic hysteresis 80−19869
quartz, high-grade low-temp. impurity band IR absorption spectra 79−56825
quartz, hydrothermal crystn., new natural nutrient sources 77−8738
quartz, ion beam etching, for SAW refl. struct. fabrication, role of redeposition 77−56123
quartz, magnetoelec. reson. *(Russian)* 79−42904
quartz, non-crystalline characteristics after ion implantation *(French)* 77−73117
α-quartz, obs. of reversible elastic Dauphine twinning 78−87684
quartz, optical SHG with surface plasmons 78−18008
quartz, piezo quasi-mosaic struct. effect obs. on X-ray diffr. *(Russian)* 77−89349
quartz, piezoelec. and gamma-ray diffr. props. 77−20801
α-quartz, piezoelec. consts. determ. from dynamical X-ray diffr. curves 77−77153
quartz, piezoelectric surface wave velocity, flexural biasing state influence 79−56730
quartz, resonant powder, stimulated phonon echo, ang. and powder depend. 79−8093
quartz, SAW generation, use of analytical calc. for semi-infinite piezoelec. 78−51809
quartz, smoky, γ-irrad., electric dipolar echoes 80−20604
quartz, surface acoustic waves power densities approximation 77−79987
quartz, surface quality, determ. using Ag diffusion and neutron-activation method 79−51401

piezoelectric materials continued
quartz, synthetic, characterisation by IR adsorption 79−56824
quartz, synthetic, precision meas. of elastic and piezoelectric charact. 78−6638
quartz, vacancy attenuation of elastic waves at high temp. 79−86846
quartz, var. of elastic consts. under gamma irradiation 77−36180
quartz, with metallic overlay films for temp. compensation, SAW device appls. 80−79043
quartz crystal, γ-irradiated, US shear wave propag., beat obs. 77−43283
quartz crystal, charact., operation mode and struct. *(German)* 79−61306
quartz crystal, influence of tabs thickness and resonating props. 78−18140
quartz crystal, new method of freq. spectrum determ. and appls. 78−23402
quartz crystal, oscillating charact., nucl. and X-irrad. effects 79−78626
quartz crystals, oscillating, surface patterns obs., energy trapping appl. 80−71323
quartz crystals with TTC-cut *(Danish)* 80−60504
α-quartz dislocation free and low dislocation, prep. by hydrothermal crystallisation 78−72712
quartz ferrobielastic twinning, electrical and acoustic emissions 79−56731
quartz fundamental elastic constants, temp. derivatives 79−55810
quartz fused, refractive index distrib. normal to polished surface, ellipsometric meas. 79−86965
quartz lattice constants, impurity effects 80−39034
quartz oscillating crystals, electron contrast effects in SEM 78−88255
quartz plates, acoustic reson. vibr., Berg-Barrett X-ray diffr. method 80−40063
α-quartz plates vibrating in thickness, doubly rotated, zero polarizing effect 80−55038
quartz resonators, thickness-mode, thermal stress effects on reson. freq., theory 80−50272
quartz rotated Y-cuts, higher-order effects of initial deform. on cryst. vibrs. 77−46862
quartz substrate covered with metal or quartz powder, dynamic SAW reflecting struct. 80−74565
quartz synthetic crystals, observation of growth defects by light scatt. tomography 78−71743
quartz wedge, reflection, transmission and conversion of normally incident SAW 80−2257
quartz with zero temp. coeff. of delay, SAW propag. charact. 80−75420
Rochelle salt, crystal, X-ray topographic obs. of localised vibr. 79−24264
Rochelle salt, electromechanical behaviour, influence of ferroelec. phase transitions 77−8510
Rochelle salt, mechanoluminescence and crack mobility, charge prod. during fracture 78−88370
Rochelle salt, phonon echos in SiO_2, ADP, KDP, and Rochelle salt *(Japanese)* 79−51213
Rochelle salt-ammonium Rochelle salt mixed cryst., elastic props., piezoelec. reson. method 78−76390
SAW device materials development 78−6636
SAW devices and temperature compensation techniques 80−74614
SAW generation on semi-infinite piezoelec. solid 78−51809
shape-dependent damping 80−93242
smectic liquid crystal, piezoelectric domains, free energy minimisation and Euler eqns. calc. 77−51319
specific directions of plane elastic waves in thin quartz crystal plates 80−92601
synthetic polymer films, acoustoelectric transducers appl. *(Italian)* 79−98577
Tanane, ferroelec. mol. cryst., strong piezoelec. coupling 80−75942
temperature compensated materials with high piezoelectric coupling 77−40184
TGS, under electrostatic field, magnitude of neutron diffr. enhancement due to piezoelec. effect *(Chinese)* 79−51907
TGSe, ferroelec., effect of gamma irradiation on dielec., piezoelec. and elastic props. 77−43943
thermopiezoelectric material, monoclinic symmetry, surface wave propag. 80−44403
thickness waves, dispersion charact. near cutoff freqs. 79−19841
tourmaline, elastic consts. by US phase-comparison method 80−2108
tourmaline, resonator, eleetroelastic constants, elec. field induced freq. shift study 80−20597
transmitters and receivers for medical ultrasonics 80−76819
US vibration visualization using IR telethermography 78−33966
vinylidene-fluoride-trifluoroethylene copolymer, piezoelectricity 80−88930
wave propag. in medium of hexagonal symmetry 79−28042
weak piezoelectric materials, piezoelec. const. determ., reson. method *(German)* 78−92025
ABO_3-type crystal, electro-opt. effect, theoretical treatment 78−76427
β-AgI, piezoelectric ionic cryst., US investigation 79−77689
$AgNa(NO_2)_2$, complex piezoelectric constant, meas. by interferometric method, at frequencies up to 50 kHz 79−63270
$Ag_3SbS_3(AsS_3)$, electroacoustic echo, ultrasonic wave attenuation *(Russian)* 80−88280
$\alpha AlPO_4$ as SAW substrate material, piezoelec. props. 80−80710
α-$AlPO_4$, berlinite, H_2O conc. determ. by Raman scatt. 80−76572
$AlPO_4$, berlinite, piezoelectric coupling for SAW applications 79−56055
α-$AlPO_4$, berlinite, SAW velocity and piezoelec. coupling obs. 79−56056
α-$AlPO_4$, berlinite, X-axis boule cut SAW props. 79−56061
$AlPO_4$, berlinite material for SAW devices 79−56735
$AlPO_4$ hydrothermal synthesis 78−60562
$AlPO_4$, piezoelectric coupling of temp. compensated cuts, calc. 78−13869
$B_{12}GeO_{20}$, cryst. powder, phonon electroacoustic echo signal storage 78−68055
$Ba_{0.8}Ca_{0.08}Pb_{0.12}TiO_3$, piezoelectric ceramic solid soln. *(Polish)* 77−55755
$Ba_{0.95}Ca_{0.005}TiO_3$, piezoelectric ceramic solid soln. *(Polish)* 77−55755
$(Ba_{0.95}Ca_{0.05})TiO_2+CaCO_3$ (0.75%), piezoelectric ceramic solid soln. *(Polish)* 77−55755
$Ba(NO_2)_2.H_2O$, hexagonal, piezoelec., electro-optic, dielec., elastic, thermoelastic props., space groups 78−76388
$Ba_2Si_2TiO_8$, elastic consts., thermal expansion and piezoelec. props. 77−85651
$Ba_2Si_2TiO_8$, fresnoite, SAW props., expt. and calc. 78−43229
$Ba_2Si_2TiO_8$, fresnoite single cryst. SAW charact. 79−37913

piezoelectric materials continued
$Ba_2Si_2TiO_8$ fresnoite, characts. for SAW devices 79−82430
$Ba_{2-x}Sr_xTiSi_2O_8$, piezoelec. crysts., SAW characts. 80−84354
$BaTiO_3$ ceramic, electromechanical coupling caused by electrostriction, reson. props. meas. 77−20802
$BaTiO_3$ ceramic, piezoelectric effect due to polarisation, expt. *(Polish)* 77−77151
$BaTiO_3$, ceramic, secondary electron emission yield 79−91546
$BaTiO_3$, electro-opt. effect, theoretical treatment 78−76427
$BaTiO_3$, ferroelectric ceramic, dielec., piezoelec. and elastic props., orientational contrib. 78−68468
$BaTiO_3$, fractographic features of fatigue 79−52374
$BaTiO_3$, photoferroelec., lighting effect on deform. and stresses 78−43802
$BaTiO_3$, piezoceramic, nonlinear piezoeffect 79−42900
$BaTiO_3$, piezoceramic, elastic normal wave propagation, phase transitions *(Russian)* 80−40067
$BaTiO_3$, piezoelectric ceramic solid soln. *(Polish)* 77−55755
$BaTiO_3$, polycrystalline ferroelectric, grain-size dependent props. 80−71352
$BaTiO_3$, polydomain ferroelec. crysts., phys. consts., self consistent calcs. 80−88942
$BaTiO_3$:Al, 0.05-0.3 wt.%, ceramic dielectric, dielec. and mech. props. 79−8091
$BaTiO_3$-Ni ferrite, piezoelectric-piezomagnetic sintered two-phase composite, magnetoelec. conversion 77−12181
$Ba_2TiSi_2O_8$, fresnoite, Czochralski growth and phys. props. 78−3026
BeO, wurtzite-type crystals, lattice dynamics including the effect of electronic extension 80−59586
$Bi_{12}FeO_{20}$, longitudinally vibrated bars, reson. freq., DC elec. field effects, elastic coupling polarising correction terms 80−60503
$BiGeO_{20}$, photocurrent oscills. in pulsed illumination rel. to piezoelec. props. 80−80325
$Bi_{12}GeO_{20}$, and CdS, separated, coupling of propagating SAW 78−38929
$Bi_{12}GeO_{20}$, elastic wave leakage across gap between piezoelectrics 78−6204
$Bi_{12}GeO_{20}$, electromech. props. 79−38455
$Bi_{12}GeO_{20}$, finite amplitude SAW distorted rippling profiles, optical probing obs. 80−34287
$Bi_{12}GeO_{20}$, piezoelec. resonator, electroelastic coeffs. 77−52020
$Bi_{12}GeO_{20}$ plate cut along (110) axis, torsional thickness oscillations calc. *(Czech)* 77−55754
$Bi_{12}GeO_{20}$, secondary electron emission yield 79−91546
$Bi_{12}GeO_{20}$-CdS, air gap coupled system, SAW energy transfer 77−11774
$Bi_{12}SiO_{20}$ crystal, piezoelec. and SAW props. 80−75949
$Bi_{12}SiO_{20}$, laevorotatory, cryst. struct., absolute piezoelec. d_{14} coeff. 79−94974
$Bi_{12}SiO_{20}$, pulling large crystals 79−11507
$Bi_{12}SiO_{20}$ surface and pseudosurface wave props. 79−46908
$BiTaO_4$, cryst. growth. hydrothermal method 77−8736
$Bi_{1-x}Te_xO_{3/2+x/2}$ ($0.33 \leq x \leq 0.50$) solid solutions, low temp. phase stable at 20 degrees C, properties *(French)* 79−55886
$Ca_{12}Al_{14}O_{33}$, piezoelectric material, cryst. growth and characterisation 79−99825
CdO-TeO_2 system, partial phase diagrams 78−84784
$Cd_{14-x}P_4S_{24-2x}I_{2x}$, icosahedral structs., synthesis and characts. 77−1107
CdS, semicond. piezoelec. crysts., US investigation of acoustoelectric characts. 77−1456
CsD_2AsO_4, shorted and free single crysts., piezoelec. coupled soft mode, Brillouin scatt. meas. 77−52109
CsH_2AsO_4, shorted and free single crysts., piezoelec. coupled soft mode, Brillouin scatt. meas. 77−52109
$Cs_2S_2O_6$, hexagonal, piezoelec., electro-optic, dielec., elastic, thermoelastic props., space groups 78−76388
$Cs_2S_2O_6$, piezoelectric, crystal struct. studied by X-ray diffr. 80−100208
CuCl, mech. vibrs. in piezoelec. solid, excitation by light pulses 80−75305
CuCl third-order elastic and piezoelec. constants 79−46739
Fe complex, Fe^{2+} chelate of hydrazinecarboxylic acid, Mossbauer effect, cryst. field splitting 79−78591
GaAs, crystal, piezoelectric oscills. meas. by laser interferometry 77−118
$KBrO_3$, trigonal, elastic, thermoelastic and dynamic piezoelec. props., US vel. meas. 77−32328
$K_2Cd_2(SO_4)_3$, piezoelec. langbeinite-type, cryst. struct. and ferroelastic transform. 78−6036
$K_2Cd_2(SO_4)_3$, piezoelectric, cryst. struct., near ferroelastic transition 78−42984
KD_2PO_4, neutron scattering from coupled polar-elastic waves 80−92623
KH_2PO_4 electro-optic modulator crysts., piezoelec. induced acoustic transients 80−70316
KH_2PO_4, kinetics of growth from aqueous soln. 78−6838
KH_2PO_4, neutron critical scatt. in struct. transition due to homogeneous crystal deform. 79−42922
KH_2PO_4, phonon echos in SiO_2, ADP, KDP, and Rochelle salt *(Japanese)* 79−51213
KH_2PO_4, polarisation effect in piezoelectric executing longitudinal vibs. 79−1741
KH_2PO_4 type crysts., microhardness, expt. determ. 79−24603
KH_2PO_4, under electrostatic field, magnitude of enhancement of neutron diffr. due to piezoelec. effect *(Chinese)* 79−51907
KIO_3, cryst. struct. 79−19234
$K_{2.85}Li_{1.55}Nb_{5.11}O_{15}$, elastic and piezoelec. props. 79−15403
$K_xLi_{1-x}NbO$ films, epitaxial growth by melting on $K_{1.5}Bi_{1.0}Nb_{5.1}O_{15}$ substrate 79−33204
$(KNa)NbO_3$ ceramic, piezoelectric effect due to polarisation, expt. *(Polish)* 77−77151
$K_{1-x}Na_xTaO_3$, quantum ferroelec., elastic compliance, impurity effects 79−99835
$KNbO_3$, piezoelec. and electrostrictive coeffs. 77−85653
K_2SeO_4, elastic compliance anomalies 80−45010
$KTa_{1-y}Nb_yO_3$, quantum ferroelec., elastic compliance, impurity effects 79−99835
$KTaO_3$, electromech. props. and electron tunnelling 78−23403
$3La(IO_3)_3.HIO_3.7H_2O$, pyroelec., cryst. struct. 79−1410
$3La(IO_3)_3.HIO_3.7H_2O$, pyroelec. p_3 and piezoelec. d_{33} coeffs. 79−19840
(Li, Na)NbO_3 ceramic, dielectric and electromechanical props. 77−40183
(Li,Na)NbO_3, polycryst. disc, temp. and time dependent dielec. props. 77−81060
piezoelectric materials continued
$LiClO_4.3D_2O$, hexagonal, piezoelec., electro-optic, dielec., elastic, thermoelastic props., space groups 78−76388
$LiClO_4.3H_2O$, absolute sign of piezoelec. d_{33} and pyroelectric p_3 coeffs. 78−43793
$LiClO_4.3H_2O$, hexagonal, piezoelec., electro-optic, dielec., elastic, thermoelastic props., space groups 78−76388
LiF, compressed crystals, inhomogeneous elec. field due to piezoelectric effect 80−55044
Li_2GeO_3, acoustic props., intrinsic piezoeffect, US absorpt. coeffs. *(Russian)* 80−29692
Li_2GeO_3, melt-grown single crysts., polar twins, piezoelec. meas., etching behaviour 79−32999
Li_2GeO_3 piezoelectric glass ceramic, recrystallisation, pyroelectric response, permittivity 80−80703
Li_2GeO_3, pure, and Si- and Mg-doped, impurity effects on elastic and piezoelec. props. 79−47388
$Li_{1-x}H_xIO_3$, dielec. behaviour, Raman and IR spectra 77−32357
$Li_{1-x}H_xIO_3$, piezoelectric props., space charge effects 78−6637
$LiHSeO_3$, X-ray cryst. struct. determ. 80−28966
α-$LiIO_3$, cryst. growth of high piezoelec. and optical quality 78−31313
α-$LiIO_3$, cryst. growth by conc. convection of soln. 78−72716
$LiIO_3$, elastic wave leakage across gap between piezoelectrics 78−6204
α-$LiIO_3$, neutron diffr. intensity enhancement under DC field, investig. 80−10462
$LiIO_3$, piezoelec. coated with semicond. film, Bleustein-Gulyaev wave amplification 79−61309
α-$LiIO_3$, piezoelec. mat. for acoustooptic cells, piezoelectric transducers 78−95575
$LiIO_3$, polarisation effect in piezoelectric executing longitudinal vibs. 79−1741
α-$LiIO_3$, single cryst., opt. and physicochem. props. 77−8566
α-$LiIO_3$, single crysts., light diffr. under DC field 80−11367
$LiIO_3$, transverse gap elastic waves, expt. 80−59576
$LiIO_3$, US wave tunnelling across piezoelectric gap 78−87857
$Li_{1-x}Na_xNbO_3$, LPE, growth and temp. coeff. of SAW velocity 78−43227
$LiNbO_3$ acoustic waveguide, nonlinear interaction of elastic waves with reson. *(Russian)* 78−6206
$LiNbO_3$, acousto-photorefractive effect 77−88878
$LiNbO_3$, anisotropy and phase velocities of prop. of elastic waves 79−1478
$LiNbO_3$, chemical, struct. and physical props., book contrib. 79−69783
$LiNbO_3$, crysts., elec. field influence on hypersonic wave propag. 80−44668
$LiNbO_3$, Czochralski grown single crysts., cellular interface and struct. due to constitutional supercooling *(Chinese)* 79−51026
$LiNbO_3$, damping of LF elastic vibrs., internal friction meas. 79−28043
$LiNbO_3$ delay line, bulk wave generation due to nonlinear interaction of SAW 79−42359
$LiNbO_3$, diffr. effects from very narrow surface wave transducers 78−22240
$LiNbO_3$, diffusion of Co, Ni, Zn and Cu and its effect on acoustic velocity 77−84847
$LiNbO_3$, effects of He ion implantation on SAW propag. 80−75421
$LiNbO_3$, electroacoustic correlation memory effect 78−88001
$LiNbO_3$, electroacoustic coeffs. 79−69564
$LiNbO_3$ fibre, vibrations 78−31156
$LiNbO_3$, finite difference anal. of SAW 80−75423
$LiNbO_3$, γ-irradiated and annealed, elastic and piezoelectric props. 78−2807
$LiNbO_3$, hypersonic wave attenuation, temp. depend. long wavelength phonons 78−18710
$LiNbO_3$ interfaces, SAW reflection, light scatt. meas. 80−34286
$LiNbO_3$, ion-beam etching, for SAW refl. struct fabrication, role of redeposition 77−56123
$LiNbO_3$, LPE on $LiTaO_3$ substrate, using Li_2O-V_2O_5 flux 78−44031
$LiNbO_3$, line acoustical waves anal. 78−34692
$LiNbO_3$, low freq. Raman scatt. spectra of polaritons, photographic recording 79−73952
$LiNbO_3$, opposed interaction of acoustic waves 77−24360
$LiNbO_3$, parametric phonon echo obs. 80−59588
$LiNbO_3$, partial waves of SAW, direct meas. by light scatt. 78−66994
$LiNbO_3$, phase and amplitude relations between fundamental and second harmonic SAW 77−69157
$LiNbO_3$, photocond. induced by N_2 laser, piezoelec. reson., acoustic wave rel. determ. *(Japanese)* 78−2521
$LiNbO_3$, photoelasticity tensor, including piezoelectrooptic interaction correction, Brillouin scatt. 77−24820
$LiNbO_3$, photoinduced grating contrib. to acoustic wave vel. 77−77154
$LiNbO_3$, piezoceramic, elastic normal wave propagation, phase transitions *(Russian)* 80−40067
$LiNbO_3$, piezoelec., SAW interaction with secondary electrons 80−80708
$LiNbO_3$, piezoelec. layer, non-cryst. characts. after ion implantation *(French)* 77−73117
$LiNbO_3$, piezoelectric stress const. determ. by impact loading technique 77−69778
$LiNbO_3$, piezoelectric surface wave velocity, flexural biasing state influence 79−56730
$LiNbO_3$, piezoelectric plate resonator, acoustic correl. 79−76929
$LiNbO_3$ piezoelectric coeff. and permittivity meas., small-sample method 80−15981
$LiNbO_3$ piezoelectric plate, direct and indirect elastic wave excitation *(Russian)* 80−34858
$LiNbO_3$ powder, RF field depend. of memory echoes 79−8095
$LiNbO_3$, refractive index, temp. depend. over 300 to 620 nm *(Russian)* 78−56451
$LiNbO_3$, SAW, suppression of harmonic generation by ZnO thin-film loading 80−84355
$LiNbO_3$, SAW convergence props. 80−24726
$LiNbO_3$, SAW conversion to bulk plate modes in shallow gratings 80−1385
$LiNbO_3$ SAW device, obs. of bulk waves and surface waves through side planes of several cuts 78−71238
$LiNbO_3$, SAW generation, use of analytical calc. for semi-infinite piezoelec. 78−51809
$LiNbO_3$, SAW propagation and scatt., finite difference anal. 80−20595
$LiNbO_3$, shock loaded above Hugoniot elastic limit, elec. and mech. response 78−19411
$LiNbO_3$ substrate, covered with metal or quartz powder, dynamic SAW reflecting struct. 80−74565

piezoelectric materials continued
$LiNbO_3$ substrate for InSb films, prep. and props. 80−35093
$LiNbO_3$, surface acoustic waves power densities approximation 77−79987
$LiNbO_3$, surface elastic wave propag. in piezoelec. plate, elec. screening effect *(Russian)* 79−14999
$LiNbO_3$, tapped SAW delay line, coupling with CdS bulk wave 77−1289
$LiNbO_3$, temp. coeff. of freq. determ. 80−75316
$LiNbO_3$, use as surface acoustic wave devices 78−91525
$LiNbO_3$, wedge fabrication for line acoustic wave propag., using cleavage method 78−30818
$LiNbO_3$, X-ray determ. of piezoelec. coeff. 77−8511
$LiNbO_3$, Y-Z cut, surface to bulk mode wave conversion, at interfaces ang. spectrum meas. 78−47652
$LiNbO_3$, Y-cut, plasma ion-acoustic waves excitation by piezoelectric surface acoustic wave 80−10381
$LiNbO_3$:He^+, ion implanted SAW guides, air-gap Si convolver data 78−42500
$LiNbO_3$:phosphor, piezoelec., interaction with SAW, excitation of electrolum. 79−60615
$LiNbO_3$-CdS, layered structure, acoustoelectric surface current kinetics 78−43232
$LiNbO_3$-CdS layer structure, temp. depend. of acoustoelectric current 79−7867
$LiNbO_3$-CdS separated medium convolver, illumination effects 77−72766
$LiNbO_3$-CdSe, piezoelec.-semicond. layer struct., acoustic-wave-induced increase in cond. 77−59307
$LiNbO_3$-CdSe structure, electroacoustic effects and signal convolution 80−10098
$LiNbO_3$-InSb layer structures, fabrication and use in SAW amplification 79−41540
$LiNbO_3$-InSb struct., electroacoustic interaction temp. depend. 79−69336
$LiNbO_3$-liquid-CdS-liquid-$LiNbO_3$ structure, acoustic wave propag. and amplification 77−42654
$LiNbO_3$-Ni, layered structure, mag. control of surface elastic waves 77−20666
$LiNbO_3$-p-Si, frequency doubling of the two-pulse and three-pulse echoes in surface acoustic waves 79−69335
$LiNbO_3$-Si, acoustoelectronic memory, effect of band-bending 80−70771
$LiNbO_3$-Si(CdTe) structure, acoustoelectronic interaction between SAW and transverse drift current 77−69424
Li_2SiO_3, Czochralski growth and charact. 79−91577
Li_2SiO_3, melt-grown single crysts., polar twins, piezoelec. meas., etching behaviour 79−32999
Li_2SiO_4, piezoelectric glass ceramic, recrystallisation, pyroelectric response, permittivity 80−80703
$LiTaO_2$ and SiO_2/$LiTaO_3$ struct., Rayleigh waves, piezoelectric leaky surface waves, temp. depend. 79−46905
$LiTaO_3$, crysts., elec. field influence on hypersonic wave propag. 80−44668
$LiTaO_3$, electroacoustic coeffs. 79−69564
$LiTaO_3$, low freq. Raman scatt. spectra of polaritons, photographic recording 79−73952
$LiTaO_3$, piezoelectric resonator characterisation 78−95550
$LiTaO_3$, rotated Y-cut, SH and Rayleigh surface waves 79−46910
$LiTaO_3$ thin plate temperature characteristics 77−39141
$LiTaO_3$-SiO_3, temp. compensated SAW device fabrication 79−76923
$MgAl_2O_4$ spinel material for SAW devices 79−56735
NH_4Cl, ferroelastoelectric poling, differing piezoelec. props. of domain states 77−16102
NH_4Cl, piezoelec. effect near nonferroelastic phase transition 80−66116
$NH_4H_2PO_4$, phonon echos in SiO_2, ADP, KDP, and Rochelle salt *(Japanese)* 79−51213
NH_4NBeF_4, successive phase transitions, dielec. and optical props. obs. 80−50275
$(NH_4)_6Sb_4(SO_4)F_{12}$, dielec. props. and phase transitions 79−69765
$(Na,Li)NbO_3$, ceramics, electrophys. and struct. props. near morphotropic transition 78−2816
$(Na,Li)NbO_3$ ceramic, optimum prep. conditions and characterisation 78−3079
NaCl, piezoelectric effect 79−69779
NaCl, uniform deformation and birefringence in nonuniform elec. field *(Russian)* 79−87396
$NaClO_3$, cryst. growth from soln., selective etching technique for observation of dislocations 79−19251
$NaClO_3$ single crystals, change of elastic constants by gamma radiation 78−63800
Na_2CoGeO_4, single cryst. growth and study of their piezoelec. and elastic props. 79−4906
$Na(H_3O)[I(OH)_3O_3]$, piezoelec. and pyroelec. ionic displacements 79−38456
$Na_{0.5}K_{0.5}NbO_3$, piezoelectric ceramic solid soln. *(Polish)* 77−55755
$NaNH_4SeO_4.2H_2O$, polarisation effect in piezoelectric executing longitudinal vibs. 79−1741
$Na_5W_3O_9F_5$, phase transitions obs. *(French)* 80−6516
$NdNbO_4$, cryst. growth rel. to investig. of PbO-KF-B_2O_3-PbNdTiNbO$_7$ cross section 77−86004
PVF_2, film, origin of pyroelectricity 79−99828
PVF_2, film, static and dynamic pyroelectric coeffs. from 90-370K 79−99827
PVF_2 thin film SAW tranducers for 8 MHz delay line 80−58876
$(Pb,Sr)(Zr,Ti)O_3$, piezoceramic, effect of glass additions on props. during hot pressing 79−24475
$Pb_{0.6}Ba_{0.4}Nb_2O_3$, piezoelectric ceramic solid soln. *(Polish)* 77−55755
$PbBi_2Nb_2O_9$ ceramic, grain oriented, dielectric and piezoelectric props. 79−42896
$Pb(Cu_{1/4}Nb_{3/4})O_3$-$Pb(Li_{3/4}Nb_{3/4})O_3$-$PbTiO_3$-$PbZrO_3$, piezoelec. ceramic materials for SAW devices 79−11390
$Pb(Cu_{1/4}Nb_{3/4})O_3$-$Pb(Li_{1/4}Nb_{3/4})O_3$-$PbTiO_3$-$PbZrO_3$, optimisation of composition for SAW devices 79−33609
$Pb(Fe_{1/2}Nb_{1/2})O_3$-La_2O_3(CeO_2) ferroelec. ceramics, electrophysical props. 78−35099
$Pb_5Ge_3O_{11}$ bonded Pb(Zr,Ti)O_3 composites, piezoelec. props. 79−78629
$Pb_2KNb_2O_5$, SAW props., rel. to device appl. 78−71923
$Pb_2KNb_5O_{15}$ material for SAW devices 79−56735
$Pb_2KNb_5O_{15}$ piezoelectric coupling for SAW applications 79−56055
$Pb_2KNb_5O_{15}$, strong electromechanical coupling of SAW 78−63919

piezoelectric materials continued
$Pb(Mg_{1/3}Nb_{2/3})O_3$-$PbTiO_3$-$PbZrO_3$ ceramics, HF filters appl. additives effect obs. *(Japanese)* 80−60507
$Pb(Mg_{1/3}Nb_{2/3})O_3$-$PbTiO_3$-$PbZrO_3$, piezoelec. PCM ceramic, formation process *(Japanese)* 77−85978
$Pb(Mg_{1/3}Nb_{2/3})O_3$-$PbTiO_3$-$PbZrO_3$, piezoceramics for high frequency use 78−95555
$PbNb_2O_3$, piezoelectric ceramic solid soln. *(Polish)* 77−55755
$PbNb_2O_6$ ceramic, piezoelectric effect due to polarisation, expt. *(Polish)* 77−77151
$PbNb_2O_6$, O defects and elec. props. anomalies 79−42898
PbNdTiNbO$_7$, cryst. growth rel. to investig. of PbO-KF-B_2O_3-PbNdTiNbO$_7$ cross section 77−86004
$Pb(Sb_{1/3}Mn_{2/3})O_3$-$PbTiO_3$-$PbZrO_3$, remanent dielec. polarisation of poled ceramic, heat treatment 79−87390
$PbSc_{0.5}Nb_{0.5}O_3$, single cryst., dielec. props. 80−66126
$Pb_5(SiO_4)(VO_4)_2$ cryst. growth and elastic props., appl. in acousto-optical devices 78−19660
$Pb_{0.94}Sr_{0.06}Ti_{0.47}Zr_{0.53}O_3$, piezoelectric ceramic, stress relax., time depend. deformation 80−60899
$Pb_xSr_{1-x}(Zr,Ti,Nb)O_3$, hydrophone ceramic, effect of one-dimensional uniaxial stress 80−80705
$(Pb_{0.95}Sr_{0.05}(Zr_{0.53}Ti_{0.47})O_3)_{99\%}+Ta_2O_5(Nb_2O_5)$ piezoelectric ceramic solid soln. *(Polish)* 77−55755
Pb(Ti, Zr)O_3, piezoelectric-ferroelectric ceramic, polarisation processes, X-ray obs. 80−34847
Pb(Ti,Zr)O_3 solid solutions, phase coexistence discrepancies 80−96662
$PbTiO_3$ ceramics, temp.-compensated, for SAW appl. 80−15355
$PbTiO_3$, ferroelectric ceramic, dielec., piezoelec. and elastic props., orientational contrib. 78−68468
$PbTiO_3$, piezoceramics for high frequency use 78−95555
$PbTiO_3$-$PbZrO_3$-$In(Li_{3/5}W_{2/5})O_3$, piezoelec. ceramic characteris. for surface wave filters 78−95215
$PbTiO_3$-$PbZrO_3$-$Pb(Ni_{1/3}Sb_{2/3})O_3$ solid solutions, dielec. and electromech. anomalies *(German)* 77−20800
$PbTiO_3$-$PbZrO_3$-$PbNb_{2/3}Zn_{1/3}O_3$(-$PbNb_{2/3}Co(Mg)_{1/3}O_3$) solid solutions, dielec. and piezoelec. props. 79−87393
$PbTiO_3$-$Pb(Fe_{1/2}Nb_{1/2})O_3$ based modified ceramics, struct. and elec. props. 79−87392
$PbTiO_3$-$Pb(Fe_{1/2}Nb_{1/2})O_3$-$PbZrO_3$, with additions, exam. of electrical characteristics 80−2698
$xPbTiO_3+(1-x)PbCd_{1/3}Nb_{2/3}O_3$, phase transition spread, polarisation relaxation, dielectric susceptibility *(Russian)* 80−75922
$PbTi_xZr_{1-x}O_3$, sound velocity temp. coefficients 77−12315
Pb(Z,Ti,Mg,W)O_3, low-Q ceramics, props. and transducer appl. 80−75944
Pb(Zc,Ti)O_3 crystal, appl. to identification of resonant frequencies of rotating beams 79−81824
Pb(Zn,Ti)O_3 piezoelectric electrically deformable diffraction grating 80−78963
$Pb(Zn_{1/3}Nb_{2/3})O_3$-$PbTiO_3$-$PbZrO_3$ ceramics, HF filters appl. additives effect obs. *(Japanese)* 80−60507
Pb(Zr,Ri)O_3:Ni-silicon rubber flexible composite pyroelectric, dielectric props. 80−80704
Pb(Zr,Ti,Nb)O_3 ceramics, rel. dielec. const. and piezoelec. props. rel. to porosity 79−11388
Pb(Zr,Ti,Sn)O_3 ceramics, ferroelec., doped with tri- and pentavalent oxides, piezoelectric props. 78−19413
Pb(Zr,Ti)O_2 ceramic, surface barrier electroreflectance, hysteresis, ageing 80−80752
Pb(Zr,Ti)O_3, ceramic, coexistence of tetragonal and rhombohedral phases 77−7845
Pb(Zr,Ti)O_3 ceramics, low field depoling charact. 77−8492
Pb(Zr, Ti)O_3 ceramic, appl. in electrically controllable diffr. grating for parallel polarised light refl. 77−39026
Pb(Zr,Ti)O_3 ceramic, permittivity and resonant frequency ageing, space charge field effects 77−85657
Pb(Zr,Ti)O_3 ceramic-polyvinylidene fluoride composite film, complex piezoelec. props. 78−64323
Pb(Zr,Ti)O_3 ceramics, shock depoling, pulse charging of nanofarad capacitors 79−42913
Pb(Zr,Ti)O_3, ceramic vibrator, resonant freq. temp. stability *(Chinese)* 79−47386
Pb(Zr,Ti)O_3 ceramics, piezoelectric charact. *(French)* 79−56727
Pb(Zr,Ti)O_3 ceramic, interconnected porous, props. 80−43579
Pb(Zr, Ti)O_3 ceramics, low temp. sintering, elec. and mech. props. 80−71616
Pb(Zr,Ti)O_3 ceramics with ladder type struct., prep. and props. 80−75945
Pb(Zr,Ti)O_3 ceramics, DC field sintering preparation, piezoelectric props., ageing behaviour 80−81211
Pb(Zr,Ti)O_3 disc, SH_0 waveguide spiral delay line charact. 77−72123
Pb(Zr,Ti)O_3 fibre arrays in epoxy cement, ferroelectric ceramic-plastic composites 80−81015
Pb(Zr,Ti)O_3 film, prep. by electron beam evaporation technique 77−1809
Pb(Zr,Ti)O_3, fracture and deform. 80−79870
Pb(Zr,Ti)O_3 internally electroded multilayers, piezoelectric props., permittivity, transducers 80−80672
Pb(Zr,Ti)O_3, PCD ceramic, pyroelectric props. 80−100635
Pb(Zr, Ti)O_3, piezoceramic, explosive synthesis 77−16525
Pb(Zr,Ti)O_3 piezoceramic, phase transition under shock loading *(Russian)* 77−69041
Pb(Zr,Ti)O_3, piezoceramic, nonlinear piezoeffect 79−42900
Pb(Zr,Ti)O_3, piezoelectric material, effect of processing on props. *(Polish)* 77−85655
Pb(Zr,Ti)O_3, piezoelec., compositional fluctuation and props. 78−18742
Pb(Zr,Ti)O_3, piezoelectric bimorph, quasistatic response exam. 78−43794
Pb(Zr,Ti)O_3 piezoelectric ceramic, CeO_2 additive effect on struct. and props. 79−52140
Pb(Zr,Ti)O_3, piezoelectric ceramics, low fluence neutron irrad. effects 80−92564
Pb(Zr,Ti)O_3, polarisation effect on deform. and strength, Curie pt. region 79−42902
Pb(Zr,Ti)O_3, prep. and reactivity from butoxide precursors 78−84749
Pb(Zr,Ti)O_3, research grade, hydrophone ceramic, effect of one-dimensional uniaxial stress 80−80705
Pb(Zr,Ti)O_3, synthesis from cryochem. mixtures, chem. reacts. in sublimation drying 79−11538

piezoelectric materials continued
$Pb(Zr,Ti)O_3$ type 1 ceramic, appl. in Langevin type sonar transducer, performance characts. 80−79095
$Pb(Zr,Ti)O_3$:La(Cd,W), electro-optical ferroelec. ceramic, secondary electron emission yield 79−91546
$Pb(Zr,Ti)O_3$:Mn ceramics, anomalous dielec. losses 79−42892
$Pb(Zr,Ti)O_3$-epoxy resin composite piezoelec. relax. due to ionic cond. 77−36179
$Pb(Zr,Ti)O_3$-$Pb_3Ge_5O_{11}$ ceramic, sintering conditions rel. to piezoelec., dielec. props., microstruct. 77−16252
$Pb(Zr_{0.53},Ti_{0.47})O_3$, piezoelec. ceramic, HF filter appl. *(Korean)* 79−27472
$Pb(ZrTi)O_3$ ceramic, piezoelectric effect due to polarisation, expt. *(Polish)* 77−77151
$Pb(ZrTi)O_3$ type piezoelectric ceramics, compressive properties 79−33612
$Pb(Zr_{0.42}Ti_{0.58})O_3$, hot-pressed piezoelec. ceramic, effect of nonferroelectric phase 77−43936
$Pb(Zr_{0.52}Ti_{0.48})O_3$, polycrystalline ferroelectric, grain-size dependent props. 80−71352
$Pb(Zr_{1-x}Ti_x)O_3$ ceramics, double isovalent substitution effect on piezoelectric characts. *(French)* 79−51908
$Pb(Zr_{1-x}Ti_x)O_3$ solid solution, piezoelectric ceramic, prop. improvement by multiple substitution 80−80702
$Pb(Zr_xTi_{1-x})O_3$, high density, sol-gel technique prep., piezoelec. props. 80−20596
$Pb(Zr_xTi_{1-x})O_3$, temp. coeff. of resonant freq. as function of Zr/Ti composition *(Chinese)* 78−68454
$Rb_6Sb_4(SO_4)_3F_{12}$, dielec. props. and phase transitions 79−69765
SO_2, lattice dynamics, rigid mol. model 80−44266
SiO_2, phase an amplitude relations between fundamental and second harmonic SAW 77−69157
SiO_2, phonon echos in SiO_2, ADP, KDP, and Rochelle salt *(Japanese)* 79−51213
Sr Nb_2O_6, crystallography, polymorphism and isomerism, X-ray diffr. and DTA study 80−100216
$Sr_{0.5}Ba_{0.5}Nb_2O_3$ piezoelectric transducer, SAW props. 80−79037
$Sr_{0.5}Ba_{0.5}Nb_2O_6$, ferroelec., dielec. behaviour 78−80309
$Sr_x(Na_{0.5}Bi_{0.5})_{1-x}$ solid solutions, piezoelec. and ferroelec. props. *(French)* 80−108158
$Sr_4NaLiNb_{10}O_{30}$, electro-optic, pyroelec., dielec. and piezoelec. props. *(Chinese)* 79−69810
$Sr_4NaLiNb_{10}O_{30}$, single cryst. growth, Czochralski method *(Chinese)* 79−74078
$Sr_xPb_{1-x}(Zr_{0.545}Ti_{0.455})O_3$, piezoelec. resonator, preparation and props. *(Rumanian)* 80−28402
$SrTiO_3$, thermal expansion near displacive phase transition meas. 77−12345
TGSe:D,L-α-alanine crysts. with large unipolarity, dielec., piezoelec., elastic props. and internal friction 79−33615
TiO_2, rutile, ferroelectric ceramic, dielec., piezoelec. and elastic props., orientational contrib. 78−68468
Tl_3TaSe_4, for SAW devices, temp. compensated cuts with zero power flow 77−12313
Tl_3VS_4, for SAW devices, temp. compensated cuts with zero power flow 77−12313
Tl_3VS_4, growth of inclusion free crystals, for surface wave and bulk wave acoustic devices 80−25549
ZnO films US transducers obtained by DC diode sputtering, dielec. breakdown props. 80−40066
ZnO, piezoelec. films produced by gas transport reaction, US excitation efficiency 80−2700
ZnO thin film SAW filters 79−23157

piezoelectric oscillations
acoustic surface waves, power densities approximation 77−79987
acoustoelectric wave excitation in piezoelec. crystals by narrow metallic electrodes 79−69777
antisymmetric vibrs. of plate, dispersion eqn. homogeneous solns. 78−10846
antisymmetric waves in unbounded plate with axisymm. electrodes 77−32329
ceramic, excitation of acoustoelectric oscills. by ionising radiation 78−56191
ceramic, statically compressed layer, electrical energy of instantaneous discharges *(Russian)* 78−39503
ceramic, TsTS-19, dynamic peizoelec. modulus *(Russian)* 79−28681
ceramic vibrator, resonant freq. temp. stability anal. *(Chinese)* 78−68454
cholesteric liquid crystal layer, piezoelectric effect due to shear vibration 77−85656
conference, ferroelectric materials and their applications, Kyoto, Japan, Nov. 17-19, 1977 79−19846
coupled resonators, depend. of interresonator coupling coeff. on orientation of electrodes *(Czech)* 77−46860
crystal, X-ray refl., oscill. elec. field effects 79−78625
cylindrical shell, inhomogeneous, torsional wave motion 80−60506
elastic wave oscillator and filter design 77−19470
electromechanical filter torsional mode transducer analysis 77−27436
energy trapping methods of thickness extension and thickness shear modes 80−15980
external friction reduction by forced piezoelec. oscillation 80−92096
forced torsional vibrations of a semi-infinite piezoelectric medium of (622) class 79−51910
infinite crystal under thermal field, vibr. wave propag. 78−68455
laser beam deflector, basic characts., multielement 77−54808
laser beam deflector, bimorph, theory and expt. 77−54807
multielectrode composite piezoceramic bar, reson. and antireson. freqs. and equivalent elec. cct. 77−46877
nonsymmetric vibrations of piezoelectric ceramic rings polarized along the thickness 80−7299
normal mode responses of linear materials with hexagonal symmetry 77−90103
periodic coupling of piezoelec. and magnetoelastic surface waves 78−10269
piezoceramic disc resonators, dispersion of thickness vibrs. 78−22237
piezoelectrics, elastic wave leakage across gap 78−6204
plate, infinite, critical reflection of antisymm. SH waves 77−34990
plate, loaded, thickness normal modes, generalised orthogonality conditions 78−90585

piezoelectric oscillations continued
polarisable dielectric crystals, mean internal stress pot. *(Italian)* 79−65797
polyvinylidene fluoride film, acoustic loss factor and piezoelectric coupling coeff. 77−81058
polyvinylidene fluoride film, piezoelectricity, importance of metal-polymer interface 78−76391
powder, memory echo, dipolar field contrib. 80−84700
powder, polarisation echo, long memory times 77−8516
quartz, freq. shifts under gamma irradiation 77−36180
quartz, second-order phenomena and polarising effect with plates of orientation 78−72463
quartz crystal, influence of tabs thickness and resonating props. 78−18140
quartz crystal, new method of freq. spectrum determ. and appls. 78−23402
quartz crystal, oscill. props., mag. field effects 77−59516
quartz crystal, oscillating characts., nucl. and X-irrad. effects 79−78626
quartz crystal, weak anharmonic modes detection, multicryst. reson. freqs. 77−81061
quartz crystal resonators in overtones of coupled thickness shear and thickness twist, anal. 79−81673
α-quartz plate frequency changes rel. to electroelastic tensor and second-order phenomena 78−60398
quartz plates, acoustic reson. vibr., Berg-Barrett X-ray diffr. method 80−40063
quartz rotated Y-cuts, higher-order effects of initial deform. on cryst. vibrs. 77−46862
α-quartz twinning and tailored domain patterns 77−40197
quartz/Permalloy two-layer disc, bending reson. vibrs. *(Russian)* 77−24797
resonances of unbounded plate with circular electrodes 77−84175
resonators, executing longitudinal vibs., polarisation effect 79−1741
rod, depolarising-field effect, longitudinal effect extensional vibration 78−95551
rods, hexagonal crystal symmetry, wave propagation 78−56429
SAW attenuation due to thin film finite conductivity and air loading 77−31154
SAW velocity rel. to uniaxial biasing stresses 77−27416
semiconductor, generation in LF electric field 78−64068
surface excitation by far IR laser beam 79−46906
surface piezoacoustic waves, interaction with two-dimens. plasmons, appl. to MOS structs. 79−28683
surface waves in crystals, theory in symm. form 78−10848
thermopiezoelectric laminae, coated with electrodes, two dimens. vibr. theory 78−35092
thermopiezoelectricity, general eqns. 80−7297
thickness vibrations, digital computer simulation 77−88998
thin piezoceramic discs with split electrodes, asymmetric vibrs. 80−34857
transducers of tall, narrow elements of acoustic imaging array, vibration mode 80−74690
transient response of infinite piezoelec. plate on elastic medium to pot. pulse 78−52442
unplated piezoceramic plate frequency response meas. 78−248
viscosity meas. method, 40 kHz 78−59519
width-extensional vibration energy trapping by complex branches of dispersion curves 79−51911
$BaTiO_3$ polydomain crystals, dielec. props. 78−43827
$Bi_{12}GeO_{20}$ plate cut along (110) axis, torsional thickness oscillations calc. *(Czech)* 77−55754
GaAs crystal, vibrs. meas. by laser interferometry 77−118
KH_2PO_4, KD_2PO_4 crystals used for laser control, acoustic vibr. suppression 78−1363
$LiNbO_3$ acoustic conversion, piezoelect. surface wave behaviour at discontinuities 77−31198
$LiNbO_3$ fibre, vibrations 78−31156
$LiNbO_3$, photocond. induced by N_2 laser, piezoelec. reson., acoustic wave rel. determ. *(Japanese)* 78−2521
PLZT pyroelectric detectors, piezoelectric oscillations, in response to CO_2 laser pulses 79−61305
PLZT pyroelectric detectors, delayed onset of piezoelec. oscills. 80−75953
$PbMg_{1/3}Nb_{2/3}O_3$, ferroelec., crit. electron-phonon phenomena and diffuse phase transition in elec. field 79−38497
$Pb(Zr,Ti)O_3$ ceramic, permittivity and resonant frequency ageing, space charge field effects 77−85657
Si, mechanical Q meas., low temps. 78−48118

piezoelectric resonators *see crystal resonators*

piezoelectric semiconductor materials *see piezoelectric semiconductors*

piezoelectric semiconductors
acoustic wave combinatorial scatt. by electrons *(Russian)* 77−11963
acoustic wave propag., nonlinear theory, soln. by perturbation techniques 78−57796
acoustic waves, amplification and vel. change, due to external temp. gradient 78−84260
acoustic waves, longitudinal, amplification 78−76114
acoustic waves parametric excitation 79−47128
acoustic waves synchronisation 77−11964
acoustoelectric current, second harmonics 80−80329
acoustoelectric effect, effect of diffusion of charge carriers *(Russian)* 80−65633
acoustoelectric effects, nonlinear 77−69382
acoustoelectric interactions on cylindrical surfaces 80−6914
acoustoelectric surface phonon-conduction electron interaction 79−42360
acoustohelicon waves, parametric excitation 79−38135
Auger recombination, phonon assisted, scatt. mechanisms 77−85804
Brillouin scattering theory, acoustic phonon conduction electron interaction 77−40255
cascade capture of carriers by attractive impurity centres, cross section 78−56157
circular cylinder, scatt. of plane axial-shear wave 78−2806
cyclotron resonance linewidth, quantum-limit 80−7171
cyclotron-phonon resonance due to polarisation scatt. from photons 79−95649
deformable semiconductors, integral forms of the balance laws 79−38453
degenerate, transverse magnetoresist. in strong field, quantum effect 80−80299

piezoelectric semiconductors continued
degenerate semiconductors, hot electron transport in parabolic energy bands, kinetic theory, transport coeffs. 80−29412
diffraction transverse acoustoelectric effect 77−35967
dissipative, amplification of spin waves 79−24000
electro-optical and nonlinear-optical materials, review 80−74450
film, mobility of hot electrons 78−56247
film, quantum acoustoelec. interaction, thickness depend. *(Russian)* 79−47126
film, quantum acoustoelectric interaction 79−15197
film, Rayleigh wave amplification, quantum theory approach 77−69158
film, surface mode phonon amplification, theory 78−34691
film, surface phonon amplification 77−31864
frequency mixing of acoustic waves in oscillatory and DC elec. fields, theory 77−35966
heavily doped compensated piezoelectric semiconductor, sound absorpt. coeff. calc. *(Russian)* 79−15194
II-VI semiconductors, heteroepitaxial, for SAW and electro-optic device appl., prep. and props., book contrib. 79−83134
III-V compounds, piezoelec. coupling and dislocations 79−91377
III-V crystals, thermally enhanced diffusion of point defects near dislocations during device operation 79−90820
III-V semiconductors, heteroepitaxial, for SAW and electro-optic device appl., prep. and props., book contrib. 79−83134
III-V semiconductors, piezoelectric induced polarization charge distribs. around point defects 79−56725
III-V semiconductors, stress-induced elec. props. of point defects, piezoresistance effect 79−56726
information storage in piezoelectric semiconducting single crystals 78−15101
inhomogeneous, amplification of acoustic wave 79−69561
inhomogeneous, longitudinal phonon-plasmon interaction 79−56156
inhomogeneous semiconductor, acoustoelectric interaction, elec. cond. 79−95453
interaction of acoustic waves and microwave radiation fields: depletion and mixing effects 79−90056
light anomalous transmission, sound-induced, below plasma edge 78−68475
α-$LiIO_3$ powders, temp. depend. of electro-acoustic echo 80−66115
magnetised heavily doped piezoelectric semicond., hybrid mode parametric excitation 80−29427
magnetised semiconductor plasma, EM wave amplitude modulation and demodulation 80−84482
memory-correlator cells employing acoustically induced charge hologram in piezoelectric semiconductors 78−86290
n-type, heavily doped, laser beam modulational instability 79−99570
n-type, magnetoactive, Brillouin instability in magnetostatic field 80−78909
nondegenerate, interaction between electrons and strong piezoelec. wave *(Russian)* 77−90106
nonlinear acoustic noise amplification theory, phonon distrib. function basis 78−47837
nonlinear interaction of quasicollinear acoustic waves 77−59306
nonlinear noise amplification 78−60167
optical absorption by polaron, external static elec. field depend. 77−85158
optical absorption by polaron, interacting with acoustic modes 77−59547
optical image storage and scanning in multilayer struct. using surface acoustic waves 79−55238
oscillations of piezosemiconductor plates, charged particle beam modulated, energy losses *(Russian)* 80−2259
parametric instability of acoustic waves in high freq. elec. field and transverse mag. field 79−65521
photocurrent in quantising magnetic field in presence of nonequilibrium photoelectrons, spectral oscill. and energy relax. by interaction with acoustic phonons 79−91100
photoelasticity and acousto-optic diffr. 80−29715
piezoelectric nondegenerate semicond., magnetoacoustic effects of nonparabolic band struct. 80−96948
piezoelectric semiconductor SAW convolver, convolution voltage enhancement due to carrier transverse drift 80−1381
piezoresistance of grain boundaries 78−51995
plasma, modulational instability of far IR laser 79−47117
plasma, parametric excitation of helicon and acoustic waves 80−107837
plasmon enhanced sound amplification in mag. field 77−39900
polar materials, appl. to SAW and other devices 80−66114
polarisation echo *(Russian)* 78−15099
recombination at deep traps 79−38100
resonant microwave absorption by electrons in strong piezoacoustic wave 77−85270
SAW amplification 79−46907
SAW convolver, convolution voltage enhancement due to carrier transverse drift 80−1381
SAW convolver, effect of transverse drift of carriers on operation, theory and expt. 80−14529
SAW convolver, efficiency 78−18124
scattering anisotropy in longit. quantizing mag. fields 78−26890
second acoustic harmonic generation and explosive instability of acoustoelectronic waves 77−43669
shock waves and acoustoelec. domains 77−32049
slow shift SAW in attenuating piezo-electric and piezosemicond. surface structs. 78−79872
sound attenuation, effect of strong doping 80−2120
stationary acoustic wave nonlinear theory 77−76878
stimulated Brillouin scatt. in magnetised semiconductor plasma 80−33085
stimulated Brillouin scatt. of laser radiation 79−95793
stimulated Brillouin scattering of helicon waves 79−99571
Stoneley wave amplification at interface between piezoelectric semicond. and dielectric crystal 79−19441
superlattice formation, periodic pot. 78−19142
surface electroacoustic wave excitation by drifting cond. electrons 77−66083
surface phonon acoustoelectric interaction, elastic anisotropy effects 80−6610
surface piezoelectric shear wave, two-dimens. electron plasma interaction *(Russian)* 79−19842
thermopiezosemiconductor critical drift velocity for US amplification 78−60169
ultrasound amplification, hard regime 77−89810

piezoelectric semiconductors continued
US absorption of moderate freq., electron distrib. function perturbation 77−55587
US amplification, influence of thermal quenching of photocond. 77−4410
US attenuation, carrier conc. dependence 78−72206
US attenuation, polarisation of Maxwell-Wagner relaxation oscillators 80−44670
US ionisation of shallow impurities 77−43538
US parametric amplification effects, contributions to nonlinear material coefficients 80−34144
US wave amplification at intermediate freq. in const. elec. field *(Russian)* 77−35965
vibrating membrane of piezoresistive semicond., current amplification 78−75025
wave discontinuities, growth 80−34488
weakly inhomogeneous, theory of sound absorption 80−15574
Wigner crystal, long-wavelength excitations in strong mag. fields 79−82533
wurtzite structure, transport in longit. quantizing mag. field 78−26891
zinc-blende semiconductors, quantum resonances in valence bands under uniaxial stress 79−99480
ZnO, film, reactively RF sputtered, anal. of texture 78−67921
Ag_3SbS_3, pyrargyrite, US absorption, influence of illumination, photocond. and photoabsorption of sound 79−42153
Ag_5SbS_4, electron absorption and dispersion of ultrasound velocity 80−15197
Ag_3SbS_3. piezoelec. semicond., residual cond., ultrasound photoabsorpt. *(Russian)* 78−72465
n-AlSb, acoustoelectric effect due to piezoelectrically active wave 80−80331
$BaTiO_3$, ohmic noble metal contacts using In_2O_3 layer 79−42638
$Bi_{12}GeO_{20}$, $Bi_{12}SiO_{20}$, IR reflection spectra studies of lattice vibrations 79−99879
CdS, acoustic-wave-induced increase in cond. 77−59307
CdS, acoustoelec. interaction, influence of surface pot. 77−1455
CdS, acoustoelectric interaction at wave reflection points 78−2528
CdS, acoustoelectronic current SHG 80−6916
CdS, and $Bi_{12}GeO_{20}$, separated, coupling of propagating SAW 78−38929
CdS, Bleustein-Gulyaev wave transmission charact. at corner 77−59197
CdS, carrier density nonlinearity of interacting acoustic fluxes 77−51781
CdS crystal, SAW amplification, bulk and acoustic noise 80−39637
CdS crystal growth with strong long-lived polarisation echoes 79−43113
CdS crystal with thin photoproduced semiconducting layer, tests of convolver on transverse surface waves 77−42646
CdS, elastic, piezoelec. and dielec. props. 80−108157
CdS, elastic, piezoelectric, and dielec. props., 4.2 to 300K 80−60508
CdS, elastic wave propag., in hexagonal piezoelec. crysts. *(Russian)* 77−69777
CdS, electroacoustic interaction obs. 77−11966
CdS film, second harmonic generation by transverse acoustic wave 77−51782
CdS, flexural waves in resonator platelets, synchronous amplification and generation 78−84527
CdS, frequency mixing of acoustic waves in oscillatory and DC elec. fields, theory 77−35966
CdS, heavily doped compensated piezoelectric semiconductor, sound absorpt. coeff. calc. *(Russian)* 79−15194
CdS, intensity fluctuations of nonlinearly amplified phonons, Brillouin scatt. meas. 77−90163
CdS, low resist. single cryst., photodeform. mechanism 77−89806
CdS, nonlinear electronic absorption of US waves 79−15196
CdS, obs. of acoustically induced space charge gratings 77−7203
CdS, obs. of forbidden Brillouin scatt. near exciton reson. 78−15180
CdS, parametric interaction of acoustic surface waves *(French)* 77−62083
CdS, photocond., acoustoelec. fluctuations 79−24022
CdS, photocond. cryst. characterisation of electron-trap responsible for acoustic holographic echoes *(French)* 79−19544
CdS, photocond. meas. using surface wave acoustoelec. current 77−8131
CdS, photoconducting, surface acoustic noise amplification by carrier drift 78−72208
CdS, photoconductive, transverse electric current effect on SAW propagation 79−47127
CdS, piezoelec. polycryst. film layer struct., acoustic harmonic generation 77−89812
CdS, piezoelectric semicond., acoustoelectric current of Lamb waves *(Russian)* 77−89815
CdS plates, noise amplification as function of drift field intensity, conductivity and freq. *(Russian)* 79−73556
n-CdS, polaron effective mass, DC Hall effect meas. 78−39037
CdS, SAW absorpt., effect of transverse electron drift 77−76879
CdS SAW convolver, effect of transverse drift of carriers on operation 80−14529
CdS, SAW meas. of surface elec. props. 77−20387
CdS, SAW superheterodyne amplification 77−55589
CdS, single crysts., US luminesc. obs. 80−76092
CdS, space charge distribution at elastic wave propag. *(Russian)* 77−77150
CdS, stimulated Mandelstam-Brillouin scatt. on acoustic phonon amplification *(Russian)* 80−71437
CdS, surface elastic wave propag. in piezoelec. plate, elec. screening effect *(Russian)* 79−14999
CdS, thin film transducers, electromechanical coupling meas. by light diffr. 77−23840
CdS, thin plates, piezosemiconductors, second harmonic acoustoelectric current obs. 80−80329
CdS, transverse acoustoelec. effect, for SAW optical image scanning 77−11001
CdS, ultrasound amplification, hard regime 77−89810
CdS:Cu, US absorpt. in heavily doped piezoelec. semicond. 79−11189
CdS-Au Schottky diode, elec. props. under stress 79−15222
CdS-Au structure, work function of {0001} faces of CdS, effect of piezoelec. props. 78−23164
CdS-ZnTe, acoustoelectric domain injection across interface, propag. loss, elastic consts. 77−51778
CdS(Se), piezoelec. semicond., sound absorption 80−60051
CdSe, heavily doped compensated piezoelectric semiconductor, sound absorpt. coeff. calc. *(Russian)* 79−15194
CdSe, wave propag. 79−28042

piezoelectric semiconductors continued
Cds, photoconductive, convolution voltage enhancement due to carrier transverse drift in SAW convolver 80−1381
$(CuCr_2S_4)_x$-$(Cu_{0.5}In_{0.5}Cr_2S_4)_{1-x}$ solid solution, piezoelectric effect, X-ray struct. anal. *(Russian)* 80−15978
$Cu_{0.5}In_{0.5}Cr_2S_4$, piezoelectric effect, X-ray struct. anal. *(Russian)* 80−15978
$CuPbBiS_3$ aikenite, low-temperature phase, electrophysical props. 77−47822
$CuPbSbS_3$, electron-phonon interactions, temp. depend. 77−51464
GaAs, absorption edge broadening by piezoelec. phonon fields 77−16302
n-GaAs epitaxial film, surface mode phonon amplification, numerical analysis 78−34691
GaAs film, piezoelec. semicond., cascade capture of carriers by attractive impurity centres, cross sections 78−56157
n-GaAs film, surface phonon amplification 77−31864
GaAs, high press. electron transport props., three band model 80−15516
n-GaAs, non-equilibrium acoustic phonon generation by hot electrons 80−6477
n-GaAs, nonlinear interaction of acoustic waves with microwave elec. fields 79−42593
GaAs, piezoelec. coupling and dislocations 79−91377
GaAs, piezoelectric constant due to bond bending, electron redistribution effect 79−38457
n-GaAs, piezoelectric semiconductor, influence of acoustic phonon disturbances on conductivity 78−91697
GaAs powder, RF field depend. of memory echoes 79−8095
GaAs, SAW meas. of surface elec. props. 77−20387
n-GaAs, strain sensitivity of specimens obtained from pressed powders 77−36177
GaAs:Cr excess electron lifetime determ. by US method *(Czech)* 77−20336
n-GaP, acoustoelectric effect due to piezoelectrically active wave 80−80331
GaP, piezo-modulated spectroscopic investigation of N and N-N pairs, bound exciton 77−66474
GaP-Au Schottky diode, elec. props. under stress 79−15222
GaSb, piezoresistive vibrating circular membrane, reflectance light modulation 80−97232
n-GaSb, stress-induced elec. props. of point defects, piezoresistance effect 79−56726
n-Ge, piezoresistance with deform. axis symm. rel. to all const. energy ellipsoids 77−55533
Ge, piezoresistive vibrating circular membrane, reflectance light modulation 80−97232
Ge single cryst., radiation piezoelec. effect 78−19419
Ge single crystals, photopiezoelectric effect under elastic deform. 80−107856
InSb, acoustoelectric effect at 77K 78−72209
n-InSb, acoustoelectric instability, effect of nonparabolic band struct. 79−60875
n-InSb, acoustohelicon waves, parametric excitation 79−38135
InSb, amplification and vel. change of acoustic waves due to external temp. gradient 78−84260
n-InSb, Brillouin instability in magnetostatic field 80−78909
n-InSb, carrier temp. effect on transverse phonon-helicon interaction 77−15886
n-InSb, dynamical light scatt. from dielec. bulk waves, appl. of phenomenological theory 79−69829
n-InSb, HF EM and acoustic oscill. generation in LF electric field 78−64068
n-InSb, helicons, parametric decay 80−34472
n-InSb, longitudinally magnetized, laser beam modulational instability, phonon-helicon interaction 79−56254
p-InSb, quantum resonances in valence band under uniaxial stress, far IR meas. 79−99481
n-InSb, SBS of laser radiation in presence of mag. field, ion acoustic wave nonlinearity 80−45091
n-InSb, stationary energy transport velocity of light scattered from bunched solid-state plasma 79−95720
n-InSb, stimulated Brillouin scattering of helicon waves 79−99571
n-InSb, transversely magnetised, parametric instability of acoustic waves 79−65521
n-InSb, ultrasound modulation in mag. field 79−69196
n-InSb, Wigner cryst., long-wavelength excitations in strong mag. fields 79−82533
InSb-$LiNbO_3$ struct., electroacoustic interaction temp. depend. 79−69336
Se, elastic and piezoelec. consts., US phase vel. meas. 79−86834
Se, SAW propag. on Y-cut plate and X-axis 80−75313
Se, SAW vel. and electromech. coupling factor 80−75422
Se, trigonal, acoustoelectric current saturation 80−60053
Se, trigonal, low temp. sp. ht. and elastic consts., piezoelec. effect influence on phonons 80−54404
Se_xTe_{1-x}, acoustoelectric current saturation 80−60053
SiC, absorption of US waves 78−72210
SiC, acoustic props. study at 9.43 GHz 80−65169
SiC, sound absorption 78−88000
Te, acousto-optic props. at 10.6 μm 79−91401
Te, acousto-optical props. at wavelength of 10.6 μm 80−76001
Te, acoustoelectric current flow, acoustic refraction effect 79−19637
Te, acoustoelectric domain induced transparency near 11 micron 77−85727
Te, carrier density nonlinearity of interacting acoustic fluxes 77−51781
Te, dislocations influence on galvanomag. props. 80−54722
Te, elastic and piezoelec. consts., US phase vel. meas. 79−86834
Te, screw-dislocation-induced scatt. and acceptor states, galvanomag. and optical expts. 77−28142
Te, trigonal, electronic and optical props., press. depend., self consistent pseudopotential formalism 79−65838
Tl_3TaS_4, piezoelec. semicond., acoustic wave generation, amplification material appl. *(Russian)* 78−72464
ZnO, Bleustein-Gulyaev wave transmission characts. at corner 77−59197
ZnO, elastic, piezoelec. and dielec. props. 80−108157
ZnO film, longit. elastic wave attenuation, 9.4 GHz 78−18888
ZnO film, sputtering using Zn target, technique and characterisation 78−3040
ZnO film on Corning 7059 glass and Si, SAW transducer appl. 80−80138
ZnO film on glass substrate, high-rate deposition using DC reactive magnetron sputtering 80−80978

piezoelectric semiconductors continued
ZnO film on ozidised Si, optical measure of acoustic quality 80−80893
ZnO, influence on frequency-temp. coeff. of SAW devices 80−79066
ZnO, intensity fluctuations of nonlinearly amplified phonons, Brillouin scatt. meas. 77−90163
ZnO piezoelec. film, fabrication and appl. *(Japanese)* 78−23616
ZnO, piezoelec. powder, dynamic polarisation echoes 78−52443
ZnO, RF sputtered epitaxial film, appl. to integrated optics 77−14821
ZnO thin film SAW device manufacture, sputtering system and film characterisation 78−95692
ZnO/quartz for SAW device materials, expt. study of props. 80−80050
ZnO/SOS monolithic SAW amplifier 78−6205
ZnO/Si acoustoelectric devices, magnetron discharge sputtering prep. 80−80332
ZnO-Au-epoxy resin, and ZnO-Au-fused quartz transducers, λ/4-mode operation, theory *(Japanese)* 78−30145
ZnO-SiO_2-Si layered structure, SAW props., anal. 77−62729
ZnS, elec. struct., piezoelec. consts. *(Chinese)* 79−56122
ZnS film on Corning 7059 glass and Si, SAW transducer appl. 80−80138
ZnS, surface acoustic wave modes 78−2352
ZnS-MgS, exam. of piezoelectric props. and elastic compliances, as function of MgS conc. 79−95709
ZnSe 79−38457

piezoelectric thin films
conference, ferroelectric materials and their applications, Kyoto, Japan, Nov. 17-19, 1977 79−19846
elastic wave vel. control *(Russian)* 79−61310
polar polymer, piezoelectricity and pyroelectricity 80−7267
poly(vinylidene fluoride), piezoelec. response depend. on phase I vol. fraction 80−20593
poly(vinylidene fluoride), poled, piezoelec. activity and field-induced cryst. struct. transitions 80−20592
β-poly(vinylidene fluoride), single cryst. orientation, piezoelec. 80−20591
poly(vinylidene fluoride), strong piezoelec. under high press. annealing 80−11344
poly(vinylidene fluoride) piezoelectric film, Lamb and shear wave propagation *(French)* 80−44256
poly-vinylidene fluoride-co-tetrafluoroethylene, dipolar theory applications to piezoelectric props. 79−78627
polyvinylidene fluoride, anisotropy and temp. depend. of piezoelec. consts. 77−1640
polyvinylidene fluoride, piezoelec., nonlinear dynamic response 80−75946
polyvinylidene fluoride, plasma poling, piezoelec. and pyroelec. responses 80−71296
polyvinylidene fluoride, polarisation and depolarisation processes 80−11318
polyvinylidene fluoride, poled, short duration unipolar stress pulse detection, generation 80−106695
polyvinylidene fluoride, uniaxially stretched and corona poled, piezoelec. meas. 80−25311
polyvinylidene fluoride, US atten. at high freqs. 79−65798
polyvinylidene fluoride film, acoustic wave reson. meas. 77−81058
polyvinylidene fluoride film, shear props. by piezoelectric resonance 79−99824
polyvinylidene fluoride films, HF US absorpt. meas., 300 to 1500 MHz 80−74667
polyvinylidene fluoride films for SAW transducers on Si substrates 80−74618
polyvinylidene fluoride foil, piezoelectric effect, 100 Hz acoustic and NMR meas. 78−60396
polyvinylidene fluoride piezoelectric film, Lamb and SH wave attenuation *(French)* 80−79196
PVC foil, piezoelectric effect, 100 Hz acoustic and NMR meas. 78−60396
pyroelectric effects, origin 78−88258
quartz, film acoustic surface waveguides, electrically controllable polarisation conversion and its appl. 79−76924
semiconductor, Rayleigh wave amplification, quantum theory approach 77−69158
semiconductor, surface mode phonon amplification, theory 78−34691
semiconductor, surface phonon amplification 77−31864
silk fibroin, oriented, piezoelec. consts. temp. dispersions 80−11345
third-order piezoelectric and dielec. consts. meas. using surface acoustic waves *(Japanese)* 80−55042
TsTS polarized ceramic film, Lamb waves near. crit. freq. study *(Russian)* 78−52039
unidirectional SAW transducer and filter 78−46879
vinylidene fluoride-trifluoroethylene film, cryst. phase transition 80−66120
vinylidenefluoride/tetrafluoroethylene copolymer, piezoelect. and pyroelect. response rel. to dipole polarisation 80−7267
ZnO, film, reactively RF sputtered, anal. of texture 78−67921
AlN, piezoelectric film, low temp. growth by RF reactive planar magnetron sputtering method 80−76175
Bi_2O_3 compound films for SAW devices and filters *(Japanese)* 77−73116
$Bi_{12}SiO_{20}$:Nd, light absorpt. and transmission spectra, photoluminescence spectrum, optical absorpt. coeff. 79−74001
Bi_2WO_6, RF sputtering, possible piezoelec., pyroelec. and photolithography appl. 77−15705
CdS, piezoelec. polycryst. film layer struct., acoustic harmonic generation 77−89812
CdS transducers, testing, via light diffr. by acoustic waves 77−23840
n-GaAs epitaxial film, surface mode phonon amplification, numerical analysis 78−34691
$K_xLi_{1-x}NbO$ films, epitaxial growth by melting on $K_{1.5}Bi_{1.0}Nb_{5.1}O_{15}$ substrate 79−33204
$Li_{1-x}Na_xNbO_3$, LPE, growth and temp. coeff. of SAW velocity 78−43227
$LiNbO_3$, film, Lamb waves near. crit. freq. study *(Russian)* 78−52039
$LiNbO_3$, LPE on $LiTaO_3$ substrate, using Li_2O-V_2O_5 flux 78−44031
$LiNbO_3$, spontaneous parametric scatt. line profile, IR absorpt. coeffs. 80−25377
$LiNbO_3$:Na^+ (Co^{2+}, Zr^{4+}), LPE growth from Li_2O-V_2O_5 flux, X-ray and acoustic characterisation 80−15383
$Pb(Zr,Ti)O_3$ film, prep. by electron beam evaporation technique 77−1809
ZnO epitaxial film with smooth surface from CVD onto a sputtered ZnO film on sapphire, waveguide appl. 78−56588

piezoelectric thin films continued
ZnO film, longit. elastic wave attenuation, 9.4 GHz 78−18888
ZnO film, RF sputtered, characterization for SAW transducers 80−80138
ZnO, film, SAW resonators 78−83199
ZnO film on glass substrate, high-rate deposition using DC reactive magnetron sputtering 80−80978
ZnO films for SAW devices and filters *(Japanese)* 77−73116
ZnO films US transducers obtained by DC diode sputtering, dielec. breakdown props. 80−40066
ZnO formed by RF reactive ion-plating 79−83140
ZnO, on concave Au substrate, transducer for focusing microwave ultrasound 77−7276
ZnO, optical measure of acoustic quality 80−80893
ZnO, RF planar-magnetron sputtered, characterisation 80−96751
ZnO, SAW devices appl. for HF range *(Japanese)* 80−53598
ZnO sputtered films, vertical electrode config. to avoid contamination 79−69982
ZnO thin film SAW device manufacture, sputtering system and film characterisation 78−95692
ZnO thin-film loading of $LiNbO_3$, suppression of SAW harmonic generation 80−84355
ZnO/quartz for SAW device appls., expt. study of props. 80−80050
ZnO/Si using magnetron discharge sputtering, acoustoelectric device appls. 80−80332
ZnO-Si structure, MIS and SAW propag. characts. 78−30988
ZnO-SiO_2-Si layered structure, SAW props., anal. 77−62729
ZnO-SiO_2-Si layered films for SAW devices and filters *(Japanese)* 77−73116
ZnS film, RF sputtered, characterization for SAW transducers 80−80138

piezoelectric transducers
400 MHz to 2.3 GHz acousto-optic deflectors 79−50416
accelerometer appl., using ceramic piezoelectric materials 79−6100
accelerometers, construction and appls. 79−50686
acoustic defectoscopes, low freq., elec. simulation of compound piezoelec. transducers 80−102956
acoustic emission measurement transducers, comparison of piezoelec. and optical sensors 79−14192
acoustic field homogeneity enhancement 77−68358
acoustic Lamb wave focusing devices 80−79093
acoustic microscope appl. 80−1387
acoustic signal distortion, piezoelec. transducers 80−87637
acoustically loaded, expt. method for equivalent circuit parameter determination 78−51036
acousto-optic devices, transducer bandwidth, layer thickness determ. *(Chinese)* 80−53593
acousto-optic modulator for optical fibres 79−98499
acoustoelectric coupled, variational principle for soln. of nonlinear acoustoelectronic problems 78−90621
amplitude and phase statistical dispersion 77−68357
amplitude-freq. and transient characts., when radiating US waves 78−36996
amplitude-frequency and phase-frequency curves 79−68531
amplitude-frequency response determ. for acoustic emission 80−87699
analysis, application of chain matrix of a four-pole 77−42679
annular array search units, potential appl. in conventional US testing systems 80−35446
aperiodic piezoelectric transducers, ceramic, structure and operating principles 78−85109
arbitrarily electroded piezoelec. plate acoustic spatial response determ. 80−99910
automatic acoustic emission analysis system with programmed control *(Russian)* 78−46866
automatic setup for continuous meas. of internal friction and elastic moduli of solids 80−108652
bandwidth enlargement, for NDT 78−71257
bandwidth improvement using thin layers 79−64481
bar transducer under influence of body force, response 77−72125
basic parameters, comparison of specified field and self consistent field methods 79−94442
biological and medical appls. 80−19205
biological temperature telemetry, domestic fowl appl. 78−57152
bolt clamped Langevin longitudinal transducer *(Japanese)* 79−27483
bolt-clamped Langevin type transducer, effect of surface conditions on performance *(Japanese)* 80−48543
broad-band acoustic transducer design 78−51029
broadband, production 80−61044
broadband piezotransducers, comparative anal. and power ratings 80−5904
broadband SAW delay lines using weakly piezoelectric substrates 78−22230
capacitative appl. to elimination of transducer bond correction in US wave vel. meas. 77−46873
ceramic, design and appls. 77−12314
ceramic, LF characts., consequences for Fabry-Perot interferometry 80−86390
ceramic, two methods of increasing bandwidth 78−54357
ceramic buzzers for high sound levels 80−92005
ceramic cylinders, short axially polarized annular, calculation of equivalent circuit parameters 80−5901
ceramic piezoelectric transducer, anomalous radiation pattern due to parasitic Lamb wave generation 80−96170
ceramic plates, expt. data for design of line arrays, medical diagnostics appl. 77−84099
ceramic transformers, optimal transducer design *(Japanese)* 77−13770
characteristics deviation 79−98581
complex vibratory systems, matrices of parameters for six-pole equivalent circuits 77−68304
component of acoustic microscope, for phase imaging in refl. 78−30136
composite, of low freq. acoustic flaw detector, natural freq. calc. 80−89450
composite piezoelectric US transducer, finite element simulation 79−41541
composite piezoelectric US transducer, finite element simulation *(Japanese)* 79−68537
composite piezotransducer for LF acoustic inspection using electrical models 80−104393
composite strip piezoceramic US receiving array 78−42511

piezoelectric transducers continued
composite tapered bar transducers, derivation of fund. relations 78−90620
connectivity and piezoelectric-pyroelectric composites 78−80290
contactive, spectrum of natural freqs. 80−69623
CW Doppler bloodflow meas., perivascular transducer effect on accuracy 77−90825
cylindrical, influence on spectrum of natural freqs. 80−87694
cylindrical ceramic radiating transducers, dynamic eqns. 79−86315
cylindrical piezoceramic transducer, increase of bandwidth via two transition layers 77−14871
cylindrical transducer in near-critical flow, influence of acoustic surface vibrs. on drag. 78−5729
damping by multilayer front face 79−55301
depolarised, by heat treatment, for improved resoln. 80−104196
development trends and appl. *(German)* 80−52186
disc impedance meas. and US transducer CAD program 79−46157
distortion measurement 77−10006
double-diffused MOS transducer, detection of acoustic waves 77−80043
dual-gate depletion-mode FET/piezoelectric film transducer 79−50563
dual-mode transducer and liq. acoustic line, testing of bulky irregular objects 78−56855
dynamic lumped parameters of composite piezoelectric transducers 78−18142
echo ultrasonometer, implantable, for organ dimension meas. 77−90866
electret applications, book contrib. 80−80709
electric field, nonuniform, expt. study 80−102955
electroacoustic sensitivity of radially polarized ceramic cylinders as a function of frequency 79−15402
electroacoustic transducers using piezoelectric polyvinylidenefluoride films for diaphragm material 80−10100
electromagnetic cavity resonator, excitation and detection of acoustic waves 80−33399
electromechanical physical/mech. parameters effect on characts. *(Bulgarian)* 77−61060
electromechanical polygonal ring, analysis of influence of oscillatory modes on transducer characts. 80−87697
electron stream effects on material with semiconducting boundary layer 78−19414
electronically scanned US diagnostic systems, electromechanical coupling coeff. for plank-shaped transducers 80−33383
EM transducer dynamic range optimisation 77−19506
energy balance for impedance calc. 78−36993
energy method for impedance calculation, extension of Auld's method 77−72126
epidural intracranial pressure meas. by piezoresist. transducer *(German)* 78−85404
equivalent circuit with inhomogeneous acoustic load 79−32174
equivalent parameter study in resonance thickness meas. 78−54340
excitation at odd subharmonics 79−98583
eye fine movement recording through closed eyelid 78−35988
farfield angular radiation pattern generated from arrayed piezoelectric transducers using finite element anal. 80−33401
ferroelectric cylinders, radially polarised, electroacoustic sensitivity calc. by normal-mode methods 77−62131
flexural piezoelectric bimorph vibrator, spurious response suppression *(Japanese)* 78−59233
flexural-extensional behavior of composite piezoelectric circular plates 80−58879
flowmeter appl., Danfoss 80−6172
focusing type, pulsed operation 79−68539
force transducers, calibration by absolute impulsive method 80−105627
force-frequency measuring gauge based on oscillating quartz crystal 80−31727
force-voltage charact. calc. due to point force application at piezoelement centre 77−2643
frequency characteristic control 79−94446
frequency response, meas. using an acoustooptic modulator 80−38023
grating-array acoustic-surface-wave transducers and reflectors 80−58884
HF piezoceramic array, acoustical decoupling characts. of onionskin paper backing material 79−81675
HF strain transducer for acoustic wave signal processing 77−88991
HF vibration measurement using time-average electronic speckle pattern interferometry system 80−37966
high power applications in gases 79−23165
history in America (up to 1940) 77−45665
hydraulic materials-testing system with 10-nm positional accuracy 78−85065
hydroacoustic transducers of fixed operating freq., elec. imped. matching *(Croatian)* 79−55287
hydrophone calibration appl. modified balancing method 77−11097
hydrophone performance, geometric factors 77−50846
hydrophones using piezoelectric polymer, for large receiver arrays 80−14540
impact motion acceleration transducer system with mechanical waveguide, anal. of processes 79−30436
impedance, eqn. for energy balance of piezoelec. medium 79−28684
included scanner for corner reflector acoustic channel 80−106705
input electrical impedance expression, internal loss correction 78−53101
inspection of plane parallel objects, with oblique bottom immersion chamber 78−53111
inspection using piezoelect. 80−104392
interdigital excitation of surface waves on basal plane of a semi-infinite hexagonal piezoelec. cryst. 78−22244
interdigital transducer for Lamb wave devices for AM, influence of electrical termination 79−41549
interdigital transducer in layered anisotropic semiconducting struct., elec. input admittance matching 78−22238
interdigital transducer models for synthesis of SAW transversal filters 80−5897
interdigital transducer on piezoelectric half space, spectrum of emanating acoustic waves 80−79044
interdigital transducers, quasiacoustic wave propagation, field theory anal. 78−66998
intracorneal adhesion of human skin measurement, diagnostic appl. 77−48819
laser frequency stabilisation, piezoceramic transducer freq. response *(Russian)* 79−10315
LAW transducer made with $LiNbO_3$ 80−5854
layered, generalized orthogonality of normal modes 80−58885

piezoelectric transducers continued
$LiNbO_3$ wedge waveguide apodised interdigital transducer evaluation 77−27451
liquid acoustic parameters and density determ. *(Russian)* 78−49799
liquid atomisation, using US resonators *(German)* 79−66359
LMFBR, coolant start of boiling detection by acoustic method 78−86646
long, experimental investigation of field 78−49822
low frequency US flaw detector appl. 79−98580
manufacture and testing 79−23174
Mason's model for piezoelectric plate transducers 78−33979
materials, high-temp. long duration appl. 80−43586
mechanical response in piezoelectric transducer with current in semiconducting boundary layer 78−18139
mechanical stress meas., advantages *(Russian)* 78−70114
medical imaging, ceramic and PVF_2 transducers compared 79−57734
medical ultrasonics, transmitters and receivers from piezoelectric materials 80−76819
microphones with rigidly supported piezopolymer membranes 80−64330
micropositioning appl. *(German)* 80−8967
microwave ultrasound in liquid generation, $\lambda/4$-mode operation, effective attenuation analysis *(Japanese)* 78−30145
miniature, for transient soft body contact stress problems 80−8975
modulation transducers for alternating pressures 78−77891
mosaic transducer, monolithic, utilising trapped energy modes 77−19504
mosaic transducers for GHz bandwidth bulk acoustic delay line 80−74657
multilayered, amplitude-freq. characts. anal., to determine acoustic emission receiver configuration 78−42507
NDT method, with computerised vibrational spectroscopy 78−29105
noise suppression and prevention for shock and vibration meas. 80−22353
oblique entry probes for examining pipe welds, determination of optimal inclination angles for piezoelectric plates 78−76808
oceanography, bonded flexure transducers mobile sand grains underwater detect. 78−96192
operation, 40 kHz, Doppler alarm, leak detection appl. *(Italian)* 78−42508
optically controlled piezoelectric transducers for ultrasonic volume waves 79−18662
optically-controlled acoustic transducers, piezoelect. and electrostrictive 80−74638
optimisation using acoustic emission transducers 80−48539
optimum size determ. *(Russian)* 79−88943
opto-acoustic transducer structs., recent investigations 80−74688
opto-acoustic transducers, improved equivalent cct. 80−74658
optoacoustic monitor for optically pumped far IR laser 80−102729
oral force monitoring, thin bite element 77−48888
outdoor noise monitoring microphone installation and calibration *(Japanese)* 78−42504
parameter measuring technique 78−72989
parameters testing equipment 79−50555
part inspection with surface temp. up to 500°C 79−98584
phonon beams, GHz range, excitation and detect. 78−43080
photoacoustic effect in piezoelectric ceramics 80−84252
photoacoustic signal detection 78−54467
piezoceramic, blind reading aid using conversion of optical images into vibrotactile 80−85533
piezoceramic, optoacoustic effect obs., in optical fibre 80−48423
piezoceramic aperiodic transducer, mech. load study 80−87700
piezoceramic bar transducers, inhomogeneous, analysis using Reissner mixed variational principle 79−64479
piezoceramic benders, circular, bond stresses 78−21124
piezoceramic cardiovascular acceleration transducer 79−39536
piezoceramic microwelding transducer component oscillation amplitudes 79−26046
piezoceramic transducers, transient charact. 80−106704
piezoceramic transducers for generation of acoustic pulses having prescribed shape 80−87691
piezoceramic tubes with capped or shielded ends, sensitivity above omnidirectional freq. range 78−1534
piezoelectric micrometer for precision movement in optical alignment applics. 77−65017
piezoelectromechanical type, hysteresis reduction method *(Bulgarian)* 77−62129
piezoelectromechanical type with several inputs, bimorphplates description *(Bulgarian)* 77−62130
piezojunction tunnel transducers for hydrostatic pressure *(Polish)* 78−89470
piezometer ring design 77−15142
piezoresistive accel. transmitter mech. designs *(German)* 79−12792
plate transducer, electrical response under influence of body force 77−58520
plates with rectangular electrodes, two-dimensional energy trapping 77−27458
polar polymers for transducers 79−23162
polarised polyvinylidene fluoride film, piezoelectric transducer 80−75993
polarized dielectric appl. *(French)* 79−51902
polymer film, loudspeakers, headphones and pick-ups *(German)* 77−62128
polymer film, piezoelec. and pyroelec. response rel. to dipole polarisation 80−7267
polymer film elements, effect of acoustic radiation on equivalent circuit 79−94380
polymer flexural disc hydrophone 78−63254
polymer piezoelectric transducer appls. 79−32169
polymer sheet transducers for Rayleigh waves excitation and detection *(French)* 79−14182
polyvinylidene fluoride as transducer material 80−75947
polyvinylidene fluoride film, biaxially oriented, charact. for transducer appl. 80−88931
polyvinylidene fluoride film appl., poled, short duration unipolar stress pulse detection, generation 80−106695
polyvinylidene fluoride film polymer transducer, with US appl., durable lead attachment techniques 80−79094
polyvinylidene fluoride films, HF US absorpt. meas., 300 to 1500 MHz 80−74667
polyvinylidene fluoride foil appls. *(German)* 78−22243
polyvinylidene fluoride transducers, underwater acoustic meas. 79−14184
polyvinylidene-fluoride stretched membrane variable focus US transducer 77−39185
piezoelectric transducers continued
preparation method problems for UF-90PTs instrument, for US testing of concerete 78−90622
pressure, piezoresistive pressure pickup on IC *(German)* 77−49717
pressure bar transducer, dynamic transmitting props. *(Chinese)* 78−4605
pressure meas. appl., up to 6×10^8 N/m^2 80−31785
pressure sensor, catheter-tip, with on-chip compensation and signal processing 77−44818
pressure sensor using TsTS-19 piezoelectric ceramic 80−105670
probe, conversion ratios 80−69624
pulse frequency-response curves for a contact piezoelectric transducer 79−68538
pulse-driven, fundamental charact. 80−38210
pulsed operation, calculation of inverse Laplace transform 79−64480
pulsed opto-acoustic spectroscopy 80−62743
PVF_2 transducers for NDT 80−76476
quartz, measurement time extension using fused quartz housing 78−54354
quartz, multimodality influence on US vel. and attenuation meas. 77−11100
quartz piezosensor, construction and performance 79−88939
quartz-LZT wide-range instrument transducer, practical feasibility 78−51035
radiation and reception field investigations; piezoelectric probe, pulsed mode, Kirchhoff approx. 80−87636
radiator of longitudinal acoustic waves with an inhomogeneous elec. field 80−87693
reciprocity calibration of acoustic emission transducers 80−28401
reciprocity technique for estimating the diffuse-field sensitivity of piezoelectric transducers 80−48538
rectangular plate vibrating mode, US array appl. 77−80046
reflex hammer with peizoelec. cryst. for accurate reflex latency meas. 80−3839
resonant, construction and delay line contract, US thickness meter 78−53100
respiration monitor for children using belly-belt electronic sensor 77−56512
response equalization using low-pass filter 78−30144
response optimisation using electrical correcting circuits 77−68359
rolling ultrasonic low-frequency probe 79−98582
SAW, characterization of RF sputtered ZnO and ZnS films by X-ray diffraction anal. 80−80138
SAW phase shifter with 3 interdigital transducers 80−79062
SAW transducer, 2-phase interdigital with unidirectional props. 79−1044
SAW transducer analysis by equivalent parameter representations 78−1541
SAW transducers based on layered systems, calc. of electromech. coupling coeff. squared 80−87690
semiconductor, pre-energised nonuniform, delay rod loaded, subject to body force, mechanical response 77−27449
sensitivity determ. by impedance method 77−11104
sensitivity measurement 78−49821
shear wave transducer for use in marine sediment studies 78−63257
shear-mode acoustic wave receiving, transfer charact. 80−87696
shock wave propagation in shock tubes, investigations on suitability of piezoelectric and magnetoelastic detectors *(Polish)* 80−79351
short pulse US transducers, design and characterisation using PZT5A 78−87228
side-plated piezoceramic bar, elec. and acoustic wave propag. 77−50847
slot-effect, appl. of energy principle for calc. force upon electret *(German)* 77−3706
sonar transducer, Langevin type, made from $Pb(Zr,Ti)O_3$ type 1 ceramic, performance charact. 80−79095
SQUID coupled to piezoelectric transducer, detection of gravitational waves 78−21218
strain gauge, for clinical recording of ocular microtremor 78−96109
strain transducer, diffused MOS device 77−5825
surface excitation 79−76935
surface excited, charge density distrib. determ. method 79−94447
surface excited, operation in radiation mode 80−33407
surface excited, operation in reception mode 80−33408
surface excited, thick, acoustic fields 80−102957
surface excited, thick, transient, pulse and amplitude-frequency charact. 80−102958
surface excited, US field 80−64331
surface-skimming bulk wave excitation, analysis using Green's function formulation 80−53519
synthetic polymer films, acoustoelectric transducers appl. *(Italian)* 79−98577
tangentially polarized cylindrical transducers, intrinsic noise 79−94441
tapered piezoelectric bar transducer with transverse polarisation of piezoceramic, acoustic props. 78−1537
temperature field calculation on transmitter chips *(German)* 78−77888
testing, using high-power DUMILOAD device 77−3707
thickness mode, front face mech. impedance effects 77−31197
thickness mode, method for stress const. determ. 79−14187
thickness mode piezoelec. US probe design factors 79−68540
thickness vibrator, digital computer simulation 77−88998
thickness-extensional trapped energy mode transducer array, increased bandwidths and mode shapes 80−74633
thin film unidirectional SAW transducer and filter 78−46879
Tonpilz, design using nonlinear goal programming 80−106696
transducer, performance calc. 80−77771
transformation factor, effect of DC field 80−5903
transmit/receive 2D ceramic piezoelectric arrays, construction and performance, medical, NDT appls. 78−87223
triaxial cell, for measuring occlusal force by human teeth *(German)* 78−20303
triaxial vector accelerometry for quantifying tremor and ataxia 78−28116
two-dimensional monolithic mosaic transducer array 79−46156
UD-24 instrument, piezoelec. US transducers 80−108664
ultrasonic pulsed measuring instrums., signal shape anal. 80−87678
underwater transducers materials, suitability of polyvinylidene fluoride 78−1531
unidirectional SAW transducers, 3-phase equivalent cct. model 80−74627
unidirectional transducer used in SAW grating-resonator filter, behaviour 80−5877
US, design, US imaging equipment appl. 78−9525

piezoelectric transducers continued
US, discs attached to metal rods and metal plates 80−96166
US, for acoustic emission measurement in NDT 80−28375
US aperiodic sensor, fabrication and design problems 77−77713
US array technology, 2-D, state of art review 77−844
US biomedical low-loss wideband for noninvasive appls., charact. 78−48846
US flowmeter output characteristic linearity 78−42685
US hydrophone, cylindrical, theoretical shape of directional pattern 79−81609
US imaging biomedical micro-array technology for improved image quality *(German)* 80−98052
US inclined probe, construction improvements 80−33411
US inertial transducer, rotational perturbation detection appl. 78−9524
US meas. with piezoelectric transducers, absolute calibration 80−79099
US phase flowmeter, pulsating flow rate meas. error evaluation 77−72388
US power output meas. using modulated radiation pressure 78−59230
US pulsed fields, from thick piezoelectric disc immersed in petrol *(French)* 80−53512
US receiving array having power response 80−74653
US reflection from transducer with coupling layer *(German)* 79−10440
US scanners, phased-array, angular response of piezoelectric elements 79−64471
US strip transducers with nondirectional sound radiation *(German)* 79−98576
US surface excited thick piezoelectric transducer, output current form 80−87701
US telemetry for monitoring heart/respiration rate and body/skin temp. of scuba divers 77−90929
US testing appl., of glass-reinforced plastics, use of protective coatings for dry-entry transmission 77−90563
US transducer, thick, operating as radiator or receiver, performance charcts. 80−35484
US transducer, US energy meas. for echography 80−36044
US transducer element tuning 80−87684
US transducers, energy and spectral evaluations of broadband excitation 80−35485
US transducers, integrated acousto-optical effect prod. by pulsed sound fields 77−31193
US transducers, surface-driven, input impedance calc. 80−35493
vacuum piezoceramic transducer for 760 to 10^{-3} torr 78−86283
VHF piezoelectric transducer-delay line systems 77−7277
vibration and pressure transducer design for nuclear reactor environment 78−823
vibration electronic damping in optical structures 79−50372
vibration mode in tall, narrow elements of acoustic imaging array 80−74690
vibrocontact, performance calc. 80−77771
water-loaded, air-backed discs, impulse response 79−27482
wedge-shaped transducer, ang. displacement of sound beam 77−35009
wedge-type backing 79−41546
wedged, with improved signal-to-scattered-noise ratio 79−3880
wide-band projecting transducer 77−84096
wideband, US field intensity meas. appl. *(Russian)* 80−38209
wideband, with inhomogeneous electric field 77−31196
wideband excitation of surface elastic waves in microwave range 80−10105
ZnO, microwave acousto-optical device applic., 0.2 to 18 GHz 77−58465
AlN, piezoelectric film, low temp. growth by RF reactive planar magnetron sputtering method 80−76175
$BaTiO_3$, ferroelectric polydomain crysts., piezoresonance effects, appl. as transducer 79−4779
CdS thin film transducers, testing via light diffr. by acoustic waves 77−23840
n-InSb, noise, round trip acousto-electronic amplification, anodic piezoelectric transducer *(Russian)* 78−23139
KH_2PO_4 electro-optic modulator crysts., piezoelec. induced acoustic transients 80−70316
$LiIO_3$ and quartz, acoustic field distrib., Bragg diffr. method 80−97231
$LiIO_3$ crystal elastic, piezoelec., dielectric and acoustic props. 79−46740
α-$LiIO_3$, piezoelec. mat. for acoustooptic cells, piezoelectric transducers 78−95575
$LiIO_3$, Z-cut cryst., appl. as wide band transducer in US pulse-phase interferometer 77−14868
$LiNbO_3$, very narrow surface wave transducer, acoustic diffr. effects 78−22240
Mn low-impedance stress gauges for precision measurement in severe shock-wave environments 80−38367
PVF_2 film US transducers, review *(Japanese)* 79−98579
PZT-polymer flexible composite transducer 78−80291
$Pb(Ti,Zr)O_3$, ceramic disc stack piezoelec. transducer, performance charcts. 77−37843
$Pb(Zc,Ti)O_3$ crystal, appl. to identification of resonant frequencies of rotating beams 79−81824
$Pb(Zr,Ti)O_3$ ceramic, interconnected porous, props. 80−43579
$Pb(Zr,Ti)O_3$ fast transducer driving Fabry-Perot optical switch 79−86251
$Pb(Zr,Ti)O_3$ internally electroded multilayers, piezoelectric props., permittivity, transducers 80−80672
$Pb(Zr,Ti)O_3$:Mn, crystal struct. and electrophysical props., piezotransformer props. 78−43806
$Pb(ZrTi)O_3$ ceramic transducer for generation and detection of unipolar stress pulses 80−64328
SbSI materials, piezoelectric props. rel. to use as electroacoustic transducers 78−52445
Si filamentary piezoresistor for pulsed wave process meas. 78−57980
Si force transducer, extraluminal meas. of oviduct contractile activity 77−40805
Si, mechanical Q meas., low temps. 78−48118
Si miniature biomedical piezoresistive pressure transducer *(German)* 80−37016
Si piezoresistive accelerometer power transfer factor *(German)* 80−37017
Si piezoresistive coefficient calc. and meas. *(German)* 80−39571
$Sr_{0.5}Ba_{0.5}Nb_2O_3$ piezoelectric transducer, SAW props. 80−79037
Yb stress transducer, piezoresistive effects 77−68539
ZnO film concave transducer, for focusing microwave ultrasound 77−7276
ZnO films US transducers obtained by DC diode sputtering, dielec. breakdown props. 80−40066

piezoelectric transducers continued
ZnO interdigital transducer, efficient bulk-wave excitation in layered media 77−69156
^{67}Zn spectrometer, double freq. interferometer for absolute velocity calibration of piezoelectric transducer 80−37146

piezoelectricity
see also electrostriction; piezoelectric devices; piezoelectric materials; piezoelectric oscillations
acoustic activity and other effects due to spatial dispersion in piezoelec. cryst. 78−2808
acoustic activity in crystals which show piezoelec. effect 78−26631
acoustic gap waves between two piezoelectric half spaces 78−50970
acoustic harmonic, excitation and energy flux in piezoelec. cryst. 79−15404
acoustic wave passage through gap between piezoelectrics coated with insulating films 79−28187
acoustic wave propagation, group vel. charcts. 80−92613
acoustic waves, parametric excitation in presence of electron currents *(Russian)* 80−80328
acousto-EM wave propag. modes, hexagonal crystals *(Spanish)* 77−4602
acoustoelectrical waves, double refl.- and birefr. in piezoelec. cryst. 80−11047
anelastic loss, specimen geometry effect 79−78624
anisotropic media, piezomagnetoelectric effects 80−25174
asymptotic analysis of the electroelastic state of a thin piezoelectric layer *(Russian)* 79−8094
axis of highest activity, meas. apparatus 77−55753
backward waves and acoustic scanning, nonlinear interaction of vol. and surface waves 80−79040
backward-wave-mode thickness vibration energy trapping by piezoelectric reaction control 79−56728
band structure, calc. using Euwema PWG method with X_α approx. 78−15106
bending elements with passive substrate layer, static force/deflection calc. *(German)* 77−77152
bending of peizoelectric multilayer plates with uniform elec. field, anal. 80−40064
biomaterial, isotropic, induced piezoelec. 77−13048
biomembranes, lipid-protein interactions, flexoelectric effects 78−92600
Bleustein-Gulyaev surface waves behaviour in periodically corrugated piezoelectric medium 80−87616
Bleustein-Gulyaev wave amplification in piezoelec. coated with semicond. film 79−61309
Bleustein-Gulyaev wave propag. charcts. at surface imperfections 78−43226
Bleustein-Gulyaev wave transmission charcts. at corner 77−59197
bone, distrib. of induced elec. activity in bent long bone 78−3541
bone, distrib. of piezoelec. effects in bent long bone, anal. model 77−36983
bone, human cortical, local piezoelec. polarisation as function of stress freq. 77−32933
bone, human cortical, US properties and microtexture 80−51144
bone, piezoelectric, dielectric and elastic constants, rel. to temp. and hydration 77−16946
bone, role of stress-gradient effects 80−67113
bone, strain-related potentials, freq. depend., effect of meas. system parameters 80−16991
bone, stress generated potentials at osteon level 78−31837
bone, stress generated potentials rel. to collagen piezoelectricity 77−32932
bone, stress generated pots., linear piezoelec. model 80−3688
bone, US exposure, effect of sample rot. 78−80913
bone, wave propag. in piezoelectric two-layered cylindrical shell with hexagonal symmetry 78−55487
bone piezoelectric effect, theoretical anal. 79−70567
bone piezoelectric response obs., freq. depend. 79−92287
bone stress wave detection using piezoelec. effect, non-invasive technique 78−31948
capacitance type AC dilatometer for piezoelectric and electrostriction const. meas. 80−77747
cavitation bubbles in water, elec. pulses production 79−47407
ceramic, nonlinear charge release under uniaxial press. 80−80706
ceramic blocks, TsTS-23, TBk-3, TsTSNV-1, longit. piezoelec. effect and moduli 78−56430
ceramic cylinders, LF voltage-press. sensitivity 78−2805
ceramic plates, bending strains, electromechanical transformation, energetic method of calc. *(Ukrainian)* 80−71320
ceramics, electromechanical energy conversion in nonuniformly deformed bodies *(Russian)* 78−19418
charge storage, charge transport and electrostatics conference, Kyoto, Japan (Oct. 78) 80−7252
chitin, in lobster shell and apodeme, piezoelec. rel. to remodelling 78−64929
cholesteric liquid crystal, piezoelectric coeffs., Onsager theory, interparticle pot. and first moment vector 77−24264
cholesteric liquid crystals with vibration 78−6013
cholesteric liquid crysts., electrodynamics, continuum theory 80−6356
cholesterol derivatives, piezoelec. rel. to atherosclerosis 77−78076
collagen structures, piezoelec. effect, in rel. to mol. struct. 80−41100
complex piezoelectric constant, meas. by interferometric method, at frequencies up to 50 kHz 79−63270
complex reciprocity theorem for multiregions with piezoelectic media and surface impedance 79−61307
conference, ferroelectric materials and their applications, Kyoto, Japan, Nov. 17-19, 1977 79−19846
constant deformable dielectrics, coupled mechanoelectric fields, piezoelectricity and Lamb problem 80−58899
coupled surface electroacoustic waves 78−2355
crystal, optical and acoustic prop. interactions, including piezoelec. effects 77−4621
crystal classes, artificial poling procedures and transducer appls. 77−12314
crystal nonlinear electroacoustics, dynamical eqns. and constitutive relations 79−56734
crystals, class $C_{6v}(C_{4v})$, shear wave scatt. by low resist. cylinder and cylindrical void 78−95113
crystals, rel. between nonlinear piezoelec. coeffs. 79−47389
crystals, variation of phase vel. and wave struct. of finite amplitude SAW 78−95219

piezoelectricity continued
cubic crystal, surface acoustic wave modes 78−2352
cubic crystal/cubic crystal interface, transverse surface acoustoelec. wave propag., due to electrostriction 77−66082
cylindrical crystal surfaces, influence of piezoelectric effect of transverse SAW 78−94479
cylindrical shell, finite, torsional wave propagation 78−56428
cylindrical shell, longitudinal wave propagation 78−92026
p-decyloxbenzylidene p'-amino 2-methyl butyl cinnamate, smectic A to C transition, Landau theory 77−84906
dicalcium strontium propionate, cryst. symmetry in low temp. phase 79−37693
dielectric and piezoelectric relax., difference between 78−72458
dielectric relaxation time determ., piezostimulated current curves, theoretical and exptl. anal. methods 78−92020
dielectrics, deformable, polarisation gradient elasticity theory, coupled mechano-electric fields 80−55037
dielectrics, piezoelectricity, mechano-electric coupled fields, polarisation gradient 80−75940
diglycine nitrate, cryst. growth, dielec. and electromech. props. 80−2701
DOBAMBC, chiral smectic, flexoelectric effect and polarisation props. *(Russian)* 80−15002
dynamically loaded deformable dielectric material with memory, elec. responses 77−36176
echos of piezoelectric powder *(French)* 78−72462
elastic dielectric, constitutive eqns. 77−8512
elastic equilibrium of a piezoelectric cylindrical body with random anisotropy *(Russian)* 79−61308
elastic wave propag. and interaction with charge carriers, appl. of hardened elastic moduli *(Russian)* 78−35095
elastic wave propagation in hexagonal crysts. *(Russian)* 77−69777
elastic wave with struct. of EM wave in piezoelectric media *(Russian)* 77−16251
electrets, piezo- and pyroelectric props. 80−80685
electrets and dielectrics, conf., Sao Carlos, Brazil, Sept. (1975) 80−7251
electric polarisation effects on piezoelec. and photoelastic interactions *(German)* 78−35091
electrical discharge from arbitrarily deformed bodies, theory *(Ukrainian)* 80−11341
electrical response of relaxing dielectrics compressed by shock waves, axial mode problem 78−80280
electro-acoustic effects on phase vels. of acoustic and EM waves *(French)* 79−15401
electroacoustic echo, phase amplitude depend. *(Russian)* 80−7298
electroacoustic echo, thermodynamic theory 78−19420
electroacoustic echo at doubled freq. in piezoelectrics 78−15100
electroacoustic echo effect, tensor description 78−19103
electroacoustic echo form. in powders by FM mechanism 78−19421
electroacoustic echoes and long-time storage in piezo- and ferroelectrics 79−38454
electroacoustic parametric interactions 79−1740
electroelastic plane wave propagation in piezoceramic medium *(Russian)* 77−55752
electroelasticity for piezoelectric medium with cuts, 2-D boundary value problems 80−71319
electroelasticity problems, numerical soln. 80−80707
electron stream effects on material with semiconducting boundary layer 78−19414
electron-hole droplet, motion damping, impurity and piezoelec. scatt. 78−67951
energy balance of piezoelectric, inc. impedance of piezoelectric transducer 79−28684
epoxy resin-ferroelectric $Pb(Zr,Ti)O_3$ composite, dielec., elastic and piezoelec. consts. 77−8515
ferroelastoelectric poling, differing piezoelec. props. of domain states 77−16102
ferroelectric ceramic, axially loaded, nature of elec. field and resulting voltage 78−72468
ferroelectric ceramic, shock induced polarisation 77−48133
ferroelectric ceramics, 1-D linear dynamic electromechanical responses 79−47397
ferroelectric ceramics, elastic and piezoelec. eigenstate spaces 79−42901
ferroelectric ceramics, materials and dielec. props., review 80−75957
ferroelectric piezomaterials, pyrochlore struct. high sound-propagation velocity 78−43791
ferroelectric theory and dynamics, optical, acoustic electro-optical props., Brillouin zone struct. 80−11347
flexure and twisting of thin plate with elliptic opening *(Russian)* 77−66456
flexure of thin plates, integer polynomial solns. *(Russian)* 78−52444
forced torsional vibrations of a semi-infinite piezoelectric medium of (622) class 79−51910
Gulyaev Blustein wave excitation by developing defects *(Russian)* 78−56030
Gulyaev-Bleustein wave excitation, wave field structure 79−19442
harmonic generation in piezoelectric crystals under the action of homogeneous external fields 79−32121
hypersound resonant excitation by 2-dimens. plasmons *(Russian)* 79−78032
III-V crystals, piezoelectric effect due to dislocations 77−81059
III-V semiconductors, piezoelectric induced polarization charge distribs. around point defects 79−56725
III-V semiconductors, stress-induced elec. props. of point defects, piezoresistance effect 79−56726
inhomogeneous piezoelectric body, thermopiezoelec. problem 79−33611
inhomogeneous piezoelectrics, electromechanical props. prediction 80−103919
insulating crystals, piezoelec. potentials of dislocations 80−20594
ionic single crystals, elec.-mech. coupling of dislocations 78−75676
line acoustical waves anal. 78−34692
linear transversely isotropic media, normal mode response, boundary effects 78−52441
liquid crystals, piezoelectric effect 78−6635
liquid crystals, piezoelectric effect use as light modulator 80−83679
lithium ammonium tartrate monohydrate elastic props., piezoelec. reson. method meas. 77−63370
Love wave propagation in polarised piezoceramic supports *(Russian)* 77−69039
macroscopic quadrupole effects as method of obs. of struct. transforms in crysts. 80−71321
magnetoelectric resonances in piezoelectrics *(Russian)* 79−42904

piezoelectricity continued
MBBA, nematic liq. cryst., flexoelectric and dielec. relax. behaviour 78−94979
MBBA, nematic liq. cryst., transverse electrooptic effect 79−94897
mechanical disturbances in piezoelectric slab from periodic elec. field, body force, const. heat flow 78−19412
mechanical properties meas., piezoelec. method, for small sandwich specimen 77−54939
molecular crystals, polariton spectra and lattice dynamics 80−49313
nematic layer, piezoelec. instability, threshold characts. *(Russian)* 77−24800
nematic liquid crystal, flexo-electric domains 78−43792
nematic liquid crystal, piezoelectric coeffs., Onsager theory, interparticle pot. and first moment vector 77−24264
nematic liquid crystal, piezoelectric effect 79−90551
nonlinear electroacoustics, fundamentals and appl. 80−34489
nonlinear electroacoustics of dielec., piezoelec., and pyroelec. crysts. 78−79155
nonlinear electromechanical coefficients 78−80292
nonlinear response to plane waves of uniaxial strain 77−12316
nylon 11, pyroelectricity and piezoelectricity 77−69780
order-disorder type ferroelectrics, piezoelec. and elastic props. 77−12318
organic crystals for SHG, selection and characterisation 77−3626
orthorhombic crystals, triboluminescence and piezoelectric behaviour 79−95861
osteon system piezoelec. polarisation model 78−3540
parametric echoes, description and demonstration 79−42903
parametric interaction of EM and acoustic waves in solids, theory 78−60166
4-n-pentyl phenyl-4(4-pentyl benzoyloxy)3-chlorobenzoate, liq. cryst., flexoelectric and dielec. relax. behaviour 78−94979
phonon echo in crystals 77−1641
phonon echo in travelling and standing wave regimes in piezoelectrics 77−8521
phonon echoes and long-time storage in piezoelectric powders *(Japanese)* 80−70330
phonon electroacoustic echo under acoustic reson. conditions *(Russian)* 77−48131
photoacoustic detection, theory and expt. 80−90904
photovoltaic effect, phonon mechanism 79−7862
piezo-stimulated current spectra 77−69767
piezoceramic medium, electroelastic waves, magnetic accompanying effects *(Russian)* 79−28680
piezoceramic plate, electroelastic equilibrium *(Russian)* 78−43795
piezoceramics, converters of shock wave mech. energy into elec. power 80−61429
piezochemiluminescent, piezochemomagnetic and piezochemovoltaic effects *(Russian)* 77−85820
piezoelectric-semiconductor, layer struct. transverse acoustoelectric effect 79−69565
piezopolarons and condensons, temp. and screening effects on effective mass 77−43521
piezostimulated currents, new method for exam. of dielec. relax. 78−10847
plate, elastic surface wave propag., elec. screening effect *(Russian)* 79−14999
PMMA, shock induced polarisation, dielec. const., dipole lifetime rel. to particle velocity *(French)* 77−69776
polar polymer, piezoelectric response rel. to dipole polarisation 80−7267
polar polymer, piezoelectricity and pyroelectricity 80−7267
polarisation echo, physical nature 77−1635
polaron lifetime, elimination of IR divergence 78−76007
poly-gamma-benzylglutamate, oriented films, piezoelectric relax. 77−24798
polyacrylonitrile, elec. polarisation 80−7275
polymer, piezoelectricity and pyroelectricity, review 77−8514
polymer film transducer, piezoelec. and pyroelec. response rel. to dipole polarisation 80−7267
polymer materials, piezoelectricity and pyroelectricity and anal. *(Japanese)* 78−88257
polymers, elec. props. and morphology, correl. review 78−43786
polymers, electrical phenomena, nature and appl., book contrib. 80−50254
polypropylene, electron bombarded, radical formation, piezoelectric and pyroelectric effects, ESR study 80−7169
polyvinylidene fluoride, amorphous, low temp. anomalies 78−30724
polyvinylidene fluoride, bending piezoelectricity 77−12319
polyvinylidene fluoride, biaxially stretched film, corona charging and piezoelec. effect 78−88256
polyvinylidene fluoride, elec. field induced phase changes 79−11387
polyvinylidene fluoride, film, piezoelec. relax. 79−87394
polyvinylidene fluoride, piezoelec. and pyroelec. props., struct. model 79−11386
polyvinylidene fluoride, piezoelec. consts. calc. 80−103918
polyvinylidene fluoride, piezoelec. parameters versus bias field strength 79−91376
polyvinylidene fluoride, piezoelectric effect formation due to injection process, TSC *(French)* 80−34856
polyvinylidene fluoride, suitability as underwater transducer material 78−1531
polyvinylidene fluoride, thermodynamical model, applications *(French)* 80−39315
polyvinylidene fluoride, uniaxially stretched, piezoelec. and pyroelec. 77−40181
polyvinylidene fluoride film, anisotropy and temp. depend. of piezoelec. consts. 77−1640
polyvinylidene fluoride film, hysteresis and dipolar orientation 80−97217
polyvinylidene fluoride film, shear props. by piezoelectric resonance 79−99824
polyvinylidene fluoride film, stretched, struct. and elec. props. 79−90572
polyvinylidene fluoride films, corona-charged, struct. changes, piezo- and pyroelec. props. 79−11389
polyvinylidene fluoride films, corona-poled, piezoelectricity *(Japanese)* 80−55040
polyvinylidene fluoride films, stretched and rolled, electrostriction and piezoelectric effects *(Japanese)* 80−55041
polyvinylidene fluoride-tetrafluoroethylene, ferroelectric props. 79−42929
powder, mech. of long-time phase memory 79−42899
powder, polarisation echo for system of anharmonic oscillators *(Russian)* 77−81062
powder, RF dynamic polarisation echo obs. 77−16254

piezoelectricity continued
powder, three pulse echo, mechanism contribs. 78−68444
powder material US pulse echoes and suppression 77−28520
powders, explanation of polarisation echo by dislocation mechanism *(Russian)* 77−36181
protein-methylglyoxal complex, electronic props., energy band cond. 79−24936
PVFD, electret, polarisation process 80−7273
PZT/polymer composites, simplified fabrication 80−40323
quartz, complex piezoelectric constant, meas. by interferometric method, at frequencies up to 50 kHz 79−63270
quartz, piezo quasi-mosaic struct. effect obs. on X-ray diffr. *(Russian)* 77−89349
quartz, piezoelec. and gamma-ray diffr. props. 77−20801
α-quartz, piezoelec. consts. determ. from dynamical X-ray diffr. curves 77−77153
quartz, synthetic, precision meas. of elastic and piezoelectric characts. 78−6638
quartz-bearing rocks, search for piezoelec. effect 77−73728
rare earth compounds, $RNaMTa_5O_{15}$ (R=rare earth, M=K, Rb, Tl, Cs), relative stability of struct. types, and piezoelec. props. *(French)* 80−49206
Rayleigh wave propag. near Curie temp., ferroelec. cryst. with piezoeffect 77−89630
resonance method for determ. of small piezeoelec. consts. *(German)* 78−92025
Rochelle salt, crystal, X-ray topographic obs. of localised vibr. 79−24264
Rochelle salt, electromechanical behaviour, influence of ferroelec. phase transitions 77−8510
SAW propagating in two separated piezoelec. media, coupling 78−38929
SAW propagation, temp. coeffs., piezoelectric coupling in quartz, $LiNbO_3$, $LiTaO_3$, Tl_3VS_4 *(French)* 78−35093
semi-infinite crystal, surface wave solns. nonexistence example 80−6611
semiconductor, absorpt. and amplification of US at moderate freq. 78−19102
semiconductor, nondegenerate, interaction between electrons and strong piezoelec. wave *(Russian)* 77−90106
semiconductor-piezoelectric corrugated boundary, reflected acoustic wave amplification *(Russian)* 78−30819
semiconductor-piezoelectric structure, SAW attenuation and transverse acoustoelec. field 78−10516
semiconductor-piezoelectric structure, vol. acoustic wave excitation in non-linear interaction with surface waves 80−69582
semiinfinite heated piezoelectric slab, tangential elec. field excitation, soln. 77−14656
shear SAW amplification in periodic structures on solids 79−90055
shear surface waves, generalised 80−92770
shock compression of solids, review 80−24534
shocked piezoelectric disc as Maxwell solid 78−15098
slab with dissipative characteristics, disturbances 80−25310
smectic helixing crystal, dielec. props., temp. and freq. depends. *(Russian)* 78−60380
smectic liquid crystals, piezoeffects and ferroelectric phenomena 79−32883
sodium ammonium tartrate, improper ferroelec. transition anomalies 78−19430
sodium benzoylacetonate, piezoelectricity, transition of 70°C 79−8092
sound waves, energy flow and group vel. in piezoelec. cryst. 77−39633
spinning disc of radially inhomogeneous piezoelectric material, transient voltages and stresses 80−55039
stimulated Raman effect in cubic piezoelectric single cryst., coupled wave dispersion *(German)* 79−36963
Stoneley wave amplification between two piezoelecs. separated by thin semicond. film 79−14998
superlattices, plasmons, two-dimens., due to piezoelec. effect 80−92845
surface modes, acoustic wave propagation in piezoelec. crysts. 80−20026
surface polaron states, polaron-phonon interactions in piezoelectric crystal 80−70790
surface wave anal. using orthogonal functions 78−51810
surface wave propagation in homogeneous piezoelectric halfspace 79−3970
surface waves, perturbation anal. of attenuation and dispersion 78−47653
surface waves on cubic cryst., slowness surface Gaussian curvature 79−77887
surface waves on cubic crystals, energy propagation props. 78−51811
surface waves on semiinfinite crystal, asymptotic expressions 78−51812
TGS:α-alanine, piezoelectric props., ferroelec. phase existence *(Russian)* 79−47387
TGS, electromech. coupling of surface acoustic waves near ferroelec. transition 78−19415
TGS, piezoelectric resonance spectra in 17 to 60 MHz range 77−16269
TGSe, ferroelec., effect of gamma irradiation on dielec., piezoelec. and elastic props. 77−43943
thermal fluctuations in piezoelectric plate *(Russian)* 78−76389
thermo-piezoelectric material, time depend. harmonically changing plane wave propag. anal. 80−15977
thermo-piezoelectricity, of polarised annular disc, deformation due to prescribed temp. distrib. 80−2699
thermoelasticity with piezoelectric effects, dynamic reciprocal theorem 78−83242
thermopiezoelectric laminae, coated with electrodes, two dimens. vibr. theory 78−35092
thermopiezoelectricity, uniqueness theorem 79−73884
thickness vibration of piezoelectric plate, natural freq. spectrum 80−15979
thin anisotropic layer, electroelastic equilibrium 80−28429
thin plate, electroelastic equilib. anal. *(Russian)* 78−19417
torsional wave propag. in infinite piezoelec. cylinder (622) cryst. class 80−87642
tourmaline, resonator, electroelastic constants, elec. field induced freq. shift study 80−20597
transition radiation of Gulyaev-Bleustein SAW in piezocrystals 78−43231
variational limits on piezoelectric problem parameters 79−81594
vibrating piezoelectric solid, perturbation theory for linear electroelastic eqns. 79−1739
vibrations, waves, flexure, fracture, fundamental equations 80−60505
vinylidene-fluoride-trifluoroethylene copolymer, piezoelectricity 80−88930
piezoelectricity continued
vinylidenefluoride/tetrafluoroethylene copolymer, piezoelect. and pyroelect. response rel. to dipole polarisation 80−7267
wurtzite type crystals, bond ionicity anisotropy and spontaneous distortion 77−19900
wurtzite-type crystals, lattice dynamics including the effect of electronic extension 80−59586
zinc-blende semiconductors, quantum resonances in valence bands under uniaxial stress 79−99480
zincblende crystals, internal strain and piezoelectric coefficient 78−39505
zincblende-type crystals, electromodulation, piezomodulation, theory 80−93281
$AgNa(NO_2)_2$, complex piezoelectric constant, meas. by interferometric method, at frequencies up to 50 kHz 79−63270
Au-CdS, Schottky junction, surface defects, photovoltaic, piezoelectric and V-I characteristics *(French)* 80−49898
BN, cubic, energy band and piezoelec. calcs. 78−72071
$Ba_{0.92}Ca_{0.08}TiO_3$ ceramic, uniaxial stress effects, US dilatometric and dielec. meas. 78−52454
$Ba_2Si_2TiO_8$, elastic consts., thermal expansion and piezoelec. props. 77−85651
$BaTiO_3$ a-domain crystals, domain struct. influence on physical consts. 79−69798
$BaTiO_3$, c-domain cryst., HF dispersion of permittivity 78−60379
$BaTiO_3$, ferroelectric polydomain crysts., piezoresonance effects, appl. as transducer 79−4779
$BaTiO_3$, nonpiezoelec. dielec., light-sensitive Rayleigh wave generation by surface piezoelectricity 78−43228
$BaTiO_3$, piezoceramic, nonlinear piezoeffect 79−42900
$BaTiO_3$ polydomain crystals, dielec props. 78−43827
$BaTiO_3$:Al, 0.05-0.3 wt.%, ceramic dielectric, dielec. and mech. props. 79−8091
$Ba_2TiSi_2O_8$, fresnoite, Czochralski growth and phys. props. 78−3026
$Bi_{12}GeO_{20}$, elastic and piezoelectric consts., thermal expsn. 78−31157
$Bi_{12}GeO_{20}$, electromech. props. 79−38455
$Ca_{12}Al_{14}O_{33}$, piezoelectric material, cryst. growth and characterisation 79−99825
$Ca_2MTa_5O_{15}$(M=K, Rb, Tl, Cs), relative stability of struct. types, and piezoelec. props. *(French)* 80−49206
$Cd_2MTa_5O_{15}$ (M=K, Rb, Tl, Cs), relative stability of struct. types, and piezoelec. props. *(French)* 80−49206
CdS, elastic, piezoelec. and dielec. props. 80−108157
CdS, low resist. single cryst., photodeform. mechanism 77−89806
CdS polycrystalline films, high strain sensitivity 80−93017
CdS-Au Schottky barrier, piezoelec. effect due to mech. bending 77−69779
CdS-Au structure, work function of {0001} faces of CdS, effect of piezoelec. props. 78−23164
$Ce(CO_3)_5^{6-}$, in Na and guanidinium salts, struct./props. correlation *(French)* 78−95032
$CsCuCl_3$, phys. props. 77−62511
$CsCuCl_3$, piezoelectricity, Jahn-Teller type phase transform. 80−40065
CsH_2AsO_4, elastic props., photoelasticity near ferroelectric phase transition 80−29107
$Cu_3B_7O_{13}Cl(Br)$, piezoelectric, elastic and electromechanical coefficients *(French)* 78−39504
CuCl, interface supercond., piezoelec. hypothesis 80−60128
$DyVO_4$, Jahn-Teller transition, improper antiferroelectricity rel. to sublattice piezoelec. coupling 77−24802
n-GaAs, strain sensitivity of specimens obtained from pressed powders 77−36177
GaP-Ag(Au), Schottky barrier, stress effects on elec. props. 80−34512
n-GaSb, stress-induced elec. props. of point defects, piezoresistance effect 79−56726
$Gd_2(MoO_4)_3$, nonlinear piezoelec. coeffs. near phase transition 79−95710
$Gd_2(MoO_4)_3$, piezoelectric and electrostriction coeffs. near ferroelastic transition *(French)* 77−40182
p-Ge, piezo Hall effect meas. 80−96883
Ge, radiation piezoelec. effect, EMF generation under α-irrad. and uniaxial deform. 77−12320
Ge single cryst., radiation piezoelec. effect 78−19419
HCN crystals, polarition spectra and lattice dynamics 80−49313
p-InSb, quantum resonances in valence band under uniaxial stress, far IR meas. 79−99481
$K_2Cd_2(SO_4)_3$, ferroelastic phase transition, X-ray diffr. and dielec. temp. depend. meas. 79−55882
KCl, temp. depend. of dislocation charge, piezoelec. defect technique 78−22733
KD_2PO_4, neutron scattering from coupled polar-elastic waves 80−92623
$KH_{2(1-x)}D_{2x}PO_4$, photoelasticity and electrooptic effects at forbidden deform. *(Russian)* 78−35117
KH_2PO_4, electro-optic modulators, transient acoustic waves 79−59809
KH_2PO_4, Pockels' const., linear electro-optic consts., sign of piezoelectric const. 78−60425
KH_2PO_4 powder, dynamic polarisation echoes 79−4773
$K_{2.89}Li_{1.55}Nb_{5.11}O_{15}$, elastic and piezoelec. props. 79−15403
$K_2Mn_2(SO_4)_3$, elastic props. using piezoelec. reson. and US vel. meas. 80−15180
$KNbO_3$, piezoelec. and electrostrictive coeffs. 77−85653
$KTaO_3$, electromech. props. and electron tunnelling 78−23403
$KTaO_3$, nonpiezoelec. dielec., light-sensitive Rayleigh wave generation by surface piezoelectricity 78−43228
$3La(IO_3)_3.HIO_3.7H_2O$, pyroelec. p_3 and piezoelec. d_{33} coeffs. 79−19840
(Li,Na)NbO_3, polycryst. disc, temp. and time dependent dielec. props. 77−81060
$LiClO_4.3H_2O$, pyroelec. and piezoelec. coeffs., struct. refinement 78−18602
LiF, charged dislocations, comprehensive deform. effects on charge, elec. field 79−14815
LiF, compressed crystals, inhomogeneous elec. field due to piezoelectric effect 80−55044
Li_2GeO_3, acoustic props., intrinsic piezoeffect, US absorpt. coeffs. *(Russian)* 80−29692
Li_2GeO_3, components of elastic, piezoelec. and permittivity tensors meas. 77−8518
Li_2GeO_3, pure, and Si- and Mg-doped, impurity effects on elastic and piezoelec. props. 79−47388
$Li_{1-x}H_xIO_3$, piezoelectric props., space charge effects 78−6637
$LiNbO_3$ piezoelectric plate, direct and indirect elastic wave excitation *(Russian)* 80−34858

piezoelectricity continued
$LiNbO_3$, polydomain, nonstoichiometric crysts., elastic, piezoelec., dielec. constants. 77−8513
$LiNbO_3$, X-ray determ. of piezoelec. coeff. 77−8511
lithium ammonium tartrate monohydrate ferroelastic phase transition *(Japanese)* 79−77747
$(NH_4)_2BeF_4$, elastic compliance, US attenuation and piezo-coeffis., 170 and 190K 79−51918
NH_4Cl, piezoelec. effect near nonferroelastic phase transition 80−66116
$NH_4H_2PO_4$ crystal, ferroelectricity, spontaneous polarisation obs. 79−28687
$Na_9(Al_6Si_6O_{24})(OH)_2.6H_2O$, hydrosodalite, ferroelec. transition, pyro- and piezoelec. activity 79−15421
NaCl, electric field induced by homogeneous stresses 80−11343
NaCl, piezoelectric effect 79−69779
NaCl, uniform deformation and birefringence in nonuniform elec. field *(Russian)* 79−87396
Na_2CoGeO_4, single cryst. growth and study of their piezoelec. and elastic props. 79−4906
$Na(H_3O)[I(OH)_3O_3]$, piezoelec. and pyroelec. ionic displacements 79−38456
$NaND_4SeO_4.2D_2O$, nonlinear electromechanical props. above Curie temp. 79−33610
$NaNO_2$, band struct., polarisation and piezoelec. consts. calc. 78−52448
$Ni_3B_7O_{13}I$, shear modulus anomalous temp. depend. 78−43061
PLZT ferroelec. ceramics, piezoelec. props. 79−42897
$Pb_5Ge_3O_{11}$ bonded $Pb(Zr,Ti)O_3$ composites, piezoelec. props. 79−78629
$PbNb_{0.5}Sc_{0.5}O_3$, ceramic, dielec. props. 79−11392
$Pb_{0.94}Sr_{0.06}(Ti_{0.47}Zr_{0.53})O_3$-NiO, modified, dielec. and piezoelec. props. 80−11342
$PbTiO_3$ single crystals, dielectric permittivity meas., piezoelectric dispersion 79−99817
$PbTiO_3$-$PbZrO_3$-$PbNb_{2/2}Zn_{1/3}O_3$(-$PbNb_{2/3}Co(Mg)_{1/3}O_3$) solid solutions, dielec. and piezoelec. props. 79−87393
$PbTiO_3$-$Pb(Fe_{1/2}Nb_{1/2})O_3$ based modified ceramics, struct. and elec. props. 79−87392
$PbTiO_3$-$Pb(Fe_{1/2}Nb_{1/2})O_3$-$PbZrO_3$, with additions, exam. of electrical characteristics 80−2698
$PbTi_xZr_{1-x}O_3$, ferroelec., electric field depend. of contour mode reson. 77−12351
$Pb(Zr,Ti,Nb)O_3$ ceramics, rel. dielec. const. and piezoelec. props. rel. to porosity 79−11388
$Pb(Zr,Ti,Sn)O_3$ ceramics, ferroelec., doped with tri- and pentavalent oxides, piezoelectric props. 78−19413
$Pb(Zr,Ti)O_3$ ceramics, low field depoling charact. 77−8492
$Pb(Zr,Ti)O_3$, ceramic, axially loaded, nature of elec. field and resulting voltage 78−72468
$Pb(Zr,Ti)O_3$ ceramic/polymer, composite systems, piezoelec. props. 79−99823
$Pb(Zr,Ti)O_3$ ceramics, space charge field meas. by ferroelec. domain switching current, piezoelec. reson. freq. ageing charact. 80−7296
$Pb(Zr,Ti)O_3$ ceramic, interconnected porous, props. 80−43579
$Pb(Zr,Ti)O_3$ ceramics with ladder type struct., prep. and props. 80−75945
$Pb(Zr,Ti)O_3$, excitation of mechanical vibr. by ionising radiation beams 77−24799
$Pb(Zr,Ti)O_3$, internally electroded with Pt, resonance behaviour 80−84701
$Pb(Zr,Ti)O_3$, piezoceramic, nonlinear piezoeffect 79−42900
$Pb(Zr,Ti)O_3$, piezoelectric bimorph, quasistatic response exam. 78−43794
$Pb(Zr,Ti)O_3$, shock wave compressed, dielec. props. 77−48139
$Pb(Zr, Ti)O_3$-epoxy resin composite piezoelec. relax. due to ionic cond. 77−36179
$RbH_3(SeO_3)_2$, crystal lattice monoclinic distortion determ. by phase transition from elec. meas. results 79−73887
$RbH_3(SeO_3)_2$, piezoelectric effect, near nonintrinsic ferroelectric phase transition 78−2815
SbSI, absorption edge, elec. field effect rel. to ferroelec. props. 80−97240
Se, elastic and piezoelec. consts., US phase vel. meas. 79−86834
SiO_2, and $SiO_{0.7}$, amorphous sputtered thin film, US anomalies, 0.5-300K 80−34145
SiO_2 film, thermally grown or sputtered, electrostriction and piezoelectricity 77−12010
$Sr_{0.5}Ba_{0.5}Nb_2O_6$ crystals, ferroelec., dislocation free, pyroelec. props. 79−42907
$Sr_{0.5}Ba_{0.5}Nb_2O_6$, ferroelec., primary pyroelectricity 77−63371
$Sr_{0.61}Ba_{0.39}Nb_2O_6$, electromechanical props., permittivity, elastic compliance, piezoelectric moduli 80−29691
$Sr_2MTa_5O_{15}$ (M = K, Rb, Tl, Cs), relative stability of struct. types, and piezoelec. props. *(French)* 80−49206
$Sr_4NaLiNb_{10}O_{30}$, electro-optic, pyroelec., dielec. and piezoelec. props. *(Chinese)* 79−69810
$Tb_2(MoO_4)_3$, nonlinear piezoelec. coeffs. near phase transition 79−95710
Te, elastic and piezoelec. consts., US phase vel. meas. 79−86834
Te, piezo-Hall effect from 4.2 to 77K 77−76848
Te, piezoelectrical free-carrier scatt. by screw dislocations, Hall effect and cond. meas. 80−24926
TeO_2 piezoelec. powder, orientation depend. of memory echo 78−35094
$Th(CO_3)_5^{6-}$, in Na and guanidinium salts, struct./props. correlation *(French)* 78−95032
Ti_2O_3, piezoresistivity and semiconductor-semimetal transition 79−42595
ZnO, chemisorption of O_2, charge transfer obs. by surface piezoelec. effect 77−89824
ZnO, elastic, piezoelec. and dielec. props. 80−108157
ZnO, piezoelec. films produced by gas transport reaction, US excitation efficiency 80−2700
ZnO, piezoelec. powder, dynamic polarisation echoes 78−52443
ZnS-MgS, exam. of piezoelectric props. and elastic compliances, as function of MgS conc. 79−95709

piezoreflectance
anthracene, single cryst., piezomodulated reflection spectra 79−61392
cholesteryl myristate, press. depend. of cholesteric pitch near cholesteric-smectic A phase transition 77−68918
cholesteryl oleyl carbonate, press. depend. of cholesteric pitch near cholesteric-smectic A phase transition 77−68918
graphite, magnetoreflection under press., Landau level transitions 80−50303

piezoreflectance continued
graphite, magnetoreflectivity in high fields under press., energy band parameters 79−61346
graphite, piezoreflectivity, 3 to 6 eV 79−47472
III-V semiconductors, conduction-band struct. from reflectivity meas. when subject to mechanical strain 79−42449
semiconductor energy gap measurement, piezo-reflection-retrotransmission technique *(French)* 77−28545
tetracene single crystals, Davydov splitting, press. depend., phase transition obs. 78−27250
transition metal dichalcogenides, modulation spectroscopy obs. 78−80377
zincblende-type crystals, electromodulation, piezomodulation, theory 80−93281
Bi, magnetoreflectivity in high fields under press., energy band parameters 79−61346
$CdCr_2Se_4$, modulated piezoreflection spectra 80−97237
CdTe, luminescence and reflect. investig. of excitons, stress and Zeeman splitting 77−40281
CuBr, piezo-optical effects on excitons, importance of k-linear terms 79−95802
GaAs Schottky-barrier, linear and quadratic electroreflectance, minicomputer-controlled meas. 80−97241
$GaAs_{1-x}P_x$-GaP heterostructure, photomodulation spectroscopic exam. 77−40257
$Ga_xIn_{1-x}P$, band struct. enhancement of indirect transitions, piezoreflectance meas. 77−20823
GaSb, piezoresistive vibrating circular membrane, reflectance light modulation 80−97232
Ge, at E_1 and $E_1+\Delta_1$ edges, high mag. field 77−77245
Ge, piezoresistive vibrating circular membrane, reflectance light modulation 80−97232
InP:Bi, uniaxial stress effect on free and Bi-bound excitons 79−56854
n-InSb, conduction-band struct. from reflectivity meas. when subject to mechanical strain 79−42450
$MoS_2(Se_2)$, effect of uniaxial stress on excitonic optical spectra 78−84606
$Sm_{1-x}La_xS$, press.-induced semicond.-metal transition, refl. and lattice compression meas. 77−62826
$Sm_{1-x}Y_xS$, press.-induced semicond.-metal transition, refl. and lattice compression meas. 77−62826
Te, trigonal, electronic and optical props., press. depend., self consistent pseudopotential formalism 79−65838
TlBr, piezoreflectance of first exciton band obs. 78−64347
TlCl, piezoreflectance of first exciton band obs. 78−64347
TlCl, piezoreflectance spectra of first exciton band 77−12357
$WS_2(Se_2)$, effect of uniaxial stress on excitonic optical spectra 78−84606
ZnTe films, internal stress effect on fund. refl. spectra 80−60701

piezoresistance
anisotropy of hopping conduction, percolation theory 78−72156
anthracene, excess electron and excess hole cryst., band struct., drift and Hall mobilities, depend. on press. 79−60709
diamond indentor-anvil system, resist.-vs-press. relations 79−77681
diffused Si pressure transducer, stress conc. at transverse gauges 78−12711
diffusion layers, piezoresist. coefficient determ. allowing for two-dimens. impurity distribution *(Russian)* 78−6374
hexagonal metals, deformed, resistivity changes calcs. 80−44564
III-V semiconductor, anisotropic carrier mobility due to dislocations 78−60124
III-V semiconductor, local resist. near dislocations, eqns. 78−60123
III-V semiconductors, conduction-band struct. from reflectivity meas. when subject to mechanical strain 79−42449
III-V semiconductors, stress-induced elec. props. of point defects, piezoresistance effect 79−56726
III-V semiconductors transport parameters, review 79−19587
inhomogeneous strain field scatt. deform. potential, theory 77−35905
n-InSb, anomalous Hall effect, stress depend. 80−65598
Manganin stress gauges, technique for calibrating effect of resistive hysteresis on dynamic piezoresistive coeff. 79−54118
metal films, strain coeffs. of resist., size effect 79−42673
metal-GaAs(GaP), Schottky barrier diodes, elec. props. under mech. stress 80−11087
metallic film, strain coeffs. of resist., deduced from effective Fuchs-Sondheimer model and relax. time model 79−78222
metallic film, strain coeffs. of resist., general Fuchs-Sondheimer expressions 78−52107
metallic glasses, elec. resist., press. depend. 80−96841
minerals, up to 60 kbar *(German)* 80−31032
MOSFET, piezoresistivity effects and use as press. transducers 80−4695
piezoelectric crystals piezoresist. of grain boundaries 78−51995
plastically deformed compound semiconductors, electronic transport and opt. props. of dislocations 80−80212
polyacetylene, pristine and doped, press. effects on resist. 80−103698
polyethylene films, low density, γ-irrad., elec. cond., effect of elongation 79−4564
potassium acetylacetonate, polycryst., elec. cond., pyroelectricity, phase transition, UV spectrum 78−76392
Schottky-barrier structs., surface barrier current instability, uniaxial crystal compression 80−20310
semiconductor, anisotropic conductivity and ambipolar drift noise 77−20375
semiconductor, carrier capture cross section by attractive Coulomb centres, piezoelec. scatt. 78−72170
semiconductor, low-symmetry, modelling of elec. props. 78−19036
semiconductor, piezogalvanomagnetic effects measurement at low temps., apparatus with stabilised dynamic load 77−67458
semiconductor, piezoresistive, vibrating membrane, current amplification 78−75025
semiconductor piezogalvanomagnetic effects at low temp., meas. installation 77−41625
shock compression of solids, review 80−24534
Si:B, isolated A^+ states under high compressive stress, long wavelength photocond. spectra 79−60765
n-SiC, 6H and 15R polytypes, (0001) plane, influence of uniaxial mechanical stress on resist. anomaly 78−10445
strain gauges, biaxial gauge factors 80−52185
TCNQ ion-radical salts, strain sensitivity 79−65461
thermal strains, effect of support, theory 80−88647
TTF-TCNQ, elec. cond., role of librations 79−19580

piezoresistance continued
TTF-TCNQ, metallic cond. press. depend., single particle phonon scatt. description 79−69503
TTF-TCNQ, metallic conductivity press. depend. thermal expansion effects 79−69502
TTF-TCNQ complex salt press. dependence elec. cond. at low temps. *(Japanese)* 79−87090
n-$AgInSe_2$, press.-induced compensation, resist. expts. 78−30919
Ag_2Te, liq., elec. cond. at high temps. and pressures 79−11119
Al, resistivity, press. depend., calc. 80−20151
n-$Al_xGa_{1-x}As$ epitaxial films, elec. cond. press. depend. 79−56337
Au, effect of press. on resistivity 78−79978
Au-CdS Schottky diode, elec. props. under stress 79−15222
Au-Cr Kondo alloy, effect of press. on resistivity 78−79978
Au-GaP Schottky diode, elec. props. under stress 79−15222
B, β-rhombohedral, elec. cond. due to uniaxial press. pulse 78−39110
Ba I-Ba II phase boundary, Ba I fusion curve peak at high press. *(Russian)* 80−2165
Bi whiskers, elec. resist. under strain *(Russian)* 79−91164
Bi whiskers, electron transition on simple extension, elec. resist. and magnetoresist. meas. *(Russian)* 80−29422
$Bi_{1-x}Sb_x$, band inversion under press., Fermi surface anisotropy, galvanomag. meas. 77−51637
$Bi_{2-x}Sb_xTe_3$, solid soln. film on mica substrate, effect of stresses on elec. cond. 78−51859
n-Bi_2Te_3, magnetoresist. under uniaxial stress 77−35956
Bi_2Te_3, Shubnikov-de Haas effect and Hall coeff., high press. effect 77−51767
Bi_2Te_3-Sb_2Te_3 film, cond., galvanomag. Seebeck and Nernst-Ettingshausen effects under press., band model 77−47907
n-$CdGeAs_2$:In(Te), resist. and Hall coeff. meas., influence of press. 77−47810
$Cd_xHg_{1-x}Te$, electron mobility and conc. near gapless state, influence of hydrostatic press. 79−65486
$Cd_xHg_{1-x}Te$, low temp. piezoresistance, Hall effect, elec. cond., plastic flow 80−6844
$Cd_xHg_{1-x}Te$, uniaxially compressed, deform. effects, elec. resist. 78−39114
CdS, even acoustoelec. current due to Lamb waves, freq. depend. 80−20256
CdS, plastically deformed cryst. with dislocation slip band, residual cond. 80−6839
Ce, TCR up to 15 kbar *(French)* 79−95383
CoS_2, narrow-band ferromag., high press. effect on anomalous elec. resist. 80−70698
Cr-Co (4.0 at.%) alloy, antiferromag., disappearance of resist. min. under press., and press. coeff. of T_N 80−10960
Cr-Fe (0.6 at.%), antiferromag., anomalous press. effect on resist. minimum 79−15138
Cr-V-Fe alloy, resistivity minimum, press. effect 79−38043
$CrAs_{0.42}Sb_{0.58}$, mag. and struct. transitions under press., elec. resist. meas. 78−27038
Cu, electrical resistivity, linear strain effect at elevated temps. 79−91022
Cu film, strain coeff. of resist., film thickness and grain size depend. 77−55620
Cu-Mn alloy, manganin, hysteresis-corrected calibration under shock loading 80−74818
CuCl powder compacts, DC voltage depend. resist. under press. 80−80334
Cu_2S, electromechanical props. *(Russian)* 79−11117
$Cu_{40}Zr_{60}$, amorphous alloys, supercond. transition temp., press. depend. 80−84524
EuB_6, electrical transport under press. 79−87101
EuB_6, resist., Hall effect, and magnetoresist. under hydrostatic press., 4.2 to 300K 80−96879
$Eu_{1-x}^{2+}Eu_x^{3+}N_xO_{1-x}$, resist., pressure depend., semicond.-metal transition obs. 79−78104
$Eu_{1-x}^{2+}Nd_x^{3+}N_xO_{1-x}$, resist., pressure depend., semicond.-metal transition obs. 79−78104
EuO, hydrostatic press. effects on elec. resist. in temp. range 3 to 300K 79−23968
EuO, magnetic semiconductor, piezoresistance effect, 4.2 to 300K 80−34450
EuO, transmission and resistivity, stress modulation effect near Curie temperature 80−96874
EuO:Gd, elec. cond. under hydrostatic press., Curie temp. 80−96881
$Eu_{0.98}Sm_{0.02}O$, ferromag. semicond., elec. cond. meas. 80 to 370K, press. effect to 20 kbar 77−51751
$Fe_{0.2}Co_{0.8}S_2$, narrow-band ferromag., high press. effect on anomalous elec. resist. 80−70698
α-Fe_2O_3, elec. resist. and phase transition under shock compression 80−72496
Fe_2O_3, hematite crystal, press. depend. of elec. resistivity and contacts 79−65476
Fe_2SiO_4, elec. cond. under defined thermodynamic activities, up to 20 kbar, 340-1100°C 80−6832
Fe_2SiO_4, fayalite, elec. cond. obs. under shock compression 80−81873
n-GaAS, plastic deform. effect on elec. props. 77−28178
GaAs, elec. effects of dislocations 79−82586
GaAs, electron irrad. induced defect levels, hydrostatic press. effect 80−92858
n-GaAs, influence of uniaxial stress on low field resist. 78−87976
GaAs, p-n junction, piezotunnel current *(Russian)* 77−47890
p-GaAs, piezoresistance, relax. time for heavy and light holes determ. 79−19599
GaAs, piezoresistance and conduction band minima 78−51993
GaAs, Schottky barrier diodes, strain sensitivity mechanism 79−38165
p-GaAs, strain sensitivity, piezoresistance *(Russian)* 79−82585
GaAs, three level cond. band struct., uniaxial stress effects, resist. and Gunn effect threshold meas. 77−85137
n-GaAs, transferred electron effects under hydrostatic press. 78−26871
GaP, influence of shear deform. on interband interaction 78−39116
GaP, scatt. mech., mobility tensor 80−6826
n-GaP, uniaxially deformed, piezoresist. exam. of donor levels 77−4346
GaSb, piezoresistive vibrating circular membrane, reflectance light modulation 80−97232
n-GaSb, stress-induced elec. props. of point defects, piezoresistance effect 79−56726
GaTe, transport properties under hydrostatic pressure 80−75589
Ga_2Te_3, liq., elec. resistivity meas. up to 30 kbar 79−38070

piezoresistance continued
P- Ge, acceptor wavefunctions in spherical approx. and piezoresist. 80−29405
Ge, covalent semicond., piezoresistance coeffs. of holes, temp. depend. 77−39847
Ge, deformed at relatively low temps., Hall effect 79−82612
n-Ge, elec. cond., effect of shock waves *(Russian)* 78−87979
Ge, electron mobility in Δ_{1c} minima, temp. depend. 79−65473
p-Ge, hopping transport at high mag. field at uniaxial stress 79−95412
n-Ge, longit. piezoresist., in strong elec. field 78−56147
Ge, low-temp. dislocation cond. mechanism in plastically-deformed pure samples 80−15527
n-Ge, modelling of elec. props. 78−19036
Ge, multivalley struct., helical instability *(Russian)* 79−47101
Ge, oscillistor effect in strong mag. fields, ambipolar drift and breakdown 78−2511
Ge, piezoresistance, energy and momentum relax. of charge carriers 78−47786
n-Ge, piezoresistance under mechanical stress, rel. to cond. band minima 80−6836
n-Ge, piezoresistance with deform. axis symm. rel. to all const. energy ellipsoids 77−55533
Ge, piezoresistive vibrating circular membrane, reflectance light modulation 80−97232
n-Ge, plastic deformation, impurities and dislocations interaction, cond. *(Russian)* 79−47100
Ge, plastically deformed low temp. cond. *(Russian)* 80−6831
Ge, plastically deformed under high temp. creep conditions, elec. props. 80−92915
p-Ge, stretched along ⟨111⟩ axis, bulk negative differential cond. and current oscills., 78K 79−19601
p-Ge, strong uniaxial deform. at low temps., piezoresist. 78−19038
p-Ge, uniaxial compression influence on carrier heating by weak electric field 80−10978
n-Ge, uniaxially deformed, longitudinal magnetoresist. in quantising mag. field 79−15168
n-Ge, uniaxially stretched along [111] axis, negative differential conductance 77−51759
Ge:Al(B), uniaxially stressed, photoionisation of acceptors, impurity photocond. meas. 78−10509
n-Ge:Au piezoresistance in presence of deep levels, stress anisotropy 80−10979
Ge:Cu, press. effect on energy spectrum of carriers, elec. cond. and Hall coeff. expts. 79−23930
Ge:Ga, uniaxially stressed, far IR photocond. meas. 78−10496
Ge:Li-O, donor complex EPR and photoelectron piezoelectric spectra, dynamic tunnelling 79−1711
HMTSF-TNAP, elec. cond. under press. 78−84200
$Hg_{1-x}Cd_xTe$, zero-bandgap state induced by press., galvanomag. props. 77−47725
HgTe, uniaxially compressed, anomalous magnetoresist. and band crossing 79−65501
I, metallic, mol. and monatomic phase, elec. resist. at high press. and low temp. 80−65638
n-InAs, magnetophonon resonance under hydrostatic press. 77−47832
$InAs_{1-x}P_x$, high field instabilities, press. and comp. depends. 78−26873
$In_{1-x}Ga_xAs_yP_{1-y}$, evidence for alloy scatt. from press. induced changes of electron mobility 80−88548
n-InP, high field props. under high press. 78−26872
n-InP, transferred electron effects under hydrostatic press. 78−26871
InP, transferred electron effects under high press. 80−34453
n-InP:Cr, press. depend. of elec. resist. and Cr ionisation energy 80−80281
n-InSb, characts. of Gunn effect 77−55538
InSb, current-voltage characteristics at room temperature and high hydrostatic pressure 80−88560
n-InSb, elec. cond., press. dependence 80−6830
n-InSb, Hall effect and magnetoresist. in extreme quantum limit, stress depend. 80−11021
p-InSb, influence of plastic bending on galvanomag. props. 79−28349
p-InSb, negative magnetoresist. under press. 80−20224
p-InSb, negative piezomagnetoresist. and Hall effect meas., antiferromag. order form. 78−19061
n-InSb, quantum magnetophonon oscills. of piezoresist. 77−15880
n-InSb, undoped, press. induced slow relax. of free electron conc., Hall coeff. meas. 77−47833
p-InSb, uniaxially deformed, mag. field induced semicond.-metal transition 79−95457
InSb:Cr, press. effects on transport props. 78−56146
InSb:Ge, uniaxially compressed, anisotropy of elec. props. 78−19035
InSb:S(Se)(Te), reson. states and reson. scatt., elec. props. 80−49738
InSb:Te, anomalous anisotropy of magnetoresist. and g-factor 77−47831
n-In_2Se, influence of hydrostatic press. on elec. cond. and Hall coeff. 77−55552
In_4Se_3 layer crystal, three-dimensionalization of transport effects 79−73514
In_2Te_3, liq., elec. resistivity meas. up to 30 kbar 79−38070
K-Rb, dil., calc. of press. depend. of low-temp. transport props. 78−30905
$KTa_{0.7}Nb_{0.3}O_3$, pressure-induced resistance and colour change obs. 80−75608
$MgSiO_3$, elec. cond. under defined thermodynamic activities up to 20 kbar, 340-1100°C 80−6832
$Na_{1.9}V_{12}O_{29.7}$, press. depend. of elec. cond., semicond.-metal phase transition obs. 78−64072
$NbCl_4$, high press. elec. resistivity 80−29404
NbO, high press. elec. resistivity, semiconductor to semiconductor transition 80−29404
NbO_2, high press. elec. resistivity, phase transition 80−29404
$NbSe_3$, Fermi surface, press. effects, Shubnikov-de Haas effect meas. at 1.5K 80−20068
Ni-Y, amorphous, elec. resist., press. depend. 80−96841
Ni_2SiO_2, elec. cond. under defined thermodynamics activities, up to 20 kbar, 340-1100°C 80−6832
$Pb_{1-x}Ge_xTe$:Ga, influence of hydrostatic compression on elec. props. 79−73516
PbO_2 compressed powder magnetoresistance and apparent carrier mobility 80−35669
n-PbSe, pressure induced transition to gapless state 78−2533
$Pb_{1-x}Sn_xSe$, band struct. and transport props., hydrostatic press. effects 80−15452

piezoresistance continued
n-$Pb_{1-x}Sn_xSe$, single crysts. and diodes, elec. props. under high press. 77−47809
$Pb_{0.82}Sn_{0.18}Te$, film, effect of hydrostatic pressure on props. 80−70862
$Pb_{0.82}Sn_{0.18}Te$ films, piezoresist. effect 79−38197
$Pb_{1-x}Sn_xTe$ film n- and p-type 78−6465
p-$Pb_{1-x}Sn_xTe$ piezoresistance, temp. and conc. depend. *(Russian)* 79−1601
p-$Pb_{1-x}Sn_xTe$, single crysts. and diodes, elec. props. under high press. 77−47809
$Pb_{1-x}Sn_xTe$:In, carrier spectroscopic g-factors, magnetoresistance, temp. depend. 80−6705
Pd complex, tetrabenzo tetra-azacyclohexadecine, I_2 oxidation product, synthesis and characterization 79−47900
Pd film on Melinex, resistance-strain behaviour, island struct. effects 77−55621
Pd_2F_6, evidence of an electronic transition under high press. *(French)* 79−42596
$Pd_{82-x}V_xSi_{18}$, metallic glasses, effect of press. on elec. resist. 80−6805
$Pd_{30}Zr_{70}$, amorphous alloys, supercond. transition temp., press. depend. 80−84524
S, dielectric to metal transition at ultrahigh dynamic press. *(Russian)* 79−60881
$(SN)_x$, tensile and piezoresist. expts. 78−15447
$(SN)_x$, uniaxial stress effect on room temp. elec. cond. 77−39826
Sb, carrier density at press. up to 80 kbar, magnetoresist. and Hall effect obs. 79−73534
Sb, current carrier concentration charge, under pressure *(Russian)* 79−7824
Si (100) inversion layers, effective masses, Shubnikov-de Haas oscills. under mechanical stress 77−43625
n-Si, deform. pot. shear const. determ. 77−15763
n-Si, drag thermoelec. power, anisotropy parameter determ., piezoresist. meas. 80−20235
Si, heat treated, spin-depend. recomb. at dislocations 79−47122
n-Si, influence of deform. on capture of electrons by divacancies 77−1449
Si inversion layer, press. depend. of struct. of field effect mobility 78−60216
n-Si, inversion layers, many-valley electron-phonon interactions, piezoresistance, anisotropic cond., Shubnikov-de Haas oscillations 78−52096
Si inversion layers, piezoresistance 77−35935
Si inversion layers, stress and intersubband correlation 78−60227
Si, multivalley struct., helical instability *(Russian)* 79−47101
n-Si, piezoresist. effect, influence of temp. and impurity conc. *(German)* 77−62924
n-Si, piezoresist. rel. to piezothermoelec. power, electron-phonon drag region 80−70737
Si, piezoresistance, energy and momentum relax. of charge carriers 78−47786
Si piezoresistive coefficient calc. and meas. *(German)* 80−39571
n-Si, plastically deformed, donor action of dislocations, elec. props. 79−11126
Si, plastically deformed, spin-depend. charge transport 80−6895
n-Si, quadratic piezoresistance, ang. depend. *(Russian)* 78−47782
n-Si, shear deformed, Smith-Herring and mobility change piezoresistance 80−6842
n-Si, surface quantum oscills. in inversion layers under uniaxial press. 78−88041
n-Si, uniaxially deformed, intervalley scatt., 78-300K 77−20330
Si:B, piezothermoelec. power 78−56173
Si:B, polycryst. film, piezoresistive gauge factor 77−12029
p-Si:B, reduction of vibration noise, suitable orientation of element, rel. to crystallographic axes 79−11123
p-Si:B, total piezoresist. tensor, 20 to 300K 78−19037
Si:Li, strongly doped, gas-liq. type transition 77−43600
n-Si:P, piezoresist. under strong uniaxial elastic deform. 77−15858
n-Si:P, piezothermoelec. power in electron-phonon drag region, anisotropy 80−70738
Si:P dislocation p-n junctions, capacitive props. 80−20300
p-Si:P implanted films, piezoresist. stress tensors, ion dose depend., −80 to 120°C 80−100538
n-Si:P(Sb)(As), characts. of piezoresist. 77−51750
n-Si:Zn,P, local deform. of cryst. lattice, charact. parameters or recomb. waves 77−4386
n-Si-Ag Schottky barrier diodes, excess current mechanism under uniaxial press. 78−91771
SiC (6H), space group determ. 78−2090
n-SiC, cubic, piezoresistance meas. under hydrostatic compression 77−4344
n-SiC, polytypes, temp. depend. of piezoresist. constants 79−11125
SiC polytypes deformed, resist. anisotropy in (0001) plane 80−20198
α-SiC:B(Be)(Ga), piezoresist. rel. to acceptor levels 78−60129
Si(100) inversion layers, magnetoelec. and piezoresist. evidence for mobility domains 77−4447
SmS, crit. point for isostructural black to metallic phase transition, thermoelec. power meas. 78−60174
SmS, semiconducting, piezoresistance at 80K 80−59990
Sn_2S_3, resistivity, Mossbauer spectra, press. effects 79−73862
TaN film, press. depend. of elec. props. appl. to press. meas. 79−78241
Te, liq., elec. resistivity meas. up to 30 kbar 79−38070
Te, thin film, deformation sensitivity coeff. 79−95524
Te, two types of carriers 80−60013
Te, undoped, elec. cond., magnetoresist. and Hall meas., hydrostatic press. effect 77−47830
Te:Sb, impurity states and impurity conduction, hydrostatic pressure 80−39521
Ti, polycrystal, discontinuous electrical resistivity, low temp. active straining *(Russian)* 80−103666
Ti_2O_3, semicond., effect of stress on elec. resist. 78−34832
TiS_2, elect. resist. at room temp., press. depend. to 80 kbar 80−49730
TiS_2, transport props. under press. 79−95410
$TiSe_2$, CDW transition temp. and transport props. pressure depend. 79−99550
$TiSe_2$, transport props. under press. 79−95410
p-TlInSe, piezoresist. effect 77−35942
Tl_2Te, liq., elec. resistivity meas. up to 30 kbar 79−38070
TmSe, elec. resist. under press. at very low temp. 80−96878
U_3P_4, press. effects on elec. resist. and Curie temp. 80−75559
VSe_2, press. depend. of CDW transitions, role of Coulomb correlations, elec. props. 78−87927

piezoresistance continued
Yb foil gauge, lateral compressive stresses meas. in shock-loaded PMMA 80−103007
Yb stress transducer, piezoresistive effects 77−68539
Zn, $2^1/_2$ order phase transition, magnetoresist. anisotropy change under stress *(Russian)* 77−62907
ZnS, plastically deformed, anisotropic cond. 78−56143
ZnSe, dislocation motion, influence on elec. cond. 79−15149

piezoresistive devices *see piezoelectric devices*

piles (nuclear fission) *see fission reactors*

pinch effect
θ-pinch, electron temp. meas. by Thompson scatt. with ruby laser *(Chinese)* 79−37552
θ-pinch, with axial current-carrying rod, light scatt. diagnostics *(Russian)* 77−11395
θ-pinch energy loss, electron temp. meas. by Thomson laser scatt. *(Chinese)* 80−54028
θ-pinch plasma with antiparallel trapped mag. field axial behaviour 79−41857
accelerator, coaxial with external mag. field, rot. and pinch 77−7603
anomalous transport processes in radially compressed reversed-field configurations, numerical simulation 80−64689
arc plasma processes, appl. of mag. pinch force 77−15258
belt pinch, diffusion processes, impurity and neutral gas effects, 3-fluid model 77−24057
belt pinch, equilib. and stability, theory and expt. 77−43042
belt pinch, high-β plasma with impurities and neutrals, transport 77−11317
belt pinch, high-temp. plasma stability 77−24161
belt pinch, MHD stability, numerical anal. 77−43049
belt pinch, MV shock compression and millisecond confinement 77−24165
belt pinch, numerical computation, diffuse equilib. config. 78−30471
belt pinch, shock compression in toroidal geometry 78−67399
belt pinch, shock heated weakly compressed high-temp. plasma 77−24164
belt pinch, stable equilib. form., initial conditions effects 77−24163
belt pinch, strongly elongated, free-boundary MHD equilib. 78−5912
belt pinch, temp. and density meas. by Thomson scatt. 77−27734
belt pinch, TENQ, energy confinement, beta limit 77−43033
belt pinch IIa, energy confinement, MHD stability 77−43029
belt pinch IIa, high-β Tokamak equilib., stability and transport 79−10690
Belt Pinch IIa, transport phenomena, density profiles 80−24219
belt pinch plasma, electron density profile, multichannel laser scatt. diagnostics 77−31514
belt pinches, transport and radiation studies 80−28798
belt shaped screw pinch, reactor design study 80−13857
Bennett pinch, reverse B_z pinch, MHD stability 77−11384
beta pinch shock heating of toroidal collisionless plasma 77−76138
collisionless flow and end loss from a high-energy theta-pinch plasma 80−92365
Columbia Torus-1 belt pinch high beta toroidal device, preionisation, optimisation 80−92368
compact reverse-field pinch for small demonstration fusion reactor 80−95413
continuous flow pinch, model and computer simulation 77−80343
continuous flow pinch, single-fluid one-dimensional radial compression theory 77−3975
cylindrical foil in air, elec. explosion, high current shunt pinch props. 79−64950
dense pinch, electron-positron pair production in EM field *(Russian)* 80−100092
diffuse, equilib. density and mag. field profiles determ. using magnetoacoustic oscills. 80−48986
diffuse, magnetohydrostatic equilibria, circ. cylindrical, internal modes stability 80−43957
diffuse linear pinch, dispersion differential eqn. in MHD, approx. 80−64694
diffuse pinch, electrothermal stability anal. of fully ionised plasma 80−43901
diffuse pinch, energy equilib., classical scalar cond. and neo-classical models 80−24208
diffuse pinch, energy equilibria and plasma-wall boundary condition 79−1321
diffuse pinch, field reversal, model 77−58886
diffuse pinch, tearing mode stable configuration 78−63578
diffuse theta-pinch, ion temp. meas. *(Japanese)* 80−87951
diodes, relativistic, time depend. ion and pinched electron flow 77−89330
double-theta pinch, numerical computation, diffuse equilib. config. 78−30471
electrode discharge, nonhydrodynamic pinch compression, kinetics and D^+ focusing *(Russian)* 80−38689
electron beam, intense, relativistic, high energy ion collective accel., localised pinch model 78−87460
electron beam diode, pinched relativistic, large ion current meas. 77−31428
electron beam transport, beyond diode, Z-pinch plasma 77−87874
EM field oscillations near plasma focus and Z-pinch *(Russian)* 78−79458
energy spectra of accelerated deuterons in a plasma focus 80−103110
ETA-BETA II, reverse field pinch, expt. tests and performance 80−102312
Eta-Beta II, reverse field pinch toroidal machine, design parameters 80−13851
ETA-BETA II RFP, diffuse pinch, temp. and confinement results 80−74028
ETA-BETA II RFP, vacuum system design and operation 80−95450
fast shock heating, of electrons and ions, in high-voltage belt pinch 77−72462
field reversed pinches, microinstability effect on MHD stability 80−79460
field reversed theta pinch, model for angular rotation 80−37596
finite Larmor radius corrections, calc. technique 79−32764
finite Larmor radius equations in an arbitrary near-theta pinch geometry 78−71523
Fiscatron fusion reactor principle, Z-pinch device using ^{6}LiD 78−78492
focus plasma, pinch column form. and stability 80−96380
fusion plasma experiments, vacuum developments 79−63260
fusion reactor based on θ-pinch with a liner 77−34443

pinch effect continued
fusion reactors, design, and alternative fusion concepts, systems studies 80−27805
Garching belt pinch MHD equilibria, cylindrical slab model 78−34353
Garching Belt-Pinch IIa, effect of q on confinement and stability 80−96384
H-pinch discharge, quasistationary, EM characts. and energy balance, erosion plasma generator 80−19630
H-pinched discharge, low-current, optical, elec. and erosion studies 77−35417
HBTX1A experimental reversed field pinch machine, parameters and layout 80−13850
helical theta pinch, equilib. and stability at low compression ratio 77−43044
helically symmetric plasmas, guiding centre 79−1336
helt pinch, stable 3 dimens. MHD equilib., numerical model anal. 77−27665
high beta pinches, mag. field diffusion, hybrid model calcs. 77−24152
high current RFP devices and the pulsed RFP reactor 80−79556
high velocity plasma fluxes 80−87860
high-beta, hard core, magneto-viscous resistive tearing of cylindrical flux surfaces 80−1831
high-beta collisionless plasma, hybrid kinetic model, equilib. and stability props. 77−24138
high-beta pinch, kinetic behaviour, anomalous transport and unstable MHD modes 77−76163
high-density, post-implosion anomalous transport, lower hybrid drift instability 77−24056
high-density Z-pinch experiment pulse power supply, design and operation 80−70028
hypocycloidal pinch apparatus, dense plasma production diagnostics, high laser beam absorption 77−43051
hypocycloidal pinch laser radn. absorpt., heating appl. 77−27679
implosion heating experiment, Faraday rot. meas. 77−39456
inert gas high-current discharges, Z-pinch dynamic and radiative characts. 80−19631
intense relativistic electron beam focusing with large aspect ratio diodes 77−23610
ion beam, intense, supercompression in collapsing pinch 77−80379
ion energy distribution in plasma focus during second pinch compression 80−75070
ion self-pinch formulae 80−1833
kink instability, hydromagnetic, dynamical shear stabilisation, by nonlinear mode coupling 79−50858
large aspect-ratio terawatt diode with heated and unheated anode, electron and ion current flow 79−10675
laser induced magnetically enhanced reactor, LIME 78−58434
laser irradiated plasma focus, neutron emission *(Japanese)* 78−38538
LASL toroidal reversed-field pinch programme, energy loss meas. 80−23127
Lausanne belt pinch, plasma stability 77−43028
Levitron, crit. tilts calcs. 79−73025
levitron, min.-average-B, analytical model 79−50876
linear pinch plasma, extreme UV spectra of light impurity ions, appl. of grazing incidence spectrometer 80−59276
linear theta pinch Isar II, low compressed high-β stellarator, surface effects 77−76161
linear Z-pinch, outer 2s-shell electron excitation emission of C-, N-, and O-impurity ions 78−22113
linearised Vlasov-fluid model for sharp boundary screw pinch 79−60168
magnetic pinch discharge, superstrong mag. field prod. 79−90444
magnetoacoustic oscillations in a finite-beta current carrying plasma column 80−1771
magnetoacoustic wave, absorpt. in high-beta plasma *(German)* 80−10430
magnetoplasma compressor, operating modes, pinch description 77−84531
Magoya high-beta toroidal θ-pinch STP and CCT, confinement obs. 77−43041
MHD nonlinear mode structure 77−974
MHD pinch, resistive, nonequilib. stability 79−50877
microinstabilities in field reversed Z pinches, persistence of MHD stability 80−87872
micropinch in a high-current diode, review 80−103183
multi-coil mag. probe in plasma diagnostics, reliability assessment 79−55544
multicharged ion heating in Z-pinch, column compression, temp. and density *(Russian)* 80−64754
neo-Z-pinch, mag. fusion appls. 80−103180
non-cylindrical, optimal parameters, anal. and numerical calc. *(Russian)* 78−59644
paramagnetic spheromak formation in a combined zee and theta pinch 80−92372
PIACE-R1, design fabrication and testing 80−92378
pinch-tormac, device using theta pinches and tormac-like end sections 80−24213
pinched beam diode, geometrical focusing of intense ion beams 78−58898
plasma, infinitely conducting, pinch effect, dynamical accumulation towards neutral line of magnetic field 80−83977
plasma focus, Al ion acceleration *(Russian)* 79−77415
plasma focus, electron density distrib., N_2 laser interferometric study, X-ray and neutron emission 78−87479
plasma shell, cylindrical, apparatus for production 80−106948
plasma-pinch configurations, one-dimens. equilibrium-diffusion code 78−75401
plasmatron channel, spatial-temporal pulsations of arc plasma pinch 80−24210
plastic deform after pinch effect *(Russian)* 78−27563
polystyrene microspheres in theta-pinch, ablation rates 78−18436
relativistic electron beam, diode compression 77−24197
relativistic electron beam collective ion acceleration, localised pinch model, simulation 78−9826
relativistic electron beam diode, annular cathode, pinching rot. and reflexing in axial mag. field 78−9860
relativistic electron beam diode, anode scatt. effects on electron pinch radius 77−68877
relativistic electron beam diode, low impedance, pinch profile, X-ray diagnostics 77−24207
relativistic electron beam diode, pinched, particle simulation code and ion current reduction 77−68878
pinch effect continued
relativistic electron beam pinch formation in low impedance diodes 77−72510
resistive MHD instabilities, diffuse pinch configs., numerical study 77−58853
reverse field pinch, Faraday rot. diagnostics for internal mag. field 80−43976
reverse pinch effect cavity pulsed light source for photolysis 78−87114
reverse-field pinch, MHD simulation 78−5920
reversed field, heating, diffusion, stability 77−43036
reversed field, MHD instabilities, diffusion 77−39451
reversed field, TPE-1, stable equilibria 77−43037
reversed field configuration, equilibrium and stability and confinement props. 80−87932
reversed field configuration, with minimum pot. energy, sharp boundary model calcs. 77−24153
reversed field expt. and 3-D numerical and analytical study 77−43035
reversed field high β pinch, analytic models, MHD stability 78−59642
reversed field pinch, ATHENE and EUROPA codes calcs. 77−24151
reversed field pinch, burn stability 78−58467
reversed field pinch, config. evolution 77−24150
reversed field pinch, expt. and comp. studies 80−23128
reversed field pinch, fully programmed or Z-pinch relax., helical kink instability 77−27703
reversed field pinch, high current density operation 79−10692
reversed field pinch, HTBX I, stability 77−24143
reversed field pinch, kink instability, optical and electrical meas. 77−24188
reversed field pinch, MHD turbulence model 77−24144
reversed field pinch, nonlinear saturation of tearing mode 79−73028
reversed field pinch, numerical studies 80−87931
reversed field pinch, reactor burning calcs. 77−23253
reversed field pinch, resistive and MHD instability, unstable central region 77−27704
reversed field pinch, RFX constructional details 80−91277
reversed field pinch, tearing mode MHD eqns., linear and non-linear calc. 77−27705
reversed field pinch, time evolution calcs. using 1-d MHD equilib. and diffusion code 78−30466
reversed field pinch, toroidal equilibria 77−24148
reversed field pinch config. of ETL TPE-1, current fast programming 77−27702
reversed field pinch expt. in small compact torus STP-1 80−75043
reversed field pinch machines, plasma stability anal. 80−24214
reversed field pinch reactor, 600 MWe, plasma physics and reactor parameters 79−71976
reversed field pinch reactor, choice of parameters for 600 MW net electrical output 78−58471
reversed field pinch reactor, physical principles, design, operation and plasma stability 78−58470
reversed field pinch reactor, preliminary engineering design 78−58472
reversed field pinch reactor 78−58433
reversed field pinch toroidal fusion reactor 79−71977
reversed field pinches, bibliography, 1958-75 77−24171
reversed field pinches, mag. field meas. in plasma toroidal systems 80−49004
reversed field pinches, theory and experiments, review 77−24126
reversed ultra fast theta pinch, mag. wave heating of Tokamak 77−35364
reversed-field configuration generated by a rotating relativistic electron beam 78−71524
reversed-field pinch, formation, relaxation and heating studies 80−24215
reversed-field pinch, in STP-1, using new external-field programming, MHD instability 80−28803
reversed-field pinch, numerical computation, diffuse equilib. config. 78−30471
reversed-field pinch burn dynamics, global computer code 78−63579
reversed-field pinch plasma model 80−87935
REXIMPLO expt., quasi-spherical plasma compression 80−79546
RFX field system design 78−54884
rod pinch diodes, intense electron-beam pinch form. and propag., ion generation 79−14589
RTPR, Bondarenko formalism to account for resonance self-shielding effects 77−23300
sausage instability EM fields particle accel. in pinch *(Russian)* 79−7474
screw, SPICA, β-control 77−27709
screw pinch, finite Larmor radius stabilisation, resonant particle effects 80−54020
screw pinch, force free current induction by boundary displacements 79−32796
screw pinch, force-free fields, numerical computation, diffuse equilib. config. 78−30471
screw pinch, gross instability, high-β plasma column motion, feedback stabilisation 77−27699
screw pinch, high-β, perturbation theory on guiding centre plasmas 79−72999
screw pinch, high-β, perturbation theory on spectrum of ideal magneto-hydrodynamic 79−72999
screw pinch, m=1 motion determ. by probes and streak photographs 77−15239
screw pinch, MHD equilib. eqns., rigid-drift assumption soln. 79−60179
screw pinch, reactor design parameters 77−23254
screw pinch, sharp boundary, short wavelength instabilities, Vlasov fluid theory 77−58883
screw pinch, sharp boundary Vlasov fluid model, finite Larmor radius stabilisation 77−58882
screw pinch, sharp boundary Vlasov fluid stability anal. 77−24071
screw pinch, stable 3 dimens. MHD equilib., numerical model anal. 77−27665
screw pinch, time-depend. MHD eqns., numerical solns. 77−24154
screw pinch, toroidal plasma current decay and profile 77−24167
screw pinch, TPE-1a, quasi-steady equilib. 77−43038
screw pinch 'SPICA', equilib. and stability of high-β plasmas 79−98992
screw pinch noncircular discharge, initial phase 77−76179
screw pinch stability, CGL model 77−19743
screw pinches, high density plasma confinement, comparison with high-beta Tokamaks 77−24128
screw pinches, sharp-boundary, m=1 and m=2 instabilities, finite gyroradius effects 77−19748
screw-pinch, equilibrium and stability 80−87934

pinch effect continued
screw-pinch configs., collisionless, hybrid-kinetic stability props. of high-beta plasmas 80−43871
screw-pinch high-β Tokamak, field generation using transverse rotating mag. field 80−19606
Scylla IV-P linear theta-pinch, material end plugging 78−55744
Scyllac, equilibrium and stability, MHD three dimensional soln. 77−24131
Scyllac, MHD flow, numerical computation 77−80282
Scyllac, MHD stability δW calc. correction 77−65856
Scyllac, theta pinch implosion, gross plasma motion model and feedback stabilisation 77−24141
Scyllac equilibria, analytic and numerical studies 77−72474
Scyllac feedback stabilisation 77−24129
Scyllac feedback-sector expt. 77−72473
Scyllac sector feedback stabilisation expt., engng. aspects of on-line operation 77−23268
Scyllac toroidal theta pinch, diagnostics by laser scatt., interferometry and selfluminosity obs. 77−24185
self-pinched beam, with distributed energy, radial expansion 80−19609
sharp boundary pinch kink mode, linearly unstable MHD, nonlinear behaviour 78−67339
sharp boundary Vlasov-fluid screw pinch, free and forced m=0 oscillations 80−38636
sheet pinch, equilib. flow effect on resistive tearing mode 79−1335
signular magnetic field lines and line crossing in pinch layers, space plasma appl. 79−14590
simulation model 78−1884
spheromak formation by theta pinch 80−106962
spheromak plasma config. form. by combined Z- and θ-pinch discharges 80−43955
stabilizing passive shell and active feedback windings in reverse field pinch fusion reactors 80−18666
staged theta pinch, physics and technology problems 77−27696
straight and helical θ-pinches with low compression ratio, wall stabilisation 77−27697
streak mode interferometric study of plasma focus 79−73042
super pinch in thermonucl. microexplosion, gamma-ray laser pumping 80−28186
superpinch implosion, isentropic compression of thermonuclear plasma 78−5032
tearing and reconnection of magnetic fields 79−23446
TERP noncircular toroidal pinch, turbulent heating 77−24162
thermonuclear plasma, pulsed, high-density, neutron diagnostics 79−90462
theta, plasma heating mechanism obs. and analysis *(Japanese)* 80−1818
theta pinch, Alfven wave heating 78−75379
theta pinch, closed, balanced by transverse current *(Russian)* 78−1879
theta pinch, dielectronic recomb. rates of Fe IX, X, XI 78−71525
theta pinch, electron densities from Thomson scatt. and He-Ne laser interferometry 79−86615
theta pinch, end-plugged, energy and particle confinement 79−82088
theta pinch, Fe impurity effective dielectronic recombination rates meas. 80−79570
theta pinch, field reversed, ion beam injection, fusion appl. 79−22476
theta pinch, H plasma, mag. piston study *(Russian)* 80−83971
theta pinch, hot linear, end plugging effect on instability and parameters 80−24223
theta pinch, linear, end losses, stoppering, instabilities and heating 80−24224
theta pinch, linear, end plugging by high mass number plasmas 77−68851
theta pinch, linear, with strong and fast rising mag. field 80−24222
theta pinch, low density, step-like mag. piston 80−103182
theta pinch, low density plasma, microinstabilities 80−79496
theta pinch, mag. pulse penetration, Alfven velocity scaling 80−33803
theta pinch, microinstability and anomalous transport, kinetic and numerical study 77−76162
theta pinch, $N^{+,2+,3+}$ lines Stark broadening, He(II) line diagnostics 80−24249
theta pinch, nonlinear wave propag., soliton form. 79−46442
theta pinch, plasma rot., MHD spectrum of instabilities 78−59582
theta pinch, plugged, thermal end loss 80−1836
theta pinch, radial oscills. of plasma density and mag. field, light scatt. and probe obs. 80−14937
theta pinch, reversed field config. by Z-discharge 79−4168
theta pinch, reversed-field, formation and adiabatic compression in imploding liners 78−30465
theta pinch, rigidly rotating, Vlasov fluid stability 80−28794
theta pinch, rot. instability 78−71522
theta pinch, spark channel quasi-spherical compression, electron temp. 80−87920
theta pinch classical electrodynamics description 79−90436
theta pinch coil, quasi-static potential distributions *(Japanese)* 78−38523
theta pinch coil, quasistatic electric field reduction, using shell with slits *(Japanese)* 78−30474
theta pinch discharge, radial EM energy flow and plasma heating power 80−64747
theta pinch fusion reactor, switching technology for supercond. mag. energy storage system 77−23285
theta pinch implosion dynamics, ionisation rate enhancement by two step process 77−58885
theta pinch implosion heated fusion and fusion-fission reactor linear confinement 77−74983
theta pinch plasma density radial profile measurements using quasiquadrature interferometer 80−70038
theta pinch plasma with no bias field, fluctuating fields, spectroscopic obs. 77−11398
theta pinch pulse rapid heating of Tokamak 77−76132
theta-pinch, 10.6 μm interferometry and Faraday rot. meas. 77−80358
theta-pinch, ablation rates of spherical polystyrene pellets in plasma 77−89265
theta-pinch, axial heat flux limit effects 79−10636
theta-pinch, azimuthal mag. field, relativistic electron runaway, bremsstrahlung diagnostics *(Russian)* 78−9818
theta-pinch, bumpy, finite wavelength stability 77−24146
theta-pinch, bumpy, guiding centre plasma stability 77−24147
theta-pinch, bumpy, wall stabilisation 78−1875
theta-pinch, CO_2 laser beam focused in axial direction 77−76148
pinch effect continued
theta-pinch, collisionless, high-beta, anisotropy-driven EM modes, finite Larmor radius effects 80−1830
theta-pinch, collisionless neutral current layer, ion energy spectrum meas. *(Russian)* 77−68874
theta-pinch, conical, electrodeless injection, dynamics of plasma in longit. mag. field 79−55479
theta-pinch, cool, intense relativistic electron beam interaction 78−51334
theta-pinch, cross-field instabilities, nonlocal anal. 77−24137
theta-pinch, D_2 fill in Scylla IV-P, plasma parameters and end-loss 78−1880
theta-pinch, density, azimuthal mag. field effects, laser interferometric meas. 77−11406
theta-pinch, double, plasma motion 77−11383
theta-pinch, double, stabilised, toroidal plasma production, probe diagnostics 78−63576
theta-pinch, election parallel thermal conductivity, reduction using waves 79−10637
theta-pinch, electron heating in turbulent neutral layer *(Russian)* 80−10361
theta-pinch, end loss, diagnostics 77−89286
theta-pinch, end loss, ideal MHD model 77−47248
theta-pinch, end plugging by pulsed mirrors 79−14602
theta-pinch, end plugs, energy confinement increase 78−51336
theta-pinch, end-loss, reduction with quartz end plugs, Scylla IV-P 77−89292
theta-pinch, fast, axial ion energy distrib., particle and probe diagnostics 78−59655
theta-pinch, fast, double-frame hologram interferometer meas. of density 79−19097
theta-pinch, field-reversal, expts. 78−14196
theta-pinch, groove type drift turbulence, Lagrangian description *(Russian)* 77−72448
theta-pinch, guiding centre plasma stability, press. anisotropy effects 77−1008
theta-pinch, heat propag. across mag. field, magnetothermal waves 77−42999
theta-pinch, helical, with low compression ratio 78−26313
theta-pinch, high β, plasma evolution and thermonuclear yield 77−89287
theta-pinch, high density linear system, fusion power appls. 77−23255
theta-pinch, high-beta plasma discharge, spectroscopic meas. 77−24186
theta-pinch, high-energy, linear, quartz end plug effects 77−76184
theta-pinch, holographic interferometry 77−22591
theta-pinch, hot, linear, end-loss meas. 77−89291
theta-pinch, incomplete preionis. effects 78−83600
theta-pinch, linear, 14 MeV neutron source appls. 77−23332
theta-pinch, linear, end loss reduction by solid and plug 77−89293
theta-pinch, linear, end losses simulated by numerical technique 77−89295
theta-pinch, linear, material end plugging 77−76183
theta-pinch, linear, microinstability onset, anomalous resistivity, electron heating and MHD oscills. 77−27698
theta-pinch, linear, RF oscill. multiple mirror stabilisation and heating 77−89290
theta-pinch, linear, solid end plugs and mag. mirrors, fusion reactor 77−89294
theta-pinch, linear, time-depend. MHD flow eqns., numerical obs. 77−24155
theta-pinch, long wavelength m=1 MHD instability 77−72485
theta-pinch, low-energy, end losses obs. 77−24157
theta-pinch, medium density, large diameter, medium voltage, implosion meas. 77−24140
theta-pinch, MHD, for fixed internal currents, const. press. model 79−41863
theta-pinch, MHD unstable continuous spectrum, noncircular rotating θ pinch 79−94779
theta-pinch, modified bumpy torus, stability 78−83594
theta-pinch, neutral current sheet, electron energy distrib. meas. 80−43954
theta-pinch, nonthermal density fluctuations, laser scatt. diagnostics 78−59679
theta-pinch, Pharos device with end stoppering, homogeneity, stability 78−34360
theta-pinch, plasma rot. during implosion, directional probe obs., model 78−1877
theta-pinch, post-implosion phase, electron temp. and density meas., mag. field profiles 77−31522
theta-pinch, pulsed, ignition in single turn solenoid 79−55538
theta-pinch, pulsed, plasma loss from very short pinch 77−89297
theta-pinch, rapidly rot., equilib. 77−1007
theta-pinch, reverse field expts., equilibrium, confinement, stability 80−28787
theta-pinch, rotating, mechanism, MHD anal. 77−24135
theta-pinch, Scylla I-C, laser beam-plasma interaction 77−24090
theta-pinch, Scyllac toroidal config. theory, review 77−24125
theta-pinch, seeded with high-Z elements, VUV, X-ray and laser holography diagnostics 77−35381
theta-pinch, sheath broadening by lower hybrid drift instability 77−31429
theta-pinch, simulation of lower hybrid drift instability 77−24070
theta-pinch, slit metal vessels for fast discharge, mag. bias fields 78−38520
theta-pinch, small diameter plasma, axial laser heating 78−87467
theta-pinch, spectral line classification of Ar^{n+} ions 79−6896
theta-pinch, staged, implosion heating 77−72473
theta-pinch, striated corona, theory 79−41897
theta-pinch, strong fast growing mag. field, pre-ionisation effects *(Russian)* 80−33800
theta-pinch, toroidal, ion heating, diagnostics 77−62381
theta-pinch, toroidal, sharp boundary dynamical model instabilities, feedback 77−51216
theta-pinch, toroidal multiple mirror field, high-beta, opt. obs. 77−24136
theta-pinch, ultra-fast, mag. field distrib. diagnostics, electron density *(Japanese)* 78−55753
theta-pinch, with closed helical mag. axis, equilib. obs. 77−24158
theta-pinch coil Em field calc. *(Japanese)* 78−9817
theta-pinch device for modelling fusion reactor operation 78−89972
theta-pinch fusion system with liner exploded by thermonuclear neutrons 80−79547
theta-pinch implosion, numerical models including classical and anomalous transport 77−24139

pinch effect continued
theta-pinch implosions, ion refl., hybrid Vlasov-fluid model 77−15229
theta-pinch linear, fusion reactor concept 78−5042
theta-pinch machines, computer modelling 79−10703
theta-pinch machines, linear, computer model of plasma 77−89296
theta-pinch mag. piston-plasma interaction, pot. fine struct. *(Russian)* 78−9798
theta-pinch modelling by hybrid numerical models, turbulence effect 77−31510
theta-pinch plasma, multiple pass CO_2 laser heating, density profile, diagnostics 79−60160
theta-pinch reactor, fast feedback stabilisation 77−23269
theta-pinch reactor, first wall environment 77−30661
theta-pinch Ti ion injection by CO_2 laser, spectroscopic anal. 80−79577
theta-pinches, linear, interconnected 78−47154
thin skin pinch, anisotropic conducting wall effect on instabilities 80−28800
thin-skin pinch, stability, influence of thick conducting liner and superconducting wall, dispersion relation 80−64766
Tokamak plasma, new pinch effect and electron heat loss 79−32798
Tokamaks, transport losses, computer modelling and scaling 80−28612
toroidal belt pinch, dynamics, equilib., heating, numerical simulation 77−24168
toroidal belt pinch, two-dimens. MHD simulation 77−19751
toroidal equilibrium, noncircular sharp boundary plasma pinch form. 77−24166
toroidal equilibrium of reversed field pinch 78−26318
toroidal magnetic field reversal in pinches 78−26319
toroidal magnetic field self reversal 77−27706
toroidal magnetic pumping method, efficiency *(Russian)* 80−10401
toroidal pinch, current reduction and reversal 77−58887
toroidal pinch, dynamic stabilisation by oscill. toroidal field 77−27700
toroidal pinch, radial oscills. damping 78−30476
toroidal pinch discharge, preionisation phase, numerical computation 80−64696
toroidal pinch equil. config., nonlinear operator eqn., optimisation soln. 78−59649
toroidal pinch experiments, using perforated shell-type coil 79−86598
toroidal pinch systems, numerical anal. using programs in FORTRAN-D *(Japanese)* 78−5910
toroidal reverse field pinch, fusion reactor concept 78−5042
toroidal reversed field pinch, lower hybrid drift instability, mag. shear effect 78−67397
toroidal reversed field pinch reactor, engineering desing 80−13856
toroidal reversed field pinches, toroidal effects on force free magnetostatic soln. 78−67391
toroidal reversed-field pinches, current, temp., confinement time scaling 77−43078
toroidal screw pinch, MHD kink instabilities 77−19742
toroidal screw pinch, Spica, current decay, stability 77−43040
toroidal Z-pinch plasmas, drift kinetic equation 78−91147
TRISOPS IV machine, high temp. high press. plasma prod. by vortex ring compression 78−71504
two stage ion heating, plasma injection with theta heating 77−76139
two-stage ion heating obtained in rapid theta-compression expt. 78−22520
two-stage ion heating obtained in rapid theta-compression expt. 78−22521
ultrarelativistic beam anlaysis assuming classical ideal-gas statistics, algorithm 78−63003
vacuum arc, high-current, mag. constriction effects prior to anode vapour release 77−68888
Vlasov equilibria, local Maxwellian velocity distribution 80−87928
X-ray emission in pinched discharges, runaway electron model 79−46497
Z discharge between electrodes, relax., toroidal config. possibility 80−28802
Z discharge relaxation between electrodes 80−75089
Z-pinch, azimuthal mag. field meas. using Faraday rot. 78−9832
Z-pinch, constriction due to radiation losses *(Russian)* 78−30473
Z-pinch, contraction actuated by radiation losses 77−1009
Z-pinch, current sheath struct., mag. probe and numerical model *(Russian)* 78−59645
Z-pinch, dense, strong optical attenuation of ruby laser 77−84520
Z-pinch, dense plasma, Hα line profile, density meas. 80−43987
Z-pinch, fast discharge, plasma target form., laser irrad. 80−38683
Z-pinch, gas puff device, X-ray spectra, plasma form. 79−94816
Z-pinch, gas-embedded, α-heating, deformations and kink instability 77−24149
Z-pinch, HBTX 1, ion temp., total radiated energy 77−27729
Z-pinch, HBTX 1 reversed field, Thomson scatt. diagnostics 77−27730
Z-pinch, high current density generation for electron beam fusion 77−67870
Z-pinch, high current discharge in Xe, heating efficiency 78−47152
Z-pinch, high density, Hβ line spectra 78−18445
Z-pinch, high density, pulse power supply 79−14603
Z-pinch, high density, Schlieren meas. 77−11408
Z-pinch, high plasma density, conceptual fusion reactor 78−5015
Z-pinch, high-density, form. regimes 78−59652
Z-pinch, imploding Al liner, soft X-ray spectroscopy 78−14198
Z-pinch, liner implosion, MHD model calcs. 78−67392
Z-pinch, liner implosion non-adiabatic dynamics, MHD computer simulation 77−84488
Z-pinch, m=1 mode dynamic stabilisation, HF current 77−24142
Z-pinch, mag. field fast recomb. through plane pinch current sheet 80−38695
Z-pinch, noncylindrical, electrode domain, mag. field penetration *(Russian)* 77−11382
Z-pinch, noncylindrical, failure of current envelope and escape of shock wave near metallic surface *(Russian)* 78−55741
Z-pinch, noncylindrical, strongly rotating plasma dynamics 79−77354
Z-pinch, optimum, stability calcs. *(Russian)* 80−106956
Z-pinch, overdense, He plasma, laser-driven hydrodynamic perturbation, shock density struct. 79−77385
Z-pinch, particle orbits, diamag., energy balance, Lawson criterion 78−79454
Z-pinch, plane, mag. field null region parallel current effect *(Russian)* 78−91137
Z-pinch, plasma production, streak, X-ray and vis. photographic obs. 78−38522
Z-pinch, rotating, energy balance *(Russian)* 80−14924
Z-pinch, sausage instability nonlinear evolution 77−19752

pinch effect continued
Z-pinch, stabilised, reversed current effect 80−79539
Z-pinch dense H plasma, emission spectrum thermal equilibrium departure 79−82094
Z-pinch discharge, electron temp. and density variation obs. 78−75426
z-pinch discharge, spectral line shape, high-density effects 79−73038
Z-pinch dynamic evolution, simulation expts. 79−60185
Z-pinch for CO_2 laser pellet simulation expts. 78−55742
Z-pinch gas discharge, Hall effect influence on plasma dynamics 77−51218
Z-pinch high density plasma, EM radiation transmission intensity depend. 79−60145
Z-pinch high density plasma, spectroscopic analysis 79−98980
Z-pinch high density plasma spectroscopic analysis 79−98981
Z-pinch in HBTX-1, large amplitude helical kink instability and field reversal 78−42783
Z-pinch plasma, focused ion beam microinstability, pellet fusion appl. 79−32785
Z-pinch plasma, heating by CO_2 laser beam 78−34348
Z-pinch plasma, interaction with CO_2 laser radiation 80−48919
Z-pinch thermonucl. imploding liner, model calcs. 77−74995
Z-pinch tunnelling instability and finite Langmuir ion radius, MHD anal. *(Russian)* 77−47168
Z-pinch turbulence spectroscopic detection and anal. *(Russian)* 80−100098
Z-pinch type plasma focus, ion accel., numerical study 78−91142
Z-pinch ultradense plasma, density dynamics, interferometric meas. 79−77413
Z-pinches, fast radiating, at medium press., physical features of dynamics *(Russian)* 79−37526
Z-pinches of intense energy density driven by high-voltage storage lines 80−24216
Z-pinches of intense energy-density driven by high voltage storage lines 80−87952
Zeta, reversed field pinch, expt. results 77−27707
ZT-1 reversed field pinch, derated mode MHD stability and diffusion 77−27701
ZT-1 reversed field pinch, ion temp. meas. 77−27728
ZT-40, modelling in G2M diffusion code 80−79557
ZT-40, reverse field pinch engineering prototype 80−102316
ZT-40, toroidal pinch, power supply crowbar transformer, low leakage and high current 80−102322
ZT-40, toroidal Z-pinch, circuit design and plasma simulation 78−54961
ZT-S expt., pitch programming 80−87933
ZT-S reversed field pinch simulations 80−83993
Al laser plasma, high-Z, temp. meas. from bremsstrahlung emission 80−87914
Ar ion laser discharge, current modulation 77−46717
Ar, Z-pinch determ. by intrinsic stimulated emission 78−26311
CO_2 laser system, pulsed, for fusion research 80−58556
DyI_3/CsI/Hg arc, oscillations induced by external mag. field, arc constriction 79−60205
Ge, electron-hole liquid, pinch effect 78−87993
Ge, electron-hole plasma, destruction of pinch channel by longit. mag. field *(Russian)* 77−80802
H Z-pinch plasma, strong optical attenuation, shadowgraph meas. 78−26294
He, ultradense reproducible Z-pinch, for laser-pellet interaction simulation, characterisation 78−30463
He Z-pinch, ionisation and radiation dynamics simulation 78−83606
InSb, pinch effect at room temp. 80−65615
Li wire high energy density exploding plasma, holographic interferometry, self pinching, charge density 79−77436
Si, p-i-n structures, pinch effect expt. obs. 79−90971
Z-pinch, noncylindrical, dynamics and particle accel. mechanism 77−76170
Zn, plastic deform after pinch effect *(Russian)* 78−27563

pincushion distortion *see aberrations*

Piobert lines *see Luder's bands*

pion-baryon interactions
see also pion-baryon scattering; pion-hyperon interactions; pion-nucleon interactions
$\Delta S=0$ baryon-π amplitudes, Melosh transformation 78−12857
$SU(4)_W$ symmetry, dibaryon coupling constants for γ, π and baryon interactions *(Russian)* 80−13329
N$\pi\pi$ system, s-wave final state interactions 80−57638
$\pi C \rightarrow \pi C'$, constraints due to PCAC and charmed-baryon couplings 79−89082
πd interactions at large momentum transfers 77−13972
$\pi d \rightarrow NN$, near threshold, effect of nucleon small components, nucleon pole diag. 77−30423
$\pi^- d \rightarrow d\pi^- \pi^- \pi^+$ at 9 GeV/c, $\pi^- \pi^- \pi^+$ system decay 77−22766
$\pi^- d \rightarrow \gamma nn$, capture rate calc. in impulse approx. 77−82763
$\pi^- d \rightarrow \pi^0 nn$, expt. and theory, $\pi^- d \rightarrow$all branching ratio 77−41858
$\pi\Sigma$ two channel system, Y_0^* (1405) couplings, K-matrix parametrizations 78−21452

pion-baryon scattering
see also pion-baryon interactions; pion-hyperon scattering; pion-nucleon scattering
πd amplitude near ΔN threshold, use of Argand diagrams for distinguishing time and pseudoresonances 79−36097
pion-charmed baryon scatt. and coupling strengths, superconvergence sum rules 80−52532
resonance scattering interaction region, props. of baryon resonances 77−41856
pd forward elastic amplitude in non-overlapping potentials model 78−45943
πd elastic scatt., high energy and large angle, πN amplitude anal., Glauber model 77−30442
πd elastic scatt., relativistic three-body calc. 77−74715
πd scatt. in (3,3) reson. region, relativistic description 77−57558
$\pi^- d \rightarrow \pi^- pn$, 1 GeV/c, reaction 77−57559
$\pi^+ p \rightarrow \pi^+ (\pi N)$ 16 GeV/c diffr. process, Drell-Hiida-Deck model anal. 77−61326

pion decay
σ-model with quarks of π decays and π electromag. form factor 79−22100
decay constant, EM form factor, quark EM self-energy on QCD 80−37242
galactic processes rel. to gamma-ray astronomy *(Polish)* 77−70999

pion decay continued
general relativity, ratio of neutral to charged π decay lifetimes 79−49513
leptonic, radiative corrections 77−38162
mesonic octet decays, chiral QFT description using one loop approx. *(Russian)* 79−63471
QCD, lattice-gauge theory calc. of π and ρ-meson decay consts. 78−74154
quantum field theory with chiral Lagrangian 77−65110
radiative decay amplitude, low-energy expansion, currents, sum rules 80−52509
μ-e universality constraints, implications for SU(2)×U(1) gauge models of π decay 79−9368
$\pi\to e\mu$ and possible violation of e-μ universality 77−2739
$\pi\to e\nu_e\gamma$, isospin-breaking, chiral limit, conserved-vector-current violation, σ model 80−62988
$\pi\to e\nu\gamma$, branching ratio, axial vector form factor determ. 78−74247
$\pi\to e\nu\gamma$, isospin violation in form factor, induced by current quark mass 80−32069
$\pi\to e\nu\gamma$, modified quark loop model, form factors, struct. functions, radiative decay 80−91088
$\pi\to e\nu\gamma$, PCAC and quark model 77−30366
$\pi\to e\nu\gamma$, SU(3)×SU(3) σ-model predictions, comparison with expt. 77−10243
$\pi\to e\nu\gamma$, vector form factor, quark masses and isospin breaking 79−13111
$\pi\to e\nu\gamma$ and SU(3)×SU(3) σ-model 80−78054
$\pi\to l\nu_e\gamma(l\nu_e l'^{+}l'^{-})$ in review of weak-EM decays *(Russian)* 77−2818
$\pi\to l\nu\gamma$, struct. constants of mesons in quark diagram model *(Russian)* 79−30717
$\pi\to\mu\mu$, mesonic wave functions at zero point *(Chinese)* 77−10242
π^0, neutral weak current effect on decay mode Weinberg-Salam model, P-violation contrib. 78−86450
$\pi^0\to 2\gamma$, decay width as signal for nuclear matter phase transition, Primakoff effect 80−86842
$\pi^0\to 2\gamma$, Han-Nambu and SUB quark models, modified, appl. to spin statistics 80−22562
$\pi^0\to 2\gamma$, tensor-trace and triangle anomalies 80−73709
$\pi^0\to 2\gamma$ decay rates from γN amplitudes, N EM polarisabilities 77−18289
$\pi^0\to 2\gamma$ in reaction $\pi^-p\to\omega n$, $\omega\to\pi^0\gamma$, $\pi^0\to 2\gamma$, differential cross sections 79−93464
$\pi^0\to 3\gamma$, C-noninvariant decay, branching ratio upper limit 80−47297
$\pi^0\to 3\gamma$, C-noninvariant decay 78−82203
$\pi^0\to 4\gamma$, upper limit to branching ratio 78−93882
$\pi^0\to 4\gamma$ allowed decay search, branching ratio upper limit 80−47298
π^0 decay, Compton electron scatt., 0.1 to 5.0 GeV 79−397
$\pi^0\to e^+e^-$, branching ratio meas. 78−41538
$\pi^0\to e^+e^-$, decay probabilities in strong electromagnetic field *(Russian)* 79−80825
$\pi^0\to e^+e^-$, decay rate, comparison with unitarity calcs. 78−4853
$\pi^0\to e^+e^-$, form factor slope meas. 78−41537
$\pi^0\to e^+e^-$, neutral-current anal. 78−8658
$\pi^0\to\gamma$Ps, Ps=orthopositronium, π^0 lifetime, O(α) EM correction *(Russian)* 79−45089
$\pi^0\to\gamma e^+e^-$, form factor slope calc., VDM 78−58181
$\pi^0\to\gamma\gamma$, μe universality and μ number nonconservation in rare decays 80−42445
$\pi^0\to\gamma\gamma$, u-d quark mass difference effects, form factors 79−89159
$\pi^0\to\gamma\gamma(\pi^+\pi^-\gamma)$, chiral quark model anal. *(Russian)* 80−105900
$\pi^0\to\nu\bar{\nu}$, neutrino mass test 79−93406
$\pi^0\to x\gamma_1$ in 2x-dimensional space time 80−52510
$\pi^+\to e^+\nu_e\gamma$, decay rate calc. in SU(2)×SU(2) sigma model 78−8659
$\pi^+\to e^+\nu\gamma$, u-d quark mass difference effects, form factors 79−89159
$\pi^+\to e^+\nu\gamma$ calculation using field-current identity *(Chinese)* 77−34149
$\pi^+\to\mu^+\nu$, muon momentum, weak interactions and lepton number conservation 80−42444
$\pi^+\to\mu^+\nu$, μe universality and μ number nonconservation in rare decays 80−42445
$\pi^+\to\mu^+\nu_\mu$, at rest, μ^+ momentum meas. 78−45911
$\pi^+\to\mu^+\nu_\mu$, muon momentum meas. 80−37253
$\pi^\pm$ decay, gauge theory, radiative corrections to μ-e universality 77−10244
$\pi^\pm\to e^\pm\nu$, Higgs bosons, effects on experimental observables, and fermion mass scale 80−32061
$\pi^\pm\to\mu^\pm\nu$, Higgs bosons, effects on experimental observables, and fermion mass scale 80−32061
$\pi^0\to\gamma\gamma$ in $\pi^-p\to\pi^+p\pi^+\pi^-\pi^0$ 4 GeV inclusive interaction 79−54357
π^0 decay in supernova shell, gamma-ray emission 80−101602
$^1H(\pi^-,\gamma\gamma)n$, off-mass shell πN amplitude, $\pi^0\to\gamma\gamma$ amplitude, chiral Lagrangian model 79−93669

pion-hyperon interactions
see also pion-hyperon scattering
No entries

pion-hyperon scattering
see also pion-baryon interactions
compilation of coupling constants and low-energy parameters 79−22159
$\pi\Sigma$ scattering amplitude, sum rules for $\pi\Sigma$ reson. parameters *(Russian)* 79−22137

pion interactions *see lepton-hadron interactions; meson-meson interactions; photon-hadron interactions; pion-baryon interactions; pion-nucleus reactions; pion-pion interactions*

pion-nucleon interactions
see also pion-nucleon scattering; pion-proton interactions
100 GeV/c, multiplicities and pseudorapidity distrib. 78−82241
π^-+nucleus interaction, 50 GeV, pion associative multiplicities anal. *(Russian)* 77−46191
$\pi N\to\rho X$, trajectory data, reson. and scatt. regions, compatibility *(Russian)* 78−8703
σ term in hybrid chiral bag model, PCAC and SU(3)×SU(3) symmetry violation 80−78096
abnormal states of nuclear matter, instability rel. to pion condensation *(Russian)* 78−37302
bound nucleon-pion scatt. at medium energies, impulse approx. 77−23108
charmed meson prod. at 12.4-15.0 GeV/c 77−6176
chiral symmetry and pion condensation, review book contrib. 80−437
compilation of integrated cross sections 79−89187
conference on few body systems and nuclear forces, Graz, Austria (Aug. 1978) 79−67567
Conference on meson-nuclear physics, Houston, USA (Mar. 1979) 79−85489
constituent quark model and production of particles from nuclear targets 80−380
Coulomb corrections, phase shift anal., S-matrix theory, below 300 MeV 79−85325
coupling constant from chiral Lagrangian 77−88001
coupling constant from simultaneous anal. of all invariant amplitudes using rational series 78−58199
cross-sections related by sum rules, pomeron hypothesis, heavy-quark channels and threshold predictions 78−89755
deep inelastic scatt., total cross section unitarity bound 80−37294
deep inelstic pp, πN, eN scatt., lepton-hadron relation, multiparticle prod. phenomena, average multiplicities 78−37247
exotic channels in fragmentation region, early scaling 77−18361
fibre bundles almost complex manifold approach, curvature form 78−12915
field theoretic treatment of pion-nucleus scatt. 78−29505
finite-range effects in the πNN, πNΔ and $\pi\Delta\Delta$ vertices 79−22129
hadron interactions, effective radius quantum number depend., quark sum rules *(Russian)* 80−102062
high energy γ-quanta generation efficiency *(Russian)* 79−45105
higher-twist effects in QCD, deep inelastic scattering and the Drell-Yan process 80−102020
inclusive distribution of longit. velocities in range 20 to 200 GeV *(Russian)* 77−57578
inclusive hadroproduction of μ pairs, 39.5 GeV/c $\pi^\pm$, K^+, p, $\bar{p}$ beams on Cu target 78−62470
inelastic diffraction, unitarity bounds, evaluation including real parts 77−82724
inelastic scatt. in Fermi liquid, nucleon-nucleon interaction effects 80−22862
isoscalar current and mag. moment operators, pion-exchange contrib. 77−67636
low energy calcs. in OPEM 77−54117
low energy interaction, field theoretic approach 79−67602
low energy scattering, one particle exchange model, spin 3/2 particle 78−4873
meson field theory, second quantisation, in linear and angular momentum bases 77−22633
meson-nuclear physics, International Topical Conf. 77−6436
multiperipheral n-particle prod., KNO scaling deviation at high energies *(Russian)* 77−34141
muon pair production with low masses *(Russian)* 79−89212
neutral current, P-violation in nuclear transitions 79−13243
non-perturbative effects, quantum field theory, modified normalisation conditions 80−9089
non-radiative absorption by single nucleon in nuclei, pion condensation 77−42000
nuclear matter, πN effective interaction, pion propagator modification 77−2927
nuclear matter, pion propagator optical pot. Pauli blocking corrections 77−22919
nuclear matter, quasiclassical model of meson condensation *(Russian)* 80−5086
nucleus-π^+ total cross-section, nuclear density and π-N off-shell amplitude effect 77−3050
off-energy-shell continuation of the two-body T-matrix in the presence of resonances 79−67604
one nucleon absorption of slow pions, pion condensate effect *(Russian)* 78−8765
optical potential, slow π in nuclear matter, P-wave screening Lorentz-Lorenz factor *(Russian)* 77−6335
P-wave interaction, effect of non-condensed pions in nuclear medium 79−13237
parity-violating nucleon-pion amplitude in unified gauge-invariant models 77−6070
partial wave anal. in first and second resonance regions below 1.0 GeV/c 77−6145
pseudoscalar and pseudovector coupling to bound Dirac nucleon 78−25073
quark jet multiple production in π-Al collisions 80−9188
s-channel resonance prod. in πN scatt., amplitude zeros in Mandelstam plane 80−73686
s-wave pion-nucleon phase shifts in Pade approximation using ε, ρ, f, N, Δ 79−67603
scattering amplitude in nuclear medium at nuclear matter density 78−29500
separable interactions for πN and $\pi\pi$ scatt., three-body problems 78−78113
solidification of nucleon system, π^0 condensation, πN P-wave interaction 78−54715
SU(2)×SU(2) pion and nucleon field theory, covariant perturbative expansion 77−5983
$d\pi\to pn\pi$, total cross sections 79−85510
$d\pi^\pm\to pn\pi^\pm$, 350 MeV break-up, differential cross sections 79−85509
Δ resonance shifts, simple model 77−82829
$\gamma N\Delta_{33}$ form factors in πN collisions 79−63515
J/Ψ prod., valence- and sea-quark distribs., deep inelastic scatt. and Drell-Yan processes 79−13069
N(1360)Γ<67 resonance, πN channel, dibaryon pp resonance systematics 80−68481
N$\to\Delta$(1232) electromagnetic transition form factor and pion-nucleon dynamics at moderate energies 80−57598
N form factor, isovector, meson field theory, pseudoscalar πN interaction 80−62986
NNπ partial violating amplitude, short distance effects, PCAC 77−57557
N$\pi\to$Nπ and N$\pi\pi$, resonance region $s^{1/2}$=1380-1740 MeV, partial wave anal. 77−61315
N$\pi\to$Nπ*, diffractive process, Pomeron current model 77−87958
N$\pi\to$N$\pi\pi$, isobar model rescattering effects, unitarity corrections 79−71762
N$\pi\pi$ dynamics, medium energy, dispersion relations, isobar expansion for πN 80−4917
N$\pi\pi$ medium energy dynamics from πN, isobar model rescatt. corrections 80−4918
$pd\to\nu\pi d\pi^+\pi^+\pi^-$, 19 GeV/c, two and three pion coherent prod. 79−36095

pion-nucleon interactions continued
pp⇄dπ$^+$, 3.2 GeV, forward scatt. relativistic study, reaction cross-section 79−97633
(π,πN), quasi-elastic scatt., N knockout, coincidence measurement optimum conditions 79−76027
π condensation induced density oscillations, infinite nuclear matter and pions atoms calcs. 78−70476
π double recharging in nuclei with change of strangeness *(Russian)* 79−89332
π resonances, Peierls-Yoccoz projection applied to satellite meson coherent state 79−26345
π-Be, associative production of D^0 mesons, with muons 55 GeV/c *(Russian)* 79−3060
π$^-$-nucleus interactions, 40 GeV/c, multiparticle production 80−5173
π$^\pm$ N 200, 280 GeV on Pt target, γ resonance prod. 79−93460
π$^\pm$(π^0) condensation in nuclear medium, possible coexistence 79−36181
π$^-$+A→p+anything, A=C, Al, Ti, Cu, Cd, Pb, inclusive backward emission of protons, 1.5 to 9.0 GeV *(Russian)* 77−10278
π$^-$+C, 40 GeV/c, secondary particle multiplicity off several nucleons *(Russian)* 78−484
π$^-$+C(Al)(Cu)(Pb)(H), 3.7 Gev/c, incoherent prod. of ρ^0 mesons *(Russian)* 78−33084
π+d→2N in Δ-resonance region, 100-300 MeV *(Russian)* 78−33083
π$^-$+emulsion, 200 GeV/c, charm particle decay due to neutral currents *(Russian)* 79−22146
π$^-$+emulsion nuclei, 50 GeV/c multiplicities of secondary charged particles *(Russian)* 78−46116
π$^-$+nucleus→π$^+$π$^-$π$^-$+nucleus, 8.9, 12.9, 15.1 GeV/c, resonance behaviour of coherently prod. A$_1$, A$_3$ mesons 78−50047
π∓U interaction at 55 GeV/c, search for long lived heavy mesons *(Russian)* 80−5029
π$^-$Be→D^{0}D^{0}X, pair production at 55 GeV/c *(Russian)* 79−3059
πd, 15 GeV, separation of ΔΔ and NN components of d 78−12933
πd, compilation of integrated cross sections 79−89187
πd, nonadiabatic effects in inelastic scatt., Green's function technique *(Russian)* 79−9402
πd→A$_1$d, double scatt. at high energy, unstable particle scatt. amplitude 78−45929
πd elastic scatt.,high energy and large angle, πN amplitude anal., Glauber model 77−30442
πD→pp, generalised Low eqn. approach to reaction matrix 79−85491
π$^-$d, 360 GeV/c, multiplicity distribs. and double scatt. effects 78−66165
π$^-$d, charge multiplicity distribs., parity tests 79−97602
π$^-$d, multiplicity distrib. data, simple non-interacting fireball model 79−3178
π$^-$d→(p$_s$)X^{--}p, 13.2 GeV, search for charge −2 mesons 78−66167
π$^-$d→Δ$^-$p, high energy, backward Δ$^-$ prod. mech., Δ^{++}-Reggeon exchange *(Russian)* 79−97637
π$^-$d high multiplicity interactions at 21 GeV/c 78−4879
π$^-$d→nn, mechanism, cross-sections, EM form factors 79−89181
π$^-$d→nn, nnγ, nnπ^0, neutral reactions, 224 MeV cross-sections 78−54651
π$^-$d→π$^-$ pn final state interactions and d breakup for 438 MeV/c π$^-$ impulse *(Russian)* 80−18145
π$^-$d→π$^+$X, screening effect of protons in deuterons *(Russian)* 77−267
π$^-$d→π$^+$X$^-$, 2.6 GeV/c, d proton screening correction and Glauber parameter 80−9175
π$^+$d, 4 GeV/c, cross sections for strange particle prod. 79−17753
π$^+$d, 6 to 100 GeV/c, P$_\perp$ distribs. of K^0, π$^-$, ρ^0, f, equilibrium temp. 79−49540
π$^+$d interactions, strange-particle cross-sections at 4 GeV/c 78−89734
π$^+$d→p(N*,Δ$^+$), 1-5 GeV, inclusive cross-sections 77−6157
π$^+$d→pp, 40-60 MeV, ang. distribs., D-state admixture 77−2864
π$^+$d→pp, calc. including form factor at absorption and scatt. vertex 77−6155
π$^+$d→pp, meson exchange currents, effects on pion absorption 79−85287
π$^+$d→pp amplitude, choice of πNN vertex 79−75795
π$^+$d→pp′, effect of form factors on disintegration 77−6156
π$^\pm$d, three body systems, review of recent theoretical anal. 79−80842
π$^\pm$d, total cross section determ., 200 to 370 GeV/c 79−26352
π$^+$^{4}He→π$^-$ 4p; 1.5 to 2.0 GeV/c, cross sections, momentum spectra, ang. distrib. Δ resonances prod. 77−65237
πN, 50-200 GeV/c, multiparticle production, multiplicities, cross sections and ang. distribs. 80−86768
πN, π$^+$d, 100 GeV/c, charged-particle multiplicity distribs. 78−33101
πN, ψ hadronic prod., lepton pair ang. distribs., cross section χ contribution 80−42487
πN, strength of parity violation in vector meson dominance 79−71653
πN→(ρ,Ω)N, Regge model with derivative relations between S-channel helicity amplitudes 77−74713
πN→A$_2$N, ρ and f Regge exchanges, an interpretation 79−63531
πN charge exchange scatt., Regge pole, model calcs. 80−102071
πN charge exchange scatt. saturation, trajectory props. *(Russian)* 79−89186
πN collisions, N→Nπ$^-$ diffractional dissociation, Deck mechanism *(Russian)* 80−86699
πN coupling, parity violating, weak and EM interaction model anal. 79−67599
πN coupling in Δ(1231) isobar region, pion index of refraction, self-energy in low density limit 80−42554
πN dilepton prod. quark-parton distribs., Drell-Yan model 79−17752
πN field theoretic aspects, disconnectedness problem 79−85335
πN forces, in free space and nuclear matter 77−23115
πN four invariant amplitudes at low energy, simultaneous analysis of effective resonance poles 79−67598
πN→γπN, recoil corrections to static model, interaction current 78−25072
πN high-energy collision yields, evidence for composite quark model *(Russian)* 79−9636
πN in nucleus, diffraction dissociation, dip and kink structs., differential cross sections 80−95284
πN interactions at low energy, theoretical anal. 79−85326
πN→J/ψ+X, 27 and 40 GeV, total (J/ψ) production cross sections on Cu target *(Russian)* 78−25249
πN→KΣ*, isospin restrictions on spin density matrices *(Russian)* 77−30446
πN→K+hyperon, hypercharge exchange reactions in quasieikonal model *(Russian)* 79−3041
πN→lX, quark structure functions for hadrons, Drell-Yan model anal. 78−21476
pion-nucleon interactions continued
πN low energy partial wave anal., cross sections, Δ^0 and Δ^{++} 80−52531
πN→μ$^+$μ$^-$X, longitudinal photon polarisation from helicity ang. distrib. 80−5025
πN→μ$^+$μ$^-$X, π-struct. function determ. 79−63553
πN→Nπ(π), √s=1.3 to 2.0 GeV, K-matrix fits 78−66151
πN→Nππ, 1.65-1.97 GeV, partial wave anal. including π-exchange 78−66148
πN→Nππ, 1.65-1.97 GeV/c^2, πN resonance coupling to Δπ and ρN channels 78−66149
πN off-shell t-matrix, P-wave states calc. 77−61205
πN→π$^+$π$^-$N, 4-17 GeV/c, ρ^0 and f prod. mech. 80−436
πN→πΔ, finite energy sum rules and duality 77−22763
πN→πX, dual fermion model for inclusive single particle distribs. 78−86446
πN→π(Nπ) diffraction dissociation, role of nucleon exchange 77−38192
πN→ππΔ, S-wave prod. determ. 78−45972
πN→ππN, 16 GeV/c, model for diffractive scatt. 77−50014
πN→ππN, 1.3 to 1.8 GeV, interference of isobars, partial wave anal. 79−63519
πN→ππN, alternative soft-pion approaches 77−26541
πN→ππN, fifth order perturbation theory prod. amplitudes, isobar models 77−54088
πN→ππN, importance of analyses, t-channel effects, isobar model validity 77−22776
πN→ππN, isobar formalism, one-pion-exchange partial-wave cross sections 77−87957
πN→ππN, kinematic singularity free helicity amplitudes, crossing matrix anal. props. 80−95285
πN→ππN, off-shell phase shift anal. of ππ→ππ amplitude 77−2867
πN→ππN, π prod. near threshold, s-wave ππ parameters 77−38197
πN→ππN or ππΔ, ππ scatt. amplitude, current algebra 78−62455
πN→ππN reaction, scattering lengths, data compared to prediction *(Russian)* 79−93459
πN→ππN reaction amplitude reconstruction in relativistic energy region *(Russian)* 79−13173
πN→ρδ, or ωΔ, polarisation, selection rule on ang. momentum transfer 77−34180
πN scatt. amplitude, two pion exchange three nucleon pot. and nuclear matter 79−40877
πN scattering, chiral dynamics and asymptotical restrictions, sum rules *(Russian)* 78−17047
πN semi-inclusive reactions at 40 GeV/c, single particle correls., π$^\pm$ and γ struct. functions *(Russian)* 77−82792
πN t-matrix, half-shell theory, generalised to all partial waves 79−85330
πN total cross section sum rule, reln. of sea quark distrib. and pomeron 79−63441
π$^-$N, 150 GeV/c, prod. of J/ψ and ψ′ mesons 79−40804
π$^-$N, 16, 22 GeV, dimuon prod. parton intrinsic transverse momentum, QCD perturbation 80−63037
π$^-$N, 217 GeV, dimuon prod., prod. of γ associated with χ→ψγ 79−36081
π$^-$n, 40 GeV/c, charge multiplicity in forward and backward hemispheres *(Russian)* 77−265
π$^-$n, 40 GeV/c, cross sections of Λ and K prod. *(Russian)* 77−6184
π$^-$N, 40 GeV/c, leading and conserved mesons *(Russian)* 78−45987
π$^-$n, 40 GeV/c, many pion systems in inclusive reactions, transverse momentum effects *(Russian)* 80−57654
π$^-$N, 40 GeV/c, many-nucleon interactions, secondary π$^\pm$ spectra *(Russian)* 79−97638
π$^-$n, 40 GeV/c, multiplicity of secondary charged particles *(Russian)* 77−34190
π$^-$n, 40 GeV/c, secondary neutron average number, charge exchange coeffs., n inelasticity coeffs. *(Russian)* 80−32132
π$^-$n, 40 GeV/c, semi-inclusive π$^\pm$ transverse momentum distributions, statistical model anal. *(Russian)* 79−13174
π$^-$n, 40 GeV/c, two-particle charged and γ rapidity correls. 77−18335
π$^-$N, 40 GeV/c in ^{12}C, multinuclear inclusive process correlation functions *(Russian)* 80−68500
π$^-$N, 50 GeV, rapidity gap correlations, cluster emission model studies 79−93469
π$^-$N, 50 GeV/c, multiple pion production, role of clusters 77−34199
π$^-$n, diffr. dissoc. in ππ collisions *(Russian)* 78−29356
π$^-$N, in ^{12}C, 40 GeV, secondary charged particle multiplicities *(Russian)* 79−3184
π$^-$N, in ^{12}C, 40 GeV/c, one- and multi-nucleon interactions, secondary charged particle multiplicity *(Russian)* 80−83013
π$^-$N, in C, 5 GeV/c, π^0 and n inclusive spectra, cascade model *(Russian)* 80−68490
π$^-$N, Λ hyperon prod. cross section, momentum and ang. distribs. *(Russian)* 80−42497
π$^-$N→D^{-*}+charmed baryon, generalised quark line rule, SU$_4$ symm. scheme 78−54614
π$^-$N→D*$^-$+X, 10.5 GeV/c, near threshold 78−37249
π$^-$N→γX, 50 GeV, gamma prod. characteristics in emulsion reactions 80−68492
π$^-$N in Be, 150, 175 GeV/c, high mass muon pair prod., Drell-Yan QCD corrections 80−13343
π$^-$N in Ne, 25, 50 GeV/c, secondary particle multiplicity and multiple scatt. model anal. *(Russian)* 80−83014
π$^-$N interactions, 50 GeV/c, inclusive charged π prod. in nuclear emulsion anal. 78−66168
π$^-$N→J/ψ+X, 43 GeV/c, cross-sections for W, Cu, Be targets 78−25089
π$^-$N→J(ψ)+X, 27 and 40 GeV/c total cross-section for Cu nucleus 78−25088
π$^-$N→μ$^+$μ$^-$X, 27, 40 GeV, cross sections and differential distribs. *(Russian)* 78−89919
π$^-$N→μ$^+$μ$^-$X, K$^-$/π$^-$ structure function ratio using Drell-Yan process 80−86718
π$^-$N→μ$^+$μ$^-$+hadrons, 225 GeV, ψ and charm prod. 78−25092
π$^-$n→p$_{forward}$X^{--}, search for nonstrange exotic mesons, baryon exchange 77−50015
π$^-$n→pX^{--}, 21, 205 and 360 GeV/c, reggeised one-pion-exchange 80−57649
π$^-$n→pions+X, 40 GeV/c, transverse pion momenta depend. on secondary particle multiplicity *(Russian)* 78−33103
π$^-$n→pπ$^-$π^0 or ρ$^-$π$^-$ p, 5, 9 GeV/c, model independ. anal. of final states 78−25071
π$^-$n→π$^-$π$^-$p, 15 GeV/c diffr. dissociation and N* prod. by pomeron exchange 77−41865

pion-nucleon interactions continued
$\pi^-n \to \pi^-\pi^-p$, cross section at 226, 250, 312 MeV 78−50046
$\pi^-N \to \psi X$, 225 GeV, bottom meson pair production limit 80−73750
$\pi^-N \to \eta^0(\omega)X$ at 40 GeV/c, cross sections 77−18359
$\pi^-n \to \rho^0\pi^-n$, 9 GeV exchange Deck model anal. 80−47322
π^-n semi-inclusive interaction, 40 GeV/c, charge distribution *(Russian)* 77−74739
π^-N semi-inclusive reactions at 40 GeV/c, structure functions *(Russian)* 77−61332
π^0N, 82 to 182 MeV, total cross section determ. *(Russian)* 79−22122
π^+n, 195 GeV/c, inclusive π^+/π^- ratio and quark distributions 79−54367
π^+n, 195 GeV/c, single particle inclusive distribs. 79−75804
$\pi^+N \to e^+e^-$, 830 MeV/c, comparison with recent data 77−87996
$\pi^+n \to K^-K^+p$, 6 GeV/c, f, f' and A_2^0 interference 77−253
$\pi^+n \to K^-K^+p$, characteristics of S-wave $\bar{K}K$ enhancement at 1300 MeV 77−6158
$\pi^+n \to K^-K^+p$, f,f' mesons, high statistics study at 6 GeV/c 77−79279
$\pi^+n \to p_{slow}+x$, 195 GeV/c, triple Regge model anal., dominant π exchange 78−54657
$\pi^+n \to pX$, 100 to 400 GeV/c, slow-proton prod., Regge trajectory 80−22646
$\pi^+n \to p(\pi^+\pi^-)s$, direct channel diagram of $(\pi^+\pi^-)s$ atom prod. *(Chinese)* 79−81308
$\pi^+n \to p\pi^0$, quantum chromodynamics and P-odd effects *(Russian)* 79−89172
$\pi^+n \to p\pi^+\pi^-$, 9 GeV/c, channel separation using transversity parameter 78−74273
$\pi^+n \to \pi^+X$, 195 GeV/c, hierarchy of mean multiplicities 79−36112
$\pi^+n \to \pi^+\pi^-p$, $(\rho^0+\omega^0)$, comparative study of ρ^0, ω, $K^{*0}(890)$ and $\bar{K}^{*0}(890)$ production 78−58200
$\pi^+n \to \rho^0X$, 6.0 GeV/c, comparison with $K^-p \to \bar{K}^{*0}X$ 77−30459
$\pi^\pm N$, 16 GeV, dimuon prod., $q\bar{q}$ annihilation contrib., exact scaling deviations 79−89196
$\pi^\pm N$, 200 GeV/c, dimuon prod. cross section, Drell-Yan predictions, struct. functions 80−37300
$\pi^\pm n$, high-energy, react. differences and annihilations 78−74279
$\pi^\pm N$, ψ hadronic production, gluon contrib. in QCD framework 78−78139
$\pi^\pm n \to (p\pi^-)\pi^\pm$, 5.1, 9 GeV/c, neutron diffr. dissoc. 77−74714
$\pi^\pm N \to K^-K^+N$, 6 GeV/c, ϕ-meson prod. 77−26540
$\pi^\pm N \to \mu^+\mu^-X$, 225 GeV/c, muon pair prod., $q\bar{q}$ annihilation model 79−63552
$\pi^\pm N \to \mu^+\mu^-X$, 225 GeV/c, muon pair prod., 2 to 11 GeV/c^2, differential cross section 79−67612
$\pi^\pm N \to \omega(N,\Delta)$, EM mixing effects, dynamics of vector meson prod. *(Russian)* 78−58191
$\pi^\pm N \to \rho^0X$, inclusive cross sections and spin density matrices, 3-Reggeon model anal. *(Russian)* 79−80858
$\pi^\pm N \to \rho^\pm\gamma N$, bremsstrahlung in vector meson prod. at high energy *(Russian)* 79−80851
πNN form factor; relativistic calc. of $\Delta(1232)$ contribution to imaginary part *(Korean)* 80−47292
πNN vertex function, dispersion theory calc. 77−57509
π^-nn stable bound state, Heitler-London-Pauling variational method 79−13151
π^-p, 40 GeV/c, charge transfer distrib. and π cluster prod. 77−34184
$\pi^-p \to \pi^0n$, $\pi^-p \to \eta n$, 6-200 GeV, charge exchange amplitude energy behaviour 77−22800
$\pi^-p \to \pi^0n$ reaction for large transmitted momenta, 40 GeV/sec *(Russian)* 78−12934
$\pi\pi NN$ partial-wave amplitudes, interior dispersion relations 77−82758
$\pi\pi\pi$ absorpt. in nucl. matter 78−50049
ρ trajectory intercept, energy depend. 78−45959
ρ-meson intermediate states in πN scatt. Chew-Low theory modifications 79−479
$C+\pi^-$, 40 GeV/c, two-particle correls., rapidities, ang. distribs. *(Russian)* 78−17251
$^{12}C+\pi^-$, 40 GeV/c, multiplicity distribs. of secondary charged particles, Glauber model calcs. *(Russian)* 78−17252
$^{12}C(\pi^-,\pi^\pm)X$, 40 GeV, multiparticle prod. mechanism, various model predictions 79−573
$Cu+\pi^- \to \psi X$, 16, 22 GeV, cross section, quark fusion model 79−36278
$^3H(\pi^\pm,\pi^\mp)$, 232-252 MeV charge exchange differential cross section 80−37401
$\pi^-d \to \gamma nn$, n-n scatt. length from photon spectra 79−67600
πN vertex function with off-shell nucleon 77−71530
$\pi^-N \to \mu^+\mu^-X$, lepton ang. distrib. calc. by QCD 79−26303
$\pi^\pm n$, mean charged multiplicity, energy depend., modified Heisenberg ~ calcs. 79−40806

pion-nucleon scattering
see also pion-nucleon interactions; pion-proton scattering
(3,3) reson. in $^{13}C(\pi^+,\pi^0)^{13}N$, eikonal cross-section calc. 77−18609
(3,3) reson. in $^{13}C(\pi^+,\pi^0)^{13}N$, optical model calc. 77−18610
(3,3) reson. in $^{13}C(\pi^+,\pi^0)^{13}N$ 77−18608
(3,3) reson. in $^{40}Ca(\pi,\pi N)$, WKD approx. validity 77−18615
(3,3) resonance region phase shifts and diffractive nature of π-nucleus scatt. 77−6462
$\pi N \to \pi(N\pi)$ diffr. process, $N\pi$ absorbed two-component model 77−18254
$\pi N \to \rho X$, trajectory data, reson. and scatt. regions, compatibility *(Russian)* 78−8703
amplitudes, singularities of zero trajectories, dual model predictions 80−63021
analytical props. of scatt. amplitude, localisable quantum field theory *(Russian)* 77−74603
backward elastic, polarisation, peripherality measure, intermediate energy 77−2862
baryon reson. spectrum in dual model 77−18318
Chew-Low model, πN vertex function 78−8686
Chew-Low model, covariant theory of off shell πN scatt. 77−6151
chiral symmetry and the NN interaction, book contrib. 79−97669
compilation of coupling constants and low-energy parameters 79−22159
Coulomb-nuclear interference polarisation in high energy large momentum transfer hadron reactions 77−79282
current algebra appl. to low-energy scatt. 77−18319
Deck model, rescattering effects for diffr. dissociation of hadrons 78−4844
differential cross-section zeros, reson. identification 77−82693

pion-nucleon scattering continued
diffractional approx., few-nucleon nuclei, nuclear structure *(Russian)* 78−650
elementary particle scattering, phenomenological approach to the inverse problem 79−49498
EM effects in high energy scatt. 78−93906
EM nucleon form factor sidewise dispersion relations, inelastic effects 78−82212
energy-dependent phase shift analysis of pion-nucleon scattering below 400 MeV 78−86455
field theoretic treatment of pion-nucleus scatt. 78−29505
field theory model, linear wave eqn. with energy-depend. pot. 77−18317
final state theorem extension, anal. of accurate low energy expts. 77−65172
form factor determ. in modified Chew-Low model 77−6152
form factor in Chew-Low theory 78−41574
forward scattering amplitude, method for testing analyticity 77−57462
forward scattering amplitudes, axiomatic lower bound *(Russian)* 78−78211
forward scattering amplitudes, high energy, integral axiomatic upper bounds for coupling const., logarithmic sensitivity *(Russian)* 77−13984
generalised reaction matrix, elastic and charge exchange polarisations *(Russian)* 77−50013
high-energy, effect of anomalous mag. moments in quantum field theory 78−465
integral axiomatic restrictions *(Russian)* 77−79224
isovector exchange, $NN \to NN\pi$ comparison with πN elastic scatt. 78−37189
local phenomenological potentials, 0-250 MeV scatt. 78−70400
low energy, determ. of low eqn. 78−8688
low energy, local and nonlocal pots., reaction matrix anal., inverse scatt. 78−8684
low energy nonresonant amplitudes, t- and u-channel structure 77−38193
low energy scatt., subtracted form of Low eqn. 78−66150
low energy scatt. amplitudes, current algebra constraints 77−38196
low-energy, nonlinear chiral dynamics description *(Russian)* 78−17043
nonlinear chiral dynamics of s- and p-wave scatt., superpropagators *(Russian)* 77−38198
off-mass shell model, calc. of finite-energy sum rules using partial wave anal. 79−63517
off-mass-shell, field theoretic aspects pion-nucleus physics 77−10325
P-wave amplitudes, high-energy contribs. 77−41857
P-wave interaction, anal. based on PCAC and σ-commutator 79−85334
Pade approximants and πN scattering 80−22634
parity-violating scatt. amplitude calc. using soft-pion techniques 79−75787
partial conservation of axial vector current limit, on shell corrections 77−18201
partial wave amplitudes coupled channel anal. 80−42495
partial wave anal. 1.6 to 10 GeV, possible high spin resonances in Argand plots 78−70403
partial wave analysis, high energy behaviour large momentum transfer region 79−22130
partial wave analysis, S- and P-wave scatt. lengths 80−63019
partial wave analysis 80−42494
partial wave sum rules application 77−10204
phase shifts in $\Delta(3,3)$ region, model using particle poles and current algebra 77−6146
phase-shifts, low energy, threshold parameter determ. 77−88002
pion condensation in neutron matter: effects of pion-nucleon scattering 79−26388
potential determination using Newton-Sabatier method, inverse scatt. problem 78−89731
pseudoresonance Argand loops *(Russian)* 79−9354
quantum field theory approach, standard reduction techniques, calc. of scatt. amplitude 80−42570
radiative corrections, tables 79−26335
relativistic potl. theory appl., corrections to πN off energy shell T-matrix elements 77−6154
resonance damping in nuclear matter 77−10350
scattering amplitudes with positive imaginary parts, theory 77−71466
scattering lengths from invariant amplitudes in terms of rational analytic series 79−45099
separable potl. model, form factors 77−6153
sigma term from threshold data 80−57633
sigma term related to scatt. length, Altarelli-Cabibbo-Maiani relation derivation 80−57632
special coherent states and scatt. phase shifts, meson field theory 79−67601
spin flip dynamics and inclusive processes *(Russian)* 78−41589
static nucleon, soln. to eqn. using Schauder's principle 77−41859
$SU(2)\times SU(2)$ chiral symmetric Lagrangian description of low energy πN and NN scatt. 79−26251
sum rules, finite-energy, three component duality 80−82996
two component Pomeron, πN, kN, NN forward scatt. amplitudes 80−37245
zero trajectories of invariant πN amplitudes 80−102067
$d(\pi,\pi)d$, differential cross section, investigation of ΔN interaction in the deuteron 79−67597
n-hadron amplitudes from p-hadron and d-hadron amplitudes in Glauber-model 77−22803
$N\pi \to N^*\pi$, Gribov-Morrison rule as kinematic effect 77−49999
π+light nuclei, high energy cross section calc., complex ang. momentum theory *(Russian)* 78−46067
πd, 142, 180 MeV, covariant three-body calc. 77−6450
πd, comparison of Faddeev eqn. approach with optical potential 79−76030
πd, elastic differential cross section, Faddeev calc. and π-absorption 79−75793
πd, impulse approx. calc. of scatt. in resonance region 77−6452
πd, low energy scattering theory *(Russian)* 79−54460
πd, multiple scatt. formalism 77−6451
πd, relativistic effects in deuteron alignment 78−25068
πd backward scatt. and inelastic intermediate states, ω meson prod. *(Russian)* 78−41579
πd elastic scatt., 142 MeV, elastic cross section and polarisation observables 79−75791
πD elastic scatt., 47.5-256 MeV, single scatt. contrib. 77−67671
πd elastic scatt., dibaryon resonance effects on differential cross section, Glauber model 79−97634

pion-nucleon scattering continued
πd field theoretical model, effective semi-relativistic three-body problem 78−86454
πd low energy scatt., Afnan-Thomas anal. with exclusion principle 79−75792
πd multiple scatt., kinematical ambiguities anal. 77−22764
πd polarised scatt., dibaryon resonance signals in excitation functions 80−9181
πd→πd, 141 to 260 MeV backward elastic scatt. in (3,3) reson. region 79−85531
πd→πd, 47 MeV, differential elastic cross section 79−85530
πd quasielastic and inelastic rescattering as cumulative particle prod. source *(Russian)* 79−22340
πd scatt., 142 MeV, polarisation observables 78−78210
πd scatt., and NN covariant dynamics 77−6449
πd scatt., effect of genuine π absorpt. and emission 79−17939
πd scatt., relativistic kinematic effects 78−8685
πd semi relativistic field theroretical model, extended Fadde'ev and Amado-Lovelace eqns. 78−89729
πd-scattering length calc., on basis of Faddeev's equations *(Russian)* 78−33082
$\pi^{\pm}$d, 47 MeV, elastic scatt. differential cross section 79−75794
πN, 6-200 GeV, amplitude anal. in impact parameter representation, non-zero polarisation, shell struct. *(Russian)* 80−86752
πN, Low eqn. approx. soln., field theory propagator modification 79−85546
πN, null plane current anticommutators, sum rules and appls. 80−52436
πN backward scattering amplitudes, superconvergence and nonlinear dispersion relations 78−468
πN channels, relativistic parametrization of separable pots. 79−63518
πN coupling constant determ. using forward dispersion relations 79−45098
πN elastic amplitude, off-shell behaviour, and separable potential model 79−85327
πN elastic scatt., nonstatic model for nuclear reactions 80−102125
πN low energy partial wave anal., cross sections, Δ^0 and Δ^{++} 80−52531
πN low energy scatt. amplitudes, partial wave N/D techniques 79−85331
πN low energy scatt. from N, Δ poles, low energy theorems 80−86751
πN off shell scatt. and πNN vertex function 79−85333
πN off shell scatt. near Δ resonance, parameter free form factor 80−9168
πN partial wave anal. using dispersion relations, threshold to 10 GeV/c 77−22768
πN phase shifts, possible pole in πNN vertex function 79−85332
πN→πN, EM corrections, calc. by general dispersion reln. method 79−9378
πN→πN, universal function for large angle cross sections of exclusive hadronic reactions 77−50010
πN scatt., isospin violation from π^0-η mixing, partial wave anal., N*(1540) struct. 80−27426
πN scatt. amplitudes used in ππ scatt. length calc. 78−45952
πN scattering amplitudes, theoretical ambiguities and isotopic invariance *(Russian)* 79−9404
πN scattering lengths, statistical approach, data representation by analytic functions 77−10279
πN small angle scatt., polarisation, quasi-potential approach 77−45993
πN T-matrix, off-shell model of scattering amplitude 79−414
$\pi^+ n \rightarrow \pi^+ \pi^- p$, 15 GeV/c, longit. phase space anal., ρ^0, f^0, Δ^0, N* 77−74727
$\pi^{\pm}$N, 2-15 GeV/c, in Ge, Si, influence of channelling on scattering 80−73729
$\pi^{\pm}$n backward elastic scatt. 20-40 GeV, Regge theory description, angular distrib., radiative corrections 78−62461
πNN vertex function and off-mass-shell πN scatt. 80−73739
πNN vertex operator for πN elastic scatt. phase shift calcs. 77−54118
πNσ commutator, discussion using dynamical theory of πN amplitude 79−22134
$\pi^{\pm}$p, <280 GeV/c dual absorptive model of elastic scatt. 79−63529
^{12}C, pion rescattering after ^{12}C(e,e'π$^+$)^{12}B, near threshold 78−13065
^{3}He (π, π) Δ(1236) resonance region, Watson multiple scatt. series. integral eqns. 80−37402

pion-nucleus reactions
for inelastic pion-nucleus scattering, see "pion-nucleus scattering" see also pion-nucleon interactions
π^-+nucleus interaction, 50 GeV, pion associative multiplicities anal. *(Russian)* 77−46191
A=6to 14, radiative pion capture, mag. dipole resonance excitation in 1p shell nuclei 78−74408
absorption, energy dependent mean free path length for star formation 77−23393
absorption and prod. of mesons, overview 79−85492
absorption and production expts., review 77−10435
absorption data compilation 77−18619
absorptive s-wave pion-nucleus optical pot., energy dependence 79−54418
barionic cumulative effect in nuclei collective nature *(Russian)* 79−22339
binding effects in optical pot. of pion in nucleus 78−41685
channelling, modulation of high energy interactions 80−37373
charge exchange reactions 79−59093
charged particle yields from π^- capture in biologically significant materials 80−12201
Chew-Low eqn., no crossing approx. 78−82396
clusterisation and secondary particle correl. *(Russian)* 78−33133
coherent particle prod. cross-sections at 200 GeV/c 77−18360
collective tube model, credibility of criticism by Azimov et al., effects of target fragmentation 78−93982
conference on few body systems and nuclear forces, Graz, Austria (Aug. 1978) 79−67567
conference on few body systems and nuclear forces, Graz, Austria (Aug. 1978) 79−80880
conference on high energy physics and nuclear struct. Vancouver, Canada (Aug. 1979) 80−41936
Conference on meson-nuclear physics, Houston, USA (Mar. 1979) 79−85489
credibility of criticism by Azimov et al., misuse of CTM 78−93980
deep inelastic reacts. in isobar model 78−41779
deformed nuclei, absorption of slow π^-, mesic atoms 80−78321

pion-nucleus reactions continued
distorted waves, 100 to 200 MeV, difference between Schrodinger and Klein-Gordon wave functions 78−94033
double charge exchange in heavy nuclei, pion condensation 77−79402
elastic pion double charge exchange, NN correlations in nuclear medium 77−10449
emulsion nuclei, 200 GeV/c inelast. interactions 78−8860
emulsion nuclei, 20 TeV, balloon-borne chamber, Monte Carlo simulation 80−9309
emulsion nuclei+π^-, correlations between secondaries 77−57654
emulsions, 50 GeV π^- beam collisions, pion cluster prod. 77−46190
fast particle production on nuclei in quark model *(Russian)* 79−6612
few-body systems, reaction mechanisms 77−23115
field theoretic aspects pion-nucleus physics 77−10325
field theoretic treatment of pion-nucleus scatt. 78−29505
field theory, chiral symmetry and pion-nucleus interactions 79−80961
fissionability, target mass depend. for π, γ, α, p, cascade-evaporation and liquid drop calcs. *(Russian)* 80−106089
fragmentation, clustering and absorption mechanisms in p and π induced reactions 79−6546
Frankel events observation in streamer chamber 79−85505
Glauber screening eqns. in fast backward particle prod. in high energy processes, role of short range nucleus struct. 79−63670
high energy reactions, secondary particle multiplicity 79−93597
high-energy, correlation between fast target protons and hadron+nucleon collisions 78−41681
high-energy similarity of pion and proton induced reactions 77−67747
impact parameter anal. of coherent and incoherent pion prod. 77−2870
inclusive distribution of longit. velocities in range 20 to 200 GeV *(Russian)* 77−57578
inclusive reactions, pion annihilation 77−6446
intermediate energy nuclear physics, review of recent expts. 78−50061
intermediate state of ρ-propagation in static model 79−67781
intranuclear cascade model for high energy (up to 1000 GeV) reactions 78−70498
isobar doorway model, pion absorpt. optical potential 79−85420
isobar model for pion induced reactions, proton spectrum 77−18617
isobar propagation and collective effects, pion-nucleus and photonuclear investigation 80−22676
low energy π capture, quasideuteron absorption dominant mechanism 79−6701
meson exchange current effects in hadron-nucleus scatt. 79−26380
meson-nuclear phys. in 1979, current status and new development 79−85490
meson-nuclear physics, International Topical Conf. 77−6436
multiple-scattering theory 77−82967
multiplicity of charged particles, 200 GeV/c *(Russian)* 78−29509
multiplicity of secondary particles, 7 GeV/c *(Russian)* 77−88146
non-radiative absorption by single nucleon in nuclei, pion condensation 77−42000
nuclear critical opalescence, pion field and condensation 80−42559
one nucleon absorption of slow pions, π-condensate effect *(Russian)* 77−30639
one nucleon absorption of slow pions, pion condensate effect *(Russian)* 78−8765
optical model of low-energy reactions 77−6460
particle momenta spectra fits from streamer chamber expt. with two temp. Boltzmann model 79−85507
photoemulsion nuclei, π^+ absorption, up to 114 MeV, nuclear scaling *(Russian)* 78−25247
pion condensation and the pion-nuclear interaction, book contrib. 80−485
pion condensation in nuclear matter, book contrib. 80−484
pion photoproduction and radiative capture 78−50213
pion-nucleon vertex function with one nucleon off shell 79−40966
pion-nucleus scatt. and absorption amplitudes, composite particle struct. 79−67778
proton semileptonic decay in nuclei, pion attenuation 80−47286
quark-parton model, relation between low mass dimuon and meson prods. 78−41477
radiative capture, current algebra model with hard pions *(Russian)* 77−74890
radiative capture on light nuclei, partial transitions, shell model calc. 77−57693
radiological imaging, use of inelastic high energy particle interactions 80−61675
reaction mechanisms, at low energy and near 3.3 reson. region 79−80958
reaction mechanisms, nuclear environment and models 80−42700
relativistic pot. models for π absorpt. and prod., equivalence theorem 77−74884
resonant total cross sections in strong absorpt. model 77−23114
review, medium energy pion-nucleus absorption and scattering, pion condensation 78−8858
s-d shell nuclei, 70 MeV pion interactions, cascade evaporation model 77−10444
S-wave π absorption, off shell effects, effect on π-nucleus optical pot. 78−70566
s-wave absorpt., optical potl. calc. 77−10439
s-wave absorption, sensitivity to off-shell props. of πN scatt. 77−50158
S-wave pion-nucleus dynamics in the σ+ω model 79−89245
secondary particle correlations, 3.7 GeV/c *(Russian)* 77−79404
secondary shower particles angular distribs., in 200 GeV reactions *(Russian)* 78−25252
single charge exchange and inelastic scatt. cross sections relationship 80−102204
single-charge-exchange in isobar doorway model, comparison with ^{12}C(π$^+$,π^0)^{13}N 77−41999
spallation cross-section, systematics 79−6716
three-nucleon systems, props. and interactions 79−71805
three-pion prod. on complex nuclei with 23 GeV/c π^- 78−82392
threshold pion absorption in nuclei 78−82390
total cross section, A-depend. shift of peak 78−33226
total cross section data from LAMPF and BNL, (3,3) resonance 77−10436
total cross section treatment for (3,3) resonance region 80−42703
total cross-section depend. on nuclear density and π-N off-shell amplitude near (3,3) 77−3050
total cross-sections, contrib. of quasi-elast. scatt. 78−78417
total cross-sections, strong absorpt., N*(3,3) resonance 77−10442
total cross-sections in (3,3) resonance region 77−10437

pion-nucleus reactions continued
total inelastic cross sections, 2 to 6 GeV/c, various nuclei *(Russian)* 78−46113
total pion absorption cross section, A depend., proton yields 80−106081
truncated pion-nucleon amplitudes and pion-nucleus interactions 80−68708
two particle correlations at 200 GeV/c for secondary particles *(Russian)* 78−46112
$^{12}C+\pi^-$, 40 GeV/c, leading particle spectrum and bremsstrahlung model *(Russian)* 78−41781
^2H target, expt. to observe excited states of nucleons in nuclei *(French)* 79−3179
$^2H(\pi^+,pp)$, pion absorpt., effect of $\rho\pi$ exchange currents *(Korean)* 80−47402
$(\pi^-,2n)$, π absorption study by subsequent particle emission observation 79−85493
$(\pi^-,2n)$ reaction on ^6Li, ^{10}B, ^{12}C, ^{14}N and ^{16}O 77−10440
$(\pi^-,2n)$ struct. and reaction information, two hole states, direct mechanism 79−85496
$(\pi^+,2p)$ quasi two particle scaling, momentum distrib. from statistical model *(Russian)* 79−40968
$(\pi,2\pi)$, possible probe for pion condensation precursor phenomena 80−78330
(π^+,d), DWBA cross section *(Chinese)* 80−27673
(π,f), emulsion nuclei, prod. cross section for ^1H, ^2H, ^3H *(Russian)* 79−67801
(π^-,f), at rest, exciton model 78−94042
(π,γ), A=14 nuclei, isospin T=2, 1 and 0 collective resonances, shell model 80−510
(π,γ), cross sections from Boltzmann eqn. 79−89330
(π,γ), γ-transitions on and off line 80−37912
(π,γ), inverse pion photoprod., level struct. determ. 80−22863
(π,γ), π electromag. processes, theoretical aspects 80−22822
(π^-,γ), 1p nuclei M2 giant resonance calcs. 80−22784
(π^-,γ), 1p shell nuclei, response function comparison with (e,e') 80−63143
(π^-,γ), 1p shell nuclei, spin-dipole excitations, shell model calcs. 79−17935
(π^-,γ), absorpt. on light nuclei, resonance states 77−14189
(π^-,γ), high spin isomer state excitation, review 79−49569
(π^-,γ), pion absorption by two nucleon cluster, high spin state excitation probability 79−49570
(π^-,γ), unified description of direct and resonance processes 78−86551
$(\pi,\gamma\gamma)$, pion condensation studies status report 79−85524
$(\pi^-,\gamma\gamma)$, existence test for pion condensation 79−85525
$(\pi,\gamma X)$ reactions on ^{28}Si, ^{60}Ni, 70 MeV pions, expts. with pion beams of Saclay Linac *(French)* 79−572
(π,N), wave function orthogonality, bound state to continuum transitions 78−78335
(π^-,n), π threshold prod. and absorption, pseudoscalar-pseudovector equivalence 79−80877
(π,NN) reaction for nuclear struct. studies, one- and two-nucleon models 77−18629
(π^-,NN), low energy pion absorption, $\sigma+\omega$ model, optical pots., real $\rho^2(r)$ pot. 80−83125
(π^-,nn), S-wave and p-wave absorptive pion-nucleus optical pot. 80−27677
(π,p), A=12-181, proton yields, number of nucleons involved in pion absorption 80−63209
(π^-,p) process, cross section, at. number depend., 1.43 GeV/c *(Russian)* 77−30638
(π^+,p), differential cross-section, current theories 77−6445
(π^+,p) near (3,3) resonance region, isobar doorway model 78−41778
(π,π) single and double charge exchange in resonance region, geometrical limit 80−86930
(π^-,π^0) absorpt. by complex nuclei 77−88174
(π^+,π^-) A=9-32, 180 MeV 80−105960
(π^+,π^-) reactions on light nuclei, micron spectrometer for meas. with energy resolution of 1 MeV for 400 MeV/c momentum 78−13368
(π^+,π^0), isobar-doorway model optical pot. appl. to isospin nonzero nuclei 80−52699
(π^+,π^0), isobaric analogue state obs. in CH_2, ^7Li, ^{13}C, ^{27}Al, ^{58}Ni, ^{90}Zr, ^{120}Sn, ^{208}Pb 80−106078
(π^+,π^0) inclusive reacts., 100 MeV, π^0 detection from γ-ray spectra 78−33222
$(\pi^\pm,\pi^0)$ 50-200 MeV, single charge exchange, total charge exchange cross section 79−93663
(π,π'), use in nuclear struct. determ. studies, review 79−85527
$(\pi,\pi d)$ 115 MeV, light emulsion nuclei, integral reaction and differential cross sections *(Russian)* 79−13351
$(\pi,\pi He)$ 115 MeV, light emulsion nuclei, integral reaction and differential cross sections *(Russian)* 79−13351
$(\pi,\pi N)$ cross-sections, nucleon charge exchange 77−10443
$(\pi,\pi N)$ knockout reaction, nonanalogue nucleon charge exchange transitions 79−22336
$(\pi,\pi n)$ reaction on light nuclei near (3,3) resonance 77−14182
$(\pi,\pi N)$ reactions, nuclear structure effects, modified semiclassical model 77−34348
$(\pi,\pi p)$, emulsion light nuclei, 112 MeV, cross sections and mechanisms *(Russian)* 79−97733
$(\pi,\pi p)$ 60 MeV, light photoemulsion nuclei, direct knock-out model anal. *(Russian)* 79−54461
$(\pi^+,\pi^0 p)$, 170 MeV, light nuclei *(Russian)* 78−41782
$(\pi^+,\pi^+ p)$, strong absorpt. model for π induced knockout reactions 78−74404
$(\pi^+,\pi^+ p)$ quasi two particle scaling, momentum distrib. from statistical model *(Russian)* 79−40968
$(\pi^-,\pi^+\pi^-\pi^-)$, 8.9, 12.9, 15.1 GeV/c, resonance behaviour of A, A_3 mesons coherently produced on nuclei 78−50047
$(\pi,\pi X)$, multi-nucleon removal processes, reaction mechanisms 79−85520
$(\pi,\pi^+ X)$, 4.3 GeV/c, inclusive pion prod., nuclear mass number depend. 79−76029
$(\pi^-,\psi C\bar{C})$, $\psi\to\mu^+\mu^-$, $C\bar{C}\to\mu^\pm\nu X$, 225 GeV/c, search for extra μ 80−82967
$(\pi^-,\psi X)$, 225 GeV, bottom meson pair production limit 80−73750
(π,X), 50-300 MeV, pion reaction mode status, absorption and inelastic scatt. 80−42701
(π,X), effective S-wave πNN interaction, effects in nuclear matter 80−105985
(π^-,X), 1.75-6.5 GeV/c, total inelasic and knock-out cross sections, nuclear RMS radius *(Russian)* 80−32175
pion-nucleus reactions continued
(π^-,X), 20, 37 GeV/c, ang. distribs., multiplicity distribs. and particle correlations 79−93664
(Π^-,X), in emulsion, 50 GeV, charged particle multiplicity obs. 80−5172
(π^-,X), n and charged particle emission following π^- capture 80−73867
(π^-,X), z=6, 7, 8, 35, 47, charged heavy particle emission after pion capture *(Russian)* 80−69271
(π^-,X) slow pion capture in deformed nuclei, effects on high spin state excitation 80−18345
(π^+,X), 85 to 245 MeV, capture cross sections for Li, C, Al, Fe, Nb, Bi 80−73869
$(\pi^\pm,X)$, absorption cross section in range 20 to 280 MeV for Al, Ti, Cu, Sn, Au nuclei 80−78327
$(\pi,X\gamma)$ reaction at 70 MeV on s-d shell nuclei 78−29504
(π^-,Xn), stopped pion induced nuclear fission, two-step model anal. 79−59097
π double recharging in nuclei with change of strangeness *(Russian)* 79−89332
Π field in nuclei, μ absorpt. and doubly radiative Π absorpt. as probes 77−88063
π-atomic states in A=12-52, nuclear structure influence, doorway processes 80−99588
π^-, radiative capture, branching ratio with respect to stopped π^- absorpt. 78−89914
π^- absorption, meas. of neutrons and charged particles 77−10450
π^- absorption at rest, high spin state excitation, π-condensation and Δ^{++} *(Russian)* 80−86927
π^- capture at rest, exptl. method for pion discrimination and absolute counting 80−5432
π^- interactions in nucl. emulsions, 65 GeV/c, γ quanta production 78−13160
π^--emulsion interaction, 50 GeV/c , charge particle multiplicity 78−46109
π^--nucleus, 3.9 GeV/c, backward proton emission *(Russian)* 77−38302
π^--nucleus, one-particle inclusive distribs. of $\pi^\pm$ at 50 GeV *(Russian)* 77−50162
π^+ interactions, 10-254 MeV, in emulsion stacks 78−13166
$\pi^\pm$ absorption cross section on nuclei, 60-280 GeV/c 79−22293
$\pi+A\to p+X$, effect of short range pairing correl. in cumulative nucleon prod. *(Russian)* 79−30794
$\pi^-+A\to p+$anything, A=C, Al, Ti, Cu, Cd, Pb, inclusive backward emission of protons, 1.5 to 9.0 GeV *(Russian)* 77−10278
π^-+C, 40 GeV/c, secondary particle multiplicity off several nucleons *(Russian)* 78−484
$\pi^-+{}^{12}C$, 40 GeV/c, partial inelasticity factors determ. *(Russian)* 78−33227
$\pi+d\to 2N$ in Δ-resonance region, 100-300 MeV *(Russian)* 78−33083
$\pi+$emulsion nucleus, 60 to 200 GeV, shower particle multiplicity distrib. parametrisations 78−62524
π^-+emulsion, 50 GeV/c^{-1}, pseudo-rapidity distrib. of fast secondaries 79−9631
π^-+emulsion collisions, charged particle multiplicity distrib., high energy, KNO scaling 78−70568
π^-+emulsion nuclei, 50 GeV/c multiplicities of secondary charged particles *(Russian)* 78−46116
π^-+emulsion nuclei, shower ang. distribs., anisotropy coeffs. multiple prod. mechanism 10^{10} to 10^{13} eV/nucleon *(Russian)* 77−79385
π^-+nucleus, inclusive at 3.9 GeV/c, Λ Feynman scaling obs. *(Russian)* 79−9635
π^-+nucleus, multiple charged-particle generation in inclusive reactions at 40 GeV 79−76022
$\pi^-+\text{nucleus}\to(3\pi)^-+\text{nucleus}$, 15 GeV/c, diffractive dissociation *(Russian)* 78−25250
π^-+photoemission nuclei, search for new short lived particles *(Russian)* 77−88180
π^-+Xe, 3.5 GeV/c, π^0 correlations *(Russian)* 77−82760
πA high-energy collision yields, evidence for composite quark model *(Russian)* 79−9636
π^-A, 3.7 GeV, correlation parameter between π^- emitted backwards and forwards *(Russian)* 78−45984
$\pi^-A\to\pi^0X$ with $\Delta(1240)$ slow isobar intermediate prod. in heavy nuclei, cross section *(Russian)* 78−89917
πd, compilation of integrated cross sections 79−89187
π^+d, 4 GeV/c, cross sections for strange particle prod. 79−17753
π^3He^3H coupling constant estimation, Chew-Low eqn. 77−3051
π^3He^3He coupling, estimation methods 79−63599
π^3He^3He coupling on basic of PCAC 80−32196
πN in nucleus, diffraction dissociation, dip and kink structs., differential cross sections 80−95284
πN scattering amplitude in nuclear medium at nuclear matter density 78−29500
π^-N, 50 GeV, inelasticity factors, energy separated particles *(Russian)* 78−25251
$\pi^-Ne\to$neutral hadron+X, 200 GeV/c, n and $\bar{n}$ prod. 77−18349
$\pi^-p\to J/\psi+n$ or $\chi+n$, 27-40 GeV/c, nuclear proton, upper limit on cross section *(Russian)* 78−78218
$(\pi^\pm X)$ total cross sections, shadowing and antishadowing effects 79−9632
ψ meson prod. by π^--mesons with momentum 43 GeV/sec in Be, Cu and W nuclei *(Russian)* 78−8863
ρ-meson intermediate states in πN scatt. Chew-Low theory modifications 79−479
Ag $(\pi,\alpha X)$, 70 MeV, α cross sections and energy spectra, intranuclear cascade calcs. 79−575
$Al+\pi^-$, 0.75 GeV/c, neutron energy spectra meas. 79−67777
$Al+\pi^-$, 3.7 GeV/c, proton spectra *(Russian)* 78−41785
$Al+\pi^-$, 40 GeV/c, multiparticle production 80−5173
$Al+\pi^-$, 7 GeV/c hadron multiple prod. *(Russian)* 79−22298
$Al+\pi^\pm$, 125 MeV, true absorpt. and scatt. 79−63705
$Al+\pi^\pm$, 200 GeV, jet production 79−54438
$^{22}Al(\pi,p\gamma\gamma)$, 190 MeV, quasi-free single nucleon removal, p and π spectra 79−85519
^{27}Al, 355 MeV, ratio of π^+ and π^- cross sections from coincidence meas. 78−29501
$^{27}Al+\pi^-$, γ-π^- coincidence spectra, 190 MeV 78−89913
$^{27}Al(\pi,^\pm X\gamma)$, 190, 220 MeV, multinucleon removal cross sections and γ-ray spectra, binding energy effects 79−3183
$^{27}Al(\pi,\pi' p)$, 255 MeV, quasielastic knockout, proton yield, $\sigma(\pi^+)/\sigma(\pi^-)$ cross section ratio 80−32305

pion-nucleus reactions continued
^{27}Al(π,xγ), gamma ray coincidence spectra, nuclear surface clustering evidence 79−6707
^{27}Al(π^-, pxγ), 300 MeV, proton-gamma ray coincidence spectra 79−6704
^{27}Al(π^-,Xγ) 230 MeV reactions near Δ(1232) resonance 77−6465
^{27}Al(π^-,π^- n) and (π^-, π^-p+π^0n), knockout reactions, cross sections, nucleon charge exchange model 78−25246
^{27}Al($\pi^\pm$,p), (π^+,d), E=100, 220 MeV p and d spectra meas. 78−648
^{27}Al($\pi^\pm$,$\pi^\pm$N), 180-255 MeV, quasielastic pion scatt. coincidence expt. interpretation, impulse approx. 80−68704
^{27}Al($\pi^\pm$,$\pi^\pm$X), 190 MeV, multiparticle removal occurring as separate particles, cluster removal 79−85498
^{27}Al($\pi^\pm$,$\pi^\pm$xγ), 300 MeV, pion-gamma coincidence spectra 79−6705
^{27}Al(π^+,xγ), 300 MeV, gamma-ray coincidence spectra, clustering evidence 79−6706
Al(π,X), 125 MeV, absorption cross section in 3:3 resonance region 79−85543
Al(π,X), quark jet multiple production 80−9188
Al(π,αX), 70 MeV, α cross sections and energy spectra, intranuclear cascade calcs. 79−575
A(π^+,2p)B*, effect of nuclear form factors *(Russian)* 78−25248
A($\pi^\pm$,$\pi^-\pi^0$)A, possibility of investigating $\gamma\pi\to\pi\pi$ and $\rho(\rho')\to\pi\gamma$ processes *(Russian)* 79−9639
^{75}As, stopped π^- absorpt. 77−38299
^{75}As, stopped π^- absorption, in beam and activation γ-ray spectroscopy 79−40960
Au (π,αX), 70 MeV, α cross sections and energy spectra, intranuclear cascade calcs. 79−575
Au fragmentation by 294 MeV π^+, excitation function for ^{24}Na prod. 77−38301
^{197}Au ($\pi\pm$,$\pi\pm$N), 100-300 MeV, activation cross section, π^+/π^- cross section ratio 79−89329
^{197}Au, stopped π^- absorpt. 77−38299
^{197}Au, stopped π^- absorption, in beam and activation γ-ray spectroscopy 79−40960
^{197}Au(π^-, xn), single and correlated n spectroscopy, nuclear temp. 79−6713
^{197}Au($\pi^\pm$, spallation), 100-300 MeV, cross sections for products A=167-196 80−27619
^{197}Au($\pi^\pm$,x), 176-368 MeV, ^{24}Na fragment emission excitation functions cascade-evaporation anal. 79−6553
Au(π^-,X), stopped π^- capture, product nuclei distribs., isomeric yield ratios, neutron multiplicity 77−18625
^{10}B(π^-,2n), neutron-pair emission characts., excitation energy spectra 78−13159
^{10}B(π^-,2n), stopped pion absorption 78−25243
^{10}B(π^-,n), single neutron emission induced by stopped π^- in 1p shell nuclei 79−59089
Be, 200 GeV/c, forward inclusive prod. spectra of K_s, Λ^0, $\bar{\Lambda}^0$, n, 200 GeV/c 78−82393
Be+π^-, 43 GeV/c, inclusive J/ψ prod., A-depend. 78−62581
Be+π^-, 7 GeV/c hadron multiple prod. *(Russian)* 79−22298
Be+π^-, associative production of D^0 mesons with muons, 55 GeV/c *(Russian)* 79−3060
Be+$\pi^-\to D^0\bar{D}^0$X, pair production at 55 GeV/c *(Russian)* 79−3059
Be+π^+, 150 GeV, inclusive muon pair prod. parameters, statistical interpretation 79−30820
^{9}Be π capture, two-photon emission obs. 79−26460
^{9}Be(π, πN), 60 and 300 MeV, γ-ray meas. 78−41780
^{9}Be(π,X), X=γ, $\gamma\gamma$, e^+e^-, rare pion absorption modes, theoretical and expt. results 80−42698
^{9}Be(π^-, γ), photon spectra meas. with SIN pairspectrom. 77−10446
^{9}Be(π^-,2n), neutron-pair emission characts., excitation energy spectra 78−13159
^{9}Be(π^-,2n), stopped pion absorption 78−25243
^{9}Be(π^-,n), single neutron emission induced by stopped π^- in 1p shell nuclei 79−59089
^{9}Be(π^-,πN), 1 GeV/c, heavy fragment knockout process, ^{8}Li ang. distribs. 80−106036
Be(π^-, Ψ), 43 GeV, A dependence of inclusive distrib. *(Russian)* 78−45983
Bi, π^- absorption *(Russian)* 78−46115
Bi+$\pi^\pm$, 125 MeV, true absorpt. and scatt. 79−63705
^{209}Bi, pion$^-$ capture, high spin states and neutron multiplicities meas. 78−54806
^{209}Bi, π^- capture, p, d and α inclusive prod. spectra 79−22338
^{209}Bi, stopped π^- absorption, in beam and activation γ-ray spectroscopy 79−40960
Bi(π,X), 125 MeV, absorption cross section in 3:3 resonance region 79−85543
C (π^-,p) 1.5-5 GeV/c, cumulative proton polarisation *(Russian)* 80−86896
C, absorpt. of stopped π^-, charged particle energy spectra meas. 78−33224
C, π^- interactions at 5 GeV, spectra investigs. using propane bubble chamber *(Slovak)* 77−42214
C, π^+ absorption in flight, 80-140 MeV, absorption cross section 79−85494
C+π, 40 GeV/c, π interference *(Russian)* 78−41784
C+π, 40 to 280 MeV, second order optical pot., effect of short range correls. 78−74407
C+π^-, 3.7 GeV/c, proton spectra *(Russian)* 78−41785
C+π^-, 40 GeV/c, two-particle correls., rapidities, ang. distribs. *(Russian)* 78−17251
C+π^-, 5 GeV/c, pp correlations *(Russian)* 80−9316
C+π^-, 7 GeV/c hadron multiple prod. *(Russian)* 79−22298
C+π^-, elastic and coherent cross-section at 40 GeV/c using propane bubble chamber 80−27524
C+π^- 40 GeV/c, multiparticle production 80−5173
C+π^- collision data, 40 GeV/c, comparison with Bialkowski, Chiu and Tow model 78−58305
C+π^- inclusive K^0-meson production cross section *(Russian)* 78−82394
C+$\pi^\pm$, 125 MeV, true absorpt. and scatt. 79−63705
C+$\pi^\pm$, 225 GeV/c, J/ψ and ψ'(3.7) prod. study using muon pair meas. 77−57694
C+$\pi^\pm$, massive muon pair prod., test of Drell Yan model 77−57695
^{12}C (π,X), X=γ, $\gamma\gamma$, e^+e^-, rare pion absorption modes, theoretical and expt. results 80−42698
^{12}C ($\pi^\pm$, $\pi^\pm$d), 180 MeV, cross-section ratios 80−32308

pion-nucleus reactions continued
^{12}C ($\pi^\pm$, $\pi^\pm$t), 180 MeV, cross section ratios 80−32308
^{12}C, π capture, two-photon emission obs. 79−26460
^{12}C, π^- capture, p, d and α inclusive prod. spectra 79−22338
^{12}C, π^- capture reactions, neutron spectra determ. by 2 and 4 nucleon cluster expansions 79−6703
^{12}C, π^+ absorption in flight, cross section, 91-143 MeV 80−63212
^{12}C, π^+ induced two nucleon removal 78−25242
^{12}C, rescatt. effects in 2p bound π-absorpt. 79−36275
^{12}C, total cross section, Glauber theory in microscopic α-cluster model 79−13346
^{12}C+π, 5 GeV/c, momentum spectra and mechanism of proton emission *(Russian)* 79−89334
^{12}C+π, 60-120 MeV, p-wave optical pot., cross sections, Chew-Low model 78−70567
^{12}C+π^-, 4 GeV/c, general characts. of secondary π inclusive prod. *(Russian)* 78−78421
^{12}C+π^-, 40 GeV, secondary charged particle multiplicities *(Russian)* 79−3184
^{12}C+π^-, 40 GeV/c, cross sections of Λ and K prod. *(Russian)* 77−6184
^{12}C+π^-, 40 GeV/c, effect of nucl. transparency *(Russian)* 78−54805
^{12}C+π^-, 40 GeV/c, leading and conserved mesons *(Russian)* 78−45987
^{12}C+π^-, 40 GeV/c, multiplicity distribs. of secondary charged particles, Glauber model calcs. *(Russian)* 78−17252
^{12}C+π^-, 40 GeV/c, $\pi^\pm$ momentum and ang. distribs. *(Russian)* 77−50164
^{12}C+π^-, 40 GeV/c, secondary charged particles multiplicity *(Russian)* 77−50163
^{12}C+π^-, 40 GeV/c, secondary charged particle inclusive spectra, $\pi^\pm$ struct. functions *(Russian)* 78−89921
^{12}C+π^-, 40 GeV/c, total disintegration, emission angles and momenta of fragments *(Russian)* 78−89920
^{12}C+π^-, 5 GeV/c, charged π emission space-time characts. *(Russian)* 78−78422
^{12}C+π^-, KNO scaling, automodel behaviour of multiplicity distrib. as function of inelasticity factor *(Russian)* 79−89213
^{12}C+$\pi^-\to$p+X, 40 GeV/c π^- momentum *(Russian)* 79−89335
^{12}C+$\pi^\pm$, proton spectra, cross section, π. absorpt. mechs. 78−25239
^{12}C(π, 2γ), limit on 2γ/1γ branching ratio 77−10447
^{12}C(π, πN), 60 and 300 MeV, γ-ray meas. 78−41780
^{12}C(π^-, πp)^{11}B, knockout reaction, cross section ratio $\sigma(\pi^+,\pi^0\mathrm{p})/\sigma(\pi^-,\pi^0\mathrm{p})$ meas. 80−32254
^{12}C(π,X), angular distrib. of inelastic diffusion of $\pi^\pm$ *(French)* 80−47507
^{12}C(π,X), deep inelastic, π and Δ optical pot. effects, semiclassical transport model 80−52698
^{12}C(π,X), Kalinkin-Shmonin model, expt. data 80−86931
^{12}C(π,γ), photon spectrum from generalised Helm model 79−76023
^{12}C(π,$\gamma\gamma$)X, two-photon decay branching ratios 77−88179
^{12}C(π,p), limit on pion-condensate strength 77−71625
^{12}C(π,p)^{11}Be, captive rate probabilities to bound states 77−18614
^{12}C(π,π'), obs. of enhanced ^{12}C excitation by inelastic π scatt. on πN(3,3) reson. 79−17938
^{12}C($\pi\,\gamma\gamma$), branching ratio, ang. correlation 79−85526
^{12}C(π^-, 2γ), doubly radiative capture theory, branching ratio and ang. correlations 80−9314
^{12}C(π^-, e^+e^-)^{12}B, 164 MeV, estimation of cross-section *(Russian)* 79−89333
^{12}C(π^-, γ), pion$^-$ radiative capture probab. *(Russian)* 80−42538
^{12}C(π^-, γ)^{12}B*, excitation of collective states, shell model 80−22652
^{12}C(π^-, NN), bound π absorpt., HF wave functions, branching ratios, ang. distrib. 78−54803
^{12}C(π^-, X), 40 GeV/c, cumulative pions and nucleus total disintegration probability *(Russian)* 80−57807
^{12}C(π^-, X), 40 GeV/c, many-nucleon interactions, secondary $\pi^\pm$ spectra *(Russian)* 79−97638
^{12}C(π^-, X), (X=p, d, t, ^{3}He, ^{4}He, ^{6}Li, ^{7}Li), emitted particle energy spectrum following pion stopping 79−93666
^{12}C(π^-,X), 40 GeV/c, hadron emission into backward hemisphere *(Russian)* 79−59094
^{12}C(π^-,X), 40 GeV/c, $\pi^\pm$ rapidity distribs., fast and slow particle components *(Russian)* 79−40969
^{12}C(π^-,X), 40 GeV/c, secondary neutron average number, charge exchange coeffs., n inelasticity coeffs. *(Russian)* 80−32132
^{12}C(π^-,2n), neutron-pair emission characts., excitation energy spectra 78−13159
^{12}C(π^-,2n), stopped pion absorption 78−25243
^{12}C(π^-,γ), gamma-ray meas. with SIN pairspectrom. 77−10523
^{12}C(π^-,n), single neutron emission induced by stopped π^- in 1p shell nuclei 79−59089
^{12}C(π^-,n), stopped pion, neutron energy spectra, mean energies and multiplicities 80−9311
^{12}C(π^-,nn) or ^{12}C(π^-,pn), rescatt. effects in stopped pion absorpt. 78−29498
^{12}C(π^-,p)^{11}Be, absorption at rest. expts. with pion beams of Saclay Linac *(French)* 79−572
^{12}C(π^-,π^-)^{12}C*, 4.5 GeV/c, gamma-ray decay obs., nucl. polarisation anal. 77−30636
^{12}C(π^-,π^-p)^{11}B, 170 MeV, comparison with dispersion theory calcs. *(Russian)* 77−50161
^{12}C(π^-,π^+)X, 40 GeV, multiparticle prod. mechanism, various model predictions 79−573
^{12}C(π^+, π^+p), 100, 180 MeV, knock out reaction, cross section and pion distortion in DWIA 80−91167
^{12}C(π^+,X), 85-245 MeV, true absorption and scatt. in (3,3) resonance region 80−102207
^{12}C(π^+,2p), cluster effects in in-flight π^+ capture 78−89916
^{12}C(π^-,$\alpha\pi^+$)^{8}Be, 112 MeV, pole approx. anal., knock out reaction mechanism *(Russian)* 78−86553
^{12}C(π^+,d)^{10}C, transitions to low lying states in ^{10}C 78−46110
^{12}C(π^+,p^{3}He), cluster effects in in-flight π^+ capture 78−89916
^{12}C(π^+,p), 90 and 180 MeV, ang. distrib. meas. 79−85502
^{12}C(π^+,p)^{11}C, 49.3 MeV, transitions confirm multistep processes 78−46110
^{12}C(π^-,p)^{11}C near (3,3) resonance region, appl. of isobar doorway model 78−41778
^{12}C(π^+,pd), cluster effects in in-flight π^+ capture 78−89916
^{12}C(π^+,π^+), 180 MeV, I^+ T=0,1 collective states anal. 79−85540
^{12}C(π^+,π^++p)^{11}B, 100 MeV, cross-section meas. 78−29510

pion-nucleus reactions continued
$^{12}C(\pi^+,\pi^+\alpha)$, 60 MeV, ^{8}Be cross sections and ang. distribs., direct knock-out model anal. *(Russian)* 80−27620
$^{12}C(\pi^+,\pi^+p)$, 100, 130 MeV, quasi-elastic scatt. cross section 80−102208
$^{12}C(\pi^+d)$, DWBA cross section formula, PWBA differential cross section *(Chinese)* 80−22861
$^{12}C(\pi^\pm,\pi^\pm N)$, 291 MeV, quasielastic scatt., differential cross sections, Monte-Carlo data fit 80−68703
$^{12}C(\pi^\pm,\pi^\pm d)$, ^{10}B, 180 MeV, isospin effects in (3/2, 3/2) resonance region 79−85365
$^{12}C(\pi^\pm,X)$, 100-250 MeV, ^{12}C production yield ratio with ^{13}C and ^{16}O 79−85516
$^{12}C(\pi^\pm,X)$, 180, 290 MeV, quasielastic scatt., differential cross section 79−85518
$^{12}C(\pi^\pm,\pi^\pm N)$, 180-255 MeV, quasielastic pion scatt. coincidence expt. interpretation, impulse approx. 80−68704
$^{12}C(\pi^\pm,\pi^\pm)$, 148 to 226 MeV, ang. distrib. around (3,3) reson. 79−85537
$^{12}C(\pi^\pm,\pi^\pm)$ local energy shift effects 79−85511
$^{12}C(\pi^\pm,\pi^+p)^{11}B$, 180 MeV, isospin effects in (3/2, 3/2) resonance region 79−85365
$^{12}C(\pi^\pm,\pi^\pm p)^{11}B$, 180 MeV, π^+ to π^- cross-section ratio 80−73868
$^{12}C(\pi^\pm,\pi^\mp)$, 290 MeV, double charge exchange cross sections 80−18348
$^{12}C(\pi^\pm,\pi^\mp)$, 290 MeV, inclusive double charge exchange, differential cross sections 79−93662
$^{12}C(\pi^\pm,\pi N)$, 200 MeV, $^{11}C/^{11}B$ mirror level pair cross sections 79−67665
$^{12}C(\pi^\pm,\pi N)$, 40-600 MeV, excitation functions and absolute cross sections 80−18226
$^{12}C(\pi^\pm,\pi N)^{12}C$(4.44 and 15.11 MeV), test of outgoing nucleon analogue charge exchange 78−25238
$^{13}C(\pi^+,\pi^0)$, angle integrated cross section, optical pot., n and p radius differences 80−32307
$^{13}C(\pi,\pi N)$, 60 and 300 MeV, γ-ray meas. 78−41780
$^{13}C(\pi,np)^{11}Be$, capture rate probabilities to bound states 77−18614
$^{13}C(\pi^+,\pi^{+orb})$, 120-226 MeV, inelastic scatt, and charge exchange, coupled channels calcs. 80−57804
$^{13}C(\pi^+,p)$, 90 and 180 MeV, ang. distrib. meas. 79−85502
$^{13}C(\pi^+,\pi^0)$, 0-300 MeV, cross sections, pion-nucleus optical pot. including nuclear Hamiltonian 80−68706
$^{13}C(\pi^+,\pi^0)$, 150 MeV, single charge exchange, isobaric analogue state excitation, cross sections 80−42544
$^{13}C(\pi^+,\pi^0)$, total cross section energy depend., first order optical pots. 79−76028
$^{13}C(\pi^+,\pi^0)^{13}N$, 70-230 MeV, calc. of cross section, using multistep contributions within modified eikonal formalism 78−21609
$^{13}C(\pi^+,\pi^0)^{13}N$, charge-exchange transition vertex, optical pot. 77−6461
$^{13}C(\pi^+,\pi^0)^{13}N$, DWIA, isovector correls. 78−29499
$^{13}C(\pi^+,\pi^0)^{13}N$, eikonal model cross-section calc. near (3,3) reson. 77−18609
$^{13}C(\pi^+,\pi^0)^{13}N$, Pauli and short range correls. near (3,3) reson. 77−18608
$^{13}C(\pi^+,\pi^0)^{13}N$ in (3,3) reson. region, optical model calc. 77−18610
$^{13}C(\pi^\pm,X)$, 100-250 MeV, ^{12}C production yield ratio with ^{12}C 79−85516
$^{14}C(\pi\gamma)$, collective resonances, A=14 isobaric states, shell model predictions 79−85386
$^{40}C(\pi,\gamma X)$, short-range 4-N correls. 77−18613
Ca isotopes, neutron RMS radii from pion total cross-sections 77−57589
$^{A}Ca(\pi^-,\pi^-N)$, A=40, 44, 48, 291 MeV, quasielastic scatt., differential cross sections, Monte-Carlo data fit 80−68703
$^{A}Ca(\pi^\pm,X)$, A=40, 44, 48, 180, 290 MeV, quasielastic scatt., differential cross section 79−85518
$^{A}Ca(\pi^\pm,\pi^\pm)$, A=40,42,44,48, 180 MeV (in)elastic scatt. differential cross-sections, Pauling blocking 79−85539
$^{A}Ca(\pi^-,\pi^+)$, A=40, 44, 48, 290 MeV, inclusive double charge exchange, differential cross sections 79−93662
$^{A}Ca(\pi^\pm,\pi^\mp)$, A=40,44,48, 290 MeV, double charge exchange cross sections 80−18348
^{40}Ca, π^- capture, p, d and α inclusive prod. spectra 79−22338
$^{40}Ca(\pi^-,2n)$, absorpt. at rest, ^{38}K excitation spectrum and distrib. 78−66322
$^{40}Ca(\pi^+,\pi^+)$, 241 and 163 MeV, giant resonance studies 79−85512
$^{40}Ca(\pi^\pm,\pi N)$, 200 MeV, $^{39}Ca/^{39}K$ mirror level pair cross sections 79−67665
$^{48}Ca(\pi^-,\pi^0)$, excitation of collective modes and high-spin states, DWA calcs. 77−10448
$^{48}Ca(\pi^\pm,\pi^\pm)$, optical pot. ambiguities, neutron radius determ. 79−17872
$Ca(\pi^\pm,X)$, stopped π^-, fast $\pi^\pm$, 180, 220 MeV, interactions near $\Delta(1232)$ resonance 79−6712
$Cd+\pi^-$, 0.75 GeV/c, neutron energy spectra meas. 79−67777
$Cd+\pi^-$, 7 GeV/c hadron multiple prod. *(Russian)* 79−22298
$Cd(\pi^-,X)$, 0 MeV, A=111, 112, E2 nuclear resonance effects, γ and X-ray meas. 78−41774
^{59}Co, stopped π^- absorption, in beam and activation γ-ray spectroscopy 79−40960
$C(\pi,X)$, 125 MeV, absorption cross section in 3:3 resonance region 79−85543
$C(\pi^-,X)$, 3 GeV/c, n inclusive spectra, neutron yield *(Russian)* 80−13510
$C(\pi^+,2p)$, 112 MeV, reaction mechanism *(Russian)* 78−29508
$C(\pi,\alpha X)$, 70 MeV, α cross sections and energy spectra, intranuclear cascade calcs. 79−575
$C(\pi^-,n)$ spectrum obs. and calc. 79−17933
$C(\pi^\pm,\pi^\pm X)$, X=He or d, 170 MeV, cross sections and ang. distribs., direct knockout mechanism *(Russian)* 80−86887
$C(\pi^+,\pi^+d(He))$, 60 MeV, cross sections, momentum and ang. distribs. *(Russian)* 77−74888
$C(\pi,\pi p)$, 170 MeV, two stage and knock out contribs., π^+,π^- spallation differences *(Russian)* 80−68632
$C(\pi^-,\pi^-p)$, nuclear photoemulsion obs. at E_π=115 MeV, ang. distribs. and cross sections *(Russian)* 79−13352
$Cr+\pi$, 200 GeV, multiparticle production in emulsion 79−40967
$^{52}Cr(\pi,X)$, angular distrib. of inelastic diffusion of $\pi^\pm$ *(French)* 80−47507
$^{52}Cr(\pi^\pm,\pi^\pm)$, 180 MeV, ang. distrib. around (3,3) reson. 79−85537
$Cr(\pi^-,\pi^0)$, 200 MeV, deexcitation γ spectra, transitions in ^{52}Mn 78−89912
$^{133}Cs(\pi,p)$, stopped π^- ^{132}I yield and γ-ray spectra 80−86857
$^{133}Cs(\pi^-p)$ stopped π, ^{132}I isomer and gamma-ray spectrum 80−78199

pion-nucleus reactions continued
$Cu+\pi^-$, 27, 40 GeV, cross sections and differential distribs. for muon pair prod. *(Russian)* 78−89919
$Cu+\pi^-$, 27, 40 GeV/c, muon pair production with low masses *(Russian)* 79−89212
$Cu+\pi^-$, 3.7 GeV/c, proton spectra *(Russian)* 78−41785
$Cu+\pi^-$, 43 GeV/c, inclusive J/ψ prod., A-depend. 78−62581
$Cu+\pi^-$, 7 GeV/c hadron multiple prod. *(Russian)* 79−22298
$Cu+\pi^-$, inclusive interaction, $J(\psi)$ prod. cross sections at 27 and 40 GeV/c 78−25088
$Cu+\pi^-$ 40 GeV/c, multiparticle production 80−5173
$Cu+\pi^-\rightarrow J/\psi+X$ *(Russian)* 78−25249
$Cu+\pi^-\rightarrow\mu^+\mu^-X$, 16, 22 GeV, quark annihilation model interpretation, scaling 79−36277
$Cu(\pi^-,\Psi)$, 43 GeV, A dependence of inclusive distrib. *(Russian)* 78−45983
$Cu(\pi^-,X)$, 3 GeV/c, n inclusive spectra, neutron yield *(Russian)* 80−13510
$Cu(\pi^-,X)$, stopped pions, radioactive product yields 80−83126
$Cu(\pi^-,p)$ 1.5-5 GeV/c, cumulative proton polarisation *(Russian)* 80−86896
$Cu(\pi^-,\psi'(3700))$, 50 GeV, formation cross-sections *(Russian)* 80−106082
$Cu(\pi^-$, spallation) 0.6, 0.9, 1.2 GeV, T=1/2 resonances, Na, Sc and Co rel. yields 80−5109
$Cu(\pi^-$, spallation), 500, 1570 MeV, product relative yields, charge dispersion and mass yield 79−6554
$Cu(\pi^\pm$, spallation), 50-350 MeV, radioactive residual nuclei prod. cross sections at (3,3) resonance 79−3130
$^{19}F(\pi^-,\pi^-n)$ and $(\pi^-,\pi^-p+\pi^0n)$ knockout reactions, cross sections, nucleon charge exchange model 78−25246
$^{19}F(\pi^-,X\gamma)$, 230 MeV reactions near $\Delta(1232)$ resonance 77−6465
$Fe+\pi^-$, 0.75 GeV/c, neutron energy spectra meas. 79−67777
$Fe+\pi^\pm$, 125 MeV, true absorpt. and scatt. 79−63705
$Fe(\pi,X)$, 125 MeV, absorption cross section in 3:3 resonance region 79−85543
Ge, 15 GeV/c protons, nucl. interactions under random and channelling conditions in single crystals 79−13348
$^{76}Ge(\pi^+xn)^{76-x}As$, 100, 180 MeV, product formation cross section 80−42705
$H+\pi^\pm$, 200 GeV, jet production 79−54438
$H+\pi^\pm$, 50-30 MeV, total cross section meas. 77−6437
$H+\pi^\pm$, A=1,2, total cross sections, charge independ. and symm. 78−66321
$^{1}H(\pi^-,\gamma n)$ differential cross-sections in $\Delta(1232)$ region 79−93665
$^{1}H(\pi^-,X)$, 40 GeV/c, hadron emission into backward hemisphere *(Russian)* 79−59094
$^{1}H(\pi^-,\gamma)$, effective range theory parameters a_{nn} and r_{nn} 79−85381
$^{1}H(\pi^-,\gamma\gamma)n$, off-mass shell πN amplitude, $\pi^0\rightarrow\gamma\gamma$ amplitude, chiral Lagrangian model 79−93669
$^{2}H+\pi$, coupled channel theory 78−13157
$^{2}H+\pi$, elastic scatt., absorpt., model using coupled channel eqns., exact soln. 77−88176
$^{2}H+\pi^-$, multiplicity distrib. data, simple non-interacting fireball model 79−3178
$^{2}H+\pi^-\rightarrow\pi^0nn$, rest capture branching ratio, impulse approx. 78−62957
$^{2}H+\pi^+$, proton spectra, cross section, π. absorpt. mechs. 78−25239
$^{2}H(\pi,2n\gamma)$, final state interactions, n+n scatt. parameters 78−25245
$^{2}H(\pi,n\pi)$, total cross sections 79−85510
$^{2}H(\pi,p)^{1}H$, threshold to 3,3 resonance region, disintegration model containing absorption 77−88177
$^{2}H(\pi,p)p$, absorptive P-wave pion-nucleus optical pot. 79−22327
$^{2}H(\pi,p)p$, cross sections, Faddeev like eqns., absorption effects for scatt. 80−86928
$^{2}H(\pi,p)p$, reactive two body contrib. to pion-nucleus optical pot. 80−9313
$^{2}H(\pi,p)p$ in resonance region, theoretical models 80−83123
$^{2}H(\pi,pp)$, generalised Low eqn. approach to reaction matrix 79−85491
$^{2}H(\pi,pp)$, pion absorption in field theory using Low equation 79−67779
$^{2}H(\pi,\pi)^{2}H$, impulse approx., three-body helicity formalism 77−74885
$^{2}H(\pi^-,n)n$, mechanism, cross-sections, EM form factors 79−89181
$^{2}H(\pi^-,n\gamma)n$, n-n scatt. length from γ spectrum 78−62576
$^{2}H(\pi^-,\pi^-p)n$, 438 GeV/c, break up process, kinematic variables, np final state interaction *(Russian)* 80−52701
$^{2}H(\pi^-,\gamma n)n$, effective range theory parameters a_{nn} and r_{nn} 79−85381
$^{2}H(\pi^-,n\gamma)n$, multiple scatt. corrections, off-shell rescatt. effects, effective range 80−83127
$^{2}H(\pi^+,p)p$, $p\pi$ exchange current effects on pion absorption, cross section enhancement 80−57803
$^{2}H(\pi^+,p)^{1}H$, total cross section, ang. distribs. and asymmetry parameters 80−63182
$^{2}H(\pi^+,p)p$, pion absorption, absorptive P-wave pion-nucleus optical pot. 79−76031
$^{2}H(\pi^+,p)p$, pionic disintegration, absorptive π-nucleus optical pot., microscopic model 80−99191
$^{2}H(\pi^+,pp)$ 40, 50 and 60 MeV, absolute differential cross sections, ang. distrib. polynomial fit 78−70571
$^{2}H(\pi^+,\pi^-)X^-$, 2.6 GeV/c, d proton screening correction and Glauber parameter 80−9175
$^{2}H(\pi^\pm,p\pi^\pm)$, 340 MeV/c, reaction mechanisms and isospin effects 80−32306
$^{2}H(\pi^\pm,p\pi^\pm)n$, 350 MeV break-up, differential cross sections 79−85509
$^{3}H(\pi^-,\gamma)3n$, rest π, resonance branching ratio, bound state upper limit 80−99162
$^{3}H(\pi^-,3n)$, final state continuum spectra, hyperspherical basis 77−26590
$^{3}H(\pi^+,\gamma)^{3}He$ 79−80959
$^{3}H(\pi^\pm,\pi^0)^{3}He$, elastic scatt., charge exchange and symmetries, and ^{3}H, ^{3}He form factors meas. 79−80959
$He+\pi$, compilation of integrated cross sections 79−89187
$He+\pi$, fragment and pion multiplicities 77−18620
$He+\pi$, particle multiplicity correlations in streamer chamber 79−85506
$He+\pi^\pm$, 1.5 to 2.5 GeV interactions in streamer chamber 79−6709
$^{3}He(\pi,\Gamma)^{3}H$, model calc. of Panofsky ratio 77−14190
^{3}He, liquid, pionic K X-ray transition energies and Lorentzian widths 80−78727
^{3}He Panofsky ratio meas., $\omega(\pi^-,\pi^0)/\omega(\pi^-,\gamma)$ 79−76034
^{3}He, π^- nonradiative absorption at rest 79−76035
$^{3}He(\pi^-,\pi^0)$, 200 MeV, single charge exchange, isobaric analogue state excitation, cross sections 80−42544
$^{3}He(\pi^-,\gamma)^{3}H$, Panofsky ratio and axial vector form factor 79−574

pion-nucleus reactions continued
^{3}He(π^-,γ)^{3}H, radiative capture rate and threshold π photoprod.; Panofsky ratio from ^{3}He(π^-,π^0) 79−13350
^{3}He(π^-,n)^{2}H, 100, 200 and 290 MeVs differential cross sections 78−33223
^{3}He(π^-,π^0), form factor sensitivity in Glauber multiple scatt. formalism 80−105964
^{3}He(π^-,π^0)^{3}H, elastic scatt., charge exchange and symmetries, and ^{3}H, ^{3}He form factors meas. 79−80959
^{3}He(π^-,π^0)^{3}H, isobaric analogue state ang. distrib. 79−85508
^{3}He(π^-,π^0)^{3}H, optical potential in momentum representation 80−78324
^{3}He(π^-,π^0)^{3}H, Panofsky ratio and axial vector form factor 79−574
^{3}He(π^+,3p), final state continuum spectra; hyperspherical basis 77−26590
^{3}He$\pi^-\rightarrow$nd, ^{3}He$\pi^-\rightarrow$n+n+p, two nucleon absorpt. model 78−41776
^{4}He (π^-, π^-p), 5GeV/c, quasielastic scatt., cross section, form factor, final state interactions 80−99190
^{4}He, π scatt. and absorption, microscopic calc. 79−85501
^{4}He+π^-, coupled channel method, determ. of total cross sections 79−36281
^{4}He+π^-, excitation of Δ-nuclear states 77−88093
^{4}He+π^-, pion absorption, isobar formation in streamer chamber 79−85504
^{4}He+π^+, 110, 160 MeV, cross section ratio of (π^+,π^+p) to (π^+,π^-n)+(π^+,π^0p) reactions 78−74403
^{4}He+π^+, 120-165 MeV, non-elastic interaction 79−76041
^{4}He+$\pi^+\rightarrow\pi^+\pi^-$ppd, 1.7 GeV/c, cross section, Δ(1232) and ρ(770) resonance prod. 78−89911
^{4}He+$\pi^\pm$, proton spectra, cross section, π. absorpt. mechs. 78−25239
^{4}He(π,X), 120, 145, 165 MeV, total and differential cross sections 80−78326
^{4}He(π,πX)^{3}H, 5 GeV, nucleon isobar content in He using impulse approx. 79−36276
^{4}He(π^-,n)^{3}H, 100, 200 and 290 MeVs differential cross sections 78−33223
^{4}He(π^-,n)T, neutron energy spectrum determ. 79−6702
^{4}He(π^-,π^-X)^{3}H, 5 GeV, nucleon isobar prod. and knockout 80−42709
^{4}He(π^-,π^-x)He, 5 GeV, recoil spectrometer meas. 78−90011
^{4}He(π^-,π^-x)^{3}H, 5 GeV, recoil spectrometer meas. 78−90011
^{4}He(π^+,3p)^{1}H, 98-156 MeV, cross-section comparison with models 77−18612
^{4}He(π^+,3pn), quasideuteron absorption in non-radiative capture 79−85495
^{4}He(π^+,π^-)4p, 1.5 to 2.0 GeV/c, cross sections, momentum spectra, ang. distrib. Δ resonances prod. 77−65237
^{4}He(π^+,π^0p), 120-165 MeV, isobaric resonance excitation, total inelastic cross section 79−85427
^{4}He(π^+,π^+p), 120-165 MeV, 3 nucleon exchange in knock-out reactions, cross sections 79−85437
^{4}He(π^+,π^0p)^{3}He, 105 to 135 MeV, cluster effects 79−85513
^{4}He(π^+,π^+2n2p), 120-165 MeV, total cross section, multiple scatt. processes 79−85517
^{4}He(π^+,π^+n), 120-165 MeV, isobaric resonance excitation, total inelastic cross section 79−85427
^{4}He(π^+,π^+n), 120-165 MeV, 3 nucleon exchange in knock-out reactions, cross sections 79−85437
^{4}He(π^+,π^+n)^{3}He, cluster effects 79−85513
^{4}He(π^+,π^+p), 120-165 MeV, isobaric resonance excitation, total inelastic cross section 79−85427
^{4}He(π^+,π^+p)^{3}H, 135 to 155 MeV, cluster effects 79−85513
^{4}He(π^+,$\pi^\pm$p), 120-165 MeV, 3 nucleon exchange in knock-out reactions, cross sections 79−85437
^{4}He($\pi^\pm$,$\pi^\mp$) double charge exchange, model development 77−54259
^{4}He($\pi^\pm$,$\pi^\mp$)4(p,n), ang. distrib. and cross-section calc. 77−23109
^{A}He, A=3,4, pionic, scatt. lengths and 1s width charge exchange contribs. calcs. 79−17934
^{A}He(π^-n), A=3,4, 50-290 MeV, cross section, energy depend. 79−85521
Hg(π^-,X), stopped π^- capture, product nuclei distribs., isomeric yield ratios, neutron multiplicity 77−18625
^{165}Ho, aligned, pion cross-section meas. in (3,3) reson. region 78−29507
^{165}Ho(π^-,X), 175 MeV/c, monopole and quadrupole strong interaction effects in pionic atoms 78−41777
^{165}Ho(π^-,xn), two-nucleon absorpt. mechanism calc. 77−18618
H(π^-, π^0), Panofsky ratio meas. with TRIUMF pion^0 spectrum 77−14192
^{115}In, π^- capture, p, d and α inclusive prod. spectra 79−22338
Li+$\pi^\pm$, 125 MeV, true absorpt. and scatt. 79−63705
^{6}Li, radiative π capture from 1s level, partial rates 79−3180
^{6}Li(e,e′), 76-141 MeV, form factors, appl. to (π^-,γ), phenomenological model 80−83068
^{6}Li(π^-, γ), photon spectra meas. with SIN pairspectrom. 77−10446
^{6}Li(π^-,n), single neutron emission induced by stopped π^- in 1p shell nuclei 79−59089
^{6}Li(π^+, 2p), 85 MeV, ang. depend. of cross section *(Russian)* 77−34349
^{7}Li+$\pi^-\rightarrow^{4}$He+^{3}n (or ^{3}He+^{4}n), search for neutron nuclei *(Russian)* 77−74889
^{7}Li(π, πN), 60 and 300 MeV, γ-ray meas. 78−41780
^{7}Li(π,π'), 164 MeV, ang. distrib., cross sections 79−85532
^{7}Li(π,πn)^{6}Li, 50-290 MeV, cross-section meas. 77−6463
^{7}Li(π^-, γ), photon spectra meas. with SIN pairspectrom. 77−10446
^{7}Li(π^-, t)^{4}H, study of particle-unstable state ^{4}H, branching ratio 79−93528
^{7}Li(π^-,X), π^--capture at rest, isotopic yield distribs., T-T coincidence, ^{4}H formation 79−85497
^{7}Li(π^-,n), single neutron emission induced by stopped π^- in 1p shell nuclei 79−59089
^{7}Li(π^+, 2p), 85 MeV, ang. depend. of cross section *(Russian)* 77−34349
^{7}Li(π^+,2p), cluster effects in in-flight π^+ capture 78−89916
^{7}Li(π^+,p^{3}He), cluster effects in in-flight π^+ capture 78−89916
^{7}Li(π^+,pd), cluster effects in in-flight π^+ capture 78−89916
^{7}Li(π^+,π^-)^{7}Be, distorted wave impulse calc., optical pot., multiple scatt. 78−50138
^{7}Li(π^+,π^0), 90 to 210 MeV, ^{7}Be 429 keV 1/2$^-$ excited state, cross section 78−647
^{7}Li(π^+,π^0)^{7}Be, DWIA isovector correls. 78−29499
^{7}Li($\pi^\pm$,πN)^{6}Li* cross-section ratios, N charge exchange model 77−54257
pion-nucleus reactions continued
^{A}Li (π^-,2n), A=6,7, recoil momentum, excitation energy distribs. and neutron momenta 79−67780
^{A}Li(π^+,p), A=6,7, 75 and 175 MeV, ang. distrib. 79−85503
^{A}Li(πp), A=6, 7, 75, 175 MeV, diffential cross sections, reaction mechanisms 80−78332
Li(π,X), 125 MeV, absorption cross section in 3:3 resonance region 79−85543
^{175}Lu(π^-,X), 230 MeV/c, monopole and quadrupole strong interaction effects in pionic atoms 78−41777
^{2}M+π, resonances near ΔN threshold, Argand diagrams 78−62582
^{24}Mg($\pi^\pm$,πN), 200 MeV, ^{23}Mg/^{23}Na mirror level pair cross sections 79−67665
^{25}Mg($\pi\pm$, $\pi\pm$N), 100-300 MeV, activation cross section, π^+/π^- cross section ratio 79−89329
^{14}N(π^-,2n), neutron-pair emission characts., excitation energy spectra 78−13159
^{14}N(π^-,2n)^{12}C, ^{12}C excitation spectrum 77−10451
^{14}N(π^-,n), single neutron emission induced by stopped π^- in 1p shell nuclei 79−59089
^{14}N(π^-,n), stopped pion, neutron energy spectra, mean energies and multiplicities 80−9311
^{14}N(π^-,xγ), recoil momentum spectrum of ^{12}C* using deexcitation γ rays Doppler broadened 77−54256
^{15}N(π^+, π^0)^{15}O, isobar hole model calc. of single charge exchange 79−85523
Nb+$\pi^\pm$, 125 MeV, true absorpt. and scatt. 79−63705
^{93}Nb(π^-,X), stopped π^-, ^{86,87}Y^{m,g} isomeric yield ratios and γ-spectra 80−86857
Nb(π,X), 125 MeV, absorption cross section in 3:3 resonance region 79−85543
Ne+π, fragment and pion multiplicities 77−18620
Ne+π, particle multiplicity correlations in streamer chamber 79−85506
Ne+π^-, 25 and 50 GeV, multiplicity of charged particles 78−62575
Ne+π^+, 10.5 GeV/c multiplicities and inclusive moment and rapidity spectra 78−8862
Ne+π^+ 1.5 to 2.5 FeV interactions in stream chamber 79−6710
Ne+π 10.5 GeV/c, recoil nucleon spectra, tube model anal. 77−61458
^{20}Ne+π^-, pion absorption, isobar formation in streamer chamber 79−85504
Ni+π, E$_\pi$=0, 45 MeV γ-ray spectra, prod. cross-section for residual nuclei meas. 78−649
^{A}Ni($\pi^\pm$,xγ), 100-200 MeV, prompt and delayed γ spectra, nuclide yields 79−22332
^{60}Ni+π, 70 MeV, γ+charged particle coincidence spectroscopy, cross section, p multiplicity 78−46111
^{62}Ni+$\pi^\pm$, proton spectra, cross section, π. absorpt. mechs. 78−25239
^{62}Ni(π^-,p),($\pi^\pm$,d), E=100, 220 MeV, p and d spectra meas. 78−648
Ni(π,αX), 70 MeV, α cross sections and energy spectra, intranuclear cascade calcs. 79−575
Ni(π^+, π^-), 200 MeV, deexcitation γ spectra, transitions in ^{58,60}Cu 78−89912
N(π^+,2p), 112 MeV, reaction mechanism *(Russian)* 78−29508
N(π^+,π^+d(He)), 60 MeV, cross sections, momentum and ang. distribs. *(Russian)* 77−74888
N(π,πp), 170 MeV, two stage and knock out contribs., π^+,π^- spallation differences *(Russian)* 80−68632
N($\pi\pm$, $\pi^\pm$ X), X=He or d, 170 MeV, cross sections and ang. distribs., direct knockout mechanism *(Russian)* 80−86887
^{A}O(π^+,π^-), A=16,18, cross section and ang. distribs., Glauber and coherent fluctuation models *(Chinese)* 80−102211
^{A}O(π^+,π^-)Ne, A=16,18; 95 to 145 MeV, π double charge exchange, differential cross section 78−70573
^{16}O, 2p bound π absorpt, p-wave rescattering terms for light nuclei 78−70575
^{16}O, pion photoproduction and radiative capture 78−50213
^{16}O, π^+ induced four nucleon removal 78−25242
^{16}O, two nucleon emission following bound pion absorption 78−82395
^{16}O+π, total cross section calc., complex momentum theory anal. with $\alpha_{\rho^0}>1$ *(Russian)* 79−9638
^{16}O(π,2N), bound 2p pion absorpt., microscopic description, NN correls. 78−94030
^{16}O(π,γ), continuum shell model, strongly excited resonances, nucleon emission 78−94031
^{16}O(π,γn), direct and resonance reaction unified shell model, n, γ spectra 80−52696
^{16}O(π,πp), 163 MeV, coincidence expt. 80−78334
^{16}O(π^-, 2n), stopped π, ^{14}N levels and excitation energies, kinematically complete investigation 80−99128
^{16}O(π^-, γ), photon spectra meas. with SIN pair-spectrom. 77−14191
^{16}O(π^-, γ)^{16}N, capture rate, A=16 ground and excited states 78−17105
^{16}O(π^-,γ), one and two neutron emission, decay channels 79−45300
^{16}O(π^-,γn), γ-spectrum and γ-n ang. correlation function from continuum shell model 78−86551
^{16}O(π^-,γn)^{15}N, information from radiative π capture coincidence spectra 78−86550
^{16}O(π^-,n), stopped pion, neutron energy spectra, mean energies and multiplicities 80−9311
^{16}O(π^-,π^-p)^{15}N, 170 MeV, comparison with dispersion theory calcs. *(Russian)* 77−50161
^{16}O(π^+,p)^{15}O, 66 MeV, ang. distrib. meas. 77−10438
^{16}O(π^+,p)^{15}O, 66 MeV pions, expts. with pion beams of Saclay Linac *(French)* 79−572
^{16}O(π^+,π^-), 140 MeV, nuclear structure effects on cross section 78−17246
^{16}O(π^+,π^-), 240 MeV, double charge exchange cross section 79−85515
^{16}O(π^+,π^-), 240 MeV, integrated and doubly differential cross sections 80−68702
^{16}O(π^+,π^-)^{16}Ne, 145 MeV, non-analogue π double charge exchange 77−67773
^{16}O($\pi^\pm$,X), 100-250 MeV, ^{12}C production yield ratio with ^{12}C 79−85516
^{18}O(π,X), angular distrib. of inelastic diffusion of $\pi^\pm$ *(French)* 80−47507
^{18}O(π,π^-), ^{18}Ne cross section, excitation function and double isobaric analogue state 80−27596
^{18}O(π^-, γ) photon spectra meas. with SIN pair-spectrom. 77−14191
^{18}O(π^-,π^+), 164 MeV, ^{18}C mass excess and discrete nuclear states 79−13196

pion-nucleus reactions continued
$^{18}O(\pi^+,\pi^-)$, 140 MeV, nuclear structure effects on cross section 78−17246
$^{18}O(\pi^-,\pi^-)$, 164 MeV, ^{18}Ne analogue and nonanalogue states, π double charge exchange form factors 80−13405
$^{18}O(\pi^-,\pi^-)^{18}Na$, nuclear struct. effects 78−37380
$^{18}O(\pi^+,\pi^-)^{18}Ne$, 148, 187 MeV, ^{18}Ne ground state obs. 77−74883
$^{18}O(\pi^+,\pi^-)^{18}Ne$ double-charge-exchange, isobaric analogue transition 77−38300
$^{18}O(\pi^+,\pi^-)^{18}Ne(GS)$, optical model calc. including ^{18}F intermediate state coupling, cross section 79−13349
$^{18}O(\pi^\pm,\pi^\pm')$, 180 MeV, ang. distrib. around (3,3) reson. 79−85537
$\pi^+,2p)$, 112 MeV, reaction mechanism *(Russian)* 78−29508
$O(\pi^-,\gamma)$, ^AN, A=16,18, E1 and M2 giant resonance excitation 79−89280
$O(\pi^-,n)$ spectrum obs. and calc. 79−17933
$O(\pi^\pm,\pi^\pm X)$, X=He or d, 170 MeV, cross sections and ang. distribs., direct knockout mechanism *(Russian)* 80−86887
$O(\pi^+,\pi^+d(He))$, 60 MeV, cross sections, momentum and ang. distribs. *(Russian)* 77−74888
$O(\pi,\pi p)$, 170 MeV, two stage and knock out contribs., π^+,π^- spallation differences *(Russian)* 80−68632
$O(\pi^-,\pi^-p)N$, nuclear photoemulsion obs. at E_π=115 MeV, ang. distribs. and cross sections *(Russian)* 79−13352
Pb, π^- absorption *(Russian)* 78−46115
$Pb+\pi^-$, 0.75 GeV/c, neutron energy spectra meas. 79−67777
$Pb+\pi^-$, 3.7 GeV/c, proton spectra *(Russian)* 78−41785
$Pb+\pi^-$, 7 GeV/c hadron multiple prod. *(Russian)* 79−22298
$Pb+\pi^-$ 40 GeV/c, multiparticle production 80−5173
^{208}Pb, 355 MeV, ratio of π^+ and π^- cross sections from coincidence meas. 78−29501
$^{208}Pb(\pi,\pi'p)$, 255 MeV, quasielastic knockout, proton yield, $\sigma(\pi^+)/\sigma(\pi^-)$ cross section ratio 80−32305
$^{208}Pb(\pi^-,\Gamma)$, RPA calc. of partial and total capture rates 78−74409
$^{208}Pb(\pi^-,^4n)$, 120 MeV, tetraneutron possible existence, cross section and lifetime bounds 79−40958
$^{208}Pb(\pi^\pm,\pi^\pm N)$, 180-255 MeV, quasielastic pion scatt. coincidence expt. interpretation, impulse approx. 80−68704
$Pb(\pi^-,X)$, 3 GeV/c, n inclusive spectra, neutron yield *(Russian)* 80−13510
$Pb(\pi^-,p)$ 1.5-5 GeV/c, cumulative proton polarisation *(Russian)* 80−86896
^{108}Pd, repulsive P-wave interaction, nucl reson. meas. 77−14195
^{110}Pd, repulsive P-wave interaction, nucl. reson. meas. 77−14195
$Pt(\pi^-,X)$, stopped π^- capture, product nuclei distribs., isomeric yield ratio, neutron multiplicity 77−18625
(π, X), theoretical approaches, in $\Delta(1232)$ energy regime 79−80960
π^-, stopped absorption by A=80-240 nuclei, spallation, fission, new isotope synthesis 77−6459
^{32}S, (π,γ), shell model anal. 78−89910
$^{32}S+\pi^-$, 70 MeV, modification of ISOBAR-EVA prompt-γ code 77−18616
$^{32}S(\pi,\gamma X)$, short-range 4-N correls. 77−18613
$^{45}Sc(\pi^-,X)$, stopped π^-, yields and γ-rays 80−86857
$^{76}Se(\pi^-,xn)^{76-x}As$, 100, 180 MeV, product formation cross section 80−42705
^{28}Si $(\pi^\pm,X\gamma)$, 190, 220 MeV, multinucleon removal cross sections and γ-ray spectra, binding energy effects 79−3183
$^{28}Si(\pi,X)$, angular distrib. of inelastic diffusion of $\pi^\pm$ *(French)* 80−47507
$^{28}Si(\pi,n\gamma)$, neutron spectra from coincidence expts. 79−85499
$^{28}Si(\pi^+,\pi^{+\prime})$, 162 MeV, high spin particle-hole state excitation 79−85541
$^{28}Si(\pi^\pm,\pi^\pm)$, 130 to 226 MeV, ang. distrib. around (3,3) reson. 79−85537
$Sn+\pi^\pm$, 225 GeV/c, J/ψ and $\psi'(3.7)$ prod. study using muon pair meas. 77−57694
$Sn+\pi^\pm$, massive muon pair prod., test of Drell Yan model 77−57695
^{181}Ta, pion$^-$ capture, high spin states and neutron multiplicities meas. 78−54806
$^{181}Ta+\pi^\pm$, proton spectra, cross section, π. absorpt. mechs. 78−25239
$^{181}Ta(\pi^\pm,p)$, $(\pi^\pm,d)$, E=100, 220 MeV, p and d spectra meas. 78−648
$Ta(\pi^-,X)$, stopped pions, radioactive product yields 80−83126
$Th+\pi^-$, neutron multiplicity distrib. *(Russian)* 78−41783
$^{232}Th(\pi^-,f)$, resting pions, delayed fission search *(Russian)* 80−52704
Tl, π^- absorption *(Russian)* 78−46115
$U+\pi^-$, 7 GeV/c hadron multiple prod. *(Russian)* 79−22298
$^{238}U(\pi^-,f)$, resting pions, delayed fission search *(Russian)* 80−52704
$U(\pi^-,X)$, 3 GeV/c, n inclusive spectra, neutron yield *(Russian)* 80−13510
$^{51}V(\pi^-,X\gamma)$ 230 MeV reactions near $\Delta(1232)$ resonance 77−6465
$W+\pi$, 200 GeV, multiparticle production in emulsion 79−40967
$W+\pi^-$, 43 GeV/c, inclusive J/ψ prod., A-depend. 78−62581
$W(\pi^-,\Psi)$, 43 GeV, A dependence of inclusive distrib. *(Russian)* 78−45983
$Xe+\pi$, 2.34-10.0 GeV, π^0 and proton characteristics *(Russian)* 77−3052
$Xe+\pi^-$, 3.2 GeV/c, π^0, η, ω, f meson prod. determ. of meson-N total cross sections *(Russian)* 79−22122
$Xe+\pi^-$, π^0 prod. anal., possible existence of abnormal nuclear density 77−54143
$Xe+\pi^-$ 3.2 GeV/c, intermediate Δ^- prod. in π^0 and η prod. *(Russian)* 79−36280
$Xe+\pi^-$ inclusive K^0-meson production cross section *(Russian)* 78−82394
$Xe+\pi^+$, 2.34 GeV/c, p emission, nucleon Fermi motion 77−18628
$Xe+\pi^+\rightarrow p+...$, 2.34 GeV/c, proton angular distrib., shock-wave effect *(Russian)* 77−38304
$Xe(\pi,X)$, 2.34 to 9 GeV/c, multiple particle prod. and hadron formation time *(Russian)* 79−80957
$Xe(\pi,p)$, E_π=2.34 and 3.5 GeV/c, energy and angular distrib. obs. *(Russian)* 79−9633
$Xe(\pi^+,pX)$, 2.34 GeV/c, gauge props. of proton emission *(Russian)* 77−38303
$Xe(\pi^+,p\pi^0)$, E_π=2.34 GeV/c, momentum distrib. function estimate for internuclear nucleons *(Russian)* 79−9634
$^{90}Zr(\pi^+,\pi^{+\prime})$, 241 and 163 MeV, giant resonance studies 79−85512

pion-nucleus scattering
see also pion-nucleon scattering
3,3 resonance region, Δ-isobar dynamics, optical potential and RPA calcs. 77−34347
$^{12}C(\pi^\pm,\pi^{\pm\prime})$, isospin mixing doublet, possible isospin mixing matrix element extraction 79−85364
$^{16}O(\pi^+,\pi^+)$, 50 MeV, Lorentz-Lorenz effect 78−17247
$\Delta(1232)$ isobar propagation in nuclear matter 77−10349
A=1, 2, 3, 4, 12, 16 nuclei, intermediate energies, collective isobaric resonance 80−63208
amplitude determ. using derivative sum rules and dispersion relations 77−10373
annihilation nonlocality effects in the pion optical potential, dependence of (π,π) cross section 79−85550
Born series rearrangement in model space, resolvent operator expansion 80−13422
bound nucleon-pion scatt. at medium energies, impulse approx. 77−23108
Coulomb effects in inelastic pion-nucleus scattering, eikonal model description 79−76025
coupled-channel model of low energy scatt. 79−76040
deformed aligned nuclei and low energy pions, total cross section, pion condensation effect 77−61456
differential cross section calculation program modification 79−54457
differential cross sections, calculator program modification for differing p and n radii 79−54456
diffractional approx., few-nucleon nuclei, nuclear structure *(Russian)* 78−650
dispersion relation anal. of low-energy π-nucl. forward elastic scatt. 77−14200
elastic, appl. of multiple scatt. theory in resonance region 77−6438
elastic, pion-nuclear T-matrix calc., isobar hole model anal. 79−59090
elastic low energy scatt., corrections to multiple scatt. series 77−6439
Feshbach-Villars formalism and pion-nucleon scattering, relativistic scatt. theory, T-matrix 80−63211
few nucleon problems, Hamiltonian approach 77−6448
field theoretic T-matrix 77−6324
field theoretic treatment of pion-nucleus scatt. 78−29505
finite nuclei, Δ-resonance self energy, Fermi broadening, π-nucleus optical pot. 80−68707
giant multipole resonances and inelastic pion scattering 79−85426
higher order optical potential and effective Δ-nucleus potential in (3,3) resonance region 77−10378
impulse approx. in peripheral region for elastic scatt. 79−507
intermediate energy nuclear physics, review of recent expts. 78−50061
intermediate state of ρ-propagation in static model 79−67781
Israel Physical Society 1980 annual meeting, Rehovot, Israel (April 1980) 80−94909
Lee model evaluation of scatt. operator 79−22328
Lee model use in pion-nucleus scatt. theory testing 80−78325
light nuclei, micron spectrometer for meas. with energy resolution of 1 MeV for 400 MeV/c momentum 78−13368
Lorentz-Lorenz effect and ρ^2 terms in pion-nucleus scattering 78−82391
Lorentz-Lorenz effects in low energy scatt. 77−46151
low energy, E<80 MeV, scatt. review 79−85529
low energy π-nucleus scattering, optical pot., quasideuteron model calcs. 78−74406
low energy scatt., cross-section 79−3181
low energy scatt., second order density effect, Lorentz-Lorenz pot. 78−8861
Low eqn., multiple scatt. effects 77−41998
lowest order optical pot. containing π emission and absorption effects 80−73865
many-body theory, low-energy elastic regime 79−36279
meson-nuclear phys. in 1979, current status and new development 79−85490
microscopic calculation of absorption channels in pion elastic scattering from light nuclei 79−76039
microscopic calculations of medium corrections to pion-nuclear elastic scattering 78−78418
microscopic theory, review 80−47511
momentum space optical pot. computer code PIPIT 77−38298
momentum space optical potl. code, PIPIT 77−6442
multiple Coulomb scattering angle meas. 50 to 200 GeV/c 80−9315
multiple scattering theory *(Russian)* 79−49640
nonrelativistic QFT formulation, Low eqn., optical pot. definition 79−6700
nuclear isobars elastic scatt., appl. to pion-nucleus interaction *(Russian)* 79−45297
nuclear structure studies around (3,3) resonance, review 79−85528
nucleon Fermi motion, numerical approx. in momentum-space calc. 79−45302
off-shell ambiguities and phenomenological optical potentials 78−37379
optical pot., first order, remarks on calculations 77−46150
optical pot., hole-line expansion and Pauli principle 77−18627
optical pot., off shell sensitivity, repulsive correl. 77−71626
optical potential, p-wave absorptive pot. and higher-order corrections 79−45303
optical potential for low energy scatt. 79−40965
optical potl. for low and medium energies 77−6443
p-wave π absorpt. on two nucleons and low energy π-nucleus scatt. 79−76038
P-wave pion absorption on two nucleons and low-energy pion-nucleus scattering 78−78416
Pauli blocking effects in low-energy scatt. 77−6441
Pauli suppression of Born amplitude, effect on (3,3) resonance 77−6323
pion condensation in nuclear matter, book contrib. 80−484
pion-nucleus scatt. and absorption amplitudes, composite particle struct. 79−67778
pions and isobars in nuclei−an overview, (π,π) and nuclear forces 79−85373
radiative corrections to elastic scatt. 77−67772
relativistic potl. theory appl., corrections to πN off energy shell T-matrix elements 77−6154
review, medium energy pion-nucleus absorption and scattering, pion condensation 78−8858
s-wave amplitude, test of new threshold expansion using dispersion relns. 77−6325
scattering by nuclear pion cloud, significance 79−85372
scattering lengths in multiple scatt. theory, binding corrections 78−651

pion-nucleus scattering continued
single charge exchange and inelastic scatt. cross sections relationship 80−102204
total cross-sections, contrib. of quasi-elast. scatt. 78−78417
total cross-sections as test of pion condensate existence, ≈1.2 GeV 78−17249
use in nuclear struct. determ. studies, review 79−85527
d(π,π)d, differential cross section, investigation of ΔN interaction in the deuteron 79−67597
Δ(33) interaction with nucleus, effective shell model pot., pion scatt. test 80−32202
Δ spreading potential in pion-nucleus scatt., optical model approach 79−85422
^{2}H(π,π), covariant NN dynamics 77−6449
^{4}He(π^{+}, π^{-})^{4}He*, coupled channel method, determ. of total cross sections 79−36281
(π,π), A>2 nuclei, three rung ladder graph, singularity curves 80−32303
(π,π), Coulomb effects in pion Klein-Gordon eqn. 79−93668
(π,π), cross section calc., comparison of factorisation approx. taking account of nucleon Fermi motion 78−29497
(π,π), elastic scatt. amplitude anal., use in DWIA 79−85544
(π,π), elastic scatt. relativistic kinematics, differential cross sections 80−63210
(π,π), light nuclei near threshold, π mass difference effects, nuclear K-matrix 80−27674
(π,π), Low eqn. approx. soln., field theory propagator modification 79−85546
(π,π), many-body response problem, reaction channel m-croscopic treatment 79−85547
(π,π), phase shifts in (3,3) resonance region and diffractive nature 77−6462
(π,π), relativistic Schrodinger and Klein-Gordon optical models, off-shell sensitivity 80−5175
(π,π), Weinberg chiral Lagrangian nonlinear terms, nuclear binding, optical pot. 80−78329
(π,π),(3,3) resonance region, Brown-Rho bag model descript. 80−57806
(π,π) elastic and inelastic, approx. four particle eqns. *(Russian)* 78−86554
(π,π) elastic scatt., covariant theory, first and second order optical pots. 79−85545
(π,π) elastic scatt., reaction mechanisms, structure information and neutron radii 80−42702
(π,π) elastic scatt. on light nuclei, optical pot. and scatt. amplitude model *(Russian)* 78−89918
(π,π) near (3,3) region, statistical theory transport eqn. 79−85552
(π,π) optical pot., possible local field correction from resonant scatt. cross section 79−85421
(π,π) P-wave absorptive and dispersive effects, nuclear matter considerations 79−85558
(π^{-},π^{-}) on Li, Be, C, Al, Cu, Sn, Pb, 30 to 50 GeV/c, nuclear radii, real/imaginary forward scatt. amplitude ratio *(Russian)* 77−34351
(π^{-},π^{0}) at rest, branching ratios, model anal. 77−10445
(π^{+},π^{+or0}) inelastic reactions, cross sections from Boltzmann eqn. 79−89330
(π$^{\pm}$, π$^{\pm}$), slow mesons, anal. using effective quasi-potential *(Russian)* 77−34350
(π$^{\pm}$,π$^{\pm}$) from Be, C, Al, Cu, Sn, Pb, 70, 125, 175 GeV/c 80−83128
(π,π′), 1p shell targets, DWIA calcs., strong transitions, isospin effects 80−42708
(π,π′), collective transitions, giant resonances, isospin content and spin transfer 80−42580
(π,π′), particle-hole state excitation, field theory calcs. *(Russian)* 80−37318
(π, π′) many body QFT framework anal., final state particle-hole correlations 80−13508
(π,π′) momentum space DWIA study 79−85551
(π$^{\pm}$,π$^{\pm}$), π^{-} nuclear response enhancement, continuum effects, stretched state isospin mixing 80−86929
(π,π′), microscopic Fermi liquid approach 79−26459
(π,X), 50-300 MeV, pion reaction mode status, absorption and inelastic scatt. 80−42701
π^{-}-mesonic atom, π^{-}-nucleus optical pot. information 79−85559
π$^{\pm}$ 162 MeV elastic scatt., ang. distribs., diffraction patterns, optical model calcs. 78−58309
π^{-} + ^{12}C, 40 GeV/c, partial inelasticity factors determ. *(Russian)* 78−33227
πd coherent scattering expts., book contrib. 79−21889
πN low energy scatt., subtracted form of Low eqn. 78−66150
πN T-matrix, off-shell model of scattering amplitude 79−414
π$^{\pm}$p, 2-9.5 GeV/c, wide angle elastic scatt., differential cross section 80−73730
ρ meson exchange anal. 78−82397
Al (π$^{\pm}$,π$^{\pm}$), 65-215 MeV forward scatt. amplitudes 79−85533
^{10}B(π^{+},π^{0}), 1st order pion-nucleus pot. calc. 77−23113
^{9}Be(π,π), ang. distribs., optical model calcs. 78−58308
^{9}Be(π$^{\pm}$,π$^{\pm}$) elastic and inelastic quadrupole scatt., 162 MeV, rot. and optical model anal. 79−6714
^{A}C(π,π′), A=12, 13, ∼180 MeV, isospin mixing, levels, excitation functions and ang. distribs. 80−42543
^{A}C(π^{-},π^{-}), (A=12,13), 29.2 and 49.5 MeV, neutron radii determ. 79−97653
^{A}C(π^{-},π^{-}), A=12,13, 49.5 and 29 MeV, differential cross sections 79−85534
^{A}C(π$^{\pm}$,π$^{\pm}$), A=12,13, 180 MeV near (3,3) reson., nuclear RMS radii determ. 79−85538
^{12}C, elast. and inelastic scatt., Glauber theory in microscopic α-cluster model 79−13346
^{12}C, penetration range, 200 MeV to 2 GeV *(French)* 78−4964
^{12}C, quasielastic π scatt., recoil proton spectra obs. 77−14198
^{12}C-π wavefunctions and inelastic scatt., optical model with Kisslinger pot. 77−18611
^{12}C+π, P-wave pion absorption on two nucleons and low-energy pion-nucleus scattering 78−78416
^{12}C+π optical potl. at 50 MeV 77−6440
^{12}C+π optical potl. improved calcs. 77−6334
^{12}C+π^{-}, multiple scattering theory with separate treatment of proton and neutron 79−45301
^{12}C+π^{+}, 50 MeV, off-shell ambiguities and phenomenological optical potentials 78−37379
^{12}C+π^{+}(π^{-}) elastic and inelastic scatt. at 148 MeV 77−50159
pion-nucleus scattering continued
^{12}C(π, π) elastic and inelastic, nonstatic effects in isobar doorway model 79−80955
^{12}C(π,π′), 4.5 GeV/c 2^{+} scatt., Glauber theory 77−88175
^{12}C(π,π′), A* excitation, A* model unified description 80−102205
^{12}C(π,π′), collective resonances 78−78415
^{12}C(π,π′), enhancement near (3,3) resonance 79−85535
^{12}C(π,π′), monopole scatt., opt. pot., coupled-channel formalism 78−94034
^{12}C(π,π′)^{12}C*, giant dipole resonance, Glauber theory 77−6467
^{12}C(π,π′γ), 30-150 MeV, calc. π-γ ang. correls. 77−10452
^{12}C(π,π), 1.12 GeV, covariant optical model, nucl. struct. calc. 77−14197
^{12}C(π,π), 200 to 400 MeV, domination by giant isobaric resonances 79−67776
^{12}C(π,π), 24-110 MeV, optical pot., quasideuteron model calcs. 78−74406
^{12}C(π,π), 260, 280 MeV, elastic and inelastic differential cross sections from Glauber theory *(Chinese)* 79−59092
^{12}C(π,π), 260 MeV, short range correlations from Glauber multiple diffraction theory *(Chinese)* 80−102210
^{12}C(π,π), doorway, isobar model 77−10434
^{12}C(π,π), effects of off-shell two body amplitudes 79−85327
^{12}C(π,π), elastic and inelastic, recoil effects 79−85555
^{12}C(π,π), hadron induced semicoherent scatt., excitation of ^{12}C(2^{+}, 4.4 MeV) level 78−70569
^{12}C(π,π), many body effects in resonant scatt. 78−94029
^{12}C(π,π), model which reduces to eikonal approx. 77−6444
^{12}C(π,π), nonlinear meson dynamics and binding corrections, optical pots. 80−106080
^{12}C(π,π), pionic resonance fluorescence in Δ(33) region 79−85554
^{12}C(π,π), total cross section, density distribs. and ray bending effects 80−47509
^{12}C(π,π) 28 to 260 MeV, corrections to optical potential, role of ρ^{2} term 78−70574
^{12}C(π,π) cross section calc., comparison of factorisation approx. taking account of nucleon Fermi motion 78−29497
^{12}C(π,π) elastic scatt., π^{+},π^{-} diffr. minima differences 77−61459
^{12}C(π,π)^{12}C, 50 MeV, optical potential with kinematic, absorption and correl. corrections 77−50157
^{12}C(π^{-}, π^{-}′), P$_{33}$ resonance region, elastic cross section, Coulomb nuclear interference 77−23110
^{12}C(π^{-}, π^{-}), 29 MeV, differential cross section, ang. distrib. 79−3182
^{12}C(π^{-},π^{-}), 40 GeV, semi-coherent elastic scatt., angular distrib. 80−68701
^{12}C(π^{-},π^{-}), 60-90 MeV, backward scatt. cross-sections 77−18630
^{12}C(π^{-},π^{-})^{12}C*, 20 to 40 GeV/c, semicoherent elastic scatt. 80−5174
^{12}C(π^{+},π^{+}), 28.4, 38.6, 48.9 MeV, ang. distribs. meas. 78−41775
^{12}C(π^{-},X), 85-245 MeV, true absorption and scatt. in (3,3) resonance region 80−102207
^{12}C(π^{+},π^{+}′), 100-291 MeV, cross sections and ang. distribs., spin and isospin transfer 80−52697
^{12}C(π^{+},π^{+}), 0-300 MeV, cross sections, pion-nucleus optical pot. including nuclear Hamiltonian 80−68706
^{12}C(π^{+},π^{+}), 148 MeV, inelastic scatt., 15.1 MeV (1^{+}) state, differential cross section 78−89792
^{12}C(π^{+},π^{+}), 23-35 MeV, elastic backward scatt. 79−17940
^{12}C(π^{+},π^{+}), 40 MeV, differential cross sections and strength parameters, optical model fit 80−18347
^{12}C(π^{+},π^{+}), 49.9 MeV, differential cross sections, partial wave and optical model anal. 79−22333
^{12}C(π^{+},π^{+}), 50 MeV, DWBA, calcs. 77−50156
^{12}C(π^{+},π^{+}), elast. and inelast. scatt., 50 MeV, ang. distrib. determ. optical model and DWBA 79−45304
^{12}C(π^{+},π^{+}), phase shift equivalent optical pots., π wave-function constraint 79−9629
^{12}C(π$^{\pm}$, π$^{\pm}$), 162, 226 MeV, elastic cross sections around πN (3,3) resonance region 78−13164
^{12}C(π$^{\pm}$, π$^{\pm}$), model Coulomb corrections in eikonal 80−5171
^{12}C(π$^{\pm}$, π$^{\pm}$), resonance region, first order optical pot. calcs. 79−40957
^{12}C(π$^{\pm}$,π$^{\pm}$′), 162 MeV, strongly isospin-mixed 79−93505
^{12}C(π$^{\pm}$,π$^{\pm}$), 162 MeV, large scale elastic and inelastic scatt. near πN(3,3) resonance 79−40961
^{13}C(π,π′), 162 MeV, pure n and p transitions, differential cross sections 80−5040
^{13}C(π,π), elastic and inelastic near πN(3.3) reson. 80−73870
^{13}C(π^{+}, π^{+or0}), 120-226 MeV, inelastic scatt, and charge exchange, coupled channels calcs. 80−57804
^{13}C(π^{+},π^{0}) 1st order pion-nucleus pot. calc. 77−23113
^{13}C(π^{+},π^{0})^{13}N, Pauli and short range correlations 77−3049
^{13}C(π^{+},π^{0})^{13}N, two-body correlation effects 77−88178
^{13}C(π^{+},π^{0})^{13}N$_{g.s.}$, (3,3) resonance region, importance of two-step processes in multiple scatt. treatment 77−6464
^{13}C(π$^{\pm}$,π$^{\pm}$), near πN (3,3) resonance, 180 MeV, collective states and cross sections 80−13507
^{A}Ca, A=40, 44, pionic X-rays and neutron radius 79−36802
^{A}Ca(π,π), A=40,48, 40-241 MeV, first and second order optical pots., resonance behaviour 80−68624
^{A}Ca(π$^{\pm}$,π$^{\pm}$), A=40,42,44,48, 180 MeV (in)elastic scatt. differential cross-sections, Pauling blocking 79−85539
^{A}Ca(π$^{\pm}$,π$^{\pm}$), A=40,48, 180 MeV near (3,3) reson., nuclear RMS radii determ. 79−85538
^{40}Ca (π$^{\pm}$, π$^{\pm}$), model Coulomb corrections in eikonal 80−5171
^{40}Ca, penetration range, 200 MeV to 2 GeV *(French)* 78−4964
^{40}Ca+π$^{\pm}$, multinucleon removal, prompt de-excitation γ-spectra obs. 79−6708
^{40}Ca(π,π^{+}′), 50 MeV, energy spectra and cross sections 78−25241
^{40}Ca(π,πN) at (3,3) reson., WKD approx. validity 77−18615
^{40}Ca(π,π), nuclear matter distribs., density depend. HF anal. 79−487
^{40}Ca(π,π), pionic resonance fluorescence in Δ(33) region 79−85554
^{40}Ca(π,π)^{40}Ca, 50 MeV, optical potential with kinematic, absorption and correl. corrections 77−50157
^{40}Ca(π^{+},π^{+}), 40 MeV, differential cross sections and strength parameters, optical model fit 80−18347
^{40}Ca(π^{-},π^{-}), 115, 240 MeV, cross sections, Coulomb effects 78−62579
^{40}Ca(π$^{\pm}$,π$^{\pm}$), 65 MeV, ang. distrib. 79−85536
^{40}Ca(π$^{\pm}$,π$^{\pm}$), 65-215 MeV forward scatt. amplitudes 79−85533
^{40}Ca(π$^{\pm}$,π$^{\pm}$), elastic and inelastic scatt., energy and A-depend. 78−54802
^{40}Ca(π$^{\pm}$,π$^{\pm}$), resonance region, first order optical pot. calcs. 79−40957
^{48}Ca(π,π), nuclear matter distribs., density depend. HF anal. 79−487

pion-nucleus scattering continued
Ca($\pi^{\pm}$,$\pi^{\pm}$), 130 MeV, A=40,48, π^{+}, π^{-} cross sections, neutron radius 78−25240
Ca(π^{+},π^{+}'), 163,241 MeV, giant quadrupole resonances 79−40893
C(π^{+},π^{+}p)C, 170 MeV, direct-knock-out dominant mechanism *(Russian)* 77−61460
^{52}Cr($\pi^{\pm}$,$\pi^{\pm}$), 180 MeV near (3,3) reson., nuclear RMS radii determ. 79−85538
^{63}Cu, quasielastic π scatt., recoil proton spectra obs. 77−14198
Cu($\pi^{\pm}$,$\pi^{\pm}$), 65-215 MeV forward scatt. amplitudes 79−85533
Fe(π^{+},π^{+}) elast. and inelast. scatt., 50 MeV, ang. distrib. determ. optical model and DWBA 79−45304
^{1}H(π^{+},$\pi^{+}\gamma$), 269, 298, 324 MeV, radiative scatt. cross section, internal emission and recoil corrections 80−57805
^{2}H (π^{+}, π^{+}), low energies, Coulomb interaction *(Russian)* 80−83129
^{2}H+π, coupled channel theory 78−13157
^{2}H+π, crossed pion absorpt. contrib. to scatt. length 77−10433
^{2}H+π, elastic scatt., absorpt., model using coupled channel eqns., exact soln. 77−88176
^{2}H+π, high energy cross section calc., complex ang. momentum theory *(Russian)* 78−46067
^{2}H(π, π) 25-180 MeV, three body calc. up to (3,3) resonance, polarisations 79−40964
^{2}H(π,π,) low energy scatt., Afnan-Thomas anal. with exclusion principle 79−75792
^{2}H(π,π)„ pole terms and absorption in p-wave πd interaction 80−86932
^{2}H(π,π), 140-260 MeV, (3,3) region, tensor force, cross sections, pol. parameters 80−68641
^{2}H(π,π), 141 to 260 MeV backward elastic scatt. in (3,3) reson. region 79−85531
^{2}H(π,π), 142, 180 MeV, covariant three-body calc. 77−6450
^{2}H(π,π), 142, 256 MeV, form factor−backward scatt. correlation, tensor polarisation 80−99189
^{2}H(π,π), 343-637 MeV/c, elastic differential cross section meas. 78−50215
^{2}H(π,π), 47 MeV, differential elastic cross section 79−85530
^{2}H(π,π), (3,3) resonance region, three body relativistic eqns., cross section calcs. 78−74405
^{2}H(π,π), Brueckners R-matrix model for absorptive scatt. 77−6457
^{2}H(π,π), comparison of Faddeev eqn. approach with optical potential 79−76030
^{2}H(π,π), Coulomb effects in elastic scatt., approx. treatment 79−85548
^{2}H(π,π), dibaryon resonances in Glauber model anal. *(Russian)* 79−89331
^{2}H(π,π), effect of genuine π absorpt. and emission 79−17939
^{2}H(π,π), elastic differential cross section, Faddeev calc. and π-absorption 79−75793
^{2}H(π,π), elastic scatt., charge exchange, deuteron disintegration, three-particle rel. eqns. 78−37381
^{2}H(π,π), exchange of ρ-mesons 78−21610
^{2}H(π,π), expt. and theoretical work, present status, model testing, πN interaction 80−42699
^{2}H(π,π), Faddeev calcs. 77−18622
^{2}H(π,π), graph summation method 77−18624
^{2}H(π,π), high energies, total cross sections from refined Glauber model 80−78322
^{2}H(π,π), high energy total cross section in Glauber model 80−18346
^{2}H(π,π), impulse approx. calc. of scatt. in resonance region 77−6452
^{2}H(π,π), low energy scatt. absorption effects, cross sections, Faddeev like equations 80−86928
^{2}H(π,π), low energy scattering theory *(Russian)* 79−54460
^{2}H(π,π), medium energy elastic scatt. amplitudes, covariant multiple scatt. model convergence test 80−42710
^{2}H(π,π), modified Glauber amplitude anal., differential and total cross sections 79−22334
^{2}H(π,π), multiple scatt. calc. 78−29506
^{2}H(π,π), multiple scatt. formalism 77−6451
^{2}H(π,π), NΔ interaction anal., D* model 78−29503
^{2}H(π,π), off-shell pion-nucleon amplitude multiple-scatt. calc. 77−79401
^{2}H(π,π), pion absorption effect from threshold to resonance 80−99193
^{2}H(π,π), pion-deuteron scatt. length 78−58306
^{2}H(π,π), polarised d, dibaryon resonance signals in excitation functions 80−9181
^{2}H(π,π), relativistic description, πN waves, NN rescatt., ρ-exchange, π absorption and emission 80−9310
^{2}H(π,π), relativistic Faddeev calc. 80−102066
^{2}H(π,π), scatt. length, exchange current contrib. 80−78328
^{2}H(π,π) 142 MeV, three-body calc. 78−37378
^{2}H(π,π) constrained phase anal. from NNπ system relativistic 3-body theory 77−61457
^{2}H(π,π) correction in (3,3) resonance region for differential cross section 79−97732
^{2}H(π,π) elastic scatt., multiple scatt. calcs. 77−18623
^{2}H(π,π)^{4}H, 142 MeV, elastic cross section and polarisation observables 79−75791
^{2}H(π^{-}, π^{-}), 552 MeV/c, elastic differential cross section Glauber theory anal. *(Russian)* 80−52700
^{2}H(π^{-},π^{-}), 1.57, 1.66 and 1.76 GeV/c elastic hack scatt. cross section energetic shape struct. *(Russian)* 80−47510
^{2}H(π^{-},π^{-}), 438 MeV/c, differential and total cross sections 79−76026
^{2}H(π^{+}, π^{+}), 49 MeV, P-wave dispersive contrib. π and ρ rescatt. 80−78331
^{2}H(π^{+},π^{+}), 130 to 350 MeV, 180° scatt. 80−78335
^{2}H(π^{+},π^{+}), tensor polarisation and cross section at 180° 80−5116
^{2}H($\pi^{\pm}$,$\pi^{\pm}$), 140-260 MeV, backward scatt., differential cross sections 80−99194
^{2}H($\pi^{\pm}$,$\pi^{\pm}$), 47 MeV, elastic scatt. differential cross section 79−75794
^{2}H+π scatt. lengths, charge exchange combinations 79−40962
^{3}H($\pi^{\pm}$,$\pi^{\pm}$), 232, 252, 295 MeV/c, forward angle scatt., nuclear struct. and π reaction models 79−76032
^{3}H($\pi^{\pm}$,$\pi^{\pm}$), elastic scatt., charge exchange and symmetries, and ^{3}H, ^{3}He form factors meas. 79−80959
^{4}H(π,π), differential cross-sections calc. 77−6458
^{A}H(π^{+}, π^{+}), A=1,2, 130-280 MeV, 180° excitation function, dibaryon resonance signals 80−68619
^{3}He+$\pi_{3}^{\pm}$, dispersion relations, determ. of π^{3}He^{3}H coupling constant 78−58307
^{3}He+π^{-}, strong interaction shift, multiple scatt. and absorptive effects, calc. 78−62958
^{3}He(π,π), 1 GeV, backward scatt., nonstable meson-nucleon interaction cross section, resonance *(Russian)* 80−68559

pion-nucleus scattering continued
^{3}He(π,π), 145, 180, 195 MeV, differential cross section, mesonic exchange effects, form factors, optical pot. 79−85376
^{3}He(π,π), 68-154 MeV, single and double collision differential cross section calcs. *(Russian)* 80−106083
^{3}He(π,π), elastic interactions in JINR high press. streamer chamber, triggering system 80−102400
^{3}He(π,π), elastic interactions in JINR high press. streamer chamber, selection criteria 80−102401
^{3}He(π,π), optical model calc. 77−6454
^{3}He(π,π), optical potential in momentum representation 80−78324
^{3}He(π,π), role of spin isospin effects in Δ(1236) resonance domain *(Russian)* 78−78423
^{3}He(π,π) in Δ_{33} reson. region, differential cross section, comparison with model calcs. 77−18621
^{3}He(π^{-},π^{-}), 145, 180 and 195 MeV, relationship to ^{3}He(e,e) 80−78323
^{3}He(π^{-},π^{-}), 68 MeV, differential cross section 78−33221
^{3}He(π^{-},π^{-}), low energies, scatt. lengths and phase shift calcs., inelastic process contribs. 79−54459
^{3}He(π^{-},π^{0})^{3}H, large angle charge exchange scatt. differential cross section 79−22331
^{3}He($\pi^{\pm}$,$\pi^{\pm}$), 232, 252, 295 MeV/c, forward angle scatt., nuclear struct. and π reaction models 79−76032
^{3}He($\pi^{\pm}$,$\pi^{\pm}$), elastic scatt., charge exchange and symmetries, and ^{3}H, ^{3}He form factors meas. 79−80959
^{3}He($\pi^{\pm}$,$\pi^{\pm}$), low energy, scatt. lengths, approx. pot. 4-body eqns. 79−76033
^{4}He, π scatt. and absorption, microscopic calc. 79−85501
^{4}He+π, effects of pion absorption 79−22341
^{4}He+π, high energy cross section calc. complex ang. momentum theory *(Russian)* 78−46067
^{4}He+π^{-}, multiple scattering theory with separate treatment of proton and neutron 79−45301
^{4}He(π, π), elastic data inconsistencies and dispersion relations above 33 resonance 80−68700
^{4}He(π,π), 1.12 GeV, covariant optical model, nucl. struct. calc. 77−14197
^{4}He(π,π), 200 to 400 MeV, domination by giant isobaric resonances 79−67776
^{4}He(π,π), 24-110 MeV, optical pot., quasideuteron model calcs. 78−74406
^{4}He(π,π), 60-260 MeV, energy-independ. phase shift anal. 78−41773
^{4}He(π,π), 75-260 MeV, dibaryon contrib. to πNN cluster 79−89328
^{4}He(π,π), (3,3) region, multiple scatt. theory study by optical pot. method *(Russian)* 80−13509
^{4}He(π,π), backward dispersion relations and phase shift anal. 79−63703
^{4}He(π,π), derivative sum rule and scatt. parametrisation 79−76037
^{4}He(π,π), dispersion relations for forward scatt. logarithm 78−17243
^{4}He(π,π), elastic interactions in JINR high press. streamer chamber, selection criteria 80−102401
^{4}He(π,π), exchange of ρ-mesons 78−21610
^{4}He(π,π), extraction of Breit-Wigner parameters from p-wave, isohelion existence 77−6455
^{4}He(π,π), forward scatt. amplitude, imaginary part in unphysical region 77−14194
^{4}He(π,π), low energy, first order optical pot., Pauli principle corrections, nuclear binding 80−27675
^{4}He(π,π), lowest order optical model 77−6456
^{4}He(π,π), microscopic calc. of medium corrections 78−78418
^{4}He(π,π), model which reduces to eikonal approx. 77−6444
^{4}He(π,π), multiple scatt. formalism, dynamics of πN resonances 77−6447
^{4}He(π,π), multiple scatt. anal. at medium energies 77−26791
^{4}He(π,π), optical model calc. 77−6454
^{4}He(π,π), pion-nuclear T-matrix calc., isobar hole model anal. 79−59090
^{4}He(π,π), single scatt. optical pot., Pauli principle and binding effects on cross section 80−86933
^{4}He(π,π) 28 to 260 MeV, corrections to optical potential, role of ρ^{2} term 78−70574
^{4}He(π,π) in Δ_{33} reson. region, differential cross section, comparison with model calcs. 77−18621
^{4}He(π,π)^{4}He, 3,3 resonance region, Δ-isobar dynamics 77−34347
^{4}He(π,π)^{4}He, eikonal and quasi-eikonal models in complex ang. momentum plane *(Russian)* 77−50160
^{4}He(π^{-},π^{-}), 110-260 MeV, cross section, phase shifts 78−54804
^{4}He(π^{-},π^{-}), 1.12 GeV, multiple scatt. theory 77−6466
^{4}He(π^{-},π^{-}), 20-280 MeV, phase shift anal. 77−18641
^{4}He(π^{-},π^{-}), 51-260 MeV, dynamical and fixed scatterer approx. calcs. 78−25244
^{4}He(π^{-},π^{-}), total cross section, improved optical pot., second order correction 79−22330
^{4}He(π^{-},π^{-})^{4}He, 51-260 MeV, nuclear-Coulomb interf. calc. using optical model phase shift anal. 77−54199
^{4}He(π^{-}, $\pi^{\pm}$), resonance region, first order optical pot. calcs. 79−40957
^{4}He($\pi^{\pm}$,$\pi^{\pm}$), 30-70 MeV, backward scatt. cross-sections 77−18630
^{4}He($\pi^{\pm}$,$\pi^{\pm}$), 51 MeV, three body systems, review of recent theoretical anal. 79−80842
^{4}He($\pi^{\pm}$,$\pi^{\pm}$), differential cross section 78−33221
^{A}He(π,π), A=3, 4, low energy scatt. length and phase calcs. 80−47508
^{A}He($\pi^{\pm}$,$\pi^{\pm}$), A=3,4, 260 to 310 MeV, differential cross sections 80−99192
He(π,π), absorpt. effects in resonance region 79−76036
He(π^{-},π^{-}), 1.12 GeV, multiple scatt. anal., optical model potl. 77−6453
He(π,π)He, Glauber model applicability near Δ_{33} reson. region 77−14193
^{165}Ho(π,π), aligned deformed nuclei, cross sections and diffractive minima from eikonal approx. 80−22860
Ho($\pi^{\pm}$,$\pi^{\pm}$), 65-215 MeV forward scatt. amplitudes 79−85533
^{7}Li(π,π), 164 MeV, ang. distrib., cross sections 79−85532
^{7}Li(π,π), elastic and inelastic, nuclear struct. effects in optical model 77−23112
^{7}Li(π^{+},π^{0}), 1st order pion-nucleus pot. calc. 77−23113
^{A}Li(π^{-},π^{+}), A=6, 7, 50 MeV, optical model anal., core+valence neutron model, isotopic effects 79−6715
^{24}Mg($\pi^{\pm}$,$\pi^{\pm}$) 180 MeV elastic and inelastic scatt., optical model and DWBA calcs. 78−89915
^{26}Mg($\pi^{\pm}$,$\pi^{\pm}$'), pion spectra, absolute cross section 80−78333
^{92}Mo($\pi^{\pm}$,$\pi^{\pm}$), 180 MeV, octupole transitions 79−85542
^{58}Ni(π,π), 162 MeV, elastic and inelastic ang. distribs., optical and PWIA anals. 80−42706
^{58}Ni(π,π), ang. distribs., optical model calcs. 78−58308

pion-nucleus scattering continued
^{60}Ni($\pi^+,\pi^{+\prime}$), 50 MeV, energy spectra and cross sections 78−25241
^{A}O(π,π), 163 MeV, A=16, 18, comparison of π^+ and π^- scatt. at (3,3) resonance 78−86552
^{A}O(π^-,π^-), (A=16,18), 29.2 MeV, neutron radii determ. 79−97653
^{A}O(π^-,π^-), A=16,18, 29 MeV, differential cross sections 79−85534
^{A}O($\pi^\pm,\pi^\pm$), A=16, 18, resonance region, proton and neutron distribs. 80−91195
^{16}O+π, optical potential, p-wave absorptive pot. and higher-order corrections 79−45303
^{16}O($\pi,\pi^\pm$), 115, 240 MeV, cross sections, Coulomb effects 78−62579
^{16}O(π,π'), ~180 MeV, isospin mixing, levels, excitation functions and ang. distribs. 80−42543
^{16}O(π,π'), excitation of collective modes and high-spin states, DWA calcs. 77−10448
^{16}O(π,π), 1.12 GeV, covariant optical model, nucl. struct. calc. 77−14197
^{16}O(π,π), 200 to 400 MeV, domination by giant isobaric resonances 79−67776
^{16}O(π,π), 40-342 MeV, second order optical pot. parameters 79−22337
^{16}O(π,π), binding effects in optical model with S-wave interaction 77−14196
^{16}O(π,π), Coulomb-nuclear interference, extracted Bethe phase 77−10441
^{16}O(π,π), nonlinear meson dynamics and binding corrections, optical pots. 80−106080
^{16}O(π,π), pionic resonance fluorescence in Δ(33) region 79−85554
^{16}O(π,π), T-matrix from isobar-hole model, many-body corrections, optical pot. parameter 80−9312
^{16}O(π,π), three-body model of πN interaction using finite binding pots. 80−42707
^{16}O(π,π) low energy p-wave optical pot., absorptive part from isobar-hole model 79−85556
^{16}O(π,π) optical pot., local field correction 80−68705
^{16}O(π,π)^{16}O, microscopic isobar-hole calc. doorway states 78−4965
^{16}O($\pi^+,\pi^{+\prime}$), 50 MeV, energy spectra and cross sections 78−25241
^{16}O(π^+,π^+), 40 MeV, differential cross sections and strength parameters, optical model fit 80−18347
^{16}O(π^+,π^+), 50 MeV, partial wave amplitude anal. 79−22335
^{16}O(π^+,π^+), 50-340 MeV, isobar hole doorway states, collective Δ-hole states 79−85350
^{16}O(π^+,π^+), 80-340 MeV, ang. distribs. of cross-sections determ. 78−33225
^{16}O(π^+,π^+) 40 and 49.7 MeV, differential cross sections, partial wave and optical model anal. 78−70570
^{16}O(π^-,π^-) elast. and inelast. scatt., 50 MeV, ang. distrib. determ. optical model and DWBA 79−45304
^{16}O($\pi^\pm,\pi^\pm$), P_{33} resonance region, elastic cross section, Coulomb nuclear interference 77−23110
^{16}O($\pi^\pm,\pi^\pm$), elastic scatt., complex amplitude anal., phase 78−62580
^{16}O(π^-,π^-), resonance region, first order optical pot. calcs. 79−40957
^{16}O(π^-,π^-), Coulomb-nuclear interference, new anal. method 78−21608
^{18}O+$\pi^+(\pi^-)$, elastic and inelastic scatt., angular distrib., 180 MeV, comparison with ^{28}Si 78−94035
^{18}O+π^+, inelastic and elastic scatt., neutron-proton radius differences and isovector deform. 79−40963
^{18}O(π,π'), 164 MeV, yrast state and level excitation, DWIA calcs., shell model context 80−42526
^{18}O(π,π'), 230 MeV, neutron deform. param. determ. 78−29502
^{18}O(π,π'), mirror state EM decay rates, multipole matrix element isospin decomposition 79−36190
^{18}O(π,π'), momentum space DWIA calcs., DWIA validity, shell model sensitivities 79−85553
^{18}O($\pi^-,\pi^{-\prime}$) ^{18}O(2^+), DWIA anal. with microscopic form factors, effective charges 79−85549
^{18}O($\pi^\pm,\pi^\pm$), correlation effects, Glauber theory anal. 79−85514
^{18}O($\pi^\pm,\pi^\pm$) inelastic scatt., core polarisation effects from Glauber theory 79−75962
^{19}O($\pi^\pm,\pi^\pm$), 180 MeV near (3,3) reson., nuclear RMS radii determ. 79−85538
O($\pi^\pm,\pi^\pm$), A=16,18, elastic and inelastic scatt., energy and A-depend. 78−54802
O(π^+,π^+p)O, 170 MeV, direct-knock-out dominant mechanism *(Russian)* 77−61460
^{208}Pb (π^-,π^-), 29 MeV, elastic differential cross-section 79−71872
^{208}Pb, quasielastic π scatt., recoil proton spectra obs. 77−14198
^{208}Pb(π,π), 162 MeV, elastic and inelastic ang. distribs., optical and PWIA anals. 80−42706
^{208}Pb(π,π), ang. distribs., optical model calcs. 78−58308
^{208}Pb(π,π), many body effects in resonant scatt. 78−94029
^{208}Pb(π,π), total cross section, density distribs. and ray bending effects 80−47509
^{208}Pb(π,π)^{208}Pb, 50 MeV, optical potential with kinematic, absorption and correl. corrections 77−50157
^{208}Pb($\pi^+,\pi^{+\prime}$), 50 MeV, energy spectra and cross sections 78−25241
^{208}Pb(π^+,π^+), 40 MeV, differential cross sections and strength parameters, optical model fit 80−18347
^{208}Pb($\pi^\pm,\pi^\pm$), 80, 116 MeV, elastic and inelastic, optical and collective model anal. 79−22329
^{208}Pb($\pi^\pm,\pi^\pm$), elastic and inelastic scatt., energy and A-depend. 78−54802
Pb($\pi^\pm,\pi^\pm$), 65-215 MeV forward scatt. amplitudes 79−85533
($\pi^-,\pi^{-\prime}$) 40 GeV/c, secondary particle multiplicities as function of number of π^-p collisions *(Russian)* 78−89922
(π, X), theoretical approaches, in Δ(1232) energy regime 79−80960
^{32}S(π,π), many body effects in resonant scatt. 78−94029
^{32}S(π,π), total cross section, density distribs. and ray bending effects 80−47509
^{2}Si($\pi^\pm,\pi^{\pm\prime}$) 130, 180, 226 MeV, πN(3), region, inelastic transitions, optical and DWIA anal. 79−97677
^{28}Si+$\pi^+(\pi^-)$, elastic and inelastic scatt., angular distrib., 180 MeV, comparison with ^{18}O 78−94035
^{28}Si(π,π'), momentum space DWIA calcs., DWIA validity, shell model sensitivities 79−85553
^{28}Si(π,π), 162 MeV, elastic and inelastic ang. distribs., optical and PWIA anals. 80−42706
^{28}Si($\pi^\pm,\pi^{\pm\prime}$), 162 MeV, excitation of high-spin particle-hole states 79−93667
^{28}Si($\pi^\pm,\pi^\pm$), 180 MeV near (3,3) reson., nuclear RMS radii determ. 79−85538
Si(π,π), ang. distribs., optical model calcs. 78−58308

pion-nucleus scattering continued
Si(π^+,π^+), elast. and inelast. scatt., 50 MeV, ang. distrib. determ. optical model and DWBA 79−45304
^{119}Sn(π^-,π^-), smooth cutoff model angular distrib. 77−10376
^{120}Sn(π,π), many body effects in resonant scatt. 78−94029
^{120}Sn(π,π), total cross section, density distribs. and ray bending effects 80−47509
Sn($\pi^\pm,\pi^\pm$), 65-215 MeV forward scatt. amplitudes 79−85533
^{51}V($\pi,\pi'\gamma$), 200 MeV, ^{51}V levels 78−21611
^{89}Y(π,π'), 163, 240 MeV, giant resonance pionic excitation 80−52561
^{89}Y(π,π'), giant reson. excitation 80−73834
^{90}Zr(π,π'), 226 MeV, giant reson. examination 80−73871
^{90}Zr(π,π)^{90}Zr, 50 MeV, optical potential with kinematic, absorption and correl. corrections 77−50157
^{90}Zr(π^+,π^+), 40 MeV, differential cross sections and strength parameters, optical model fit 80−18347

pion-pion interactions
see also pion-pion scattering
3π dynamics, two-body unitarity and analyticity 77−18205
cluster transverse momenta, effect on short range two-particle correlations 78−37237
coupled integral eqns. for scatt. at all energies 78−49982
crossing symmetric amplitude with Regge poles 78−54621
form factor and propagator bounds *(German)* 80−37265
high energy two-particle interactions, scaling 78−4878
lectures, theory and expt. results, analyticity, unitarity, phase-shifts, current algebra 77−50008
linear chain decay, pion coherence, Bose-Einstein symm. 77−49921
Pauli principle effect in nuclear matter, exchange of interacting two pions 78−12983
resonances, dominant, pole positions, partial waves 80−63020
separable interactions for πN and $\pi\pi$ scatt., three-body problems 78−78113
π^- ^{12}C, 40 GeV/c, Λ and K_1^0 inclusive distribs. *(Russian)* 77−34196
π^-p→n+kπ^0 (k=1 to 5), 1.3 to 3.8 GeV/c, differential and total cross-sections 80−83000
π^-p→ne^0, 1.3 to 3.8 GeV/c, differential and total cross-sections 80−83000
$\pi\pi$, diffr. dissoc. *(Russian)* 78−29356
$\pi\pi\to\gamma\gamma$, analyticity bounds for pion EM polarizabilities and threshold values 79−13157
$\pi\pi\to\gamma\gamma$, ρ EM polarisabilities difference contribs. 79−3023
$\pi\pi\to K\bar{K}$, dispersion model, matrix N/D method *(Russian)* 78−45954
$\pi\pi\to K\bar{K}$, I=0 state scatt. amplitude 77−18325
$\pi\pi\to K\bar{K}$, low energy cross sections *(Chinese)* 80−52535
$\pi\pi\to K\bar{K}$, modified K-matrix formalism for meson-meson scatt. amplitudes 77−82774
$\pi\pi\to K\bar{K}$, pion and kaon EM radius, low-energy approx. 78−50033
$\pi\pi\to K\bar{K}$ amplitude in the unphysical region, hyperbolic dispersion curves 79−9407
$\pi\pi\to K\bar{K}$ study via π^-p→$K_S^0K_S^0$n at 8.9 GeV/c 77−22796
$\pi\pi\to N\bar{N}$, helicity amplitude, extrapolation of $S^{I=0}$-wave 80−91112
$\pi\pi\to N\bar{N}$, partial-wave amplitudes using hyperbolic dispersion relations 77−30284
$\pi\pi\to\pi\omega$, ρ'(1250) meson and two channel $\pi\pi$, $\pi\omega$ problem, N/D method *(Russian)* 80−37297
$\pi\pi\to\pi\pi\pi$, fifth order perturbation theory prod. amplitudes, isobar model 77−54088
$\pi^-\pi^0$-interaction, energetically independent phase anal. in π^-p→$\pi^-\pi^0$p reaction *(Russian)* 77−88007
$\pi^0\pi^0$ S wave, bounds on absorptive part 77−67674
$\pi^+\pi^-$ atomic bound states and $\pi\pi$ scatt. lengths in H_2 gas target, X-ray spectra 77−27206
$\pi^+\pi^-\to K_S^0K_S^0$ scatt. cross section meas. 78−82240
$\pi^+\pi^-\to\pi^0\pi^0$, mass distribs. calc. 78−41586
$\pi^+\pi^-\to\pi^0\pi^0$ cross-section from π^-p→$\pi^0\pi^0$n at 2.01 GeV/c 78−21461
$\pi^+\pi^-\to\pi^+\pi^+\pi^-$, cross section meas. for quad-pion mass region 1.5 to 1.9 GeV 77−67675
$\pi^\pm\pi^\pm\to$mesons, multimeson inclusive spectra and recombination model, multiquark structure functions, predictions 80−73751
$\pi\pi N\bar{N}$ partial-wave amplitudes, interior dispersion relations 77−82758
$\pi\pi\pi$ system, relativistic dynamics in ω channel 78−21360
ρ production amplitude phase shift, S-channel unitary relations *(Russian)* 78−74278
ρ resonance, N/D calc., rebuttal of criticism 77−71462

pion-pion scattering
see also pion-pion interactions
amplitude, unitarity, analyticity, crossing symmetry props., partial waves 80−57641
chiral symmetry, dispersion method of self-consistent description *(Russian)* 79−93459
coupled integral eqns. for scatt. at all energies 78−49982
cross-section from π^-n→pX^{--}, reggeised one-pion-exchange 80−57649
crossing symmetric amplitude with Regge poles 78−54621
crossing symmetric unitary Regge representation 77−10201
crossing symmetry and unitarity, spectral functions 77−6165
cut extrapolation method for data anal., crossed channel Mandelstam cuts, symm. $\pi\pi$ scatt. 77−49867
elastic scatt., asymptotic total cross sections and positivity 80−13334
elastic scatt. at complex energies, stable unbiased analytic extrapolation 79−13155
form factor at s<$(m_\omega + m_\pi)^2$, influence of $\pi\omega$ inelastic channel 77−2838
geometrical scaling at inelastic threshold, appl. to K^+p, $\pi\pi$, Kπ 77−22797
geometrical scaling at inelastic threshold 77−18323
high complex energies, $\pi\pi$ scatt. amplitudes with isospin 1 or 2 77−67631
isospin decomposition of three pion scatt. amplitude, partial-wave anal. 77−6061
low energy, quantum field theory with chiral Lagrangian 77−65110
minimal K-matrix model, three pion enhancements 77−6060
off-shell phase shift anal. of $\pi\pi\to\pi\pi$ amplitude extracted from $\pi N\to\pi\pi N$ 77−2867
P-wave scatt. length, absolute bound 77−57563
partial wave construction, analytic crossing symmetric 77−87919
partial wave dispersion relation with inelastic cut, $\pi\pi$ scatt. in 1 GeV region 78−4877
partial wave equations, analyticity domain of $\pi\pi$ scatt. amplitudes 79−2956

pion-pion scattering continued
partial-wave $\pi\pi$ amplitudes, Roy eqns., proof of soln. existence 78−70310
phase shift analysis, imposed analyticity effects 79−418
phase shifts, nonlinear σ model Pade calcs. 78−8695
Roy's equations for scatt. amplitudes, mathematical props. 77−71463
Roy's S- and P-wave eqns., manifold of solns. 78−66154
Roy eqns., multiple solns., N/D method on finite interval 78−16949
Roy eqns., regularisation with smooth cut off 78−29271
Roy eqns., S- and P-wave scatt., constraints and correl. 78−21460
Roy equations, iterative solutions, N/D equations 79−36098
S-wave π-π scattering lengths in the (8,8) symmetry-breaking scheme 79−17759
s-wave scattering length bounds 77−57562
S-wave scattering lengths *(Russian)* 79−54358
scattering by nuclear pion cloud, significance 79−85372
self-interactions, nonperturbative, scatt. amplitudes containing only convergent integrals 80−68480
sum rules on crossing-symmetry basis 77−57467
t-channel isospin-1 scatt. amplitude, crossing constraints 77−67592
universal curve for $\pi\pi$ scatt. lengths, optimal extrapolation techniques 77−46080
p-resonance production, quasipotential approach, linear σ-model 80−86755
π, EM form factor and P-wave isovector $\pi\pi$ phase-shift data consistency 79−3025
π EM radius, low-energy approx., comparison with kaon radius 78−50033
π^0-π^0 partial wave amplitudes, crossing symmetric dispersion relations 78−50048
$\pi\pi$, ρ-meson contrib. in broken chiral symmetry model, phase shifts and lengths *(Russian)* 80−86756
$\pi\pi$ amplitude from $\pi N\rightarrow\pi\pi N(\Delta_1)$ review and implications for current algebra developments 78−62455
$\pi\pi$ elastic scatt., exclusive and almost exclusive process asymptotic behaviour, renormalisation group 80−42464
$\pi\pi$ P-wave anal., ρ pole parameters 77−46079
$\pi\pi\rightarrow\pi\pi$, dispersion model, matrix N/D method *(Russian)* 78−45954
$\pi\pi\rightarrow\pi\pi$, I=0 state scatt. amplitude 77−18325
$\pi\pi\rightarrow\pi\pi$, modified K-matrix formalism for meson-meson scatt. amplitudes 77−82774
$\pi\pi\rightarrow\pi\pi$, operator dual model for bound relativistic quark based mesons *(Russian)* 79−9408
$\pi\pi\rightarrow\pi\pi$, ρ(1250) meson and two channel $\pi\pi$, $\pi\omega$ problem, N/D method *(Russian)* 80−37297
$\pi\pi$ resonances, anal. of asymptotical sum rules *(Russian)* 79−54359
$\pi\pi$ S-wave phase shift, lower bounds, ϵ^0 and ρ poles 78−45953
$\pi\pi$ scatt. length, interior dispersion relations 78−45952
$\pi\pi$ scatt. lengths, rigorous phenomenological anal. 80−102070
$\pi\pi$ scattering amplitudes, Veneziano model representation 79−26313
$\pi^-\pi^+$ scattering length, effective radius approx. *(Russian)* 77−34178
$\pi^0\pi^0$ amplitude bounds 77−34107
$\pi^0\pi^0$ amplitude construction, approx. scheme from analyticity, crossing symmetry and unitarity *(German)* 80−91111
$\pi^0\pi^0$ amplitudes, construction from axiomatic requirements 77−38201
$\pi^0\pi^0$ coupling constant bounds as function of D-wave scatt. length 77−2866
$\pi^0\pi^0\rightarrow\pi^0\pi^0$, axiomatic bound, scatt. amplitude, optimality 78−41585
$\pi^0\pi^0$ scatt., axiomatic constraint optimality, lower bounds 80−32124
$\pi^0\pi^0$ scatt. amplitude, new method for deriving absolute bounds 77−6059
$\pi^+\pi$, QCD, one-gluon-exchange, resonating group method, soft-core approx. 80−63025
$\pi^+\pi^-$ scatt., 1.0-1.8 GeV, phase shift anal. 78−8694
ρ-meson N/D calc. in Veneziano model 77−67627
S*, bias free pole search in S-wave $\pi\pi$ scatt. 79−58976

pion production
A(d,π)X, relativistic energies, Glauber theory 77−30540
accelerators, linear and cyclic, production, uses and properties of π *(French)* 80−63417
baryon resonance decay, π emission, quark model, widths, amplitudes, sum rules 77−57534
baryonium muliquark system model of fireball, high energy pion production 79−97603
black holes in binary stellar systems, π meson prod. and gamma emission during accretion 80−17608
bootstrap model, probability of cumulative prod. *(Russian)* 77−46028
charged current induced weak one pion prod., form factors from PCAC 80−18129
coherent π^0,ρ^0 meson prod., test for neutral weak currents of exotic space-time struct. 79−75715
coherent diffractive excitation of protons into $p\pi^+\pi^-$, 20.8 GeV/c *(Russian)* 77−34187
coherent pion prod. in high energy heavy ion collisions, pion laser 80−73856
compressed zone evolution in high energy nuclear collisions, pion characts. 79−26447
condensation and neutron star dynamics 79−67047
conference, 11th Masurian school in nuclear physics, Mikolajki, Poland (Aug.-Sept. 1978) 79−63605
conference on few body systems and nuclear forces, Graz, Austria (Aug. 1978) 79−67567
conference on few body systems and nuclear forces, Graz, Austria (Aug. 1978) 79−80880
Conference on meson-nuclear physics, Houston, USA (Mar. 1979) 79−85489
conversion target for Saclay electron linear accelerator, reliable pion prod. 77−54384
cosmic ray-nucleus reacts., 20 TeV, balloon-borne chamber, Monte Carlo simulation 80−9309
cosmic rays EAS growth, fragmentation and pionisation ranges significance in inclusive spectra 79−84614
cumulative, electroproduction from d, effect of rescatt., scaling effects *(Russian)* 78−74265
cumulative effects, phenomenological model for pion prod. and elastic scattering involving deuterons 78−58267
cumulative production in hadron-nucleus collisions *(Russian)* 78−607
degenerate matter, pionisation *(Russian)* 77−91558
diffractive hadronic reactions, statistical description of multipion prod. 80−95260
double pion photoprod., correction to Chew-Low model amplitude 77−2844
Drell-Yan trigger, hadronic prod. of dilepton pairs and muons 78−37182
dynamical model for multiplicity distribs. in πp and pp-collisions, pion prod. 78−21469
$e^+e^-\rightarrow\pi^+\pi^-(\pi^0\omega)$, ρ'(1250) description, EM form factors, bound states, N/D method *(Russian)* 80−42465
electron linear accelerators, appls. *(Japanese)* 78−78533
electropion prod., deep inelastic scatt. and struct. from electron coincidence expts. at Stanford 80−22821
electroproduction, inclusive particle ratios on H and D targets 77−18291
electroproduction, light cone dispersion sum rules, axial vector currents 78−41556
electroproduction, near threshold, inelastic response functions 78−33172
electroproduction, quark-parton model, fragmentation functions 79−13136
electroproduction, quark-parton model consistency 77−79254
electroproduction, test of quark parton model 77−57488
electroproduction at threshold, weak form factors 79−22107
electroproduction cross-section, six-fermion interaction const. and neutral currents *(Russian)* 77−34147
electroproduction in protons, two-pion radius and axial mass determ. *(Russian)* 77−10267
electroproduction inclusive particle ratios 78−37217
electroproduction inclusive processes, quark fragmentation function ratio determ. 77−61294
electroproduction of low energy π^+, from ^{3}He 78−21545
elementary properties, general review 79−85340
energy distrib. in multiple hadron prod., case for discrete fireball mass spectrum 77−57499
exclusive one-pion prod., ν-induced neutral current channels 78−54624
expanding fireball in high energy heavy ion reactions, pion radiation 80−5155
fireball model anal. of small and large P_t pion distribs., ISR energies 77−38211
fireballs, quantum-statistical chain decay, pion clusters 78−430
galactic processes rel. to gamma-ray astronomy *(Polish)* 77−70999
hadron+hadron, high-energy, inclusive spectra of secondary pions, Feynman scaling and statistical model 80−42502
hadron+hadron, jet production, large transverse momentum 80−42503
hadron+nucleus, spatial temporal development, nuclear hadronic cascades 80−63040
hadron-nucleus collisions, backward particle emission, energy depend. 78−25236
hadronic collisions, violation of Feynman scaling, central region, fragmentation, mixed two component model 77−26551
heavy ion collisions, high energy, depend. of total pion prod. cross sections on eqn. of state 78−41772
heavy ion collisions, pion prod. depend. on pion charge 80−37392
heavy ion collisions, pion spectra, Coulomb distortion in final state EM interaction 80−13497
heavy ion reactions below 500 MeV, pion prod. and absorpt. 79−40952
heavy-ion collisions, π prod. and multiplicity at 100-280 MeV/nucleon 77−65234
heavy-ion collisions, threshold prod., calc. of effective NN collision cross sections 77−46185
(H1,πX), 125-400 MeV/N, low energy 0° pion prod., charge ratio 80−95324
high energy inelastic hadron reactions, π prod., scaling law, fireball model 78−74287
high energy nuclear collisions, pion multiplicity calc., target at. no. depend., statistical model anal. *(Russian)* 79−9425
high-energy collisions, primary particles causality and unitarity breakdown 77−57486
identical pion interference when emitted from sources of different sizes *(Russian)* 79−93466
inclusive electroproduction, quark-parton model comparison with expt. data 78−37218
inclusive interactions, double Reggeon representation of energy depend. of cross sections *(Russian)* 77−74737
inclusive particle production in C+p and W+p reactions, nuclear size depend. 77−46168
inclusive resonance prod., Bose interference effects 77−38210
inclusive super-fast prod. in relativistic deuteron-proton and nucleus collisions 77−18362
intensification of pion beams by highly excited nuclear matter with inverse population *(Russian)* 79−49595
intranuclear cascade model reply to criticism 77−71501
intranuclear-cascade model, criticism 77−71500
inverse pion electroprod. in $\pi^-p\rightarrow e^+e^-n$ 276 MeV, model independ. anal. *(Russian)* 77−61317
LAMPF high power pion prod. target mechanism 77−83387
light nuclei (p,π^+) reactions, π distortion effect on asymmetry 78−50176
mass quantisation, pion prod. in pp, np, πp *(French)* 78−25059
meson dipion cascade decays, current algebra techniques, pole plus remainder model, chiral symmetry breaking and QCD 80−62972
meson reson. elasticities belonging to a dual spectrum, multipion channel coupling 77−38136
meson-nucleon collisions, pion spectra forward-backward asymmetry, fragmentation effects, meson reson. decay 78−86457
multi π systems, mass distrib. using information theory method 78−82250
multiparticle production, quasi-classical description of isospin conservation 78−58134
multipion production, π^- multiplicity distrib. and $\pi^-\pi^-$ correlation function, collective phenomena search 79−85485
multiple scattering in hadron-nucleus interactions, enhancement of Bose-Einstein symmetrisation effects 78−58271
multiple-collision model for pion prod. in relativistic nucleus-nucleus collisions 78−37365
multiplicative processes, ρ^0 meson formation cross section, pion prod., multiperipheral cluster model *(Russian)* 78−17067
multiplicity distributions of charged π in 2 GeV/nucleon ^{12}C, ^{16}O induced reactions in nuclear emulsions 78−66297
n-particle decay of dual resonance, decay width, multiplicity distrib., multipion channels 78−16997
neutron stars, pion condensate form. rel. to cooling 80−77443
nuclear absorption and prod. of mesons, overview 79−85492

pion production continued
nuclear backward π^+ prod., momentum depend., scaling, Monte Carlo calcs. 79−13305
nuclear collisions, central, standard deviation of π multiplicity, *(Russian)* 80−73864
nuclear collisions, coherent π production *(French)* 80−78311
nuclear collisions, pion multiplicity and nonlinear effects in pion production, NN inelastic interactions *(Russian)* 80−52637
nuclear matter, non-Abelian Cherenkov radiation of pions from a fast nucleon 79−40865
nuclear matter, pion propagation and production 79−80893
nuclear multi-particle rescatt. effects, cumulative π, p, K prod. *(Russian)* 80−52638
nuclear photoprod. near threshold 77−14101
nuclear pion prod. with heavy ions, statistical approach, pion interferometry 79−85487
nucleon+nucleus collisions cumulative pion prod., inelastic rescatt. contrib., statistical bootstrap model *(Russian)* 78−54766
nucleon+nucleus reactions, semiclassical models, multiple scatt., nucleon recoil 77−2996
nucleon-nucleus reactions, π cumulative prod., cluster model 77−41968
nucleus+π^+ 11.7 GeV/c, impact parameter anal. of coherent and incoherent pion prod. 77−2870
nucleus+nucleus high energy studies at Berkeley Bevalac, expt. data, theoretical predictions 77−50144
nucleus-nucleus reactions, pion production, Fermi motion effects, multiplicity distribs. and inclusive cross sections 79−93622
pair production in two-photon e^-e^+ events 77−71523
phase space critical surface of pions produced in inclusive π^-p interactions *(Russian)* 80−18154
phenomenological analysis of single pion photoproduction in the first resonance region 78−89721
photo and electroproduction in first πN-reson. region, production amplitudes up to 500 MeV, review *(Russian)* 78−54636
photoproduced pion inclusive distrib. in QCD, recombination model 79−85303
photoproduction, double polarisation meas. up to 2.5 GeV 77−34163
photoproduction, final state theorem extension, anal. of accurate low energy expts. 77−65172
photoproduction, multichannel N/D model fit, Δ^+ pole parameters 77−10265
photoproduction, weak interaction induced parity violating assymetries 79−71758
photoproduction $\leq$450 MeV, one-particle exchange model 79−13135
photoproduction amplitudes, Pade approximants and dispersion relation solns. 80−91096
photoproduction and electroproduction from nuclei, thresholds from pseudoscalar and pseudovector Lagrangian densities 78−29449
photoproduction in E<450 MeV region, dispersion relations, CT invariance, review, book contrib. 80−47311
photoproduction in first resonance region, one particle exchange model 78−4864
photoproduction in large cosmic-ray showers 80−4214
photoproduction near threshold, interior dispersion relations appls. 78−93889
photoproduction of π^+ and π^- from protons and neutrons, 250 to 790 MeV, cross section features 77−46053
photoproduction on N, multipole $E_{1+}^{(3/2)}$ and its double zero at reson. $\Delta(1232)$ 79−40790
photoproduction on nuclei, current algebra model with hard pions *(Russian)* 77−74890
photoproduction on nuclei in $\Delta(1236)$ region, nonrelativistic operator 77−41949
photoproduction on polarised nucleons above 3 GeV 77−34164
physical pion low energy electro- and photoprod., Ward identity, chiral symmetry breaking struct. 80−5003
physical pion low energy photo- and electroprod., photoprod. phenomenology, quark mass 80−5004
pion electroproduction from the nucleon near threshold 80−68651
pion photoproduction and radiative capture 78−50213
pionisation influence on beam hardness, beam evolution eqns. for hadronic processes *(Russian)* 80−42407
pionisation region gauge invariance violation for hadrons, K and γ in EAS *(Russian)* 79−40676
polarised photoproduction of single pions, even wave harmonic oscillator theory 79−40791
pp→πX, large P_T π prod., QCD theory 78−45861
primary cosmic ray spectrum and scaling consts. for pion prod. spectrum derivation 77−25897
proton accelerator π factories, multidisciplinary role 78−21791
proton-nucleus inclusive single particle prod. of $\pi^\pm$, $K^\pm$ and $p^\pm$ at 28.5 GeV 77−18346
proton-nucleus reactions, large momentum pion prod. nuclear density fluctuation 77−38267
QCD effects, parton transverse momenta, large-p_T hadron prod. 78−66083
quantum-chromodynamic predictions for inclusive spin-spin asymmetries at large transverse momentum 79−49472
quark jet fragmentation, large momentum transfer reactions, implication of large vector meson prod. 79−345
radiation therapy, Stanford Medical Pion Generator, simultaneous multiport irradiation planning 79−20647
rapid pionisation model, inclusive spectra height and average multiplicity growth *(Russian)* 78−89763
relativistic heavy ion collisions, pion sources, discussion 79−59086
relativistic heavy ion collisions, pion volume emission from Δ (1232) decay 79−93651
relativistic heavy ion reactions, 1.05-7.52 GeV, π prod., statistical interpretation 79−570
relativistic heavy-ion collisions, π^- multiplicity distribs., collective tube model 78−89902
relativistic heavy-ion collisions, two-pion to single-pion inclusive data ratio, pion source parameters 79−3171
relativistic light ion collisions, two-fireball model improvements, p and π spectra 80−5158
relativistic nuclear collisions, π interferometry observation, source space time struct. 79−13324
relativistic nuclei collisions, nuclear pionisation phenomena *(Russian)* 79−6696
relativistic nucleon-nuclei collisions *(Russian)* 78−25201
pion production continued
relativistic pot. models for π absorpt. and prod., equivalence theorem 77−74884
resonant decay, identical pion prod. correl. *(Russian)* 77−228
rising π inclusive cross section as series of threshold effects, multiperipheral model 78−93918
S-wave, off shell effects, field theoretic model 78−70566
seagull effect in π semi-inclusive distribs. by information theory, p_L-p_T correlations 78−86458
simultaneous pion and meson resonance production, correl. jet model 78−86456
SIN πE3 channel, pion prod. meas. 80−74056
single π photo and electroprod., theoretical anal., fixed-t dispersion relations 77−22743
single π prod., review and implications for current algebra developments 78−62455
single pion photoproduction between threshold and 16 GeV, multipole and amplitude anals. 79−3031
single pion production in antineutrino induced charged current interactions 79−36063
soft π prod. in e^+e^- annihilations, nucleon pole term 79−36090
sum rules for π inclusive reactions, π bremsstrahlung 78−45811
superdense celestial bodies, pionisation effect rel. to eqn. of state 80−67773
temperature dependence of threshold for pion condensation in neutron matter 79−45197
three-pion prod. on complex nuclei with 23 GeV/c π^- 78−82392
threshold photoprod., exchange currents, equivalence theorem 77−79321
threshold photoprod., research at Saclay 77−82917
threshold pion electroproduction, nuclear response surface 78−93989
transverse momentum correls. in cluster model 77−38134
uncorrelated jet model, quantum statistical correls., Bose-Einstein statistics, pion prod. 78−16992
uncorrelated jet model at high energy, quantum statistics, soft pion prod. 78−16995
uncorrelated jet model with Bose-Einstein statistics for π prod. anal. 78−82172
vacuum polarisation in strong fields, π condensation 79−314
vertex function anal., prod. and absorpt. in nucl. reactions 78−12989
weak neutral current, gauge theory model predictions 79−13014
weak neutral current π prod., comparison of gauge theory models 78−82139
weak neutral current coupling const. from νN single pion prod. data anal. 77−13911
weak neutral current couplings calc. of u and d quarks, π prod. data 78−54603
(α,πX), π multiplicity dispersion in nuclear collisions *(Russian)* 79−54443
αN, 0.1-1.21 TeV, multiple pion production, role of clusters 77−34199
(d,π), 4.2, 4.5 GeV/N, pion multiplicities and theoretical models, review 80−42657
(d,π) reactions, prod. cross sections near threshold, non-nucleon model 77−41976
d(γ,π^0)d differential cross section, investigation of ΔN interaction in the deuteron 79−67597
D→K$\pi l\nu$, charm-changing weak hadronic current, models 80−57585
D^0→$K^-\pi^+$, quark total number conservation, D^+ lifetime longer than D^0 80−57590
D^0→$K^-\pi^+\pi^-$, obs. in 3.77 GeV e^+e^- annihilation 78−37206
D^0→$\bar{K}^0\pi^0$, $\Delta T=1$ constraints and final state interactions 80−95267
D^0→$\bar{K}^0\pi^0$, quark total number conservation, D^+ lifetime longer than D^0 80−57590
D^0→K^+K^-, $\pi^+\pi^-$, branching ratio, $\Delta I=1/2$ rule violation, colour radius interactions calc. 79−93412
D^+→$\bar{K}^0\pi^+$, quark total number conservation, D^+ lifetime longer than D^0 80−57590
d+nucleus→π+X, inelastic rescatt. contrib. to cumulative meson prod. *(Russian)* 77−61334
dA→π^-+X, scaling invariance of interactions of relativistic nuclei, the cumulative effect *(Russian)* 79−93611
DD pα, 1300 to 2300 MeV, π^0 photoproduction, double polarisation parameters 80−13317
dd→π^0X, large transverse momentum, π^0 prod. cross section, ISR energies 79−3055
dp→dp$\pi^+\pi^-$, 11.9 GeV/c, d* effect and resonance prod. 77−22805
δ(980)→$\pi\gamma\gamma$, radiative decay width using a vector dominance model 78−82205
δd→π^0, multiple scatt. contrib. to threshold photoprod. 80−73718
δd→π^+nn, final state interaction effects *(Russian)* 78−41558
(e,e'$\pi^\pm$), threshold production 79−85452
(e,e'π), π electromag. processes, theoretical aspects 80−22822
(e,e'$\pi^\pm$), near threshold, reactions on ^{3}He, ^{6}Li, ^{11}B, ^{12}C and ^{16}O 77−10388
e+p→e'n+π^+, σ_L, σ_U separation, π EM form factor 77−79269
ed, charged pion forward electroprod. at $Q^2=1.0(GeV/c)^2$, $\pi^\pm$ cross section ratio 79−93434
ed, $K^\pm/\pi^\pm$ ratio and symmetry props. of quark- parton model, fragmentation functions 78−93888
ed→e'$p_s p\pi^-$, 0.70 and 1.35 GeV^2, cross section 77−10264
e^-d→$e^-\pi^+$nn, e^-d→$e^-\pi^-$pp, forward prod. of single pions in resonance region 78−37219
e^+e→$\pi^+\pi^-\gamma$, virtual electrons bremsstrahlung photon, Feynman diagrams, Weizsacker-Williams approx. 80−52484
e^+e^-→ hadrons, 1.6 GeV, total cross section, pion multiplicity 77−49983
e^+e^- annihilation, 3.6-5.2 GeV, charged π, K, N inclusive prod. 79−30743
e^+e^- annihilation, DD τ decay, large timelike Q^2, conservation of vector current and current algebra 78−78155
e^+e^- annihilation, inclusive pion spectra, parton fragmentation model 77−18305
e^+e^-→e^+e^-X, X=e^+e^-, $\mu^+\mu^-$, $\pi^+\pi^-$, η', photon-photon interactions, QED test 79−93425
e^+e^-→$e^+e^-\pi$ 79−13142
e^+e^-→$e^+e^-\pi^0$, beam polarisation effects on cross section 77−61269
e^+e^-→$e^+e^-\pi^+\pi^-$, beam polarisation effects on cross section 77−61269
e^+e^-→γ^*→γ+hadrons, QCD predictions 80−63009
e^+e^-→$\gamma\pi^0$, inclusive production, 4.9 to 7.4 Gev, cross sections 78−89723
e^+e^-→hadrons, 12, 30 GeV, π,k,p,$\bar{p}$ production 80−105916
e^+e^-→hadrons, 1.35 to 2.125 GeV, hadronic cross sections 79−58968

pion production continued
e^+e^-→hadrons, 53 GeV², $\pi^\pm$ and $K^\pm$ cross sections, scaling 78−78201
e^+e^- inclusive hadron prod., polarisation and p nonconservation asymmetries, π, $K^\pm$, $D^\pm$ prod. 80−78084
e^+e^-→K^+K^-, 1.6 GeV, total cross-section meas., pion form factors determ. 77−46064
e^+e^-→L^-L^+→ pions, test for chirality of heavy-lepton current 77−18308
e^+e^-→$\mu 3\pi$, above 6 GeV, inference of τ decay 78−50042
e^+e^-→$n\pi$, jet struct., lightlike (zero mass) quarks anal. 79−63496
e^+e^-→$p\pi^-\bar{n}$, partial conservation of axial flow *(Russian)* 78−8681
e^+e^-→$p\pi^0\bar{p}$, partial conservation of axial flow *(Russian)* 78−8681
e^+e^-→$\omega\pi^0$, OZI rule violation and cryptoexotic mesons 79−71760
e^+e^-→$\pi^+\pi^-$, 0.78 to 1.34 GeV, π form factor meas. 78−33076
e^+e^-→$\pi^+\pi^-$, 400 MeV, pion form factors *(Russian)* 79−3034
e^+e^-→$\pi^+\pi^-$, near threshold, π form factor *(Russian)* 80−4996
e^+e^-→$\pi^+\pi^-$, vector meson dominance anal. for π form factor 78−70370
e^+e^-→$\pi^+\pi^-$(K^+K^-), $\sqrt{s}$=1.5 GeV, EM timelike form factors for π and K 80−91089
e^+e^-→$\pi^+\pi^-\pi^0$, 1.45-1.875 GeV, ω behaviour at 1.55 GeV 80−82984
e^+e^-→$\pi^+\pi^-\pi^0$, 750-1100 MeV, ω and ϕ meson interference 80−105910
e^+e^-→$\pi^+\pi^-\pi^0$, neutral current and one-photon graph interf. 77−87990
e^+e^-→$\pi^+\pi^-\pi^0$, ϕ meson mass meas., $\omega\phi$ interference obs. *(Russian)* 78−45935
e^+e^-→$\pi^+\pi^-\pi^0$, weak neutral current effects, asymmetries 77−6139
e^+e^-→$\pi^+\pi^-\pi^+\pi^-$, 1.45-1.875 GeV, ρ behaviour at 1.55 GeV 80−82984
e^+e^-→$\pi^+\pi^-\pi^+\pi^-$, 890-1100 MeV, cross section, πA_1 prod., ϕ branching ratio 79−36087
e^+e^-→$\pi^+\pi^-\pi^+\pi^-$ cross section, current algebra calc., props. of hadronic axial vector current 79−17742
e^+e^-→$\pi^\pm X$, 13 and 25 GeV², cross sections, scaling 77−49989
e^+e^-→$\pi^\pm X$, at CERN ISR with x=0 77−18303
e^+e^-→$\pi^\pm X$, weak neutral-current effects 77−13968
e^+e^-→πX, soft π prod., PCAC hypothesis, current algebra commutator relations 78−33075
e^+e^-→π+anything, statistical model anal., two-parameter fit 77−6138
e^+e^-→$\tau^+\tau^-$→cascade π and ρ, parity violation from weak and EM interaction interference *(Chinese)* 79−49504
e^+e^-→$x\pi$, even G parity hadronic cross section, $\rho'(1600)$ 2π branching ratio 78−12921
eN, pion production, vector-like theories *(Russian)* 78−37221
eN→$e'\pi^\pm X$, longitudinal-transverse separation 77−49977
en→$en\pi$, pol. e, P-odd asymmetry and cross sections, SU(2)xU(1), SU(3)xU(1) calcs. *(Russian)* 80−62998
eN→$e\pi_s$+X, test of soft-pion theorem in inclusive pion electroprod. 79−17739
eN→$e\pi^\pm X$, ^1H, ^2H targets, π^+/π^+ ratio, Q^2 to 4 GeV² 77−74693
en→$e\pi^\pm X$, π^+/π^- ratio meas. 77−18295
eN→$e\pi^\pm X$, sum rules for polarised N 78−89718
eN→$e\pi\Delta$, low energy, ΔN axial form factors soft-pion theory 78−70380
eN→$e\pi$N, π form factor determ. 78−66128
eN inelasticcatt., low energy pion electroprod. and hadron form factors, book 79−85306
e^-N, inclusive pion production due to γq→$\pi q'$ process, quark-parton model *(Russian)* 80−78073
e^-N→e^-Nπ, electromag. and weak process from weak neutral current interaction *(Russian)* 78−45928
e^-N→$e^-\pi X$, high Q^2 cross-section meas. 78−21439
ep, 20.5 GeV, inclusive π^0 electroprod. in deep inelastic region 80−52520
ep, K^+/π^+ ratio and symmetry props. of quark- parton model fragmentation functions 78−93888
ep→4π or 2π, 1.6 GeV region, spontaneously broken gauge theory model 77−2845
ep→eNπ, $\gamma^+p\Delta^+(1231)$ vertex transition form factor *(Russian)* 80−37269
ep→$e'n\pi^+$, 0.06-1.35 GeV², cross section 77−10263
ep→$ep\pi^0$, $-k^2$=0.88 (GeV/c)², comparison with various models 77−18294
ep→$ep\pi^0$, coincidence electroproduction of single neutral pions in the resonance region at q^2=0.5 (GeV/c)² 79−89168
ep→$ep\pi^0$, elastic π^0 electroprod. above resonance region, cross section, direction 78−62412
ep→$ep\pi^0$ or $en\pi^+$, threshold cross section slope, form factors, π axial mass and radius 78−62411
ep→$ep\pi^+\pi^-$, exclusive ρ^0 prod. by virtual photons 79−22113
ep→ex^{++}n, longitudinal and transverse contribs., π^+ EM form factor 78−66126
ep→$e\pi^+$n, scalar transverse separation 77−18296
ep→$e\pi^\pm X$, π^+/π^- ratio meas. 77−18295
ep→$e\pi^\pm$+anything, π^+, π^- structure function behaviour, various W and Q values 77−10262
ep→π^0X, duality and finite energy sum rules 80−42477
η→$3\pi^0$, decay rate, up quark masslessness 79−40761
η→$\pi^+\pi^-\pi^0$, decay width 78−70362
η→$\pi\pi\gamma$, quark loop model, SU(3) splitting of quark masses 80−62990
η^0-π^0 mixing effects and ΔS=1 nonleptonic weak decays 80−4991
η'→$\eta\pi\pi$, current algebra calcs. with symmetry breaking, inconsistency with expt. 79−13114
f'(1514)→2π, decay amplitudes, OZI rule, dispersion relations, intermediate states contribs. 79−383
(γ,$p\pi^-$) reaction on nuclei, investigation using 2-arm spectrometric arrangement 79−711
(γ,π), few body pion photoprod. in Δ-resonance, region 80−42636
(γ,π), light nuclei near threshold, π mass difference effects, nuclear K-matrix 80−27674
(γ,π), photopion reaction sensitivity to optical pot. 80−78278
(γ,π), π electromag. processes, theoretical aspects 80−22822
(γ,Π) in nuclear matter, optical pot. and Fermi gas model, Li, Be appl. 79−36230
(γ,π^0), near threshold photoprod. on ^1H and ^2H, cross section calcs. 78−25174
(γ,$\pi^\pm$), low energy photoprod., emission ang. depend. *(Russian)* 80−57769
(γ,$\pi^\pm$), threshold production 79−85452
(γ,π^-p), detector system and ccts. 78−877
(γ, πX), 4.2, 4.5 GeV/N, pion multiplicities and theoretical models, review 80−42657
γ→$\pi\pi$, threshold-450 MeV, energy dependent multipole anal. 80−78082

pion production continued
γ→$\pi\omega$, transition and π form factors, p'(1200) resonance *(Russian)* 79−22098
γ→$\pi\pi$, EM radius, low-energy approx. comparison with kaon 78−50033
γ+d→p+n+π^0, interactions of nucleons in final state 78−37220
γ+N→N+π, spatial parity nonconservation in π-meson photoproduction *(Russian)* 77−61301
γd→nnπ^+, cross-section and asymmetry ratios in region of first resonance *(Russian)* 78−78196
γd→nnπ^+, threshold form factors 79−85453
γd→pn, EM properties of πNN system, virtual π reabsorption 79−22109
γd→ppπ^-, cross section, double pion photoprod. on one nucleon 78−70378
γd→π^0d, 1 to 10 MeV above threshold 79−85454
γd→π^0d, 450 MeV cross section asymmetry *(Russian)* 79−89171
γd→π^0d, meson-exchange currents in photomesic reactions, relativistic many-body theory 80−422
γd→π^0d, recoil deuteron polarisation statistical tensors anal. 78−74348
γd→$\pi^\pm$NN, off-energy shell photoprod. amplitudes for reactions on bound neutrons 80−421
$\gamma\gamma$→$\pi\pi$, inelasticity effects for real photons in e^+e^- collisions 77−67667
$\gamma\gamma$→$\pi\pi$ amplitude, coupled channel calc. of final state interactions 77−2809
$\gamma\gamma$→$\pi\pi$ scalar-isoscalar amplitude and p EM polarisability 77−82743
γ ^{3}He→$\pi^+\pi^-{}^3$He, E<800 MeV, gauge-invariant one-pion-exchange model 77−18298
γN, exclusive photoprod. reactions, Okubo-Zweig-Iizuka rule 80−95277
γN, inclusive pion production due to γq→$\pi q'$ process, quark-parton model *(Russian)* 80−78073
γN, $\pi^\pm$ photoprod., low energy, emission ang. depend. *(Russian)* 80−57769
γN→$\pi^\pm$+anything, 9-18 GeV, forward hemisphere 77−6134
γN→Nπ, mag. dipole photoexcitation, singular integral eqns., polynomial ambiguity 80−57608
γN→Nπ, P-odd effects, weak interaction *(Russian)* 78−54638
γN→Nπ, P-odd multipole amplitude, dispersion relations *(Russian)* 79−93435
γn→n$\pi^+\pi^-$, threshold to 1 GeV, Δ production 77−26532
γn→pπ^-, to 500 MeV, multipole anal. near P_{33} reson. *(Russian)* 77−74695
γn→p$\pi^-\pi^0$, threshold to 1 GeV, Δ production 77−26532
γN→$\phi\pi^0$N, diffractive photoprod., OZI rule violation and cryptoexotic mesons 79−71760
γn→π^-p, 0.9-1.65 GeV, pol. γ, cross section asymmetry *(Russian)* 80−86728
γn→π^-p, 250 to 500 MeV, multipole anal. *(Russian)* 77−10266
γn→π^-p, 700 MeV, polarised neutrons, target asymmetry meas. 77−13967
γn→π^-p, 700 to 1200 MeV, recoil proton polarisation 80−78075
γn→π^-p, 850 MeV, target asymmetry meas. 78−21438
γn→π^-p, cross section determ. from 20-100 MeV meas. on π^-p→γn reaction *(French)* 79−411
γn→π^-p, proton polarisation in $^2H(\gamma,np)$ *(Russian)* 78−41700
γn→π^-p reaction cross-section asymmetry in photon energy range 0.9 to 1.65 GeV *(Russian)* 80−32108
γn→$\pi^-\pi^0$p, Chew-Low amplitude correction 77−2844
γN→π^+X, QCD cross sections 80−73715
γN→π^+n, meas. of asymmetries and cross sections using 16 GeV linearly polarised photons 80−13318
γn→π^+p, π^+n, π^-p, $K^+\Lambda$, $K^+\Sigma^0$ final state comparisons above resonance region 80−105906
γN→$\pi\Delta$, low energy prod. and Δ-N axial transition vertex 77−49981
γN→$\pi\Delta$, meas. of asymmetries and cross sections using 16 GeV linearly polarised photons 80−13318
γN→$\pi\Delta$ reaction amplitude, equivalence theorems *(Russian)* 80−52522
γN→$\pi\Delta$(1232), multipole amplitudes, dispersion relations 80−5002
γN→πN, backward π prod., effective pole model phenomenological study 79−3030
γN→πN, dispersion rels. by method of Pade approx. 77−34166
γN→πN, fixed Regge singularities 77−74694
γN→πN, P-odd partial amplitudes, dispersion relns. *(Russian)* 79−85304
γn→$\rho^0(p\pi^-)$, 7.5 GeV, cross channel isospin amplitude meas. and anal. 77−18299
γn to 5.3 GeV, multipion and strange particle prod., reson. 77−10261
Γ_{pol}N→$\pi^\pm$N, weak neutral interactions, QCD renormalisation 79−93433
γp, π^0 prod. in resonance region, asymm. *(Russian)* 78−17031
γp→$K^+K^-\pi^+$p, photoprod. at CERN SPS and search for charmed mesons 79−26336
γp→$K^+K^-\pi^+\pi^-$p, 20-70 GeV, $K^+K\pi$ threshold enhancment 80−78076
γp→Nπ, 250-500 MeV, multipole anal. *(Russian)* 77−246
γp→Nπ, position and residue of the pole in the $M_{1+}^{(3/2)}$ amplitude *(Russian)* 79−22112
γp→nπ^+, cross-section and asymmetry ratios in region of first resonance *(Russian)* 78−78196
γp→nπ^+, differential cross sections meas., 500-930 MeV 77−79271
γp→nπ^+, multipole anal. by regularisation method *(Russian)* 77−82753
γp→nπ^+, multipole anal. in region of first reson. 80−22622
γp→nπ^+, photoprod. of π^+ by unpolarised and linearly polarised photons 77−46055
γp→nπ^+, pion photoprod. using coherent bremsstrahlung beam and polarised proton target *(Russian)* 79−80830
γp→nπ^+ 340 MeV, cross section asymmetry *(Russian)* 79−63487
γp→nπ^+ reaction, with polarised protons and photons at 340 MeV *(Russian)* 79−89170
γp→nπ^+ section asymmetry, pion-proton twin birth contribution *(Russian)* 80−47308
γp→nπ^+, 340 MeV, pol. p, first resonance region, π^+ photoprod., T-asymmetry *(Russian)* 80−62997
γp→pX, 710 to 950 MeV, momentum spectrum of recoil protons 79−22108
γp→pπ^0, 500 MeV, double polarisation expt. *(Russian)* 77−74696
γp→pπ^0, multipole anal. in region of first reson. 80−22622
γp→pπ^0, photoproduction, in low-energy region, complex multipole amplitudes 80−68463
γp→pπ^0, pion photoprod. using coherent bremsstrahlung beam and polarised proton target *(Russian)* 79−80830

pion production continued
$\gamma p \rightarrow p\pi^0$, quantum chromodynamics and P-odd effects *(Russian)* 79−89172
$\gamma p \rightarrow p\pi^0(n\pi^+)$, to 500 MeV, multipole anal. near P_{33} reson. *(Russian)* 77−74695
$\gamma p \rightarrow p\pi^+\pi^-$, 710 to 950 MeV, cross section determ. from momentum spectrum of recoil protons 79−22108
$\gamma p \rightarrow p\pi^+\pi^-$, 710 to 950 MeV, cross section determ. from momentum spectrum of recoil protons 79−22108
$\gamma p \rightarrow p\pi^0$, differential cross sections meas., 500-930 MeV 77−79271
$\gamma p \rightarrow \pi^0 X$, invariant cross section at large p_T, hard scatt. model 80−22621
$\gamma p \rightarrow \pi^0$+jet+X, perturbative QCD predictions 79−89165
$\gamma p \rightarrow \pi^0(p^+)p$, energy independ. multipole anal. through second resonance region 78−62410
$\gamma p \rightarrow \pi^0 p$, 0.6 to 1.8 GeV, backward angles, η-cusp 80−57609
$\gamma p \rightarrow \pi^0 p$, 0.9 to 1.2 GeV, ang. distribs. of differential cross section 77−87982
$\gamma p \rightarrow \pi^0 p$, 1 to 10 MeV above threshold 79−85454
$\gamma p \rightarrow \pi^0 p$, 1.0 and 1.1 GeV, forward prod. on polarised protons 77−74692
$\gamma p \rightarrow \pi^0 p$, 1.4 GeV, differential cross section meas. 80−42476
$\gamma p \rightarrow \pi^0 p$, 250 to 500 MeV, multipole anal. *(Russian)* 77−10266
$\gamma p \rightarrow \pi^0 p$, 360-500 MeV, secondary proton polarisation meas. *(Russian)* 78−54637
$\gamma p \rightarrow \pi^0 p$, 390-975 MeV, differential cross section 80−86725
$\gamma p \rightarrow \pi^0 p$, 400 to 1142 MeV, recoil proton polarisation 80−82981
$\gamma p \rightarrow \pi^0 p$, 450 to 800 MeV, proton polarisation, Walker-type anal., $P_{11}(1470)$, $D_{13}(1470)$, $S_{11}(1535)$ resonances 80−73721
$\gamma p \rightarrow \pi^0 p$, below 1 GeV, polarised target asymmetry meas., comparison with phenomenological anal. 78−62409
$\gamma p \rightarrow \pi^0 p$, differential cross sections at large angles, 2-6 GeV 78−37214
$\gamma p \rightarrow \pi^0 p$, E_γ=1.3 to 2.1 GeV polarisation parameter meas. 79−80829
$\gamma p \rightarrow \pi^0 p$, high energies, semiempirical amplitude anal. dispersion relations and Regge poles 80−86726
$\gamma p \rightarrow \pi^0 p$, proton polarisation vector components *(Russian)* 79−85305
$\gamma p \rightarrow \pi^0$, low energies, complex amplitudes in s- and p-wave approx. 80−102053
$\gamma p \rightarrow \pi^+ n$, 0.5-0.8 GeV, ang. distrib. of polarised target asymmetry 77−34165
$\gamma p \rightarrow \pi^+ n$, 1.35-1.65 GeV, pol. γ, resonance energy region, cross section asymmetry *(Russian)* 80−86727
$\gamma p \rightarrow \pi^+ n$, 250 to 500 MeV, multipole anal. *(Russian)* 77−10266
$\gamma p \rightarrow \pi^+ n$, 520 to 2250 MeV, meas. of Σ, T, and P polarisation parameters 79−75778
$\gamma p \rightarrow \pi^+ n$, 600-1875 MeV, pol.p and γ, G and H polarisation parameters 80−99105
$\gamma p \rightarrow \pi^+ n$, 850 MeV, target asymmetry meas. 78−21438
$\gamma p \rightarrow \pi^+ n$, π^+ form. asymm. near first πn resonance *(Russian)* 78−66124
$\gamma p \rightarrow \pi^+ n$, $\pi^+ n$, $\pi^- p$, $K^+\Lambda$, $K^+\Sigma^0$ final state comparisons above resonance region 80−105906
$\gamma p \rightarrow \pi^+ n$ below 1.02 GeV, polarized target asymm. meas. 78−17029
$\gamma p \rightarrow \pi^+\pi^- p$, Chew-Low amplitude correction 77−2844
$\gamma p \rightarrow \pi^+\pi^- p$, Lagrangian model, polarised and unpolarised photons 78−17028
$\gamma p \rightarrow \pi^+\pi^-\pi^0\pi^0 p$, 20-70 GeV, $\omega\pi^0$ state enhancement at 1.25 GeV 80−78078
$\gamma p \rightarrow \pi^+\pi^-\pi^+\pi^-\pi^+\pi^- p$, diffractive production, jet-like structure 80−57606
$\gamma p \rightarrow \pi^0 X$, duality and finite energy sum rules 80−42477
$\gamma p \rightarrow \pi N$ multipole isotopic anal., soln. irregular behaviour near P_{33} resonance *(Russian)* 80−5005
$\gamma p \rightarrow \pi X$, large p_T, perturbative QCD 80−86723
$\gamma p \rightarrow \pi\pi N$, 710-950 MeV 79−63484
$\gamma p \rightarrow \rho'(1500)p$, $\rho'(1500) \rightarrow \pi^+\pi^-\pi^+\pi^-$, photoprod. at CERN SPS and search for charmed mesons 79−26336
$\gamma p \rightarrow V^0 p$, one-pion exchange contrib., vertex corrections 78−50039
$\gamma\gamma p \rightarrow \pi^0 p$, phase shift anal., shrinking photon, geometrical duality 77−87983
$\gamma\rho \rightarrow \pi^+\pi^- p$, 20-70 GeV, dipion enhancemment, $\rho'(1600)$ observation 80−78079
$^2H(\gamma,\pi^0)$, near threshold, total and differential cross-sections 77−14106
$J/\psi \rightarrow K_S K^-\pi^+$, low lying resonance saturation 79−54338
$J/\psi \rightarrow 3\pi$, low lying resonance saturation 79−54338
(K^-,π), Σ hypernuclei production 79−85392
(K^-,π^-), hypernuclei generation, γ-spectroscopy and lifetimes 79−75890
(K^-,π^-), strange giant resonance, DWIA calc. 77−14187
(K^-,π^-), strangeness exchange reactions, CERN 79−85561
(K^-,π^-) reaction on ^{9}Be, ^{12}C, ^{16}O, ^{32}S, and ^{40}Ca 77−14183
$K \rightarrow \pi l\nu_l$, form factor, parameter-free hard-meson prediction via current algebra sum rules 77−49954
$K \rightarrow \pi\pi\gamma\gamma$, scalar meson model for radiative decays involving $\delta(980)$ 78−82204
$K \rightarrow \pi\pi\pi\gamma$, scalar meson model for radiative decays involving $\delta(980)$ 78−82204
$K^+ \rightarrow \pi^- + \pi^0 + \pi^0$, π^+ meson energy spectrum below 30 MeV 78−12906
$K^+ \rightarrow \pi^+\pi^- e^+\nu$, $\pi\pi$ energy, phase shift difference, hadronic current form factors, scatt. length 77−41840
$K^+ \rightarrow \pi^+\pi^0\pi^0$, decay matrix element parameters expt. determ. 77−13956
$K^+ \rightarrow \pi^+\pi^+\pi^-$, meas. of π^+ spectrum below 30 MeV 77−6115
$K^\pm \rightarrow \pi^\pm\gamma\gamma$, scalar meson model for radiative decays involving $\delta(980)$ 78−82204
$K_2^0 \rightarrow k\pi$, k=2 or 3, Racah time reversal, a C,P,T scheme 80−78056
$K_L \rightarrow \pi^- \mu^+\nu_\mu$, transverse polarisation of μ, violation of time-reversal invariance 80−68448
$K_L^0 \rightarrow \pi^0\gamma\gamma$, scalar meson model for radiative decays involving $\delta(980)$ 78−82204
$K_L^0 \rightarrow \pi^+ + \pi^- + \pi^0$, matrix element for data fit, branching ratio 77−38165
$K_L \rightarrow \pi^+\pi^-\pi^0$ Dalitz plot 78−4859
$K_L \rightarrow \pi^+\pi^-\pi^0$, matrix element expt. study *(Russian)* 78−78174
$K_S \rightarrow \pi^+\pi^-\gamma$, branching ratio and photon spectrum meas. 77−2828
$K^*(892) \rightarrow K\pi\pi$, decay width upper limit 78−78177
$K^*(1420) \rightarrow K^*(892)\pi^+\pi^-$, partial width for decay mode 78−78177
$K^- d \rightarrow \pi^- \Lambda p$, anal. of Λp enhancement at 2.129 GeV in cross section meas. 79−22141
$K^- d \rightarrow \pi^- \Lambda p$, low energy Faddeev calc. 79−85341
$K^- d \rightarrow \pi^- \Lambda p$, pole in $^3S_1$ hyperon-nucleon scattering amplitudes 80−102068
$K^- d \rightarrow \pi^- \Lambda p$ breakup process, appl. of Faddeev eqns. 79−75797
$K^- d \rightarrow \pi\Lambda p$, ΣN bound state and Λp enhancement 80−47326

pion production continued
$K^+ d$ inclusive reactions, 4.6 GeV/c, topological cross sections, π^-, K^0, Λ prod. 77−50004
$K^- {}^4He \rightarrow \pi^- {}^4_\Lambda He$, final state interaction model, Muskhelishvili Omnes eqn. soln., πmomentum distrib. 77−30285
$\bar{K}N \rightarrow \Sigma\pi$, 1520-1745 MeV, partial wave anal. 77−18324
$K^- n \rightarrow (\Sigma\pi)^-$, 680-840 MeV/c differential cross-sections 77−18324
$K^- N \rightarrow K^- N\pi$, diffractive excitation at 14.3 GeV/c and 500-1500 GeV/c 77−6175
$K^- N \rightarrow K^- N\pi\pi$, diffractive excitation at 14.3 GeV/c and 5n0/1500 GeV/c 77−6175
$K^- N \rightarrow \Lambda\pi(\Sigma\pi)$, review 79−85339
$K^- n \rightarrow \pi^- \Sigma^0$, 1750-2200 MeV, partial wave anal. 77−79280
$K^- n \rightarrow \pi^0 \Sigma^-$, 1750-2200 MeV, partial wave anal. 77−79280
$\bar{K}p$, 70 GeV/c, total and differential cross-sections for π and K production 80−63050
kp, large P_T pion^0 prod., meson structure functions, quark distrib. functions 80−86714
$Kp \rightarrow \pi^- \Sigma^+$, exchange degeneracy in hypercharge exchange reacts. 78−41581
$Kp \rightarrow \pi(K)(p)X$, 4-250 GeV/c, Pomeron factorisation 77−14005
$K^- p$, 32 GeV/c, exclusive reactions, diffractive dissociation processes, $\pi^+\pi^-$ and K^+K^- prod. 80−86760
$K^- p$, neutral channel cross section meas., 1470 to 1560 MeV CM energy 78−82237
$K^- p \rightarrow (\bar{K}\pi\pi)^- p$, 4.2 GeV/c, partial wave anal. in Q region 80−13330
$K^- p \rightarrow \Lambda\pi^+\Sigma^\pm$, 4.2 GeV/c, differential cross sections 77−30431
$K^- p$ interaction at 32 GeV/c 78−482
$K^- p \rightarrow K_S{}^0\pi^+\pi^- n$, 6 GeV/c, K* and Q_2 signals, partial wave anal. 80−86754
$K^- p \rightarrow K^- p\pi^0$, amplitude calc. for soft pion emission, using PCAC 79−13153
$K^- p \rightarrow K^- p\pi^+\pi^-$, 14 GeV/c, peripherally prod. π, possible preequilibrium π evaporation 79−80850
$K^- p \rightarrow K^-\pi^-\pi^+ p$, 10, 14.3 and 16 GeV/c, partial wave anal. of $p\pi^+\pi^-$ system 78−82251
$K^- p \rightarrow K^-\pi^0 p$, c.m. energy 1775 to 1957 MeV 79−22138
$K^- p \rightarrow K^-\pi^0 p$, cm. energy 1775 to 1957 MeV 79−3046
$K^- p \rightarrow K^-\pi^+ n$, c.m. energy 1775 to 1957 MeV 79−22138
$K^- p \rightarrow K^-\pi^+ n$, cm. energy 1775 to 1957 MeV 79−3046
$K^- p \rightarrow K^-\pi^+\pi^- p$, 10, 14.3, 16 GeV/c, partial wave anal. of $(K\pi\pi)^-$ system in the L-region 79−17764
$K^- p \rightarrow \bar{K}^0\pi^- p$, 4.2 GeV/c, multichannel anal. 80−73736
$K^- p \rightarrow \bar{K}^0\pi^- p$, 4.2 GeV/c, non-charge exchange $\bar{K}^0\pi^-$ prod., spin-parity struct., mass 78−45949
$K^- p \rightarrow \bar{K}^0\pi^- p$, c.m. energy 1775 to 1957 MeV 79−22138
$K^- p \rightarrow \bar{K}^0\pi^- p$, cm. energy 1775 to 1957 MeV 79−3046
$K^- p \rightarrow \bar{K}^0\pi^+\pi^- n$, 10 GeV/c, partial wave anal. of $(\bar{K}^0\pi^+\pi^-)$ system 78−45969
$K^- p \rightarrow \Lambda^0\pi^0$, strong reaction asymmetry and mass quantisation, particle struct. *(French)* 79−3043
$K^- p \rightarrow \lambda$+pions, 4.2 GeV/c, multiplicities, hadronic temps. and ang. distribs. in $K\bar{K}$, $\bar{p}p$ annihilations 79−45101
$K^- p \rightarrow \Lambda(\Sigma)K^0, K^\pm\pi^\pm$, 4.2 GeV/c, 1550 MeV, I=1 enhancement in $(\Lambda\pi)$ and $(\Sigma\pi)$ systems 78−89735
$K^- p \rightarrow \Lambda\pi^0$, 6 GeV/c, baryon exchange reactions, ηNN coupling constant, Λ polarisation, nucleon-Regge exchange 80−78098
$K^- p \rightarrow \Lambda\pi^0$ baryon Regge exchange, FESR anal. 80−63022
$K^- p \rightarrow \Lambda\pi^+\pi^-$, 4.2 GeV/c, ρ-ω interference 77−30429
$K^- p \rightarrow \Lambda\pi^+\pi^-$, CM energies 1.65 to 1.72 GeV 77−41861
$k^- p \rightarrow \Lambda\pi^+\pi^-$, partial wave anal. in $\Lambda(1520)$ region, Λ partial decay widths *(Russian)* 80−32131
$K^- p \rightarrow pK^0\pi^-\pi^0$, 10 GeV/c, dynamical mechanism from cluster anal. *(Russian)* 80−42499
$K^- p \rightarrow \pi^-\Sigma^+$ 79−93462
$K^- p \rightarrow \pi^-\Sigma^+$ and $\pi^+ p \rightarrow K^+\Sigma^+$, exchange degeneracy 80−57634
$K^- p \rightarrow \pi^-\Sigma^\pm(1385)$, 1775-2170 MeV, partial wave anal. 78−54653
$K^- p \rightarrow \pi^- Y^+$, $Y^+ = \Sigma^+$ or $Y^{*+}(1385)$, 7 GeV/c, hypercharge exchange in line-reversed $\pi^+ p$ and $K^- p$ 80−82998
$K^- p \rightarrow \pi^- Y^*(1385)$, 11.5 GeV/c, confirmation of exchange degeneracy predictions in line reversed reacts. 78−82247
$K^- p \rightarrow \pi^0\Lambda$, 4.2 GeV/c, total and differential cross sections, forward production peaks 79−40801
$k^- p \rightarrow \pi^0\Lambda(1520)$, 1.71 to 2.17 GeV, partial wave analysis 78−29352
$K^- p \rightarrow \pi^- X$, 100, 200 GeV/c high transverse momentum π^0 prod., quark scatt. 78−45976
$K^- p \rightarrow \pi^-\Sigma^-$, box diagram calcs. unitarity corrections in strong interactions 80−91110
$K^- p \rightarrow \pi^-\Sigma^+$ 78−82239
$K^- p \rightarrow \pi^+\pi^-\pi^0\Lambda$, 4.2 GeV/c, partial-wave anal. of 3π system 77−82770
$K^- p \rightarrow \pi^-\Sigma^\pm(1385)$, 1775-2170 MeV, partial wave anal. 79−6348
$K^- p \rightarrow \pi\Sigma(1385)$, 4.2 GeV/c, total and differential cross sections 77−41860
$K^- p \rightarrow \pi X$, 32 GeV/c, struct. functions *(Russian)* 77−264
$K^- p \rightarrow \Sigma^-\pi^+$, backward differential cross section 80−63024
$K^- p \rightarrow \Sigma^-\pi^+\omega$, 4.2 GeV/c, B (1235) backward prod., $\pi^+\omega$ mass enhancement 78−89736
$K^- p \rightarrow \Sigma^-\pi^+\pi^-\pi^+$, 4.15 GeV/c, nondiffractive A_1 production, double-Regge model 80−78097
$K^- p \rightarrow \Sigma^0\pi^+\pi^-$, 4.2 GeV/c, ρ-ω interference 77−30429
$K^- p \rightarrow \Sigma^\pm\pi^\mp$, 1.934-2.516 GeV/c, reson. states identification 77−38200
$K^- p \rightarrow \Sigma^+\pi^\pm$, threshold and below, ratio of $\Sigma^-\pi^+$ to $\Sigma^+\pi^-$ production 78−70407
$K^0 p \rightarrow \Lambda^0\pi^+\pi^+\pi^-$, 1.5 to 2.5 GeV, effective mass distrib. 77−22792
$K^0 p \rightarrow \Sigma^0\pi^+\pi^+\pi^-$, 1.5 to 2.5 GeV, effective mass distrib. 77−22792
$K^0 p \rightarrow \Sigma^\pm\pi^\mp\pi^+\pi^+$, 1.5 to 2.5 GeV, effective mass distrib. 77−22792
$K^+ p$, two-particle inclusive and semi-inclusive correls. at 32 GeV/c *(Russian)* 77−88020
$K^+ p \rightarrow K^0(\pi^+)$+anything, 32 GeV/c, associated multiplicities *(Russian)* 77−34197
$K^+ p \rightarrow K^0 p\pi^+$, 3 to 16 GeV/c, resonance production, cross sections and density matrix elements 78−17048
$K^+ p \rightarrow K^0 p\pi^+$, resonance production at 5, 8.25, and 16 GeV/c 78−12931
$K^+ p \rightarrow K^0\pi^+ p$, 32 GeV/c, non-diffractive two body channel contributions 79−75801
$K^+ p \rightarrow K^+ p2\pi^+2\pi^-$, 16 GeV/c, azimuthal correls., Bose Einstein symmetrization effects 78−37239
$K^+ p \rightarrow K^+ p\pi^+\pi^-$, 2.7 to 32 GeV/c, impact parameter bounds, energy and effective mass dependence 80−57640
$K^+ p \rightarrow K^+ p\pi^+\pi^-\pi^0$, 8.2 and 16 GeV/c cross section determ. 77−22808

pion production continued
$K^+p\to K^+\pi^+\pi^+p$, 32 GeV/c, non-diffractive two body channel contributions 79−75801
$K^+p\to K^+\pi^+\pi^+\pi^-n$, 8.2 and 16 GeV/c cross section determ. 77−22808
$K^+p\to\pi^-X$, 32 GeV/c, associated average charged particle multiplicities 77−2882
$K^+p\to\pi^-X$, 8.2-32 GeV/c, transverse momentum distribs. *(Russian)* 77−30467
$K^+p\to\pi^-X^{+++}$ inclusive double-charge-exchange π^- prod., 100 GeV/c 78−37250
$K^+p\to\pi^-\pi^-X$, 32 GeV/c, two-pion correlations, Monte Carlo model 80−83008
$K^+p\to\pi^-\pi^-X$, inclusive distribs. in statistical model, correl. function 77−18354
$K^+p\to\pi^0X$, 32 GeV/c, inclusive and semi-inclusive distributions of π^0 80−27525
$K^+p\to\Sigma^+\pi^+$, strong reaction asymmetry and mass quantisation, particle struct. *(French)* 79−3043
$K^+p\to K_S^0\pi^+p$, 10 GeV/c, $K\pi$ prod., two arm spectrometer studies 78−50052
$K^+p\to K^+p\pi^+\pi^-$, study of low-mass $p\pi\pi$ system 77−22781
$K^+p\to K^\pm\pi^+\pi^-p$, 13 GeV/c, mass depend. of $1^+K^*\pi$ and ρK partial waves 78−8705
$K_L^0p\to K_S^0p(\pi^+\Lambda)(\pi^+\Sigma^0)(\pi^+\pi^0\Lambda)$, differential and polarisation cross sections near 550 MeV/c 79−17757
$K_L^0p\to K_S^0p\pi^+\pi^-$, 1.5 to 2.5 GeV, effective mass distrib. 77−22792
$K_L^0p\to K_S^0\pi^+\pi^-p$, up to 17 GeV/c, $Q^0\bar{Q}^0$ prod., cross sections 80−32129
$K_L^0p\to\Lambda^0\pi^+$, 1605 to 1910 MeV, differential and channel cross section meas. 79−75768
$K_s^0\pi^+\pi^+\pi^-$ narrow peak at 2.6 GeV in 12 GeV/c pp interactions 77−30452
$^6Li(\gamma,\pi^+)^6He$, cross-section determ. 77−14100
$lN\to l'\pi X$, semi-inclusive deep inelastic scatt. cross sections, higher twist effects 80−32105
Λ^0, neutral strange-particle prod. by 300 GeV protons in Be, Cu, Pb 79−17905
$\Lambda_c^+\to pK^0\pi^+\pi^-$, kaonic decay observation, prod. rates 79−26332
(n,pπ⁻), 100 to 300 GeV, coherent neutron dissociation on nuclei 78−29465
(n,pπ⁻) reactions on nuclei, 8 to 24 GeV/c, coherent diffractive prod., cross sections 78−41711
(N,π^-), π^- production by nucleons on light nuclei, estimate of energy consumption *(Russian)* 79−80943
$n\to p\pi^-\pi^0$, diffractive dissociation induced by 12 GeV K^- 79−40805
$N\to\pi N$, diffraction dissociation, two-component model 79−3037
$n+C\to(n^*\to\Delta\pi)X$, 45 GeV, production cross section 77−82795
$n+N\to(n^*\to\Delta\pi)X$, 45 GeV, decay prob. 77−82795
$nd\to(p\pi^-)d$, 26.6 GeV/c coherent interaction, peripherality of nucleon diffr. dissoc. 79−45108
$nd\to(p\pi^-)d$, diffr. dissoc. and interactions of diffractive produced systems 79−45107
NN, 0.25-42.3 TeV, multiple pion production, role of clusters 77−34199
$NN\to(N\pi)N$, Deck-model baryon-exchange contribs. 77−49933
$N\bar{N}\to(\pi,\rho,\omega,f)$, statistical model 80−102028
$N\bar{N}$ annihilation, even-odd ratio in multipion prod. 77−22755
$N\bar{N}$ annihilation to pions 78−25060
$N\bar{N}$ annihilations, statistical bootstrap model anal. 78−37224
NN dynamics at medium energies, elastic and inelastic scatt., unitary model 80−63101
NN interactions, inclusive pion production, low transverse momentum distrib., cluster model 77−67684
$NN\to NN(N\pi)$, isobar and peripheral model anal., and unified theory 79−80841
$NN\to NN\pi$, anal. via nonrelativistic field theory with HBE 79−85317
$NN\to NN\pi$, effect of π-baryon from factors on ang. depend. of cross sections 79−85318
$NN\to NN\pi$, lowest order Feynman diagram calc. 79−63508
$NN\to NN\pi$, polarization analysis of reactions with four spin-1/2 particles 80−86745
$N\bar{N}\to N\pi N$, 9 GeV/c, isospin cross sections, differential anal. 80−431
$N\bar{N}\to$pions, direct channel scheme based on statistical bootstrap, low-energy region 78−12924
$nn\to\pi^-d$, matrix element for s-wave pion prod. 77−6142
$nn\to\pi^-d$, π-production amplitude mass extrapolation 77−74709
$NN\to\pi X$, expt. review of π-prod. by (un)polarised nucleons on few-nucleon systems 79−80944
$N\bar{N}\to\pi n$, parametrisation of branching ratios 79−26341
$N\bar{N}\to\pi\pi,\rho$ EM polarisabilities difference contribs. 79−3023
$N\bar{N}\to\pi\pi$, $Q^2\bar{Q}^2$ resonances using MIT bag and ^3Po models 78−58171
$N\bar{N}\to\bar{\pi}\pi\pi$, kinematic singularity free helicity amplitudes, crossing matrix anal. props. 80−95285
NN semi-inclusive reactions, secondary pion production, 1000 GeV, scaling phenomena 79−22157
$N\bar{N}$ system, single γ and π emission rates, meson quantum number assignments 78−78208
np, Lorentz-invariant method, 24 and 70 GeV/c interactions, including pionisation 79−80848
$Np\to(N\pi)p$, diffraction dissociation, absorptive effects 80−5009
$np\to(p\pi^-)p$ diffractive dissociation, struct. in momentum transfer 77−13992
np collisions, at 800 MeV, model tests 77−18316
$np\to d(\pi\pi)^0$, threshold to 3 GeV/c, effective Hamiltonian for ABC effect 77−65168
$np\to d\pi^-$, 350-550 MeV, d ang. distrib. 79−75784
$np\to d\pi^0$, 795 MeV, test of isospin invariance 79−75786
$np\to d\pi^0$, nuclear forces charge symmetry test 80−5071
$np\to d\pi^+\pi^-$, 1.73 GeV, $\pi^+\pi^-$ effective mass spectrum anomaly *(Russian)* 79−67570
$np\to d\pi^+\pi^-$, 1.73GeV/c effective mass spectrum $(\pi^+\pi^-)$, narrow enhancements 80−86741
np interactions, 460-580 MeV, π^+ prod. 79−75785
$np\to nn\pi^+$, 790 MeV, deviation from T=1 matrix element, π centre of mass ang. distrib. 78−70392
$np\to pp\pi^-$, 11.9 GeV/c, differential cross section 77−22805
$np\to pp\pi^-$, 790 MeV, deviation from T=1 matrix element, π centre of mass ang. distrib. 78−70392
$np\to p\pi^-_{\pi^+}p$, neutron dissociation reaction, 50 to 300 GeV/c 79−17765
$np\to p\pi^+\pi^+\pi^-\pi^-n$, 5.1 GeV/c, $p\pi^+\pi^+(n\pi^-\pi^-)$ combination effective mass distrib. singularity *(Russian)* 79−67569
pion production continued
$np\to\pi^0d$, differential cross sections for 470-590 MeV, ang. distribs. 80−57628
$\bar{n}p$ reactions in Gargamelle, charged and neutral pion prod. 78−462
$N\pi\to N\pi\pi$, isobar model rescattering effects, unitarity corrections 79−71762
$N\pi\pi$ dynamics, medium energy, dispersion relations, isobar expansion for πN 80−4917
$N\pi\pi$ medium energy dynamics from πN, isobar model rescatt. corrections 80−4918
ν, $\bar{\nu}$ charged current induced one pion weak prod., I=1/2 resonant contrib. 80−47274
ν and $\bar{\nu}$ inclusive processes for neutral currents, sea quark effects, meson prod. 79−22088
$\nu(\bar{\nu})$ charged current induced one π prod., model total cross sections 80−4979
$\nu(\bar{\nu})$ N interactions, π charge distrib., isospin and V,A struct. of weak neutral currents 77−38157
$\nu(\bar{\nu})N\to\nu(\bar{\nu})NN\pi^0$, charged neutral current ratios with $\nu N\to\mu N''\pi^0$ 77−22727
$\nu(\bar{\nu})p$ elastic and quasielastic scatt., neutral current isospin props. 77−2812
$\nu+N\to\nu+N+\pi$, six-fermion interaction const. and neutral currents *(Russian)* 77−34147
$\nu+n\to\nu+p+\pi$, six-fermion interaction const. and neutral currents *(Russian)* 77−34147
$\bar{\nu}N$, K^0 and π^- prod. rates, SU(3) symmetry violation in quark jet 80−82966
νN, semi inclusive π prod., angular asymmetries in QCD 79−9360
$\bar{\nu}N$, single π^0 or π^- prod., neutral current interactions 78−41527
$\nu n\to=\nu p\pi^-$, neutral current process, excitation function, cross section ratio 80−78053
$\nu n\to\mu^-n\pi^+$, weak current isospin struct. study 79−49507
$\nu n\to\mu^-p\pi^0$, weak current isospin struct. study 79−49507
$\bar{\nu}n\to\mu^+n\pi^-$, effects of second-class weak currents in $\Delta(1236)$ reson. region 78−8656
$\nu N\to\mu N''\pi^0$, charged/neutral current ratios with $\nu N\to\nu N'\pi^0$ 77−22727
$\nu N\to\mu N\pi$, high energy behaviour, light cone commutators, PCAC calcs. 78−37199
$\nu N\to\mu N\pi$, PCAC anal. in 1st reson. region 77−82730
$\nu N\to\nu N\pi\pi$, neutral-current cross sections for double-pion production by neutrinos 79−17712
$\nu n\to\nu n\pi^0$, neutral current induced one-pion production, Weinberg-Salam structure 80−52454
$\nu n\to\nu p\pi^-$, expt. results comparison to theory 80−102038
$\nu n\to\nu p\pi^-$, neutral current induced one-pion production, Weinberg-Salam structure 80−52454
$\nu n\to\nu p\pi^-$, threshold pion prod., photon-neutrino weak coupling theory 77−67642
$\nu N\to\nu\pi X$, scale breaking effects 79−40770
$\nu N\to\nu x_\mu$ neutral current coupling 77−74673
$\nu N\to\pi^\pm\Delta$, dynamical model 79−401
$\nu_\mu N\to\mu^-N\pi$, cross sections and invariant mass distribs., inelastic charged current reactions 79−71742
νp interactions, globality prop. of charged multiplicity, pion prod., lepton-hadron relation 77−2813
$\nu p\to\mu^-\Delta 3\pi^+\pi^-$, E>10 GeV, inclusive 79−376
$\nu p\to\mu^-p\pi^+$, cross section above 1 GeV 79−9362
$\nu p\to\mu^-p\pi^+$, effects of second-class weak currents in $\Delta(1236)$ reson. region 78−8656
$\nu p\to\mu^-p\pi^+$, weak current isospin struct. study 79−49507
$\nu p\to\mu^-\pi^+p$, E>5 GeV, cross-section meas. 78−93872
$\bar{\nu}p\to\mu^+p\pi^-$, 5-70 GeV, cross section, I=1/2 prod. amplitude 80−62962
$\nu p\to\nu n\pi^+$, neutral current induced one-pion production, Weinberg-Salam structure 80−52454
$\nu p\to\nu p\pi^0$, neutral current induced one-pion production, Weinberg-Salam structure 80−52454
νp pion prod. by weak neutral currents, PCAC calcs. in various charge modes 77−26508
$\nu p\to\pi$, threshold to 450 MeV, energy depend. multipole anal. 80−32110
ω^*-ϕ^* interference in multi π prod., origin of Iizuka-Zweig-Okubo rule violation 78−70324
(p,pπx) reaction, pion production, flucton mechanism anal. 79−6590
(p,π), 4.2, 4.5 GeV/N, pion multiplicities and theoretical models, review 80−42657
(p,π), exclusive single nucleon transfer, theoretical status 80−42652
(p,π), hopes and realities, review, book contrib. 80−73849
(p,π), pion prod. in proton-nucleus collisions, expt. and theoretical results, book contrib. 79−75991
(p,π), polarised p, light nuclei, cross sections, ang. distribs. and anal. power 79−85460
(p,π) reactions near threshold, relativistic effects in one-nucleon model 77−34302
(p,π^-), nuclear size dependence of π^- prod., unified pattern 78−82349
(p,π^+), 1p-shell nuclei, inclusive cross sections near threshold 79−85462
(p,π^+), 8-16 MeV, inclusive cross sections near threshold, A depend. 80−27644
(p,π^+), differential cross-section, current theories 77−6445
(p,π^+), light nuclei, 0.5-10 MeV, total cross sections near pion Coulomb barrier 80−32280
(p,π^+), polarised p, 200 MeV, p distortion and asymmetries 79−22285
(p,π^+), π threshold prod. and absorption, pseudoscalar-pseudovector equivalence 79−80877
(p,π^+) reaction anal. at momentum transfer below 600 MeV/c 77−79376
$(p,\pi^\pm)$, 320-800 MeV protons on ^2H to ^{10}B targets, coherent pion production *(French)* 79−533
$(p,\pi^\pm)$, 585 MeV, A=1-208, differential cross section and pol. parameter 80−106056
$(p,\pi^\pm)$, 585 MeV, cross sections, polarisation parameter for H, D, Be, C, O, Al, Ni, Cu, Mo, Pb targets 80−73848
(p,π^+), 154 MeV, production on ^{10}B, ^{13}C, ^{14}N, ^{25}Mg, ^{28}Si, ^{32}S and ^{40}Ca 77−10391
(p,πx) in emulsion, 70 GeV/c, Lorentz invariant kinematical anal. 80−47474
(p,π^+X), 4.3 GeV/c, inclusive pion prod., nuclear mass number depend. 79−76029
(p,X), 200 GeV/c in emulsion, fireball parameters and π emission 80−95317
(P,X), 22.6 GeV/c, pion p_T distrib. in emulsion 80−95319

pion production continued
(p,X), 400 GeV, A=6-180, $\bar{p},\pi^{\pm}$ and $K^{\pm}$ backward prod., invariant cross sections 80−102188
(p,X), 70 GeV/c *(Russian)* 80−52681
(p,X), inclusive pion prod., forward and backward π spectra 79−85484
(p,X), pion production, Fermi motion effects, multiplicity distribs. and inclusive cross sections 79−93622
$\bar{p}$ annihilation in nucl. emulsion, statistical theory of multiple prod. *(Spanish)* 77−67669
$\bar{p}$ annihilations in heavy liquid bubble chamber, effects of complex nuclei reactions 77−79373
p-nucleus 0.8-4.89 GeV collisions, energy depend. of 180° prod. of $\pi^{\pm}$ 80−22834
p+Be(Cu), 70 GeV, π^+, K^+, p large p_T yields *(Russian)* 77−82778
p+d→π+t, 470 MeV, importance of NN→NNπ in backward scatt. peak at 470 MeV 79−30744
p+e→π+N, form factor determ. *(Russian)* 79−9382
p+H target, high transverse momentum π^0 and jets prod. 78−70417
p+nucleus, (p,π^+) cross-section calc. model 77−61422
p+nucleus, inclusive π prod., 0.78 to 5 GeV, relation to NN π prod. 78−78384
p+nucleus collisions, cumulative pion production models, comparison 78−13092
p+Z→π^+(K,p,$\bar{p}$)X, 28.5 Gev/c, invariant cross-sections, for P_T 0.75-2.25 GeV/c 77−30456
pA→π^-+X, scaling invariance of interactions of relativistic nuclei, the cumulative effect *(Russian)* 79−93611
pd, 70 GeV, $\pi^{\pm}$, $K^{\pm}$, p, $\bar{p}$ prod. with 0.5-2.2 GeV/c transverse momenta, yield ratio, QCD *(Russian)* 80−83012
pd, rescattering effects in 19 GeV/c interactions, $\Delta\Delta$ component of D 80−42500
pd→(Nπ)$^+$d, Deck model anal. 77−22757
pd→($p\pi^+\pi^-$)d, diffr. dissoc. and interactions of diffractive produced systems 79−45107
$\bar{p}$D annihilation, pion rescatt. effect at intermediate energies 80−5010
pd collision, 19 GeV/c one, two and three pion prod., cross sections 77−71537
pd→dπ^+n, 585 MeV, Glauber theory, NN and NΔ amplitudes 78−62525
pd interaction, single particle distribs. with large momentum transfer at 3.3 GeV/c *(Russian)* 78−41596
pd→ndπ^+, 585 MeV, reaction mechanisms 79−548
pd→$p_s\pi^+\pi^-\pi^-\pi^0$, 0.4 to 0.9 GeV/c, meson resonance production 79−93447
pd→pd$\pi^+\pi^-$, 19 GeV/c, two and three pion coherent prod. 79−36095
pd→pd$\pi^+\pi^-\pi^0$, 19 GeV/c, two and three pion coherent prod. 79−36095
pd→p$\pi^+\pi^-$d, interference phenomena in coherent production, nucleon diffractive amps., helicity-flip 80−47329
pd→π^0X, large transverse momentum, π^0 prod. cross section, ISR energies 79−3055
pd→$\pi^{\pm}$($K^{\pm}$)pX, 11.75 GeV/c, meas. of left-right asymmetry far inclusive $\pi^{\pm}$, $K^{\pm}$, p prod., polarised p-beam 79−22155
pd→πd$\pi^+\pi^-$, 19 GeV/c, two and three pion coherent prod. 79−36095
pd→tπ^+, 750 MeV, T=1 NN phase shifts and total cross section 80−22630
pn, 195 GeV/c, inclusive π^+/π^- ratio and quark distributions 79−54367
pN, 22.6 GeV in emulsion, cluster size in pionisation region 80−78099
pN, 67 GeV/c, in Be, Al, Cu, inclusive $\pi^{\pm}$, $K^{\pm}$, p, $\bar{p}$ prod. cross sections *(Russian)* 80−86769
pN, 67 GeV/c, nuclear targets, $\pi^{\pm}$, $K^{\pm}$, p,$\bar{p}$ yields *(Russian)* 80−68501
pN, 70 GeV, forward prompt muon yield, μ/π yield ratio *(Russian)* 79−97641
pN, 70 GeV in emulsion, pion cluster obs. 80−86762
pn→3$\pi^-2\pi^+$, 1.0 to 1.6 GeV/c, like pion interference 77−26538
pn→d($\pi\pi$)^0, effective two body interaction Hamiltonian, missing mass, ABC effect 78−70388
pN→N$\pi\Delta$(1236) above 6 GeV, crossed channel isospin amplitude anal. 79−6346
pN→pnπ^+ (and similar), Δ(1236) isobar prod. 78−21443
$\bar{p}$n→$\bar{p}p\pi^-$, 2.98 GeV/c, Δ^{--} prod. in additive quark model framework 80−52529
pN→π^-X, 3.95 to 9.7 GeV/c, inclusive π^- prod. below 62 mrad *(Russian)* 79−49538
pN→π^-pX, 9 GeV/c, inclusive π^-p prod. below 188 mrad *(Russian)* 79−49538
pN→π^0X, 200-400 GeV/c, inclusive π^0 prod. over large X_T and X_F ranges 80−37310
$\bar{p}$n→$\pi^+\pi^-\pi^-$, 1.09 to 1.43 GeV, spin-parity function, Veneziano model anal. 79−13148
$\bar{p}$n→$\pi^+\pi^-\pi^-$, 2.98 GeV/c, Dalitz plot 79−80835
pN→πX, intermediate $\bar{p}$ contrib. to backward π prod. *(Russian)* 80−13326
$\bar{p}$n→xπ, temperature parameter for thermal-like emission spectra, fluctuations 80−68482
pp, 205 GeV/c, invariant-mass depend. of correl. functions 77−34181
pp, 24 GeV/c, final states with large transverse momentum particle, π and N emission 79−13159
$\bar{p}p$, 2.32 GeV/c, cross-sections, C-invariance, π and ρ^0 multiplicities anal. 78−41569
pp, 400 GeV/c, inclusive and semiinclusive prod. of π^0, K_s^0, Λ^0, $\bar{\Lambda}^0$, Σ^0, $\bar{\Sigma}^0$, η^0, ω^0 79−93472
pp, 405 GeV/c, pion local number distrib. fluctuations, higher order correlations 80−18152
pp, 69 GeV/c, charged backward π prod., inclusive baryon resonance prod. cross section *(Russian)* 79−30760
pp, 70 GeV, $\pi^{\pm}$, $K^{\pm}$, p, $\bar{p}$ prod. cross sections, QCD-parton model anal. *(Russian)* 80−63044
$\bar{p}p$, 8.8 GeV/c, exclusive annihilation processes, cross sections, quark model anal. 80−105920
$\bar{p}p$, 9.1 GeV/c, single pion prod. anal. 78−54645
pp, $\sqrt{s}$=30.6, 53.2 GeV, direct photon prod., γ/π^0 ratio 79−71771
pp, final state struct. prod. in association with large transverse momentum π^0 79−45115
pp, final states containing high p_T π^0 at CERN ISR 79−45119
pp, ISR energies, high p_T π^0 and single photon events, associated charged particle multiplicity 80−63039
pp, large P_T pion^0 prod., meson structure functions, quark distrib. functions 80−86714
pion production continued
pp, Lorentz-invariant method, 24 and 70 GeV/c interactions, including pionisation 79−80848
pp, $\bar{p}p$, fireball mass and pion multiplicity 78−45974
$\bar{p}p$, $\pi^{\pm}$ inclusive prod., annihilation component estimation 77−82790
$\bar{p}p$, $\pi^{\pm}$ inclusive spectra, comparison with Monte Carlo quark-parton model 79−30755
$\bar{p}p$, soft-pion amplitude for π^0 emission 78−41570
$\bar{p}p$, three-body annihilations, rel. to quark rearrangement model 78−21444
$\bar{p}p$ 14.75 GeV/c, search for $K_s^0\pi^{\pm}\pi^+\pi^-$ resonance near 2.6 GeV/c 78−74289
$\bar{p}p$→$2\pi^+2\pi^-$, 5.7 GeV/c, pion ang. distribs., ρ^0, f^0, prod. rates 77−2857
$\bar{p}p$→$2\pi^+2\pi^-\pi^0$, 0 to 700 MeV/c, interference correls. between like pions 77−61311
pp→($p\pi^+$)($p\pi^-$), 23-63 GeV, charge exchange double dissociation reaction anal., $\Delta^{++}\Delta^0$ prod. 79−6350
pp→($p\pi^+$)($p\pi^-$), observation of charge exchange double dissociation 78−25079
pp→($p\pi^+\pi^-$)($p\pi^+\pi^-$), 24 GeV/c, double diffraction dissociation reaction, cross sections, mass spectra 78−93908
pp→($p\pi^+\pi^-$)($p\pi^+\pi^-$), s-depend. of double diffraction dissociation 78−25084
pp→(π^+n)p, π energy and transverse momentum distrib., DHD model with nucleon exchange *(Russian)* 80−13327
pp→(π^+,K^+,p,d)X, 6 and 11.8 GeV/c, polarised proton, L-R asymmetry meas. 77−30455
$\bar{p}p$ annihilation, 100 GeV/c, general features of charged particle prod. 79−75803
$\bar{p}p$ annihilation, π^+, π^- and π^0 probability distrib. 78−41604
$\bar{p}p$ annihilation at rest, maximum final particle momentum projection direction reference frame 77−57553
$\bar{p}p$ annihilation mechanisms, 2.5 to 9.1 GeV/c, pion prod., quasi two body process 78−17039
$\bar{p}p$ annihilations, multipion distrib., statistical bootstrap model 80−68472
pp collision inclusive spectra, fast pionisation at high energies, z-scaling *(Russian)* 80−47339
pp collisions, 300 GeV, correlations between neutral and charged pions 79−36115
pp collisions, azimuthal correl. of high $\rho_T\pi^0$ and η with second π^0 79−85347
pp collisions, charged and neutral multiplicities associated with large transverse momentum π^0s 79−3058
pp collisions, correl. of neutral and charged pions, multiparticle prod. mech. 78−8708
pp collisions, high momentum $\pi^{\pm}$ and $K^{\pm}$ prod., 45 GeV, cross sections 78−93910
pp collisions, large transverse momentum pions prod., correls., fireball model 78−66174
pp collisions, multiplicities of pion, kaon or proton prod. at ISR 77−259
pp collisions, thermodynamical approach to few body hadronic interactions, pion prod. 77−74704
pp→dπ, 400 to 600 MeV, production cross sections 80−78091
pp→dπ^+, 0.8 GeV, differential cross section and polarisation asymmetries 80−27519
pp→dπ^+, 305 to 425 MeV, differential cross section meas., d-wave π production contrib. 78−62440
pp→dπ^+, 305 to 425 MeV, differential cross section and analysing power, using polarised protons 79−36094
pp→dπ^+, 750 MeV, T=1 NN phase shifts and total cross section 80−22630
pp→dπ^+, 800 MeV, comparison between expt. momentum spectra and theoretical models 78−62441
pp→dπ^+, 800 MeV 77−6141
pp→dπ^+, deuteron polarisation, isobar model anal. 79−49535
pp→dπ^+, differential cross section, polarisation asymm., threshold to 750 MeV 78−54648
pp→dπ^+, differential cross-section and polarisation 78−8683
pp→dπ^+, P-wave meson prod., calc. of total and differential cross section 77−6143
pp→dπ^+, polarised beam and target, NΔ intermediate states, coupled channel method 79−9392
pp→dπ^+ or pπ^+n, 800 MeV, cross sections, n-p final state interactions 78−70387
pp→$\Delta^{++}p\pi^-$, 4 GeV/c, mass spectra, ang. distribs. and momentum transfer *(Russian)* 80−42489
pp→$\Delta^{++}\pi^-$p, polarised proton, spin effects in SU(3) and quark model 77−30399
pp→eπX, 10-25 GeV, anomalous behaviour of direct electrons 77−14004
pp fragmentation at high energies, quark constituents 77−34185
pp inclusive and semiinclusive interactions, 69 GeV/c, π^+, π^- and p prod. 77−79289
pp inclusive interactions, phenomenological model of pion prod. *(Russian)* 79−30763
pp inclusive interactions, π^0 prod. at large p_T at CERN ISR 79−13168
$\bar{p}p$ inclusive prod. of π^-,η,ρ^0,ω,f, mesons at 0.7 GeV/c 77−65170
$\bar{p}p$ inclusive $\pi^{\pm}$ prod., 100 GeV/c, R-distrib. 77−50028
pp inclusive reacts., charged particle associated multiplicities at ISR energies 78−21473
pp inelastic, 28.5 GeV.c^{-1}, particle generation mechanisms, multiperipheral cluster model anal. *(Russian)* 79−9424
pp inelastic collisions, ρ-dominance in collision model 78−37238
$\bar{p}p$ interaction at 22.4 GeV/c, identical pion pair interference obs. *(Russian)* 79−9420
pp interactions, 28.5 GeV/c, central prod. of π cluster, props. 77−10287
pp interactions, π^- multiplicity distribs. *(Russian)* 78−41742
pp interactions π^0 inclusive resolved high p_T meas. at CERN ISR 79−63555
pp jet prod., π^0 fragments, jet fragmentation function and momentum 80−443
pp→$K_s^0\pi^-$+anything, 28.4 GeV/c, cross-sections and mass distribs. meas. 77−38212
$\bar{p}p$→$K^0{}_SK^0{}_S$+pions, 700-760 MeV/c, $K^0{}_SK^0{}_S$ threshold enhancement in final states 78−82228
pp multipion production, charge correl. cluster effect *(Chinese)* 77−57500
pp multiplicity distrib. formula in 10-405 GeV range 77−13998
pp→NNπ^+, consideration of p→nπ^+ forbidden reaction threshold case 78−62442
$\bar{p}p$→nπ's, multiplicity distrib. and charmed meson hadronic decays 77−10288

pion production continued
pp→pX, 28.5 GeV/c, π charge multiplicity, scaling and Hagedorn temp. 77−26553
pp→pX or $\pi^{\pm}$X, 7.9 GeV/c, polarised target, spin depend. 79−3056
pp→p(nπ^+), 28.5 GeV/c, t-depend. and struct. 77−22802
pp→p(pπ^0), 28.5 GeV/c, t-depend. and struct. 77−22802
pp→p(p$\pi^+\pi^-$)(nπ^+)(pπ^0), polarised protons at 6 GeV/c, low mass enhancements 77−30400
pp→pions, 102, 400 GeV/c, transverse momentum props. 78−8713
$\bar{p}$p→pions, 1.6 GeV/c, branching ratio meas. 78−17038
pp→pnπ^+, 19 GeV/c, nucleon dissociation and spectator concept 77−30447
pp→pnπ^+, 800 MeV 77−6141
pp→pnπ^+, mass spectra at 28.5 GeV/c 77−22801
pp→pnπ^+, two nucleon mechanism for pion production 79−85286
$\bar{p}$p→$\bar{p}$p2$\pi^+2\pi^-$, 100 GeV/c, diffraction and ρ^0 prod. in exclusive interactions 78−93909
pp→ppπ^0, 800 MeV, Δ^+ prod., π and ρ exchange 79−85316
pp→ppπ^0, 800 MeV 77−6141
pp→ppπ^0, mass spectra at 28.5 GeV/c 77−22801
$\bar{p}$p→$\bar{p}$pπ^+($\bar{n}$pπ^-), 8.8 GeV/c, one pion prod. cross sections, Deck model anal. 80−105919
pp→pp$\pi^+\pi^-$, $s^{1/2}$=31 GeV, double pomeron exchange, dipion mass 77−13993
$\bar{p}$p→$\bar{p}$p$\pi^+\pi^-$, 100 GeV/c diffraction and Δ^{++} prod. in exclusive interactions 78−93909
pp→pp$\pi^+\pi^-$, double Pomeron exchange, 23.4 to 63.4 GeV 79−3050
$\bar{p}$p→$\bar{p}$p$\pi\pi$, 12 GeV/c, final state diffraction dissociation, cross section 80−99109
pp→pπ^+n, 800 MeV, Δ^{++} prod. and cross sections 79−22294
pp→π^-X, polarised p, inclusive π^- scatt. asymmetries near X=0 79−63541
pp→π^-X, search for new long lived particles with masses 1.4 to 3.0 GeV at CERN ISR 79−40810
pp→π^-X^{+++} inclusive double-charge-exchange π^- prod., 100 GeV/c 78−37250
$\bar{p}$p→π^-X(ΔX), 22.4 GeV/c, test of factorisation hypothesis for leading Regge trajectories *(Russian)* 79−49561
$\bar{p}$p→$\pi^-\pi^+$, 10.1 GeV 78−66160
$\bar{p}$p→$\pi^-\pi^+$, 1.0 to 2.2 GeV/c, polarisation parameter meas. 77−74711
$\bar{p}$p→$\pi^-\pi^+$, 1.0 to 2.2 GeV/c, polarisation parameter 77−87995
$\bar{p}$p→$\pi^-\pi^+$, 6 GeV/c, differential cross sections, line reversal symmetry test for baryon exchange 78−78202
$\bar{p}$p→$\pi^-\pi^+$, amplitude anal., 2020 to 2580 MeV/c^2, spin 3, 4 and 5 mesons 77−41853
$\bar{p}$p→$\pi^-\pi^+$, amplitude anal., meson prod. in 2020-2580 MeV/c^2 region 77−46075
$\bar{p}$p→$\pi^-\pi^+$, differential cross-section zeros 77−38191
$\bar{p}$p→$\pi^-\pi^+$, polarised targets, $\bar{p}$ parity meas. 77−2860
$\bar{p}$p→$\pi^-\pi^+$($\pi^+\pi^-$), 1-2 GeV/c, partial wave determ. and resonance struct. 79−93449
pp→$\pi^-\pi^+$pp, 800 MeV, integrated cross section meas. near threshold 78−62441
pp→π^0, large transverse momentum jets investig. at 52.4, 62.7 GeV 80−18151
pp→π^0X, 100, 200 GeV/c high transverse momentum π^0 prod., quark scatt. 78−45976
pp→π^0X, 100 and 200 GeV, ang. depend. of π^0 prod. 78−41603
pp→π^0X, 50-400 GeV, cross sections, 0.3 to 4 GeV/c π^0 transverse momenta 77−18350
pp→π^0X, 52.7, 62.4 GeV, inclusive prod. at very large p_T at the ISR 79−71769
pp→π^0X, 53, 63 GeV, inclusive π^0 prod. at very large transverse momenta 78−45980
pp→π^0X, intermediate $p_\perp$ distribution through a QCD resummation mechanism 80−83010
pp→π^0X, large transverse momentum, π^0 prod. cross section, ISR energies 79−3055
pp→π^0X, parton model, polarised proton, large p_T π^0 prod. asymm. 78−12936
pp→π^0X, pol.p, 24 GeV/c, high $p_T\pi^0$ prod., spin. depend. 80−105935
pp→π^0X, scaling in the mean hypothesis and Feynman variable energy depend. 80−42501
pp→π^0X/π^-p→π^0X ratio at high-p_T, quark model explanation 77−10290
$\bar{p}$p→π^0+X, 4.6, 9.1 GeV/c, inclusive total, topological and invariant differential cross sections 79−408
pp→π^0+X, large p_T-π^0 spectra, quark model anal. 78−89756
pp→π^0+X, π^0 prod. at large p_T, parton model 77−46090
pp→π^0+X, secondary neutral pion-nucleon flux ratio at atm. top 80−8500
pp→π^0+anything, $\sqrt{s}$=52.7 and 62.4 GeV, prod. of high transverse momentum π^0s 78−78226
pp→π^0+anything, large p_T, clustered parton model 77−67688
$\bar{p}$p→$\pi^0\eta$, 1.1-2.0 GeV/c, differential cross sections in T and U meson region 79−9393
pp→$\pi^0\pi^0$, up to 10 GeV/c, correlation of momentum of π^0 pairs 80−5011
pp→$\pi^0\pi^0$X, ISR π^0-π^0 azimuthal correlation data, comments 80−52543
pp→$\pi^0\pi^0$X, large p_T, azimuthal correlations 78−89749
$\bar{p}$p→π^+X, 22.4 GeV/c, invariant cross section, average multiplicity and annihilation spectra 79−6354
pp→π^+X, non-plateau behaviour in central region 77−6182
pp→π^++X, inclusive reactions, ISR energies, scaling variable 77−50021
pp→π^+d, 400-800 MeV, anal. by neutron exchange, ΔN intermediate states, diproton resonances 80−27518
pp→π^+d, 515 and 575 MeV, spin depend. parameter meas. 80−73734
pp→π^+d, di-proton resonances 80−22631
pp→π^+d, interaction anal. by neutron exchange Born terms, ΔN states, diproton resonances 79−93391
pp→π^+d, NΔ(1232) state contrib., K matrix theory anal. 80−5013
pp→π^+d, SIS, 578 MeV, pol. beam and target, spin depend. parameters 80−42651
pp→π^+d, up to 1 GeV, differential cross section using polarised beam and target 79−17748
pp→π^+pn, 1 GeV/c, momentum spectra ang. depend., one-particle-exchange model comparison *(Russian)* 77−10276
pp→π^+pn, 800 MeV, comparison between expt. momentum spectra and theoretical models 78−62441
$\bar{p}$p→$\pi^+\pi^-$, 6 GeV/c, differential cross sections, line reversal symmetry test for baryon exchange 78−78202
pion production continued
$\bar{p}$p→$\pi^+\pi^-$, isospin decomposition 79−9394
$\bar{p}$p→$\pi^+\pi^-$, polarised target, charge parity determ. 77−57567
$\bar{p}$p→$\pi^+\pi^-$ 6.2 GeV/c, ang. distrib. 77−18330
$\bar{p}$p→$\pi^+\pi^-$X, 100 GeV/c, tests of factorisation in Pomeron and Reggeon exchange 77−74731
pp→$\pi^+\pi^-(K^+K^-)$, 1.0-2.2 GeV/c, polarisation parameter 77−30401
pp→$\pi^+\pi^-\pi^+\pi^-\pi^0$, 1950 MeV/$c^2$, experimental evidence 80−27516
$\bar{p}$p→$\pi^+\pi^-\pi^+\pi^-\pi^0$, 1950 MeV/$c^2$, properties evidence for $\bar{p}$p→$\omega^0\rho^0$ 80−27517
$\bar{p}$p→$\pi^{\pm}K_s^0X^{\mp}$, low energy, thermodynamical anal. of charged pion momentum spectra 77−65169
pp→$\pi^{\pm}$X, charge ratio for cosmic pion spectrum in atmosphere 78−28463
pp→$\pi^{\pm}$X, primary proton energy rel. to pion energy, Landau parameter 79−54364
pp→$\pi^{\pm}$+X, 100-400 GeV, expt. techniques and data analysis 78−58216
pp→$\pi^{\pm}(K^{\pm})$pX, 11.75 GeV/c, meas. of left-right asymmetry far inclusive $\pi^{\pm}$, $K^{\pm}$, p prod., polarised p-beam 79−22155
pp→$\pi^{\pm}\pi^{\mp}$+anything, 69 GeV/c, study of rapidity gaps *(Russian)* 77−54125
pp→$\pi^{\pm}\pi^+$X, 24 GeV, high transverse momentum inclusive interaction 79−13169
pp→π^0X reaction, quark-quark inelastic collision model *(Russian)* 80−32141
$\bar{p}$p→πX, 22.4 GeV/c, charged particle spectra 77−13997
pp→πX, 24 GeV/c, direct γ-yield 77−14003
$\bar{p}$p→πX, 9.1 GeV/c, topological and channel cross-sections 77−30415
pp→πX, crucial spin tests of QCD approaches to large transverse momentum processes 79−63558
pp→πX, large P_T, transversely polarised beam and target, QCD predictions 79−49553
pp→πX, large-P_T reactions in broken color gauge theory 80−95292
pp→πX, Pomeron struct., effects on one particle inclusive cross sections 79−89210
pp→πX, $\pi^{\pm}$ average transverse momentum energy depend., scaling relation 80−91116
pp→π+anything, pion spectrum at top of atmosphere 78−53780
pp→π(K)(p)X, 4-250 GeV/c, Pomeron factorisation 77−14005
$\bar{p}$p→$\pi\pi$, 1-2 GeV/c, Barrelet zero anal., resonant struct. 80−73735
$\bar{p}$p→$\pi\pi$, 1-2 GeV/c, resonance region, partial waves, positivity constraints 80−99107
pp→$\pi\pi$, πp, π^-p, double differential cross-section meas. 77−82776
pp→$\pi\pi$X, $\sqrt{s}$=63 GeV, high momentum meson correlations 80−32138
pp reacts. at 205 GeV/c, one, two, and three particle distribs. 78−8716
pp scatt., eikonal mechanisms at high energy 78−82256
pp scatt., intermediate energy, polarised p, three body model 79−67590
$\bar{p}$p→xπ, model of excited hadronic matter 78−74288
pp→xπX, QCD radiation and mean scaling, longitudinal and transverse momentum 80−42405
P_1P_2→P_3N_4+mesons, 28.5 GeV/c, space-time extension of centrally produced matter, intensity interferometer technique 77−50017
$p\pi^+\pi^-$ systems in coherent and incoherent p-nucleus collisions, 18.6 GeV/c 77−41866
ϕ(1020)→3π, decay amplitudes, OZI rule, dispersion relations, intermediate states contribs. 79−383
$\phi\rightarrow\pi\gamma$, SU(3)×SU(3) algebra, appl. to ground state mesons, coupling constraints and decay rate 78−58183
$\phi\pi$ prod. in e^+e^- annihilation and diffractive photoprod., 4 quark state signature 79−6324
(π,π^+X), 4.3 GeV/c, inclusive pion prod., nuclear mass number depend. 79−76029
π→5π, diffr. dissoc. at 16 GeV/c 78−82252
π dispersion relation in nuclear matter using ν+nucleus reactions 79−488
π pairs, dynamical and Bose-Einstein inclusive correlations, from cluster decay 78−62463
π photoprod. at intermediate energy, review 78−50061
π photoproduction reacts. on few body systems and Δ-N interaction 79−71842
π^- clinical facilities, linear accelerator selection 79−20645
π^- semi-inclusive cross sections to 300 GeV/c in pp 77−13999
π^--emulsion nuclei collisions, 50 GeV, cluster prod. 77−46190
π^0, photoprod. in $^{12}C(\gamma,\pi^0p)$ at 0.7-1.65 GeV, cross section asymmetry meas. *(Russian)* 80−63164
π^0 coherent photoprod. on ^{4}He, screening corrections and rescatt. *(Russian)* 78−41697
π^0 correlations from π^-+Xe at 3.5 GeV/c *(Russian)* 77−82760
π^0 electroproduction, test of quark parton model 78−8672
π^0 emission by protons with anomalous mag. moment in const. EM field, Furry formalism *(Russian)* 78−410
π^0 high p_T prod. ang. depend., inclusive cross sections, scaling 80−91119
π^0 inclusive photoprod. and quark-parton model 78−78189
π^0 pairs, high transverse momentum, azimuthal correlations 78−62469
π^0 photoprod. from complex nucl. targets 77−82905
π^0 photoproduction, Regge poles and cuts 78−66127
π^0 photoproduction and nonhadronic duality 77−67661
π^0 photoproduction from protons, 0.7-1.45 GeV, polarised target asymmetry 77−46054
π^0 photoproduction on H, 300 and 310 MeV 79−527
π^0 photoproduction on H at 320 MeV 77−22742
π^0 prod. at large p_T, pp and $\pi^{\pm}$p collision 77−79287
π^0 prod. in π^-p inclusive interaction, 5 GeV/c *(Russian)* 78−45946
π^0 production by ν and $\bar{\nu}$ neutral currents, comparison 79−49509
π^0 production in $\bar{p}$p annihilation 79−63507
π^0/η prod. ratio at high transverse momenta 78−41602
π^+ electroproduction, transverse and longitudinal cross-section separation, pion radius 77−38179
π^+ prod. on ^{27}Al and ^{51}V 78−21543
$\pi^{\pm}$ coherent prod., differential cross sections meas. by SPES I 79−75983
$\pi^{\pm}$ inclusive distribs. in π^--nucleus reactions at 50 GeV *(Russian)* 77−50162
$\pi^{\pm}$ inclusive prod., central region factorization for cross section 79−6353
$\pi^{\pm}$ photoprod. cross sections calc. 77−82762
$\pi^{\pm}$ production, large p_T, pp and pd interactions, 200 to 400 GeV 77−22815
π+H target, high transverse momentum π^0 and jets prod. 78−70417
πd quasielastic and inelastic rescattering as cumulative particle prod. source *(Russian)* 79−22340
π^-d→d$\pi^-\pi^-\pi^+$ at 9 GeV/c, $\pi^-\pi^-\pi^+$ system decay 77−22766

pion production continued
π^- d→π^+X^-, 2.6 GeV/c, d proton screening correction and Glauber parameter 80−9175
π^+d, 15 GeV, neutral three pion resonance prod., pure I=1 exchange 80−57644
π^+d, 15 GeV/c, many-pion prod. and resonant prod. cross sections 80−22642
π^+d, 6 to 100 GeV/c, $P_\perp$ distribs. of K^0, π^-, ρ^0, f, equilibrium temp. 79−49540
πN→$\pi^+\pi^-$N, 4-17 GeV/c, ρ^0 and f prod. mech. 80−436
πN→πX, dual fermion model for inclusive single particle distribs. 78−86446
πN→π(Nπ) diffraction dissociation, role of nucleon exchange 77−38192
πN→$\pi\pi\pi$N, alternative soft-pion approaches 77−26541
πN→$\pi\pi$N, importance of analyses, t-channel effects, isobar model validity 77−22776
πN→$\pi\pi$N, isobar formalism, one-pion-exchange partial-wave cross sections 77−87957
πN→$\pi\pi$N, kinematic singularity free helicity amplitudes, crossing matrix anal. props. 80−95285
πN→$\pi\pi$N, π prod. near threshold, s-wave $\pi\pi$ parameters 77−38197
πN→$\pi\pi$N reaction amplitude reconstruction in relativistic energy region *(Russian)* 79−13173
πN single and double diffractive prod., monopole transitions and slope-mass relation 77−38152
π^-n, 40 GeV/c, many pion systems in inclusive reactions, transverse momentum effects *(Russian)* 80−57654
π^-N, 40 GeV/c, many-nucleon interactions, secondary $\pi^\pm$ spectra *(Russian)* 79−97638
π^-n, 40 GeV/c, two-particle charged and γ rapidity correls. 77−18335
π^-N, 50 GeV/c, multiple pion production, role of clusters 77−34199
π^-N, in C, 5 GeV/c, π^0 and n inclusive spectra, cascade model *(Russian)* 80−68490
π^-N interactions, 50 GeV/c, inclusive charged π prod. in nuclear emulsion anal. 78−66168
π^-n→$\pi^-\pi^-$p, 15 GeV/c diffr. dissociation and N* prod. by pomeron exchange 77−41865
π^+n, 195 GeV/c, inclusive π^+/π^- ratio and quark distributions 79−54367
π^+n→$\pi^+\pi^-$p, 15 GeV/c, longit. phase space anal., ρ^0, f^0, Δ^0, N* 77−74727
πNN dynamics, Faddeev approach, 0-1200 MeV pp scatt. 80−57625
πp, large P_T pion^0 prod., meson structure functions, quark distrib. functions 80−86714
πp charged particle and γ two-particle correls. at 40 GeV/c *(Russian)* 77−74736
πp multiplicity distrib. formula in 10-405 GeV range 77−13998
πp→p$\pi^0\pi^0$, medium energy, cross section *(Japanese)* 77−41847
πp→π^0X, 100 and 200 GeV, ang. depend. of π^0 prod. 78−41603
πp→π^0+anything, large p_T, clustered parton model 77−67688
πp→π^0p, 650 and 700 MeV, angular depend. of secondary p polarisation *(Russian)* 78−78191
πp→πX, high p_T π^0 prod., leading particle contrib., QCD calcs. 80−73746
πp→π(K)(p)X, 4-25 GeV/c, Pomeron factorisation 77−14005
π^-p, 100, 200, 360 GeV/c, inclusive prod. of π^0, K_S^0, Λ^0, $\bar{\Lambda}^0$, cross sections 80−73745
π^-p, 100 GeV/c, π^0 and η inclusive prod. in all neutral mode 79−13165
π^-p, 200, 300 GeV, relative π^+, K^+, p, $\bar{p}$ prod., charge ratios, high p_T 80−47335
π^-p, 200 GeV/c, valence and sea quark distribs. in the pion, quark recombination model 79−63556
π^-p, 40 GeV, charged π correl. rapidity depend. 77−88011
π^-p, 40 GeV/c, charge transfer distrib. and π cluster prod. 77−34184
π^-p, 40 GeV/c, identical π interference *(Russian)* 78−472
π^-p, 40 GeV/c, many pion systems in inclusive reactions, transverse momentum effects *(Russian)* 80−57654
π^-p, 40 GeV/c, multi-pion systems and transverse momenta, differential cross sections *(Russian)* 80−32142
π^-p, charged-neutral pion prod. correl. in 5-205 GeV/c range 77−13996
π^-p, diffractive and non-diffractive, 40 GeV/c, momentum and ang. characts. *(Russian)* 77−50034
π^-p, large p_T inclusive π^0 prod., quark subprocesses 77−2885
π^-p→($\pi^+\pi^-\pi^0$)n, 12, 15 GeV/c, partial wave anal. of neutral 3π system, A-meson prod. 78−58207
π^-p→$\eta\pi^+\pi^-$n, D, E, and δ mesons obs. at 12 and 15 GeV/c 79−3052
π^-p→$\eta\pi^+\pi^-$n, axial vector and pseudoscalar resonances near 1.275 GeV, D mesons 79−30747
π^-p inclusive reactions, 147 GeV/c, average charged particle multiplicities 79−40818
π^-p interactions, 5 and 40 GeV, inclusive struct. functions of γ, $\pi^\pm$, K^0, and Λ *(Russian)* 79−80856
π^-p→$K_s^0K^+\pi^-$n, 3.95 GeV/c, E(1420) quantum numbers and branching ratio 80−95286
π^-p→$K^-K^+\pi^0$n, D, E, and δ mesons obs. at 12 and 15 GeV/c 79−3052
π^-p→$K^-K^+\pi^0$n, D, E, and δ mesons, obs. at 12 and 15 GeV/c 79−9410
π^-p→n+kπ^0 (k=1 to 5), 1.3 to 3.8 GeV/c, differential and total cross-sections 80−83000
π^-p→n$\pi^+\pi^-$, 8 GeV/c, backward meson and baryon reson. prod. 79−415
π^-p→$p_{fast}\pi^+\pi^-\pi^-$, 9, 12 GeV/c, backward meson prod., quasi two body processes, A_1^-, A_2^- prod. 79−413
π^-p→p$\pi^+\pi^-\pi^-$, impact param. anal. at 9 and 12 GeV/c 78−8706
π^-p→π^-_{fast}+X^+, 147 GeV/c, differential cross sections, triple Regge anal. 79−40811
π^-p→π^-+X^+, associated multiplicity increase with transverse momentum *(Russian)* 77−46092
π^-p→$\pi^-p\pi^+\pi^-\pi^0$, 4.5 GeV, $\Delta\pi\pi$ system study 79−93453
π^-p→$\pi^-\pi^-$X, 50 GeV/c, $\pi^-\pi^-$ low mass system, cross sections and S-wave phase shifts 79−71766
π^-p→$\pi^-\pi^-\pi^+$+, 13 GeV, prism-plot anal. 79−36109
π^-p→$\pi^-\pi^-\pi^+$p, 147 GeV/c, diffraction dissociation 77−2869
π^-p→$\pi^-\pi^-\pi^+$p, 25 GeV/c, boson states 77−30451
π^-p→$\pi^-\pi^-\pi^+$p, 63, 94 GeV/c, A_2 meson prod. from partial wave anal. 80−37303
π^-p→$\pi^-\pi^-\pi^+$p, 63, 94 GeV/c, A_1 meson existence from partial wave anal. 80−37304
π^-p→$\pi^-\pi^-\pi^+$p, 63, 94 MeV/c, A_3 meson, 3π resonances in 2^- partial waves 80−37305
pion production continued
π^-p→$\pi^-\pi^-\pi^+\pi^0$p, 11.2 GeV/c, study of A_2^- decay to eta+pion$^-$ 77−22806
π^-p→$\pi^-\pi^+$n, 203-357 MeV, integrated cross section, chiral symmetry breaking parameter 80−32125
π^-p→$\pi^-\pi^+$n, below 1400 MeV, PS11 contrib. threshold K-matrix, chiral symmetry breaking 80−32126
π^-p→$\pi^-\pi^+$n, narrow epsilon resonance under rho 80−5021
π^-p→$\pi^-\pi^+$n, S-wave dipion production 78−25069
π^-p→$\pi^-\pi^+\pi^-$p, partial-wave anal., analyticity and unitarity 77−88000
π^-p→π^0X, 5 GeV/c, associative multiplicity of charged particles as function of missing mass squared *(Russian)* 79−22136
π^-p→$\pi^0(\eta)$+anything, absorptive corrections using Regge pole amplitude 77−38204
π^-p→$\pi^-\pi^0$n, 200, 240 MeV, total near-threshold cross section, isotopic amplitudes *(Russian)* 80−37296
π^-p→$\pi^0\pi^0$n, 6, 8, 12 GeV, $\pi^0\pi^0$ S wave and I=0 amplitude 80−18144
π^-p→$\pi^-\pi^+$X$^-$, 2.6 GeV/c, d proton screening correction and Glauber parameter 80−9175
π^-p→$\pi^+\pi^-$n, 12, 15 GeV/c, $\pi^+\pi^-$ ang. distrib. in mass range 0.8 to 2.2 GeV/c^2 78−66164
π^-p→$\pi^+\pi^-$n, 17.2 GeV/c, model independent partial wave anal. of $\pi^+\pi^-$ prod. at low 4-momentum transfer 79−54363
π^-p→$\pi^+\pi^-$n, 17.2 GeV/c meas. with transversely polarised target 77−30449
π^-p→$\pi^+\pi^-$n, 17.3 GeV/c, polarised p, $\pi^+\pi^-$ partial wave anal. for low four-momentum transfer 79−63533
π^-p→$\pi^+\pi^-$n, 1.33-1.38 GeV, isobar prod. near threshold, isobar model partial wave anal., bag model 79−93456
π^-p→$\pi^+\pi^-$n, amplitude anal. of $\pi\pi$ scatt. 1.0 to 2.08 GeV, f, g, h mesons 79−3042
π^-p→$\pi^+\pi^-$n, polarization measurements and a narrow ε(750) 79−63514
π^-p→$\pi^+\pi^-$n, $\pi\pi$ scatt. partial wave anal. f, g and h mesons 80−5015
π^-p→$\pi^+\pi^-$n, rescattering effects, π ang. and momentum distribs. 78−93903
π^-p→$\pi^+\pi^-$n reaction near threshold, cross-section estimation at 190 and 200 MeV *(Russian)* 77−2865
π^-p→$\pi^+\pi^-\pi^-$n, D, E, and δ mesons obs. at 12 and 15 GeV/c 79−3052
π^-p→$\pi^\pm$X, 40 GeV/c, charge asymmetry as function of charged multiplicity and transverse momentum 79−40807
π^-p→πX, 40 GeV/c, p_T correls. of identical pions *(Russian)* 77−74735
π^-p semi-inclusive 40 GeV/c, charged particle and γ correls. *(Russian)* 77−34195
π^+p, 10.5 GeV/c, π^0 prod. anal. 78−41608
π^+p, 16 GeV/c, transverse energy spectra of hadrons 77−38209
π^+p, 32 GeV/c, π and ρ^0 inclusive prod., f and η cross section estimates *(Russian)* 80−68499
π^+p, 4 GeV/c, γ and π^0 production 79−80844
π^+p, 6 to 100 GeV/c, $P_\perp$ distribs. of k^0, π^-, ρ^0, f, equilibrium temp. 79−49540
π^+p, inclusive yields, transverse spectra, of nonstrange mesons, direct π prod. 78−4886
π^+p 3.6 GeV/c, nonstrange and single pion final state cross-section meas. 77−50001
π^+p→($\pi^+\pi^-\pi^0$)Δ^{++}, 16 GeV/c, partial wave anal., ω^* and A_2^0 80−63033
π^+p→$\Delta^{++}\pi^+\pi^-\pi^0$, 15 GeV/c, A_1, A_3 and A_4 prod. 77−82780
π^+p→four prong final states, 10.3 GeV/c, resonance prod. cross-sections 78−74276
π^+p→γX, 16 GeV/c, inclusive π^0 prod. multiplicities 77−41867
π^+p interaction, pion prod., direct and by meson resonance decay 78−29365
π^+p→n$\pi^+\pi^+\pi^+\pi^-$, reaction, extraction from background 78−880
π^+p→p$\pi^+\pi^+\pi^-$, 16 GeV/c, A_1, A_3 and A_4 prod. 77−82780
π^+p→π^-X^{+++} inclusive double-charge-exchange π^- prod., 100 GeV/c 78−37250
π^+p→$\pi^+p\pi^0$, 1 GeV, N^{*+}, N^{*+} and ρ^+ prod., single π distribs. 77−74716
π^+p→$\pi^+p\pi^0\pi^0$, 4 GeV/c, study of $\Delta^{++}\pi^0\pi^0$ events, comparison with $\pi^+\pi^-$ data 79−22132
π^+p→$\pi^+p\pi^0\pi^0$($\pi\pi^0$), 3.5 GeV/c, cross-sections meas. 77−71527
π^+p→$\pi^+p\pi^+\pi^-\pi^0$, 4 GeV, inclusive π^0 and γ production data 79−54357
π^+p→$\pi^+\pi^-\Delta^{++}$, narrow epsilon resonance under rho 80−5021
π^+p→$\pi^+\pi^-\Delta^{++}$, polarization measurements and a narrow ε(750) 79−63514
π^+p→$\pi^+\pi^-\Delta^{++}$, S-wave dipion production 78−25069
π^+p→$\pi^+\pi^+$n, 12.5 GeV, meas. and anal. of $\pi^+\pi^-$ system 77−82788
π^+p→$\pi\pi$N, 1.4-1.7 GeV, isobar model partial wave anal., baryon resonance decay 80−86750
π^+p, 100 GeV/c, inclusive charged-pion prod. 78−33102
$\pi^\pm$p, 100 GeV/c, π^0 and η inclusive prod. in triple Regge region 79−13164
$\pi^\pm$p 100 GeV/c, π^0 and η inclusive prod., triple Regge theory test 79−6349
$\pi^\pm$p interactions, π^0 multiplicities, 10.5, 15 MeV, differential cross sections 78−41597
$\pi^\pm$p→p$\pi^\pm\pi^+\pi^-$, 16 GeV/c, dynamical mechanism from cluster anal. *(Russian)* 80−42499
$\pi^\pm$p→π^0X, 100, 200 GeV/c high transverse momentum π^0 prod., quark scatt. 78−45976
$\pi^\pm$p→π^0X, 14 GeV/c, test of limiting fragmentation hypothesis 77−18355
$\pi^\pm$p→$\pi^0\pi^0$+X, direct and indirect pair production 79−9419
$\pi^\pm$p→$\pi^\pm$+anything, 16 and 100 GeV/c, high transverse momentum, charge asymm. 77−18339
$\pi^\pm$p→$\pi^\pm\pi^0$p, phase anal. of $\pi^+\pi^0$ and $\pi^-\pi^0$ interactons *(Russian)* 79−30748
$\pi\pi$ correlations in multiperipheral resonance prod. model 78−45891
$\pi^+\pi^-$ from ρ decay following diffractive ρ muoprod. in μp reactions 77−30391
$\pi^+\pi^-$→$\pi^+\pi^0\pi^0$ cross-section from π^-p→$\pi^0\pi^0$n at 2.01 GeV/c 78−21461
$\pi^+\pi^-$→$\pi^+\pi^+\pi^+\pi^-$, cross section meas. for quad-pion mass region 1.5 to 1.9 GeV 77−67675
$\pi^-\pi^-\pi^-$ correlation functions, Mueller scheme with Bose-Einstein statistics 78−93915
$\pi^\pm$single particle distribs. in pp, πp collisions, transverse momentum, rapidity depend. hard scatt. models 78−29361
ψ→3π, ρ recurrences, quantitative study 77−79266

pion production continued
ψ (3100) decay, inclusive γ and π^0 momentum spectra, direct γ prod. at large x 80−42466
$\psi' \rightarrow \psi + 2\pi$, decay width dynamical calc. 77−18278
$\tau \rightarrow 3\pi\nu$ decay, current algebra calcs. 79−30764
$\tau \rightarrow \nu_\tau n\pi$, T-violation effects, neutrino mass *(Russian)* 80−95294
$\tau \rightarrow \nu\rho\pi$ decay parameters from PCAC and current algebra, A_1 characts. 80−37314
$\tau \rightarrow \rho\pi\nu_\tau$, quark model, current algebra model, divergence of axial vector current 80−57655
$\tau^- \nu_\tau \pi^- \gamma$, π form factors, axial-vector and structure dependent, vector meson dominance model 80−62989
Ag(Fe,f), central collisions, nucleon characteristics, nuclear pionisation in complete fission *(Russian)* 79−80963
^{107}Ag+p, 24 GeV/c, in nucl. emulsion, particle emission freq. variation 78−37335
Al+p, 200 GeV/c, relative yields of $\pi^\pm$, $K^\pm$, p, $\bar{p}$ 78−93995
Al+p, 600 MeV, pion production, energy spectra, A depend. *(Russian)* 78−17213
^{27}Al(e,e'π^+), energy and ang. distribs. of πs, low lying residual states 78−54740
^{27}Al(γ,π^+) and ^{27}Al(e,e'π^+), 130 to 580 MeV, cross sections, impulse approx., multipole decomp. 77−54206
Al(α, $\chi\pi$), 18 GeV, π multiplicity distrib. 79−97713
Al(p,$\bar{p}\pi^-$), 10 GeV, $\bar{p}$ weak absorpt., $\bar{p}$ and π^- yields *(Russian)* 79−75987
(Ar, π^-X), 800 MeV/A, π^- energy and ang. distribs., firestreak and hard scatt. model anal. 80−13498
^{40}Ar+various nuclei, negative pion production, 0.4-2.1 GeV/nucleon 78−37364
^{197}Au(γ,π^-xn), threshold to 750 MeV, activation method determ. of yields, and expt. mean cross sections 79−54430
Au(p,$\bar{p}\pi^-$), 10 GeV, $\bar{p}$ weak absorpt., $\bar{p}$ and π^- yields *(Russian)* 79−75987
^{A}B(p,π^+), A=10,11, 200 MeV, pion energy spectra for discrete final states, cross sections 80−106057
^{10}B(p, π^+)^{11}B, 140 to 200 MeV, π^+ ang. distrib., energy depend. 79−63667
^{10}B(p,π^+), 320-605 MeV, cross sections, pion exchange model anal. 80−27676
^{10}B(p,π^+), differential cross sections, DWBA calc. 79−85415
^{10}B(p,π^+), near threshold, reaction energy dependence 79−85461
^{10}B(p,π^+)^{11}B, 163 to 186 MeV, expt. and theoretical study of π^+ prod. 79−59061
^{10}B(p,π), microscopic model anal., stripping model test for (d,p) 79−85436
^{11}B(γ,π^-)^{11}C, 142.0-169 MeV, cross-section near threshold 77−6348
^{138}Ba(γ,π^-xn)La, 150-300 MeV, pion production cross sections calc. 80−9287
Be+p, 200 GeV/c, relative yields of $\pi^\pm$, $K^\pm$, p, $\bar{p}$ 78−93995
Be+p, high mass symmetric hadron and pion pair prod., scaling props. 79−22291
^{9}Be, π^+ electroprod., distorted wave impulse approx. anal. 79−17894
^{9}Be(K$^-$, π^-)$^9_\Lambda$Be*, ang. distribs. of strangeness exchange reactions, PWIA anal. *(Chinese)* 79−80956
^{9}Be(e,e'π^+), energy and ang. distribs. of πs, low lying residual states 78−54740
^{9}Be(e,π^+), 1848 MeV, virtual photon spectrum, virtual photon theory test 80−102183
^{9}Be(e,$\pi^\pm$), 10 MeV π, of PWIA calcs. 79−93607
^{9}Be(γ,π^+), 100-800 MeV, cross section, surface prod. model anal. 80−47466
^{9}Be(γ,π^+), threshold to 175 MeV, total cross sections, DWIA anal. 80−13459
^{9}Be(γ,π), photoabsorption and sum rules, structure, RMS radius, polarisability and exchange parameters 80−22686
^{9}Be(p,π^-)^{10}C, 613 MeV, residual nucleus excitation levels, cross section 78−78383
^{9}Be(p,π^+), 320-605 MeV, cross sections, pion exchange model anal. 80−27676
^{9}Be(p,$\pi^\pm$), 800 MeV, ^{10}Be, ^{10}C ang. distribs. to isobaric analogue states cross section ratio 79−89274
^{9}Be(p,$\pi^\pm$), 800 MeV, ang. distribs. 79−85463
^{9}Be(p,π), 200 MeV, proton distortion and asymmetries 79−85464
Be(p,$\bar{p}\pi^-$), 10 GeV, $\bar{p}$ weak absorpt., $\bar{p}$ and π^- yields *(Russian)* 79−75987
Br(Fe,f), central collisions, nucleon characteristics, nuclear pionisation in complete fission *(Russian)* 79−80963
^{79}Br+p, 24 GeV/c, in nucl. emulsion, particle emission freq. variation 78−37335
(C, π^-X), 800 MeV/A, π^- energy and ang. distribs., firestreak and hard scatt. model anal. 80−13498
C, photoproduction of negative pions, 510 to 750 MeV 78−74347
C+p, 600 MeV, pion production, energy spectra, A depend. *(Russian)* 78−17213
C+p(d)(α)(^{12}C), 4.2 GeV/N, multiple π^- prod., mean multiplicity *(Russian)* 80−27647
^{A}C(p,π^+), A=12,13, 200 MeV, pion energy spectra for discrete final states, cross sections 80−106057
^{A}C(p,$\pi^\pm$), A=12,13, 200 MeV, analogue and nonanalogue state cross sections 80−99130
^{12}C, π^+ electroprod., distorted wave impulse approx. anal. 79−17894
(^{12}C, πX), 4.2, 4.5 GeV/N, pion multiplicities and theoretical models, review 80−42657
^{12}C+^{12}C, 800 MeV/nucleon, two-fireball model for p and π inclusive spectra 79−13323
^{12}C+π^-, 4 GeV/c, general characts. of secondary π inclusive prod. *(Russian)* 78−78421
^{12}C+π^-, 40 GeV/c, $\pi^\pm$ momentum and ang. distribs. *(Russian)* 77−50164
^{12}C+π^-, 40 GeV/c, secondary charged particle inclusive spectra, $\pi^\pm$ struct. functions *(Russian)* 78−89921
^{12}C+π^-, 5 GeV/c, charged π emission space-time characts. *(Russian)* 78−78422
^{12}C+various nuclei, negative pion production, 0.4-2.1 GeV/nucleon 78−37364
^{12}C(^{12}C,X), two fireball model, pp correlations and inclusive pion spectrum 80−68694
^{12}C(^{3}He,π^0), 180, 200 MeV, inclusive prod. cross section 77−6410
^{12}C(^{4}He,π^0), 710 MeV, inclusive neutral pion prod. cross section 77−6410

pion production continued
^{12}C(a,X), a=p,d,^{4}He,^{12}C, 4.2 GeV/c, multitudes of secondary negative particles, momentum distrib. ratios *(Russian)* 80−63178
^{12}C(e, $\pi^\pm$), 17 and 29 MeV 79−63659
^{12}C(e,e'π^+), energy and ang. distribs. of πs, low lying residual states 78−54740
^{12}C(e,e'π^+)^{12}B, near threshold, equivalent photon approx., Kroll-Ruderman term 78−13065
^{12}C(e,e'πs) threshold prod. at 280 MeV, π^+/π^- ratio 77−41957
^{12}C(e,eπ), total cross section from square reaction matrix element *(Russian)* 80−32271
^{12}C(e,$\pi^\pm$), 10 MeV π, of PWIA calcs. 79−93607
^{12}C(e,π), charged π electroprod. near threshold, data anal. 78−66266
^{12}C(γ, π^-)^{12}N$_{gs}$, threshold prod., 15.11 MeV M1 form factor 78−62519
^{12}C(γ, π^-p), final state interaction, plane and distorted wave momentum distrib. 80−18286
^{12}C(γ,π^-), 160-250 MeV, total cross section from elementary Hamiltonian model 80−18292
^{12}C(γ,π^-), (γ,π^-p), knockout p interaction, optical model and quasifree π photoprod. mechanism *(Russian)* 80−42638
^{12}C(γ,π^-), model yield calc. 77−14107
^{12}C(γ,π^-), near (3,3) resonance, differential cross-section meas. 77−10385
^{12}C(γ,π^-), threshold to 360 MeV, total cross sections in Δ region 80−13457
^{12}C(γ,π^-), total cross section calc. in impulse approx. 80−13458
^{12}C(γ,π^-)^{12}N, near threshold, total cross section 77−14104
^{12}C(γ,π^-)^{12}N, threshold to reson., total and differential cross sections 79−85456
^{12}C(γ,π^-)^{12}N, total cross-section anal. 77−14102
^{12}C(γ,π^-)^{12}N, total cross section calc., Δ(1232) contrib. 80−91175
^{12}C(γ,π^-)^{12}N$_{g.s.}$, near threshold, total cross section calc. 78−50152
^{12}C(γ,π^-p), 340-380 MeV, quasi-free photoprod., impulse and shell model anal. *(Russian)* 80−5124
^{12}C(γ,π^-p), final state interaction, distorted and plane wave momentum distribs. 80−78275
^{12}C(γ,π^0), pionic and EM A* resonance excitation 80−91160
^{12}C(γ,π^0)^{12}C, 220-360 MeV, phenomenological isobar doorway model calcs., total cross section 79−525
^{12}C(γ,π^+)^{12}B, nuclear critical opalescence study 80−105988
^{12}C(γ,π^-)^{12}B, spin flip transition strength 77−14103
^{12}C(γ,π^+)^{12}B$_{g.s.}$, 0-4 MeV, pion photoprod. cross section 80−42637
^{12}C(γ,π^+)^{12}C, up to 175 MeV, total cross sections, DWIA anal. 79−59049
^{12}C($\gamma,\pi^\pm$), PWIA anal. 77−14108
^{12}C(k$^-$, π^-)$^{12}_\Lambda$C, strangeness exchange reaction, ground state ang. distrib., 11 MeV excitation 79−85560
^{12}C(k$^-$,π^-)$^{12}_\Lambda$C, Λ-nuclear spin-orbit coupling, ΛN effective interaction 79−85562
^{12}C(p,π^-)^{13}O, 613 MeV, residual nucleus excitation levels, cross section 78−78383
^{12}C(p,π^+), optical model orthogonality constraints for bound and continuum waves 79−89306
^{12}C(p,π^+)^{13}C, π distortion effect on asymmetry, polarised protons 78−50176
^{12}C(p,π^+)^{13}C, relativistic pion stripping formalism 78−41717
^{12}C(π^-, X), 40 GeV/c, cumulative pions and nucleus total disintegration probability *(Russian)* 80−57807
^{12}C(π^-, X), 40 GeV/c, many-nucleon interactions, secondary $\pi^\pm$ spectra *(Russian)* 79−97638
^{12}C(π^-,X), 40 GeV/c, hadron emission into backward hemisphere *(Russian)* 79−59094
^{12}C(π^-,X), 40 GeV/c, $\pi^\pm$ rapidity distribs., fast and slow particle components *(Russian)* 79−40969
^{12}C(π^-p) in Δ(1232) region, differential yield, impulse and shell model anal. *(Russian)* 79−67744
^{13}C(K$^-$, Π^-) ^{13}C$_\Lambda$, ang. distribs. of strangeness exchange reactions, PWIA anal. *(Chinese)* 79−80956
^{13}C(p,π^-), 185 MeV, differential cross section, two-nucleon model *(Chinese)* 79−59069
^{40}Ca(^{40}Ar, π^+X), 1.05 GeV/nucleon 79−63693
^{40}Ca(^{40}Ca,x), relativistic, compression and pion distrib., Monte Carlo calc. 80−73853
^{40}Ca(p, π^+)^{41}Ca, 140 to 200 MeV, π^+ ang. distrib., energy depend. 79−63667
^{40}Ca(p,nπ^+), $\simeq$500 MeV, NNπ vertex function 79−59066
^{40}Ca(p,π^+), 163 to 186 MeV, expt. and theoretical study of π^+ prod. 79−59061
^{40}Ca(p,π^+), differential cross sections, DWBA calc. 79−85415
^{40}Ca(p,π^+), near threshold, reaction energy dependence 79−85461
^{40}Ca(p,π^+)^{41}Ca, relativistic pion stripping formalism 78−41717
C($\alpha,\chi\alpha$), 18 GeV, π multiplicity distrib. 79−97713
Cl (Ar, π^-X), 250, 400 MeV/A, pion yield near threshold 80−18344
Cl(Ar,X), 0.4-1.8 GeV/u, multipion prod. energy depend. 80−106065
C(p,π^+) 240 MeV inclusive pion production *(Russian)* 80−86908
C(p,π^+), 400-500 MeV, cross-sections meas. 77−10392
Cu (p,π^+) 240 MeV inclusive pion production *(Russian)* 80−86908
Cu+p, 600 MeV, pion production, energy spectra, A depend. *(Russian)* 78−17213
Cu(^{20}Ne,π^+), 800 MeV/N, doubly differential cross sections and ang. distribs. 80−9305
Cu(α, $\chi\pi$), 18 GeV, π multiplicity distrib. 79−97713
Cu(γ,π^-), quasifree photoprod. cross sections 79−75972
Cu(p,$\bar{p}\pi^-$), 10 GeV, $\bar{p}$ weak absorpt., $\bar{p}$ and π^- yields *(Russian)* 79−75987
Cu(p,π^+), 400-500 MeV, cross-sections meas. 77−10392
D+hadron, inclusive π, N spectra in high energy hadronic reactions, d fragmentation region *(Russian)* 78−54809
D(p,π^+)T, 410, 605, 809 MeV, pion angular distrib. 78−29466
e^+e^- annihilation, quark jets, transverse momentum profile 80−57621
ep$\rightarrow$enπ^+, forward π^+ electroprod. in Δ(1232) resonance region 79−22115
$\gamma_{virtual}$ hadron$\rightarrow\pi^\pm$ anything, sum rules using PCAC 77−34161
(HI,X), inclusive pion prod., forward and backward π spectra 79−85484
(HI,π), π radiation from relativistic heavy ion 80−73863
^{1}H(γ,π^0), 1 to 10 MeV above threshold 79−85454
^{1}H(γ,π^0), polarised γ, 0.76-1.3 GeV, asymmetry meas. in photoprod. cross section *(Russian)* 79−59051
^{1}H(γ,π^+), 3.4-18 GeV, πNN form factor and differential cross sections, one pion exchange 80−68526

pion production continued
^{1}H(n,d)π^0, 459, 648, 802 MeV, relative diff. cross section and ang. distrib. 80−52671
^{1}H(n,π^0)^{2}H, differential cross sections for 470-590 MeV, ang. distribs. 80−57628
^{1}H(n,π^0)^{2}H, nuclear forces charge symmetry test 80−5071
^{1}H(p,pπ^+)n, 800 MeV, Δ^{++} prod. and cross sections 79−22294
^{1}H(p,π^+)^{2}H, Low eqn. approx. soln., field theory propagator modification 79−85546
^{1}H(p,π^+)^{2}H, pol. p, total cross section, ang. distribs. and asymmetry parameters 80−63182
^{1}H(p,π^+)^{2}H, SIS, 578 MeV, pol. beam and target, spin depend. parameters 80−42651
^{1}H(p,π^+)pn, polarised p, 305, 330 MeV, pion production differential cross section 79−67754
^{1}H(π^-,X), 40 GeV/c, hadron emission into backward hemisphere *(Russian)* 79−59094
^{2}H(δ,π^0), multiple scatt. contrib. to threshold photoprod. 80−73718
^{2}H(e,eπ), total cross section from square reaction matrix element *(Russian)* 80−32271
^{2}H(γ, pp)π^-, high momenta of emitted nucleons 78−70512
^{2}H(γ, π^-)nn, excitation function, cross-section, threshold π^+ prod. 77−26670
^{2}H(γ,nnπ^+), threshold form factors 79−85453
^{2}H(γ,p)n, EM properties of πNN system, virtual π reabsorption 79−22109
^{2}H(γ,π^-p)^{1}H, π^--p coincidence obs., mechanism and rescatt. effects *(French)* 79−3133
^{2}H(γ,π^0), 1 to 10 MeV above threshold 79−85454
^{2}H(γ,π^0), 300 to 700 MeV, differential cross sections, partial wave analysis *(Japanese)* 78−17177
^{2}H(γ,π^0), 450 MeV cross section asymmetry *(Russian)* 79−89171
^{2}H(γ,π^0), coherent photoprod., binding effects and threshold amplitude calc. 80−32264
^{2}H(γ,π^0), cross section and threshold effects using dynamical γN→Nπ^0 model 80−27627
^{2}H(γ,π^0), impulse approx. calc. of differential cross-section 77−18524
^{2}H(γ,π^+), 1-4 MeV, cross-section meas. 78−21544
^{2}H(γ,π^+), threshold prod., excitation function 77−14105
^{2}H(γ,π^+)2n, π^+ energy spectra and emission angle *(Russian)* 79−40903
^{2}H(γ,π^+)2n, threshold to 22 MeV, bremsstrahlung yield and total cross section 80−9288
^{2}H(γ,π^+)2n cross section, threshold charged photopion prod. operator props. 79−89292
^{2}H(γ,π^+)nn, n-n final state interaction effects 80−102181
^{2}H(γ,π^+)nn, photoprod. near threshold, nucleus axial props. rel. to nucleon spin-fip *(French)* 79−522
^{2}H(γ,π^+)nn, threshold cross-section, impulse approx. 77−38256
^{2}H(γ,$\pi^\pm$), photprod. on neutrons effect of Fermi motion 78−74349
^{2}H(γ,π), impulse approx. and π rescattering effects 77−6346
^{2}H(γ,π), threshold photoprod. cross sections, elementary nucleonic amplitudes 80−22812
^{2}H(n,π^-), 400-580 MeV, differential cross sections and ang. distribs. 80−86906
^{2}H(n,π^-)^{3}He, 400 to 580 MeV at backward pion angles 80−73847
^{2}H(p, dπ^+)n, 585 MeV, d momentum spectra 78−41718
^{2}H(p,dπ^+), 800 MeV, pion prod. with spectator neutron, cross section 80−9294
^{2}H(p,nπ^+), 585 MeV, differential cross sections, reaction mechanisms 79−548
^{2}H(p,π^+), 400, 470, 600 MeV, microscopic model calcs., reaction cross section 79−40916
^{2}H(p,π^+), 400-470 MeV, backward π differential cross sections and anal. power 80−86905
^{2}H(p,π^+), polarised p, 305, 330 MeV, pion production differential cross section 79−67754
^{2}H(p,π^+)^{3}H, 400, 470, 600 MeV, differential cross section using isobar model 80−9291
^{2}H(p,π^+)^{3}H, studied via pp→π^+d amplitude and triangle graph 77−38265
^{2}H(p,π^+)^{3}H, pion prod. models for medium energies 77−18563
^{3}H(γ,π^0), 0-8 MeV, cross sections, taking π rescatt. amplitudes into account 78−78364
^{3}H(γ,π^0)^{3}H, polarisation effects 180 to 700 MeV, impulse approx. calcs. *(Russian)* 80−37368
^{3}H(t,π^-), π^- production by nucleons on light nuclei, estimate of energy consumption *(Russian)* 79−80943
^{A}H(γ,π^0), A=1, 2, 1-10 MeV, photoprod. yields, DWIA anal., dipole photoprod. amplitudes 80−68645
^{3}He, threshold pion photoproduction and radiative capture, π-^{3}He-^{3}H coupling constant 79−40962
^{3}He(N,πX), expt. review of π-prod. by (un)polarised nucleons on few-nucleon systems 79−80944
^{3}He(e,π^+)^{3}H, cross section from t recoil cross section meas. 79−6574
^{3}He(γ,π^0), 0-8 MeV, cross sections, taking π rescatt. amplitudes into account 78−78364
^{3}He(γ,π^0), 1 to 10 MeV above threshold 79−85454
^{3}He(γ,π^0), cross section and threshold effects using dynamical γN→Nπ^0 model 80−27627
^{3}He(γ,π^0), polarisation effects 180 to 700 MeV, impulse approx. calcs. *(Russian)* 80−37368
^{3}He(γ,π^0)^{3}He, polarisation effects 180 to 700 MeV, impulse approx. calcs. *(Russian)* 80−37368
^{3}He(γ,π^+) near threshold, photoprod. yield and transition matrix element 79−89291
^{3}He(γ,π^+)^{3}H, exchange current effects, two body processes 79−71839
^{3}He(γ,π^+)^{3}H, Fermi motion and off-shell effects, impulse approx. 80−27626
^{3}He(γ,π^+)^{3}H, threshold π prod., and axial vector form factor 79−574
^{3}He(γ,π^+)^{3}H, threshold form factors 79−85453
^{3}He(γ,π^+)^{3}H cross section near threshold , 80−83093
^{3}He(γ,π^-), (3,3) resonance region, nuclear wave functions, kinematics 78−78361
^{3}He(γ,π), threshold photoprod. cross sections, elementary nucleonic amplitudes 80−22812
^{3}He(p,π^+)^{4}He, 300-400 MeV, virtual pion exchange 77−74848
^{3}He(p,π^+)^{4}He, 415, 716 MeV, DWIA calcs. of differential cross-section 77−6359
^{3}He(π^-,γ)^{3}H, radiative capture rate and threshold π photoprod., Panofsky ratio from ^{3}He(π^-,π^0) 79−13350

pion production continued
^{4}He+p, 8.56 GeV/c, two pronged events, cross sections and prod. features 79−3152
^{4}He(γ, π^0), relative cross section depend. on pion parity *(Russian)* 78−66129
^{4}He(γ,pπ^-), π^--p coincidence obs., mechanism and rescatt. effects *(French)* 79−3133
^{4}He(γ,π^0), 1 to 10 MeV above threshold 79−85454
^{4}He(γ,π^0), differential cross section, complex momenta theory for nondiffractive processes *(Russian)* 80−32266
^{4}He(γ,π^0), impulse approx. for differential cross sections in resonance region *(Russian)* 78−41698
^{4}He(γ,π^0), P-odd effects, Regge and boson pole interference *(Russian)* 79−6564
^{4}He(γ,π^0), polarisation effects 180 to 700 MeV, impulse approx. calcs. *(Russian)* 80−37368
^{4}He(γ,π^0), reaction cross section meas. equipment 78−29694
^{4}He(p,nπ^+), 18.6 GeV, invariant mass distrib., double Regge pole model comp. 79−3144
^{4}He(p,nπ^+), ≃500 MeV, NNπ vertex function 79−59066
^{4}He(p,nπ^+), pion prod. operator non-relativistic approx. 79−85500
^{4}He(p,nπ^+), pion prod. operator non-relativistic approx. 80−27640
^{4}He(p,pπ^0), 18.6 GeV, invariant mass distrib., double Regge pole model comp. 79−3144
^{A}He(γ,π^0), A=3, 4, 1-10 MeV, photoprod. yields, DWIA anal., dipole photoprod. amplitudes 80−68645
H(ϕ,π^0), 350 MeV, differential cross sections 78−86527
K (Ar, π^+X), 250, 400 MeV/A, pion yield near threshold 80−18344
K(Ar,X), 0.4-1.8 GeV/u, multipion prod. energy depend. 80−106065
K^+p→$\pi^\pm$X, 32 GeV, topological cross sections 80−102085
^{6}Li+α, 18 GeV/c, π^- multiplicity distribs. *(Russian)* 78−41742
^{6}Li(^{3}He,π^-), 910 MeV, π^- doubly coherent prod., inclusive π spectra 79−85481
^{6}Li(^{3}He,π^-)^{9}C, 910 MeV, doubly coherent π prod. 80−13487
^{6}Li(α, $\chi\pi$), 18 GeV, π multiplicity distrib. 79−97713
^{6}Li(α,π^+)^{6}He, threshold prod. in α-d cluster model 77−79356
^{6}Li(γ,π^+), cross-section calc. 78−17248
^{6}Li(γ,π^+)^{6}He, analysis using current algebra model with rigid π-mesons *(Russian)* 77−14112
^{6}Li(γ,π^+)^{6}He, photoprod. near threshold, nucleus axial props. rel. to nucleon spin-fip *(French)* 79−522
^{6}Li(γ,π^+)^{6}He, threshold to 7 MeV, cross sections rel. to proton target 77−54207
^{6}Li(γ,π^0)^{6}Li*(3.56 MeV), partial photoproduction reactions, large momentum transfer anal., form factor choice 80−22808
^{6}Li(k$^-$,π^-)$^{6}_{\Lambda}$Li, strangeness analogue reson. 79−85566
^{6}Li(p,dπ^+)^{5}He, 800 MeV, momentum spectra enhancement 77−10395
^{6}Li(p,π^+)^{7}Li, 600 MeV, comparison with π,p exchange calcs. 77−79377
^{7}Li(γ,π^-), threshold to 360 MeV, total cross sections in Δ region 80−13457
^{7}Li(γ,π^-), total cross section calc. in impulse approx. 80−13458
^{A}Li, A=6,7, π^+ electroprod., distorted wave impulse approx. anal. 79−17894
^{A}Li(γ,π), A=6, 7 80−22686
Li(e,e$'\pi^+$), A=6,7, energy and ang. distribs. of πs, low lying residual states 78−54740
^{26}Mg(p,π^+), isobar configuration effects, p→$\Delta^0\pi^-$ model, ang. distribs. *(Chinese)* 80−47484
(n,pπ^-), neutron coherent dissociation using nuclear targets, comparison of expt. data with Deck model 79−89309
^{14}N(γ,π^-), DWIA anal., wave function and π optical pot. effects on cross section 80−63168
^{14}N(γ,π^-)^{14}C, threshold, impulse approx. anal. 77−14109
^{14}N(γ,π^-)^{14}O, 145-325 MeV, Gamow-Teller suppression and M1 radiative widths 80−52609
^{14}N(γ,π^+), anomalous $^{14}N_{gs}$→$^{14}C_{gs}$ transition, Kroll Ruderman terms 80−63167
Na(^{20}Ne,π^+), 800 MeV/N, doubly differential cross sections and ang. distribs. 80−9305
(Ne, π^-X), 800 MeV/A, π^- energy and ang. distribs., firestreak and hard scatt. model anal. 80−13498
Ne+$\pi^\pm$, 10.5 GeV/c multiplicities and inclusive moment and rapidity spectra 78−8862
(^{20}Ne, π^+X), 400 MeV/N, pion prod. doubly differential cross sections and ang. distrib. 80−32299
^{20}Ne+α, 18 GeV/c, π^- multiplicity distribs. *(Russian)* 78−41742
^{20}Ne+emulsion nuclei, evidence against copious threshold pion prod. 78−37362
^{20}Ne+emulsion nuclei, Monte Carlo simulation pion and proton multiplicities 78−37363
Ne(α, $\chi\pi$), 18 GeV, π multiplicity distrib. 79−97713
^{A}Ni(p,π^+), A=58, 64, 660 MeV, pion energy spectra, isotopic effects *(Russian)* 80−42669
^{16}O, pion photoproduction and radiative capture 78−50213
^{16}O, π^+ electroprod., distorted wave impulse approx. anal. 79−17894
(^{16}O, πX), 4.2, 4.5 GeV/N, pion multiplicities and theoretical models, review 80−42657
^{16}O+emulsion nuclei, 75-200 MeV/nucleon, pion and proton multiplicities 78−37363
^{16}O(e,e$'\pi^+$), energy and ang. distribs. of πs, low lying residual states 78−54740
^{16}O(e,e$'\pi$s) threshold prod. at 280 MeV, π^+/π^- ratio 77−41957
^{16}O(e,e), T=1 level form factors, Helm model, pion photoprod. and muon capture appls. 80−52553
^{16}O(e,π^+), 180.4 MeV, virtual photon spectrum, virtual photon theory test 80−102183
^{16}O(e,$\pi^\pm$), 10 MeV π, of PWIA calcs. 79−93607
^{16}O(e,π), charged π electroprod. near threshold data anal. 78−66266
^{16}O(γ,π^0) coherent photoprod. in isobar-hole formalism, DWIA comparison 79−89290
^{16}O(γ,π^+), 200-350 MeV, cross sections, DWIA anal. 80−106048
^{16}O(γ,π^+), differential cross section from elementary Hamiltonian model 80−18292
^{16}O(γ,π^+), threshold to 175 MeV, total cross sections, DWIA anal. 80−13459
^{16}O(k$^-$,π^-)$^{16}_{\Lambda}$O, Λ-nuclear spin-orbit coupling, ΛN effective interaction 79−85562
^{16}O(p,π^+)^{17}O, polarised protons, π distortion effect on asymmetry 78−50176
(p,n) for A between 27 and 238, 800 MeV, n prod. systematics, π associated cross section 79−3153

pion production continued
Pb+p, 600 MeV, pion production, energy spectra, A depend. *(Russian)* 78−17213
Pb(^{12}C,X), 1-2 GeV/n, central collision threshold phenomena, pion prod. 80−95326
Pb(^{20}Ne,π^+), 800 MeV/N, doubly differential cross sections and ang. distribs. 80−9305
^{208}Pb (Ar, π^+X), 250, 400 MeV/A, pion yield near threshold 80−18344
^{208}Pb+^{40}Ar, 1.8 GeV/nucleon, appl. of multiple-collision model for pion prod. 78−37365
^{208}Pb+Ar, 1.8 GeV/nucleon, fireball model calc. of π-multiplicity distribs. 78−37366
^{208}Pb(^{3}He,π^0), 200 MeV, inclusive neutral pion prod. cross section 77−6410
^{208}Pb(p,π^+), 180 MeV, ang. distribs., discrete states, differential cross section 79−13298
^{208}Pb(p,π^+), differential cross sections, DWBA calc. 79−85415
^{208}Pb(p,π^+)^{209}Pb, 160 MeV, ang. distributions 78−37345
^{208}Pb(p,π), microscopic model anal., stripping model test for (d,p) 79−85436
Pb(α, $\chi\pi$), 18 GeV, π multiplicity distrib. 79−97713
Pb(γ,π^+), quasifree photoprod. cross sections 79−75972
$\bar{p}$p, 5.7 GeV/c, nonannihilation channels Δ^{++}, $\bar{\Delta}^{++}$, Δ^0, $\bar{\Delta}^0$ prod. cross sections 80−27515
pp collisions, multiplicity distribs. in impact parameter space, multi-Regge model 77−14001
pp→p$\pi\pi$, exclusive pion prod. OPE and VME amplitudes 79−85336
pp→pp$\pi^+\pi^-$, 12, 24 GeV/c, p dissociation into ($p\pi^+\pi^-$), partial wave anal. 79−22148
$\bar{p}$p→$\pi^+\pi^-$, 5.7 GeV/c, two-pion correls., interference effects 80−32116
pp→$\pi^+\pi^-$X, QCD testing by high energy hadroprod. of lepton pairs 79−26343
πd→π^0d, 350-500 MeV, differential cross section asymm., impulse approx. with pion rescatt. terms 77−30389
^{A}Sn(p,π^+), A=112, 124, 660 MeV, pion energy spectra, isotopic effects *(Russian)* 80−42669
Ta+p(d)(α)(^{12}C), 4.2 GeV/N, multiple π^- prod., mean multiplicity *(Russian)* 80−27647
^{181}Ta+^{12}C, 4.2 GeV/N, identical pion$^-$ interference effect, generation range determ. *(Russian)* 80−42695
^{181}Ta+α, 4.2 and 5.15 GeV, central nuclear collisions, pion multiplicity calc. *(Russian)* 79−59079
^{181}Ta(a,X), a=p,d,^{4}He, ^{12}C, 4.2 GeV/c, multitudes of secondary negative particles, momentum distrib. ratios *(Russian)* 80−63178
^{51}V(e,e'π^+) and ^{51}V(γ,π^+), 130 to 580 MeV, cross sections, impulse approx., multipole decomp. 77−54206
Xe+π^-, 3.2 GeV/c, π^0, η, ω, f meson prod. determ. of meson-N total cross sections *(Russian)* 79−22122
Xe+π^- 3.2 GeV/c, intermediate Δ^- prod. in π^0 and η prod. *(Russian)* 79−36280
^{89}Y(e,e'π^+), energy and ang. distribs. of πs, low lying residual states 78−54740
^{90}Zr (p,π^+), 180 MeV, ang. distribs., discrete states, differential cross section 79−13298
^{90}Zr(p,π^+), differential cross sections, DWBA calc. 79−85415
^{90}Zr(p,π^+)^{91}Zr, 160 MeV, ang. distributions 78−37345

pion-proton inclusive interactions
absorption role in πp and pp multiplicity differences 78−66172
beam fragmentation region, vector and tensor meson prod., Mueller-Regge formalism 78−17057
charged particle and γ two-particle correls. at 40 GeV/c *(Russian)* 77−74736
collective tube model, credibility of criticism by Azimov et al., misuse of CTM 78−93980
cross section meas. for 100-3000 GeV using hadron-Fe collisions 79−49549
dynamical model for multiplicity distribs. in πp and pp-collisions, pion prod. 78−21469
estimate of ω, ϕ and baryonium mixing at t≈0 79−40814
exchange degeneracy evidence, Kp and πp total cross sections anal. 77−82796
Feynman-gas model for semi-inclusive processes, πp appl., multiperipheral model predictions *(Russian)* 78−435
fireball characteristics in 400 GeV/c πN collisions 78−58173
hadronic multiple prod. and average charged multiplicity, strato-gluon mechanism in pp, Kp, πp *(Chinese)* 80−22586
hadronic two-jet events, momentum unbalance, parton transverse momentum 80−57652
inclusive struct. functions of γ, $\pi^\pm$, K^0, and Λ *(Russian)* 79−80856
large p_t hadron production, lowest subprocess model, two body reactions 78−4887
meson fragmentation region, meson spectra, quark cascade model 77−67689
meson prod. with large transverse momentum, effective gluon model 78−8717
meson production at large p_T, comparison with pp results 77−50030
multiparticle rapidity clustering in 200 GeV/c π^-p interactions 78−54658
multiplicity distrib. formula in 10-405 GeV range 77−13998
neutral particle production in 4 to 2100 GeV interactions, review *(Russian)* 80−68489
one-dimensional cascade model of interacting nuclei using Glauber theory 78−17233
phase space critical surface of pions produced in inclusive π^-p interactions *(Russian)* 80−18154
pion prod., charged-neutral correl. in 5-205 GeV/c 77−13996
quantum chromodynamics, hadroprod. of lepton pairs and real photons 78−50056
quark cascade model, inclusive meson and baryon spectra in pp, πp, e^+e^- 77−50025
quark model and π^+p-pp multiplicity difference 79−40813
resonance pion prod., Bose interference effects 77−38210
thermodynamic model calcs. of single particle distribs. 77−30453
total cross section behaviour at high energies 77−67683
transverse energy spectra of hadrons 77−38209
ap→cX, a, c=$\pi^\pm$, $K^\pm$, p, $\bar{p}$, low P_t hadron fragmentation at 100, 175 GeV/c 79−85346
η/π^0 prod. ratio at high transverse momenta 78−41602
NN off-shell annihilation obs. at 8 and 16 GeV/c 77−38208

pion-proton inclusive interactions continued
pp→π^0X/π^-p→π^0X ratio at high-p_T, quark model explanation 77−10290
π production, direct and by meson resonance decay in π^+p interactions 78−29365
π^0 prod. at large p_T, pp and $\pi^\pm$p collision 77−79287
π^-+emulsion nuclei, 50 GeV/c multiplicities of secondary charged particles *(Russian)* 78−46116
π+H target, high transverse momentum π^0 and jets prod. 78−70417
π^-+p→Λ+X, relative scale invariance *(Russian)* 77−88003
π^-+p→p+μ+X, 200 and 240 GeV, charmed, particle forward prod. search 77−22818
π^-N semi-inclusive reactions at 40 GeV/c, structure functions *(Russian)* 77−61332
πp, large P_T pion^0 prod., meson structure functions, quark distrib. functions 80−86714
πp→ X, cross-section and quark energy distrib. 77−22813
πp→K(p)X, 50-175 GeV, Regge parametrisation 77−14002
πp→$\mu^+\mu^-$X, quark transverse momentum effect in bag model 80−86668
πp→π^0X, 100 and 200 GeV, ang. depend. of π^0 prod. 78−41603
πp→π^0+anything, large p_T, clustered parton model 77−67688
πp→πX, 5 GeV, nucleon isobar content in He using impulse approx. 79−36276
πp→πX, high p_T π^0 prod., leading particle contrib., QCD calcs. 80−73746
πp→πX or ρ^0X, central region, Regge Mueller approach, inclusive cross sections *(Russian)* 78−58218
πp→π(K)(p)X, 4-25 GeV/c, Pomeron factorisation 77−14005
πp→ψX, 70 GeV to ISR energies, pion exchange model anal. *(Russian)* 79−40823
π^-p, 100, 200, 360 GeV/c, inclusive prod. of π^0, K_S^0, Λ^0, $\bar{\Lambda}^0$, cross sections 80−73745
π^-p, 100 GeV/c, inclusive meson and strange particle prod., energy partition 80−95289
π^-p, 100 GeV/c, π^0 and η inclusive prod. in all neutral mode 79−13165
π^-p, 11.2 GeV/c, longit. and azimuthal correls. between meson pairs, ρ-meson effects 77−6180
π^-p, 147 GeV/c, neutral particle prod., K_S, Λ, $\bar{\Lambda}$, γ, multiplicity scaling form 80−22645
π^-p, 15 and 147 GeV/c, impact parameter anal. of multiparticle prod. 79−30758
π^-p, 16 GeV/c, inclusive $\bar{K}^{*0}$ (890) inclusive prod. 78−8710
π^-p, 200, 300 GeV, relative π^+, K^+, p, $\bar{p}$ prod., charge ratios, high p_T 80−47335
π^-p, 200 GeV/c, charge struct. of events anal. 77−18356
π^-p, 200 GeV/c, valence and sea quark distribs. in the pion, quark recombination model 79−63556
π^-p, 250 GeV/c, inclusive prod. of neutral strange particles, K^0_s, Λ, $\bar{\Lambda}$ 78−21479
π^-p, 340 GeV, associated charm prod. evidence, $D^\pm$ prod. 80−86767
π^-p, 360 GeV/c, total and elastic cross-sections meas., charged-particle multiplicity distrib. anal. 77−18357
π^-p, 40 GeV/c, associated multiplicity dependence on transverse momentum *(Russian)* 77−74738
π^-p, 40 GeV/c, associative multiplicity of charged particles, automated behaviour of spectra *(Russian)* 77−10295
π^-p, 40 GeV/c, charge multiplicity in forward and backward hemispheres *(Russian)* 77−265
π^-p, 40 GeV/c, charge particle asymmetry and quark model *(Russian)* 77−266
π^-p, 40 GeV/c, dispersion of longit. rapidity distribs., multiperipheral cluster model anal. *(Russian)* 78−17063
π^-p, 40 GeV/c, leading and conserved mesons *(Russian)* 78−45987
π^-p, 40 GeV/c, many pion systems in inclusive reactions, transverse momentum effects *(Russian)* 80−57654
π^-p, 40 GeV/c, multi-pion systems and transverse momenta, differential cross sections *(Russian)* 80−32142
π^-p, 40 GeV/c, particle prod. with large transversal momenta *(Russian)* 78−41609
π^-p, 40 GeV/c, semi-inclusive $\pi^\pm$ transverse momentum distributions, statistical model anal. *(Russian)* 79−13174
π^-p, 40 GeV/c interactions, charge asymmetry depend. on transversal momenta *(Russian)* 78−54662
π^-p, 4.85 GeV/c, strange particle prod., absolute and topological cross-sections *(Russian)* 77−254
π^-p, 5 GeV, spectra investigs. using propane bubble chamber *(Slovak)* 77−42214
π^-p, 5-40 GeV/c, distribs. of total multiplicity of secondary particles *(Russian)* 77−22820
π^-p, 70 GeV/c, direct electron prod. from charm particle pair decay, e/π ratio 80−105928
π^-p, 70 GeV/c, directly produced electrons from charmed D particle decay, cross sections 80−73755
π^-p, charged and neutral multiplicities at 205 GeV/c 77−71544
π^-p, diffractive and non-diffractive, 40 GeV/c, momentum and ang. charcts. *(Russian)* 77−50034
π^-p, inclusive Δ^{++}(1232) prod. at 147 GeV/c 79−17772
π^-p, large p_T inclusive π^0 prod., quark subprocesses 77−2885
π^-p, multiple production processes regularities, Monte Carlo model 80−102082
π^-p, semi-inclusive distrib., 21 GeV/c, multiplicity and rapidity 78−21482
π^-p 5 GeV/c interactions, inclusive distrib. of Γ^0 and K^0_1 *(Russian)* 78−54652
π^-p→($\bar{p}$p)X^0, narrow p$\bar{p}$ state search 80−78102
π^-p collisions, charged particle multiplicity, Bose distrib. 77−50022
π^-p→Δ^{++}X, 100, 200, 360 GeV/c, δ^{++} inclusive and semi-inclusive prod. cross sections 79−40817
π^-p→Δ^{++}(1232), 15 GeV/c, multiplicity distrib. determ. 78−45982
π^-p→ηX, pseudoscalar meson prod. in triple Regge region, absorpt. corrections 78−78228
π^-p→f^0X, tensor meson prod. in triple Regge region, cut corrections 77−46087
π^-p→γX, 5 GeV/c, invariant struct. function *(Russian)* 77−74717
π^-p→γX, large angle real photon prod. at large p_T, QCD anal. 80−22644
π^-p→γ+X, 5 GeV/c, scaling obs. *(Russian)* 78−45986
π^-p inclusive interactions, ρ^0, ω, f-mesons prod. cross section *(Russian)* 78−33098
π^-p inclusive reactions, 147 GeV/c, average charged particle multiplicities 79−40818

pion-proton inclusive interactions continued
π^-p interactions, 15 GeV/c, vector meson prod., polarisation props. 78−37251
π^-p interactions, 15 GeV/c, K^0_s, Λ, $\bar{\Lambda}$ prod., Regge anal. 78−45981
π^-p interactions at 40 GeV/c, cluster field features *(Russian)* 79−9421
π^-p interactions at 6 GeV/c, inclusive strange particle production 79−93454
$\pi^-p\rightarrow K^0_S$, Λ, $\bar{\Lambda}$, prod. in 16 GeV/c interactions 80−37308
$\pi^-p\rightarrow K^0X$, 205 GeV/c cross-sections 77−71544
$\pi^-p\rightarrow K^0+X$, 4.9-40 GeV/c inclusive and semi-inclusive distribs. *(Russian)* 78−41610
$\pi^-p\rightarrow\Lambda K^++X^-$, 4.35, 4.85 GeV/c, mass spectra of N* resonances *(Russian)* 77−6159
$\pi^-p\rightarrow\Lambda+X$, 4.9-40 GeV/c inclusive and semi-inclusive distribs. *(Russian)* 78−41610
$\pi^-p\rightarrow\Lambda(\bar{\Lambda})X$, 205 GeV/c cross sections 77−71544
π^-p multiparticle prod. at 147 GeV/c, inclusive and semi-inclusive charge struct. 79−58980
$\pi^-p\rightarrow\mu^+\mu^-+$hadrons, $\pi^-p\rightarrow$hadrons, quark-parton model 78−74222
$\pi^-p\rightarrow$neutral hadron+X, 200 GeV/c, n and $\bar{n}$ prod. 77−18349
$\pi^-p\rightarrow p_{slow}+X^-$, 147 GeV/c, differential cross sections, triple Regge anal. 79−40811
$\pi^-p\rightarrow pX$, 12 GeV/c, absorbed Mueller-Regge model for backward inclusive p prod. 80−73752
$\pi^-p\rightarrow pX$, 40-240 GeV, B^- boson missing mass search between 2 and 12.5 GeV 79−93473
$\pi^-p\rightarrow pX$, inclusive backward proton cross sections, calc. program adaptation 80−9185
$\pi^-p\rightarrow px^-$ interaction, 40 GeV, azimuthal correlations *(Russian)* 78−58217
$\pi^-p\rightarrow\phi X$, 16 GeV/c, cross-section 77−61330
$\pi^-p\rightarrow\pi^-_{fast}+X^+$, 147 GeV/c, differential cross sections, triple Regge anal. 79−40811
$\pi^-p\rightarrow\pi^-X$, 30-60 GeV/c, inclusive cross sections, resonance effects *(Russian)* 79−67615
$\pi^-p\rightarrow\pi^-X$, triple Pomeron coupling, Reggeon treatment 80−68488
$\pi^-p\rightarrow\pi^-+X^+$, associated multiplicity increase with transverse momentum *(Russian)* 77−46092
$\pi^-p\rightarrow\pi^-(\pi^0)X$, 40 GeV, three reggeon approach, multiperipheral model evidence *(Russian)* 79−30761
$\pi^-p\rightarrow\pi^-p+$anything, 40 GeV/c, two-pomeron interaction cross section *(Russian)* 77−6186
$\pi^-p\rightarrow\pi^-\pi^-X$, 50 GeV/c, $\pi^-\pi^-$ low mass system, cross sections and S-wave phase shifts 79−71766
$\pi^-p\rightarrow\pi^-\pi^+\pi^-X$, 200 GeV/c, three particle correl. 79−9415
$\pi^-p\rightarrow\pi^0X$, 5 GeV/c, associative multiplicity of charged particles as function of missing mass squared *(Russian)* 79−22136
$\pi^-p\rightarrow\pi^0X$, 5 GeV/c, inclusive distribs. *(Russian)* 78−45946
$\pi^-p\rightarrow\pi^0X$, helicity, non-flip amplitude in phase modified absorpt. model 77−79288
$\pi^-p\rightarrow\pi^0X$, large P_T collisions, quark cascade model anal. 79−36110
$\pi^-p\rightarrow\pi^0X$, large p_T processes, pion exchange model anal. *(Russian)* 80−27527
$\pi^-p\rightarrow\pi^0X$, pseudoscalar meson prod. in triple Regge region, absorpt. corrections 78−78228
$\pi^-p\rightarrow\pi^0+X$, 5 GeV/c, scaling obs. *(Russian)* 78−45986
$\pi^-p\rightarrow\pi^0(\eta)+$anything, absorptive corrections using Regge pole amplitude 77−38204
$\pi^-p\rightarrow\pi^+X$, double charge exchange at high energies *(Russian)* 77−82793
$\pi^-p\rightarrow\pi^\pm X$, 40 GeV/c, charge asymmetry as function of charged multiplicity and transverse momentum 79−40807
$\pi^-p\rightarrow\pi X$, 40 GeV/c, p_T correls. of identical pions *(Russian)* 77−74735
$\pi p^-\rightarrow\psi+X$, $\psi(3.1)$ inclusive prod. in fragmentation region 79−13150
$\pi^-p\rightarrow\rho^0+X$, 100-360 GeV, cross sections 79−40816
$\pi^-p\rightarrow\rho^0\pi^-X$, diffractive contrib. in multi-Regge factorisation 80−73753
π^-p semi-inclusive 40 GeV/c, charged particle and γ correls. *(Russian)* 77−34195
π^-p semi-inclusive interaction, 40 GeV/c, charge distribution *(Russian)* 77−74739
$\pi^-p\rightarrow\Sigma^\pm+$anything, 4.35 and 4.85 GeV/c, inclusive spectra *(Russian)* 77−13977
$\pi^-p\rightarrow V^0X$, 5 GeV/c, cross-section meas. *(Russian)* 77−61331
π^+p, 10.5 GeV, inclusive and direct photon prod. 80−5024
π^+p, 10.5 GeV/c, π^0 prod. anal. 78−41608
π^+p, 16 GeV, ρ^+, ρ^-, ρ^0 inclusive prod., cross sections, quark model 78−93912
π^+p, 32 GeV/c, elastic scatt. and multiplicities, total and differential cross sections *(Russian)* 80−52548
π^+p, 32 GeV/c, inclusive strange particle prod., Σ^+, K_S^0, Λ and $\bar{\Lambda}$ cross sections 80−52541
π^+p, 32 GeV/c, π and ρ^0 inclusive prod., f and η cross section estimates *(Russian)* 80−68499
π^+p, 32 GeV/c, slow proton and $\Delta^{++}(1236)$ inclusive prod. *(Russian)* 80−63046
π^+p, 4 GeV/c, γ and π^0 production 79−80844
π^+p, 60 GeV/c, cross-sections and charged-particle multiplicity meas. 77−30463
π^+p, inclusive yields, transverse spectra, of nonstrange mesons, quark model 78−4886
π^+p, π multiplicity and asymmetric fireballs 79−93474
π^+p, π^+ structure from two jet events, parton scatt. anal. 79−49491
$\pi^+p\rightarrow\Delta^{++}(1236)$, Λ^0, 100 GeV/c, one-meson-exchange mechanism anal. 78−8712
$\pi^+p\rightarrow f+X^{++}$ 8 GeV/c, reaction anal. 79−93457
$\pi^+p\rightarrow\gamma X$, 16 GeV/c, inclusive π^0 prod. multiplicities 77−41867
$\pi^+p\rightarrow K^0_SX$, 147 GeV/c, cross-section, scaling 80−52539
$\pi^+p\rightarrow K^+X$, pion struct. function from low p_T hadron prod. 79−13129
$\pi^+p\rightarrow K^+X$, π struct. function from low p_T hadron prod. 79−45123
$\pi^+p\rightarrow K^{*\pm}(892)X$, 16 GeV/c 80−86765
$\pi^+p\rightarrow\Lambda X$, 147 GeV/c, cross-section, scaling 80−52539
$\pi^+p\rightarrow\pi^-X$, double charge exchange at high energies *(Russian)* 77−82793
$\pi^+p\rightarrow\pi^-X^{+++}$ inclusive double-charge-exchange π^- prod., 100 GeV/c 78−37250
$\pi^+p\rightarrow\pi^+p\pi^+\pi^-\pi^0$, 4 GeV, inclusive π^0 and γ production data 79−54357
$\pi^+p\rightarrow\rho^0X^{++}$, 8 GeV/c, reaction anal. 79−93457
$\pi^+p\rightarrow\Sigma^+(1385)+X$, 16 GeV/c, spin density matrix of $\Sigma^+(1385)$ by statistical tensor method 78−37235
$\pi^\pm$p, 100 GeV/c, inclusive charged-pion prod. 78−33102

pion-proton inclusive interactions continued
$\pi^\pm$p, 100 GeV/c, π^0 and η inclusive prod. in triple Regge region 79−13164
$\pi^\pm$p, 130, 200 GeV, jet prod. cross sections, QCD anal. and scale breaking 80−99111
$\pi^\pm$p, 147 GeV/c, inclusive Δ^{++} prod., cross section energy depend. 80−57651
$\pi^\pm$p, 150 GeV/c, multiparticle prod., quark parton model anal. 79−30756
$\pi^\pm$p, 200 GeV/c, high p_T charged particle prod. and correlations 79−89199
$\pi^\pm$p, 200 GeV/c, high p_T jet prod., QCD expt. test 79−89200
$\pi^\pm$p, fireball model, universal scaling function 80−57646
$\pi^\pm$p, high energy, mean charged hadron multiplicity, modified Heisenberg approach 78−45988
$\pi^\pm$p, high-energy, react. differences and annihilations 78−74279
$\pi^\pm$p, π^+/π^- inclusive ratio in quark recombination model 80−102022
$\pi^\pm$p 100 GeV/c, π^0 and η inclusive prod., triple Regge theory test 79−6349
$\pi^\pm$p and pp collisions, charged particle average multiplicities comparison, quark model *(Russian)* 78−17065
$\pi^\pm p\rightarrow\Delta^{++}(1232)+X$, 16 GeV/c, cross sections 78−66169
$\pi^\pm p\rightarrow e^+e^-$, 18 GeV, direct pair prod. meas. 79−427
$\pi^\pm p\rightarrow e^+e^-+X$, direct and indirect pair production 79−9419
$\pi^\pm p\rightarrow e^\pm X$, 18 GeV/c, expt. results from SLAC 78−89748
$\pi^\pm$p interactions, π^0 multiplicities, 10.5, 15 MeV, differential cross sections 78−41597
$\pi^\pm p\rightarrow\mu^+\mu^-X$, 15.5 GeV/c, expt. results from SLAC 78−89748
$\pi^\pm p\rightarrow p+$anything, 6 GeV/c, unitary bounds on ang. distribs. 77−30466
$\pi^\pm p\rightarrow\pi^0X$, 100, 200 GeV/c high transverse momentum π^0 prod., quark scatt. 78−45976
$\pi^\pm p\rightarrow\pi^0X$, 14 GeV/c, test of limiting fragmentation hypothesis 77−18355
$\pi^\pm p\rightarrow\pi^0X(\eta X)$, inclusive multi-Pomeron corrections in the Regge-eikonal model 79−63557
$\pi^\pm p\rightarrow\pi^\pm+$anything, 16 and 100 GeV/c, high transverse momentum, charge asymm. 77−18339
$\pi^\pm p\rightarrow\pi^\pm+$anything, 50 to 175 GeV/c, cross sections, factorisation 77−50027
$\pi^\pm p\rightarrow\pi^\pm(\pi^0)+$anything, beam fragmentation region, scatt. asymm. *(Russian)* 77−79292
$\pi^\pm$p reactions, μ prod., Drell Yan prod. of intermediate vector bosons 78−29364
$\pi^\pm$single particle distribs. in pp, πp collisions, transverse momentum, rapidity depend. hard scatt. models 78−29361
π^+p, 100 GeV, topological cross-sections and multiplicity distribs. meas. 77−30464
$\pi^\pm$p, 100 and 175 GeV/c, inclusive scatt. results from Fermilab single arm spectrometer 78−89746

pion-proton interactions
see also pion-proton inclusive interactions; pion-proton scattering
$\pi^+p\rightarrow\pi^+p\phi$, 3.75 GeV/c, φ production angular distrib. and derived cross sections 78−58201
$\pi^-p\rightarrow\delta^-p$, $\pi^+\pi^-\pi^-\gamma\gamma$ backgrounds produced near the δ^- mass region 80−9182
characteristics at 40 and 10^4 GeV, comparison 77−61335
charge exchange reactions, model of ρ Regge trajectory 78−37226
charge-exchange differential cross-sections, unitarity bounds 77−30422
clusters, search using rapidity gap method *(Russian)* 78−41517
correlation between π and accompanying large transverse momentum particle *(Russian)* 80−86758
cross-section asymptotic limit, structure functions, Adler's sum rule and improved scaling variable 77−41843
electron pair prod. at 4.0 GeV 77−38199
fragmentation model and minimal rule 78−25019
hadronic reaction total cross sections, correl. between maxima positions, and hadronic spectroscopy *(Russian)* 79−54356
high-mass resonance enhancement by large transverse momenta selection 77−2871
identical pion interference when emitted from sources of different sizes *(Russian)* 79−93466
KNO scaling, automodel behaviour of multiplicity distrib. as function of inelasticity factor *(Russian)* 79−89213
meson diffraction dissociation and helicity conservation, Deck model description 77−38153
meson production, Δ exchange, 4 GeV/c 78−74275
meson resonances, new, search in μ channel in 11.46 GeV/c interactions 80−22641
missing mass counter experiment, non-reproducibility of data 77−22762
pion-quark scattering model for lepton pair production from qq̄ annihilation 79−13056
quark parton model, total cross sections 78−45859
quasi-potential reconstruction, scatt. theory inverse problems *(Russian)* 80−5016
radiative scattering, calc. of polarisation asymmetries using Lagrangian isobar model 79−89184
real photon prod. at large p_T, QCD and CIM anals., jets 79−89185
soft-photon anal. of πp bremsstrahlung 78−25076
strange axial vector meson non-diffracture prod. in Kp and πp interactions 80−32122
strange particle production in π^-p interactions at 5 GeV *(Russian)* 79−3040
strong exchange degeneracy analysed in Kp and πp reactions, pomeron behaviour 78−41515
two-body hypercharge exchange reactions, planar and nonplanar, cross section energy depend. 79−75790
Δ, I=3/2 high mass enhancement in 10.3 GeV/c π^+p interactions 78−66117
η and ω prod. at 10 and 16 GeV/c 77−34191
$\eta'\rightarrow\mu^+\mu^-\gamma$, in π^-p interactions at 25 and 33 GeV/c, form factors *(Russian)* 80−4984
Kp/πp total cross section ratios in SU(3) 77−46089
$p\pi^-\rightarrow$baryons by diquark-quark fusion model 80−102065
$p\pi^-$ interaction, K+hyperon prod., mass quantisation anal. *(French)* 78−70401
φ prod. in 19 GeV/c interactions, test of Zweig rule 77−2874
π prod. in pp, np, πp interactions, mass quantisation *(French)* 78−25059
$\pi^-p\rightarrow\pi^0n$, cross-section over momentum range 1.5 to 40 GeV/c *(Russian)* 79−89195

pion-proton interactions continued

$\pi^- + p \rightarrow e^+e^- + n$, 276 MeV, model independent anal. *(Russian)* 77−61317
πp, 16 GeV/c, diffr. dissoc. into $\bar{K}K^*$, $\bar{K}^*K$ 78−41594
πp, 16 GeV/c, diffr. dissoc. $\pi \rightarrow 5\pi$ 78−82252
πp, 16-GeV/c, dimuon production and obs. of low-mass continuum 78−37236
πp, beauty prod. total cross section from perturbative QCD 80−32080
πp, direct photon prod., Compton and annihilation process contrib. 80−105925
πp, inelastic charge exchange scatt., diffraction approach, convergent polynomial expansion, scaling 80−78095
πp, massive lepton pair prod., pion exchange model anal., quark parton interpretation *(Russian)* 80−82993
$\pi p \rightarrow 2\pi^+\pi^-\pi^0 p$, diffractive dissociation at 16 GeV *(Russian)* 80−22639
$\pi p \rightarrow (\pi\rho)p$, A_1 reson. diffr. prod., unitary coupled-channel anal. 78−8687
$\pi p \rightarrow (\rho\pi)p$, A_2 diffractive prod., Deck model and Pomerons 79−71733
$\pi p \rightarrow (\rho\pi)p$, diffr. dissociation, Deck model and helicity conservation 77−30344
$\pi p \rightarrow A_2 p$, diffractive process, possible one-photon exchange extraction *(Russian)* 78−444
$\pi p \rightarrow A_2 p$, diffractive prod. and Reggeon-photon coupling analogy 78−45890
$\pi p \rightarrow \Lambda K$, associated prod. of strange particles at resonance energies 77−22775
$\pi p \rightarrow \rho p$, 6 GeV/c, differential cross sections, line reversal symmetry test for baryon exchange 78−78202
$\pi p \rightarrow \Sigma K$, associated prod. of strange particles at resonance energies 77−22775
$\pi^- p$, 150 GeV/c, leading particles and diffraction dissociation, 2-, 4- and 6-prong events 80−68486
$\pi^- p$, 16 GeV/c, narrow width boson of mass 2.95 GeV obs. 78−17056
$\pi^- p$, 16 GeV/c, $\bar{\Xi}^-$ and anti-Ξ^+ prod. 79−45113
$\pi^- p$, 16 GeV.c^{-1}, strange particle production, CERN 2m H_2 bubble chamber data *(Russian)* 79−9413
$\pi^- p$, 2-14 GeV/c, total cross section, narrow baryon search 80−105922
$\pi^- p$, 200 GeV, inclusive $\Delta^{++}(1232)$ prod. 78−21478
$\pi^- p$, 200 GeV/c, inelastic diffractive-dissociation cross section 79−22151
$\pi^- p$, 21 GeV, prompt e^- associated with strange particle in strong interaction, direct evidence 79−419
$\pi^- p$, 225 GeV, search for correlated neutral strange particles and muon prod. 77−260
$\pi^- p$, 25, 33 GeV/c, mass spectrum, $\eta' \rightarrow \mu^+\mu^-\gamma$, branching ratio 80−27498
$\pi^- p$, 25 GeV/c, $\mu^+\mu^-\gamma$ mass spectrum, obs. of $\eta \rightarrow \mu^+\mu^-\gamma$ decay *(Russian)* 79−22090
$\pi^- p$, 360 GeV/c, direct e^+e^- pair prod. in liquid H, comparison with QED calcs. 77−10285
$\pi^- p$, 40 GeV, charged π correl. rapidity depend. 77−88011
$\pi^- p$, 40 GeV/c, elastic and inelastic exclusive reactions, cross sections *(Russian)* 77−67677
$\pi^- p$, 40 GeV/c, identical π interference *(Russian)* 78−472
$\pi^- p$, 40 GeV/c, multiplicity of secondary charged particles *(Russian)* 77−34190
$\pi^- p$, 40 GeV/c, secondary neutron average number, charge exchange coeffs., n inelasticity coeffs. *(Russian)* 80−32132
$\pi^- p$, 9 and 12 GeV/c, backward ω^0 and η^0 prodn 79−45100
$\pi^- p$, analysis of partial and topological cross sections at 5 GeV/c *(Russian)* 77−50002
$\pi^- p$, charged multiplicity with strange particle prod., 4.9 to 205 GeV/c 77−18334
$\pi^- p$, comparison of expt. distrib. of rapidity intervals, 60 GeV, with multiperipheral cluster model *(Russian)* 77−34189
$\pi^- p$, χ_J P-wave charmonium states, hadronic prod. cross section 80−37292
$\pi^- p$, Q production, Breit-Wigner parameters, decay modes 77−57560
$\pi^- p \rightarrow (\bar{p}n)p$, 12 GeV/c, peripheral $\bar{p}n$ prod. and decay ang. distribs. 78−33096
$\pi^- p \rightarrow (\pi^+\pi^-)n$, 17.2 GeV/c, role of A_1 exchange, Regge pole exchange 77−61325
$\pi^- p \rightarrow (\pi^+\pi^-\pi^0)n$, 12, 15 GeV/c, partial wave anal. of neutral 3π system, A-meson prod. 78−58207
$\pi^- p$ backward scattering, $S_{\parallel}$ partial wave amplitude near ηn prod. threshold 77−34176
$\pi^- p$ charge-exchange amplitude zeros from a Barrelet analysis between 1.4 and 2.3 GeV 79−13152
$\pi^- p \rightarrow \chi n$, 40 GeV/c, prod. of $\chi(2.85)$ particles *(Russian)* 78−45963
$\pi^- p \rightarrow D^0\bar{D}^0 n$, 40 GeV, D^0 hadronic decay, search for associated prod. of charmed particles 77−13990
$\pi^- p \rightarrow D^0\bar{D}^0 n$, 40 GeV/c, search for associative prod. of charmed hadrons *(Russian)* 77−6178
$\pi^- p \rightarrow d\bar{p}$, 9, 12 GeV/c, double-baryon exchange mechanism 77−82761
$\pi^- p$ Drell-Yan lepton pair prod. processes, π structure function and scaling phenomena 80−405
$\pi^- p \rightarrow \delta^- p$, near production threshold, nonobs. of $\delta^- \rightarrow \pi^+\pi^-\pi^-$ enhancement 79−13113
$\pi^- p \rightarrow \Delta^+(1236)\pi^-$, 3.0 to 5.5 GeV/c, differential cross section, fluctuations 77−22774
$\pi^- p \rightarrow e^+e^- n$, 164 MeV, differential cross section for inverse pion electroprod. *(Russian)* 79−80845
$\pi^- p \rightarrow e^+e^- n$, 275 MeV, nucleon and pion form factors *(Russian)* 77−82764
$\pi^- p \rightarrow e^+e^- n$, dispersion theory anal., pion and nucleon form factors *(Russian)* 77−10253
$\pi^- p \rightarrow e^+e^- n$, induced pseudoscalar nucleon form factor, current algebra appl. *(Russian)* 78−78212
$\pi^- p \rightarrow e^+e^- n$, induced pseudoscalar nucleon form factor, current algebra framework 79−22131
$\pi^- p \rightarrow e^+e^- n$, S and D-wave resonances parameters in quasi-threshold kinematic config. 79−63516
$\pi^- p \rightarrow \eta_{charmed} + n$, generalised quark line rule, SU_4 symm. scheme 78−54614
$\pi^- p \rightarrow \eta^0 n$, 3.3 GeV/c, differential cross section, helicity-flip amplitude *(Russian)* 78−45945
$\pi^- p \rightarrow \eta^0 n$, $d\sigma/dt$ Fermilab data, estimate of ρ-A_2 exchange degeneracy breaking 79−13162
$\pi^- p \rightarrow \eta^0 n$, Regge-pole model anal. 77−74719
$\pi^- p \rightarrow \eta^0\pi^+\pi^- n$, D, E, and δ mesons obs. at 12 and 15 GeV/c 79−3052
$\pi^- p \rightarrow \eta'n$, 15-40 GeV/c, differential cross section and singlet-octet mixing angle 79−54361
$\pi^- p \rightarrow \eta'n$, cross-section over momentum range 15 to 40 GeV/c *(Russian)* 79−89194
$\pi^- p \rightarrow \eta'n$, rare decay modes near production threshold of η^- 80−9171
$\pi^- p \rightarrow \eta'n$, Regge pole model with phenomenological residue functions 80−102077
$\pi^- p \rightarrow \eta(\eta')n$, 8.45 GeV/c, differential cross section ratio, η' decay branching 80−78094
$\pi^- p \rightarrow \eta\eta n$, 40 GeV/c, production cross sections and $\eta\eta$ angular distribs. *(Russian)* 78−78223
$\pi^- p \rightarrow \gamma\gamma n$, radiative decay widths for $\rho \rightarrow \pi\gamma$, $\omega \rightarrow \pi\gamma$ 78−467
$\pi^- p \rightarrow \eta n$, 1171 to 2267 MeV/c polarised cross section meas., partial wave anal. in resonance region 79−89182
$\pi^- p \rightarrow \eta n$, 15 to 40 GeV/c, study of $\eta \rightarrow 2\gamma$ 79−58978
$\pi^- p \rightarrow \eta n$, 15-40 GeV/c, cross sections and spin-flip amplitudes *(Russian)* 79−67609
$\pi^- p \rightarrow \eta n$, 40 GeV/c, large momentum transfer, differential cross-section meas. *(Russian)* 78−33094
$\pi^- p \rightarrow \eta n$, cross-sections to 40 GeV/c *(Russian)* 77−34182
$\pi^- p \rightarrow \eta n$, quark-line rule for η-η' complex 77−30330
$\pi^- p \rightarrow \eta n$, Reggeon field theory, behaviour of A_2 trajectory 80−22594
$\pi^- p \rightarrow \eta n$, tensor-exchange amplitude and polarisation determ. 78−45962
$\pi^- p \rightarrow \eta\pi^+\pi^- n$, axial vector and pseudoscalar resonances near 1.275 GeV, D mesons 79−30747
$\pi^- p \rightarrow \gamma\gamma n$, near threshold, perturbation theory estimates, branching ratio and ang. distrib. 79−89183
$\pi^- p \rightarrow \gamma\gamma n$, search for η_c 79−22150
$\pi^- p \rightarrow \gamma\gamma n$, tree diagrams from chiral invariant Lagrangian model 79−85337
$\pi^- p \rightarrow \gamma n$, capture rate calc. 77−82762
$\pi^- p \rightarrow \gamma n$, differential cross-sections in $\Delta(1232)$ region 79−93665
$\pi^- p \rightarrow \gamma n$, radiative capture, parameter meas. between 20 and 100 MeV by Saclay Linac *(French)* 79−411
$\pi^- p$ inelastic diffractive scatt., 33 to 60 GeV/c *(Russian)* 78−41591
$\pi^- p$ inelastic interactions at 205 GeV/c, three-fireball model, computer simulation 78−474
$\pi^- p \rightarrow J/\psi + n$ or $\chi + n$, 27-40 GeV/c, nuclear proton, upper limit on cross section *(Russian)* 78−78218
$\pi^- p \rightarrow k_S^0 K_S^0 n$ for $\pi\pi \rightarrow K\bar{K}$ 8.9 GeV/c study 77−22796
$\pi^- p \rightarrow K_S^0 K^- p$, 10 GeV/c, spin 4 meson reson. prod. 78−50050
$\pi^- p \rightarrow K_1^0 K_1^0 n$, 40 GeV/c *(Russian)* 77−261
$\pi^- p \rightarrow K_1^0 K_1^0 n$, 50 GeV/c, cross section, ang. distrib., mass spectrum *(Russian)* 77−34186
$\pi^- p \rightarrow K_s^0 K^\pm \pi^\mp n$, 3.95 GeV/c, E(1420) quantum numbers and branching ratio 80−95286
$\pi^- p \rightarrow K^- K_S^0 p$, 10 GeV/c, isospin 1 meson reson. prod. 78−50051
$\pi^- p \rightarrow K^- K_S^0 p$, 9.8 and 18.8 GeV, decay ang. distribs. and differential cross sections 79−17754
$\pi^- p \rightarrow K^- K^0 p$, 10 GeV/c, A_2 and g reson. prod. 78−82230
$\pi^- p \rightarrow K^- K^0 p$, double Regge exchange phenomenology 79−3008
$\pi^- p \rightarrow K^- K^+ n$, 6 GeV/c, f, f' and A_2^0 interference 77−253
$\pi^- p \rightarrow K^- K^+ n$, characteristics of S-wave $K\bar{K}$ enhancement at 1300 MeV 77−6158
$\pi^- p \rightarrow K^- K^+ n$, f,f' mesons, high statistics study at 6 GeV/c 77−79279
$\pi^- p \rightarrow K^- K^+ \pi^0 n$, D, E, and δ mesons obs. at 12 and 15 GeV/c 79−3052
$\pi^- p \rightarrow K^0\Lambda$, 3.5 GeV/c, Λ polarisation, high statistics meas. 80−57637
$\pi^- p \rightarrow K^0\Lambda$, threshold to 2350 MeV/c, partial wave anal. of world data 77−87997
$\pi^- p \rightarrow K^0\Lambda$, threshold to 2350 MeV, partial wave analysis 78−29349
$\pi^- p \rightarrow K^0\Lambda^0$, 1375 to 2375 MeV, new results and anal. 80−438
$\pi^- p \rightarrow K^0\Lambda^0$, 1400 to 2380 MeV/c, differential cross sections and polarisations, partial wave anal. 78−70405
$\pi^- p \rightarrow K^0\Lambda^0$, up to 1334 MeV/c, cross sections and polarisation, energy depend, phase shift anal. 78−70404
$\pi^- p \rightarrow K^0\Lambda^0$, up to 1334 MeV/c, differential cross sections and polarisation, phase shift anal. 79−412
$\pi^- p \rightarrow K^0\Lambda^0$ up to 2.375 GeV/c, resonance parameters, partial wave anal. 80−32133
$\pi^- p \rightarrow K^0\Lambda(1520)$ or $K^0(\Sigma(1385)/\Lambda(1405))$, 8.0, 10.7, 15.7 GeV/c, cross sections 77−38194
$\pi^- p \rightarrow K^0\Sigma^0$, 1395 to 2375 MeV/c, differential cross-section and polarisation meas. 80−9183
$\pi^- p \rightarrow K^0\Sigma^0$, 1395 to 2375 MeV/c, differential cross-section and polarisation 80−57635
$\pi^- p \rightarrow K^0\Sigma^0$, threshold to 1334 MeV/c, differential cross-section and polarisation 78−89733
$\pi^- p \rightarrow K^0\Sigma^0$, threshold to 1334 MeV/c, differential cross section and polarisation data 79−17755
$\pi^- p \rightarrow K^+K^-K^+K^- n$, 22.6 GeV/c, ϕ prod., Okubo-Zweig-Iizuka rule test 78−89743
$\pi^- p \rightarrow K^+K^- n$, 10 GeV/c, obs. of new structure in K^+K^- system at 2.20 GeV, width approx. 200 MeV 79−80843
$\pi^- p \rightarrow K^+K^- n$, 62 GeV, spin-5 boson resonance at 2300 MeV 80−102078
$\pi^- p \rightarrow K^+\Sigma^- n$, 5 and 8 GeV, differential cross section 78−21456
$\pi^- p \rightarrow K^+\Sigma^-$, backward scatt. at 3.5 GeV/c, polarisation parameter meas., isospin anal. 78−41572
$\pi^- p \rightarrow K^+(K^{*+})\Sigma^{*-}(1385)$, 4.35 and 4.85 GeV/c, backwared prod. of $\Sigma^{*-}(1385)$ *(Russian)* 77−6160
$\pi^- p \rightarrow \bar{K}KN$, S-wave anal., scalar mesons and branching ratios 80−13328
$\pi^- p \rightarrow K^{*0}(890)\,\Lambda^0/\Sigma^0$, 10 GeV/c, K^{*0} polarisation meas. in hypercharge exchange reaction 80−63017
$\pi^- p \rightarrow \Lambda K$, low energy, amplitude anal., Lagrangian model 80−82995
$\pi^- p \rightarrow \Lambda K^0$ or $\Lambda K^*(890)$, 8 GeV/c, differential cross section, Λ polarisation 77−34175
$\pi^- p \rightarrow \Lambda K^0(K^{*0})$, 3-6 GeV/c, Regge theory of baryon exchange 78−25074
$\pi^- p \rightarrow M^- p$, meson missing mass determ., electronic techniques 79−59315
$\pi^- p \rightarrow M^0 n$, meson missing mass determ., electronic techniques 79−59315
$\pi^- p \rightarrow N^{*0}\pi^0$, 9, 12 GeV/c, nucleon exchange obs. 77−71529
$\pi^- p \rightarrow n e^+ e^-$ virtual photon polarisation, PCAC anal. 78−12930
$\pi^- p \rightarrow n k_S^0 K_S^0$, 6, 7 GeV/c, cross section, decay ang. distribs. and S-wave amplitude 79−49539
$\pi^- p \rightarrow n\pi^-\pi^-\pi^+\pi^+$, 12 GeV/c, Δ^-, ρ and f prod., baryon exchange 79−423
$\pi^- p \rightarrow n\pi^-\pi^+$, 12 GeV/c, ρ and f prod., differential cross section, baryon exchange 79−423

pion-proton interactions continued
$\pi^-p \to n\pi^-\pi^+\pi^0$, 12 GeV/c, ω prod., differential cross section, baryon exchange 79−423
$\pi^-p \to n\pi^0_s$ in water, H-bond breaking *(Russian)* 79−94866
$\pi^-p \to n\pi^+\pi^-$, 8 GeV/c, backward meson and baryon reson. prod. 79−415
$\pi^-p \to \omega n$, 15-40 GeV/c, cross sections and density matrix elements *(Russian)* 80−37302
$\pi^-p \to \omega n$, 15-40 GeV/c, differential cross sections meas. 79−93464
$\pi^-p \to \omega n$, 20-200 GeV/c, prod. cross section, Regge formalism test 77−26546
$\pi^-p \to \omega n$, 6 GeV/s, abnormal polarisation effect in Ar, two-Reggeon exchange model *(Russian)* 77−10282
$\pi^-p \to \omega n$, c.m. momentum 40 to 200 MeV/c, cross section meas. 79−75789
$\pi^-p \to \omega n$, Reggeon cuts and reaction description *(Russian)* 78−45947
$\pi^-p \to \omega\pi^- p$, 11.2 GeV/c, partial wave anal. of g-meson prod. 78−78220
$\pi^-p \to p_{fast}\pi^+\pi^-\pi^-$, 9, 12 GeV/c, backward meson prod., quasi two body processes, A_1^-, A_2^- prod. 79−413
$\pi^-p \to p_{forward}X^-$, search for nonstrange exotic mesons, baryon exchange 77−50015
$\pi^-p \to p\pi^+\pi^-\pi^-$, 9 and 12 GeV/c, backward enhancement in A_1 region and A_2 prod. 78−45970
$\pi^-p \to pFpn$, M^- state in pn search, M^0 state decay 79−36108
$\pi^-p \to pd$, 10 and 16 GeV/c, cross section meas. 78−21466
$\pi^-p \to$ pions + X, 40 GeV/c, transverse pion momenta depend. on secondary particle multiplicity *(Russian)* 78−33103
$\pi^-p \to \bar{p}pn$, 10 and 16 GeV/c, anal. of $\bar{p}p$ and $\bar{p}n$ pairs 79−75788
$\pi^-p \to p\bar{p}n$, 18 GeV, $p\bar{p}$ resonant state partial wave anal. 80−32134
$\pi^-p \to pp\bar{p}\pi^-$, narrow $p\bar{p}$ reson. at 2020 MeV, 2200 MeV 77−67682
$\pi^-p \to p\bar{p}\pi p$, 16 GeV/c, high statistics search for 2.95 GeV $\bar{p}p\pi^-$ mass enhancement 79−85344
$\pi^-p \to p\pi^-$, 6 GeV/c, differential cross sections, line reversal symmetry 78−41564
$\pi^-p \to p\pi^-$, 6 GeV/c, differential cross sections, line reversal symmetry test for baryon exchange 78−78202
$\pi^-p \to p\pi^-\pi^-$, 4 GeV/c backward scatt., interference between $I_u=1/2$ and $I_u=3/2$ baryon exchange amplitudes 78−70412
$\pi^-p \to p\pi^-\pi^0$, 9 and 12 GeV/c, backward e^- prod. 78−8704
$\pi^-p \to p\pi^+\pi^-\pi^-$, 16 GeV/c, prism plot anal., reaction mechs. 77−6174
$\pi^-p \to p\pi^+\pi^-\pi^-$, impact param. anal. at 9 and 12 GeV/c 78−8706
$\pi^-p \to p\rho^-$, 6 GeV/c, line reversed reaction, Δ exchange, ρ^- decay 78−12926
$\pi^-p \to \phi n$, 1.6-2.0 GeV/c, total cross-section 77−87998
$\pi^-p \to \phi n$, OZI rule violation in central region 77−61262
$\pi^-p \to \phi n$, quark line rule, violations 80−52530
$\pi^-p \to \phi n$, study of second-order hadronic process 79−22135
$\pi^-p \to \phi n$, violation of Iizuka-Okuba-Zweig rule 77−65173
$\pi^-p \to \phi\phi n$, 22.6 GeV/c, cross section meas. 78−37242
$\pi^-p \to \pi^-p\pi^+\pi^-$, 3.93 GeV/c, prism plot anal. 78−54650
$\pi^-p \to \pi^-p\pi^+\pi^-\pi^0$, 4.5 GeV, $\Delta\pi\pi$ system study 79−93453
$\pi^-p \to \pi^-\phi p$, 10 GeV/c, prod. cross section meas. 77−65174
$\pi^-p \to \pi^-\pi^-\pi^+ + $, 13 GeV, prism-plot anal. 79−36109
$\pi^-p \to \pi^-\pi^-\pi^+ p$, 147 GeV/c, diffraction dissociation 77−2869
$\pi^-p \to \pi^-\pi^-\pi^+ p$, 63, 94 GeV/c, A_2 meson prod. from partial wave anal. 80−37303
$\pi^-p \to \pi^-\pi^-\pi^+ p$, 63, 94 GeV/c, A_1 meson existence from partial wave anal. 80−37304
$\pi^-p \to \pi^-\pi^-\pi^+ p$, 63, 94 MeV/c, A_3 meson, 3π resonances in 2^- partial waves 80−37305
$\pi^-p \to \pi^-\pi^-\pi^+\pi^0 p$, 11.2 GeV/c, study of A_2^- decay to eta + pion$^-$ 77−22806
$\pi^-p \to \pi^-\pi^-\pi^+\pi^0 p$, 11.2 GeV/c, anal. of $\omega\pi^-$ system prod. 77−88012
$\pi^-p \to \pi^-\pi^0 p$, energetically independent phase anal. of $\pi^-\pi^0$-interaction *(Russian)* 77−88007
$\pi^-p \to \pi^-\pi^+ n$, 203-357 MeV, integrated cross section, chiral symmetry breaking parameter 80−32125
$\pi^-p \to \pi^-\pi^+ n$, below 1400 MeV, PS11 contrib. threshold K-matrix, chiral symmetry breaking 80−32126
$\pi^-p \to \pi^-\pi^+ n$, narrow epsilon resonance under rho 80−5021
$\pi^-p \to \pi^-\pi^0 n$, S-wave dipion production 78−25069
$\pi^-p \to \pi^-\pi^+ n(\rho^0+\omega)$, comparative study of ρ^0, ω, $K^{*0}(890)$ and $\bar{K}^{*0}(890)$ production 78−58200
$\pi^-p \to \pi^-\pi^+\pi^- p$, partial-wave anal., analyticity and unitarity 77−88000
$\pi^-p \to \pi^-\pi n$, $\pi^+\pi^-$ angular distrib. in invariant mass region 78−58209
$\pi^-p \to \pi^0 n$, 15 to 40 GeV/c, differential cross sections, (non)spin-flip amplitude parametrisation 79−75800
$\pi^-p \to \pi^0 n$, 40 GeV/c, large momentum transfer, high statistics meas. 78−17053
$\pi^-p \to \pi^0 n$, 400-600 MeV, forward scatt. differential cross sections 78−93902
$\pi^-p \to \pi^0 n$, 618-2724 MeV, differential cross section and polarisation meas. 77−6162
$\pi^-p \to \pi^0 n$, charge exchange parameter meas. between 20 and 100 MeV by Saclay Linac *(French)* 79−411
$\pi^-p \to \pi^0 n$, charge exchange polarisation, Gribov Reggeon calculus, derivative rule, absorpt. model alternative 77−46076
$\pi^-p \to \pi^0 n$, differential cross section and charge independence principle 78−17045
$\pi^-p \to \pi^0 n$, $d\sigma/dt$ Fermilab data, estimate of ρ-A_2 exchange degeneracy breaking 79−13162
$\pi^-p \to \pi^0 n$, helicity nonflip amplitude in Reggeon calculus 77−22765
$\pi^-p \to \pi^0 n$, polarisation meas. 617 to 2267 MeV/c 79−9401
$\pi^-p \to \pi^0 n$, $\pi^0 \to \gamma\gamma$, 618-2724 MeV/c pions, high statistics differential cross sections meas. 77−13973
$\pi^-p \to \pi^0 n$, resonance region, differential cross section, polarisation parameter 77−22773
$\pi^-p \to \pi^0 n$, secondary trajectories propagators in Reggeon field theory, interacting Reggeons and Pomerons 79−40764
$\pi^-p \to \pi^0 n$ or ηn, nondiffractive reactions, scaling of differential cross sections 78−62462
$\pi^-p \to \pi^0 n$ or γn, Panofsky ratio for pions, meas. using liquid H target 77−50000
$\pi^-p \to \pi^0\pi^0 n$, 10 GeV, $\pi^0\pi^0$ mass distribs. calc. 78−41586
$\pi^-p \to \pi^0\pi^0 n$, 200, 240 MeV, total near-threshold cross section, isotopic amplitudes *(Russian)* 80−37296
$\pi^-p \to \pi^0\pi^0 n$, 6, 8, 12 GeV, $\pi^0\pi^0$ S wave and I=0 amplitude 80−18144
$\pi^-p \to \pi^0\pi^0 n$, matrix element calc. and verification *(Russian)* 79−9396
$\pi^-p \to \pi^0\pi^0 n(\pi^0\gamma n)$, 270 MeV, γ-ray spectra, cross-sections meas. *(Russian)* 77−22767

pion-proton interactions continued
$\pi^-p \to \pi^+ X^-$, 2.6 GeV/c, d proton screening correction and Glauber parameter 80−9175
$\pi^-p \to \pi^+\pi^- 3\gamma n$, obs. of $\eta' \to \omega\gamma$ decay rate 77−74683
$\pi^-p \to \pi^+\pi^- n$, 12, 15 GeV/c, $f^0(1270)$ prod. cross sections, decay density matrix elements 78−33095
$\pi^-p \to \pi^+\pi^- n$, 12, 15 GeV/c, $\pi^+\pi^-$ ang. distrib. in mass range 0.8 to 2.2 GeV/c^2 78−66164
$\pi^-p \to \pi^+\pi^- n$, 17.2 GeV/c, model independent partial wave anal. of $\pi^+\pi^-$ prod. at low 4-momentum transfer 79−54363
$\pi^-p \to \pi^+\pi^- n$, 17.2 GeV/c meas. with transversely polarised target 77−30449
$\pi^-p \to \pi^+\pi^- n$, 17.3 GeV/c, polarised p, $\pi^+\pi^-$ partial wave anal. for low four-momentum transfer 79−63533
$\pi^-p \to \pi^+\pi^- n$, 1.33-1.38 GeV, isobar prod. near threshold, isobar model partial wave anal., bag model 79−93456
$\pi^-p \to \pi^+\pi^- n$, amplitude anal. of $\pi\pi$ scatt. 1.0 to 2.08 GeV, f, g, h mesons 79−3042
$\pi^-p \to \pi^+\pi^- n$, polarization measurements and a narrow $\varepsilon(750)$ 79−63514
$\pi^-p \to \pi^+\pi^- n$, $\pi\pi$ scatt. partial wave anal. f, g and h mesons 80−5015
$\pi^-p \to \pi^+\pi^- n$, $\pi\pi$ scatt. phases near threshold, pseudoperipheral approx. *(Russian)* 79−71763
$\pi^-p \to \pi^+\pi^- n$, rescattering effects, π ang. and momentum distribs. 78−93903
$\pi^-p \to \pi^+\pi^- n$ ($K^+K^- n$), 1.98, 2.41 GeV/c, pole parameters determ. 78−25075
$\pi^-p \to \pi^+\pi^- n$ reaction near threshold, cross-section estimation at 190 and 200 MeV *(Russian)* 77−2865
$\pi^-p \to \pi^+\pi^-\pi_0 p$, phase of Deck model 77−22709
$\pi^-p \to \pi^+\pi^-\pi^0 n$, 12, 15 GeV/c, prod. of A_2^0 (1310) and ω^* (1675) 78−74283
$\pi^-p \to \pi^+\pi^+\pi^-\pi^- n$, D, E, and δ mesons obs. at 12 and 15 GeV/c 79−3052
$\pi^-p \to \pi^+\pi^+\pi^-\pi^- n$, D, E, and δ mesons, obs. at 12 and 15 GeV/c 79−9410
$\pi^-p \to \psi n$, 8.2-9.8 GeV/c, upper limit on prod. cross-section determ. 78−41578
$\pi^-p \to \psi n$, generalised Veneziano models 80−22638
$\pi^-p \to \rho^0_0 n$, 17 GeV, polarised target, partial wave analysis 79−45106
$\pi^-p \to \rho^0_0 n$, Reggeon cuts and reaction description *(Russian)* 78−45947
$\pi^-p \to \rho^0\pi^- p$, Reggeised Deck model, Steinmann relation 78−45973
$\pi^-p \to \rho\pi p$, three body phenomenology for elementary particle systems 79−80846
$\pi^-p \to X^- p$, background produced near δ meson mass region 79−36096
$\pi^-p \to X^- p$, study of $\delta(970)$ meson 79−9428
$\pi^-p \to X^0 n$, $\pi^+\pi^-$ decay mode anal. 77−67670
$\pi^-p \to X^0 n$, $X^0 \to \gamma\gamma$, 15 and 40 GeV/c, cross sections *(Russian)* 77−34183
$\pi^-p \to X^0 n$, $X^0 \to \gamma\gamma$, four-momentum transfer region 0.38-0.79 (GeV/c)^2 77−67656
$\pi^-p \to Xn$, 40 GeV/c, $X(2.85) \to 2\gamma$ obs. 78−25047
π^+p, 10 to 16 GeV/c, hypercharge-exchange reactions 80−13335
π^+p, 16 GeV, reaction impact parameter, expt. methods of estimation 79−13158
π^+p, 16 GeV/c, narrow mass enhancement at 1.36 GeV in diffractive (πN) systems 79−45109
π^+p, 4.2 GeV/c, topological cross sections *(Russian)* 78−89732
π^+p, 6 to 100 GeV/c, $P_\perp$ distribs. of k^0, π^-, ρ^0, f, equilibrium temp. 79−49540
π^+p, angular correl. reson. prod. effect at 16 GeV/c 77−88014
π^+p, strange-particle cross-sections at 10.3 GeV/c 77−87999
π^+p 3.6 GeV/c, nonstrange and single pion final state cross-section meas. 77−50001
$\pi^+p \to 3\pi^+\pi^- n$, diffractive dissociation at 16 GeV *(Russian)* 80−22639
$\pi^+p \to (K^+K^-\pi^-)p$, $K\bar{K}^*$ mass enhancement 77−26547
$\pi^+p \to (N\pi)^-\pi^+\pi^+\pi^-$, 4.5 GeV centre-of-mass energy, resonance prod. 78−70402
$\pi^+p \to (\pi^+p\bar{p})p$ 50 GeV/c, narrow baryonium states, diffractive prod. cross sections 80−442
$\pi^+p \to (\pi^+\pi^-)\Delta^{++}$ 16 GeV/c, amplitude anal. in rho region 78−66163
$\pi^+p \to (\pi^+\pi^-\pi^0)\Delta^{++}$, 16 GeV/c, partial wave anal., ω^* and A_2^0 80−63033
$\pi^+p \to (\rho^0,\omega)\Delta^{++}(1238)$, q_L=7.1 GeV/c, role of new exchanges *(Russian)* 79−54355
π^+p collisions at 10.5 GeV/c, new neutral particle search 77−50012
$\pi^+p \to \bar{D}^0 C_1^{++}$, 4.5 GeV, prod. cross sections, decay branching ratios 78−41576
$\pi^+p \to \Delta_f^{++}\bar{p}p$, 9.8 GeV/c, narrow $\bar{p}p$ state search 80−57636
$\pi^+p \to \Delta^{++}\pi^+\pi^-\pi^0$, 15 GeV/c, A_1, A_3 and A_4 prod. 77−82780
$\pi^+p \to e^+e^-$, 4.0 GeV/c, direct and via ρ^0, ω^0 decay 77−26542
$\pi^+p \to \eta\Delta^{++}$, quark-line rule for η-η' complex 77−30330
$\pi^+p \to$ four prong final states, 10.3 GeV/c, resonance prod. cross-sections 78−74276
$\pi^+p \to K^+K_S^0 p$, forward A_2^+ prod. at 12.7 GeV/c 79−22149
$\pi^+p \to K^+\Sigma^+$, 1.721 to 1.954 GeV c.m. energy, cross section, ang. distrib., polarisation 78−4872
$\pi^+p \to K^+\Sigma^+$, 4, 7, 11.5, 70 GeV/c, weak exchange degeneracy, Navelet-Stevens model generalisation 79−93462
$\pi^+p \to K^+\Sigma^+$, 7 and 11.6 GeV/c, Σ^+ polarisation meas. 78−41573
$\pi^+p \to K^+\Sigma^+$, exchange degeneracy in hypercharge exchange reacts. 78−41581
$\pi^+p \to K^+\Sigma^+$, exchange degeneracy in hypercharge exchange reacts. 78−82239
$\pi^+p \to K^+\Sigma^+$ and $K^-p \to \pi^-\Sigma^+$, exchange degeneracy 80−57634
$\pi^+p \to K^+\Sigma^+$ and line reversed reaction $K^-p \to \pi^-\Sigma^+$, simple Regge pole model 80−78093
$\pi^+p \to K^+\Sigma^+(1385)$, 16 GeV/c, spin density matrix of $\Sigma^+(1385)$ by statistical tensor method 78−37235
$\pi^+p \to K^+Y^+$, $Y^+=\Sigma^+$ or $Y^{*+}(1385)$, 7 GeV/c, hypercharge exchange in line-reversed π^+p and K^-p 80−82998
$\pi^+p \to K^+Y^*$, 11.5 GeV/c, line reversed reaction, $Y^*(1385)$ diff. cross section and decay ang. distribs. 79−89193
$\pi^+p \to K^+Y^*(1385)$, 11.5 GeV/c confirmation of exchange degeneracy predictions in line reversed reacts. 78−82247
$\pi^+p \to K^{*+}(890)Y^+$, $Y^+=\Sigma^+$ or $Y^{*+}(1385)$, 7 and 11.5 GeV/c, hyperon polarisation, vector meson decay angular distribs. 80−82997
$\pi^+p \to \Lambda K^+\pi^-$, 10.3 GeV/c, p diffractive dissociation into ΛK^+ and $(\Sigma K)^+$ 78−45966
$\pi^+p \to \Lambda K x\pi$, 10.3 GeV/c, threshold enhancements in ΛK mass spectra 78−74284

pion-proton interactions continued
$\pi^+p\rightarrow$meson resonances, 15 GeV/c, SLAC bubble-chamber expt. 78−41595
$\pi^+p\rightarrow n\pi^+\pi^+\pi^+\pi^-$, reaction, extraction from background 78−880
$\pi^+p\rightarrow\omega\Delta^{++}(1236)$ 16 GeV/c, cross-sections, spin-density matrix elements 77−10284
π^+p phase shift anal., 1.3-2.4 GeV, continuum ambiguity 77−22778
π^+p polarisation near backward direction, partial waves anal., comparison with model predictions 77−30421
$\pi^+p\rightarrow p\pi^+$, 6 GeV/c, differential cross sections, line reversal symmetry test for baryon exchange 78−78202
$\pi^+P\rightarrow p\pi^+\pi^+\pi^-$, 15 GeV/c, A_1, A_3 and A_4 prod. 77−82780
$\pi^+p\rightarrow p\pi^+\pi^+\pi^-$, 3.1 GeV.c^{-1}, contrib. of reson. states of cross section, Regge pole exchange model anal. *(Russian)* 79−9403
$\pi^+p\rightarrow\pi^0\Delta^{++}(1236)$, $\eta\Delta^{++}$, $\eta'\Delta^{++}$, 16 GeV/c, cross-sections, spin density matrix elements determ. 78−21467
$\pi^+p\rightarrow\pi^+(\pi^+n)$, 16 GeV/c, prod. and decay processes, Drell-Hiida-Deck model predictions 77−41864
$\pi^+p\rightarrow\pi^+(\pi^+n)$, partial-wave struct. of Drell-Hiida-Deck amplitude in diffractive πN system 77−41863
$\pi^+p\rightarrow\pi^+pp\bar{p}$, 10.3 GeV/c, Δ^{++} prod. obs. 78−21453
$\pi^+p\rightarrow\pi^+p\pi^0$, 1 GeV, N^{*+}, N^{*+} and ρ^+ prod., single π distribs. 77−74716
$\pi^+p\rightarrow\pi^+p\pi^0$, p diffractive dissociation, ρ^+ prod., one-pion-exchange model 78−21451
$\pi^+p\rightarrow\pi^+p\pi^0\pi^0$, 4 GeV/c, study of $\Delta^{++}\pi^0\pi^0$ events, comparison with $\pi^+\pi^-$ data 79−22132
$\pi^+p\rightarrow\pi^+p\pi^0\pi^0$, $\Delta^{++}\pi^0\pi^0$ event selection, 4 GeV/c, comparison with $\pi^+\pi^-$ data prediction 78−82232
$\pi^+p\rightarrow\pi^-p\pi^+\pi^0(p\pi^0)$, 3.5 GeV/c, cross-sections meas. 77−71527
$\pi^+p\rightarrow\pi^+\pi^-\Delta^{++}$, 7.1 GeV/c, model-independ. anal. 78−17044
$\pi^+p\rightarrow\pi^+\pi^-\Delta^{++}$, narrow epsilon resonance under rho 80−5021
$\pi^+p\rightarrow\pi^+\pi^-\Delta^{++}$, polarization measurements and a narrow $\varepsilon(750)$ 79−63514
$\pi^+p\rightarrow\pi^+\pi^-\Delta^{++}$, S-wave dipion production 78−25069
$\pi^+p\rightarrow\pi^+\pi^-\pi^0n$, 12 and 15 GeV, partial wave analysis, spin, parity production 78−29359
$\pi^+p\rightarrow\pi^+\pi^+n$, 12.5 GeV, meas. and anal. of $\pi^+\pi^-$ system 77−82788
$\pi^+p\rightarrow\pi\pi N$, 1.4-1.7 GeV, isobar model partial wave anal., baryon resonance decay 80−86750
π^+p radiative scatt., bremsstrahlung peak in Δ^{++} resonance region, mag. moment from low energy theorem 78−45944
$\pi^+p\rightarrow\rho^0\Delta^{++}$, 3.75 GeV/c, amplitude anal., t-depend. 78−74274
$\pi^+p\rightarrow\rho^0\Delta^{++}$, quasi eikonal model anal., πP cut contribution, enhancement coefficients *(Russian)* 79−40798
$\pi^+p\rightarrow\rho^0\Delta^{++}$ or $\omega\Delta^{++}$, positivity conditions in joint vector-meson Δ prod. 77−13975
$\pi^+p\rightarrow\rho^0\Delta^{++}(1236)$ or $\omega\Delta^{++}(1236)$, 10.3 GeV/c, cross-section meas. 78−82248
$\pi^+p\rightarrow\rho^0\Delta^{++}(\omega\,\Delta)$, $\Delta I=1$ rule, model tests from polarisation expts. 77−30471
$\pi^+p\rightarrow\Sigma^+(1385)K^+(K^{*+}(890))$ 10.3 GeV.c, Y*K and Y*K* prod. 79−49544
$\pi^+p\rightarrow\Sigma Kx\pi$, 10.3 GeV/c, threshold enhancements in ΛK mass spectra 78−74284
$\pi^\pm p$, 14 GeV/c, N diffr. dissoc., bubble-chamber anal. 78−66175
$\pi^\pm p$, 16 GeV, anomalous prod., f and A_2^0 tensor mesons as source 78−70411
$\pi^\pm p$, 16 GeV/c, $\delta(970)$ and D(1285) prod. and decay, branching ratios 77−46084
$\pi^\pm p$, 18 GeV/c, prod. limits on impaired electrons or positrons 78−45967
$\pi^\pm p$, A meson prod., Regge model, polarisation anal. 78−41577
$\pi^\pm p$, effective radius and total cross sections Pomeranchuk theorem confirmation *(Russian)* 78−89737
$\pi^\pm p$, high-energy, react. differences and annihilations 78−74279
$\pi^\pm p$, total cross section determ., 200 to 370 GeV/c 79−26352
$\pi^\pm p\rightarrow\Delta K^+\pi^\pm$, proton dissociation in 3-body final states 79−85338
$\pi^\pm p\rightarrow p\pi^+\pi^\pm\pi^-$, 16 GeV/c, clustering, multidimens. study using Yang variables 80−5020
$\pi^\pm p\rightarrow p\pi^\pm\pi^+\pi^-$, 16 GeV/c, dynamical mechanism from cluster anal. *(Russian)* 80−42499
$\pi^\pm p\rightarrow\pi^\pm+X$, 140-175 GeV, differential cross-section meas. 77−18345
$\pi^\pm p\rightarrow\pi^\pm(N\pi)^+$, 16 GeV/c, spin-parity anal. of diffractively prod. low-mass Nπ 78−17055
$\pi^\pm p\rightarrow\pi^+\pi^0p$, phase anal. of $\pi^+\pi^0$ and $\pi^-\pi^0$ interactons *(Russian)* 79−30748
$\pi^\pm p$ reactions, 16 GeV/c, strange particle prod. in 3 and 4 body final states 78−475
$\pi^\pm p\rightarrow\rho^\pm p$, radiative corrections and vacuum pole exchange *(Russian)* 79−58964
$\Pi^-\rho\rightarrow\bar{p}d$, $\bar{p}$ prod. obs. near 3.75 GeV/c threshold momentum 80−52533
$\pi^+\rho\rightarrow\Delta^{++}\pi^+\pi^-\pi^0$, 15 GeV/c, $\omega'(1675)$ prod. 78−37241
$\pi^-p\rightarrow\eta n$, 724-2723 MeV/c, differential cross sections, baryon resonance non-zero couplings 79−71761
$\pi^-p\rightarrow\eta n$, Fermilab energy, Regge pole model 79−17762
$\pi^-p\rightarrow\gamma n$, n-n scatt. length from photon spectra 79−67600

pion-proton scattering
see also pion-proton interactions
backward πN scattering at 3.5 GeV/c, data anal. by Regge type models 77−61314
Bounds on slope of diffraction peak and zeros of absorptive differential cross sections 78−74282
bremsstrahlung, near Δ resonance, external emission dominance 77−10280
Chou-Yang model, π form factor 78−45960
cross sections, large angle, fluctuations, 2-9 GeV/c 78−37228
differential cross section and phase shifts, 20-96 MeV 77−6147
differential cross section energy dependence, large angles, 2-9.7 GeV/c 78−37227
differential cross sections, 400-590 MeV/c 77−6148
diffractional approx., few-nucleon nuclei, nuclear structure *(Russian)* 78−650
elastic, methodics of identification in bubble chamber *(Rumanian)* 79−63520
elastic and charge exchange, resonance region, data amalgamation 77−22770
elastic scattering, relativistically invariant scaling law 77−13986
forward scattering amplitudes, zeros and low energy parameters 79−9400

pion-proton scattering continued
forward symmetric amplitude, asymptotic parametrisation by continuous moment sum rules 77−18341
hadron-nucleon total cross-section, regularities and systematics 77−38205
high energy diffraction scatt., model with shielded pomeron, pp, πp, Kp investigation 78−17004
impact param. anal. in range 50-175 GeV/c 77−22799
impact parameter representation *(Russian)* 80−5019
large angle scatt. of particles with spin, nonautomodel corrections, Logunov-Tavkhelidze quasipot. approach *(Russian)* 79−54360
large momentum transfer, multiple-scattering model, three-quark proton 80−63031
partial wave anal., 0.8-2.0 GeV/c, resonance parameters, existence of $D_{35}(1925)$ 77−22771
polarisation meas., 100 GeV 79−63527
spin-flip amplitude in 300GeV elastic scatt. 79−93461
string model, string geometrical shape and overlapping functions 79−13073
ZGS, strong interaction counter expts. 80−91305
πp, quark-diquark elastic scatt., diquark fragments, large transverse momentum baryon production 80−47330
$\pi p\rightarrow\eta n$, pion-nucleon charge exchange scatt. and scaling of differential cross section 79−26348
$\pi p\rightarrow p+$pions, average transverse momentum, baryon exchange 77−30448
$\pi p\rightarrow\pi p$, polarisation phenomena in hadron collisions at small momentum transfer *(Russian)* 78−58196
$\pi p\rightarrow\pi p\gamma$, 269, 298, 324 MeV 79−22133
$\pi p\rightarrow\pi p\gamma$, 298 Mev, non-relativistic calc. 77−71528
π^-p, 1180 to 1360 MeV, polarisation parameter 77−61316
π^-p, 12 to 24 GeV, leading effective trajectories, residues, anal. 79−421
π^-p, 2-14 GeV/c, total cross section, narrow baryon search 80−105922
π^-p, 360 GeV/c, total and elastic cross-sections meas., charged-particle multiplicity distrib. anal. 77−18357
π^-p, 40 GeV/c, forward elastic scatt. amplitude, real/imaginary part ratio *(Russian)* 79−22147
π^-p, 9, 12 GeV/c, backward elastic scatt. 77−82761
π^-p, cross section, multiple scatt. model anal. 79−36105
π^-p, diffraction scatt. slope parameter oscillation, lines of zeros, convergent polynomial expansion 79−93455
π^-p, elastic and coherent cross-section at 40 GeV/c using propane bubble chamber 80−27524
π^-p, elastic backscattering, 25 to 38 GeV/c *(Russian)* 77−54121
π^-p, elastic differential cross-sections at 8 and 16 GeV/c 77−71536
π^-p, in C, 40 GeV/c, secondary particle multiplicities *(Russian)* 78−89922
π^-p, slope of forward diffraction peaks 79−36103
π^-p, unitarity violation at 100 GeV 79−71764
π^-p backward elastic, 2.93 and 3.25 GeV/c, polarisation meas. 77−2863
π^-p backward elastic scatt., 3.5 GeV/c, polarisation parameter, isospin anal. 77−13974
π^-p backward scatt., 1.28-3.0 GeV/c, cross-sections, ang. distrib. meas. 78−41575
π^-p charge exchange scatt. from 618-2267 MeV/c, polarisation meas. 77−30420
π^-p differential cross section, diffraction peak compatibility with unitary bounds 79−97610
π^-p elastic differential cross section, 0.4 to 2.15 GeV/c 77−22772
π^-p elastic scatt., 2.22-3.5 GeV/c, backward polarisation 80−82999
π^-p elastic scatt., 30-140 GeV/c, differential cross section in Coulomb interference region 78−89741
π^-p elastic scatt., 3.42-5.03 GeV, narrow baryon search in differential cross section 80−105921
π^-p elastic scatt., 450-560 MeV, polarisation parameter *(Russian)* 80−37295
π^-p elastic scatt., cross section meas. across threshold 79−75789
π^-p elastic scatt. at 490 and 600 MeV, polarisation parameter meas. *(Russian)* 80−42496
π^-p elastic scatt. near η threshold, cusp discontinuity, nonspin-flip elastic amplitude 80−22635
π^-p elastic scattering, 2 GeV/c region, high precision meas. 80−91109
$\pi^-p\rightarrow\eta n$, ρ and A_2 exchange amplitudes, 2.5-200 GeV/c 77−34174
$\pi^-p\rightarrow p\pi^-$, 3.0 to 5.5 GeV/c, differential cross section, fluctuations 77−22774
$\pi^-p\rightarrow p\pi^-$, backward scatt. cross sections at 25, 38 GeV/c 77−50009
$\pi^-p\rightarrow\pi^-p$, 291.5 and 308 MeV, polarisation parameters meas. 79−6347
$\pi^-p\rightarrow\pi^-\pi^-\pi^+p$, 25 GeV/c, boson states 77−30451
$\pi^-p\rightarrow\pi^0n$, 20-200 GeV, pure ρ-Regge-pole exchange model in forward direction 77−38203
$\pi^-p\rightarrow\pi^0n$, charge exchange polarisation parameter meas., 617 to 2267 MeV/c 78−82231
$\pi^-p\rightarrow\pi^0n$, pion-nucleon charge exchange scatt. and scaling of differential cross section 79−26348
$\pi^-p\rightarrow\pi^0n$, pure $\rho+\rho'$ Regge-pole anal. for 20-200 GeV/c forward scatt. 78−8702
$\pi^-p\rightarrow\pi^0n$, ρ and A_2 exchange amplitudes, 2.5-200 GeV/c 77−34174
π^+p, 32 GeV/c, elastic scatt. and multiplicities, total and differential cross sections *(Russian)* 80−52548
π^+p, 47.9 MeV, differential cross section and phase shifts 79−22123
π^+p, 4.4-6.0 GeV/c, slope of forward strong interaction peak 77−30424
π^+p, anal. of reson. multipoles, γ-ray spectra calc. *(Russian)* 79−26346
π^+p, Born amplitude, unitarity sufficiency condition 79−86068
π^+p, elastic scatt., 6 and 12 GeV/c, polarisation meas. using CERN polarised d target 79−49542
π^+p, elastic scatt. 50 to 200 GeV peripheral Pomeron explanation 79−40803
π^+p, elastic scatt. in Coulomb-nuclear interf. region at 42.5 and 52.2 GeV/c 77−18332
π^+p, nonrelativistic scatt., Coulomb corrections 80−82994
π^+p, scattering amplitudes, integral axiomatic restrictions *(Russian)* 77−82685
π^+p, spin rotation parameter meas. in 45 GeV/c scatt. *(Russian)* 77−6169
π^+p, up to 10 GeV/c, partial wave anal. using impact parameter approach, Δ resonances 77−22769
π^+p at 45 GeV/c, polarisation parameter *(Russian)* 77−34179
π^+p backward scatt., 1.25-2.0 GeV/c, differential cross section meas. 78−37229
π^+p elastic differential cross section, 0.4 to 2.15 GeV/C 77−22772

pion-proton scattering continued
π^+p elastic partial wave amplitude construction from knowledge of Barrelet zeros 77−22777
π^+p elastic scatt., phase shift Coulomb corrections 79−67605
π^+p elastic scattering, 100 GeV/c, polarisation meas. 77−30440
π^+p forward scatt. amplitude, analytic parametrisation of high energy crossing 77−57568
π^+p inelastic diffr. scatt. at 42.5 and 52.2 GeV/c *(Russian)* 77−82777
π^-p→pπ^- and $\bar{p}$p→$\pi^-\pi^+$ line reversed channels, 6 GeV/c, differential cross section comparison 77−74708
π^+p→π^+p, high energy, polarisation, spin correls., s-channel helicity amplitudes 77−30435
π^+p→π^+p, parameter meas. between 20 and 100 MeV by Saclay Linac *(French)* 79−411
π^+p→π^+pγ, 165 MeV, monotonically decreasing photon energy spectrum, no $\Delta^{++}(1232)$ bump 80−68476
π^+p scatt., 291.4 and 310.0 MeV, polarisation parameter 78−41571
$\pi^\pm$p, 0 to 350 MeV, elastic and charge-exchange scatt., partial wave anal., Δ resonances, review 80−63018
$\pi^\pm$p, 100 GeV/c, polarisation parameters and ang. distribs. for elastic scatt. 80−95287
$\pi^\pm$p, 100 GeV/c scatt., polarisation param. meas. 77−71534
$\pi^\pm$p, 2-9 GeV/c, large angle elastic scatt. cross sections, parton and bootstrap model test 78−78209
$\pi^\pm$p, 269 MeV, 298 MeV, bremsstrahlung cross-section and soft-photon theorem 78−89730
$\pi^\pm$p, 29.1 to 89.4 MeV, differential cross sections 79−85329
$\pi^\pm$p, 378 to 625 MeV/c, differential cross section meas. 79−85328
$\pi^\pm$p, 39, 44.5 GeV/c, differential cross section meas. 77−74720
$\pi^\pm$p, 40-45 GeV, Regge anal. differential cross sections *(Russian)* 78−25081
$\pi^\pm$p, 50, 100, 200 GeV/c. differential cross sections meas. 77−18329
$\pi^\pm$p, elastic differential and total cross-sections, 50 to 175 GeV/c 77−74721
$\pi^\pm$p, elastic scatt. and diffractive dissociation, Regge model with $\alpha_P(0)>1$ *(Russian)* 80−57630
$\pi^\pm$p, peripheral reaction model, large angle behaviour 78−442
$\pi^\pm$p backward elastic, polarisation, peripherality measure, intermediate energy 77−2862
$\pi^\pm$p backward elastic scatt., 30-90 GeV/c, cross section u and momentum depend. 80−18146
$\pi^\pm$p elastic and charge exchange, electromagnetic corrections, dispersion relation method 77−38195
$\pi^\pm$p elastic scatt., 1.9-9.5 GeV, test of parton and statistical bootstrap models 78−89728
$\pi^\pm$p elastic scatt., 400 to 590 MeV/c, cross sections *(Russian)* 77−10281
$\pi^\pm$p elastic scatt., 420-640 MeV, differential cross sections, charge exchange isospin boundaries *(Russian)* 79−40800
$\pi^\pm$p elastic scatt., charge exchange, partial wave anal., Δ mass splitting, P_{33} resonance 78−29348
$\pi^\pm$p elastic scatt., dominant exchanges using Reggeon-photon coupling analogy 78−78204
$\pi^\pm$p elastic scattering, 39, 44.5 GeV/c, polarisation, spin rot. meas. 77−30438
$\pi^\pm$p elastic scattering, amplitude anal., σ trajectory 78−33081
$\pi^\pm$p elastic scattering, energy depend. of interaction radius 77−67679
$\pi^\pm$p forward elastic scattering, differential cross section anal. outside Coulomb interference region 77−67678
$\pi^\pm$p forward scatt. amplitude real parts 78−41588
$\pi^\pm$p large angle elastic scatt., preasymptotic effects 79−26347
$\pi^\pm$p large angle elastic scatt., 20, 30 GeV/c, dimension counting rule test 80−83003
$\pi^\pm$p→$\pi^\pm$pγ, 269-324 MeV, cross-sections, bremsstrahlung energy and ang. depend. 77−6149
π^+p→π^+pγ, 298 MeV, bremsstrahlung cross sections, model calcs. 77−6150
$\pi^\pm$p→$\pi^\pm$p$\pi^+\pi^-$, partial wave anal. of low-mass p$\pi^+\pi^-$ system 78−25070

pion scattering *see lepton-hadron scattering; meson-meson scattering; photon-hadron scattering; pion-baryon scattering; pion-nucleus scattering; pion-pion scattering*

pions
σ model, $SU_2\times SU_2$, modified Goldberger-Treiman relation, pseudoscalar form factor 80−27421
axial vector form factor from current algebra, π PCAC and covariant threshold electroprod. amps. 80−414
Bethe Salpeter wave function in ladder model, bound state of spin $^1/_2$ quarks 77−18176
biomedical experiences with π^-, conf., Brugg-Windisch, Switzerland (Dec. 1978) 80−22138
Cabibbo angle universality and association with K, π and D meson mass 79−12974
cancer therapy, pion range shifter 77−32953
charge radius, coloured quark field theory 80−62945
compositeness from wave function renormalisation constant 80−101997
confinement scheme, gauge model 78−45841
deep inelastic structure functions in massive quark model 80−86717
dimensions, mass, elec. and mag. moments *(French)* 80−13305
dose and LET distributions due to neutron and photons from stopped $pion^-$ 77−52878
dosimetry, charged particle emission from π^- capture 78−40337
dosimetry, in vivo, using Al activation 80−46060
electromagnetic mass differences and radial excitations of ρ-A_1-π system 79−40775
EM form factor, asymptotic behaviour in scale-invariant quark model 78−37211
EM form factor, dispersion theoretic study, meas., charge radius 77−67652
EM form factor and P-wave isovector $\pi\pi$ phase-shift data consistency 79−3025
EM form factor asymptotics in QCD perturbation theory, partonic interpretation *(Russian)* 80−62984
EM form factor factorisation and asymptotic behaviour in QCD 80−91090
EM form factor zeros 77−6126
EM formfactor, upper bounds on derivatives 77−6125
EM mass difference, up quark mass effect on Dashen's formula 79−63461
EM mass difference to N, in Nambu-Jona-Lasinio model 79−93415
EM mass differences, quark behaviour 79−58941
EM mass shifts, asymptotic bounds and causality conditions 80−73704
EM mass shifts, quark-parton model, SU_3 quark triplet 80−42459
EM props., dressed quark model *(Russian)* 80−52508
EM radius, low-energy approx. $\pi\pi\to\pi\pi$, $\pi\pi\to K\bar{K}$, $\gamma\to\pi\pi$, $\gamma\to K\bar{K}$ 78−50033
exchange, lepton-hadron relation and the nucleon-nucleon potential 79−22207
form factor, ω and ϕ effects G-parity violation 79−35963
form factor, expt. behaviour, influence of left-hand cut on second Riemann sheet 80−13304
form factor, inelastic effect of $\omega\pi^0$ channel calc. 77−46062
form factor, large-Q^2 behaviour, Bethe-Salpeter eqn. 77−6002
form factor, resonant space and time like, radiative correction, ρ resonance interference 79−54341
form factor, Roy's eqn., inelastic effects 78−8669
form factor and asymptotic behaviour 79−30734
form factor and Bloom-Gilman duality 79−9352
form factor and charge radius data anal., inconsistency, indistinguishable models 77−38170
form factor extraction from high energy scatt., Chou-Yang model 77−6127
form factor from vector meson dominance anal. of $e^+e^-\to\pi^+\pi^-$ 78−70370
form factor via π^-p→e$^+$e$^-$n 275 MeV *(Russian)* 77−82764
form factors, dispersion theory anal. of π^-p→e$^+$e$^-$n cross sections *(Russian)* 77−10253
form factors, hadron distributions in quark jets 79−54317
form factors, in QCD, light cone Bethe-Salpeter eqn. soln. 79−80827
form factors, Omnes-Muskhelishvili eqns. with inelastic unitarity 79−9371
form factors in quantum chromodynamics, asymptotic form *(Russian)* 78−17021
gas, thermodynamical functions 77−64995
hadron building blocks, pionic mass intervals in narrow and S-state resonances 80−105875
high p_T jet pairs, parton-parton scattering and π quark struct. functions 80−47248
inertial mass, quaternion field theory of matter 78−24702
LAMPF biomedical project, pion beam development 79−79629
longitudinal struct. function, exclusive and almost exclusive process asymptotic behaviour, renormalisation group 80−42464
magnetic polarisability using gauge and relativistic invariance 78−4861
mammalian cells, lethally damaged, proliferation obs. after irrad. by various particles 80−108971
mass determ., 2-level vac. polarisation concept 79−40766
mass determ. via pionic-atom transitions 77−10297
mass difference, Bars-Halpern-Yoshimura unified gauge model, perturbative calc. 77−10251
mass difference between neutral and charged pions, strong gravity coupling const. determ. 77−22715
mass in improved static bag model 80−73667
mass shifts 78−45920
mass-sum rule, Veneziano-type amplitudes π and K mesons 78−74180
masses in QCD lattice gauge theory 80−4928
meson condensation and two photon emission in hadron capture by nuclei and heavy-ion collisions 79−3109
microdosimetry of the pion beam at TRIUMF 80−109037
modified quark loop model, form factors, struct. functions, radiative decay 80−91088
nonlinear chiral models for pion field, many dimensional solitons 78−4792
nonlinear chiral theory, renormalisations 77−65112
phase transition and multiplicity distrib. in Feynman gas model with Bose statistics *(Russian)* 78−89683
plastic scintillator telescope for pion beam monitor in (π^-,γ) experiments 79−49913
polarisabilities of hadrons, quark models 77−82703
polarisability of pions 78−456
polarizabilities of proton and pion, sum rule relation *(Russian)* 79−93420
potential model, Dirac eqn. with linear confining pot., symmetric model, π^0 and ρ^0 79−364
QCD exclusive processes, π, K, ρ form factors, hadronic wavefunction evolution eqns. 80−18135
QCD spectrum calcs. in lattice gauge theory using Wilson's fermion method, massless π 79−367
quark effective-bare mass distinction, pion peculiarity 78−12866
quark model with 4 quarks pseudoscalar meson masses 77−46021
radii determination using geometrical model of hadron hadron collisions 79−89137
radiobiology of π^- beams at Rutherford Lab., 1971-76 77−13003
radiotherapy, simulated treatment planning for Stanford Medical Pion Generator 77−86634
radiotherapy appls., review *(Japanese)* 78−40321
radiotherapy studies with nucl. emulsions 78−73219
relativistic gas, kinetic props., non-equilib. statistical operator method 79−30718
Santilli's model for hadron constituents number, computation simple approach 80−42389
SIN high resolution pion channel and spectrometer 79−22517
soft pion theorems, non-leptonic weak interactions, book contrib. 78−78163
stopping power ratios meas. for 60 MeV positive or negative pions 79−83847
straton model, bound states of mesons, average radii, pion appl. *(Chinese)* 78−78150
straton model, near-flat-bottom interaction pot., wave function of pseudoscalar meson *(Chinese)* 78−82167
structure function, comparison between results from ep→epX and Kuti-Weisskopf model *(Russian)* 80−13291
structure function and scaling phenomena in Drell-Yan lepton pair prod. processes 80−405
structure function determ. in two-jet calorimeter experiment at Fermilab 79−45116
structure function expt. determ., quark distrib. 79−89154
structure function from deep-inelastic scatt. on virtual particles 77−18292
structure function from nucleon low energy relation 80−52507
structure functions, prediction in quark cascade model 79−36033

pions continued
structure functions from ep→epX interactions *(Russian)* 79−22097
structure functions from inclusive prod. data, nonstrange quark distribs. 80−86715
SU_3 couplings of scalar mesons to two pseudoscalars, S* to $\pi\pi$ and ε to $K\bar{K}$ 80−22580
testes, mice, comparative effects of various radiations on weight loss and spermatogenic stem-cell survival 80−108976
Thomas-Fermi type picture of EM struct. 80−9170
three pion states, permutation group S_3 irreducible representation 79−17635
valance quark distribs. in π, K, D, Regge trajectories, SU(3), SU(4) breaking 79−30703
wave function renormalisation const., upper bounds 78−74215
$e^+e^-\rightarrow\pi^+\pi^-$, near threshold, π form factor *(Russian)* 80−4996
$e^+e^-\rightarrow\pi^+\pi^-(K^+K^-)$, $\sqrt{s}$=1.5 GeV, EM timelike form factors for π and K 80−91089
$e\pi$ inelastic scattering, asymptotic bounds on π form factor 78−12917
η−π^0, effects of EM mixing on pn mass difference *(Russian)* 78−74255
$\gamma\pi$ high multipole polarisabilities from Compton scatt. amplitudes 79−85301
NN scattering in nonAbelian gauge theory, π-, ρ-, and ω-exchange, scalar Pade approx. 79−67573
π condensation, vacuum instability in external fields 78−50114
π form factors, axial-vector and structure dependent, vector meson dominance model 80−62989
π radius and EM mass difference from phenomenological form factor 77−65156
π^-, absorpt. length in Fe in range 15<E<140 GeV 80−894
π^-, effect on brain vascular permeability of neonatal rats 80−26275
π^-, effects on mouse embryo pronuclear zygote stage 80−26274
π^-, energy deposition spectra and radiation therapy appl. 80−26363
π^-, long-term effects on female mice rel. to X-rays 80−26273
π^-, pre-clinical studies at TRIUMF 80−26264
π^-, presence in heavy nuclei, binding energy calcs. 78−82275
π^-, RBE and OER values from Vicia Faba root growth inhibition obs. 80−26271
π^-, radiation therapy, in vivo beam localisation by positron activation 80−72316
π^-, radiobiological evaluation of suitability for tumour therapy 80−67166
π^-, suitability for use in radiotherapy, radiobiological obs. 80−26338
π^- and π^+, stopping density distribs. in 1 and 2 dimensions 80−26340
π^- EM form factor meas. 78−17020
π^- in heavy atomic nuclei *(Russian)* 78−25139
π^- irradiation of Chinese hamster cells, OER 79−88126
π^- mass, influence on limit of ν_μ mass 77−14619
π^- radiation therapy dose calcs., Monte Carlo computer program 80−46061
$\pi^0,\pi^\pm$ EM polarisabilities, sum rules, coloured quark field theory 80−57561
π^+, nonadiabatic motion stability in mag. confinement system, numerical simulation 77−61646
π^+, π^- structure function behaviour in ep→e$\pi^\pm$+anything, various W and Q values 77−10262
π^+ structure from two jet events, parton scatt. anal. of π^+p and pp 79−49491
π^3He^{3}H coupling constant estimation, Chew-Low eqn. 77−3051
πN coupling in Δ(1231) isobar region, pion index of refraction, self-energy in low density limit 80−42554
πNN form factors for one off-shell nucleon, dispersion relation calc. 79−9373
π^-p elastic interactions, methodics of identification in bubble chamber *(Rumanian)* 79−63520
$\pi\pi$ coupling constant bounds as function of D-wave scatt. length 77−2866
ρ-π puzzle, possible soln. in neutrino-nucleon inelastic scatt. and weak neutral currents 79−17714
$\rho\pi$ system, resonance-particle prod. amplitude phase shift, S-channel unitary relations *(Russian)* 78−74278
$\rho\pi$ system effective Lagrangian *(Russian)* 77−6036
σ model, pion condensation, use of chiral symmetries 79−296
σ model, pion condensation, use of chiral symmetries, reply to comments 79−297
^{1}H, pionic, pion mass high accuracy meas. from transitions 80−106406
π^-, fast, effects obs. on channelling in cryst. *(Russian)* 77−84812
Ti, pionic, pion mass high accuracy meas. from transitions 80−106406
pipe diffusion *see diffusion in solids*
pipeline processing
binary tree-based image processor architecture 79−72524
Cytocomputer biomedical image analysis 79−92419
multiple microprocessors for continuous patient monitoring 80−26389
nerve fibre counting by pipeline multiminicomputer image processing 80−109013
nuclear fusion plasma simulation with parallel pipeline programming 79−68947
pitch detection *see acoustic variables measurement*
PIXE *see ion microprobe analysis*
plages *see Sun*
planet Mercury *see Mercury (planet)*
planetary atmospheres
absorption line variation across planetary disc with inhomogeneous atm. 80−8569
aerobraking for planetary orbit missions 80−109338
angular momentum of seasonally condensing atmospheres, appl. to Mars 80−26735
banding, hydrodynamic mechanism 79−44386
chemical composition rel. to surface temp., simplified model 79−84695
circular polarization of sunlight reflected from planetary atmospheres 78−28558
circulation, estimated characts. 77−17393
climatic change on terrestrial planets, review 79−53742
cometary nuclei or asteroids interaction with planetary atms., rel. to 1908 Tunguska event 78−49378
coronas, collisional model for spectral line profiles 78−77508
diffuse reflection, adding algorithm for Markov chain radiative transfer formalism 80−21902
diffuse reflection and transmission in accordance with phase function $^3/_4(1+\cos^2\Theta)$ 79−44353
planetary atmospheres continued
diffuse reflection and transmission of light, soln. for three-term phase function *(Russian)* 77−13260
diffuse reflection by semi-infinite atmosphere *(Russian)* 77−82008
diffuse reflection problem, invariance principles and integral eqns. for radiation fields in plane atmosphere 80−67559
diffuse reflection problem for combination of Rayleigh and isotropic scatt., exact soln. 79−84661
diurnal average photodissoc. rates determ. 77−78311
dust grains in outer planetary magnetospheres, physical and dynamical processes 80−41745
Eddington approx. range of validity 78−12086
energy balance of rot. planet in solar flux 80−26765
entry probes heat shield ablation, C excited electronic states contrib. to transport props. 80−23326
entry probes objectives, atmospheric composition and structure obs. 77−49267
equation of transfer for optical depths >100, soln. method 78−96414
erosion of planetary and satellite atmospheres, by energetic atomic particles 80−72736
ethane, long path photoelec. absorpt. spectra 4200-10600 Å, appl. to Uranus 77−83592
evolution of interior, atm., ocean, Viking mission Mars information, appl. to Earth 77−78709
evolution rel. to H_2 ortho-para ratio in primitive solar nebula 78−89233
exospheres, collisionless, satellite atoms depletion by radiation press. 79−96933
exospheres, vel. distrib. function 77−82136
exploration methods appl. to Venus, Mars and giant planets *(Czech)* 78−32374
exponential turbulence and light bending during occultation 80−17513
flow of rot. liq., western boundary currents and detached layers 80−81984
formation from N_2 reservoir, solar nebula NH_3 synthesis, kinetic model 80−62041
giant planet, convective instability of fluid layers 80−56754
giant planet atmospheres, IR radiation, review 80−8568
giant planets, atmospheric thermal structs. 79−84735
giant planets, detectability of liq. methane, laboratory optical absorpt. spectra meas. 80−93278
giant planets, H_2 (4,0), S(1) quadrupole line intensity and pressure shift, laboratory meas. 78−90178
giant planets, methane and ethane 1380 to 1600 Å photoabsorpt. cross sections 78−90181
giant planets, radiowave refraction 80−98608
gravitational field of planet, kinetic eqn. soln. for gas 78−16322
greenhouse effect for Earth, Venus and Jupiter 80−101544
Hartmann boundary layer control of spin-up of stratified, conducting fluid 77−42923
Hermaean magnetosphere, compression by solar wind 79−96936
HF radio occultation meas., phase screen concept 80−56735
ice clathrate as source of atmospheres on terrestrial planets 78−28557
ice evaporation rel. to ice-covered rivers on Mars 80−17526
inert gases in terrestrial planet atmospheres, accretion from protoplanetary nebula 80−109385
interstellar cloud material contrib. 79−25698
inverse multiple scatt., approx. models, limb darkening and phase curves 79−44388
investigation by mass spectrometer-molecular beam expt. 78−49327
Io, atm. vertical struct. vars. *(Russian)* 77−78714
Io, brightness increase after eclipse, colour TV obs. 77−87318
Io, cometary ionosphere model 78−69738
Io, form. of Na clouds and regolith by micrometeoroid impact 80−77330
Io, gaseous SO_2 identified and upper limits for other gases 79−92704
Io, Na I D_2 emission line profiles, var. with orbital phase angle and mag. latit. 78−4139
Io, non-linear standing Alfven wave current system 80−72869
Io, plasma torus, ion density spatial distrib. 80−72861
Io, SHF radioemission and radiation belts *(Russian)* 80−36565
IO, SO_2, frost IR spectra and deposition processes 80−77331
IO, SO_2 atmosphere stability 79−92705
Io, SO_2 model atmos. and ionosphere 80−72853
Io, volcanic activity model based on plasma obs. 80−72870
Io's torus, charged particle radial diffusion 80−72859
Io interacting with jovian magnetosphere, model 80−36563
Io Na cloud, distrib. implications 80−46464
Io Na D-line emission, comparison of observed and theoretical line profiles 78−93145
Io plasma disc, model of plasma injection 80−72860
Io plasma torus, effects on Jupiter kilometric radiation spatial and temporal distrib. 80−77328
ion exchange with the solar wind for planets with negligible intrinsic magnetic fields 79−40050
ion-molecule reactions, review 78−33563
ionospheres, ionic reactions in lab. and planetary atmospheres 80−59168
ionospheres of major planets, review of pre-Voyager knowledge 80−90351
IR laser heterodyne spectroscopy for trace gases remote detect. 78−61606
isotope abundances 79−58284
Jovian planets, ortho-para equilib. of H_2 78−28574
Jupiter, $^{12}CH_4(^{13}CH_4)$ ν_4 band, line parameters, 7.7 micron transmission 78−85894
Jupiter, $^{15}N/^{14}N$ ratio from 10 to 13 μ spectrum 79−8876
Jupiter, β Scorpii occultation, turbulent scatt. 77−37562
Jupiter, absorption in blue and UV 79−40125
Jupiter, acetylene abundance 78−16337
Jupiter, acetylene formation, by photolysis or thunderstorms 79−66957
Jupiter, atm. circulation and weather 77−22134
Jupiter, atmosphere coloration due to Si compounds 80−51689
Jupiter, atmosphere map at 2400 Å from Voyager 2 obs. 80−77336
Jupiter, atmosphere optical parameters latit. vars. from 0.6 to 1.1 μ spectrophotometry 80−46468
Jupiter, atmospheric aerosol props. from near IR polarisation studies 78−85899
Jupiter, atmospheric comp. and cloud struct. deduced from absorpt. bands in refl. sunlight 80−56758
Jupiter, atmospheric comp. rel. to near IR spectral albedo 80−31242
Jupiter, atmospheric constituents rel. to 5-8 μm obs. 77−29711
Jupiter, atmospheric constitution, struct. and dynamics 80−105186

planetary atmospheres continued
Jupiter, atmospheric methane and ammonia abundance photoelectric obs. 77−33397
Jupiter, atmospheric probe, mass loss, shape change, real-gas aerodynamic effects 78−4055
Jupiter, atmospheric probe vehicles, SiO boundary layer surface opacity 79−45641
Jupiter, atmospheric structure and 5 μ limb-darkening 79−25539
Jupiter, aurora due to protons, nightside 80−85890
Jupiter, auroral hot spots, Io- and Europa-related, longit. asymm. 79−75138
Jupiter, auroral hot spots obs. 78−16333
Jupiter, bounce averaged synchrotron loss in dipole field 77−87316
Jupiter, C/H, $^{12}CH_4/^{13}CH_4$ ratios determ. from near-IR spectra 77−9698
Jupiter, charged particles accel. rel. to decametric radiation modulation by Io 78−89110
Jupiter, chemical structure of deep atmosphere 78−45270
Jupiter, circular polarisation of 1.4 GHz emission from radiation belts 77−37556
Jupiter, circulation and thermal regime, survey 80−8584
Jupiter, circulations in atmosphere rel. to terrestrial turbulence and baroclinic instability 79−40132
Jupiter, cloud distrib. between Voyager 1 and 2 missions, 5 micron obs. 80−77345
Jupiter, cloud features, pre-Voyager velocity data 79−92710
Jupiter, cloud microphysics anal. 79−16853
Jupiter, cloud structure and vel. fields 79−92712
Jupiter, CO abundance 78−49374
Jupiter, CO obs. at 5 μm, airborne spectroscopic obs. 78−36491
Jupiter, CO thermochemistry, implications for atm. convection 78−36500
Jupiter, comp. and temp. struct. from Voyager 1 IR obs. 80−26790
Jupiter, constituents, comparison with Saturn, visible obs. *(French)* 80−101550
Jupiter, cosmic ray ionization 80−17538
Jupiter, current disc of magnetosphere, modeled using Pioneer 10 data 80−101551
Jupiter, D abundance 78−45265
Jupiter, D/H and C/H ratios from methane-d_1 spectrum 78−28572
Jupiter, dawn magnetodisc, energetic electrons 79−70987
Jupiter, dayside magnetosphere, departure from rigid co-rotation 79−96957
Jupiter, decametric and hectometer radio emission obs. 80−67644
Jupiter, decametric harmonic radiation generation 77−45353
Jupiter, decimetric radio spectrum, 1975 December 77−60718
Jupiter, density model and total reflection of light *(Italian)* 79−21221
Jupiter, differential rotation, convective instability and geostrophic mode of motion 77−17426
Jupiter, differential rotation, eqns. of momentum variation in convective shell 77−25978
Jupiter, disturbances and dislocations, triggering factors 80−72867
Jupiter, dust in magnetosphere derived from Io volcanoes 80−85889
Jupiter, dynamical activity in 1975, photographic and photoelec. obs. 79−21224
Jupiter, effect of rot. on inflated magnetosphere, similarity model 78−57492
Jupiter, effective transport coeffs. of plasma in LTE approx. 78−1801
Jupiter, electron density profiles, Voyager 1 radio occultation meas. 79−96953
Jupiter, electrons pitch angle distrib. in radiation belt 77−33402
Jupiter, EM noise and radiowave propag. below 100 kHz in atm., equatorial region 80−26782
Jupiter, energetic electron flux and synchrotron power 77−71056
Jupiter, energetic particle flux modulation rel. to current disc penetrations in magnetosphere 79−44404
Jupiter, energetic particles recirculation in magnetosphere 78−89108
Jupiter, energetic protons in magnetosphere 79−101111
Jupiter, equatorial atmosphere, Voyager obs. of small-scale waves 79−92713
Jupiter, equatorial belt, spectrophotometry in 0.6-1.1 μm range 79−96960
Jupiter, evidence for telluric value of $^{12}C/^{13}C$ atmospheric ratio 78−20723
Jupiter, far IR spectrum, depend. on atm. vertical thermal struct. 77−60713
Jupiter, far IR spectrum showing NH_3 rotational bands 78−85891
Jupiter, fast moving bright spot obs. in North Temperate Current C 80−67640
Jupiter, field-aligned currents in magnetosphere, Pioneer 10 and 11 obs. 77−25975
Jupiter, future spacecraft missions 77−37564
Jupiter, GeH_4, ν_3 and 2 ν_3 bands, high resolution IR spectra 78−37636
Jupiter, GeH_4, ν_3 fundamental, theoretical absolute J-manifold intensities 78−74707
Jupiter, GeH_4 abundance from IR spectrum anal. 78−61791
Jupiter, GeH_4 IR laser sideband obs., ro-vibr. struct., isotope shifts, line widths 79−72306
Jupiter, Great Red Spot, atmosphere baroclinic model, solitary waves on unsymmetric shear flow 80−82266
Jupiter, Great Red Spot, super hurricane model *(German)* 77−9704
Jupiter, Great Red Spot and South Temperature Belt white spots motion and struct. 77−67065
Jupiter, Great Red Spot as plane vortex with elliptical nucleus 77−53466
Jupiter, H_2 2-O quadrupole spectrum obs. 77−45351
Jupiter, H_2 content from spectral line equivalent width *(Russian)* 78−12143
Jupiter, H_2 quadrupole lines in spectrum 79−70990
Jupiter, H_2 rotational quadrupole lines, theoretical brightness temps. 78−7917
Jupiter, Hα auroral activity obs. 77−45350
Jupiter, H I Lyman α emission, Voyager 2 EUV obs. 80−77338
Jupiter, H Lyman-α brightness, longit. asymm. 80−72852
Jupiter, H quadrupole absorption, spatial and temporal variations 77−37561
Jupiter, haze layers, Voyager 1 obs. from UV to IR 79−92714
Jupiter, high spectral resolution obs. between 30 and 50 μm 80−46462
Jupiter, hydrocarbon and H I photochemistry rel. to Lyman alpha albedo 80−105194
planetary atmospheres continued
Jupiter, inhomogeneous atmospheric model anal., H_2 4-0 S(1) line 77−71054
Jupiter, inner magnetosphere, L dependence of protons radial diffusion coeff. 78−16339
Jupiter, inner plasmasphere, possible source by photoionisation of Io's H I ring 77−60715
Jupiter, Io torus and magnetosphere Birkeland currents 80−105198
Jupiter, ionisational nonequilib. shock layer effects on entry heating 77−25979
Jupiter, ionosphere, daytime electron temp. calc. 77−25972
Jupiter, ionosphere, effect of electron precipitation, Pioneer 10 and 11 S band occultation obs. 77−56871
Jupiter, ionosphere, electron collision processes with hydrogenic ions 79−72424
Jupiter, ionosphere, energetic electrons precip. fluxes upper limit 79−75143
Jupiter, ionosphere, hydrocarbons, semiempirical electron impact ionis. cross-sections 78−1089
Jupiter, ionospheric Na, deposition and sputtering on Io 79−44405
Jupiter, ionospheric plasma MHD in Great Red Spot region *(Russian)* 79−37466
Jupiter, IR absorpt. profiles of GeH_4, computer simulation 78−81584
Jupiter, IR and visible spectrum, C/H ratio 79−48729
Jupiter, IR imaging in 8-14 μ spectral region 77−41350
Jupiter, IR multiple freq. sounding of anomalous clouds 79−2515
Jupiter, IR obs. by Fourier transform spectroscopy 78−61747
Jupiter, IR radiation absorpt. induced by press., mol. collision between CO_2, N_2, O_2 *(Russian)* 80−56600
Jupiter, IR spatial scans 80−82268
Jupiter, IR spectral obs., 800-1000 cm^{-1} 78−16336
Jupiter, IR spectrum, 17-25 μ, comparison with thermal struct. models 77−45348
Jupiter, light polarization and scattering 79−96814
Jupiter, lightning flashes, first results, geometric reduction 79−96952
Jupiter, lossy radial diffusion model of linear magnetosphere 79−53764
Jupiter, low order effect of cosmic ray albedo neutron decay (CRAND) input 78−45271
Jupiter, Lyman α albedo, Copernicus UV obs. 80−94747
Jupiter, Lyman α albedo rel. to solar activity 80−98601
Jupiter, mag. tail, traversal by Voyager 2 and Saturn, 1981 prospects 80−12706
Jupiter, magnetoplasmadisc, struct. and props. 80−12704
Jupiter, magnetosheath sunward flow, depend. on solar wind press. 80−72857
Jupiter, magnetosphere, 1.79-2.15 MeV protons residence lifetimes in equatorial region 80−26785
Jupiter, magnetosphere, current sheet plasma 79−84731
Jupiter, magnetosphere, energetic electrons ten-hour modulation phase 80−26784
Jupiter, magnetosphere, high β plasma in dynamic current sheet 79−16872
Jupiter, magnetosphere, Io torus, latitudinal plasma oscills. 80−85892
Jupiter, magnetosphere, low energy electron obs. comments 77−71053
Jupiter, magnetosphere, low-energy charged particle environment, Voyager 1 first look 80−26797
Jupiter, magnetosphere, mode coupling of Z-mode waves, decametric radiation source 77−29537
Jupiter, magnetosphere, particle flux ang. distrib. in rot. system 77−9700
Jupiter, magnetosphere, planetary spin period accel. of particles 77−9701
Jupiter, magnetosphere, plasma sheet theory 77−64697
Jupiter, magnetosphere, radial diffusion of energetic particles 77−9702
Jupiter, magnetosphere, radial diffusion of Io-injected plasma 79−75144
Jupiter, magnetosphere, S nebula 77−87315
Jupiter, magnetosphere, stability of electron shell distrib. to parallel propag. plasma waves 78−4032
Jupiter, magnetosphere, tailward directed ion beam 80−72854
Jupiter, magnetosphere, time dependent model of current sheet 79−16875
Jupiter, magnetosphere and bow shock, Voyager 2 magnetometer obs. 80−77339
Jupiter, magnetosphere and nonthermal radio emission, exploration methods *(Czech)* 78−32374
Jupiter, magnetosphere compression by solar wind 79−12429
Jupiter, magnetosphere corotation lag, inertial limit, theory 80−41660
Jupiter, magnetosphere electron fluxes rel. to Io Na emission region morphology 77−49329
Jupiter, magnetosphere energetic ions and electrons Voyager 2 obs. 80−77342
Jupiter, magnetosphere longit. asymm. and energetic particles periodic escape 77−25973
Jupiter, magnetosphere low energy plasma, Voyager obs. 80−72855
Jupiter, magnetosphere shape and field, model 80−72868
Jupiter, magnetosphere trapped energetic particle spectrum 80−72711
Jupiter, magnetospheric effects of Io's wobbling flux tube and surface cond. 80−26783
Jupiter, magnetospheric plasma wave propag., CMA diagrams 77−87317
Jupiter, magnetotail, solar wind interaction 79−96956
Jupiter, magnetotail structure inferred from plasma obs. 80−72864
Jupiter, mean temp. struct. from far IR spectral obs. 80−17540
Jupiter, methane absorpt. interpretation 77−29707
Jupiter, methane and NH_3 bands, longitudinal variability, visible obs. 80−82270
Jupiter, methane and NH_3 bands spectropolarimetry, 6800-8200 Å 79−66955
Jupiter, methane band photometry, absolute reflectivity, centre-to-limb vars. 79−53759
Jupiter, methane band photometry, SEB and STrZ reflectivity, atm. models 79−53760
Jupiter, methane emission at 76 GHz correl. with decameter activity 78−4140
Jupiter, methylamine prod. and distrib. 77−64693
Jupiter, microwave spectrum 78−85889
Jupiter, NH_3, spatial distrib. from optical band strengths and curves of growth 80−46386
Jupiter, NH_3 6450 A absorption band obs. 77−33396
Jupiter, NH_3 abundance from visible obs. 80−82269
Jupiter, NH_3 and PH_3 photochemistry in stratosphere 77−53463
Jupiter, NH_3 atmospheric abundance 78−12142

planetary atmospheres continued
Jupiter, NH_3 column density from high resolution spectra around 80 μm 78−45267
Jupiter, NH_3 photochemistry 77−45354
Jupiter, NH_3 spectral line meas. using 10μm superheterodyne receiver 78−16335
Jupiter, NH_3 vertical density profiles from IR and radioelectric emissivity data 80−82267
Jupiter, of UV (1200-1900 Å) spectrum and minor constituents abundances 77−25974
Jupiter, outer magnetosphere, solar wind dynamic press. variations 77−71051
Jupiter, outer magnetosphere, solar wind magnetic field variations 77−71052
Jupiter, outer magnetosphere, temporal var. in heavy ion plasma 78−61787
Jupiter, outer magnetosphere neutral sheet, relativistic electron accel. 77−17424
Jupiter, particle trapping rel. to internal magnetic field geometry 78−28575
Jupiter, particles, environments and possible ecologies 77−33394
Jupiter, PH_3 absorpt. in 5 μm window 80−31243
Jupiter, PH_3 obs. at 5 μ 77−33393
Jupiter, PH_3 photolysis and abstraction reactions 79−66327
Jupiter, Pioneer 10 and 11 obs. of magnetic field orientation in ionosphere 79−25540
Jupiter, Pioneer 10 imaging data for prominent belt and zone, haze particles 78−45269
Jupiter, planetary meteorology rel. to weather and climate on Earth 79−84697
Jupiter, plasmapause theory rel. to Io as ion source 77−22133
Jupiter, plasmasphere, stop zones for decametric radiation 77−2368
Jupiter, plasmasphere, thermal struct. 78−93148
Jupiter, plasmasphere models 78−77517
Jupiter, polar regions limb darkening obs. and atmospheric props. 79−62790
Jupiter, probe entry, Rankine-Hugoniot eqns., soln. using reduction-of-ionisation-pot. 77−9651
Jupiter, probe heat shield C vaporisation 79−1264
Jupiter, production and interaction of solitary waves 78−36496
Jupiter, proton flux along magnetic field lines in middle magnetosphere 79−53763
Jupiter, protons accel. at 32 Jovian radii in outer magnetosphere 78−57489
Jupiter, quasi-geostrophic model of circulation 80−41761
Jupiter, radiation belts and atmosphere, Pioneer 10 ratio obs. 79−35179
Jupiter, radiation-induced cooling 78−85885
Jupiter, radio brightness distrib. across disc. 77−87319
Jupiter, radio emission, mag. field, energisation, comparison with pulsars 80−46466
Jupiter, radioemission, short-duration bursts, magnetospheric EM cyclotron instability mechanism 78−7919
Jupiter, radioemission at 100 kHz, from magnetosphere 80−85891
Jupiter, Red Spot 90 day oscill. rel. to position of Mercury 77−82158
Jupiter, role of P in upper atmosphere 79−40130
Jupiter, S II forbidden line emission round planet, distrib. and intensity 80−85885
Jupiter, S II torus, longitudinal asymmetry visible spectra 80−82271
Jupiter, S Nebula, temp. anisotropy 80−17539
Jupiter, scavenging reactions of acetylene and ethylene for P containing radicals 78−81582
Jupiter, simulation, synthesis of UV photoprod. organic solids, mol. anal. 78−69740
Jupiter, spacecraft entry, modelling by H_2-He mixture 78−71413
Jupiter, spectral determ., lab. obs. of ethane $^RQ_0$ branch intensity in ν_9 fundamental 77−6856
Jupiter, spectral emission of upper atm., Galatry profile 77−78642
Jupiter, spectrophotometric and polarimetric obs. *(Russian)* 77−71050
Jupiter, spectroscopic results *(French)* 77−33403
Jupiter, stratosphere, NH_3 mixing ratio 79−16874
Jupiter, struct. and comp. models, aerosols occurrence *(Russian)* 77−53465
Jupiter, surface condition and cooling rate 77−29714
Jupiter, temp. struct. from inversion of IR spectral meas. 79−75141
Jupiter, temp. struct. recovery from inversion of thermal radiance data 77−82154
Jupiter, temporal characts., IR obs., north-south temp. asymm. 80−41760
Jupiter, thermal profiles and NH_3 distribs. from IR spectral meas. 79−40126
Jupiter, thermal struct. from Voyager 2 IR obs. 80−77335
Jupiter, thermal structure from IR spectral meas., filtered iterative inversion method 78−7918
Jupiter, thermodynamics of trace elements 79−66956
Jupiter, trace constituents upper limits from 5 μm spectrum anal. 78−61790
Jupiter, transport props. 78−57490
Jupiter, turbulent mixing coeff. and homopause height 78−49354
Jupiter, upper atmosphere aerosol content from Ganymede eclipse obs. 77−41349
Jupiter, upper atmosphere temperature, Voyager 1 meas. 80−17536
Jupiter, upper layer struct. model *(Russian)* 77−25976
Jupiter, UV emission from excited atoms and molecules 78−40865
Jupiter, vertical cloud struct. from 5 μm meas. 77−29710
Jupiter, Voyager 1, photographic obs. of atmosphere struct. and motions 80−26788
Jupiter, Voyager 1 EUV obs. 80−26792
Jupiter, Voyager 1 meas. of ionic species in magnetosphere 79−96955
Jupiter, Voyager 1 obs. 79−96948
Jupiter, Voyager 1 results 80−4293
Jupiter, Voyager I results, diverse features 79−84738
Jupiter, Voyager low energy charged particle expt. results 80−98605
Jupiter, Voyagers to test magnetic anomaly model of magnetosphere 79−44403
Jupiter, whistler mode chorus obs. and Io torus implications 80−72862
Jupiter, whistler obs. by Voyager 1, lightning detect. 79−84733
Jupiter, whistler propagation in magnetosphere, theory 80−72863
Jupiter, wind vector, eddy mmtm. and energy conversion obs. 80−72851
Jupiter, zonal vel. and texture from Voyager 1 images 79−92711
Jupiter as source of electrons observed at Earth orbit 80−90357

planetary atmospheres continued
Jupiter atmosphere, cloud struct. and C/H ratio from methane line profiles near 1.1 μ 80−62067
Jupiter atmosphere, organic compounds hot-atom synthesis 79−101109
Jupiter atmosphere, origin of differential rot. 80−46467
Jupiter atmosphere and ionosphere, Voyager 1 preliminary radio profiles 80−26791
Jupiter atmospheric, review 78−32377
Jupiter cloud configurations, Pioneer and Voyager obs. interpretation in time-depend. framework 80−26787
Jupiter cloud morphology, monitoring by 5 micron IR imaging during Voyager 1 encounter 80−26799
Jupiter cloud zones, IR obs. 77−29712
Jupiter clouds spectropolarimetry, lines equivalent widths information content 80−31215
Jupiter corotating magnetosphere, self-consistent model 78−89109
Jupiter diffuse aurora, influence of plasma injection from Io 80−4289
Jupiter equatorial regions, light and dark spots lifetimes and motions 78−57493
Jupiter Great Red Spot, depend. on solar activity 79−101110
Jupiter inner magnetosphere, O^+ forbidden emission detect. 80−51687
Jupiter inner magnetosphere, revised Pioneer 10 absolute electron intensities 77−37563
Jupiter inner magnetosphere, whistler mode noise 78−89112
Jupiter ionosphere, decametric radiation sources locations 79−75148
Jupiter ionosphere, electron accel. rel. to S-bursts obs. at 32 MHz 78−36498
Jupiter ionosphere, electron stream accel. in Io flux tube rel. to S-bursts 78−36499
Jupiter ionosphere, electrons accel. rel. to S-bursts freq. drift meas. at different freqs. 80−85888
Jupiter ionosphere, secondary electrons 79−75140
Jupiter ionosphere, spectral broadening meas. by Pioneers 10 and (11) 80−109391
Jupiter ionosphere, Voyager 2 occultation, radio obs. 80−77337
Jupiter ionosphere and magnetosphere, Cotton-Mouton effect rel. to decametre radio emission modulation 80−67643
Jupiter magnetodisc, props. from mag. field meas. 79−58297
Jupiter magnetopause motion, longitudinal control 78−49375
Jupiter magnetosphere, centrigugal distortion by equatorially confined current sheet 79−40134
Jupiter magnetosphere, comparison of Earth-based and Pioneer results 78−12076
Jupiter magnetosphere, contrib. of water products from Galilean satellites 78−45268
Jupiter magnetosphere, diffusion coefficients determ. from Io observed effects 78−32388
Jupiter magnetosphere, electrodynamic interaction with Io 78−81583
Jupiter magnetosphere, electron pitch-angle diffusion by whistler mode waves near Io plasma torus 80−4290
Jupiter magnetosphere, electrons pitch angle distrib. rel. to 1.4 GHz emission circular polarisation 77−64692
Jupiter magnetosphere, electrostatic waves obs. 80−72865
Jupiter magnetosphere, equatorial confinement and vel. space distrib. of satellite ions 77−53464
Jupiter magnetosphere, HF and LF events from Voyager 2 obs. 80−77344
Jupiter magnetosphere, impulsive penetration of solar wind filamentary plasma elements 77−78581
Jupiter magnetosphere, Io interaction with plasma torus 80−98604
Jupiter magnetosphere, kilometric radiation ray tracing 80−72866
Jupiter magnetosphere, kilometric radiation spatial and temporal studies 80−77328
Jupiter magnetosphere, nonlinear phase bunching effects on extraordinary mode decametric emission 77−2366
Jupiter magnetosphere, particle accel. 79−12428
Jupiter magnetosphere, plasma and mag. field perturbations due to Galilean satellites perturbations 80−46465
Jupiter magnetosphere, plasma cloud injection from Io, S and O ions discontinuities 80−90358
Jupiter magnetosphere, plasma corotation lag from Voyager 1 obs. 80−90361
Jupiter magnetosphere, plasma sheet self-consistent model 78−57494
Jupiter magnetosphere, plasma waves from Voyager 2, radio obs. 80−77343
Jupiter magnetosphere, proton bombardment effects on Io refl. spectrum 79−96950
Jupiter magnetosphere, radial diffusion eqn. for collision-affected plasma 78−49310
Jupiter magnetosphere, relativistic particles rel. to linear polarisation at 6, 11 and 21 cm 77−87313
Jupiter magnetosphere, S plasma discontinuities 80−4291
Jupiter magnetosphere, solar wind interaction rel.to non-Io-related radio emission 78−57491
Jupiter magnetosphere, theory of Io-modulated decametric radio S-bursts *(Russian)* 80−8582
Jupiter magnetosphere, thermal electron density 79−40133
Jupiter magnetosphere, Voyager 1 obs. of energetic ions and electrons 80−26798
Jupiter magnetosphere, Voyager 1 planetary radio astronomy obs. 80−26796
Jupiter magnetosphere, Voyager 1 plasma wave obs. 80−26795
Jupiter magnetosphere, Voyager 1 studies preliminary results 80−26793
Jupiter magnetosphere, Voyager 2 obs. of hot plasma environment 80−77341
Jupiter magnetosphere 80−72858
Jupiter magnetosphere and bow shock, plasma densities from Voyager 2 obs. 80−77340
Jupiter magnetosphere disturbed by Ganymede, Voyager-2 obs. 80−72856
Jupiter magnetosphere energetics comparison with terrestrial magnetosphere 79−58201
Jupiter magnetosphere plasma observations, Voyager 1 initial results 80−26794
Jupiter magnetosphere-satellite interactions, aspects of energetic charged particle loss 80−36566
Jupiter meteorology, large-scale moist convection 77−37555
Jupiter mid-magnetosphere, equatorial protons instability 80−67642
Jupiter NH_3 distrib. and photochemical products 77−67063
Jupiter outer magnetosphere, charged particles energisation 78−89111

planetary atmospheres continued
Jupiter probe, mass and shape var. due to aerodynamic heating 79−84630
Jupiter radiation belt, erosion of Ganymede atmosphere by energetic atomic particles 80−72736
Jupiter radiation belts, particle fallout mechanism for Io local gas emission *(Russian)* 80−82275
Jupiter radiation belts, review 79−58296
Jupiter spectrum, obs. from 1500 to 2000 Å with IUE 80−56752
Jupiter stratosphere, acetylene photopolymers aerosol 80−31244
Jupiter subliming boundary layer flow, simulation 78−65545
Jupiter surface, equatorial jet stream form. due to cylindrical shear layer 78−16340
Jupiter thermosphere, heating by soft electrons precip. 77−82157
Jupiter tropical and temperate belts, 0.6 to 1.1 μm spectrophotometry, brightness distrib. and atmosphere optical parameters 79−92715
Jupiter two phase NH_3 stratiform clouds 77−25977
Jupiter upper atmosphere, heating by solar wind energy 77−37471
Jupiter upper atmosphere, photochemical models 80−36567
Jupiter upper atmosphere CO, extraplanetary source 78−93144
Jupiter wind, correl, with Earth surface winds questioned 79−25290
Jupiter zonal flow, baroclinic instabilities 80−31245
Juptier, $^{74}GeH_4$ transition moment for ν_3 79−72363
kinetic energy of atm. circulation of slowly rotating planet, appl. to Venus 77−13261
Laplace's tidal eqn. asymptotic eigensolns for rapidly rot. planet 77−33166
lidar temperature profiling technique 77−33352
light reflection, transmission and absorpt. coeffs. of double layers 77−6999
light scattering, by optically thin spherically symmetric atmosphere rel. to brightness at zenith near terminator 80−109382
light scattering, meas. via laser beam *(Russian)* 79−44365
light scattering by optically thin inhomogeneous spherically symmetric atmosphere 80−67600
magnetoatmospheric instabilities, max. growth rates 77−53573
magnetosphere boundary layer phenomena 80−36776
magnetosphere interaction with plasma flow, review of studies 78−65496
magnetospheres, effect on cosmic ray propag. 80−101517
magnetospheres, energetic particle accel., lab. and space expts. 77−5400
magnetospheres, magnetic field determ., by solar coronal plasma and solar wind interactions *(Dutch)* 77−67054
magnetospheres, plasma physics, book 79−84696
magnetospheres, props. of dust in plasma environment 80−26930
magnetospheres and radio emissions, conf. Snowmass, Colorado, USA (Aug. 1978) 80−41939
magnetospheres of Jupiter, Saturn and Uranus, review 78−12145
major planets, Raman scatt. in atmospheres 78−28571
Mars, 1877-1971 dust storms and polar cap recession rate correl. *(Italian)* 77−91461
Mars, 1971 dust clouds physical characts. 79−84704
Mars, 1971 dust storm, diurnal thermal tide, topography effects 77−45341
Mars, 1973, dust storm, maps from hourly photographs 77−5477
Mars, ^{15}N enrichment rel. to cosmic ray interactions in early solar system 78−73669
Mars, ^{40}Ar origin 77−64687
Mars, abundance of volatiles, comparison with Earth, rel. to meteoritic source 78−36482
Mars, aeolian activity rel. to variable surface features obs. during Viking mission 78−20678
Mars, aerosol characts. from isophotes 77−29699
Mars, air mass along ray in spherical model 77−29688
Mars, Ar content of atmosphere, Viking 1 X-ray fluorescence spectroscopy 77−13270
Mars, Ar degassing models 77−29700
Mars, atm. struct. and extinction from ϵ Geminorum occultation obs. 78−7898
Mars, atm. struct. expt. on Viking spacecraft, techniques, instruments and accuracy 77−13205
Mars, atm. tides, evidence from occultation of ϵ Geminorum 77−37550
Mars, atmosphere boundary layer, momentum and heat turbulent flux, Viking 1 obs. 80−72810
Mars, atmosphere density long-term vars. rel. to watery past 80−17527
Mars, atmosphere dust content rel. to longit. var. of 2.8 cm brightness temp. 80−105191
Mars, atmosphere model and water vapour distrib. 79−40113
Mars, atmosphere opacity, 1977 obs. from Viking 80−41753
Mars, atmosphere-regolith exchange of CO_2, rel. to atm. press. and response to insolation changes 78−73668
Mars, atmospheric aerosol props. from Viking lander imaging data 78−20698
Mars, atmospheric dust, Viking Orbiter obs. of opposition effect 79−25536
Mars, atmospheric expts. by Viking project 78−20611
Mars, atmospheric Kr and Xe, Viking obs. 77−56856
Mars, atmospheric oblateness from ϵ Geminorum occultation obs. 77−5483
Mars, atmospheric opacity during July-November 1976, Viking orbiter obs. 78−20676
Mars, atmospheric parameters from Mars 6 descent module radio data 77−33386
Mars, atmospheric rare gases relative concs., effects on regolith adsorption 78−49358
Mars, atmospheric refr. rel. to occultation of ϵ Geminorum, (1976 April 8) 77−53567
Mars, atmospheric struct. from occultation of ϵ Geminorum (1976 April 8) 77−37545
Mars, atmospheric struct. Viking obs. 78−20691
Mars, atmospheric water vapour adsorption on regolith 78−65540
Mars, capture of phobos and Deimos by protoatmospheric drag 79−40110
Mars, carbonate formation, CO_2 pressure and H_2O abundance effects 78−61778
Mars, chemical composition deduced from twilight glow obs. 80−56739
Mars, climate, past, present and future 78−7900
Mars, climate oscills., latitude depend. and oscill. spectra 80−90355
Mars, climatology from Viking 1 after 20 sols 77−17409
Mars, cloud formations, reflectivity time var., visible photometry obs. 80−72840
Mars, cloud microphysics anal. 79−16853
planetary atmospheres continued
Mars, cloud obs. by Mars 2 in 0.36 to 1.38 μ range 77−53450
Mars, cloud positions during 1907-73 period, topographic control 78−36479
Mars, CO_2 atmosphere erosion by solar wind energetic atomic particles 80−72736
Mars, CO_2 ice clouds, brightness temp. and radiative props. 80−105192
Mars, CO_2 IR heterodyne spectroscopy 77−41344
Mars, CO_2 photoionisation and photoelectron energy distrib. in thermosphere 79−2506
Mars, CO 115 GHz microwave line detect. 77−74000
Mars, CO abundance calc. 77−33387
Mars, comp. of surface layer 78−20706
Mars, composition and structure, Viking 1 results 77−13265
Mars, composition at surface, Viking 1 lander preliminary analysis 77−13268
Mars, composition model 78−69721
Mars, cosmic-ray interactions with rocks and atmosphere, gamma-ray spectra 77−53448
Mars, crater ejecta emplacement, atmos. effects 80−56747
Mars, crater generated lee waves 80−72824
Mars, cusp of magnetosphere, to explain Mars 5 mag. and plasma obs. 80−51685
Mars, data from Viking spacecraft 78−61779
Mars, discrete wind events at Viking-2 site during northern summer 79−16859
Mars, diurnal composition var. model 79−84702
Mars, diurnal props. of clouds over Tharsis volcanoes 80−94738
Mars, diurnal variations of surface layer meteorological parameters, Viking Lander sites 79−88615
Mars, dust affecting surface and atmos. heating 80−67625
Mars, dust and ice hazes, Mariner 9 TV limb obs. 79−5772
Mars, dust clouds and frictional generation of glow discharges 77−78708
Mars, dust clouds physical props., surface layer particles mean radius 78−45258
Mars, dust storm 1971-2, Mariner 9 IR spectra, composition and particle size distribs. 77−41345
Mars, dust storm of 1971, cloud form., multicolour TV photometry obs. 80−101546
Mars, dust storms, opacity from Viking IR thermal mapping 80−82253
Mars, dust storms 77−49324
Mars, dust storms interplay with perennial ice cover rel. to polar landscapes evolution 79−84721
Mars, dust storms monitoring using atm. transparency meas. *(Russian)* 78−36481
Mars, dynamical phenomena during June-November 1976, Viking orbiter imaging results 78−20675
Mars, electron cooling by electron impact excitation of CO_2 78−57481
Mars, energetic electrons absorpt. by Ar gas 77−31420
Mars, exospheric density and escape fluxes of atomic isotopes 79−5771
Mars, exploration by Viking orbiters 78−20612
Mars, extratropical cyclones, Viking Orbiter 1 obs. during summer season 79−44398
Mars, frontal systems during N polar hood passage over lander site before dust storm 79−84718
Mars, general circulation model, including dust and topography 80−90354
Mars, global dust storms, exploration methods *(Czech)* 78−32374
Mars, grain saltation estimation 77−17398
Mars, H_2O vapour, comparison of spacecraft meas. 79−8871
Mars, H_2O vapour high-altitude profile 79−8869
Mars, impact ejecta trajectories, drag and gravity effects, analytic solns. 78−40854
Mars, integral photometry rel. to global dust storms 78−61780
Mars, ion and electron temps. in upper atm. 79−16862
Mars, ionosphere, $(CO_2)_2^+$ photodissoc., lab. mass spectra 77−6867
Mars, ionosphere, normal horizontal gradient effects on radio signals phase meas. 77−29691
Mars, ionosphere, post-Viking model 79−25532
Mars, ionosphere, proton affinities and cluster ion stabilities in CO_2 and CS_2 77−77760
Mars, ionosphere and magnetosphere interaction with solar wind 80−72835
Mars, isothermal atmosphere model from ϵ Geminorum occultation obs. 78−57482
Mars, isotope ratios and noble gas upper limits 77−17408
Mars, isotopic N composition rel. to past history 77−17406
Mars, isotopic ratios and minor constituents from Mariner 9 77−82142
Mars, large-scale dynamics, heat transfer by baroclinic eddies and topographically forced long waves 78−45255
Mars, latits. of polar hood boundaries rel. to surface heights 77−5482
Mars, lightning in atmosphere, chemical impact 79−96940
Mars, low latitude circulation 77−41343
Mars, lower atm., O_3 distrib. and photochemistry 79−35169
Mars, lower atmosphere modelling, multilayer radiative transfer 80−46451
Mars, magnetic minerals, obs. by Viking extended mission 80−72830
Mars, magnetosphere, effect of Deimos 80−41752
Mars, meteorological results from Viking 2 77−53455
Mars, microwave absorption 77−71045
Mars, mirages, possibility of Viking lander obs. 77−29693
Mars, N_2 dayglow prediction 77−53452
Mars, N atom loss rate, calc. 80−46452
Mars, neutral upper atmosphere composition, Viking obs. 77−56857
Mars, numerical circulation model with topography for S.Hemisphere 77−5480
Mars, O_2 dayglow and O_3 abundance latit. var. 79−53750
Mars, O_3 global distrib. 77−78710
Mars, O_3 layer and two aerosol layers detect. by Mars 5 spacecraft UV obs. 78−49357
Mars, O_3 vertical distrib., Mariner 9 UV spectral obs. 79−66952
Mars, O I dayglow red emission at 630 nm 80−62063
Mars, O isotopes, implications for evolution of volatiles 77−17400
Mars, occultation of ϵ Geminorum, 1976 April 8, atm. temp. var. *(French)* 77−53449
Mars, occultation of ϵ Geminorum, atmosphere temp. profiles 79−2508
Mars, occultation of ϵ Geminorum, planetary atm. temp. struct. determ. 77−87306
Mars, occultation of ϵ Geminorum 77−60702
Mars, optical props. during 1971 dust storm 77−13274
Mars, optical props. during 1971 dust storm *(Russian)* 78−93138

planetary atmospheres continued
Mars, palaeoclimate and enhanced atmospheric CO_2 80−46450
Mars, phase function, July to November 1976, rel. to atmospheric condensate phenomena 78−20677
Mars, photochemistry and evolution, Viking obs. 78−20692
Mars, photochemistry of atmosphere 77−91458
Mars, photochemistry of CO_2-H_2O-N_2 atmosphere 77−29692
Mars, photodesorption from mineral surfaces and effects on atmospheric stability 78−7903
Mars, photoelectron fluxes in ionosphere 79−53751
Mars, photoelectrons caused by solar photons of less than 80 Å 80−56744
Mars, photosynthetic microorganism response, model 79−40114
Mars, phys. parameters calc. *(French)* 78−7901
Mars, physics of atmosphere, surface and interior, book 79−101104
Mars, planetary meteorology rel. to weather and climate on Earth 79−84697
Mars, polar areas, volatiles behaviour, model 78−49363
Mars, possible surface reactions, Viking biology expts. simulation 78−7904
Mars, primitive atm. and implications for channel form. 78−65543
Mars, primitive atmosphere temp. history with reducing greenhouse effect 77−87031
Mars, probe optimal entry trajectories with two-dimensional control 77−91400
Mars, radiation-induced cooling 78−85885
Mars, radiative equilibrium temp. affected by O_3 80−72827
Mars, relative humidity 80−72826
Mars, released volatiles 80−17524
Mars, review 77−13273
Mars, review of surface and atmosphere *(Russian)* 78−20667
Mars, role in shaping of planetary surface 78−7905
Mars, saltation threshold, interparticle force, surface roughness and low atm. density effects 77−5478
Mars, sand blown by wind, threshold windspeed 80−72811
Mars, scale height and temp. profiles from ϵ Geminorum occultation obs. 78−53853
Mars, seasonal press. variations *(French)* 77−29687
Mars, seasonal var. of O_3 density 79−70984
Mars, significance for volatile storage and atmospheric history of CO_2 adsorption and capillary condensation on clays 80−72833
Mars, soil transport by winds 80−31228
Mars, solar wind and supernova, rel. to atmospheric evolution, implications of Viking data 77−87307
Mars, solar wind interaction with ionosphere, electrodynamic model 79−84624
Mars, solar wind sputtering rel. to mass loss 78−53855
Mars, south polar region eolian features rel. to polar vortex, seasonal var. 80−31227
Mars, spacecraft final descent vel. control in atm., autonomous navigation algorithm 77−29620
Mars, spectral line shape of O following dissociative excitation 80−105097
Mars, spiral clouds, Viking Orbiter images during 1978 northern summer 79−75133
Mars, static stability and thermal wind in atmosphere of variable comp. 79−84720
Mars, structure from Viking 2 entry meas. 77−56858
Mars, sulphate aerosol formation from volcanoes, and deposition 80−72828
Mars, surface and atmosphere temps., Viking obs. 77−56868
Mars, surface atmospheric pressure, Viking 1 lander verification of radio occultation meas. 77−22129
Mars, surface condensates obs. during winter at Viking 2 lander site 79−80265
Mars, surface meteorological results, Viking 1 and 2 landers 78−20702
Mars, suspended dust particles props. and effects 79−84717
Mars, tephigram of CO_2 atmosphere 78−73671
Mars, thermal radiative transfer, numerical modelling 80−8574
Mars, thermal regime, long wavelength radiation fluxes 77−33385
Mars, thermosphere, heat sources prod. by solar UV radiation absorpt. 77−25965
Mars, travelling thermal wave effect on circulation 80−8388
Mars, troposphere, radio beam curvature effect on phase meas. 78−49118
Mars, turbulent mixing coeff. and homopause height 78−49354
Mars, upper atmosphere absorption of solar UV, interaction model 80−56746
Mars, upper atmosphere composition and struct. from Viking neutral mass spectrometers 78−20689
Mars, upper atmosphere structure and dynamics, review 77−33382
Mars, upper atmosphere structure from Viking spacecraft expts. 79−25534
Mars, upper atom. temp. struct. from ϵ Geminorum occultation obs. 79−53749
Mars, UV spectra and photometry by TD1A and OAO-2 satellites 77−91459
Mars, Viking 1 landing and early expt. results 77−2362
Mars, Viking 1 preliminary meteorological results 77−13266
Mars, Viking lander preliminary findings *(German)* 77−78711
Mars, Viking Meteorology Experiment 77−33384
Mars, Viking orbiter imaging expt., preliminary results 77−17401
Mars, Viking radio occultation meas. of atmosphere and topography 78−20687
Mars, Viking-1 meteorological meas. 77−29686
Mars, water vapour adsorption on regolith hygroscopic minerals 78−65541
Mars, water vapour global seasonal var. and implications for permafrost 79−84714
Mars, water vapour mapping expt., Viking preliminary results 77−13263
Mars, water vapour obs. from Viking orbiters 78−20682
Mars, water vapour vertical distrib. 79−84713
Mars, waves or turbulence evidence from occultation of ϵ Geminorum 79−53748
Mars, wind activity detect. by seismometer at Viking Lander 2 site 79−84703
Mars, wind blown deposits, silt-clay electrostatic aggregates 80−21940
Mars, wind erosion, yardang evidence 80−67623
Mars, wind patterns rel. to sand sea (erg) in north polar region 80−67624
Mars, wind speed requirements for particle motion 77−5479
planetary atmospheres continued
Mars, wind streaks, seasonal and secular var., Mariner 9 and Viking obs. 80−67622
Mars, windblown particle abrasion, erosion of quartz and basaltic sand 80−17525
Mars, winds rel. to crater streaks in Chryse Planitia, early Viking results 78−65534
Mars atmosphere, coupling between thermal tides and dust storms 79−84719
Mars atmosphere descent trajectories using parachute-rocket system for soft landing 78−69640
Mars atmosphere diurnal tide, influence of Martian polar caps 79−96943
Mars atmosphere dust, Viking orbiter imaging obs. 79−84707
Mars atmosphere phenomena during major dust storms, meas. at surface 79−84708
Mars atmosphere pressure, annual cycle meas. by Viking landers 1 and 2 80−72812
Mars atmosphere thermal IR properties, 15 μm band meas. 79−84710
Mars atmosphere thermal IR properties, dust and ice clouds detect. from Viking IRTM spectral meas. 79−84712
Mars atmosphere thermal IR properties, global behaviour at 7, 9, 11 and 20 μm 79−84709
Mars atmosphere thermal IR properties, local dust clouds effects 79−84711
Mars atmospheres, Viking orbiters radio occultation meas. during one Martian year 80−72836
Mars atmospheric, review 78−32377
Mars atmospheric pressure, seasonal var. as affected by S polar cap 79−84716
Mars descent vehicle, aerodynamic braking arc control algorithm 79−84629
Mars dusty atmosphere, solar heating rates 78−85878
Mars equatorial thermosphere, struct. and dynamics 77−53451
Mars ionosphere, theoretical model in light of Viking obs. 78−96419
Mars ionosphere, Viking retarding potential analyzer obs. 78−20690
Mars magnetosphere, Mars 2 and 3 evidence 78−49361
Mars magnetosphere, Mars 3 evidence re-examined 78−49359
Mars magnetosphere, Mars 5 evidence re-examined 78−49360
Mars magnetotail direction, Mars 5 evidence 78−49362
Mars meteorology, obs. during three seasons at surface 78−89096
Mars orbit emplacement using atmospheric braking, control algorithm 78−69639
Mars polar cap winds, numerical model 79−96942
Mars surface and atmosphere, IR thermal mapping by Viking 77−13264
Mars thermosphere, depend. of struct. on solar activity 77−64686
Mars thermosphere, effects of energetically produced O_2^+ on ion temps. 79−96945
Mars upper atmosphere, composition and struct., Viking obs. 77−53453
Mars upper atmosphere, H Lyman α radiation meas. with absorpt. cell spectrophotometer 78−28519
Mars upper atmosphere isotopic composition, Viking 1 obs. 77−17405
Martian atmosphere, W.W. Campbell's spectroscopic study 77−71047
mass spectrometry, for atmos. composition 80−8518
Mattauch-Herzog mass spectrometer, small, with improved high pressure performance 79−8795
Mercury, atm. comp. from Mariner 10 data 77−9684
Mercury, bow shock and magnetosphere obs., Mariner 10 plasma electron expt. 77−60700
Mercury, He exosphere model based on Mariner 10 UV spectrometer data 78−77509
Mercury, magnetosphere, fit to scaled down geomagnetic field 77−87299
Mercury, magnetosphere model 80−36531
Mercury, Monte Carlo modelling of exosphere 78−96416
Mercury, occultation expt. by Mariner 10 UV spectrometer 77−67023
Mercury, simple mols. prod. by solar wind irradiation 78−16324
Mercury, surface interaction with exospheric atmosphere 78−49351
Mercury, Venus and Mars development and structure *(German)* 77−67055
Mercury airglow, Mariner 10 UV spectrometer expt. 77−64611
Mercury exosphere simulation, Monte Carlo methods 80−67588
Mercury exosphere simulation, Monte Carlo methods 80−67589
Mercury magnetic field and magnetosphere, Mariner 10 obs. 78−12131
Mercury magnetosphere and mag. field, Mariner 10 obs. and theory 80−36530
Mercury magnetospheric mag. field model 77−45336
meteorite entry, expansion, decel. and intense shock wave emission 77−37584
methane, ^{12}C and ^{14}C, line parameters for ν_2 and ν_4 bands, isotope shifts, appln. to planetary atmospheres 80−95622
methane, absorption and press. coeffs., 4500-10500 Å, band model calcs., astronomy appls. 77−83593
methane, liq., optical consts. meas. in IR, possible planetary cloud cover component 78−64341
methane, photoabsorpt. cross sections, 1400-1850 Å spectral region 77−46572
methane(-H_2), long path photoelec. absorpt. spectra 4200-10600 Å, appl. to Uranus 77−83592
methane 6819 Å line interpretation rel. to inhomogeneous scattering models for Uranus and Neptune 78−53871
MHD wave propagation, in presence of rot. and variable mag. field 79−40024
microwave absorption in atmosphere of giant planets induced by collisions of H molecules 80−90350
Milne problem for inhomogeneous atm. 79−21179
mixed fluid, nonlinear internal wave formation from gravitational collapse 80−33619
mm wavelength spectral lines detectability 79−5769
Moon, ionosphere/exosphere modulation by solar wind and EUV radiation 77−17390
multiple scattering in atmosphere with rough surface, azimuth-independent case 78−12085
multiple scattering of light, Hovenier's exit function eqn., numerical props. 80−62054
Neptune, 5-20 micron obs. rel. to upper atmosphere temp. inversion 78−32393
Neptune, albedo and brightness temp., 5 μm IR obs. 80−82300
Neptune, ammonia and water vapour contents 80−90366
Neptune, atmosphere radiative props. rel. to thermal evolution, comparison with Uranus 78−85903
Neptune, atmospheric changes from IR photometry 78−40869

planetary atmospheres continued
Neptune, atmospheric struct. from stellar occultation obs. (1980 August 21) 80−109395
Neptune, effective temp. from IR photometry 78−32394
Neptune, evidence for optically thin high-altitude cloud form. 77−53469
Neptune, ionosphere model, ionization 78−4142
Neptune, IR refl. spectrum, evidence for weather 77−53468
Neptune, limb brightening in 7300 Å methane band, photometry obs. 80−82297
Neptune, methane and ethane emission detect. rel. to warm thermal inversion layer 78−16344
Neptune, mixing ratios of methane, ethane and acetylene in stratosphere 80−51692
Neptune, props. from IR spectrum from 0.8 to 2.5 microns 80−21946
Neptune, thermal profile, supersaturated stratospheric methane 79−40137
Neptune atmosphere, equatorial flow model rel. to rot. 80−67653
Neptune atmosphere, UV albedo meas. 80−82295
occultation studies, wavelength depend. of turbulence effects on refr. angles 79−48697
occultations of stars, wave optics of central spot 77−67053
optically thick, radiative transfer eqn., direct soln. 77−41170
origin, of atmospheres of Earth and planets *(Chinese)* 79−16846
origin, Pioneer Venus gas comp. meas. implications 80−51678
origin, theory based on protoplanetary cloud history 80−12549
outer planets, abundance of photochem. produced organic compounds, lab. simulation 79−75142
outer planets, abundance ratios determ. method, appl. to Jupiter 79−84734
outer planets, atm. dynamics 79−75125
outer planets, IR absorpt. spectrum of monodeuterated methane, appl. 77−42318
outer planets, magnetospheric plasma as energy source for space instrumentation 77−64605
outer planets, probing using Raman effect 77−87277
outer planets, review 77−5470
outer planets, sources of UV absorpt. in spectra 77−41353
outer planets, Voyager spacecraft mission 78−49289
physics of atmospheres, book 79−62568
Pioneer Venus spacecraft programme 78−61707
plasma wake of dipole antenna entering planetary atmosphere, cylindrically stratified model 79−48647
plasma-neutral gas interaction in cosmic physics 78−69669
plasmas, new concept for EM and electrostatic waves detect. 77−9549
Pluto, image tube spectra, 6800-9000 Å, search for possible atm., methane upper limit 79−16880
Pluto, surface and atmosphere from 1.4-1.9 μm spectrum 80−46480
polarisation state, aerosol and Rayleigh scatt. 77−49171
probe flight characts., scale model expts., for Mars, Venus, Jupiter, Saturn 78−7854
probes for hostile atmospheres and surfaces 78−4065
propeller spindown of rotating magnets, torque calc. 79−8831
radiation field, in plane parallel atmosphere involving energy sources *(Russian)* 77−91417
radiation field calc. in homogeneous semi-infinite atm. with isotropic scatt. *(Russian)* 77−70991
radiation field in deep layers of semi-infinite medium with elongated phase function *(Russian)* 79−35129
radiation field in optically thick atmosphere near reflecting surface 77−25962
radiation propagation through turbulent planetary atmospheres, effects of inhomogeneous background 78−69679
radiation redistrib., diffuses reflection effects 78−53819
radiation transfer in plane atmospheres, nonlinear eqns. in linear transfer problems 79−62741
radiative flux calcs. for asymm. phase functions, delta-M method 78−32338
radiative transfer, a^m and b^m functions of anisotropic scatt. 77−56848
radiative transfer, anisotropic light scatt. in inhomogeneous atmosphere with small true absorpt. 79−62742
radiative transfer, exact soln. of diffuse refl. and transmission problem in Rayleigh scatt. 79−35116
radiative transfer, key eqn. exact soln., Laplace transform and linear singular operators method 80−67536
radiative transfer, Markov chain formalism 78−36447
radiative transfer, polarised, in flat geometry media, soln. symm. 79−21180
radiative transfer, soln. of equation for Rayleigh's phase function by principle of invariance 79−84660
radiative transfer, synthetic scattering phase function 80−98541
radiative transfer, time-dependent, exact soln. of integro-differential eqn. via Laplace transform 80−94703
radiative transfer, two stream approx. 80−109383
radiative transfer, unified treatment of reflected and transmitted intensities in plane-parallel atmosphere 78−85838
radiative transfer albedo problem in inhomogeneous isotropically scatt. atmospheres 80−36398
radiative transfer in atmosphere of finite optical thickness, standard problem 80−51646
radiative transfer in finite atmosphere, exact soln. of basic eqn. via Laplace transform 80−94702
radiative transfer in grey diurnally insolated atmosphere 77−22060
radiative transfer in isotropically scatt. semiinfinite atm. 77−13232
radiative transfer in planetary atmosphere, F_N method for polarisation studies 80−98540
radiative transfer in semi-infinite Rayleigh scattering atmosphere, exact soln. 79−35112
radiative transfer in spherical shell atmosphere, asymmetric phase functions 79−2500
radiative transfer in spherical shell atmospheres, appl. to Venus, line form. level 80−17487
radiative transfer multidimens., appl. to Venus and Mars 77−64638
radiative transfer multiple nonstationary scatt. with curved surfaces 77−29641
radiative transfer transport equation with scattering albedo $\omega_0<1$, exact soln. 79−35111
radio occultation concept, origin and implementation 77−45316
radio spectroscopy by automatic interplanetary stations *(Russian)* 77−91442
radio transmission diffraction effects 77−64682
radiometry in quasi-isotropic atmosphere 80−90345
planetary atmospheres continued
radiowave propag. for composition anal. 79−21204
radiowave propag. under superrefraction, complex geometrical optics *(Russian)* 78−49353
radiowave refraction during transillumination of planetary atmospheres 78−96413
radiowaves refraction attenuation 80−4280
rapidly rotating magnetosphere, interchange stability 77−17423
Rayleigh atmosphere single-scatt. albedo, determ. from polarisation meas. 79−35117
Rayleigh scattering in plane-parallel optically thick atmosphere 77−73947
Rayleigh scattering in spherical shell atmospheres 78−85872
Rayleigh scattering transport eqn. exact soln. by Laplace transform and Wiener-Hopf technique 79−8827
Rayleigh-scattering dense atmosphere with true absorpt., single-scatt. albedo determ. method 80−94704
reducing atmospheres, bimolecular reactions of positive ions, laboratory studies 77−63896
remote sensor, high resolution Fourier transform spectropolarimetry 78−57469
remote sounding, new inversion method 80−12677
research developments 78−69720
response to heat sources and perturbations *(Chinese)* 80−85748
Rossby solitary waves, theory 78−1678
satellite atmospheres, possible existence 78−96415
satellite particle exospheres of planets, appl. to Earth 79−101097
Saturn, 5-8 μm photometry 77−29711
Saturn, ammonia and N mixing ratio in troposphere 80−94748
Saturn, at. H cloud formed by photo sputtering of ring ice 80−46475
Saturn, atmospheric aerosol props. from near IR polarisation studies 78−85899
Saturn, atmospheric comp. rel. to near IR spectral albedo 80−31242
Saturn, Axel dust props., Mie theory 77−37565
Saturn, C/H, $^{12}CH_4/^{13}CH_4$ ratios determ. from near-IR spectra 77−9698
Saturn, constituents, comparison with Jupiter, visible spectra obs. *(French)* 80−101550
Saturn, deuterated methane obs. in 5 μm spectrum 79−25543
Saturn, equatorial atmosphere, radiative portion model 77−37566
Saturn, evidence for telluric value of $^{12}C/^{13}C$ atmospheric ratio 78−20723
Saturn, far IR photometry, atm. thermal models 79−75151
Saturn, far IR spectrum, PH_3 and NH_3 absorpt. lines 78−12147
Saturn, H_2 2-O quadrupole spectrum obs. 77−45351
Saturn, H_2 content from spectral line equivalent width *(Russian)* 78−12143
Saturn, H_2 quadrupole lines in spectrum 79−70990
Saturn, HD detect. at 6063.88 Å, D/H abundance ratio calc. 78−57495
Saturn, imaging, photometry and polarimetry obs. from Pioneer 11 probe 80−82289
Saturn, inhomogeneous models 78−12149
Saturn, ionisational nonequilib. shock layer effects on entry heating 77−25979
Saturn, ionosphere, chem. and phys. props., model calcs. 80−26801
Saturn, ionosphere model, ionization 78−4142
Saturn, IR spectrum, 17-25 μ, comparison with thermal struct. models 77−45348
Saturn, latit. differences in cloud layer struct. 78−20725
Saturn, limb darkening and brightness temp., 1.30 cm interferometry obs. 80−82279
Saturn, long term variation of H_2 and methane absorpt. 77−71058
Saturn, Lyman α emission from disc and ring system 78−12150
Saturn, magnetopause influenced by Jupiter's mag. tail 80−12706
Saturn, magnetosphere, trapped radiation belts, particle absorpt., Pioneer 11 obs. 80−82287
Saturn, magnetosphere interaction with solar wind, Pioneer 11 obs. 80−82282
Saturn, methane and NH_3 in outer atmosphere, obs. and model *(Russian)* 77−33406
Saturn, NH_3 abundance from visible obs. 80−82269
Saturn, NH_3 vertical density profiles from IR and radioelectric emissivity data 80−82267
Saturn, physical props. of atmosphere upper layers *(Russian)* 78−40867
Saturn, Pioneer 11 investig. 80−46476
Saturn, Pioneer 11 IR radiometry obs. 80−82290
Saturn, ring system-ionosphere interaction 80−94751
Saturn, rings effect on direct solar radiation reaching top of atm. 79−70992
Saturn, seasonal phenomena from $3\nu_3$ methane band obs. 80−26803
Saturn, stratospheric seasonal climate model 79−75150
Saturn, struct. and comp. models, aerosols occurrence *(Russian)* 77−53465
Saturn, temp. inversion model 78−12148
Saturn, thermal profile from IR meas. inversion 78−4144
Saturn, upper clouds, NH_3 frost near IR refl. spectra 79−8135
Saturn, upper neutral atm. and ionosphere, vertical struct., Pioneer 11 radius occultation obs. 80−82293
Saturn, UV photometry from Pioneer 11 probe 80−82288
Saturn, UV spectra and photometry by TD1A and OAO-2 satellites 77−91459
Saturn, visual mapping and photometering, 1973-4 period 77−87321
Saturn atmosphere, acetylene detect. using IUE satellite 79−48731
Saturn atmosphere, origin of differential rot. 80−46467
Saturn atmosphere, temp. distrib. from spatially resolved IR obs. at 10 and 20 μm 79−84741
Saturn ionosphere, spectral broadening meas. by Pioneer (11) 80−109391
Saturn magnetosphere, bowshock and magnetopause detect. by Pioneer 11, mag. field determ. 80−82283
Saturn magnetosphere, cosmic ray cutoff rigidities 80−72873
Saturn magnetosphere, energetic ions and electrons, Pioneer 11 obs. 80−82286
Saturn magnetosphere, interactions with satellites and rings 80−82285
Saturn magnetosphere, trapped radiation, absorpt. by satellites and ring, Pioneer 11 obs. 80−82284
Saturn NH_3 atmospheric abundance 78−12142
Saturn radiation belt protons, rings ice particles sputtering 78−89116
Saturn rings vicinity, origin of Lyman-alpha emission 79−12430
Saturn upper atmosphere, struct. from Titan eclipse light curve 80−90362

planetary atmospheres continued
scattering cross section of radiowaves reflected from planet with spherically symmetrical atmosphere 80−21935
shear flow/topography interaction, in homogeneous rot. fluid 79−55354
six channel radiometer for spectral investigations *(Russian)* 77−29468
solar nebula evolution, giant planet formation, gaseous envelope instability 79−12415
solar radiation diffusive reflection by plane parallel planetary atmosphere 77−5471
space probe or meteorite reentry, mass loss and shape change with radiative heating 80−31198
spacecraft braking problem in Jupiter atmosphere, ballistic and navigation aspects 80−61981
spacecraft deep radio occultations and evolute flashes, planetary atms. struct. determ. 79−53731
spacecraft entry, body shape for minimal radiative heat inflow *(Russian)* 78−77457
spacecraft entry, transport props. of monatomic C rel. to heat shield ablation 78−87424
spacecraft meas., review 78−69719
spectra, anisotropic scatt. effects 77−2357
stellar occultation data, effects of photon noise and initial conditions 78−28530
stellar occultations, turbulence effects on refr. angles 78−61773
stellar occultations by turbulent atmospheres, heuristic scatt. model 77−37534
stellar occultations by turbulent atms., wave-optical theory 78−61772
temperature depend. of possible S_8 IR bands 77−29709
temperature inversion, thermodynamics of gravitating fermions 79−57994
temperature perturbations, radiative damping 78−32163
terrestrial planets, atmosphere formation by impact 77−45335
terrestrial planets, planetary development *(Hungarian)* 77−73987
terrestrial planets atmospheres, origin by shock degassing during accretion stage *(Russian)* 79−101099
thermal convection approximations 79−35127
thermal escape, assoc. non-Maxwellian effects 79−80264
thermal escape of molecules, non-Maxwellian effects 80−46419
thermospheres, turbulence effects 79−88610
Titan, 16-30 μm spectroscopy 80−56760
Titan, atm. vertical struct. vars. *(Russian)* 77−78714
Titan, atmosphere organic chemistry, review 80−90364
Titan, inhomogeneous scattering model of atmosphere 79−44406
Titan, N_2 atmosphere evolution 79−30005
Titan, optical props. and vertical distrib. of aerosols in atmosphere 80−46471
Titan, search for H_2 (3,0) S1 line in spectrum 78−4143
transfer equation, in semi-infinite atmosphere with albedo ($\omega>1$) 80−82184
turbulence determ. from radio occultations of spacecraft 80−94734
turbulence effects on atmospheric profiles derived from radio occultations 77−60696
turbulence effects on occultations, power spectra of phase and intensity fluctuations 79−40104
turbulence effects on profiles from Doppler meas. of occultations 79−2498
turbulence effects on profiles from intensity meas. of occultations 79−2499
turbulence effects on radio propag. during occultation 78−85871
turbulent scatt. in exponential atmosphere, wave-optical soln. 77−60590
two layer model, parameters determ. from obs. of absorpt. bands 78−24480
Uranus, 5-20 micron obs. rel. to upper atmosphere temp. 78−32393
Uranus, albedo and brightness temp., 5 μm IR obs. 80−82300
Uranus, albedo and spectral features from IR obs. 80−82299
Uranus, ammonia and water vapour contents 80−90366
Uranus, appl. of methane band-model parameters to visible and near IR spectrum 80−98609
Uranus, atmosphere radiative props. rel. to thermal evolution, comparison with Neptune 78−85903
Uranus, D/H ratio from visible spectra obs. 80−82296
Uranus, D/H ratio meas. 78−57497
Uranus, disc profiles, narrow waveband, 6000-8500 Å region 79−66960
Uranus, H_2 quadrupole lines detect. in spectrum 78−93149
Uranus, H_2 rotational quadrupole lines, theoretical brightness temps. 78−7917
Uranus, HD detect. at 6063.88 Å, D/H abundance ratio calc. 78−57495
Uranus, ionosphere model, ionization 78−4142
Uranus, limb and polar brightening at 7300 Å 77−56873
Uranus, limb brightening within methane 7300 Å band 78−85902
Uranus, methane absorpt. band in spectrum 78−45275
Uranus, methane band limb-brightness obs. rel. to atmospheric struct. 79−84742
Uranus, microwave brightness temp. increase 78−93150
Uranus, NH_3 depletion evidence 78−53870
Uranus, props. from IR spectrum from 0.8 to 2.5 microns 80−21946
Uranus, rotation periods rel. to methane band strength var. 78−49376
Uranus, saturation model of atmospheric structure 77−60723
Uranus, thermal structure from IR meas. 78−36509
Uranus, unsuccessful search for ethane emission 78−16344
Uranus, whole-disc optical polarization meas. 77−45356
Uranus atmosphere, equatorial flow model rel. to rot. 80−67653
Uranus atmosphere, UV albedo meas. 80−82295
Uranus atmosphere model, methane cloud 77−37567
Uranus clouds, particle comp. 80−31253
Uranus magnetosphere, plasma dynamics in mag. field laboratory simulation 79−16757
Uranus radiation belt protons, rings ice particles sputtering 78−89116
Uranus upper atmosphere, mean temp. and temp. vars. 80−46477
Uranus upper atmosphere, struct. from SAO 158687 occultation obs. 80−17547
Uranus upper atmosphere, temp. struct. 79−62791
Venus, acoustic-gravity waves in thermosphere 80−17520
Venus, aerosol distrib. changes, 1972-75 period 77−64681
Venus, aerosol model 80−101545
Venus, anal. of wind vel. meas. from Venera spacecraft data 77−29683
Venus, atmosphere and review of studies of planet *(Russian)* 77−25966
Venus, atmosphere circulation and ionisation rel. to rot. period 79−70977
Venus, atmosphere radio occultation obs. and surface bistatic radiolocation by Venera-9 and (Venera-10) 79−48698

planetary atmospheres continued
Venus, atmosphere radio transirradiation by Venera 9 and 10 satellites 77−82140
Venus, atmosphere structure instruments on Pioneer entry probes 80−67562
Venus, atmosphere thermal balance 77−73994
Venus, atmospheric conditions and clouds theory *(German)* 77−25968
Venus, atmospheric constitution, struct. and dynamics 80−105186
Venus, atmospheric dynamics, winds, circulation and turbulence 77−78706
Venus, atmospheric parameters meas. by Venera 9 and 10 descent vehicles 77−78597
Venus, atmospheric temp. and press. from high resolution IR spectra 77−60701
Venus, atmospheric tidal torque rel. to rot. dynamic evolution since form. 80−56742
Venus, attached and detached bow shocks 77−37541
Venus, boundary layer structure, Venera 9 and 10 obs. 77−78688
Venus, bow shock observations, 4th Dec. 1978 80−41747
Venus, chemical comp., Venera 12 gas chromatography *(Russian)* 79−66948
Venus, chemical composition deduced from twilight glow obs. 80−56739
Venus, chemistry of lower atm. prior to Pioneer Venus mission 79−16857
Venus, circulation development and vars., Mariner 10 TV pictures 78−57479
Venus, Cl+SO_2 reaction significance 79−84353
Venus, cloud and temp. struct., from 12-20 μm spectrum 79−66946
Venus, cloud cover obs. and recording 78−49355
Venus, cloud layer model, Venera-10 optical meas. interpretation *(Russian)* 79−21215
Venus, cloud layer moisture, Venera 4 ionization densimeter meas. 77−33379
Venus, cloud microphysics anal. 79−16853
Venus, cloud microstructure, optical props., H_2SO_4 atmosphere-aerosol study 80−72808
Venus, cloud microstructure 80−46431
Venus, cloud model using radiative transfer theory 77−82138
Venus, cloud optical properties and atmos. layered struct. 80−51681
Venus, cloud particles, Venera 9 and 10 nephelometric meas. 77−78695
Venus, cloud particles phase function, Mariner 10 data 79−40105
Venus, cloud patterns, waves and convection 77−5473
Venus, cloud properties from airborne obs. of near-IR reflectivity spectrum 78−53850
Venus, cloud structure, high-contrast UV detail 80−51682
Venus, clouds, aerosol size distrib., coagulation sedimentation and turbulent mixing effects 77−71041
Venus, clouds, anisotropic scattering model 78−53852
Venus, clouds, coagulation effects on droplet size distrib. 77−67056
Venus, clouds, IR absorption and scattering, particle size dispersion effect 80−109384
Venus, clouds, IR radiation, Venera 9 and 10 radiometer meas. 77−78699
Venus, clouds, Mueller scatt. matrices for nonspherical particles 78−90366
Venus, clouds, review 77−73993
Venus, CO_2, IR absorption, extrapolation from liquid to gas 77−493
Venus, CO_2 8689 Å band high-dispersion spectroscopy near superior conjunction 79−75129
Venus, CO_2 band spectroscopic obs. at 7820 Å 77−37540
Venus, CO_2 equivalent widths, phase variation obs. 77−37539
Venus, CO_2 IR absorpt. bands, 3900-10000 cm^{-1}, assignment 78−7896
Venus, CO_2 IR spectrum, laboratory expt. 77−3362
Venus, CO_2 line profiles, phase variation 77−82139
Venus, CO_2 lines equivalent widths, multiple scatt. calcs. 78−4095
Venus, CO_2 photoionisation and photoelectron energy distrib. in thermosphere 79−2506
Venus, composition, physical characteristics, optical properties 79−92690
Venus, composition and structure, Pioneer results 80−46230
Venus, composition and structure 77−73992
Venus, cyclic and diurnal vars. in thermosphere and exosphere 80−51683
Venus, dark face, atmospheric constitution, pictures from NASA Venus Pioneer space vehicle *(French)* 80−94735
Venus, dayside ion comp. dynamic effects, Pioneer obs. of ionsphere 79−48703
Venus, dayside ion composition, Pioneer meas. of ionosphere 79−48702
Venus, dayside ion densities 80−46444
Venus, daytime, density, press. and temp., Venera radio probing results 79−80253
Venus, daytime magnetosphere 79−96937
Venus, daytime topside ionosphere, plasma transport 78−4131
Venus, diffr. effects in radio transmission 77−64682
Venus, dynamical processes, three-dimens. model 78−32376
Venus, dynamics from power spectrum anal. of Mariner 10 images 79−53746
Venus, early evolutionary stages in atm. and climate 79−8696
Venus, electrical discharges *(Russian)* 79−66950
Venus, electron cooling by electron impact excitation of CO_2 78−57481
Venus, electron obs. and ion flows, Pioneer orbiter plasma analyzer expt. 80−46448
Venus, electron temp. and densities, Pioneer Orbiter meas. of ionosphere 79−48705
Venus, equatorial and polar limb-darkening 79−88613
Venus, equatorial IR brightness diurnal vars., obs. during 1975 apparition 79−16858
Venus, exosphere, hydrogen Lyman α emission 80−105188
Venus, exosphere, nonthermal H population, Venera Lyman α obs. 78−93136
Venus, exospheric density and escape fluxes of atomic isotopes 79−5771
Venus, far IR photometry, atm. thermal models 79−75151
Venus, flow of solar wind behind planet, model 80−98531
Venus, Fresnel refl. of Sun estimates 77−87305
Venus, H_2O content from narrow band photometry data 79−62779
Venus, H_2SO_4 aerosol cloud model implications 78−3312
Venus, H_2SO_4 aerosols characts. from isophotes, spacecraft obs. 78−81575
Venus, H distrib. and escape, charge exchange effects 77−29674
Venus, height depend. of temp., 52-90 km altitude, model 79−8866
Venus, high resolution Fourier transform spectropolarimetry 78−57469

planetary atmospheres continued
Venus, high spectral resolution ground-based obs. in 450 to 1250 cm^{-1} region 77−91456
Venus, hothouse theory of recent cosmological catastrophe 80−41749
Venus, impact ejecta trajectories, drag and gravity effects, analytic solns. 78−40854
Venus, implications of ^{36}Ar excess 80−12700
Venus, induced magnetosphere 79−84699
Venus, information from equivalent widths in spectropolarimetry 79−70976
Venus, internal gravity waves 79−5770
Venus, interpretation of weak spectral absorpt. lines 78−24481
Venus, ionopause, shocked solar wind viscous flow behaviour 79−75068
Venus, ionopause altitude variability model 79−75128
Venus, ionosphere, CO_2 and CO electron vibr. cooling rates 80−41750
Venus, ionosphere, comprehensive model 78−57480
Venus, ionosphere, day and nighttime radio sounding meas. from Venera 9, 10 spacecraft 79−8867
Venus, ionosphere, distrib. of elec. currents induced by solar wind interaction 77−64683
Venus, ionosphere, ion comp., photochemical and thermal diffusion control 80−46445
Venus, ionosphere, magnetic flux rope obs. by Pioneer Orbiter 79−70980
Venus, ionosphere, plasma diagnostics meas. by Venus Orbiter *(German)* 79−96941
Venus, ionosphere, thermal structure and energy influx 80−46443
Venus, ionosphere and airglow, calcs., Pioneer Venus prospects 78−89092
Venus, ionosphere energetics, model based on Pioneer obs. 79−75127
Venus, ionospheric diurnal ion comp. vars., Pioneer orbital meas. 80−46440
Venus, IR brightness temp., daytime minima 80−77309
Venus, IR emission spectrum, 17-38 μm, aqueous H_2SO_4 droplets in CO_2 atm. 78−40855
Venus, IR image and thermal struct. at time of Pioneer Venus probe encounter 79−48714
Venus, IR polarization interpretation 79−53745
Venus, IR radiation absorpt. induced by press., mol. collision between CO_2, N_2, O_2 *(Russian)* 80−56600
Venus, IR spectrometer obs. on Venera 9 and 10 spacecraft 77−78698
Venus, kinetic energy of atm. circulation 77−13261
Venus, light polarization and scattering 79−96814
Venus, lighting conditions in 0.5-1.1 μ range, Venera 9 and 10 meas. 77−78696
Venus, lightning discharges, frequency of occurrence 80−56743
Venus, lightning in atmosphere, chemical impact 79−96940
Venus, liquid content of lower clouds, Mariner 10 radio occultation data 79−40106
Venus, luminous flux from Sun, meas. from Venera-9 and Venera-10 77−37544
Venus, magnetic field and magnetosphere 80−56737
Venus, magnetosphere, evidence for boundary layer and magnetotail from Mariner 10 obs. 77−9686
Venus, magnetosphere, solar wind interaction 80−41687
Venus, magnetosphere press. balance, outside dayside ionopause 80−90353
Venus, Mariner 10 photometric obs. 77−29685
Venus, Mariner 10 radio occultation obs., pressure-temp. profiles 78−28563
Venus, Mariner 10 UV images normalisation 77−56850
Venus, microwave absorption in 21-117 GHz range 77−71040
Venus, model from radio, radar and occultation obs. 80−46420
Venus, nephelometer on Pioneer Venus Sounder and small probes 80−67511
Venus, net radiation meas. by Pioneer small probe 80−46435
Venus, neutral atmosphere, radio sounding meas., Venera-9, 10 spacecraft 79−8868
Venus, night airglow excitation, O_2 Herzberg II bands 77−41340
Venus, nightside ionopause config. 79−80256
Venus, nightside ionosphere, electron currents meas. in optical shadow by Venera satellites 78−4133
Venus, nightside ionosphere, electron temp. and density models 80−46442
Venus, nightside ionosphere, formation process, ionization, mixing ratios 80−41751
Venus, nightside ionosphere, Pioneer orbiter radio occultations 80−46441
Venus, nightside ionosphere origin and maintenance 77−2359
Venus, nighttime, radiowave fluctuation and turbulence, Venera radioscopy data 79−80254
Venus, nighttime atm. radioscopy by Venera 9 and 10 probes 79−62777
Venus, nighttime ionosphere, electron interaction in optical umbra 79−80259
Venus, nighttime ionosphere, two freq. radioscopy by Venera 9 and 10 probes 79−62778
Venus, nighttime luminescence, CO molecule identification 77−78702
Venus, nighttime luminescence, Venera 9 and 10 spectroscopic obs. 77−78701
Venus, NO production by lightning in clouds, odd N chem. reactions 80−26768
Venus, noble gases *(German)* 79−58289
Venus, O_2, $^1\Delta g \rightarrow {}^3\Sigma g^-$ band, prod. mechanisms 80−82251
Venus, O_2, Ar, CO abundances, error of Pioneer Venus chromatography obs. 80−105189
Venus, $O_2(^1\Delta)$ airglow and nightglow emission 80−17515
Venus, O_2 airglow emission from atom recomb. 79−31576
Venus, orographically scattered gravity waves 77−67057
Venus, oxidation state of atmosphere and crust from Pioneer Venus results 80−98586
Venus, photoelectrons and electron temps. in ionosphere 78−77511
Venus, photoelectrons caused by solar photons of less than 80 Å 80−56744
Venus, photoelectrons energy deposition 77−9687
Venus, Pioneer Bus neutral gas mass spectrometer 80−67513
Venus, Pioneer Differential Long Baseline Interferometry expt., wind meas. 80−67578
Venus, Pioneer gas chromatograph analyses, laboratory simulation 80−46362
Venus, Pioneer meas. of physical props. up to 200 km altitude *(French)* 80−46421
Venus, Pioneer nephelometer expts. results 80−46430
Venus, Pioneer obs., first report 79−84701

planetary atmospheres continued
Venus, Pioneer orbiter cloud photopolarimeter investigation 79−48713
Venus, Pioneer Orbiter cloud photopolarimeter meas. 78−57429
Venus, Pioneer Orbiter obs. of lightning 79−70979
Venus, Pioneer Orbiter radiometer (VORTEX) 80−67504
Venus, Pioneer small probes net flux radiometer expt. 80−67512
Venus, Pioneer Sounder Probe gas chromatograph 80−67507
Venus, Pioneer Sounder Probe neutral gas mass spectrometer 80−67506
Venus, Pioneer Sounder Probe Particle Size Spectrometer 80−67510
Venus, Pioneer Sounder Probe Solar Flux Radiometer 80−67508
Venus, Pioneer Venus magnetic field meas. on dayside ionosphere 79−48700
Venus, Pioneer Venus Orbiter neutral gas mass spectrometer expt. 80−67502
Venus, Pioneer Venus results, surface and atmosphere 80−17523
Venus, Pioneer-Venus, Venera 11 and 12 research results on atmosphere and surface topography *(German)* 79−80260
Venus, planetary meteorology rel. to weather and climate on Earth 79−84697
Venus, plasma wake, viscous flow 77−87302
Venus, plasma waves, solar wind interaction, Pioneer electric field meas. 79−48701
Venus, polar clearing in clouds, Pioneer Orbiter 1 obs. at 11.5 μm 79−70978
Venus, polar ionosphere, Pioneer orbiter radio occultations, electron density 79−48706
Venus, polarisation variation over disc, comment 77−2358
Venus, press. and density for different chem. comps. *(French)* 79−21214
Venus, radar obs. of atmos., soil and relief 80−36537
Venus, radiance meas. using Pioneer Venus Solar Flux Radiometer 80−82198
Venus, radiation-induced cooling 78−85885
Venus, radiative fluxes and equilib. temp. profile *(Russian)* 77−91455
Venus, radiative transfer, far IR opt. consts. of H_2SO_4 droplets 77−8574
Venus, radiative transfer, line form. level 80−17487
Venus, radiative transfer in 2.86-4.16 μm window 79−8863
Venus, reality of strong winds 77−29682
Venus, retrograde rot., Fabry-Perot meas. 78−65525
Venus, retrograde zonal winds below clouds 80−46436
Venus, review of Venera data 80−72804
Venus, role of gaseous S_2, S_3, S_4 and H_2S_n 80−17518
Venus, rotation of upper atmosphere *(French)* 80−36534
Venus, S chemistry and thermodynamics 79−44391
Venus, scatt. solar radiation in cloud layer, multiple scatt. theory inversion 79−8865
Venus, scattered solar radiation, day sky spectrum, Venera meas. 80−56573
Venus, scattering coeff. from Venera 9 and 10 photometry 80−8572
Venus, scattering layer over absorbing clouds, Venera 9 and 10 UV photometry 77−78700
Venus, scattering layers above visible clouds vertical structure 79−62775
Venus, SO_2 detect. in UV spectrum 79−62781
Venus, solar radiation spectral comp. rel. to Venera 9 and 10 illumination meas. 79−88612
Venus, solar wind interaction with ionosphere, electrodynamic model 79−84624
Venus, spectral detection of SO_2 and CS_2 *(French)* 79−62776
Venus, spectral line profiles and phase curves for Rayleigh scatt. 77−29684
Venus, spectral line shape of O following dissociative excitation 80−105097
Venus, spin and atmospheric tides 77−87301
Venus, spin evolution 80−46423
Venus, stratospheric large-scale turbulence, model 80−12699
Venus, struct. and comp. from refl. sunlight polarisation calc. and obs. 80−36533
Venus, subcloud lower atmosphere, IR radiation absorption calc. method 77−53446
Venus, sulphur chemical cycles, involving S, sulphite, sulphide and sulphate 80−50837
Venus, sunlight absorption 80−46434
Venus, surface layer turbulence from Venera 9 and 10 data 79−62780
Venus, surface reflections of Pioneer Venus descent vehicles radio emission, atm. data 80−105187
Venus, surface wind vel., Venera 9 and 10 anemometer meas. 77−78692
Venus, temp., cloud structure and dynamics from IR remote sensing 80−46429
Venus, thermal anomalies persistence and size 78−85876
Venus, thermal contrast from Pioneer probe data 80−46229
Venus, thermal IR temperature maps anal. 78−89094
Venus, thermal radiation fluxes altitude distrib. in subcloud atm. 77−29676
Venus, thermal radiative transfer, numerical modelling 80−8574
Venus, thermal radiometry by Venera 9 and 10 of cloud tops 80−46424
Venus, thermal regime, exploration methods *(Czech)* 78−32374
Venus, thermal structure and major ion comp. of ionosphere, Venus Orbiter retarding potential analyzer obs. 79−48704
Venus, thermosphere, comp. meas., temp. profile and homopause altitude 79−48707
Venus, thermosphere, heat sources prod. by solar UV radiation absorpt. 77−25965
Venus, thermosphere and exosphere, Pioneer Venus 1 drag meas. 79−48709
Venus, thermosphere during daytime, nitrogen chemistry 80−17517
Venus, thermosphere eddy coeffs. and lower atmosphere He content 79−80255
Venus, tidal theory and torque balance 80−46422
Venus, troposphere, chem. model, vertical zoning, comp., diurnal vars. 78−45251
Venus, troposphere, circulation calc. using 20-layer model *(Russian)* 77−33380
Venus, turbulence from Pioneer multiprobe radio scintillations 80−46437
Venus, turbulent mixing coeff. and homopause height 78−49354
Venus, ultraviolet photometry and cloud struct., Venera obs. 80−56738
Venus, undercloud atm. spectral struct. and thermal radiation spatial distrib. *(Russian)* 77−29678
Venus, upper atm., rot., photographs 1927-1975 in UV *(French)* 79−2504
Venus, upper atm. barotropic instability, model 78−89091

planetary atmospheres continued
Venus, upper atm. temp. and dynamics from Pioneer Orbiter IR radiometer meas. 80−26766
Venus, upper atmosphere, aerosol layer obs. from polarimetry 80−90352
Venus, upper atmosphere, diffusion model 79−2505
Venus, upper atmosphere density from Pioneer orbiter drag meas. 79−48710
Venus, upper atmosphere neutral composition, Pioneer quadrupole mass spectrometer obs. 79−48708
Venus, upper atmosphere neutral gas comp., diurnal vars. 80−46427
Venus, upper atmosphere structure and dynamics, review 77−33382
Venus, UV cloud images from pioneer orbiter 80−46432
Venus, UV cloud model from polarimetric obs. 80−82250
Venus, UV markings, Venera 9 cloud top data analysis 80−17521
Venus, UV markings contrast spectral depend. 79−62783
Venus, UV markings space-time relationships 77−5472
Venus, UV nightglow and thermospheric circulation 80−46428
Venus, Venera 11 and 12 first results *(Russian)* 79−35165
Venus, Venera 11 and 12 mass spectrometer meas. of lower atmosphere *(Russian)* 79−66947
Venus, Venera 9 and 10 aerodynamics and dynamics during motion in atmosphere 77−91399
Venus, Venera 9 and 10 radio transmissions near limb 77−78694
Venus, Venera-8 optical meas. interpretation 79−8864
Venus, vortex circulation, Mariner 10 polar stereographic UV images 79−35167
Venus, wake region, ionosheath plasma diffusion model 79−80257
Venus, whistler mode wave absorption in ionosphere 80−46446
Venus, wind speed meas. by anemometers on Venera-9 and Venera-10 probes 77−37542
Venus, wind vel. and turbulence, Venera 9 and 10 Doppler meas. 77−78693
Venus, winds, spectroscopic obs., techniques and data reduction 79−75130
Venus, zonal winds vertical extent 78−85875
Venus airglow, Mariner 10 UV spectrometer expt. 77−64611
Venus atmosphere, anal. by automatic interplanetary stations (Venera-4, 5, 6 and 8) 78−28520
Venus atmosphere, C and N species prod. by thunderstorms 80−98587
Venus atmosphere, dynamics rel. to Earth-synchronous rot. 79−25531
Venus atmosphere, IR extinction meas. from Pioneer Venus IR radiometer expt. 79−48719
Venus atmosphere, radio waves attenuation investigation by bistatic radar method 80−62061
Venus atmosphere, results of solar flux radiometer expt. aboard Pioneer Venus multiprobe mission 79−48718
Venus atmosphere, scattered solar radiation fluxes spectral and altitude distrib. 80−62059
Venus atmosphere, SO_2 detect. by IUE 79−101101
Venus atmosphere, SO_2 distrib. and implications 79−101100
Venus atmosphere, struct., and light, heat and wind regimes from space vehicles 80−62062
Venus atmosphere and surface, investigation by radiosounding from Venera 9 and 10 satellites 80−101543
Venus atmosphere profile from Mariner 10 radio occultation, statistical and computational uncertainties 79−96938
Venus atmosphere structure up to 110 km, Pioneer Venus entry probes preliminary results 79−48715
Venus atmospheric, review 78−32377
Venus atmospheric precipitation, props. and possibilities of detect. 80−56741
Venus atmospheric scatt., effect of varying scale height of scatt. particles 77−29679
Venus bow shock, comments 77−71042
Venus bow shock, depend. on solar wind strength 80−41748
Venus bow shock, Pioneer magnetometer obs. 80−36535
Venus cloud cover, obs. by Venera 9 orbiter 80−51680
Venus cloud layer, optical model from spectral photometric data from entry probes and orbiters 78−4130
Venus cloud layer, struct. according to Venera 9 televised pictures 80−67604
Venus cloud layer, Venera 9 and 10 narrow-band photometric probing 77−78697
Venus cloud tops UV spectroscopy, initial results from Pioneer Venus orbiter 79−48711
Venus cloud-top, thermal asymmetry 77−53447
Venus clouds, H_2SO_4 aerosol medium IR optical props. and spectrum 78−65526
Venus clouds, particle size distrib. meas. 79−48717
Venus clouds, Pioneer Venus nephelometer expt. preliminary results 79−48716
Venus clouds, UV absorbers, Pioneer data 80−46433
Venus clouds, UV absorbers identification 78−20665
Venus clouds spectropolarimetry, lines equivalent widths information content 80−31215
Venus cloudy layer, TV observation of UV and violet region from Venera station orbiter *(Russian)* 79−53747
Venus day sky spectrum, Venera 11 and 12 spectrophotometric obs. *(Russian)* 79−66949
Venus dayglow spectrum, 1250 to 1430 Å, Pioneer Venus obs. 80−77311
Venus daytime ionosphere, two freq. radioscopy results from Venera 9 and (Venera 10) 78−4129
Venus daytime ionosphere, two-freq. radio transillumination data using Venera-9, 10 probes 80−21936
Venus daytime ionosphere, Veneras 9 to 10 dual-freq. radio occultation expts. studies 79−96939
Venus dust ring, evidence from Venera 9, 10 obs. 79−75131
Venus environment, plasma wave investigation by Pioneer Venus Orbiter 80−67497
Venus exosphere, hot hydrogen origin 80−36536
Venus exosphere non-thermal H, ionospheric source and H budget 79−12416
Venus exosphere temperature, consequences of day-to-night var. 79−35164
Venus ionosphere, characts. and interaction with solar wind 77−73995
Venus ionosphere, electron temp. probe on Pioneer Venus Orbiter 80−67500
Venus ionosphere, mag. flux ropes nature *(Russian)* 80−77313
Venus ionosphere, Pioneer Venus Orbiter planar retarding potential analyser plasma expt. 80−67501
planetary atmospheres continued
Venus ionosphere, struct. of solar wind interaction region from ion flux characts. meas. 78−4051
Venus ionosphere, thermal diffusion calcs. 80−72806
Venus ionosphere composition, meas. by ion mass spectrometers on Pioneer Venus Bus and Orbiter 80−67499
Venus ionosphere solar wind interaction, review of present understanding 79−58288
Venus line profiles and curves of growth for isotropic scatt. 77−37538
Venus lower atmosphere composition, anal. by gas chromatography 79−48721
Venus lower atmosphere composition, preliminary results from Pioneer Venus 79−48720
Venus lower atmospheric layer, appl. of penetrative convection model *(Russian)* 78−24335
Venus magnetic tail, unipolar induction effects 80−62060
Venus mesosphere and thermosphere temp. struct., day-night variations 77−33381
Venus middle atmosphere, IR remote sounding from Pioneer orbiter 79−48712
Venus nightglow spectrum, $O_2(C^3\Delta_u$ to $a^1\Delta_g)$ 79−16856
Venus nighttime ionosphere, two-freq. sounding by Venera-9 and Venera-10 probes 77−37543
Venus plasma environment, study via plasma analyser expt. on Pioneer Venus Orbiter 80−67498
Venus radiative transfer of solar radiation, model based on Venera 10 data *(Russian)* 80−12698
Venus retrograde winds, possible periodic vars. 79−25530
Venus solar wind interaction region, plasma meas. using wide-angle instruments on (Venera 9 and 10) 77−91396
Venus stratosphere, retrograde rotation meas. with Fabry-Perot radial vel. spectrometer 79−44389
Venus thermosphere, Ar isotope abundances upper limits 80−4281
Venus thermosphere, depend. of struct. on solar activity 77−64686
Venus thermosphere, H global circulation and distrib. 78−89093
Venus upper atmosphere, N detect. 80−77310
Venus upper atmosphere mean circulation, diagnostic model using remote temp. soundings 79−58287
Venus wind velocities, vector determ. by radio interferometry 79−48722
vertical structure, general props. 78−4128
Voigt line width, empirical fits 77−22059
Voyager imaging experiment 78−24427
Voyager IR spectroscopy and radiometry experiments 78−24428
Voyager low energy charged particle experiment 78−20618
Voyager magnetic field experiment 78−24431
Voyager mission objectives 78−24426
Voyager photopolarimeter experiment 78−20616
Voyager planetary radioastronomy experiment 78−24433
Voyager plasma experiment 78−20617
Voyager plasma wave system 78−24432
Voyager radio science experiment 78−24430
Voyager UV spectrometer experiment 78−24429
windblown dust, threshold speeds and particle sizes 77−45083
C I UV fluoresc. from CO_2 photodissoc., rel. to Mars and Venus 79−13776
CO_2, electron energy deposition, excitation, ionization and heating, Venus and Mars appl. 79−45857
H distribution and escape, charge exchange effects 77−29674
H, He glow phenomena, effects of solar spectral lines modification by interplanetary medium 79−66973
H/D ratio in planetary atmospheres, determ. from CH_3D 9613 Å band 78−86861
H_2 (4,0) and (3,0) S(1) lines, absorption strengths 79−16852
HD 4-0 and 5-0 bands, absorption strengths in outer planet atmospheres 80−43059
H_2O, IR continuum absorpt. due to librational mode of dimer 78−66542
HeH_2, collision induced dipole IR spectra, ab initio SCF LCAO calc. 79−89737
NH_4OH, aerosols existence in planetary atms., IR reflectivity spectra, Kramers-Kronig anal. 78−68500
PH_3 photochemistry 77−16807
SO_2 IR absorption spectra *(Russian)* 79−25328

planetary nebulae
8 to 13 micron spectrophotometry, of six planetary nebulae 80−22057
10 micron properties, obs. 79−48879
49+88.1°, halo planetary nebula, photoionisation models and chemical abundances 80−109507
60−7°1, radial vel. meas. of central star FG Sagittae rel. to binary star model 80−98664
108−76.1°, halo planetary nebula, photoionisation models and chemical abundances 80−109507
108-76°1, new halo planetary nebula, chemical abundances 77−45510
158+17°1, new nearby object on POSS E-print 80−98701
A 21 (YM 29), planetary nebula model with strong stellar wind *(Russian)* 78−32559
Abell 30, Abell 78, unusual central struct. obs. 80−51855
Abell 30, obs. of ejected material from central star 80−82474
Abell 30 and 78, photometry and spectroscopy 77−91602
Abell 46, central star found to be eclipsing binary 80−73027
Abell 46, IUE spectroscopic obs. of eclipsing binary nucleus 80−98693
Abell 63, eclipsing binary central star UU Sagittae 78−93304
abundances of He, Ne, Ar, N, and Cl 80−109532
abundances of Ne, Ar and Cl rel. to O 79−5887
AFCRL 618, thermal radio emission from young planetary nebula 78−12343
atomic and molecular data for planetary nebulae, heavy particle processes 80−109528
BD+30°3639, IR spectrum 77−22297
BD+30° 3639, S III 18.7 μ fine-struct. forbidden line obs. 77−37637
bibliographical index for period (1965 to 1976) 78−12106
bipolar nebulae, photographic photometry *(Russian)* 77−13447
bipolar nebulae, study of general phenomenon 78−41026
birthrate in solar neighbourhood 77−13423
Butterfly Nebula M2-9 rel. to Be stars and protoplanetaries 79−48887
catalogue, of new and misclassified planetary nebulae 80−109378
central star evolutionary scenario towards white dwarf stage, composition effect 80−109427
central stars, Cassegrain image-tube scanner obs. of spectra 77−22214
central stars, evolution 78−12325
central stars, spectra, temps., binaries and peculiar stars 80−109435

planetary nebulae continued
central stars, spectrogram analysis 79−97001
central stars, temps. determ. rel. to nebulae evolution 80−67724
central stars, UV radiation meas. 78−28679
central stars, UV spectral obs. from TD-1 satellite 80−31300
central stars, visible and near IR spectra 77−78785
central stars, Zanstra temps. and effective temps. relation 79−88654
central stars of planetary nebulae, kinematics 80−51762
central stars of solar mass, evolution 80−109428
central stars temperatures, determ. from nebulae ionic abundance ratios 79−2565
central stars variability, UV obs. 78−36668
chemical abundance determ. from weak diagnostic spectral lines 80−109531
chemical abundances, spectrophotometric results 78−36663
chemical comp., network of models 79−48900
classification according to abundance, chem. kinetic and spatial props. 80−109509
classification according to chemical abundance 80−109530
Cn 3-1, emission line obs. 77−33621
control stars temperatures, determ. from forbidden O III lines 78−41015
cosmic dust in planetary nebulae, theoretical data review 80−109536
V1016 Cygni, proto-planetary nebula mass ejection rel. to photometric and spectroscopic evolution 78−85947
V1016 Cygni, single star model, possible forming planetary nebula 77−60762
detection rates in globular clusters 80−26950
distance scale, new, rel. to galactic distrib. 80−67819
distance scale, rel. to white dwarf birth rate 78−20867
distance scale of planetary nebulae, meas. methods 80−109521
distances, determ. through nebular ionised mass/nebula radius relation 80−101625
distances, new synthetic scale 78−89240
dust in planetary nebulae, observational review 80−109535
dust model for IR emission 80−56900
dust temperature and mass, IR photometry obs. 80−94850
dust to gas ratio and internal extinction 77−45519
ejection by stellar He shell flashes, theory rel. to planetary distance scale 78−24540
electron density from forbidden line ratios, evolutionary changes 77−78861
electron temperatures, determ. from radio continuum obs. 78−41027
element abundance and classification, implications for galaxy abundance 80−109530
element abundances, He/H, N/O and ^{3}He, implications for previous evolution 80−105237
emission line intensities for small ang. size moderate excitation nebulae 79−21407
emission line object, spectral obs., possible planetary nebula 77−49451
emission line objects in LMC *(French)* 78−69875
emission mechanisms and spectral features 79−67080
ESO 263-PN 02, spectroscopic obs. 80−101626
ESO/Uppsala survey of ESO(B) Atlas of southern sky, fifth list containing 2395 objects 78−20653
ESO/Uppsala survey of ESO(b) Atlas of southern sky, fourth list, 2920 objects 77−26059
ESO/Uppsala survey of ESO (B) Atlas of S. sky, pt.VII 80−56722
ESO/Uppsala survey of ESO (B) Atlas of southern sky, sixth list containing 3162 objects 79−8850
EUV spectra of young planetary nebulae 79−35336
evolution, analytical survey of spectrophotometric data 77−26045
evolution, implications of nuclei temps. and masses 80−82344
evolution after central star ejection, review 80−109533
excitation classes of planetary nebulae in Magellanic Clouds 77−91611
expanding molecular envelopes around evolved stars, CO emission line obs. 77−22219
extinction rel. to turbulent interstellar medium in Galaxy 80−62220
Fabry-Perot interferometry 78−4323
faint new planetary nebula discovery near NGC 6401 globular cluster 77−49461
far UV flux determ. from nebula ionisation state 80−72945
forbidden line and optical continuum electron temps. comparison 79−30105
formation, by thermonuclear explosion of stellar degenerate C core 78−36558
formation, model involving pulsation-convection coupling in late-type stars 77−13356
formation, role of Mira-type pulsation 80−26928
formation and C detonation supernova models, mass limits 79−17053
formation models, implications for Fe condensation 79−40238
formation with close binary nuclei 79−71097
Fornax dwarf galaxy, detection and props. of identified planetary 78−41005
G326.3−1.8, peculiar supernova remnant, two nearby planetary nebulae discoveries 79−25675
G339.2−0.4, supernova remnant or planetary nebula, radio and optical obs. 80−22104
galactic centre, 1415 MHz obs. 79−71096
galactic centre direction, new object detect. *(French)* 79−21434
galactic centre distribution radio obs. 77−17667
galactic centre field, planetary nebulae and Wolf-Rayet stars identifications 80−8674
galactic centre planetary nebulae, radio search, implications of flux density distrib. 80−56913
galactic stellar subsystems, kinematical model 77−13402
Galaxy chemical evolution, role of planetary nebulae 80−109541
HBV 475 (V1329 Cygni), high-excitation emission lines obs. 78−40955
HD 138403, emission line spectrum 77−67100
He2-442, UVRK photometry and spectroscopic obs. *(Russian)* 80−94817
He 1-3, misidentification correction 79−62895
He 2-111, giant halo with very high vels. discovery 79−25691
He 2-36, A-type central star 79−17064
Helix Nebula, abundance anomalies 78−86001
high-excitation, IUE satellite obs. 80−94860
IC 2149, absolute spectrophotometry in near IR 77−17669
IC 2149, extinction and radio struct. 77−41402
IC 2149, two-photon emission of H in UV spectrum 77−22301
IC 3568, struct. and internal extinction 80−31338
IC 418, C abundance from visible and IUE obs. 80−82451
planetary nebulae continued
IC 418, IR spectra, heated dust emission, atomic emission lines 80−46629
IC 418, near-IR spectroscopic obs. 80−4421
IC 418, search for absorpt. in CO fourth positive system 80−46647
IC 418, structure from electronographic data 79−35339
IC 418, UV spectra and C abundance 80−67832
IC 4593, absolute spectrophotometry in near IR 77−17669
IC 4593, emission line obs. 77−33621
IC 4997, compact planetary nebula, rapid emission-line vars. origin 79−92838
IC 4997, O III 4363 Å forbidden line/Hγ intensity ratio vars. 78−86003
IC 4997, O III 4363 Å/Hγ ratio reversal 79−92821
IC 4997, [O III] 4363 Å line intensity in variable planetary nebula 78−8100
interaction with interstellar medium, disruption timescale calcs. 79−101179
interstellar extinction, average model, from planetary nebulae obs. 80−62221
interstellar extinction from planetary nebulae optical and radio obs. 77−22295
interstellar medium, ionisation, heating and stirring, role of planetary nebulae, review 80−109540
ion recombination and level populations, resolution of ang. momentum states 77−45529
ionisation, influence of He shell flashes in nuclei 80−73021
ionisation models rel. to spectra, theory 80−109529
IR emission, advances in obs. and review of line and continuum radiation 80−109525
IR emission lines in 12 faint objects *(French)* 78−12337
IR radiation energy balance 77−13424
IR stars, dust obs. suggesting evolution of planetary nebulae 77−41404
K648, halo planetary nebula, low Ar abundance meas. 80−82443
K648, halo planetary nebula, spectrophotometry and element abundances 78−41011
K 648, halo planetary nebula, photoionisation models and chemical abundances 80−109507
kinematics, radial vel. meas. in galactic anticentre direction 80−46633
kinematics from radial velocities 78−45385
kinematics of galactic objects 80−26948
LMC N25, planetary nebula in red globular cluster NGC 1852 77−17668
local space density and formation rate 77−17652
low excitation planetary nebulae of small ang. size, spectral studies 80−17646
low-excitation nebulae, effective temps. of exciting stars 77−13427
in M15, possible second planetary nebula detect. in Hα 77−17655
M1-2, possible eclipsing binary central star 80−105239
M1-67 possible H II region, internal motions 79−92841
M1-76, possible forbidden line BQ star 79−84847
M1-78, possible planetary nebula, struct. at 15.4 GHz 78−41025
M2-9, compact planetary nebula, search for 1612 MHz OH maser 80−12774
in M31 (Andromeda galaxy), astrometric catalogue 79−40087
in M31 (Andromeda galaxy), identifications and photometry 78−28737
in M31 (Andromeda Galaxy) and companions, planetary nebulae props. 80−109520
M32-1, in M32, Hα/Hβ ratio shows that M32 is in front of (M31) 78−93394
M32-1, in M32, spectrophotometry and filter photometry 79−25664
M4-18, emission line spectra of peculiar object 79−84846
M4-18, spectroscopic obs. of compact object 80−67829
in M87, extended emission from large number of nebulae *(Russian)* 80−77492
M 1-2, emission line obs. 77−33621
M 2-9, structural changes (1952-78) 80−82456
Magellanic Clouds, chemical comp. of planetary nebulae 77−37632
in Magellanic Clouds, identification, luminosity function and numbers 80−67815
Magellanic Clouds, lists of planetary nebulae 79−58405
in Magellanic Clouds, space distrib., excitation classes and comps. 80−109519
major axes correl. with interstellar mag. field direction, hydromagnetic model 80−82473
materials motion around a source whose luminosity changes 79−12394
models, theoretical, low to medium excitation objects 80−67817
moderately bright, spectroscopic study 79−84835
molecules, abundances and IR spectra 78−53998
morphology and struct. 80−109534
MWC 17, emission line star, dense planetary nebula like object 77−45449
Mz 3 (p-K 331−1°1), obs. of bipolar nebula, possible protoplanetary 78−45376
nearby object in Lynx found on POSS E-print 80−98701
new and known planetary nebulae, on plates taken with 1.2 m Schmidt telescope 77−45530
new object in Monoceros 78−86002
new planetary nebulae discoveries with low surface brightness 78−16496
NGC 1360, central star found to be spectroscopic binary 77−45494
NGC 1360, central star radial vel. obs. 80−4350
NGC 147, Local Group galaxy, identifications and radial vels. of planetary nebulae 77−33596
NGC 185, Local Group galaxy, identifications and radial vels. of planetary nebulae 77−33596
NGC 2346 and 3132, A-type central stars 79−17064
NGC 2346 and 3132, A-type central stars of planetary nebulae, radial vel. study 78−81629
NGC 3132, central star is visual binary 78−20859
NGC 3242, 7009, 6210, high excitation planetary nebulae, high dispersion EUV obs. 80−77466
NGC 3242, UV emission lines, Copernicus obs., upper limits 79−12501
NGC 4361, unusual high excitation nebula, theoretical model, chem. comp. 80−22060
NGC 6210, 6543, 6572, spectroscopic obs. using multichannel analogue detector system 78−36461
NGC 6210, absolute spectrophotometry in near IR 77−17669
NGC 6302 chem. composition 78−96525
NGC 650/ 80−17639
NGC 6527, 7027, [O III] 88.35 microns and [O I] 63.2 microns fine struct. lines search 80−12794

planetary nebulae continued
NGC 6543, emission line obs. 77−33621
NGC 6543, lightcurve oscills. of BD+66°1066 nucleus 79−75223
NGC 6543, planetary nebula nucleus, periodicity disclaimed due to telescope periodic drive error 79−92763
NGC 6543, struct. 78−20869
NGC 6572, 6891, 7662, near IR spectrophotometry 78−8105
NGC 6572, IR spectra, heated dust emission, atomic emission lines 80−46629
NGC 6720, O III 5007 Å forbidden line obs., vel. structure 78−61909
NGC 6720 (Ring Nebula), monochromatic isophotometry 77−53673
NGC 6720 (Ring Nebula), strong forbidden N II emission and element abundances 77−26035
in NGC 6822, irregular galaxy, planetary nebula spectrophotometry and comp. 80−41867
NGC 6826 nucleus, UV spectrum obs. by International Ultraviolet Explorer (IUE) 78−96474
NGC 6853, probable binary central star from proper motion obs. 77−49434
NGC 6853, spectroscopic obs., element abundances 77−53667
NGC 6853 (Dumb-bell Nebula), complex motions of neutral and ionised gas 78−24539
NGC 6853 (Dumbbell Nebula), ionization and abundances 78−45390
NGC 7009, spectral comparisons of ring and ansae 79−71101
NGC 7027, 0.9-2.7 μ spectrum 77−2461
NGC 7027, 16-38 μ spectral obs. and dust model 78−93354
NGC 7027, 4 to 8 micron spectrum 78−12333
NGC 7027, anal. of low excitation emission lines 77−64823
NGC 7027, astrometric position meas. with small Schmidt telescope 78−73749
NGC 7027, C abundance 77−87526
NGC 7027, C III spectral lines, IUE obs. 79−71089
NGC 7027, charge transfer reaction rate rel. to forbidden Ne II 12.8 μ emission 80−56701
NGC 7027, continuum obs. and electron temp. 77−2462
NGC 7027, density gradient 77−87513
NGC 7027, dust model for IR emission 80−56900
NGC 7027, effect of dust on [O II] emission 80−8667
NGC 7027, far IR obs. 77−22288
NGC 7027, forbidden Mn V transitions identification 78−50496
NGC 7027, H_2 emission spatial distrib. obs. 80−98698
NGC 7027, He I 2.0 μm line strength rel. to He I 584 Å transfer problem 80−67550
NGC 7027, identification of central star 79−67008
NGC 7027, interstellar extinction, 164-2170 nm obs. 79−67082
NGC 7027, ionization struct., charge transfer reactions 78−36671
NGC 7027, ionization struct. and comp. 78−28745
NGC 7027, IR emission lines from molecules in grain mantles 78−36670
NGC 7027, IR spectrum 77−22297
NGC 7027, Mg abundance gradient 80−41875
NGC 7027, microns unidentified feature, high resolution spectra 80−82466
NGC 7027, near IR obs. 78−73748
NGC 7027, physical conditions and CNO elements abundances 80−82459
NGC 7027, radio recomb. line obs. 77−9780
NGC 7027, S III 18.7 μ fine-struct. forbidden line obs. 77−37637
NGC 7027, S IV and Ne II IR emission line obs. 79−21400
NGC 7027, search for vibrationally excited H_2 emission 78−93346
NGC 7027, struct. from electronographic obs. 80−12789
NGC 7027, UV emission line spectrum rel. to interstellar reddening, IUE obs. 78−96524
NGC 7027 and NGC 7293, spectral obs. *(Russian)* 78−61897
NGC 7293 (Helix nebula), complex struct. due to mass losing binary companion 79−48895
NGC 7293 (Helix Nebula), microstructures *(Russian)* 78−93344
NGC 7293 (Helix Nebula), obs. of [O I] λ6300 vel. field 78−12340
NGC 7662, Ne IV forbidden $^2D \rightarrow {}^4S$ lines obs. in UV spectrum 79−48896
NGC 7662, photoionisation model with charge transfer reactions rel. to emission-line spectrum 80−62233
NGC 7662, rocket UV spectrum and models 78−28746
nuclei parameters for 8 objects, evolutionary stage *(Russian)* 79−21404
O-type planetary nuclei, atmospheric props. 78−4206
O-type planetary nuclei, spectral classification, magnitudes, distances 78−4203
O/H ratios, meas. rel. to Galaxy O enrichment 80−105328
observation, list of bright nebulae 77−87514
observations and theory, IAU Symposium 76, Ithaca, New York, USA (1977 June 6 to 10) 80−105435
optical positions, meas. for 345 objects 77−5551
optical studies, review of recent advances 80−109522
origin, red giant stellar wind/circumstellar nebula interaction model 78−36674
origin and early evolution 79−62893
origin from giant stars, internal struct. and evolution 80−109537
origin from molecular envelopes of late-type giant stars 78−40940
outer layers structural properties and dynamics 78−8104
P-K 164+31°1, spectroscopic obs., identification 77−74123
peculiar central stars, spectroscopic characts. 77−87405
photoelectric filter photometry of 25 objects 77−9781
photoelectric spectrophotometry of emission lines, abundances 78−81677
photoionisation models for gaseous nebulae with optically thin condensations 80−36693
photoionization models for gaseous nebulae 79−21392
physical characteristics of field and galactic centre nebulae, rel. to evolution 78−54029
physical parameters, from absolute flux densities for emission lines in 6000-11000 Å range 80−51857
physical processes, advances in theory 80−109527
PK 108−76°1, 49+88°1, halo planetary nebulae, low Ar abundances meas. 80−82443
PK 181+1.1, very low surface brightness planetary nebula near galactic anticentre, discovery 79−17049
PK 60−7°1, nebula around FG Sagittae, spectrophotometric study 79−40240
PK 6-2°1, photoelec. spectrophotometry, N and He overabundance 77−78849
planetary nebulae central stars, atmospheric models 80−109434
planetary nebulae continued
planetary nebulae central stars, spectra, temps., binaries and peculiar stars 80−109435
PN 108-76°1, halo planetary nebula, element abundances 78−41011
PN 173+3.1, near galactic anticentre, coords., radial vel. and orbit 80−105309
PN 49+88°1, halo planetary nebula, spectrophotometry and element abundances 78−41011
possible probable and true planetary nebulae detected since 1966 78−16495
proto-planetary nebulae, props. and comparison with planetary nebulae 80−109538
RX Puppis, peculiar emission-line object, physical model 78−61871
radial vels. in LMC, catalogue 79−101089
radio and optical structure, comparison using 6 cm data 79−75262
radio emission, advances in obs. 80−109526
radio flux densities at 2.7 GHz 79−58394
radio mapping with Very Large Array 79−21196
radiofrequency recombination lines, computation of b_n factors 77−64832
refractory elements gas-phase abundances, hot stellar wind model 80−109516
review 77−17665
review 78−16510
review of characts. and evolution 78−32560
runaway planetary nebula ejection from M32 80−46626
FG Sagittae, 1975-8 spectral obs. of peculiar variable 80−72959
FG Sagittae, anomalous planetary nebula, spectrophotometry and UBV photometry (1968 to 1977) 79−88687
HM Sagittae, emission line variable, near IR spectrum *(Russian)* 78−81637
HM Sagittae, emission variable as embryonic planetary nebulae 77−56950
HM Sagittae, emission-line variable and radio source, as planetary nebula progenitor 78−28706
HM Sagittae, eruptive BQ forbidden line star, evolution to planetary nebula 78−20835
HM Sagittae, near emission-line object, optical and IR obs. and relation to planetary nebulae 78−36575
HM Sagittae, near-IR spectrographic obs. of young object 80−94810
FG Sagittae, photometric radius and pulsation mass 78−36576
HM Sagittae, planetary nebula excited by Wolf-Rayet star, spectrum 78−54003
HM Sagittae, possible proto-planetary, emission line widths 78−45389
HM Sagittae, proto-planetary nebula mass ejection rel. to photometric and spectroscopic evolution 78−85947
FG Sagittae, spectrum of assoc. nebula 78−49498
HM Sagittae, UBV changes and planetary nebula emission lines 77−71120
FG Sagittae, UBV photometry and spectroscopic obs. 77−71119
HM Sagittae, variable emission object, spectrophotometry 80−17599
HM Sagittae, young planetary nebula, 2.8 cm flux density secular increase 79−67025
HM Sagittae as young planetary nebula 79−48801
SchuWe-3, spectroscopic obs. 80−101626
Sharpless 176, large nearby planetary nebula, radius and distance determ. 77−87503
Simeiz 22, planetary nebula model with strong stellar wind *(Russian)* 78−32559
SMC, faint planetary nebulae identification 79−17081
southern, radio obs. at 5 GHz 79−58396
southern, red-sensitive objective-prism survey list of suspected objects 78−77496
in southern hisphere, IR and SHF obs. 80−90496
southern planetary nebulae, new discoveries 77−64667
southern planetary nebulae identifications 77−22302
spatial structure investigation by mathematical modelling, appl. to (NGC 7662) *(Russian)* 79−101188
spectra at visible, radio and IR wavelengths *(Italian)* 77−91604
spectra correction for interstellar absorpt., typical spectrum derivation 77−53677
spectral line intensity ratios evolution 77−64820
spectrophotometry, emission line intensities, physical conditions 78−36651
statistical props., graphical presentation 78−77589
statistical props. of central stars, spectral types and absolute magnitudes 77−87504
statistics of spatial and velocity distrib., review 80−109518
stellar planetary nebulae, southern, with emission lines, observational data 80−41843
stellar planetary nebulae, VLA obs. 80−22056
Stephenson's planetary nebula, optical, near IR and radio obs., position 79−67086
structural development, theory 77−64746
survey of Palomar Sky Survey E-prints 80−82460
truncated composite shell models, appl. to emission line fluxes 79−25677
ultraslow novae explosions, rel. to planetary nebulae form. *(Russian)* 78−77564
unidentified 3.3 μ emission feature obs. 77−33601
UV emission line spectra, excitation mechanisms *(Italian)* 78−32550
UV observations, accuracy and interpretation 80−109524
UV observations, review 80−109523
UV photometric obs., interstellar extinction determ. 77−17660
UV spectra, review of obs. 79−92843
19 W32 and 43, galactic centre planetary nebulae search 80−90506
Webb Society handbook 80−8743
^{22} Ne neutron source effects on Mg and Ne abundances 78−49430
C IV 1550 Å lines fluxes, meas. and theory rel. to C abundances 79−17051
CNO abundances, central stars masses, and origin of Population II planetaries 78−85992
Fe abundances from forbidden Fe VI emission 79−8970
Fe abundances in gaseous nebulae, from forbidden Fe III and Fe VI lines intensities 78−53806
Fe and C gas phase abundances 78−28744
H I Lyman α line formation in expanding spherical planetary nebula 79−30110
H II, region observational props. connected with planetary nebulae 80−109539
H Lyman α line formation, effects of nebula geometry 78−20871
H_2 emission detect. from 5 objects 78−20879
He abundance enhancement 78−93376

planetary nebulae continued
He enrichment 79−21380
He enrichment 79−35326
He I 584 Å in quasars and gaseous nebulae, line transfer problem and line strength 80−67550
He II, Lyman α photons absorpt. rel. to forbidden lines intensities 80−67833
He, N, O abundances of planetary nebulae in Magellanic Clouds 78−4338
He^+ radio recombination lines, stimulated emission 78−8092
N abundance enhancement 78−93376
N enrichment 79−35326
OH emission from planetary nebulae, search 79−48787
S abundances, determ. from IR line meas. 80−82444
S abundances in 20 galactic planetaries from spectrophotometry 78−45375

planetary rings *see planetary satellites*

planetary satellite atmospheres *see extraterrestrial atmospheres; planetary satellites*

planetary satellites
see also Moon
1966 S 2, positional obs., 1980 March 15 80−85893
1966 S 2 and 1980 S 15-18, separations from Saturn 80−67645
1978 P 1, speckle interferometric obs. (1980 June) 80−101553
1978 P 1, speckle obs. rel. to orbital radius and system mass and density 80−109394
1979 J 1 and 2, Voyager 1 imagery analysis 80−67639
1979 J 1 discovery by Voyager 2 camera 80−77334
1979 J 1-3, satellite periods from Voyager 1 and 2 data 80−105196
1980 S 10, precise positions, 1980 March 15 to 16, and relation to Dione 80−85893
1980 S 1, 3, 6, 25, new Saturnian satellites, positional obs., (1980 March 9 to 14) 80−94749
1980 S 2, new Saturnian satellite, discovery and possible orbital periods 80−46473
1980 S 3, 13, positional obs. (1980 March 15 and 16) 80−85893
1980 S 7 to 14, Saturnian satellites, obs. (1980 March 13 to April 8) 80−62068
Amalthea, 1976-8 absolute astrometric posn. 79−62789
Amalthea, effect of proximity to Roche limit on dynamical behaviour of ejecta 80−98592
Amalthea (J V), UBV photoelectric photometry near greatest W. elongation 78−36493
Amatthea, coupled to Jovian ionosphere 80−72869
analytical satellite theory in extended phase space 80−67524
artificial, zero angle approx. of orientation *(Russian)* 79−12381
artificial Martian satellite, meas. error and optimal trajectory 77−53409
asteroid satellites, discovery from occultations of stars 80−4286
asteroids, satellite detect. from occultation obs. 80−67629
astrometry, equatorial coords. for 1972-4 period *(French)* 78−81577
atmospheres, possible existence 78−96415
axisymmetric, periodic motion rel. to centre of mass in evolutionary circular orbit 80−21899
Bode's law and the 'missing moons' of Saturn 79−58480
Callisto, brightness temp. at 1.3 cm wavelength 77−67062
Callisto, diameter from lunar occultation meas. during 1977 January 1 disappearance event 78−45272
Callisto, evolution and surface age 80−56755
Callisto, evolution from derived crustal description 80−82265
Callisto, icy crater model to explain radar scatt. results 78−61789
Callisto, identification of water frost 78−4141
Callisto, IR emission spectra 80−82264
Callisto, surface affected by internal processes 80−21944
capture due to gas drag in primordial circumplanetary envelopes 79−53741
Cassini's laws and rotational motion of triaxial satellites 79−8812
celestial mechanics, modification of Szebehely eqn. 78−24447
Charon, Pluto's satellite, discovery and review of data (book) 80−82591
Charon, Pluto's satellite 79−30006
Charon (1978 P 1), occultation on 1980 April 6 probable 80−67651
Charon (1978 P 1), probable stellar occultation, 1980 April 6, min. dia. 80−62071
Charon (1978 P 1), satellite of Pluto, positions and dynamical parameters 80−62069
Charon (1978 P 1), stellar occultation obs., 1980 April 6, rel. to satellite dia. and struct. 80−94754
Charon (1978 P 1) probably no occultation of star on 1980 April 6, ephemeris 80−62070
circumplanetary swarm accumulation model 78−28549
comets ejection hypothesis, celestial mechanical aspects 80−62080
commensurabilities in solar system 80−109418
65 Cybele, occultation of AGK3+19°599, discovery of 1979 (65) 1 possible satellite 80−31237
Deimos, 100 years since discovery, review of studies 78−73670
Deimos, 37 positional photographic obs. during 1973 October at Pulkovo *(Russian)* 78−28568
Deimos, capture by photoatmospheric drag 79−40110
Deimos, effect on magnetosphere of Mars 80−41752
Deimos, evidence for strong interaction with solar wind 79−8787
Deimos, loose material downslope movement obs. 80−94737
Deimos, photographic positional obs. with Ukrainian Academy 400 mm astrography *(Russian)* 79−44395
Deimos, photometry from Viking orbiter images 80−72838
Deimos, spacecraft imaging 78−89102
Deimos, spectral evidence for carbonaceous chondrite surface comp. 80−41754
Deimos, surface features map and props. 80−31224
Deimos, surface morphology, comp. and props. 78−89103
Deimos, surface photometry 77−29696
Deimos, Viking Orbiter imaging results 79−35170
despun satellites, global tectonics 77−60698
direct and retrograde orbits, limiting radii and appl. to solar system and stellar systems 79−88572
Earth, debris belt creation by artificial satellites collisions 78−89035
Earth, ring system form. assoc. with Eocene terminal event 80−76890
Earth, search for natural or artificial objects located at Earth-Moon libration points 80−98647
Earth/Moon system, satellite aided capture of external body 79−75087
Elara radius and albedo 77−33399
Enceladus, IR photometry rel. to presence of water frost 78−12146
Enceladus, near IR spectra and JHK photometry 80−56761
ephemerides representation by Chebyshev polynomials *(Russian)* 79−16800
escape or capture duration, simple lower bound 79−2475
Europa, diameter from lunar occultation meas. during 1977 January 1 disappearance event 78−45272
Europa, ice crater model to explain radar scatt. results 78−61789
Europa, liquid water layer beneath ice crust, model 80−26780
Europa, UV emissions and possibility of O and H clouds 79−5775
evolution of planetary and satellite systems, computer program 80−77308
evolution of planetary rings, satellite formation model 78−53845
fluid drops as cosmological models, stellar evolution, solar system origin, planetary geology 80−73086
formation, physiochemical mechanism 79−8857
formation, unified theory for objects from meteors to stars 77−9739
formation by successive contractions of planetary gas discs 78−85863
formation from self-similar discs 79−80248
formation of planetary and satellite systems 79−21209
formation of regular satellite systems and major planet rings 80−41746
formation process, conservation laws and mass distrib. 78−81565
Fourier transform spectroscopy appl. to remote identification of solids in solar system 77−87273
Galilean satellites, 12.6 cm radar obs. 77−71057
Galilean satellites, 1976-8 relative posns. 79−62789
Galilean satellites, Amalthea, Voyager 1 results 80−4293
Galilean satellites, as plasma source in Jupiter corotating magnetosphere 78−89109
Galilean satellites, astrometric obs. in (1977) 79−48728
Galilean satellites, astrometric position determ. *(French)* 80−77326
Galilean satellites, astrometric position determ. 80−77327
Galilean satellites, astrometry using image photometric anal. technique. *(French)* 80−85880
Galilean satellites, contrib. of water products to Jupiter magnetosphere 78−45268
Galilean satellites, de Sitter ephemerides rel. to Jupiter oblateness 77−29715
Galilean satellites, diameters from Pioneer data 78−85893
Galilean satellites, dynamical coupling of periodic systems, resonance *(French)* 77−73938
Galilean satellites, dynamo mag. fields possible strengths 79−16873
Galilean satellites, eclipse spectrophotometry 79−96949
Galilean satellites, eclipses rel. to light hesitation determ. by Romer *(Danish)* 77−57140
Galilean satellites, ephemeris using Samson's theory *(French)* 78−16334
Galilean satellites, icy crater model to explain radar scatt. results 78−61789
Galilean satellites, improved ephemerides for Voyager mission 80−62066
Galilean satellites, interior structure from possible flyby meas. 78−36495
Galilean satellites, Jupiter Orbiter Mission CCD camera 80−85859
Galilean satellites, masses from Pioneer 10 and Pioneer 11 tracking data 77−37554
Galilean satellites, max. permissible exospheric temps. calc. 79−70989
Galilean satellites, mutual phenomena during 1979, obs. 79−80266
Galilean satellites, mutual phenomena in 1979 *(French)* 79−12427
Galilean satellites, near IR spectra rel. to surface composition 79−35180
Galilean satellites, orbital evolution rel. to Jupiter tidal Q 77−29713
Galilean satellites, orbits from numerical integration *(French)* 80−26779
Galilean satellites, photometric eclipses anal. rel. to theory of motion 78−53864
Galilean satellites, Pioneer 10 and 11 photographs 77−9699
Galilean satellites, pole positions 79−66954
Galilean satellites, position determ. in 1978 using Double Zeiss Astrograph *(French)* 80−72809
Galilean satellites, positioned within dipole-like Jovian mag. field, rel. to form. 79−2516
Galilean satellites, positions obtained in 1978 at ESO-La Silla *(French)* 80−21943
Galilean satellites, radar obs. during 1976, results 78−61788
Galilean satellites, rel. to Jupiter magnetosphere centrifugal distortion by equatorial current sheet 79−40134
Galilean satellites, role in restricted Jupiter orbiter problem 77−13216
Galilean satellites, spectral reflectivities in 0.32-0.86 μ range 79−35181
Galilean satellites, surface features from Voyager 2 obs. 80−72871
Galilean satellites, water ice existence, IR spectral reflectance obs. 80−82263
Galilean satellites as CO source in upper atmosphere of Jupiter 79−40128
Galilean satellites ions in Jupiter magnetosphere, equatorial confinement and vel. space distrib. 77−53464
Galilean satellites magnetospheres, plasma and mag. field perturbations 80−46465
Galilean satellites motion theory 77−45352
Galilean satellites of Jupiter, orbits long period behaviour 78−40864
Galilean satellites of Jupiter 79−5777
Galilean satellites volcanism and rotation, influence of Jupiter mag. field 80−31247
Ganymede, atmosphere erosion by radiation belt energetic atomic particles 80−72736
Ganymede, brightness temp. at 1.3 cm wavelength 77−67062
Ganymede, diameter from lunar occultation meas. during 1977 January 1 disappearance event 78−45272
Ganymede, effect on Jupiter magnetosphere, Voyager 2 obs. 80−77341
Ganymede, evolution and surface age 80−56755
Ganymede, icy crater model to explain radar scatt. results 78−61789
Ganymede, O atmosphere stability 77−29708
Ganymede, phase curve and surface microstructure from Voyager 1 photopolarimetry 79−96958
Ganymede, stellar occultation obs. by Voyager 1 rel. to exospheric atmosphere 80−26792
Ganymede, surface affected by internal processes 80−21944
Ganymede, surface model and characts. from radar obs. 80−90359
Ganymede, wake turbulence rel. to field-aligned currents in Jupiter magnetosphere 77−25975
Ganymede disturbing Jovian magnetosphere 80−72856
Ganymede image restoration by maximum entropy method 77−60624
gas condensation chemistry 79−35155
gravitational fields, inform. theory appl. 78−53835
gravitational heating of interior during form. process 80−36529

planetary satellites continued
532 Herculina, occultation of SAO 120774, discovery of 1978 (532) 1 possible satellite 78−69734
532 Herculina satellite, age and lifetime 79−40122
Himalia, radius and albedo 77−33399
hydrostatic tides, theory, Earth, planets and satellites appl. 79−84075
Hyperion, IR photometry rel. to membership of new class of satellites 78−12146
Hyperion, near IR spectra and JHK photometry 80−56761
Hyperion, radius and albedo from 20 μ obs. 79−40136
Iapetus, brightness and B−V colour index 77−60719
Iapetus, eclipse by Saturn's ring shadows, predictions 77−91472
Iapetus, eclipse by shadow of Saturn and rings (19-20 October 1977) 78−16342
Iapetus, eclipses by Saturn and its rings, 1977, Oct. 77−91471
Iapetus, eclipses by Saturn and rings, 1977 Oct. 19-20 and 1978 Jan. 7-8 predictions 77−53467
Iapetus, near IR reflectivity of dark and light faces 80−26800
Iapetus, normal reflectance from lunar occultation obs. 78−85897
Iapetus, radius from 1974 March 30 lunar occultation 78−36505
Iapetus, relative reflectance meas. at 1.6 and 2.2 μm 80−98607
Iapetus, theory of motion, perturbations 78−28577
Iapetus eclipses by Saturn's ring A, photometric confirmation of Encke division 78−45273
icy interiors and surfaces evolution 78−61771
icy satellites, mass-radius relationships 80−31222
internal satellite, in new kind of three-body problem 78−45210
Io, 5 micron variability 80−46463
Io, 'volcanic' outbursts, elec. current origin explanation 80−82276
Io, absorpt. bands in near IR spectrum 79−5776
Io, active volcanic eruptions and hot spots, Voyager 1 discoveries 79−40131
Io, albedo distrib. on surface 79−53761
Io, albedo stability and colour markings, historical meas. 79−96951
Io, atm. vertical struct. vars. *(Russian)* 77−78714
Io, atmosphere, review 77−5470
Io, atmospheric models with NH_3, N_2 and Na 77−37559
Io, bright dawn terminator due to thermoluminesc. 78−96425
Io, brightness increase after eclipse, colour TV obs. 77−87318
Io, charged particle absorpt. in Jupiter's magnetosphere 77−25971
Io, cometary ionosphere model 78−69738
Io, contrib. to Jupiter low-energy charged particle environment, Voyager 1 first look 80−26797
Io, contrib. to Jupiter magnetosphere energetic ions and electrons, Voyager 1 obs. 80−26798
Io, correlation of posteclipse brightening with major solar flares 78−28573
Io, currently active volcanism discovery 80−26789
Io, effect on S II ring round Jupiter 80−90360
Io, erosional scarps 79−92699
Io, evidence of SO_2 from UV obs. 80−36561
Io, flux tube wobbling and surface cond. effects on Jupiter's decametric emission and magnetosphere 80−26783
Io, form. of Na clouds and regolith by micrometeoroid impact 80−77330
Io, gaseous SO_2 identified and upper limits for other gases 79−92704
Io, global SO_2 abundance upper limit 80−77332
Io, H_2O loss and anhydrous surface form. 79−53756
Io, implications of Na and K salts spectral refl, changes and luminesc. during proton bombardment 79−96950
Io, indirect link with forbidden S II emission variability round Jupiter 80−85885
Io, influence on Jupiter S-bursts 78−36499
Io, intense transient brightening obs. near 5 micrometres 79−101113
Io, interaction with Jupiter mag. field, Voyager 1 preliminary results 80−26793
Io, interaction with plasma torus 80−98604
Io, ion source for Jupiter magnetosphere rel. to plasmapause theory 77−22133
Io, IR refl. spectra, 2.8-5.2 μm 80−56756
IO, IR reflectance spectrum, absorption features 79−92706
Io, local gas emission mechanism *(Russian)* 80−82275
Io, long term light vars. *(Italian)* 78−93147
Io, melting by tidal dissipation 80−4292
Io, modulation of Jupiter decametric radiation, charged particles accel. 78−89110
Io, morphology of Na emission region 77−49329
Io, Na cloud, comparison of models and two-dimens. images 79−12426
Io, Na cloud, first photographs 78−32389
Io, Na cloud direct images 78−61792
Io, Na cloud distrib. and intensity 78−36494
Io, Na deposition and sputtering rel. to Jupiter's ionosphere 79−44405
Io, Na I D_2 emission line profiles, var. with orbital phase angle and mag. latit. 78−4139
Io, Na I D-line emission synoptic obs. 77−13281
Io, non-linear standing Alfven wave current system 80−72869
Io, periodic variations obs. in Na and K clouds 78−4138
Io, phase and beaming effects on Jupiter decametric radiation 78−89114
Io, phase motion and Jovian decametric source locations 78−40866
Io, phase profile for S-bursts in Jupiter decametric radio emission 78−20722
Io, pictures of Na cloud 79−12425
Io, Pioneer 10 probe and Earth based obs. *(French)* 77−74006
Io, plasma cloud injection into Jupiter magnetosphere, S and O ions discontinuities 80−90358
Io, plasma injection influence on diffuse Jovian aurora 80−4289
Io, plasma sheath electrons rel. to Jupiter modulated decametric radio S-bursts *(Russian)* 80−8582
Io, plasma torus, ion density spatial distrib. 80−72861
Io, plasma torus implications of whistler mode chorus obs. 80−72862
Io, possible source of Jupiter's inner plasmasphere 77−60715
Io, post eclipse brightening, BV photometry 77−37560
Io, reflectance spectrum, evidence for sublimates and adsorbates 79−92707
Io, role of SO_2 in volcanism 79−92700
Io, search for colour changes and brightening upon eclipse reappearance 77−91469
Io, SHF radioemission and radiation belts *(Russian)* 80−36565
IO, SO_2 atmosphere stability 79−92705
Io, SO_2 frost IR spectra and deposition processes 80−77331
Io, SO_2 frost or adsorbate on surface, IR spectrum 79−92708
Io, SO_2 model atmos. and ionosphere 80−72853
planetary satellites continued
Io, source mechanism for Jovian decametric radiation 77−45349
Io, spectrum, S-containing mixtures and surface albedo 79−40127
Io, sulphur chemical cycles, involving S, sulphite, sulphide and sulphate 80−50837
Io, surface albedo rel. to laboratory samples 78−53865
Io, surface and environs, magmatic-volatile model 80−17537
Io, surface composition, comparison of observed and lab. reflectance spectra 77−60716
Io, surface composition 77−87314
Io, surface flows of quenched molten S 79−92703
Io, terrain units, map from Voyager 1 data 79−92696
Io, thermal and EM phenomena *(French)* 77−60714
Io, trapped electrons accel. rel. to S-bursts freq. drift meas. at different freqs. 80−85888
Io, visible spectrum, search for new features 79−35185
Io, volcanic activity model based on plasma obs. 80−72870
Io, volcanic eruption plumes 79−92698
Io, volcanic features 79−92697
Io, volcanic plume dynamics 79−92701
Io, volcanic resurfacing rates rel. to volatiles 79−92702
Io, volcanism, sulphur as volatile material 80−51688
Io, volcanoes as source of magnetosphere dust 80−85889
Io's torus, charged particle radial diffusion 80−72859
Io and Jovian radio S-bursts source of 2.5-35 MHz radiation 80−36562
Io interacting with jovian magnetosphere, model 80−36563
Io interaction with environment, Jupiter Voyager imagery analysis 80−105197
Io Na cloud, distrib. implications 80−46464
Io Na cloud, monochromatic imaging using filters, slitless (multislit) spectrograph, and interferometers 79−8840
Io Na cloud, obs. rel. to Jupiter magnetosphere thermal electron density 79−40133
Io Na cloud, solar radiation press. as cause of east-west asymmetries 80−36560
Io Na D-line emission, comparison of observed and theoretical line profiles 78−93145
Io plasma disc, model of plasma injection 80−72860
Io plasma torus, auroral hiss obs. (by Voyager 1) 79−92709
Io plasma torus, effects on Jupiter kilometric radiation ray tracing 80−72866
Io plasma torus, electrons pitch-angle diffusion by whistler mode waves 80−4290
Io plasma torus, radiative cooling and spectra 80−72850
Io plasma torus, Voyager 1 EUV spectrum obs. 80−26792
Io plasma torus, Voyager 1 plasma waves obs. 80−26795
Io plasma torus, Voyager 1 radio astronomy obs. 80−26796
Io plasma torus model in whistler propagation study 80−72863
Io plasma torus props. from Voyager EUV data 80−82262
Io plasma-torus and Jupiter magnetosphere Birkeland currents 80−105198
Io surface composition, implications of Na and K doped NH_3 frosts reflectance spectra 78−84561
Io tidal heating rel. to Galilean satellites orbital reson. locks 79−75145
Io torus, latitudinal plasma oscills. 80−85892
Io torus, plasma density from Voyager 1 occultation 80−77337
Io torus, Voyager 2 EUV obs. 80−77338
Io-Jupiter electrodynamic interaction, theory 78−81583
Io-related decametric radiation, geometrical beaming model for Jupiter 79−101112
Io-related Jovian radio emission, S-bursts occurrence with L-bursts and freq. upper limit 80−85887
Io-related radio emission, Jovian longitudinal control 79−30004
Jupiter, astrometric obs. of faint satellites during 1975-6 opposition 79−75139
Jupiter, auroral hot spots, Io- and Europa-related, longit. asymm. 79−75138
Jupiter, capture problem in celestial mechanics 78−77477
Jupiter, data from Voyager 2 on Jovian system 79−84740
Jupiter, eclipses of Galilean moons, obs. program 77−9703
Jupiter, Galilean from Voyager spacecraft 80−56759
Jupiter, Galilean satellite predictions by Galileo 79−88784
Jupiter, Galilean satellites, 1975-6 astrometric obs. 80−4288
Jupiter, Galilean satellites diverse features, Voyager I results 79−84738
Jupiter, micrometeorite impact, ion emission on satellite surfaces 80−77362
Jupiter, mutual eclipses and occultations of satellites, diameter calculation *(Swedish)* 79−92695
Jupiter, Na I emission from region C_2, Na transport from Io 79−53758
Jupiter, narrow rings, origin and location 80−56764
Jupiter, orbital and solar resonance of inner three Galilean satellites 80−56753
Jupiter, photometry of Io, Europa and Callisto, 1976 to 1979, possible solar variability detect. 80−98623
Jupiter, ring and Galilean satellites, origin 79−84736
Jupiter, ring and Galilean satellites, Voyager 2 IR obs. 80−77335
Jupiter, ring system, summary of recent research 80−72875
Jupiter, ring system, Voyager 2 obs. 80−12707
Jupiter, rings, Voyager I obs. *(French)* 80−82281
Jupiter, satellite orbits, three dimens. periodic orbit determ. 80−67526
Jupiter, speckle patterns, image retrieval 77−22100
Jupiter, surface meteoroid bombardment effects on satellite light curves 80−26786
Jupiter, triple shadow phenomena caused by Galilean satellites (AD 1900-2100) ephemerides 80−67641
Jupiter, Voyager 1 data summary *(Russian)* 80−82274
Jupiter, Voyager 1 obs. of Galilean satellites and Amalthea 79−96948
Jupiter, Voyager 1 photographic obs. of ring, Amalthea and Galilean satellites 80−26788
Jupiter, Voyager colour photographs of Amalthea and Galilean satellites *(German)* 79−96959
Jupiter, Voyager I encounter, general description of planet and satellites environment 80−12642
Jupiter, Voyagers 1 and 2, general results 80−17542
Jupiter's ring, Pioneer 11 obs. 79−88620
Jupiter's ring detect. at 2.2 μm 79−66958
Jupiter auroral hot spots at foot of Io-associated flux tube 78−16333
Jupiter faint satellites, astrometric obs. during 1976 to 1977 opposition 80−26778
Jupiter faint satellites (VI-XIII), astrometric obs., (1974 to 1977) 78−89107

planetary satellites continued
Jupiter fictitious satellites motion, long-period effects at 1/1 reson. 78−85830
Jupiter inner satellites, interaction with 79−58296
Jupiter inner satellites, mutual phenomena in 1979, ephemerides 78−53866
Jupiter magnetosphere-satellite interactions, aspects of energetic charged particle loss 80−36566
Jupiter major satellites, thermal structs. from Voyager 1 IR obs. 80−26790
Jupiter orbiter motion and risk of collision with Galilean satellites 77−2322
Jupiter outer satellites, origin rel. to libration-point capture theory 77−29636
Jupiter ring, dust EM scatt. lifetimes 80−82273
Jupiter ring, Voyager 1 detection 79−40131
Jupiter ring system, dust derived from Io volcanoes 80−85889
Jupiter satellite orbits, post-Newtonian effects 79−101054
Jupiter XIII, precise positions during 1975-76 opposition 77−64691
Jupiter XIII, rel. to satellite system struct. 77−67066
Jupiter/Ganymede, Jupiter/Callisto systems, satellite aided capture of external body 79−75087
Leda (Jupiter XIII), continuation ephemeris (1978 Sept.-1979 May) 78−69739
Leda (Jupiter XIII), ephemeris for 1977/78, Aug.-Apr. 77−82156
Leda (Jupiter XIII), orbit and ephemeris for 1974-2000 period 79−8875
Leda (Jupiter XIII), precise positions for 1976 Nov. 2 and Dec. 13 77−22135
magnetic moments, two predictions from scaling law test 80−21934
major planets, satellite systems form. 78−69714
major satellites of outer planets, internal structs. 79−62770
Mars, crater density interpretation 80−82252
Mars, ring production by destruction of Phobos 79−66951
Mars moons, dynamical evolution and origin 78−89104
Mars satellites, history of discovery 78−89099
Mars satellites, orbits and perturbations 78−89100
Martian satellite mass estimation from multiple Viking Orbiter encounters 77−56831
Martian satellites, effect of proximity to Roche limit on dynamical behaviour of ejecta 80−98592
Martian satellites, history of discovery and positional obs. (1877 to 1977) 78−89101
Martian satellites, origin by impact rupture of single body 77−64704
mean motions, distrib. rel. to development of solar system 77−91451
18 Melpomene, occultation of SAO 114159; discovery of 1978 (18) 1 possible satellite 79−16870
18 Melpomene, occultation of SAO 114159, secondary extinction event obs. rel. to 1978 (18) 1, possible satellite 80−56749
Mercury, escape of natural satellite 78−16323
Mercury, natural satellites escape rel. to planet's slow rot. 79−25529
Mimas, effect on Saturn's magnetic field *(Russian)* 80−94752
Mimas and Tethys, orbital theory including perturbs. 80−36568
minor planet satellite observations, reliability 80−46460
Miranda, influence on struct. of Uranian ring system 78−4148
Miranda (Uranus V), appulse to BD−14°3996 on 1977, March 10, predictions 77−2369
motion in vicinity of triangular libration points 78−12488
mutual phenomena of Jupiter's satellites (1973 Sept.-1974 Jan.) 79−40129
N-body problem, dynamical coupling of periodic systems, resonance *(French)* 77−73938
Neptune, ring, observational evidence in 1846-7 from Lassell and Challis 80−67652
Neptune, satellite system and origin of Pluto rel. to encounter with massive body 79−84743
Neptune II (Nereid), ephemeris, (1978 May 12 to September 19) 78−53873
Neptune ring, history of obs. 78−69745
Neptune/Triton system, satellite aided capture of external body 79−75087
Nereid, ephemeris continuation (1977, May-October) 77−49330
Nereid (Neptune II), ephemeris (1979 May-Sept.) 79−53770
Nereid (Neptune II), ephemeris (1980 March 2 to September 8) 80−46481
nomenclature, the case against mythological names 77−37533
nomenclature for unconfirmed satellites 79−16877
Oberon, near IR spectra and JHK photometry, mass and dia. measurement 80−56761
orbit, calc. for almost circular-near equatorial plane situation *(Russian)* 77−82115
orbit determination method by filter technique *(French)* 79−101050
orbit stability in restricted three-body problem 79−21162
orbit-orbit resonances in satellite systems, varieties and similarities 78−4093
orbital evolution due to tidal dissipation in major planets 79−40103
orbital resonances in solar system, review 77−25998
orbital stability, Hill's concept generalisation 79−92656
orbiter probe mission, 1981, planning 78−4056
orbits, third and fourth-order perturbations rel. to flattening of planet 80−67529
outer Galilean satellites, convection in ice crusts, effect on surface relief 79−84730
outer planets, Voyager spacecraft mission 78−49289
outer planets and satellites form. theory *(Chinese)* 78−69712
outer solar system satellites, identification of new class 78−12146
pendulum like systems, diagrammatic transition theory 79−44342
Phobos, 100 years since discovery, review of studies 78−73670
Phobos, 20 positional photographic obs. during 1973 October at Pulkovo *(Russian)* 78−28568
Phobos, capture by photoatmospheric drag 79−40110
Phobos, composition, evidence for carbonaceous chondrite surface from spectral anal. 78−49365
Phobos, equilibrium figures 77−33388
Phobos, evidence for carbonaceous chondritic composition from multicolour obs. with Viking lander cameras 78−49366
Phobos, first encounter by Viking Orbiter-1, mass and density determ. 78−49364
Phobos, grooves distrib., morphology and possible origin 80−72837
Phobos, Marsshine and shape/size determ. 79−44396
Phobos, mass from Viking Orbiter radio tracking data, density estimate 78−32380
planetary satellites continued
Phobos, mass from Viking Orbiter radio tracking data 78−32379
Phobos, modelling and mapping 79−40115
Phobos, of grooves, cratering hypothesis supported 78−57484
Phobos, orbital inclination evolution 80−67628
Phobos, origin of grooves, seismic effects of large meteoroid impact *(Russian)* 78−69754
Phobos, photometry and origin of dark markings on crater floors 79−16861
Phobos, photometry from Viking orbiter images 80−72838
Phobos, props., comp. and origin *(Norwegian)* 78−36478
Phobos, scale model using Mariner 9 obs. and solar simulation technique 78−28566
Phobos, spacecraft imaging 78−89102
Phobos, striations as evidence for tidal stress 77−78707
Phobos, surface density of impact craters 77−37547
Phobos, surface features map and props. 80−31224
Phobos, surface morphology, comp. and props. 78−89103
Phobos, surface photometry 77−33389
Phobos, Viking 1 Orbiter, encounter, trajectory analysis 80−12641
Phobos and Deimos, Mariner and Viking pictures 77−41347
Phobos and Deimos, preliminary results from Viking obs. 78−20681
Phobos and Deimos, Viking imaging, primary mission overview 78−20680
Phobos and Deimos, Viking photographs, surface features 79−21218
Phobos and Deimos 77−49323
Phobos and Deimos orbital evolution 80−26770
Phobos surface grooves, hybrid origin 80−31229
Phobos transit of Mars viewed by Viking cameras 78−69723
Phoebe, near IR spectra and JHK photometry 80−56761
Phoebe (Saturn IX), orbital motion 1904 to 1969 and Saturn mass determ. 79−88621
planetary geodetic control using natural satellite imaging 79−70959
Pluto, 1978 P 1, cosmogonical implications *(Chinese)* 79−84744
Pluto, 1978 P 1, discovery of possible satellite, ephemeris 78−69744
Pluto, 1978 P 1, possible satellite, orbit and eclipses ephemeris 78−93152
Pluto, 1978 P 1, possible satellite, Pluto image elongation obs. 78−81586
Pluto, 1978 P 1, satellite, obs. 78−85900
Pluto, Charon, account of discovery 80−12708
Pluto, discovery of satellite considered *(Swedish)* 79−92716
Pluto, satellite obs. *(Czech)* 80−31252
Pluto and its satellite, physical parameters and current research, review *(French)* 79−70994
Pluto-Charon, tidal evolution 80−26806
polarimetry of particulate surfaces 78−58011
polytropic satellite in central orbit, Roche problem and appl. to Saturn's rings 80−82179
position meas. for Uranus, Neptune, Jupiter and Saturn satellites 78−81573
resonance rotation stability 79−96897
resonant orbits about Jupiter, Periodic Comet Boethin (1975 I) case 80−72883
retrograde satellites, existence in restricted three-body problem, effect of mass ratio 77−13210
Rhea, normal reflectance from lunar occultation obs. 78−85897
Rhea, planetary, 1976 to 1979, rel. to possible solar variability detect. 80−98623
ring systems, review of physical studies 80−72874
ring systems and Saturn C-ring structure 78−81574
ring systems around giant planets, origin 78−32373
ring systems of Jupiter, Saturn and Uranus, radii and origins 79−84737
rings, Keplerian systems, collisional evolution, improved general theory 79−21152
rings, radiative transfer and multiple scatt. shadowing effect, theory 79−29987
rings, review 79−101096
satellite-satellite resonances, origin 79−16867
saturn, 1966 December and 1980 March positions for five satellites 80−94750
Saturn, 1978 opposition astrometric obs. of satellites 79−75149
Saturn, 1979 S 3, discovery of possible satellite 80−26802
Saturn, 1980 March Pic du Midi obs. 80−67646
Saturn, 1980 S 24 and 1966 S 2, 1980 April obs. 80−82280
Saturn, absorpt. of trapped radiation, Pioneer 11 obs. 80−82284
Saturn, absorption of particles, ring and satellite discoveries, Pioneer 11 obs. 80−82287
Saturn, astrometric obs. from McCormick Observatory (1977) 80−105200
Saturn, astrometric results from 1974 lunar occultations of satellites 78−36506
Saturn, D-ring (1973 September) 79−96966
Saturn, external gravit. field, tidal perturbs. due to rings, mass of rings calc. 79−35189
Saturn, F-ring and new satellite, Pioneer II discoveries 80−8585
Saturn, faint satellites existence, reexamination of evidence 79−16877
Saturn, interactions with magnetosphere 80−82285
Saturn, mutual eclipses and occultations of satellites, diameter calculation *(Swedish)* 79−92695
Saturn, narrow rings, origin and location 80−56764
Saturn, obs. of possible new satellite 78−7921
Saturn, orbital elements of satellites rel. to Saturn 's position and mass 77−74007
Saturn, outer ring and five possible new satellites discovery 80−46472
Saturn, outer ring search, 1979 November obs. 80−17543
Saturn, particle flux, Pioneer 11 meteoroid detector obs. 80−82291
Saturn, ring system, summary of recent research 80−72875
Saturn, ring system-ionosphere interaction 80−94751
Saturn, rings, four colour phase curves, analysis 80−4295
Saturn, rings, history and perturbation anal. *(French)* 80−82281
Saturn, rings, International Planetary Patrol obs. and data reduction 80−4294
Saturn, satellite analyses and electronographic obs. (1980 March) 80−77346
Saturn, satellite associated clouds, Pioneer UV photometry obs. 80−82288
Saturn, satellite masses calc. 77−56872
Saturn, satellite surfaces and interiors, review 80−4297
Saturn, satellites and exterior ring obs. (1980 Feb.-March) 80−51690
Saturn, satellites and rings, imaging, photometry and polarimetry obs. from Pioneer 11 probe 80−82289

planetary satellites continued
Saturn, satellites I-IX, astrometry obs. from McDonald Observatory (1975-1976) 80−105199
Saturn, surface meteoroid bombardment effects on satellite light curves 80−26786
Saturn, wavy deformation of rings caused by gravitational perturbations 78−57496
Saturn's rings, apparent and true thickness 79−21225
Saturn's rings, Cassini division formation, reson. with Mimas 78−61796
Saturn's rings, effect on direct solar radiation reaching top of atm. 79−70992
Saturn's rings, far IR spectral obs. 78−16341
Saturn's rings, structure from refl. sunlight polarization obs., disc of rock bodies 79−53767
Saturn's rings, thickness caused by satellite and solar perturbs. and planetary precession 80−36569
Saturn's rings, vel. dispersion calc. 78−61795
Saturn's rings, vertical struct. and thickness 79−53769
Saturn's rings gravit. field 77−87320
Saturn's rings optical thickness, nearby faint satellites obs., possible new satellite 79−16876
Saturn A and B rings, surface brightness obs. *(Russian)* 80−72872
Saturn A-ring, azimuthal brightness var. and particles size 78−32391
Saturn B-ring, optical reflectance polarimetry (1958-76 obs.) 79−44408
Saturn B-ring, optical reflectance polarimetry interpretation 80−31248
Saturn D-ring methane 890 nm band obs. 79−44407
Saturn E-ring, obs. during (March 1980) 80−67647
Saturn E-ring rel. to Enceladus orbit, max. density from CCD obs. 80−94750
Saturn equatorial satellites motion, appl. of problem of four fixed centres 78−28493
Saturn F-ring, discussion based on Pioneer 11 obs. 80−105202
Saturn innermost satellites, separations and times of elongation, (1980 February 29 to March 18) 80−56762
Saturn ring disappearances (1600 to 2100) 80−72876
Saturn ring E, inferences from obs. of radiation belt particles 80−41762
Saturn ring system, brightness enhancements rel. to existence of supposed satellites (1980 S 7 and 23) 80−94749
Saturn ring system, ephemeris for Earth ring plane crossing (1979 October 27) 79−101115
Saturn ring system, far UV spectrum and reflectivity rel. to comp. 78−53867
Saturn ring system, numerical simulation of systems of colliding bodies in gravit. field 77−29634
Saturn ring system, statistical mechanics of Keplerian orbits 78−20625
Saturn ring system, thickness from low tilt angle photometry 79−35186
Saturn rings, 3 mm obs. and props. 80−46470
Saturn rings, aperture synthesis study at 3.71 cm wavelength 79−96963
Saturn rings, brightness temp., 1.30 cm interferometry obs. 80−82279
Saturn rings, ice photo-sputtered to form at. H cloud 80−46475
Saturn rings, ice sputtering by radiation belt protons 78−89116
Saturn rings, interferometric obs. at 3.71 cm wavelength 79−96962
Saturn rings, IR brightness and eclipse cooling obs. 80−56763
Saturn rings, IR brightness scans 80−90363
Saturn rings, maintenance by planet gravit. quadrupole moment 78−53869
Saturn rings, model constraints from radar obs. of polarisation and albedo 80−82277
Saturn rings, near IR polarisation studies 78−85899
Saturn rings, new ring detection by focal coronograph *(French)* 80−72772
Saturn rings, Pioneer 11 investig. 80−46476
Saturn rings, structure and origin 78−73674
Saturn rings, unilluminated side, 20 μm brightness temp. 80−109392
Saturn rings, vertical struct. and thickness 80−4296
Saturn rings and icy satellites, formation, stability and observability of amorphous ice coverings 79−35188
Saturn rings azimuthal brightness vars., obs. at tilt angle (B∼11.°5) 79−48732
Saturn rings diffuse reflection, mutual shadowing effect classical calc. extensions 79−84666
Saturn rings thickness, photometric determ. 79−66959
Saturn rings vicinity, origin of Lyman-alpha emission 79−12430
Saturn satellite orbits, post-Newtonian effects 79−101054
Saturn satellites, positional photographic obs. at Pulkovo, (1971 to 1974) *(Russian)* 79−96965
Saturn satellites mutual phenomena in 1979-1980, ephemerides 78−53868
Saturn/Titan system, satellite aided capture of external body 79−75087
Saturnian rings mechanics, transversal viscosity effects on colliding bodies systems in gravit. field 77−67026
shapes and gravitational moments of tidally and rot. distorted objects 79−53757
solar system origin theories, critical review *(Chinese)* 77−22117
spin-orbit resonance, mathematical aspects 79−12389
stability limits for satellite motion 79−21163
synchronous rotation theory *(Russian)* 78−93134
Tethys, effect on Saturn's magnetic field *(Russian)* 80−94752
thermal evolution of small planetary bodies, convection modes 80−26764
three-body problem, doubly-averaged elliptical restricted, trajectories 80−46376
three-body problem, elliptic, Jacobian integral development *(German)* 79−92655
tidal friction in planet-satellite systems of solar system, secular effects 79−8860
tidal interactions, consequences and inferences 77−87297
tidal torques on circumbinary accretion discs, theory, commensurable satellites form. appl. 79−70952
Titan, 16-30 μm spectroscopy 80−56760
Titan, atm. vertical struct. vars. *(Russian)* 77−78714
Titan, atmosphere, review 77−5470
Titan, atmosphere organic chemistry, review 80−90364
Titan, Axel dust props., Mie theory 77−37565
Titan, brightness changes, solar activity effects 79−75177
Titan, brightness temp. at 6 cm wavelength 79−101114
Titan, contaminant terrestrial microorganisms, limitations to growth 77−41355
Titan, detectability of liq. methane, laboratory optical absorpt. spectra meas. 80−93278
Titan, dynamo mag. fields possible strengths 79−16873
Titan, inhomogeneous scattering model of atmosphere 79−44406
planetary satellites continued
Titan, IR spectrum from 0.8 to 2.5 microns 80−21946
Titan, Kuiper bands detect. in spectrum 78−85898
Titan, long term light vars. *(Italian)* 78−93147
Titan, N_2 atmosphere evolution 79−30005
Titan, NH_3 atmospheric abundance 78−12142
Titan, normal reflectance from lunar occultation obs. 78−85897
Titan, optical props. and vertical distrib. of aerosols in atmosphere 80−46471
Titan, photochemistry of hydrocarbons in atm. 79−53766
Titan, search for H_2 (3,0) S1 line in spectrum 78−4143
Titan, secular brightness increase, 1972-76 period 78−16346
Titan, sources of UV absorpt. in spectrum 77−41353
Titan, spectral reflectivity in 0.32-0.86 μ range 79−35181
Titan, suspected near IR variability 80−46469
Titan, upper ionosphere photoionisation 77−60720
Titan (Saturn VI) eclipse, 1979 December 20, photometric obs. 80−31250
Titan atmosphere, non-Maxwellian effects assoc. with H_2 thermal escape 79−80264
Titan atmosphere, photochemical aerosols identification 80−31249
Titan atmosphere, photochemical models 80−36567
Titan atmospheric aerosol distribution, constraint 79−96964
Titan eclipse by Saturn, light curve obs. rel. to Saturn upper atmosphere struct. 80−90362
Titan-Hyperion orbit-orbit resonance, appl. of spin-orbit theory 78−24451
Titan-Hyperion orbital resonance origin, observational test 79−25542
Titan-Hyperion resonances and close approaches, restricted three-body problem anal. 80−77347
Titania, near IR spectra and JHK photometry, mass and dia. measurement 80−56761
Titania and Oberon, IR photometry rel. to membership of new class of satellites 78−12146
Titius Bode Rule for solar planets and planetary satellites, c.f. Bohr atomic orbitals 79−101057
Titius-Bode law expt. *(Swedish)* 78−85870
topographic changes on airless bodies, meteorite impact and ejecta deposition 78−65523
Triton, diameter and reflectance, spectral and radiometric obs. 80−17546
Triton, image tube spectra, 6800-9000 Å, search for possible atm., methane upper limit 79−16880
Triton, IR photometry rel. to membership of new class of satellites 78−12146
Triton, narrow band spectrophotometry 79−16879
Triton, satellite with atmosphere, IR spectrum obs. 80−21945
true circular orbit 80−46368
Umbriel, near IR spectra and JHK photometry, mass and dia. reassessment 80−56761
Uranus, ϵ-ring, variable width and ellipticity, orbital considerations 78−40870
Uranus, evidence for satellite belt from SAO 158687 occultation 77−29718
Uranus, Laplace relation and satellites masses 77−5492
Uranus, mass estimate of proposed sixth satellite 79−35190
Uranus, narrow rings, origin and location 80−56764
Uranus, new satellite occultation of SAO 158687, Kavalur obs. 77−53473
Uranus, occultations of stars by rings, existence of rings confirmation and radii calc. 78−53872
Uranus, ring system, struct. from photoelec. obs. of 5AO 158687 occultation 80−77348
Uranus, ring system, summary of recent research 80−72875
Uranus, ring system, theory, orbital reson. with Ariel, Titania and Oberon 77−64698
Uranus, rings, nature and origin, orbital resonance 79−96967
Uranus, rings, occultation obs. *(French)* 80−82281
Uranus, rings, possible obs. by William Herschel 79−48733
Uranus, rings, size, shape and periods of rotation *(French)* 79−48735
Uranus, rings origin, orbital reson. effects 78−53874
Uranus, satellite rings, KAO obs. of SAO 158687 occultation 77−53471
Uranus, satellite rings, Perth Observatory obs. of SAO 158687 occultation 77−53472
Uranus, satellite rings occultation of SAO 158687, discovery accounts 77−74009
Uranus, satellites and rings, albedo and spectral features from IR obs. 80−82299
Uranus ϵ ring, precession 80−26804
Uranus ring, form. and stability 80−82302
Uranus ring occultation possibilities for two faint 11-12 mag. stars 77−56875
Uranus ring system, obs. of occulation of (SAO 158687) 77−67068
Uranus ring system, quantitative anal. of Dermott-Gold theory 78−4147
Uranus ring system, reality of occultation events a to g, 1980 August 15 to 16 questioned 80−109396
Uranus ring system, statistical mechanics of Keplerian orbits 78−20625
Uranus rings, as volatile material in satellite orbits, model 80−26807
Uranus rings, BD−15° 3969 occultation obs. 78−89118
Uranus rings, colours and magnitudes of stars occulted during (1977 to 1980) 78−16277
Uranus rings, discovery, SAO 158687 occultation on 1977 March 10 78−69743
Uranus rings, geometric albedo upper limit 78−36510
Uranus rings, ice sputtering by radiation belt protons 78−89116
Uranus rings, obs. of stellar occultation, (1980 August 15 to 16) 80−98610
Uranus rings, occultation of SAO 158687, 1977 March 10, photoelec. obs. and anal. *(Chinese)* 78−69657
Uranus rings, occultation of SAO 158687, 1977 March 10, photoelec. obs. 79−30007
Uranus rings, optical search 77−67067
Uranus rings, prediction in 1972 based on Alfven critical vel. effect 79−2518
Uranus rings, radii and widths from 1978 April 10 occultation of SAO 158687 79−8878
Uranus rings, radii from SAO 158687 occultation 78−89117
Uranus rings, reson. orbit theory and prediction of undiscovered satellite 78−81585
Uranus rings, S/N ratios for stellar occultations, 1977-80 period 78−32392

planetary satellites continued
Uranus rings, theory 79−21226
Uranus rings discovery *(Danish)* 78−69742
Uranus satellite belt, numbers and positions from SAO 158687 occultation 77−33408
Uranus satellite ring system, new features from Kavalur photoelectric record of SAO 158687 occultation 78−12152
Uranus satellite rings, occultation of SAO 158687 77−37568
Uranus satellites, astrometric obs. 80−67654
Uranus satellites, narrow band spectrophotometry of Ariel, Umbriel, Titania and Oberon 79−16879
UV spectra, International Ultraviolet Explorer (IUE) obs. 78−93133
Venus, dust ring possibility from Venera 9 and 10 spectroscopy 80−8573
Venus, escape of natural satellite 78−16323
Venus, natural satellites escape rel. to planet's slow rot. 79−25529
Venus, small satellite as source of dust ring obs. by (Venera 9, 10) 79−75131
Voyager imaging experiment 78−24427
Voyager IR spectroscopy and radiometry experiments 78−24428
Voyager magnetic field experiment 78−24431
Voyager mission objectives 78−24426
Voyager photopolarimeter experiment 78−20616
Voyager plasma experiment 78−20617
Voyager plasma wave system 78−24432
Voyager radio science experiment 78−24430
Voyager UV spectrometer experiment 78−24429
Io, Na and H clouds 77−64695
Io, Na D-emission photography using Mach-Zehnder interferometer 77−60617
Io, Na I, Ca I, Fe I, and Mg I emission lines in spectrum 79−21223

planetoids *see asteroids*

planets
see also asteroids; comets; Earth; Jupiter; Mars; Mercury (planet); Neptune; planetary satellites; Pluto; Saturn; Uranus; Venus
1978 annual review of Earth and planetary sciences 79−5437
accretion dynamics, computer simulation, sensitivity to initial conditions 77−82131
accretion model of planet formation rel. to minor planet size 78−12137
accretion of terrestrial planets, gravitational N-body problem 78−53846
accretion rates, implications of ^{36}Ar excess on Venus 80−12700
accumulation model, numerical expts. results *(Russian)* 80−8557
accuracy of Ptolemaic and Copernican theories using curve fitting techniques 78−32325
AGU conference, June 1979, Washington, DC, USA 80−8732
American Astron. Soc., Division for Planetary Sciences, 11th-Annual meeting (Clayton, Missouri, 23-26 October 1979) 80−36760
angular momentum and magnetic moment from superheavy hadrons 80−26843
Annual review of Earth and planetary sciences, vol.5 77−64174
asteroids and planets X, conference (Tucson, March 1979) 80−31406
astrometric observations, phase reduction formulae *(Russian)* 79−96891
astrometric observations via Danjon astrolabe 77−64651
astrometry, daytime obs., anomalous refr. and personal errors meas. 78−24441
astrometry, equatorial coords. for 1972-4 period *(French)* 78−81577
astrometry, meridian obs. of major and minor planets, (1974-1977) 78−69660
astrometry with Danjon astrolabe, review *(French)* 80−94715
atmospheres, response to heat sources and perturbations *(Chinese)* 80−85748
atmospheres of Earth and planets, origin *(Chinese)* 79−16846
Barnard's star, analysis of and possible planetary system 78−81657
Barnard's star, astrometric obs. 1916-1976, sexagintennial report 77−45432
Barnard's star, evidence for planetary companions 78−81656
basalts, redox state 78−77217
basic properties, rel. to anthropic principle of cosmology and physical world struct. 79−48973
with biospheres, criteria for evolution of technology 77−71018
Bode's law of planetary magnetism, re-evaluation 78−40853
brightness temperatures in far IR, recalibration 77−9683
capture into resonance rotation, tidal friction 77−78620
chemically peculiar (CP) stars formation, planetesimal impact hypothesis 78−20834
circumstellar disks and planetary formation 79−58321
close encounter computation, new method 79−35099
collisions and interactions in early solar system 77−73977
cometary contribution 79−58300
comets capture by Laplace scheme, orbital elements statistical consequences 78−53888
comets capture by planets, Laplace hypothesis 78−28592
comets ejection hypothesis, celestial mechanical aspects 80−62080
composition, rel. to mass distrib. in solar nebula and planetary system 78−12109
computer simulations of planetary system evolution 80−94733
conducting sphere rotating in time independ. homogeneous mag. field, unipolar induction *(German)* 78−17836
conference (Boston, MA, 28 October, 1977) 79−53740
conference on planetary sciences, Rome, Italy (Apr. 1979) 80−77537
conjunctions, rel. to solar activity cycles and terrestrial palaeoclimatic record 77−78401
conjunctions and Maya chronology 78−36470
conjunctions rel. to Mayan dates in AD 293-1237 period 77−17392
convective dynamo, models 78−89090
core cooling by subsolidus mantle convection 80−36278
crater doublets expected frequency 78−61777
crater morphology from impact spacecraft imagery 80−62052
crater size-freq. data presentation and analysis, standard techniques 79−44387
cratered terrain, thermal regimes and impact melt 77−2125
cratering, as key to system history 77−82132
cratering by meteorite impact 79−21244
61 Cygni, unseen companions, max. entropy spectral anal. of period data *(Russian)* 78−69841
degenerate substellar bodies, role of chemical immiscibilities 78−69798
density structure, max. entropy inversion 80−67602
despun planets, global tectonics 77−60698
diameter meas. by occultation obs., teaching expt. 78−12457
dielectric props. of lunar and planetary surfaces 77−60678
differential rotation, gravitational effects 79−8862

planets continued
differentially rotating models, gravit. field and figure 78−7893
dispersal of solar nebula by solar wind with Sun in T Tauri stage 77−5467
dust-covered planetary surface, polarimetric model 79−25528
dynamical control of interplanetary bodies, resonances and close encounters 80−82260
dynamo theorems 80−81810
dynamo theory for mag. field generation *(German)* 78−40852
dynamos in interior driven by gravitational settling 80−36246
early accumulation and planetesimal relative rels. 79−58283
Earth and planetary sciences, annual review (volume 7) 79−84070
education, Kepler's third law, synodic period statement 77−87601
electrically conducting fluid core location from external mag. obs. 78−32248
electrically-conducting fluid, mag. flux linkage, planetary dynamo theory 80−8536
electrically-conducting fluid, mag. flux linkage, relativistic case, planetary dynamo theory 80−12655
elliptical galaxies, lack of spiral arms and lifebearing planets 77−64845
energy balance of rot. planet with atmosphere in solar flux 80−26765
ephemerides, direct computation method *(French)* 78−7862
ephemerides, effect of star catalogue coord. system orientation errors *(Russian)* 80−51640
equatorial parameters determ., theory 80−4282
eucrite parent asteroid, bulk composition, planetary evolution bearing 80−56786
evolution, solar influence 78−49348
evolution of planetary and satellite systems, computer program 80−77308
evolution rel. to analysis of lunar and terrestrial rocks *(French)* 79−88355
evolution rel. to H_2 ortho-para ratio in primitive solar nebula 78−89233
exploration, achievements and planned missions 79−62710
exploration, invited discourse before sixteenth general assembly of IAU 78−12076
exploration by spacecraft 80−105146
exploration methods, appl. to planetary atmospheres and solar nebula theory *(Czech)* 78−32374
exploration programs, United States 78−77461
external potential, determ. using gravity vector anomaly *(Russian)* 77−33375
extra-solar planetary systems, detection by Space Telescope 80−109356
extrasolar, direct imaging with space telescope during stationary occultations 78−85858
extrasolar, search for unseen and sub-stellar companions of nearby stars, astrometry 79−30092
extrasolar Earthlike planets, topography 78−61889
extrasolar planetary systems, direct imaging 80−82426
extrasolar planetary systems, dynamical instability and detection 80−82429
extrasolar planetary systems, multiplicity of solar-type stars 77−13386
extrasolar planetary systems, origin, comparison with close binary systems, and freq. 79−5859
extrasolar planets, astrometric photoelectric detection equipment 80−56882
extrasolar planets detection, imaging theory 77−29882
extrasolar systems, detection using space-borne interferometers 80−109357
extrasolar systems, search strategies 80−46615
far IR and submillimetre obs. 77−71037
ferroelectric phases, high press. studies 78−69334
figure, Clairaut-Laplace-Lyapunov problem 77−25963
figures, hydrostatic equilib. eqn. numerical soln. 79−62773
flattening, gravit. pot. expansion rel. to satellite orbits third and fourth-order perturbations 80−67529
fluid sphere interior soln., const. gravitational mass density in general relativity 77−79015
formation, appl. of statistical mechanics of perturbed Keplerian orbits 77−49269
formation, behaviour of system of particles at high press. 77−87261
formation, current theories and problems 79−84685
formation, implications of origin of large interstellar grains towards ρ Ophiuchi 80−41870
formation, mechanism of early growth 78−28547
formation, physiochemical mechanism 79−8857
formation, planetesimal theory origin 77−87623
formation, primordial solar nebula struct. and evolution 80−62042
formation, unified theory for objects from meteors to stars 77−9739
formation as adiabatic phase transition, isoentropic model 80−26763
formation as isothermal phase transition, elementary model 79−62771
formation by coalescence, averaging of orbital eccentricities 77−17388
formation by successive contractions of solar nebula 78−85863
formation from self-similar discs 79−80248
formation from solar nebulae, mass transprt processes in rotating dust cloud 80−8556
formation in binary star systems, Goldreich-Ward planetesimal accretion 78−61883
formation in collapsing protostellar cloud, dust dynamics 79−58401
formation in relation to interstellar clouds and star form., plasma physics theory 78−73744
formation models 80−62058
formation of planetary and satellite systems 79−21209
formation of planetary system, Titius-Bode law 80−62057
formation process, conservation laws and mass distrib. 78−81565
formation with Fe cores in early solar system 78−85869
four-body problem, restricted planetary case 80−41742
Fourier transform spectroscopy appl. to remote identification of solids in solar system 77−87273
Fulton's orrery, 19th century instrument to demonstrate planetary system motions 78−69695
gamma-ray emission, observational and physical review 79−80373
gas condensation chemistry 79−35155
general planetary theory in elliptic variables 77−13212
general relativity test, planets observed by astrometric and radiometric methods 78−45552
geodetic control using natural satellite imaging 79−70959
giant gaseous protoplanets, interaction with primitive solar nebula 80−56727
giant planet evolution, theory 80−56734

planets continued
giant planet interiors, dense fluid mixture of nuclei, phase separation calcs. 77−56849
giant planets, 1.4 mm obs., effective temps. 77−87312
giant planets, atmospheric thermal structs. 79−84735
giant planets, detectability of liq. methane, laboratory optical absorpt. spectra meas. 80−93278
giant planets, gravitational effects on comet orbits evolution 80−98613
giant planets, origin of ring systems 78−32373
giant planets, representation of perturbations due to Pluto *(French)* 80−26724
giant planets, satellite escape or capture duration 79−2475
giant planets, second order perturbs. *(French)* 79−12385
giant planets' atmospheres, bimolecular reactions of positive ions, laboratory studies 77−63896
giant planets and white dwarfs 79−16955
giant planets second-order perturbations, semi-major axis secular vars. *(French)* 79−2474
gravitational attraction of planet of arbitrary oblateness 77−91424
gravitational fields, inform. theory appl. 78−53835
gravitational forces on Earth, effect on earthtides and earthquakes 79−100817
gravitational heating of interior during form. process 80−36529
gravitational potential at planet physical surface, satellite model applicability 79−62774
gravitational quadrupoles *(Russian)* 79−58285
gravitational spectra, determ. from planetary orbiters tracking 80−41744
gravitational spectra from direct measurements 80−30978
growth in protoplanetary nebula *(Russian)* 78−69715
habitable planets in Galaxy, number 79−40221
habital planets around multiple stars, computer simulations 79−2559
heavy viscous liquid forming thin shell on planet in circular orbit, Navier Stokes eqns. soln. *(Russian)* 78−65782
heliocentric planetary alignments correl. with Chinese earthquakes 77−5136
heliogenic model of origin, and lunar volcanism *(French)* 77−64671
hydrostatic ellipticity calculation algorithm 80−62055
hydrostatic tides, theory, Earth, planets and satellites appl. 79−84075
impact craters, relative prod. rates on different planets 77−60699
impact craters, use of equivalency in estimation of historical size distrib. 78−45250
inner planetary systems, stability 79−70975
inner planets, second order perturbation theory *(French)* 80−72801
inner planets orbits, discrepancies in motions of perihelia 80−67531
intenal structure, series soln. of Lane-Emden problem 78−36559
interior differentiation processes, trace elements as probes 80−98584
interior equations of state, theoretical, comparison using high-compression exptl. data 79−20779
interiors, condensed matter physics 80−77307
interiors, effects of ferroelectric phase transitions 77−53045
interiors, generalisation of Vashchenko Zubarev formula for Gruneisen parameter 80−90030
internal structure is general relativity 78−57477
interstellar gases, planetary focusing effects 77−5494
interstellar planetesimals, capture by solar system rel. to terrestrial catastrophism 80−31043
IR astronomy development progress *(German)* 77−67138
IR brightness temps. at 1 mm wavelength 79−2496
Jacobi's virial eqn. soln. for celestial bodies 79−8832
jet stream formation in early solar system 78−69711
Jovian planet interior heat production 80−98606
Kepler's laws of planetary motion, conservation principles 77−13538
LF radio survey by RAE 2 77−49321
limb-darkening of planetary solids near opposition, laboratory study 78−36477
lithosphere global TRM in presence of central dipole field, theory 80−31223
Love numbers of giant planets 78−16338
lunar and planetary science, ninth conference, Houston, Texas, (1978 March 13 to 17) 80−17711
lunar occultations, obs. at Cracow in 1974-75 period 77−33363
magnetic field, hydromagnetic phenomena described by elec. currents 80−36495
magnetic field, spherical dynamo with anisotropic-α effect 80−81809
magnetic field as probe of interior structure 80−36528
magnetic field calculation of cosmological bodies 79−12399
magnetic field of rot. body, model 80−82249
magnetic field origin, conf., Nov. 1978, Texas USA 80−36234
magnetic fields, apparent source depths 78−57478
magnetic fields, cosmological interpretation 80−46714
magnetic fields, dimensional anal., simple model 79−58286
magnetic fields, effect of photon mass 77−33477
magnetic fields, spacecraft meas. 79−2503
magnetic fields, survey of expt. data 78−73664
magnetic fields driving forces, theory 79−16854
magnetic moments, two predictions from scaling law test 80−21934
magnetism of planets, review 80−98585
major planets, estimate of stellar perturbs. in motion 77−78621
major planets, Raman scatt. in atmospheres 78−28571
mass-radius relations for cold spherical body, relativistic effects 80−26730
massess of largest bodies and vels. during accumulation *(Russian)* 79−35160
massive planet in asteroid belt, existence and removal, Ovenden's hypothesis 79−2502
massive protoplanets orbital stability in terrestrial planet region 79−66931
mean motions, distrib. rel. to development of solar system 77−91451
meridian obs. with photoelectric multislit micrometer, disc centre determ. 77−53443
meteorite bombardment evidence *(Russian)* 79−101098
meteorite impact ejecta, depend. of mass and energy lost on planetary escape vel. 78−45295
meteorite impacts, review 79−8884
methane, 4350-10600 Å bands, intensity profile, vibr. assignments, rel. to major planets spectra 78−42084
methane, liquid, vibrational overtone spectrum, planetary appls. 79−2497
MHD dynamo theory of mag. field *(French)* 79−35161
Mie-Gruneisen equation of state, appl. to planetary interiors 78−29072
millimetre temps. of planets, galactic and extragalactic sources 78−28556
missing planet origin of asteroids rejected 78−69732
motion equations, integration, Taylor-Steffensen series appl. *(Russian)* 78−49352
motion of major planets, numerical study 79−92657
motion reproduced by planetarium gear mechanisms 80−4258
N-body problem, dynamical coupling of periodic systems, resonance *(French)* 77−73938
NASA planetary missions planning 79−5732
neutron-gamma techniques for planetary exploration 79−53728
non-solar planets, cosmic ray Cherenkov photons effect on IR interferometric search 80−98523
nonsolar planets, detect. via spinning 78−85977
observational ephemeris, 1977, September to October *(French)* 77−87241
occultations, mutual events in AD 1557 to 2230 period 79−88611
occultations of stars, wave optics of central spot 77−67053
orbit determ. by Lambert 80−42024
orbit stability in binary systems, Hill's method appl. 80−94834
orbital eccentricity, effects of encounters with preplanetary bodies 78−7894
orbital elements from Munich meridian obs. (1941-61) *(German)* 80−77306
orbital motion calc. method 77−53411
orbital resonances in solar system, review 77−25998
orbital semi-major axes, higher order stability in restricted three body problem 77−13208
orbital speed, in Kepler ellipse, theory 77−70984
orbital stability, Hill's concept generalisation 79−92656
orbits, analytical method for asteroid belt effects 79−75082
orbits, computation using Chebychev polynomials and appl. to minor planets *(French)* 80−61997
orbits, perturbations by solar companion star 78−12198
orbits major axes invariability, applicability of Poisson's theorem in heliocentric variables *(French)* 78−85829
origin, initial rotation periods and relative formation times *(Chinese)* 80−105182
origin, large, late-stage planetesimals growth 79−96931
origin, monograph 78−32625
origin, new tidal theory 78−93131
origin of planetary systems, model comparisons 80−17508
origins rel. to trace elements in shergottite meteorites 79−44420
osculating elements reduction to proper elements for entire solar system 80−21897
outer, probing using Raman effect 77−87277
outer planets, abundance ratios determ. method, appl. to Jupiter 79−84734
outer planets, mass removal from early solar system 78−53841
outer planets, projected plans for Voyager 1 and 2 probes *(French)* 77−70976
outer planets, Voyager spacecraft mission 78−49289
outer planets and satellites form. theory *(Chinese)* 78−69712
outer solar system, mass distrib. and planet form. 80−77349
outermost, observing in 1977, prospects 77−56874
particulate surfaces, multiple light scatt. effects, lab. expt. 78−58912
peridotite-H_2O-CO_2 system, phase relationships, rel. to planetary mantles 78−77506
perihelion advance in post-Newtonian gravitation with correction 77−70986
perihelion shift, Lorentz-invariant theory of gravit. rel. to general relativity *(German)* 78−29030
perihelion shift, predictive relativistic mechanics for gravitational interaction 77−2541
periodic systems dynamical coupling, particular case of homographic soln. 80−36480
perturbations of cometary orbits, rel. to long-period comets inclination and perihelion latit. distribs. 80−101563
perturbations of Quadrantid meteor stream, rel. to long-term orbital evolution 80−17551
perturbing planet coordinates, expression through perturbed planet eccentric anomaly 80−67530
photographs and spacecraft imagery, digital recording and image processing in data centres 77−78676
photometric properties, theory 80−67601
planetary sciences, AAS meeting (Honolulu, 19-22 January 1977) 78−4127
planetesimals, collisional growth and relative vel. 80−82247
planetesimals in primitive solar system, statistical behaviour 78−93130
planetesimals long-term behaviour and planets formation 77−91450
planetesimals to planets: numerical simulation of collisional evolution 78−85861
planetsimal aggregation during solar system form., numerical expts. 78−69713
plasma flow around planets, collisionless hydrodynamics rel. to Larmor freq. 78−69637
position measurements, photographic image expansion estimation *(Russian)* 77−71007
position obs., phase corrections 79−8861
positional catalogue from photoelectric meridian obs. 77−91453
positions, low-precision formulae 80−61990
positions calc. using programmable pocket calculator *(Norwegian)* 78−69700
propeller spindown of rotating magnets, torque calc. 79−8831
protoplanetary bodies, generalised coagulation eqn. 77−25958
protoplanetary core formation by rain-out of Fe drops 79−66932
protoplanetary disc nebula disruption by T Tauri-like solar wind 80−36516
protoplanetary eruptive evolution and comets 79−70969
protoplanetary nebula, grain accretion time and mass limit 77−73976
protoplanetary orbits, effects of resisting medium 77−73978
protoplanets, isolated giant gaseous, struct. and evolution 79−75123
Ptolemaic system, success as kinematic predictor of planetary positions 77−78941
pyroxenes from planetary basalt, silicate mineralogy study 80−72802
radar obs. technique *(Spanish)* 79−5759
radio source mapping using VLBI *(Japanese)* 80−21927
radio wave emission, obs. during JIKIKEN (EXOS-B) satellite initial phase *(Japanese)* 80−94675
radiowaves reflected from planet with spherically symmetrical atmosphere 80−21935

planets continued
rapidly rotating planets, form. of closest satellites and Saturn ring system 78−53869
rectangular coordinates, approximation via Chebyshev polynomials *(Russian)* 80−62033
reflectance meas. in thermal emission region, thermal component removal 80−17497
regolith dissipation during cratering, stochastic model 79−70974
regolith reprocessing by cratering, erosion of material layer which loses charact. props. 80−62053
relativistic celestial mechanics, astron. meas. and coord. systems 80−36481
relativistic effects verification, comparison of obs. results with theoretical data *(Russian)* 79−80209
resonance rotation stability 79−96897
rigid bodies, translational-rotational motion eqns. in osculating elements 78−28495
ring formation, particle size distribs. 77−41338
ring structures, rock mechanics theory 77−64675
ring systems, review of physical studies 80−72874
rotating self-gravitating fluid sphere with uniform distrib. of heat sources, MHD convective instability 77−29264
rotation, ang. moments mass depend. rel. to self-similarity 80−36490
rotation and figure of giant planets 79−96934
rotation origin, tidal hypothesis 79−8859
rotation rate, approx. analytical theory 77−60697
rotational alignment in nuclei and planets 80−90636
WZ Sagittae, recurrent nova, physical parameters and evolution to star+-planet system 78−85948
satellites accumulation, circumplanetary swarm model 78−28549
scintillation at Earth's night horizon, Salyut 4 obs. 77−9590
secular planetary theory of first order up to fourth power in eccentricities and inclinations 79−96894
shape of planets and Sun due to rot., equipot. surface 77−13541
shock degassing of planetesimal *(Russian)* 79−70973
solar activity, planetary influence refuted *(French)* 78−69770
solar nebula, charged dust accretion rel. to Fe, stone and planetesimal formation 78−28548
solar nebula evolution, giant planet formation, gaseous envelope instability 79−12415
solar system evolution from preplanetary gas disc, rel. to crystallisation and cryst. struct. *(German)* 78−93129
solar system formation, supernova trigger, evidence from meteorites isotopic anomalies 78−77499
solar system origin theories, critical review *(Chinese)* 77−22117
solar wind flow past planets, axisymm. implicit blunt body computation technique 78−96370
solar wind interaction with non-magnetic bodies 78−49270
solar wind sputtering rate 80−85835
solid-state convection in planetary interiors, numerical methods 79−84693
Space Shuttle, small planetary missions 80−109339
spectra, anisotropic scatt. effects 77−2357
spectrograph for planetary studies 77−73954
spin angular momentum distrib. explanation 80−41741
spin motion and axial inclination *(Italian)* 79−21210
stability, three-body problem using hydrodynamical model 77−87245
star of Bethlehem, possible triple conjunction of Saturn and Jupiter 77−13256
Star of Bethlehem, role of planetary conjunctions in 7 and 6 BC 79−67136
stars cold satellites searching via speckle interferometry, coherent optical system appl. *(Russian)* 80−12672
stars possessing Earthlike planets, prevalence in Universe 80−41735
stars with companions, statistics 77−91572
stellar multiplicity and planetary systems 79−44564
stellar planetary systems, spectrographic search 77−78827
structure, global seismic effects of basin-forming impacts 78−12122
surface elemental anal. via orbital gamma-ray spectroscopy 79−12412
surface layers, validity of radiative-conductivity, theory 77−17354
surface material, high-energy particle interactions, gamma-ray production, simulation 78−16318
surface roughness effect on transmission of microwave radiation through planetary surface 79−75126
surface scattering of bistatic radar signals 80−41743
surface shape determ. from limb photographs by spacecraft 79−8845
surface structure of terrestrial planets *(Russian)* 78−73346
surfaces, appl. of statistical methods 80−101540
surfaces, exploration by radar 78−73663
surfaces brightness characts. calc. method 79−62754
survival following supernovae in planetary systems 80−56860
swirling particle fluids, computer studies, evolution of planetary-type bodies 79−35121
synodic periods rel. to climatic changes in China 80−85741
terrestrial, basin and crater form., oscillating peak model 80−101539
terrestrial, climatic change, review 79−53742
terrestrial, cores formation, history and energetics 79−84694
terrestrial, cratered surface entropy 80−101541
terrestrial, early evolutionary stages in atm. and climate 79−8696
terrestrial, origin and evolution *(German)* 77−71039
terrestrial, solid convection, conf., Moffett Field, California, USA (Dec 1977) 79−84691
terrestrial, solid-state convection, obs. evidence 79−84692
terrestrial, subsolidus convective cooling histories 79−66939
terrestrial, thermal evolution, calc. 79−2501
terrestrial group, limiting masses, distances and accumulation times 79−8858
terrestrial planets, core formation 80−17514
terrestrial planets, internal struct. evolution, calc. 77−82137
terrestrial planets, mag. fields 78−12125
terrestrial planets, nearby meteoric dust distrib. mathematical modelling 79−96976
terrestrial planets, struct. 77−87298
terrestrial planets accretion, shock degassing rel. to atmospheres origin *(Russian)* 79−101099
terrestrial planets and meteorites C, N and noble gases, origin and abundances 78−28559
terrestrial planets gravitational potentials, convergence of expansion in spherical harmonics 78−24479
terrestrial planets interior evolution 77−53444
theoretical studies, developments in 1973-6 period 78−77505
planets continued
thermal convection in heterogeneous planetary interior 79−30001
thermal evolution of small planetary bodies, convection modes 80−26764
thermal mantle convection, mechanical boundary conditions 79−20782
thermal radiation intensity field modelling; principles 80−62056
thermodynamics of black planet, surface Carnot interaction 80−85877
three-body problem, model for close encounters in planetary system 78−61718
tidal dissipation in solid cores of major planets 79−40103
tidal friction rel. to Solar System stability 80−82233
tidal gravitational field and anholonomic coords. 79−34723
tidal interactions, consequences and inferences 77−87297
tidal potentials rel. to Maunder sunspot minimum 77−33376
tidal theory of solar activity 79−30034
tidal torques on circumbinary accretion discs, theory, commensurable satellites form. appl. 79−70952
tides, mechanical interpretation of solar activity *(French)* 78−20787
Titius Bode Rule for solar planets and planetary satellites, c.f. Bohr atomic orbitals 79−101057
Titius-Bode law, existence of space for more than ten planets 78−40851
Titius-Bode law, Piagetian learning cycle for astronomy study unit 80−51985
Titius-Bode relation, modified 79−84684
topographic changes on airless bodies, meteorite impact and ejecta deposition 78−65523
transneptunian planets, implications of solar system origin, nature of long-period comets 79−8856
triple conjunction rel. to Star of Bethlehem *(French)* 79−84923
turbulent convection within rapidly rotating superadiabatic fluids with horizontal temperature gradients 78−90913
turbulent protoplanets, non-volatile compound segregation 79−62772
turbulent thermal convection in presence of rot. and mag. field, stellar and planetary dynamos appl. 80−6042
unseen companions of Ci 182354 and Wolf 1062, astrometric anals. 78−16459
Uranus-Neptune general planetary theory, short-periodic term elimination 79−75153
UV spectra, International Ultraviolet Explorer (IUE) obs. 78−93133
viscous coupling in a spherical body of temperature-dependent viscosity [planetary interiors] 79−21211
volcanism and thermal tectonics on one-plate planets 78−77507
Voyager mission to outer planets 79−62718
Voyagers 1 and 2, missions and prospects 78−7859
wave tilt sounding of multilayered structures on planetary surfaces 80−61926
white dwarf planetary companions, detection by direct photometry from space telescope 79−71076
X-ray and gamma-ray remote sensing spectrometers, data analysis system for planetary mission appl. 79−12411
C, primordial retention by terrestrial planets 79−40102
Fe-Ni-Si cores, form. 78−12112
H-He fluid planets, dynamics and He distrib. 78−28555
H-He fluid planets, phase diagram and transport props. 78−28554
$^{15}N/^{14}N$ ratio rel. to solar nebula differentiation 80−36519

planimeters *see area measurement*

planning
see also town and country planning
accident investigation, advance prep. 78−57083
acoustic planning of plants, technical and economic advantages 80−3561
analytical instrument use and planned acquisitions 78−88684
BWR power plant turbine building, radiation protection, calc. and obs. 78−74461
computed tomography, USA government regulation of use 80−17104
computerised electron beam treatment planning algorithms 79−100733
computerised tomography planning issues (in 1975 and 1976) 80−17103
Earth obs. systems, planning, design and control 79−58220
electrification of rural areas, energy economies and national policies, in developing countries 79−48042
electron beam dosimetry for treatment planning 80−3817
electron beam treatment planning, patient specific data acquisition 79−100731
electron beam treatment planning, symposium, Cincinnati, USA (July 1977) 79−100730
electron beam treatment planning and execution, for 10 to 35 MeV beams 79−100732
electron beam treatment planning for 1 to 10 MeV beams 79−100735
electron beam treatment planning system, absorption equivalent thickness factor 79−100734
energy, in Arab world, with aid of computer 80−26122
energy demand and conservation in USA, National Energy Plan impact 80−26121
energy modelling for policy anal. 79−83578
energy planning, national, optimisation model 79−57350
energy requirements in United States in year 2000 for stable social progress 79−79385
environment protection when siting power station, temp. and humidity meas. methods *(French)* 79−12318
environmental systems control, transient finite element and linear programming method 79−57497
European computer network, engineering design computer packages, teaching 80−31465
European Space Agency remote sensing programme activities and plans 79−70885
experiment, appl. to calibration of X-ray radiometric analyser 80−61186
experiment, appl. to superconducting magnetic systems 79−67352
experiment, optimum plans calc. on convex polyhedrals 80−57084
fast particle therapy status and prospects in Europe 79−20641
flood control planning 78−81245
fusion reactor, TFTR, preoperational test plan, manpower loading and scheduling 80−102340
geoscientific maps for planning 79−84080
integrated surface physics and chemistry laboratory planning for automation 79−67269
materials testing by statistical methods *(German)* 80−93725
neutron radiation therapy, treatment planning corrections 79−20637
neutron radiotherapy planning and radiation quality definition 80−12246
nuclear plant reliability data system, quality control program in design planning 79−97774
nuclear power plant, Virgil C., startup, conduct of operations, organisation and personnel 80−63340

planning continued
nuclear power plant *(Korean)* 78−54819
nuclear power plants, capital cost considerations, optimum plant size 80−63416
nuclear power plants, startup, staffing program, scope, tasks, resources, constraints, anal., implementation 80−63341
oncology, radiation, use of computers review 79−25098
operating theatre X-ray installation planning 79−92339
operational environmental satellite system, next phase planning, USA 79−5728
optical system tolerancing plan activities and documents 80−48382
optics industry, business side, conf., San Diego, USA (Aug. 1978) 79−81354
Project Manager organisation in nuclear plant turnover and startup 80−63339
radio studio acoustics for SDR's Stuttgart Broadcasting House *(German)* 78−71243
radioactive effluent monitoring, symposium, Portoroz (1977) 78−89985
radiography, equipment needs for radiology department, math. model 78−65107
Radiological Emergency Response Planning and Preparedness Training Programmes, USA 78−57079
radiotherapy treatment planning, FORTRAN program for optimisation using complication probability factor 80−81686
sea use plan concepts and criteria 80−46203
solar power investment programme for small national state or political subdivision of large state, review 79−66403
space orbiter vehicle, Space Shuttle, project planning 79−84641
space research, computerised planning in ESA 80−4223
space research, forward-looking financial planning in ESA 80−4221
space research, investment planning in ESA 80−4222
standard sample homogeneity evaluation, optimal obs. planning 80−93721
United States' Pacific Northwest Electric Utility, strategic solar energy planning program 79−48101
waste nuclear material disposal planning and difficulties *(German)* 78−86630
water quality management planning in coastal zone, stratified water circulation forecasting 79−5543
water utilisation system, area wide multimodal system, nonlinear goal programming model 79−57518
wind power exploitation on large scale, physical planning aspects in Holland 80−61241
X-ray departments, General Hospitals, planning standards 78−92741

plants (industrial) *see industrial plants*

plants (power) *see power plants*

plasma
see also electromagnetic wave propagation in plasma; plasma-beam interactions; plasma impurities; plasmons; relativistic plasmas; solid-state plasma
aether drag and radiation press. in dispersive medium 79−35124
antenna in magnetoplasma, radiation patterns 80−43933
astrogeophysical plasmas, current instability in reconnecting current sheets 77−37486
astronomical plasmas, dielectronic recombination review 80−46391
astronomical plasmas, MHD, monograph 78−40816
astronomy, plasma physics *(Russian)* 78−89057
astrophysical, charged particle accel. by MHD shock waves 80−101532
astrophysical, cosmic ray particles pitch angle scatt. and Fermi accel. 78−53775
astrophysical, high temp., thermal bremsstrahlung radiation 80−94697
astrophysical, instability of self-gravitating isotropic pressure plasma 80−72763
astrophysical, nonrelativistic electrons interaction with radiation in mag. field 80−109354
astrophysical, population of excited atomic states in emission spectra 77−25940
astrophysical, stability of anisotropic jet 77−17353
astrophysical, super-Alfvenic particle streaming 80−31206
astrophysical, thermodynamic inconsistency of modified Saha eqn. at high press. 78−36450
astrophysical aspects 79−16820
astrophysical beam-plasma system, entropy theorem and plasma waves spontaneous emission 78−69677
astrophysical clouds, comptonisation of X-rays, radiation spectra 80−85850
astrophysical collisionless homogeneous plasma, strong EM waves waveform, polarisation and non-linear effects 78−53809
astrophysical compressible plasma, current sheet self-similar resistive decay 80−1755
astrophysical dense plasmas, transport coeffs. 80−77280
astrophysical dense plasmas nuclear reactions, simple classical fluids theory 80−75141
astrophysical inhomogeneous medium, polarised radiation transfer 80−99607
astrophysical plasma, elec. field around rot. mag. dipole 78−45141
astrophysical plasma, phase transfer, optical spectral line emission bursts *(Russian)* 80−77286
astrophysical plasma, rotating, effect of suspended particles on gravit. instability 80−109347
astrophysical plasma, shock accel. of galactic cosmic rays 80−82155
astrophysical plasma, shock accel. of particles, review 80−82192
astrophysical plasma, turbulent bremsstrahlung of Langmuir waves 80−62009
astrophysical plasma in steady-state ionisation balance, radiative power loss 79−82063
astrophysical plasmas, accuracy of ion density computation during rarefied flow around bodies 79−50849
astrophysical plasmas, charge transfer rel. to Si lines appl. as spectral diagnostics 80−41717
astrophysical plasmas, conduction mode var. and inertial conductivity 77−84407
astrophysical plasmas, di-electronic recombination *(French)* 80−82188
astrophysical plasmas, distrib. function of particles accelerated by Alfven waves, self-similar solns. 79−32757
astrophysical plasmas, electron impact excitation coeff. for highly ionised ions 77−7510
astrophysical plasmas, energy release, flares and particle acceleration in close binary system *(Russian)* 80−73005

plasma continued
astrophysical plasmas, energy spectrum of particles accelerated near singular line of mag. field *(Russian)* 80−90332
astrophysical plasmas, $H+H^-$ assoc. detachment collisions 79−44351
astrophysical plasmas, head-on approximation in second harmonic emission 79−41803
astrophysical plasmas, hydromagnetic surface waves theory 79−25462
astrophysical plasmas, laboratory expts. on dense matter in laser driven fusion 80−75077
astrophysical plasmas, mag. field line reconnection via clouds-in-cells model 77−84490
astrophysical plasmas, max. growth rates of magnetoatmospheric instabilities 77−53573
astrophysical plasmas, mirror instability, mag. field first adiabatic invariant breaking 80−67546
astrophysical plasmas, nonthermal processes in diffuse magnetised plasmas, wave physics, book 80−105446
astrophysical plasmas, particle streaming at speeds greater than Alfven velocity 79−40068
astrophysical plasmas, prod. of pulses of charact. energy, solar flares appls. 77−78736
astrophysical plasmas, shock waves post-collisional propag. and amplification *(Russian)* 79−44360
astrophysical plasmas, X-ray spectral lines profile evolution due to Comptonisation 79−66916
astrophysical plasmas in mag. and gravitational fields, MHD separation of high energy plasma 80−67547
astrophysical plasmas radio emission, probability of occurrence of stable pulses 78−42737
astrophysical self-gravitating plasma with finite ion gyroviscosity effects rotating layer instability 80−56706
astrophysical shearing plasma, magneto-ionic rays propag. 79−84659
astrophysical stationary plasmas, He-like ions line intensities 78−53811
astrophysics, dense plasmas and nuclear reactions theory 80−77281
astrophysics, EM mode coupling in inhomogeneous magnetised plasma 77−84435
astrophysics, plasma transfer eqn. in inhomogeneous magnetised plasma 77−84436
astrophysics, relativistic modes of tearing instability in background plasma 80−62012
astrophysics and plasma computing conference 77−29639
at mag. equator, rel. to vertical E×B plasma drift vel. 80−36435
atmosphere, phenomena induced by charged particle beams obs. 80−17443
atomic level population of plasma, Jeffries' level population ratios and Seaton's cascade matrix 80−52934
α Aurigae (Capella), coronal line emission in soft X-ray spectrum 78−93228
auroral arcs, plasma transverse Kelvin-Helmholtz instability rel. to electrostatic turbulence 77−53287
auroral E-layer, plasma lines meas. 79−25386
auroral electrojet, nonpotential waves 77−49212
auroral ionosphere, collisional ion cyclotron waves 77−29574
auroral oval, dayside, plasma density rel. to neutral wind profiles between 115 and 175 km altitude 80−98494
auroral plasma, electrostatic V-shocks approximate equipotentials 80−21870
auroral zone, nighttime scintillation localised enhancements struct. 80−98506
B-type stars hot circumstellar plasma, constraints from XUV obs. 78−93232
black holes, magnetosphere, charge particle trapping 78−57573
Cassiopeia A, electron kinetic instability rel. to radio spectrum secular flattening 80−101637
celestial bodies, magnetosphere interaction with plasma flow, review of studies 78−65496
chemistry in gas, liq., or solid state 79−79241
chemistry of plasmas *(Czech)* 79−47924
circumterrestrial plasma faraday inverse effect *(Russian)* 80−4190
coherent structures in fluids, appl. to plasma physics, review 79−10621
collective effects and pulsar emission models 79−25461
collisionless gravitating systems, gravitational pot. nonlinear eqns. determ., astrophysical appl. 80−67560
collisionless magnetized cosmic plasmas, non-resistive electric potential drops 80−31204
collisionless plasma, signature of parallel elec. fields 78−77439
colloidal plasmas in space: some aspects of condensation and growth of solids 79−41795
Comet Kohoutek (1973 XII), plasma irregularities in tail 77−13285
Comet Morehouse (1908 III) tail, helical waves theory 80−4305
comet tails, hydromagnetic models 80−56773
cometary, acceleration in solar wind, rel. to ion-acoustic turbulence *(Russian)* 80−106923
cometary plasma acceleration, role of mag. structs. 80−46486
cometary plasma tails, general morphology rel. to Swan Cloud, 1974 January 11 in Comet Kohoutek (1973 XII) 80−98612
cometary tail, mag. field size 79−88626
cometary tails, small-scale turbulence theory 79−44411
comets plasma tails, disconnection rel. to mag. field line reconnection at interplanetary sector boundaries 78−93155
comets plasma tails disruption, triggering by flute instability 78−93156
comets type I tails, ray struct. and electrodynamical forces *(Russian)* 79−101119
conference, general congress, Societe Francaise de Physique, Toulouse, France (June 1979) 80−77536
conference, plasma science, New York, USA (May 1977) 77−84396
conference, trends in physics, York, England (Sep. 1978) 80−31416
conference on ionised gas physics, Dubrovnik, Yugoslavia (Aug.-Sept. 1978) 80−36779
conference on phenomena in ionised gases, Grenoble, France (July 1979) 80−36767
conference on plasma science, Monterey, CA, USA (May 1978) 79−37442
coronal active region, differential emission measure exponential depend. on temp. and struct. 78−53917
cosmic plasma environments, immersed dust props. 80−26930
cosmic plasma physics, appl. to interstellar clouds and star form. 78−73744
cosmic plasma physics and double radiosources 78−69898
cosmic plasma properties from magnetospheric research, use in astrophys. 78−93051

plasma continued
cosmic turbulent plasma, depolarisation of EM waves 77−17358
Crab nebula, magnetoparametric instabilities theory 79−8829
Crab nebula, parametric plasma instabilities 78−45220
Crab Nebula, wisps struct. rel. to nonlinear plasma effects 79−25682
Crab pulsar magnetosphere, nonlinear space charge waves rel. to coherent radio emission 77−41386
D-region plasma density measurement, rocket borne expt. 78−45126
degenerate electron-neutron plasma, energy release mechanism 77−74790
degenerate stars, force-free mag. fields stability 78−49425
discharge, impulse-type cathode streamer, emitted photons estimation *(Japanese)* 79−32845
dust grains in hot gas 79−92820
E-region, plasma densities rel. to cross-polar cap horizontal currents 77−45230
E-region of ionosphere, effective electron collision frequency 79−58153
Earth bow shock, conference, Strasbourg, France (1978 August 31 to September 1) 80−82573
Earth bow shock, current-driven instabilities in laminar perpendicular shock 78−77430
Earth bow shock, initial ISEE mag. field obs. 80−90307
Earth bow shock, kinetic models of shocks in collisionless plasmas 80−90330
Earth bow shock, plasma props. in quasi-parallel, quasi-laminar shock 77−37484
Earth bow shock plasma, possible generation mechanisms of low-freq. waves (≲50 Hz) 80−90312
near-Earth plasma, 0 to 100 keV, quantitative models review 80−36459
Earth plasma sheet, magnetised plasma slow convection theory 80−109312
electric currents in cosmic plasmas 78−12094
electron flows stabilisation 80−109411
electrons, from heated oxide cathode, multiphoton laser absorption 80−6224
energy build-up and release in astrophysical plasmas 80−46395
equatorial electrojet, multifreq. HF radar studies of plasma instabilities in Africa 78−36370
EUV spectrum of hot, optically-thin interstellar plasma 78−81665
extended extragalactic radio sources, relativistic parametric instabilities 78−24561
F_2-layer field-aligned and field-perpendicular vels. theory 78−85760
F-region, artificial control of equatorial spread-F irregularities 78−69602
F-region, diffusion-recomb. parameters 77−13156
F-region, effects of E-region coupling on Perkins spread-F instability 78−40755
F-region, interhemispheric ion transport induced by neutral zonal winds 80−98509
F-region, nocturnal, heights over Arecibo, band struct. 79−66863
F-region, plasma ambipolar diffusion eqn. in gravit. field 77−78562
F-region, plasma line data rel. to photoelectron energy loss and spectral features 77−45227
F-region, two-dimensional Rayleigh-Taylor mode theory for spread-F bubbles 78−88986
F-region plasma cloud, intermediate wavelength E×B gradient drift instability 80−105114
F-region plasma clouds, high-altitude limit of gradient drift instability 78−88984
F-region striated Ba clouds, electron density struct. meas. 78−88974
fluctuations in nonstationary nonequilibrium system, near instability boundary *(Russian)* 79−19034
galactic corona, prod. and heating mechanism 80−82492
galactic spiral structure formation, plasma density wave analogy *(Russian)* 77−13470
galaxy bridges and jets, hydromagnetic break-up into aligned objects 77−49475
Galilean satellites magnetospheres, plasma and mag. field perturbations 80−46465
geophysical compressible plasma, current sheet self-similar resistive decay 80−1755
geophysical plasmas, accuracy of ion density computation during rarefied flow around bodies 79−50849
geophysical plasmas, mag. field line reconnection via clouds-in-cells model 77−84490
geophysical plasmas radio emission, probability of occurrence of stable pulses 78−42737
geophysical self-gravitating plasma with finite ion gyroviscosity effects rotating layer instability 80−56706
geophysical shearing plasma, magneto-ionic rays propag. 79−84659
geophysics EM mode coupling in inhomogeneous magnetised plasma 77−84435
geosynchronous plasma, analytical simulation 79−84594
gravitating magnetised plasma, nonlinear Poynting flux 80−26736
high β plasmas, hydromagnetic waves propag. and damping 80−17482
impurity ions on rational magnetic surfaces, convection and diffusion, collisional multifluid model 80−28615
intercluster intergalactic medium, theory for expanding cosmologies 80−4426
intergalactic hot gas in clusters of galaxies, distrib. 79−17089
intergalactic plasma, rel. to diffuse X-ray background spectrum from 3 to 50 keV 80−41916
interplanetary, turbulent, Volterra integral eqns. for charged particle transport 78−8225
interplanetary collisionless shock waves, thickness 80−90314
interplanetary integrated electron content, Mars 4-7 meas. 77−53383
interplanetary magnetic holes, theory 79−29961
interplanetary medium, fields and plasmas in outer solar system 79−58213
interplanetary medium, first evidence and early studies of Earth bow shock 80−85816
interplanetary medium, inner solar system mag. fields and plasmas rel. to coronal holes 79−58212
interplanetary medium, low-freq. waves obs. in vicinity of Earth bow shock 80−90311
interplanetary medium, mag. field large-scale struct. rel. to Alfven waves 79−29962
interplanetary medium, solar nonrelativistic electron diffusion mechanism 77−53349
interplanetary medium, solar type III radio bursts nonlinear stability 80−26826

plasma continued
interplanetary medium, theory of magnetic shocks in collisionless plasma 80−85854
interplanetary plasma, flow rel. to Forbush decreases struct. 77−91385
interplanetary plasma, scintillation pattern rearrangements 79−96879
interplanetary plasma field characteristics of directional discontinuities 77−29722
interplanetary plasma flow from strong flare, 1972, August 4 to 5, struct. rel. to mag. storm 79−53653
interplanetary plasma flow hydromagnetic struct. rel. to geomag. Pc 1 pulsations 78−45142
interplanetary plasma flows from strong flares, props. and nature of mag. regions 77−91397
interplanetary plasma flux from strong flare rel. to magnetospheric disturbances 78−73600
interplanetary plasma inhomogeneities, anisotropy *(Russian)* 80−36468
interplanetary plasma regime, rel. to cosmic ray storm symmetrical equator-pole anisotropy obs. 78−89020
interplanetary plasma stream of August 4, 1972, hydromagnetic struct. 78−28475
interplanetary plasma turbulence spectrum, determ. from radio sources scintillation spectra 80−46361
interplanetary shock, assoc, plasma wave turbulence obs. 79−53700
interplanetary shock waves, influence on solar particle events 77−49250
interplanetary shock waves, parameters correl. with energetic storm particle events 79−35079
interplanetary shock waves in turbulent medium, energetic particles interaction 80−4210
interplanetary turbulent plasma, radio imagery 79−92645
interplanetary wake of Venus, plasma electron obs. 78−77510
interstellar hot plasma clouds, contrib. to diffuse soft X-ray brightness distrib. 79−53942
interstellar hot plasma in Hercules, O VII emission line obs. in diffuse soft X-rays 79−25759
interstellar plasmas, ion chemistry 80−62254
Io plasma torus, effects on Jupiter kilometric radiation ray tracing 80−72866
Io plasma torus, effects on Jupiter kilometric radiation spatial and temporal distrib. 80−77328
Io torus, Voyager 2 EUV obs. 80−77338
Io torus props. from Voyager EUV data 80−82262
ion-beam plasma and compensated ion beam propagation, review 77−80317
ionosphere, Alfven waves boundary condition 79−53611
ionosphere, antenna in plasma, Debye screening and electron conc. nonuniformity 78−69563
ionosphere, artificial excitation of plasma inhomogeneities 80−36450
ionosphere, auroral, field-normal plasma-line scatt. detect. expt. 78−73580
ionosphere, auroral convection over $60° \leq \Lambda \leq 75°$ from Millstone Hill incoherent scatter 80−67454
ionosphere, auroral zone, irregularities, simultaneous rocket probe, scintillation and incoherent scatter radar obs. 80−94640
ionosphere, Ba clouds striation 77−9607
ionosphere, controlled expt. with rocket-borne plasma gun 78−57424
ionosphere, current collection by long wire in near-Earth orbit 79−25438
ionosphere, daytime positive storm effects at middle latits., prod. by travelling atmospheric disturbances 79−25394
ionosphere, differences between regions of upflowing and outflowing current 79−100999
ionosphere, diffusion and heat flow eqns. with large temp. differences between interacting species 79−66857
ionosphere, diffusion of weakly ionized multiconstituent plasma 78−57384
ionosphere, drifting plasmon simulation, electrostatic waves 80−53965
ionosphere, effect of finite conductivities on axisymmetric toroidal Alfven wave resons. 79−75035
ionosphere, effect of HF-induced plasma instabilities on electron temps. 78−40756
ionosphere, effect of recomb. processes and plasma nonisothermability on thermal parametric instability 80−61967
ionosphere, effect on obs. of solar type III radio bursts 80−72904
ionosphere, effects of induced and combination scatt. on propag. of strong radio waves 77−91345
ionosphere, elec. fields and plasma convection in dayside auroral oval 80−98501
ionosphere, electrostatic field struct. in wake of body in rarefied plasma flow 77−91402
ionosphere, electrostatic waves obs. in unstable polar cap 79−29927
ionosphere, energetic particle meas. within structs. responsible for auroral accel. processes 79−53644
ionosphere, equatorial, plamsa density bubbles obs. by (ESRO-4) 80−4194
ionosphere, equatorial, plasma bubbles and irregularities in nighttime F-region 77−87156
ionosphere, equatorial daytime topside, plasma temps. and ion dynamics 79−84584
ionosphere, equatorial spread-F irregularities drifting patches rel. to spatial reson. mechanism 79−21095
ionosphere, F-layer plasma tubes in polar region, model 78−28391
ionosphere, Injun 5 low-energy plasma obs. during major mag. storm 78−88987
ionosphere, ion cyclotron wave spectrum generated by Ba injection 79−53648
ionosphere, ion cyclotron waves critical-level behaviour 80−6238
ionosphere, large-scale plasma stratification during vertical sounding 77−17273
ionosphere, lower, plasma processes rel. to atmosphere mass distrib. by latitude 80−90115
ionosphere, lower hybrid drift instabilities, electron collisional effects 80−101484
ionosphere, lower hybrid drift instability 80−46343
ionosphere, near-wake struct. of Atmosphere Explorer C (AE-C) satellite, parametric investigation 79−53647
ionosphere, nighttime equatorial, Rayleigh-Taylor and wind-driven instabilities 79−96855
ionosphere, nonlinear interaction with microwaves from solar power satellite, theoretical anal. *(Japanese)* 80−94634
ionosphere, nonlinear mixing as a plasma density probe 78−77406
ionosphere, parametric generation of oscills. during EM sounding from Alouette and Isis satellites 77−60510

plasma continued
ionosphere, particle precipitation rel. to convection in plasma sheet 79−88544
ionosphere, plasma bubbles spatial relationship with 1 m equatorial spread-F irregularities 80−67457
ionosphere, plasma convection at high latitudes, model rel. to incoherent scatter obs. 80−72687
ionosphere, plasma instabilities obs. in multiple pump heating expt. 78−57382
ionosphere, plasma meas. during Western European Winteranomaly Campaign 78−45125
ionosphere, plasma motion in depleted regions at equator 80−12605
ionosphere, probe-created plasma disturbances rel. to Spacelab proposed low-energy meas. 78−77458
ionosphere, radio waves interaction nonstationary processes *(Russian)* 78−93028
ionosphere, radio waves self action, nonstationary theory *(Russian)* 79−48604
ionosphere, rapid subauroral ion drifts obs. by Atmosphere Explorer C 80−4188
ionosphere, role in time dispersion of EM pulses 80−94645
ionosphere, simultaneous obs. of field-aligned currents and plasma drift vels. by Atmosphere Explorer C 80−72681
ionosphere, small-scale irregularity structs. assoc. with subtrough density gradients, Ogo 6 obs. 78−40753
ionosphere, sound propagation, weakly ionised quasihydrodynamics approx. *(Russian)* 77−82079
ionosphere, stimulated Brillouin scatt. theory 77−37478
ionosphere, struct. of electrostatic field in wake of spherical satellite 77−60509
ionosphere, subsonic wave-ionised plasma interaction, electron density study 80−4183
ionosphere, theory of coherent parametric instabilities excited by two or more pump waves 78−57381
ionosphere, thermal parametric instability at freqs. close to electron gyrofreq. 80−46344
ionosphere, topside, low-energy plasma, Injun 5 Lepedea obs. 78−77408
ionosphere, topside, plasma bubbles near dawn terminator 79−101016
ionosphere, topside, thermal plasma enhancements rel. to auroral electrojets 77−9617
ionosphere, Tordo 1 polar cusp Ba plasma injection expt. 78−77402
ionosphere, upper, small-scale stratification, influence of strong radio wave with amplitude modulation 79−12330
ionosphere, VLF triggered emissions, beam-plasma instability appl. 79−14564
ionosphere, wave meas. via satellite-borne cross-power spectrum analysers 80−94621
ionosphere, whistler pulse self-distortion in plasma 79−46456
ionosphere, whistlers group vel. in two-ion plasma 78−87452
ionosphere above Arecibo, HF-enhanced plasma line height 78−28392
ionosphere conductivity, limits of applicability of formulae of mean free path theory 77−60512
ionosphere E_s-layer, Langmuir wave propag. and enhanced plasma line 79−29928
ionosphere equatorial spread-F, high freq. drift waves with wavelengths below ion gyroradius 78−88973
ionosphere F-region, Rayleigh-Taylor instability rel. to equatorial irregularities 77−29566
ionosphere four-component plasma, ion vels. 77−13154
ionosphere high-latitude electrostatic turbulence, polarisation, freq. and wavelengths 78−88981
ionosphere modification, plasma densities in artificially created equatorial spread-F 78−88972
ionosphere multicomponent plasma, electron wave transform. into ion wave during quasilongit. propag. 78−73572
ionosphere multispecies flows, transport eqns. mathematical struct. 78−47084
ionosphere negative storms, plasma density vars. simulation using neutral comp. data 79−25393
ionosphere plasma, long metallic tethers electrodynamics 78−69652
ionosphere plasma clouds, deform. and striation, multilevel model with recomb. chemistry 77−25834
ionosphere plasma clouds, late time striation spectra 77−25836
ionosphere plasma conductivity, kinetic theory 79−53609
ionosphere small-scale plasma scatt. intensity, modulation trough 79−58159
ionosphere turbulent polar cusp, temps. and low-energy particles and Kelvin-Helmholtz instability 78−96343
ionosphere upper layers, drift instability generation by action of strong radio wave 77−91344
ionosphere-protonosphere, plasma fluxes, ATS-6 obs. 78−28409
ionosphere/magnetosphere, coherent anomalous resist. in region of electrostatic shocks 80−4189
ionospheric plasma props. around S. Atlantic geomagnetic anomaly region *(Japanese)* 80−72695
ionsphere, region of intense plasma wave turbulence, on auroral field lines 77−45228
JIPP T-II plasma, soft X-ray spectrum meas. 79−55554
Jupiter, magnetosphere, high β plasma in dynamic current sheet 79−16872
Jupiter, magnetosphere, low-energy charged particle environment, Voyager 1 first look 80−26797
Jupiter, magnetosphere energetic ions and electrons Voyager 2 obs. 80−77342
Jupiter, outer magnetosphere, temporal var. in heavy ion plasma 78−61787
Jupiter corotating magnetosphere, self-consistent model 78−89109
Jupiter inner magnetosphere, O^+ forbidden emission detect. 80−51687
Jupiter inner magnetosphere, whistler mode noise 78−89112
Jupiter ionosphere, decametric radiation sources locations 79−75148
Jupiter ionosphere, peak electron concs. from Voyager 1 preliminary radio profiles 80−26791
Jupiter ionosphere and Io torus, Voyager 1 and 2 radio occultation obs. 80−77337
Jupiter magnetosphere, contrib. of water products from Galilean satellites 78−45268
Jupiter magnetosphere, electron pitch-angle diffusion by whistler mode waves near Io plasma torus 80−4290
Jupiter magnetosphere, electrostatic waves obs. 80−72865
Jupiter magnetosphere, HF and LF events from Voyager 2 obs. 80−77344
plasma continued
Jupiter magnetosphere, influence of Io plasma injection on Jovian diffuse aurora 80−4289
Jupiter magnetosphere, Io interaction with plasma torus 80−98604
Jupiter magnetosphere, kilometric radiation ray tracing 80−72866
Jupiter magnetosphere, kilometric radiation spatial and temporal studies 80−77328
Jupiter magnetosphere, MHD wave interactions rel. to particle accel. 79−12428
Jupiter magnetosphere, plasma cloud injection from Io, S and O ions discontinuities 80−90358
Jupiter magnetosphere, plasma corotation lag from Voyager 1 obs. 80−90361
Jupiter magnetosphere, plasma sheet self-consistent model 78−57494
Jupiter magnetosphere, plasma waves from Voyager 2, radio obs. 80−77343
Jupiter magnetosphere, S plasma discontinuities 80−4291
Jupiter magnetosphere, theory of Io-modulated decametric radio S-bursts *(Russian)* 80−8582
Jupiter magnetosphere, Voyager 1 planetary radio astronomy obs. 80−26796
Jupiter magnetosphere, Voyager 2 obs. of hot plasma environment 80−77341
Jupiter magnetosphere and bow shock, plasma densities from Voyager 2 obs. 80−77340
Jupiter magnetosphere energetics comparison with terrestrial magnetosphere 79−58201
Jupiter magnetosphere plasma observations, Voyager 1 initial results 80−26794
Jupiter mid-magnetosphere, equatorial protons instability 80−67642
Jupiter outer magnetosphere, similarity model of rot. effects 78−57492
near-Jupiter plasma, Voyager 1 plasma wave obs. 80−26795
Jupiter radiation belts, review 79−58296
laboratory, magnetosphere, and astrophysical plasma knowledge interaction 80−59166
laboratory and space plasmas, conference, Nagoya, Japan (1977 December 8 to 9) 80−4470
laser, new free electron laser 79−98329
laser plasma, He-like ions (Z=12-19), $1s^2\ {}^1S_0$-$1s3p\ {}^1P_1$ lines satellites obs. 79−22640
lower ionosphere, collision freqs. for use in continuum momentum eqns. 77−87171
M87 jet, magnetised plasma clouds model 78−54055
magnetic tail, plasma flow pulsations obs. 78−77436
magnetised, high-cond. mag. tearing 77−7527
magnetised cold plasma, bounded volume, natural oscillations 77−76077
magnetodisc, props. from mag. field meas. 79−58297
magnetopause, plasma acceleration evidence for reconnection 80−26701
magnetopause, rot. simple and shock waves in anisotropic plasma 77−91369
magnetopause Kelvin-Helmholtz instability, effect of finite ion Larmor radius 79−80096
magnetoplasma, hot collisionless, resonant excitation of upper hybrid wave by two EM beams 79−77384
magnetoplasma, Kelvin-Helmholtz instability 79−23407
magnetoplasma, modulation instability of whistler waves 77−72450
magnetoplasma, solitary ion-acoustic wave propag. exact stationary solns. 79−19010
magnetosheath, dayside, plasma press. anisotropy and mirror instability 77−37483
magnetosheath, electrostatic turbulence meas. 79−66881
magnetosheath, energetic plasma ions obs. 79−21106
magnetosheath, plasma depletion obs. at dayside magnetopause 79−66876
magnetosheath, plasma meas. by International Sun-Earth Explorers 1 and 2 quadrispherical LEPEDEAS 78−85801
magnetosheath, Prognoz 4 obs. of $\lesssim$2 MeV electrons and cold plasma 80−90296
magnetosheath, turbulence rel. to solar wind ion injections in morning auroral oval 80−98502
magnetosheath and solar wind, magnetospheric energetic electrons bursts correl. with geomag. activity 79−80095
magnetosheath plasma, props. during August 1972 77−25904
magnetosphere, adiabatic plasma convection in tail plasma sheet 79−25408
magnetosphere, Alfven and compressional waves coupling 78−89001
magnetosphere, Alfven waves excitation by bouncing electron beams rel. to nightside mag. pulsations 80−4203
magnetosphere, anomalous resist. in geomag. tail region 79−12353
magnetosphere, auroral radiation generation theory 79−75051
magnetosphere, beam-plasma interaction expt. using electron beam from JIKIKEN satellite *(Japanese)* 80−94655
magnetosphere, cause of plasma sheet thinning during substorms 80−72705
magnetosphere, characteristics rel. to plasma density gradients near L=4 77−25878
magnetosphere, critical electron pitch angle anisotropy for chorus generation 77−2308
magnetosphere, current instability on short wave drift oscills., nonlinear theory *(Russian)* 80−53981
magnetosphere, current interruption in collisionless plasma by non-linear electrostatic waves 79−75052
magnetosphere, dayside magnetopause, mechanism of plasma penetration and electron escape 78−61672
magnetosphere, detached plasma regions, wave propagation characts., instability phenomena 77−25880
magnetosphere, distant geomagnetic tail, Pioneer 7 and 8 obs. 77−64548
magnetosphere, double layers and electrostatic shocks review 80−36460
magnetosphere, drift instabilities assoc. with particles in ring current and plasma sheet inner edge 79−12351
magnetosphere, drift-mirror instability 77−49229
magnetosphere, dynamic equilib. plasma configurations 77−5397
magnetosphere, early results of GEOS-1 keV plasma expt. 79−35068
magnetosphere, effect of bounce resons. on Alfven waves generation outside plasmasphere 79−12344
magnetosphere, elec. currents in hot adiabatic plasma 78−89002
magnetosphere, elec. field around rot. mag. dipole 78−45141
magnetosphere, elec. field in VLF to HF range, EXOS-B obs. 80−67478
magnetosphere, electron accel. in array of auroral arcs 78−36357
magnetosphere, electron density and temp. meas. by GEOS-1 mutual impedance expt. 79−35071

plasma continued
magnetosphere, electron density meas. via International Sun-Earth Explorers 78−85803
magnetosphere, electron pitch angle diffusion instabilities rel. to pulsating aurora 3 Hz modulation 79−25391
magnetosphere, electrostatic field struct. in wake of body in rarefied plasma flow 77−91402
magnetosphere, electrostatic instabilities 78−34286
magnetosphere, electrostatic shocks, double layers and anomalous resistivity 78−45152
magnetosphere, electrostatic shocks as source of discrete auroral arcs 78−45153
magnetosphere, EM instabilities in anisotropic loss-cone plasma 77−87185
magnetosphere, EM wave propag. and instabilities 77−87186
magnetosphere, enhancement of EM ion cyclotron instability by cold plasma, computer simulation 77−33287
magnetosphere, fluid description of hot collisionless plasma and double-adiabatic approximation limits 78−75262
magnetosphere, frontside boundary layer obs. and reconnection problem 78−89010
magnetosphere, GEOS-1 meas. of electric and magnetic wave fields and cold plasma parameters 79−48620
magnetosphere, hiss generation beyond plasmapause by magnetosonic waves 77−82085
magnetosphere, hot tenuous plasmas, fireballs and boundary layers in magnetotail 78−77438
magnetosphere, hydromag. energy spectra depend. on solar wind vel. and interplanetary mag. field direction 80−67476
magnetosphere, hydromagnetic oscills. coupling modes in non-uniform finite press. plasmas 79−21108
magnetosphere, hydromagnetic pulsations generation by Kelvin-Helmholtz instability 78−73584
magnetosphere, International Sun-Earth Explorer 1 and 2 fast plasma expt. 78−85800
magnetosphere, inverse loss cone electrons temp. anisotropy relaxation due to interaction with electrostatic waves *(Russian)* 80−109314
magnetosphere, ion cyclotron instability rel. to energy depend. of ring current proton precip. 77−78565
magnetosphere, ion-cyclotron wave amplification for typical radial profiles of magnetospheric parameters 77−25886
magnetosphere, ISEE plasma obs. of subsolar magnetopause 79−40034
magnetosphere, JIKIKEN (EXOS-B) satellite stimulated plasma wave expts. *(Japanese)* 80−94649
magnetosphere, LF ion acoustic perturbation emission in presence of stationary whistler turbulence 77−49242
magnetosphere, long-period geomag. oscills. rel. to energetic particle fluxes modulation 79−25407
magnetosphere, low energy electrons and protons obs. 78−36407
magnetosphere, low-energy plasma obs. at synchronous orbit 78−77435
magnetosphere, macroscopic elec. fields 78−49238
magnetosphere, mag. field-aligned pot. drops due to electrostatic ion cyclotron turbulence 78−45155
magnetosphere, mag. reconnection rel. to plasma accel., heating and shock form. 78−40773
magnetosphere, MHD torsional oscills. in orthogonal curvilinear coordinates rel. to micropulsations 79−80097
magnetosphere, microscopic plasma processes rel. to reconnection 78−61676
magnetosphere, microstructure and plasma interactions at magnetopause 78−61673
magnetosphere, mode of propag. electrostatic plasma waves and radio waves determ. using stimulated plasma wave results *(Japanese)* 80−94650
magnetosphere, multi-harmonic electron cyclotron instabilities 78−87442
magnetosphere, natural radio emissions identification by Geos I 78−53774
magnetosphere, one-dimensional gasdynamical model of convection 78−81508
magnetosphere, open model plasma populations 80−90295
magnetosphere, outer radiation zone struct. in simple model 77−25877
magnetosphere, particle accel. by MHD surface waves rel. to auroral arc form. 77−9621
magnetosphere, plasma comp. expt. on International Sun-Earth Explorer A 78−85810
magnetosphere, plasma condensations diagnostics from mag. field records on geostationary satellite 79−58189
magnetosphere, plasma convection rel. to model current system for high-latit. mag. activity 79−92636
magnetosphere, plasma density sensitive instabilities 77−25879
magnetosphere, plasma diagnostics via trigger VLF emission 78−45149
magnetosphere, plasma dynamics in mag. field laboratory simulation 79−16757
magnetosphere, plasma injection and diamagnetism 79−80085
magnetosphere, plasma mantle and ionospheric plasmas, field aligned distrib. 78−57406
magnetosphere, plasma meas. by Prognoz-4, ions and electrons in disturbance 77−41271
magnetosphere, plasma parameters along satellite trajectories 80−8490
magnetosphere, plasma sheet press. anisotropies 78−89009
magnetosphere, plasma sheet thinnings, plasma flow 78−28432
magnetosphere, polar, electrostatic H^+ cyclotron waves near one Earth radius altitude 78−45154
magnetosphere, polar cap convection after interplanetary mag. field becomes northward 80−94658
magnetosphere, polar cap plasma flow entry region longit. position 80−67472
magnetosphere, polar cusp, Hawkeye 1 obs. 78−77422
magnetosphere, proton-cyclotron instabilities in non-uniform loss-cone plasma 80−90286
magnetosphere, radio and plasma waves obs. during JIKIKEN (EXOS-B) satellite initial phase *(Japanese)* 80−94675
magnetosphere, region of intense plasma wave turbulence on auroral field lines 77−45228
magnetosphere, role of hot plasma in convection 78−32297
magnetosphere, simulation of plasma beam-mag. dipole interactions 77−7585
magnetosphere, solar wind plasma penetration of magnetopause 78−61675
magnetosphere, thermal/suprathermal plasmas obs. by GEOS-1 S-302 expt. 79−35070
plasma continued
magnetosphere, three-dimens. meas. by ISEE spacecraft 79−40035
magnetosphere, topology of geomag. tail and plasma sheet 77−53331
magnetosphere, toroidal line resons. rel. to continuous (Pc 3,4) pulsations in European sector 80−21877
magnetosphere, transport coeffs. for plasma with quasicollisions 78−71440
magnetosphere, turbulent generation of electrostatic fields 78−28439
magnetosphere, variability of plasma sheet dynamics assoc. with substorms 80−98518
magnetosphere, VLF plasma waves obs. and comparison with high energy electron flux by EXOS-B satellite *(Japanese)* 80−94652
magnetosphere, VLF whistlers propag. in directions near reson. cone rel. to electron temp. 77−82086
magnetosphere, whistler modes, obliquely propagating 77−80288
magnetosphere, whistler pulse self-distortion in plasma 79−46456
magnetosphere axisymmetric toroidal Alfven wave resonances, effect of finite ionosphere conds. 79−75035
magnetosphere boundary layer, field-aligned currents theory 80−67473
magnetosphere cold plasma diagnostics using satellite meas. of VLF signals from ground transmitters 77−49183
magnetosphere convection, variability of S_q vars. field magnetically conjugate structs. 79−58191
magnetosphere dayside cleft, mag. field perturbations rel. to interplanetary mag. field 79−40023
magnetosphere dayside cusp region, plasma props. 79−12352
magnetosphere dynamics during auroral electrojet events, from energetic electron intensity changes at synchronous orbit 79−66882
magnetosphere electron density, small scale struct. from plasma resons. on-line tracking 79−35073
magnetosphere energetics, comparison with Jovian magnetosphere 79−58201
magnetosphere entry layer, plasma obs. by HEOS 2 satellite 78−61669
magnetosphere geomag. tail, distrib. of B_y 79−80091
magnetosphere high-latitude electrostatic turbulence, polarisation, freq. and wavelengths 78−88981
magnetosphere ion composition dynamics, GEOS mass spectrometer obs. 79−35069
magnetosphere longitudinal currents, dynamic processes in turbulence development 80−67469
magnetosphere low-β plasma, evidence for two-dimensional inertial turbulence 78−36399
magnetosphere near-Earth plasma, Alfven waves stimulated excitation by pulsed radio emission 79−58192
magnetosphere near-Earth plasma sheet, search for mag. neutral line from Imp 6 mag. field obs. 78−89007
magnetosphere physics, advances with GEOS-1 (conference, Innsbruck, Austria, 1978) 79−35066
magnetosphere physics, review 79−12356
magnetosphere plasma, hot ion component rel. to electron component, obs. and implications 79−80106
magnetosphere plasma density, GEOS-1 relaxation sounder meas. 79−35072
magnetosphere plasma density and temperature, GEOS-1 multi-expt. determ. 79−35074
magnetosphere plasma mantle, magnetotail boundary layer obs. 78−61670
magnetosphere plasma sheet, form. resulting from plasma mantle dynamics 79−40022
magnetosphere plasma sheet, plasma flows and mag. field vectors during substorms 78−96357
magnetosphere plasma sheet, plasma flows rel. to discrete auroras occurrence and lifetimes 80−67447
magnetosphere plasma wave investigation by International Sun-Earth Explorer 1 and 2 78−85802
magnetosphere polar cusp, low-freq. pulsations possible generation mechanism 79−53657
magnetosphere ring current plasma injection, correl. with solar wind parameters 78−96363
magnetosphere tail, explosive tearing mode reconnection 78−88992
magnetosphere tail, intense oscills., modulation instability at lower hybrid reson., strongly turbulent plasma *(Russian)* 78−59563
magnetosphere VLF triggered emissions, beam-plasma instability appl. 79−14564
magnetospheric and space plasma physics (1966-76) *(Japanese)* 78−24410
magnetotail, Alfven wave generation via proton accelerator 78−73582
magnetotail, distant, lower-hybrid-drift wave turbulence 79−25399
magnetotail, expected reconnection signatures 78−96361
magnetotail, hot tenuous plasmas, fireballs and boundary layers rel. to substorm processes 78−32300
magnetotail, localised induced elec. field 77−53329
magnetotail, obs. of hot tenuous plasmas, fireballs and boundary layers 77−29588
magnetotail, plasma waves obs. 77−29592
magnetotail lobe plasma, double-peaked ion spectra as evidence for massive ions 78−32299
magnetotail magnetic current sheets, effect of press. anisotropy on equilib. struct. 79−12354
magnetotail plasma flow during plasma sheet expansions, Vela 5, 6 and Imp 6 obs. 77−49240
magnetotail plasmas, magnetic fields and magnetic reconnection 79−75049
matter-antimatter boundary layers, theory 77−49284
meteor plasma diffusion, geomagnetic field effect expt. *(Russian)* 78−61814
meteor trails, influence of recomb. on under-dense radio-meteor data 79−80279
meteor trial, diffusion of weakly ionised plasma filament forming angle with mag. field 79−53610
meteors ionisation columns, initial radii meas. 80−94762
middle atmosphere, plasma densities and comp. during winter anomaly 78−45191
molecular plasma, solitary population-inversion wave in drift-superheating instability 77−15191
multicharged ion thermal charge exchange reaction, rel. to astrophysics 80−63815
near-Earth plasma, elec. fields penetration along geomag. force lines, electrostatic approach applicability 80−4178
neutral sheet effect on magnetospheric plasma 77−49243
neutron star, magnetised, atmosphere, cyclotron line form. 79−48839

plasma continued
neutron star, neutrino-pair bremsstrahlung in hot plasma, strong mag. field 78−61878
neutron star atmosphere, normal mode anal. of interchange instability at magnetopause 77−13376
neutron star interior plasma, mag. field rel. to pulsar periods long-term changes 80−22029
neutron star magnetosphere, plasma dynamics and accretion, fate of sinking filaments 80−51798
neutron stars plasma accretion, interaction with mag. field and accretion flow hydrodynamics 80−109452
nonlinear magnetoacoustic waves, damping, simulation 78−79423
nonlinear optimisation algorithms 80−18623
NP 0532 magnetosphere, cyclotron instability rel. to origin of radiation *(Russian)* 80−8645
particle acceleration in collisionless shocks, astrophysical systems 80−31208
particles of disperse material, and plasma fluxes, heat exchange calcs. *(Russian)* 80−23997
pinch, thin skin type, anisotropic conducting wall effect on instabilities 80−28800
planetary atmosphere, dipole antenna plasma wake, cylindrically stratified model 79−48647
planetary magnetospheres, radial diffusion eqn. for collision-affected plasma 78−49310
planetary nebulae, hydromagnetic model for major axes correl. with interstellar mag. field 80−82473
planetary nebulae, recomb. and level populations of ions, resolution of ang. momentum states 77−45529
plasma column, ultra-high current, electron collisionless motion 79−64824
plasma star model for QSOs, analysis 79−58437
plasmapause, 1-30 Hz waves generation by reson. electron instability 78−49235
plasmapause, electron density profile meas. stimulated plasma wave results *(Japanese)* 80−94650
plasmapause, ion cyclotron waves rel. to proton precip. and stable auroral red arc form. 78−49197
plasmapause, shocks and solitons 77−25840
plasmapause, spontaneous polarization of a turbulent magnetized plasma 80−19580
plasmapause as plasma sheath, min. thickness 77−25842
plasmapause physics, conf., Grenoble, 1975, Aug. 77−25838
plasmapause steady state positions from McIlwain's electric field models 77−25839
plasmasphere, corotation electric field 77−25841
plasmasphere, Coulomb collision-induced photoelectron trapping by geomag. field 79−8739
plasmasphere, global morphology of light ions from ESRO-4 satellite 77−25844
plasmasphere, mid-latitude, nighttime electron content, geophysical disturbance effects, 1974 August to November 80−94642
plasmasphere, parameter determ. from geomagnetic pulsation amplitudes 77−25847
plasmasphere, wave-particle interactions, ELF-HF obs. from EXOS-B 80−67467
plasmasphere asymmetry in noon-midnight direction from Prognoz satellites 77−25843
plasmasphere hot zone, Prognoz ion temp. meas. 77−25845
polarisation transfer in inhomogeneous magnetised plasma, comments and reply 79−96905
propagation in gas breakdown near laser-irrad. target *(Russian)* 79−55476
protonosphere, plasma flux rel. to positive ionospheric storms worldwide distrib. 79−44290
pulsar, plasma coupling, boundary conditions 80−94823
pulsar atmosphere with arbitrary mag. and rot. axes, qualitative features 78−57569
pulsar constrained atmosphere, min. energy state 79−25622
pulsar force-free magnetospheres, temp. stabilisation of instabilities 77−49413
pulsar magnetosphere, behaviour of plasma and mag. lines of rot. system 78−20848
pulsar magnetosphere, instability 78−53976
pulsar magnetosphere, magnetoactive plasma equilib. in gravit. field *(Russian)* 80−26895
pulsar magnetosphere, radio propag. effects on pulsar emission polarisation 79−75235
pulsar magnetosphere pair prod. 79−44515
pulsar magnetospheres, narrowband versus broadband emission processes rel. to luminosities 80−51797
pulsar magnetospheres, propag. effects in shearing field-free plasma rel. to microstruct. 80−17483
pulsar magnetospheres, quasi-steady, Vlasov-Maxwell eqns. 77−13375
pulsar magnetospheres, stellar-wind model for plasma-EM fields 80−22031
pulsar magnetospheres, vacuum gaps 79−30082
pulsar magnetospheres physics, limitations on force-free approximation 77−5541
pulsar open magnetosphere, plasma instabilities as source of coherent radio emission 80−82403
pulsar plasma, MHD, Lorentz covariant eikonal method 77−27663
pulsar polar cap, inhomogeneous struct. and radiation processes 79−25623
pulsars, finite force face cold plasma atm. models, plasma differential rot. 80−77378
pulsars charge-separated magnetospheres, props. 78−40981
pulsars force-free wind zone, stability 78−49468
QSOs, plasma laser star model, analysis 79−58437
QSOs, plasma laser star model 78−96558
quasar plasma-laser star model, O VI and He II emission lines 77−45597
quasars, coherent curvature radiation driven by plasma waves 77−60848
quasars, theory of H line emission from dense plasmas 80−51900
radiation opacity in dense plasma 80−26731
radiation transfer through moving astrophysical plasmas 78−65489
radiation transfer through moving inhomogeneous media 78−65490
radio galaxies, extended, multiple ejection theory 77−45592
radio galaxies, radiation transfer, dynamics, stability and evolution of synchrotron plasmon, book 78−24564
radio sources, beam and cloud stability 80−67893
plasma continued
radio sources, double, extragalactic, plasmons ejection models rel. to source separation depend. on redshift 80−22096
radio sources, extended, extragalactic, MHD instabilities and electron accel. 80−27000
radio sources, extragalactic, double, hypersonic plasma cloud model gas dynamics 79−67107
radio sources, extragalactic, radio emission from intense EM beam-plasma system 79−84663
radio sources, physical conditions in compact heads 80−51892
radiogalaxy, particle acceleration and plasma heating by turbulent Alfven waves 77−13227
radiogalaxy M87 jet, internal shocks in plasma beam 78−93416
radiosources, decay excitation of plasma turbulence and nonlinear radiative transfer 77−17707
radiosources, plasma physics, particle accel. and flux vars. 77−13479
RF energy absorption by hot ion-electron plasma *(Japanese)* 79−77404
rockets, RF discharge produced plasma rel. to payload charge neutralisation during electron beam emission 80−77258
Saturn, magnetosphere interaction with solar wind, Pioneer 11 obs. 80−82282
Saturn magnetosphere, plasma density from rings Lyman-alpha emission 79−12430
Scorpius X-1, optically thick hot plasma model for X-ray, optical and radio emission 78−16576
Scorpius X-1, thermal bremsstrahlung from hot plasma 20-75 keV obs. 80−98741
selections from 1977 Comments on Modern Physics, book 79−30181
solar active regions, differential emission measure solns. errors 79−12397
solar active regions, skinning process stability of mag. field 77−53521
solar active regions magnetic fields, appl. of new approach to force-free field 80−62011
solar atmosphere, acoustic waves interaction with mag. flux tubes 80−85911
solar atmosphere, charged particle accel. in flares in presence of microturbulence 77−53528
solar atmosphere, dynamics of fast electron cloud travelling through plasma 77−996
solar atmosphere, dynamo action in thin slab 79−44430
solar atmosphere, electrostatic ion-cyclotron heating 80−51708
solar atmosphere, evidence for neutral H continuous absorpt. above transition region 79−92738
solar atmosphere, force-free mag. fields evolution, nonequilib. states and preflare stage 80−105213
solar atmosphere, force-free mag. fields time evolution 78−85843
solar atmosphere, mag. flux ropes equilib. and stability *(Russian)* 80−8617
solar atmosphere, MHD fluctuations due to magnetosonic wave propag. in warm plasma 80−77275
solar atmosphere, non-force-free mag. fields in magnetohydrostatic equilib. 79−92733
solar atmosphere, nonequilib. plasma density diagnostics via C III EUV lines 78−53899
solar atmosphere, nonrelativistic stream propag. rel. to type III radio bursts 78−28623
solar atmosphere, particle accel. rel. to spectral features in hard X-ray and radio events 77−45369
solar atmosphere, physical parameters determ. from X-ray images quantitative interpretation 79−40085
solar atmosphere, plasma effects on spectral lines in radio emission 78−96466
solar atmosphere, plasma motion accompanying force-free mag. fields evolution 78−12176
solar atmosphere, plasma processes rel. to microwave bursts and large-scale mag. fields 79−2536
solar atmosphere, plasma turbulence rel. to flares development 77−17476
solar atmosphere, radio emission polarised zebra struct. interpretation 78−96467
solar atmosphere, rope structure of rising mag. field *(Russian)* 78−40898
solar atmosphere, stability of mag. flux element in horizontally stratified compressible, plasma 78−28610
solar atmosphere, struct. of turbulent shock wave propagating across mag. field 79−40166
solar atmosphere, type III radio bursts fundamental emission 80−36603
solar corona, Alfven and magnetoacoustic wave mode coupling, cold plasma approx. 78−12178
solar corona, Bernstein waves coherent nonlinear interaction rel. to type IV continuum bursts 77−53529
solar corona, bounce-reson. instability rel. to type IV radio emission pulsations 78−89161
solar corona, collisionless cond. front prod. by rapid heating rel. to hard X-ray bursts 79−44427
solar corona, density determ. from Fe IX lines 79−44429
solar corona, double plasma reson. rel. to radio bursts of drifting pairs type 78−24502
solar corona, electron beam dynamics in plasma 77−78759
solar corona, electron beam injections rel. to type IV radio burst quasi-periodic struct. 80−62097
solar corona, electron scatt. hypothesis for type V radio bursts 77−45378
solar corona, EM loss-cone instability rel. to type IV radio emission *(Russian)* 78−77528
solar corona, fast electrons stream free dispersal with nonsteady injection 80−17568
solar corona, fast mode waves evanescence 78−89147
solar corona, heating by ion acoustic waves 78−4181
solar corona, holes, temp. decrease, plasma density effect on wave absorpt. *(Russian)* 80−77374
solar corona, hydromagnetic surface waves dissipation 80−21904
solar corona, instabilities of trapped particles in magnetic fields 78−61823
solar corona, intensity ratios of fine-struct. components of H like ions reson. lines 80−101581
solar corona, interchange instability rel. to mag. flux-tubes heating and reconnection 77−56894
solar corona, Langmuir instabilities rel. to type III radio bursts 77−2404
solar corona, Langmuir turbulence rel. to quasi-stable particle accel. and type I radio bursts *(Chinese)* 80−105220
solar corona, Langmuir waves emission 78−57515

plasma continued
solar corona, mag. field from Crab nebula polarised radioemission occultation obs. *(Russian)* 78−77527
solar corona, plasma flow along sheared mag. arches 80−62092
solar corona, plasma heating by anomalous current dissipation 78−53895
solar corona, plasma parameters in long-duration X-ray event, Skylab obs. 77−29741
solar corona, polar plume X-ray anal. 79−12455
solar corona, singular lines of one-dimensional force-free mag. field *(Russian)* 79−48670
solar corona, tearing instability, high cond. theory 77−7527
solar corona, three dimensional Langmuir wave instabilities rel. to type III radio bursts 77−2404
solar corona, type II radio emission origin 79−92750
solar corona, type IV decimetre bursts theory 77−2400
solar corona, X-ray photographs anal. and interpretation 79−40086
solar corona magnetic traps, plasma instability periodical regimes *(Russian)* 80−8616
solar corona quasi-static loops, numerical modelling with uniform energy input 80−21958
solar corona streamer, drift pair radio burst theory 79−25558
solar coronal holes, models of flows 79−58313
solar coronal loops, heating by Alfvenic surface waves reson. absorpt. 79−16905
solar coronal loops, stability 79−101132
solar coronal loops, temp. and density struct. 78−89155
solar coronal loops, thermal instabilities in magnetically confined plasmas 80−36600
solar coronal plasma turbulent pulsations, efficiency of four-plasmon interactions in radar signal refl. 80−101582
solar flare, electron density determ. from X-ray spectra obs. 80−82326
solar flare, EUV and X-ray obs. of thermal phase 79−8886
solar flare, transient plasma X-ray spectra, electron density and temp. diagnostics 80−77368
solar flare accelerated particles, nucl. composition and Coulomb losses 80−72913
solar flare heated filament, mass motions 77−29770
solar flare plasma, evaporative cooling 78−40890
solar flare plasma, heat transfer theory 79−40168
solar flare plasma, Langmuir turbulence spectrum estimate from X-ray obs. 80−82329
solar flare plasma, new atomic data for Fe^{19+} spectra 80−67545
solar flare plasma, physical parameters and dynamics from X-ray and XUV emission 78−12175
solar flare plasma flows, thermal character of instability leading to condensation form. 78−57524
solar flare plasma non-stationary heating by non-thermal electrons 77−17455
solar flare plasma physics, explosive phase 77−17514
solar flares, compressible mag. field reconnexion theory 80−6226
solar flares, electron beam diagnostic 80−26827
solar flares, electrostatically unstable heat flow and its consequences 78−20804
solar flares, Fe XXIV-XXV X-ray lines wavelengths rel. to hot plasma motions 80−21973
solar flares, Fe XXV dielectronic satellite line spectra as measure of non-thermal electron energy distribs. 80−21911
solar flares, hard X-ray sources diagnostics 78−89159
solar flares, He-like ions line intensities for non-stationary plasmas 78−53812
solar flares, kinetic processes theory 78−85920
solar flares, mag. field energy dissipation in neutral current sheets 78−26250
solar flares, mag. pumping of energy into nonequilib. turbulent plasma as energy source 77−78764
solar flares, mag. reconnection rel. to plasma accel., heating and shock form. 78−40773
solar flares, plasma column merging, simulation expt. *(Japanese)* 80−31269
solar flares, plasma equilib. conditions from high-resolution X-ray spectra 80−26837
solar flares, plasma turbulence hypothesis confirmation from H spectral lines *(Russian)* 79−16925
solar flares, protons stochastic accel. 80−21953
solar flares, transient plasma X-ray lines, rate coeff. determ. 80−72903
solar flares, trigger mechanism for emerging flux model 78−89162
solar flares, unstable arch model 77−91507
solar flares, X-ray line spectra from transient plasma 80−98626
solar flares collective plasma effects assoc. with particle streams continuous injection model 80−21954
solar flares experimental simulation, merging of two current carrying plasma columns *(Japanese)* 80−94775
solar flares nonthermal electron beams, reverse currents effects on dynamics and X-ray bremsstrahlung 80−51711
solar moving type IV radio bursts, shock and plasmoid models 79−40174
solar plasmas density determination, N III and O IV intersystem multiplets appl. 80−31264
solar system plasma physics, magnetospheres, book 79−84696
solar system plasma physics, plasma processes, book 79−84625
solar system plasma physics, solar and solar wind, book 79−84782
solar transition zone, nonresonant heating mechanism *(Chinese)* 80−85921
solar type III radio burst sources, plasma wave clumping origin 80−21959
solar wind, Alfven instabilities in streaming plasmas with anisotropic press. 77−49259
solar wind, Alfven waves, non-linear interaction with compressive fast magnetosonic waves 80−105142
solar wind, alignment of plasma anisotropies and mag. field direction 78−32311
solar wind, anisotropic struct. of plasma irregularities obs. using interplanetary scintillations 80−67489
solar wind, charge particle diffusion in presence of Alfven waves and perpendicular particle flux 77−84406
solar wind, current sheets resistive instabilities 80−4218
solar wind, deceleration upstream from Earth bow shock rel. to diffuse upstream ions origin 80−98528
solar wind, density and mag. field orientation rel. to magnetopause three-dimensional shape 79−101029
solar wind, dynamic mag. struct. of large amplitude Alfvenic vars. 80−72734

plasma continued
solar wind, effect on terrestrial weather *(Swedish)* 79−79910
solar wind, EGD positive ion expt. on International Sun-Earth Explorer B 78−85805
solar wind, electron density meas. via International Sun-Earth Explorers 78−85803
solar wind, energetic particle meas. upstream of Earth bow shock 80−90308
solar wind, flow around magnetosphere rel. to magnetopause position 78−49236
solar wind, He^+ flux after interplanetary shock, Imp 7 obs. 80−101520
solar wind, heat flux regulation by whistler instability 77−45277
solar wind, International Sun-Earth Explorer 1 and 2 fast plasma expt. 78−85800
solar wind, International Sun-Earth Explorer 1 solar wind expt. 78−85800
solar wind, interplanetary plasma turbulence 79−53693
solar wind, low freq. continuum from ISEE 3, thermal electrostatic noise, LF obs. 80−101519
solar wind, mag. fields and flows between 1 and 0.3 AU during Helios 1 primary mission 79−29963
solar wind, magnetosonic instability driven by alpha particle beam 79−35089
solar wind, MHD shock waves numerical simulation 78−77449
solar wind, MHD solitons theory 80−4217
solar wind, MHD turbulence props. 80−61977
solar wind, microinstability onset and its consequences 77−87222
solar wind, models with Alfven waves 79−16789
solar wind, monochromatic non-WKB Alfven waves, normals evolution 80−101521
solar wind, multispacecraft obs. of microscale fluctuations 77−87224
solar wind, nature of small-scale inhomogeneities 78−45173
solar wind, nonlinear Langmuir waves during Type III radio bursts 78−93173
solar wind, obs. of backstreaming protons near Earth bow shock 80−90309
solar wind, obs. of flows associated with hot heavy ions 80−51635
solar wind, obs. of fully developed anisotropic MHD turbulence 80−94669
solar wind, passage of low-freq. wave packet across stand-off shock front 78−45138
solar wind, plasma analyser for Pioneer Jupiter missions 77−67024
solar wind, plasma comp. expt. on International Sun-Earth Explorer A 78−85810
solar wind, plasma fluid aspects 80−90313
solar wind, plasma instability theory 79−96877
solar wind, plasma motion through comet coma 78−49391
solar wind, plasma obs. during August 1972 solar-terrestrial events 77−25902
solar wind, plasma parameters rel. to magnetospheric ring current plasma injection 78−96363
solar wind, plasma props. during August 1972, near-Earth obs. 77−25904
solar wind, plasma wave elec. fields obs. by Helios 1 77−37492
solar wind, plasma wave investigation by International Sun-Earth Explorer 1 and 2 78−85802
solar wind, plasma/cosmic rays energy exchange depend. on cosmic rays radial gradient orientation *(Russian)* 79−53682
solar wind, plasmadynamical processes review *(German)* 80−109323
solar wind, proton temp. heliocentric gradient from Pioneer 10 obs. 79−40052
solar wind, protons non-bi-Maxwellian distrib. function rel. to ion cyclotron instability 78−96375
solar wind, second harmonic radiation and related nonlinear phenomena in type III bursts 78−7958
solar wind, self consistent soln. of three-fluid model 78−57418
solar wind, stream interaction regions, microscale instabilities 80−72739
solar wind, thin layered field aligned currents distrib. 79−12375
solar wind, time-depend. two-fluid model with thermal cond. 79−92643
solar wind, upstream, obs. of two distinct populations of bow shock ions 79−21124
solar wind, upstream particle events close to bow shock and 200 R_E upstream 80−77247
solar wind, vars. in plasma characts. near D sheets 77−29616
solar wind, wave propag. rel. to vel. correl. with geomag. Pc 3-4 activity 78−73585
solar wind corotating interaction regions, energetic particles shock accel. 80−82159
solar wind filamentary plasma elements, penetration into magnetospheres of Earth and Jupiter 77−78581
solar wind high-speed streams, proton-driven EM instabilities 79−53701
solar wind interaction regions, N-S mag. field component solar cycle dependent configurations 80−98529
solar wind ion acoustic waves, high-resolution spectrograms 79−96878
solar wind microinstabilities in moderately inhomogeneous plasma 77−87223
solar wind multispecies flows, mathematical struct. of transport equations 78−47084
solar wind near Mars, Mars 2 plasma and magnetic meas. 77−53384
solar wind plasma fluctuations, Ogo 5 meas. 78−57420
solar wind plasma radial expansion in 0.3-1 AU range 79−21121
solar wind turbulent plasma, radio wave propag. meas. using three satellites 80−101518
solar X-ray flares, Skylab obs. rel. to physical parameter profiles 80−17561
space plasma, mass discrimination effects in mass spectrometers ion and neutral extraction 80−4230
space plasma, non-ducted whistler-mode signal parametric decay 80−6239
space plasmas, electron beam-plasma discharge at low press. and mag. field strengths 78−42769
space plasmas, new concept for EM and electrostatic waves detect. 77−9549
space plasmas, nonstationary processes study via incoherent response method, phase fluctuations effects 78−45184
space plasmas, VLF signals preprocessing on spacecraft 77−64609
spacecraft charging by magnetospheric plasmas, effects, counter measures 77−22035
spectra emissivity, at electron cyclotron freq., theory 79−72996
spin-flip and normal synchrotron radiation from rot. charge in mag. plasma 80−28153

plasma continued
SS 433, plasma clouds props. and nature of system *(Russian)* 80−36647
Stark profile of H-like ions, Lyman lines in dense plasma 79−82048
stellar, in strong mag. field, neutrino pair emission, photon-neutrino coupling theory 77−17548
stellar, rotating Hall plasma, self gravitational instability, MHD stability 80−14890
stellar atmosphere, nonequilib. plasma density diagnostics via C III EUV Lines 78−53899
stellar atmospheres, higher order fluid eqns. for multicomponent nonequilib. plasma 80−105156
stellar atmospheres, MHD waves propag. in mag. flux tube 78−69789
stellar coronal plasma, EUV spectra and contribs. to diffuse EUV background 80−62324
stellar evolved C cores, nuclear energy generation rates and energy dissipation 80−82339
stellar interiors, thermonuclear reaction rate enhancement due to strong screening, ionic mixtures case 80−36613
stream, electron distribution function, probe diagnostics 80−14935
Sun, coronal and transition zone plasma evolution during 1973 August 9 compact flare 79−5792
Sun, EUV spectra and solar atmosphere plasma diagnostics 79−30050
Sun, plasma hydrodynamic motion in convective element intrinsic mag. field 80−101583
Sun, use of MHD pulses as diagnostic technique 80−109405
supernova remnants, shock-heated plasma temp. determ. 78−65676
superradiation from non-ideal plasmas in electric field 80−38568
Swiss Physical Society, autumn sessions 78−72053
tetrafluoromethane, plasma etching of $Si_3N_4(SiO_2)$ in dry processing, active etchant species 80−79581
thermal emission of an optically thick plasma containing a strong magnetic field 79−25469
thermodynamics of low-temp. plasma with nonequilibrium ionisation, review 80−96343
Tokamak, runaway-driven kinetic instabilities 78−75290
topside ionosphere, anomalous resistivity of auroral plasma 77−5389
Tycho supernova remnant, X-ray line emission rel. to plasma ionisation equilib. 80−46636
upper atmosphere and solar-terrestrial relations, introduction to aerospace environment, book 80−8466
Uranus magnetosphere, plasma dynamics in mag. field laboratory simulation 79−16757
Venus, plasma meas., from Mariner 5, reexamination 79−80258
Venus environment, plasma wave investigation by Pioneer Venus Orbiter 80−67497
Venus environment, study via plasma analyser expt. on Pioneer Venus Orbiter 80−67498
Venus ionosphere, electron temp. probe on Pioneer Venus Orbiter 80−67500
Venus ionosphere, flute instability, mag. flux rope development *(Russian)* 80−77313
Venus ionosphere, Pioneer Venus Orbiter planar retarding potential analyser plasma expt. 80−67501
very-low-q discharges in DIVA confinement and MHD characts. 80−64765
white dwarf degenerate cores, thermomagnetic instability conditions 80−77395
X-ray pulsars atmospheres, possible vacuum signature in spectra 80−27015
X-ray source accretion disc interaction with mag. field, plasma diffusion across Alfven surface 78−93461
X-ray sources, compact, plasma oscills. rel. to radio emission 80−62317
Ar discharge, population processes of 4p levels, perturbation influence 80−38565
Ar, enhanced microwave scatt. at upper hybrid freq. 77−7548
Ar-Br_2, positive column at. state densities 80−44007
Ba^+ clouds in upper atmosphere, striation struct. due to presence of BaO flow 77−25833
CO-N_2 plasma mixture decay, effective recombination coeffs. *(Russian)* 77−47144
CO_2-N_2-He, vol. discharge, negative ions effect 80−14956
F isoelectronic sequence, spectra and energy levels 79−93948
Fe-H multicomponent, confined atom-, and Debye Huckel-, Thomas-Fermi-Dirac models 77−24053
H, spectral broadening by low-freq. elec. field in dense plasma 79−98026
H_2 pulsed arc, dense plasma, Balmer spectrum near photorecombination threshold, press. depend. 80−38569
H_2, UV spectral radiance calibration *(French)* 78−12774
H_Λ line width in at. H atmosphere, shock tube absorption meas. 79−64834
Hα(Dα) plasma red shift meas. in Ar arc, ion dynamic depend. 80−10364
He, hollow-cathode type discharge, spectroscopic obs., laser light source appl. 80−59335
He I 4^3D, ^3F-2^3P line struct., in low-press. linear discharge 79−14523
Hg, liq. sound vel. near metal-nonmetal transition, up to 1600°C and 2000 kg/cm^2 80−39222
Kr afterglow plasma, electron energy distrib. funtion 80−38748
$^{14}N^{15}N+O$ plasma, isotope fractionation under simulated space conditions 78−73623
Ne superradiation propagation through reson.-absorbing positive column plasma, pulse shape change 79−4117
O discharge, capacitatively-coupled, RF, low-press., spatial and temporal emission 79−27847
O_2-N_2 plasma mixture decay, effective recombination coeffs. *(Russian)* 77−47144
Xe, radiation imprisonment of $1s_4$ resonance line 79−82115

plasma accelerators *see collective accelerators*

plasma applications
see also plasma arc spraying; plasma deposition; plasma devices
accel. of projectiles to hypervelocities using series of imploded annular plasma discharges 80−74042
adhesion improvement by gas-plasma contaminant removal 79−39112
AES, SpectraScan III system using high-energy Ar plasma excitation and high-resolution spectrometry 79−96382
arc welding, plasma flow effect on weld pool obs., using basic- and cellulose-coated electrodes 79−7496

plasma applications continued
ashing technique for energy dispersive X-ray analysis of biological specimens in SEM 78−24199
atomic emission analysis, inductively coupled plasma, spectral characteristics 79−70394
atomic emission spectroscopy using inductively coupled plasma, multielement method for liquids and dissolved solids 79−96395
atomic fluoresc. spectroscopy inductively coupled plasma as atomisation cell 77−12839
borsic fibre reinforced Al, hot pressed forged, plasma sputtered *(Russian)* 78−35330
chemistry, nonequilib. plasma, diat. mol. excited state population in diffusion approx. 80−19553
chemistry, review 77−48644
chromatography, baseline corrector for boxcar integrator instruments 77−52717
cumulative plasmadynamic discharge, dynamics and radiation, UV source appls. *(Russian)* 79−55578
cutting at elevated press., underwater appl. 78−87507
cutting metals and alloys, improved plasma torch design 79−8401
cutting with additional heating of plasma-forming gas 80−24267
CVD, RF plasma activated, kinetic model 78−27416
DC plasma excitation source, interference effects 80−86434
deposition of ZrO_2 electrodes for MHD generator 77−39474
deuteron beam generation, 1 to 5 MeV, by plasma focusing *(Russian)* 77−38537
direct energy conversion, CO_2 laser to HV elec. energy 77−88834
direct flow plasma reactor, working of phosphate *(Russian)* 80−55663
electron source with high brightness, emitter and beam parameters 80−106218
element mass separation mechanism in plasma discharge in intersecting fields *(Russian)* 80−14943
emission spectroscopy, analytical, using inductively coupled Ar plasma 79−39257
emission spectroscopy, use of plasma jet and aerosol desolvation system 77−86425
etching, end point detection by optical emission spectroscopy 80−50733
etching control using optical reflection methods 79−57127
expanding plasma, gain on transitions of hydrogenic ions 78−17918
explosive plasma compressor, production of Cu-Fe metastable solid solutions *(Russian)* 77−90289
ferrite reduction using plasma methods *(Russian)* 80−7700
film deposition from metal plasmas 78−6859
fissioning plasma from gas phase nucl. reactor, appl. 80−64794
flow of gas meas., with fluctuating pressures and temperatures, transit time of spark charged plasma cloud determ. *(German)* 80−14861
flowing afterglow plasma ion source, appls. 80−87955
fluorescence spectrometry, inductively coupled plasmas as excitation sources 80−43999
gas chromatography, evaluation of microwave-induced plasma in He, as element-selective detector 77−81450
gas mixture, separation in travelling mag. field in discharge 79−64927
gaseous core reactor neutronics, proliferation potential, and resource utilisation 79−9716
gaseous core reactor nonproliferation features 79−9740
gaseous core reactor U plasma radiative temp. calc. 79−9807
glass substrate, glow discharge effect on surface props. and struct. 78−85201
glass thermopolishing, by use of low temp. plasma radiation *(Russian)* 80−45406
glow polymerisation, thin organic polymer coating technique *(German)* 77−12774
hydrogel pilocarpine release rate control by plasma polymerisation 77−60284
ignition of constant-current vacuum arcs, plasma stream cathode spot excitation 80−75111
industrial utilisation, synthesis, powder, metallurgical and surface treatments, review *(French)* 80−96398
integrated circuit, plasma-removal of polymeric layers 80−1851
internal combustion engine, ignition by plasma jet 78−38555
intraresonator absorption spectroscopy in plasma jet, laser stimulation optimisation 80−77881
ion beam, polarised, obtained from laser-produced plasma using polarised target *(Russian)* 77−38536
ion-to-electron conversion dynodes, prep. by plasma anodisation 77−1887
ionic cleaning, plasma accelerator with closed drift of electrons for ion beam formation *(Russian)* 79−38993
isotope separation, impulse plasma centrifuge with circulation, theory *(Russian)* 80−38553
isotope separation, plasma ion cyclotron reson. 77−10787
isotope separation by ponderomotive force effect near ion-cyclotron reson. 80−43998
isotope separation in rotating plasma, ^{6}Li enrichment, using ultracentrifuge method *(Japanese)* 79−41248
laser beam cut off device, expanding supersonic plasma 79−68412
laser pulse detector, fast nondamageable, using gaseous plasma 80−95138
laser with plasma Q-switch 80−28259
laser-plasma ion source for ion implantation in solids 80−78474
liquid crystal alignment by O_2 RF plasma exposed solid surfaces 77−76307
liquid crystal alignment on plasma-synthesized polymer films 77−76308
low press. high frequency induction plasma, cleaning and polishing of glass and Pt-Ir substrates *(Russian)* 78−35578
mass separation by weakly ionised plasma centrifuge 80−106985
materials preparation, plasma chemistry of heterogeneous systems 80−61100
melting furnace, for steel industry, development in GDR *(German)* 78−22522
metal, plasma-arc refining remelting calc. *(Russian)* 78−18463
metal oxide reduction by electron cyclotron reson. plasma of H, model study on discharge cleaning 80−76548
metal oxide reduction using plasma methods *(Russian)* 80−7700
metal refractory single crystal growth by plasma heating *(Russian)* 78−35292
metal surface, plasma cleaning and etching, removal of C 80−97645
metal surface cleaning, by electron cyclotron resonance plasma of H 79−47821
metal surface hardening by plasma nitriding 79−8400
metal vapour production by plasmo-chemical reaction in elec. discharge *(Russian)* 77−63913

plasma applications continued
metal wire plasma sputtering mechanism *(Russian)* 77−52538
metal-containing plasma polymerised fluorocarbon films, deposition, struct., and polymerisation mechanism 79−78928
metal-vapour recombination lasers using segmented plasma excitation 80−74370
metallurgy, powder, using low-temperature plasma *(Bulgarian)* 78−52715
methane, conversion in H_2 plasma flow, Monte Carlo study 78−61010
microwave induced plasma discharge, emission source appls. 78−32880
microwave noise source, Ar, new similarity rules 77−55177
microwave plasma discharge, appl. to passivation of metals by polymerisation 78−64762
microwave surface wave plasma at atmospheric press., trace gas anal. by optical emission spectroscopy 79−50868
microwave surface wave plasma production and appl. 79−19059
microwave-induced He(Ar) plasma cavity, excitation source for optical emission spectroscopy 77−44567
negative photoresist, RF O_2 plasma stripping, visible spectra 77−40591
negative photoresists, RF O_2 plasma stripping, optical detect. systems 77−40585
neutral beam production using negative ions 80−28696
nitriding in glow discharges, influence on phase comp. and plasticity of diffusion layer *(Russian)* 80−76400
oxidation of Si, magnetoactive O^+ plasma 80−38831
oxidation of SiC in glow discharges at high temp. 77−25174
oxide film prod. by pulsed evap., capacitor prod. and characts. *(Russian)* 78−60584
PET fibres, adhesivity improvement by plasma surface treatment 79−15823
plasma arc refining melting, allowing two phase region and plotting distrib. functions *(Russian)* 78−31358
plasma chemistry, conf., Rome, Italy (Sept. 1975) 78−3336
plasma chemistry, history, diagnostics, production, organic cmpd. synthesis 80−61099
plasma etching techniques in semiconductor manufacture 79−20238
plasma polymerisation, pulsed RF discharge 77−56227
plasma science conference, Montreal, Canada (June 1979) 79−90380
plasma-electron beam discharge, reacting substances *(Russian)* 77−47272
plasma-laser amplifier, 11-16 micron 10^{11} W cm^{-2} pump beam 77−88861
plasmochemical synthesis, powder dispersion control 80−55332
plasmochemical synthesis, powdered infusible compounds, props. 80−55330
polyester fibres, plasma surface treatment, ESR detect. of free radicals 79−15824
polyethylene films, plasma surface treatment, ESR detect. of free radicals 79−15824
polyethylene terephthalate fabric, surface struct., props. rel. to plasma surface treatment 78−95831
polymerisation, pulsed RF discharge 77−56227
polymerisation and polymer surface treatment 77−70198
polymerisation by glow discharge method, formation mech. *(Japanese)* 80−61094
polymerized dielectric thin films deposited by glow discharge, time-dependent props. 77−63564
polymers, plasma surface treatment and plasma induced grafting 79−15825
polypropylene films, plasma surface treatment, ESR detect. of free radicals 79−15824
powder grains, melting, in plasma flame 79−60200
powder metallurgy, production of composites 77−90295
powder polydisperse, heating and vaporisation in plasma stream *(Russian)* 77−59707
processing and heating applications colloquium, London (May 1979) 79−94822
processing apparatus, RF discharge plasma conditions 77−72521
quantitative elemental analyses by plasma emission spectroscopy 79−57337
quiescent equilibrium plasma, aberrationless high-perveance ion beam extraction 79−90472
radial electric field, appearance in source plasma due to beam extraction 79−45500
radial electric field generation, in rot. plasma 79−55480
reaction product spatial separation, in plasma chemistry reactor, neutral beam relax. 79−64926
reactor components and vessels, underwater plasma arc and explosive cutting 79−9922
reduction technology, low temp., present state and future prospects *(Russian)* 78−18462
refractory dielectric coatings appl. using electrodeless capacitor HF plasmotron 77−69984
restoration, evaporation and melting of materials in high temp. gas flow *(Russian)* 80−39271
RF etching, ion energy *(French)* 79−46495
RF plasma etching, ion energy 79−73049
rotating plasma, separation of metals 78−75436
ruby laser, power enhancement by intracavity plasma 80−53330
semiconductor fabrication, CVD technology trends 78−19670
semiconductor structures and devices, plasma etching methods *(Slovak)* 80−40564
silicone membrane progesterone release rate control by plasma polymerisation 77−60285
spatial mass separation of neutral atoms, in rot. weakly ionised plasma *(Russian)* 79−3590
spectroscopic jet light source, intensity distribs., OH band rot. temp. 77−44555
spectroscopy, inductively coupled Ar plasma, development, technique and appls. 79−35839
sputtering, interaction of particles in liquid phase *(Russian)* 78−35306
steel, austenitic stainless, high N, plasma arc remelting, processing parameters and props. 80−16336
steel, C, melting, N_2 absorpt., CO form. influence *(Russian)* 79−39193
steel, plasma thermochemical treatment 79−94823
styrene, plasma polymerisation, polymer struct., NMR 77−25264
surface treatment, low-pressure plasma applications 79−94824
surface treatment by glow discharge, struct. changes in vacuum deposited metal coatings *(Russian)* 79−15852
theoretical scaling laws, implications 80−28805
thermal plasma engineering in metallurgy, inorganic materials technology 78−3070
thin oxide films, form. in microwave plasma 80−76382
transition metal carbide, behaviour in Cs or K plasma 77−20979
triode plasma etching 79−47789
underwater wet plasma wetting in pressurized water 78−7090
welding and cutting, benefits 77−39478
xylene, plasma polymerisation deposition and ESR of trapped free radicals 79−83455
Al film, and native oxide film, etching in carbon tetrachloride plasmas 80−76407
Al plasma etching, undercutting phenomena 80−97635
AlN, plasmochemical synthesis, powder dispersion control 80−55332
AlN powder, plasma synthesized, sintering behaviour, props. and struct. 79−100097
AlN powder, synthesis in low-temp. plasma 80−16257
AlN synthesis, temp. distrib. in plasma-chemical reactor 77−59730
Al_2O_3, polymorphic transformations rel. to prep. under low-temp. plasma conditions 77−40419
Al_2O_3, powder grains, melting, in plasma flame 79−60200
Ar MHD arcjet, recombination lasing 77−65588
Ar plasma, inductive coupled, pyrolysis of hydrocarbons for coating nuclear fuel particles *(German)* 80−18585
B fibre reinforced H, hot pressed forged, plasma sputtered *(Russian)* 78−35330
BN, high-temp. plasmochem. synthesis, control of props. 80−55333
BN production, powdered, in arc plasma *(Chinese)* 79−98999
CO_2 electroionisation laser plasma mirror, soft X-ray emission for biological radiography 79−43983
CO_2 laser, mode locking obs. by intracavity plasma injection 80−83624
CO_2 laser modulation, plasma injection into cavity 80−83626
CO_2 laser power variation detection via plasma tube impedance changes 80−69437
CoO, plasma reduction melting *(Russian)* 78−31359
Cu, metal surface cleaning, by electron cyclotron resonance plasma of hydrogen 79−47822
Fe-Al powder cpds., prep. in low-temp. plasma, struct. props. 77−44192
GaAs film plasma oxidation process 77−77614
H plasmochemical prod. by H_2O decomposition in non-equilib. plasma 80−45773
H prod. from CO_2+steam, plasmochem. cycle 80−45772
LaF_3, VUV luminescence, conference, Moscow, USSR (Apr. 1978) 80−62378
Li, isotope separation by plasma centrifuge, static characts. anal. *(Japanese)* 80−5326
MoB_2, hexagonal, form. by plasma heating and props. 79−28996
NiO, plasma reduction melting *(Russian)* 78−31359
Si, amorphous, hydrogenation using DC and HF plasma treatment 80−59497
Si compounds, plasma etching, gas flow-rate depend. 80−97603
Si, etching in He-F_2 plasma, etch rates, mass spectra, direct ion sampling study 80−79510
Si purification, plasma melting zone technique *(French)* 80−89141
Si purification, plasma melting zone technique, optimisation *(French)* 80−89142
Si selective anodic oxidation in O_2 plasma 80−108610
Si_3N_4 antireflection coating for solar cells, reactive plasma process for forming metal grid patterns 80−93990
$Si_3N_4(SiO_2)$ plasma etching, plasma processes involved in dry processing using CF_4 active etchant species 80−79581
SiO_2, etching in He-F_2 plasma, etch rates, mass spectra, direct ion sampling study 80−79510
SiO_2, reduction by C using a plasma, thermodynamic computer anal. 77−40530
SiO_2, reduction by RF induction plasma torch., Si form. 78−11186
SiO_2 relief, plasma etching, tapered wall prod. 80−97606
SiO_2, substrate, glow discharge effect on surface props. and struct. 78−85201
SiO_2, surface reactivity modification by Ar/O_2 plasma treatment 78−64890
Sn-SnO_x-Sn tunnelling junctions, fabrication by modified RF plasma oxidation method 80−103787
TiC-WC-TaC carbide mixture in plasma reactor *(German)* 77−1819
$TiCl_4$, reduction in steady beam-plasma discharge 80−100099
TiN-VN alloys, synthesis in low-temp. plasma, phys.-chem. props. *(Russian)* 79−38761
TiN_2, ultrafine synthesis in RF plasma, X-ray diffr. chem. and electron microscopy anal. 79−70026
U plasma fueled reactor, use as power supply for nuclear pumped laser system 80−63247
V slag enrichment by oxide reduction during plasma melting *(Russian)* 78−52716
W, heat resistant particles in low temp. Ar plasma, heating, melting, vaporisation *(Russian)* 80−40384
W, powder, produced by plasma regeneration *(Russian)* 78−31360
Xe isotope separation in HF discharge, thermodiffusion *(Russian)* 77−46649
Xe-He(Ne), gas mixture, element and isotope separation in impulse plasma centrifuge *(Russian)* 80−38725
ZrN, plasma-formed, ESCA and supercond. transition temp. 78−19697

plasma arc sprayed coatings
adhesion, ASTM test 80−50812
aerospace appls. 78−44026
applications to design 78−35588
carburizing in glow discharge methane plasma 79−11724
consolidation by laser remelting 80−93697
electronic and domestic appl., cooking plates with high abrasion and corrosion resistance *(Japanese)* 80−55558
ferrite film, prop. by plasma jet spraying microstruct. and magnetic props. 78−6546
fused coating, strength of adhesion to base by gas flame soldering 78−23894
metal hot sprayed deposit adhesion quality factors 79−83365
metals, prep. by plasma arc spraying and characterisation 79−23873
Nichrome-silicate glass-CaF_2 multicomponent self-lubricating coating, prep. by plasma spraying, and props. 80−40604
polymer, struct. investig. by multiple-external-refl. method 78−6235
powder sprayed materials, control of mech. props. 80−11560

plasma arc sprayed coatings continued
process instability, effect on struct. and mech. props. of coatings 77−56131
refractory oxides, prep. by plasma arc spraying and characterisation 79−23873
steel, 30KhGSA, fatigue strength under fretting corrosion, effect of plasma-sprayed coatings *(Russian)* 78−11394
steel, medium C, 45, fatigue strength increase by plasma steel coatings, fretting corrosive cond. 79−15875
ultramicrostructure and porosity 79−82500
weakening effect in constructional materials *(Russian)* 78−31547
wear resistant coatings, operating principles and applications *(French)* 80−76418
Al, effect of Si substrate surface conditions and impact velocity of sprayed particles 80−21145
Al plasma sprayed coating adhesion to mild steel, substrate pretreatment effect 79−83391
Al sintered powder coatings, form. and behaviour under particle bombard. 80−35029
Al, steel substrate, microstructural investigation and oxidation effects 78−11426
Al-Ni mixed-powder-based plasma-sprayed coatings, strength characts. 77−12548
Al-Si coatings, form. and behaviour under particle bombard. 80−35029
Al_2O_3 and Al_2O_3-Y_2O_3, plasma spraying, microstruct., porosity and adhesion 77−32710
Al_2O_3 based coating produced from separated flow vacuum arc plasma *(Russian)* 78−31548
Al_2O_3, composite base ceramic coating, hot pressed, H_2 permeability 77−56164
Al_2O_3, form. and behaviour under particle bombard. 80−35029
Al_2O_3-TiO_2, prep. by plasma arc spraying and characterisation 79−23873
Be, erosion rates under H^+ ion bombard., fusion reactor appls. 80−39179
Be, plasma spray/sinter technique, Ar, satellite support structures, appls. 78−7079
Co-Cr-W-C, hardfaced coating for high temp. liquid Na service, deposition and wear 77−32724
Co-Cr-W-C, wear-resistant coating alloy, carbide form. and decomp. 77−32711
Co-Mo-Cr-Si, plasma and detonation coatings, Laves- and carbide-strengthened, comparative props. 78−15562
Cr, powder, plasma deposition for production of contact portions of cermet electric heating element 78−11364
CrC, plasma sprayed coating 78−68835
Cr_3C_2, $Cr_{23}C_6$, plasma sprayed coatings for gas-cooled reactor appl. 79−24676
Cr_xC_y-(Ni-Cr), for gas cooled reactor heat exchangers, factors affecting performance 80−40609
$MgAl_2O_4$-Al_2O_3 powder prep., for plasma arc spraying, coating props. 77−66612
Ni, effect of Si substrate surface conditions and impact velocity of sprayed particles 80−21145
Ni-Co-Cr-Al-Y, metallurgical characts. and oxidation behaviour 80−40618
Ni-Cr-Al coatings, corrosion and thermal shock resist. in diesel engines 79−24675
Ni-Mo-Cr-Si, plasma and detonation coatings, Laves- and carbide-strengthened, comparative props. 78−15562
(NiCo)-Cr-Al-Y/ZrO_2-Y_2O_3 plasma sprayed ceramic coating for turbine engine components 80−40616
$NiCr_2O_4$, plasma-sprayed coatings, props. 77−59999
Nichrome, plasma spray coatings, relaxation phenomena 80−19876
Sm-Co, amorphous, plasma-sprayed, role of Ar or H_2 atm. in mag. props. and crystn., rel. to H_2 storage 80−64898
$SmCo_5$, high coercivity isotropic plasma-sprayed magnet, eutectoid decomp. 80−80568
$SmCo_5$, isotropic plasma-sprayed high coercivity magnet, eutectoid decomp. 80−75810
$SrZrO_3$ coatings, plasma-sprayed, spectral emittance *(French)* 78−26709
TaC-NiC, powder for plasma arc spray coating appl. 78−15591
Ti alloy substrate, Ni-Cr plasma spray coated, interface interaction 77−21323
TiB_2, erosion rates under H^+ ion bombard., fusion reactor appls. 80−39179
TiC, erosion rates under H^+ ion bombard., fusion reactor appls. 80−39179
TiO_2, wear against grey cast Fe 79−34155
VBe_{12}, erosion rates under H^+ ion bombard., fusion reactor appls. 80−39179
W, effect of Si substrate surface conditions and impact velocity of sprayed particles 80−21145
W, plasma coating, thick, struct. and mech. props. 77−28716
W, plasma spray coatings, relaxation phenomena 80−19876
WC, plasma sprayed coating 78−35592
WC, plasma sprayed coating 78−68835
WC-TiC, powder for plasma arc spray coating appl. 78−15591
WC-TiC-Co, powder for plasma arc sprayed coating 78−15591
WC-TiC-TaC, powder for plasma arc spray coating appl. 78−15591
Y_2O_3, coating for graphite crucible used in melting U 77−32712
Zr-based thermal barrier coating evaluation 80−40619
ZrO_2, plasma sprayed coatings, elec. cond. and gas permeability 79−82478
ZrO_2, stabilised, coating for turbine components, degradation due to internal stresses 79−24671
ZrO_2, stabilized, thermal barrier coating system, spectral emission and absorpt., 300 to 1590K 79−24672
ZrO_2, stabilized by Y_2O_3, corrosion and thermal shock resist. in diesel engines 79−24675

plasma arc spraying
coatings and composite materials 78−3247
contamination of plasma arcs by electrode vapour 77−65924
dielectric coatings appl. using electrodeless capacitor HF plasmotron 77−69984
electronic and domestic appl., cooking plates with high abrasion and corrosion resistance *(Japanese)* 80−55558
energy characteristics of straight and reversed polarity guns 79−41887
Euroflamm facility for thermal spraying in pure Ar atm. 77−32709

plasma arc spraying continued
frequency analyses application 79−83359
gas turbine airfoils, protective coatings, degradation characts. and methods of application 79−24670
gas turbines high-temperature corrosion protective coating appl. 77−12728
glow discharge cleaning effectiveness rel. to base material atomisation rate *(Russian)* 80−20797
metals, prep. by plasma arc spraying and characterisation 79−23873
Nichrome-silicate glass-CaF_2 multicomponent self-lubricating coating, prep. by plasma spraying, and props. 80−40604
powder, effect of thermal power of jet on heating and deposition on substrate 77−59959
process parameters, dimensionless complex parameters appl. 80−66426
production process equipment, present state and future prospects *(Russian)* 78−22518
projection plasma arc, transferred or not transferred, for anti-wear surfacing *(French)* 80−76418
protective coating plasma polymerisation in vacuum chamber 79−70183
refractory oxides, prep. by plasma arc spraying and characterisation 79−23873
thermal plasma transport phenomena, conf., Odeillo-Font-Romeu, France (Sept. 1975) 78−1798
torch anode design improvement to increase deposition efficiency 79−87750
utilisation in research work 79−83117
ZrO_2 powders, stabilised, for plasma spray-coatings 80−20869
Ag, plasma arc srapying, chem. reaction with plasma gases 80−66427
Al_2O_3-TiO_2, prep. by plasma arc spraying and characterisation 79−23873
Cr-Al_2O_3 powder targets for plasma-ion spray deposition of resistance films 80−84897
Cu, plasma arc srapying, chem. reaction with plasma gases 80−66427
Mo-N, nonporous metal production accompanying arc plasma nitriding *(Russian)* 80−7712
N_2 shielding gas use and other improvements 77−21296
Ni alloys, self-fluxing, interaction with oxygen 79−61774
Ni, plasma arc srapying, chem. reaction with plasma gases 80−66427
Ni-Al thermally reactive powder, particle heating dynamics during plasma deposition 80−16179
Ni-Cr-Al_2O_3 powder targets for plasma-ion spray deposition of resistance films 80−84897
SiC fibre reinforced Al, plasma-formed semifinished products, props. 80−84890
Ti, plasma arc srapying, chem. reaction with plasma gases 80−66427
TiC, plasma arc srapying, chem. reaction with plasma gases 80−66427
W, plasma arc srapying, chem. reaction with plasma gases 80−66427
Y_2O_3, ceramic structs., thin-walled fabrication, plasma spraying technique 79−33978
Zn, plasma arc srapying, chem. reaction with plasma gases 80−66427
Zr, plasma arc srapying, chem. reaction with plasma gases 80−66427
Zr-Cu, amorphous alloy, sheet production by plasma spray quenching 77−44193

plasma-beam interactions
see also electromagnetic wave propagation in plasma; plasma production and heating by laser beam
2XIIB neutral beam injection confinement expts., stream stabilization 77−76164
acoustic pressure generation by laser beams 79−18575
Alfven wave excitation, by fast particles in a finite press. plasma of adiabatic traps 78−79424
Alfven waves, ion beam effect on stability *(Russian)* 78−38468
alpha particle beam incident on fully ionised H plasma, energy loss and stopping power 80−64742
alpha particles, satellite interactions with Alfven waves in Tokamak, quasi-linear theory 77−42995
alpha-particles, in high-density plasma, energy loss, dielec. function calcs. 77−89273
amplifying modes and feedback oscills., strong fields 77−68806
atomic beam scatt., local mass spectra diagnostics of admixture ions *(Russian)* 77−19774
beam instabilities, periodic regimes *(Russian)* 80−53999
beam instability, in weakly ionised high-density plasma, Langmuir oscill. interactions *(Russian)* 78−26271
beam instability, nonlinear theory in collisional plasma 79−82061
beam relaxation, influence of modulation instability 78−75367
beam-induced currents in toroidal plasma 80−28808
beam-isotropic plasma system, quasi linear relaxation *(Russian)* 78−22515
beam-plasma discharge formation without mag. field, role of HF velocity modulation 78−75370
beam-plasma heating, transverse beam motion 79−19051
beam-plasma instability, effect of a plasma density gradient, fluid equation anal. 79−4156
bounded cold plasma stream, polarisation current and moving dielec. modes 77−19722
bounded unmagnetised plasma, Buneman instability and current limitation 78−75311
bremsstrahlung of relativistic electron collision with heavy ions 78−75376
Brillouin and Raman scattering of an extraordinary mode in a magnetized plasma 80−92269
Buneman instability nonlinear saturation 80−79467
butane RF plasma, initial etching prior to deposition of C 79−66224
Cerenkov interaction between obliquely propagating whistler wave and electron beam, computer simulation 80−43937
charge exchange meas. in Tokamak plasma, active beam method 80−48991
charged particle beam, collisional interaction with H target of arbitrary ionisation level 78−93095
charged particle transport, energy deposition, in hot plasma, moment method calc. 78−22458
charged particle with relativistic vel. in plasma cylinder, energy loss rate 77−31485
classical collisional theory of beam-driven plasma currents 80−87906
coherent microemission excited by relativistic electron beam in solid-state plasma *(Russian)* 77−15205
coherent millimetric radiation from relativistic beam-plasma instabilities 77−39435

plasma-beam interactions continued
coherent radiation from modulated electron beam in residual gas 77−594
cold beam, nonlinear interaction, numerical simulation 77−51201
cold beam-weakly collisional plasma, amplitude oscills. destruction 80−28695
cold electron beam in pure runaway regime, collective drag and instabilities 80−83949
collective field acceleration of heavy ions with intense relativistic electron beam 79−50863
collision plasma beam instability, nonlinear theory *(Russian)* 79−19049
collisionless relaxation of a plasma with an unstable electron distribution function 79−19052
column embedded by rotating ion beam 80−28690
column rot. and particle transport, travelling EM wave and neutral beam heating *(Russian)* 79−27798
contra-streaming electron beams, RF emission in beam-plasma and beam-beam interaction 78−45137
contrastreaming electron beams in magnetoplasma, nonlinear anal. 78−94918
conversion between cold plasma modes in inhomogeneous plasma possible plasma heating 79−77397
counter stream type beam-plasma interaction, quenching of plasma oscill. 78−5882
counter streaming electron beam instability, stabilisation 78−1849
counter-streaming electron beam instability 77−62376
counterstreaming ion beam plasma device, standing oscills., due to electron-ion instability 78−26305
cross-field-current driven lower-hybrid instability from electron beam injection, ion heating 77−65860
curved relativistic electron beam, instability in plasma *(Russian)* 78−87456
cyclotron maser, high-current and plasma filled, theory 78−17890
cyclotron wave excitation in spiral electron beam interaction 79−64843
deflagration wave in slab target, form. by ion beam 80−28628
deflagration wave in spherical target, form. by ion beam 80−28629
density profile near laser-plasma critical surface, flux limited thermal cond. effects 80−87857
destruction of trapping oscillations 78−71501
deuteron beam relaxation, charge exchange, instability, in 2-component Tokamak *(Russian)* 80−53997
discharge, electron kinetics, charge particle finite lifetime effect 80−92404
discharge, electron kinetics, deexcitation processes effect 80−92405
discharge, in supersonic gas jet flowing into high vacuum *(Russian)* 79−55583
discharge, near Zarnitsa-2 rocket, parameter estimation *(Russian)* 78−26357
discharge disruption by transverse electric field *(Russian)* 78−1846
discharge dynamics, calculations of plasma energy and particle balance 80−28847
discharge for plasmochemical reactions *(Russian)* 79−37508
dispersion relation for charge and current compensated relativistic electron beam-plasma system 78−83580
dissipative beam instability, anomalous beam energy loss *(Russian)* 79−60156
DITE Tokamak, beam driven current meas. 80−106940
DIVA, methane pulsed injection into DIVA Tokamak, transport props. 78−79411
double beam interaction with plasma theory 80−48901
double sheaths, force balance and density criteria 78−91116
E-layer formation by intense electron beam injection 78−34351
efficiency, wave HF press. effects *(Russian)* 80−10395
electric double layer, electron velocity distrib. on high pot. side 80−70010
electromagnetic emission, near geometric mean plasma frequency, mechanism 79−82066
electron and ion beam instability in plasma-beam interaction 78−5888
electron beam, 35 keV, <30A, stabilisation of drift instability by lower-hybrid waves 77−51182
electron beam, anomalous relativistic deposition in dense plasma, coupling efficiency 77−84457
electron beam, anomalous wave amplification *(Russian)* 78−87463
electron beam, caviton interactions 78−22517
electron beam, coherently radiating, radiation press. at surface 78−9314
electron beam, collisional relax. on injection into plasma 80−64738
electron beam, Coulomb collisions in mag. field, polarised radiation enhancement *(Russian)* 80−54002
electron beam, density modulated, phase focusing *(Russian)* 77−80318
electron beam, distrib. function deform., electron wave suppression 77−15209
electron beam, effect on pump-driven quasi-modes 78−30450
electron beam, energy coupling to expanding thick-shelled target 80−96365
electron beam, enhanced energy deposition, interferometric obs., simulation 77−31490
electron beam, entropy theorem and plasma waves spontaneous emission 78−69677
electron beam, explosive wave interaction near stability boundary 77−11358
electron beam, fast, relax. in thermionic converter, cross sections energy depend. 80−43939
electron beam, fluctuations in plasma with Lorentzian vel. distrib. *(Russian)* 77−19669
electron beam, fluid treatment of runaway electrons in strong elec. fields 80−33812
electron beam, freely propagating, ion oscill. excitation *(Russian)* 80−1815
electron beam, high current, ion acceleration using gas lens *(Russian)* 77−19721
electron beam, high energy, relax. in weakly ionised plasma with few collisions *(Russian)* 80−14909
electron beam, high-current, causing press. reduction in air afterglow 80−28867
electron beam, high-current, relax. dynamics, modulation instability of noise *(Russian)* 77−31487
electron beam, high-power, relax. oscillations 80−64744
electron beam, impinging on plasma surface, nonlinear interaction *(Russian)* 79−55519
electron beam, in bounded plasma, spectra of Cherenkov instabilities *(Russian)* 79−77402
plasma-beam interactions continued
electron beam, in inhomogeneous plasma, space charge wave generation 79−41845
electron beam, injection into neutral gas, plasma channel form., numerical model *(Russian)* 79−55540
electron beam, instabilities, orbit perturbation theory 78−5885
electron beam, instability *(Russian)* 78−1847
electron beam, instability due to whistler mode EM waves 79−14564
electron beam, intense rotating relativistic, pitch angle meas. 78−1902
electron beam, interaction with mag. mirror, ion heating and beam trapping 78−9795
electron beam, ion neutralisation, probe beam diagnostics 79−27157
electron beam, ion-sound turbulence driven by return current 78−34314
electron beam, ion-sound turbulence wave dynamics 78−38489
electron beam, kinetic, quasilinear relax., self-similar solns. 80−64702
electron beam, low current passage through gases, peculiarities 80−38812
electron beam, modulated, stability *(Russian)* 78−38510
electron beam, modulated relativistic, space focusing *(Russian)* 78−67373
electron beam, monochromatic, excitation of and attenuation of nonlinear waves in waveguide *(Russian)* 77−47220
electron beam, nonlinear convective and oscill. instabilities, simulation models 78−34338
electron beam, nonlinear induced modulated transparency, mechanism 78−34341
electron beam, oblique wave excitation in semifinite magnetoactive plasma with metal screen 78−26306
electron beam, plane, stability in spatially-limited plasma *(Russian)* 79−98923
electron beam, proton beam form. and plasma oscills. *(Russian)* 78−29207
electron beam, radiation of nonlinear and quasielectrostatic instabilities *(French)* 77−65880
electron beam, relativistic, anomalous energy deposition into solid low-Z target 80−48906
electron beam, relativistic, diocotron modes, magnetic shear stabilisation 80−54006
electron beam, relativistic, dissipative Cerenkov instability, oscill. modes, quasi-linear theory *(Russian)* 78−59564
electron beam, relativistic, electrostatic trapping in mag. mirror 77−24120
electron beam, relativistic, energy distrib. 78−5883
electron beam, relativistic, excitation of rippled plasma resonators 80−48902
electron beam, relativistic, heating and induced turbulence of Langmuir and EM waves *(Russian)* 77−62378
electron beam, relativistic, intense, high energy ion collective accel., localised pinch model 78−87460
electron beam, relativistic, intense, rot. in plasma, μs microwave radiation bursts 79−73018
electron beam, relativistic, interaction with air 80−48904
electron beam, relativistic, interaction with plasma filled waveguide *(Russian)* 78−59605
electron beam, relativistic, magnetoplasma heating, anomalously fast electron-ion energy transfer 78−38515
electron beam, relativistic, plasma filled waveguide, induced field dynamics, beam reson. interaction *(Russian)* 78−59616
electron beam, relativistic, producing electron-positron plasma 79−19053
electron beam, relativistic, propag. in strong mag. field *(Japanese)* 80−91737
electron beam, relativistic, rotating in background plasma, coherent radiation 78−42767
electron beam, relativistic, shock focusing in implosions of inertial fusion model targets 79−49832
electron beam, relativistic, stationary state in ionised gas, force-free motion 79−13887
electron beam, relativistic, sub-critical current, turbulent interaction, anomalously high energy loss *(Russian)* 78−59615
electron beam, relativistic, surface EM wave excitation 77−79734
electron beam, relativistic, turbulence excitation 79−32786
electron beam, relativistic instability in variable dissipation level plasma *(Russian)* 80−19594
electron beam, scatt. and energy broadening 77−62373
electron beam, soliton characts., reson.-like struct. 78−79429
electron beam, supercritical vel. pot. wave amplification, organic plasma *(Russian)* 78−1851
electron beam, test particle diffusion and scatt. in turbulent collisionless plasma 78−38508
electron beam, thin, field-aligned, stability in plasma 77−76124
electron beam, three dimens. quasilinear relax. *(Russian)* 80−83947
electron beam, tubular, EM wave excitation in plasma-filled waveguide *(Russian)* 79−37507
electron beam, unstable, whistler wave propag. along reson. cone, diagnostics 77−31484
electron beam, use for plasma chemistry *(Russian)* 77−47272
electron beam (relativistic)-plasma interaction, transverse mag.-field induced enhanced energy deposition 77−62377
electron beam accel., ignition of thermonuclear microexplosions 77−27686
electron beam and partially ionised plasma, axial mag. field, bea m energy distrib. 78−47131
electron beam charge neutralization, hydrodynamic approx. 78−47132
electron beam confinement time enhancement of ions in laser-produced plasma 78−38518
electron beam delay, strong turbulence, ballistic modes and Langmuir solitons *(Russian)* 77−76111
electron beam dispersion by localised electric field 77−76121
electron beam dissipative instability in plasma waveguides with diffuse boundaries *(Russian)* 77−15212
electron beam driven Tokamaks, review 80−99317
electron beam emission from rockets, beam-plasma discharge ignition rel. to payload charge neutralisation 80−77258
electron beam excitation of pot-surface oscillations, linear theory of beam instability 79−37505
electron beam excitation of surface oscillations in plasma waveguide *(Russian)* 77−39431
electron beam excited discharge plasma, relax., atom. press. 79−37569
electron beam excited plasma, modulation instability of Langmuir waves *(Russian)* 77−35361

plasma-beam interactions continued
electron beam explosive instability in helical resonator, RF emission 79−55520
electron beam fusion of D-T pellets, neutronics and photonics 80−52781
electron beam generated electron plasma oscillations, quenching by low freq. externally applied wave 80−24160
electron beam generated plasma, collision process kinetics *(Russian)* 79−37444
electron beam heating and beam energy distrib. in E-region approximated plasma 80−103163
electron beam heating model 79−73019
electron beam heating of a mirror confined plasma, diode mag. field gradient effect 80−54009
electron beam in channel, stationary states of cylindrical electron beam 79−55046
electron beam in isotropic plasma, EM wave radiation 80−19591
electron beam in semirestricted magneto-active plasma, excitation of surface vibrations *(Bulgarian)* 78−34334
electron beam in Zn vapour, plasma prod. and beam interaction 78−47133
electron beam injection, ω_{ci} instability confined plasma 78−47114
electron beam injection, beam-plasma discharge at low press. and mag. field strengths 78−42769
electron beam injection, energy transfer, heating 77−76129
electron beam injection into inhomogeneous magentised plasma 77−76117
electron beam instability in solar type III radio bursts, nonlinear stabilisation 80−26826
electron beam interaction, instability 79−64877
electron beam interaction, nonrelativistic, modulated, fast EM wave conversion, in waveguide 77−84455
electron beam interaction, numerical simulation 78−91120
electron beam interaction, soft X-ray and UHF meas. *(Russian)* 79−32825
electron beam interaction with EM wave, stochastic oscill. *(Russian)* 79−46460
electron beam interaction with strong turbulent plasma 79−14563
electron beam interaction with toroidal plasma column, interferometric and probe diagnostics 77−24100
electron beam irradiation of Au foil, mag. enhanced energy deposition 79−86591
electron beam nonlinear interaction, hot-cathode discharge double layer 78−34337
electron beam penetration, double layer form., Buneman and Pierce instabilities, collisionless regime 80−10398
electron beam plasma discharge, in crossed elec. and mag. field *(Russian)* 78−87458
electron beam produced inert gas plasmas, UV to near IR laser lines 80−92334
electron beam production of plasma in hollow collector, plasma props. 79−27794
electron beam propagation in plasma channels for ICF reactors 80−1812
electron beam relax. *(Russian)* 79−68935
electron beam relaxation, partially ionised plasma, kinetic approach 78−59618
electron beam relaxation in high density weakly ionised gas *(Russian)* 80−106943
electron beam self-focusing decline by gas breakdown, avalanche and plasma cond. effects 78−18420
electron beam space charge wave in mag. field, cyclotron damping 79−46459
electron beam stabilised mirror confined gas, hot electron population study 80−100089
electron beam stimulated wave instability, nonlinear dynamics *(Russian)* 77−19720
electron beam stopping process in hydrodynamic stage of streaming instability, boundary value treatment 80−103164
electron beam transport, beyond diode, Z-pinch plasma 77−87874
electron beam waves+plasma waves, nonlinear interactions 80−38670
electron beam-cold plasma interaction, nonlinear wave growth and instability, simulation 77−89300
electron beam-magnetoplasma, radiation at or near electron plasma frequency, transverse modes 80−106942
electron beam-N_2 plasma, isolation foil effect, numerical method 79−7469
electron beam-neutral gas interaction, SEEBIE expt., Thomson scatt. diagnostics 77−24111
electron beam-plasma accel. heating, by propag. direction-decreasing density 77−89275
electron beam-plasma discharge, characts. in crossed elec. and mag. fields *(Russian)* 80−10396
electron beam-plasma discharge, crossed field confinement 78−79445
electron beam-plasma discharge, of initially neutral gas 80−54004
electron beam-plasma discharge prod. H ion beam 77−6593
electron beam-plasma discharge shaping, by HF beam modulation, approx. nonlinear theory *(Russian)* 77−47219
electron beam-plasma interaction, electron wave cavity form. 77−35358
electron beam-plasma interaction, in strong Langmuir turbulence region *(Russian)* 80−1811
electron beam-plasma interaction, instability development *(Russian)* 78−55727
electron beam-plasma interaction, obs. of decay instability of beam plasma wave 79−27793
electron beam-plasma interaction, RF emission, oscill. nodes and instabilities 77−24099
electron beam-plasma interaction, theory of nonlinear wave interaction explosively unstable 78−59591
electron beam-plasma interaction in magnetosphere, JIKIKEN satellite expt. *(Japanese)* 80−94655
electron beam-plasma interactions in turbulence regime, phenomenological model 80−6260
electron beam-plasma ion source, optimum discharge parameters 78−59617
electron beam-plasma low freq. instability, cyclotron oscills. *(Russian)* 80−33783
electron beam-plasma system, electrostatic waves, nonlinear Landau damping 77−76055
electron beam-plasma system, explosive instabilities 78−51318
electron beam-plasma system, explosive instability 79−19050
electron beam-plasma system, explosive instability 80−1813
plasma-beam interactions continued
electron beam-plasma system, nonlinear Landau damping of electrostatic waves *(Japanese)* 77−42972
electron beam-plasma system, Simon short-circuit effect, freq. shift 80−96366
electron beam-produced plasma, pot. meas. by two-electrode probe 78−51354
electron beam-produced supercooled He plasma, emission spectrum 77−84501
electron beam-sliding spark plasma device, physical props. 78−5974
electron beam-slow wave interaction in plasma filled waveguide, signal spatial evolution 77−11362
electron beam-vaporised metal surface interaction, 0.4-5 mA ion beam extraction 77−84456
electron beam-whistler soliton interaction in external mag. field, appl. solar wind 77−11360
electron beam-whistler wave nonlinear interaction, computer simulation 77−3938
electron beams, counter-streaming in stationary background, longitudinal mode instability 78−26273
electron beams, counterstreaming, nonlinear development of electromagnetic filamentation instability 79−64852
electron beams, illustration of analogy between negative energy waves and anomalous Doppler effect 77−65881
electron beams, interaction with bounded magnetised plasma *(Russian)* 78−59624
electron beams, relativistic, theoretical scheme for axial compression 80−96367
electron beams, stability in plasma 80−1814
electron burst relaxation in fluctuating plasma, formal dynamical model 78−83579
electron cloud travelling through plasma, dynamics 77−996
electron cyclotron harmonic waves excited by helical electron beam, time depend. 77−31455
electron cyclotron harmonic waves excited in helical electron beam-plasma system 78−1848
electron cyclotron instability, nonlinear development, lower hybrid oscill. effects 78−30437
electron flux-driven ion acoustic instability in Q-machine, probe diagnostics 80−33765
electron heating by relativistic electron beam 77−15213
electron impact generated ion charge state densities analytical approx. calcs. *(German)* 79−82075
electron oscillation in radial potential well effect on beam interactions *(Russian)* 80−14912
electron pulse in cold, dense plasma, energy loss 77−19725
electron rot. relativistic beam, formation of closed mag. field line confinement 77−84458
electron rot. relativistic beam in magnetised plasma, Vlasov equilib. *(Russian)* 77−84452
electron stopping model and secondary-electron distrib. in weakly ionised gas 80−6263
electron stream, sheared, in semi-infinite plasma, reson. instability 80−48868
electron streams, in solar corona, Langmuir instabilities rel. to type III radio bursts 77−2404
electron streams, thick-target, relax. and bremsstrahlung, Legendre expansion, solar X-ray flares appl. 79−70950
electron wave suppression in relation to deformation of electron beam distrib. function 79−1324
electron waves, naturally excited and externally applied 79−90419
electron-beam heating, modulated beam, parametric lower-hybrid instability 78−91127
electron-beam inertial confinement expts. at Valduc *(French)* 80−48907
electron-beam maintained flowing N_2 discharge, cathode shape effect 79−27850
electron-beam plasma, equilibria accessibility, multiple equilibria, nonlinear calc. *(Russian)* 77−84451
electron-beam scattering in partially ionised He(Ar), diagnostic technique 80−28824
electron-beam sliding spark device, C^{4+} plasma, soft X-ray emission, no superradiant gain 78−79444
electron-beam-heating from foilless diode 80−103168
electron-beam-ion two-stream instability initiated turbulent state, 3-dimens. vel. diffusion 78−59595
electron-beam-sustained discharge, plasma contraction by mag. field of current 80−100115
electron-ion oscillating discharge, excitation of EM oscill. in plasma zone 77−55188
electrostatic instability of electron Bernstein wave 77−11333
electrostatic ion cyclotron instability driven by a deflected ion beam 80−87879
electrostatic ion cyclotron instability driven by parallel ion beam injection 77−51176
electrostatic ion-cyclotron instability, ion beam excited 77−68781
electrostatic simulation code, one-dimensional 77−58888
electrostatic wave coupled multicomponent plasma, formation, evolution diffusion 77−84460
electrostatic wave energy in beam-plasma system 78−18397
electrostatic waves, nonlinear Landau damping 77−15186
electrostatic waves generated by ion-beams, shock-like waves 78−59621
EM instabilities, in beam-plasma, renormalization procedure 79−41813
EM instabilities in plasma with anisotropic press. *(Russian)* 78−22503
EM modes excitation in waveguide 78−1844
EM radiation, direct generation mechanism in beam-plasma system 80−54007
EM right-handed Gaussian beam excitation of plasma wave 79−55495
EM soliton propagation in nonequilibrium dispersive media *(Russian)* 80−106933
EM surface oscillation excitation in semirestricted plasma by relativistic electron beams *(Russian)* 79−14561
EM wave amplification in plasma filled waveguide *(Russian)* 77−68801
energetic charged particles, slowing-in distrib. of Maxwellian thermonuclear plasma 79−90418
energetic test ions, energy loss to plasma electrons 79−94804
energy balance in PLT Tokamak 80−28733
energy deposition of fast ions in plasma, Green's function calc. methods 79−14559
energy lost by fast electrons in laser plasma 80−103165
energy transfer in laser (or particle) beam produced plasmas 80−38680
equilibrium accessibility 78−26304

plasma-beam interactions continued
equilibrium of electron bunches exciting nonlinear plasma wave 78−75369
excitation of coherent EM radiation by relativistic beam in plasma surrounded by wall 78−67370
explosive instabilities in cold beam-plasma system 77−15210
explosive instability due to helical electron beam 77−68807
explosive instability in electron beam-plasma system 77−84454
explosive magnetic field generation due to EM incident radiation, laser plasma mechanism 80−6253
fast charged particle beam density effect on stopping in matter 78−14180
fast deuteron beam, in 2-component Tokamak, quality factor calcs. *(Russian)* 78−87500
fast electron beam, suppression in plasma in strong EM wave field *(Russian)* 80−53998
fast ion beam, Alfven wave excitation in Tokamak *(Russian)* 80−53999
fast ion beam, in Tokamak plasma, quasilinear relax. *(Russian)* 78−87457
fast ion beams, quasilinear relax. in non-circular cross-section Tokamak *(Russian)* 80−106938
fast ion excitation of monochromatic Alfven waves *(Russian)* 77−19718
fast ion Fokker-Planck code FIFPC 78−34342
fast ions, behaviour during H-neutral-beam-injection in large Tokamak plasma 80−28713
fast ions in laser-produced plasma, nonlinear plasma-wave interaction 80−24183
fast proton injection, nonlinear evolution of ion cyclotron waves in magnetospheric plasma *(Russian)* 79−55490
fast test particles, slowing down, energy distrib. and spectra in infinite plasma 77−58870
fast test particles, slowing down, energy distrib. and spectra in finite plasma 77−58871
feedback beam-plasma interaction and suppression of oscillation 78−75368
field reversal experiment in 2XIIB 80−28732
field-reversed ion layer, beam driven instabilities 79−64893
field-reversed mirror startup by neutral beam injection 79−86605
finite element approx., wave-particle interaction in weakly turbulent plasmas 77−39422
fluctuating plasma, one-dimens. kinetic beam-plasma instability 79−32784
focus plasma, pinch column form. and stability 80−96380
fusion device surface effects on neutral beam injector and beam direct convertor operation 80−47719
fusion pellet plasma, multi-GeV heavy ion beam, filamentation instability 78−89976
fusion plasma in beam driven Tokamak, Fokker-Planck/transport analyses 80−28826
fusion reactor, beam-driven bumpy torus 80−42859
fusion reactor, TFTR Tokamak, plasma generation and confinement 80−42864
fusion reactor, two-component and hot-ion Tokamaks 80−42863
fusion reactor cavity design, compact electron beam or light ion beam reactor using nonspherical blast waves 80−9405
fusion reactor cavity gas response to particle beam target explosions 80−37602
fusion system, imploding liq. metal liner, rot. electron beam stabilisation 77−74994
fusion-neutron production in D-beam-heated PLT plasmas 80−28807
gas discharge, fast processes in beam-plasma interaction 79−64879
Gaussian beam in plasma, nonuniform ripple growth 79−23429
glow discharge, intense electron beam maintained, N_2 oxidation and collective interactions 79−32841
glow discharge, pulsed, externally maintained, by electron beam 78−79490
group velocity direction of unstable Cernekov beam-plasma modes 79−10674
harmonic generation, three wave coupling 77−19726
heating in toroidal plasmas 80−24239
heating mechanism study in high-beta plasma using ion beams 77−5962
heavy ion beam probe on LITE deep well mag. baseball device 77−84518
heavy ion beam-induced ion-acoustic turbulence *(Russian)* 80−106923
heavy-particle acceleration by charge-density waves in vacuum and in plasma 80−70044
HF electric field, nonlinear behaviour just before beam-plasma discharge initiation 80−87904
HF noise and transport in electron-beam-heated plasma *(Russian)* 77−55174
high current pulsed electron beam injection, oscills. excitation *(Russian)* 77−11361
high current relativistic electron beam retardation distance *(Russian)* 80−14911
high toroidal mode number stability of beam-induced tensor press. Tokamak 80−10378
hot plasma, space pot. distrib. meas. by fast neutral beam method 80−48970
hot-beam plasma, finite geometry effect, instability growth rate, quasistatic approx. 77−51200
hybrid reactor blanket, secondary neutron streaming in plasma vacuum cavities 80−95416
ICF reactor mats., particle-beam-driven, critical environmental considerations 80−32444
implosion, by pulsed electron beam accelerator, 4TW, laser and X-ray obs. 80−1816
impulsive electron beam, axial injection into SF_6, discharge and oscill. 80−59316
impurity atom diffusion, laser fluorescence study 79−68955
impurity injected beam, edge cooling by super-banana limiter 80−43940
inert gas electron beam excited plasma UV absorpt. by diatoms 79−68907
inertial confinement, by laser and electron beams, conf. summary 77−76174
inertial confinement fusion energy with particle beams 77−83074
inertial fusion appls. 80−59250
inertial fusion by oscillating relativistic electron beams in magnetic mirror *(French)* 79−54595
inhomogeneous beam-plasma system, continuous oscill. spectrum *(Russian)* 80−106937
plasma-beam interactions continued
inhomogeneous electron flux approaching cold plasma, surface wave excitation *(Russian)* 78−87459
inhomogeneous plasma, electron beam quasilinear relax. dynamics *(Russian)* 79−27791
instabilities, oscillating, single and counterstreaming beams 77−72455
instabilities in plasma media with absorption 80−64743
instability, satellite excitation 77−42981
instability in plasma slab due to plasma-beam interaction 78−71474
intense, avoidance of current limitations, fusion, ion accel. appls. 79−45898
intense electron current and secondary plasma formation in H plasma discharge 79−64929
intense EM beam-plasma system, radio emission 79−84663
intense ion beam propag. in z-discharge plasma channels, straight and tapered 80−83948
intense relativistic electron beam, trajectories and beam heating of toroidally confined plasma 78−63572
intense relativistic electron beam-plasma system, coupled transverse oscillations, kinetic description 80−64741
intense relativistic pulsed electron beam appls. in plasma phys. *(Dutch)* 78−30452
interior modes, feedback stabilization using RF loaded particle beams 77−31453
ion acceleration, by plasma waves excited by electron beams *(Russian)* 78−71500
ion acceleration by intense relativistic electron beams, one-dimensional electrostatic model 78−75374
ion acceleration by space charge waves in straight-line electron beam 80−103166
ion acceleration from gas by electron beam impact 77−593
ion acceleration in plasma by steady state field, UV and X-ray laser amplification 80−28187
ion acoustic solitons in beam plasma system with nonisothermal electrons generated by ion-beam 80−103151
ion beam, 26 keV, trapped in Tokamak, RF wave heating 78−59627
ion beam, 60 MeV, high-press. plasma production, electron props. diagnostics *(French)* 80−10407
ion beam, accelerated multiply charged ions, current generation *(Russian)* 77−58872
ion beam, cross-field injection, propag. and energy deposition, heating appl. 78−5881
ion beam, dispersion relation of ion Bernstein wave 77−62375
ion beam, EM instability excitation 78−30451
ion beam, energetic, propag. through fusion target chamber, stability 78−26303
ion beam, explosively unstable waves, pump field method obs. 80−92333
ion beam, fast, production technology, use in laboratory and space expts. 78−5889
ion beam, fast, quasilinear relax. in two-component Tokamak, Coulomb collisions 79−37509
ion beam, light, propag. in plasma channel 80−75064
ion beam, parametric excitation of ion acoustic (electrostatic ion cyclotron) waves 80−38591
ion beam, propag. and defocusing in plasma background 77−11359
ion beam, reactive medium instability of space charge wave 78−18421
ion beam, relativistic, nonlinear low freq. EM wave excitation, plasma oscillatory props. *(Russian)* 78−59614
ion beam, stochastic heating by lower hybrid waves 79−98933
ion beam, turbulent plasma, laboratory and space plasma comparison 78−5945
ion beam, vel.- or density-modulated, spatial evolution of wave propag. 79−37510
ion beam, velocity modulation, spatial evolution 77−47223
ion beam, velocity-modulated, steepening and breaking in phase space 80−54005
ion beam , collisionless interaction in transverse mag. field, lower hybrid longit. oscills. *(Russian)* 77−47222
ion beam collisionless relax. *(Russian)* 79−68933
ion beam deceleration, mag. field form. *(Russian)* 78−38464
ion beam deviation, plasma boundary neutralisation surface depend. *(Russian)* 78−59613
ion beam driven instability, in magnetised plasma, light scatt. obs. 79−77424
ion beam dynamics in dense plasma with current 78−75377
ion beam energy relax. in turbulent plasma 78−79443
ion beam excitation of ion-cyclotron waves, ion heating 78−34335
ion beam excitation of ion-cyclotron waves, ion heating 78−34336
ion beam expansion due to ion cyclotron wave interactions 79−31786
ion beam focusing in dense plasma with 100 A to 10 kA current *(Russian)* 77−7561
ion beam induced plasma currents, kinetic theory 79−32746
ion beam injection, heating and acoustic instabilities 79−60154
ion beam injection, instabilities 77−19724
ion beam injection, MHD instability 77−76113
ion beam injection, self-oscillations, feedback mechanism, ion-ion stability excitement 79−50864
ion beam interaction in mag. field, beam relax., nonlinear stages, heating *(Russian)* 77−47217
ion beam interaction perpendicular to external mag. field, lower hybrid instability 77−39434
ion beam modes propag. in double plasma 79−98924
ion beam production from interaction with Nd:YAG laser radiation bursts 80−106939
ion beam propagation, plasma oscill., effect on transverse phase vol. 78−38509
ion beam relax., modulation instability at lower hybrid reson., strongly turbulent plasma *(Russian)* 78−59563
ion beam scatt. by shear Kelvin-Helmholtz wave interactions 79−14562
ion beam scattering by ion-acoustic turbulence 80−6262
ion beam shear-Alfven instability in two component Tokamak 79−60119
ion beam slowing down and relax. by electrostatic ion cyclotron wave excitation 77−76115
ion beam system, 4-wave interaction, positive (negative) energy electrostatic ion waves 80−48884
ion beam thermalisation in turbulent plasma 77−76114
ion beam with rotational and axial motion, thermal equilibrium props. 80−53934
ion beam-plasma, effect on ion acoustic soliton characts. 77−89271
ion beam-plasma collective interactions, high current-density 80−75066
ion beam-plasma interaction system investig. 79−77401

plasma-beam interactions continued
ion beam-plasma system, absolute and convective instabilities of electrostatic ion cyclotron waves 77−68774
ion beam-plasma system, absolute and convective instabilities of electrostatic ion cyclotron waves 80−64740
ion beam-plasma system, absolute instabilities of electrostatic ion cyclotron waves 78−9793
ion beam-plasma system, dispersion relation 79−46485
ion beam-plasma system, explosive instability 77−15208
ion beam-plasma system, higher-order modes of space charge waves 80−69992
ion beam-plasma system, parametric instabilities at unstable electrostatic ion cyclotron waves 79−14535
ion beam-plasma system, self-oscills. due to 2 stream ion-ion instability 77−76123
ion beam-plasma system wave propag. in cylindrical geometry 80−38592
ion beam-plasma system with nonisothermal electrons, ion-acoustic solitary waves 80−33784
ion beam-plasma systems, ion-electron instability 78−91118
ion beam-plasma wave modes, ion beam deceleration by ion acoustic turbulence 78−42771
ion beam-slab target interaction, deflagration waves form. 80−24184
ion beam-spherical target, deflagration wave 80−28694
ion beam-stabilisation of ion acoustic instability in Q-machine 80−33766
ion beams, compensated, handling and expts. *(Russian)* 79−46461
ion beams, direct energy conversion with space-charge compensation 78−87461
ion bunching in electronic space-charge regions 77−3955
ion cyclotron instability induced by perpendicular beam injection into a plasma 79−14565
ion cyclotron waves and high-energy protons, nonlinear interaction in Earth's magnetosphere *(Russian)* 80−17444
ion density, in ionising beams 78−83582
ion density in ionising beams, appl. 78−83583
ion flux nonlinear interaction 77−76116
ion optics, high current beam extracted from plasma, iteration scheme 78−50693
ion ring, field-reversed, anomalous decay of induced electron current 80−24206
ion source, max. current calc. 77−11356
ion-acoustic noise excited by ion-beam, suppression by external RF field 79−77396
ion-acoustic solitons, amplification by an ion beam 78−83554
ion-beam optimal focusing, compensated beams in plasma *(Russian)* 77−76109
ion-beam perpendicular injection, anomalous slowing, quasilinear and trapping regimes 78−1850
ion-beam plasma and compensated ion beam propagation, review 77−80317
ion-beam-driven lower-hybrid instability, anomalous beam slowing 79−41816
ion-beam-excited electrostatic ion cyclotron instability obs. 78−75310
ion-beam-plasma system, ion cyclotron harmonic instabilities *(Japanese)* 78−91124
ion-cyclotron harmonic waves excitation by interacting ion beam 77−3956
ion-cyclotron instability, parametric depend., beam injection, Tokamak stability 78−47110
ion-cyclotron node-whistler mode instability, role in parallel shock wave structs. 77−42994
ion-cyclotron wave, driven unstable by cold-ion beam, nonlinear stabilisation 79−98925
ion-injection caused inhomogeneity spreading, weakly ionised current-carrying magnetoplasma 78−71445
ionised gases, conf., Berlin, E.Germany (Sept. 1977) 78−63615
ionosphere, discharge around rocket following injection of electron beam 77−78570
ionosphere, partially coherent radiation by charged particle beams 78−28407
ionosphere, VLF waves, natural and elecron-beam producted, rocket obs. 78−7829
ionospheric plasma, electron beam expansion and propag., space shuttle expt. 78−7830
ISX-B, neutral beam power system 80−91283
JXFR, neutral beam injection system, gas-beam interaction secondary particles 80−106227
kink mode stability 77−76120
Kyoto beam-plasma type ion source, ion extraction system 78−66007
Langmuir oscillations, amplification, suppression by charged particle in magnetoplasma 79−37482
Langmuir soliton excitation by monoenergetic electron beam *(Russian)* 79−77381
Langmuir waves, large amplitude, nonlinear Landau damping and form. of standing nonlinear waves 80−92292
Langmuir waves, nonlinear interaction at beam input 79−50866
large amplitude wave-electron interaction, enhancement by DC elec. field, simulation 79−90420
light emission from atom beam-plasma interactions, temp. and density meas. 77−72454
light-ion beams for fusion programme at NRL 78−59042
linear effects of wave propag. in plasmas, review 78−14149
longitudinal waves in magnetoactive plasma, nonlinear scatt. probability 78−22471
loss-cone modes in ripple-assisted neutral beam injection, stability 77−76059
low density runaway beam, interaction with cavity modes 79−77398
low pressure plasma system, design and operating characteristics 79−64880
low temp. plasma ionisation by fast electron beam, effective cross section calc. 79−14572
lower hybrid wave excitation by electron beam, body waves 78−34287
lower hybrid wave excitation by electron beam, surface waves 78−34288
magnetic compression of relativistic electron beams, transmission through mag. mirror 77−1012
magnetic field instability of plasma in EM beam 80−64745
magnetic field reversal induced by intense rotating electron beam in initially neutral gas 78−42768
magnetically confined afterglow/at. beam, technique for α ion+atom cross section determ. 77−34750
magnetically insulated coaxial line, ion beam effects 80−87297
plasma-beam interactions continued
magnetised beam-plasma system, instability of Trivelpiece mode 77−62374
magnetised plasma, in open plane periodic waveguide, reson. emission 78−26299
magnetised plasma filled open periodic waveguide kinetic theory of reson. radiation *(Ukrainian)* 77−51197
magnetized inhomogeneous plasma, wave reson. and conversion 80−92313
magnetosphere, polar region, VLF noise generation by electron beams 78−4039
Maxwellian thermonuclear plasma, quantum mechanical slowing in distrib. of energetic charged particles 79−86588
megavolt and megampere diagnostic techniques for pulsed power particle beam fusion drivers 80−49010
MFTF, neutral beam module component design and development 80−91270
MFTF, start up neutral beam power supply system 80−91281
MFTF, sustaining neutral beam power supply, cct. anal. using ASTAP and EMTP codes 80−91284
MFTF, sustaining neutral beam power supply system, modelling with ASTAP code 80−91285
MHD surface wave excitation by charged particle beams 77−55157
microwave excitation in plasma-filled waveguide 77−47224
microwave field spatial distrib., visible emission polaris. 78−67372
mirror machine, 2XIIB, neutral-beam-injected, field reversal expts. 79−86589
modulated beam stability *(Russian)* 79−90421
modulated electron beam in inhomogeneous isotropic plasma, nonlinear wave generation 78−1852
modulated electron beams, instability, spatially separated in plasma 80−70012
modulated hollow beam, excitation of semi-infinite plasma cylinder radiation calcs. 77−39433
modulated relativistic electron beam-plasma interactions, instability, heating 79−98929
modulation of 10 keV ion beam 77−42993
molecular gas heating in electron beam maintained discharge 79−27804
multidipole plasma, origin and confinement of energetic ions 78−91123
multiflow beam-plasma system, potential waves profile regulation *(Russian)* 79−37511
negative ion beam decompensation effect *(Russian)* 79−68934
negative ion beam instability spatial development in rarefield gas *(Russian)* 80−92314
negative mass instability, electrostatic numerical simulation 77−89261
neutral atoms−Tokamak plasma, Alfven wave stabilisation by collisional dissipation 77−55138
neutral beam driven convective loss cone instability 77−89269
neutral beam generation, negative ion revolving multiple beam instabilities *(French)* 80−47798
neutral beam heating, flux-conserving-Tokamak equilibria 77−11381
neutral beam heating in the Princeton Large Torus 80−106950
neutral beam induced reverse electron currents, Levitron obs. 78−59620
neutral beam injection, 26 keV, Tokamak, resulting ion beam RF heating 78−59627
neutral beam injection, charge exchange and ionis. rate coeffs., analytical approx. 79−86590
neutral beam injection, energetic ion distrib. 77−19723
neutral beam injection, neutron prod. in Maxwellian D ion plasma, ion temp. diagnostics appls. 80−49005
neutral beam injection and gas puffing into ORMAK, effect on impurity behaviour 79−64878
neutral beam injection expts. on Tokamak plasma at ORNL 80−28809
neutral beam injection for Doublet III, two-gap magnet design and performance 80−92379
neutral beam injection heating, in PLT 79−82074
neutral beam injection heating in JIPP-II Tokamak 80−28710
neutral beam injection heating in Tokamaks, review 80−28729
neutral beam injection in electrostatic plasma-confinement experiments in a tandem mirror system 80−70025
neutral beam injection in JIPP T-II, investig. 80−28810
neutral beam injection in Tokamak, impurities and elec. field effects 77−65883
neutral beam injection in Tokamaks, review of technology progress 80−28731
neutral beam injection into Doublet III device 79−94805
neutral beam injection systems based on negative ions, review 80−42852
neutral beam injector, simulation of neutral particle transport 80−37600
neutral beam injector research and development, in USA 77−76118
neutral beam production using negative ions 80−28696
neutral beam scattering for density and temperature 78−59668
neutral beam US development program and review 80−92348
neutral beam-heated PLT plasma, neutron emission meas. 79−68954
neutral beam-injected mirror-confined plasma transport 78−22461
neutral beam-sustained field reversed mirror fusion test facility 80−43962
neutral beam-sustained tandem mirror reactors, fusion power reactor and fusion-fission hybrid reactor 80−42856
neutral beams in mag. fields, enhanced reionisation loss 77−68808
neutral injection, prod. of H^- ions from accel. cluster ions for neutral beam 77−65376
neutral injection heating of CLEO stellarator−theory and experiment 80−28755
neutral injection heating of Cleo stellarator 80−28714
neutral injection instability, kinetic, criteria for anisotropic plasma 80−38627
neutral injection kinetics, Monte Carlo anal., local liberation to wall 77−42992
neutral injection parameters and beam line design for TEXTOR 80−28811
neutral-beam injection electron heating in Oak Ridge ORMAK 77−80323
neutral-beam requirements for compression-boosted ignited Tokamak plasmas 78−78494
neutral-beam-driven current evolution in Tokamak plasmas 80−28712
neutral-beam-injected O impurities in 2XIIB mag. mirror 79−37547
neutron flux pumped gamma-ray laser 80−28186
non-resonantly growing waves in beam-plasma system 79−60155
non-self sustained discharge current, gas purity effects 80−38845
nonlinear amplification of waves in beam-plasma system *(Russian)* 78−5886

plasma-beam interactions continued
nonlinear beam-plasma interaction, freq. shift, growth rate 78−59619
nonlinear beam-plasma interaction, simple model 77−89268
nonlinear evolution of the bump-on-tail instability for electron beam in plasma 80−6248
nonlinear interaction, electron collisions effect 78−14181
nonlinear interaction of charged particle beam *(Russian)* 78−38507
nonlinear interaction of cold beam and weakly collisional plasma, simulation 79−32783
nonlinear Landau damping of electrostatic waves in electron beam-plasma system 79−14525
nonlinear mode coupling and saturation of decay instability in ion beam-plasma system 80−83931
nonlinear monochromatic wave, source of particles effect *(Russian)* 78−9779
nonlinear plasma, excitation of large amplitude regular oscills. by modulated electron beam *(Russian)* 78−5887
nonlinear potential oscillations, of cold unbounded plasma, charged particle beam effects *(Russian)* 79−55492
nonlinear theory for electron beams *(Russian)* 79−50867
nonlinear wave amplification in a beam-plasma system 78−91103
nonlinear wave particle interaction 78−34339
nonlinear wave stimulation by injecting electron clusters into plasma *(Russian)* 77−7562
nonlinear waves in modulated electron beam-plasma system *(Russian)* 78−26264
nonlinearly stabilised beam propag., simulation 78−18422
oblique Langmuir solitons under free path conditions *(Russian)* 80−79477
Ormak, confinement and neutral beam injection obs. 77−43022
oscillation suppression by wave perturbation on beam distribution function 77−80316
overneutralised electron beams in metal vapour, ion focusing theory and expt. 78−75366
parametric amplifier, nonlinear hydrodynamic amplifier 79−23462
parametric instability produced by relativistic electron beam in plasma 77−89274
parametric instability thresholds in modulated electron-beam plasma system 77−68792
parametric oscillations in electron beam-plasma system 79−27792
particle acceleration *(Russian)* 77−68805
particle and momentum source response of Tokamak plasma 80−6261
particle beam-plasma interaction, ion-acoustic turbulence effects 78−91121
particle-beam fusion experiments for fusion ignition, pellet compression and long solenoid approaches, breakeven experiments 80−47720
Penning discharge, fast processes in beam-plasma interaction 79−64879
peripheral suppressor grid recovery systems for Tokamaks 80−28813
PETULA device, electron beam interaction, UHF radiation *(Russian)* 78−38532
planar diode, electron beam instabilities, finite ion mass and electron velocity spread effects 77−31483
plasma confinement, relativistic electron beam ring experiments 80−28691
in plasma filled waveguide in axial mag. field 79−41841
in plasma-filled waveguide, beam geometry and mag. self-field effects 79−41842
polarized light interferometer for laser fusion studies 80−31855
ponderomotive laser-plasma effects subject to strong magnetic fields and collisions 80−87905
positive ions in plasma formed by dense beam of negative ions in gas, drift mechanism *(Russian)* 80−103160
potential oscillations excitation with electron beams 78−30419
Princeton Large Torus, unbalanced neutral beam injection, toroidal plasma rot., Doppler shift meas., confinement times 79−77400
production and flow of plasma in ion beams 80−28624
protium beam injection into protium-deuterium plasmas, fusion neutron production 79−23430
pulsar, radio emission mechanism model, by electron/positron-magnetosphere EM interaction 78−8036
pulsar radio emission from relativistic electron beams 77−5540
pulsars, relativistic beam-plasma system, electrostatic excitation level 77−9762
pulsed neutron source creation by laser/relativistic-electron-beam plasma heating 78−74527
pulsed non self maintained discharge, ionisation, high electron beam current effects *(Russian)* 80−14951
pulsed thermonuclear reactor, ignition of D-T target using electron beams 79−71955
quasi stationary waves exam. on periodic injection of electron bunches *(Russian)* 78−47134
quasi-longitudinal waves, excitation in magnetised plasma waveguide by electron beam 78−87462
quasilinear relaxation of dissipative instability of relativistic beam in bounded plasma 80−38671
radial electric field, appearance in source plasma due to beam extraction 79−45500
radiation emission from electron beam excited strongly turbulent plasma 80−53943
radiation in presence of DC field, beam-wave energy conversion 79−68932
radiative collapse of a relativistic electron-positron plasma to ultrahigh densities 80−14929
Raman backscatter in high temperature, inhomogeneous plasmas 80−92268
reactive instability, nonlinear evolution, wave coupling effects 79−41844
reactive-medium instability, transition to inverse Landau damping obs. 77−35359
relativisitc electron beam, reverse current damping *(Russian)* 78−1800
relativistic, intense, unneutralised electron beams, adiabatic eqns. of state for plasma interaction 79−77399
relativistic beam, excitation of Langmuir oscills., modulation instability *(Russian)* 79−4155
relativistic beam, slow wave excitation in waveguide 77−11364
relativistic beam generation of EM waves in plasma *(Russian)* 78−75364
relativistic beam of oscillators, collective slowing down *(Russian)* 77−11365
relativistic charged particle beam, monochromatic EM wave excitation in magnetoactive plasma *(Russian)* 78−87464

plasma-beam interactions continued
relativistic electron beam, 20 MeV, interaction in dense plasma 79−41846
relativistic electron beam, causing reversed field configuration plasma in metal tube 78−91114
relativistic electron beam, combined reson. in corrugated waveguide *(Russian)* 80−10394
relativistic electron beam, current multiplication during propagation 79−41843
relativistic electron beam, D-D target, thermonucl. reaction, neutron and proton prod. 80−37575
relativistic electron beam, deceleration in dense plasma, simulation 77−998
relativistic electron beam, EM instability collisional effects 80−64725
relativistic electron beam, energy deposition in high temp. targets 79−4157
relativistic electron beam, heating, reverse current, persisting EM radiation obs. 78−9796
relativistic electron beam, high-current, propag. along plasma channels *(Russian)* 78−87455
relativistic electron beam, in bounded anisotropic plasma, Cerenkov instabilities spectra *(Russian)* 78−38506
relativistic electron beam, in plasma focus, form., interaction dynamics *(Russian)* 79−4154
relativistic electron beam, intense, coupled dipole oscills. 80−64739
relativistic electron beam, interaction with EM surface waves 79−60153
relativistic electron beam, irrad. of anode foil plasma, ion accel. *(Russian)* 80−54000
relativistic electron beam, mag. confined plasma form. inside imploding liners 79−60175
relativistic electron beam, of high intensity and short pulse width, return beam 78−59622
relativistic electron beam, plasmochemical action in N_2, degradation spectrum calcs. *(Russian)* 79−37536
relativistic electron beam, propag. in air, exploding beam preformed plasma column 77−87875
relativistic electron beam, propag. in inhomogeneous plasma, instability 78−9797
relativistic electron beam, propag. in vac., ion accel. from anode plasma 80−47790
relativistic electron beam, quasitransverse oscills. excitation, anomalous Doppler effect *(Russian)* 79−55518
relativistic electron beam, regular transverse plasma oscills. stimulation, nonlinear theory *(Russian)* 77−47218
relativistic electron beam, reverse current amplification *(Russian)* 78−26302
relativistic electron beam, scattering by mag. field errors and beam-induced waves 78−38514
relativistic electron beam, short pulsewidth, plasma heating, microwave emission 78−5884
relativistic electron beam, slow space-charge wave propag. 80−1115
relativistic electron beam, stability in inhomogeneous plasma 77−39432
relativistic electron beam, stimulated Raman scatt., parametric mode coupling 77−89272
relativistic electron beam, surface filamentation 78−67369
relativistic electron beam, transport, oscills. 77−7559
relativistic electron beam, Vlasov eqn. in plasma medium 80−14910
relativistic electron beam collective ion acceleration, localised pinch model, simulation 78−9826
relativistic electron beam heated plasma, Thomson scattering system 78−75421
relativistic electron beam heating, beam scatt. 79−37519
relativistic electron beam high current ring form., for plasma confinement 77−76168
relativistic electron beam hybrid reactor, parametric anal. of conceptual design 79−76121
relativistic electron beam in magnetised plasma, relax. processes, nonlinear theory, instability *(Russian)* 80−103162
relativistic electron beam in plasma, relaxation *(Russian)* 80−103161
relativistic electron beam in plasma filled channel, wall instabilities 79−86123
relativistic electron beam in plasma-filled waveguide 78−5879
relativistic electron beam induced fusion *(Japanese)* 78−1859
relativistic electron beam induced heating 80−43942
relativistic electron beam induced turbulence and heating, review 80−38672
relativistic electron beam initiated plasma, optical meas. *(Japanese)* 80−48914
relativistic electron beam injection, ion heating investig., density depend. *(Russian)* 77−11372
relativistic electron beam injection, sheet beam model 79−7468
relativistic electron beam injection, uniform mag. field plasma, space charge neutralisation *(Russian)* 77−19719
relativistic electron beam injection into plasma, development of dissipative two-stream instability 80−19593
relativistic electron beam injection into waveguide, charge and current neutralisation *(Russian)* 78−26301
relativistic electron beam interaction, field reversal 79−10713
relativistic electron beam interaction in bounded plasma *(Russian)* 78−26300
relativistic electron beam interaction plasma electron heating 78−63573
relativistic electron beam interaction with plasma in strong mag. field 78−75372
relativistic electron beam propag., numerical simulation 77−997
relativistic electron beam relax. in inhomogeneous plasma *(Russian)* 77−76110
relativistic electron beam relaxation, modulation instability influence *(Russian)* 77−35360
relativistic electron beam rot. in plasma, coherent curvature radiation, two-stream instability 80−19590
relativistic electron beam transmission through strong mag. field in gases 80−48900
relativistic electron beam transport and reflection from ionisation front 78−75371
relativistic electron beam with variable charge neutralisation degree, equil. state 80−59249
relativistic electron beam-EM wave interaction under autoresonance conditions *(Russian)* 80−54001
relativistic electron beam-plasma instability, macro-and microscopic models 80−75065

plasma-beam interactions continued
relativistic electron beam-plasma interaction, efficiency increase *(Russian)* 78−34340
relativistic electron beam-plasma system, stability theory for finite geometries 79−68919
relativistic electron beam/electrostatic wave interaction 78−75375
relativistic electron beams, collective accel., beamfront velocity effects 80−75063
relativistic electron beams, EM instability and stopping power of plasma 80−92289
relativistic electron beams, nonlinear theory of stimulated scatt. of waves *(Russian)* 79−60157
relativistic electron beams, plasma prod. from diatomic gases, mag. field diffusion 80−83955
relativistic electron beams, propag. in a transverse mag. field *(Russian)* 78−22516
relativistic electron beams in plasma-filled waveguide, microwave radn. generation *(Russian)* 79−14566
relativistic electron flux absorpt. by preheated plasma *(Russian)* 77−84453
relativistic electrons, bremsstrahlung instability *(Russian)* 78−47103
relativistic plasma, longit. waves and beam instability *(Russian)* 79−60158
relativistic runaway electrons, induced EM emission around plasma freq., plasma density effects 79−82065
relativistic self-focused electron beam, hose instability meas. 78−83544
relativistic self-pinched electron beam, Bennett profile, resistive hose instability 78−83543
relativistic tangential electron beam-semirestricted plasma collision, dissipation instability *(Bulgarian)* 78−34333
relativitic electron beam, relaxation tangential to semi-bound plasma 79−37506
relaxation of relativistic electron beam in plasma with random density inhomogeneities 77−11357
resonance absorption, self-consistent density profiles for obliquely incident light 80−64758
resonant excitation of slow low-freq. waves by opposite moving electron beams *(Russian)* 80−92336
resonator, electron-beam excited, explosive instability 80−28693
return current response to external beam current in mag. field 77−15211
reversed-field configuration generated by a rotating relativistic electron beam 78−71524
RF emission, plasma wave scatt. by ion-acoustic waves in nonequilib. plasma 80−64733
rF instabilities driven by neutral beam injection, review 80−28757
rotating proton layer, transient magnetic field reversal 80−70027
runaway electrons, enhanced drag by radiation 80−10397
sheath, modulated beam injection transition radiation intensity calc. 77−11363
simulation, explosive instability 79−27821
single-stage accelerated ion beams from plasma, ion optics 78−1147
solar electrons-interplanetary plasma wave interaction, numerical anal. 78−7853
solar flares, plasma heating by energetic nonthermal electrons, theory 77−53505
solar type III radio bursts caused by high-density electron beam, numerical simulation 79−84779
soliton formation, finite amplitude Langmuir type, existence region 77−84422
space and laboratory plasma charged particle-beam interactions workshop 78−7821
space charge neutralisation 79−45507
space simulation beam-plasma discharge, plasma diffusion 79−60108
space-charge wave instability of spiral beam-plasma system in nonuniform mag. field 80−1760
spark, in vac., high-press. local plasma regions production, X-ray and hologram diagnostics 79−19104
spherator, FM-1 energy loss rates of injected energetic ions 77−89270
spiral beam-plasma system, instability, effect of nonuniformity of mag. field 80−48899
spiral electron beam-EM wave interaction, plasma effects *(Russian)* 77−76125
spiral electron beam-plasma system, fast cyclotron wave instability 79−14536
stabilisation of explosive instability and heating of plasma ions by modulated particle flux *(Russian)* 77−3939
stationary discharge, ionisation, high electron beam current effects *(Russian)* 80−14951
steady-state space charge blowup and recovery of intense ion beams 79−1323
stimulated bremsstrahlung of electrons, strong optical field influence 78−59623
stimulated Brillouin scattering from pre-ionised plasma 80−92267
stimulated ion Compton backscattering in laser plasma interaction 80−79511
stochastic heating of ion beams by lower hybrid waves 78−83586
stopping power of plasma in electron beam-plasma system meas. 77−84450
strong electron beam-plasma interaction in mag. mirror field, microwave generation *(Russian)* 77−11355
strong turbulence effects on the kinetic beam-plasma instability 80−59207
strongly magnetised plasma collisional relax. of ion beam 80−33785
strongly turbulent stabilization of electron beam-plasma interactions 80−59251
superbanana limiter as a possible edge cooling scheme 80−92362
supercritical velocity beam interaction with finite amplitude wave, instability *(Russian)* 77−31486
superthermal electron beam, relax. due to Coulomb collisions in plasma 80−106941
surface oscillation cyclotron excitation, electron beam cyclotron instability *(Russian)* 80−54008
surface wave dispersion, stabilisation by HF electric field 78−91117
tandem mirrors, ambipolar pot-enhancement by neutral beam injection 79−94806
temporal growth of filamentation instability of a Gaussian laser beam in a plasma 79−50865
test particle dynamics in turbulent magnetoplasma 79−14614
TFR, high power neutral beam injection and ion power balance, anomalous heat conduction 78−82511
TFR, ion energy balance, heating by fast neutral injection 77−43023

plasma-beam interactions continued
TFTR, neutral beam power system 80−91282
theta-pinch, cool, intense relativistic electron beam interaction 78−51334
Thomson scatt. from thermal plasma, intensity depend. frequency shift 78−42770
Tokamak, flux-conserving cylindrical equilib. evolution with adiabatic compression and beam heating 80−28799
Tokamak, fusion power reactor design 77−74982
Tokamak, impurity control by neutral-beam injection 80−32494
Tokamak, neutral beam injection, low density ignition scenarios 80−48937
Tokamak, neutral beam-heated, parametric scaling 80−10406
Tokamak, noncircular cross section, fast neutral atom injection, collective processes, Alfven waves *(Russian)* 77−47221
Tokamak, T-11, fast neutral beam injection, heating 77−42991
Tokamak fusion reactors, neutral beam driven, physical basis and engineering parameters, review 77−54360
Tokamak neutral injection heating, high energy ion production 79−32788
Tokamak plasma, beam driven currents, trapped electrons effect 80−70011
Tokamak plasma, radial current distrib. meas. using neutral Li beam 78−30488
Tokamak radial transport, multi-regime model including neutral beam injection 77−65840
Tokamaks, neutral-beam injection, USA research 80−27808
toroidal plasmas, beam driven currents, trapped electrons effect 80−70011
toroidal plasmas, beam induced currents 80−92335
toroidal relativistic beams, kink instability, shear Alfven modes 77−76122
torsatrons, neutral beam injection calcs. 80−48949
transverse Cherenkov mode nonlinear stabilisation by external mag. field 80−38642
trapped particle oscillations, destruction, simulation by TWT 77−31462
trapping dynamics, in weak cold beam plasma instability, DC elec. field effects 78−83581
turbulence, nonstationary, elec. field pulsations, nonlinear differential eqn. 77−42983
turbulence, wave power spectral distrib. 78−14163
turbulent electron beam plasma interactions, PN calc., numerical anal. 79−14560
turbulent heating by runaway electron beams, Tokamask plasma 79−73020
Twin Beam Mirror, effect of hot beam injection angle 80−48939
twin beam mirrors, effect of hot beam injection angle 78−58466
two component plasma electron beam nonlinear stabilisation, diamagnetic and VHF obs. *(Russian)* 79−27759
two-beam gain saturation in an electron-ion beam without capture of electrons 78−94919
two-stage-discharge ion source 79−90423
two-stream ion-ion instability in axially bounded ion beam-plasma system 78−91119
ultra-high current carrying column, generalised Bennett equilib. and particle orbit anal. 78−83598
ultrarelativistic beam quasilinear relativistic plasma relax. in strong mag. field, magnetobremsstrahlung *(Russian)* 80−38669
ultrarelativistic electron beam in pulsar atmospheres, mechanism for radio emission 78−20847
ultrarelativistic particle beam in relativistic plasma, emission due to mag. bremsstrahlung 80−46390
unshielded plasma waveguide excitation by modulated electron beam 80−79512
VEGA device, electron beam interaction, UHF radiation *(Russian)* 78−38532
velocity angle scattering of a relativistic electron beam during transport through plasma 80−92337
velocity modulated neutralised ion beam, evolution in potential wells, ion density distrib. *(Russian)* 80−100082
velocity space ring plasma instability, magnetised ion interaction, Vlasov theory 79−77368
velocity space ring plasma instability, magnetised ion interaction, electrostatic and EM simulations 79−77369
visible and UV high intensity spectral lines, in electron beam-produced plasma 79−73012
VLF hiss in plasma penetrated by electron beam 78−26293
volume discharge, instability with electron beam at front of accelerating pulse 79−10739
wave dispersion in presence of relativistic beam 80−19592
wave excitation by electron beams, modulated and unmodulated 77−7560
wave interaction, dispersion and higher order nonlinear effects 78−71502
wave-particle interaction in the late beam-plasma instability 80−28692
waveguide, plasma-filled, electron beam interaction, spatial evolution of complex EM modes, collision effects 79−14556
waveguide, plasma-filled, two-stream instability nonlinear evolution, numerical simulation 80−43938
weakly collisional inhomogeneous plasmas, cyclotron resonance destruction, cyclotron drift instabilities 79−77372
whistler mode waves, temp. anisotropy and beam type instabilities 77−3937
wide electron beam, quasielastic relax. into finite thickness plasma layer *(Russian)* 80−54003
Z-pinch plasma, focused ion beam microinstability, pellet fusion appl. 79−32785
Al ion acceleration in plasm focus *(Russian)* 79−77415
Al target, in air, pulsed CO_2 laser irrad., thermal response and plasma characts. 79−86595
Ar, ion confinement and heating, by negative plasma potentials produced by supplemental electron emission 79−41861
Au pellet fusion target-particle beam system, radiative opacity 80−10365
Ba ion beam, plasma optical diagnostics 79−94815
CO_2 decomposition, plasma radiolysis by high current relativistic electron beam 79−91947
CO_2, dissoc. in nonequilib. plasma of stationary plasma-beam discharge *(Russian)* 79−99006
CO_2 gas laser, glow discharge electron irrad. rel. to output characts. 79−64198
CO_2 relativistic electron beam transport at low pressures 78−75373
Cu anode splitting by electron beam in X-ray regime of Z-pinch 78−5932

plasma-beam interactions continued
Cu, surface, electron stimulated desorption, glow discharge treatment 79−65964
$D^+ + Rb \rightarrow D^{-,0} + Rb$, equil. fraction of D^- ions, charge transfer cross section 77−65375
Fe XXII, XXIV, XXV, charge exchange recomb. in Princeton large torus during beam heating 80−100067
H atoms, injection into hot plasma, ionic mixtures, local X-ray diagnostics *(Russian)* 77−35401
H, change in spectral line intensity of multiply charged ions *(Russian)* 78−58814
H glow discharge, electron macroscopic props. *(Russian)* 80−92403
H plasma beam, electron macroscopic props. *(Russian)* 80−92403
H^- and H electron loss in plasma target 78−67371
H^+, intense beam generation, appl. to controlled fusion 77−76119
$H + O^{8+} \rightarrow H^+ + O^{7+*}$, during neutral beam injection into Tokamak 77−58899
H_2 beam discharge, electron kinetics in collisionless non-equilibrium plasma 80−92402
H_2, fast electron retardation, ionisation cascade, degradation spectra, anal. *(Russian)* 79−27741
H_2 plasma, neutral H ats. penetration, kinetic theory 79−32782
H(D) neutral beam injection expts., PLT and ISX 80−28812
He cryogenic glow discharge, effect of laser radiation (10.6 μm) 80−64803
He, fast electron retardation, ionisation cascade, degradation spectra, anal. *(Russian)* 79−27741
He I beam-plasma discharge, optical radiation polarisation 78−67478
He ion beam plasma inhomogeneous system, microinstabilities 78−91122
He plasma-electron beam, electron cyclotron instability, nonlinear time development, k-spectrum 77−76210
He relativistic electron beam transport at low pressures 78−75373
He-Ne gas laser, glow discharge electron irrad. rel. to output characts. 79−64198
N_2, electron beam energy distrib., excitation and ionisation model, Monte Carlo method *(Russian)* 79−27790
N_2, electron beam sustained high press. discharge, time behaviour of recomb. coeff. 80−10447
N_2 relativistic electron beam transport at low pressures 78−75373
N_2-CO_2-H_2O gasdynamic laser mixture, electron beam diagnostics 77−83845
Nz, electron beam sustained discharge, performance 78−75365
O_2, electron beam energy branching, discrete energy loss method 80−48905
O_2 injection, TFR Tokamak current plateau, effect on Mo impurity 78−22565
Ti XX 80−100067

plasma collision processes
see also plasma transport processes; plasma-wall interactions
2-species finite-sized particles plasma, collisional effects 77−11308
ablation of hydrogen pellet in fusion plasma, scaling law 77−35354
acceleration effects in resonant interaction of laser beam and ions 80−10390
acceleration statistics during successive charge interchanges *(Russian)* 78−1789
acoustic wave interaction, diagnostics appl. 78−83541
air, glow discharge plasma, electron energy balance 77−43092
air, weakly-ionised, secondary electron distrib., produced by electron source distrib. 80−6211
air plasma, gas-discharge, meas. of electron energy loss distrib. 77−35418
air plasma, radiowave interaction, electron velocity, collision cross-section depend. 80−103155
air wake, hypersonic, ionised, free electron attachment coeff. meas. 79−27835
Alcator and Rector devices, collisional regimes 77−43024
Alfven mode, current driven, electron-ion collisions and full dispersion function, numerical anal. 80−64726
Alfven wave instability, neutral at. heated Tokamak, collisional dissipation stabilisation 77−55138
alkali metal, thermal plasma, data on collisional transition probabilities from 1000 to 8000K 77−72406
alkali metal atoms, charge exchange, exciplex or excimer form. in plasma 80−75026
alkali metal plasma, effect of elastic electron scatt. by at. excited states on conductivity 78−42715
alkali metal vapour-H plasma, charge exchange role in optical props. 80−59284
alpha-particle heating in an open-field-line plasma 80−48908
ambipolar electron and ion diffusion in collisional plasma in RF electric field 80−6220
amplitudes oscillations destruction in weakly collisional plasma-cold beam system 80−28695
anisotropic collisional plasma half space, interaction of penetrating EM waves 78−55724
anomalous electron-ion energy exchange, trapped electron mode 77−68739
anomalous intensity ratios in H like L_α doublet in optically thick laser prod. plasmas 80−103186
anomalous resistivity of turbulent plasma in strong electric field 79−72989
anomalous transport of ions, in weakly ionised plasma, high-freq. field effects 78−63549
antenna system, radiation from plasma column in glass tube excited by waveguide 79−50860
arc plasma, temp. meas. by submillimeter diagnostic technique 80−38853
astrophysical plasmas, di-electronic recombination *(French)* 80−82188
atom-ion collisions, in hollow cathode discharge, limit angle, corpuscular diagnostics 79−55454
atomic and molecular cross-section data for controlled thermonuclear fusion devices 77−68741
atomic and molecular processes involving ionic-covalent nonadiabatic coupling, review 80−38535
atomic collision processes and X-ray and UV lasers 80−64787
atomic collisions, cross sections, Maxwellian rate coeffs. 78−51279
atomic cross sections, calc. using effective Feynman diagrams 80−38566
atomic elastic electron scatt. cross section, Glauber approx. modification 78−25700

plasma collision processes continued
atomic ion-electron recomb. in presence molecules, appl. to HCl 80−28601
atomic O, form. and recomb. in U-tube downstream from DC discharge 78−67333
atomic processes for mag. fusion research, data status, review 80−42851
ballistic compressor, nonideal plasma generation, Coulomb interactions, theory 78−87466
ballooning and tearing instabilities 80−28651
banana drift diffusion, Tokamak mag. field with ripples, model collision operator 77−65839
beam instability, nonlinear theory in collisional plasma 79−82061
beam-plasma system, electron relax. in weakly ionised plasma with few collisions *(Russian)* 80−14909
beam-plasma system, nonlinear wave-particle interaction 78−34339
Bernstein waves, propagation in inhomogeneous plasma, dispersion rel., quasi-linear equations, diffusion coeff. determ. 80−75044
binary collision model for plasma simulations, Monte Carlo method particle code 78−9824
binary correlation and convergent collision integral for a plasma 79−41792
binary inelastic collisons, inverse bremsstrahlung absorpt. in large radiation field, Born approx. calcs. 78−42222
bottleneck calculation for collisional radiative recomb. coeffs. for Li-like ions 80−53942
bremsstrahlung, electron-electron, nonequilib. weakly ionised plasma, time depend. 77−11323
bremsstrahlung, stimulated, multiphoton, electron-electron collisions effect 77−76039
broadening of free-bound radiation thresholds, expt. results for Cl^-, I^- and Br^- 80−53940
charge exchange in collisions of multi-charged ions *(Russian)* 79−98859
charge exchange meas. in Tokamak plasma, active beam method 80−48991
charge exchange neutrals, emitted from rot. plasma, meas. 80−106979
charge particle potential scattering, in presence of mag. and laser field 79−81248
charged particle energy loss in turbulent plasma 77−84400
charged particle potential scattering in laser field, eikonal theory 79−81249
chemical reactions, rate coeffs., database creation, DATSTOR 80−48846
chemical reactions in plasma of given chemical content, computer generation, REACS 80−48844
chemical species within plasma, number density variation with time, numerical model, PLASKEM 80−48845
chemistry of plasmas, appl. to IC fabrication 79−79252
classical oscillators, parametrically excited, appl. to plasma interactions 80−33729
cold plasma, Alfven shock waves in presence of effective electron-ion collisions 78−26286
cold plasma, density short wave perturbation, elastic electron-atom collision 78−47119
cold plasma blanket, collisional transport model 77−72466
cold-banket systems, boundary layer analysis 80−28605
colliding plasma evolution, EM computer simulations 80−87926
collision operator for 1D plasma, verification by simulation, heat cond. 79−27823
collisional drift modes, anomalous skin effect, enhanced particle penetration during fuelling, nonlinear theory 80−64703
collisional ionization rate coefficients 79−14518
collisional plasma, modulation instability, turbulence by const. wave pumping *(Russian)* 80−103139
collisional plasma heating rate by mag. pumping, asymmetric RF field 77−7569
collisional transport in Tokamaks, particle and heat sources effect 78−83529
collisionless relaxation of a nonequilibrium distribution of waves and particles 79−19028
colloidal plasma theory, electron droplet collision temp. 77−3914
column and surrounding liq. interaction, quantitative anal. under quasiisothermal conditions 80−38788
complex form., electron-nearest ion interaction, effect on elec. cond. *(Russian)* 78−1788
Compton effect and pair production *(Russian)* 77−24052
conductance theory, quantum-statistical, of nonideal plasmas 80−79440
conductivity, nonideal nondegenerate plasma, dynamic model 78−26238
Coulomb collisions, rel. to MHD wave damping in sunspots 77−5514
Coulomb collisions in degenerate plasma in quantising mag. field, photon absorpt. *(Russian)* 78−55715
Coulombic scatt. of charged particle by random distrib. as two-body process 77−38789
coupled mode equations, linearised, space time solns. 80−87884
current instability on short wave drift oscills., nonlinear theory *(Russian)* 80−53981
current-driven collisional drift and Alfven instabilities in sheared mag. field 80−92286
cusp fields, plasma confinement time investigation using Monte Carlo simulation, collision effects 80−64770
cylindrical pellet in plasma, ablation flow linear stability anal. 80−1738
damping of electrostatic high freq. oscills., nonlinear Schrodinger eqn., appl. to high freq. electrostatic plasma oscills. 77−7530
DC current, collisionless limit, induced by travelling wave, collision term based calc. 78−1806
DC plasma jet, NO synthesis, chem. kinetics obs. 80−38728
dense ionised plasma, thermodynamic props., electron screening corrections 77−972
dense plasma XUV transition Doppler broadening suppression, collisional-radiative model 80−19614
density fluctuation in collisional plasma 80−75053
density-dependent ion lines, excited levels collision relaxation rates calcs. 78−18458
deterministic description of atomic processes 80−59169
deuteron beam relaxation, charge exchange, instability, in 2-component Tokamak *(Russian)* 80−53997
diagnostic techniques for fluctuations 80−49002
diatomic molecules vibr. excited state population in nonequilib. plasma, rel. to plasma chem. 80−19553
diatomic species nonequilibrium dissoc., numerical and analytical results compared 78−71428

plasma collision processes continued
dielectric response and energy loss in intermediate quantum plasma 80−38541
dielectron recombination, secondary ionis. effects *(Russian)* 80−53922
dielectronic recombination, elec. microfield effects, Stark approx. calcs. 77−11311
dielectronic recombination and ionisation equilib., influence of autoionisation and excitation 77−15160
dielectronic recombination through the forbidden levels, low density and T_e highly ionised plasma 80−43850
dielectronic satellite spectra, electron collisions, corona model theory 80−59188
differential ion flux vector meas. technique 78−18459
diffuse discharge, HV, anodic region anal. at 10 to 400 mm Hg 77−43094
diffusion in velocity space, assoc. with mag. moment nonadiabatic changes 77−3920
dilute low-temperature plasma, ionisation in presence of solid phase and alkali metal component 77−42989
dipolar molecule plasma, in elec. field, electron mobility and electron atom collisions 77−76029
discharge, molecular dissociation on bombardment by low energy electrons 80−43845
discharge, pulsed ionisation initiated, non-self-maintained, instability 79−86572
discharge plasma, diffusion regime, elec. sheath theory 80−1810
dissipative trapped electron instability dispersion relation, ion-ion collisions in Tokamaks 78−34290
dissipative trapped electron modes, in torus, impurity effect on LF drift modes 77−55139
dissipative trapped ion instability and anomalous transport 78−22483
dissociation equilibrium, phase space allocation 79−27746
dissociative recombination of H_3O^+ and D_3O^+ at elevated electron and gas temperatures, rate coeff. determ. 80−63747
draft waves driven by temperature gradients, ballooning limit 80−106917
drift and trapped electron instabilities, in systems with mag. shear 80−28648
drift collisional tearing mode, stabilisation by coupling with ion-acoustic wave 78−59589
drift instability, electron-ion heat exchange and electron thermal conduct. effects 77−984
drift instability, electrostatic current-driven, scaling law for high density and high current Tokamaks 80−38691
drift instability, local and nonlocal theories comparison 80−19574
drift mode, current driven, electron-ion collisions and full dispersion function, numerical anal. 80−64726
drift wave turbulence, dissipative, current driven, in Tokamak plasma 80−38587
drift waves, collisional, shear stabilization 79−86577
drift-cyclotron instability, collisional effects 77−55144
drift-kinetic evolution of collisional plasmas in tori 77−72409
duoplasmatron, discharge plasma, negative ion form. and extraction 77−7511
elastic electron+neutral atom in weakly ionised plasma unstable modes anal. 80−38606
electric double layer, electron velocity distrib. on high pot. side, electron-electron interactions 80−70010
electric field compression near a plasma electrode 80−64736
electric LF microfield distribs., two-temp. plasma containing multiply charged ions 77−58843
electrical conductivity of high-density, shock-heated Ar and Xe plasmas 80−38557
electrical conductivity tensor for H_2O_2 plasma in mag. field *(Russian)* 80−87864
electrical discharge, deionisation, caused by internal surfaces, dispersion model anal. *(Russian)* 78−5961
electrical discharge, deionisation of low press. plasma in gas discharge gap, elec. strength *(Russian)* 78−1921
electrical resistivity, in structureless H plasma, weak electron-ion interaction 77−47154
electromagnetic wave interaction with varying plasma 78−75346
electron and ion collisions in lower ionosphere, collision freqs. for use in continuum momentum eqns. 77−87171
electron beam, Coulomb collisions in mag. field, polarised radiation enhancement *(Russian)* 80−54002
electron beams, modulated, non-linear oscillation theory *(Russian)* 80−106898
electron collision effect on wave-breaking in cold plasma 80−96353
electron collision freq. diagnostics, by EM impulse reflection 78−42817
electron collision frequency, determ. by coil probe method 77−1016
electron collision frequency, effective, in ionosphere E-region 79−58153
electron collision frequency in nonuniform column, RF coil probe determ. 78−18446
electron collision rates and distribution functions in O_2 glow discharge 79−10631
electron collisions, role in trapped electron fast-ion induced shortwave modes *(Russian)* 77−47176
electron collisions during electron beam heating 79−7471
electron collisions effect on plasma-beam nonlinear interaction 78−14181
electron density fluctuation spectrum, very high collision freq. effects 80−87847
electron dissociative attachment of mol. plasma in crossed electric and mag. fields 78−5847
electron distribution function, electron-electron interaction effects in external field 80−1739
electron distribution function, steady state response to applied electric field, e−e collisions 80−83883
electron distribution relaxation numerical study for CO_2-N_2-He discharges 80−54070
electron energy distrib., relax. in elec. field, at. excitation rate 78−34266
electron energy distrib. function, Coulomb collision effects, in Xe plasma 80−38532
electron energy distrib. relaxation after sudden elec. field application 78−71425
electron energy loss by ionisation and excitation of atoms in plasma 80−33732
electron ensemble, collision-dominated final periodic state and adjustment 78−71426
electron ensemble, collisional relax. and elec. field heating, stationary states transition times *(German)* 77−68736
electron ensemble, weak turbulence, diffusion and collisions in elec. and mag. fields *(German)* 78−83564
electron ensemble behaviour in HF elec. field, low-ionised nonisothermal plasma *(German)* 79−77383
electron ensemble in variable electric field, vel. distrib. relax. 78−34259
electron fluctuation spectrum and drift instabilities in partially ionised plasmas, collision freq. effects 80−53924
electron gas, screening of ionic motions by electronic background 80−64678
electron hole-electron hole interactions in magnetised plasma loaded waveguide 80−38661
electron hole-Korteweg-de Vries soliton interactions in magnetised plasma loaded waveguide 80−38661
electron impact excitation coeff. for highly ionised ions 77−7510
electron impact width of plasma lines, approximative semiclassical formula 80−43972
electron kinetic eqn. allowing for exchange correlations 78−71437
electron neutral collision frequency from breakdown measurements in crossed electric and magnetic fields 79−14517
electron plasma, classical, dispersion relation, RPA method 79−55481
electron plasma, impurity screening effects in intermediate degeneracy region 80−14882
electron plasma column, transport across mag. field to thermal equilib. 79−37531
electron plasma waves, nonlinear evolution equation including collision effects 79−82056
electron resonant, effects on trapped electron instabilities 77−7528
electron scattering, from a centre of force in strong mag. fields 78−75256
electron stopping model and secondary-electron distrib. in weakly ionised gas 80−6263
electron stopping power, Ray-Hora theory 78−75257
electron three-body recomb., Fokker-Planck extension 77−62332
electron transfer between multicharged ions and neutral targets 77−72407
electron velocity distrib., collisions *(Russian)* 78−1790
electron velocity distrib. function relax., time depend. electric field *(German)* 77−31424
electron waves, broad-band, nonlinear Landau damping 77−89246
electron-electron collisions, neutral atom momentum relax. *(Russian)* 79−18997
electron-ion anomalously fast energy transfer, relativistic electron beam magnetoplasma heating 78−38515
electron-ion collision freq. from EM wave dispersion *(Russian)* 77−47211
electron-ion collisions, stimulated multiphoton bremsstrahlung 79−19007
electron-ion impact ionisation, improved Bethe approx. 77−84399
electron-ion pairs, correlated pairs, effect on conductivity 78−26249
electron-ion recombination, involving collective excitation, dynamic polarisation calcs. *(Russian)* 79−55451
electron-ion recombination coefficient in afterglow, continuity equation, numerical solution 80−28598
electron-ion recombination in ambient electron and neutral gases 80−38531
electron-ion turbulence in collision dominated regime, ionospheric turbulence meas. appl. 79−48605
electron-neutral collision effects on ionisation wave in He plasma 80−43846
electron-neutral collision freq., effect on electron temp. relax. 78−51280
electron-neutral collisions, calc. with respect to momentum transfer, new approach to Boltzmann collision integral 80−92255
electron-neutral particle collision in nonlinear plasma, for Ohm's law coeffs. 79−98857
electron-proton interaction, two-body sum over states of static screened Coulomb pot. 78−55714
electron-sheath collision, laser absorpt. inverse bremsstrahlung prod. 77−58877
electrons, fast, isotropisation distance for elastic scatt. 78−30407
electrons, stopping power, quantum diffraction effects 78−91064
electrons, transport laser fusion plasma, Fokker-Planck eqn. 78−22462
electrons interaction with Langmuir waves, Legendre expansion of quasi-linear eqns. 78−30418
electrostatic drift wave instability, in sheared mag. fields 79−37483
electrostatic instabilities role in critical ionisation vel. mechanism 78−67355
electrostatic ion waves, collisional damping 77−11335
electrostatic plasma probe, neuron membrane physical analogue 80−79573
electrostatic wave, electron Landau damping and electron collisions, Fokker-Planck model 78−47111
electrothermal stability anal. of fully ionised plasma, diffuse pinch 80−43901
elementary reactions in thermonuclear fusion plasmas 79−85762
EM instability of relativistic electron beam penetrating in infinite plasma, collisional effects 80−64725
EM ion cyclotron instability in current-carrying collisional plasma 77−15187
EM pulse absorpt., collision process effects 78−9791
EM surface wave attenuation in unmagnetised RF plasma column 77−42986
EM wave, low-freq., collisional effects on propag. 78−75349
EM wave resonance tuning of magnetoactive plasma *(Russian)* 80−83914
emission spectra, semibounded weakly ionised plasma, collisions effect *(Russian)* 77−89232
energetic test ions, energy loss to plasma electrons 79−94804
energy loss due to binary collisions in a relativistic plasma 80−24127
energy transfer collision freq. in turbulently heated plasma with ion-acoustic instability 80−10399
enhanced line radiation from active molecular plasmas due to electron collision induced instability 78−71491
excitation rate, weakly ionised plasma, strong external field 77−62333
excitations of wave modes and energy loss by charged particle passing through plasma sheet 78−38473
excited atom reactions, in Ne afterglows, rate consts. meas. 79−64826
excited atoms, radial distrib., prod. by surface wave *(French)* 80−96349
excited atoms population distribs., collisional transitions effect 79−90373
excited gas, resonant optical discharge 80−92343
expanding laser produced plasma, three body recomb. 77−3962

plasma collision processes continued
expansion in vacuum, recombining plasma temp. and electron density time depend. 77−24064
explosive instabilities, nonlinear perturbation 80−59199
explosive instability of one dimensional weak mag. field *(Russian)* 80−14896
fast electron beam, suppression in plasma in strong EM wave field *(Russian)* 80−53998
fast ion deceleration in accretion column 80−38530
Fermi acceleration, inertial confinement 77−72488
finite bandwidth radiation, nonlinear dissipation near electron cyclotron harmonic resonances 80−28670
fission fragment generated plasma, electron distrib. function, effect of collisions and diffusion 77−23653
fission fragments generated plasma, electron distrib. function 77−19731
flame, electron-neutral energy exchange in AC field 77−42519
fluctuation level saturation in magnetised plasma with anisotropic vel. distrib. *(Russian)* 78−59593
four-wave interactions in warm magnetised plasma, Lagrangian formalism 77−76056
free electron recombination, arbitrary nonequilibrium stationary distribution calcs. *(Russian)* 80−53947
free expansion of slightly ionized plasma *(Russian)* 80−1740
fusion chain reactions, kinetics, high electron temps., interactions with D-T plasma 80−68945
fusion possibilities and plasma confinement and interactions in mag. config. Tokamak, review *(French)* 80−54017
fusion reaction rate increase in plasma strongly perturbed by longitudinal wave 80−27815
fusion-generated alpha particles driven plasma transport 78−83533
glow discharge, cathode dark space ionisation avalanche with cold cathode *(Russian)* 80−84013
glow discharge, electron velocity distribution function relax., periodic behaviour in highly modulated elec. field 79−64935
glow discharge, high press., collision freq. meas. 77−55184
glow discharge cathode region microscopic model 78−67524
glow discharge plasma, corpuscular diagnostic method of metastable atoms, review *(Czech)* 80−24241
glow discharge sheath RF impedance, scatt. and ionisation effects 79−86630
guided waves in hot collisional uniaxial plasma 80−53995
gyro-kinetic equation with collisions, toroidal geometry appl. 77−51222
H Lyman-α line core, effect of emitter ion dynamics 77−47161
halide ions, recombination, exciplex or excimer form. in plasma 80−75026
harmonics generation in inhomogeneous plasma *(Russian)* 80−83916
He I and II radiation enhancement in mag. field, nonlocal thermodynamic equilib. 80−10366
HF discharge, ionisation overheat instability in EM wave field *(Russian)* 80−106990
HF electric field effect simulation, Coulomb collisions, weighted particle method *(Russian)* 77−3981
high melting particle heating, melting and vaporisation in hot gas 80−6201
high temperature plasma, impurity ionis. equilib., radiative cooling 78−42712
high temperature plasma, physics, book 80−98767
high-Z emitters in ultradense plasmas, hydrogenic profiles, perturbing ion effects 80−79566
hollow cathode arc discharge, electron energies, excitation and ionisation speeds *(German)* 78−91170
hollow-cathode arc discharge, electron energy distrib. and ionisation velocity 78−67534
hollow-cathode discharge alignment, electron collisions 79−64944
homogeneous bimolecular plasmachemical reactions, nonequilib. kinetics 78−63634
hot collisional plasma filled waveguide, wave propag. 80−92331
hydrogenic atoms and ions, degenerate state transitions, plasma waves, Stark effect 79−72389
hydrogenic ion lines, red shift in plasma 80−103128
hydromagnetic waves, nonlinear, in two-electron temp. plasma 79−98884
impurities in collision-dominated regime, transport props. 78−5850
impurity diffusion, in Tokamak in collision regime, neutral injection effects *(Russian)* 78−26247
impurity diffusion and heat transfer, in neoclassical regime, neutral injection effects *(Russian)* 78−26248
impurity diffusion eqn., with ionisation and recombination source terms 78−30409
impurity ions in Tokamaks, charge transfer excitation 79−4103
impurity ions on rational magnetic surfaces, convection and diffusion, collisional multifluid model 80−28615
inelastic collision frequency, polarisation effects *(Russian)* 77−3918
inert gas afterglow, excimer form., VUV emission obs. at low press. 80−38755
inert gas arc, low-voltage, ionis. mechanism 79−27852
inert gas DC discharge, ionis. wave wavelength, electron gas state depend. 78−1918
inert gas discharge, electrophoresis anal. using plasma kinetic eqns. 77−43100
inert gas plasma, weakly ionised, photon echo relax. obs. in RF discharge 80−43986
inert gas stationary afterglow obs. of singly charged atomic ions, three-body rate coeffs. 80−38757
instability, current-driven, link-like, in magnetised collisional plasma 77−80284
instability, electrostatic, parametric, due to thermal coupling 80−79465
inward particle transport by plasma collective modes 79−55543
ion+molecule, interstellar species form. radiative assoc., reaction types 80−31348
ion+neutral atom collisions, partially ionised plasma, turbulence, power spectrum var. with press. 80−38645
ion acceleration in expanding rarefied plasma 79−41799
ion acoustic wave, large amplitude coherent, heating mechanism 79−23432
ion and electron temps. equilibration rate, quantum effects 80−24133
ion beam scattering by ion-acoustic turbulence 80−6262
ion beam thermalisation in turbulent plasma 77−76114
ion composition of plasma of pulsed discharge in He, H_2^+ current time evolution 80−54046
ion current magnetic field reversal, electron effects 79−10638

plasma collision processes continued
ion distribution in collisional HF-discharge in RF range *(Russian)* 80−106986
ion drift velocity in EM fields, charge transfer effect 78−83527
ion energy loss to electrons, high energy test ions 78−91065
ion excited level population probabilities, steady- vs. quasisteady-state models 80−24128
ion excited level population probabilities, steady-state, appl. to H-like ions 80−19552
ion interactions in weakly ionised plasma through acoustic field, plasmoid existence 79−27776
ion interactions in weakly ionised plasma through phonon exchange in neutral gas 79−27775
ion recombination rate in boundary layer 79−1286
ion scatt., suprathermal, by partially ionised impurities, measurement of Z_{eff} 80−54039
ion sources, fundamental and special physical processes 80−32559
ion velocity, distrib. diagnostics by neutral particle time-of-flight spectra 78−67439
ion velocity space diffusion in controlled ion wave turbulence, ion wave echo probe obs. 77−43079
ion-acoustic shock waves, in multi-electron temp. collisional plasma 77−7523
ion-acoustic-solitons, dissipative effect on formation 77−84419
ion-ion collision stabilisation of drift instability, plasma-electron beam interaction 77−51182
ion-ion diffusion, 2D boundary-value problem, multiple mirror expt. 77−84411
ion-sound soliton-resonant particle interactions *(Russian)* 80−14880
ionisation and recombination processes simulation 79−14604
ionisation cross sections and rate coeffs. for partially ionised gas 79−46422
ionisation dynamics of CO_2 laser prod. plasma, spectrosc. obs. 80−43968
ionisation of atoms by electrons, thermal, direct continuum transitions role *(Russian)* 79−98858
ionisation of H plasma in uniform elec. field *(Russian)* 80−53923
ionisation wave, kinetic theory 78−22454
ionised emitters, electron impact broadened lines, quantum mech. interference effects 77−42282
ionised gas, slow electron momentum transfer cross section in mag. field, RF cond. meas. 79−82030
ionosphere, collision frequencies, recomb. coeffs., rel. to resistivity of semiconductors and metals 79−8742
ionospheres, ionic reactions in lab. and planetary atmospheres 80−59168
ions, electron impact excitation close-coupling formalism, perturbative treatment 80−48091
ions, multicharged, cross sections for electron impact ionis. 78−37746
ions, multiply-charged, dielectronic collisional recombination rate, effect on level populations 79−1287
ions, positive, dielectronic recomb. in plasma generalised cascade theory 80−43851
isotropic plasma, metastable atoms, equilib. distrib. function 78−91068
kinetic equation for electron gas in strong fields and inhomogeneities 79−72986
kinetic equations for collisional plasma model 77−42963
kinetic reactions, pulsed afterglow technique obs. in Ar-II plasma 80−48854
kinetics, in electron beam generated plasma *(Russian)* 79−37444
L-2 stellarator, ohmic heating discharges with gas puffing 80−79593
Landau damping and oscills., linearized Vlasov-Hermite system, non-analytic initial perturbation 77−89245
Langmuir turbulence, HF energy dissipation *(Russian)* 78−5873
Langmuir wave eqn., steady state shockwave solns. 77−68799
Langmuir wave interference, electron collisions *(Russian)* 80−69970
Langmuir waves, collisional damping in collisionless limit 78−34295
Langmuir waves, modified decay, collisions effect *(Russian)* 77−27672
laser beam filamentation in collisional plasma, theory 77−84440
laser beam filamentation in strongly ionised magnetoplasma 78−26291
laser beam-plasma interaction nonlinear force, generalised derivation of Stamper term 79−37502
laser fusion plasma, HF EM wave swelling effect near crit. density 77−84443
laser plasma jets in conical targets, collision influence in final stages of expansion 79−14584
laser produced plasma, wavelength effect on absorpt. and ionis. 77−27654
laser scatt. in plasma 80−83905
laser target, Monte Carlo (hybrid) suprathermal electron transport 80−24200
laser targets, dynamics, 2-D three-temperature MHD model 80−70014
laser-fusion regime, plasma transport, extension of Braginskii system of fluid equations 80−53935
LF waves, plasma ionisation instability, dispersion rel. *(Russian)* 78−83519
light scattering, by plasmas with ionised impurities, collision effects 79−41835
line broadening in atomic and ionic emissions from plasmas *(French)* 80−79434
line broadening theory, screening process dynamics *(Russian)* 80−69988
line emission, radiative and collisional broadening in laser heated plasma 77−47159
long time confinement of pure electron plasma, max. confinement time 80−48954
long-wavelength modes and anomalous transport in toroidal magnetoplasmas 80−28613
low ionised anisothermal plasma, ionising electron collision kinetics *(German)* 80−33730
low temp. plasma ionisation by fast electron beam, effective cross section calc. 79−14572
low-frequency oscillations, in plasma with negative ions, collision effects 78−87448
lower-hybrid waves in collisional plasmas with field-aligned current, instability 80−75045
Lyman-α line wings, contribution of proton perturbers 78−67325
Lyman-α transition, line broadening, ion dynamics effects 78−42801
magnetic field instability of plasma in EM beam 80−64745
magnetic field line reconnection, neutral layer with Petschek slow shocks 79−50851
magnetic field operation, in resonant absorption of light 79−73013
magnetic fields of hot dense plasmas, particle probes sensitivity 80−70037

plasma collision processes continued
magnetic mirror, collisional loss of electrostatically confined species in a magnetic mirror 78−79455
magnetic pulse penetration into plasma, theta pinch geometry, Alfven velocity scaling 80−33803
magnetic trap, with helical mag. axis, plateau and banana diffusion regimes 80−10425
magnetised turbulent plasma, nonlinear current density, collisional contribs. 78−63567
magnetized sphere interaction with supersonic plasma flow 78−59608
magnetoacoustic nonlinear dispersive waves in collisional plasma 77−72424
magnetoplasma, weakly ionised, perturbational heating in oscill. elec. field, collisional relax. and Boltzmann eqn. 79−37515
magnetosheath, effective collision freq. in medium with MHD turbulence 78−28420
mass renormalization in stochastic acceleration of particles *(Russian)* 80−100066
metal vapour laser, afterglow electron energy balance 79−76678
metastable molecule excitation and ionization, electron microphysical determ. collision frequencies *(German)* 79−41793
methane, ion-molecule reactions in glow discharge, mass spectrometric obs. 78−63627
MHD generators, non-equilib., electron collision freq. rel. to ionisation instability 77−72506
MHD plasma, dense, ionisation and radiation dynamics, simulation 78−83606
MHD switch-on shocks, ionis., heating 77−80320
microcanonically distributed plasma, reduced distrib. functions 80−28604
microwave probe, semispherical monopole, input admittance thermal noise *(Russian)* 77−76196
Microwave reflexion in rectangular waveguides by high pressure RF plasma columns 80−43975
minor confined high beta reactor, simple binary collision theory 79−86603
mirror, plasma confinement time investigation using Monte Carlo simulation, collision effects 80−64770
mixture, binary, low ionised, electron kinetics, collision processes influence *(German)* 79−14519
modelling of plasma with collisions, macroparticle method 79−18996
modes and ballooning in magnetically confined plasmas 80−28650
modulational instability in Langmuir and ion-acoustic turbulence, collisional excitation 77−24086
molecular electron imact excitation, rot. transitions *(Russian)* 79−76524
Monte Carlo Lorentz collision operator 77−76028
moving collisional plasma and moving plasma with intrinsic spatial dispersion, emission of longit. waves 80−87848
moving electron plasma, interaction of large-amplitude plasma waves 79−98899
multicharged ion and nucleus electron capture during collisions *(Russian)* 80−87850
multicharged ion thermal charge exchange reaction, rel. to astrophysics 80−63815
multiphoton inverse bremsstrahlung, plasma laser absorpt. coeff., correspondence principle method 79−32749
multiple ion plasma, Pfirsch Schluter regime, classical transport and friction coeffs. 77−55130
multiply charged ion, electron capture into different excited states in plasma 80−64679
negative ion production and density meas. in low-press. plasma 79−64825
neoclassical transport of multispecies toroidal plasma in collisionality regimes 77−47152
neutral atom kinetics, near Tokamak discharge chamber wall *(Russian)* 79−4102
neutral atom transport, computer code SPUDNUT 80−48962
neutral beam heating in the Princeton Large Torus 80−106950
neutral beam injection, charge exchange and ionis. rate coeffs., analytical approx. 79−86590
neutral gas-moving magnetised plasma interaction, Alfven critical vel. 78−69670
neutral gas-plasma interaction in cosmic physics 78−69669
neutral injection kinetics, Monte Carlo anal., local liberation to wall 77−42992
neutral particles, interaction with wall and plasma, kinetic description 78−59658
nonattaching gas, irrad., in infinite cylindrical cell, space charge and wall effects 77−68737
nonequilibrium ionisation and recombination processes in laser-produced plasmas 79−41794
nonequilibrium plasma, kinetic theory of spectral line broadening 80−59187
nonideal plasma, elem. excitations and macroscopic props., review 80−43842
nonisothermal plasma electron ensemble, nonstationary behaviour, kinetic description 80−59171
nonlinear collisional drift instability, numerical analysis 78−91091
nonlinear dielectric perturbation, wave and particle interactions 80−38593
nonlinear interaction of cold beam and weakly collisional plasma, simulation 79−32783
nonlinear Langmuir wave, collisional damping in rarefied plasma 78−22484
nonlinear transport due to collisional drift wave 77−72417
nonlinear wave phenomena, collisional and weakly collisional cases 77−11346
nonneutral electron plasma, transport due to electron-atom collisions 78−67318
nonthermal plasma, H and H-like ion populations, collisional radiative recomb. and ionis. 78−38450
nonthermal plasma, quasistationary state population, relax. times 77−3916
ohmic heating of plasmas in closed magnetic systems 80−28756
optical line emission, Doppler broadened axially symmetric plasma, interpretation model 78−75276
optically thin plasmas, steady state populations, relaxation times 79−55561
orifice flow, wall interactions in mol. flow regime, for diagnostics 79−23449
plasma collision processes continued
partially ionised fluid, thermal instability, compressibility and collisional effects 78−55693
partially ionised plasma, resistivity reduction due to ionisation and recombination 78−63545
particle and momentum source response of Tokamak plasma 80−6261
particle dynamics in low freq. EM waves, magnetosphere particle flux in inhomogeneous plasma 80−1804
particle orbit in magnetic field, guiding-centre Hamiltonian, arbitrary gyration 80−1834
particle scattering by low freq. waves, effective scatt. freq., eval. method 80−83882
Penning discharge, ion heating and collisional energy loss 77−72519
phase transition in elec. discharge plasma between parallel plates, compression by recomb. press. 80−64799
pinched discharges, runaway electron model for X-ray emission 79−46497
plasma diffusion in stochastic mag. fields, rare collision effects *(Russian)* 79−77342
plasma lasers in molecular medium, thermal ionisation and recomb. *(Russian)* 78−22118
plasma multitemperature mixtures, Maxwell-Grad moment method calcs. 77−47134
plasma temperature anisotropy relaxation due to binary encounters 77−39404
plasma-wave dispersion rels., modification due to magnetic monopoles, pulsar emission 79−75704
ponderomotive effects and magnetic field generation in radiation plasma interaction 80−28680
ponderomotive laser effects in collisional plasma transport 80−38562
population inversion due to plasma expansion into ambient gas, electron cooling 80−96363
positive column, metastable atom radial transport at various electron distribs., atom+atom collision effects 80−44037
positive column of glow discharge of electronegative gas, molecular excitation and ionisation by electron collisions 80−49031
positive ion bunches, gas neutralisation, without mag. field *(Russian)* 79−27744
positive ion kinetics in cathode fall of abnormal glow discharge 79−14626
powders, spark elutriation into plasma spectrochem. anal. *(German)* 78−68959
propagation of electromagnetic and electroacoustic waves through compressible fully ionised warm plasma 77−992
propane-air laminar flame plasmas interaction with microwave TM_{010} mode in combustion bomb cavity 80−53939
pulsed HP glow discharges, time-resolved electron-neutral collision frequency meas. 77−39498
pulsed limiter discharge, multicomponent nonideal plasma, chem. composition 80−19657
pycnonuclear reactions, pair correlation function in dense plasma 79−67001
quasicollisions model for particle scattering on plasma turbulent pulsations appl. to transport coeffs. determ. 78−71440
quasistatic theory for negative ion free-bound radiation threshold broadening 80−53941
radial diffusion, eqn. for collision-affected plasma 78−49310
radiation coupling, kinetic model, collisions effect 78−34262
radiation instability and heavy ion cluster formation in multicomponent plasma 79−64849
radiation-driven ionisation fronts, head-on collisions, temp. jump ratio 77−3915
radiative electron capture anal. by ion channelling techniques 77−35350
radiative emission rates for low- and medium-Z elements in high temp. plasmas 80−103125
radiative recombination coefficients, in low-density plasmas 77−62334
radiowaves interaction, thermic excitation of parametric instability, controlled 80−24164
rare gas plasmas, energetic binary collisions 79−77337
rarefied electron gas, space depend. electron transport by integral approach 80−92257
Rayleigh-Taylor instability, MHD flow of composite medium, variable viscosity 78−1813
reaction product spatial separation, in plasma chemistry reactor, neutral beam relax. 79−64926
recombination, isotope enrichment due to reson. trapping 77−58203
recombination coefficients *(Russian)* 79−50847
recombination decay, in electron beam generated He plasma, Ne addition effects 78−59545
recombination in laser-prod. plasma 80−106871
recombination in the free vacuum expansion of a complex plasma 79−64827
relativistic Boltzmann theory, reduction of collision integrals 80−79560
relativistic plasma collisions instability *(Russian)* 80−83913
relativistic plasma test particle energy loss, unified theory 78−71530
relativistic statistical mechanics 79−82039
relativistic two-stream instability, nonlinear state electron ion collisions effect 78−26280
resistive modulation instability 79−77378
resistivity, trapped electron regime, collisional theory 77−84412
resistivity anomalous, generated by ion-acoustic turbulence, collision freq.-turbulence spectrum relation 78−14205
resonance interaction of particles trapped by a plasma wave *(Russian)* 78−26236
resonant charge exchange, polarisation effect 80−43859
resonant ion charge exchange collective modes 80−33736
RF discharge, effective electron collision freq., energy dissipation, press. depend. *(Russian)* 77−19784
RF discharge, electrode sheath 80−44052
RF discharge plasma, recombination and diffusion coeffs. 77−7594
RF driven currents in steady state Tokamak reactors 80−28687
RF plasma excitation, appl. to ion plating 79−69995
rotary symmetry plasma, magnetohydrodynamic eqns. and plasma wall effect *(German)* 79−68909
rotating plasma, in mirror trap, equilib. state *(Russian)* 78−75259
rotational and gas temps., rel. in low press. mol. plasma 80−6215
Rutherford scattering, in homogeneous mag. field *(German)* 78−75258
Rydberg atom, electron collisions 80−63833
scattering spectra from weakly ionised plasmas calc. *(German)* 79−77347
screening in one dimens. plasma 80−65478

plasma collision processes continued
self absorption of He like satellite lines in high density fusion plasmas 80−64776
self-gravitating composite plasma with finite Larmor radius, hydromagnetic stability 77−62350
self-sustained gas discharge, mol. vibr. relax. effect on thermal stability 80−10358
shear stabilisation of collisional drift instability 78−59569
sheath, collision-dominated, analysis of voltage drop 77−24098
sheath edge theory is weakly ionised collision dominated plasma 80−43935
silent discharge, excited species reactions, discharge channel characts., numerical simulation 80−38813
simulation of plasma afterglow by computer code GLOWCODE 77−39480
single atomic collision relative level populations, thermal equilib. 80−1743
single particle motion in 1-component strongly coupled plasma 80−48847
slightly dissipative plasma, helical flux and other integral variants 77−65833
solar emission lines of NeV, MgVII, SiIX, SXI, population levels as function of electron density and temp. 80−21963
solar flare plasma non-stationary heating by non-thermal electrons 77−17455
solar wind, collisional theory of anisotropic plasma 78−53782
spectra-line profiles, weakly turbulent plasma unified electron broadening theory 77−58848
spectral line broadening, correlations in quantum theory 77−7514
spectral line profile of low-press. afterglow plasma in mag. field 80−6285
spherical Langmuir probe, appl. to collisional plasma, theory 78−18460
spherical probe in stationary collision dominated isothermal plasma, kinetic theory 77−47264
spontaneous superradiance in plasma flow 77−3470
SS Si, surface, plasma etching in CF_4-H_2 glow discharge, AES meas. 79−98922
Stark broadening of isolated Sn II lines in cool plasma, semi-empirical calcs. 80−59186
stellarator, superbanana diffusion of plasma, effect of fluctuating elec. field 77−62330
stopping power of a nonequilibrium plasma for incident alpha particles 80−64742
stratified partially ionised plasma, stability in mag. field, cond. and viscosity effects 78−26276
strongly magnetised plasma collisional relax. of ion beam 80−33785
submillimetre diagnostics, active, of Ar arc, data numerical anal. 80−48979
superdense plasmas, spectroscopic diagnostics, at. collisions 78−63538
supersonic colliding plasma jets, hot dense plasma formation, hydrodynamic model *(Russian)* 80−38676
superthermal electron beam, relax. due to Coulomb collisions in plasma 80−106941
surface wave spectrum, surface impedance with specular-diffuse particle scattering 77−24058
tearing instability kinetic theory, collisional to collisionless regimes 77−84425
temperate multi-species plasma around ion cyclotron freq. range, plane wave propagation 80−75050
temperature anisotropy relaxation due to binary encounters 77−39404
thermal ionisation, single-step ionis. role, diffusion approx. 80−43843
thermal parametric instability, effect of recomb. processes 80−61967
thermalisation of energetic charged particles in fusion plasma, QED effects 77−65834
thermionic convertor in diffusion mode, V-I characts., Coulomb collisions effects 77−7604
thermodynamical functions for dense multicomponent plasmas, electron-proton plasma appl. 80−38548
thermonuclear plasma surrounded by cold blanket, density profiles, thermo-elec. forces effect 79−31189
thermonuclear target, calc. of charged particle spectra by Monte Carlo method *(Russian)* 79−37445
theta pinch implosion dynamics, ionisation rate enhancement by two step process 77−58885
theta-pinch Ti ion injection by CO_2 laser, spectroscopic anal. 80−79577
thin foil layered targets, Rayleigh-Taylor instability in laser irradiation 80−87876
third-harmonic generation in collisional plasma, self-focusing effect 77−7550
Thomson scattering cross-sections, in strong mag. field 79−55453
three-body electron attachment to O in nonself maintained discharge *(Russian)* 80−14881
Tokamak, anomalous diffusion with light and heavy impurities, drift wave depend. 80−64677
Tokamak, fusion reactor, axisymmetric, slowing-down alpha particle loss, Monte-Carlo calc. 78−59653
Tokamak, high-density regime performance, scaling laws 77−11380
Tokamak, large poloidal beta, MHD stability, collisional and anomalous trapped particle diffusion 77−24055
Tokamak, Macrotor, metallic impurity suppression by electron injection 79−32781
Tokamak, Pfirsch-Schluter friction on H^+ 78−34272
Tokamak, two-component, fast beam ions quasilinear relax., Coulomb collisions 79−37509
Tokamak fusion reactor, thermonuclear instabilities α-particle interactions 77−88281
Tokamak plasma, highly ionised Mo ions, recomb. and ionisation rate coeffs. determ. 78−71427
Tokamak plasma effective charge, high electron density with impurities, X-ray obs. *(Russian)* 77−19762
Tokamaks, computer simulation of trapped electron modes 80−106874
Tokamaks, divertor, refuelling methods, pellet-plasma interaction 80−28841
Tokamaks, dynamics of H, He, O reactions, corona model, spectroscopy diagnostics *(German)* 79−60103
transition radiation emitted due to the presence of intense EM beam 79−86586
transport collision frequencies, integration of empirical data 79−25969
transport collision frequencies, temp. depend. by approx. method 79−25970
plasma collision processes continued
trapped α-particles, quasilinear relax. in Tokamak reactor, during cyclotron magnetoacoustic instability *(Russian)* 79−55487
trapped electron instabilities, collisional effects 78−26279
trapped electron instability, mag. curvature drift driven, collision effects 77−55142
trapped electron instability, turbulence, unstable mode dynamics anal. 80−33761
Tuman 2, adiabatic mag. field, compression heating, ion energy balance 77−51238
turbulence generating mechanism in weakly collisional plasma 77−11340
turbulence induced by plasma-electric current interaction in focus expt., laser diagnostics 80−24171
turbulent H plasma, n-α line Stark profiles, plasmon-atom collision 77−24084
turbulent plasma, impinged charged particle, linear response theory 80−64727
turbulently heated plasma electron cyclotron radiation, spectral line width collisional broadening 78−34369
two electron temp. plasma, collisional and Landau damping of ion-acoustic waves 80−19572
two-body charged particle collision, reson. effects 77−15159
two-electron capture processes in plasma containing multiply charged ions 80−43854
two-level atoms interacting with free electron gas, dynamics by 2-D model 78−26237
two-particle effective pot., for dense hydrogeneous plasma near 10K 80−38533
two-stream plasma, thermalisation *(Russian)* 79−4119
unification equilibrium and radiative energy loss rates for C, N and O ions 78−87430
velocity orthogonal function representation for distrib. function of collisional plasma 77−42962
vibrational kinetics and plasma characts. in CO-N_2 discharge 80−59331
Vlasov equilibria, local Maxwellian velocity distribution 80−87928
wave damping 77−11337
wave penetration into half-space collisional plasma 80−106928
waveguide, plasma-filled, electron beam interaction, spatial evolution of complex EM modes, collision effects 79−14556
waves, fast, compressional, near ion cyclotron freq., collisional effects, damping 79−50854
weakly nonideal inert gas impulse plasma, Coulomb cross-section calcs. 80−103113
X-ray spectral density determ., effect of collisions on dielectronic satellite intensity *(Russian)* 77−62348
Al plasma, X-ray photoabsorpt. coeff. 79−27754
Al surface, multiply charged ion interactions, laser plasma 80−70007
Al, vacuum arc, excited state density theory 80−100107
Al_2O_3 powder, injected into induction plasma, particle temp. and trajectory 78−59607
Al(XII) and (XIII) reson. line trapping in laser-heated plasma, source distrib. diagnostics 78−42730
Ar afterglow, line radiation of plasma in early afterglow 80−38745
Ar afterglow, spectra and microphotograms, dissociative recombinations 78−26365
Ar arc, non-LTE, electron balance, temp. and density *(French)* 78−1796
Ar arc discharge, neutral system collisional radiation model 78−67535
Ar atom populations in partially ionised flat plate boundary layer 77−65847
Ar discharge, recombination coefficient meas. under diffusion-recombination conditions of plasma decay *(Russian)* 78−26324
Ar, electron-atom bremsstrahlung continuum, afterglow decay *(German)* 78−83626
Ar hollow cathode arc, in mag. field up to 2 k0e, plasma parameters 80−6306
Ar, inelastic collisions between excited states, Chapman-Engskog procedure, electron energy distrib. 79−68902
Ar ion system, collisional radiative model 78−71080
Ar, low voltage arc, ionisation waves, hydrodynamical model including inelastic interaction 78−87563
Ar, metastable $^3P_2$ deactivation in afterflow, plasma characts. 78−55769
Ar plasma, boundary layer low-press., kinetic evolution of $3p^5$ 4s level *(French)* 77−80279
Ar plasma, collision-dominated electron relax., heating, at. transitions 78−18373
Ar, plasma, electron-ion recombination in extinguishing arc 78−59687
Ar, plasma, electron-ion recombination, 300 to 500K, in discharge tube 78−59714
Ar plasma, inductively coupled, excitation transfer between plasma and impurities *(French)* 78−14211
Ar plasma, low density, shock-heated, effective collision freq. calcs., electron temp. meas. 80−75025
Ar plasma, optical props., visible, near-IR region, using shock tube 79−55471
Ar plasma, thermal equilibrium properties, estimation 78−1793
Ar, plasma column of hollow cathode arc, collisional model of ion system 80−38749
Ar plasma interaction with flat anode 78−71497
Ar plasma jet, collisional line broadening, oscill. strengths of reson. lines 77−75106
Ar plasma jet, surrounded by Ar, He, N_2, H_2 gases, recombinations in decaying jet 78−9753
Ar, precursor phenomena ahead of shock wave *(French)* 77−24087
Ar, weakly-ionised, collisional drift instability 80−53977
B IV, ionisation rate coeff. in θ-pinch plasma, spectral meas. 77−6911
C oxides, glow discharge, excitation and ionisation mech., elec. and optical obs. *(Russian)* 78−59695
C V, ionisation rate coeff. in θ-pinch plasma, spectral meas. 77−6911
CO discharge, electron energy distrib. and kinetic coeffs., ground-state mols. 80−43867
CO discharge, electron energy distrib. and kinetic coeffs., vibr. excited mols. 80−43868
CO electrical discharge laser, vibr. excitation rate levels and energy balance 79−81413
CO-He-O_2 gas discharge laser plasma, positive ion generation mechanism *(Russian)* 79−99005
CO-N_2 plasma mixture decay, effective recombination coeffs. *(Russian)* 77−47144
CO_2, dissoc. in high-press. nonequilib. plasma 79−15991
CO_2 dissociation in a nonequilibrium plasma 80−87851

plasma collision processes continued
CO_2-He-Cs glow discharge, quenching cross section of resonant Cs(6P) state by CO_2 mols. 80−43860
CO_2-N_2-He, non-self-sustained plasma discharge instability, electron collisions *(Russian)* 77−76050
CO_2-N_2-He-O_2 discharge mixture, three body electron attachment to O_2 80−64779
CO_2(-He) discharge, UV-initiated, electron ion recomb. and CO_2 dissoc. 80−44068
Ca plasma, Knudsen discharge, longitudinal mag. field, emission polaris. 77−76211
Ce, arc, excitation and ionis. in nonequilib. plasma 78−18461
Ce, gas discharge, two-photon ionis. by laser light 78−87534
Cl III, Stark broadening of isolated lines by plasma 78−9116
Cr, gas-phase, plasma, sputtering and beam-foil excitations 80−32820
Cr ions in Tokamak plasmas, spectroscopy and atomic physics 80−53938
Cs, discharge, hot cathode diode, low-press., initial stage transient processes 78−51382
Cs, electron-atom momentum transfer cross sections, from plasma electron thermal conductivity 78−42224
Cs, nonideal plasma press. ionisation, short range forces, thermodynamic props. 80−33733
Cs plasma, decay in presence of N_2, population inversion 79−55455
Cs plasma discharge, positive column constriction, ion conversion effect 80−44020
Cs plasma in vacuum diode, pre-discharge, electron impact excitation line emission polarisation 78−47170
Cs-He afterglow, spectral emission from excited Cs ions, 380-750 nm 79−82116
Cs-He plasma, steady-state discharge, role of inelastic collisions, spectroscopic diagnostics 78−42709
Cs-N_2 discharge, Cs_2^+ form. rate, mass spectra obs., N_2 press. depend. 79−27853
Cs-N_2 plasma, collision recomb. of charged particles *(Russian)* 77−80373
cu, laser light absorpt. by plasma with very steep density gradient 80−96348
D-T thermonuclear plasma, neutron collision diagnostics *(Russian)* 77−34471
D+PTFE, DF* prod., Fourier transform IR spectroscopy 80−87105
D+T, guiding centre distrib. spatial separation, reaction rate enhancement 80−33737
Eu^+ metastable states in discharge plasma, anomalously high speed deexcitation, modulation of induced radiation obs. 80−44014
F II, Stark broadening of isolated lines by plasma 78−9116
F_2, electron dissociative attachment rate consts. at 300 and 500K in discharge 80−43849
Fe IX, X, XI, dielectronic recomb. rates in θ-pinch plasma 78−71525
Fe ions in Tokamak plasmas, spectroscopy and atomic physics 80−53938
Fe multiply-charged ions, radiative cooling of Tokamak plasma 77−19677
Fe XXII, XXIV, XXV, charge exchange recomb. in Princeton large torus during beam heating 80−100067
Fe^{n+} forbidden spectral lines, in PLT Tokamak, diagnostics of localised high-temp. regions 79−98958
H Balmer lines, plasma-broadening in wall-stabilised arc, low electron density 80−43891
H, collisional energy level transition rate, in RF plasma, fluoresc. meas. 77−38726
H, dense plasma, ionisation, master eqn. analytical soln. 78−59544
H, excited state electron and ion quantum scatt. cross sections, dipole approx. *(Russian)* 79−6996
H I (3^1P^0−2^1S) line, Stark broadening parameters, modified adiabatic theory, electron scatt. phase shifts 80−43879
H, in hot plasma, elementary excitation spectrum, exchange and polarisation effects 80−43892
H, ion equilib. density, in low press. system 78−9752
H ion sources, high current, ion species computs. 77−42209
H ion sources, plasma reaction cross sections data 77−38538
H, ions recomb. and level populations, resolution of ang. momentum states 77−45529
H line Stark broadening, role of ion dynamics simulation 80−24144
H, Lyman-α Stark broadening, dynamic screening effects 78−18386
H, optically thin plasma, UV spectral emission coeff., quantum statistics of recomb. continuum *(Russian)* 79−77348
H, partly ionised plasma, ionised collisions effect on thermal cond. *(Russian)* 78−47093
H, pellet ablation in thermonuclear plasma, reactor refuelling 77−88282
H, pellet ablation in thermonuclear plasma, electron space charge and refuelling 77−88283
H plasma, departures of electron energy distrib. from Maxwellian rel. to electron collisions 77−80266
H plasma, departures of electron energy distrib. from Maxwellian rel. to collisional ionisation 77−80274
H plasma, high-temp., proton neutralisation cross-section by impurity ions *(Russian)* 77−11310
H plasma, recombining, weakly ionised, population inversion 80−87849
H plasma, thermal emission and Debye shielding 80−64692
H radiative recombination in quasistationary thermonuclear plasma *(Russian)* 77−39465
H, recombining plasma, population inversion using collisional-radiative model 79−46423
H solid pellet evaporation in plasma *(Japanese)* 79−94772
H, Stark broadening, model microfield methods calcs. 80−92274
H-like metastable ions, de-excitation in laser plasma *(Russian)* 77−7597
$H+O^{8+}\rightarrow H^+ + O^{7+}$*, during neutral beam injection into Tokamak 77−58899
$H^+ + He(1^1S)$, $He(n^1P)$ excitation cross sections computation 79−94070
H_2 glow discharge with variable degrees of dissoc., diffusion theory of positive column 80−44018
H_2 monoplasmatron arc plasma, electrokinetic parameters space distrib. *(Russian)* 80−53925
H_2 plasma collision-dominated electron distrib. function with turbulent heating 78−71509
H_2 solid pellet ablation rate in plasma 77−65878
H_2-H mixture positive column, static electric charact. 78−67500
H_2-He, hollow cathode effect in cylindrical geometry *(French)* 80−33842
H_2+He(Ne), gas discharge plasma, H_2 dissoc. excitation, cross section anal. 80−33735

plasma collision processes continued
$H_{\alpha,\beta}$ lines, dense plasma Stark broadened central struct., comment 77−23464
$H_{\alpha,\beta}$ lines, dense plasma Stark broadened central struct., reply 77−23465
$H_{\alpha,\beta}$ lines, Stark broadened, central struct., in dense plasma 77−6722
HCl, in nonequilib. plasma, electron energy distrib. function and dissoc. kinetics 80−11882
$H_2(D_2)$, electron dissociative attachment rates, rot. (vibr.) excitation depend. 80−43848
H_2O electron collision cross sections behind shock wave in plasma 77−11309
$H(^2S)+Ar(^3P_{0,2})$, energy transfer collisions, Lyman-α emission profile obs., in microwave discharge and reaction cell 80−58359
$H(1s)+O^{8+}(He^{2+})(H^+)$, charge transfer, 0.025-200 keV/amu 79−22823
He (n=3, 4) singlet states quenching by N_2 in low-press. glow discharge 80−49030
He afterglow, collision processes rate coeffs. 77−24221
He afterglow, Rydberg states collisional radiative transfer, He^+ electronic recombination 77−62401
He, afterglow of low-press. glow discharge, recombination processes 78−26366
He, afterglow of pulsed discharge, elec. and optical meas. 78−26329
He afterglow plasma, $He(2^3S_1)+e\rightarrow He(1^1S_0)+e+KE$, rate const., electron energy distrib. 78−71571
He, collisional excitation transfer for $3^{1,3}P$ and D states 80−106387
He, collisional radiative model, reson. optical pumping, plasma diagnostics appl. 79−37459
He, electron energy distrib. and collisions during decay, peculiarities 78−63621
He flow discharge, intermediate press., positive column conc. of ions and metastables 80−44017
He glow dishcharge, low press., excitation transfer and quenching of n=3 excited states 80−38743
He, hollow cathode, 1-4 torr, population of excited levels, excitation and decay mechanisms 77−80267
He I, Stark broadening of 3965 Å line in plasma jet 79−98023
He II plasma, spectral line shifts, electron collision induced 80−106879
He in transient plasma, excitation transfer between excited states 78−70914
He, photon echoes obs., collisional relax. on $2^3S_1-3^3P_{012}$ 79−19089
He, plasma, afterglow and inertial expansion, numerical soln. of relax. kinetics 77−27769
He plasma, collisional-radiative recombination 77−58841
He plasma, cooling, nonequilib.-ionised radiating ats. 77−76128
He plasma, cryogenic, oscill. excitation by hot electrons 79−55493
He plasma, electron-impact widths and shifts of neutral He lines 79−27753
He, plasma afterglow, stepwise excitation, electron energy distrib. and density at metastable states 77−84413
He plasma collisional-radiative model, appl. to positive column 79−64836
He plasma expansion, supersonic, population inversion 79−27755
He, Stark broadened 4121 Å and 4437 Å lines in plasma, electron impact effects 77−27025
He, Stark broadening in plasma, close electron collisions effect 77−23459
He, strongly ionised plasma, impact radiative recomb. rate 78−59546
He^+, excitation in hollow cathode discharge, rel. to plasma electron density and temp. 77−7589
He-$CO_2(O_2)$ volume discharges, electron recombination and attachment 77−19799
He-Cd, glow discharge, collision rates calcs. 77−68882
He-Cd discharge, principal Cd ionis. mechanism, radial profiles meas. 77−27758
He-Cd plasma, in discharge tube, excitation mechanism obs. 78−30479
He-Hg plasma, prod. by nucl. radiation, charge exchange effects 77−24103
He-Hg RF discharge, atomic ionis. and excitation, spectral line intensities 78−26334
He-like ions, collisional excitation in stationary plasmas rel. to line intensities 78−53811
He-like ions, spectral broadening in plasma, theory, high-Z 80−6223
He-Ne, afterglow of low-press. glow discharge, recombination processes 78−26366
He-Ne gas mixture plasma, role of charge exchange in form. of optical props. 80−28600
He+group II metal atoms, gas discharge plasma, Penning ionisation, cross section anal. 80−33735
He+He, (2^3S) and (2^1S) metastable states, direct and assoc. ionisation rate consts. in afterglow, electron energy spectra 79−13812
He_2^+ recombination, high-temp., in plasma jet *(French)* 80−43861
Hel, low density suprathermal field fluctuations and high energy electrons 80−1847
^{3}He-Hg (−Kr)+^{3}He(n,p)T, high press. plasma excitation, luminesc. spectra 80−38719
Hg plasma, molecular dynamics model for atom-electron interactions 78−42708
Hg plasma formation by strong Hg line irrad., mechanism 78−83585
Hg positive column, high press., excimer densities and destruction mechanisms 78−5967
Hg vapour, optically pumped positive columm, collisional processes 78−87499
Hg-Ar, low press. discharge positive column ionisation processes 78−75445
Hg+Hg, gas discharge plasma, collision cross section anal. 80−33735
K discharge plasma, K_2 excited mols. form. by K(4P) collisions 80−44013
K plasma, DC conductivity, electron collision cross sections 77−3469
K^- and K_2^- form. and decay in discharge plasma *(Russian)* 79−90374
K-Kr, afterglow of laser plasma, fluoresc. spectra 79−19085
K_2^+ ion formation in low press. K discharge plasma 80−43862
K_n^+, ion formation in elec. discharge, n=2-6, 10^{-3}−1 torr. *(Russian)* 79−77448
Kr gas discharge plasma, electron impact depolarization 80−43847
Kr hollow cathode discharge, multiply charged and mol. ion prod. and loss 79−46499
KrF* excimer laser, discharge pumped, influence of electron-F_2 collisions 78−42326
Mg, hollow cathode discharge, excitation mechanisms of triplet state atoms and decay obs. 80−44015

plasma collision processes continued
Mg+Ar(Xe), plasma, near reson. charge exchange, spectra *(German)* 77−31425
Mo, ionisation equilibrium, radn. losses, in high temp. plasma 77−72422
Mo^{29+} to $^{39+}$, photoionis. cross sections, radiative recomb. rate coeffs., rel. to plasma diagnostics 80−52953
Mo^{32+}, dielectronic recomb. rate coeffs. in plasma 80−43853
Mo^{38+}, dielectronic recomb. rate coeffs. in plasma 80−43852
N afterglow plasma, diffusion and recombination, microwave cavity expts. 79−90479
N discharge, externally maintained, instability growth time, associative ionisation 80−6254
N plasma, ionis. and radiation characts. 78−71459
N recombination, in transient plasma 78−83521
N_2, beam and glow discharge type, macroscopic props., kinetic eqns. 80−43864
N_2, DC low press. positive column, electron distrib. function superelastic electron collision depend. 79−46498
N_2, diffuse plasma, population densities of triplet states, correl. with electron impact processes 80−43966
N_2, electron beam sustained high press. discharge, time behaviour of recomb. coeff. 80−10447
N_2, high-pressure vol. discharge, stepwise ionisation processes quasi-stationary stage characts. *(Russian)* 77−27756
N_2 molecular plasmas, electron kinetics *(German)* 78−91171
N_2, pink afterglow, ionisation and ion conversion mechanisms 78−63624
N_2 plasma, electron distrib. function, kinetic coeffs. *(Russian)* 78−38451
N_2 plasma, electronic excitation levels in gas-discharge 80−24280
N_2 plasma heating in electrodeless RF capacitative discharge, mechanism, impurity effect 80−59312
N_2, plasmochemical action of relativistic electron beam, calc. by degradation spectrum method *(Russian)* 79−37536
N_2 positive column, superelastic collisions and electron distrib. function 80−1858
N_2, Rayleigh-Lewis and pink afterglows, mechanisms 78−63622
N_2, translational energy transfer rate, after pulsed discharge, interferometric obs. *(Russian)* 78−26322
N_2^+, excitation in RF discharges *(French)* 77−61868
N_2-Ar plasma, coupled thermal-chem. relax., thermodynamic nonequilib. 78−34265
N_2-H_2 mixture, glow discharge, ionisation and excitation obs. 78−67505
N_2-H_2 plasma, transport coeffs. and collision processes *(German)* 79−23395
N_2-Ne, positive column, electron vel. distrib. function *(German)* 78−1885
N_2-Ne glow discharge, energy balance, ionis. collisions *(German)* 78−34263
N_2-Ne glow discharge, kinetic eqn., transport coeff., collision freq., mean energy *(German)* 78−34261
$N(^2D,^2P)$ metastable production by electron collisions in DC glow discharge 80−59274
NF_3, electron dissociative attachment rate consts. at 300 and 500K in discharge 80−43849
Na arc plasma, dense, high-temp., near-reson. light scatt., collision-induced fluoresc. 77−1019
Na-Ne, low press. discharge positive column, multistep ionisation 78−75446
Ne, 2p levels prod. by dissoc. recomb. in afterglow, recomb. coeff., level population 80−43855
Ne afterglow, 1s atom prod. by recombination, press. depend. 78−59716
Ne afterglow, diffusion, collisions, decay freqs., fluoresc. obs., calcs. 78−59715
Ne afterglow plasma, 2p levels collisional transfer coeffs., laser excitation obs. 80−43856
Ne, electron-atom bremsstrahlung continuum, afterglow decay *(German)* 78−83626
Ne, excited atoms reactions in pure afterglow, plasmas using resonance absorpt. spectrometry 80−33835
Ne gas discharge plasma, electron impact depolarization 80−43847
Ne, low ionised anisothermal plasma, ionising electron collision kinetics *(German)* 80−33731
Ne, low press. discharge positive column, multistep ionisation 78−75446
Ne, luminesc. discharge, loss mechanisms *(French)* 78−9877
Ne, metastable level deactivation by electron collision in low press. discharge 78−83520
Ne, negative afterglow, pulse excited, at. spectral lines, microwave quenching 78−63591
Ne, negative glow discharge recomb. at. excitation *(Russian)* 77−76225
Ne plasma, electron collision ionisation, electron kinetic behaviour during elec. field perturbation *(German)* 80−64676
Ne, RF discharge, emission modulation due to fast electron distrib. time variation 79−41900
Ne, temporal decay, electron distrib. function and macroscopic parameters relax. 78−18374
Ne Townsend discharge, Ne_2^+ form. and destruction 80−38747
Ne VI, VII and VIII, total collisional ionis. rates in plasma 77−19102
Ne-He and Ne negative afterglows, microwave quenching and recombination processes, Ne spectral emission 77−80307
Ne-Hg RF discharge, atomic ionis. and excitation, spectral line intensities 78−26334
Ne-N_2, energy transfer, H^+ ion beam produced plasma, ion density and temp. 80−38539
Ni ions in Tokamak plasmas, spectroscopy and atomic physics 80−53938
O^{6+}, line emissions from He-like ions, electron params., ion diffusion in Tokamak plasmas 79−4114
O^{6+}-He^{2+} collisions, electron capture and impact ionisation cross sections, loss of alpha particle in Tokamak plasmas 79−68936
O^-+N_2, electron detachment, collision with vibr. excited mols. 79−54961
O^-+O_2, electron detachment, collision with vibr. excited mols. 79−54961
O^++H, cold dense H plasma, charge exchange, impurity losses, Monte Carlo simulation 78−34260
O_2 discharge, conditions, self-consistent electron energy distrib. functions calc. 80−38746
O_2, discharge, nonequilib. vibr. population, dissoc. rate, role of ats. and dissoc. 79−64933
O_2 electron attachment in non-self-maintained discharge, plasma decay obs. 80−43844
O_2 electron binding in N_2 plasma, mechanism 79−55452

plasma collision processes continued
O_2 plasma, UV continuum spectra, mol. recomb. of ground state atoms 78−91078
O_2, RF discharge, moderate press., O production kinetics 79−64934
O_2-N_2 plasma mixture decay, effective recombination coeffs. *(Russian)* 77−47144
O_2^-+N_2, electron detachment, collision with vibr. excited mols. 79−54961
O_2^-+O_2, electron detachment, collision with vibr. excited mols. 79−54961
Rb-Cs plasma, electron collision induced charge exchange *(Russian)* 77−68740
SF_6 axially blown arc, current-zero behaviour, theoretical model 80−38789
Si surface reacting with H plasma, low-press. 79−47968
Ti plasma impurity, atom-electron collisions in inner discharge column *(Russian)* 80−38529
Ti XX 80−100067
U^++$U(U^+)(U^{2+})$, elastic scatt. in plasma, interaction pots. and momentum transfer 80−38534
Xe afterglow, $6s'(^1/_2)_0$, $6s'(^1/_2)_1$ at. states, collisional relax., population decay 78−63617
Xe afterglow, radiative and collisional deexcitation of reson. states, absorpt. and emission obs. 80−38742
Xe, in gas discharge, collisional excitation, radiation lifetimes, macroscopic alignment obs. 80−33734
Xe, plasma afterglow, spectral features, 450-900 nm 79−23404
Xe, plasma shock front, elementary processes 80−19581
Xe precursors, associative ionisation and photoionisation, relative contrib., electron density prediction 80−43858
Xe, pulsed discharge, superheating instability, effect of secondary ionisation 77−55189
Xe_2^+, dissoc. recomb. in afterglow, rate coeff., excited state prod. 77−46647
Xe_2^+ excimer form. in pulsed discharge, visible emission obs. 80−38754
Zn, gas-phase, plasma, sputtering and beam-foil 80−32820

plasma confinement
see also magnetic traps; pinch effect; plasma focus; plasma impurities; plasma-wall interactions
absolute dissipative drift-wave instabilities in Tokamaks 80−92296
accelerator, stationary erosion elec. arc type, with mag. cathode spot confinement, flow *(Russian)* 79−98996
additional heating in Tokamaks, specific diagnostics review 80−28753
adiabatic equilibrium calculations of major-radius compression in a Tokamak 80−106964
adiabatic invariant J, finite-β effect in axisymmetric tokamaks 80−79538
adiabatic magnetic compression of field-reversing E layers 79−82089
adiabatic plasma containment on mag. force lines by self-generated electrostatic field 77−84474
adiabatic toroidal compressor, power balance anal., electron density and temp. diagnostics 77−51219
advanced fuel bumpy tori studies 78−58430
advanced fuel fusion reactor, SURMAC, employing axisymmetric surface mag. confinement 78−58431
Alcator, high-density and collisional plasma regimes 77−43024
Alcator A Tokamak, soft X-ray imaging 80−73563
Alcator high density Tokamak, ion temp. profile reconstruction *(Russian)* 80−106959
Alcator Tokamak, energy balance, MHD activity 80−28838
Alcator Tokamak, heat loss, mag. fluctuation mechanism 79−1292
Alcator tokamak, low q operations 79−60173
alpha-particle heating in high density D-T plasma 80−28735
alpha-particles, confinement in Tokamak with noncircular cross-section *(Russian)* 79−37525
anomalous diffusion and transport beta limits in dense Tokamak plasmas 79−72993
anomalous drift wave transport in high temp. plasmas, thermodynamic stability 80−69980
anomalous electron pseudo-classical transport with coherent electrostatic wave propag. 80−24137
anomalous transport in toroidal geometry 78−79453
anomalous trapped ion transport in Tokamaks, 2-dimens. fluid calcs. 78−30412
anomalous turbulent resistivity at high drift vels., rel. to confinement and fluctuations in toroid 80−24139
antiparallel structure build-up and stability in systems with mag. barrier 80−92371
ASDEX divertor Tokamak, status and design principles 80−13847
Asperator NP-3, nonplanar helical mag. axis system, line of force, toroidal effect 80−70020
Asperator NP-L stellarator, mag. field config. meas. 80−92367
astron, current cancellation, incoming electron pulse density spreading 77−1013
astron exponential rigid rotor equilibria, excluding untrapped particles 78−67395
Astron type equilibrium in absence of applied mag. field 79−64899
atomic processes determining the plasma-wall interaction 80−59247
atomic processes for mag. fusion research, data status, review 80−42851
axial heating of mag. confined plasma by CO_2 laser 78−14182
axially symmetric plasma, two-fluid equilib. theory 77−80345
axially symmetric toroidal system, Ohm's law in banana regime *(Russian)* 79−4164
axisymmetric high-beta tandem-mirror reactor, MHD stability 80−75042
axisymmetric mirror machines, long thin approx., stability and field singularity 80−83933
axisymmetric plasma equilib. MHD eqn., exact solns. 77−65898
axisymmetric plasma equilibrium, stability 80−106915
axisymmetric ring method of complementary variational principles appl. to equilib. condition *(French)* 77−7579
axisymmetrical field-reversed equilib. of arbitrary ion gyroradius, stability 79−32802
ball lightning, radiation emission, cluster plasma 77−2219
ball lightning, turbulent plasma sphere, rel. to confinement in fusion reactor 80−32516
ballooning instability in bumpy torus, hot electron annulus effect 80−53983
ballooning stable profiles in circular Tokamaks 80−92317
beam-induced currents in toroidal plasma 80−28808

plasma confinement continued
beam-induced tensor pressure Tokamak equilibria 80−106965
Belt Pinch Screw Reactor, neutronics characteristics 80−18624
betatron resonance instability, axisymm. field reversed system 79−68917
bi-conical system of concentric explosive compression of D-T 79−50880
bi-liner method for implosive compression of plasma 79−50881
bifurcated Tokamak equilibria, helical flux invariance, current shrinking and disruption 78−34359
bipolar injection in spherical geometry, multiple pot. well struct. 78−26315
blanket boundary layer, high-density gas, localised drift mode stability 80−43956
Bohm-type thermal losses from high-β plasma 80−38679
boundary condition for computational MHD 78−1811
boundary conditions for simulation plasma in mag. field 78−26321
boundary conditions for space charge surface layer at electrode plasma boundary, particle flux *(Russian)* 78−55736
braided field, transport of density, current, electron heat, fluid and particle models 78−30410
bumpy torus, ELMO, equilib., stability, confinement 77−24145
bumpy torus, inward ion transport, strong elec. field effects 78−63548
bumpy torus, NBT-I, effective toroidal curvature, error field, electron beam diagnostics 80−24237
bumpy torus (ELMO), radial transport eqn. in one-dimens., const. edge neutral flux 79−98956
Bumpy Torus plasma, NASA Lewis, optimisation and scaling of ion heating 77−24110
bundle divertor, mag. config., wall impurity removal for Tokamak 77−65901
bundle divertor for ILB advanced fuel Tokamaks, designs. appls. 78−62618
centrifugal relativistic electron beam, equilibria and stability 79−90451
chaotic motion theories with appl. to controlled fusion research, review 78−93605
charged particle confinement, by transverse EM waves, theory 77−55145
charged particle motion, near a neutral line, nonadiabatic effects 78−1878
Cherenkov adsorption of azimuthal EM travelling waves, magnetoactive heating and containment *(Russian)* 80−38675
circular waveguide, hot-beam plasma interaction finite geometry effect, quasistatic approx. 77−51200
classical energy confinement, in Alcator tokamak 79−60172
CLEO stellarator, low and zero current plasma confinement 80−83983
closed mag. field line confinement with rot. relativistic electron beam 77−84458
closed magnetic field line plasma system form. using intense relativistic electron beams 77−24122
closed-line magnetic field approach to plasma confinement, in toroidal systems 78−42792
cold-ended dense liner-fusion plasma, equilib. profiles calc. 77−19745
colliding plasma evolution, EM computer simulations 80−87926
collisionless drift waves in Tokamaks analytic eigenvalue eqns. 80−6246
collisionless plasma, polarisation by single-mode pot. drift wave 80−106920
collisionless tearing modes, wider than 'current channel' 79−7456
Columbia Torus-1 belt pinch high beta toroidal device, preionisation, optimisation 80−92368
column, confinement by ablation front from cold gas plug 80−28793
column, HF field effect on diffusion and convection 80−103173
column, wave coupling in non-neutral plasma 80−75054
column compressed by mag. field, multichord corpuscular diagnosis *(Russian)* 79−4190
column-wall interactions in Tokamak, in-situ meas. on PDX 80−59248
compact reverse-field pinch for small demonstration fusion reactor 80−95413
compact toroidal configuration, heating and confinement principles 80−24185
compact toroidal ignition experiment, support struct. anal. by numerical code 80−106167
compression efficiency by supersonic heavy liner 77−19749
compression expt. high-aperture laser lens 79−14076
computer models of magnetically confined plasmas, review 77−11388
conference, controlled fusion and plasma physics, Oxford, England (Sept. 1979) 80−77545
conference, fusion technology, Padova, Italy (Sep. 1978) 80−8741
conference on fusion reactor materials [Miami Beach, Florida, Jan. 1979] 80−31407
conference on fusion research and plasma physics, Innsbruck, Aug. 1978 80−27033
containment vessels, backscatt. and sputtering from pocket and finned structs., Monte Carlo computation 79−14558
controlled nuclear fusion, progress and problems review 79−36415
controlled nuclear fusion development, confinement and laser ignition 79−31176
convective amplification of drift waves and thermal fluctuation levels in a stable plasma 80−83932
convective cell nonlinear excitation and anomalous diffusion, in inhomogeneous plasma 80−79468
convex analysis and variational inequalities *(Japanese)* 80−77606
coupled explosion current plasma compression, numerical anal. 79−50884
coupled explosion-current compression of plasma, self-similar approximation 79−50883
cryogenic rings, current induction and decay 80−106972
CT6B Tokamak, measurement of plasma column displacement 80−84001
CTR plasmas, review of parametric processes 78−30430
Culham Levitron, drift island diffusion 80−59267
current density profile control in JIPP-II Tokamak, preprogramming method 79−86565
current density profile measurements in the Proto-Cleo torsatron 80−83995
current driven dissipative drift wave turbulence in Tokamak plasma, finite-β and quasilinear effects 79−98913
current driven modes, cold mantle systems, stability props. 80−92287
current layer, mag. field struct. fast rearrangement *(Russian)* 77−68842
current-convective instability stabilisation by mag. field *(Russian)* 77−3930
cylindrical magnetic surface force free system for high-temp. plasma confinement *(Russian)* 78−42793
plasma confinement continued
cylindrical rotating P-layer, electrostatic stability props. 79−64851
cylindrical system with heavy inertial layer, neutron yield, explosion-induced D-T compression 80−68944
cylindrically confined cold plasma, overdense and steep density, plane EM wave scattering 80−70005
cylindrically symmetric mirror plasma, shear stabilisation 80−83978
D-shaped toroidal field coil, design 79−9225
DC octupole in toroidal geometry, dissipative trapped electron mode and collisional drift wave 78−51293
dense plasma generation by ionised gaseous filament explosion 78−71507
dense plasma ionisation and cohesion, critical density and press., approx. formulas 80−59253
deuterium-tritium thermonuclear ignition, high current density approach, expt. 78−54874
diagnostics of local parameters of ions in Tokamak-4 plasma *(Russian)* 79−32824
diamagnetic frequency profile effects on toroidal drift waves 79−41821
diffuse pinch, energy equilib., tensor cond. model 80−24209
diffusion, time-dependent, in toroidal geometry, finite element code 77−84410
diffusion in toroidal traps, anomalous electron viscosity *(Russian)* 80−48956
diffusion reduction by plasma rotation and ion dissipative effects 80−38696
direct energy conversion and control of unstable burn by cyclic major radius compression and decompression 80−87936
discharge, light emission efficiency, electrostatic confinement effects 80−33752
dispersion relation for instability hindrance in a magnetically confined plasma with finite press. 80−59221
disruptions in Tokamaks and small scale turbulence 80−59266
disruptive instability in TO-1 Tokamak, feedback stabilisation *(Russian)* 79−55546
dissipative trapped electron modes, in torus, impurity effect on LF drift modes 77−55139
dissipative trapped-ion mode, nonlinear saturation by mode coupling 77−19688
DITE, low Q discharges 80−92374
DITE bundle convertor, density meas. 80−92373
DITE phase II neutral injection system investig. 80−28814
DITE Tokamak, beam driven current meas. 80−106940
DIVA, metal-impurity, confinement, discharges 80−28843
DIVA Tokamak, q=1 mag. surface noncircular cross-section, in low-q discharge 80−100090
double tearing instability, nonlinear evolution 78−67348
Doublet IIA, doublet config. control, electron density, confinement time 77−80341
Doublet IIA, m=1 oscills., internal disruptions, impurity line emission 77−58898
Doublet III, noncircular toroidal plasma confinement expt. 79−49846
Doublet III, noncircular toroidal Tokamak, design and construction 79−49847
draft waves driven by temperature gradients, ballooning limit 80−106917
drift Alfven waves in Tokamaks, instability 78−79431
drift and trapped electron instabilities, in systems with mag. shear 80−28648
drift cyclotron loss cone mode stabilisation, by l.f. density fluctuations 78−47116
drift instability, current-driven, sheared mag. field, finite-beta effect on transport 80−28617
drift instability, electrostatic current-driven, scaling law for high density and high current Tokamaks 80−38691
drift instability stabilisation by RF elec. field in inhomogeneous plasma, kinetic theory 79−55536
drift motion in curved mag. field with rot. transform 80−1754
drift surfaces in linear and axisymmetric magnetic fields 79−14599
drift wave, low freq., pseudoclassical diffusion in Tokamak *(Chinese)* 80−69990
drift waves, shear damping in large aspect ratio Tokamak 80−6242
drift-kinetic evolution of collisional plasmas in tori 77−72409
drift-tearing instabilities in Tokamaks 79−98912
E layer, cusp injected, equilib. props. and limiting current behaviour 78−83601
E layer, nonrelativistic nonneutral, Vlasov equilib. and electrostatic stability 77−7580
E-layer formation by intense electron beam injection 78−34351
EBT, ray tracing near electron cyclotron freq. 80−103178
EBT heating, electron-cyclotron absorption and microwave propagation 80−64749
EBT reactor, new design arising from plasma research 80−27806
ECR ion source, extracted ions charge state distrib., confinement times 80−24268
electrode discharge, nonhydrodynamic pinch compression, kinetics and D^+ focusing *(Russian)* 80−38689
electrode power loading in high current ion sources 80−27858
electromagnetic confinement, stationary plasma parameter calcs. *(Russian)* 78−83603
electron and ion rings, strong, truncated exponential-rigid-rotor model, fusion confinement 79−41860
electron beam inertial confinement thermonuclear fusion 80−27803
electron beam propagation in plasma channels for ICF reactors 80−1812
electron beam ring, relativistic, toroidal magnetic configs. 80−28691
electron cyclotron emission from Tokamak plasmas with mildly superthermal electrons 80−92270
electron cyclotron frequency expts. in 15X-B Tokamak, temp. rel. to heating power 80−48912
electron cyclotron radiation from a high density Tokamak 80−92266
electron cyclotron resonance heating of Tokamak plasmas, fluctuations and instability 80−83956
electron heat diffusion coefficient, in Tokamak, meas. by sawtooth oscill. obs. 79−64911
electron plasma, finite-length thermal equilib. 79−32801
electron plasma column, transport across mag. field to thermal equilib. 79−37531
electron ring production, in preionised gas, ion accumulation 77−65905
electron-beam inertial confinement expts. at Valduc *(French)* 80−48907
electron-beam-sustained discharge, plasma contraction by mag. field of current 80−100115
electron-free plasma confinement in RF quadrupole field 78−71517

plasma confinement continued
electron-optical Feniks streak camera, quick change dyanamic processes application 79−50391
electrostatic and magnetostatic particle simulation models in three dimensions 79−64903
electrostatic confinement in EM trap, ion current decay *(Russian)* 80−79543
electrostatic confinement of a plasma torus in a magnetic field *(Russian)* 80−1825
electrostatic double layers, lab. expt. 79−60177
electrostatic end plugging, open-ended mag. confinement system 78−55743
electrostatic ion stoppering in mag. mirror field 78−1871
electrostatic levitation, control and transport in high rate, low cost production of inertial confinement fusion targets 80−47723
electrostatic plasma-confinement experiments in a tandem mirror system 80−70025
electrostatic Trivelpiece-Gould modes in a torus 80−38609
electrostatic wave, stochastic ion motion, mag. field config. depend. 80−59229
electrostatic wave propagation near lower hybrid freq. in toroidal plasma NOVA-I *(Japanese)* 79−82055
electrostatically focused ions, spherical potential profile, meas. 80−64762
electrostatically plugged spindle cusp, density and decay time, microwave interferometry 77−58881
elliptic column, MHD spectrum 77−31451
elliptic column instability, mag. surface separatrix, 2-D MHD eqns. *(Russian)* 77−51212
elliptic equilibria in MHD approx., cylindrical topology, non-axisymmetric toroids 77−51213
elliptical plasma source, radiation emission distrib. 80−103124
ELMO, bumpy torus, self-consistent operating point calcs. 79−85779
ELMO bumpy torus, ambipolar diffusion 80−38552
ELMO Bumpy Torus, electron cyclotron heating, density and temp. 80−28780
Elmo bumpy torus., performance, point model calcs. 79−98962
ELMO Bumpy Torus, ray tracing near electron cyclotron freq. 80−83975
ELMO bumpy torus, transport, scaling 77−72415
ELMO bumpy torus, transport and scaling simple neoclassical pt. model 78−22459
ELMO bumpy torus design 78−58429
elongated cylinder, nonlinear MHD instabilities and convection, simulation 77−24169
EM field orthonormal decomposition, duality and complex vectorial space in anisotropic media 80−28754
EM wave in inhomogeneous magnetoactive plasma, total absorpt. effect *(Russian)* 80−106944
EM wave penetration into magnetically confined plasma, anomalous skin-effect 79−64873
EM waves in plane inhomogeneous plasma in presence of mag. field shear, appl. to plasma diagnostics *(Russian)* 80−103140
end loss from a high-beta plasma column 80−79537
end stoppering by the reversed field multiple-mirror concept 79−10687
energy balance in PLT Tokamak 80−28733
energy confinement comparison of ohmically heated stellarators to Tokamaks 80−92360
energy confinement scaling and poloidal beta in high density Tokamaks 80−96381
equilibria in elongated field-reversed plasma 80−14926
equilibrium, in l=2 stellarator, mag. bump effects *(Russian)* 80−54019
equilibrium and stability, strong magnetic shear effect, anal. 80−14925
equilibrium and stability of high-β toroidal multipoles 80−64769
equilibrium currents, effect on separatrix characts. in l=3 stellarator 80−64706
equilibrium equation exact soln. for plasma ring *(French)* 78−26312
equilibrium form of a steady plasma 78−67396
equilibrium in highly collisional toroidal regime 80−28796
ERASMUS, low aspect ratio Tokamak, characts., RF expts. 79−99000
erosion magnetoplasma compressor, stabilisation of electron temp. in compression region 79−19057
Eta Beta machine, spark gap switches charact. *(Italian)* 79−55533
exact Vlasov equilibria for field-reversing rings 80−87925
exploding liner gas confinement, liner velocity effects 80−79541
external conducting sheets, stability effects on mag. contained plasmas 80−1787
external s-polarized pump wave, stability of electromagnetic plasma confinement *(Russian)* 79−41856
extraordinary mode radiation, induced emission in Tokamaks 79−64838
EXTRAP, properties 78−18439
fast ion beams, quasilinear relax. in non-circular cross-section Tokamak *(Russian)* 80−106938
fast ions, behaviour during H-neutral-beam-injection in large Tokamak plasma 80−28713
fast rising mag. field with long pulse duration for plasma expts. 77−2672
fast wave heating via mode conversion and ICRF scaling 80−28815
fast-liner reactor, fusion power from fast imploding liners 79−76119
fast-magnetosonic-wave heating of the conceptual NUWMAK Tokamak reactor 80−6264
FE Tokamak, ray trajectory and ion absorption of LH waves 80−28671
Ferromak helical magnetic configuration using ferromagnetic materials 79−82090
field line integration for MHD equilibria near a closed magnetic field line 78−59651
field reversal experiment in 2XIIB 80−28732
field reversed, force-free equilib. with mass flow 79−60186
field reversed geometries, particle orbits 79−60187
field reversed ion layer in background plasma, stability props. 79−77370
field reversed mirror configuration, sustaining a toroidal current 80−28804
field reversing electron and proton layers, recent results 80−28789
field-reversed ion layer, beam driven instabilities 79−64893
field-shaping coil, double layer system 78−42785
filament ellipticity, energy lifetime in T-8 apparatus *(Russian)* 80−87930
finite beta reduction of lower hybrid drift instability 77−42978
finite-beta effects on drift wave turbulence and particle confinement 80−38652
flow driven by fusion-generated alpha particles 79−14592

plasma confinement continued
fluid-wall inertial confinement fusion reactor concept, tritium breeding control 79−85773
flute oscillation suppression, regulator synthesis *(Russian)* 80−24212
flute perturbations, open mag. confinement system with radial elec. field 78−51338
flux conserving Tokamak equilibrium, local analytical approach 79−90437
flux conserving Tokamak MHD equilibrium evolution 80−75088
force-free analytical three dimensional toroidal MHD-equilibria of arbitrary cross section 80−106885
Frascati Tokamak, 1MJ plasma focus dynamics, neutron production scaling 80−24220
free boundary eigenvalue problem in plasma confinement *(French)* 77−67200
free transit time of ions confined by quadrupole RF field, using Poisson process 77−62392
free-boundary equilibrium of a high-β Tokamak 80−92376
FT Tokamak, electron energy replacement time and total energy containment time 80−28836
FT Tokamak, scaling of energy confinement time for discharges with Z_{eff}=1 80−92363
FT-1 Tokamak, discharges in low density plasma *(Russian)* 80−106958
fusion and fusion-fission reactors, high-density linear confinement systems 77−74983
fusion development status, review, energy balance, confinement, designs *(German, English)* 77−67874
fusion energy prod. by plasma vortex struct. compression 79−9888
fusion in D-T macrosamples using CO_2 lasers 78−82507
fusion plasma, confinement scalings determ. 78−17431
fusion plasma, D-T, reaction rate with suprathermal ions, ^{6}Li seeded 79−676
fusion plasma, impurity radiation loss, for corona equilib. 78−91074
fusion plasma in beam driven Tokamak, Fokker-Planck/transport analyses 80−28826
fusion plasma source, PROMETHEUS, potential mirror concepts for materials testing 77−83431
fusion possibilities and plasma confinement and interactions in mag. config. Tokamak, review *(French)* 80−54017
fusion power, plasma and the controlled thermonuclear reaction, review of practical problems of energy prod. 79−93826
fusion products in Tokamak plasma, deposition and thermalisation 80−83895
fusion reactor, alternative confinement approaches, literature survey 78−87477
fusion reactor, gas insulated plasma boundary layers, ballooning modes stability 80−10415
fusion reactor, Jupiter, with multi-trap EM trap 77−34444
fusion reactor, low MP metal partially disintegrated superhigh field solenoid *(Russian)* 77−7584
fusion reactor, PLT, fusion-produced T confinement 79−98955
fusion reactor, reversed-field-pinch, superconducting windings 80−27804
fusion reactor, stationary turbulence as confinement layer 77−68844
fusion reactor alternative magnetic confinement systems 78−58428
fusion reactor design and economics, confinement physics effects 78−50358
fusion reactor divertor collector plate, pot. drop across electrostatic plasma sheath 80−13833
fusion reactor inertially confined plasma, charged particle energy deposition 77−83081
fusion reactor magnetic confinements, international collaboration 80−63390
fusion reactor performance calc., with linear magnetic liner 79−50885
fusion reactor plasma heating and confinement, review 80−63388
fusion reactor [conf. Madison, WI, USA, Oct. 1977] 79−71957
fusion reactors, basic problems rel. to extraterrestrial plasmas 78−69672
fusion reactors, conf. summary 77−74997
fusion reactors, design, and alternative fusion concepts, systems studies 80−27805
fusion reactors, divergent impulsive crossflow over packed columnar arrays 80−47702
fusion reactors, field-reversing E- and P-layers, generation and stability 77−74988
fusion reactors, magnetic confinement research developments 80−13844
fusion reactors conceptual design, review 77−57749
fusion system, imploding liq. metal liner, rot. electron beam stabilisation 77−74994
fusion system, with rot. stabilised liq.-liner, finite liner compressibility effects 79−18036
fusion system stability and dynamic properties transfer function anal. 79−93825
fusion Tokamak reactor, driven, two-component and hot ion, modes of operation 80−42863
fusion tokamak reactors, status and prospects 80−102292
fusion-fission magnetically confined reactors, review 80−74019
fusion-neutron production in D-beam-heated PLT plasmas 80−28807
Garching Belt-Pinch IIa, effect of q on confinement and stability 80−96384
gas blanket confinement in fusion reactor, drift mode instabilities 78−18403
gross energy confinement times, in ISX-A Tokamak 79−37533
guiding centre orbits and topology of noncircular axisymm. Tokamak plasmas 80−6227
guiding centre plasma, equilib. configs. 77−31500
guiding centre theory, to second order in gyroradius, tokamak orbits 78−51332
gyro-kinetic equation with collisions, toroidal geometry appl. 77−51222
gyrokinetic modes, spatial struct. in toroidal geometry 80−79489
gyrotron for electron-cyclotron heating in large Tokamaks 80−28751
heating by EM wave transmission in mag. field *(Russian)* 80−103167
heating by HF field near lower hybrid freq., in Tokamak *(Russian)* 77−55159
heating in toroidal plasmas 80−24239
heavy ion beam inertial confinement fusion, US programme 80−23136
heavy-ion beam inertial-confinement fusion, commercial power generation 79−6762
helical equilibrium of current carrying column 77−72445
helical field config. for plasma confinement in very deep mag. well 77−35376
helical magnetic fields, mass flow stabilisation, MHD stability 77−24133
helical solenoid, neoclassical diffusion 78−94893

plasma confinement continued
helical system, MHD instabilities 80−1829
helically symmetric equilib. of current-carrying finite beta plasma 77−43019
helically symmetric equilib. of current-carrying plasma 77−68852
helically symmetric plasmas, guiding centre 79−1336
Heliotron D, confinement of ohmically heated plasmas 79−50879
Heliotron DM and D devices, RF heating 77−72469
Heliotron E, helical coil design, mag. field perturbations 80−99300
Heliotron E, neutral beam injector ion source power supply 80−99333
Heliotron E, vacuum chamber construction using electron beam welding 80−106180
Heliotron E project for fusion reactor plasma confinement *(Japanese)* 79−81077
Heliotron-D device, Joule current inhibition 79−99001
Heliotron-E, physical aspects, outline 79−99002
Helmholtz equation, solutions in toroidal coordinates 79−46467
hexapole Tokamak, axisymmetric jumps, interpretation 80−106966
HF EM field, turbulent model of plasma column *(Russian)* 80−83915
high beta MHD theory, stellarator equilibrium and stability, mirror traps and reverse field machines 80−28778
high beta plasma surrounded by cond. shell, dynamic stabilisation 80−96354
high beta Tokamak heating 80−28730
high beta toroidal device, preionisation, optimisation 80−92368
high density, in multiple mirror 80−92364
high field laser heated solenoids 79−60161
high field tokamak, plasma energy balance and classical ion thermal cond., Joule heating *(Russian)* 79−27797
high magnetic field behaviour of solids and plasmas, conference, Cambridge, MA, USA (Sept. 1978) 79−60667
high temperature in Tokamak, stabilisation *(Russian)* 79−82103
high temperature plasma heat insulation by electric and magnetic fields *(Russian)* 79−14600
high toroidal mode number stability of beam-induced tensor press. Tokamak 80−10378
high voltage opening switch using spoiled electrostatic confinement 80−103205
high-β flux-conserving equilibria, with supercond. metal shell, stability anal. 80−10428
high-β tokamak, ballooning mode instability theory *(Russian)* 79−27757
high-β Tokamak states, accessibility, transport model 79−64829
high-β Tokamaks, with anisotropic press., dynamics calcs. 79−73027
high-beta, with elongated cross-sections, MHD stability anal. 77−24170
high-beta column, in linear solenoid, end-loss calcs. 77−24156
high-beta flux conserving equilibrium, resistive magnetic flux diffusion 80−87873
high-beta Tokamak plasma, stability to ballooning modes 80−75091
high-beta Tokamaks surrounded by force-free fields 78−91141
high-beta toroidal plasma, stable confinement in levitated octupole 80−75090
high-press. flux conserving Tokamak equilibria, theory 77−27695
high-temp. regimes, simulation and confinement scaling 80−38673
hot cathode reflex discharge in cusp and uniform mag. fields 78−67456
HT-6 Tokamak, mass spectroscopic diagnostics *(Chinese)* 79−98990
hybrid reactors, fuel production for fission reactors, fuel cycle options 80−27812
hypercompression of matter by thermonuclear miniexplosion 79−50882
ICF reactor, first wall protection schemes 80−32437
ICF reactor fuel pellet fabrication techniques and quality factors, optical systems 80−32436
ICF reactors, material implications of design and system studies 80−32431
ICF targets, laser driven, materials problems 80−32438
ICF targets, semiconductor process technology for mass production 80−32439
ideal MHD equilibria of diffuse high-β stellarator 79−64897
ideal-MHD kink and ballooning modes, depend. on plasma shape and profiles 79−64846
imploding plasmas, mag. field generation, Nernst refrigeration 80−79526
implosion and reflection of coalesced shocks, self similar analytic solns. 78−55735
implosion of dense liner at medium vel., fast fusion reactor, energy regime 77−74996
implosions, mag. field generation due to Nernst refrigeration 79−27811
impurity behaviour during neutral beam injection and gas puffing into ORMAK 79−64878
impurity ions in Tokamaks, charge transfer excitation 79−4103
impurity spatial and time distrib. in JIPP T-II tokamak, vis. spectrosc. meas. 79−86619
impurity transport, neoclassical theory 79−98873
incompressible nondissipative MHD turbulence in spheromak, stable equilib. statistical states 79−60134
inertial, Fermi acceleration 77−72488
inertial, in fusion reactors, design constraints 79−49858
inertial confinement, advanced engineering requirements, review 80−95421
inertial confinement, by laser and electron beams, conf. summary 77−76174
inertial confinement, ion-beam wet-wood-burners using limited mass targets 80−102301
inertial confinement, reaction gains, reheat calcs., collective model 78−59664
inertial confinement, SOLASE laser fusion reactor design and its technological implications 79−71974
inertial confinement, USA research 80−78448
inertial confinement fusion, A-FLINT advanced-fuel pellet design 80−23125
inertial confinement fusion, appl. of intense charged particle beams overlap 80−91242
inertial confinement fusion, high yield Li injection fusion energy convertor 79−85772
inertial confinement fusion at NRL, laser and ion drivers 80−23131
inertial confinement fusion at Osaka, laser energy drivers, REB fusion research 80−23135
inertial confinement fusion energy with particle beams 77−83074
inertial confinement fusion gains using collective model for electrodynamic laser compressions 80−23138
inertial confinement fusion generating remote systems, laser driver sources 79−9886
plasma confinement continued
inertial confinement fusion mag. wall reactor cavity concept, new plasma model 79−86602
inertial confinement fusion power system, nuclear pumped laser coupling 79−85775
inertial confinement fusion research at Los Alamos, recent progress 80−23133
inertial confinement fusion target, density in fuel region by activation anal. 80−33807
inertial fusion reactors, feedback-controlled laser-guided pellets 80−73997
inertial-confinement ion-beam wet-wood-burner fusion neutron source 80−32489
initial confinement fusion, use of black-body radiation as fusion driver 80−91241
instability suppression by external turbulence introduction 79−32768
interchange instability in sheared mag. field, ion Larmor radius effects 77−62357
internal disruption in Tokamak, relax. oscills., self-consistent model *(Russian)* 80−53957
internal helical modes, m>1, in Tokamak with small shear and high plasma press. *(Russian)* 80−10371
ion beam shear-Alfven instability in two component Tokamak 79−60119
ion layer confined by mag. field, rigid rotor equilib. 77−47249
ion resonance instability, strong self-elec. field influence, nonneutral column 78−34301
ion ring, field-reversed, anomalous decay of induced electron current 80−24206
ion ring, mag. compression 77−72486
ion ring dynamics, angular momentum conservation 79−41864
ion sources, large vol. mag. multipole development 80−27857
ion temp. and parametric decay development in RF-generated stellarator plasma 80−79436
ion-ion hybrid damping in D_2-H_2 plasma 79−77361
ion-mixing mode and model for density rise in confined plasma 79−98862
ionisation waves in bounded low-temp. plasma 79−94794
ions, high energy tail formation associated with lower hybrid heating 79−98940
ISX-A Tokamak, plasma confinement and impurity flow reversal 80−28770
ISX-B Tokamak, intense heating, plasma position and current, feedback control modeling 80−33802
JAERI large Tokamak, fast acting movable rail limiters, R and D programme *(Japanese)* 79−13524
JAERI large Tokamak JT-60, vacuum vessel R and D programme *(Japanese)* 79−13523
JET plasma, diagnosis using electron cyclotron emission 79−98991
JET project description 78−58399
JFT-2 Tokamak, large scale fluctuation mode mixing, probe, interferometric obs., MHD anal. 78−67312
JIPP T-II torus, neutral gas injection and plasma current control, suppression of major disruption 80−28839
KEMP-II confinement machine, potential calc. 77−15225
kink instabilities of a field reversed ion ring with a toroidal magnetic field 80−1758
kink instability, internal MHD, sufficient cond. *(Chinese)* 80−43897
large aspect-ratio terawatt diode with heated and unheated anode, electron and ion current flow 79−10675
laser compression of inertially confined plasmas, future energy developments 80−23120
laser fusion, for electrical power generation 77−26867
laser fusion, HYLIFE reactor chamber response to fusion microexplosion 79−89499
laser fusion, plasma confinement, laser compression, Li activation *(German)* 80−52783
laser fusion 78−59635
laser fusion plasma, computer simulation of Weibel-like instability effects 79−14581
laser fusion reactor design, pellet X-ray spectra calc. 79−36410
laser heating and mag. compression of plasma in fast solenoid 79−46463
laser inertial containment, principles and problems *(French)* 80−78437
laser solenoid fusion concept 78−58435
laser-driven fusion, validity of hydrodynamic approximation 80−75087
laser-fusion plasma confinement, α-emission recoil force effect 80−6275
laser-produced plasma, supercrit. density modifications due to reson. RF cavity field 79−50875
Levitron, crit. tilts calcs. 79−73025
levitron, enhanced plasma loss due to ohmic heating currents 77−72460
linear devices, energy end loss, kinetic approach 77−76186
linear magnetic solenoid reactor plasmas, dynamic behaviour 80−64751
linearised gyro-kinetics, particle to guiding centre variables transformation 78−91081
linked Min-B config. with high-shear mag. surface 77−65900
LINUS, imploding liq. liner system, engineering anal. 80−99315
LINUS conceptual reactor 78−58432
longitudinal current excitation in plasma loop, 'mag. projectile' as mag. flux carrier 79−19079
low frequency parametric processes in magnetically confined plasmas 80−28827
low Z impurity transport in Tokamaks, simulation 79−55468
low-β plasmas, turbulence, spectral struct., Bhom diffusion coeffs., determ. 80−106924
low-beta compressible limit, resistive tearing mode, finite Larmor radius effect 77−72487
low-beta plasma column, RF current-dynamic shear stabilisation of hydromag. instability 79−46454
low-Z impurities radiation during RF heating in ATC 80−28816
lower hybrid heating in JIPP T-II tokamak plasma, obs. 79−86617
lower hybrid wave turning point location, nonuniform magnetoplasma 80−79473
lower hybrid waves, ray trajectory and ion absorpt. in Tokamak 80−28667
lower hybrid waves, trajectories and damping in Tokamak plasma 80−83922
magnetic configuration parameters, apparatus with spatial axis *(Russian)* 79−98949
magnetic confinement, 2D 79−60167
magnetic confinement, alternative mag. configurations for commercial fusion reactor development 79−71949

plasma confinement continued
magnetic confinement of finite-β plasma, 'second' stability region 79−82084
magnetic confinement system, surface problems caused by dissolved H_2 80−57946
magnetic confinement time, primary ionizing electron, meas. method for multidipole system 78−55739
magnetic containment testing for JET 78−54870
magnetic field aligned electric fields in adiabatic plasma 78−1873
magnetic field analysis in complex geometry *(French)* 80−79535
magnetic field effects on plasma motion in ring container, entropy 78−59553
magnetic field line reconnection, expts. and anal. 78−1874
magnetic field line trajectory calc., Kolmogorov Arnold Moser surface 80−59263
magnetic field measurement in toroidal plasma systems 80−49004
magnetic field penetration through slits in ideal shield 80−78745
magnetic field perturbations due to hole in conducting wall 77−47246
magnetic field plasma compression, stabilized imploding liner 79−60174
magnetic field reconnection, in collisionless plasma, electron Landau reson. 79−50852
magnetic fields for surface containment, magnet array 77−3973
magnetic fields of hot dense plasmas, particle probes sensitivity 80−70037
magnetic flux diffusion in imploding liquid liners 78−34361
magnetic insulation of vacuum lines 77−27711
magnetic island, m=2, high-energy runaway orbits 80−64767
magnetic island coalescence, 2-dimens. MHD eqns. 80−64695
magnetic islands coalescence instability 77−31511
magnetic mirror drift cone mode stabilisation with warm plasma, radial normal mode calc. 78−51294
magnetic quadrupole field, MHD equilib. 77−31507
magnetic reconnection, plasma confinement and jetting 79−10704
magnetic reconnection in collisionless plasma 79−82051
magnetic shear stabilisation of drift waves 77−72427
magnetic shear stabilisation of lower hybrid drift instabilities 77−42979
magnetic surface destruction in divertor region attributed to discrete struct. of mag. coils 77−31498
magnetic surface with free boundary, eqn. soln. based on one-dimens. model *(Chinese)* 77−76159
magnetic surfaces in DC toroidal octupole field, mag. field perturbation effects 77−62390
magnetic surfaces in the reversed-field geometry 79−7476
magnetic trap, ambipolar, hydrodynamic plasma equilib. *(Russian)* 79−98951
magnetically confined afterglow/at. beam, technique for α ion+atom cross section determ. 77−34750
magnetically confined plasma, creation inside imploding liners using relativistic electron beams 79−60175
magnetically confined plasma, external conducting open sheet, stability effects 80−92302
magnetically confined plasma, high temp., transport processes, numerical soln. 80−19559
magnetically confined plasmas, ballooning modes 80−6231
magnetically confined plasmas, expressions for nonclassical energy and particle flows 80−75031
magnetically confined plasmas, parametric instabilities in laser heating 78−18432
magnetically confined plasmas, theory 79−98963
magnetically insulated diode, coaxial geometry, one-, two-species equilib., electron and ion flow 77−58905
magnetised plasma, hot, unstable behaviour, in contact with cold wall 79−1333
magnetised plasma, in dielectric chamber with thermionic emitter, enhanced diffusion 79−64901
magneto-viscous resistive tearing of cylindrical flux surfaces 80−1831
magnetoacoustic oscills., in toroidal plasma, comparison with cylindrical plasmas, numerical calcs. 80−33760
magnetohydrostatic diffuse high-β equilib. 79−10691
magnetohydrostatic equilibria, circ. cylindrical, internal modes stability, in diffuse pinch 80−43957
magnetosonic resonance heating in the Erasmus Tokamak 80−28720
major disruptions in the TOSCA Tokamak 80−83979
maser emission, by plasma produced electrons orbiting a positively charged wire 80−92272
materials development for fusion 80−33804
maximum constriction phase of a weakly ionized discharge in helium 79−90486
maximum energy-confinement time in joule-heated Tokamaks 79−37532
Maxwell equation, solutions in toroidal coordinates 79−46467
Mercier criterion for a finite-pressure plasma in arbitrary-shaped magnetic axis configurations 79−37534
MHD asymptotic stationary regimes, inertial effects with infinite conductivity 77−15175
MHD codes, linear and nonlinear, plasma instabilities, PL1 programs 77−76040
MHD eqns. and confinement studies in closed magnetic configurations 79−98964
MHD equilibria, secular instability in mag. quadrupole field 80−53982
MHD equilibria, stability criterion 79−14534
MHD equilibria, stochastic stability 79−77414
MHD equilibria in mag. quadrupole field, secular instability 80−10427
MHD equilibria three-dimens., elliptical-centred 79−37535
MHD equilibrium, with axisymmetry and noncircular cross section, free boundary soln. to eqn. *(Chinese)* 80−59260
MHD equilibrium and stability, triangular deformation elliptic cross section *(Chinese)* 80−53950
MHD equilibrium and stability in three dimens. configurations 80−28776
MHD equilibrium of plasma confined in spherical microwave cavity 79−68911
MHD equilibrium of plasma confined in spherical microwave cavity 79−68912
MHD equilibrium with elliptic free-boundary, limiter and current profile effects 79−37529
MHD ideal equilibria, computer codes, review 77−27712
MHD instabilities, nonlinear behaviour calcs., numerical techniques 77−27659
MHD spectrum of straight plasma column with arbitrary cross section, finite element calc. 77−11327
MHD stability, computational aspects 77−27690
plasma confinement continued
MHD stability in diffuse high-β l=1 equilibria 77−19746
MHD stability of toroidal plasma, for localised displacement 79−73030
Microtor Tokamak, LF microturbulence, far IR laser scatt. 80−96362
microwave cavity confinement, MHD stability, elementary mode polaris. cjaracts. 77−43050
migma, localised MeV d^+ trapping observation, density and confinement time meas. 79−14596
migma electron velocity space distrib. function strapping 77−83091
migma ion distrib. in phase space, shaping 77−83090
Migma IV high energy fusion apparatus 77−83075
migmacells II and III advanced fuel expts., orbit diagnostics and lifetime meas. 77−83088
Min-B, β-ratio low pressure plasma in linked magnetic wells 78−30468
minidisruptions of current carrying plasma, ion-ion and kinetic effects 79−60178
minimum beta at ignition, analytic calcs. for transport scaling laws 79−71947
mirror fusion test facility, supercond. coils for plasma confinement field 79−36402
mirror fusion test facility, supercond. magnet prod. system 79−36408
mirror fussion test facility, supercond. Yin-Yang coil fabrication 79−36403
mirror machine, 2XIIB, neutral-beam-injected, field reversal expts. 79−86589
mirror machine, enhanced plasma confinement by MHD oscillation 80−24205
mirror plasma confinement, recent developments *(Japanese)* 79−7475
mirror system, fusion superconducting magnet development 77−26869
mirror trap, PR-6, drift loss-cone instability stabilisation by cold ions addition 79−32800
mirror-torus hybrid, two-energy-component plasma 77−15223
Mirror-Torus-System-1 with divertor mag. field, plasma density and depolarisation current 80−70022
modes and ballooning in magnetically confined plasmas 80−28650
moving plasmoid reactors using advanced fuel, modularisation 80−99312
multi-dipole device, spatial potential variations rel. to anomalous ion temperature 79−90378
multichambered neutral beam line, self-consistent background gas density calc. 78−34352
multichannel configuration, relativistic electron beam driven inertial fusion, transport calcs. 78−75268
multidipole device, primary electron effective MFP meas. 77−24183
multidipole plasma, origin and confinement of energetic ions 78−91123
multimode instability control by state feedback 79−77357
multiple magnet system for homogeneous steady state plasma 78−59660
multipole confinement experiments, summary 79−90434
multipole fusion confinement with 2 MA levitated superconducting coil 80−106191
Nagoya Bumpy Torus, confinement studies 80−78445
NASA Lewis Bumpy Torus, high pot., characts. 77−65904
negative shear ferromak for stabilization of current disruptions in toroidal discharge 80−106971
neoclassical current in a toroidally-confined multispecies plasma 78−83528
neoclassical transport theory, for toroidal axisymmetric plasma, moment eqn. calcs. 78−42724
Nernst-Wienecke equilibrium in linear magnetized plasmas 79−94812
neutral beam injection expts. on Tokamak plasma at ORNL 80−28809
neutral beam injection heating, in PLT 79−82074
neutral beam injection heating in Tokamaks, review 80−28729
neutral beam injection in JIPP T-II, investig. 80−28810
neutral beam injection in Tokamaks, review of technology progress 80−28731
neutral injection parameters and beam line design for TEXTOR 80−28811
neutral-beam-driven current evolution in Tokamak plasmas 80−28712
non-neutral plasmas, confinement props. 80−38688
nonlinear ideal MHD equilib. in axisymmetric systems 78−1876
nonlinear kink instabilities in Tokamaks surrounded by force-free fields 80−43909
nonlinear phenomena by the Tokamak helical mode evolution 80−92398
nonmagnetic dense thermonucl. plasma confinement, electron beam heating 77−76171
nonneutral electron beam propagation in inhomogeneous mag. field, stability 77−24175
nonthermal radiation emission, in Tokamak plasma, at plasma frequency 78−42732
nuclear fusion, basic concepts 77−34451
nuclear fusion potential 77−75000
numerical simulation of disruptions and loss in Tokamak plasma 80−70026
NUWMAK fusion reactor, toroidal field magnet system 79−36406
octopoles, for advanced fuel cycle fusion reactors 79−76144
octupole, trapped-electron and trapped-ion regimes, diffusion, fluctuations 77−72416
Ohmic current driven MHD instability in Heliotron-D device 80−38640
ohmic heating of plasmas in closed magnetic systems 80−28756
open field line geometry, end plugging, end loss scaling 77−68855
optimal feedback control of plasma parameters in Tokamak 79−64891
Ormak, confinement and neutral beam injection obs. 77−43022
ORMAK, impurity and surface studies 77−31517
ORMAK, plasma equilib. feedback control 77−3976
oscillations of radially confined round beam, stability and distrib. function 80−53966
paramagnetic spheromak formation in a combined zee and theta pinch 80−92372
paramagnetism in RF mag. field, expt., theory and simulation 80−6225
parametric instabilities, in thin radially inhomogeneous plasma column 79−7457
particle confinement scaling experiments in the Culham Levitron 80−92361
particle diffusion across mag. fields, stable profile for nonlinear diffusion eqns. 78−22456
particle drift absence in translationally symmetric mag. fields 79−37454
particle orbit in magnetic field, guiding-centre Hamiltonian, arbitrary gyration 80−1834
PCX facility, intense laser radiation effects on mag. confined plasma 78−66405
Penning discharge, ion heating and collisional energy loss 77−72519
peripheral suppressor grid recovery systems for Tokamaks 80−28813

plasma confinement continued
Petula Tokamak, Transit Time Magnetic Pumping heating 80−28739
Pharos II, Naval Research Lab. inertial confinement fusion programme 78−59042
PIACE-R1, design fabrication and testing 80−92378
pinch-tormac, device using theta pinches and tormac-like end sections 80−24213
plasma column, position control system, stability 80−106982
plasma confinement in mirror and cusp fields, Monte Carlo simulation 80−96379
plasma confinement mag. field, computer simulation of finite linear multi-pole with closed ends 77−35382
plasma physics, and controlled nuclear fusion, conf., Berchtesgaden (1976) 77−43020
plasma simulation, splines and higher order interpolations 79−64902
plasma-surface interactions in Tokamaks, review 79−73017
PLT Tokamak, neutral beam heating 80−28701
PLT Tokamak, ohmically heated plasmas, radiation, impurity effects, instability and particle transport 80−28833
PLT tokamak discharge, ion temp., X-ray Doppler broadening determ. 79−27830
poloidal rotation velocity determ. in FT-1 Tokamak *(Russian)* 80−19565
polymer-coated laser fusion targets, compression to 10×liq. DT density 80−83964
preionisation in discharge regime in Tokamak *(Russian)* 80−54018
PRETEXT, poloidal field coil code, expt. verification 80−92377
Princeton Large Torus, unbalanced neutral beam injection, toroidal plasma rot., Doppler shift meas., confinement times 79−77400
propagation of a wide ion beam into a magnetic barrier, Vlasov equilib. model anal. 79−90439
Proto-Cleo torsatron, vac. mag. surfaces shape, electron beam diagnostics 79−73035
proton rings, mag. compression, computer simulation 78−22548
PULSATOR I Tokamak, wall analysis, impurities 77−31515
Pulsator Tokamaks, modulated runaway losses and effects of helical dipole field 80−28845
pulsed e.m. confinement system, electron ionised plasma, particle lifetime 77−1014
pulsed high-beta plasmas, conference, Abingdon, Oxon., England (Sept. 1975) 77−24123
pulsed ion diode, self mag. insulation 77−65918
pulsed Tokamak reactor, poloidal mag. field design 80−13858
pure electron plasma long time confinement, max. confinement time 80−48954
Q-machine, control of plasma pot. distrib. with electron emissive limiter 77−19744
Q-machine, flute instability excitation 79−46441
Q-machine, plasma potential control with electron-emissive grid 77−39446
Q-machine, single ended, collisionless plane diode model 79−7478
quadrupole magnetic field, density and potential fluctuations obs. 78−91146
quasisteady, scaling laws rel. to fusion reactor operation 79−27812
radial boundary layers, diffusing toroidal equilibria 77−89285
radiation emission spatial distrib. reconstruction in torous 80−103123
radiation losses from T-10 Tokamak, pyroelectric detect. *(Russian)* 80−53936
radiation-held plasma, stability 78−71526
Rayleigh-Taylor instability, in curved mag. field, excitation and control 78−47113
Rayleigh-Taylor modes of rot. MHD equilib., shear stabilisation 79−27813
reactor, Tokamak, fuel injection, dynamic burn control 1-D transport code 80−68948
reactor, Tokamak, toroidal magnetic field ripple, burn control 80−63375
reactor ignition, overheated underdense Tokamak plasma, two-zone model and 1-D transport code 80−63376
realistic Vlasov slab equilibria with magnetic shear 79−90440
rectangular finite-β system, kink instability 77−76070
Rector, axisymm. toroidal plasma, MHD props. 77−43024
relativistic charge particle confinement by EM wave 78−38524
relativistic electron beam high current ring form., for plasma confinement 77−76168
relativistic electron beam ring, facilities of Nagoya University Plasma Physics Institute 78−5919
relativistic electron beam ring, landing on equilib. orbit 77−35375
relativistic electron rings, translation and stacking 77−87877
relativistic toroidal plasma, equil. and circular rotation *(French)* 77−15222
renormalised Vlasov turbulence 80−19579
resistive instability of tearing modes, equilib. flows 79−27816
resistive internal helical mode near the instability threshold *(Russian)* 79−98948
resistive internal helical modes, mag. field configs. *(Russian)* 77−19741
resistive MHD instabilities, diffuse pinch configs., numerical study 77−58853
resistive plasma column, reconnecting mode, moment eqns. treatment 78−22493
return current response to external beam current in mag. field 77−15211
reversed current effect in stabilised Z-pinch 80−79539
reversed field configuration, equilibrium and stability and confinement props. 80−87932
reversed field configuration plasma in metal tube, induced by relativistic electron beam 78−91114
reversed field confinement by rotating relativistic electron beam 80−92370
reversed magnetic fields induced by a rotating e-beam 80−28790
reversed-current ion ring reactor, image current interaction 79−85778
reversed-field pinch plasma model 80−87935
RF cavity with magnetic mirrors, computer simulation of confine 78−59648
RF confinement near critical density, computer simulation 77−72492
RF confinement of plasma near critical density, computer simulation 77−24178
RF driven current generation by lower hybrid waves in Tokamak 80−103116
RF flux control of toroidal plasma 80−38582
RF heating of toroidal plasma, review 79−98939
RF plugging, nonadiabatic, in cusped field, ion heating effect 78−59656
RF plugging and heating, rel. to plasma impedance 80−96378
plasma confinement continued
RF plugging and heating of magnetised sheet plasma 79−19075
RF quadrupole field, lifetimes of confined ions, influence of buffer gas *(French)* 77−35378
RFC-XX, cusp end plugging MW quasi-steady wide band RF system 80−13880
rigid-rotor equilib. of magnetically confined nonneutral plasma 77−72484
ring, equilib. condition, complementary variational principles 78−51335
rotamak, compact torus generated by rot. mag. field 80−83980
rotating ion layer in external mag. field, equilib. props. 79−14598
rotating plasma, axially symmetric, continuous MHD spectrum 79−60180
rotating plasma column, non-ideal MHD equations 78−59592
rotating plasma reactors, longitudinal confinement, stability equilibrium and heating problems 80−74001
rotating proton layer, transient magnetic field reversal 80−70027
runaway electron diffusion and power balance in Tokamak moderate density discharges 80−28609
runaway electrons in toroidal discharges 79−64892
Saturn stellarator-torsatron, collisionless plasma diffusion 77−1011
scaling and similarity laws 78−94932
scaling laws 78−5915
screw pinch, force free current induction by boundary displacements 79−32796
screw-pinch, equilibrium and stability 80−87934
screw-pinch high-β Tokamak, field generation using transverse rotating mag. field 80−19606
Scyllac, computational plasma MHD for stable equilibria 77−84478
Scyllac, m=1 waves propag. 78−5865
Scyllac, theta pinch implosion, gross plasma motion model and feedback stabilisation 77−24141
Scyllac fusion test reactor design 77−23252
segmented compact Tokamak reactor, poloidal field coil system 80−13866
self confinement in highly ionised plasma 77−31495
self-similar power-driven expansion into vac. problem, approximate solns. 80−79540
semi-stellarator field stabilization of Tokamak plasma 80−6245
Shafranov equation, solutions in toroidal coordinates 79−46467
shape stability for plasma in standing EM field 80−28795
sheaf instability at moderate densities, anomalous ion heating *(Russian)* 80−43922
shear Alfven wave heating experiments in heliotron D 80−28716
short-circuit effect in a bounded plasma 79−27820
simulation models, three dimens., for cylindrical and toroidal plasmas 78−1884
single particle trajectories in axisymmetrical EM fields 77−80342
skin current heating of toroidal plasma 80−28715
slightly dissipative plasma, helical flux and other integral variants 77−65833
SLPX, supercond. long pulse expt., design features 80−13854
small aspect ratio tokamak, high press. equilibria 79−4174
small-aspect-ratio, small-major-radius Tokamak reactors 78−79452
soft X-ray emission from Tokamak low β mag. confinement systems 80−48959
solid H_2 pellet ablation, in Tokamak plasma 77−89264
Sorb-ac wafer pumps, behaviour in plasma machines, review 78−70627
space potential on Elmo bumpy torus, ion-beam probe 78−67414
space-charge double layers, anal. using fluid theory 80−75062
spatial distribution of impurities and H neutrals in ELMO bumpy torus 79−55559
spherator, FM-1, magnetic islands obs. 77−15232
spherator, FM-1 energy loss rates of injected energetic ions 77−89270
Spherator with purely poloidal magnetic field, MHD stability 79−98961
Spheromak, MHD stability 79−41859
spheromak, toroidal reactor low aspect ratio limit 80−23139
spheromak formation by theta pinch 80−106962
spheromak plasma config. form. by combined Z- and θ-pinch discharges 80−43955
spheromaks, nonlinearly stable equilibrium statistical states 80−53975
split magnetic surface config., electron instability *(Russian)* 77−68843
stabilisation of low-m kink modes in Tokamak 79−64890
stability criteria, closed field lines system rot. transform *(Russian)* 77−3972
stability criterion for plasma equilibria with tensor pressure 79−1334
stability in toroidal axisymmetric system *(German)* 80−28792
static stability, equilibrium config., stray field effects in Tokamaks *(Chinese)* 77−76158
stationary MHD eqns. for rotating toroidal plasma 80−92278
stellarator, current carrying, m=1 kink instability, nonlinear props. 78−63566
stellarator, current-carrying, kink and tearing mode MHD instability 78−22539
stellarator, current-carrying, plasma energy content *(Russian)* 78−1870
stellarator, FLR stabilisation, MHD configs. with zero rot. transform 77−72472
stellarator, helical plasma equilib. 77−27710
stellarator, high β, feedback stabilised 79−19074
stellarator, high-β, finite gyroradius stabilisation of MHD modes 78−26314
stellarator, high-β equilibria with three helical beta fields, numerical expt. 80−10426
stellarator, high-beta, feedback stabilisation and equilibrium of 120° torus sector 78−75404
stellarator, hybrid, MHD stability anal., plasma press. depend. *(Russian)* 77−47241
stellarator, ISAR T1-B, m=2 instability, finite Larmor radius stabilisation 77−31506
stellarator, Isar T1-B, m=2 mode collision-dominated stability obs. 77−24130
stellarator, l=2, without longitudinal current, equilib., stability 77−31509
stellarator, laser plasma expansion 77−76177
stellarator, mag. surface destruction due to finite press. plasma *(Russian)* 78−22545
stellarator, mag. surfaces destruction near separatrix 78−30475
stellarator, MHD instabilities 78−14154
stellarator, non-circular cross section, MHD equilibria 78−5914
stellarator, noncircular cross section, MHD equilib. 78−9820
stellarator, nonlinear props. of m=1 internal kink mode 78−94908

plasma confinement continued
stellarator, ohmically heated, comparison with Tokamak 77−11371
stellarator, plasma diffusion *(Russian)* 79−32747
stellarator, plasma losses, quasi-neoclassical law 80−79544
stellarator, Proto-Cleo, electron beam transit-time mag. pumping 77−19754
stellarator, RF heated, quasi steady state currents, mag. field perturbation obs. *(Russian)* 77−47256
stellarator, Saturn, current-free transport processes, drift modes effect 80−19605
stellarator, Saturn, transient electric field effect on collisionless diffusion *(Russian)* 78−26245
stellarator, three-turn, transverse mag. field effect on axial mag. surfaces 77−19747
stellarator, twisted coils in linear config., rot. transform angle of mag. field 77−47247
stellarator, Uragan-2, equilib. and HF heating 77−72459
stellarator, with 3 mag. axes, Doublestar, numerical study 78−91140
stellarator field with twisted coils, rot. transform angle 77−68853
stellarator fields, review 78−30467
stellarator geometry, superbanana orbits for 3.5 MeV alpha particles 80−24231
stellarator limiting equilibrium plasma pressure with mag. shear *(Russian)* 79−4166
high-β stellarator with l=3, stability 77−7529
stellarator with ohmic heating currents 77−72467
stellarator with ohmic plasma heating, magnetic surface distortion by helical current perturbation *(Russian)* 77−15236
stellarator with spatial mag. axis, equilib., MHD stability 77−72470
stellarator-multipole toroidal hybrid mag. configs., codes and simulation 77−55163
stellarator-Tokamak hybrid system, JIPP T-II, feedback control 77−72468
stellarators, controlled thermonuclear fusion expts. at Kharkov Inst., Ukrainian SSR *(Russian)* 79−13526
stellarators, high-beta, toroidal equilib., m=1 mode 77−24124
stellarators, magnetic hill effects on equilibrium 80−79558
stellerator and torsatron, l=3 trap mag. config., axial region mag. surface struct. 77−51214
stimulated Compton scatt., Bose condensation and onset of final equilib. state 77−51193
stochastic magnetic field, Kolmogorov entropy for motion 79−60183
stochastic orbits in Tokamak, statistical description, low freq. fluctuations 80−59265
straight l=1 config., equilib., stability 77−1006
superbanana limiter as a possible edge cooling scheme 80−92362
superconducting fusion magnets for mirror systems 79−36401
superconducting magnet system appls. *(Slovak)* 78−87474
superconducting magnet systems 77−19759
superconducting magnets, magnetic confinement of plasmas in fusion reactors 79−23441
superconducting magnets for fusion reactor, safety and structural aspects 77−26874
superconducting toroidal coil, TESPE, for Tokamak fusion plasma containment 79−54223
supra-thermal trapped electron quasi-linear diffusion, mag. drift reson. and Alfven wave excitation *(Russian)* 79−27748
surface mag. field confinement of high-β plasma, toroidal current stabilisation 78−67401
surface magnetic field configurations, free boundaries 77−19750
surface problems in controlled fusion *(Chinese)* 79−97904
T-10, ohmic heating, plasma confinement study 80−28768
T-11 Tokamak, neutral beam injection, plasma heating and stability 80−28702
T-tube plasma, influence of boundary layer on H_γ line 80−48862
Takamak plasma density profiles from electron cyclotron radiation spectra 80−103179
tearing instability, m=1, kinetic and finite beta effects 78−67398
tearing mode saturation, poloidal number greater than 1 77−68845
tearing modes, nonlinear interaction in highly resistive tokamaks 79−64855
tearing modes, unified theory 80−19607
tearing modes with mag. braiding 80−10429
tearing-mode activity for hollow current profiles 79−55498
Texas turbulent torus, turbulent heating effects 79−90442
TEXTOR, interferometric and polarimetric diagnostics 80−70039
TEXTOR vessel, plasma position, feedback control calcs., response time behaviour 79−98959
TFR, ion energy balance, heating by fast neutral injection 77−43023
TFR, reduced fusion neutron production 78−63577
TFR 600 Tokamak, plasma confinement, low effective plasma charge 80−28769
TFR discharge, energy balance obs. 77−43021
TFR Tokamak, ion cyclotron instability, microwave scatt. obs. 78−71473
TFR Tokamak at ionisation equilibrium, heavy impurities 80−106970
theoretical scaling laws, implications 80−28805
thermonuclear fusion and the Tokamak, review *(Italian)* 79−31177
thermonuclear ignition, inertially confined fusion, high density effects 80−86981
thermonuclear microexplosion reactor, heavy ion beam ignition and inertial confinement 79−59252
theta pinch, tearing and reconnection of magnetic fields 79−23446
theta-pinch, collisionless, high-beta, anisotropy-driven EM modes, finite Larmor radius effects 80−1830
theta-pinch, fast, axial ion energy distrib., particle and probe diagnostics 78−59655
theta-pinch, Pharos device with end stoppering, homogeneity, stability 78−34360
thin line cusp magnetoplasma sheath, RF feedback stabilisation 80−70009
Tokamak, accuracy of plasma displacement meas. using mag. probes 77−19766
Tokamak, adiabatic compression, impurity ions line radn. meas. 77−43075
Tokamak, adiabatic toroidal compressor, safety factor meas. 79−19091
Tokamak, Alcator, electron cyclotron emission, polarisation freq. depend. 80−33808
Tokamak, Alcator, high-density D_2 discharge parameters obs. 78−18438
Tokamak, Alcator scaling, transport model 78−75406
Tokamak, Alfven waves, interaction with trapped electrons *(Russian)* 77−11338
plasma confinement continued
Tokamak, alpha transport and blistering of first wall 79−19069
Tokamak, anisotropic high-β stability to ballooning modes 78−91143
Tokamak, anomalous transport, dissipative trapped-ion instability 77−72420
Tokamak, arbitrary cross section, equilib., stability 77−19755
Tokamak, asymmetrical collisional tearing mode growth rate, variational treatment 79−32803
Tokamak, ATC, bistable equilib., mag. pumping appl. 77−65903
Tokamak, ATC, electron density fluctuations, safety factor 77−43074
Tokamak, ATC, free expansion expt. 78−30469
Tokamak, axially symmetric, α-particle escape in nucl. fusion, azimuthal distrib. *(Russian)* 77−18694
Tokamak, axisymm. MHD instability, feedback stabilisation 78−87484
Tokamak, axisymmetric instabilities, time depend. simulation 79−10702
Tokamak, bundle divertor, charged-particle orbit and cross-field diffusion 78−42784
Tokamak, collisional, multispecies transport 77−19674
Tokamak, confinement and stability, effects of shaping and compression of plasma 80−28772
Tokamak, counterstreaming-ion, plasma refuelling and heating 77−71693
Tokamak, current profile from mag. diaphragm *(Russian)* 78−71520
Tokamak, current rise, two-dimens. fluid simulation 77−72491
Tokamak, cylindrical, high β flux conserving equilib. 79−19073
Tokamak, cylindrical, ideal MHD equilib., uniqueness theorems 79−32795
Tokamak, diffusion of runaway electrons across mag. field 78−87480
Tokamak, discharge development *(Russian)* 77−68809
Tokamak, disruptive instability fine struct., X-ray diagnostics 77−43073
Tokamak, DITE, divertor and injection expts. 77−72478
Tokamak, DITE, high-density discharge regime, with Ti gettered walls 78−22544
Tokamak, DIVA, divertor expt. 79−10688
Tokamak, DIVA, impurity shielding and sweeping out, axisymm. divertor 78−86685
Tokamak, DIVA, metal impurities anal. 79−64906
Tokamak, DIVA, radiation loss and power balance, pyroelectric detection 78−86684
Tokamak, DIVA divertor and JFT-2 expts., impurities 77−72501
Tokamak, divertor expts. for controlling plasma-wall interactions 78−94125
Tokamak, Doublet IIA, temporal and spatial behaviour of plasma props. 77−43030
Tokamak, drift cyclotron instabilities driven by ion temperature gradient 79−10654
Tokamak, drift tearing modes 78−75289
Tokamak, drift wave convective amplification enhancing transport 79−37488
Tokamak, drift wave propag. and convective growth 79−60137
Tokamak, drift-wave turbulence effect on mag. struct. 78−22501
Tokamak, E×B plasma divertor 79−19076
Tokamak, electron cyclotron heating, Bernstein modes, Vlasov dispersion relation 80−33809
Tokamak, electron energy confinement, simulation predictions 79−64898
Tokamak, electron energy confinement time, direct determ. 78−9834
Tokamak, elliptic flux-conserving, plasma equilib. 79−10695
Tokamak, elongated, vertical stability 79−14594
Tokamak, energy confinement times 79−10693
Tokamak, equilib. and radial stability 78−9819
Tokamak, equilibrium and stability, time-depend. three dimensional MHD calc. 77−24131
Tokamak, Erasmus, small aspect ratio, stable equilib. conds. 77−43034
Tokamak, external mag. field structs., high-β equilib. 77−72479
Tokamak, fast ion injection, energy amplification 77−71692
Tokamak, Fe^{n+} forbidden spectral lines, for diagnostics of localised regions 79−98958
Tokamak, finite shear, ballooning modes 78−5918
Tokamak, finite-orbit effects on non-pot. oscills. 77−15228
Tokamak, flux-conserving, inductive effects 79−41862
Tokamak, flux-conserving cylindrical equilib. evolution with adiabatic compression and beam heating 80−28799
Tokamak, flux-conserving equilib. in neutral beam heating 77−11381
Tokamak, fusion power reactor design 77−74982
Tokamak, fusion reactor, axisymmetric, slowing-down alpha particle loss, Monte-Carlo calc. 78−59653
Tokamak, H_2 breakdown condition 79−14569
Tokamak, heavy-impurity re-cycling and power loss at limiter 78−22543
Tokamak, helical, alpha particle absolute confinement condition 78−42782
Tokamak, helical instability, mag. shaping effect 78−42781
Tokamak, helical winding, effect of HF current on discharge 78−87485
Tokamak, high β_J, m=1 mode, internal helical instability suppression *(Russian)* 79−98947
Tokamak, high beta, axially symmetric diffuse column, equilib. and stability anal. 77−24132
Tokamak, high beta, hot plasma preparation 77−999
Tokamak, high beta, MHD stability 77−68849
Tokamak, high beta, theory 78−25324
Tokamak, high beta, transport and radiation studies 80−28798
Tokamak, high energy α-particle flux at walls due to mag. field rippling *(Russian)* 77−68841
Tokamak, high energy electrons in low density regime 79−98905
Tokamak, high-β, stability props. calc. model. 77−84484
Tokamak, high-β small aspect ratio, probe and laser beam meas. 77−27733
Tokamak, high-beta, equilibria and m=1 kink ballooning mode nonlinear evolution 80−24236
Tokamak, high-beta, instabilities, rel. to screw pinch 77−24128
Tokamak, high-beta, time evolution, MHD simulation using flux coords. 77−24134
Tokamak, high-beta, with force-free currents, MHD stability 78−87481
Tokamak, high-beta limitation by instabilities during rapid heating 77−39448
Tokamak, high-beta limitation by instabilities during rapid heating 77−39449
Tokamak, high-density regime performance, scaling laws 77−11380
Tokamak, highly elongated and non-circular cross section equilib., axisymmetric instabilities 77−72482
tokamak, horizontal plasma position control by feedforward-feedback system with digital computer 80−75093

plasma confinement continued
Tokamak, HP flux-conserving equilibria 77−35379
Tokamak, hydromag. kink mode instability, dynamic shear stabilisation, by nonlinear mode coupling 79−50858
Tokamak, hydromagnetic stability 78−30428
Tokamak, ignited plasma, temp. control by toroidal field ripple 78−5033
Tokamak, impurity conc. and time evolution 77−51156
Tokamak, impurity instabilities *(Russian)* 77−68763
Tokamak, impurity radiation loss effects 78−22465
Tokamak, impurity transport *(Russian)* 80−106957
Tokamak, initial stage of discharge development 77−72476
Tokamak, inner mode relax. oscills., numerical model, electron thermal cond. distrib. *(Russian)* 77−47242
Tokamak, internal disruptions, sawtooth oscills. 78−47147
Tokamak, internal helical mode stability, by MHD approx. *(Russian)* 78−91139
Tokamak, internal kink mode, numerical study 80−48953
Tokamak, internal m=1 kink modes 77−15231
Tokamak, ion temp. by Fe^{19+} forbidden line 78−83602
Tokamak, ISX, dynamics and feedback control 78−71528
Tokamak, JFT-2, gross particle confinement characts. by boundary plasma, electrostatic probe diagnostics 79−32822
Tokamak, JFT-2, particle and heat transport during lower hybrid heating 80−70021
Tokamak, JIPP T-11, with pulsed gas injection 78−71527
Tokamak, kink modes nonlinear evolution 77−19753
Tokamak, large, optimum config. of poloidal field coils 79−23464
Tokamak, large aspect ratio, ballooning stability boundaries 79−1332
Tokamak, large aspect ratio, two-fluid energy principle 79−19078
Tokamak, large mag. islands as disruption mode 79−27819
Tokamak, large mag. islands as disruption mode 79−27818
Tokamak, large poloidal beta, MHD stability, collisional and anomalous trapped particle diffusion 77−24055
Tokamak, limiter-scrape-off layer, kinetic theory 78−14193
Tokamak, local stability criteria, multipole field effects *(Chinese)* 77−39445
Tokamak, local toroidal and poloidal current density meas. 77−27732
Tokamak, localised MHD modes, shape optimisation 79−98954
Tokamak, low-beta and high-beta regime stable to ballooning modes 80−75083
Tokamak, lower hybrid wave refl. from lower hybrid surface, toroidal effect 79−27770
Tokamak, LT-3, disruptive instability, spectroscopic observations 78−87483
Tokamak, LT-3, helical MHD modes during disruptive instability 77−76063
Tokamak, LT-3, runaway electron transport 77−11316
Tokamak, Macrotor, mag. fluctuations 79−60184
Tokamak, mag. field penetration through cylindrical resistive shell 79−14595
Tokamak, mag. surface destruction 79−67150
Tokamak, magnetic extraction of runaway electrons 78−34362
Tokamak, major disruption suppression by tearing modes stabilisation 80−10422
Tokamak, major disruptions mechanism 79−7477
Tokamak, mathematical model, poloidal fields improvement in plasma stability *(Russian)* 78−51339
Tokamak, metal impurities due to arcing 78−42787
Tokamak, metal impurity reduction by working gas injection 80−106963
Tokamak, MHD flow in Li blanket *(Russian)* 78−47146
Tokamak, microinstability theory, review 78−75292
Tokamak, multiplication of accelerated electrons *(Russian)* 79−46471
Tokamak, neutral density profile 79−14520
Tokamak, neutrals and impurities toroidal transport code 77−72490
Tokamak, non-circ. cross section, Alfven instability stabilisation *(Russian)* 78−26260
Tokamak, non-circular, cross-sectional shape control 77−43031
Tokamak, non-circular cross-section, axisymmetric modes 77−72481
Tokamak, non-circular cross-section, Doublet III design optimisation 77−72480
Tokamak, noncirc., axisymmetric modes wall stabilisation, simulation 78−67394
Tokamak, noncirc. cross-section, local, ideal and resistive stability 78−22540
Tokamak, noncircular, reactor size plasma MHD equilib. calc. 77−24121
Tokamak, noncircular cross-section, high-β, anisotropic equilib. 80−24238
Tokamak, nonlinear helical perturbations 77−51221
Tokamak, nonlinear ideal MHD equilib. 78−1876
Tokamak, nonlinear perturbation, feedback effect *(Russian)* 80−83967
Tokamak, nonlinear saturation of dissipative trapped electron instability 77−84429
Tokamak, nonlinear stability to free boundary kink modes 77−1010
Tokamak, O trapping and removal, discharge cleaning 78−22541
Tokamak, odd drift modes, effect of trapped electrons *(Russian)* 77−43055
Tokamak, ohmically heated, comparison with stellarator 77−11371
Tokamak, ohmically heated, empirical scaling laws for confinement 79−23442
Tokamak, optimum conceptual scaling 78−54908
Tokamak, pellet fuelling, effects of transport on injection 79−89501
Tokamak, Petula, low-Z materials effect on plasma characts. 77−72477
Tokamak, plasma compression, runaway electron behaviour, excitation, X-ray obs. *(Russian)* 78−38531
Tokamak, plasma density anal., electron and ion density control methods 78−47145
Tokamak, plasma equilib., ferromagnet-saturation effects, numerical simulation 78−18440
Tokamak, plasma equilib., nonlinear boundary value problem 79−19080
JFT-2a Tokamak, plasma equilib. with separatrix mag. surface 77−7581
Tokamak, plasma MHD equilib., var. method *(Russian)* 80−106960
Tokamak, plasma paramagnetism, expt. obs 80−54021
Tokamak, plasma position dynamics 78−66420
Tokamak, plasma simulation using nonuniform spatial mesh technique 77−79478
Tokamak, PLT, current profile evolution effect on plasma-limiter interaction and energy confinement time 80−10420
Tokamak, PLT, disruptive instabilities, X-ray study 78−89974
Tokamak, PLT, expt. results 77−43072
plasma confinement continued
Tokamak, PLT, fast-wave heating of two-ion plasma through minority cyclotron reson. damping 80−24194
Tokamak, PLT, microinstabilities, microwave scatt. meas. 78−67413
Tokamak, poloidal divertor expt., stabilisation of the axisymmetric instability 79−4171
Tokamak, poloidal field distrib. meas. by far IR polarimetry 78−42810
Tokamak, poloidal field induced Faraday rot. 79−10716
Tokamak, press. upper limit 77−58884
Tokamak, radiative and particle power losses, bolometric meas. 80−73996
Tokamak, reactor size, diffusive losses and scaling law 78−87478
Tokamak, recycling processes 78−94126
Tokamak, relativistic runaway electron beams 77−51223
Tokamak, resistive perturbations, energy principle 77−43053
Tokamak, review of controlled fusion *(German)* 77−34425
Tokamak, runaway electron discharge MHD stability 78−75303
Tokamak, runaway electron instability, non-thermal microwave radn. 80−1842
Tokamak, runaway regime, single particle trajectories 77−80342
Tokamak, sawtooth oscills. 78−47150
Tokamak, scaling law, appl. to JIPP T-II device 78−47155
Tokamak, scrape-off layer in poloidal field divertor 79−68944
Tokamak, shape optimisation of surface current model 79−10689
Tokamak, sharp-boundary model, axisymmetric MHD instability anal. 77−51217
Tokamak, shell-less octapole, positional behaviour of plasma column 77−84475
Tokamak, simulation model 78−1884
Tokamak, small aspect ratio, flat current noncircular, unstable MHD spectrum 80−69989
Tokamak, small aspect ratio, MHD spectrum calc. 77−72483
Tokamak, space-depend. thermal stability of reacting plasma 79−19068
Tokamak, square or inverse-dee, equilibria, axisymmetric instability and stabilisation 79−73029
Tokamak, stability of internal helical mode, high press. plasma *(Russian)* 78−91138
Tokamak, stability w.r.t. slip motions 77−15227
Tokamak, start-up phase, plasma impurities effects 77−14265
Tokamak, steady-state diffusion, particle loss 78−22457
tokamak, stochastic ion heating by lower hybrid wave 80−28707
Tokamak, stochastic particle orbits, statistical description 80−79466
Tokamak, superconducting, toroidal simulation 77−62394
Tokamak, surface effects and impurity production 78−94127
Tokamak, surface interactions and conditioning techniques 78−94124
Tokamak, surface processes in plasma-wall interactions 78−94121
Tokamak, T-10, plasma parameters 77−43071
Tokamak, T-10, stainless steel limiter expts. in ohmic heating region *(Russian)* 80−83969
Tokamak, T-11, fast neutral beam injection, heating 77−42991
Tokamak, T-4, corpuscular diagnostics by charge exchange of plasma ions at artificial target *(Russian)* 80−83968
Tokamak, tearing mode coupling 78−14192
Tokamak, tearing mode suppression by feedback system *(Russian)* 78−22535
Tokamak, temp. drift instabilities 77−19687
Tokamak, TFR, internal disruptions and current breakdown, X-ray diagnostics 77−43027
Tokamak, TFR, low-freq. oscill. struct. during current disruptive instability 78−22564
tokamak, TFR, plasma confinement exam. 79−60169
Tokamak, TFR, variable-radius Mo and graphite limiters 78−63600
Tokamak, time evolution of mass flow 79−23444
Tokamak, toroidal field ripple effect on particle and energy transport 77−11315
Tokamak, TOSCA, magnetic islands and disruption 79−23456
Tokamak, TOSCA, shaping and compression expts. 77−43032
Tokamak, trapped electron instability, 2-dimens. eigenvalue problem, anal. soln. 78−83549
Tokamak, trapped particle modes, parametric excitation, instabilities, HF pump effect 77−24177
Tokamak, trapped-electron dissipative mode, two-dimens. spatial struct. 77−51175
Tokamak, trapped-ion residual instabilities 77−47185
Tokamak, trapped-particle instabilities, linear and nonlinear theory 77−72429
Tokamak, Tuman-2, current channel mag. compression *(Russian)* 78−38455
Tokamak, Tuman-2A, plasma compression particle diagnostics, density and temp. *(Russian)* 80−38677
Tokamak, two-dimens. MHD simulation 77−19751
Tokamak, two-dimens. transport, theory 79−64896
Tokamak, upgraded DIVA, ion temp. charact. 78−63584
Tokamak, wall protection from hard disruptions 77−31508
Tokamak, weakly localized two-dimensional drift modes 80−53970
Tokamak, zero-dimens. transport model, variable density profile 79−7479
Tokamak 'blister' divertor, enhanced toroidal field ripple trapping 78−59654
Tokamak (Alcator), driven lower-hybrid waves, light scatt. study 80−1835
Tokamak and CTR reactors, mobile diaphragm operation mode *(Russian)* 80−83966
Tokamak and stellarator, progress in experiments 78−94122
Tokamak apparatus, resistive shell, penetration of time-varying vertical and horizontal mag. fields 78−63575
Tokamak apparatus, toroidal inhomogeneity of vertical field 78−9816
Tokamak axisymmetric equilib., flux surface shape and current profile optimization resistive interchange stability 77−84480
Tokamak boundary in contact with limiter 78−5913
Tokamak contamination, comparison of different refuelling methods 78−94133
Tokamak device, control coil optimum design, nonlinear optimisation 77−27744
Tokamak devices, series coupled power crowbar system *(Japanese)* 78−55755
Tokamak discharge, breakdown phase, ionis. time, mag. flux requirement *(German)* 78−34363
Tokamak discharge, current mixing and mag. surface tearing in initial stages *(Russian)* 79−4165
Tokamak discharge, initial stage, theory *(Russian)* 78−38512

plasma confinement continued
Tokamak discharge, transient behaviour, electrohydrodynamical model 80−48952
Tokamak discharge dynamics, dominated by trapped electron instability 79−55537
Tokamak divertor scrape-off width, mag. perturbation effect 78−59657
Tokamak elliptic, neoclassical transport 78−14135
Tokamak equilib., impurity radn. effect on power balance 77−72465
Tokamak equilib., non-circ. cross section, current peaking effect 78−5916
Tokamak equilibria, with fixed boundaries, MHD stability 78−71477
Tokamak equilibrium, high-β, second order effects 80−70024
Tokamak equilibrium, inverse problem, iterative metric method 80−106883
Tokamak experimental power reactor, burn cycle dynamics, confinement scaling laws and heating 77−23263
Tokamak experimental results, review 79−98968
Tokamak experiments and apparatus, review 79−98967
Tokamak expts. survey, apparatus, techniques, containment times, plasma instabilities 78−59662
Tokamak fusion devices, likelihood of success 80−52784
Tokamak fusion power generation 78−74472
Tokamak fusion reactor, RF injection for refuelling and impurity control 80−87921
Tokamak fusion reactor, TFTR, plasma generation and confinement 80−42864
Tokamak fusion reactor, wall bombarding high energy α-particle characts., drift *(Russian)* 77−47214
Tokamak fusion reactor plasma, trapped α-particle cyclotron instability 79−73024
Tokamak fusion reactors, doublet research, plasma shape control, MHD stability 80−28837
Tokamak fusion reactors, neutral beam driven, physical basis and engineering parameters, review 77−54360
Tokamak fusion reactors, plasma modelling and first wall interaction phenomena 77−30660
Tokamak fusion reactors, refuelling pellets, self-propulsion force exerted by anisotropic ablation 80−106969
Tokamak Fusion Test Reactor, conceptual digital computer control systems 77−23281
Tokamak generated W radiation, Ag I isoelectronic sequence identification 80−83981
Tokamak high beta stability 80−96383
tokamak impurity-control techniques 80−75082
Tokamak internal disruption development mechanism, mag. island growth, simulation 78−26317
Tokamak limiter, surface observation, infrared techniques 80−38693
Tokamak limiter surface temp. meas. 79−98984
Tokamak liner destruction model, by runaway electrons, nonlinear dynamics 77−84481
Tokamak LT-3, hollow current profile form. 77−72500
Tokamak LT-3, plasma rot. meas. by Doppler shift of spectral lines 79−19087
Tokamak magnetic confinement, recent progress in Tokamak expts. for fusion energy prod., review 79−71948
Tokamak magnetic confinement expts., conf. summary 77−76172
Tokamak magnetic confinement theory, conf. summary 77−76173
Tokamak modes, MHD theory, drift effects *(Russian)* 79−37477
Tokamak orbits, topology 80−28806
Tokamak plasma, extreme UV impurity study, radiation power loss 78−42803
Tokamak plasma, LF electrostatic instability in cylindrical collisionless plasma 79−10696
Tokamak plasma, light-impurity-free plasma, Au-shell surface and Ti gettered burial chamber 78−42786
Tokamak plasma, Pulsator I, disruptive instability, origin 77−43026
Tokamak plasma, Pulsator I, high density, props. and stability 77−43025
Tokamak plasma, real and simulated, impurity behaviour 78−94128
Tokamak plasma, resistive ballooning mode eqn. 79−14597
Tokamak plasma, RF driven electron currents for confining poloidal field 78−91145
Tokamak plasma, vertical stability, finite cond. effects 79−4162
Tokamak plasma equilib. by finite elements, book contrib. 79−32805
Tokamak plasma equilibrium, feedback control 78−55738
Tokamak plasma isolated from limiter by pulsed multipole field 79−19071
Tokamak plasma model position control model 80−92383
Tokamak plasma transport codes, neutral atoms 79−98875
Tokamak plasma-wall interaction, appl. of fluoresc. spectroscopy 79−23451
Tokamak plasmas, advanced-fuel, ignition and thermal stability 80−86970
Tokamak plasmas, turbulent heating by runaway electron beams, plasma instability 79−73020
Tokamak power plants, impact of technology and maintainability on economic aspects 80−27807
Tokamak radial transport, scrape off effect 79−90443
Tokamak radiation, near plasma freq., three-wave mechanism 79−37464
Tokamak radiation and Kadomtsev-Pogutse instability 79−37463
Tokamak reactor, impurity control, divertor and gas blanket model 79−90445
Tokamak reactor, short-pulse D-T, burn phase control 79−86604
Tokamak reactor with high-temperature blanket 80−27809
Tokamak reactor with injection of deuterium and tritium ions, calc. of characts. 78−37447
Tokamak reactors, prod. of noncircular discharge, ohmic heating expts. (Doublet III) 80−52785
Tokamak resistive kink modes, stabilisation of optimised current profiles 77−24069
Tokamak resistive toroidal equilibria, anomalous resistivity and thermal cond. 78−83595
Tokamak short-wave instabilities of trapped electrons 77−19756
Tokamak studies in the USSR 80−74022
Tokamak synchrotron emission and runaway electron distrib., time evolution 77−39447
Tokamak T-4, poloidal field oscills., microwave noise *(Russian)* 78−22536
Tokamak TFR, electron temp. and density relax. 77−51235
Tokamak TM-3, fan anisotropy, accelerated electron distrib. function anisotropy *(Russian)* 79−37476
plasma confinement continued
Tokamak TO-1, feedback system effect on plasma parameters *(Russian)* 80−103174
Tokamak toroidal divertor, weak field perturbation 78−51337
Tokamak toroidal field coils, reduction of bending moments 80−47697
Tokamak transport codes, present status 79−98874
Tokamak with destroyed mag. surfaces, electron thermal conductivity 78−30411
Tokamak with field-shaping coil systems, MHD equilib. 78−94930
Tokamak with horizontally elongated cross sections, equilib. and stability 78−75405
Tokamak with magnetic limiter, positional instabilities 77−11386
Tokamak with non-circular cross-section, ballooning modes, stability *(Russian)* 80−103141
Tokamak with vertically elongated cross sections 78−94931
Tokamak-4, electron density and temp. distribs., q=5.4 stability margin mode *(Russian)* 77−47240
Tokamak-fusion reactors, He exhaust 80−75084
tokamak-like equilibria at beta close to unity 80−19604
Tokamaks, Alfven nonlinear gravit. drift waves and β limitations 80−92369
Tokamaks, arbitrary cross section, high-β equilibria categorisation 79−64888
Tokamaks, computer simulation of trapped electron modes 80−106874
Tokamaks, CT-8, mag. field design *(Chinese)* 80−43995
Tokamaks, elongated, axisymm. MHD stability 78−86683
Tokamaks, energy confinement scaling, Frascati Torus results 80−79536
Tokamaks, high-β, expt. and comp. studies 80−23128
Tokamaks, high-beta, heating, confinement, dynamics studies 80−24218
Tokamaks, injected ion loss due to spatial field ripple 80−92321
Tokamaks, kink and tearing modes 79−98910
Tokamaks, lower hybrid heating, simulation using BALDUR 1-D transport code 80−92339
Tokamaks, lower hybrid resonance cones 80−28791
Tokamaks, LT-3 and LT-4, plasma physics research at the Australian National University 79−99003
Tokamaks, magnetic islands, tearing modes 80−28846
Tokamaks, merging, model 79−60166
Tokamaks, MHD stability and reactor requirements 79−98911
Tokamaks, neutral-beam injection, USA research 80−27808
Tokamaks, nonlinear drift tearing modes 80−53971
Tokamaks, position instability analysis, effective mode approx. 80−103145
Tokamaks, transport computation, heating, treatment of neutral gas, and impurities, review 79−98966
Tokamaks, transport losses, computer modelling and scaling 80−28612
Tokamaks, TUMAN and TOSCA, minor radius compression expts. 77−68820
Tokamaks of arbitrary cross section, wall stabilized high β equilibria 77−84477
tokamaks with elongated cross section, MHD stability 79−90441
Tokamaks with iron core transformer, self-consistent MHD equilibria 80−19608
Tokapole II, poloidal divertor, plasma production and confinement studies 80−18602
Topolotron, plasma cross section reconstruction, Farey dissection optimization, computer anal. 77−84523
Tormac, Gaussian HeII 4686 Å spectral lines, Doppler and Stark broadening effect, turbulence 80−106980
Tormac DT fusion reactor, power gain and net output 78−58402
Tormac toroidal line cusp theory, research at Princeton Univ. 77−24160
toroid, alpha-particles anomalous diffusion in nonlinear trapped-ion regime 77−11319
toroid, anomalous transport model in high density regimes 77−11389
toroid, ballooning mode topology 78−5917
toroid, cold plasma blanket, collisional transport model 77−72466
toroid, dissipative trapped ion instability, nonlinear stabilisation 77−11331
toroid, electron beam landing on equilib. orbit 77−68850
toroid, energy principle and kink instability 79−10650
toroid, geometrical effects on turbulent diffusion 79−27751
toroid, high mode number plasma stability 79−19072
toroid, ion-acoustic instability, current-driven, quenching in trapped electron regime 77−31460
toroid, laser prod. and heated D plasma 77−76152
toroid, lower hybrid decay ray trajectories 79−19022
toroid, magneto-acoustic oscills. 79−19026
toroid, nonlinear axisymmetric equilibria in MHD approx. 78−18437
toroid, ohmic heating current effect on confinement time 77−68854
toroid, with self-consistent electric field, equilib. plasma config. *(Russian)* 78−22537
toroid equilib. and stability, computational method, book 79−14601
toroid with vanishing press. grad., MHD stability 78−14195
toroidal, axisymmetric, guiding-centre simulation 77−27713
toroidal, azimuthal plasmal rot., classical transport processes, hydrodynamic eqn. *(Russian)* 80−33746
toroidal, edge cooling by super-banana limiter, injected impurity beam orbits 80−43940
toroidal, equilib., external analytic solns., Wangerin transform calcs. *(Chinese)* 78−91136
toroidal, overlapping and stochasticity, critical limits 80−59268
toroidal, supplementary heating, France, review 77−24101
toroidal axisymmetric equilibria, particle diffusion by mag. perturbations 80−14927
toroidal axisymmetric hybrid system, plasma equilib. 77−11387
toroidal bicusp (Tormac), plasma containment, props. 77−24159
toroidal cavity partially filled with anisotropic dissipative plasma, wave excitation from antenna 77−24097
toroidal config., peeling stability criterion 79−98953
toroidal confinement system, excitation of reson. 79−90406
toroidal cross section, α-particle confinement 80−1828
toroidal devices, electron runaway prod., kinetic eqn. 78−47148
toroidal diffuse equilib. config., pinches, Tokamak 78−30471
toroidal diffusion, ambipolarity paradox 78−63547
toroidal diffusion vel., fluid inertia effect 79−4113
toroidal discharge, adiabatic compression heating 77−68821
toroidal discharge, dynamic stabilisation in weak longit. mag. field *(Russian)* 78−87476
toroidal discharge, minimum energy state 80−44058
toroidal discharge stability, conducting viscous fluid model 77−24127
toroidal discharges, equilib., generalised energy principle 77−43039

plasma confinement continued
toroidal equilib. anal., azimuthal symmetry, second order inverse aspect ratio effect 77−43052
toroidal equilibria with z asymmetric cross section 79−82087
toroidal equilibrium, MHD stability to axisymmetric modes 77−76176
toroidal equilibrium, noncircular sharp boundary plasma pinch form. 77−24166
toroidal equilibrium of stationary plasma flow 77−55162
toroidal field, D-shaped and circular coils stress distrib. 77−3974
toroidal field coil, 10 Tesla 77−27692
toroidal filament, stabilisation of current instabilities by feedback method *(Russian)* 77−76185
toroidal high-β plasma, liner compression 77−26877
toroidal mag. field, computer simulation of electron clouds 77−27715
toroidal mag. field, thermal cond. with stochastic inhomogeneity *(Russian)* 80−83973
toroidal magnet for FINTOR 1 fusion reactor 77−27694
toroidal magnetic configuration calc., with modified spatial magnetic axis *(Japanese)* 77−89283
toroidal magnetic confinement, progress, rel. to fusion reactor requirements 80−59261
toroidal magnetic field, new lens system 77−67535
toroidal magnetic system, impurities, cleaning methods 78−22546
toroidal MHD configuration, equilib. and stability near mag. axis 77−11390
toroidal MHD stability, complex mag. configs., Mercier's criterion 77−89289
toroidal multipole, nonlinear plasma diffusion 77−68751
toroidal pinch discharge, preionisation phase, numerical computation 80−64696
toroidal pinch equil. config., nonlinear operator eqn., optimisation soln. 78−59649
toroidal pinch experiments, using perforated shell-type coil 79−86598
toroidal plasma, bumpy, radial DC elec. field on particle transport 78−59646
toroidal plasma, classical diffusion 78−71443
toroidal plasma, compression, appl. of plasma focus device 80−43996
toroidal plasma, convective cells and transport anal. 80−24229
toroidal plasma, criteria for stability of surface preserving modes 79−14591
toroidal plasma, eigenvalue problem and nonlinear evolution of kink modes 80−24234
toroidal plasma, He^{2+} confinement, optimisation of axisymm. config. 79−10697
toroidal plasma, internal kink mode 78−91144
toroidal plasma, magnetised, steady current generation by RF travelling field 77−11313
toroidal plasma, rapid thermal transport from turbulent skin layer to core 78−59659
toroidal plasma, resistive MHD mode and sawtooth oscill., nonlinear evolution 80−24235
toroidal plasma, sharp boundary, MHD stability 77−11385
toroidal plasma, sharp boundary, wall stabilisation 78−42788
toroidal plasma, slide-away regime, quasilinear theory 79−98960
toroidal plasma, trapped-electron instability, numerical simulation 78−94933
toroidal plasma, vertical displacement instability *(Chinese)* 80−1824
toroidal plasma column, general soln. of linear equilib. eqn. *(French)* 77−89284
toroidal plasma compression, computer model, appl. to topolotron 77−15233
toroidal plasma compression by imploding plasma liner 80−33811
toroidal plasma in high β Tokamak, struct. of force-free mag. fields, equilib. model *(Japanese)* 79−82086
toroidal plasma MHD stability, mag. axis curvature modulation effects 77−84487
toroidal plasma with applied electric fields, confinement optimisation 78−9821
toroidal plasma with nonplanar mag. axis, MHD equilib., diffusion 77−84486
toroidal plasma-containing system, EM oscill. spectrum 80−79471
toroidal plasmas, equilib. energy principle with global invariants 80−92366
toroidal plasmas, nonlinear heating by lower hybrid waves 79−90422
toroidal plasmas, theory of neutral injection heating 79−98938
toroidal reactors, confinement scaling, effect on economy and unit size 80−13860
toroidal relativistic electron beam ring, equilib. config. 77−65906
toroidal resistivity calc. 79−98965
toroidal shells, conducting mag. field 77−3514
toroidal solenoids, helically wound, form factor calcs. 80−100091
toroidal stellarator, longit. current in plasma, mag. surfaces *(Russian)* 77−39450
toroidal stellarator, single particle motion, computer code 80−28818
toroidal SURMACS, high-β plasma confinement 79−7473
toroidal system, low density plasma electrostatic pot. 77−80340
toroidal system, low-collisionality regime, particle/energy confinement times, β-depend. 78−75409
toroidal system, MHD plasma control by feedback and HF fields 80−28781
toroidal system, trapped particle instability, shear stabilisation 77−68848
toroidal systems, gradient B drift instability 77−62391
toroidal systems, magnetic field topology 77−19757
toroidal trap, filling with laser plasma 77−76153
toroidal trap, MHD stability in near-axial region *(Russian)* 78−38521
toroidal trap, plasma rot. effect on neoclassical transport of impurities *(Russian)* 80−83972
toroidally confined plasma, intense relativistic electron beam heating, and electron beam trajectories 78−63572
toroidally linked mirror system, ballooning instabilities 78−22542
torroidal equilibria, highly elongated axisymmetric, MHD stability, numerical anal. 77−43049
torsatron, superconducting mag. engineering design 80−99297
torsatrons, mag. surfaces, particle orbits, neutral injection 80−79551
torsatrons, toroidal vacuum fields, particle orbits 80−79445
TORTUR II, turbulent skin heating of toroidal plasma 79−98992
TORTUR toroidal device, plasma confinement and skin currents 77−76180
torus, axisymmetric, MHD intercharge modes, anisotropic press. effects 77−15230
torus, drift wave eigenmodes, nonlocalisation by mag. shear 78−34302
plasma confinement continued
torus, effect of elliptical cross-section on collisionless trapped-particle instability 77−39417
torus, modified bumpy, equilib., stability 77−72475
torus, self-consistent electrostatic field calc. 78−42789
torus, trapped ion mode driven by ion mag. drift reson. 77−31452
torus plasma, fluctuation induced particle transport, strong DC elec. and mag. fields 77−89322
torus with three coil arrangements, simulation 78−18434
TOSCA Tokamak, plasma shape and position meas. 79−73039
transition from Pastukhov to collisional confinement in a magnetic and electrostatic well 80−103181
transport processes in toroidal stellarators and torsatrons 79−90381
transverse convective ion transport in Tokamak, kinetic description 80−6214
trapped ion mode, ion motion, overlapping bounce resons. effect 77−76069
trapped particle anomalous transport in Tokamak, scaling laws 80−103115
trapped particle modes, HF pump effects 77−31499
traps with helical mag. axis, neoclassical diffusion 77−31430
travelling magnetic field use in equilibrium control 77−19758
Tuman 2, adiabatic mag. field, compression heating, ion energy balance 77−51238
turbulent plasma in toroidal plasma, optical diagnostics and thermal transport 79−73023
two-stream plasma, thermalisation *(Russian)* 79−4119
ultra-high current carrying column, generalised Bennett equilib. and particle orbit anal. 78−83598
ultra-high-current plasma column, electron collisionless motion 79−64824
ultrahigh vacuum tranfer system, 15 cm diameter, for remote plasma-wall interaction expts. 80−86327
US magnetic fusion program, survey 80−91249
Vlasov equilibria, local Maxwellian velocity distribution 80−87928
Vlasov-Maxwell equilibria, exact solns. with sheared mag. fields 77−3977
VLF heating methods, thermonuclear prospects, review 80−28738
wall confined shock heated fusion reactor, design 80−99314
wall layer kinetic theory for weakly ionised plasma 79−1330
wall-confined liner-compressed plasma, transport calcs. 78−63546
wall-plasma interface region, cross field thermal losses, simulation 78−59609
wave trajectories and electron cyclotron heating in Tokamak plasmas 80−83923
waveguide, confinement by high power excitation 77−31497
weak magnetic fields, B=0 pts. *(Russian)* 77−3978
weakly-ionised plasma, magnetised, unstable oscillations, influence on radial electric field *(Russian)* 80−103175
weakly-ionised plasma diffusion in apparatus with spatial axis *(Russian)* 80−1826
Z-pinch turbulence spectroscopic detection and anal. *(Russian)* 80−100098
Zeta plasma, field line reconnection and density fluctuations 80−69975
ZT-S reversed field pinch simulations 80−83993
Al_2O_3, limiter and liner, results in Tokamak Petula 79−655
Ar full circle arc, mass flow field investig. 80−38797
Ar, ion confinement and heating, by negative plasma potentials produced by supplemental electron emission 79−41861
$Ar^{16,17+}$ filled glass shell, symmetric laser compression 80−64759
B_xH_y compounds, doubly-isotopic, laser driven nuclear fusion, energy release 78−78499
Ba^+ ion cloud containment in RF trap, <50 ions, optical sideband cooling 78−75407
Cd laser produced plasma recombination laser, power output enhancement by plasma confinement 80−63989
D diffusion studies by pulsed injection in Tokamak plasma 80−28611
D plasmas, laser prod., interaction with mag. fields 77−76151
D-^{3}He, confined by levitating supercond. ring, neutron effects 80−47715
D-D fusion reactor plasmas, pure and catalysed, thermal stability 80−24207
D-T linear mag. fusion device, particle end loss reduction 78−33289
D-T Tokamak, high-density, ohmically-heated, transport calcs. 80−24142
D-T toroidal plasma, steady state, thermally self-sustained by thermonuclear fusion reaction 77−83080
D_2 fusion reactors, catalysed, power balance calc., plasma confinement 80−42847
D_2-filled cone, fusion neutron generation using explosive implosion of polyethylene shell 78−82510
DT fusion plasma, free expansion hydrodynamics 78−70629
Fe XV, line intensity and linewidths at high electron density, generalised population ratio 80−99481
H, ACT-1 toroidal plasma, externally launched ion Bernstein wave 80−106967
H^+, intense beam generation, appl. to controlled fusion 77−76119
H_2 Tokamak plasma, Doppler temp. and particle confinement time from H_α-line meas. 78−55737
H(D) neutral beam injection expts., PLT and ISX 80−28812
He plasma beam-transverse mag. barrier interaction, collisionless electrostatic shock 77−80339
Ne plasma, compression, spectra, temp. and density calc. model 78−59663
Ti spongy metallic protective gettered coating for thermonuclear reactor walls *(Russian)* 80−106154
Ti, Tokamak plasma, atomic struct., highly ionized states 80−75086
U plasmas, fissioning, for space vehicle power, propulsion, terrestrial appls. 77−3145
UF_6, high temp. fissioning plasma core reactors, fluid mechanical confinement 80−63248
UF_6, plasma confinement expts. appl. to plasma core reactor 77−23190

plasma containment *see plasma confinement*

plasma density
acoustic wave interaction, diagnostics appl. 78−83541
adiabatic compression in multistage heating cycle causing increase in plasma density 79−98937
afterglow, diffusion controlled, density decay 79−7442
afterglow, electron energy distrib., radial variation 78−71570
air, flowing, glow discharge, negative ion density increase with press. 80−28821
air, RF discharge, electron temp. and density 78−51371

plasma density continued
air flow in plasma generator, radn. parameters meas. 79−68952
air-water vapour mixture, electron conc. and conductivity behind strong shock wave 80−48890
Alcator high density Tokamak, ion temp. profile reconstruction *(Russian)* 80−106959
Alcator tokamak, low q operations 79−60173
Alcator Tokamak high-density discharge, parameters for D_2, neutron emission 78−18438
alpha-particle heating in high density D-T plasma 80−28735
ambipolar electron and ion diffusion in collisional plasma in RF electric field 80−6220
angle and polarisation dependent intense light absorption, theoretical interpretation 78−59638
anomalous conductivity and electron heating, in two-stream unstable plasma 80−6219
anomalously resistive phase, spiky density fluctuations and relax oscill., microwave scatt. obs. 80−38547
Ar, plasma rotating, weakly ionised, diagnostics 79−82122
arc, density and temp. meas. 78−1937
arc, electron density determ. by IR laser transmission meas. 79−7491
arc, plasma parameters, probe and spectral meas. 80−24273
arc plasma, atmospheric, electron density meas. by two-wavelengths interferometry *(Japanese)* 80−38720
arc plasma, low-temp. diagnostics by scatt. and resonance fluorescence 78−67482
arc plasma, stabilised by N_2 injection through porous wall, thermodynamic nonequilib., plasma parameters 79−86629
astrophysical plasma, highly ionized, ionization equilib. validity 80−21906
asymmetric electron density profile, interferometric meas., laser-created plasma 80−75085
at. emission obs. of plasma props. 80−19021
atmospheric pressure plasma flow, boundary layer charged particle density profiles 80−38571
automatic recording system of probe meas. for plasma parameters *(Japanese)* 79−41870
background plasma density minimum for plasma-grounded electron beam targets 77−7564
beam-plasma discharge, characts. in crossed elec. and mag. fields *(Russian)* 80−10396
beam-plasma instability, one-dimens. kinetic, in fluctuation plasma 79−32784
belt pinch, shock heated weakly compressed high-temp. plasma 77−24164
Belt Pinch IIa, transport phenomena, density profiles 80−24219
belt pinch plasma, electron density profile, multichannel laser scatt. diagnostics 77−31514
Berkeley multifilament ion source, plasma characts. 79−94807
breakdown, ionising wave propag. mechanisms 80−83941
Brillouin backscatt. depend. on density scale lengths near crit. density 80−43888
broadening of free-bound radiation thresholds, expt. results for Cl^-, I^- and Br^- 80−53940
bundle divertor, Tokamak plasma, scrape off layer density decrease, model 80−28851
capillary discharge, with evaporable wall, plasma parameters axial distrib. *(Russian)* 78−75280
capillary discharge with vaporising wall, plasma parameters axial distrib., model 79−64943
caviton dynamics at crit. density 80−106909
caviton generation in plasma reson. region *(Russian)* 80−53926
cavitons, highly nonlinear states in plasmas, expt. obs. 80−6233
cavitons in laser irradiated fusion plasmas, EM wave propag., supersonic density humps 80−24178
charge carrier density, enhancement by probing RF voltage signals 77−58891
charged particle density, mag. field effect *(Russian)* 78−22552
classical plasma dynamics 80−83888
coaxial cylindrical discharge tube, diffusion plasma column density and pot. distribs. 79−41797
coaxial plasma source, optical meas. 78−1895
coherence function concept extension to quadratic models 79−72987
cold mantle, density scaling laws 80−83889
cold plasma, density short wave perturbation, elastic electron-atom collision 78−47119
collective plasma density fluctuations, far IR scatt. apparatus obs. 79−32818
collisional plasma charge density diagnostics using single Langmuir probe 79−50888
collisionless flow and end loss from a high-energy theta-pinch plasma 80−92365
collisionless plasma, hydrodynamics, decay of initial density discontinuity *(Russian)* 77−3921
collisionless plasma expansion and fast ion generation at plasma-vacuum boundary 80−59257
column, diagnostics by TE_{0mn} reson. cavities, geom. factors 77−15237
column, magnetised, electron density and electron collision freq. determ. by coil probe method 77−1016
column, scattered microwave pattern meas. 77−35384
column compressed by mag. field, multichord corpuscular diagnosis *(Russian)* 79−4190
column electron density radial profile, modified laser interferometry 78−67429
combustion product plasma, electron conc. and mobility determ. by HCN laser submillimetric interferometry 78−1889
conducting sphere in quiescent slightly ionised plasma, exact solution 79−86564
confinement of LiH plasmas, decay, density measurement 79−46470
conical waves from scatt. laser radiation, pot. electron density determ. *(Russian)* 78−59667
continuous optical discharge, diagnostics 80−43947
continuum, flowing (nonflowing), mass discrimination effects in ion extraction 77−63979
corona, discharge pulses, field strength and electron density calcs. 80−38814
corona, laser induced microsphere, electron density profile, interaction and transport profile 80−107008
corona discharge, electron density meas. by microwave resonant cavity method 77−68881
plasma density continued
critical density surface, CO_2 laser radiation reson. absorption and surface instability 80−48859
critical surface density profiles, radial stability 79−55460
current density, local, mag. probe and Thomson scatt. meas., using Spitzer-Harm distrib. 78−18451
current layer, electron and density distribs. holographic interferograms *(Russian)* 77−47257
current sheet, near line of zero mag. field, numerical anal. *(Russian)* 80−83908
current sheet generation in rarefied plasma, mag. flux plasma trap appls. 80−38698
cyclotron harmonic waves props. from perpendicular dispersion relation 80−38612
cyclotron self-absorption in two-temp. plasma, temp. and density meas. 80−48987
D-T plasma model, uniqueness and linear stability of operating points 80−14897
DC arc plasma, alterations in spectral line intensities due to external mag. fields 80−79621
DC arc plasma, axial mass transport, added particle distrib. 79−86640
Debye screening modifications in ponderomotive effects 80−33777
deexcitation wave emission and thermal fluctuations of inhomogeneous plasma *(Russian)* 80−106892
dense, X-ray emission diagnostics in hypocycloidal pinch 77−43051
dense plasma, diagnostics of two-wavelength optical absorpt. 79−98978
dense plasma focus, ruby laser holographic diagnostics *(Japanese)* 80−100097
dense plasma ionisation and cohesion, critical density and press., approx. formulas 80−59253
density meas. by interferometer 78−55748
density rise model and ion mixing mode in confined plasma 78−79409
determination of equilib. density using magnetoacoustic oscills. in diffuse pinch 80−48986
diagnostic technique, CW Ar laser, radiation scatt. 78−38536
diagnostic technique using self reversed deuterium D_α line 78−55746
diagnostics, laser beam-ion acoustic wave interactions, excitation and interference 78−34326
diagnostics, scattered radiation intensity fluctuation method *(Russian)* 80−14932
diagnostics by laser light scatt. *(German)* 77−7599
diagnostics by short-circuit effect 79−23460
diagnostics using mutual and self impedance meas. *(French)* 78−14208
dielectric response function, density fluctuations effects 78−30413
dielectron recombination, electron density effect *(Russian)* 79−98856
diffuse pinch, energy equilib., classical scalar cond. and neo-classical models 80−24208
diode, high-current, ion effects on electron storage *(Russian)* 77−7600
discharge, electron density and temp. profiles, Langmuir probe meas. *(French)* 78−30482
discharge, grazing, incomplete gas temp. and electron density diagnostics 79−55600
discharge, HF, self-acting field effect on spatial distrib., appl. to He *(Russian)* 79−99007
discharge, pulsed, density perturbations, laser beam diagnostics 79−7498
discharge, pulsed ionisation initiated, non-self-maintained, instability 79−86572
discharge, RF, gamma regime, ionis. balance and plasma characts., model 80−44022
discharge, running striation excitation, metastable atoms lifetime influence 80−38760
discharges, high current, press., conductivity meas. 80−38793
dispersed heterogeneous system, electron conc. calc. method 78−38452
distribution function, probe meas., ionis. wave irregularity effect 77−47255
distribution meas., using Michelson interferometer *(Japanese)* 78−42820
DITE bundle convertor, density meas. 80−92373
DITE phase II neutral injection system investig. 80−28814
DITE Tokamak, beam driven current meas. 80−106940
DIVA, scrape off layer, multigrid energy analyser applications 80−33818
double layers, stability, density criterion 79−68931
double layers from ion acoustic instability numerical simulation 80−59220
double-layer, steady-state, fluid theory 80−43873
Doublet III, plasma density, shaping and characteristics 80−74018
drift cyclotron loss cone mode, warm plasma effects 79−68904
drift instability stabilisation by RF elec. field in inhomogeneous plasma, kinetic theory 79−55536
drift wave instability, due to nonuniform density gradient in sheared mag. field 79−23415
drift-dissipative waves, weakly ionised plasma, column steady state 80−38613
dual laser interferometer for plasma density measurements on large Tokamaks 78−71542
ECR as a diagnostic for mirror trap plasma 80−38709
eigenmodes, universal, in collisionless plasma slab 80−38581
electrode contact processes, microplasma diagnostics 80−59325
electrodynamic mechanisms of limitation of the electron concentration in a laser spark *(Russian)* 80−59333
electron, microwave p-i-n diode modulator, transient plasma instability meas. *(German)* 80−87942
electron, Thomson scatt. meas. in JIPP T-II device 79−23461
electron and at. excited states densities in laser prod. He plasma 80−38710
electron and ion density control methods for Tokamak 78−47145
electron beam, relativistic, intense, rot. in plasma, μs microwave radiation bursts 79−73018
electron beam, relativistic, stationary state in ionised gas, force-free motion 79−13887
electron beam, relativistic, with inhomogeneous ion density, self-consistent model 80−43247
electron beam controlled discharge, cathode density waves 80−38798
electron beam fusion compression targets, fuel preconditioning studies 79−81076
electron beam stabilised mirror confined gas, hot electron population study 80−100089
electron beam-neutral gas interaction, SEEBIE expt., Thomson scatt. diagnostics 77−24111
electron conc. determ. from EM wave propag. *(Russian)* 79−4150

plasma density continued
electron concentration balance in wave field, profile stabilisation *(Russian)* 78−22497
electron cyclotron emission in ALCATOR Tokamak 78−5935
electron cyclotron frequency sub-harmonic effect on wave absorpt. in Tokamak Thor 80−28686
electron cyclotron heating in Tokamaks: experiments and prospects 80−28749
electron cyclotron heating rate, density depend. 79−10678
electron densities from Thomson scatt. and He-Ne laser interferometry 79−86615
electron density, determ. by spectral line width, at oscill. strength effects 77−51230
electron density, determ. from He I Stark widths and He-Ne laser interferometry 77−80374
electron density, interferometric meas. 78−67479
electron density, meas, in unmagnetised plasma, self-oscill. probe method 80−19611
electron density, meas. using three-laser intercavity interferometer 77−80357
electron density, multi-pulse ruby laser recording of temporal evolution by light scatt. 80−14938
electron density, spectroscopic meas. during arc discharge extinction *(French)* 77−80361
electron density and mag. field meas. by far IR polarimeter-interferometer 79−32817
electron density and temp., adiabatic toroidal compressor, power balance anal. 77−51219
electron density and temp. distribs., Tokamak-4, q=5.4 stability margin mode *(Russian)* 77−47240
electron density determ. by CO_2 laser 90° collective scatt. 78−67433
electron density determ. by globally convergent method for partially ionised plasma 80−53929
electron density determ. using microwave interferometers, modulated transmission and reflection types comparison 79−37546
electron density distrib. in focus device 79−10711
electron density distrib. meas. *(Russian)* 78−22550
electron density fluctuations, homodyne method with CO_2 laser 79−68957
electron density fluctuations in cold plasma, effective dielec. permeability *(Russian)* 80−32882
electron density in high-temp. gas flows, homodyne multiray interferometer technique 79−86609
electron density meas. by EM wave propag. in magnetised plasma column 80−43974
electron density meas. by far IR laser beam deflection 80−48966
electron density meas. by far IR laser beam deflection 80−59296
electron density meas. by two-freq. band microwave interferometer 80−83890
electron density meas. in shock generated plasma by light interferometry 80−48981
electron density meas. in vac. arcs at anode spot form. threshold 79−55552
electron density profile determ. by neutral beam probing 79−4186
electron density profile evaluation from integrated meas. 79−77418
electron density variation influence on excitation temp. in rapidly varying plasma 80−38537
electron distribution function, meas. by direct differentiation of probe charact. 77−68860
electron energy distribution 78−67465
electron heating due to MHD shock wave, electron temp. and density 79−14588
electron oscillation in radial potential well effect on beam interactions *(Russian)* 80−14912
electron plasma, finite-length thermal equilib. 79−32801
electron plasma, impurity screening effects in intermediate degeneracy region 80−14882
electron plasma wave, finite amplitude, nonlinear behaviour, sideband instability, electron distrib. function 78−38480
electron standing wave, stationary density variation 77−76065
electron temp. meas., continuous, automatic, using double Langmuir probe 80−43977
electron temperature and density for plasma parameters typical for tokamak boundary region, meas. method 79−55560
electron temperature and density in Ar behind reflected shock waves 80−38549
electron temperature and electron density in low density magnetised plasma by probe method 80−48848
electron vel. distrib. in reflex discharge, Thomson scatt. meas. 78−34368
electron wave, guided, on planar plasma slab, propag. and attenuation charcts., dissipative processes 80−38608
electron-beam-sustained discharge, plasma contraction by mag. field of current 80−100115
electron-density structures in laser-produced plamas at high irradiances 79−82041
electron-ion anomalously fast energy transfer, relativistic electron beam magnetoplasma heating 78−38515
electron-positron counterstreaming beams plasma, relativistic, radiative collapse to ultrahigh densities 79−60188
electronic multiplication in nonuniform elec. field 79−86559
electrostatic confinement in EM trap, ion current decay *(Russian)* 80−79543
electrostatic plasma-confinement experiments in a tandem mirror system 80−70025
electrostatic probe meas. 77−39464
electrostatic turbulence, variable density and pressure, two-fluid model and geostrophic approx. 80−53986
ELMO bumpy torus, collisional regime, radial transport 79−41801
ELMO Bumpy Torus, electron cyclotron heating, density and temp. 80−28780
EM emission around plasma freq. induced by relativistic runaway electrons, effect of plasma density inhomogeneity 79−82065
EM macroparticle acceleration, high press. gas temp. density 80−79583
EM oscill. spectrum, toroidal plasma-containing system 80−79471
EM pulse, conversion to Langmuir wave in plasma 80−92308
EM resonant properties of laser-prod. plasmas 80−43928
EM wave interaction, density profile steepening at reson. absorpt., hydrodynamic model 79−46434
EM wave resonant absorption, due to DC mag. field parallel to density gradient 80−19563
EM wave self action during modulation instability *(Russian)* 80−14905
plasma density continued
EM wave self-action during thermal modulation instability of high hybrid oscills. *(Russian)* 80−53980
EM waves incident on warm plasma half-space dual propag. and absorpt., density and temp. depend. 80−75048
equilibrium and transport in 2+*e*-dimensional two-components plasmas 79−55470
equilibrium in highly collisional toroidal regime 80−28796
estimation method for electron temp. and density in ^{3}He plasma and ^{3}He-Ar plasma 80−64785
excited atoms population distrib., electron-density variation influence 78−87431
expansion into vacuum, ion acceleration 80−6228
exploding liner gas confinement, liner velocity effects 80−79541
explosive magnetic field generation due to EM incident radiation, laser plasma mechanism 80−6253
F-150 device, multiframe laser interferometry for investigation of plasma dynamics 78−83614
far IR interferometry 78−47183
far IR laser scatt. meas. of nonthermal density fluctuations 80−59297
far-IR emission anal. 77−31521
Faraday rot. meas. in high-β fusion expts., plasma electron density and mag. field determ. 80−49008
Faraday tarotion, effects of pulsewidth 78−71540
fast interferometer diagnostics using N_2 laser 78−87489
fast IR laser interferometry, electronic density fluctuation meas. 80−49000
filament ellipticity, energy lifetime in T-8 apparatus *(Russian)* 80−87930
finite amplitude lower hybrid frequency wave propagation, effects *(Russian)* 79−55489
first wall materials, effect on Tokamak plasmas 80−38692
fission reactor, gas-discharge, fuel element component conc., plasma temp. profile instabilities 80−63253
flame, diffusion type, oppositely directed jets, elec. props. 78−56896
fluctuation amplitudes in mag. mirror device, microwave meas. 77−3985
fluctuation evaluation by microwave interferometry 78−67437
fluctuation of density in collisional plasma 80−75053
fluctuation spectrum 78−18377
fluctuations, collective spectrum 77−47148
fluctuations, laser heterodyne meas. 77−15246
fluctuations, microwave scatt. 79−98985
fluctuations, microwave scatt. obs. 80−48851
fluctuations associated with EM wave nonlinear quasioptics in DC mag. field *(Russian)* 79−98914
fluctuations in ATC Tokamak 77−43074
fluctuations meas. by laser scatt. from turbulence 77−39469
fluctuations of density, one-component plasma, mode-coupling theory 79−23398
fluctuations study by small angle CO_2 laser scatt. 80−59285
focal region of intense laser beam in tenuous plasma, spatial and temporal electron and ion density variations 80−53989
focus, Mather-type machines, temp., density, neutron and X-ray emission charcts. 77−24184
free electron recombination, arbitrary nonequilibrium stationary distribution calcs. *(Russian)* 80−53947
FT Tokamak, non-thermal electron distrib. function 80−83891
FT-1 Tokamak, discharges in low density plasma *(Russian)* 80−106958
FT-1 Tokamak, electron density and temp. radial distrib. laser scatt. obs. *(Russian)* 78−59666
fusion mirror reactors, finite orbit treatment of plasma buildup 80−37631
fusion possibilities and plasma confinement and interactions in mag. config. Tokamak, review *(French)* 80−54017
fusion reactor, gas insulated plasma boundary layers, ballooning modes stability 80−10415
fusion reactor lower hybrid heating, nonuniform density, particle simulation model 78−14185
fusion reactors, superheating-diffusion instability, thermonuclear burn 80−32500
fusion system stability and dynamic properties transfer function anal. 79−93825
fusion Tokamak experiments, H(D) recycling model, influence on discharge behaviour 80−10393
fusion-neutron production in D-beam-heated PLT plasmas 80−28807
gas discharge columns with electron prod. and loss rates linear and quadratic in electron density, electron density distribs. 80−96400
gas flow, partly ionised, electron density and conc. meas. method *(Russian)* 77−55172
gas jet target with electron beam heating, plasma density meas. 77−39457
gas stream with dispersive impurity, initial region boundaries, impurity velocities *(Russian)* 80−100069
glow discharge, electric probe diagnostics, sputtering of appl. 78−71537
glow discharge, large amplitude striations, electron conc. variation 77−89342
glow discharge instability in N_2-CO_2 non self sustained ionisation source, mechanism 80−38819
Grill phase tracking during density increase in Tokamaks 80−28762
Hall current and gyroviscosity effect on conducting, rotating viscous plasma stability 80−75041
He I and II radiation enhancement in mag. field, nonlocal thermodynamic equilib. 80−10366
heating in lower hybrid freq. range, temp., ion diffusion 80−83954
heterodyne CO_2-laser interferometer with direct phase readout for meas. electron line densities in plasmas 80−1848
heterodyne quadrature interferometer for simultaneous measurements of plasma density along several chords 78−67416
HF discharge, ionisation overheat instability in EM wave field *(Russian)* 80−106990
HF discharge, plasma density and electron temp. meas. using Langmuir probe *(Russian)* 79−37559
HFS brightness ratios of impurity metal 77−89310
high current relativistic electron beam retardation distance *(Russian)* 80−14911
high density directed plasma, source, design, charcts., numerical model 80−38538
high melting particle heating, melting and vaporisation in hot gas 80−6201
high pressure optical discharges, density and temp. meas. 80−48931

plasma density continued
high velocity jets generated by plasma focus and shock-wave expt., temp. and density meas. *(Russian)* 80−106882
high-density effects on plasma spectroscopy 78−75429
high-density pulsed plasma, laser interferometry 78−67430
highly-dispersed aerosol, nonisothermal, thermionic electron density function determ. 78−91066
hollow cathode arc, plasma column parameters *(French)* 78−9885
holographic study of laser prod. plasma at 10.6 μm 80−38685
hydrodynamic wave description including electron spin 80−38643
ICRF heating in TFR, preliminary obs. and further development prospects 80−28741
ICRF heating optimisation in PLT 80−28742
impedance of magneto-acoustic wave launching antenna 80−24180
implosion plasma, exploded-wire array, X-ray line spectra 79−55457
impulse spark study using two-wavelength interferometry 80−86391
inductively coupled plasma, temp. and electron density, optical meas. 78−67417
inert gas ion laser, high voltage-low press. discharges, stationary props. 80−92400
inert gas mixtures, high-press., collisional radiative recomb. 80−63595
inhomogeneity spreading in weakly ionised current-carrying plasma 78−71445
inhomogeneous plasma, relativistic electron beam propagation effects 78−9797
inhomogeneous plasmas, resonant microwave absorption, nonlinear effects 79−94793
interferometer for density meas., 10^{19}-10^{22} m^{-3}, and simple hydrocyanic acid 0.337 mm 78−5922
interferometry techniques for high β-plasma density meas., holographic and coupled cavity laser methods 80−49006
internal disruption in Tokamak, relax. oscills., self-consistent model *(Russian)* 80−53957
ion acoustic soliton propag. in two-electron temp. plasma 80−33767
ion acoustic waves, linear and nonlinear, cold electron density effects 78−30441
ion beam probe diagnostic system for EBT 77−84513
ion beam-created high-press. plasma, electron props. diagnostics *(French)* 80−10407
ion beam-plasma system wave propag. in cylindrical geometry 80−38592
ion composition of plasma of pulsed discharge in He, H_2^+ current time evolution 80−54046
ion cyclotron resonance heating in multiple mirror machine 77−24108
ion cyclotron wave, in density stratified magnetoplasma, crit. level behaviour 80−6238
ion density and temp., cusp field with RF plugging, appl. thermonucl. plasma 77−76169
ion density fluctuations and vel. distrib. in presence of ion cyclotron waves 79−19090
ion oscillation excitation by freely propagating electron beam *(Russian)* 80−1815
ion pressure discharge theory in the strong ionisation regime 80−38734
ion sheath diagnostics using elastic surface waves *(Japanese)* 77−89266
ion temp. and density meas. in direct current octopole by induced optical fluoresc. 80−14939
ion temperature of low density plasmas by two-probe method 78−55749
ion turbulence in laser heated plasma 78−42807
ion-acoustic holes in a two-electron-temperature plasma 80−59205
ion-acoustic instability, ion tail formation and saturation 80−38610
ion-acoustic plasma turbulence, two-dimensional electron density spectra 78−75479
ion-acoustic turbulence and heat-flux limitation, in laser-heated plasma 78−18453
ion-acoustic turbulence-plasma interactions and electron spectrum in electric fields 80−38617
ion-acoustic wave excitation by two Gaussian laser beams, density profile modification 79−19006
ion-mixing mode and model for density rise in confined plasma 79−98862
ionisation instability mode of plasma accelerator, probe method for electron distrib. function determ. 80−19612
ionosphere, gradient-drift instability, nonlinear effects 80−36455
ionosphere, lower hybrid drift instability 80−46343
ionosphere, nonlinear mixing as a plasma density probe 78−77406
ionosphere, total electron content, ATS-6 radio beacon expt. meas. 77−2303
ionospheric plasma disturbance due to earthquakes and volcanic eruptions 80−36453
ions in steady-state plasma, excited levels population probabilities, asymptotic behaviour 80−79438
JAERI Tokamak, Ti coating for improved plasma characts. 80−24232
jet carrying solid particles, electrophysical props. 80−24134
jets, intersecting, gas-dynamic accel. in compression zone, optical and spectroscopic obs. 77−51247
JIPP T-II Tokamak, current density profile control 80−32493
JIPP T-II tokamak plasma, Mo impurity diffusion during H_2 gas puffing 80−28602
L-2 stellarator, current equilibrium and effective ion charge 80−24228
L-2 stellarator, ohmic heating discharges with gas puffing 80−79593
L-2 stellarator, ohmic heating ion component characts. and particle lifetimes *(Russian)* 78−59547
Langmuir finite amplitude wave passage through plasma wave density barrier 79−86579
Langmuir probe characteristics at low plasma densities, numerical analysis 78−63592
Langmuir soliton excitation by monoenergetic electron beam *(Russian)* 79−77381
large-diameter column, diagnostics by TE_{0mn} reson. cavities, geom. factors 77−15237
laser beam self-focusing, electron density for swelling 77−42985
laser created plasma, interferometer for electron density meas. 80−48983
laser emission intensity reduction near solid target surface *(Russian)* 80−38681
laser fusion, progress at Lawrence Livermore Lab., USA 80−57945
laser fusion expts., tamper temp. and compression, simultaneous proton and α-particle meas. 78−83607
laser interferometer, optoelectronic modulation for electron density variation meas. in IR 80−4762
laser interferometry density meas. on refuelling by solid H pellets in rotating plasma 79−4188
laser irradiated plasmas, flow effects on density profiles 78−18429
plasma density continued
laser light resonant and collisional absorpt., heating, density profiles 78−38527
laser microplasma, electron, atom and ion density determ. *(German)* 77−7588
laser plasma, 1/4 crit. density region, harmonic generation expts. *(Russian)* 77−7578
laser plasma, electron density determ. from X-ray spectra of multiply charged K ions 78−94938
laser plasma, Langmuir probe meas. of parameters and expsn. 78−18456
laser plasma density profile modification by ponderomotive force 78−59634
laser plasma electron density, Stark-broadened line wings of H-like ions 78−79462
laser plasma expansion and rethermalisation in uniform mag. field 78−30458
laser plasmas, wave absorpt. and superreflectivity due to EM struct. resonances 80−24177
laser prod., interferometric exam. 77−3986
laser produced, heated by 10^{-10} sec. pulses, X-ray emission spectra 77−51239
laser produced plasma, structure of XUV emitting regions 80−54038
laser produced plasma density profile meas. using Wollaston prism interferometer 80−48973
laser produced plasma expansion, ion emission, hot, cold electron density, temp. ratios 78−71513
laser radiation, intense, transmission through overdense plasma 79−10671
laser radiation reson. absorption, incidence ang. and polaris. depend. 78−9805
laser spark absorpt. and laser pulse contraction meas. using dye lasers 80−48988
laser spark evolution, thermal wave propag. and shock form. 79−90455
laser target, Monte Carlo (hybrid) suprathermal electron transport 80−24200
laser-compressed plasma, density measurement by X-ray line shift *(German)* 80−48967
laser-imploded target, spatially-resolved X-ray spectra diagnostics 79−37543
laser-irradiated glass shell plasma, electron temp. and density, Si X-ray emission diagnostics *(Chinese)* 80−38718
laser-irradiated plasma, soliton form. at crit. density 80−6267
laser-produced, multicharged He-like ion intercomb. line diagnostics 78−9106
laser-produced plasma, electron density diagnostics by multicharged ion K-spectra, review 79−64908
laser-produced plasma, electron density meas. using holographic microinterferometer 80−43964
laser-produced plasma, ion acceleration in presence of density profile steepening 80−14923
laser-produced plasma, light press. effects, steady-state mdoel 77−47234
laser-produced plasma, supercrit. density modifications due to reson. RF cavity field 79−50875
laser-produced plasmas, microwave diagnostics, electron density 78−9845
Lausanne belt pinch, plasma stability 77−43028
linear electron-ion beams, particle density, longit. mag. field effects 77−50597
linear magnetic solenoid reactor plasmas, dynamic behaviour 80−64751
low-density plasmons, electron temp. meas. by He spectrosc. 80−103192
low-pressure discharge anode sheath in crossed fields, electron density distrib. 78−75424
low-pressure pulsed Hg discharge, props. 79−64916
low-temperature plasma, in mag. field, density, probe determ. 78−67418
low-Z impurities radiation during RF heating in ATC 80−28816
lower hybrid heating in JIPP T-II tokamak plasma, obs. 79−86617
lower hybrid resonance cone propag., density fluctuations effect 78−59583
lower hybrid RF emission, meas. by antenna 78−9852
lower hybrid wave accessibility, effect of density gradient 80−1794
lower hybrid wave excitation, of mirror mag. field plasma 79−19054
lower hybrid wave scattering by density fluctuations 79−94792
lower hybrid wave turning point location, nonuniform magnetoplasma 80−79473
lower hybrid waves, quasi-optical beam self-action in magnetoplasma 80−38657
magnetic driving energy of the collisional tearing modes 80−92301
magnetic field measurement in inhomogeneous plasma, probe laser beam depolaris. effects 78−67411
magnetic mirror, injected plasma particle refl. (trapping), quiescent (turbulent) plasma 80−48955
magnetic mirror trap, open, with min. B, LF oscills. 80−38708
magnetic mirrors, density, increase due to transverse energy increase 79−64889
magnetic pinch discharge, superstrong mag. field prod. 79−90444
magnetic pulse penetration into plasma, theta pinch geometry, Alfven velocity scaling 80−33803
magnetically confined arc, axial density and temp. var. 78−5966
magnetically confined plasmas, expressions for nonclassical energy and particle flows 80−75031
magnetized inhomogeneous plasma, wave reson. and conversion 80−92313
magnetoplasma, nonuniform, simulation, initial particle loadings 79−46473
magnetoplasma, overdense, anomalous penetration of laser radiation, upper hybrid and whistler modes 79−77386
magnetoplasma wave, quasistatic density perturbation, universal formula 79−60131
magnetoplasmadynamic arcjet, density meas. by CO_2, laser interferometry 80−59277
maximum constriction phase of a weakly ionized discharge in helium 79−90486
maximum energy-confinement time in joule-heated Tokamaks 79−37532
measurement, for plasma in EM trap *(Russian)* 78−5944
measurement by HCN laser interferometer 77−39467
measurement by Michelson laser interferometer *(Russian)* 78−38534
measurement by modulated submillimetric laser interferometer 77−39466
measurement by optical density comparison at two freq. *(Russian)* 78−22554
measurement using AM active microwave method 80−87948

plasma density continued
measurement using microwave interference signals from 0 to n.360° phase meas. *(German)* 80−6278
measurement using modulated submm. laser interferometer 77−7586
measurements, via quadrature interferometer 78−1900
metal plasma prod. by exploding wire, X-ray diagnostics 78−5909
metal vapour production by sputtering in hollow-cathode discharge 80−1868
metal vapour-inert gas arc discharges, heavy particle distrib. 80−38782
methane pyrolysis, AC arc discharge plasma temp., electron density meas. 79−87843
MHD accelerator, thermodynamic props., mag. field strength, Hall currents in arc region 77−65917
MHD flow, plane, in hyperbolic mag. field, mag. field line reconnection 79−32755
MHD switch-on shocks, ionis., heating 77−80320
Michelson interferometry diagnostics 78−1890
micropinch in a high-current diode, review 80−103183
microtearing modes and anomalous transport in Tokamaks, self consistent calc. 80−59222
microwave beam interaction, intense, with low temp. plasma flow, space distrib. 80−38578
microwave dynamic interaction, probe diagnostics 80−19584
microwave interferometer for electron density meas. on T-II plasma device 78−55754
microwave plasma, electron density determ. at atm. press. by hot wave method 77−35420
microwave plasma generation at atm. pressure, departure from LTE 78−67597
microwave plasma source, helical slow-down structs., electron density 78−18424
Microwave reflexion in rectangular waveguides by high pressure RF plasma columns 80−43975
microwaves, critical surface phenomena 78−51313
MIGMA IV, stability study of plasma density buildup 79−13522
Mirror-Torus-System-1 with divertor mag. field, plasma density and depolarisation current 80−70022
mixed ion plasma general ambipolar diffusion theory 78−94897
modification in 10^6 W cm^{-2} ablated microballoons, optical diagnostic technique 78−14206
modulated mol. beam of Sn_2, for density and neutral gas press. meas. 77−27735
modulational instability of ion acoustic waves in the presence of density gradients 79−64840
molecular lines role in plasma satellites, H_2 (He_2) obs. 80−44053
multi-chord particle diagnostics of a plasma column *(Russian)* 80−1840
multi-ion system, modulation instability of ion acoustic waves 80−69996
multi-region global transport model for Tokamaks 80−92264
multicharged ion heating in Z-pinch, column compression, temp. and density *(Russian)* 80−64754
multidipole plasma density 78−94929
multifilament plasma source, multipole mag. field effects on characts. 79−46462
multiposition Thomson scatt., determ. of electron density and temp. profiles 80−48977
naphthalene-He photoionis. plasma, CO_2 additive effect 80−10359
narrow inhomogeneous layer, surface wave-incident radiation nonlinear interaction 80−100080
negative ion beam instability spatial development in rarefield gas *(Russian)* 80−92314
negative wave momentum density in plasma 80−79463
neutral atom distribution near wall, temp. grad. effect 80−19555
neutral density meas. from charge exchange expt. 78−91153
neutral density profile, absolute meas. by H_α line reson. fluorescence 80−24250
neutral density profile for Tokamaks 79−14520
neutral injection heating of Cleo stellarator 80−28714
neutral injection parameters and beam line design for TEXTOR 80−28811
neutral-beam-driven current evolution in Tokamak plasmas 80−28712
non-Debye plasma, single electron density of states 78−34264
non-equilibrium, energy density determ. via short-time pulsed probe analyser 77−15240
non-LTE plasma props. and at. processes, medium to high press. 80−59170
non-stationary resonant reflectivity of plasmas, model calcs. 80−14903
noncircular Tokamak, time evolution of elongation ratio and Mirnov oscill. 80−64763
nonequilibrium, electron density diagnostics via C III EUV Lines 78−53899
nonideal plasma, elem. excitations and macroscopic props., review 80−43842
nonideal plasma thermodynamic functions and transport deviations 78−75273
nonlinear interaction, electron collision freq., self-consistent eqn. *(Russian)* 80−75055
nonlinear scattering of upper hybrid laser radiation by electron Bernstein modes in a plasma 80−64720
nonstationary plasma, anomalous radiation intensity 80−87898
nonuniform column, electron density determ. by RF coil probe 78−18446
normal atom conc. determ. by resonance line broadening with Hg press. 80−43883
oblique Langmuir solitons under free path conditions *(Russian)* 80−79477
ohmic heating in Frascati Tokamak, preliminary results 80−28734
ohmically heated plasma, in JFT-2 Tokamak, Thomson scatt. meas. 79−50890
optical line emission, Doppler broadened, axially symmetric, plasma, interpretation model 78−75276
optically thin plasmas, steady state populations, relaxation times 79−55561
oscillating arc plasma, optical characts., H_α spectral line profile *(Russian)* 77−19775
overdense column, reson. microwave absorpt. 80−64732
p-polarised EM wave struct. near point of reflection *(Russian)* 80−103118
parameter determ. by two beams of submillimetre waves *(Russian)* 78−22556
parametric modulation of density of laser plasma near crit. surface *(Russian)* 79−4108
plasma density continued
pellet refuelling of a divertor Tokamak 80−91247
Penning discharge plasma, residual gas density and elec. potential profile meas. 78−67485
phase transition in elec. discharge plasma between parallel plates, compression by recomb. press. 80−64799
pinched high velocity plasma fluxes 80−87860
plasma, emission and absorption coeff. at high electron density 80−103121
plasma, H_3^+ ion density decay, mass spectral obs. 77−3987
plasma, magnetised, double-layer characts. meas. 80−43874
plasma, ohmically heated in Tokamak and stellarator 77−11371
plasma focus, electron density distrib., N_2 laser interferometric study, X-ray and neutron emission 78−87479
plasma production modified magnetron discharge facility 78−75380
plasma with negative cond., electron conc. distrib., stability *(Russian)* 78−55722
plasmasphere, electron content determ. via radio beacon studies 77−45229
plasmasphere, total electron content, ATS-6 radio beacon expt. meas. 77−2303
plateau effect on inverse bremsstrahlung 80−43894
polarisation of picosecond excited continuous X-ray radiation *(Russian)* 80−59190
polyethylene filament, plasma prod. by staged laser heating, optical obs. 77−89321
polymer-coated laser fusion targets, compression to 10×liq. DT density 80−83964
ponderomotive craters, in phased waveguide array plasma, form. by microwave irrad. 80−83885
positive column, density oscills. due to negative ions, metastable atom model 78−1799
positive column, ion motion, radial pot. distrib. 79−55599
positive column, ionisation and temp. effect on charged particle profile and density 80−79596
positive column, irregular ionisation wave electron density rel. to light intensity variations 78−67520
positive column, of pulsed Hg-Ar discharge, electron energy distrib. calcs. 79−64919
positive column, subnormal, ion and electron radial distrib., theoretical description 80−79598
positive column of high-voltage diffuse discharge, nonstationary processes 80−64802
positive ion collection by probe in collisional plasma, density determ. 78−51352
pressure, virial kinetic definition, spherical geometry calcs. *(French)* 80−69973
Princeton large torus, multi-channel TV-Thomson scatt., apparatus, mech. aspects 78−54932
probe meas. near plasma edge in Alcator 79−7489
profile modification by light pressure in spherical geometry 78−59636
profile modification by ponderomotive force 78−59634
profile modifications at critical density 78−59550
profile near laser-plasma critical surface, flux limited thermal cond. effects 80−87857
profile self-steepening in laser plasma, interferometry 78−5938
profiling by interferometry with rapid spatial scanning, and Thomson scatt. of short laser 80−49014
Pulsator Tokamak, electron density limitation 80−96385
pulse discharge, in H_2 and/or N_2 *(Russian)* 77−27753
pulsed discharge plasma, quasistationary stage props., calc. method 78−38560
pulsed high-pressure microwave discharge, electron density and elec. field calcs. 77−76238
pulsed limiter discharge, multicomponent nonideal plasma, chem. composition 80−19657
pulsed micro-discharges, optical interferometry obs. 80−38804
pycnonuclear reactions, and pair correl. function in dense plasma 78−32445
Q-machine, single ended, collisionless, steady-state parameters and Buneman instability 80−59227
quadrupole ion store, spatial distribution of ions derived by phase space anal. 80−95185
quasi steady high beta plasma in multiple mirror machine, density oscill., stability obs. 80−28663
quiescent equilibrium plasma, aberrationless high-perveance ion beam extraction 79−90472
radial electron concentration profile determ. by microwave resonator method *(German)* 79−86608
radial electron density gradient in electronegative gas in discharge plasma 78−87433
radial stability of density profiles for obliquely incident light 80−92350
radiation cooling of high-β plasma 78−1807
radiation induced shock tube flow nonuniformities in ionising Ar 80−43865
radiation intensity calcs. in vacuum UV region *(Russian)* 80−48861
radiation-pressure effects in laser-plasma interactions, interferometric diagnostics 78−38540
radiative collapse of a relativistic electron-positron plasma to ultrahigh densities 80−14929
rarefied flow around point charge, particle distrib. function and density 78−26256
rarefied plasma, density discontinuity effect on kinetics *(Russian)* 79−37451
rarefied plasma flow, degree of nonisothermality, probe meas. 80−24243
rarefied plasma flow around bodies, ion density computation accuracy 79−50849
Rayleigh-Taylor instability generation of mag. fields, effects on laser fusion 79−19025
reactive plasma, optical emission spectroscopy, emission intensities and reactive density, correl. method 80−92385
recovery electric strength, effect of plasma parameters 80−6294
reference temp. method for determ. densities and plasma temp. 77−84510
relativistic systems, Bogolyubov equation hierarchy, plasma wave radiation damping 79−77377
resonance absorption, self-consistent density profiles for obliquely incident light 80−64758
resonance fluorescence method for plasma diagnostics, at. density and temp. meas. 80−49001
resonant absorption in Ar plasma at thermal equilib. 80−1799

plasma density continued
resonant excitation of slow low-freq. waves by opposite moving electron beams *(Russian)* 80−92336
resonant scattering of Lyman alpha radiation as a neutral density diagnostic for fusion plasmas 78−83612
resonator method, distributed-coupling system 77−1017
resonator method, mode selection by absorbing rings 77−1018
reverse field pinch, Faraday rot. diagnostics for internal mag. field 80−43976
RF discharge plasmas, mag. field effects, probe and microwave meas. 77−7594
RF inductively coupled, diagnostic meas. 77−39453
RF plasma etching, ion energy *(French)* 79−46495
RF probe meas. 79−86612
RF sputtering 79−87578
rotation influence on kink instability, compressibility *(Russian)* 80−48887
runaway electron diffusion and power balance in Tokamak moderate density discharges 80−28609
runaway relativistic electron scatt. on oscills. in Tokamak *(Russian)* 80−48849
S microwave radiation induced prod. and heating, electron temp. and density *(Spanish)* 79−98926
Saha equation, first order estimate for He plasma 80−19554
scattering spectra from weakly ionised plasmas calc. *(German)* 79−77347
Schlieren measurements of plasma kinematics during current disruptions in Tokamaks 80−92395
secondary beam production by two EM beams interaction, appl. heating and diagnostics 77−11352
self absorption of He like satellite lines in high density fusion plasmas 80−64776
self similar cooling wave, effective thermal cond. *(Russian)* 80−14908
self-oscillating mode origination in nonequilib. magnetised plasma 79−86568
sheaf instability at moderate densities, anomalous ion heating *(Russian)* 80−43922
shock generated turbulence, obs. in mag. plasma by CO_2 laser scatt. 80−84003
shock heated dense plasma, density, temp. and press. determ. 79−32819
single particle motion in 1-component strongly coupled plasma 80−48847
slow wave struct., nonlinear coupling with lower hybrid waves near plasma surface 80−92309
solar corona, plasma radiowave fluctuations and turbulence, Venus 10 radio transmission expt. 79−80295
solar flar spectra, high dielectronic satellite lines analysis for plasma props. calc. 80−12728
solar plasmas density determination, N III and O IV intersystem multiplets appl. 80−31264
solar transition zone, electron density, energy balance and press. from EUV spectra 80−21957
soliton generation at resonance and density modification in laser irrad.-plasma 78−14172
source, dielec. chamber, plasma flow characts. optimisation 80−38574
space charge ionising waves, high velocity propagation 80−87889
space-resolved extreme UV spectroscopy of C laser produced plasma 79−50889
spark, in vac., high-press. local plasma regions production, X-ray and hologram diagnostics 79−19104
spark, underwater, integrated bulk plasma characts. 79−27857
spectral line meas. 77−23467
spectroscopic diagnostics, book contrib. 77−51242
spectroscopic effects in dense and ultradense plasmas, review 80−43990
spectroscopic electron density meas., hot point low induction vacuum spark gas *(Russian)* 80−92390
spectroscopic source, inductively coupled, analyte excitation temp. and electron density distribs. 77−40592
spherical probe meas. in mag. field 77−31526
SPICA, impurity radiation, density and temp. 80−87859
stability of stationary inhomogeneous electron temp. distrib. states and electrodynamic params. *(Russian)* 78−42749
steady state plasma, electron temp. and density meas. system 78−87490
stellarator, Wendelstein-VII A, charge exchange atoms yield, elliptic cross-section effect *(Russian)* 79−98950
stimulated Brillouin backscatter saturation for long CO_2 laser pulses 80−19582
stimulated Brillouin scatt., efficient saturation due to nonlinear ion wave decay 79−86585
stimulated Brillouin scatt., saturated steady-state refl., density depend. 80−53945
stratified plasma, obliquely propag. extraordinary microwave Budden tunnelling 80−48895
stream incident on flat metal target, boundary layer struct. 77−76106
stream incident on flat metal target, boundary region optical diagnostics 77−76107
submillimetre diagnostics, active, of Ar arc, data numerical anal. 80−48979
supercritical density profiles of CO_2-laser-irradiated microballoons 80−14918
superdense glow discharge, effect of transverse magnetic field on ion concentration 80−87972
superdense plasmas, spectroscopic diagnostics, at. collisions 78−63538
superradiation from non-ideal plasmas in electric field 80−38568
supersonic flowing continuum plasma, triple probe method applied to direct display of parameters in supersonic flowing continuum plasma 79−60191
supersonic jet, ionisation in Mach disc, submillimeter laser interferometry diagnostics 80−14934
suprathermal electric microfields and plasma parameters in crit. vel. rot. plasma 79−60198
suprathermal electrons, self-generated mag. fields, laser plasma 78−5902
surface contamination of EM trap, effect on plasma density 78−9822
surface modes in magnetized fully ionized plasma 80−38550
surfatron produced electron density and temp. microwave meas. 80−43965
Takamak plasma density profiles from electron cyclotron radiation spectra 80−103179
target impurity effect on laser produced expansion, ion spectrography 80−43945
temperature and density diagnostics of laser prod. plasma 78−51360

plasma density continued
temporal var., soft X-ray absorpt. obs. 77−1015
TFR, reduced fusion neutron production 78−63577
TFR, soft X-ray diagnostics 77−51234
theoretical scaling laws, implications 80−28805
thermal instability, mag. field generated, in laser heated plasma, hydrodynamic effects 80−96355
thermionic diodes, planar low press. gas discharges, plasma regime, plasma characts. 79−77435
thermonuclear dense plasma, neutron diagnostics, book contrib. 80−24253
thermonuclear ignition, inertially confined fusion, high density effects 80−86981
thermonuclear plasma, radn. losses at impurities, $n_e\tau$ parameter *(Russian)* 79−68908
thermonuclear plasma surrounded by cold blanket, density profiles, thermo-elec. forces effect 79−31189
theta pinch, low density, step-like mag. piston 80−103182
theta pinch, $N^{+,2+,3+}$ lines Stark broadening, He(II) line diagnostics 80−24249
theta pinch, radial oscills. of plasma density and mag. field, light scatt. and probe obs. 80−14937
theta pinch plasma density radial profile measurements using quasiquadrature interferometer 80−70038
theta-pinch, 10.6 μm interferometry and Faraday rot. meas. 77−80358
theta-pinch, density, azimuthal mag. field effects, laser interferometric meas. 77−11406
theta-pinch, fast, double-frame hologram interferometer meas. of density 79−19097
theta-pinch, high-beta plasma discharge, spectroscopic meas. 77−24186
theta-pinch, low-energy, end losses obs. 77−24157
theta-pinch, nonthermal density fluctuations, laser scatt. diagnostics 78−59679
theta-pinch, post-implosion phase, electron temp. and density meas., mag. field profiles 77−31522
Thompson scattering for electron beam and plasma diagnostics *(Russian)* 80−54031
Thomson scatt. pathways calibration, rel. to diagnostics *(French)* 80−43886
Thomson scattering meas. of heating process 80−59272
Thomson scattering with high background level of plasma scattering 80−43979
TM-3 Tokamak, electron density and temp., microwave, cond. and diamagnetism obs. 77−15247
Tokamak, Doublet IIA, temporal and spatial behaviour of plasma props. 77−43030
Tokamak, edge effects and impurities, influence on thermal stability 80−87892
Tokamak, fast-wave heating, ray-tracing anal. 79−41848
Tokamak, JFT-2, gross particle confinement characts. by boundary plasma, electrostatic probe diagnostics 79−32822
Tokamak, JFT-2, scrape-off layer, particle and energy fluxes, probe and IR obs. 78−59690
Tokamak, large magnetic field ripples, electric probe meas. 80−83976
Tokamak, LT-3, stable discharge, ion temp. and energy balance, UV polychromator meas. 77−65914
Tokamak, neutral beam-heated, parametric scaling 80−10406
Tokamak, PLT, expt. results 77−43072
Tokamak, reactor size, diffusive losses and scaling law 78−87478
Tokamak, relax. during internal disruptions 77−51235
Tokamak, T-10, plasma parameters 77−43071
Tokamak, T-4, corpuscular diagnostics by charge exchange of plasma ions at artificial target *(Russian)* 80−83968
Tokamak, Thomson scatt. diagnostics, far IR lasers development, review 80−24242
Tokamak, Thomson scatt. meas. *(Russian)* 77−27738
Tokamak diagnostics, review 78−47163
Tokamak discharge, breakdown phase, ionis. time, mag. flux requirement *(German)* 78−34363
Tokamak discharge microwave preionisation at electron cyclotron resonance 80−83896
Tokamak electron temp. and density profiles from electron cyclotron radiation spectra 80−59293
Tokamak fusion reactor geometry, optimum plasma parameters rel. to reactor parameters 79−76140
Tokamak magnetic confinement, recent progress in Tokamak expts. for fusion energy prod., review 79−71948
Tokamak plasma, density profile, laser interferometry 78−5928
Tokamak plasma, Thomson scatt. method using pulsed ruby laser 79−10720
JFT-2a Tokamak plasma with separatrix mag. surface, density and temp. 77−7581
Tokamak reactors, neutral beam injection, energy and power requirements 80−91243
Tokamak TFR, Thomson scattering system based on two-detector spectrometers 80−32426
Tokamak TO-1, feedback system effect on plasma parameters *(Russian)* 80−103174
Tokamak transport codes, one-dimens., poloidal divertor simulation 79−37539
Tokamak-4, $q=5.4$ stability margin mode *(Russian)* 77−47240
Tokamaks, density upper limit from thermal stability data 80−18600
toroidal kink instability, noncirc. cross section, nonlinear phase obs., probe diagnostics 79−60182
toroidal plasmas, high temp., electron cyclotron emission meas. by mesh filter method 80−75101
toroidal reversed-field pinches, current, temp., confinement time scaling 77−43078
transient setting of ponderomotive nonlinearity, self-focusing and plasma-wave excitation 79−77387
transition layer between two magnetized plasmas 80−24136
transverse p-polarized surface wave excitation causing density disturbances *(Russian)* 79−41856
triple probe method for meas. plasma parameters in low-density flowing collisionless plasma 78−1898
tubular flow reactor, ion density and Z_{eff} profiles, neutral beam attenuation technique 80−6282
Tuman-2A, plasma compression particle diagnostics, density and temp. *(Russian)* 80−38677
turbulent reactor, power law distribs., cosmic ray source model *(Russian)* 78−26244

plasma density continued
turbulently heated, electron distrib. anisotropy, X-ray diagnostics 78−59682
two-component plasma, density fluctuations, time depend. 77−80272
two-plasmon decay, profile modification, produced by 10.6 micron radiation, at $^1/_4$-crit. density 79−19061
two-plasmon decay instability, nonlinear saturation and recurrence 79−82057
two-stage ion heating obtained in rapid theta-compression expt. 78−22521
UHF discharge plasma, parametrically excited relaxation oscills. 80−53978
UHF discharge with preliminary locally ionised gaseous medium 80−38851
unmagnetised plasma, quasilinear theory of parametric processes 79−94787
UV photoplasma, electron density, microwave meas. 80−75097
vacuum arc in Cu cathode region, current parameters, theory 80−54068
vacuum spark, electron density, interferometric meas. 78−5962
variational principal in relativistic magnetic fluid dynamics, Lagrangian density 79−73031
velocity diffusion eqns., high-energy tail formation 78−71455
W VII-A stellarator, Ohmic heating, energy and particle confinement 80−24226
wave, finite amplitude, nonlinear behaviour, sideband instability, electron distrib. function 78−38480
wave heating at electron cyclotron harmonics in toroidal plasmas 80−28727
whistler wave ducting caused by antenna actions 78−59586
whistler wave trapping in density crest 80−53984
X-ray diagnostics, hot lab. and astrophysical plasma 80−59282
X-ray line radiation from cylindrical Al plasma, calc. model 80−64777
X-ray monochromatic images for hot plasma ion and temp. distrib. 80−64772
Z-discharge plasma, low-temp., time evolution, diagnostics 79−37548
Z-pinch, gas puff device, X-ray spectra, plasma form. 79−94816
Z-pinch, HBTX 1, ion temp., total radiated energy 77−27729
Z-pinch, HBTX 1 reversed field, Thomson scatt. diagnostics 77−27730
Z-pinch, high density, Hβ line spectra 78−18445
Z-pinch, high density, Schlieren meas. 77−11408
Z-pinch, high-density, form. regimes 78−59652
Z-pinch, imploding Al liner, soft X-ray spectroscopy 78−14198
Z-pinch, overdense, He plasma, laser-driven hydrodynamic perturbation, shock density struct. 79−77385
Z-pinch, plane, mag. field null region parallel current effect *(Russian)* 78−91137
Z-pinch dense H plasma, emission spectrum thermal equilibrium departure 79−82094
Z-pinch discharge, electron temp. and density variation obs. 78−75426
Z-pinch discharge, interferometry 77−35394
z-pinch discharge, spectral line shape, high-density effects 79−73038
Z-pinch high density plasma, spectroscopic analysis 79−98980
Z-pinch high density plasma spectroscopic analysis 79−98981
Z-pinch plasma, density and temp., spectroscopic meas. 79−4181
Z-pinch plasma, interferometry 80−6277
Z-pinch turbulence spectroscopic detection and anal. *(Russian)* 80−100098
Z-pinch ultradense plasma, density dynamics, interferometric meas. 79−77413
Zeta plasma, field line reconnection and density fluctuations 80−69975
Al plasma, hot dense homogeneous, X-ray production rate and ionisation state density, calc. 78−71458
Al resonance line profiles, influence of boundary layer of Al-seeded shock heated plasma 80−43876
Al target, CO_2 laser irrad., 10^6-10^8 W cm^{-2}, diagnostics 77−89281
Al target, in air, pulsed CO_2 laser irrad., thermal response and plasma characts. 79−86595
Al XIII, hot pinched plasma, Lyman series Stark profiles, electron density determ. 78−51348
Ar afterglow, spectra and microphotograms, dissociative recombinations 78−26365
Ar arc, non-LTE, electron balance, temp. and density *(French)* 78−1796
Ar arc, plasma parameters determ. by laser scatt. 79−32812
Ar arc discharge, neutral system collisional radiation model 78−67535
Ar arc plasma, circuit-breaking, anode layer, optical diagnostics 77−80351
Ar arc plasma, decaying, temporal changes of particle densities and temps. 79−64940
Ar, arc plasma, MTE continuum emission coeff. relation for atom. press. 77−31432
Ar arc plasma, partial LTE for lower excited levels of ArI 80−79565
Ar atmospheric arc plasma deviation from LTE 78−67604
Ar boundary layer electrostatic probe meas. *(Japanese)* 78−5933
Ar constricted discharge, electron density and temp. and gas temp., iterative method *(German)* 78−83627
Ar, decaying plasma arc, electron disappearance mechanism 80−38765
Ar decaying pulsed discharge plasma, acoustic waves density modulation 80−103143
Ar discharge, ion density profile, reson. laser light meas. 80−92401
Ar discharge, pulsed, weakly ionised, neutrals effect, interferometric obs. 79−27854
Ar, emission coeff., high press. peculiarities 77−43067
Ar, formation in crossed electric and magnetic fields, optical spectra 80−79452
Ar HF torch discharge, spectral diagnostics 79−14607
Ar highly ionised low press. plasma produced in pulsed discharge, characts. *(French)* 77−58901
Ar hollow cathode arc, in mag. field up to 2 k0e, plasma parameters 80−6306
Ar, ionising boundary layer in shock-tube side-wall flow 79−60144
Ar negative glow fast electron density rel. to discharge pressure and current 78−67528
Ar, optical breakdown at 10.6 μm near plasma layer boundary 79−60165
Ar plasma, continuum radiation, temp. and charged particle concs. from line intensities and widths 77−68867
Ar plasma, electron density, microwave refl. meas. 78−59674
Ar plasma, interferometric study of density and electron conc. behind shock waves 78−1888

plasma density continued
Ar, plasma, jet, optical studies using Schlieren and shadow methods 80−59279
Ar plasma, RF prod., mag. field effect on props. *(Korean)* 79−50869
Ar plasma, shock-compressed, thermophysical and gasdynamic characts. 77−43016
Ar, plasma arc, dynamic charact., electron energy relaxation effect 80−38774
Ar, plasma column of hollow cathode arc, collisional model of ion system 80−38749
Ar plasma density meas. by Langmuir probe and microwave interferometer 80−28819
Ar plasma jet, electron temp. and density determ. 79−41875
Ar plasma jet, turbulent, radiowave interaction 77−989
Ar plasma parameters, microwave scanning technique 80−64773
Ar, positive column, contracted, electron density, temp., elec. field, line emission 80−6311
Ar, positive column, contracted, balance equations anal. 80−6312
Ar, slightly ionised, ion density meas. with hollow probe 77−15242
Ar, stationary striations as bifurcation phenomenon 79−32767
Ar, stream electrons, at atm. press., electrical parameters *(Russian)* 80−53930
Ar wall-stabilised arc electron and heavy-particle temp. variations 78−67602
$Ar^{16,17+}$ filled glass shell, symmetric laser compression 80−64759
Ar-C arc, C I lines Stark broadening, electron density and temp. meas. 77−10634
Ar-H_2S plasma, spectroscopic study, electron density, ionis. temp. meas. 77−19764
Ar-He plasma, electron temp. and density meas., to check diffusion calc. 79−27749
Ar-N_2 mixtures, DC arc, energy balance of electrons 78−42797
Ar-Xe, shock wave dynamic compression, thermodynamic props. *(Russian)* 80−53931
ArI, highly excited atomic levels, spectral-line-blending study in high-density plasma 80−48969
Au, thin foil, enhanced electron energy deposition heated, soft X-ray vacuum UV spectra 80−80901
B II, Stark shift, shock tube meas. 77−50403
beta measurements in high-β fusion experiments from magnetic flux and luminosity profiles 80−49007
C arc in air, electron density meas. by CO_2 laser interferometry *(Japanese)* 80−28822
C plasma, spectral and absorpt. coeffs. 80−69985
C VI, laser plsma, electron density profile, Stark broadening meas. of vac. UV lines 78−59684
CO-N_2-^{3}He, nucl. reactor active zone, plasma and sustained discharge props. 80−5729
CO_2, decaying discharge plasma, contraction in const. elec. field, profiles of gas density and temp. *(Russian)* 79−37447
CO_2 gas laser, glow discharge electron irrad. rel. to output characts. 79−64198
CO_2 laser beam scatt. by microscopic fluctuations in plasma density 80−79574
CO_2 TEA laser produced, spectral analysis of emission, charact. parameters determ. *(German)* 78−38516
CO_2-N_2-^{3}He, laser, plasma diagnostics of media capable of lasing in nucl. reactor environment 79−10279
CO_2+H+Xe plasma, elec. parameters, Xe effects *(Russian)* 77−84507
Cd-Ar low-pressure discharge column, energy balance obs. 78−67504
Cl_2-arc, low temp., visible and IR continuum radiation 80−38784
Cs fully-ionised plasma hollow-cathode arc discharge theory 78−67533
Cs, Knudsen arc, electron beam heating and ionisation 80−75114
Cs photoplasma, effect of H_2 impurities *(Russian)* 77−35320
Cs plasma, decay in presence of N_2, population inversion 79−55455
Cs, prod. by resonant light irrad., density profile 77−7563
CsI-Hg-Ar discharge, high-press., temp. and plasma comp. determ. 79−10709
Cu arc, fluctuating, diagnostics using spectral-image photographs *(Japanese)* 79−41896
cu, laser light absorpt. by plasma with very steep density gradient 80−96348
Cu vapour laser, non heated, kinetic processes 80−37999
D, high current pulse discharge investig. *(Russian)* 78−47171
D-T Tokamak, high-density, ohmically-heated, transport calcs. 80−24142
D_2 discharge, high current, pulsed, plasma composition, temp., electron density, press., spectral diagnostics 79−55459
D_2 plasma, isolated, CO_2 laser-produced, holographic interferometry diagnostics 80−24254
DyI_3-Hg arc discharge plasma, spectroscopic study 80−54033
Fe XV, line intensity and linewidths at high electron density, generalised population ratio 80−99481
H arc, electron density, interferometric determ., refr. index calc. in high press. 80−24284
H atomic radial profile in FT-1 Tokamak, reson.-fluoresc. meas. 79−90467
H Balmer lines, plasma-broadening in wall-stabilised arc, low electron density 80−43891
H beam production in maser dissociator, performance characts. 78−87034
H dense thermal plasma, radiation emission 80−103120
H, Hα line profile as plasma density meas. 80−43987
H, ion equilib. density, in low press. system 78−9752
H line broadening and shift due to plasma ions *(Russian)* 80−96350
H, plasma, collisional depopulation rate of n=2 level, laser plasma method 78−79463
H, plasma, in θ-pinch with axial current-carrying rod, light scatt. diagnostics *(Russian)* 77−11395
H plasma, laser produced, characterisation meas. 78−67409
H plasma, thermal emission and Debye shielding 80−64692
H plasma target investig. *(Russian)* 80−106981
H, recombining plasma, population inversion using collisional-radiative model 79−46423
H spark, laser-triggered, electron densities meas. 80−106975
H^-, density meas. by photodetachment 80−48976
H^- surface ion source, plasma parameters, diagnostics 78−9849
H-like ions, emission spectrum, depend. on electron density in laser plasma 79−27248
H^+-He^{2+}, strongly coupled ionic mixture, density fluctuations, timer depend. 77−80272

plasma density continued
H_2 hot-iron plasma, ion temp. and electron density depend. studied by laser light scatt. and emission spectroscopy 80−96342
H_2 monoplasmatron arc plasma, electrokinetic parameters space distrib. *(Russian)* 80−53925
H_2 plasma, radial density and temp. profiles, using magnetoacoustic oscills. 79−19082
H_2, plasma, resonance fluorescence diagnostics 80−48971
H_2-He plasma, shock-heated, relax. distance and equilib. electron density diagnostics 77−24180
H_2-N_2 glow discharge, positive column, electron energy-distrib. spatial variation 77−47294
$H_{\alpha,\beta}$ lines, Stark broadened, central struct., in dense plasma 77−6722
H_α line Stark profiles in low-density arc, exptl. discrepancies 78−67470
H_δ line profile for plasma microfield distrib. function reconstruction 78−71539
Hα and Hβ, Stark profiles, ion-motion effect 80−63592
He afterglow, collision processes rate coeffs. 77−24221
He collisional plasma, classical diffusion in large amplitude density fluctuations presence 78−18381
He diffusion plasma column in coaxial cold cathode discharge, radial distrib. of electron density 77−51237
He discharge, medium press., contraction mechanism, inhomogeneous heating 80−44024
He discharge, RF, plasma parameters and volt-ampere characts., two discharge regimes 80−44016
He, electron distribution function relaxation in high freq. gas breakdown *(Russian)* 80−14957
He flow, RF discharge test obs. 80−44028
He, hollow-cathode type discharge, spectroscopic obs., laser light source appl. 80−59335
He I line profiles, ion motion effect in low electron density plasma 80−43877
He I Stark widths 77−80374
He II, 4686 Å Stark broadened profile, electron density and temp. meas. 77−23460
He II, Doppler and Stark broadened lines, electron density and ion temp. meas. 78−67407
He II, stationary population inversion between low lying levels of He^+ in recombining plasma 77−84494
He II, Z-pinch plasma, Stark broadened profile, 4686 Å, electron density and temp. 77−84495
He II 4686 Å line, Stark profile meas. in high density plasma 80−96390
He II 4686 Å Stark broadened profile, electron density and temp. meas. 77−23460
He modulated positive column, elec. and optical props. 77−27765
He plasma, cryogenic, recombination decay *(Russian)* 79−4104
He, plasma, in θ-pinch with axial current-carrying rod, light scatt. diagnostics *(Russian)* 77−11395
He plasma, laser heating, spectroscopic meas. 77−76205
He, plasma, non-equilib., of strong current pulse discharge, diagnostics *(Russian)* 78−75271
He plasma chemical device, integrated electron density meas., interferometric method 79−55548
He plasma He I 4471 Å line profile obs. at high electron density 78−67472
He plasma in electron beam-excited discharge, atm. press., relax. obs. and model 79−37569
He positive column comp. at intermediate press. 80−19646
He, positive column plasmas, metastable atom density meas. by improved self absorpt. method 80−87968
He pulsed arc, Thomson scatt. diagnostics 80−24297
He, RF field bursts in density wells 79−60143
He, spark prod. by short laser pulses, spectroscopic meas. of temp. and electron density 77−43086
He, ultradense reproducible Z-pinch, for laser-pellet interaction simulation, characterisation 78−30463
He, usual glow and hollow-cathode discharges, negative glow, spectroscopic obs. 77−72516
He^+, excitation in hollow cathode discharge, rel. to plasma electron density and temp. 77−7589
He-Cd, usual glow and hollow-cathode discharges, negative glow, spectroscopic obs. 77−72516
He-Cd^+ laser discharge, positive column, non-Maxwellian electron energy distrib., electron density determ. 77−84493
He-Cd^+ positive column laser discharge, ion density 77−68885
He-Co_2-Xe plasma discharge electron conc. and temp., optical diagnostics method 79−41871
He-Hg RF discharge, atomic ionis. and excitation, spectral line intensities 78−26334
He-I^+ laser discharge, positive column, particle densities 80−103215
He-Kr^+ ion laser, microwave-pulse-excited, spectroscopic expts. 77−71973
He-Ne gas laser, glow discharge electron irrad. rel. to output characts. 79−64198
He-Ne modulated positive column, elec. and optical props. 77−27765
He-Ne plasma He I 4471 Å line profile obs. at high electron density 78−67472
He-Xe plasma, in mag. field, effect of CO_2 mol. addition on plasma parameters 77−42965
^3He plasma, prod. by products of $^3He(n,p)^3H$ in nucl. reactor, props. 77−76146
Hg, high-pressure discharge, temp. and electron density meas. *(French)* 78−59705
Hg low-pressure pulse-modulated discharge optical and electrical parameters 78−67491
Hg-Tl-I discharges, 50 Hz, axial segregation effect on elec. field strength 80−59320
K, positive column, ion distrib. function for each species using probe 78−55752
K-Kr, afterglow of laser plasma, fluoresc. spectra 79−19085
K_2O-Al_2O_3-$2SiO_2$-BaO plasma emitter 80−96368
Kr glow discharge, electron energy distrib. function, electrical characts. investig. 80−24279
Kr plasma, shock-heated, continuum radiation emission coefficient meas. 79−64835
Kr-Cl_2 mixture, glow discharge positive column, electron energy distrib. and rates of inelastic processes, negative Cl ions form. 80−19632
Kr-N_2 plasma, afterglow ion prod. and loss processes 77−11401
Kr^+-He, microwave-pulse-excited, internal plasma parameters, time variation 77−38858

plasma density continued
Kr(-He) arc, wall-stabilised, atm. press. 79−46503
Li wire high energy density exploding plasma, holographic interferometry, self pinching, charge density 79−77436
Mg plasma, heated by ruby laser pulses, X-ray emission spectrum 80−64781
Mo, arc, vac., stabilised, plasma props. 78−51384
Mo XLI, Mo XL, X-ray emission from vacuum-spark plasma 78−41991
N discharge, externally maintained, instability growth time, associative ionisation 80−6254
N, plasma, Stark broadening, photoelec. obs. 77−23463
N_2 afterglow, chem. reactions rel. to plasma props, appl. to toluene polymerisation 80−3346
N_2 arc, plasma parameters determ. by laser scatt. 79−32812
N_2 arc, spectroscopic meas. w.r.t. LTE 77−19786
N_2 arc plasma, recombination with gas glow, spectroscopic diagnostics 77−7626
N_2 arc plasma, stabilised by gas injection, thermochem. nonequil., particle excitation, vibr. temps. 80−19634
N_2, dense gas near metallic target, laser spark *(Russian)* 80−38682
N_2, diffuse plasma, population densities of triplet states, correl. with electron impact processes 80−43966
N_2 discharge, electron shock wave formation, numerical simulation 80−38777
N_2 high intensity arc anode region, temp., current density, flow field, numerical anal. 78−9827
N_2 plasma, electron temp. and conc. meas., complete LTE 77−65908
N_2 plasma, spatial distrib. in transverse-discharge supersonic stream, continuum theory and probe meas. 80−48866
N_2 plasma jet, spectroscopic obs., electron temp. 77−31512
N_2 positive corona into spark, prebreakdown phase, spectroscopic anal. 80−38790
N_2, streamer discharge, spatial and temporal spectroscopy 78−5971
N_2-He plasma, laser produced, high press. amplified stimulated emission 80−78843
N_2-methane, rapidly developing discharge, streak camera records interpretation 80−59280
$N(^2D,^2P)$ metastable ats. prod. in N_2 DC glow discharge 80−38758
$N(^2D,^2P)$ metastable production by electron collisions in DC glow discharge 80−59274
Na high-pressure arc, time-depend. plasma temp. meas. 77−68866
Na vapour, electron and ion beam transportation channel form., reson. saturation based laser ionis. 79−77410
Na-Ne-Ar AC discharge, positive column 77−39487
Na-Xe, high-pressure discharge, electron density, interferometric meas. 78−75415
Nd:glass laser irradiated fusion targets, time and space resolved harmonic emission 79−82095
Ne discharge positive column in longitudinal mag. field, metastable atom radial density distrib. obs. 78−67496
Ne, electron energy distrib., relax. process 78−30507
Ne filled glass microballoons, laser imploded, compressed core density meas. by X-ray continuum edge shift 79−10705
Ne like ions, population inversion, gain estimate for 40 to 80 nm range transitions 77−75482
Ne, nuclear induced plasma, simulated 80−64786
Ne plasma, electron collision ionisation, electron kinetic behaviour during elec. field perturbation *(German)* 80−64676
Ne plasma, generated by 200 MeV protons, electron density and electron temp. 78−22568
Ne positive column plasmas, metastable atom density meas. by improved self absorpt. method 80−87968
Ne, streamer plasma characts., cond., plasma density and field strength calcs. *(Russian)* 77−47262
Ne-Hg RF discharge, atomic ionis. and excitation, spectral line intensities 78−26334
Ne-N_2, energy transfer, H^+ ion beam produced plasma, ion density and temp. 80−38539
O_2 discharge plasma, metastable states role, two step ionisation, electron densities and transition pts. 80−44019
O_2 glow discharge, positive column contraction characts. 79−90483
O_2-injected TFR Tokamak current plateau, laser diagnostics 78−22565
SF_6 high-current arc props., influence of electrode material 78−71592
SF_6, particle densities in decaying plasma 78−75442
SiH_4 discharge, low pressure, plasma parameters, relevance to Si film deposition 80−44030
Ti density, in DC sputtering discharge by atomic absorpt. spectroscopy 80−43973
Xe discharges, electrodeless, UHF in waveguide rel. to DC characts. 80−38762
Xe plasma, shock-compressed, thermophysical and gasdynamic characts. 77−43016
Xe precursors, associative ionisation and photoionisation, relative contrib., electron density prediction 80−43858
Xe, pulse gas discharge, high-intensity, energy storage and temp. in channel 78−1926
Xe, s-p transitions, Stark consts. and oscill. strengths, shock tube meas. 80−18822
Xe, wall-stabilised plasma, temp. and press. of high press. plasma *(German)* 79−23450
Y_2O_3 plasma, eqn. of state investig. 80−75027

plasma deposited coatings
elastic properties, acoustic meas. *(Russian)* 80−97519
ferrite films, influence of heating support on struct. and props. *(Russian)* 79−78445
ferrites, plasma sputtering, struct. props. and phys.-chem. transform. *(Russian)* 79−38739
fluorocarbon polymer thin films for lubrication of Au contact surfaces 80−89157
glow discharge polymerisation double probe meas. and contamination effects 77−70300
inorganic thin films, plasma-promoted deposition 79−78896
low-pressure plasma applications to surface treatment 79−94824
organo tin polymers, glow discharge formed, interface composition and adhesion 79−82467
organo-tin polymer films, glow discharge prep., comp. determ. by XPS and AES 80−35109
oxide, pore size distrib. and permeability 79−24641
oxide, RF plasma deposition on glass or $In_{2-x}Sn_xO_{3-y}$, and liq. cryst. aligning props. 77−48350

plasma deposited coatings continued
polyacrylonitrile, adhesion to plastics 80−50745
polymer, RF plasma deposition on glass or $In_{2-x}Sn_xO_{3-y}$, and liq. cryst. aligning props. 77−48350
polymer film, adhesion to plastics 80−50745
polymer layer, glow deposition rate obs. in DC discharges 78−68633
polymer thin film growth by glow discharge polymerisation, temp. depend. 78−68632
polymerized dielectric thin films deposited by glow discharge, time-dependent props. 77−63564
polysiloxane plasma polymerised film growth on GaAs substrate, dry etching process 80−25575
polystyrene, adhesion to plastics 80−50745
rare-earth aluminate, scandate and zicronate films, film coatings, electrophys. props. w.r.t. prep. technology 80−60781
temperature measurement of spherical or near-spherical particles in plasma stream 80−21138
thermoregulating plasma coatings, UV irrad. influence on optical parameters *(Russian)* 80−40259
thin film stoichiometry adjustment by mag. field 79−78900
vinyltrimethoxy silane, plasma polymerised, abrasion resist. antirefl. coating for polycarbonate 77−42635
VLSI multilayer metallisation interlayer dielectrics, CVD films 80−45235
Ag, electron beam plasma sputtered coatings on KCl substrate, islet struct. *(Russian)* 80−39460
Al, electron beam plasma sputtered coating, islet struct. *(Russian)* 80−39460
Al, film deposition from metal plasmas 78−6859
Al, film on Si(111) substrate, struct., props. depend. on vapour flow, ionisation *(Russian)* 80−75453
Al metallization of semiconductor devices by high rate magnetron/plasmatron sputtering 79−28919
Al-Zn-Mg plasma sputtered, mech. props. rel. to heat treatment *(Russian)* 80−40387
AlN film, Si doping by DC glow discharge 78−19674
AlN films, RF glow discharge deposited, current-voltage characts. 80−84515
Al_2O_3, glass resistant, plasma coating props. 79−34164
Al_2O_3, ion condensing metal plasma stream, coating microhardness, chemical reactions 79−42426
Al_2O_3-NiCr composite, plasma sputtering of electroheating coatings, elec props. *(Russian)* 80−108350
$As_{2-x}S_{3+x}$, hydrogenated chalcogenide glasses, prep. by plasma decomposition 80−49735
$As_{2-x}Se_{3+x}$, hydrogenated chalcogenide glasses, prep. by plasma decomposition 80−49735
B films, prep. by H reduction of BCl_3, struct. and hardness 80−54543
B, protective coatings for first wall, prep. by means of low press. plasma CVD 80−35103
B:H amorphous films, optical band gap, thermal treatment effect 80−93415
B_xCy, protective coatings for first wall, prep. by means of low press. plasma CVD 80−35103
BN, high temp. reactive plasma deposition, struct., resist., and dielec. const. meas. 77−7988
C, amorphous film, spin resonance, IR spectra, microhardness 80−71157
C, diamond-like, mech. props. 79−90924
C, diamond-like, produced by RF glow discharge of hydrocarbon gases, props. and coating rates 80−21146
C diamondlike layers, RF plasma deposited, frictional props. 80−71762
C film, amorphous, growth under ion impact in butane plasma, and IR transparency 78−52688
C film, diamond-like, produced in butane plasma, XPS anal. and elec. props. 79−82484
C films, diamond-like, on Si, colour chart 80−97366
i-C, hard coating preparation by ion beam methods 80−25579
CeO_2, plasma deposition of crysts. and their characterisation 80−20800
Cr-C, deposited by hollow cathode discharge, characterisation 78−11371
Cr-C, hard coating preparation by ion beam methods 80−25579
Cr-N, deposited by hollow cathode discharge, characterisation 78−11371
Cu, film deposition from metal plasmas 78−6859
Cu-Fe, explosive plasma sputtered coatings, struct. and props. *(Russian)* 80−100783
Fe_4N, hard coating preparation by ion beam methods 80−25579
Fe_2O_3, plasma sputtered coatings, oxide dissociation, coating props., struct. and composition *(Russian)* 80−54577
GaAs oxide growth kinetics and physical props. 79−77937
GaAs, plasma-grown oxides, physical props., Auger and IR spectral anal. 79−91821
GaAs-plasma grown oxide interface, new resonant ellipsometric technique for characterisation 79−40606
GaN, plasma deposition and elec. cond. 78−60585
GaP, plasma deposition and elec. cond. 78−60585
HfO_2, plasma deposition of crysts. and their characterisation 80−20800
InO_3:Sn transparent conducting films, homeotropic orientation of liquid crystals *(Russian)* 80−108181
Mn-Cr-Ti layers on low C steel, composite, residual stresses rel. to arc-spraying parameters *(German)* 80−104077
MoN_x, ion condensing metal plasma stream, coating microhardness, chemical reactions 79−42426
Nb films, supercond. props. and electronic density of states *(Russian)* 79−28439
Ni-Cr alloy (20 wt.%), on steel, struct. and mech. props. 79−96222
Ni-Cr-Si, corrosion and failure mechanisms of coatings for gas turbine applications 79−29284
Re, films, from $Re_2(CO)_{10}$ vapour decomp. 80−20799
S-based amorphous semicond. film, prep. by plasma decomp. of H_2S-N_2-NH_3, and characterisation 80−80422
Si, amorphous, elec. props., ion implantation effects 80−79828
Si, amorphous, glow discharge deposited, mobility edge calc. 80−80220
Si, amorphous, glow discharge produced, defect creation, high optical excitation 80−97327
Si, amorphous, glow-discharge, optically detected mag. reson., annealing and substrate temp. effects 80−20519
Si, amorphous, photovoltaic cell, plasma deposited, horizontally multilayered struct. 80−50964
Si, amorphous, plasma-deposited, H_2 evolution, mass spectrometry and RHEED obs. 78−72050
Si, amorphous, prep. by glow discharge decomposition method *(Japanese)* 77−81226
plasma deposited coatings continued
Si, amorphous, production by glow-discharge method *(Japanese)* 77−90283
Si amorphous film, film, glow discharge deposited, refl. spectra and dielec. function 80−50360
Si, amorphous film, plasma preparation 78−72740
Si, amorphous film, plasma-deposited, photoluminesc. and EPR meas. 79−4864
Si, amorphous film, RF plasma deposition from $SiCl_4$-H_2, characterisation 80−66435
Si, amorphous films, halogenated and hydrogenated, elec. and optical props. 80−97016
Si, amorphous glow discharge films, H_2 content, elec. props., and photostability 80−25577
Si and Si:H amorphous films, porosity and oxidation of evap., sputtered and plasma-deposited films 80−10838
Si film, amorphous, structural comparison of evaporated and glow discharge samples 77−62778
Si films, polycryst., glow discharge deposited below 250°C, struct. and morphology 80−49535
Si, glow discharge film decomposed from silane, on amorphous substrate, elec. cond., RHEED study 80−20044
Si plasma deposited amorphous hydrogenated film, optical props., annealing effect 79−56874
Si polycrystalline films, characts. 80−80988
Si:F,H, amorphous, glow discharge deposited elec. props. and device aspects 80−44744
Si:H, amorphous, defect creation and H evolution 80−50392
Si:H, amorphous, dopant conc., glow discharge optical spectroscopy 80−49546
Si:H, amorphous, exodiffusion of H, EPR expts. 80−49102
Si:H, amorphous, glow discharge deposited, thermal dehydrogenation, IR spectra 80−44442
Si:H, amorphous, glow discharge deposited, laser annealing 80−49104
Si:H, amorphous, plasma deposited, cond. adsorbate and insulating layer effects 80−49749
Si:H, amorphous, plasma-deposited, effect of DC elec. field superimposed during deposition 80−44643
Si:H, amorphous, prep. by RF glow discharge decomp. of SiH_4, optical props. and H conc. 80−15416
Si:H, amorphous film, prep. by plasma decomp. of SiH_4 under mag. field, and characterisation 80−45239
Si:H, amorphous films, plasma-deposited, defect states, IR, ESR, and refractive index meas. 79−65944
Si:H,F,O amorphous, plasma deposited, comp. and optical props. 80−50441
Si:H amorphous film, microstruct., SEM and TEM obs. 80−10801
Si:H amorphous film, plasma-deposited, growth morphology and defects 80−44128
Si:H amorphous film, plasma-deposited, elec. and comp. heterogeneity 80−44745
Si:H amorphous film, prop. by glow discharge deposition, and plasma parameter effects on props. 80−45240
Si:H amorphous films, conductivity and temp. dependence of optical gap 80−100462
Si:H amorphous films, effects of glow-discharge prep. conditions on H content 79−46969
Si:H amorphous films, IR spectrum and struct. 80−97277
Si:H amorphous films, role of Ar in deposition process, IR absorpt. and photocond. meas. 80−50321
Si:H amorphous glow discharge film, optical absorpt., near IR region 79−87518
a-Si:H film, glow discharge deposited, H profiles, doping level 80−84202
Si:O,H amorphous, electronic and struct. props. 80−50391
Si:P, heavily doped, glow-discharge-produced, elec. and optical props 80−2497
Si-B amorphous film, plasma deposited, characterization 79−69828
Si-containing inorganic films, for microelectronics appls., plasma deposition and characterisation 79−78904
Si-F-H:P, film, dark cond., struct., Raman scatt. 80−88588
Si-H, amorphous, on Nb or W, spectrally selective absorber, IR spectra 80−26164
Si-H, amorphous, plasma-deposited, H evolution and defect creation 80−44914
Si-H, amorphous, thermal stability and decomp. kinetics 80−24758
Si-H, amorphous plasma deposited film, H content and density 79−82472
Si-H:P amorphous film, dark cond., struct., Raman scatt. 80−88588
Si-Ti-Cr system, plasma coating on Nb, alloy substrates, radiating power 79−60529
Si_xAs_{1-x}:H, amorphous system, struct. and defects, Raman and EPR meas. 80−49103
Si_xB_{1-x} films, anal. of H ratios and profiling using nucl. techniques and Rutherford backscatt. 80−61202
$Si_{1-x}C_x$:H glow discharge films, local atomic struct., XPS and AES study 80−93448
$Si_xC_{1-x}H_z$ amorphous films, IR absorpt. bands 80−100705
$Si_xC_yH_z$ films, reactive plasma deposited, comp., IR anal., and optical props. 79−95945
SiN film, elastic stiffness and thermal expansion coeffs. 80−107451
SiN_x, composition and characterisation, optical and elec. props. 80−15401
SiN_x films, plasma-deposited, radial wafer-to-wafer uniformity 80−104073
SiN_x films, process and props. 80−80986
SiN_z, plasma deposited, H content meas. 78−63949
Si_3N_4 and SiO_2 on InP, interface props., n-channel MOSFET action 80−93003
Si_3N_4 facet coating, GaAs-GaAlAs TJS lasers, high power density single mode operations 79−86186
Si_3N_4, film, H_2 concentration profile, chem. bonding 79−33205
Si_3N_4 films, plasma deposited over substrate steps, fast etching phenomenon 79−34168
Si_3N_4, hard coating preparation by ion beam methods 80−25579
Si_3N_4 off-stoichiometric plasma-deposited layer, AES evaluation of comp. 78−26781
Si_3N_4, surface passivation of GaAs and interface props. 80−93005
Si_3N_4:H, film, impurity profile determ. by 1.2 MeV proton-proton scatt. 80−49256
SiO_x thin films, deposition and characterisation study 80−80133

plasma deposited coatings continued
Si_xO_{1-x} films, anal. of H ratios and profiling using nucl. techniques and Rutherford backscatt. 80−61202
Sm-Co deposit, arc plasma sprayed, crystal and micro struct. exam. 79−28248
ThO_2, plasma deposition of crysts. and their characterisation 80−20800
TiN_x, ion condensing metal plasma stream, coating microhardness, chemical reactions 79−42426
Ti_3N_4 plasma condensation on steel and carbide *(Russian)* 80−20796
WC, explosive plasma sputtered coatings, struct. and props. *(Russian)* 80−100783
ZrO_2, plasma deposited, porosity, gas permeability and dielectric strength 79−52125
ZrO_2, plasma deposition of crysts. and their characterisation 80−20800

plasma deposition
anodisation of metals and semiconductors, model 79−28952
benzene, plasma polymerisation in glow discharge, thin film IR and free radical EPR obs. 80−2964
carbonaceous film, deposition on RF target in butane plasma 77−16507
ceramics coating by physical vapour deposition processes *(Japanese)* 80−55306
chemistry of plasmas, appl. to IC fabrication 79−79252
diamond, reactive pulse plasma crystallisation 79−95938
dielectric thin film, polymerisation on carrier foils in discharge plasma *(German)* 77−16508
film deposition, ion beam techniques 80−11564
films, preparation using low pressure plasmas 77−40361
flame spraying techniques 79−94825
glow discharge phenomena in plasma etching and plasma deposition 79−69993
heating and evaporation of disperse particles in plasma, calcs. *(Russian)* 77−21021
high energy beam deposition in CO/He and Ar/Kr/F_2 gas mixtures 80−63999
inorganic thin films, review 80−50564
ion plating, evaporation sources, gaseous media, and transport modes 80−80984
IR thin film plasma deposition processes 80−87466
LPCVD-type plasma-enhanced deposition system [for semiconductor wafer processing] 80−60791
macroparticles elimination from plasma stream, using curved plasma duct 80−33826
optical fibre plasma activated CVD, influence of substrate temp. 80−48475
optical fibre preparation by Ar plasma augmented vapour deposition 80−48478
optical fibre preparation using RF plasma deposition 78−55479
optical fibres, plasma augmented vapour deposition 80−69561
optical fibres prepared by plasma-augmented vapour deposition 79−50451
organic film, synthesis and characterisation, review 79−91584
oxide film, RF plasma deposition on glass or $In_{2-x}Sn_xO_{3-y}$, and liq. cryst. aligning props. 77−48350
plasma processing apparatus, RF discharge plasma conditions 77−72521
polymer film, RF plasma deposition on glass or $In_{2-x}Sn_xO_{3-y}$, and liq. cryst. aligning props. 77−48350
polymer layer, glow deposition rate obs. in DC discharges 78−68633
polymer thin film growth by glow discharge polymerisation, temp. depend. 78−68632
polymeric electret films, produced in HF discharge, props. *(Russian)* 80−20578
polymerisation on solid substrate in RF discharge 80−2963
polymorphous thin film production in HF discharge 80−1855
pulsed plasma generator applic. *(Russian)* 77−21037
quartz, thin film deposition, by low pressure high freq. induction plasma *(Russian)* 79−69992
reactor for materials research good processing 77−40362
semiconductor film growth, multilayer systems, spectroscopic ellipsometry, review 80−103603
semiconductor IC production, plasma CVD equipment for insulating films 80−25572
sputtering, particle velocity and disperse composition *(Russian)* 80−40258
styrene, plasma polymerisation in glow discharge, thin film IR and free radical EPR obs. 80−2964
techniques, comparison between electron beam evaporation and high rate with plasmatron 78−11110
thin film growth measurement using galvanically separated quartz monitor probe *(German)* 80−11576
thin films, deposition techniques, review 80−80964
torch anode design improvement to increase deposition efficiency 79−87750
vinyltrimethoxy silane, plasma polymerised, abrasion resist. antirefl. coating for polycarbonate 77−42635
VLSI processing, radiation, and hardening 79−24088
BN, deposition of wurtzite type layers, by reactive pulse plasma crystallisation 79−28953
BN film, high temp. reactive plasma deposition, struct., resist., and dielec. const. meas. 77−7988
C, diamond like, reactive pulse plasma crystallisation 79−95938
C film, amorphous, growth under ion impact in butane plasma, and IR transparency 78−52688
C, film with random struct. growth from ion impact damage in butane plasma 79−83139
CdTe, sputtered film, electrode effects in AC characts. from equivalence impedance meas. of metal-CdTe-Al struct. 79−82686
CeO_2, plasma deposition of crysts. and their characterisation 80−20800
Cr coatings, plasma-chemical deposition using transport reactions *(Russian)* 80−16191
GaAs, selective plasma oxidation, interface props. 80−100933
GaAs thin films, reactively sputtered, ESCA/XPS study 80−97430
GaN, deposition from plasma reactor, organo-metallic and donor-acceptor complex exchange in HF plasma 80−38839
GaN, plasma deposition and elec. cond. 78−60585
GaP, plasma deposition and elec. cond. 78−60585
HfO_2 crystallite growth from oxide plasmas, growth morphology 80−59417
HfO_2, plasma deposition of crysts. and their characterisation 80−20800
Ni wire plasma sputtering with W particles, coagulation, struct. and particle size *(Russian)* 80−40260

plasma deposition continued
P, amorphous, prepared by chem. transport in low-press. H_2 plasma, radial distrib. function 80−64899
S-based amorphous semicond. film, prep. by plasma decomp. of H_2S-N_2-NH_3, and characterisation 80−80422
Si, amorphous film, glow discharge deposition, rate enhancement by mag. field 80−65412
Si, amorphous film, plasma preparation 78−72740
Si film, glow discharge deposition, SiH_4 discharge parameters obs. 80−44030
Si film, prep. by plasma-induced CVD from $SiCl_4$-H_2 79−83132
a-Si p-i-n and c-Si p-n junction solar cells, design concept differences 80−94031
Si polycrystalline films, characts. 80−80988
Si solar cells, polycrystalline, from recrystallized plasma deposited thin films 80−104509
Si:H, amorphous, control and anal. of deposition, using plasma spectroscopy 80−45230
Si:H, amorphous film, prep. by plasma decomp. of SiH_4 under mag. field, and characterisation 80−45239
Si:H, plasma-deposited amorphous film, proton mag. reson. 80−44931
Si:H amorphous, plasma-deposited, luminesc. decay 79−73989
Si:H amorphous film, prop. by glow discharge deposition, and plasma parameter effects on props. 80−45240
Si:H amorphous films, optoelectronic behaviour depend. on impurity incorporation during plasma deposition 80−49804
Si-containing inorganic films, for microelectronics appls., plasma deposition and characterisation 79−78904
SiH_4-He, reaction mechanisms of RF glow discharge deposition process 79−95944
SiN_x films, plasma enhanced CVD, props., meas. and interpretations 80−80987
SiN_x films, process and props. 80−80986
Si_3N_4 layers, RF plasma deposition and props. 79−43155
Si_3N_4, MIS struct. form. by reactive deposition on n-InSb substrates, C/V meas. 80−103752
Si_3N_4 passivation planar plasma deposition system, productivity increase 80−40269
$Si_xN_yH_z$ film, prep. from plasma-induced CVD from Si-NH_3 79−83132
SiO_2 liq. cryst. alignment films prod. by RF plasma beam technique 80−76198
SiO_2 nonporous film, plasma deposition method, appl. to semicond. device manufacture *(Russian)* 80−16197
SiO_2 thin films, plasma deposition in prod. planar reactor 80−2966
SiO_x thin films, deposition and characterisation study 80−80133
ThO_2 crystallite growth from oxide plasmas, growth morphology 80−59417
ThO_2, plasma deposition of crysts. and their characterisation 80−20800
UO_2 crystallite growth from oxide plasmas, growth morphology 80−59417
ZnS, thin film deposition, by low pressure, high freq. induction plasma *(Russian)* 79−69992
ZrO_2 crystallite growth from oxide plasmas, growth morphology 80−59417
ZrO_2, plasma deposition of crysts. and their characterisation 80−20800
ZrO_2-Y_2O_3 microspheres, stabilised, from HF air plasma, struct. 79−78917

plasma devices
see also magnetohydrodynamic convertors; plasma diodes; plasma focus; plasma guns; stellarators; Tokamak devices
2X11B, drift cone mode stabilisation with warm plasma, radial normal mode calc. 78−51294
ablation type magnetoplasma compressor, mech. of plasma focus formation 78−79478
AC electrodeless narrow gap discharge, anal. and plasma display design 80−70063
AC plasma display panel wall charge magnitude and distribution probe 78−67487
accelerator, 0.2TW proton pulse generation 77−22618
accelerator, coaxial, current sheet shape 78−83621
accelerator, coaxial, HF field meas., energy removal *(Russian)* 77−3997
accelerator, coaxial, motion and shape of snowplough sheets 78−59689
accelerator, coaxial, multi-component plasma dynamics *(Russian)* 78−22576
accelerator, coaxial, propagating plasma sheath, mag. field meas. 79−90474
accelerator, coaxial *(Russian)* 78−26337
accelerator, coaxial with external mag. field, rot. and pinch 77−7603
accelerator, compensated ion beams, ion dynamics *(Russian)* 77−47274
accelerator, electrodynamic, end-fire type, limiting operating conditions 79−55575
accelerator, electrodynamic, modulated, optimum operating conditions 77−27749
accelerator, end-fire type, high-current discharge effects, anode damage 79−27839
accelerator, Hall type, cathode region mag. field effects, elec. and thermal characts. 77−62412
accelerator, Hall-current type, drift instability dispersion relations 77−19705
accelerator, impulsive, investigation under cosmic conditions 77−53399
accelerator, linear rail type, plasma cluster ionised front vel., theory 79−46494
accelerator, microwave generation by RF instabilities, discharge voltage depend. 77−7538
accelerator, open single lens Hall current type, characts. 77−55178
accelerator, stationary erosion elec. arc type, with mag. cathode spot confinement, flow *(Russian)* 79−98996
accelerator, steady-state, intermediate power, I-V characts., discharge parameters 78−1913
accelerator, two-stage, with closed electron drift, auxiliary mag. lens effect *(Russian)* 77−47271
accelerator with pre-ionised Cs, closed electron drift, and extended accel. zone, I-V characts. 80−14944
accelerators, current sheet dynamics, interferometry and probe meas. 78−26351
accelerators, technical appls. 79−60203
ACT-1, current generation by unidirectional lower hybrid wave 80−92306

plasma devices continued
adiabatic toroidal compressor, power balance anal., electron density and temp. diagnostics 77−51219
antenna, focusing hog-horn antenna for microwave diagnostics in plasma machines 80−96395
arc, DC, wall-stabilised, plasma source for biological soln. spectrochem. anal. 80−41343
arc, low press., large cross section anode plasma with constricted channels, broad electron beam prod. 80−38840
arc furnace, ignition and stabilisation *(French)* 78−47187
Astron Accelerator, 5 MeV, 400 A, 500 MHz modulation system for beam energy 77−24202
Astron ion ring configurations, adiabatic compression of ion rings and associated plasma, kinetic theory 79−46469
auto-resonant ion acceleration concept, computer simulation 77−24208
automatic feedback parameter analogue simulation 78−26336
automatic initiator for microwave induced plasma 78−88682
beam-plasma ion source, max. current calc. 77−11356
bimetallic electrodes for plasma torches, Cu to W joining methods 80−24266
bragg effects in microwave transmission through stationary plasma structures 80−83944
branch divertor for Tokamaks *(Russian)* 80−54051
bundle divertor, Tokamak plasma, scrape off layer density decrease, model 80−28851
capacitor, coaxial and planar magnetoplasma, impedance characts. 78−42837
capacitor, impedance of warm inhomogeneous magnetoplasma capacitor 79−41886
capillary charge torch, flow deflection mechanism *(Russian)* 78−83539
cathode plasma dispersion in transverse mag. field *(Russian)* 79−98997
centrifuge, crossed-field, ion wind effect on separation 80−79591
centrifuge, enhanced isotope separation in crossed E×B fields 79−18305
centrifuge, isotope and element separation mechanism 80−6291
centrifuge, rotating plasmas, balance and separation processes 78−1911
centrifuge, weakly ionised, for mass separation 80−106985
chemical reactor, methane-H_2 system, exptl. and thermodynamic investig. *(French)* 78−15698
chemical reactors for surface layer removal, regime parameters *(Russian)* 80−54050
chromatograph/mass spectrometer column overload prevention valve 80−16748
chromatograph/mass spectrometer sample overload protection 79−39237
chromatograph/mass spectrometer simultaneous electron impact/chem. ionisation carrier gas mixture 79−30600
closed-line magnetic field approach to plasma confinement, in toroidal systems 78−42792
cluster accelerator, external mag. field influence 80−6287
coaxial accelerator, current density distrib. 78−26352
coaxial accelerator, propag. vel. and shape of luminous front 78−22578
coaxial plasma accelerator, neutron yield meas. *(Russian)* 78−38551
collective ion acceleration by controlled motion of virtual cathode in relativistic electron beam 77−24210
collective ion acceleration by cyclotron of space charge waves in relativistic electron beam 77−24204
collective ion acceleration following relativistic electron beam injection into low press. gas 77−24209
collector, hollow, electron beam deceleration-produced plasma props. 79−27794
conference on fusion research and plasma physics, Innsbruck, Aug. 1978 80−27033
conference on plasma science, Monterey, CA, USA (May 1978) 79−37442
crossed field tube for high power on-off switching 77−24222
crossed-field plasma centrifuge, effect of ion wind on separation 79−31722
Culham Levitron, drift island diffusion 80−59267
current controller, precise, 0-5 mA, for moderate density plasma diagnostics 79−46483
current multiplier, gas discharge device, current amplification 80−49018
cutting at elevated press., underwater appl. 78−87507
direct energy space charge based convertor, numerical simulator 77−35406
display panel, short-gap atm. discharge with needle-sphere electrodes 77−4008
DITE phase II neutral injection system investig. 80−28814
double column plasma reactor, source of chemical reagents *(French)* 77−1023
double plasma and other synthesised plasma devices, adjustment of ion energy distribution 80−19625
duopigatron, preacceleration effects on ion beam transmission effects 78−87005
duopigatron plasma generator, emission aperture shape effect on ion optics 78−5956
ECR ion source, extracted ions charge state distrib., confinement times 80−24268
electron beam for vacuum metallurgy *(Japanese)* 78−18465
electron beam switch, microwave energy compression 80−96396
electron emitter with constricted arc discharge, characts., anode spots effects 80−70040
electron gun, coaxial, electron flux formation in strong mag. field *(Russian)* 79−98998
electron gun, glow-discharge type, with plane-frustrum cold cathode, characts. 79−7495
electron gun, pulsed, plasma emitter, ≥50 kA, ≥95% transmission coeff. 77−18134
electron gun, with plasma anode, high intensity microsecond electron beam *(Russian)* 78−21271
electron gun use of glow discharge lamp for Auger spectroscopy 77−31027
electron gun with plasma cathode and built-in gas generator 80−106947
ELMO Bumpy Taurus, trapped-particle instabilities 79−31184
ELMO bumpy torus, collisional regime, radial transport 79−41801
ELMO bumpy torus, macroscopic MHD stability and beta limit 79−31186
EM macroparticle acceleration, high press. gas temp. density 80−79583
EM radiation detection at long wavelength, by glow discharges 78−58035
EM shock tube for obtaining short pulses of visible radiation, plasma flow anal. 78−1909
plasma devices continued
equilibrium of plasma without shell, impurities outside coronal equilibrium and hollow profiles, MAKOKOT code 80−28774
erosion magnetoplasma compressor, stabilisation of electron temp. in compression region 79−19057
evaporating-wall high-current discharged, pulsed press. 79−27838
fast gas valve for gas injection into vacuum 78−74011
fast H gas injection system for plasma physics expts. 78−71550
field reversed mirror configuration, sustaining a toroidal current 80−28804
field-shaping coil, double layer system 78−42785
focus discharge in Mather accelerator 80−24257
focused flow device, one-dimens. radial compression theory 77−3975
front-end electroreactive accelerators, appl. to study of Earth magnetosphere 77−53400
furnace, modified plasma torch type, doped MgO single crysts. growth *(Japanese)* 79−95923
furnace, smelting, burning arcs interaction 78−1944
furnaces, mineralogy and extractive metallurgy appls. *(French)* 80−28849
fusion, international fusion technology program 80−95423
fusion reactor, beam and plasma direct converters 80−42861
fusion reactor, Princeton large torus 3-coil test 78−54945
fusion reactor, toroidal device with nonplanar mag. axis, magnet and coil engineering 78−55009
fusion reactor engineering, conf. San Francisco, USA (Nov. 1979) 80−91248
fusion reactor Zephyr experiment, toroidal chamber, ASDEX project *(German)* 80−73992
Garching belt pinch MHD equilibria, cylindrical slab model 78−34353
gaseous core reactor, basis for direct nucl. pumped gas laser 78−33725
gaseous core reactor, fission fragment effect on electron energy distrib., radiative transport 77−24062
gaseous core reactor, laboratory scale UF_6 plasma confinement expt. 77−23190
gaseous core reactor, UF_6 technology 78−33254
gaseous core reactor based on U plasma core, present research 78−33244
gaseous core reactor with U-fuelling, preliminary expts. 78−33243
gaseous nuclear reactor with RF heated UF_6 fuel 77−23189
generator, ignition conditions for power superposition between two generators *(French)* 78−9799
generator, one-dimens. model 79−64881
generator arc chamber, hydrodynamic struct. 80−1817
glow discharge, detector for millimeter rad., cyclotron reson. effect on sensitivity 78−62222
graphic display, large-area, selection circuitry 78−38556
grid controlled switching element, stationary conducting state 79−77430
grid controlled switching element, stationary conducting state, arc conditions 79−77431
gyrotron 50 GHz design considerations 80−28728
gyrotron for electron-cyclotron heating in large Tokamaks 80−28751
gyrotron power source development in MM wavelength range 80−28852
gyrotrons, space charge phenomena 80−28868
Hall accelerator, azimuthal drift current, induction meas. method 79−23465
Hall accelerator, direct flow, I-V characts. 78−26350
Hall accelerator, electrothermal instabilities, current conduction 77−51159
Hall accelerator, four-lens, pure ion beam struct. 78−66441
Hall accelerator, ion current oscills. *(Russian)* 79−98995
Hall accelerator, point and jet ionis. modes 78−26349
Hall accelerator, variations in performance when using He gas *(Russian)* 80−103195
Hall accelerator, with extended accel. zone, high freq. plasma waves 78−67441
Hall accelerator, with extended accel. zone, ion stream modulation at exit 78−79480
Hall current accelerator, with extended accelerator zone, local plasma props. meas. 79−64917
Hall plasma accelerator, using Cd vap. 78−71553
Hall quasistationary axial plasma accelerator, with anode layer, characts. *(Russian)* 79−4193
Hall-current accelerator beam, plasma-optical focusing 77−7605
heavy-particle acceleration by charge-density waves in vacuum and in plasma 80−70044
Heliotron D, confinement of ohmically heated plasmas 79−50879
Heliotron D, shear Alfven wave heating expts. 80−28716
Heliotron-D, low freq. shear Alfven wave heating, diagnostics 78−1858
Heliotron-D device, Joule current inhibition 79−99001
Heliotron-E, physical aspects, outline 79−99002
heterogeneous plasma discharge, spatial information modelling and processing algorithms 78−14229
high-current multirod cathode, influence of absorption effects on characts. 80−20756
high-current travelling wave plasma accelerator appl. to plasma-wall interactions 78−5954
high-energy plasma technology, equipment, cold plasma prod. *(Russian)* 78−51367
hollow cathode, through-flow arc mode 79−27837
hot cathode, for plasma and electron physics in underground laboratory 79−35480
HV glow discharge as plasma electron source, characts. 80−44031
ICP torch design method, using hydrodynamic flow patterns 80−24256
induction plasma torch, temps. and velocities effects of cool central gas feed 78−94942
induction-coupled plasma system, use for spectrochem. anal., calibr. 77−90708
inductively coupled plasma for atomic emission spectroscopy, multielement method for liquids and dissolved solids 79−96395
inductively coupled plasma torch configurations 77−82608
inductively coupled plasma-AES, present and future position in analytical chem., review 80−7887
inductor plasma-filled, producing liq. metal MHD in trough *(Russian)* 79−1259
inert gas rotating arc meas. in plasma centrifuge 78−75438
injector, plasma parameter determ. by laser light scatt. *(Russian)* 78−22573
ion acceleration from turbulent plasma by electron beam 77−10137
ion accelerator, two-stage and axial, with plasma anode layer 79−71561

plasma devices continued
ion accelerator with closed Hall current, eqns. of motion *(Russian)* 77−47273
ion optical system, ion beam collimation quality determ. 77−10138
ion source, cold cathode, for mass spectrometry 80−42293
ion source, FEBIAD, plasma and beam characteristics 78−66002
ion source, IBM-5, without external mag. field 80−5428
ion source, stationary, 50 to 400 eV range 79−97469
ion source anode layer struct. with closed Hall current, anomalous cond. effects *(Russian)* 77−46437
ion source discharge, stable, theory 79−31278
ion source using HF glow discharge, temp. and electron density profile meas. *(German)* 78−70221
ion sources, large vol. mag. multipole development 80−27857
ion-acoustic instability oscillations in collisionless single ended Q-machine 80−38731
isotope separation, rotating plasma, skewed mag. and elec. fields *(Russian)* 78−70969
isotope separation in rot. plasma column of hollow cathode discharge 78−75454
JET, control system, communications, diagnostics, data storage and anal., NORD computers 80−68943
JIPP T-II, lower hybrid wave heating 80−28722
JIPP T-II, neutral beam injection, investig. 80−28810
JXFR, neutral beam injection system, gas-beam interaction secondary particles 80−106227
large volume magnetic multipole plasma source, operating characts. 80−100084
laser beam cut off device, expanding supersonic plasma 79−68412
laser electron accelerator, mechanism 79−81103
laser pulse amplifier using induced Raman or Brillouin processes 80−1279
laser-plasma source, for pulsed X-ray lithography 79−30636
lens, unipotential, for proton beam focusing 79−41326
lens for ion-beam, focusing and form. of intensive beam *(Russian)* 78−21270
Levitron, fluctuations, diffusion and beam-induced currents 80−28616
levitron, min.-average-B, analytical model 79−50876
Levitron, neutral beam induced reverse electron current 78−59620
levitron, overlapping and stochasticity, critical limits 80−59268
light source, inductively-coupled plasma, for optical emission spectrometry *(Japanese)* 79−48020
light sources of high radiation intensity 80−19084
linear accelerator, rail type, plasma cluster ionised front propag. vel. meas. 79−10665
linear plasma induction accelerator, high current ion beam source *(Russian)* 78−21272
liquid metal plasma valve circuit breaker, 15 kA-30 kV, fusion reactor application 78−74488
LITE deep well mag. baseball, heavy ion beam probe 77−84518
magnetic confinement, structural anal., combined interactive/batch computer environment 80−91255
magnetic field configurations, analytical and numerical methods 79−86623
magnetic flux trap, loop probe meas. in Ar(Kr) 79−14621
magnetocumulative generator, megampere pulse shaping, explosively compressed plasma column *(Russian)* 78−1912
magnetoplasma compressor, cathode potential drop, plasma flow *(Russian)* 78−22577
magnetoplasma compressor, construction and applications 79−32831
magnetoplasma compressor, impurity separation in channel, numerical investig. *(Russian)* 79−37467
magnetoplasma compressor, operating modes, pinch description 77−84531
magnetoplasma compressor, operating modes, probe diagnostics 77−84530
magnetoplasma compressor compression region struct. streak and framing camera diagnostics 77−84532
magnetoplasmadynamic accelerators, anode power 78−71546
magnetoplasmadynamic accelerators, flowfield and performance 77−3996
magnetron, with split electrodes, radial ion (electron) cluster rot., fusion appl. 78−17415
magnetron ion source, Penning phenomena effects on Hg ionisation in plasma 79−18069
maser dissociator, H beam production performance characts. 78−87034
mass separator, plasma-optical model, optical props. optimisation 78−16894
mass separator, with 3-parameter focusing, plasma optical model 78−9855
materials development for fusion 80−33804
MHD generator, coal-fired, mol. beam mass spectrometric sampling system 80−52358
MHD generator, open cycle, with shaped magnetic induction, theory of nonuniform electrical conduction 80−28831
MHD generator performance, plasma effective Ohm's law due to anisotropic inhomogeneities 78−67316
microwave noise source, Ar, new similarity rules 77−55177
microwave plasma sources, F atom prod. for HF chem. laser 78−22140
microwave-induced He(Ar) plasma cavity, excitation source for optical emission spectroscopy 77−44567
mirror machine end-loss processes, review 77−55164
MITE accelerator, long self-magnetically insulated power transport expts. 79−90471
multidipole, appl. to provide source for magnetized plasma column 80−33810
multifilament plasma source, multipole mag. field effects on characts. 79−46462
multipurpose reactor for materials research and processing 77−40362
NASA Lewis Bumpy Torus, high pot., characts. 77−65904
nonisothermal vertical impinging jets of differing momentum, one and two phase *(Russian)* 77−72511
nonstationary MHD plasma flow, in coaxial accelerator in condensed media 79−60204
optical shutters, fast acting, for Nova laser fusion reactor 78−66854
PARODIE device for construction of large size homogeneous stationary plasma *(French)* 78−14223
Penning discharge, ion heating mechanism *(Rumanian)* 78−59710
peripheral suppressor grid recovery systems for Tokamaks 80−28813
periplasmatron discharge development at FAR for JET 80−99380
PIACE-R1, design fabrication and testing 80−92378
plasma devices continued
pinch experiment, high energy Cu foil fuse for implosion in multimegajoule region 77−24218
plasma sheath, nonequilibrium, intense ion beam extraction 77−89267
plasma torch behaviour during laser irrad. of Pb surface *(Russian)* 78−87506
plasmatron, erosive slot-shaped, plasma jet form. *(Russian)* 78−75437
plasmotron, DC, high-power, long-operating, coaxial elec. arc, principles 78−42832
polychlorinated biphenyls waste disposal by pyrolysis, plasma torch appl. 80−76487
position control system for plasma column, stability 80−106982
Proto-Cleo torsatron, vac. mag. surfaces shape, electron beam diagnostics 79−73035
puffatron, charge exchange neutrals, emitted from rot. plasma, meas. 80−106979
pulsator, accumulation of impurities and stability behaviour in high density regime 80−28835
pulsed electrodynamic plasma accelerator for prod. of intense microsecond pulses of low-energy electrons 79−90476
pulsed electron source 77−46439
pulsed erosion jet, energy characts., heat flow distribution *(Russian)* 80−33825
pulsed induction discharge, Hall effect 79−64833
pulsed plasma light source for vacuum UV to visible regions 77−45877
quantometer, quantitatively coupled, for emission spectrochem. anal. *(Japanese)* 78−83624
rail accelerator, ambient medium heating expt. 78−75439
rail accelerator, ambient medium heating in tube 78−63599
reflection triode, prod. of high current ion beams *(Russian)* 80−83230
reflex tetrode, ion beam extraction anal. 80−48903
resonant helical divertor 77−62411
review, laboratory plasma devices 80−79589
RF induction discharge excitation source for at. emission spectroscopy 79−87919
RF induction plasma torch, temp., elec. cond., efficiency values from mag. probe meas. 78−42836
RF ion source, 15 cm diameter, stable working conditions calcs. 78−86388
RF plasma torch, temp. distribution and EM field, one dimensional analysis, using finite element method 80−24264
RINGBOOG II, cold plasma blanket research 79−98992
rocket engine, laser evaporated target, nozzle for impulse augmentation 79−23439
rotating plasma device, G-II device for plasma research *(Japanese)* 80−70042
scalpel, A or He, animal surgery studies 77−52912
Scyllac, computational plasma MHD for stable equilibria 77−84478
self-accelerating microwave ion and plasma sources 78−66000
shutter for multichannel Nd:glass laser 80−64088
small-aspect-ratio, small-major-radius Tokamak reactors 78−79452
source, dielec. chamber, plasma flow characts. optimisation 80−38574
space charge lens for high current ion beams 78−55075
space plasma chamber, design and appls. *(Japanese)* 77−22039
spark, high voltage, resistive phase 78−67453
spectrometer plasma torch, high-power operation 79−40621
spheroimak devices, magnetohydrostatic equilibrium config. 80−83965
stationary magnetoplasmadynamic source, elec. and thermal characteristics 80−14915
steady-state rotating plasma, for mass separation of elements *(Russian)* 78−25732
surface heat treatment using plasma torch with rectangular jet 77−27751
surface heater, magnetically scanned, appls. 79−94826
surface-plasma Penning source, intense H^- beam production, ion-optical characts. 79−13892
switch, grid-controlled Cs-Ba discharge, spontaneous current cutoff 80−19626
switch, plasma-jet-triggered, 10 to 100 kV operation 79−55574
switch, triggered vacuum gap, plasma buildup and breakdown delay 79−73048
switches, high press. surface discharge, review 80−103208
switches, laser triggered gap switches as heavy duty high speed switches *(Japanese)* 78−94940
switching, fast-opening, for use with relativistic electron beam diode 77−47275
thermionic convertor, elec. power density on optimisation 79−10723
thermionic emission triode, with auxiliary discharge, rectifying parameters 79−64925
thermionic plasma converter, overneutralised, instability simulation 79−14619
thermonuclear fusion research, economic factors 80−73991
thermonuclear ignition by means of compact devices *(Italian)* 80−52778
thermonuclear target, transport of relativistic electron beam *(Russian)* 78−38552
thin-film thermometer for meas. of transient plasma heat fluxes in divertor assembly 78−18447
three-electrode DC Ar plasma source for optical emission spectrometry 80−62735
three-rails accelerator, one cluster regime 80−6288
Tokamak gettering, Ti thin films, H absorption and desorption, Auger electron spectrosc. 80−75092
Tokamak plasma, line spectra of highly ionised heavy atoms 80−79567
Tokamak reactors, role of α-particles review 80−86971
Tokamak Thor, discharge, electron distribution function, laser Thomson scatt. 80−59327
Tokamaks, PLT and PDX, X-ray diagnostics 80−75104
Topolotron, plasma cross section reconstruction, Farey dissection optimization, computer anal. 77−84523
torch, as spectroscopic light source, optical emission and at. absorpt. appls. 77−51243
torch, reduced size inductively coupled, operation mode and detection limit 80−43994
torch, RF, particle heating 77−68810
torch, with water stabilisation of elec. arc, features 77−72505
torch cutting-punch machine for steel panels 78−18466
torch for cutting metals and alloys, improved design with double arc protection 79−8401
torch plasmatron, high-freq., burning regimes *(Russian)* 80−38723

plasma devices continued
torch with magnetically traversed arc for surface heat treatment 79−32832
Tormac DT fusion reactor, power gain and net output 78−58402
toroidal fusion reactor, common problems in control system software design 77−23282
toroidal plasmas, axisymmetric, high mode number stability 80−28642
toroidal solenoids, helically wound, form factor calcs. 80−100091
TPD-plasma, optical escape factors and population densities 79−37460
triode, reflex, anode design for ion beam impedance collapse 78−9862
triple plasma devices, for strong double layers obs. in mag. field 79−60177
tritium filling and monitoring apparatus for particle beam inertial confinement fusion targets 80−57949
underwater plasma weld cooling 79−1932
valve for high-power conversion/switching, liq. metal cathode, design features 78−9865
waveguide containing relativistic electron beam, slow cyclotron wave 80−106983
welding and cutting appl., benefits 77−39478
welding torch with ring nozzles, shielding gas discharge modelling 79−7497
Wisconsin supported toroidal octupole, ion cyclotron reson. heating 77−89276
Ar inductively-coupled RF plasma torch, computer model 78−71559
Ar plasma source in TM_{010} cavity, for soln. anal. 79−48032
CO_2 laser-plasma amplifier, 11-16 μm range 78−22173
Cs plasma thermoelectronic laser energy convertor 78−90421
Cs thermionic converter, auxiliary discharge to reduce voltage drop 79−10724
Cs-Ba triode arc switch, high-current, low-voltage, pulsed control 78−71551
H, ACT-1 toroidal plasma, externally launched ion Bernstein wave 80−106967
H, atomic beam prod. at. 90 to 500 eV from surface plasma source 80−38729
H plasma target investig. *(Russian)* 80−106981
H^-, ion source, CW plasma device, current maximisation 79−22521
H_2O, as dielectric insulator *(Russian)* 78−75430
He plasma chemical device, integrated electron density meas., interferometric method 79−55548
^{3}He-Xe, nucl. pumped laser plasma, distrib. functions 79−36880
Li plasma dynamic laser, using supersonic nozzle, population inversion, excitation cross section 78−50760
SF_6-N_2-Ar mixture high-current multispark discharge switching characteristic 78−67444
U enrichment by plasma centrifuge, partial pressure distrib. obs. 78−74501
U enrichment by plasma centrifuge, rotational velocity meas. 78−74502
U plasma fission reactor, for space vehicle power, propulsion, terrestrial appls. 77−3145
W high-current multicavity thermionic cathode, erosion mechanisms, sputtering 79−55570
ZrD, electrodes with externally ignited vacuum arc, source of D^+ ions 80−33845

plasma diagnostic techniques
see also plasma probes
Abel inversion applied to plasma spectroscopy, interactive method 79−23447
absolute wave amplitude determ., Langmuir probe RF coupling 78−75425
acid phthalate curved crystal spectrograph, diffraction efficiency calc. method 80−79630
acoustic wave interaction, diagnostics appl. 78−83541
acoustic wave temp. determ., pulsed discharge inhomogeneous gas heating 77−55175
active beams for charge exchange meas., Tokamak plasma diagnostics appls. 80−48991
active particle beam systems for meas. of plasma pot., current and impurity profiles 80−48990
active spectroscopy of 4-photon scatt. in cold plasma *(Russian)* 80−1839
active-recording X-ray crystal spectrometer for laser induced plasmas 77−3993
advanced magnetic confinement fusion, plasma neutron diagnostic techniques with good spatial and energy resolution 79−46478
afterglow, electron energy distrib. meas., Langmuir probe characteristics 77−80350
Agat, streak image camera with picosecond time resolution used in plasma investig. 80−38717
air, hypersonic wake, electron recomb. coeff., temp. depend. meas. 79−27834
air arc temp. meas. by N_2^+ integrated emission coeffs. 80−59314
air blast circuit breaking arcs, elec. grad. using plasma probe methods 78−87527
ALVAND 2 diagnostic Tokamak construction 78−14217
AM active microwave method for density meas. 80−87948
analyzing signals, generation for cosmic plasma investig. 79−90469
arc discharge, cathode spot high current density meas., expt. 78−9879
arc plasma flow, velocimetry methods 80−43992
arc spectrography, applic. of equidensitometry *(German)* 77−1962
arcs characts. meas. temp. and particle densities determ. *(French)* 80−19651
atom concentration determ. *(Russian)* 77−56305
atom temperature measurements using thermal diffusion 80−43985
atomic profile determ., Fourier analysis, deconvolution of Fabry-Perot interferograms *(French)* 80−48972
automated diagnostics 79−94820
axially symmetric plasma, error estimate of optical diagnostic methods 77−84500
beam-foil spectra, heavy metal contaminants, rel. abundance and charge stable comp. diagnostics 79−46480
bremsstrahlung attenuation obs., electron distrib. anisotropy, turbulently heated plasma 78−59682
broadband UV detect. in Tokamak using photoelectric effect and photodiode array 79−90464
calorimeter for absorbed energy meas. in laser prod. plasma 78−5942
calorimetric system for recording plasma blowoff and scattered light distributions from laser plasmas 80−59287

plasma diagnostic techniques continued
cellulose nitrate film, ion track density, quantitative assessment using Fourier transform techniques 79−86610
cellulose nitrate film ion data, dark-field illum. image recording photographic method 80−70031
Ceratron multiplier, for plasma diagnostics on charge-exchanged fast atoms, local counting efficiency 77−51233
coaxial line, open-ended, for microwave diagnostics 77−27736
coherent four-photon light scatt. by ionic sound 79−14618
collective electric field fluctuations of two-temp. electron gas nonthermal plasma 80−43882
collective oscills. in toroidal plasma, microwave scatt. diagnostic technique, review 80−48863
collective plasma density fluctuations, far IR scatt. apparatus obs. 79−32818
concentration determ., metal atoms, HFS intensity redistrib. method 77−84498
conference, high temp. plasma diagnostics, Tennessee, USA (Jan. 1976) 77−31528
corpuscular diagnostic method of metastable atoms in glow discharge plasma, review *(Czech)* 80−24241
corpuscular techniques and devices, SM magnetic trap investigation example 77−43069
current controller and rapid sweep electric probe characts. generator 79−46483
current transport at the surface of a hollow cathode, current distrib. technique 80−54048
data acquisition system for Texas Turbulent Torus 78−4601
DC plasma atomic emission spectrometry system, characterisation of interelement enhancement effect 80−89549
dense plasma, thin struct. component intensity ratios for H-like ions *(Russian)* 77−76194
density and mag. field profile determs. in diffuse pinch using magnetoacoustic oscills. 80−48986
density fluctuation evaluation by microwave interferometry 78−67437
density meas. by interferometer 78−55748
density meas. by Langmuir probe and microwave interferometer 80−28819
density measurement by short-circuit effect 79−23460
density measurement of laser-compressed plasma, X-ray line shift *(German)* 80−48967
density measurements, via quadrature interferometer 78−1900
density profiling by interferometry with rapid spatial scanning, and Thomson scatt. of short laser pulse 80−49014
DFS-8 spectrograph, attachment for oscillographic recording of line shapes 80−105721
differential ion flux vector meas. technique 78−18459
diffraction radiation characts. of an open conducting periodic struct., temp. and elect. conc. determ. *(Ukrainian)* 80−70004
diffusion, of heat and particles, due to collisionless drift instability, probe diagnostics 78−59555
digital bispectral analysis and its applications to nonlinear wave interactions 79−73036
digital interferometer, 2 mm wave, for Tokamak discharges in upgraded DIVA 78−75417
digital spectral techniques in plasma fluctuation diagnostics 80−49003
diode, field-emission type, Thomson-scatt. diagnostics 80−43988
discharge, Tesla coil type, temp. diagnostics from OH $A \rightarrow X$ intensity meas. 79−64939
discharge studies using UHV systems, reliable gate valves 79−54147
discharge tube with transparent hollow cathode, spectroscopic meas. 79−1368
discharge velocity meas. using photomultipliers 79−19086
dispersion interferometer, with coherent response for multifreq. interrogation of interplanetary plasma 77−22038
DITE Tokamak re-cycling expts., interferometry, mass spectrometry and C thermal desorption probe 78−34356
double-pass rapid-scanning Fourier transform spectrometer, appl. to Tokamak plasma 80−59299
drifting magnetoplasma, new interf. pattern near reson. cones 77−35398
dual laser interferometer for plasma density measurements on large Tokamaks 78−71542
dynamic thermocouple technique for temp. meas., electronic insertion 77−76203
Earth's neighbourhood, investigation of origins of plasma using OPEN program 80−109318
echo effect, appl. to particle distrib. function regeneration *(Russian)* 80−14933
ECR as a diagnostic for mirror trap plasma 80−38709
electrode method *(Russian)* 78−14200
electron beam in solar flares, diagnostic 80−26827
electron concentration and temp., in He-Xe-Co_2 plasma, optical method 79−41871
electron current component meas. method for hollow cold cathode 80−54043
electron density and mag. field meas. by far IR polarimeter-interferometer 79−32817
electron density determ. by globally convergent method for partially ionised plasma 80−53929
electron density determ. using microwave interferometers, modulated transmission and reflection types comparison 79−37546
electron density display with resonance cone RF probe 77−62404
electron density meas. by EM wave propag. in magnetised plasma column 80−43974
electron density meas. by far IR laser beam deflection 80−59296
electron density meas. in shock generated plasma by light interferometry 80−48981
electron density of laser-produced plasma from multicharged ion K-spectra, review 79−64908
electron density profile evaluation from integrated meas. 79−77418
electron density radial profile measurements using Mach Zehnder CW multichannel interferometer 79−75581
electron detect. using p-i-n photodiode, time resolution 79−14608
electron energy determ. using analogue computer and Langmuir probe 78−14212
electron energy distrib. function measurement by probe, cct. for potential fluctuation compensation in plasma 80−54041
electron energy distribution function, freq. dependence of AC method 79−64907
electron temp., time and space var., determ. from electron cyclotron emission meas. in Tokamak plasma 80−48996

plasma diagnostic techniques continued
electron temperature and density for plasma parameters typical for tokamak boundary region, meas. method 79−55560
electronic instrum. for determ. of electron energy distrib. function of afterglows 79−32840
electrons nonthermal energy distribs. meas., Fe XXV dielectronic satellite spectra appl. 80−21911
electrostatic energy analyser, data interpretation 78−42813
electrostatic particle analyser, optimisation and performance 78−42815
EM impulse reflection from cold mgnetoplasma, charact. parameters diagnostics 78−42817
EM wave scatt., homodyne method for detecting asymmetric spectra 79−14611
emission spectroscopy, background reduction method using flame atomic absorpt. 79−16069
estimation method for electron temp. and density in ^{3}He plasma and ^{3}He-Ar plasma 80−64785
EUV spectra and solar atmosphere plasma diagnostics 79−30050
Fabry-Perot interferometer, submillimetre range 77−3990
Fabry-Perot interferometer appls. 80−59302
Fabry-Perot scanning interferometer, SKIF-1, for spectral-line profiles of plasma sources 79−17476
Fabry-Perot spectrometer, pulsed plasma emitted line profile meas. for vel. determ. 79−41869
far IR 2-D plasma interferometry evaporographic and pyroelec. recording 78−5929
far IR interferometry, for plasma density measurement 78−47183
far IR laser scatt. meas. of nonthermal density fluctuations 80−59297
far IR lasers appl. and detection systems in controlled fusion research 78−47182
far IR Michelson interferometry based on fast plasma scanning 77−31513
far IR systems, for plasma studies 78−47185
far IR technology and applications, conf., Reston, USA, (Apr. 1977) 78−45711
Faraday cup collector for positive, negative and neutral flux meas. 78−87494
Faraday cups for laser plasmas, evaluation 78−5941
Faraday rot. diagnostics of laser gas discharge plasma 80−43981
Faraday rotation, mag. field determ. in hot plasma *(Rumanian)* 80−87950
Faraday rotation meas., implosion heating expt. 77−39456
fast photography, appl. to electron beam produced plasma 77−39458
fast streak or frame camera appl. to plasma dynamics in plasma focus device 79−68950
field visualisation technique applied to sub-mm diagnostics of axisymmetric plasma 80−43980
flame, microwave-emission diagnostics, propane-O_2 flame obs. 80−45503
flash X-radiography system for electron beam generated plasma 78−51358
flow velocity, meas. using reson. ionisation velocimeter 79−82002
fluctuations, LF, diagnostics by probes and optical line radiation 79−64905
fluctuations, methods for diagnostics 80−49002
FM-1 spherator, microwave scatt., drift wave turbulence 77−65912
formation dynamics of underexpanded supersonic erosive laser plasma flare, high speed techniques 80−48923
formation of plasma in fusion devices, at. and plasma processes, diagnostic techniques 80−48915
Fourier transform spectrometer, double-pass rapid-scanning 80−103190
Fourier transform spectroscopy appl., far IR 78−58069
Frascati experiment, neutron yield determ. Ag-activated Geiger counter calibration 80−99409
free-free transitions, mutiphoton, energy absorption laser pulse shape-independ. 80−43184
fusion plasma in mag. confinement, review of required diagnostic techniques 79−71951
fusion reactor, diagnostics of radial plasma transport rate, data acquisition and handling system 78−54937
fusion reactor mechanical diagnostics, techniques in fluctuating mag. fields 78−54946
fusion reactors, interferometric phase detection system, using high speed digital techniques 78−62629
galvanic detection of optical absorpt. in gas discharge 77−15251
gas blast circuit breaking arc, arc diameter, RF technique 78−87528
gas temp. meas. in glow discharge in capillary using thermocouples *(Russian)* 78−59694
Gaunt factor temp. depends., from Ar II and Ca II Stark widths 78−87491
grating double monochromator, GDM 1000, spectral anal. of low intensity emissions 79−80701
grazing incidence spectrograph-monochromator with focusing toroidal mirror 79−75617
grazing incidence spectrometry, photometric calibration of 1.0 m spectrometer 80−92386
grazing incidence X-ray microscopy, of laser fusion targets 78−47178
Hall accelerator, azimuthal drift current, induction meas. method 79−23465
hard X-ray energy and flux meas. for 50 keV to 10 MeV range 80−48992
heat flow in plasma jet, calorimetric probe for *(Russian)* 78−12698
heavy ion beam probe on LITE deep well mag. baseball device 77−84518
heavy ion beam probe system, for deep mag. well device 78−59669
heavy ion beam probe system 78−9850
heterodyne quadrature interferometer for simultaneous measurements of plasma density along several chords 78−67416
heterodyne receiver, meas. of electron cyclotron emission from hot plasmas 79−90463
high energy ion analyser for laser produced plasma studies 77−51236
high resolution X-ray optics, for astronomical and laboratory sources 78−45766
high temperature metrological cooperation between USSR and GDR *(German)* 78−4622
high-press. discharge lamps, theory and diagnostics methods 78−9829
hollow cathode arc, Langmuir probe meas. for discharge model 78−87533
hollow cathode discharge, particle diagnostics with mass spectrometer 79−46476
hollow cathode stationary afterglow apparatus, for at. props. studies 78−63619

plasma diagnostic techniques continued
hologram interferometry, for laser spark diagnostics 79−64921
holographic interferometry, double pulsed time differential method 77−22591
holographic interferometry, of laser fusion plasma, picosec. 79−46492
holographic microinterferometer to meas. plasma electron densities and other transparent objects 80−43964
holographic time-differential cine interferometry of gas discharge plasma 80−38716
holography, anomalous dispersion methods, for anal. of spatially inhomogeneous objects 79−63303
homodyne sub-mm interferometer for plasma diagnosis 79−32811
hot plasma, space pot. distrib. meas. by fast neutral beam method 80−48970
hot spot distribution, significance for interpretation of laser produced plasma expts. 78−55732
image convertor and spectral analyser device for low-temp. plasma diagnosis 79−4180
image convertor camera, for laser and laser-plasma diagnostics 78−38550
images, two dimensional, techniques for reconstruction from projections 79−90453
IMPATT source, frequency-stabilised, 115 GHz 80−67573
impurity concentrations on wall during Tokamak discharges, laser probing technique 80−49013
incoherent Thomson scattering techniques 80−48999
inductive oscillometry, field difference theory 78−51342
inductively coupled plasma spectrometer, data processing using APL 79−17501
inert gas hollow cathode arc, mol. beam sampling of metastable atoms as electron temp. probe 80−43967
inert gas plasma, weakly ionised, photon echo relax. obs. in RF discharge 80−43986
injection of small solid particles, giving local hot Tokamak plasma parameters *(Russian)* 78−30486
instabilities, obs. via 1-300 kHz multichannel spectral analyser 77−39455
instrument distortion elimination, Abel transformation of functions *(Russian)* 77−7598
insulator surface flashover in vacuum, electro-optical meas. 80−38823
interferometer, rapid spatially scanning IR heterodyne, for plasma diagnostics appl. 79−49275
interferometer for density meas., 10^{19}-10^{22} m^{-3}, and simple hydrocyanic acid 0.337 mm 78−5922
interferometer for electron density meas. on laser created plasma 80−48983
interferometric measurement of cryogenic laser fusion target uniformity 78−47158
interferometry techniques for high β-plasma density meas., holographic and coupled cavity laser methods 80−49006
interplanetary plasma meas. by modulation method, amplifiers sensitivity increase 79−92676
intraresonator absorption spectroscopy in plasma jet, laser stimulation optimisation 80−77881
ion beam probe diagnostic system for EBT 77−84512
ion beam probe diagnostic system for EBT 77−84513
ion detection by channel electron multiplier 78−5375
ion detector, Daly-type, plasma ion energy meas. 78−22570
ion energy analyser, electrostatic, 0.5-30 keV, appl. to polyethylene plasma 78−91157
ion energy analysis on a plasma focus device, rel. to fusion plasmas 79−90465
ion energy and momentum spectrometer with high resolution, for investigating expanding laser blow-off plasmas 80−86495
ion extraction from plasma, stagnation point, mass discrimination effects 79−35886
ion flux in glow discharge, $\lesssim$1.2 kG field, double probe meas. effects *(German)* 77−31534
ion mass spectra, local admixture ion content after at. beam scatt. *(Russian)* 77−19774
ion probe system, monochromatic, highly collimated, 0.5 to 5.0 MeV 79−46482
ion scatt., suprathermal, by partially ionised impurities, measurement of Z_{eff} 80−54039
ion sheath diagnostics using elastic surface waves *(Japanese)* 77−89266
ion temp. meas. using light scatt. techniques 77−84492
ion temperature profile meas. using charge-exchange neutral anal. 80−48850
ion velocity, distrib. diagnostics by neutral particle time-of-flight spectra 78−67439
ionising shock waves due to laser, superfast optical methods *(Russian)* 78−71535
ionospheric electron densities meas., by radio wave scattering, using artificial plasma inhomogeneities *(Russian)* 79−5636
ionospheric waveform distortion by microwave scatt. 79−50859
IR and millimetric waves and applications, conf., Miami Beach, USA (Dec. 1979) 80−57009
IR holography at 10.6 μm for laser diagnostics 80−84007
IR scanning heterodyne interferometry for pulsed fusion reactors 77−84525
IR time resolved spectroscopy passive image dissector 77−41705
jet impinging on metal surface, interferometric temp. meas., <5000K 78−87498
jet reaction meter, use of inductive transducer 77−11399
Josephson junctions, applications in plasma physics 80−103194
Knudsen converter low energy electron reflection from thermionic cathode, mag. field depend. 80−19627
Langmuir probe technique for flame temp. meas. 77−24181
large Tokamaks, particle and photon meas. 79−46479
laser amplitude calibration from Raman spectra, for diagnostics *(Russian)* 80−38702
laser feedback interferometer for electron density meas. 79−2813
laser fusion, image convertor camera optical measurement 78−38549
laser fusion diagnostics, techniques and appl. 80−49009
laser fusion expts., calorimeters for meas. of ions, X-rays and scatt. radiation 78−16800
laser fusion programme diagnostics, plasma physics on micron and picosecond scale 79−23452
laser interferometer, optoelectronic modulation for electron density variation meas. in IR 80−4762
laser interferometric system 77−19770

plasma diagnostic techniques continued
laser intraresonator diagnostics, appl. to He-Ne plasma 77−84499
laser multi-frame interferometry for investigation of dynamics in pulse plasma 78−83615
laser plasma, 5-20 keV X-ray emission spectrum investigation using nucl. emulsions 80−92392
laser plasma, produced by CO_2 laser beam, picosec. diagnosis 79−46491
laser plasma electron density, Stark-broadened line wings of H-like ions 78−79462
laser plasma X-ray spectroscopic diagnostics using high-quality quartz and Si crystals 79−68953
laser produced plasma density profile meas. using Wollaston prism interferometer 80−48973
laser radiation scatt. from CW Ar laser, low-temp. plasma diagnostics 78−38536
laser-Doppler velocimetry in ionized gases, review 80−48975
laser-fusion program, LLL, X-ray diagnostic instrumentation 77−76213
laser-produced expanding plasma, diagnosis with charge collectors 77−19771
laser-produced plasmas, spectra simplification by electro-optic gating of radiant emission 78−22561
lasers, far IR, developed for Tokamak plasma Thomson scatt. diagnostics, review 80−24242
Lecher wire interferometer, 30 GHz, ion-acoustic wave meas. 78−5946
local optical observation of cylindrical plasma *(French)* 77−15244
local spectroscopy methods, rational algorithm selection to treat expt. data 78−51346
low temp. plasma diagnostics by reson. Rayleigh scatt. 80−48980
low temperature plasma, laser light scatt. methods 78−87497
low-pressure discharge anode sheath in crossed fields, electron density distrib. 78−75424
luminescence spectroscopy for gases excited by products of neutron nuclear reactions 80−26074
Mach-Zehnder heterodyne interferometer, RF phase reference 77−26390
Mach-Zender twin-wave laser interferometer for plasma diagnostics 78−4687
magnetic field determ. from charged particle beam defl. 80−28825
magnetic field measurement in inhomogeneous plasma, probe laser beam depolaris. effects 78−67411
magnetic field measurement in toroidal plasma systems 80−49004
magnetic tape method obs. of self generated mag. fields 80−64775
magnetically insulated ion diode, ion beam diagnostics 80−48974
magnetically shielded sampling technique, for plasma diagnostics in medium-press. magnetoplasma 78−22560
magnetobremsstrahlung emission, in toroidal plasma, electron diagnostics 80−48997
mass spectrometer-probe diagnostics of non-thermal plasma wall ion energy distrib. 78−9846
megavolt and megampere diagnostic techniques for pulsed power particle beam fusion drivers 80−49010
metal halide discharges, horizontal burning, parameter meas. techniques 80−38802
MFTF, plasma diagnostics system 80−95444
MHD generator, K addition atoms, automatic system for conc. meas. 79−50892
MHD power generators, combustion products plasma characterisation, generator channel flow, diagnostic techniques 80−43993
Michelson interferometer with CO_2 laser for density meas. *(Russian)* 78−38534
microcoded, aperture imaging, appl. to laser plasma diagnosis 80−24251
microfield cross spectrum meas. with two dipole antennas, theory 77−51227
microwave diagnostics, nonlinear interaction of two beams 79−73044
microwave emission spectra of low temp. plasma, electron vel. distrib. determ. 78−47167
microwave interference signals from 0 to n.360° phase meas. for plasma density meas. *(German)* 80−6278
microwave interferometer, freq. stabilized, laser prod. plasma density decay meas. 77−84524
microwave interferometer for meas. phase shifts with high resolution 77−3994
microwave optics for microwave scatt. expt. *(Japanese)* 79−37551
microwave p-i-n diode modulator, transient plasma instability meas. *(German)* 80−87942
microwave plasma detector system for gas chromatography/emission spectroscopy in environmental pollution studies 80−26070
microwave propag. const. determ. in temperate plasma, slab line technique 80−53992
microwave propagation effects in randomly ionized plasma, experimental system 79−27784
Microwave reflexion in rectangular waveguides by high pressure RF plasma columns 80−43975
microwave resonator method for radial electron conc. profile determ. *(German)* 79−86608
mirror machine diagnostics 80−48958
MM and subMM wave appl. in 100-1000 GHz range 80−17962
modulated mol. beam of Sn_2, for density and neutral gas press. meas. 77−27735
molecular lines role in plasma satellites, $H_2(He_2)$ obs. 80−44053
momentum meas. by ballistic and torsion pendulums in laser-produced plasmas 78−83611
monochromator, visible, scanning drive, for fusion reactor 78−54940
monochromators, grazing incidence and normal incidence, intensity calibration in VUV for plasma diagnostics 80−48995
monopole as microwave probe for diagnostics *(Russian)* 77−76196
multi-channel integrator for plasma magnetic-probe meas. 78−75413
multi-pulse ruby laser recording of temporal evolution of electron density and temp. 80−14938
multichannel atomic analyser, with automatic data recording, for TM-3 Tokamak 78−67420
multichannel charge-exchange energy analyser with high time resolution, plasma energy spectrum 79−41882
multichannel HCN laser interferometer for Tokamak plasma diagnostics 78−5928
multichannel system electronics for pulsed plasma source optical diagnostics 79−77425
multiframe ps holography appl. to high power laser effects in dielectrics 78−26328
multiposition Thomson scatt., determ. of electron density and temp. profiles 80−48977
neutral atom energy analysis, 200 eV-10 keV range 77−83763
plasma diagnostic techniques continued
neutral atom multichannel energy spectrometer, 0.3-10 keV, for fast pulsed expts. 79−73037
neutral beam probing-spectroscopic method, for electron density profile 78−63590
neutral beam scattering, space and time resolution of density and temp. 78−59668
neutral particle analyser for 200 eV to 30 keV range 79−14609
neutral particle energy analyser, 10-channel ion temp. meas. 77−19765
neutral particle spectrometer for measuring ion temperatures *(Chinese)* 79−37553
neutral-particle analyzer system, multichannel, for anal. of charge-exchange flux from magnetically-confined plasma 80−4804
Neutron diagnostics for pulsed high-density thermonuclear plasmas 79−90462
neutron production in Maxwellian D ion plasmas, ion temp. diagnostics appls. 80−49005
nonlinear EM wave scattering 77−11350
nuclear activation techniques for pulsed ion beams 77−84514
optical diagnostics of laser fusion plasmas 77−89305
optical escape factor, rel. to thermalisation length 79−86611
optical image synchronisation with electrical parameters 80−31919
optical line emission, Doppler broadened, axially symmetric, plasma, interpretation model 78−75276
optical measurement of laser-driven imploding shock wave *(Japanese)* 77−43066
optical methods for submillimetric and millimetric diapason EM waveband *(Russian)* 79−1338
optical scattering of light by atoms, techniques theory 80−54044
optical spectroscopy for diagnostics and process control during glow discharge etching and sputter deposition 79−15606
optical system, fully automatic, for meas. of vol. emission coeff. of radiation 77−58893
optical systems for diagnostics of laser produced plasmas 80−10434
optical temp. meas. evaluation by computer 78−91150
optically thick plasma, two-dimens. radiation restoration rel. to local diagnostics 80−43885
optogalvanic double-resonance spectroscopy 80−57385
orifice flow, wall interactions in mol. flow regime 79−23449
oscillating slit mechanism, for H isotope ratio determ. in microwave induced plasma 79−41868
paramagnetism of plasma in RF field 79−46490
particle densities, neutral and charged, using electron beam scatt., in partially ionised He(Ar) 80−28824
particle velocity distrib. variation with distance, rel. to temp. diagnostics 79−77419
particle-beam fusion experiments for fusion ignition, pellet compression and long solenoid approaches, breakeven experiments 80−47720
Penning discharge plasma, residual gas density and elec. potential profile meas. 78−67485
photographic UF-VR film, exposed to soft X-rays, quantum discrimination efficiency and sensitivity 80−22499
photopreionisation-stabilised discharge scheme for nanosecond excitation of dye vapour and metal halide plasmas 79−98982
picosecond X-ray chronoscopy 78−38546
picosecond X-ray spectral studies 78−38547
pin diode detector array, obs. of X-rays 78−47174
pitch angle meas. of intense rotating relativistic electron beam 78−1902
plasma chemistry, diagnostic techniques 78−3338
plasma chemistry, history, diagnostics, production, organic cmpd. synthesis 80−61099
plasma column position detector, using segmented photodiode 78−1901
plasma density IF phase meas. using three-mirror interferometer 78−75414
plasmascope, opto-electronic method for vel. meas. in thermal plasmas 77−39462
plastic scintillators, quenched, sub-nanosecond 77−54419
polychromator based on MDR-2 monochromator 78−5924
position detection and control, in Tokamaks, interferometric method 80−1850
potential measurement using plasma probe at 'floating' potential 79−37541
pressure sensor using TsTS-19 piezoelectric ceramic 80−105670
probe, elec. highly negative, in flowing continuum plasma, ion sheath 77−72493
probe characteristic in highly ionised plasma, transition region 78−79474
probe characteristics for cool plasma, electron saturation current 78−79473
probe current modulation, electron distrib. determ., finite amplitude distortion, instrumental function 78−47168
probe-tube microphone, press. fluctuation meas. in flowing combustion plasma 78−18443
Proto-Cleo torsatron, vac. mag. surfaces shape, electron beam diagnostics 79−73035
pulse generator, variable duration and synchronised, Nd:YAG regenerative amplifier 79−45967
pulse hollow cathode discharge, time resolved high resolution spectroscopy 80−38759
pulsed electrostatic probes as diagnostic for transient plasma 78−94937
pulsed submillimetre fluoromethane laser for diagnostics 77−19307
radial carrier density profiles, determ. using microwave resonators *(German)* 78−47160
ram effect for conducting cylinder in drifting plasma 80−54029
rapid-scan polarising Michelson interferometer and InSb detector calibration 80−59305
ray phase determ., probing radiation transmittivity modulus for plasma column 80−38658
real-time spectral analysis methods, applicability and constraints *(Russian)* 77−31525
refraction into a nonlinear medium: wave profiles and hysteresis 80−43395
resonance fluorescence diagnostics, of high temp. H_2 plasma 80−48971
resonance fluorescence method for plasma diagnostics, at. density and temp. meas. 80−49001
resonant optical schlieren system for plasma flow studies 78−5940
reverse field pinch, Faraday rot. diagnostics for internal mag. field 80−43976
RF coil probe, electron density and collision freq. determ. in nonuniform column 78−18446
ring aperture antenna in plasma, input admittance anal. 78−38542

plasma diagnostic techniques continued
rocket nozzle, static electricity form., gasdynamic and electrophysical parameters determ. 79−40060
rotation meas. by perturbed mag. field phase slip between X-ray and field detectors 80−48982
rotation speed measurement, in external magnetic field *(German)* 78−42821
sampling techniques for long-wavelength electron wave dispersion evolution meas. 80−6283
scanning multiple collector electrostatic analyzer with application to plasma potential measurement 79−73046
scattered radiation intensity fluctuation method *(Russian)* 80−14932
secondary emission, absorber covered graphite Faraday cup, 1.5 MeV proton beam study 78−9864
self absorption of He like satellite lines in high density fusion plasmas 80−64776
self-generated mag. fields, two-dimens. distrib., laser-plasma reson., mag. tape irradiation 79−41877
shearing interferometer for dense laser prod. inhomogeneous plasma *(Russian)* 80−83994
shiva and Argus target diagnostics vacuum systems 79−81079
Shiva laser fusion facility, target diagnostic system, data acquisition and anal. 78−51366
six solenoid oscillometer for non-intrusive LF positive-glow plasma diagnostics 78−51343
slot-shaped erosion plasmatron for spectroscopy of low-temp. plasma 79−94821
soft X-ray analysers for pulsed-source emissions 80−31957
soft X-ray emission from Tokamak low β mag. confinement systems 80−48959
soft X-ray imaging instrument for the Alcator A Tokamak 80−73563
soft X-ray spectra meas., using intrinsic Ge detector 77−51232
solar corona diagnostics with broad-band X-ray imaging systems, physical parameter method 78−49414
solar emission lines of NeV, MgVII, SiIX, SXI, population levels as function of electron density and temp. 80−21963
solar flares, XUV electron density diagnostics 79−88633
solar plasmas density determination, N III and O IV intersystem multiplets appl. 80−31264
sounding with finite-radiation-pattern source *(Russian)* 78−59606
space potential measurements with particle beam probes 80−84006
space- and time-resolved VUV spectroscopic measurements 79−80700
space-time correlation functions for vel. space diffusion coeff. using probes 78−59595
Spacelab Picpab expt., phenomena induced by charged particle beams obs. 80−17443
spark channel formation in strong mag. field, Kerr cell obs., plasma model *(Russian)* 78−59693
spark plasma ion source effects on mass spectroscopic quantitative anal. 79−14631
spatial imaging detector system for pulsed plasma extreme ultraviolet diagnostics 80−33821
spatial temp. distrib. meas., interference filter photographic method 78−67332
spectral line profile, least-squares approx. 79−23458
spectral method for electron temp. meas. in Tokamak discharges 77−76198
spectral method for temperature field determ., in asymmetrical plasmas *(Czech)* 80−38704
spectral source profiling using Reticon photodiode array 77−63999
spectrograph, grazing incidence, stigmatic obs. of laser-produced plasmas 79−73041
spectrophotometer, compact, plasma diagnostics 300 to 2500Å 79−64904
spectroscopic effects in dense and ultradense plasmas, review 80−43990
spectroscopic escape factor, approaches to evaluation 79−90387
spectroscopic escape factor, defn. and evaluation 79−90385
spectroscopic escape factor, radiative decay 79−90386
spectroscopic system for laser prod. plasma meas. *(French)* 77−62396
spectroscopy techniques development, review 80−43991
stigmatic spectrograph image intensifier system for low light levels 78−93767
stimulated Brillouin scatt. in laser plasma expts., review 79−10706
streak camera, proximity-focused, subpicosecond 77−5938
streak camera, wide dynamic range, proximity focusing, visible and X-ray recording 77−89304
streak camera intensified CCD readout system, sensor props. 79−27825
streak mode interferometric study of plasma focus 79−73042
submillimetre diagnostics, active, of Ar arc, data numerical anal. 80−48979
submillimetre laser interferometer system, for plasma density meas. 77−7586
subMM compensation-type interferometer to receive probing radiation for optically dense plasmas 80−54037
subpicosecond proximity-focused streak camera, for X-ray and visible light 77−79183
subpicosecond X-ray streak camera, for laser-fusion diagnostics 78−42822
Sun, use of MHD pulses as diagnostic technique 80−109405
superheterodyne tracking cct. for mm-wave measurements 80−59288
surface interaction process, simple plasma device for obs. 77−27723
surface physics techniques for Tokamak plasma diagnosis 78−94936
surfatron produced electron density and temp. microwave meas. 80−43965
synchronised diagnostic laser pulse system for laser fusion 78−51365
temperature distributions of powder particles in plasma stream, method and apparatus 78−14210
temperature measurement method using probe, of laser-produced plasma 79−27831
temperature measurement methods *(Hungarian)* 79−46477
temperature of molecular plasma, Raman Q-branch intensity 79−37545
temperature structures of astrophysical plasmas, derivation from X-ray spectra, use of a priori information 78−20778
temporal and spatial meas. of RF electric field in magnetized plasma using emissive probe 80−54042
TEXT data acquisition, multichannel AD subsystem 78−54936
TFTR, diagnostic interface systems, problems 78−62626
TFTR, general arrangement of diagnostics 80−95445
TFTR, neutron spectrometer mech. design 80−95498
thermal sensitive paper for intense, relativistic electron beam dynamics diagnostic 78−83619
plasma diagnostic techniques continued
thermoanemometric sounding, ion energy accommodation coeff. meas. in rarefied plasma 80−16722
thermonuclear events, high-yield, in Shiva Nova laser facility, diagnostic instrumentation 79−41034
theta pinch, emission line time histories, impurity ion dielectronic recombination rates 80−79570
theta pinch plasma density radial profile measurements using quasiquadrature interferometer 80−70038
theta pinch plasma with no bias field, fluctuating fields, spectroscopic obs. 77−11398
theta-pinch, fast, double-frame hologram interferometer meas. of density 79−19097
Thompson scattering for electron beam and plasma diagnostics *(Russian)* 80−54031
Thomson 90° scatt. system 78−5947
Thomson parabola ion analyzer for laser-plasma studies 79−1343
Thomson scatt. apparatus, using laser beam, to determine electron temp. and density in plasma 78−34367
Thomson scatt. pathways calibration, rel. to diagnostics *(French)* 80−43886
Thomson scattering, 4-channel spectral analyser 80−31905
Thomson scattering, in DITE Tokamak, electron temp. and density, pulsed rube laser 79−10720
Thomson scattering, multi-channel TV apparatus, PLT machine, mech. aspects 78−54932
Thomson scattering, triple grating polychromator 77−43059
Thomson scattering diagnostic system, analogue data processing circuits 78−87488
Thomson scattering from an anisotropic plasma 79−60112
Thomson scattering multipass laser system for Tokamaks 77−76189
Thomson scattering system for relativistic electron beam heated plasma 78−75421
three-laser intercavity interferometer 77−80357
three-mirror image rotator use in laser produced plasma expt. 80−33814
time gated spectroscopy, appl. to electron beam produced plasma 77−39458
time-gated optical imaging system meas. of laser target emitted light angular distrib. 80−79572
time-resolved X-ray pinhole photography, of compressed laser fusion targets 78−38548
Tokamak, JET, far IR interferometer design 80−59295
Tokamak, LT-3, stable discharge, ion temp. and energy balance, UV polychromator meas. 77−65914
Tokamak, mean ion temp. diagnostics at wall by ion beam surface modification anal. 79−46457
Tokamak, PLT, electron cyclotron radiation Fourier transform diagnostics 80−59292
Tokamak, recomb.-induced neutral particle flux, ion temp. diagnostic method 79−32799
Tokamak, rot. Soller slit system, electron temp. and spatial distrib., soft X-rays meas. *(Russian)* 77−47260
Tokamak electron temp. and density profiles from electron cyclotron radiation spectra 80−59293
Tokamak far IR Fourier transform spectroscopic Michelson interferometer 80−59294
Tokamak far IR Fourier transform spectroscopy resolution limits 80−59298
Tokamak fusion reactor, TFTR, plasma generation and confinement 80−42864
Tokamak plasma spectroscopy, optical filters appl. 78−26326
Tokamak plasma-wall interaction, appl. of fluoresc. spectroscopy 79−23451
Tokamak plasmas, measurement of electron cyclotron emission using fast response InSb subMM detector 80−27347
Tokamak poloidal field, EM wave polarisation diagnostic method 78−59683
Tonks-Dattner resonances, appls. to plasma diagnostics 78−83618
toroidal, modulated submillimetre-laser polarimeter for meas. of Faraday rotation 79−46474
toroidal mirror fabrication for soft X-ray imaging 78−41384
toroidal plasmas, high temp., electron cyclotron emission meas. by mesh filter method 80−75101
transient plasma heat fluxes in divertor assembly, meas. by thin-film thermometer 78−18447
trifluoromethane plasma etching of SiO_2, optical spectroscopy appl. 80−87940
trigger system, optically isolated, for pulsed high voltage plasma expt. 77−41650
turbulence levels behind electrostatic shockwave, fast ion beam diagnostics *(Russian)* 79−98974
turbulence meas. with spectrum analyzer and differential amplifier 77−43081
turbulence spectrum reconstruction from light propag. time correlation function 77−19178
two-dimensional spectral line emission reconstruction as a plasma diagnostic 78−67415
two-frequency dispersion interferometers for space plasma nonuniformity 79−70964
UHF nonequilibrium plasma diagnostics by atomic bremsstrahlung continuum 78−67483
uniformly redundant array imaging of laser driven compressions, preliminary results 79−60189
UV holographic microinterferometer and probe beam design for plasma probing 80−59270
UV radiometric standards, gas discharges, plasma diagnostics appls. 80−47088
vacuum monochromator, grazing-incidence, absolute calibration using Tokamak discharges 78−87492
velocity distribs. in field-free plasmas, effect of finite analyser size on distrib. functions 79−55562
vibration-insensitive He-Ne laser interferometer for plasma electron density meas. 79−14610
wake, hypersonic, free electron distrib., RF method 79−27833
wave diagnostics in Venus environment, by Pioneer Venus Orbiter instrument 80−67497
wide energy range mass spectrograph for diagnostics of fast pulsed sources 79−37549
X-ray and visible streak camera for subpicosecond laser fusion diagnostics 77−18122

plasma diagnostic techniques continued
X-ray calibration of Kodak RAR 2490 film, appl. to laser plasma expts. 77−35383
X-ray catoptrical crossed-mirror imaging at grazing incidence 80−77923
X-ray coded imaging of relativistic electron beam targets 78−47179
X-ray detector with subnanosecond time response 78−86741
X-ray diagnostics, hot lab. and astrophysical plasmas 80−59282
X-ray diagnostics, plasmas in PLT and PDX Tokamaks 80−75104
X-ray diagnostics for electron beam fusion programme 78−47181
X-ray emission from laser produced plasma, diagnostic methods for spatio-temporal obs. *(French)* 78−14209
X-ray emission in laser imploded targets, three-dimens. reconstruction 80−79563
X-ray emission of Tokamak plasma, reconstruction accuracy 79−77422
X-ray emission spectrum of plasma focus meas., using Ross filters and Si detectors 80−59273
X-ray images with submicron resolution, optical simulation of technique 78−34366
X-ray imaging, conf., Reston, USA (Apr. 1977) 78−45762
X-ray imaging, for laser fusion programme 78−47173
X-ray imaging, MOS solid-state detector arrays 78−47180
X-ray imaging, two dimens. monochromatic, of laser produced plasma 79−60193
X-ray line shift for high density laser produced plasma diagnostics 80−64778
X-ray measurements using self-scanning Si diode array 77−41739
X-ray microradiographs of laser fusion targets, improved image analysis techniques 80−79562
X-ray microscopy, coded imaging techniques, of laser fusion plasmas 78−47177
X-ray photography of laser plasma, using quartz analyser crystal 77−35403
X-ray pinhole camera, emission recording from laser generated plasma 77−80364
X-ray pinhole imaging techniques for electron beam fusion 78−47176
X-ray pinhole microphotography, time-resolved, of laser compressed targets 77−62395
X-ray radiography appl. of chamber with plasma focus *(Russian)* 77−7592
X-ray recording focusing spectrograph for laser plasma 78−1891
X-ray shadowgraphing for laser produced plasma 77−89311
X-ray spectra spatial resolution recording by spherical crystal analyser 78−74114
X-ray spectrograph, convex curved crystal, ray tracing 79−35900
X-ray spectrograph, high luminosity, electron temp. determ. from continuous recomb. radiation 79−64924
X-ray spectrograph, high-luminosity, vertical focusing, for laser plasma diagnostics 78−51355
X-ray spectrograph with spherically bent cryst. analyser, for laser plasma diagnostics 77−76212
X-ray spectrographs, flat and convex curved cryst., wavelength calibration 79−40649
X-ray spectrometer, high-speed, multichannel, bremsstrahlung of hot electron component obs. 80−57445
X-ray streak camera, high time resolution, with X-ray microscope *(French)* 78−42823
X-ray streak photography, pinhole imaging, laser produced plasma 77−15245
X-ray stream camera, ultrafast X-ray diagnostics for laser fusion experiments 77−79185
X-rays monitoring by nanosecond 5-200 keV X-ray spectrometer 77−26447
XUV emission as a diagnostic of laser-heated plasmas 80−48994
Z-pinch, dense plasma, Hα line profile, density meas. 80−43987
zone-plate coded imaging of laser-produced plasmas 77−55167
zone-plate coded imaging on microscopic scale 77−54673
Al coated glass microballoon targets for laser implosion expt., search for shell disintegration 80−33792
Al(XII) and (XIII) reson. line trapping in laser-heated plasma, source distrib. diagnostics 78−42730
Ar plasma diagnostic method for partial LTE 78−67606
Ar plasma radiation obs., line and continuous spectra *(French)* 80−19619
CO_2 1KJ laser system for laser-plasma interaction expts. 78−5502
CO_2 TEA laser electrical excitation rates, theory and expt. 78−71078
CsI photocathodes, efficiency evaluation for soft X-ray diagnostics 80−57442
Cu, surface, C and H ion bombardment, secondary electron emission coeff. experimental technique 79−78804
Cu-like ions, 4s-4p reson. lines and transitions obs. by means of laser prod. plasma, appl. to Tokamaks 80−99468
CuI photocathodes, efficiency evaluation for soft X-ray diagnostics 80−57442
Fe XXV, He-like, dielectronic satellite spectrum, electron temp. diagnostics in plasma 79−82098
H atom analyser using Cs heat pipe, low energy appl. 80−70043
H beam production systems, 3 to 15 keV 79−18315
H concentration by 121.6 nm reson. fluoresc. from Kr 3rd harmonic generation *(Russian)* 77−79895
H, plasma, collisional depopulation rate of n=2 level, laser plasma method 78−79463
H, UV light source, 121.5-121.6 nm *(Russian)* 78−25942
H-atom injector, pulse recharging type, features 78−79460
H-like ions in laser-produced plasma, Balmer fine struct. (broadening) 80−48860
H_2 plasma, diagnostics using reson. multiphoton ionis. 80−58640
He, electron-beam-produced supercooled plasma, emission spectrum 77−84501
He non-equilib. plasma diagnostics, PLTE model and steady state attainment 80−38715
He-Ne laser Michelson interferometer for electron density meas. 77−35394
Hg arc plasma, azimuthal RF cond. meas. by eddy current effect, expt. 77−1029
Kr, UV light source, 121.5-121-6 nm *(Russian)* 78−25942
Li beam probing for density profile meas. 79−4186
LiF curved crystal spectrograph, diffraction efficiency calc. method 80−79630
Mo, beam-foil spectra, 5-55 nm, using 22-200 MeV beams, rel. to Tokamak impurities 79−46481

plasma diagnostic techniques continued
Mo^{29+} to $^{39+}$, photoionis. cross sections, radiative recomb. rate coeffs., rel. to plasma diagnostics 80−52953
Nd:YAG laser multipass cell for Raman scatt. diagnostics 80−1231
Ne spectral line broadening as diagnostic for compressed laser fusion targets 79−98979
UF_6, high temp. fissioning plasma core reactors, fluid mechanical confinement 80−63248
Zn-like ions, 4s-4p reson. lines and transitions obs. by means of laser prod. plasma, appl. to Tokamaks 80−99468

plasma diagnostics
see also plasma density; plasma diagnostic techniques; plasma diagnostics by laser beam; plasma temperature
Abel integral eqn. solution by orthogonal polynomials 78−67436
ablative acceleration of laser-irradiated thin-foil targets 79−71952
absorption in laser-produced plasma expts. 80−14931
accelerator, electrodynamic, modulated, optimum operating conditions 77−27749
accelerator, microwave generation by RF instabilities, discharge voltage depend. 77−7538
accelerator, pulsed coaxial, electron density and temp., from X-ray emission spectra 77−27750
acoustic noise in electric arcs, arc temp. meas. appl. *(French)* 80−28865
additional heating in Tokamaks, specific diagnostics review 80−28753
adiabatic compression in Tokamak, impurity ions line radn. meas. 77−43075
AF glow discharge positive column, stratification obs. 78−67509
afterglow discharge, electron-atom bremsstrahlung, time decay 78−63620
afterglow functions, multistop method investig., dead time registration effects *(Russian)* 79−10719
air, DC point-to-plane elec. discharge, temp. patterns, Michelson interferometry 80−54061
air, flowing glow discharge, negative ion density, probe and gasdynamic thermometer diagnostics 80−28821
air, high current discharge temp. and density 77−62427
air, high-current discharge, current-carrying zone investig., induction method *(Russian)* 78−26355
air, laser-initiated ionisation channels, form., charact. 77−89345
air, RF discharge, electron temp. and density 78−51371
air, shock heated plasma, nonequilib. submillimetre emission *(Russian)* 78−1869
air blast arc, post-zero current and power loss meas. 79−19106
air breakdown by CO_2 laser radiation near solid target *(Russian)* 77−84472
air breakdown plasma relax. near target, microwave method 79−86616
air discharge, HF, bipolar, reduced-press, elec. macroparameter diagnostics 80−1854
air flow in plasma generator, radn. parameters meas. 79−68952
air glow plasma, X-band heterodyne generation by microwave mixing 77−35391
air high-current discharge cond. zone, HF mag. field probe 78−71589
air plasma, gas-discharge, meas. of electron energy loss distrib. 77−35418
air plasma, optical emission, localised oscill. mode obs. 80−83903
air wake, hypersonic, ionised, free electron attachment coeff. meas. 79−27835
Alcator, electron cyclotron emission, polarisation freq. depend. 80−33808
Alcator, geometrical and elec. props., rel. to THOR 79−98993
Alcator A Tokamak, spatial profiles of light impurity ions 80−48948
alkali metal, dense arc plasma, elec. and heat conds., two-probe diagnostics 80−38560
alkali metal vapour-H plasma, charge exchange role in optical props. 80−59284
alkali-metal hollow cathode arc, low-press. current limiting 80−6304
anomalous conductivity and electron heating, in two-stream unstable plasma 80−6219
anomalous glow discharge Faraday dark space, electron vel. distrib., Langmuir probe meas. 80−44040
anomalous intensity ratios in H like L_α doublet in optically thick laser prod. plasmas 80−103186
anomalous turbulent resistivity at high drift vels., rel. to confinement and fluctuations in toroid 80−24139
anomalous turbulent resistivity at high drift vels., toroidal plasma 80−24138
anomalously resistive phase, spiky density fluctuations and relax oscill., microwave scatt. obs. 80−38547
Ar, plasma rotating, weakly ionised, diagnostics 79−82122
arc, DC, transferred, for refractory refining, initiation and performance charact. 78−9866
arc, electrical charact., effects of laminar and turbulent flows 80−1870
arc, high current, anodes processes, plasma pot., probe meas. 77−19801
arc, high-current, graphite cathode vaporisation, composition and temp. spectral determ. 78−14228
arc, of Cs-film coated hollow cathode, intermediate press. operation 80−6305
arc, plasma parameters, probe and spectral meas. 80−24273
arc, pulsed, high-current, initial anode heat flux meas. and modelling 79−50903
arc, quasi-steady-state, in orifice air flow 77−68887
arc, wall-stabilised, N atom Stark broadened VUV lines 78−90107
arc appearance; metal vap. columnar arc instability in mag. fields up to 67 kA 78−9893
arc discharge, heat flux and current density dstrib. in heat spot *(Russian)* 79−14625
arc discharges, periodic processes, spectral emission charact., vidicon system investig. *(Russian)* 78−9848
arc electrode processes thermodynamic approach *(Russian)* 77−27755
arc hollow cathode, diagnostics 80−44043
arc in porous channel, thermoelectric charact. 79−32835
arc plasma, spectral line intensity, comp. changes effects *(Russian)* 78−75452
arc plasma, temp. meas. by submillimeter diagnostic technique 80−38853
arc plasma electron density meas., high-pressure, by strioscopy and IR absorption *(French)* 80−19620
arc roots, high current, vaporisation effect 78−30496
arcs, helical form model 80−103199

plasma diagnostics continued
arcs, spectral line intensities, discharge mode effects *(Russian)* 77−89343
Asperator NP-L stellarator, mag. field config. meas. 80−92367
atom-ion collisions, in hollow cathode discharge, limit angle, corpuscular diagnostics 79−55454
atomic particle stripping analysers with solid and gaseous targets 79−1341
atomic processes, absolute spectral intensity meas. technique and other applications *(Croatian)* 79−10707
Au foil, 8 ns laser pulse-target interactions, ion-expansion struct. 79−14575
audio signal amplitude modulation, negative ion current effect 77−84515
axisymmetric plasma Abel eqn. soln. accuracy, using Pearce method 77−84506
axisymmetric plasma spectral emission and absorpt. coeffs., algorithm 79−37461
Balmer Hβ line profiles, mag. field effects on afterglow plasma 80−1849
barycentric velocity, time-of-flight mass spectrometric meas. 77−43063
beam-plasma discharge, characts. in crossed elec. and mag. fields *(Russian)* 80−10396
beam-plasma discharge, microwave field spatial distrib., visible emission polaris. 78−67372
beam-plasma system, ionic mixtures, local X-ray diagnostics *(Russian)* 77−35401
beam-plasma system, pot. meas. using two-electrode probe 78−51354
beam-plasma system, unstable, whistler wave propag. along reson. cone, diagnostics 77−31484
beam-plasma system enhanced energy deposition, interferometric obs., simulation 77−31490
beat heating, system, using double-barrelled laser 78−67386
belt pinch, shock heated weakly compressed high-temp. plasma 77−24164
belt pinch, temp. and density meas. by Thomson scatt. 77−27734
Berkeley multifilament ion source, plasma characts. 79−94807
Beta-II, magnetised coaxial plasma gun mechanical design and construction 80−91271
bipolar oscillatory spark discharges, vapour mixing and energy transfer 79−73050
blistering, in Al; Cu, Si, by plasma focus discharge deuterons, anal. 77−35351
Blumlein-type transverse fast discharge, voltage meas. 80−19642
bremsstrahlung attenuation obs., electron distrib. anisotropy, turbulently heated plasma 78−59682
bremsstrahlung X-rays emitted from electron cyclotron reson. plasma, degree of polarisation 80−87944
Brillouin backscatt. depend. on density scale lengths near crit. density 80−43888
broadening of free-bound radiation thresholds, expt. results for Cl^-, I^- and Br^- 80−53940
bumpy torus, NBT-I, effective toroidal curvature, error field, electron beam diagnostics 80−24237
BWO appl., 110 to 170 GHz, using Sm-Co ring magnets *(German)* 80−105684
capillary discharge jet, displacement meas. 79−94817
cathode fall in electron beam controlled stationary non-self-sustained discharges 78−71613
charge carrier density, enhancement by probing RF voltage signals 77−58891
charge exchange neutrals, emitted from rot. plasma, meas. 80−106979
charge exchange neutrals, spectrum, meas. in rot. plasma 80−38706
charge exchange neutrals detection based on H_2^+ negative surface ionisation on ThO_2 80−6280
charge-exchange at. spectrum, Tuman 2 mag. compression heating, ion energy balance 77−51238
circuit breaking arc column electrical conductivity meas., microcomputer appl. *(French)* 80−28864
cluster accelerated by coaxial gun, spectroscopic struct. and mass determin. 77−80349
cluster accelerated by plasma gun, decay 78−30489
cluster acceleration and decay in coaxial gun, obs. 78−63603
cluster ionised front, in rail-type linear accelerator, propag. vel. meas. 79−10665
coaxial accelerator, current density distrib. 78−26352
coaxial cold cathode discharge, props. of medium press. diffusion plasma column 77−51237
coaxial cylindrical discharge tube, diffusion plasma column density and pot. distribs. 79−41797
coaxial plasma guns, breakdown phase, optical and elec. meas. 80−70036
coaxial plasma source, optical meas. 78−1895
coefficients of viscosity of a gaseous plasma 80−43875
coherence wave spectra, freq. averaging effects, digital simulation 77−35390
coherent four-wave scatt. 80−28681
coherent wave particle interaction in Q-machine plasma, electrostatic analyser diagnostics 80−59226
cold cathode arc starting, probe and high speed photography obs. 80−38832
cold collisional plasma, current distrib. and input impedance of antenna of revolution 77−24096
collectively accelerated protons, nucl. activation, time-of-flight, and foil activation meas. 79−4195
collisional plasma rotating inside cylindrical annulus, anal. and diagnostics appls. 78−22466
Columbia Torus-1 belt pinch high beta toroidal device, preionisation, optimisation 80−92368
column compressed by mag. field, multichord corpuscular diagnosis *(Russian)* 79−4190
column equilibrium in octopole Tokamak without conducting shell 79−41858
combustion products, noise temp. meas. using contactless capacitive convertor 78−9830
combustion-driven implosion, spectroscopic study 78−14189
complex plasma layer, optical diagnostics algorithms 78−67435
computational model for spectral and radiative characts. in Kr and Xe arcs 80−64812
conductivity and eqn. of state, exploding Cs wire plasma 78−26323
conference, high temp. plasma diagnostics, Tennessee, USA (Jan. 1976) 77−31528
plasma diagnostics continued
conference, inertial confinement fusion, San Diego, USA, (Feb. 1978) 78−46171
conference, New York, USA (Oct. 79) 80−73093
conference, physics of ionised gases, Dubrovnik, Yugoslavia, (Aug.-Sep. 1976) 77−42961
confinement of LiH plasmas, decay, density measurement 79−46470
continuous emission, ionisation potential lowering and total excitation cross section of atmospheric thermal plasma 80−38705
continuous emission spectrum *(Russian)* 77−84508
continuous optical discharge, diagnostics 80−43947
continuum absorpt. and emission spectra of nonideal plasmas, approx. calcs. 80−75035
controlled thermonuclear fusion expts. *(Spanish)* 79−63805
controlled thermonuclear fusion with submillimetric plasma diagnostics 77−38416
corona, discharge pulses, field strength and electron density calcs. 80−38814
corona, laser-induced plasma, interferometric meas. *(Russian)* 78−1886
corona discharge, computing process for electrons and ions distribution determ. 79−4204
corona discharge, electron density meas. by microwave resonant cavity method 77−68881
corona system, under neg. direct and pulsed voltage, characts. 79−19107
corpuscular diagnostics by charge exchange of plasma ions at artificial target, in Tokamak T-4 *(Russian)* 80−83968
CT6B Tokamak, measurement of plasma column displacement 80−84001
cumulative plasmadynamic discharge, dynamics and radiation, UV source appls. *(Russian)* 79−55578
current density in ionised gas in macroscopic field, direct meas. by Stark broadening of H lines *(French)* 78−9839
current density profile determ. using ordinary and extraordinary microwaves 78−75419
current disruption, in Tokamak plasmas, schlieren signal meas. from millimetre waves 80−48998
current distrib. and voltage in vacuum arc 78−30508
current field characts. diagnostics, freq. shift in microwave cavity flow 77−62406
current generation by electrostatic travelling waves in collisionless magnetised plasma 80−53976
current profile, meas. by probes 78−75416
current sheath struct. diagnostics, fast particle beams, deuterated polyethylene fusion, plasma focus 77−76206
current sheet, mag. field struct. rearrangement, electron accel., X-ray probe obs. *(Russian)* 78−38530
current sheet dynamics in accelerator, interferometry and probe meas. 78−26351
current sheets in staged focus 78−14225
current sheets in staged focus 78−14226
current source duration in laser-produced plasmas 78−1862
current-driven collisionless drift instability 80−14893
cyclotron emission spectrum, electron temp. 77−76208
cyclotron harmonic waves props. from perpendicular dispersion relation 80−38612
cyclotron radiation from magnetically confined plasmas, review 80−38722
cyclotron radiation from turbulently heated plasma 77−84502
cyclotron resonance and magnetoplasma phenomena at IR and microwave frequencies, review 79−61224
cyclotron resonant gas breakdown with 1.22-mm $^{13}CH_3F$ laser 79−55549
cyclotron self-absorption in two-temp. plasma, temp. and density meas. 80−48987
cylindrical conducting body, supersonic plasma cross-flow, stagnation region meas. 79−32810
cylindrical foil in air, elec. explosion, high current shunt pinch props. 79−64950
cylindrical plasma, wave tracing and short-wave diagnostics 77−76100
D_α spectral profile measurements on TFR plasmas 80−92397
data acquisition system assembly for pulsed fusion experiments 80−49011
DC arc plasma, meas. of conc. ratio of component atoms *(Russian)* 77−27754
dense plasma, H_β line red shift expt. 78−67473
dense plasma, spectral series degeneracy 80−19622
dense plasma focus, strong subnanosecond field variations 80−70035
dense plasma focus Julich I, neutronics, fusion plasma investigation 77−35396
dense plasma XUV transition Doppler broadening suppression, collisional-radiative model 80−19614
density, temp., determ. using magneto-acoustic oscills. 77−80354
density and temp. profiles near plasma edge in Alcator 79−7489
density and temperature meas. by coherent antiStokes Raman scatt. *(German)* 79−27321
density fluctuations, microwave scatt. 79−98985
density fluctuations, microwave scatt. obs. 80−48851
density measurement, for plasma in EM trap *(Russian)* 78−5944
density measurements in magnetosphere 79−35072
density modification in 10^6 W cm^{-2} ablated microballoons, optical diagnostic technique 78−14206
density modifications, supercrit., of laser-produced plasma, due to reson. RF cavity field 79−50875
density profile of Z-pinch plasma, interferometry 80−6277
density profile self-steepening in laser plasma, interferometry 78−5938
density profiling, high speed interferometer 77−1021
density spatial distribution pulsation by modulation of reflected wave *(Russian)* 77−62409
density-dependent ion lines, excited levels collision relaxation rates calcs. 78−18458
deuteron beam time-amplitude characts. in plasma focus *(Russian)* 79−82099
dielectric chamber, short-circuit effect, diffusion and stability obs. 78−71446
dielectronic satellite spectra, electron collisions, corona model theory 80−59188
differential emission measure solutions, errors 79−12397
diffuse discharge, HV, anode drop meas. in transverse air flow 77−39483
diffuse pinch, energy equilib., tensor cond. model 80−24209
diffuse theta-pinch, ion temp. meas. *(Japanese)* 80−87951

plasma diagnostics continued
diffusion, of heat and particles, due to collisionless drift instability, probe diagnostics 78−59555
diffusion of charged particles along mag. neutral line 80−6218
diffusive plasma transport across mag. field, expt. methods *(Russian)* 79−1294
direct extraction H^- sources, prod. and destruction in magnetron and duoplasmatrons 77−23340
discharge, capillary pulse type, spectral chronographic-equidensitometric diagnostics 80−44055
discharge, grazing, incomplete gas temp. and electron density diagnostics 79−55600
discharge, hollow cathode effect with axial elec. field *(French)* 79−60209
discharge, hollow-cathode, radiation signals in weak mag. field 78−70789
discharge, hollow-cathode type, cathode fall width determ. with fixed shadow probe 80−24292
discharge, low-pressure, shape and width of ion line, use on diagnostic 77−35386
discharge, maser atomic H source, H_2 dissoc. meas. 79−86637
disruptive instability fine struct. in Tokamak, X-ray diagnostics 77−43073
dissociative recombination of H_3O^+ and D_3O^+ at elevated electron and gas temperatures, rate coeff. determ. 80−63747
DIVA, scrape off layer, multigrid energy analyser applications 80−33818
divertor fluxes in stellarators and torsatrons, azimuthal distrib. 80−6216
Doppler temp. measurements in TFR Tokamak using spectral scanning in VUV, monochromator design 80−38703
dosimetry of impulse fluxes of ionising radiation, use of microwave methods 77−25557
double layers from ion acoustic instability numerical simulation 80−59220
double plasma arc, rotation in graphite tube 78−71599
Doublet IIA, m=1 oscills., internal disruptions, impurity line emission 77−58898
drift and current flow of charged particle along mag. neutral line 80−1749
drift wave freq. profiles, Doppler model 78−71471
drift wave instability, current-driven, θ-probe obs. 80−59204
drift wave spectra modulation due to HF fields 80−38624
drive pulses, from unidirectional motion, laser action on solid target *(Russian)* 77−1003
duoplasmatron anode plasma, ion temp. 80−6292
dye laser emission, from laser spark, nonlinear absorpt. meas. 79−64922
dynamic Stark effect in H_δ and neutral He spectral lines for elec. field strength meas. in waveguide 80−69103
EBT, ray tracing near electron cyclotron freq. 80−103178
ECR fundamental ordinary mode absorption and emission, in PLT 80−43943
education, plasma diagnostics using commercial gas tubes 77−87597
electric arc, horizontal, in inhomogeneous mag. field, mass spectrometric anal. 80−79620
electric arcs, temperature estimation from self-reversed spectral lines 80−75110
electric discharge with disc cathode in He flow, spectrosc. investig. 80−64809
electric double layers in magnetised plasma column 79−55555
electric field fluctuations spectrum, laser fluoresc. spectroscopy meas. 80−87946
electric field intensity meas. in stabilised arc, plate probe meas. 80−75095
electric field of laser prod. plasma in air *(Russian)* 79−37555
electric fields, in hot cathode discharge double layer, electron beam diagnostics 78−34337
electrical conductivity of high-density, shock-heated Ar and Xe plasmas 80−38557
electrical conductivity of nonideal high-press. plasma, Ar arc IR continuum absorption obs. 80−38558
electrical discharge in vacuum, ion emission, mass spectrometric obs. *(French)* 78−1919
electrode contact processes, microplasma diagnostics 80−59325
electrode vapour conc. meas. from light scatt. in air arc plasma 78−30505
electrodeless discharge, medium press., in rapidly pulsed high freq. field *(Russian)* 79−55581
electrodynamic mechanisms of limitation of the electron concentration in a laser spark *(Russian)* 80−59333
electron and at. excited states densities in laser prod. He plasma 80−38710
electron and heavy particle temp. difference in Ar arc, laser interferometry 80−38766
electron and ion energy distribs., laboratory and space plasma comparison 78−5945
electron and ion temps., Thomson scatt., and neutron emission obs., Tokamak discharge 78−18438
electron and plasma density distribs., in current layer, holographic interferograms *(Russian)* 77−47257
electron beam, ion neutralisation, probe beam diagnostics 79−27157
electron beam controlled discharge, cathode density waves 80−38798
electron beam current meas. in gas 80−38523
electron beam diagnostics by neutron radiation spectra, applied to accelerated electrons in Tokamaks *(Russian)* 78−22555
electron beam diode, pinched relativistic, large ion current meas. 77−31428
electron beam energy distrib. in plasma 78−5883
electron beam fusion compression targets, fuel preconditioning studies 79−81076
electron beam heating and beam energy distrib. in E-region approximated plasma 80−103163
electron beam impact on hemispherical target, implosion dynamics 77−47228
electron beam interaction, soft X-ray and UHF meas. *(Russian)* 79−32825
electron beam interaction with toroidal plasma column, interferometric and probe diagnostics 77−24100
electron beam irradiated pellet, holographic interferometry of plasma blowoff vel. and density 77−23279
electron beam produced plasma, fast photography, emission spectroscopy 77−39458
plasma diagnostics continued
electron beam stabilised mirror confined gas, hot electron population study 80−100089
electron beam-formed plasma potential, two-electrode probe diagnostics *(Russian)* 80−1841
electron beam-neutral gas interaction, SEEBIE expt., Thomson scatt. diagnostics 77−24111
electron beam-plasma accel. heating, by propag. direction-decreasing density 77−89275
electron beam-plasma interaction, microwave obs. 78−9796
electron beam-plasma interaction, RF emission, oscill. nodes and instabilities 77−24099
electron beams, relativistic intense solid, cyclotron maser instability 79−55494
electron conc. determ. from EM wave propag. *(Russian)* 79−4150
electron concentration, ion current, in relativistic electron beam oscill. diode 78−9861
electron concentration in pulse discharge plasma in H_2 and/or N_2 *(Russian)* 77−27753
electron cyclotron emission characts., high-density TFR plasma 77−62400
electron cyclotron emission in ALCATOR Tokamak 78−5935
electron cyclotron emission in steady state inhomogeneous plasma 80−48864
electron cyclotron frequency expts. in 15X-B Tokamak, temp. rel. to heating power 80−48912
electron cyclotron heating in Tokamaks: experiments and prospects 80−28749
electron cyclotron plasma radiation, in L-2 stellarator *(Russian)* 79−4178
electron cyclotron resonance, emission, from Princeton Large Tokamak, diagnostic appls. 77−80280
electron cyclotron resonance plasma, production of multiply-charged ions, X-rays and charge state distribs. meas. 80−43941
electron density, dense plasma, Stark broadened $H_{\alpha,\beta}$ line struct. 77−6722
electron density, determ. by spectral line width, at oscill. strength effects 77−51230
electron density, determ. from He I Stark widths and He-Ne laser interferometry 77−80374
electron density, from multicharged He-like ion intercomb. lines, in laser plasma 78−9106
electron density, in reson. laser radiation absorption of lasers-generated plasma 78−9805
electron density, meas. using three-laser intercavity interferometer 77−80357
electron density, scattered microwave pattern meas. 77−35384
electron density, spectroscopic meas. during arc discharge extinction *(French)* 77−80361
electron density, temp., and distrib. function, in ion beam-created high-press. plasma *(French)* 80−10407
electron density, TFR Tokamak disruptive instability oscill. struct., mag. probe and X-ray diagnostics 78−22564
electron density, X-ray emission, dense plasma production by hypocycloidal pinch 77−43051
electron density and temp., adiabatic toroidal compressor, power balance anal. 77−51219
electron density and temp., microwave, cond. and diamagnetism obs. in TM-3 Tokamak 77−15247
electron density and temp. distribs., Tokamak-4, q=5.4 stability margin mode *(Russian)* 77−47240
electron density and temp. in magnetosphere, GEOS-1 mutual impedance expt. meas. 79−35071
electron density and temp. meas. using spectral line density ratios 78−14203
electron density and temp. profiles, Langmuir probe meas. in sputtering DC discharge *(French)* 78−30482
electron density by EM wave scatt., identification problem 78−71532
electron density determ. from X-ray spectra of multiply charged K ions 78−94938
electron density diagnostics using self reversed deuterium D_α line 78−55746
electron density fluctuation amplitudes in mag. mirror device, microwave meas. 77−3985
electron density fluctuations in ATC Tokamak plasma 77−43074
electron density for solar flares, XUV spectrum diagnostics 79−88633
electron density in electron beam sustained discharge, electron neutral inverse bremsstrahlung 78−63604
electron density meas. by EM wave propag. in magnetised plasma column 80−43974
electron density meas. by two-freq. band microwave interferometer 80−83890
electron density meas. in Tokamak plasma, far IR waveguides for interferometers 79−73034
electron density meas. in vac. arcs at anode spot form. threshold 79−55552
electron density of laser plasma, XUV spectra of O-like ions 79−1340
electron density of Z-pinch discharge, interferometry 77−35394
electron density profile, resonator method, distributed-coupling system 77−1017
electron density profile, resonator method, mode selection by absorbing rings 77−1018
electron density profile by neutral Li beam probing 79−4186
electron distrib., Langmuir probe effect on meas. 78−83609
electron distribution function, in low-temp. low press. plasma, meas. methods *(Czech)* 78−71534
electron distribution function, plasma stream, probe diagnostics 80−14935
electron distribution relaxation numerical study for CO_2-N_2-He discharges 80−54070
electron distributions, bremsstrahlung linear polaris. obs., in mag. field *(Russian)* 77−47158
electron emission, 1 MeV, from CO_2 laser heated plasma 79−90468
electron emission from microwave irrad. plasma slab 77−84503
electron energy, continuum X-ray emission obs. of laser beam-target energy deposition 78−22563
electron energy, high, in ns dense gas discharge, particle diagnostics 79−60210
electron energy distrib., DC glowing discharge rel. to microwave discharge, in N_2, probe meas. *(Russian)* 77−47280
electron energy distrib., Druyvesteyn method 78−30481

plasma diagnostics continued
electron energy distrib. functions determ. by second derivative method *(Russian)* 78−51356
electron energy distrib. meas. by electrostatic probe, plasma drift effect 79−86613
electron energy distrib. of relativistic plasma in mag. mirror, synchrotron radn. meas. 79−10717
electron energy distribution function meas. using delay line differentiator *(Japanese)* 80−84002
electron energy distribution in a low-pressure RF discharge 80−87979
electron energy distributions in a sputtering discharge *(French)* 79−55557
electron energy spectrum, local meas., X-ray method 78−9842
electron energy transport into layered targets irradiated by CO_2-laser light 80−69979
electron heat diffusion coefficient, in Tokamak, meas. by sawtooth oscill. obs. 79−64911
electron heat diffusivity, ORMAK Tokamak, X-ray emission obs. 77−31524
electron heating due to MHD shock wave, electron temp. and density 79−14588
electron long-wavelength wave dispersion evolution meas., sampling technique 80−6283
electron pressure, geological materials in DC arc, determ. by spectrographic manometry 78−16796
electron relaxation to Maxwellian energy distribution, in low-press. Hg discharge 79−64949
electron synchrotron emission from Tokamak plasma 77−43076
electron synchrotron emission from Tokamak plasmas 77−43077
electron temp. in medium press. flowing positive column with vol. recomb. 78−87561
electron temp. meas., continuous, automatic, using double Langmuir probe 80−43977
electron temp. meas. by soft X-ray energy anal., pulse pileup effects 79−64910
electron temp. meas. using thermal cyclotron radiation emission, from Alcator tokamak 79−60171
electron temperature, in HF plasma, meas. by spectroscopic and double probe methods 77−65910
electron temperature, O_2-injected TFR Tokamak current plateau, Thomson scatt. 78−22565
electron temperature, plasma press., energy lifetime, in T-9 Tokamak *(Russian)* 77−68863
electron temperature, time history meas. of impurities line emission 77−15241
electron temperature and density, TFR hot plasma, soft X-ray diagnostics 77−51234
electron temperature and density relax. during internal disruptions in Tokamak 77−51235
electron temperature determ., semi-analytical eqn. for X-ray absorpt. curve 77−27722
electron temperature in glow discharge in transverse mag. field, spectrosc. method meas. 80−87855
electron temperature in plasma cluster, coaxial gun accel., spectroscopic diagnostics *(Czech)* 77−24182
electron temperature measurements from cyclotron emission in T-10 Tokamak 80−19617
electron transport, determ. from pulsed arc meas. 77−47157
electron transport induced by drift wave fluctuations, microwave scatt. 78−94894
electron velocity distrib. determ. during strong turbulence 79−60196
electron velocity distribution during Landau damping of slow electrostatic waves 78−9774
electron velocity distribution function in plasma jet, light scatt. meas. 79−4183
electron-beam inertial confinement expts. at Valduc *(French)* 80−48907
electron-cyclotron emission spectra from Princeton Large Torus 77−89314
electron-density structures in laser-produced plamas at high irradiances 79−82041
electronic temperature, low, of weakly magnetised plasma meas. 77−68870
electrostatic analyser, high-energy ion form., turbulent current discharge 77−19785
electrostatic fluctuation in stochastic ion heating, twin capacitative probes meas. 78−34347
electrostatic ion analysers for laser prod. plasma detection, space charge effects 80−96392
electrostatic plasma-confinement experiments in a tandem mirror system 80−70025
electrostatic trapping of intense relativistic electron beam in magnetic mirror 77−24172
electrostatic wave packet, nonlinear evolution in collisionless plasma, probe obs. 77−62358
electrostatic wave radiation near lower hybrid freq. 77−84430
electrostatic waves in drifting ionospheric simulation 80−53965
electrostatic well accumulation of multicharged ions in mag. mirror plasma by electron cyclotron reson. 79−32804
electrostatically plugged spindle cusp, density and decay time, microwave interferometry 77−58881
elliptical plasma source, radiation emission distrib. 80−103124
EM beams interaction, secondary wave prod., diagnostics appl. 77−11352
EM field modification meas. in turbulent plasma 77−42987
EM trap confinement, microwave investig. *(Russian)* 80−10416
EM waves in plane inhomogeneous plasma in presence of mag. field shear, appl. to plasma diagnostics *(Russian)* 80−103140
EM waves nonlinear mixing as density probe 78−77406
EM-implosion generation of pulsed high energy density plasma 78−94927
emission from excited metal atoms in cathode region of discharge in air 78−1939
emission from plasma formed in proton beam collision with Al target 80−53946
emission line shapes from a rotating ring radiator 80−83998
emission spectra, of Hg plasma near photorecomb. threshold, high press. effects *(Russian)* 78−38545
emission spectra of atoms and molecules accelerated by stationary external field *(Russian)* 77−3319
energy balance, in L-2 stellarator, with ohmic heating *(Russian)* 79−4179

plasma diagnostics continued
energy balance in PLT Tokamak 80−28733
energy distribution of electrons heated by laser light absorpt., simulation and test particle methods 80−48963
energy partitioning, in magnetoplasma, relativistic electron beam heating 78−38515
energy transport, in laser produced plasma, X-ray obs. 78−75269
ERASMUS, low aspect ratio Tokamak, charact., RF expts. 79−99000
ERASMUS Tokamak data acquisition system, program struct. 80−49012
EUV and X-ray high resolution spectra from laser produced plasma 77−84522
excited atom reactions, in Ne afterglows, rate consts. meas. 79−64826
excited atoms, near-reson. Rayleigh scatt. obs. 77−3992
expanding laser-produced plasma, radiative transfer line intensities and stimulated emission 77−3988
exploded-wire plasma, inner-shell X-ray spectra 77−27720
exploding foil, theory of expt. determ. of potential drop 78−71515
exploding metal foil plasmas, short term radiative processes obs. 79−82083
exploding wires, continuum radiation, spectral radiant intensity meas. 78−91134
exploding-pusher-tamper areal density, neutron activation meas. 80−91237
extreme UV spectroscopy of the 2XIIB neutral-beam-heated fusion mirror machine 80−74002
far IR laser interferometer, for low temp. plasma diagnostic techniques 77−58895
Faraday rot. meas. in high-β fusion expts., plasma electron density and mag. field determ. 80−49008
Faraday tarotion, effects of pulsewidth 78−71540
fast atom fluxes in Alcator Tokamak 79−10715
fast electron energy spectra and preheating of laser irrad. target 79−55528
fast ion beam vel. distrib. meas. with probe 79−13890
fast ion energy spectra from laser prod. plasma 79−73033
fast neutral diagnostics of heated plasma, temp. determ. 77−68875
fibre-optic data transmission systems 80−79571
field ion samples in Tokamak plasma, impurities study 79−98971
Filippov dense focus, time and space resolved neutron emission meas. 77−58896
fine struct. of plasma satellites of He 492.2 nm line 80−59235
fission-fragment-generated plasma, theory of spectroscopic diagnostics 78−34374
flash lamp, discharge-channel development, effect of reflected shock waves, photographic obs. 77−43093
flashtubes, plasma-wall interaction, spectroscopic meas. 79−77421
flow over flat plate, flush probe studies 80−1845
flow through blocked picket fence mag. trap, Langmuir probe meas. 77−51220
fluctuation diagnostics, digital time series anal. techniques 78−5951
fluid-ion cyclotron instability, pulsed CO_2 radiation scatt. obs., theory 77−31461
flush probe studies of plasma flow over flat plate 80−24147
flute modes, similar freq., simultaneous feedback stabilisation 80−103146
focus, 1 kJ, neutron-, ion-, and electron-energy spectra 77−35404
focus, collapse phase, luminous front time evolution, spectrosc. obs. 78−42816
focus, current sheath evolution; optical and elec. diagnostics 77−76207
focus, effective ion temperature, determ. by nucl. reaction rate in D_2-^{3}He mixture *(Russian)* 79−27824
focus, emission spectrum, 10-350 eV, by photoemission scintillation spectra *(Russian)* 77−80367
focus, heating by TEA CO_2 laser, neutron enhancement *(Japanese)* 78−9808
focus, high energy deuteron intensity and ang. distrib. 78−59671
focus, instability enhanced X-ray and neutron emissions 77−62399
focus, Mather-type machines, temp., density, neutron and X-ray emission charact. 77−24184
focus, suprathermal microwave radiation, temporal, spectral and ang. distrib. 78−18450
focus, time-resolved X-ray photography 77−27718
focus apparatus, staged, current-sheet dynamics, X-ray and fusion-neutron emission intensities 79−4160
focus device, interferograms, neutron and X-ray emission 77−27726
focus dynamics with powerful laser interaction during MHD stage, diagnostics 80−48924
focus electron kinematics, accel. and hard X-ray prod., relativistic numerical anal. 77−58897
focused relativistic electron beam discharge into thin target, EUV emission 78−47162
focusing hog-horn antenna for microwave diagnostics in plasma machines 80−96395
FOM Instituut voor Plasmafysica, Jutphaas, expts., 1977, review 79−98992
forbidden lines in dense plasma, detectability 78−5856
Frascati 1 MJ plasma focus facility, deuteron energy distrib. 80−87957
free-burning arc continuous radiation rel. to electrode erosion 78−71578
frequency shift of TM_{omo} mode due to anisotropic temp. effect 77−84517
FT Tokamak, non-thermal electron distrib. function 80−83891
fusion experiments application conf., Varenna, Italy (Sept. 1978) 80−48989
fusion plasma, RF phased waveguide heating, thermal eddies form. 80−24193
fusion plasma in beam driven Tokamak, Fokker-Planck/transport analyses 80−28826
fusion plasma particle diagnosis 77−35397
fusion possibilities and plasma confinement and interactions in mag. config. Tokamak, review *(French)* 80−54017
fusion reactor, MFTF, supervisory control and diagnostics system, database management system 80−99326
fusion reactor, MFTF, supervisory control and diagnostics system, database management system, data structs. 80−99327
fusion targets, space time implosion charact., X-ray obs. 77−27725
fusion-plasma neutron fission and activation of U fuels 79−13521
gas discharge, mass spectrometry, corrections 79−82100
gas discharge in crossed fields, obs. 78−75471
gas filled microballoon targets, laser produced implosion dynamics 80−24198

plasma diagnostics continued
gas flow, nonequilib. ionisation and Hall EMF 80−69981
gas flow, partly ionised, electron density and conc. meas. method *(Russian)* 77−55172
gas jet target with electron beam heating, plasma density meas. 77−39457
gas mixture, reacting, atom conc. reson. absorb. meas., microwave discharge lamp calibration 79−92032
gas RF breakdown, time-resolved studies 78−79485
gas temperature measurement from mol. emission spectra in glow discharge 79−55558
gas-discharge plasma, in axisymm. mag. field, plasma flow diagnostic meas. 77−35419
gaseous impurity origin, meas. by mass spectroscopy in JFT-2 Tokamak 79−1339
generator arc chamber, hydrodynamic struct. 80−1817
glass microballoon, laser irradiated, time resolved spectroscopy of second harmonic emission 79−23457
glass microballoon imploded by laser, X-ray transmission analysis *(French)* 80−54011
glass-Al, layered target, reduced thermal cond., X-ray meas. 77−31523
glow discharge, crossed-field type, electron energy distrib. diagnostics 79−27851
glow discharge, electric probe diagnostics, sputtering of appl. 78−71537
glow discharge, gas temp. meas. by fluoresc. spectroscopy 78−18467
glow discharge, intermediate pressure, voltage-current characts. 79−55604
glow discharge, mass-energy anal. of ions. near cathode 77−84563
glow discharge, temp. meas. using electronic rot.-vibr. mol. spectra *(Russian)* 78−71575
glow discharge, tube impedance with and without metal cover 78−67508
glow discharge characterisation 78−71536
glow discharge characts. meas. for sputtering appl. 78−72726
glow discharge in transverse gas flow causing population inversion, discharge struct. 78−78992
glow discharge plasma line emission intensity calc. and meas. 78−67526
glow discharge sputtering diagnostics, optical spectroscopy 78−72666
glow discharges, atomic and ionic spectral line excitation in cathodic region *(Russian)* 78−63611
graphite hollow cathode glow discharge C conc. determ. 80−44032
graphite vapour cloud, laser-prod., temp. conditions investig. 80−59290
grid influence, on low-voltage Cs arc plasma in 3-electrode system 80−38844
gyromagnetic props. of cold plasma, calc. and expt. 77−84415
H-pinched discharge, low-current, optical, elec. and erosion studies 77−35417
Hall accelerator plasma stream, electron temp. using Xe-optical thermometer 78−79475
Hall effect in toroidal discharge, investig. 80−38701
harmonic emission mechanisms, three-halves, from laser-produced plasma 80−59283
harmonic generation in Nd:glass laser produced plasmas 78−30480
He I and II radiation enhancement in mag. field, nonlocal thermodynamic equilib. 80−10366
heat transfer rates to flat plate from normally-impinging N plasma jet 80−75061
heating experiments, diagnostics, turbulent heating example 80−49015
heating mechanism obs. and analysis, with fast theta pinch *(Japanese)* 80−1818
HF discharge, near electrode region, spectra 80−38833
HF discharge in inert gas, optical diagnostics, bremsstrahlung 78−9871
HF electric field, nonlinear behaviour just before beam-plasma discharge initiation 80−87904
HF induced discharge, gasdynamic parameters meas. and calc. 78−94934
HF noise and transport in electron-beam-heated plasma *(Russian)* 77−55174
high beta toroidal device, preionisation, optimisation 80−92368
high current, high press. discharges, conductivity meas. 80−38793
high current vacuum arc, with axial mag. field, current distrib. meas. 78−87572
high temperature, radiation loss measurement due to ions impurity 77−7613
high voltage Penning discharge reflex system, confinement in mag. mirror field 79−86600
high-current vacuum discharge, cathode region mag. field effects, elec. and thermal characts. 77−62412
high-density effects on plasma spectroscopy 78−75429
high-energy ions from Nd laser produced plasma, asymptotic energy distrib. meas. 77−89303
high-energy laser cavity diagnostics, holographic subtraction technique 77−19285
high-power neutral beam, spectral resolution by optical diagnostics 80−33819
high-Z emitters in ultradense plasmas, hydrogenic profiles, perturbing ion effects 80−79566
HIP-1 hot ion plasma, effect of anode-cathode geometry on performance characts. 77−24112
hollow cathode arc discharge, balance equations for active zone processes *(German)* 79−68963
hollow cathode discharge, expt. determ. of Ar and Ne metastable atom conc. *(French)* 77−31540
hollow cathode discharge with variable voltage 80−59336
hollow cathode glow discharge, state of equilib., spectroscopic meas. 80−19647
hollow cathode inert gas discharge, excitation and ionis. mechanisms, spectra obs. 77−15261
hollow-cathode discharge alignment, electron collisions 79−64944
hollow-cathode glow discharge, fast electron current, electrostatic vel. analyzer diagnostics 79−27856
homogeneity and stability, theta-pinch Pharos device, time-resolved photography 78−34360
hot-electron plasma in simple mirror, stability, X-ray diagnostics 77−24176
HT-6 Tokamak, mass spectroscopic diagnostics *(Chinese)* 79−98990
HV nonosecond transient meas. from pulsed low inductance gas discharge, Kerr effect 78−51380
hypersonic plasma streams, microwave emission obs. 79−14617
ICF targets, material response and implosion dynamics obs. 78−58477
impedance meas. at lower hybrid freq. 78−47165
implosive shock wave, prod. by laser, eval. of attained temp. 79−73022

plasma diagnostics continued
impulse spark study using two-wavelength interferometry 80−86391
impurities, far-IR emission anal. 77−31521
impurities, spectroscopic meas. 79−10714
impurities in DIVA divertor and JFT-2 confinement 77−72501
impurities in DIVA Tokamak, spectroscopic meas. 79−27826
impurities origin, Diva Tokamak, arcing, ion sputtering, evap. 78−59691
impurity behaviour during neutral beam injection and gas puffing into ORMAK 79−64878
impurity conc. and time evolution in Tokamak, optical meas. 77−51156
impurity density in DITE Tokamak, soft X-ray meas. 80−19616
impurity deposition in ISX-Tokamak, time resolved measurements 80−38694
impurity profiles from VUV spectroscopy of TFR Tokamak plasma 78−51349
impurity spatial and time distrib. in JIPP T-II tokamak, vis. spectrosc. meas. 79−86619
in temperature, total radiated energy from HBTX 1 Z-pinch 77−27729
inductively coupled plasma, temp. and electron density, optical meas. 78−67417
inert gas, electron density determ. from spectral line meas. 77−23467
inert gas afterglow, excimer form., VUV emission obs. at low press. 80−38755
inert gas afterglow plasmas, cyclotron emission and electron thermalisation 77−84545
inert gas discharge, moderate press., visible and UV radiation spectrum 77−31533
inert gas discharge, spatial mass division in crossed elec.-mag. field *(Russian)* 78−5960
inert gas halides, excimer emission from electron beam produced plasma 80−43887
inert gas ion laser, high voltage-low press. discharges, stationary props. 80−92400
inert gas ion laser discharge, energy balance 78−74884
inert gas plasma, electron-beam produced, laser action of ionized and neutral atomic lines 80−106929
inert gas plasmas, prod. by U fission fragments in nucl. reactor props. 77−76147
inert gas positive discharge column, at. temp., interferometric meas. 77−35427
inert gas stationary afterglow obs. of singly charged atomic ions, three-body rate coeffs. 80−38757
inhibited electron thermal cond. in plasma from microwave laser irrad. targets, laser intensity threshold Z-depend. 80−48928
inhomogeneous plasma, collisionless emission of radiation *(Russian)* 77−3926
instability meas. by mm wave scatt. in turbulent plasma *(French)* 78−34373
intense relativistic pulsed electron beam appls. in plasma phys. *(Dutch)* 78−30452
interferogram numerical processing, for axially symm. plasma discharge 77−27717
interferometer phase detection using LSI-11 microcomputer and high-speed digital techniques 78−71545
interferometric data inversion, cylindrically symmetric refractionless plasmas 79−90459
International Sun Earth Explorer 1, electron spectrometer expt. 78−85809
International Sun-Earth Explorer 1, solar wind expt. 78−85800
International Sun-Earth Explorer 1 and 2, fast plasma expt. 78−85800
International Sun-Earth Explorer 1 and 2, plasma wave investigation 78−85802
International Sun-Earth Explorer B, EGD positive ion expt. 78−85805
International Sun-Earth Explorers 1 and 2, quadrispherical LEPEDEAS for plasma meas. 78−85801
interplanetary wave expt. on International Sun-Earth Explorer C spacecraft 78−85794
interstellar medium, far IR fine structure line obs. 80−62253
ion acoustic test waves in magnetized plasma, meas. by 30 GHz Lecher wire interferometer 78−1903
ion acoustic turbulence in a large-volume plasma 78−67354
ion acoustic wave, parametric decay instability 79−23413
ion beam, intense neutralised, ballistic focusing obs. 78−9859
ion beam scattering by ion-acoustic turbulence 80−6262
ion beam-plasma interaction system investig. 79−77401
ion beam-plasma system, dispersion relation 79−46485
ion charge distribution, in 10.6 micron heated laser induced plasma, X-ray diagnostics 80−6271
ion component energy anal. in moving plasma 77−80366
ion component studies with monopole mass spectrometer 78−5926
ion composition of plasma of pulsed discharge in He, H_2^+ current time evolution 80−54046
ion composition of pulsed discharge plasma, optical, probe, mass spectroscopic anal. 80−33840
ion confinement time, in pulsed laser-produced plasma 78−38518
ion current density modulation, in Hall accelerator with extended accel. zone 78−79480
ion current from Penning discharge ion source, depend. on mag. field and anode diameter 80−54072
ion cyclotron resonance heating in multiple mirror machine 77−24108
ion density, temporal var., soft X-ray absorpt. obs. 77−1015
ion density and temp., cusp field with RF plugging, appl. thermonucl. plasma 77−76169
ion density fluctuations and vel. distrib. in presence of ion cyclotron waves 79−19090
ion diagnostics study of plasma from laser beam focused on Z>5 targets 77−68868
ion diode, intense, mag. insulated, ion beam focusing, particle diagnostics 78−9858
ion emission from laser plasma, secondary electron emission effects on detect. efficiency 80−100096
ion energy distribution, electrostatic retarding field energy analyser 80−70032
ion energy radial profiles in ATC Tokamak, charge exchange meas. 79−10712
ion energy selection by parallel-plate electrostatic analyser 78−83610
ion formation and relative yields from laser prod. plasma, mass spectra, appls. *(Russian)* 78−59631
ion heating, in toroidal theta-pinch, diagnostics 77−62381
ion sheath effect on Bernstein mode waves excitation and detect. 77−7518

plasma diagnostics continued
ion source using HF glow discharge, temp. and electron density profile meas. *(German)* 78−70221
ion spectra, high-energy, periodical modulations, emitted by 1 kJ plasma focus 80−59310
ion temp. determination, Abel transform and Doppler effect appl. *(Japanese)* 77−80348
ion temp. meas., 10-channel neutral particle energy analyser 77−19765
ion temperature, and plasma pot., in electron beam produced plasma in hollow collector 79−27794
ion temperature, He II Doppler broadening meas. in ZT-1 pinch 77−27728
ion temperature, in Tokamak plasma, X-ray Doppler broadening determ. 79−27830
ion temperature, meas., ion cyclotron instabilities 77−68871
ion temperature, spectroscopic meas. in plasma with RF and neutral beam heating 78−5934
ion temperature characteristics of upgraded DIVA Tokamak device 78−63584
ion temperature determ., appl of secondary electron emission to energy anal. of energetic neutrals 80−59278
ion temperature determ. from Doppler profiles 78−79466
ion temperature diagnostic system design and operation at Princeton 78−54942
ion temperature distrib. determ. from impurity lines Doppler broadening 79−27827
ion temperature in scrape-off layer, Katsumata probe meas. 78−75418
ion temperature meas. in ring-shaped T-9 Tokamak *(Russian)* 77−68862
ion velocity distribution, in rot. plasma, Doppler broadening meas. 79−50894
ion velocity space diffusion and ion-cyclotron oscill. enhancement in mirror confined plasma 77−24059
ion velocity space diffusion in controlled ion wave turbulence, ion wave echo probe obs. 77−43079
ion-acoustic current driven instability, in collisionless Q-machine plasma 79−32770
ion-acoustic current driven wave in turbulently heated plasma, microwave meas. 77−72441
ion-acoustic current driven wave in turbulently heated plasma, microwave meas. 78−5937
ion-acoustic dispersion relation, microwave scatt. meas. 78−14215
ion-acoustic dissemination in moving plasma jet 80−38707
ion-acoustic instability, current-driven quenching in trapped electron regime 77−31460
ion-acoustic instability, electron flux driven, in Q-machine, probe diagnostics 80−33765
ion-acoustic instability, time- and freq.-resolved spectra 78−5948
ion-acoustic instability stabilisation by ion beam in Q-machine, probe diagnostics 80−33766
ion-acoustic plasma turbulence, two-dimensional electron density spectra 78−75479
ion-acoustic waves detection using 30 GHz Lecher wire interferometer 78−5946
ion-acoustic waves in two electron temp. plasma, collisional and Landau damping 80−19572
ion-cyclotron instability meas. in mirror-confined plasma 77−3991
ion-ion hybrid damping in D_2-H_2 plasma 79−77361
ion-sound waves in turbulently heated plasma, parallel and perpendicular propag., microwave obs. 79−14612
ionisation and heating by MHD switch-on shocks 77−80320
ionisation dynamics of CO_2 laser prod. plasma, spectrosc. obs. 80−43968
ionisation waves in plasma columns, microwave detect. 78−79461
ionised emitters, electron impact broadened lines, quantum mech. interference effects 77−42282
ionised gas, H_α-, H_α-line Stark broadening, space charge field 77−39409
ionised gas, slow electron momentum transfer cross section in mag. field, RF cond. meas. 79−82030
ionised gases, conf., Berlin, E.Germany (Sept. 1977) 78−63615
ions, multicharged, in plasma produced by laser, spectral line profiles *(French)* 80−79528
ions, multiply ionised, electron impact line width, semiclassical formula 80−43972
IR, nonthermal, and X-ray emission from exploding wire plasmas 79−4187
IR plasma temperature unit, 10000 to 15000K, USSR special standard 77−31519
IR schlieren and absorpt. methods for dense plasma 78−79465
IR thermography of high-power neutral beam target 80−33820
jet, absolute spectral brightness measurement 80−28832
jet, laser Doppler anemometry *(French)* 77−43070
jet, pulse, characts. w.r.t. IR spectra *(Russian)* 79−32826
jet, radiative parameters, temp., electron density *(Russian)* 78−38459
jet, supersonic, vel. meas. using Doppler shift *(French)* 78−14207
jet, swirled, natural gas injection effect on temp. and vel. fields 79−90473
jet, thermal and electrical meas. 78−5931
JET plasma, diagnosis using electron cyclotron emission 79−98991
jets, absolute spectral brightness, space-time distribs. *(Russian)* 79−27836
jets, intersecting, gas-dynamic accel. in compression zone, optical and spectroscopic obs. 77−51247
JFT-2 Tokamak, large scale fluctuation mode mixing, probe, interferometric obs., MHD anal. 78−67312
JIPP T-II, electron cyclotron emission meas. using double-pass optical spectrometer 80−54035
JIPP T-II tokamak plasma, Mo impurity diffusion during H_2 gas puffing 80−28602
JIPP-T-II Tokamak plasma, time resolved spatial profiles of impurities 80−48950
kinetic reactions, pulsed afterglow technique obs. in Ar-II plasma 80−48854
kink instability in reversed field pinches, optical and electrical meas. 77−24188
Knudsen arc ignition, plasma form. kinetics, spectroscopic and probe obs. 80−38808
Kr I, 5871 Å line, transition probability meas. in shock wave plasma 77−3291
L-2 stellarator, ohmic heating ion component characts. and particle lifetimes *(Russian)* 78−59547
plasma diagnostics continued
laboratory, magnetosphere, and astrophysical plasma knowledge interaction 80−59166
Langmuir probe diagnostics of non-equipotential plasma *(Russian)* 78−83608
Langmuir probe transitional characts., effect of ion distrib. and electron relaxation *(Russian)* 79−7486
Langmuir turbulence meas., forbidden transition satellites 80−38714
Langmuir turbulence spectrum, optical polarisation meas. *(Russian)* 78−22572
Langmuir waves, driven by electron-ion decay instability, scattered spectrum 80−43970
large-diameter column, diagnostics by TE_{0mn} reson. cavities, geom. factors 77−15237
laser, high-press. ioniser-sustainer, far IR absorpt. determ. of electron densities 77−14695
laser driven fusion, microshell implosion α-particle and proton meas. 77−10486
laser driven implosions, hydrodynamic instabilities 80−64756
laser energy deposition, 1.06 μm irrad. of parylene disc, X-ray and particle diagnostics 77−43010
laser energy deposition in planar target, expansion and X-ray emission obs. 78−9810
laser flame, far UV line emission of multiply charged ions *(Russian)* 78−75420
laser fusion, 4 TW system 78−74471
laser fusion, CO_2 single beam irrad., diagnostics 78−51329
laser fusion expts., tamper temp. and compression, simultaneous proton and α-particle meas. 78−83607
laser fusion implosion, subns, fast Fourier transform streak photography diagnostics 79−71945
laser fusion implosion, X-ray diagnostics 78−51362
laser fusion ion temp. meas., neutron time of flight techniques 78−17413
laser fusion targets, spatially resolved α-emission 77−68811
laser heated magnetoplasma, X-ray meas. of electron temp. 77−31493
laser heated plasma, suprathermal electrons, 511 keV photon detect. 77−62336
laser imploded Ne microballoon, X-ray shadowgraphy 79−14579
laser imploded targets, compressed core density and radius, X-ray spectroscopy meas. calcs. 78−59685
laser ion-source, form of ion pulses depend. on plasma characts. *(German)* 77−185
laser irradiated plasma, electron energy profile steepening, polarimetry obs. 78−34349
laser irradiated plasma focus, neutron emission *(Japanese)* 78−38538
laser irradiation rel. to emitted current distrib. 77−15217
laser light absorption, by planar plasmas, polarisation and ang. depend. 77−76096
laser microplasma, electron, atom and ion density determ. *(German)* 77−7588
laser plasma, 1/4 crit. density region, harmonic generation expts. *(Russian)* 77−7578
laser plasma, 5-20 keV X-ray emission spectrum investigation using nucl. emulsions 80−92392
laser plasma, backscattered light pulse shape depend. 80−10431
laser plasma, backscattered radiation, spectral-time meas. *(Russian)* 78−42812
laser plasma, Brillouin backscatter depend. on pulse amplitudes, timing, target and geometry 79−77417
laser plasma, electron density and temp., spectroscopic diagnostics, book contrib. 77−51242
laser plasma, electrostatic fields, generated by intense 1.06 μm laser 79−46465
laser plasma, free-free X-ray bremsstrahlung prod., intensity and polarisation anisotropy 77−89320
laser plasma, high energy ion prod., obs. 77−89318
laser plasma, high Z target, time resolved X-ray spectra 79−27807
laser plasma, radn. induced perturbations, sidelight fluctuations 79−82080
laser plasma, resonant line satellites, abnormal intensity *(Russian)* 77−3995
laser plasma, shock waves, ionis. radn. 77−80327
laser plasma, spectral analysis 77−76204
laser plasma as UV light source, grooved TA target 79−19096
laser plasma drop, $3\omega_0/2$ harmonic generation, plasma corona local diagnostics *(Russian)* 78−22567
laser plasma focus, interferometry and luminosity meas. 78−47161
laser plasma spectra, Mg XII resonance line at 8.42 Å, new satellite line structure 78−53912
laser plasmas, ultrahigh speed diagnosis of corona parameter *(Russian)* 78−1899
laser prod. plasma, emission and spectral absorpt. meas. *(French)* 78−9806
laser prod. plasma, radiation press. effects, interferometric meas. 78−51325
laser produced plasma, CO_2 TEA laser-solid interaction, spectral analysis of emission, charact. parameters determ. *(German)* 78−38516
laser produced plasma, energy absorpt., IR and plasma calorimetric meas. 79−90456
laser produced plasma, fine-scale structs. 79−19062
laser produced plasma, interferometric exam. 77−3986
laser produced plasma, props. at high irradiance levels 78−55733
laser produced plasma, radiation obs. 78−22562
laser produced plasma, radiation press. effects, interferometric diagnostics 78−38540
laser produced plasma, self-generated mag. field 79−98943
laser produced plasma, self-generated mag. fields 79−77423
laser produced plasma, simultaneous meas. of current and mag. field 77−1001
laser produced plasma, solid in high press. gas atm. in elec. field, spatial struct. *(Russian)* 80−83962
laser produced plasma, spontaneous mag. field generation, simulation and expt. 79−46472
laser produced plasma, spontaneous mag. field struct. *(Russian)* 77−62402
laser produced plasma, structure of XUV emitting regions 80−54038
laser produced plasma, transient ionising regime, X-ray emission obs. 79−55550
laser produced plasma, X-ray, electron and ion emission 77−58879
laser produced plasma, X-ray generation, mag. field effect 77−19740

plasma diagnostics continued
laser produced plasma corona development, X-ray streak camera obs. 77−15245
laser produced plasma from layered target 78−9812
laser produced plasma heated by 10^{-10} sec. pulses, X-ray emission spectra 77−51239
laser produced plasma parameters determ. from shape of single optically thick line profile 80−103191
laser radiation, anomalous transmission in overdense plasma 78−38499
laser radiation absorption polarisation and ang. depend., reson. absorpt. process obs. 77−76094
laser radiation energy loss to resonantly accelerated ions X-ray meas. of energy distrib. 80−10413
laser spark, diagnostics using hologram interferometer 79−64921
laser spark evolution, thermal wave propag. and shock form. 79−90455
laser spark produced shock wave, IR and microwave thermal radiation *(Russian)* 78−38533
laser spectroscopy in intense magnetic fields 80−62738
laser supported detonation waves, initiation 78−63568
laser target, spherical irradiation, expt. data anal. method 78−1904
laser target irradiation in high mag. fields 78−8989
laser thermonuclear fusion, shell target parameters meas. using X-ray schlieren method 80−14942
laser transmittance in high-Z thin plasma, energy transport 77−80333
laser-imploded target, spatially-resolved X-ray spectra diagnostics 79−37543
laser-irradiated glass shell plasma, electron temp. and density, Si X-ray emission diagnostics *(Chinese)* 80−38718
laser-matter interactions, automatic treatment of data *(French)* 78−42830
laser-produced high-Z plasma, X-ray diagnostics 80−75074
laser-produced multiple-charged ions, pressure dependence, microwave meas. *(Japanese)* 80−10412
laser-produced plasma, continuum X-ray emission spectra 77−55171
laser-produced plasma, high-energy charged particle diagnostics, rel. to nucl. fusion products 77−24190
laser-produced plasma, props. meas. *(Korean)* 80−96373
laser-produced plasma, spectral line shape and intensity, multicharged ion obs. 80−10435
laser-produced plasma, suprathermal electron effects, sheath generation effects on implosion dynamics 77−24191
laser-produced plasma, X-ray bremsstrahlung and fast ion meas. 78−5936
laser-produced plasma, X-ray spectra 80−75075
laser-produced plasma, X-ray spectrometry, for energy transport diagnostics *(French)* 80−43982
laser-produced plasma continua, for absorpt. spectroscopy in VUV and XUV 80−75094
laser-produced plasma electron temp. determ. by Langmuir probes remote from target 78−75427
laser-produced plasma induced shock wave interferometric obs. 78−75428
laser-produced plasmas, microwave diagnostics, electron density 78−9845
laser-produced plasmas, pinhole imaging of fast ions 77−80347
laser-produced plasmas, spontaneous mag. fields, Faraday rot. obs. 78−59680
laser-target interaction expt., backscattered light and harmonic generation, spectral anal. 78−59676
laser-target interaction products, calorimetry 78−51361
light emission from atom beam-plasma interactions, temp. and density meas. 77−72454
light impurities, diagnostics in T-4 Tokamak plasma *(Russian)* 80−10432
light scattering from laser produced plasma 77−11397
light total absorption method for inhomogeneous layer *(Russian)* 77−65911
line broadening in atomic and ionic emissions from plasmas *(French)* 80−79434
line broadening in high density plasma, H_α and H_β line profiles *(Japanese)* 77−43065
line radiation emission, from hot dense Al plasma 80−79456
line-focus plasma, laser produced, coherent far IR radiation 78−42806
linear pinch plasma, extreme UV spectra of light impurity ions, appl. of grazing incidence spectrometer 80−59276
linear turbulently heated plasma, secondary emission detector obs. 80−75100
local intensities, reconstruction by statistical regularisation, theory 77−11400
local ion distrib. function, neutral density profile, temp. determ. 77−31520
low frequency parametric processes in magnetically confined plasmas 80−28827
low temperature inhomogeneous dense plasmas, optical diagnostics 80−75096
low-β plasma, strong turbulence in rot. column 78−94915
low-density plasma, deionisation between electrodes, pot. difference effects 77−51162
low-density plasma, reabsorbed radiation polarisation in mag. field 78−67426
low-density plasma highly-excited level population calc. 78−67326
low-density plasmons, electron temp. meas. by He spectrosc. 80−103192
low-pass interference filters for Tokamak plasma diagnostics 80−64783
low-pressure pulsed Hg discharge, props. 79−64916
low-pressure RF discharge electron temp. probes 78−67542
low-temperature plasma jet, vel. meas. by obs. brightness inhomogeneities 77−43062
low-voltage pulse discharge plasma, radial temp. distrib. and chem. comp. determ. *(Russian)* 78−71544
low-Z elements, satellite lines in laser produced plasma 78−42802
low-Z impurities in PLT Tokamak, radiative power loss 78−91155
lower hybrid cones, trajectory meas., mag. field line determ. 80−33817
lower hybrid freq., reson. cones, wave and particle meas. 77−65913
lower hybrid heating in JIPP T-II tokamak plasma, obs. 79−86617
lower hybrid RF emission, meas. by antenna 78−9852
lower hybrid wave excitation, of mirror mag. field plasma 79−19054
lower hybrid wave propag. and parametric decay in WEGA Tokamak 80−28725
lower hybrid waves detection by microwave scatt. 78−87493
Lyman-α, line broadening calc. 80−43984
Lyman-α line broadening, of H and hydrogenic ions in dense plasmas 78−42811

plasma diagnostics continued
Lyman-α line core, effect of emitter ion dynamics 77−47161
Lyman-α line shape of high-z emitters, effect of fine struct. splitting in ultradense plasmas 79−64912
Lyman-α Stark profile, Stark broadening theory, in dense equilib. plasma 77−84505
Lyman-α transition, line broadening, ion dynamics effects 78−42801
Macrotor Tokamak, laser-induced desorption of impurities from walls, spectral anal. 78−59681
magnetic dipole transitions in TiXIV, TiXV, TiXVII ground state terms in Tokamak discharge 80−63575
magnetic diverters for experimental Tokamaks and fusion reactors 80−18621
magnetic field of longitudinal current, meas. using open microwave reson. 78−9844
magnetic field perturbation obs., quasi steady state currents in RF heated stellarator *(Russian)* 77−47256
magnetic field strength meas. in high density plasma, spectrosc. method 80−1843
magnetic flux conservation, test using radially resolving diamag. loop 78−12734
magnetic flux trap, loop probe meas. in Ar(Kr) 79−14621
magnetic mirror confined non-neutral electron clouds, electrostatic modes, probe diagnostics 79−46466
magnetic mirror experiments, measuring MeV ions from fusion reactions 80−6281
magnetic mirror plasma, transfer function meas. 77−51215
magnetic mirror trap, open, with min. B, LF oscills. 80−38708
magnetic pickup for spontaneous magnetic fields meas. near laser plasma 80−24246
magnetic signal interpretation, relativistic electron beam heated plasma, dynamical model 77−42997
magnetically confined arc, axial density and temp. var. 78−5966
magnetoacoustic wave resonance, generation and detection by single antenna 78−5950
magnetoactive plasma, high-freq. electric effect on atomic spectra 78−9761
magnetoplasma compressor, operating modes, probe diagnostics 77−84530
magnetoplasma compressor compression region struct. streak and framing camera diagnostics 77−84532
magnetosphere, electron density meas. via International Sun-Earth Explorers 78−85803
magnetosphere cold plasma diagnostics using satellite meas. of VLF signals from ground transmitters 77−49183
magnetospheric physics, simulation expts. 79−88549
mass spectroscopy of Q-switched Nd^{3+} laser produced plasma *(Russian)* 79−78817
megagauss magnetic field profile, in laser-prod. plasma, Faraday rot. and interferometric meas. 78−79471
metal, TEA CO_2 laser prod. plasma, charge collection meas. 77−19739
metal impurities, DITE Tokamak plasma, N-ion backscatt. anal. 79−4182
metal plasma prod. by exploding wire, X-ray diagnostics 78−5909
metal surface in strong electrostatic field, ps laser pulse plasma 77−62389
metal target interaction, plasma stream, boundary layer struct., particle diagnostics 77−76106
metal target interaction, plasma stream, boundary region optical diagnostics 77−76107
metal-halide arc, laser Raman scatt. determ. of local density 77−11424
metallic atoms separation in rot, plasma, spectral meas. 79−98988
metastable atoms in arc burning in argon, local densities meas. *(French)* 77−4017
methane, ion-molecule reactions in glow discharge, mass spectrometric obs. 78−63627
methane pyrolysis, AC arc discharge plasma temp., electron density meas. 79−87843
MFTF, supervisory control and diagnostics system software 80−99324
mFTF plasma diagnostics Data Acquisition System 80−99319
MHD accelerator, thermodynamic props., mag. field strength, Hall currents in arc region 77−65917
MHD convertor, U-25, diagnostics system data processing 78−26339
MHD generator, discharge struct. 78−91166
MHD modes in Tokamaks, X-ray techniques 78−47175
MHD turbulence, interferometric meas. in toroidal pinches 77−27731
micro-Fresnel zone plates for coded X-ray imaging of laser produced plasmas 78−42814
microarc atmospheric pressure glow discharge, operating characts, obs. 79−82106
microchannel plate photomultipliers for plasma diagnostics 79−41077
microinstabilities in PLT Tokamak, microwave scatt. meas. 78−67413
micrometal plasma, capable of igniting combustible mixtures, N_2 laser induced, interferometric study 77−89278
microscopy of laser fusion plasma, Fresnel zone structs. 78−51359
microtearing modes and anomalous transport in Tokamaks, self consistent calc. 80−59222
Microtor Tokamak, LF microturbulence, far IR laser scatt. 80−96362
microwave, electron density profile leading edge data., algorithm 79−41880
microwave bundle transmission, plasma column, dielectric const. and r depend. *(Russian)* 77−3983
microwave discharge, fast wave emission diagnostics 80−92391
microwave dynamic interaction, probe diagnostics 80−19584
microwave emission from transformed electrostatic oscills. 77−76209
microwave heating in ELMO Bumpy Torus, anal. 80−28829
microwave holographic imaging through random aberrating media 77−3551
microwave induced plasma, mixed-gas low-pressure, excitation conditions 77−62422
microwave interferometer for electron density meas. on T-II plasma device 78−55754
microwave noise from poloidal field oscills. in Tokamak T-4 *(Russian)* 78−22536
microwave plasma, electron density determ. at atm. press. by hot wave method 77−35420
microwave plasma diagnostic interferometer with fourfold signal passage 78−87487
microwave plasma discharge, electron energy distrib. function *(Russian)* 77−11415

plasma diagnostics continued
microwave plasma generation at atm. pressure, departure from LTE 78−67597
microwave plasma interaction, reson. and thermoelec. mag. fields obs. 77−27678
microwave radiation from turbulently heated plasmas 77−43080
microwave scattering at upper hybrid freq., diagnostics appls. 77−7548
migmacell II, Si detector for fusion products 77−83089
migmacells II and III advanced fuel expts., orbit diagnostics and lifetime meas. 77−83088
molecular beam mass spetrometric sampling system, ion concs. in coal-fired MHD plasmas 80−52358
molecular beam production, by pulsed plasma injector, diagnostic obs. 77−65548
molecular beam sampling of hollow-cathode discharge plasma, fast neutral source 77−68865
molecular electron imact excitation, rot. transitions *(Russian)* 79−76524
molecular laser processes, mm. and submm. microwave spectroscopy 78−13685
momentum generation in high-current arc 78−71586
moving arc, microcrater current and spectral fluctuations, simultaneous meas. 80−38828
moving media, monochromatic radiation absorpt., effects calcs. 77−76101
multi-chord particle diagnostics of a plasma column *(Russian)* 80−1840
multicharged ions, in laboratory plasma, spectroscopy 80−24255
multicharged ions in laser plasma *(Russian)* 79−1344
multicomponent inhomogeneous plasma, spectroscopic analysis 78−67425
multidipole device, primary electron effective MFP meas. 77−24183
multifilament plasma source, multipole mag. field effects on charact. 79−46462
multimillion degree plasma high resolution spectroscopy 77−65915
multimirror experiment, linear, trapped electron instability 79−60181
multiple species ion energy analyser for laser-induced plasma expts. 78−55750
multiply charged ion interactions with Al surface, laser induced plasma 80−70007
multiply charged ions, X-ray spectra in laser plasmas, 1.5-15 Å 78−13462
multiwave picosecond interferometry, of CO_2-laser produced plasma 77−89319
$N^{+,2+,3+}$ lines Stark broadening, He(II) line diagnostics in theta pinch plasma 80−24249
negative grid pulse effects, on Knudsen Cs arc discharge plasma 80−38843
negative ion production and density meas. in low-press. plasma 79−64825
neutral density meas. from charge exchange expt. 78−91153
neutral density profile, absolute meas. by H_α line reson. fluorescence 80−24250
neutral fraction of unmagnetized plasma, 6MKh1S mechanotron meas. of rotation field 78−5925
neutral high power beams, optical diagnostics 80−92394
neutral particle detector and spectrometer for plasma diagnostics 79−23455
neutron and X-ray emission diagnostics, 120 and 20 kV focus device dynamics 77−74990
neutron and X-ray sources space-time struct., scintillator diagnostics, plasma focus 77−74993
neutron emission, obs. and mechanism in plasma focus device 79−90475
neutron emission from Mather-type plasma focus 79−19084
neutron emission measurement, in beam-heated PLT plasma, rel. to ion temp. 79−68954
neutron yield, plasma temp., energy deposition of relativistic electron beam 78−5894
noise temperature meas. by induction converter 77−65909
non-Maxwellian electron plasma distrib., produced by large-amplitude electrostatic wave 78−75299
nonequilibrium plasma flow, wave conversion to EM radiation 78−75281
nonideal plasma, measured props. and nonideality influence 80−43869
nonlinear phenomena by the Tokamak helical mode evolution 80−92398
nonlinear pressure forces for laser radiation in plasma, experimental confirmation 80−28682
nonneutral plasma microstate, synchrotron radn. meas. 79−46486
nonuniform column, electron density and collision freq. determ. by RF coil probe 78−18446
nuclear generated plasmas, ^3He and $^{235}UF_6$ excitation, spectra obs. 80−83997
ohmically heated plasma in Tokamak and stellarator 77−11371
open cycle MHD generator, channel metal surfaces, elec. charact. of boundary layer 77−39473
optical detector correlation measurements of turbulent ionization and ion-acoustic waves 80−59329
optical diagnostic multichannel apparatus 79−50896
optical diagnostics, Abel integral eqn. numerical soln. 79−7488
optical diagnostics using Ba ion beam 79−94815
optical measurements on plasma initiated by a relativistic electron beam *(Japanese)* 80−48914
optically thin plasmas, steady state populations, relaxation times 79−55561
optogalvanic effect charact. in discharge plasmas 78−63583
ORMAK, impurity and surface studies 77−31517
oscillating arc plasma, optical charact., H_α spectral line profile *(Russian)* 77−19775
parallel electric fields in collisionless plasma, particle signature 78−77439
paramagnetism in RF mag. field, expt., theory and simulation 80−6225
parameter determ. by two beams of submillimetre waves *(Russian)* 78−22556
parametric decay spectrum of heating near LH frequency in Petula 80−28761
parametric heating near lower hybrid frequency in Petula 80−28760
parametric instabilities in weakly-inhomogeneous hot plasmas 80−28828
partial discharge spectra meas. by multichannel amplitude analyser system *(Italian)* 80−33847
particle and energy balance by corpuscular diagnostics 80−92399
particle diagnostics of laser-produced plasma, space charge effects 78−63581
particle distribution function, diagnosis using echo effect *(Russian)* 80−14933

plasma diagnostics continued
parylene discs, 1.06 μm laser irrad., plasma prod. processes 78−18431
PDX Tokamak, Ti density meas. using Ti XVII forbidden line 80−32496
Penning discharge, study of hot plasma obtained *(Rumanian)* 79−7504
Penning discharge ion source with hollow cathode, HF instabilities 80−43997
phase transitions in dense, capillary discharge plasma, doubly-charged ions effects *(Russian)* 77−35429
photorecombination spectra, nonideality effect 79−82046
picket fence cusped mag. field, electrostatic self-plugging 79−27815
pinched electron beam prod. expanding gas bubbles, fast photography obs. 80−79564
Pioneer Jupiter missions, solar wind plasma analyser 77−67024
planar streak tube, for X-ray and optical cameras, laser fusion appls. 78−59686
plasma, emission and absorption coeff. at high electron density 80−103121
plasma focus, hard X-rays indicating electron beam 79−14613
plasma focus, nonthermal processes, neutron spectra 78−42804
plasma focus, radiation spectrum in quantum energy range, 0.64-350 eV 79−19094
plasma focus, vac. UV emission meas. using ionisation chamber 77−80370
plasma focus discharge, elec. charact., rel. to hard radiation pulses, time correls. *(Russian)* 78−38528
plasma focus X-ray spectra meas. with time resolution 77−43064
plasma optical transparency evaluation, line broadening effect 80−79453
plasma science conference, Montreal, Canada (June 1979) 79−90380
plasma spectroscopy, broadband stable detector 78−87495
plasma vibrational spectroscopy, data gathering and processing system 79−31737
plasma-surface interactions in Tokamaks, review 79−73017
plasmatron spray, parameters meas. *(French)* 77−35402
plasmatrons, mono- and duo-, anode space-charge sheath charact. rel. to ion source 79−55576
plastic film, laser energy transport, X-ray, ion emission, scatt. light diagnostics 77−24117
plastic targets, anisotropic production of laser-plasma soft X-rays and fast electrons 78−38517
PLT, Fe-charge state distrib. by Bragg cryst. X-ray spectroscopy 79−68956
PLT, ion temp. radial profile meas., neutron flux, Doppler broadening and charge exchange 78−79469
PLT Tokamak, W ion soft X-ray emission effects 78−83537
PLT Tokamak cyclotron radiation Fourier transform spectral analysis 79−32815
polarization and millisecond spectral measurements of electron cyclotron emission from DITE Tokamak 80−92396
polarized light interferometer for laser fusion studies 80−31855
poloidal asymmetry obs., in impurity-ion UV emission, grad B drift 78−26331
poloidal field induced Faraday rot. in Tokamak plasma 79−10716
poloidal rotation velocity determ. in FT-1 Tokamak *(Russian)* 80−19565
polyethylene, laser irrad., mol. emission from unionised gas 78−42777
polyethylene, laser-prod. plasma, space-resolved extreme UV emission 80−54015
polyethylene, X-ray emission spectra of CO_2 laser-irrad. targets, nonlinear processes 80−33793
polyethylene fibre explosion, neutron and energetic ion emission 78−5927
polyethylene filament, plasma prod. by staged laser heating, optical obs. 77−89321
polyethylene irradiated by Nd-glass laser, high energy ion anal. 77−51236
polyethylene layered target, laser produced plasma, expsn., X-ray meas. 77−80326
polymer breakdown plasma analysis, mass-spectrometric installation 78−88670
polymer-coated laser fusion targets, compression to 10×liq. DT density 80−83964
polystyrene coated Al, laser produced plasma energy transport 77−11375
polystyrene slab, electron emission from Nd laser prod. plasma 79−98944
population inversion in FM-1 spherator 77−7048
positive column, in pulsed low-pressure Hg discharge, radial distributions 79−64920
positive column, in transverse mag. field, plasma parameter diagnostics 79−19103
positive column, of pulsed Hg-Ar discharge, electron energy distrib. calcs. 79−64919
positive column of F glow discharge, elec. props. 79−50916
positive corona electrode, negative ion counterflow, elec. field strength meas. 80−38817
positive ion collection by probe in collisional plasma, density determ. 78−51352
potential measurement using scanning multiple collector electrostatic analyzer 79−73046
potential perturbation due to grid or probe 78−47166
pressure, pulsed, in high-current evaporating-wall discharge 79−27838
Princeton Large Tokamak, D electrodisintegration neutron spectrum 77−84521
Princeton Large Torus, unbalanced neutral beam injection, toroidal plasma rot., Doppler shift meas., confinement times 79−77400
probe, digitised random signal analysis method, power spectrum, phase vel. 77−84509
probe analysis, electron reflection and secondary emission 79−98977
probe cct. used in pulsed plasma diagnostics 80−87947
probe diagnostics of nonstationary plasma, anal. *(Russian)* 78−38535
probe measurements correction in RF plasma 78−26333
production, initial stage, Q-switched laser in N_2, plasma parameters obs. *(German)* 79−55531
profile inversion of simple plasmas and nonuniform regions, three-pole reflection coeff. 77−3984
proton beam energy and current, collective acceleration in intense relativistic electron beams 78−9864
proton behaviour in JFT-2 Tokamak, charged-exchanged fast ion anal. 78−51341
PULSATOR, impurities in high density regime 80−79579
PULSATOR I Tokamak, wall analysis, impurities 77−31515

plasma diagnostics continued
pulsed, floating Langmuir double probe electronic cct. 77−62403
pulsed discharge plasma, quasistationary stage props., calc. method 78−38560
pulsed EUV diagnostics using spatial imaging detector system 80−33821
pulsed HP glow discharges, time-resolved electron-neutral collision frequency meas. 77−39498
pulsed micro-discharges, optical interferometry obs. 80−38804
pulsed microwave inert gas discharge, ion composition, mass spectra 79−14616
pulsed plasma source temperature calibration spectropyrometer 77−7590
pulsed radiation emission from focused plasma 77−27727
pulsed X-rays from hot plasma, appl. of thermoluminescent detectors 79−7484
pulsed Xe discharges, in quartz chamber, elec. cond. meas. 79−55605
radial ion energy measurements in a fast theta pinch 78−67412
radial oscillation and electron temp. in toroidal pinch plasma 78−26272
radial oscillations damping in toroidal pinch 78−30476
radial structure in Ar and He discharges, spectral anal. 77−31541
radiation efficiency coeff. *(Russian)* 77−27655
radiation intensity calcs. in vacuum UV region *(Russian)* 80−48861
radiation losses from T-10 Tokamak, pyroelectric detect. *(Russian)* 80−53936
radiation temp. of weakly ionised gas discharge *(Russian)* 78−59697
radiation temperature of proton beam induced plasma 80−100094
radiative transfer in pulsed laser plasma-target interactions 79−7487
Raman scattered light, in laser plasma, magnetic fields and line splitting *(Russian)* 79−55510
random EM wave field in magnetoplasma, anal. of six component meas. 79−27782
random linear electrostatic waves, cross spectrum measurement in isotropic Maxwellian plasma 79−46450
rare earth metal plasmas, absorpt. spectra continua, 40 to 2000 Å 78−54471
rarefied plasma, density meas. by electron beam probe 77−35385
rarefied plasma flow, degree of nonisothermality, probe meas. 80−24243
ray tracing near electron cyclotron reson., finite temp. effect 80−53994
reactive hot gas thermodynamics and diagnostics 78−76865
reactive ion etching RF discharge plasma deceleration filter 78−41370
reactive plasma, optical emission spectroscopy, emission intensities and reactive density, correl. method 80−92385
reactive sputter etching, plasma gas temp. determ. 78−63586
reflectance of laser-produced plasmas, angle and polarisation depend. 78−18452
refraction in randomly inhomogeneous plasma, diagnostics using geometric-optical approx. calcs. 78−9843
relativistic electron beam diode, low impedance, pinch profile, X-ray diagnostics 77−24207
relativistic electron beam diode, medium current 77−46443
relativistic electron beam discharges, thin targets, spatially resolved VUV emission 77−89323
relativistic electron beam interaction, field reversal 79−10713
relativistic electron beam pinch formation in low impedance diodes 77−72510
relativistic electron beams in conical diodes, flow meas. 79−77416
relativistic magnetised plasma, negative absorpt. and energy distrib. function of hot electrons 79−4143
relativistic Thomson scatt. by fusion plasma 79−77420
residual gas anal., using computer controlled mass analyser, in ISX-A Tokamak 79−82096
resistivity and heating, high drift vels., particle diagnostics 78−38541
resonance cone trajectory, focused, nonlinear modification, probe diagnostics 80−10379
resonance lines of highly ionised Ti, Cr, Fe, and Ni in PLT discharge 79−68941
resonance scattering in an argon high current low pressure discharge 80−38735
resonant absorption in Ar plasma at thermal equilib. 80−1799
resonant Balmer line irrad. of H plasma, theory and laser spectrosc. meas. 80−75099
resonant HF radiation, from stationary discharge in Hg vapour *(Russian)* 79−55580
resonant multiphoton optogalvanic spectroscopy, diagnostics appls. to D plasma 79−23448
resonant scattering meas. 77−47269
resonant scattering of Lyman alpha radiation as a neutral density diagnostic for fusion plasmas 78−83612
retarding field energy analyser for beam-plasma system 77−35392
retarding potential analyzer for Pioneer-Venus Orbiter Mission 79−58251
reversed field pinch, expt. and 3-D numerical anal. 77−43035
reversed field pinches, electrical diagnostics 77−39451
review of high press. diagnostics 77−47268
RF discharge plasma skin effect counteraction by external mag. field 78−67543
RF discharge plasmas, mag. field effects, probe and microwave meas. 77−7594
RF discharge-plasma interaction, energy exchanges, magnetoacoustic wave generation 78−30485
RF induction plasma torch, temp., elec. cond., efficiency values from mag. probe meas. 78−42836
RF ion source 15 cm stable working region determ. 78−75381
RF lower hybrid heating, ion meas. 77−65916
RF lower-hybrid heating of ATC Tokamak 77−65891
RF plasma, gas rotational temp. determ. 79−90458
RF plasmas for semiconductor device processing, spectroscopic anal. 78−63589
RF preionisation in Tokamak Thor, plasma ignition conditions and density profiles 78−71538
RF probe meas. of electron density and temp. 79−86612
RF radiation emission from laser produced plasmas 78−42800
RF sputtering, impedance matching networks, experimental and design information 80−50555
RF voltage in plasma probe sheath, effect on electron energy distrib. meas. 80−54045
ring cusp, plasma width meas. 80−87927
rotating critical vel. plasma, particle vels. obs. 77−65846
rotating high current arc, hot wake investigation 80−1862
rotating plasma, at high Hartmann number 79−41806
rotating plasma, heating and diagnostics by induced poloidal currents 78−18449
plasma diagnostics continued
rotating proton beam, generation and propag. 79−6217
rotation, of theta pinch plasma column, directional probe obs. 78−1877
rotation of plasma in Tokamak LT-3, spectral lines Doppler shift 79−19087
runaway electron instability, non-thermal microwave radn. 80−1842
runaway electrons, X-ray obs. in Tuman-2 Tokamak *(Russian)* 78−38531
safety factor in adiabatic toroidal compressor Tokamak 79−19091
scattered light LF fluctuations meas. method 78−75412
Schlieren measurements of plasma kinematics during current disruptions in Tokamaks 80−92395
scrape-off layer of Tokamak, probe meas. 78−91156
screening efficiency of the scrape off plasma in the shadow of a poloidal limiter 80−79576
screw pinch, m=1 motion determ. by probes and streak photographs 77−15239
screw pinch, SPICA, β-control, Thomson scatt., X-ray emission and probe meas. 77−27709
Scyllac toroidal theta pinch, diagnostics by laser scatt., interferometry and selfluminosity obs. 77−24185
self-generated mag. fields in laser plasma 79−98970
self-generated mag. fields in laser prod. plasma 78−34350
self-generated magnetic field in CO_2 laser produced CD_2 target plasma, press. depend. 78−26310
semiconductor materials, RF plasma etching, optical emission obs. 77−51226
sheath, metal probe-gas discharge plasma boundary, impedance parameter variations 77−58869
shock heated dense plasma, density, temp. and press. determ. 79−32819
shock-heated dense plasma, continuum radiation and optical transmittance diagnostics 80−24202
short-wave plasma diagnostics, EM diffr. on cylindrical column 77−80376
shortwave thermal radiation, diagnostics *(Russian)* 77−47258
soft X-ray diagnostics, Gaunt factor effect 79−19093
soft X-ray diagnostics of CO_2 laser-produced magnetoplasmas 79−60192
soft X-ray emission, from picosecond laser plasma 77−55169
soft X-ray emission during neutron emission from plasma focus 77−24187
soft X-ray population inversion in laser plasmas, reson. photoexcitation, photon-assisted processes 80−87378
soft X-ray spectrometry at high count rates 79−31310
soft X-ray spectrum of hot optically thin plasma, interstellar medium appl. 78−34275
solar coronal plasma density, determ. from reson. lines fine struct. components 80−101581
solar flares, Fe XXI 1354 Å obs. from Skylab rel. to ionisation equilib. calcs. 80−21956
solar flares, hard X-ray sources diagnostics 78−89159
solar flares primary energy release region, plasma radiation diagnostics 79−84777
solar wind, electron density meas. via International Sun-Earth Explorers 78−85803
solar wind expt. on International Sun-Earth Explorer C spacecraft 78−85788
solid breakdown, pulsed, plasma form. blow off, shock waves 77−27688
space charge field, spatio-temporal distrib. determ. in breakdown 80−38771
space charge phenomena in gyrotrons 80−28868
space plasmas, new concept for EM and electrostatic waves detect. 77−9549
space plasmas, VLF signals preprocessing on spacecraft 77−64609
space potential, new method of determ., using electron density and mean electron energy *(Russian)* 78−22557
space potential determ. and storage in fast changing plasma 80−87949
space potential measurements with particle beam probes 80−84006
space potential on Elmo bumpy torus, ion-beam probe 78−67414
spark, in vac., high-press. local plasma regions production, X-ray and hologram diagnostics 79−19104
spark discharge plasma electron temperature, time development 77−11394
spatial distribution and species content of laser ablated polystyrene planar target 78−9811
spatial distribution of impurities and H neutrals in ELMO bumpy torus 79−55559
spatial emission profiles from inductively coupled plasma, matrix effects 80−75036
spatially resolved suprathermal X-ray emission from laser-fusion targets 80−48984
spectra, overlapping doublet, escape factor 80−96391
spectra from plasmas induced by ^3He or $^{235}UF_6$ reactions 80−64784
spectral diagnostics of plasma object with known contours 80−1846
spectral line emission from C-H plasmas generated by TEM_{10} laser pulses 80−43969
spectral line intensity, arc plasma temp. depend. 77−29079
spectral line profile of low-press. afterglow plasma in mag. field 80−6285
spectral line widths in HF plasma diagnostics 79−10708
spectral lines, complex level shift 78−26253
spectral lines of laser produced plasma, space depend. shift 80−6268
spectral radiation distribution at elevated press. 79−82047
spectral transitions, 50 to 150 Å, Fe to Br range with 15-24 lost electrons 77−80369
spectroscopic diagnostics of plasmas in space and the laboratory 80−38721
spectroscopic electron density meas., hot point low induction vacuum spark gas *(Russian)* 80−92390
spectroscopy, systematic errors due to light refraction 77−47270
spectroscopy role in basic props. meas. 77−58900
spherical plasma, optically thick resonance line 77−7572
spherical shell targets, laser-driven compression and neutron generation obs. 77−42188
spontaneous magnetic field, target size and struct. depend. 80−1819
stainless steel laser irradiated, plasma cloud radiation absorpt. and diagnostics *(Russian)* 78−59632
Stark broadening of isolated Sn II lines in cool plasma, semi-empirical calcs. 80−59186
Stark effect and four-quantum transitions, very strong stochastic electric fields 78−9760
Stark profiles of plasma-broadened He I and He II lines 79−46489

plasma diagnostics continued
Stark shift by inhomogeneous strong E field, X-ray Lyman profile 80−106977
static field spectrograph for laser induced plasma expts. 77−26427
stationary nonequilibrium distributions of ions produced in the interaction with an electron thermostat *(Russian)* 80−64684
stationary RF discharges of stellarator configuration, meas. with ion sensitive probe 79−60194
statistically inhomogeneous plasma, diagnostics by modulated EM wave *(Russian)* 78−38544
steel target-supersonic plasma impact effect, X-ray diagnostics 79−32780
stellarator, Wendelstein-VII A, charge exchange atoms yield, elliptic cross-section effect *(Russian)* 79−98950
stimulated Brillouin backscattering, mag. confined plasma 78−51307
stimulated Raman and Thomson scatt., beat-wave electron trapping 78−51308
stopping power of a nonequilibrium plasma for incident alpha particles 80−64742
stratified pulsed discharge, struct. and emission 79−64946
strong Langmuir turbulence for electron plasma waves, plasma diagnostics appl. 80−48889
student experiments on elec. cond. and similarity laws 78−24605
submillimeter wave polarimeter, for plasma diagnostics 78−91158
submillimetre background emission from Tokamaks 78−47102
supercritical density profiles of CO_2-laser-irradiated microballoons 80−14918
superdense plasma, X-ray emission, plasma diagnosis *(Russian)* 78−30487
superdense plasmas, spectroscopic diagnostics, at. collisions 78−63538
superradiation from non-ideal plasmas in electric field 80−38568
superradiation from non-ideal plasmas in electric field 80−83904
supersonic stream, incident on metal surfaces, emission 77−76105
suprathermal electric microfields and plasma parameters in crit. vel. rot. plasma 79−60198
surface erosion by plasma stream, ejected particle vel., Doppler vel. meas. 78−59610
surface impurities, in ISX-A Tokamak, AES obs. 79−82097
surface magnetic cusps, error in plasma leak meas. 79−60197
surfatron produced electron density and temp. microwave meas. 80−43965
sustained optical discharges in molecular gases 80−100085
symmetrical implosion system, charged reaction products, electrostatic field effects 80−32499
synchrotron emission from runaway electrons in TM-3 Tokamak 77−15247
synchrotron radiation from high temp. plasmas 79−98994
T-10 Tokamak, plasma X-ray emission 80−28840
T-4 Tokamak, impurity ion diagnosis, C nuclei absolute content *(Russian)* 79−14615
T-tube plasma, influence of boundary layer on H_γ line 80−48862
Takamak plasma density profiles from electron cyclotron radiation spectra 80−103179
target in air, CO_2-TEA laser breakdown, average temp. depend. on physico-chemical target props. 77−19738
temperature, density, Thomson scatt. in reversed field pinch on HBTX 1 77−27730
temperature, Doppler broadening meas. in ZT-1 toroidal pinch 77−19773
temperature, HF fluctuations, in stream of vortical plasmatron, holographic interferometry obs. 77−43068
temperature, ion and electron, turbulent heating mechanism in T-5M toroid *(Russian)* 77−47259
temperature, spectroscopic meas., ionis. rate const. 77−47143
temperature and density, HFS brightness ratios of impurity metal 77−89310
temperature and density diagnostics of laser prod. plasma 78−51360
temperature dependence on laser flux 79−50895
temperature determination from H_2 and D_2 molecular band intensities in low pressure plasma 80−37896
temperature determination on basis of cyclotron absorption in inhomogeneous mag. field *(Russian)* 77−80375
temperature distribution, vac. arc plasma, fault current limiter mode 78−9851
temperature distribution in jet, spectroscopic meas. *(Korean)* 77−80355
temperature fields, local equilib. in emissive medium, reconstruction 79−41874
temperature fluctuations, turbulent, microwave blackbody spectrum obs. 78−1897
temperature from recombination continuum, bremsstrahlung emission 79−50887
temperature meas. from H_2 and D_2 mol. band intensities 79−98986
temperature meas. in cross-flow arcs 78−22559
temperature meas. in inhomogeneous plasmas appl. of Bartels' theory of radiation 80−53948
temperature measurement, by vibr. Raman intensity, 500-2000K 79−37436
temperature measurement, charge separation and target voltages in laser-produced plasmas 78−5896
temperature profile, air discharge channel, high-current pulsed 77−27768
temporal development and properties, of microwave produced overdense plasma in coaxial discharge 79−55565
test particle dynamics in turbulent magnetoplasma 79−14614
Texas Experimental Torus, data acquisition and processing system 77−24217
Texas Turbulent Torus, energetic ion production, temporal and spatial evolution 78−1855
TEXTOR, interferometric and polarimetric diagnostics 80−70039
TEXTOR, mag. diagnostics and monitoring systems data acquisition 80−99320
TFR, electron cyclotron frequency emission and transmission meas. 80−79575
TFR, ICRF heating obs. by all metal antenna 80−18606
TFR 600, ^2H ion flux, temp., and density meas. 80−48940
TFR 600 Tokamak, soft X-ray meas., mag. topology near $q=1$ surface 80−79580
TFR machine, impurity behaviour, radiation losses and wall effects 77−31516
TFR Tokamak, ion cyclotron instability, microwave scatt. obs. 78−71473
TFR Tokamak, soft X-ray spectrum, forbidden lines 78−79470
plasma diagnostics continued
thermal density fluctuations, light scatt. using CW CO_2 laser and heterodyne detection 78−59677
thermal end loss from plugged theta pinch 80−1836
thermal fluctuations and leaking radiation from laser-produced plasma 80−87953
thermal induction plasma, energy balance, calorimetric meas. 78−59625
thermonuclear dense plasma, neutron diagnostics, book contrib. 80−24253
thermonuclear fusion plasmas, elem. processses and role of atomic, ionic and mol. data 80−14916
thermonuclear neutron pulse, electron beam generated, scintillator-photomultiplier response 78−51357
thermonuclear plasma, ion temp. determ. 77−11405
theta pinch, tearing and reconnection of magnetic fields 79−23446
theta-pinch, 10.6 μm interferometry and Faraday rot. meas. 77−80358
theta-pinch, azimuthal mag. field, relativistic electron runaway, bremsstrahlung diagnostics *(Russian)* 78−9818
theta-pinch, collisionless neutral current layer, ion energy spectrum meas. *(Russian)* 77−68874
theta-pinch, D_2 fill in Scylla IV-P, plasma parameters and end-loss 78−1880
theta-pinch, double, stabilised, toroidal plasma production, probe diagnostics 78−63576
theta-pinch, end loss, diagnostics 77−89286
theta-pinch, end-loss, reduction with quartz end plugs, Scylla IV-P 77−89292
theta-pinch, fast, axial ion energy distrib., particle and probe diagnostics 78−59655
theta-pinch, high-beta plasma discharge, spectroscopic meas. 77−24186
theta-pinch, high-energy, linear, quartz end plug effects 77−76184
theta-pinch, low-energy, end losses obs. 77−24157
theta-pinch, medium density, large diameter, medium voltage, implosion meas. 77−24140
theta-pinch, neutral current sheet, electron energy distrib. meas. 80−43954
theta-pinch, nonthermal density fluctuations, laser scatt. diagnostics 78−59679
theta-pinch, seeded with high-Z elements, VUV, X-ray and laser holography diagnostics 77−35381
theta-pinch, ultra-fast, mag. field distrib. diagnostics, electron density *(Japanese)* 78−55753
theta-pinch Ti ion injection by CO_2 laser, spectroscopic anal. 80−79577
thin foils, for particle diagnostics, resolution anal. 77−7595
thin wire target, props. of plasma prod. by counter incident double laser beam irrad. in uniform mag. field 79−94810
Thompson scattering for electron beam and plasma diagnostics *(Russian)* 80−54031
Thomson scattering, temp. distrib. and electron conc. meas. in Tokamak *(Russian)* 77−27738
Thomson scattering meas. of heating process 80−59272
THOR Tokamak, geometrical and elec. props., rel. to Alcator 79−98993
thyratrons, nanosecond discharge of the H_2 plasma deionisation, spectroscopic study *(Slovak)* 77−47279
time of flight spectroscopy of fast ions from laser-prod. plasma 77−76190
time-resolved X-ray spectroscopy of laser-produced plasmas 80−84004
Tokamak, Alcator, effect of wall temp. on O, N and C impurities, spectroscopic diagnostics 79−41840
Tokamak, ATC, ion heating in ion cyclotron freqs. 77−68812
Tokamak, DITE, arcing, time-resolved meas. 80−10436
Tokamak, DITE expt., plasma surface interaction program 77−31503
Tokamak, DIVA, metal impurities anal. 79−64906
Tokamak, DIVA, radiation loss and power balance, pyroelectric detection 78−86684
Tokamak, Doublet IIA, temporal and spatial behaviour of plasma props. 77−43030
Tokamak, Fe^{19+} forbidden line, ion temp. 78−83602
Tokamak, helical winding, effect of HF current on discharge 78−87485
Tokamak, impurity ionis. degree and diagnostics accuracy, electron distrib. depend. *(Russian)* 79−98973
Tokamak, ion temp. scaling, using 10-channel neutral particle energy analyser 77−72496
Tokamak, JFT-2, gross particle confinement charact. by boundary plasma, electrostatic probe diagnostics 79−32822
Tokamak, JFT-2, particle and heat transport during lower hybrid heating 80−70021
Tokamak, JFT-2, scrape-off layer, particle and energy fluxes, probe and IR obs. 78−59690
Tokamak, large magnetic field ripples, electric probe meas. 80−83976
Tokamak, lower-hybrid-freq. heating, parametric instabilities 79−90426
Tokamak, LT-3, disruptive instability, spectroscopic observations 78−87483
Tokamak, LT-3, ion heating by disruptive instability, ion temp. particle diagnostics 79−86593
Tokamak, PLT, beam-heated, neutron emission profiles 78−63588
Tokamak, PLT, expt. results 77−43072
Tokamak, PLT, fast-wave heating of two-ion plasma through minority cyclotron reson. damping 80−24194
Tokamak, poloidal field distrib. meas. by far IR polarimetry 78−42810
Tokamak, small, TOSCA, sawtooth oscills., X-ray diagnostics 79−41817
Tokamak, T-10, plasma parameters 77−43071
Tokamak, TFR, internal disruptions and current breakdown, X-ray diagnostics 77−43027
Tokamak, TFR-600, surface conditioning and mass spectroscopy 79−672
Tokamak, time resolved heat flux to wall meas., sheath model with secondary electron emission 78−79468
Tokamak, TM-3, near wall region, Langmuir probe obs. *(Russian)* 77−47261
Tokamak, TOSCA, magnetic islands and disruption 79−23456
Tokamak (Alcator), driven lower-hybrid waves, light scatt. study 80−1835
Tokamak Alcator C far IR emission diagnostics of electron temp. 80−59291
Tokamak apparatus, resistive shell, penetration of time-varying vertical and horizontal mag. fields 78−63575
Tokamak diagnostics, review 78−47163
Tokamak discharge, impurity emission spectra for diagnostics 77−11403
Tokamak electron cyclotron emission spectrometry by plasma-scanned Michelson interferometer 79−32814

plasma diagnostics continued
Tokamak energy loss determ., fast time resolution bolometer *(Russian)* 77-76193
Tokamak experiments and apparatus, review 79-98967
Tokamak expts. survey, apparatus, techniques, containment times, plasma instabilities 78-59662
Tokamak FT-1, lower-hybrid heating using decelerating system, neutrals diagnostics *(Russian)* 79-98927
Tokamak Fusion Test Reactor diagnostic penetrations, neutron streaming calc. 79-9877
Tokamak Fusion Test Reactor neutron collimator design 79-9876
Tokamak limiter surface temp. meas. 79-98984
Tokamak microwave discharges, refraction losses, from measured plasma density profiles 78-22549
Tokamak model shell, shell current and vertical field meas. 77-76201
Tokamak plasma, confinement time meas. 80-87945
Tokamak plasma, direct determ. of electron energy confinement time 78-9834
Tokamak plasma, extreme UV impurity study, radiation power loss 78-42803
Tokamak plasma, highly ionised Mo ions, recomb. and ionisation rate coeffs. determ. 78-71427
Tokamak plasma, line spectra of highly ionised heavy atoms 80-79567
tokamak plasma, new atomic data for Fe^{19+} spectra 80-67545
Tokamak plasma, Ni, Cr and Fe NeI-like ions, mag. quadrupole lines 79-13662
Tokamak plasma, radial current distrib. meas. using neutral Li beam 78-30488
Tokamak plasma, Thomson scatt. with repetitively Q-switched ruby laser 80-59271
Tokamak plasma boundary, particle energy meas., calibration method 79-98983
Tokamak plasma effective charge, high electron density with impurities, X-ray obs. *(Russian)* 77-19762
Tokamak plasma spectroscopic diagnostics, Fe ion resonance-line intensity meas 80-48993
Tokamak plasmas, cyclotron radiation, diagnostic tool *(Dutch)* 78-30472
tokamak-10, ion energy balance, neutron flux and atom energy spectra, obs. and model *(Russian)* 79-27795
Tokamak-4 plasma, meas. of local parameters of ions *(Russian)* 79-32824
Tokamaks, dynamics of H, He, O reactions, corona model, spectroscopy diagnostics *(German)* 79-60103
Tokamaks, electron freq. rad. spontaneous emission 80-53944
Topolotron, plasma cross section reconstruction, Farey dissection optimization, computer anal. 77-84523
Tormac, Gaussian HeII 4686 Å spectral lines, Doppler and Stark broadening effect, turbulence 80-106980
toroidal discharge, optical meas. of primary avalanche 80-54059
toroidal kink instability, noncirc. cross section, nonlinear phase obs., probe diagnostics 79-60182
toroidal plasma, enhanced diffusion, electrostatic drift modes, ohmic heating effects obs. 77-19702
toroidal reversed-field pinches, current, temp., confinement time scaling 77-43078
torus plasma, fluctuation induced particle transport, strong DC elec. and mag. fields 77-89322
TOSCA Tokamak, plasma shape and position meas. 79-73039
Townsend avalanche, vacuum UV spectra 80-64810
TPD-plasma, optical escape factors and population densities 79-37460
transparency changes of plasma burst in intense optical radiation, direct meas. 78-9807
transport coefficients determ. from high press. arc meas. 77-47156
transport functions by precision arc expts., H Balmer spectrum 80-103187
transverse HF discharge, electron energy distrib. from spectra *(Russian)* 80-84012
trapped electron instability, feedback diagnostic 78-51350
trapped electrons, test charge pot. in single wave case 80-24247
TTT, current penetration and resistivity, probe diagnostics 79-32821
Tuman-2A, plasma compression particle diagnostics, density and temp. *(Russian)* 80-38677
turbulent AC arc, temp. diagnostics, radial distribs. 77-24240
turbulent heating of magnetic mirror confined plasma, rel. to Buneman instability 77-24106
turbulent interaction fronts in laser produced counterstreaming plasma 79-41807
turbulent ion heating enhancement via spatial mag. field variations, catalytic scheme 77-24107
turbulent plasma, electron distribution function, correlation anal. 79-14547
turbulent plasma, magnetised, line shape of optical satellites 80-75098
turbulent plasma in toroidal plasma, optical diagnostics and thermal transport 79-73023
turbulent plasma jet, radiowave interaction and electron density fluctuation 77-989
turbulently heated plasma electron cyclotron radiation, spectral line width collisional broadening 78-34369
turbulently heated toroidal plasma discharge, microwave spectra obs. 79-50893
two component plasma electron beam nonlinear stabilisation, diamagnetic and VHF obs. *(Russian)* 79-27759
two ion components, meas. by collective laser scatt. 80-92388
two phase flow, particle velocity optical meas. *(Russian)* 80-54032
two-plasmon decay, profile modification, produced by 10.6 micron radiation, at $^1/_4$-crit. density 79-19061
UHF radiation from electro beam interaction in VEGA device *(Russian)* 78-38532
UHF radiation from electron beam interaction in PETULA device *(Russian)* 78-38532
ultrahigh vacuum tranfer system, 15 cm diameter, for remote plasma-wall interaction expts. 80-86327
unipolar arc 79-1357
unipolar pulsed LCD discharge, spectrum, time scanning 80-64774
unstable turbulent ionisation waves, two dimensional Fourier spectroscopy 80-38646
Uragan-2, ohmic heating, hard X-ray emission from electron-wall interaction *(Russian)* 77-47215
UV continuum source, use of laser generated plasmas 79-94314
UV photoion density meas. 78-51340

plasma diagnostics continued
UV photoplasma, electron density, microwave meas. 80-75097
vacuum arc in Cu cathode region, current parameters, theory 80-54068
vacuum diode, plasma expansion study by spectroscopic method 79-55551
vacuum spark, electron density, interferometric meas. 78-5962
vacuum UV emission from low temp. air plasma, investig. 80-69982
velocity diffusion, three-dimens., in two-stream turbulence, probe diagnostics 78-59595
velocity of plasma species in pulse EM accelerator, time distrib. *(Russian)* 77-47267
Venus ionosphere, Pioneer Venus Orbiter planar retarding potential analyser plasma expt. 80-67501
Venus ionosphere, plasma diagnostics meas. by Venus Orbiter *(German)* 79-96941
Venus plasma environment, study via plasma analyser expt. on Pioneer Venus Orbiter 80-67498
vibrational kinetics and plasma characts. in CO-N_2 discharge 80-59331
Voigt profile, Lorentz component true halfwidths and line intensities 80-87943
volume recombination coeff. meas. method, in Ne positive column, ionis. role 77-51252
Voyager plasma experiment 78-20617
Voyager plasma wave system 78-24432
VUV imaging of laser prod. plasma 78-51363
W VII-A stellerator, line emission, poloidal and toroidal asymmetry 80-79578
wall conditioning by low power discharge in ISX-A Tokamak, AES and residual gas anal. 79-90438
water, vapour RF discharge, low press., afterglow, spherical plasmoid, optical diagnostics 78-38568
wave dispersion relation determ. by microwave scatt. 79-27829
wave group velocity measurement by FM technique 79-73047
wave number spectrum parameter estimation form fixed probe pair data 79-82062
wavelength scaling experiments in CO_2 and Nd:glass laser-produced plasma 77-24116
waves detection in turbulent plasma by satellites of forbidden He transitions *(Russian)* 78-18391
weakly nonideal dense plasma, elec. conductance obs. 78-71447
weakly-ionised plasma diffusion in apparatus with spatial axis *(Russian)* 80-1826
whistler wave damping, dipole antenna obs., large magnetoplasma 78-34327
whistler wave trapping in density crest 80-53984
wire explosion plasma production, diagnostics by Bartels method 79-10686
X-ray absorption lines, signature for preheat level in non-explosive laser implosions 80-106978
X-ray analysis, appls., conf., Denver, USA (Aug 1975) 77-56307
X-ray and fast ion emission in CO_2 laser target interaction *(French)* 77-80352
X-ray and fast ion spectra from laser plasma, thermal conduction 78-5899
X-ray and neutron emission from staged plasma focus 78-14220
X-ray and particle energy meas. in laser-plasma interaction 78-42799
X-ray bremsstrahlung polarisation and anisotropy, evidence of suprathermal electron fluxes 80-103193
X-ray continuum meas., theory of foil-absorption techniques 79-23459
X-ray deconvolution method from hot plasmas 80-54030
X-ray diagnostics appl. to laser induced fusion, review 77-55176
X-ray emission, electron temp. meas. 80-103127
X-ray emission, generated by Q-switched ruby laser, 10^{12} W/cm^2 78-75389
X-ray emission, laser produced plasma, self-generated mag. field effect 77-43011
X-ray emission, soft, from laser produced plasma 78-14213
X-ray emission, superthermal, from CO_2-laser-produced plasmas 79-90454
X-ray emission characteristics of CO_2 laser produced plasmas 78-9828
X-ray emission characts. of laser-produced plasmas, X-ray camera development 77-54031
X-ray emission from Au impurities in H_2 DIVA Tokamak plasma 79-32820
X-ray emission from CO_2 laser created plasmas 77-89306
X-ray emission from CO_2 laser generated plasma, time-resolved photography 77-80364
X-ray emission from laser compression expts. 78-5905
X-ray emission from laser prod. plasma, spatially resolved spectroscopy 78-78930
X-ray emission from plasma focus, anisotropic and collimated 78-26330
X-ray emission from plasma focus, space and time resolved meas. 79-4185
X-ray emission from plasma focus in puffed gas 78-14219
X-ray emission from plasma produced by laser irradiation 79-98989
X-ray emission spectra, of exploded wire plasma 77-68872
X-ray energy distribution, plasma focussed, nuclear emulsion study 78-83620
X-ray intensity from plasma focus, high energy electrons trajectory 78-42808
X-ray line emission from single and multiple exploding wires 77-84519
X-ray line radiation from cylindrical Al plasma, calc. model 80-64777
X-ray line radiation from laser produced plasma, ang. distrib. 77-15238
X-ray line spectra from exploded-wire array, plasma temp. and density 79-55457
X-ray microscope, axisymmetric grazing incidence, for laser fusion diagnostics, imaging characts. 78-75422
X-ray monochromatic images for hot plasma ion and temp. distrib. 80-64772
X-ray obs. by array of pin diode detectors 78-47174
X-ray output and operating characts. of plasma focus 78-14224
X-ray production, polarisation meas. in laser plasma 77-47266
X-ray production by laser plasma in strong elec. field 80-70034
X-ray shadowgraphy of laser driven implosions 80-92393
X-ray spectra from exploded-wire plasmas, spatial resolution techniques 78-14188
X-ray spectra of plasma produced by subns laser pulses *(Russian)* 78-9847
X-ray spectra of plasmas produced by 250 ps laser pulses 77-19769
X-ray spectral density determ., effect of collisions on dielectronic satellite intensity *(Russian)* 77-62348

plasma diagnostics continued
X-ray spectrometry of laser compressed microballoons 80−87954
X-ray spectroscopy, high temperature plasma, autoionisation states 77−31434
X-ray spectroscopy of plasma from laser irrad. glass spheres 78−51364
X-rays from laser prod. plasma, K_α emission 79−90460
X-rays from laser prod. plasma *(Russian)* 79−46488
Z_{eff}, TFR hot plasma, soft X-ray diagnostics 77−51234
Z_{eff} values, in T-10 column central zone, Thomson scatt. obs. *(Russian)* 79−55545
Z-discharge plasma, low-temp., time evolution, diagnostics 79−37548
Z-pinch, azimuthal mag. field meas. using Faraday rot. 78−9832
Z-pinch, current sheath struct., mag. probe and numerical model *(Russian)* 78−59645
Z-pinch, gas puff device, X-ray spectra, plasma form. 79−94816
Z-pinch, high density, Hβ line spectra 78−18445
Z-pinch, imploding Al liner, soft X-ray spectroscopy 78−14198
Z-pinch, plasma production, streak, X-ray and vis. photographic obs. 78−38522
Z-pinch dense H plasma, emission spectrum thermal equilibrium departure 79−82094
Z-pinch discharge, electron temp. and density variation obs. 78−75426
z-pinch discharge, spectral line shape, high-density effects 79−73038
Z-pinch plasma, density and temp., spectroscopic meas. 79−4181
Z-pinch turbulence spectroscopic detection and anal. *(Russian)* 80−100098
Z-pinches of intense energy-density driven by high voltage storage lines 80−87952
Ag, laser produced soft X-ray spectra, transitions 77−15171
Al, CO_2 laser produced plasma, fast particle emission 78−42805
Al discharge, hollow cathode with pulse feeding, spectroscopic study 78−34377
Al, evap. by long pulse Nd laser, spectroscopy 78−14201
Al foil, 8 ns laser pulse-target interactions, ion-expansion struct. 79−14575
Al laser plasma, laser beam self-focusing, X-ray emission 79−82064
Al, laser produced plasma, X-ray spectroscopy 77−72502
Al laser produced plasma, expsn., X-ray meas. 77−80326
Al, laser-heated plasma, reson. line emission, spatial and spectral intensities 77−39460
Al, laser-prod. plasma, space-resolved extreme UV emission 80−54015
Al, laser-produced, X-ray line emission spatial resolution, shadow technique 77−35400
Al, laser-produced, X-ray spectrum, time depend. *(Russian)* 77−55173
Al, laser-produced plasma, population inversion between Al^{11+} levels, X-ray lines obs. 78−38539
Al plasma, laser produced, origin of K_α radiation 78−9833
Al reflective target, momentum and energy transfer pulse duration/polarisation depend., torsion pendulum diagnostics 80−43952
Al target, CO_2 laser irrad., 10^6-10^8 W cm^{-2}, diagnostics 77−89281
Al target, in air, pulsed CO_2 laser irrad., thermal response and plasma characts. 79−86595
Al target, laser irradiated, X-ray emission in presence of high elec. field 79−94818
Al target, relativistic electron beam impact, vac. UV emission 77−47263
Al, X-ray emission spectra of CO_2 laser-irrad. targets, nonlinear processes 80−33793
Al XIII, hot pinched plasma, Lyman series Stark profiles, electron density determ. 78−51348
Ar, afterflow stability boundaries, plasma oscillation modes in mag. field 78−38486
Ar, afterglow, pulsed discharge, acoustic oscills. in emitted radiation 77−89309
Ar afterglow, spectra and microphotograms, dissociative recombinations 78−26365
Ar arc, high-press., in longitudinal mag. field, spiral wall characts. 77−65919
Ar arc, Lyman-α wings Stark broadening 77−27721
Ar arc discharge, parameters variation during extinction obs., by spectroscopy and laser interferometry *(French)* 80−19653
Ar arc plasma, decaying, temporal changes of particle densities and temps. 79−64940
Ar, arc plasma, MTE continuum emission coeff. relation for atom. press. 77−31432
Ar arc plasma, partial LTE for lower excited levels of ArI 80−79565
Ar arc plasma, transition probabilities, continuum emission coeffs., electron density 77−51228
Ar arc plasmas, steady-state and decaying, mol. gas impurities 80−103177
Ar atmospheric arc plasma deviation from LTE 78−67604
Ar, atmospheric arc-jet plasma, ζ-function evaluation, near 10^4K 77−84497
Ar cascade arc light emission, effect of pulsed microwave field 78−67599
Ar cold plasma generator, optical emission spectra and elec. parameters *(Ukrainian)* 78−67374
Ar constricted discharge, electron density and temp. and gas temp., iterative method *(German)* 78−83627
Ar, continuum radn. meas., 120 to 340 nm 77−58894
Ar DC magnetron discharge, spectroscopic obs. 80−44010
Ar, decaying plasma arc, electron disappearance mechanism 80−38765
Ar decaying pulsed discharge plasma, acoustic waves density modulation 80−103143
Ar discharge, ion density profile, reson. laser light meas. 80−92401
Ar discharge, luminous channel form. meas. 79−64945
Ar discharge, population processes of 4p levels, perturbation influence 80−38565
Ar, discharge, pulsed, neutron species spatial distrib., laser beam diagnostics 78−38543
Ar discharge, pulsed, weakly ionised, neutrals effect, interferometric obs. 79−27854
Ar discharge, recombination coefficient meas. under diffusion-recombination conditions of plasma decay *(Russian)* 78−26324
Ar, Doppler temp. from linewidth, in inductively coupled plasma 77−43083
Ar, effects of Joule heating on plasma heat transfer 77−72412
Ar, electric arc with liq. K cathode, parameters, cathode sheath model 77−4003
Ar, emission coeff., high press. peculiarities 77−43067
Ar, glow discharge, spectral line excitation, cold cathode region 77−84552
plasma diagnostics continued
Ar, HF discharge, arc type, spectral parameters 80−1873
Ar HF discharge, excited atoms and metastable state densities meas. 79−14606
Ar HF torch discharge, spectral diagnostics 79−14607
Ar high density plasma, highly excited atomic levels, spectral-line-blending study 80−48969
Ar, high-frequency discharge, spectral parameters meas. *(Russian)* 79−10742
Ar high-pressure arc plasma, IR continuum emission obs. 78−71604
Ar high-pressure plasma elec. conductivity obs. 78−71448
Ar highly ionised low press. plasma produced in pulsed discharge, characts. *(French)* 77−58901
Ar hollow cathode arc, in mag. field up to 2 k0e, plasma parameters 80−6306
Ar II, magnetically confined plasma, pulsating ion laser action 78−78994
Ar, in rot. steady state centrifuge, rot. rate and temp. diagnostics *(Russian)* 78−5923
Ar inductively coupled RF plasma, spatial distrib. of temp. and number densities of electrons, atoms and ions 77−68873
Ar, ionising boundary layer in shock-tube side-wall flow 79−60144
Ar jet, under press., heavy particles temp. meas. *(French)* 78−9841
Ar, low press. discharge afterglow, dissoc. recombination, microwave diagnostics 78−9876
Ar low temp. plasma flow, interaction with intense microwave beam 80−38654
Ar magnetic helical arc electrode, for MHD generator, visible, RF and probe diagnostics 78−9867
Ar, metastable $^3P_2$ deactivation in afterflow, plasma characts. 78−55769
Ar, metastable atom density changes during arc interruption 77−51250
Ar, optical breakdown at 10.6 μm near plasma layer boundary 79−60165
Ar plasma, 14000K, continuum emission coeff., laser spark temp. meas. 77−31527
Ar plasma, Ar III and IV lines, Stark broadening, Gaunt factor calcs. 77−51231
Ar plasma, collision-dominated electron relax., heating, at. transitions 78−18373
Ar plasma, continuum radiation, temp. and charged particle concs. from line intensities and widths 77−68867
Ar plasma, electron density, microwave refl. meas. 78−59674
Ar plasma, electron temp. meas., microwave technique 78−26325
Ar, plasma, electron-ion recombination in extinguishing arc 78−59687
Ar, plasma, H impurity, equilib. state of highly ionised plasma 78−83597
Ar plasma, hypersonic nozzle, radiation field characts. 77−84340
Ar plasma, inductively coupled, excitation transfer between plasma and impurities *(French)* 78−14211
Ar plasma, interferometric study of density and electron conc. behind shock waves 78−1888
Ar, plasma, ion energy level populations in crossed elec. and mag. fields 78−67428
Ar plasma, microwave absorption at singularity, parametric satellite excitation obs. 77−51194
Ar plasma, negative plasma potentials produced by supplemental electron emission, Langmuir probe diagnostics 79−41861
Ar, plasma, one-phase and two-phase jets, non-equilibrium in initial region *(Russian)* 77−31518
Ar plasma, optical props., visible, near-IR region, using shock tube 79−55471
Ar, plasma, population density meas. in free jet expansion flow 77−27737
Ar plasma, RF prod., mag. field effect on props. *(Korean)* 79−50869
Ar plasma, RF surface wave form., metastable atom density meas. 77−58890
Ar plasma, wall stabilised arc, spectroscopic temp. and radiation standard 77−76199
Ar plasma jet, collisional line broadening, oscill. strengths of reson. lines 77−75106
Ar plasma jet, electron temp. and density determ. 79−41875
Ar plasma jet, emission of electron-neutral atom bremsstrahlung *(French)* 78−26332
Ar plasma parameters, microwave scanning technique 80−64773
Ar, positive column, contracted; electron density, temp., elec. field, line emission 80−6311
Ar, positive column, local transverse mag. field, striation freq. spectra, microwave probe 78−87562
Ar, pulsed highly ionised low press. discharge 77−62398
Ar pulsed plasma, elec. cond. obs. at 10 atm and 15000K 78−71449
Ar RF discharge plasma, magnetically stabilised, electron temp. using optical spectroscopy *(German)* 78−63582
Ar, radiative energy loss in shock tube 77−19768
Ar, shock compressed, radn. emission *(Russian)* 79−37554
Ar, sputtering glow discharge, metastable and reson. states density meas. *(French)* 80−14955
Ar, stream electrons, at atm. press., temp. and conc. from study of electrical parameters *(Russian)* 80−53930
Ar supersonic jet, radiation in magnetoplasmadynamic source 77−35329
Ar UHF discharge, spectral meas., Ar II lasing lines 79−99016
Ar, vac. UV emission profile, temp., spectroscopic meas. 77−51229
Ar wall-stabilised arc electron and heavy-particle temp. variations 78−67602
Ar XVIII Lyman-α line Stark broadening, hot dense laser-produced plasma 77−11402
Ar, Z-pinch determ. by intrinsic stimulated emission 78−26311
$Ar^{16,17+}$ filled glass shell, symmetric laser compression 80−64759
Ar:K seeded plasma, temperature diagnostics 78−67427
Ar:S, plasma, atomic S lines above first ionisation limit 78−25462
Ar-air, transformer plasmatron, LF discharge, electrical and energy props. 80−103200
Ar-air arc, stabilised, spectroscopic methods of temp. meas. *(Russian)* 80−38854
Ar-C arc, C I lines Stark broadening, electron density and temp. meas. 77−10634
Ar-H plasma, electron density meas. rel. to AR I 3949 Å Stark width 79−63954
Ar-H_2, elec. breakdown, time and space resolved spectra 78−18470
Ar-H_2S plasma, spectroscopic study, electron density, ionis. temp. meas. 77−19764

plasma diagnostics continued
Ar-He plasma, electron temp. and density meas., to check diffusion calc. 79−27749
Ar-He plasma, ion acoustic soliton form., mechanism 78−18457
Ar-He plasma, thermal diffusion of neutral species in plasma jet, 2000-4000K 79−32742
Ar-hexamethyldisiloxane, glow discharge positive column ion mass spectra identification 80−38834
Ar-N_2 mixtures, DC arc, energy balance of electrons 78−42797
As_2O_3, multiple reactions by single electron impact 78−22037
Au, radiation from beam-foil excitation and Tokamak produced plasmas 79−54828
B II, Stark shift, shock tube meas. 77−50403
B III, IV, laser produced plasma, satellite spectra 78−5165
B IV, ionisation rate coeff. in θ-pinch plasma, spectral meas. 77−6911
Be expanding laser-produced plasma, recombination effects 78−94935
Be II, III, laser produced plasma, satellite spectra 78−5165
Be IV, line broadening and self-absorpt. in laser prod. plasma 78−17615
Be isoelectronic series, Z=22-34, spectral lines from laser prod. plasma 77−50388
Be, stigmatic obs. with grazing-incidence spectrograph 79−73041
C foil, laser plasma, mol. ions studied by mass spectrosc. 79−90429
C III EUV lines, rel. to density diagnostics in non-equilib. plasmas 78−53899
C IV, V, laser produced plasma, satellite spectra 78−5165
C influx flow rate in ohmically heated plasma, C line meas. 77−15243
C, laser plasma, time resolved electron temp. *(Russian)* 78−22566
C oxides, glow discharge, excitation and ionisation mech., elec. and optical obs. *(Russian)* 78−59695
C spectra from CO_2 laser prod. plasmas 80−38711
C V, ionisation rate coeff. in θ-pinch plasma, spectral meas. 77−6911
C VI, laser produced, electron density profile, Stark broadening meas. of vac. UV lines 78−59684
C VI, n=3 and n=2 levels population inversion, possible extreme UV laser 77−7073
C VI laser produced plasma, transient population inversion at 18.2 nm 79−41876
C^{4+} plasma, soft X-ray emission, electron-beam sliding spark device 78−79444
C^{5+}, plasma expansion, Balmer spectrum intensity inversion, charge transfer pumping 78−34371
CN molecular bands in N_2 and air-O_2 arcs, CN origin, band identification 80−38803
CO laser, chem. composition of plasma, room temp. 77−83866
CO laser, mass spectra of positive ions in discharge plasma 77−89315
CO-Ar, glow discharge, ion cluster in positive column, ion mass spectra diagnostics 80−38752
CO-He-O_2, species concentrations in glow discharge and afterglow, mass spectra, laser conditions 78−14241
CO-He($-O_2$), glow discharge ion cluster in positive column, ion mass spectra diagnostics 80−38752
CO_2, decaying discharge plasma, contraction in const. elec. field *(Russian)* 79−37447
CO_2 laser beam scatt. by microscopic fluctuations in plasma density 80−79574
CO_2 laser discharge, positive ion processes, mass spectrometric obs. 77−89337
CO_2 laser discharge, TEA, glow form. and glow-to-arc transitions, high speed camera obs. 78−25846
CO_2 laser prod. microballoon plasma, fast ion emission 80−103172
CO_2 lasers, CO_2-CO-N_2-He, ionisation wave, slow changes, dispersion curves 80−38822
CO_2 plasma, 10000-13000K, VUV continuum radiation 78−91152
CO_2 plasma, atm. press. opt. props., 400-1200 nm spectral range and 10^4-2×10^4K temp. 80−33753
CO_2 plasma, spectral absorpt. coeffs., atm. press. meas. *(Russian)* 77−89316
CO_2-He, species concentrations in glow discharge and afterglow, mass spectra, laser conditions 78−14241
CO_2-laser radiation filamentation in underdense H_2 plasma, X-ray diagnostics 80−14941
CO_2-N_2-He, fluorescent IR radiation from glow discharge 78−94386
CO_2-N_2-He mixture volumetric glow discharge formation at atm. pressure 78−71615
CO_2-N_2-He-O_2 discharge mixture, three body electron attachment to O_2 80−64779
CO_2+H+Xe plasma, elec. parameters, Xe effects *(Russian)* 77−84507
CO_2+N_2+He, glow discharge positive ion species identification *(Russian)* 80−84014
Ca, Doppler temp. from linewidth, in inductively coupled plasma 77−43083
Ca II, reson. line broadening in shock tube plasma 77−35393
Ca, laser produced plasma, vac. UV emission 77−80372
Ca plasma, Knudsen discharge, longitudinal mag. field, emission polaris. 77−76211
Cd, CO_2 laser produced plasma evolution, laser possibility 77−80325
Cd-Ar low-pressure discharge column, energy balance obs. 78−67504
Ce, arc, excitation and ionis. in nonequilib. plasma 78−18461
Cl I, wall-stabilised arc, absolute transition probabilities, 5300-6850 Å 78−9105
Cl VII, in laser heated plasma, emission intensity anomalies, 58-78 Å *(Russian)* 77−46521
Cl VUV line emission from TFR-600 Tokamak 79−98987
Cl X-ray emission spectra, detect. from Alcator-A Tokamak 80−92389
Cl^- free-bound continuum radiation threshold broadening obs. 78−71579
Cl_2-arc, low temp., visible and IR continuum radiation 80−38784
Co, X-ray transitions in laser produced plasma 80−100093
Cr, arc, steady, vac., plasma ion mass and energy diagnostics 78−51385
Cr from Tokamak-produced plasma, $2s^22p^k$-$2s2p^{k+1}$ transitions in F I to Be I isoelectronic sequences 80−37765
Cr, X-ray spectra in Tokamak-10 facility plasma *(Russian)* 78−9837
Cr, X-ray transitions in laser produced plasma 80−100093
Cr(II) lines, oscill. strengths in 2413-2718 Å wavelength range 80−106294
Cs arc, low-voltage hot-cathode, plasma production and props., review 77−27766
Cs, atomic excited states population in arc 78−26368
Cs discharge, high-press., pulsed, in capillary energy balance diagnostics 77−65920
Cs discharge plasma, optogalvanic effect characts. 78−63583

plasma diagnostics continued
Cs I, excited level populations, relative spectral line intensities *(Spanish)* 78−51344
Cs, photoplasma, optical excitation in radiation diffusion conditions 78−55227
Cs plasma, elec. cond. and eqn. of state, behind reflected shock wave 78−42716
Cs plasma, generation by adiabatic compression, elec. cond. and thermodynamic parameters meas. 80−59180
Cs plasma, in thermionic convertor, spectroscopic meas. of Cs I *(Japanese)* 77−58902
Cs, plasma diagnostics by wire explosion 78−71516
Cs plasma elec. conductivity meas. 78−71450
Cs plasma in thermionic converter, mass spectrometric study of positive and negative ions 79−19083
Cs plasma in vacuum diode, pre-discharge, electron impact excitation line emission polarisation 78−47170
Cs, resonantly excited in cylindrical discharge plasma, effective lifetimes 78−79413
Cs, thermionic converter, ion species mass anal. 77−89344
Cs thermionic convertor, pulsed, plasma parameters, operating characts. 80−6293
Cs vapour, plasma production by weak CW laser beam at 6010 Å 77−62388
Cs-Ba, high current Knudsen arc discharge, spontaneous extinction, optical diagnostics 80−44044
Cs-CO_2-He glow discharge, quenching cross section of resonant Cs(6P) state by CO_2 mols. 80−43860
Cs-He plasma, steady-state discharge, role of inelastic collisions, spectroscopic diagnostics 78−42709
Cs-N_2 discharge, Cs_2^+ form. rate, mass spectra obs., N_2 press. depend. 79−27853
Cs-N_2 plasma, collision recomb. of charged particles *(Russian)* 77−80373
CsI-Hg-Ar discharge, high-press., temp. and plasma comp. determ. 79−10709
Cu accelerated plasma, velocity meas. using fast-scanning Fabry-Perot spectrometer 79−41869
Cu anode splitting by electron beam in X-ray regime of Z-pinch 78−5932
Cu, arc, steady, vac., plasma ion mass and energy diagnostics 78−51385
Cu discharge, hollow cathode in pulse mode, spectral lines and intensities 78−34376
Cu, excited states population in high-current hollow-cathode discharge *(Russian)* 77−35421
Cu foil, 8 ns laser pulse-target interactions, ion-expansion struct. 79−14575
Cu plasma, laser-produced high energy X-ray bremsstrahlung, evidence of reson. absorpt. 78−42776
Cu-Ne laser, spectral lines emission of gas-discharge pulse plasma 79−31883
Cu-Ne mixture, 3-20 kHz pulse discharge obs. 78−71092
CuBr laser, tunable dye laser radiation, gas temp. atomic density meas. technique 79−82037
D, high current pulse discharge investig. *(Russian)* 78−47171
D ion energy spectrum from plasma focus discharge 78−14218
D plasma in laser target, neutron meas. 77−7596
D-T fuel temperature in laser fusion targets, neutron energy spectra obs. 77−89317
D-T thermonuclear plasma, neutron collision diagnostics *(Russian)* 77−34471
D_2 in shell target, laser compressed, particles meas. 77−62408
D_2-^{3}He, filled microspheres, implosion expts. 78−59672
D_2-^{3}He mixture plasma focus, ion temp. 78−5953
DT, in glass shell, spectrum and absolute yield of α-particles 77−79482
DyI_3-Hg arc discharge plasma, spectroscopic study 80−54033
Eu^+ metastable states in discharge plasma, anomalously high speed deexcitation, modulation of induced radiation obs. 80−44014
F spectral lines, neutral, in shock tube plasma, Stark widths and shifts 78−9117
Fe, arc, steady, vac., plasma ion mass and energy diagnostics 78−51385
Fe discharge, hollow cathode in pulse mode, spectral lines and intensities 78−34376
Fe exploded wire, X-ray line emission and plasma conditions 78−59670
Fe from Tokamak-produced plasma, $2s^22p^k$-$2s2p^{k+1}$ transitions in F I to Be I isoelectronic sequences 80−37765
Fe, highly ionised, 1s to 3p Kβ-like X-ray spectrum 77−50394
Fe, highly ionised laser prod. plasma, extreme UV line profiles of expansion velocities 78−14199
Fe IX, X, XI, effective dielectronic recombination rates in H plasma, emission time histories 80−79570
Fe, laser prod. plasma, study by UV spectroheliography 78−22529
Fe, X-ray spectra in Tokamak-10 facility plasma *(Russian)* 78−9837
Fe XXII,XXIII, Be I and B I like spectra from laser-produced plasma, classification 78−67410
Fe^{n+} forbidden spectral lines, in PLT Tokamak, diagnostics of localised high-temp. regions 79−98958
H arc axial ground state population meas. 78−67598
H atom density, resonance fluorescence method *(Russian)* 78−9838
H Balmer lines, plasma-broadening in wall-stabilised arc, low electron density 80−43891
H, Balmer-α line profiles and polarisations in strong mag. field 77−6729
H dense thermal plasma, radiation emission 80−103120
H flux to walls, ang. and time resolved meas. techniques 79−674
H flux to walls of fusion reactor, novel meas. technique 78−29640
H high power arc, standard source of continuum radiation, 53-92 nm 80−44054
H isotope separation in DC-arc plasma, mass spectrometric anal. 79−90457
H, L_β reson. line Stark broadening in equilib. plasma 79−32823
H line broadening and shift due to plasma ions *(Russian)* 80−96350
H line shape, joint electron and ion influence *(Russian)* 78−9762
H lines, effect of reduced mass in Stark broadening *(Russian)* 77−79578
H lines, electron width and shift *(Russian)* 78−67421
H, Lyman-α Stark broadening, dynamic screening effects 78−18386
H, n-α line Stark profiles, large θ-discharge 77−24084
H pellet-rotating plasma interaction, spectroscopic anal. 78−18455
H, plasma, in θ-pinch with axial current-carrying rod, light scatt. diagnostics *(Russian)* 77−11395
H plasma, K impurities, optical props. 80−103119

plasma diagnostics continued
H plasma, laser produced, characterisation meas. 78−67409
H, plasma distribution function inference from optical spectra 78−67406
H radiative recombination in quasistationary thermonuclear plasma *(Russian)* 77−39465
H spark, laser-triggered, electron densities meas. 80−106975
H, Stark profiles, anisotropy of HF noise, turbulent plasma 78−1896
H Z-pinch plasma, strong optical attenuation, shadowgraph meas. 78−26294
H^-, density meas. by photodetachment 80−48976
H^- surface ion source, plasma parameters, diagnostics 78−9849
H-inert gas laser spark, emission spectra 79−82119
H-like ions, emission spectrum, depend. on electron density in laser plasma 79−27248
H-like ions, spectral line intensity, density depend., plasma diagnostic appls. 78−83617
H-like ions in laser plasma, X-ray emission intensities of reson. line satellites 77−80371
H-like light ion resonance line broadening and absorption in laser prod. plasmas 79−19088
H-like metastable ions, de-excitation in laser plasma *(Russian)* 77−7597
$H+O^{8+}\rightarrow H^+ + O^{7+*}$, during neutral beam injection into Tokamak 77−58899
H_2 arc, at. and mol. no. densities meas. by VUV spectroscopy 79−94828
H_2 arc plasma Balmer spectrum decay and two-fluid model 78−67603
H_2 discharge plasma, laser-induced transient striations obs. 79−27785
H_2, electron swarms transport parameters meas., nonuniformities effect 78−83613
H_2 gas target, laser-induced parametric instabilities, diagnostics 78−51345
H_2, Lyman system nonsaturated laser line intensity obs. 78−71089
H_2 molecular lines, in H_β region, in low press. afterglow discharge 79−60199
H_2 plasma, radial density and temp. profiles, using magnetoacoustic oscills. 79−19082
H_2 plasma development in 2kJ focus discharge accelerator, optical image structs. 79−82076
H_2 plasma reactor design, heat transfer and flow 80−38697
H_2 pulsed arc, dense plasma, Balmer spectrum near photorecombination threshold, press. depend. 80−38569
H_2 Tokamak plasma, Doppler temp. and particle confinement time from H_α-line meas. 78−55737
H_2-D_2-He, microwave discharge lamp, H and D Lyman-α line shapes 79−80698
H_2-He plasma, shock-heated, relax. distance and equilib. electron density diagnostics 77−24180
H_2-SiH_4, glow discharge, emission spectroscopy of Si H 80−69984
H_3^+ ion density decay, mass spectral obs. 77−3987
$H_{\alpha,\beta}$ lines, dense plasma Stark broadened central struct., comment 77−23464
$H_{\alpha,\beta}$ lines, dense plasma Stark broadened central struct., reply 77−23465
H_α and H_β spectral profiles from neutral beams and plasmas in high mag. fields 80−83999
H_α and H_β Stark profiles in LF turbulent plasma 77−7593
H_α line shape, plasma broadened, fine struct. effects at low electron densities 78−62765
H_β line profile for plasma microfield distrib. function reconstruction 78−71539
HCN laser processes, mm. and submm. microwave spectroscopy 78−13685
$H_2(D_2)$-Ne-He(Ar) plasma, combustion driven shock tube, H_β central struct., ion mass effect 78−26327
$H_3O^+(H_2O)_n$ formation in vacuum spark, mass spectrometer expt. 79−32844
Hα and Hβ, Stark profiles, ion-motion effect 80−63592
Hα(Dα) plasma red shift meas. in Ar arc, ion dynamic depend. 80−10364
He afterglow, Rydberg states collisional radiative transfer, He^+ electronic recombination 77−62401
He, afterglow of pulsed discharge, elec. and optical meas. 78−26329
He, afterglow produced by microwave surfaguide, spectroscopic diagnostic, electron and He_2 rot. temp. 80−44042
He, arc plasma Stark profile, heavy-particle temp. 79−46484
He, collisional radiative model, reson. optical pumping, plasma diagnostics appl. 79−37459
He continuum radiation, 109 to 540 nm, meas. in arc plasma *(German)* 80−106932
He continuum radiation emission obs. to near vacuum UV 78−71582
He, cryogenic discharge, interferometer meas. of neutral gas temp. 78−1924
He DC discharge electron free streaming wave propagation obs. 78−75314
He discharge, EM fields near antenna, probe diagnostics 77−24095
He, discharge, level populations, time resolved spectra 77−80391
He discharge, VUV continuum kinetics 79−94827
He, discharge plasma, dynamical studies, pulse repetition rates effects 77−62397
He, duoplasmatron arc, ionisation meas., line intensity ratios 80−54060
He, fast electron energy distrib. in positive column and negative glow 80−38764
He glow discharge, n=3 sublevel quenching and energy transfer, laser perturbation method 80−44060
He glow discharge, negative-luminesc. plasma, electron energy distrib. from line intensities and probe obs. 80−49033
He glow discharge with constriction, electrokinetic and optical charact. axial distribs. *(Russian)* 77−80393
He HF discharge double-probe meas. 78−67541
He high-current pulse discharge plasma partial LTE disturbances 78−67600
He high-current pulse discharge plasma kinetic and dynamic processes 78−67601
He I, 4471 Å line profile in various plasmas, ion perturbation effects 78−94214
He I, exptl. line profiles near 4471.5 Å 77−6725
He I, plasma, excited atoms, near-reson. Rayleigh scatt. obs. 77−3992
He I, spectral line shift and Stark broadening in plasma 77−18843
He I line profiles, ion motion effect in low electron density plasma 80−43877
He I line profiles with forbidden components induced by fluctuating fields in small theta pinch plasma 77−80353

plasma diagnostics continued
He I neutral line broadening meas. 78−18448
He I plasma arc, spectral line profiles, $\lambda\lambda$=4471 Å and 4922 Å *(French)* 78−83625
He I plasma lines, Stark broadening, quantum mechanical calcs. 80−43880
He I satellite line shape, stochastic theory 78−38460
He II, 4686 Å Stark broadened profile, electron density and temp. meas. 77−23460
He II, Doppler and Stark broadened lines, electron density and ion temp. meas. 78−67407
He II, reson. line Stark broadening and plasma polarisation shift 77−1020
He II, Stark broadening of VUV transitions at 304, 1215, 1640 Å 78−66506
He II, Z-pinch plasma, Stark broadened profile, 4686 Å, electron density and temp. 77−84495
He II 4686 Å line, Stark profile meas. in high density plasma 80−96390
He, impurity ion emissions in vacuum UV 500 to 1500 Å region *(Japanese)* 77−80363
He, in rot. steady state centrifuge, rot. rate and temp. diagnostics *(Russian)* 78−5923
He, laser plasma, spectroscopic meas. *(French)* 77−62396
He like ions with Z=12-23, reson. line satellite intensities in laser plasma X-ray emission 79−10718
He, low press. discharge, electron free streaming waves expansion 80−79595
He, low pressure, line spectrum, mol. transisions effects 79−60212
He, microwave discharge, electrodynamic and spectral charact. *(Russian)* 77−11413
He, microwave discharge, emission processes, steady-state kinetic calcs. 77−68880
He, photon echoes obs., collisional relax. on $2^3S_1-3^3P_{012}$ 79−19089
He plasma, electron density, determ. by emission coeff. and Stark broadening *(German)* 77−58903
He, plasma, in θ-pinch with axial current-carrying rod, light scatt. diagnostics *(Russian)* 77−11395
He plasma, laser heating, spectroscopic meas. 77−76205
He plasma, low-density, electron temp. determ. from He I 3889 Å and 5016 Å line intensities 80−96394
He, plasma, non-equilib., of strong current pulse discharge, diagnostics *(Russian)* 78−75271
He plasma, recombining, method of determ. of electron temp., electron density and ion density 77−84494
He, plasma, stationary recombining, population inversion inferred from intensity meas. 78−9836
He plasma He I 4471 Å line profile obs. at high electron density 78−67472
He plasma in electron beam-excited discharge, atm. press., relax. obs. and model 79−37569
He plasma-electron beam, electron cyclotron instability, nonlinear time development, k-spectrum 77−76210
He, positive column plasmas, metastable atom density meas. by improved self absorpt. method 80−87968
He pulsed arc, Thomson scatt. diagnostics 80−24297
He pulsed discharge, He_2 mol. formation in early afterglow, time-resolved spectra 78−63585
He, pulsed elec. discharge, high-current, diagnostics and nonequilib. state 79−64942
He, quasicontinuous discharge, at high press., spectral obs. *(Russian)* 78−26356
He, relaxation time determ. for establishing quasisteady state population 78−59639
He, spark prod. by short laser pulses, spectroscopic meas. of temp. and electron density 77−43086
He, Stark broadening satellite transitions, in turbulent plasma 77−61759
He, Stark effect on optically excited plasma atoms in static mag. field 78−66505
He supersonic jet, radiation in magnetoplasmadynamic source 77−35329
He, ultradense reproducible Z-pinch, for laser-pellet interaction simulation, characterisation 78−30463
He, usual glow and hollow-cathode discharges, negative glow, spectroscopic obs. 77−72516
He, Voigt profile, line absorpt. calcs. of 388.9 nm triplet, 501.6 nm singlet lines 78−90123
He^+, excitation in hollow cathode discharge, rel. to plasma electron density and temp. 77−7589
He^+, He_2^+ and metastable He and He_2 densities in afterglow, mass spectroscopy 77−24221
He-Ar-H arc plasma, nonequilib. effects, spectroscopic diagnostics 77−76191
He-Cd, afterglow, Cd^+ excited state prod. by Penning and charge exchange reactions 77−15252
He-Cd, usual glow and hollow-cathode discharges, negative glow, spectroscopic obs. 77−72516
He-Cd discharge, principal Cd ionis. mechanism, radial profiles meas. 77−27758
He-Cd plasma, in discharge tube, excitation mechanism obs. 78−30479
He-Cd vapour excitation in hollow cathode discharge 80−64815
He-Cd^+ positive column laser discharge, ion density 77−68885
He-Cs plasma, HF instability in crossed fields, obs. 78−75305
He-Cu discharge, Cu ion laser, at. emission obs. of plasma props. 80−19021
He-Hg afterglow plasma, time resolved double probe study 78−18444
He-Hg plasma, prod. by nucl. radiation, charge exchange effects 77−24103
He-Hg RF discharge, atomic ionis. and excitation, spectral line intensities 78−26334
He-Kr^+ ion laser, microwave-pulse-excited, spectroscopic expts. 77−71973
He-like ions, spectral line intensity, density depend., plasma diagnostic appls. 78−83617
He-like ions in laser prod. plasma, anomalous intensity ratios of reson. to intercombination lines 79−23454
He-N_2 mixture, plasma created by electron beam, spectral composition *(Russian)* 78−30453
He-N_2 plasma, N_2 $B^3\Pi_g$ state excitation, role of long lived states, luminesc. 80−37829
He-Ne, glow discharges, AC cataphoresis meas. using light spectrometry 79−60096
He-Ne discharge, striation oscills., spectral width variations 77−62429

plasma diagnostics continued
He-Ne laser, transition probabilities of Ne spectral lines at 352, 363, 345 and 543 nm 78−25851
He-Ne laser plasma, line profiles meas. by optogalvanic spectroscopy 78−62233
He-Ne plasma He I 4471 Å line profile obs. at high electron density 78−67472
He-Xe plasma, in mag. field, effect of CO_2 mol. addition on plasma parameters 77−42965
He_2^+ recombination, high-temp., in plasma jet *(French)* 80−43861
HeI, low density suprathermal field fluctuations and high energy electrons 80−1847
^{3}He plasma, prod. by products of $^3He(n,p)^3H$ in nucl. reactor, props. 77−76146
^{3}He-Hg (−Kr)+$^3He(n,p)T$, high press. plasma excitation, luminesc. spectra 80−38719
Hg 40.8 MHz discharge electrode space-charge sheath thickness obs. 78−67547
Hg arc, continuum radiation meas. 77−62416
Hg continuous spectra at series limit $6p'\ ^3P_2$ *(French)* 77−88413
Hg, optically pumped positive column, E-I charcts. 80−44035
Hg plasma, spectral line strength, charge density effect 79−73040
Hg plasma flow, electron temp. determ. from partial LTE populations 80−24248
Hg positive column, high press., excimer densities and destruction mechanisms 78−5967
Hg-Ar, HF discharge, electron energy distrib. and atom ionisation processes 80−44048
Hg-He(Ar), modulated discharge, elec. and optical props. 77−7627
Hg-Sn halide arc, molecular optical absorption obs. 78−75457
K plasma, DC conductivity, electron collision cross sections 77−3469
K plasma in arc and capillary devices, optical props. 80−24244
K, positive column, ion distrib. function for each species using probe 78−55752
K positive column discharge plasma, neg. ion prod. 78−59712
K, resonantly excited in cylindrical discharge plasma, effective lifetimes 78−79413
K-H plasma, low temp. discharge, ion constitution mass spectra *(Russian)* 77−4000
K-Kr, afterglow of laser plasma, fluoresc. spectra 79−19085
K_2^+ ion formation in low press. K discharge plasma 80−43862
Kr hollow cathode discharge, multiply charged and mol. ion prod. and loss 79−46499
Kr I lines from wall-stabilised arc measurements, transition probabilities 78−22569
Kr, ionising shock wave refl., interferometric meas. 79−55553
Kr plasma, shock-heated, continuum radiation emission coefficient meas. 79−64835
Kr, reson. levels relax. consts. determ. by alignment method in discharge 79−26936
Kr-Cl_2 mixture, glow discharge positive column, electron energy distrib. and rates of inelastic processes, negative Cl ions form. 80−19632
Kr-N_2 plasma, afterglow ion prod. and loss processes 77−11401
Kr-Xe, glow discharges, AC cataphoresis meas. using light spectrometry 79−60096
Kr(-He) arc, wall-stabilised, atm. press. 79−46503
KrF*, electron beam controlled laser, plasma processes 79−930
Li I (2p-4d, 4f, 4p) line broadening in electrolytic plasma *(French)* 78−1892
Li wire, optical meas. of laser detonated shock waves 78−42798
Mg plasma, heated by ruby laser pulses, X-ray emission spectrum 80−64781
Mg XII, electron temp. determ. of laser plasma from continuous recomb. radiation 79−64924
Mg+Ar(Xe), plasma, near reson. charge exchange, spectra *(German)* 77−31425
Mn XVII to Mn XXII ions spectrum emitted by Tokamak produced plasma 80−10437
Mo, arc, steady, vac., plasma ion mass and energy diagnostics 78−51385
Mo, arc, vac., stabilised, plasma props. 78−51384
Mo impurity and injected O_2 distribs., TFR Tokamak current plateau, VUV obs. 78−22565
Mo X-ray emission spectra, detect. from Alcator-A Tokamak 80−92389
Mo XIII-XVIII, spectrum 20 to 90 Å from laser-prod. plasma and low-inductance vac. spark 80−102473
Mo XLI, Mo XL, X-ray emission from vacuum-spark plasma 78−41991
Mo XV to Mo XXXIII identification in soft X-ray spectrum of TFR Tokamak 77−72504
Mo XXXI-XXXIV spectra from exploded Mo wire plasmas 79−1295
N arcs, spectroscopic meas. rel. to LTE 77−76200
N I plasma jet, spectroscopic diagnostics, Stark broadening and shift, study 80−38727
N, nonequilibrium plasma, thermocouple diagnostics 80−103188
N, plasma, Stark broadening, photoelec. obs. 77−23463
N V, ionis. rate meas. in theta-pinch plasma, VUV obs. 78−26254
N V, VI, laser produced plasma, satellite spectra 78−5165
N^{2+}, spectral line breadth in molecular nonequilibrium plasma *(Russian)* 80−48044
N^{4+}, 2s-2p excitation absolute cross sections by electron impact, rate coeffs. temp. depend. 79−94087
N_2 afterglow, chem. reactions rel. to plasma props, appl. to toluene polymerisation 80−3346
N_2, afterglow, short-lived, electron and ion density enhancement obs. 78−63625
N_2 arc, magnetically stabilised cross-flow, temp. and flow fields meas. 80−54054
N_2 arc, spectroscopic meas. w.r.t. LTE 77−19786
N_2 arc plasma, recombination with gas glow, spectroscopic diagnostics 77−7626
N_2, barrier discharge, struct., spectral anal. *(Russian)* 77−21463
N_2, diffuse plasma, population densities of triplet states, correl. with electron impact processes 80−43966
N_2 discharge, effect of Cs additive on I-V charcts. 79−32813
N_2, discharge, elec. and optical props. calcs. *(Russian)* 79−10741
N_2 discharge, non-Boltzmann vibr. level populations, CARS determ. 78−5968
N_2 discharge plasma, ionic comp., mass spectra meas. *(Russian)* 78−22571
N_2 discharge plasma, radial distrib. profile of atom conc., Lewis-Rayleigh afterglow radiation 77−89312

plasma diagnostics continued
N_2, fission fragment excitation, delayed coincidence spectroscopy 77−24189
N_2, glow discharge, DC, low-press., translational/rot. temps. relation 78−38454
N_2, glow discharge, decay instability and contraction, interferometric and photographic obs. *(Russian)* 78−59696
N_2 glow discharge, neutral components comp., mass spectroscopy study *(Russian)* 80−10439
N_2, homogeneous overvolted discharge, electron density evolution 79−1359
N_2, laser-irrad. freely expanding jet, electron temp. and spontaneous mag. field meas. 77−84469
N_2, microwave discharge at high press., vibr. excitation *(French)* 78−14239
N_2 non-LTE, pulsed discharge, I-V characteristic obs. 78−71618
N_2 plasma, 10000-13000K, VUV continuum radiation 78−91152
N_2 plasma, 18000-45000K, continuum emission coeff., laser spark temp. meas. 77−31527
N_2 plasma, electron temp. and conc. meas., complete LTE 77−65908
N_2, plasma, in graphite reactor, temperature distribution *(Russian)* 77−51241
N_2 plasma, non-equilib., excited species, vibr.-rot. anal. fluoresc. obs. 80−54034
N_2, plasma, pulsed discharge, component conc. radial distrib. determ. *(Russian)* 77−21462
N_2, plasma created by electron beam, spectral composition *(Russian)* 78−30453
N_2, plasma discharge stream, rarefied, diagnostics using sounding and UHF interferometry 79−41872
N_2 plasma jet, spectroscopic obs., electron temp. 77−31512
N_2 positive column, gas temp., interferometric diagnostics, heat cond. calc. 79−32834
N_2 positive corona into spark, prebreakdown phase, spectroscopic anal. 80−38790
N_2, streamer discharge, spatial and temporal spectroscopy 78−5971
N_2, translational energy transfer rate, after pulsed discharge, interferometric obs. *(Russian)* 78−26322
N_2 vibrational levels stepwise excitation, effect on electron energy balance in He-N_2-CO_2 discharge 80−54071
N_2-Ar corona dishcharge, convection and mixing, atm. press., mass spectra obs. 80−1853
N_2-CO_2-H_2O gasdynamic laser mixture, electron beam diagnostics 77−83845
N_2-H_2 arc, bent and rot., flow mechanism 80−70047
N_2-He, barrier discharge, struct., spectral anal. *(Russian)* 77−21463
N_2-methane, rapidly developing discharge, streak camera records interpretation 80−59280
N_2-O_2 mixture transient discharges, RF techniques 80−70067
$N(^2D,^2P)$ metastable ats. prod. in N_2 DC glow discharge 80−38758
$N(^2D,^2P)$ metastable production by electron collisions in DC glow discharge 80−59274
NH_3 glow discharge, electron energy distrib. and negative ions *(Russian)* 79−7499
$N_2(N_2+Ar)$ pulse excited microwave discharge diagnostics at moderate press. 78−9873
N_2O laser, mass spectra of positive ions in discharge plasma 77−89315
N_2O-He, species concentrations in glow discharge and afterglow, mass spectra, laser conditions 78−14241
Na arc plasma, dense, high-temp., local conc. determ. by near-reson. Rayleigh scatt. 77−1019
Na D line emission from shock generated sodium halide plasmas 77−47265
Na, high press. arc, plasma spectral change mechanism 79−82093
Na high-pressure arc, time-depend. plasma temp. meas. 77−68866
Na I, reson. line broadening in shock tube plasma 77−35393
Na, nonequilib. excited-level population in inhomogeneous plasma 77−3917
Na-like ions, Kr-Mo, 2-3 transitions, plasma X-ray spectra classification 79−37544
Na-Ne-Ar AC discharge, field strength, electron props., radiated power 77−39487
Na-Xe, high-pressure discharge, electron density, interferometric meas. 78−75415
Nd:glass laser irradiated fusion targets, time and space resolved harmonic emission 79−82095
Ne, $1s_5$ level density meas. by fluorescence, effect of dye laser intensity 78−67474
Ne, 4 MHz discharge, electron energy distrib., probe diagnostics 78−38566
Ne afterglow, diffusion, collisions, decay freqs., fluoresc. obs., calcs. 78−59715
Ne afterglow, recombination processes, microwave quenching 79−14624
Ne atom, temp. in hollow cathode laser discharge 79−7490
Ne, discharge, excitation mechanisms investig. using radial distrib. of excited atoms 80−38744
Ne, discharge, low-press., atom densities of first excited state 80−38750
Ne discharge, spectral line intensity radial distrib. 78−5930
Ne discharge, wavenumber spectra of turbulent ionisation waves 78−71541
Ne, early afterglow, electron temp. at few torr press. *(French)* 77−4013
Ne, electron energy distrib. meas. in moving striations 77−55191
Ne, excited atoms concentration determ., in high-frequency and glow discharges *(Russian)* 80−70050
Ne, excited atoms reactions in pure afterglow, plasmas using resonance absorpt. spectrometry 80−33835
Ne filled glass microballoons, laser imploded, compressed core density meas. by X-ray continuum edge shift 79−10705
Ne, glow discharge, ionisation waves, regular and irregular, correlation meas. 78−1917
Ne, glow discharge, turbulent ionisation waves, correlation meas. 78−67519
Ne HF discharge plasma electron energy distrib. 78−67540
Ne II line Stark broadening in pulsed arc, obs. 78−67469
Ne II lines from pulsed arc plasma, Stark broadening 78−66504
Ne, in glass microbubble, laser-imploded, compression, X-ray emission 78−18454
Ne, low press. discharge, electron free streaming waves expansion 80−79595
Ne, low press. discharge afterglow, dissoc. recombination, microwave diagnostics 78−9876

plasma diagnostics continued
Ne medium-pressure discharge, electron temp. radial profile meas. by electron-atom bremsstrahlung continuum 78−67497
Ne microballoon, laser compression, X-ray emission diagnostics of explosive pusher mode 79−54598
Ne microballoon spectra, density-sensitive dielectronic satellite lines 79−72270
Ne, negative afterglow, pulse excited, at. spectral lines, microwave quenching 78−63591
Ne, nuclear induced plasma, simulated 80−64786
Ne plasma, generated by 200 MeV protons, electron density and electron temp. 78−22568
Ne positive column, high-press., optical and probe diagnostics 78−51383
Ne, positive column, mol. ion conc. determ. 77−58913
Ne, positive column, radial distrib. of excited atoms *(French)* 78−14237
Ne positive column plasmas, metastable atom density meas. by improved self absorpt. method 80−87968
Ne pulsed transverse discharge, spectrosc. absorpt. investig with nanosec. time resolution *(Russian)* 80−64782
Ne, RF discharge, emission modulation due to fast electron distrib. time variation 79−41900
Ne, streamer plasma characts., cond., plasma density and field strength calcs. *(Russian)* 77−47262
Ne Townsend discharge, Ne_2^+ form. and destruction 80−38747
Ne, Townsend discharge afterglow, decay rate of metastable ats. 80−44011
Ne VI, VII and VIII, total collisional ionis. rates in plasma 77−19102
Ne X Lyman-α line Stark broadening, hot dense laser-produced plasma 77−11402
Ne-Ar, glow discharges, AC cataphoresis meas. using light spectrometry 79−60096
Ne-Ar discharge, transient cataphoresis, time depend. 80−38753
Ne-He DC glow discharge electron density decay, microwave cavity obs. 78−91167
Ne-Hg RF discharge, atomic ionis. and excitation, spectral line intensities 78−26334
Ne-like ions, Kr-Mo, 2-3 transitions, plasma X-ray spectra classification 79−37544
Ne-N_2 mixture, plasma created by electron beam, spectral composition *(Russian)* 78−30453
Ne-Ne and Ne, negative afterglows, microwave quenching and recombination processes, Mo emission 77−80307
Ni from Tokamak-produced plasma, $2s^22p^k$-$2s2p^{k+1}$ transitions in F I to Be I isoelectronic sequences 80−37765
Ni, X-ray transitions in laser produced plasma 80−100093
O atom concentration, in O_2, $(CO)(CO_2)$ glow discharge, mass spectrometric determ. *(Russian)* 78−87512
O impurities, neutral-beeam-injected, in 2XIIB mag. mirror 79−37547
O, impurity radiation, metastable transitions in Tokamak, modified coronal model 78−26255
O low-pressure discharge, plasma atomic species, mass spectrometric obs. 78−67502
O VI, ionis. rate meas. in theta-pinch plasma, VUV obs. 78−26254
O VII, laser produced plasma, satellite spectra 78−5165
O^-, spectra in pure O arc plasma, 2000-9000 Å, 9000K 79−32750
O^{6+}, line emissions from He-like ions, electron params., ion diffusion in Tokamak plasmas 79−4114
O-like ions, spectral line intensity, density depend., plasma diagnostic appls. 78−83617
O_2 plasma, 10000-13000K, VUV continuum radiation 78−91152
O_2 plasma, UV continuum spectra, mol. recomb. of ground state atoms 78−91078
OH radicals in glow discharge, rot. levels distrib., temp. meas. 78−47169
$OH(^2\Pi)$, rot and translational temps. in gas discharge 78−5243
Pb, mass ejection from shocked surface during fusion 78−47186
Pb, X-ray emission spectra of CO_2 laser-irrad. targets, nonlinear processes 80−33793
Pt, laser produced plasma, Ni-like X-ray spectrum 80−43983
Rb, resonantly excited in cylindrical discharge plasma, effective lifetimes 78−79413
S (S-He) discharges, stability, emission spectra 80−107003
SF_6 circuit breaking arc investigation *(Japanese)* 78−55768
SF_6, high-current discharge plasma column, radiation charact. and struct. *(Russian)* 80−106989
SF_6, high-temp. circuit-breaking arc, axial and radial heat transport 79−19105
SF_6 plasma column, in Maecker type arc, diagnostics and model *(French)* 80−19652
SF_6-inert gas mixture, high power cylindrical spark discharge, dynamic and visible charact. 80−64816
SI II, Stark broadened linewidths, plasma diagnostics and stellar spectra appls. 77−84496
Si III, EUV spectra in solar transition zone rel. to energy balance and press. 80−21957
Si III, IV, Stark line broadening in pulsed arc, plasma diagnostics 78−944
Si lines as spectral diagnostics for astrophysical plasmas, effect of charge transfer 80−41717
Si^+ lines, from plasma, Stark broadening 79−4189
Si:H, amorphous, control and anal. of deposition, using plasma spectroscopy 80−45230
Sn I, Sn II, wall-stabilised arc, absolute transition probabilities, 5300-6850 Å 78−9105
Sr, atoms and ions in discharge, temp. and conc. determ, by spectral line shapes *(Russian)* 78−14214
Sr, Doppler temp. from linewidth, in inductively coupled plasma 77−43083
Ta, plasma produced by pinched relativistic electron beam impact on foil 79−77403
Ta XLVI(XLVII), $3d^k$-$3d^{k-1}npnf$ transitions in laser plasma 78−9108
Ti, arc, steady, vac., plasma ion mass and energy diagnostics 78−51385
Ti density, in DC sputtering discharge by atomic absorpt. spectroscopy 80−43973
Ti II, oscillator strengths from combined hook and emission expts. 80−87081
Ti, laser prod. plasma, study by UV spectroheliography 78−22529
Ti, laser produced plasma, vac. UV emission 77−80372
Ti, laser-prod. plasma, space-resolved extreme UV emission 80−54015
Ti spectral line excitation by 100 eV electrons in inner discharge columm *(Russian)* 80−38529

plasma diagnostics continued
Tl, axial distrib. in unipolar arc discharge, influence of Li conc. 80−19656
Tl-Xe, electric discharge excitation of Tl in high-press. Xe 80−49025
U enrichment by plasma centrifuge, rotational velocity meas. 78−74502
U, hollow cathode discharge, opto-galvanic spectroscopy-electron temp., isotope ratio analysis 79−77437
UF_6, emission and absorpt. spectra at 80 to 600 nm, decomp. products 77−23212
UF_6, plasma confinement expts. appl. to plasma core reactor 77−23190
UF_6, plasma expts. related to plasma core reactors 78−8977
V XX, Be I like spectra from laser-produced plasma, classification 78−67410
W, radiation from beam-foil excitation and Tokamak produced plasmas 79−54828
W radiation from Tokamak-produced plasmas 78−9835
W XX to XXXV spectra and spatial distrib. in PLT Tokamak 78−55747
W-glass discs, 1.06 μm laser irrad., plasma prod. processes 78−18431
Xe, continuum absorpt. coeff., in shock tube, determ. 77−39463
Xe discharges, electrodeless, UHF in waveguide rel. to DC characts. 80−38762
Xe, ns. discharge, energy balance, optical meas. 78−1935
Xe, plasma, optical props., wall erosion products effects calcs. 78−47164
Xe, plasma afterglow, spectral features, 450-900 nm 79−23404
Xe, plasma column in flashtube, characts. and parameters 80−54053
Xe, pulse gas discharge, high-intensity, energy storage and temp. in channel 78−1926
Xe, reson. levels relax. consts. determ. by alignment method in discharge 79−26936
Xe, Townsend discharge, electron energy distrib. functions 79−4198
Xe Townsend discharge electron energy distrib. obs. 78−67549
Xe, wall-stabilised plasma, temp. and press. of high press. plasma *(German)* 79−23450
Xe-^{3}He plasma, plasma parameters determ. 80−54047
Xe_2^+ excimer form. in pulsed discharge, visible emission obs. 80−38754
Y_2O_3 capillary discharge plasma, temp., radiation screening elimination 80−64682
Zn I, relative populations in arc, sputtering and gas phase collisions 80−934

plasma diagnostics by laser beam
θ-pinch, electron temp. meas. by Thompson scatt. with ruby laser *(Chinese)* 79−37552
absorption, z-depend., stimulated backscatter processes in laser plasma 80−43944
absorption coeff. spatial distrib., laser scanning method *(Russian)* 78−22551
air, laser-induced breakdown over long distances 80−33795
air gap, drift vel. meas. of ionized particles 80−24298
air plasma, TEA CO_2 laser-produced, using solid targets, induced shock waves 80−64729
Alcator Tokamak, IR laser probing 80−10433
amplitude calibration from Raman spectra *(Russian)* 80−38702
anomalous transport in turbulent electron heating 78−14216
arc, density and temp. meas. 78−1937
arc, electron density determ. by IR laser transmission meas. 79−7491
arc discharge, flow vel. meas. using laser Doppler velocimetry 77−80360
arc plasma, atmospheric, electron density meas. by two-wavelengths interferometry *(Japanese)* 80−38720
arc plasma, low-temp. diagnostics by scatt. and resonance fluorescence 78−67482
arc plasma electron density, interferometric meas. 78−67479
arc quasistationary plasma, scatt. diagnostics using periodically pulsed UV lasers 78−67481
arc thermal ion spectrum, meas. by CW CO_2 laser 90° scatt. 78−67480
arcs characts. meas. temp. and particle densities determ. *(French)* 80−19651
asymmetric electron density profile, interferometric meas., laser-created plasma 80−75085
atomic absorption spectra, high freq. Stark effect 80−23359
atomic collision processes and X-ray and UV lasers 80−64787
axially symmetric plasma, error estimate of optical diagnostic methods 77−84500
Balmer series transitions for laser plasma diagnostics 80−64780
beat heating, system, using double-barrelled laser 78−67386
belt pinch, shock heated weakly compressed high-temp. plasma 77−24164
Bragg cell heterodyne interferometry of fast plasma events 77−11404
chemically reacting non-LTE plasma, elementary reactions 78−3337
column electron density radial profile, modified laser interferometry 78−67429
combination scattering method 80−79569
combustion product plasma, electron conc. and mobility determ. by HCN laser submillimetric interferometry 78−1889
conference, high temp. plasma diagnostics, Tennessee, USA (Jan. 1976) 77−31528
conical waves from scatt. laser radiation, pot. electron density determ. *(Russian)* 78−59667
current changing plasma in Tokamak, Thomson scatt. and local current density determ. 77−27724
current density, local, mag. probe and Thomson scatt. meas., using Spitzer-Harm distrib. 78−18451
current sheet formation, in Ar plasma, cineholographic obs. *(Russian)* 78−38529
CW far-infrared laser scattering from a laboratory plasma ion acoustic wave 80−106974
dense plasma, diagnostics of two-wavelength optical absorpt. 79−98978
dense plasma, laser scatt. 78−67408
dense plasma focus, ruby laser holographic diagnostics *(Japanese)* 80−100097
density distribution meas., using Michelson interferometer *(Japanese)* 78−42820
density fluctuations, laser heterodyne meas. 77−15246
density fluctuations meas., spatial distrib. 78−34372
density fluctuations study by small angle CO_2 laser scatt. 80−59285
density meas. on refuelling by solid H pellets in rotating plasma, laser interferometry 79−4188
density profiling by interferometry with rapid spatial scanning, and Thomson scatt. of short laser pulse 80−49014
diode, field-emission type, Thomson-scatt. diagnostics 80−43988

plasma diagnostics by laser beam continued
discharge, pulsed, density perturbations, laser beam diagnostics 79−7498
drift wave freq. profiles, Doppler model 78−71471
dual laser interferometer for plasma density measurements on large Tokamaks 78−71542
effective cross section and space charge, preionised gas laser induced breakdown 80−48930
electron and ion temps., Thomson scatt., and neutron emission obs., Tokamak discharge 78−18438
electron densities from Thomson scatt. and He-Ne laser interferometry 79−86615
electron density, determ. from He I Stark widths and He-Ne laser interferometry 77−80374
electron density, in O_2-injected TFR Tokamak current plateau interferometric diagnostics 78−22565
electron density and temp. determ. from laser scatt. *(German)* 77−7599
electron density determ., in collisionless plasma, by CO_2 laser 79−41879
electron density determ. by CO_2 laser 90° collective scatt. 78−67433
electron density distrib. meas. *(Russian)* 78−22550
electron density fluctuations, homodyne method with CO_2 laser 79−68957
electron density fluctuations, laser scatt. by turbulence 77−39469
electron density fluctuations in ATC Tokamak plasma 77−43074
electron density in high-temp. gas flows, homodyne multiray interferometer technique 79−86609
electron density in hollow cathode discharge, laser heterodyne meas. 78−30483
electron density in pulsed laser discharges, interferometric meas. 80−96393
electron density meas. by far IR laser beam deflection 80−48966
electron density meas. by far IR laser beam deflection 80−59296
electron density meas. by HCN laser interferometer 77−39467
electron density meas. by modulated submillimetric laser interferometer 77−39466
electron density measurement by laser light scatt., calib. by Raman scatt. 77−35399
electron density measurement using feedback-stabilized fractional fringe CO_2 laser interferometer 79−75582
electron density using fast N_2 laser interferometer, dense plasma 78−87489
electron directed velocity meas., optimised method using laser scatt. incoherent regions 80−79561
electron temperature and density, Thomson scatt. in JIPP T-II device 79−23461
electron temperature and density of laser prod. plasma 78−30458
electron temperature meas. by Thomson laser scatt., θ-pinch energy loss *(Chinese)* 80−54028
electron temperature meas. by Thomson scatt. 79−19092
electron temperature profile meas. by Thomson scatt. with single laser shot *(French)* 78−9840
electron vel. distrib. in reflex discharge, Thomson scatt. meas. 78−34368
electrooptically switched multipass system 77−89302
EM field during metal evap. at laser focus, RF signal recording obs. 80−59281
emission spectra, satellite lines of He-like ions in laser prod. plasma 79−86618
energy partitioning, in magnetoplasma, relativistic electron beam heating 78−38515
enhanced laser-plasma backscatt. due to prepulse radiation 78−18428
Fabry-Perot laser interferometer for plasma density meas. in unsteady flow 77−68869
far IR 2-D plasma interferometry evaporographic and pyroelec. recording 78−5929
far IR diagnostic quartz beam splitters 77−39470
far IR interferometry, for plasma density measurement 78−47183
far IR laser scatt. meas. of nonthermal density fluctuations 80−59297
far IR lasers, development for Thomson scatt. diagnostics of Tokamak plasma, review 80−24242
far IR lasers appl. and detection systems in controlled fusion research 78−47182
far IR systems, for plasma studies 78−47185
far IR two-dimensional plasma interferometry with evaporographic and pyroelec. recording 77−39468
fast IR laser interferometry, electronic density fluctuation meas. 80−49000
feedback interferometer with phase quadrature using two-mode He-Ne laser 79−2813
focus, beam deviation method 78−55745
focus, Mather-type machines, temp., density, neutron and X-ray emission characts. 77−24184
focus device, maximum compression phase 79−10711
focused plasma, electron density distrib., N_2 laser interferometric study, X-ray and neutron emission 78−87479
free-free transitions, mutiphoton, energy absorption laser pulse shape-independ. 80−43184
FT-1 Tokamak, electron density and temp. radial distrib. laser scatt. obs. *(Russian)* 78−59666
glass microballoons, laser imploded dynamics, X-ray streak camera study 79−68937
glass targets, laser-produced plasma X-ray spectral lines identification *(Chinese)* 80−54036
glow discharge, high press., collision freq. meas. 77−55184
Heliotron-D, low freq. shear Alfven wave heating, diagnostics 78−1858
heterodyne CO_2-laser interferometer with direct phase readout for meas. electron line densities in plasmas 80−1848
heterodyne quadrature interferometer for simultaneous measurements of plasma density along several chords 78−67416
HF discharge diagnostics with Fabry-Perot interferometer, apparatus function 78−9872
high energy CO_2-laser pulse, interaction with liquid and solid targets, optical investigations 78−42829
high-density pulsed plasma, laser interferometry 78−67430
high-power submillimetric laser oscillator-amplifier system design 77−38927
holographic interferometry system for plasma flow phenomena, Ba II ion density meas. 78−55751
holographic microinterferometer to meas. plasma electron densities and other transparent objects 80−43964
holographic schlieren investigation of laser-induced plasma density 77−72503
holographic study of laser prod. plasma at 10.6 μm 80−38685

plasma diagnostics by laser beam continued
hot plasma, mag. field direction determ., by light scatt. 78−67434
image convertor and spectral analyser device for low-temp. plasma diagnosis 79−4180
implosion, by pulsed electron beam accelerator, 4TW, laser and X-ray obs. 80−1816
implosion heating experiment, Faraday rot. meas. 77−39456
impurity atom diffusion, laser fluorescence study 79−68955
impurity concentration meas. from laser fluoresc. lines *(Russian)* 78−1887
impurity concentrations on wall during Tokamak discharges, laser probing technique 80−49013
incoherent Thomson scattering techniques 80−48999
injector, plasma parameter determ. by laser light scatt. *(Russian)* 78−22573
interferential laser Doppler velocimetry in HF plasma jet *(French)* 77−89307
interferometer for density meas., 10^{19}-10^{22} m^{-3}, and simple hydrocyanic acid 0.337 mm 78−5922
interferometry, multiframe, using inorganic liquid laser 77−30211
intracavity method for optical densities meas., dynamic range extension 79−9231
ion acoustic wave-CO_2 light scatt. 78−34325
ion beam driven instability, in magnetised plasma, light scatt. obs. 79−77424
ion density fluctuations, CO_2 laser heated plasma, Thomson scatt. meas. 78−42807
ion temp. and density meas. in direct current octopole by induced optical fluoresc. 80−14939
ion temp. meas. by 10.6 μ scatt. from thermal fluctuations 78−67431
ion-acoustic fluctuations, CO_2 laser study 80−83946
ion-acoustic wave dispersion, pulsed CO_2 laser scatt. meas. 79−27828
ion-acoustic wave excitation and interference by laser beam 78−34326
IR holography at 10.6 μm for laser diagnostics 80−84007
IR impulse holography and interferometry, appls. *(Russian)* 77−14678
jet form. by focusing laser beam on plane target, investigation using wavefront method 80−75103
JIPP T-II device, electron temp. meas. using Thomson scatt. method 79−50891
Langmuir turbulence, laser excited, in dense plasma focus, light scatt. obs. 77−7591
laser beam-plasma interaction, in mag. field, breakdown, heating, trapping, fusion, diagnostics, book contrib. 77−51196
laser created plasma, interferometer for electron density meas. 80−48983
laser fusion, shadowgraph and interferometry experiments, with ten-picosecond light source 78−42824
laser fusion diagnostics, techniques and appl. 80−49009
laser fusion plasma 77−89305
laser implosion microballoons, X-ray line radiation diagnostics *(Chinese)* 80−6279
laser interferometry in plasma-focus device for investigation of plasma dynamics 78−83614
laser irradiated plasma, electron energy profile steepening, polarimetry obs. 78−34349
laser irradiated solid target, picosecond microphotography 78−42828
laser plasma, high speed multiframe interferometry 78−1905
laser plasma focus, interferometry and luminosity meas. 78−47161
laser prod. plasma, fine diagnostics by induced Compton scatt. 78−59673
laser produced plasma, laser light scatt., ang. distrib. 77−15215
laser produced plasma, ultraviolet probing with picosecond pulses 78−42827
laser radiation parametric decay into plasma waves, Thomson scatt. meas. 78−30484
laser scattering from large Tokamak plasmas, signal-to-noise scaling 78−42809
laser spark absorpt. and laser pulse contraction meas. using dye lasers 80−48988
laser-heated plasma with large temp. gradient, ion acoustic turbulence, reduced thermal cond. 80−53987
laser-produced plasma, application of synchronised ultrashort Nd:glass laser pulse 78−42825
laser-produced plasma motion and lateral energy flow meas. 80−75102
low-power laser radiation scatt., low-temp plasma, appl. to N_2 and Ar *(Russian)* 79−98975
Mach-Zender twin-wave laser interferometer for plasma diagnostics 78−4687
magnetic field diagnosis by scatt. radiation spectral comp. *(Russian)* 80−28823
magnetic field direction meas. by laser light scatt. 77−80365
magnetic field measurement in inhomogeneous plasma, probe-laser beam depolaris. effects 78−67411
magnetic field measurement in toroidal plasma systems 80−49004
magnetoplasmadynamic arcjet, density meas. by CO_2, laser interferometry 80−59277
methanol far IR laser, twin optically pumped 80−59306
methanol laser, twin optically pumped far IR, use in plasma diagnostics 80−54049
methanol twin optically pumped far IR laser 80−103189
MHD plasma, by holographic interferometry and Fourier filter correlation, Hungarian progress report 80−48965
Michelson interferometer, in-cavity, high electron density resolution 79−2811
Michelson interferometer with CO_2 laser for density meas. *(Russian)* 78−38534
Michelson interferometry diagnostics 78−1890
miniature exploding foil, pulsed laser stereophotography 78−41364
momentum transfer to target from laser prod. plasma, schlieren and shadow photographs 77−58889
moving plasma filament, submillimetric complex transmission coefficient meas. 78−67424
multi-pulse ruby laser recording of temporal evolution of plasma parameters by light scatt. 80−14938
multichannel HCN laser interferometer for Tokamak plasma diagnostics 78−5928
multichannel scattering diagnostics, density profile meas. in belt pinch plasmas 77−31514
multiframe laser interferometer system, meas. of rapidly varying processes 79−85166
multiframe ps holography appl. to high power laser effects in dielectrics 78−26328

plasma diagnostics by laser beam continued
multiframing interferometer and appl. to plasma focus expt. 80−4761
multiple-pass laser heating of a short plasma column 80−38684
nonequilibrium microwave discharge, light scattering meas. 77−62405
ohmically heated plasma, in JFT-2 Tokamak, Thomson scatt. meas. 79−50890
optical interferometry for laser diagnosis of plasmas, review *(Russian)* 77−11409
optical mixing in light scatt. expts. 79−4184
optically-pumped submillimetre oscillator, for plasma diagnostics 78−47184
parameter meas. using submillimeter methods 77−72498
particle density, laser interferometric obs. 78−86324
particle density in high density pulsed plasmas, laser interferometric determ. *(German)* 78−18442
plane scattering wave form., electron stream diagnostics 77−15248
plasma density IF phase meas. using three-mirror interferometer 78−75414
plasma focus, turbulence, light scatt. obs., pinch break-up 77−24083
polarised submillimeter interferometer, features 77−72499
polythene pellet evaporation by CO_2 laser, multiple-frame laser shadow photography 77−80359
probing radiation Raman scatt. *(Russian)* 80−19618
pulse plasma diagnosis using laser multi-frame interferometry 78−83615
pulse recording using photomultiplier with capacitive load 79−37542
pulsed CO_2 laser scatt. from ion-acoustic wave, heterodyne detection 77−35389
pulsed coherent radiation source, 118 nm 80−106572
pulsed submillimeter laser with optical pumping appl., construction and expt. parameters 80−58565
pulsed submillimetre fluoromethane laser for diagnostics 77−19307
rapid events, photographic study by picosecond techniques 78−42826
Rayleigh scattering in air 79−1342
reacting gas flow, laser induced fluoresc. meas. 77−76011
reflection losses from plane target, optical calorimetry 78−9809
refractive index measurements using laser differential interferometer 77−55170
resonant CO_2 laser radiation absorption and surface instability at crit. density surface 80−48859
resonant laser emission in plasma, atomic absorpt. line contours, Stark effect *(Russian)* 77−76195
resonant optical schlieren system for plasma flow studies 78−5940
reversed field pinch, expt. and 3-D numerical anal. 77−43035
scattering diagnostics, time depend. plasma parameters 78−51351
scattering experiments with periodic 1.06 μm Nd:YAG laser and Si avalanche detector 78−51347
scattering of CW Ar laser, radiation, low-temp. plasma diagnostics 78−38536
scattering spectra recording using self-terminating-transition lasers 79−64923
Scyllac toroidal theta pinch, diagnostics by laser scatt., interferometry and selfluminosity obs. 77−24185
selective excitation spectroscopy, particle kinetics 78−82046
self-generated mag. fields, two-dimens. distrib., laser-plasma reson., mag. tape irradiation 79−41877
SHG in laser plasma, review 80−53993
shock generated turbulence, obs. in mag. plasma by CO_2 laser scatt. 80−84003
shock wave implosion, laser-driven, optical meas. technique *(Japanese)* 77−43066
solid target-intense CO_2 laser beam nonlinear interaction, radiation obs. 78−22562
space-resolved extreme UV spectroscopy of C laser produced plasma 79−50889
spark, in vac., high-press. local plasma regions production, X-ray and hologram diagnostics 79−19104
spectral measurements of $3/2\omega_0$ harmonic for laser plasma parameter determ. *(Russian)* 77−43014
spectroscopy techniques development, review 80−43991
stellarator, Isar T1-B, m=2 mode collision-dominated stability obs. 77−24130
stimulated Brillouin backscatter from theta pinch 78−67359
stroboscopic method for picosecond diagnostics of rapid processes 78−47159
submillimetre laser Thomson scatt. system 77−84526
submillimetric-wave laser Thomson scatt. ion temp. diagnostic implementation in Tokamak 80−59301
supersonic jet, ionisation in Mach disc, submillimeter laser interferometry diagnostics 80−14934
survey of laser appls. in metrology *(German)* 77−698
synchronised diagnostic laser pulse system for laser fusion 78−51365
temperature and electron density, determ. by optical density comparisons, at two freq. *(Russian)* 78−22554
temperature meas. on laser heating of solid surface *(Russian)* 78−47172
thermal conductivity, laser-heated plasma, heat-flux limitation, laser-beam scatt. diagnostics 78−18453
thermal ion fluctuations determ. by cooperative Thomson scatt. 77−47254
thermal plasma fluctuations, CO_2 laser scatt., spectrally resolved meas. 77−84504
thermometry, review *(German)* 77−14734
thermonuclear plasmas, HCN CW laser source *(German)* 77−10948
theta pinch, radial oscills. of plasma density and mag. field, light scatt. and probe obs. 80−14937
theta-pinch, D_2 fill in Scylla IV-P, plasma parameters and end-loss 78−1880
theta-pinch, density, azimuthal mag. field effects, laser interferometric meas. 77−11406
theta-pinch, fast, double-frame hologram interferometer meas. of density 79−19097
theta-pinch, post-implosion phase, electron temp. and density meas., mag. field profiles 77−31522
theta-pinch, pulsed, plasma loss from very short pinch 77−89297
theta-pinch, seeded with high-Z elements, VUV, X-ray and laser holography diagnostics 77−35381
theta-pinch plasma, multiple pass CO_2 laser heating, density profile, diagnostics 79−60160
Thomason scattering and refractivity methods 77−35371
Thompson longitudinal scatt., current density meas. in Tokamak-type devices 77−19767
plasma diagnostics by laser beam continued
Thompson scattering diagnostics of low density plasmas, Nd:glass laser system 80−96388
Thomson 90° scatt. system 78−5947
Thomson scatt. apparatus, using laser beam, to determine electron temp. and density in plasma 78−34367
Thomson scatt. diagnostics using optical multichannel analyser 78−67432
Thomson scatt. pathways calibration, rel. to diagnostics *(French)* 80−43886
Thomson scattering, in DITE Tokamak, electron temp. and density, pulsed rube laser 79−10720
Thomson scattering, multi-channel TV apparatus, PLT machine, mech. aspects 78−54932
Thomson scattering, rot. Raman calibration 80−1844
Thomson scattering, triple grating polychromator 77−43059
Thomson scattering from an anisotropic plasma 79−60112
Thomson scattering multipass laser system for Tokamaks 77−76189
Thomson scattering system for relativistic electron beam heated plasma 78−75421
Thomson scattering with high background level of plasma scattering 80−43979
Tokamak, adiabatic plasma compression, impurity spectra and Thomson scatt. *(Russian)* 77−76192
Tokamak, Doublet IIA, temporal and spatial behaviour of plasma props. 77−43030
Tokamak, far IR laser collective scatt. system 80−59300
Tokamak, high-β small aspect ratio, probe and laser beam meas. 77−27733
Tokamak electron density meas., non-interferometric FIR scheme 80−14936
Tokamak magnetic field meas. using laser light scattering 78−34370
Tokamak plasma-wall interaction, appl. of fluoresc. spectroscopy 79−23451
Tokomak plasmas, new developments in laser diagnostics 78−22558
toroidal bicusp (Tormac), plasma containment, props. 77−24159
toroidal controlled fusion poloidal mag. field meas. by far IR Faraday rotation 80−59303
toroidal plasma, modulated submillimetre-laser polarimeter for meas. of Faraday rotation 79−46474
tubular flow reactor, ion density and Z_{eff} profiles, neutral beam attenuation technique 80−6282
turbulence in shock waves, investigation by anal. of scattered laser light 77−3940
turbulence induced by plasma-electric current interaction in focus expt., laser diagnostics 80−24171
turbulence meas. by CO_2 laser light collective scatt. 80−84005
turbulent heating, current penetration and electron temp., Thomson scattering obs. 79−4158
ultra-fast detectors for laser fusion diagnostics, quenched plastic scintillator with microchannel plate photomultiplier 80−74084
Z-discharge plasma, low-temp., time evolution, diagnostics 79−37548
Z-pinch, dense, strong optical attenuation of ruby laser 77−84520
Z-pinch, high density, Schlieren meas. 77−11408
Z-pinch, overdense, He plasma, laser-driven hydrodynamic perturbation, shock density struct. 79−77385
Z-pinch high density plasma, spectroscopic analysis 79−98980
Z-pinch high density plasma spectroscopic analysis 79−98981
Z-pinch plasma, interaction with CO_2 laser radiation 80−48919
Z-pinch ultradense plasma, density dynamics, interferometric meas. 79−77413
Al plasma, laser produced, reflectance meas. 80−79568
Ar arc, high current, interferometric and spectroscopic study 80−59275
Ar arc, plasma parameters determ. by laser scatt. 79−32812
Ar arc discharge, parameters variation during extinction obs. *(French)* 80−19653
Ar discharge, optogalvanic and excited state photoionisation signals, space charge effects 80−14947
Ar, discharge, pulsed, neutron species spatial distrib., laser beam diagnostics 78−38543
Ar discharge plasma laser interferometry 77−19770
Ar, hollow cathode arc discharge, collective scatt. meas., turbulence 80−48978
Ar, plasma, jet, optical studies using Schlieren and shadow methods 80−59279
Ar plasma, shock tube data on radiative cooling, IR laser techniques 78−79472
C arc in air, electron density meas. by CO_2 laser interferometry *(Japanese)* 80−28822
CO_2 1KJ laser system for laser-plasma interaction expts. 78−5502
CO_2 laser, pulsed low-pressure far IR, appls. 80−53332
CO_2 laser beam-diagnostics techniques, laser beam parameter monitoring 80−64089
CO_2 laser light interaction with high temp. plasma *(Japanese)* 79−82101
CO_2 laser system, pulsed, for fusion research 80−58556
CO_2 long-pulse 2 GW single longit. mode source for laser-matter expts. 80−78860
Cu, laser-produced plasma X-ray spectral lines identification *(Chinese)* 80−54036
D_2 plasma, isolated, CO_2 laser-produced, holographic interferometry diagnostics 80−24254
DCN waveguide lasers, optimised 190/195 μm, radiation source for plasma diagnostics 80−99709
D_2O vapour high-power 385 μm laser oscillator 80−69422
Fe-Ar low press. flow discharge, axial density profiles of sputtered cathode atoms 80−49029
H arc, electron density, interferometric determ., refr. index calc. in high press. 80−24284
H arc, laser Thomson scatt., ion temp. determ. 79−23453
H atomic radial profile in FT-1 Tokamak, reson.-fluoresc. meas. 79−90467
H atoms, Rayleigh scatt. from n=2 states, fusion plasma diagnostics appls. 80−43002
H, local population values, reson. laser scatt. *(Russian)* 77−19763
H, plasma, collisional depopulation rate of n=2 level, laser plasma method 78−79463
H^- density measurement by photodetachment 79−73045
H_2 arc plasma, forward scatt. at 10 μm using light mixing to meas. ion temp. 77−89313
H_2, plasma, resonance fluorescence diagnostics 80−48971

plasma diagnostics by laser beam continued
H_2 plasma diagnostics by reson. multiphoton ionis. 80−58640
H_2-He plasma, shock-heated, relax. distance and equilib. electron density diagnostics 77−24180
HCN laser, temporal coherence meas., comparison of TGS pyroelec. detector with W-C point contact diode 80−31871
He (n=3, 4) singlet states quenching by N_2 in low-press. glow discharge 80−49030
He, collisional radiative model, reson. optical pumping, plasma diagnostics appl. 79−37459
He discharge, time-resolved population meas. using N_2-laser-pumped dye lasers 77−80362
He plasma chemical device, integrated electron density meas., interferometric method 79−55548
He-Ne laser and interferometer systems *(Czech)* 80−87941
He-Ne laser plasma, metastable at. and electron density diagnostics 77−84499
Hg vapour discharges, high-press., e-beam initiated, laser absorpt. meas. 80−92412
Mo^{13+}, determination of spectrum using low-inductance spark and laser-produced plasma 80−19610
N^{4+}, electron-impact ionisation rate coeffs. in theta-pinch plasma 79−41878
N_2 arc, plasma parameters determ. by laser scatt. 79−32812
N_2, low pressure discharge, gas temp., laser interferometric meas. *(German)* 79−68951
Na-Ne plasma, near-reson. dye laser scatt. and two-photon absorpt. 77−39459
Nd:YAG laser pulse tailoring/synchronization system for laser-plasma interaction expt. 79−98404
Ne afterglow plasma, 2p levels collisional transfer coeffs., laser excitation obs. 80−43856
Ne discharge, time-resolved population meas. with N_2-laser-pumped dye lasers 77−80362
O^{5+}, electron-impact ionisation rate coeffs. in theta-pinch plasma 79−41878
Xe, s-p transitions, Stark consts. and oscill. strengths, shock tube meas. 80−18822

plasma diodes
Aarhus modified negative ion source 79−81109
anode space-charge sheath characts. rel. to ion source, mono- and duoplasmatron 79−55576
bilateral emission plasmatron as radiation source for spectral analysis *(Russian)* 77−48744
coaxial plasmatron, characteristics *(Russian)* 80−59311
coaxial plasmatron, Cu electrode degradation by arc spot, thermal shock and surface cracks 79−14629
coaxial plasmatron, heat exchange in gas dynamical canal at high press. *(Russian)* 79−68962
collective field accelerator, vac. diode with relativistic electron beam operation 77−24201
collective ion acceleration in diode with insulated anode 80−14005
cylindrical diode, magnetically insulated, cathode plasma props., electron beam prod. *(Russian)* 77−74550
cylindrical for charged particle beam generation and focusing 77−67532
DC melting plasmatron, low pressure characts. *(Russian)* 78−94945
DC plasmatron with axially-blown arc, optimisation *(Russian)* 77−39476
diffusion diode, current oscills., overneutralisation and diffusion instability 77−24199
diode, field-emission type, Thomson-scatt. diagnostics 80−43988
direct extraction H^- sources, prod. and destruction in magnetron and duoplasmatrons 77−23340
discharge, filled with H plasma, intense electron current and secondary plasma formation 79−64929
display devices *(Japanese)* 79−68961
double cylindrical, production of radially convergent proton beam 78−9856
double-focusing, rel. to single-focusing, importance of anode plasma effects 78−91159
Duopigatron metal ion source, currents and lifetime 77−18724
duoplasmatron, discharge plasma, negative ion form. and extraction 77−7511
duoplasmatron, H ion species produced in high current ion sources computs. 77−42209
duoplasmatron, pulsed valve for anode opening 79−68109
duoplasmatron anode plasma, ion temp. 80−6292
duoplasmatron for Ar ion source, props. 78−74523
duoplasmatron hollow cathode ion source, bakeable 77−6602
duoplasmatron ion source, D ion mass, energy, current density distribs. 77−23339
Duoplasmatron ion source, magnetic topography 77−57783
duoplasmatron ion source for secondary ion mass spectrometry 79−85196
duoplasmatron ion source in KEK-PS 77−83390
duoplasmatron pulsed ion source, >1 A *(French)* 77−65374
duoplasmatron sputter source for multiply charged ions from solids 78−66446
electric arc plasmatron for low-press. supersonic plasma jet prod. *(Russian)* 78−14221
electron accelerator, electron beam power increase by inductive accumulator 78−33339
electron accelerator, high current diode, mag. insulation and parasitic current, contraction instability *(Russian)* 77−58906
electron beam diode, repetitively pulsed 79−76164
electron beam transport, beyond diode, Z-pinch plasma 77−87874
electron emission temperature, streaming plasma in laser vac. diode 78−91162
electron flow stability *(Russian)* 78−1906
electron processes, in collisionless diode, linear theory 80−38730
field emission medium energy diode, electron flow, HF oscills. 80−79582
field reversing E-layers, translation and compression in magnetically insulated diode 80−14017
flat, with cathode filament, theory 80−103197
flowing-gas laser plasmotron, expt. and theory 79−27843
foil-less, appl. to rel. beam accel. from pulsar polar cap 80−17604
foilless diodes, hollow relativistic electron beam generation 79−76170
heat flux across plasma diode 77−84542
heat transfer in a plasmotron channel 78−83622
heavy ion collective acceleration at Univ. of Maryland 79−76163

plasma diodes continued
HF plasmatron, electrodeless capacitor, applying refractory dielectric coatings 77−69984
high current diodes, mag. cut-off 77−47276
high current short bremsstrahlung pulse sources 80−5400
high-current diode, ion effects on electron storage *(Russian)* 77−7600
hollow discharge duoplasmatron, H^- source 77−26432
hollow discharge duoplasmatron H^- energy spectra 77−79490
HV vac. diode, electron beams, numerical anal. 77−27748
inert gas duoplasmatron, ion source 80−32560
intense relativistic electron beam, $\nu/\gamma \sim 1$ diode characteristics 77−15249
ion diode, intense, mag. insulated, design review 78−9857
ion diode, intense, mag. insulated, ion beam focusing, particle diagnostics 78−9858
ion sheath motion, computer simulation 77−15207
Lambshift polarised H^- and $^2H^-$ source at Giessen polarisation facility 77−65372
large aspect-ratio terawatt diode with heated and unheated anode, electron and ion current flow 79−10675
light gate, prevention of laser damage by back-reflected light 78−87057
Luce diode, acceleration mechanisms in single and multiple stage collective vacuum diodes 79−76168
magnetically insulated diode, coaxial geometry, one-, two-species equilib., electron and ion flow 77−58905
magnetically insulated diode, controlling hollow electron beam current with shielding beam 80−9437
magnetically insulated diode, hollow electron beam pot. 80−70046
magnetically insulated diode, superdense MeV proton beam generation 80−14017
magnetically insulated diodes for prod. of intense proton beams 80−14004
magnetically insulated ion diode, ion beam diagnostics 80−48974
micropinch in a high-current diode, review 80−103183
Multiduoplasmatron, Multiduopigatron, ion *(French)* 78−26348
negative ion high current beams, source plasma parameters determ. 77−83376
neutral beam injectors, fast, for TFR 77−76140
particle beam interactions with plasma, inertial fusion appls. 80−59250
Periplasmatron, ion source for neutral beam injection systems 78−54915
periplasmatron, neutral beam injectors, multi-aperture extraction systems 80−42301
pinched beam diode, geometrical focusing of intense ion beams 78−58898
pinched electron beam diode, ballistic focusing of intense neutralised ion beam 78−9859
pinched electron beam diode, proton current density meas. using biased charge collecting probe 77−55166
pinched relativistic electron beam diode, large ion current meas. 77−31428
planar, electron beam instabilities, finite ion mass and electron velocity spread effects 77−31483
planar diode in self-pinch mode, production and focusing of intense ion beam 77−24206
plasmation, high-power elec. arc AC generator, phys. processes and parameters 80−19623
plasmatron, 2 MW, for generation of high-press. high-temp. hydrogen flows 77−58904
plasmatron, coaxial, transversely blown electric arc *(Russian)* 80−24265
plasmatron, discharge stabilised, by gas blown through porous wall 80−75105
plasmatron, electric arc fluctuation with vortical arc stabilisation *(Russian)* 78−30493
plasmatron, high freq. torch discharge calcs., burning regimes *(Russian)* 80−38723
plasmatron, high-temperature arc heating of gas *(Czech)* 79−68958
plasmatron, industrial *(Russian)* 78−30492
plasmatron, linear, 3-phase, current and voltage characts. *(Russian)* 77−84535
plasmatron, vortical, HF temp. fluctuation obs. in N_2 plasma stream, holographic interferometry 77−43068
plasmatron as thermionic energy converter 77−84537
plasmatron channel, spatial-temporal pulsations of arc plasma pinch 80−24210
plasmatron channel arc, laminar axial core flow, strong localised disturbance effect 78−91178
plasmatron discharges, pretreatment of metallic substrates improved for vacuum deposition 78−76604
plasmatron for semiconductor surface treatment *(Russian)* 79−77428
plasmatron gas average enthalpy, forced heat exchange calcs. *(Russian)* 80−38724
plasmatron heater, use in apparatus for high-temp. gas flow meas. *(Russian)* 77−39368
plasmatron melting arc in Ar and CO_2 atmosphere, performance characts., MHD calcs. *(Russian)* 80−38573
plasmatron spray, parameters meas. *(French)* 77−35402
plasmatron with arc chamber of variable radius, characts. meas. 77−35407
plasmatron with interelectrode insert, characts. 80−44009
plasmatron with interelectrode insert, output electrode turbulent heat transfer 78−71555
plasmotron, capacitative, optimisation 79−55568
plasmotron, thermal and elec. characts., depend. on channel radius and flow 78−1910
plasmotron, two-jet type, thermal and V-I characts. 78−55757
Poisson-Boltzmann eqns. soln. using stochastic transport theory *(Russian)* 77−84533
proton intense beam production, ~1 MeV, pinched electron-beam diode 77−10521
pulsed ion diode, self mag. insulation 77−65918
pulsed mag. diodes for intense ion beam prod. 77−71707
reflex diode, relativistic electron beam, enhanced deposition, mag. and elec. fields effects calcs. 77−31491
reflex triode system for generation of intense magavolt proton beam 77−24203
relativistic diodes, time depend. ion and pinched electron flow, computer simulation 77−89330
relativistic electron beam, diode compression 77−24197
relativistic electron beam, kinetic energy conversion to EM energy 78−1915
relativistic electron beam, propag. in air, exploding beam preformed plasma column 77−87875

plasma diodes continued
relativistic electron beam diode, annular cathode, pinching rot. and reflexing in axial mag. field 78−9860
relativistic electron beam diode, anode scatt. effects on electron pinch radius 77−68877
relativistic electron beam diode, low impedance, pinch profile, X-ray diagnostics 77−24207
relativistic electron beam diode, medium current 77−46443
relativistic electron beam diode, pinched, particle simulation code and ion current reduction 77−68878
relativistic electron beam diode, use of plasma-filled fast-opening switch 77−47275
relativistic electron beam diodes, closure vels. and bipolar flow, B_z mag. fields 77−89331
relativistic electron beam diodes, time depend. effects, emission schemes 77−89329
relativistic electron beam focusing using axial loads 78−18464
relativistic electron beam oscill. diode, ion beam production 78−9861
relativistic electron beam pinch formation in low impedance diodes 77−72510
relativistic electron beams in conical diodes, flow meas. 79−77416
RF plasmatron with external electrodes and longitudinal forced gas flow 77−19778
ring gap plasmatron for high rate sputtering 77−40368
slot-shaped erosion plasmatron for spectroscopy of low-temp. plasma 79−94821
space charge limited current flow in coaxial cylinders, potentials up to 15 MV 77−39477
spherical diode, ion beam production and focusing using self-pinched electron flow 77−24205
spherical magnetically insulated diode for production of intense focused ion beams 79−85200
stability criterion, numerical anal. of one-dimens. Knudsen plasma nonlinear oscills. 78−79433
symmetric double diode, time depend. theory and computer simulation of electron and ion flow 77−24065
thermal cathode, emission cooling *(Russian)* 80−54052
thermal plasma engineering in metallurgy, inorganic materials technology 78−3070
thermionic convertor, ignited noble gas triode, arc drop elimination 77−24213
thermionic convertor, long, cylindrical, current density distrib. 78−71552
thermionic diode, cylindrical current-density distrib. 78−79479
thermionic diode, ignited mode, interelectrode space and sheath anal. 77−24212
thermionic diode, wall-to-wall theory, sheath anal. 77−24211
transformer plasmatron design *(Russian)* 78−14222
two-stream plasmatron flow structure obs. and optimisation 78−71556
two-stream plasmatron for treating dispersed materials *(Russian)* 78−22575
X-ray source, high power microsecond electron beam 80−52378
Ar ion duoplasmatron source, new target ion source system for short lived nuclei meas. 78−66449
Ar, plasma, ion energy level populations in crossed elec. and mag. fields 78−67428
Ar-air, transformer plasmatron, LF discharge, electrical and energy props. 80−103200
Cs diode with W emitter, current oscills. at low emitter temp. *(Russian)* 78−5952
Cs plasma in vacuum diode, pre-discharge, electron impact excitation line emission polarisation 78−47170
H^+ beam, 0.5 TW pulses, production with spherically focusing mag. insulated diode 79−31288
H_2 monoplasmatron arc plasma, electrokinetic parameters space distrib. *(Russian)* 80−53925
I^- beam, duoplasmatron ion source for SIMS, Ar-I_2 medium 77−18123
W multicavity cathode operation 78−75433

plasma filled waveguides
Alfven waves, torsional, axisymmetric, discrete/continuous spectra, appl. to waveguide 78−59587
antenna system, radiation from plasma column in glass tube excited by waveguide 79−50860
beam-plasma interaction, in plasma filled waveguide in axial mag. field 79−41841
beam-plasma interaction, in plasma-filled waveguide, beam geometry and mag. self-field effects 79−41842
beam-plasma system in waveguide, EM modes excitation 78−1844
Cerenkov instabilities spectra, of relativistic electron beam, in bounded anisotropic plasma *(Russian)* 78−38506
circular waveguide, hot-beam plasma interaction finite geometry effect, quasistatic approx. 77−51200
coaxial plasma waveguide system, (m=1), EM wave propag. and absorpt. 77−89263
coherent microemission excited by relativistic electron beam in solid-state plasma *(Russian)* 77−15205
collision freq. effect on parallel plane waveguide 78−14176
collisionless, dispersion relations *(Chinese)* 77−58865
collisionless plasma, microwave electron acceleration, waveguide obs. 80−43932
column waveguide, time varying, laser beam propagation 78−94916
confinement by high power excitation 77−31497
corrugated, relativistic electron beam interaction, combined reson. *(Russian)* 80−10394
cyclotron maser, high-current and plasma filled, theory 78−17890
cylindrical waveguide filled with uniaxial, collisional, hot and moving plasma, dispersion for TE and TM modes 80−106934
diffraction radiation characts. of an open conducting periodic struct., temp. and elect. conc. determ. *(Ukrainian)* 80−70004
discharge, UHF, propag. at reduced press. *(Russian)* 79−99008
discrete modes of a system subject to an inhomogeneous, high-frequency force 80−43237
dissipative instability in plasma waveguides with diffuse boundaries *(Russian)* 77−15212
electron beam excitation of surface oscillations in plasma in metal cylindrical waveguide *(Russian)* 77−39431
electron beam interaction, nonrelativistic, modulated, fast EM wave conversion, in waveguide 77−84455
electron beam interaction, spatial evolution of complex EM modes, collision effects 79−14556
plasma filled waveguides continued
electron beam-slow wave interaction in plasma filled waveguide, signal spatial evolution 77−11362
electron beams, interaction with bounded magnetised plasma *(Russian)* 78−59624
electron nonlinear waves in strongly magnetised plasma 80−79472
electron plasma, war, isotropic, drifting, waveguide modes, relativistic electrodynamical study 79−77393
electron plasma waves in cylindrical waveguide 79−4134
electron wave, guided, on planar plasma slab, propag. and attenuation characts., dissipative processes 80−38608
EM wave amplification, electron beam-plasma interaction *(Russian)* 77−68801
EM wave cyclotron absorption in plasma-filled waveguide in nonuniform mag. field 78−51315
EM wave excitation by tubular electron beam in plasma-filled waveguide *(Russian)* 79−37507
EM wave freq. spectra dispersion eqn. numerical anal., relativistic electron beam interaction *(Russian)* 78−59605
EM wave propagation, effect of inhomogeneities 80−19585
EM wave resonance tuning of magnetoactive plasma *(Russian)* 80−83914
enhanced radiation beams from three annular plasma layers coaxial line excitation 80−53996
experimental simulation 79−23427
field config., charge density wave and internal wave *(Russian)* 77−3924
fusion plasma, RF phased waveguide heating, thermal eddies form. 80−24193
Grill phase tracking during density increase in Tokamaks 80−28762
guided electron plasma waves, propag. along cylinder, dissipative processes effects 80−92332
harmonic generation at microwave frequency in bounded magnetoplasma 80−48897
high power level plasma waveguide mode excitation 79−41839
hot collisional uniaxial plasma, guided waves, TM mode dispersion rel. 80−53995
ICR heating in T-10 Tokamak under weak dissipation conditions 80−28759
ICRF heating in Macrotor Tokamak 80−28744
impedance of magneto-acoustic wave launching antenna 80−24180
ion acoustic wave, excited by EM rad. press. 78−26298
laser beam in plasma waveguide, absorpt. effects, normal mode anal. 79−64871
laser beam propagation in plasma waveguide, normal mode anal. of oscillating Gaussian soln. 79−4145
linear accelerators, plasma waveguides appl. as accelerating structures 80−9438
lower hybrid region, antenna impedance 80−28664
lower hybrid reson., slow TM mode excitation by antenna waveguides *(Russian)* 77−47227
lower hybrid self-trapping at RF gas breakdown 80−38850
lower hybrid wave heating in JIPP T-II 80−28722
lower-hybrid waves, focusing and channelling during HF-breakdown of gas *(Russian)* 80−106890
magnetic-insulation wave front struct. 79−55517
magnetised plasma filled open periodic waveguide kinetic theory of reson. radiation *(Ukrainian)* 77−51197
magnetised plasma loaded waveguide, interaction between solitary structures 80−38661
magnetoplasma column in waveguide, wave packet bifurcation 77−7556
MHD m=0 torsional waves, propag. and interaction 77−65850
microwave cavity, partially filled with temp.-anisotropic uniform hot plasma, eigenmodes 78−75362
microwave discharge, fast wave emission diagnostics 80−92391
microwave excitation by electron beam in plasma-filled waveguide 77−47224
microwave harmonic generation in plasma-filled waveguide 80−1798
microwave induced steady-state overdense plasma production, near coaxial discharge dipole reson. 79−55523
Microwave reflexion in rectangular waveguides by high pressure RF plasma columns 80−43975
modes of warm transversely-drifting electron plasma in strong mag. field 79−50861
multilayered plasma columns excitation with mag. current ring, radiation pattern 77−7557
negative mass instability, nonlinear development, effect on intense microwave generation 78−75285
nonlinear distortion of amplitude-modulated microwave 80−28683
nonlinear electron plasma waves in magnetised plasma waveguide 80−38662
nonlinear EM wave propag. 77−991
nonlinear lower-hybrid waveguide in plasma, stability 80−19578
nonlinear wave attenuation, excited by monochromatic electron beam *(Russian)* 77−47220
open plane periodic waveguide, reson. emission of magnetised plasma 78−26299
parallel-plate, excitation analysis 77−62371
parametric decay spectrum of heating near LH frequency in Petula 80−28761
parametric instabilities of waves in bounded magnetised plasma 77−68772
ponderomotive craters, in phased waveguide array plasma, form. by microwave irrad. 80−83885
potential oscillations excitation with electron beams 78−30419
power flow in relativistically moving anisotropic warm plasma filled waveguide 78−55725
power reflection, transmission and absorption coefficients for a moving plasma slab in a rectangular waveguide 80−106925
propagation and attenuation characts. 78−67367
quasi-longitudinal waves, excitation in magnetised plasma waveguide by electron beam 78−87462
radiation from waveguide, rel. to plasma wave scatt. by ion-acoustic oscills. 80−87886
radiation pattern of open ended waveguide in air core surrounded by annular plasma column 78−67366
rectangular, nonlinear mixing of microwaves 79−77394
relativistic electron beam injection into waveguide, charge and current neutralisation *(Russian)* 78−26301
relativistic electron beam interaction 78−5879
relativistic electron beam interaction in bounded plasma *(Russian)* 78−26300

plasma filled waveguides continued
relativistic electron beam reson. interaction, induced field dynamics *(Russian)* 78−59616
relativistic electron beam/electrostatic wave interaction 78−75375
relativistic electron beams in plasma-filled waveguide, microwave radn. generation *(Russian)* 79−14566
resonance cone reflection and plasma-filled waveguide modes 78−67365
resonator, electron-beam excited, explosive instability 80−28693
reversed field configuration plasma in metal tube, induced by relativistic electron beam 78−91114
RF coupling gaps, mutual interaction 77−58867
RF emission, plasma wave scatt. by ion-acoustic waves in nonequilib. plasma 80−64733
self-influence of magneto-acoustic waves in a plane plasma waveguide *(Russian)* 79−41815
slow surface wave propag. in solid-plasma waveguide effect of dielec. material 79−50862
slow wave excitation, by relativistic beam, in waveguide 77−11364
slow-fast mode conversion effect on lower hybrid slow mode excitation 80−28668
solitary structures in magnetised plasma loaded waveguide 80−48878
soliton propag. and deformation in magnetised plasma filled waveguide, modification by reson. particles 79−77395
temporal development and properties, of microwave produced overdense plasma in coaxial discharge 79−55565
TM modes in lossy plasma filled waveguides 79−23423
TM modes propag. in parallel plane waveguide filled with moving collisional plasma 79−82072
two-stream instability, nonlinear evolution, numerical simulation 80−43938
UHF discharge with preliminary locally ionised gaseous medium 80−38851
uniaxial anisotropic relativistic warm plasma, EM wave propag. and attenuation 80−59246
warm moving plasma in plane parallel waveguide, TE modes 77−80314
wave heating at electron cyclotron harmonics in toroidal plasmas 80−28727
wave propag. in hot collisional plasma filled waveguide 80−92331
wave radiation by oscillating electric dipole in moving warm plasma 80−87868
Woods' MHD waveguide, guided modes, locally excited MHD waves, wave eqn. 77−51199
H, ACT-1 toroidal plasma, externally launched ion Bernstein wave 80−106967

plasma flow
see also plasma focus; plasma magnetohydrodynamics
ablation by laser, front structure, numerical hydrodynamic-heat flow simulation 79−64883
ablation due to supersonic flow, electron heat transfer mech. 78−71496
ablative acceleration of laser-irradiated thin-foil targets 79−71952
acceleration, velocity, meas. method for solid particles *(Russian)* 78−94903
acceleration in nonuniform mag. fields 77−58849
acceleration of plasma formed by relativistic electron beam 77−27657
accelerator, electrodynamic, modulated, optimum operating conditions 77−27749
accelerator, linear rail type, plasma cluster ionised front vel., theory 79−46494
accelerator, stationary erosion elec. arc type, with mag. cathode spot confinement, flow *(Russian)* 79−98996
acoustic instability of flow in MHD channel 79−64842
air discharge, turbulent flow stabilisation effect *(Russian)* 79−99010
air flow glow discharge, voltage, current oscills. 79−55585
air wake, hypersonic, electron recomb., temp. depend. meas. 79−27834
air wake, hypersonic, ionised, free electron attachment coeff. meas. 79−27835
Alfven and magnetoacoustic vortices *(Russian)* 77−80302
anisotropic plasma dynamics, uniqueness theory 78−79415
Ar, plasma rotating, weakly ionised, diagnostics 79−82122
arc discharge, flow vel. meas. using laser Doppler velocimetry 77−80360
arc lamps, Hg vertical, Hg plus I, metal halide, convection effects study 80−6299
arc nozzle clogging theory 80−38791
arc plasma flow, velocimetry methods 80−43992
arc plasma flow-cold electrode gap, electric breakdown *(Russian)* 78−34280
arcs, wall-stabilised, free recovery with imposed laminar and turbulent flows 80−59321
Astron type equilibrium in absence of applied mag. field 79−64899
astrophysical plasma, highly ionized, ionization equilib. validity 80−21906
atmospheric pressure plasma flow, boundary layer charged particle density profiles 80−38571
atomic O, form. and recomb. in U-tube downstream from DC discharge 78−67333
auroral arc, energy source for electron accel. and field-aligned currents 77−9593
auroral plasma, turbulent acceleration by electrostatic waves *(Russian)* 80−53952
backflow of quasiparticles, dynamics of one-component plasma 79−27614
barycentric velocity, time-of-flight mass spectrometric meas. 77−43063
beam-plasma discharge, in supersonic gas jet flowing into high vacuum *(Russian)* 79−55583
Bohm-type thermal losses from high-β plasma 80−38679
boundary acceleration in intense UV radiation field *(Russian)* 77−35334
boundary layer flow, past heated cylinder, in radial mag. field *(Russian)* 77−47170
bunch enlargement in vac. *(Russian)* 80−83907
Buneman-Farley instability, nonlinear decay interactions 80−38616
capillary charge torch, flow deflection mechanism *(Russian)* 78−83539
capillary discharge, with evaporable wall, plasma parameters axial distrib. *(Russian)* 78−75280
capillary discharge with vaporising wall, plasma parameters axial distrib., model 79−64943
centrifuges, fluid flow analysis, third-order differential equation solution *(Japanese)* 80−53949
Cerenkov instability of nonuniform flows *(Russian)* 78−26263

plasma flow continued
channel flow, coaxial, compressive, viscous, thermal and elec. cond. effects *(Russian)* 77−3927
charged particle acceleration in finite temp. plasma *(Russian)* 77−51163
charged particle propag. in parabolic intensity profile laser beam, isotope separation appl. 79−54984
coaxial channel flow of accelerators and compressors, two-dimens., simulation 80−19566
collisionless flow and end loss from a high-energy theta-pinch plasma 80−92365
collisionless flow of unmagnetised plasmas around extended bodies 78−79416
collisionless plasma, expansion into vac., ion accel., instability devel. electron heat flow 80−38575
collisionless plasma expansion into a vacuum, particle simulation 79−82054
collisionless plasma in curved mag. field 78−67329
collisionless plasma motion in gasdynamic approx. 79−27756
collisionless shocks, ions nonfluid behaviour at high Mach numbers 80−90330
column rot. and particle transport, travelling EM wave and neutral beam heating *(Russian)* 79−27798
compression of superdense eqn. of state and boundary press. profile, simulation 78−83589
computer models 77−76045
conducting gas flow in high current electric arcs, calc. methods and numerical anal. 79−90478
constricted glow discharge in transverse air flow 80−24278
continuous flow pinch, single-fluid one-dimensional radial compression theory 77−3975
continuous optical discharge, diagnostics 80−43947
continuous optical discharge convective flow, thermogasdynamic instability 78−75397
convective cell formation and EM drift wave turbulence 80−24168
converging shock and thermal waves, numerical study 77−62282
Coriolis forces, effect on Hall currents and Rayleigh-Taylor instability 79−41809
critical surface, enhanced stimulated Brillouin scatt. due to light refl. 80−1750
current shell axial motion in plasma focus 77−7517
curved plasma optical system, plasma stream transport *(Russian)* 78−87439
cyclotron instabilities of streams, Nyquist criteria *(Chinese)* 79−73001
cylindrical conducting body, supersonic plasma cross-flow, stagnation region meas. 79−32810
deflagration wave, in laser compression 79−23419
dense plasma, coaxial acceleration and plasmochemistry *(Russian)* 78−92482
density plateau effect on inverse bremsstrahlung 80−43894
diagnostics using Al, Cu, Si, blistering by plasma focus discharge deuterons anal. 77−35351
differential charging and sheath asymmetry of nonconducting spacecraft due to plasma flows 79−12378
differential ion flux vector meas. technique 78−18459
diffusion in toroidal traps, anomalous electron viscosity *(Russian)* 80−48956
diffusion reduction by plasma rotation and ion dissipative effects 80−38696
discharge, flow patterns, rot. forces, numerical anal. 78−34380
discharge in air, pulsed, high-current, channel temp. profile 77−27768
discharge tube shape, flow velocity, effect on electron temp. of medium pressure positive column 79−64941
discharge under transverse convection conditions 80−24272
double probe theory for a low-density flowing collisionless plasma 79−37470
drift motion, in curved mag. field, conducting boundary effects 77−47174
drifting magnetoplasma, new interf. pattern near reson. cones 77−35398
EHD of three component medium with shock waves, unidimens. flow *(Russian)* 77−35250
eigenvalue problem for Lagrangian systems 77−49601
electric fields and currents in plasma for flow in space-periodic mag. field *(Russian)* 77−47172
electromotive force generated by driven plasma motions 77−19680
electron acceleration to mildly relativistic energies by strong turbulence 77−31437
electron cloud, thermalised, expansion 77−7516
electron directed velocity meas., optimised method using laser scatt. incoherent regions 80−79561
electron plasma with zero temp., fluid mechanics eqns. invariant solns. 79−90272
electron-ion plasma, equilib. and stratification in gravit. field *(Russian)* 79−29988
electron-ion turbulence in collision-dominated regime, ionospheric turbulence meas. appl. 79−48605
electrostatic energy analyser, data interpretation 78−42813
electrostatic probe continuum plasma, stagnation pt. current collection, numerical calc. 77−3989
electrostatic stagnation point probes in flowing plasma, Knudsen no. effect 78−1893
EM field induced resultant drift inwards from boundary, in D-T plasma 80−38577
EM radiation from line source in moving magnetoplasma sheath, saddle point approx. 77−51189
EM wave interaction, density profile steepening at reson. absorpt., hydrodynamic model 79−46434
emission from hypersonic plasma-plane obstruction zone *(Russian)* 77−84449
entrainment of weakly-ionised plasma by rot. EM field *(Russian)* 77−19679
expanding into vacuum, bremsstrahlung radiation intensity *(Russian)* 79−7448
expanding laser-produced plasma, radiative transfer line intensities and stimulated emission 77−3988
expansion in vacuum, recombining plasma temp. and electron density time depend. 77−24064
expansion into vacuum, ion acceleration 80−6228
expansion of exploding plasmas, multiple-bounce and snowplough models 78−34281
expansion of gaseous plasma 79−46437

plasma flow continued
expansion of nonneutral plasma into vac. 79−77350
fast electron production in plasma jet, suppression in laser-plasma *(Russian)* 79−14583
flows with higher-order eqns., MacCormack's method extension 79−3987
flush probe studies of plasma flow over flat plate 80−24147
flux anisotropies in guiding centre plasma 79−50850
focusing in axially symmetric mag. field *(Russian)* 78−1809
free-burning arcs, simple theory 80−6297
fusion reactors, divergent impulsive crossflow over packed columnar arrays 80−47702
gas, optical breakdown in intense annular beam from CO_2 laser, flow-concentration effects 79−64886
gas discharge, perturbation by longitudinal turbulence 80−24271
gas flow, nonequilib. ionisation and Hall EMF 80−69981
gas stream with dispersive impurity, initial region boundaries, impurity velocities *(Russian)* 80−100069
gas-discharge plasma, in axisymm. mag. field, plasma flow diagnostic meas. 77−35419
generator arc chamber, hydrodynamic struct. 80−1817
glow discharge, high press. probe meas., current-voltage characts. 79−90466
guiding centre orbits and topology of noncircular axisymm. Tokamak plasmas 80−6227
heat exchange of low-temp. plasma with wall, longitudinal mag. field effect 80−33781
heat transfer in flowing low-temperature plasma, theory 79−72991
heat transfer in interaction of electric arc with longitudinal gas flow 77−11189
HF one-dimens. motion, symmetry 77−35333
high current arc, turbulence 78−47197
high density directed plasma, source, design, characts., numerical model 80−38538
high temperature gas flow, electric-arc heater apparatus *(Russian)* 77−39368
high-current free-burning arcs, magnetically-driven plasma flow model 78−71588
high-temperature MHD generator, shock tube plasma source 77−35372
highly-ionised positive column under free-fall and ambipolar diffusion conditions 78−67490
hollow electron beam pot. in magnetically insulated diode 80−70046
holographic interferometry system for plasma flow phenomena, Ba II ion density meas. 78−55751
hydrodynamic Cherenkov instability, electron flow-surface wave interaction *(Russian)* 77−72440
hydrodynamic eauation for weakly coupled one-component plasma 79−90390
hydrodynamic stability near front of thermal wave 77−80283
hypersonic plasma streams, microwave emission obs. 79−14617
implosion, ablative, laser driven, struct. and scaling laws from stationary flow model 77−43008
implosion heating, numerical modelling of Los Alamos expt. 77−43056
impurity diffusion, in Pfirsch-Schluter regime, suppression by plasma rotation *(Russian)* 79−98867
impurity separation, in channel of magnetoplasma compressor, numerical investig. *(Russian)* 79−37467
impurity transport, neoclassical theory 79−98873
instability near pipe wall, ref. to MHD generator 77−35330
interplanetary space, collisionless hydrodynamics rel. to Larmor freq., plasma flow around planets 78−69637
ion acoustic wave propagation, electron-ion plasma, Grad's thirteen moment approximation 79−50857
ion beam extraction from flowing plasma 80−18044
ion beam generation increase through moving plasma boundary 80−63439
ion flux in glow discharge, ≤1.2 kG field, double probe meas. effects *(German)* 77−31534
ion source, high current, plasma supply to extraction region, theory and expt. 80−14023
ion velocity distribution, in rot. plasma, Doppler broadening meas. 79−50894
ion-acoustic turbulence, in rarefied plasma flow, Langmuir probe meas. *(Russian)* 79−55547
ionised gas, nonequilibrium, supersonic, corner expansion flow, physical aspects 80−1639
ionised gas flow, magnetohydrodynamic, supersonic, struct. rel. to mag. field *(Russian)* 77−27656
ionised mixture, dense, binary, dynamical props., statistical mechs. 80−43895
ionosphere, plasma flow, var. in topside and F-layer, ionospheric-protonospheric interaction model calcs. 80−4180
ionosphere, simulation of satellite flight using synthesised plasmas *(French)* 78−16269
ionosphere and magnetosphere, adiabatic potential transitions properties in polar regions 79−5713
ionospheric rocket-borne mass spectrometer, Monte Carlo prediction of +ve ion collection 80−8459
isotropic inhomogeneous moving plasma column, cross polarisation of scatt. EM waves 79−98917
jet, supersonic, vel. meas. using Doppler shift *(French)* 78−14207
jet, swirled, natural gas injection effect on temp. and vel. fields 79−90473
jet mixing with surrounding gas, effect of sound radiation 79−82053
JIPP T-II tokamak plasma, Mo impurity diffusion during H_2 gas puffing 80−28602
laminar stead state flow, vel. meas. using total-head pressure probe 77−43060
laser, recombination dynamic H plasma, freely expanding, from supersonic nozzle 77−19240
laser beam ablation characts., flat target, steady-state model 77−68839
laser created plasma, ponderomotive force, mag. fields and hydrodynamics *(French)* 77−80281
laser irradiated plasmas, flow effects on density profiles 78−18429
laser light reflection enhancement from expanding laser prod. plasma, Brillouin scatt. 77−3963
laser plasma, Langmuir probe meas. of parameters and expsn. 78−18456
laser plasma expansion and rethermalisation in uniform mag. field 78−30458
laser produced plasma, extreme UV line profiles of expansion profiles 78−14199
laser produced plasma, transition from isentropic to isothermal expansion 80−92279
laser produced plasma expanding into mag. field, oscill. modes 77−51178
laser produced plasma expansion, ion emission, hot, cold electron density, temp. ratios 78−71513
laser produced plasmas, self-consistent profile modification in underdense region 80−75038
laser supported absorption waves, momentum transfer to surface, flowfield model 80−14921
laser-driven fusion, validity of hydrodynamic approximation 80−75087
laser-fusion regime, plasma transport, extension of Braginskii system of fluid equations 80−53935
laser-generated, ion beam production from interaction with Nd:YAG laser radiation bursts 80−106939
laser-induced plasma expansion, radiation press. effects, self-similar model 79−94778
laser-irradiated solid target, nonlinear dynamics 80−28767
laser-produced plasma, hydrodynamic stead-state solns. in planar geometry 79−37522
laser-produced plasma, light press. effects, steady-state mdoel 77−47234
laser-produced plasma, microsphere implosion, symm. and stability of thermally generated mag. field 77−24118
laser-produced plasma ejection from thin capillaries, expt. 78−75395
layer expansion near barrier irradiated by laser in high density gas 80−70016
linear gasdynamic confinement system 80−48957
low density magnetised plasma wake, perturbations 79−41808
low-density plasma, deionisation between electrodes, pot. difference effects 77−51162
low-energy electron microsecond pulse prod. from dense plasmoids 79−90476
low-temperature plasma jet, vel. meas. by obs. brightness inhomogeneities 77−43062
macroparticles elimination from plasma stream, using curved plasma duct 80−33826
magnetic barrier, stationary flows *(Russian)* 77−11326
magnetic field formation, by hydrodynamic motion or ion beam deceleration *(Russian)* 78−38464
magnetic mirror, injected plasma particle refl. (trapping), quiescent (turbulent) plasma 80−48955
magnetically confined plasma, numerical computation 77−80282
magnetically insulated diode, coaxial geometry, one-, two-species equilib., electron and ion flow 77−58905
magnetised, expanding, gaskinetic press. 77−45394
magnetised plasma interaction with neutral gas, threshold vel. 80−59241
magnetized sphere interaction with supersonic plasma flow 78−59608
magnetoacoustic disturbance, hydrodynamic instability in nonuniform plasma flow *(Russian)* 80−1766
magnetoplasma compressor, operating modes, pinch description 77−84531
magnetoplasma compressor, operating modes, probe diagnostics 77−84530
magnetoplasma compressor compression region struct. streak and framing camera diagnostics 77−84532
magnetosphere interaction with plasma flow, review of studies 78−65496
mass separation in rotating weakly ionised plasma *(Russian)* 80−1745
merging of magnetic fields with field-aligned plasma flow components 78−79417
metal surface, high-intensity laser beam interaction 80−19600
metal target interaction, plasma stream, boundary layer struct., particle diagnostics 77−76106
metal target interaction, plasma stream, boundary region optical diagnostics 77−76107
metallic atoms separation in rot, plasma, spectral meas. 79−98988
MFTF, plasma streaming system, description 80−91280
MHD conversion channel, anal. by finite difference method 78−22470
MHD convertor channel flow 80−24261
MHD generator, combustion-driven, boundary-layer profile meas. 77−24194
MHD generator channel, turbulent MHD boundary layer 77−43085
MHD instability of laminar plasma stream *(Chinese)* 79−73002
MHD radial channel flow, in 2-dimens. mag. field, numerical simulation *(Russian)* 77−47171
microwave beam interaction, intense, with low temp. plasma flow, space distrib. 80−38578
microwave flowing plasma source, power absorpt. characts. 77−84464
momentum transfer, driven by fusion-generated alpha particles 79−14592
moving cold magnetised plasma, wave propag., polarisation relations and dispersion eqns. 80−64723
moving plasma, four-dimens. constitutive relations 79−37537
moving plasma in an electric shock tube with pulsed gas injection 79−77355
multi-component plasma dynamics in coaxial accelerator *(Russian)* 78−22576
multispecies flows, transport eqns. mathematical struct. 78−47084
multistreaming, fluid codes viability 77−15173
nonequilibrium gas relaxation in supersonic nozzle, analysis method 80−74941
nonequilibrium ionised boundary-layer flow, numerical anal. 77−11324
nonequilibrium plasma flow, wave conversion to EM radiation 78−75281
nonlinear interaction, electron collision freq., self-consistent eqn. *(Russian)* 80−75055
nonlinear interactions and hydrodynamics in HF field *(Russian)* 80−53951
nonneutral plasma expansion 78−9766
nozzle boundary layer equations for laser heated flow, similarity soln. 77−31355
numerical methods in fluid dynamics, conference, Tbilisi, USSR (June 1978) 80−17717
orifice flow, wall interactions in mol. flow regime, for diagnostics 79−23449
parametric instability stabilisation in nonstationary plasma *(Russian)* 78−1831
partially ionised gas flow over body, plasma form. at surface 78−75378
particle interactions in turbulent plasma flow on surface-melted substrate *(Russian)* 77−31482
photoabsorption convection in horizontal tube, unsteady-state convection, num. investig. 80−33594

plasma flow continued
plasma dynamics, Soviet literature growth and duplication parameters *(Russian)* 80−59191
plasma stream, magnetized, simulation of plasma flow over object 79−10679
plasmatron, discharge stabilised, by gas blown through porous wall 80−75105
polarisation of picosecond excited continuous X-ray radiation *(Russian)* 80−59190
poloidal rotation velocity determ. in FT-1 Tokamak *(Russian)* 80−19565
positive column, hydrodynamic contraction due to longitudinal turbulent flow 78−67510
positive columns composed of mixed ion plasma, general ambipolar diffusion theory 78−94897
Princeton Large Torus, unbalanced neutral beam injection, toroidal plasma rot., Doppler shift meas., confinement times 79−77400
probe, elec. highly negative, in flowing continuum plasma, ion sheath 77−72493
probe meas. of flow over flat plate 80−1845
production and flow of plasma in ion beams 80−28624
pulsed erosion jet, energy characts., heat flow distribution *(Russian)* 80−33825
pulsed laser-generated impulse on a surface in supersonic flow 80−48917
quasistatic compressional flow, arbitrarily low rate, plasma parameters temp. depend. 77−27658
radiation induced shock tube flow nonuniformities in ionising Ar 80−43865
radiation pressure dominated plasma flow 80−1763
ram effect for conducting cylinder in drifting plasma 80−54029
rarefied electron-ion plasma flow around point charge, particle distrib. function and density 78−26256
rarefied plasma flow, degree of nonisothermality, probe meas. 80−24243
rarefied plasma flow, external mag. field effect on electrostatic field struct. in wake of disc. 79−10648
rarefied plasma flow around bodies, ion density computation accuracy 79−50849
rarefied plasma flow around body, electrostatic field struct. in wake 77−91402
relativistic electron beams, laminar flow equilib. 77−51224
relativistic streaming plasma, generalised Ohm's Law, pulsar magnetosphere relevance 78−9823
resistive hose instability in relativistic electron beam 80−67947
resonance absorption, self-consistent density profiles for obliquely incident light 80−64758
resonant optical schlieren system for plasma flow studies 78−5940
RF medium pressure flowing positive column plasma, electron temp. 78−59549
rocket engine, laser evaporated target, nozzle for impulse augmentation 79−23439
rotating, nonlinear wave interaction 79−60123
rotating critical vel. plasma, particle vels. obs. 77−65846
rotating plasma, charge exchange neutrals, spectrum 80−38706
rotating plasma, spatial distrib. derivation, ionic components in reson. ionic cyclotron instability *(Russian)* 78−47117
rotating ternary, element separation, degrees of ionis. effects 77−15174
rotation, of theta pinch plasma column, directional probe obs. 78−1877
rotation speed measurement, in external magnetic field *(German)* 78−42821
scalar partial differential eqns., variational principles 79−30255
screw pinch, gross instability, high-β plasma column motion, feedback stabilisation 77−27699
screw pinch, m=1 motion determ. by probes and streak photographs 77−15239
Scyllac, theta pinch implosion, gross plasma motion model and feedback stabilisation 77−24141
seeded combustion gas near cold electrodes, MHD boundary layer 80−48865
self-excited cumulative flow, compression dynamics and heating *(Russian)* 78−22469
self-gravitating plasma with finite ion gyroviscosity effects rotating layer instability 80−56706
self-gravitating rotating plasma, gyroviscosity effects 78−5860
self-similar expansion of a plasma into a vacuum 80−28623
shear flow, electrostatic instability, theory and appl. to magnetopause and solar wind 80−96359
shear flow, influence on magneto-ionic rays propag. 79−84659
shear flow in mag. field, stability 78−26197
sheath criterion generalisation, sonic ion wave at boundary 77−3954
Shuttle/Spacelab platform in near Earth ionospheric plasma, aerodynamics 80−8517
slow convection of magnetised plasma, appl. to Earth plasma sheet 80−109312
slow ion, effect on ion and electron current distrib., electron temp. 77−24063
solar atmosphere, plasma motion accompanying force-free mag. fields evolution 78−12176
solar flare plasma flows, in strong mag. field, gas dynamics 78−57524
source, dielec. chamber, plasma flow characts. optimisation 80−38574
spatial temp. distrib. meas., interference filter photographic method 78−67332
spatial waves nonlinear modulation in steady plasma flow 77−31444
spontaneous superradiance of at. and mol. ions 77−3470
stabilisation in transverse mag. field 79−64839
stability in axial mag. field *(Russian)* 78−26258
steady-state conditions in transverse mag. field, shock waves *(Russian)* 78−9765
stochastic acceleration by electrostatic wave near ion cyclotron harmonics 77−42980
stochastic acceleration by electrostatic wave propag. near ion cyclotron harmonics 77−39421
stream density through mag. mirror, reduction by HF rot. dipole mag. field *(Russian)* 77−47244
streaming in crossed fields, conductivity tensor calc. using correl. function of microscopic current 77−19675
subsonic flow in MHD channel, acoustic stability 78−9764
subsonic flows, in closed field lines regions of coronal-interplanetary space 78−28624
Sun, adiabatic flow in coronal loops 80−56803
supersonic, interaction with meteorites, ablation process lab. modelling 77−87351
plasma flow continued
supersonic dense stream, shock braking processes, radiation-gasdynamic obs. 80−19635
supersonic flow around conducting bodies, inductive interaction *(Russian)* 79−27789
supersonic flow in generator channel, with slanted entrance stream 79−77429
supersonic flowing continuum plasma, triple probe method applied to direct display of parameters in supersonic flowing continuum plasma 79−60191
supersonic low-density flow, electrostatic field struct. in wake of sphere 77−60509
supersonic plasma jet, current carrying-interaction with coaxial mag. field *(German)* 79−77356
supersonic plasma-steel target impact effect, boundary layer role 79−32780
supersonic stream, incident on metal surfaces, emission 77−76105
supersonic-subsonic flow transition, shock form. and propag. 77−47173
supersonic-subsonic flow transition, shock formation, enhancement by microwaves 77−65845
surface wave reson. instability in inhomogeneous plasma stream 77−24078
symmetric double diode, time depend. theory and computer simulation of electron and ion flow 77−24065
TE glow discharge, influence of fluid-dynamic phenomena 78−71619
thermal instability, mag. field generated, in laser heated plasma, hydrodynamic effects 80−96355
theta-pinch, groove type drift turbulence, Lagrangian description *(Russian)* 77−72448
theta-pinch, high-energy, linear, quartz end plug effects 77−76184
theta-pinch, linear, material end plugging 77−76183
Thompson scattering for electron beam and plasma diagnostics *(Russian)* 80−54031
Tokamak, noncircular cross-section, high-β, anisotropic equilib. 80−24238
Tokamak transport codes, one-dimens., poloidal divertor simulation 79−37539
Tokamaks and reactors, applic. of bundle divertors, collisionless exhaust flow 80−27814
toroidal equilibrium of stationary plasma flow 77−55162
toroidal plasma, convective cells and transport anal. 80−24229
toroidal trap, plasma rot. effect on neoclassical transport of impurities *(Russian)* 80−83972
transverse shear flow in magnetised plasma, rel. to auroral Kelvin-Helmholtz instability 77−53287
turbulent acceleration by electrostatic waves, in Earth's auroral plasma *(Russian)* 80−53952
turbulent interaction fronts in laser produced counterstreaming plasma 79−41807
turbulent skinned discharge, thermalisation of directed motion of plasma fluxes *(Russian)* 77−11373
turbulent stream of high temp. gas with particles, modelling *(Russian)* 80−38572
two fluid theory for flow of fully ionised plasma, initial value problem *(German)* 80−53954
two phase flow, particle velocity optical meas. *(Russian)* 80−54032
two-component laser-produced plasma, similarity flows 78−83591
two-dimensional flow in entrance region of channel with Hall and ion slip currents 77−42968
two-stream plasma, thermalisation *(Russian)* 79−4119
two-stream plasmatron flow structure obs. and optimisation 78−71556
UHF discharge with preliminary locally ionised gaseous medium 80−38851
vacuum arc plasma flow in plasma-optical system *(Russian)* 80−106992
vacuum far-ultraviolet light source, hypersonic flow with plasma focus *(Russian)* 77−49789
velocity driven modes in dense partially ionized plasmas, stability aspects 80−1792
velocity measurement using Langmuir probe, flame or plasma sheath 79−46475
velocity measurements in thermal plasmas, via new opto-electronic method 77−39462
velocity-shear flute instability of plasma flowing along curved mag. field 77−31459
Venus, plasma wake, viscous flow 77−87302
viscosity of H plasma *(Russian)* 80−53953
vortex, heating and cooling dynamics *(Russian)* 80−1753
vortex formation by baroclinic vector in laser-pellet interaction 79−14580
wake, hypersonic, free electron distrib., RF method 79−27833
wake model of fast moving body in plasma and its effects 79−77353
waveguide, rectangular, filled with uniaxial anisotropic relativistic warm plasma, EM wave propag. and attenuation 80−59246
welding arc, EM forces effect on plasma flows, calc. 80−83912
welding arcs, gas velocity fields modelling 80−75039
Ar arcjet plume, freely expanding, excited state distrib. function 79−98881
Ar arcs in supersonic flow, numerical analysis 80−38776
Ar atom populations in partially ionised flat plate boundary layer 77−65847
Ar boundary layer electrostatic probe meas. *(Japanese)* 78−5933
Ar full circle arc, mass flow field investig. 80−38797
Ar, ionised gas flow, heat transfer to sphere, appl. dimensionless rels. 77−35331
Ar, ionising boundary layer in shock-tube side-wall flow 79−60144
Ar, laser-initiated plasma, gasdynamic instabilities and convective flow parameters 78−22525
Ar low temp. plasma flow, interaction with intense microwave beam 80−38654
Ar plasma, shock-compressed, thermophysical and gasdynamic characts. 77−43016
Ar plasma, supersonic nonequilib. corner expansion flow, electron and particle temp. 77−89235
Ar plasma, viscosity determ. by stabilised elec. arc. 79−41873
Ar, stabilised electric arc, laminar plasma flow section, length and characts. 78−91177
Ar-Cs plasma stream, electrodynamic braking with strong MHD interaction 78−9763
Ar-He plasma, thermal diffusion factors, binary mixture hypothesis 79−27749

plasma flow continued
Ar-He plasma, thermal diffusion of neutral species in plasma jet, 2000-4000K 79−32742
CO_2 laser, continuous, fast flowing, thermal discharge contraction *(Russian)* 79−99009
H pellet in plasma, transonic flow in ablation cloud 79−1322
H pellet in plasma, transonic flow in ablation cloud 80−64735
H-constricted discharge, mag. field effects and cross-currents *(Russian)* 77−68761
H_2 plasma flow, methane conversion in plasma, Monte Carlo study 78−61010
H_2 plasma reactor design, heat transfer and flow 80−38697
He, gas discharge flow, contracted strata rel. to turbulence 78−1923
He, plasma, afterglow and inertial expansion, numerical soln. of relax. kinetics 77−27769
He plasma expansion, supersonic, population inversion 79−27755
He, RF discharge test obs. 80−44028
He-Ar mixture, mass separation with rot. plasma 79−13842
Hg plasma flow, electron temp. determ. from partial LTE populations 80−24248
Kr, hollow-cathode glow discharge with gas flow 78−67532
N glow discharge, volt-ampere charact. in gas flow *(Russian)* 80−106991
N_2 arc, magnetically stabilised cross-flow, temp. and flow fields meas. 80−54054
N_2 high intensity arc anode region, temp., current density, flow field, numerical anal. 78−9827
N_2, inductively coupled plasma discharge, temp. and vel. profiles 77−4004
N_2 plasma, spatial distrib. in transverse-discharge supersonic stream, continuum theory and probe meas. 80−48866
N_2, plasma discharge stream, rarefied, diagnostics using sounding and UHF interferometry 79−41872
N_2 plasma jet anode root behaviour rel. to hollow-anode thermal insulation 78−71554
N_2H_4 production from NH_3 in atmospheric press. electron-beam controlled discharge 80−38799
O_2-sseded Ar plasma supersonic free jet expansion flow, population density measurements *(Japanese)* 80−96351
Si compounds, plasma etching, gas flow-rate depend. 80−97603
SiO_2, plasma etching, gas flow-rate depend. 80−97603
TiC plasma-chemical synthesis, depend. on geometric and flow rate parameters *(Russian)* 80−40677
Xe plasma, shock-compressed, thermophysical and gasdynamic characts. 77−43016

plasma focus
1 kJ plasma focus, neutron-, ion-, and electron-energy spectra 77−35404
1-MJ plasma focus expt., neutron yield, current distrib., scaling law 77−74991
ablation type magnetoplasma compressor, mech. of plasma focus formation 78−79478
breakup-initiated shockfront development in 2-kJ plasma focus discharge 80−70001
closed poloidal heliotron, accelerated electron focusing *(Russian)* 80−106961
collapse phase, luminous front time evolution, spectrosc. obs. 78−42816
compression phase focus current, mag. probe meas. 78−5939
current carrying double layer production in focus device 80−83953
current sheath dynamics, mag. tension and thickness 77−76108
current sheath evolution; optical and elec. diagnostics 77−76207
current sheath struct. diagnostics, fast particle beams, deuterated polyethylene fusion 77−76206
current sheets in staged focus 78−14225
current sheets in staged focus 78−14226
current shell axial motion 77−7517
current structure, fast particle generation *(Russian)* 80−48913
dense plasma focus, formed in plasma erosion accelerator, radiation props. 78−67440
dense plasma focus, ruby laser holographic diagnostics *(Japanese)* 80−100097
dense plasma focus, strong subnanosecond field variations 80−70035
dense plasma focus, thermonucl. erosion of wall materials 77−23273
dense plasma focus devices matching with fission reactors 78−37436
dense plasma focus Julich I, neutronics, fusion plasma investigation 77−35396
deuteron beam generation, 1 to 5 MeV, by plasma focusing *(Russian)* 77−38537
deuteron beam time-amplitude characts. *(Russian)* 79−82099
development, model, neutron radiation *(Russian)* 78−22519
device, efficient operation, upper press. limit 77−84529
device with inductive energy storage, plasma prod. 79−77427
diagnostics, laser beam deviation method 78−55745
diagnostics, Mather-type machines, temp., density, neutron, and X-ray emission characts. 77−24184
discharge, elec. characts., rel. to hard radiation pulses, time correls. *(Russian)* 78−38528
discharge in Mather accelerator 80−24257
discharges, electron and deuteron beam energy spectra 80−24262
dynamics, anomalous cond. effect *(Russian)* 78−87475
dynamics with powerful laser interaction during MHD stage, diagnostics 80−48924
effective ion temperature, determ. by nucl. reaction rate in D_2-^3He mixture *(Russian)* 79−27824
electron beam accel., ignition of thermonuclear microexplosions 77−27686
electron density distrib., N_2 laser interferometric study, X-ray and neutron emission 78−87479
electron kinematics, accel. and hard X-ray prod., relativistic numerical anal. 77−58897
EM field oscillations near plasma focus and Z-pinch *(Russian)* 78−79458
emission spectrum, 10-350 eV, by photoemission scintillation spectra *(Russian)* 77−80367
energy spectra of accelerated deuterons in a plasma focus 80−103110
F-150 device, multiframe laser interferometry for investigation of plasma dynamics 78−83614
fast high voltage plasma focus, current and neutron yield scaling 80−64752
fast streak or frame camera appl. to plasma dynamics in plasma focus device 79−68950

plasma focus continued
filament formation, proposed mechanism 78−14227
Filippov dense focus, time and space resolved neutron emission meas. 77−58896
Filippov plasma focus apparatus fundamental characteristics *(Japanese)* 77−51244
formation in axially symmetric mag. field *(Russian)* 78−1809
Frascati 1 MJ plasma focus facility, deuteron energy distrib. 80−87957
Frascati experiment, neutron yield determ. Ag-activated Geiger counter calibration 80−99409
Frascati Tokamak, 1MJ plasma focus dynamics, neutron production scaling 80−24220
fusion, plasma focus as large fluence neutron source 77−88315
fusion plasma focus as high intensity neutron source 77−83433
hard X-rays indicating electron beam 79−14613
heating by laser beam 77−76154
heating by TEA CO_2 laser, neutron enhancement *(Japanese)* 78−9808
heating by TEA CO_2 laser and anomalous absorpt. obs. *(Japanese)* 77−43013
high velocity jets generated by plasma focus and shock-wave expt., temp. and density meas. *(Russian)* 80−106882
hypocycloidal pinch apparatus, dense plasma production diagnostics, high laser beam absorption 77−43051
instability enhanced X-ray and neutron emissions 77−62399
intense relativistic electron beam focusing with large aspect ratio diodes 77−23610
ion energy analysis on a plasma focus device, rel. to fusion plasmas 79−90465
ion energy distribution in plasma focus during second pinch compression 80−75070
ion spectra, high-energy, periodical modulations, emitted by 1 kJ plasma focus 80−59310
KEMP-II confinement machine, potential calc. 77−15225
Langmuir turbulence, laser excited, in dense plasma focus, light scatt. obs. 77−7591
laser compression of advanced H-^{11}B fuel, reaction feasibility 77−83084
laser compression of advanced H-^{11}B fuel, reaction feasibility 77−83085
laser fusion power plants, design and operating characts. of optical system 79−76136
laser irradiated, neutron yield enhancement 77−62386
laser light absorption in high temp. plasma 77−76090
laser light interaction with high temp. plasma *(Japanese)* 79−82101
laser plasma focus, interferometry and luminosity meas. 78−47161
laser produced, as laser pulse clipper and optical isolator 77−65601
laser produced line-focus plasma, coherent far IR radiation 78−42806
low-energy, neutron yield props., filling press. depend. 77−74992
magnetic field configurations, analytical and numerical methods 79−86623
magnetoplasma compressor, erosion type, focus zone, nonideal plasma, strong shock waves 78−91161
magnetoplasma compressor, radial limitation of focal zone, dynamic, energy, spectral characts. 79−55477
Mather geometry, high energy deuteron intensity and ang. distrib. 78−59671
Mather type, diagnostics results 77−27726
Mather type PF devices, optimisation using 2D snow plow code 80−87956
maximum compression phase, laser diagnostics 79−10711
MHD 2D calcs. 78−9767
MHD 2D calcs. 78−9768
MHD calcs., two dimens., in the Mahler geometry 79−4120
microinstabilities, current driven, suprathermal microwave emission and soft X-rays obs. 77−89328
modified magnetron discharge facility 78−75380
neutron and X-ray emission diagnostics, 120 and 20 kV focus device dynamics 77−74990
neutron and X-ray flashes during long-lasting current pulse 78−63601
neutron and X-ray sources space-time struct., scintillator diagnostics 77−74993
neutron emission, obs. and mechanism 79−90475
neutron emission from Mather-type plasma focus 79−19084
neutron emission parameters 80−24221
neutron production, recent developments to increase yield 79−14567
neutron production in dense focus 77−74989
neutron production in dense plasma focus, mechanisms 79−90435
neutron yield scaling lasers, recent research 80−24263
neutron yield to electromechanic work correlation in Mather-type device 77−15250
nonthermal processes, neutron spectra 78−42804
overneutralised electron beams in metal vapour, ion focusing theory and expt. 78−75366
pinch column form. and stability 80−96380
plane shock formation, plasma focus zone, magnetoplasma compressor, dynamic model 78−83569
plasma boiler moving in ambient plasma, fusion reaction rate enhancement 79−18038
plasma gun behaviour, contraction at electrode end, and neutron radiation 78−30490
prepulse discharges in high current accelerator diodes with double shaping line 80−5399
pulsed high-β devices, CTR radiation test facilities appls. 77−23256
pulsed neutron source creation by laser/relativistic-electron-beam plasma heating 78−74527
pulsed radiation emission 77−27727
radiation spectrum in quantum energy range, 0.64-350 eV 79−19094
relativistic electron beam, in plasma focus, form., interaction dynamics *(Russian)* 79−4154
self-inductance changes in plasma focus 77−27651
self-trapped cylindrical laser beams, radial intensity profile and nonlinear wavenumber shift 80−1802
sheath driven targets, simulation 80−48898
soft X-ray emission during neutron emission 77−24187
solid density plasma production by plasma focus discharge 78−87465
staged focus apparatus, staged, current-sheet dynamics, X-ray and fusion-neutron emission intensities 79−4160
streak mode interferometric study of plasma focus 79−73042
suprathermal microwave radiation, temporal, spectral and ang. distrib. 78−18450
toroidal plasma, compression, appl. of plasma focus device 80−43996
turbulence, light scatt. obs., pinch break-up effects 77−24083

plasma focus continued
turbulence induced by plasma-electric current interaction in focus expt., laser diagnostics 80−24171
upper-hybrid reson. absorpt. of laser in plasma focus, backscatter 80−28621
vacuum far-ultraviolet light source, hypersonic flow with plasma focus *(Russian)* 77−49789
vacuum UV emission meas. using ionisation chamber 77−80370
X-ray and neutron emission from staged plasma focus 78−14220
X-ray emission, superthermal, from CO_2-laser-produced plasmas 79−90454
X-ray emission from plasma focus, anisotropic and collimated 78−26330
X-ray emission from plasma focus, space and time resolved meas. 79−4185
X-ray emission from plasma focus in puffed gas 78−14219
X-ray energy distribution, nuclear emulsion study 78−83620
X-ray generator for X-ray diffr. studies of polycrystalline materials, nanosecond exposure times 77−89348
X-ray intensity from plasma focus, high energy electrons trajectory 78−42808
X-ray output, operating characts. 78−14224
X-ray photography, time-resolved 77−27718
X-ray radiography appl. of chamber with plasma focus *(Russian)* 77−7592
yield enhancement, high and low density mode operation 77−27746
Z-pinch type plasma focus, ion accel., numerical study 78−91142
Al ion acceleration *(Russian)* 79−77415
D ion energy spectrum from plasma focus discharge 78−14218
D_2-^{3} He mixture, neutron yield ratios, ion temp. 78−5953
H_2 plasma development in 2kJ focus discharge accelerator, optical image structs. 79−82076
N_2, electric breakdown, vol. discharge with external photoionisation, plasma focus spark channel *(Russian)* 80−38738
^{A}U, A=235, 238, fission and activation by fusion plasma neutrons 79−13521
Z-pinch, noncylindrical, dynamics and particle accel. mechanism 77−76170

plasma generation *see plasma production*

plasma guns
analysis for plasma guns for spraying 80−38732
arc plasma gun for metal cutting, transient performance, obs. 80−49017
Berkeley multifilament ion source, plasma characts. 79−94807
Beta-II, magnetised coaxial plasma gun mechanical design and construction 80−91271
coaxial, accelerated plasma cluster decay 78−30489
coaxial, critical ionis. vel., dynamics 78−30494
coaxial, steady-state fluid model 79−60201
coaxial gun, plasma cluster accel., decay, obs. 78−63603
coaxial gun acceleration of plasma cluster, spectroscopic determ. of electron temp. *(Czech)* 77−24182
coaxial neutral particle source, for heavy ion collective accelerator 77−75013
coaxial plasma guns, breakdown phase 80−70036
compact 5×10^{12} A/s rail-gun pulser for laser plasma shutter 80−70017
electrodeless injection, dynamics of plasma in longit. mag. field 79−55479
electron-beam ion source 78−83584
energy characteristics of straight and reversed polarity guns 79−41887
gas injected washer plasma gun 80−100083
MFTF, plasma streaming system, description 80−91280
microwave surface wave plasma at atmospheric press. 79−50868
plasma focusing, gun behaviour 78−30490
pulsed coaxial, X-ray emission diagnostics 77−27750
resistive anisotropic plasma jet, stability 78−69667
reversed field mirror reactors, startup using coaxial plasma guns, scaling laws 80−99279
rocket-borne plasma gun, use in controlled ionospheric experiment 78−57424
self-pulsing operation, circuit theory anal. 77−27747
simulation of electron optical system, plasma boundary anal. 78−67442
solid pellet acceleration using plasma gun 79−90470
vacuum arc plasma flow in plasma-optical system *(Russian)* 80−106992
Ba rail gun for plasma injection 80−59255
C high-intensity pulsed source, for ion injector 79−89512

plasma heating
see also plasma focus; plasma production and heating by laser beam
2XIIB magnetic mirror device, neutral beam injection 80−28782
200 kV Blumlein transmission line for Tokamak plasma heating, calc. and obs. 79−55521
absorption of axially asymmetric EM waves, in inhomogeneous plasma 77−55156
accelerator, closed Hall current discharge, anode sheath struct. 77−76215
active burn control of nearly ignited plasmas 80−48909
additional heating in Tokamaks, specific diagnostics review 80−28753
adiabatic compression heating in toroidal discharges 77−68821
adiabatic heating combining minor and major radii compression of toroidal plasma 78−94922
air, pulsed corona discharge channel fast heating process 78−67560
air, shock heated plasma, nonequilib. submillimetre emission *(Russian)* 78−1869
air-core Tokamak, optimisation of ohmic heating coil configurations 80−14914
Alcator, high density regimes, numerical simulation 77−68858
Alfven and magnetoacoustic wave heating for fusion plasmas 80−24188
Alfven resonance effects on magnetosonic modes in large Tokamaks 79−73006
Alfven wave, shear, low freq., heating in Heliotron-D, diagnostics 78−1858
Alfven wave energy transformation and heating by acoustic waves for stimulated Mandelstam-Brillouin scatt. *(Russian)* 77−11328
Alfven wave heating, helical launching struct., Proto-Cleo stellarator 77−72456
Alfven wave heating, nonlinear processes 80−28718
Alfven wave heating, plasma resistive effects 78−1857
Alfven wave heating 77−68817
Alfven wave heating in Proto-Cleo stellarator 77−7565
Alfven wave heating in Proto-Cleo stellarator 78−9802
Alfven wave heating in Proto-Cleo stellarator 78−83587
Alfven wave heating in toroidal plasma 80−28740

plasma heating continued
Alfven wave heating of a theta pinch 78−75379
Alfven wave heating of high beta plasma 77−39436
Alfven wave heating of inhomogeneous plasma by collisionless damping, initial value problem soln. 79−64864
Alfven wave resonant mode conversion, kinetic processes 77−19730
Alfven waves, appls. to plasma heating in linear and toroidal geometries 79−10676
alpha particle heating, loss, cross sections for O^{q+}-He^{2+} collisions 79−68936
alpha particle heating of fast-solenoid fusion reactor plasma, self-consistent anal. 79−31187
alpha particle orbits in radially nonuniform slender plasma column, multigroup rep. 80−53921
alpha-particle heating, compact expts. proposals 77−62379
alpha-particle heating in an open-field-line plasma 80−48908
alpha-particle heating in high density D-T plasma 80−28735
anomalous, turbulence onset due to velocity gradient driven flute instabilities 77−39414
anomalous heating by ion sound turbulence 78−67378
anomalous turbulent resistivity at high drift vels., rel. to confinement and fluctuations in toroid 80−24139
anomalous turbulent resistivity at high drift vels., toroidal plasma 80−24138
antenna waveguide, slow TM mode excitation at lower hybrid reson. *(Russian)* 77−47227
arc heating, equilib. in gas-melt system *(Russian)* 79−37512
arcs, elec., high-current, conducting gas flow anal. *(Russian)* 79−32754
ASDEX, 30 kA ohmic heating system, tests and performance 80−13848
asymmetric plasma resistivity, creation using waves 80−103171
atmospheric positive streamer corona, primary wave emission, secondary electron emission 80−44008
atomic processes for mag. fusion research, review 80−42851
axial asymmetrical electromagnetic field, plasma heating under double ICR conditions *(Russian)* 79−14573
axial shock heating applied to compact toroid plasma formation 80−95402
background plasma density minimum for plasma-grounded electron beam targets 77−7564
beam-induced tensor pressure Tokamak equilibria 80−106965
beam-plasma heating, transverse beam motion 79−19051
beam-plasma interaction, high current electron beam trapping and ion heating 78−9795
beam-plasma interaction, ion beam, stochastic heating by lower hybrid waves 79−98933
beat frequency heating, mag. field effects 77−76144
beat frequency heating by circularly polarized microwaves 77−65882
beat heating by two Gaussian beams in extraordinary mode 80−64746
belt pinch, diffusion processes, impurity and neutral gas effects, 3-fluid model 77−24057
belt pinch, high-temp. plasma stability 77−24161
belt pinch, shock compression in toroidal geometry 78−67399
belt pinch, shock heated weakly compressed high-temp. plasma 77−24164
belt pinch plasma, preheating discharge optimisation, laser scatt. diagnostics 77−31514
Berkeley multicusp ion source for use with TFTR neutral beam injector, characts. 80−54040
Bernstein dispersion relation for oblique propagation 80−75052
Bernstein waves, propagation in inhomogeneous plasma, dispersion rel., quasi-linear equations, diffusion coeff. determ. 80−75044
beta pinch shock heating of toroidal collisionless plasma 77−76138
Bohm-type thermal losses from high-β plasma 80−38679
boundary layer flow, past heated cylinder, in radial mag. field *(Russian)* 77−47170
Bumpy Torus plasma, NASA Lewis, optimisation and scaling of ion heating 77−24110
burn period plasma current maintenance, rectifying first wall, cct. anal. 80−102307
capillary discharges, ohmic superheating in dense plasma 77−35362
channel flow, coaxial, compressive, viscous, thermal and elec. cond. effects *(Russian)* 77−3927
chaotic motion theories with appl. to controlled fusion research, review 78−93605
charged particle acceleration and diffusion in stochastic mag. field 80−43872
charged particle beam appls. in long solenoid reactors 77−67893
charged particle trajectories in radial electric and uniform axial magnetic fields 79−77336
charged particle transport, energy deposition, in hot plasma, moment method calc. 78−22458
chemically reactive arc-heated gas flow, ion saturation current fluctuation probe 78−63574
Cherenkov adsorption of azimuthal EM travelling waves, magnetoactive heating and containment *(Russian)* 80−38675
circuit-breaking arc radiative transfer, magnetic stability, and turbulent heat exchange 78−75482
CLEO stellarator, heating, confinement and fluctuations 80−24225
cluster ion mean specific size, effects of break-up ratios and distrib. functions of specific size 80−75068
cold electron plasma waves, finite extent, reson. decay, fusion appls. 78−38485
cold plasma blanket in linear fusion reactor, heating 79−59258
collective phenomena and anomalous resistance, electron current drift velocity *(Russian)* 80−24140
collisional drift modes, anomalous skin effect, enhanced particle penetration during fuelling, nonlinear theory 80−64703
collisional plasma heating rate by mag. pumping, asymmetric RF field 77−7569
collisionless plasma, microwave electron acceleration, waveguide obs. 80−43932
column, heating by shaped pulse of magnetoacoustic waves *(Russian)* 79−55522
column compressed by mag. field, multichord corpuscular diagnosis *(Russian)* 79−4190
column rot. and particle transport, travelling EM wave and neutral beam heating *(Russian)* 79−27798
combustion bomb microwave cavity, electrically loaded with propagating flame front electron plasma, theory and expt. 79−20369
compact fusion ignition experiments, designs, numerical computation 80−13853

plasma heating continued
compact toroidal configuration, heating and confinement principles 80−24185
complex ray analysis for plasmas 80−83902
composite discharge plasma, rate of heating of dry air as function of voltage and density *(Russian)* 79−37513
compressible liner implosion, stability, soluble model 79−27810
compressible liquid shell, rot. stabilised implosion, dynamics 79−27809
compression, isentropic, optimal, reversed time numerical method, solid pellet implosion 78−79446
compression by electric field, rel. to limiting value of ion-acoustic plasma oscills. *(Russian)* 77−11369
compression by profiled explosion, neutron output 80−13782
compression clamping, controlled thermal runaway 77−67890
compressional Alfven wave heating, plasma source 79−27802
concentric compression of plasma, possibility of generating singular densities 77−68840
conference, controlled fusion and plasma physics, Oxford, England (Sept. 1979) 80−77545
conference, Varenna, Italy, (Sept. 1976) 77−65885
conference, Varenna, Italy (Sept. 1977) 79−98869
conference on fusion research and plasma physics, Innsbruck, Aug. 1978 80−27033
consecutive microsecond pulse ion beams from reflex tetrode ion source 79−41323
controlled thermonuclear fusion, contemporary state of research 79−680
convective plasma loss by ion-cyclotron RF field, elimination by mode control 80−83957
coupling to the fast wave at lower hybrid frequencies 80−75069
cross-field heating of ions, mechanism 78−1856
cross-field-current driven lower-hybrid instability from electron beam injection, ion heating 77−65860
CTR neutral-beam injection system, plasma source design 77−24105
current carrying plasma, trapping and build-up of HF turbulent noise *(Russian)* 77−3957
current driven instabilities, anomalous effects 78−91096
current structure, fast particle generation *(Russian)* 80−48913
currents in short pulsed high current electron beam injection into initially neutral gases 80−33749
cusp field with RF plugging, appl. thermonucl. plasma 77−76169
cutting with additional heating of plasma-forming gas 80−24267
cyclotron heating in short adiabatic traps *(Russian)* 78−5890
cyclotron self-absorption in two-temp. plasma, temp. and density meas. 80−48987
cylindrical ion implosion fusion using radially convergent beams 80−23137
cylindrical system with heavy inertial layer, neutron yield, explosion-induced D-T compression 80−68944
dense plasma focus, formed in plasma erosion accelerator, radiation props. 78−67440
dense plasma turbulent heating expts. 78−75386
diagnostics, turbulent heating example 80−49015
discharge dynamics, calculations of plasma energy and particle balance for T-10 Tokamak 80−28847
dissipation phenomena formalism diffusion and heating applications 79−4111
dissociative recombination of H_3O^+ and D_3O^+ at elevated electron and gas temperatures, rate coeff. determ. 80−63747
distortion of the thermal-ion distribution during neutral-injection heating 80−103169
DITE, neutral injection heating 80−92347
DIVA, scrape off layer, multigrid energy analyser applications 80−33818
double plasma and other synthesised plasma devices, adjustment of ion energy distribution 80−19625
Doublet III, neutral beam injection system, overview and status 80−13868
Doublet III, neutral beam injection system, parametric study 80−13869
Doublet III, ohmic heating E-coil vacuum breaker system, function and operation 80−102323
drift cone instability suppression by electron heating in adiabatic traps *(Russian)* 80−53959
drift wave stabilisation in collisionless plasma, by lower-hybrid waves 78−51296
duopigatron ion source, extraction electrode, hole geometry optimisation 78−32921
duoPIGatron ion source for plasma heating 77−67534
dynamics of heating and cooling of a plasma vortex *(Russian)* 80−1753
Earth bow shock, ion and electron heating two stream instability 77−53320
EBT, ray tracing near electron cyclotron freq. 80−103178
EBT heating, electron-cyclotron absorption and microwave propagation 80−64749
EBT reactor, new design arising from plasma research 80−27806
ECR fundamental ordinary mode absorption and emission, in PLT 80−43943
election parallel thermal conductivity, reduction using waves 79−10637
electric field heated nonisothermal plasma, nonstationary electron behaviour, kinetic description 80−59171
electron acceleration by localised electric field 77−76142
electron acceleration during reson. absorpt. 78−14184
electron and ion heating by neutral injection in the DITE tokamak 78−67376
electron and ion waves, excitation by two or more pump waves 78−57381
electron beam, anomalous relativistic deposition in dense plasma, coupling efficiency 77−84457
electron beam, quasilinear relaxation of dissipative instability of relativistic beam in bounded plasma 80−38671
electron beam, relativistic, heating and induced turbulence of Langmuir and EM waves *(Russian)* 77−62378
electron beam, relativistic, intense, high energy ion collective accel., localised pinch model 78−87460
electron beam, relativistic, magnetoplasma heating, anomalously fast electron-ion energy transfer 78−38515
electron beam (relativistic)-plasma interaction, transverse mag.-field induced enhanced energy deposition 77−62377
electron beam controlled discharge, cathode density waves 80−38798
electron beam fusion, pulsed power requirements for breakeven 77−23278
plasma heating continued
electron beam fusion compression targets, fuel preconditioning studies 79−81076
electron beam fusion of D-T pellets, neutronics and photonics 80−52781
electron beam heating, electron energy distrib. 79−7471
electron beam heating and beam energy distrib. in E-region approximated plasma 80−103163
electron beam heating model 79−73019
electron beam heating of a mirror confined plasma, diode mag. field gradient effect 80−54009
electron beam induced fusion, power requirements for target implosion expt. 77−23277
electron beam inertial confinement thermonuclear fusion 80−27803
electron beam injection, energy transfer, heating 77−76129
electron beam injection into inhomogeneous magentised plasma 77−76117
electron beam interaction, dispersion characts. modification 78−30450
electron beam irradiated pellet, holographic interferometry of plasma blowoff vel. and density 77−23279
electron beam propagation in plasma channels for ICF reactors 80−1812
electron beam-N_2 plasma, isolation foil effect, numerical method 79−7469
electron beam-plasma accel. heating, by propag. direction-decreasing density 77−89275
electron cyclotron frequency expts. in 15X-B Tokamak, temp. rel. to heating power 80−48912
electron cyclotron heating, Bernstein modes, Vlasov dispersion relation 80−33809
electron cyclotron heating, superthermal electrons 80−64753
electron cyclotron heating and wave trajectory in toroidal plasmas 78−47137
electron cyclotron heating and wave trajectory in toroidal plasmas 80−28726
electron cyclotron heating for bumpy torus 79−14574
electron cyclotron heating in Elmo bumpy torus, review 80−28750
electron cyclotron heating in high density toroidal plasmas 79−37517
electron cyclotron heating in Tokamaks: experiments and prospects 80−28749
electron cyclotron heating in toroidal plasmas, wave trajectories 80−38678
electron cyclotron heating in toroidal systems 77−76141
electron cyclotron heating of high-β toroidally confined plasmas, ISX-B expt. 80−37588
electron cyclotron heating rate, density depend. 79−10678
electron cyclotron plasma heating, abnormal resist. *(Russian)* 77−7567
electron cyclotron plasma radiation, in L-2 stellarator *(Russian)* 79−4178
electron cyclotron resonance heating of Tokamak plasmas, fluctuations and instability 80−83956
electron cyclotron resonance plasma, metal surface cleaning *(Japanese)* 80−16572
electron distrib. function in slide-away regime 77−68823
electron ensemble, collisional relax. and elec. field heating, stationary states transition times *(German)* 77−68736
electron heating, ion cyclotron influence in min-B mirror trap 80−79521
electron heating and anomalous conductivity, in two-stream unstable plasma 80−6219
electron heating by energetic neutral-beam injection in Oak Ridge ORMAK 77−80323
electron heating by ion acoustic turbulence 79−90424
electron heating by Langmuir waves, with induced l-s scatt. *(Russian)* 80−10403
electron heating by relativistic electron beam 77−15213
electron heating due to kinetic shear Alfven wave 79−90425
electron heating due to MHD shock wave, electron temp. and density 79−14588
electron heating within interaction zones of simple high-speed solar wind streams 79−25426
electron Landau damping of lower hybrid waves 78−42741
electron plasma cooling by cyclotron radiation 80−69986
electron plasma waves, sum-freq. excitation, energy transfer efficiency 78−38496
electron slide-away regime in high temp. plasma 77−68822
electron temp. control in double plasma device 77−35363
electron tubes, power capabilities *(French)* 78−9801
electron velocity distrib. determ. during strong turbulence 79−60196
electron velocity distribution, behaviour in periodic elec. field *(German)* 79−10632
electron wave coupling and propag. using phased waveguide arrays, heating appl. 78−5863
electron-beam heating, modulated beam, parametric lower-hybrid instability 78−91127
electron-beam inertial confinement expts. at Valduc *(French)* 80−48907
electron-beam-heating from foilless diode 80−103168
electron-cyclotron wave heating in Tokamak, cyclotronic attenuation energy loss calc. *(Russian)* 77−47225
electron-ion collisions, stimulated multiphoton bremsstrahlung 79−19007
electrons heating in lower ionosphere by horizontal lightning discharges 80−90283
electrostatic large amplitude standing wave, particle stochastic motion 79−77406
electrostatic wave, magnetised plasma charged particle stochastic accel. 80−59230
electrostatic wave, stochastic acceleration near ion cyclotron freq. 77−65868
electrostatic wave absorption by Landau damping at low power levels 78−9774
electrostatic wave heating of charged particles, wave perpendicular to mag. field 78−63565
electrostatic wave propagation to lower hybrid reson. in mag. field with shear 77−80285
ELMO bumpy torus, ambipolar diffusion 80−38552
ELMO Bumpy Torus, electron cyclotron heating, density and temp. 80−28780
ELMO Bumpy Torus, microwave coupling 80−99328
ELMO Bumpy Torus, ray tracing near electron cyclotron freq. 80−83975
EM field, electron energy spectrum control 78−47135
EM field orthonormal decomposition, duality and complex vectorial space in anisotropic media 80−28754

plasma heating continued
EM pump wave parametric decay into electron electrostatic waves, simulation 77−19683
EM right-handed Gaussian beam excitation of plasma wave 79−55495
EM wave absorption in randomly inhomogeneous collisionless plasma at resonance frequencies *(Russian)* 78−59598
EM wave heating, reson. high-freq. dissipation, temp. anomaly 79−73016
EM wave heating at parametric cyclotron resonance 78−18425
EM wave in inhomogeneous magnetoactive plasma, total absorpt. effect *(Russian)* 80−106944
EM wave resonant absorption, theory and expt. 78−75353
EM waves incident on warm plasma half-space dual propag. and absorpt., density and temp. depend. 80−75048
energetic neutral beams, development to MW power level of controlled thermonuclear research 79−45508
energy balance, electron runaway, electric field effect on temp. relax. 77−970
energy balance, in L-2 stellarator, with ohmic heating *(Russian)* 79−4179
energy balance in PLT Tokamak 80−28733
energy confinement comparison of ohmically heated stellarators to Tokamaks 80−92360
energy end loss from linear devices, kinetic approach 77−76186
energy end loss scaling in open field line geometry with end plugging 77−68855
energy exchange anal., neutral beam injection, Ohmic heating, and turbulent plasma 78−5895
energy flow and absorption along resonance cones near the lower hybrid 79−77405
energy of a turbulent, current-carrying plasma in a strong electric field 80−79514
energy transfer in laser (or particle) beam produced plasmas 80−38680
Engineering Test Facility/International Tokamak Reactor, plasma physics characts. 80−95420
enhanced plasma loss due to secondary currents, Tokamaks and non-Ohmic stellarators 77−65884
ERA compression system, IPP-Japan 80−95490
excited gas, resonant optical discharge 80−92343
explosion compression of plasma up to critical values of thermonuclear microfusion 77−67872
explosion compression of plasma up to critical values of thermonuclear microfusion 77−67873
explosion compression profiled via nonhomogeneous external layer 78−22534
explosion-induced compression, continuous profiling 78−51330
explosion-induced profiling of plane shock wave through layer systems 78−51331
explosive instability collision mode stabilisation by drifting effects, Thirring instability *(Russian)* 80−43920
fast electron prod., microwave expt. simulating laser-plasma interaction 77−58850
fast ion Fokker-Planck code FIFPC 78−34342
fast ion injection in Tokamak, energy amplification 77−71692
fast ions, behaviour during H-neutral-beam-injection in large Tokamak plasma 80−28713
fast shock heating, of electrons and ions, in high-voltage belt pinch 77−72462
fast wave damping in ion cyclotron freq. range, heating appl. 77−65867
fast wave heating in ion cyclotron freq. range 77−65890
fast wave heating via mode conversion and ICRF scaling 80−28815
fast-magnetosonic-wave heating of the conceptual NUWMAK Tokamak reactor 80−6264
fast-wave heating of reactor plasma, two freq. regions consideration 77−67884
Fermi acceleration and RF heating 80−33790
field reversal experiment in 2XIIB 80−28732
field reversed mirror neutral beam startup, hybrid plasma code simulation 80−99313
fluctuating plasma, Trivelpiece-Gould mode parametric decay 78−75321
flute instability, HF electrostatic field driven, dispersion eqn. 79−46440
focus, 2D MHD calcs. 78−9767
FT Tokamak, RF additional heating system 80−13879
FT-1 Tokamak, electron cyclotron heating expt. 80−75071
FT-1 Tokamak, lower hybrid heating, energy balance 80−79523
FT-1 Tokamak, lower hybrid plasma heating 80−28700
fused metal foil operating switch for inductively driven plasma implosions generation 80−70018
fusion chain reactions, kinetics, high electron temps., interactions with D-T plasma 80−68945
fusion device surface effects on neutral beam injector and beam direct convertor operation 80−47719
fusion energy production, adiabatic heating, by compressible fast liner 79−31182
fusion plasma, RF phased waveguide heating, thermal eddies form. 80−24193
fusion plasma focus as high intensity neutron source 77−83433
fusion plasma heating by D injection, D^- form. *(French)* 79−94080
fusion plasma in beam driven Tokamak, Fokker-Planck/transport analyses 80−28826
fusion products in Tokamak plasma, deposition and thermalisation 80−83895
fusion reactor, BBC CQK 200-4 modulator tube for sustaining neutral beam power supply 80−99290
fusion reactor, doublet Tokamak, parallel connected ohmic heating coil 78−54930
fusion reactor, effects of suprathermal alpha particles, phase-space grouping techniques 77−79479
fusion reactor, High Voltage Switch Tube, for Neutral Beam Power System 80−99291
fusion reactor, MFTF, neutral beam source development 80−102368
fusion reactor, ohmic heating energy storage for power reactor, costing 78−58495
fusion reactor, rectangular plasma generator, advanced ion source for ion injectors 80−99376
fusion reactor cavity design, compact electron beam or light ion beam reactor using nonspherical blast waves 80−9405
fusion reactor implosion heating coil, radially fed, design, fabrication 78−55006
fusion reactor lower hybrid heating, nonuniform density, particle simulation model 78−14185
plasma heating continued
fusion reactor neutral beam injection, comparison of series and shunt regulation for power supply 77−23271
fusion reactor plasma heating and confinement, review 80−63388
fusion reactor problems *(German)* 78−50298
fusion reactor with dense plasma confined by crimped mag. field. 77−34442
fusion reactors, basic problems rel. to extraterrestrial plasmas 78−69672
fusion reactors, neutral beam design for plasma heating 80−13836
fusion reactors, quasi-stationary, Tokamak type, HF methods 77−34445
fusion system, with rot. stabilised liq.-liner, finite liner compressibility effects 79−18036
fusion-neutron production in D-beam-heated PLT plasmas 80−28807
gas jet target with electron beam heating, plasma density meas. 77−39457
Gaussian laser beam propagation in overdense plasma, self-focusing 79−55513
Grill phase tracking during density increase in Tokamaks 80−28762
gun injection heating of Tokamak 78−94923
gyrotron 50 GHz design considerations 80−28728
gyrotron for electron-cyclotron heating in large Tokamaks 80−28751
harmonic oscillating two-stream instability in lower-hybrid heating 79−1311
heat flow, quasilinear model for micro-unstable Tokamak 77−76033
heat flow and diffusion in Tokamak, quasi-linear theory 79−98871
heat flux limitation in an ion-acoustic instability-induced turbulent plasma 79−7472
heating and refuelling by injection in ASDEX divertor Tokamak 77−67889
heating at const. impedance 79−14568
heating expts. in Japan, summary 80−28737
heating in lower hybrid freq. range, temp., ion diffusion 80−83954
heating in toroidal plasmas 80−24239
heavy elements, isentropic explosion compression by 'soft' layer effect 77−43017
heavy ion beam inertial confinement fusion, US programme 80−23136
Heliotron D, confinement of ohmically heated plasmas 79−50879
Heliotron D, RF heating, equilibrium and stability 80−28777
Heliotron-E, physical aspects, outline 79−99002
HF discharge, ionisation overheat instability in EM wave field *(Russian)* 80−106990
HF electric field heating, stochastic method *(Russian)* 77−3958
HF gyrotrons appl. to tokamak plasma heating 79−60159
HF heating, EM wave retardation by large diameter helices, theory, expt. 79−32787
HF heating by MHD waves of finite press. plasma *(Russian)* 80−83950
HF heating in Tokamaks, fast wave propag. at lower hybrid reson. *(Russian)* 77−7566
HF heating in Tokamaks and stellarators, review 80−28736
HF heating in Uragan-2 stellarator 77−72459
HF heating of plasma column, at freqs. below electron cyclotron freq. 78−91125
HF heating of Tokamak plasma *(Russian)* 77−7571
HF magnetoacoustic heating of T-4 Tokamak 77−76137
HF noise and transport in electron-beam-heated plasma *(Russian)* 77−55174
HF plasma generation, electron heating, nonlinear kinetic theory 80−44041
high beta Tokamak heating 80−28730
high current relativistic electron beam retardation distance *(Russian)* 80−14911
high density plasma, thermonuclear reaction wave, propag. stages, computer simulation 78−742
high density plasma, turbulent heating, rapid current penetration 78−51320
high field ignition test reactor using adiabatic compression 79−89500
high field tokamak, plasma energy balance and classical ion thermal cond., Joule heating *(Russian)* 79−27797
high magnetic field behaviour of solids and plasmas, conference, Cambridge, MA, USA (Sept. 1978) 79−60667
high melting particle heating, melting and vaporisation in hot gas 80−6201
high n flux fusion heating, $^6Li(n,t)^4He$ use 78−89975
high power microwave pulse interaction with thermally ionised laboratory plasma 80−10409
high power MM wave source−gyrotron *(Japanese)* 80−23654
high power neutral injectors, review 80−18656
high-β plasma, heating mechanism study by ion beams 77−5962
high-frequency heating of inhomogeneous plasma in $\omega \geq \omega_{Hi}$ freq. range *(Russian)* 80−106946
high-temp. regimes, simulation and confinement scaling 80−38673
HIP-1 hot ion plasma, effect of anode-cathode geometry on performance characts. 77−24112
hollow cathode inert gas discharge, excitation and ionis. mechanisms, spectra obs. 77−15261
hot electron prod., anomalous absorpt., inverse bremsstrahlung 77−68833
hot plasma preparation for high beta Tokamak 77−999
hot-electron plasma in simple mirror, stability, X-ray diagnostics 77−24176
hot-ion-mode ignition in a Tokamak reactor 80−73999
hybrid waves, lower, backscatter, effect of waveguide boundary conditions 80−64709
ICR heating in T-10 Tokamak under weak dissipation conditions 80−28759
ICRF heating, preliminary results in DIVA 80−28758
ICRF heating in Macrotor Tokamak 80−28744
ICRF heating in TFR, preliminary obs. and further development prospects 80−28741
ICRF heating in TFR at the ion-ion hybrid resonance 80−74020
ICRF heating of D^+ plasma with H^+ minority component in DIVA 80−18601
ICRF heating of H-D Tokamak plasma under harmonic resonance 80−28719
ICRF heating of toroidal plasma, linearly- rel. to circ.-polarised RF field efficiency 80−28711
ICRF heating optimisation in PLT 80−28742
ignition device for plasma column 79−98936
ignition test reactor with high field operation 79−71965
ignitor experiment, multistage heating cycles 79−98937

plasma heating continued
implision heating in staged theta-pinch 77−72473
imploding liner fusion, USA expt. and theoretical studies 80−23129
implosion and reflection of coalesced shocks, self similar analytic solns. 78−55735
implosion heating, numerical modelling of Los Alamos expt. 77−43056
implosion heating experiment, Faraday rot. meas. 77−39456
impurities radiation balance, neutral injection heating *(Russian)* 79−46435
impurity diffusion and heat transfer, in neoclassical regime, neutral injection effects *(Russian)* 78−26248
impurity effects and control, neutral beam injection, computational models for large Tokamaks 80−28773
inert gas afterglow plasmas, cyclotron emission and electron thermalisation 77−84545
inert gas electron beam excited plasma UV absorpt. by diatoms 79−68907
inertial confinement, black body radiation implosion in ablator, driver, gas, pellet system 80−73990
inertial confinement fusion, Angara 5 features and design principles, accel. module 80−63384
inertial confinement fusion, pulsed power aspects, overview 80−63382
inertial confinement fusion at NRL, laser and ion drivers 80−23131
inertial fusion by oscillating relativistic electron beams in magnetic mirror *(French)* 79−54595
inertial-confinement ion-beam wet-wood-burner fusion neutron source 80−32489
inhomogeneous RF plasma, absorption and parametric decay of extraordinary waves 80−59206
injection heating in DITE Tokamak 77−72478
injection systems at Princeton plasma lab. 77−68825
instability, electrostatic, parametric, due to thermal coupling 80−79465
instability onset time in heated layers 77−72461
intense ion beam propag. in z-discharge plasma channels, straight and tapered 80−83948
intense negative ion beams from N_2 cluster ions, size specification 78−87006
intense relativistic pulsed electron beam appls. in plasma phys. *(Dutch)* 78−30452
ion acoustic wave, large amplitude coherent, heating mechanism 79−23432
ion beam, cross-field injection, propag. and energy deposition, heating appl. 78−5881
ion beam injection, direct energy conversion with space-charge compensation 78−87461
ion beam injection, heating and acoustic instabilities 79−60154
ion beam injection, instabilities 77−19724
ion beam interaction in mag. field, beam relax., nonlinear stages, heating *(Russian)* 77−47217
ion beam-plasma, effect on ion acoustic soliton characts. 77−89271
ion beam-plasma collective interactions, high current-density 80−75066
ion beam-slab target interaction, deflagration waves form. 80−24184
ion cyclotron drift instability driven by cross-field electron current, plasma heating 78−51290
ion cyclotron heating, Tokamaks and mirrors, quasilinear model 78−59626
ion cyclotron heating by azimuthally rotating RF fields, in toroidal plasma 80−28721
ion cyclotron instability induced by perpendicular beam injection into a plasma 79−14565
ion cyclotron reson. heating, Wisconsin supported toroidal octupole 77−89276
ion cyclotron resonance heating in multiple mirror machine 77−24108
ion cyclotron slow mode wave ion motion and plasma heating 77−7509
ion cyclotron waves, oscillating two-stream instability, RF heating of tokamak plasma 80−1779
ion extractor electrode CAD *(Japanese)* 78−86680
ion heating, in toroidal theta-pinch, diagnostics 77−62381
ion heating and fine struct. of potential accompanying magnetic piston-plasma interaction *(Russian)* 78−9798
ion heating and ion acoustic turbulence 77−11370
ion heating by coherent ion-acoustic wave 78−94924
ion heating by current driven turbulence in inhomogeneous plasma 80−33791
ion heating by current-driven turbulence in inhomogeneous plasma 80−96370
ion heating by electrostatic waves across mag. field 77−65894
ion heating by injected ion beam 78−34335
ion heating by injected ion beam 78−34336
ion heating by lower hybrid mode, nonlinear theory 77−42998
ion heating by nonlinear ion-acoustic waves excited by whistlers and Alfven waves 79−82060
ion heating by white noise signals, in double plasma devices 79−82077
ion heating due to collisionless drift-wave turbulence 80−106949
ion heating in presence of ion cyclotron instabilities 77−68871
ion heating in slide-away regime, electrostatic modes 77−68795
ion source, electron backstream to source plasma region 80−96369
ion temp. and parametric decay development in RF-generated stellarator plasma 80−79436
ion temperature, spectroscopic meas. in plasma with RF and neutral beam heating 78−5934
ion temperature scaling, using 10-channel neutral particle energy analyser 77−72496
ion-acoustic heating, renormalised turbulence theory 77−988
ion-acoustic instability ohmic heating, ion/electron temps. formulae 77−7570
ion-acoustic resonant oscills., collision integral under strong turbulence conditions *(Russian)* 77−47231
ion-acoustic turbulence, scaling laws and asymptotic states 79−60141
ion-cyclotron and first harmonic heating of large Tokamak 77−51204
ion-cyclotron and ion-ion hybrid reson. heating 78−22523
ion-cyclotron drift instability driven by cross-field current 77−35341
ion-ion hybrid damping in D_2-H_2 plasma 79−77361
ion-ion hybrid resonance damping and heating in the ERASMUS Tokamak 80−92345
ion-sound waves in turbulently heated plasma, parallel and perpendicular propag., microwave obs. 79−14612
ionosphere, electron distrib. rel. to production rate and heating 80−105103
ionosphere, heating by powerful radio emission with random modulation of carrier freq. 80−109310

plasma heating continued
ionosphere, radiowave heating rel. to form. of mid-latit. E_s-layer 77−60514
ions, high energy tail formation associated with lower hybrid heating 79−98940
ISX-B, electron cyclotron microwave heating 80−99329
ISX-B, high power neutral beam injection studies 80−79545
ISX-B, neutral beam power system 80−91283
ISX-B Tokamak, intense heating, plasma position and current, feedback control modeling 80−33802
Japanese Tokamak research, impurity control, low-q discharge, scaling law, RF heating 80−74015
JET, additional heating systems 77−68834
JET additional heating power supply and protection 78−66391
JET project description 78−58399
JFT-2 Tokamak, plasma heating near lower hybrid frequency 80−28698
JIPP T-II, simultaneous neutral beam injection and lower hybrid heating 80−79516
Joule heating and Lorentz force effects in gravity waves generated from auroral electrojet 78−28393
Joule heating effect on plasma heat transfer 78−38513
JXFR, neutral beam injection system, gas-beam interaction secondary particles 80−106227
klystron development, UHF, 600 kW, stability and durability improvement *(German)* 80−106211
L-2 stellarator, ohmic heating discharges with gas puffing 80−79593
L-2 stellarator, ohmic heating ion component characts. and particle lifetimes *(Russian)* 78−59547
Langmuir turbulence, relativistic electron increase with heating *(Russian)* 79−27799
Langmuir turbulence, statistical theory 80−38647
Langmuir turbulence driven by constant pumping 78−75341
Langmuir wave excitation by two pumping waves, convective instability *(Russian)* 80−14904
large-volume plasmas, prod. and heating using plasma return current discharge 78−94920
LHR frequency range waves interactions in octopole Tokamak 80−28724
linear compression of plasma vortex 80−64755
linear magnetic solenoid reactor plasmas, dynamic behaviour 80−64751
linear theta pinch Isar II, low compressed high-β stellarator, surface effects 77−76161
linear turbulently heated plasma, secondary emission detector obs. 80−75100
linear wave props., parametric decay, heating 78−42758
localised lower hybrid wave enhancement of drift waves 78−67343
long time confinement of pure electron plasma, max. confinement time 80−48954
low freq. axisymmetric pumping, collisionless heating for toroidal plasma 77−76134
low frequency heating wave, parametric instabilities induction in mag. confined plasma 80−24187
low frequency parametric processes in magnetically confined plasmas 80−28827
low-frequency plasma instability, high frequency electrostatic eigenmode drive 79−60118
lower hybrid cones, trajectory meas., mag. field line determ. 80−33817
lower hybrid decay wave ray trajectories, ergodic behaviour 79−19022
lower hybrid drift instability, cross-field electron current, ion heating 79−23414
lower hybrid frequency heating by wave absorpt. 77−68815
lower hybrid heating, collective effects 79−14570
lower hybrid heating, nonlinear pump wave absorption, Tokamak appls. 78−34344
lower hybrid heating, parametric excitation 77−68816
lower hybrid heating experiments in JFT-2 Tokamak 80−28747
lower hybrid heating in inhomogeneous mag. fields 79−37489
lower hybrid heating in JIPP T-II tokamak plasma, obs. 79−86617
lower hybrid heating in toroids, US experimental program, review 80−28748
lower hybrid heating of toroidally confined plasma, transport, theory 78−42723
lower hybrid pump wave two-dimens. depletion by quasi-mode excitation 78−67344
lower hybrid radiation coupling at plasma edge 77−76143
lower hybrid reson. heating, canted mag. mirror electron cyclotron reson. plasma 77−19727
lower hybrid resonance heating, RF breakdown of resonators, 0.8-0.9 GHz 77−84564
lower hybrid resonance heating in WEGA Tokamak, effectiveness study 80−28746
lower hybrid resonance heating mechanisms and effects 79−98931
lower hybrid resonance heating theory of Tokamak plasmas 80−28745
lower hybrid RF heating, parametric instabilities 77−24102
lower hybrid RF heating, parametric oscillations 78−30432
lower hybrid wave excitation, by periodic slow E waves, appl. RF heating 77−62360
lower hybrid wave excitation, of mirror mag. field plasma 79−19054
lower hybrid wave heating, alumina loaded antenna 79−4159
lower hybrid wave heating, electron distrib. function *(Russian)* 80−83951
lower hybrid wave heating, quasilinear effects 80−28763
lower hybrid wave heating in Alcator-A Tokamak 79−82078
lower hybrid wave heating in Doublet IIA 80−28723
lower hybrid wave heating in JIPP T-II 80−28722
lower hybrid wave heating simulation in nonuniform plasma 80−64771
lower hybrid wave in nonuniform density plasma, propagation and heating 79−90402
lower hybrid wave propag. and parametric decay in WEGA Tokamak 80−28725
lower hybrid wave scattering by density fluctuations, effect on Tokamak plasma heating 79−94792
lower hybrid waves, filamentation and spatial attenuation in Tokamaks 80−28665
lower hybrid waves, nonlinear behaviour, near linear mode-conversion point 80−53963
lower hybrid waves, nonlinear evolution 79−64857
lower hybrid waves, propag. in toroidal plasma 80−83927
lower hybrid waves, ray trajectory and ion absorpt. in Tokamak 80−28667

plasma heating continued
lower hybrid waves, trajectories and damping in Tokamak plasma 80−83922
lower hybrid waves penetration and linear absorpt. 77−65869
lower ionosphere, heating by radio waves rel. to nonlinear focusing 77−60511
lower-hybrid wave absorption in the presence of simultaneous density and magnetic field gradients 79−94790
magnetic accumulation in plane liner, flux loss and equiv. cct. 79−14571
magnetic field diffusion, on nonuniform Lagrangian mesh, exact energy conversion 78−91080
magnetic fusion program in US, recent exptl. results 79−85781
magnetic mirror, injected plasma particle refl. (trapping), quiescent (turbulent) plasma 80−48955
magnetic mirror ion confinement increases, Joule heating 80−83985
magnetic mirror plasma, field compression method in which field is propagating wave 79−98957
magnetic pinch discharge, superstrong mag. field prod. 79−90444
magnetic reconnection, plasma accel., heating and shock form. 78−40773
magnetised plasma electron heating in parametric modulation instability 78−75384
magnetised sheet plasma, sheath reson., RF plugging 77−15206
magneto-acoustic resonance heating in the ion-cyclotron frequency domain 79−98932
magneto-acoustic wave, finite-amplitude, heating characts. *(Russian)* 77−11368
magnetoacoustic heating by ion Landau damping 80−92341
magnetoacoustic oscillation excitation in strongly inhomogeneous plasma 80−38641
magnetoacoustic oscillations, parametric decay in cylindrical plasma 80−24157
magnetoplasma, intense EM wave absorption, numerical results 80−43890
magnetoplasma, weakly ionised, perturbational heating in oscill. elec. field, collisional relax. and Boltzmann eqn. 79−37515
magnetoplasma coaxial Gaussian EM beams cross-focusing, plasma wave generation 79−32779
magnetosonic cavity mode absorpt. 79−19055
magnetosonic resonance heating in the Erasmus Tokamak 80−28720
magnetosonic wave excitation in toroidal plasma, probe meas. 77−65866
magnetosonic wave heating, near ion cyclotron freq. 77−51203
magnetosonic waves in presence of lower hybrid turbulence and heating 78−26281
materials development for fusion 80−33804
melting furnace, for steel industry, development in GDR *(German)* 78−22522
metallurgical industry appl. 77−42996
MFTF, sustaining neutral beam power supply, cct. anal. using ASTAP and EMTP codes 80−91284
MFTF, sustaining neutral beam power supply system, modelling with ASTAP code 80−91285
MHD equilibrium and stability, triangular deformation elliptic cross section *(Chinese)* 80−53950
MHD fast electron generation in shock waves propagating along magnetic fields *(Russian)* 77−990
MHD generator current density and elec. field dependence on plasma thermodynamic pulsation *(Polish)* 77−80268
MHD switch-on shocks, ionis., heating 77−80320
microwave absorption, expt. 78−75383
microwave excitation, upper hybrid reson. region, appl. heating *(Russian)* 77−3943
microwave field power transfer efficiency under electron cyclotron reson. condition 78−9789
microwave heating, toroidal mag. plasma, direct current generation 78−34271
microwave heating in ELMO Bumpy Torus, anal. 80−28829
microwave heating of plasma in EM trap *(Russian)* 80−10400
microwave high-power absorption localisation, cold cylindrical plasma column 78−51319
microwave surface wave plasma at atmospheric press. 79−50868
microwave trajectory and electron cyclotron heating, toroidal plasma 78−59628
minor radius compression expts. in TUMAN and TOSCA devices 77−68820
mirror fusion plasma, electron heating using external power 78−87482
mirror trapped ions under instability around ion cyclotron frequency, enhanced heating 78−5892
modulated relativistic electron beam-plasma interactions, instability 79−98929
modulation instability in magnetised plasma waves nonlinear development during heating *(Russian)* 78−47118
molecular beams, intense condensed, for injector for heating and fuelling of toroidal plasma expt. 77−24179
molecular gas heating in electron beam maintained discharge 79−27804
motional impedance and heating of low resistive plasmas 80−14913
multicharged ion heating in Z-pinch, column compression, temp. and density *(Russian)* 80−64754
multidipole plasma, origin and confinement of energetic ions 78−91123
multijet mixing chamber of plasma heating unit, heat exchange calcs. *(Russian)* 77−68813
multimegawatt gyrotron design for controlled thermonuclear reactor heating 80−59256
multiple stage cluster beam ionizer 79−67425
MW impulse generator system, for ion cyclotron heating, fusion reactor 78−70635
negative ion source and beam development for fusion reactor ignition 79−45411
Nernst-Wienecke equilibrium in linear magnetized plasmas 79−94812
neutral beam and RF heating systems for Argonne expt. power reactor 77−67891
neutral beam generation, negative ion revolving multiple beam instabilities *(French)* 80−47798
neutral beam heating, flux-conserving-Tokamak equilibria 77−11381
neutral beam heating in the Princeton Large Torus 80−106950
neutral beam injection, 120 keV, ion source 80−91357
neutral beam injection, 24 MW 400 keV H beam 80−91356
neutral beam injection, energetic ion distrib. 77−19723
neutral beam injection, energy and power requirements 80−91243
neutral beam injection, fuelling profiles effect on plasma transport props. 80−19596
plasma heating continued
neutral beam injection, impurity contaminated Tokamak 80−9403
neutral beam injection, RF instabilities, review 80−28757
neutral beam injection, ripple-assisted, loss-cone modes, stability 77−76059
neutral beam injection and adiabatic compression heating in TFTR device 77−65332
neutral beam injection expts. in ORMAK 77−68829
neutral beam injection expts. on Tokamak plasma at ORNL 80−28809
neutral beam injection heating, computer simulation, Monte Carlo method 77−68859
neutral beam injection heating, in PLT 79−82074
neutral beam injection heating in JIPP-II Tokamak 80−28710
neutral beam injection heating in Tokamaks, review 80−28729
neutral beam injection heating in toroidal mag. field with new lens system 77−67535
neutral beam injection in JIPP T-II, investig. 80−28810
neutral beam injection in Tokamak, impurities and elec. field effects 77−65883
neutral beam injection in Tokamaks, review of technology progress 80−28731
neutral beam injection into mirror machines 77−68830
neutral beam injection systems, beam intensity distribs. 77−34055
neutral beam injection systems based on negative ions, review 80−42852
neutral beam injection systems for reactors and advanced expts. 77−67886
neutral beam injection USA research 80−27808
neutral beam injector research and development, in USA 77−76118
neutral beam injectors, fast, for TFR 77−76140
neutral beam line for plasma heating, stray particle loss near deflection magnet 80−47794
neutral beam module component design and development for MFTF 80−91270
neutral beam source, 40 kV for TMX, engineering design 80−91358
neutral beam system for Princeton Large Torus 78−9019
neutral beam US development program and review 80−92348
neutral beam-heated PLT plasma, neutron emission meas. 79−68954
neutral beams in mag. fields, enhanced reionisation loss 77−68808
neutral high power beams, optical diagnostics 80−92394
neutral injection, in thermonuclear reactor 77−67888
neutral injection, prod. of H^- ions from accel. cluster ions for neutral beam 77−65376
neutral injection, quasiperpendicular, in Frascati Tokamak 77−68831
neutral injection heating, ion power balance 77−67887
neutral injection heating of CLEO stellarator−theory and experiment 80−28755
neutral injection heating of Cleo stellarator 80−28714
neutral injection heating of large Tokamaks and reactors 77−68828
neutral injection heating of toroidal plasmas, theory 79−98938
neutral injection heating of Wendelstein VII A stellarator 77−68832
neutral injection heating systems for ORMAK 77−68827
neutral injection parameters and beam line design for TEXTOR 80−28811
neutral injection systems at Princeton plasma lab. 77−68826
neutral-beam requirements for compression-boosted ignited Tokamak plasmas 78−78494
neutral-beam-driven current evolution in Tokamak plasmas 80−28712
neutron production in Maxwellian D ion plasma, ion temp. diagnostics appls. 80−49005
non-stochastic heating by electrostatic waves 78−47136
non-stochastic heating of magnetized plasma by electrostatic wave 80−10405
noncircular Tokamak, heating by collisional slowing of fast ions 80−95403
nonlinear conversion, EM radiation to ion-acoustic waves, near plasma reson. *(Russian)* 78−5859
nonlinear cross-field ion acoustic instability and plasma heating 80−83928
nonlinear dissipation, effect on heating under strong Langmuir turbulence conditions *(Russian)* 78−34346
nonlinear effects in propagation of lower hybrid waves in a plasma 80−10380
nonlinear heating by lower hybrid waves 79−90422
nonlinear interaction, four-wave systems, differential eqns. 77−80319
nonlinear ion-sound waves excitation, by whistlers and Alfven waves *(Russian)* 79−27783
nonlinear stability problems, two-time method, dissipation scalings, ohmic heating 80−53967
nonlinear wave-plasma coupling at the lower hybrid frequency 79−94791
nuclear fusion, basic concepts 77−34451
octupole, lower hybrid heating and mode conversion 80−6265
Ohmic, in stellarator fields, review 78−30467
ohmic and neutral injection heating in PLT device 77−65888
ohmic heating, electron power balance, TFR device 77−67885
ohmic heating current effect on confinement in toroid 77−68854
ohmic heating currents, enhanced plasma loss in levitron 77−72460
ohmic heating in Frascati Tokamak, preliminary results 80−28734
ohmic heating in L-2 stellarator 77−72458
ohmic heating in magnetic bottle, mag. field aligned currents 78−18426
ohmic heating in stellarator fusion reactor 77−65333
Ohmic heating in stellarator Uragan-2, MHD-instability and limiting currents *(Russian)* 80−106881
ohmic heating in stellarators *(Russian)* 79−19058
ohmic heating in W VII A stellarator 77−72457
Ohmic heating of plasma in apparatus with spatial axis, MHD-instability *(Russian)* 80−106945
ohmic heating of plasmas in closed magnetic systems 80−28756
ohmic heating system for TFTR Tokamak 78−55017
ohmic heating to ignite fusion in stellarator 78−8978
Ohmic pumping by means of externally driven tearing modes 80−28706
ohmically heated plasma, in JFT-2 Tokamak, Thomson scatt. meas. 79−50890
ohmically heated Tokamak and stellarator plasmas, comparison 77−11371
optical phonons heating, stimulated combinational scattering, nonlinear effects *(Russian)* 78−34343
Ormak, confinement and neutral beam injection obs. 77−43022
oscillations, in lower-hybrid range, of bounded plasma 80−24162
overdense column, reson. microwave absorpt. 80−64732
paramagnetism in RF mag. field, expt., theory and simulation 80−6225
paramagnetism of plasma in RF field 79−46490

plasma heating continued
parameters and regimes in Thor Tokamak 77−68824
parametric absorption of EHF radiation in magnetoactive plasma *(Russian)* 79−32790
parametric cyclotron resonance 77−27234
parametric decay instability, finite pump band width effects 77−80297
parametric decay spectrum of heating near LH frequency in Petula 80−28761
parametric heating near lower hybrid frequency in Petula 80−28760
parametric instabilities, effect of finite-bandwidth pump 78−22495
parametric instabilities and ion heating in a two-ion species plasma 80−28708
parametric instabilities in hot plasma near lower hybrid freq. 77−65870
parametric instabilities in hot plasma near lower hybrid freq. 77−65871
parametric instability produced by relativistic electron beam in plasma 77−89274
parametric instability thresholds in modulated electron-beam plasma system 77−68792
parametric resonance at lower hybrid freq., electron heating 77−43000
parametrically turbulent plasma heating *(Russian)* 78−59630
particle acceleration by intense microwave irrad. 77−47230
particle beam-plasma interaction, ion-acoustic turbulence effects 78−91121
PDX neutral beam injector development 80−99375
Penning discharge, ion heating and collisional energy loss 77−72519
Penning discharge, study of hot plasma obtained *(Rumanian)* 79−7504
perpendicular collisionless shock, ion dynamics and heating, numerical anal. 77−51186
PETULA Tokamak, lower hybrid heating expts. 80−83958
Petula Tokamak, lower hybrid waves, plasma heating and nonlinear effects 80−28697
Petula Tokamak, transit time magnetic pumping 80−24186
pinch, reversed field config., heating, diffusion, stability 77−43036
pinch experiment, high energy Cu foil fuse for implosion in multimegajoule region 77−24218
plasma-wall heat transfer, fusion appls. 77−11367
PLT, fusion neutron yield during D neutral beam injection 80−79522
PLT, ICRF heating for two-ion regime 80−83959
PLT, neutral beam injection, power input and plasma temp. reconciliation 80−106224
PLT, neutral beam injection and ICRF heating, charge exchange meas. 80−83892
PLT, ohmic heating system operation 78−66401
PLT, start-up phase, volt-second consumption 80−18603
PLT neutral beam injection, impurity studies expt. ORMAK 78−58438
PLT neutral particle injectors 78−58437
PLT Tokamak, neutral beam heating 80−28701
PLT Tokamak, ohmically heated plasmas, radiation, impurity effects, instability and particle transport 80−28833
potential oscillations, parametric excitation in magnetised collisionless plasma *(Russian)* 79−55484
power flow and electron Landau damping of lower hybrid waves in cylindrical plasma 79−94784
prepulse discharges in high current accelerator diodes with double shaping line 80−5399
Princeton Large Torus, unbalanced neutral beam injection, toroidal plasma rot., Doppler shift meas., confinement times 79−77400
processing and heating applications colloquium, London (May 1979) 79−94822
pulsed erosion jet, energy characts., heat flow distribution *(Russian)* 80−33825
pulsed neutron source creation by laser/relativistic-electron-beam plasma heating 78−74527
pulsed power acceleration for fusion reactor ignition 80−63383
pump frequency oscillations, obs. in multiple pump ionospheric heating expt. 78−57382
Q-machine, single ended, collisionless plane diode model 79−7478
R-OM stellarator, MHD resonant HF heating 80−79518
radial ion energy measurements in a fast theta pinch 78−67412
radiation due to gas layer impact against obstacle at very high vel. 80−19602
radiation-driven ionisation fronts, head-on collisions, temp. jump ratio 77−3915
radiogalaxy, particle acceleration and plasma heating by turbulent Alfven waves 77−13227
radiowaves interaction, thermic excitation of parametric instability, controlled 80−24164
rail accelerator, ambient medium heating in tube 78−63599
rarefied plasma, heat propag. across mag. field, magnetothermal waves 77−42999
rarefied plasma, mag. field rapid penetration, magneto-acoustic shock waves, super-Alfven penetration *(Russian)* 78−59554
reactor, Tokamak, fuel injection, dynamic burn control 1-D transport code 80−68948
reactor, Tokamak, toroidal magnetic field ripple, burn control 80−63375
reactor ignition, overheated underdense Tokamak plasma, two-zone model and 1-D transport code 80−63376
recombining plasma, excited levels, population kinetics 79−90376
reflection coefficients of stationary shock waves on rigid wall for profiled pressure 78−51303
reflex discharge, device for generation, confinement and plasma heating *(Rumanian)* 78−47151
reflex triode with uniform ion flow 79−98928
relativistic electron beam, energy deposition in plane solid low Z target 78−5894
relativistic electron beam, energy transfer, axial variation 80−87909
relativistic electrón beam, scattering by mag. field errors and beam-induced waves 78−38514
relativistic electron beam, short pulsewidth, plasma heating, microwave emission 78−5884
relativistic electron beam diodes, wave shaping, numerical study 80−87911
relativistic electron beam heated plasma, mag. signal interpretation, dynamical model 77−42997
relativistic electron beam heated plasma, Thomson scattering system 78−75421
relativistic electron beam heating, beam scatt. 79−37519
relativistic electron beam heating, magnetosonic wave emission 77−51206
relativistic electron beam heating, return current processes 77−51205
plasma heating continued
relativistic electron beam heating, secondary parametric instabilities 78−26307
relativistic electron beam induced fusion *(Japanese)* 78−1859
relativistic electron beam induced heating 80−43942
relativistic electron beam induced turbulence and heating, review 80−38672
relativistic electron beam injection, ion heating investig., density depend. *(Russian)* 77−11372
relativistic electron beam injection 77−76130
relativistic electron beam injection 77−76131
relativistic electron beam interaction, relevance to space shuttle expts. 78−9796
relativistic electron beam interaction plasma electron heating 78−63573
relativistic electron beam interaction with plasma in strong mag. field 78−75372
relativistic electron beams as plasma heating mechanism for solenoid systems 80−24190
relativistic electron-cyclotron heating, computer numerical anal. by averaging methods 77−27716
resonant EM wave absorpt. in inhomogeneous plasma 77−68804
reversed field pinch, config. evolution 77−24150
reversed ultra fast theta pinch, mag. wave heating of Tokamak 77−35364
reversed-field pinch, formation, relaxation and heating studies 80−24215
review of heating expts. in Japan 77−65889
RF, helical quadrupole field, MHD helical oscills., torus 77−76135
RF, torch, trajectory and temp. history of injected particle 77−68810
RF and neutral beam heating of current-free stellarators 80−28853
RF and neutral beam plasma heating 77−65331
RF and neutral injection heating, recent developments 77−65886
RF anomalous penetration in collisionless plasma 80−64730
RF antenna, coupling theory 78−91128
RF discharge, electron heating and ionisation, rate eqns. 77−24237
RF discharge plasma skin effect counteraction by external mag. field 78−67543
RF discharge-plasma interaction, energy exchanges, magnetoacoustic wave generation 78−30485
RF driven current generation by lower hybrid waves in Tokamak 80−103116
RF electric fields in ion cyclotron excitation of multispecies plasma 80−1803
RF energy coupling by magneto-acoustic waves in toroidal plasma 80−28743
RF energy dissipation in plasma reson. conditions, collisionless mech. *(Russian)* 77−47226
RF heated multi-ion plasma, heating of selected ion 78−59629
RF heated Tokamak plasma, waveguide array excited lower hybrid fields 78−42773
RF heating, conclusions from Varenna conference (1977) 79−98935
RF heating, elevated electron temp. plasma *(German)* 79−27806
RF heating, limitation of RF elec. field by partially ionised blanket 78−42774
RF heating, mode conversion process, localised absorption 80−103170
RF heating, slow waves launched into overdense plasma by phased waveguide 79−64882
RF heating, state of art in France and European community 77−47232
RF heating at lower-hybrid freq. 77−65893
RF heating based on Fermi acceleration, expt. 79−27801
RF heating based on Fermi acceleration, theory 79−27800
RF heating in ATC, low-Z impurity radiation 80−28816
RF heating in Heliotron DM and D devices 77−72469
RF heating in low hybrid freq. band, exciting system design *(Russian)* 77−51202
RF heating in stationary systems, electron cyclotron reson. and lower hybrid regimes 79−98930
RF heating limitations, Alfven's critical ionisation velocity phenomena 80−28717
RF heating near lower hybrid freq. in Tokamak 77−68814
RF heating of dense plasma in magnetic field 77−19732
rF heating of fusion plasma *(Japanese)* 80−92338
RF heating of magnetically confined plasma, anomalous skin-effect 79−64873
RF heating of magnetized rarefied plasma 80−24195
RF heating of toroidal plasma, review 79−98939
RF heating studies at Grenoble laboratory 77−65887
RF heating using Grill waveguide array, theory 77−65892
RF heating with helical coupler 79−23431
RF intense heating, energy confinement 80−38674
RF intense localised field, magnetised plasma particle and wave heating 77−84462
RF ion heating, near to lower hybrid freq. 77−62380
RF ion parametric heating, near lower hybrid freq., turbulence, instability 77−62382
RF lower hybrid heating, ion meas. 77−65916
RF lower-hybrid heating of ATC Tokamak 77−65891
RF oscillation ponderomotive accel. of electrons in elec. double layer 80−70010
RF plasma heating, effect of wall corrugations on lower hybrid wave spectrum 80−33787
RF plasma heating, resonant surface accessibility, surface wave role 80−92346
RF plasma heating, stochasticity role 80−28752
RF plasma heating, surface wave role, resonant surface accessibility 80−75072
RF plugging, nonadiabatic, in cusped field, ion heating effect 78−59656
RF plugging and heating, rel. to plasma impedance 80−96378
RF plugging and heating of magnetised sheet plasma 79−19075
RF-method for currentless plasma production and heating 80−79519
rotating plasma, heating and diagnostics by induced poloidal currents 78−18449
rotating plasma reactors, longitudinal confinement, stability equilibrium and heating problems 80−74001
runaway electrons quasilinear relaxation, HF heated tokamak plasma 77−65837
S microwave radiation induced prod. and heating, electron temp. and density *(Spanish)* 79−98926
Sandia Labs. particle beam fusion programme 80−23134
Scyllac configuration, toroidal theta-pinch theory, review 77−24125
Scyllac fusion test reactor design 77−23252

plasma heating continued
second-harmonic generation of upper-hybrid radiation in a plasma 80−79506
self heating and saturation due to numerical instabilities 80−75067
self similar cooling wave, effective thermal cond. *(Russian)* 80−14908
self-excited cumulative flow, compression dynamics and heating *(Russian)* 78−22469
sheaf instability at moderate densities, anomalous ion heating *(Russian)* 80−43922
shear Alfven wave heating experiments in heliotron D 80−28716
shock heated dense plasma, density, temp. and press. determ. 79−32819
shock heated plasma, Al-seeded, boundary layer influence on Al I reson. line profiles 80−43876
shock heating mechanism of laser prod. plasma *(Russian)* 77−80334
shock waves, implosive and re-explosive, plasma parameters 80−48891
shock-heated dense Ar, Kr and Xe plasmas, calc. of equilibrium props. *(Japanese)* 80−79513
shock-heated dense plasma, continuum radiation and optical transmittance diagnostics 80−24202
shock-heated high-density Ar(Xe) plasmas, elec. cond. 80−38557
shock-heated plasma, interaction with nozzle-shaped mag. field 79−55478
short-circuit effect in a bounded plasma 79−27820
shortwave thermal radiation, diagnostics *(Russian)* 77−47258
simulation of neutral beam injection heating 77−79476
skin current heating of toroidal plasma 80−28715
skin heating in Frascati Tokamak 77−84461
small-aspect-ratio torus for demonstrating thermonuclear ignition 79−71966
solar atmosphere, heating of chromosphere and corona by sound waves 79−21246
solar atmosphere, shock heating and emission lines form. 77−56889
solar chromosphere, temperature distribution, acoustic wave heating 77−53508
solar corona, emerging mag. flux-tubes heating by interchange instability 77−56894
solar corona, heating by fast electron streams 80−105228
solar corona, loop heating by fast mode MHD waves 80−41801
solar flare plasma non-stationary heating by non-thermal electrons 77−17455
solar flares, plasma heating by energetic nonthermal electrons, theory 77−53505
solar quiescent prominences, heating and cooling, calc. 80−12738
solar wind electron heating at Earth's bow shock, high temporal resolution obs. 79−58197
solar wind heating by heat conduction driven ion acoustic instability 77−78591
Soviet Tokamaks review *(Russian)* 79−4192
spectroscopic electron density meas., hot point low induction vacuum spark gas *(Russian)* 80−92390
spherator, FM-1 energy loss rates of injected energetic ions 77−89270
spherical implosion, of coalesced weak shocks, approx. anal. soln. 77−55161
spherical implosions, instability growth and saturation simulation 77−79480
stabilisation of explosive instability and heating of plasma ions by modulated particle flux *(Russian)* 77−3939
steady-state space charge blowup and recovery of intense ion beams 79−1323
stellarator, current turbulent ion heating, modulation stability 80−79525
stellarator, ohmic heating current, inductorless excitation *(Russian)* 79−98864
stellarator, RF heated, quasi steady state currents, mag. field perturbation obs. *(Russian)* 77−47256
stellarator reactor, possibility of medium energy neutral beam injection 77−31489
stellarator W VII-A, neutral injection 80−83960
stellarator with ohmic heating currents 77−72467
stellarator with ohmic plasma heating, magnetic surface distortion by helical current perturbation *(Russian)* 77−15236
stellarators, controlled thermonuclear fusion expts. at Kharkov Inst., Ukrainian SSR *(Russian)* 79−13526
stochastic heating, relativistic electron generation *(Russian)* 80−83952
stochastic heating model 77−68818
stochastic heating of ion beam by lower hybrid waves 78−83586
stochastic heating of plasmas in inhomogeneous magnetic fields 80−59231
stochastic ion heating, by lower hybrid waves in Tokamak plasma 78−91126
stochastic ion heating, by perpendicular propag. electrostatic obs. 77−80322
stochastic ion heating, ion acoustic wave fluctuations obs., correlation time 78−34347
stochastic ion heating by a perpendicularly propagating electrostatic wave 80−10410
stochastic ion heating by an electrostatic wave in a sheared magnetic field 80−79520
stochastic ion heating by electrostatic wave in sheared mag. field 80−28705
stochastic ion heating by lower hybrid wave 80−28707
stochastic ion heating of turbulent plasma 77−47229
stratified plasma, obliquely propag. extraordinary microwave Budden tunnelling 80−48895
strong Langmuir turbulence, soliton flash, turbulent ion heating and relax. oscills. 78−1834
subsonic electron fluid and small spark formation 80−38792
Sun, coronal plasma heating during flares, ionisation and reverse currents 79−5793
Sun, coronal thermal stability during fast mode wave heating 80−90397
Sun, quasiperiodic microwave bursts and adiabatic heating 80−51713
superdense plasma, X-ray emission, plasma diagnosis *(Russian)* 78−30487
supernova remnants, shock-heated plasma temp. determ. 78−65676
supplementary heating in toroidal plasmas in France, review 77−24101
suprathermal electric microfields and plasma parameters in crit. vel. rot. plasma 79−60198
surface EM wave, propag. allowing for electron heating *(Russian)* 78−34321
surface heating, density rippling, and propagation cones in high-power lower-hybrid heating 80−92342
plasma heating continued
surface mag. field confinement of high-β plasma, toroidal current stabilisation 78−67401
T-10, ohmic heating, plasma confinement study 80−28768
T-10 Tokamak, plasma thermal-loss process and behaviour of impurities 79−27805
T-11 Tokamak, neutral beam injection, plasma heating and stability 80−28702
T-4 tokamak, ion cyclotron heating, obs. *(Russian)* 79−27796
tearing mode instabilities and suppression by lower hybrid fields 80−28666
temperate multi-species plasma around ion cyclotron freq. range, plane wave propagation 80−75050
TERP noncircular toroidal pinch, turbulent heating 77−24162
Texas turbulent heating experiment, fast crowbar switching system 77−23260
Texas Turbulent Torus, energetic ion production, temporal and spatial evolution 78−1855
Texas turbulent torus, turbulent heating effects 79−90442
TFR, electron cyclotron heating, computer simulation 80−79517
TFR, high power neutral beam injection and ion power balance, anomalous heat conduction 78−82511
TFR, ICRF heating obs. by all metal antenna 80−18606
TFR, ion energy balance, heating by fast neutral injection 77−43023
TFTR, neutral beam power system 80−91282
theoretical scaling laws, implications 80−28805
theory and expt. at Kharkov Inst., Ukrainian SSR *(Russian)* 79−14544
thermal energy transport, scaling laws 77−68754
thermal enhancement of plasma by EM wave transmission in mag. field *(Russian)* 80−103167
thermal induction plasma, energy balance, calorimetric meas. 78−59625
thermal ion distribution distortion by neutral injection heating 80−92344
thermal parametric instability in non-uniform plasma, theory *(Russian)* 79−27760
thermal transport from turbulent skin layer to plasma core in heating 77−31492
thermalisation of energetic charged particles in fusion plasma, QED effects 77−65834
thermalisation of fast magnetoacoustic waves near cut-off freq. *(Russian)* 77−47178
thermionic advanced convertor with auxiliary ionisation, microwave heating 77−24216
thermonuclear energy prod. by imploding pre-heated plasma 77−10489
thermonuclear fusion and the Tokamak, review *(Italian)* 79−31177
thermonuclear fusion plasmas, elem. processses and role of atomic, ionic and mol. data 80−14916
thermonuclear ignition by means of compact devices *(Italian)* 80−52778
thermonuclear plasma, ion temp. determ. 77−11405
thermonuclear target, electron beam heating and compression 77−42185
thermonuclear toroidal plasmas, heating methods 79−98934
theta pinch, fast, plasma macroscopic behaviour obs. and analysis *(Japanese)* 80−1818
theta pinch, linear, end losses, stoppering, instabilities and heating 80−24224
theta pinch, reversed-field, formation and adiabatic compression in imploding liners 78−30465
theta pinch, spark channel quasi-spherical compression, electron temp. 80−87920
theta pinch discharge, radial EM energy flow and plasma heating power 80−64747
theta pinch implosion dynamics, ionisation rate enhancement by two step process 77−58885
theta pinch plasma, absorpt. of magnetoacoustic waves *(German)* 80−10430
theta pinch pulse rapid heating of Tokamak 77−76132
theta-pinch, cool, intense relativistic electron beam interaction 78−51334
theta-pinch, electron heating in turbulent neutral layer *(Russian)* 80−10361
theta-pinch, linear, microinstability onset, anomalous resistivity, electron heating and MHD oscills. 77−27698
theta-pinch, linear, RF oscill. multiple mirror stabilisation and heating 77−89290
theta-pinch, medium density, large diameter, medium voltage, implosion meas. 77−24140
theta-pinch, neutral current sheet, electron energy distrib. meas. 80−43954
theta-pinch, strong fast growing mag. field, pre-ionisation effects *(Russian)* 80−33800
theta-pinch, with fast rising mag. fields 78−5891
theta-pinch plasma column, design of Marshall implosion coil for shock heating 77−23267
Thomson scattering meas. of heating process 80−59272
time independent ionisation structure, radiation heated plasma, numerical methods 79−7470
TM-1-MH Tokamak, HF heating expts. 80−79527
TNS, air core and Fe core ohmic heating systems 78−66402
TNS, electron cyclotron heating startup system, design 80−99330
TNS fusion reactors, negative-ion neutral-beam system design for plasma heating 80−13837
Tokamak, 26 keV trapped ion beam, RF wave heating 78−59627
Tokamak, adiabatic plasma compression, impurity spectra and Thomson scatt. *(Russian)* 77−76192
Tokamak, ATC, ion heating in ion cyclotron freqs. 77−68812
Tokamak, counterstreaming-ion, plasma refuelling and heating 77−71693
Tokamak, fast-wave heating, ray-tracing anal. 79−41848
Tokamak, flux-conserving cylindrical equilib. evolution with adiabatic compression and beam heating 80−28799
Tokamak, full dispersion relation for warm magnetoplasma near electron cyclotron freq. 77−68773
Tokamak, fusion power reactor design 77−74982
Tokamak, fusion reactor, axisymmetric, slowing-down alpha particle loss, Monte-Carlo calc. 78−59653
Tokamak, heating by accelerated neutralised change carriers *(German)* 78−67377
Tokamak, heating by pulsed elec. fields, hot ion prod. 80−24192
Tokamak, ion heating by transit time mag-pumping, exptl. evidence 78−5893
Tokamak, JFT-2, parametric heating by RF near lowr hybrid freq. 80−70023

plasma heating continued
Tokamak, JFT-2, particle and heat transport during lower hybrid heating 80−70021
Tokamak, low-beta and high-beta regime stable to ballooning modes 80−75083
Tokamak, lower hybrid heating to ignition 80−18605
Tokamak, lower-hybrid-freq. heating, parametric instabilities 79−90426
Tokamak, LT-3, ion heating by disruptive instability, ion temp. particle diagnostics 79−86593
Tokamak, neutral beam injection, low density ignition scenarios 80−48937
Tokamak, neutral beam-heated, parametric scaling 80−10406
Tokamak, octopole, obs. of RF driven plasma current 80−48910
Tokamak, Petula, vac. vessel and RF coils for compressional transit time mag. pumping heating 78−70634
Tokamak, plasma heating at lower hybrid freq., numerical treatment 79−60139
Tokamak, PLT, beam-heated, neutron emission profiles 78−63588
Tokamak, PLT, fast-wave heating of two-ion plasma through minority cyclotron reson. damping 80−24194
Tokamak, relativistic electron beam injection 80−87910
Tokamak, RF heating by lower-hybrid wave electron Landau damping 80−19595
Tokamak, second harmonic electron cyclotron resonance heating 80−64750
Tokamak, T-10, stainless steel limiter expts. in ohmic heating region *(Russian)* 80−83969
Tokamak, T-11, fast neutral beam injection, heating 77−42991
Tokamak, Texas turbulent torus, turbulent heating model 79−37518
Tokamak, Vlasov plasmas, geometrical optics approach to electron-cyclotron frequency heating 80−14917
Tokamak and tandem mirror reactors, neutral beam injection and superconducting magnets 80−63391
Tokamak apparatus for turbulent heating of plasma *(Japanese)* 78−1914
Tokamak data processing, no. of computers required 80−59252
Tokamak design, TORUS II SUPRA 79−37527
Tokamak discharge microwave preionisation at electron cyclotron resonance 80−83896
Tokamak experimental power reactor, burn cycle dynamics, confinement scaling laws and heating 77−23263
Tokamak FT-1, lower-hybrid heating using decelerating system, neutrals diagnostics *(Russian)* 79−98927
Tokamak fusion ignition, lower hybrid heating system 78−70636
Tokamak fusion reactor, steady-state, lower hybrid wave-driven, design constraints 80−10424
Tokamak fusion reactors, doublet research, plasma shape control, MHD stability 80−28837
Tokamak fusion reactors, stable equilibria using supplemental heating 80−91244
Tokamak heating by fast magnetosonic wave excitation 80−24189
Tokamak heating by plasma column mixing, electrotech. method 79−32789
Tokamak ignition equilibria and thermal stability 80−74005
tokamak induction heating coils, 50 kA prototype superconducting cable, critical current 80−106196
Tokamak installation, supplementary RF heating *(Czech)* 80−24258
Tokamak lower hybrid heating by HF field *(Russian)* 77−55159
Tokamak magnetic confinement, recent progress in Tokamak expts. for fusion energy prod., review 79−71948
Tokamak neutral injection heating, high energy ion production 79−32788
Tokamak plasma, edge cooling during RF heating, high-Z impurity prevention 78−67400
Tokamak plasma, h.f. heating and abnormal resist. *(Russian)* 77−1000
Tokamak plasma, lower hybrid wave propag. and damping, numerical study 80−64698
Tokamak plasma, quasi-mode parametric excitations in lower-hybrid heating 80−64748
Tokamak plasma, RF power coupling antennae for ion cyclotron heating 80−13878
Tokamak plasma power coupling by 500 KW RF amplifier 80−13877
Tokamak plasmas, advanced-fuel, ignition and thermal stability 80−86970
tokamak power reactor, electron cyclotron reson. heating by gyrotrons 80−99331
Tokamak power reactor, electron-cyclotron-reson.-heated, characts. 79−31188
Tokamak power reactor, steady state, lower hybrid wave driven 80−48945
Tokamak radial transport, multi-regime model including neutral beam injection 77−65840
Tokamak reactor, beam-driven, nucl. reactions among energetic ions 77−34469
Tokamak reactor, cycled, energy optimisation of burn phase 77−38406
Tokamak reactor, short-pulse D-T, burn phase control 79−86604
Tokamak reactor, thermal stabilisation by controlled ejection of fusion α-particles 77−38408
Tokamak reactor, thermal thermonucl. instability 77−74986
Tokamak reactors, prod. of noncircular discharge, ohmic heating expts. (Doublet III) 80−52785
Tokamak turbulent heating current penetration, poloidal profiles and anomalous transport 77−55158
Tokamak with poloidal divertor, discharge startup 80−48942
tokamak-10, ion energy balance, neutron flux and atom energy spectra, obs. and model *(Russian)* 79−27795
Tokamaks, gas breakers for ohmic heating circuits 78−66396
Tokamaks, high-beta, heating, confinement, dynamics studies 80−24218
Tokamaks, lower hybrid heating, simulation using BALDUR 1-D transport code 80−92339
Tokamaks, non-circular, shaping and internal structure 80−28842
Tokamaks, transport computation, heating, treatment of neutral gas, and impurities, review 79−98966
topside ionosphere, ion heating by electrostatic ion cyclotron waves 80−12606
Tormac, confinement system, magnetoacoustic heating studies 80−24217
Tornado traps, rotating plasma operation 77−15226
toroidal belt pinch, dynamics, equilib., heating, numerical simulation 77−24168
toroidal bicusp (Tormac), plasma containment, props. 77−24159
toroidal confinement system, excitation of reson. 79−90406
plasma heating continued
toroidal magnetic pumping method, efficiency *(Russian)* 80−10401
toroidal plasma, enhanced diffusion, electrostatic drift modes, ohmic heating effects obs. 77−19702
toroidal plasma, ion temp. control by neutral injection 79−37514
toroidal plasma, quasispherical liner compression 80−92381
toroidal reactors, α heating 80−13861
toroidally confined plasma, intense relativistic electron beam heating, and electron beam trajectories 78−63572
torsatrons, mag. surfaces, particle orbits, neutral injection 80−79551
torsatrons, neutral beam injection calcs. 80−48949
TORTUR I, heating by current driven turbulence 80−24191
TORTUR II, turbulent skin heating of toroidal plasma 79−98992
TORTUR toroidal device, plasma confinement and skin currents 77−76180
transient microwave heating of ionised media, exact solns. 77−19728
Transit Time Magnetic Pumping heating in Petula Tokamak 80−28739
TTMP heating 77−68753
TTMP heating 77−68819
TTT, current penetration and resistivity, probe diagnostics 79−32821
Tuman 2, adiabatic mag. field compression heating, ion energy balance 77−51238
Tuman-2A, plasma compression particle diagnostics, density and temp. *(Russian)* 80−38677
Tuman-2A Tokamak, ohmic heating and compression of plasma 80−28703
turbulence, current-driven 78−9803
turbulent, anomalous transport 78−14216
turbulent, in plasma betatron 77−76126
turbulent, ion-acoustic dispersion relation meas. 78−14215
turbulent, resistivity enhancement by LF self-modulation of electron plasma modes 78−9759
turbulent, wave dispersion relation determ. by microwave scatt. 79−27829
turbulent current discharge, high energy ion form., electrostatic analyser 77−19785
turbulent heating, current penetration and electron temp., Thomson scattering obs. 79−4158
turbulent heating, cyclotron radiation obs. 77−84502
turbulent heating, electric field penetration for nonlinear current saturating elec. cond. 77−24109
turbulent heating, emitted microwave radn. 77−43080
turbulent heating, flat top electron distrib. effect, with ion-acoustic instability 80−10399
turbulent heating, thermalisation freq. 77−39440
turbulent heating and transport in Tokamak plasma, theory 77−72421
turbulent heating by runaway electron beams, Tokamask plasma 79−73020
turbulent heating mechanism, in T-5M toroid, ion and electron temp. diagnostics *(Russian)* 77−47259
turbulent heating of large toroidal plasma, scaling problems 77−19729
turbulent heating of magnetic mirror confined plasma, rel. to Buneman instability 77−24106
turbulent heating of plasma with transverse current, mechanism *(Russian)* 77−80324
turbulent heating through skin layer, torus 77−76133
turbulent ion heating by superposed multipole field in Tokamak 79−19071
turbulent ion heating enhancement via spatial mag. field variations, catalytic scheme 77−24107
turbulent plasma, impinged charged particle, linear response theory 80−64727
turbulent resistivity, particle diagnostics 78−38541
turbulent skinned discharge, thermalisation of directed motion of plasma fluxes *(Russian)* 77−11373
turbulently heated plasma, current driven ion-acoustic wave 78−5937
turbulently heated plasma electron cyclotron radiation, spectral line width collisional broadening 78−34369
turbulently heated toroidal plasma discharge, microwave spectra obs. 79−50893
two stage ion heating, plasma injection with theta heating 77−76139
two-stage ion heating obtained in rapid theta-compression expt. 78−22520
two-stage ion heating obtained in rapid theta-compression expt. 78−22521
UHF pulse heating and brightening of weakly ionised lab. plasma *(Russian)* 77−39437
UHF TV klystron, pulsed operation for lower hybrid heating in ATC machine 78−66404
Uragan-2, ohmic heating, charged particle anomalous diffusion, turbulence, gravitational drift instability *(Russian)* 77−47150
Uragan-2, ohmic heating, hard X-ray emission from electron-wall interaction *(Russian)* 77−47215
VLF heating methods, thermonuclear prospects, review 80−28738
W VII-A stellarator, neutral injection, heating efficiencies, deposition profiles 80−79524
W VII-A stellarator, Ohmic heating, energy and particle confinement 80−24226
wall confined shock heated fusion reactor, design 80−99314
wave heating at electron cyclotron harmonics in toroidal plasmas 80−28727
wave trajectories and electron cyclotron heating in Tokamak plasmas 80−83923
waveguide array for lower hybrid wave excitation 80−48911
WEGA stellarator, lower hybrid heating 80−79515
Wega tokamak, HF heating at low hybrid freq. 77−76136
Wega Tokamak, lower hybrid heating 80−28699
Wendelstein VII-A, neutral beam injectors, performance 80−99389
whistler wave ducting caused by antenna actions 78−59586
Z-pinch, gas-embedded, α-heating, deformations and kink instability 77−24149
Z-pinch, high current discharge in Xe, heating efficiency 78−47152
Z-pinch, liner implosion non-adiabatic dynamics, MHD computer simulation 77−84488
Z-pinches of intense energy density driven by high-voltage storage lines 80−24216
α-particle heating of subignited plasma 80−92340
D plasma, explosion fusion, optimisation of Ar admixture 79−41031
Al foil in quartz dust, electrical explosion for accelerator application 80−6314

plasma heating continued
Ar arc heating, high-pressure complex heat exchange expt. *(Russian)* 80−75112
Ar, effects of Joule heating on plasma heat transfer 77−72412
Ar, ion confinement and heating, by negative plasma potentials produced by supplemental electron emission 79−41861
Ar plasma, collision-dominated electron relax., heating, at. transitions 78−18373
C influx flow rate in ohmically heated plasma, C line meas. 77−15243
CO_2, laser, semi-self-sustained discharge, optical homogeneity, mol. gas heating 80−37990
CO_2-N_2-H, laser discharge circuit parameters, effect on energy imput mode 77−75476
Cs discharge, high-press., pulsed, in capillary energy balance diagnostics 77−65920
Cs, exploding wire, striations produced at supercrit. press. 79−64952
Cs, Knudsen arc, electron beam heating and ionisation 80−75114
Cs plasma, ohmic heating, electrical conduction temp. depend. 78−71442
(D,T), reaction rate parameter, temp. dependence, fusion process in Maxwellian DT plasma 80−59254
D, compression and heating by shell, thermonuclear neutron output *(Russian)* 77−371
D plasma, density optimisation in conical system for explosion fusion 79−41032
D source, magnetically insulated, pulsed, peak beam parameters 80−32548
D^- ion source for high voltage neutral beams for fusion reactors 80−99379
D-D fusion reactor plasmas, pure and catalysed, thermal stability 80−24207
D-H plasma, HF heating by magnetoacoustic waves *(Russian)* 77−3960
D-T concentric plasma compression, optimum output of fusion neutrons 79−41030
D-T fusion plasma, parametric noise effect on temp. stability 77−39439
D-T fusion reactor core plasma, α-particle heating, dynamic characts. 77−74985
D-T plasma, density optimisation in conical system for explosion fusion 79−41032
D-T plasma ball, critical continuously shaped concentric explosive compression, approx. estimate 78−87473
D-T plasmas, ignition toroidal expt., equilibrium configs. and heating 80−28704
D-T Tokamak, high-density, ohmically-heated, transport calcs. 80−24142
D-T tokamak plasma effect of particle confinement and recycling on thermally stable regions 79−97900
$D^+ + Rb \rightarrow D^{-,0} + Rb$, equil. fraction of D^- ions, charge transfer cross section 77−65375
D_2 plasma, compression by microfusion explosion, expt. biconical system 80−13783
DT-Pu plasma, neutron induced fission, plasma heating effect 80−27800
Fe XXII, XXIV, XXV, charge exchange recomb. in Princeton large torus during beam heating 80−100067
GaAs, oxide layers prepared by anodic, thermal and plasma oxidation, in-depth profiles and annealing effects 79−61768
H, ACT-1 toroidal plasma, externally launched ion Bernstein wave 80−106967
H plasma, magnetic piston study in theta-pinch *(Russian)* 80−83971
H^+, intense beam generation, appl. to controlled fusion 77−76119
H-D plasma, fast magnetosonic wave mode conversion, in Tokamak 77−72436
H_2 beam discharge, electron kinetics in collisionless non-equilibrium plasma 80−92402
H_2, highly turbulent, produced by magnetically rotated arc 80−38769
H_2, ohmic heating, ionization meas., axial discharge 78−38511
H_2 plasma collision-dominated electron distrib. function with turbulent heating 78−71509
H_2-He plasma, shock-heated, relax. distance and equilib. electron density diagnostics 77−24180
He discharge, medium press., contraction mechanism, inhomogeneous heating 80−44024
He plasma, cooling, nonequilib.-ionised radiating ats. 77−76128
He plasma, cryogenic, oscill. excitation by hot electrons 79−55493
He+H_2 microwave plasma, pulsed high current heating at atm. press. 78−55728
K plasma, magnetic-mirror-trapped, heating with array of hot W wires 80−33789
N glow discharge, volt-ampere charact. in gas flow *(Russian)* 80−106991
N_2 discharge, anomalous heating *(Russian)* 80−1866
N_2, discharge, excitation efficiency of rot. and vibr. levels, heating due to elastic collisions and relax. 80−38751
N_2 plasma heating in electrodeless RF capacitative discharge, mechanism, impurity effect 80−59312
Ti XX 80−100067
Ti-Si_3N_4 system, reactions under heating and plasma conditions 79−95988
U plasma, RF heated for gaseous nucl. reactor, handling technology 77−23189
UF_6, high temp. fissioning plasma core reactors, fluid mechanical confinement 80−63248
Xe, electron gas shock heated, associative ionisation and photoionisation, rel. contribs. 80−43858
Xe, plasma shock front, elementary processes 80−19581

plasma impurities
see also plasma-wall interactions
active particle beam systems for meas. of plasma pot., current and impurity profiles 80−48990
Alcator A Tokamak, spatial profiles of light impurity ions 80−48948
alkali metal seeded plasma, calc. of thermal nonequilib. near-electrode region 77−55186
alkaline impurity, source function in combustion products flow *(Russian)* 77−56301
arcing and surface damage in DITE Tokamak, SEM obs. 78−59611
atomic processes determining the plasma-wall interaction 80−59247
atomic processes for mag. fusion research, review 80−42851
belt pinch, diffusion processes, impurity and neutral gas effects, 3-fluid model 77−24057
bundle divertor, mag. config., wall impurity removal for Tokamak 77−65901

plasma impurities continued
bundle divertor, Tokamak plasma, scrape off layer density decrease, model 80−28851
charge transfer excitation, of impurity ions in Tokamaks 79−4103
collision-dominated regime, transport props. 78−5850
collisional transport in Tokamaks, particle and heat sources effect 78−83529
Columbia Torus-1 belt pinch high beta toroidal device, preionisation, optimisation 80−92368
combustion product plasma, electron conc. and mobility determ. by HCN laser submillimetric interferometry 78−1889
combustion products plasma with mixed alkali impurities, elec. cond. calc. 79−86621
concentration and time evolution, numerical analysis 77−51156
concentration determ., metal atoms, HFS intensity redistrib. method 77−84498
concentration meas. from laser fluoresc. lines *(Russian)* 78−1887
concentrations on wall during Tokamak discharges, laser probing technique 80−49013
conductivity, electrical, classical, plasma impurities, Sonin polynomial distrib. function *(Russian)* 80−83894
conference on fusion research and plasma physics, Innsbruck, Aug. 1978 80−27033
current-convective instability in plasma with impurities *(Russian)* 77−68748
DC arc plasma, axial mass transport, added particle distrib. 79−86640
density and temperature by neutral beam scatt., space and time resolution 78−59668
deposition of plasma impurities, in ISX-Tokamak, time resolved measurements 80−38694
diagnostics, soft X-rays, hot TFR plasma 77−51234
diffusion, 1-dimens. code, impurity eqns. inclusion 77−15169
diffusion, in Pfirsch-Schluter regime, suppression by plasma rotation *(Russian)* 79−98867
diffusion, simultaneous, of impurities in Tokamak-like plasma 77−72413
diffusion eqn., with ionisation and recombination source terms 78−30409
diffusion in Pfirsch-Schluter regime *(Russian)* 78−26246
diffusion in Tokamak in Pfirsch-Schluter regime 77−35322
dilute low-temperature plasma, ionisation in presence of solid phase and alkali metal component 77−42989
discharge cathode sheath, weakly ionised impurities effect *(Russian)* 78−22582
dissipative trapped electron modes, in torus, impurity effect on LF drift modes 77−55139
dissipative trapped ion instability, circulating ion resons. and impurity effects, local limit 78−79427
DITE Tokamak, impurity density, soft X-ray meas. 80−19616
DIVA, metal-impurity, confinement, discharges 80−28843
divertor expt. for control in DIVA 79−662
divertorless Tokamaks, limiter pumping system 80−95463
Doublet IIA, m=1 oscills., internal disruptions, impurity line emission 77−58898
drift cyclotron instabilities, ion impurity effects 77−985
drift waves, multispecies plasma, nonlinear behaviour, turbulence, diffusion 78−59588
DTHR, advanced bundle divertor design 80−99281
electric LF microfield distribs., two-temp. plasma containing multiply charged ions 77−58843
electron dissociative attachment of mol. plasma in crossed electric and mag. fields 78−5847
electron plasma, impurity screening effects in intermediate degeneracy region 80−14882
elementary reactions in plasma fusion, diffusion, contamination bremsstrahlung and electrostatic forces *(German)* 79−46429
elementary reactions in thermonuclear fusion plasmas 79−85762
equilibrium of plasma without shell, impurities outside coronal equilibrium and hollow profiles, MAKOKOT code 80−28774
far-IR emission anal. 77−31521
fast neutral diagnostics of heated plasma, temp. determ. 77−68875
field ion samples in Tokamak plasma, impurities study 79−98971
first wall materials, effect on Tokamak plasmas 80−38692
flow reversal expt., result anal. 80−106875
flux and differential wall changes, in Alcator-A Tokamak, surface probes 80−38664
fusion devices, controlled, surface effects, conf., San Francisco, USA (Feb. 1976) 77−30659
fusion plasma, impurity radiation loss, for corona equilib. 78−91074
fusion plasma, Lawson criterion for impurity losses, energy balance eq. *(Korean)* 78−17414
fusion possibilities and plasma confinement and interactions in mag. config. Tokamak, review *(French)* 80−54017
fusion reactor, impurity and gas throughput control 78−54907
fusion reactor, STARFIRE project, impurity control system 80−102345
fusion reactor neutral gas fuelling; control of impurities and α-particles 79−76128
fusion reactor plasma impurity control using neutral gas blankets 80−13835
gas stream with dispersive impurity, initial region boundaries, impurity velocities *(Russian)* 80−100069
heavy metal contaminants, rel. abundance and charge stable comp. diagnostics by beam-foil spectroscopy 79−46480
heavy-impurity control by light-impurity radiation, wall layer cooling 77−65879
high beta toroidal device, preionisation, optimisation 80−92368
high temperature plasma, impurity ionis. equilib., radiative cooling 78−42712
high-pressure atomic and molecular impurities, preionisation by UV irrad. of surface discharge 80−38847
high-Z emitters in ultradense plasmas, hydrogenic profiles, perturbing ion effects 80−79566
ICRF heating, preliminary results in DIVA 80−28758
ICRF heating in TFR, preliminary obs. and further development prospects 80−28741
impurity atom diffusion, laser fluorescence study 79−68955
impurity control and plasma transport in plasma-edge region 80−13832
impurity density distrib., energy loss and diffusion in Tokamaks 77−65838
injected beam, edge cooling by super-banana limiter 80−43940
instabilities in Tokamak *(Russian)* 77−68763
ion component energy anal. in moving plasma 77−80366

plasma impurities continued
ion scatt., suprathermal, by partially ionised impurities, measurement of Z_{eff} 80−54039
ion temperature distrib. determ. from impurity lines Doppler broadening 79−27827
ion-drift wave eigenmodes in sheared mag. field, impurity effects 80−43911
ions on rational magnetic surfaces, convection and diffusion, collisional multifluid model 80−28615
ISX Tokamak, arcing obs. 80−33836
ISX-A Tokamak, plasma confinement and impurity flow reversal 80−28770
ISX-B impurity study program, in situ Tokamak expts. 80−37589
ISX-B noncircular Tokamak for expts. on the physics of high-β toroidally confined plasmas 80−37588
ISX-B tokamak, design of bundle divertor expt. 80−102341
ISX-B Tokamak for impurity study expts., program objectives 80−37587
JET project description 78−58399
JFT-2 Tokamak, impurity ion sputtering 80−79554
JIPP T-II tokamak plasma, Mo impurity diffusion during H_2 gas puffing 80−28602
JIPP T-II torus, neutral gas injection and plasma current control, suppression of major disruption 80−28839
JIPP-T-II Tokamak plasma, time resolved spatial profiles of impurities 80−48950
laser plasma, two component impurities *(Russian)* 78−22527
light impurities, diagnostics in T-4 Tokamak plasma *(Russian)* 80−10432
light scattering, by plasmas with ionised impurities, collision effects 79−41835
line emission, time history meas. for electron temp. determ. 77−15241
line radiation meas. of adiabatic compression in Tokamak 77−43075
linear reactor system with impurity-seeded multiple-mirror end plug 78−78493
low Z impurity transport in Tokamaks, simulation 79−55468
low-frequency instabilities in Tokamak due to trapped ions *(Russian)* 79−4125
low-Z impurities in PLT Tokamak, radiative power loss 78−91155
low-Z impurities radiation during RF heating in ATC 80−28816
low-Z impurity elements, radiative energy losses calcs. 77−39411
lower-hybrid wave absorption in the presence of simultaneous density and magnetic field gradients, impurity effects 79−94790
macroparticles elimination from plasma stream, using curved plasma duct 80−33826
magnetic confinement system, surface problems caused by dissolved H_2 80−57946
magnetic limiter effect on impurity content in Tokamak 79−661
metal impurities, DITE Tokamak plamsa, N-ion backscatt. anal. 79−4182
metal snow liberated from wall, cooling effects 78−71494
metal snow liberated from wall, cooling effects 78−71495
metal-seeded rotating plasma 80−1746
metallic atoms separation in rot, plasma, spectral meas. 79−98988
methane pulsed injection into DIVA Tokamak, transport props. 78−79411
MFTF, plasma buildup, contaminant control 80−95461
MHD generator plasma with addition of N_2, stability 79−19014
microarcing studies in low temp. RF-plasma 80−96407
moderate-Z impurity elements, radiative energy losses calcs. 77−39411
multi-ion species plasma, diffusion due to drift wave fluctuations 77−68752
multicharged ions in laser plasma *(Russian)* 79−1344
multiple mirror end plug, for linear fusion reactor, impurity seeded 78−63580
multiply charged, electron capture into different excited states in plasma 80−64679
naphthalene-He photoionis. plasma, CO_2 additive effect 80−10359
neo-Z-pinch, mag. fusion appls. 80−103180
neutral beam injection and gas puffing into ORMAK, effect on impurity behaviour 79−64878
neutral beam injection expts. on Tokamak plasma at ORNL 80−28809
neutral beam injection heating in JIPP-II Tokamak 80−28710
neutral beam injection in Tokamak, impurities and elec. field effects 77−65883
numerical modelling of effects in Tokamak expts. 79−659
ORMAK, impurity and surface studies 77−31517
PDX Tokamak, surface analysis station 80−79586
Pfirsch-Schluter transport, temp. screening effect 77−76035
plasma, charged particle energy losses, homogeneous superhigh freq. elec. field and ion polarisation effects *(Russian)* 79−90384
PLT, D_2 flux and energy incident on probe, power balance, impurity generation 80−79553
PLT, Fe-charge state distrib. by Bragg cryst. X-ray spectroscopy 79−68956
PLT edge plasma, lower limits for parallel impurity fluxes 79−1320
PLT Tokamak, ohmically heated plasmas, radiation, impurity effects, instability and particle transport 80−28833
PLT Tokamak, W ion soft X-ray emission effects 78−83537
powder particles in plasma stream, temp. distribs. meas. method and apparatus 78−14210
production during plasma-fusion reactor wall interaction *(Russian)* 78−25325
profiles, from VUV spectroscopy of TFR Tokamak plasma 78−51349
pulsator, accumulation of impurities and stability behaviour in high density regime 80−28835
PULSATOR, impurities in high density regime 80−79579
PULSATOR I Tokamak, wall analysis, impurities 77−31515
radiation balance, neutral injection heating *(Russian)* 79−46435
radiation from impurities in Tokamak or mag. mirror reactor plasmas 78−5857
reactor ignition, overheated underdense Tokamak plasma, two-zone model and 1-D transport code 80−63376
reduction of effective sputtering yield by honeycomb structures, appl. to fusion reactor first wall design 79−23440
residual gas anal., using computer controlled mass analyser, in ISX-A Tokamak 79−82096
rotating plasma reactors, longitudinal confinement, stability equilibrium and heating problems 80−74001
scrape-off layer of Tokamak, probe meas. 78−91156
simulation of impurity peak positions in TFR discharges 78−91149
Soviet Tokamaks review *(Russian)* 79−4192
plasma impurities continued
spatial distribution of impurities and H neutrals in ELMO bumpy torus 79−55559
spectroscopic meas. in DIVA Tokamak 79−27826
spectroscopic meas. of impurity contamination 79−10714
superbanana limiter as a possible edge cooling scheme 80−92362
surface contamination of EM trap, effect on plasma density 78−9822
surface erosion from plasma solid interaction 80−38665
surface impurities, in ISX-A Tokamak, AES obs. 79−82097
T-10, ohmic heating, plasma confinement study 80−28768
T-10 Tokamak, plasma thermal-loss process and behaviour of impurities 79−27805
T-10 Tokamak, plasma X-ray emission 80−28840
T-12 Tokamak with two axisymmetric divertors, characteristics of divertor 80−28844
T-4 Tokamak, impurity ion diagnosis, C nuclei absolute content *(Russian)* 79−14615
temperature and density, HFS brightness ratios of impurity metal 77−89310
TEXTOR, technical materials for first wall 77−34430
TEXTOR program at KFA, Julich 77−31505
TFR 600 Tokamak, plasma confinement, low effective plasma charge 80−28769
TFR machine, impurity behaviour, radiation losses and wall effects 77−31516
TFR Tokamak at ionisation equilibrium, heavy impurities 80−106970
TFTR Flexibility Modification, in-torus surface pumping, Ti and Zr/Al gettering 80−95451
thermonuclear plasma, radn. losses at impurities, $n_e\tau$ parameter *(Russian)* 79−68908
theta-pinch Ti ion injection by CO_2 laser, spectroscopic anal. 80−79577
Thor Tokamak, wall conditioning by cleaning H discharges 80−78440
time-resolved spatial profile in JIPP T-II tokamak, vis. spectrosc. meas. 79−86619
Tokamak, adiabatic plasma compression, impurity spectra and Thomson scatt. *(Russian)* 77−76192
Tokamak, Alcator, effect of wall temp. on O, N and C impurities, spectroscopic diagnostics 79−41840
Tokamak, anomalous diffusion with light and heavy impurities, drift wave depend. 80−64677
Tokamak, DITE, impurity ion concentrations and diffusion, spectroscopic measurement 80−28771
Tokamak, DITE, plasma and impurity fluxes on walls 80−28688
Tokamak, DIVA, impurity shielding and sweeping out, axisymm. divertor 78−86685
Tokamak, DIVA, mag. divertor action for impurity control 79−4196
Tokamak, DIVA, metal impurities anal. 79−64906
Tokamak, DIVA divertor and JFT-2 expts., impurities 77−72501
Tokamak, edge effects and impurities, influence on thermal stability 80−87892
Tokamak, heavy-impurity re-cycling and power loss at limiter 78−22543
Tokamak, high-density regime performance, scaling laws 77−11380
Tokamak, impurity beam trapping instability 77−34428
Tokamak, impurity behaviour, MHD activity influence *(Russian)* 79−98866
Tokamak, impurity control *(Japanese)* 79−82085
Tokamak, impurity control by neutral-beam injection 80−32494
Tokamak, impurity flow and H recycle effects, from wall ion beam anal. 79−46457
Tokamak, impurity ionis. degree and diagnostics accuracy, electron distrib. depend. *(Russian)* 79−98973
Tokamak, impurity transport *(Russian)* 80−106957
Tokamak, JFT-2, plasma parameter improvement by Ti gettering 79−671
Tokamak, Macrotor, metallic impurity suppression by electron injection 79−32781
Tokamak, metal impurities due to arcing 78−42787
Tokamak, metal impurity reduction by working gas injection 80−106963
Tokamak, Pfirsch-Schluter friction on H^+ 78−34272
Tokamak, PLT, current profile evolution effect on plasma-limiter interaction and energy confinement time 80−10420
Tokamak, start-up phase, plasma impurities effects 77−14265
Tokamak, surface effects and impurity production 78−94127
Tokamak, TFR, variable-radius Mo and graphite limiters 78−63600
Tokamak, TFR-600, surface conditioning and mass spectroscopy 79−672
Tokamak collisional plasmas, poloidal asymmetry of impurity spectral line emission 80−32485
Tokamak discharge, anomalous drift-wave transport anal. 79−32745
Tokamak discharge, impurity emission spectra for diagnostics 77−11403
Tokamak discharge chamber, AES anal. *(Russian)* 79−4163
Tokamak equilib., impurity radn. effect on power balance 77−72465
Tokamak first wall, angular effects in sputtering by H ions of 304 stainless steel 79−46458
Tokamak first wall low-Z materials, impurity radiation from medium density plasmas 79−55472
Tokamak for surface and impurities studies 77−31531
Tokamak fusion devices, secondary ion emission, appl. to impurity control 80−37584
Tokamak fusion reactor, RF injection for refuelling and impurity control 80−87921
Tokamak fusion reactors, model of impurity control techniques 78−17428
Tokamak impurity problems, atomic and mol. struct. and collision data, review 80−43959
tokamak impurity-control techniques 80−75082
Tokamak limiter, surface observation, infrared techniques 80−38693
Tokamak plasma, edge cooling during RF heating, high-Z impurity prevention 78−67400
Tokamak plasma, extreme UV impurity study, radiation power loss 78−42803
Tokamak plasma, light-impurity-free plasma, Au-shell surface and Ti gettered burial chamber 78−42786
Tokamak plasma, line spectra of highly ionised heavy atoms 80−79567
Tokamak plasma, Ni, Cr and Fe NeI-like ions, mag. quadrupole lines 79−13662
Tokamak plasma, Pulsator I, high density, props. and stability 77−43025
Tokamak plasma, real and simulated, impurity behaviour 78−94128
Tokamak plasma effective charge, high electron density with impurities, X-ray obs. *(Russian)* 77−19762

plasma impurities continued
Tokamak plasma-wall interaction, appl. of fluoresc. spectroscopy 79−23451
Tokamak plasmas containing momentum sources, impurity transport 80−48935
Tokamak reactor, impurity control, divertor and gas blanket model 79−90445
Tokamak reactor, impurity diversion through ambient boundary layer flow 80−19603
Tokamak reactor design, influence of physics parameters 79−36414
Tokamak scrape-off plasma, metal impurity recycling effect 80−10421
Tokamak TO-1, feedback system effect on plasma parameters *(Russian)* 80−103174
Tokamak transport codes, one-dimens., poloidal divertor simulation 79−37539
Tokamak-like plasma, impurity radiation, nonhydrodynamic coronal model calcs. 77−31433
Tokamaks, large, impurity effects and control, neutral beam injection, computational models 80−28773
Tokamaks, transport computation, heating, treatment of neutral gas, and impurities, review 79−98966
Tokamaks and reactors, applic. of bundle divertors, collisionless exhaust flow 80−27814
toroidal magnetic system, impurities, cleaning methods 78−22546
toroidal transport code for neutrals and impurities in Tokamak 77−72490
transport, in Tokamak reactor *(German)* 77−34425
transport, neoclassical theory 79−98873
transport calculations for a wall-confined liner-compressed plasma 78−63546
transport coeffs., neoclassical, for ion and impurity species 78−14137
transport in plateau to Pfirsch-Schluter regimes 77−35323
transport processes in high-β plasma with impurities and neutrals 77−11317
trapped-ion instability, transport coeff., impurity ions effect 77−76057
UV emission poloidal asymmetry obs., grad B drift 78−26331
wall released impurity transport in limiter scrape off layer of Tokamak 79−670
wall-stabilised arc conductivities with Cu vapour contamination 78−75458
Al_2O_3 powder, injected into induction plasma, particle temp. and trajectory 78−59607
Ar arc plasmas, steady-state and decaying, mol. gas impurities 80−103177
Ar plasma, H impurity, equilib. state of highly ionised plasma 78−83597
Ar plasma, inductively coupled, excitation transfer between plasma and impurities *(French)* 78−14211
Ar, plasma arc discharge, contamination near Cu electrode *(French)* 79−77443
Au, impurity radiation loss effects 78−22465
Au X-ray emission, in H_2 DIVA Tokamak plasma 79−32820
C component determ. in He and propane glow discharges 80−44032
C influx flow rate in ohmically heated plasma, C line meas. 77−15243
Cl VUV line emission from TFR-600 Tokamak 79−98987
Cr, X-ray spectra in Tokamak-10 facility plasma *(Russian)* 78−9837
Cs photoplasma, effect of H_2 impurities *(Russian)* 77−35320
Cs, trace identification in neutral-beam research 80−95401
D plasma, high current pulse discharge investig. *(Russian)* 78−47171
D-T plasmas, ignition toroidal expt., equilibrium configs. and heating 80−28704
DT multiple mirror reactor, power balance, impurities 77−74998
Fe IX, X, XI, effective dielectronic recombination rates in H plasma, emission time histories 80−79570
Fe, impurity atoms in hot plasma, radiation energy loss 78−18441
Fe, impurity radiation loss effects 78−22465
Fe ions, radiation losses in high temp. plasma 77−19678
Fe multiply-charged ions, radiative cooling of Tokamak plasma 77−19677
Fe, X-ray spectra in Tokamak-10 facility plasma *(Russian)* 78−9837
Fe XXV, He-like, dielectronic satellite spectrum, electron temp. diagnostics in plasma 79−82098
H discharges, chem. interaction with fusion reactor materials, impurities 77−35357
H isotope trapping, materials exposed to high power discharges in PLT 80−37576
H, L_β reson. line Stark broadening in equilib. plasma 79−32823
H plasma, high-temp., proton neutralisation cross-section by impurity ions *(Russian)* 77−11310
H-like ions in laser-produced plasma, Balmer fine struct. (broadening) 80−48860
H_2 contamination in He plasma, satellites of He 492.2 nm line, fine struct. interpretation 80−59235
$H(1s)+O^{8+}(He^{2+})(H^+)$, charge transfer, 0.025-200 keV/amu 79−22823
He plasma, impurity ion emissions in vacuum UV 500 to 1500 Å region *(Japanese)* 77−80363
He-like ions, spectral broadening in plasma, theory, high-Z 80−6223
He-Xe plasma, in mag. field, effect of CO_2 mol. addition on plasma parameters 77−42965
InI, in AC metal halide discharge, atomic plasma characts., a priori method 80−44034
KOH, MHD plasma mol., pot. energy curves and dipole moment, bond lengths 78−71462
Mo, beam-foil spectra, 5-55 nm, using 22-200 MeV beams, rel. to Tokamak impurities 79−46481
Mo, effect of O_2 injection in TFR Tokamak current plateau 78−22565
Mo emission in He-Ne and Ne negative afterglow 77−80307
Mo impurity flux, time resolved, in DITE Tokamak 80−63373
Mo, impurity radiation loss effects 78−22465
Mo, ionisation equilibrium, radn. losses, in high temp. plasma 77−72422
Mo XXXI-XXXIV spectra from exploded Mo wire plasmas 79−1295
N V, ionis. rate meas. in theta-pinch plasma, VUV obs. 78−26254
N^{4+}, 2s-2p excitation absolute cross sections by electron impact, rate coeffs. temp. depend. 79−94087
N^{4+}, electron-impact ionisation rate coeffs. in theta-pinch plasma 79−41878
N_2 discharge, effect of Cs additive on I-V characts. 79−32813
N_2 plasma heating in electrodeless RF capacitative discharge, mechanism, impurity effect 80−59312
N_2-Cu thermal plasma, effect of Cs on intensity of spectral lines, quantitative spectral anal. appl. *(German)* 78−30417
plasma impurities continued
Na, trace identification in neutral-beam research 80−95401
NaI, in AC metal halide discharge, atomic plasma characts., a priori method 80−44034
Ne, impurity flow reversal effect in Tokamak plasma 79−7446
O, impurity radiation, metastable transitions in Tokamak, modified coronal model 78−26255
O, impurity radiation loss effects 78−22465
O, in 2XIIB mag. mirror, neutral-beam-injected 79−37547
O ions, radiation losses in high temp. plasma 77−19678
O, line emission temp. meas. in LT-3 Tokamak 77−65914
O trapping and removal, Microtor Tokamak, low-temp. H plasma 78−22541
O VI, ionis. rate meas. in theta-pinch plasma, VUV obs. 78−26254
O^{5+}, electron-impact ionisation rate coeffs. in theta-pinch plasma 79−41878
$O^+ + H$, cold dense H plasma, charge exchange, impurity losses, Monte Carlo simulation 78−34260
Pb particles, evaporation in arc plasma, integral eqn. method calcs. 78−1942
SF_6, high-temp. circuit-breaking arc, Cu impurity effect on heat transport 79−19105
Si, impurity atoms in hot plasma, radiation energy loss 78−18441
Ti, atom-electron collisions in inner discharge column *(Russian)* 80−38529
Ti density meas. in PDX Tokamak using Ti XVII forbidden line 80−32496
Ti impurity flux, time resolved, in DITE Tokamak 80−63373
TlI, in AC metal halide discharge, atomic plasma characts., a priori method 80−44034
W, impurity radiation loss effects 78−22465
W radiation from Tokamak-produced plasmas 78−9835
W XX to XXXV spectra and spatial distrib. in PLT Tokamak 78−55747

plasma in solids *see solid-state plasma*

plasma instability
see also plasma oscillations
2XIIB mirror, quasilinear model, stability of larger scaled machines 77−76165
2XIIB neutral beam injection confinement expts., stream stabilization 77−76164
ω_{ci} instability, suppression by electron beam injection in mirror confined plasma 78−47114
ablating fluid, model of Rayleigh-Taylor stability 78−34303
absolute dissipative drift-wave instabilities in Tokamaks 80−92296
absorptive instabilities in parametric back-scatt. of light 78−22510
accelerator, microwave generation by RF instabilities, discharge voltage depend. 77−7538
acoustic instability of flow in MHD channel 79−64842
acoustic instability of plasma flow in MHD generator channel *(Russian)* 77−89234
acoustic stability of subsonic flow in MHD channel 78−9764
adiabatic invariant J, finite-β effect in axisymmetric tokamaks 80−79538
adiabatic trap, charged particles motion, mag. field inhomogeneity effect, drift instability *(Japanese)* 77−43054
advanced fuel fusion reactor wall loading limitations and stability index beta 80−99311
air, discharge, high-current, nanosecond, explosive cathode processes and contraction 80−10449
air, non-self-sustained discharge plasma ionisation instability obs. 78−71609
air, non-self-sustaining discharge, ionisation instabilities *(Russian)* 78−26268
air, wall-stabilised arc, step and sinusoidal current change response 80−103209
air discharge, turbulent flow stabilisation effect *(Russian)* 79−99010
air flow glow discharge, voltage, current oscills. 79−55585
air plasma, optical emission, localised oscill. mode obs. 80−83903
Alfven, Tokamak reactor toroidal effects, direct mag. field approx. *(Russian)* 77−51166
Alfven instabilities in streaming plasmas with anisotropic press., appl. to solar wind 77−49259
Alfven instability in magnetosphere, theory rel. to auroral radiation generation 79−75051
Alfven instability stabilisation in non-circ. cross section of Tokamak *(Russian)* 78−26260
Alfven ion cyclotron mode in diffuse high-beta plasmas, local stability 80−92294
Alfven mode, current driven, electron-ion collisions and full dispersion function, numerical anal. 80−64726
Alfven nonlinear gravit. drift waves and β limitations in Tokamaks 80−92369
Alfven wave decay instability in hot plasma, two liq. hydrodynamic approx. *(Russian)* 79−7452
Alfven wave instability, neutral at. heated Tokamak, collisional dissipation stabilisation 77−55138
Alfven wave instability, reson. interaction with fast ions, finite-β plasma 78−51299
Alfven wave instability excitation by trapped α-particles 77−65855
Alfven wave perturbed plasma, fast magnetoacoustic wave interaction, instability phenomena 77−62351
Alfven wave-fast ion beam instability, in two-component Tokamak, Coulomb collisions 79−37509
Alfven waves, excitation of convective cells in plasma *(Russian)* 78−47097
Alfven waves, finite amplitude circularly polarised, instability 78−28502
Alfven waves, finite-amplitude circularly polarised, instability 79−4122
Alfven waves, ion beam effect on stability *(Russian)* 78−38468
Alfven waves, satellite, interaction with α-particles in Tokamak, quasi-linear theory 77−42995
Alfven waves generation outside plasmasphere, effect of bounce resons. 79−12344
Alfven waves in finite-β current carrying plasma, monoenergetic fusion product effects 78−91101
Alfven waves modulational instability, solitons 78−59576
Alfven waves shear driven instability 77−72433
Alfven-ion cyclotron instability, physical mechanism, computer simulation 77−72437

plasma instability continued
Alfven-ion cyclotron instability, stabilisation in inhomogeneous media 80−59210
Alfven-ion-cyclotron instability for axially bounded plasma 80−1788
alpha particles interaction with mag. plasma fluctuations in D-T reaetor 80−24204
in ambipolar traps, appl. to fusion reactors *(Russian)* 79−55535
amplitudes oscillations destruction in weakly collisional plasma-cold beam system 80−28695
anisotropic guiding centre plasma, stability props., rel. to Suydam function 79−64854
anisotropic plasma, cyclotron and electrostatic instabilities criteria 80−38627
anisotropic plasma jet, instability due to finite Larmor radius 77−17353
anisotropic plasma with two-dimens. inhomogeneity, absolute parametric instability *(Russian)* 77−62362
anomalous absorption of UHF radiation in electron cyclotron resonance range *(Russian)* 80−1807
anomalous cross-field transport, due to electrostatic fluctuations, theories 79−98870
anomalous drift wave transport in high temp. plasmas, thermodynamic stability 80−69980
anomalous laser radiation absorption near plasma critical density, acoustic instability 79−19063
anomalous plasma transport due to electron temp. gradient instability 80−33813
anomalous Tokamak radial transport, large mode number tearing and twisting modes 80−1747
anomalous transport effects in magnetically confined plasma columns 78−42725
anomalous transport from plasma waves 80−59182
anomalous transport processes in radially compressed reversed-field configurations, numerical simulation 80−64689
anomalous viscosity due to EM instability in turbulent plasma 80−106901
anomalous viscosity due to EM instability in turbulent plasma, nonlinear theory 80−106902
antiparallel structure build-up and stability in systems with mag. barrier 80−92371
arc, cylindrically symmetric, atm. press., steady-state stability model 78−38561
arc, helical in stabilising channel in mag. field 79−60206
arc column, helical instability limits 78−71564
arc column helical instability in axial mag. field, damping and RF-DC discharge 78−71595
arc discharge, low pressure, electrical noise in longitudinal mag. field *(Russian)* 79−10730
arc stability, energy balance with charge conservation 77−11417
astron exponential rigid rotor equilibria, excluding untrapped particles 78−67395
astron ion ring, stability against poloidal perturbations 78−83599
Astron kink stability, toroidal mag. field 79−19077
auroral plasma, stability, parallel and perpendicular propag. of electrostatic waves 79−35040
auroral plasma, turbulent acceleration by electrostatic waves *(Russian)* 80−53952
axis encircling ion gyro-instability 80−79494
axis encircling ion gyroinstability 80−64715
axisymmetric, in Tokamak equilib. 77−72482
axisymmetric high-beta tandem-mirror reactor, MHD stability 80−75042
axisymmetric mirror machine, MHD stable confinement possibilities 80−83988
axisymmetric mirror machines, long thin approx., stability and field singularity 80−83933
axisymmetric modes in non-circular cross-section Tokamaks 77−72481
axisymmetric plasma equilib. MHD eqn., exact solns. 77−65898
axisymmetric Tokamak plasma MHD equilibria and Mercier local stability criterion 78−51333
axisymmetrical field-reversed equilib. of arbitrary ion gyroradius, stability 79−32802
azimuthal angle of T-D mode induced scatt. from parametric ion-acoustic wave 78−75322
ball lightning, quantum mech. theory *(German)* 78−16082
ballooning and tearing instabilities 80−28651
ballooning criterion for multipoles 80−43915
ballooning effect in flute oscillations and plasma stability limits in ambipolar trap *(Russian)* 80−106955
ballooning instabilities in toroidally linked mirror systems 78−22542
ballooning instability boundaries in circular Tokamak 80−6241
ballooning instability in bumpy torus, hot electron annulus effect 80−53983
ballooning limit of non-circular small aspect ratio Tokamak 80−28801
ballooning mode in Tokamak, shear effects *(Russian)* 79−98890
ballooning mode topology 78−5917
ballooning modes, MHD theory, applic. to JET 80−28639
ballooning modes in low-beta and high-beta Tokamak 80−75083
ballooning modes in Tokamak with finite shear 78−5918
ballooning stable profiles in circular Tokamaks 80−92317
ballooning trapped electron mode, linear and nonlinear theory 80−28656
ballooning trapped-electron mode overlapping many rational surfaces 80−28618
beam cyclotron instability in geomag. tail region, anomalous resist. prod. 79−12353
beam instability, nonlinear theory in collisional plasma 79−82061
beam plasma collective instability, relativistic electron beam turbulence excitation 79−32786
beam plasma system, interaction efficiency, wave HF press. effects *(Russian)* 80−10395
beam propagation, turbulent nonlinear stabilisation, simulation 78−18422
beam relaxation, influence of modulation instability 78−75367
beam trapping dynamics, in weak cold beam plasma instability, DC elec. field effects 78−83581
beam-plasma, explosive instabilities, wave-wave coupling 77−15210
beam-plasma expt. in strong mag. field 77−68806
beam-plasma instability, destruction of trapping oscillations 78−71501
beam-plasma instability, effect of a plasma density gradient, fluid equation anal. 79−4156
beam-plasma instability, one-dimens. kinetic, in fluctuation plasma 79−32784
plasma instability continued
beam-plasma instability singularities, anomalous Doppler effect 80−75040
beam-plasma interaction, in plasma filled waveguide in axial mag. field 79−41841
beam-plasma interaction, in plasma-filled waveguide, beam geometry and mag. self-field effects 79−41842
beam-plasma oscill. instabilities, single and counterstreaming beams 77−72455
beam-plasma reactive instability, nonlinear evolution, wave coupling effects 79−41844
beam-plasma stability *(Russian)* 79−90421
beam-plasma system, cold beam, nonlinear interaction, numerical simulation 77−51201
beam-plasma system, dissipative beam instability *(Russian)* 79−60156
beam-plasma system, electron cyclotron instability, nonlinear development, lower hybrid oscill. effects 78−30437
beam-plasma system, electrostatic instability of electron Bernstein wave 77−11333
beam-plasma system, electrostatic wave energy, weakly explosive instability 78−18397
beam-plasma system, explosive instability due to helical electron beam 77−68807
beam-plasma system, finite amplitude wave instability, interaction with supercritical vel. beam *(Russian)* 77−31486
beam-plasma system, high-current electron beam, relax. dynamics, modulation instability of noise *(Russian)* 77−31487
beam-plasma system, instability *(Russian)* 78−1847
beam-plasma system, instability due to whistler mode EM waves 79−14564
beam-plasma system, ion beam injection, instabilities 77−19724
beam-plasma system, kink mode stability 77−76120
beam-plasma system, quasitransverse oscills. excitation by relativistic electrons, anomalous Doppler effect *(Russian)* 79−55518
beam-plasma system, reactive medium instability of space charge wave of ion beam 78−18421
beam-plasma system, reactive-medium instability, transition to inverse Landau damping obs. 77−35359
beam-plasma system, velocity-modulated ion beam, spatial evolution 77−47223
belt pinch, equilib. and stability, theory and expt. 77−43042
belt pinch IIa, high-β Tokamak equilib., stability and transport 79−10690
Bennett pinch, reverse B_z pinch, MHD stability 77−11384
beta limits for Tokamak experiments 80−83937
betatron resonance instability, axisymm. field reversed system 79−68917
BGK type waves, instability condition for unmagnetised and magnetised plasmas 77−31447
book, handbook on plasma instabilities (vol.I) 77−24080
bounce-resonance instability in solar corona, effects on type IV radio emission pulsations 78−89161
bounded unmagnetised plasma, Buneman instability and current limitation 78−75311
bremsstrahlung instability of relativistic electrons *(Russian)* 78−47103
Brillouin amplification, convective, in homogeneous plasma slab 77−24089
broadband noise effect on ion cyclotron waves 77−68778
bump-in-tail instability-generated turbulence, phase space -ranulation due to mode-mode coupling 80−38651
bump-on-tail instability, single-mode saturation, mobile ions 77−31458
bump-on-tail instability with immobile ions, single-mode saturation 77−7525
bumpy torus, ELMO, equilib., stability, confinement 77−24145
Buneman's instability, in hot ion plasma, theory 78−79422
Buneman and Pierce instability, double layer from. in collisionless plasma 80−10398
Buneman instability, and anomalous resistivity, amplitude saturation 78−75300
Buneman instability, nonlinear saturation 77−24068
Buneman instability and steady-state parameters in collisionless single ended Q-machine 80−59227
Buneman instability nonlinear saturation 80−79467
Buneman-Farley instability, nonlinear decay interactions 80−38616
Bunemann instability in presence of mag. field 80−6234
centrifugal relativistic electron beam, equilibria and stability 79−90451
Cerenkov instabilities spectra, of relativistic electron beam, in bounded anisotropic plasma *(Russian)* 78−38506
Cerenkov instability of nonuniform flows *(Russian)* 78−26263
channelling instability stabilisation, by mag. HF oscills. and magnetoacoustic waves *(Russian)* 77−47177
chaotic motion theories with appl. to controlled fusion research, review 78−93605
charged particle motion, in axially symm. trap, stability *(Russian)* 78−71519
circuit related instability of a plasma discharge 79−73056
circuit-breaking arc radiative transfer, magnetic stability, and turbulent heat exchange 78−75482
CLEO stellarator, heating, confinement and fluctuations 80−24225
coherent millimetric radiation from relativistic beam-plasma instabilities 77−39435
coherent parametric instabilities excited by two or more pump waves, appl. to ionosphere 78−57381
coherent waves in nonlinear medium, nonresonant interaction, eqns. system development and examples *(Czech)* 80−24149
cold cathode reflex arc, LF plasma instabilities *(French)* 77−62415
cold electron beam in pure runaway regime, collective drag and instabilities 80−83949
cold electron plasma waves, finite extent, reson. decay, fusion appls. 78−38485
cold mantle plasma current and mag. curvative driven modes, non-adiabatic stability anal. 80−33772
cold plasma, density short wave perturbation, elastic electron-atom collision 78−47119
collapse instability nature in Tokamak, surface currents *(Russian)* 80−92310
colliding relativistic plasma instabilities with relativistic temps. *(Russian)* 80−83913
collisional drift instability, local and nonlocal theories comparison 80−19574
collisional drift instability, shear stabilisation 78−59569

plasma instability continued
collisional drift modes, anomalous skin effect, enhanced particle penetration during fuelling, nonlinear theory 80−64703
collisional drift modes rel. to equatorial spread-F, artificial control technique 78−69602
collisional ion cyclotron instability, in auroral ionosphere 77−29574
collisional plasma, filamentation of laser beam, theory 77−84440
collisional plasma, modulation instability, turbulence by const. wave pumping *(Russian)* 80−103139
collisionless contact discontinuity, stability, astrophys. appls. 80−62002
collisionless drift instability, discrete unstable modes, transition to turbulence, theory and expt. 80−59240
collisionless drift instability, localised by electron temp. gradients 79−60129
collisionless drift modes in sheared slab geometry, stability props. 80−1786
collisionless electrostatic drift waves, linear theory, space plasma appls. 79−1305
collisionless mirror instability, of equatorial protons in Jupiter mid-magnetosphere 80−67642
collisionless plasma, expansion into vac., ion accel., instability devel. electron heat flow 80−38575
collisionless plasma, polarisation by single-mode pot. drift wave 80−106920
collisionless plasma, reunification of mag. field in plane layer *(Russian)* 77−58860
collisionless plasma current layer, tearing instability due to EM wave *(Russian)* 78−71465
collisionless plasma modulation instability, nonthermal radiation spectrum obs. 78−75320
collisionless sheath stability 80−106936
collisionless tearing mode, in plasma slab, stationary mag. field reconnection 78−83545
collisionless tearing mode, nonlinear evolution 77−58855
collisionless tearing modes, wider than 'current channel' 79−7456
collisionless tearing modes and enhanced transport; simulation 79−86607
collisionless trapped-particle instability, effect of elliptical cross-section of torus determ. 77−39417
collisionless universal instability, stability of bound eigenmode solns., convective modes 78−71472
collisonal drift wave instability, multimode stabilisation by dynamic feedback 78−79419
column equilibrium in octopole Tokamak without conducting shell 79−41858
complex eigenvalues, variation principles 79−21527
composite rotating plasma, gravitational instability, including Larmor radius, Hall currents, collisions 77−60591
compressible dissipative magnetoplasma, energy principle for stability criteria 78−91084
compressible liner implosion, stability, soluble model 79−27810
computerised analysis, collaboration collection report 80−73106
conductor, MHD kink instability 80−6307
conductors with MHD sausage instabilities, elec. resist. 80−100076
cone instability suppression in mag. mirror by profiled mag. field *(Russian)* 77−51167
confined waves with ergodic ray trajectories, instability condition 80−14894
continuous optical discharge convective flow, thermogasdynamic instability 78−75397
contracted positive column head oscillations 78−67516
convective, electron waves nonlinear propag. 78−1825
convective cell excitation by Bernstein waves *(Russian)* 80−53961
convective cell modes, parametric excitation by lower hybrid wave 77−55136
convective cells form. by modulational instability 79−98903
convective instability, harmonic generation and anomalous absorpt. in pumping wave decay *(Russian)* 80−14889
convective instability and nonaxisymmetric waves, in weakly ionised plasma in strong mag. field 79−90397
convective instability in inhomogeneous mag. field 78−67340
convective-like modes in plasma slab with mag. shear 77−68783
cool regions in relativistic plasmas: thermal instabilities 80−17486
counter streaming electron beam instability, stabilisation 78−1849
counter-streaming electron beam instability 77−62376
counter-streaming electron beams in stationary background, longitudinal mode instability 78−26273
counter-streaming instabilities, electrostatic wave oblique propag. 78−59577
counter-streaming plasma, electrostatic instability, theory and simulation 78−59578
counterstreaming electron beams, plasma form. and oscill. excitation 77−27687
coupled intensity deviations from stationary nonlinear state, space and time soln. 80−48882
coupled Langmuir and ion-acoustic solitary waves, theory of two-dimensional stability 78−38476
coupled Langmuir and ion-acoustic solitons, instability 78−75294
coupled mode equations, linearised, space time solns. 80−87884
coupled resistive g/ion temperature gradient instability 80−79481
coupled three wave system, instability saturation, bifurcations and strange attractor 80−59233
criterion for absolute instability of a wave in a nonuniform medium 80−106903
critical surface density profiles, radial stability 79−55460
cross field instability in equatorial electrojet over Africa, multifreq. HF radar studies 78−36370
cross-field plasma ion acoustic instability in asymptotic quasilinear limit 79−77379
cross-field-current driven lower-hybrid instability from electron beam injection, ion heating 77−65860
crossed field two-stream instability in polar cap ionosphere, electrostatic waves obs. 79−29927
crossed-field discharge plasma instabilities, obs., 10 kHz to 2 GHz 78−75306
crossfield instability in collisional magnetoplasma, dispersion, spectral chracts. 77−31464
current carrying magnetised plasma, parametric resonance 79−68918
current convective instability in auroral zone, rel. to localised nighttime scintillation enhancements 80−98506
current convective instability in diffuse aurora 79−70907
plasma instability continued
current density distrib. in terms of heating rate and plasma stability 79−98937
current disruption, in Tokamak plasmas, schlieren signal meas. from millimetre waves 80−48998
current driven collisional drift and Alfven instabilities in sheared mag. field 80−1795
current driven electromagnetic ion cyclotron instability 79−32762
current driven instabilities, anomalous effects 78−91096
current driven instabilities rel. to fast particle emission 77−19707
current driven modes, cold mantle systems, stability props. 80−92287
current instability, in reconnecting current sheets 77−37486
current instability on short wave drift oscills., nonlinear theory *(Russian)* 80−53981
current interruption mechanism in collisionless plasma 78−42721
current-carrying plasma sheet stability 79−60133
current-convective instability in plasma with impurities *(Russian)* 77−68748
current-convective instability stabilisation by mag. field *(Russian)* 77−3930
current-driven collisional drift and Alfven instabilities 79−46445
current-driven collisional drift and Alfven instabilities in sheared mag. field 80−92286
current-driven collisional drift instability in sheared mag. field 79−27765
current-driven collisionless drift instability 80−14893
current-driven EM modes, dispersion relation 79−41825
current-driven HF drift wave, inhomogeneous plasma instability 80−59204
current-driven instabilities, in laminar perpendicular shock 78−77430
curved relativistic electron beam, instability in plasma *(Russian)* 78−87456
cyclotron, Alfven waves self-modulation in magnetosphere *(Russian)* 78−40765
cyclotron, bounce effects caused by trapped alpha particles 77−76060
cyclotron decay instability saturation 78−26278
cyclotron instabilities of streams, Nyquist criteria *(Chinese)* 79−73001
cyclotron instability, mag. field longit. inhomogeneity effect, magnetosphere *(Russian)* 77−3929
cyclotron instability, magnetized electron plasma, anisotropic temp. 77−65851
cyclotron instability, quasilinear relativistic plasma relax. in strong mag. field, magnetobremsstrahlung *(Russian)* 80−38669
cyclotron instability, rel. to magnetosphere VLF noise intensity modulation by MHD oscills. 78−45139
cyclotron instability in magnetosphere of pulsar NP 0532, rel. to origin of radiation *(Russian)* 80−8645
cyclotron instability in solar atmosphere, rel. to radio emission polarised zebra struct. 78−96467
cyclotron instability in solar corona, rel. to radio bursts of drifting pairs type 78−24502
cyclotron instability with anisotropic kinetic temp., Nyquist diagrams *(Chinese)* 80−28627
cyclotron maser instability, linear and self-consistent nonlinear theory 77−38847
cyclotron maser instability, quasi-linear theory, calc. of microwave generation efficiency 80−1783
cyclotron maser instability, self-consistent theory for intense hollow electron beams 79−4129
cyclotron maser instability for general mag. harmonic number, appl. to electron beam propag. 79−4130
cyclotron maser instability in intense hollow electron beams, effect of energy and axial momentum spreads 80−1782
cyclotron oscillations of a large-Larmor-radius plasma 78−67338
cyclotron radiation emitted perpendicularly to mag. field, stability 77−72439
cyclotron wave instability in spiral electron beam-plasma system 79−14536
cyclotron waves, self-trapping instability 77−76067
cylindrical pellet in plasma, ablation flow linear stability anal. 80−1738
cylindrical rotating P-layer, electrostatic stability props. 79−64851
cylindrically symmetric mirror plasma, shear stabilisation 80−83978
D-T plasma model, uniqueness and linear stability of operating points 80−14897
Debye screening modifications in ponderomotive effects 80−33777
decay dissipative instability of surface Langmuir wave in semibounded plasma *(Russian)* 80−38583
decay instabilities in inhomogeneous plasma, trapped wave effects *(Russian)* 79−98893
decay instability of laser radiation in a magnetoplasma 80−1781
dense expanding plasma, laser radiation absorpt. 79−90417
dense plasma clarification by strong EM wave self-action 78−75360
dense relativistic electron gas, EM response in strong mag. fields, particle polarisation, mode struct. 80−43963
density gradient instabilities, in neutral inhomogeneous guiding-centre plasma, anal. calcs. 77−47190
destabilization of drift-universal eigenmodes by toroidal effects 80−103148
deuteron beam relaxation, charge exchange, instability, in 2-component Tokamak *(Russian)* 80−53997
diagnostics, via 1-300 kHz mutlichannel spectral analyser 77−39455
dielectric chamber, short-circuit effect, diffusion and stability obs. 78−71446
diffuse linear pinch, dispersion differential eqn. in MHD, approx. 80−64694
diffuse pinch, energy equilib., classical scalar cond. and neo-classical models 80−24208
diffusion across mag. field, mode transition process in collisional drift waves 77−80275
diffusion diode, current oscills., overneutralisation and diffusion instability 77−24199
diocotron-instability pulses, discharge current and electron loss effects 77−62423
direct Langmuir collapse, virial theory 78−79430
discharge, HF, stability under strong skin effect *(Russian)* 78−14242
discharge, pulsed ionisation initiated, non-self-maintained, instability 79−86572
discharge in crossed E and H fields, low-freq. instability 78−18475
discharge positive column, instability, of ionic component, amplification factor, dispersion eqn. 78−14232
dispersion relation for instability hindrance in a magnetically confined plasma with finite press. 80−59221

plasma instability continued
disruption, tearing and kink modes, limit of safety factor in JFT-2 Tokamak 80−38589
disruptions, internal, precursors of, tearing mode 80−28652
disruptive, in Tokamak reactor *(German)* 77−34425
disruptive, low freq. oscills. in TFR Tokamak 78−22564
disruptive instability, helical MHD modes in LT-3 Tokamak 77−76063
disruptive instability fine struct. in Tokamak, X-ray diagnostics 77−43073
disruptive instability in quasistationary MHD configuration *(Russian)* 79−55485
disruptive instability in TO-1 Tokamak, feedback stabilisation *(Russian)* 79−55546
dissipative and reactive mode transfer functions in linear multi-mirror expt. 78−63558
dissipative balloon non-threshold modes *(Russian)* 80−70000
dissipative breaking instability, stabilising influence of plasma flow *(Russian)* 78−91106
dissipative Cerenkov instability, oscill. modes, quasi-linear theory for relativistic electron beam *(Russian)* 78−59564
dissipative Cherenkov instability in relativistic electron beam, theory *(Russian)* 77−47251
dissipative drift modes in weakly ionised plasma, parametric study, dynamic stabilisation 79−64841
dissipative drift-wave instabilities, mag. shear effects, theory 78−75297
dissipative gravitating two-fluid plasma, stability 79−21171
dissipative instability, quasilinear relax. of relativistic electron beam in metal sheath bounded plasma 80−38671
dissipative instability of 1-dimens. force-free mag. field *(Russian)* 80−53956
dissipative parametric instabilities, in a strongly ionized plasma *(Russian)* 78−30422
dissipative trapped electron instability, nonlinear saturation 79−19018
dissipative trapped electron instability, spectral formulation 78−91095
dissipative trapped electron instability, turbulence theory 78−71482
dissipative trapped electron instability dispersion relation, ion-ion collisions in Tokamaks 78−34290
dissipative trapped electron instability in toroidal geometry, DC octupole obs. 78−51293
dissipative trapped electron instability ion Landau damping, finite Larmor radius effects 78−51297
dissipative trapped electron mode, overlapping many rational surfaces, asymptotic theory 79−98907
dissipative trapped electron modes, in torus, impurity effect on LF drift modes 77−55139
dissipative trapped ion instability, circulating ion resons. and impurity effects, local limit 78−79427
dissipative trapped ion instability, nonlinear stabilisation 77−11331
dissipative trapped ion instability and anomalous transport 78−22483
dissipative trapped particle instability, Connor-Hastie-Taylor transformation *(Russian)* 80−33759
dissipative trapped particle instability, quasi-linear and nonlinear theory 78−26277
dissipative trapped-electron drift tearing modes, theory 77−84428
dissipative trapped-ion instability, anomalous transport in Tokamak 77−72420
dissipative trapped-ion mode, nonlinear saturation by mode coupling 77−19688
disturbance propag. in relativistic Vlasov plasma 77−72426
divertor injection Tokamak experiment, plasma stability, energy and particle transport, and hydrogen recycling 80−28834
double layer, existence and stability of trapped Langmuir modes 80−6236
double layer formation in multiple plasma device 80−83897
double layers, electric field collapse phenomena, Buneman instability *(Russian)* 80−79476
double resonance parametric excitation due to zero and finite wavenumber pumps 77−31443
double tearing mode, linear anal. 80−92277
Doublet IIA, m=1 oscills., internal disruptions, impurity line emission 77−58898
draft waves driven by temperature gradients, ballooning limit 80−106917
drift, collisional instability, mag. shear stabilisation 78−18412
drift, stabilisation by RF electric fields at lower hybrid freq. 78−9784
'drift' thermonuclear instabilities in Tokamak reactor *(Russian)* 78−25326
drift Alfven and double tearing instabilities, nonlinear evolution 78−67348
drift Alfven waves, convective cells form. by modulational instability 79−77364
drift Alfven waves in Tokamaks, instability 78−79431
drift and sausage, noncylindrical Z-pinch dynamics, particle accel. mechanism 77−76170
drift and tearing eigenmodes, variational theory 78−71468
drift and trapped electron instabilities, in systems with mag. shear 80−28648
drift collisional tearing mode, stabilisation by coupling with ion-acoustic wave 78−59589
drift cone instability suppression by electron heating in adiabatic traps *(Russian)* 80−53959
drift cone mode, stabilisation at finite beta by warm plasma 77−7533
drift cone mode instability simulation 80−83930
drift cone mode stabilisation with warm plasma, radial normal mode calc. 78−51294
drift cone modes, electron stabilisation in mirror plasmas 77−72430
drift current-driven in self-induced and external mag. shear field 78−18411
drift cyclotron and lower-hybrid drift instabilities with magnetic shear 79−10651
drift cyclotron instabilities, ion impurity effects 77−985
drift cyclotron instabilities, temp. grad. and electron gyroradius effects 79−10653
drift cyclotron instabilities driven by ion temp. gradient 79−10654
drift cyclotron instability, nonlinear dynamics 78−30433
drift cyclotron instability with HF applied mag. field 78−51298
drift cyclotron loss cone instability, identification, suppression by RF field 78−18394
drift cyclotron loss cone instability, nonlinear saturation 80−83929
drift cyclotron loss cone instability, stabilisation by addition of cool plasma 77−7526

plasma instability continued
drift cyclotron loss cone mode stabilisation, by l.f. density fluctuations 78−47116
drift cyclotron loss cone mode stabilisation in mirror machines 79−27814
drift cyclotron loss-cone mirror instability, HF mag. field interaction 80−6249
drift dissipative instabilities, modified dispersion equation 79−1299
drift dissipative instability in two-temp. plasma 77−80298
drift dissipative modes, dynamic stabilization by oscill. azimuthal mag. field 77−47186
drift instabilities, collisionless, theory and numerical simulation 78−47106
drift instabilities, density grad., oblique propag. at zero beta 78−71470
drift instabilities, magnetospheric, assoc. with particles in ring current and plasma sheet inner edge 79−12351
drift instabilities of magnetised plasma in RF elec. field 77−24081
drift instability, collisional, nonlinear behaviour, limit cycle 77−39418
drift instability, collisionless, heat (particle) diffusion, probe diagnostics 78−59555
drift instability, collisionless, nonlinear saturation 77−68785
drift instability, collisionless, numerical simulation 78−59665
drift instability, current-driven, sheared mag. field, finite-beta effect on transport 80−28617
drift instability, electron-ion heat exchange and electron thermal conduct. effects 77−984
drift instability, electrostatic current-driven, scaling law for high density and high current Tokamaks 80−38691
drift instability, generation by action of strong radio wave on ionosphere upper layers 77−91344
drift instability, non-local, of current-carrying plasma with temp. inhomogeneities 78−59580
drift instability, stabilisation by lower-hybrid waves, electron beam-plasma interaction 77−51182
drift instability in Hall current plasma accelerator, dispersion relations 77−19705
drift instability stabilisation by RF elec. field in inhomogeneous plasma, kinetic theory 79−55536
drift instability-caused turbulence, anomalous diffusion, convective cell form. 77−43058
drift loss-cone instability, stabilisation in Pr-6 mirror trap by cold ions injection 79−32800
drift mode, current driven, electron-ion collisions and full dispersion function, numerical anal. 80−64726
drift mode, localised, in high density gas balnket boundary layer 80−43956
drift mode instability, plasma-neutral gas interaction effects 78−18403
drift turbulence theory in mag. field with shear, nonlinear wave packet formation *(Russian)* 79−77376
drift wave eigenmodes, effect of finite ion Larmor radius *(Chinese)* 80−103133
drift wave in sheared mag. field, stable eigenvalues 78−38484
drift wave instabilities, effects of hot electrons 79−7453
drift wave instability, current-driven 80−1770
drift wave instability, due to nonuniform density gradient in sheared mag. field 79−23415
drift wave instability, nonlocal collisionless, toroidal curvature effects 80−38588
drift wave instability, nonuniform density grad. in sheared mag. field 79−7461
drift wave instability in weakly ionised plasma, radial elec. field effects 78−59568
drift wave plasma instability, rel. to small-scale ionospheric irregularities assoc. with subtrough density gradients 78−40753
drift wave stabilisation by HF applied electric field 77−19701
drift wave stabilisation in collisionless plasma, by lower-hybrid waves 78−51296
drift wave stability, toroidal mode coupling effects 78−83547
drift wave stability and, drift-Alfven waves 79−37488
drift wave stability and transport theory in fusion systems 80−28653
drift wave stability in axisymmetric toroidal plasma 77−65858
drift wave turbulence, dissipative, current driven, in Tokamak plasma 80−38587
drift waves, collisional, shear stabilization 79−86577
drift waves, eigenmodes with arbitrary radial wavelengths, stability 80−64710
drift waves, instability in AC elec. field, wave growth rate and dispersion relation 80−48886
drift waves, stabilisation by lower hybrid waves of finite wavenumber 80−53968
drift waves, strongly dispersive, modulation instability, convective cell formation 80−38635
drift waves and steepened structs. in equatorial spread-F 79−2431
drift waves and trapped particle modes, non-Hermitian radial mode eqns. 77−89244
drift waves in turbulent plasma 78−1830
drift-Alfven mode stability, local theory 79−19012
drift-Alfven wave coupling, destabilisation 77−19694
drift-cone instabilities in mirror-confined plasma 80−28630
drift-cone mode stabilisation in PR-6 mirror by RF power injection 79−90399
drift-cyclotron, potential feedback control 77−19689
drift-cyclotron instability, collisional effects 77−55144
drift-cyclotron instability, feedback stabilisation, appl. to polar cusp plasma 78−7838
drift-cyclotron instability, rel. to high freq. drift waves in ionsophere equatorial spread-F 78−88973
drift-dissipative instability, excitation suppression by weak transverse mag. field *(Russian)* 80−33829
drift-dissipative instability of inhomogeneous plasma in mag. field, review 77−7536
drift-dissipative instability suppression in lower-hybrid pump wave field 80−106921
drift-mode stability analysis for the Tandem Mirror 80−64704
drift-superheating instability, mol. plasma, solitary population-inversion wave 77−15191
drift-tearing instabilities in Tokamaks 79−98912
drift-tearing modes in a Tokamak plasma 78−75289
drift-wave eigenmodes, current-driven, stability criteria 79−32769
driftwaves, self focusing and mag. field stabilisation *(Russian)* 77−47180

plasma instability continued
E×B drift instability, in nonuniform elec. field, particle aspect anal. 78−18407
E×B instability in bounded plasma, harmonic eqns. 77−51171
E×B instability in topside ionosphere, rel to plasma bubbles near dawn terminator 79−101016
E layer, nonrelativistic nonneutral, Vlasov equilib. and electrostatic stability 77−7580
e-layer, negative mass instability in electron ring accelerator rel. to microwave generation 77−83797
E-region, unstable polar cap, rocket-borne wave, field and plasma obs. 77−21978
Earth bow shock, ion and electron heating two stream instability 77−53320
EBT, neoclassical operating points, stability anal., sign of self consistent radial ambipolar field 78−30425
eigenmode analysis for inhomogeneous Vlasov plasma 79−90392
eigenmodes, universal, in collisionless plasma slab 80−38581
electric arc, self magnetic field, kink instability, plasma jets production *(Polish)* 80−19662
electric field compression near a plasma electrode 80−64736
electric field penetration in plasma with nonlinear current saturating cond. 77−19672
electrojets, Doppler spectra of current-driven plasma instabilities 79−58163
electromagnetic filamentation instability, nonlinear development 79−64852
electromagnetic ion cyclotron instability, particle anal. 79−94781
electron 2-dimens. classical plasma, dielec. response function 77−39403
electron accelerator, high current diode, mag. insulation and parasitic current, contraction instability *(Russian)* 77−58906
electron and ion beam instability in plasma-beam interaction 78−5888
electron beam, plane, stability in spatially-limited plasma *(Russian)* 79−98923
electron beam, relativistic, diocotron instability 80−27853
electron beam, relativistic, diocotron modes, magnetic shear stabilisation 80−54006
electron beam, relativistic, rotating, filamentary instabilities 77−76187
electron beam, relativistic instability in variable dissipation level plasma *(Russian)* 80−19594
electron beam excitation of pot-surface oscillations, linear theory of beam instability 79−37505
electron beam excited plasma, modulation instability of Langmuir waves *(Russian)* 77−35361
electron beam explosive instability in helical resonator, RF emission 79−55520
electron beam in circ. waveguide electrostatic instability in rippled magnetic field 80−19588
electron beam interaction, instability 79−64877
electron beam interaction, numerical simulation 78−91120
electron beam interaction with plasma, explosive wave interaction near stability boundary 77−11358
electron beam relaxation in high density weakly ionised gas *(Russian)* 80−106943
electron beam runaway instability in a Tokamak, kinetic theory 78−30427
electron beam space charge wave in mag. field, cyclotron damping 79−46459
electron beam stabilised mirror confined gas, hot electron population study 80−100089
electron beam stimulated wave instability, nonlinear dynamics *(Russian)* 77−19720
electron beam stopping process in hydrodynamic stage of streaming instability, boundary value treatment 80−103164
electron beam-cold plasma interaction, nonlinear wave growth and instability, simulation 77−89300
electron beam-magnetoplasma, radiation at or near electron plasma frequency, transverse modes 80−106942
electron beam-plasma instability, orbit perturbation theory 78−5885
electron beam-plasma interaction, electron wave cavity form. 77−35358
electron beam-plasma interaction, instability development *(Russian)* 78−55727
electron beam-plasma interaction, obs. of decay instability of beam plasma wave 79−27793
electron beam-plasma interaction, RF emission, oscill. nodes and instabilities 77−24099
electron beam-plasma low freq. instability, cyclotron oscills. *(Russian)* 80−33783
electron beam-plasma system, explosive instability 79−19050
electron beam-plasma system, explosive instability 80−1813
electron beams, counterstreaming, self-consistent computation of explosive instability 78−22494
electron beams, modulated, non-linear oscillation theory *(Russian)* 80−106898
electron beams, relativistic, striations in density distrib. rel. to plasma column instability 80−24154
electron beams, relativistic intense solid, cyclotron maser instability 79−55494
electron Bernstein modes, nonlinear scatt. of upper hybrid laser radiation 80−64720
electron bunch, relativistic, instability in reson. storage chamber 77−54381
electron burst relaxation in fluctuating plasma, formal dynamical model 78−83579
electron current driven ion wave instability, excitation, electrode type effects 80−38603
electron cyclotron harmonic waves excited by helical electron beam, time depend. 77−31455
electron cyclotron harmonic waves excited in helical electron beam-plasma system 78−1848
electron cyclotron instability on Jupiter rel. to diffuse aurora, influence of plasma injection from Io 80−4289
electron cyclotron instability suppression by selective cyclotron damping 80−83939
electron cyclotron resonance heating of Tokamak plasmas, fluctuations and instability 80−83956
electron dissociative attachment of mol. plasma in crossed electric and mag. fields 78−5847
electron fluctuation spectrum and drift instabilities in partially ionised plasmas, collision freq. effects 80−53924
electron heat conductivity, magnetic field line diffusion 80−28641
plasma instability continued
electron instability in split mag. surface config. *(Russian)* 77−68843
electron kinetic instabilities in solar wind 78−96369
electron kinetic instability in Cassiopeia A, rel. to radio spectrum secular flattening 80−101637
electron magnetised plasma, stability in circularly polarised EM wave field 80−87897
electron plasma, EM instability reduction of thermal flux, simulation 78−75272
electron plasma, parametric instability excitation by high-freq. EM waves 79−19031
electron plasma cooling by cyclotron radiation 80−69986
electron plasma wave, finite amplitude, nonlinear behaviour, sideband instability, electron distrib. function 78−38480
electron plasma wave coupling with LF wave 77−55134
electron rot. relativistic beam in magnetised plasma, Vlasov equilib. *(Russian)* 77−84452
electron runaway affect on ordinary and extraordinary modes in inhomogeneous plasma 80−28669
electron solitary holes, in magnetised collisionless plasma, form. and coalescence 79−32741
electron tearing mode instability in collisional plasma *(Russian)* 78−22477
electron temperature gradient driven microtearing mode 80−96361
electron trapping by plasma waves *(Russian)* 78−22474
electron-beam heating, modulated beam, parametric lower-hybrid instability 78−91127
electron-beam plasma, equilibria accessibility, multiple equilibria, nonlinear calc. *(Russian)* 77−84451
electron-beam-ion two-stream instability initiated turbulent state, 3-dimens. vel. diffusion 78−59595
electron-electron two-stream instability, intense relativistic electron beam interaction 78−51334
electron-ion decay instability in laser prod. plasma, backscatter diagnostics 80−43944
electron-ion instability, standing oscills. form. in counterstreaming ion beam plasma device 78−26305
electron-ion two-stream unstable plasma, anomalous cond., electron heating 80−6219
electron-plasma waves excited by cavity modulation instability investigation 80−19567
electron-positron plasma, produced by relativistic electron beam, waves, microinstabilities, collective positron accel. 79−19053
electronegative gas discharge, spontaneous oscills. 80−87977
electronegative gas glow discharge, plasma instability boundary conditions *(Russian)* 80−38739
electrophotoionised discharge, inert gases-halide mols. laser mixtures, current voltage characts. 80−38821
electrostatic, in anti-loss-cone plasma 78−34286
electrostatic, two-stream, two-dimens., nonlinear evolution, Vlasov eqn. numerical evolution 79−73032
electrostatic beam-plasma instability, axial wave electric field 78−5883
electrostatic bounce modes in mirror plasmas 80−1790
electrostatic cyclotron harmonic instability, in magnetosphere, theory and expt. 79−29945
electrostatic drift instability of Tokamak plasmas 80−96358
electrostatic drift wave instability, in sheared mag. fields 79−37483
electrostatic flow shear instability, theory and appl. to magnetopause and solar wind and appl. to 80−96359
electrostatic flute mode instability in magnetosphere, rel. to turbulent generation of electrostatic fields 78−28439
electrostatic heat flux instabilities, linear Vlasov dispersion relation 78−79420
electrostatic instabilities, crossfield-current-driven 77−31442
electrostatic instabilities in magnetosphere, rel. to electron accel. in auroral arcs array 78−36357
electrostatic instabilities role in critical ionisation vel. mechanism 78−67355
electrostatic instability, ion-cyclotron, current-driven, TFR Tokamak 80−64711
electrostatic ion cyclotron electron drift instability anal. using linear Vlasov dispersion reln. 80−1780
electrostatic ion cyclotron instability driven by a deflected ion beam 80−87879
electrostatic ion cyclotron instability driven by parallel ion beam injection 77−51176
electrostatic ion cyclotron wave, nonlinear propag. and modulational instability 78−1823
electrostatic ion cyclotron waves, modulational instability, auroral plasma 79−62643
electrostatic ion cyclotron waves, parametric excitation in two-ion-species plasma 77−76068
electrostatic ion cyclotron waves and ion acoustic waves, parametric instabilities 80−38591
electrostatic ion-cyclotron instability, EM effects 78−22488
electrostatic ion-cyclotron instability, ion beam excited 77−68781
electrostatic ion-cyclotron instability in magnetopause, rel. to rot. waves in anisotropic plasma 77−91369
electrostatic ion-cyclotron instability in solar atmosphere, rel. to coronal heating 80−51708
electrostatic microinstabilities, transport theory 80−79443
electrostatic mode whistler instability in solar wind, criterion 79−96877
electrostatic parametric instability, due to thermal coupling 80−79465
electrostatic perturbations, axisymm., cylindrical rot. plasma 77−65849
electrostatic solitary drift waves, modulational instability 78−91105
electrostatic temperature and gradient drift instabilities, linear Vlasov dispersion relation 79−90400
electrostatic Trivelpiece-Gould modes in a torus 80−38609
electrostatic wave near ion cyclotron harmonic, stochastic ion accel. 77−42980
electrostatic waves in magnetosphere, rel. to inverse loss cone electrons temp. anisotropy relaxation *(Russian)* 80−109314
electrostatically unstable heat flow in solar flares, and its consequences 78−20804
electrothermal instabilities in Hall accelerator 77−51159
electrothermal instability in Hall disc generator, ion fly wheel effect 79−4191
electrothermal stability anal. of fully ionised plasma, diffuse pinch 80−43901
elliptic column instability, mag. surface separatrix, 2-D MHD eqns. *(Russian)* 77−51212

plasma instability continued
ELMO Bumpy Taurus, trapped-particle instabilities 79−31184
ELMO bumpy torus, macroscopic MHD stability and beta limit 79−31186
Elmo bumpy torus, MHD spectrum, global instabilities, staircase model 79−73000
elongated cylinder, nonlinear MHD instabilities and convection, simulation 77−24169
EM cyclotron instability, effect of plasma drift 79−60150
EM cyclotron instability in hot plasma 78−34294
EM drift waves, nonlinear instability threshold amplitude 78−34305
EM electron cyclotron instability, axial and azimuthal bunching mechanisms 78−51295
EM field orthonormal decomposition, duality and complex vectorial space in anisotropic media 80−28754
EM fluctuations, anomalous ion loss 79−1312
EM instabilities, heat flux reduction 78−67320
EM instabilities, in beam-plasma, renormalization procedure 79−41813
EM instabilities, k, B_0, second order theory 78−38483
EM instabilities, proton-driven, in high-speed solar wind streams 79−53701
EM instabilities, thermal flux reduction 79−14529
EM instabilities in anisotropic loss-cone plasma 77−87185
EM instabilities in plasma with anisotropic press. *(Russian)* 78−22503
EM instabilities in solar corona, rel. to scatt. hypothesis for type V radio bursts 77−45378
EM instability excitation in beam-plasma system 78−30451
EM instability in counterstreaming plasmas in mag. field 78−22508
EM instability in substorm mode saturation by mag. trapping 78−24412
EM instability of relativistic electron beam penetrating in infinite plasma, collisional effects 80−64725
EM instability threshold for mag. neutral sheet 78−38500
EM instability threshold in mag. neutral sheet 78−14160
EM ion cyclotron instability in current-carrying collisional plasma 77−15187
EM ion cyclotron instability in magnetosphere, enhancement by cold plasma 77−33287
EM ion-cyclotron instability, EM particle simulation codes 78−1883
EM ion-cyclotron instability, nonlinear aspects 78−5870
EM ion-cyclotron instability vs. electrostatic ion-cyclotron instability 78−22486
EM loss-cone instability, rel. to solar type IV radio emission *(Russian)* 78−77528
EM lower hybrid instability driven by solar wind heat flux, threshold 79−88559
EM oscill. spectrum, toroidal plasma-containing system 80−79471
EM proton cyclotron instability, max. convective growth rate modifications 77−80290
EM wave absolute two plasmon parametric decay 77−76091
EM wave amplified scattering, in presence of singular point, exptl. obs. *(Russian)* 78−79439
EM wave decay instability in magnetoactive plasma *(Russian)* 78−14175
EM wave decay interaction in semi-bounded plasma *(Russian)* 77−7543
EM wave decay into two plasmons *(Russian)* 78−26290
EM wave dissipation and superstrong turbulence in inhomogeneous plasma *(Russian)* 80−83919
EM wave parametric absorption in plasma turbulence, instability effects *(Russian)* 77−7551
EM wave parametric decay to electrostaatic wave, mode coupling of modulational instabilities 80−24161
EM wave propagation and instabilities in magnetosphere 77−87186
EM wave self action during modulation instability *(Russian)* 80−14905
EM wave self-action during thermal modulation instability of high hybrid oscills. *(Russian)* 80−53980
EM wave stimulated backscattering in bounded dissipative plasma, nonlinear theory 77−7547
EM wave stimulated combinational scatt. and particle trapping 78−75358
EM waves, extraordinary parametric decay into two upper hybrid plasmons 80−43904
energetic particle trapping by Alfven wave instabilities 80−31205
energy lifetime of plasma, T-3 scaling law, in Tokamaks 80−28635
enhanced line radiation from active molecular plasmas due to electron collision induced instability 78−71491
enhanced losses due to collisionless drift waves, dynamic stabilisation effects 80−14888
equation of state, quantum statistical theory, degeneration, electron-hole plasma thermal instability 78−91627
equatorial electrojet and assoc. plasma instabilities 79−8750
equilibrium and stability, iron core influence in fusion reactor TFR 600 80−23150
equilibrium and stability of high-β toroidal multipoles 80−64769
equilibrium and transport in $2+\varepsilon$-dimensional two-components plasmas 79−55470
equilibrium currents, effect on separatrix characts. in l=3 stellarator 80−64706
equilibrium of electron bunches exciting nonlinear plasma wave 78−75369
equilibrium of plasma without shell, impurities outside coronal equilibrium and hollow profiles, MAKOKOT code 80−28774
ERA compression system, IPP-Japan 80−95490
expansion into vacuum, ion acceleration 80−6228
exploding wire, structural inhomogeneity and MHD sausage instability, arc chains, grain size and annealing 79−41904
exploding wire discharge, thermal instability of elec. cond. in metal vap. 78−1868
explosive, stabilisation and heating by modulated particle flux *(Russian)* 77−3939
explosive electrostatic wave instability in nonlinear medium 78−42757
explosive instabilities, nonlinear perturbation 80−59199
explosive instabilities in electron beam-plasma system 78−51318
explosive instability collision mode stabilisation by drifting effects, Thirring instability *(Russian)* 80−43920
explosive instability in electron beam-plasma system 77−84454
explosive instability of one dimensional weak mag. field *(Russian)* 80−14896
explosive magnetic field generation due to EM incident radiation, laser plasma mechanism 80−6253
explosive-type, resonantly interacting wave system 77−72443
explosive-type, space-time evolution of resonantly interacting wave system 77−35343
explosively unstable waves, in ion beam-plasma system, pump field method obs. 80−92333
external conducting sheets, stability effects on mag. contained plasmas 80−1787
external kink-mode, maximising beta in tokamak with force-free current layer 77−43043
external s-polarized pump wave, stability of electromagnetic plasma confinement *(Russian)* 79−41856
F-region, electron-ion collisions effects 78−45097
F-region field-aligned irregularity excitation and thermal parametric instability 78−77419
fan instability, in Tokamak, accelerated electron distrib. function anisotropy *(Russian)* 79−37476
fast charged particle beam density effect on stopping in matter 78−14180
fast electron prod. by parametric instability, finite bandwidth control 77−58850
fast shock heating, of electrons and ions, in high-voltage belt pinch 77−72462
feedback controller development 79−50853
feedback stabilisation of flute oscills. in direct traps *(Russian)* 77−47184
field reversed ion layer in background plasma, stability props. 79−77370
field reversed pinches, microinstability effect on MHD stability 80−79460
field-reversed ion layer, beam driven instabilities 79−64893
field-reversed mirrors, stability of low-frequency modes 79−86606
field-reversing electron ring generation in RECE Christa, millisec. lifetime, mag. probe meas. 77−24173
filamentation, due to compressional Alfven wave in laser heating 77−35342
filamentation, Langmuir turbulence effect 77−35347
filamentation instability, laser beam interacting with ion-acoustic wave 79−41838
filamentation instability, spatial growth in collisionless magnetoplasma 77−80311
filamentation instability, temporal growth, EM beam of freq. up to plasma reson. freq. 78−51304
filamentation instability caused by incident microwave 77−31473
filamentation instability growth, EM wave propag. 78−1841
filamentation instability of EM wave, spatial growth 78−51311
filamentation instability of extraordinary and ordinary modes in a magnetoplasma 78−83575
filamentation instability of laser beam in inhomogeneous plasma, preferential heating 80−19568
finger ring Tokamak, plasma stability region *(Russian)* 77−51165
finger-ring Tokamak T-12, poloidal divertor mag. config. MHD and vertical stability effects *(Russian)* 78−59643
finite Larmor radius corrections, calc. technique 79−32764
finite Larmor radius equations in an arbitrary near-theta pinch geometry 78−71523
finite-β collisional plasma, temp. fluctuations and wave induced losses with draft-Alfven instability 77−3934
finite-β plasma, crit. conditions for drift, drift-Alfven and drift-tearing instabilities in sheared mag. field 80−64699
finite-beta effects on drift cyclotron instability 79−64856
fire-hose, dynamic stabilisation by magneto-acoustic wave 78−42750
firehose instabilities, finite ion Larmor radius modifications 79−73003
fission reactor, gas-discharge, fuel element component conc., plasma temp. profile instabilities 80−63253
flame, plasma, with rectangular cross section, prod. by nozzle *(Japanese)* 78−47108
flat current sheet, rupture criteria 79−1293
flow, hydrodynamic stability near front of thermal wave 77−80283
fluctuating forces in plasmadynamics 79−68913
fluctuation diagnostics, digital time series anal. techniques 78−5951
fluctuation level saturation in magnetised plasma with anisotropic vel. distrib. *(Russian)* 78−59593
fluctuations in nonstationary nonequilibrium system, near instability boundary *(Russian)* 79−19034
fluctuations of localised plasmons under action of EM pumping wave *(Russian)* 77−76078
fluid-ion cyclotron instability, pulsed CO_2 radiation scatt. obs., theory 77−31461
flute, laser produced plasma column in uniform mag. field 80−38687
flute instabilities, velocity gradient driven 77−39414
flute instability, as trigger mechanism for cometary plasma tails disruption 78−93156
flute instability, HF electrostatic field driven, dispersion eqn. 79−46440
flute instability, hollow axisymmetric mirror, MHD stable, multipole field stabilization *(Russian)* 80−33801
flute instability excitation in Q-machine 79−46441
flute interchange mode stability, finite-β, hot electron plasma with cold components 78−67341
flute mode axial feedback stabilisation in mirror reactor 77−80344
flute mode stabilisation by axial feedback in multiple mirror 78−75408
flute modes, similar freq., simultaneous feedback stabilisation 80−103146
flute oscillations stability in ambipolar traps *(Russian)* 79−46452
flute perturbations, open mag. confinement system with radial elec. field 78−51338
focus, heating by TEA CO_2 laser, neutron enhancement *(Japanese)* 78−9808
focus, instability enhanced X-ray and neutron emissions 77−62399
focus, suprathermal microwave radiation, temporal, spectral and ang. distrib. 78−18450
focus plasma, CO_2 laser irradiated, neutron yield enhancement 77−62386
force-free magnetic fields in degenerate stars, stability 78−49425
forced oscills. generated by point antenna, drifting plasma *(French)* 80−79470
frequency response investigation as automatic control problem 79−10649
FT-1 Tokamak, discharges in low density plasma *(Russian)* 80−106958
fusion energy program, mirror approach 80−42855
fusion pellet ablation layer, Rayleigh-Taylor stability 78−58473
fusion possibilities and plasma confinement and interactions in mag. config. Tokamak, review *(French)* 80−54017

plasma instability continued
fusion products, thermalisation orbits, wall-loadings and microinstabilities 77−88284
fusion reactor, field-reversed mirror 80−42857
fusion reactor, gas insulated plasma boundary layers, ballooning modes stability 80−10415
fusion reactor, using toroidally-linked mirrors 80−42858
fusion reactors, field reversed mirrors 80−43961
fusion reactors, liquid metal linear implosion systems with blade lattice for rotational stabilisation 80−73994
fusion reactors, superheating-diffusion instability, thermonuclear burn 80−32500
fusion systems, solenoidal, instability-driven anomalous transport, review 78−22460
g×B instability in finite Larmor radius plasma, multiple time scale anal. 80−53972
galactic spiral structure formation, plasma density wave analogy *(Russian)* 77−13470
Garching Belt-Pinch IIa, effect of q on confinement and stability 80−96384
gas discharge instability near electrode 80−70064
gas discharge positive column plasma, absolute and convective instabilities of helical waves *(Russian)* 79−37478
gas flow, nonequilib. ionisation and Hall EMF 80−69981
gas-dynamic pulsation effects on turbulent gas flow discharges *(Russian)* 79−7500
Gaussian beam in plasma, nonuniform ripple growth 79−23429
Gaussian laser beam propagation in overdense plasma, self-focusing 79−55513
Gaussian ripple on uniform EM beam, growth on magnetoplasma 79−19041
generalized lower-hybrid-drift instability and modified two-stream instability, unified theory 80−1777
glow discharge, attachment instability suppression by rot. elec. field 79−64954
glow discharge, ionisation instability, stabilising effect of turbulent transport processes *(Russian)* 78−59698
glow discharge, ionisation overheat instability in alternating fields, h.v. pulse stabilisation *(Russian)* 78−91175
glow discharge, nonselfsustained, comp. and stability, peeling-off, ionisation and recomb. effects *(Russian)* 77−11414
glow discharge, positive column stability in stationary regimes 79−41893
glow discharge, sticking instability *(Russian)* 78−38559
glow discharge, superheating ionisation instability with rot. elec. field 80−79611
glow discharge instability in N_2-CO_2 non self sustained ionisation source, mechanism 80−38819
glow discharge stability, high-power mol. laser, book contrib. 77−50650
Goldreich-Keeley radiative instability, physical mechanism 79−12400
gradient drift instability, rel. to electron density struct. in F-region striated Ba clouds 78−88974
gradient drift instability in F-region, high-altitude limit 78−88984
gradient drift instability in ionospheric clouds, rel. to late time striation spectra 77−25836
gradient driven azimuthal ion acoustic waves 79−41812
gradient-driven instability 78−75291
gravitational, Larmor radius effects 78−1826
gravitational drift instability, charged particle anomalous diffusion in Uragan-2 *(Russian)* 77−47150
gravitational field effect on EM radiation propag., instability *(Russian)* 77−3946
gravitational instability of composite plasma, effect of gyroviscosity and ion viscosity 77−87255
gravitational instability of rot. plasma, effect of suspended particles 80−109347
gravitational instability of self-gravitating isotropic press. plasma theory 80−72763
grooved instability, self-adjusting feedback system for stabilisation *(Russian)* 77−68767
group velocity direction of unstable Cernekov beam-plasma modes 79−10674
growing mode instabilities, obs. in multiple pump ionospheric heating expt. 78−57382
growth rates, MHD and guiding centre plasma models comparison 77−42969
gutter modes, in pulsar magnetosphere 78−53976
gyrokinetic modes, spatial struct. in toroidal geometry 80−79489
Hall current and gyroviscosity effect on conducting, rotating viscous plasma stability 80−75041
harmonic generation, in moving plasma *(Russian)* 78−87449
harmonic oscillating two-stream instability in lower-hybrid heating 79−1311
heat and particle fluxes, inhomogeneous plasma, current driven drift wave effects 78−94901
heat flow and diffusion in Tokamak, quasi-linear theory 79−98871
heat flux limitation by ion-acoustic instability 80−92304
heat flux limitation in an ion-acoustic instability-induced turbulent plasma 79−7472
heat instability in mol. glow discharge, mol. relax. vel. const. determ. *(Russian)* 78−5959
heated layers, instability onset time 77−72461
heavy-particle acceleration by charge-density waves in vacuum and in plasma 80−70044
helical equilibria, stability code ERATO 80−79493
helical hydrodynamic instability, retrograde motion effects in plasma column *(Russian)* 77−982
helical instability in magnetised positive column 77−35344
helical instability in Tokamak, mag. shaping effect 78−42781
helical kink in reversed field pinch 77−27703
helical modes, of solar mag. flux ropes *(Russian)* 80−8617
helical perturbation in Tokamak, freq. entrapment *(Russian)* 80−10369
helical system, current-carrying, m=1 reconnecting mode, nonlinear calc. 80−6243
helical theta pinch, equilib. and stability at low compression ratio 77−43044
helically symmetric plasmas, guiding centre 79−1336
Heliotron D, RF heating, equilibrium and stability 80−28777
hexapole Tokamak, axisymmetric jumps, interpretation 80−106966
HF convective loss cone instability in short mirror machines 79−90401
HF discharge, EM wave ionisation instability model 78−67512
plasma instability continued
HF discharge, ionisation overheat instability in EM wave field *(Russian)* 80−106990
HF excited instabilities in ionosphere 78−45130
HF instability of runaway electron distrib. 79−4131
HF oscillations *(Russian)* 78−18410
HF-induced plasma instabilities in ionosphere, effect on electron temps. 78−40756
high beta MHD theory, stellarator equilibrium and stability, mirror traps and reverse field machines 80−28778
high beta plasma surrounded by cond. shell, dynamic stabilisation 80−96354
high beta stellarator, l=2,3 helical fields, stabilisation effects 80−28779
high beta stellarator stability theory 80−28797
high density plasma in multiple mirror, low freq. instability 80−48870
high density plasma stability in multiple mirror 80−79483
high energy electron induced instabilities, in Tokamak low density regime 79−98905
high frequency oscillations in bounded thermally produced plasma 78−38481
high frequency turbulent instability in magnetosphere, magnetoacoustic waves generation 77−13187
high mode number stability of an axisymmetric toroidal plasma 79−19072
high pressure, HF discharges and DC arcs in $H_2(D_2)$(inert gas), instability obs. 80−38807
high temperature mag. confined plasma, transport processes, instability 77−68755
high temperature plasma, physics, book 80−98767
high toroidal mode number stability of beam-induced tensor press. Tokamak 80−10378
high-β collisionless plasmas, velocity shear instabilities 77−35339
high-β flux-conserving equilibria, with supercond. metal shell, stability anal. 80−10428
high-β skin current Tokamak, axially symmetric displacement stability 77−65899
high-β tokamak, ballooning mode instability theory *(Russian)* 79−27757
high-β Tokamak dynamics, reduced MHD eqns., linear, nonlinear stability 77−84479
high-β Tokamaks, with anisotropic press., dynamics calcs. 79−73027
high-beta, with elongated cross-sections, MHD stability anal. 77−24170
high-beta flux conserving equilibrium, resistive magnetic flux diffusion 80−87873
high-beta pinch, kinetic behaviour, anomalous transport and unstable MHD modes 77−76163
high-beta plasmas, energy anisotropy instabilities, comparison of various kinetic and fluid descriptions 79−1310
high-beta Tokamak plasma, stability to ballooning modes 80−75091
high-beta toroidal plasma, stable confinement in levitated octupole 80−75090
high-density electrode discharge stability in very strong mag. field 78−75478
high-n ballooning theory, stability of axisymmetric tokamak equilib. 80−64705
highly ionised plasma, nonlinear effects in excitation of mag. field *(Russian)* 79−55502
hollow cathode arc with reduced gas flow, operation mode 80−38783
hollow cathode glow discharge, state of equilib., spectroscopic meas. 80−19647
hot-beam plasma, finite geometry effect, instability growth rate, quasistatic approx. 77−51200
hydrodynamic, in laser-driven ablative implosion 78−5900
hydrodynamic Cherenkov instability, electron flow-surface wave interaction *(Russian)* 77−72440
hydromagnetic instability, self gravitating finite conducting viscous plasma 79−23406
hydromagnetic Kelvin-Helmholtz instability in cometary tails, rel. to small-scale turbulence 79−44411
hydromagnetic stability of Tokamak plasma 78−30428
hydromagnetic surface waves, dissipation by reson. conversion 80−21904
ICRF heating, preliminary results in DIVA 80−28758
ideal-MHD ballooning modes, stability of finite-beta plasmas 79−64845
ideal-MHD kink and ballooning modes, depend. on plasma shape and profiles 79−64846
imploding liquid metal liner dynamic stabilisation 79−89494
imploding plasma liners, MHD instability effects 80−75081
impulsive instabilities in solar atmosphere, rel. to microwave bursts fast structs. 79−2536
impurity beam trapping instability in Tokamak 77−34428
impurity drift instability of dissipative type 78−1822
impurity instabilities in Tokamak *(Russian)* 77−68763
inert gas halide lasers, e-beam sustained, glow discharge stability 79−55117
inhomogeneous plasma, parametric trapping of EM waves *(Russian)* 78−9780
inhomogeneous plasma, relativistic electron beam propagation effects 78−9797
inhomogeneous plasma, unstable normal modes prod. by mag. shear 77−7532
inhomogeneous plasma stream in mutually perpendicular fields, nonlinear theory 78−57796
instability meas. by mm wave scatt. in turbulent plasma *(French)* 78−34373
instability of two dimensional waves, critical drift velocities, oscill. growth factor *(Russian)* 80−106922
intense relativistic electron beam-plasma system, coupled transverse oscillations, kinetic description 80−64741
interaction of plasma with strong EM wave, efficient transformation of radiation frequency 80−106931
interchange instabilities induced by gravity 78−91076
interchange instability at magnetopause of accreting magnetised neutron star, normal mode anal. 77−13376
interchange instability in sheared mag. field, ion Larmor radius effects 77−62357
interchange instability in solar corona rel. to mag. flux-tubes heating and reconnection 77−56894
interchange stability of axisymmetric field reversed equilibria 80−59214
interior modes, feedback stabilization using RF loaded particle beams 77−31453

plasma instability continued
internal disruption in Tokamak, relax. oscills., self-consistent model *(Russian)* 80−53957
internal feedback caused by variation of plasma pot. in bounded plasma 80−43906
internal helical modes, m>1, in Tokamak with small shear and high plasma press. *(Russian)* 80−10371
internal instability, m=1, kinetic theory 79−1309
internal kink instability, nonlinear props. in stellarator 78−94908
internal kink mode in Tokamaks 80−92318
internal m=1 helical mode, feedback suppression in Tokamak 80−19577
internal m=1 kink mode 78−94909
internal m=1 kink modes in Tokamak 77−15231
internal resistive modes, (m=1, n=1) and (m=2, n=1) MHD eqns. linear anal., toroidal coupling 77−43048
ion acoustic, strongly magnetised plasma collisional relax. of ion beam 80−33785
ion acoustic instability, electron distrib. meas. 77−19691
ion acoustic instability, renormalised kinetic theory for long range oscills. 79−27773
ion acoustic instability in polar cap ionosphere, rel. to plasma flow entry region position 80−67472
ion acoustic instability in solar corona, nonlinear saturation rel. to coronal heating 78−4181
ion acoustic stability anal. of Earth's bow shock 78−81506
ion acoustic wave, parametric decay instability 79−23413
ion acoustic waves and solitons in plasma, stability anal. 79−60128
ion beam, neutralised, ion-acoustic instability in transverse mag. field 79−13891
ion beam, neutralised, LF wave dispersion, instability in weak mag. field *(Russian)* 79−98888
ion beam driven instability, in magnetised plasma, light scatt. obs. 79−77424
ion beam injection, heating and acoustic instabilities 79−60154
ion beam injection, MHD instability 77−76113
ion beam injection, self-oscillations, feedback mechanism, ion-ion stability excitement 79−50864
ion beam interaction in mag. field, beam relax., nonlinear stages, heating *(Russian)* 77−47217
ion beam shear-Alfven instability in two component Tokamak 79−60119
ion beam-plasma system, absolute and convective instabilities of electrostatic ion cyclotron waves 77−68774
ion beam-plasma system, absolute and convective instabilities of electrostatic ion cyclotron waves 80−64740
ion beam-plasma system, absolute instabilities of electrostatic ion cyclotron waves 78−9793
ion beam-plasma system, dispersion relation of ion Bernstein wave 77−62375
ion beam-plasma system, explosive instability 77−15208
ion beam-plasma system, parametric instabilities at unstable electrostatic ion cyclotron waves 79−14535
ion beam-plasma system, self-oscills. due to 2 stream ion-ion instability 77−76123
ion beam-plasma system wave propag. in cylindrical geometry 80−38592
ion beam-plasma systems, ion-electron instability 78−91118
ion cyclotron, ion density fluctuations and vel. distrib. 79−19090
ion cyclotron beam-whistler instability in shock wave 77−7540
ion cyclotron drift instability driven by cross-field electron current, plasma heating 78−51290
ion cyclotron EM wave instability, oblique, due to monoenergetic fusion alphas 79−37491
ion cyclotron instability, in TFR Tokamak, microwave scatt. obs. 78−71473
ion cyclotron instability, noise and quiet start methods in particle simulation 77−89301
ion cyclotron instability in magnetosphere ring current, rel. to energy depend. of proton precip. 77−78565
ion cyclotron instability in solar wind, influence of protons non-bi-Maxwellian distrib. function 78−96375
ion cyclotron instability induced by perpendicular beam injection into a plasma 79−14565
ion cyclotron parametric instability in multispecies plasma, theory 77−68775
ion cyclotron waves, oscillating two-stream instability, RF heating of tokamak plasma 80−1779
ion cyclotron waves, parametric excitation in plasma containing two types of ions 78−30440
ion Langmuir wave, modulation instability *(Russian)* 78−71475
ion loss due to low frequency instabilities 80−6217
ion noise instability propag., weakly ionised plasma, dispersion eqn. *(German)* 77−31439
ion oscillations, self-modulation 77−80303
ion pressure gradient driven drift modes; 3-dimens. fluid simulation 80−103150
ion resonance instability, influence of finite ion Larmor radius and equilib. self elec. fields 78−83556
ion resonance instability, nonneutral plasma column, finite ion Larmor radius effects 78−38482
ion resonance instability, strong self-elec. field influence, nonneutral column 78−34301
ion ring, field-reversed, anomalous decay of induced electron current 80−24206
ion ring, precessional mode stabilisation using general mag. multipole field 77−24174
ion stream, instability during charge interchange in gas *(Russian)* 77−7519
ion surface waves stimulated by vol. plasma waves, parametric interaction 78−42751
ion temp. and parametric decay development in RF-generated stellarator plasma 80−79436
ion wave, rel. to Brillouin backscatter saturation in underdense plasma target 80−14886
ion wave instability, current-driven, nonlinear development 77−62353
ion wave packet, nonlinear, modulational instability, expt. 77−65853
ion waves, two-stream ion-ion instability in axially bounded ion beam-plasma system 78−91119
ion-acoustic, electron flux limitation of laser energy deposition 77−39419
ion-acoustic, in presence of HF oscills. 78−18398
ion-acoustic, in turbulent plasma, ion-tail form. effect on resistivity 80−10360
plasma instability continued
ion-acoustic, in turbulently heated plasma, flat top electron distrib. effect 80−10399
ion-acoustic, time- and freq.-resolved spectra 78−5948
ion-acoustic cross-field current-driven instability 78−14144
ion-acoustic current driven instability, in collisionless Q-machine plasma 79−32770
ion-acoustic drift instability, parametric excitation and suppression 77−39416
ion-acoustic fluctuations heating, laser beam absorption mechanism 77−51209
ion-acoustic heat flux instability, second-order theory 79−60125
ion-acoustic instability, current-driven, quenching in trapped electron regime 77−31460
ion-acoustic instability, double layer form., numerical simulation 80−59220
ion-acoustic instability, electron flux driven, in Q-machine, probe diagnostics 80−33765
ion-acoustic instability, enhanced ion-damping 79−94783
ion-acoustic instability, ion tail formation and saturation 80−38610
ion-acoustic instability in positive column of DC discharge 78−67335
ion-acoustic instability in solar wind, wave-particle interactions rel. to particle vel. distribs. *(German)* 80−109323
ion-acoustic instability ohmic heating, ion/electron temps. formulae 77−7570
ion-acoustic instability oscillations in collisionless single ended Q-machine 80−38731
ion-acoustic instability stabilisation by ion beam in Q-machine, probe diagnostics 80−33766
ion-acoustic instability supression by microwave field 78−71466
ion-acoustic parametric decay instability in plasma with $\beta>1$ 77−975
ion-acoustic standing wave instability, electron current driven 78−42742
ion-acoustic turbulence, current driven 78−59594
ion-acoustic turbulence generated anomalous resistivity, collision freq.-turbulence spectrum relation 78−14205
ion-acoustic turbulence spectra 78−14145
ion-acoustic wave, in collisionless plasma, modulational instability, ion temp. effect 79−60132
ion-acoustic wave, modulational instability 77−89254
ion-acoustic wave, modulational instability in turbulent phonon field 78−18395
ion-acoustic wave, oblique modulation stability 77−19697
ion-acoustic wave, parametric decay imstability caused by finiteness of pump wave amplitude 78−22482
ion-acoustic wave modulation instability, effect of finite ion temp. 79−1307
ion-acoustic waves, energy props. in stable and unstable plasmas 79−68916
ion-acoustic waves, modulational instability in two electron temp. plasma 78−75301
ion-acoustic-like instabilities in solar wind at 1 AU 78−89032
ion-acoustically turbulent plasma, cond., solar corona appl. 79−19027
ion-beam-excited electrostatic ion cyclotron instability obs. 78−75310
ion-beam-plasma system, ion cyclotron harmonic instabilities *(Japanese)* 78−91124
ion-cyclotron, in mirror-confined plasma 77−3991
ion-cyclotron drift instability driven by cross-field current 77−35341
ion-cyclotron instability, parametric depend., beam injection, Tokamak stability 78−47110
ion-cyclotron instability driven by oppositely directed proton streams in magnetosphere 79−62690
ion-cyclotron ion temp. meas. 77−68871
ion-cyclotron node-whistler mode instability, role in parallel shock wave structs. 77−42994
ion-cyclotron oscills., electrostatic, nonlinear interaction causing modulational instability 77−89248
ion-cyclotron turbulence modulation by LF perturbations 78−91108
ion-cyclotron wave, driven unstable by cold-ion beam, nonlinear stabilisation 79−98925
ion-drift wave eigenmodes in sheared mag. field, impurity effects 80−43911
ion-ion hybrid waves in collisional two-species current carrying plasma, instability 79−90394
ion-ion two stream instability, quasi-neutral particle simulation model 78−47157
ion-mixing mode and model for density rise in confined plasma 79−98862
ionisation by high-speed electrons formed from parametric instabilities 78−75333
ionisation instability, dispersion rel. *(Russian)* 78−83519
ionisation instability, in non-equilib. MHD generators 77−72506
ionisation instability development for plasma with variable direction of mean current 78−83558
ionisation instability in H plasma, due to departures of electron energy distrib. from Maxwellian 77−80274
ionisation instability mode of plasma accelerator, probe method for electron distrib. function determ. 80−19612
ionisational instabilities of EM wave in homogeneous high-freq. discharge *(Russian)* 78−34382
ionising instability of laser heating plasma *(Russian)* 78−1815
ionosphere, artificial spread-F generation by parametric instability 77−45247
ionosphere, equatorial spread F, nonlinear theory of collisional Rayleigh-Taylor instability 78−32270
ionosphere, equatorial spread-F, plasma instabilities obs. by Spacelab-borne Langmuir probe 77−21947
ionosphere, instabilities and fine struct. 80−21869
ionosphere, lower hybrid drift instability 80−46343
ionosphere, morphological studies of rising equatorial spread F bubbles 78−77410
ionosphere, plasma disturbance by extraordinary wave 77−29542
ionosphere, shortwave drift-dissipative instability, caused by EM wave *(Russian)* 77−47179
ionosphere plasma interaction with gravity waves, elec. field and current prod. 80−61957
ISX-A Tokamak, plasma equilibrium position dynamics 79−77360
JAERI Tokamak, Ti coating for improved plasma characts. 80−24232
Jeans' gravitational instability of an anisotropic plasma with generalised polytropic equations of state *(Italian)* 79−94780
jet, hydromagnetic stability 78−1827

plasma instability continued
JFT-2 Tokamak, large scale fluctuation mode mixing, probe, interferometric obs., MHD anal. 78−67312
JIPP T-II torus, neutral gas injection and plasma current control, suppression of major disruption 80−28839
Jupiter, short duration radiobursts model 77−13279
Kadomtsev-Pogutse instability and Tokamak radiation 79−37463
Kelvin-Helmholtz hydromagnetic instability, plane tangential discontinuity, dispersion eqn. *(Russian)* 79−7451
Kelvin-Helmholtz instability, finite ion Larmor radius effect 79−1300
Kelvin-Helmholtz instability at magnetopause, rel. to magnetosphere hydromag. energy spectra 80−67476
Kelvin-Helmholtz instability in comet tails, appl. to helical waves in Comet Morehouse (1908 III) 80−4305
Kelvin-Helmholtz instability in ionosphere turbulent polar cusp, evidence from low-energy particles 78−96343
Kelvin-Helmholtz instability in magnetoplasma 79−23407
Kelvin-Helmholtz instability in magnetosphere, appl. to hydromagnetic pulsations 78−73584
Kelvin-Helmholtz instability of magnetopause, effect of finite ion Larmor radius 79−80096
Kelvin-Helmholtz instability through porous medium of two superposed plasmas 80−106886
kinetic ballooning modes, theory 80−79484
kinetic equations for low frequency instabilities in inhomogeneous plasmas 80−83886
kinetic processes in solar flares, theory 78−85920
king instability, in rectangular finite-β system 77−76070
kink, current disruption *(Russian)* 78−1819
kink, hydromagnetic, in low-beta plasma, column, dynamic shear stabilisation by RF current 79−46454
kink, hydromagnetic, in Tokamak (pinch) plasmas, dynamical shear stabilisation, nonlinear 79−50858
kink, in high-β Tokamak, probe and laser beam meas. 77−27733
kink, in reversed field pinches, optical and electrical meas. 77−24188
kink instabilities of a field reversed ion ring with a toroidal magnetic field 80−1758
kink instabilities of a plasma column with elliptical cross-section 80−79495
kink instability, compressibility effect *(Russian)* 77−68764
kink instability, imperfectly conducting plasma *(Russian)* 77−68765
kink instability, internal MHD, sufficient cond. *(Chinese)* 80−43897
kink instability, m=1, in current carry stellarator, nonlinear props. 78−63566
kink instability and energy principle in toroidal plasma 79−10650
kink instability saturation of current carrying column 77−72445
kink mode in toroidal plasma 78−91144
kink mode stability regime in toroidal plasma, wall stabilisation 78−42788
kink modes, nonlinear evolution in Tokamak 77−19753
kink-like, current-driven, in magnetised collisional plasma 77−80284
Knudsen plasma, one-dimens., bounded, nonlinear oscills., numerical method 78−79433
Landau modes, higher order, in water-bag and 2-Maxwellian plasmas 80−38601
Langmuir and dispersive ion acoustic waves, coupled nonlinear Schrodinger eqn. 79−77362
Langmuir collapse, dimensionality and dissipation 80−87880
Langmuir field, localised, in plasma, temporal evolution 79−90405
Langmuir localised perturbation, spontaneous radiation emission 80−69987
Langmuir modulational instability, nonlinear development 79−32761
Langmuir oblique solitons, self-contraction in free path regime *(Russian)* 80−43921
Langmuir oscillations, interactions in weakly ionised high-density plasma, beam instability *(Russian)* 78−26271
Langmuir oscills., modulational instability, in EM wave field 80−38618
Langmuir running wave instability and damping, at different amplitudes and phase velocity 80−38620
Langmuir soliton excitation by monoenergetic electron beam *(Russian)* 79−77381
Langmuir soliton solns. with high nonlinearities, energy principle 80−24156
Langmuir solitons, generation and collapse, numerical study 77−68784
Langmuir standing wave, stability and kinetic effects *(Russian)* 77−80299
Langmuir standing waves instability, one dimens., soliton and collapse, numerical expt. 80−38619
Langmuir turbulence, modulating instability wave, nonlinear dynamics, solitons *(Russian)* 77−47196
Langmuir turbulence, numerical modelling, solitons, nonlinear interactions 80−70030
Langmuir turbulence, stationary 78−14164
Langmuir turbulence, statistical theory 80−38647
Langmuir turbulence, strong, transition *(French)* 80−28674
Langmuir turbulence and modulational instability 78−75335
Langmuir turbulence and modulational instability in unmagnetised, completely ionised plasma 79−37496
Langmuir wave, 3D parametric decay into Langmuir and longit. LF waves *(Japanese)* 77−42971
Langmuir wave, acoustic turbulence effect on collapse 79−14549
Langmuir wave collapse in mag. field, instability-caused cavity *(Russian)* 78−1817
Langmuir wave excitation by two pumping waves, convective instability *(Russian)* 80−14904
Langmuir wave quasicollapse, one-dimens., under parametric and modulation instabilities 77−42982
Langmuir waves, driven by electron-ion decay instability, scattered spectrum 80−43970
Langmuir waves, in solar corona, rel. to type IV decimetre bursts 77−2400
Langmuir waves, oblique, localised, in inhomogeneous plasma, parametric excitation *(Russian)* 79−98885
Langmuir waves, obliquely modulated, stability in collisional plasmas 78−22480
Langmuir waves, three-dimensional instabilities in solar corona rel. to type III radio bursts 77−2404
Langmuir-wave modulation instability in electron beam self-induced transparency 78−34341
large-amplitude Langmuir wave instability 78−75325
laser, free electron, relativistic, rippled static mag. field, simulation, waves and instability 77−54686
laser beam self-focusing effect on filamentation instability 78−51305
laser beam-plasma interaction, in mag. field, breakdown, heating, trapping, fusion, diagnostics, book contrib. 77−51196
laser discharge, high-power, stabilisation with mag. field 80−99739
laser driven implosions, hydrodynamic instabilities 80−64756
laser fusion configuration, magnetic field generation by Rayleigh-Taylor instability 78−58476
laser fusion plasma, computer simulation of Weibel-like instability effects 79−14581
laser imploded spherical targets, stability 78−5906
laser implosion prepulse large amplitude backscatter instability with struct. pulse 77−80332
laser irrad. plasmas, single and double frequency reson. heating, unstable oscills. *(Chinese)* 77−76149
laser irradiated plasma focus, neutron emission *(Japanese)* 78−38538
laser light parametric absorpt., convective parametric instability 80−100073
laser plasma, convective parametric decay instability 80−64722
laser plasma, critical surface filamentation and parametric instability 78−47140
laser plasma, magnetic instability and spontaneous generation of mag. fields 79−60164
laser produced plasma, parametric instabilities in two electron temp. plasma *(Japanese)* 80−96377
laser produced plasma, parametric instability, laser fusion research 77−88762
laser produced plasma, three halves harmonic spectra, time resolved obs. 80−79529
laser-driven implosion, Rayleigh-Taylor instability, nonlinear development, calcs. 78−58475
laser-matter interaction, absorption processes, parametric instabilities 79−46464
laser-pellet irradiation, two-plasmon decay instability, soliton form. role 78−1842
laser-plasma interaction, spikon lifetime 80−14922
laser-produced plasma, microsphere implosion, symm. and stability of thermally generated mag. field 77−24118
laser-produced plasma, two-plasmon decay and generation of $3\omega_0/2$ harmonic *(Russian)* 77−89279
Lausanne belt pinch, plasma stability 77−43028
Levitron, fluctuations, diffusion and beam-induced currents 80−28616
LF instabilities of warm plasma driven by field-aligned currents 77−31449
linear and nonlinear wave transformation and absorpt. in inhomogeneous plasma capacitor 77−76046
linear effects of wave propag. in plasmas, review 78−14149
linear electron-ion beams, particle density, longit. mag. field effects 77−50597
linear stability of high-m drift-tearing modes 80−64716
linear wave props., parametric decay, heating 78−42758
linearised Vlasov-fluid model for sharp boundary screw pinch 79−60168
linearly unstable mode stabilisation by reson. nonlinear coupling to damped modes 80−59234
local sufficient condition for MHD stability in closed line systems 80−83910
localised drift-Alfven mode instability due to current density gradient 80−19571
localised modes in inhomogeneous Vlasov plamsa 78−83563
localised plasma perturbations, fluctuations in parametrically stable plasma *(Russian)* 79−37474
localised pumping-excited waves, parametric instability, nonlinear stage 80−38622
localised structures and anomalous DC resist. 77−58846
long-wavelength modes and anomalous transport in toroidal magnetoplasmas 80−28613
longitudinal plasma wave, threshold amplitude for onset of instability 80−1793
longitudinal self-consistent large amplitude wave stability in absence of large-scale mag. field 79−32759
loss-cone modes in ripple-assisted neutral beam injection, stability 77−76059
low density magnetised plasma wake, perturbations 79−41808
low frequency current-driven modes, stability in boundary layer of gas-insulated plasmas 79−98909
low frequency heating wave, parametric instabilities induction in mag. confined plasma 80−24187
low frequency parametric processes in magnetically confined plasmas 80−28827
low-β interchange instability, finite Larmor radius effects, sheaths 77−84426
low-β plasma, strong turbulence in rot. column 78−94915
low-frequency instabilities in Tokamak due to trapped ions *(Russian)* 79−4125
low-frequency plasma instability, high frequency electrostatic eigenmode drive 79−60118
low-frequency Rayleigh-Taylor modes rel. to equatorial spread-F, artificial control technique 78−69602
lower hybrid, in ion beam-plasma interaction 77−39434
lower hybrid and ion cyclotron waves, nonlinear modulation 78−75295
lower hybrid cones, nonlinear development 78−34306
lower hybrid drift, laser produced plasma column in uniform mag. field 80−38687
lower hybrid drift, sheath broadening in theta pinches 77−31429
lower hybrid drift instabilities, mag. curvature and ion distrib. function effects 77−19698
lower hybrid drift instability, cross-field electron current, ion heating 79−23414
lower hybrid drift instability, growth rate reduction by finite beta 77−42978
lower hybrid drift instability, mag. shear effect in toroidal reversed field pinch 78−67397
lower hybrid drift instability, nonlinear stabilization by electron resonance broadening 78−34307
lower hybrid drift instability, particle simulation 78−67404
lower hybrid drift instability, quasilinear stabilisation 78−83548
lower hybrid drift instability, strong flute, theta-pinch simulation 77−24070

plasma instability continued
lower hybrid drift instability, Tormac sheath, inhomogeneity and mag. shear influences 78−34299
lower hybrid drift instability at low vels., stability calc. 77−84424
lower hybrid drift instability in laser prod. plasma 79−27764
lower hybrid drift instability stabilisation by mag. shear 77−42979
lower hybrid heating, collective effects 79−14570
lower hybrid heating experiments in JFT-2 Tokamak 80−28747
lower hybrid instability, ion-beam-driven, anomalous beam slowing 79−41816
lower hybrid instability nonlinear injected ion beam anomalous slowing 78−1850
lower hybrid large-amplitude waves, filamentation 77−80294
lower hybrid mode, nonlinear theory, ion heating 77−42998
lower hybrid oscillating two stream instability, in plasma with mag. shear 79−90395
lower hybrid parametric instabilities, nonuniform pump waves, Tokamak appls. 78−34344
lower hybrid parametric instabilities, unified formalism 77−89251
lower hybrid wave decay into EM wave, parametric instabilities 77−31457
lower hybrid wave turbulence effect on tearing mode instability 80−92322
lower hybrid waves, current-driven electrostatic ion-cyclotron instability 80−103149
lower hybrid waves, modulation instability growth rates 80−48881
lower hybrid waves, parametric decay, ion nonlinearity effect 79−37485
lower hybrid waves in toroidal discharge, parametric decay 80−38596
lower-hybrid pump wave, growing instability threshold 77−89237
lower-hybrid waves in collisional plasmas with field-aligned current, instability 80−75045
lower-hybrid-drift instability, rel. to high freq. drift waves in ionosphere equatorial spread-F 78−88973
lower-hybrid-drift wave turbulence in distant magnetotail, theory 79−25399
m=1 cyclotron-mode klystron instability 79−73005
m=1 instability, toroidal theta-pinch, Scyllac ordering, dynamical model 77−51216
m=1 waves propagating in Scyllac 78−5865
m=2 instability in stellarator, finite Larmor radius stabilisation 77−31506
macroscopic instability of magnetoacoustic solitons *(Russian)* 77−47200
magnetic bottle, ohmic heating, mag. field aligned currents 78−18426
magnetic driving energy of the collisional tearing modes 80−92301
magnetic field generation by intense Langmuir plasma waves 80−38623
magnetic field instability of plasma in EM beam 80−64745
magnetic field measurement in toroidal plasma systems 80−49004
magnetic field self-excitation by intense EM radiation, mag. instability *(Russian)* 79−14582
magnetic flux element stability in horizontally stratified compressible plasma, solar atmosphere appls. 78−28610
magnetic mirror, injected plasma particle refl. (trapping), quiescent (turbulent) plasma 80−48955
magnetic piston interaction with nonmagnetised plasma 80−38630
magnetic reconnection and m=1 oscills. in current carrying plasmas 78−71463
magnetic tearing instability, high cond. theory 77−7527
magnetically confined plasma, external conducting open sheet, stability effects 80−92302
magnetically confined plasma, numerical computation of MHD flow in Scyllac 77−80282
magnetically confined plasma, transport processes and instabilities 77−72419
magnetically confined plasmas, ballooning modes 80−6231
magnetically confined plasmas, parametric instabilities in laser heating 78−18432
magnetised, parametric instabilities with well separated freq. *(Chinese)* 80−106887
magnetised beam-plasma system, instability of Trivelpiece mode 77−62374
magnetised non-uniform plasma, with density depend. fluctuations 79−41831
magnetised plasma, evolution, numerical soln. of hybrid Vlasov-fluid model 79−90452
magnetised plasma, hot, unstable behaviour, in contact with cold wall 79−1333
magnetised plasma electron heating in parametric modulation instability 78−75384
magnetised plasma stability in large amplitude circularly polarised wave, dispersion relations 80−59223
magnetized plasma parametric resonance in non-monochromatic pump-wave 80−38598
magneto-acoustic macroscopic soliton instability growth rate, dispersion eqn. *(Russian)* 78−59562
magneto-active plasma, theory of turbulence 78−83567
magneto-parametric instabilities, two-fluid model 80−85851
magneto-viscous resistive tearing of cylindrical flux surfaces 80−1831
magnetoacoustic disturbance, hydrodynamic instability in nonuniform plasma flow *(Russian)* 80−1766
magnetoacoustic oscillations, parametric decay in cylindrical plasma 80−24157
magnetoacoustic oscills., in toroidal plasma, comparison with cylindrical plasmas, numerical calcs. 80−33760
magnetoactive plasma, modulational instability caused by Langmuir oscillations 80−92297
magnetoactive plasma parametric instability in HF wave generated field *(Russian)* 78−59566
magnetoatmospheric instabilities, max. growth rates 77−53573
magnetohydrodynamic stability noncompact operator spectrum approx. *(German)* 77−68759
magnetoparametric instabilities, appl. to Crab Nebula 78−61727
magnetoparametric instabilities, appl. to Crab nebula 79−8829
magnetoplasma, optimisation of plasma quiescence 79−1304
magnetoplasma compressor, erosion type, focus zone, nonideal plasma, strong shock waves 78−91161
magnetoplasma stability against EM perturbations in presence of gravit. field 77−41295
magnetosonic waves, instability driven by alpha particle beam in solar wind 79−35089
magnetosonic waves in magnetosphere, rel. to hiss generation beyond plasmapause 77−82085

plasma instability continued
magnetosphere, Alfven wave stimulation by trapped electrons, geomag. pulsation generation *(Russian)* 77−22003
magnetosphere, antiloss cone instability 77−25867
magnetosphere, drift-mirror instability 77−49229
magnetosphere, elec. field induced instability 77−70942
magnetosphere, electrostatic ion-cyclotron instability during quiet times and auroral proton precip. 77−33256
magnetosphere, instabilities due to antiloss cone *(Russian)* 79−21105
magnetosphere, modified two-stream instability, EM effects 77−70946
magnetosphere, plasma instability theory for anisotropic vel. distribs. *(Russian)* 78−12053
magnetosphere, plasma waves and instabilities in polar cusp 78−12058
magnetosphere, proton-cyclotron harmonics, instability due to anti-loss core proton distribs. 80−56678
magnetosphere, ring current and antiloss cone drift instability 77−22016
magnetosphere, shear instability: auroral arc deformation and anomalous momentum transport 78−77433
magnetosphere, structure and stability properties 78−77440
magnetospheric whistler parametric instability, pitch-angular electron scatt. *(Russian)* 78−77420
major disruptions in the TOSCA Tokamak 80−83979
many-wave explosive instability 77−80296
marginal stability anal., anomalous transport, profiles, coeffs. and turbulence level calc. 77−47175
marginal stability in solar flares, assoc. with particle streams continuous injection model 80−21954
mass flow stabilisation in helical mag. fields, MHD stability 77−24133
medium beta plasma with velocity gradients, dispersion relation for drift waves 80−64719
Mercier criterion for a finite-pressure plasma in arbitrary-shaped magnetic axis configurations 79−37534
metal vapour columnar arc instability, mag. fields effect, up to 67 kA 78−9893
MHD, generalised Lorenz eqns., strange attractors 80−59232
MHD, in belt pinch IIa, energy confinement 77−43029
MHD, in high-current evaporating-wall discharge, causing pulsed press. 79−27838
MHD, in toroid with vanishing press. grad. 78−14195
MHD, stability code, ERATO, convergence of solns. 80−83906
MHD, toroidal axisymmetric config., vacuum potential energy change, spectral codes 80−87869
MHD, unstable continuous spectrum, noncircular rotating θ pinch 79−94779
MHD 3-dimens. stable equilib., numerical model anal. 77−27665
MHD codes, linear and nonlinear, plasma instabilities, PL1 programs 77−76040
MHD devices, plasma ionization instability, dynamic suppression, switching modelling 80−59308
MHD eqn., stability, transport calc. for high-beta Tokamaks 80−28848
MHD equilibria, secular instability in mag. quadrupole field 80−53982
MHD equilibria, stability criterion 79−14534
MHD equilibria, stochastic stability 79−77414
MHD equilibria in mag. quadrupole field, secular instability 80−10427
MHD equilibrium and spectrum, ideal 79−98883
MHD equilibrium and stability, triangular deformation elliptic cross section *(Chinese)* 80−53950
MHD equilibrium and stability in three dimens. configurations 80−28776
MHD equilibrium of plasma confined in spherical microwave cavity 79−68911
MHD equilibrium of plasma confined in spherical microwave cavity 79−68912
MHD equilibrium problem, inversion of variables method *(Russian)* 79−4118
MHD gamma-instability, in spheres and cylinders *(Russian)* 77−76044
MHD generator, arc switching near electrodes, elec. current oscills. 79−55569
MHD generator, channel, near electrode-free wall, plasma instability, flow inhomogeneity effect 78−26338
MHD generator, conductivity and power output ionization stability, and boundary layer effects 80−1752
MHD generator, non-equilibrium, ionisation instability, finite boundary layer effect calc. 79−19098
MHD generator plasma with addition of N_2, stability 79−19014
MHD ideal equilibria, computer codes, review 77−27712
MHD instabilities, large computational programs, comparative numerical studies, Tokamaks 78−79425
MHD instabilities, nonlinear behaviour calcs., numerical techniques 77−27659
MHD instabilities, stabilisation in current-carrying stellarator 79−86582
MHD instabilities in current carrying stellarator, stabilisation 79−64848
MHD instabilities in extended extragalactic radio sources, rel. to electron accel. 80−27000
MHD instabilities in helical system 80−1829
MHD instabilities in stellarator 78−14154
MHD instability, rel. to development of solar flares 77−17476
MHD instability in galaxy bridges and jets, rel. to breakup into aligned objects 77−49475
MHD instability in magnetosphere, particle accel. by surface waves rel. to aurora 77−9621
MHD instability in nonuniform plasma, kinetic theory 77−15190
MHD instability in reversed field pinches 77−39451
MHD instability of laminar plasma stream *(Chinese)* 79−73002
MHD instability stabilisation by force free mag. fields 80−83911
MHD kink stability, convection effects, MHD boundary layer anal. 80−1762
MHD localised ballooning mode, kinetic anal. 78−75298
MHD modes, linearly unstable, nonlinear behaviour, appl. to pinch kink modes 78−67339
MHD nonlinear mode struct. in pinch 77−974
MHD sausage instability, wavelength determ. from voltage pulse in exploding wire 77−47238
MHD spectrum of instabilities due to plasma rot. in theta pinch 78−59582
MHD spectrum of straight plasma column with arbitrary cross section, finite element calc. 77−11327
MHD stability, computational aspects 77−27690
MHD stability, local, for equilib. plasma configs. 79−10659
MHD stability analysis of axisymm. surface current model equilibria for $N=0$ and $n\neq0$ modes 80−92276

plasma instability continued
MHD stability criteria for localised displacements 80−28645
MHD stability in diffuse high-β l=1 equilibria 77−19746
MHD stability in toroidal trap near-axial region *(Russian)* 78−38521
MHD stability of a helical magnetic field of arbitrary amplitude 79−86578
MHD stability of high beta Tokamak 77−68849
MHD stability of runaway electron discharge in Tokamaks 78−75303
MHD stability of toroidal plasma, for localised displacement 79−73030
MHD stability to axisymmetric modes in toroidal equilib. 77−76176
MHD toroidal plasma stability, mag. axis curvature modulation effects 77−84487
MHD turbulence, three-dimens. soln. in cylindrical geometry 78−67351
MHD waves, modulation instability *(Russian)* 77−89259
MHD waves in stellar atmospheres, dynamic instability in mag. flux tube 78−69789
MHD waves parallel to mag. field, modulational instability 77−15181
MHD-instability and limiting currents during Ohmic heating in stellarator Uragan-2 *(Russian)* 80−106881
MHD-instability on ohmic heating in apparatus with spatial axis *(Russian)* 80−106945
micro-unstable Tokamak, quasilinear model, diffusion, heat flow 77−76033
microinstabilities, Alfven-type drift oscills. 78−22496
microinstabilities, in moderately inhomogeneous plasma 77−87223
microinstabilities, low frequency, simulation model 78−38525
microinstabilities current driven, in plasma focus, suprathermal microwave emission and soft X-ray obs. 77−89328
microinstabilities in field reversed Z pinches, persistence of MHD stability 80−87872
microinstabilities in inhomogeneous plasma with incident α-particle beam, effect on stopping power 80−64742
microinstabilities in plasma slab, drift waves 78−14156
microinstabilities in PLT Tokamak, microwave scatt. meas. 78−67413
microinstability, onset in solar wind and its consequences 77−87222
microinstability theory in Tokamaks, review 78−75292
microtearing modes and anomalous transport in Tokamaks, self consistent calc. 80−59222
microtearing modes and anomalous transport in Tokamaks 80−92316
microwave dynamic interaction, probe diagnostics 80−19584
microwave generation by negative-mass instability in ultrarelativistic plasma 78−51289
microwave heating in ELMO Bumpy Torus, anal. 80−28829
microwave p-i-n diode modulator, transient plasma instability meas. *(German)* 80−87942
migma ion distrib. in phase space, shaping 77−83090
MIGMA IV, stability study of plasma density buildup 79−13522
mirror confinement, magnetic-curvature-driven interchange instability 79−41865
mirror drift cone stability simulation with loss-cone ions 80−1789
mirror fusion reactor, convective loss-cone instability is absolute 79−64900
mirror fusion test facility 80−43962
mirror instabilities, finite in Larmor radius modifications 79−73003
mirror instability in dayside magnetosheath, rel. to pressure anisotropy 77−37483
mirror instability in magnetosheath, rel. to plasma depletion at dayside magnetopause 79−66876
mirror plasma, drift cyclotron loss cone instability, localised cold plasma effect 79−32797
mirror plasma, hot electron ring, conducting wall stabilisation 78−1881
mirror trapped ions under instability around ion cyclotron frequency, enhanced heating 78−5892
mirror-drift-cone and convective-loss-cone instabilities, strong inhomogeneities effect 77−89250
mirror-drift-cone instability, nonlocal hybrid-kinetic stability anal. 80−24230
MITE accelerator, long self-magnetically insulated power transport expts. 79−90471
mode converted lower hybrid solitons, stability in parametric regions 80−92303
mode crossing stability, Lagrangian nondegenerate fluid or Vlasov plasma 78−42735
modes and ballooning in magnetically confined plasmas 80−28650
modified bumpy torus, theta pinch, stability, theory 78−83594
modulated electron beams, instability, spatially separated in plasma 80−70012
modulated relativistic electron beam-plasma interactions, instability, heating 79−98929
modulation instability, in weakly ionised magnetoactive plasma *(Russian)* 79−98892
modulation instability, Langmuir turbulence, isotropic oscills. and energy flux nonlinear freq. shift *(Russian)* 79−27778
modulation instability, linear and nonlinear theories, inverse dispersive media *(Russian)* 79−19032
modulation instability and inhomogeneous Langmuir fields in plasma *(Russian)* 80−106894
modulation instability and nonlinear waves *(Russian)* 78−22476
modulation instability and plasma electrodynamic characteristics 80−38621
modulation instability and strong turbulence in materials with inverse dispersion *(Russian)* 77−62359
modulation instability at lower hybrid reson., strongly turbulent plasma, macroscopic effects of collapse *(Russian)* 78−59563
modulation instability in a magnetic field 79−98906
modulation instability in magnetised plasma waves nonlinear development during heating *(Russian)* 78−47118
modulation instability in nonlinear ion-acoustic waves in collisional plasma 77−24067
modulation instability influence on relativistic electron beam relax. *(Russian)* 77−35360
modulation instability of Langmuir wave due to electron oscill. *(Russian)* 77−47182
modulation instability of relativistic plasma, rel. to pulsars radio radiation *(Russian)* 77−22258
modulation instability of turbulent spectra *(Russian)* 79−37472
modulation instability of whistler waves 77−72450
modulation instability saturation, narrow beam of radio waves in magnetised plasma *(Russian)* 77−47203
modulational, Langmuir turbulence 78−51302
plasma instability continued
modulational instability for electron plasma wave, computer simulation 79−32766
modulational instability growth, for randomised initial conditions 78−18406
modulational instability in Langmuir and ion-acoustic turbulence, collisional excitation 77−24086
modulational instability of electron and ion waves 77−76054
modulational instability of elliptically polarised EM waves 78−14167
modulational instability of ion acoustic waves in the presence of density gradients 79−64840
modulational instability of nonlinear wave propagation in relativistic plasmas 80−106911
modulational instability of two transverse waves, cold plasma 79−32765
modulational instability produced by Langmuir turbulence in a magnetic field 80−1759
molecular discharge, externally sustained, thermal instability 77−58915
molecular gas ionisation instability, in CW discharge, suppressed by varying elec. field 79−23476
molecular gas plasma dissociative thermal, vibr. instabilities *(Russian)* 78−83561
multi-harmonic electron cyclotron instabilities, theory 78−87442
multi-ion system, modulation instability of ion acoustic waves 80−69996
multifilament plasma source, multipole mag. field effects on characts. 79−46462
multimirror experiment, linear, trapped electron instability 79−60181
multimode instability control by state feedback 79−77357
multimode plasma instabilities, dynamic feedback stabilisation 78−79419
multiple-mirror confined plasma, interchange modes stabilisation 78−42790
multiple-mirror plasmas, MHD stabilisation 80−6244
negative conductivity plasma, electronic conc. distrib. *(Russian)* 78−55722
negative ion beam instability spatial development in rarefield gas *(Russian)* 80−92314
negative mass instability, electrostatic numerical simulation 77−89261
negative mass instability, nonlinear development, effect on intense microwave generation 78−75285
negative shear ferromak for stabilization of current disruptions in toroidal discharge 80−106971
negative-mass instability, relativistic nonneutral E-layer, axial energy spread effect 78−42745
neutral beam driven convective loss cone instability 77−89269
neutral beam generation, negative ion revolving multiple beam instabilities *(French)* 80−47798
neutral current layer, tearing mode instability and mag. field line reconnection *(Russian)* 78−91087
non self sustained repetitively pulsed discharge in N_2-CO_2 and N_2, instability obs. 80−38820
non-equilib. plasma, spontaneously radiating layer, quasi-static surface instability, energy relations *(Russian)* 78−59558
non-linear tearing mode, numerical code for tokamak 77−43046
non-self-sustained discharge plasma, thermal instability development, laser appls. 78−71611
nonequilibrium plasma, fast Langmuir soliton possibility 78−75340
nonequilibrium plasma, ionis. instability 78−75283
nonequilibrium plasma slab, global instability 78−71474
nonequilibrium weakly ionised plasma, de-excitation and stability 78−38453
nonhomogeneous plasma in radiating field, absolute dissipative instability *(Russian)* 77−19681
nonideal plasma, elem. excitations and macroscopic props., review 80−43842
nonisothermal plasma, parametric absorpt. of laser emission *(Russian)* 77−80312
nonlinear, conversion of EM radiation to ion-acoustic waves near plasma reson. *(Russian)* 78−5859
nonlinear 3-wave interaction, mag. electron plasma, water bag distrib. 77−76072
nonlinear and quasielectrostatic, radiated by finite plasma-electron beam system *(French)* 77−65880
nonlinear collisional drift instability, numerical anal. 78−71479
nonlinear collisional drift instability, numerical analysis 78−91091
nonlinear convective and oscill. instabilities, beam-plasma system, simulation models 78−34338
nonlinear cross-field ion acoustic instability and plasma heating 80−83928
nonlinear electrostatic 4-wave interaction, positive (negative) energy waves, explosive instability 80−48884
nonlinear evolution of exploded wire plasma, numerical simulation 78−83605
nonlinear evolution of the bump-on-tail instability for electron beam in plasma 80−6248
nonlinear heat and particle transport due to collisional drift waves 78−71444
nonlinear heating by lower hybrid waves, two stream and ion-cyclotron instabilities 79−90422
nonlinear helical MHD instability in toroidal plasma, stability criteria *(Russian)* 78−5862
nonlinear helical perturbation in Tokamak, dynamics, mag. probe obs. *(Russian)* 80−53958
nonlinear interaction, near linear stability boundary, non-equilib. media 78−59591
nonlinear interaction of cold beam and weakly collisional plasma, simulation 79−32783
nonlinear interaction with laser beam, modulational instability 78−59603
nonlinear ion-sound waves excitation, by whistlers and Alfven waves *(Russian)* 79−27783
nonlinear Kelvin-Helmholtz instability in hydromagnetics 79−90393
nonlinear kink instabilities in Tokamaks surrounded by force-free fields 80−43909
nonlinear Landau damping by cascading, saturation 77−76066
nonlinear Landau damping in mirror plasmas 79−27766
nonlinear Langmuir wave modulation, in collisionless plasma 77−89256
nonlinear Langmuir wave modulation in weakly magnetized plasmas 79−4133
nonlinear lower-hybrid waveguide in plasma, stability 80−19578
nonlinear magnetostatic modes and twisting modes with magnetic islands 80−106900
nonlinear microinstabilities, review 78−14150

plasma instability continued
nonlinear mode coupling and saturation of decay instability in ion beam-plasma system 80−83931
nonlinear mode coupling between stable and unstable waves, growth rate modulation 78−1829
nonlinear mode coupling instability saturation, bifurcations and strange behaviour 80−48873
nonlinear mode coupling model equations, topological struct. 80−75056
nonlinear periodic waves stability in plasmas 80−38615
nonlinear propag. of EM wave, modulational instability 79−19047
nonlinear Rayleigh-Taylor instability in partially ionized plasma and the equatorial spread-F 79−16748
nonlinear resonance instability in ionosphere, rel. to small-scale plasma scatt. modulation trough 79−58159
nonlinear saturation of two unstable modes, survival competition 78−34298
nonlinear stability in nonuniform mag. field 78−38472
nonlinear stability problems, two-time method, dissipation scalings, ohmic heating 80−53967
nonlinear theory of beam instability in collision plasma *(Russian)* 79−19049
nonlinear theory of collisional drift-waves in toroidal geometry and anomalous skin effects in Tokamaks 80−92320
nonlinear theory of unstable plane waves and solitons 80−87888
nonlinear three wave mode coupling, instability saturation 80−87881
nonlinear time-dependent hydromagnetic model, spatial and temporal finite-difference techniques 80−59192
nonlinear transparency due to modulation instability *(Russian)* 78−59604
nonlinear transport instability in diffusive plasma 78−59584
nonlinear two-stream, in high-field electron drift, particle diagnostics 78−38541
nonlinear unstable longitudinal oscillations, parametric excitation in magnetoactive plasma *(Russian)* 78−18390
nonlinear vibrational excitation waves in a molecular plasma with negative ions *(Russian)* 79−27777
nonlinear wave, excitation and attenuation by monochromatic electron beam in waveguide *(Russian)* 77−47220
nonlinear wave effects, comparison of theory and experiment, review 79−7460
nonlinear wave solutions, stability 79−14533
nonlinear waves, in cold two-component plasma, decay instabilities 77−35346
nonlinear waves at upper hybrid reson. parametric excitation 79−23418
nonneutral electron beam propagation in inhomogeneous mag. field, stability 77−24175
nonresistive plasma, magnetic kinks in astrophysics 79−27763
nonuniform Langmuir fields, evolution and modulation instability 80−38599
numerical simulation of disruptions and loss in Tokamak plasma 80−70026
oblique Langmuir solitons under free path conditions *(Russian)* 80−79477
octupole, levitated, instabilities in trapped ion regime 77−68847
octupole, lower hybrid heating and mode conversion 80−6265
odd drift modes, effect of trapped electrons *(Russian)* 77−43055
Ogra-3 mirror device, loss mechanism due to cyclotron instabilities 80−28788
Ohmic current driven MHD instability in Heliotron-D device 80−38640
ohmic heating, electron power balance, TFR device 77−67885
ohmic heating of plasmas in closed magnetic systems 80−28756
one-dimensional strong Langmuir turbulence, modulational disturbance spectra 78−75339
open trap plasmas, electronic loss layer formation, low freq. oscill. anomalous electron diffusion *(Russian)* 79−90383
open traps, axially symmetric, transverse particle losses 80−28784
optical props. of thin plasma layer, parametric turbulence effects *(Russian)* 77−58864
ordinary EM waves hydrodynamic instability, rel. to Jupiter Io-modulated decametric radio S-bursts *(Russian)* 80−8582
origin of galaxies in expanding Universe, plasma cond. and instabilities, MHD soln. 80−62283
oscillating two-stream instability, rel. to solar type III radio bursts nonlinear stability 80−26826
oscillations, in lower-hybrid range, of bounded plasma 80−24162
oscillations of radially confined round beam, stability and distrib. function 80−53966
oscillations spatial mode stabilisation algorithms 80−64721
overdense column, reson. microwave absorpt. 80−64732
overheat acoustic instability in pulsed laser discharge *(Russian)* 80−103142
overheating instability, HF EM field effect 78−9771
overheating instability in solar active regions, critical mag. field gradient 77−53521
parallel velocity shear instabilities in an inhomogeneous plasma 79−82050
parameteric interactions in random media 77−27671
parametric, due to lower hybrid RF heating 78−30432
parametric, effect of particle drift motion 78−34293
parametric, fast electron production calcs. 77−55146
parametric, general quasi-linear theory 79−60130
parametric, in modulated electron-beam plasma system 77−68792
parametric, laser prod. plasma at high laser intensity 78−5903
parametric, LF ion-acoustic surface waves *(Russian)* 77−68766
parametric, microwave p-i-n diode modulator, transient plasma instability meas. *(German)* 80−87942
parametric, modulating instability in nonuniform pump field *(Russian)* 77−76048
parametric, purely-growing, at near-critical densities 77−15182
parametric, saturation by anomalous diffusion 78−14161
parametric, saturation by nonlinear four-Langmuir-wave coupling 78−42748
parametric, saturation in a strong electromagnetic field *(Russian)* 78−22475
parametric, turbulence evolution with two characteristic wavelength scales 77−80305
parametric, turbulent noise, electric field pulsations 77−42983
parametric, with electrostatic Langmuir pump wave 77−19700
parametric decay and Brillouin backscatt. instabilities, IR laser induced 77−47187
plasma instability continued
parametric decay in homogeneous plasma, pumping wave struct. absolute instability *(Russian)* 77−47183
parametric decay instabilities, higher-order nonlinearities 78−79432
parametric decay instabilities in magnetoplasma 78−9787
parametric decay instabilities in UHF discharge due to inhomogeneity parallel to pump field 80−19644
parametric decay instability, finite pump band width effects 77−80297
parametric decay instability, obs. by scatt. of laser beam from plasma 77−80309
parametric decay instability, stabilisation by nonlinear shift of Langmuir wave freq. *(Russian)* 77−72425
parametric decay instability at ion-ion hybrid reson. 77−65864
parametric decay instability near lower hybrid resonance 78−18399
parametric decay instability saturation near lower hybrid freq. 77−68777
parametric decay interaction, three-wave, threshold behaviour, bounded inhomogeneous plasma 78−42746
parametric decomposition absolutely unstable *(Russian)* 79−41829
parametric double instability in magnetised plasma 77−24074
parametric effects, energy equation considerations 78−91100
parametric excitation of longitudinal waves *(Russian)* 78−34282
parametric excitation of nonlinear oscillations by inhomogeneous electric field *(Russian)* 78−22478
parametric excitation of purely growing instabilities by EM wave 77−47188
parametric instabilities, cascade saturation induced by monochromatic driver pump 80−79491
parametric instabilities, effect of finite-bandwidth pump 78−22495
parametric instabilities, in thin radially inhomogeneous plasma column 79−7457
parametric instabilities, mag. shear effect on Bernstein waves 79−19019
parametric instabilities, nonlinear turbulence theory, pump field to plasmon conversion 77−24085
parametric instabilities, of commensurable and incommensurable nonlinear plasma waves 79−66915
parametric instabilities, review *(German)* 77−31440
parametric instabilities, spatial turbulence effect 79−27767
parametric instabilities, spectra and appl. to Crab nebula 78−45220
parametric instabilities, theory 78−14151
parametric instabilities and ion heating in a two-ion species plasma 80−28708
parametric instabilities and lower hybrid RF heating in Tokamak 77−24102
parametric instabilities excitation in HF discharge 78−34285
parametric instabilities in hot plasma near lower hybrid freq. 77−65870
parametric instabilities in hot plasma near lower hybrid freq. 77−65871
parametric instabilities in weakly-inhomogeneous hot plasmas 80−28828
parametric instabilities of inhomogeneous plasma in presence of long-wave low frequency oscillations *(Russian)* 80−103136
parametric instabilities of waves in bounded magnetised plasma 77−68772
parametric instabilities set up by EM radiation in non-uniform magnetoactive plasma *(Russian)* 80−106889
parametric instability, anomalous heating by strong EM field 77−11377
parametric instability, appearance of stochasticity on decay confinement *(Russian)* 78−51300
parametric instability, drift waves convective cells, shear nonlinear excitation *(Russian)* 80−38585
parametric instability, during ion parametric heating near lower hybrid freq. 77−62382
parametric instability, exact soln. for non-uniform plasma and pumping field *(Russian)* 80−83920
parametric instability, near lower hybrid reson., ion-acoustic turbulence effect *(Russian)* 79−4126
parametric instability, space-time random fluctuations 78−30431
parametric instability, thermal fluctuation effect in inhomogeneous plasma *(Russian)* 80−106897
parametric instability, two-plasmon, two-dimensional relax. 78−5866
parametric instability and Langmuir quasicollapse, two-dimensional calc. 78−75329
parametric instability aperiodic, stabilisation of nonlinear freq. shift 77−65873
parametric instability damping by high power elec. field pumping *(Russian)* 77−7553
parametric instability depend. on laser line-width, time-depend. theory 79−60138
parametric instability development, supplementary plasma ionisation *(Russian)* 80−24150
parametric instability due to a low frequency whistler wave 80−83926
parametric instability excitation by electron cyclotron waves in column 77−65862
parametric instability excited by two pump waves 78−59572
parametric instability in Crab Nebula, rel. to wisps struct. 79−25682
parametric instability in ionosphere, rel. to generation of plasma waves by extraordinary RF wave 77−13153
parametric instability in magnetised plasma 77−27662
parametric instability of inhomogeneous plasma, with pump wave strong coupling 78−94912
parametric instability of stimulated Raman backscatt. of circ. polarised EM waves 79−37465
parametric instability produced by relativistic electron beam in plasma 77−89274
parametric instability saturation *(Korean)* 79−7455
parametric instability saturation by electrostatic daughter wave nonlinear decay 80−53945
parametric instability saturation with multi-connected pump region *(Russian)* 77−68768
parametric instability stabilisation in nonstationary plasma *(Russian)* 78−1831
parametric interaction of waves in nonuniform pump field 77−24073
parametric ion-acoustic instability, dispersion eqn. 77−76047
parametric Langmuir turbulence, two pump wave excitation, plasmon nonlinear stabilisation *(Russian)* 78−83565
parametric magnetosonic turbulence, evolution of fluctuations into electrostatic and acoustic waves 77−11342
parametric phenomena in inhomogeneous plasma 77−47193
parametric phonon excitation and turbulence 78−75342
parametric processes in CTR plasmas, review 78−30430
parametric reson. between EM waves and electron surface modes *(Russian)* 78−34320
parametric resonance at lower hybrid freq., electron heating 77−43000

plasma instability continued
parametric scatt. of intense EM wave, ultrarelativistic plasma 77−84489
parametric scattering instability, photon helicity conservation 77−31478
parametric two-plasmon instability, Langmuir wave decay, numerical anal. 78−14152
parametric wave excitation in bounded systems 80−6252
parametrically excited instabilities, time evolution 78−9786
parametrically excited waves, collective oscill. and instability of single freq. state *(Russian)* 79−19033
parametrically unstable plasma, solitons 78−63563
parametrically unstable plasma eqns. and solitons 78−75324
partially ionised fluid, thermal instability, compressibility and collisional effects 78−55693
partially ionised plasma, thermal instability, Hall currents 78−63551
particle and heat fluxes, inhomogeneous plasma, effect of current driven drift waves 78−94898
particle beam instabilities in plasma media with absorption 80−64743
peeling instability in toroidal MHD equilibrium configuration 80−79488
pellet heated by multi-GeV heavy ions, filamentation instability 78−89976
Penning cold-cathode discharge, m=0 mode instability investigation 79−98894
Penning discharge ion source with hollow cathode, HF instabilities 80−43997
Penning discharge plasma, electron vel. distrib., rot. instability effect *(Russian)* 77−80301
Penning discharges, high-pressure, low-frequency instabilities, role of temp. gradient 79−37567
periodical regimes in solar mag. traps, rel. to solar radio pulsations *(Russian)* 80−8616
Perkins instability in nocturnal ionosphere, rel. to F-region height bands over Arecibo 79−66863
Perkins spread-F instability, effects of E-region coupling 78−40755
Pierce and Buneman instability, double layer from. in collisionless plasma 80−10398
pinch, reversed field config., heating, diffusion, stability 77−43036
pinch, reversed-field type, in STP-1, using new external-field programming, MHD instability 80−28803
pinch, thin-skin, stability, influence of thick conducting liner and superconducting wall, dispersion relation 80−64766
pinch implosion, post-implosion anomalous transport, lower hybrid drift instability 77−24056
planar diode, electron beam instabilities, finite ion mass and electron velocity spread effects 77−31483
planar shock wave, annular vortex damping *(Russian)* 79−10667
plane parallel flow stability in magnetized plasma, velocity shear instability 79−37468
plasma, ion cyclotron beam-whistler mode instability in parallel shocks 78−14148
plasma bunch, stability, breaking 78−9785
plasma focus, recent developments to increase neutron yield 79−14567
plasma mirror machines, computer simulation of field reversal 78−26316
plasma torch behaviour during laser irrad. of Pb surface *(Russian)* 78−87506
plasma transport, anomalous, electron temp. gradient instability 80−75034
plasma-beam system, surface wave dispersion, stabilisation by HF electric field 78−91117
plasma-beam system simulation, explosive instability 79−27821
plasmatron with interelectrode insert, characts. 80−44009
plasmon scatt. by electrons in intense EM field, instability 77−72434
PLT Tokamak, ohmically heated plasmas, radiation, impurity effects, instability and particle transport 80−28833
poloidal mode ballooning of trapped electron instability 80−28657
position instability analysis, effective mode approx. in Tokamak 80−103145
positional stability of a current-carrying plasma in an l=2 stellarator field 80−106906
positive column, density oscills. due to negative ions, metastable atom model 78−1799
positive column, of electroneg. gas, transverse stability, effect of dissoc. attachment 79−23475
positive column, striation dynamics, velocity/amplitude correlation 78−67517
positive column of high-voltage diffuse discharge, nonstationary processes 80−64802
potential double layers, form. and stability in double plasma beam system 77−11336
potential small-scale instabilities of inhomogeneous plasma in crossed electric and magnetic fields 80−79492
potential waves in cold plasma, parametric instability *(Russian)* 78−91088
precursor whistler mode plasma turbulence formation in parallel shock waves 80−24172
pressure anisotropy stabilisation of axisymmetric mirror machines 79−4169
pressure driven ballooning modes, numerical studies 80−92282
primary electron-gas ionization sustained discharges in incompletely ionised plasma 79−50910
proton-cyclotron instabilities, in non-uniform loss-cone magnetospheric plasma 80−90286
pseudo-classical transport, nonlinear theory of collisionless drift instability 79−94774
pulsar electron-positron plasma *(Russian)* 80−36656
pulsar polar caps as foil-less diodes, nonneutral relativistic beam accel. 80−17604
pulsar rotating magnetosphere, charge bunching mechanism for coherent curvature radiation 77−33538
pulsars coherent radio radiation by antenna mechanisms, theory 77−49414
pulsator, accumulation of impurities and stability behaviour in high density regime 80−28835
Pulsator Tokamak discharges with AC modulation 80−96386
Pulsator Tokamaks, modulated runaway losses and effects of helical dipole field 80−28845
pumped electron-ion plasma modulational instabilities due to relativistic electron mass variations 79−77363
purely growing instability, ionospheric, rel. to Langmuir waves propag. and E, enhanced plasma line 79−29928
Q machine plasma with localised strong electric field, LF instability investigation 78−79418
plasma instability continued
Q-machine, control of plasma pot. distrib. with electron emissive limiter 77−19744
Q-machine, plasma potential control with electron-emissive grid 77−39446
Q-machine plasma with strong localised elec. field, LF instability obs. 78−71480
quasi steady high beta plasma in multiple mirror machine, density oscill., stability obs. 80−28663
QUISTOR, space charge and ion stability 80−86487
radial electric field, appearance in source plasma due to beam extraction 79−45500
radial stability of density profiles for obliquely incident light 80−92350
radiation instability and heavy ion cluster formation in multicomponent plasma 79−64849
radiation-held plasma, stability 78−71526
radiative relativistic instability in accelerated plasma 79−77367
raman side-scatter instability in nonuniform plasma 79−32751
Rayleigh instability, analog, with liqs. *(Russian)* 79−98889
Rayleigh Taylor instabilities, wind-driven, in nighttime equatorial ionosphere, rel. to spread-F recurrence 79−96855
Rayleigh-Taylor, direct determ. in laser-pellet fusion expt., fast Fourier transform technique 79−71945
Rayleigh-Taylor, in inertial-confinement fusion targets 77−51174
Rayleigh-Taylor, in resistive MHD pinch 79−50877
Rayleigh-Taylor bubbles in equatorial ionosphere 78−77409
Rayleigh-Taylor growth stabilisation by thermal conduction 77−15180
Rayleigh-Taylor imploding shell instability dynamic stabilisation by laser modulation 77−47233
Rayleigh-Taylor instability, diffuse-boundary 78−94911
Rayleigh-Taylor instability, effect of Coriolis force 79−41809
Rayleigh-Taylor instability, in curved mag. field, excitation and control 78−47113
Rayleigh-Taylor instability, MHD flow of composite medium, variable viscosity 78−1813
Rayleigh-Taylor instability, rel. to F-region equatorial irregularities 77−29566
Rayleigh-Taylor instability for impulsively accelerated shells in pellet fusion 77−62384
Rayleigh-Taylor instability generation of mag. fields, effects on laser fusion 79−19025
Rayleigh-Taylor instability in imploding foil plasma, two dimens. simulation 78−47156
Rayleigh-Taylor instability in topside ionosphere, rel. to plasma bubbles near dawn terminator 79−101016
Rayleigh-Taylor instability in toroidal plasma compression by imploding plasma liner 80−33811
Rayleigh-Taylor instability stabilisation mechanism, NRL fusion programme 78−59042
Rayleigh-Taylor mode, nonlinear, and ionosphere spread-F bubbles, two-dimensional theory 78−88986
Rayleigh-Taylor modes of rot. MHD equilib., shear stabilisation 79−27813
reactor, Tokamak, toroidal magnetic field ripple, burn control 80−63375
real gas discharge, thermodynamic stability 80−38852
relativistic beam, excitation of Langmuir oscills., modulation instability *(Russian)* 79−4155
relativistic beam generation of EM waves in plasma *(Russian)* 78−75364
relativistic electron beam, high-current, reson. ion accel., nonlinear instabilities *(Russian)* 77−11329
relativistic electron beam, intense, coupled dipole oscills. 80−64739
relativistic electron beam in magnetised plasma, relax. processes, nonlinear theory, instability *(Russian)* 80−103162
relativistic electron beam in plasma, coherently radiating, radiation press. at surface 78−9314
relativistic electron beam injection into plasma, development of dissipative two-stream instability 80−19593
relativistic electron beam rot. in plasma, coherent curvature radiation, two-stream instability 80−19590
relativistic electron beam-plasma instability, macro-and microscopic models 80−75065
relativistic electron beam-plasma system, stability theory for finite geometries 79−68919
relativistic electron beams, EM instability and stopping power of plasma 80−92289
relativistic MHD growth and decay discontinuities 80−92280
relativistic nonneutral E layer, negative-mass instability 77−68856
relativistic parametric instabilities, in extended extragalactic radio sources 78−24561
relativistic plasma, longit. waves and beam instability *(Russian)* 79−60158
relativistic self-focused electron beam, hose instability meas. 78−83544
relativistic self-pinched electron beam, Bennett profile, resistive hose instability 78−83543
relativistic tangential electron beam-semirestricted plasma collision, dissipation instability *(Bulgarian)* 78−34333
relativistic transverse cold plasma waves, nonlinear, linearly polarised, stability 80−6235
relativistic two-stream instability, nonlinear state electron ion collisions effect 78−26280
relativistically covariant formulation in theory of plasma stability 80−75046
relativitic electron beam, relaxation tangential to semi-bound plasma 79−37506
resistive anisotropic jet, astrophysical asepcts 78−69667
resistive axisymmetric modes for doublets, stability, numerical parameter obs. 78−79421
resistive EM ion cyclotron instability 78−87444
resistive g mode, parallel viscosity influence 80−79486
resistive hose instability in relativistic electron beam 80−67947
resistive instability in low-β plasma cylinder 77−80289
resistive instability of tearing modes, equilib. flows 79−27816
resistive internal helical mode near the instability threshold *(Russian)* 79−98948
resistive internal kink mode 77−68793
resistive ion-ion-hybrid instability in current-carrying plasmas 79−37487
Resistive lower-hybrid instability in current-carrying plasmas 78−71467
resistive m=2 tearing instability, linear and non-linear props., numerical study 77−42974

plasma instability continued
resistive MHD instabilities, diffuse pinch configs., numerical study 77−58853
resistive MHD instabilities, in solar flare unstable arch model 77−91507
resistive MHD instabilities of current sheets, appl. to solar wind 80−4218
resistive modulation instability 79−77378
resistive tearing m=1 instability turbulent modification 80−43916
resistive tearing mode, influence of diffusion 78−34297
resistive-g and ion temp. gradient in sheared magnetic field 80−64708
resonance instability, inhomogeneous plasma stream, surface waves 77−24078
resonance instability of small-scale perturbations *(Russian)* 77−89260
resonant CO_2 laser radiation absorption and surface instability at crit. density surface 80−48859
resonant electron instability near plasmapause, rel. to 1-30 Hz waves generation 78−49235
resonant instability of semi-infinite plasma with sheared electron stream 80−48868
resonator, electron-beam excited, explosive instability 80−28693
reverse loss-cone instability in ambipolar trap *(Russian)* 80−106893
reversed field configuration, equilibrium and stability and confinement props. 80−87932
reversed field pinch, HTBX I, stability 77−24143
reversed field pinch, nonlinear saturation of tearing mode 79−73028
reversed field pinch, resistive and MHD instability, unstable central region 77−27704
reversed field pinch, tearing mode MHD eqns., linear and non-linear calc. 77−27705
reversed field pinch expt. in small compact torus STP-1 80−75043
reversed field pinch machines, plasma stability anal. 80−24214
reversed field pinch reactor, physical principles, design, operation and plasma stability 78−58470
reversed field pinches, theory and experiments, review 77−24126
reversed-current ion ring reactor, image current interaction 79−85778
reversed-field pinch plasma model 80−87935
RF emission, plasma wave scatt. by ion-acoustic waves in nonequilib. plasma 80−64733
RF heating in stationary systems, electron cyclotron reson. and lower hybrid regimes 79−98930
rF instabilities driven by neutral beam injection, review 80−28757
ripple loss of fast ions in a large Tokamak 80−92382
rotating Hall plasma, self gravitational instability, MHD stability 80−14890
rotating plasma, MHD stability criterion 80−79487
rotating plasma, spatial distrib. derivation, ionic components in reson. ionic cyclotron instability *(Russian)* 78−47117
rotating plasma column, non-ideal MHD equations 78−59592
rotating plasma reactors, longitudinal confinement, stability equilibrium and heating problems 80−74001
rotation influence on kink instability, compressibility *(Russian)* 80−48887
rotation instability on collisionless FLR plasma, nonlinear theory 80−79485
rotation of magnetised nonuniform plasma, MHD ordering 80−33756
rotational stabilization of a spiral instability in a plasma with an immobile boundary 80−38644
runaway electron induced microscopic instabilities *(Chinese)* 80−103134
runaway electron instability, non-thermal microwave radn. 80−1842
runaway electrons, X-ray obs. in Tuman-2 Tokamak *(Russian)* 78−38531
runaway electrons in collective electric fields 78−67313
runaway electrons quasilinear relaxation, HF heated tokamak plasma 77−65837
runaway rates in plasmas, const. in Kruskal-Bernstein theory 78−9773
runaway-driven kinetic instabilities in Tokamaks 78−75290
satellite plasma sheaths, streaming instabilities, elec. equilib., one-dimens. particle simulation 77−22036
sausage, nonlinear evolution in Z-pinch 77−19752
sausage instability EM fields particle accel. in pinch *(Russian)* 79−7474
scattering decay of electron whistler-ion quasimode parametric coupling 78−18401
screw, Ne wall stabilised arc column in longit. mag. field 78−87551
screw instability boundary, small perturbation effect 77−35335
screw instability of finite cond. gas *(Russian)* 80−92311
screw pinch, finite Larmor radius stabilisation, resonant particle effects 80−54020
screw pinch, gross instability, high-β plasma column motion, feedback stabilisation 77−27699
screw pinch, sharp boundary, short wavelength instabilities, Vlasov fluid theory 77−58883
screw pinch, sharp boundary Vlasov fluid model, finite Larmor radius stabilisation 77−58882
screw pinch, sharp boundary Vlasov fluid stability anal. 77−24071
screw pinch 'SPICA', equilib. and stability of high-β plasmas 79−98992
screw pinch stability, CGL model 77−19743
screw pinches, high density plasma confinement, comparison with high-beta Tokamaks 77−24128
screw pinches, sharp-boundary, m=1 and m=2 instabilities, finite gyroradius effects 77−19748
screw-pinch, equilibrium and stability 80−87934
screw-pinch configs., collisionless, hybrid-kinetic stability props. of high-beta plasmas 80−43871
Scyllac, computational plasma MHD for stable equilibria 77−84478
Scyllac, equilibrium and stability, MHD three dimensional soln. 77−24131
Scyllac, MHD stability δW calc. correction 77−65856
Scyllac, theta pinch implosion, gross plasma motion model and feedback stabilisation 77−24141
Scyllac configuration, toroidal theta-pinch theory, review 77−24125
Scyllac feedback stabilisation 77−24129
Scyllac sector feedback stabilisation expt., engng. aspects of on-line operation 77−23268
secondary parametric instabilities in relativistic electron beam heating 78−26307
self consistent circ. polarised waves, stability 79−14526
self heating and saturation due to numerical instabilities 80−75067
self-consistent EM wave stability in warm plasma 79−32763
self-gravitating composite plasma with finite Larmor radius, hydromagnetic stability 77−62350
plasma instability continued
self-gravitating rotating plasma, gyroviscosity effects 78−5860
self-gravitational instability of plasma rotating layer, effects of finite ion gyroviscosity 80−56706
self-oscillating mode origination in nonequilib. magnetised plasma 79−86568
self-sustained gas discharge, mol. vibr. relax. effect on thermal stability 80−10358
semi-self-maintained gas discharge, ionisation instability theory 78−67511
semi-stellarator field stabilization of Tokamak plasma 80−6245
shape stability for plasma in standing EM field 80−28795
sheaf instability at moderate densities, anomalous ion heating *(Russian)* 80−43922
shear Alfven wave, heat flux instability 80−43893
shear flow in mag. field, stability 78−26197
shear flow stability and Alfven waves in magnetised plasma 80−96360
shear stabilisation of drift oscills., ionic viscosity influence *(Russian)* 77−84432
sheared systems, low-β plasma, MHD intercahnge instability 80−64717
sheath, qpprox. model analysis of steady state situation 80−43934
sheet pinch, equilib. flow effect on resistive tearing mode 79−1335
shortwave trapped electron modes, fast ion-induced, electron collisions role *(Russian)* 77−47176
sideband, growth rates, nonlinear Vlasov eqn. 77−19696
sideband instability, nonlinear large-amplitude wave evolution, simulation 78−83546
sideband instability, review 77−47194
sideband instability in large amplitude wave, computer simulation 80−38602
slope reversal of a monotonically decreasing electron tail in a strong magnetic field 78−67347
slow-fast mode conversion effect on lower hybrid slow mode excitation 80−28668
small aspect ratio tokamak, high press. equilibria 79−4174
solar corona, instabilities of trapped particles in magnetic fields 78−61823
solar flare plasma flows, thermal character of instability leading to condensation form. 78−57524
solar flare plasma instability and turbulence, review 80−62100
solar wind, stability against whistler mode, anal. of proton to α-particle vel. ratio 79−2453
solar wind, stream interaction regions, microscale instabilities 80−72739
solar wind kinetic instability due to electron nonthermal props. 80−41691
solitary kinetic Alfven wave stability, one dimensional nonlinear case 80−1776
solitons, stability to transverse perturbations 77−51180
space-charge wave instability of spiral beam-plasma system in nonuniform mag. field 80−1760
spatial channelling instability modes, suppression by feedback *(Russian)* 77−47243
spectral distrib., modulation of plasma noise 80−38648
spherical implosions, instability growth and saturation simulation 77−79480
spherical laser plasma, hydrodynamic instability and spontaneous mag. field generation *(Russian)* 78−38519
spheroidal low aspect ratio plasma configurations, MHD equilibrium and stability 80−1791
spheroimak devices, magnetohydrostatic equilibrium config. 80−83965
spheromak, ideal MHD stability 80−92281
Spheromak fusion reactors, MHD equilib. and stability, numerical anal. 80−74000
spheromaks, nonlinearly stable equilibrium statistical states 80−53975
spiral beam-plasma system, instability, effect of nonuniformity of mag. field 80−48899
stabilisation of low-m kink modes in Tokamak 79−64890
stabilisation of modulation instability, fast Langmuir solitons generation *(Russian)* 78−38470
stability criteria, closed field lines system rot. transform *(Russian)* 77−3972
stability criterion for feedback control of unstable waves 77−5671
stability criterion for plasma equilibria with tensor pressure 79−1334
stability of Bernstein-Greene-Kruskal equilibria, spatially inhomogeneous Vlasov equilibrium 80−1778
stabilizing passive shell and active feedback windings in reverse field pinch fusion reactors 80−18666
stable route to the high β_p regime 80−92319
static stability, equilibrium config., stray field effects in Tokamaks *(Chinese)* 77−76158
stationary inhomogeneous electron temp. distrib. states and electrodynamic params. *(Russian)* 78−42749
stationary plasma jet, explosive instability stabilisation *(Russian)* 78−63562
stationary stratified HF discharge in plane wave fields 78−67513
stellarator, current-carrying, kink and tearing mode MHD instability 78−22539
stellarator, high-β, finite gyroradius stabilisation of MHD modes 78−26314
stellarator, Isar T1-B, m=2 mode collision-dominated stability obs. 77−24130
stellarator, MHD equilibrium and stability of plasma in toroidal geometry, 3-D computer code 80−70041
stellarator, Saturn, drift oscills. characts., high shear stabilisation *(Russian)* 79−98887
stellarator fields, m=2 tearing mode, linear growth rate 80−75037
stellarator plasma, drift instability stabilisation by AC elec. field *(Russian)* 79−7459
high-β stellarator with l=3, stability 77−7529
stellarator with spatial mag. axis, equilib., MHD stability 77−72470
stellarators, equilibrium and stability calcs. 80−83982
stimulated backscattering of electromagnetic ordinary waves from extraordinary waves below the upper hybrid frequency 79−32748
stimulated radiation, leaking normal mode spectra, cold plasma cylinder 77−89231
stimulated Raman and Brillouin scatt., static mag. field effects 80−6258
stimulated Raman scattering of EM wave, finite-wavelength, dielectric tensor determination 79−64876
stochastic instability control in tokamak by pulsed RF modulation 80−59245

plasma instability continued
stochastic instability theory applics. to nonlinear plasma systems, review *(Czech)* 80−38580
stochastic mag. field fluctuations, self-consistent model 80−100074
straight and helical θ-pinches with low compression ratio, wall stabilisation 77−27697
stratified partially ionised plasma, stability in mag. field, cond. and viscosity effects 78−26276
striations in narrow He-Ne discharges 80−38736
in strong circularly polarised EM wave field, anal. *(Russian)* 77−7544
strong turbulence effects on the kinetic beam-plasma instability 80−59207
strongly turbulent stabilization of electron beam-plasma interactions 80−59251
superheat-ionisation stability in glow discharge, stabilised by RF elec. field 79−19112
suppression by cold plasmas 79−46470
suppression by external turbulence introduction 79−32768
suppression by feedback method automatic control, stabilisation methods 78−63564
suprathermal electric microfields and plasma parameters in crit. vel. rot. plasma 79−60198
surface instability of bounded simulation plasma in mag. field 78−26321
surface mag. field confinement of high-β plasma, toroidal current stabilisation 78−67401
surface MHD waves in arc discharge, low freq. spectrum, instabilities *(Russian)* 77−68762
surface modes, in collisional electron plasma 77−58858
surface oscillation cyclotron excitation, electron beam cyclotron instability *(Russian)* 80−54008
surface waves, HF, parametric excitation using slanted, incident EM waves *(Russian)* 80−87874
SW parametric instability of inhomogeneous plasma, semi-bounded by vac. *(Russian)* 80−83917
system with trapped particles, satellite excitation 77−42981
T-11 Tokamak, neutral beam injection, plasma heating and stability 80−28702
T-6 Tokamak, disruptive instability growth, mag. field perturbation struct. and dynamics *(Russian)* 78−59560
tandem mirror physics, fusion plasma confinement 80−43960
tearing, twisting and ballooning modes in finite-β plasmas 80−28649
tearing instability, current shear effect in relativistic stream superposition model 80−24155
tearing instability, m=1, kinetic and finite beta effects 78−67398
tearing instability in background plasma, relativistic modes 80−62012
tearing instability in cylindrical plasma configurations *(Russian)* 80−10370
tearing instability kinetic theory, collisional to collisionless regimes 77−84425
tearing mode, low-m, stabilization 77−65857
tearing mode coupling in Tokamak 78−14192
tearing mode instabilities and suppression by lower hybrid fields 80−28666
tearing mode interactions 79−41823
tearing mode mag. island struct. rot., diagnostics theory 80−48982
tearing mode magnetic reconnection, explosive, in magnetosphere tail, theory 78−88992
tearing mode suppression by feedback system *(Russian)* 78−22535
tearing modes, evolution in Tokamak plasma 77−84427
tearing modes, ion dynamics effects, eigenmode eqns. 80−59212
tearing modes, nonlinear interaction in highly resistive tokamaks 79−64855
tearing modes, unified theory 80−19607
tearing modes with mag. braiding 80−10429
tearing-mode activity for hollow current profiles 79−55498
tearing-mode instability, Alfven pulse-excited, mag. field lines reconnection dynamics *(Russian)* 80−1768
tearing-mode instability in a field-reversed ion layer 80−53969
teating modes, nonlinear quenching of diamagnetic and gyroviscous effects 79−64847
temperature drift instabilities in Tokamak plasmas 77−19687
temperature gradient drift wave eigenmodes stability in sheared mag. field 80−43914
temporal growth of filamentation instability of a Gaussian laser beam in a plasma 79−50865
TERP noncircular toroidal pinch, turbulent heating 77−24162
test electron transport in stochastic mag.-field, principles and problems 79−77341
theory and expt. at Kharkov Inst., Ukrainian SSR *(Russian)* 79−14544
thermal, time evolution, temp. profiles 78−14147
thermal convection instabilities of spherically symmetric plasmas *(Chinese)* 80−1774
thermal flux reduction, in laser-irrad. plasma, EM instabilities effects 78−59641
thermal instabilities in magnetically confined plasmas, appl. to solar coronal loops 80−36600
thermal instability, in self-sustaining gas discharge *(Russian)* 79−55582
thermal instability, mag. field generated, in laser heated plasma, hydrodynamic effects 80−96355
thermal instability, of compressible plasma, finite Larmor radius effect 78−91085
thermal instability of ionosphere due to power transmitting satellite 77−25826
thermal instability of plasma column, flat glow discharge with convective cooling 77−24232
thermal modulation instability in a weakly ionized plasma, nonlinear stage *(Russian)* 80−38586
thermal modulational instability and stratification 78−75332
thermal parametric instability, effect of recomb. processes 80−61967
thermal parametric instability in non-uniform plasma, theory *(Russian)* 79−27760
thermal parametric instability in nonuniform plasma, nonlinear theory *(Russian)* 79−27761
thermal plasma fluctuations, CO_2 laser scatt., spectrally resolved meas. 77−84504
thermal thermonucl. instability in Tokamak reactor 77−74986
thermal-convective instability of partially ionized plasma, radiative transfer, medium porosity and collisional effects 80−67538
thermic excitation of parametric instability, controlled, radiowaves interaction 80−24164
plasma instability continued
thermionic plasma converter, overneutralised, instability simulation 79−14619
thermionic triode, oscills. in low press. inert gas discharge 80−79590
thermomagnetic instability of inhomogeneous plasma *(Russian)* 80−28660
thermonuclear Alfven instability stabilisation in high press. tokamak, mag. surface distortion *(Russian)* 79−27758
thermonuclear cone microinstabilities and anomalous alpha-particle losses in Tokamaks 80−28636
thermonuclear fusion and the Tokamak, review *(Italian)* 79−31177
thermonuclear fusion plasma, laser coupling and implosion 77−43006
thermonuclear instability and fueling, cold plasma layer surface fueling source 80−59196
theta pinch, hot linear, end plugging effect on stability and parameters 80−24223
theta pinch, linear, end losses, stoppering, instabilities and heating 80−24224
theta pinch, low density, step-like mag. piston 80−103182
theta pinch, microinstability and anomalous transport, kinetic and numerical study 77−76162
theta pinch, rigidly rotating, Vlasov fluid stability 80−28794
theta pinch, rot. instability 78−71522
theta pinch, tearing and reconnection of magnetic fields 79−23446
theta-pinch, bumpy, finite wavelength stability 77−24146
theta-pinch, bumpy, guiding centre plasma stability 77−24147
theta-pinch, bumpy, wall stabilisation 78−1875
theta-pinch, cross-field instabilities, nonlocal anal. 77−24137
theta-pinch, groove type drift turbulence, Lagrangian description *(Russian)* 77−72448
theta-pinch, high-energy, linear, quartz end plug effects 77−76184
theta-pinch, linear, microinstability onset, anomalous resistivity, electron heating and MHD oscills. 77−27698
theta-pinch, long wavelength m=1 MHD instability 77−72485
theta-pinch, reverse field expts., equilibrium, confinement, stability 80−28787
theta-pinch, toroidal multiple mirror field, high-beta, opt. obs. 77−24136
theta-pinch reactor, fast feedback stabilisation 77−23269
thin foil layered targets, Rayleigh-Taylor instability in laser irradiation 80−87876
thin line cusp magnetoplasma sheath, RF feedback stabilisation 80−70009
three-dimensional MHD equilibria with shear, ballooning modes 78−71476
three-wave parametric decay instability 77−89252
threshold criteria for instabilities, caused by ion-acoustic waves and EM wave interactions *(Russian)* 78−22505
TO-1 Tokamak, kink instability, feedback stabilisation 80−28634
Tokamak, anomalous diffusion with light and heavy impurities, drift wave depend. 80−64677
Tokamak, asymmetrical collisional tearing mode growth rate, variational treatment 79−32803
Tokamak, axisymm. MHD instability, feedback stabilisation 78−87484
Tokamak, axisymmetric instabilities, time depend. simulation 79−10702
Tokamak, confinement and stability, effects of shaping and compression of plasma 80−28772
Tokamak, destabilizing effect of width and limiting plasma press. *(Russian)* 79−7458
Tokamak, edge effects and impurities, influence on thermal stability 80−87892
Tokamak, electron energy confinement, simulation predictions 79−64898
Tokamak, equilibrium and stability, time-depend. three dimensional MHD calc. 77−24131
tokamak, field line reconnection and disruptive instability 77−43045
Tokamak, helical winding, effect of HF current on discharge 78−87485
Tokamak, high β_J, m=1 mode, internal helical instability suppression *(Russian)* 79−98947
Tokamak, high beta, axially symmetric diffuse column, equilib. and stability anal. 77−24132
tokamak, high-beta, equilib. and stability, theory and expt. 77−43042
Tokamak, high-beta, equilibria and m=1 kink ballooning mode nonlinear evolution 80−24236
Tokamak, high-beta, with force-free currents, MHD stability 78−87481
Tokamak, high-beta limitation by instabilities during rapid heating 77−39448
Tokamak, high-beta limitation by instabilities during rapid heating 77−39449
tokamak, horizontal plasma position control by feedforward-feedback system with digital computer 80−75093
Tokamak, ideal MHD stability 80−59216
Tokamak, internal helical mode stability, by MHD approx. *(Russian)* 78−91139
Tokamak, internal kink mode, numerical study 80−48953
Tokamak, JFT-2, parametric heating by RF near lowr hybrid freq. 80−70023
Tokamak, large aspect ratio, ballooning stability boundaries 79−1332
Tokamak, large aspect ratio, two-dimens. drift-wave stability 80−79479
Tokamak, large aspect ratio, two-fluid energy principle 79−19078
Tokamak, large mag. islands as disruption mode 79−27819
Tokamak, large mag. islands as disruption mode 79−27818
Tokamak, large poloidal beta, MHD stability, collisional and anomalous trapped particle diffusion 77−24055
Tokamak, local stability criteria, multipole field effects *(Chinese)* 77−39445
Tokamak, lower-hybrid-freq. heating, parametric instabilities 79−90426
Tokamak, LT-3, disruptive instability, spectroscopic observations 78−87483
Tokamak, LT-3, ion heating by disruptive instability, ion temp. particle diagnostics 79−86593
Tokamak, major disruption suppression by tearing modes stabilisation 80−10422
Tokamak, non circular, small-aspect-ratio, high mode number ballooning instabilities, max. β-value 80−73995
Tokamak, noncirc., axisymmetric modes wall stabilisation, simulation 78−67394
Tokamak, noncirc. cross-section, local, ideal and resistive stability 78−22540
Tokamak, noncircular, reactor size plasma MHD equilib. calc. 77−24121
Tokamak, nonlinear perturbation, feedback effect *(Russian)* 80−83967
JFT-2a Tokamak, plasma equilib. with separatrix mag. surface 77−7581

plasma instability continued
Tokamak, PLT, disruptive instabilities, X-ray study 78−89974
Tokamak, poloidal divertor expt., stabilisation of the axisymmetric instability 79−4171
Tokamak, sharp-boundary model, axisymmetric MHD instability anal. 77−51217
Tokamak, small aspect ratio, flat current noncircular, unstable MHD spectrum 80−69989
Tokamak, space-depend. thermal stability of reacting plasma 79−19068
Tokamak, square or inverse-dee, equilibria, axisymmetric instability and stabilisation 79−73029
Tokamak, stability of internal helical mode, high press. plasma *(Russian)* 78−91138
Tokamak, stochastic particle orbits, statistical description 80−79466
Tokamak, T-10, stainless steel limiter expts. in ohmic heating region *(Russian)* 80−83969
Tokamak, TOSCA, magnetic islands and disruption 79−23456
Tokamak, trapped electron instability, 2-dimens. eigenvalue problem, anal. soln. 78−83549
Tokamak and CTR reactors, mobile diaphragm operation mode *(Russian)* 80−83966
Tokamak axisymmetric equilib., flux surface shape and current profile optimization resistive interchange stability 77−84480
Tokamak discharge, transient behaviour, electrohydrodynamical model 80−48952
Tokamak discharge dynamics, dominated by trapped electron instability 79−55537
Tokamak experimental results, review 79−98968
Tokamak expts. survey, apparatus, techniques, containment times, plasma instabilities 78−59662
Tokamak first wall low-Z materials, impurity radiation from medium density plasmas 79−55472
Tokamak fusion reactor, thermonuclear instabilities α-particle interactions 77−88281
Tokamak fusion reactor plasma, trapped α-particle cyclotron instability 79−73024
Tokamak fusion reactors, doublet research, plasma shape control, MHD stability 80−28837
Tokamak fusion reactors, stable equilibria using supplemental heating 80−91244
Tokamak high beta stability 80−96383
Tokamak high temperature plasma stabiliser *(Russian)* 79−82103
Tokamak hydromagnetic stability, ideal and resistive, review 78−34358
Tokamak ignition equilibria and thermal stability 80−74005
Tokamak machine with iron cct., flux mapping and current distrib. 79−41866
Tokamak MHD processes, Kadomtsev-Pogutse eqns. numerical simulation, kink modes and internal disruption 77−43047
Tokamak modes, MHD theory, drift effects *(Russian)* 79−37477
Tokamak plasma, LF electrostatic instability in cylindrical collisionless plasma 79−10696
Tokamak plasma, Pulsator I, disruptive instability, origin 77−43026
Tokamak plasma, Pulsator I, high density, props. and stability 77−43025
Tokamak plasma, resistive ballooning mode eqn. 79−14597
Tokamak plasma, Thomson scatt. with repetitively Q-switched ruby laser 80−59271
Tokamak plasma, vertical stability, finite cond. effects 79−4162
Tokamak plasmas, advanced-fuel, ignition and thermal stability 80−86970
Tokamak plasmas, turbulent heating by runaway electron beams, plasma instability 79−73020
Tokamak resistive kink modes, stabilisation of optimised current profiles 77−24069
Tokamak synchrotron emission and runaway electron distrib., time evolution 77−39447
Tokamak thermonuclear reactor, MHD modes drift phenomena, kinetic method *(Russian)* 80−1827
Tokamak TO-1, feedback system effect on plasma parameters *(Russian)* 80−103174
Tokamak TO-1, stabilisation of helical instability by feedback *(Russian)* 78−30443
Tokamak trapped particles, interaction in amplitude moderated RF fields 80−79497
Tokamak with horizontally elongated cross sections, equilib. and stability 78−75405
Tokamak with magnetic limiter, positional instabilities 77−11386
Tokamak with non-circular cross-section, ballooning modes, stability *(Russian)* 80−103141
Tokamaks, ballooning modes and pressure limits 80−28647
Tokamaks, computer simulation of trapped electron modes 80−106874
Tokamaks, elongated, axisymm. MHD stability 78−86683
Tokamaks, feedback stabilisation of magnetic islands 80−28638
Tokamaks, high-β, MHD stability limits 80−28643
Tokamaks, high-pressure, MHD-mode stability, high wave number 80−28644
Tokamaks, ideal MHD mode stabilisation and optimisation 80−79480
Tokamaks, injected ion loss due to spatial field ripple 80−92321
Tokamaks, kink and tearing modes 79−98910
Tokamaks, magnetic islands, tearing modes 80−28846
Tokamaks, MHD beta limits, dependence on current density and pressure profiles, num. calc. 80−28637
Tokamaks, MHD stability and reactor requirements 79−98911
Tokamaks, non-circular, shaping and internal structure 80−28842
Tokamaks, non-circular, stability and beta limits 80−28646
Tokamaks, nonlinear drift tearing modes 80−53971
tokamaks with elongated cross section, MHD stability 79−90441
Tokamaks with large-aspect-ratio, stability, two-fluid dissipative theory 80−28640
Tokapole II, non-circular Tokamak, axisymmetry instability 80−87877
Tonks-Dattner resonances, appls. to plasma diagnostics 78−83618
toroidal, equilib., external analytic solns., Wangerin transform calcs. *(Chinese)* 78−91136
toroidal axisymmetric plasma, ideal and resistive ballooning modes 80−83936
toroidal axisymmetric system *(German)* 80−28792
toroidal config., peeling stability criterion 79−98953
toroidal filament, stabilisation of current instabilities, by feedback method *(Russian)* 77−76185
toroidal geometry, characterisation of the essential spectrum of an operator rel. to plasma stability *(French)* 80−92284
plasma instability continued
toroidal kink instability, noncirc. cross section, nonlinear phase obs., probe diagnostics 79−60182
toroidal pinch, dynamic stabilisation by oscill. toroidal field 77−27700
toroidal pinch experiments, using perforated shell-type coil 79−86598
toroidal plasma, criteria for stability of surface preserving modes 79−14591
toroidal plasma, eigenvalue problem and nonlinear evolution of kink modes 80−24234
toroidal plasma, sharp boundary, MHD stability 77−11385
toroidal plasma, trapped-electron instability, numerical simulation 78−94933
toroidal plasma, vertical displacement instability *(Chinese)* 80−1824
toroidal plasmas, axisymmetric, high mode number stability 80−28642
toroidal plasmas, MHD instabilities 80−38579
toroidal relativistic beams, kink instability, shear Alfven modes 77−76122
toroidal screw pinch, MHD kink instabilities 77−19742
toroidal screw pinch, Spica, current decay, stability 77−43040
toroidal system, MHD plasma control by feedback and HF fields 80−28781
toroidal systems, gradient B drift instability 77−62391
toroidal theta pinch fusion reactor for investigating plasma instability problems, expt. 77−23251
transverse Cherenkov mode nonlinear stabilisation by external mag. field 80−38642
transverse circularly polarised self-consistent large amplitude wave stability, in large-scale mag. field 79−32760
transverse instability in plasma column 78−5869
transverse ion-acoustic and antidrift waves in magnetised plasma, stability 77−55147
transverse Kelvin-Helmholtz instability, suppression by lower hybrid turbulence 77−65861
transverse Kelvin-Helmholtz instability in magnetised plasma, appl. to auroral arcs 77−53287
trapped α-particles, quasilinear relax. in Tokamak reactor, during cyclotron magnetoacoustic instability *(Russian)* 79−55487
trapped electron instabilities, collisional effects 78−26279
trapped electron instabilities, reson. electron effects 77−7528
trapped electron instability, feedback diagnostic 78−51350
trapped electron instability, mag. curvature drift driven, collision effects 77−55142
trapped electron instability, nonlinear saturation 79−14531
trapped electron instability, turbulence, unstable mode dynamics anal. 80−33761
trapped electron shear-Alfven instability, stabilisation by temp. gradient 80−28599
trapped electrons in Tokamak, short wave instabilities at high pressure 77−19756
trapped ion eigenmodes, two dimens. anal. 80−83935
trapped ion mode, ion motion, overlapping bounce resons. effect 77−76069
trapped ion mode driven by ion mag. drift reson. 77−31452
trapped ion mode excitation in Tokamak *(Russian)* 78−38467
trapped particle anomalous transport in Tokamak, scaling laws 80−103115
trapped particle instability in Tokamaks, book 78−83562
trapped particle instability in toroid, shear stabilisation 77−68848
trapped particle instability threshold 77−980
trapped particle instability threshold 77−981
trapped particle modes, HF pump effects 77−31499
trapped particle modes, parametric excitation, instabilities, HF pump effect 77−24177
trapped-electron cyclotron instability, in Tokamak, 2-dimens. eigenvalue problem, analytic soln. 78−30434
trapped-electron dissipative mode, two-dimens. spatial struct. 77−51175
trapped-electron instability dissipation, nonlinear saturation, in Tokamak 77−84429
trapped-ion instability, transport coeff., impurity ions effect 77−76057
trapped-ion residual instabilities in Tokamak 77−47185
trapped-particle instabilities, linear and nonlinear theory 77−72429
Trivelpiece-Gould-modes, axial inhomogeneous plasma 79−23405
Tuman-2A Tokamak, ohmic heating and compression of plasma 80−28703
turbulence, finite-β, universal mode, Alcator scaling 79−90408
turbulence generating mechanism in weakly collisional plasma 77−11340
turbulence induced by plasma-electric current interaction in focus expt., laser diagnostics 80−24171
turbulent convective transport in a plasma 80−28606
turbulent destabilization and saturation of the universal drift mode in a sheared magnetic field 79−37455
turbulent diffusion in plasma with high-energy ions, thermonuclear case 77−971
turbulent heating, electric field penetration for nonlinear current saturating elec. cond. 77−24109
turbulent heating of magnetic mirror confined plasma, rel. to Buneman instability 77−24106
turbulent heating of plasma with transverse current, mechanism *(Russian)* 77−80324
turbulent plasma, parametric instabilities, anomalous energy absorpt., dispersion eqn. 80−92291
turbulently heated toroidal plasma discharge, microwave spectra obs. 79−50893
twisting modes 79−60135
two component plasma electron beam nonlinear stabilisation, diamagnetic and VHF obs. *(Russian)* 79−27759
two Langmuir wave parametric decay instability, self-trapped EM pump wave effects 80−96357
two stream instability in equatorial electrojet over Africa, multifreq. HF radar studies 78−36370
two-component ionic fluids, temp. depend. of plasma freq. 78−47115
two-component laser-produced plasma, similarity flows 78−83591
two-fluid dissipative plasma, energy principle in Lagrangian form, tearing modes 78−42794
two-ion component plasma, growth rates and stability regions 77−55141
two-plasmon decay, profile modification, produced by 10.6 micron radiation, at $^1/_4$-crit. density 79−19061
two-plasmon decay in CO_2-laser-plasma interaction 79−1326
two-plasmon decay instability, nonlinear saturation and recurrence 79−82057

plasma instability continued
two-stream, causing electron emission in microwave irrad. plasma 77−84503
two-stream and Buneman instability stabilisation mechanism, hot plasma 77−983
two-stream instability, in force-free pulsar wind zone 78−49468
two-stream instability, in neutralised electron ring 78−25357
two-stream instability, occurrence in collisionless shocks at high Mach numbers 80−87893
two-stream instability, thin layer waves modes 77−62361
two-stream instability in plasmas with arbitrary orientation of magnetic field 80−41715
two-stream nonsymmetric instability 77−31446
two-stream plasma, development of instability of dispersed waves *(Russian)* 80−103138
ubiquitous mode, theory 77−68794
ultralow frequency oscill. in trapped electron regime 80−1784
universal drift instability, magnetic gradient effects 79−60117
universal drift instability from single-particle approach 79−19023
unmagnetised plasma, quasilinear theory of parametric processes 79−94787
unstable continuous spectrum and ballooning modes 80−19569
unstable oscillations, sheared toroidal mag. field procedure for reconciling oscillation characts. with periodicity 78−34309
unstable turbulent ionisation waves, two dimensional Fourier spectroscopy 80−38646
upper hybrid turbulence, kinetic modulational instability 77−42984
vacuum arc cathode plasma interaction with transverse mag. fields 78−75468
variational methods for complex eigenfrequencies 80−28631
velocity driven modes in dense partially ionized plasmas, stability aspects 80−1792
velocity space ring plasma instability, magnetised ion interaction, Vlasov theory 79−77368
velocity space ring plasma instability, magnetised ion interaction, electrostatic and EM simulations 79−77369
velocity-shear flute instability of plasma flowing along curved mag. field 77−31459
vertical stability in elongated Tokamak, numerical study 79−14594
vibrational kinetics and plasma characts. in CO-N_2 discharge 80−59331
Vlasov equilibria, local Maxwellian velocity distribution 80−87928
Vlasov plasma mathematical model 79−55503
Vlasov stability, particle reson. effects in axisymm. field reversal config. 78−83553
Vlasov-Maxwell equilibria, exact solns. with sheared mag. fields 77−3977
VLF electrostatic emissions form. mechanism in high latit. F-region 78−93037
volume discharge, instability with electron beam at front of accelerating pulse 79−10739
W VII-A (2,1) tearing mode depend. on stellarator field 80−79550
W VII-A stellarator, m=2 mode at q=2 80−24227
wake model of fast moving body in plasma and its effects 79−77353
warm fluid magnetoplasma, automated calc. of parametric instability 79−50855
wave excitation mechanisms and harmonic generation in laser produced plasma *(Russian)* 77−11339
wave growth, stability anal., particle distrib. functions and transport theory 80−43903
wave heating at electron cyclotron harmonics in toroidal plasmas 80−28727
wave-particle interaction, in cyclotron reson. region, trapped particle effects 77−51164
wave-particle interaction in the late beam-plasma instability 80−28692
wave-particle interactions instability in magnetosphere tail plasma sheet, rel. to adiabatic convection 79−25408
wave-particle transport from electrostatic instabilities 80−83898
waveguide, plasma-filled, two-stream instability nonlinear evolution, numerical simulation 80−43938
waveguides with diffuse boundaries, electron beam dissipative instability *(Russian)* 77−15212
weakly collisional inhomogeneous plasmas, cyclotron resonance destruction, cyclotron drift instabilities 79−77372
weakly inhomogeneous magnetic field amplification by plasma wave 80−24166
weakly ionised cylindrical plasma, nonlinear stability 79−27772
weakly ionised plasma in DC field, non-zero neutrals temp., unstable modes anal. 80−38606
weakly ionised plasma stability in strong DC elec. field 78−75308
Weibel instabilities, temp. anisotropy driven, statistical thermodynamics 80−75047
Weibel instability, nonlinear theory 79−60122
whistler instability, solar wind heat flux regulation 77−45277
whistler instability in solar wind, rel. to nature of small-scale inhomogeneities 78−45173
whistler mode instability in magnetosphere, critical electron pitch angle anisotropy for chorus generation 77−2308
whistler mode waves, temp. anisotropy and beam type instabilities 77−3937
whistler wave, filamentation instability due to ponderomotive force 79−14538
whistler wave decay, into upper sideband and low-freq. waves 79−73007
whistlers, scattering, nonlinear, by lower hybrid and ion Bernstein modes 80−43929
Z discharge relaxation between electrodes 80−75089
Z-pinch, gas-embedded, α-heating, deformations and kink instability 77−24149
Z-pinch, m=1 mode dynamic stabilisation, HF current 77−24142
Z-pinch in HBTX-1, large amplitude helical kink instability and field reversal 78−42783
Z-pinch plasma, focused ion beam microinstability, pellet fusion appl. 79−32785
Z-pinch tunnelling instability and finite Langmuir ion radius, MHD anal. *(Russian)* 77−47168
Zakharov equations derivation for higher electron non-linearities in Langmuir collapse dynamics 80−43919
zero-mode, new parametric decay instability in external electric field 77−15184
Zeta plasma, field line reconnection and density fluctuations 80−69975
ZT-1 reversed field pinch, derated mode MHD stability and diffusion 77−27701

plasma instability continued
Ar DC discharge plasma parametric instabilities near lower hybrid frequency *(Japanese)* 79−7450
Ar, dynamic stabilisation of dissipative drift modes by oscillating azimuthal mag. field 78−18396
Ar hollow cathode arc, in mag. field up to 2 k0e, plasma parameters 80−6306
Ar ion laser, He, Ne, impurity effects, ignition enhancement and instability suppression 79−13948
Ar, laser-initiated plasma, gasdynamic instabilities and convective flow parameters 78−22525
Ar, stationary striations as bifurcation phenomenon 79−32767
Ar, weakly-ionised, collisional drift instability 80−53977
Ar^+ ion laser, plasma instability, suppression by He admixture 79−64204
Ar-N_2(CO), non-self-sustained discharge instability, negative differentiated cond. *(Russian)* 80−38740
CO discharge, low-pressure laser striation obs. 78−66814
CO-Ar mixture non-self-sustained discharge instability obs. 78−71612
CO_2 laser, vibrational control in stabilisation of ionisation-thermal instability 77−19302
CO_2-N_2 electroionisation laser mixture, ionisation instability of semi self maintaining discharge 80−63971
CO_2-N_2-He, non-self-sustained plasma discharge instability, electron collisions *(Russian)* 77−76050
Co_2:He:N, glow discharge instability in afterglow 80−6313
Cs, exploding wire, striations produced at supercrit. press. 79−64952
Cu arc, fluctuating, diagnostics using spectral-image photographs *(Japanese)* 79−41896
Cu II, laser construction and performance, novel hollow cathode discharge structs. 80−38000
D plasma, nonuniform Vlasov, linear normal modes of electrostatic perturbations, calc. method 77−42977
D-D fusion reactor plasmas, pure and catalysed, thermal stability 80−24207
D-D plasma interaction with relativistic electron beam, thermonucl. reaction, neutron and proton prod. 80−37575
D-T fusion plasma, parametric noise effect on temp. stability 77−39439
D-T plasmas, ignition toroidal expt., equilibrium configs. and heating 80−28704
D-T tokamak plasma effect of particle confinement and recycling on thermally stable regions 79−97900
DyI_3/CsI/Hg arc, oscillations induced by external mag. field, arc constriction 79−60205
EM wave generation, spontaneous, in plasmas with electron thermal flux 77−84418
H laser plasma, parameteric instability depend. on laser line-width, time-depend. theory 79−60138
H_2 gas target, laser-induced parametric instabilities, diagnostics 78−51345
H_2, plasma, thermally anisotropic, cyclotron instabilities 78−1814
He ion beam plasma inhomogeneous system, microinstabilities 78−91122
He plasma-electron beam, electron cyclotron instability, nonlinear time development, k-spectrum 77−76210
He spark, cathode spot conversion kinetics 80−44067
He-Cs, turbulent plasma, characts., electron energy balance *(Russian)* 79−27779
He-Cs plasma, HF instability in crossed fields, obs. 78−75305
He+H_2 microwave plasma, pulsed high current heating at atm. press., MHD instability 78−55728
Kr-F_2 mixture, preionised electric discharge stability 79−64865
KrF laser, e-beam sustained, glow discharge stability 79−55117
N discharge, externally maintained, instability growth time, associative ionisation 80−6254
N, glow discharge instability in afterglow 80−6313
N_2, a.c. discharge, stability *(Russian)* 78−26358
N_2 electron-beam-sustained discharge stability model 78−71608
N_2, glow discharge, decay instability and contraction, interferometric and photographic obs. *(Russian)* 78−59696
N_2 glow discharge, semi-self maintained, stability *(Russian)* 79−27845
N_2, non-self-maintained discharge, high press., ionisation instability, pulse discharge train *(Russian)* 77−47282
N_2, non-self-maintained glow discharge ionisation instability, vibr. states excitation calc. 77−19805
N_2-Ar mixture non-self-sustained discharge instability obs. 78−71612
N_2-CO_2, N_2 non-self-maintained discharge, high press., ionisation instability, pulse discharge train *(Russian)* 77−47282
N_2-CO_2 mixture non-self-sustained discharge ionisation instabilities, obs. 78−71610
N_2-O_2 nonselfsustaining discharge plasma, current establishment/relax. processes, rel. to CO_2 laser *(Russian)* 79−99011
Na-Ne-Ar discharge low-press., instability 78−9868
Ne discharge, ionisation wave, phase instability and disintegration obs. 78−67518
SF_6 gas, dispersion relation of spontaneous oscill., unstable regions 80−1875
Xe, pulsed discharge, superheating instability, effect of secondary ionisation 77−55189

plasma interactions *see plasma collision processes*

plasma jets
absolute spectral brightness, space-time distribs. *(Russian)* 79−27836
absolute spectral brightness measurement 80−28832
a.c. arc, cross electrode type, operating characts. *(Japanese)* 77−1022
aerosol jet, electrophysical props. 80−24134
air plasma jet, calorimetric probe for local heat flux measurements 77−43061
air plasma jet of induction plasma generator, SiO_2 particle movement and heating *(Russian)* 80−7522
anisotropic plasma jet, stability 77−17353
arc, macroscopic behaviour *(Japanese)* 77−24228
arc furnace, ignition and stabilisation *(French)* 78−47187
arc jet, effect of negative ions on I-V, enthalpy, cond. characts. 77−24235
arc spraying of powder, effect of thermal power of jet on heating and deposition on substrate 77−59959
arcjet operation, transitional behaviour 79−37556
atomic emission spectroscopy, discharge current and gas flow rate influence *(Czech)* 80−26081
atomiser, thermal characteristics 77−51246
calormetric probe for determ. of heat flow *(Russian)* 78−12698

plasma jets continued
capillary discharge jet, displacement meas. 79−94817
cluster accelerated by coaxial gun, spectroscopic struct. and mass determin. 77−80349
cumulative plasmadynamic discharge, dynamics and radiation, UV source appls. *(Russian)* 79−55578
DC plasma jet, NO synthesis, chem. kinetics obs. 80−38728
diagnostics, thermal and electrical meas. 78−5931
electric arc, self magnetic field, kink instability, plasma jets production *(Polish)* 80−19662
electron velocity distribution function in plasma jet, light scatt. meas. 79−4183
emission from hypersonic plasma-plane obstruction zone *(Russian)* 77−84449
fast electron production in plasma jet, suppression in laser-plasma *(Russian)* 79−14583
flame, heat transfer to stationary sphere 80−33824
galaxy bridges and jets, hydromagnetic break-up into aligned objects 77−49475
gas-discharge plasma, in axisymm. mag. field, plasma flow diagnostic meas. 77−35419
H plasma jet, calc. of temp. and trajectory of particles in nonisothermal jet *(Russian)* 80−7514
heat exchange in multijet mixing chamber of plasma heating unit *(Russian)* 77−68813
heat exchange with blunt body near stagnation point 79−77103
heat exchange with obstacle 78−47130
heat transfer in plasma multijet mixing chamber *(Russian)* 77−84534
heat transfer rates to flat plate from normally-impinging N plasma jet 80−75061
heat transfer to rotating water-cooled cylindrical wall *(French)* 80−28850
heterogeneous medium, interactions of laser radiation 80−28765
high velocity jets generated by plasma focus and shock-wave expt., temp. and density meas. *(Russian)* 80−106882
hollow cathode gasdynamic jet carrying excited metal atoms as spectral light source and chemical reactor 79−46493
hydromagnetic stability 78−1827
hypersonic plasma jet discharge, highly effective radiation sources prod. using freq. doubled pulses 79−93235
hypersonic plasma jet discharge, pulsed radiation source *(Russian)* 78−74073
impinging on metal surface, interferometric temp. meas., <5000K 78−87498
impulse plasma jet volume and time distrib. parameters 78−71558
interferential laser Doppler velocimetry in HF plasma jet *(French)* 77−89307
intersecting, gas-dynamic accel. in compression zone, optical and spectroscopic obs. 77−51247
ion-acoustic dissemination in moving plasma jet 80−38707
ionosphere, energetic electron efflux, caused by plasma jet injection from rocket *(Russian)* 79−5701
laser beam focused in plane target, jet form., investigation using wavefront method 80−75103
laser beams interacting nonlinearly, causing enhanced electron density fluctuations 79−98920
laser Doppler anemometry *(French)* 77−43070
laser plasma jets in conical targets, collision influence in final stages of expansion 79−14584
low temperature, decomposition and reduction of SiO_2 *(German)* 80−45499
low-temperature plasma jet, vel. meas. by obs. brightness inhomogeneities 77−43062
magnetic reconnection, plasma confinement and jetting 79−10704
magnetoplasmadynamic arcjet, density meas. by CO_2 laser interferometry 80−59277
MHD, in welding arcs, gasdynamic characts. *(Russian)* 78−47191
mixing of jet with surrounding gas, effect of sound radiation 79−82053
MPD arcjet, effect of strong mag. field on physical processes 77−89324
nonisothermal vertical impinging jets of differing momentum, one and two phase *(Russian)* 77−72511
plasma focus, vac. UV emission meas. using ionisation chamber 77−80370
plasma spraying, coatings and composite materials 78−3247
plasmatron spray, parameters meas. *(French)* 77−35402
powder condensation growth, math. model of jet-plasma treatment process *(Russian)* 80−7513
powder grains, melting, in plasma flame 79−60200
production in dielectric breakdown of solids *(Russian)* 78−22524
pulse, characts. w.r.t. IR spectra *(Russian)* 79−32826
pulsed erosion jet, energy characts., heat flow distribution *(Russian)* 80−33825
quasisteady uniform jet, form. by slot-shaped erosive plasmatron *(Russian)* 78−75437
radiative parameters, temp., electron density *(Russian)* 78−38459
rarefied plasma flow, degree of nonisothermality, probe meas. 80−24243
reaction intensity meter, use of inductive transducer 77−11399
reactive hot gas thermodynamics and diagnostics 78−76865
slot-shaped erosion plasmatron for spectroscopy of low-temp. plasma 79−94821
source, dielec. chamber, plasma flow characts. optimisation 80−38574
spark machining, heat and mass transfer 79−1369
spectral analysis of fission reactor materials 80−19624
spectroscopic light source, intensity distribs., OH band rot. temp. 77−44555
stabilization of jet on axis of plasma chem. reactor *(Russian)* 79−50899
stationary plasma jet, explosive instability stabilisation *(Russian)* 78−63562
supersonic, damaging of metals, mech. momentum role 80−2065
supersonic, ionisation in Mach disc, submillimeter laser interferometry diagnostics 80−14934
supersonic, prod. by electric arc plasmatron *(Russian)* 78−14221
supersonic, vel. meas. using Doppler shift *(French)* 78−14207
supersonic colliding plasma jets, hot dense plasma formation, hydrodynamic model *(Russian)* 80−38676
supersonic jets of magnetoplasmadynamic source plasma, gasdynamic struct. of initial section 77−35332
supersonic plasma jet, current carrying-interaction with coaxial mag. field *(German)* 79−77356
surface heat treatment using plasma torch with rectangular jet 77−27751
swirled, natural gas injection effect on temp. and vel. fields 79−90473
switch, plasma-jet-triggered, 10 to 100 kV operation 79−55574
temperature distribution by spectroscopic measurement *(Korean)* 77−80355
thermal plasma engineering in metallurgy, inorganic materials technology 78−3070
turbulent, electrostatic probe meas. at atm. press., mean values determ. *(Russian)* 77−51240
underwater wet plasma wetting in pressurized water 78−7090
Z-pinch, gas puff device, X-ray spectra, plasma form. 79−94816
Ag cylinder implosion plasma and vapour jet deposition recording 78−75400
Al target bombardment in vacuum by microsecond laser pulses, plasma parameters 79−64884
Al_2O_3, powder grains, melting, in plasma flame 79−60200
Ar, appl. to emission spectroscopy, flame stability improvement 77−86425
Ar arcjet plume, freely expanding, excited state distrib. function 79−98881
Ar, atmospheric arc-jet plasma, ζ-function evaluation, near 10^4K 77−84497
Ar, emission of electron-neutral atom bremsstrahlung *(French)* 78−26332
Ar, heat transfer and hydrodynamic struct. 79−14521
Ar jet-transferred DC arc for refractory refining, initiation and performance characts. 78−9866
Ar jets, single- and two-phase, non-equilib. in initial zones 79−82102
Ar laminar plasma jet, H_2 diffusion obs. 78−71557
Ar MHD arcjet, recombination lasing 77−65588
Ar magnetoplasmadynamic arcjet, recomb. lasing 80−48218
Ar one-phase and two-phase jets, non-equilibrium in initial region *(Russian)* 77−31518
Ar, optical studies using Schlieren and shadow methods 80−59279
Ar plasma, hypersonic nozzle, radiation field characts. 77−84340
Ar, plasma, population density meas. in free jet expansion flow 77−27737
Ar plasma jet, electron temp. and density determ. 79−41875
Ar supersonic jet, radiation in magnetoplasmadynamic source 77−35329
Ar, surrounded by Ar, He, N_2, H_2 gases, recombinations in decaying jet 78−9753
Ar, turbulent, radiowave interaction and electron density fluctuation 77−989
Ar, under press., heavy particles temp. meas. *(French)* 78−9841
Ar-He plasma, thermal diffusion of neutral species in plasma jet, 2000-4000K 79−32742
ArH exciplex emission obs. in rarefied Ar-H_2 plasma jet *(French)* 80−48054
Cs hollow-cathode plasma jet source 77−84463
H levels, population inversion, in supersonic H-Ar plasma jet 79−3417
Hα and Hβ, Stark profiles, ion-motion effect 80−63592
He I 447.1 and 492.2 nm lines, ion motion effects on Stark profiles 80−69105
He supersonic jet, radiation in magnetoplasmadynamic source 77−35329
He_2^+ recombination, high-temp., in plasma jet *(French)* 80−43861
N, high intensity arcs, anode contraction region modeling 80−103210
N I plasma jet, spectroscopic diagnostics, Stark broadening and shift, study 80−38727
N_2, appl. to prep. of ultra-fine TiN powder *(Japanese)* 78−72757
N_2, arc jet enthalpy meas. by fast miniature total calorimetric probe 78−67486
N_2 plasma jet anode root behaviour rel. to hollow-anode thermal insulation 78−71554
N_2, spectroscopic obs., electron temp. 77−31512
N_2-CO_2-H_2O gasdynamic laser mixture, electron beam diagnostics 77−83845
TaN, cubic phase formation from hexagonal by plasma jet heating 78−84726
TiC plasma-chemical synthesis, depend. on geometric and flow rate parameters *(Russian)* 80−40677
TiC, ultrafine powder prep. by plasma jet *(Japanese)* 77−52273
Xe, radiating, bulk energy distrib. 80−75107
Y_2O_3 capillary discharge plasma, temp., radiation screening elimination 80−64682

plasma magnetohydrodynamics
accelerator, pulsed, nonstationary 2-dimensional MHD soln. in coax. channel *(Russian)* 77−27745
accelerator, thermodynamic props., mag. field strength, Hall currents in arc region 77−65917
accelerators, electrodynamic characts. 80−64788
acoustic instability of plasma flow in MHD generator channel *(Russian)* 77−89234
adiabatic motion in dipole mag. field in presence of longit. electrostatic fields, plasma parameters 79−77349
Alcator A Tokamak, disruptive MHD activity during plasma current rise 80−32487
Alcator Tokamak, energy balance, MHD activity 80−28838
Alfven fluctuations in inhomogeneous nonequilib. plasma *(Russian)* 79−4123
Alfven ion cyclotron waves, in finite length plasma, differential eqn. 78−91097
Alfven pulse-excited instability in neutral sheet, mag. field lines reconnection dynamics *(Russian)* 80−1768
Alfven resonance effects on magnetosonic modes in large Tokamaks 79−73006
Alfven shock evolution is classical MHD *(French)* 78−18352
Alfven wave excitation, by fast particles in a finite press. plasma of adiabatic traps 78−79424
Alfven waves, collapse, energy transfer mechanisms *(Russian)* 77−76075
Alfven waves, finite amplitude circularly polarised, instability 78−28502
Alfven waves, nonlinear self-precession and wavenumber shift 80−10389
Alfven waves, soln. for MHD equations, properties *(Russian)* 80−106891
Alfven waves collisionless damping in inhomogeneous plasma, initial value problem soln. 79−64864
Alfven-ion-cyclotron instability for axially bounded plasma 80−1788

plasma magnetohydrodynamics continued
alkali metal-inert gas, inhomogeneous mixture, nonequilib. processes under conditions of T-layer form. 78−91079
anisotropic MHD turbulence in solar wind, obs. 80−94669
anisotropic plasma, relativistic MHD 80−92380
anisotropically conducting plasma in inhomogeneous elec. and mag. fields, current calc. *(Russian)* 80−74995
anomalous transport due to long-lived fluctuations, hydrodynamic contrib. 77−15165
anomalous transport processes in radially compressed reversed-field configurations, G1M/HYBRID quasi-equilib. MHD code 80−64689
arc, helical in stabilising channel in mag. field 79−60206
arc, plasma, of free jet laminar core, axial flow, strong localised disturbance effect 78−91178
arc heater, rotating mag. field interaction with gas stabilised discharge 78−71598
arc plasma motion in flat and labyrinth channel, velocity calc. 79−4121
arc plasma processes, appl. of mag. pinch force 77−15258
arc tunnel, formation of high speed quasisteady plasma flow *(Japanese)* 80−10367
arc voltage-current charact., MHD eqns. anal. 80−38815
arcjet, density meas. by CO_2 laser interferometry 80−59277
arcjet operation, transitional behaviour 79−37556
arcs, elec., high-current, conducting gas flow anal. *(Russian)* 79−32754
asymptotic stationary regimes, inertial effects with infinite conductivity 77−15175
axisymmetric plasma, ideal MHD spectrum, finite hybrid elements method 78−42734
axisymmetric plasma equilib. MHD eqn., exact solns. 77−65898
axisymmetric plasma stream, interaction with inhomogeneous mag. field 78−67331
axisymmetric Tokamak plasma MHD equilibria and Mercier local stability criterion 78−51333
axisymmetric toroidal MHD equilibria, numerical determ. 79−82091
ballooning mode, kinetic anal. 78−75298
ballooning mode topology 78−5917
ballooning modes in Tokamak with finite shear 78−5918
belt pinch, high-temp. plasma stability 77−24161
belt pinch, strongly elongated, free-boundary MHD equilib. 78−5912
Bennett pinch, reverse B, pinch, MHD stability 77−11384
boundary condition for computational MHD, plasma confinement 78−1811
boundary layer flow, past heated cylinder, in radial mag. field *(Russian)* 77−47170
boundary layer on flat plate with aligned magnetic field *(French)* 78−1808
boundary layer with travelling mag. field and Hall currents 78−94904
cathode, sheaths in K_2CO_3 seeded petroleum MHD combustion plasma 80−87870
channel flow rel. to element distrib. in capacitative energy store 79−86569
channel with Hall and ion slip currents, forced convective heat transfer 80−33823
charged particles drifts in mag. field with arbitrary spatial var. 80−46382
coal-fired MHD generator, molecular beam mass spectrometric sampling system 80−52358
coaxial channel flow of accelerators and compressors, two-dimens., simulation 80−19566
coherent wave interaction with MHD turbulence *(Russian)* 78−1833
cold magnetised plasma, radiation pressure forces 78−79437
collective plasma effects in solar flares, assoc. with particle streams continuous injection model 80−21954
collective resonant transformer accelerators, beam instabilities 79−76174
collisional magnetoplasma, crossfield instability, dispersion, spectral characts. 77−31464
collisional plasma rotating inside cylindrical annulus, two-species MHD anal. 78−22466
collisionless kinetic eqn. expansion in inhomogeneous mag. field *(Russian)* 77−31438
collisionless plasma, Chew-Goldberger-Low theory with finite Larmor radius corrections 80−75024
collisionless plasma fluid model and cosmic plasmas elec. current systems 79−84658
collisionless plasma in curved mag. field 78−67329
column embedded by rotating ion beam, instability 80−28690
combustion product plasma, discharge on cooled Cu electrodes, rel. to erosion damage in MHD channels 78−1925
compressible magnetic-field reconnexion 80−6226
compression, using EM self drives for captive liners 78−9769
computer simulation method for axisymmetric toroidal plasma 77−27713
conductivity rel. to boundary layer during internal cooling in MHD generator *(Russian)* 78−38557
conductors with MHD sausage instabilities, elec. resist. 80−100076
conference, Varenna, Italy (Sept. 1977) 79−98869
conference on fusion research and plasma physics, Innsbruck, Aug. 1978 80−27033
confinement studies in closed magnetic configurations and MHD eqns. 79−98964
controlling factors, field line reconnexion by localized enhancement of resistivity 79−72998
convection, two velocity hydrodynamic eqn. solution *(Russian)* 80−79459
convection in force-free mag. field, mechanism for chem. separation in cosmic plasmas 79−35125
convective instability in inhomogeneous mag. field 78−67340
convective-like modes in plasma slab with mag. shear 77−68783
cosmic ray scatt. in stochastic mag. field, solar wind fluctuations, above 1 GeV 78−61689
Couette flow, Hall and ion-slip effects, heat transfer 79−94726
coupled explosion current plasma compression, numerical anal. 79−50884
current discharge plasma, mag. reconnection temporal evolution near mag. neutral line 79−32756
current disruption, in Tokamak plasmas, schlieren signal meas. from millimetre waves 80−48998
current driven drift modes in plasma slab with sheared mag. field 79−77366
current sheet, near line of zero mag. field, numerical anal. *(Russian)* 80−83908
plasma magnetohydrodynamics continued
current sheet in compressible plasma, self-similar resistive decay 80−1755
current-driven collisional drift and Alfven instabilities in sheared mag. field 80−92286
cyclotron harmonic waves and resonance cone, around antenna in magnetoplasma 78−91098
cylindrical centrifuge, boundary-value problem at arbitrary mag. Reynolds no. 77−68760
cylindrical inductive MHD pump, external mag. field, dipole calcs. *(Russian)* 77−3884
diagnostics by holographic interferometry and Fourier filter correlation 80−48965
diamagnetic boundary layers, kinetic theory, rel. to solar wind 77−9642
diffuse high β l=1 equilibria, MHD stability 77−19746
diffuse linear pinch, dispersion differential eqn. in MHD, approx. 80−64694
diffusion due to mag. field fluctuations 80−1761
discharge, cylindrical, rotation by elec. and mag. fields, isotope separation appl. 77−39486
discharge, evaporating-wall high-current type, pulsed press., MHD instability 79−27838
discharge dynamics, calculations of plasma energy and particle balance 80−28847
disruptions, internal, precursors of, tearing mode 80−28652
disruptive instability in quasistationary MHD configuration *(Russian)* 79−55485
DITE, low Q discharges 80−92374
double plasma arc, rotation in graphite tube 78−71599
double tearing mode, linear anal. 80−92277
double-layer forward shocks, in MHD fluid, particle simulation code investig. 78−38491
drift motion, in curved mag. field, conducting boundary effects 77−47174
drift motion in curved mag. field with rot. transform 80−1754
drift turbulence theory in mag. field with shear, nonlinear wave packet formation *(Russian)* 79−77376
drift wave instability, due to nonuniform density gradient in sheared mag. field 79−23415
drift-mode stability analysis for the Tandem Mirror 80−64704
dynamical grid method for time-dependent simulations of axisymmetric instabilities in tokamaks 79−10702
dynamo action in thin slab, appl. to solar atmosphere 79−44430
EBT, toroidal MHD equilibrium 80−87871
electric and diffusion current generation by EM field, moving media 77−76097
electric fields and currents in plasma for flow in space-periodic mag. field *(Russian)* 77−47172
electrical conductivity, weakly ionised flowing plasma, crossed elec. and mag. fields 79−1291
electrodynamic and gravitational effects of Proca stresses in astrophys. 78−93098
electromechanical simulation averaging of EM fields in channel flow 79−77277
electron gas with external mag. field, Vlasovs equation with mollified density 80−1756
electron heat conductivity, magnetic field line diffusion 80−28641
electron-hole plasma, subject to crossed fields, propagation and spreading 78−76102
electrons acceleration by weak MHD turbulence, energy spectrum, radiosources appl. 79−88582
electrostatic perturbations, axisymm., cylindrical rot. plasma 77−65849
electrothermal waves, in nonequilibrium MHD plasma, dispersion relation 79−98904
elliptic equilibria in MHD approx., cylindrical topology, non-axisymmetric toroids 77−51213
Elmo bumpy torus, MHD spectrum, global instabilities, staircase model 79−73000
elongated cylinder, nonlinear MHD instabilities and convection, simulation 77−24169
EM wave, low-freq., collisional effects on propag. 78−75349
energetic charged particles transport mode in mag. fluctuations superposed on diverging mean field 79−50848
energy lifetime of plasma, T-3 scaling law, in Tokamaks 80−28635
equilibria, secular instability in mag. quadrupole field 80−53982
equilibria, stochastic stability 79−77414
equilibria, three-dimens., elliptical-centred 79−37535
equilibria in mag. quadrupole field 77−31507
equilibrium, with axisymmetry and noncircular cross section, free boundary soln. to eqn *(Chinese)* 80−59260
equilibrium and spectrum, ideal 79−98883
equilibrium and stability in three dimens. configurations 80−28776
equilibrium of plasma confined in spherical microwave cavity 79−68911
equilibrium of plasma confined in spherical microwave cavity 79−68912
equilibrium problem, inversion of variables method *(Russian)* 79−4118
equilibrium with elliptic free-boundary, limiter and current profile effects 79−37529
exploded wire plasma nonlinear evolution, numerical simulation 78−14197
exploding wire burst phase, simulation by one-dimens. MHD code 80−75080
explosive instability of one dimensional weak mag. field *(Russian)* 80−14896
Faraday MHD generator-operating region 80−103132
fast electron generation in shock waves propagating along magnetic fields *(Russian)* 77−990
fast field reconnection, in astrophysics 77−53424
fast magnetic field line reconnection in elec. cond. incompressible fluid 77−55097
field line integration for MHD equilibria near a closed magnetic field line 78−59651
field reversed pinches, microinstability effect on MHD stability 80−79460
finger-ring Tokamak T-12, poloidal divertor mag. config. MHD and vertical stability effects *(Russian)* 78−59643
finite Larmor radius equations in an arbitrary near-theta pinch geometry 78−71523
finite-β plasma, crit. conditions for drift, drift-Alfven and drift-tearing instabilities in sheared mag. field 80−64699
flow, numerical simulation 80−6229
flow stabilisation in transverse mag. field 79−64839

plasma magnetohydrodynamics continued
flow stability in axial mag. field *(Russian)* 78−26258
fluid simulation of plasmas, MHD particle code 79−68948
flux conserving Tokamak MHD equilibrium evolution 80−75088
focus dynamics with powerful laser interaction during MHD stage, diagnostics 80−48924
force-free analytical three dimensional toroidal MHD-equilibria of arbitrary cross section 80−106885
force-free magnetic fields, resistive evolution, in 1-dimens. slab geometry 79−68910
force-free magnetic fields, time evolution 78−85843
freezing-in condition for mag. field and current sheets 78−75277
fusion plasma, MHD behaviour computation *(Japanese)* 79−31178
fusion plasma prod. by electrically exploded liquid threads, MHD instability 77−15220
gamma-instability, in spheres and cylinders *(Russian)* 77−76044
Garching belt pinch MHD equilibria, cylindrical slab model 78−34353
general relativistic plasma MHD conservation laws, black hole rot. energy 79−2685
general relativistic plasma sphere with central gravitating mass, MHD eqns. 80−6276
generalised Lorenz eqns., strange attractors 80−59232
generator, local characts., transverse current inhomogeneity in MHD channel 80−24146
generator channel, turbulent MHD boundary layer 77−43085
glow discharge, MHD gas movement near anode spots 80−1869
gravitational instability of rot. plasma, effect of suspended particles 80−109347
guiding centre plasma and MHD models comparison 77−42969
guiding-centre plasma, conservation eqn. in phase space 79−98880
gun-injected plasma dynamics, along longit. mag. field 79−55479
gyromagnetic props. of cold plasma, calc. and expt. 77−84415
Hall current and gyroviscosity effect on conducting, rotating viscous plasma stability 80−75041
Hamilton's principle for hydromagnetic fluid with free boundary 78−94905
helical field config. for plasma confinement in very deep mag. well 77−35376
helical hydrodynamic instability, retrograde motion effects in plasma column *(Russian)* 77−982
helical magnetic field, arbitrary amplitude, MHD stability 79−86578
Heliotron D, RF heating, equilibrium and stability 80−28777
HF discharge plasma, effect of mag. field on alternating elec. field *(Russian)* 79−37559
HF heating by MHD waves of finite press. plasma *(Russian)* 80−83950
high beta MHD theory, stellarator equilibrium and stability, mirror traps and reverse field machines 80−28778
high beta stellarator, l=2,3 helical fields, stabilisation effects 80−28779
high temperature plasma, physics, book 80−98767
high-β Tokamak dynamics, reduced MHD eqns., linear, nonlinear stability 77−84479
high-β Tokamaks, with anisotropic press., dynamics calcs. 79−73027
high-beta, with elongated cross-sections, MHD stability anal. 77−24170
high-beta column, in linear solenoid, end-loss calcs. 77−24156
high-beta flux conserving equilibrium, resistive magnetic flux diffusion 80−87873
high-beta pinch, kinetic behaviour, anomalous transport and unstable MHD modes 77−76163
high-beta pinch, one-dimens. equilibrium-diffusion code 78−75401
high-beta Tokamaks surrounded by force-free fields 78−91141
high-n ballooning theory, stability of axisymmetric tokamak equilib. 80−64705
highly ionised plasma, nonlinear effects in excitation of mag. field *(Russian)* 79−55502
hollow axisymmetric mirror, MHD stable, multipole field stabilization *(Russian)* 80−33801
hydrodynamic wave description including electron spin 80−38643
hydromagnetic eqns. for infinitely long plasma cylinder, unstable soln., pulsar mag. fields 80−96352
hydromagnetic rarefaction waves and free expansion in collision-free strongly magnetised plasma 80−38594
ideal equilibria, computer codes, review 77−27712
ideal MHD equilibria of diffuse high-β stellarator 79−64897
ideal MHD instabilities, large computational programs, comparative numerical studies, Tokamaks 78−79425
ideal-MHD ballooning modes, stability of finite-beta plasmas 79−64845
ideal-MHD kink and ballooning modes, depend. on plasma shape and profiles 79−64846
imploding plasma liners, MHD instability effects 80−75081
incompressible nondissipative MHD turbulence in spheromak, stable equilib. statistical states 79−60134
incompressible nonviscous plasma flow, analogy to Stokes flow *(Italian)* 79−19008
incompressible viscous fluid, MHD flow past accelerated plate, Hall effects 80−92275
induction MHD machine, mech. strengthened channel, EM processes anal. *(Russian)* 77−24198
inhomogeneous plasma, unstable normal modes prod. by mag. shear 77−7532
instabilities, current-driven, in E, turbulent acceleration 77−19707
instabilities, nonlinear behaviour calcs., numerical techniques 77−27659
instabilities in stellarator 78−14154
instabilities spectrum due to plasma rot. in theta pinch 78−59582
instability, hydromagnetic, in low-beta plasma column, dynamic shear stabilisation by RF current 79−46454
instability, secular, in mag. quadrupole field, of MHD equilibria 80−10427
instability and Ohmic heating of plasma in apparatus with spatial axis *(Russian)* 80−106945
instability in nonuniform plasma, kinetic theory 77−15190
instability in reversed field pinches 77−39451
instability of laminar plasma stream *(Chinese)* 79−73002
integral invariants and quasi-MHD nonlinear dissipation 79−98882
interchange instabilities induced by gravity 78−91076
interchange stability of axisymmetric field reversed equilibria 80−59214
internal m=1 helical mode, feedback suppression in Tokamak 80−19577
interplanetary medium, slow MHD shock waves 78−12068
interplanetary plasma wave propagation, magnetoacoustic wave transverse to mag. field 80−12629
plasma magnetohydrodynamics continued
interplanetary shock wave propag., numerical soln. of two dimensional problem *(Russian)* 77−41277
interplanetary space, collisionless hydrodynamics rel. to Larmor freq., plasma flow around planets 78−69637
ion acoustic solitons in collisionless multi-ion plasmas 79−77351
ion acoustic wave radiation due to oscill. point charge *(French)* 80−43900
ion beam, pulsed, incident on mag. barrier, virtual anode form. 80−103131
ion beam injection, MHD instability 77−76113
ion beam shear-Alfven instability in two component Tokamak 79−60119
ion ring, precessional mode stabilisation using general mag. multipole field 77−24174
ion-acoustic waves, soln. for MHD equations, properties *(Russian)* 80−106891
ionisation and radiation dynamics of dense MHD plasmas, simulation 78−83606
ionising MHD shock wave propag., in nonuniform medium 78−5874
ionization instability, dynamic suppression, switching modelling of MHD device 80−59308
ionosphere, vertical displacement during substorms 80−4184
ISX-A Tokamak, plasma confinement and impurity flow reversal 80−28770
JET, ballooning modes, MHD theory 80−28639
jet, hydromagnetic stability 78−1827
jets, in welding arcs, gasdynamic characts. *(Russian)* 78−47191
JFT-2 Tokamak, large scale fluctuation mode mixing, probe, interferometric obs., MHD anal. 78−67312
JFT-2a Tokamak, plasma MHD with separatrix mag. surface 77−7581
Kelvin-Helmholtz hydromagnetic instability, plane tangential discontinuity, dispersion eqn. *(Russian)* 79−7451
kinetic equation for electron gas in strong fields and inhomogeneities 79−72986
king instability, in rectangular finite-β system 77−76070
kink instabilities of a field reversed ion ring with a toroidal magnetic field 80−1758
kink instability, hydromag., in Tokamak (pinch) plasma, dynamic shear stabilisation, nonlinear 79−50858
kink instability, internal MHD, sufficient cond. *(Chinese)* 80−43897
kink stability, convection effects, MHD boundary layer anal. 80−1762
large aspect ratio expansion, toroidal magnetofluid equilibria, anisotropic pressure 78−26257
large-scale flow along mag. lines of force, elec. fields and currents 77−55132
laser created plasma, ponderomotive force, mag. fields and hydrodynamics *(French)* 77−80281
laser generated plasma, expansion, pulsed mag. field effects, interferometric studies 77−58876
laser plasmas, strong mag. field effects, review *(Russian)* 78−38462
laser target behaviour, anal. in CASTOR 2 code 79−86594
laser targets, dynamics, 2-D three-temperature MHD model 80−70014
laser thermonuclear fusion, review 77−34449
laser-heated exploding wires, X-ray emission 79−10685
line sources, elec. and mag., interaction with moving magnetoplasma slab, EM radiation 80−67537
linear and nonlinear ideal MHD codes, plasma instability, PL1 programs 77−76040
linear induction MHD machine, elec. cond. body motion in mag. field *(Russian)* 77−7468
linear induction MHD pump, DC, mag. field obs. *(Russian)* 77−7469
linearised gyro-kinetics, particle to guiding centre variables transformation 78−91081
linearly unstable MHD modes, nonlinear behaviour, appl. to pinch kink modes 78−67339
local sufficient condition for MHD stability in closed line systems 80−83910
long-wave oscillation damping calc. *(Russian)* 78−75302
long-wavelength modes and anomalous transport in toroidal magnetoplasmas 80−28613
Lorentz covariant eikonal method, dispersion relation, for cold one-component plasma 77−27663
magnetic barrier, stationary flows *(Russian)* 77−11326
magnetic circuit, field calcs. *(Russian)* 77−3883
magnetic dipole radiation field, hot magnetoplasma *(Russian)* 78−30416
magnetic dynamo, MHD turbulence, perturbational method 79−90389
magnetic dynamo action in two-dimens. turbulent MHD 77−51161
magnetic field diffusion, on nonuniform Lagrangian mesh, exact energy conversion 78−91080
magnetic field effects on plasma motion in ring container, entropy 78−59553
magnetic field energy dissipation, in neutral current sheets 78−26250
magnetic field line reconnection, neutral layer with Petschek slow shocks 79−50851
magnetic field line reconnection by resistivity, localised enhancement 78−22467
magnetic field line reconnection in collisionless plasma 77−47167
magnetic field line reconnection in magnetotail 79−80102
magnetic field line reconnection mechanisms in collisionless plasma 79−77352
magnetic field lines reconnection, clouds-in-cells plasma model 77−84490
magnetic field lines reconnection in plasma, astrophys., geophys. and lab. appl. *(Russian)* 78−91083
magnetic field reconnection, in collisionless plasma, electron Landau reson. 79−50852
magnetic field-line reconnection by localised enhancement of resist. 77−65843
magnetic flux element stability in horizontally stratified compressible plasma, solar atmosphere appls. 78−28610
magnetic flux ropes on Sun, equilib. and stability *(Russian)* 80−8617
magnetic force lines reconnection in high press. plasma 77−89233
magnetic island coalescence, 2-dimens. MHD eqns. 80−64695
magnetic islands coalescence 80−19564
magnetic pulse penetration into plasma, theta pinch geometry, Alfven velocity scaling 80−33803
magnetic reconnection, plasma accel., heating and shock form. 78−40773
magnetic reconnection and m=1 oscills. in current carrying plasmas 78−71463
magnetic reconnection in collisionless plasma 79−82051

plasma magnetohydrodynamics continued
magnetic tearing instability, high cond. theory 77—7527
magnetic trap, ambipolar, hydrodynamic plasma equilib. *(Russian)* 79—98951
magnetic-field-aligned elec. currents in cold collisionless plasma 79—1298
magnetically driven tranverse shock waves, precursor photoionis. model 77—31471
magnetised plasma, hot, unstable behaviour, in contact with cold wall 79—1333
magnetised plasma motion in a homogeneous mag. field *(Russian)* 79—37466
magneto-acoustic oscillations in a toroidal plasma 79—19026
magneto-acoustic waves, soln. for MHD equations, properties *(Russian)* 80—106891
magneto-viscous resistive tearing of cylindrical flux surfaces 80—1831
magnetoacoustic disturbance, hydrodynamic instability in nonuniform plasma flow *(Russian)* 80—1766
magnetohydrostatic equilibria, circ. cylindrical, internal modes stability, in diffuse pinch 80—43957
magnetopause, MHD flow, elec. field generation 78—40760
magnetoplasma compressor, radial limitation of focal zone, dynamic, energy, spectral characts. 79—55477
magnetoplasma wave, quasistatic density perturbation, universal formula 79—60131
magnetospheric simulation expts. 80—46347
magnetostatic mode and cross-field electron transport 78—83538
mass flow stabilisation in helical mag. fields, MHD stability 77—24133
matter-antimatter plasma, boundary layer model with mag. neutral sheet 78—53807
Mercier criterion for a finite-pressure plasma in arbitrary-shaped magnetic axis configurations 79—37534
merging of magnetic fields with field-aligned plasma flow components 78—79417
merging of two current carrying plasma columns, solar flare exptl. simulation *(Japanese)* 80—94775
metal vapour columnar arc instability, mag. fields effect, up to 67 kA 78—9893
MHD channel, frame-type, two-dimens. elec. effects, numerical parametric soln. 78—42834
MHD combustion, operating mode aspects 78—18388
MHD equilibrium and stability, triangular deformation elliptic cross section *(Chinese)* 80—53950
MHD generator, channel, near electrode-free wall, plasma instability, flow inhomogeneity effect 78—26338
MHD generator, characteristics improvement, using current parallel to magnetic field 80—1751
MHD generator, conductivity and power output ionization stability, and boundary layer effects 80—1752
MHD instabilities, stabilisation in current-carrying stellarator 79—86582
MHD instability stabilisation by force free mag. fields 80—83911
MHD waves segregation in ideal medium 78—87440
MHD-instability and limiting currents during Ohmic heating in stellarator Uragan-2 *(Russian)* 80—106881
microinstabilities in field reversed Z pinches, persistence of MHD stability 80—87872
microwave cavity confinement, MHD stability, elementary mode polaris. cjaracts. 77—43050
minimum energy solutions, Clebsch representations 79—14524
mirror machine, enhanced plasma confinement by MHD oscillation 80—24205
mode crossing stability, Lagrangian nondegenerate fluid or Vlasov plasma 78—42735
modulation instability of MHD waves *(Russian)* 77—89259
modulational instability produced by Langmuir turbulence in a magnetic field 80—1759
most probable states in MHD 79—60114
motion in H-constricted discharge, mag. field effects and cross-currents *(Russian)* 77—68761
motion in weakly rippled mag. field *(Russian)* 77—68758
moving magnetic rotator radiating MHD waves, reaction force 78—34312
multifluid Tokamak transport code, two dimens., time evolution 77—58880
multiple-mirror plasmas, MHD stabilisation 80—6244
neutron stars, postglitch behaviour of quantum plasma 79—35289
non-force-free solar mag. fields in magnetohydrostatic equilib., anal. 79—92733
nonequilibrium MHD power generation using nonseeded AR plasma 77—24196
nonequilibrium plasma, two-temp., expanding in disc-shaped channel, hypersonic MHD interactions 80—10368
nonequilibrium plasma MHD flow between parallel discs, tangential vel. effects 80—64697
nonideal MHD, energy principles, Tokamaks and stellarators 77—76042
nonlinear Alfven waves, in hot plasma, struct. and stability *(Russian)* 79—37473
nonlinear axisymmetric MHD equilibria, numerical soln. 80—79461
nonlinear helical MHD instability in toroidal plasma, stability criteria *(Russian)* 78—5862
nonlinear hydromagnetic waves in two-electron temp. plasma 79—98884
nonlinear ideal MHD equilib. in axisymmetric systems 78—1876
nonlinear Kelvin-Helmholtz instability in hydromagnetics 79—90393
nonlinear magnetoacoustic waves, damping, simulation 78—79423
nonlinear phenomena in MHD and Hall effect 79—72988
nonlinear stability problems, two-time method, dissipation scalings, ohmic heating 80—53967
nonlinear time-dependent hydromagnetic model, spatial and temporal finite-difference techniques 80—59192
nonresistive plasma, magnetic kinks in astrophysics 79—27763
nonstationary MHD plasma flow, in coaxial accelerator in condensed media 79—60204
nonstationary plasma acceleration, dielec. ablation effects *(Russian)* 77—11325
nonstationary two-dimensional MHD flow, in radial channel, theory *(Russian)* 78—75279
nova outburst, equatorial belt formation, plasma current rings model, double adiabatic MHD 80—67757
numerical simulation, variational approach 80—28625
oscillations, MHD ensemble, interaction with quasiuniform mag. field, sunspots 77—76041

plasma magnetohydrodynamics continued
one-dimensional force-free magnetic field, singular lines *(Russian)* 79—48670
optically thin medium, weak MHD discontinuity propag. 79—46438
origin of galaxies in expanding Universe, plasma cond. and instabilities, MHD soln. 80—62283
parallel velocity shear instabilities in an inhomogeneous plasma 79—82050
paramagnetism of plasma in RF field 79—46490
parametric absorption of EHF radiation in magnetoactive plasma *(Russian)* 79—32790
particle acceleration by MHD shock turbulence 80—87894
peeling instability in toroidal MHD equilibrium configuration 80—79488
perturbation theory on guiding centre plasmas 79—72999
perturbation theory on spectrum of ideal magnetohydrodynamic 79—72999
perturbations and completeness of solns. 78—1810
perturbations due to localised flows, eddy theorem 79—41822
perturbations for finite magnetic Reynolds number 80—1757
pinch, resistive, MHD, nonequilib. stability 79—50877
pinch, reversed-field type, in STP-1, using new external-field programming, MHD instability 80—28803
pinch effect, dynamical accumulation towards neutral line of magnetic field 80—83977
plane flow in hyperbolic mag. field, mag. field line reconnection 79—32755
plane parallel flow stability in magnetized plasma, velocity shear instability 79—37468
plane wavepropag. in rarefied, radiative elect. anisotropic plasma *(Italian)* 79—94777
plane waves in rarefied, radiative, elect. anisotropic plasma, small perturbation eqns. *(Italian)* 79—94776
plasma column, influence of external mag. axial field on an autocompression, review *(Rumanian)* 80—24148
plasma focus, 2D MHD calcs. 78—9767
plasma focus, 2D MHD calcs. 78—9768
plasma focus, fast high voltage, current and neutron yield scaling 80—64752
plasma focus, MHD calcs., two dimens., in the Mahler geometry 79—4120
plasma loop expansion, self similar solutions *(Russian)* 79—72955
plasmadynamic continuum sources 79—27803
plasmatron melting arc in Ar and CO_2 atmosphere, performance characts., MHD calcs. *(Russian)* 80—38573
ponderomotive effects, kinetic theory 79—32740
power flow in relativistically moving anisotropic warm plasma filled waveguide 78—55725
power generators, combustion products plasma characterisation, generator channel flow, diagnostic techniques 80—43993
Poynting's theorem for inhomogeneous moving media reconsidered 79—48661
pressure driven ballooning modes, numerical studies 80—92282
pressure fluctuations in flowing combustion plasma, meas. by probe-tube microphone 78—18443
probe characteristics, in synthesised magnetoplasma stream 79—77426
pulsed isothermal plasma generator plant for study of MHD flows 78—1907
quasi-linear equation of plasma in mag. field, appl. to mirror confinement 79—1297
radial boundary layers, diffusing toroidal equilibria 77—89285
radial channel flow, in 2-dimens. mag. field, numerical simulation *(Russian)* 77—47171
radial electric field generation, in rot. plasma 79—55480
radiative interaction of electron gas in mag. field, distrib. function 79—60116
radio galaxies, plasma hydromagnetics and hydromagnetic stability 78—24564
rarefied plasma, mag. field rapid penetration, magneto-acoustic shock waves, super-Alfven penetration *(Russian)* 78—59554
Rayleigh-Taylor instability, MHD flow of composite medium, variable viscosity 78—1813
Rayleigh-Taylor modes of rot. MHD equilib., shear stabilisation 79—27813
relativistic cylindrical shock propagation through a magnetic field 79—94796
relativistic degenerate electron plasma, dielectric response in mag. field, plasma oscillations 80—54022
relativistic MHD, shock waves 78—9770
relativistic MHD growth and decay discontinuities 80—92280
relativistic MHD symmetric flows eqn. of motion *(Russian)* 80—83992
relativistic plasma, hydrodynamic free expansion into vacuum 77—3980
relativistic shock waves 77—24035
relativistically streaming plasma, flux conservation, MHD and force-free approxs. 79—19081
residual force equation soln. by three dimens. code 80—28622
resistive drift-Alfven waves in sheared magnetic fields 79—77365
resistive internal helical modes, mag. field configs. *(Russian)* 77—19741
resistive MHD instabilities, diffuse pinch configs., numerical study 77—58853
resistive MHD instabilities of current sheets, appl. to solar wind 80—4218
resistive steady states of elliptical cross-section plasmas 79—98872
reverse-field pinch, MHD simulation 78—5920
reversed field high β pinch, analytic models, MHD stability 78—59642
reversed field pinch, nonlinear saturation of tearing mode 79—73028
reversed field pinch expt. in small compact torus STP-1 80—75043
rotary symmetry plasma, magnetohydrodynamic eqns. and plasma wall effect *(German)* 79—68909
rotating ion layer in external mag. field, equilib. props. 79—14598
rotating plasma, at high Hartmann number 79—41806
rotating plasma, axially symmetric, continuous MHD spectrum 79—60180
rotating plasma, MHD stability criterion 80—79487
rotating plasma, viscous dynamics 78—91082
rotating plasma, weakly ionised, rot. vel. and ion cond., obs. and MHD theory 80—38576
rotating plasma between coaxial electrodes 79—32753
rotating plasma column, non-ideal MHD equations 78—59592
rotating plasma disc form. in radially directed Ar arc 77—76216
rotating plasmas, balance and separation processes 78—1911
rotation of a classical toroidal plasma 80—59193

plasma magnetohydrodynamics continued
rotation of magnetised nonuniform plasma, MHD ordering 80−33756
screw pinch, finite Larmor radius stabilisation, resonant particle effects 80−54020
screw pinch, time-depend. MHD eqns., numerical solns. 77−24134
Scyllac, computational plasma MHD for stable equilibria 77−84478
Scyllac, equilibrium and stability, MHD three dimensional soln. 77−24131
Scyllac, MHD stability δW calc. correction 77−65856
Scyllac configuration, toroidal theta-pinch theory, review 77−24125
Scyllac theta-pinch, sharp boundary dynamical model 77−51216
secondary shock wave formation by supersonic flow decleration in mag. field 79−90410
seeded combustion gas near cold electrodes, MHD boundary layer 80−48865
self-generated fields by currents driven by electron press. grad. 78−1794
self-gravitating composite plasma with finite Larmor radius, hydromagnetic stability 77−62350
self-gravitational instability of plasma rotating layer, effects of finite ion gyroviscosity 80−56706
self-oscillating mode origination in nonequilib. magnetised plasma 79−86568
shear Alfven wave, heat flux instability 80−43893
shear Alfven wave heating experiments in heliotron D 80−28716
shear Alfven waves, quasi-linear theory 80−64714
shear flow in mag. field, stability 78−26197
shear flow stability and Alfven waves in magnetised plasma 80−96360
sheared systems, low-β plasma, MHD intercahnge instability 80−64717
sheet discharge, MHD flow analysis *(Chinese)* 79−72997
shock, MHD, superadiabatic excitation in collisionless plasma 80−79503
shock production of steady flow in axisymmetric mirror 77−84414
shock wave, isomagnetic compression shock occurrence, critical parameters 77−76085
shock wave, transverse, ionising, possible structs., neutrals photoionis. effects 78−75343
shock wave collisions, anal. theory, vel., incidence angle and mag. field effects 77−7415
shock wave propag., counter wave form. in spatially varying mag. field *(Russian)* 77−24088
shock wave-induced plasma current, transverse mag. field interaction, simulation 78−38463
shock waves, MHD, propag., in nonuniform plasma, simulation 77−76084
shock waves in solar corona, rel. to type II radio emission 79−92750
shock waves in turbulent medium, energetic particles interaction 80−4210
shock-heated plasma, interaction with nozzle-shaped mag. field 79−55478
signular magnetic field lines and line crossing in pinch layers, space plasma appl. 79−14590
simulation of laser beat freq. heated plasma 77−11392
slab-shaped magnetoplasma excitation by magnetic current line sources 78−55717
solar active regions, magnetised expanding plasma, gaskinetic press. 77−45394
solar flares, radiative, mechanical and mag. energy release 79−53797
solar wind flow past planets, axisymm. implicit blunt body computation technique 78−96370
solitons, upper hybrid, formation from MHD perturbations 79−90348
space-charge wave instability of spiral beam-plasma system in nonuniform mag. field 80−1760
Spherator with purely poloidal magnetic field, MHD stability 79−98961
spheroidal low aspect ratio plasma configurations, MHD equilibrium and stability 80−1791
spheromak, ideal MHD stability 80−92281
Spheromak, MHD stability 79−41859
Spheromak fusion reactors, MHD equilib. and stability, numerical anal. 80−74000
spirally-wound pump, EM processes in secondary medium, model *(Russian)* 77−3881
stabilisation of low-m kink modes in Tokamak 79−64890
stability, computational aspects 77−27690
stability analysis of axisymm. surface current model equilibria for N=0 and n≠0 modes 80−92276
stability and energy confinement in belt pinch IIa 77−43029
stability code, ERATO, convergence of solns. 80−83906
stability criteria, closed field lines system rot. transform *(Russian)* 77−3972
stability criteria for localised displacements 80−28645
stability criterion for symmetric MHD equilib. 79−14534
stability in toroid with vanishing press. grad. 78−14195
stability in toroidal axisymmetric system *(German)* 80−28792
stability in toroidal trap near-axial region *(Russian)* 78−38521
stability noncompact operator spectrum approx. *(German)* 77−68759
stability of high beta Tokamak 77−68849
stability of runaway electron discharge in Tokamak 78−75303
stability of Tokamak plasma 78−30428
stable MHD fluctuations theory development *(Russian)* 80−24145
star formation and interstellar clouds, impact of cosmic plasma physics 78−73744
stationary frozen-in coordinate system 78−40761
stationary magnetoplasmadynamic source, elec. and thermal characteristics 80−14915
stationary MHD eqns. for rotating toroidal plasma 80−92278
statistical mechanics, transport coeffs. 77−15166
steady flow, shock and soliton solutions 77−15172
stellarator, current-carrying, kink and tearing mode MHD instability 78−22539
stellarator, FLR stabilisation, MHD configs. with zero rot. transform 77−72472
stellarator, high-β, finite gyroradius stabilisation of MHD modes 78−26314
stellarator, hybrid, MHD stability anal., plasma press. depend. *(Russian)* 77−47241
stellarator, MHD equilibrium and stability of plasma in toroidal geometry, 3-D computer code 80−70041
stellarator, non-circular cross section, MHD equilibria 78−5914
stellarator, noncircular cross section, MHD equilib. 78−9820
stellarator equations of motion calcs. 80−103198
stellarator fields, m=2 tearing mode, linear growth rate 80−75037
high-β stellarator with l=3, stability 77−7529

plasma magnetohydrodynamics continued
stellarator with spatial mag. axis, equilib., MHD stability 77−72470
stochastic mag. field fluctuations, self-consistent model 80−100074
strange attractor for MHD flow 80−59194
stratified partially ionised plasma, stability in mag. field, cond. and viscosity effects 78−26276
subsonic flow in MHD channel, acoustic stability 78−9764
supernova outburst, relativistic particles generation, kinetics *(Russian)* 79−21319
supersonic conducting gas stream, interaction with mag. field, numerical simulation 80−6230
supersonic flow around conducting bodies, inductive interaction *(Russian)* 79−27789
supersonic flow in generator channel, with slanted entrance stream 79−77429
supersonic flow of combustion products, nonequilibrium physicochemical processes, open-cycle MHD generator 80−103196
supersonic ionised gas flow struct. rel. to mag. field *(Russian)* 77−27656
supersonic jets of magnetoplasmadynamic source plasma, gasdynamic struct. of initial section 77−35332
supersonic MHD generator, working body thermodynamic props., chem. kinetics effect 78−91163
surface hydromagnetic waves, dissipation 80−21904
surface wave propagation, on plasma column, mag. current excitation 78−1821
tearing mode magnetic reconnection, explosive, in magnetosphere tail, theory 78−88992
TFR 600 Tokamak, plasma confinement, low effective plasma charge 80−28769
theoretical plasma mechanics, book 80−27048
thermal mode ray trajectory in inhomogeneous magnetoplasma 80−106884
thermal radiation flux distribution from electrodynamic gas heater *(Russian)* 79−18678
thermal-convective instability of partially ionized plasma, radiative transfer, medium porosity and collisional effects 80−67538
thermomagnetic shock waves, in nonequilib. plasma 77−27676
theta pinch, radial oscills. of plasma density and mag. field, light scatt. and probe obs. 80−14937
theta-pinch, double, stabilised, toroidal plasma production, probe diagnostics 78−63576
theta-pinch, end loss, ideal MHD model 77−47248
theta-pinch, linear, time-depend. MHD flow eqns., numerical obs. 77−24155
theta-pinch, long wavelength m=1 MHD instability 77−72485
theta-pinch, MHD, for fixed internal currents, const. press. model 79−41863
theta-pinch, rotating, mechanism, MHD anal. 77−24135
Thomson scattering, rot. Raman calibration 80−1844
three-dimensional MHD equilibria with shear, ballooning modes 78−71476
Tokamak, cylindrical, ideal MHD equilib., uniqueness theorems 79−32795
Tokamak, equilibrium and stability, time-depend. three dimensional MHD calc. 77−24131
Tokamak, fusion power reactor design 77−74982
Tokamak, high-beta, equilibria and m=1 kink ballooning mode nonlinear evolution 80−24236
Tokamak, high-beta, MHD eqn., stability, transport calc. 80−28848
Tokamak, high-beta, time evolution, MHD simulation using flux coords. 77−24134
Tokamak, high-beta limitation by instabilities during rapid heating 77−39448
Tokamak, high-beta limitation by instabilities during rapid heating 77−39449
Tokamak, HP flux-conserving equilibria 77−35379
Tokamak, ideal MHD stability 80−59216
Tokamak, impurity behaviour, MHD activity influence *(Russian)* 79−98866
Tokamak, inner mode relax. oscills., numerical model, electron thermal cond. distrib. *(Russian)* 77−47242
Tokamak, internal kink mode, numerical study 80−48953
Tokamak, large poloidal beta, MHD stability, collisional and anomalous trapped particle diffusion 77−24055
Tokamak, localised MHD modes, shape optimisation 79−98954
Tokamak, magnetic island formation and evolution, MHD eqns. soln. *(Russian)* 77−47169
Tokamak, nonlinear helical perturbations 77−51221
Tokamak, plasma MHD equilib., var. method *(Russian)* 80−106960
Tokamak, poloidal divertor expt., stabilisation of the axisymmetric instability 79−4171
Tokamak, sharp-boundary model, axisymmetric MHD instability anal. 77−51217
Tokamak, small aspect ratio, flat current noncircular, unstable MHD spectrum 80−69989
Tokamak, small aspect ratio, MHD spectrum calc. 77−72483
Tokamak, two-dimens. MHD simulation 77−19751
Tokamak, with nonmonotonic current profile, mag. island dynamics *(Russian)* 79−98879
Tokamak blanket, liq. Li module stresses due to changing poloidal mag. field 80−95435
Tokamak circuit, mag. interactions with plasma 78−22468
Tokamak discharge, initial stage, theory *(Russian)* 78−38512
Tokamak discharge, transient behaviour, electrohydrodynamical model 80−48952
Tokamak doublet geometry, shape control of doublets 80−48943
Tokamak equilibria, with fixed boundaries, MHD stability 78−71477
Tokamak equilibrium, inverse problem, iterative metric method 80−106883
Tokamak fusion reactors, doublet research, plasma shape control, MHD stability 80−28837
Tokamak hydromagnetic stability, ideal and resistive, review 78−34358
Tokamak modes, MHD theory, drift effects *(Russian)* 79−37477
Tokamak orbits, topology 80−28806
Tokamak plasma, control systems, construction and simulation study *(Japanese)* 80−100100
Tokamak plasma equilib. by finite elements, book contrib. 79−32805
Tokamak reactor design, influence of physics parameters 79−36414
Tokamak simulation, equivalent cct. model and mag. field diffusion eqns. 77−84409

plasma magnetohydrodynamics continued
Tokamak thermonuclear reactor, MHD modes drift phenomena, kinetic method *(Russian)* 80−1827
Tokamak with field-shaping coil systems, MHD equilib. 78−94930
Tokamaks, ballooning modes and pressure limits 80−28647
Tokamaks, high-β, MHD stability limits 80−28643
Tokamaks, high-pressure, MHD-mode stability, high wave number 80−28644
Tokamaks, ideal MHD mode stabilisation and optimisation 80−79480
Tokamaks, large, impurity effects and control, neutral beam injection, computational models 80−28773
Tokamaks, MHD beta limits, dependence on current density and pressure profiles, num. calc. 80−28637
Tokamaks, MHD stability and reactor requirements 79−98911
Tokamaks, non-circular, shaping and internal structure 80−28842
Tokamaks, non-circular, stability and beta limits 80−28646
tokamaks with elongated cross section, MHD stability 79−90441
Tokamaks with iron core transformer, self-consistent MHD equilibria 80−19608
Tokamaks with large-aspect-ratio, stability, two-fluid dissipative theory 80−28640
Tokapole II, non-circular Tokamak, axisymmetry instability 80−87877
toroid, nonlinear axisymmetric equilibria in MHD approx. 78−18437
toroidal axisymmetric config., vacuum potential energy change, spectral codes 80−87869
toroidal belt pinch, two-dimens. MHD simulation 77−19751
toroidal equilibria with z asymmetric cross section 79−82087
toroidal equilibrium, MHD stability to axisymmetric modes 77−76176
toroidal equilibrium, noncircular sharp boundary plasma pinch form. 77−24166
toroidal equilibrium of stationary plasma flow 77−55162
toroidal MHD stability, complex mag. configs., Mercier's criterion 77−89289
toroidal pinch discharge, preionisation phase, numerical computation 80−64696
toroidal plasma, eigenvalue problem and nonlinear evolution of kink modes 80−24234
toroidal plasma, resistive MHD mode and sawtooth oscill., nonlinear evolution 80−24235
toroidal plasma, sharp boundary, MHD stability 77−11385
toroidal plasma column, general soln. of linear equilib. eqn. *(French)* 77−89284
toroidal plasma in high β Tokamak, struct. of force-free mag. fields, equilib. model *(Japanese)* 79−82086
toroidal plasma MHD stability, mag. axis curvature modulation effects 77−84487
toroidal plasma with nonplanar mag. axis, MHD equilib., diffusion 77−84486
toroidal plasmas, axisymmetric, high mode number stability 80−28642
toroidal plasmas, MHD instabilities 80−38579
toroidal screw pinch, MHD kink instabilities 77−19742
toroidal system, MHD plasma control by feedback and HF fields 80−28781
torroidal equilibria, highly elongated axisymmetric, MHD stability, numerical anal. 77−43049
torus, axisymmetric, MHD intercharge modes, anisotropic press. effects 77−15230
torus, MHD helical oscills. in torus, RF helical quadrupole heating 77−76135
Transit Time Magnetic Pumping heating in Petula Tokamak 80−28739
transverse MHD shock waves 79−10666
transverse waves propag. along axisymm. mag. field in nonhomogeneous plasma, WKB kinetic theory 78−42740
turbulence, 2-D, hydrodynamic and plasma applications, dynamical eqns., diffusion, MHD, superfluidity, review 80−69769
turbulence, axisymmetric 79−19035
turbulence, forced and dissipative, eqns. of motion, 2-D MHD flow 77−65844
turbulence, high-beta, 2-dimens. MHD 77−15193
turbulence, interferometric meas. in toroidal pinches 77−27731
turbulence, numerical simulation and closure techniques 79−90343
turbulence, two dimens. stationary states in non-dissipative limit 80−24169
turbulence, two-dimens., cylindrical nondissipative model 79−32772
turbulence rel. to form. time of isotropic particle vel. distrib., magneto-sheath appls. 78−28420
turbulent flow, of ionised plasma effect of mag. field and elec. current 79−60115
turbulent MHD, three-dimens. soln. in cylindrical geometry 78−67351
turbulent shock wave propagation in solar atmosphere across mag. field, struct. 79−40166
twist transport in force-free mag. flux tubes, appl. to solar prominences 78−40813
two-dimensional flow in entrance region of channel with Hall and ion slip currents 77−42968
two-dimensional mag. flux shell model for MHD simulations of cylindrically symmetric plasmas 80−1838
two-fluid dissipative plasma, energy principle in Lagrangian form, tearing modes 78−42794
universal drift instability, magnetic gradient effects 79−60117
unstable continuous spectrum, noncircular rotating θ pinch 79−94779
vacuum arc anode spot, ion currents and interaction with axial mag. fields 78−75469
vacuum arc cathode plasma interaction with transverse mag. fields 78−75468
vacuum arc retrograde motion in mag. field, Hall effect study 80−6315
variational principal in relativistic magnetic fluid dynamics, Lagrangian density 79−73031
very-low-q discharges in DIVA confinement and MHD characts. 80−64765
vibrations in toroidal confinement with special parameter distrib. 80−83909
Vlasov plasma, ponderomotive force and linear susceptibility 77−76043
vortices, force-free, interaction 79−37469
wake of body moving rapidly in rarefied magnetised plasma 78−67330
wall-stabilized arc, in transverse magnetic field, velocity and temperature field determination 78−38569
wave growth and decay in high temp. gas 80−79458
wave propagation in inhomogeneous media, calc. allowing for finite cond. *(Russian)* 78−63553
plasma magnetohydrodynamics continued
waves in magnetised plasma, kinetic eqn., velocity Fourier transform solution of a model collision operator 79−94785
weak mag. field driven arc velocity and configuration obs. 78−71596
weak magnetic fields, B=0 pts. *(Russian)* 77−3978
weakened fusion plasma in MHD channel, generation aspects 79−43778
weakly ionised plasma, in mag. field, diffusion, boundary conditions effects *(Russian)* 78−75278
Z-pinch, liner implosion, MHD model calcs. 78−67392
Z-pinch, liner implosion non-adiabatic dynamics, MHD computer simulation 77−84488
Z-pinch, noncylindrical, strongly rotating plasma dynamics 79−77354
Z-pinch tunnelling instability and finite Langmuir ion radius, MHD anal. *(Russian)* 77−47168
Ar arcjet, recombination lasing 77−65588
Ar discharge rotating plasma column LF oscillations 78−71481
Ar high-pressure helical arc phase velocity in longitudinal mag. field 78−71594
Ar induction HF discharge plasma in crossed fields, with Cs seeding, Hall parameter 79−55465
Ar magnetoplasmadynamic arcjet, recomb. lasing 80−48218
Ar plasma, operating characts., numerical study 78−67309
Ar supersonic jet, radiation in magnetoplasmadynamic source 77−35329
Ar-Cs plasma stream, electrodynamic braking with strong MHD interaction 78−9763
CO_2-N_2 electroionisation laser mixture, ionisation instability of semi self maintaining discharge 80−63971
Cs plasma probe meas. in mag. field 78−63597
Cs-Xe solar-pumped MHD excimer laser, modelling 80−95873
H plasma, dense, produced by conic electrode source, mag. field effect on flow 77−58873
H plasma, freely expanding, population inversion obs. 80−95877
H_2 plasma, MHD and transverse ionising shock waves, jump conditions, ionis. effects 79−32775
He supersonic jet, radiation in magnetoplasmadynamic source 77−35329
KOH, MHD plasma mol., pot. energy curves and dipole moment, bond lengths 78−71462
Li, blanket, for Tokamak thermonuclear reactor, MHD flow modelling *(Russian)* 78−47146
N_2-H_2 arc, bent and rot., flow mechanism 80−70047
Z-pinch, noncylindrical, dynamics and particle accel. mechanism 77−76170

plasma measurement techniques *see plasma diagnostic techniques*

plasma oscillations
see also plasma waves
Alfven and magnetoacoustic wave heating for fusion plasmas 80−24188
Alfven fluctuations in inhomogeneous nonequilib. plasma *(Russian)* 79−4123
Alfven oscillations in magnetosphere, theory rel. to auroral radiation generation 79−75051
alpha particles interaction with mag. plasma fluctuations in D-T reactor 80−24204
anharmonic oscillator description 77−3936
anomalous absorption of UHF radiation in electron cyclotron resonance range *(Russian)* 80−1807
anomalous laser radiation absorption near plasma critical density, acoustic instability 79−19063
anomalously resistive phase, spiky density fluctuations and relax oscill., microwave scatt. obs. 80−38547
arc discharges, periodic processes, spectral emission characts., vidicon system investig. *(Russian)* 78−9848
auroral electron beam, plasma oscill. reemission, radiowave generation mechanism *(Russian)* 78−40724
axial eigenmodes for long-$\lambda_\parallel$ waves in plasmas bounded by sheaths 80−28655
axially-symmetric ambipolar trap, flute oscills. stability limits *(Russian)* 80−103176
axisymmetric plasma equilibrium, stability 80−106915
beam-plasma expt. in strong mag. field 77−68806
beam-plasma instability, destruction of trapping oscillations 78−71501
beam-plasma system, electron cyclotron instability, nonlinear development, lower hybrid oscill. effects 78−30437
beam-plasma system, instability *(Russian)* 78−1847
beam-plasma system, nonlinear convective and oscill. instabilities, simulation models 78−34338
beam-plasma system, oscill. suppression by wave perturbation on beam distrib. function 77−80316
beam-plasma system, oscills. excitation *(Russian)* 77−11361
beam-plasma system, quasitransverse oscills. excitation by relativistic electrons, anomalous Doppler effect *(Russian)* 79−55518
beam-plasma system, relativistic electron beam, transport, oscills. 77−7559
beam-plasma system, trapped particle oscillations, destruction, simulation by TWT 77−31462
cavitons, particle beam interactions 78−22517
Chirikov-Taylor model, turbulent diffusion calc. 80−79469
classical electron liquid, longitudinal props. 79−98897
classical one-component plasma, self-motion and collective behaviour 77−80271
coated semiconductor spheres, surface modes, plasmon oscills. 80−54730
collective oscills. in toroidal plasma, microwave scatt. diagnostic technique, review 80−48863
collisional plasma, modulation instability, turbulence by const. wave pumping *(Russian)* 80−103139
constricted glow discharge in transverse air flow 80−24278
contracted positive column head oscillations 78−67516
control by linear feedback system *(Russian)* 78−38469
converging nonlinear resonance cones 79−94789
counter stream type beam-plasma interaction, quenching of plasma oscill. 78−5882
counterstreaming electron beams, plasma form. and oscill. excitation 77−27687
counterstreaming ion beam plasma device, standing oscills., due to electron-ion instability 78−26305
coupled localized electron-plasma waves and oscillatory ion-acoustic perturbations 78−67349
current instability on short wave drift oscills., nonlinear theory *(Russian)* 80−53981
cyclotron absorption, temp. determ. method *(Russian)* 77−80375
cyclotron heating in short adiabatic traps *(Russian)* 78−5890

plasma oscillations continued
cyclotron oscillations of a large-Larmor-radius plasma 78−67338
DC corona discharge in rarefied air, coherent ion plasma oscillations 77−76230
decay instability of EM oscillations, in inhomogeneous plasma with turning points *(Russian)* 79−4124
dielectric friction in plasma, harmonic oscillator and rigid dipole dielectrics, collective plasma oscills. 80−53928
diffusion diode, current oscills., overneutralisation and diffusion instability 77−24199
dispersion equation, low-frequency plasma instability, high frequency electrostatic eigenmode drive 79−60118
disruption, tearing and kink modes, limit of safety factor in JFT-2 Tokamak 80−38589
dissipative parametric instabilities, in a strongly ionized plasma *(Russian)* 78−30422
distribution function for inhomogeneous plasma 80−59218
Doublet IIA, m=1 oscills., internal disruptions, impurity line emission 77−58898
drift, shear effect on turbulent diffusion 77−76082
drift cyclotron instability, nonlinear dynamics 78−30433
drift oscillation spectra, LF, modification in HF elec. pump field *(Russian)* 80−1767
drift-dissipative instability suppression in lower-hybrid pump wave field 80−106921
drift-dissipative waves, weakly ionised plasma, column steady state 80−38613
dynamic plasma discharge microwave oscillation expt. 77−84433
E×B oscills. in bounded plasma, harmonic eqns. 77−51171
echo in semi-bounded plasma, electrostatic sheath potential profiles for boundary 80−64712
echo oscillations in relativistic plasma *(Russian)* 80−53990
electric field penetration, nonlinear, in plasma layer *(Russian)* 77−89236
electrodeless discharge in air, count rate emission and exposure time 79−64936
electron, in relativistic plasma, dispersion relations in mag. field 78−34364
electron, nonlinear damping 79−37480
electron beam excitation of pot-surface oscillations, linear theory of beam instability 79−37505
electron beam excitation of surface oscillations in plasma in metal cylindrical waveguide *(Russian)* 77−39431
electron beam generated electron plasma oscillations, quenching by low freq. externally applied wave 80−24160
electron beam interaction with EM wave, stochastic oscill. *(Russian)* 79−46460
electron beam produced, proton beam form. *(Russian)* 78−29207
electron beam-plasma interaction, RF emission, oscill. nodes and instabilities 77−24099
electron beam-plasma low freq. instability, cyclotron oscills. *(Russian)* 80−33783
electron beams, modulated, non-linear oscillation theory *(Russian)* 80−106898
electron cyclotron heating in toroidal plasmas, wave trajectories 80−38678
electron cyclotron reson. in inhomogeneous mag. field integral eqn. *(Russian)* 80−33758
electron fluid long wavelength ballooning modes, destabilization by finite trapped beta 79−68914
electron gyroresonance cyclotron oscillation propagation obs. in nonuniform mag. field 78−75351
electron longitudinal oscills. in plasma with cut-off Maxwellian vel. distrib. 77−31445
electron nonlinear waves in strongly magnetised plasma 80−79472
electron oscill., Langmuir wave modulation instability *(Russian)* 77−47182
electron oscillation in radial potential well effect on beam interactions *(Russian)* 80−14912
electron oscillations, in hot plasma with non-Maxwellian vel. distrib. *(Portuguese)* 78−83557
electron oscillations in fully ionized plasma 79−41814
electron oscillations in nonideal plasma 78−94907
electron oscillations in static electric field 78−22487
electron waves, modulated, dispersive, evolution in low-density Q-machine plasma 79−86575
electron-acoustic, nonlinear scatt., plasma ions effect 77−72438
electron-eigen oscills. and ballistic modes 78−22472
electron-free plasma confinement in RF quadrupole field 78−71517
electronic oscillations in relativistic plasma, hydrohydrodynamic model *(Russian)* 78−79434
electrostatic, conversion to EM waves near plasma freq. 79−37462
electrostatic, mag. field modulation excitation *(Russian)* 79−60107
electrostatic, mode coupling, collective coord. calcs. 77−976
electrostatic forced oscills., drift effects, multiple water bag model. *(French)* 77−58857
electrostatic high frequency oscills., damped nonlinear Schrodinger eqn. calcs. 77−7530
electrostatic trapping of intense relativistic electron beam in magnetic mirror 77−24172
electrostatic waves in drifting ionospheric simulation 80−53965
ELF ion plasma oscills. in Nike-Apache rocket apogee region in ionosphere 79−40012
EM oscill. spectrum, toroidal plasma-containing system 80−79471
EM surface oscillation excitation in semirestricted plasma by relativistic electron beams *(Russian)* 79−14561
EM wave in inhomogeneous magnetoactive plasma, total absorpt. effect *(Russian)* 80−106944
EM wave self-action during thermal modulation instability of high hybrid oscills. *(Russian)* 80−53980
EM waves, nonlinear generation in electron-positron plasma *(Russian)* 80−106973
explosive emission diode, plasma pot. oscills., probe diagnostics 80−6284
fast ion beam, in Tokamak plasma, quasilinear relax. *(Russian)* 78−87457
feedback beam-plasma interaction and suppression of oscillation 78−75368
feedback stabilisation of flute oscills. in direct traps *(Russian)* 77−47184
field emission medium energy diode, electron flow, HF oscills. 80−79582
finite plasma cylinder oscillations in external mag. field 78−42738
plasma oscillations continued
fluctuations in nonstationary nonequilibrium system, near instability boundary *(Russian)* 79−19034
flute, suppression by regulator with cross feedback *(Russian)* 78−26262
flute oscillation suppression by automatic EM control *(Russian)* 78−30464
flute oscillations and plasma stability limits in ambipolar trap, ballooning effect *(Russian)* 80−106955
flute oscillations stability in ambipolar traps *(Russian)* 79−46452
flute oscillations suppression, regulator synthesis *(Russian)* 80−24212
forced oscills. generated by point antenna, drifting plasma *(French)* 80−79470
forced radial magnetoacoustic oscillations, of fully ionised plasma with partially ionised shell 78−18405
FT-1 Tokamak, lower hybrid plasma heating 80−28700
gas discharge streamer propagation mechanism based on plasma vibrs. *(Russian)* 77−84546
glow discharge, reaction oscills. freq. eqn. derivation, expt. and numerical calc. 77−1027
Hall accelerator, ion current oscills. *(Russian)* 79−98995
helical MHD oscillations, dynamic props. obtained from amplitude-phase freqs. *(Russian)* 77−89258
hemispherical monopole surrounded by plasma layer, Tonks-Dattner reson. and input admittance 80−87887
HF, in nonequilib. plasma accelerator *(Russian)* 77−3997
HF, ion-acoustic instability 78−18398
HF instability *(Russian)* 78−18410
HF magnetoacoustic heating of T-4 Tokamak 77−76137
HF oscillations and electron beam relax. in homogeneous gas-discharge plasma 80−38614
HF second-step discharge meas. and equivalent cct. 79−7505
high current low voltage arc discharge *(Russian)* 79−55579
high frequency oscillations in bounded thermally produced plasma 78−38481
high mode number stability of an axisymmetric toroidal plasma 79−19072
higher surface modes near plane metal-vacuum interface, RPA calc. 78−42760
hydrodynamic eauation for weakly coupled one-component plasma 79−90390
hydromagnetic oscillations coupling modes in non-uniform finite pressure plasmas, two-fluids model 79−21108
inhomogeneous beam-plasma system, continuous oscill. spectrum *(Russian)* 80−106937
inhomogeneous electron flux approaching cold plasma, surface wave excitation *(Russian)* 78−87459
inhomogeneous plasma column, reson. props., control using probing UHF signal *(Russian)* 77−76051
instability of two dimensional waves, critical drift velocities, oscill. growth factor *(Russian)* 80−106922
intense relativistic electron beam-plasma system, coupled transverse oscillations, kinetic description 80−64741
internal disruption in Tokamak, relax. oscills., self-consistent model *(Russian)* 80−53957
ion acoustic instability, renormalised kinetic theory for long range oscills. 79−27773
ion beam, neutralised, LF plasma wave dispersion *(Russian)* 79−98888
ion beam injection, self-oscillations, feedback mechanism, ion-ion stability excitement 79−50864
ion beam propagation, plasma oscill., effect on transverse phase vol. 78−38509
ion beam-plasma ion beam, collisionless interaction in transverse mag. field, lower hybrid longit. oscills. *(Russian)* 77−47222
ion beam-plasma system, self-oscills. due to 2 stream ion-ion instability 77−76123
ion cyclotron waves, oscillating two-stream instability, RF heating of tokamak plasma 80−1779
ion Langmuir wave, modulation instability *(Russian)* 78−71475
ion oscillation excitation by freely propagating electron beam *(Russian)* 80−1815
ion oscillations, self-modulation 77−80303
ion thermal conductivity, anomalous, drift oscills. effects *(Russian)* 79−23403
ion waves, two-stream ion-ion instability in axially bounded ion beam-plasma system 78−91119
ion-acoustic, gradient-driven instability 78−75291
ion-acoustic current driven instability, in collisionless Q-machine plasma 79−32770
ion-acoustic fluctuations, CO_2 laser study 80−83946
ion-acoustic instability oscillations in collisionless single ended Q-machine 80−38731
ion-acoustic limiting value, effect of electron gas heating during elec. field compression *(Russian)* 77−11369
ion-acoustic oscillations, in inhomogeneous plasma layer, high freq. radiation excitation *(Russian)* 78−26270
ion-acoustic oscillations in intense EM field *(Russian)* 79−55483
ion-cyclotron, non-electrostatic, spontaneous excitation, threshold electron drift 80−38625
ion-cyclotron instability driven by oppositely directed proton streams in magnetosphere 79−62690
ion-cyclotron oscillations, simultaneous enhancement with ion vel. space diffusion in mirror confined plasma 77−24059
ion-cyclotron oscillations in mag. mirror device, microwave meas. 77−3985
ion-cyclotron oscills., electrostatic, nonlinear interaction causing modulational instability 77−89248
ion-cyclotron wave, driven unstable by cold-ion beam, nonlinear stabilisation 79−98925
ionic sound, coherent four-photon light scatt., plasma diagnostics method 79−14618
ionisation wave, obs. of phase modulation 80−69993
ionisation waves, half subharmonic excitation in glow discharge, positive column 80−44006
ionization-diffusion oscillations in glow discharge plasma, rel. to stepwise ionization 78−1927
ionosphere, parametric excitation by strong radiowave 77−17283
ionosphere, photoelec. distrib. determ. from plasma line intensity meas. 77−41259
ionospheric plasma, electrostatic cyclotron oscillation, photoionisation *(Russian)* 78−63552
ISX-A Tokamak, plasma equilibrium position dynamics 79−77360

plasma oscillations continued
kink modes, free boundary, nonlinear stability of Tokamak 77—1010
Knudsen plasma, one-dimens., bounded, nonlinear oscills., numerical method 78—79433
Landau damping, application of Laplace transform inversion, for teachers 79—21496
Landau damping, relaxation of initial excitation *(Russian)* 78—55721
Langmuir, excited by relativistic electron beam *(Russian)* 77—35360
Langmuir electronic oscills., Vlasov kinetic eqn. 78—14133
Langmuir oscillation collapse in supersonic regime, forbidden energy *(Russian)* 80—14895
Langmuir oscillations, amplification, suppression by charged particle in magnetoplasma 79—37482
Langmuir oscillations, interactions in weakly ionised high-density plasma, beam instability *(Russian)* 78—26271
Langmuir oscills., 2-dimens. distribs., critical rate of collapse *(Russian)* 80—106896
Langmuir oscills., modulational instability, in EM wave field 80—38618
Langmuir stimulated oscills., finite amplitude, in plasma reson. region *(Russian)* 77—62363
Langmuir turbulence, isotropic oscills. and energy flux nonlinear freq. shift *(Russian)* 79—27778
Langmuir turbulence, modulation perturbation spectrum 80—33776
Langmuir turbulence, numerical modelling, solitons, nonlinear interactions 80—70030
Langmuir turbulence in upper hybrid resonance region, external electric field effects *(Russian)* 79—73010
Langmuir waves, induced nonthreshold scatt. on HF oscills. in inhomogeneous plasma *(Russian)* 80—53960
Langmuir waves, nonperiodic oscillations 80—48888
Langumir perturbation, emission of EM radiation, plasma freq. harmonics 78—34292
laser electron accelerator, mechanism 79—81103
laser irrad. plasmas, single and double frequency reson. heating, unstable oscills. *(Chinese)* 77—76149
laser produced plasma expanding into mag. field, oscill. modes 77—51178
laser-target impact, HF oscill. excitation *(Russian)* 80—92353
linear electron plasma test wave, wavenumber oscills., standing wave effects 78—38478
linear longitudinal oscillations in multicomponent plasma, damping and dispersion 77—19703
linearized Vlasov-Hermite system, non-analytic initial perturbation 77—89245
localised pumping-excited waves, parametric instability, nonlinear stage 80—38622
long wavelength modes, longitudinal, microscopic theory 77—89239
long wavelength modes, transverse, microscopic theory 77—89238
long-wave oscillation damping calc. *(Russian)* 78—75302
long-wave oscillations, hydrodynamic action calc. of damping 77—31427
longitudinal oscillations, kinetic theory 78—75319
low freq. quasipotential oscills., magnetoactive plasma, freq. and attenuation *(Russian)* 77—47181
low frequency oscills. during disruptive instability in TFR Tokamak 78—22564
low-freq. oscillation spectrum in weakly ionised plasma 80—87885
low-frequency instabilities in Tokamak due to trapped ions *(Russian)* 79—4125
low-frequency oscillations, in plasma with negative ions, collision effects 78—87448
lower hybrid oscillating two stream instability, in plasma with mag. shear 79—90395
lower hybrid waves, current-driven electrostatic ion-cyclotron instability 80—103149
lower-hybrid range oscillations in bounded plasma 80—24162
mach cones induced by fast heavy ions in electron plasma 79—14546
magnetic field parametric generation under intense irrad. *(Russian)* 79—77412
magnetic filament with diffused boundary, anomalous damping 78—75331
magnetic mirror confined non-neutral electron clouds, electrostatic modes, probe diagnostics 79—46466
magnetic mirror trap, open, with min. B, LF oscills. 80—38708
magnetic reconnection and m=1 oscills. in current carrying plasmas 78—71463
magnetised cold plasma, bounded volume, natural oscillations 77—76077
magneto-acoustic, density and temp. determ. 77—80354
magneto-acoustic oscillations, pressure and viscosity effects 80—79464
magneto-acoustic oscillations in a toroidal plasma 79—19026
magnetoacoustic, used for equilib. plasma density and mag. field profile determs. 80—48986
magnetoacoustic oscillation excitation in strongly inhomogeneous plasma 80—38641
magnetoacoustic oscillations, two-component plasma, numerical calcs. 78—59567
magnetoacoustic oscillations in a finite-beta current carrying plasma column 80—1771
magnetoacoustic oscillations in current-carrying plasma column 78—30438
magnetoacoustic oscills., in bounded plasmas, viscous damping 80—38605
magnetoacoustic oscills., in toroidal plasma, comparison with cylindrical plasmas, numerical calcs. 80—33760
magnetoactive plasma, modulational instability caused by Langmuir oscillations 80—92297
magnetoplasma, weakly ionised, perturbational heating in oscill. elec. field, collisional relax. and Boltzmann eqn. 79—37515
magnetosphere tail, intense oscills., modulation instability at lower hybrid reson., strongly turbulent plasma *(Russian)* 78—59563
memory function, coupling of single particle and collective modes 77—68749
MHD generator, channel, near electrode-free wall, plasma instability, flow inhomogeneity effect 78—26338
MHD helical oscills. in torus, RF helical quadrupole heating 77—76135
MHD oscills. ensemble, interaction with quasiuniform mag. field, sunspots 77—76041
MHD spectrum in small aspect ratio Tokamaks 77—72483
MHD torsional oscills. of magnetosphere rel. to micropulsations, orthogonal curvilinear coordinates theory 79—80097
microtearing modes and anomalous transport in Tokamaks, self consistent calc. 80—59222
microwave emission from transformed electrostatic oscills. 77—76209
plasma oscillations continued
microwave excitation, upper hybrid reson. region, appl. heating *(Russian)* 77—3943
mirror machine, enhanced plasma confinement by MHD oscillation 80—24205
mode dispersion, in weakly and strongly coupled one component plasma 77—51181
modulational instability produced by Langmuir turbulence in a magnetic field 80—1759
multicomponent plasma, linear longit. oscill. damping and dispersion, development of turbulence 77—51185
negative ion beam instability spatial development in rarefield gas *(Russian)* 80—92314
non-potential oscills., finite-orbit effects in Tokamak 77—15228
noncircular Tokamak, time evolution of elongation ratio and Mirnov oscill. 80—64763
nonisothermal plasma, parametric absorpt. of laser emission *(Russian)* 77—80312
nonlinear, model from statistical data, control system appl. *(Russian)* 78—83560
nonlinear acoustic, laser diagnostics 77—19770
nonlinear dissipation, effect on heating under strong Langmuir turbulence conditions *(Russian)* 78—34346
nonlinear electron oscillations, driven by EM wave 79—64850
nonlinear electrostatic, multiple water bag model 79—14532
nonlinear longitudinal, parametric excitation of magnetoactive plasma *(Russian)* 78—18390
nonlinear lower-hybrid waveguide in plasma, stability 80—19578
nonlinear oscills. in warm plasma with initial vel. perturbations 77—15179
nonlinear plasma, excitation of large amplitude regular oscills. by modulated electron beam *(Russian)* 78—5887
nonlinear potential oscillations, of cold unbounded plasma, charged particle beam effects *(Russian)* 79—55492
nonlinear theory of beam instability in collision plasma *(Russian)* 79—19049
nonlinear theory of unstable plane waves and solitons 80—87888
nonlinear wave packet acceleration and slowing down 80—59203
normal mode analysis, eigenfunctions and adjoint functions 78—42744
oblique Langmuir solitons under free path conditions *(Russian)* 80—79477
OGRA-3 installation, large plasma density during feedback stabilisation, unstable oscills. characts. *(Russian)* 77—47245
Ogra-3 mirror device, loss mechanism due to cyclotron instabilities 80—28788
open trap plasmas, electronic loss layer formation, low freq. oscill. anomalous electron diffusion *(Russian)* 79—90383
oscillating two-stream and parametric decay instabilities in a weakly magnetized plasma 80—38637
oscillation centres and mode coupling in non-uniform Vlasov plasma 79—90448
Pade approximation to wave amplitude 79—73004
parametric excitation, HF drift oscills., weakly ionised nonuniform plasma *(Russian)* 77—3928
parametric excitation of charge density fluctuations in classical and quantum electron-hole plasmas 79—50856
parametric excitation of nonlinear oscillations by inhomogeneous electric field *(Russian)* 78—22478
parametric instabilities of inhomogeneous plasma in presence of long-wave low frequency oscillations *(Russian)* 80—103136
parametric modulation of density of laser plasma near crit. surface *(Russian)* 79—4108
parametric oscillations in electron beam-plasma system 79—27792
parametric oscillations in ionosphere, generation during EM sounding from Alouette and Isis satellites 77—60510
parametric resonance in a weakly turbulent relativistic electron plasma 79—55539
parametric stimulation of longitudinal oscills. by transverse-longitudinal RF waves *(Russian)* 78—5876
parametrically excited relaxation oscills. in UHF discharge 80—53978
parametrically excited waves, collective oscill. and instability of single freq. state *(Russian)* 79—19033
partially ionised fluid, thermal instability, compressibility and collisional effects 78—55693
Penning discharge ion source with hollow cathode, HF instabilities 80—43997
Penning discharge plasma, electron vel. distrib., rot. instability effect *(Russian)* 77—80301
plasma waves, self channelling effects, localised plasma regions *(Russian)* 79—77375
plasma-beam interaction, nonlinear theory *(Russian)* 79—50867
positive column, density oscills. due to negative ions, metastable atom model 78—1799
potential double layers, highly nonlinear states in plasmas, expt. obs. 80—6233
potential oscillations, parametric excitation in magnetised collisionless plasma *(Russian)* 79—55484
potential oscillations excitation with electron beams 78—30419
primary electron-gas ionization sustained discharges in incompletely ionised plasma 79—50910
probkotron plasma stabilisation system, automatic, against flute oscills. *(Russian)* 80—24211
Pulsator Tokamaks, modulated runaway losses and effects of helical dipole field 80—28845
pump frequency oscillations, obs. in multiple pump ionospheric heating expt. 78—57382
Q-machine, plasma potential control with electron-emissive grid 77—39446
quasi steady high beta plasma in multiple mirror machine, density oscill., stability obs. 80—28663
quasi-two-dimensional system, hydrodynamic theory 78—38477
radial oscillations damping in toroidal pinch 78—30476
radiation from waveguide, rel. to plasma wave scatt. by ion-acoustic oscills. 80—87886
relativistic, covariant theory 79—19011
relativistic beam, excitation of Langmuir oscills., modulation instability *(Russian)* 79—4155
relativistic degenerate electron plasma, dielectric response in mag. field, plasma oscillations 80—54022
relativistic degenerate electron plasma, oscillations, dielectric response function 78—87486

plasma oscillations continued
relativistic electron beam, intense, coupled dipole oscills. 80−64739
relativistic electron beam dissipative Cerenkov instability, oscill. modes, quasi-linear theory *(Russian)* 78−59564
relativistic ion beam-plasma interaction, plasma oscillatory props., EM wave excitation *(Russian)* 78−59614
relativistic isotropic plasma, EM and electrostatic oscills. 80−54026
relativistic particle ring, coherent oscillations, Vlasov eqn. 78−55060
relativistic plasma, oscillations, dispersion relations, electron fluid model approx. calcs. 78−1882
relativistic tangential electron beam-semirestricted plasma collision, dissipation instability *(Bulgarian)* 78−34333
relativitic electron beam, relaxation tangential to semi-bound plasma 79−37506
relaxation oscillations in high-power electron beam-plasma system 80−64744
relaxational oscillations of plasma wave energy, in solar mag. traps *(Russian)* 80−8616
resistive modulation instability 79−77378
resistive plasma column, reconnecting mode, moment eqns. treatment 78−22493
resonant excitation of slow low-freq. waves by opposite moving electron beams *(Russian)* 80−92336
resonant fields, in magnetoactive plasma *(Russian)* 78−18392
RF oscillation ponderomotive accel. of electrons in elec. double layer 80−70010
runaway relativistic electron scatt. on oscills. in Tokamak *(Russian)* 80−48849
sawtooth, in Tokamak 78−47147
sawtooth, in Tokamak 78−47150
scattering of two longitudinal oscillations into single transverse wave, radiation emission and dynamics 77−58861
self-oscillating mode origination in nonequilib. magnetised plasma 79−86568
sharp boundary Vlasov-fluid screw pinch, free and forced m=0 oscillations 80−38636
shear stabilisation of drift oscills., ionic viscosity influence *(Russian)* 77−84432
solar electron plasma oscillations assoc. with type III radio bursts 77−37592
sonic-Langmuir solitons, formation, interaction, inverse scatt. method 77−27664
spatially inhomogeneous singular spectra of weak turbulence *(Russian)* 77−27673
stabilisation of spatial mode, algorithm 80−64721
stability and distrib. function influence on eigenoscillations 80−53966
stability of the longitudinal oscillations of a bunched beam propagating in a vacuum chamber with reactive impedance 79−85849
stellarator, Saturn, drift oscills. characts., high shear stabilisation *(Russian)* 79−98887
stimulated Raman and Thomson scatt., beat-wave electron trapping 78−51308
in strong circularly polarised EM wave field, anal. *(Russian)* 77−7544
strong Langmuir turbulence, soliton flash, turbulent ion heating and relax. oscills. 78−1834
surface oscillation cyclotron excitation, electron beam cyclotron instability *(Russian)* 80−54008
surface oscillations parametric excitation 78−30420
surface vibration excitation, electron beam in semirestricted magnetoactive plasma *(Bulgarian)* 78−34334
T-10, ohmic heating, plasma confinement study 80−28768
T-12 Tokamak with two axisymmetric divertors, characteristics of divertor 80−28844
theta pinch, radial oscills. of plasma density and mag. field, light scatt. and probe obs. 80−14937
theta-pinch, linear, microinstability onset, anomalous resistivity, electron heating and MHD oscills. 77−27698
three-dimensional stationary plasmon distributions 77−68796
Tokamak, confinement and stability, effects of shaping and compression of plasma 80−28772
Tokamak, destabilizing effect of width and limiting plasma press. *(Russian)* 79−7458
Tokamak, inner mode relax. oscills., numerical model, electron thermal cond. distrib. *(Russian)* 77−47242
Tokamak, sawtooth oscillations, mag. islands and disruptions 80−83940
Tokamak, small, TOSCA, sawtooth oscills., X-ray diagnostics 79−41817
Tokamak experimental results, review 79−98968
Tokamak plasma, Pulsator I, disruptive instability, origin 77−43026
Tokamaks, feedback stabilisation of magnetic islands 80−28638
Tokamaks, magnetic islands, tearing modes 80−28846
toroidal discharge, dynamic stabilisation in weak longit. mag. field *(Russian)* 78−87476
toroidal pinch discharge, preionisation phase, numerical computation 80−64696
toroidal pinch plasma, damping of radial oscill. 78−26272
toroidal plasma, resistive MHD mode and sawtooth oscill., nonlinear evolution 80−24235
transverse, regular, stimulation by relativistic electron beam, nonlinear theory *(Russian)* 77−47218
transverse instability in plasma column 78−5869
transverse plasma oscillations, linearised Vlasov-Maxwell eqn. solns. 79−90398
turbulence pulsations, quasilinear theory 78−26283
turbulent heating of plasma with transverse current, mechanism *(Russian)* 77−80324
turbulent plasma, plasmon gas oscillations *(Russian)* 78−47120
UHF discharge with preliminary locally ionised gaseous medium 80−38851
ultralow frequency oscill. in trapped electron regime 80−1784
unbiquitous mode, theory 78−5864
unneutralized electron cloud injection and containment in bumpy toroidal mag. field 80−64761
unstable oscillations, sheared toroidal mag. field procedure for reconciling oscillation characts. with periodicity 78−34309
very-low-q discharges in DIVA confinement and MHD characts. 80−64765
viscous damping of magnetoacoustic oscillations in cold, bounded cylindrical plasma 80−24151
Vlasov equation, two dimens., numerical soln., multistep technique 78−1795
Vlasov linearised collisionless eqn. soln. 78−30423
plasma oscillations continued
Vlasov theory, linear approx., electron distrib. initial value problem 77−84423
wave dispersion in presence of relativistic beam 80−19592
wavebreaking amplitudes in inhomogeneous plasma, temp. depend. 79−68915
weak Langmuir turbulence, in nonuniform plasma, spectral intensities *(Russian)* 79−55504
weakly-ionised plasma, magnetised, unstable oscillations, influence on radial electric field *(Russian)* 80−103175
whistler mode signals generation in presence of enhanced fluctuations in plasmas 80−92293
whistler wave, large amplitude oscillation by high power microwaves 80−43913
whistler wave trapping in density crest 80−53984
Al, plasma oscillations in oxide free Al clusters 78−2510
Ar, afterflow stability boundaries, plasma oscillation modes in mag. field 78−38486
Ar, afterglow, pulsed discharge, acoustic oscills. in emitted radiation 77−89309
Ar arc, high-press., in longitudinal mag. field, spiral wall characts. 77−65919
Ar discharge rotating plasma column LF oscillations 78−71481
Ar, laser-initiated plasma, gasdynamic instabilities and convective flow parameters 78−22525
Ar, weakly ionised plasma turbulence in longitudinal mag. field 78−75338
CO_2 laser, vibrational control in stabilisation of ionisation-thermal instability 77−19302
Co, $K\beta_{1,3}$ X-ray emission spectra, low energy plasmon satellites 80−19560
Cs-Ba discharge, high-current, low-press., spontaneous current cutoff 80−19626
Cu, $K\beta_{1,3}$ X-ray emission spectra, low energy plasmon satellites 80−19560
D-T plasmas, ignition toroidal expt., equilibrium configs. and heating 80−28704
$DyI_3/CsI/Hg$ arc, oscillations induced by external mag. field, arc constriction 79−60205
H line broadening and shift due to plasma ions *(Russian)* 80−96350
H_2 plasma, radial density and temp. profiles, using magnetoacoustic oscills. 79−19082
He plasma, cryogenic, oscill. excitation by hot electrons 79−55493
He-Ar plasma, linear longit. oscill. damping and dispersion, development of turbulence 77−51185
He-Cs discharge plasma, high freq. oscills. in crossed elec. and mag. fields *(Russian)* 77−15189
Hg discharge, radial distrib. of low-freq. oscills. *(Russian)* 78−1928
Ne, discharge streamer propagation mechanism based on plasma vibrs. *(Russian)* 77−84546
SF_6, discharge and oscill. due to axial injection of impulsive electron beam 80−59316
SF_6 gas, dispersion relation of spontaneous oscill., unstable regions 80−1875
SF_6 gas, low press., excitation of nonlinear wave by repeated pulsed electron beam 80−87878
Si, non thermal laser induced ordering, plasma life time, phonon interactions 80−84481

plasma probes
see also Langmuir probes
AC plasma display panel wall charge magnitude and distribution probe 78−67487
air blast circuit breaking arcs, elec. grad. using plasma probe methods 78−87527
alloy components, sputtering, in plasma, probe method obs. 79−55564
antenna, circular aperture, induced HF thermal noise calc. 78−87496
arc tracks in T-10 Tokamak, wall erosion by unipolar arcs 80−64811
arcs, wall-stabilised, free recovery with imposed laminar and turbulent flows 80−59321
Berkeley multicusp ion source for use with TFTR neutral beam injector, characts. 80−54040
calorimetric probe for local heat flux measurements in plasma jet 77−43061
calormetric probe for determ. of heat flow *(Russian)* 78−12698
charged particle density, mag. field effect *(Russian)* 78−22552
chemically reactive arc-heated gas flow, ion saturation current fluctuation probe 78−63574
Columbia Torus-1 belt pinch high beta toroidal device, preionisation, optimisation 80−92368
computer processing of probe measurements 80−62640
conducting bodies in ionised multicomponent gas, electric effects, method of separation 80−96389
conductivity meas. in flowing plasma, pulsed probe method 78−1894
continuum theory for ionised gas interaction with emitting surface 78−14204
cooled electric probes in dense plasma, thermal diffusion effects 80−92384
current collection, appl. to long wire in near-Earth orbit 79−25438
current collection by spherical Langmuir probes drifting in a collisionless plasma 78−83616
current density, local, mag. probe and Thomson scatt. meas., using Spitzer-Harm distrib. 78−18451
current density profile measurements in the Proto-Cleo torsatron 80−83995
current-voltage characts., probe meas. correction in RF plasma 78−26333
cylinder short-wave probe, inverse diagnostics problem formation 78−67423
cylindrical hollow cathode negative glow, fast electron angular distrib. obs. 78−67529
cylindrical probe, electron current second derivative calc. algorithm 78−63594
cylindrical probe, in collisionless magnetoplasma, upper bound current 78−91154
DC probe voltage deviation caused by probe current drawing across plasma resistance, compensation cct. 80−54041
delay line differentiator for meas. of electron energy distrib. function *(Japanese)* 80−84002
diagnostic techniques for fluctuations 80−49002
diffusion type, cylindrical, in mag. field, floating pot. calc. 80−10438

plasma probes continued
directional double probe, rot. obs. during implosion in theta-pinch column 78−1877
directional planar plasma probe for energetic plasma electron anal. 79−9062
discharge, luminesc. lamp. external and internal probe meas. 80−43978
disruptive instability in TO-1 Tokamak, feedback stabilisation *(Russian)* 79−55546
double electric probe with VHF decoupling and telemetry, plasma parameter determ. *(Russian)* 79−7485
double probe electron temp. and density meas., semiautomatic system 78−87490
double probe theory for a low-density flowing collisionless plasma 79−37470
electric field determ. in plasmas with turbulence using emissive floating probe 79−86614
electric field measurement in corona discharges 80−33822
electric field prod. in air near laser spark, probe obs. *(Russian)* 80−59334
electric probe in weakly ionised and rarefied plasma *(Russian)* 80−24252
electrical conductivity of low-temp. alkali plasma, weak probing signal method meas. 80−48968
electrical feedthrough for probe meas. in vacuo 78−71543
electrical probe, using discrete stepped pulse generator 77−39454
electrical probes, in dynamic plasma, theory, math. anal. 77−43082
electron conc. and temp. approximate formulae 78−63596
electron current, at plasma-electrode interface in transverse mag. field, probe obs. 79−64914
electron current at spherical probe, theory 79−55556
electron density, in mag. field, spherical probe meas. 77−31526
electron density, meas. in unmagnetised plasma, self-oscill. probe method 80−19611
electron density and electron collision freq. determ. by coil probe method 77−1016
electron density determ. by electrostatic probe 77−39464
electron distrib. function, probe meas., ionis. wave irregularity effect 77−47255
electron distribution function, meas. by direct differentiation of probe charact. 77−68860
electron distribution function in ionis. instability mode of plasma accelerator 80−19612
electron energy distrib. functions determ. by second derivative method *(Russian)* 78−51356
electron energy distribs. in front of and behind plasma sheath 77−76202
electron energy distribution function, probe meas. in Ar afterglow 79−60195
electron energy distribution function in flame plasma, probe meas. 79−60190
electron reflection in probe analysis of plasmas 79−64913
electron temp. determ., floating double probe and renewed method 77−80356
electron temperature, in HF plasma, meas. by spectroscopic and double probe methods 77−65910
electron temperature and electron density in low density magnetised plasma by probe method 80−48848
electron temperature meas. in ionosphere by high-freq. probe method 79−92632
electronic temperature, low, of weakly magnetised plasma meas. 77−68870
electrostatic, in synthesised magnetoplasma stream 79−77426
electrostatic, reference temp. method for determ. densities and temp. 77−84510
electrostatic cylindrical probe, ion saturation current rel. to plasma confining wall *(Russian)* 77−27719
electrostatic cylindrical probe in collisionless magnetoplasma, theory 77−19772
electrostatic double probes, behaviour in intense RF fields 78−59675
electrostatic plasma probe, neuron membrane physical analogue 80−79573
electrostatic probe, electron temp. meas., surface pot. var. effect 78−14202
electrostatic probe, for metastable atom conc., He and Ar plasma jets *(French)* 79−98972
electrostatic probe characteristics in a magnetic field, ellipsoidal probe in diffusion regime 80−33815
electrostatic probe continuum plasma, stagnation pt. current collection, numerical calc. 77−3989
electrostatic probe current in dense externally maintained plasma 79−27832
electrostatic probe for ion energy anisotropy meas. in magnetised plasma 79−10710
electrostatic probe in a magnetic field 79−55563
electrostatic probe meas. in mag. field *(Russian)* 78−22553
electrostatic probe meas. in turbulent jets at atm. press., mean values determ. *(Russian)* 77−51240
electrostatic stagnation point probes in flowing plasma, Knudsen no. effect 78−1893
Elmo Bumpy Torus heavy ion probe 80−59286
emissive probe, potential meas. in magnetised gas 80−100095
emissive probe using CO_2 laser-heated emission of electrons from C-coated metal surface 80−6270
emitting in synthesised magnetoplasma stream 79−77426
enthalpy meter, optimum dimensions 77−35387
explosive emission diode, plasma pot. oscills., probe diagnostics 80−6284
fast ion beam vel. distrib. meas. with probe 79−13890
field visualisation technique applied to sub-mm diagnostics of axisymmetric plasma 80−43980
field-reversing electron ring generation in RECE Christa, millisec. lifetime, mag. probe meas. 77−24173
flame measurements, probe material effect on results 80−19613
flat-saturating gridded probe, ion flux meas. 77−11396
floating double probe, magnetised DC discharge plasma, anomalous resist. 78−87434
floating double probe for determ. of plasma electron temp. *(Japanese)* 77−80368
focus, Mather-type machines, temp., density, neutron and X-ray emission charact. 77−24184
focus current, compression phase, mag. probe meas. 78−5939
formation of plasma in fusion devices, at. and plasma processes, diagnostic techniques 80−48915
fusion reactor, diagnostics of radial plasma transport rate, data acquisition and handling system 78−54937
glow discharge, high press. probe meas., current-voltage charact. 79−90466
glow discharge, investigation with cylindrical hollow cathode in Ne and He *(Russian)* 80−28856
glow discharge, large amplitude striations, electron conc. variation 77−89342
glow discharge polymerisation double probe meas. and contamination effects 77−70300
Hall current accelerator, with extended accelerator zone, local plasma props. meas. 79−64917
hemispherical antenna as microwave plasma probe 78−67438
high beta toroidal device, preionisation, optimisation 80−92368
high-current constricted-arc anode heat balance obs. 78−71499
high-pressure nonstationary plasma, cylindrical and spherical probe diagnostics 78−63598
high-pressure plasma, probe meas. for different probe and plasma temps. 79−82092
high-Q resonant probe for plasma wave diagnostics 78−9831
hollow cathode, MPD arc config., 0.25-30 kA, current and pot. distribs. 78−9869
hollow cathode arc, plasma column parameters *(French)* 78−9885
hollow cathode discharge, electron temp meas. 78−67445
hot spot distribution, significance interpretation of laser produced plasma expts. 79−98945
inductively coupled RF plasma, excitation, ionisation and electron temps. and positive ion conc. meas. 77−39453
instantaneous triple-probe method for direct display of plasma parameters in low density continuum plasma 80−84000
ion acoustic wave excitation with array of wire probes 79−37492
ion current and charact. by non-self-maintained ionisation 80−38713
ion current and disturbance region size, numerical calc. *(Russian)* 78−91151
ion density meas. in slightly ionised Ar 77−15242
ion extraction by small orifice probe, sheath effects 80−59307
ion sheath, convection sustained, struct., probe meas. 78−14179
ion temp. meas. in rarefied drifting plasma 77−84511
ion temperature determ. in mag. field, gridded probe method 80−70033
ion-acoustic turbulence, in rarefied plasma flow, Langmuir probe meas. *(Russian)* 79−55547
ion-acoustic wave excitation with probes 77−68780
ion-acoustic wave meas. with probes, antenna charact. 78−5949
ion-acoustic waves, probe excited in multidipole plasma device 78−42739
ionised gas flow contaminated with macroscopic particles, charged particle density meas. 77−68864
ionosphere probes, plasma disturbances creation rel. to Spacelab proposed low-energy meas. 78−77458
ionospheric plasma probe measurements, commutable source of ref. voltages 80−31192
ionospheric structure studies by space vehicle obs. 79−53540
JFT-2 Tokamak, large scale fluctuation mode mixing, probe, interferometric obs., MHD anal. 78−67312
Langmuir probe sweeping circuit 80−83996
large Debye length probe theory in continuum plasma, exptl. studies 78−38537
laser fusion diagnostics, techniques and appl. 80−49009
laser produced plasma, self-generated mag. fields 79−77423
laser-produced plasma, simultaneous meas. of current flow and mag. field 77−24192
loop antenna, electron plasma wave radiator and detector, exptl. obs. 77−51198
low pressure gas discharge meas. 80−96412
low-frequency impedance, of probe in dense plasma 79−64918
low-temperature plasma, in mag. field, density, probe determ. 78−67418
low-temperature plasma, in mag. field, electron temp. and plasma pot., probe determ. 78−67419
lower hybrid frequency propagation in FT-1 Tokamak *(Russian)* 79−55482
magnetic field, effect on charact. of floating RF plasma probe 79−64915
magnetic fields of hot dense plasmas, particle probes sensitivity 80−70037
magnetic induction, in cylindrical geometry, Fourier components 77−65907
magnetically shielded sampling probe, for plasma diagnostics in medium-press. magnetoplasma 78−22560
magnetoplasma, interaction of amplitude modulated microwave, plasma waves excitation 77−3947
magnetosonic wave excitation in toroidal plasma, probe meas. 77−65866
magnetotail dynamic structure simulation by powered double probe *(Japanese)* 79−25406
metal atom density, in coal plasma, probe determ. 77−62407
metal probe-gas discharge plasma boundary, impedance parameter variations 77−58869
microwave, hemispherical monopole, charact. 80−19621
microwave beam, reson. interaction, mag. field self-generation, probes obs. 77−35353
microwave discharge, plasma probe charact. affected by microwaves 79−10733
microwave plasma interaction, reson. and thermoelec. mag. fields obs. 77−27678
multi-channel integrator for plasma magnetic-probe meas. 78−75413
multi-coil mag. probe in plasma diagnostics, reliability assessment 79−55544
multi-electrode probe for orbit-limited current meas. 78−59678
multimode EM probe, appl. to wall region 79−94819
negative electrostatic probe, energy transfer from ions and electrons 78−79464
negative glow plasma, contact electrode charging time meas. 78−67525
negative ion current collection, effect on audio signal amplitude modulation 77−84515
negatively-biased cylindrical probe characteristics at medium pressure 78−63593
neutral beam probe, ion temp. meas. *(Japanese)* 80−19615
Nier-Bernas type ion source, factors affecting cathode performance 77−18723
non-self-maintained discharge, plasma probe currents 78−63631
nonlinear effects in the vicinity of a radiofrequency probe 80−48985

plasma probes continued
nonlinear helical perturbation in Tokamak, dynamics, mag. probe obs. *(Russian)* 80−53958
organic surface contaminants, anal. by plasma chromatography-mass spectroscopy, and Raman microprobe technique 80−108773
oxy-acetylene combustion products, seeded, elec. cond. rel. to MHD power generation 77−3922
parameter determination, by low-freq. modulation of probe potential *(Russian)* 79−37540
perturbed plasma region near probe, numerical calc. *(Russian)* 79−98976
pinched electron beam diode, proton current density meas. using biased charge collecting probe 77−55166
plasma-wall sheath, secondary electrons, Langmuir probe obs. 80−92387
positive column, axial elec. field and electron temp. in transverse mag. field 78−9880
positive ion extraction by an anodic orifice probe 80−38712
potential measurement using probe at 'floating' potential 79−37541
potential perturbation due to grid or probe 78−47166
probe characteristic in highly ionised plasma, transition region 78−79474
probe characteristics for cool plasma, electron saturation current 78−79473
probe current modulation, electron distrib. determ., finite amplitude distortion, instrumental function 78−47168
propane flame plasma, Langmuir probe teaching expt. 78−12456
pulsed electrostatic probes as diagnostic for transient plasma 78−94937
pulsed plasma diagnostics, double probe cct. 80−87947
quadrupole and double sphere dipole probe meas. for electron density and temp. diagnostics *(French)* 78−14208
quadrupole probe, plasma electron temp. appl., transfer impedance rel. to electrode radius *(French)* 77−68861
rapid sweep electric probe characts. generator 79−46483
resistivity anomalous, generated by ion-acoustic turbulence, collision freq.-turbulence spectrum relation 78−14205
resonance characteristics of sounding rocket impedance probe data *(Japanese)* 77−17271
resonance probe applications in geophys. and in laboratory *(Chinese)* 80−90226
reversed current effect in stabilised Z-pinch 80−79539
reversed field pinch, expt. and 3-D numerical anal. 77−43035
RF, for space pot. meas. in medium press. plasma 77−72497
RF discharge plasmas, mag. field effects, probe and microwave meas. 77−7594
RF double probe technique for resonance cone observations 79−46487
RF plasma utilisation in sputtering and surface reactions 78−84714
RF probe, directional, for flowing plasma conductivity meas. 78−51353
RF probe, ion sheath effects on impedance characts. 78−42818
RF probe sheath, finite thickness effect 80−43971
RF voltage in plasma probe sheath, effect on electron energy distrib. meas. 80−54045
RF-floated electrostatic probes in RF plasmas, press. depend. of electron temp. 77−47253
satellite and spherical probe, static and dynamic behaviour of sheaths, simulation 77−25907
screw pinch, m=1 motion determ. by probes and streak photographs 77−15239
screw pinch, SPICA, β-control, Thomson scatt., X-ray emission and probe meas. 77−27709
second derivative of probe charact. meas. by delay circuit 77−39461
sheath, planar continuum with regeneration and convection of ionis., probe meas. 77−80315
sheath thickness to Debye length ratio for slightly ionised continuum plasma 80−70008
shooting, for high-density plasma 80−33816
short-time pulsed probe analyser, appl. to non-equilib. plasmas 77−15240
single-ended Q-machine, method for axial pot. 79−73043
space plasma electron energy distrib. function meas. by probe *(Japanese)* 78−28474
space potential, new method of determ., using electron density and mean electron energy *(Russian)* 78−22557
space potential location, in large Debye length stationary plasma 80−14940
space probe, automatic setting of range of amplifying path 77−67019
space simulation plasma chamber, elec. field meas. with double probes, atm. appl. 79−64909
spatially resolved electrical probes, wall stabilised arc meas. 77−84516
spherical, in corona discharge, I-V characts. 78−79467
spherical electrostatic probe in continuum plasma, analytical models 77−55168
spherical ion acoustic soliton excitation by conducting probe 79−90461
spherical Langmuir probe, appl. to collisional plasma, theory 78−18460
spherical probe, in slightly ionised continuum plasma, electrostatic characts. 77−76197
spherical probe, slightly ionised continuum, current-pot. curves 77−72494
spherical probe in stationary collision dominated isothermal plasma, kinetic theory 77−47264
temperature and space potential, in mag. field 79−19095
temperature sheaths, probes and electrodes in MHD plasma 78−55726
temporal and spatial meas. of RF electric field in magnetized plasma using emissive probe 80−54042
theta pinch, radial oscills. of plasma density and mag. field, light scatt. and probe obs. 80−14937
theta pinch discharge, radial EM energy flow and plasma heating power 80−64747
theta-pinch, low-energy, end losses obs. 77−24157
theta-pinch, post-implosion phase, electron temp. and density meas., mag. field profiles 77−31522
Tokamak, accuracy of plasma displacement meas. using mag. probes 77−19766
Tokamak, high-β small aspect ratio, probe and laser beam meas. 77−27733
Tokamak, local toroidal and poloidal current density meas. 77−27732
Tokamak current profile meas. by neutral beam probe *(Japanese)* 80−96397
tokamak probe diagnostics allowing for asymmetry 79−41881
toroidal reversed-field pinches, current, temp., confinement time scaling 77−43078
total-head pressure probe, plasma flow vel. meas. method 77−43060

plasma probes continued
triple probe method applied to direct display of parameters in supersonic flowing continuum plasma 79−60191
triple probe method for meas. plasma parameters in low-density flowing collisionless plasma 78−1898
triple-probe method for direct display of plasma parameters 77−35395
twin probe, characts. investigation under DC and HF fields 77−7587
two-electrode probe, electron beam-formed plasma, pot. diagnostics *(Russian)* 80−1841
UHF discharge plasma parameter meas., three-probe method 78−63630
water vapour, electron energy distrib. function, electron sink and plasma resist. effect *(Russian)* 80−106987
wave number spectrum parameter estimation form fixed probe pair data 79−82062
waves, lower hybrid, in octopole Tokamak, ray trajectories 80−64707
Ar negative glow fast electron density rel. to discharge pressure and current 78−67528
Ar plasma jet, surrounded by Ar, He, N_2, H_2 gases, recombinations in decaying jet 78−9753
Ar^+ laser plasma, localised probe diagnostics 79−55113
C electrodes, used in emission spectrography, isotopic labelling study *(Hungarian)* 80−106976
CO_2-N_2-^3He, laser, plasma diagnostics of media capable of lasing in nucl. reactor environment 79−10279
Cs plasma probe meas. in mag. field 78−63597
Cu plasma, produced by CO_2 laser beam irrad. of solid, expansion of spontaneous mag. field 77−72495
H, contracted low-press. arc, electron energy distrib. 78−18477
H isotope separation in DC-arc plasma, mass spectrometric anal. 79−90457
H_2 plasma ion temperature determ. in mag. field, gridded probe method 80−70033
H_2-N_2 glow discharge, positive column, electron energy-distrib. spatial variation 77−47294
He discharge, probe meas. 77−47292
He glow discharge, negative-luminesc. plasma, electron energy distrib. from line intensities and probe obs. 80−49033
He-Cd^+ laser discharge, positive column, non-Maxwellian electron energy distrib., electron density determ. 77−84493
He-Cs plasma, HF instability in crossed fields, obs. 78−75305
He-Kr^+ laser, microwave-pulse-excited, internal plasma parameters, time variation 77−38858
He-O_2 DC discharge, electron distrib. function 80−92407
Hg discharge, positive column, elec. probe for diagnostics, teaching appl. 79−62979
Hg vapour, optically pumped positive columm, collisional processes 78−87499
Hg-vapour plasma, RF, probe diagnosis *(Russian)* 78−75423
K, discharge plasma, anomalous bright 5730 Å band excitation mechanism 78−67475
Mo impurity flux, time resolved, in DITE Tokamak 80−63373
N cooled discharge plasma electron energy distrib. function 78−63633
N_2, arc jet enthalpy meas. by fast miniature total calorimetric probe 78−67486
N_2 plasma, spatial distrib. in transverse-discharge supersonic stream, continuum theory and probe meas. 80−48866
N_2-Ne, positive column, electron vel. distrib. function *(German)* 78−1885
Ne afterglow plasma, electron energy distrib. function 78−63587
Ne, nuclear induced plasma, simulated 80−64786
O plasma electron energy distribution obs. 78−63595
O_2, electron energy distrib. function, electron sink and plasma resist. effect *(Russian)* 80−106987
Ti impurity flux, time resolved, in DITE Tokamak 80−63373
Xe, pulsed high frequency discharge, energy spectrum and electron density meas. *(Russian)* 78−26354

plasma production
see also exploding wires and foils; plasma production and heating by laser beam
40 kV neutral beam injector, modified duoPIGatron ion source 79−68117
ablation of hydrogen pellet in fusion plasma, scaling law 77−35354
accelerated Mach wave in nonhomogeneous cumulation cone 79−68925
accelerator, linear rail type, plasma cluster ionised front vel., theory 79−46494
air, atmospheric, cylindrically converging blast waves 80−92180
air, plasma, optical absorpt. coeff. at 1000 atm, 13000K, N_2^+ photodissoc. 80−64691
anodic plasma production and ion acceleration in coaxial diode with mag. insulation *(Russian)* 80−10402
arc, vac., fast plasma jet production from cathode spot 80−6309
arc production process equipment, present state and future prospects *(Russian)* 78−22518
atmospheric positive streamer corona, primary wave emission, secondary electron emission 80−44008
ball lightning, elec. discharge into sand layer expts., erosion-discharge model 78−81322
ball lightning, quantum mech. theory *(German)* 78−16082
ball lightning, radiation emission, cluster plasma 77−2219
ballistic compressor, nonideal plasma generation, Coulomb interactions, theory 78−87466
beam discharge for apparatus with spatial axis, weakly ionised plasma diffusion *(Russian)* 80−1826
beam-plasma discharge, near Zarnitsa-2 rocket, parameter estimation *(Russian)* 78−26357
Berkeley multifilament ion source, plasma characts. 79−94807
biconical profiled explosion-induced compression of matter 79−67938
cathode energy conditions in explosive electron emission 79−19111
coaxial lower hybrid plasma source capable of producing pulsed plasmas 80−33788
collective interactions, effects in high current discharge 79−55603
combustion-driven implosion, spectroscopic study 78−14189
concentric discharge, in controllable ion gun with high brightness 77−87871
conical slow wave antenna, plasma source using electron cyclotron resonance heating 78−42775
convergent neutral beam expts., particle distribs., ionisation 78−14183
counterstreaming electron beams, plasma form. and oscill. excitation 77−27687
crossed field plasma discharges characts. 80−100116

plasma production continued
CTR neutral-beam injection system, plasma source design 77−24105
current carrying double layer production in focus device 80−83953
current structure, fast particle generation *(Russian)* 80−48913
currents in short pulsed high current electron beam injection into initially neutral gases 80−33749
cylindrical foil, elec. explosion, current distrib. in high current shunting discharge 79−41855
cylindrical plasma shell, apparatus for production 80−106948
dense H_2 plasma generator, thermonuclear research appl. 77−34448
dense plasma, diagnostics of two-wavelength optical absorpt. 79−98978
dense plasma generation by ionised gaseous filament explosion 78−71507
dense plasma ionisation and cohesion, critical density and press., approx. formulas 80−59253
dense plasma source, with high-current discharge 78−9888
development in focus discharge accelerator, optical image structs. 79−82076
diatomic gases, plasma prod. by relativistic electron beams mag. field diffusion 80−83955
dielectric surfaces in evacuated cavities, plasma release due to electron irrad., transport characts. 80−33786
direct extraction H^- sources, prod. and destruction in magnetron and duoplasmatrons 77−23340
disc LaB_6 cathode for plasma production in magnetic field 80−106951
discharge development in Tokamak *(Russian)* 77−68809
discharge tube shape, flow velocity, effect on electron temp. of medium pressure positive column 79−64941
discharges, sustained by uniform ionisation source, props. 78−71605
duoPIGatron ion source, plasma studies 77−76145
duopigatron plasma generator, emission aperture shape effect on ion optics 78−5956
duoplasmatron ion source, D ion mass, energy, current density distribs. 77−23339
dust particles fast impact on Au or W target, ion comp. rel. to micrometeoroid detect. 77−39438
electric discharge, in air, pulsed, high-density, between parallel plates 80−1857
electric furnaces, investig. of gas conditions *(Russian)* 78−94921
electron beam, enhanced energy deposition, interferometric obs., simulation 77−31490
electron beam, relativistic, anomalous energy deposition into solid low-Z target 80−48906
electron beam, relativistic, interaction with air 80−48904
electron beam (relativistic)-target interaction, self mag. field effects on energy deposition 78−83588
electron beam fusion, pulsed power requirements for breakeven 77−23278
electron beam fusion, X-ray pinhole imaging techniques 78−47176
electron beam fusion compression targets, fuel preconditioning studies 79−81076
electron beam fusion programme, hard X-ray diagnostics 78−47181
electron beam fusion target, Rayleigh-Taylor instability 77−51174
electron beam generated plasma, collision process kinetics *(Russian)* 79−37444
electron beam ignition of plasma discharge in high density gas *(Russian)* 78−1853
electron beam impact on hemispherical target, implosion dynamics 77−47228
electron beam in gas, current meas. 80−38523
electron beam in Zn vapour, plasma prod. and beam interaction 78−47133
electron beam induced fusion, power requirements for target implosion expt. 77−23277
electron beam irradiated pellet, holographic interferometry of plasma blowoff vel. and density 77−23279
electron beam irradiated target, generated plasma props. 78−51321
electron beam irradiation of Au foil, mag. enhanced energy deposition 79−86591
electron beam plasma discharge, in crossed elec. and mag. field *(Russian)* 78−87458
electron beam produced inert gas plasmas, UV to near IR laser lines 80−92334
electron beam produced plasma, fast photography, emission spectroscopy 77−39458
electron beam produced plasma, IF emission spectrum and form. kinetics 80−102533
electron beam production of plasma in hollow collector, plasma props. 79−27794
electron beam targets, thick-shell shock-focusing 78−30454
electron beam-formed plasma potential, two-electrode probe diagnostics *(Russian)* 80−1841
electron beam-neutral gas interaction, SEEBIE expt., Thomson scatt. diagnostics 77−24111
electron beam-produced plasma, visible and UV high intensity spectral lines 79−73012
electron beam-vaporised metal surface interaction, 0.4-5 mA ion beam extraction 77−84456
electron cyclotron resonance plasma, production of multiply-charged ions, X-rays and charge state distribs. meas. 80−43941
electron density meas. in shock generated plasma by light interferometry 80−48981
electron distribution function and ionisation in space-depend. theory 80−38545
electron-free plasma form. *(French)* 78−1854
electron-positron plasma, produced by relativistic electron beam, waves, microinstabilities, collective positron accel. 79−19053
electronic excitation and ionisation temp. meas. in ICP Ar source, H_2O vapour effects 80−75028
electrostatic wave coupled multicomponent plasma, formation, evolution diffusion 77−84460
EM implosion of foil, SHIVA pulsed radn. source expt. 78−14190
emission from plasma formed in proton beam collision with Al target 80−53946
exploded wire, nonlinear evolution, numerical simulation 78−83605
exploded wire plasma nonlinear evolution, numerical simulation 78−14197
exploding wire, dense metal plasma, X-ray diagnostics 78−5909
exploding wire, inner shell X-ray spectra 77−27720
exploding wire, MHD sausage instability wavelength determ. 77−47238
exploding wire, nonthermal IR and X-ray emission 79−4187
exploding wire, X-ray emission spectra 77−68872
plasma production continued
exploding wire burst phase, simulation by one-dimens. MHD code 80−75080
exploding wire discharge, thermal instability of elec. cond. in metal vap. 78−1868
explosion induced compression, neutron yield optimisation in crucial systems 80−5328
explosion induced conical system, internal break even possibilities 79−94811
explosion-induced longitudinal-cylindrical compression of plasma 79−89496
explosive emission multiple-tip cathodes, improved stability 79−64887
explosive implosion of variable density shell, neutron generation in a plane system 79−18035
explosive implosion of variable density shell into conical region, neutron output determ. 79−22454
explosive instability collision mode stabilisation by drifting effects, Thirring instability *(Russian)* 80−43920
extended high-current discharge, initiation by long laser spark *(Russian)* 80−10404
extremely dense plasma generation by cylindrical cumulative compression 78−71508
field reversed mirror neutral beam startup, hybrid plasma code simulation 80−99313
fission fragment generated plasma, electron distrib. function, effect of collisions and diffusion 77−23653
fission fragment generated plasma, kinetic model 77−31488
fission fragment generated plasma, kinetic modelling 77−23644
fission fragments, electron distrib. function 77−19731
fission-fragment-generated plasma, theory of spectroscopic diagnostics 78−34374
fission-fragment-generated plasma from interaction in neutral gas 78−34345
fissioning high pressure gas, expt. for generation in gaseous core reactor 77−23191
flame, plasma, with rectangular cross section, prod. by nozzle *(Japanese)* 78−47108
flow and production in ion beam 80−28624
focus device with inductive energy storage, plasma prod. 79−77427
focused relativistic electron beam discharge into thin target, EUV emission 78−47162
formation of plasma in fusion devices, at. and plasma processes, diagnostic techniques 80−48915
fusion plasma prod. by electrically exploded liquid threads, MHD instability 77−15220
fusion reactor, neutral beam injector mag. cusp plasma source, design and fabrication 80−99377
fusion reactor, rectangular plasma generator, advanced ion source for ion injectors 80−99376
gas discharge ion source, high energy characts. 78−42772
gas jet target with electron beam heating, plasma density meas. 77−39457
generator, ignition conditions for power superposition between two generators *(French)* 78−9799
generator, one-dimens. model 79−64881
generator arc chamber, hydrodynamic struct. 80−1817
glass cell plasma production by pulsed discharge development, finite difference soln. 78−67559
H-pinch discharge, quasistationary, EM characts. and energy balance, erosion plasma generator 80−19630
Hall accelerator plasma stream, electron temp. using Xe-optical thermometer 78−79475
heating in lower hybrid freq. range, temp., ion diffusion 80−83954
high current discharge from cold LaB_6 cathode 80−107011
high current plasma source, multirod cathode design 78−26308
high current short bremsstrahlung pulse sources 80−5400
high melting particle heating, melting and vaporisation in hot gas 80−6201
high temperature plasma, applic. of concept of vortex gas tunnel 77−84459
high-energy plasma technology, equipment, cold plasma prod. *(Russian)* 78−51367
hollow cathode discharge, H_2 prod. in H_2O vap. plasma 78−75441
hollow cathode discharge plasma, entry of Co, Ni, Ti, V, Cr, Fe and Mn 79−41891
hollow-cathode arc discharge, electron energy distrib. and ionisation velocity 78−67534
hollow-cathode multipole boundary ion source, IBIS, plasma prod. and containment system 78−74521
hot cathode, for plasma and electron physics in underground laboratory 79−35480
hot cathode reflex discharge in cusp and uniform mag. fields 78−67456
hot dense plasma generation for fast wave propag. 78−14186
hypervelocity and temperature amplification in exploding composite wires 79−41853
imploding plasma liners, MHD instability effects 80−75081
imploding spherical shells, acoustic amplification 79−10683
implosion, by pulsed electron beam accelerator, 4TW, laser and X-ray obs. 80−1816
inert gas electron beam excited plasma UV absorpt. by diatoms 79−68907
inert gas halides, excimer emission from electron beam produced plasma 80−43887
inert gas plasma, electron-beam produced, laser action of ionized and neutral atomic lines 80−106929
inert gas plasmas, prod. by U fission fragments in nucl. reactor props. 77−76147
inertial confinement, black body radiation implosion in ablator, driver, gas, pellet system 80−73990
insulator surface flashover in vacuum, electro-optical meas. 80−38823
intense electron beam, stable extraction from plasma, neutralisation method 77−24104
ion beam current from multidipole source, increase by injection of primary electrons 77−79489
ion beam-created high-press. plasma, electron props. diagnostics *(French)* 80−10407
ion beams impurity production by gas discharge source, cathode material testing 79−86592
ion source, electron backstream to source plasma region 80−96369
ion source, two-stage discharge type, operational characts. 80−47797

plasma production continued
ion-acoustic instability, electron flux driven, in Q-machine, probe diagnostics 80−33765
ion-acoustic instability stabilisation by ion beam in Q-machine, probe diagnostics 80−33766
Knudsen arc ignition, plasma form. kinetics, spectroscopic and probe obs. 80−38808
large area plasma source for ion extraction array 77−84465
large volume magnetic multipole plasma source, operating characts. 80−100084
large-volume plasmas, prod. and heating using plasma return current discharge 78−94920
laser-heated exploding wires, X-ray emission 79−10685
layer produced by moving ionis. source, EM wave propag. *(Russian)* 78−1836
layered shell explosive implosion into D-plasma region of compression 79−22455
long plasma column production, by efficient surface wave launcher 79−32836
low temp. plasma ionisation by fast electron beam, effective cross section calc. 79−14572
low-temperature plasma production by electron beam ionisation of gas mixture 80−87908
Mach wave parameters in cumulation cone 79−18034
magnetic accumulation in plane liner, flux loss and equiv. cct. 79−14571
magnetic field reversal induced by intense rotating electron beam in initially neutral gas 78−42768
magnetic mirror reflex discharge, device for generation, confinement and heating of hot plasma *(Rumanian)* 78−47151
magnetic multipole line-cusp plasma generator for neutral beam injectors 79−19056
magnetically confined plasma, creation inside imploding liners using relativistic electron beams 79−60175
magnetron ion source, influence of gas press. on charge comp. of emitted ion beam 79−37516
MFTF, start up neutral beam power supply system 80−91281
microwave discharge, supersonic flow in waveguide, electron densities, possible laser 80−38842
microwave discharge technique, plasma prod. for ion source 78−327
microwave excitation structures, surface wave, plasma production and appl. 79−19059
microwave field power transfer efficiency under electron cyclotron reson. condition 78−9789
microwave flowing plasma source, power absorpt. characts. 77−84464
microwave induced steady-state overdense plasma production, near coaxial discharge dipole reson. 79−55523
microwave O^{+} plasma, magnetoactive, for oxidation of Si 80−38831
microwave plasma production at atm. press., surface wave propag. method 80−10408
microwave plasma source, helical slow-down structs., electron density 78−18424
microwave surface wave plasma at atmospheric press., production and appls. 79−50868
mirror-confined plasma, large-radius, high-beta 80−87907
modified magnetron discharge facility 78−75380
molecular beam production, by pulsed plasma injector, diagnostic obs. 77−65548
motional impedance and heating of low resistive plasmas 80−14913
multidipole device, primary electron effective MFP meas. 77−24183
multifilament plasma source, multipole mag. field effects on characts. 79−46462
multimode ion source characts., plasma density and ion loss investigation 78−55080
multiple-wire implosion in transmission line generators, hot plasma efficient prod. 80−48929
with multiply ionised species 78−75388
negative partial-discharge inception voltage in compressed SF_6 *(German)* 79−94829
neutron generation by implosion of D_2 gas target 78−54869
non-Debye plasma generation by impulse compression 78−71505
non-Debye plasma generation methods and props. 78−75387
nonideal plasma, measured props. and nonideality influence 80−43869
nonideal plasma generation, by electrolyte impulse diaphragmic discharge 78−71506
nuclear generated plasmas, ^{3}He and $^{235}UF_6$ excitation, spectra obs. 80−83997
nuclear induced plasmas and nuclear pumped lasers, conf., Orsay, France (May 1978) 80−62393
optical measurements on plasma initiated by a relativistic electron beam *(Japanese)* 80−48914
partially ionised gas flow over body, plasma form. at surface 78−75378
particle-beam-induced fusion, inertial confinement 77−42184
pellet fusion by relativistic pinched electron beams, beam propag. expt. 77−68163
pellet fusion targets, fast protons energy deposition 78−58404
pellet heated by multi-GeV heavy ions, filamentation instability 78−89976
Penning discharge plasma source, form. mechanism 78−18423
periplasmatron ion source for intense neutral beam 80−99380
pinched electron beam prod. expanding gas bubbles, fast photography obs. 80−79564
plasma chemistry, history, diagnostics, production, organic cmpd. synthesis 80−61099
plasma compression for microfusion, bilinear systems, thermodynamic optimisation 79−67939
plasma focus, recent developments to increase neutron yield 79−14567
plasma stream, magnetized, simulation of plasma flow over object 79−10679
plasmadynamic continuum sources 79−27803
plasmotron, DC, high-power, long-operating, coaxial elec. arc, principles 78−42832
polyethylene fibre explosion, neutron and energetic ion emission 78−5927
prepulse discharges in high current accelerator diodes with double shaping line 80−5399
propane flame plasma, Langmuir probe teaching expt. 78−12456
pulsed erosion jet, energy characts., heat flow distribution *(Russian)* 80−33825
pulsed plasma generation by surface wave 78−75385
pulsed plasma source temperature calibration spectropyrometer 77−7590
plasma production continued
Q-machine, single ended, collisionless, steady-state parameters and Buneman instability 80−59227
Q-machine plasma, coherent wave particle interaction 80−59226
quiescent plasma, prod. by RF discharge 77−7568
quiet plasma, in mag. field, produced by transverse diffusion from RF discharge 78−79448
radiation temperature of proton beam induced plasma 80−100094
Rayleigh-Taylor instability in imploding foil plasma, two dimens. simulation 78−47156
reflex discharge, plasma quiescence 80−64806
reflex tetrode, ion beam extraction anal. 80−48903
relativistic electron beam, anomalous interaction with solid target 80−28709
relativistic electron beam, energy deposition in plane solid low Z target 78−5894
relativistic electron beam, enhanced deposition, mag. and elec. fields effects calcs. 77−31491
relativistic electron beam, focusing and energy transfer on to target 77−42186
relativistic electron beam discharges, thin targets, spatially resolved VUV emission 77−89323
relativistic electron beam target design, jacket material and design, Monte Carlo method 78−17416
relativistic electron beam-solid target interaction, fusion induction 77−42187
relativistic monoenergetic electron beam in atmosphere, plasma formation and collective interaction *(Russian)* 79−77407
reversed field mirror reactors, startup using coaxial plasma guns, scaling laws 80−99279
RF device description 77−80321
RF plasma etching, ion energy *(French)* 79−46495
RF preionisation in Tokamak Thor, plasma ignition conditions and density profiles 78−71538
RF produced mag. confined nonneutral electron plasma 79−10677
RF sources, effect of an axial magnetic field on an improved constricted source 79−1325
rotating, steady fully ionised plasma in crossed fields 78−79445
rotationally stabilized liquid liner implosion for fusion plasma production 77−23274
S microwave radiation induced prod. and heating, electron temp. and density *(Spanish)* 79−98926
sheath driven targets, simulation 80−48898
shock tube plasma source for high-temperature MHD generator 77−35372
shock wave induced fusion, multiple refraction problems in layered medium 80−5330
shock wave produced plasma, electron and ion thermal diffusion effects 80−48891
single slit plasma source, consumption of fuel for singly charged ions 78−67379
solid breakdown, pulsed, plasma form. blow off, shock waves 77−27688
solid density plasma production by plasma focus discharge 78−87465
solving transient process in electrical explosion of conductor in restricted volume of liquid *(Russian)* 80−100088
source characteristics for chem. reactors *(French)* 78−11605
spark, vac., high-press. local plasma regions production, X-ray and hologram diagnostics 79−19104
spark plasma ion source effects on mass spectroscopic quantitative anal. 79−14631
spatial emission profiles from inductively coupled plasma, matrix effects 80−75036
spectra from plasmas induced by ^{3}He or $^{235}UF_6$ reactions 80−64784
spherical implosion, compression and self similar motion of coalesced shocks 78−9815
spherical implosions, instability growth and saturation simulation 77−79480
stationary magnetoplasmadynamic source, elec. and thermal characteristics 80−14915
steady-state rotating plasma, for mass separation of elements *(Russian)* 78−25732
strong ion ring, production in long pulse ion accelerator, effect of mirror rise time 77−24113
supersonic colliding plasma jets, hot dense plasma formation, hydrodynamic model *(Russian)* 80−38676
supersonic jets of magnetoplasmadynamic source plasma, gasdynamic struct. of initial section 77−35332
surface plasma source, H^{-} ion form. and secondary electrons *(Russian)* 78−71503
surfatron low-pressure RF plasma source 78−67548
surfatron produced electron density and temp. microwave meas. 80−43965
targets for laser and electron beam fusion, design space 79−18037
thermal plasma engineering in metallurgy, inorganic materials technology 78−3070
thermionic diodes, planar low press. gas discharges, plasma regime, plasma characts. 79−77435
thermionic diodes, planar low press. gas discharges, space charge regime, volt-ampere characts. 79−77434
thermonuclear combustion in plasma with electron thermal cond. *(Russian)* 78−13319
thermonuclear fusion plasmas, elem. processses and role of atomic, ionic and mol. data 80−14916
thermonuclear neutron pulse, electron beam generated, scintillator-photomultiplier response 78−51357
thermonuclear target, electron beam heating and compression 77−42185
theta-pinch, pulsed, ignition in single turn solenoid 79−55538
Tokamak discharge, initial stage, theory *(Russian)* 78−38512
Tokamak fusion reactor, TFTR, plasma generation and confinement 80−42864
Tokamak plasma, light-impurity-free plasma, Au-shell surface and Ti gettered burial chamber 78−42786
Tokamak plasma startup system, for fusion reactor 78−62612
Tokamak power reactors, initiation pulse prod. methods in ohmic heating circuits 78−55730
Tokapole II, poloidal divertor, plasma production and confinement studies 80−18602
toroidal pinch experiments, using perforated shell-type coil 79−86598
TP-D plasma source, production of low-energy high-current ion beam 77−57424
Triplemafios multicharged heavy ion source *(French)* 78−9800

plasma production continued
TRISOPS IV machine, high temp. high press. plasma prod. by vortex ring compression 78−71504
turbulent plasma, impinged charged particle, linear response theory 80−64727
two-stage-discharge ion source 79−90423
vacuum breakdown in elec. field in range (5-7)×10^6 V/cm 80−87973
weakly ionised plasma electron electrodynamics charact., pulsed ionisation source *(Russian)* 79−7444
wire explosion plasma production, diagnostics by Bartels method 79−10686
X-ray coded imaging of relativistic electron beam targets 78−47179
Z-pinch, gas puff device, X-ray spectra, plasma form. 79−94816
Z-pinch, plasma production, streak, X-ray and vis. photographic obs. 78−38522
Al foil in quartz dust, electrical explosion for accelerator application 80−6314
Al target, relativistic electron beam impact, vac. UV emission 77−47263
Ar cold plasma generator, optical emission spectra and elec. parameters *(Ukrainian)* 78−67374
Ar, electric arc with liq. K cathode, parameters, cathode sheath model 77−4003
Ar emission source for gas chromatography 79−74438
Ar, fission fragment energy deposition kinetics rel. to nucl. pumped laser 77−23652
Ar plasma, RF prod., mag. field effect on props. *(Korean)* 79−50869
Ar plasma, RF surface wave form., metastable atom density meas. 77−58890
Ar plasma, shock-compressed, thermophysical and gasdynamic charact. 77−43016
Ar, plasma, shock-compressed optical props. 79−23426
Ar-Kr(Xe)(N_2), electron beam ionis., low temp. plasma prod. 80−87908
Ar-liquid K cathode arc, dense plasma prod., cathode erosion rate estimation *(French)* 80−44056
Ar-N_2 mixture, fission fragment energy deposition kinetics, rel. to nucl. pumped laser 77−23652
Ar-Xe plasma, shock wave dynamic compression, thermodynamic props. *(Russian)* 80−53931
Au, thin foil, enhanced electron energy deposition heated, soft X-ray vacuum UV spectra 80−80901
Cr from Tokamak-produced plasma, $2s^22p^k$-$2s2p^{k+1}$ transitions in F I to Be I isoelectronic sequences 80−37765
Cs arc, low-voltage hot-cathode, plasma production and props., review 77−27766
Cs discharge, high-press., pulsed, in capillary energy balance diagnostics 77−65920
Cs hollow-cathode plasma jet source 77−84463
Cs plasma, generation by adiabatic compression, elec. cond. and thermodynamic parameters meas. 80−59180
Cs plasma in vacuum diode, pre-discharge, electron impact excitation line emission polarisation 78−47170
Cs plasma source for ARAKS expt. 79−21142
Cs, prod. by resonant light irrad., density profile 77−7563
D-Ar mixture, effect of Ar admixture on plasma temp. 79−37446
D-fusion, shock wave induced, Ar admixture optimisation 80−5329
D-T compression, explosion-induced, thermonuclear avalanche reaction 78−47144
D-T explosion induced compression, neutron yield 79−67940
D-T explosion induced compression, neutron yield, thermal conduction effects 79−67941
D-T plasma, thermonuclear reaction product kinetics effect on parameters 80−5327
DT plasma in biconical system, neutron generation by shell implosion 79−37524
Fe from Tokamak-produced plasma, $2s^22p^k$-$2s2p^{k+1}$ transitions in F I to Be I isoelectronic sequences 80−37765
H plasma, dense, produced by conic electrode source, mag. field effect on flow 77−58873
H^-, production by Hall accelerator in Cs vapour, space-charge effects 78−67375
H_2, breakdown condition in JFT-2 Tokamak 79−14569
H_2 pellet-plasma interaction, neutral gas shielding model 79−23428
H_2, solid pellet ablation in plasma 80−19589
$H_2(D_2)$-Ne-He(Ar) plasma, combustion driven shock tube, H_β central struct., ion mass effect 78−26327
He, afterglow produced by microwave surfaguide, spectroscopic diagnostic, electron and He_2 rot. temp. 80−44042
He, microwave discharge as source of atmospheric pressure plasma 77−35416
He, plasma, non-equilib., of strong current pulse discharge, diagnostics *(Russian)* 78−75271
He plasmas, produced by pulsed electron cyclotron reson. discharge in poloidal heliotron type mag. field 77−76127
He, ultradense reproducible Z-pinch, for laser-pellet interaction simulation, characterisation 78−30463
He-H_2 strongly supercooled quasistationary plasma prod. by intense electron beam in dense gas *(Russian)* 77−89277
He-Hg plasma, prod. by nucl. radiation, charge exchange effects 77−24103
He-N_2 mixture, plasma created by electron beam, spectral composition *(Russian)* 78−30453
He-Ne mixture, electron beam prod. plasma decay, appl. to laser pumping 79−41847
^{3}He plasma, prod. by products of ^{3}He(n,p)^{3}H in nucl. reactor, props. 77−76146
Hg plasma formation by strong Hg line irrad., mechanism 78−83585
K_2O-Al_2O_3-$2SiO_2$-BaO plasma emitter 80−96368
LaB_6 hollow cathode for dense plasma production 78−55729
Li plasma, elec. cond. at 12.5-50 MPa, (7-50)×10^3K 80−64685
Li wire high energy density exploding plasma, holographic interferometry, self pinching, charge density 79−77436
N_2, electron beam produced, plasma, energy distribution of electrons 77−3959
N_2 glow discharge, variable current penetration mechanism 79−55584
N_2, plasma created by electron beam, spectral composition *(Russian)* 78−30453
Ne plasma, generated by 200 MeV protons, electron density and electron temp. 78−22568
Ne-N_2, energy transfer, H^+ ion beam produced plasma, ion density and temp. 80−38539

plasma production continued
Ne-N_2 mixture, plasma created by electron beam, spectral composition *(Russian)* 78−30453
Ni from Tokamak-produced plasma, $2s^22p^k$-$2s2p^{k+1}$ transitions in F I to Be I isoelectronic sequences 80−37765
O_2, electron beam energy branching, discrete energy loss method 80−48905
Pb, mass ejection from shocked surface during fusion 78−47186
SF_6 gas, low press., excitation of nonlinear wave by repeated pulsed electron beam 80−87878
Ta foil, plasma production by pinched relativistic electron beam impact 79−77403
U plasma, present research status with appl. to gaseous core reactors 78−33244
U-He plasma, radiation-induced, electron energy distrib. 77−24054
Xe plasma, shock-compressed, thermophysical and gasdynamic charact. 77−43016

plasma production and heating by laser beam
500 keV fast ion acceleration mechanism 78−75391
ablating fluid, model of Rayleigh-Taylor stability 78−34303
ablation front structure, numerical hydrodynamic-heat flow simulation 79−64883
ablation waves, mag. field generation in inhomogeneous plasma 77−11344
ablative acceleration model for moderate laser intensities 80−92351
ablative acceleration of laser-irradiated thin-foil targets 79−71952
ablative implosion, hydrodynamic stability 78−5900
ablative laser fusion implosion, scaling laws and spatial struct. 80−87915
ablative mode compression experiments of spherical targets by glass laser GEKKO IV *(Japanese)* 80−100086
absorption, z-depend., stimulated backscatter processes 80−43944
absorption and ionisation in laser-prod. plasma, wavelength effect 77−27654
absorption and reflection processes of laser irrad. pellets 78−30457
absorption in laser-produced plasma expts. 80−14931
absorption of laser radn., heating appl. 77−27679
absorption processes, parametric instabilities 79−46464
acceleration of thin foil targets under intense laser irradiation 80−92356
advanced lasers for fusion, review 79−18435
aerosol, plasma production by CO_2 laser beam, brightening channel 80−6272
aerosol induced breakdown in air, two-dimensional modelling 79−90368
air, laser-evaporated microplasma radial glow and temp. distrib. 78−67387
air, laser-induced breakdown over long distances 80−33795
air, optical breakdown, initation by absorbing water droplets 80−10352
air, optical breakdown near metal target by laser beam 80−6209
air, optical breakdown threshold reduction near dielectric surface 77−51211
air, optical detonation threshold, press. depend. rel. to Ar 79−23438
air, optical discharge maintenance by giant laser pulse with extended tail 79−23478
air, plasma, slow burning gasdynamics, due to Nd laser beam *(Russian)* 80−108715
air, supersonic radiation waves, excitation by CO_2 laser 79−90433
air-at Ti surface, optical breakdown, interferometric investigation 80−100064
air breakdown by CO_2 laser radiation near solid target *(Russian)* 77−84472
air breakdown initiated by particle in laser beam 77−58875
air breakdown initiated on aerosol, IR laser pulse *(French)* 79−73021
air breakdown near solid surface, thermal stress cracking effects reducing threshold 79−69924
air breakdown plasma, effect on absorpt. coeff. of metal target irradiated by CO_2 laser 79−52052
air breakdown plasma relax. near target, microwave method 79−86616
air exploded by focused laser, emission processes affecting development of explosion 79−7417
air near solid dielectric surface, reduction of laser breakdown threshold 79−77446
air plasma, CO_2 laser interaction with plane target *(French)* 78−9806
air plasma, laser-produced, decay time *(Russian)* 79−98941
air plasma, TEA CO_2 laser-produced, using solid targets, induced shock waves 80−64729
air-plasma interaction and surface shielding, evaporation wave and gasdynamic effects *(Russian)* 78−22532
Alfven wave, compressional, in laser heating of plasmas, filamentation instability 77−35342
alkali halide surface light emission, 10.6 μm laser pulse irradiation *(Russian)* 78−27352
alkali hydride arc, laser initiated, H^- production 80−32550
amplifier module radiation heating at DELFIN 80−92359
angle and polarisation dependent intense light absorption, theoretical interpretation 78−59638
anomalous absorption, interaction of laser with laser produced plasma 77−19734
anomalous absorption by focusing TEA CO_2 laser light on solid targets, higher harmonics generation *(Japanese)* 77−43012
anomalous energy flux and deposition in laser prod. plasma 77−3965
anomalous heating by strong EM field, parametric instability 77−11377
anomalous heating of laser prod. plasma 77−27689
anomalous intense laser radiation transmission through overdense plasma 79−10671
anomalous laser radiation absorption near plasma critical density, acoustic instability 79−19063
ANTARES and advanced CO_2 laser-fusion systems 80−32502
asymmetric electron density profile, interferometric meas., laser-created plasma 80−75085
attenuation of 10.6 μm retropulse in fusion system, by elec. initiated laser-driven plasma 77−34424
Au foil, 8 ns laser pulse-target interactions, ion-expansion struct. 79−14575
axial heating with CO_2 lasers 77−43001
backscatter from laser plasma, optical ray retracing effects 78−91133
backscattered light and harmonic generation in CO_2 laser-target interaction expt., spectral anal. 78−59676
backscattered light pulse shape depend. 80−10431
backscattered radiation, spectral-time meas. *(Russian)* 78−42812
Balmer series transitions for laser plasma diagnostics 80−64780
beat heating, system, using double-barrelled laser 78−67386

plasma production and heating by laser beam continued
beat heating in plasmas using CO_2 lasers 80−43950
book, principles of laser plasmas, for graduate students and researchers 77−50647
breakdown phenomena 78−75390
breakdown plasma form. dynamics in gaseous media, IR optics element surface breakdown 79−45986
breakdown processes, effects of spherical aberration and multiphoton absorpt. 77−84473
Brillouin backscatter depend. on pulse amplitudes, timing, target and geometry 79−77417
caviton dynamics at crit. density 80−106909
cavitons in laser irradiated fusion plasmas, EM wave propag., supersonic density humps 80−24178
cellulose nitrate film ion data, dark-field illum. image recording photographic method 80−70031
charge particle potential scattering, in presence of mag. and laser field 79−81248
charge separation and target voltages in laser-produced plasmas 78−5896
charged particle diagnostics, high-energy, rel. to nucl. fusion products 77−24190
charged particle potential scattering in laser field, eikonal theory 79−81249
clean fusion concepts, survey 77−83082
collective behaviour, in laser plasma expts. 77−43005
collisional absorption of two beams, inverse bremsstrahlung, heating 78−26292
collisional plasma, mixed mode operation, cross-focusing 80−83945
collisionless plasma expansion and fast ion generation at plasma-vacuum boundary 80−59257
column development and heating, by intense CO_2 laser radiation *(French)* 78−47142
compressed laser fusion targets, time resolved X-ray pinhole photography 78−38548
compression, laser-induced, expt. and theoretical obs. 77−43003
compression of hollow microspheres *(Russian)* 77−11379
compression of superdense eqn. of state and boundary press. profile, simulation 78−83589
compression pulses for spherical laser targets 78−5904
compressional density profiles, flow effects in laser irrad. plasmas 78−18429
compressive plasma fusion in D-T macrosamples by CO_2 laser 78−82507
concentric hyperdetonation shock wave 79−7464
conference, inertial confinement fusion, San Diego, USA, (Feb. 1978) 78−46171
conference on fusion reactor materials [Miami Beach, Florida, Jan. 1979] 80−31407
confined plasma column, soft X-ray lasing action conditions 80−74346
confinement of LiH plasmas, decay, density measurement 79−46470
continuous optical discharge, diagnostics 80−43947
continuous optical discharge convective flow, thermogasdynamic instability 78−75397
continuous X-ray radiation, picosecond ruby laser heating *(Russian)* 80−75079
continuum source, laser-produced plasma, for absorpt. spectroscopy in VUV and XUV 80−75094
controlled nuclear fusion development, confinement and laser ignition 79−31176
convective parametric decay instability in a laser plasma 80−64722
conversion between cold plasma modes in inhomogeneous plasma possible plasma heating 79−77397
corona, laser induced microsphere, electron density profile, interaction and transport profile 80−107008
corona, laser-induced plasma, interferometric meas. *(Russian)* 78−1886
corona development, X-ray streak camera obs. 77−15245
corona parameters, ultrahigh speed diagnosis *(Russian)* 78−1899
crater formation and reson. absorpt. of focused laser light 79−23436
critical parameters corresponding to thermonuclear physical threshold 78−83593
critical surface filamentation and parametric instability 78−47140
CTR hydrodynamics calcs. 77−79477
current source duration in laser-produced plasmas 78−1862
current-carrying channels, laser prod., for guidance of elec. discharge 78−71568
curvature effects in laser plasma interactions 80−43948
curvature radiation, from laser heated dense plasma, spectrum 79−41834
CW laser beam stablisation by spatially dependent absorption 79−76740
cyclotron resonant gas breakdown with 1.22-mm $^{13}CH_3F$ laser 79−55549
D_2 target fabrication for laser fusion *(Japanese)* 78−8971
Debye screening modifications in ponderomotive effects 80−33777
decay instability of laser radiation in a magnetoplasma 80−1781
deflagration in laser plasma 79−19064
deflagration wave, in laser compression 79−23419
deflagration waves supported by thermal radiation 80−64757
dense expanding plasma, laser radiation absorpt. 79−90417
dense laser plasma, deceleration and scatt. of epithermal electrons 77−84471
dense matter, laser driven fusion, laboratory expts. 80−75077
dense plasma, laser scatt. 78−67408
dense plasma column, high-power irrad., electron temp. increase 79−86597
dense plasma XUV transition Doppler broadening suppression, collisional-radiative model 80−19614
density decay meas., freq. stabilized microwave interferometer 77−84524
density measurement of laser-compressed plasma, X-ray line shift *(German)* 80−48967
density modification in 10^6 W cm^{-2} ablated microballoons, optical diagnostic technique 78−14206
density profile deformation and efficiency of resonance absorpt. in nonuniform plasma *(Russian)* 79−4148
density profile meas. using Wollaston prism interferometer 80−48973
density profile modification by light pressure in spherical geometry 78−59636
density profile modification by ponderomotive force 78−59634
density profile modifications at critical density 78−59550
density profile self-steepening in laser plasma, interferometry 78−5938
detonation waves, laser supported, initiation 78−63568
deuteron source, laser-plasma 80−78475
diagnosis of expanding plasma using charge collectors 77−19771
plasma production and heating by laser beam continued
diagnosis of laser-produced plasma using stigmatic grazing-incidence spectrograph 79−73041
diagnostics, X-ray line shift of seeded Ne 80−64778
diagnostics by high speed multiframe interferometry 78−1905
diagnostics by induced Compton scatt. 78−59673
diagnostics for laser fusion programme, plasma physics on micron and picosecond scale 79−23452
diagnostics of laser plasma, 1/4 crit. density region, harmonic generation expts. *(Russian)* 77−7578
diagnostics of laser prod. plasma 77−76204
diagnostics of plasma produced in static electric field 77−58879
diagnostics of pulsed HF laser produced plasma 78−55733
diagnostics via Faraday cups, evaluation 78−5941
diagnostics with EUV and X-ray high resolution spectra 77−84522
dielectric, multiframe ps holography 78−26328
dielectric medium, optically transparent, avalanche ionis., recomb. effect 80−7295
dielectric surface, photoinduced surface discharge 80−88929
direct conversion of CO_2 laser energy to HV electrical energy using laser-produced plasma 78−18427
double layer spherical targets, implosion process under laser irradiation 80−92354
double-diffusion hot-electron transport in self-consistent E and B fields 79−23437
dual beam module for nuclear fusion expts. 77−19336
dynamic response to laser modulations, in CW laser prod. Cs plasma 80−14920
effective cross section and space charge, preionised gas laser induced breakdown 80−48930
ejection from thin capillaries, expt. 78−75395
electric field of laser prod. plasma in air *(Russian)* 79−37555
electric field pattern calcs. in laser produced plasma *(German)* 80−54014
electrodynamic mechanisms of limitation of the electron concentration in a laser spark *(Russian)* 80−59333
electron and at. excited states densities in laser prod. He plasma 80−38710
electron density, Stark-broadened line wings of H-like ions 78−79462
electron density and temp., spectroscopic diagnostics, book contrib. 77−51242
electron density determ. from X-ray spectra of multiply charged K ions 78−94938
electron density diagnostics by multicharged ion K-spectra obs., review 79−64908
electron distrib. function and quasi-static EM fields, transport coeffs. 77−55160
electron distribs., resonantly heated, props. 78−30462
electron emission, 1 MeV, from CO_2 laser heated plasma 79−90468
electron emission temperature, streaming plasma in laser vac. diode 78−91162
electron energy profile steepening, polarimetry obs. 78−34349
electron energy transport into layered targets irradiated by CO_2-laser light 80−69979
electron flux limitation due to ion-acoustic instability 77−39419
electron gas, nonequilib. heating, hot electron spectra 79−55529
electron temp. determ. by Langmuir probes remote from target 78−75427
electron thermal conduction, kinetic description 77−24060
electron transport, high energy, numerical modelling *(Japanese)* 80−96346
electron-density structures in laser-produced plamas at high irradiances 79−82041
electron-energy transport in laser-produced plasmas 80−6266
electron-ion temperature difference in short plasma column 77−72463
electronic instrumentation for laser fusion reactor research 78−78498
electrostatic droplet source suitable for laser targets 77−34074
electrostatic fields, generated by intense 1.06 μm laser 79−46465
electrostrictive forces, hydrodynamic code calc. 77−65896
elliptical Gaussian beam, propagation and focusing anal. 79−50873
EM resonant properties of laser-prod. plasmas 80−43928
EM-implosion generation of pulsed high energy density plasma 78−94927
emission of multiply charged ions from plasma produced by CO_2 laser 80−9445
emission spectra, satellite lines of He-like ions in laser prod. plasma 79−86618
emission spectrum, resonant line satellites, abnormal intensity *(Russian)* 77−3995
emitted current distrib. rel. to irrad. distrib. 77−15217
energy absorption, in laser produced plasma, IR and plasma calorimetric meas. 79−90456
energy absorption, meas. via differential calorimeter 78−5942
energy absorption and mag. compression of plasma in fast solenoid 79−46463
energy absorption model, wave amplitudes and particle distribs. 77−47235
energy distribution of electrons heated by laser light absorpt., simulation and test particle methods 80−48963
energy transfer in laser (or particle) beam produced plasmas 80−38680
energy transport, in laser produced plasma, X-ray obs. 78−75269
enhanced Brillouin scattering, Gaussian laser beam in hot collisionless plasma 79−94799
enhanced laser-plasma backscatt, due to prepulse radiation 78−18428
erosion plasma burst, effect of dynamic stresses 80−79532
evolution model, theory and expt. 79−94808
expanding laser produced plasma, three body recomb. 77−3962
expanding laser-produced plasma, radiative transfer line intensities and stimulated emission 77−3988
expansion, ion energy distrib., charge transfer effects 80−106953
expansion and rethermalisation in uniform mag. field 78−30458
expansion into mag. field, oscill. modes 77−51178
expansion of laser plasma in stellarator fields 77−76177
expansion stages, scatter of branches, ultimate ionisation *(Russian)* 78−22531
exploding pusher target, computer simulation *(Japanese)* 80−96376
exploding-pusher-tamper areal density, neutron activation meas. 80−91237
explosive magnetic field generation due to EM incident radiation, laser plasma mechanism 80−6253

plasma production and heating by laser beam continued
explosive-pusher-type laser compression experiments with neon-filled microballoons 80−23132
extended plasma source for short wavelength amplifiers, open channel technique 78−79447
far IR lasers appl. and detection systems in controlled fusion research 78−47182
fast electron energy spectra and preheating of laser irrad. target 79−55528
fast electron prod., microwave expt. simulating laser-plasma interaction 77−58850
fast electron production, continuum X-ray emission diagnostics 78−22563
fast electron production in plasma jet, suppression in laser-plasma *(Russian)* 79−14583
fast electrons, resistive inhibition from laser prod. plasma in low density Au target 80−87916
fast electrons, X-rays and ions, motion evaluation 80−19557
fast expansion, fast ion ambipolar accel. 78−47141
fast ion, ion emission from laser generated plasma, Child's law 79−60163
fast ion emission, reson. absorpt., laser generated plasma 78−42779
fast ion emission *(Russian)* 79−55532
fast ion energy spectra from laser prod. plasma 79−73033
fast ion generation in laser-target interactions, model 77−3964
fast ion obs. in laser plasma *(Russian)* 77−58878
fast ion production, simple model anal. 78−22530
fast ion production by laser light press. 77−7574
fast ion stream production, protuberant shock wave form. in atm. 77−27674
fast ions from laser-produced plasmas, pinhole imaging 77−80347
fast ions in laser-produced plasma, nonlinear plasma-wave interaction 80−24183
fast-ion emission from CO_2-laser pulse-produced plasma 79−68939
fast-ion emission from laser-produced plasma, suppression 77−1002
feedback controlled particle suspension system for laser initiated target expt. mag. mirror fusion facility 78−1864
feedback laser fusion using direct nucl. pumped laser 78−58445
filament ellipticity, energy lifetime in T-8 apparatus *(Russian)* 80−87930
filamentation instability of laser beam in inhomogeneous plasma, preferential heating 80−19568
fine-scale structures, due to CO_2 laser stimulation 79−19062
flat target, X-ray bremsstrahlung prod., intensity and polarisation anisotropy 77−89320
flowing-gas laser plasmotron, expt. and theory 79−27843
focus, heating by TEA CO_2 laser, neutron enhancement *(Japanese)* 78−9808
focus, high density, as laser pulse clipper and optical isolator 77−65601
focus dynamics with powerful laser interaction during MHD stage, diagnostics 80−48924
focus heating by TEA CO_2 laser and anomalous absorpt. obs. *(Japanese)* 77−43013
focus plasma, CO_2 laser irradiated, neutron yield enhancement 77−62386
focusing of laser, max. absorpt. on spherical target 77−3967
foil irradiated at 1.06 and 0.53 μm, ablation rate and heat penetration 79−90432
formation dynamics of underexpanded supersonic erosive laser plasma flare, high speed techniques 80−48923
four-channel laser system with four-ellipsoidal-mirror set-up for focusing laser beams 79−94276
framed particles, automatic selection of polymer shells for laser targets 77−80336
free convection in photoabsorption in liqs., gases and plasmas 77−11191
fusion, CO_2 single beam irrad., diagnostics 78−51329
fusion, developments for future energy involving lasers 80−23120
fusion, glass microballoon selection, wall thickness and uniformity meas. 78−87469
fusion, laser initiated, X-ray diagnostics appls., review 77−55176
fusion, non-classical aspects, Zhabotinsky effect and communications theory 77−38404
fusion, progress at Lawrence Livermore Lab., USA 80−57945
fusion, truncated Maxwellian electron vel. distrib., ion expsn. 78−51326
fusion, wavelength scaling 78−51328
fusion and fusion-fission reactors, high-density linear confinement systems 77−74983
fusion application 77−6563
fusion by laser, Nova scientific feasibility experiment 79−49863
fusion by laser, present state of research *(French)* 78−29645
fusion by laser 78−59635
fusion comparative review of high-power lasers 77−7062
fusion control, future prospects in electrotechnology *(French)* 78−37446
fusion diagnostics with axisymmetric grazing incidence X-ray microscope 78−75422
fusion energy generation, plasma confinement, laser compression, Li activation *(German)* 80−52783
fusion experiment alignment accuracy meas. 78−55731
fusion expts. at Osaka, pellet compression 78−50300
fusion HYLIFE reactor chamber response to fusion microexplosion 79−89499
fusion ignition, laser-driven isentropic hollow-shell implosion 79−31183
fusion implosion, laser-driven stable implosion scheme 79−4161
fusion implosion and target interaction physics 77−88276
fusion ion temp. meas., neutron time of flight techniques 78−17413
fusion microballoon wall-thickness meas. 77−50289
fusion pellet implosion dynamics, high compression, hinged ramp pulse 78−41859
fusion plasma, computer simulation of Weibel-like instability effects 79−14581
fusion plasma, HF EM wave swelling effect near crit. density 77−84443
fusion plasma, non-stochastic heating by electrostatic waves 78−47136
fusion plasma, penetration length of alpha particles 77−15214
fusion plasma, synchronised diagnostic laser pulse system 78−51365
fusion plasma confinement, α-emission recoil force effect 80−6275
fusion plasma diagnostics, picosec. holographic interferometry 79−46492
fusion plasma production by CO_2 laser *(Japanese)* 79−14586
fusion plasma simulation, hydrodynamical behaviour *(Chinese)* 80−1823
fusion processes, Lagrangian vs. Eulerian framework 77−50284
fusion reaction, laser-induced *(German)* 77−65328
fusion reactor, design of 20 tesla pulsed solenoid 77−23270
plasma production and heating by laser beam continued
fusion reactor, laser plasma simulation code, PHD-IV 78−59640
fusion reactor, tubular, controlled fusion *(Italian)* 77−26868
fusion reactor advanced H-^{11}B fuel, reaction feasibility 77−83084
fusion reactor advanced H-^{11}B fuel, reaction feasibility 77−83085
fusion reactor appl. 77−26867
fusion reactor program, LLL, X-ray diagnostic instrumentation 77−76213
fusion studies, microshell implosion, α-particle and proton meas. 77−10486
fusion target, energy transport 78−47143
fusion target, fast ions 78−51327
fusion target, laser-irrad., mag. field transport, nonlocal conduct. effects, simulation 78−59637
fusion target, loading and kinematic positioning 78−58487
fusion target illumination reduction, enhanced stimulated Raman plasmon scatt. 77−84470
fusion target implosion, laser compression efficiency, wavelength depend. calcs. 77−35369
fusion target insertion system 78−46172
fusion target interactions at 10.6 μm 77−88274
fusion target support fibre, heated by return current 79−45416
fusion target uniformity, interferometric meas. 78−47158
fusion targets, H isotopes condensation 77−42190
fusion targets, six-beam irrad. and implosion, laser focus depend. 80−14919
fusion targets, space time implosion charact., X-ray obs. 77−27725
fusion targets, spatially resolved α-emission 77−68811
fusion technology 78−754
fusion with 1000 times compression, and kiloJoule laser energy *(German)* 78−41858
gas, high pressure, near solid target, laser plasma evolution 80−96375
gas, optical breakdown in intense annular beam from CO_2 laser, flow-concentration effects 79−64886
gas breakdown, laser radiation induced, book contrib. 77−51256
gas breakdown, multiply-charged plasma, temp. kinetics and population levels *(Russian)* 80−106952
gas breakdown model *(German)* 78−87472
gas breakdown model 80−1821
gas breakdown near metal target, CO_2 laser pulse focus effect 79−52051
gas breakdown near solid targets, by pulsed CO_2 laser radiation *(Russian)* 78−26362
gas filled microballoon targets, laser produced implosion dynamics 80−24198
gas target IR irrad., hydrodynamic expansion simulation 79−55524
gasdynamic pressure on target in CO_2 laser radiation 78−1867
gaseous target fast electron resonant accel. mechanism 77−19737
Gekko IV, four beam phosphate glass laser system for fusion expts. 78−46650
German laser fusion programme, results for Asterix III and Nd-lasers 78−63136
glass, ZhS-12 type, optical discharge, dynamics and props. 79−61471
glass laser high power system for thermonuclear fusion *(Japanese)* 78−8970
glass laser targets, microspherical, processing method in floating state 77−80337
glass microballoon, laser irradiated, time resolved spectroscopy of second harmonic emission 79−23457
glass microballoon imploded by laser, X-ray transmission analysis *(French)* 80−54011
glass microballoon target, D_2-filled, laser-driven shock wave 78−41856
glass microballoons, laser driven compression, calc. results *(Chinese)* 79−63807
glass microballoons, laser imploded dynamics, X-ray streak camera study 79−68937
glass microbubbles, Ne gas permeabilities distrib. 77−35367
glass microshell, high-power glass laser interaction 78−9804
glass microsphere heating, $3/2\omega_0$ harmonic generation by Nd laser radiation *(Russian)* 77−43014
glass microspheres, separation by diameters and wall thicknesses to obtain correct. laser-target shells 78−8969
glass shell target, electron temp. and density, Si X-ray emission diagnostics *(Chinese)* 80−38718
glass target, spherical-shell, energy absorpt., expt. determ. 80−54016
glass targets, laser-produced plasma X-ray spectral lines identification *(Chinese)* 80−54036
glass-CO_2-hybrid laser system for plasma prod. and heating in mag. traps 80−24196
graphite vapour cloud, laser-prod., temp. conditions investig. 80−59290
grazing incidence X-ray microscopy, of laser fusion targets 78−47178
Group IV photolytic laser expts., for fusion research 78−63101
Group VIA photolytic laser systems, for fusion research 78−59002
halide vapour, discharge, potential fusion laser systems 78−63074
harmonic emission mechanisms, three-halves, from laser-produced plasma 80−59283
harmonic generation in 10 μm laser-produced plasma, intensity depend. 79−55506
harmonic generation in laser prod. plasma 77−84438
harmonic generation in Nd:glass laser produced plasmas 78−30480
heat flux limitation by magnetic field curvature in laser-plasma interaction 80−43951
heat front penetration depth, heat transport wavelength depend. 80−48926
heat-flux limitation and ion-acoustic turbulence, optical diagnostics 78−18453
heating, flux-limited thermal cond. 77−76155
heating and dispersion conditions, for laser plasma with two component impurities *(Russian)* 78−22527
heating and ionisation in presence of strong UV and X-radiation 78−71512
heating by shortwave laser pulses, electron thermal conduct. effect 77−1005
heating of plasma focus 77−76154
Helios gas laser system, ICF expt. program as LASL 80−32501
heterogeneous medium, interactions of laser radiation 80−28765
High Density Z-pinch pulse power supply 79−14603
high energy CO_2-laser pulse, interaction with liquid and solid targets, optical investigations 78−42829
high energy ion prod. in laser irrad. CH_2 target 77−89318
high field laser heated solenoids 79−60161
high intensity laser-matter coupling in vac. 79−90430

plasma production and heating by laser beam continued
high power laser appl. *(French)* 80−13785
high pressure optical discharges, density and temp. meas. 80−48931
high Z target, time resolved X-ray spectra 79−27807
high-energy ions from Nd laser produced plasma, asymptotic energy distrib. meas. 77−89303
high-power non-self-sustained discharge with ionisation by repetitive electrodeless pulses 78−71514
high-power pulsed laser requirements and performances 78−83592
high-Z disc targets, 1.06 μm laser radiation interaction 80−6269
high-Z plasma, X-ray diagnostics 80−75074
holographic study of laser prod. plasma at 10.6 μm 80−38685
hot electron energy relaxation and transport *(Japanese)* 80−96347
hot spot distribution, significance for interpretation of laser produced plasma expts. 78−55732
hot spot distribution, significance in interpretation of laser produced plasma expts. 80−1820
hot spot distribution, significance interpretation of laser produced plasma expts. 79−98945
hybrid-wavelength laser system, spherical solid target, computer anal. 80−48920
hydrodynamic instabilities in laser driven implosions '80−64756
hydrodynamic stead-state solns. in planar geometry 79−37522
hypercompression of matter by thermonuclear miniexplosion 79−50882
hypocycloidal pinch apparatus, dense plasma production diagnostics, high laser beam absorption 77−43051
ice, surface, interaction of laser burst, possible appl. 80−7444
ICF reactor fuel pellet fabrication techniques and quality factors, optical systems 80−32436
ICF reactors, pellet and laser beam space-time interaction system study 80−13802
ICF targets, laser driven, materials problems 80−32438
ICF targets, semiconductor process technology for mass production 80−32439
imaging space-time-density contours in gas, overlapping pulse technique 80−73320
imploded glass microspheres, numerical modelling 77−24115
imploded spherical targets, stability 78−5906
imploded target, spatially-resolved X-ray spectra diagnostics 79−37543
imploding spherical shells, acoustic amplification 79−10683
implosion, ablative, laser driven, struct. and scaling laws from stationary flow model 77−43008
implosion, laser-induced, expt. and theoretical investigation 77−43002
implosion expts. 78−58490
implosion studies, laser-matter interactions at Limeil 80−92357
implosive shock wave, prod. by laser, eval. of attained temp. 79−73022
induced shock wave interferometric obs. 78−75428
inert gas hydride laser, use two-step nucl. fusion dissipative confinement of doubly isotopic boron hydrides 78−82506
inert gases, supersonic radiation waves, excitation by CO_2 laser 79−90433
inertial confinement, advanced engineering requirements, review 80−95421
inertial confinement, by laser and electron beams, conf. summary 77−76174
inertial confinement, temporally shaped laser pulse generation 78−50831
inertial confinement fusion, high yield Li injection fusion energy convertor 79−85772
inertial confinement fusion, pulsed power aspects, overview 80−63382
inertial confinement fusion at NRL, laser and ion drivers 80−23131
inertial confinement fusion at Osaka, laser energy drivers, REB fusion research 80−23135
inertial confinement fusion gains using collective model for electrodynamic laser compressions 80−23138
inertial confinement fusion generating remote systems, laser driver sources 79−9886
inertial confinement fusion power system, nuclear pumped laser coupling 79−85775
inertial confinement fusion reactor, appl. PWR fuel rod reenriching 80−106174
inertial confinement fusion research at Los Alamos, recent progress 80−23133
inertial confinement fusion research system of high power lasers *(Japanese)* 80−5324
inertial confinement fusion target, formation of uniform solid fuel layers 80−95432
inertial confinement fusion targets 78−50299
inertial fusion reactors, feedback-controlled laser-guided pellets 80−73997
inertial fusion results from Shiva 80−92358
inhibited electron thermal cond. in plasma from microwave laser irrad. targets, laser intensity threshold Z-depend. 80−48928
inhomogeneous laser-generated plasma, resonantly enhanced elec. field props. 80−33796
initial stage, Q-switched laser in N_2, plasma parameters obs. *(German)* 79−55531
instabilities, parametric, in two electron temp. plasma *(Japanese)* 80−96377
instabilities in laser produced plasma column in uniform mag. field 80−38687
intense field QED in continuous medium, appl. to Thomson scatt. and Cherenkov radiation 80−27435
interferometric exam. 77−3986
intracavity laser breakdown plasma, laser short pulse generation 78−37924
inverse bremsstrahlung, radial expansion effect, quasistatic model 79−37520
inverse bremsstrahlung absorption intensity depend., in inhomogeneous standing wave, laser fusion appls. 78−67382
inverse bremsstrahlung energy absorption in laser-irradiated plasmas 79−37521
inverse bremsstrahlung heating, Coulomb screening effect 79−68940
inverse-bremsstrahlung absorption rate in an intense laser field 80−24201
ion acceleration in presence of density profile steepening 80−14923
ion beam, polarised, obtained from laser-produced plasma using polarised target *(Russian)* 77−38536
ion beam production from interaction with Nd:YAG laser radiation bursts 80−106939
ion confinement in pulsed laser-produced plasma 78−38518

plasma production and heating by laser beam continued
ion density fluctuations, CO_2 laser heated plasma, Thomson scatt. meas. 78−42807
ion diagnostics study of plasma from laser beam focused on Z>5 targets 77−68868
ion emission, plasma expansion, hot, cold electron density, temp. ratios 78−71513
ion emission from laser plasma, longit. mag. field effects *(Russian)* 80−54012
ion emission from laser plasma, secondary electron emission effects on detect. efficiency 80−100096
ion energy, non-thermal, scaling, in laser generated plasma 78−63550
ion energy selection by parallel-plate electrostatic analyser 78−83610
ion formation and relative yields from laser prod. plasma, mass spectra, appls. *(Russian)* 78−59631
ion source for MI-1309 mass spectrometer 79−21849
ion-acoustic fluctuations heating, laser beam absorption mechanism 77−51209
ion-acoustic wave excitation by two Gaussian laser beams, density profile modification 79−19006
ion-source, form of ion pulses depend. on plasma characts. *(German)* 77−185
ionisation dynamics of C plasmas, importance of photoexcitation 78−91130
ionisation dynamics of CO_2 laser prod. plasma, spectrosc. obs. 80−43968
ionisation in rapidly changing plasma, numerical integration of ionisation rate eqns. 78−55734
ionisation process computer simulation code, atomic transition processes 80−28764
ionised gases, conf., Berlin, E.Germany (Sept. 1977) 78−63615
ionising instability of laser heating plasma *(Russian)* 78−1815
ions, fast, J×B accel. in laser-target interactions 78−83590
ions, multicharged, in plasma produced by laser, spectral line profiles *(French)* 80−79528
ions, multiply charged, production by CO_2 laser-condensed media impact *(Russian)* 77−47236
IRIS implosion experiment experience using four-beam system *(French)* 78−14187
isolator for retropulse in CO_2 laser amplifier chain 79−22959
isotope enrichment due to reson. trapping in recombining plasma 77−58203
isotope separation using plasma heating at two-ion resonance 77−23579
jet form. by focusing laser beam on plane target, investigation using wavefront method 80−75103
jet production from solid target, absolute spectral brightness obs. *(Russian)* 79−27836
jets in conical targets, collision influence in final stages of expansion 79−14584
KMSF laser implosion fusion programme, neutron yield and peak fuel density 80−23130
L-2 stellarator, solid H_2 pellet injection parameters and effects 80−28775
Langmuir probe meas. of parameters and expsn. 78−18456
Langmuir soliton generation at crit. density with HF pump 80−6267
Langmuir waves, driven by electron-ion decay instability, scattered spectrum 80−43970
lase fusion, wavelength scaling, benefits of lasers with wavelength less than one micron 80−75073
laser, multiple-beam pellet irradiance, diffraction analysis 78−50845
laser beam re-entry into laser prod. plasma 79−55526
laser beam thermal coupling, edge effect due to plasma growth 78−9813
laser beam with retractable focus, ionis. path form. in gases 79−18992
laser beam-plasma interaction, in mag. field, breakdown, heating, trapping, fusion, diagnostics, book contrib. 77−51196
laser beat heating, temp. effects 77−51210
laser breakdown of air initiated from dust particle, laser beam shutter 79−68412
laser compression expts., X-ray emission 78−5905
laser diagnostics, probing radiation Raman scatt. *(Russian)* 80−19618
laser driven fusion, teaching approach 80−42012
laser driven implosion, anomalous interaction 78−8986
laser driven inertial confinement fusion, pulse power technology 80−63385
laser driven plasma, vacuum insulation against suprathermal electrons 80−18598
laser emission intensity reduction near solid target surface *(Russian)* 80−38681
laser energy absorpt. in practical target illumination schemes 79−23434
laser flame, far UV line emission of multiply charged ions *(Russian)* 78−75420
laser fusion, 4 TW system 78−74471
laser fusion, critical surface bubbles and corrugations 77−11376
laser fusion, electron thermal cond., plasma hydrodynamic calcs. 77−68750
laser fusion, energy flux limitation by ion acoustic turbulence, anomalous transport coeffs. 77−43009
laser fusion, energy transport, implosion, pellet design study by GEKKO II glass laser *(Japanese)* 79−14585
laser fusion, image convertor camera optical measurement 78−38549
laser fusion, interaction and transport processes, continuous pulse shaping 80−28766
laser fusion, scattered energy focusing 77−84467
laser fusion, shadowgraph and interferometry experiments, with ten-picosecond light source 78−42824
laser fusion, suprathermal electron transport, dual treatment 80−18599
laser fusion cryogenic target characterisation by wavefront shearing interferometer 80−74008
laser fusion DT target, conical, for implosion studies with CO_2 laser 79−41849
laser fusion experiments at KMSF 80−92355
laser fusion exploding pusher targets, theoretical performance model 79−82081
laser fusion expts., tamper temp. and compression, simultaneous proton and α-particle meas. 78−83607
laser fusion implications of resonance absorption and associated electrostatic field pressure 80−24176
laser fusion implosion, X-ray diagnostics 78−51362
laser fusion microsphere targets, nondestructive anal. using rot. Raman spectroscopy 80−50896
laser fusion physical processes, investigation 80−74024
laser fusion power plant, conceptual design 79−71975

plasma production and heating by laser beam continued
laser fusion power plants, design and operating characts. of optical system 79−76136
laser fusion reactor, wetted-first-wall, falling liq. film 78−66408
laser fusion reactor materials, fusion microexplosion emission, resulting problems 77−30663
laser fusion reactor targets, energy partition and neutron spectra 78−58451
laser fusion reactors, conceptual, first wall response to energy deposition 77−34429
laser fusion research, present (1977) status *(Japanese)* 78−37439
laser fusion target chamber, stimulated Raman scatt. 79−9873
laser fusion targets, electrolytic and electroless plating of discrete microparticles 79−15841
laser implosion, of structured pellet, model 79−10684
laser implosion microballoons, X-ray line radiation diagnostics *(Chinese)* 80−6279
laser induced plasma profiles, theory rel. to simulation 77−35368
laser induced thermonuclear fusion, turbulent mixing effect on shell target compression *(Russian)* 80−5332
laser interaction and implosion at Centre d'Etudes de Limeil 80−24197
laser irradiated solid target, picosecond microphotography 78−42828
laser light absorpt. by ion acoustic turbulence in laser prod. plasma 79−4144
laser light absorption, by planar plasmas, polarisation and ang. depend. 77−76096
laser light parametric absorpt., convective parametric instability 80−100073
laser light reflection enhancement from expanding laser prod. plasma, Brillouin scatt. 77−3963
laser light resonant and collisional absorpt., heating, density profiles 78−38527
laser light scattering, ang. distrib. 77−15215
laser microplasma, electron, atom and ion density determ. *(German)* 77−7588
laser penetration of solids, induced press. and impulse effect 79−19060
laser plasma, 5-20 keV X-ray emission spectrum investigation using nucl. emulsions 80−92392
laser plasma, radn. induced perturbations, current and press. fluctuations 79−82079
laser plasma, radn. induced perturbations, sidelight fluctuations 79−82080
laser plasma, spontaneous mag. fields of dipole configuration *(Russian)* 79−77411
laser plasma, struct. features of 2 ω_0 and 3/2 ω_0 harmonics *(Russian)* 77−11366
laser plasma compression, computer simulation of implosion struct. *(Japanese)* 79−14587
laser plasma from solid target 77−47237
laser plasma-target interface breakdown 77−89282
laser plasmas, strong mag. field effects, review *(Russian)* 78−38462
laser plasmas, wave absorpt. and superreflectivity due to EM struct. resonances 80−24177
laser produced plasma, spontaneous mag. field generation, simulation and expt. 79−46472
laser produced plasma, three halves harmonic spectra, time resolved obs. 80−79529
laser produced plasma, ultraviolet probing with picosecond pulses 78−42827
laser pulse irrad. of metallic targets, absorpt. studies 80−79455
laser radiation, nonlinear scatt. by fast ion waves in plasma 80−106916
laser radiation conversion into X-rays in laser prod. plasma 77−76150
laser radiation distrib. characteristic determ. in vicinity of focus 79−50871
laser radiation energy loss to resonantly accelerated ions 80−10413
laser solenoid fusion concept 78−58435
laser solenoid radiation test facility 77−83430
laser spark absorpt. and laser pulse contraction meas. using dye lasers 80−48988
laser spark evolution, thermal wave propag. and shock form. 79−90455
laser spark produced shock wave, IR and microwave thermal radiation *(Russian)* 78−38533
laser spatial intensity distrib. effect on ablated polystyrene target plasma characts. 78−9811
laser spherical heating, combination scatt. diagnostics 80−79569
laser supported absorption waves, momentum transfer to surface, flowfield model 80−14921
laser supported detonation waves, radial losses effect on propag. 77−35366
laser systems for high temp. plasma prod. 80−19599
laser target interaction in air, shock wave diffr., reflection *(Chinese)* 80−83961
laser target irradiation in high mag. fields 78−8989
laser thermonuclear fusion, review 77−34449
laser-controlled thermonuclear fusion, expt. studies *(Russian)* 77−24114
laser-erosion plasma, kinetics in its later stage, i.e. after laser pulse 80−64760
laser-fusion, KMSF group results 77−54358
laser-fusion diagnostics, subpicosecond X-ray streak camera 78−42822
laser-fusion pellet injection accuracies, accelerations and deflections 79−85774
laser-fusion system, multibeam, illumination and energy deposition 79−98429
laser-gas interaction, neutral atom inverse bremsstrahlung, laser induced electron avalanche *(French)* 78−26309
laser-heated plasma, energy deposition, bremsstrahlung spectra calcs. 77−3968
laser-heated plasma, energy deposition, Gaunt factor calcs. 77−7576
laser-heated plasma, energy deposition, suprathermal electron calcs. 77−7577
laser-irradiated target, electron accel. by reson. 80−75076
laser-matter interactions, automatic treatment of data *(French)* 78−42830
laser-pellet irradiation, two-plasmon decay instability, soliton form. role 78−1842
laser-plasma interaction and ablative acceleration of thin foils at 10^{12}-10^{15} W/cm^2 80−83963
laser-produced plasma, application of synchronised ultrashort Nd:glass laser pulse 78−42825
laser-produced plasma, continuum X-ray emission spectra 77−55171
laser-produced plasma, light press. effects, steady-state mdoel 77−47234
plasma production and heating by laser beam continued
laser-produced plasmas, light absorpt., mag. fields and hot electron physics 77−43004
laser-produced plasmas, spontaneous mag. fields, Faraday rot. obs. 78−59680
laser-target impact, HF oscill. excitation *(Russian)* 80−92353
lateral energy transport from laser prod. plasma 80−59258
layer expansion near barrier irradiated by laser in high density gas 80−70016
layered target, 10 μm laser prod. plasma 78−9812
light angular distrib. emitted from laser target, time-gated optical imaging system meas. 80−79572
light scattering from laser produced plasma 77−11397
line emission, radiative and collisional broadening in laser heated plasma 77−47159
line-focus plasma, laser produced, coherent far IR radiation 78−42806
linear discharge, laser initiated, electron density meas. by far IR laser beam deflection 80−48966
long column heating, theoretical anal. 77−3961
long laser pulse irradiation of pellet plasma, 10^{12}-10^{15} W cm^{-2} 3 nsec pulses 79−86596
low Z plasma, 1.06 μm low pulse reson. absorption 80−87903
low-Z elements, satellite lines in laser produced plasma 78−42802
lower hybrid drift instability in laser prod. plasma 79−27764
LTE validity condition for laser prod. plasma 78−79450
luminar-combustion wave, shock parameters near detonation threshold 80−6256
macroparticle accel. by laser induced ablation pressure, wavelength scaling 77−76156
Macrotor Tokamak, laser-induced desorption of impurities from walls, spectral anal. 78−59681
magnetic field, self-generated, in laser produced plasma, X-ray emission diagnostics 77−43011
magnetic field effect, plasma prod. from solid target in gas atm. 77−19740
magnetic field effects on laser generated plasma expansion, interferometric studies 77−58876
magnetic field generation in laser-produced plasma 80−77818
magnetic field parametric generation under intense irrad. *(Russian)* 79−77412
magnetic field self-excitation by intense EM radiation, mag. instability *(Russian)* 79−14582
magnetic instability and spontaneous generation of mag. fields 79−60164
magnetic radiative force in laser prod. plasma 78−5901
magnetic tape method obs. of self generated mag. fields 80−64775
magnetically confined plasma, axial heating by CO_2 lasers 78−14182
magnetically confined plasma, laser heating, radial expansion effect 77−39442
magnetically confined plasma, laser heating 77−7575
magnetically confined plasmas, parametric instabilities in laser heating 78−18432
magnetoplasma, CO_2 laser produced, soft X-ray diagnostics 79−60192
magnetoplasma, CO_2 laser produced, stimulated Brillouin scatt. 79−60162
magnetoplasma, hot collisionless, resonant excitation of upper hybrid wave by two EM beams 79−77384
magnetothermal phenomena *(Russian)* 80−33798
mass spectrometric analysis, high-yield laser ion source with plasma focusing 78−61097
matched plasma heating mode with moving boundaries 78−59633
maximum energy flux in collisonless plasma, comparison with free molecular gas motion 80−6221
maximum transport vels., obs. and theory 78−67385
mechanical response to giant laser pulse, recoil impulse meas. 80−80910
megagauss magnetic field profile, in laser-prod. plasma, Faraday rot. and interferometric meas. 78−79471
metal, TEA CO_2 laser prod. plasma, charge collection meas. 77−19739
metal, transient heating by microsecond-duration CO_2 laser pulses with air plasma ignition 79−69915
metal foil, destruction by laser pulse in presence of plasma cloud *(Russian)* 77−80338
metal foil, high-Z, and polyethylene foil and double layer, transmittance, energy transport 77−80333
metal foil, laser pulse heating enhancement with pulsed air jet *(Russian)* 78−22533
metal surface, flash mechanism caused by monochromatic laser radiation 79−95878
metal surface, high-intensity laser beam interaction 80−19600
metal surface, transient heating by CO_2 laser pulses with air-plasma ignition 79−98942
metal surface in strong electrostatic field, ps laser pulse plasma 77−62389
metal surface irradiated by laser, pulsed, plasma to wall energy transfer 79−60152
metal surface micro-inhomogeneity effect on optical breakdown of gas 80−48922
metal target heating by CO_2 laser pulses, breakdown initiation in vapour 79−91540
metal vaporisation by laser irrad., effect of plasma 79−1800
metal vaporisation centres, erosion accompanying simultaneous action of laser emission and ultrasound *(Russian)* 80−7442
metal vapour, flow vel. of ions 79−82002
metal vapour production by sputtering in hollow-cathode discharge 80−1868
metallic ion generation, multiple charged, using TEA-CO_2 laser irradiation *(Japanese)* 77−79197
metallic target, post-crit. stationary plasma form. by TEA-CO_2 laser irrad. 77−1004
metallic target, self-generated mag. fields 78−34350
metallic target, self-generated mag. fields due to laser field 79−27808
MHD model, 2-D three-temperature, for dynamics of laser target 80−70014
MHD propulsion, by laser radiation absorption 77−3998
MHD simulation of laser beat freq. heated plasma 77−11392
micro-Fresnel zone plates for coded X-ray imaging of laser produced plasmas 78−42814
microballoon, of Né, X-ray shadowgraphy 79−14579
microdiscs, energy transport to rear surface under high laser irrad. 80−33797
micrometal plasma, capable of igniting combustible mixtures, N_2 laser induced 77−89278

plasma production and heating by laser beam continued
microscopy of laser fusion plasma, Fresnel zone structs. 78−51359
microshell compression by fast ions generated by laser radiation 78−22526
microshell laser implosion, critical density surface expsn. 78−5907
microsphere implosion, symm. and stability of thermally generated mag. field 77−24118
microsphere plasma, density profile indicating inhibited transport 79−41850
microwave diagnostics of laser-produced plasmas, electron density 78−9845
miniexplosion, critical masses in fission-fusion hybrid systems 77−3158
mirror-damage thresholds for laser-fusion pulse shapes 78−74467
momentum meas. by ballistic and torsion pendulums 78−83611
momentum transfer to target from laser prod. plasma, schlieren and shadow photographs 77−58889
Monte Carlo (hybrid) suprathermal electron transport 80−24200
multicharged ions in laser plasma *(Russian)* 79−1344
multicharged plasma, heated by laser radiation, ionis. and recomb. 80−19597
multicomponent laser plasma, soft X-ray population inversion by resonant photoexcitation 79−10680
multicomponent spherical plasma cloud expansion in vacuum 78−75393
multiphoton absorption, in collisionless turbulent plasma 79−82082
multiphoton inverse bremsstrahlung, plasma laser absorpt. coeff., correspondence principle method 79−32749
multiple-charged ions, pressure dependence *(Japanese)* 80−10412
multiple-laser-beam expts., Compton-induced refl. 77−993
multiple-pass laser heating of a short plasma column 80−38684
multiply charged laser plasma, rapid cooling, possible short-wavelength radiation generation 79−41852
multipole confinement of ion laser produced plasma 80−83974
multiwave picosecond interferometry, of CO_2-laser produced plasma 77−89319
N- and S-modes of self-similar compression of finite mass of plasma 78−42778
nanosecond pulse-target interactions, prepulse effects 77−89280
neutron emission from laser irrad. plasma focus *(Japanese)* 78−38538
non-linear theory of collective processes in laser-pellet interaction and soliton generation 80−24199
non-uniform laser plasma, stimulated Raman light scatt. spectrum *(Russian)* 80−106926
nonequilibrium ionisation and recombination processes in laser-produced plasmas 79−41794
nonequilibrium stationary particle distributions *(Russian)* 77−11312
nonlinear absorption by optical mixing, temp. effects 77−15218
nonlinear dynamics of laser irradiated solid target 80−28767
nonlinear inverse bremsstrahlung and heated-electron distributions 80−48927
nonlinear laser forces, acting on electrons of tenuous plasma 79−41837
nonlinear properties and dynamics of laser prod. plasma, for fusion research 77−88762
nonlinear scattering of upper hybrid laser radiation by electron Bernstein modes in a plasma 80−64720
nonperturbative analytic approach, Pade approximants 78−20951
nonquadratic plasma waveguide, propag. of highly aberrated laser beams 77−84441
nonstationary plasma turbulence in parametric resonances 77−11378
Nova: the laser fusion scientific feasibility experiment 78−59040
NOVA, high speed rot. mech. shutter design for pre-pulse protection 80−96032
Nova, mechanical design, overview 80−91279
NOVA, pulsed power control system, fibre-optic multi-tapped computer bus 80−95443
NOVA laser facility and future programs for fusion reactor ignition 80−37590
Nova laser system design for fusion 78−46652
nozzle boundary layer equations for laser heated flow, similarity soln. 77−31355
nuclear fusion, 1979 developemnt trends and supercompression *(Czech)* 80−23122
nuclear fusion expts., calorimeters for meas. of ions, X-rays and scatt. radiation 78−16800
nuclear pumped laser fusion blanket optimisation in space and time 80−37616
OMEGA fusion Nd:glass laser system 78−50811
OMEGA laser system, design parameters, performance 78−46655
OMEGA laser system for fusion expts. 78−46649
Omega laser system for fusion studies, Rochester Univ. 78−59041
opaque targets in air, pulsed laser heating 77−52204
optical breakdown wave form. and propag. in gases 79−90411
optical diagnostics of laser fusion plasmas 77−89305
optical discharges by laser radiation, continuous equilib. plasma maintenance 80−59259
optical emission after laser-induced breakdown 77−58836
optical meas. of temp. on laser heating of solid surface *(Russian)* 78−47172
optical measurements of plasma motion and lateral energy flow 80−75102
optical system for laser induced plasma compression 80−14382
optical systems for diagnostics of laser produced plasmas 80−10434
parametric instabilities at high laser intensity 78−5903
parametric instability depend. on laser line-width, time-depend. theory 79−60138
parametric modulation of density of laser plasma near crit. surface *(Russian)* 79−4108
parametric resonance in a weakly turbulent relativistic electron plasma 79−55539
parametrically absorbing laser plasma during implosion *(Russian)* 78−1861
paraxial self focusing theory, EM wave propagation in plasma 79−94304
particle diagnostics of laser-produced plasma, space charge effects 78−63581
parylene, solid, 1.06 μm laser radiation interaction 78−91132
parylene disc, 1.06 μm laser beam irrad., beam and plasma diagnostics, 2D simulation 77−43010
parylene disc, Brillouin scattering reduction 1.06 μm beam at large focal spot 78−18430
parylene disc, high-power glass laser interaction 78−9804
parylene discs, 1.06 μm laser irrad., plasma prod. processes 78−18431

plasma production and heating by laser beam continued
PCX facility, intense laser radiation effects on mag. confined plasma 78−66405
pellet compression, X-ray images with submicron resolution 78−34366
pellet implosion, laser coupling wavelength depend., hydrodynamic code simulation 77−51208
pellet implosion, scheme for stable implosio n, asymptotic theory derived 78−29649
pellet implosions, laser coupling wavelength depend. 78−30459
pellet targets, laser beam interaction obs. 77−43007
perturbations accompanying compression of shell target by laser radiation *(Russian)* 78−13321
Pharos II, Naval Research Lab. inertial confinement fusion programme 78−59042
photon drag of electrons *(Russian)* 78−18433
physical processes for plasma prod., heating for thermonuclear fusion 77−35371
picosecond X-ray chronoscopy 78−38546
picosecond X-ray spectral studies 78−38547
pinholes irradiated by Nd:glass laser pulses, plasma closure phenomena 79−89946
planar laser explosion near a target in air 80−19601
planar metallic targets, absorption of laser radiation 79−87528
planar targets, laser beam interaction obs. 77−43007
plasma focus, interferometry and luminosity meas. 78−47161
plasma profiles, relativistic correction to ponderomotive force 78−91131
plasma torch behaviour during laser irrad. of Pb surface *(Russian)* 78−87506
plastic film, laser energy transport, X-ray, ion emission, scatt. light diagnostics 77−24117
plastic target disintegration and vaporisation 77−39443
plastic targets, anisotropic production of laser-plasma soft X-rays and fast electrons 78−38517
plexiglass compression by profiled opposite laser beams 78−47139
polarisation and ang. of reson. absorption by planar targets 78−9810
polarisation of picosecond excited continuous X-ray radiation *(Russian)* 80−59190
polarization-dependent energy transport in laser-produced plasmas 78−67380
polyethylene, expanding plasma, high power CO_2 laser radiation interaction 78−47138
polyethylene, laser irrad., mol. emission from unionised gas 78−42777
polyethylene, laser-prod. plasma, space-resolved extreme UV emission 80−54015
polyethylene, laser-produced plasma, momentum transfer and interaction phenomena of high power CO_2 laser 80−48921
polyethylene, production of large warm plasmas by staged laser heating 77−19733
polyethylene, time of flight spectroscopy of fast ions 77−76190
polyethylene, X-ray emission spectra of CO_2 laser-irrad. targets, nonlinear processes 80−33793
polyethylene filament, plasma prod. by staged laser heating, optical obs. 77−89321
polyethylene irradiated by Nd-glass laser, high energy ion anal. 77−51236
polyethylene layered target, laser produced plasma, expsn., X-ray meas. 77−80326
polyethylene pellets, heating using CO_2 laser 79−1331
polymer shells in laser fusion 78−8987
polymer-coated laser fusion targets, compression to 10×liq. DT density 80−83964
polymeric laser fusion targets, cryogenic fuel config. 78−8988
polystyrene coated Al, energy transport through plastic 77−11375
polystyrene slab, electron emission from Nd laser prod. plasma 79−98944
polythene pellet evaporation by CO_2 laser, multiple-frame laser shadow photography 77−80359
ponderomotive force, mag. fields and hydrodynamics of laser created plasmas *(French)* 77−80281
ponderomotive force, relativistic corrections 77−65897
ponderomotive force in a gas-dynamical description of laser-induced plasmas 78−79449
population inversion due to plasma expansion into ambient gas, electron cooling 80−96363
positive, negative and neutral fluxes of expanding, laser produced plasma 78−87494
prepulse damage to targets and alignment verification 79−54593
prepulse large amplitude backscatter instability with struct. pulse 77−80332
probe diagnostics for simultaneous meas. of current flow and mag. field 77−24192
probee investigations of the electric fields produced in air near a laser spark *(Russian)* 80−59334
profiled cylindrical explosion-laser compression up to hyperhigh densities 77−68837
profiled shock wave disintegration at cumulation point 79−7463
propagation in gas breakdown near laser-irrad. target *(Russian)* 79−55476
properties meas. *(Korean)* 80−96373
pulse detector, fast nondamageable, using gaseous plasma 80−95138
pulse plasma diagnosis using laser multi-frame interferometry 78−83615
pulse profiling in high power lasers for fusion, methods 79−50870
pulse profiling in high power lasers for fusion, pulse evolution in amplifiers 79−50872
pulse shaping effects on interaction processes in laser prod. plasmas 80−43946
pulse-heated sheet targets, thermal transient analysis, obs. of plasma spreading 77−84468
pulsed heating profile width and total coupling changes with pulse length and press. 80−71520
pulsed intense metal ion beam from laser-produced plasma 77−26433
pulsed laser heating of thick opaque targets in air 79−14576
pulsed laser interaction under high-pressure He ambient *(Russian)* 78−51322
pulsed laser-generated impulse on a surface in supersonic flow 80−48917
pulsed neutron source creation by laser/relativistic-electron-beam plasma heating 78−74527
PVA target, spherical-shell, energy absorpt., expt. determ. 80−54016
radial stability of density profiles for obliquely incident light 80−92350
radiant emission, spectra simplification by electro-optic gating 78−22561
radiation absorption in magnetoplasma, rel. to laser fusion 80−92273

plasma production and heating by laser beam continued
radiation diffraction in high power low system, theory and expt. 79−90431
radiation pressure effects in plasma prod., interferometric meas. 78−51325
radiation-pressure effects in laser-plasma interactions, interferometric diagnostics 78−38540
radiative transfer in pulsed laser plasma-target interactions 79−7487
rapid events, photographic study by picosecond techniques 78−42826
rare earth metal plasmas, absorpt. spectra continua, 40 to 2000 Å 78−54471
rarefaction shocks in laser plasma corona 79−19037
Rayleigh-Taylor growth stabilisation by thermal conduction 77−15180
Rayleigh-Taylor imploding shell instability dynamic stabilisation by laser modulation 77−47233
Rayleigh-Taylor instability for impulsively accelerated shells in pellet fusion 77−62384
Rayleigh-Taylor instability generation of mag. fields, effects on laser fusion 79−19025
reactor-laser for disintegrating thermonuclear plasma 80−19598
reflectance, of laser pulses on laser produced plasmas 79−73015
reflectance of laser-produced plasmas, angle and polarisation depend. 78−18452
reflection losses from plane target, optical calorimetry 78−9809
reflection of laser plasma from hot shield, expt. 80−33782
reflectivity and temp., scaling laws of laser plasma 80−87913
reheating effects, electron stopping power theory appl. 78−75257
relativistic self focusing from laser irrad. target, MeV and GeV ion prod. 78−51323
resonance absorpt. and optimum focusing of axisymmetrically polarised laser beam, spherical plasma *(Russian)* 78−1863
resonance absorption, in laser-produced plasma, X-ray bremsstrahlung emission obs. 78−59559
resonance absorption, self-consistent density profiles for obliquely incident light 80−64758
resonance absorption in CO_2 laser-plane targets interaction experiments 80−106954
resonance laser radiation absorption, incidence ang. and polaris. depend. 78−9805
resonance saturation for coupling laser energy into plasma 79−77408
resonant absorption, at high laser intensity, hot electron spectra, theory 77−80331
response to ponderomotive forces from laser pulse 77−47207
retropulse isolation, laser-target using aperture in vacuum 78−9388
review 77−19735
review of heating expts. in Japan 77−65889
review of laser radiation interaction phenomena 80−43953
RF radiation emission from laser produced plasmas 78−42800
rocket engine, nozzle for impulse augmentation 79−23439
scaling laws for plasma production and pellet acceleration by laser 79−55527
screening of graphite, polished Al targets in air, CO_2 laser radiation refl. 80−25500
second harmonic emission spectrum, from laser produced plasma 79−90416
second harmonic emission spectrum, near threshold 80−87912
second harmonic generation suppression effect *(Russian)* 80−87899
self-focusing generation of high laser flux densities in laser prod. plasma 78−18413
self-generated mag. fields, two-dimens. distrib., laser-plasma reson., mag. tape irradiation 79−41877
self-generated mag. fields in laser plasma 79−98970
self-generated magnetic field distrib., near laser-plasma reson. interaction region 80−10414
self-generated magnetic field in CO_2-laser-produced plasma 79−98943
self-generated magnetic field in laser-produced plasmas, metallic target 79−41851
self-generated magnetic fields 79−77423
self-similar motion of laser fusion plasma, energy absorpt. 77−76157
self-similar motion of laser half-space plasma, deflagration regime 79−10682
self-similar motion of laser half-space plasma, thermal wave and intermediate regime 79−14578
shearing interferometer for dense laser prod. inhomogeneous plasma *(Russian)* 80−83994
sheath inverse bremsstrahlung, electron-sheath collision, laser absorpt. 77−58877
shell, self-similar implosion 77−31494
shell, thin-walled spherical, for laser-fusion reactor, Taylor instability evolution *(Russian)* 77−46400
shell target compression and heating, numerical modelling *(Russian)* 78−1860
shell target irradiated by laser, compression dynamics *(Russian)* 78−79451
shells, creation of finite perturbations by use of laser beam 79−18849
SHG in laser plasma *(Russian)* 79−86587
SHG in laser plasma 80−53993
SHIVA, 30 TW Nd glass laser system for inertial confinement fusion 79−22978
Shiva, laser-target and laser isolation 78−59035
Shiva alignment systems 78−59033
Shiva fusion laser, development of components and subsystems 78−5491
Shiva high-radiance nd-doped disc laser amplifiers 78−59036
Shiva laser, 25 MJ energy storage and delivery system 78−59038
Shiva laser beam diagnostics 78−59037
Shiva laser computer control system 78−59034
Shiva laser fibre-optic digital links 79−85804
Shiva laser fusion facility, target diagnostic system, data acquisition and anal. 78−51366
SHIVA laser optical component manufacture and testing 79−22980
Shiva laser performance, nominal interstage beam energy, power 78−59032
Shiva mechanical systems 78−63135
Shiva Nd:glass laser system, for fusion expts. 78−50812
Shiva optical system 78−59039
shock heating mechanism of laser prod. plasma *(Russian)* 77−80334
shock tube plasma heating using TEA CO_2 laser, refraction anal. 77−24119
shock wave front, plasma column lateral expansion 77−80329
shock wave implosion, laser-driven, optical meas. technique *(Japanese)* 77−43066

plasma production and heating by laser beam continued
shock wave reflection in acoustic cavity 77−65895
shock waves, ionis. radn., laser prod. plasma 77−80327
shock-tube plasma, propag. and energy absorpt. characts. of CO_2 laser beam 77−62385
shocks, imploding, cylindrical and spherical, fusion yield estimation 80−79530
short plasma column, two temp. effects, electron-ion effect, comment 78−67383
short plasma column, two temp. effects, electron-ion effect, reply 78−67384
short-pulse laser backscatter from gas target 80−79454
short-wave emission, initial plasma parameters 80−99692
silicate glass darkening due to UV radiation from laser produced plasma jet 78−52598
simulation of two freq. laser prod. heating 78−67381
single and double frequency reson. heating, unstable oscills. *(Chinese)* 77−76149
slab laser ablation characts., steady-state model 77−68839
soft X-ray emission, from picosecond laser plasma 77−55169
soft X-ray population inversion in laser plasmas, reson. photoexcitation, photon-assisted processes 80−87378
Solase laser fusion reactor, wall protection scheme 78−58491
SOLASE laser fusion reactor design and its technological implications 79−71974
solid, high energy plasma generation 77−68835
solid in high press. gas atm. in elec. field, spatial struct. *(Russian)* 80−83962
solid target, unidirectional plasma motion, drive pulse meas. *(Russian)* 77−1003
solid target-intense CO_2 laser beam nonlinear interaction, radiation obs. 78−22562
spark in focused laser beam, and continuous optical discharge, numerical study 79−14632
spark plasma deionisation stage, laser radiation absorption obs. 78−75398
spatially resolved suprathermal X-ray emission from laser-fusion targets 80−48984
spectral analysis of emission of CO_2 TEA laser produced plasma, charact. parameters determ. *(German)* 78−38516
spectral line emission from C-H plasmas generated by TEM_{10} laser pulses 80−43969
spectral line shape and intensity, multicharged ion obs. on laser-produced plasma 80−10435
spectral lines in plasma, space depend. shift 80−6268
spectral transitions, 50 to 150 Å, Fe to Br range ions with 15-24 lost electrons 77−80369
spectrochemical analysis, plasma obtained without supplementary elec. discharges *(Russian)* 77−29081
spectroscopic observation of laser produced plasma, XUV emitting region struct. 80−54038
spectroscopic system for laser prod. plasma meas. *(French)* 77−62396
specular reflection of light from laser-produced plasmas 79−37456
sphere, energetics of laser compression, rel. to controlled fusion *(French)* 77−15216
spherical implosions, instability growth and saturation simulation 77−79480
spherical irradiation, expt. data anal. method 78−1904
spherical irradiation of target by high power laser beams 77−15219
spherical laser plasma, classical optics and light press. 78−59601
spherical laser plasma, fast ion generation by ion-acoustic turbulence 77−80330
spherical laser plasma, hydrodynamic instability and spontaneous mag. field generation *(Russian)* 78−38519
spherical multipole magnetic trap, plasma containment 80−87937
spherical plasma, optically thick resonance line 77−7572
spherical plasma, simplified theoretical model 77−62387
spherical shell targets, laser-driven compression and neutron generation obs. 77−42188
spherical target preparation and placement in laser forces by cryogenic device 77−80335
spherically symmetric absorption (reflection), simulation 78−51285
spikon lifetime 80−14922
spindle-cusp container, laser-produced high-β plasma 78−59650
spontaneous mag. field form. in laser plasma, opto-electric effect *(Russian)* 80−54013
spontaneous magnetic field, target size and struct. depend. 80−1819
spontaneous magnetic field generation associated with laser-produced plasmas in presence of ambient gas 80−10411
spontaneous magnetic fields in laser produced plasma *(Russian)* 77−62402
spontaneous magnetic fields in laser-induced plasma 79−32793
spontaneously generated magnetic field, laser produced plasma *(Rumanian)* 78−51324
staged heating using laser irrad. and mag. compression 77−19736
staged laser heating of a magnetically confined plasma 80−92352
stainless steel laser irradiated, plasma cloud radiation absorpt. and diagnostics *(Russian)* 78−59632
startup system for magnetic fusion 77−18704
static field spectrograph for laser induced plasma expts. 77−26427
steady convective states in field of continuous laser radiation 79−14212
steady state ablation model of laser target slabs 78−9814
steel, mild, laser microspectral anal. 80−108769
steel, moving target in N_2-Ar-He, action of laser beam at high pressures, surface hardening *(Russian)* 78−94925
steel, trace element anal., spectra of laser plasma 78−88691
stimulated Brillouin backscatter saturation for long CO_2 laser pulses 80−19582
stimulated Brillouin backscattering, Faraday rot. effect 78−71511
stimulated Brillouin scatt. in laser plasma expts., review 79−10706
stimulated Raman and Brillouin scatt., static mag. field effects 80−6258
stochastic (white noise) analysis of resonant absorption in laser generated plasma 79−50874
striated filamentary sparks produced by a CO_2 TEA laser 80−24288
stroboscopic method for pizosecond diagnostics of rapid processes 78−47159
strongly coupled classical plasmas in laser fusion and astrophysics, review 79−10634
supercompression of structured slab, laser deposition time depend., heat cond. effect 77−51207

plasma production and heating by laser beam continued
supercritical density modifications due to reson. RF cavity field 79−50875
supercritical density profiles of CO_2-laser-irradiated microballoons 80−14918
superelastic laser energy conversion, efficient plasma heating 80−96372
superthermal electrons, temp. and fraction estimation 80−1822
suprathermal electron effects, sheath generation effects on implosion dynamics 77−24191
suprathermal electrons, self-generated mag. fields, laser plasma 78−5902
suprathermal electrons in laser-heated plasma, 511 keV photon detect. 77−62336
surface impact of beam, in air, plasma press. *(Russian)* 78−91129
surface irradiation shielding time with CO_2 laser beam, appl. to Al and graphite 79−55530
surface plasma formation by HF and DF laser radiation, threshold conditions 79−10681
surface pressures from laser supported detonations 77−68836
sustained optical discharges in molecular gases 80−100085
switches, laser triggered gap switches as heavy duty high speed switches *(Japanese)* 78−94940
sychrotron-like X-radiation produced by intense laser beam heating 78−67322
symmetrical implosion system, charged reaction products, electrostatic field effects 80−32499
target, cylindrical shell, thermal vibrs., general soln. 80−95433
target behaviour, anal. in CASTOR 2 code 79−86594
target failure accompanying oblique incidence of laser radiation *(Russian)* 78−94926
target impurity effect on laser produced expansion, ion spectrography 80−43945
target in air, CO_2-TEA laser breakdown, average temp. depend. on physico-chemical target props. 77−19738
targets for laser and electron beam fusion, design space 79−18037
TEA-CO_2 laser pulse interaction with dense H plasma 80−38683
TEA-CO_2 laser-metallic target system, plasma target coupling 80−48925
temperature and density diagnostics of laser prod. plasma 78−51360
temperature dependence on laser flux 79−50895
temperature gradient-caused ion acoustic turbulence and reduced thermal cond. 80−53987
temperature measurement method using probe, of laser-produced plasma 79−27831
temperature versus laser flux, scaling law 79−90427
thermal conduction, flux-limited, in laser prod. plasma 78−5899
thermal conduction, strongly flux-limited, modified LASNEX calc. 79−37523
thermal coupling of 2.8-μm laser radiation to metal targets 80−76107
thermal flux reduction, in laser-irrad. plasma, EM instabilities effects 78−59641
thermal instability, mag. field generated, in laser heated plasma, hydrodynamic effects 80−96355
thermonuclear fusion appls. *(Spanish)* 79−26748
thermonuclear fusion by laser, Soviet progress report *(Russian)* 77−26878
thermonuclear fusion by lasers, state-of-the-art review *(Japanese)* 78−21768
thermonuclear fusion by lasers, theory, computer simulation, expt. 77−34440
thermonuclear fusion plasma, laser coupling and implosion 77−43006
thermonuclear fusion problems and progress 78−74500
thermonuclear laser-heated solenoid expt., numerical simulation 78−75394
thermonuclear reactions, laser compressed, thermalising and electrodynamic coupling 77−11374
thermonuclear synthesis with high power lasers *(Russian)* 77−26879
theta-pinch, CO_2 laser beam focused in axial direction 77−76148
theta-pinch, Scylla I-C, laser beam-plasma interaction 77−24090
theta-pinch, small diameter plasma, axial laser heating 78−87467
theta-pinch plasma, multiple pass CO_2 laser heating, density profile, diagnostics 79−60160
theta-pinch Ti ion injection by CO_2 laser, spectroscopic anal. 80−79577
thin target in air, pulse-laser heating 80−2902
thin wire target, props. of plasma prod. by counter incident double laser beam irrad. in uniform mag. field 79−94810
Thomson scatt. from thermal plasma, intensity depend. frequency shift 78−42770
three-mirror image rotator use in laser produced plasma expt. 80−33814
time of flight spectroscopy of fast ions 77−76190
time-resolved spectroscopy and microanalysis 77−43015
time-resolved X-ray spectroscopy of laser-produced plasmas 80−84004
toroidal trap filling with laser plasma 77−76153
transient ionising regime of laser produced plasma, X-ray emission obs. 79−55550
transition from isentropic to isothermal expansion 80−92279
transition from isentropic to isothermal expansion in laser-produced plasmas 80−87918
transition radiation emitted due to the presence of intense EM beam 79−86586
transparency changes of plasma burst in intense optical radiation, direct meas. 78−9807
transparent dielectric, laser induced plasma at surface 80−79531
transparent dielectric optical breakdown, thermal instability *(Russian)* 77−55854
transparent solid target, self-focusing effect on plasma generation 78−30460
triggered solid dielectric switches with low jitter and inductance 80−54066
triggered switching of solid insulated spark gap 80−54065
turbulent interaction fronts in laser produced counterstreaming plasma 79−41807
two beam CO_2 laser Lekko II expts. *(Japanese)* 80−100087
two dimens. supersonic plasma frontwave propag., intense laser on gas 78−87470
two-component laser-produced plasma, similarity flows 78−83591
two-dimensional Lagrangian calculation of a laser-heated solenoid 80−54027
two-plasmon decay, profile modification, produced by 10.6 micron radiation, at $^1/_4$-crit. density 79−19061
two-plasmon decay and generation of $3\omega_0/2$ harmonic *(Russian)* 77−89279

plasma production and heating by laser beam continued
uniformly redundant array imaging of laser driven compressions, preliminary results 79−60189
upper-hybrid reson. absorpt. of laser in plasma focus, backscatter 80−28621
upper-hybrid-resonance absorption of laser radiation, magnetised plasma 77−72451
UV continuum source, use of laser generated plasmas 79−94314
UV light source using grooved Ta target reson. absorpt. of emission 79−19096
vacuum interface sheath struct. of laser prod. plasma 78−5908
vacuum UV emission and absorption from laser-induced plasmas, target geometry effects *(Russian)* 77−47164
variable-Z target, 1.06 μm laser radiation interaction 78−91132
vortex formation by baroclinic vector in laser-pellet interaction 79−14580
VUV imaging of laser prod. plasma 78−51363
water, interaction of laser bursts, possible appl. 80−7444
wave excitation mechanisms and harmonic generation in laser produced plasma *(Russian)* 77−11339
wavelength dependence of energy absorption in laser-plasmas 80−87917
wavelength scaling experiments in CO_2 and Nd:glass laser-produced plasma 77−24116
X-ray absorption lines, signature for preheat level in non-explosive laser implosions 80−106978
X-ray and fast ion emission in CO_2 laser target interaction *(French)* 77−80352
X-ray and particle energy meas. in laser-plasma interaction 78−42799
X-ray bremsstrahlung, fast ion and suprathermal electron energies 78−5936
X-ray bremsstrahlung polarisation and anisotropy, evidence of suprathermal electron fluxes 80−103193
X-ray detector with subnanosecond time response 78−86741
X-ray emission, electron temp. meas. 80−103127
X-ray emission, generated by Q-switched ruby laser, 10^{12} W/cm^2 78−75389
X-ray emission, soft, from laser produced plasma 78−14213
X-ray emission, superthermal, from CO_2-laser-produced plasmas 79−90454
X-ray emission characteristics of CO_2 laser produced plasmas 78−9828
X-ray emission from CO_2 laser created plasmas 77−89306
X-ray emission from CO_2 laser generated plasma, time-resolved photography 77−80364
X-ray emission from laser prod. plasma 78−42780
X-ray emission from laser produced plasma, diagnostic methods for spatio-temporal obs. *(French)* 78−14209
X-ray emission from laser produced plasma heated by 10^{-10} sec. pulses 77−51239
X-ray emission from plasma produced by laser irradiation 79−98989
X-ray emission in laser imploded targets, three-dimens. reconstruction 80−79563
X-ray imaging, for laser fusion programme 78−47173
X-ray imaging, MOS solid-state detector arrays 78−47180
X-ray imaging, two dimens. monochromatic, of laser produced plasma 79−60193
X-ray laser plasma population inversion evidence 78−74893
X-ray lasers, plasma, production, optical transitions of multiply charged ions, population inversion, review 77−19227
X-ray line profiles, Stark broadening 78−42733
X-ray line radiation from laser produced plasma, ang. distrib. 77−15238
X-ray measurement of electron temp., laser heated magnetoplasma 77−31493
X-ray microradiographs of laser fusion targets, improved image analysis techniques 80−79562
X-ray microscopy, coded imaging techniques, of laser fusion plasmas 78−47177
X-ray pinhole microphotography, time-resolved, of laser compressed targets 77−62395
X-ray pinhole photography of the target pellet in laser fusion *(Chinese)* 79−97458
X-ray production, polarisation meas. in laser plasma 77−47266
X-ray production by laser plasma in strong elec. field 80−70034
X-ray shadowgraphing for laser produced plasma 77−89311
X-ray shadowgraphy of laser driven implosions 80−92393
X-ray source for synchrotron radiation research and microradiography 80−320
X-ray spectra of laser-produced plasma 80−75075
X-ray spectra of plasma produced by subns laser pulses *(Russian)* 78−9847
X-ray spectra of plasmas produced by 250 ps laser pulses 77−19769
X-ray spectrograph, high-luminosity, vertical focusing, for laser plasma diagnostics 78−51355
X-ray spectrometry of laser compressed microballoons 80−87954
X-ray spectrometry of laser-plasma, energy transport diagnostics *(French)* 80−43982
X-ray spectroscopic diagnostics using high-quality quartz and Si crystals 79−68953
X-ray spectroscopy of plasma from laser irrad. glass spheres 78−51364
X-rays from laser prod. plasma, K_α emission 79−90460
X-rays from laser prod. plasma *(Russian)* 79−46488
XUV lasing, gain-verification problem 78−71086
Z-pinch for CO_2 laser pellet simulation expts. 78−55742
Z-pinch plasma, heating by CO_2 laser to temp. of 200 eV 78−34348
Z-pinch plasma, interaction with CO_2 laser radiation 80−48919
Ag, laser produced soft X-ray spectra, transitions 77−15171
Al, CO_2 laser produced plasma, fast particle emission 78−42805
Al coated glass microballoon targets for laser implosion expt., search for shell disintegration 80−33792
Al, diagnosis, spatial resolution of X-ray emission by shadow technique 77−35400
Al, evap. by long pulse Nd laser, spectroscopy 78−14201
Al, expanding plasma, high power CO_2 laser radiation interaction 78−47138
Al, film, reflection coeff., effects of plasma bursts prod. 78−56547
Al foil, 8 ns laser pulse-target interactions, ion-expansion struct. 79−14575
Al foil, burn-through by laser-driven ablation 80−33794
Al, IR laser reflectance, anomalous absorpt., plasma ignition 80−7439
Al in air, gasdynamic processes, recoil impulse 77−35370
Al laser plasma, high-Z, temp. meas. from bremsstrahlung emission 80−87914

plasma production and heating by laser beam continued
Al laser plasma, laser beam self-focusing, X-ray emission 79−82064
Al laser produced plasma, expsn., X-ray meas. 77−80326
Al, laser-heated plasma, reson. line emission, spatial and spectral intensities 77−39460
Al, laser-prod. plasma, space-resolved extreme UV emission 80−54015
Al, laser-produced, X-ray spectrum, time depend. *(Russian)* 77−55173
Al, laser-produced plasma, population inversion between Al^{11+} levels, X-ray lines obs. 78−38539
Al, laser-produced plasma, momentum transfer and interaction phenomena of high power CO_2 laser 80−48921
Al, light interaction with solid at extreme intensities 77−80328
Al microdisc targets for single beam laser expts., prod. method 78−1865
Al plasma, laser produced, origin of K_α radiation 78−9833
Al plasma, laser produced, reflectance meas. 80−79568
Al reflective target, momentum and energy transfer pulse duration/polarisation depend., torsion pendulum diagnostics 80−43952
Al surface, pulsed CO_2 laser interaction at oblique incidence 80−48916
Al target, CO_2 laser irrad., 10^6-10^9 W cm^{-2}, diagnostics 77−89281
Al target, in air, pulsed CO_2 laser irrad., thermal response and plasma characts. 79−86595
Al target, laser irradiated, X-ray emission in presence of high elec. field 79−94818
Al target, light propag. in plasma vapour, 10.6 μm laser 79−23435
Al target, momentum transfer, cratering, and blow-off plasma ang. distrib. 78−5898
Al target, multiple-pulse thermal coupling at 3.8 μm wavelength 80−96371
Al target, nanosecond laser pulse-target interactions, prepulse effects 77−89280
Al target, spatial distrib. of heating by laser-ignited air plasmas 79−23433
Al target bombardment in vacuum by microsecond laser pulses, plasma parameters 79−64884
Al target in air, plasma form. due to CO_2 laser pulse interaction 80−96374
Al, X-ray emission spectra of CO_2 laser-irrad. targets, nonlinear processes 80−33793
Al, X-ray spectroscopy, plasma parameters, oscillator strengths 77−72502
Ar, CW optical discharge in laser plasmatron mode 80−75078
Ar continuous optical discharge maintenance in applied mag. field 78−75396
Ar gas, high pressure, interaction with Q-switched ruby laser, obs. 79−55525
Ar high press. gases, laser spark, breakdown and radiation supported shock waves 79−32791
Ar high-pressure breakdown by Nd:glass laser radiation 78−75399
Ar, holographic schlieren density study 77−72503
Ar, laser oscill. obs. in transversely initiated laser produced plasma 77−88696
Ar laser-evaporated microplasma radial glow and temp. distrib. 78−67387
Ar, laser-initiated plasma, gasdynamic instabilities and convective flow parameters 78−22525
Ar, optical breakdown at 10.6 μm near plasma layer boundary 79−60165
Ar, optical detonation threshold, press. depend., rel. to air 79−23438
Ar plasma development by laser radiation absorption 78−75392
Ar, preionised, CO_2 laser induced breakdown press. and pre-ionisation depend., cascade model 80−54010
Ar, recomb. laser in expanding CO_2 laser prod. plasma, 1.79 μm laser oscill. 77−88698
$Ar^{16,17+}$ filled glass shell, symmetric laser compression 80−64759
B III plasma, efficient heating by superelastic laser energy conversion 80−96372
B_xH_y compounds, doubly-isotopic, laser driven nuclear fusion, energy release 78−78499
B_2O_3 laser-produced plasmas, isotopic enhancement 80−92349
Be expanding laser-produced plasma, recombination effects 78−94935
Br II, plasma form. at KBr surface due to CO_2 laser irrad. 78−60534
C foil, laser irrad., mol. ions studied by mass spectrosc. 79−90429
C, laser plasma, time resolved electron temp. *(Russian)* 78−22566
C plasma, laser produced, anomalous mag. field reversal, two-dimens. numerical results 78−87471
C spectra from CO_2 laser prod. plasmas 80−38711
C target, CO_2 laser irrad. in strong mag. field, mass loss and plasma blow off 78−30455
C VI, laser produced, electron density profile, Stark broadening meas. of vac. UV lines 78−59684
C VI laser produced plasma, transient population inversion at 18.2 nm 79−41876
CD_2, laser plasma, ion energy distrib. 78−30461
CD_2, laser produced, X-ray photography using quartz analyser crystal 77−35403
CD_2 target plasma, CO_2 laser produced, press. depend. of self-generated mag. field 78−26310
CF_3I, I laser medium, UV absorption profile modification by vibr. excitation, for fusion ignition 78−58717
CH_2, laser plasma, ion energy distrib. 78−30461
CO-O_2-SF_6, efficient CO_2 laser radiation 3rd harmonic generation, for fusion ignition 78−59087
CO_2 electron beam controlled laser, emission pulse synchronisation with plasma mirror 79−89930
CO_2 laser, Antares system, 100 kJ, for fusion expts. 78−46665
CO_2 laser, target bombardment, plasma shock wave production and propagation 79−64885
CO_2 laser Antares system, power amplifier module 78−46666
CO_2 laser Antares system, optical design and anal. 78−46667
CO_2 laser Antares system, energy extraction, pulse shaping 78−46668
CO_2 laser beam, nonlinear interaction with plasma 78−59603
CO_2 laser fusion development 79−49859
CO_2 laser fusion effort at Los Alamos Scientific Lab. 78−33290
CO_2 laser fusion target alignment 78−46706
CO_2, laser intensity distrib., hot spot detect. using Ag halide film 78−82945
CO_2 laser plasma shutter, transmission cut-off time depend. on breakdown intensity 80−6259
CO_2 laser prod. microballoon plasma, fast ion emission 80−103172
CO_2 laser produced plasmas, picosecond development of high harmonic emission 79−90391

plasma production and heating by laser beam continued
CO_2 laser system, pulsed, for fusion research 80−58556
CO_2 laser-gas target interaction, two-plasmon decay 79−1326
CO_2 laser-heated electron emission from C-coated metal surface, appl. to emissive probe meas. 80−6270
CO_2 laser-induced plasma heated at 10.6 micron, nonequilib. ionis. 80−6271
CO_2 laser-produced plasma-initiated neutral gas recomb. lasers 80−48286
CO_2 long-pulse 2 GW single longit. mode source for laser-matter expts. 80−78860
CO_2, supersonic radiation waves, excitation by CO_2 laser 79−90433
Ca, laser produced plasma, vac. UV emission 77−80372
Cd, CO_2 laser produced plasma evolution, laser possibility 77−80325
Cd, laser oscill. at 5378 Å obs. 77−3569
Cd laser produced plasma recombination laser, power output enhancement by plasma confinement 80−63989
Cd plasma, laser action via recombination process 79−94217
Cl II, plasma form. at NaCl surface due to CO_2 laser irrad. 78−60534
Cl VII, in laser heated plasma, emission intensity anomalies, 58-78 Å *(Russian)* 77−46521
Cl VII, transitions in laser heated plasma, intensity anomalies obs. 58 to 78 Å 78−1214
Cs vapour, plasma production by weak CW laser beam at 6010 Å 77−62388
Cu, CO_2 laser beam irrad., expansion of spontaneous mag. field in plasma 77−72495
Cu foil, 8 ns laser pulse-target interactions, ion-expansion struct. 79−14575
Cu, high energy X-ray bremsstrahlung, evidence of reson. absorpt. in laser-produced plasma 78−42776
cu, laser light absorpt. by plasma with very steep density gradient 80−96348
Cu, laser-produced plasma X-ray spectral lines identification *(Chinese)* 80−54036
Cu target, simultaneous meas. of current and mag. field 77−1001
Cu-like ions, 4s-4p reson. lines and transitions obs. by means of laser prod. plasma, appl. to Tokamaks 80−99468
D fuel pellets, laser acceleration for injection into thermonuclear reactor *(Russian)* 80−52779
D, fusion pellet, conical, neutron production 79−22467
D pellet, ionisation by Nd laser irrad. 80−43949
D pellet, laser prod. plasma, multiple heating 77−76152
D pellet, plasma density distrib. prod. by ruby laser irradiation 77−3966
D pellets, ionisation by Nd laser radiation 80−70015
D plasma, amplification of laser implosion velocity 79−68938
D plasma in laser target, neutron meas. 77−7596
D plasma neutron generation by CO_2 laser implosion of polyethylene shell into conical region 78−87468
D plasma prod., interaction with mag. fields 77−76151
D, shell target compression on laser heating *(Russian)* 80−47718
D, solid, plasma formation by ultrashort laser prepulse 77−72464
D-T ball, laser driven compression with profiled explosion induced precompression 77−68838
D-T filled laser fusion microballoon targets, fuel content characterisation and press. retention meas. 79−54594
D-T fuel temperature in laser fusion targets, neutron energy spectra obs. 77−89317
D-T microsphere, concentric cumulation of laser generated fast ions 78−30456
D-T pellets surrounded by high density shells, implosion characts. 77−3969
D-T spheres, fusion neutron heating, Monte-Carlo anal. 77−6553
D-T target, laser pulse compression, thermonucl. reaction initiation *(Russian)* 77−23249
D_2 filled glass microspheres for multibeam laser-target expts. 78−82509
D_2 freely falling pellets, plasma prod. by Nd:glass laser irrad. 77−58874
D_2 in shell target, diagnostic methods 77−62408
D_2 isolated energetic plasma prod. by CO_2 laser 79−14577
D_2 plasma, isolated, CO_2 laser-produced, holographic interferometry diagnostics 80−24254
D_2-^3He, filled microspheres, implosion expts. 78−59672
DT gas-filled shell, cryogenic, laser fusion 78−8985
DT glass microballoon, Ne seeded, compression by CO_2 laser 79−22466
DT, in glass shell, spectrum and absolute yield of α-particles 77−79482
DT laser compression, computer simulation, shock and thermal waves *(Chinese)* 79−90428
DT laser-driven plasma, thermonuclear burn wave with electron- and α-conductivities 77−18698
DT plasma, amplification of laser implosion velocity 79−68938
DT reaction rate in laser fusion pellets, effect of high energy ion loss 80−32495
Fe, highly ionised laser prod. plasma, extreme UV line profiles of expansion velocities 78−14199
Fe, laser prod. plasma, study by UV spectroheliography 78−22529
Fe XVII to Fe XXI spectra, 8 to 18 Å, emitted from plasma after laser heating 78−25464
Fe XXII,XXIII, Be I and B I like spectra from laser-produced plasma, classification 78−67410
H, C VI, cylindrical plasma, XUV gain calc. 79−72995
H compression, conservative scheme for eqns. of gas dynamics *(Russian)* 79−50755
H, laser breakdown and propag., 2D-simulation 78−5921
H laser plasma, parameteric instability depend. on laser line-width, time-depend. theory 79−60138
H plasma, laser produced, characterisation meas. 78−67409
H-like ions, emission spectrum, depend. on electron density in laser plasma 79−27248
H-like ions in laser plasma, X-ray emission intensities of reson. line satellites 77−80371
H-like light ion resonance line broadening and absorption in laser prod. plasmas 79−19088
H_2 gas target, laser-induced parametric instabilities, diagnostics 78−51345
H_2 gas target, stimulated Brillouin scatt., press. depend. 78−42764
HF, high-energy laser, energy extraction, beam quality, for fusion ignition 78−63102
HF laser, Phoenix oscillator-amplifier system, laser-beam characts., rel. to plasma heating 79−76701
HF laser conceptual design for laser fusion 79−86192
HF laser possible use as laser-fusion drivers 79−22979

plasma production and heating by laser beam continued
He, gas, laser-induced breakdown cyclotron reson. at low press. 79−60100
He, high press., laser plasma optically pumped by focusing CO_2 laser beam with axicon 79−32792
He, laser induced tunnelling, avalanche initiating electron prod. 77−39441
He, laser plasma, spectroscopic meas. *(French)* 77−62396
He like ions with Z=12-23, reson. line satellite intensities in laser plasma X-ray emission 79−10718
He plasma, heating, spectroscopic meas. 77−76205
He, relaxation time determ. for establishing quasisteady state population 78−59639
He, spark prod. by short laser pulses, spectroscopic meas. of temp. and electron density 77−43086
He, tenuous plasma, electron accel. by ponderomotive forces 79−77409
He, underdense gas breakdown by laser pulse, backscatt. and beam refr. 78−5897
He-like ions in laser prod. plasma, anomalous intensity ratios of reson. to intercombination lines 79−23454
He-like ions of third sequence elements, blue satellite to resonance lines 80−70013
I laser, high-power, beam quality, gain saturation effect, for fusion ignition 78−63149
I laser, possible use as laser-fusion drivers 79−22979
K I, II, plasma form. at KBr surface due to CO_2 laser irrad. 78−60534
K-Kr, afterglow of laser plasma, fluoresc. spectra 79−19085
KCl, cryst., optical breakdown plasma effects 77−66558
KCl, cryst., plasma prod. by laser impact, effect on surface 78−1866
Kr, laser oscill. obs. in transversely initiated laser produced plasma 77−88696
Kr, recomb. laser in expanding CO_2 laser prod. plasma, 3.07 μm laser oscill. 77−88698
KrF laser beam, Raman pulse compression, for fusion expts. 78−59086
Li wire, optical meas. of laser detonated shock waves 78−42798
Li^+, doubly excited autoionis. resons., laser prod. plasma absorption spectra obs. 77−50392
Mg plasma, heated by ruby laser pulses, X-ray emission spectrum 80−64781
Mg XII, electron temp. determ. of laser plasma from continuous recomb. radiation 79−64924
Mg XII resonance line at 8.42 Å, new satellite line structure 78−53912
Mo ions, X-ray emission spectra, from laser produced plasma, line identification via HF calcs. 78−33459
Mo XIII-XVIII, spectrum 20 to 90 Å from laser-prod. plasma and low-inductance vac. spark 80−102473
N_2, dense gas near metallic target, laser spark *(Russian)* 80−38682
N_2, dense molecular gas, breakdown due to laser radiation, numerical simulation 80−38686
N_2, laser induced tunnelling, avalanche initiating electron prod. 77−39441
N_2, laser-irrad. freely expanding jet, electron temp. and spontaneous mag. field meas. 77−84469
N_2-He plasma, laser produced, high press. amplified stimulated emission 80−78843
NH_3 pellet, magnetic mirror fusion using CO_2 laser start-up plasma system 77−62383
NH_3 pellet generation system for Baseball II-T target plasma expt. 77−39444
Na I, plasma form. at NaCl surface due to CO_2 laser irrad. 78−60534
Na, neutral atom production by pulsed laser heating 77−85848
Na vapour, electron and ion beam transportation channel form., reson. saturation based laser ionis. 79−77410
NaCl, cryst., optical breakdown plasma effects 77−66558
NaCl, cryst., plasma prod. by laser impact, effect on surface 78−1866
Nd^{3+} laser plasma, Q-switching, use in physical experiments *(Russian)* 79−78817
Nd:BeF_2 glass lasers for fusion expts. 78−46661
Nd:glass, fluorophosphate glass for fusion lasers 78−46660
Nd:glass laser development and laboratory work 78−94395
Nd:glass laser irradiated fusion targets, time and space resolved harmonic emission 79−82095
Nd:glass lasers, optimisation for 1-10 ns pulses operation 78−46651
Nd:YAG laser pulse tailoring/synchronization system for laser-plasma interaction expt. 79−98404
Nd:YAG short-pulse oscillator, for Shiva 78−63134
Ne filled glass microballoons, laser imploded, compressed core density meas. by X-ray continuum edge shift 79−10705
Ne, in glass microbubble, compression, X-ray emission 78−18454
Ne microballoon, laser compression, X-ray emission diagnostics of explosive pusher mode 79−54598
Ne-like multicharged ions, vacuum UV lasing action 78−1213
OCS laser, two-quantum excitation, photolysis, energy transfer, for fusion expts. 78−59003
Pb, mass ejection from shocked surface during fusion 78−47186
Pb, X-ray emission spectra of CO_2 laser-irrad. targets, nonlinear processes 80−33793
Pt, laser produced plasma, Ni-like X-ray spectrum 80−43983
Si, laser-heated, bremsstrahlung spectra, Gaunt factor calcs. 77−3968
SiO_2, high temp. plasma, emissivity and opacity, photon group means 77−7573
SiO_2, laser-fusion microballoon, expansion density profile, 10.6 μm irrad. 78−86686
T breeding and burning within laser compressed pellets 77−83103
Ta XLVI(XLVII), $3d^k$-$3d^{k-1}$npnf transitions in laser plasma 78−9108
Tb-Al-Cl vapour complex, fusion laser gain medium 78−63073
$TbCl_3$-$AlCl_3$, vap., high-energy laser medium props., for fusion ignition 78−63075
$TbCl_3$-$AlCl_3$ vap. complex, kinetics and laser fusion pot. 79−98343
Ti, laser prod. plasma, study by UV spectroheliography 78−22529
Ti, laser produced plasma, vac. UV emission 77−80372
Ti, laser-prod. plasma, space-resolved extreme UV emission 80−54015
Tl, neutral atom production by pulsed laser heating 77−85848
V XX, Be I like spectra from laser-produced plasma, classification 78−67410
W-glass discs, 1.06 μm laser irrad., plasma prod. processes 78−18431
W_2O-P_2O_5, glass, 1.06 μm laser radiation interaction 78−91132
Xe, fast ionisation waves, supported by laser beam *(Russian)* 78−22528
Xe, laser oscill. obs. in transversely initiated laser produced plasma 77−88696

plasma production and heating by laser beam continued
Xe low threshold supersonic emission waves and effect on laser beam 79−27780
Xe, plasma-recombination laser, CO_2 laser prod. using periodic pumping 79−45927
Xe, recomb. laser in laser prod. plasma, 2.03, 2.65, 3.43 and 3.65 μm laser oscills. 77−88698
XeF(B) nuclear pumping, candidate laser fusion driver 79−86171
YAG:Nd laser pulses, mutual exchanges with plasma *(German)* 80−48918
Zn-like ions, 4s-4p reson. lines and transitions obs. by means of laser prod. plasma, appl. to Tokamaks 80−99468

plasma sheaths
see also plasma confinement
accelerator, closed Hall current discharge, anode sheath struct. 77−76215
accelerator, coaxial, propagating plasma sheath, mag. field meas. 79−90474
accelerator, coaxial with external mag. field, rot. and pinch 77−7603
air, discharge, high-current, nanosecond, explosive cathode processes and contraction 80−10449
anode sheath, crossed field low press. discharge in magnetron and Penning cell 77−11432
anode sheath in a strong transverse magnetic field 80−6310
anode sheath in high pressure high current arc 78−67467
arc, high-intensity, anode boundary layer, one-dimens. anal. 80−96401
arc, sheath structure at an emitting electrode 79−55606
arc, transient, contracted, cold-cathode, in mag. field, charact. 80−24291
arc, vac., anode spot and ion form., review 77−80382
arc discharge, high current, anode near-electrode layer, spot formation and sheath breakdown 80−38835
axial eigenmodes for long-λ_b waves in plasmas bounded by sheaths 80−28655
background plasma density minimum for plasma-grounded electron beam targets 77−7564
beam injection, transition radiation intensity calc. 77−11363
breakdown to glow transition in plasma filled gap 80−100105
breakup-initiated shockfront development in 2-kJ plasma focus discharge 80−70001
cathode, sheaths in K_2CO_3 seeded petroleum MHD combustion plasma 80−87870
cathode sheath, ion field effect on field emission charact. 77−66582
collision-dominated, analysis of voltage drop 77−24098
collisionless sheath eqns., neg./positive bias similarity transforms. *(Japanese)* 78−34332
collisionless sheath stability 80−106936
convection sustained ion sheath, struct., probe meas. 78−14179
CTR devices, surface effects related to voltage breakdown 77−35356
dipole antenna entering planetary atmosphere, plasma wake cylindrically stratified model 79−48647
discharge, RF, gamma regime, ionis. balance and plasma charact., model 80−44022
discharge plasma, diffusion regime, elec. sheath theory 80−1810
double layers, stability, density criterion 79−68931
double sheaths, force balance and density criteria 78−91116
edge theory is weakly ionised collision dominated plasma 80−43935
effective boundary conditions for plasma in mag. field near electrode 80−38668
electric arc with liq. K cathode, parameters, cathode sheath model 77−4003
electric field averaging at cathode in space charge sheath 77−19806
electric sheath and presheath in a collisionless, finite ion temperature plasma 80−64737
electrode, geometrically developed electron refl. at plasma boundary, kinetic coeff. 80−24182
electrodynamically accelerated, physical models *(Rumanian)* 78−51317
electron energy distribs. in front of and behind plasma sheath 77−76202
electron-sheath collision, laser absorpt. inverse bremsstrahlung prod. 77−58877
electrostatic double layers, review 78−67368
EM radiation from line source in moving magnetoplasma sheath, saddle point approx. 77−51189
focus, current sheath dynamics, mag. tension and thickness 77−76108
focus, current sheath evolution; optical and elec. diagnostics 77−76207
focus, current sheath struct. diagnostics, fast particle beams, deuterated polyethylene fusion 77−76206
fusion reactor divertor collector plate, pot. drop across electrostatic plasma sheath 80−13833
glow discharge, intense electron beam maintained, N_2 oxidation and collective interactions 79−32841
glow discharge, laterally spreading, short, edge struct. 80−59328
glow discharge sheath RF impedance, scatt. and ionisation effects 79−86630
grid, electrostatic wave launching, nonlinear steady-state structs. 78−42766
high-beta, formation, theoretical analysis 78−59612
high-current, low/intermediate press. arc, anode sheath and pot. drop 79−41901
high-current arc, positive anode pot. drop 79−41902
highly conducting core sheath formation, flat 3-zone description *(German)* 79−41890
hollow cathode arc with fully ionized dense plasma, V-I charact. and other props. 79−14627
integro-differential eqns., nonlinear, nonlocal, soln. formalism 80−43936
intense electron beam, stable extraction from plasma, neutralisation method 77−24104
Io, plasma sheath electrons rel. to Jupiter modulated decametric radio S-bursts *(Russian)* 80−8582
ion acoustic waves, at plasma sheath 77−7531
ion acoustic waves excited by boundary sheaths 77−62355
ion density, in ionising beams 78−83582
ion magnetron scaling law 79−27855
ion sheath diagnostics using elastic surface waves *(Japanese)* 77−89266
ion sheath expansion into collision-dominated plasma 78−38505
ion sheath motion in plasma diode, computer simulation 77−15207
ion sheaths, effect on RF excitation of electrostatic Bernstein mode waves 77−7518
ion-acoustic soliton, refl. from sheath around negatively biased grid 78−38479

plasma sheaths continued
jellium, one-dimensional, wall effects 79−46468
laser produced plasma, vacuum interface sheath struct. 78−5908
laser-produced plasma, suprathermal electron effects, sheath generation effects on implosion dynamics 77−24191
low temp. dense plasma electrode phenomena, review 80−33743
low-β interchange instability, finite Larmor radius effects, sheaths 77−84426
low-density plasma, deionisation between electrodes, pot. difference effects 77−51162
low-pressure discharge anode sheath in crossed fields, electron density distrib. 78−75424
lower hybrid drift instability, Tormac sheath, inhomogeneity and mag. shear influences 78−34299
magnetised sheet plasma, sheath reson., RF plugging 77−15206
magnetosheath effects on cylindrical Langmuir probes 80−28820
metal probe-gas discharge plasma boundary, impedance parameter variations 77−58869
metal vapour production by sputtering in hollow-cathode discharge 80−1868
metallic sphere in radially inhomogeneous sheath, EM wave backscattering anal. *(Russian)* 77−7558
negatively-biased cylindrical probe characteristics at medium pressure 78−63593
nonequilibrium, intense ion beam extraction 77−89267
nonlinear effects in the vicinity of a radiofrequency probe 80−48985
nonselfmaintained discharge, current voltage characts. 80−44045
open-system plasma mag. confinement, effect of time-variable boundaries on end loss 79−37530
parallel-plate sputtering system deposition rate model 79−87579
Penning discharge, cathode sheath, RF impedance study 80−106935
Penning-type HV discharge, ionis. average freq. in anode sheath 80−44012
planar continuum sheath, regeneration and convection of ionis., probe meas. 77−80315
plasma flow velocity measurement, Langmuir probe method 79−46475
plasmatrons, mono- and duo-, anode space-charge sheath characts. rel. to ion source 79−55576
probe, diffusion type, cylindrical, in mag. field, floating pot. calc. 80−10438
probe, elec. highly negative, in flowing continuum plasma, ion sheath 77−72493
probe, RF, ion sheath effects on impedance characts. 78−42818
probe, small orifice type, sheath effects on ion extraction 80−59307
probe ion current and charact. by non-self-maintained ionisation 80−38713
probee investigations of the electric fields produced in air near a laser spark *(Russian)* 80−59334
pulsar polar caps as foil-less diodes, nonneutral relativistic beam accel. 80−17604
reflex discharge, diocotron-instability pulses, current and electron loss effects 77−62423
RF discharge, electrode sheath 80−44052
RF probe sheath, finite thickness effect 80−43971
RF sheath in self-sustained plasmoids, size and disappearance analysis 80−44026
RF voltage in plasma probe sheath, effect on electron energy distrib. meas. 80−54045
satellite and spherical probe, static and dynamic behaviour of sheaths, simulation 77−25907
satellite plasma sheaths, streaming instabilities, elec. equilib., one-dimens. particle simulation 77−22036
secondary electrons in plasma-wall sheath, Langmuir probe obs. 80−92387
shape in coaxial accelerator 78−22578
sheath criterion generalisation, sonic ion wave at boundary 77−3954
solid surface interaction, electrostatic sheath equations, inc. heating, ion mobility and ion recomb. 80−1808
space-charge double layers, anal. using fluid theory 80−75062
spacecraft surface plasma sheath, space charge neutralisation 77−87240
spherical antenna covered with isotropic plasma layer, radiation characts. 80−14907
stability, approx. model analysis of steady state situation 80−43934
targets, sheath driven, simulation 80−48898
temperature measurement method using probe, of laser-produced plasma 79−27831
temperature sheaths, probes and electrodes in MHD plasma 78−55726
thermionic advanced convertor with auxiliary ionisation, microwave heating 77−24216
thermionic convertors sheath operating mechanism effects 80−30507
thermionic diode, ignited mode, interelectrode space and sheath anal. 77−24212
thermionic diode, wall-to-wall theory, sheath anal. 77−24211
thickness to Debye length ratio for slightly ionised continuum plasma 80−70008
thin line cusp magnetoplasma sheath, RF feedback stabilisation 80−70009
Tokamak, JFT-2, scrape-off layer, particle and energy fluxes, probe and IR obs. 78−59690
Tokamak, Macrotor, metallic impurity suppression by electron injection 79−32781
Tokamak, time resolved heat flux to wall meas., sheath model with secondary electron emission 78−79468
Tormac DT fusion reactor, power gain and net output 78−58402
Z-pinch, current sheath struct., mag. probe and numerical model *(Russian)* 78−59645
Z-pinch, high current discharge in Xe, heating efficiency 78−47152
Z-pinch gas discharge, Hall effect influence on plasma dynamics 77−51218
Al plasma anodisation forming voltage limitation mechanism *(Japanese)* 80−16579
Ar arc plasma, circuit-breaking, anode layer, optical diagnostics 77−80351
Co_2-N_2-He, pulsed discharge with temp. and density gradient in cathode sheath 79−41899
Cs-Ba discharge, high-current, low-press., spontaneous current cutoff 80−19626
H_2, solid, ablation by magnetised plasma, semi-empirical calc. 80−38666
He spark, cathode spot conversion kinetics 80−44067
He-Ne waveguide lasers, HF discharge stability 79−18401
plasma sheaths continued
Hg 40.8 MHz discharge electrode space-charge sheath thickness obs. 78−67547
Li plasma, electrode pot. layer characts., surface ionisation and Schottky effects 77−15260

plasma shock waves
ablation waves, mag. field generation in inhomogeneous plasma 77−11344
accelerated Mach wave in nonhomogeneous cumulation cone 79−68925
adiabatic switch-on shock wave, in collisionless plasma, relativistic distrib. function *(Russian)* 79−55505
aerosol induced breakdown in air, two-dimensional modelling 79−90368
air, optical detonation threshold, press. depend. rel. to Ar 79−23438
air, optical discharge maintenance by giant laser pulse with extended tail 79−23478
air, shock heated plasma, nonequilib. submillimetre emission *(Russian)* 78−1869
air plasma, optical absorpt. coeff. at 1000 atm, 13000K, N_2^- photodissoc. 80−64691
air plasma, TEA CO_2 laser-produced, using solid targets, induced shock waves 80−64729
air-water vapour mixture, electron conc. and conductivity behind strong shock wave 80−48890
Alfven shock evolution is classical MHD *(French)* 78−18352
blast type cosmic phenomena, gasdynamical models and two-dimens. unsteady computs. 77−60565
blast wave computations using the flux-corrected transport algorithm 79−77184
blast waves produced by a time-dependent energy source 80−14898
breakdown, ionising wave propag. mechanisms 80−83941
breakup-initiated shockfront development in 2-kJ plasma focus discharge 80−70001
charge separation effect on shock wave struct. *(Russian)* 77−80306
cluster ionised front, in rail-type linear accelerator, propag. vel. meas. 79−10665
cold collisionless plasma with random inhomogeneous density distrib. 80−70002
collisionless, isomagnetic discontinuity form., dissipative mechanism *(Russian)* 78−38492
collisionless, precursor struct. model 79−1313
collisionless anisotropic plasma, shock waves, Zemplen's thermodynamic theorem 77−68798
collisionless shocks, kinetic models 80−90330
collisionless shocks, simulation and laboratory expts. 80−87893
collisions, anal. theory, vel., incidence angle and mag. field effects 77−7415
compressible magnetic-field reconnexion 80−6226
compression by profiled explosion, neutron output 80−13782
compressive plasma fusion in D-T macrosamples by CO_2 laser 78−82507
concentric compression of plasma, possibility of generating singular densities 77−68840
concentric hyperdetonation shock wave 79−7464
converging shock and thermal waves, numerical study 77−62282
counter wave form., propag. in spatially varying mag. field *(Russian)* 77−24088
critical surface, enhanced stimulated Brillouin scatt. due to light refl. 80−1750
current sheet, near line of zero mag. field, numerical anal. *(Russian)* 80−83908
deflagration wave, in laser compression 79−23419
deflagration wave formed by ion beam in spherical target 80−28694
dense plasma, diagnostics of two-wavelength optical absorpt. 79−98978
discharge, high current, shock wave parameters, radn. effects *(Russian)* 77−7620
drift waves, finite amplitude, propag. in collisional plasma, shock wave profile 77−27669
Earth bow shock, obs. of quasi-parallel, quasi-laminar struct. 77−37484
EHD of three component medium with shock waves, unidimens. flow *(Russian)* 77−35250
eigenoscillations of ion cyclotron beam whistler turbulence 77−7540
electrical conductivity of high-density, shock-heated Ar and Xe plasmas 80−38557
electron density meas. in shock generated plasma by light interferometry 80−48981
electron temperature and density in Ar behind reflected shock waves 80−38549
electrostatic, double layer stability 80−6236
electrostatic, turbulence levels diagnostics by fast ion beam *(Russian)* 79−98974
electrostatic shock wave, energy dissipation and turbulence processes *(Russian)* 79−7465
electrostatic shock-like wave, hemispherical 79−41828
electrostatic shocks, double layers and anomalous resistivity in magnetosphere 78−45152
electrostatic shocks in ionosphere, differences between regions of upflowing and outflowing current 79−100999
electrostatic shocks in ionosphere/magnetosphere, role of coherent anomalous resistivity 80−4189
electrostatic V-shocks in auroral plasma, approximate equipotentials 80−21870
EM shock tube plasma heating using TEA CO_2 laser, refraction anal. 77−24119
erosion plasma burst, effect of dynamic stresses 80−79532
explosion compression of plasma up to critical values of thermonuclear microfusion 77−67872
explosion compression of plasma up to critical values of thermonuclear microfusion 77−67873
explosion-induced compression, continuous profiling 78−51330
explosion-induced compression for thermonuclear microfusion, power station parameters 78−82508
explosion-induced profiling of plane shock wave through layer systems 78−51331
explosions in two-component plasma with thermal energy and heat flux relax., similarity transformation 77−19710
Faraday MHD generator-operating region 80−103132
fast ion deceleration in accretion column 80−38530
Fermi acceleration by shock waves in astrophysical plasmas 80−31207
finite ion temperature effects on strongly nonlinear ion acoustic solitons 79−41811

plasma shock waves continued
flash lamp, discharge-channel development, effect of reflected shock waves, photographic obs. 77−43093
flow in transverse mag. field *(Russian)* 78−9765
fusion model targets, inertial confinement, shock focusing in implosions 79−49832
fusion reactor cavity design, compact electron beam or light ion beam reactor using nonspherical blast waves 80−9405
gas blast circuit breakers, three nozzle arc models, review 79−27862
gas-ionising detonation wave, spatially-polarised struct., rel. to mag. viscosity *(Russian)* 77−39361
head-on collisions between radiation-driven fronts with self-consistent absorpt. 77−27675
heating dense Ar, Kr and Xe plasmas, calc. of equilibrium props. *(Japanese)* 80−79513
heating front produced by laser, vel. in magnetically confined plasma 77−7575
heavy elements, isentropic explosion compression by 'soft' layer effect 77−43017
high density plasma, thermonuclear reaction wave, propag. stages, computer simulation 78−742
high energy CO_2-laser pulse, interaction with liquid and solid targets, optical investigations 78−42829
high velocity jets generated by plasma focus and shock-wave expt., temp. and density meas. *(Russian)* 80−106882
hot gas plasma, building up compression rings by dielectric spark discharge in layers of liquid 78−38493
hydromagnetic waves, nonlinear, in two-electron temp. plasma 79−98884
imploding shocks in plasma, approx. analytical solns. 80−83942
implosion and reflection of coalesced shocks, self similar analytic solns. 78−55735
implosive shock wave, prod. by laser, eval. of attained temp. 79−73022
impulse spark study using two-wavelength interferometry 80−86391
interplanetary, and Forbush effect fine structure 77−53366
interplanetary medium, slow MHD shock waves 78−12068
interplanetary medium, type II radiobursts and shock waves 80−56690
interplanetary shock passage and protons and α-particles in solar wind 77−33301
interplanetary shock wave propag., numerical soln. of two dimensional problem *(Russian)* 77−41277
ion beam driven instability, in magnetised plasma, light scatt. obs. 79−77424
ion cyclotron beam-whistler mode instability in parallel shocks 78−14148
ion-acoustic and Langmuir coupled waves with trapped ions, envelope shock soln. 77−19686
ion-acoustic solitons in multicomponent plasma, with negative ions 79−41827
ion-acoustic turbulence, in rarefied plasma flow, Langmuir probe meas. *(Russian)* 79−55547
ion-acoustic waves nonlinear propag., shock wave struct. 77−68782
ion-cyclotron node-whistler mode instability, role in parallel shock wave structs. 77−42994
ionising MHD shock wave propag., in nonuniform medium 78−5874
ionising MHD shock wave struct., electron atom-ion temps., mag. field *(Russian)* 77−7541
ionising shock wave, in transverse mag. field *(Russian)* 77−89161
ionising shock waves in EM field 79−64867
ionising shock waves in EM field in supersonic flow *(Russian)* 77−89155
ionising shock waves in transverse mag. field *(Russian)* 78−59597
ionising shock waves theory *(Russian)* 79−94797
isomagnetic compression shock occurrence, critical parameters 77−76085
jump conditions derivation, electrons and ions, across collisionless perpendicular shock 77−3941
jump-inhomogeneous medium, homogenisation by a reflectionless shock-wave 78−83568
Korteweg de Vries equation, shock-like solns. for plasma response to piston driver 77−51187
laminar perpendicular shock, current-driven instabilities 78−77430
Langmuir wave eqn., steady state shockwave solns. 77−68799
laser fast ion driven protuberant shock wave 77−27674
laser fusion exploding pusher targets, theoretical performance model 79−82081
laser gas breakdown, shock and ionisation waves, photographic absorpt. obs. 80−87967
laser irradiated solid target, picosecond microphotography 78−42828
laser plasma, shock waves, ionis. radn. 77−80327
laser prod. plasma, shock heating mechanism *(Russian)* 77−80334
laser produced plasma, mag. field effect, laser-supported detonation wave 77−19740
laser produced plasma, momentum transfer, cratering, and blow-off plasma ang. distrib. 78−5898
laser produced plasma, momentum transfer to target, spherical blast wave theory 77−58889
laser produced plasma, shock wave reflection in acoustic cavity 77−65895
laser spark evolution, thermal wave propag. and shock form. 79−90455
laser spark ignited near conducting target *(Russian)* 78−9884
laser spark produced shock wave, IR and microwave thermal radiation *(Russian)* 78−38533
laser supported detonation waves, initiation 78−63568
laser supported detonation waves, radial losses effect on propag. 77−35366
laser-driven imploding shock wave, optical meas. *(Japanese)* 77−43066
laser-driven isentropic hollow-shell implosion, ignition problem 79−31183
laser-erosion plasma, kinetics in its later stage, i.e. after laser pulse 80−64760
laser-produced plasma induced shock wave interferometric obs. 78−75428
laser-supported detonation waves, influence on drilling of Cu with CO_2 laser pulses 79−28866
layer expansion near barrier irradiated by laser in high density gas 80−70016
limit shock waves, nonlinear MHD waves 79−77382
luminar-combustion wave, shock parameters near detonation threshold 80−6256
luminous detonation wave, plasma column lateral expansion 77−80329
Mach wave generation, two stage process 79−68924
magnetic field line reconnection, neutral layer with Petschek slow shocks 79−50851
magnetic piston interaction with nonmagnetised plasma 80−38630
plasma shock waves continued
magnetic shocks in collisionless plasma, theory 80−85854
magnetically driven tranverse shock waves, precursor photoionis. model 77−31471
magneto-acoustic solitons, macroscopic instability *(Russian)* 77−47200
magnetohydrodynamic supersonic ionised gas flow struct. rel. to mag. field *(Russian)* 77−27656
magnetoplasma compressor, erosion type, focus zone, nonideal plasma, strong shock waves 78−91161
magnetosphere, modified two-stream instability, EM effects 77−70946
Marshall implosion coil for shock heating 77−23267
MHD, propag., in nonuniform plasma, simulation 77−76084
MHD fast electron generation in shock waves propagating along magnetic fields *(Russian)* 77−990
MHD shock, superadiabatic excitation in collisionless plasma 80−79503
MHD shock front, EM radiation emission, rel. to solar radio bursts *(Russian)* 77−87259
MHD shock waves in solar wind, numerical simulation 78−77449
MHD shock waves in turbulent medium, energetic particles interaction 80−4210
MHD shocks in solar corona, rel. to type II radio emission 79−92750
MHD shocks in thermally-conducting medium 78−59581
MHD simulation, shock wave-induced plasma, transverse mag. field interaction 78−38463
MHD switch-on shocks, ionis., heating 77−80320
micrometal plasma, capable of igniting combustible mixtures, N_2 laser induced 77−89278
multiframe ps holography appl. to high power laser effects in dielectrics 78−26328
nonequilibrium effects on shock struct. in ionised gas 77−19709
nonequilibrium ionised boundary-layer flow, numerical anal. 77−11324
nonlinear-wave propagation in a proton-electron plasma coupled with a strong radiation field 80−48872
nonstationary two-dimensional MHD flow, in radial channel, theory *(Russian)* 78−75279
optical breakdown wave form. and propag. in gases 79−90411
optically thin medium, weak MHD discontinuity propag. 79−46438
outer planetary atmosphere, ionisational nonequilib. shock layer effects on entry heating 77−25979
parametric excitation by pump mag. field in high temp. plasma 77−65859
particle acceleration by MHD shock turbulence 80−87894
particle simulation code investig. 78−38491
perpendicular collisionless shock, ion dynamics and heating, numerical anal. 77−51186
photodetonation and supersonic radiation wave propag. in Xe plasma *(Russian)* 80−10385
physical quantities from conservation eqns., anisotropic plasma 77−65874
planar shock wave, annular vortex damping *(Russian)* 79−10667
plane shock formation, plasma focus zone, magnetoplasma compressor, dynamic model 78−83569
planetary probe shock layer thermodynamics, reduction-of-ionisation-pot. model 77−9651
plasma, emission and absorption coeff. at high electron density 80−103121
plasma, supersonic-subsonic flow transition, shock formation, enhancement by microwaves 77−65845
plasmapause, shocks and solitons 77−25840
plexiglass compression by profiled opposite laser beams 78−47139
precursor whistler mode plasma turbulence formation in parallel shock waves 80−24172
profiled shock wave disintegration at cumulation point 79−7463
radiation induced shock tube flow nonuniformities in ionising Ar 80−43865
radiation transfer in reson. medium, Fokker-Planck eqn. coeffs. depend. on shock wave intensity *(Russian)* 79−37453
rarefaction shocks in laser plasma corona 79−19037
rarefied plasma, mag. field rapid penetration, magneto-acoustic shock waves, super-Alfven penetration *(Russian)* 78−59554
rarefied plasma in mag. field, transport props. *(Russian)* 77−47201
reflection by elliptic cylinder *(Russian)* 78−26287
reflection coefficients of stationary shock waves on rigid wall for profiled pressure 78−51303
reflectionless passage through region of jump-like nonhomogeneity 77−42870
relativistic, MHD 78−9770
relativistic cylindrical shock propagation through a magnetic field 79−94796
retrograde ionizing waves in coaxial accelerator 78−42761
rotational shock waves, in anisotropic plasma 77−91369
second-kind explosive shock wave propagating after implosive shock wave collapse 80−48891
secondary shock wave formation by supersonic flow decleration in mag. field 79−90410
self-excited cumulative flow, compression dynamics and heating *(Russian)* 78−22469
sheath, electrodynamically accelerated, physical models *(Rumanian)* 78−51317
shock-heated dense plasma, continuum radiation and optical transmittance diagnostics 80−24202
slow mode shock layer, form. as result of mag. reconnection 78−40773
solar flare region heated by electron stream 77−71079
solar flares, radiative, mechanical and mag. energy release 79−53797
solar hard X-ray flares, impulsive electron acceleration, theory 77−29749
solar hard X-ray flares, impulsive electron acceleration inferences from obs. 77−29748
solar wind, cosmic ray interaction 77−53346
solar wind flow past planets, axisymm. implicit blunt body computation technique 78−96370
solid breakdown, pulsed, plasma form. blow off, shock waves 77−27688
solitary quasishock compression waves in vel.-modulated ion beam *(Russian)* 80−28679
space plasma discontinuities, shocks and neutral layers 79−60106
spherical implosion, of coalesced weak shocks, approx. anal. soln. 77−55161
stabilisation of explosive instability and heating of plasma ions by modulated particle flux *(Russian)* 77−3939
steady flow, shock and soliton solutions 77−15172
steady flow production, by shock, in mirror 77−84414

plasma shock waves continued
structure, at re-entry speeds, in Ar 80−43927
structure of a shock front, completely ionized plasma, unmagnetized and magnetized *(Russian)* 79−19038
supercompression of structured slab, laser deposition time depend., heat cond. effect 77−51207
supernova remnants, shock-heated plasma temp. determ. 78−65676
supernova shock waves structure 77−17603
supersonic dense stream, shock braking processes, radiation-gasdynamic obs. 80−19635
supersonic flowing continuum plasma, triple probe method applied to direct display of parameters in supersonic flowing continuum plasma 79−60191
supersonic jet, ionisation in Mach disc, submillimeter laser interferometry diagnostics 80−14934
supersonic plasma-steel target impact effect, boundary layer role 79−32780
supersonic-subsonic flow transition, shock form. and propag. 77−47173
surface discharge plasma, UV pulse form. by EM shock wave front 77−58917
surface pressures from laser supported detonations 77−68836
switch-on nonstationary, shock wave struct., dissipative electron transport influence 78−5875
thermomagnetic shock waves, in nonequilib. plasma 77−27676
theta pinch, spark channel quasi-spherical compression, electron temp. 80−87920
Thomson scattering, rot. Raman calibration 80−1844
trans-relativistic shock relations, numerical solns. 80−31202
transverse ionising shock wave, soln. for problem of nonstationary evolution of magnetic struct. 80−70003
transverse ionising shock wave struct., neutrals photoionis. effects 78−75343
transverse magnetic field effects, review 80−103153
transverse MHD shock waves 79−10666
transverse shock wave structure, dispersion, oscillations *(Russian)* 77−11345
turbulence in shock waves, investigation by anal. of scattered laser light 77−3940
turbulent shock wave propagation in solar atmosphere across mag. field, struct. 79−40166
two dimens. supersonic plasma frontwave propag., intense laser on gas 78−87470
two-stage cumulation method 79−68923
wall confined shock heated fusion reactor, design 80−99314
weakly ionised gas, heavy ion seeded, theory 79−60006
Z-pinch, high-density, form. regimes 78−59652
Z-pinch, noncylindrical, failure of current envelope and escape of shock wave near metallic surface *(Russian)* 78−55741
Z-pinch, overdense, He plasma, laser-driven hydrodynamic perturbation, shock density struct. 79−77385
Al foil, burn-through by laser-driven ablation 80−33794
Al target, in air, pulsed CO_2 laser irrad., thermal response and plasma characts. 79−86595
Ar high press. gases, laser spark, breakdown and radiation supported shock waves 79−32791
Ar, ionising boundary layer in shock-tube side-wall flow 79−60144
Ar, optical breakdown at 10.6 μm near plasma layer boundary 79−60165
Ar, optical detonation threshold, press. depend., rel. to air 79−23438
Ar, partially ionised, shock wave struct. 79−14550
Ar, photoexcitation and photoionisation ahead of strong shock wave *(French)* 77−19708
Ar plasma, interferometric study of density and electron conc. behind shock waves 78−1888
Ar plasma, optical props., visible, near-IR region, using shock tube 79−55471
Ar plasma, shock tube data on radiative cooling, IR laser techniques 78−79472
Ar plasma, shock-compressed, thermophysical and gasdynamic characts. 77−43016
Ar, plasma, shock-compressed optical props. 79−23426
Ar, precursor phenomena ahead of shock wave *(French)* 77−24087
Ar, radiative energy loss in shock tube 77−19768
Ar, reflected shock wave, press. anal. at Mach numbers of 10 to 35 77−15060
Ar-Cs plasma stream, electrodynamic braking with strong MHD interaction 78−9763
Ar-H_2O mixture, thermally ionised behind shock wave, cross section for collisions of electron with H_2O 77−11309
Ar-Xe, shock wave dynamic compression, thermodynamic props. *(Russian)* 80−53931
CO_2, temp. and press. relax. behind shock wave, M=10-30 78−38490
CO_2 laser, target bombardment, plasma shock wave production and propagation 79−64885
Ca II, reson. line broadening in shock tube plasma 77−35393
Cs nonideal plasma thermodynamic props., shock wave obs. 78−71434
Cs plasma, elec. cond. and eqn. of state, behind reflected shock wave 78−42716
Cs plasma elec. conductivity meas. 78−71450
D-T plasma ball, critical continuously shaped concentric explosive compression, approx. estimate 78−87473
D-Xe plasma, shock-wave struct., heavy doping effects *(Russian)* 77−11343
D_2 plasma, compression by microfusion explosion, expt. biconical system 80−13783
DT laser compression, computer simulation, shock and thermal waves *(Chinese)* 79−90428
DT pellets, laser-driven fusion, imploding shocks 80−79530
H plasma, dense, produced by conic electrode source, mag. field effect on flow 77−58873
H_2 plasma, MHD and transverse ionising shock waves, jump conditions, ionis. effects 79−32775
H_2, transverse ionising shock wave, soln. for problem of nonstationary evolution of magnetic struct. 80−70003
H_2(D_2)-Ne-He(Ar) plasma, combustion driven shock tube, H_2 central struct., ion mass effect 78−26327
He plasma beam-transverse mag. barrier interaction, collisionless electrostatic shock 77−80339
Kr, ionising shock wave refl., interferometric meas. 79−55553
Li wire, optical meas. of laser detonated shock waves 78−42798
plasma shock waves continued
N_2 discharge, electron shock wave formation, numerical simulation 80−38777
Na I, reson. line broadening in shock tube plasma 77−35393
Pb, mass ejection from shocked surface during fusion 78−47186
SF_6-inert gas mixture, high power cylindrical spark discharge, dynamic and visible charact. 80−64816
Xe low threshold supersonic emission waves and effect on laser beam 79−27780
Xe plasma, shock-compressed, thermophysical and gasdynamic characts. 77−43016
Xe, plasma shock front, elementary processes 80−19581
Xe precursors, associative ionisation and photoionisation, relative contrib., electron density prediction 80−43858
Y_2O_3 capillary discharge plasma, temp., radiation screening elimination 80−64682

plasma simulation
acceleration of plasma formed by relativistic electron beam 77−27657
acceleration system, two stage, in megawatt power ion source, numerical simulation for design 78−94941
afterglows, simulation by computer code GLOWCODE 77−39480
Alfven-ion cyclotron instability, physical mechanism, computer simulation 77−72437
anomalous electron pseudo-classical transport with coherent electrostatic wave propag. 80−24137
anomalous plasma transport due to electron temp. gradient instability 80−33813
auroral arcs formation and V-potential double layers 80−103185
axisymmetric plasma, ideal MHD spectrum, finite hybrid elements method 78−42734
axisymmetric toroidal MHD equilibria, numerical determ. 79−82091
ballooning instability in bumpy torus, hot electron annulus effect 80−53983
beam propagation, turbulent nonlinear stabilisation, simulation 78−18422
beam-magnetic dipole interactions, magnetosphere plasma simulation 77−7585
beam-plasma system, cold beam, nonlinear interaction, numerical simulation 77−51201
beam-plasma system, nonlinear convective and oscill. instabilities, simulation models 78−34338
beam-plasma system, trapped particle oscillations, destruction, simulation by TWT 77−31462
beam-plasma system enhanced energy deposition, interferometric obs., simulation 77−31490
belt pinch, diffusion processes, impurity and neutral gas effects, 3-fluid model 77−24057
Bernstein modes, two dimens. electrostatic particle simulation 78−71531
binary collision model for plasma simulations, Monte Carlo method particle code 78−9824
boundary conditions for simulation plasma in mag. field 78−26321
Buneman instability nonlinear saturation 80−79467
Cerenkov interaction between obliquely propagating whistler wave and electron beam, computer simulation 80−43937
channel formation, by electron beam injection into neutral gas, numerical model *(Russian)* 79−55540
charge distortion on a wire in a warm plasma 78−55274
charged fluids near freezing point, static dielectric behaviour, simulation 78−56417
classical one-component plasma, screening pot., lattice model 78−22453
coaxial channel flow of accelerators and compressors, two-dimens., simulation 80−19566
coherence wave spectra, freq. averaging effects, digital simulation 77−35390
colliding plasma evolution, EM computer simulations 80−87926
collision operator for 1D plasma, verification by simulation, heat cond. 79−27823
collisionless plasma expansion into a vacuum 79−82054
collisionless tearing modes and enhanced transport, simulation 79−86607
compression of superdense eqn. of state and boundary press. profile, simulation 78−83589
computer models of magnetically confined plasmas, review 77−11388
computer simulation, statistical mechs., for teachers 78−62014
continuous flow pinch, model and computer simulation 77−80343
controlled Tokamak plasma 80−59269
convective diffusion and heat transport, kinetic effects 79−10644
convective diffusion and heat transport, kinetic effects 79−27750
Coulombic system with multipole series, Monte Carlo simulation *(Russian)* 77−62339
counter-streaming plasma, electrostatic instability, theory and simulation 78−59578
critical surface, enhanced stimulated Brillouin scatt. due to light refl. 80−1750
critical surface density profiles, radial stability 79−55460
cross-field electron heat transport due to high frequency electrostatic waves 80−53932
current penetration, magnetostatic code, anomalous heating, heat transport, microinstabilities 78−38526
current rise in Tokamak, two-dimens. fluid simulation 77−72491
cusp fields, plasma confinement time investigation using Monte Carlo simulation, collision effects 80−64770
density profile modification by light pressure in spherical geometry 78−59636
desorption of TiD_2 films formed during simulated Tokamak gettering cycles 80−34296
diffusion, random function two-time correlation functions 79−46428
diffusion time scale Tokamak code, G2M, two dimens. 78−42795
diffusional expansion across mag. field, modelling problem *(Russian)* 80−48964
diodes, relativistic, time depend. ion and pinched electron flow, computer simulation 77−89330
discharge, axially symmetric, narrow, at high overvoltage, computer simulation 79−19101
discrete Poisson eqn. soln. with complicated boundaries, appl. to KEMP-II machine 77−15225
double layer spherical targets, implosion process under laser irradiation 80−92354
double layers, numerical simulation 79−14605
double layers from ion acoustic instability numerical simulation 80−59220

plasma simulation continued
drift cone mode instability simulation 80−83930
drift instabilities, collisionless, theory and numerical simulation 78−47106
drift instability, collisionless, numerical simulation 78−59665
drift instability-caused turbulence, anomalous diffusion, convective cell form. 77−43058
Duoplasmatron discharge resonance radiation emission model 78−67477
dynamical grid method for time-dependent simulations of axisymmetric instabilities in tokamaks 79−10702
EBTR, parametric anal. of thermonuclear burn dynamics and energy balance 80−37597
electric double layer, electron velocity distrib. on high pot. side 80−70010
electric double layer form. and dynamics, simulation 80−48855
electron beam, relativistic, rotating, filamentary instabilities 77−76187
electron beam-cold plasma interaction, nonlinear wave growth and instability, simulation 77−89300
electron beam-plasma interactions in turbulence regime, phenomenological model 80−6260
electron cloud containment in toroidal mag. field 77−27715
electron cross-field heat transport caused by HF electrostatic wave 80−28619
electron current at spherical probe, theory 79−55556
electron plasma, EM instability reduction of thermal flux, simulation 78−75272
electron plasma wave, computer simulation of modulational instability 79−32766
electron temperature meas. by impurities line emission time history 77−15241
electrostatic and magnetostatic particle simulation models in three dimensions 79−64903
electrostatic two-dimens. model for bounded plasma slab 79−55542
electrostatic waves in drifting ionospheric simulation 80−53965
elongated cylinder, nonlinear MHD instabilities and convection, simulation 77−24169
EM instabilities, thermal flux reduction 79−14529
EM particle simulation codes, initial noise, quiet start 78−1883
EM pump wave parametric decay into electron electrostatic waves 77−19683
EM wave resonant absorpt., electron acceleration 77−76142
EM waves, delay line simulation, wave propag. in dispersive and attenuating media 80−82606
energy distribution of electrons heated by laser light absorpt., simulation and test particle methods 80−48963
exploded wire plasma nonlinear evolution, numerical simulation 78−14197
exploding pusher laser fusion 79−54596
externally driven magnetic reconnection and a powerful magnetic energy converter 79−68949
fast electrons, resistive inhibition from laser prod. plasma in low density Au target 80−87916
field reversed mirror neutral beam startup, hybrid plasma code simulation 80−99313
finite-size particle method, numerical criteria to test real system equivalence 77−11393
fluid simulation of plasmas, MHD particle code 79−68948
focal region of intense laser beam in tenuous plasma, spatial and temporal electron and ion density variations 80−53989
fusion blanket neutronics, acceleration of Monte Carlo simulation 77−23280
fusion reactor, effects of suprathermal alpha particles, phase-space grouping techniques 77−79479
fusion reactor, laser plasma simulation code, PHD-IV 78−59640
fusion reactor, microscopic behaviour and neutral beam heating of Tokamak 77−79476
fusion reactor, TEXT, poloidal field power systems, design and anal. 80−102328
fusion reactor, toroidal field ripple effects, computer simulation 78−54892
fusion reactor lower hybrid heating, nonuniform density, particle simulation model 78−14185
fusion reactors, field reversed mirrors 80−43961
fusion systems, solenoidal, instability-driven anomalous transport, review 78−22460
fusion target implosion, laser compression efficiency, wavelength depend. calcs. 77−35369
fusion targets design space, burn code 79−18037
gas discharges, electron swarm motion, computer simulation 77−89339
glow discharge cathode region microscopic model 78−67524
guiding center plasma with gravitational or gradient drifts 80−38632
guiding-centre simulation of toroidal plasma 77−27713
gyrating charged particle beam compression, modeling with finite circuit element code 80−14930
heat transport, computer simulation 80−28817
heating by two freq. laser 78−67381
helicon solitons, interaction and formation 77−7537
HF electric field effect simulation, Coulomb collisions, weighted particle method *(Russian)* 77−3981
high density plasma, thermonuclear reaction wave, propag. stages, computer simulation 78−742
hot plasma preparation for high beta Tokamak 77−999
identification problems 78−71532
implosion heating, numerical modelling of Los Alamos expt. 77−43056
impurity conc. and time evolution in Tokamak, optical meas. 77−51156
impurity peak positions in TFR discharges 78−91149
inertial confinement fusion mag. wall reactor cavity concept, new plasma model 79−86602
inverse bremsstrahlung absorption intensity depend., in inhomogeneous standing wave, laser fusion appls. 78−67382
inward particle transport by plasma collective modes 79−55543
ion acoustic wave, large amplitude, initial freq. shift 80−28661
ion beam extraction, computer simulation, finite element method 80−96387
ion cyclotron heating, Tokamaks and mirrors, quasilinear model 78−59626
ion cyclotron instability, noise and quiet start methods in particle simulation 77−89301
ion pressure gradient driven drift modes; 3-dimens. fluid simulation 80−103150
ion sheath motion in plasma diode, computer simulation 77−15207

plasma simulation continued
ion source trajectory computation, computer simulation 78−71510
ion-acoustic turbulence, scaling laws and asymptotic states 79−60141
ion-acoustic wave packet propag., nonlinear, longer wavelength wave generation, simulation 78−14157
ion-acoustic waves, linear response to impulse 79−14541
ion-acoustic waves, nonlinear freq. shift and modulation, computer simulation 77−68789
ion-acoustic waves, nonlinear self-modulation, expt. and simulation 78−42743
ion-acoustic waves, nonlinear self-modulation 78−14155
ion-acoustic waves, trapped particles, harmonic generation 77−76188
ionic and plasma cluster equilibrium and kinetic props., computer simulation 78−71533
ionisation and recombination processes simulation 79−14604
KEMP-II confinement machine, potential calc. 77−15225
kinematic model of strong turbulence in plasma with relaxed closure *(French)* 79−10701
kinetic effects in plasma resonance in weak fields 78−83532
kinetic theory for fluctuations and noise 79−27822
kink modes, nonlinear evolution in Tokamak 77−19753
Langmuir turbulence, fast electron tails form. *(Russian)* 79−68922
Langmuir turbulence, numerical modelling, solitons, nonlinear interactions 80−70030
Langmuir wave evolution, three dimensional kinetic model, Vlasov eqn. calcs. 80−43923
Langmuir wave quasicollapse, one-dimens., under parametric and modulation instabilities 77−42982
large amplitude wave-electron interaction, enhancement by DC elec. field, simulation 79−90420
laser compression expts., X-ray emission 78−5905
laser fusion, critical surface bubbles and corrugations 77−11376
laser fusion, parameter study of exploding pusher target *(Japanese)* 80−96376
laser fusion configuration, magnetic field generation by Rayleigh-Taylor instability 78−58476
laser fusion plasma, computer simulation of Weibel-like instability effects 79−14581
laser fusion simulation, hydrodynamical behaviour *(Chinese)* 80−1823
laser fusion theory, computer simulation, expt. 77−34440
laser heated electron distribs., props. 78−30462
laser heated gas target plasma, hydrodynamic expansion simulation 79−55524
laser heated microsphere plasma, density profile indicating inhibited transport 79−41850
laser heated plasma, heat-flux limitation and ion-acoustic turbulence 78−18453
laser imploded glass microspheres, numerical modelling 77−24115
laser imploded targets, compressed core density and radius, X-ray spectroscopy meas. calcs. 78−59685
laser induced plasma profiles, theory rel. to simulation 77−35368
laser light, intense, ang. and polaris. depend. absorption, theoretical interpretation 78−59638
laser light absorpt. and scatt. in laser fusion plasma 78−51312
laser light absorpt. by short wavelength ion turbulence 77−35352
laser light absorpt. due to self-generated mag. fields 78−14170
laser light absorption with self-generated magnetic field 77−24092
laser light resonant and collisional absorpt., heating, density profiles 78−38527
laser plasma compression, computer simulation of implosion struct. *(Japanese)* 79−14587
laser produced, ionisation process computer simulation code, atomic transition processes 80−28764
laser produced plasma, self-generated mag. field effects, X-ray diagnostics 77−43011
laser produced plasma, spontaneous mag. field generation, simulation and expt. 79−46472
laser spatial intensity distrib. effect on ablated polystyrene target plasma characts. 78−9811
laser-driven ablation, exptl. obs. and numerical simulations 79−4177
laser-heated exploding wires, X-ray emission 79−10685
laser-induced plasma expansion, radiation press. effects, self-similar model 79−94778
laser-irradiated fusion target, mag. field transport, nonlocal conduct. effects 78−59637
laser-produced plasma, spherically symmetric absorption (reflection) 78−51285
laser-target, Monte Carlo (hybrid) suprathermal electron transport 80−24200
linear multipole, plasma simulation, finite element model 80−1837
low power Tokamak experimental fusion power plant, scoping studies with empirical scaling, SISYFUS code 80−102309
low Z impurity transport in Tokamaks, simulation 79−55468
lower hybrid drift instability, particle simulation 78−67404
lower hybrid wave heating simulation in nonuniform plasma 80−64771
lower hybrid wave propag., numerical simulation 79−55541
lower hybrid waves, excitation in finite plasma, simulation 79−41820
magnetic field effects, boundary conditions 80−10392
magnetic field lines reconnection, clouds-in-cells plasma model 77−84490
magnetic reconnection, plasma confinement and jetting 79−10704
magnetised plasma, evolution, numerical soln. of hybrid Vlasov-fluid model 79−90452
magnetised plasma, hybrid simulations of quasineutral phenomena 78−67403
magnetosonic wave propag., computer simulation and theoretical anal. 78−5861
magnetosphere, enhancement of EM ion cyclotron instability by cold plasma, computer simulation 77−33287
magnetospheric physics, simulation expts. 79−88549
magnetospheric plasma convection, numerical simulation 79−62679
magnetostatic particle code, Darwin's formulation of Maxwell's eqns. 77−27714
MAKOKOT simulation code 79−98969
Mather type PF devices, optimisation using 2D snow plow code 80−87956
maximum energy flux in collisonless plasma, comparison with free molecular gas motion 80−6221
MHD, numerical simulation, variational approach 80−28625
MHD channel flow, averaging of EM fields by electromech. simulation 79−77277
MHD channel flow, numerical simulation 80−6229

plasma simulation continued
MHD codes, linear and nonlinear, plasma instabilities, PL1 programs 77−76040
MHD generator, diagonal channel equivalent energy circuit 79−55571
MHD ideal equilibria, computer codes, review 77−27712
MHD instabilities, large computational programs, comparative numerical studies, Tokamaks 78−79425
MHD plasma, dense, ionisation and radiation dynamics 78−83606
MHD radial channel flow, in 2-dimens. mag. field, numerical simulation *(Russian)* 77−47171
MHD shock waves, double layer upstream shocks, particle simulation code investig. 78−38491
MHD simulation of laser beat freq. heated plasma 77−11392
MHD turbulence, numerical simulation and closure techniques 79−90343
microinstabilities, low frequency, simulation model 78−38525
migmacell II fusion products spectra anal. 77−83089
mirror, plasma confinement time investigation using Monte Carlo simulation, collision effects 80−64770
mirror drift cone stability simulation with loss-cone ions 80−1789
mirror machines, computer simulation of field reversal 78−26316
modelling of plasma with collisions, macroparticle method 79−18996
Monte Carlo simulation of classical 2-D one component plasma 79−94814
multidimensional quasineutral plasma simulation model 79−7481
multifluid Tokamak transport code, two dimens., time evolution 77−58880
multistreaming, fluid codes viability 77−15173
negative mass instability, electrostatic numerical simulation 77−89261
neutral atom transport, computer code SPUDNUT 80−48962
neutral beam injection heating, computer simulation, Monte Carlo method 77−68859
neutral gas transport in infinite cylindrical plasma, Tokamak model, Monte Carlo algorithm 78−79459
neutral injection heating of Wendelstein VII A stellarator 77−68832
non-linear tearing mode, numerical code for tokamak 77−43046
nonequilibrium MHD duct with resistive electrodes, computer simulation, performance characts. calc. 77−72509
nonlinear evolution of exploded wire plasma, numerical simulation 78−83605
nonlinear interaction of cold beam and weakly collisional plasma, simulation 79−32783
nonlinear magnetoacoustic waves, damping, simulation 78−79423
nonlinear wave interactions, symbolic computation code MACSYMA 77−27660
nonlinear wave-particle interaction in magnetosonic mode, pure sinusoidal wave model 78−26320
nonlinear waves excited near resonance, computer simulation 77−72435
nonthermal O plasma stationary states 78−63544
nonuniform magnetoplasma, initial particle loadings 79−46473
nuclear fusion plasma simulation with parallel pipeline programming 79−68947
numerical simulation in fluid dynamics 80−17805
numerical simulation of anomalous transport processes in radially compressed reversed-field configurations 80−64689
numerical simulation of disruptions and loss in Tokamak plasma 80−70026
one-dimensional electrostatic simulation code, plasma wave problem, plasma-beam instability problem 77−58888
paramagnetism in RF mag. field, expt., theory and simulation 80−6225
paramagnetism of plasma in RF field 79−46490
particle beam-plasma interaction, ion-acoustic turbulence effects 78−91121
particle simulation, drift wave theory, anomalous transport 77−72428
parylene disc, 1.06 μm laser beam irrad., beam and plasma diagnostics, 2D simulation 77−43010
pellet fusion by relativistic pinched electron beams, beam propag. expt. 77−68163
phase space granulation due to mode-mode coupling, in instability generated turbulence 80−38651
plasma confinement in mirror and cusp fields, Monte Carlo simulation 80−96379
plasma laser light absorption, simulation 77−11347
plasma wall interaction in ATC during high power neutral beam injection 77−31502
plasma-beam interaction radiation in presence of DC field, beam-wave energy conversion 79−68932
plasma-beam system simulation, explosive instability 79−27821
plasma-weak electron beam interaction, numerical simulation 78−91120
positive column, striation dynamics, velocity/amplitude correlation 78−67517
proton beam, intense, space charge neutral, trapping in mag. mirror, simulation 78−9825
proton ring, static compression and trapping, simulation 77−84491
proton rings, mag. compression, computer simulation 78−22548
proton rings in mag. mirrors, computer simulation 78−67405
quasi-neutral particle simulation model for ion wave propag. and two-stream instability 78−47157
Raman backscatter in high temperature, inhomogeneous plasmas 80−92268
Rayleigh-Taylor instability generation of mag. fields, effects on laser fusion 79−19025
Rayleigh-Taylor instability in imploding foil plasma, two dimens. simulation 78−47156
relativistic electron beam, deceleration in dense plasma, simulation 77−998
relativistic electron beam collective ion acceleration, localised pinch model, simulation 78−9826
relativistic electron beam diode, pinched, particle simulation code and ion current reduction 77−68878
relativistic electron beam propag., numerical simulation 77−997
relativistic electron-cyclotron heating, computer numerical anal. by averaging methods 77−27716
relativistic plasma, cyclotron radiation interaction computer model 78−30478
relativistic plasma code instability due to Lorentz force 79−7482
resonant absorption of laser light, by magnetised plasma 78−51309
resonant absorption of light, generation of static mag. field 77−31480
resonant particle effects in Langmuir and whistler waves, long-time-scale plasma simulation 78−42796
reverse-field pinch, MHD simulation 78−5920

plasma simulation continued
reversed field pinch, ATHENE and EUROPA codes calcs. 77−24151
reversed field pinch, expt. and 3-D numerical anal. 77−43035
reversed-field pinch burn dynamics, global computer code 78−63579
RF cavity with magnetic mirrors, computer simulation of confine 78−59648
RF confinement near critical density, computer simulation 77−72492
RF confinement of plasma near critical density, computer simulation 77−24178
ripple loss of fast ions in a large Tokamak 80−92382
rotating proton layer, transient magnetic field reversal 80−70027
runaway electrons, enhanced drag by radiation 80−10397
runaway electrons in strong elec. fields, fluid treatment 80−33812
satellite and spherical probe, static and dynamic behaviour of sheaths, simulation 77−25907
satellite plasma sheaths, streaming instabilities, elec. equilib., one-dimens. particle simulation 77−22036
self-focusing generation of high laser flux densities in laser prod. plasma 78−18413
semiclassical two-component plasma, strong-coupling regime 79−7483
sheath, collision-dominated, analysis of voltage drop 77−24098
sheath driven targets, simulation 80−48898
shock wave-induced plasma current, transverse mag. field interaction, simulation 78−38463
shock waves, MHD, propag., in nonuniform plasma, simulation 77−76084
sideband instability, nonlinear large-amplitude wave evolution, simulation 78−83546
sideband instability in large amplitude wave, computer simulation 80−38602
silent discharge, excited species reactions, discharge channel characts., numerical simulation 80−38813
small amplitude wave propagation, stratified media, mathematical model 79−60147
solar flares experimental simulation, merging of two current carrying plasma columns *(Japanese)* 80−94775
solar wind, disturbances caused by charged Helios spacecraft 78−24416
soliton, Langmuir, one-dimensional, propag., interactions and generation 77−43057
space plasma chamber, design and appls. *(Japanese)* 77−22039
space simulation studies 79−58217
spatial grid effects reduction using higher order multipoles and splines 78−91148
spherical implosions, instability growth and saturation simulation 77−79480
spherical laser plasma, fast ion generation by ion-acoustic turbulence 77−80330
splines and higher order interpolations 79−64902
strong turbulence effects on the kinetic beam-plasma instability 80−59207
supersonic conducting gas stream, interaction with mag. field, numerical simulation 80−6230
symmetric double diode, time depend. theory and computer simulation of electron and ion flow 77−24065
Tandem Mirror Reactor startup and shutdown, simulation and control 80−99277
Tandem Mirror Reactor steady state, simulation and control 80−99278
TEA-CO_2 laser pulse interaction with dense H plasma 80−38683
tearing modes, nonlinear interaction in highly resistive tokamaks 79−64855
TFR, electron cyclotron heating, computer simulation 80−79517
thermal conduction, flux-limited, in laser prod. plasma 78−5899
thermal conductivity and viscosity, one-component plasma, mol. dynamics study 79−23402
thermionic diodes, planar low press. gas discharges, plasma regime, plasma characts. 79−77435
thermionic diodes, planar low press. gas discharges, space charge regime, volt-ampere characts. 79−77434
thermionic plasma converter, overneutralised, instability simulation 79−14619
thermonuclear laser-heated solenoid expt., numerical simulation 78−75394
theta pinch, low density, step-like mag. piston 80−103182
theta-pinch, linear, end losses simulated by numerical technique 77−89295
theta-pinch, linear, material end plugging 77−76183
theta-pinch, lower hybrid drift instability 77−24070
theta-pinch implosion, numerical models including classical and anomalous transport 77−24139
theta-pinch implosions, ion refl., hybrid Vlasov-fluid model 77−15229
theta-pinch machines, computer modelling 79−10703
theta-pinch machines, linear, computer model of plasma 77−89296
theta-pinch modelling by hybrid numerical models, turbulence effect 77−31510
three dimensional particle simulation models for cylindrical and toroidal plasmas 78−1884
time integration in plasma simulation, analysis 79−50886
Tokamak, electron energy confinement, simulation predictions 79−64898
Tokamak, high beta, axially symmetric diffuse column, equilib. and stability anal. 77−24132
Tokamak, high-beta, equilibria and m=1 kink ballooning mode nonlinear evolution 80−24236
Tokamak, high-beta, time evolution, MHD simulation using flux coords. 77−24134
Tokamak, inner mode relax. oscills., numerical model, electron thermal cond. distrib. *(Russian)* 77−47242
Tokamak, large mag. islands as disruption mode 79−27818
Tokamak, large mag. islands as disruption mode 79−27819
Tokamak, noncirc., axisymmetric modes wall stabilisation, simulation 78−67394
Tokamak, plasma equilib., ferromagnet-saturation effects, numerical simulation 78−18440
Tokamak, plasma simulation using nonuniform spatial mesh technique 77−79478
Tokamak, superconducting, toroidal simulation 77−62394
Tokamak, TFR, current plateau, O_2 injection effect on Mo impurity 78−22565
Tokamak, two-dimens. MHD simulation 77−19751
Tokamak fusion reactors, mathematical simulation of plasma equibilbrium and power supply operating conditions 79−76125

plasma simulation continued
Tokamak internal disruption development mechanism, mag. island growth, simulation 78−26317
Tokamak MHD processes, Kadomtsev-Pogutse eqns. numerical simulation, kink modes and internal disruption 77−43047
Tokamak model shell, shell current and vertical field meas. 77−76201
Tokamak neutral low energy transport, multigroup discrete ordinate methods, ANISN simulation code 78−34269
Tokamak plasma, control systems, construction and simulation study *(Japanese)* 80−100100
Tokamak plasma, neutral atom transport by multigroup methods, time reduction techniques 78−18385
Tokamak plasma, real and simulated, impurity behaviour 78−94128
Tokamak plasma model position control model 80−92383
Tokamak power reactor, burn cycle dynamics, confinement scaling laws and heating 77−23263
Tokamak radial transport, multi-regime model including neutral beam injection 77−65840
Tokamak reactor, short-pulse D-T, burn phase control 79−86604
Tokamak simulation, equivalent cct. model and mag. field diffusion eqns. 77−84409
Tokamak transport codes, one-dimens., poloidal divertor simulation 79−37539
Tokamak transport phenomena numerical computation codes 77−27691
Tokamak transport simulation models 77−79474
tokamak-like equilibria at beta close to unity 80−19604
Tokamaks, computer simulation of trapped electron modes 80−106874
toroidal belt pinch, dynamics, equilib., heating, numerical simulation 77−24168
toroidal belt pinch, two-dimens. MHD simulation 77−19751
toroidal plasma, eigenvalue problem and nonlinear evolution of kink modes 80−24234
toroidal plasma, quasispherical liner compression 80−92381
toroidal plasma, resistive MHD mode and sawtooth oscill., nonlinear evolution 80−24235
toroidal plasma, trapped-electron instability, numerical simulation 78−94933
toroidal plasma compression, computer model, appl. to topolotron 77−15233
toroidal stellarator, single particle motion, computer code 80−28818
toroidal transport code for neutrals and impurities in Tokamak 77−72490
torus with three coil arrangements, simulation 78−18434
Townsend discharge, macroscopic quantities, Boltzmann eqn. and Monte Carlo calcs. 80−38848
transport model for Alcator, high density regimes 77−68858
turbulence, Duffing's eqn. governed system 79−10664
turbulence, strong, Langmuir, review 80−59237
turbulence development and decay mechanisms, wave interactions, analogue simulation *(Russian)* 79−7462
turbulence generating mechanism in weakly collisional plasma 77−11340
turbulent plasma, electron/ion energy distribs., laboratory and space plasma comparison 78−5945
two-dimensional Lagrangian calculation of a laser-heated solenoid 80−54027
two-dimensional mag. flux shell model for MHD simulations of cylindrically symmetric plasmas 80−1838
two-plasmon decay instability, nonlinear saturation and recurrence 79−82057
unstable drift waves, in sheared mag. field, simulation study 79−86574
Vlasov and water-bag models, self similar solns., simulation 78−26242
Vlasov equation, two-dimens., numerical soln., appl. to electrostatic instability and monochromatic wave 79−73032
wall-plasma interface region, cross field thermal losses, simulation 78−59609
wave, monochromatic in 1-dimens. plasma, amplitude oscills. 78−87443
wave-plasma interaction, boundary conditions, refl. coeffs. 77−24094
waveguide, plasma-filled, two-stream instability nonlinear evolution, numerical simulation 80−43938
waveguide and cavity filled with plasma, expt. simulation 79−23427
whistler wave, in nonuniform mag. field, test particle correlation, simulation 79−37486
whistler wave-electron beam nonlinear interaction, computer simulation 77−3938
X-ray streak camera electrode design using a plasma simulation code 79−30632
Z-pinch, current sheath struct., mag. probe and numerical model *(Russian)* 78−59645
Z-pinch, liner implosion non-adiabatic dynamics, MHD computer simulation 77−84488
Z-pinch dynamic evolution, simulation expts. 79−60185
ZT-40, toroidal Z-pinch, circuit design and plasma simulation 78−54961
ZT-S reversed field pinch simulations 80−83993
Ar arc discharge, neutral system collisional radiation model 78−67535
Ar-Xe, shock wave dynamic compression, thermodynamic props. *(Russian)* 80−53931
C plasma, laser produced, anomalous mag. field reversal, two-dimens. numerical results 78−87471
D-^{3}He, driven Tokamak fusion reactor, plasma parametric studies and appl. 80−42865
DT laser compression, computer simulation, shock and thermal waves *(Chinese)* 79−90428
H, laser breakdown and propag., 2D-simulation 78−5921
H line Stark broadening, role of ion dynamics simulation 80−24144
H, plasma distribution function inference from optical spectra 78−67406
He glow discharge, electron behaviour in cathode fall, Monte Carlo simulation 78−1941
He, ultradense reproducible Z-pinch, for laser-pellet interaction simulation, characterisation 78−30463
Hg plasma, molecular dynamics model for atom-electron interactions 78−42708
N_2 high intensity arc anode region, temp., current density, flow field, numerical anal. 78−9827
Ne plasma, compression, spectra, temp. and density calc. model 78−59663
Ne-Ar, high press. mixture, AC discharges, one-dimensional numerical simulation 78−67451
O silent discharge, numerical simulation 78−63629

plasma temperature
θ-pinch, electron temp. meas. by Thompson scatt. with ruby laser *(Chinese)* 79−37552
AC arc, temp. diagnostics, radial distribs. 77−24240
AC discharges between isolated electrodes, gas temp. depend. 80−38800
active burn control of nearly ignited plasmas 80−48909
adiabatic compression in multistage heating cycle causing increase in plasma temp. 79−98937
air, DC point-to-plane elec. discharge, temp. patterns, Michelson interferometry 80−54061
air, laser-evaporated microplasma radial glow and temp. distrib. 78−67387
air, RF discharge, electron temp. and density 78−51371
air, wall-stabilised arc, step and sinusoidal current change response 80−103209
air arc temp. meas. by N_2^+ integrated emission coeffs. 80−59314
air flow in plasma generator, radn. parameters meas. 79−68952
air plasma flow in channel inlet zone, local heat transfer 80−64687
Alcator A Tokamak, disruptive MHD activity during plasma current rise 80−32487
Alcator high density Tokamak, ion temp. profile reconstruction *(Russian)* 80−106959
anisotropic plasma, cyclotron and electrostatic instabilities criteria 80−38627
anisotropy relaxation due to binary encounters 77−39404
Ar, plasma rotating, weakly ionised, diagnostics 79−82122
arc, DC, AC, for spectrochem. anal., correlation between anal. signals, plasma parameter changes 79−52828
arc, density and temp. meas. 78−1937
arc, high-intensity, anode boundary layer, one-dimens. anal. 80−96401
arc, plasma parameters, probe and spectral meas. 80−24273
arc, quasi-steady-state, in orifice air flow 77−68887
arc plasma, electrical conductivity and temp. distrib. in insulating channels 79−23401
arc plasma, electron and heavy particle temp. difference 80−38766
arc plasma, low-temp. diagnostics by scatt. and resonance fluorescence 78−67482
arc plasma, stabilised by N_2 injection through porous wall, thermodynamic nonequilib., plasma parameters 79−86629
arc plasma, temp. meas. by submillimeter diagnostic technique 80−38853
arcs, elec., high-current, conducting gas flow anal. *(Russian)* 79−32754
asymmetrical plasma diagnostics, by spectral method *(Czech)* 80−38704
at. emission obs. of plasma props. 80−19021
atom temperature measurements using thermal diffusion 80−43985
atomic ion-electron recomb. in presence molecules, appl. to HCl 80−28601
auroral arcs formation and V-potential double layers 80−103185
automatic recording system of probe meas. for plasma parameters *(Japanese)* 79−41870
axially symmetric plasma, error estimate of optical diagnostic methods 77−84500
belt pinch, shock heated weakly compressed high-temp. plasma 77−24164
Berkeley multifilament ion source, plasma characts. 79−94807
bremsstrahlung attenuation obs., electron distrib. anisotropy, turbulently heated plasma 78−59682
bremsstrahlung X-rays emitted from electron cyclotron reson. plasma, degree of polarisation 80−87944
bunch enlargement in vac. *(Russian)* 80−83907
capillary discharge, high-current, magnetogasdynamic regime 79−86628
capillary discharge, with evaporable wall, plasma parameters axial distrib. *(Russian)* 78−75280
capillary discharge with vaporising wall, plasma parameters axial distrib., model 79−64943
charge exchange neutrals, emitted from rot. plasma, meas. 80−106979
circuit-breaking arc radiative transfer, magnetic stability, and turbulent heat exchange 78−75482
coaxial gun acceleration of plasma cluster, spectroscopic determ. of electron temp. *(Czech)* 77−24182
cold plasma, density short wave perturbation, elastic electron-atom collision 78−47119
collective electric field fluctuations of two-temp. electron gas nonthermal plasma 80−43882
collective phenomena and anomalous resistance, electron current drift velocity *(Russian)* 80−24140
collisionless flow and end loss from a high-energy theta-pinch plasma 80−92365
collisionless magnetoplasma, EM wave conversion to extraordinary wave 80−79451
column and surrounding liq. interaction, quantitative anal. under quasiisothermal conditions 80−38788
column compressed by mag. field, multichord corpuscular diagnosis *(Russian)* 79−4190
combustion product plasma, electron conc. and mobility determ. by HCN laser submillimetric interferometry 78−1889
continuous emission, ionisation potential lowering and total excitation cross section of atmospheric thermal plasma 80−38705
continuous optical discharge, diagnostics 80−43947
continuous X-ray radiation, picosecond ruby laser heating *(Russian)* 80−75079
coupled resistive g/ion temperature gradient instability 80−79481
cross-field plasma ion acoustic instability in asymptotic quasilinear limit 79−77379
CT-6 Tokamak device, development, test operation *(Chinese)* 80−87919
current structure, fast particle generation *(Russian)* 80−48913
cyclotron emission spectrum, electron temp. 77−76208
cyclotron instability with anisotropic kinetic temp., Nyquist diagrams *(Chinese)* 80−28627
cyclotron self-absorption in two-temp. plasma, temp. and density meas. 80−48987
D-T plasma model, uniqueness and linear stability of operating points 80−14897
DC arc plasma, alterations in spectral line intensities due to external mag. fields 80−79621
Debye screening modifications in ponderomotive effects 80−33777
dense plasma, diagnostics of two-wavelength optical absorpt. 79−98978
determination from H_2 and D_2 mol. band intensities 79−98986
determination from H_2 and D_2 molecular band intensities in low pressure plasma 80−37896

plasma temperature continued
determination on basis of cyclotron absorption in inhomogeneous mag. field *(Russian)* 77−80375
diagnostic error using finite size electrostatic analyser, field-free plasma 79−55562
diagnostics, scattered radiation intensity fluctuation method *(Russian)* 80−14932
diagnostics of LF plasma fluctuations by probes and optical line radiation 79−64905
diagnostics of temperature fields, local equilib. in emissive medium, reconstruction 79−41874
diagnostics using particle vel. distrib., variation with distance 79−77419
dielectric response function, density fluctuations effects 78−30413
diffuse discharge, current constriction near anode in combustion product plasma 80−103201
diffuse pinch, energy equilib., classical scalar cond. and neo-classical models 80−24208
diffuse theta-pinch, ion temp. meas. *(Japanese)* 80−87951
diffusion, steady-state, boundary electron temp. and current density in Tokamak 78−22457
diffusion cooling, electron energy balance 78−5852
discharge, capillary pulse type, spectral chronographic-equidensitometric diagnostics 80−44055
discharge, grazing, incomplete gas temp. and electron density diagnostics 79−55600
discharge, hollow cathode effect with axial elec. field *(French)* 79−60209
discharge, ns, in dense gas, high energy electrons 79−60210
discharge, pulse, low voltage, radial temp. distrib., chem. composition determ. 79−50845
discharge, RF, gamma regime, ionis. balance and plasma characts., model 80−44022
discharge, Tesla coil type, temp. diagnostics from OH A→X intensity meas. 79−64939
discharge in air, pulsed, high-current, channel temp. profile 77−27768
discharges, high current, press., conductivity meas. 80−38793
dissociative recombination of H_3O^+ and D_3O^+ at elevated electron and gas temperatures, rate coeff. determ. 80−63747
distortion of the thermal-ion distribution during neutral-injection heating 80−103169
distribution, vac. arc plasma, fault current limiter mode 78−9851
distribution in jet, spectroscopic meas. *(Korean)* 77−80355
DIVA, scrape off layer, multigrid energy analyser applications 80−33818
Doppler broadening meas. in ZT-1 toroidal pinch 77−19773
double-layer, steady-state, fluid theory 80−43873
double-pass rapid-scanning Fourier transform spectrometer meas. in Tokamak plasma 80−59299
drift cyclotron instabilities, temp. grad. and electron gyroradius effects 79−10653
drift cyclotron loss cone mode, warm plasma effects 79−68904
drift instability, non-local, of current-carrying plasma with temp. inhomogeneities 78−59580
drift instability stabilisation by RF elec. field in inhomogeneous plasma, kinetic theory 79−55536
drift waves, multispecies plasma, nonlinear behaviour, turbulence, diffusion 78−59588
drift-dissipative waves, weakly ionised plasma, column steady state 80−38613
duoplasmatron anode plasma, ion temp. 80−6292
EBT expts., simple annulus power balance 80−48947
ECR as a diagnostic for mirror trap plasma 80−38709
ECR fundamental ordinary mode absorption and emission 80−43943
edge cooling using superbanana limiter 80−92362
electric arc, horizontal, in inhomogeneous mag. field, mass spectrometric anal. 80−79620
electric arcs, temperature estimation from self-reversed spectral lines 80−75110
electric field pattern calcs. in laser produced plasma *(German)* 80−54014
electrical conductivity of high temp. imperfect gas *(Russian)* 80−100072
electrical conductivity of high-density, shock-heated Ar and Xe plasmas 80−38557
electrode contact processes, microplasma diagnostics 80−59325
electrolyte pulsed discharge, radiation and equilib. composition 78−5975
electron, microwave p-i-n diode modulator, transient plasma instability meas. *(German)* 80−87942
electron, Thomson scatt. meas. in JIPP T-II device 79−23461
electron beam heating, electron energy distrib. 79−7471
electron conc. and temp. approximate formulae 78−63596
electron concentration balance in wave field, profile stabilisation *(Russian)* 78−22497
electron cyclotron emission from Tokamak plasmas with mildly superthermal electrons 80−92270
electron cyclotron emission in ALCATOR Tokamak 78−5935
electron cyclotron frequency expts. in 15X-B Tokamak, temp. rel. to heating power 80−48912
electron density and temp., adiabatic toroidal compressor, power balance anal. 77−51219
electron density and temp. distribs., Tokamak-4, q=5.4 stability margin mode *(Russian)* 77−47240
electron density and temp. meas. using spectral line density ratios 78−14203
electron density and temp. profiles, Langmuir probe meas. in sputtering DC discharge *(French)* 78−30482
electron density determ. by CO_2 laser 90° collective scatt. 78−67433
electron density diagnostics using self reversed deuterium D_α line 78−55746
electron directed velocity meas., optimised method using laser scatt. incoherent regions 80−79561
electron energy balance in Hall accelerator *(Russian)* 79−55456
electron energy distrib. in nonstationary plasma column 79−18998
electron energy distrib. of relativistic plasma in mag. mirror, synchrotron radn. meas. 79−10717
electron heat diffusivity, ORMAK Tokamak, X-ray emission obs. 77−31524
electron heating due to MHD shock wave, electron temp. and density 79−14588
electron oscillations, in hot plasma with non-Maxwellian vel. distrib. *(Portuguese)* 78−83557
plasma temperature continued
electron plasma, impurity screening effects in intermediate degeneracy region 80−14882
electron plasma relax. characts., 3-30 eV 80−79612
electron plasma waves in a two-temperature plasma 80−92285
electron temp., time and space var., determ. from electron cyclotron emission meas. in Tokamak plasma 80−48996
electron temp. determ., floating double probe and renewed method 77−80356
electron temp. in medium press. flowing positive column with vol. recomb. 78−87561
electron temp. meas., continuous, automatic, using double Langmuir probe 80−43977
electron temp. meas. by soft X-ray energy anal., pulse pileup effects 79−64910
electron temp. relax. in afterglow plasma 78−51280
electron temperature, multi-pulse ruby laser recording of temporal evolution by light scatt. 80−14938
electron temperature, plasma press., energy lifetime, in T-9 Tokamak *(Russian)* 77−68863
electron temperature and density for plasma parameters typical for tokamak boundary region, meas. method 79−55560
electron temperature and density in Ar behind reflected shock waves 80−38549
electron temperature and electron density in low density magnetised plasma by probe method 80−48848
electron temperature and ion composition, allowance for excited states 78−30408
electron temperature dependence of ion beam-induced currents 79−32746
electron temperature determ., semi-analytical eqn. for X-ray absorpt. curve 77−27722
electron temperature difference in flow core of MHD accelerator channel 79−10722
electron temperature gradient driven microtearing mode 80−96361
electron temperature in glow discharge in transverse mag. field, spectrosc. method meas. 80−87855
electron temperature meas. by impurities line emission time history 77−15241
electron temperature meas. by Thomson laser scatt., θ-pinch energy loss *(Chinese)* 80−54028
electron temperature meas. in ionosphere by high-freq. probe method 79−92632
electron temperature measurements from cyclotron emission in T-10 Tokamak 80−19617
electron temperature profile meas. by Thomson scatt. with single laser shot *(French)* 78−9840
electron vel. distrib. in reflex discharge, Thomson scatt. meas. 78−34368
electron velocity distrib. determ. during strong turbulence 79−60196
electron velocity distribution, behaviour in periodic elec. field *(German)* 79−10632
electronegative gas glow discharge, plasma instability boundary conditions, electron temp. *(Russian)* 80−38739
electronic excitation and ionisation temp. meas. in ICP Ar source, H_2O vapour effects 80−75028
electrostatic, slow,, Landau damping at low power levels 78−9774
electrostatic plasma-confinement experiments in a tandem mirror system 80−70025
electrostatic probe, electron temp. meas., surface pot. var. effect 78−14202
electrostatic probe for ion energy anisotropy meas. in magnetised plasma 79−10710
ELMO bumpy torus, collisional regime, radial transport 79−41801
ELMO Bumpy Torus, electron cyclotron heating, density and temp. 80−28780
EM macroparticle acceleration, high press. gas temp. density 80−79583
EM waves incident on warm plasma half-space dual propag. and absorpt., density and temp. depend. 80−75048
emission line shapes from a rotating ring radiator 80−83998
equilibrium in highly collisional toroidal regime 80−28796
erosion magnetoplasma compressor, stabilisation of electron temp. in compression region 79−19057
estimation method for electron temp. and density in ^{3}He plasma and ^{3}He-Ar plasma 80−64785
excitation temperature of rapidly varying plasma 80−38537
excited atoms population distrib., electron-density variation influence 78−87431
expansion into vacuum, ion acceleration 80−6228
exploding liner gas confinement, liner velocity effects 80−79541
Fabry-Perot interferometer meas. 80−59302
far IR lasers appl. and detection systems in controlled fusion research 78−47182
fast electron convective heat transfer and thermal escape *(Russian)* 80−1744
fast neutral diagnostics of heated plasma, temp. determ. 77−68875
fast-ion emission from CO_2-laser pulse-produced plasma 79−68939
filament ellipticity, energy lifetime in T-8 apparatus *(Russian)* 80−87930
fission reactor, gas-discharge, fuel element component conc., plasma temp. profile instabilities 80−63253
floating double probe for determ. of plasma electron temp. *(Japanese)* 77−80368
fluctuations, turbulent, microwave blackbody spectrum obs. 78−1897
focus, effective ion temperature, determ. by nucl. reaction rate in D_2-^{3}He mixture *(Russian)* 79−27824
focus, Mather-type machines, temp., density, neutron and X-ray emission characts. 77−24184
Fourier transform spectrometer, double-pass rapid-scanning, for plasma diagnostics 80−103190
free electron recombination, arbitrary nonequilibrium stationary distribution calcs. *(Russian)* 80−53947
free expansion of plasma with two electron temperatures 79−90377
free-burning arcs, simple theory 80−6297
frequency shift of TM_{omo} mode due to anisotropic temp. effect 77−84517
FT-1 Tokamak, electron density and temp. radial distrib. laser scatt. obs. *(Russian)* 78−59666
fusion mirror reactors, finite orbit treatment of plasma buildup 80−37631
fusion plasma boundary layer 77−47216

plasma temperature continued
fusion possibilities and plasma confinement and interactions in mag. config. Tokamak, review *(French)* 80−54017
fusion reactors, superheating-diffusion instability, thermonuclear burn. 80−32500
fusion research plasma temp. increase 80−18607
fusion system stability and dynamic properties transfer function anal. 79−93825
gas breakdown, multiply-charged plasma, temp. kinetics and population levels *(Russian)* 80−106952
gas temp. meas. in glow discharge in capillary using thermocouples *(Russian)* 78−59694
gas temperature measurement from mol. emission spectra in glow discharge 79−55558
gas-discharge plasma, in axisymm. mag. field, plasma flow diagnostic meas. 77−35419
gaseous core reactor U plasma radiative temp. calc. 79−9807
Gaunt factor temp. depends., from Ar II and Ca II Stark widths 78−87491
glow discharge, crossed-field type, electron energy distrib. diagnostics 79−27851
glow discharge, electric probe diagnostics, sputtering of appl. 78−71537
glow discharge, superheating ionisation instability with rot. elec. field 80−79611
glow discharge, temp. meas. using electronic rot.-vibr. mol. spectra *(Russian)* 78−71575
gradient drift wave eigenmodes stability in sheared mag. field 80−43914
graphite arc, in Ar flow, meas. of anode voltage drop 80−84022
graphite vapour cloud, laser-prod., temp. conditions investig. 80−59290
H-pinched discharge, low-current, optical, elec. and erosion studies 77−35417
Hall accelerator plasma stream, electron temp. using Xe-optical thermometer 78−79475
He I and II radiation enhancement in mag. field, nonlocal thermodynamic equilib. 80−10366
heating in lower hybrid freq. range, temp., ion diffusion 80−83954
HF discharge, ionisation overheat instability in EM wave field *(Russian)* 80−106990
HF discharge, plasma density and electron temp. meas. using Langmuir probe *(Russian)* 79−37559
HF induced discharge, gasdynamic parameters meas. and calc. 78−94934
HFS brightness ratios of impurity metal 77−89310
high pressure optical discharges, density and temp. meas. 80−48931
high temperature plasma, impurity ionis. equilib., radiative cooling 78−42712
high velocity jets generated by plasma focus and shock-wave expt., temp. and density meas. *(Russian)* 80−106882
high-pressure plasma, probe meas. for different probe and plasma temps. 79−82092
high-temp. regimes, simulation and confinement scaling 80−38673
highly ionised plasma, nonlinear effects in excitation of mag. field *(Russian)* 79−55502
highly-ionised positive column under free-fall and ambipolar diffusion conditions 78−67490
hollow cathode arc, plasma column parameters *(French)* 78−9885
ICRF heating in TFR, preliminary obs. and further development prospects 80−28741
impedance of magneto-acoustic wave launching antenna 80−24180
implosion plasma, exploded-wire array, X-ray line spectra 79−55457
implosive shock wave, prod. by laser, eval. of attained temp. 79−73022
inductively coupled plasma, temp. and electron density, optical meas. 78−67417
inert gas hollow cathode arc, mol. beam sampling of metastable atoms as electron temp. probe 80−43967
inert gas ion laser, high voltage-low press. discharges, stationary props. 80−92400
inert gas mixtures, high-press., collisional radiative recomb. 80−63595
inert gas plasmas, prod. by U fission fragments in nucl. reactor props. 77−76147
inert gas positive discharge column, at. temp., interferometric meas. 77−35427
internal disruption in Tokamak, relax. oscills., self-consistent model *(Russian)* 80−53957
ion acoustic soliton propag. in two-electron temp. plasma 80−33767
ion acoustic wave radiation due to oscill. point charge *(French)* 80−43900
ion acoustic waves, linear and nonlinear, cold electron density effects 78−30441
ion and electron temps. equilibration rate, quantum effects 80−24133
ion beam probe diagnostic system for EBT 77−84513
ion beam-created high-press. plasma, electron props. diagnostics *(French)* 80−10407
ion component energy anal. in moving plasma 77−80366
ion density and temp., cusp field with RF plugging, appl. thermonucl. plasma 77−76169
ion energy analysis on a plasma focus device, rel. to fusion plasmas 79−90465
ion energy radial profiles in ATC Tokamak, charge exchange meas. 79−10712
ion pressure discharge theory in the strong ionisation regime 80−38734
ion temp. and density meas. in direct current octopole by induced optical fluoresc. 80−14939
ion temp. meas. by 10.6 μ scatt. from thermal fluctuations 78−67431
ion temp. meas. in rarefied drifting plasma 77−84511
ion temperature, and plasma pot., in electron beam produced plasma in hollow collector 79−27794
ion temperature, in Tokamak plasma, X-ray Doppler broadening determ. 79−27830
ion temperature, meas., ion cyclotron instabilities 77−68871
ion temperature, neutral beam probe meas. *(Japanese)* 80−19615
ion temperature, of beam-heated PLT plasma, neutron emission meas. 79−68954
ion temperature, spectroscopic meas. in plasma with RF and neutral beam heating 78−5934
ion temperature characteristics of upgraded DIVA Tokamak device 78−63584
ion temperature determ., appl of secondary electron emission to energy anal. of energetic neutrals 80−59278
ion temperature determ. from Doppler profiles 78−79466
ion temperature determ. in mag. field, gridded probe method 80−70033
plasma temperature continued
ion temperature diagnostic system design and operation at Princeton 78−54942
ion temperature distrib. determ. from impurity lines Doppler broadening 79−27827
ion temperature in scrape-off layer, Katsumata probe meas. 78−75418
ion temperature meas. in ring-shaped T-9 Tokamak *(Russian)* 77−68862
ion temperature measurement using stimulated Brillouin and Compton scatt. 77−58892
ion temperature of low density plasmas by two-probe method 78−55749
ion temperature profile meas. using charge-exchange neutral anal. 80−48850
ion-acoustic solitary waves, ion temp. and higher order contrib. effects 79−46439
ion-acoustic wave, in collisionless plasma, modulational instability, ion temp. effect 79−60132
ion-acoustic waves freq. and damping from dispersion relations 80−69991
ion-sound waves in turbulently heated plasma, parallel and perpendicular propag., microwave obs. 79−14612
ionosphere, electron temp. distrib., approx. expressions using vertical rockets data 80−12599
ionosphere, lower hybrid drift instability 80−46343
jet, absolute spectral brightness measurement 80−28832
jet, laser Doppler anemometry *(French)* 77−43070
jet, radiative parameters, temp., electron density *(Russian)* 78−38459
jet, swirled, natural gas injection effect on temp. and vel. fields 79−90473
jets, intersecting, gas-dynamic accel. in compression zone, optical and spectroscopic obs. 77−51247
JFT-2 Tokamak, radiation loss meas. using thin-film thermometer 80−47698
JIPP T-II, electron cyclotron emission meas. using double-pass optical spectrometer 80−54035
JIPP T-II device, electron temp. meas. using Thomson scatt. method 79−50891
JIPP T-II plasma, soft X-ray spectrum meas. 79−55554
L-2 stellarator, ohmic heating discharges with gas puffing 80−79593
L-2 stellarator, ohmic heating ion component characts. and particle lifetimes *(Russian)* 78−59547
Langmuir double modulation probe, current ratio optimisation 79−48576
Langmuir system, kinetic theory of mag. field generation 80−69974
Langmuir wave excitation by two pumping waves, convective instability *(Russian)* 80−14904
laser flux dependence 79−50895
laser fusion expts., tamper temp. and compression, simultaneous proton and α-particle meas. 78−83607
laser heated electron distribs., props. 78−30462
laser heated plasma, heat-flux limitation and ion-acoustic turbulence 78−18453
laser irradiated dense plasma column, dynamics 79−86597
laser plasma, 1/4 crit. density region, harmonic generation expts. *(Russian)* 77−7578
laser plasma, high Z target, time resolved X-ray spectra 79−27807
laser plasma, Langmuir probe meas. of parameters and expsn. 78−18456
laser plasma, reflectivity and temp., scaling laws 80−87913
laser plasma electron density, Stark-broadened line wings of H-like ions 78−79462
laser plasma expansion and rethermalisation in uniform mag. field 78−30458
laser plasmas, ultrahigh speed diagnosis of corona parameter *(Russian)* 78−1899
laser produced, heated by 10^{-10} sec. pulses, X-ray emission spectra 77−51239
laser produced plasma, lateral energy transport 80−59258
laser produced plasma, radiation press. effects, interferometric diagnostics 78−38540
laser produced plasma, temperature versus laser flux, scaling law 79−90427
laser produced plasma, transient ionising regime, X-ray emission obs. 79−55550
laser produced plasma expansion, ion emission, hot, cold electron density, temp. ratios 78−71513
laser-generated, ion beam production from interaction with Nd:YAG laser radiation bursts 80−106939
laser-heated plasma with large temp. gradient, ion acoustic turbulence, reduced thermal cond. 80−53987
laser-imploded target, spatially-resolved X-ray spectra diagnostics 79−37543
laser-irradiated glass shell plasma, electron temp. and density, Si X-ray emission diagnostics *(Chinese)* 80−38718
laser-irradiated target, electron accel. by reson. 80−75076
laser-produced high-Z plasma, X-ray diagnostics 80−75074
laser-produced plasma, temp. meas. method using probe 79−27831
laser-produced plasma, X-ray spectra 80−75075
laser-produced plasma electron temp. determ. by Langmuir probes remote from target 78−75427
LASL toroidal reversed-field pinch programme, energy loss meas. 80−23127
Lausanne belt pinch, plasma stability 77−43028
linear gasdynamic confinement system 80−48957
linear turbulently heated plasma, secondary emission detector obs. 80−75100
low-density plasmons, electron temp. meas. by He spectrosc. 80−103192
low-pressure pulsed Hg discharge, props. 79−64916
low-pressure RF discharge electron temp. probes 78−67542
low-temperature plasma, in mag. field, density, probe determ. 78−67418
low-temperature plasma, in mag. field, electron temp. and plasma pot., probe determ. 78−67419
low-voltage pulse discharge plasma, radial temp. distrib. and chem. comp. determ. *(Russian)* 78−71544
low-Z impurities radiation during RF heating in ATC 80−28816
magnetic pinch discharge, superstrong mag. field prod. 79−90444
magnetically confined arc, axial density and temp. var. 78−5966
magnetically confined plasmas, expressions for nonclassical energy and particle flows 80−75031
magnetised plasma, electric current and electron temp. distribs. *(Russian)* 77−35319
magnetoplasma, nonuniform, simulation, initial particle loadings 79−46473

plasma temperature continued
maximum constriction phase of a weakly ionized discharge in helium 79−90486
maximum energy flux in collisonless plasma, comparison with free molecular gas motion 80−6221
measurement, by vibr. Raman intensity, 500-2000K 79−37436
measurement in cross-flow arcs 78−22559
measurement on laser heating of solid surface *(Russian)* 78−47172
metal snow liberated from wall, cooling effects 78−71494
metal snow liberated from wall, cooling effects 78−71495
methane pyrolysis, AC arc discharge plasma temp., electron density meas. 79−87843
MHD generator channel electrode surface temp. selection, effect of working body props. 79−55573
MHD wave growth and decay in high temp. gas 80−79458
Michelson interferometry diagnostics 78−1890
microwave beam interaction, intense, with low temp. plasma flow, space distrib. 80−38578
microwave cavity, partially filled with temp.-anisotropic uniform hot plasma, eigenmodes 78−75362
microwave plasma generation at atm. pressure, departure from LTE 78−67597
mirror plasma, drift cyclotron loss cone instability, localised cold plasma effect 79−32797
molecular beam sampling of hollow-cathode discharge plasma, fast neutral source 77−68865
molecular electron imact excitation, rot. transitions *(Russian)* 79−76524
multi-chord particle diagnostics of a plasma column *(Russian)* 80−1840
multi-ion system, modulation instability of ion acoustic waves 80−69996
multi-region global transport model for Tokamaks 80−92264
multichannel HCN laser interferometer for Tokamak plasma diagnostics 78−5928
multicharge heavy ion emission from strong-current low induction discharge plasma *(Russian)* 80−14033
multicharged ion heating in Z-pinch, column compression, temp. and density *(Russian)* 80−64754
multicomponent multiply ionised plasma, mean radiation paths calc. 80−33754
multimirror experiment, linear, trapped electron instability 79−60181
multiply charged laser plasma, rapid cooling, possible short-wavelength radiation generation 79−41852
multiposition Thomson scatt., determ. of electron density and temp. profiles 80−48977
neutral atom distribution near wall, temp. grad. effect 80−19555
neutral beam heating in the Princeton Large Torus 80−106950
neutral beam injection heating in JIPP-II Tokamak 80−28710
neutron production in Maxwellian D ion plasmas, ion temp. diagnostics appls. 80−49005
noncircular Tokamak, time evolution of elongation ratio and Mirnov oscill. 80−64763
nonideal plasma, elem. excitations and macroscopic props., review 80−43842
nonlinear drift wave evolution, model eqn. 80−100075
nonlinear interaction, electron collision freq., self-consistent eqn. *(Russian)* 80−75055
nonthermal electron energy distribs. measured by Fe XXV satellite lines 80−21911
nonthermal O plasma stationary states 78−63544
normal atom conc. determ. by resonance line broadening with Hg press. 80−43883
ohmic heating in Frascati Tokamak, preliminary results 80−28734
ohmically heated plasma, in JFT-2 Tokamak, Thomson scatt. meas. 79−50890
optical line emission, Doppler broadened, axially symmetric, plasma, interpretation model 78−75276
optical temp. meas. evaluation by computer 78−91150
parametric instability, thermal fluctuation effect in inhomogeneous plasma *(Russian)* 80−106897
Pfirsch-Schluter transport, temp. screening effect 77−76035
plasmatron, vortical, HF temp. fluctuation obs. in N_2 plasma stream, holographic interferometry 77−43068
PLT, Fe-charge state distrib. by Bragg cryst. X-ray spectroscopy 79−68956
PLT, ion temp. radial profile meas., neutron flux, Doppler broadening and charge exchange 78−79469
PLT, neutral beam injection, power input and plasma temp. reconciliation 80−106224
PLT, neutral beam injection and ICRF heating, charge exchange meas. 80−83892
polarisation and ang. of reson. absorption by planar targets 78−9810
polarisation of picosecond excited continuous X-ray radiation *(Russian)* 80−59190
population inversion due to plasma expansion into ambient gas, electron cooling 80−96363
positive column, axial elec. field and electron temp. in transverse mag. field 78−9880
positive column, electron temp. with two- and three-body vol. recomb. 80−19645
positive column, in transverse mag. field, plasma parameter diagnostics 79−19103
positive column, ionisation and temp. effect on charged particle profile and density 80−79596
positive column with vol. recomb., electron temp. characts. 77−84401
positive columns composed of mixed ion plasma, general ambipolar diffusion theory 78−94897
potential variations in multi-dipole device rel. to anomalous ion temperatures 79−90378
powder particles in plasma stream, temp. distribs. meas. method and apparatus 78−14210
power flow and electron Landau damping of lower hybrid waves in cylindrical plasma 79−94784
probe diagnostics, temp. and space pot. in mag. field 79−19095
probe meas. near plasma edge in Alcator 79−7489
pulsed erosion jet, energy characts., heat flow distribution *(Russian)* 80−33825
pycnonuclear reactions, and pair correl. function in dense plasma 78−32445
quadrupole and double sphere dipole probe meas. for electron density and temp. diagnostics *(French)* 78−14208
quantum effects on temp. relax. 80−28603
plasma temperature continued
radiation cooling of high-β plasma 78−1807
radiation intensity calcs. in vacuum UV region *(Russian)* 80−48861
radiation plasma, diffusion-recombination distribution of free carrier concentration *(Russian)* 78−79408
radiation temperature of proton beam induced plasma 80−100094
radiative emission rates for low- and medium-Z elements in high temp. plasmas 80−103125
ram effect for conducting cylinder in drifting plasma 80−54029
Raman Q-branch intensity, for mol. plasma 79−37545
rarefied plasma flow, degree of nonisothermality, probe meas. 80−24243
ray tracing near electron cyclotron reson., finite temp. effect 80−53994
recombination continuum estimate of temp., bremsstrahlung emission 79−50887
recovery electric strength, effect of plasma parameters 80−6294
reference temp. method for determ. densities and plasma temp. 77−84510
relativistic electron beam, energy deposition in plane solid low Z target 78−5894
relaxation, in external mag. field 78−1797
relaxation processes in plasmas with magnetic field 79−46426
resonance absorpt. and optimum focusing of axisymmetrically polarised laser beam, spherical plasma *(Russian)* 78−1863
resonance fluorescence method for plasma diagnostics, at. density and temp. meas. 80−49001
resonant absorption in Ar plasma at thermal equilib. 80−1799
reverse field pinch, Faraday rot. diagnostics for internal mag. field 80−43976
RF discharge-plasma interaction, energy exchanges, magnetoacoustic wave generation 78−30485
RF medium pressure flowing positive column plasma, electron temp. 78−59549
RF probe meas. 79−86612
rotational and gas temps., rel. in low press. mol. plasma 80−6215
runaway electron critical velocity in magnetised gas *(Chinese)* 80−87845
runaway electron diffusion and power balance in Tokamak moderate density discharges 80−28609
S microwave radiation induced prod. and heating, electron temp. and density *(Spanish)* 79−98926
scattered light LF fluctuations meas. method 78−75412
self similar cooling wave, effective thermal cond. *(Russian)* 80−14908
sheaf instability at moderate densities, anomalous ion heating *(Russian)* 80−43922
shock heated dense plasma, density, temp. and press. determ. 79−32819
shock-heated dense plasma, continuum radiation and optical transmittance diagnostics 80−24202
short plasma column, two temp. effects, electron-ion effect, comment 78−67383
short plasma column, two temp. effects, electron-ion effect, reply 78−67384
shortwave thermal radiation, diagnostics *(Russian)* 77−47258
soft X-ray diagnostics, Gaunt factor effect 79−19093
solar flares, Fe XXI 1354 Å obs. from Skylab rel. to ionisation equilib. calcs. 80−21956
solar transition zone, electron density, energy balance and press. from EUV spectra 80−21957
space charge ionising waves, high velocity propagation 80−87889
space-resolved extreme UV spectroscopy of C laser produced plasma 79−50889
spark, in vac., high-press. local plasma regions production, X-ray and hologram diagnostics 79−19104
spark, underwater, integrated bulk plasma characts. 79−27857
spark discharge plasma electron temperature, time development 77−11394
spatial temp. distrib. meas., interference filter photographic method 78−67332
spectral line intensity, arc plasma temp. depend. 77−29079
spectral line meas. 77−23467
spectroscopic diagnostics, book contrib. 77−51242
spectroscopic source, inductively coupled, analyte excitation temp. and electron density distribs. 77−40592
spherical probe, slightly ionised continuum, current-pot. curves 77−72494
SPICA, impurity radiation, density and temp. 80−87859
stainless steel laser irradiated, plasma cloud radiation absorpt. and diagnostics *(Russian)* 78−59632
stationary inhomogeneous electron temp. distrib. states and electrodynamic params. *(Russian)* 78−42749
stationary nonequilibrium distributions of ions produced in the interaction with an electron thermostat *(Russian)* 80−64684
stellarator, Wendelstein-VII A, charge exchange atoms yield, elliptic cross-section effect *(Russian)* 79−98950
submillimetre diagnostics, active, of Ar arc, data numerical anal. 80−48979
submillimetric-wave laser Thomson scatt. ion temp. diagnostic implementation in Tokamak 80−59301
superradiation from non-ideal plasmas in electric field 80−38568
supersonic dense stream, shock braking processes, radiation-gasdynamic obs. 80−19635
supersonic flowing continuum plasma, triple probe method applied to direct display of parameters in supersonic flowing continuum plasma 79−60191
suprathermal electrons, self-generated mag. fields, laser plasma 78−5902
surfatron produced electron density and temp. microwave meas. 80−43965
sustained optical discharges in molecular gases 80−100085
T-10 Tokamak, electron cyclotron emission meas. 80−92375
T-tube plasma, influence of boundary layer on H_γ line 80−48862
target in air, CO_2-TEA laser breakdown, average temp. depend. on physico-chemical target props. 77−19738
temperature and electron density, determ. by optical density comparisons, at two freq. *(Russian)* 78−22554
temperature drift instabilities in Tokamak plasmas 77−19687
temperature meas. in inhomogeneous plasmas appl. of Bartels' theory of radiation 80−53948
temperature scale, 10000 to 15000K, construction using plasma spectral density measurements 79−30470
TFR, soft X-ray diagnostics 77−51234
TFR 600, ^2H ion flux, temp., and density meas. 80−48940

plasma temperature continued
TFR plasma temp. measurement using spectral scanning in VUV, monochromator design 80−38703
theoretical plasma mechanics, book 80−27048
thermal, time evolution, temp. profiles 78−14147
thermal induction plasma, in finite cylinder, 2-dimens. analysis 77−55128
thermal plasma, heat transfer to neighbouring walls or electrodes 78−1804
thermionic diodes, planar low press. gas discharges, plasma regime, plasma characts. 79−77435
thermonuclear dense plasma, neutron diagnostics, book contrib. 80−24253
thermonuclear fusion, breakeven condition on hot-ion mode 80−78439
thermonuclear plasma, ion temp. determ. 77−11405
theta pinch, $N^{+,2+,3+}$ lines Stark broadening, He(II) line diagnostics 80−24249
theta pinch, spark channel quasi-spherical compression, electron temp. 80−87920
theta-pinch, axial heat flux limit effects 79−10636
theta-pinch, fast, axial ion energy distrib., particle and probe diagnostics 78−59655
Thompson scattering diagnostics of low density plasmas, Nd:glass laser system 80−96388
Thompson scattering for electron beam and plasma diagnostics *(Russian)* 80−54031
Thomson scatt. diagnostics using optical multichannel analyser 78−67432
Thomson scatt. meas. of electron temp. 79−19092
Thomson scatt. pathways calibration, rel. to diagnostics *(French)* 80−43886
Thomson scattering, multi-channel TV apparatus, PLT machine, mech. aspects 78−54932
Thomson scattering from an anisotropic plasma 79−60112
Thomson scattering meas. of heating process 80−59272
Thomson scattering with high background level of plasma scattering 80−43979
thyratrons, nanosecond discharge of the H_2 plasma deionisation, spectroscopic study *(Slovak)* 77−47279
Tokamak, Alcator, high-density D_2 discharge parameters obs. 78−18438
Tokamak, edge effects and impurities, influence on thermal stability 80−87892
Tokamak, electron energy confinement, simulation predictions 79−64898
Tokamak, fast-wave heating, ray-tracing anal. 79−41848
Tokamak, JFT-2, gross particle confinement characts. by boundary plasma, electrostatic probe diagnostics 79−32822
Tokamak, LT-3, ion heating by disruptive instability, ion temp. particle diagnostics 79−86593
Tokamak, mean ion temp. diagnostics at wall by ion beam surface modification anal. 79−46457
Tokamak, metal impurity reduction by working gas injection 80−106963
Tokamak, neutral beam-heated, parametric scaling 80−10406
Tokamak, PLT, expt. results 77−43072
Tokamak, PLT, fast-wave heating of two-ion plasma through minority cyclotron reson. damping 80−24194
Tokamak, reactor size, diffusive losses and scaling law 78−87478
Tokamak, recomb.-induced neutral particle flux, ion temp. diagnostic method 79−32799
Tokamak, relax. during internal disruptions 77−51235
Tokamak, T-10, plasma parameters 77−43071
Tokamak, T-4, corpuscular diagnostics by charge exchange of plasma ions at artificial target *(Russian)* 80−83968
Tokamak, temp. fluctuations and heat transfer 80−74003
Tokamak, Texas turbulent torus, turbulent heating model 79−37518
Tokamak, TFR, variable-radius Mo and graphite limiters 78−63600
Tokamak, Thomson scatt. diagnostics, far IR lasers development, review 80−24242
Tokamak, TM-3, near wall region, Langmuir probe obs. *(Russian)* 77−47261
Tokamak Alcator C far IR emission diagnostics of electron temp. 80−59291
Tokamak diagnostics, review 78−47163
Tokamak discharge microwave preionisation at electron cyclotron resonance 80−83896
Tokamak electron temp. and density profiles from electron cyclotron radiation spectra 80−59293
Tokamak far IR Fourier transform spectroscopy resolution limits 80−59298
Tokamak fusion reactor, ignited operation regimes 80−10423
Tokamak fusion reactor, steady-state, lower hybrid wave-driven, design constraints 80−10424
Tokamak ignition equilibria and thermal stability 80−74005
Tokamak magnetic confinement, recent progress in Tokamak expts. for fusion energy prod., review 79−71948
Tokamak modes, MHD theory, drift effects *(Russian)* 79−37477
Tokamak plasma, Thomson scatt. method using pulsed ruby laser 79−10720
Tokamak power reactor, steady state, lower hybrid wave driven 80−48945
Tokamak reactor, neoclassical regime, stationary temp. profile 77−74987
Tokamak reactor design, influence of physics parameters 79−36414
Tokamak scrape-off plasma, metal impurity recycling effect 80−10421
Tokamak TFR, Thomson scattering system based on two-detector spectrometers 80−32426
Tokamak TO-1, feedback system effect on plasma parameters *(Russian)* 80−103174
Tokamak transport codes, one-dimens., poloidal divertor simulation 79−37539
Tokamak-4, $q=5.4$ stability margin mode *(Russian)* 77−47240
Tokamak-4 plasma, meas. of local parameters of ions *(Russian)* 79−32824
Tokamaks, PLT and PDX, X-ray diagnostics 80−75104
toroidal plasma, ion temp. control by neutral injection 79−37514
toroidal plasmas, high temp., electron cyclotron emission meas. by mesh filter method 80−75101
transition from isentropic to isothermal expansion in laser-produced plasmas 80−87918
transition layer between two magnetized plasmas 80−24136
transport functions by precision arc expts., H Balmer spectrum 80−103187
plasma temperature continued
triple probe method for meas. plasma parameters in low-density flowing collisionless plasma 78−1898
triple-probe method for direct display of plasma parameters 77−35395
Tuman-2A, plasma compression particle diagnostics, density and temp. *(Russian)* 80−38677
turbulent heating mechanism, in T-5M toroid, ion and electron temp. diagnostics *(Russian)* 77−47259
turbulent plasma, electron distribution function, correlation anal. 79−14547
two electron temp. plasma, collisional and Landau damping of ion-acoustic waves 80−19572
two-electron temp. plasma, ion acoustic holes 80−59205
two-fluid equilibrium, axially symm. plasma, inertial effects 78−51282
two-stage ion heating obtained in rapid theta-compression expt. 78−22520
two-stage ion heating obtained in rapid theta-compression expt. 78−22521
two-temperature He plasma, transport props. 80−92260
UHF discharge with preliminary locally ionised gaseous medium 80−38851
unmagnetised plasma, quasilinear theory of parametric processes 79−94787
Venus ionosphere, plasma diagnostics meas. by Venus Orbiter *(German)* 79−96941
wall-stabilized arc, in transverse magnetic field, velocity and temperature field determination 78−38569
wave dispersion in presence of relativistic beam 80−19592
wavebreaking amplitudes in inhomogeneous plasma, temp. depend. 79−68915
weakly ionised plasma in DC field, non-zero neutrals temp., unstable modes anal. 80−38606
whistler damping near electron gyrofreq. due to cold-plasma injection, rel. to magnetosphere 80−28659
X-ray continuum meas., theory of foil-absorption techniques 79−23459
X-ray diagnostics, hot lab. and astrophysical plasma 80−59282
X-ray emission, electron temp. meas. 80−103127
X-ray emission, superthermal, from CO_2-laser-produced plasmas 79−90454
X-ray monochromatic images for hot plasma ion and temp. distrib. 80−64772
Z_{eff} values, in T-10 column central zone, Thomson scatt. obs. *(Russian)* 79−55545
Z-pinch, gas puff device, X-ray spectra, plasma form. 79−94816
Z-pinch, HBTX 1, ion temp., total radiated energy 77−27729
Z-pinch, HBTX 1 reversed field, Thomson scatt. diagnostics 77−27730
Z-pinch, high density, Hδ line spectra 78−18445
Z-pinch, imploding Al liner, soft X-ray spectroscopy 78−14198
Z-pinch dense H plasma, emission spectrum thermal equilibrium departure 79−82094
Z-pinch discharge, electron temp. and density variation obs. 78−75426
Z-pinch plasma, density and temp., spectroscopic meas. 79−4181
Z-pinches of intense energy-density driven by high voltage storage lines 80−87952
ZT-1 reversed field pinch, derated mode MHD stability and diffusion 77−27701
Al laser plasma, high-Z, temp. meas. from bremsstrahlung emission 80−87914
Al plasma, hot dense homogeneous, X-ray production rate and ionisation state density, calc. 78−71458
Al target, in air, pulsed CO_2 laser irrad., thermal response and plasma characts. 79−86595
Al target bombardment in vacuum by microsecond laser pulses, plasma parameters 79−64884
Al, vacuum arc, excited state density theory 80−100107
Ar, afterglow, pulsed discharge, acoustic oscills. in emitted radiation 77−89309
Ar arc, non-LTE, electron balance, temp. and density *(French)* 78−1796
Ar arc, plasma parameters determ. by laser scatt. 79−32812
Ar arc plasma, decaying, temporal changes of particle densities and temps. 79−64940
Ar arc plasma, partial LTE for lower excited levels of ArI 80−79565
Ar arc plasma, transition probabilities, continuum emission coeffs., electron density 77−51228
Ar atmospheric arc plasma deviation from LTE 78−67604
Ar boundary layer electrostatic probe meas. *(Japanese)* 78−5933
Ar constricted discharge, electron density and temp. and gas temp., iterative method *(German)* 78−83627
Ar decaying arc, numerical simulation 80−38767
Ar, decaying plasma arc, electron disappearance mechanism 80−38765
Ar discharge, ion density profile, reson. laser light meas. 80−92401
Ar, discharge, pulsed, neutron species spatial distrib., laser beam diagnostics 78−38543
Ar discharge, pulsed, weakly ionised, neutrals effect, interferometric obs. 79−27854
Ar, formation in crossed electric and magnetic fields, optical spectra 80−79452
Ar full circle arc, mass flow field investig. 80−38797
Ar HF torch discharge, spectral diagnostics 79−14607
Ar hollow cathode arc, in mag. field up to 2 kOe, plasma parameters 80−6306
Ar III, in pulsed arc plasma, ξ, factor determ. 79−4116
Ar, in rot. steady state centrifuge, rot. rate and temp. diagnostics *(Russian)* 78−5923
Ar, ionising boundary layer in shock-tube side-wall flow 79−60144
Ar jet, under press., heavy particles temp. meas. *(French)* 78−9841
Ar laser-evaporated microplasma radial glow and temp. distrib. 78−67387
Ar one-phase and two-phase jets, non-equilibrium in initial region *(Russian)* 77−31518
Ar, optical breakdown at 10.6 μm near plasma layer boundary 79−60165
Ar plasma, continuum radiation, temp. and charged particle concs. from line intensities and widths 77−68867
Ar plasma, electron temp. meas., microwave technique 78−26325
Ar plasma, inductively coupled, excitation transfer between plasma and impurities *(French)* 78−14211
Ar plasma, low density, shock-heated, effective collision freq. calcs., electron temp. meas. 80−75025
Ar plasma, RF prod., mag. field effect on props. *(Korean)* 79−50869

plasma temperature continued
Ar plasma, supersonic nonequilib. corner expansion flow, electron and particle temp. 77−89235
Ar plasma, wall stabilised arc, spectroscopic temp. and radiation standard 77−76199
Ar, plasma arc, dynamic charact., electron energy relaxation effect 80−38774
Ar plasma arc, wall-confined, nonequilibrium effects 80−70058
Ar plasma jet, electron temp. and density determ. 79−41875
Ar plasma jet, surrounded by Ar, He, N_2, H_2 gases, recombinations in decaying jet 78−9753
Ar plasma radiation obs., line and continuous spectra *(French)* 80−19619
Ar RF discharge plasma, magnetically stabilised, electron temp. using optical spectroscopy *(German)* 78−63582
Ar, stream electrons, at atm. press., electrical parameters *(Russian)* 80−53930
Ar, vac. UV emission profile, temp., spectroscopic meas. 77−51229
Ar wall-stabilised arc electron and heavy-particle temp. variations 78−67602
$Ar^{16,17+}$ filled glass shell, symmetric laser compression 80−64759
Ar:K seeded plasma, temperature diagnostics 78−67427
Ar-He plasma, electron temp. and density meas., to check diffusion calc. 79−27749
Ar-N_2 mixtures, DC arc, energy balance of electrons 78−42797
C, laser plasma, time resolved electron temp. *(Russian)* 78−22566
C plasma, spectral and absorpt. coeffs. 80−69985
CO_2, decaying discharge plasma, contraction in const. elec. field, profiles of gas density and temp. *(Russian)* 79−37447
CO_2 plasma, atm. press. opt. props., 400-1200 nm spectral range and 10^4-2×10^4K temp. 80−33753
CO_2-N_2-^{3}He, laser, plasma diagnostics of media capable of lasing in nucl. reactor environment 79−10279
CO_2(-He) discharge, UV-initiated, electron ion recomb. and CO_2 dissoc. 80−44068
Cl_2-arc, low temp., visible and IR continuum radiation 80−38784
Cs plasma, decay in presence of N_2, population inversion 79−55455
Cs(Ar-Cs) plasmas, electron momentum transfer cross section, cyclotron reson., temp., cond., and vel. meas. 80−106930
CsI-Hg-Ar discharge, high-press., temp. and plasma comp. determ. 79−10709
Cu arc, fluctuating, diagnostics using spectral-image photographs *(Japanese)* 79−41896
Cu-Ne, hollow cathode laser discharge, spectroscopic temp. meas. 79−7490
CuBr laser, tunable dye laser radiation, gas temp. atomic density meas. technique 79−82037
D, high current pulse discharge investig. *(Russian)* 78−47171
D-Ar mixture, effect of Ar admixture on plasma temp. 79−37446
D-T fuel temperature in laser fusion targets, neutron energy spectra obs. 77−89317
D-T fusion plasma, parametric noise effect on temp. stability 77−39439
D-T tokamak plasma effect of particle confinement and recycling on thermally stable regions 79−97900
D+PTFE, DF* prod., Fourier transform IR spectroscopy 80−87105
D_2 discharge, high current, pulsed, plasma composition, temp., electron density, press., spectral diagnostics 79−55459
D_2-^{3} He mixture, neutron yield ratios, ion temp. 78−5953
DyI_3-Hg arc discharge plasma, spectroscopic study 80−54033
Fe XXV, He-like, dielectronic satellite spectrum, electron temp. diagnostics in plasma 79−82098
H arc, laser Thomson scatt., ion temp. determ. 79−23453
H atom analyser using Cs heat pipe, low energy appl. 80−70043
H dense thermal plasma, radiation emission 80−103120
H, plasma, collisional depopulation rate of n=2 level, laser plasma method 78−79463
H plasma, laser produced, characterisation meas. 78−67409
H plasma, thermal emission and Debye shielding 80−64692
H plasma plane and cylindrical layer emission field calc. *(Russian)* 80−33755
H, recombining plasma, population inversion using collisional-radiative model 79−46423
H^- surface ion source, plasma parameters, diagnostics 78−9849
H_2 arc plasma, forward scatt. at 10 μm using light mixing to meas. ion temp. 77−89313
H_2 hot-iron plasma, ion temp. and electron density depend. studied by laser light scatt. and emission spectroscopy 80−96342
H_2 plasma, radial density and temp. profiles, using magnetoacoustic oscills. 79−19082
H_2, plasma, resonance fluorescence diagnostics 80−48971
H_2 plasma ion temperature determ. in mag. field, gridded probe method 80−70033
H_2 plasma reactor design, heat transfer and flow 80−38697
H_2-D_2-He, microwave discharge lamp, H and D Lyman-α line shapes 79−80698
H_2-SiH_4, glow discharge, emission spectroscopy of Si H 80−69984
H_β line profile for plasma microfield distrib. function reconstruction 78−71539
$H_2(D_2)$, electron dissociative attachment rates, rot. (vibr.) excitation depend. 80−43848
Hα and Hβ, Stark profiles, ion-motion effect 80−63592
He, afterglow, intermediate press., plasma discharge parameter time depend. calc. 79−19102
He afterglow plasma, $He(2^3S_1)+e\rightarrow He(1^1S_0)+e+KE$, rate const., electron energy distrib. 78−71571
He, afterglow produced by microwave surfaguide, spectroscopic diagnostic, electron and He_2 rot. temp. 80−44042
He, arc plasma Stark profile, heavy-particle temp. 79−46484
He, cryogenic discharge, interferometer meas. of neutral gas temp. 78−1924
He diffusion plasma column in coaxial cold cathode discharge, radial distrib. of electron density 77−51237
He discharge, medium press., contraction mechanism, inhomogeneous heating 80−44024
He discharge, RF, plasma parameters and volt-ampere characts., two discharge regimes 80−44016
He II, 4686 Å Stark broadened profile, electron density and temp. meas. 77−23460
He II, Doppler and Stark broadened lines, electron density and ion temp. meas. 78−67407
plasma temperature continued
He II, stationary population inversion between low lying levels of He^+ in recombining plasma 77−84494
He II, Z-pinch plasma, Stark broadened profile, 4686 Å, electron density and temp. 77−84495
He II 4686 Å line, Stark profile meas. in high density plasma 80−96390
He II 4686 Å Stark broadened profile, electron density and temp. meas. 77−23460
He, in rot. steady state centrifuge, rot. rate and temp. diagnostics *(Russian)* 78−5923
He plasma, cryogenic, recombination decay *(Russian)* 79−4104
He plasma, ion state and electron temperature in high-current pulsed discharge *(Russian)* 79−27844
He plasma, laser heating, spectroscopic meas. 77−76205
He plasma, low-density, electron temp. determ. from He I 3889 Å and 5016 Å line intensities 80−96394
He positive column, magnetised, temps. of charged particles, nonlinear effect of ionis. waves 80−44023
He pulsed arc, Thomson scatt. diagnostics 80−24297
He, pulsed elec. discharge, high-current, diagnostics and nonequilib. state 79−64942
He, spark prod. by short laser pulses, spectroscopic meas. of temp. and electron density 77−43086
He, ultradense reproducible Z-pinch, for laser-pellet interaction simulation, characterisation 78−30463
He-Co_2-Xe plasma discharge electron conc. and temp., optical diagnostics method 79−41871
He-H_2 strongly supercooled quasistationary plasma prod. by intense electron beam in dense gas *(Russian)* 77−89277
He-Ne waveguide laser, discharge plasma theory, max. output intensity depend. on discharge tube radius 79−55110
He_2 high press. afterglows, reviews 80−64823
^{3}He plasma, prod. by products of $^3He(n,p)^3H$ in nucl. reactor, props. 77−76146
Hg plasma flow, electron temp. determ. from partial LTE populations 80−24248
Hg plasma formation by strong Hg line irrad., mechanism 78−83585
Hg-Tl-I discharges, 50 Hz, axial segregation effect on elec. field strength 80−59320
K-Kr, afterglow of laser plasma, fluoresc. spectra 79−19085
K_2O-Al_2O_3-$2SiO_2$-BaO plasma emitter 80−96368
Kr water-cooled arc lamp, anode, temp. distrib. along length, anode geometry effects 80−106994
Kr^+-He, microwave-pulse-excited, internal plasma parameters, time variation 77−38858
Mg plasma, heated by ruby laser pulses, X-ray emission spectrum 80−64781
Mg XII, electron temp. determ. of laser plasma from continuous recomb. radiation 79−64924
Mo, arc, vac., stabilised, plasma props. 78−51384
Mo XLI, Mo XL, X-ray emission from vacuum-spark plasma 78−41991
N, high intensity arcs, anode contraction region modeling 80−103210
N, plasma, Stark broadening, photoelec. obs. 77−23463
N_2 afterglow, chem. reactions rel. to plasma props, appl. to toluene polymerisation 80−3346
N_2 arc, plasma parameters determ. by laser scatt. 79−32812
N_2 arc, spectroscopic meas. w.r.t. LTE 77−19786
N_2 arc plasma, stabilised by gas injection, thermochem. nonequil., particle excitation, vibr. temps. 80−19634
N_2, diffuse plasma, population densities of triplet states, correl. with electron impact processes 80−43966
N_2 discharge, electron shock wave formation, numerical simulation 80−38777
N_2, glow discharge, DC, low-press., translational/rot. temps. relation 78−38454
N_2, laser-irrad. freely expanding jet, electron temp. and spontaneous mag. field meas. 77−84469
N_2, low pressure discharge, gas temp., laser interferometric meas. *(German)* 79−68951
N_2, low-pressure DC discharge positive column, vibration temp. radial distrib. 78−67499
N_2 plasma, electron distrib. function, kinetic coeffs. *(Russian)* 78−38451
N_2 plasma, electron temp. and conc. meas., complete LTE 77−65908
N_2, plasma, in graphite reactor, temperature distribution *(Russian)* 77−51241
N_2 plasma, non-equilib., excited species, vibr.-rot. anal. fluoresc. obs. 80−54034
N_2 plasma jet, spectroscopic obs., electron temp. 77−31512
N_2 positive column, gas temp., interferometric diagnostics, heat cond. calc. 79−32834
N_2 positive corona into spark, prebreakdown phase, spectroscopic anal. 80−38790
N_2, RF plasma, gas rotational temp. determ. 79−90458
N_2, streamer discharge, spatial and temporal spectroscopy 78−5971
N_2-Ar plasma, coupled thermal-chem. relax., thermodynamic nonequilib. 78−34265
N_2-CO_2-H_2O gasdynamic laser mixture, electron beam diagnostics 77−83845
N_2-H_2 arc, bent and rot., flow mechanism 80−70047
Na, high press. arc, plasma spectral change mechanism 79−82093
Na high-pressure arc, time-depend. plasma temp. meas. 77−68866
Na-Ne-Ar AC discharge, positive column 77−39487
Na-Xe, high-pressure discharge, electron density, interferometric meas. 78−75415
Ne medium-pressure discharge, electron temp. radial profile meas. by electron-atom bremsstrahlung continuum 78−67497
Ne, nuclear induced plasma, simulated 80−64786
Ne plasma, generated by 200 MeV protons, electron density and electron temp. 78−22568
Ne-N_2, energy transfer, H^+ ion beam produced plasma, ion density and temp. 80−38539
OH radicals in glow discharge, rot. levels distrib., temp. meas. 78−47169
SF_6 axially blown arc, current-zero behaviour, theoretical model 80−38789
SF_6, high-temp. circuit-breaking arc, axial and radial heat transport 79−19105
SF_6 plasma column, in Maecker type arc, diagnostics and model *(French)* 80−19652

plasma temperature continued
SF_6 plasma thermodynamic props. at arc extinction temp. and pressures 80−79435
SF_6-inert gas mixture, high power cylindrical spark discharge, dynamic and visible charact. 80−64816
SiH_4 discharge, low pressure, plasma parameters, relevance to Si film deposition 80−44030
Sr, atoms and ions in discharge, temp. and conc. determ, by spectral line shapes *(Russian)* 78−14214
Ta, plasma produced by pinched relativistic electron beam impact on foil 79−77403
UI plasma, absolute emission coeff. 80−64693
Xe discharges, electrodeless, UHF in waveguide rel. to DC characts. 80−38762
Xe, pulse gas discharge, high-intensity, energy storage and temp. in channel 78−1926
Xe, s-p transitions, Stark consts. and oscill. strengths, shock tube meas. 80−18822
Xe, wall-stabilised plasma, temp. and press. of high press. plasma *(German)* 79−23450
Y_2O_3 capillary discharge plasma, temp., radiation screening elimination 80−64682
Y_2O_3 plasma, eqn. of state investig. 80−75027

plasma theory
see also Debye-Huckel theory
ω_{pe} radiation emission from Tokamaks, mechanism 78−51286
adiabatic invariant J, finite-β effect in axisymmetric tokamaks 80−79538
adiabatic to stochastic motion transition, Kolmogorov Arnold Moser surface 80−59175
aerosol, highly-dispersed, nonisothermal, thermionic electron density function determ. 78−91066
aerosol induced breakdown in air, two-dimensional modelling 79−90368
afterglow, electron energy distrib., radial variation 78−71570
alkali metal plasma, effect of elastic electron scatt. by at. excited states on conductivity 78−42715
alkali metal-inert gas, inhomogeneous mixture, nonequilib. processes under conditions of T-layer form. 78−91079
ambipolar plasma traps, resonance particle diffusion 79−86601
ambipolar traps, transport processes, neo-classical theory *(Russian)* 78−71518
amplification of radiation near cyclotron frequency due to electron population inversion 80−92271
anisotropic plasma, kinetic evolution theory 80−28608
anisotropic plasma dynamics, uniqueness theory 78−79415
anomalous electron diffusion, thermal mag. fluctuations 78−83531
anomalous heat conductivity for a weakly ionized plasma in a strong magnetic field 80−100070
arc, Elenbaas-Heller eqn. solution by analogy 78−71584
arc, high-press. gas blast, local thermal recovery, current zero model calcs. 78−9892
arc, laminar flow, equilib. composition deviation 80−24274
arc, sheath structure at an emitting electrode 79−55606
astron exponential rigid rotor equilibria, excluding untrapped particles 78−67395
astronomical magnetic fields modification by plasma mechs., review 77−73946
atomic and molecular processes involving ionic-covalent nonadiabatic coupling, review 80−38535
atomic cross sections, calc. using effective Feynman diagrams 80−38566
atomic energy level broadening in turbulent plasma, retardation effects in motion of quantum systems 77−60975
atomic physics algorithm for transient ionis. and recombination 78−5846
atomic processes for mag. fusion research, data status, review 80−42851
atomic transitions, dense plasma, modified quantum defect method, Ar appl. 80−38570
autoionisation lines, attenuation, function of electron density 78−18387
backflow of quasiparticles, dynamics of one-component plasma 79−27614
backscattering, nonlinear theory, adiabatic approx. 77−68757
ball lightning, plasma bunch description, stationary state, energy supply, occurrence 78−44969
ball lightning, quantum mech. theory *(German)* 78−16082
ballistic wave transformation kinetic effects *(Russian)* 80−38584
BBGKY hierarchy, scaling method of kinetic eqn. derivation 78−54286
bifurcation numerical method *(French)* 80−24129
binary ionic highly dissymmetric mixtures, phase separation 79−46425
black holes, magnetosphere, charge particle trapping 78−57573
bottleneck calculation for collisional radiative recomb. coeffs. for Li-like ions 80−53942
bound states, lifetime and level shift 77−62331
bound states, of particle in static screened Coulomb pot., anal. calc. 79−10633
boundary conditions at surface of plasma emitter of ions 78−87432
boundary layer, charge separation region, pot. distrib. *(Russian)* 77−76030
bounded medium, nonlinear parametric reson., limit cycle solns. 80−19071
Breit-Darwin plasma, close to equilib., coarse-grained Hamiltonian description 78−63541
bremsstrahlung, plasma, in mag. field, electron distrib. depend., diagnostics *(Russian)* 77−47158
bremsstrahlung, stimulated, multiphoton, electron-electron collisions effect 77−76039
bremsstrahlung cross-sections, 1- and 2-photon, Debye shielding corrections 80−106157
bremsstrahlung emission coefficient in the dipole approx., in magnetised plasma 80−19562
bremsstrahlung of fast particles, collective effects 79−10645
bremsstrahlung spectrum, mag. field effects 78−67323
bunch enlargement in vac. *(Russian)* 80−83907
canonical ensemble partition function, incorporation of long range electrostatic effects 78−21065
charge distortion on a wire in a warm plasma 78−55274
charged fluids near freezing point, static dielectric behaviour, simulation 78−56417
charged hard spheres in neutralising background, radial distrib. function 77−33936
charged particle, relativistic, polaris. loss in external HF elec. field *(Russian)* 78−26240

plasma theory continued
charged particle energy losses, homogeneous superhigh freq. elec. field and ion polarisation effects *(Russian)* 79−90384
charged particle in mag. field superimposed by EM wave, parametric cyclotron resonance 77−27234
charged particle motion in reson. conditions, asymptotic theory *(Russian)* 77−84397
chemically reacting polyatomic plasma, kinetic model eqns. 78−26243
Cherenkov radiation from charge separated magnetic plasma 77−47163
Choquard nonlinear eqn. minimising soln. existence and uniqueness 78−67315
classical electron gas theory 79−17335
classical one-component plasma, correl. functions, perturbation calcs. 77−68747
classical one-component plasma, dynamical struct. factor and velocity autocorrelation function 78−71430
classical one-component plasma, melting parameter 78−47092
classical one-component plasma, n-bubble graph series 77−35317
classical one-component plasma, screening pot., lattice model 78−22453
classical one-component plasma, self-motion and collective behaviour 77−80271
classical one-component rare plasma, non-linear electron distrib. around massive positively charged particle 79−55458
classical oscillators, parametrically excited, appl. to plasma interactions 80−33729
coaxial cylindrical discharge tube, diffusion plasma column density and pot. distribs. 79−41797
coefficients of viscosity of a gaseous plasma 80−43875
coherence function concept extension to quadratic models 79−72987
coherent wave particle interaction in Q-machine plasma, electrostatic analyser diagnostics 80−59226
cold plasma, props. in general relativity theory, spherical approx. *(French)* 77−45786
cold semi-infinite plasma, three wave interaction 80−79462
cold-banket systems, boundary layer analysis 80−28605
collective radio-emission from plasmas 80−46392
colliding relativistic plasma instabilities with relativistic temps. *(Russian)* 80−83913
collisional relax. of electron beam injected into plasma, Fokker-Planck eqn. anal. 80−64738
collisionless drift wave eigenmodes, in sheared mag. field, WKBJ method calcs. 78−83552
collisionless emission of radiation *(Russian)* 77−3926
collisionless magnetized cosmic plasmas, non-resistive electric potential drops 80−31204
collisionless plasma, Chew-Goldberger-Low theory with finite Larmor radius corrections 80−75024
collisionless plasma, hydrodynamics, decay of initial density discontinuity *(Russian)* 77−3921
collisionless plasma expansion and fast ion generation at plasma-vacuum boundary 80−59257
collisionless universal instability, stability of bound eigenmode solns., convective modes 78−71472
colloidal plasma theory, electron droplet collision temp. 77−3914
column under ion free flight conditions *(Russian)* 79−86560
complex dielectric function long wave limit, Coulomb systems with bound states, elec. cond. 80−33738
complex nonlinear impedance of flat antenna 80−103130
composite formation, in equilib. plasmas 79−41800
composite particle ensemble, fixed ion plasma model, projection technique 77−27649
composition of equilibrium plasma 79−1288
compressible magnetic-field reconnexion 80−6226
compression of superdense eqn. of state and boundary press. profile, simulation 78−83589
computational model for spectral and radiative characts. in Kr and Xe arcs 80−64812
conductance theory of nonideal plasmas 80−33745
conducting bodies in ionised multicomponent gas, electric effects, method of separation 80−96389
conducting sphere in quiescent slightly ionised plasma, exact solution 79−86564
conference on plasma intrinsic stochasticity, Cargese, France (June 1979) 80−59174
continuous emission, ionisation potential lowering and total excitation cross section of atmospheric thermal plasma 80−38705
continuum spectra, role of excited and unstable negative ions 77−65842
convective amplification of drift waves and thermal fluctuation levels in a stable plasma 80−83932
convective diffusion and heat transport, kinetic effects 79−10644
cooling time, plasma with $\beta \gg 1$, dimens. estimates 78−83525
correlation function, long time asymptotic behaviour, influence of waves on relax. processes *(Chinese)* 80−59195
correlation measurements of turbulent ionization and ion-acoustic waves 80−59329
Coulomb bridge graphs in $2+\epsilon$ dimensions 80−24131
Coulomb system, two-dimensional, props. 77−62337
Coulomb systems, equilib. distrib. functions expansion in power of density 80−64681
Coulomb systems, thermodynamic function calc. in grand canonical ensemble calc. 77−35315
Coulomb systems, thermodynamic functions, phase transitions 79−85108
Coulombic scatt. of charged particle by random distrib. as two-body process 77−38789
Coulombic system with multipole series, Monte Carlo simulation *(Russian)* 77−62339
coupled intensity deviations from stationary nonlinear state, space and time soln. 80−48882
coupled waves in stratified Chew-Goldberger-Low plasma 80−87875
critical surface density profiles, radial stability 79−55460
critical transition to stochasticity 80−57202
current generation by electrostatic travelling waves in collisionless magnetised plasma 80−53976
current production by rotating mag. fields 80−79442
current sheet, near line of zero mag. field, numerical anal. *(Russian)* 80−83908
current sheet in compressible plasma, self-similar resistive decay 80−1755
current-carrying plasma, discontinuous transitions 78−9754
cyclotron emissivity of plasma of arbitrary density 77−47162
cyclotron radiation emission, from Alcator tokamak 79−60171

plasma theory continued
D-T plasma model, uniqueness and linear stability of operating points 80−14897
damped double solitons in the nonlinear Schrodinger equation 79−64853
Debye screening, no evidence for Hγ red shift 79−31369
Debye thermodynamics for the two-dimensional one-component plasma 80−43866
decaying plasma, nonequilib. props. during afterglow modulation by acoustic waves 80−103144
degenerate plasma consisting of heavy neutral particles, gasdynamic eqns. and one-dimens. collisionless motion 78−63543
dense electron gas response at any degeneracy, RPA calcs., plasma modes, screening 78−36930
dense ionised plasma, thermodynamic props., electron screening corrections 77−972
dense plasma, atomic energy level deform. and eqn. of state 78−71435
dense plasma afterglow, theory 78−9882
dense plasma focus, formed in plasma erosion accelerator, radiation props. 78−67440
dense plasma ionisation and cohesion, critical density and press., approx. formulas 80−59253
dense relativistic electron gas, EM response in strong mag. fields, particle polarisation, mode struct. 80−43963
density rise model and ion mixing mode in confined plasma 78−79409
diatomic asymmetric mol., vibr. self-ionisation and recomb. *(Russian)* 77−79700
dielectric friction in plasma, harmonic oscillator and rigid dipole dielectrics, collective plasma oscills. 80−53928
dielectric permeability of a nonideal plasma 79−32739
dielectric permeability of inhomogeneous plasma *(Russian)* 79−94771
dielectric permittivity determin., of strongly inhomogeneous media *(Russian)* 77−89227
dielectric response and energy loss in intermediate quantum plasma 80−38541
dielectric response function, density fluctuations effects 78−30413
dielectron recombination, electron density effect *(Russian)* 79−98856
dielectronic recombination rates, ionization equilib. and radiative energy loss rates for Ne, Mg, S ions in low density plasma 79−68903
diffusion fluxes, thermal cond., chem. reactive plasma 77−47142
diffusion of electrons through excited atomic or ionic states, role of collective interactions 80−79433
dilute electron plasma kinetic eqns. in coherent region 78−75264
direct Langmuir collapse, virial theory 78−79430
discharge plasma, diffusion regime, elec. sheath theory 80−1810
discharges, high-freq., unipolar and electrodeless capacitively-coupled, excited at atm. press., appls. 80−1861
dispersed heterogeneous system, electron conc. calc. method 78−38452
dispersion function, multipole approx., modified asymptotic Pade method 80−48853
dispersion function, two-pole approx. based on modified Pade approximant 79−82040
dispersion relation for instability hindrance in a magnetically confined plasma with finite press. 80−59221
dispersion rels., variational nature of eigenvalue problems with a parameter 79−77338
dissipation phenomena formalism, diffusion and heating applications 79−4111
dissipative non-Hamiltonian dynamical system, stochastic props. and strange attractors 80−57200
dissipative trapped electron mode, overlapping many rational surfaces, asymptotic theory 79−98907
dissociation equilibrium, phase space allocation 79−27746
Doppler profiles, optical escape factors, in spherical, cylindrical and plane parallel geometries 78−47101
double layer formation in multiple plasma device 80−83897
double layers modelled by numerical integration of Vlasov-Poisson system 80−92290
double-layer, steady-state, fluid theory 80−43873
drift cyclotron loss cone instability, nonlinear saturation 80−83929
drift waves, finite-β-modified, in sheared mag. field 78−91092
drift waves, nonlinear stabilisation, weak turbulence theory 79−98908
drift-kinetic evolution of collisional plasmas in tori 77−72409
dynamical polarisability at long wavelengths, strongly coupled one-component plasma 79−82059
effective dielectric permeability of cold plasma with electron density fluctuations *(Russian)* 80−32882
eikonal expansion of the Vlasov-Maxwell equations valid near cyclotron resonance 80−92300
electric field, HF, influence on electron ensemble in low-ionised non-isothermal plasma *(German)* 79−77383
electric field and struct. of weakly ionised plasma near charged spheroid *(Russian)* 77−47145
electric field penetration in plasma with nonlinear current saturating cond. 77−19672
electric LF microfield distribs., two-temp. plasma containing multiply charged ions 77−58843
electric pot. distrib. in plasma 80−106876
electric response function, two-component quantum plasma 79−37452
electrical conductivity, weakly ionised flowing plasma, crossed elec. and mag. fields 79−1291
electrical double layers, strong, exptl. obs. 78−30435
electrodynamic mechanisms of limitation of the electron concentration in a laser spark *(Russian)* 80−59333
electroionised discharges, theory 80−38816
electrolyte pulsed discharge, radiation and equilib. composition 78−5975
electromagnetic confinement, stationary plasma parameter calcs. *(Russian)* 78−83603
electromagnetic emission, near geometric mean plasma frequency, mechanism 79−82066
electromagnetic fields of non-equilibrium plasmas 80−6210
electromagnetic ion cyclotron instability, particle anal. 79−94781
electromagnetic wave backscattering across mag. field in bounded plasma 79−90415
electron and plasma stream reflection at a nonadiabatic mirror 80−87929
electron autoreson. accel. at nonlinear ECR in growing mag. field 80−87867
electron beam-magnetoplasma, radiation at or near electron plasma frequency, transverse modes 80−106942
electron cloud in equilib., mag. field effect, pot. and space charge distrib. 80−92410
plasma theory continued
electron cyclotron emission from thermal plasmas 79−55473
electron cyclotron emission from Tokamak plasmas with mildly superthermal electrons 80−92270
electron cyclotron emission in steady state inhomogeneous plasma 80−48864
electron cyclotron radiation from a high density Tokamak 80−92266
electron density determ. by globally convergent method for partially ionised plasma 80−53929
electron density fluctuation spectrum 78−18377
electron density fluctuations, collective spectrum 77−47148
electron distrib. function for plasma in const. elec. field 79−4106
electron distribution function and ionisation in space-depend. theory 80−38545
electron distribution function in rapidly changing elec. field *(Russian)* 78−1792
electron distribution in a free HF plasma column, anomalous skin effect *(Russian)* 80−1741
electron distribution relaxation numerical study for CO_2-N_2-He discharges 80−54070
electron dynamics in random field, dense Hg plasma conductivity appl. 80−14885
electron emission temperature, streaming plasma in laser vac. diode 78−91162
electron energy balance in Hall accelerator *(Russian)* 79−55456
electron energy distrib., relax. in elec. field, at. excitation rate 78−34266
electron energy distrib. in nonstationary plasma column 79−18998
electron energy distribution, in r.f. elec. field 78−67363
electron energy distribution function in afterglow discharge 79−10725
electron energy distribution function in very nonuniform elec. field 80−38556
electron fluid turbulence, one-dimens., statistical formulation 78−49751
electron gas, nonequilib. heating, hot electron spectra 79−55529
electron impact generated ion charge state densities analytical approx. calcs. *(German)* 79−82075
electron kinetic coefficients, of H plasma, interpolation calcs. *(Russian)* 78−71429
electron kinetic eqn. allowing for exchange correlations 78−71437
electron kinetic eqn. for plasma with strong inter-ion interaction and electron exchange correlation 80−48857
electron kinetics in const. and varying field *(Russian)* 80−53927
electron liquid, 2-dimens., cluster expansion 79−55461
electron oscillations, in hot plasma with non-Maxwellian vel. distrib. *(Portuguese)* 78−83557
electron plasma, nonlinear singular structs. for collisionless phase space fluids *(French)* 77−62335
electron plasma, pure, liquefaction and crystallisation 78−18376
electron plasma in mag. field, photon absorpt. quantum mechanical treatment 79−1296
electron plasma wave, guided propag. in plasma slab, dissipation effects 79−46447
electron plasma waves, toroidal Trivelpiece-Gould modes 80−33770
electron processes, in collisionless diode, linear theory 80−38730
electron runaway distrib. in Tokamaks, positive slope 78−5849
electron solitary holes, in magnetised collisionless plasma, form. and coalescence 79−32741
electron streams, thick-target, relax. and bremsstrahlung, Legendre expansion, solar X-ray flares appl. 79−70950
electron temp. relax. in afterglow plasma 78−51280
electron temperature and ion composition, allowance for excited states 78−30408
electron transport in dense nondegenerate plasma, thermal cond. *(Russian)* 79−98865
electron vel. distrib. in weakly ionised plasma 78−5848
electron velocity distrib., collisions *(Russian)* 78−1790
electron velocity distrib. function relax., time depend. electric field *(German)* 77−31424
electron velocity distribution, behaviour in periodic elec. field *(German)* 79−10632
electron wave dispersion relation in two-temperature plasma 79−86580
electron waves, beat radiation 80−43314
electron waves beat-driven optical free electron laser 80−43315
electron-electron collisions, neutral atom momentum relax. *(Russian)* 79−18997
electron-ion pairs, correlated pairs, effect on conductivity 78−26249
electron-ion recombination in ambient electron and neutral gases 80−38531
electron-neutral particle collision in nonlinear plasma, for Ohm's law coeffs. 79−98857
electron-positron counterstreaming beams plasma, relativistic, radiative collapse to ultrahigh densities 79−60188
electron-proton interaction, two-body sum over states of static screened Coulomb pot. 78−55714
electronic excitation and ionisation temp. meas. in ICP Ar source, H_2O vapour effects 80−75028
electronic multiplication in nonuniform elec. field 79−86559
electrophysical properties of non-equilibrium aerosol plasma 80−38543
electrostatic binding energy, relation to elementary consts. 78−47089
electrostatic plasma turbulence, entropy definition 77−76081
elementary processes and chem. reactions, review *(Czech)* 80−24126
elliptic problems involving a free boundary 80−24130
EM wave emission and induced absorption by thermal level ion acoustic fluctuations 79−37462
EM wave scattering in plasma with strong Langmuir turbulence, anal. *(Russian)* 77−76088
EM wave spontaneous emission, quasistatic surface excitation spectra 77−24061
EM waves in magneto-active plasma, group velocity direction 80−59201
emission, appl. to solar radio bursts *(Russian)* 78−14139
emission coefficient distribution, calculation methods *(German)* 78−91071
emission lines, broadening and displacement during nonlinear transfer in turbulent plasma *(Russian)* 77−91418
emission spectra, semibounded weakly ionised plasma, collisions effect *(Russian)* 77−89232
enclosed plasma spatial distrib. *(Russian)* 78−51283
energy balance, electron runaway, electric field effect on temp. relax. 77−970
energy lost by fast electrons in laser plasma 80−103165
energy transfer, macroscopic single-fluid plasma 78−42714

plasma theory continued
energy transfer direction, power solns. of kinetic eqns. for waves and particles 77−15164
enhanced fluctuations in semi-infinite plasma, HF elec. field 78−91069
equation of state, activity expansion *(Chinese)* 80−43863
equation of state, for classical 1-component plasma 80−83887
equation of state, quantum statistical theory, degeneration, electron-hole plasma thermal instability 78−91627
equation of state for a partially degenerate plasma 79−60104
equation of state of nonideal plasma 78−75261
equilibrium in free boundary case, variational principle calcs., wall interaction *(Chinese)* 80−69972
ergodic adiabatic invariants, goodness 79−71352
evolution and enhanced relax. of plasma in uniform mag. field 78−59551
excitation of high-frequency waves with mixed polarization by streaming energetic electrons 80−1773
excitation spectrum of relativistic quantum plasma, covariant Wigner function approach 80−87938
excitation temperature of rapidly varying plasma 80−38537
excited atom concentration distrib. near absorbent boundary 78−67327
excited atoms population distrib., electron-density variation influence 78−87431
excited atoms population distribs., collisional transitions effect 79−90373
excited levels populations, in nonequilib. Li plasma *(Russian)* 77−62349
expanding laser-produced plasma, radiative transfer line intensities and stimulated emission 77−3988
expanding plasma, gain on transitions of hydrogenic ions 78−17918
extraordinary mode radiation, induced emission in Tokamaks 79−64838
fast electron convective heat transfer and thermal escape *(Russian)* 80−1744
fast electrons, distrib. function, elec. field effects *(Russian)* 79−98860
fast Langmuir solitons existence in non-equilibrium plasma 80−38604
Fermi systems of charged particles, collective variables method 79−88873
fluctuation-dissipative relation in nonlinear electrodynamics *(Russian)* 78−79410
fluctuations, LF, diagnostics by probes and optical line radiation 79−64905
fluctuations, long-lived, anomalous transport, hydrodynamic contrib. 77−15165
fluctuations, long-lived, anomalous transport 77−19673
fluctuations, nonlinear EM, in nonequilib. plasma *(Russian)* 78−9756
fluctuations, plasma with power distrib. of particles, time variation *(Ukrainian)* 77−72408
fluctuations in plasma with Lorentzian vel. distrib., electron beam interaction *(Russian)* 77−19669
fluctuations of density and current, mode-coupling theory 79−23398
flute instability, HF electrostatic field driven, dispersion eqn. 79−46440
flux anisotropies in guiding centre plasma 79−50850
focus, neutron radiation, model *(Russian)* 78−22519
focusing resonance cones 78−71431
Fokker-Planck eqn., integration method 78−91067
forbidden lines in dense plasma, detectability 78−5856
free energy, exchange quantum correction, one-component plasma 78−47091
free expansion of plasma with two electron temperatures 79−90377
free plasma column in gas at high pressure 78−75477
free plasma filament in high press. gas *(Russian)* 77−84405
free-burning arc isothermal-channel theory 78−71587
free-free Gaunt factor calc. 79−60113
fusion plasma, D-T, reaction rate with suprathermal ions, ^{6}Li seeded 79−676
fusion reactor, time-dependent tandem mirror confinement, start-up and alpha particle build-up 80−10419
fusion system, with rot. stabilised liq.-liner, finite liner compressibility effects 79−18036
fusion system stability and dynamic properties transfer function anal. 79−93825
galactic masers, role of plasma effects in generating high-vel. and symmetric spectral features 80−31378
gas-blanketed plasma, boundary layer press. balance and diffusion 78−18380
generalised flux theorem for relativistic plasma, covariant forms 77−55165
generalised mean spherical approx. and thermodynamics 79−98861
generalised Ohm's law, for unsteady state of partially ionised gases 80−38542
generalised Rosenbluth pot., Balescu-Lenard eqn. friction and diffusion coeffs., wave effects 78−38457
geometrical optics formalism 80−83925
glow discharge, electron velocity distribution function relax., periodic behaviour in highly modulated elec. field 79−64935
glow discharge, positive column stability in stationary regimes 79−41893
glow discharge, tube impedance with and without metal cover 78−67508
gyrokinetic equation for low and high frequency problems 79−19003
gyrokinetic modes, spatial struct. in toroidal geometry 80−79489
harmonics generation in inhomogeneous plasma *(Russian)* 80−83916
He I and II radiation enhancement in mag. field, nonlocal thermodynamic equilib. 80−10366
heat and particle fluxes, inhomogeneous plasma, current driven drift wave effects 78−94901
heat conduction and magnetic field induction in the presence of cold- and hot-electron Maxwellian distributions 79−60109
helical stellarator, Asperator NP-3, toroidal discharge forbidden region 80−79592
HF plasma generation, electron heating, nonlinear kinetic theory 80−44041
high beta plasma surrounded by cond. shell, dynamic stabilisation 80−96354
high density directed plasma, source, design, characts., numerical model 80−38538
high melting particle heating, melting and vaporisation in hot gas 80−6201
high temperature plasma, impurity ionis. equilib., radiative cooling 78−42712
high Z plasma, high temp., opacity calcs., W, U appls. 78−79414
high-β tokamak, ballooning mode instability theory *(Russian)* 79−27757
high-n ballooning theory, stability of axisymmetric tokamak equilib. 80−64705
highly degenerate multicomponent plasma thermodynamic props. 80−33739
hollow cathode arc discharge, balance equations for active zone processes *(German)* 79−68963
hollow cathode arc with fully ionized dense plasma, V-I characts. and other props. 79−14627
homogeneous bimolecular plasmachemical reactions, nonequilib. kinetics 78−63634
hot collisionless plasma, fluid description and limits to double-adiabatic approximation 78−75262
hot dense plasma, change from Fermi-Dirac statistics to strong coupling at $kT=mc^2$ 78−55716
hot electron plasma, with cold components, flute-interchange mode stability, finite-β 78−67341
hot plasma, mag. field direction determ., by light scatt. 78−67434
hydrodynamic action, functional integration method appl., wave damping 77−31427
hydrodynamic eauation for weakly coupled one-component plasma 79−90390
hydrogenic plasma, statistical mechs. of composite particles, projection technique 78−47090
hydrogenic plasmas and fluids, transverse dielec. function, excitation spectrum 78−67311
imploding plasmas, mag. field generation, Nernst refrigeration 80−79526
implosions, mag. field generation due to Nernst refrigeration 79−27811
impurity radiation from medium density plasmas in Tokamak or mag. mirror reactors 78−5857
impurity radiation loss effects on Tokamak expts. 78−22465
incompressible nondissipative MHD turbulence in spheromak, stable equilib. statistical states 79−60134
induced Compton scatt. from nonlinear charges, nonlinear classical theory 77−68857
inert gas ion laser, high voltage-low press. discharges, stationary props. 80−92400
inert gas plasma, emission continua, photoionis. cross sections, absorption coeffs. 300-10000 Å 78−42731
inert gas plasma, free-bound continuum determ. using photoionis. cross sections calc. 80−43878
inert gas plasma, thermodynamic functions, composition, and elec. cond., calc. method 79−32738
inhomogeneous diffusion equation, analytical solns. 77−55129
inhomogeneous plasma, generation of higher harmonics of resonant radiation 80−106880
inhomogeneous plasma column, reson. props., control using probing UHF signal *(Russian)* 77−76051
inhomogeneous plasma equilibria, linearised anal. 79−50878
inverse bremsstrahlung, Lorentz model 77−35327
inverse bremsstrahlung for intense radn. fields 78−51288
inverse-bremsstrahlung absorption rate in an intense laser field 80−24201
ion acceleration in expanding rarefied plasma 79−41799
ion acoustic instability, renormalised kinetic theory for long range oscills. 79−27773
ion acoustic soliton, Boussinesq eqn. description 79−46449
ion acoustic solitons in collisionless multi-ion plasmas 79−77351
ion acoustic wave, self excited, in hot plasma, dispersion theory 80−92283
ion acoustic waves, linear and nonlinear, cold electron density effects 78−30441
ion clusters, equilib. props. and struct., Monte Carlo calcs. *(Russian)* 79−27745
ion distribution function, ion drift rate *(Russian)* 78−1791
ion energy loss to electrons, high energy test ions 78−91065
ion excited level population probabilities, steady- vs. quasisteady-state models 80−24128
ion excited level population probabilities, steady-state, appl. to H-like ions 80−19552
ion microfield distrib. function, quantum-statistical calc. *(Russian)* 77−65836
ion pressure discharge theory in the strong ionisation regime 80−38734
ion recombination in low-density ambient gas, variational principle, equiv. to quasiequilib. condition 79−37443
ion system, internal energy, Debye temp. function, Monte Carlo method data 77−35314
ion temp. and parametric decay development in RF-generated stellarator plasma 80−79436
ion-acoustic Korteweg de Vries solitary waves in plasma with density, temp. gradients 78−55720
ion-acoustic pulse generation by 2 EM pulses at difference freqs. in collisionless plasma 80−79475
ion-acoustic turbulence, current-driven in weakly ionised plasma, quasilinear theory 79−41830
ion-acoustic waves freq. and damping from dispersion relations 80−69991
ion-sound soliton-resonant particle interactions *(Russian)* 80−14880
ionic and plasma cluster equilibrium and kinetic props., computer simulation 78−71533
ionic fluid, equilib. props. using corresponding states concepts 79−27889
ionic lines, isolated, Stark broadening function *(French)* 77−23462
ionic structure in high density plasma, screening effects 77−7513
ionic system with mild repulsion, Monte Carlo calc. 78−94891
ionisation equilibrium in partially degenerate plasmas 79−94813
ionisation of H plasma in uniform elec. field *(Russian)* 80−53923
ionisation wave, kinetic theory 78−22454
ionisation-recombination kinetics in equilib. plasma 79−90371
ionisation-recombination kinetics in ionising plasma 79−90372
ionised relaxation dissipation of waves in low-temp. plasma *(Russian)* 78−1816
ionised system theory, general Mayer graph estimates, long range behaviour 79−46424
ionosphere, perturbation of collisional plasma by opposing EM wave, anal. *(Russian)* 77−9605
ions, multiply-charged, dielectronic collisional recombination rate, effect on level populations 79−1287
ions in steady-state plasma, excited levels population probabilities, asymptotic behaviour 80−79438
irreversible ponderomotive effects 79−60105
isotropic plasma, metastable atoms, equilib. distrib. function 78−91068
isotropic plasma, reciprocity theorem 78−8254
jellium, one-dimensional, wall effects 79−46468

plasma theory continued
KdV eqn. with damping, rational solns., appl. to plasma physics 79−27743
kinetic, magnetised plasma, Fokker-Planck coeffs. 77−72410
kinetic, Rosenbluth pots. for magnetised plasma 77−58842
kinetic eqn. for electron runaway prod. in toroids 78−47148
kinetic eqns. and fluctuations in μ space 77−89230
kinetic equation, for plasma in strong high freq. EM field 80−38540
kinetic equation, multiple spatial scaling, weak coupling approx. 77−80269
kinetic equation for two-dimens. guiding centre plasma 78−26241
kinetic equation in the kinetic region of the dilute and nonuniform electron plasma 80−103109
kinetic equation including strong fields and inhomogeneities 80−38544
kinetic equations for collisional plasma model 77−42963
kinetic equations for low frequency instabilities in inhomogeneous plasmas 80−83886
kinetic equations in theory of transport props. of fully ionised gases 79−10640
kinetic expressions for transport coeffs. 77−27652
kinetic reactions, pulsed afterglow technique obs. in Ar-II plasma 80−48854
kinetic theory, one-component plasma, nonlocal shear viscosity, long-time behaviour 77−35321
kinetic theory for fluctuations and noise, computer simulation 79−27822
kinetic theory of collective plasma excitations evolution, plasmadynamical state 77−15163
kinetic theory of impurity diffusion in Pfirsch-Schluter regime 77−72414
kinetic theory of neutrals in a bounded plasma slab with inhomogeneous ion temperature and density 80−87861
kinetic theory of the collisional scrape off layers 80−79439
kinetic transport properties of a bumpy torus with finite radial ambipolar field 79−55469
Knudsen plasma, one-dimens., bounded, nonlinear oscills., numerical method 78−79433
Korteweg-de Vries eqn. and 2nd Painleve transcendent, boundary value problem in plasma theory 80−69971
Landau equation, non-Markovian terms 80−79432
Landau equation for weakly coupled gases soln. for homogeneous plasma relaxation 79−41798
Landau-Fokker-Planck eqn., for arbitrary statistics, relativistic and nonrelativistic case 80−36935
Langmuir soliton EM wave scatt., theory *(Russian)* 80−38564
Langmuir solitons, transverse instability 80−6250
Langmuir turbulence, optical satellites 79−60111
Langmuir turbulence, statistical theory 80−38647
Langmuir turbulence in upper hybrid resonance region, external electric field effects *(Russian)* 79−73010
Langmuir wave-particle interactions, microscopic Lagrangian description, warm plasma 78−42755
laser beam absorption, anomaly due to two-plasmon decay 79−1318
laser beam inverse bremsstrahlung heating, Coulomb screening effect 79−68940
laser beam with retractable focus, ionis. path form. in gases 79−18992
laser produced plasma, wavelength effect on absorpt. and ionis. 77−27654
laser produced plasma expansion, ion emission, hot, cold electron density, temp. ratios 78−71513
laser radiation absorption, by dense plasma, polarisation depend. 77−62368
laser-driven fusion, validity of hydrodynamic approximation 80−75087
laser-heated plasma, energy deposition, bremsstrahlung spectra calcs. 77−3968
laser-heated plasma, energy deposition, Gaunt factor calcs. 77−7576
laser-heated plasma, energy deposition, suprathermal electron calcs. 77−7577
laser-irradiated plasma, soliton form. at crit. density 80−6267
laser-plasma interaction, spikon lifetime 80−14922
Lie transform, approach to classical perturbation theory, plasma physics appl. 78−93510
line emission, radiative and collisional broadening in laser heated plasma 77−47159
line radiation transfer, Grad moment method 79−98877
linear response theory of elec. cond. of nonideal plasma 79−64832
linear Z-pinch, outer 2s-shell electron excitation emission of C-, N-, and O-impurity ions 78−22113
liquid metal perturbation theory, extension to dense partially ionised plasmas 80−75500
local mean field theory, basis problems 80−92253
local thermodynamic equilibrium 78−18379
localised modes in inhomogeneous Vlasov plamsa 78−83563
long wavelength modes, space-time correlation functions 78−9772
low density non ideal plasma, two particle energy shift 79−14516
low pressure Ar plasmas near wall, kinetics study *(French)* 80−28689
low voltage inert gas arc theory 80−38809
low-density plasma highly-excited level population calc. 78−67326
low-temperature plasma atomic level population density computation 78−71461
low-Z impurity elements, radiative energy losses calcs. 77−39411
lower hybrid resonance heating theory of Tokamak plasmas 80−28745
Lyapunov characteristic exponents and stochasticity 80−59177
Lyapunov characteristic numbers and Kolmogorov entropy, stochasticity of dynamical systems 80−59178
macroparticles theory of Dupree, critical exam. *(French)* 77−15161
magnetic dipole radiation field, hot magnetoplasma *(Russian)* 78−30416
magnetic field, force-free, resistive evolution, in cylindrical geometry 80−6212
magnetic field distortion near an ablating H_2 pellet, effect on Tokamak reactor refuelling 80−64734
magnetic field line trajectory calc., Kolmogorov Arnold Moser surface 80−59263
magnetic fields modulation excitation *(Russian)* 79−60107
magnetic island, m=2, high-energy runaway orbits 80−64767
magnetic piston interaction with nonmagnetised plasma 80−38630
magnetic properties in strong field for one-component plasma 80−100068
magnetic reconnection in collisionless plasma 79−82051
magnetic Rosenbluth potentials, generalised to include wave effects 78−94896
magnetically confined plasmas, theory 79−98963
plasma theory continued
magnetised plasma, electric current and electron temp. distribs. *(Russian)* 77−35319
magnetised plasma, evolution, numerical soln. of hybrid Vlasov-fluid model 79−90452
magnetised plasma filled open periodic waveguide kinetic theory of reson. radiation *(Ukrainian)* 77−51197
magnetised plasma interaction with neutral gas, threshold vel. 80−59241
magnetised plasma kinetic theory, kinetic eqn. derivation 77−47147
magnetised plasma stability in large amplitude circularly polarised wave, dispersion relations 80−59223
magneto-viscous resistive tearing of cylindrical flux surfaces 80−1831
magnetoactive plasma, effect on a plane disc, impedance calcs. 80−1809
magnetoplasma, hot collisionless, resonant excitation of upper hybrid wave by two EM beams 79−77384
Mandel'shtam-Brillouin scattering, induced, from laser plasma, spectrum *(Russian)* 79−98876
many component plasmas with self consistent field, variational principles and canonical theory 80−87856
many-electron atoms plasma, quantum statistical theory of recomb. continuum *(Russian)* 78−34279
many-electron ion plasma, thermodynamic functions calcs. 80−103108
Maxwell-Klimontovich equations for turbulent plasma, renormalisation 80−79500
Maxwell-Vlasov equations, in region exterior to perfectly cond. infinite cylindrical antenna 78−1843
Maxwell-Vlasov system, boundary value problem 79−19001
Mayer-Salpeter nodal expansion, extension to two-component high-temp. plasma 77−35318
mean spherical model 80−87846
mechanics, book 80−27048
metal halide arc, energy balance 79−77440
MHD, generalised Lorenz eqns., strange attractors 80−59232
MHD eqns. and confinement studies in closed magnetic configurations 79−98964
MHD equilibrium, with axisymmetry and noncircular cross section, free boundary soln. to eqn. *(Chinese)* 80−59260
MHD generator, supersonic, working body thermodynamic props., chem. kinetics effect 78−91163
microfield in nonideal plasma 77−68743
microwave cavity, partially filled with temp.-anisotropic uniform hot plasma, eigenmodes 78−75362
mixture, binary, low ionised, electron kinetics, collision processes influence *(German)* 79−14519
model connection, hydrodynamic, water bag and Vlasov models 79−4107
moderate-Z impurity elements, radiative energy losses calcs. 77−39411
modified Saha equation at high press. thermodynamic inconsistency 78−36450
monochromatic Langmuir wave amplification by electron beam in nonlinear plasma *(Russian)* 77−76112
Mossbauer effect in magnetised plasma, applic. to gamma-ray lasers 80−28186
moving plasma, four-dimens. constitutive relations 79−37537
moving plasma filament, submillimetric complex transmission coefficient meas. 78−67424
MTE continuum emission coeff. relation, appl. to Ar arc 77−31432
multicomponent, confined atom-, and Debye Huckel-, Thomas-Fermi-Dirac models 77−24053
multicomponent, modified Thomas-Fermi-Dirac statistical models 78−18378
multicomponent multiply ionised plasma, mean radiation paths calc. 80−33754
multilayered plasma columns excitation with mag. current ring, radiation pattern 77−7557
multiple mirror mag. trap ion distrib. function, high energy tail 78−83596
N particle Coulomb system, eqn. of state, virial theorem calcs. *(French)* 80−64680
negative diffusion of ion energy, magnetised plasma, drift-wave fluctuations 78−94902
negative grid pulse effects, on Knudsen Cs arc discharge plasma 80−38843
negative wave momentum density in plasma 80−79463
neoclassical point model, stability analysis 78−30425
neutral beam production using negative ions 80−28696
neutral injection heating of toroidal plasmas, theory 79−98938
neutral particle balance in nonequilib. plasma, excited atoms effect 79−27747
neutral particles, interaction with wall and plasma, kinetic description 78−59658
neutral particles transport calc. in high temp. plasma *(Japanese)* 79−82045
non-Debye plasma, single electron density of states 78−34264
non-equilib. plasma, spontaneously radiating layer, quasi-static surface instability, energy relations *(Russian)* 78−59558
non-LTE, props. and at. processes, medium to high press. 80−59170
non-LTE line transfer, excited atom diffusion effects 77−31435
nonequilibrium plasma, fast Langmuir soliton possibility 78−75340
nonequilibrium plasma, kinetic eqn. for waves and wave scatt. *(Russian)* 78−14174
nonequilibrium plasma, kinetic theory of spectral line broadening 80−59187
nonequilibrium plasma, nonlinear wave interaction and stationary fluctuation spectrum *(Russian)* 78−14153
nonequilibrium plasma chemical reaction kinetics 78−76863
nonequilibrium stationary particle distributions *(Russian)* 77−11312
nonequilibrium weakly ionised plasma, de-excitation and stability 78−38453
nonideal alkali plasmas, ionis. equilib. 77−39401
nonideal plasma, electron degeneracy, Monte Carlo calcs. 77−35316
nonideal plasma, elem. excitations and macroscopic props., review 80−43842
nonideal plasma, measured props. and nonideality influence 80−43869
nonideal plasma theory, using Hellmann pseudopotential 78−75260
nonideal plasma thermodynamic functions and transport deviations 78−75273
nonisothermal plasma electron ensemble, nonstationary behaviour, kinetic description 80−59171
nonisothermal rarefied plasma, transport processes and Lenard-Balescu eqn. 80−6222
nonlinear coupling of three waves in non-uniform plasma 80−6237

plasma theory continued
nonlinear dielectric perturbation, wave and particle interactions 80−38593
nonlinear diffusion, Okuda-Dawson scaling 78−67321
nonlinear elliptic eigenvalue problems, convergence of inverse iteration method 79−40353
nonlinear mode coupling model eqns., topological struct. 78−75304
nonlinear oscillator systems, primary resonances do not overlap 80−59176
nonlinear problem, a priori estimation and rearrangement *(French)* 79−55450
nonlinear problem variational soln. *(French)* 78−63539
nonlinear processes in magnetised plasma, nonstationary HF pressure *(Russian)* 80−106895
nonlinear susceptibilities of magnetised plasma *(Russian)* 79−50846
nonlinear theory of unstable plane waves and solitons 80−87888
nonlinear wave envelope equations for plasma physics, Fourier's method convergence 79−55463
nonlinear-wave propagation in a proton-electron plasma coupled with a strong radiation field 80−48872
nonstationary MHD plasma flow, in coaxial accelerator in condensed media 79−60204
nonstationary plasma column, Schottky's diffusion theory 78−91174
nonthermal O plasma stationary states 78−63544
nonthermal plasma, H and H-like ion populations, collisional radiative recomb. and ionis. 78−38450
nonthermal radiation emission, in Tokamak plasma, at plasma frequency 78−42732
nonthermal radiation emission from toroidal plasma, at electron plasma freq. 79−98878
Ohm's law for partially ionised plasma *(Chinese)* 79−90375
one component plasma, dynamical struct. factor, collective modes 80−28607
one component plasma, isothermal compressibility 79−10635
one component plasma, mag. props. 79−86558
one component plasma fluid, derivation of eqn. of state in strong coupling 80−33741
one conponent plasma, charged hard sphere theory 80−106873
one-component high density plasma at intermediate wave numbers, collective excitations 78−67314
one-component plasma, dipolar and ionic electrically neutral, correl. condits. 78−4573
one-component plasma, internal energy, mean spherical approx., asymptotic form 80−1742
one-component plasma in two and three dimens., static props., semi-analytic theory 80−87853
one-component-plasma approx. scheme, quadratic compressibility sum rule 78−42713
one-dimensional inhomogeneous plasma, ion and electron vel.-space distribs., Vlasov eqn. 78−51281
optical line emission, Doppler broadened axially symmetric plasma, interpretation model 78−75276
optical measurements on plasma initiated by a relativistic electron beam *(Japanese)* 80−48914
optical scattering of light by atoms, techniques theory 80−54044
optically thick plasma, two-dimens. radiation restoration rel. to local diagnostics 80−43885
optically thin plasmas, He II excited states, role of direct ionisation excitation 80−102579
optimal feedback control of plasma parameters in Tokamak 79−64891
oscillations, in lower-hybrid range, of bounded plasma 80−24162
oscillations, normal mode analysis, eigenfunctions and adjoint functions 78−42744
overheating instability, HF EM field effect 78−9771
pair correlations in a two-component plasma 79−7443
paramagnetism in RF mag. field, expt., theory and simulation 80−6225
partially ionised plasma, generalised Ohm's law *(Chinese)* 78−14131
partially ionised plasma, kinetic fluctuations *(Russian)* 78−59552
partially ionised plasma, theory of dielectric constant 80−59173
particle and heat fluxes, inhomogeneous plasma, effect of current driven drift waves 78−94898
particle motion, regular and stochastic, Hamiltonian formalism 80−59167
particle orbit in magnetic field, guiding-centre Hamiltonian, arbitrary gyration 80−1834
particle orbits in ion rings 80−92254
particle transport in HF heated magnetised plasma 80−87863
particle trapping, detrapping and acceleration, in single wave, magnetoplasma 77−68738
particle velocity distrib. functions in nonuniform background, iterative calc. 78−71438
particle-wave interactions, cyclotron reson. vel. shift, wave propag. effects 80−33774
pellet ablation in hot plasmas, mag. shielding 79−14557
pendulum, bounce resonance and Kolmogorov entropy 80−57199
phase transition in elec. discharge plasma between parallel plates, compression by recomb. press. 80−64799
photoionisation absorption spectra, photorecombination radiation, for dense nonideal plasma 78−26252
photon escape probabilities for Stark-broadened Lyman series lines 80−24143
photon gas, steady state nonequilibrium distribution *(Russian)* 79−4110
photon kinetic equation for Doppler line broadening, soln. 78−9751
photon soliton and fine structure due to nonlinear Compton scattering 80−10363
photorecombination spectra, nonideality effect 79−82046
planetary and stellar magnetospheres, conf., Snowmass, Colorado, USA (Aug. 1978) 80−41939
plasma, ion drift velocity in EM fields, charge transfer effect 78−83527
plasma column, ultra-high current, electron collisionless motion 79−64824
plasma diffusion in stochastic mag. fields, rare collision effects *(Russian)* 79−77342
plasma dispersion for strong coupling 80−103111
plasma science conference, Montreal, Canada (June 1979) 79−90380
plasmadynamical modes, macroscopic, two-fluid description 77−15162
polarisability, long wavelength limits and compressibility sum rules 77−84404
polarisation shift effect in high-density plasmas 78−79412
polarisation transfer in inhomogeneous magnetised plasma, comments and reply 79−96905

plasma theory continued
ponderomotive effects, kinetic theory 79−32740
ponderomotive force, nonreson. EM wave spatial effects, kinetic perturbation theory 78−18417
ponderomotive potential for magnetised particle produced by low-freq. magnetoplasma wave 79−64859
population densities of excited states of H-like ions, computer program 77−39402
population inversion, soft X-ray transitions in cooling plasma, H-like ions 78−87437
population inversion in H-like ions, CR model 79−10647
positive column, density oscills. due to negative ions, metastable atom model 78−1799
positive column, electron temp. characts. 77−11419
positive column, excitation and ionisation mechanism *(Japanese)* 79−4105
positive column, ion motion, radial pot. distrib. 79−55599
positive column, ionisation and temp. effect on charged particle profile and density 80−79596
positive column, of electroneg. gas, transverse stability, effect of dissoc. attachment 79−23475
positive column with vol. recomb., electron temp. characts. 77−84401
positive columns composed of mixed ion plasma, general ambipolar diffusion theory 78−94897
potential distribution, stationary plasma, allowing for space-charge density depend. *(Russian)* 77−47146
Poynting's theorem for inhomogeneous moving media reconsidered 79−48661
Poynting's theorem for moving media, Lerche's relativistic theory 79−48660
pressure, virial kinetic definition, spherical geometry calcs. *(French)* 80−69973
primordial lepton gas, elec. cond., Landau, Boltzmann eqn. calcs. *(French)* 80−75030
probe vicinity, perturbed plasma, numerical calc. *(Russian)* 79−98976
probee investigations of the electric fields produced in air near a laser spark *(Russian)* 80−59334
pulsed current voltage characteristics of a thermally produced plasma 80−38554
pycnonuclear reactions, and pair correl. function in dense plasma 78−32445
pycnonuclear reactions, pair correlation function in dense plasma 79−67001
Q-machine, single ended, collisionless plane diode model 79−7478
quantum plasma, convergence formalism 79−18999
quantum plasma, HF conductivity 79−19000
quantum two-component plasma third sum rule and local mean-field theory 78−5982
quasioptics and anisotropic and dispersive media 80−38567
quasistatic theory for negative ion free-bound radiation threshold broadening 80−53941
quasistationary distribution functions for kinetic eqns. 78−9755
quasistationary O plasma, non-LTE props. calcs. *(German)* 77−58844
radial distribution function for two-component plasma 79−37448
radial distribution function of fluid, quantum corrections 77−3906
radial distribution functions and bound electronic energy levels in H plasma 79−37450
radial electron density gradient in electronegative gas in discharge plasma 78−87433
radiation, appl. to spectral anal. 79−55475
radiation continuous spectrum from inert gas plasma 78−42729
radiation cooling of high-β plasma 78−1807
radiation coupling, kinetic model, collisions effect 78−34262
radiation efficiency coeff. *(Russian)* 77−27655
radiation emission, in N LTE plasma 77−39410
radiation emission from localised current source in magnetoplasma 78−34276
radiation emission spatial distrib. reconstruction in torous 80−103123
radiation from source in magnetoactive plasma, appl. to cyclotron and multipole radn. 77−51190
radiation from warm plasma column with open ended coaxial ine 80−106878
radiation intensity, local values by Abel eqn. *(Russian)* 78−91072
radiation losses from impurities in high temp. plasma 77−19678
radiation plasma, diffusion-recombination distribution of free carrier concentration *(Russian)* 78−79408
radiation pressure, Thomas-Fermi eqn. of state, high temp., coupling to high-density electron plasma 77−3925
radiative cooling rates, high-temp. low-density plasma $2 \leq Z \leq 92$ 78−83534
radiative emission rates for low- and medium-Z elements in high temp. plasmas 80−103125
radiative plasma with anisotropic permittivity, developing wavefronts 80−43896
radiative processes in relativistic plasmas, appl. to kinetic theory of free-electron lasers 78−42316
radiowave generation by gyrosynchrotron and Langmuir-wave processes, solar and stellar appl. 79−21172
rarefied plasma, density discontinuity effect on kinetics *(Russian)* 79−37451
rarefied plasma in HF field, drift-kinetic eqn. *(Russian)* 77−27650
real gas discharge, thermodynamic stability 80−38852
recombination in the free vacuum expansion of a complex plasma 79−64827
recombination magnetic field effect 78−38449
recombining plasma, excited levels, population kinetics 79−90376
reflex triode system, generation of intense microwave radiation by relativistic electron beam 80−14887
regularised long wave equation, numerical studies 80−53964
relativistic Boltzmann theory, entropy production, reference frame 78−22547
relativistic Boltzmann theory, reciprocal relations, transport props. 78−30477
relativistic collisionless plasma, EM perturbation of relativistic Vlasov-Maxwell eqns. 79−90449
relativistic degenerate electron plasma, dielec. response function 78−71529
relativistic electron power law spectra in random mag. field 80−24240
relativistic magnetised Vlasov-Maxwell plasma, current responses 79−90450
relativistic plasma, kinetic equation, fully convergent 80−54025

plasma theory continued
relativistic quantum electrodynamical plasmas, covariant Wigner function calcs. 79−4175
relativistic transverse cold plasma waves, nonlinear, linearly polarised, stability 80−6235
relativistically covariant formulation in theory of plasma stability 80−75046
relativistically streaming plasma, flux conservation, MHD and force-free approxs. 79−19081
relaxation processes in plasmas with magnetic field 79−46426
renormalized kinetic theory of nonequilibrium many-particle classical systems 79−82038
resistive evolution of force-free mag. fields, rel. to anisotropic diffusion 79−90382
resistive steady states of elliptical cross-section plasmas 79−98872
resistivity, of turbulent plasma, with ion-acoustic instability, ion-tail form. effect 80−10360
resonance cone, in inhomogeneous magnetoplasma column, theoretical anal. 80−83884
resonance cone surface, nonlinear eqn. modification for magnetised plasma 80−33740
resonance radiation effect on electron emission of metal wall in boundary layer *(French)* 79−37504
resonant absorption in Ar plasma at thermal equilib. 80−1799
resonant absorption of laser light, by magnetised plasma 78−51309
resonant charge exchange, polarisation effect 80−43859
resonant wave-particle interaction, at half-integer cyclotron harmonics 78−78871
reversed current effect in stabilised Z-pinch 80−79539
RF electric field in inhomogeneous magnetised plasma column 78−83522
RF sputtering 79−87578
rotating plasma column, effect on radiation pattern of elec. current source 77−62345
rotation instability on collisionless FLR plasma, nonlinear theory 80−79485
runaway electron diffusion and power balance in Tokamak moderate density discharges 80−28609
runaway electron motion in momentum space, multicomponent plasma 79−37449
runaway electron tail, self-consistent theory 77−62338
runaway electrons in collective electric fields 78−67313
Saha's ionisation eqn. soln., input for opacity calcs. 77−39412
Saha equation, first order estimate for He plasma 80−19554
scaling method for obtaining kinetic eqns. from BBGKY hierarchy 77−45785
scattering amplitude due to elec. current ring surrounding plasma column in semiconductor plasma 79−37457
screening efficiency of the scrape off plasma in the shadow of a poloidal limiter 80−79576
screening in one dimens. plasma 80−65478
screening potential, of classical one-component plasma, lattice model 79−82043
second harmonic emission spectrum from laser prod. plasma near threshold 80−87912
self magnetic field generation by interaction with intense microwave radiation 79−27788
self-consistent kinetic theory of stochasticity 80−59179
self-generated fields by currents driven by electron press. grad. 78−1794
self-generated magnetic field in laser-produced plasmas, metallic target 79−41851
self-generated magnetic fields and harmonic emission 80−38546
self-localised EM fields in dense gas *(Russian)* 78−26239
semiinfinite plasma interaction with charged nonrelativistic particle 77−38110
sheath, electrodynamically accelerated, physical models *(Rumanian)* 78−51317
shock wave, transverse, ionising, possible structs., neutrals photoionis. effects 78−75343
shock waves, collisionless anisotropic plasma, Zemplen's thermodynamic theorem 77−68798
simulation of impurity peak positions in TFR discharges 78−91149
singular magnetic field lines, theory 79−4109
Singwi-Tosi-Land-Sjolander approximation correl. function, config.-space anal. 79−90379
Singwi-Tosi-Sjolander approximation, pair correl. function, k-space solns. and thermodynamic props. 79−94770
slab-shaped magnetoplasma excitation by magnetic current line sources 78−55717
slightly dissipative plasma, helical flux and other integral variants 77−65833
slightly ionised inert gas plasma, hollow arc discharge in cylindrical hollow cathode, theory 80−38810
small overdense plasma particle Thomson-like RF scatt., linear perturbation theory 80−48858
soft X-ray spectrum of hot optically thin plasma, interstellar medium appl. 78−34275
soft X-ray transitions, population inversion of H-like ions 77−62346
solar emission lines of NeV, MgVII, SiIX, SXI, population levels as function of electron density and temp. 80−21963
solar flare continuum events, m wavelength obs., emission mechanism 79−21248
solar transition zone, electron density, energy balance and press. from EUV spectra 80−21957
solid surface interaction, electrostatic sheath equations, inc. heating, ion mobility and ion recomb. 80−1808
soliton dynamics in nonintegrable systems, classical solns. 78−28996
space plasma discontinuities, shocks and neutral layers 79−60106
space potential determ. and storage in fast changing plasma 80−87949
spectra emissivity, at electron cyclotron freq., theory 79−72996
spectra-line profiles, weakly turbulent plasma unified electron broadening theory 77−58848
spectral broadening, for H-like ions 79−46431
spectral emissivity at electron cyclotron frequency 78−91077
spectral line broadening, correlations in quantum theory 77−7514
spectral line broadening, nonthermal RPA plasma, collective effects 79−46433
spectral line broadening due to Coulomb interaction *(Russian)* 79−86567
spectral line contours, 'hollow' source functions 78−9554
spectral line profiles, plasma carrying sound waves 78−38461
plasma theory continued
spectral line width variation within Stark broadened multiplets 78−91073
spectral lines in hot dense matter, photoabsorpt. cross sections 77−7515
spectral radiation distribution at elevated press. 79−82047
spectroscopic escape factor, approaches to evaluation 79−90387
spectroscopic escape factor, defn. and evaluation 79−90385
spectroscopic escape factor, radiative decay 79−90386
spectroscopy, Abel integral eqn. soln. *(French)* 78−30415
spin polarisation in mag. field *(Russian)* 80−33744
spiral electromagnetic waves, Landau and Cerenkov damping in mag. plasma, theory *(Russian)* 78−71486
spontaneous emission, near electron plasma freq., in runaway-electron-tail plasma 78−75275
spontaneous synchrotron emission 78−91075
sputtered atoms, LTE in excitation process 80−35037
stabilisation of low-m kink modes in Tokamak 79−64890
Stark broadening in thermal plasmas 77−47165
Stark broadening in turbulent plasma 77−47166
Stark broadening of isolated Sn II lines in cool plasma, semi-empirical calcs. 80−59186
Stark broadening of neutral lines 78−46299
Stark profile H-like ions, Lyman lines in dense plasma 79−82048
stationary nonequilibrium distributions of ions produced in the interaction with an electron thermostat *(Russian)* 80−64684
stellarator, Wendelstein-VII A, charge exchange atoms yield, elliptic cross-section effect *(Russian)* 79−98950
stimulated radiation, leaking normal mode spectra, cold plasma cylinder 77−89231
stimulated Raman and induced Compton scatt., nonlinear kinetics 77−35328
stimulated transitions between highly excited levels, rel. to anomalous Balmer decrement 78−5176
stochastic equations of motion for plasma particles 80−38551
stochastic permittivity effect of finite-amplitude elec. field 78−71436
strings in heavy-light gas mixture, self induced particle separation *(Russian)* 80−79441
strongly coupled classical plasmas in laser fusion and astrophysics, review 79−10634
strongly coupled multicomponent plasmas, statics and thermodynamics 80−33742
strongly coupled one-component plasma, shear viscosity, microscopic theory 77−51157
strongly coupled two-component plasmas, approx. schemes 77−19671
submillimetre background emission from Tokamaks 78−47102
sum rules and dynamical correlations in classical one-component plasma 79−55462
super-convergent adiabatic invariants with resonant denominators by Lie transforms 79−1289
superradiation from non-ideal plasmas in electric field 80−83904
superthermal electrons, behaviour in scrape-off layer of DIVA 78−30495
symmetric solutions of a plasma physics equation *(French)* 79−23396
synchrotron emissivity near electron cyclotron and upper hybrid freqs. 78−14140
synchrotron radiation from relativistic electron circ. orbits in magnetoplasma 79−55474
synchrotron radiation spontaneous emission from relativistic electrons, kinetic theory 77−72489
synchrotron turbulent reactor, relativistic electrons spectrum in nonsteady radiosources 79−40071
synchrotron-transient radiation of charged particle in plasma with random inhomogeneities, spectrum 78−45213
temperature anisotropy relaxation due to binary encounters 77−39404
temperature relaxation, in external mag. field 78−1797
temperature relaxation, quantum effects 80−28603
test charge problem in bounded plasma 77−80270
test particle in mag. field, pot. 80−106872
test particle potential in external homogeneous magnetic field 80−43870
theoretical physics at Kharkov Inst., Ukrainian SSR *(Russian)* 79−12558
thermal conductivity and thermal diffusion coefficient of high-temp. plasma in mag. field 80−92256
thermal conductivity and viscosity, one-component plasma, mol. dynamics study 79−23402
thermal equilib., plasma containing negative ions 77−68746
thermal equilibrium, single atomic collision relative level populations 80−1743
thermal equilibrium in plasmas containing negative ions 77−19670
thermal induction plasma, in finite cylinder, 2-dimens. analysis 77−55128
thermal parametric instability in non-uniform plasma, theory *(Russian)* 79−27760
thermionic-weakly ionised plasma, compact static isothermal, stationary transport process of charge carriers, continuum theory *(German)* 78−14138
thermodynamic equilib., multiphoton processes 77−47212
thermodynamic properties quantum-mech. one-component plasma, high density metallic region 77−84403
thermodynamic props. of relativistic quantum scalar plasma 78−75410
thermodynamic quantities, lower bounds, one-component plasma, two- and three-dimens. 79−68905
thermodynamic quantitites, of d-dimensional one-component plasma, d-dimens. Coulomb interaction 79−82042
thermodynamical functions for dense multicomponent plasmas, electron-proton plasma appl. 80−38548
thermodynamics, two-dimens. plasma 77−3919
thermodynamics and correlation functions 80−24132
thermodynamics and structure of two-component classical plasma, mean spherical approx. 80−64683
thermodynamics of nonideal low-temp. plasma *(Russian)* 77−80273
thermodynamics of nonideal low-temperature multicomponent plasma: chemical model 79−41796
thermonuclear fusion plasmas, effect of nucl. elec. quadrupole moments 78−83524
thermonuclear fusion plasmas, elem. processses and role of atomic, ionic and mol. data 80−14916
thermonuclear plasma, H_2 fuel pellet ablation, atomic processes effect 80−18596
thermonuclear plasma, radn. losses at impurities, $n_e\tau$ parameter *(Russian)* 79−68908
thermonuclear react. rates, computation with STEEP code 78−18375

plasma theory continued
thermonuclear reactions in laser fusion, emitted particle spectra, Monte Carlo calcs. *(Russian)* 80−52780
theta-pinch, collisionless, high-beta, anisotropy-driven EM modes, finite Larmor radius effects 80−1830
Thomas-Fermi model, review 77−84
Thomas-Fermi screened Coulomb systems, thermodynamic props. calcs. 77−67399
Thomas-Fermi thermodynamic functions, quantum and exchange corrections *(Russian)* 77−9953
Thomson cross sections, vacuum polaris. effects 79−10646
Thomson scatt. from plasma with Spitzer-Harm electron distrib. function 78−51287
Thomson scattering, collision-dominated, negative ions effect 78−45118
Thomson scattering from an anisotropic plasma 79−60112
time-dependent processes in collisionless plasma, anal. numerical calcs. 80−87858
Tokamak, impurity behaviour, MHD activity influence *(Russian)* 79−98866
Tokamak, impurity ionis. degree and diagnostics accuracy, electron distrib. depend. *(Russian)* 79−98973
Tokamak, nonaxisymmetric, reduced fusion neutron production 78−63577
Tokamak, recomb.-induced neutral particle flux, ion temp. diagnostic method 79−32799
Tokamak, TFR, runaway discharge, cyclotron radiation spectra interpretation 79−41805
Tokamak cyclotron radiation spectrum, dielec. props. contrib. 79−41804
Tokamak fusion reactor, ignited operation regimes 80−10423
tokamak medium field ignition test reactor, plasma engineering 78−58419
Tokamak radiation, near plasma freq., three-wave mechanism 79−37464
Tokamak radiation and Kadomtsev-Pogutse instability 79−37463
Tokamaks, energy confinement scaling, Frascati Torus results 80−79536
Tokamaks, neutral beam heated, radial transport/Fokker-Planck model 77−15224
Tonks-Dattner resonances, appls. to plasma diagnostics 78−83618
toroidal plasma, 2-D neutral H transport 78−59661
toroidal plasma, slide-away regime, quasilinear theory 79−98960
toroidal resistivity calc. 79−98965
transformation group techniques appl. to nonlinear fluid and plasma eqns. *(French)* 80−77623
transport coefficients in partially ionised gas mixture, approx. method 79−72991
transport coeffs., relativistic Boltzmann theory, variational method 78−47096
transport collision frequencies, integration of empirical data 79−25969
transport collision frequencies, temp. depend. by approx. method 79−25970
transport fluxes across magnetic field, EM fluctuation effects 78−94899
transport processes caused by magnetic flutter, assoc. with drift waves 79−86561
transverse convective ion transport in Tokamak, kinetic description 80−6214
transverse wave packet, 3-dimens., nonlinear evolution in hot plasma, ion-acoustic wave effect 80−43899
transverse waves in magnetoplasma subjected to stochastic mag. field, normal mode approach 80−75049
turbulence, Duffing's eqn. governed system 79−10664
turbulence, kinetic equation, stationary distribs., symmetry group 77−35348
turbulence, Markovian expansion, theory 78−79435
turbulent diffusion of toroidal plasma, geometrical effects 78−94900
turbulent heating, flat top electron distrib. effect, with ion-acoustic instability 80−10399
turbulent plasma, anomalous EM wave electron radiation 80−43889
turbulent plasma, kinetic theory of binary correlations 78−26285
turbulent plasma collective modes, sum-rule anal. 80−59238
two component plasma cluster, scatt. *(Russian)* 78−47088
two dimensional real matter, low density free energy in canonical thermodynamics plasmas 80−87852
two-component plasma, density fluctuations, time depend. 77−80272
two-component plasma, mean spherical model 80−87854
two-fluid dissipative plasma, energy principle in Lagrangian form, tearing modes 78−42794
two-fluid equilibrium, axially symm. plasma, inertial effects 78−51282
two-particle bound state, lifetimes and level shifts 78−75265
two-particle effective pot., for dense hydrogeneous plasma near 10K 80−38533
two-temp. electron-ion plasma with mirror reflection, EM fluctuations, space charge correl. *(Russian)* 78−59548
ultra-high current carrying column, generalised Bennett equilib. and particle orbit anal. 78−83598
unification equilibrium and radiative energy loss rates for C, N and O ions 78−87430
unmagnetised plasma, quasilinear theory of parametric processes 79−94787
vacuum polarisation, influence on radiation propagation in plasma *(Russian)* 78−47100
velocity autocorrelation function, long time behaviour 77−84402
velocity autocorrelation function in a strongly coupled, magnetized, pure electron plasma 80−6213
velocity diffusion, three-dimens., in two-stream turbulence 78−59595
virial pressure of classical one-component plasma 80−38536
Vlasov and water-bag models, self similar solns., simulation 78−26242
Vlasov equation, numerical solution, with filtering in time 79−82036
Vlasov equation, two-dimens., numerical soln., appl. to electrostatic instability and monochromatic wave 79−73032
Vlasov plasma, linearisation, optimal control 80−53920
Vlasov theory for magnetised plasma, coherent state approach 80−64675
Vlasov-Poisson eqn., space-time approach 78−83523
voltage tensor for plasma in HF EM and constant elec. fields *(Russian)* 78−63540
wave energy density and wave momentum density of species in collisionless plasma 80−79437
wave interactions, nonlinear, microscopic Lagrangian description, warm magnetoplasma 78−42754
wave packets in dispersive media, main signal and precursor approx. 80−24158
wave propagation, linear, dispersion relation, microscopic Lagrangian description, warm magnetoplasma 78−42753

plasma theory continued
weakly ionised gas, kinetic theory of electron component 77−47132
weakly ionised plasma in DC field, non-zero neutrals temp., unstable modes anal. 80−38606
weakly nonideal inert gas impulse plasma, Coulomb cross-section calcs. 80−103113
weakly-ionised, three-component, ionis. equilib. instability 80−10877
Weibel instabilities, temp. anisotropy driven, statistical thermodynamics 80−75047
whistler-Alfven turbulence interaction 80−75058
X-ray emission from laser prod. plasma 78−42780
X-ray emission from optically thin plasmas, abundance effects on continuum spectrum 78−53814
X-ray emission spectrum, multiple Compton scatts. effect, Monte Carlo calcs. 78−96389
X-ray line profiles, Stark broadening in laser plasma 78−42733
X-ray spectra from laser fusion reactor pellets 79−36410
X-ray spectroscopy, high temp. plasma 77−31434
Z-pinch, constriction due to radiation losses *(Russian)* 78−30473
Z-pinch, plane, mag. field null region parallel current effect *(Russian)* 78−91137
Z-pinch, rotating, energy balance *(Russian)* 80−14924
Z-pinch dense H plasma, emission spectrum thermal equilibrium departure 79−82094
Zakharov equations derivation for higher electron non-linearities in Langmuir collapse dynamics 80−43919
Al plasma, hot dense homogeneous, X-ray production rate and ionisation state density, calc. 78−71458
Al plasma, X-ray photoabsorpt. coeff. 79−27754
Al resonance line profiles, influence of boundary layer of Al-seeded shock heated plasma 80−43876
AlO, in arc, normalised temperature, localised emission, aureoles *(German)* 77−62413
Al(XII) and (XIII) reson. line trapping in laser-heated plasma, source distrib. diagnostics 78−42730
Ar arc, non-LTE, electron balance, temp. and density *(French)* 78−1796
Ar arc plasma, partial LTE for lower excited levels of ArI 80−79565
Ar, dense plasma, complex refractive index 79−23397
Ar, glow discharge, spectral line excitation, cold cathode region 77−84552
Ar plasma, boundary layer low-press., kinetic evolution of $3p^5$ 4s level *(French)* 77−80279
Ar plasma, constricted electric arc, iteration method anal. 79−90484
Ar plasma, operating characts., numerical study 78−67309
Ar plasma, recombination, kinetics of stimulated atomic populations *(Russian)* 78−87436
Ar plasma, spectral line blending of excited at. levels 77−76038
Ar:K seeded plasma, temperature diagnostics 78−67427
Ar-H_2 plasma, thermodynamic properties 78−63542
Ar-He plasma, thermal diffusion factors, binary mixture hypothesis 79−27749
Ar-He plasma, thermal diffusion factor, 2000-4000K, binary mixture hypothesis 79−32743
Ar-N_2-H_2 plasma equilibrium compositions and thermodynamic props. 78−71433
Ar-Xe, shock wave dynamic compression, thermodynamic props. *(Russian)* 80−53931
ArI, highly excited atomic levels, spectral-line-blending study in high-density plasma 80−48969
C plasma, continuous absorpt. coeffs. 80−10362
C VI, XUV gain in expanding cylindrical plasma 77−15170
CN, in arc, normalised temperature, localised emission, aureoles *(German)* 77−62413
CO discharge, electron energy distrib. and kinetic coeffs., ground-state mols. 80−43867
CO-He-O_2 gas discharge laser plasma, positive ion generation mechanism *(Russian)* 79−99005
CO_2-N_2-He, vol. discharge, negative ions effect 80−14956
Ca plasma, Knudsen discharge, longitudinal mag. field, emission polaris. 77−76211
Cl III, Stark broadening of isolated lines by plasma 78−9116
Cl^- radiative detachment threshold effect of plasma microfield 78−71580
Cr ions in Tokamak plasmas, spectroscopy and atomic physics 80−53938
Cs, dense plasma near saturation line elec. cond. 80−38559
Cs fully-ionised plasma hollow-cathode arc discharge theory 78−67533
Cs, photoplasma, optical excitation in radiation diffusion conditions 78−55227
Cs plasma, elec. cond. and eqn. of state, behind reflected shock wave 78−42716
Cs, plasma, eqn. of state, 30-140 atm, 3000-4000K, by adiabatic compression 78−14132
Cs plasma, eqn. of state 78−42711
Cs, plasma, highly ionised, conductivity and eqn. of state 78−26323
Cs-He plasma, steady-state discharge, role of inelastic collisions, spectroscopic diagnostics 78−42709
Cu, vapour laser emission, pulse characteristics rel. to plasma parameters 78−71090
Cu-N mixture, partially ionised, transport and thermodynamic props. 77−80276
F II, Stark broadening of isolated lines by plasma 78−9116
Fe ions in Tokamak plasmas, spectroscopy and atomic physics 80−53938
H, 2S level population calc. in turbulent plasma *(Russian)* 78−25451
H atom, spectral line broadening, ion dynamic effects 79−46432
H, dense plasma, ionisation, master eqn. analytical soln. 78−59544
H I (3^1P^0−2^1S) line, Stark broadening parameters, modified adiabatic theory, electron scatt. phase shifts 80−43879
H II region, H137β/109α intensity ratio interpretation 80−31344
H, in hot plasma, elementary excitation spectrum, exchange and polarisation effects 80−43892
H, ions recomb. and level populations, resolution of ang. momentum states 77−45529
H line curvilinear trajectories and Stark broadening 78−67324
H line shape, joint electron and ion influence *(Russian)* 78−9762
H lines in plasma, Stark broadening, review 78−42001
H, Lyman-α Stark broadening, dynamic screening effects 78−18386
H, optically thin plasma, UV spectral emission coeff., quantum statistics of recomb. continuum *(Russian)* 79−77348
H, pair correlations down to r=0 80−14883
H plasma, recombining, weakly ionised, population inversion 80−87849

plasma theory continued
H plasma, spectral intensity near series limit, taking into account sub-barrier ionisation *(Russian)* 77−31436
H plasma form., in arc discharge, dissoc. excitation role 77−84398
H plasma hemispheric layer total radiation calc. *(Russian)* 78−34278
H, quasi-nonideal, comp. analysis 77−72411
H, Stark broadened profiles, model electronic microfields 78−13468
H, Stark broadening, model microfield methods calcs. 80−92274
H, Stark profile, ion motion, model microfields 78−13469
H, Zeeman levels orientation by reson. radn. in turbulent plasma *(Russian)* 79−98028
H^- affinity radiation, theoretical study of negative absorption 80−38001
H-like atoms, Stark broadening, ion dynamics correction to unified classical path theory 79−76382
H-like atoms and ions, statistical equilib. among sublevels in non-LTE plasma 77−31426
H-like ions, Lyman α self absorption, effect in quantum 2 and 3 states in recombining plasmas 78−37605
H-like ions, reson. doublet component intensities in optically thin laser plasma *(Russian)* 78−38458
H-like plasma, instantaneous population densities of excited levels 77−47149
H^+-He^{2+}, strongly coupled ionic mixture, density fluctuations, timer depend. 77−80272
H^+-He^{2+} mixture, fully ionised, two-component plasma, mean spherical model 80−87854
He, afterglow, intermediate press., plasma discharge parameter time depend. calc. 79−19102
He, discharge plasma, dynamical studies, pulse repetition rates effects 77−62397
He, hollow cathode, 1-4 torr, population of excited levels, excitation and decay mechanisms 77−80267
He I, He II, population densities in TPD plasma machine, collisional-radiative model 77−47160
He I, II excited state population densities in non-LTE plasmas 78−67328
He I overlapping lines, model microfield method·Stark profiles, ion dynamics effect 79−82049
He I satellite line shape, stochastic theory 78−38460
He, plasma, afterglow and inertial expansion, numerical soln. of relax. kinetics 77−27769
He plasma, electron-impact widths and shifts of neutral He lines 79−27753
He plasma, ion state and electron temperature in high-current pulsed discharge *(Russian)* 79−27844
He plasma, Stark effect in 3-D stochastic elec. fields and static mag. field 78−5855
He plasma collisional-radiative model, appl. to positive column 79−64836
He plasma in electron beam-excited discharge, atm. press., relax. obs. and model 79−37569
He-Cs mixture discharge, B-invariant transformation theory 78−67503
He-like ions, level populations and line intensities for stationary plasmas 78−53811
He-like ions, line intensities for non-stationary plasmas 78−53812
Hg plasma formation by strong Hg line irrad., mechanism 78−83585
K, low-temperature plasma atomic level population density computation 78−71461
Li plasma, elec. cond. at 12.5-50 MPa, $(7\text{-}50)\times10^3$K 80−64685
Li-D equation of state under extreme conditions, solid state to plasma region 80−69976
LiH plasma, phase transition 78−42710
Mo XXXI-XXXIV spectra from exploded Mo wire plasmas 79−1295
N arc, radiation transport 78−79486
N, electron impact collisions in nonlinear plasma, 100 to 10000K 79−98857
N plasma, ionis. and radiation characts. 78−71459
N_2 arc vacuum UV radiation loss calc. 78−71581
N_2, beam and glow discharge type, macroscopic props., kinetic eqns. 80−43864
N_2 discharge, anomalous heating *(Russian)* 80−1866
N_2, low-pressure DC discharge positive column, vibration temp. radial distrib. 78−67499
N_2 plasma, electron distrib. function, kinetic coeffs. *(Russian)* 78−38451
N_2 positive column, superelastic collisions and electron distrib. function 80−1858
N_2 vibrational levels stepwise excitation, effect on electron energy balance in He-N_2-CO_2 discharge 80−54071
N_2-Ar plasma, coupled thermal-chem. relax.; thermodynamic nonequilib. 78−34265
N_2-Cu thermal plasma, effect of Cs on intensity of spectral lines, quantitative spectral anal. appl. *(German)* 78−30417
N_2-H_2 plasma, transport coeffs. and collision processes *(German)* 79−23395
N_2-Ne glow discharge, energy balance, ionis. collisions *(German)* 78−34263
N_2-Ne glow discharge, kinetic eqn., transport coeff., collision freq., mean energy *(German)* 78−34261
N_x ground state, second virial coeffs. calcs., 6000 to 20000K 77−14524
Na isoelectronic sequence, dielectronic recombination rate coeffs., 2-10^3 eV 80−10357
Na plasma, optical properties 79−4115
Ne, electron energy distrib., relax. process 78−30507
Ne, electron impact collisions in nonlinear plasma, 100 to 10000K 79−98857
Ne like multiply charged ion transitions, stimulated emission possibility in far UV 79−10292
Ni ions in Tokamak plasmas, spectroscopy and atomic physics 80−53938
Ni plasma, X-ray transport 79−64837
O glow discharge atomic radial distribution obs. 78−67501
O, impurity radiation, metastable transitions in Tokamak, modified coronal model 78−26255
O VUV emission rates in quasi-resistive and slide-away regimes in Thor Tokamak 78−83536
O_2 discharge, conditions, self-consistent electron energy distrib. functions calc. 80−38746
O_2, discharge, nonequilib. vibr. population, dissoc. rate, role of ats. and dissoc. 79−64933
O_2 glow discharge, DC, particle concs. calc. 80−1859

plasma theory continued
O_2 plasma, UV continuum spectra, mol. recomb. of ground state atoms 78−91078
O_2, RF discharge, moderate press., O production kinetics 79−64934
Si, laser-heated, bremsstrahlung spectra, Gaunt factor calcs. 77−3968
U gas mixture plasmas, electron energy distrib., radiation source 77−46225
U plasma, fission fragment effect on electron energy distrib., radiative transport 77−24062
U-He plasma, radiation-induced, electron energy distrib. 77−24054
^{235}U, opacity and radiative energy current calc., 5000-8000K 78−83535
Xe, arc, wall-stabilised, dynamic analysis, radiation transport 80−44066
Xe, continuum absorpt. coeff. 77−39463
Xe discharge plasma spectral and integral characteristics calc. 78−71583
Xe I level deviation from Boltzmann population in steady-state plasma 78−67605
Xe, plasma shock front, elementary processes 80−19581
Xe precursors, associative ionisation and photoionisation, relative contrib., electron density prediction 80−43858
Xe, total emission coeff., line contrib. 79−77346
Y_2O_3 plasma, eqn. of state investig. 80−75027

plasma thermocouples *see plasma devices; thermocouples*

plasma torches *see plasma devices*

plasma transport processes
see also Vlasov equation
1-MJ plasma focus expt., neutron yield, current distrib., scaling law 77−74991
ablative laser fusion implosion, scaling laws and spatial struct. 80−87915
absorption of axially asymmetric EM waves, in inhomogeneous plasma 77−55156
accelerator, closed Hall current discharge, anode sheath struct. 77−76215
accelerator, conical, plasma cluster vel. calc., snow-plough and erosive models *(Russian)* 80−27839
active particle beam systems for meas. of plasma pot., current and impurity profiles 80−48990
adiabatic trap, charged particles motion, mag. field inhomogeneity effect, drift instability *(Japanese)* 77−43054
aerosol plasma, cond. determ. 79−55464
air, wall-stabilised arc, step and sinusoidal current change response 80−103209
air arc discharge high-temp. transport obs. 78−71577
air blast arc, post-zero current and power loss meas. 79−19106
air flow glow discharge, voltage, current oscills. 79−55585
air gap, drift vel. meas. of ionized particles 80−24298
air high-current discharge cond. zone, HF mag. field probe 78−71589
air plasma, radiowave interaction, electron velocity, collision cross-section depend. 80−103155
air plasma flow in channel inlet zone, local heat transfer 80−64687
air-water vapour mixture, electron conc. and conductivity behind strong shock wave 80−48890
Alcator, high density regimes, numerical simulation 77−68858
Alcator Tokamak, heat loss, mag. fluctuation mechanism 79−1292
Alfven mode, current driven, electron-ion collisions and full dispersion function, numerical anal. 80−64726
Alfven waves, excitation of convective cells in plasma *(Russian)* 78−47097
Alfven waves in finite-β current carrying plasma, monoenergetic fusion product effects 78−91101
Alfven waves in inhomogeneous plasma, collisionless damping rel. to energy transport 79−64864
alkali metal, dense arc plasma, elec. and heat conds., two-probe diagnostics 80−38560
alkali metal plasma, effect of elastic electron scatt. by at. excited states on conductivity 78−42715
alkali metal seeded plasma, calc. of thermal nonequilib. near-electrode region 77−55186
alkali-metal hollow cathode arc, low-press. current limiting 80−6304
alkaline impurity, source function in combustion products flow *(Russian)* 77−56301
alpha particle orbits in radially nonuniform slender plasma column, multi-group rep. 80−53921
alpha particle transport in thermonuclear Tokamak plasma 78−94895
alpha particles anomalous interaction with dissipative trapped-ion mode 78−5851
alpha transport and blistering of first wall in Tokamak 79−19069
alpha-particle heating in an open-field-line plasma 80−48908
alpha-particles anomalous diffusion in nonlinear trapped-ion regime of fusion reactor 77−11319
alpha-particles energy spectrum resulting from turbulent diffusion 77−11318
ambipolar diffusion eqn. in gravit. field, analytical solns. appl. to F-region 77−78562
ambipolar diffusion in nonuniform plasma with different positive ion components 79−23400
ambipolar electron and ion diffusion in collisional plasma in RF electric field 80−6220
ambipolar plasma traps, resonance particle diffusion 79−86601
ambipolar traps, transport processes, neo-classical theory *(Russian)* 78−71518
anisotropic plasma, kinetic evolution theory 80−28608
anisotropic resistivity across mag. field, effect of ion-acoustic turbulence 80−59236
anode sheath in high pressure high current arc 78−67467
anomalous, due to EM drift wave fluctuations 78−26251
anomalous, electron temp. gradient instability 80−75034
anomalous conductivity and electron heating, in two-stream unstable plasma 80−6219
anomalous cross-field transport, due to electrostatic fluctuations, theories 79−98870
anomalous diffusion and transport beta limits in dense Tokamak plasmas 79−72993
anomalous drift wave transport in high temp. plasmas, thermodynamic stability 80−69980
anomalous electron diffusion, thermal mag. fluctuations 78−83531
anomalous electron pseudo-classical transport with coherent electrostatic wave propag. 80−24137
anomalous electron transport equations for ion sound and related turbulent spectra 78−67319

plasma transport processes continued
anomalous glow discharge Faraday dark space, electron vel. distrib., Langmuir probe meas. 80−44040
anomalous heat conductivity for a weakly ionized plasma in a strong magnetic field 80−100070
anomalous plasma diffusion across a strong magnetic field 79−72994
anomalous plasma transport due to electron temp. gradient instability 80−33813
anomalous resistivity, effects on collisionless shocks structure 80−87893
anomalous resistivity, multiple electron beams evolution 78−83530
anomalous resistivity in magnetosphere, rel. to electrostatic shocks and double layers 78−45152
anomalous resistivity of turbulent plasma in strong electric field 79−72989
anomalous skin effect conditions 78−67544
anomalous thermal transport in turbulent skin layer, ion-acoustic waves mechanism 78−5853
anomalous Tokamak radial transport, large mode number tearing and twisting modes 80−1747
anomalous transport, particle simulation, drift wave theory 77−72428
anomalous transport due to EM fluctuations across mag. field 79−32744
anomalous transport due to long-lived fluctuations, general formalism 77−19673
anomalous transport due to long-lived fluctuations, hydrodynamic contrib. 77−15165
anomalous transport effects in magnetically confined plasma columns 78−42725
anomalous transport from plasma waves 80−59182
anomalous transport in Tokamak, dissipative trapped-ion instability 77−72420
anomalous transport in toroidal geometry 78−79453
anomalous transport in turbulent electron heating 78−14216
anomalous transport model, scaling laws 77−68754
anomalous transport of ions, in weakly ionised plasma, high-freq. field effects 78−63549
anomalous transport processes in radially compressed reversed-field configurations, numerical simulation 80−64689
anomalous trapped ion transport in Tokamaks, 2-dimens. fluid calcs. 78−30412
anomalous turbulent resistivity at high drift vels., rel. to confinement and fluctuations in toroid 80−24139
anomalous turbulent resistivity at high drift vels., toroidal plasma 80−24138
anomalous viscosity due to EM instability in turbulent plasma 80−106901
anomalous viscosity due to EM instability in turbulent plasma, nonlinear theory 80−106902
arc, cathode region, easily ionised admixture effects calcs. 79−14633
arc, core formation, temp. profiles and elec. power input 77−24241
arc, Elenbaas-Heller eqn. solution by analogy 78−71584
arc, high press., convection 78−59701
arc, of Cs-film coated hollow cathode, intermediate press. operation 80−6305
arc, pulsed, high-current, initial anode heat flux meas. and modelling 79−50903
arc, tanh conductivity model, thermal and electrical characts. 78−42846
arc, tank conductivity model, electrode geometry effects 78−42845
arc AC, in longitudinal gas flow, periodic regime, exact soln. 77−27767
arc discharge, dense plasma, radiative thermal cond. and elec. cond. coeffs. determ. 80−75033
arc discharge, heat flux and current density dstrib. in heat spot *(Russian)* 79−14625
arc in air, transport coeffs. meas. 78−59709
arc nozzle clogging theory 80−38791
arc plasma, electrical conductivity and temp. distrib. in insulating channels 79−23401
arc plasma cross-section, narrow insulating slot 77−72515
arcs, elec., high-current, conducting gas flow anal. *(Russian)* 79−32754
Asperator NP-3, toroidal device with nonplanar mag. axis, current equilib. 80−48932
astronomical rarefied magnetoactive plasma, polarised radiation transfer 79−92669
astrophysical, magnetospheric, and lab. plasma knowledge interaction 80−59166
asymmetric plasma resistivity, creation using waves 80−103171
atom-molecule anisotropic interaction pot. influence on transport cross sections, appl. to He-alkali dimer 80−9677
axial particle drift in the positive column of a discharge 80−100113
axially symmetric toroidal system, Ohm's law in banana regime *(Russian)* 79−4164
backflow of quasiparticles, dynamics of one-component plasma 79−27614
ball lightning, turbulent plasma sphere, model eqns. for current and heat flux 80−32516
ballooning trapped-electron mode overlapping many rational surfaces 80−28618
banana drift diffusion, Tokamak mag. field with ripples, model collision operator 77−65839
beam discharge, electron kinetics, charge particle finite lifetime effect 80−92404
beam discharge, electron kinetics, deexcitation processes effect 80−92405
beam-induced currents in toroidal plasmas 80−92265
beam-plasma interaction, test particle diffusion and scatt. in turbulent collisionless plasma 78−38508
belt pinch, diffusion processes, impurity and neutral gas effects, 3-fluid model 77−24057
belt pinch IIa, high-β Tokamak equilib., stability and transport 79−10690
Belt Pinch IIa, transport phenomena, density profiles 80−24219
belt pinches, transport and radiation studies 80−28798
Bernstein waves, propagation in inhomogeneous plasma, dispersion rel., quasi-linear equations, diffusion coeff. determ. 80−75044
Birkeland currents, and limits to double-adiabatic approximation for hot collisionless plasma 78−75262
Bohm diffusion coeff., free trajectory derivation 79−10641
boundary conditions for space charge surface layer at electrode plasma boundary, particle flux *(Russian)* 78−55736
boundary layer effect on transport phenomena in MHD generators 79−23463
breakdown wave propagation in ionised gas in nanosecond discharges 80−87890

plasma transport processes continued
bumpy torus, inward ion transport, strong elec. field effects 78−63548
bumpy torus (ELMO), radial transport eqn. in one-dimens., const. edge neutral flux 79−98956
bumpy torus plasma, weak vertical mag. field effect on fluctuation induced transport 80−48946
bunch enlargement in vac. *(Russian)* 80−83907
Buneman instability nonlinear saturation 80−79467
burn period plasma current maintenance, rectifying first wall, cct. anal. 80−102307
capillary discharge, with evaporable wall, plasma parameters axial distrib. *(Russian)* 78−75280
caviton dynamics at crit. density 80−106909
channel flow, coaxial, compressive, viscous, thermal and elec. cond. effects *(Russian)* 77−3927
charged fluids near freezing point, static dielectric behaviour, simulation 78−56417
charged particle acceleration and diffusion in stochastic mag. field 80−43872
charged particle diffusion in presence of Alfven waves, perpendicular particle flux 77−84406
charged particle diffusion in turbulent mag. field 77−70989
charged particle drift motion under resonance conditions 80−38611
charged particle transport, multigroup formalism to solve Fokker-Planck eqn. 80−68159
charged particle transport theory, discrete and continuous interactions 79−55467
charged particles, energy and momentum, Vlasov equilib. in KEMP II EM trap *(French)* 77−43018
Chirikov-Taylor model, turbulent diffusion calc. 80−79469
classical diffusion equation soln. for fully ionised plasma 80−103114
classical diffusion in large-aspect toroidal plasmas 78−71443
classical one-component plasma, transport coeffs. 78−9757
classical plasma diffusion 77−72418
classical to vortex diffusion transition in levitated octupole 77−35326
classical transport processes in azimuthally rot. plasma *(Russian)* 80−33746
closed poloidal heliotron, accelerated electron focusing *(Russian)* 80−106961
coefficients determ. from high press. arc meas. 77−47156
coefficients of viscosity of a gaseous plasma 80−43875
coherent anomalous resistivity, in region of ionosphere/magnetosphere electrostatic shocks 80−4189
coherent nonlinear transport, in strongly unstable plasma 77−39405
cold plasma blanket, collisional transport model 77−72466
cold plasma blanket for Tokamak, heat diffusion and temp. profile 77−65902
cold turbulent plasma blanket, anomalous heat transport 80−18604
cold-banket systems, boundary layer analysis 80−28605
collapse instability nature in Tokamak, surface currents *(Russian)* 80−92310
collective behaviour, in laser plasma expts. 77−43005
collective electric field fluctuations of two-temp. electron gas nonthermal plasma 80−43882
collective ion acceleration by relativistic electron cloud *(Russian)* 80−48961
collective phenomena and anomalous resistance, electron current drift velocity *(Russian)* 80−24140
collision operator for 1D plasma, verification by simulation, heat cond. 79−27823
collision-dominated regime of axisymmetric toroidal plasma 77−76034
collisional divertor scrape-off layer in Tokamak, plasma transport 80−28614
collisional drift modes, anomalous skin effect, enhanced particle penetration during fuelling, nonlinear theory 80−64703
collisional transport in Tokamaks, particle and heat sources effect 78−83529
collisionless diffusion, in 'Saturn' stellarator-torsatron 77−1011
collisionless drift modes, graphical method for finding complex roots of nonlinear eqn. 80−33762
collisionless plasma fluid model and cosmic plasmas elec. current systems 79−84658
collisionless shocks, kinetic models 80−90330
collisionless tearing modes and enhanced transport, simulation 79−86607
collisionless universal instability, stability of bound eigenmode solns., convective modes 78−71472
column, HF field effect on diffusion and convection 80−103173
column rot. and particle transport, travelling EM wave and neutral beam heating *(Russian)* 79−27798
combustion product plasma, electron conc. and mobility determ. by HCN laser submillimetric interferometry 78−1889
combustion products plasma with mixed alkali impurities, elec. cond. calc. 79−86621
compact fusion ignition experiments, designs, numerical computation 80−13853
complex dielectric function long wave limit, Coulomb systems with bound states, elec. cond. 80−33738
concentration perturbation spreading in weakly ionised magnetoplasma, ambipolar diffusion *(Russian)* 77−47151
conductance theory, quantum-statistical, of nonideal plasmas 80−79440
conductance theory of nonideal plasmas 80−33745
conducting bodies in ionised multicomponent gas, electric effects, method of separation 80−96389
conducting sphere in quiescent slightly ionised plasma, exact solution 79−86564
conduction and dielectric problems in turbulent plasma, linear response theory 78−71432
conduction heat loss scaling in open field line geometries 78−14136
conduction mode variation and inertial conductivity 77−84407
conductivity, effect of correlated electron-ion pairs 78−26249
conductivity, electrical, classical, plasma impurities, Sonin polynomial distrib. function *(Russian)* 80−83894
conductivity, nonideal nondegenerate plasma, dynamic model 78−26238
conductivity and viscosity, effect on stratified partially ionised plasma stability in mag. field 78−26276
conductivity calc., Renormalisation Group method 78−71457
conductivity meas., directional RF probe design 78−51353
conductivity meas. in flowing plasma, pulsed probe method 78−1894
conductivity of inhomogeneous plasma with nonlinear ionis. waves 78−42718
conductivity of ionosphere plasma, kinetic theory 79−53609

plasma transport processes continued
conductivity of ionospheric plasma, applicability limits of mean free path theory formulae 77−60512
conductivity sum rules in two component plasma 77−39406
conductivity tensor, Grad's moment eqns. 77−58847
conductivity tensor of streaming plasma in crossed field 77−19675
conductivity tensors in collisionless plasma 79−72990
conference, physics of ionised gases, Dubrovnik, Yugoslavia, (Aug.-Sep. 1976) 77−42961
conference, Varenna, Italy (Sept. 1977) 79−98869
conference on fusion research and plasma physics, Innsbruck, Aug. 1978 80−27033
confinement in multislit EM trap, model description *(Russian)* 80−96382
continuous X-ray radiation, picosecond ruby laser heating *(Russian)* 80−75079
convection in magnetosphere tail lobes, rel. to plasma sheet form. 79−40022
convective amplification of universal drift modes 80−59208
convective cell excitation by Bernstein waves *(Russian)* 80−53961
convective cell nonlinear excitation and anomalous diffusion, in inhomogeneous plasma 80−79468
convective cells and anomalous plasma diffusion *(Russian)* 78−71439
convective cells form. by modulational instability 79−98903
convective cells of drift waves, plasma with shear, nonlinear excitation mechanism *(Russian)* 80−38585
convective diffusion and heat transport, kinetic effects 79−10644
convective diffusion and heat transport, kinetic effects 79−27750
convective instability, harmonic generation and anomalous absorpt. in pumping wave decay *(Russian)* 80−14889
convective instability and nonaxisymmetric waves, in weakly ionised plasma in strong mag. field 79−90397
convective plasma loss by ion-cyclotron RF field, elimination by mode control 80−83957
cooled electric probes in dense plasma, thermal diffusion effects 80−92384
Coriolis forces, effect on Hall currents and Rayleigh-Taylor instability 79−41809
corona, laser induced microsphere, electron density profile, interaction and transport profile 80−107008
corona, multifluid behaviour between elec.-stressed spherical cathode and spherical anode 80−10443
corona discharge current oscillations and role of excited atoms 78−67590
corona system, under neg. direct and pulsed voltage, charcts. 79−19107
Coulomb system, two-dimensional, props. 77−62337
coupled resistive g/ion temperature gradient instability 80−79481
critical-velocity rotating plasma interaction with neutral gas, obs. 78−75344
cross-field electron heat transport due to high frequency electrostatic waves 80−53932
cross-field electron transport due to thermal electromagnetic fluctuations 80−92258
CT-6 Tokamak device, development, test operation *(Chinese)* 80−87919
Culham Levitron, drift island diffusion 80−59267
current carrying double layer production in focus device 80−83953
current carrying plasma, helically symmetric equilib. 77−68852
current channel magnetic compression, in Tuman-2 Tokamak *(Russian)* 78−38455
current conduction in Hall accelerator, electrothermal instabilities 77−51159
current contraction in near-anode region of combustion product plasma 78−75267
current controller, precise, 0-5 mA, for moderate density plasma diagnostics 79−46483
current density, local, mag. probe and Thomson scatt. meas., using Spitzer-Harm distrib. 78−18451
current density and electric field fluctuations 78−38456
current density determ. by Thomson scatt. 77−27724
current density meas. by longitudinal Thompson scatt. in Tokamak-type devices 77−19767
current density profile control in JIPP-II Tokamak, preprogramming method 79−86565
current density profile determ. using ordinary and extraordinary microwaves 78−75419
current density profile diagnostics by modulated laser Faraday rot. polarimetry 79−46474
current density profile measurements in the Proto-Cleo torsatron 80−83995
current discharge plasma, mag. reconnection temporal evolution near mag. neutral line 79−32756
current disruption, in Tokamak plasmas, schlieren signal meas. from millimetre waves 80−48998
current disruption accompanied by kink instability *(Russian)* 78−1819
current distribution in hollow-cathode arc discharge 78−67537
current driven electromagnetic ion cyclotron instability 79−32762
current driven instabilities, anomalous effects 78−91096
current field charcts. diagnostics, freq. shift in microwave cavity flow 77−62406
current fluctuations, discharge contractions, in combustion products plasma 80−14953
current fluctuations, one-component plasma, mode-coupling theory 79−23398
current generated by alpha-particle loss in Tokamak reactors 80−106877
current generation, DC, during microwave toroidal mag. plasma heating 78−34271
current generation by electrostatic travelling waves in collisionless magnetised plasma 80−53976
current generation by unidirectional lower hybrid wave in ACT-1 80−92306
current instability, in reconnecting current sheets 77−37486
current instability on short wave drift oscills., nonlinear theory *(Russian)* 80−53981
current interruption in collisionless plasma, by non-linear electrostatic waves 79−75052
current interruption mechanism in collisionless plasma 78−42721
current multiplication, during relativistic electron beam propag. 79−41843
current peaking effect on non-circ. Tokamak equilib. 78−5916
current penetration, magnetostatic code, anomalous heating, heat transport, microinstabilities 78−38526
plasma transport processes continued
current production by rotating mag. fields 80−79442
current profile, meas. by probes 78−75416
current reduction and reversal in toroidal pinch 77−58887
current rise in Tokamak, two-dimens. fluid simulation 77−72491
current sheet, near line of zero mag. field, numerical anal. *(Russian)* 80−83908
current sheet in compressible plasma, self-similar resistive decay 80−1755
current sheets resistive MHD instabilities, appl. to solar wind 80−4218
current structure, fast particle generation *(Russian)* 80−48913
current susta-ning by RF travelling field in collisional toroidal plasma 78−47094
current sustaining by RF field 78−30414
current transport at the surface of a hollow cathode, current distrib. technique 80−54048
current-carrying finite beta plasma, helically symmetric equilib. 77−43019
current-carrying plasma, Thomson scatt., current density 78−51287
current-carrying plasma sheet stability 79−60133
current-convective instability in plasma with impurities *(Russian)* 77−68748
current-driven collisional drift instability in sheared mag. field 79−27765
current-driven HF drift wave, inhomogeneous plasma instability 80−59204
currents, ion beam-induced, kinetic theory 79−32746
currents in short pulsed high current electron beam injection into initially neutral gases 80−33749
curvature effects in laser plasma interactions 80−43948
curved plasma optical system, plasma stream transport *(Russian)* 78−87439
cyclotron radiation transport in plasmas by neutron transport techniques 80−38660
cyclotrons resonance maser, Vlasov-Maxwell eqns., guided wave field theory 80−14309
cylindrical conducting body, supersonic plasma cross-flow, stagnation region meas. 79−32810
DC arc, for emission spectroanal., transport mechanism 78−22464
DC arc plasma, axial mass transport, added particle distrib. 79−86640
DC current, collisionless limit, induced by travelling wave, collision term based calc. 78−1806
DC toroidal current RF travelling field driven, radial profile 78−75270
deflagration wave, in laser compression 79−23419
dense nondegenerate plasma, electron transport, thermal cond. *(Russian)* 79−98865
dense nonideal plasma, Coulomb interaction problem 78−71451
dense pinch, electron-positron pair production in EM field *(Russian)* 80−100092
dense plasma afterglow, theory 78−9882
density, current, electron heat, through braided magnetic field, fluid and particle models 78−30410
density rise model and ion mixing mode in confined plasma 78−79409
detached shock wave, elect. cond. in ionised Ar 79−10592
dielectric chamber, short-circuit effect, diffusion and stability obs. 78−71446
dielectric constant for ion-acoustic waves in turbulent plasma 77−986
dielectric constant for ion-acoustic waves in turbulent plasma 77−987
dielectric response and energy loss in intermediate quantum plasma 80−38541
dielectric response function, density fluctuations effects 78−30413
dielectric response function of 2-dimens. electron plasma 77−39403
dielectric surfaces in evacuated cavities, plasma release due to electron irrad., transport charcts. 80−33786
diffuse decay of ionised gas in cylinder with non-conducting walls 77−27653
diffuse discharge, current constriction near anode in combustion product plasma 80−103201
diffuse electrical gas discharge, in turbulent flows 79−94834
diffuse pinch, energy equilib., classical scalar cond. and neo-classical models 80−24208
diffuse pinch, energy equilib., tensor cond. model 80−24209
diffusion, 1-dimens. code, impurity eqns. inclusion 77−15169
diffusion, anomalous, due to dissipative trapped ion instability 77−11331
diffusion, anomalous, due to drift instabilities 78−47106
diffusion, anomalous, parametric instability saturation 78−14161
diffusion, collisionless, in Saturn stellarator, transient electric field effect *(Russian)* 78−26245
diffusion, cross-field, in Tokamak with bundle divertor 78−42784
diffusion, eqns. with large temp. differences between interacting species, ionosphere appls. 79−66857
diffusion, fluctuations, trapped-electron and trapped-ion regimes in octupole 77−72416
diffusion, heat flow, quasilinear model for micro-unstable Tokamak 77−76033
diffusion, neoclassical, in traps with helical mag. axis 77−31430
diffusion, nonadiabatic, in geometric mirrors, higher order adiabatic invariants 77−68846
diffusion, of weakly ionised plasma filament in mag. field 79−53610
diffusion, quasilinear, in solar mag. traps, rel. to plasma instability periodical regimes *(Russian)* 80−8616
diffusion, random function two-time correlation functions 79−46428
diffusion, simultaneous, of impurities in Tokamak-like plasma 77−72413
diffusion, steady-state, boundary electron temp. and current density in Tokamak 78−22457
diffusion, time-dependent, in toroidal geometry, finite element code 77−84410
diffusion, turbulent, geometrical effects in toroidal plasma 79−27751
diffusion, turbulent, in multicomponent plasma *(Russian)* 78−22455
diffusion across mag. field, mode transition process in collisional drift waves 77−80275
diffusion across mag. field effect of ion-acoustic turbulence 80−59236
diffusion and ang. momentum transfer, across X-ray source accretion disc Alfven surface 78−93461
diffusion and drift in F-region, electron loss coeffs. calcs. 77−13156
diffusion and particle motion in mag. mirrors 77−15234
diffusion broken ambipolarity in drift wave turbulence 79−64828
diffusion coeff., drift waves, in sheared mag. field 77−76079
diffusion coeff., mass separation effect 77−76032
diffusion coeff. for turbulent plasma 78−5854
diffusion coeff. in Tokamak scrape-off layer 78−91156
diffusion coefficient scaling in $\epsilon \rightarrow 1$ plasma 77−76037

plasma transport processes continued
diffusion coefficient scaling in levitated octupole 77−35325
diffusion cooling in afterglow, electron energy balance 78−5852
diffusion diode, current oscills., overneutralisation and diffusion instability 77−24199
diffusion due to mag. field fluctuations 80−1761
diffusion equations, basis for confinement scaling and similarity laws derivation 78−94932
diffusion fluxes, thermal cond., chem. reactive plasma 77−47142
diffusion in divertor scrape-off layer in Tokamak 79−667
diffusion in divertor scrape-off layer of Tokamak 79−668
diffusion in finite amplitude wave 77−68753
diffusion in low-beta devices, finite element analysis 77−80277
diffusion in reversed field pinches 77−39451
diffusion in stellarator *(Russian)* 79−32747
diffusion in toroidal plasma with nonplanar mag. axis 77−84486
diffusion in toroidal traps, anomalous electron viscosity *(Russian)* 80−48956
diffusion in Uragan-2, turbulence and gravitational drift instability *(Russian)* 77−47150
diffusion in velocity space, assoc. with mag. moment nonadiabatic changes 77−3920
diffusion of charged particles along mag. neutral line 80−6218
diffusion of electrons through excited atomic or ionic states, role of collective interactions 80−79433
diffusion of fast electron in presence of mag. field 77−84408
diffusion of impurities in Pfirsch-Schluter regime 77−35322
diffusion of multi-ion species plasma due to drift wave fluctuations 77−62341
diffusion of multi-ion species plasma due to drift wave fluctuations 77−68752
diffusion of nonequilib. plasma in mag. field, boundary conditions 78−42722
diffusion rate, meas. by trapped particle echoes in mirror machine 77−35324
diffusion rates, automatic computation, stellar interiors appl. 78−57434
diffusion reduction by plasma rotation and ion dissipative effects 80−38696
diffusion spreading of weak inhomogeneities in ionospheric according to electrostatic approx. 80−4187
diffusion through magnetic fields, fluid inertia effect 79−4113
diffusion time scale Tokamak code, G2M, two dimens. 78−42795
diffusional expansion across mag. field, modelling problem *(Russian)* 80−48964
diffusive plasma transport across mag. field, expt. methods *(Russian)* 79−1294
dilute electron plasma kinetic eqns. in coherent region 78−75264
discharge, two-temperature, transport eqns., transient phenomena 80−96402
discharge current, in electrodeless RF discharges in gas mixtures 80−44029
discharge plasma, diffusion regime, elec. sheath theory 80−1810
discharge with external ionis., electric strength and elec. cond. 78−91180
discharges, high current, press., conductivity meas. 80−38793
dissipation phenomena formalism, diffusion and heating applications 79−4111
dissipative trapped electron instability, turbulence theory 78−71482
dissipative trapped ion instability and anomalous transport 78−22483
distribution of particles in stochastic fields 80−79448
disturbance propag. in relativistic Vlasov plasma 77−72426
DITE Tokamak, beam driven current meas. 80−106940
DIVA, metal-impurity, confinement, discharges 80−28843
DIVA, methane pulsed injection into DIVA Tokamak, transport props. 78−79411
divertor fluxes in stellarators and torsatrons, azimuthal distrib. 80−6216
divertor injection Tokamak experiment, plasma stability, energy and particle transport, and hydrogen recycling 80−28834
double layer formation in multiple plasma device 80−83897
double layers, electric field collapse phenomena, Buneman instability *(Russian)* 80−79476
double layers from ion acoustic instability numerical simulation 80−59220
double-diffusion hot-electron transport in self-consistent E and B fields 79−23437
double-layer, steady-state, fluid theory 80−43873
drift and current flow of charged particle along mag. neutral line 80−1749
drift and trapped electron instabilities, in systems with mag. shear 80−28648
drift equations for fully ionised binary and ternary plasmas 77−47140
drift instability, current-driven, sheared mag. field, finite-beta effect on transport 80−28617
drift instability, electron-ion heat exchange and electron thermal conduct. effects 77−984
drift instability, non-local, of current-carrying plasma with temp. inhomogeneities 78−59580
drift instability-caused turbulence, anomalous diffusion, convective cell form. 77−43058
drift kinetic equation, num. soln. 80−59172
drift loss cone instability in inhomogeneous mag. field 80−48934
drift mode, current driven, electron-ion collisions and full dispersion function, numerical anal. 80−64726
drift of positive ions in plasma formed by dense beam of negative ions in gas *(Russian)* 80−103160
drift wave, low freq., pseudoclassical diffusion in Tokamak *(Chinese)* 80−69990
drift wave collisionless turbulence, renormalised dielectric function 78−51292
drift wave particle flux, wave amplitude rel. to plasma density 79−4137
drift wave stability and transport theory in fusion systems 80−28653
drift wave turbulence and convective cell formation 80−43925
drift waves, instability in AC elec. field, wave growth rate and dispersion relation 80−48886
drift waves, multispecies plasma, nonlinear behaviour, turbulence, diffusion 78−59588
drift-wave eigenmodes, current-driven, stability criteria 79−32769
drift-wave turbulence effect on mag. struct. and electron transport in Tokamak 78−22501
E layer, cusp injected, equilib. props. and limiting current behaviour 78−83601
early afterglow, higher diffusion modes 78−1802

plasma transport processes continued
EBT, neoclassical transport 80−32488
EBT, radial transport in collisionless electron regimes 80−32491
effective conductivity, in high current low voltage arc discharge, oscills. effects *(Russian)* 79−55579
effective conductivity tensor, effect of spherical anisotropic inclusions 77−55546
effective transport coeffs. of plasma in LTE approx. 78−1801
election parallel thermal conductivity, reduction using waves 79−10637
electric and diffusion current generation by EM field, moving media 77−76097
electric current generation by EM radiation 78−71492
electric currents in hot adiabatic plasma, theory 78−89002
electric discharge with disc cathode in He flow, spectrosc. investig. 80−64809
electric double layer form. and dynamics, simulation 80−48855
electric double layer motion 80−33751
electric field compression near a plasma electrode 80−64736
electric field pattern calcs. in laser produced plasma *(German)* 80−54014
electric field penetration in plasma with nonlinear current saturating cond. 77−19672
electric response function, two-component quantum plasma 79−37452
electrical and heat conductivity, H transport functions by precision arc expts. 80−103187
electrical breakdown, local, of highly ionised gas flow 79−41894
electrical conductivities of plasma in uniform mag. field, complementary variational principles 79−46430
electrical conductivity, complementary variational principles 79−46427
electrical conductivity, Coulomb interactions effect 78−42719
electrical conductivity, effect of electron-nearest ion collision complex form. *(Russian)* 78−1788
electrical conductivity, effect of monochromatic finite amplitude ion acoustic wave 78−91070
electrical conductivity, of nonideal plasma, linear response theory 79−64832
electrical conductivity, weakly ionised flowing plasma, crossed elec. and mag. fields 79−1291
electrical conductivity computation, partially-ionised gas 79−86563
electrical conductivity of high temp. imperfect gas *(Russian)* 80−100072
electrical conductivity of high-density, shock-heated Ar and Xe plasmas 80−38557
electrical conductivity of low-temp. alkali plasma, weak probing signal method meas. 80−48968
electrical conductivity of nonideal high-press. plasma, Ar arc IR continuum absorption obs. 80−38558
electrical conductivity of partially ionised gas, calc. method 77−42967
electrical conductivity temp. depend., working fluid for MHD generator 79−4194
electrical conductivity tensor, relativistic, EM radiation propag. in strong gravit. field *(Russian)* 77−3945
electrical conductivity tensor for H_2O_2 plasma in mag. field *(Russian)* 80−87864
electrode discharge, nonhydrodynamic pinch compression, kinetics and D^+ focusing *(Russian)* 80−38689
electron acceleration, by mag. field energy dissipation in neutral current sheets 78−26250
electron acceleration in a plasma resonance field *(Russian)* 79−98868
electron autoreson. accel. at nonlinear ECR in growing mag. field 80−87867
electron back diffusion, Monte-Carlo calc. 77−68884
electron beam, relativistic, limiting current 77−51224
electron beam, relativistic, strong mag. field, transverse energy determ. by bremsstrahlung 77−62344
electron beam (relativistic)-plasma interaction, transverse mag.-field induced enhanced energy deposition 77−62377
electron beam propagation in plasma channels for ICF reactors 80−1812
electron beam random walk diffusion in stellerator 77−19754
electron beam self-focusing decline by gas breakdown, avalanche and plasma cond. effects 78−18420
electron beam stabilised mirror confined gas, hot electron population study 80−100089
electron beams, modulated, non-linear oscillation theory *(Russian)* 80−106898
electron collisions and vel. distrib. in elec. field, Boltzmann eqn. 77−30115
electron cond. losses in end-plugged plasma 78−51336
electron cross-field heat transport caused by HF electrostatic wave 80−28619
electron current, at plasma-electrode interface in transverse mag. field, probe obs. 79−64914
electron current component meas. method for hollow cold cathode 80−54043
electron cyclotron emission from Tokamak plasmas with mildly superthermal electrons 80−92270
electron cyclotron plasma heating, abnormal resist. *(Russian)* 77−7567
electron diffusion, identification problem 78−71532
electron diffusion by positive ion, waveguide theory *(French)* 77−74240
electron distribution function, electron-electron interaction effects in external field 80−1739
electron distribution in a free HF plasma column, anomalous skin effect *(Russian)* 80−1741
electron drift threshold for nonelectrostatic ion cyclotron oscills. spontaneous excitation 80−38625
electron dynamics in random field, dense Hg plasma conductivity appl. 80−14885
electron emission temperature, streaming plasma in laser vac. diode 78−91162
electron energy distribution function in very nonuniform elec. field 80−38556
electron energy radial distrib., in molecular gas discharge plasmas *(French)* 80−48852
electron energy transport into layered targets irradiated by CO_2-laser light 80−69979
electron ensemble, weak turbulence, diffusion and collisions in elec. and mag. fields *(German)* 78−83564
electron ensemble behaviour in HF elec. field, low-ionised nonisothermal plasma *(German)* 79−77383
electron heat conductivity, magnetic field line diffusion 80−28641

plasma transport processes continued
electron heat diffusion coefficient, in Tokamak, meas. by sawtooth oscill. obs. 79−64911
electron heat diffusivity, ORMAK Tokamak, X-ray emission obs. 77−31524
electron heat transport in Tokamak with helical perturbations 78−47095
electron holes, theory, anal. soln. 80−48879
electron kinetic eqn. for plasma with strong inter-ion interaction and electron exchange correlation 80−48857
electron oscillation in radial potential well effect on beam interactions *(Russian)* 80−14912
electron oscillations in fully ionized plasma 79−41814
electron plasma, EM instability reduction of thermal flux, simulation 78−75272
electron plasma, partially degenerate, at high temp., Compton scatt. opacity 77−11322
electron plasma column, transport across mag. field to thermal equilib. 79−37531
electron plasma externally launched diocotron mode-induced transport across mag. field 78−9758
electron plasma waves, unidirectional, current generation 79−82058
electron runaway effect in dense plasma *(Russian)* 77−39407
electron temperature gradient driven microtearing mode 80−96361
electron temperature meas. by Thomson laser scatt., θ-pinch energy loss *(Chinese)* 80−54028
electron thermal conductivity in Tokamak with destroyed mag. surfaces 78−30411
electron thermal energy transport in high temperature plasma 79−68906
electron thermoconductivity, impurities transport *(German)* 77−34425
electron transfer coeff., mol. dynamic method 78−71441
electron transport, determ. from pulsed arc meas. 77−47157
electron transport, high energy, numerical modelling *(Japanese)* 80−96346
electron transport, in spherically symmetric plasma, model 78−59557
electron transport induced by drift wave fluctuations 78−94894
electron-beam-ion two-stream instability initiated turbulent state, 3-dimens. vel. diffusion 78−59595
electron-energy transport in laser-produced plasmas 80−6266
electron-ion plasma, stimulated bremsstrahlung light absorption *(Russian)* 78−87438
electronegative gas plasma, negative ion ambipolar diffusion coeffs. 80−44046
electrons, adiabatic convection in magnetosphere tail plasma sheet 79−25408
electrons transport, in laser fusion plasma, Fokker-Planck eqn. 78−22462
electrostatic confinement in EM trap, ion current decay *(Russian)* 80−79543
electrostatic drift wave instability, in sheared mag. fields 79−37483
electrostatic microinstabilities, transport theory 80−79443
electrostatic probe characteristics in a magnetic field, ellipsoidal probe in diffusion regime 80−33815
electrostatic wave coupled multicomponent plasma, formation, evolution diffusion 77−84460
elementary reactions in plasma fusion, diffusion, contamination bremsstrahlung and electrostatic forces *(German)* 79−46429
ELMO bumpy torus, ambipolar diffusion 80−38552
ELMO bumpy torus, collisional regime, radial transport 79−41801
ELMO Bumpy Torus, electron cyclotron heating, density and temp. 80−28780
ELMO Bumpy Torus, radial transport in collisionless regimes 80−79447
ELMO bumpy torus, transport, scaling 77−72415
EM field induced resultant drift inwards from boundary, in D-T plasma 80−38577
EM field orthonormal decomposition in anisotropic media, duality and vector space 80−28620
EM fluctuations, affecting transport across mag. field 78−94899
EM macroparticle acceleration, high press. gas temp. density 80−79583
EM resonant properties of laser-prod. plasmas 80−43928
enclosed plasma spatial distrib. *(Russian)* 78−51283
energetic charged particle transport, moment method 78−22458
energetic charged particles transport mode in mag. fluctuations superposed on diverging mean field 79−50848
energy balance, electron runaway, electric field effect on temp. relax. 77−970
energy confinement comparison of ohmically heated stellarators to Tokamaks 80−92360
energy confinement scaling and poloidal beta in high density Tokamaks 80−96381
energy deposition of fast α particles in a fully ionized deuterium-tritium plasma 80−92259
energy flow and absorption along resonance cones near the lower hybrid 79−77405
energy lifetime of plasma, T-3 scaling law, in Tokamaks 80−28635
energy of a turbulent, current-carrying plasma in a strong electric field 80−79514
energy transport, in laser produced plasma, X-ray obs. 78−75269
energy transport from 1.06 μm and 0.53 μm laser plasmas interactions at 10^{15} W cm^{-2} 80−92261
enhanced losses due to collisionless drift waves, dynamic stabilisation effects 80−14888
enhanced plasma loss due to secondary currents, Tokamaks and non-Ohmic stellarators 77−65884
entropy production by anomalous drift wave transport 78−75263
equilibrium and transport in 2+ε-dimensional two-components plasmas 79−55470
excited gas, resonant optical discharge 80−92343
exploding wire discharge, thermal instability of elec. cond. in metal vap. 78−1868
externally driven magnetic reconnection and a powerful magnetic energy converter 79−68949
fast electron convective heat transfer and thermal escape *(Russian)* 80−1744
fast electrons, X-rays and ions, motion evaluation in laser produced plasma 80−19557
Fermi acceleration and particle pitch angle scatt., appl. to cosmic rays 78−53775
field emission medium energy diode, electron flow, HF oscills. 80−79582
field reversed mirror confinement, finite gyro-radius effects 80−83989
field reversed mirrors, fusion product energy distribs. 80−37595
field-aligned currents, driving LF instabilities 77−31449

plasma transport processes continued
fission fragment generated plasma, electron distrib. function, effect of collisions and diffusion 77−23653
fission fragments generated plasma, electron distrib. function 77−19731
fission reactor, gas-discharge, fuel element component conc., plasma temp. profile instabilities 80−63253
fissioning plasma from gas phase nucl. reactor, appl. 80−64794
flame plasma with presence of current, EM radiation obs. *(Russian)* 80−103126
flashlamp discharges, anomalous plasma resistivity 78−87508
flat current sheet, rupture criteria 79−1293
fluctuation diagnostics, digital time series anal. techniques 78−5951
fluctuations in plasma with Lorentzian vel. distrib., electron beam interaction *(Russian)* 77−19669
flux motion in curvilinear plasmo-optical system *(Russian)* 80−83893
focus, current sheath evolution; optical and elec. diagnostics 77−76207
focus, current sheath struct. diagnostics, fast particle beams, deuterated polyethylene fusion 77−76206
focus current, compression phase, mag. probe meas. 78−5939
focus device dynamics, 120 and 20 kV, neutron and X-ray emission diagnostics 77−74990
focus dynamics, anomalous cond. effect *(Russian)* 78−87475
Fokker-Planck linearized collision operator appls. 77−3923
Fokker-Planck-Coulomb systems, collective modes, 1-dimens. case 77−45809
formation of plasma in fusion devices, at. and plasma processes, diagnostic techniques 80−48915
free trajectory derivation of (Bohm) diffusion coeff., comments and reply 80−1748
free-free Gaunt factor calc. 79−60113
free-standing discharge, ATC Tokamak 78−30469
frequency dependent transport coeffs., two-fluid plasma 77−15167
FT Tokamak, non-thermal electron distrib. function 80−83891
fueling and thermonuclear instability, cold plasma layer surface fueling source 80−59196
fusion inertial confinement plasmas, energetic charged fusion product slowing 80−37594
fusion plasma in beam driven Tokamak, Fokker-Planck/transport analyses 80−28826
fusion plasma reaction rates, velocity-space methods 77−79475
fusion plasma rotation induced by 3.5 MeV alpha-particle losses 78−18384
fusion plasma transport, unified slowing down theory 78−18383
fusion possibilities and plasma confinement and interactions in mag. config. Tokamak, review *(French)* 80−54017
fusion products, thermalisation orbits, wall-loadings and microinstabilities 77−88284
fusion products in Tokamak plasma, deposition and thermalisation 80−83895
fusion reactor, diagnostics of radial plasma transport rate, data acquisition and handling system 78−54937
fusion reactor, exhaust to divertor target by collisionless processes 79−63808
fusion reactor inertial confinement pellets, neutronics modelling 80−37593
fusion reactor inertially confined plasma, charged particle energy deposition 77−83081
fusion reactor pellet re-fuelling feasibility 80−91246
fusion systems, solenoidal, instability-driven anomalous transport, review 78−22460
fusion target, laser-irrad., mag. field transport, nonlocal conduct. effects, simulation 78−59637
fusion-generated alpha particles driven plasma transport 78−83533
gas flow, nonequilib. ionisation and Hall EMF 80−69981
gas-blanketed plasma, boundary layer press. balance and diffusion 78−18380
gas-discharge cathode region transfer process simulation, Monte Carlo method 78−71600
generalised Rosenbluth pot., Balescu-Lenard eqn. friction and diffusion coeffs., wave effects 78−38457
glass-Al, layered target, reduced thermal cond., X-ray meas. 77−31523
glow discharge, high press. probe meas., current-voltage characts. 79−90466
glow discharge, ionisation instability, stabilising effect of turbulent transport processes *(Russian)* 78−59698
graphite arc, in Ar flow, meas. of anode voltage drop 80−84022
guiding center drift equations in mag. coordinate system 80−87865
guiding centre orbits and topology of noncircular axisymm. Tokamak plasmas 80−6227
Hall accelerator, azimuthal drift current, induction meas. method 79−23465
Hall accelerator, ion current oscills. *(Russian)* 79−98995
Hall accelerator, with extended accel. zone, ion stream modulation at exit 78−79480
Hall current and gyroviscosity effect on conducting, rotating viscous plasma stability 80−75041
heat and particle diffusion, due to collisionless drift instability, probe diagnostics 78−59555
heat and particle fluxes, inhomogeneous plasma, current driven drift wave effects 78−94901
heat and particle transport, nonlinear, due to collisional drift waves 77−80278
heat conduction, microinstabilities in moderately inhomogeneous plasma 77−87223
heat conduction and magnetic field induction in the presence of cold- and hot-electron Maxwellian distributions 79−60109
heat conduction over plasma density step 79−7447
heat exchange of low-temp. plasma with wall, longitudinal mag. field effect 80−33781
heat flow, eqns. with large temp. differences between interacting species, ionosphere appls. 79−66857
heat flow and diffusion in Tokamak, quasi-linear theory 79−98871
heat flux limitation by ion-acoustic instability 80−92304
heat flux reduction by electromagnetic instabilities 78−67320
heat transfer, 1976 literature review 78−5740
heat transfer, in wall region of reactor Tokamak *(Russian)* 78−87501
heat transfer bibliography 78−63425
heat transfer rates to flat plate from normally-impinging N plasma jet 80−75061
heat transport, computer simulation 80−28817

plasma transport processes continued
heat transport on plasma with mega-Gauss magnetic fields, enhancement 78−34273
heat wave propagation in fully ionised plasma *(Russian)* 80−24141
heat waves, linear mag. fusion device, particle end loss reduction 78−33289
heating by shortwave laser pulses, electron thermal conduct. effect 77−1005
heating in lower hybrid freq. range, temp., ion diffusion 80−83954
heating in toroidal plasmas 80−24239
heavy ion complex mobility in cool plasma 77−62343
Heliotron-D device, Joule current inhibition 79−99001
HF noise and transport in electron-beam-heated plasma *(Russian)* 77−55174
HF oscillations and electron beam relax. in homogeneous gas-discharge plasma 80−38614
high beta pinches, mag. field diffusion, hybrid model calcs. 77−24152
high current vacuum arc, with axial mag. field, current distrib. meas. 78−87572
high density directed plasma, source, design, characts., numerical model 80−38538
high density plasma, thermonuclear reaction wave, propag. stages, computer simulation 78−742
high density plasma, turbulent heating, rapid current penetration 78−51320
high density plasma interaction with a strong EM wave, Green's function method calcs. 80−48885
high field tokamak, plasma energy balance and classical ion thermal cond., Joule heating *(Russian)* 79−27797
high melting particle heating, melting and vaporisation in hot gas 80−6201
high temperature mag. confined plasma, transport processes, instability 77−68755
high-β plasma with impurities and neutrals in belt pinch 77−11317
high-β Tokamak states, accessibility, transport model 79−64829
high-beta pinch, kinetic behaviour, anomalous transport and unstable MHD modes 77−76163
high-temp. regimes, simulation and confinement scaling 80−38673
high-temperature plasma, elec. cond. in uniform mag. field 79−4112
higher-order Chapman-Enskog theory for electrons 80−38561
highly-ionised free-fall positive column, differential eqn. system 78−67489
highly-ionised positive column under free-fall and ambipolar diffusion conditions 78−67490
hollow arc cathode, with highly ionised dense plasma, props. 79−64951
hollow cathode arc with fully ionized dense plasma, V-I characts. and other props. 79−14627
hollow cathode arc with reduced gas flow, operation mode 80−38783
hollow current profile form. in Tokamak LT-3 77−72500
hollow electron beam pot. in magnetically insulated diode 80−70046
hollow-cathode glow discharge, fast electron current, electrostatic vel. analyzer diagnostics 79−27856
hollow-cathode low-pressure discharge critical current determ. 78−67538
hot plasma resistivity, minimum cutoff 80−28610
hydrocarbon fuels, universal formula for elec. cond. of combustion-products plasma 79−19004
hydrocarbon fuels combustion prod. plasma with alkali impurity, elec. cond. 79−55466
hydromagnetic rarefaction waves and free expansion in collision-free strongly magnetised plasma 80−38594
ICRF heating in TFR, preliminary obs. and further development prospects 80−28741
implosion heating, numerical modelling of Los Alamos expt. 77−43056
impurities in collision-dominated regime, transport props. 78−5850
impurity atom diffusion, laser fluorescence study 79−68955
impurity control and plasma transport in plasma-edge region 80−13832
impurity density distrib., energy loss and diffusion in Tokamaks 77−65838
impurity diffusion, in Pfirsch-Schluter regime, suppression by plasma rotation *(Russian)* 79−98867
impurity diffusion, in Tokamak in collision regime, neutral injection effects *(Russian)* 78−26247
impurity diffusion and heat transfer, in neoclassical regime, neutral injection effects *(Russian)* 78−26248
impurity diffusion eqn., with ionisation and recombination source terms 78−30409
impurity diffusion in Pfirsch-Schluter regime, kinetic theory 77−72414
impurity diffusion in Pfirsch-Schluter regime *(Russian)* 78−26246
impurity effects and control, neutral beam injection, computational models for large Tokamaks 80−28773
impurity flow reversal expt., result anal. 80−106875
impurity ion UV emission poloidal asymmetry obs., grad B drift 78−26331
impurity ions effect on transport coeff. 77−76057
impurity ions on rational magnetic surfaces, convection and diffusion, collisional multifluid model 80−28615
impurity transport, neoclassical theory 79−98873
impurity transport in plateau to Pfirsch-Schluter regimes 77−35323
inert gas arc, low-voltage, ionis. mechanism 79−27852
inert gas ion laser, high voltage-low press. discharges, stationary props. 80−92400
inert gas plasma, thermodynamic functions, composition, and elec. cond., calc. method 79−32738
inert gases, atomic alignment in positive column *(Russian)* 80−87981
inert gases, metastable atom diffusion, state decay, VUV obs. from discharge afterglow 80−44061
inhibition of transport, 1.06 μm laser beam irrad. of parylene disc 77−43010
inhomogeneity spreading in weakly ionised current-carrying plasma 78−71445
inhomogeneous diffusion equation, analytical solns. 77−55129
inhomogeneous diffusion equations, analytic solutions, and diffusion coeffs. 78−34267
inhomogeneous plasma, LF EM turbulence effects 79−86583
inhomogeneous strongly magnetised plasma, quasilinear diffusion, particle transport and electrostatic oscillations 78−42723
integral invariants and quasi-MHD nonlinear dissipation 79−98882
inward particle transport by plasma collective modes 79−55543
ion acceleration in anode foil plasma, irrad. by relativistic electron beams *(Russian)* 80−54000

plasma transport processes continued
ion acceleration in coaxial diode with mag. insulation *(Russian)* 80−10402
ion acceleration in expanding rarefied plasma 79−41799
ion acoustic solitary waves in presence of HF elec. field 77−62342
ion acoustic wave, self excited, in hot plasma, dispersion theory 80−92283
ion acoustic wave propagation, electron-ion plasma, Grad's thirteen moment approximation 79−50857
ion acoustic wave radiation due to oscill. point charge *(French)* 80−43900
ion acoustic waves method of plasma potential meas. 80−59289
ion and electron current distrib. in plasma wind tunnel, slow ion effects 77−24063
ion and impurity species, neoclassical transport coeffs. 78−14137
ion beam with rotational and axial motion, thermal equilibrium props. 80−53934
ion composition of plasma of pulsed discharge in He, H_2 current time evolution 80−54046
ion current from Penning discharge ion source, depend. on mag. field and anode diameter 80−54072
ion current in electron beam-formed plasma, two-electrode probe meas. *(Russian)* 80−1841
ion current magnetic field reversal, electron effects 79−10638
ion drift speed into plasma sheath, rel. to acoustic waves propag. 77−7531
ion heating by current driven turbulence in inhomogeneous plasma 80−33791
ion heating by current-driven turbulence in inhomogeneous plasma 80−96370
ion loss due to low frequency instabilities 80−6217
ion motion, nonlinear, in slow ion cyclotron mode 77−7509
ion motion, superadiabatic and stochastic, in mirror-machine plasma, in presence of electrostatic wave 80−53933
ion pressure discharge theory in the strong ionisation regime 80−38734
ion ring, field-reversed, anomalous decay of induced electron current 80−24206
ion sheath, convection sustained, struct., probe meas. 78−14179
ion source anode layer struct. with closed Hall current, anomalous cond. effects *(Russian)* 77−46437
ion thermal conductivity, anomalous, drift oscills. effects *(Russian)* 79−23403
ion transport in electrical discharge 78−87435
ion velocities, in four-component ionospheric plasma 77−13154
ion velocity space diffusion and ion-cyclotron oscill. enhancement in mirror confined plasma 77−24059
ion velocity space diffusion in controlled ion wave turbulence, ion wave echo probe obs. 77−43079
ion wave effects in open cylindrical magnetoplasma device, turbulent thermal insulation 80−106914
ion wind, in plasma centrifuge, isotope separation appls. 79−31722
ion-acoustic instability, electron flux driven, in Q-machine, probe diagnostics 80−33765
ion-acoustic instability stabilisation by ion beam in Q-machine, probe diagnostics 80−33766
ion-acoustically turbulent plasma, cond., solar corona appl. 79−19027
ion-beam perpendicular injection, anomalous slowing, quasilinear and trapping regimes 78−1850
ion-ion diffusion, 2D boundary-value problem, multiple mirror expt. 77−84411
ion-sound soliton-resonant particle interactions *(Russian)* 80−14880
ion-sound turbulence, current-driven, from electron beam interaction, wave dynamics 78−38489
ion-sound turbulence driven by return current from electron beam interaction 78−34314
ionization-diffusion oscillations in glow discharge plasma, rel. to stepwise ionization 78−1927
ionosphere plasma interaction with gravity waves, elec. field and current prod. 80−61957
isotope separation, HF stationary discharge, travelling mag. field, barodiffusion separation 80−44049
isotope separation, impulse plasma centrifuge with circulation, theory *(Russian)* 80−38553
isotope separation by ponderomotive force effect near ion-cyclotron reson. 80−43998
JET, transport calcs. for approach to ignition 80−92263
jet carrying solid particles, electrophysical props. 80−24134
Jupiter, bounce averaged synchrotron loss in dipole field 77−87316
kinematic model of strong turbulence in plasma with relaxed closure *(French)* 79−10701
kinetic effects in plasma resonance in weak fields 78−83532
kinetic equations in theory of transport props. of fully ionised gases 79−10640
kinetic expressions for transport coeffs. 77−27652
kinetic reactions, pulsed afterglow technique obs. in Ar-H plasma 80−48854
kinetic theory, for dense plasmas transport coeffs. 80−77280
kinetic transport properties of a bumpy torus with finite radial ambipolar field 79−55469
Landau equations, complete difference schemes *(Russian)* 79−77343
Langmuir oblique solitons, self-contraction in free path regime *(Russian)* 80−43921
Langmuir system, kinetic theory of mag. field generation 80−69974
Langmuir wave evolution, three dimensional kinetic model, Vlasov eqn. calcs. 80−43923
Langmuir waves, collisional damping in collisionless limit 78−34295
laser beam filamentation in strongly ionised magnetoplasma 78−26291
laser driven plasma, vacuum insulation against suprathermal electrons 80−18598
laser field effect on transport coeffs. 78−67317
laser fusion, electron thermal cond., plasma hydrodynamic calcs. 77−68750
laser fusion, energy flux limitation by ion acoustic turbulence, anomalous transport coeffs. 77−43009
laser fusion, interaction and transport processes, continuous pulse shaping 80−28766
laser fusion, suprathermal electron transport, dual treatment 80−18599
laser fusion target, energy transport 78−47143
laser heated microsphere plasma, density profile indicating inhibited transport 79−41850

plasma transport processes continued
laser heated plasma, electron thermal conduction, kinetic description 77−24060
laser plasma, magnetothermal phenomena *(Russian)* 80−33798
laser plasma, radn. induced perturbations, current and press. fluctuations 79−82079
laser plasmas, hot electron energy relaxation and transport *(Japanese)* 80−96347
laser produced plasma, heat front penetration depth, heat transport wavelength depend. 80−48926
laser produced plasma, maximum transport vels., obs. and theory 78−67385
laser produced plasma, maximum vels., obs. and theory 78−67385
laser produced plasma, simultaneous meas. of current and mag. field 77−1001
laser produced plasma, strongly flux limited thermal cond., modified LASNEX calc. 79−37523
laser radiation, intense, transmission through overdense plasma 79−10671
laser target, Monte Carlo (hybrid) suprathermal electron transport 80−24200
laser targets, dynamics, 2-D three-temperature MHD model 80−70014
laser transmittance in high-Z thin plasma, energy transport 77−80333
laser-fusion regime, plasma transport, extension of Braginskii system of fluid equations 80−53935
laser-pellet plasma, electron distrib. function and quasi-static EM fields, transport coeffs. 77−55160
laser-produced plasma, hydrodynamic stead-state solns. in planar geometry 79−37522
laser-produced plasma, simultaneous meas. of current flow and mag. field 77−24192
laser-produced plasma, X-ray spectrometry, for energy transport diagnostics *(French)* 80−43982
Levitron, fluctuations, diffusion and beam-induced currents 80−28616
limiting current in steady state diffusion-recombination discharge 78−67466
linear compression of plasma vortex 80−64755
linear effects of wave propag. in plasmas, review 78−14149
linear gasdynamic confinement system 80−48957
linear reactor system with impurity-seeded multiple-mirror end plug 78−78493
localised structures and anomalous DC resist. 77−58846
long time confinement of pure electron plasma, max. confinement time 80−48954
long-wavelength modes and anomalous transport in toroidal magnetoplasmas 80−28613
longitudinal current excitation in plasma loop, 'mag. projectile' as mag. flux carrier 79−19079
longitudinal current generation and relax. in stellarator *(Russian)* 80−10418
longitudinal electrical resistivity in magnetic field, shielding effect *(Chinese)* 80−69977
low pressure HF discharge, anomalous cond. mag. field effects 80−44047
low Z impurity transport in Tokamaks, simulation 79−55468
low-β plasmas, turbulence, spectral struct., Bhom diffusion coeffs., determ. 80−106924
low-frequency impedance, of probe in dense plasma 79−64918
low-frequency transport processes in lower ionosphere, collision freqs. for continuum momentum eqns. 77−87171
lower hybrid heating of toroidally confined plasma, transport, theory 78−42723
lower hybrid wave scattering by density fluctuations 79−94792
magnetic cusp, relativistic electron beam driven inertial fusion, transport calcs. 78−75268
magnetic diverters for experimental Tokamaks and fusion reactors 80−18621
magnetic field, force-free, resistive evolution, in cylindrical geometry 80−6212
magnetic field effects, boundary conditions, computer simulation 80−10392
magnetic field effects on plasma motion in ring container, decreasing entropy 78−59553
magnetic flutter causing transport phenomena 79−86561
magnetic island coalescence, 2-dimens. MHD eqns. 80−64695
magnetic mirrors Hamiltonians of particle motion, canonical transforms. 80−33748
magnetic pinch discharge, superstrong mag. field prod. 79−90444
magnetic Rosenbluth potentials, generalised to include wave effects 78−94896
magnetic trap, open, axially symmetric, reson. particle diffusion, homogeneous model *(Russian)* 79−98952
magnetic trap, with helical mag. axis, plateau and banana diffusion regimes 80−10425
magnetic-field-aligned elec. currents in cold collisionless plasma 79−1298
magnetically confined plasma, high temp., transport processes, numerical soln. 80−19559
magnetically confined plasma, transport processes and instabilities 77−72419
magnetically confined plasmas, expressions for nonclassical energy and particle flows 80−75031
magnetically insulated diode, coaxial geometry, one-, two-species equilib., electron and ion flow 77−58905
magnetised column, drift dissipative waves, LF oscills., anomalous diffusion and equilib. 80−33769
magnetised DC discharge plasma, pot. difference meas., anomalous resist. 78−87434
magnetised plasma, double-layer characts. meas. 80−43874
magnetised plasma, electric current and electron temp. distribs. *(Russian)* 77−35319
magnetised plasma, hot, unstable behaviour, in contact with cold wall 79−1333
magnetised plasma, in dielectric chamber with thermionic emitter, enhanced diffusion 79−64901
magneto-electrostatic reactor, power gain factor 80−48933
magneto-electrostatic traps, classical transport processes *(Russian)* 78−75403
magneto-ionic energy transport in shearing plasma, rays propag. 79−84659
magneto-viscous resistive tearing of cylindrical flux surfaces 80−1831

plasma transport processes continued
magnetoacoustic oscillations in current-carrying plasma column 78−30438
magnetoplasma, intense EM wave absorption, numerical results 80−43890
magnetoplasma, plasma wave generation and SHG by Gaussian EM beam 79−37479
magnetoplasma, weakly ionised, perturbational heating in oscill. elec. field, collisional relax. and Boltzmann eqn. 79−37515
magnetoplasma, with anisotropic inhomogeneities, effective Ohm's law, appl. to MHD generator performance 78−67316
magnetoresistance, due to density or concentration inhomogeneities 78−47099
magnetostatic mode and cross-field electron transport 78−83538
marginal stability anal., anomalous transport, profiles, coeffs. and turbulence level calc. 77−47175
mass renormalization in stochastic acceleration of particles *(Russian)* 80−100066
mass separation in rotating weakly ionised plasma *(Russian)* 80−1745
maximum energy flux in collisonless plasma, comparison with free molecular gas motion 80−6221
maximum energy-confinement time in joule-heated Tokamaks 79−37532
Maxwellian thermonuclear plasma, quantum mechanical slowing in distrib. of energetic charged particles 79−86588
megavolt and megampere diagnostic techniques for pulsed power particle beam fusion drivers 80−49010
memory function, coupling of single particle and collective modes 77−68749
memory function, transverse current correlations in classical one component plasma 78−94892
metal plasma prod. by exploding wire, X-ray diagnostics 78−5909
metal surface, high-intensity laser beam interaction 80−19600
metal-seeded rotating plasma 80−1746
MHD accelerators, electrodynamic characts. 80−64788
MHD boundary layer on flat plate with aligned magnetic field *(French)* 78−1808
MHD channel, anisotropically conducting plasma in inhomogeneous elec. and mag. fields, current calc. *(Russian)* 80−74995
MHD channel with Hall and ion slip currents, forced convective heat transfer 80−33823
MHD combustion, operating mode aspects 78−18388
MHD devices, plasma ionization instability, dynamic suppression, switching modelling 80−59308
MHD eqn., stability, transport calc. for high-beta Tokamaks 80−28848
MHD eqns. and confinement studies in closed magnetic configurations 79−98964
MHD equilibria, secular instability in mag. quadrupole field 80−53982
MHD equilibrium with elliptic free-boundary, limiter and current profile effects 79−37529
MHD flow, plane, in hyperbolic mag. field, mag. field line reconnection 79−32755
MHD generator, characteristics improvement, using current parallel to magnetic field 80−1751
MHD generator, conductivity and power output ionization stability, and boundary layer effects 80−1752
MHD generator, diagonal electrode config., nonuniform conductivity in boundary layer, effect on local characts. 77−39471
MHD generator, plasma interelectrode breakdown, model 79−55572
MHD generator, plasma turbulence in combustion channel 80−75057
MHD generator channel electrode surface temp. selection, effect of working body props. 79−55573
MHD oscills. ensemble, interaction with quasiuniform mag. field, sunspots 77−76041
microcanonically distributed plasma, reduced distrib. functions 80−28604
microtearing modes and anomalous transport in Tokamaks, self consistent calc. 80−59222
microtearing modes and anomalous transport in Tokamaks 80−92316
migma electron velocity space distrib. function strapping 77−83091
migma ion distrib. in phase space, shaping 77−83090
mirror devices, axial particle transport, finite mean free path effects 80−83900
mirror plasma, quasilinear transport model 77−76181
Mirror-Torus-System-1 with divertor mag. field, plasma density and depolarisation current 80−70022
motion of the cathode spot of a vacuum arc 80−54069
moving plasma, four-dimens. constitutive relations 79−37537
multi-ion system, modulation instability of ion acoustic waves 80−69996
multi-region global transport model for Tokamaks 80−92264
multichannel configuration, relativistic electron beam driven inertial fusion, transport calcs. 78−75268
multicomponent plasma, ion-acoustic resist. 80−10383
multifluid Tokamak transport code, two dimens., time evolution 77−58880
multimirror experiment, linear, trapped electron instability 79−60181
multiphase medium plasma dynamics, Soviet literature growth and duplication parameters *(Russian)* 80−59191
multiple ion plasma, Pfirsch Schluter regime, classical transport and friction coeffs. 77−55130
multispecies flows, transport eqns. mathematical struct. 78−47084
multispecies plasma with biMaxwellian distribs. 79−77339
multispecies tokamak plasma containing multiple charge state ions, neoclassical transport 79−77340
multispecies transport in collisional Tokamaks 77−19674
multitemperature mixtures, Maxwell-Grad moment method calcs. 77−47134
negative diffusion of ion energy, magnetised plasma, drift-wave fluctuations 78−94902
negative diffusion of perpendicular ion energy in magnetised plasma, mode coupling 79−41802
negative grid pulse effects, on Knudsen Cs arc discharge plasma 80−38843
neoclassical coefficients, ELMO bumpy torus, one dimens. radial transport eqn. 78−42727
neoclassical conductivity, numerical integration for Tokamak 77−65841
neoclassical current in a toroidally-confined multispecies plasma 78−83528
neoclassical diffusion in helical solenoids 78−94893
neoclassical transport in elliptic Tokamak 78−14135
neoclassical transport of multispecies plasma, mixed regime with several collisional species 78−34274

plasma transport processes continued
neoclassical transport of multispecies toroidal plasma in collisionality regimes 77−47152
neoclassical transport theory, for toroidal axisymmetric plasma, moment eqn. calcs. 78−42724
neutral atom transport, computer code SPUDNUT 80−48962
neutral beam induced reverse electron currents, Levitron obs. 78−59620
neutral beam injection, fuelling profiles effect on plasma transport props. 80−19596
neutral beam injector, simulation of neutral particle transport 80−37600
neutral-beam-injected mirror-confined plasma transport 78−22461
neutral current layer, tearing mode instability and mag. field line reconnection *(Russian)* 78−91087
neutral current layer dissociation, external plasma effect *(Russian)* 78−18409
neutral gas transport in infinite cylindrical plasma, Tokamak model, Monte Carlo algorithm 78−79459
neutral particles transport calc. in high temp. plasma *(Japanese)* 79−82045
neutral radiant gas, kinetic eqns. with allowance for radiation polarisation 79−23399
neutral transport, one-group treatment 77−39408
neutral-beam-driven current evolution in Tokamak plasmas 80−28712
non-Debye plasma generation methods and props. 78−75387
non-linear transport equations: Properties deduced through transformation groups 80−4680
non-LTE line transfer, excited atom diffusion effects 77−31435
non-self sustained discharge current, gas purity effects 80−38845
nonclassical diffusion across a mag. field *(Chinese)* 78−67390
nonideal plasma, electric conductivity up to 10^6K 80−103112
nonideal plasma, elem. excitations and macroscopic props., review 80−43842
nonideal plasma, measured props. and nonideality influence 80−43869
nonideal plasma thermodynamic functions and transport deviations 78−75273
noninteracting electrons, in strong elec. field, distrib. function, mean values *(Russian)* 78−87984
nonisothermal rarefied plasma, transport processes and Lenard-Balescu eqn. 80−6222
nonlinear diffusion, Okuda-Dawson scaling 78−67321
nonlinear diffusion across mag. field of toroidal multipole 77−68751
nonlinear diffusion in exploding wires 78−14191
nonlinear fluctuation-dissipation theorem, nonpotential perturbation fields *(Russian)* 80−59225
nonlinear heat and particle transport due to collisional drift waves 78−71444
nonlinear interaction, electron collision freq., self-consistent eqn. *(Russian)* 80−75055
nonlinear inverse bremsstrahlung and heated electron distributions 80−43930
nonlinear inverse bremsstrahlung and heated-electron distributions 80−48927
nonlinear kink instabilities in Tokamaks surrounded by force-free fields 80−43909
nonlinear magnetostatic modes and twisting modes with magnetic islands 80−106900
nonlinear phenomena in MHD and Hall effect 79−72988
nonlinear scattering of upper hybrid laser radiation by electron Bernstein modes in a plasma 80−64720
nonlinear transport due to collisional drift wave 77−72417
nonlinear transport instability in diffusive plasma 78−59584
nonlinear wave phenomena, collisional and weakly collisional cases 77−11346
nonlocal shear viscosity, long-time behaviour, microscopic approach 77−35321
nonneutral and quasineutral diffusion of weakly ionised multiconstituent plasma 78−57384
nonneutral electron plasma, transport due to electron-atom collisions 78−67318
nonselfmaintained discharge, current voltage characts. 80−44045
nonstationary plasma column, Schottky's diffusion theory 78−91174
nuclear fusion reaction effect on diffusion and thermal cond. 77−76031
numerical simulation of disruptions and loss in Tokamak plasma 80−70026
Ohm's law, electrical conductivity, turbulence effect 78−22463
Ohm's law coefficients, in nonlinear plasma, from electron-neutral particle collisions 79−98857
oHM's law in turbulent plasmas and beta limitations by anomalous diffusion 79−77344
ohmic heating in Frascati Tokamak, preliminary results 80−28734
ohmic heating of plasmas in closed magnetic systems 80−28756
open trap plasmas, electronic loss layer formation, low freq. oscill. anomalous electron diffusion *(Russian)* 79−90383
open traps, axially symmetric, transverse particle losses 80−28784
origin of galaxies in expanding Universe, plasma cond. and instabilities, MHD soln. 80−62283
oxy-acetylene combustion products, seeded, elec. cond. rel. to MHD power generation 77−3922
parametric instability, general quasi-linear theory 79−60130
parametric interaction of waves in plasma with random large-scale inhomogeneities *(Russian)* 80−103137
parametric resonance in a weakly turbulent relativistic electron plasma 79−55539
partially ionised gas mixture, transfer coeffs. by approx. method 79−72991
particle and energy balance by corpuscular diagnostics 80−92399
particle and energy transport, toroidal field ripple effect in Tokamak 77−11315
particle and heat fluxes, inhomogeneous plasma, effect of current driven drift waves 78−94898
particle diffusion across mag. fields, stable profile for nonlinear diffusion eqns. 78−22456
particle diffusion coeff., higher-order corrections 78−59556
particle drift absence in translationally symmetric mag. fields 79−37454
particle number conservation in charged particles diffusive transport 78−75266
particle scattering on plasma turbulent pulsations, quasicollisions model rel. to transport coeffs. 78−71440
particle streaming at speeds greater than Alfven velocity, astrophysical appls. 79−40068
particle transport in HF heated magnetised plasma 80−87863
particle transport phenomena, theory, book 79−63176
Pfirsch-Schluter particle diffusion, modification by reson. mag. perturbation 79−64830
Pfirsch-Schluter transport, temp. screening effect 77−76035
Pfirsch-Schluter transport modification by poloidally asymmetric sources 78−42726
PHAEDRUS RH heated tandem mirror, single particle orbits 78−79456
pinch, resistive, MHD, nonequilib. stability 79−50877
pinch, reversed field config., heating, diffusion, stability 77−43036
pinch implosion, post-implosion anomalous transport, lower hybrid drift instability 77−24056
plasma, ion drift velocity in EM fields, charge transfer effect 78−83527
plasma decay under constant voltage *(Russian)* 80−106988
plasma diffusion in stochastic mag. fields, rare collision effects *(Russian)* 79−77342
plasma reactors, laminar and turbulent transport model *(German)* 77−11321
plasmadynamical modes, macroscopic, two-fluid description 77−15162
plasmotron, thermal and elec. characts., depend. on channel radius and flow 78−1910
plasmotron, two-jet type, thermal and V-I characts. 78−55757
plastic film, laser energy transport, X-ray, ion emission, scatt. light diagnostics 77−24117
PLT Tokamak, ohmically heated plasmas, radiation, impurity effects, instability and particle transport 80−28833
polarisation of picosecond excited continuous X-ray radiation *(Russian)* 80−59190
polarization-dependent energy transport in laser-produced plasmas 78−67380
poloidal mode ballooning of trapped electron instability 80−28657
ponderomotive laser effects in collisional plasma transport 80−38562
ponderomotive laser-plasma effects subject to strong magnetic fields and collisions 80−87905
position instability analysis, effective mode approx. in Tokamak 80−103145
positive column, ionisation and temp. effect on charged particle profile and density 80−79596
positive column, metastable atom radial transport, effect of wall boundary conditions 78−67493
positive column, metastable atom radial transport at various electron distribs., atom+atom collision effects 80−44037
positive column, metastable atom transport, excitation rate radial variation, flux to wall calc. 80−44038
positive column, subnormal, ion and electron radial distrib., theoretical description 80−79598
positive column constriction, cryogenic discharge, ambipolar wall diffusion 78−18468
positive column gas discharge with external ionisation, voltage-current characts. 80−96408
positive column of high-voltage diffuse discharge, nonstationary processes 80−64802
positive columns composed of mixed ion plasma, general ambipolar diffusion theory 78−94897
positive-ion distribution in a strong electric field, steady state kinetic eqn. 80−33844
potential small-scale instabilities of inhomogeneous plasma in crossed electric and magnetic fields 80−79492
prepulse discharges in high current accelerator diodes with double shaping line 80−5399
pressure, virial kinetic definition, spherical geometry calcs. *(French)* 80−69973
primordial lepton gas, elec. cond., Landau, Boltzmann eqn. calcs. *(French)* 80−75030
pseudo-classical transport, nonlinear theory of collisionless drift instability 79−94774
pseudo-classical transport, particle and energy flux, electron trapping by drift waves 79−94773
pulsar magnetospheres, anomalous energy dissipation from limitations on force-free approximation 77−5541
pulsed current voltage characteristics of a thermally produced plasma 80−38554
pulsed DC glow discharge, cataphoresis eqns. 78−67506
pulsed e.m. confinement system, electron ionised plasma, particle lifetime 77−1014
pulsed Xe discharges, in quartz chamber, elec. cond. meas. 79−55605
pure electron plasma, waves and transport 80−38563
quantum plasma, HF conductivity 79−19000
quasi neutral plasma expansion, fluid model approach 80−33747
quasicollisional plasma, transport coeffs., appl. to magnetosphere 78−71440
quiet plasma, in mag. field, produced by transverse diffusion from RF discharge 78−79448
radial boundary layers, diffusing toroidal equilibria 77−89285
radial diffusion, eqn. for collision-affected plasma 78−49310
radial electric field, appearance in source plasma due to beam extraction 79−45500
radiation temperature of proton beam induced plasma 80−100094
radiative heat transfer effect on MHD discontinuity propag. in optically thin medium 79−46438
radiative power loss, from plasmas in steady state ionisation balance 79−82063
Ramsauer-Townsend effect, partially ionised gas elec. cond. 78−67458
randomly inhomogeneous cond. medium in mag. field 80−19558
rarefied electron gas, space depend. electron transport by integral approach 80−92257
rarefied ionised gas, ion transport in strong elec. field 77−51155
rarefied plasma, mag. field rapid penetration, magneto-acoustic shock waves, super-Alfven penetration *(Russian)* 78−59554
Rayleigh-Taylor instability generation of mag. fields, effects on laser fusion 79−19025
reactor, Tokamak, fuel injection, dynamic burn control 1-D transport code 80−68948
reactor ignition, overheated underdense Tokamak plasma, two-zone model and 1-D transport code 80−63376
reduction and inversion due to plasma rotation and ion-neutral friction 80−79444
reflex discharge, diocotron-instability pulses, current and electron loss effects 77−62423
relativistic Boltzmann theory, reciprocal relations, transport props. 78−30477

plasma transport processes continued
relativistic Boltzmann theory, reduction of collision integrals 80−79560
relativistic Boltzmann theory, transport coeffs., variational method 78−47096
relativistic Boltzmann theory, viscous phenomena 78−34365
relativistic charged particle motion in Tokamaks, electric field and slowing down effects 80−92262
relativistic collisionless plasma, EM perturbation of relativistic Vlasov-Maxwell eqns. 79−90449
relativistic degenerate electron gas in strong mag. field 77−80346
relativistic electron beam injected into drift tube, limiting currents 79−10699
relativistic electron beam injection, uniform mag. field plasma, space charge neutralisation *(Russian)* 77−19719
relativistic electron beams, gradB transport, bunching and focusing 80−96345
relativistic electron beams, theoretical scheme for axial compression 80−96367
relativistic magnetised Vlasov-Maxwell plasma, current responses 79−90450
relativistic statistical mechanics 79−82039
relativistic streaming plasma, generalised Ohm's Law, pulsar magnetosphere relevance 78−9823
relativistic two component plasma, conductivity sum rules 77−19761
relativistically streaming plasma, flux conservation, MHD and force-free approxs. 79−19081
renormalised Vlasov turbulence 80−19579
resistance, anomalous, its nonlinear electrothermal runaway rel. to fast particle emission 77−19707
resistive effects in Alfven wave heating 78−1857
resistive evolution of force-free mag. fields, rel. to anisotropic diffusion 79−90382
resistive hose instability in relativistic electron beam 80−67947
resistive internal helical mode near the instability threshold *(Russian)* 79−98948
resistive internal kink mode 77−68793
resistive plasma, response to external current field 78−34268
resistive steady states of elliptical cross-section plasmas 79−98872
resistive tearing mode, influence of diffusion 78−34297
resistivity, anomalous, and Buneman instability, amplitude saturation 78−75300
resistivity, anomalous, in turbulently heated plasma with ion-acoustic instability 80−10399
resistivity, in structureless H plasma, weak electron-ion interaction 77−47154
resistivity, localised enhancement, mag. field-line reconnection 78−22467
resistivity, of turbulent plasma, with ion-acoustic instability, ion-tail form. effect 80−10360
resistivity, trapped electron regime, collisional theory 77−84412
resistivity, turbulent, at high drift vels., particle diagnostics 78−38541
resistivity anomalous, generated by ion-acoustic turbulence, collision freq.-turbulence spectrum relation 78−14205
resistivity enhancement by LF self-modulation of electron plasma modes 78−9759
resistivity phenomena in multi-ion plasma with ion-acoustic turbulence 80−48856
resistivity reduction in partially ionised plasma due to ionisation and recombination 78−63545
resonant collective processes, wave and particle accel. into increasing plasma gradient 77−47153
resonant excitation of slow low-freq. waves by opposite moving electron beams *(Russian)* 80−92336
resonant medium with small degree of ionisation, radiation transfer mechanism *(Russian)* 79−37453
return current processes in heating by electron beam 77−51205
return current response to external beam current in mag. field 77−15211
reversal field mirror, alpha-particle effects 78−58468
reverse current damping by relativistic electron beam *(Russian)* 78−1800
reversed field pinch, config. evolution 77−24150
reversed field pinch, numerical studies 80−87931
reversed-field pinch plasma model 80−87935
RF current dynamic shear stabilisation of low-beta plasma column hydromag. instability 79−46454
RF discharge, electrode sheath 80−44052
RF discharge plasma, recombination and diffusion coeffs. 77−7594
RF discharge plasma skin effect counteraction by external mag. field 78−67543
RF driven current generation by lower hybrid waves in Tokamak 80−103116
RF driven currents in steady state Tokamak reactors 80−28687
RF induction plasma torch, temp., elec. cond., efficiency values from mag. probe meas. 78−42836
RF plugging and heating, rel. to plasma impedance 80−96378
RF voltage in plasma probe sheath, effect on electron energy distrib. meas. 80−54045
RINGBOOG II, toroidal discharges with cold blankets 80−83901
rotating plasma, heating and diagnostics by induced poloidal currents 78−18449
rotating plasma, viscous dynamics 78−91082
rotating plasma, weakly ionised, rot. vel. and ion cond., obs. and MHD theory 80−38576
runaway electron critical velocity in magnetised gas *(Chinese)* 80−87845
runaway electron motion in momentum space, multicomponent plasma 79−37449
runaway electron transport in LT-3 Tokamak 77−11316
runaway electrons quasilinear relaxation, HF heated tokamak plasma 77−65837
runaway electrons radial transport in ORMAK 79−10639
runaway relativistic electron scatt. on oscills. in Tokamak *(Russian)* 80−48849
screw instability of finite cond. gas *(Russian)* 80−92311
screw pinch, force free current induction by boundary displacements 79−32796
screw pinch, toroidal plasma current decay and profile 77−24167
screw-pinch configs., collisionless, hybrid-kinetic stability props. of high-beta plasmas 80−43871
Scyllac configuration, toroidal theta-pinch theory, review 77−24125
self similar cooling wave, effective thermal cond. *(Russian)* 80−14908
plasma transport processes continued
self-diffusion, in classical one-component plasma, microscopic theory 77−55131
self-generated fields by currents driven by electron press. grad. 78−1794
self-generated magnetic field in laser-produced plasmas, metallic target 79−41851
self-inductance changes in plasma focus 77−27651
self-oscillating mode origination in nonequilib. magnetised plasma 79−86568
separable solutions for Tokamak plasma transport 77−51158
shear stabilisation of drift oscills., ionic viscosity influence *(Russian)* 77−84432
shear viscosity of strongly coupled 1-component plasma, kinetic theory 79−10643
sheath broadening in theta pinches, lower hybrid drift instability 77−31429
shock wave, collisionless, turbulent ion viscosity *(Russian)* 78−38492
shock wave, laminar to turbulent boundary layer transition, effect on current flow 79−41709
shock wave produced plasma, electron and ion thermal diffusion effects 80−48891
shock wave struct., dissipative electron transport influence 78−5875
shock waves in rarefied plasma in mag. field, transport props. *(Russian)* 77−47201
shock-radiative recombination rate in afterglow of He plasma 79−4205
short-circuit effect in a bounded plasma 79−27820
Simon short-circuit effect used for density diagnostics 79−23460
single particle motion in 1-component strongly coupled plasma 80−48847
skin current heating of toroidal plasma 80−28715
slow convection of magnetised plasma, appl. to Earth plasma sheet 80−109312
solar nonrelativistic electron diffusion mechanism in interplanetary medium 77−53349
solar wind plasma kinetics 77−91512
space plasma turbulence and nonlinear waves, anomalous electrical resistivity 79−60142
space simulation beam-plasma discharge, plasma diffusion 79−60108
spark, underwater, integrated bulk plasma characts. 79−27857
spatial diffusion coeff., unmag. collisional plasma, from ion-acoustic turbulence data 78−42728
spectroscopic electron density meas., hot point low induction vacuum spark gas *(Russian)* 80−92390
sphere spark gap, impulse wave investigation *(French)* 79−50900
spheromak plasma config. form. by combined Z- and θ-pinch discharges 80−43955
stationary turbulence regions and anomalous resist. in magnetosphere plasma 80−38649
statistical mechanics, transport coeffs. 77−15166
steady state transport and scaling in ELMO bumpy torus 78−22459
steady-state currents driven by collisionally damped lower-hybrid waves 80−38639
steady-state Tokamak reactors with RF driven currents 80−27818
stellarator, current turbulent ion heating, modulation stability 80−79525
stellarator, ohmic heating current, inductorless excitation *(Russian)* 79−98864
stellarator, Saturn, current-free transport processes, drift modes effect 80−19605
stellarator, Saturn, microwave plasma, electron thermal cond. 79−19005
stellarator geometry, superbanana orbits for 3.5 MeV alpha particles 80−24231
stellarators, particle orbits and toroidal vacuum fields 80−79450
stellarators, toroidal vacuum fields, particle orbits 80−79445
stochastic mag. field fluctuations, self-consistent model 80−100074
stochasticity due to mag. perturbations in axisymmetric geometries 80−87866
stopping power of a nonequilibrium plasma for incident alpha particles 80−64742
strings in heavy-light gas mixture, self induced particle separation *(Russian)* 80−79441
strong current discharge with reverse current in optically opaque plasma *(Russian)* 77−31544
strongly coupled one-component plasma, shear viscosity, microscopic theory 77−51157
student experiments on elec. cond. and similarity laws 78−24605
supercompression of structured slab, laser deposition time depend., heat cond. effect 77−51207
supersonic plasma-steel target impact effect, boundary layer role 79−32780
superthermal electron beam, relax. due to Coulomb collisions in plasma 80−106941
supra-thermal trapped electron quasi-linear diffusion, mag. drift reson. and Alfven wave excitation *(Russian)* 79−27748
suprathermal electron fluxes, evidence from X-ray bremsstrahlung polarisation and anisotropy 80−103193
surface impedance of plasma cylinder with anomalous skin effect, energy loss calc. 78−47098
surface ion acoustic waves in non isothermal gas layer *(Russian)* 80−87891
surface mag. field confinement of high-β plasma, toroidal current stabilisation 78−67401
surface wave spectrum, surface impedance with specular-diffuse particle scattering 77−24058
surfatron produced electron density and temp. microwave meas. 80−43965
swarm diffusion tensor rel. to mobility 78−71454
tandem mirror plasmas, alpha particle dynamics 80−83986
Tandem mirror reactors, anomalous and classical transport effect 80−13862
tandem mirrors, analytic approx. to resonant plateau transport coeff. 80−32486
target impurity effect on laser produced expansion, ion spectrography 80−43945
tearing instability, current shear effect in relativistic stream superposition model 80−24155
tearing modes with mag. braiding 80−10429
test electron transport in stochastic mag. field, principles and problems 79−77341
test particle dynamics in turbulent magnetoplasma 79−14614
test particle potential in external homogeneous magnetic field 80−43870

plasma transport processes continued
TFR, high power neutral beam injection and ion power balance, anomalous heat conduction 78−82511
TFR, reduced fusion neutron production 78−63577
TFR 600 Tokamak, electron heat transport anomaly 80−79449
thermal conduction, flux-limited, in laser prod. plasma 78−5899
thermal conduction stabilisation of Rayleigh-Taylor growth 77−15180
thermal conductivities and coefficients of thermal diffusion of high temp. plasma 80−64690
thermal conductivity, laser-heated plasma, heat-flux limitation, laser-beam scatt. diagnostics 78−18453
thermal conductivity, reduced in laser-heated plasma with large temp. gradient 80−53987
thermal conductivity and thermal diffusion coefficient of high-temp. plasma in mag. field 80−92256
thermal conductivity and viscosity, one-component plasma, mol. dynamics study 79−23402
thermal conductivity reson. helical mag. field effects calcs. in Tokamak 77−47155
thermal convection instabilities of spherically symmetric plasmas *(Chinese)* 80−1774
thermal duction, flux-limited, in laser heated plasma 77−76155
thermal energy transport model in high density regimes of toroidal plasma 77−11389
thermal flux reduction by EM instabilities 79−14529
thermal ion distribution distortion by neutral injection heating 80−92344
thermal mode ray trajectory in inhomogeneous magnetoplasma 80−106884
thermal parametric instability, effect of recomb. processes 80−61967
thermal plasma, heat and mass transfer 78−1805
thermal plasma, heat transfer to neighbouring walls or electrodes 78−1804
thermal plasma transport phenomena, conf., Odeillo-Font-Romeu, France (Sept. 1975) 78−1798
thermal transport due to ion-acoustic waves 79−10642
thermal transport from turbulent skin layer to plasma core in heating 77−31492
thermal wave front, plasma flow stability 77−80283
thermionic converter, ignited mode, internal phenomena and output characteristic *(Japanese)* 80−3527
thermionic convertor, ignited mode, electron energy distrib. meas. of Cs plasma *(Japanese)* 80−3528
thermionic convertors, effect of electron thermal conductivity, theory 80−40892
thermionic plasma converter, overneutralised, instability simulation 79−14619
thermionic triode, oscills. in low press. inert gas discharge 80−79590
thermionic-weakly ionised plasma, compact static isothermal, stationary transport process of charge carriers, continuum theory *(German)* 78−14138
thermonuclear cone microinstabilities and anomalous alpha-particle losses in Tokamaks 80−28636
thermonuclear plasma surrounded by cold blanket, density profiles, thermo-elec. forces effect 79−31189
theta pinch, closed, balanced by transverse current *(Russian)* 78−1879
theta pinch, microinstability and anomalous transport, kinetic and numerical study 77−76162
theta-pinch, electron heating in turbulent neutral layer *(Russian)* 80−10361
theta-pinch, linear, microinstability onset, anomalous resistivity, electron heating and MHD oscills. 77−27698
theta-pinch, neutral current sheet, electron energy distrib. meas. 80−43954
theta-pinch description form classical electrodynamics 79−90436
theta-pinch implosion, numerical models including classical and anomalous transport 77−24139
third-harmonic generation in collisional plasma, self-focusing effect 77−7550
thyratrons, nanosecond discharge of the H_2 plasma deionisation, spectroscopic study *(Slovak)* 77−47279
time-dependent transport processes, for two-component plasma 80−38555
Tokamak, Alcator scaling, transport model 78−75406
Tokamak, anomalous diffusion of α-particles due to trapped ion mode 80−48951
Tokamak, arbitrary cross-section, self consistent two dimens. transport eqns. 79−49842
Tokamak, diffusion of runaway electrons across mag. field 78−87480
Tokamak, DITE, impurity ion concentrations and diffusion, spectroscopic measurement 80−28771
Tokamak, drift wave convective amplification enhancing transport 79−37488
Tokamak, effect of fuel pellet injection velocity on energy parameters 80−32490
Tokamak, electron energy confinement, simulation predictions 79−64898
Tokamak, electrostatic drift waves, numerical anal. of instability and transport 80−48871
Tokamak, energetic ion slowing and transport coeff. by Makokot code 80−83899
Tokamak, fast electron intensive transverse migration *(Russian)* 78−18382
Tokamak, high β_J, m=1 mode, internal helical instability suppression *(Russian)* 79−98947
Tokamak, high beta, transport and radiation studies 80−28798
Tokamak, impurity behaviour, MHD activity influence *(Russian)* 79−98866
Tokamak, impurity transport *(Russian)* 80−106957
Tokamak, inner mode relax. oscills., numerical model, electron thermal cond. distrib. *(Russian)* 77−47242
Tokamak, JFT-2, particle and heat transport during lower hybrid heating 80−70021
Tokamak, JFT-2, scrape-off layer, particle and energy fluxes, probe and IR obs. 78−59690
Tokamak, large magnetic field ripples, electric probe meas. 80−83976
Tokamak, large poloidal beta, MHD stability, collisional and anomalous trapped particle diffusion 77−24055
Tokamak, local toroidal and poloidal current density meas. 77−27732
Tokamak, neutral beam-heated, parametric scaling 80−10406
Tokamak, Pfirsch-Schluter friction on H^+ 78−34272
Tokamak, physics of burn control 80−37599
plasma transport processes continued
Tokamak, PLT, current profile evolution effect on plasma-limiter interaction and energy confinement time 80−10420
Tokamak, ray tracing in axisymmetric toroidal coords. 77−84476
Tokamak, reactor size, diffusive losses and scaling law 78−87478
Tokamak, small ignition, with neutral injection heating, transport calculations 80−9409
Tokamak, T-4, corpuscular diagnostics by charge exchange of plasma ions at artificial target *(Russian)* 80−83968
Tokamak, temp. fluctuations and heat transfer 80−74003
Tokamak, Texas turbulent torus, turbulent heating model 79−37518
Tokamak, time resolved heat flux to wall meas., sheath model with secondary electron emission 78−79468
Tokamak, trapped electron modes, cross-section elongation effects 78−59585
Tokamak, with nonmonotonic current profile, mag. island dynamics *(Russian)* 79−98879
Tokamak axisymmetric equilib., flux surface shape and current profile optimization resistive interchange stability 77−84480
Tokamak current profile meas. by neutral beam probe *(Japanese)* 80−96397
Tokamak device, eddy currents induced in vacuum vessel, anal. 80−1832
Tokamak discharge, anomalous drift-wave transport anal. 79−32745
Tokamak discharge, current mixing and mag. surface tearing in initial stages *(Russian)* 79−4165
Tokamak discharge microwave preionisation at electron cyclotron resonance 80−83896
Tokamak doublet geometry, shape control of doublets 80−48943
Tokamak fusion reactor, steady-state, lower hybrid wave-driven, design constraints 80−10424
Tokamak fusion reactors, doublet research, plasma shape control, MHD stability 80−28837
Tokamak fusion reactors, neutral beam injector penetrations, limiting neutron streaming, neutron flux calc. 80−95400
Tokamak internal disruption development mechanism, mag. island growth, simulation 78−26317
Tokamak magnetic confinement theory, conf. summary 77−76173
Tokamak model shell, shell current and vertical field meas. 77−76201
Tokamak neutral low energy transport, multigroup discrete ordinate methods, ANISN simulation code 78−34269
Tokamak plasma, beam driven currents, trapped electrons effect 80−70011
Tokamak plasma, edge cooling during RF heating, high-Z impurity prevention 78−67400
Tokamak plasma, heated turbulently, elec. cond. 78−42720
Tokamak plasma, h.f. heating and abnormal resist. *(Russian)* 77−1000
Tokamak plasma, neutral atom transport by multigroup methods, time reduction techniques 78−18385
Tokamak plasma, new pinch effect and electron heat loss 79−32798
Tokamak plasma, runaway electrons and current dirve 80−74004
Tokamak plasma, superthermal fusion products, α-particle transport theory 78−66417
Tokamak plasma, vertical stability, finite cond. effects 79−4162
Tokamak plasma transport codes, neutral atoms 79−98875
Tokamak plasmas containing momentum sources, impurity transport 80−48935
Tokamak radial transport, multi-regime model including neutral beam injection 77−65840
Tokamak radial transport, scrape off effect 79−90443
Tokamak reactor, impurity control, divertor and gas blanket model 79−90445
Tokamak reactor, neoclassical regime, stationary temp. profile 77−74987
Tokamak reactor design, influence of physics parameters 79−36414
Tokamak reactor with turbulent transport coeff., energy balance 79−71953
Tokamak reactors, neutral beam injection, energy and power requirements 80−91243
Tokamak refuelling by pellet injection, transport processes effects 80−38699
Tokamak resistive toroidal equilibria, anomalous resistivity and thermal cond. 78−83595
Tokamak scrape-off plasma, metal impurity recycling effect 80−10421
Tokamak simulation, equivalent cct. model and mag. field diffusion eqns. 77−84409
Tokamak TO-1, feedback system effect on plasma parameters *(Russian)* 80−103174
Tokamak transport codes, present status 79−98874
Tokamak transport eqns., nonlinear partial differentials, soln. technique 80−19556
Tokamak transport simulation models 77−79474
Tokamak turbulent heating current penetration, poloidal profiles and anomalous transport 77−55158
Tokamak with poloidal divertor, discharge startup 80−48942
Tokamak-fusion reactors, He exhaust 80−75084
tokamak-like equilibria at beta close to unity 80−19604
Tokamaks, arbitrary cross section, high-β equilibria categorisation 79−64888
Tokamaks, divertor, refuelling methods, pellet-plasma interaction 80−28841
Tokamaks, lower hybrid heating, simulation using BALDUR 1-D transport code 80−92339
Tokamaks, magnetic islands, tearing modes 80−28846
Tokamaks, neutral beam heated, radial transport/Fokker-Planck model 77−15224
Tokamaks, transport computation, heating, treatment of neutral gas, and impurities, review 79−98966
Tokamaks, transport losses, computer modelling and scaling 80−28612
Tokamaks with shear, scaling law for trapped ion anomalous diffusion 80−32492
toroidal axisymmetric equilibria, particle diffusion by mag. perturbations 80−14927
toroidal diffusion, ambipolarity paradox 77−31431
toroidal diffusion, ambipolarity paradox 78−63547
toroidal mag. field, thermal cond. with stochastic inhomogeneity *(Russian)* 80−83973
toroidal plasma, 2-D neutral H transport 78−59661
toroidal plasma, bumpy, radial DC elec. field on particle transport 78−59646
toroidal plasma, convective cells and transport anal. 80−24229
toroidal plasma, enhanced diffusion, electrostatic drift modes, ohmic heating effects obs. 77−19702

plasma transport processes continued
toroidal plasma, magnetised, steady current generation by RF travelling field 77−11313
toroidal plasma, Monte Carlo treatment for neutral particle transport 80−33750
toroidal plasma, resistive MHD mode and sawtooth oscill., nonlinear evolution 80−24235
toroidal plasma, stationary current excitation by wide spectrum waves *(Russian)* 79−98863
toroidal plasmas, beam driven currents, trapped electrons effect 80−70011
toroidal plasmas, beam induced currents 80−92335
toroidal screw pinch, Spica, current decay, stability 77−43040
toroidal stellarators and torsatrons, viability as fusion reactors 79−90381
toroidal system, low-collisionality regime, particle/energy confinement times, β-depend. 78−75409
toroidal transport code for neutrals and impurities in Tokamak 77−72490
toroidal trap, plasma rot. effect on neoclassical transport of impurities *(Russian)* 80−83972
toroidal Z-pinch plasmas, drift kinetic equation 78−91147
torsatron, stochastic elec. field effect on transport of low collision freq. plasma 80−79446
torsatrons, mag. surfaces, particle orbits, neutral injection 80−79551
torsatrons, neutral beam injection calcs. 80−48949
torsatrons, particle orbits and toroidal vacuum fields 80−79450
torsatrons, toroidal vacuum fields, particle orbits 80−79445
torus plasma, fluctuation induced particle transport, strong DC elec. and mag. fields 77−89322
transient setting of ponderomotive nonlinearity, self-focusing and plasma-wave excitation 79−77387
transition from isentropic to isothermal expansion in laser-produced plasmas 80−87918
transition layer between two magnetized plasmas 80−24136
transport collision frequencies, integration of empirical data 79−25969
transport collision frequencies, temp. depend. by approx. method 79−25970
transport of atoms in arc electrode channel *(Russian)* 77−52725
transverse convective ion transport in Tokamak, kinetic description 80−6214
trapped electron instability, turbulence, unstable mode dynamics anal. 80−33761
trapped electron shear-Alfven instability, stabilisation by temp. gradient 80−28599
trapped particle anomalous transport in Tokamak, scaling laws 80−103115
TTT, current penetration and resistivity, probe diagnostics 79−32821
Tuman-2A Tokamak, ohmic heating and compression of plasma 80−28703
turbulence, finite-β_e universal mode, Alcator scaling 79−90408
turbulent convective transport in a plasma 80−28606
turbulent destabilization and saturation of the universal drift mode in a sheared magnetic field 79−37455
turbulent diffusion, shear effect, drift oscills. 77−76082
turbulent diffusion in plasma with high-energy ions, thermonuclear case 77−971
turbulent diffusion of toroidal plasma, geometrical effects 78−94900
turbulent diffusion regimes along the pitch angle in a geomagnetic trap *(Russian)* 79−55534
turbulent heating, electric field penetration for nonlinear current saturating elec. cond. 77−24109
turbulent heating and transport in Tokamak plasma, theory 77−72421
turbulent plasma, anomalous DC resistivity *(Japanese)* 77−42966
turbulent plasma, convective transport *(Russian)* 78−75336
turbulent plasma, self-consistent framework for the calc. of transport coefficients 79−1290
turbulent plasma blanket, anomalous heat transport 80−83224
turbulent plasma in toroidal plasma, optical diagnostics and thermal transport 79−73023
turbulent shock wave propagation in solar atmosphere across mag. field, struct. 79−40166
two phase flow, particle velocity optical meas. *(Russian)* 80−54032
two-dimensional, in Tokamak, theory 79−64896
two-dimensional convection, strong turbulence theory 77−76083
two-temperature He plasma, transport props. 80−92260
vacuum arc in Cu cathode region, current parameters, theory 80−54068
variable property heat transfer to single sphere in high temp. surroundings 80−14884
velocity angle scattering of a relativistic electron beam during transport through plasma 80−92337
velocity diffusion eqns., high-energy tail formation 78−71455
velocity distrib. function of light ions in heavy gas in elec. field 78−83526
velocity modulated neutralised ion beam, evolution in potential wells, ion density distrib. *(Russian)* 80−100082
velocity space ring plasma instability, magnetised ion interaction, Vlasov theory 79−77368
velocity-space diffusion in perpendicularly propag. electrostatic wave 80−59228
viscosity, fourth approx. for multicomponent plasma 77−15168
viscosity, rel. to hydromagnetic surface waves dissipation 80−21904
viscosity of partly ionised gas simplified calc. expressions 79−18983
Vlasov eqn. for vel. depend. interactions and pair-wise central pot. 78−34270
Vlasov equation, coherent state approach, quantum effects calcs. 78−1803
Vlasov equilibria, local Maxwellian velocity distribution 80−87928
Vlasov plasmas, geometrical optics approach, Tokamak appl. 80−14902
Vlasov-Maxwell equilibria, exact solns. with sheared mag. fields 77−3977
volume forces in weakly ionized plasmas 79−73055
W VII-A stellarator, particle and energy transport 80−83222
wall released impurity transport in limiter scrape off layer of Tokamak 79−670
wall stabilised arc, current step changes, conductance transient effects 78−87547
wall-confined liner-compressed plasma, transport calcs. 78−63546
wall-plasma interface region, cross field thermal losses, simulation 78−59609
wall-stabilised arc conductivities with Cu vapour contamination 78−75458
plasma transport processes continued
water vapour, electron energy distrib. function, electron sink and plasma resist. effect *(Russian)* 80−106987
wave growth, stability anal., particle distrib. functions and transport theory 80−43903
wave-particle transport from electrostatic instabilities 80−83898
weakly ionised gas, electron energy distrib. 79−82028
weakly ionised gas transport theory 78−75274
weakly ionised plasma electron electrodynamics characts., pulsed ionisation source *(Russian)* 79−7444
weakly nonideal dense plasma, elec. conductance obs. 78−71447
weakly nonideal inert gas impulse plasma, Coulomb cross-section calcs. 80−103113
weakly turbulent collisionless plasma, anomalous transport coeffs. 78−71453
weakly-ionised plasma diffusion in apparatus with spatial axis *(Russian)* 80−1826
Wigner distribution function, transport equations, inhomogeneous dispersive medium 80−53214
X-ray line radiation from cylindrical Al plasma, calc. model 80−64777
Z-discharge plasma, low-temp., time evolution, diagnostics 79−37548
Z-pinch, high-density, form. regimes 78−59652
Z-pinch, mag. field fast recomb. through plane pinch current sheet 80−38695
Z-pinch, overdense, He plasma, laser-driven hydrodynamic perturbation, shock density struct. 79−77385
Z-pinch gas discharge, Hall effect influence on plasma dynamics 77−51218
Z-pinch turbulence spectroscopic detection and anal. *(Russian)* 80−100098
ZT-1 reversed field pinch, derated mode MHD stability and diffusion 77−27701
ZT-40, modelling in G2M diffusion code 80−79557
ZT-S reversed field pinch simulations 80−83993
α particles slowing down diffusion in fusion reactor gas *(Chinese)* 80−87862
Al, plasma, transfer eqn. soln. using freq. and angle averaged photon escape probabilities 80−64688
Ar afterglow, line radiation of plasma in early afterglow 80−38745
Ar arc, non-LTE, electron balance, temp. and density *(French)* 78−1796
Ar arcs in supersonic flow, numerical analysis 80−38776
Ar, decaying arc, electron cooling, diffusion, ionisation and recombination processes 80−33841
Ar decaying arc, numerical simulation 80−38767
Ar discharge, electron swarm characts. 79−77441
Ar discharge, ion density profile, reson. laser light meas. 80−92401
Ar, effects of Joule heating on plasma heat transfer 77−72412
Ar, formation in crossed electric and magnetic fields, optical spectra 80−79452
Ar full circle arc, mass flow field investig. 80−38797
Ar high-pressure plasma elec. conductivity obs. 78−71448
Ar hollow cathode arc, in mag. field up to 2 k0e, plasma parameters 80−6306
Ar induction HF discharge plasma in crossed fields, with Cs seeding, Hall parameter 79−55465
Ar jet, heat transfer and hydrodynamic struct. 79−14521
Ar laminar plasma jet, H_2 diffusion obs. 78−71557
Ar, low-press. glow discharge, elec. characts. of positive column 80−100112
Ar plasma, constricted electric arc, iteration method anal. 79−90484
Ar, plasma, one-phase and two-phase jets, non-equilibrium in initial region *(Russian)* 77−31518
Ar plasma, shock-compressed, thermophysical and gasdynamic characts. 77−43016
Ar plasma, thermal equilibrium properties, estimation 78−1793
Ar plasma, viscosity determ. by stabilised elec. arc. 79−41873
Ar pulsed plasma, elec. cond. obs. at 10 atm and 15000K 78−71449
Ar, stream electrons, at atm. press., temp. and conc. from study of electrical parameters *(Russian)* 80−53930
Ar two-temp. plasma, kinetic theory calcs. of transport props. 78−14134
Ar-Cs plasma, HF induction discharge, Hall effect *(Russian)* 77−43101
Ar-He plasma, thermal diffusion factors, binary mixture hypothesis 79−27749
Ar-He plasma, thermal diffusion of neutral species in plasma jet, 2000-4000K 79−32742
Ar-He plasma, thermal diffusion factor, 2000-4000K, binary mixture hypothesis 79−32743
Ar-N_2 plasma, diffusion separation N_2 dissociation 77−76036
Ar-N_2(CO), non-self-sustained discharge instability, negative differentiated cond. *(Russian)* 80−38740
Ar+H_2, plasma, transport coeff. calcs., 2000-25000K 77−11314
BH plasma, hot, proton and deuteron transport calc., moment method 78−22458
CO discharge, electron energy distrib. and kinetic coeffs., ground-state mols. 80−43867
CO discharge, electron energy distrib. and kinetic coeffs., vibr. excited mols. 80−43868
CO_2 laser, continuous, fast flowing, thermal discharge contraction *(Russian)* 79−99009
CO_2-N_2-He gas mixtures, time-of-flight meas. of electron transport parameters 78−94387
Co_2:He:N, glow discharge instability in afterglow 80−6313
Cs, dense plasma, elec. and radiative heat cond. evaluation 78−71452
Cs, dense plasma, ionisation equilib. and cond., ion clusters effects 80−75032
Cs, dense plasma near saturation line elec. cond. 80−38559
Cs, electron-atom momentum transfer cross sections, from plasma electron thermal conductivity 78−42224
Cs, photoplasma, optical excitation in radiation diffusion conditions 78−55227
Cs plasma, elec. and radiative thermal conds., expt. data anal. method 78−42717
Cs plasma, elec. cond. and eqn. of state, behind reflected shock wave 78−42716
Cs plasma, elec. cond. meas. 79−64831
Cs plasma, generation by adiabatic compression, elec. cond. and thermodynamic parameters meas. 80−59180
Cs, plasma, highly ionised, conductivity and eqn. of state 78−26323
Cs plasma, in thermionic convertor, spectroscopic meas. of Cs I *(Japanese)* 77−58902

plasma transport processes continued
Cs plasma, ohmic heating, electrical conduction temp. depend. 78−71442
Cs plasma elec. conductivity meas. 78−71450
Cs vapour, electrical cond. near saturation point 80−69967
Cs(Ar-Cs) plasmas, electron momentum transfer cross section, cyclotron reson., temp., cond., and vel. meas. 80−106930
Cu exploding foils, rapid mag. energy transfer, conductivity law *(French)* 78−91135
Cu-N mixture, partially ionised, transport and thermodynamic props. 77−80276
D diffusion in the Tokamak plasma, pulsed injection obs. 80−28611
D-T magnetoplasma, fusion effects on diffusion and thermal cond. 77−67883
D-T plasma, Monte Carlo anal. of particle spectra 79−72992
D-T reactor, neoclassical transport props., model 77−68756
D-T steady state Tokamak reactor, neoclassical diffusion 77−3159
D-T Tokamak, high-density, ohmically-heated, transport calcs. 80−24142
H atoms in cylindrical hydrogenic plasma, transport code 78−51284
H glow discharge, electron macroscopic props. *(Russian)* 80−92403
H, HF discharge, gas breakdown, electron diffusion eqn. exact soln. 80−19658
H neutral atoms in H plasma slab, kinetic theory 79−19002
H, partly ionised plasma, ionised collisions effect on thermal cond. *(Russian)* 78−47093
H plasma, K impurities, optical props. 80−103119
H plasma, magnetic piston study in theta-pinch *(Russian)* 80−83971
H plasma beam, electron macroscopic props. *(Russian)* 80−92403
H plasma target investig. *(Russian)* 80−106981
H solid pellet evaporation in plasma *(Japanese)* 79−94772
H^-, surface plasma source, prod. by H atom backscatt. from cesiated W 77−3953
H_2 beam discharge, electron kinetics in collisionless non-equilibrium plasma 80−92402
H_2 electron swarms transport parameters meas., nonuniformities effect 78−83613
H_2, electron transport coeffs. at high E/N values 79−94835
H_2 glow discharge with variable degrees of dissoc., diffusion theory of positive column 80−44018
H_2, partially ionised, thermal cond. 79−86562
H_2 plasma, neutral H ats. penetration, kinetic theory 79−32782
H_2 transport in toroidal plasma using multigroup discrete ordinates methodology 80−69978
H_2-$H_2O(Cl_2)$, diffusion in stratified positive column, impurity effects 77−11320
H_2-He gas mixtures, 1000-25000K, transport property correlations 80−75029
^2H-^3H ionised plasma, fast α particle energy deposition, transport eqn. 80−100071
Hα and Hβ, Stark profiles, ion-motion effect 80−63592
He collisional plasma, classical diffusion in large amplitude density fluctuations presence 78−18381
He, collisional plasma, vortex diffusion, shear effect 79−32773
He constricted glow discharge, space charge double layer influence obs. 78−67492
He, electron distribution function relaxation in high freq. gas breakdown *(Russian)* 80−14957
He I 447.1 and 492.2 nm lines, ion motion effects on Stark profiles 80−69105
He I line profiles, ion motion effect in low electron density plasma 80−43877
He, low press. discharge, electron free streaming waves expansion 80−79595
He plasma, ion state and electron temperature in high-current pulsed discharge *(Russian)* 79−27844
He, plasma, non-equilib., of strong current pulse discharge, diagnostics *(Russian)* 78−75271
He pulsed arc, Thomson scatt. diagnostics 80−24297
He-Cs, turbulent plasma, characts., electron energy balance *(Russian)* 79−27779
He-Na mixture, low-pressure discharge, radial cataphoresis obs. 78−67507
He-O_2 DC discharge, electron distrib. function 80−92407
He-Xe plasma, in mag. field, effect of CO_2 mol. addition on plasma parameters 77−42965
Hg arc plasma, azimuthal RF cond. meas. by eddy current effect, expt. 77−1029
Hg dense weakly ionised plasma, molecular dynamics 78−71456
Hg low-pressure arc, positive column, heat flow processes 80−24135
Hg, plasma, dense weakly ionised, thermo EMF, calc. 80−64686
Hg plasma, molecular dynamics model for atom-electron interactions 78−42708
Hg vapour high-pressure lamps with Sn halide additives, chemical transport obs. 78−71576
K plasma, DC conductivity, electron collision cross sections 77−3469
KOH, MHD plasma mol., pot. energy curves and dipole moment, bond lengths 78−71462
Kr, low-press. glow discharge, elec. characts. of positive column 80−100112
Kr, plasma, high-press. arc discharge, elec. cond. 80−59181
Li plasma, elec. cond. at 12.5-50 MPa, (7-50)×10^3K 80−64685
Mo impurity anomalous diffusion simulation, TFR Tokamak current plateau, O_2 injection effect 78−22565
N afterglow plasma, diffusion and recombination, microwave cavity expts. 79−90479
N glow discharge, volt-ampere charact. in gas flow *(Russian)* 80−106991
N, glow discharge instability in afterglow 80−6313
N, high intensity arcs, anode contraction region modeling 80−103210
N_2, beam and glow discharge type, macroscopic props., kinetic eqns. 80−43864
N_2, diffusion approx. of Boltzmann eq. for slow electrons 79−82044
N_2 discharge, anomalous heating *(Russian)* 80−1866
N_2, electron transport coeffs. at high E/N values 79−94836
N_2 glow discharge, variable current penetration mechanism 79−55584
N_2, inductively coupled plasma discharge, temp. and vel. profiles 77−4004
N_2 plasma, electron distrib. function, kinetic coeffs. *(Russian)* 78−38451
N_2 positive column, gas temp., interferometric diagnostics, heat cond. calc. 79−32834
plasma transport processes continued
N_2 positive corona into spark, prebreakdown phase, spectroscopic anal. 80−38790
N_2, stationary beam discharge plasma, electron kinetics 80−38775
N_2, vibr. excited, electron distrib. function, temp., drift vel., kinetic coeffs. *(Russian)* 79−7445
N_2, weakly ionised, electron transport coeffs., Boltzmann eqn. anal. *(Japanese)* 80−59183
N_2-Cu arc plasma, transport coeffs. 80−96344
N_2-H_2, high-temp. plasma, transport coeff. calcs. 77−62340
N_2-H_2 plasma, transport coeffs. and collision processes *(German)* 79−23395
N_2-Ne glow discharge, kinetic eqn., transport coeff., collision freq., mean energy *(German)* 78−34261
N_2-O_2 gas mixture, weakly ionised, electron transport coeffs. anal. *(Japanese)* 80−59184
N_2-O_2 nonselfsustaining discharge plasma, current establishment/relax. processes, rel. to CO_2 laser *(Russian)* 79−99011
Na, nonequilib. excited-level population in inhomogeneous plasma 77−3917
Ne afterglow, diffusion, collisions, decay freqs., fluoresc. obs., calcs. 78−59715
Ne discharge, Boltzmann eqn., numerical study 77−35424
Ne discharge, numerical study 79−32838
Ne, impurity flow reversal effect in Tokamak plasma 79−7446
Ne, low press. discharge, electron free streaming waves expansion 80−79595
Ne, low press. discharge, kinetics and column impedance *(German)* 77−58845
Ne plasma, electron collision ionisation, electron kinetic behaviour during elec. field perturbation *(German)* 80−64676
Ne, positive column contraction under diffusion-recombination conditions 80−24293
Ne, streamer plasma characts., cond., plasma density and field strength calcs. *(Russian)* 77−47262
Ne^+, radiating ions, velocity distrib. symm. in hollow cathode discharge, charge and momentum transfer 79−73054
Ne-Ar discharge, transient cataphoresis, time depend. 80−38753
Ne-H-H_2 mixture, positive column characts. and comparison with approx. diffusion theory 80−44025
O^{6+}, line emissions from He-like ions, electron params., ion diffusion in Tokamak plasmas 79−4114
O_2 discharge, electron gas, transport coeff. and energy distrib. function calcs. 77−68742
O_2, electron energy distrib. function, electron sink and plasma resist. effect *(Russian)* 80−106987
O_2, weakly ionised, electron transport coeffs., Boltzmann eqn. anal. *(Japanese)* 80−59183
SF_6 axially blown arc, current-zero behaviour, theoretical model 80−38789
SF_6 gas blast breaker, current zero meas. 80−38795
SF_6, high-temp. circuit-breaking arc, axial and radial heat transport 79−19105
SF_6-inert gas mixture, high power cylindrical spark discharge, dynamic and visible charact. 80−64816
SF_6+H_2 mixture, equilib. composition and transport props., 300 to 15000K 77−24051
U plasma, fission fragment effect on electron energy distrib., radiative transport 77−24062
UF_6, thermodynamic functions and elec. cond. at 1000 to 11000K and 0.1 to 100 atm. 77−42964
Xe discharge, HF, with propag. EM wave, isotope distrib. *(Russian)* 77−76235
Xe, electrical conductivity beyond critical point, intermediate density between gas plasma and solid *(Russian)* 80−20265
Xe isotope separation in HF discharge, thermodiffusion *(Russian)* 77−46649
Xe, plasma, high-press. arc discharge, elec. cond. 80−59181
Xe plasma, shock-compressed, thermophysical and gasdynamic characts. 77−43016
Xe-He(Ne), gas mixture, element and isotope separation in impulse plasma centrifuge *(Russian)* 80−38725
Z-pinch, noncylindrical, dynamics and particle accel. mechanism 77−76170
Zn afterglow diffusion coeff. for metastable Zn atoms 77−23542

plasma turbulence
AC arc, temp. diagnostics, radial distribs. 77−24240
acoustic waves dispersion in turbulent medium 80−10384
adiabatic modifications to theory 79−90407
adiabatic modifications to turbulence theories 78−34315
air blast arc, post-zero current and power loss meas. 79−19106
air discharge, turbulent flow stabilisation effect *(Russian)* 79−99010
Alfven turbulence in extended extragalactic radio sources, rel. to electron accel. 80−27000
Alfven wave turbulence, interaction with whistler wave turbulence 80−64728
Alfven wave turbulence in interplanetary plasma, spatial fluctuation spectra 79−53693
Alfven wave turbulence in solar flares, rel. to protons stochastic accel. 80−21953
alpha-particles energy spectrum resulting from turbulent diffusion 77−11318
amplification of ion cyclotron waves via high frequency electron plasma wave turbulence 80−92305
anisotropic MHD turbulence in solar wind, obs. 80−94669
anomalous absorption of UHF radiation in electron cyclotron resonance range *(Russian)* 80−1807
anomalous electron transport equations for ion sound and related turbulent spectra 78−67319
anomalous EM wave electron radiation 80−43889
anomalous resistivity of turbulent plasma in strong electric field 79−72989
anomalous thermal transport in turbulent skin layer, ion-acoustic waves mechanism 78−5853
anomalous transport from plasma waves 80−59182
anomalous turbulent resistivity at high drift vels., rel. to confinement and fluctuations in toroid 80−24139
anomalous turbulent resistivity at high drift vels., toroidal plasma 80−24138

plasma turbulence continued
anomalous viscosity due to EM instability in turbulent plasma 80−106901
anomalous viscosity due to EM instability in turbulent plasma, nonlinear theory 80−106902
anomalously resistive phase, spiky density fluctuations and relax oscill., microwave scatt. obs. 80−38547
arc column in free turbulent jet, electric field strength 80−49021
arc in channel with distributed gas flow, positive column anal. *(Russian)* 80−14949
arcs, wall-stabilised, free recovery with imposed laminar and turbulent flows 80−59321
astrophysical sources, radiation distrib. functions calc. 77−70990
astrophysical synchrotron reactor as RF source *(Russian)* 78−4098
atomic energy level broadening in turbulent plasma, retardation effects in motion of quantum systems 77−60975
average trajectories, kinetic description 77−72447
ball lightning, turbulent plasma sphere, model eqns. for current and heat flux 80−32516
ballooning trapped electron mode, linear and nonlinear theory 80−28656
beam propagation, turbulent nonlinear stabilisation, simulation 78−18422
beam-plasma system, nonlinear convective and oscill. instabilities, simulation models 78−34338
beam-plasma turbulence, wave power spectral distrib. 78−14163
beta pinch shock heating of toroidal collisionless plasma 77−76138
bump-in-tail instability-generated turbulence, phase space -ranulation due to mode-mode coupling 80−38651
Buneman instability, nonlinear saturation 77−24068
chaotic motion theories with appl. to controlled fusion research, review 78−93605
charged particle, impinged, linear response theory 80−64727
charged particle energy loss in turbulent plasma 77−84400
charged-particle systems, strongly correlated, theory 77−68797
Chirikov-Taylor model, turbulent diffusion calc. 80−79469
circuit-breaking arc quenching, effects 79−27861
circuit-breaking arc radiative transfer, magnetic stability, and turbulent heat exchange 78−75482
circumsolar plasma, Venera 10 radio signal spectral meas. 80−109326
clumps as enhanced correlations and turbulent Debye screening 78−91110
coherent wave interaction with MHD turbulence *(Russian)* 78−1833
cold plasma, strongly turbulent, second harmonic generation 77−55133
collective modes, sum-rule anal. 80−59238
collective phenomena and anomalous resistance, electron current drift velocity *(Russian)* 80−24140
collisional drift modes, anomalous skin effect, enhanced particle penetration during fuelling, nonlinear theory 80−64703
collisional plasma, modulation instability, turbulence by const. wave pumping *(Russian)* 80−103139
collisional plasma, turbulence generating mechanism 77−11340
collisionless plasma, polarisation by single-mode pot. drift wave 80−106920
collisionless plasma modulation instability, nonthermal radiation spectrum obs. 78−75320
collisionless turbulent plasma, random phase wave, soluble nonMarkovian system model 78−87450
Compton scattering of transverse waves by relativistic electrons, effect on plasma turbulent reactors 80−51644
convective cell excitation by Bernstein waves *(Russian)* 80−53961
convective cells and anomalous plasma diffusion *(Russian)* 78−71439
convective transport *(Russian)* 78−75336
correlation function based on trapping *(French)* 77−89262
correlation measurements of turbulent ionization and ion-acoustic waves 80−59329
current carrying plasma, trapping and build-up of HF turbulent noise *(Russian)* 77−3957
current discharge, high energy ion form., electrostatic analyser 77−19785
current driven dissipative drift wave turbulence in Tokamak plasma, finite-β and quasilinear effects 79−98913
dense plasma turbulent heating expts. 78−75386
density fluctuations, microwave scatt. obs. 80−48851
development and decay mechanisms, wave interactions, analogue simulation *(Russian)* 79−7462
diagnostic techniques for fluctuations 80−49002
diagnostics, turbulent heating example 80−49015
dielectric and conduction problems, linear response theory 78−71432
diffuse electrical gas discharge, in turbulent flows 79−94834
diffusion, geometrical effects in toroidal plasma 79−27751
diffusion, shear effect, drift oscills. 77−76082
diffusion coeff. for turbulent plasma 78−5854
diffusion coefficients of low frequency electromagnetic turbulent plasma 80−28677
diffusion in multicomponent plasma *(Russian)* 78−22455
digital spectral techniques in plasma fluctuation diagnostics 80−49003
direct interaction approximation and plasma turbulence theory 79−19036
discharges, high current, press., conductivity meas. 80−38793
discrete unstable modes, transition to turbulence, theory and expt. 80−59240
dispersion equation for inhomogeneous plasma 78−75337
dispersion relations, Dupree's resonance function 79−60124
disruptions in Tokamaks and small scale turbulence 80−59266
dissipative non-Hamiltonian dynamical system, stochastic props. and strange attractors 80−57200
dissipative trapped electron instability, turbulence theory 78−71482
dissipative trapped ion instability and anomalous transport 78−22483
drift cyclotron loss cone mode, warm plasma effects 79−68904
drift instability-caused turbulence, anomalous diffusion, convective cell form. 77−43058
drift turbulence theory in mag. field with shear, nonlinear wave packet formation *(Russian)* 79−77376
drift wave collisionless turbulence, renormalised dielectric function 78−51292
drift wave fluctuations, induced electron transport 78−94894
drift wave fluctuations, spectral distrib. 77−7534
drift wave theory, plasma turbulence, Kolmogorov spectrum analogy 79−73011
drift wave turbulence, diffusion broken ambipolarity 79−64828
drift wave turbulence, dissipative, current driven, in Tokamak plasma 80−38587
drift wave turbulence, exact Gaussian soln. 80−92325
drift wave turbulence, nonlinear behaviour and turbulence spectra 80−19573
drift wave turbulence and convective cell formation 80−43925
drift waves, multispecies plasma, nonlinear behaviour, turbulence, diffusion 78−59588
drift waves, nonlinear stabilisation, weak turbulence theory 79−98908
drift waves in turbulent plasma 78−1830
drift waves in turbulent plasma with magnetic shear 78−75330
drift-cone mode stabilisation in PR-6 mirror by RF power injection 79−90399
drift-wave turbulence, possible inverse cascade behaviour 79−32774
drift-wave turbulence, role of clumps 78−67352
drift-wave turbulence, spectrum cascade by mode coupling 79−14548
drift-wave turbulence effect on mag. struct. and electron transport in Tokamak 78−22501
Duffing's equation governed system, for random and chaotic phenomena 79−10664
Dupree-Weinstock theory, applied mag. field *(French)* 77−47198
Dupree-Weinstock theory, orbit function convergence 78−67353
E×B turbulence in magnetosphere, rel. to generation of electrostatic fields 78−28439
E-region, over India, turbulence obs. in electron density fluctuations 77−9609
electric field compression near a plasma electrode 80−64736
electric field determ. in plasmas with turbulence using emissive floating probe 79−86614
electron acceleration by strong plasma turbulence 79−4140
electron acceleration to mildly relativistic energies by strong turbulence 77−31437
electron and ion energy distribs., laboratory and space plasma comparison 78−5945
electron beam delay, strong turbulence, ballistic modes and Langmuir solitons *(Russian)* 77−76111
electron beam interaction with strong turbulent plasma 79−14563
electron beam-plasma interactions in turbulence regime, phenomenological model 80−6260
electron beams, counterstreaming, self-consistent computation of explosive instability 78−22494
electron bunch, relativistic, instability in reson. storage chamber 77−54381
electron cyclotron radiation from turbulently heated plasma 78−34369
electron density fluctuations, in tail of Comet Kohoutek (1973 XII) 77−13285
electron distribution anisotropy, turbulently heated plasma, X-ray diagnostics 78−59682
electron distribution function, correlation anal. 79−14547
electron ensemble, weak turbulence, diffusion and collisions in elec. and mag. fields *(German)* 78−83564
electron fluid, one-dimens., statistical formulation 78−49751
electron heating, anomalous transport 78−14216
electron long-wavelength wave dispersion evolution meas. in turbulent column 80−6283
electron plasma, strongly turbulent, EM scattering 77−55150
electron velocity distrib. determ. during strong turbulence 79−60196
electron waves, broad-band, nonlinear Landau damping 77−89246
electron-beam-ion two-stream instability initiated turbulent state, 3-dimens. vel. diffusion 78−59595
electron-free plasma confinement in RF quadrupole field 78−71517
electron-ion turbulence in collision dominated regime, ionospheric turbulence meas. appl. 79−48605
electrons acceleration by weak MHD turbulence, energy spectrum, radiosources appl. 79−88582
electrostatic, in parametric instability, general quasi-linear theory 79−60130
electrostatic, nonlinear dispersion relation and fluctuation spectrum 77−65872
electrostatic, random function two-time correlation functions 79−46428
electrostatic ion cyclotron turbulence in ionosphere/magnetosphere, rel. to coherent anomalous resistivity 80−4189
electrostatic ion cyclotron turbulence in magnetosphere, rel. to mag. field-aligned pot. drops 78−45155
electrostatic plasma turbulence, entropy definition 77−76081
electrostatic shock wave, energy dissipation and turbulence processes *(Russian)* 79−7465
electrostatic turbulence, variable density and pressure, two-fluid model and geostrophic approx. 80−53986
electrostatic Vlasov plasma 77−58862
electrostatic Vlasov turbulence, iterative soln. 80−10375
electrostatic wave turbulence along auroral field lines, obs. 77−45228
electrostatic wave turbulence in magnetosheath, meas. 79−66881
electrostatic waves, turbulent acceleration in Earth's auroral plasma *(Russian)* 80−53952
EM, LF, effects on spatially inhomogeneous plasma 79−86583
EM drift wave turbulence and convective cell form. 80−24168
EM field modification meas. in turbulent plasma 77−42987
EM pulses, Thomson scatt. by random fluctuations, self-focusing effects 78−83573
EM turbulent acceleration rel. to fast particle emission 77−19707
EM wave depolarisation in plasma with MHD turbulence *(Russian)* 80−103154
EM wave dissipation and superstrong turbulence in inhomogeneous plasma *(Russian)* 80−83919
EM wave parametric absorption in plasma turbulence, instability effects *(Russian)* 77−7551
EM wave parametric decay into two plasmons, nonlinear saturation mechanism efficiency *(Russian)* 77−11349
EM wave propag. 79−14553
EM waves nonlinear transfer, emission lines broadening and displacement *(Russian)* 77−91418
energetic particles, interaction with shock wave front in turbulent medium 80−4210
energy of a turbulent, current-carrying plasma in a strong electric field 80−79514
evolution equation, asymptotic soln. to Cauchy problem *(Russian)* 77−35349
excitation by relativistic electron beam 79−32786
fine struct. of plasma satellites of He 492.2 nm line 80−59235

plasma turbulence continued
finite bandwidth radiation, nonlinear dissipation near electron cyclotron harmonic resonances 80−28670
finite element approx., wave-particle interaction in weakly turbulent plasmas 77−39422
finite-β_e universal-mode turbulence and Alcator scaling 79−90408
finite-beta effects on drift wave turbulence and particle confinement 80−38652
fluctuations, LF, diagnostics by probes and optical line radiation 79−64905
fluctuations, wave-number spectrum moments, correlation method for estimation 78−16732
fluid-like turbulence, rel. to Fermi acceleration and particle pitch angle scatt. 78−53775
FM-1 spherator, microwave scatt., drift wave turbulence 77−65912
focus, current sheath struct. diagnostics, fast particle beams, deuterated polyethylene fusion 77−76206
formation of plasma in fusion devices, at. and plasma processes, diagnostic techniques 80−48915
fusion reactor, stationary turbulence as confinement layer 77−68844
fusion reactors, turbulent plasma blanket 79−59259
gas blast circuit breakers, three nozzle arc models, review 79−27862
gas discharge, perturbation by longitudinal turbulence 80−24271
gas-dynamic pulsation effects on turbulent gas flow discharges *(Russian)* 79−7500
glow discharge, 20 to 200 m/s air current *(Russian)* 77−65921
glow discharge, ionisation instability, stabilising effect of turbulent transport processes *(Russian)* 78−59698
guiding center plasma with gravitational or gradient drifts 80−38632
harmonic generation, in moving plasma *(Russian)* 78−87449
heat exchange of low-temp. plasma with wall, longitudinal mag. field effect 80−33781
heat flux limitation in an ion-acoustic instability-induced turbulent plasma 79−7472
heating, collision integral under strong ion-acoustic turbulence conditions *(Russian)* 77−47231
heating, current driven ion-acoustic wave 78−5937
heating, electric field penetration for nonlinear current saturating elec. cond. 77−24109
heating, emitted microwave radn. 77−43080
heating, in plasma betatron 77−76126
heating, Ohmic and neutral beam injection, energy exchange anal. 78−5895
heating, thermalisation freq. 77−39440
heating, turbulent, flat top electron distrib. effect, with ion-acoustic instability 80−10399
heating by current-driven turbulence 78−9803
heating cyclotron radiation obs. 77−84502
heating mechanism in T-5M toroid, ion and electron temp. diagnostics *(Russian)* 77−47259
heating of large toroidal plasma, scaling problems 77−19729
heating of plasma with transverse current, mechanism *(Russian)* 77−80324
heavy ion beam-induced ion-acoustic turbulence *(Russian)* 80−106923
helicon solitons, interaction and formation 77−7537
helicons *(Russian)* 79−55488
HF anisotropic noise, H Stark profiles 78−1896
HF EM field, turbulent model of plasma column *(Russian)* 80−83915
high current arc, turbulence 78−47197
high density plasma, turbulent heating, rapid current penetration 78−51320
high freq. rad. field in turbulent plasma 80−38648
high frequency turbulent instability in magnetosphere, magnetoacoustic waves generation 77−13187
hydromagnetic turbulence in high β plasmas, collisionless damping by hydromagnetic waves 80−17482
implosion heating, numerical modelling of Los Alamos expt. 77−43056
incoherent weak turbulence in solar wind, rel. to second harmonic radiation in type III bursts 78−7958
incompressible nondissipative MHD turbulence in spheromak, stable equilib. statistical states 79−60134
inhomogeneous RF plasma, absorption and parametric decay of extraordinary waves 80−59206
inhomogeneous strongly magnetised plasma, quasilinear diffusion, particle transport and electrostatic oscillations 78−42723
instability induced by plasma-electric current interaction in focus expt., laser diagnostics 80−24171
instability meas. by mm wave scatt. in turbulent plasma *(French)* 78−34373
instability suppression by external turbulence introduction 79−32768
interaction fronts in laser procuced counterstreaming plasma 79−41807
interchange mode turbulence, spectral cascade processes 80−33775
interplanetary plasma turbulence, radio imagery 79−92645
interstellar, maser effect in H I 21 cm line *(Russian)* 79−88727
ion acceleration from turbulent plasma by electron beam 77−10137
ion acoustic, electron heating 79−90424
ion acoustic, resistivity phenomena in multi-ion plasma 80−48856
ion acoustic turbulence in a large-volume plasma 78−67354
ion acoustic turbulence in laser-heated plasma with large temp. gradient 80−53987
ion beam, neutralised, ion-acoustic instability in transverse mag. field 79−13891
ion beam energy relax. in turbulent plasma 78−79443
ion beam scattering by ion-acoustic turbulence 80−6262
ion beam thermalisation in turbulent plasma 78−76114
ion beam-plasma wave modes, ion beam deceleration by ion acoustic turbulence 78−42771
ion cyclotron beam whistler turbulence in collisionless shock waves, eigenoscills. 77−7540
ion cyclotron wave turbulence, nonlinear effects, lab. expt., magnetosphere appl. 80−24170
ion heating and ion acoustic turbulence 77−11370
ion heating by current driven turbulence in inhomogeneous plasma 80−33791
ion heating by current-driven turbulence in inhomogeneous plasma 80−96370
ion heating due to collisionless drift-wave turbulence 80−106949
ion heating enhancement via spatial mag. field variations, catalytic scheme 77−24107
ion sound soliton-Langmuir wave interactions *(Russian)* 80−100077
ion turbulence in laser heated plasma 78−42807
plasma turbulence continued
ion velocity space diffusion in controlled ion wave turbulence, ion wave echo probe obs. 77−43079
ion wave instability, current-driven, nonlinear development 77−62353
ion wave turbulence, anomalous DC resistivity *(Japanese)* 77−42966
ion-acoustic, effect of turbulence on anisotropic resistivity and particle transport across mag. field 80−59236
ion-acoustic current driven wave in turbulently heated plasma, microwave meas. 77−72441
ion-acoustic heating, renormalised turbulence theory 77−988
ion-acoustic instability, ion tail formation and saturation 80−38610
ion-acoustic plasma turbulence, two-dimensional electron density spectra 78−75479
ion-acoustic plasma turbulence with pump wave *(Russian)* 77−76080
ion-acoustic turbulence, collisional excitation of modulational instability 77−24086
ion-acoustic turbulence, current driven 78−59594
ion-acoustic turbulence, current-driven in weakly ionised plasma, quasilinear theory 79−41830
ion-acoustic turbulence, in rarefied plasma flow, Langmuir probe meas. *(Russian)* 79−55547
ion-acoustic turbulence, quasilinear evolution excited by return current 80−79502
ion-acoustic turbulence, rel. to mag. field energy dissipation in neutral current sheets 78−26250
ion-acoustic turbulence, scaling laws and asymptotic states 79−60141
ion-acoustic turbulence, test wave propag. 78−91090
ion-acoustic turbulence and heat-flux limitation, in laser-heated plasma 78−18453
ion-acoustic turbulence generated anomalous resistivity, collision freq.-turbulence spectrum relation 78−14205
ion-acoustic turbulence in magnetoplasma 79−10663
ion-acoustic turbulence in solar corona, four-plasmon interactions rel. to radar signal refl. 80−101582
ion-acoustic turbulence spectra 78−14145
ion-acoustic turbulence-plasma interactions and electron spectrum in electric fields 80−38617
ion-acoustic wave, dispersion relation calc. 78−26284
ion-acoustic wave, dispersion relation calc. 78−63554
ion-acoustic wave, modulational instability in turbulent phonon field 78−18395
ion-acoustic wave turbulence absorption; NRL fusion programme 78−59042
ion-acoustic wave turbulence spectrum in large volume plasma 78−5871
ion-acoustically turbulent plasma, cond., solar corona appl. 79−19027
ion-cyclotron turbulence modulation by LF perturbations 78−91108
ion-sound turbulence, current-driven, from electron beam interaction, wave dynamics 78−38489
ion-sound turbulence driven by return current from electron beam interaction 78−34314
ion-sound turbulent heating 78−67378
ionosphere, diagnostics, by EM wave propag. obs. 78−45032
ionosphere, velocity shear driven turbulence 77−9608
isotropic turbulence spectra with plasmon condensate 77−47199
jet, electrostatic probe meas. at atm. press., mean values determ. *(Russian)* 77−51240
kinematic model of strong turbulence in plasma with relaxed closure *(French)* 79−10701
kinetic Alfven waves, coherent, anomalous damping 77−31469
kinetic equation, stationary distribs., symmetry group 77−35348
kinetic theory of binary correlations 78−26285
Kolmogorov turbulent spectrum, direct interaction model 78−18275
Langmuir, adiabatic interaction with ion-acoustic waves *(Russian)* 80−1765
Langmuir, effect on Brillouin backscatt. and filamentation instability 77−35347
Langmuir, strong, simulations review 80−59237
Langmuir and EM waves, turbulence induced by relativistic electron beam in mag. field *(Russian)* 77−62378
Langmuir and ion acoustic wave coupling, turbulence spectra, light absorption 80−87902
Langmuir envelope solitons in turbulent plasma 78−67334
Langmuir oscillation collapse in supersonic regime, forbidden energy *(Russian)* 80−14895
Langmuir oscills., modulational instability, in EM wave field 80−38618
Langmuir plasma, self-magnetised collapse dynamics 80−92327
Langmuir soliton theory, Lagrangian density and conservation laws, strongly turbulent plasma 77−51169
Langmuir turbulence, collisional excitation of modulational instability 77−24086
Langmuir turbulence, fast electron tails form. *(Russian)* 79−68922
Langmuir turbulence, HF energy dissipation *(Russian)* 78−5873
Langmuir turbulence, ion sound upconversion, comments 80−92324
Langmuir turbulence, isotropic oscills. and energy flux nonlinear freq. shift *(Russian)* 79−27778
Langmuir turbulence, large-scale, renormalisation group method 80−38650
Langmuir turbulence, laser excited, in dense plasma focus, light scatt. obs. 77−7591
Langmuir turbulence, modulating instability wave, nonlinear dynamics, solitons *(Russian)* 77−47196
Langmuir turbulence, modulation perturbation spectrum 80−33776
Langmuir turbulence, numerical modelling, solitons, nonlinear interactions 80−70030
Langmuir turbulence, optical satellites 79−60111
Langmuir turbulence, relativistic electron increase with heating *(Russian)* 79−27799
Langmuir turbulence, renormalisation method and singularities 77−80304
Langmuir turbulence, review 78−51302
Langmuir turbulence, stationary 78−14164
Langmuir turbulence, statistical theory 80−38647
Langmuir turbulence, strong, transition *(French)* 80−28674
Langmuir turbulence and modulational instability 78−75335
Langmuir turbulence and modulational instability in unmagnetised, completely ionised plasma 79−37496
Langmuir turbulence driven by constant pumping 78−75341
Langmuir turbulence in galactic masers, role in generating high-vel. and symmetric spectral features 80−31378
Langmuir turbulence in solar corona, four-plasmon interactions rel. to radar signal refl. 80−101582

plasma turbulence continued
Langmuir turbulence in solar corona, rel. to quasi-stable particle accel. and type I radio bursts *(Chinese)* 80−105220
Langmuir turbulence in upper hybrid resonance region, external electric field effects *(Russian)* 79−73010
Langmuir turbulence meas., forbidden transition satellites 80−38714
Langmuir turbulence of relativistic plasma in strong mag. field *(Russian)* 80−28678
Langmuir turbulence spectrum, optical polarisation meas. *(Russian)* 78−22572
Langmuir wave, acoustic turbulence effect on collapse 79−14549
Langmuir wave collapse, acoustic turbulence effect 79−37481
Langmuir wave evolution, three dimensional kinetic model, Vlasov eqn. calcs. 80−43923
Langmuir wave turbulence in solar type III radio bursts, nonlinear stabilisation 80−26826
Langmuir waves, induced nonthreshold scatt. on HF oscills. in inhomogeneous plasma *(Russian)* 80−53960
Langmuir waves, nonperiodic oscillations 80−48888
Langmuir waves, numerical modelling of 1-D turbulence, acoustic oscillations effect *(Russian)* 80−103135
Langmuir waves, turbulent bremsstrahlung process 80−62009
laser beam self-focused in turbulent plasma, average field 80−79505
laser diagnostics, probing radiation Raman scatt. *(Russian)* 80−19618
laser fusion, energy flux limitation by ion acoustic turbulence, anomalous transport coeffs. 77−43009
laser irradiated plasmas, flow effects on density profiles 78−18429
laser light absorpt., turbulence 78−47128
laser light absorpt. by ion acoustic turbulence in laser prod. plasma 79−4144
laser light absorpt. by short wavelength ion turbulence 77−35352
laser light absorption and harmonic generation 78−75359
laser plasma, convective parametric decay instability 80−64722
laser plasma, diagnostics in 1/4 crit. density region, harmonic generation expts. *(Russian)* 77−7578
laser scattering, electron density fluctuations meas. 77−39469
LF modes, laser heterodyne meas. 77−15246
light re-emission, in parametrically turbulent laser plasma *(Russian)* 79−55509
linear response theory, ion-acoustic waves dielectric const. 77−986
linear response theory, ion-acoustic waves dielectric const. 77−987
linear response theory of turbulent magnetised plasma 77−47197
linear turbulently heated plasma, secondary emission detector obs. 80−75100
localised pumping-excited waves, parametric instability, nonlinear stage 80−38622
low pressure plasma, two-dimens. turbulent convection 80−28676
low-β plasma, strong turbulence in rot. column 78−94915
low-β plasmas, turbulence, spectral struct., Bhom diffusion coeffs., determ. 80−106924
lower hybrid heating, collective effects 79−14570
lower hybrid resonance cone propag., density fluctuations effect 78−59583
lower hybrid turbulence spectrum, amplitude-freq. nonlinear cut-off *(Russian)* 79−37494
lower hybrid wave turbulence effect on tearing mode instability 80−92322
lower hybrid waves resonance interaction with turbulent plasma 78−30445
lower-hybrid turbulence filamentation by adiabatic perturbations 78−22500
lower-hybrid-drift wave turbulence in distant magnetotail, theory 79−25399
magnetic dynamo, MHD turbulence, perturbational method 79−90389
magnetic dynamo action in two-dimens. turbulent MHD 77−51161
magnetic mirror, injected plasma particle refl. (trapping), quiescent (turbulent) plasma 80−48955
magnetic mirror confined plasma, turbulent heating, rel. to Buneman instability 77−24106
magnetised non-uniform plasma, with density depend. fluctuations 79−41831
magnetised plasma, pseudo three dimen. electrostatic turbulence, stationary spectrum 78−91109
magnetised turbulent plasma, nonlinear current density, collisional contribs. 78−63567
magneto-active plasma, theory of turbulence 78−83567
magnetoacoustic turbulence, collision free mechanism *(Russian)* 78−22502
magnetoacoustic wave turbulence in interplanetary plasma, spatial fluctuation spectra 79−53693
magnetoactive plasma, modulational instability caused by Langmuir oscillations 80−92297
magnetosonic turbulence in interplanetary medium, evidence from plasma inhomogeneities anisotropy *(Russian)* 80−36468
magnetosonic waves in presence of lower hybrid turbulence and heating 78−26281
magnetosphere, conductivity anisotropy and effects 77−13182
magnetosphere, electrostatic ion loss-cone waves nonlinear generation 77−41269
magnetosphere, lower hybrid turbulence, nonlinear LF spectrum cutoff 78−4041
magnetosphere, strong Langmuir turbulence as source of km-wide RF radiation *(Russian)* 77−9630
marginal stability anal., anomalous transport, profiles, coeffs. and turbulence level calc. 77−47175
Markovian expansion, theory 78−79435
mass renormalization in stochastic acceleration of particles *(Russian)* 80−100066
Maxwell stress tensor in turbulent medium, calc. *(Russian)* 78−71483
Maxwell-Klimontovich equations for turbulent plasma, renormalisation 80−79500
MHD, 2-dimens., for high-beta turbulence 77−15193
MHD, two dimens. turbulence, stationary states in non-dissipative limit 80−24169
MHD fast electron generation in shock waves propagating along magnetic fields *(Russian)* 77−990
MHD flow, 2-D, eqns. of motion, dissipative, forced turbulence 77−65844
MHD generator, plasma turbulence in combustion channel 80−75057
MHD generator, turbulence of combustion products in channel 79−64866
MHD generator channel, turbulent MHD boundary layer 77−43085
MHD oscills. ensemble, interaction with quasiuniform mag. field, sunspots 77−76041
MHD turbulence, axisymmetric 79−19035
MHD turbulence, generalised Lorenz eqns., strange attractors 80−59232
MHD turbulence, interferometric meas. in toroidal pinches 77−27731
MHD turbulence, numerical simulation and closure techniques 79−90343
MHD turbulence, three-dimens. soln. in cylindrical geometry 78−67351
MHD turbulence, two-dimens., cylindrical nondissipative model 79−32772
MHD turbulence in Jupiter magnetodisc, rel. to plamsa transport into outer magnetosphere 79−58297
MHD turbulence in solar wind, props. 80−61977
MHD turbulence rel. to form. time of isotropic particle vel. distrib., magnetosheath appls. 78−28420
MHD turbulent dynamo problem *(Russian)* 78−63501
micro-turbulence in solar atmosphere, rel. to charged particles accel. in solar flares 77−53528
Microtor Tokamak, LF microturbulence, far IR laser scatt. 80−96362
mode coupling coefficients, for magnetised turbulent plasma 78−79432
modulation instability and strong turbulence in materials with inverse dispersion *(Russian)* 77−62359
modulation instability at lower hybrid reson., strongly turbulent plasma *(Russian)* 78−59563
modulation instability of turbulent spectra *(Russian)* 79−37472
modulational instability produced by Langmuir turbulence in a magnetic field 80−1759
monochromatic wave injection, turbulent spectrum modification, dispersion relation 77−31467
multicharged ion heating in Z-pinch, column compression, temp. and density *(Russian)* 80−64754
multicomponent plasma, ion-acoustic resist. 80−10383
multicomponent plasma, linear longit. oscill. damping and dispersion, development of turbulence 77−51185
non-linear oscillators, development of Kolmogorov spectrum 79−60140
nonequilibrium plasma, fast Langmuir soliton possibility 78−75340
nonequilibrium plasma, nonlinear wave interaction and stationary fluctuation spectrum *(Russian)* 78−14153
nonequilibrium turbulence in solar atmosphere, mag. pumping as flare energy source 77−78764
nonhomogeneous plasma in radiating field, absolute dissipative instability *(Russian)* 77−19681
nonideal plasma, elem. excitations and macroscopic props., review 80−43842
nonlinear dissipation, effect on heating under strong Langmuir turbulence conditions *(Russian)* 78−34346
nonlinear interaction of intense HF EM field with Langmuir waves in turbulent plasma 80−53988
nonlinear magnetosonic waves in finite conductivity isothermal plasma, asymptotic method 79−77374
nonlinear media, kinetics of HF and LF waves *(Russian)* 79−4444
nonlinear wave effects, comparison of theory and experiment, review 79−7460
nonstationary, elec. field pulsations, nonlinear differential eqn. 77−42983
nonstationary plasma turbulence in parametric resonances 77−11378
Ohm's law, electrical conductivity, turbulence effect 78−22463
oHM's law in turbulent plasmas and beta limitations by anomalous diffusion 79−77344
ohmic heating of plasmas in closed magnetic systems 80−28756
one-dimensional strong Langmuir turbulence, modulational disturbance spectra 78−75339
onset, due to velocity gradient driven flute instabilities, anomalous heating 77−39414
optical props. of thin plasma layer, parametric turbulence effects *(Russian)* 77−58864
overdense column, reson. microwave absorpt. 80−64732
parametric, pumping wave harmonics generation *(Russian)* 78−26266
parametric instabilities, nonlinear turbulence theory, pump field to plasmon conversion 77−24085
parametric instabilities, spatial turbulence effect 79−27767
parametric instability, near lower hybrid reson., ion-acoustic turbulence effect *(Russian)* 79−4126
parametric instability, turbulence evolution with two characteristic wavelength scales 77−80305
parametric instability, two-plasmon, two-dimensional relax. 78−5866
parametric instability aperiodic, stabilisation of nonlinear freq. shift 77−65873
parametric instability damping by high power elec. field pumping *(Russian)* 77−7553
parametric instability saturation *(Korean)* 79−7455
parametric instability saturation with multi-connected pump region *(Russian)* 77−68768
parametric interaction of waves in plasma with random large-scale inhomogeneities *(Russian)* 80−103137
parametric Langmuir turbulence, two pump wave excitation, plasmon nonlinear stabilisation *(Russian)* 78−83565
parametric magnetosonic turbulence, evolution of fluctuations into electrostatic and acoustic waves 77−11342
parametric phonon excitation and turbulence 78−75342
parametric phonon-turbulence from circ. polaris. UHF waves *(German)* 78−34316
parametric resonance in a weakly turbulent relativistic electron plasma 79−55539
parametric turbulence, due to EM wave decay 77−31470
parametric turbulence nonlinearity relax. *(Russian)* 77−55149
parametric turbulence of inhomogeneous plasma layer *(Russian)* 79−68921
parametric turbulence of particles emitted by a laser plasma *(Russian)* 80−53985
parametric wave interactions, random inhomogeneities effect 77−68788
parametrically turbulent plasma heating *(Russian)* 78−59630
parametrically unstable plasma, solitons 78−63563
PARODIE device for construction of large size homogeneous stationary plasma *(French)* 78−14223
partially ionised plasma, strong turbulence 80−79499
particle acceleration by intense microwave irrad. 77−47230
particle acceleration by MHD shock turbulence 80−87894
particle beam-plasma interaction, ion-acoustic turbulence effects 78−91121

plasma turbulence continued
particle interactions in turbulent plasma flow on surface-melted substrate *(Russian)* 77−31482
perturbation of coherent wave-particle reson. 78−26274
perturbed orbit theories, approximations and elementary effects 78−71484
photon diffusion, stochastic, in unstable, turbulent, magnetoplasma 79−48662
photon interaction with a turbulent medium 79−82068
planar Langmuir solitons, 3-dimens., stability 80−46827
plasma, turbulent, parametric instabilities, anomalous energy absorpt., dispersion eqn. 80−92291
plasma convective cells of drift waves, plasma with shear, nonlinear excitation mechanism *(Russian)* 80−38585
plasma focus, recent developments to increase neutron yield 79−14567
plasma focus, turbulence, light scatt. obs., pinch break-up 77−24083
plasma reactors, laminar and turbulent transport model *(German)* 77−11321
plasmatron with interelectrode insert, output electrode turbulent heat transfer 78−71555
plasmon condensate, nonlinear statistical theory 77−47192
plasmon gas oscillations *(Russian)* 78−47120
positive column, striation dynamics, velocity/amplitude correlation 78−67517
precursor whistler mode plasma turbulence formation in parallel shock waves 80−24172
propagators and trajectories, asymptotic, in plasma turbulence theory 79−90409
pseudo three dimens., magnetized nonuniform plasma comparison with ATC Tokamak 78−38488
pulsations, quasilinear theory 78−26283
quantum mechanical Vlasov eqn. 78−83566
quasicollisions model for particle scattering on plasma turbulent pulsations appl. to transport coeffs. determ. 78−71440
quasilinear thoery, mode coupling 80−79498
radiation emission from electron beam excited strongly turbulent plasma 80−53943
radiosources, decay excitation of plasma turbulence and nonlinear radiative transfer 77−17707
random acceleration problem, Novikov-Furutsu theorem 78−59596
random density inhomogeneity effects on nonlinear ion-acoustic waves, envelope characts. 77−19684
rarefied plasma, mag. field rapid penetration, magneto-acoustic shock waves, super-Alfven penetration *(Russian)* 78−59554
reactor, power law distribs., cosmic ray source model *(Russian)* 78−26244
reactor power distrib., energy and particle flux directions *(Ukrainian)* 78−93104
relativistic electron beam induced turbulence and heating, review 80−38672
relativistic electron beam turbulent interaction, anomalously high energy loss *(Russian)* 78−59615
relativistic electron spectra, Compton effect *(Russian)* 77−19760
relativistic plasma, modulation instability rel. to pulsars radio radiation *(Russian)* 77−22258
renormalised Vlasov turbulence 80−19579
renormalized Compton scattering and nonlinear damping of collisionless drift waves 80−69998
resistive tearing m=1 instability turbulent modification 80−43916
resistivity, of turbulent plasma, with ion-acoustic instability, ion-tail form. effect 80−10360
resistivity, turbulent, at high drift vels., particle diagnostics 78−38541
reversed field pinch, MHD turbulence model 77−24144
Rossby wave turbulence, exact Gaussian soln. 80−92325
Rossby wave turbulence, nonlinear behaviour and turbulence spectra 80−19573
runaway electron diffusion and power balance in Tokamak moderate density discharges 80−28609
shock generated turbulence, obs. in mag. plasma by CO_2 laser scatt. 80−84003
shock wave, collisionless, turbulent ion viscosity *(Russian)* 78−38492
shock wave propagating in solar atmosphere across mag. field, struct. 79−40166
shock waves, turbulence investigation by anal. of scattered laser light 77−3940
shockwave, electrostatic, turbulence levels diagnostics by fast ion beam *(Russian)* 79−98974
skin heating in Frascati Tokamak 77−84461
solar atmosphere, plasma turbulence rel. to flares development 77−17476
solar corona, plasma radiowave fluctuations and turbulence, Venus 10 radio transmission expt. 79−80295
solar corona, turbulence triggering during fast flux emergence 78−45304
solar flare particles pulsed accel., plasma turbulence, ion-acoustic and Langmuir waves 78−96450
solar flare plasma instability and turbulence, review 80−62100
solar flares, kinetic processes and plasma turbulent state 78−85920
solar flares nonrelativistic electrons accel. by strong plasma turbulence 78−7954
solar flares primary energy release region, plasma radiation diagnostics 79−84777
solar type III radio bursts fundamental radiation rel. to coronal low freq. turbulence 79−84778
solar wind, Venera 10 radiowave spectral width meas. 79−88560
solar wind at Jupiter, bow shock, Voyager 1 plasma wave turbulence 79−96954
solar wind density fluctuations near Sun from Pioneer 6 spectral broadening meas. 77−13199
solar wind upstream of Earth bow shock, nonlinear plasma processes 80−85833
soliton, Langmuir, one-dimensional, propag., interactions and generation 77−43057
solitons, laser physics appls. 80−48333
solitons, nonlinear normal mode theory 80−48875
sonic-Langmuir solitons, formation, interaction, inverse scatt. method 77−27664
space plasma turbulence and nonlinear waves, weak turbulence theory, plasmon turbulence 79−60142
space-time formulation 77−11341
spatial diffusion coeff., unmag. collisional plasma, from ion-acoustic turbulence data 78−42728

plasma turbulence continued
spatially inhomogeneous singular spectra of weak turbulence *(Russian)* 77−27673
spectra-line profiles, weakly turbulent plasma unified electron broadening theory 77−58848
spectrum analyzer and differential amplifier for turbulence meas. 77−43081
spectrum modification by monochromatic wave injection 77−19706
spectrum reconstruction from light propag. time correlation function 77−19178
spherical laser plasma, fast ion generation by ion-acoustic turbulence 77−80330
spontaneous polarization of a turbulent magnetized plasma 80−19580
Stark broadening in turbulent plasma 77−47166
stationary MHD eqns. for rotating toroidal plasma 80−92278
stationary spectrum of strong turbulence, magnetised nonuniform plasma 77−72446
stationary turbulence regions and anomalous resist. in magnetosphere plasma 80−38649
statistical theory, quantum mechanical approach 80−43926
stellarator, current turbulent ion heating, modulation stability 80−79525
stellarator, Saturn, current-free transport processes, drift modes effect 80−19605
stimulated radiation, leaking normal mode spectra, cold plasma cylinder 77−89231
stochastic ion heating, ion acoustic wave fluctuations obs., correlation time 78−34347
stochastic ion heating of turbulent plasma 77−47229
stream of high temp. gas with particles, modelling *(Russian)* 80−38572
strong Langmuir turbulence, soliton flash, turbulent ion heating and relax. oscills. 78−1834
strong Langmuir turbulence for electron plasma waves, plasma diagnostics appl. 80−48889
strong turbulence and anomalous diffusion in mag. field 80−59239
strong turbulence effects on the kinetic beam-plasma instability 80−59207
strong turbulence fluctuations in partially ionised plasma, power spectrum var. with press. 80−38645
strong turbulence theory, Boltzmann plasma 79−41832
strongly turbulent stabilization of electron beam-plasma interactions 80−59251
subsonic electron fluid and small spark formation 80−38792
sum rules and collective modes in a turbulent plasma 80−6255
synchrotron turbulent reactor, relativistic electrons spectrum in nonsteady radiosources 79−40071
temperature fluctuations, turbulent, microwave blackbody spectrum obs. 78−1897
TERP noncircular toroidal pinch, turbulent heating 77−24162
test charge moving in turbulent plasma, rate of energy loss 78−5872
test electron transport in stochastic mag. field, principles and problems 79−77341
test particle dynamics in turbulent magnetoplasma 79−14614
Texas Turbulent Torus, energetic ion production, temporal and spatial evolution 78−1855
Texas turbulent torus, turbulent heating effects 79−90442
theory and expt. at Kharkov Inst., Ukrainian SSR *(Russian)* 79−14544
thermal parametric instability in non-uniform plasma, theory *(Russian)* 79−27760
thermal transport from turbulent skin layer to plasma core in heating 77−31492
theta-pinch, electron heating in turbulent neutral layer *(Russian)* 80−10361
theta-pinch, groove type drift turbulence, Lagrangian description *(Russian)* 77−72448
theta-pinch modelling by hybrid numerical models, turbulence effect 77−31510
Tokamak, far IR laser collective scatt. system 80−59300
Tokamak, Texas turbulent torus, turbulent heating model 79−37518
Tokamak apparatus for turbulent heating of plasma *(Japanese)* 78−1914
Tokamak discharge, anomalous drift-wave transport anal. 79−32745
Tokamak plasma, heated turbulently, elec. cond. 78−42720
Tokamak plasma, turbulent heating and transport theory 77−72421
Tokamak radiation, near plasma freq., three-wave mechanism 79−37464
Tokamak reactor with turbulent transport coeff., energy balance 79−71953
Tokamak turbulent heating current penetration, poloidal profiles and anomalous transport 77−55158
Tokamaks, disruptions and turbulence 80−28675
Tormac, Gaussian HeII 4686 Å spectral lines, Doppler and Stark broadening effect, turbulence 80−106980
toroidal plasma, optical diagnostics and thermal transport 79−73023
toroidal plasma, rapid thermal transport from turbulent skin layer to core 78−59659
toroidal plasma discharge, turbulently heated, microwave spectra obs. 79−50893
TORTUR I, heating by current driven turbulence 80−24191
TORTUR II, turbulent skin heating of toroidal plasma 79−98992
TORTUR toroidal device, plasma confinement and skin currents 77−76180
torus, turbulent heating through skin layer 77−76133
transport coeffs. calc. for weakly turbulent plasma 79−1290
transport in plasma, turbulent, convective, kinetic equations 80−28606
transverse Kelvin-Helmholtz instability, suppression by lower hybrid turbulence 77−65861
trapped electron instability, nonlinear saturation 79−14531
trapped electron instability, turbulence, unstable mode dynamics anal. 80−33761
trapped electrons, test charge pot. in single wave case 80−24247
TTT, current penetration and resistivity, probe diagnostics 79−32821
turbulence, 2-D, hydrodynamic and plasma applications, dynamical eqns., diffusion, MHD, superfluidity, review 80−69769
turbulence, nonlinear interaction of magneto-sound waves 78−45134
turbulent diffusion in plasma with high-energy ions, thermonuclear case 77−971
turbulent diffusion of toroidal plasma, geometrical effects 78−94900
turbulent diffusion regimes along the pitch angle in a geomagnetic trap *(Russian)* 79−55534
turbulent electron beam plasma interactions, PN calc., numerical anal. 79−14560

plasma turbulence continued
turbulent flow, of ionised plasma effect of mag. field and elec. current 79−60115
turbulent heating, current penetration and electron temp., Thomson scattering obs. 79−4158
turbulent heating by runaway electron beams, Tokamask plasma 79−73020
turbulent particle propagator in mag. field 79−4141
turbulent plasma, magnetised, line shape of optical satellites 80−75098
turbulent plasma, wave scintillations, fourth-order moment eqn., astrophys. appl. 80−46381
turbulent plasma blanket generation, in Tokamak plasma *(Russian)* 79−55566
turbulent reactors, relativistic electrons accel. and cosmic radiosources nonlinear spectra 79−8824
two dimensional guiding centre plasma, cut-off 77−31468
two-dimensional convection, strong turbulence theory 77−76083
two-dimensional inertial turbulence, in cosmic-scale low-β magnetospheric plasma 78−36399
two-stream plasma, thermalisation *(Russian)* 79−4119
universal drift mode, turbulent destabilisation and saturation in sheared mag. field 79−37455
unstable turbulent ionisation waves, two dimensional Fourier spectroscopy 80−38646
upper hybrid turbulence, kinetic modulational instability 77−42984
Uragan-2, ohmic heating, charged particle anomalous diffusion, turbulence, gravitational drift instability *(Russian)* 77−47150
Vlasov eqn., time linear statistics for nonlinear turbulence eqns. 77−65835
vortex-acoustic ion wave turbulence, statistical mechanics 80−92326
vortices in cosmic plasma, depolarisation of EM waves 77−17358
vortices in laser-produced plasmas 80−79501
wake model of fast moving body in plasma and its effects 79−77353
wave number spectrum parameter estimation form fixed probe pair data 79−82062
wave propag., nonlinear theory *(Russian)* 78−14165
wave turbulence associated with interplanetary shock, obs. 79−53700
waves, transverse and longitudinal, interaction in highly turbulent plasma 77−19704
waves detection in turbulent plasma by satellites of forbidden He transitions *(Russian)* 78−18391
weak Langmuir turbulence, in nonuniform plasma, spectral intensities *(Russian)* 79−55504
weak turbulence, of nonisothermal plasma, due to Langmuir wave-ion acoustic wave interaction *(Russian)* 79−37495
weak turbulence theory, low phase vel. induced wave scatt. 77−55148
weakly turbulent collisionless plasma, anomalous transport coeffs. 78−71453
whistler mode turbulence in Jupiter magnetosphere, Voyager 1 plasma wave obs. 80−26795
whistler mode turbulence near Io plasma torus, electron pitch-angle diffusion 80−4290
whistler-Alfven turbulence interaction 80−75058
Z-pinch turbulence spectroscopic detection and anal. *(Russian)* 80−100098
Zakharov equations derivation for higher electron non-linearities in Langmuir collapse dynamics 80−43919
Ar arcs in supersonic flow, numerical analysis 80−38776
Ar, hollow cathode arc discharge, collective scatt. meas., turbulence 80−48978
Ar, jet, radiowave interaction and electron density fluctuation 77−989
Ar, weakly ionised plasma turbulence in longitudinal mag. field 78−75338
CO_2 laser light collective scatt. meas. 80−84005
H glow discharge, electron macroscopic props. *(Russian)* 80−92403
H, n-α line Stark profiles, large θ-discharge 77−24084
H plasma, magnetic piston study in theta-pinch *(Russian)* 80−83971
H plasma beam, electron macroscopic props. *(Russian)* 80−92403
H, Zeeman levels orientation by reson. radn. in turbulent plasma *(Russian)* 79−98028
H_2 beam discharge, electron kinetics in collisionless non-equilibrium plasma 80−92402
H_2 plasma collision-dominated electron distrib. function with turbulent heating 78−71509
H_2, produced by magnetically rotated arc 80−38769
H_α and H_β Stark profiles in LF turbulent plasma 77−7593
He, collisional plasma, vortex diffusion, shear effect 79−32773
He, gas discharge flow, contracted strata rel. to turbulence 78−1923
He I satellite line shape in plasma, stochastic theory 78−38460
He, parametric plasma turbulence, soliton struct. obs. 79−60143
He plasma, Stark shift and line broadening in 3-D stochastic laser field 78−50502
He, Stark broadening satellite transitions, in turbulent plasma 77−61759
He-Ar plasma, linear longit. oscill. damping and dispersion, development of turbulence 77−51185
He-Cs, turbulent plasma, characts., electron energy balance *(Russian)* 79−27779
Ne discharge, ionisation wave, phase instability and disintegration obs. 78−67518
Ne discharge, wavenumber spectra of turbulent ionisation waves 78−71541
Ne, glow discharge, turbulent ionisation waves, correlation meas. 78−67519
Z-pinch, noncylindrical, dynamics and particle accel. mechanism 77−76170

plasma-wall interactions
see also plasma impurities
ablation due to supersonic flow, electron heat transfer mech. 78−71496
ablation stabilised arc theory 80−70072
advanced fuel fusion reactor wall loading limitations and stability index beta 80−99311
air, afterglow plasma, interaction with glass, Cu, steel walls, calorimetric method obs. 78−14177
air, wall-stabilised arc, step and sinusoidal current change response 80−103209
air plasma flow in channel inlet zone, local heat transfer 80−64687
alumina confined arc, ablation-induced effects 80−70073
anomalous transport processes in radially compressed reversed-field configurations, numerical simulation 80−64689
arc furnaces, stabilisation methods *(German)* 78−75402
arcing and surface damage in DITE Tokamak, SEM obs. 78−59611
arcs, wall-stabilised, free recovery with imposed laminar and turbulent flows 80−59321
ASDEX divertor expt. 77−31504
ATC during high power neutral beam injection 77−31502
atomic and surface physics, conf., Salzburg, Austria (Feb. 1980) 80−57010
atomic processes determining the plasma-wall interaction 80−59247
blanket, NOEL (No External Leak), thermal anal. and tests 80−95459
blanket boundary layer, high-density gas, localised drift mode stability 80−43956
boundary condition, energy equilibria in diffuse pinch 79−1321
bundle divertor, mag. config., wall impurity removal for Tokamak 77−65901
capillary discharge, with evaporable wall, plasma parameters axial distrib. *(Russian)* 78−75280
capillary discharge with vaporising wall, plasma parameters axial distrib., model 79−64943
cold plasma blanket for Tokamak, heat diffusion and temp. profile 77−65902
combustion product plasma, discharge on cooled Cu electrodes, rel. to erosion damage in MHD channels 78−1925
containment vessels, backscatt. and sputtering from pocket and finned structs. 79−14558
contamination due to H ion sputtering of Tokamak stainless steel first wall 79−46458
controlled fusion devices conf., Abingdon, England (April 1978) 78−94917
controlled thermonuclear fusion, surface effects 77−26866
CT-6 Tokamak plasma props. *(Chinese)* 80−103159
CTR devices, surface effects related to voltage breakdown 77−35356
CTR first wall design, surface phenomena importance 77−34431
CTR first-wall irradiation environment, appl. of dual-ion accelerator 78−13325
CTR first-wall materials, ionisation-assisted damage processes 77−34432
current disruption, in Tokamak plasmas, schlieren signal meas. from millimetre waves 80−48998
DC glow discharge in tube with walls of different catalytic activity 80−100103
deflagration wave in slab target, form. by ion beam 80−28628
deflagration wave in spherical target, form. by ion beam 80−28629
dense plasma focus, thermoncl. erosion of wall materials 77−23273
depth profile of near surface C contaminant in implanted first wall 77−34433
discharge, light emission efficiency, electrostatic confinement effects 80−33752
discharge cleaning in JFT-2 Tokamak, AES 78−51316
discharge sparking potential dependence on nature of the wall 78−67552
Diva, metal impurities origin, arcing ion sputtering, evap. 78−59691
divertor expts. for control in Tokamaks 78−94125
Doublet III, limiter performance, design and material selection 80−106162
earth reentry exposure, simulated, effect on mech. props., oxidation of ThO_2 dispersion hardened alloys, Haynes 188 and Hastelloy X 79−5086
electrical discharge, deionisation, caused by internal surfaces, dispersion model anal. *(Russian)* 78−5961
electrical discharge, deionisation of low press. plasma in gas discharge gap, elec. strength *(Russian)* 78−1921
electron beam-sliding spark plasma device, X-ray microscopy appls. 78−5974
electron current, at plasma-electrode interface in transverse mag. field, probe obs. 79−64914
electron cyclotron reson. ion source with permanent mags., plasma-wall interaction expts. 80−99378
electron emission, secondary, effect on energy transport to limiter of Tokamak 79−3236
electron plasma waves, refl. from flat plane boundary 77−58852
electrostatic sheath equations, inc. heating, ion mobility, and ion recomb. 80−1808
EM surface wave diffr. by inhomogeneity in plasma-dielectric boundary 77−24075
emission from hypersonic plasma-plane obstruction zone *(Russian)* 77−84449
equilibrium in free boundary case, variational principle calcs., wall interaction *(Chinese)* 80−69972
external conducting sheets, stability effects on mag. contained plasmas 80−1787
flashtubes, plasma-wall interaction, spectroscopic meas. 79−77421
flow instability near pipe wall, ref. to MHD generator 77−35330
fusion device, angular and time resolved energetic H flux to walls, measurement techniques 79−674
fusion device surface effects on neutral beam injector and beam direct convertor operation 80−47719
fusion devices, controlled, surface effects, conf., San Francisco, USA (Feb. 1976) 77−30659
fusion plasma boundary layer 77−47216
fusion reactor, fusion-product bombardment of first wall 77−38409
fusion reactor, impurity and gas throughput control 78−54907
fusion reactor, plasma-wall interaction, permissible degree criterion 78−89981
fusion reactor divertor collector plate, pot. drop across electrostatic plasma sheath 80−13833
fusion reactor first wall material, sputtering coeff. calcs., 1 keV H^+, D^+, T^+ and He^+ *(Russian)* 77−8697
fusion reactor first wall materials, surface resist. 80−42853
fusion reactor first-wall, struct. anal. for high temp. performance 78−13326
fusion reactor materials, surface anal. in Princeton Large Torus 77−57743
fusion technology, surface studies 80−23149
fusion Tokamak experiments, H(D) recycling model, influence on discharge behaviour 80−10393
gas-discharge plasma, interaction with thin quartz glass layer *(Russian)* 78−14178
gaseous impurity origin, meas. by mass spectroscopy in JFT-2 Tokamak 79−1339
geometrically extended electrode, charged particle and energy fluxes 78−79442

plasma-wall interactions continued
heat exchange of low-temp. plasma with wall, longitudinal mag. field effect 80−33781
heat transfer, fusion appls. 77−11367
heat transfer, in wall region of reactor Tokamak *(Russian)* 78−87501
heat transfer rates to flat plate from normally-impinging N plasma jet 80−75061
heat transfer to rotating water-cooled cylindrical wall *(French)* 80−28850
high enthalpy plasma from explosive source, cavity and channel inner surface interaction 79−98946
high intensity laser-matter coupling in vac. 79−90430
high-current travelling wave plasma accelerator appl. 78−5954
impurity concentrations on wall during Tokamak discharges, laser probing technique 80−49013
impurity flux and differential wall changes, in Alcator-A Tokamak, surface probes 80−38664
impurity introduction mechanism, fusion temps., review 77−42990
inert gas, low-press. discharge, electron energy distrib., elec. field and electron wall loss effects 80−24294
inhomogeneous plasmas, resonant microwave absorption, nonlinear effects 79−94793
intense ion source discharge, delay of arc starvation saturation 78−79457
ion beam analysis of surface modifications in Tokamaks, review 79−46457
ion microanalysis and implantation applied to fusion surface research 79−45405
jellium, one-dimensional, wall effects 79−46468
jet, heat exchange with obstacle 78−47130
JFT-2a Tokamak, plasma behaviour with separatrix mag. surface 77−7581
Kharkov stellarators, plasma-wall interactions 80−79552
laser impact, air-plasma layer interaction and surface screening *(Russian)* 78−22532
laser-driven ablation, exptl. obs. and numerical simulations 79−4177
linear theta pinch Isar II, low compressed high-β stellarator, surface effects 77−76161
low pressure Ar plasmas near wall, kinetics study *(French)* 80−28689
macrotor, metal influx 79−650
magnetic confinement system, surface problems caused by dissolved H_2 80−57946
magnetic field effects, computer simulation 80−10392
magnetic mirror 2XIIB, first wall surface conditions control 77−31501
magnetised plasma, hot, unstable behaviour, in contact with cold wall 79−1333
magnetised plasma, in dielectric chamber with thermionic emitter, enhanced diffusion 79−64901
magnetoactive plasma, effect on a plane disc, impedance calcs. 80−1809
magnetoplasma compressor, radial limitation of focal zone, dynamic, energy, spectral characts. 79−55477
metal, time resolved impurity conc. in DITE Tokamak using RBS anal. 79−1329
metal snow liberated from wall, cooling effects 78−71494
metal snow liberated from wall, cooling effects 78−71495
metal surface irradiated by laser, pulsed, plasma to wall energy transfer 79−60152
metal target interaction, plasma stream, boundary layer struct., particle diagnostics 77−76106
metal target interaction, plasma stream, boundary region optical diagnostics 77−76107
MFTF, end loss region high energy plasma gettering 80−102343
MHD equilibrium with elliptic free-boundary, limiter and current profile effects 79−37529
MHD generator, local characts., transverse current inhomogeneity in MHD channel 80−24146
mirror fusion reactor design, hybrid fusion-fission reactor, surface bombardment rates 77−30662
multimode EM probe, appl. to wall region 79−94819
narrow inhomogeneous layer, surface wave-incident radiation nonlinear interaction 80−100080
negative ion emission in electrode layer of low-temp. plasma 80−70006
neutral atom kinetics, near Tokamak discharge chamber wall *(Russian)* 79−4102
neutral injection kinetics, Monte Carlo anal., local liberation to wall 77−42992
neutral injection parameters and beam line design for TEXTOR 80−28811
neutral particle distrib., Maxwellian plasma, singular eigenfunctions 77−76104
neutral particles, interaction with wall and plasma, kinetic description 78−59658
nonexponential Debye shielding rel. to electrode-plasma pot. difference 80−100081
orifice flow, wall interactions in mol. flow regime, for diagnostics 79−23449
ORMAK, first wall, surface impurities and cleaning techniques 77−34435
ORMAK, impurity and surface studies 77−31517
ORMAK, normal discharge energy loss to wall and limiter 78−34355
oscillations, low frequency, growth, limit of safety factor in JFT-2 Tokamak 80−38589
particle interactions in turbulent plasma flow on surface-melted substrate *(Russian)* 77−31482
pellet ablation in plasma 80−19589
perspex confined arc, ablation-induced effects 80−70073
plasma recycling at surfaces using self-consistent model 77−35355
plasma surface interaction program of DITE Tokamak expt. 77−31503
plasma-surface interactions in Tokamaks, review 79−73017
PLT, vacuum vessel wall surface conditions, long term changes 79−653
PLT edge plasma, lower limits for parallel impurity fluxes 79−1320
polymer surface interaction process, simple plasma device for obs. 77−27723
positive column, in transverse mag. field, plasma parameter diagnostics 79−19103
positive column, metastable atom radial transport, effect of wall boundary conditions 78−67493
positive column, metastable atom transport, excitation rate radial variation, flux to wall calc. 80−44038
positive column constriction, cryogenic discharge, ambipolar wall diffusion 78−18468
plasma-wall interactions continued
primary electron-gas ionization sustained discharges 79−50910
Princeton Large Torus Tokamak, appl. of high-field surface and techniques 79−68942
propagation of a wide ion beam into a magnetic barrier, Vlasov equilib. model anal. 79−90439
PULSATOR I Tokamak, wall analysis, impurities 77−31515
Q-enhanced mirror fusion system 78−94130
quark surface in pinch discharge 79−1319
radiation blistering, material distortion *(Russian)* 77−76160
radiation plasma, diffusion-recombination distribution of free carrier concentration *(Russian)* 78−79408
random solid, light ion backscattering energy spectra calcs. 78−72655
reactive plasma, optical emission spectroscopy, emission intensities and reactive density, correl. method 80−92385
reactive sputtering of low-Z materials by H_n^+, expts. rel. to plasma-wall interactions, review 77−48297
reduction of effective sputtering yield by honeycomb structures, appl. to fusion reactor first wall design 79−23440
reflection coeffs. for light ion-surface interaction, review *(Russian)* 80−38663
reflection of laser plasma from hot shield, expt. 80−33782
residual gas anal., using computer controlled mass analyser, in ISX-A Tokamak 79−82096
resistive axisymmetric modes for doublets, stability, numerical parameter obs. 78−79421
resonance radiation effect on electron emission of metal wall in boundary layer *(French)* 79−37504
RINGBOOG II, cold plasma blanket research 79−98992
rotary symmetry plasma, magnetohydrodynamic eqns. and plasma wall effect *(German)* 79−68909
runaway electron bombardment of limiter during Tokamak startup 77−30666
scrape-off layer in Tokamak with divertor, plasma transport 80−28614
scrape-off layer of poloidal limiter, transport code calcs. rel. to plasma parameters 79−669
secondary electrons in plasma-wall sheath, Langmuir probe obs. 80−92387
self similar cooling wave, effective thermal cond. *(Russian)* 80−14908
sheath, integro-differential eqns., nonlinear, nonlocal, soln. formalism 80−43936
sheath edge theory is weakly ionised collision dominated plasma 80−43935
slow wave propag., plasma/dielectric wall 77−51183
solid H pellet interaction with magnetised plasma 80−78451
sputtered metal density meas. by atomic fluorescence spectroscopy 78−67422
sputtering, heavy-impurity control by light-impurity radiation, wall layer cooling 77−65879
sputtering yield meas. on first wall materials of thermonuclear fusion devices *(Japanese)* 77−85865
steel, stainless, 305, surface composition changes with plasma discharges 77−34434
steel, stainless, H recycle from Tokamak walls using plasma-wall interaction simulator 78−94131
steel, stainless, spatial distribution of limiter material and impurities on the first wall of TFR 400 79−651
substance evaporation into DC arc plasma, kinetics *(Ukrainian)* 80−33780
supersonic plasma-steel target impact effect, boundary layer role 79−32780
supersonic stream, incident on metal surfaces, emission 77−76105
surface erosion, sputtering, unipolar arcs, heat pulses 80−38665
surface erosion by plasma stream, ejected particle vel., Doppler vel. meas. 78−59610
surface erosion phenomena in CTR appl. 77−71695
surface excitations in metal-contiguous isotropic electron plasma 80−38667
surface impurities, in ISX-A Tokamak, AES obs. 79−82097
surface impurities during start up and early operation of ISX-A, surface anal. with sample transfer 79−654
surface problems in controlled fusion *(Chinese)* 79−97904
surface processes 78−94121
TEXTOR, plasma wall interaction experimental studies, design features 80−13845
TEXTOR, plasma-wall interaction study reactor, mechanical struct. design 80−13846
TEXTOR, technical materials for first wall 77−34430
TEXTOR program at KFA, Julich 77−31505
TFR machine, impurity behaviour, radiation losses and wall effects 77−31516
thermal losses, cross-field, in wall-plasma interface region, simulation 78−59609
thermal plasma, heat transfer to neighbouring walls or electrodes 78−1804
theta-pinch reactor, first wall environment 77−30661
Tokamak, Alcator, effect of wall temp. on O, N and C impurities, spectroscopic diagnostics 79−41840
Tokamak, alpha transport and blistering of first wall 79−19069
Tokamak, axially symmetric, α-particle escape in nucl. fusion, azimuthal distrib. *(Russian)* 77−18694
Tokamak, blanket and first wall design concept, thermal and hydraulic anal. 80−95460
Tokamak, cold layer formation, wall protection 78−30470
Tokamak, current transitions at plasma-wall interface 80−83984
Tokamak, DITE, plasma and impurity fluxes on walls 80−28688
Tokamak, DITE H conc. meas. in walls and limiters 78−94136
Tokamak, electrically isolated target, formation of arcing, role of runaway electrons 80−64764
Tokamak, fusion power reactor design 77−74982
Tokamak, heavy-impurity re-cycling and power loss at limiter 78−22543
Tokamak, high energy α-particle flux at walls due to mag. field rippling *(Russian)* 77−68841
Tokamak, ISX-A, wall conditioning by low power discharge, AES and residual gas anal. 79−90438
Tokamak, Macrotor, metallic impurity suppression by electron injection 79−32781
Tokamak, metal impurities due to arcing 78−42787
tokamak, plasma-wall-divertor model 78−58462
Tokamak, PLT, current profile evolution effect on plasma-limiter interaction and energy confinement time 80−10420

plasma-wall interactions continued
Tokamak, surface effects and impurity production 78−94127
Tokamak, surface interactions and conditioning techniques 78−94124
Tokamak, TFR, variable-radius Mo and graphite limiters 78−63600
Tokamak, time resolved heat flux to wall meas., sheath model with secondary electron emission 78−79468
Tokamak, TM-3, near wall region, Langmuir probe obs. *(Russian)* 77−47261
Tokamak, wall protection from hard disruptions 77−31508
Tokamak boundary in contact with limiter 78−5913
Tokamak devices, blistering and flaking by He atoms 78−86690
Tokamak discharge chamber, AES anal. *(Russian)* 79−4163
Tokamak experimental power reactor, burn cycle dynamics, confinement scaling laws and heating 77−23263
tokamak first wall, 3.5 MeV alpha bombardment 78−58463
Tokamak first wall, fusion product bombardment 78−5019
Tokamak first wall low-Z materials, impurity radiation from medium density plasmas 79−55472
Tokamak first-wall characterisation by in situ Auger electron spectroscopy 78−5022
Tokamak for surface and impurities studies 77−31531
Tokamak fusion reactor, electron emission effect at divertor target 79−660
Tokamak fusion reactor, impurity control and plasma transport in plasma-edge region 80−13832
Tokamak fusion reactor, wall bombarding high energy α-particle characts., drift *(Russian)* 77−47214
Tokamak fusion reactors, model of impurity control techniques 78−17428
Tokamak fusion reactors, plasma modelling and first wall interaction phenomena 77−30660
Tokamak fusion test reactor, thermal response of first wall limiters 80−79585
Tokamak impurity problems, atomic and mol. struct. and collision data, review 80−43959
Tokamak ISX-A, impurity expts. 79−1328
Tokamak IT-60, first wall design and related expts. 79−673
Tokamak liner destruction model, by runaway electrons, nonlinear dynamics 77−84481
Tokamak plasma-wall interaction, appl. of fluoresc. spectroscopy 79−23451
Tokamak reactor, first wall coating materials and techniques 78−8974
Tokamak reactors and structural materials 80−32428
Tokamak transport simulation models 77−79474
Tokamak wall, model of unipolar arc 79−657
Tokamaks, column wall interactions, in-situ meas. on PDX 80−59248
Tokamaks, review 78−94123
toroidal cavity partially filled with anisotropic dissipative plasma, wave excitation from antenna 77−24097
TORTUR II, turbulent skin heating of toroidal plasma 79−98992
transient gas feed in Tokamak discharges, numerical investigation of build-up phase of neutral H layer near wall 78−94135
transient neutral gas interactions with plasmas and walls 78−94134
ultrahigh vacuum tranfer system, 15 cm diameter, for remote plasma-wall interaction expts. 80−86327
unipolar arc damage in hot, dense D plasma 79−3235
Uragan-2, ohmic heating, hard X-ray emission from electron-wall interaction *(Russian)* 77−47215
viscous damping of magnetoacoustic oscillations in cold, bounded cylindrical plasma 80−24151
weakly ionised plasma, in mag. field, diffusion, boundary conditions effects *(Russian)* 78−75278
Al foil, burn-through by laser-driven ablation 80−33794
Al, sputtered by He^+, photon emission, dose depend. 77−8695
Al target, spatial distrib. of heating by laser-ignited air plasmas 79−23433
Al_2O_3, D plasma interaction, surface structure, chemistry and resistivity changes 78−53010
Al_2O_3, plasma interactions in PETULA Tokamak *(French)* 77−62372
Ar plasma, constricted electric arc, iteration method anal. 79−90484
B_4C, chem. erosion by H-plasma, first wall of fusion reactor 77−36676
C bonding to Tokamak walls, XPS studies 80−80942
C^+, on metal surface, removal by Ar^+ impact, 20-30 keV, in plasma 77−76103
Ga, liq. surface tension affected by low temp. plasma 79−33160
H discharges, chem. interaction with fusion reactor materials, impurities 77−35357
H flux to walls of fusion reactor, novel meas. technique 78−29640
H trapping studies in fusion first wall materials 79−45407
H^-, surface plasma source, prod. by H atom backscatt. from cesiated W 77−3953
H_2, neutral, behaviour calc. in wall region of high temp. plasma, wall interaction 77−35377
H_2 plasma reactor design, heat transfer and flow 80−38697
H_2, solid, ablation by magnetised plasma, semi-empirical calc. 80−38666
He, afterglow plasma, interaction with glass, Cu, steel walls, calorimetric method obs. 78−14177
He, hollow cathode, 1-4 torr, population of excited levels, excitation and decay mechanisms 77−80267
In, liq. surface tension affected by low temp. plasma 79−33160
LiD end plug, in linear theta pinch, effect on confinement props. 79−82088
N, high intensity arcs, anode contraction region modeling 80−103210
N_2, afterglow plasma, interaction with glass, Cu, steel walls, calorimetric method obs. 78−14177
Ne positive column, wall loss in transverse mag. field 78−55767
Ni, self-sputtering yields, low energy, rel. to plasma-wall interaction in fusion devices 78−56553
O bonding to Tokamak walls, XPS studies 80−80942
SF_6 plasma interaction with solid polymer, emission-spectra 80−87960
SiC, chem. erosion by H-plasma, first wall of fusion reactor 77−36676
SiO_2, surface, plasma etching in CF_4-H_2 glow discharge, AES meas. 79−98922
Ti, D bombarded surface, ion fraction and energy anal. of sputtered particles 77−36345
UF_6, high temp. fissioning plasma core reactors, fluid mechanical confinement 80−63248
V, D bombarded surface, sputtered particles, ion fraction and energy anal. 77−36345

plasma-wall interactions continued
Xe, plasma, optical props., wall erosion products effects calcs. 78−47164
Y, D bombarded surface, ion fraction and energy anal. of sputtered particles 77−36345

plasma waves
see also magnetohydrodynamic waves; plasma oscillations; plasma shock waves
absolute dissipative drift-wave instabilities in Tokamaks 80−92296
absolute wave amplitude determ., Langmuir probe RF coupling 78−75425
absorption, causal correl. with helicon dispersion 79−32758
acoustic excitation in conducting gas, action at a distance 79−86571
acoustic interactions of ions in weakly ionised plasma, plasmoids 79−27776
acoustic stability of subsonic flow in MHD channel 78−9764
acoustic wave excitation by ion-acoustic waves 77−39415
acoustic wave generation by backward Alfven wave in plasma layer *(Russian)* 77−11328
acoustic wave interaction, diagnostics appl. 78−83541
acoustic wave propagation in inhomogeneous mag. fields 79−60121
acoustic waves dispersion in turbulent medium 80−10384
active molecular plasmas, electromagnetic fluctuations 78−63560
air, supersonic radiation waves, excitation by CO_2 laser 79−90433
Alfven, current driven, electron-ion collisions and full dispersion function, numerical anal. 80−64726
Alfven, long, circ. polarised, 2-component nonlinear Schrodinger eqn. calcs. 80−48883
Alfven and magnetoacoustic wave heating for fusion plasmas 80−24188
Alfven ion cyclotron waves, in finite length plasma, differential eqn. 78−91097
Alfven nonlinear gravit. drift waves and β limitations in Tokamaks 80−92369
Alfven pulse-excited instability in neutral sheet, mag. field lines reconnection dynamics *(Russian)* 80−1768
Alfven resonance effects on magnetosonic modes in large Tokamaks 79−73006
Alfven surface waves, propag. along cylindrical plasma columns 80−106913
Alfven wave, fast, inhomogeneous plasma, mode conversion and tunnelling 78−34300
Alfven wave accelerated particles, bremsstrahlung radiation losses rel. to self-similar soln. for distrib. function 80−56702
Alfven wave damping in nonuniform plasma, continuous spectrum phase mixing 78−47112
Alfven wave emission from Sun rel. to anomalous acceleration of minor ions in the solar wind 78−77453
Alfven wave excitation, by fast particles in a finite press. plasma of adiabatic traps 78−79424
Alfven wave excitation by fast ion beam in two-component Tokamak, Coulomb collisions 79−37509
Alfven wave heating, nonlinear processes 80−28718
Alfven wave heating in toroidal plasma 80−28740
Alfven wave instability excitation by trapped α-particles 77−65855
Alfven wave turbulence, interaction with whistler wave turbulence 80−64728
Alfven wave turbulence in interplanetary plasma, spatial fluctuation spectra 79−53693
Alfven wave turbulence in solar flares, rel. to protons stochastic accel. 80−21953
Alfven waves, appls. to plasma heating in linear and toroidal geometries 79−10676
Alfven waves, circular polarisation, propagation in mag. field, spiky soliton 80−28662
Alfven waves, circularly polarised, spiky soliton soln. to nonlinear evolution eqn. 80−38590
Alfven waves, exact, nonlinear, existence of solitons 80−24159
Alfven waves, in stochastic mag. field, Khasminskii's theorem 80−59198
Alfven waves, nonlinear self-precession and wavenumber shift 80−10389
Alfven waves, resonant absorption 80−92323
Alfven waves, sheared, current-carrying plasma, transient growth 79−41824
Alfven waves, soln. for MHD equations, properties *(Russian)* 80−106891
Alfven waves, torsional, axisymmetric, discrete/continuous spectra, appl. to waveguide 78−59587
Alfven waves collisionless damping in inhomogeneous plasma, initial value problem soln. 79−64864
Alfven waves generated by an inverted plasma energy distribution 78−85775
Alfven waves in streaming plasmas with anisotropic press., appl. to solar wind 77−49259
Alfven-ion-cyclotron instability for axially bounded plasma 80−1788
Alfvenic particle streaming in astrophysical plasmas 80−31206
amplification of ion cyclotron waves via high frequency electron plasma wave turbulence 80−92305
amplification of radiation near cyclotron frequency due to electron population inversion 80−92271
amplitude oscillations, of monochromatic wave in 1-dimens. plasma, simulation 78−87443
anisotropic collisionless plasma, wave propagation in presence of mag. field 79−41833
anisotropic plasma with two-dimens. inhomogeneity, absolute parametric instability *(Russian)* 77−62362
anomalous absorption of UHF radiation in electron cyclotron resonance range *(Russian)* 80−1807
anomalous cross-field transport, due to electrostatic fluctuations, theories 79−98870
anomalous transport effects in magnetically confined plasma columns 78−42725
anomalous transport from plasma waves 80−59182
antenna, oblate spheroidal, radiation and reception characts. for electron plasma waves 78−42765
antenna radiation patterns in laboratory plasma in whistler wave regime 77−27685
approximate theory for large-amplitude wave propag. 77−65854
asymmetric plasma resistivity, creation using waves 80−103171
atmospheric positive streamer corona, primary wave emission, secondary electron emission 80−44008
atomic emission in solar atmosphere, effect on spectral lines in radio emission 78−96466

plasma waves continued
auroral arc, intense vel. shear and assoc. electrostatic waves 77−70911
auroral kilometric radiation coherent generation by nonlinear beatings between electrostatic waves 80−26691
auroral plasma, stability, parallel and perpendicular propag. of electrostatic waves 79−35040
auroral plasma, turbulent acceleration by electrostatic waves *(Russian)* 80−53952
auroral radio echo, ion-acoustic, short term characts. 78−45080
axial eigenmodes for long-$\lambda_{\parallel}$ waves in plasmas bounded by sheaths 80−28655
axisymmetric toroidal Alfven wave resonances in ionosphere, effect of finite ionosphere conds. 79−75035
azimuthal angle of T-D mode induced scatt. from parametric ion-acoustic wave 78−75322
ballistic wave transformation kinetic effects *(Russian)* 80−38584
ballooning mode in Tokamak, shear effects *(Russian)* 79−98890
ballooning trapped-electron mode overlapping many rational surfaces 80−28618
barrier penetration, in inhomogeneous magnetised plasma 79−19030
beam instability, nonlinear theory in collisional plasma 79−82061
beam-plasma, explosive instabilities, wave-wave coupling 77−15210
beam-plasma, relativistic electron beam relax. Langmiur waves diffusion 77−11357
beam-plasma interaction, ion beam, stochastic heating by lower hybrid waves 79−98933
beam-plasma interaction, test particle diffusion and scatt. in turbulent collisionless plasma 78−38508
beam-plasma nonlinear interaction, electron collisions effect 78−14181
beam-plasma reactive instability, nonlinear evolution, wave coupling effects 79−41844
beam-plasma system, electron beam on surface, nonlinear interaction *(Russian)* 79−55519
beam-plasma system, electron waves, naturally excited and externally applied 79−90419
beam-plasma system, electrostatic wave energy, weakly explosive instability 78−18397
beam-plasma system, explosive instability due to helical electron beam 77−68807
beam-plasma system, finite amplitude wave instability, interaction with supercritical vel. beam *(Russian)* 77−31486
beam-plasma system, harmonic generation by three wave coupling 77−19726
beam-plasma system, nonlinear amplification of waves *(Russian)* 78−5886
beam-plasma system, nonlinear wave-particle interaction 78−34339
beam-plasma system, oscill. suppression by wave perturbation on beam distrib. function 77−80316
beam-plasma system, unstable, whistler wave propag. along reson. cone, diagnostics 77−31484
beam-plasma system, wave interaction, dispersion and higher order nonlinear effects 78−71502
beam-plasma turbulence, wave power spectral distrib. 78−14163
beat heating in plasmas using CO_2 lasers 80−43950
Bernstein dispersion relation for oblique propagation 80−75052
Bernstein large amplitude waves, enhanced damping 77−35338
Bernstein mode radiation, oblique mag. field *(French)* 78−91086
Bernstein modes, two dimens. electrostatic particle simulation 78−71531
Bernstein modes in electron cyclotron heating of Tokamak, Vlasov dispersion eqn. 80−33809
Bernstein modes radiation coupling in ring plasma 77−89253
Bernstein waves, convective cell excitation *(Russian)* 80−53961
Bernstein waves, parametric decay, whistler mode radiation generation 77−76095
Bernstein waves, parametric instabilities, mag. shear effect 79−19019
Bernstein waves, propagation in inhomogeneous plasma, dispersion rel., quasi-linear equations, diffusion coeff. determ. 80−75044
Bernstein waves in solar corona, coherent nonlinear interaction rel. to type IV continuum bursts 77−53529
BGK type waves, instability condition for unmagnetised and magnetised plasmas 77−31447
boson soliton collisions in plasma, nonlinear scatt. 79−27768
bounded medium, nonlinear parametric reson., limit cycle solns. 80−19071
breakdown wave propagation in ionised gas in nanosecond discharges 80−87890
Brillouin and Raman scattering of an extraordinary mode in a magnetized plasma 80−92269
Buneman-Farley instability, nonlinear decay interactions 80−38616
caviton, dissipative three-dimens. Langmuir soliton, formation *(Russian)* 80−83943
caviton dynamics at crit. density 80−106909
caviton generation in plasma reson. region *(Russian)* 80−53926
cavitons in laser irradiated fusion plasmas, EM wave propag., supersonic density humps 80−24178
Cerenkov interaction between obliquely propagating whistler wave and electron beam, computer simulation 80−43937
channelling instability stabilisation, by mag. HF oscills. and magnetoacoustic waves *(Russian)* 77−47177
charged particle confinement, by transverse EM waves, theory 77−55145
Cherenkov radiation, prod. by unstable plasma wave coupling in ionosphere 79−40003
circular plate electron plasma wave antennas, exact directional patterns 78−30449
circularly polarised, in a weak stochastic mag. field, damping coeff. 78−34291
cnoidal waves, nonlinear, using perturbation theory 79−10662
coherence wave spectra, freq. averaging effects, digital simulation 77−35390
coherent curvature radiation driven by plasma waves in quasars 77−60848
coherent nonlinear wave interaction, book 78−30444
coherent three-wave interaction, phase integral 79−60127
coherent wave interaction with MHD turbulence *(Russian)* 78−1833
coherent wave particle interaction in Q-machine plasma, electrostatic analyser diagnostics 80−59226
coherent waves in nonlinear medium, nonresonant interaction, eqns. system development and examples *(Czech)* 80−24149
coherent waves interaction in stochastic mag. field 78−42752
cold, electrostatic, ion-cyclotron waves and ion-ion hybrid resonances 79−60136
plasma waves continued
cold electron plasma waves, finite extent, reson. decay, fusion appls. 78−38485
cold electron plasma waves, parametric decay, convective loss effect 80−38634
cold plasma dispersion surfaces 79−60120
collective behaviour, in laser plasma expts. 77−43005
collective ion acceleration by cyclotron of space charge waves in relativistic electron beam 77−24204
collective motion of electrons deduced from shift of lower oblique reson. freq. 79−55499
collisional drift wave, nonlinear unstable, asymptotic expansion 77−35337
collisional drift wave obs. in DC octupole in toroidal geometry 78−51293
collisional drift waves, nonlinear heat and particle transport 77−80278
collisional ion cyclotron waves, in auroral ionosphere 77−29574
collisionless drift modes, graphical method for finding complex roots of nonlinear eqn. 80−33762
collisionless drift modes in sheared slab geometry, stability props. 80−1786
collisionless drift wave eigenmodes, in sheared mag. field, WKBJ method calcs. 78−83552
collisionless drift wave in Vlasov plasma, nonlocal anal. 80−43910
collisionless drift waves in Tokamaks analytic eigenvalue eqns. 80−6246
collisionless electrostatic drift waves, linear theory, space plasma appls. 79−1305
collisionless plasma, polarisation by single-mode pot. drift wave 80−106920
collisionless plasma current layer, tearing instability due to EM wave *(Russian)* 78−71465
collisionless relaxation of a nonequilibrium distribution of waves and particles 79−19028
comet tails, type 1, helical waves 77−78716
compressional Alfven wave heating, plasma source 79−27802
compressional waves, fast, near ion cyclotron freq., collisional effects, damping 79−50854
confined waves with ergodic ray trajectories, instability condition 80−14894
convective amplification of drift waves and thermal fluctuation levels in a stable plasma 80−83932
convective amplification of universal drift modes 80−59208
convective cell nonlinear excitation and anomalous diffusion, in inhomogeneous plasma 80−79468
convective cells, nonlinear excitation by interchange modes and spectrum cascade processes 80−69997
convective cells and anomalous plasma diffusion *(Russian)* 78−71439
convective cells form. by modulational instability 79−98903
convective instability and nonaxisymmetric waves, in weakly ionised plasma in strong mag. field 79−90397
converging ion acoustic soliton excitation in double plasma type device 80−106907
converging nonlinear resonance cone trajectories 80−92299
Coriolis force influence on LF waves in rotating plasmas 78−75309
correlation function, long time asymptotic behaviour, influence of waves on relax. processes *(Chinese)* 80−59195
coupled Langmuir and ion-acoustic solitary wave, unstable to perturbation 79−19013
coupled Langmuir and ion-acoustic solitary waves, theory of two-dimensional stability 78−38476
coupled Langmuir and ion-acoustic solitons, instability 78−75294
coupled localized electron-plasma waves and oscillatory ion-acoustic perturbations 78−67349
coupled mode equations, linearised, space time solns. 80−87884
coupled three wave system, instability saturation, bifurcations and strange attractor 80−59233
coupled waves in stratified Chew-Goldberger-Low plasma 80−87875
coupling coefficients for circ. polarised wave in cold plasma 78−18400
coupling of waves in cold nonuniform magnetoplasma 80−43918
coupling to the fast wave at lower hybrid frequencies for plasma heating 80−75069
criterion for absolute instability of a wave in a nonuniform medium 80−106903
cross-field electron heat transport due to high frequency electrostatic waves 80−53932
Culham Levitron, drift island diffusion 80−59267
Culham Levitron, electrostatic fluctuations 80−79482
current carrying magnetised plasma, parametric resonance 79−68918
current carrying plasma, trapping and build-up of HF turbulent noise *(Russian)* 77−3957
current driven collisional drift and Alfven instabilities in sheared mag. field 80−1795
current driven dissipative drift wave turbulence in Tokamak plasma, finite-β and quasilinear effects 79−98913
current driven drift modes in plasma slab with sheared mag. field 79−77366
current driven instabilities, anomalous effects 78−91096
current generation by electrostatic travelling waves in collisionless magnetised plasma 80−53976
current-driven collisional drift and Alfven instabilities 79−46445
current-driven kink-like instability in collisional plasma 77−80284
cyclotron harmonic absorption via the Green's function for the mode conversion-tunneling equation 78−75296
cyclotron harmonic wave, props. prediction from perpendicular dispersion relation 80−1772
cyclotron harmonic wave propag. by antenna 79−4152
cyclotron harmonic waves and resonance cone, around antenna in magnetoplasma 78−91098
cyclotron harmonic waves props. from perpendicular dispersion relation 80−38612
cyclotron radiation emitted perpendicularly to mag. field, stability 77−72439
cyclotron wave excitation in spiral electron beam interaction 79−64843
cyclotron wave instability in spiral electron beam-plasma system 79−14536
cyclotron waves, diamagnetism *(Russian)* 79−98901
cyclotron waves, self-trapping instability 77−76067
cyclotron waves in bounded magnetoplasma 80−48869
cyclotron-harmonic wave propag. in spiraling electron beam 77−19685
cylindrical soliton-like waves, slow and fast, obs. 80−28654

plasma waves continued
damping, plasma waves generated by EM wave linear conversion 77−11337
decay instabilities in inhomogeneous plasma, trapped wave effects *(Russian)* 79−98893
decay instability of laser radiation in a magnetoplasma 80−1781
decay of a lower-hybrid wave to two lower-hybrid waves 80−87883
decaying plasma, nonequilib. props. during afterglow modulation by acoustic waves 80−103144
deexcitation wave emission and thermal fluctuations of inhomogeneous plasma *(Russian)* 80−106892
deflagration wave formed by ion waves, energy from fusion reaction effects 80−79478
deflagration wave in slab target, form. by ion beam 80−28628
deflagration wave in spherical target, form. by ion beam 80−28629
delay line simulation, wave propag. in dispersive and attenuating media 80−82606
density fluctuation in collisional plasma 80−75053
destabilization of drift-universal eigenmodes by toroidal effects 80−103148
detection in turbulent plasma by satellites of forbidden He transitions *(Russian)* 78−18391
diamagnetic frequency profile effects on toroidal drift waves 79−41821
dielectric response and energy loss in intermediate quantum plasma 80−38541
difference frequency wave generation in magnetoplasma, by coaxial Gaussian beams cross focusing 79−32779
diffraction, at a metallic grid *(Russian)* 79−37471
diffuse boundary plasma, ordinary wave excitation under anomalous skin effect conditions 77−15204
diffusion across mag. field, mode transition process in collisional drift waves 77−80275
diffusion of multi-ion species plasma due to drift wave fluctuations 77−62341
digital spectral techniques in plasma fluctuation diagnostics 80−49003
dipole excitation of ion waves 77−3950
direct Langmuir collapse, virial theory 78−79430
discharge positive column, instability, of ionic component, amplification factor, dispersion eqn. 78−14232
discontinuous wave pattern observed with ionisation waves, cusp catastrophe model 79−60126
discrete unstable modes, transition to turbulence, theory and expt. 80−59240
dispersion equations in moving media, relativistic electrodynamics 80−57089
dispersion function for anisotropic longitudinal waves 80−14891
dispersion relation determ. by microwave scatt. 79−27829
dispersion relation for charge and current compensated relativistic electron beam-plasma system 78−83580
dispersion relation for nonuniform magnetised plasmas 77−15183
dispersion relations, Dupree's resonance function 79−60124
dispersive wave trains, near-linear, two-time procedure for higher order modulation 78−65788
dispersive waves, nonlinear mixing 77−22428
disruptions, internal, precursors of, tearing mode 80−28652
dissipative balloon non-threshold modes *(Russian)* 80−70000
dissipative drift-wave instabilities, mag. shear effects, theory 78−75297
dissipative trapped electron instability, spectral formulation 78−91095
double layers modelled by numerical integration of Vlasov-Poisson system 80−92290
double resonance parametric excitation due to zero and finite wavenumber pumps 77−31443
double resonance parametric process, exptl. study 77−62352
draft waves driven by temperature gradients, ballooning limit 80−106917
drift, collisional, nonlinear transport 77−72417
drift, collisional instability, mag. shear stabilisation 78−18412
drift, current driven, electron-ion collisions and full dispersion function, numerical anal. 80−64726
drift, dissipation by ionised relax. in low-temp. plasma *(Russian)* 78−1816
drift Alfven waves, convective cells form. by modulational instability 79−77364
drift Alfven waves in Tokamaks, instability 78−79431
drift and tearing eigenmodes, variational theory 78−71468
drift and trapped-electron modes, 2D spatial struct. 78−91094
drift cone mode, stabilisation at finite beta by warm plasma 77−7533
drift cyclotron instability, nonlinear dynamics 78−30433
drift cyclotron loss cone mode, warm plasma effects 79−68904
drift dissipative, LF oscills., anomalous diffusion and equilib. 80−33769
drift in Hall current plasma accelerator, dispersion relations 77−19705
drift instabilities of magnetised plasma in RF elec. field 77−24081
drift instability, collisionless, nonlinear saturation 77−68785
drift instability, electron-ion heat exchange and electron thermal conduct. effects 77−984
drift instability, electrostatic current-driven, scaling law for high density and high current Tokamaks 80−38691
drift mode in Tokamak, wave anal. 77−89255
drift mode instability, plasma-neutral gas interaction effects 78−18403
drift solitons, LF, 2D stability 77−84431
drift turbulence theory in mag. field with shear, nonlinear wave packet formation *(Russian)* 79−77376
drift wave, collisional, nonlinear evolution, successive bifurcations to chaotic state 80−33773
drift wave, HF, current-driven inhomogeneous plasma instability 80−59204
drift wave, low freq., pseudoclassical diffusion in Tokamak *(Chinese)* 80−69990
drift wave, nonlinear theory for collisionless nonuniform plasma 77−15177
drift wave collisionless turbulence, renormalised dielectric function 78−51292
drift wave eigenmodes, effect of finite ion Larmor radius *(Chinese)* 80−103133
drift wave eigenmodes, in torus, nonlocalisation by mag. shear 78−34302
drift wave eigenvalues, variational calc. 79−68920
drift wave equations, numerical solution by invariant bedding 80−10374
drift wave fluctuations, induced electron transport 78−94894
drift wave fluctuations, multi-ion species plasma diffusion 77−68752
drift wave fluctuations, spectral distrib. 77−7534
drift wave freq. profiles, Doppler model 78−71471
plasma waves continued
drift wave in sheared mag. field, stable eigenvalues 78−38484
drift wave instability, current-driven 80−1770
drift wave instability, due to nonuniform density gradient in sheared mag. field 79−23415
drift wave instability, nonlocal collisionless, toroidal curvature effects 80−38588
drift wave instability, nonuniform density grad. in sheared mag. field 79−7461
drift wave linear dispersion eqn. including temp. fluctuation 80−10376
drift wave particle flux, wave amplitude rel. to plasma density 79−4137
drift wave spectra modulation due to HF fields 80−38624
drift wave stabilisation by HF applied electric field 77−19701
drift wave stabilisation in collisionless plasma, by lower-hybrid waves 78−51296
drift wave stability, toroidal mode coupling effects 78−83547
drift wave stability and, drift-Alfven waves 79−37488
drift wave stability and transport theory in fusion systems 80−28653
drift wave stability in axisymmetric toroidal plasma 77−65858
drift wave theory, particle simulation, anomalous transport 77−72428
drift wave theory, plasma turbulence, Kolmogorov spectrum analogy 79−73011
drift wave turbulence, diffusion broken ambipolarity 79−64828
drift wave turbulence, dissipative, current driven, in Tokamak plasma 80−38587
drift wave turbulence, exact Gaussian soln. 80−92325
drift wave turbulence and convective cell formation 80−43925
drift wave turbulence in FM-1 spherator, microwave scatt. 77−65912
drift waves, collisional, shear stabilization 79−86577
drift waves, collisionless, in Vlasov plasma, WKB type eigenmode anal. 79−4139
drift waves, convective cells, nonlinear excitation mechanism with shear *(Russian)* 80−38585
drift waves, eigenmodes with arbitrary radial wavelengths, stability 80−64710
drift waves, finite amplitude, propag. in collisional plasma, shock wave profile 77−27669
drift waves, finite-β-modified, in sheared mag. field 78−91092
drift waves, high freq., with wavelengths below ion gyroradius, in ionosphere equatorial spread-F 78−88973
drift waves, initial value problem by non-Hermitian radial mode eqns. 77−89244
drift waves, instability in AC elec. field, wave growth rate and dispersion relation 80−48886
drift waves, LF, electron beams and their trajectories 77−65865
drift waves, magnitude of radial electric field determ. *(Russian)* 80−103175
drift waves, microinstabilities in plasma slab 78−14156
drift waves, multispecies plasma, nonlinear behaviour, turbulence, diffusion 78−59588
drift waves, nonlinear behaviour and turbulence spectra 80−19573
drift waves, nonlinear saturation 77−68786
drift waves, nonlinear stabilisation, weak turbulence theory 79−98908
drift waves, parametric excitation, with pump near ion cyclotron freq. in two-ion-species plasma 78−91093
drift waves, scatt. by parametric interaction 78−79428
drift waves, shear damping in large aspect ratio Tokamak 80−6242
drift waves, short-circuit effects in afterglow 77−35431
drift waves, single mode, low freq., with captured electrons, spatial struct. *(Russian)* 80−10372
drift waves, solitary, excitation and propag. in ionosphere *(Russian)* 77−70915
drift waves, stabilisation by lower hybrid waves of finite wavenumber 80−53968
drift waves, stabilisation by mag. shear 77−72427
drift waves, strongly dispersive, modulation instability, convective cell formation 80−38635
drift waves, wave action 80−43908
drift waves and steepened structs. in equatorial spread-F 79−2431
drift waves in sheared mag. field, real-space quasilinear theory 77−76079
drift waves in sheared mag. field, real-space quasilinear theory 77−84416
drift waves in sheared mag. field, variational method calcs. 80−106910
drift waves in turbulent plasma 78−1830
drift waves in turbulent plasma with magnetic shear 78−75330
drift waves propag. and convective growth in Tokamaks 79−60137
drift-Alfven mode stability, local theory 79−19012
drift-Alfven wave coupling, destabilisation 77−19694
drift-Alfven waves in a sheared magnetic field, numerical anal. 79−94788
drift-dissipative waves, weakly ionised plasma, column steady state 80−38613
drift-wave eigenmodes, current-driven, stability criteria 79−32769
drift-wave turbulence, possible inverse cascade behaviour 79−32774
drift-wave turbulence, role of clumps 78−67352
drift-wave turbulence effect on mag. struct. and electron transport in Tokamak 78−22501
drift-waves, collisionless, stable eigenmodes 78−34308
drifting plasma, radiation potential of immersed point antenna 80−14906
driftwaves, self focusing and mag. field stabilisation *(Russian)* 77−47180
dynamical polarisability at long wavelengths, strongly coupled one-component plasma 79−82059
E×B effects on nonlinear mode-converted lower-hybrid waves, derivation of nonlinear differential eqn. 80−1785
EBT heating, electron-cyclotron absorption and microwave propagation 80−64749
echo, linear, in plasma with strongly inhomogeneous magnetic field 80−106919
echo, nonlinear, time-depend., in strong HF elec. field *(Russian)* 78−1818
echo of longitudinal waves in plasma layer under mirror reflection conditions *(Russian)* 77−11330
echo surface wave propagation in confined plasma *(Russian)* 77−7520
eigenmodes, universal, in collisionless plasma slab 80−38581
eikonal expansion of the Vlasov-Maxwell equations valid near cyclotron resonance 80−92300
election parallel thermal conductivity, reduction using waves 79−10637

plasma waves continued
electric field meas., forbidden transition satellites in turbulent plasma 80−38714
electric waves, linearly polarised, parametric instabilities rel. to Crab nebula 78−45220
electrical conductivity, effect of monochromatic finite amplitude ion acoustic wave 78−91070
electrical double layers, strong, exptl. obs. 78−30435
electroacoustic and cyclotron harmonic waves, effect on RF probe impedance characts. 78−42818
electromagnetic ion cyclotron instability, particle anal. 79−94781
electron, excitation by three-ring antenna, radiation characts. 78−91107
electron, relativistic effects 78−34310
electron, stability anal. 80−6240
electron, third-order Landau mode obs. 77−15188
electron acoustic solitary wave propag. in magnetoplasma 80−75051
electron and ion waves, excitation by two or more pump waves 78−57381
electron and ion waves in solar wind, elec. field meas. by Helios I 77−37492
electron beam, kinetic, quasilinear relax., self-similar solns. 80−64702
electron beam, wave amplification by spatially periodic mag. field, space charge waves 77−19158
electron beam controlled discharge, cathode density waves 80−38798
electron beam delay, strong turbulence, ballistic modes and Langmuir solitons *(Russian)* 77−76111
electron beam excited plasma, modulation instability of Langmuir waves *(Russian)* 77−35361
electron beam interaction, entropy theorem and plasma waves spontaneous emission 78−69677
electron beam interaction, numerical simulation 78−91120
electron beam stimulated wave instability, nonlinear dynamics *(Russian)* 77−19720
electron beam waves+plasma waves, nonlinear interactions 80−38670
electron beam-cold plasma interaction, nonlinear wave growth and instability, simulation 77−89300
electron beam-magnetoplasma, radiation at or near electron plasma frequency, transverse modes 80−106942
electron beam-plasma interaction, anomalous wave amplification *(Russian)* 78−87463
electron beam-plasma interaction, obs. of decay instability of beam plasma wave 79−27793
electron beam-plasma system, electrostatic waves, nonlinear Landau damping 77−76055
electron beam-plasma system, explosive instability 80−1813
electron beam-plasma system, Simon short-circuit effect, freq. shift 80−96366
electron beams, modulated, non-linear oscillation theory *(Russian)* 80−106898
electron Bernstein modes, nonlinear scatt. of upper hybrid laser radiation 80−64720
electron Bernstein waves, 3D propag. 79−55496
electron Bernstein waves, phase, group and ray velocities 79−27769
electron classical motion in wave of slowly varying amplitude 80−28658
electron collision effect on wave-breaking in cold plasma 80−96353
electron concentration balance in wave field, profile stabilisation *(Russian)* 78−22497
electron current driven ion wave instability, excitation, electrode type effects 80−38603
electron cyclotron, slope reversal of a monotonically decreasing electron tail in a strong magnetic field 78−67347
electron cyclotron absorption of the ordinary wave at normal incidence 80−19570
electron cyclotron emission from Tokamak plasmas with mildly superthermal electrons 80−92270
electron cyclotron harmonic wave instability during temp anisotropy relaxation 79−53671
electron cyclotron harmonic waves excitation, lab. expt., rel. to topside ionosphere RF sounder expt. 78−93042
electron cyclotron harmonic waves excited by helical electron beam, time depend. 77−31455
electron cyclotron harmonic waves excited in helical electron beam-plasma system 78−1848
electron cyclotron heating and wave trajectory in toroidal plasmas 80−28726
electron cyclotron heating in high density toroidal plasmas 79−37517
electron cyclotron heating in toroidal plasmas, wave trajectories 80−38678
electron cyclotron plasma heating, abnormal resist. *(Russian)* 77−7567
electron cyclotron resonance, power transfer efficiency from microwave field 78−9789
electron cyclotron wave excitation of parametric instability in plasma column 77−65862
electron diamagnetic drift, RF flux control of toroidal plasma 80−38582
electron drift velocities in positive columns, wave determination 77−76052
electron drift wave mode of Hall accelerator with extended accel. zone 78−79480
electron electrostatic wave, EM pump wave parametric decay, simulation 77−19683
electron fluid long wavelength ballooning modes, destabilization by finite trapped beta 79−68914
electron free streaming waves expansion in low press. discharges 80−79595
electron gas, screening of ionic motions by electronic background 80−64678
electron heating by Langmuir waves, with induced l-s scatt. *(Russian)* 80−10403
electron heating due to MHD shock wave, electron temp. and density 79−14588
electron Landau damping of lower hybrid waves 78−42741
electron long-wavelength wave dispersion evolution meas., sampling technique 80−6283
electron nonlinear waves in strongly magnetised plasma 80−79472
electron plasma, classical, dispersion relation, RPA method 79−55481
electron plasma, large-amplitude electrostatic wave, non-Maxwellian distrib. obs. 78−75299
electron plasma and ion-acoustic waves nonlinear coupling 79−4136
electron plasma wave, computer simulation of modulational instability 79−32766
electron plasma wave, decay to ion cyclotron wave 78−94910

plasma waves continued
electron plasma wave, finite amplitude, nonlinear behaviour, sideband instability, electron distrib. function 78−38480
electron plasma wave, guided propag. in plasma slab, dissipation effects 79−46447
electron plasma wave, reson. excitation with laser light absorption 77−24092
electron plasma wave coupling with LF wave 77−55134
electron plasma wave excitation in mag. field, transverse flux constraint 77−68771
electron plasma waves, excitation and absorpt. by fast electrons cloud 77−996
electron plasma waves, in water-bag and 2-Maxwellian plasmas 80−38601
electron plasma waves, ionospheric, excitation by strong microwaves from solar power satellite, theoretical anal. *(Japanese)* 80−94634
electron plasma waves, nonlinear evolution equation including collision effects 79−82056
electron plasma waves, refl. from flat plane boundary 77−58852
electron plasma waves, sum-freq. excitation, energy transfer efficiency 78−38496
electron plasma waves, toroidal Trivelpiece-Gould modes 80−33770
electron plasma waves, unidirectional, current generation 79−82058
electron plasma waves in a two-temperature plasma 80−92285
electron standing wave, stationary density variation 77−76065
electron trapping by plasma waves *(Russian)* 78−22474
electron wave, guided, on planar plasma slab, propag. and attenuation characts., dissipative processes 80−38608
electron wave, nondispersive, in Maxwellian plasma 79−77359
electron wave absorpt. in magnetised inhomogeneous plasma 77−15192
electron wave coupling, parametric instability saturation *(Korean)* 79−7455
electron wave coupling and propag. using phased waveguide arrays, heating appl. 78−5863
electron wave coupling between two-temp. mode and Landau mode 79−64844
electron wave dispersion relation in two-temperature plasma 79−86580
electron wave propag., plasma boundary layer effect 79−19016
electron wave propagation in inhomogeneous plasma 78−75318
electron wave suppression due to electron beam density modulation 77−15209
electron wave suppression in relation to deformation of electron beam distrib. function 79−1324
electron waves, beat radiation 80−43314
electron waves, broad-band, nonlinear Landau damping 77−89246
electron waves, excitation long low waveguiding circuit, expts. 80−1775
electron waves, higher harmonics 77−65848
electron waves, modulated, dispersive, evolution in low-density Q-machine plasma 79−86575
electron waves beat-driven optical free electron laser 80−43315
electron waves in magnetoplasma, angular dependence in Landau mode 78−22499
electron waves nonlinear propag., convective instability 78−1825
electron-acoustic mode, two-temp. electrons 78−14141
electron-cyclotron wave heating in Tokamak, cyclotronic attenuation energy loss calc. *(Russian)* 77−47225
electron-cyclotron-resonance-heated Tokamak power reactor, characts. 79−31188
electron-positron plasma, produced by relativistic electron beam, waves, microinstabilities, collective positron accel. 79−19053
electrosound waves in strong HF field, plasma with negative dielec. permeability *(Russian)* 77−31466
electrostatic, dispersion relation, quantum field theoretical approach 77−80292
electrostatic, finite amplitude, diffusion 77−68753
electrostatic, launched by grid, nonlinear steady state structs. 78−42766
electrostatic, magnetised plasma charged particle stochastic accel. 80−59230
electrostatic, non-stochastic heating 78−47136
electrostatic, nonlinear 4-wave interaction, positive (negative) energy waves, explosive instability 80−48884
electrostatic, nonlinear dispersion relation and fluctuation spectrum 77−65872
electrostatic, nonlinear Landau damping in beam-plasma system 77−15186
electrostatic, nonlinear Landau damping in electron beam-plasma system *(Japanese)* 77−42972
electrostatic, perpendicularly propag., vel.-space diffusion 80−59228
electrostatic, propag. in anisotropic plasma, HF elec. field effects, hydrodynamic eqns. *(Russian)* 78−59565
electrostatic, propag. near ion cyclotron harmonics, stochastic accel. 77−39421
electrostatic, slow,, Landau damping at low power levels 78−9774
electrostatic, stochastic heating of plasmas in inhomogeneous magnetic fields 80−59231
electrostatic, stochastic ion motion, mag. field config. depend. 80−59229
electrostatic, thermal and field-aligned-drift effects near lower oblique reson. 79−19024
electrostatic, three-wave interaction in oscillating elec. field 80−69995
electrostatic, turbulent perturbation of coherent wave-particle reson. 78−26274
electrostatic and magnetic waves in distant magnetotail, Imp 8 obs. 77−29592
electrostatic Bernstein mode waves, RF excitation, ion sheath effect 77−7518
electrostatic cyclotron harmonic instability, in magnetosphere, theory and expt. 79−29945
electrostatic daughter wave nonlinear decay, causing parametric instability saturation 80−53945
electrostatic drift instability of Tokamak plasmas 80−96358
electrostatic drift mode coupling in torus 80−59213
electrostatic drift waves, generalised non-local dispersion equation 79−90404
electrostatic drift-type modes, microinstability theory in Tokamaks 78−75292
electrostatic electron cyclotron waves from point source, angular potential patterns 79−37493
electrostatic electron wave, higher order Landau modes 77−51172
electrostatic electron wave, large amplitude, freq. shifts 77−3935
electrostatic electron wave influence on radiation incoherent scatt. cross-section 78−34311

plasma waves continued
electrostatic emissions between electron gyroharmonics in outer magnetosphere 79−16763
electrostatic envelope solitons, expt. 77−39420
electrostatic H^+ cyclotron waves near one Earth radius altitude in polar magnetosphere 78−45154
electrostatic instability in counter-streaming plasma 78−59578
electrostatic ion cyclotron electron drift instability anal. using linear Vlasov dispersion reln. 80−1780
electrostatic ion cyclotron modes, finite amplitude, in collisionless magnetoplasma 79−64858
electrostatic ion cyclotron nonlinear wave, in RF plugged plasma 77−72442
electrostatic ion cyclotron solitary waves 77−80291
electrostatic ion cyclotron wave, nonlinear propag. and modulational instability 78−1823
electrostatic ion cyclotron wave excitation by ion beam 77−76115
electrostatic ion cyclotron waves, modulational instability, auroral plasma 79−62643
electrostatic ion cyclotron waves, nonlinear steepening 80−31175
electrostatic ion cyclotron waves, optical detect. in auroral plasma 77−73900
electrostatic ion cyclotron waves, parametric excitation in two-ion-species plasma 77−76068
electrostatic ion cyclotron waves, scatt. of ordinary EM waves in ionosphere 79−70916
electrostatic ion cyclotron waves and ion acoustic waves, parametric instabilities 80−38591
electrostatic ion waves, collisional damping 77−11335
electrostatic ion waves, oblique propag. near ion cyclotron freq. 77−35345
electrostatic ion-cyclotron wave spectrum, in neutral beam injection-stabilised mirror device 78−9775
electrostatic Langmuir pump wave, parametric instabilities 77−19700
electrostatic large amplitude standing wave, particle stochastic motion 79−77406
electrostatic lower hybrid wave, nonlinear decay to whistler and Alfven wave pair 78−26275
electrostatic modes causing ion heating in slide-away regime 77−68795
electrostatic obliquely propag. wave, particle stochastic acceleration 79−23416
electrostatic pulse generation by two electromagnetic pulses 80−92295
electrostatic shock-like wave, hemispherical 79−41828
electrostatic simulation code, one-dimensional, Landau damping, particle retardation problems 77−58888
electrostatic single wave, particle trapping, detrapping and acceleration, magnetoplasma 77−68738
electrostatic solitary drift waves, modulational instability 78−91105
electrostatic stimulated backscatt. of EM waves, magnetised plasma 79−90413
electrostatic surface waves, HF, warm gaseous magnetoplasma half-space 77−76053
electrostatic Trivelpiece-Gould modes in a torus 80−38609
electrostatic two-dimens. model for bounded plasma slab 79−55542
electrostatic Vlasov turbulence, iterative soln. 80−10375
electrostatic wave, electron Landau damping and electron collisions, Fokker-Planck model 78−47111
electrostatic wave, HF, causing cross-field electron heat transport 80−28619
electrostatic wave, stochastic acceleration near ion cyclotron freq. 77−65868
electrostatic wave coupled multicomponent plasma, formation, evolution diffusion 77−84460
electrostatic wave decay near lower hybrid freq. 77−977
electrostatic wave excitation by RF field 77−19732
electrostatic wave excited by current pulse in warm magnetoplasma, theory 80−77240
electrostatic wave heating of charged particles, wave perpendicular to mag. field 78−63565
electrostatic wave near ion cyclotron harmonic, stochastic ion accel. 77−42980
electrostatic wave oblique propag., counter-streaming instabilities 78−59577
electrostatic wave packet, nonlinear evolution in collisionless plasma, probe obs. 77−62358
electrostatic wave propag., anomalous electron pseudo-classical transport 80−24137
electrostatic wave propag. in toroidal geometry, ray tracing 78−9782
electrostatic wave propag. near lower hybrid resonance at ionospheric heights 77−58856
electrostatic wave propagation near lower hybrid freq. in toroidal plasma NOVA-I *(Japanese)* 79−82055
electrostatic wave propagation to lower hybrid reson. in mag. field with shear 77−80285
electrostatic wave radiation near lower hybrid freq. 77−84430
electrostatic wave reflection from sharp density gradient 78−42747
electrostatic wave turbulence along auroral field lines, obs. 77−45228
electrostatic wave turbulence in magnetosheath, meas. 79−66881
electrostatic waves, distrib., energy absorpt. *(Russian)* 78−71478
electrostatic waves, in magnetosphere, GEOS-1 obs., rel. to plasma parameters 79−29944
electrostatic waves, mode conversion and collisionless absorption of EM wave 77−80308
electrostatic waves, nonlinear motion, particle trapping 80−64713
electrostatic waves, obs. in unstable polar cap ionosphere 79−29927
electrostatic waves, perpendicular propag., stochastic ion heating 77−80322
electrostatic waves, propag. across mag. field, ion heating 77−65894
electrostatic waves, turbulent acceleration in Earth's auroral plasma *(Russian)* 80−53952
electrostatic waves generated by ion-beams, shock-like waves 78−59621
electrostatic waves in drifting ionospheric simulation 80−53965
electrostatic waves in Jupiter magnetosphere, obs. 80−72865
electrostatic waves in magnetosphere, rel. to inverse loss cone electrons temp. anisotropy relaxation *(Russian)* 80−109314
electrostatic waves in space plasmas, new detect. technique 77−9549
electrostatic waves near upper hybrid reson. freq. in magnetosphere 79−84590
electrothermal waves, in nonequilibrium MHD plasma, dispersion relation 79−98904
plasma waves continued
elliptically polarised waves interaction, parametrically excited precession freq. 78−18402
ELMO Bumpy Taurus, trapped-particle instabilities 79−31184
EM, laser beam nonlinear interaction in electron stream diagnostics 77−15248
EM, nonlinear ordinary to extraordinary conversion 79−55501
EM and electrostatic modes of microinstabilities in moderately inhomogeneous plasma 77−87223
EM cyclotron wave, critical freq., effective anisotropy 78−34294
EM drift wave fluctuations, anomalous ion loss 79−1312
EM drift wave fluctuations, anomalous transport processes 78−26251
EM drift wave turbulence and convective cell form. 80−24168
EM drift waves, eigenvalues, coupled second-order differential eqns., numerical soln. method 80−94976
EM drift waves, nonlinear instability threshold amplitude 78−34305
EM excitation of plasma wave by two coaxial Gaussian beams 79−55511
EM instabilities in beam plasma, nonlinear dispersion relation 79−41813
EM ion waves in cold relativistic plasmas, astrophys. appl. 80−21910
EM ion-cyclotron wave growth rates, variation with proton vel. distrib. profiles 77−31450
EM pulse, conversion to Langmuir wave in plasma 80−92308
EM radiation from nonlinear coupling between longitudinal excitation 77−11334
EM soliton propagation in nonequilibrium dispersive media *(Russian)* 80−106933
EM standing wave and two-wave reson. interaction, precessional rot. and nonlinear effects 80−48892
EM surface oscillation excitation in semirestricted plasma by relativistic electron beams *(Russian)* 79−14561
EM surface wave diffr. by inhomogeneity in plasma-dielectric boundary 77−24075
EM wave, penetration into magnetoactive wave 79−23420
EM wave absolute two plasmon parametric decay 77−76091
EM wave dissipation and superstrong turbulence in inhomogeneous plasma *(Russian)* 80−83919
EM wave distribution in inhomogeneous plasma containing random irregularities 80−38633
EM wave emission and induced absorption by thermal level ion acoustic fluctuations 79−37462
EM wave excitation by tubular electron beam in plasma-filled waveguide *(Russian)* 79−37507
EM wave in nonuniform magnetostatic field, pondermotive effect, Hamiltonian theory 80−19575
EM wave parametric decay to electrostaatic wave, mode coupling of modulational instabilities 80−24161
EM wave penetration into half-space collisional plasma 80−106928
EM wave radiation pressure induced nonlinear perturbations of magnetised plasma 79−86570
EM wave resonance absorpt., mode conversion, relativistic effects 77−11391
EM wave resonance tuning of magnetoactive plasma *(Russian)* 80−83914
EM waves, electron-cyclotron reson., propag. at angle to non-uniform mag. field *(Russian)* 78−71487
EM waves, extraordinary parametric decay into two upper hybrid plasmons 80−43904
EM waves, large-scale localised distrib., nonlinear dynamics 79−73008
EM waves, nonlinear generation in electron-positron plasma *(Russian)* 80−106973
EM waves, parametric decay near upper hybrid freq. 78−59590
EM waves excited in rippled plasma resonator by relativistic electron beam 80−48902
EM waves in magneto-active plasma, group velocity direction 80−59201
EM waves in plane inhomogeneous plasma in presence of mag. field shear, appl. to plasma diagnostics *(Russian)* 80−103140
EM waves in space plasmas, new detect. technique 77−9549
EM waves propagating along mag. field in strongly anisotropic relativistic plasma, dispersion props. 80−67542
emission, absorption and transfer of waves in astrophysical diffuse magnetised plasmas, book 80−105446
energetic particle trapping by Alfven wave instabilities 80−31205
energy absorption model, wave amplitudes and particle distribs. for laser-prod. plasma 77−47235
energy determ. of EM or electrostatic waves 79−94786
energy transfer direction, power solns. of kinetic eqns. for waves and particles 77−15164
enhanced fluctuations in semi-infinite plasma, HF elec. field 78−91069
enhanced losses due to collisionless drift waves, dynamic stabilisation effects 80−14888
envelope soliton of random phase waves 78−26282
equilibrium of electron bunches exciting nonlinear plasma wave 78−75369
exact solitary ion acoustic waves in a magnetoplasma 80−6247
excitation by electron beams, modulated and unmodulated 77−7560
excitation by fast electron cloud and simulation of type III solar radio bursts 79−44455
excitation by Gaussian laser beam and stimulated Raman scatt. 77−27680
excitation by point sources 79−10660
excitation mechanisms and harmonic generation in laser produced plasma *(Russian)* 77−11339
excitation of high-frequency waves with mixed polarization by streaming energetic electrons 80−1773
excitation of plasma wave by right-handed Gaussian EM beam 79−55495
excitation of plasma waves, finite source excitors 79−10661
excitations of wave modes and energy loss by charged particle passing through plasma sheet 78−38473
excited atoms, radial distrib., prod. by surface wave *(French)* 80−96349
explosive instability collision mode stabilisation by drifting effects, Thirring instability *(Russian)* 80−43920
explosive wave interaction near stability boundary 77−11358
explosively unstable, in ion beam-plasma system, pump field method obs. 80−92333
extraordinary mode radiation induced gyroresonant emission 77−55143
extraordinary mode wave damping near electron cyclotron freq. in Tokamak 80−53979
extraordinary wave decaying into two lower-hybrid waves 79−19029

plasma waves continued
f_H resonance, ionospheric relax. sounding rocket expt. and interpretation 78−45129
fast ion beam, Alfven wave excitation in Tokamak *(Russian)* 80−53999
fast wave damping in ion cyclotron freq. range, heating appl. 77−65867
fast wave heating via mode conversion and ICRF scaling 80−28815
fast wave propag. in hot dense plasma 78−14186
fast-magnetosonic-wave heating of the conceptual NUWMAK Tokamak reactor 80−6264
fast-slow model conversion near ion-ion hybrid resonance 78−91102
finite amplitude lower hybrid frequency wave propagation, effects *(Russian)* 79−55489
finite amplitude solitary Alfven waves 80−53973
finite amplitude wave, regeneration beyond opacity barrier *(Russian)* 80−10387
finite bandwidth radiation, nonlinear dissipation near electron cyclotron harmonic resonances 80−28670
finite positive column moving striations, excitation and asynchronous quenching 78−67515
finite-amplitude Langmuir waves, decay and modulational instability 79−37496
finite-beta effects on drift wave turbulence and particle confinement 80−38652
fluctuating plasma, Trivelpiece-Gould mode parametric decay 78−75321
fluctuation diagnostics, digital time series anal. techniques 78−5951
fluctuation level saturation in magnetised plasma with anisotropic vel. distrib. *(Russian)* 78−59593
fluctuations of localised plasmons under action of EM pumping wave *(Russian)* 77−76078
forward ionisation waves rel. to acoustic phenomena 78−75282
four coupled plasma waves, interaction to second order 78−22491
four-wave interactions in warm magnetised plasma, Lagrangian formalism 77−76056
FT-1 Tokamak, lower hybrid plasma heating 80−28700
fully ionised plasma under gravit. field, small amplitude wave motion 78−94913
fusion reactor lower hybrid heating, nonuniform density, particle simulation model 78−14185
fusion target illumination reduction, enhanced stimulated Raman plasmon scatt. 77−84470
galactic spiral structure formation, plasma density wave analogy *(Russian)* 77−13470
gas discharge, fluid dynamics and nonlinear electron acoustic waves, book contrib. 77−80395
gas discharge positive column plasma, absolute and convective instability of helical wave, depend. on anisotropy of electron mobility *(Russian)* 79−37478
generalised Rosenbluth pot., Balescu-Lenard eqn. friction and diffusion coeffs., wave effects 78−38457
generalized lower-hybrid-drift instability and modified two-stream instability, unified theory 80−1777
generation at pump wave freq. by Gaussian EM beam 78−91112
geometrical optics formalism 80−83925
glow discharge, large amplitude striations, electron conc. variation 77−89342
gradient driven azimuthal ion acoustic waves, driven by electron diamagnetic velocity 79−41812
gravitationally unstable mode, Larmor radius effects 78−1826
group velocity measurement by FM technique 79−73047
group velocity resonance cone, interference pattern 78−14142
growing waves, energy density calcs. 80−53974
growth, stability anal., particle distrib. functions and transport theory 80−43903
guided electron plasma waves, propag. along cylinder, dissipative processes effects 80−92332
guided solitary waves from Boussinesq eqns. 80−92298
guiding center plasma with gravitational or gradient drifts 80−38632
harmonic generation, in moving plasma *(Russian)* 78−87449
harmonics generation in inhomogeneous plasma *(Russian)* 80−83916
heat and particle fluxes, inhomogeneous plasma, current driven drift wave effects 78−94901
heating mechanism study in high-beta plasma using ion beams 77−5962
heavily damped, method for determ. wave number and damping coeff. 78−63557
helical waves in tail of Comet Morehouse (1908 III), WKB approximation theory 80−4305
helicon solitons, interaction and formation 77−7537
helicons *(Russian)* 79−55488
Heliotron D, RF heating, equilibrium and stability 80−28777
HF EM field, turbulent model of plasma column *(Russian)* 80−83915
HF heating by MHD waves of finite press. plasma *(Russian)* 80−83950
HF heating in Tokamaks, fast wave propag. at lower hybrid reson. *(Russian)* 77−7566
HF heating of plasma column, at freqs. below electron cyclotron freq. 78−91125
HF induced waves in ionosphere, time vars. 78−45119
HF pressure, effect on efficiency of beam-plasma interaction *(Russian)* 80−10395
HF quasimonochromatic waves, charged particle drift motion under resonance conditions 80−38611
HF resonance cone, localised RF field 79−23412
high frequency, in Hall accelerator with extended accel. zone 78−67441
high temperature plasma, physics, book 80−98767
high-β collisionless plasmas, velocity shear instabilities 77−35339
high-beta inhomogeneous plasma, wave phenomena 77−76062
high-beta plasmas, energy anisotropy instabilities, comparison of various kinetic and fluid descriptions 79−1310
hot nonuniform magnetised plasma, wave propag. near singular regions 80−38628
hot nonuniform magnetised plasma wave propag. theory, Vlasov eqn. perturbation expansion 80−33768
hot plasma, white noise excitation, sum of ion acoustic waves 78−42736
hybrid waves, lower, backscatter, effect of waveguide boundary conditions 80−64709
hydrodynamic Cherenkov instability, electron flow-surface wave interaction *(Russian)* 77−72440
hydrodynamic wave description including electron spin 80−38643
hydromagnetic, on current-carrying plasma sheet, dispersion relation 79−60133
plasma waves continued
hydromagnetic rarefaction waves and free expansion in collision-free strongly magnetised plasma 80−38594
hydromagnetic surface waves, dissipation 80−21904
hydromagnetic waves, nonlinear, in two-electron temp. plasma 79−98884
hydromagnetic waves in high β plasmas, propag. and damping 80−17482
ICRF heating, preliminary results in DIVA 80−28758
ICRF heating in Macrotor Tokamak 80−28744
ICRF heating of H-D Tokamak plasma under harmonic resonance 80−28719
impedance of magneto-acoustic wave launching antenna 80−24180
inert gas DC discharge, ionis. wave wavelength, electron gas state depend. 78−1918
inert gas ion laser ion-acoustic wave excitation 78−74885
inert gases, supersonic radiation waves, excitation by CO_2 laser 79−90433
inhomogeneous electron flux approaching cold plasma, surface wave excitation *(Russian)* 78−87459
inhomogeneous nonlinear medium and time-varying medium, decay interaction of wave packets 80−14386
inhomogeneous plasma, approx. of confluence by reson. 80−43907
inhomogeneous plasma, parametric trapping of EM waves *(Russian)* 78−9780
inhomogeneous RF plasma, absorption and parametric decay of extraordinary waves 80−59206
instability, electrostatic, parametric, due to thermal coupling 80−79465
instability, satellite excitation 77−42981
instability of two dimensional waves, critical drift velocities, oscill. growth factor *(Russian)* 80−106922
interaction of transverse and longitudinal waves in highly turbulent plasma 77−19704
interchange mode turbulence, spectral cascade processes 80−33775
interior modes, feedback stabilization using RF loaded particle beams 77−31453
International Sun-Earth Explorer 1 and 2, plasma wave investigation 78−85802
interplanetary plasma wave propagation, magnetoacoustic wave transverse to mag. field 80−12629
interplanetary plasma wave-solar electrons interaction, numerical anal. 78−7853
interplanetary wave expt. on International Sun-Earth Explorer C spacecraft 78−85794
interstellar medium, ionisation-coupled acoustic instability 79−97044
ion acceleration, by plasma waves excited by electron beams *(Russian)* 78−71500
ion acceleration by space charge waves in straight-line electron beam 80−103166
ion acoustic, adiabatic interaction with Langmuir waves *(Russian)* 80−1765
ion acoustic cylindrical diverging soliton, transition to disperse wave 77−89257
ion acoustic fluctuation, thermal level, EM wave emission and induced absorption 79−37462
ion acoustic instability, electron distrib. meas. 77−19691
ion acoustic solitary waves in presence of HF elec. field 77−62342
ion acoustic soliton, Boussinesq eqn. description 79−46449
ion acoustic soliton charact., ion beam interaction effect 77−89271
ion acoustic soliton propag. in strong RF electric field 77−31454
ion acoustic soliton propag. in two-electron temp. plasma 80−33767
ion acoustic soliton reflection and transmission at plasma interface 80−106899
ion acoustic solitons, density gradients effect 77−31456
ion acoustic solitons in beam plasma system with nonisothermal electrons generated by ion-beam 80−103151
ion acoustic solitons in collisionless multi-ion plasmas 79−77351
ion acoustic space charge wave dispersion in neutralised ion beam *(Russian)* 79−98888
ion acoustic test waves in magnetized plasma, meas. by 30 GHz Lecher wire interferometer 78−1903
ion acoustic wave, large amplitude, initial freq. shift 80−28661
ion acoustic wave, large amplitude coherent, heating mechanism 79−23432
ion acoustic wave, parametric decay instability 79−23413
ion acoustic wave, self excited, in hot plasma, dispersion theory 80−92283
ion acoustic wave damping changes in noisy plasma 80−33757
ion acoustic wave excitation with array of wire probes 79−37492
ion acoustic wave propagation, electron-ion plasma, Grad's thirteen moment approximation 79−50857
ion acoustic wave radiation due to oscill. point charge *(French)* 80−43900
ion acoustic wave soliton soln., LF, multicomponent plasma 77−35336
ion acoustic wave-electron plasma wave interaction 78−30439
ion acoustic waves, at plasma sheath 77−7531
ion acoustic waves, diverging cylindrical, recurrence investigation 80−79474
ion acoustic waves, in presence of density gradients, modulational instability 79−64840
ion acoustic waves, ionospheric, excitation by strong microwaves from solar power satellite, theoretical anal. *(Japanese)* 80−94634
ion acoustic waves, linear and nonlinear, cold electron density effects 78−30441
ion acoustic waves, rel. to solar coronal heating 78−4181
ion acoustic waves, soliton-like, obs. of slow and fast cylindrical waves 79−37484
ion acoustic waves and solitons in plasma, stability anal. 79−60128
ion acoustic waves excited by boundary sheaths 77−62355
ion acoustic waves in solar wind, high resolution spectrograms 79−96878
ion acoustic waves in solar wind, obs. near D sheets 77−29616
ion acoustic waves method of plasma potential meas. 80−59289
ion acoustic-soliton, interpretation of expt. 78−38474
ion beam expansion due to ion cyclotron wave interactions 79−31786
ion beam modes propag. in double plasma 79−98924
ion beam-plasma collective interactions, high current-density 80−75066
ion beam-plasma system, absolute and convective instabilities of electrostatic ion cyclotron waves 80−64740
ion beam-plasma system, absolute instabilities of electrostatic ion cyclotron waves 78−9793
ion beam-plasma system, dispersion relation 79−46485
ion beam-plasma system, dispersion relation of ion Bernstein wave 77−62375

plasma waves continued
ion beam-plasma system, explosive instability 77−15208
ion beam-plasma system, higher-order modes of space charge waves 80−69992
ion beam-plasma system, parametric instabilities at unstable electrostatic ion cyclotron waves 79−14535
ion beam-plasma system wave propag. in cylindrical geometry 80−38592
ion beam-plasma wave modes, ion beam deceleration by ion acoustic turbulence 78−42771
ion bursts and free-streaming ion propagation, excited by grid 78−18393
ion cyclotron, ion density fluctuations and vel. distrib. 79−19090
ion cyclotron, stimulated backscatt. of EM waves 78−38495
ion cyclotron EM wave instability, oblique, due to monoenergetic fusion alphas 79−37491
ion cyclotron instability in solar wind 78−77547
ion cyclotron parametric instability in multispecies plasma, theory 77−68775
ion cyclotron resonance heating in multiple mirror machine 77−24108
ion cyclotron slow mode wave nonlinear ion motion 77−7509
ion cyclotron wave, in density stratified magnetoplasma, crit. level behaviour 80−6238
ion cyclotron wave turbulence, nonlinear effects, lab. expt., magnetosphere appl. 80−24170
ion cyclotron waves, ionospheric, generated by Ba injection 79−53648
ion cyclotron waves, nonlinear evolution in magnetospheric plasma, fast proton injection effects *(Russian)* 79−55490
ion cyclotron waves, oscillating two-stream instability, RF heating of tokamak plasma 80−1779
ion cyclotron waves, parametric excitation in plasma containing two types of ions 78−30440
ion cyclotron waves and high-energy protons, nonlinear interaction in Earth's magnetosphere *(Russian)* 80−17444
ion cyclotron waves at plasmapause rel. to stable auroral red arc form., proton obs. 78−49197
ion cyclotron waves in solar wind, influence of protons non-bi-Maxwellian distrib. function 78−96375
ion harmonic waves, plasma with arbitrary β, dispersion relation 78−34304
ion heating by current driven turbulence in inhomogeneous plasma 80−33791
ion heating by current-driven turbulence in inhomogeneous plasma 80−96370
ion heating by nonlinear ion-acoustic waves excited by whistlers and Alfven waves 79−82060
ion heating due to collisionless drift-wave turbulence 80−106949
ion loss due to low frequency instabilities 80−6217
ion modes in ionosphere, stimulated Brillouin scatt. theory 77−37478
ion motion, superadiabatic and stochastic, in mirror-machine plasma, in presence of electrostatic wave 80−53933
ion pressure gradient driven drift modes; 3-dimens. fluid simulation 80−103150
ion sound soliton-Langmuir wave interactions *(Russian)* 80−100077
ion sound wave parametrically excited in T-D reson., azimuthal angle of T-D mode induced scatt. 78−9790
ion stream, instability during charge interchange in gas *(Russian)* 77−7519
ion surface waves stimulated by vol. plasma waves, parametric interaction 78−42751
ion velocity space diffusion in controlled ion wave turbulence, ion wave echo probe obs. 77−43079
ion wave, far IR laser scatt. diagnostics 80−59297
ion wave, nonlinear propag., reductive perturbation theory 77−72444
ion wave, rel. to Brillouin backscatter saturation in underdense plasma target 80−14886
ion wave antennas in plasma, reciprocity reln. 77−3952
ion wave effects in open cylindrical magnetoplasma device, turbulent thermal insulation 80−106914
ion wave instability, current-driven, nonlinear development 77−62353
ion wave packet, nonlinear, modulational instability, expt. 77−65853
ion wave propag., quasi-neutral particle simulation model 78−47157
ion waves, grid-excited 78−75313
ion waves, supersonic, very large amplitude, collapse simulation 79−41819
ion-acoustic, collisional and Landau damping in two electron temp. plasma 80−19572
ion-acoustic, coupled-wave and envelope solitons 78−75334
ion-acoustic, cross field thermal transport 79−10642
ion-acoustic, dielectric const. in turbulent plasma 77−986
ion-acoustic, dielectric const. in turbulent plasma 77−987
ion-acoustic, dispersion relation in turbulently heated plasma 78−14215
ion-acoustic, dissipation by ionised relax. in low-temp. plasma *(Russian)* 78−1816
ion-acoustic, effect of turbulence on anisotropic resistivity and particle transport across mag. field 80−59236
ion-acoustic, from parametric instability, microwave p-i-n diode modulator, transient plasma instability meas. *(German)* 80−87942
ion-acoustic, harmonic generation 78−5867
ion-acoustic, heterodyne detection of scatt. pulsed CO_2 laser 77−35389
ion-acoustic, in radio aurora, two-stream instability 78−36355
ion-acoustic, ion heating mechanism 78−94924
ion-acoustic, ionic thermal effects in plasma with negative ions 77−47191
ion-acoustic, Korteweg-de Vries soliton, higher order terms in reductive perturbation theory 78−1824
ion-acoustic, linear, nondispersive, propag. in Ar-He plasma, simultaneous modes dispersion relations 77−27670
ion-acoustic, modulated, nonlinear, in inhomogeneous plasma 79−86576
ion-acoustic, near field diffr. pattern 77−68779
ion-acoustic, near plasma reson., form. by EM radiation nonlinear conversion heating *(Russian)* 78−5859
ion-acoustic, non-resonant EM pump field modification 78−67362
ion-acoustic, nonlinear, propag. in collision dominated regime 78−34283
ion-acoustic, nonlinear excitation in double plasma device 77−978
ion-acoustic, nonlinear freq. shift and modulation, computer simulation 77−68789
ion-acoustic, nonlinear propag. in collisional plasma, shock wave struct. 77−68782
ion-acoustic, nonlinear self-modulation, expt. and simulation plasma simulation 78−42743
ion-acoustic, nonlinear self-modulation 78−14155
ion-acoustic, nonresonant coupling 77−72432

plasma waves continued
ion-acoustic, oblique modulation stability 77−19697
ion-acoustic, parametric decay instability caused by finiteness of pump wave amplitude 78−22482
ion-acoustic, parametric excitation by pump mag. field in high temp. plasma 77−65859
ion-acoustic, propag. in multidimensions, Korteweg-de Vries eqn. 77−89241
ion-acoustic, recurrence of solitons, coupled mode eqns. *(Japanese)* 77−41471
ion-acoustic, refl. and absorpt. in density gradient 78−5868
ion-acoustic, refraction and convergence in plasma with temp. gradient 77−65863
ion-acoustic, resonant damping in corrugated plasma 78−67345
ion-acoustic, weakly dispersive, reductive perturbation theory, higher order terms contrib. 77−11332
ion-acoustic and ion-cyclotron parametric excitation in lower hybrid heating 77−68816
ion-acoustic and Langmuir coupled waves in presence of trapped ions 77−19686
ion-acoustic and plasmon interactions with HF solitons *(Russian)* 77−19682
ion-acoustic cnoidal waves, nonlinear propag. 79−77358
ion-acoustic coupling with drift collisional tearing mode, stabilisation, two-fluid model 78−59589
ion-acoustic current driven wave in turbulently heated plasma, microwave meas. 77−72441
ion-acoustic current driven wave in turbulently heated plasma, microwave meas. 78−5937
ion-acoustic cylindrical solitons 79−19015
ion-acoustic dispersion eqn. solution for positive column 78−75307
ion-acoustic dissemination in moving plasma jet 80−38707
ion-acoustic holes in a two-electron-temperature plasma 80−59205
ion-acoustic in weekly ionised gas, single fluid model for dipersion and damping 78−30442
ion-acoustic inelastic soliton interaction 78−51
ion-acoustic instability, ion tail formation and saturation 80−38610
ion-acoustic instability in positive column of DC discharge 78−67335
ion-acoustic instability oscillations in collisionless single ended Q-machine 80−38731
ion-acoustic Korteweg de Vries solitary waves in plasma with density, temp. gradients 78−55720
ion-acoustic Korteweg de Vries solitons 79−46446
ion-acoustic Landau, produced by RF oscill. multiple mirror stabilisation of theta pinch 77−89290
ion-acoustic large-amplitude solitons, nonstationary theory *(Russian)* 78−1820
ion-acoustic LF surface waves, parametric instability *(Russian)* 77−68766
ion-acoustic noise excited by ion-beam, suppression by external RF field 79−77396
ion-acoustic nonlinear waves, parametric excitation due to EM wave decomposition *(Russian)* 78−47104
ion-acoustic oscillations in intense EM field *(Russian)* 79−55483
ion-acoustic parametric decay instability in plasma with $\beta>1$ 77−975
ion-acoustic plasma turbulence with pump wave *(Russian)* 77−76080
ion-acoustic pulse generation by 2 EM pulses at difference freqs. in collisionless plasma 80−79475
ion-acoustic shock waves, in multi-electron temp. collisional plasma 77−7523
ion-acoustic solitary wave, third-order corrections, reductive perturbation method 80−43898
ion-acoustic solitary wave excitation in collisionless plasma *(Russian)* 78−26267
ion-acoustic solitary waves, in ion beam-plasma systems with isothermal electrons 80−33784
ion-acoustic solitary waves, ion temp. and higher order contrib. effects 79−46439
ion-acoustic solitary waves *(Czech)* 80−1764
ion-acoustic soliton, in nonuniform plasma, theory 78−30436
ion-acoustic soliton, refl. from sheath around negatively biased grid 78−38479
ion-acoustic solitons, 3-dimens. interactions 78−59570
ion-acoustic solitons, amplification by an ion beam 78−83554
ion-acoustic solitons, cylindrical, diverging, excitation by probe 77−7522
ion-acoustic solitons, dressed, dynamical processes 77−80286
ion-acoustic solitons, temporal development, initial value problem; 80−33771
ion-acoustic solitons, two-dimens. interaction 80−106908
ion-acoustic solitons in electromagnetically irrad. magnetoplasma 78−22485
ion-acoustic solitons in multicomponent plasma, with negative ions 79−41827
ion-acoustic solitons launched from plate, distortion in density gradient 79−64863
ion-acoustic solitons with a temperature gradient 80−79490
ion-acoustic surface wave, elec. field attenuation, low-freq. waves 79−64862
ion-acoustic surface wave spectrum in nonisothermal plasma *(Russian)* 80−53962
ion-acoustic turbulence, test wave propag. 78−91090
ion-acoustic turbulence-plasma interactions and electron spectrum in electric fields 80−38617
ion-acoustic wave, dispersion relation calc. in turbulent plasma 78−63554
ion-acoustic wave, in collisionless plasma, modulational instability, ion temp. effect 79−60132
ion-acoustic wave, modulational instability 77−89254
ion-acoustic wave, modulational instability in turbulent phonon field 78−18395
ion-acoustic wave, nonlinear wavenumber shift 77−15185
ion-acoustic wave, phase velocity 80−103147
ion-acoustic wave dispersion, pulsed CO_2 laser scatt. meas. 79−27828
ion-acoustic wave excitation and interference by laser beam 78−34326
ion-acoustic wave excitation by two Gaussian laser beams, density profile modification 79−19006
ion-acoustic wave excitation with probes 77−68780
ion-acoustic wave expts., low freq., antenna characts. of Langmuir probes 78−42819
ion-acoustic wave fluctuations obs., in turbulent ion heating, correlation time 78−34347

plasma waves continued
ion-acoustic wave interacting with laser beam, filamentation instability 79−41838
ion-acoustic wave interaction with longitudinal plasma wavepacket 80−1793
ion-acoustic wave meas. with probes, antenna characts. 78−5949
ion-acoustic wave modulation instability, effect of finite ion temp. 79−1307
ion-acoustic wave packet propag., nonlinear, longer wavelength wave generation, simulation 78−14157
ion-acoustic wave packets, nonlinear distortion 79−46448
ion-acoustic wave periodicity in inhomogeneous plasma 79−14527
ion-acoustic wave turbulence absorption; NRL fusion programme 78−59042
ion-acoustic wave turbulence spectrum in large volume plasma 78−5871
ion-acoustic wave-CO_2 light coherent scatt. 78−34325
ion-acoustic waves, cylindrical, finite amplitude, asymptotic development calcs. 77−47189
ion-acoustic waves, effect of ponderomotive force 78−75284
ion-acoustic waves, energy props. in stable and unstable plasmas 79−68916
ion-acoustic waves, interaction with EM waves, plasma instability *(Russian)* 78−22505
ion-acoustic waves, linear response to impulse 79−14541
ion-acoustic waves, modulational instability in two electron temp. plasma 78−75301
ion-acoustic waves, one-dimensional, stable approx. eqns. 77−89243
ion-acoustic waves, probe excited in multidipole plasma device 78−42739
ion-acoustic waves, refl. and absorpt. in density gradient 79−19017
ion-acoustic waves, soln. for MHD equations, properties *(Russian)* 80−106891
ion-acoustic waves, spectrum in 2-component plasma in quantising mag. field 79−4138
ion-acoustic waves, trapped particles, harmonic generation 77−76188
ion-acoustic waves and solitons, trapped electrons 77−19690
ion-acoustic waves and turbulent ionis., correlation meas. 80−59329
ion-acoustic waves detection using 30 GHz Lecher wire interferometer 78−5946
ion-acoustic waves excitation by 80−10381
ion-acoustic waves freq. and damping from dispersion relations 80−69991
ion-acoustic waves in presence of electron plasma waves 77−19693
ion-acoustic waves in solar wind, wave-particle interactions rel. to particle vel. distribs. *(German)* 80−109323
ion-acoustic waves in thin radially inhomogeneous plasma column 78−34289
ion-acoustic waves mechanism for anomalous thermal transport 78−5853
ion-acoustic-solitons, dissipative effect on formation 77−84419
ion-Bernstein, parametric excitation by lower hybrid pump wave 78−14143
ion-Bernstein wave, inhomogeneous plasma, mode conversion and tunnelling 78−34300
ion-cyclotron, in turbulent plasma, linear response theory 77−47197
ion-cyclotron, ion beam excitation 78−34335
ion-cyclotron, ion beam excitation 78−34336
ion-cyclotron and first harmonic heating of large Tokamak 77−51204
ion-cyclotron harmonic waves excitation by interacting ion beam 77−3956
ion-cyclotron instability, broadband noise effect 77−68778
ion-cyclotron RF field, plasma convective loss, elimination by mode control 80−83957
ion-cyclotron turbulence modulation by LF perturbations 78−91108
ion-cyclotron wave, driven unstable by cold-ion beam, nonlinear stabilisation 79−98925
ion-cyclotron wave, parametric excitation by pump mag. field, high temp. 78−67342
ion-cyclotron wave spectra dispersion eqn. numerical soln. *(Russian)* 78−59561
ion-cyclotron waves assoc. with paired electrostatic shocks in polar magnetosphere 77−29601
ion-cyclotron waves in topside ionosphere, noise source 80−101470
ion-drift wave eigenmodes in sheared mag. field, impurity effects 80−43911
ion-ion hybrid damping in D_2-H_2 plasma 79−77361
ion-ion hybrid waves in collisional two-species current carrying plasma, instability 79−90394
ion-sound resonances in crossed external electric and mag. fields 80−28626
ion-sound waves in nonisothermal plasma, diffr. by conducting semi-plane *(Russian)* 77−68770
ion-sound waves in turbulently heated plasma, parallel and perpendicular propag., microwave obs. 79−14612
ion-wave fluctuation in turbulent plasma, anomalous EM wave electron radiation 80−43889
ionisation, excitation in low-temperature plasma 78−1832
ionisation instability, dispersion rel. *(Russian)* 78−83519
ionisation wave, effect of electron neutral collisions in He plasma 80−43846
ionisation wave, freq. modulated, discontinuities creation 78−79426
ionisation wave, obs. of phase modulation 80−69993
ionisation wave irregularity, effect on electron distrib. function probe meas. 77−47255
ionisation waves, electron energy distrib. function 78−30421
ionisation waves, in positive column, wave packet propag. 80−96356
ionisation waves in axial mag. field, crit. current 78−42848
ionisation waves in bounded low-temp. plasma 79−94794
ionisation waves in plasma columns, microwave detect. 78−79461
ionosphere, electrostatic wave generation near lower hybrid reson. by LF EM wave 77−29557
ionosphere, equatorial horizontal plasma waves, HF radar obs. 79−29930
ionosphere, heating due to parametrically excited Langmuir waves, short-scale field-aligned density striations form. 79−8766
ionosphere, HF-induced plasma line rel. to field-aligned ionisation irregularities 78−88979
ionosphere, nonlinear Landau damping 80−8474
ionosphere, parallel propag. waves, stability of electron shell distrib. 78−4032
ionosphere, parametric excitation by strong radiowave 77−17283
ionosphere, pulsed RF waves, proton cyclotron echoes, generating mechanism 78−77407
plasma waves continued
ionosphere, stimulated by RF topside sounders, review 78−45128
ionosphere, VLF waves, natural and elecron-beam producted, rocket obs. 78−7829
ionosphere high latitude topside sounding, Bernstein modes propag. trajectories *(Russian)* 77−33258
ionosphere plasma interaction with gravity waves, elec. field and current prod. 80−61957
ionospheric plasma, electrostatic cyclotron oscillation, photoionisation *(Russian)* 78−63552
ionospheric plasma wave trajectories near resonance at upper hybrid freq. *(Russian)* 77−73903
Jeans' gravitational instability of an anisotropic plasma with generalised polytropic equations of state *(Italian)* 79−94780
Jupiter, magnetospheric plasma wave propag., CMA diagrams 77−87317
Kelvin-Helmholtz wave interactions, ion beam scatt. 79−14562
kilometric radiation in Jupiter magnetosphere, spatial and temporal studies 80−77328
Korteweg de Vries soliton, in slowly varying medium, theory 78−30436
Korteweg de Vries waves and solitons, three-dimens. stability 78−83540
Korteweg-de Vries solitary waves for cylindrical and spherical symmetric ion acoustic waves 79−77371
Landau damping, particle picture 78−38471
Landau damping, relaxation of initial excitation *(Russian)* 78−55721
Landau damping, Schrondinger eqn. perturbation expn. appl. 78−47124
Landau damping 78−14162
Landau damping for students, linearised eqns. of motion 78−57723
Landau damping in interaction between regular wave and noise *(Russian)* 78−47121
Landau mode wave pattern calc. 77−80300
Langmuir, 3D parametric decay into Langmuir and longit. LF waves *(Japanese)* 77−42971
Langmuir, acceleration of trapped particles 78−22490
Langmuir, adiabatic interaction with ion-acoustic waves *(Russian)* 80−1765
Langmuir, density profile modification of laser prod. plasma 78−59550
Langmuir, electron interactions Legendre expansion of quasilinear eqns. 78−30418
Langmuir, induced scattering on particles in external field 80−38648
Langmuir and dispersive ion acoustic waves, coupled nonlinear Schrodinger eqn. 79−77362
Langmuir and EM waves, turbulence induced by relativistic electron beam in mag. field *(Russian)* 77−62378
Langmuir and extraordinary waves growth, in stimulated Raman backscatt. of EM waves 79−37465
Langmuir and ion acoustic wave coupling, turbulence spectra, light absorption 80−87902
Langmuir bounded wave solns. in self-consistent density cavity *(Japanese)* 77−42973
Langmuir collapse, dimensionality and dissipation 80−87880
Langmuir envelope finite amplitude soliton form., in plasma-beam systems 77−84422
Langmuir envelope solitons in turbulent plasma 78−67334
Langmuir field, localised, in plasma, temporal evolution 79−90405
Langmuir finite amplitude wave passage through plasma wave density barrier 79−86579
Langmuir modes, trapped, in double layer, existence and stability 80−6236
Langmuir modulational instability, nonlinear development 79−32761
Langmuir multidimensional nonlinear waves 78−63555
Langmuir nonlinear standing waves 78−22481
Langmuir oblique solitons, self-contraction in free path regime *(Russian)* 80−43921
Langmuir oscillation collapse in supersonic regime, forbidden energy *(Russian)* 80−14895
Langmuir oscillations, amplification, suppression by charged particle in magnetoplasma 79−37482
Langmuir running wave instability and damping, at different amplitudes and phase velocity 80−38620
Langmuir soliton EM wave scatt., theory *(Russian)* 80−38564
Langmuir soliton excitation by monoenergetic electron beam *(Russian)* 79−77381
Langmuir soliton formation with ion-acoustic densiton emission 78−75328
Langmuir soliton generation at crit. density, laser-irrad. plasma 80−6267
Langmuir soliton solns. with high nonlinearities, energy principle 80−24156
Langmuir soliton weak EM wave scatt., Doppler shift and reflection coeff. calc. *(Russian)* 79−7467
Langmuir solitons, electron beam interaction in turbulent plasma 79−14563
Langmuir solitons, generation and collapse, numerical study 77−68784
Langmuir solitons, large amplitude, props. 79−10656
Langmuir solitons, nonlinear stability to transverse perturbations 79−14539
Langmuir solitons, stabilisation of modulation instability *(Russian)* 78−38470
Langmuir solitons, transverse instability 80−6250
Langmuir solitons *(Russian)* 79−46451
Langmuir solitons in magnetised collisionless plasma *(Russian)* 78−47122
Langmuir solitons nonlinear interaction in magnetised plasma 79−14540
Langmuir solitons with opposite vel., collisions 77−68776
Langmuir standing wave, stability and kinetic effects *(Russian)* 77−80299
Langmuir standing waves instability, one dimens., soliton and collapse, numerical expt. 80−38619
Langmuir to ion-acoustic nonlinear-conversion, electron-beam plasma interaction *(Russian)* 79−27759
Langmuir turbulence, modulating instability wave, nonlinear dynamics, solitons *(Russian)* 77−47196
Langmuir turbulence, stationary 78−14164
Langmuir turbulence in upper hybrid resonance region, external electric field effects *(Russian)* 79−73010
Langmuir wave, acoustic turbulence effect on collapse 79−14549
Langmuir wave, large amplitude, initial freq. shift 80−24167
Langmuir wave, nonlinear interaction with free-streaming perturbations, Vlasov plasma 79−32771
Langmuir wave, three dimens. parametric decay into another Langmuir and longitudinal LF wave 77−31441
Langmuir wave collapse, acoustic turbulence effect 79−37481

plasma waves continued
Langmuir wave collapse, Wentzel-Kramers-Brillouin model 80−38600
Langmuir wave collapse in mag. field, instability-caused cavity *(Russian)* 78−1817
Langmuir wave collapse in mag. field *(Russian)* 78−9776
Langmuir wave decay, two-plasmon parametric instability, numerical anal. 78−14152
Langmuir wave emission and absorpt. coeffs. due to anisotropic unmagnetized particles 78−16370
Langmuir wave eqn., steady state shockwave solns. 77−68799
Langmuir wave evolution, three dimensional kinetic model, Vlasov eqn. calcs. 80−43923
Langmuir wave excitation by relativistic electron beam *(Russian)* 80−19594
Langmuir wave excitation by two pumping waves, convective instability *(Russian)* 80−14904
Langmuir wave induced scatt. in turbulent plasma in strong external HF EM field 80−53988
Langmuir wave interference, electron collisions *(Russian)* 80−69970
Langmuir wave modulation instability due to electron oscill. *(Russian)* 77−47182
Langmuir wave phase vel. in relativistic particle beam 79−23408
Langmuir wave production, ion sound upconversion, comments 80−92324
Langmuir wave propag. in self-consistent stationary density cavities 77−15178
Langmuir wave quasicollapse, one-dimens., under parametric and modulation instabilities 77−42982
Langmuir wave turbulence in solar type III radio bursts, nonlinear stabilisation 80−26826
Langmuir wave-particle interactions, microscopic Lagrangian description, warm plasma 78−42755
Langmuir waves, cascade and collapse in 2-D 79−1308
Langmuir waves, collisional damping in collisionless limit 78−34295
Langmuir waves, driven by electron-ion decay instability, scattered spectrum 80−43970
Langmuir waves, induced nonthreshold scatt. on HF oscills. in inhomogeneous plasma *(Russian)* 80−53960
Langmuir waves, intense mag. field generation 80−38623
Langmuir waves, ionospheric, propag. rel. to enhanced plasma line in sporadic E 79−29928
Langmuir waves, large amplitude, nonlinear Landau damping and form. of standing nonlinear waves 80−92292
Langmuir waves, modified decay, collisions effect *(Russian)* 77−27672
Langmuir waves, modulated, nonlinear damping 78−51301
Langmuir waves, nonlinear, during Type III solar wind bursts, evolution 78−93173
Langmuir waves, nonperiodic oscillations 80−48888
Langmuir waves, numerical modelling of 1-D turbulence, acoustic oscillations effect *(Russian)* 80−103135
Langmuir waves, oblique, localised, in inhomogeneous plasma, parametric excitation *(Russian)* 79−98885
Langmuir waves, obliquely modulated, stability in collisional plasmas 78−22480
Langmuir waves, parametrically excited in inhomogeneous plasma 77−76073
Langmuir waves, three-dimensional instabilities in solar corona rel. to type III radio bursts 77−2404
Langmuir waves, turbulent bremsstrahlung process 80−62009
Langmuir waves, upconversion of ion-sound impossible 80−41716
Langmuir waves and anisotropic particles, Legendre-expanded quasilinear eqns. appl. 79−75089
Langmuir waves in solar corona, excitation by fast electrons stream 80−17568
Langmuir waves in solar corona, scatt. rel. to drift pair radioburst 79−25558
Langmuir waves in solar corona, wavenumber spectra rel. to electron distribs. 78−57515
Langmuir waves in spatially periodic mag. field 79−10655
Langmuir waves in Vlasov plasma, nonlinear theory, wave-particle interaction 80−64701
Langmuir waves in Vlasov plasma, nonlinear theory, wave-wave interaction 80−64700
Langmuir waves nonlinear coupling as saturation mechanism for parameter instabilities 78−42748
Langmuir waves spontaneous emission rel. to type III solar radio bursts 77−33455
Langmuir-wave modulation instability in electron beam self-induced transparency 78−34341
large amplitude, interaction with moving electron plasma 79−98899
large amplitude wave-electron interaction, enhancement by DC elec. field, simulation 79−90420
large-amplitude Langmuir wave instability 78−75325
laser, free electron, relativistic, rippled static mag. field, simulation, waves and instability 77−54686
laser gas breakdown, shock and ionisation waves, photographic absorpt. obs. 80−87967
laser light reflection enhancement from expanding laser prod. plasma, Brillouin scatt. 77−3963
laser plasma, fast ions *(Russian)* 79−55532
laser plasma, struct. features of 2 ω_0 and 3/2 ω_0 harmonics *(Russian)* 77−11366
laser radiation refl. coeff., decay on ion-acoustic and electronic-Langmuir vibrs. *(Russian)* 77−15194
laser supported absorption waves, momentum transfer to surface, flowfield model 80−14921
laser-pellet irradiation, two-plasmon decay instability, soliton form. role 78−1842
LF potential waves, parametrically excited, relativistic effects *(Russian)* 78−91089
LF wave effects on counter-streaming electron beam instability 77−62376
LF wave excitation by AM microwaves 77−62366
LF wave spectra in highly inhomogeneous plasma, damping 77−51184
LHR frequency range waves interactions in octopole Tokamak 80−28724
Liapunov stability of generalized Langmuir solitons 80−38631
linear and nonlinear wave transformation and absorpt. in inhomogeneous plasma capacitor 77−76046
linear effects of wave propag. in plasmas, review 78−14149

plasma waves continued
linear electron plasma test wave, wavenumber oscills., standing wave effects 78−38478
linear wave conversion in unmagnetised collisionless plasma 77−72431
linear wave propagation, dispersion relation, microscopic Lagrangian description, warm magnetoplasma 78−42753
linear wave props., parametric decay, heating 78−42758
localised drift-Alfven mode instability due to current density gradient 80−19571
localised lower hybrid wave enhancement of drift waves 78−67343
localised modes in inhomogeneous Vlasov plamsa 78−83563
localised structures and anomalous DC resist. 77−58846
long wave-short wave resonance equations, complete soln. for fluid mechanics and plasmas 79−37334
long wavelength modes, space-time correlation functions 78−9772
longitudinal acoustic wave, form. by energy conversion from transverse EM wave 77−68800
longitudinal modes, produced by counter-streaming electron beams in stationary background 78−26273
longitudinal self-consistent large amplitude wave stability in absence of large-scale mag. field 79−32759
longitudinal to EM wave conversion, WKB approx. 78−18389
longitudinal wave perturbation, producing increased fusion reaction rate 80−27815
longitudinal waves excitation by obliquely incident EM waves in semi-limited plasma *(Russian)* 79−1314
longitudinal waves in an electron plasma in a weak magnetic field 80−92312
longitudinal waves in magnetoactive plasma, nonlinear scatt. probability 78−22471
longitudinal waves in relativistic plasma *(Russian)* 80−54023
longitudinal waves in solar atmosphere, rel. to radio emission polarised zebra struct. 78−96467
longitudinal waves nonlinear interaction 78−59575
loop antenna radiator and detector, exptl. obs. 77−51198
low density runaway beam, interaction with cavity modes 79−77398
low frequency heating wave, parametric instabilities induction in mag. confined plasma 80−24187
low-frequency drift wave with trapped electron *(Russian)* 79−27762
low-frequency magnetoplasma wave, ponderomotive pot. for magnetised particle 79−64859
low-frequency oscillations, in plasma with negative ions, collision effects 78−87448
low-frequency waves, excitation by streaming ions via anomalous cyclotron reson. 78−83542
low-frequency waves, obs. in vicinity of Earth bow shock 80−90311
low-frequency waves (≲50 Hz), possible generation mechanisms with appl. to Earth bow shock 80−90312
low-frequency waves in solar wind, magnetosheath propag. rel. to Pc 3-4 activity 78−73585
low-hybrid wave nonlinear eqns. and solitons 78−75323
low-hybrid wave propagation and attenuation, influence of quasilinear effects *(Russian)* 78−18408
lower hybrid, absorpt., mode conversion 78−9781
lower hybrid, nonlinear distortion of propag. cones 77−89249
lower hybrid, parametric excitation of LF convective cell modes 77−55136
lower hybrid, random spectrum, resistive tearing m=1 instability turbulent modification 80−43916
lower hybrid, waveguide launching 80−10391
lower hybrid and ion cyclotron waves, nonlinear modulation 78−75295
lower hybrid cone, spatial depletion by parametric decay 77−76061
lower hybrid cones, filamentation, moving solitary envelope solutions 78−30426
lower hybrid cones, nonlinear development 78−34306
lower hybrid cones, stability anal. 80−48880
lower hybrid decay wave ray trajectories, ergodic behaviour 79−19022
lower hybrid drift waves in magnetosphere boundary layer, excitation by field-aligned currents 80−67473
lower hybrid freq., reson. cones, wave and particle meas. 77−65913
lower hybrid frequency heating by wave absorpt. 77−68815
lower hybrid frequency propagation in FT-1 Tokamak *(Russian)* 79−55482
lower hybrid large-amplitude waves, filamentation 77−80294
lower hybrid mode conversion, reson. cones damping 79−10652
lower hybrid parametric instabilities, nonuniform pump waves, Tokamak appls. 78−34344
lower hybrid propag. characts. in linear Tokamak plasma 77−7524
lower hybrid pump wave two-dimens. depletion by quasi-mode excitation 78−67344
lower hybrid region, antenna impedance 80−28664
lower hybrid reson., slow TM mode excitation by antenna waveguides *(Russian)* 77−47227
lower hybrid resonance cone propag., density fluctuations effect 78−59583
lower hybrid resonant coupling, elevated electron temp. plasma *(German)* 79−27806
lower hybrid RF emission, meas. by antenna 78−9852
lower hybrid self-trapping at RF gas breakdown 80−38850
lower hybrid solitons, envelopes in magnetic fields 80−59224
lower hybrid turbulence spectrum, amplitude-freq. nonlinear cut-off *(Russian)* 79−37494
lower hybrid wave, effect of finite wavelength of pump on parametric threshold 77−84420
lower hybrid wave, linear amplification and absorption 80−28673
lower hybrid wave, nonresonant parametric decay, quasi-modes 80−59197
lower hybrid wave, parametric decay into drift wave 77−68791
lower hybrid wave, propag. cone nonlinear distortion 77−68790
lower hybrid wave, unidirection, current generation in ACT-1 80−92306
lower hybrid wave accessibility, effect of density gradient 80−1794
lower hybrid wave damping by 26 keV ion beam trapped in Tokamak 78−59627
lower hybrid wave decay into EM wave, parametric instabilities 77−31457
lower hybrid wave excitation, by periodic slow E waves, appl. RF heating 77−62360
lower hybrid wave excitation, of mirror mag. field plasma 79−19054
lower hybrid wave excitation by active-passive waveguide array 80−48911
lower hybrid wave excitation by electron beam, body waves 78−34287

plasma waves continued
lower hybrid wave excitation by electron beam, surface waves 78−34288
lower hybrid wave heating, electron distrib. function *(Russian)* 80−83951
lower hybrid wave heating, quasilinear effects 80−28763
lower hybrid wave heating in Alcator-A Tokamak 79−82078
lower hybrid wave heating in Doublet IIA 80−28723
lower hybrid wave heating in JIPP T-II 80−28722
lower hybrid wave heating simulation in nonuniform plasma 80−64771
lower hybrid wave in nonuniform density plasma, propagation and heating 79−90402
lower hybrid wave propag., asymptotic soln. 78−47107
lower hybrid wave propag., numerical simulation 79−55541
lower hybrid wave propag. and parametric decay in WEGA Tokamak 80−28725
lower hybrid wave refl. from lower hybrid surface, toroidal effect 79−27770
lower hybrid wave scattering by density fluctuations 79−94792
lower hybrid wave turbulence effect on tearing mode instability 80−92322
lower hybrid wave turning point location, nonuniform magnetoplasma 80−79473
lower hybrid waves, collisionally damped, driving steady state electron currents 80−38639
lower hybrid waves, current-driven electrostatic ion-cyclotron instability 80−103149
lower hybrid waves, excitation in finite plasma, simulation 79−41820
lower hybrid waves, filamentation and spatial attenuation in Tokamaks 80−28665
lower hybrid waves, in octopole Tokamak, ray trajectories 80−64707
lower hybrid waves, in Petula Tokamak, plasma heating and nonlinear effects 80−28697
lower hybrid waves, in Tokamak plasma, damping mechanisms *(Russian)* 77−76076
lower hybrid waves, modulation instability growth rates 80−48881
lower hybrid waves, nonlinear behaviour, near linear mode-conversion point 80−53963
lower hybrid waves, nonlinear evolution 79−64857
lower hybrid waves, nonlinear propag. 79−1303
lower hybrid waves, parametric decay, ion nonlinearity effect 79−37485
lower hybrid waves, propag. and mode conversion 79−10658
lower hybrid waves, propag. in toroidal plasma 80−83927
lower hybrid waves, ray trajectories and ion absorpt. in Tokamaks 80−28671
lower hybrid waves, ray trajectory and ion absorpt. in Tokamak 80−28667
lower hybrid waves, stochastic ion heating 80−28707
lower hybrid waves, stochastic ion heating in Tokamak plasma 78−91126
lower hybrid waves, trajectories and damping in Tokamak plasma 80−83922
lower hybrid waves, two-dimens. self-modulation in inhomogeneous plasmas 79−90403
lower hybrid waves detection by microwave scatt. 78−87493
lower hybrid waves in coaxial double-plasma 77−84417
lower hybrid waves in inhomogeneous mag. fields, propag. and mode conversion 79−37489
lower hybrid waves in nonuniform plasmas, geometric optics 80−83924
lower hybrid waves in Tokamak, finite-sized source focusing 78−9783
lower hybrid waves in toroidal discharge, parametric decay 80−38596
lower hybrid waves launched by slow waveguiding circuits, propagation and reflection 77−89240
lower hybrid waves penetration and linear absorpt. 77−65869
lower hybrid waves resonance interaction with turbulent plasma 78−30445
lower oblique whistler resonance cone, interference struct. in Maxwellian magnetoplasma 80−59219
lower-hybrid mode-converted waves, nonlinear distortion 77−19699
lower-hybrid pump wave, growing instability threshold 77−89237
lower-hybrid wave absorption in the presence of simultaneous density and magnetic field gradients 79−94790
lower-hybrid wave excitation in RF fusion plasma heating, thermal eddies form. 80−24193
lower-hybrid wave stabilisation of drift instability, plasma electron beam interaction 77−51182
lower-hybrid waves, focusing and channelling during HF-breakdown of gas *(Russian)* 80−106890
lower-hybrid waves, Tokamak RF heating by electron Landau damping 80−19595
lower-hybrid waves in collisional plasmas with field-aligned current, instability 80−75045
lower-hybrid-drift instability in field reversed plasmas 80−59209
lower-hybrid-drift wave turbulence in distant magnetotail, theory 79−25399
m=1 waves propagating in Scyllac 78−5865
mach cones induced by fast heavy ions in electron plasma 79−14546
magnetic field generation, laser light reson. absorpt., stress tensor anal. 78−18419
magnetic field self-excitation by intense EM radiation, mag. instability *(Russian)* 79−14582
magnetic Rosenbluth potentials, generalised to include wave effects 78−94896
magnetic-insulation wave front struct., in waveguide 79−55517
magnetically confined plasmas, parametric instabilities in laser heating 78−18432
magnetised, parametric instabilities with well separated freq. *(Chinese)* 80−106887
magnetised plasma, backscatt. of laser beam from electrostatic waves 80−33779
magnetised plasma, double-layer characts. meas., wave trapping 80−43874
magnetised plasma, wave kinetic eqn., velocity Fourier transform solution of a model collision operator 79−94785
magnetised plasma electron heating in parametric modulation instability 78−75384
magnetized inhomogeneous plasma, wave reson. and conversion 80−92313
magnetized plasma parametric resonance in non-monochromatic pump-wave 80−38598
magneto plasma half space, reflected pulse, cyclotron and upper hybrid resonance freq. 78−63569

plasma waves continued
magneto-acoustic, bounce resonances in cyclotron build-up 77−76060
magneto-acoustic, dynamic stabilisation of fire-hose instability 78−42750
magneto-acoustic, nonlinear, propag. in nonuniform plasma *(Russian)* 78−26261
magneto-acoustic, nonlinear interaction with whistler turbulence 78−45134
magneto-acoustic macroscopic soliton instability growth rate, dispersion eqn. *(Russian)* 78−59562
magneto-acoustic solitons, macroscopic instability *(Russian)* 77−47200
magneto-acoustic wave excitation by electron interaction with MHD waves *(Russian)* 78−22473
magneto-acoustic waves, nonlinear coupling to HF electron cyclotron waves 77−76071
magneto-acoustic waves, soln. for MHD equations, properties *(Russian)* 80−106891
magneto-ionic rays, propag. in shearing plasma 79−84659
magnetoacoustic, shaped pulse heating of plasma column *(Russian)* 79−55522
magnetoacoustic and Alfven vortices *(Russian)* 77−80302
magnetoacoustic disturbance, hydrodynamic instability in nonuniform plasma flow *(Russian)* 80−1766
magnetoacoustic heating by ion Landau damping 80−92341
magnetoacoustic nonlinear dispersive waves in collisional plasma 77−72424
magnetoacoustic oscillations, parametric decay in cylindrical plasma 80−24157
magnetoacoustic oscills., in bounded plasmas, viscous damping 80−38605
magnetoacoustic parametric excitation by pump mag. field 77−31448
magnetoacoustic resonance in strongly inhomogeneous He plasma 80−69994
magnetoacoustic resonances, excitation in toroidal confinement system 79−90406
magnetoacoustic turbulence, collision free mechanism *(Russian)* 78−22502
magnetoacoustic wave cyclotron absorpt. in TM-1-VCh Tokamak *(Russian)* 77−7539
magnetoacoustic wave resonance, generation and detection by single antenna 78−5950
magnetoacoustic wave turbulence in interplanetary plasma, spatial fluctuation spectra 79−53693
magnetoacoustic waves, fast, RF excitation and thermalisation near cutoff freq. *(Russian)* 77−47178
magnetoactive collisional plasma, dielectric tensor, refl. index and attenuation 80−59202
magnetoactive plasma, low frequency waves excitation, relativistic effects *(Russian)* 80−103184
magnetoatmospheric waves, max. growth rates of instabilities 77−53573
magnetoplasma, hot collisionless, resonant excitation of upper hybrid wave by two EM beams 79−77384
magnetoplasma, interaction of amplitude modulated microwave, plasma waves excitation 77−3947
magnetoplasma, penetration of localised RF fields 79−94782
magnetoplasma, plasma wave generation and SHG by Gaussian EM beam 79−37479
magnetoplasma, solitary ion-acoustic wave propag. exact stationary solns. 79−19010
magnetoplasma, warm, full dispersion relations near electron cyclotron freq. 77−68773
magnetoplasma wave, quasistatic density perturbation, universal formula 79−60131
magnetosonic, coupling to fast eigenmodes, dispersion relations 78−30429
magnetosonic, cyclotron resonance damping in plasma with admixed ions 77−24079
magnetosonic and Alfven waves, transfer by solar wind 80−67490
magnetosonic cavity mode absorpt., heating 79−19055
magnetosonic cavity modes, complex plasma loading impedance meas. 80−59215
magnetosonic resonance heating in the Erasmus Tokamak 80−28720
magnetosonic solitons, one-dimens., helicon perturbation 79−7454
magnetosonic wave emission in electron beam heating 77−51206
magnetosonic wave excitation in toroidal plasma, probe meas. 77−65866
magnetosonic wave generation and damping near ion cyclotron freqs. in TFR Tokamak 77−76058
magnetosonic wave heating, near ion cyclotron freq. 77−51203
magnetosonic wave model, relativistic electron beam heated plasma, mag. signal interpretation 77−42997
magnetosonic wave parametric excitation, stimulated EM wave scatt. 78−34330
magnetosonic wave propag., computer simulation and theoretical anal. 78−5861
magnetosonic waves, instability driven by alpha particle beam in solar wind 79−35089
magnetosonic waves, phase and ray directions, astrophys. appl. 78−94906
magnetosonic waves, rel. to fine struct. of magnetic shocks in collisionless plasma 80−85854
magnetosonic waves excitation in toroidal traps *(Russian)* 79−14545
magnetosonic waves in magnetosphere, rel. to hiss generation beyond plasmapause 77−82085
magnetosonic waves in presence of lower hybrid turbulence and heating 78−26281
magnetosonic waves near Earth bow shock, propag. and transport from initial ISEE obs. 80−90307
magnetosphere, coupling across contact discontinuity in collisionless plasma 79−8780
magnetosphere, detached plasma regions, wave propagation characts., instability phenomena 77−25880
magnetosphere, electrostatic ion loss-cone waves nonlinear generation by turbulence 77−41269
magnetosphere, electrostatic ion-cyclotron instability during quiet times and auroral proton precip. 77−33256
magnetosphere, electrostatic wave trapping at freq. below proton plasma freq. *(Russian)* 77−78573
magnetosphere, ELF, VLF and LF waves obs. during large mag. storms 77−29594
magnetosphere, ion cyclotron waves and ring current ions simultaneous equatorial obs. 77−22012
magnetosphere, ion-cyclotron wave amplification for typical radial profiles of magnetospheric parameters 77−25886

plasma waves continued
magnetosphere, ISEE-1 and -2 results 79−58199
magnetosphere, lower hybrid turbulence, nonlinear LF spectrum cutoff 78−4041
magnetosphere, plasma wave emissions from auroral field lines 79−88556
magnetosphere, plasma waves and instabilities in polar cusp 78−12058
magnetosphere, polar cusp, Hawkeye 1 obs. 78−77422
magnetosphere, review 78−28451
magnetospheric whistler parametric instability, pitch-angular electron scatt. *(Russian)* 78−77420
Mandel'shtam-Brillouin scattering, induced, from laser plasma, spectrum *(Russian)* 79−98876
many-wave explosive instability 77−80296
maser emission, by plasma produced electrons orbiting a positively charged wire 80−92272
medium beta plasma with velocity gradients, dispersion relation for drift waves 80−64719
MHD, unstable continuous spectrum, noncircular rotating θ pinch 79−94779
MHD and guiding centre plasma models comparison 77−42969
MHD discontinuity propag. in optically thin medium 79−46438
MHD oscills. ensemble, interaction with quasiuniform mag. field, sunspots 77−76041
MHD plane wavepropag. in rarefied, radiative elect. anisotropic plasma *(Italian)* 79−94777
MHD plane waves in rarefied, radiative, elect. anisotropic plasma, small perturbation eqns. *(Italian)* 79−94776
MHD stability of a helical magnetic field of arbitrary amplitude 79−86578
MHD wave propagation in inhomogeneous media, calc. allowing for finite cond. *(Russian)* 78−63553
MHD wave radiation reaction, of moving magnetic rotator 78−34312
MHD waves segregation in ideal medium 78−87440
microinstabilities, low frequency, simulation model 78−38525
Microtor Tokamak, LF microturbulence, far IR laser scatt. 80−96362
microwave cavity discharge, behaviour at various press. and flow rates 79−23467
microwave heating of plasma in EM trap *(Russian)* 80−10400
minority cyclotron resonance damping in PLT two-ion plasma, fast-wave heating 80−24194
mode conversion of lower-hybrid waves 80−87882
mode converted lower hybrid solitons, stability in parametric regions 80−92303
modulated electron beam in inhomogeneous isotropic plasma, nonlinear wave generation 78−1852
modulation instability in magnetised plasma waves nonlinear development during heating *(Russian)* 78−47118
modulation instability producing sawtooth waves, inverse dispersive media *(Russian)* 79−19032
modulational instability of electron and ion waves 77−76054
modulational instability of nonlinear wave propagation in relativistic plasmas 80−106911
modulational instability of two transverse waves, cold plasma 79−32765
monochromatic, nonlinear evolution, two-dimens. Vlasov eqn. numerical soln. 79−73032
monochromatic EM wave excitation by relativistic charge particle beam in magnetoactive plasma *(Russian)* 78−87464
monochromatic Langmuir wave amplification by electron beam in nonlinear plasma *(Russian)* 77−76112
monochromatic wave, nonlinear behaviour in Vlasov plasma 78−71469
monochromatic wave injection, turbulent spectrum modification, dispersion relation 77−31467
monochromatic waves, nonlinear evolution in systems with nonuniform particle vel. distrib. *(Russian)* 79−55486
monochromatic whistler wave, nonlinear evolution in nonuniform mag. 80−43912
moving collisional plasma and moving plasma with intrinsic spatial dispersion, emission of longit. waves 80−87848
moving plasma, covariant dispersion eqns. 79−37538
moving weakly nonsteady plasma, propag. of plasma waves 80−106918
multi-dimensional space, reductive perturbation method for wave modulation *(Japanese)* 77−41472
multi-ion system, modulation instability of ion acoustic waves 80−69996
multicomponent plasma, ion-acoustic resist. 80−10383
multiflow beam-plasma system, potential waves profile regulation *(Russian)* 79−37511
narrow inhomogeneous layer, surface wave-incident radiation nonlinear interaction 80−100080
negative energy, analogy with anomalous Doppler effect 77−65881
negative wave momentum density in plasma 80−79463
non uniform Langmuir fields, evolution and modulation instability 80−38599
non-linear electron plasma waves in unmagnetised plasma 78−67337
non-linear propagation effects of relativistically strong plasma waves 79−10698
non-linear theory of collective processes in laser-pellet interaction and soliton generation 80−24199
non-linear wave interaction in plasma column, calcs. 80−1769
non-neutral column, wave coupling 80−75054
non-resonantly growing waves in beam-plasma system 79−60155
non-stochastic heating of magnetized plasma by electrostatic wave 80−10405
nonequilibrium plasma flow, wave conversion to EM radiation 78−75281
nonlinear, freq. shift, initial damping 77−19695
nonlinear, Landau damping *(Russian)* 78−22479
nonlinear, modulation instability *(Russian)* 78−22476
nonlinear, slowly varying in cold plasma 78−22489
nonlinear, stimulated by injecting electron clusters into plasma *(Russian)* 77−7562
nonlinear 3-wave interaction, mag. electron plasma, water bag distrib. 77−76072
nonlinear acoustic waves, in nonisothermal weakly ionised plasma *(Russian)* 79−55491
nonlinear Alfven wave in an ultra-relativistic electron-positron plasma 80−106905
nonlinear and quasielectrostatic, radiated by finite plasma-electron beam system *(French)* 77−65880
nonlinear beam-plasma interaction, freq. shift, growth rate 78−59619
nonlinear beam-plasma interaction, simple model 77−89268
nonlinear collisional drift instability, numerical analysis 78−91091
plasma waves continued
nonlinear coupling of three waves in non-uniform plasma 80−6237
nonlinear dispersive waves, Lagrangian method 78−1828
nonlinear drift wave evolution, model eqn. 80−100075
nonlinear effects in the vicinity of a radiofrequency probe 80−48985
nonlinear eigenfrequency shift, four wave resonant interaction *(Russian)* 78−83559
nonlinear electron density waves in plasma-filled waveguide *(Russian)* 78−26265
nonlinear electron oscillations, driven by EM wave 79−64850
nonlinear electron plasma waves in cylindrical waveguide 79−4134
nonlinear electron plasma waves in magnetised plasma waveguide 80−38662
nonlinear electron waves, sawtooth shaped struct. 78−22492
nonlinear electrostatic drift solitary waves in two species plasma 77−55135
nonlinear electrostatic drift wave, reson. electron effects 77−24066
nonlinear electrostatic waves, rel. to current interruption in collisionless plasma 79−75052
nonlinear equilibrium state of wave-beam, kinetic theory *(Russian)* 80−106888
nonlinear evolution eqn., bifurcation of solitary waves *(French)* 78−38465
nonlinear evolution of longitudinal wavepacket 80−1793
nonlinear generation of higher harmonics, pumped by low hybrid freq. *(Russian)* 78−22498
nonlinear HF waves, ion-acoustic, stationary propag. 77−58851
nonlinear interaction, four-wave systems, differential eqns., heating 77−80319
nonlinear interaction, involving zero energy waves 78−63559
nonlinear interaction, near linear stability boundary, non-equilib. media 78−59591
nonlinear interaction of three and four waves, Lagrangian formalism 78−63556
nonlinear interactions, in semi-bounded plasma, kinetic theory *(Russian)* 78−34313
nonlinear interactions, theory *(Russian)* 77−76049
nonlinear interactions and hydrodynamics in HF field *(Russian)* 80−53951
nonlinear ion acoustic wave, propag., with generation of long-wavelength waves 78−38475
nonlinear ion Langmuir wave collapse in nonisothermal plasma *(Russian)* 79−77380
nonlinear ion-acoustic, random density inhomogeneity effects, envelope characts. 77−19684
nonlinear ion-acoustic cnoidal waves, propag., perturbation theory calcs. 79−86581
nonlinear ion-acoustic wave emission from magnetised plasma boundary 80−38638
nonlinear ion-acoustic wave modulational instability in collisional plasma 77−24067
nonlinear ion-acoustic waves, interactions in cold plasma 80−38607
nonlinear kinetic equation, structural stability, soliton collisions 80−10382
nonlinear Landau damping by cascading, saturation 77−76066
nonlinear Landau damping in mirror plasmas 79−27766
nonlinear Landau damping of electrostatic waves in electron beam-plasma system 79−14525
nonlinear Langmuir wave, collisional damping in rarefied plasma 78−22484
nonlinear Langmuir wave interaction, at beam input to inhomogeneous plasma 79−50866
nonlinear Langmuir wave modulation, in collisionless plasma 77−89256
nonlinear Langmuir wave modulation in weakly magnetized plasmas 79−4133
nonlinear lower hybrid solitary waves 78−51291
nonlinear lower hybrid waves, saw-tooth struct. 78−59579
nonlinear magnetoacoustic waves, damping, simulation 78−79423
nonlinear magnetoacoustic waves in weakly inhomogeneous plasma 80−48867
nonlinear magnetoactive plasma, wave packet self-action *(Russian)* 78−38487
nonlinear magnetosonic waves in finite conductivity isothermal plasma, asymptotic method 79−77374
nonlinear media, kinetics of HF and LF waves *(Russian)* 79−4444
nonlinear microinstabilities, review 78−14150
Nonlinear mixing of two unstable coherent ionization waves 79−86573
nonlinear mode coupling, beat Hamiltonians and ponderomotive forces 79−14528
nonlinear mode coupling between stable and unstable waves, growth rate modulation 78−1829
nonlinear mode coupling instability saturation, bifurcations and strange behaviour 80−48873
nonlinear mode coupling model eqns., topological struct. 78−75304
nonlinear mode coupling model equations, topological struct. 80−75056
nonlinear mode-converted lower hybrid waves, 3-D effects 79−10657
nonlinear monochromatic wave, source of particles effect *(Russian)* 78−9779
nonlinear monochromatic wave growth in plasma-filled waveguide with electron beam 80−43938
nonlinear periodic waves stability in plasmas 80−38615
nonlinear plasma waves in solar atmosphere, rel. to type III radio bursts fundamental emission 80−36603
nonlinear polarized standing waves in a cold-electron overdense plasma 80−24163
nonlinear processes in magnetised plasma, nonstationary HF pressure *(Russian)* 80−106895
nonlinear prod. by EM wave transformation in hybrid reson. region *(Russian)* 77−62369
nonlinear propag. in complex mag. field geometry 78−14159
nonlinear propagation, lower hybrid waves, three dimensional effects 78−30424
nonlinear saturation mechanism of EM wave parametric decay into two plasmons, efficiency *(Russian)* 77−11349
nonlinear saturation of single wave by particle trapping 77−27666
nonlinear scattering of laser radiation by fast ion waves in plasma 80−106916
nonlinear Schrodinger eqn. for dispersive media, ion-acoustic and Langmuir wave appls. 77−31463
nonlinear Schrodinger equation, modified Zakharov-Shabat inverse scatt. problem 80−59200

plasma waves continued
nonlinear Schrodinger equation, transverse instability of soliton solns. 79−58561
nonlinear space charge waves, rel. to pulsars coherent radio emission 77−41386
nonlinear stability problems, two-time method, dissipation scalings, ohmic heating 80−53967
nonlinear stationary wave, excitation by electron bunches, theory *(Russian)* 79−37475
nonlinear subharmonic wave generation in nonuniform plasmas 80−106912
nonlinear superluminous periodic waves in magnetoplasma, governing eqns. 77−51173
nonlinear surface waves theory *(Russian)* 79−94795
nonlinear theory of collisional drift-waves in toroidal geometry and anomalous skin effects in Tokamaks 80−92320
nonlinear theory of propag. in turbulent plasma *(Russian)* 78−14165
nonlinear theory of unstable plane waves and solitons 80−87888
nonlinear three wave mode coupling, instability saturation 80−87881
nonlinear three-wave damped interaction, soln. 77−979
nonlinear three-wave interaction in magnetoplasma column 80−24152
nonlinear transparency due to modulation instability *(Russian)* 78−59604
nonlinear transverse waves in hot collisionless two-component plasma 77−62354
nonlinear travelling longitudinal wave in cold plasma 79−64861
nonlinear travelling waves in a homogeneous cold collisionless plasma 79−14542
nonlinear vibrational excitation waves in a molecular plasma with negative ions *(Russian)* 79−27777
nonlinear wave, excitation and attenuation by monochromatic electron beam in waveguide *(Russian)* 77−47220
nonlinear wave, statistical description of trapped particles, relax. time. 77−31465
nonlinear wave amplification in a beam-plasma system 78−91103
nonlinear wave effects, comparison of theory and experiment 79−7460
nonlinear wave fields, diffusion of action 78−81854
nonlinear wave interaction, symbolic computation code MACSYMA 77−27660
nonlinear wave interaction and stationary fluctuation spectrum, nonequilib. plasma *(Russian)* 78−14153
nonlinear wave interaction in magnetoplasma column, experimental results 80−24153
nonlinear wave interaction in rot. plasma 79−60123
nonlinear wave interaction in semibounded plasma *(Russian)* 78−67350
nonlinear wave interactions, appl. of digital bispectral anal. 79−73036
nonlinear wave interactions, microscopic Lagrangian description, warm magnetoplasma 78−42754
nonlinear wave interactions and critical fluctuations 80−38626
nonlinear wave packet acceleration and slowing down 80−59203
nonlinear wave propag., soliton form. 79−46442
nonlinear wave propag., solitons and envelope solitons 78−14158
nonlinear wave solutions, stability 79−14533
nonlinear wave-particle interaction in magnetosonic mode, pure sinusoidal wave model 78−26320
nonlinear wave-plasma coupling at the lower hybrid frequency 79−94791
nonlinear wave-wave interaction, bispectral wave anal. 77−24082
nonlinear wave-wave interaction, harmonic generation coupling coeffs. 78−5867
nonlinear wave-wave interactions, symmetry and selection rules 78−42756
nonlinear wave-wave interactions without resonance conditions 78−42757
nonlinear waves, commensurable and incommensurable, parametric instabilities 79−66915
nonlinear waves, in cold two-component plasma, decay instabilities 77−35346
nonlinear waves, propag. along magneto-plasma column 77−89247
nonlinear waves at upper hybrid reson. parametric excitation 79−23418
nonlinear waves excited near resonance, computer simulation 77−72435
nonlinear waves in cold plasma, classical Vlasov plasma description through quantum numerical methods 80−92288
nonlinear waves in electron beam-plasma system, explosive instability 79−19050
nonlinear waves in magnetised plasma, periodicity anal. 80−43902
nonlinear waves in modulated electron beam-plasma system *(Russian)* 78−26264
nonlinear-wave propagation in a proton-electron plasma coupled with a strong radiation field 80−48872
nonpotential waves, in auroral electrojet 77−49212
nonresonant decay of lower hybrid waves 80−92315
nonresonantly growing waves, energy 79−14530
nonuniform plasma, mode coupling, Lie operator calcs. 78−55718
oblique collision of ion-acoustic solitons 80−83934
oblique Langmuir solitons under free path conditions *(Russian)* 80−79477
oblique wave excitation in semifinite magnetoactive plasma with metal screen 78−26306
Ohmic pumping by means of externally driven tearing modes 80−28706
optical cavity plasma, stimulated Raman and Brillouin scatt., electrostatic and EM waves 78−34324
ordinary mode absorpt. spectrum, plasma effects 77−68787
oscillating two-stream and parametric decay instabilities in a weakly magnetized plasma 80−38637
oscillations, in lower-hybrid range, of bounded plasma 80−24162
overdense plasma, nonlinear linearly polarized standing waves 78−87447
Pade approximation to wave amplitude 79−73004
parameteric interactions in random media 77−27671
parametric decay below upper hybrid freq. 77−42975
parametric decay in a finite width pump, including the effects of three-dimensional geometry and inhomogeneity 78−67346
parametric decay in homogeneous plasma, pumping wave struct. absolute instability *(Russian)* 77−47183
parametric decay instability, stabilisation by nonlinear shift of Langmuir wave freq. *(Russian)* 77−72425
parametric decay instability at ion-ion hybrid reson. 77−65864
parametric decay of non-ducted whistler-mode signal 80−6239
parametric excitation of backward ion cyclotron wave with a pump in the lower hybrid range 79−37490
parametric excitation of coupled plasma waves 79−4128
parametric excitation of longitudinal waves *(Russian)* 78−34282
plasma waves continued
parametric generation in ionosphere by extraordinary radiowave 77−13153
parametric instabilities, spatial turbulence effect 79−27767
parametric instabilities and ion heating in a two-ion species plasma 80−28708
parametric instabilities in weakly-inhomogeneous hot plasmas 80−28828
parametric instabilities of inhomogeneous plasma in presence of long-wave low frequency oscillations *(Russian)* 80−103136
parametric instabilities of waves in bounded magnetised plasma 77−68772
parametric instabilities set up by EM radiation in non-uniform magneto-active plasma *(Russian)* 80−106889
parametric instability, appearance of stochasticity on decay confinement *(Russian)* 78−51300
parametric instability, thermal fluctuation effect in inhomogeneous plasma *(Russian)* 80−106897
parametric instability damping by high power elec. field pumping *(Russian)* 77−7553
parametric instability due to a low frequency whistler wave 80−83926
parametric instability of inhomogeneous plasma, with pump wave strong coupling 78−94912
parametric instability-induced, in relativistic electron beam heating 78−26307
parametric interaction of waves in nonuniform pump field 77−24073
parametric interaction of waves in plasma with random large-scale inhomogeneities *(Russian)* 80−103137
parametric interactions, random inhomogeneities effect 77−68788
parametric magnetosonic turbulence, evolution of fluctuations into electrostatic and acoustic waves 77−11342
parametric phonon excitation and turbulence 78−75342
parametric resonance in a weakly turbulent relativistic electron plasma 79−55539
parametric turbulence, due to EM wave decay 77−31470
parametric turbulence of inhomogeneous plasma layer *(Russian)* 79−68921
parametric wave excitation in bounded systems 80−6252
parametrically driven waves, effect of particle drift motion 78−34293
parametrically excited surface waves, phase mismatch 80−24165
parametrically excited waves, collective oscill. and instability of single freq. state *(Russian)* 79−19033
partial differential eqns., method of strained coords. 79−4127
particle and heat fluxes, inhomogeneous plasma, effect of current driven drift waves 78−94898
particle dynamics in low freq. EM waves, magnetosphere particle flux in inhomogeneous plasma 80−1804
particle scattering by low freq. waves, effective scatt. freq., eval. method 80−83882
particle-wave interactions, cyclotron reson. vel. shift, wave propag. effects 80−33774
Penning cold-cathode discharge, m=0 mode instability investigation 79−98894
Penning discharge ion source with hollow cathode, HF instabilities 80−43997
phase, ray and group vel. surfaces, magneto-ionic medium 77−65852
phase path, group path, attenuation 78−59571
phase-locked, particle motion in large amplitude wave 79−19021
phonon exchange between ions via neutral gas in weakly ionised plasma 79−27775
plasma, cartons induced by soliton flash 78−91104
plasma, ion-acoustic solitons, strongly non-linear 78−5858
plasma, transverse wave packets, momentum, mass and energy transport, solitons 78−1812
plasma, upper hybrid solitary waves, existence and propag. 78−83555
plasma waveguide, ion acoustic wave, excited by EM rad. press. 78−26298
plasmapause, electrostatic waves near upper hybrid resonance freq. 80−12616
plasmasphere, ion cyclotron waves, Hawkeye 1 obs. 77−70928
plasmon condensate, nonlinear statistical theory 77−47192
plasmon condensate, turbulence spectra 77−47199
plasmon dispersion, correlation correction 80−43917
plasmon prod. by laser light Raman conversion 78−47125
plasmon scatt. by electrons in intense EM field, instability 77−72434
ponderomotive effects, kinetic theory 79−32740
ponderomotive force in interaction between ion wave and HF elec. field 80−10373
positive column, irregular ionisation wave electron density rel. to light intensity variations 78−67520
positive column, standing striation excitation conditions 78−67514
potential wave amplification by supercritical vel. electron beam in organic plasma *(Russian)* 78−1851
potential waves in cold plasma, parametric instability *(Russian)* 78−91088
power flow and electron Landau damping of lower hybrid waves in cylindrical plasma 79−94784
produced by absorption of axially asymmetric EM waves, inhomogeneous plasma 77−55156
propagation characts. in magnetically confined nonneutral plasma 77−72484
propagation in low-temp. plasma, ionised relax. dissipative effect *(Russian)* 78−1816
propagation in moving cold magnetised plasma, polarisation relations and dispersion eqns. 80−64723
propagation in self-gravitating isotropic press. plasma theory 80−72763
propagation in two-fluid self-gravitating plasma 79−19009
propagation in unstable, turbulent magnetoplasma, stochastic photon diffusion 79−48662
propagation of circularly polarised waves in stochastic mag. field 77−973
proton-cyclotron frequency harmonic waves, rel. to instabilities in nonuniform loss-cone magnetospheric plasma 80−90286
pseudo-classical transport, nonlinear theory of collisionless drift instability 79−94774
pseudo-classical transport, particle and energy flux, electron trapping by drift waves 79−94773
pulsar magnetospheres, relativistic MHD wind or plasma wave 80−31317
pulsar synchro-Compton radiation damping of linearly polarised plasma waves 78−61877
pulsars, relativistic Langmuir soliton appls. 79−17004

plasma waves continued
pulsed reson. cone, plasma ringing with localised antenna 77−58866
pumping wave decay, convective instability, harmonic generation and harmonic generation *(Russian)* 80−14889
pumping wave harmonic generation, diagnostic of parametric turbulence *(Russian)* 78−26266
pure electron plasma, waves and transport 80−38563
quasi stationary waves exam. on periodic injection of electron bunches *(Russian)* 78−47134
quasi-electrostatic, two-stream nonsymmetric instability 77−31446
quasi-longitudinal waves, excitation in magnetised plasma waveguide by electron beam 78−87462
quasilinear theory 80−19576
quasistatic surface wave spectrum 77−84434
quasistatic waves, collective excitation in inhomogeneous anisotropic plasma, linear theory 77−39413
quasistatic waves, collective excitation in inhomogeneous anisothermic plasma, nonlinear effects 77−42970
radiation from waveguide, rel. to plasma wave scatt. by ion-acoustic oscills. 80−87886
radiation phenomena, fundamental radiation theory 78−94914
radiation phenomena, fundamental radn. theory 79−23409
radiation phenomena, radn. from point sources 79−23411
radiation phenomena, radn. from point sources 79−23410
radio emissions from plasma waves and type III solar bursts 79−44454
radiowave generation by gyrosynchrotron and Langmuir-wave processes, solar and stellar appl. 79−21172
random linear electrostatic waves, cross spectrum measurement in isotropic Maxwellian plasma 79−46450
rarefied plasma, heat propag. across mag. field, magnetothermal waves 77−42999
rarefied plasma, mag. field rapid penetration, magneto-acoustic shock waves, super-Alfven penetration *(Russian)* 78−59554
rarefied radiative plasma, surfaces ot discontinuity, nonlinear waves 78−87441
reflectionless shock wave in stratified medium 78−51193
regularised long wave equation, numerical studies 80−53964
relativistic electron beam, stimulated coherent EM wave scatt. by longitudinal electron waves *(Russian)* 77−7542
relativistic electron beam/electrostatic wave interaction 78−75375
relativistic electron beams, nonlinear theory of stimulated scatt. of waves *(Russian)* 79−60157
relativistic nonlinear electron cyclotron waves in plasmas 80−10377
relativistic plasma, linear wave props., using two fluid approx. 79−1337
relativistic plasma, longit. waves and beam instability *(Russian)* 79−60158
relativistic plasma, nonlinear dispersion relation for transverse wave 80−87939
relativistic plasma, nonlinear wave modulational instability with nonlinear Landau damping *(Russian, English)* 80−53955
relativistic self-focusing in cold plasma 79−73009
relativistic systems, Bogolyubov equation hierarchy, plasma wave radiation damping 79−77377
relativistic transverse cold plasma waves, nonlinear, linearly polarised, stability 80−6235
renormalized Compton scattering and nonlinear damping of collisionless drift waves 80−69998
resistive drift Alfven waves in sheared mag. fields 80−64718
resistive drift-Alfven waves in sheared magnetic fields 79−77365
Resistive lower-hybrid instability in current-carrying plasmas 78−71467
resistive modulation instability 79−77378
resonance absorption, in laser-produced plasma, X-ray bremsstrahlung emission obs. 78−59559
resonance cone, in inhomogeneous magnetoplasma column, theoretical anal. 80−83884
resonance cone, warm bounded magnetoplasma, damping 77−55140
resonance cone in inhomogeneous magnetoplasma column, quasistatic approx. 80−64724
resonance cone trajectory, focused, nonlinear modification, probe diagnostics 80−10379
resonance cones, in bounded plasma, for finite source 78−91099
resonance cones, nonlinear ponderomotive force effects 77−62356
resonance conversion of amplitude-modulated transverse to monochromatic wave 80−6251
resonance tunnelling in cold stratified plasma 79−41818
resonances in the ion cyclotron range in toroidal geometries 80−83938
resonant absorption of laser light, by magnetised plasma 78−51309
resonant behaviour, near lower hybrid freq., mirror config. effects 77−15202
resonant behaviour, RF waves nonlinear coupling *(German)* 77−15203
resonant collective processes, wave and particle accel. into increasing plasma gradient 77−47153
resonant excitation of slow low-freq. waves by opposite moving electron beams *(Russian)* 80−92336
resonant nonlinear three wave interaction, stationary solns. 77−76064
resonant particle effects in Langmuir and whistler waves, long-time-scale plasma simulation 78−42796
resonant wave interactions, inhomogeneous plasma 78−18404
resonant wave-particle interaction, at half-integer cyclotron harmonics 78−78871
resonantly interacting wave system, evolution of explosive-type instability 77−35343
resonantly interacting wave system, explosive-type instability 77−72443
retarded wave, RF heating in low hybrid freq. band, exciting system design *(Russian)* 77−51202
reversed ultra fast theta pinch, mag. wave heating of Tokamak 77−35364
RF coupling and mode conversions at lower hybrid resonance 77−24072
RF coupling loops, transmission line approx. 80−28672
RF discharge-plasma interaction, energy exchanges, magnetoacoustic wave generation 78−30485
RF driven current generation by lower hybrid waves in Tokamak 80−103116
RF emission, plasma wave scatt. by ion-acoustic waves in nonequilib. plasma 80−64733
RF energy coupling by magneto-acoustic waves in toroidal plasma 80−28743
RF heated Tokamak plasma, waveguide array excited lower hybrid fields 78−42773
RF heating, slow waves launched into overdense plasma by phased waveguide 79−64882

plasma waves continued
rF instabilities driven by neutral beam injection, review 80−28757
RF intense localised field, magnetised plasma particle and wave heating 77−84462
RF ion heating, near to lower hybrid freq. 77−62380
RF plasma heating, resonant surface accessibility, surface wave role 80−92346
RF waves, interactions between high and low freqs. in active medium 79−27774
Riemannian wave interaction in media without dispersion, quasi-elasticity *(Russian)* 78−9778
Rossby wave turbulence, exact Gaussian soln. 80−92325
Rossby waves, nonlinear behaviour and turbulence spectra 80−19573
rotating electron-plasma column space-charge wave propagation 77−55137
rotation influence on kink instability, compressibility *(Russian)* 80−48887
rotational simple and shock waves, in anisotropic plasma 77−91369
runaway electron tail, self-consistent theory 77−62338
scattering, enhanced Raman, from plasma wave, of Gaussian laser beam 79−86566
scattering of two longitudinal oscillations into single transverse wave, radiation emission and dynamics 77−58861
Schrodinger equation, nonlinear, conservation laws soln. method 79−63066
second harmonic emission, head-on approximation 79−41803
second harmonic generation by surface waves 79−1306
second helicon branch, relativistic electron motion, circularily polarised EM wave propag. *(Russian)* 77−47205
second order harmonic surface wave generation by fundamental wave 80−92307
second-harmonic generation of upper-hybrid radiation in a plasma 80−79506
self channelling effects, localised plasma regions *(Russian)* 79−77375
self consistent circ. polarised waves, stability 79−14526
self-consistent EM wave stability in warm plasma 79−32763
self-excited fluctuation spectra, digital bispectral anal. 78−83550
self-generated magnetic fields and harmonic emission 80−38546
self-gravitating disk, resonant interaction of three density waves 77−67130
self-gravitational instability of plasma rotating layer, growth rates wave number depend. 80−56706
self-influence of magneto-acoustic waves in a plane plasma waveguide *(Russian)* 79−41815
self-modulation by ponderomotive force, nonlinear analysis 78−75326
self-precession and freq. shift of two polarised waves 79−23417
semiconfined electron plasma, ballistic theory of echoes *(Russian)* 77−7521
sheaf instability at moderate densities, anomalous ion heating *(Russian)* 80−43922
shear Alfven wave heating experiments in heliotron D 80−28716
shear Alfven waves, quasi-linear theory 80−64714
shear flow stability and Alfven waves in magnetised plasma 80−96360
sheath criterion generalisation, sonic ion wave at boundary 77−3954
SHG in magnetoactive plasma by internal source *(Russian)* 77−58868
shock, rarefaction and heat waves, linear mag. fusion device, confinement 78−33289
sideband dispersion 79−19020
sideband instability, nonlinear large-amplitude wave evolution, simulation 78−83546
sideband instability in large amplitude wave, computer simulation 80−38602
single Langmuir solitons, perturbation anal. 80−69999
skin-effect, anomalous, in bounded plasmas 80−24173
slow Langmuir solitons, low amplitude and wavenumber behaviour 78−75293
slow mode magnetoacoustic waves at dayside magnetopause, rel. to plasma depletion 79−66876
slow space-charge wave propag. on relativistic electron beam 80−1115
slow wave excitation, by relativistic beam, in waveguide 77−11364
slow wave propag., plasma/dielectric wall 77−51183
slow wave struct., nonlinear coupling with lower hybrid waves near plasma surface 80−92309
slow wave-electron beam interaction in plasma filled waveguide, signal spatial evolution 77−11362
slow waves in plasma column, excitation condition 77−3932
slow-fast mode conversion effect on lower hybrid slow mode excitation 80−28668
solar corona, direct conversion of Langmuir waves into o-mode waves 80−72896
solar corona, electron flows stabilisation in inhomogeneous plasma 80−109411
solar corona, MHD wave mode coupling, stratified media 78−20775
solar corona, MHD waves, mode coupling, reduction of coupled eqns. 78−20776
solar corona, plasma waves conversion into transverse waves, rel. to radio bursts 77−2414
solar flare particles pulsed accel., plasma turbulence, ion-acoustic and Langmuir waves 78−96450
solar flares, nonthermal plasma wave elec. fields meas. using Stark effect 78−12193
solar flares primary energy release region, plasma radiation diagnostics 79−84777
solar photosphere, dipole-like progressive wave and magnetic field analysis 77−56905
solar radio bursts type II and II theory *(Russian)* 78−16381
solar SHF flux fluctuations from limited areas, rel. to coronal wave propag. 79−35222
solar type III radio bursts, deconvolution and decay mechanism 77−45381
solar type III radio bursts caused by high-density electron beam, numerical simulation 79−84779
solar type III radio bursts fundamental radiation rel. to coronal low freq. turbulence 79−84778
solar wind, cyclotron wave growth in bi-Maxwellian two-ion plasma 79−101040
solar wind, ion acoustic waves, Imp 6 wavelength meas. 78−40787
solar wind, ion acoustic waves and related plasma obs. 79−80182
solar wind, plasma waves rel. to second harmonic radiation in type III bursts 78−7958
solar wind, semi-empirical model 77−13201

plasma waves continued
solar wind at Jupiter, bow shock, Voyager 1 plasma wave turbulence 79−96954
solitary kinetic Alfven wave stability, one dimensional nonlinear case 80−1776
solitary nonlinear surface plasma density wave 79−98896
solitary population-inversion wave in mol. plasma, drift-superheating instability 77−15191
solitary wave, radially symm., Korteweg-de Vries eqn., spike soln. 78−47109
soliton, Langmuir, one-dimensional, propag., interactions and generation 77−43057
soliton damping, nonadiabatic stage, intermediate asymptotics *(Russian)* 77−68769
soliton damping 79−64869
soliton formation, electrostatic wave interaction upper-hybrid reson. freq. 77−76074
soliton generation at resonance and density modification in laser irrad.-plasma 78−14172
soliton ion-acoustic waves, K-dV eqn. with coord. stretchings 77−58859
soliton propag. and deformation in magnetised plasma filled waveguide, modification by reson. particles 79−77395
soliton propagation, cloud generation, in nonlinear dispersive media with weak dissipation 78−47123
soliton solutions in media with inverse dispersion 80−103152
solitons, classification of descriptions 78−75286
solitons, corresponding to localised density depressions travelling at sub-thermal speeds 77−19692
solitons, cylindrical ion-acoustic, propagation characts. 80−28632
solitons, in dispersive media, nonlinear evolution eqns. soln., review 78−60
solitons, instability, self-refraction *(Russian)* 77−11212
solitons, lecture 78−24690
solitons, nonlinear normal mode theory 80−48875
solitons, numerical modelling of Langmuir turbulence 80−70030
solitons, of finite amplitude, stability criteria 79−64860
solitons, one-dimens. coupled Langmuir-ion acoustic waves, dynamics and stability 78−34296
solitons, review 79−44755
solitons, stability to transverse perturbations 77−51180
solitons and tail generation in nonlinear dispersive media 78−75287
solitons in convective motion 79−46443
solitons in convective motion 79−46444
solitons of flexural EM waves in magnetoactive plasma *(Russian)* 80−83918
sonic-Langmuir solitons, formation, interaction, inverse scatt. method 77−27664
sound excitation long range effect in conducting plasma *(Russian)* 78−47105
sound waves, effect on spectral line profiles 78−38461
space charge ionising waves, high velocity propagation 80−87889
space charge wave propagation along moving magnetoplasma slab 80−38700
space charge wave propagation on rippled electron beams 77−3933
spatial collapse, highly nonlinear states in plasmas, expt. obs. 80−6233
spatial lower hybrid wave echoes, characts. 80−38597
spatial wave echoes at lower hybrid mode 77−89242
spatial waves nonlinear modulation in steady plasma flow 77−31444
spectrum of elliptic plasma column 77−31451
spectrum of ionospheric waves, meas. via satellite-borne cross-power spectrum analysers 80−94621
spherical ion-acoustic solitons, inelastic collision 79−77373
spherical thermal waves in laser produced plasma 80−59217
spontaneous radiation, weakly inhomogeneous plasma, charge density wave transform. *(Russian)* 77−3924
stability of the longitudinal oscillations of a bunched beam propagating in a vacuum chamber with reactive impedance 79−85849
standing electron plasma waves, amplitude dispersion 79−98900
standing periodic nonlinear waves form. 79−98895
standing waves in magnetised plasma cylinder, magnetoacoustic resonance 79−4132
stationary nonlinear interaction of HF and LF waves, density gravity generation 77−51170
stationary nonlinear waves, excitation by cold electron cluster excitation *(Russian)* 79−98891
stationary periodic waves with Hall dispersion, magnetohydrodynamic approx. *(Russian)* 77−27661
stationary space charge waves in bounded plasma 78−9777
stationary turbulence regions and anomalous resist. in magnetosphere plasma 80−38649
stellar atmospheres, magnetogravity waves propag. 79−92670
stellarator, Saturn, current-free transport processes, drift modes effect 80−19605
stimulated Brillouin scattering initiated by ponderomotive force density fluctuations 80−103129
stimulated light scattering by ion modes, space time evolution in homogeneous plasma 79−68930
stimulated plasma waves in magnetosphere, appl. to plasmapause meas. and propag. waves mode determ. *(Japanese)* 80−94650
stimulated plasma waves in magnetosphere, JIKIKEN (EXOS-B) satellite expts. *(Japanese)* 80−94649
stimulated scattering processes, saturation by electrostatic daughter waves nonlinear decay 80−79509
stimulated waves in magnetosphere, prod. by JIKIKEN electron beam-plasma interaction expt. *(Japanese)* 80−94655
stochastic ion heating by electrostatic wave in sheared mag. field 80−28705
stochastic self-modulation in nonequilib. media *(Russian)* 79−98902
strong Langmuir turbulence for electron plasma waves, plasma diagnostics appl. 80−48889
strong standing EM wave self-modulation by ponderomotive force 78−75327
strongly dispersive waves, contrib. of higher order terms in reductive perturbation theory 77−80287
submagnetosonic, lower hybrid wave solitons 79−14537
subsonic electron fluid and small spark formation 80−38792
surface EM wave interaction with relativistic electron beam 79−60153
surface heating, density rippling, and propagation cones in high-power lower-hybrid heating 80−92342
surface ion acoustic waves in non isothermal gas layer *(Russian)* 80−87891

plasma waves continued
surface Langmuir wave decay dissipative instability in semibounded plasma *(Russian)* 80−38583
surface ripples, parametric excitation in plasma column 77−51177
surface wave, high freq., in current carrying hot plasma column, kinetic model 78−42759
surface wave dispersion in plasma-beam system, stabilisation by HF electric field 78−91117
surface wave fluctuations in imhomogeneous magnetoactive plasma 77−24077
surface wave propagation, along plasma column, nonlinearity 79−41826
surface wave propagation, on plasma column, mag. current excitation 78−1821
surface wave reson. instability in inhomogeneous plasma stream 77−24078
surface wave spectrum, in inhomogeneous plasma cylinder, correl. with fluctuations 79−14543
surface wave spectrum, surface impedance with specular-diffuse particle scattering 77−24058
surface waves, form. by EM waves incident on magnetoactive plasma slab 77−3931
surface waves, HF, parametric excitation using slanted, incident EM waves *(Russian)* 80−87874
surface waves, LF, in cylindrical nonisothermal plasma column 80−6232
surface waves, solitary nonlinear behaviour 79−1302
surface waves in a homogeneous plasma sharply bounded by a dielectric 79−4135
surface waves in collisional current carrying plasma column 78−34284
surface waves on plasma half-space 77−51179
SW parametric instability of inhomogeneous plasma, semi-bounded by vac. *(Russian)* 80−83917
tearing mode instabilities and suppression by lower hybrid fields 80−28666
temperature gradient drift wave eigenmodes stability in sheared mag. field 80−43914
test waves, propag. in presence of large amplitude electron plasma wave, dispersion relations 77−7535
theoretical plasma mechanics, book 80−27048
theory and expt. at Kharkov Inst., Ukrainian SSR *(Russian)* 79−14544
thermal parametric instability in non-uniform plasma, theory *(Russian)* 79−27760
thermal parametric instability in nonuniform plasma, nonlinear theory *(Russian)* 79−27761
thermal waves in laser half-space plasma 79−14578
thermonuclear reaction wave in high density plasma 77−10487
theta pinch, low density, step-like mag. piston 80−103182
theta pinch plasma, absorpt. of magnetoacoustic waves *(German)* 80−10430
three wave interaction in cold semi-infinite plasma 80−79462
three-wave resonant eqns. with one heavily damped wave 78−14146
Tokamak, electrostatic drift waves, numerical anal. of instability and transport 80−48871
Tokamak, fast-wave heating, ray-tracing anal. 79−41848
Tokamak, large aspect ratio, two-dimens. drift-wave stability 80−79479
Tokamak, lower hybrid heating to ignition 80−18605
Tokamak, octopole, obs. of RF driven plasma current 80−48910
Tokamak, ray tracing for lower-hybrid waves 79−60139
Tokamak, trapped electron modes, cross-section elongation effects 78−59585
Tokamak (Alcator), driven lower-hybrid waves, light scatt. study 80−1835
Tokamak discharge, anomalous drift-wave transport anal. 79−32745
Tokamak fusion reactor, steady-state, lower hybrid wave-driven, design constraints 80−10424
Tokamak fusion reactor, thermonuclear instabilities α-particle interactions 77−88281
Tokamak fusion reactors, doublet research, plasma shape control, MHD stability 80−28837
Tokamak heating by fast magnetosonic wave excitation 80−24189
Tokamak plasma, lower hybrid wave propag. and damping, numerical study 80−64698
Tokamak plasma, quasi-mode parametric excitations in lower-hybrid heating 80−64748
Tokamak power reactor, steady state, lower hybrid wave driven 80−48945
Tokamak thermonuclear reactor, MHD modes drift phenomena, kinetic method *(Russian)* 80−1827
Tokamaks, lower hybrid resonance cones 80−28791
Tokamaks, nonlinear drift tearing modes 80−53971
topside ionosphere, ion heating by electrostatic ion cyclotron waves 80−12606
toroidal plasma, enhanced diffusion, electrostatic drift modes, ohmic heating effects obs. 77−19702
toroidal plasma, stationary current excitation by wide spectrum waves *(Russian)* 79−98863
toroidal plasmas, MHD instabilities 80−38579
torus plasma, fluctuation induced particle transport, strong DC elec. and mag. fields 77−89322
trajectories and electron cyclotron heating in Tokamak plasmas 80−83923
trajectory, mode conversion and electron cyclotron effects, in toroidal plasmas 78−47137
transient setting of ponderomotive nonlinearity, self-focusing and plasma-wave excitation 79−77387
transport processes caused by magnetic flutter, assoc. with drift waves 79−86561
transverse, dispersion eqn., nonlinear effects *(Russian)* 78−38466
transverse circularly polarised self-consistent large amplitude wave stability, in large-scale mag. field 79−32760
transverse envelope solitons, strongly non-linear 77−84421
transverse ion-acoustic and antidrift waves in magnetised plasma, stability 77−55147
transverse wave packet, 3-dimens., nonlinear evolution in hot plasma, ion-acoustic wave effect 80−43899
transverse waves in magnetoplasma subjected to stochastic mag. field, normal mode approach 80−75049
transverse waves propag. along axisymm. mag. field in nonhomogeneous plasma, WKB kinetic theory 78−42740
trapped α-particles, quasilinear relax. in Tokamak reactor, during cyclotron magnetoacoustic instability *(Russian)* 79−55487

plasma waves continued
trapped electron instability, mag. curvature drift driven, collision effects 77−55142
trapped electron shear-Alfven instability, stabilisation by temp. gradient 80−28599
trapped ion mode inhibition by drift wave fluctuation 80−59211
trapped particle instability in Tokamaks, book 78−83562
trapped particle modes, parametric excitation, instabilities, HF pump effect 77−24177
trapped particles, resonance interactions *(Russian)* 78−26236
trapped-ion mode, nonlinear saturation, mode coupling theory 78−87446
travelling large amplitude electron-ion in warm unmagnetized plasmas, stationary ion solution 79−41810
travelling wave-induced DC current in collisionless limit, collision term based calc. 78−1806
Trivelpiece-Gould mode propagation in axially inhomogeneous drifting plasma 78−75316
Trivelpiece-Gould mode propagation in axially inhomogeneous plasma column, WKB calc. 78−75317
Trivelpiece-Gould wave, excitation in magnetised plasma by slow waveguiding cct. 80−14892
Trivelpiece-Gould-modes, axial inhomogeneous plasma 79−23405
turbulence development and decay mechanisms, wave interactions, analogue simulation *(Russian)* 79−7462
turbulent plasma, electron distribution function, correlation anal. 79−14547
turbulent plasma, ion-acoustic wave, dispersion relation calc. 78−26284
two Langmuir wave parametric decay instability, self-trapped EM pump wave effects 80−96357
two Maxwellian plasma, electron plasma wave, higher order Landau modes 80−38601
two-plasmon decay, profile modification, produced by 10.6 micron radiation, at $^1/_4$-crit. density 79−19061
two-stream instability, thin layer waves modes 77−62361
two-stream plasma, development of instability of dispersed waves *(Russian)* 80−103138
two-temperature plasma, field eqn. of electron wave 80−28633
ULF, in magnetosphere, high latit. ground based obs. 78−49228
ultra-relativistic electron-positron plasma, macroscopic wave behaviour 80−106904
ultrarelativistic electron-positron plasma, wave prod., rel. to pulsar radiation 78−20629
unmagnetised plasma, quasilinear theory of parametric processes 79−94787
unshielded plasma waveguide excitation by modulated electron beam 80−79512
unstable drift waves, in sheared mag. field, simulation study 79−86574
unstable turbulent ionisation waves, two dimensional Fourier spectroscopy 80−38646
upper hybrid excitation by Gaussian EM beam 79−60149
upper hybrid mode emissions in magnetosphere, obs. during JIKIKEN (EXOS-B) satellite initial phase *(Japanese)* 80−94675
upper hybrid quasipotential waves, one dimensional collapse *(Russian)* 78−63561
upper hybrid solitons, in warm magnetised plasma, kinetic anal. 80−38595
upper-hybrid reson. absorpt. of laser in plasma focus, backscatter 80−28621
upper-hybrid-resonance absorption of laser radiation, magnetised plasma 77−72451
velocity modulated neutralised ion beam, evolution in potential wells, ion density distrib. *(Russian)* 80−100082
Venus environment, plasma wave investigation by Pioneer Venus Orbiter 80−67497
viscous damping of magnetoacoustic oscillations in cold, bounded cylindrical plasma 80−24151
viscous waves damping in a drifting plasma 79−55500
Vlasov eqn. for vel. depend. interactions and pair-wise central pot. 78−34270
Vlasov plasma, linear wave equation derivation for propag. at arbitrary angle 79−1301
VLF electrostatic emissions form. mechanism in high latit. F-region 78−93037
VLF excitation in ionosphere due to electron beam injection 80−12603
VLF waves, magnetospheric, obs. and comparison with high energy electron flux by EXOS-B satellite *(Japanese)* 80−94652
wake model of fast moving body in plasma and its effects 79−77353
Warm nonuniform plasma, stress tensor for high freq. wave propag. 80−33764
water bag plasma, electron plasma wave, higher order Landau modes 80−38601
wave dispersion in presence of relativistic beam 80−19592
wave packets in dispersive media, main signal and precursor approx. 80−24158
wave radiation by oscillating electric dipole in moving warm plasma 80−87868
wave-particle interaction, in cyclotron reson. region, trapped particle effects 77−51164
wave-particle transport from electrostatic instabilities 80−83898
wave-wave interaction, theory and expt. 77−47195
waveguide, plasma-filled, electron beam interaction, spatial evolution of complex EM modes, collision effects 79−14556
waveguide modes of warm transversely-drifting electron plasma in strong mag. field 79−50861
weak turbulence, of nonisothermal plasma, due to Langmuir wave-ion acoustic wave interaction *(Russian)* 79−37495
weak turbulence theory, low phase vel. induced wave scatt. 77−55148
weakly inhomogeneous magnetic field amplification by plasma wave 80−24166
weakly ionized, acoustic wave attenuation through reflection at neutral gas interface 78−55719
weakly localized two-dimensional drift modes 80−53970
whistler, large-amplitude, parametric coupling with ion quasimodes, induced instability 78−18401
whistler mode signals generation in presence of enhanced fluctuations in plasmas 80−92293
whistler mode waves near Io plasma torus, electron pitch-angle diffusion 80−4290
whistler type wave packets, interaction with energetic plasma electrons, nonlinear theory *(Russian)* 78−71464
plasma waves continued
whistler wave, filamentation instability due to ponderomotive force 79−14538
whistler wave, in nonuniform mag. field, test particle correlation, simulation 79−37486
whistler wave, large amplitude oscillation by high power microwaves 80−43913
whistler wave, modulational instability for oblique propag. to mag. field 79−27771
whistler wave damping, dipole antenna obs., large magnetoplasma 78−34327
whistler wave decay, into upper sideband and low-freq. waves 79−73007
whistler wave ducting caused by antenna actions 78−59586
whistler wave packet, propag. at ang. to mag. field, nonlinear evolution *(Russian)* 79−98886
whistler wave propagation in narrow density trough 80−38629
whistler wave solitons, classification of descriptions 78−75286
whistler wave trapping in density crest 80−53984
whistler waves, rel. to fine struct. of magnetic shocks in collisionless plasma 80−85854
whistler-Alfven turbulence interaction 80−75058
whistlers, supersonic large amplitude electron whistler-wave-ion density perturbation coupling, solitons 77−58854
Ar decaying pulsed discharge plasma, acoustic waves density modulation 80−103143
Ar low voltage arc, positive column ionisation waves, hydrodynamic model 78−79481
Ar plasma, microwave absorption at singularity, parametric satellite excitation obs. 77−51194
Ar, positive column, progressive and regressive ionisation waves *(French)* 80−43905
Ar-He plasma, ion acoustic soliton form., mechanism 78−18457
CO_2 glow discharge, acoustic wave influence on F^- forward ionisation wave 78−67521
CO_2 laser beam scatt. by microscopic fluctuations in plasma density 80−79574
CO_2, supersonic radiation waves, excitation by CO_2 laser 79−90433
H, ACT-1 toroidal plasma, externally launched ion Bernstein wave 80−106967
H, Stark profiles, anisotropy of HF noise, turbulent plasma 78−1896
H-D plasma, fast magnetosonic wave mode conversion, in Tokamak 77−72436
He DC discharge electron free streaming wave propagation obs. 78−75314
He flowing discharge, glow/arc transition and cathode-zone wave structure obs. 78−75475
He glow discharge plasma, ionis. waves in positive column 80−1876
He, low-press. weakly ionised magnetoplasma, acoustic wave generation 80−44059
He positive column, magnetised, temps. of charged particles, nonlinear effect of ionis. waves 80−44023
He, positive column ion-acoustic waves, obs. 78−75312
He positive column ionisation waves, influence of longitudinal mag. field 78−67522
Hg vapour line splitting on Tonks-Dattner reson. 80−59317
NaCl plasma, acoustic wave-coherent CO_2 light scatt. 78−34325
Ne discharge, ionis. waves coherent nonlinear coupling 79−55497
Ne discharge, ionisation wave, phase instability and disintegration obs. 78−67518
Ne discharge, wavenumber spectra of turbulent ionisation waves 78−71541
Ne, glow discharge, ionisation waves, regular and irregular, correlation meas. 78−1917
Ne, glow discharge, turbulent ionisation waves, correlation meas. 78−67519
Ne hot cathode discharge plasma, second order harmonic surface wave generation 80−38849
SF_6, discharge and oscill. due to axial injection of impulsive electron beam 80−59316
SF_6 gas, dispersion relation of spontaneous oscill., unstable regions 80−1875
SF_6 gas, low press., excitation of nonlinear wave by repeated pulsed electron beam 80−87878
Xe low threshold supersonic emission waves and effect on laser beam 79−27780
Z-pinch, noncylindrical, dynamics and particle accel. mechanism 77−76170

plasmatrons *see plasma diodes*

plasmoids *see plasma*

plasmons
see also phonon-plasmon interactions; solid-state plasma
A-15 compounds, disordered, resist. and supercond. transition temp. 80−107944
A-15 compounds, superconductivity 79−60947
acoustic wave interactions due to deformation potential *(Russian)* 80−15356
adsorbate and clean surfaces, electronic props. *(French)* 80−80344
adsorbates, core level spectra, exactly soluble limits of model 78−80459
adsorbates, surface plasmon effects on satellites in XPS 79−61493
adsorbates, XPS, plasmon effects on core level spectra 78−60547
adsorbed atom on solid surface, photoemission from valence band, surface plasmon emission, model Hamiltonian calcs. 80−50525
adsorbed atoms, relax. shifts, satellites and sum rules in electron spectroscopies 80−11539
adsorbed atoms and molecules XPS, many-body effects 80−55266
adsorbed atoms interactions, plasmon mediation in presence of metallic surface 78−71991
adsorbed atoms on metal surface, XPS satellite spectra 77−20993
adsorbed molecules, surface plasmon enhanced light absorption 80−40176
adsorbed species, plasmon versus shake-up satellites in XPS 78−48286
adsorption spectroscopy of adsorbed atoms, plasmon satellites and relax. shifts 77−59204
alkali halide film, low energy electron scatt. 78−26928
alkali metal, plasmon line width variation due to interband transitions 78−47822
alkali tungsten bronzes, struct. and supercond., acoustic plasmon exchange 79−82703
alkaline earth metals 79−28310

plasmons continued
anthracene, electron irrad., creation and evolution of excited states, scintillation obs. 78−92128
antiferromagnetic semiconductor, magnon-plasmon interaction and its effect on Raman scatt., theory 78−56302
bimetallic junctions, interface plasmon modes, theoretical anal. 80−54767
binary composites, percolation effects and sum rules in optical props. 79−69801
bound electron state in wake of swift ion in solids 77−15469
bound state of two plasmon excitations 78−39048
bound state of two plasmons, possible existence in metals and degenerate semiconductors 78−30882
cadmium arachidate monolayer, Ag(Au) substrate, reson. surface plasmon reflection 78−56536
cadmium arachidate monolayer, surface plasmon spectra, refractive index dispersion 78−64424
capacitor, parallel-plate, props. in plasmon model 79−51511
CDW distorted solid, quasi-one-dimens., charge density fluctuations and dielec. matrix 80−107726
charged Bose gas, optimal BDJ-type ground state props. 78−54295
charged particle moving in medium, electron density fluctuations, plasmons, wakes and clusters 79−47032
charged particles surface excitation system, ground-state energy 80−15462
chemisorption, image charge effects, surface plasmons 80−84381
chemisorption, image charge effects on adsorbate valence spectra, perturbational study 80−84380
classical two-dimensional electron system, correlations and plasma oscills. 79−69446
coated semiconductor spheres, surface modes, plasmon oscills. 80−54730
collective excitations, brief review of expt. and theory 77−1381
composite, metal spheres in dielec. medium, optical props., plasmon absorpt. 77−24811
cooperative emission of excited mol. monolayer into surface plasmons of metallic substrate 80−20666
coupling of molecules to surface plasmons in resonant elastic scattering 80−20102
4-cyano-4′-n-pentylbiphenyl, refr. index meas. and isotropic-nematic phase transition study, surface plasmon technique 80−84282
diamond, quasiparticle states, quantitative calc. 80−88499
dielectric, energy struct. determ. by electron absorpt. spectra 78−11040
dielectric function, inverse RPA calcs. at metal-vacuum interface 78−14789
dielectric function of Hubbard model 78−87929
dielectric layer, natural EM oscillations excitation by stream of electrons or EM field 80−34378
dielectric parabolic wedge, electrostatic edge modes 77−28231
dielectric wedge, electrostatic edge modes 77−28230
diffraction grating plasmon anomalies, energy absorpt. theory *(French)* 77−65628
dimerized organic linear chain conductor, electron mol. vibr. coupling consts. 78−14686
dispersion beyond k_c, dynamic struct. factor, calcs. 79−56157
dispersion for strong coupling 80−103111
dispersion in simple metals 78−91629
dispersion in two-metal systems 79−82656
dispersion relation, generation of 2-dimens. plasmon reson. at multiple wave vectors 78−63997
dispersive metals, metal, spatially dispersive, EM waves and plasmons, propagation 80−15549
dye in contact with Ag film, enhanced total refl. with surface plasmons 79−59694
effective interaction between two plasmons 79−51508
electrochromic ATR prism modulator 80−43440
electron beam, relativistic, intense, subjected to rippled elec. field, stimulated Raman scatt., short-wavelength plasmon prod. 79−98439
electron energy loss spectrometry, thin specimen sections, electron microscopic chemical analysis, review *(French)* 79−8469
electron excitation of plasmons and interband transitions, book 80−77555
electron gas, collective modes, ground state energy 77−66134
electron gas, complex dynamic struct. factor, theory 79−56152
electron gas, degenerate, in metal or semicond. slabs, surface plasmon damping 80−88501
electron gas, degenerate, response functions, memory function kinetic eqn. approach 79−49159
electron gas, dielectric function, dynamical exchange decoupling, plasmon dispersion, SDW and CDW 80−59900
electron gas, generator coordinate method 78−60077
electron gas, jellium model, dynamic correlations, first-order perturbation theory 80−44527
electron gas, mean free path of low energy electrons, influence of damping 78−10385
electron gas, multipole surface plasmons, bulk-selvedge coupling theory 79−28394
electron gas, quasi-one-dimensional, pair correl. function and plasmon dispersion curve 77−62851
electron gas, self consistent screening and approximate residual Landau interaction functions 79−19537
electron gas, slow ions and atoms energy loss to electronic excitation 77−84817
electron gas, two-dimensional, two-component, high-freq. cond. 80−29428
electron liquid, plasmon dispersion 78−56099
electron mean free path, stopping and straggling 78−91367
electron microscope image of crystal, influence of inelastic electron scatt. by plasmons *(French)* 77−76269
electron scattering from single cryst., bulk plasmon excitation 78−87933
electron spectroscopies and chemisorption, plasmon effects 79−33190
electron-hole droplet reson. radiation, radiative decay of surface plasmons *(Russian)* 77−62841
electron-plasmon and electron-phonon interactions in bulk and near surface, Kikuchi patterns 78−26759
EM surface wave exam. by appl. of optical technique 77−76893
EM waves, extraordinary parametric decay into two upper hybrid plasmons 80−43904
energy and interatomic interaction 77−69267
EXAFS in molecules and crystals, method for calc. of atomic phase shifts 77−48276

plasmons continued
excitation by large-angle scatt. electrons, density effect and plasmon bremsstrahlung 78−47718
excitation during X-ray scatt. 80−108297
rel. to exciton binding energy and lifetime in free carrier gas 79−33238
exciton energy levels, influence of exciton gas and electron-hole plasma 80−96795
excitonic insulator, quasi-one-dimens. 79−90966
excitonic phase, collective excitation modes under strong mag. field *(Japanese)* 77−43502
ferromagnetic semiconductor, magnon coupling to plasmons and LA phonons, s-d model 80−29536
ferromagnetic semiconductor, magnon-plasmon system 79−69659
ferromagnetic semiconductors, acoustic plasmons 80−7098
ferromagnetic semiconductors, Raman scattering of light on plasmon excitations 80−2738
field ion emission, surface plasmon excitation and Jason effect, comment 77−28699
field ion emission, surface plasmon interpretation, comment 77−28700
graphite, model of collective modes in layer cpds., appl. to electron energy loss data 77−47754
graphite, pyrolytic IR reflectance meas. 77−55781
graphite, X-ray scatt. from small particles at zero k 80−11505
graphite film, relativistic excitations by inelastic electron scatt. 77−1463
graphite film, secondary electron emission and EELS rel. to plasmons 80−50481
graphite intercalation compounds, KC_8 and CsC_8 polarised reflectance 78−31213
graphite intercalation cpds., dispersion relations of intercalate modes 80−34379
graphite-$FeCl_3$ intercalation cpd., electronic excitation spectrum, high resolution EELS meas. 80−45182
Hubbard, half-filled band model, local field correction to plasmon freq. 80−24823
Hubbard model, electrical conductivity calculation, dielectric function and plasma oscillations 78−64020
hypersound resonant excitation by 2-dimens. plasmons *(Russian)* 79−78032
image force for parallel incident particles, surface plasmon dispersion and single-particle effects 79−42602
inelastic positron scatt. in electron gas, plasmon excitation 80−92843
inert gas solids, collective excitations and EELS, calc. 80−92842
inhomogeneous media, surface plasmon dispersion, reply to comment 79−42609
inhomogeneous media, surface plasmon dispersion 77−24602
inhomogeneous media, surface plasmon dispersion 77−28229
inhomogeneous media, surface plasmon dispersion relation 79−42608
insulators, secondary electron emission, free-electron scatt. theory and plasmon theory 79−8211
insulators, theory of plasmon exciton coupling 78−23032
insulators, tightly bound, collective excitations 79−51492
interface dipolar plasmon in liq. multilayer struct., freq. and dispersion relations 77−59323
interface of two media, quasiparticle interaction 79−65532
intermediate valence metals, renormalisation of collective excitations, acoustic wave vel. near electronic transition 79−82539
ion, near metal surface, friction parameter and Brownian motion 80−15584
ion-induced X-ray prod., solid-effects 77−77326
ionic crystal-degenerate semiconductor interface, localised plasmon-optical phonon coupled modes 78−38930
jellium metal, bounded, linear response function in RPA 79−69444
jellium surface, hydrodynamic model of linear response, nonretarded limit 80−44526
Josephson junction, ultrasmall, dynamic Stark splitting 80−103790
Josephson tunnel junctions, high frequency losses 78−88083
Kane semiconductors, parametric excitation of surface waves 79−38014
Kikuchi patterns due to plasmon and phonon excitations 77−76264
laminated systems, two dimensional and surface plasmon mixing *(Russian)* 80−15466
Langmuir oscillation collapse in supersonic regime, forbidden energy *(Russian)* 80−14895
layer compound, model, collective modes 77−20255
layer metal particles, surface plasma oscillations 77−76765
layer metal particles, surface plasmons 77−1465
LEED Kikuchi pattern, contrast change due to plasmon excitation 78−34686
light emission from inelastic tunnelling spectroscopy, surface plasmon modes 79−3598
light metal, surface effects on X-ray level widths 79−47147
liquid, surface CARS 80−1280
magnetised solid state plasma, theory of neutron scattering 79−38015
many-electron system, eqn. of motion approach to plasmon-plasmon interaction 79−87052
metal, 'surf-riding' electrons on wake potential of ion beams 77−80747
metal, APW dispersion relation for plasmons 77−69265
metal, bulk and aggregated, plasma and conduction resonance dispersion 78−79952
metal, conduction band X-ray photoemission, intrinsic plasmons effects 78−39661
metal, damping of excited molecules located above surface 78−92160
metal, dynamic screening of core hole, semiclassical model 79−69445
metal, electrodynamics at boundary, including plasma waves 77−59317
metal, electron inelastic scatt., interaction effect in final state 79−69454
metal, electron-surface-plasmon scatt. using parabolic nontouching trajectory 77−28228
metal, EM props., general lecture 78−26901
metal, excitation by fast electrons of surface plasmons on spherical voids 77−11975
metal, excitation of plasmons by ion bombardment 78−34793
metal, highly reflecting, determ. of IR optical constants by surface plasmon excitation 78−76418
metal, inhomogeneous electron system, nonlocal exchange and correlation 78−56097
metal, interacting metal half spaces, effect of retarded-surface-plasmon dispersion and Van der Waals interaction 79−69452
metal, interband damping of long-wavelength plasmons 77−85165
metal, irradiated, surface plasmon modes of voids 79−60617
metal, optical functions, effect of surface roughness 78−56447
metal, periods IV, V, and VI, work function depend. on plasmon energy 78−18986

plasmons continued
metal, plasma oscills. of cond. electrons localised near point defects, contrib. to charact. losses *(Russian)* 77−43525
metal, plasmon dispersion, effect of band struct., dielec. function calc. 78−26825
metal, plasmon dispersion effect in (e,2e) process with atomic electron knockout 80−2904
metal, plasmon model for image-potential-induced surface state, appl. to positron surface states 79−19559
metal, plasmon satellite struct. in (e,2e) process 80−96809
metal, plasmon struct. in X-ray absorpt. spectra 79−38692
metal, quasi one dimens., plasmon dispersion relations, RPA and HF calcs. 78−34789
metal, secondary electron emission, Monte Carlo calc. 79−69932
metal, semi-infinite, nonlinear interaction of oppositely travelling surface plasmons 79−28393
metal, simple, long-wavelength plasmon width, pseudopot. theory 77−11864
metal, struct. induced surface plasmon polariton modes using ATR, theory 79−60890
metal, surface photoeffect, energy and angular energy distribs. 77−63535
metal, surface plasmon light emission due to low energy electron irrad. 80−34997
metal, surface plasmons *(Russian)* 79−33327
metal, surface plasmons in thin films, circular cylinder and spherical void, RPA calcs. 77−80823
metal, surface-plasmon dispersion relation from reflectivity of parallel-polarised light 79−78030
metal, ultrasoft XPS, plasmon satellite intensity 80−35058
metal, wake potential for fast ion pairs, self consistent calc. 78−34792
metal, X-ray excitation of surface plasmons on spherical voids 77−11974
metal as three-component liquid, plasma oscillations 79−99493
metal circular cylinders, inhomogeneous, non-radiative surface plasmon-polariton modes 80−29455
metal conduction electron photoemission spectrum, effect of recoil on shake-up spectra, infinite summation method 80−50526
metal film, carrier relax. time, optical determ. by surface plasmon excitation 77−1499
metal film, surface plasmons, rel. to structure-related optical charcts., visible and UV 77−55841
metal films, optical excitation, review 80−45106
metal overlays, effect on 3-D optical waveguides 78−94425
metal particles, spherical, surface plasmon dispersion relation, hydrodynamical model 78−84277
metal shallow grating diffr. efficiency, Rayleigh type and surface plasmon reson. type anomalies 79−55050
metal sphere, LF plasma reson., interband transitions effect 79−99906
metal spheres, optical surface plasmon modes, theory 78−2539
metal spheres, small, plasmon freqs., calc. by hydrodynamic theory 78−43319
metal substrate, H chemisorption, model, including image charge effects 79−73405
metal surface, electron-plasmon interaction 80−39649
metal surface, excited molecules located above surface, theory of damping 79−15203
metal surface, fast ion scatt. by plasmons, theory 80−45190
metal surface, force on moving charge, spatial dispersion effects 80−65646
metal surface, image force for fast particle 77−69939
metal surface, image-potential-induced states, plasmon model 79−78147
metal surface, light refl. from dye molecule monolayer 78−48246
metal surface, mol. vibr. energy transfer, classical EM theory 80−96806
metal surface, neutral molecule, resonance interaction 78−84279
metal surface, Nonlinear mixing of oppositely travelling surface plasmons 79−95460
metal surface, normal mode anal. of image pot. 79−33325
metal surface, plasmon mechanism for energy loss, dissoc. and orientation of fast ions excited by grazing collisions 80−11523
metal surface, reson. interaction with neutral mol. 77−80702
metal surface, rough, anomalous low-freq. Raman scatt. from localised acoustic vibrs. 80−93307
metal surface, with adsorbed at., XPS intrinsic plasmon satellites, dispersion and lifetime effects 79−56151
metal surface electrodynamics, optical refl. coeffs. and surface plasmon dispersion law 80−75619
metal surface energy, gradient corrections in interpolation formulae, surface plasmons 80−2441
metal surface or metal-metal interface, plasmon dispersion 78−52053
metal surface plasmons, direct energy transfer from excited dye mol. 79−91119
metal surface-void van der waals interaction energy 78−10036
metal-barrier-metal structures, coherent coupling of radiation by surface plasmons 77−89877
metal-barrier-metal structures, stimulated emission of surface plasmons by electron tunnelling 78−56236
metal-electrolyte boundary, electrodynamics in visible and near UV range, microscopic effects 80−45521
metal-metal contact, electron tunnelling stimulated by surface plasmons *(Russian)* 78−30974
metal-metal interface, EM wave propag., plasmon polaritons, computer simulation 78−84276
metallic film, steady-state Langmuir turbulence spectrum and turbulent energy absorption 78−26899
metallic films, adsorption studies using modulated surface plasmon reson. 79−82439
metallic rough surface, reflection loss for s and p polarised waves near surface plasmon freq. *(French)* 80−97225
metallic sphere, very small, surface plasmon dispersion, RPA 77−47886
metallic surface, collective effects in physical adsorption of inert gas atoms 79−19456
metallic surface, coupling to fluctuating atomic dipole, screening of point charge by surface plasmons 77−59217
metallic surface, dispersion of surface plasmons 80−2440
metallic surface, electrodynamics, microscopic effects *(Russian)* 80−6936
metallic surface energy, exchange and correl. contrib., wave-vector decomp. 80−75615
metallic thin film, structure-related optical characteristics in visible and UV 78−35217
plasmons continued
metallic thin films, density response function and dynamic struct. factor, nonlocal effects 79−69447
metallic thin films, fast electron scatt. with core electron excitation, plasmon satellite 79−33873
metallic thin films, optical props., effect of quench condensation 79−78773
metallic thin films, surface plasmon light scatt. 79−87517
metallic thin films *(French)* 80−60692
metallic thin layered structures, coupled surface plasmons 79−56873
metals, classical plasma frequency in long-wavelength limit, quantum correction 80−107728
metals, collective modes of void-surface coupled systems, surface plasmons 80−49642
metals, electronic transport eqns., optical cond., number conserving relaxation time approx. calcs. 80−49681
metals, inelastic scatt. of fast electron, plasma oscillations effect 80−100439
metals, nearly-free-electron, secondary electron emission, role of plasmon decay 77−81186
metals, photoelectron spectroscopy of localised levels near surfaces, scatt. effects and relax. shifts 78−15291
metals, unidimensional, plasmon freq., effect of nonuniform electron density profile *(Russian)* 80−59896
metals, X-ray photoemission line shape, Fermi surface excitations, book contrib. 79−61499
Mg, K X-ray emission spectra, double plasmon high energy satellite 80−11510
MIM structure, surface plasma oscillations, refl. coeff. and energy density repartition for p-polarised waves *(French)* 79−69606
MIM tunnel junction, surface plasmon excitation 78−10578
MIM tunnel junction, surface plasmon excitation by electron tunnelling 78−91779
MIM tunnel junctions, enhancement of light emission 77−51824
molten salt, possibility of plasmon mode obs., struct. dynamics 80−10477
monolayer, physically adsorbed, many-body interactions 78−84068
MOS inversion layers, acoustic plasmons 78−18983
multipole surface plasmons, attenuated total refl. spectra 79−78149
narrow gap semiconductor, electron-hole recomb. via plasmon emission 78−39046
narrow gap semiconductors, recombination mechanisms, review 80−96905
narrow gap semiconductors, stimulated plasmon emission 79−73461
nitromethane, dipolar plasmon, appl. calc. of solvated electron props. 77−89720
nitromethane, far IR reflection meas. and plasmon model relevance 79−33687
noble metal film, modulated surface-plasmon reson. in situ meas., O_2 adsorpt. 77−77311
non-specular conducting surfaces, classical electrodynamics 77−85280
non-specular dielectric surfaces, classical electrodynamics 77−85279
nonlinear saturation mechanism of EM wave parametric decay into two plasmons, efficiency *(Russian)* 77−11349
nonlinear surface-wave interaction, in plasmalike media, theory 80−107839
one-component high density plasma at intermediate wave numbers, collective excitations 78−67314
one-dimensional systems, exchange effects in plasmon dispersion 78−91628
one-dimensional systems, exchange effects in plasmon dispersion 79−60741
optical properties of rough surfaces, general theory and small roughness limit 77−75423
organic monolayer/metallic substrate, exciton-surface plasmon interaction 79−69569
organic thin film refractive index adjustment by absorbing dyes 80−43413
p-n junction, plasmon mechanism for secondary breakdown 78−95352
parametric instabilities, nonlinear turbulence theory, pump field to plasmon conversion 77−24085
parametric Langmuir turbulence, two pump wave excitation, plasmon nonlinear stabilisation *(Russian)* 78−83565
parametric wave excitation in semiconductor electron plasma *(Russian)* 79−33252
periodic crystals, general theory 78−26826
perovskites, d-band, model for X-ray photoelectron distrib. 79−61491
piezocrystal, interaction of two-dimens. plasmons with surface piezoacoustic waves, appl. to MOS structs. 79−28683
piezoelectric crystal, optical SHG with surface plasmons 78−18008
piezoelectric crystal, plasmon transformation into SAW 80−59903
piezoelectric semiconductor, plasmon enhanced sound amplification in mag. field 77−39900
plasma, HF soliton interaction with ion-acoustic waves and plasmons *(Russian)* 77−19682
plasma, laser beam absorpt., anomaly due to two-plasmon decay 79−1318
plasmon struct. obs. in K photoabsorpt. spectra 79−38693
polar liquids, surface dipolar plasmons, nonradiative, dispersion relations 78−6308
polar semiconductor, free carrier magnetoabsorpt. by photon-ionised impurity magnetoplasmon processes 79−38117
polar semiconductor, Raman spectra of coupled LO phonon-plasmon mode, de Haas-Shubnikov like quantum oscills. 78−43863
polar semiconductor-polar semicond. interface, optic-phonon-magnetoplasmons 78−23146
polar semiconductors, free-carrier absorpt., plasmon generation 79−4578
polar semiconductors, phonon-plasmon-polariton mode propag. at interface 79−60731
polyacetylene:AsF_5(I), pure and doped, electronic excitations, momentum depend., EELS study 80−76121
polymer films, mech. of charact. electron energy loss spectra 77−81188
polystyrene coated Ag holographic grating, Raman spectra enhancement by plasmon surface polaritons 80−80885
quantum electron plasma, EM fluctuations in external radiation field *(Russian)* 78−76013
quasi-one-dimensional metals, narrow-band, exchange-correlation effects on plasmons and on CDW instability 80−44525
Raman intensity enhancement, of pyridine adsorbed on Ag, by surface plasmons 80−7334

plasmons continued
rare earth vanadates, electron energy loss spectra, primary excitation processes in cathodolum. 79−11490
rough surface, dispersion relation for surface plasmons, quantum mechanical approach 78−72099
rough surface light scatt., vector theory, surface plasmon effects 79−59638
semiconductor, diamond structure, plasmon line shape, local field effects 78−76011
semiconductor, effect of free carriers on exciton luminescence 78−48226
semiconductor, electron scattering by layer of dislocation lines 79−78091
semiconductor, electron scattering by layer struct., geometrical resonances, plasmon and free carrier freq. 79−56212
semiconductor, exciton-plasma transition 79−28295
semiconductor, freq.- and wave-vector-depend. dielec. function 79−33253
semiconductor, inhomogenous, eigenoscills, of hot electrons in classically strong mag. field 79−73520
semiconductor, local fields, nonuniform charge distrib. 80−24826
semiconductor, magnetic, parametric down-conversion of laser beam 79−64287
semiconductor, magnetoplasmon-polariton surface modes, Voigt geometry 78−43451
semiconductor, MM wave guiding and control by surface plasmons 80−103713
semiconductor, natural EM oscillations excitation by stream of electrons or EM field 80−34378
semiconductor, non-equilibrium, acoustic plasma oscills. generation 80−96811
semiconductor, struct. induced surface plasmon polariton modes using ATR, theory 79−60890
semiconductor, zinc-blende structure, plasmon line shape, local field effects 78−76011
semiconductor plasma, isotropic heated, temp. plasmon oscills. 78−26898
semiconductor plasma, surface waves 79−1612
semiconductor superlattice, plasma oscills. in strong elec. field 80−44637
semiconductor superlattices, electroplasmon parametric resonance 80−34475
semiconductor surface plasmon dispersion, appl. to InSb 77−1464
semiconductor-insulator interface, surface wave spectrum, theory 79−19674
semiconductors, free electron scattering and dynamical cond. 78−2476
semiconductors, n-type, free carrier absorpt., ionized impurity scatt. 79−42999
semimetal, acoustic plasma wave excitation 78−10520
simple metals, photoemission theory, book contrib. 80−16159
simple metals, plasmon dispersion anal. from electron gas dielectric response 80−6761
simple metals, pseudopot. theory of k-depend. plasmon line width 77−85169
sinusoidal surface grating, surface plasmons effect on diffr. orders 77−42618
solar corona, efficiency of four-plasmon interactions in radar signal refl. from Sun 80−101582
solar selective absorbers and diffr. gratings, surface plasmons 79−14103
solid, Auger effect theory, plasmon effects in electron spectroscopies of valence state 78−56098
solid-liquid interface, optical methods of study *(French)* 80−7318
solid-state theory, introduction, book 79−33215
soliton solution in the wake interaction due to virtual plasmon exchange 80−65108
spectrum and damping, collisionless absorpt. threshold nonlinear phenomena *(Russian)* 80−49646
spherical particle, surface enhanced Raman scatt. by molecules 80−95629
spin density functional theory, linear response functions 78−67965
superconductirg thin films Cooper pains, photon scatt. on plasmons, Landau-Ginzburg theory 80−65738
superconductive mechanism in two-, three-dimens. electron systems 78−88065
superconductors, high temperature, tunnelling spectra, electron pairing anal., appl. to Nb_3Sn 79−87205
superlattice, image pot. enhancement by static elec. field 80−92846
superlattice, plasma oscill. under strong high freq. elec. field 80−10904
superlattices, plasmons, two-dimens., due to piezoelec. effect 80−92845
surface, density-density correlation function, exchange corrections 78−14786
surface, eigenmodes, Fredholm integral eqns. *(French)* 78−56195
surface, EM surface wave, energy flow and group vel., hydrodynamic approx. calcs. 78−84272
surface, momentum or energy fixed dispersion relations 78−14687
surface, on rough surfaces, dispersion relation charges 77−69394
surface, theory of non phase-matched SHG 78−72101
surface channel, quasitwo dimens. excitons and plasmons at different carrier conc. 78−60063
surface correlation energy, plasmon contrib. 77−69397
surface dielectric sum rule for electron response function 78−39184
surface enhanced Raman scattering surface plasmon model 80−108211
surface irregularities effect on dispersion and damping of surface plasmons 77−24604
surface magnetoplasmon type polaritons, LF, existence criterion in Faraday config. 80−96961
surface oscill. eigenmodes, chain of aligned spheres *(French)* 77−80821
surface plasmon dispersion relation at short wavelengths 80−96962
surface plasmon dispersion relation in presence of spatial dispersion 79−42612
surface plasmon dispersion relation in presence of surface roughness 80−65650
surface plasmon light emission induced by fast electrons on modulated surface 78−80424
surface plasmon obs. using X-ray emission 78−92146
surface plasmon oscills., eigenmodes, geometrical shapes 77−80822
surface plasmon radiation, roughness assisted, ang. distrib. 78−52521
surface plasmons, counterpropagating, for coherent SHG 80−33081
surface plasmons around cavity in semiinfinite metal *(French)* 78−56196
surface plasmons at inhomogeneous liq. metal/dielec. interface, second dispersion branch 77−32059
surface plasmons on rough surface, dispersion relation splitting 79−60739
surface polariton dispersion curve, optical obs., demonstration 80−101690
plasmons continued
surface polariton effects in spontaneous emission, effects of spatial dispersion 78−34879
surface roughness effect on image potential electron energy loss, plasmon electron scatt. 80−54748
TCNQ-HMTSeF, polarised single cryst. reflectance obs. and one-dimens. behaviour interpret. 78−6690
TCNQ-K, dielectric function of 1-dimens. Hubbard model 79−60740
TCNQ-TSef, Drude optical edge, press. depend. 79−19882
TEM energy loss anal. appl., plasmon dispersion relationships determ. 77−44100
thin surface layers, thickness and optical consts. using surface plasmon excitation 79−47533
thin-film geometry, harmonic generation of surface-plasmon nature, off-synchronous treatment 79−18475
transition metal, 3d, existence of several bulk plasmons 79−69455
transition metals, 3d electron struct. plasmons 79−77996
TTF-TCNQ, Drude optical edge, press. depend. 79−19882
TTF-TCNQ, exchange effects in plasmon dispersion 78−91628
TTF-TCNQ, plasmon spectrum, tight binding model 78−84158
tunnel junction, plasma radiation in Ag layer, expt. interpretation 77−31966
tunnel junction, small-particle type, light emission, local plasmon modes 79−19676
turbulent H plasma, n-α line Stark profiles, plasmon-atom collision 77−24084
two atom surface coupling, double reson. at plasmon freq., collective effects 80−34934
two-dimensional classical plasma, on dielectric film, collective excitations *(Russian)* 78−34788
two-dimensional electron gas, reson. excitations, using IR spectroscopy, review 79−60889
uniaxial crystal foil, electron energy loss probability at oblique incidence 80−25506
void lattice, plasma oscill. 78−10382
voids and particles, Van der Waals energy between them, from asymptotic to close contact 80−80351
wake potential of swift ions in solids 77−20257
water, electron energy deposition model, effect of 21.4 eV plasmon 77−4135
water, solvated electron, polaron coupling const. from dipolar plasmon freq. 77−89720
water, surface dipolar plasmons, nonradiative, dispersion relations 78−6308
waveguide scattering problem, comparison of two perturbation theories 80−83662
Wigner lattice, three-dimensional, detect. by Brillouin scatt. 77−36254
X-ray and synchrotron radiation inelastic scattering in crystals, review 78−39625
X-ray K- and L-emission bandwidths from characteristic electron energy loss values 79−83057
X-ray plasmon scatt. by solids, electron exchange energy influence 79−56884
X-ray plasmon scattering plasmon cut off wave vector electron exchange energy effect 80−50458
XPS from core levels, electron energy loss spectra, intrinsic and extrinsic plasmons 77−63532
XPS plasmon satellite struct., intrinsic versus extrinsic processes 77−77342
Ag (111) surface, obs. of surface plasmon splitting by electroreflectance spectroscopy 79−61338
Ag, cluster and microcrystal, matrix isolated, optical absorpt. spectra, photolysis and plasmon absorpt. 79−89820
Ag, electrode pot. effects on surface plasmon excitation 78−15149
Ag, electroreflectance spectroscopy, longitudinal surface plasmons 80−40137
Ag film, dye monolayer effect on surface plasmons, ATR obs. 79−87001
Ag film, energy transfer from excited dye mol. to surface plasmons 79−91119
Ag film, enhancement of electron photoemission by excitation of surface plasmons *(French)* 77−63524
Ag, film, lifetimes of surface plasmons 79−47143
Ag, film, plasma reson. radiation exam. *(German)* 79−69453
Ag film, substrate surface structure effects on absorptance 78−19585
Ag film, surface plasmon wave excitation of dye mol. fluoresc. emission 79−89703
Ag film on Cu(111), plasma reson. absorption in interfacial photoemission 78−15289
Ag foil, surface-plasmon resonance, roughness-induced wavelength corrections 80−108288
Ag foils, surface plasma-wave reflectance and roughness-induced scatt. 80−66228
Ag granular film, plasma reson. absorpt. by incident light 79−28850
Ag grating, surface plasmons rel. to diffr. order intensity profile, higher harmonics influence 78−25981
Ag grating, with LiF coating, surface plasmons, rel. to reson. anomalies in reflected light intensity 77−3665
Ag, nature of 3.8 eV plasmon in XPS 79−78838
Ag particles, lattice defect influence on size effect 78−88329
Ag, plasmon dispersion, d→f fine structure 77−11863
Ag, plasmons, influence of cryst. orientation on intensity, electron energy loss meas. *(German)* 79−23921
Ag rough film, multiple light scatt. of surface plasmons 77−48262
Ag rough surface, transition radiation for 77 keV electrons, surface plasmon light emission 78−60530
Ag, single cryst. film, cryst. orientation effect on EELS 78−80442
Ag surface, (111) and (100), crystallographic anisotropy in surface plasmon decay to photoelectrons 79−24052
Ag surface, optical props. of organic dye monolayers by surface plasmon spectroscopy 79−11480
Ag surface, periodically modulated, radiative decay of surface plasmons excited by fast electrons 77−24599
Ag surface, reson. interaction with dye monolayers 78−84674
Ag surface, sinusoidally modulated, light emission of nonradiative surface plasmons 77−1467
Ag, surface and volume plasmon light emission due to low energy electron scatt. 80−40177
Ag surface layers, reflectivity, contrib. of longit. polarisation waves 79−83046
Ag, surface plasma oscills., sinusoidal surface 77−73179

plasmons continued
Ag, surface plasmon dispersion relation in presence of surface roughness 80−65650
Ag, surface plasmon light emission induced by fast electrons on modulated surface 78−80424
Ag, surface-plasmon modulated reson. for adsorption studies 79−83045
Ag surfaces, Cs and Cs-O covered, surface plasma waves, ATR study 80−39451
Ag, thin layer on Al surface, surface plasmon ATR spectroscopy 79−78770
Ag thin layered structures, coupled surface plasmons 79−56873
Ag/organic dye, excited mol. decay near metal surface, energy transfer to plasmon surface polaritons 80−50440
Ag-Cd, α and β phase, XPS, effects of atomic order on band struct. 79−42440
Al (001), 100-2000 eV electron backscatt., surface and bulk plasmon losses 77−32480
Al (100), inelastic LEED at beam emergence condition 78−83690
Al (111), chemisorpt. of O 78−14593
Al (111), LEED Kikuchi pattern, contrast change due to plasmon excitation 78−34686
Al, adsorption of O_2, intrinsic and extrinsic plasmon coupling, XPS of adsorbed atoms core states 78−10278
Al, adsorption of small molecules, photoelectron spectra, surface plasmon spectroscopy 79−47148
Al, ang. depend. of plasmon loss features in XPS 78−43987
Al, Auger spectra, KLL and KLV, screening effects and plasmon gains 80−80913
Al, Auger spectra, plasmon satellite intensity 78−64432
Al, Auger spectrum, KLL, plasmon gain satellite obs. 78−76562
Al, bremsstahlung isochromat beyond Duane Hunt limit 77−73188
Al, bulk and surface plasmon loss intensities in XPS, Auger and electron energy loss spectra 79−38012
Al, characteristic energy losses on C contaminated surfaces, secondary electron spectra, AES, and EELS 79−99997
Al, deformation enhanced photoemission meas. 77−32511
Al, dielectric function pseudopot. theory, vol. plasmon dispersion 79−23917
Al, electron MFP determ. by depth and ang. depend. of inelastically scatt. electron spectra 78−92154
Al, exoelectron photoemission enhanced by slip steps, plasmon reson. theory 78−15300
Al film, (e, 2e) reaction, ang. correlation functions, plasmon satellites 79−19955
Al film, mean free path for plasmon excitation, 1.5 to 10.9 keV 78−51915
Al foil, straggling of relativistic electrons, 0-4000 eV 78−14393
Al, L_{23} shell ionisation cross-section under H^+, heavy-ion impact, Auger spectra, plasmon excitation structs. *(French)* 79−24406
Al, mean free path of electrons needed to form surface plasmons 77−51800
Al, photoemission from (100), (110), and (111) cryst. faces, surface states 79−4893
Al, photoemission study of energy depend. of bulk plasmon loss intensity 79−47035
Al, plasma oscillations in oxide free Al clusters 78−2510
Al, plasmon dispersion, dynamical exchange effects 79−51509
Al, plasmon dispersion, effect of band struct., dielec. function calc. 78−26825
Al, plasmon sideband exam. by synchrotron radiation tuning of electron escape depths, UPS 77−47755
Al, plasmon struct. obs. in K photoabsorpt. spectra 79−38693
Al, plasmon struct. of core lines in XPS meas. 77−63530
Al, plasmon-dislocation interactions, electron microscope investig. 77−15421
Al, polycryst., anisotropy of plasmon dispersion, pseudopotential method 78−23039
Al, polycrystalline, multiple plasmon excitation, in energy loss spectrum 79−4872
Al, secondary electron emission, role of plasmon decay 77−81186
Al, secondary electron emission, Monte Carlo calc. 79−69933
Al slab, fast electrons slowing down, Monte Carlo transport simulation *(French)* 78−26610
Al, small spheres, bulk plasmons damping 80−75561
Al, struct. in 1s soft X-ray appearance pot. spectrum 79−33862
Al surface, light diffr., photon excitation of compound plasmon resonances 79−28307
Al, surface plasmon dispersion, high-energy electron loss spectroscopy obs. 77−20390
Al, surface plasmon dispersion curves, splitting by Ag surface layers 78−60178
Al, ultra soft X-ray photoelectron energy loss study, plasmon loss intensities 78−23582
Al, X-ray emission spectra, high energy plasmon satellite intensities 78−64430
Al, XPS theory, core level spectra, plasmon creation 78−72701
Al-Al_2O_3-Ag tunnel junction, 4-pyridine carboxaldehyde-doped, surface enhanced Raman spectra, surface plasmons 79−98111
Al-Cu (1 wt.%) alloy, plasmon dislocation interactions, electron microscope investig. 77−15421
Al-Mg (3 and 7 at.%) alloys, plasmon-dislocation interactions, electron microscope investig. 77−15421
Al-Mn(Ni)(Cu), dil., core and valence band spectra, XPS study 80−84837
Al-Zn-Mg, grain boundary surfaces, plasmon loss satellites in Auger spectra 78−15261
As, interband, magnetorefl. for circularly polarised radiation 78−2840
Au, AES and characteristic energy loss spectra, expt. and interpretation 78−27354
Au, electrode pot. effects on surface plasmon excitation 78−15149
Au, electron tunnelling from particle, polarised light emission and plasmons 79−51685
Au film on Ag, optical constants, 4000-6000 Å, using surface plasmon optical excitation 77−69925
Au, L_β emission band, surface plasmons in X-ray emission bands 78−92146
Au small particles, size effects studied by electron energy loss anal. 79−47567
Au small particles in glass, transition cluster-solid state 79−33593
Au, surface-plasmon modulated reson. for adsorption studies 79−83045
plasmons continued
Au, with cadmium arachidate monolayer, surface plasma reson. 77−90210
Au/Al thin film, Al diffusion studied by attenuated total reflection method 80−92722
BN, chem. bonding and electronic struct., AES and SIMS meas. 80−50512
B_2O_3, chem. bonding, electronic struct., ESCA, Auger, and SIMS spectra 80−50512
Ba, ang. depend. of characteristic energy loss, surface plasmon excitation 78−2962
Ba, plasmon excitation by oblique incidence of primary electron beam of medium energy 78−18987
BaO, electron energy loss and secondary emission mechanisms, plasmon losses 78−76565
Be adsorbed layers on W(100) and (100), work function and loss spectra meas. surface and bulk plasmons 80−6638
Be, Auger spectrum, high energy plasmon satellite 79−82538
Be, conduction electron hole coupling, XPS obs. 77−28135
Be, longitudinal dielec. function calc. 77−1358
Be, plasmon struct. of core lines in XPS meas. 77−63530
Be, X-ray emission spectrum, double plasmon high energy satellite 78−72639
Be, X-ray K emission spectrum, high energy double plasmon satellite intensity calcs. 78−2944
Be, X-ray plasmon scatt., electron exchange energy influence 79−56884
Be, XPS theory, core level spectra, plasmon creation 78−72701
BeF_2, K-emission spectra, optical effects 78−64431
BeO, K-emission spectra, optical effects 78−64431
BeO, X-ray emission spectra, double plasmon high energy satellites 80−29829
Bi (0001), chemisorption of O_2, LEED, AES and electron loss meas. 79−77908
Bi, acoustic plasmon excitation 77−89793
Bi, and Bi_2O_3, AES and characteristic energy loss spectra, expt. and interpretation 78−27354
Bi, chemical shift of X-ray L-absorption edge 79−52044
BiSb, hybrid resonance in a quantising magnetic field 78−67933
C film, amorphous, surface plasmon dispersion, electron energy loss spectra meas. *(French)* 77−63504
C foil, energy loss spectra of transmitted electrons, straggling and plasmon excitation 79−95058
CO, adsorbed on jellium, surface plasmon relax. energies 80−70537
Ca, optical props., 2-11 eV 78−15191
Ca, plasmon excitation by oblique incidence of primary electron beam of medium energy 78−18987
CdS(Se)-Al function formation, coupled interface plasmons, low energy electron energy loss spectra 77−24621
Ce, renormalisation of collective excitations, acoustic wave vel. near electronic transition 79−82539
Co and its cpds., X-ray K-absorpt. edge shifts, plasmon energies correlation 80−20734
Co, X-ray K-absorpt., edges, plasma oscills. effects 77−59640
CoO (100), electron energy loss spectra exam. 78−72652
Cr and its cpds., X-ray K-absorpt. edge shifts, plasmon energies correlation 80−20734
Cr, charact. electron energy loss mechanism 79−91547
Cr, Kβ X-ray emission, plasmon satellite 77−28662
Cr, $K\beta_{1,3}$ X-ray emission spectra, low energy plasmon Kβ' satellite 79−74020
Cr, X-ray K_β emission spectrum, unpaired electrons and plasmon correlation 78−88383
CrO_3, $K\beta_{1,3}$ X-ray emission spectra, low energy plasmon Kβ' satellite 79−74020
Cr_2O_3, low energy X-ray emission satellite, unpaired election and plasmon effects 80−35007
Cs monolayer on Cu(111), dilution of electron gas by O adsorption, plasmon energy losses 79−47036
Cs-O film, metallic, on Ag substrate, photoemission, surface plasmon excitation 77−16461
Cu and its cpds., X-ray K-absorpt. edge shifts, plasmon energies correlation 80−20734
Cu, electron energy loss spectrum, complex dielec. function calc. 77−11862
Cu, surface-plasmon modulated reson. for adsorption studies 79−83045
Cu, X-ray K-absorpt. edges, plasma oscills. effects 77−59640
CuCl, possibility of excitonic dielectric-supercond. phase transition 77−43797
Dy_2S_3, optical props. and electronic struct. in fund. absorpt. region 80−80817
EuO (100), EELS, Eu valence in surface region and high energy giant reson. 80−84816
Fe, $K_{\beta 1,3}$ X-ray emission spectra, low-energy plasmon satellites 79−65957
$FeCl_3$ intercalated with graphite, stage 1, dielec. response and intraband plasmon dispersion 80−59902
$FeCl_3$-intercalated graphite, plasmon spectra 79−38011
$Fe(NH_4)_2(SO_4)_2.6H_2O$, Kβ' satellite of Kβ_1 X-ray emission line, plasmon oscill. theory 78−23556
Fe_2O_3, $K_{\beta 1}$ X-ray emission line, optical effects 79−91534
GaAs, acoustic plasmons in MOS inversion layers 78−18983
n-GaAs, coupled plasmon-LO phonon modes, Raman scatt. meas. 78−60472
GaAs, epitaxial film, amorphous and polycrystalline, vol. plasmon energy and linewidth, electron scatt. obs. 80−50482
n-GaAs, resonance enhancement of Raman scatt. by electron gas excitations 79−65878
GaP, photoexcited, Raman scatt. from plasmons 79−38541
Gd, X-ray absorpt. edge, plasmon excitation 80−7437
Ge film, volume plasmons, EELS, line shape 79−90984
Ge, inelastic X-ray scattering cross sections, in case of small momentum transfer 77−27786
Ge, magnetoplasma resonance in electron-hole drops *(Russian)* 78−79944
Ge, optical pulse transmission, pulsewidth depend., phonons and plasmons role 78−31198
Ge, pressure tuning of picosecond pulse transmission, plasmon-assisted recomb. model 77−88871
Ge, solid-state plasma, ultrafast transient response, theory and expt. 77−80748
Ge, volume plasmon, cryst. orientation influence 80−80921

plasmons continued
GeS(Se), dielec. function, optical and electron energy loss spectroscopy 78−15189
H_3BO_3, chem. bonding, electronic struct., ESCA, Auger, and SIMS spectra 80−50512
He liquid, surface electron states, two-dimens. cryst. form. 78−60006
Hg, liquid, surface plasmon dispersion 77−62978
$nHg_{1-x}Cd_xTe$, single-phonon and plasmon recomb. lifetime effect, with magnetically tuned bandgap 79−38098
$Hg_{a-x}Cd_xTe$, single-LO-phonon and -plasmon recombination channels narrow-bandgaps 78−91728
HgSe, reflectivity spectra, plasmon-LO phonon coupling, effect of interband contrib. 79−15458
In film, vol. plasmon dispersion and damping, electron energy loss spectra 79−7797
In, surface plasmon dispersion, high-energy electron loss spectroscopy obs. 77−20390
In, ultra soft X-ray photoelectron energy loss study, plasmon loss intensities 78−23582
InAs, surface space charge investig., reson. enhanced Raman scatt. 77−20849
InN, thin film, characterisation using XPS electron energy loss spectra 79−87561
In_2O_3, thin film, characterisation using XPS electron energy loss spectra 79−87561
In_2O_3:Sn, film, optical modulation effects in electroreflectance spectra 78−6800
InO_xN_y, thin film, characterisation using XPS electron energy loss spectra 79−87561
n-InSb, damped surface magnetoplasmons, theory 79−7873
InSb, epitaxial film, amorphous and polycrystalline, vol. plasmon energy and linewidth, electron scatt. obs. 80−50482
n-InSb, surface magnetoplasmons 79−19646
InSb surface magnetoplasma wave struct. 80−6934
InSb, volume plasmon dispersion, anisotropy 78−56090
K film, adsorbed on Ni (100), plasmon losses in electron energy loss spectra 79−61480
K film, splitting of surface plasmon emission spectra 79−99954
K surface, clean and O_2-exposed, X-ray and UV photoelectron spectra 78−52636
KBr film, oblique incidence transmission spectra for polarised extreme UV radiation 78−39614
KCl film, oblique incidence transmission spectra for polarised extreme UV radiation 78−39614
K_2CrO_4, $K\beta_{1,3}$ X-ray emission spectra, low energy plasmon $K\beta'$ satellite 79−74020
$K_2Cr_2O_7$, $K\beta_{1,3}$ X-ray emission spectra, low energy plasmon $K\beta'$ satellite 79−74020
$KMnO_4$, X-ray emission spectra, plasmon satellites 79−99985
$K_{1.62}Pt(C_2O_4)_2.2H_2O$, plasma resonance absorpt. from small particles 77−24841
La_2S_3, optical props. and electronic struct. in fund. absorpt. region 80−80817
Li aggregated deposits, optical props., 1-6 eV 77−66549
Li, analysis of optical consts. 77−40201
Li, cluster and microcrystal, matrix isolated, optical absorpt. spectra, photolysis and plasmon absorpt. 79−89820
Li, plasmon linewidth, k-dependent, anomalous behaviour explanation, interband transitions 78−47721
Li, plasmon satellite struct. in (e,2e) process 80−96809
Li, X-ray inelastic scatt. for $k \gtrsim 2k_F$ plasmon dispersion relation 79−15557
β-LiAl, optical dispersion, room temp. reflectance spectra 80−66195
LuH_2, electronic struct., optical studies, 0.2-5 eV, 4.2-340K 79−78005
LuH_2, electronic struct., photoelectron spectra study 80−50527
Mg, AES, KLL spectra, and plasmon struct. 79−15592
Mg, ang. depend. of characteristic energy loss, surface plasmon excitation 78−2962
Mg, Auger spectra, KLL and KLV, screening effects and plasmon gains 80−80913
Mg, Auger spectrum, KLL, plasmon gain satellite obs. 78−76562
Mg, deposits of different roughness, refl. drops and surface plasmons 77−20392
Mg film, electrom energy loss spectrum in excitation of volume plasmons 78−11043
Mg film, synchrotron radiation photoemission, plasmon loss struct. 79−28897
Mg, L_{23} shell ionisation cross-section under H^+, heavy-ion impact, Auger spectra, plasmon excitation structs. *(French)* 79−24406
Mg, $L_{23}VV$ Auger spectrum 78−39634
Mg, longitudinal dielec. function calc. 77−1383
Mg, plasmon struct. of core lines in XPS meas. 77−63530
Mg, plasmon-loss intensities in XPS, EELS and Auger spectra 80−10902
Mg, XPS, plasmon gains as monitor of incomplete relax., interference effects and sudden to adiabatic limits transition 80−66390
Mg, XPS theory, core level spectra, plasmon creation 78−72701
Mg-Cd, plasmon loss and plasmon gain, X-ray photoemission and AES 79−23918
Mn, $K\beta_{1,3}$ X-ray emission spectra, low energy plasmon $K\beta'$ satellite 79−74020
Mn, X-ray K_β emission spectrum, unpaired electron and plasmon effect 77−12468
MnO, electron energy loss spectra exam. 78−72652
MnO, $K_{\beta 5}$ X-ray emission spectrum, low energy plasmon satellite A 78−2945
MnO, $K\beta_{1,3}$ X-ray emission spectra, low energy plasmon $K\beta'$ satellite 79−74020
MnO, X-ray $K\beta$ emission spectra, unpaired electron and plasmon effects 78−19603
MnO_2, $K\beta_{1,3}$ X-ray emission spectra, low energy plasmon $K\beta'$ satellite 79−74020
MnO_2, X-ray emission spectra, plasmon satellites 79−99985
MnO_2, X-ray $K\beta$ emission spectra, unpaired electron and plasmon effects 78−19603
Mo (100) surface, clean and O_2 covered electron energy loss spectra meas. 77−16440
Mo, AES and characteristic energy loss spectra, expt. and interpretation 78−27354
Mo, charact. electron energy loss mechanism 79−91547
plasmons continued
Mo, electron-surface plasmon scattering using a parabolic non-touching trajectory 78−95328
Mo, electron-surface-plasmon scatt. using parabolic nontouching trajectory 77−28228
Mo, foil, electron energy loss spectra 80−7452
Mo, slow electron inelastic scatt., vol. and surface plasmon excitation 77−52207
N_2 film, on metal or sapphire substrates, luminescence and nonradiative energy transfer to surfaces 80−97350
NH_3, solvated electron, polaron coupling const. from dipolar plasmon freq. 77−89720
Na, AES, KLL spectra, and plasmon struct. 79−15592
Na, Auger spectra, KLL and KLV, screening effects and plasmon gains 80−80913
Na, cluster and microcrystal, matrix isolated, optical absorpt. spectra, photolysis and plasmon absorpt. 79−89820
Na film, adsorbed on Ni (100), plasmon losses in electron energy loss spectra 79−61480
Na film, slow electron bombarded, light radiation 80−40168
Na, IR and optical props., surface-plasmon-mediated absorpt. mechanism 80−93308
Na, plasmon satellite struct. in (e,2e) process 80−96809
Na, plasmon struct. of core lines in XPS meas. 77−63530
Na, X-ray emission spectra, double plasmon high energy satellites 80−29829
Na, XPS, plasmon gains as monitor of incomplete relax., interference effects and sudden to adiabatic limits transition 80−66390
Na, XPS theory, core level spectra, plasmon creation 78−72701
NaCl, energy struct. determ. by electron absorpt. spectra 78−11040
NaCl, secondary electron emission, appearance of collective and individual interactions of slow electrons 77−69948
Na_xWO_3, anomalous supercond. transition temp., electron pairing by acoustic plasmon exchange 79−56358
Na_xWO_3, cubic, final-state effects in XPS 77−90251
Na_xWO_3, intra- and interband plasmons, inelastic electron scatt. exam. 78−72098
Nb alloys, optical props., 0.1-25 eV, band models 78−10892
Nb, foil, electron energy loss spectra 80−7452
Nb_3Ge, disordered superconductor, T_c depression by acoustic plasmon overdamping 80−7020
NbN, optical props. and charact. electron energy loss spectra 79−52056
Nd_2O_3, EELS, low loss peak due to plasmon 80−79953
Nd_2S_3, optical props. and electronic struct. in fund. absorpt. region 80−80817
Ni (100), initial oxidation, electron energy loss spectra, LEED, AES, and work function meas. 79−61795
Ni (100) surface, clean and gas-covered, electron energy loss spectra 79−47570
Ni and its cpds., X-ray K-absorpt. edge shifts, plasmon energies correlation 80−20734
Ni, $K_{\beta 1,3}$ X-ray emission spectra, low-energy plasmon satellites 79−65957
NiO (100), electron energy loss spectra exam. 78−72652
NiO (100) surface, electronic states, electronic energy loss spectroscopy 78−6426
P, amorphous, stability in air, XPS study, comparison with cryst. polymorphs 80−25517
P, amorphous, XPS anal. of stability, form. of oxidised layer *(German)* 79−11496
Pb, chemical shift of X-ray L-absorption edge 79−52044
PbS, anisotropy of vol. plasmon dispersion, electron energy loss meas. 77−35878
$Pb_{1-x}Sn_xSe$ epitaxial layers, radiative and nonradiative recomb. processes 80−60670
$Pb_{0.78}Sn_{0.22}Te$, $Pb_{0.91}Sn_{0.09}Se$, radiative and nonradiative recombination 80−80849
$Pb_{1-x}Sn_xTe$, reststrahlen band, reflection spectra 79−8162
$Pb_{1-x}Sn_xTe$ solid solution, radiative recombination 79−52016
Pd-Cu-Si metallic glass, energy loss spectra and Auger spectra 78−23563
Pd-Ni-P metallic glass, energy loss spectra and Auger spectra 78−23563
PdH(D), energy loss spectra and Auger spectra 78−23563
Rb film, adsorbed on Ni (100), plasmon losses in electron energy loss spectra 79−61480
Rb_xWO_3, anomalous supercond. transition temp., electron pairing by acoustic plasmon exchange 79−56358
Re, extended X-ray abs. fine struct., L_α, L_β satellites 79−33861
ReO_3, intra- and interband plasmons, inelastic electron scatt. exam. 78−72098
$(SN)_2$, theory of plasmon excitations 77−69266
$(SN)_x$, epitaxial, optical props. and plasmon dispersion, from electron energy loss spectra 77−35882
Sb, Sb_2O_3 and Sb_2S_3, AES and characteristic energy loss spectra, expt. and interpretation 78−27354
Sc, XPS, plasmon peaks 78−6828
ScH_2, electronic struct., optical studies, 0.2-5 eV, 4.2-340K 79−78005
ScH_2, electronic struct., photoelectron spectra study 80−50527
ScH_2, optical interband struct. and low energy plasmons 78−31200
ScH_2, XPS, plasmon peaks 78−6828
Sc_2O_3, XPS, plasmon peaks 78−6828
Si (111), UHV cleaved, adsorbed O, electronic transitions 78−39183
Si, Auger spectra, KLL and KLV, screening effects and plasmon gains 80−80913
Si, bulk plasmon dispersion, electron energy loss spectra meas. 80−59899
Si, defect generation and annealing by intense subthreshold electron beam bombardment 79−51149
Si film, epitaxial growth on Si, impurities, plasmon energy loss anal. 77−31916
Si film, volume plasmons, EELS, line shape 79−90984
Si, inelastic X-ray scattering cross sections, in case of small momentum transfer 77−27786
Si inversion layer, (100) wavevector, depend. of 2D plasmon disp. relationship 78−76101
Si inversion layer, high freq. cond., Drude relax., 2D plasmons and minigaps in surface lattice 78−60230
Si, inversion layer, temp. depend. of subband energies, exchange and correlation effects 80−20281
Si inversion layer, two-dimensional magnetoplasmon 78−2440

plasmons continued
Si inversion layers, far IR transmission spectra, two-dimensional plasmons 77−76931
n-Si inversion layers, stress and temp. depend. of subband struct., plasmon-pole approx. 79−95461
Si, Kikuchi structures, energy analysis by intensity profiles *(German)* 79−7528
Si, laser induced dense plasma, dynamics 80−65612
Si, non thermal laser induced ordering, plasma life time, phonon interactions 80−84481
Si, p-i-n structures, pinch effect expt. obs. 79−90971
Si, photoemission study of energy depend. of bulk plasmon loss intensity 79−47035
Si, plasmon dispersion relation, local microscopic field effects 80−20103
Si, plasmon sideband exam. by synchrotron radiation tuning of electron escape depths, UPS 77−47755
Si, plasmons, influence of cryst. orientation on intensity, electron energy loss meas. *(German)* 79−23921
Si, surface, (111) 2×1, cleaved, O_2 adsorption, low-energy electron loss spectra 79−15840
Si, surface, Auger spectrum, high energy plasmon satellites 78−2955
Si, volume plasmon dispersion at large wave vectors, EELS 78−56094
Si, X-ray emission spectra, high energy plasmon satellite intensities 78−64430
Si, X-ray $L_{2,3}$ emission spectrum, high energy plasmon satellite 79−82538
Sn, electron energy loss spectra, differences in vol. plasmon energy recorded with low and high primary beam energies, plasmon dispersion model 79−65963
SnS(Se), dielec. function, optical and electron energy loss spectroscopy 78−15189
Sr, plasmon excitation by oblique incidence of primary electron beam of medium energy 78−18987
Ta, foil, electron energy loss spectra 80−7452
$TaSe_2$ (2H), optical absorpt., band struct., plasmons, and CDW 80−45104
$TaSe_2$(2H), plasmon behaviour at charge density wave onset 80−10900
Ti, Kβ X-ray emission, plasmon satellite 77−28662
TiH_x and $TiD_{0.9}$, surface characts., AES, EELS, SIMS, and XPS study 80−65343
TiN, optical props. at 300K 78−19466
TiO_{2-x}, plasmon and polar optical phonons 77−39794
Ti_2O_3, electronic structure from single crystal thermoreflectance spectroscopy 79−87420
TlCl, role of electron-hole interaction in optical spectra, review 80−45113
US(Se)(Te), electronic struct. and exchange band splitting, optical refl. meas. 80−66226
V, foil, electron energy loss spectra 80−7452
V, $K_{\beta 1,3}$ X-ray emission spectra, low-energy plasmon satellites 79−65957
VN, optical props. and charact. electron energy loss spectra 79−52056
W (100) surface, energy loss mechanisms in low energy electron scatt. 77−85859
W, charact. energy loss mechanism 79−91547
W, slow electron inelastic scatt., vol. and surface plasmon excitation 77−52207
WO_3 film, intra- and interband plasmons, inelastic electron scatt. exam. 78−72098
W(211), adsorption of Be, work function changes and scatt. electron energy losses 79−46947
Y, reflectivity spectrum, 3.5 to 30 eV dielectric function and plasmons 77−44014
YH_2, electronic struct., optical studies, 0.2-5 eV, 4.2-340K 79−78005
YH_2, electronic struct., photoelectron spectra study 80−50527
Zn and its cpds., X-ray K-absorpt. edge shifts, plasmon energies correlation 80−20734
ZnO, (0001) surface, clean and O adsorbed, AES and refl. electron energy loss spectra 79−46927
ZnO (000$\bar{1}$) surface, surface and bulk excitations, reflection electron energy loss spectroscopy 77−20389
ZnO, bulk and surface plasmons, single and multiple excitation 77−12474
ZnSe (110) surfaces, obs., by low-energy-electron loss spectroscopy *(Japanese)* 79−83071
ZnSe (111), low-energy electron loss spectra, bulk and surface transitions 78−11042
ZrN, optical props. and charact. electron energy loss spectra 79−52056
ZrN, optical props. at 300K 78−19466

plastic after-flow *see recovery-creep*

plastic afterflow *see recovery-creep*

plastic crystals
adamantane, cryst., vacancy formation energy, positron annihilation study 80−60706
adamantane, deuterated single plastic cryst., high-symmetry dispersion curves, coherent inelastic neutron scatt. meas. *(French)* 79−14905
adamantane, Ising, diffuse scatt., hard-core correl., weak-graph method 80−49137
adamantane, lattice dynamics in disordered phase 78−55923
adamantane, NMR, spin-lattice relax., plastic-brittle phase transform. 79−95665
adamantane, order cubic F$\bar{4}$3m phase, X-ray diffuse scatt. 78−38684
adamantane, plastic and solid-solid transitions, Raman study 80−60590
adamantane, plastic cryst., radio- and photothermoluminesc. *(Russian)* 79−11477
adamantane, plastic cryst. lattice vibr. study of phase transition 80−7355
adamantane, plastic cryst. rotational motion, quasielastic neutron scatt. study 79−41991
adamantane, plastic phase, C_4 rot. jumps, existence and uniqueness 80−88067
adamantane, plastic phase, librations, phonon branches, neutron scatt. study *(French)* 79−51222
adamantane, plastic-phase transition, cell model 77−11665
adamantane, Rayleigh scatt. of Mossbauer radiation 78−27125
adamantane, rotational motion, elastic incoherent struct. factor determ. 77−4056
adamantane, thermal cond. and heat capacity under press. 80−80008
adamantane, thermolum. curves 80−2876
2-adamantanone, cryst. struct. in plastic phase 80−88065
2-azanoradamantane N-oxyl, crystal-plastic transition, plastic crystal struct. exam. 78−2100

plastic crystals continued
benzene-fluorobenzene system, phase transitions, Raman spectra 79−91449
t-butyl bromide, elec cond., temp. depend. in liq. and plastic phases 80−1944
t-butyl chloride, elec cond., temp. depend. in liq. and plastic phases 80−1944
t-butyl chloride, rotational motions, cold neutron scatt.study 79−51023
t-butyl chloride, solid phases, mol. motion, cold neutron scatt obs. 78−26460
t-butyl chloride-d_0 and -d_9, polymorphism, Raman spectra 80−20617
dl-2,3-camphanedione, elec. cond., brittle-to-plastic region, cond. jump 78−39169
camphene, ^{13}C NMR obs. 79−95667
d-camphor, high resolution ^{13}C NMR spectra, 275 to 343K 79−56621
d-camphor, impurity size effect on self-diffusion 77−11727
d-camphor, NO diffusion, ELDOR, self-diffusion 77−1618
camphor, orientational disordering, thermodynamic props., stat. mech. model 80−96453
dl-camphor oxime, elec. cond., brittle-to-plastic region, cond. jump 78−39169
d-camphor systems, mol. reorientation dynamics, Raman spectra 78−31178
dl-camphoric anhydride, elec. cond., brittle-to-plastic region, cond. jump 78−39169
carbon tetrabromide, ^{13}C NMR in liq., FCC plastic cryst. and monoclinic cryst. 79−78549
carbon tetrabromide, Brillouin scatt., plastic-liquid transition 77−32389
carbon tetrabromide, disordered phase, neutron, diffuse scatt. 80−79717
carbon tetrabromide, disordered phase, neutron diffuse scattering 80−79716
carbon tetrabromide, plastic phase, orientational disorder 79−73115
carbon tetrabromide, solid, Raman spectrum, temp. depend. 78−52488
carbon tetrachloride, freezing and melting of stable and metastable phases 77−27984
carbon tetrachloride, liq. and plastic cryst. phases, thermodynamic props., light scatt., US propag. 78−2863
carbon tetrachloride, polymorphism, solid-solid phase transformations 77−62499
carbon tetrachloride, solid, Raman and far IR spectra 79−33680
carbon tetrachloride, thermal cond. and phase diagram under pressure 78−75893
carbon tetrafluoride, liq. and plastic crystn., Raman spectra 77−59565
critical behaviour at orientational order-disorder transitions, neutron scatt. 77−43308
cubic crystal, self-diffusion and melting 77−31803
cyclobutane-d_0(d_8), cryst. modifications, low. freq. Raman and IR spectra 80−7342
cyclohexane, FCC plastic phase, self-diffusion coefficient, 6 to −40°C, nucl. spin-lattice (spin) relax. 77−36144
cyclohexane, mol. motion, press. and temp. depend., PMR relax. obs. 78−64289
cyclohexane, NMR determ. of phase diagram 77−12210
cyclohexane, NO diffusion, ELDOR, self-diffusion 77−1618
cyclohexane, plastic and liquid crystal phase, rot. correl. func. by Raman spectroscopy 80−23403
cyclohexane, plastic phase, Brillouin scatt., elastic consts. determ. 79−24324
cyclohexane, plastic-phase, NO-doped, heterogeneous solid soln., mag. reson. evidence 78−34449
cyclohexane, rotational reorientation anisotropy near phase transition *(Russian)* 79−4261
cyclohexane, thermal cond. and sp. ht. under press. 78−22906
cyclohexane fluorinated derivatives, $C_6F_9H_3$, C_6H_{12}, mol. rot. in plastic phases 77−35495
cyclohexane-d_0(d_6), plastic crystal phase transition, mol. reorientation, Raman scatt. phonon spectra 80−20631
cyclohexanol, low temp. solid phases, far IR absorpt. spectra, 93 to 303K 79−56785
cyclohexanol, polymorphism, Raman spectroscopy 77−73138
cyclohexanol plastic cryst. phase, glass transition temp., press. depend. 80−49135
cyclohexanone, solid, phase behaviour, at press. up to 3 kbar, DTA 78−43108
cyclooctane, solid, NMR lineshape and spin-lattice relax. 77−24757
cyclopentanol, solid, phase behaviour, at press. up to 3 kbar, DTA 78−43108
cyclopentanone, solid, phase behaviour, at press. up to 3 kbar, DTA 78−43108
diamantane, molecular motions below plastic phase transition 77−24278
diamantane, NMR meas. of mol. motion 79−42858
diamantane, plastic and solid-solid transitions, Raman study 80−60590
diamantane, Raman study of three solid-state phase transition 79−51946
diamantane, structural changes within plastic phase 79−14929
1,12-dicarbaclosododecaborane, plastic solid, phase transitions, 10-320K, Raman and IR obs. 79−28744
1,2-dichloroethane, orientationally disordered crystal., mol. orientation 78−34448
dielectric constant of crystal with steric hindrance 77−24779
1,2-difluorotetrachloroethane, mol. motions and Zeeman-quadrupole cross relax., NMR obs. 79−65751
1,2-difluorotetrachloroethane, orientationally disordered, mol. reorientation, depolarised Rayleigh scatt. obs. 78−88316
dilatometer for PVT meas. of liquids and plastic crystals at low temperature 80−68208
2,2-dinitropropane-d_0(-d_6), phase polymorphism, vibrational assignments, IR and Raman study 80−16031
2,6-dioxaadamantane, plastic phase, transition and fusion thermodynamics, DSC meas. 78−75603
dipolar autocorrelation function, phonon contrib., IR absorption 78−42928
ethane, single cryst. X-ray struct. determ., plastic and monoclinic forms 78−63744
ethane, solid, mol. reorientational motions, incoherent neutron scatt. studies 80−107070
ethanol, polymorphic forms, mol. motion, NMR obs. 80−88885
ethylene-d_4, phase II struct. determ. by neutron diffr. 77−27870
fatty carboxylic acids, C_{15} to C_{19}, solid phase, ^1H and ^{13}C NMR spectra 79−95653
ferrocenecarbaldehyde, plastic cryst. state, Mossbauer spectroscopy and microscopic obs. 77−76333

plastic crystals continued
furane, crystalline, lattice vibr. 78−79694
glass transition temp., press. depend. 80−49135
hexachloroethane, surface roughening transition in vapour phase growth 78−2044
hexamethylbenzene, IR polarised spectra 79−28758
hexamethyldisilane, mol. motion, press. and temp. depend., PMR relax. obs. 78−64289
hexamethyldisilane, NMR determ. of phase diagram 77−12210
hexamethyldisilane, plastic deform., and diffusion of hexamethylethane-^{14}C 78−14510
hexamethylethane, mol. motion, press. and temp. depend., PMR relax. obs. 78−64289
linear diatomic rigid mol. chain, mol. dynamics, rot. phase transformation, struct. factors 78−26635
methane, solid, plastic phase, mol. dynamics simulation 80−79715
methane, solid, probing phase transition with Mossbauer effect in ^{57}Fe impurities 79−4751
methane, solid-state phase transitions, 5-80K, PMR spin-lattice relax. up to 3 kbar 77−40137
methane solid, spin model for orientational phase transition 78−30735
methane-d_4, critical behaviour at orientational order-disorder transitions, neutron scatt. 77−43308
methane-d_4, solid, thermodynamic props. calc. using significant structures method, 6 to 87K 80−24616
methylchloroform, polymorphism, solid-solid phase transformations 77−62499
molecular crystal, conditions of existence as mesogenous system 79−60488
molecular crystal, dynamics, neutron spectroscopy appl., review 79−42166
molecular crystals, diffusion and point defect struct., review 79−82373
molecular dynamics, long time behaviour for chain of colliding rotators 78−75602
α-N_2, computer-simulation with atomic pair pot., plastic cryst., phonon dispersion 77−7679
neopentane:tetramethyl tin, Mossbauer exam. of plastic phase transition 77−20778
neopentane:tetramethyltin, Mossbauer exam. of plastic phase transition 77−69759
neopentane, Brillouin scatt. near liq.-plastic cryst. transition 78−19495
neopentane, mol. motion in cryst., liq. and plastic phases, neutron scatt. obs. 78−6021
neopentane, plastic crysts., rot. correlation functions, neutron scatt. obs. 79−46578
neopentane, rotational motions, cold neutron scatt.study 79−51023
neopentane, solid and liq., effect of n-butane impurity on electron mobility and electron-ion recomb. 80−24984
neopentane-d_{12}, ^{13}C and ^{2}H spin-lattice relax. times, orientational and ang. momentum correl. times 79−33551
t-nitrobutane, plastic cryst., proton spin-lattice relax. time meas. 77−90058
NMR linewidths, anomalous high resoln. obs., rel. to vapour snakes 77−12218
NMR of ^{13}C, high-resolution spectra 79−38388
n-nonadecane, plastic phase, neutron quasielastic scatt. 79−51013
nondecane, Rayleigh scatt. of Mossbauer radiation 78−27125
norbornylene and norbornane, HCP plastic cryst. phases, radiotracer self-diffusion obs., monovacancy mechanism 79−33111
octaphenylcyclotetrasiloxane, phase behaviour and nucleation kinetics 80−29168
orientational disorder, group theory method 80−107091
orientational disordering, melting transitions, thermodynamic props. 80−96452
orientational disordering, thermodynamic props., stat. mech. model 80−96453
orientational dynamics, neutron scatt. data interpret. using functions derived from group theory 80−107092
orientationally disordered cryst., diffuse scatt., hard-core correl., weak-graph method 80−49137
2-oxa-6-thiaadamantane, plastic phase, transition and fusion thermodynamics, DSC meas. 78−75603
2-oxaadamantane, plastic phase, transition and fusion thermodynamics, DSC meas. 78−75603
n-paraffin, rotator phase transformation, lattice dynamics Helmholtz free energy 78−34585
phase transition and melting, dynamical model 77−84677
pivalic acid, liq. and plastic crysts., ^{13}C NMR chem. shift, temp. depend. 80−2652
pivalic acid, orientationally disordered crystal., mol. orientation 78−34448
pivalic acid, plastic cryst., self-diffusion 79−46832
polyethylene, structure formation, near and below melting point 79−65003
polyethylene oxide, peculiarities of struct. form. near below the melting point 80−54150
quinuclidine, cubic phase disorderd struct., X-ray diffr. study 79−69037
quinuclidine, plastic phase, mol. reorientations, ^{1}H and ^{14}N NMR relax. 79−69039
quinuclidine, plastic phase, rot. motion, quasielastic neutron scatt. 79−69038
Rayleigh diffuse line, k-independent, and orientational order 77−36253
Rayleigh scattering of Mossbauer radiation 78−27125
self-diffusion parameters, from anal. of NMR relax. data 79−42301
solid-solid phase transitions at high-press., DTA obs. 79−23540
succinonitrile, defects in plastic phase, positron annihilation obs. 80−11504
succinonitrile, HF electro-optical Kerr effect, orientation depend. 77−24822
succinonitrile, low entropy of fusion plastic crystal, dendritic growth, expt. test of theory 77−35842
succinonitrile, orientationally disordered crystal., mol. orientation 78−34448
succinonitrile, plastic, diffuse scatt., hard-core correl., weak-graph method 80−49137
succinonitrile, plastic and liq., NMR, ^{13}C spin-lattice relax. and ^{14}N linewidth 79−24227
succinonitrile, plastic cryst., orientational order, depolarised Rayleigh scatt. method 78−75612
succinonitrile, plastic cryst. and liq., Kerr effect for relax. kinetics 78−59768
plastic crystals continued
succinonitrile, plastic cryst. with steric hindrance, dielectric const. 77−24779
succinonitrile, plastic phase, mol. motions correlation times, incoherent neutron scatt. 80−49138
succinonitrile, plastic phase, mol. reorientation and rotational isomerization, anal. of elastic incoherent struct. factor 78−22674
succinonitrile, plastic phase, molecular reorientation, rotational isomerism, incoherent neutron scatt. study 79−51021
sulpholan, molecular solid, laboratory frame and rotating frame spin-lattice relax., pulsed NMR meas., phase transitions obs. 80−93197
tetrabromomethane, in disordered phases, IR active mode Raman line shape, dipole-dipole interaction 80−9603
tetrabromomethane, liq. and plastic cryst., rot. Brownian motion, far IR absorpt. 77−36234
tetrabromomethane, plastic phase, neutron diffr. obs. and theory 79−77533
tetrafluoromethane, in disordered phases, IR active mode Raman line shape, dipole-dipole interaction 80−9603
tetrahedral molecules, structural relationships between plastic and ordered phases 79−55681
tetramethylsilane, thermodynamic props. of polymorphic phases 77−84943
tetrebromomethane, thermal resistivity, heat capacity and phase diagram under pressure 80−65316
thermal energy storage using plastic crystal phase transitions 79−57480
2-thiaadamantane, plastic phase, transition and fusion thermodynamics, DSC meas. 78−75603
thianaphthalene, Rayleigh scatt. of Mossbauer radiation 78−27125
transition to crystal phase, mol. and lattice symm., Landau theory 78−42929
translation and rot. dynamics, microscopic Hamiltonian anal., inelastic neutron scatt. elastic consts. 78−38632
n-triacosane, chain axis cryst., quasi-elastic neutron scatt., plastic phase transform 78−6023
triamantane, plastic and solid-solid transitions, Raman study 80−60590
triethylenediamine, thermolum. curves 80−2876
trimethylacetic acid, high resolution ^{1}H and ^{13}C NMR spectra at liquid-solid phase transition 80−11281
trimethylacetic acid, ultrapure single crystal purification and growth 77−55883
trimethylphosphate, plastic and hard crysts., liq., nucl. spin-lattice relax. mol. motion 78−48065
tris(hydroxymethyl)aminomethane, plastic struct., phase transform. studied by X-ray diffr. 80−84130
t-cyanobutane, solid, uniaxial molecular reorientation, quasielastic neutron scatt. 78−42927
cyclopentane, plastic cryst. and liq. phases, thermal cond. and sp.ht., 100-300K, 0-2.1 GPa 78−34663
DCl, plastic cryst. phase, struct. and dynamics 80−92469
GeH_4, crystalline, determ. of mol. symm. from IR spectrum 78−9969
IF_6, NMR and NQR of ^{127}I and ^{19}F, solid-solid transitions and mol. motions 79−99784
KCN, plastic phase, Raman scatt. spectra *(French)* 80−11379
Li_2SO_4, fast ion conductors, X-ray diffr., neutron diffr., and Brillouin scatt. study 80−107170
methane-I plastic crystal, surface modes 78−71926
NF_3, Raman spectra, Coriolis coupling and transition dipole 78−39533
NH_4Cl, surface roughening transition in vapour phase growth 78−2044
NaCN, diffuse scatt., hard-core correl., weak-graph method 80−49137
NaCN, plastic phase, Raman scatt. spectra *(French)* 80−11379
γ-O_2, mol.-dynamic study of struct., dynamics 80−96467
O_2, two-dimensional adsorbed layer on graphite, props. calc. 80−103568
P compounds, globular, struct. criterion for plastic behaviour 78−51454
PD_3, liq. and plastic cryst. states, vibr. dephasing and correl. functions 79−69036
SF_6, plastic phase, neutron diffr. obs. and theory 79−77533
SF_6, plastic phase, orientational disorder 79−73115
SF_6, solid, NMR line shape and relax. 77−51978
SiH_4, plastic phase, rotational motion, quasi-elastic neutron scatt. study 79−51022
SiH_4, plastic phases I and II, neutron inelastic scatt. 79−7558
Te_xS_{1-x}, chemical bonding from ^{129}I and ^{125}Te Mossbauer spectra 79−73867

plastic deformation
see also Bauschinger effect; buckling; creep; ductility; elastoplasticity; kink bands; Luder's bands; necking; plastic flow; serrated yielding; shape memory effects; slip; superplasticity
acoustic emission appl. to materials testing plastic strain and growing cracks identification 80−81252
acoustic emission in brittle materials, book contrib. 78−11484
acoustic emission rel. to stacking fault energy 78−14365
acrylic plastic, deform. of rigidly clamped specimens subject to one sided cyclic heating 77−59932
acrylonitrile-butadiene-styrene copolymers, micromechanism of deform. and rupture *(German)* 80−35276
actinide carbides, lattice defects and rel. to phys. props., review 77−27874
activation volume dependence on total deformation value 78−5671
activation volume determ. by means of change in hardness 79−18836
activation volume stress depend. 80−54304
additives effect on deform. of solids, law of action 77−35628
adiabatic, shearing phenomena, review 80−50692
adiabatic shear in metals, explanation 77−14924
adsorbed molecule vibr. excitation due to plastic deform. accompanying fracture 77−15488
ageing alloys, single cryst., deform. and hardening 78−23716
aggregate, polycrystalline, grain boundary sliding contrib. to total strain 77−25114
AGR fuel cladding, development of high strength, ductile stainless steel alloys 80−45367
Al alloy 7075-T6, fatigue crack propag. rate rel. to accumulated plastic strain rate, cold work effect *(Japanese)* 79−96115
Al-alloys, influence of strain path on mech. props., orthogonal tensile paths 80−30035
alkali feldspar, deformation, plastic defects, TEM investig. 78−32066
alkali halide, deformed single cryst., dislocation struct. formation *(Russian)* 77−7733
alkali halide, doped single crystals, plastic anisotropy 78−26575
alkali halide, X-ray induced strain effects rel. to time of irrad. 78−6120

plastic deformation continued
alkali halide crystals, X-ray irradiated, luminescence during release of pressure 79−65939
alkali halides, dislocation dynamics studied by nucl. spin relax. meas. 80−108091
alkali halides, electrification by plastic deform., mechanism 78−26935
alkali halides, exposed to US waves, dislocation multiplication in original stage 78−47383
alkali-halide crystals, plastic deformation, effect of solid film coatings *(Russian)* 77−25167
alkaline silicate glass, surface layers, plasticity and microcrack formation, electron microscopy *(German)* 80−40469
alloy, dispersion hardened, particle size effect on fracture 79−43418
alloy, effect of degree of ordering *(Czech)* 77−1854
alloy, hyperplastic, diffusion coeffs. determ. during deform. 79−51298
alloy, ordered, with $L1_2$ superstructure, plastic deform. with mobile and immobile dislocations, phenomenological theory 79−7602
alloy, overaged and dispersion hardened, dislocation bowing computed from Orowan relations 77−19949
alloy, precipitation hardened, containing narrow soft zones at grain boundaries, fracture toughness 77−77553
alloy, strain rate sensitivity rel. to ductility, anomalies 77−36590
alloy, thermodynamic and structural changes in deform. twinning 78−2139
alloy, two-phase, deform. struct. and recrystallisation, review 79−34061
alloy, two-phase, recrystallisation mechanisms 79−47708
alloy, vacuum rolling at high temp. *(Russian)* 79−15708
alloy structural steel, electron fractographic pattern of fatigue fracture under cyclic loading 77−56094
alloys, austenitic, neutron irradiation effect on tensile, creep-rupture, deform., fracture props. 79−65120
alloys, brittle and plastic, energetic strength theories *(Bulgarian)* 80−38296
alloys, high temperature, creep failure criteria 80−65150
alloys, hot plastic strain, stress- strain-time dependences *(Russian)* 80−40430
alloys, industrial, stacking fault energy rel. to mech. props. *(French)* 79−43339
alloys, $L1_2$-type superstruct., anomalous temp. depend. of deform. charcts. *(Russian)* 79−20109
alloys, $L1_2$, superstructure, dislocation link strength and strain hardening at high degrees of deform. *(Russian)* 78−39792
alloys, machining damage, depth of surface layers determ. 80−85094
alloys, statistical model in conditions of monotonous cyclic loading *(Bulgarian)* 80−70296
amorphous materials, deform. processes 77−4813
amorphous metals, mech. charcts., review *(Japanese)* 77−86109
amorphous structure, computer simulation of deformation 79−7647
amorphous-crystalline substances, high temp. plastic deform. interpret. 77−35627
andalusite, shock-loaded, deform. 80−19873
anelastic deform. as internal parameter 77−33867
angled elliptic notch problem under biaxial loading, strain failure criterion 80−79235
anharmonic atomic chain breakup, molecular dynamics calcs., deformation dynamics 80−29117
anisotropic body, slip planes 78−39874
anisotropic constitutive equations of continuous media *(French)* 79−25846
anisotropic metal blanks, plastically deformable, stress/strain relations *(Russian)* 80−1438
anisotropic plasticity, theory development, expt. results 79−27553
anisotropic polycrystal, yield and tensile test meas. of plastic behaviour 77−32631
anisotropically strain deformed materials, condition for transfer to plasticity *(Russian)* 77−46940
anisotropy coefficient, effect of strain rate 77−25097
anisotropy theory based on yield function of fourth order 78−31457
annular plate under uniform compression, stability and behaviour 77−42759
anodic, and free anodic film on Al substrate, deform.-strength props. *(Russian)* 77−69203
anthracene, slip systems in deformed crysts. 79−42138
anthracene, triplet exciton trapping by dislocations 78−30871
arches, freely supported, reserve of resistance beyond limiting load *(Italian)* 79−18703
asperity models, slip-line field anal., wear and friction regimes 79−87739
asymmetric edge crack under longitudinal shear 77−80117
atomic chain, anharmonic, change in nature of vibr. produced by deformation 79−7666
austenite, quenched and tempered, effect of bainitic decomp. products on mech. props. 77−56007
austenitic stainless steel, Cr-Ni, stability, tensile and compressive strain depend., 4-373K 77−25052
austenitic steel, 17G1S struct. and austenite transformation kinetics variation on deform. *(Russian)* 79−70060
austenitic steel, ageing after deform. in pre-martensitic state, internal friction meas. *(Russian)* 77−77477
austenitic steel, hardened by thermomechanical treatment with ageing, influence of stabilisation on mech. props. *(Russian)* 77−52356
austenitic steel, mechanical properties, effect of high temp. thermomechanical treatment and post-deform. ageing *(Russian)* 78−39809
axisymmetric, slip line model *(Russian)* 78−83261
axisymmetric drawing through curved dies, heat transport anal. 77−52432
axisymmetric extrusion based on upper bound approach 78−56714
axisymmetric solids with material and geometric nonlinearities, finite element anal. 78−34037
bainite, formed from deformed austenite, morphology and mech. props. 79−43345
ballistic impact on thin plates, membrane model 78−30193
bar, elastic-plastic, large deform. anal. under repeated axial loading, small deform. theory correl. 78−59310
bar, stress meas. in dynamic deform. to plastic range 77−84158
BCC crystal, cyclic deformation, irreversible glide and shape changes 80−103356
BCC metals, influence of screw dislocations on cryst. lattice rotations during deform. *(Russian)* 78−6966
BCC metals, plastic deform., computer simulation 80−40456
BCC metals and alloys, review of plastic deformation and work hardening *(German)* 78−84946

plastic deformation continued
BCC metals and alloys plastically deformed, electron microscopy *(French)* 77−44299
BCC single crystals, plastic deformation localisation 80−54303
beam, fixed ended, exptl. behaviour under simulated uniformly distributed load 79−27540
beam, higher modal plastic response 77−50948
beam bending including transverse shear finite element anal. 79−90148
beam dynamic loading, large elastic-plastic deform., numerical anal., expt. meas. 78−1574
beams, dynamic plastic behaviour, rot. inertia and transverse shear influence 80−48601
beams, dynamic plastic response, rotatory inertia and transverse shear effects 80−5947
beams, impulsively loaded, higher modal dynamic plastic behaviour 78−90721
beams, inelastic bending under time varying moments, state variable approach 80−28439
beams, influence of transverse shear on plastic yielding 79−32287
beams thin-walled, of open cross section, finite-element model 80−74767
bending and torsion of simple geometries, subjected to cyclic loading, stress-strain analysis 78−90734
bending beam, slip line development 80−58928
bending plastic collapse, mm. cost in elastoplastic structs. 78−30197
bifurcation in elastic-plastic solids, perturbed motion of stress axes 78−90730
bifurcation theory of non-isothermic elastic-plastic deformations *(German)* 77−54892
billet shape during stamping *(Russian)* 79−98630
bimetal Nb-steel Kh18N10T with Cu interlayer, cyclic heating effect 77−16687
bimetal rolling, calc. of strains by variational method *(Polish)* 80−45323
bimetallic tube, residual stress after thermal cycling 77−90465
biological membranes and proteins, plastic deformation during freeze-cleavage, review 78−14400
blanks cogged into conical matrix, stability anal. *(Russian)* 80−43636
body with shape memory model, load displacement curves, snap springs 79−94501
bonded ductile half planes, plastic yielding through interface from cracks under antiplane deformation 77−14960
bone, compact, deform. and strength 78−24087
bone, deform. and strength, change dynamics at early stages of form. 78−7383
bone, deformation under unloading and repeated loading 78−3546
bone cements, effects of antibiotics, strain rate, temp. and age 77−60298
boudinage structures, displacement and stress distrib., finite element method 78−32078
bounded elastic body containing a crack, mode I deform., integral eqn. soln. 79−3976
α-brass, (211)[$\bar{1}$11] single crystal, rolling deform. 77−21174
α-brass, acoustic emission signals in plastic deform., amplitude distrib. *(Japanese)* 78−6978
α-brass, acoustic harmonic generation by long-range dislocation motion 79−42150
α/β brass, bicrystal, dynamic obs. of fracture phenomena 79−5040
α-brass, bicrystal, grain boundary fracture at intermediate temp. *(Japanese)* 79−15774
β-brass, bicrystal and tricrystal stress strain behaviour 77−36607
brass, Cu-Zn (39(40) wt.%), shape memory effect and martensitic transform. depend. on heating-cooling cycles *(Russian)* 80−97482
brass, deformation, tension, torsion compression test exam. *(Russian)* 78−31455
α-brass, deformation mode during rolling *(Japanese)* 79−79001
α-brass, dislocation struct., deform. *(Polish)* 80−24454
brass, FCC rolling texture origin with rolling plane parallel to {111} 79−91674
brass, high-speed strain effect on struct. and props. *(Russian)* 77−59855
brass, hot ductility and torsional deform. *(Japanese)* 79−57069
brass, LANKMts, solid soln. range of existence 77−12653
brass, M63, yield stress decrease in compression, rel. to previous elongation *(Polish)* 80−50665
brass, mechanical ratcheting, plastic theory 78−76702
brass, orientation change in (211) [$\bar{1}$11] single crystals during rolling *(Japanese)* 78−60712
brass, Pb effects 77−44310
α-brass, plane stress ductile fracture, prestrain effects 80−108532
brass, plastic deform., stress-strain relation of integral type 80−74754
brass, plastic deform. under complex loading 79−38890
brass, plastic props., room temp. to recrystallization temp., stress-strain relations, computer program 77−1865
brass, plastically deformed, phase transforms. and diffusion phenomena *(Russian)* 79−20115
β-brass, quenched single crystal, deform. and slip 79−79026
α+β brass, recovery and recrystn., positron annihilation 79−57003
α-brass, single crystal, deform. and ductility at elev. temps. *(Japanese)* 79−5012
brass, single crystal, two-way shape memory effect and other training phenomena 77−48505
brass, soft 70/30, density changes, void growth in biaxial stress fields, plastic deformation 80−71692
brass, spring alloys, microplastic deform. and endurance limit 80−81197
brass, stress corrosion cracking, effect of strain rate 79−20257
brass, tensile curve and specific value of anisotropy coeff. *(French)* 77−28867
α-β brass, two phase bicrystal, deform. and fracture at 450K 80−16409
α-β-brass, two phase bicrysts., deform. and fracture at 150K 80−16388
α-β brass, two-phase bicrystals, plastic deform. and fracture mechanism 78−84898
α-brass, with few inclusions, shear mode of ductile fracture 77−36652
brass 63 recrystallisation textures, and deformation formed by dry sliding against steel 79−91698
brass α-β two-phase bicrystals, interface sliding studies 80−54248
brass (70:30), cold rolled, optical, X-ray and TEM exam. of deformation struct., and textures 78−88500
brass positron annihilation in α and α+β phase, short-range order, clustering and lattice defects influence 79−29107
brass single crystal, martensite form. and shape memory effect mech. 78−19744

plastic deformation continued
α-β brass two-phase bicrystals, activated slip systems during yielding 78−84911
α-β-brass two-phase bicrystals, operative slip systems at 150K 79−70119
break-up of plastic bodies *(Russian)* 77−80121
brittle fracture, stability problem, three-dimensional linearised theory *(Russian)* 78−55606
brittle fracture, statistical theory, dislocation mechanism, crack propagation *(Chinese)* 80−106755
brittle materials, splitting of fracture toughness into two terms, elastic deform. and plastic deform. *(German)* 78−35468
bubble formation mechanism, on surface of deformed crystal, in liq. He, acoustic emission *(Russian)* 78−85066
buckling of elastic-plastic cylindrical panel under axial compression 78−1584
buckling strength of orthogonally stiffened plates under uniaxial compression 80−5964
Burgers circuits associated with generalized distortions 80−2014
butadiene rubber, polymer melt, extrusion at constant deformation rate 78−68744
butadiene-styrene block copolymer, oriented, isotropic, struct. changes during deformation *(Russian)* 78−88512
butt joint, tensile bond strength, effect of aspect ratio 80−50823
calcite, sound emission on dislocation annihilation *(Russian)* 80−54246
calcite rocks, plastically deformed, texture transitions 79−83227
calorimetric method for meas. change in stored energy with deformation 79−50682
dl-camphene, self-diffusion, effect of impurities, radiotracer and plastic deform. study 78−43177
camphor, rhombohedral, polycryst., compressive deform. and dynamic recrystn. 80−71698
cantilever postcollapse behaviour, strain hardening effects on large plastic deformation 79−46232
carbide fuel, deform. mech. map appl. to in-reactor deform. 77−18662
carbon steels isotropic-kinematic strengthening during plastic deform. *(Russian)* 77−20007
carbonate minerals, deform. twinning mechanisms 80−79814
carbonate rock, interrelation of flow or fracture and phase transition during deform. 80−51389
carbonmetalplastic, heating rate effect on thermal deform. in various atmos. 79−65226
cavitation erosion, observation of eroded surface by SEM 78−15536
cavitation-produced stress in solid 77−24354
cavity nucleation, by plastic deform. 79−29127
cell wall, Acetabularia, deform. rel. to genetic and geometric factors 77−56348
cell wall deform. and morphogenesis, local control of viscoelastic deform., Acetabularia 77−56349
celluloid, mech. props. under proportional load, time lapse, heating and isotropic props. effect *(Japanese)* 79−79043
celluloid, nonlinear viscoelastic deform. under superimposed hydrostatic pressure 79−34116
cellulose, nitrated, strength, deform. and disintegration, influence of stable free nitroxyl radicals 80−11717
cellulose nitrate, nonlinear viscoelastic deform., hydrostatic press. and third invariant of deviatoric stress tensor 80−93587
cement mortar, deform. charact., expt. study *(Japanese)* 78−56704
cement paste, heat-cured, recoverable and irrecoverable deform. 77−63732
cementite, in white pig Fe, deform. and fracture 77−4827
ceramic, electrical transducers for automatic recording of mechanisms occurring during drying 77−52561
ceramic, plastic deformation, grain and grain boundary processes 77−4814
ceramic materials, fine-grained, cyclic plastic deform. as cuase for thermal expansion hysteresis 80−89290
ceramic nuclear fuels, mech. props. at compressive deformation 80−651
ceramic oxide, TEM study of deform., review 79−87686
ceramic powder, thermal stresses during spheroidisation process *(Russian)* 80−40386
ceramics, mechanical behaviour, book 79−38983
ceramics, polycrystalline, stress-relaxation technique for deformation studies in four point bending 79−100200
ceramics and brittle solids, abrasive wear, role of plastic deform. and fracture 80−108594
chain of Al rings, plastic extension due to axial impact load 79−18737
chamotte concrete, alumina-based cement, thermomech. props. 78−35455
chopped glass fibre reinforced polyester resin, deformation and thermoset cure effect on heat cond. during molding 79−86325
chrome yellow, crystal lattice deform. effect on colour *(Rumanian)* 78−23422
chromorheology, new exptl. method 80−48658
circular bar of rate sensitive material, elastic-plastic tension-torsion 80−48602
circular cylinders, plastic buckling in pure bending 79−90158
circular hole in sheet metal subjected to biaxial tensile strength, plastic expansion 79−27541
circular plate resonse to central pulse loading 78−18187
circular plates, Ilyushin yield surface approx. 79−64505
circular tubes under transverse loading, expt. anal. of large deformations 77−19543
coil winding, plastic over bending, and over springing *(German)* 79−90156
cold drawing, moderate, resulting plastic deform. incompatibilities, X-ray line broadening determ. *(French)* 79−43265
cold-drawn sheet, texture changes in stamping *(Russian)* 77−90365
columns, Beck and Leipholz types, stability, shear deformation and rot. inertia effects 80−48610
complex loading of materials, plastic deform. 80−99939
composite, crack propag. *(Russian)* 77−25147
composite, thick walled rings, calc. taking into account deformation nonlinearity 77−58565
composite material, deformability surfaces 78−23792
composite material, sintered, microstrained state, opt. polarisation investig. 78−11476
composite materials, tension stability, deformation up to failure *(Russian)* 80−75289
composite materials loaded in, uniaxial tension under pressure, tensile strength eval. 78−19828
plastic deformation continued
composite ribbed cylindrical casings, stressed-deformed condition under external hydrostatic press. 78−6996
composite superconductor, flux jumps and training 80−70911
composite T-beams, repeated loading effects 77−86253
composite three-layer cylindrical shells, initial stressed and deformed state 80−102974
compressed bar, secondary plastic deformation influence beyond yield stress *(Russian)* 79−37199
compressible materials, flow behaviour 78−55573
compression struts, of nonlinear viscoelastic materal time dependent load bearing capability *(German)* 78−48474
compression tests, uniaxial, for plastic deform. *(Hungarian)* 80−97658
concrete, cracking along anchored deformed reinforcing bars 79−96122
concrete, creep, long term prediction and shrinkage from short term tests 79−20122
concrete, fatigue, load-deform. behaviour *(German)* 79−11693
concrete, heat resisting, exam. of deform. behaviour, description of testing rig and operation *(French)* 79−15720
concrete, plastic-brittle behaviour, hardening and softening constitutive eqns. 77−21270
concrete, reinforced slabs, punching shear strength under in-plane biaxial tension 80−100876
concrete, running fatigue test, determ. of loading-deform. charact. and internal damping *(German)* 77−25229
concrete continuum model for plastic-brittle fracture 79−27584
conical porthole, deep-water, deformation effect on optical characteristics 79−76859
conical shell under antisymmetric loading, compliance determ. 79−90153
conical shells, axially compressed with edge constraint, elastic and plastic buckling 78−63341
consecutive energy barrier systems, deform. kinetics 79−77672
constructional materials, constructing relationship processes of loading and deform. 78−6998
constructional materials, creep, viscosity, resist. to inelastic deform. 80−89309
contact adhesion between solids in vacuum, deform. and interfacial energy 78−22306
contact film absorption on plastic deform. of contacting bodies *(Russian)* 80−93596
contacting asperities, theoretical analysis of elastic-plastic deformation 79−95076
contacting bodies, roughness and Poisson's ratio effect on deform. 79−79122
containment vessel, cylindrical, submerged, dynamic plastic response, design formulae 80−83759
convexity condition in an elastic-plastic material *(German)* 80−106734
copolyimide glass based on benzophenone tetracarboxylic acid dianhydride 77−63720
cord reinforced rubber laminate, interlaminar-shear-strain meas. 79−57043
cord-rubber laminates, two-ply balanced, interlaminar-shear strain study 80−97526
Corson alloys, AE during tensile deform. *(Japanese)* 79−61654
corundum refractory ceramic deformation curve analysis *(Russian)* 79−90716
Cosserat theory of crystal plasticity, appl. to anal. of lattice rotations under constrained deform. *(Japanese)* 78−2189
coupled elastic-plastic boundary-value problems, rock mech. appl. 77−14918
coupling phenomena in thermoplasticity 80−87721
covalent crystal, resistance to microindentation 78−60753
Cr-Mo, martensite to ferrite transform. by fatigue deform. *(French)* 79−66056
crack, diffusive growth in plastically deforming solid 79−20182
crack, rectilinear, isolated, growing at const. rate under antiplane deform. conditions, dynamics 79−7338
crack and fracture behaviour, simultaneous acoustic emission and SEM techniques *(German)* 79−96240
crack edge tip, exact analytic soln. 80−69734
crack growth stability anal. using catastrophe theory 80−74810
crack loaded in uniform tension, yielding on inclined planes at tip 77−42780
crack tip, moving, void growth, coalescence, finite element anal., plane strain conditions 78−1609
crack tip, plastic deform., metallographic anal. by recrystn. 80−85029
crack tip, plastic yielding modelling by inclined slip planes 80−33472
crack tip, yielding on inclined slip planes 77−42781
crack tip strain distribution measurement by recrystn. *(German, English)* 77−56203
crack tips, blunt, elastic-plastic stress fiield, plane stress and plane strain *(Chinese)* 80−64469
crack tips, plastic zones during uniaxial deform. *(Russian)* 79−50655
crack tips, yielding on inclined planes 80−33525
cracked bar under torsion and shear, elastoplastic stress and strain calc. from screw dislocations 79−68654
cracked stiffened panels, biaxially loaded, elastic and elastic-plastic analysis, using finite element method 79−68656
cracking metal surface deformation obs. by interference microscopy *(German)* 77−56210
cracks, penny-shaped, ductile, dynamic effects in propagation, Hankel and Laplace transform methods 80−87741
cracks, plastic, in bending, tension, anal. 79−41623
cracktip under incipient creep deform., stress field and modified J-integral *(Japanese)* 80−103411
creep and long-term strength 77−11139
creep and plasticity, theory, microhomogeneity in plastic strain 79−14281
creep fracture, failure mechanism involving grain boundary sliding and brittle crack extension 80−97557
creep fracture model, plastic growth of cavities at tip of grain boundary wedge cracks 77−52446
creep strength of deformed material, conditions of physico-chemical action *(Russian)* 77−16703
creep test method for plastic deformation, high temp. tests *(Hungarian)* 80−97660
creeping structs. bounding solns. for load varyings above shakedown limit 77−89039
creeping structs, under load variations above shakedown limit, appl. of bounds 77−89040

plastic deformation continued
creeping structures with load variations above shakedown limit, boundary solns. 80−10156
cryolite, hydrothermal synthesis of large synthetic single crystal, props. 78−19654
β-succinic acid, cryst., slip system and dislocation detect. by etching 77−59015
crystal growth, creation of stress and dislocations *(Russian)* 80−103277
crystal inclusion, oblate spheroid, exam. of stress concentration due to inclusion 78−71281
crystal plasticity, surface effects, review 77−47505
crystal surface elastic props., surface tension tensor, volume stress *(Russian)* 80−100389
crystalline bodies, plastic strain and microcrack propag. 80−81199
crystalline material, flow during plastic deformation *(Russian)* 78−76705
crystalline materials, fracture, stress relaxation effect 80−88256
crystalline particles at sphere-plane contact, nondiffusional deform. under capillary forces 78−15329
crystallite deformation in rolling, computer simulation *(French)* 78−31421
crystals, quantum effects in plasticity 80−59561
crystals pulled from melt, thermal stresses and struct. defects 78−2041
Cu, formation of double twist boundaries during plastic deform. *(Russian)* 77−81295
Cu-Al, FCC, study of dipoles using weak-beam electron microscopy 78−22724
cubic crystals, active slip systems in plastic deform. process *(French)* 78−35431
cubic crystals, compression test, double slip kinematics 80−65005
cubic crystals, dislocation theory, soln. of eqns. *(German)* 78−38701
cubic crystals, elastic strip, moving stress sources, boundary-value problem soln. *(German)* 78−38702
cubic single crystals, hardness meas. by spherical indentation 80−16622
cyclic, exam. of reversible strain, effect on dislocation motion 78−84892
cyclic deformation folded strain relief, ionic cryst. model *(Russian)* 77−59858
cyclic loading for materials with vanishing elastic region 77−46939
cyclic plasticity for nonproportional paths, comparison with prediction of three incremental plasticity model 78−92308
cyclic strain diagrams recording under nonisothermal conditions, review 80−71830
cylinder compression at small elastico-plastic deformations *(Russian)* 79−10497
cylinder expansion under finite plane strain 78−51094
cylinder penetration of thin obstacle, 1-D approx. anal. *(Russian)* 78−30246
cylinders, discretely stiffened, buckling under axial compression 80−64408
cylinders, thin necked, thermoplastic deformations, stability analysis *(German)* 78−22281
cylindrical beam, impact effect on rigid wall *(German)* 80−106763
cylindrical ingot, continuous casting, elastic-plastic temp. stresses and deformation *(Russian)* 79−61576
cylindrical shell, loaded by concentrated force acting along the generator, load carrying ability 77−89044
cylindrical shell deform., effect of loading history on bifurcation *(Ukrainian)* 78−55578
cylindrical shell of variable wall thickness under radial external press., buckling, expt. study 79−96082
cylindrical shell under internal pressure, ductile growth of longitudinal flow 79−10530
cylindrical shells, Ilyushin yield surface approx. 79−64505
cylindrical tubes or shells, mild steel, quasi-static piercing 80−45351
damage accumulation in nonstationary low cycle rigid loading 77−16686
damage analysis under nonproportional cycling 80−97556
Debye-Sears cell lattices, DSC-1 and DSC-2, computation of coincident and near-coincident cells 77−84746
deep-drawing curves, cryst. microstruct. during deform. *(French)* 79−20066
defect dimension determination by acoustic emission 80−104381
defect dynamics, field equations, four dimensional space-time setting 80−96521
defective material, with strength, anisotropy induced by pretreatment, limiting state probability calc. 77−86123
deformable solids, fracture and hardening kinetics 80−35210
deformation heat attachment for scanning electron microscopy *(German)* 79−20297
deformation mechanism maps 80−3143
deformation resistance, depend. on hot press. working speed *(Russian)* 80−65126
deformed crystal, faulted dipoles 78−59814
deforming stress relaxation, non-uniform internal stress field effect 77−21204
delayed cracking by H_2 gathering simulations at plastically deformed notch, finite element anal. 78−31539
design plastic stress concentration factors using Ramberg-Osgood stress-strain parameters 78−63310
diamond, high press. appl. by spherical diamond indentor, plastic deform. obs. method 78−35619
diamond, natural, dislocation-N_2 impurity interaction, photoconductivity spectra, resistivity 79−91097
diamond, plastically deformed, EPR of two N atom centre 78−72408
diamond at room temperature 78−52927
diamond lattice, dynamic symmetry and plastic deform. 80−24527
dielectric, pulsed RF radiation produced by scratching *(Russian)* 78−19607
dielectric, thermal mechanism of plastic deformation and fracture by laser beam 77−11553
differential geometry of deformed crystals 80−19867
difficult-to-form metals, deformation broaching 80−108473
diffusion welded joints, creep deformation effect on characts. 80−25806
dilatant granular materials, initial planar deformation 79−41591
discoidal agglomerate, stress pattern, distributed loading effect during diametral compression test 80−60934
discontinuous deformation, statistical model 78−34566
discrete obstacle model, dislocation and stress field distrib. 80−79794
discrete structural models, plastic dynamics, finite element method 77−35056
discs, doubly-connected, elastoplastic, full yielding at collapse, noncircular shapes 80−74755
discs, doubly-connected, noncircular, full yielding at collapse, photoplastic verification 80−74756
dislocation and disclination kinetics, macroscopic theory *(Russian)* 80−49225
dislocation behaviour in fatigue 77−24352
dislocation cell form. during plastic deform., TEM obs. 80−60935
dislocation density, depend. on extent of plastic deform. and grain size *(Russian)* 78−22715
dislocation dynamics during strain rate changes *(German)* 78−18655
dislocation ensembles, local heating at low temps., parallel glide planes, temp. distribution *(Russian)* 80−29020
dislocation generation mechanism in shock wave deform. 78−43018
dislocation mobility, description using diffusion eqns. 78−38697
dislocation motion, Kê peak anal. by internal friction meas. during deform. 78−18705
dislocation pile-up formation, by Frank-Read source, emission of sound 79−37705
dislocation source activation by load impulses 78−14350
dislocation structure, high press. effects, plastic deform. *(Russian)* 80−88159
dislocation structure development near cryst. surface, kinetics 79−73167
dislocation subboundaries, collective effects accompanying migration *(Russian)* 78−14347
dislocation substructure strengthening and thermomechanical processing, conf., Las Vegas, USA, Feb. (1976) 77−84760
dislocation transformations in theory of plastic deformation 78−38703
dislocation velocity, thermal activation exam. of applied stress and temp. depend., expt. methods *(French)* 80−59474
dislocations, collective behaviour, velocity of slip band and mobile dislocation densities, HVEM study *(French)* 80−65006
dislocations, state of art review, book contrib. 80−39089
dispersed media, shock compressibility, brittle destruction 80−49303
dispersion hardened metallic matrix composite, powder metallurgically produced effective interparticle distance effects *(German)* 78−52727
drawing through die, global soln. of boundary problem 77−84157
ductile fracture, computer model based on plastic strain, fracture toughness prediction, comparison with steel data 79−32383
ductile single crystal, geometric effects in inhomogeneous deform. 79−46741
ductile single crystals, exam. of strain localisation 78−52912
ductile-brittle transition pressure, grain size effect *(Japanese)* 78−60745
Duralumin, lifetime after preliminary plastic deform., kinetic theory of strength 79−43395
Duraluminium rings, stress/strain relations, compression and tension tests, rigid plastic theory 79−34098
dynamic crack-tip fields according to deformation theory 80−64481
dynamic load response, dynamic plastic mode-form solutions 79−10499
dynamic plasticity, implicit and explicit computational schemes 78−34038
dynamic response of a slab of elastic-viscoplastic material that exhibits induced plastic anisotropy 80−83737
dynamic variation principle taking into account geometric nonlinearity 79−23227
Earth lithosphere bending at trench, elastic-perfectly plastic anal. 78−81135
EBR-II 80−13598
edge superdislocations, resist. to motion, temp. depend. expressions *(Russian)* 80−79789
elastic rings under essentially nonaxisymmetric load, large deform. 79−98637
elastic-perfectly plastic solids subjected to variable loads, plastic strain upper bounds 79−86346
elastic-plastic bodies, localisation of deformation, bifurcation modes 80−79167
elastic-plastic body, min. principles and strain uniqueness, stress fields 77−3734
elastic-plastic body, strain and stress fields, min. principles 77−3735
elastic-plastic deformation stress-strain anal., parametric linear programming method 79−37194
elastic-plastic media, nonisothermal, finite deformations, constitutive equations and numerical soln. 80−31503
elastic-plastic problems, supplementary strain method, appl. 80−96205
elastic-plastic solid, finite homogeneous deformation, bifurcation 77−62158
elastic-plastic solids, min. principles for stress and strain fields 77−879
elastic-plastic torsion, nonlinear boundary value problem 77−89043
elastic-plastic wave propagation, transmission of elastic-plastic boundaries 77−62188
elastic-viscoplastic proportional combined twist and stretch of circular bar of rate sensitive material 80−23912
elastically vibrating single crystal, simultaneous diffr. effect on rocking curve 80−107019
elasto-plastic continua, quasi-bifurcation in dynamics 78−38223
elastoplastic bodies, quasistatic deform., models, initial boundary value problems *(German)* 78−42549
elastoplastic body, deformation process bifurcation under combined loading *(Russian)* 77−54888
elastoplastic fracturing structures, boundary value rate problem, extremum theorems 80−48596
elastoplastic relaxing media, shock waves struct., distribution model 80−58961
elastoplastic strip or half-plane under moving load, residual stresses and plastic zones 80−53645
elastoplastic structure dynamic shakedown, plastic strains, upper bound principles 79−76986
elastoplastic structures, historical deform. analysis and parametric linear complementary problem 77−58563
elastoplastic structures, shakedown anal. 77−3745
elastoplastic system, dynamic deformation, internal state variables and internal forces 80−53660
elastoplastically deformed strengthened material, stress deformed state during rolling *(Russian)* 80−54299
elastoplasticity, shakedown problems for elastic plastic solids with piecewise linear yield surface 80−79173
elastoplasticity finite element anal. for large strains, natural factor displacement method 80−14580
electron microscopy, HV, in situ deform. expts. 77−52605
electron microscopy, HV, in situ obs. techniques and applics,. review *(Japanese)* 80−59351
electronic potentiometer, attachment for measuring deform. 77−17974

plastic deformation continued
Elinvar, Cr addition effect on modulus of elasticity and thermoelastic coeff. 77−90387
ELN-1 alloy, prestrain effects on strength *(Russian)* 78−11267
enamel coating on metallic base standardization of estimation of impact strength 78−23768
endochronic plasticity, appl. to structural dynamic response of radioactive waste containers 80−16407
energy based theory 78−63316
energy-balance approach to fatigue crack growth 78−90773
engineering materials, elev. temp. fatigue interactions 77−86173
engineering materials relation between deform., rupture, power-law creep 79−5020
enhanced thermal creep deformation, secondary stress cycling conditions, elastic region, LMFBR fuel rod 77−4832
epoxy, Al_2O_3-filled, shock-wave compression, 0.4-3.7 GPa 78−59856
epoxy, crosslinked, time-temp. superposition applied in creep with superimposed hydrostatic press. 77−70127
epoxy, mech. props., 20 to 300°C *(French)* 77−56018
epoxy impregnated superconducting composites, mech. props., strain effect at 4K 80−25822
epoxy resin, Cl-containing, relation between static and dynamic deform. characts 80−3137
epoxy resin, deform. rate depend. of mech. props. at cryogenic temps. 80−55456
epoxy resin, plastic deform. effect on crack propag. 80−97563
epoxy resin, plastic deform. mechanism 80−97534
epoxy resin, shear strength determ., anal. of methods 77−86107
epoxy resin DGEBA, cured with TETA, crack propag. and fractography 79−70154
epoxy resins, strain anal. by fluoresc. meas. *(French)* 79−47846
epoxy-polyglycol elastomers, fracture strength under compression 79−38929
equivalent minimal stress in forming processes *(French)* 80−38277
expansion process, associated differential geometry 79−67159
explosive forming, computer numerical simulation 80−59560
extrusion, reverse cold impact, appl. of ultrasonic radial oscillations *(Russian)* 80−97441
extrusion process using orthotropy concept of Hill, kinematically determined problems in rigid-ideal plastic *(German)* 80−1445
failure, effect of deep wedge shaped notches of small flank angle 80−48593
failure characts. of steel 15G2AFDps, effect of loading freq. and temp., SEM exam. of failure surface 78−84995
failure criterion considering stress state at crack apex 79−57113
fastener hole, cold worked, residual strain 79−29088
fatigue, high cycle, plastically prestrained materials and components *(Czechoslovakian)* 77−32680
fatigue, hydrostatic stress-sensitive relationship for biaxial stress conditions 80−74805
fatigue crack propag., in deformable media with nonlinear characteristics, model 78−63393
fatigue crack propag., plastic work role 79−79070
fatigue crack propagation, new measurement and observation techniques 80−45463
fatigue crack tip zone, highly-deformed, cyclic strain history *(Japanese)* 79−34145
fault gouge, structural changes during stable sliding and stick-slip 78−32079
faulting analysis in three dimens., strain field 78−77225
FCC and CC metals, behaviour during rolling, numerical simulation study *(French)* 78−84891
FCC crystal, grip effect and bend gliding during uniaxial tensile deform. *(Japanese)* 79−52314
FCC crystal, homogeneous deform. by glide of dislocations with imposed stresses and strains *(French)* 77−7783
FCC crystal, transient effects during tensile tests in model of correlated dislocation motion 78−38715
FCC crystals, deform. faceting of large-angle grain boundaries TEM 77−65984
FCC metal, origin of dislocations during microdeformation tests, X-ray topography 79−82226
FCC metals and alloys, macroscopic shear band contrib. to rolling texture 77−86056
FCC metals and alloys, plastically deformed, electron microscopy *(French)* 77−44301
f.c.c. polycrystals in microstrain region 77−1165
Fe-Cr-Co-Si-Mo, plastic deform. influence on structure and mag. props. *(Russian)* 79−70176
ferrite, polycrystalline, ionic diffusion and dislocation movement during creep deform. *(Japanese)* 77−28039
ferromagnet, mech. behaviour in microplastic strain region *(Russian)* 78−39838
ferromagnet, stress indication by transverse and longitudinal internal induction 77−16138
ferromagnetic ordered structures, domain structure, effect of defects, electron microscopy 78−64214
ferromagnetic solids, magnetomechanical effects, magnetostriction, hysteresis, stress, yielding, fatigue damage, crack growth *(Polish)* 80−71150
fibre, oriented, nonisothermal deform., thermomech. curves, statistical interpretation 77−32651
fibre reinforced complex structural mouldings, accurate stretch data for reinforcement, deform. 80−11694
fibre reinforced complex structural mouldings, accurate stretch data for reinforcement, deform. 80−16375
fibre reinforced composite, deform. diagram construction method, based on statistical distrib. of strength of fibres 77−52437
fibre reinforced composite, initial yield surface, in plane stressed state 77−86106
fibre reinforced composite, new, physical props. 77−8797
fibre reinforced composites, brittle zone on fibre surface, deform. and fracture 77−56104
fibre reinforced composites, deformability characteristics, reinforcement scheme effect 80−58930
fibre reinforced composites, exam. of thermal stress fracture 78−75103
fibre reinforced composites, reinforcement scheme optimisation with respect to deformability at assigned stresses 80−69689
fibre reinforced composites, stress redistribution dynamics during fibre rupture 80−64394
fibre reinforced composites, thermal cycling, elastoplastic strain calc. under action of external stresses *(Russian)* 79−38896

plastic deformation continued
fibre reinforced composites densification in free forging, exam. of specific work and kinetics 80−16218
fibre reinforced composites with high work of fracture 80−81029
fibre reinforced laminate, nonlinear response 77−70107
fibre reinforced nonlinearly elastic matrix, unidirectionally reinforced, deform., strength, and failure 80−3134
fibre reinforced resin matrix composite deform. and fracture in combined stress states 77−70106
fibrous refractory, exam. of deform. behaviour and thermal cond. *(French)* 79−15719
filament reinforced hypoeutectoid C steel, strength characts. after deform. and quenching 80−35271
filamentary crystals, complex stressed state, method of investigating mech. props. 80−3264
filler metal, deformation mechanism at brazed joint 78−80616
film, UH vacuum deform. meas. via Michelson interferometer 77−2650
fine fragmented crystals, complex struct. analysis by electron microscopy 80−104416
finite deformation elastoplasticity, strain measure decomposition 79−23223
fission reaction fuel, kinematic hardening rule of plasticity 80−42764
fission reactor materials, clad failure prediction during FBR overpower transiency, JANE code 80−78363
fission reactor materials, thermomechanical transient anal., strain-rate dependent plasticity 80−79864
flange, rigid-plastic deformation in deep drawing process, finite element anal. 79−18735
flat glass in vacuum, exam. of temp. dependence of microhardness and microstrength 78−88532
flat sheet, tensile deformation, strain rate sensitivity and necking 79−41590
flat sheets, tensile deformation analysis 80−96198
flow localisation in tensile samples, containing geometric and metallurgical defects 78−79233
fluorite, use of proton irrad. to reveal growth and deform. features 80−84216
foil, push-pull straining device for h.v. electron microscope in-situ deform. 77−4875
formulation of plasticity theory in tension and expansion space *(German)* 80−106733
fracture, appl. of continuum theory of dislocations fracture mechanics 78−67767
fracture, plane strain cumulative, criterion 79−60432
and fracture 78−88497
fracture energy rel. to inelastic behaviour 79−60429
fracture evaluation at high loading rate by extrapolation method 77−36723
fracture mech. during creep, interference microscopy exam. of 12Kh18N9, 08Kh18N10T 78−56756
fracture mechanics, plasticity, finite element anal., review 79−41612
fracture mechanics of yielding materials, review 78−31521
fracture of plastic materials under proportional straining, theory 77−35090
fracture resistance, dependence on crack length 78−67120
fracture semibrittle, damage process preceding fracture, plastic strain depend. 77−32692
fracture toughness tests, J integral, work for failure and work for plastic deform. 80−61061
fracture toughness tests, plastic zone obs., holography 77−9034
fragmented structures, dislocation and disclination kinetics *(Russian)* 80−79788
frame, plane, impulsively loaded, large deflections, mode approx. technique extension 80−83757
frames and beams, arbitrary cross-section, deflections at shakedown 78−34028
friction anal. in plastically compressed cylindrical specimen *(Polish)* 77−54897
fuel pins, fast breeder, fuel-cladding mech. interaction, obs. and anal. 80−86959
Gauss principle, in rolling theory, deformed and kinematic eqns. *(Russian)* 80−65124
genesis problem, approx. soln. of initial states and properties 77−14927
girder, circ-arc bow type, ultimate strength, plasticity *(Japanese)* 80−43631
glass, industrial cylindrical tubular elements under internal and external press., deform. and failure resistance 78−35460
glass, inorganic, cylindrical shell, with initial geometric imperfections, precritical deform. under external hydrostatic press. 77−81306
glass, mechanical destruction role of relaxation processes 80−89282
glass, stress in working zone under biaxial compression, Moire-band method 77−81369
glass, tempered, stress meas. in surface, indentation technique 77−44341
glass deformation degree rel. to optimum moulding prod. rate 79−50456
glass fibre reinforced composite, fatigue failure, role of shear deform. 78−15494
glass fibre reinforced composite, filament wound column, effect of end conditions on critical loads 77−59873
glass fibre reinforced epoxy resin interlaminar shear strength determ., anal. of methods 77−86107
glass fibre reinforced Kinel, mech. props., 20 to 300°C *(French)* 77−56018
glass fibre reinforced plastic, deform. conc. around openings due to pulse loading 78−23799
glass fibre reinforced plastic, failure due to deform., optical investigation method *(Russian)* 80−35437
glass fibre reinforced plastic, fracture dynamics 80−100906
glass fibre reinforced plastic, strain disintegration under repeated static load 80−11756
glass fibre reinforced plastic dome, anal. and expt. stress anal. 78−72813
glass fibre reinforced plastic laminates, strength and deformability, artificial ageing effect 80−60893
glass fibre reinforced plastics, relation between matrix vol. changes and mech. props. 80−11715
glass fibre reinforced polyester, filament wound pipe, winding angle effect on failure 79−43379
glass fibre reinforced polyester and epoxy resin, vacuum hardened shell, strength and deform. charact. eval. 78−48528
glass fibre-reinforced polyester cross-ply laminates, effect of resin failure strain on tensile props. 78−3212

plastic deformation continued
glass inorganic, shell, stress/strain state investigation under external hydrostatic press. 77−81370
glass reinforced laminates, damage accumulation during tensile loading 79−83262
glass reinforced plastic, acoustic emission investigation of deformation and fracture 77−16756
glass reinforced plastic, microwave determ. of mech. strains, anisotropic props. in millimeter range 77−9023
glass-fibre reinforced Al, highly deformed, microstruct. and mech. props. *(German)* 80−55489
glass-filled ABS, deform. and fracture behaviour, 293-353K 77−56077
grain boundaries, plasticity 80−65135
grain boundary as dislocation source during high temp. deform. *(Russian)* 78−15453
grain boundary crack nucleation, and growth under low cyclic stresses, dislocation mechanism 80−19811
grain boundary sliding, stresses and deform. 78−68739
grain boundary theory is independent crystal imperfections, plastic rotation, boundary continuum *(Russian)* 79−82236
granodiorite, fracture under uniaxial compression, mech. and AE meas. *(Japanese)* 78−56748
granodiorite, late Precambrian, strain anal. of shear zone 78−77223
granular materials, density hardening, compacting 79−32283
granular medium, mixed characteristic problem 80−23914
graphite, artificial, residual macrostresses 77−16642
graphite, deform. and fracture mech., high temp. effects 77−63763
graphite, ion bombarded, light gases, structural study using TEM 80−92570
graphite, nonlinear deformation, theoretical-exptl. correl. of material models 77−32626
graphite, silicized, fracture analysis, deform. 78−15530
graphite reinforced epoxy laminate plates with cracks, strain and failure anal. 79−29170
graphite reinforced epoxy laminates, cracked, deformation and failure in biaxial stress fields 79−47763
graphite structures in PBR, neutron radiation damage, mech. props., stress fields *(German)* 77−34387
graphite thermally stressed disc, nonlinear deformation 78−6964
graphites, reactor, strength and deformation under conditions of cyclic variation in load and temp. 79−43355
gravel, ice-thrusting, shear deform. 78−65347
grid method for residual deforms. meas. 77−52572
Griffith fracture tests, for plastic deform. *(Hungarian)* 80−97666
grinding, fracture and deform. mech., SEM obs. *(Japanese)* 79−15620
grinding, role of elastic and plastic behaviours *(Japanese)* 80−100868
hard metals, roll deform. effect on separating forces in cold strip rolling 80−35212
hardening medium, equations of steady-state motion 79−12597
Hastelloy-X, low cycle fatigue crack propagation at 25°C and 760°C 80−104270
HCP metals and alloys, plastically deformed, electron microscopy *(French)* 77−44300
heat evolution during cyclic deformation of a hereditary medium *(Russian)* 79−46227
heat resistant KhN80TBYuA and KHN62VMkYu, microscopic intergranular crack form. prediction in high temp. deform. 77−81325
heat-resisting alloys, VM-1 and VX-4, thermal fatigue rel. to struct. changes *(Russian)* 78−11302
helical shape extrusion from round billets 79−29102
hereditary media, nonlinear effects during deform. 79−86351
heteroepitaxial film deformation, causes and countermeasures *(Russian)* 80−49561
heteroepitaxial system, dislocation struct. at stress meas., theory 80−2017
heterogeneous materials, linear analysis 78−5664
heteroplastic material, large deform., approx. formulation of constitutive eqn. *(French)* 77−23891
heteroplastic material, plastic rate, effect of strain hardening *(French)* 77−63718
hexagonal metals, deformed, resistivity changes calcs. 80−44564
hexamethyldisilane, plastic deform., and diffusion of hexamethylethane-^{14}C 78−14510
hexamine, BCC, dislocation slip initiation 77−43222
high strain rate behaviour, incremental elastic-viscoplastic constitutive eqns. integration 80−85138
high strain rate material behaviour and testing techniques, J.D. Campbell memorial lecture 80−82627
high strain rate processes, review 80−84864
high temperature deformation for nuclear reactor design 77−3094
high temperature materials, classification and long-term strength charact. prediction 77−44324
high-alloy die steel, heat resistance and crushing strength, low-temp. thermomech. treatment effects 77−52372
high-C steel, strength characts. with controlled hardenability after bulk-surface hardening 77−56156
high-Si corrosion-resistant steel, 02Kh8N20S6, mech. props. and heat treatment 77−56003
high-temp. behaviour of inelastic metals 77−4830
hinges, large deform. expt. study 77−14919
hollow circular cylinder, expansion and contraction, strain softening with finite elastoplastic strain *(French)* 80−38283
hollow cone, mag. field strengthening in confocal motion subjected to plastic deform. 77−83787
hollow cylinder sagging, optimium equation 80−99945
hollow sphere exposed to radiation, thermoelastoplastic problem 77−14928
hollow thick-walled cylinders, stress-deformation, limiting state anal. *(Russian)* 79−27538
holographic interferometry, study of elastic and plastic deform. 77−62223
holographic summation using thermoplastic photographic plate *(Russian)* 79−22911
homogeneous material, 2D defects, interface problems 79−46674
homogeneous simple strain in elastic-plastic media, necessary and sufficient conditions 80−28427
honeycomb based composite, deform. theory 80−35250
hot metal, dynamic yield characts. during multistage deform., plastometer design 80−85135
hot plastic deform., relation between formability and deform. stress *(Czechoslovakian)* 77−32604
plastic deformation continued
HTBFR, constitutive equations of structural austenitic steels 79−6730
HTR components, design implications of inelastic structural anal. 79−6729
hybrid composite material beams, exam. of shear stress correction factors 78−46899
hydrogen embrittlement due to H-inclusion interaction 78−30664
hydrostatic pressure effects on fracture, exam. 78−60779
hydrostatically compressed crystals, crack nucleation mechanism 79−10893
ice, plastic deformation, ultrasonic wave attenuation by dislocations *(French)* 80−59564
ice Ih, dislocations, effect on physical and mechanical props. *(French)* 77−55287
ideal compressible media, elastoplastic thin walled constructional elements and shock wave interaction *(Russian)* 79−68618
ideal fibre reinforced, rigid plastic cantilever beam, impulsive loading, subsequent motion 77−80096
ideal fibre reinforced rigid plastic beams, impulsive transverse loading, control impact 77−80094
ideal fibre reinforced rigid plastic beams with end supports, impulsive transverse loading 77−80095
II-VI compounds, charged dislocations and plastic deform. 80−107264
II-VI semiconductor, charged dislocation motion during plastic deform. 79−82233
4,5-iminophenanthrene, polymorphism, X-ray diffr. and photoluminesc. obs., 77 to 300K 77−63449
impact testing machine operating over wide range of deform. rates 78−3271
impression method for plastic deforms. determ. at apex of stress concentrator, bare choice considerations 77−52571
impulsively loaded rigid plastic beam, max. residual deformations, approx. solns. *(Chinese)* 80−58916
impurity crystal, microstructural plastic instability *(Russian)* 79−99190
in plane strain displacement near crack tip at high temp., optical meas. 79−32412
incompressible solid, plane strain deformation, finite element anal. 79−1114
Inconel 718, low cycle fatigue at 298 and 823K 77−86151
Inconel 718, plastic deform., accelerated evolution of H_2 77−36594
incremental elastic-plastic constitutive eqn., principal axes rotation, shear deformation 77−19545
indentation hardness and microhardness test methods for plastic deform. *(Hungarian)* 80−97664
indenters, rigid, rough, rotating, plane strain collapse theory 80−79172
inelastic deform. mechanism, fatigue testing in air and corrosive environments *(Russian)* 79−52432
inelastic deformation, hardness law 78−46896
inelastic deformation of structures, repeated actions of load temp., structural model 77−3747
inelastic material, effect of material struct. changes 78−12562
inelastic material, ideal, theory of elastic and plastic distortions 78−12561
inelastic structural anal., thermomech. constitutive eqns. 79−6731
inhomogeneous, reference degree of deform. definition *(German)* 80−99936
inhomogeneous yielding, slip plane intersection with stress free boundary, mild steel appl. 78−5667
inorganic glass, effect of liq. medium on process of mechanical destruction 80−89283
instability, general formulation of Hart's criterion 79−47758
instability during tensile deform., numerical calc. 78−30203
instability onset in tensile samples containing defects 78−67061
integral inequality and plastic torsion anal. 80−10155
internal friction, and plastic strain rate, phenomenological rel. 80−75301
internal friction, determ. from dynamic hysteresis loop area and specimen cross section in deform. 78−23897
internal friction test method, for plastic deform. *(Hungarian)* 80−97662
internal stress, stochastic model for dip test in steady-state creep 80−58915
interparticle percolation, lateral and axial diffusion coeffs., shear cell appl. 79−61666
Invar, deformed, magnetism and temp. depend. of effective field on ^{57}Fe *(Russian)* 79−24234
Invar, dislocation motion anomaly 80−10554
Invar, magnetisation, hyperfine field, elec. resist. and X-ray linewidth, effect of deform. by cold rolling 77−48556
ionic crystal, book 77−52443
ionic crystal, point defect-dislocation interactions 78−63787
ionic crystals, dislocations, review 80−107236
iron, pure, tensile deformation behaviour under high pressure *(Japanese)* 80−16381
iron, spheroidal graphite, deformation under compression rel. to ductility 77−16639
isotropic and anisotropic raw materials, plastic pot. *(German)* 80−33474
isotropic body containing rigid plate-like inclusions, antiplane deform. *(Russian)* 77−27476
isotropic crystal temp. shear coeff. determ. 78−2190
isotropic material, modified stress deviator for plastic compressibility *(German)* 78−13914
isotropic materials, infinitesimal isothermal deformations, implicit functional representation 79−32297
isotropic solidification, plane slip line fields, construction by characteristic net method *(German)* 79−91640
j integral applications for short fatigue cracks at notches 80−38332
jump-like, polycrystals theory of jump-like plastic deform. at low temp., theory *(Russian)* 79−7291
junction growth mechanism during friction *(Japanese)* 79−32391
kaolin, -flint mixtures, polyethylene oxide additive effect on plastic strength after tempering 79−24568
Kester peak, plastic deform. effects *(Russian)* 80−29118
Kevlar 49 fibre, poly p-phenylene terephthalate, Raman spectroscopy, heat, stress, radiation effects 79−65871
Kinel 5504, mech. props. 20 to 300°C *(French)* 77−56018
kinetic analysis of stress sensitivity 77−3737
kinetic equations of failure in complex programs of cyclic loading 79−64592
Kossel diffraction, in scanning electron microscope, for plastic strain determ. in vicinity of fracture surface 79−20335
kyanite, deformed, defect struct. 77−31668

plastic deformation continued
lamellar composites, development of microplastic strain *(Russian)* 79−34102
laminar blocks with plastic deformations, instability 80−43629
laminate, deform. charact., pliability and rigidity 78−23798
laminated paper, decorative, deform. and internal stresses 79−61671
large deflections and creep problems, soln. strategy 77−42750
large deformation elastoplastic analysis of arbitrary shells, triangular finite element 78−83257
large strain inelastic anal., dynamic problems 80−38278
large viscoplastic deflections of impulsively loaded plane frames 79−18738
lattice defects influence on axial shadow figure *(Russian)* 80−25508
layer, co-indentation by two rigid punches, interference betweeen deformation zones 77−65693
limestone, high press. effects on plastic state 79−74889
limit analysis with anisotropic parabolic yield function 77−91114
lithosphere, elastic-perfectly plastic bending under generalised loading, appl. to Kuril Trench 78−73341
lithospheric slab at Kurile-northern Honshu arcs junction, mantle earthquakes rel. to deform 77−81805
LMFBR components, plastic dynamic anal., CEA-SEMT system 77−6506
LMFBR piping components, resistance to bending moments 77−6505
load-bearing structures, behaviour prediction of materials degradation 79−34133
load-deflection curve, post-buckling behaviour of Hutchinson's plastic buckling model 80−64411
loading, finite element anal. for materials with convex yield criterion *(French)* 79−10501
loading rate-temperature effects *(Russian)* 78−9570
local heating in crystals during low-temperature deformation 78−67766
localisability of deformations theory, representation 80−10163
localization into shear band, as instability of plastic flow and precursor to rupture 77−68458
low C steel, explosive-thermal treatment, sulphide cracking decrease, hydrogen embrittlement *(Russian)* 80−108477
low temperature, heating of dislocation sources 78−18660
machine for cold rolling, deformed contrete reinforcing bars for model tests 78−60924
machine tools, chip geometry and cutting forces 80−93629
machining theory, strain rate predictions in chip formation zone of intense shear 77−70277
macroscopic quadrupole effects as method of obs. of struct. transforms in crysts. 80−71321
Mars, erosional debris flow in fretted terrain, plastic deform. model 78−65537
martensite, struct. transforms. during deform. *(Russian)* 77−16606
martensitic steel, abrasive wear resistance, effect of tempering strain martensite 77−56116
material classification by brittleness and stress/deform. relationship 78−15528
mathematical prgramming methods for deform. anal. at plastic collapse 78−1572
mean strain in crysts. containing prismatic dislocation loops 77−7720
mechanical props. determ. with conic plastometer, wide moisture content range 78−11270
mechanical surface structure damage, action of plastic deformations *(French)* 80−30011
mechanics testing, lateral deform. gauge 79−57163
mechanism map, Ashby type, construction method 78−56703
mechanism map, for high temp. creep 78−35439
mechanism map 79−34109
membrane, shape and thickness distrib. under impulsive loading 77−23897
membrane action effect on plastic collapse load of circular orthotropic slabs with fixed edges 78−79225
metal, abrasive wear resistance rel. to physicomechanical props. 79−91804
metal, axisymmetric drawing simulation, numerical method development 78−30206
metal, axisymmetric plastic deformation, method of characteristics *(Russian)* 80−69682
metal, BCC, cryst. lattice change during deform., influence of boundary dislocations with different Burgers vectors *(Russian)* 77−21219
metal, BCC, deforming by {110} ⟨111⟩ and {112} ⟨111⟩ slip, lattice rotation calc. in axisymmetric flow *(Japanese)* 77−21225
metal, BCC, geometry of slip systems *(Hungarian)* 77−47463
metal, BCC, polycrystalline aggregate, prediction of plastic props., deformation by ⟨111⟩ pencil glide 80−11731
metal, brittle, ductility improvement by plating *(German)* 77−8954
metal, bulk deform. process 78−31459
metal, cracked, J-integral estimation 77−1876
metal, cubic, heavily rolled, shear band occurrence 79−34058
metal, cubic, plastic strain ratio, strain effects 77−16651
metal, damageability determ. by meas. of elastic, inelastic, internal friction charact. 79−66133
metal, deform. resist. determ., plastometer 78−7121
metal, deformation heat during forming, eqn. *(German)* 79−66105
metal, deformed, dispersion-hardening, theory of strength *(Russian)* 78−35424
metal, deformed in pressing process, temp. field modelling *(Russian)* 80−53602
metal, deformed struct. role in recrystallisation nucleation, review 79−34060
metal, degree of deform. effect on thermophys. props. at high temps. 78−26694
metal, dislocation density, positron annihilation method 77−85834
metal, dislocation dynamics study by current noise measurements 79−14813
metal, dislocation models of plastic deformation at elevated temps. 77−70139
metal, ductile, hard inclusion effect on plastic strain distrib., model meas. 77−59062
metal, ductility effects during plastic deform., rel. to struct. changes 78−23770
metal, dynamic and static response to simple compression, tension and torsion 77−28858
metal, electron state effect on mech. props. and electroplasticity 78−14725
metal, electroplastic effect 79−24589
plastic deformation continued
metal, fatigue fracture-stacking fault energy correlation *(Russian)* 78−15499
metal, FCC, cavitation erosion 77−86191
metal, FCC, deformation mechanism under high hydrostatic pressure *(Ukrainian)* 80−25758
metal, FCC, dislocation behaviour at high strain rates, US detection method, data analysis basis 80−85136
metal, FCC, low stacking fault energy, nucleation phenomena 79−90681
metal, FCC, polycrystn., fatigued, behaviour model during plastic deformation *(German)* 80−21023
metal, FCC or BCC, dislocation annihilation during tensile and cyclic deform. and limits of dislocation densities 80−34007
metal, FCC polycrystalline, work hardening, plastic deform *(Hungarian)* 77−77504
metal, fibres, cubic struct., texture form. in uniaxial deform. theory 79−24532
metal, finite elastic-plastic deformation at high temp., work hardening rule 77−4828
metal, fracture and ductile deform., microprobabilistic approach 78−64665
metal, friction during working stresses and rheological charact. at high temps. *(Russian)* 77−66702
metal, grain size and microstrain meas. from X-ray diffr. data, moment method *(Czech)* 78−31593
metal, hardening and softening during absorption fatigue in surface active medium, governing laws 77−86230
metal, heavily deformed recrystallisation 79−34062
metal, high temp. steady state creep, activation energy determ. *(Russian)* 77−50920
metal, inhomogeneous dislocation struct., model 79−90655
metal, inhomogeneous strain effects on surface props., rel. to fracture model development 77−72907
metal, internal stresses during rolling friction and their evaluation 77−28912
metal, microstructure and strength *(German)* 77−70138
metal, near surface microstructure effect, on wear 78−64730
metal, notched sheet, thickness effect on deform. and fracture under tension 79−70113
metal, pack rolling, bonding, deform. struct., small reduction before seizing 77−90503
metal, pinch effect on plastic deform. *(Russian)* 78−35426
metal, plastic, work hardening, sintered, porous, irreversible deform. 78−19849
metal, plastic deform. and sliding friction 79−87743
metal, plastic deform. mech., TEM appl. Mg, FCC metals *(French)* 77−1853
metal, plastic deformation under pulse action 77−76486
metal, plastic impact, energy absorbed by elastic waves 80−5972
metal, plastic props. investig. at elevated temps. by torsional method, review 79−43509
metal, plastic strain graph plotting at high strain rates by cutting method 77−90521
metal, plasticity at very low temperature, dislocation motion, rel. to supercond. and tunnelling *(Czech)* 77−32630
metal, polycrystalline, strain hardening, dislocation link length model 80−84953
metal, porous, densification during volume plastic deform. without work hardening 77−40402
metal, porous, stresses in deform. region during cold rolling 78−11241
metal, positron annihilation examination of recrystallisation *(German)* 77−70252
metal, resistance to plastic deform. under HF vibrs. rel. to surface treatment *(Russian)* 77−52400
metal, review *(Russian)* 78−19825
metal, self diffusion, effect of homogeneous plastic deformation *(Russian)* 77−89572
metal, sheet, numerical anal. of tensile tests 77−86101
metal, single crystal, dislocation loop formation, during deformation in quantising mag. fields *(Russian)* 80−103354
metal, single phase FCC, cyclic deform. long range stress changes 80−54308
metal, stress/strain relation from anisotropic hardening plastic pot., combined axial load/torsion 78−52896
metal, superconducting transition, effect of change of electrostatic interaction of defects 78−10610
metal, surface strain meas. by intensity of reflected light flux 77−17972
metal, Swift effect, in twisted tubes 77−28859
metal, Swift effect, rel. to stress/strain behaviour in simple compression, tension and torsion 77−28860
metal, thin sheet, tensile instability and limit strains, growth of surface roughness 77−86084
metal, thin-walled cylinder, elongation upon torsion 80−64386
metal, vacancy diffusion during plastic deform., possibility of stimulated electron emission obs. *(Russian)* 79−5007
metal, vacuum rolling at high temp. *(Russian)* 79−15708
metal, volume changes under plastic deform. *(Czech)* 77−63729
metal, work-hardening, plastic, sintered, porous, irreversible deform. 78−35459
metal and alloy polycrystals, internal friction amplitude depend. *(Russian)* 79−90726
metal and alloy surfaces, highly reflecting, pulsed laser stress phenomena 79−14015
metal and alloys, hot twisting differential method of shear stress determ. 77−56026
metal bicrystal, mech. behaviour, continuous theory of dislocations appl. 78−67717
metal billets, energy method anal. *(Russian)* 79−98629
metal cutting, chip forming mechanisms, deform. diagrams 77−28854
metal deformability, flow curves mathematical description, thermal dependence *(German)* 78−15484
metal deformation, elevated temps., effect of creep deterioration 77−3787
metal electroplastic deformation meas. pulse generator *(Russian)* 80−25931
metal extrusion process, stress and deform. distribs., elastic-plastic anal. 77−48364
metal fatigue crack initiation and preparation studies *(German)* 77−77587
metal fatigue tests for plastic deformation *(Hungarian)* 80−97665

plastic deformation continued
metal forming process, forming conditions and material characts. 80−30032
metal particles produced by gas evaporation, form., growth and interaction 80−16220
metal plastic deformation, influence of mech. vibrations 78−60722
metal powders, strip densification in forward slip zone in rolling 79−95972
metal rod, US heating to onset of plastic deform., temp. field calc. 77−69049
metal sheet, circular, impulsive press. by underwater wire explosions, dynamic plastic deform. 80−84866
metal sheet, strain propag. under non-uniformity distributed load 77−16653
metal sheets, theories of necking and limit strain calc. 79−29115
metal strip, high-speed compression, force parameters determ. *(Russian)* 80−21016
metal strip, porous, elastic aftereffect in cold rolling 80−11689
metal strip, sintered, rolling, algorithm for force and geometric parameters calc. 80−11727
metal structures, collapse load and energy absorpt., matrix anal. methods 77−35050
metal subjected to intense heat source, plastic deformation 77−86085
metal surfaces, abrasive wear theory based on shear effects 80−89363
metal systems, high voltage electron microscopy of dislocation dynamics *(Japanese)* 77−47458
metal tube, dynamic lateral compression, strain rate effects 80−83758
metal tubes, crushed between rigid plates, large deformation compression 80−66579
metal wire, plastic strain during extension, temp. gradient and high density elect. current *(Russian)* 79−57049
metal working by pressure, full scale adaptive simulation applied to computer aided management 79−79055
metallic bending springs at small mech. stress, non-elastic props. *(German)* 77−77532
metallic crystal, thermomechanical deform., analytical description 80−49391
metallic crystals, pulsed mechanical stressing, for dislocations motion study 79−52532
metallic glass, shear deform., mechanism involving dislocation glide 78−15462
metallic glasses, steady state inhomogeneous flow, microscopic mechanism 77−48476
metallic glasses, strength and stiffness 77−8899
metallic glasses, theory of plastic deformation below their transition temp. 79−29128
metallic materials, deformation process, stage-by-stage nature investigation using acoustic emission *(Russian)* 80−40434
metallic media, time-depend. inelastic anal. using constitutive relations 77−39237
metallic plates collision, plastic deform., jet form. 79−11669
metallic powder materials, deform., boundary conditions on sliding surfaces 80−60978
metals, adiabatic heating as cause of low cycle fatigue failure 77−21339
metals, aspects of impact testing, propagation of deformation 79−79111
metals, atomic mobility under pulsed loading conditions *(Russian)* 80−96684
metals, BCC, dislocation processes, straining expts., electron microscope obs. 80−29025
metals, BCC, low temp. softening 79−34113
metals, BCC, plastic deform., review 80−104213
metals, BCC, predicted rolled textures, influence of slip system and deform. model *(French)* 79−43309
metals, brittle and plastic, energetic strength theories *(Bulgarian)* 80−38296
metals, cavitation erosion 78−48538
metals, constitutive model at high strain-rate, shear modulus, yield strength 80−75292
metals, constitutive relns. 78−42544
metals, continuum props. of constitutive relationships 77−35053
metals, cubic, heavily deform., development of lattice curvature 80−81136
metals, cubic struct., numerical simulation of cross-rolling textures *(French)* 79−20061
metals, deformation resistance, rel. between uniaxial stress state and breaking stresses in shear 80−3147
metals, ductile, spall damage accumulation theory 77−70153
metals, dynamic compression testing, mech. behaviour 80−40464
metals, electroplastic deform. *(Russian)* 77−86108
metals, failure model in conditions of monotonous cyclic loading *(Bulgarian)* 80−70296
metals, fatigue resistance, processes leading to failure 80−94907
metals, FCC, yield threshold at 4.2K, effect on strain-hardening curve *(Russian)* 80−50671
metals, generalised constitutive eqns. 80−104219
metals, HCP exam. of texture and Young's modulus anisotropy, developed during deformation *(Russian)* 79−15694
metals, hot plastic deform., stress/strain/time relations *(Russian)* 80−20968
metals, in-situ deform., 200 kV STEM study 80−47155
metals, inelastic cyclic strain under nonuniform stress state conditions, residual stresses effect 80−81132
metals, longitudinal flow velocity distribution in rolling *(Russian)* 80−93575
metals, mechanical behaviour under impulse loading, model 79−52332
metals, mechanical props., testing and modelling 80−25811
metals, metallic deformation, improved boundary-integral eqn. calc. method 80−28437
metals, microinhomogeneous plastic deformation, rules 80−89307
metals, microstructural inhomogeneities resulting from high strain deformations 79−87705
metals, plant deform. and rectystallisation textures 78−68708
metals, plastically deforming at high strain rates, distrib. of temp., strain rate and strain 79−19311
metals, residual stress and deformation, due to quenching, elastic-plastic anal. *(Japanese)* 78−83268
metals, residual stress on drawing calcs. by stress state changes variational principle *(Russian)* 80−65125
metals, resist. against plastic deform. *(Bulgarian)* 80−88248
metals, stored energy determ., temp. recording method 79−87775
plastic deformation continued
metals, stress transients, at changes of electron drag during plastic deformation 79−61677
metals, structural state and physical similarity criteria *(Russian)* 79−52298
metals, submicroscopic defects, influence on HVEM in-situ expts. 80−103392
metals, time depend. inelastic deform., boundary integral eqn. calcs. 78−51090
metals, time dependent plastic deformation, thermodynamic model 80−76309
metals, volumetric plastic deform., kinematic and static parameter calcs. *(Russian)* 80−34124
metals, wave movement, resonance phenomena in deformation zone during rolling *(Russian)* 80−65123
metals and alloys, criteria for evaluation of strain hardening 77−55982
metals and alloys, polycryst., strength differential effect, temp. and strain rate sensitivity in saturation cycling 79−66094
metals and alloys, relative cavitation strength 77−12672
metals and alloys, shock wave effect on martensitic transform. *(Russian)* 80−96595
metals and alloys, strain rate history, endochronic theory of viscoplasticity 80−65122
metals and alloys, strength/ductility relation *(Japanese)* 79−29145
metals porous, mean principal stress in rolling without lateral expansion 80−25803
methane, crystalline, deform. under hydrostatic press. 77−70136
microcrack formation, disclination mech., late stages of plastic deform. 79−23674
microhardness meas. by ball dropping/recoil velocity ratio 77−81363
microplasticity measurement, applied to deform. mech. study 78−60720
microstrains distrib. in macroinhomogeneous fields *(Russian)* 80−21018
misfitting inclusion, deform. field 77−73276
misfitting inclusion, deform. field 77−77488
Mo, slip line study of pure single crystal compressively deformed at low temps. 79−43361
moire method of measurement *(Polish)* 80−69749
Moire strip attainment at specified pt. on contour of stress concentrator 77−52573
montmorillonite, mech. props. at high press., rel. to fault behaviour 79−84234
Mossbauer absorbers, deformation induced texture 80−7214
mould material deformation meas. at high temp., apparatus 78−3266
mullite, high temp. mech. props. in compression 77−56033
multibar structure strength from heteroplasticity concept *(French)* 79−18742
multilayer fibre reinforced composite, alternate hybrid stress elements for anal. 77−50926
multilayer material, vacuum rolling at high temp. *(Russian)* 79−15708
multilayer plates, optimum design for cylindrical bending 79−87698
multistory frames, elastic-plastic anal., slope deflection method 77−11137
Nb, influence of plastic strain on thermal expansion *(Russian)* 79−65220
near surface region of solid, H_2 effect on deform. and fracture, Rebinder-Westwood effect 79−39001
necking and tensile instability in material with strain hardening and strain-rate hardening 78−23717
Nimonic alloy reinforced Al, Cu and brass, laminated composites, low-temp creep singularities, structural defect changes *(Russian)* 80−11696
nine-atom model 77−7323
non-associated plasticity and elastoplasticity, rate boundary value problems, variational principles 80−87726
non-linear optimized fibre reinforced plates in bending 79−27550
noncoaxial plastic soil, steady in-plane deformation, flow conditions 79−84279
nonisothermal elastic-plastic and elastic-viscoplastic deforms., stress/strain relations 78−22276
nonisothermal theories, of plastic flow and theory of work hardening in creep 79−57077
nonlinear hereditary materials, dynamic deform. *(Russian)* 78−63319
nonlinear stress-strain rate relations, effects on deformation and fracture of materials in creep range 80−58938
nonmetallic material, mech. props., testing installation, +600 to −190°C 78−15633
nonsteady inelastic deform., stress anal. by photoviscoplasticity 79−94563
notch analysis for fracture toughness and fatigue crack propagation threshold 77−35086
notch-tip geometry, influence on stress and strain distrib. 80−33535
notched and bend specimens with equivalent geometries, cyclic deform. *(German)* 77−86271
notched flat tensile specimens, deform. zone *(German, English)* 78−64603
notched plates, monotonic and cyclic loaded, exam. of elastic-plastic stress-strain behaviour 78−63390
notched rectangular bars, notched bend test specimens, strain meas. *(German)* 78−11451
notched rectangular bars, stresses at plastic deflection *(German)* 78−34025
nuclear fuel sheath deform. following fuel power transients, simulation 78−33258
nuclear reactor, dynamic response of ducts to press. pulses, expts., finite element calcs. 77−3124
nuclear reactor, nonlinear structural dynamics of fuel elements, press. pulses, struct. models, expt. verification 77−3125
nuclear reactor core materials, plastic deform. constitutive eqns. 80−35259
nuclear reactor pressure vessels, strain measurements 80−79865
nuclear reactor structural mechanics, conf. 78−41874
nylon, steady-state deform. and its effect on struct. and morphology 78−15459
nylon 6, influence of monomer and water diluents on mech. relax. 79−4993
nylon 6, notched sheet, deform. mech., fracture, X-ray obs. *(Japanese)* 77−59863
Nylon 6, plasticized with NH_3, deformation by solid-state extrusion 80−25736
Nylon 6 fibre, shrinkage, influence of chain rupture during tensile deform. 79−34055

plastic deformation continued
nylon 6 fibres, chain rupture during tensile deform. 79−15740
oblate spheroidal inclusion, internal stress, misfit, inhomogeneity and plastic deform. 78−60701
4-n-octyloxy-4′-cyanobiphenyl, smectic A liq. cryst., elastic modulus determ., stress/strain relationships 78−91229
one-dimensional crystal, deform. and fracture simulation 78−47470
ophiolitic peridotites structures, role of young lithosphere thrusting in subduction zones 80−56446
optical fibre stress-optical degradation obs. 78−1402
optical glass K8, torsional deform. above T_g under low stresses, temp. effect 80−21052
optical glass K8, torsional deform. above Tg under low stresses 80−25804
ordered alloy, with $L1_2$ structure, dissociation of superdislocations and plastic deform. mech. *(Russian)* 78−52909
ordering alloy, $L1_2$ superstruct., superdislocation dissoc. *(Russian)* 78−48451
oriented polyethylene film, deformation band studies 77−52420
orthotropic medium, strain localisability function 79−18743
orthotropic spherical shells under blast loading, plastic response 80−33477
overthrust faulting, model of const. thickness overthrust on visco-plastic sole 80−51378
oxides, plastic deform., TEM obs. *(French)* 77−44304
Ozhennite, yield point, effect of ageing stress 77−21223
paper strip reinforced paraffin, model composite, optimum reinforced plates, tension/compression tests 77−86124
para-polyamide based fibres, struct. deform. props. 80−60928
partial disclination dipole motion under plastic deform. 79−73165
partially film coated crystal, strain field, deform. model and X-ray topography *(German)* 78−83653
particle deformation during cold isostatic pressing 78−44052
PCTFE, work to produce environmental crazing at low temps. 78−15553
pearlite, SEM obs. of tensile deform. and fracture 78−84897
pearlite ferrite, plastic anisotropy 79−91772
pentaplast, plasticised, thermal treatment effect on props. 80−40324
perfect single crystal, elastic instabilities and plastic modes *(French)* 79−28034
perforated struct., plastic strain conc., numeral calc. 77−75825
PET, IR, spectra of prefractured state 77−69032
PET, stress induced crystallisation, X-ray and light scattering obs. 79−99083
PET film, PET, transverse constriction and stresses accompanying uniaxial orientation 78−48475
PET film, relation between deform. and rotational isomerism 77−52438
PET film interatomic bond determ. by IR transmission and reflection spectroscopy 77−65958
PET films, one-way drawn, constant strain effects, IR meas. 80−60584
phenomenological theory, with mobile and immobile dislocations 78−75714
phenylone, deformability in physiological salt soln. 80−12305
phonon-phonon scattering, hydrostatic deformation effect 78−18721
photographic emulsion sensitivity, effect of mech. loads, changes in optical density *(Russian)* 79−67410
piezoelectric transducer automatic setup, for continuous meas. of internal friction and elastic moduli of solids 80−108652
piled bed, deform. character, two-dimens. model calcs. *(Japanese)* 79−34115
pinched rigid-plastic cylindrical shell, mode of collapse, geometrical parameters 79−10492
pinned dislocation arrangements, TEM obs. 77−43217
pipe, rigid-ideally plastic, immersed in fluid, internal pressure, dynamic plastic response 78−59317
pipe containing water, pressure pulse propagation 80−33475
pipe stability and plastic deform. under external couples 80−19259
pipes, straight, fracture under large deflection conditions, structural deformation 77−58615
pitch-polymer polisher layer, durability 77−34969
plagioclase feldspar, deformed, elastic twinning, TEM obs. 77−62551
plagioclase feldspar, deformed in compression, dislocation substruct. and slip, TEM obs. 77−43221
plain strain contained plastic deformation, elastic-plastic laws, finite element anal. 80−92073
plane anisotropic, in orthotropic material, theory *(German)* 77−884
plane strain deformation of strain rate sensitive materials, finite element anal. 80−1441
plane strain of ideal rigid-plastic bodies allowing for the change of boundary *(Russian)* 79−68599
plane stress crack geometries, comparison of finite element and expt. studies 77−89069
plane weakened by openings, periodic and inverse elastoplastic problems soln. 77−35055
plane-strain formulation of elastic-plastic constitutive laws 80−23918
plane-strain work hardening, meas. and anal. 80−81073
plastic, deformation speed in static tensile tests, machine rigidity effects *(German)* 78−48473
plastic deformation depend. on mag. field at 4.2K *(Russian)* 79−91754
plastic foil, Li ferrite clad, thermal deform. *(Polish)* 80−30002
plastic fracturing materials, work inequalities and stress-strain relations 80−103000
plastic material, strain hardened, yield criteria 79−14282
plastic polycrystalline body, energy criterion for failure 77−4823
plastic rate sensitivity with large deformations, simplified method for membrane action 80−64403
plastic structures, dynamic adaptation to stochastic excitation 79−1116
plastic zone, direct meas. in side grooved fracture toughness specimens 78−68864
plasticity diagram plotting by testing cylindrical samples in combined tensile tension 77−63879
plasticity theory governing relationships in stress and strain spaces 79−88812
plate, annular, limiting load determ. 80−38295
plate, elastic-plastic, flexed in its plane, stress concentrations, method of small parameter *(Russian)* 80−74759
plate, inelastic thick, dynamic response, rectangular finite element development 79−94520
plate, relaxed by holes, elastic-plastic deformation, stress state *(Russian)* 79−27545
plate, round uniformly loaded, of linearly strengthened elastoviscoplastic material, large flexures *(Russian)* 77−23894

plastic deformation continued
plate, simply supported rectangular under axial compression, creep buckling and deformation 79−68605
plate, thin, fracture toughness from plastic deform. induced thickness contraction 78−75109
plate, two-layered, with imperfect bonding, resting on fluid half-space, vibrations 80−74792
plate of plastic material, dynamic deflection 80−23915
plate perforation by projectile, comment on paper by Awerbuch et al. 79−27542
plate weakened by equal-armed cross-shaped crack, plastic strain and fracture 80−69740
plate with circular hole under dynamic loading, comparison of deform. and flow theories 79−23228
plates, infinitely extended, dynamic response to pressure pulse 77−68516
plates, plastic dynamic flexure 78−30196
plates, rectangular, hinge-supported, eccentrically applied, ultimate point load, kinematic solutions 80−53638
plates and shells, construction elements, review of physical props. 78−67056
plates and shells, dynamic plastic anal. using stress resultant finite element formulation 79−37191
plexiglas, strength in biaxial compression, testing machine 79−15899
plexiglas tube exposed to const. axial loads, deform. and creep, loading regime effect 77−90416
plug formation in plates, cylindrical projectile impact, nonlocal viscous fluid model 78−49653
plywood shallow shells, orthotropic, mech. charact., effect of restraint of sliding or expansion *(Japanese)* 77−77522
PMMA, amorphous, LF Raman modes, strain and temp. effects 77−36219
PMMA, crazing, deform. kinetics 80−84990
PMMA, electric phenomena in process of deform. and failure, role in fracture mechanism 77−44344
PMMA, glassy atactic, thermodynamic analysis of plastic deform. modes, 150 to 330K 80−84999
PMMA, large deforms. at tip of running crack, opt. interference obs. 80−85062
PMMA, molecular alignment 78−14299
PMMA, notched, sheet, deform. mech., fracture, X-ray obs. *(Japanese)* 77−59863
PMMA, orientation by extrusion, stress-optical study 78−47248
PMMA, plastic deform. by crazing *(Japanese)* 80−93619
PMMA, work to produce environmental crazing at low temps. 78−15553
PMMA with stress-raising flaw, deform. 80−25799
poly(ethylene terephthalate)-polystyrene, two-phase polymer alloy, deformation of films 78−52904
poly-m-phenylene, isophthalamide-b-dimethyl siloxane, morphology and tensile deform. 78−91263
poly-m-phenylene isophthalamide-b-ethylene oxide, morphology and tensile deform. 78−91263
p-polyamide based organic fibres, effect of temp. and deform. time, on deform. strength props. 80−11720
polyamide-polyoxirane copolymers, mechanical properties evaluated 80−11700
polybutadiene, cross linked, deform. below T_g, radical form. and crazing 79−52307
cis-1,4polybutadiene, lightly crosslinked, isothermal and nonisothermal creep 77−25106
polybutene-1 film, deform. mechanism, rheo-optical meas. 80−21041
polybutene-1 film, tubular-extended, anal. of orientational and form birefringence 80−29712
polycaproamide, deformability props. in cyclic extension-compression 79−20183
polycaproamide, oriented, molecular rearrangements during deformation, IR spectra exam. 80−7644
polycapromide, fracture, interatomic bonds deform. 79−57107
polycarbonate, amorphous, yield behaviour in oriented and unoriented condition, effect of temp. 80−97537
polycarbonate, compressive recovery behaviour 79−38919
polycarbonate, criterion for craze nucleation 78−19881
polycarbonate, deform. and failure modes, surface craze characts. 79−91753
polycarbonate, delayed yiedling under const. load 79−38906
polycarbonate, ductile, large strain cyclic deform. 80−85000
polycarbonate, glassy, temp. drop during deform. 78−15456
polycarbonate, notched sheet, deform. mech., fracture, X-ray obs. *(Japanese)* 77−59863
polycarbonate, notched specimens deform. and fracture 78−11293
polycarbonate, particles, critical stress 77−28869
polycarbonate, plane strain fracture energy instability and mixed mode crack propag. 78−68775
polycarbonate, plastic deform. by crazing 79−52310
polycarbonate, rigid plastic, yield behaviour *(Japanese)* 80−93620
polycarbonate blends, yield and deform. behaviour, impact modification 77−36572
polycrystal, elastoplastic, grain size effect on deformation curve *(Russian)* 79−51191
polycrystalline aggregate, continuous distrib. of dislocations, stress fields, movements in elastic-plastic deform. 78−75709
polycrystalline material, plasticity analysis using stat. model *(Russian)* 78−26619
polycrystalline materials, model of plastic deformation using slip 78−63802
polycrystalline metal, detect. using photoacoustic microscope 80−35435
polycrystalline metal, FCC, plastic stress-strain rels. under proportional loading 77−32627
polycrystalline metals, stored energy and strain hardening 79−82276
polycrystalline plasticity, based on dislocation processes, probabilistic approach 78−26621
polycrystalline plasticity, probabilistic approach, appl. 78−26622
polycrystals, constitutive relns. in elastic-plastic range 78−63801
polycrystals, deform. during cooling, revealed by deposited graphite layer *(Polish)* 80−25755
polycrystals, deformed, particle sizes and mean square strains *(German)* 78−3284
polycrystals, single phase, stress strain relations by X-ray diffraction *(Russian)* 80−5999
polycrystals elastic-plastic deformation, plane geometrical model and finite element calc. 80−79860

plastic deformation continued
polydiacetylene single crysts., twinning 78−23777
polyester model material, strain rate effect 79−83245
polyester resin, creep, temp. and humidity effects under shear and tensile strains 77−86105
polyethylene, amorphous-cryst., highly oriented, plastic deform. rel. to supermol. struct. *(Russian)* 79−51010
polyethylene, anisotropic surface stress 78−14562
polyethylene, chain-extended, deform. of lamellar microstruct. on drawing five-fold 77−21220
polyethylene, chain-extended, oriented, microindentation hardness 78−76728
polyethylene, cross-linked crysts., deform. mechanism 78−15469
polyethylene, cryst., transverse deform. and transverse movement of defects 80−38958
polyethylene, crystal, elastic line energies and line tensions of dislocations 79−90656
polyethylene, deformation, Hartree-Fock SCF calcs. 80−18949
polyethylene, direct ram extrusion, correl. between chain folding and tensile modulus 77−44209
polyethylene, doubly oriented, low density, deformation and structure, exam. 80−11705
polyethylene, drawn low-density, mech. and transport props. 79−74210
polyethylene, dynamic mechanical behaviour during creep to failure in uniaxial extension 78−15455
polyethylene, extruded high-density fibres, deformation and strain hardening 79−70035
polyethylene, high density, ductile, large strain cyclic deform. 80−85000
polyethylene, high density, necking stress *(Japanese)* 77−56036
polyethylene, high density, plastic deform. during hydrostatic extrusion 77−63722
polyethylene, high density, temp. change associated with adiabatic compression 77−66685
polyethylene, high density, time depend. deform. resistance 79−5019
polyethylene, high mol. wt., deformability in physiological salt soln. 80−12305
polyethylene, high oriented, deformation mechanisms of constrained chains, geometrically induced correlations of tie molecules 78−19835
polyethylene, high-density, lamellar sep. during deform. 78−23775
polyethylene, high-density, oriented, deform. mechanisms 78−44171
polyethylene, high-density, semicryst., fold-surface morphology effect on deform. processes 78−34447
polyethylene, high-density, tensile necking, specimen size and loading conditions effects 79−61672
polyethylene, high-density, thin-wall tubes, deform. and fracture processes 79−100222
polyethylene, high-density ultradrawn, extrusion ratio influence on tensile props. 79−61618
polyethylene, highly oriented by drawing, thermal cond. 78−47614
polyethylene, hip joint prosthetic component deformation meas. by holographic interferometry *(German)* 80−12302
polyethylene, hydrostatic extrusion, deform. of crystalline and amorphous, and thermosetting resins 79−38875
polyethylene, linear, γ-irrad., plastic deform. 79−56996
polyethylene, linear, draw temp. and mol. wt. effect on draw ratio and Young's modulus 80−84998
polyethylene, linear, plastic deform. behaviour 78−84910
polyethylene, linear role of recovery forces in deformation 78−48459
polyethylene, low density, α mgch. dispersion in relation to spherulite deform. mech. 80−25781
polyethylene, low density, deformed in tension, lamellar reorientations 78−84914
polyethylene, low density, rheology and molecular struct. effect on viscoelasticity 77−62227
polyethylene, notched sheet, deform. mech., fracture, X-ray obs. *(Japanese)* 77−59863
polyethylene, observation of deformation process with X-ray TV system 78−15610
polyethylene, oriented, high temp. deform. X-ray diffr. expts. 77−56028
polyethylene, oriented, shear strain, effect on struct., props. *(Russian)* 80−7656
polyethylene, rheological behaviour at high shear strain rates *(French)* 80−66574
polyethylene, roll oriented, superstructural change during uniaxial extension *(Japanese)* 77−52422
polyethylene, rolled, neck draw *(Japanese)* 77−86090
polyethylene, shish kebab structure, formation mechanism 78−14286
polyethylene, single cryst. and spherulites, microstruct., deform. micromechanisms 78−83758
polyethylene, sonic frequency vibration effect on stress relaxation 77−86072
polyethylene, steady-state deform. and its effect on struct. and morphology 78−15459
polyethylene, stress relaxation under tension and torsion 79−52290
polyethylene, struct. changes on hot-rolling 77−86051
polyethylene, struct. transform. under tension in liqs. *(Russian)* 77−51492
polyethylene, structural changes on hot-rolling 77−86052
polyethylene, structure change on uniaxial compression *(Russian)* 79−34119
polyethylene, ultra-oriented high density, shrinkage as meas. of deformation efficiency 80−40398
polyethylene, ultradrawn, electron microscope exam. of struct. after annealing 80−11662
polyethylene, ultraoriented, prep. comments 77−85983
polyethylene, uniaxially oriented, relation between deform. and rotational isomerism 77−52438
polyethylene crystals, plastic deformation, molecular mech., TEM obs. 80−21022
polyethylene extruded melt, elongational viscosity, tensile props. 78−67163
polyethylene film, melt-cast, deform. in equatorial region of spherulites, electron diffr. 77−25115
polyethylene film, TSC, 20 to 60°C 78−10826
polyethylene melt, flow with steady state and recurrent deform. 77−898
polyethylene melt, rheology and molecular struct., melt identification from mech. props. 77−11490
polyethylene spherulites, thin melt-cast films, high density, deform. process in non-equatorial regions 80−81124
polyethylene terephthalate, crazing and shear deformation on stretching in air and liquids *(Russian)* 78−88558
plastic deformation continued
polyethylene terephthalate, fracture, interatomic bonds deform. 79−57107
polyethylene terephthalate, preoriented sheet, plastic deform., anisotropic behaviour 79−8335
polyethylene terephthalate, solid, rheology, deform. 77−11140
polyethylene terephthalate film, deformation band studies 77−52420
polyethylene-propylene copolymers, branching effect on struct. and mech. props. *(Russian)* 79−52333
polyethylenes, ultra-high modulus, manufacture by drawing through conical die 80−66583
polyimide, influence of monomer and water diluents on mech. relax. 79−4993
polyimides, glassy aromatic, plastic deform. 77−48494
polyisobutylene, polymer melt, extrusion at constant deformation rate 78−68744
polymer, activation energies of fracture and deform., comparison *(Russian)* 78−11303
polymer, crystalline, in hydrostatic tension, plastic deform. of model 77−59870
polymer, deformation, failure, kinetic model *(Russian)* 78−72832
polymer, deformation, ultimate regimes for flexible chains 78−19844
polymer, deformation mechanisms of constrained chains, geometrically induced correlations of tie molecules 78−19835
polymer, deformation mechanisms of constrained chains deform. energetics of tie molecules 78−19836
polymer, deformation of interatomic bonds, IR spectral meas. 79−38918
polymer, drawing properties, role of interfibrillar tie mols. 78−76706
polymer, filled, rheology, steady state shear flow and periodic deform., relaxation time, spectra, viscosity 79−96066
polymer, fluid high, ultimate strength in unixial extension 79−38920
polymer, fracture kinetics, book 79−29222
polymer, glass transition due to plastic deform., high-molecular linear polymer of narrow molecular mass distrib. 79−96065
polymer, long-term durability prediction methods, review 79−20320
polymer, molecular mechanism of orientation 77−69033
polymer, orientational ordering rel. to mech. props. *(Russian)* 78−59766
polymer, physically nonlinear, stress relaxation during stretching 78−23754
polymer, rigid-chain, unity of deform. and spontaneous elongation mechanism 79−20138
polymer, solid, impact compression crushing at low temps. *(Japanese)* 78−7032
polymer, statistical interpretation of temp. and stress shift factor 77−65999
polymer, stress-relaxation apparatus, stress and vibration relaxation in sound frequency range 77−1905
polymer, stressed, config. free energy change due to partial crystn. of chains, distrib. of cryst. orientations 79−94923
polymer, TEM obs. 77−44305
polymer, ultimate lifetime at high loads 79−20184
polymer, viscofluid, extensional vibrorheometer 77−70257
polymer coated metal spheres, flow, degradation mechanism 77−9036
polymer crystal, local plastic deform. mech., effect of lattice defect 77−28870
polymer crystals, deform. and fracture, submicrocrack nucleation and supermod. struct. 78−52918
polymer endoprosthetic joint, fatigue life 80−40521
polymer film re-stretching, elasto-plastic behaviour calc., using finite element analysis *(Japanese)* 80−7621
polymer foil, optical props. study by photoelasticity in const. and oscillating mech. fields *(German)* 78−31168
polymer matrix, amorphous, stressed, thermodynamics of embedded crystallite deform. *(Polish)* 77−52424
polymer melts and solns., deformation, mol. motion under flow 79−41646
polymer network, small ang. neutron scatt. 79−90569
polymer processing technology, prod. of high chain extension 78−31378
polymer spherulites, deformation mechanism, linear isothermal viscoelasticity theory 80−58924
polymeric glasses, non-elastic deformation, thermodynamic and kinetic anal. 78−64604
polymers, abrasive wear resistance rel. to physicomechanical props. 79−91804
polymers, anal. of mechanics of solid phase extrusion 80−39204
polymers, construction of single relaxation time spectrum 78−44160
polymers, crystalline, oriented, drawing, load elongation behaviour, fibre composite model 79−15691
polymers, crystalline, with lattice defects, exam. of plastic deformation for 2-d models 78−68747
polymers, deformation of materials, review 78−68749
polymers, deformation under combined action of shear stress and hydrostatic pressure, testing equipment 77−56184
polymers, device for testing under hydrostatic pressure and anisotropic conditions 79−87783
polymers, filled, light scattering in deformation 80−11718
polymers, hydrostatic extrusion, deform. of crystalline and amorphous, and thermosetting resins 79−38875
polymers, nonlinear, stress relaxation under tension and torsion 79−52290
polymers, plastic deformation during freeze-cleavage, review 78−14400
polyolefins, creep 79−100221
polyoxymethylene, effects of hydrostatic press. on shear deform. 78−15457
polyoxymethylene, epitaxial growth on KBr single crystal *(Japanese)* 78−56054
polyoxymethylene, rolled, prediction of yielding behaviour 77−73306
polyoxymethylene, yielding behaviour under complex triaxial stress conditions 77−56030
polypropylene, crystalline, yield behaviour in oriented and unoriented condition, effect of temp. 80−97537
polypropylene, ductile, large strain cyclic deform. 80−85000
polypropylene, effects of hydrostatic press. on shear deform. 78−15457
polypropylene, glassy state, macrodeformation stresses, anelastic characteristics 79−52289
polypropylene, isotactic, shear induced β-form crystallisation 78−18555
polypropylene, notched sheet, deform. mech., fracture, X-ray obs. *(Japanese)* 77−59863
polypropylene, oriented, annealing, mol. mechanisms 77−12642
polypropylene, oriented, stress relaxation 77−44285

plastic deformation continued
polypropylene, preoriented isotactic sheet, mol. behaviour in uniaxial drawing *(Japanese)* 77−68928
polypropylene, stretching reduces electrical values *(German)* 79−43446
polypropylene, structure change on uniaxial compression *(Russian)* 79−34119
polypropylene, transparent film, strain anal. by scattered-light speckle photography 79−32399
polypropylene, ultrahigh modulus, tensile drawing, mol. wt. effect 80−104211
polypropylene, yielding behaviour under complex triaxial stress conditions 77−56030
polypropylene film, double-exposure speckle pattern obs. of tensile deform., displacement, Poisson's ratio and stress relax. 80−84795
polypropylene film, effect of crystallinity on deformation mechanism of biaxial stretching 77−80426
polypropylene fracture, interatomic bonds deform. 79−57107
polypropylene nonfilaments, highly drawn, plastic deform. 78−44174
polypyromelliteimide, fracture, interatomic bonds deform. 79−57107
polystyrene, amorphous, LF Raman modes, strain and temp. effects 77−36219
polystyrene, atactic, indentation recovery 80−84988
polystyrene, comparison of deformation processes in crazes and shear bands, SEM study 79−29191
polystyrene, glassy, intermol. interaction during inelastic deform., optical spectra obs. 77−59878
polystyrene, glassy, thermally activated deform. 79−20126
polystyrene, glassy state, macrodeformation stresses, anelastic characteristics 79−52289
polystyrene, high-impact type, deformation and microvoid form. 78−80602
polystyrene, isotactic crystals, plastic deformation, molecular mech., TEM obs. 80−21022
polystyrene, molecular alignment 78−14299
polystyrene, particles, critical stress 77−28869
polystyrene, shear bands, morphology and annealing behaviour 80−100873
polystyrene, shrinkability, orient. 79−11660
polystyrene, stress birefringence under nonisothermal conditions 78−15468
polystyrene, uniaxially oriented atactic, laser Raman scattering 79−73920
polystyrene-poly(styrene-b-butadiene-b-styrene) polyblends, mech. props. 78−52919
polystyrene-polyethylene block copolymer, deformation ratios, Poisson ratio and adhesion, dilatometric obs. 80−60937
polystyrenes, rubber modified, mech. props., mol. orientation effects 79−52331
polythene, stretching reduces electrical values *(German)* 79−43446
polyurethane, deform. under sheet pressworking, math. model 79−61673
polyurethane, filled, relation between static and dynamic deform. charcts. 80−3137
polyurethane, tensile fracture stress eval. for prosthetic heart valve 77−56533
polyurethane rubber, photoelastic, behaviour at elevated temps. 77−25094
porous bodies, anal. using plasticity theory 80−25802
porous material, wedge indentation hardness, slip line field theory 77−86128
porous material deformation anal. using upper bound theory, appl. to extrusion *(Japanese)* 77−46937
porous materials, constitutive eqns. 79−61667
porous materials, deform. diagram based on theory of plasticity *(Russian)* 78−88494
porous materials, deformation theory *(Russian)* 79−37189
porous materials, deformation theory of plasticity *(Russian)* 80−75291
porous materials, density variation during plastic shaping 80−84873
porous metal, yield stress variation during cold deformation 80−16395
porous metal gauze materials, struct. and hydraulic charcts. 80−11729
porous metals, plasticity, stress-strain curves, yield stresses, strain vectors 80−83738
porous solid, shear stress enhancement of void compaction 79−69182
porous solids, hot rolling, rheology, stressed state determ. 79−100194
positron annihilation radiation, ang. correl. shape, deform. effects 77−85831
powder metallurgy compact, elec. resistivity 78−64028
powder strip shaping device, deform. zone configuration effects 77−24979
power-law hardening material, small-scale yielding problem, soln. *(German)* 78−38210
Prandtl Reuss plastic material with isotropic work hardening, loading and unloading *(Japanese)* 77−8854
Prandtl-Reuss plastic material with isotropic work hardening, constitutive equations *(Japanese)* 77−4789
precipitate hardened material, intergranular cavity growth inhibition 80−50677
pressmold materials, stand for high-temp. mech.-props. test 77−56183
pressure transient analysis in piping systems including the effects of plastic deformation and cavitation 80−74775
prismatic bar, large deform. anal. for repeated axial loading 78−38207
prismatic bar hysteretic behaviour, yield condition under repeated axial loading 77−62167
prismatic specimens, method for plotting deformation fields 77−63851
PTFE, crystalline, subject to simple plane loading, limiting resistant, time and temp. factors 78−23794
PTFE, thin-wall tubes, deform. and fracture processes 79−100222
PVC, amorphous-cryst., highly oriented, plastic deform. rel. to supermol. struct. *(Russian)* 79−51010
PVC, calendering, defects in calendered films and sheets 79−8267
PVC, calendering, prediction of stress and torque 79−8266
PVC, cold drawn, plastic fracture around cavities 79−56994
PVC, crazing, deform. kinetics 80−84990
PVC, deform. temp.-time depend. props., viscoelastic linear and nonlinear regions comparative anal. 78−64600
PVC, glassy state, macrodeformation stresses, anelastic characteristics 79−52289
PVC, hard, flow zone effect on degradation, rigidity, deformation, under fatigue *(German)* 78−15471
PVC, rigid, craze and yield zones in fracture 80−50701
PVC, rigid plastic, yield behaviour *(Japanese)* 80−93620
PVC, rubber-modified, stress whitening and yield mechanism 79−8324
plastic deformation continued
PVC, stress relaxation in macrodeformation range 80−16370
PVC, tensile tests, post-yield phenomena 79−91752
PVC, uniaxially stretched, mol. orientation, birefringence, effect of plasticizers, draw ratio 77−48500
PVC film, uniaxially stretched, mol. orientation, polarised fluoresc. investig., deform. mechanism 77−52440
PVC sheet, notched, yielding 78−56708
PWR fuel cladding, long ballooning deformation following LOCA 80−660
PWR pressure components reliability and residual life evaluation and precipitation 79−20191
Pyrex glass, near-surface H embrittlement, effect on deform. and fracture props. 79−29180
pyroceramic, stress in working zone under biaxial compression, Moire-band method 77−81369
pyrolysis furnace tube, materials evaluation with creep damage model 77−52445
quartz, dislocations, elastic energy *(French)* 79−14807
quartz, dissociated a-dislocation, effect on plastic deformation 79−7610
quartz, plant deform. and recrystallisation textures 78−68708
quartz, strain amplitude depend. of internal friction, role of dislocations 77−27939
quartz, subgrain boundaries, theoret. predictions and microscopic obs. methods 80−84187
quartz, US absorption, influence of plastic deform. and electrostatic field *(Russian)* 80−39226
quartzite, deformation in Earth crust, dislocation climb mechanism 79−60425
quartzite, naturally deformed, textural and microstructural development, metallurgical approach 79−83228
quartzites, intracrystalline deform. comparison in natural and exptl. deform. 79−79830
quartzites, microscopic deform. and flow laws, South Mountain Anticline 78−77220
radiation blistering, fracture model, stress fields around lenticular bubble 79−86823
rapidly heated rigid plastic cantilever, expanding and contracting hinge concept 79−7293
rare earth oxides, microhardness anisotropy of single cryst. *(French)* 77−52489
rare earths, elastic and mechanical properties, review 79−70132
rate sensitive materials, deformation mechanics, approx. anal. technique 79−23221
rate type plastic material, with kinematic work hardening 78−15450
rate-independent plasticity, axiomatic model 80−87717
rate-sensitive materials, direct extrusion through conical dies 77−28872
Rayleigh-Taylor instability, method of generalised coords. 78−65771
reactor fuel cladding failure under reactivity initiated accident conditions *(Japanese)* 79−30955
reactor fuel cladding tube mech. props., ring compression test, finite element anal. 77−83037
reactor fuel pin tubes 79−47755
recovery creep model for stationary state of plastic yielding 77−7314
rectangular beam, freely supported with load input through rigid circular tool, deform. *(German)* 79−23218
rectangular parallelepiped compression, small elastoplastic deformation, variation anal. *(Russian)* 79−32294
rectangular plate, stability, mechanical props. dependent on strained condition *(Russian)* 79−10494
refractories, thermal shock resist. criteria calc., rel. to deformability 79−29212
refractory, rheological behaviour at high temp. *(French)* 77−56016
refractory, strength determ., taking account of stress/deform. relation 77−28965
refractory composites, fibre reinforced, directionally solidified tensile tests, in HVEM, deform. and fracture *(French)* 78−68785
refractory masses, subsidence, high temp., without load exam. using deform. during continuous heating *(French)* 79−15721
refractory metals, mech. props. and diffusion figures *(Russian)* 80−40436
refractory products, dense, high-temp. rheology *(French)* 77−32629
reinforced composites, strength and deformation anisotropy, numerical charcts. 80−38285
reinforced materials, semi-microscopic theory *(Russian)* 77−23893
reinforced UP resin laminate under dynamic stress, anisotropic, mech. behaviour determ. *(German)* 79−83268
relaxation in shock wave, slip mechanism 79−41605
Rene 95, as hot isostatically pressed (HIP) and HIP+forged, low cycle fatigue 80−25854
residual pseudo-macrostress, X-ray meas. errors due to plastic deform. 77−68544
rhomboidal steel panel, elastoplastic stress and strain diffusion 79−20128
rigid perfectly plastic strip, plane strain compression between parallel dies with slipping friction 80−48603
rigid plastic fibre reinforced plates, impulsive loading, dynamic deformations theory 79−23222
rigid plastic solids under lateral pressure, uniqueness of plain strain deformation 80−64404
rigid slider, deformational contact and friction on viscoelastic substrates 79−50677
rigid-plastic beam, shear to bending response to blast type loading 77−54891
rigid-plastic dynamics, large deformation, extremum, principle 80−53642
rigid-plastic medium, ideal, surface force strength lower limit under plain strain 80−99937
rigidly plastic media with hardening, shock-loaded, dislocation model and elastoplastic waves 79−86379
ring, pulled diametrically, finite plastic deform. *(Chinese)* 79−64525
ring sector, plastic twisting *(Russian)* 77−50923
rings, circular optimal plastic, stress/strain relations for rigid plastic material 79−34098
rings, plastic, large deforms., plasticity and hardening effects 80−43627
rock, continuum model for plastic-brittle fracture 79−27584
rock, deformation and fracture under general triaxial stress states, anisotropic dilatancy *(Japanese)* 78−56750
rock, plastic-brittle behaviour, hardening and softening constitutive eqns. 77−21270
rocks, dynamic deformation, at nonuniform triaxial loading *(Russian)* 77−56619
rocks, elastic longitudinal wave vels. during nonelastic deform. 78−61402

plastic deformation continued
rocks, fabric development simulation, appl. to quartzite 78−49015
rocks, hot, dry, hydraulically fractured linearly expanding cracks, eqns. *(Japanese)* 79−34809
rocks, props. gas cavity expansion, soil dilatation following explosion 79−8608
rocks, rheology and growth of banded perturbation structures 78−36152
rocks, time-dependent deform. not purely elastic specimens 78−32075
rod, cantilever, terminal moments, nonlinear anal. 80−74763
rod, cantilevered, with attached mass at end, plastic deform. under seismic effect *(Russian)* 80−53653
rod, elastoplastic, dynamic bending and residual deformation *(Russian)* 80−75293
rod, theory of resistance to failure of technical materials 79−10536
rod and plate, fatigue strength in bending, small number load cycles 77−86183
rod of rate-sensitive material, elastic-plastic tension-torsion analysis 80−83741
rod penetrating thick target, plastic deform.-jetting flow transition vel. 77−62163
rods and plates, strain-rate-sensitive material, elastic-plastic wave propag. mech. 80−69724
rolling, critical reduction, effect on chemicothermal treatment processes 77−70073
rolling, determ. of stress distrib. in rolled material 80−48651
rolling, inhomogeneous deformation model 80−48650
rotating discs, anisotropic, finite deform. 79−41586
rough surface, plastic deformation in mechanical contact 80−14583
rough surfaces in contact, stochastic approach to deform. mode 77−59950
round bar, tensile deformation, mathematical description 79−10500
round plate with radial and circular reinforcing ribs, load bearing capacity 79−98636
rubber, cutting resistance measurement in absence of friction 79−5035
rubber, dynamic mechanical properties models *(Polish)* 79−43349
rubber, natural, tensile fracture strength eval. for prosthetic heart valve 77−56533
rubber, strain-energy density function 80−25773
rubberized cloth, service life determ. under cyclic load 78−31535
rubberlike materials, finite plane strain deformations, finite element anal. 80−28438
ruby, temp.-time dependence of yield point by compression and extension 78−6988
sand bodies, shear bands formation, bifurcation problem 78−73362
sapphire:Ti^{4+}, plastically deformed, precipitation hardening, TEM study 80−7592
sapphire 0°, creep deform., fracture anal. 77−56035
sapphire :Ti^{4+}, deformation history effects on precipitation hardening 79−83209
sapphire disc, dynamic deform. by projectile impact, back reference holography obs. *(French)* 78−42307
screw dislocation control of plastic deformation in crystals 78−51605
sea ice, plastic deform. rel. to dynamic thermodynamic model 80−51432
sea ice, viscous law as stochastic average of plasticity 78−16028
sediment, artificial, const. vol. deform. effects on magnetisation 78−65265
SEM, combined deformation/heating stage, acoustic emission rate meas. 80−101892
SEM specimen holder, for cold tensile deform. and its appl. to Pb-Sn eutectic *(French)* 77−36704
semiconductor, anisotropic conductivity and ambipolar drift noise 77−20375
semiconductor, dislocation struct. and elec. props. 80−70201
semiconductor, plastic deformation under pulse action 77−76486
semiconductor, TEM obs. *(French)* 77−44303
semiconductor crystal, physical nature of low temp. microplastic strain *(Russian)* 79−65094
semiconductors, electron-hole drop formation, phonon wind influence *(Russian)* 80−92825
servocontrolled hydraulic hot-torsion machine for hot working studies 78−27698
shakedown of deformable plastic structure, approx. methods, fatigue 77−54900
shallow circular arch, spatial distrib. effect on dynamic snap-through 79−32318
shape-memory alloys, props. and appl. 80−30049
shaped strip, tension during rolling 78−84890
sharp crack tip, reverse shear on inclined planes 79−77023
shear band formation models, in rolling and extrusion 80−3152
shearing process, basal section profile effect 79−47754
sheet bending of additional deformation zone loading 77−23899
sheet drawing, slip line field for mid-plane cracking or splitting 80−50648
sheet material, method for strength meas. under biaxial tension 80−66717
sheet metal, finite element anal. of hydrostatic bulging 77−72186
sheet metal, limit strains, predictions from yield criterion 79−27539
sheet metal, texture heterogeneity, numerical simulation *(French)* 78−92274
sheet metal deformation, criteria for determ. of deformation limit G *(German)* 80−21000
sheets and beams, blank maximal deformations, length and thickness in plastic bending 77−19550
shell, dislocation differential geom. in 2D space 78−22719
shell, internally exploded, displacement meas. by photometric method 80−14642
shell, rectangular flexible elastoplastic, yield theory and deformation theory appl. 80−74773
shell, rigid-plastic, large deflection under impact of concentrated mass 77−54901
shell, shallow, limit analysis and optimal design *(Russian)* 77−42752
shell, shallow spherical, plastic deformation under explosive loading 80−14589
shell of revolution, corrugated, thermoelastic plastic deform. at finite displacements 80−74772
shells, complex profile, installation for deform. processes 80−81261
shells, kinematics at large strains and displacements 78−79221
shells, large inelastic deformations for arbitrary shape, TRUMP element appl. 80−92068
shells, plastic, explosive forming, computer numerical simulation 80−59560
plastic deformation continued
shells of revolution, plastic, limit anal., lower bound numerical method 78−63337
shot peening residual stress effects on plastic microstrain in isotopic media *(French)* 79−77675
silicate glasses, stabilised, exam. of stress relaxation and deformation 78−92292
silicate glasses, surface and subsurface deformation and cracking around Vickers indentations 79−29189
silicone elastomers, dental impression materials, dimens. stability, holographic and interferometric study 80−67204
silicone rubber, tensile fracture stress eval. for prosthetic heart valve 77−56533
siloxane rubber, energy investigation of softening during deform. 77−4819
simple tension test, appl. of hyperbolic theory of plasticity 77−39235
single crystal deform., texture form. 79−87651
single crystal deformation, active slip system and orientation change determ. method 79−90664
single crystals, homogeneous plastic deform. by dislocation glide *(French)* 80−84232
single crysts., fatigued age-hardenable, dislocation structure *(German)* 80−54247
sintered metal, cold forming with self aligning dies 78−11158
slip, non-crystallographic, in cubic cryst., algebraic determ. *(French)* 80−2112
slip, primary coplanar, role in deform. of FCC crystals *(Japanese)* 77−52412
slip and twinning, accompanying orientation changes 77−43273
slip morphology in dispersion hardened materials 77−4785
smooth pipe bend, plastic limit moment under in-plane bending 80−23906
snow, acoustic emission response 79−87801
snow driven by moving body, plastic wave generation *(Japanese)* 77−84186
soil, deformation of compressible elastoplastic ground 78−96198
soil, sandy moist, compressibility and plasticity during repeated shock loading 78−11885
soil, viscous nonlinear, stresses and strains 78−73363
soil mechanics, elastoplastic deformation, volumetric constitutive equation 80−53655
soil-struct., interaction initial stress finite element method 78−59313
solid, creep cavitation by vacancy diffusion 78−48471
solid, finite strain and finite rotation 78−30192
solid deformable body, residual stresses by creating holes, holographic interferometry appl. *(German)* 80−79243
solids, high energy electron emission, influence of structure and props. *(German)* 79−52317
solids, uniqueness and stability under config. depend. loading 78−30194
solids in vacuum, contact adhesion, single asperity experiments 77−11149
sound porous material, stress anal. during stretching *(Russian)* 79−76980
space frames of thin walled members, plastic collapse 77−31223
speckle correlation and interferometry for planar deformation analysis *(Dutch)* 80−32930
spheres and rough planes, in contact with normal load, numerical analysis and expt. verification *(Japanese)* 77−19575
spheres at high pressure, contact stresses and spreading resistance 78−71296
spherical material parts, defect coordinates, location via acoustic emission method 78−35626
spherical powder, particle deform. and sliding during compaction, metallographic study 79−66020
spherical shell, shallow radially ribbed, stress state, struct. parameters influence 80−14581
spinel oxide, dissociation of dislocations and plastic deform., temp. effects 79−7613
split Hopkinson pressure bar use in obtaining dynamic stress/strain data at const. strain rates *(Japanese)* 80−16630
spring strip production, flattening mill employing US and electroplastic effect 78−84941
stability concepts and conditions in tension 78−26046
stability of multilayer composites under inelastic deformations 80−99944
stainless steel, type 316, updated temp. integrity limit for FFTF driver fuel pins 77−42089
stainless steel cladding on mixed oxide nuclear fuel, deform. meas. 77−42088
statistical concepts, calc. of local peak stress effect 78−27584
statistical-kinematic analysis and limit equilibrium of systems with unilateral constraints 80−1451
stator end winding under short circuit, dynamic deform. and strength *(Japanese)* 78−11465
stator windings, failure mechanisms under thermal cycling *(Japanese)* 80−104189
steady-state, irreversible thermodynamic description 78−72831
steady-state straining 78−5669
steel; low alloy, high strength, hot compression dynamic precip. and coarsening of Nb(CN) 80−97514
steel, 0.45% C, annealed, roller, rolling contact fatigue life, effect of changing rolling direction 77−77519
steel, 0Kh16N15M3B type, He ion irradiation effect on struct. and mech. props. 78−19848
steel, 10KhSND, low cycle loading, deform. diagram *(Russian)* 78−52908
steel, 11423, cyclic stress anal. within hysteresis loop *(Czech)* 80−30031
steel, 11YuA, cold worked, heat treated, electromagnetomech. props. NDT 79−4980
steel, 12Kh1M1F, pipe with axial surface crack, resistance of failure in plastic deform. 79−100235
steel, 12Kh1MF, influence of preferrred dislocation orientation on high-temp. strength *(Russian)* 79−4999
steel, 15Kh15N5AMZ, martensitic transform., inverse, plastic deform. effect, 200 to 550°C *(Russian)* 77−73274
steel, 18H2N4WA, hot-worked, kinetics of austenite grain growth, rel. to deformation degree *(Polish)* 80−45322
steel, 30CH2GMT and 35CHG2SV, thermomechanical hardening *(Czechoslovakian)* 77−32602
steel, 3Kh2V8F, brittleness depend. on high temp. deform. at high stress. temp. *(Russian)* 80−50698

plastic deformation continued
steel, 4340, quenched, tempered, and austempered, effect of plastic strain followed by ageing on elastic limit 78−31446
steel, 45 and U7, deform. microheterogeneity and ductility 77−73309
steel, 45G17Yu3, deformed, influence of hot rolling on struct. *(Russian)* 77−25073
steel, 50N29 type, self-consistent junctions and spatial relative organisation 80−19750
steel, acoustic emission anal., during fatigue crack growth 77−56090
steel, acoustic emission in deformation, at various strain rates and sign change 78−44188
steel, acoustic-emission analysis of fracture-toughness tests 80−55596
steel, Al killed, cold rolled and recrystallised grain shape anisotropy 79−34064
steel, Al killed, density changes, void growth in biaxial stress fields, plastic deformation 80−71692
steel, Al-killed, sheets, effect of strain path changes on formability 79−43347
steel, Al-killed rolled sheet, plastic anisotropy theory based on yield function of fourth order 78−31458
steel, Al-stabilised, texture formation in continuous annealing, effect of coiling temp. of hot strip 79−91688
steel, alloy, 15KhM1 and 20KhM1, plastic deform. with thermal cycling 80−89310
steel, alloy, deformation, rapid dynamic, at −196°C 80−104220
steel, alloy, high speed, cutting tools, carbide heterogeneity change during hot extrusion 80−16390
steel, alloy, high speed, type R18, hot deformation and recrystn. 80−16391
steel, alloy, martensitic transforms. during deform. of types N28, N29, N30 and N31 78−56639
steel, alloy, Mn-Cr-Cu, exam. of ductility when deformed, alloying addition effects 78−44175
steel, alloy, Ni-Cr-Mo, alloys SNCM8, SAE 4161, heat treated, residual stress at fatigue fracture surface *(Japanese)* 78−64622
steel, alloy, Ni-Cr-Mo, exam. of transformation behaviour 78−76718
steel, alloy, rectangular beam, stress-strain anal. of cyclic plastic bending and torsion 78−90734
steel, alloy, sheet, crack-propag. resist. in heat-affected zone in presence of H, rolling direction and preliminary plastic tensile strain effects 80−60971
steel, alloy, softening process in deformed type 15GYuT, metallographs *(Russian)* 78−52840
steel, alloy, strain ageing anomalies, plastic strain mechanisms *(Russian)* 79−52300
steel, alloy, temp. profile, IR obs. during pull tests 77−44427
steel, alloy, tensile test, regulated, strength and deform. characteristic values, consistency *(German)* 80−93712
steel, alloy, type 25Gs, increasing fatigue resistance by surface plastic deformation 78−88530
steel, alloy, type 36NKhTYu, plastic deformation, effect of surface condition on initial stage 78−84929
steel, alloy 40Kh, sulphide cracking resistance, strengthening method influence 80−55577
steel, alloy A533B1, neutron irrad., flow growth characts. by acoustic monitoring 80−100918
steel, alloy maraging, type Kh13N8D2TM, conditions for formation of stable austenite 78−84868
steel, alloy St. 3sp, weld, deformation criteria of low cycle failure 78−39875
steel, alloy type 15G2AFDps describing cyclic-creep processes with parametric eqn. 79−57074
steel, austenite hot deformation influence on phase transformations 80−7606
steel, austenitic, 0Kh14AG12M, temp. depend. of mech. props. and kinetics of phase transforms. *(Russian)* 78−92297
steel, austenitic, 16H2NMB, struct., texture and mech. props. of product of transform. 78−92273
steel, austenitic, 45Kh2N12GS, post deformation holding at deform. temp. effect on struct. and strength of austenite and martensite *(Russian)* 79−1880
steel, austenitic, 70Kh5G4 martensite lattice struct. obtained by deform. *(Russian)* 78−88464
steel, austenitic, aged, stress induced martensitic transform., mech. props. *(Russian)* 79−87632
steel, austenitic, ageing and plastic deform. effect on struct. and mech. props. of N15Kh5G3T3 *(Russian)* 80−71691
steel, austenitic, alloy and stainless, fuel-element cans, deform., failure, rigid loading scheme 79−91765
steel, austenitic, Cr-Mn, Kh4G18F, microstruct. and mech. props. during tensile deform. *(Russian)* 79−20114
steel, austenitic, Cr-Mn, metastable, plasticity, contrib. of martensitic transform. during deform. *(Russian)* 80−30018
steel, austenitic, Cr-Mn-N, plastic deformation influence on internal friction, relaxation processes *(Russian)* 80−100870
steel, austenitic, Cr-Ni (18,12 wt.%), containing coarse grain boundary precipitates, thermomechanical treatment 78−27545
steel, austenitic, deform., struct., transform. kinetics hot working effects *(Russian)* 77−52361
steel, austenitic, explosive-thermal treatment, sulphide cracking decrease, hydrogen embrittlement *(Russian)* 80−108477
steel, austenitic, fatigue after plastic deform. sequences *(French)* 79−20131
steel, austenitic, high content of low melting additives, high temp. neutron irradiation embrittlement *(Russian)* 79−73218
steel, austenitic, high-temp. crack resist., B and Mo influence *(Russian)* 80−16435
steel, austenitic, intermittent loading effect on creep *(Japanese)* 79−29147
steel, austenitic, low C, struct. charact. of dynamic recrystallisation *(Czech)* 77−59813
steel, austenitic, low-C, transform. kinetics rel. to temp., deform., struct., mech. props. 79−24519
steel, austenitic, magnetisation meas. of stability 77−1579
steel, austenitic, metastable, 0Kh14AG12M, Cr-Mn and Cr-Mn-Ni, phase transform. kinetic effect on mech. props. *(Russian)* 79−34024
steel, austenitic, Mn strain hardening at room and low temps. *(German)* 79−38845
steel, austenitic, Nb modified, HSLA, interaction between recrystallisation and precipitation during high temp. determ. 79−100187
steel, austenitic, neutron irradiated, He absorption 77−51414
plastic deformation continued
steel, austenitic, Ni-Cr, precipitation strengthened, anelasticity, plastic creep limit, 823K 79−1899
steel, austenitic, Ni-Ti, alloy N35T5, ageing, magnetisation and Curie temp. depend. on plastic deform., Mossbauer studies *(Russian)* 79−69669
steel, austenitic, nitrided, creep, effect of N_2 and Ti and prior deform. 78−23789
steel, austenitic, pearlite transform. kinetics, effect of US deform. *(Russian)* 77−21136
steel, austenitic, stainless, life prediction of high temp. low cycle fatigue, strain rate effect 79−8360
steel, austenitic, types A533B and A508, acoustic emission during tensile tests, elastic and plastic deformation processes 79−74212
steel, austenitic, undergoing martensitic transform. during deform., temp. depend. of yield point *(Russian)* 77−66677
steel, austenitic Cr-Mn, $M_{23}C_6$ carbide precipitates comp., heat and thermomech. treatment influence *(Russian)* 80−40361
steel, austenitic heat-resisting, deformation and fracture rel. to grain-boundary reaction nodules 78−80591
steel, austenitic metastable, fatigue, effect of deformation-induced martensitic transformation *(Japanese)* 78−15514
steel, austenitic N31, mechanical instability in premartensitic state *(Russian)* 77−73273
steel, austenitic stainless, 08Kh18N10T, hot-worked precipitation kinetics and struct. of dispersed phases, Ti effect 80−29964
steel, austenitic stainless, 12Kh18N10T, deformed, phase comp. and props. after prolonged heating 80−30040
steel, austenitic stainless, 12Kh18N10T, intercrystalline corrosion, hot rolling effect 79−79010
steel, austenitic stainless, acoustic emission during cyclic deformation *(Japanese)* 79−43314
steel, austenitic stainless, aged and deformed, growth and dissolution of NbC particles 78−39782
steel, austenitic stainless, AISI 316 L, viscoplastic deformation under hot working conditions, struct. model 79−83278
steel, austenitic stainless, corrosion resistance in passive state, cold work effects *(Czech)* 77−59987
steel, austenitic stainless, Cr-Mn, austenite stability during deform. 77−70050
steel, austenitic stainless, deformation by hydroforming, heat treatment effects *(French)* 78−35450
steel, austenitic stainless, deformation induced cavitation, exam. 79−43363
steel, austenitic stainless, deformed plate, X-ray line profile anal. *(Japanese)* 78−7144
steel, austenitic stainless, fusion reactor blanket struct. material, low cycle fatigue behaviour 80−30073
steel, austenitic stainless, grain boundary as dislocation source during high temp. deform. *(Russian)* 78−15453
steel, austenitic stainless, grain boundary segregation studies, intergranular fracturing technique for stress corrosion cracking investigation 79−39057
steel, austenitic stainless, martensitic transform. effect during static and fatigue loading 77−52325
steel, austenitic stainless, metastable, transform. depend. ductility, temp. and deform. effects 78−3185
steel, austenitic stainless, microdeform. meas. using method of grids 80−55615
steel, austenitic stainless, Mn-Cr, austenite decomposition by deform., rel. to mech. props. *(Russian)* 78−27515
steel, austenitic stainless, partial dislocation separation and dislocation substructure, effect of applied stress 78−22727
steel, austenitic stainless, plastic deform. build-up during low cycle fatigue *(Russian)* 77−25207
steel, austenitic stainless, plastically deformed, TEM obs. *(French)* 77−44302
steel, austenitic stainless, porous fibre, sintered and compacted, mech. props. 79−15623
steel, austenitic stainless, stacking fault effect on martensitic transform. during plastic deform. *(Russian)* 80−25696
steel, austenitic stainless, stacking fault energy, effect of N 80−107279
steel, austenitic stainless, strain hardened containing N_2, low temp. props. 79−66128
steel, austenitic stainless, stress corrosion cracking in H_2SO_4-NaCl soln., Ni and N_2 effects *(Japanese)* 79−100289
steel, austenitic stainless, stressing conditions, fatigue behaviour, struct. development with plastic deform. *(French)* 78−68776
steel, austenitic stainless, struct. and mech. props. under low temp. deform. under linear and plane stress conditions 79−1902
steel, austenitic stainless, tensile prestrained, X-ray elastic const. meas. *(Japanese)* 79−66093
steel, austenitic stainless, tensile stress effect on He bublbe growth 79−87684
steel, austenitic stainless, type 304, cyclic creep during unbalanced tension-compression loading at elevated temp. 80−97545
steel, austenitic stainless, type 800, tensile creep props. rel. to intergranular microstruct. at 800°C, TEM study 79−38885
steel, austenitic stainless, type SUS 304, low cycle fatigue strength reduction factor *(Japanese)* 80−104259
steel, austenitic stainless 316, load relaxation data, comparison with Hart's deform. model 77−70091
steel, austenitic stainless AISI 304, dislocation substruct., carbide precipitation and deform. mech. map 77−70116
steel, austenitic stainless JIS type 304, tensile test at elevated temp., high velocity 77−73302
steel, austenitic stainless low-cycle fatigue, effect of mean plastic strain and stress factor 77−63766
steel, austenitic stainless sheet, texture anisotropy influence on deformation forming limits 79−91706
steel, austenitic stainless SUS 301, stress corrosion cracking susceptibility, effect of strain-induced α'-martensite *(Japanese)* 80−104335
steel, austenitic stainless type 304L, temp. depend. of acoustic emission accompanying plastic deform. 79−74217
steel, austenitic stainless type 304N, machining induced deformation transformation, mag. evaluation 79−83195
steel, austenitic stainless wires, phenomenology of cold twisted deformation *(French)* 80−21030
steel, austenitic type 110G13L, preliminary strengthening inheritance, exam. 78−44137

plastic deformation continued
steel, austenitic-ferritic Ni-Cr, 12Kh21N5T, phase and struct. transform. *(Russian)* 78−95748
steel, austenito-martensitic, struct. changes during plastic deform., mutual influence of phases *(Russian)* 80−30015
steel, C, 20 and 22K, ductility, effect of temp., deform. rate and stress state *(Russian)* 78−35428
steel, C, accelerated deform. by to H_2 absorption *(Japanese)* 79−70121
steel, C, accumulation of longitudinal strain under cyclic torsion 78−64615
steel, C, brazed butt joint, static torsional deform. 77−16657
steel, C, crack resistance, preliminary loading condition effects in crack appl. 78−56739
steel, C, deformation strength and strain rate depend. under plain strain state *(Japanese)* 80−30028
steel, C, effect of pre-straining on torsional fracture strain *(Japanese)* 80−3183
steel, C, failure mechanisms in impact fatigue 80−40493
steel, C, fatigue damage accompanying nonstationary modes of cyclical loading, coeff. of heredity *(Russian)* 79−52349
steel, C, fatigue damage accumulation and nonuniform microscopic strains, development features 79−91770
steel, C, fatigue strength and damping capacity, short term cyclic overload effect 79−66157
steel, C, fracture dynamics at high frequency loading *(Czech)* 80−45391
steel, C, hot plastic deform., vac. colour etching investigation 80−61036
steel, C, hypo-eutectoid naturally fibrous composites, strength analysis 78−3190
steel, C, low temperature strength, preliminary plastic deform. effect 80−81128
steel, C, microplastic deform. of drawn and undrawn samples *(French)* 79−1894
steel, C, natural reinforced composite 80−30039
steel, C, naval, corrosion in harbour anaerobic sediments, rolling direction and tensile stress effects 80−30135
steel, C, naval, corrosion in natural seawater, rolling direction and tensile stress effects 80−30134
steel, C, pearlite grade ShKh15, struct. transformations, hot plastic strain influence *(Russian)* 80−20927
steel, C, plastic deform., −150 to 200°C, effect on loading surface 79−66130
steel, C, plastic deform., study of loading surface. 77−44322
steel, C, predeformed, anisotropy temp. effect on yield point 78−39878
steel, C, pure ductile, yield pt. determ. from dislocation theory *(Serbian)* 79−34120
steel, C, recrystallization annealing, grain growth, effect of type of deform. 80−100847
steel, C, residual stress induced by uniaxial deform., mag. meas. 77−73390
steel, C, strain ageing and fatigue limit 80−40378
steel, C, structural strength, increase by high temp. mech. treatment with austenite isothermal decomp. 79−24555
steel, C, type 45 and 1Kh2M, fatigue strength, of notched specimens with regard for cyclic plastic strains 79−43414
steel, C, type SFVV1, low cycle fatigue strength reduction factor *(Japanese)* 80−104259
steel, C(0.2 wt.%), explosively strengthened, cause of anomalous increase in H_2 of low cycle endurance *(Russian)* 77−16729
steel, C (0.1-1.15 wt.%), fatigue under reversed tension-compression stresses, photoelasticity investig. *(German)* 78−31493
steel, C (0.21 wt.%), loading wave shape effect on deform., failure, impact tensile strength of smooth specimen *(Japanese)* 79−29146
steel, C and low alloy, mech. props. after warm extrusion 77−12668
steel, C content effect on annealing texture, plastic anisotropy and mechanical props. 80−29976
steel, C deep drawing sheets, influence of strain- and stress-ratios on preferred orientation change 79−91690
steel, C type U10A, X-ray diffr. investig. of carbide residues after deform. and tempering *(Russian)* 77−81275
steel, C-Cr (0.6, 13 wt.%), friction during working stresses and rheological charact. at high temps. *(Russian)* 77−66702
steel, C-Mn-Nb, Nb microalloying, weldable, structural, recrystallization and precipitation induced by high temp. deform. *(French)* 79−61632
steel, C-Mn-Si, dual phase, stress-strain curves, deformation behaviour 79−52324
steel, cast, type 20, exam. of strain characts. in premelting temp. range *(Russian)* 79−29140
steel, cast 20KhML, deform. resistance and low cycle fatigue in pure shear creep effect 78−3192
steel, cast structural, heat treatment and mech. working influence on mech. props. *(Russian)* 80−40392
steel, cementite decomposition during plastic deform., alloying element effects 78−84768
steel, CK10, structural, temp. and freq. depend. of stress-strain behaviour under cyclic loading *(German)* 79−38888
steel, Ck45, tension-compression tests, cyclic, macroscopic changes of length *(German)* 80−40424
steel, Ck 45, cylindrical bodies rolling over one another, plastic deformations caused by frictional forces 80−11735
steel, Co-Cr-Ni-Mo-Mn (39.65, 20.25, 15.33, 7.08, 1.9 wt.%) carbide formation during tempering after plastic deformation 80−16330
steel, cold drawn wire, anisotropic fracture *(Russian)* 77−1867
steel, cold strained, defects interaction with carbide strengthening phases, carbide decomp. degree *(Russian)* 80−84955
steel, cold worked, original struct. effect on softening during heating 80−60882
steel, cold-worked, alloying elements effect on cementite decomp. during plastic deform., Mossbauer study 79−82900
steel, cold-worked, state of cementite, nucl. gamma reson. meas., plastic deform. *(Russian)* 78−68706
steel, Cr, and Cr-Mo-Ni, austenite decomposition, deform. effects, ferrite reaction 79−1842
steel, Cr, phase transform., effect of high temp. plastic deform. *(Slovak)* 78−19837
steel, Cr, post-hotforming recrystallisation condition, use of NEOPHOT 2 and EPIQUANT 80−84949
steel, Cr, previous deformation influence on strength, ductility, in biaxial tension, low temps. 79−90718
steel, Cr (3.51, 3.74, 3.56 wt.%), bainite transform. of deformed austenite 77−32574
plastic deformation continued
steel, Cr-C, (2.14, 1.08 at.%) tempered, resistance to small plastic deformation, strain relaxation *(Russian)* 78−56698
steel, Cr-C (3.74, 0.86 wt.%), stress assisted bainitic transform. *(Czechoslovakian)* 77−32573
steel, Cr-Cu-Mn, fatigue crack propag. rate eval. by J integral method *(Japanese)* 79−8346
steel, Cr-Mn, effect of composition, plastic deformation, and heat treatment on martensitic transformation 79−100141
steel, Cr-Mn, unstable austenite, martensitic transform., effect of alloying, heat treatment, and deform. 78−19751
steel, Cr-Mn, X-ray diffr. exam. of fine struct. during deform. *(Russian)* 78−38661
steel, Cr-Mn(Ni), Mn and Ni additions, effect on corrosion resistance and hardness 80−104342
steel, Cr-Mo-V, biaxial cyclic deformation behaviour 80−21057
steel, Cr-Mo-V, creep deform. under const. and cyclic temp. 79−38914
steel, Cr-Mo-V, influence on brittle failure resistance 78−72858
steel, Cr-Mo-V, normalised and tempered, size and geometry effect on creep cracking behaviour 78−64630
steel, Cr-Mo-V (0.5, 0.5, 0.25 wt.%), creep crack growth at 565°C 77−73323
steel, Cr-Mo-V and stainless, biaxial cyclic deformation behaviour 80−16431
steel, Cr-Mo-V pressure vessel, microstruct. parameters and yielding rel. to plastic deform. 80−89318
steel, Cr-Ni (1.47, 1.48 wt.%), lath martensite microstruct. and props., cold rolling effect 80−55422
steel, Cr-Ni and Cr-Mn, laws governing discontinuous yield under tensile strain in liquid He 77−63760
steel, Cr-Ni-(Mn), mech. props. at low temp. 77−70118
steel, Cr-Ni-Mo, dynamic and static softening behaviour at hot forming temp. *(German)* 80−25728
steel, Cr-Ni-Mo-V, austenite form. during heating, influence of recrystn. during tempering *(Russian)* 80−104188
steel, Cr-V (1.5, 0.5 wt.%), ferritic, effect of temp. and microstruct. on creep damage 79−5023
steel, crack propagation, struct. effects 79−52370
steel, creep resistant, AISI 304, residual lifetime assessment by low cycle fatigue testing *(German)* 78−15485
steel, CrMoV, creep and creep strength under alternate tension/compression *(Czech)* 77−63728
steel, deform. resist., softening effects, analytical depend. calcs. *(Russian)* 80−49293
steel, deform. resist. during continuous hot rolling *(Russian)* 80−55462
steel, deformation and fracture resistance due to low-cycle fatigue in plane bending 79−66166
steel, deformation and stresses during elongation, application of Ludwig eqn. *(German)* 80−40475
steel, deformation anisotropy in yield point, precompression effects *(Russian)* 78−11268
steel, deformation at large plastic strains, work hardening rate 79−20065
steel, deformation under modified ausforming *(Japanese)* 79−11673
steel, deformation under mutual indentation in contact with Li melt *(Russian)* 77−59853
steel, deformed, Kh18N10T, ageing under gradually increasing load 77−90383
steel, deformed strain-aged St.3 and 09G2S, stress conc. susceptibility, H_2 effect 78−95774
steel, ductile fracture in presence of elongated sulphides *(French)* 80−45394
steel, ductile struct., crack propag. 78−68805
steel, elastic-plastic fracture, plastic zone correction application 79−70147
steel, En 24, Cr, V, deform. effect on decomp. of austenite, carbide precipitation 80−84938
steel, endurance, effect of surface diffusion alloying 77−81344
steel, eutectoid, anisothermal strain with phase transform., effect on tensile strength *(Russian)* 80−40431
steel, extra mild, thin sheet, biaxial tensile deform., effect on crystallographic texture *(French)* 77−59814
steel, extra mild, use of limiting forming curves, deform. distribution, assessing deep drawability *(French)* 77−21232
steel, fatigue, low cycle, test results, least square deviation method 77−63796
steel, fatigue crack tip plastic deform., X-ray diffr. investigation *(Russian)* 80−104251
steel, Fe-Mn-C austenitic, deform. twinning and mech. props. 77−59868
steel, ferrite-pearlite, ductile fracture, pearlite colony morphology and hydrostatic press. effect *(Japanese)* 78−15510
steel, ferritic martensitic, effect of ductility of second phase on ductile fracture 78−19847
steel, flat bars, stress meas. and calc. around drilled hole, with hole-gage-rosettes aid *(German)* 80−25757
steel, grain boundary strengthening mechanism 80−35207
steel, Hadfield, cast and crystallised, deform. resist. of grain boundaries *(Russian)* 77−21216
steel, hardened, exoelectron emission from torsion fatigue damage 77−86142
steel, hardness, tensile and impact props. correlation, at low temps. *(Japanese)* 77−52413
steel, heat resistant, cyclic determ. at elev. temps. 79−66125
steel, heat resistant Kh15N24VChT, microscopic intergranular crack form. prediction in high temp. deform. 77−81325
steel, heat treated, deform. due to thermal gradient *(French)* 79−61631
steel, high alloy, strain induced martensite and austenite influence on crack formation *(Russian)* 80−21007
steel, high C, 80Kh5G5 and 120N12, austenite hot deform. effect on martensitic transform. *(Russian)* 77−48434
steel, high C, type 7KhFNSh, plastic deform. influence of X-ray interference line breadth *(Russian)* 80−93599
steel, high Mn, mech. props., strain induced martensitic transform., effect of austenite predeformation 77−16649
steel, high Mn alloy G22, phase transform. during plastic deform. 77−16576
steel, high Ni, orientational variations of martensite transform. during deform of metastable austenite 78−84805
steel, high Si dual-phase, mech. props and microstruct. anal. 80−40444
steel, high speed R6M5, secondary inheritance investigation by austenite recrystallisation 77−90367

plastic deformation continued
steel, high speed R6M5K5, excess carbide size and distrib. effect on grain size 77−90356
steel, high speed tool, diffusion wear model 79−29230
steel, high strength, low alloy, response to cyclic plastic deform. 78−7035
steel, high strength, plastic deform. and fracture under tensile stress *(Russian)* 77−70100
steel, high strength 0.77%C, surface dissolution effect 77−8883
steel, high strength and low C, deformation, tension, torsion compression test exam. *(Russian)* 78−31455
steel, high-speed, 30Kh2N2SMKt, deform. effects on physicomech. props. 78−23741
steel, high-speed, cast, mech. props. at high temps. 79−20135
steel, high-speed, N effects on struct. and props. 77−59799
steel, high-strength, strain relax., model *(Spanish)* 77−73296
steel, high-strength plate with soft cladding layer, failure resistance during repeated static banding 77−44406
steel, high-strength structural type StE47, specimen geometry and plastic deform. effect on fracture mechanics *(German)* 80−66613
steel, high-temperature thermomechanical treatment, holding after deform. effect on strengthening 79−38868
steel, hollow cylinder, thick walled, effect of thermomech. treatment 80−11674
steel, HT60, fatigue crack propag. work coeff. 80−16422
steel, HY140 and HY180, fatigue crack init. at notch tip, early stage propag. *(Japanese)* 78−7021
steel, hypereutectoid, austenite dissociation depend. on strain at intercritical temps., pearlite transform. *(Russian)* 80−40362
steel, hypoeutectic, texture development from frictional stress *(German)* 78−53003
steel, inclusions effect on distrib. of local microheterogeneous deform. *(Russian)* 78−80586
steel, inelastic deform. mechanism, fatigue testing in air and corrosive environments *(Russian)* 79−52432
steel, intermediate class Kh16N6, structural aspects of work hardening 77−90369
steel, ion plated Pb film covered, Hertzian contact expt. 77−52511
steel, Kh2G2P, high-temp. plastic strain influence on austenite transformation kinetics *(Russian)* 80−21004
steel, KhN77TYuR, deform. parameters effect on plasticity and resist. to deform. 77−63750
steel, laser erosion value depend. on metallic props. anisotropy during plastic deform. *(Russian)* 78−31452
steel, leaded, resulphurised, deform. index of MnS inclusions 77−66683
steel, ledeburite, fracture during hot plastic deformation exam. 78−56755
steel, low alloy, acoustic emission during ductile fracture, isothermal tempering effect 79−83241
steel, low alloy, fatigue crack nucleation under high cycle fatigue and uniaxial loading 79−79060
steel, low alloy, hot deform. behaviour and modified ausforming *(Japanese)* 78−11244
steel, low alloy, quenched and tempered, formation of stony fracture during forging 79−79059
steel, low alloy, type 4340, quenched and tempered, effect of plastic strain followed by ageing, on torsion fatigue resistance 78−92360
steel, low alloy composite, ferrite-carbide struct., cold plastic deform. 77−90408
steel, low alloy type 10KhSND, resist. to low-cycle deformation at low temps. 79−87696
steel, low alloy-high strength, deforms. during cold crack developments in welded joints 80−81142
steel, low and medium C, dynamic and static strength, strain rate and temp. depend. of flow stress 80−85139
steel, low and medium C, fatigue failure, inelastic response, energy criterion 77−73333
steel, low C, 10Kh2G3M, development of plastic deform., slip and dislocation struct. *(Russian)* 79−15722
steel, low C, alloy, structural transform. during deform. and annealing *(Russian)* 79−91707
steel, low C, appl. of microbeam X-ray technique to plastic zone size evaluation 80−3199
steel, low C, bainitic, optimal struct., heat treatment effects 77−16624
steel, low C, brittle fracture susceptibility, low temp. deform. effects 77−56103
steel, low C, carburizing, hot plastic deform. effects 77−90377
steel, low C, cold rolled and recrystallised, containing Nb(CN) dispersion, struct. and textural aspect of deform. 79−47712
steel, low C, cold rolled sheet, Cu effect on recrystallization texture *(Chinese)* 79−74173
steel, low C, cold swaged, exam. of H_2 attack mechanisms 78−76791
steel, low C, corrosion, heat treatment and plastic deform. effects 77−63825
steel, low C, Cr-Ni (25, 25 wt.%), σ phase form., prestrain effects *(Japanese)* 78−92260
steel, low C, creep, prestrain effects *(Korean)* 77−21227
steel, low C, deformed, comp. of precipitated carbonitrides, X-ray diffr. anal. *(Russian)* 79−20051
steel, low C, dynamics of cyclic plastic deform. and fatigue life at low temps. 77−16670
steel, low C, dynamics of cyclic plastic deform. at low temps. *(Czechoslovakian)* 77−32679
steel, low C, fatigue life, variable strain ranges *(Czech)* 80−60956
steel, low C, ferrite grain size effect on cyclic stress-strain response 79−100203
steel, low C, hardness correl. with macrostress intensity under plastic strain 79−87708
steel, low C, hysteresis loop behaviour under fatigue load, dislocations model 79−74197
steel, low C, initial stages of plastic deform. *(Japanese)* 80−93618
steel, low C, low cycle fatigue, cumulative damage, absorbed plastic energy anal. 79−38932
steel, low C, Mn, recrystallisation and grain growth in hot rolling 79−47714
steel, low C, Mn-Nb, quenched and tempered, microstruct. and props. 77−36549
steel, low C, nucleation and increase of discontinuities in environment of non-metallic inclusions *(Polish)* 79−79022
steel, low C, plastic deformation by pencil glide, r-values and yield loci 80−7654
plastic deformation continued
steel, low C, plastic props., fracture, effect of strain rate in static tensile tests *(Czech)* 77−59866
steel, low C, push-pull fatigue strength, effect of tensile preload on plastic strain range *(Japanese)* 78−64625
steel, low C, quench-hardened, plastic deform. effect on mech. props. and struct. *(Russian)* 77−70102
steel, low C, quenched, hardening during explosive forming 79−87650
steel, low C, quenched, struct. and props. after plastic deform. and tempering 78−23734
steel, low C, rolling deform., effect on NbC particle size distrib. 79−47717
steel, low C, structural, AE rel. to crack tip plasticity *(Japanese)* 79−66150
steel, low C, texture hardening in maximum shear planes during expansion 79−91704
steel, low C, type 08Yu, influence of nonmetallic inclusions on microfailures, during strain *(Russian)* 79−34128
steel, low C, type En3, high strain deform., struct. and props. 80−89301
steel, low C and mild, fatigue deformation, phenomenological exam. 78−64691
steel, low C type 08KP, plastic deform. depend. on grain size *(Russian)* 80−66580
steel, low-alloy, BCC lattice, texture form. by drawing and pulling through nonpowered rolls *(Russian)* 77−25100
steel, low-alloy, plastic deform. mechanisms under dynamic loading 80−100883
steel, low-alloy, study of deformation and fracture processes by acoustic emission transient anal., SEM and optical microscopy study 79−43311
steel, low-C, ferritic, deform. microstruct., electron microscopy *(German)* 78−64589
steel, low-C, phosphorus effect on annealing texture, plastic anisotropy and mech. props. 77−25069
steel, low-C, preliminary thermomech. treatment, cold deform. effect on struct. and props. 79−38847
steel, low-C contaning Ti, sheets, recrystn. texture effects on plastic strain ratio and deep-drawing *(Chinese)* 80−66527
steel, low-temperature tempered, shock wave loading effects on mech. props. *(Russian)* 77−59857
steel, marageing, austenite formation, stability, transformation to martensite *(Russian)* 79−91646
steel, maraging, ageing kinetics and struct. of N12K7M5TYu, effect of high temp. deform. of austenite *(Russian)* 80−84960
steel, maraging, and HY-80, deform., hydrostatic pressure effect 77−36596
steel, maraging, plastic deform. effects on ageing kinetics *(Russian)* 77−77508
steel, maraging, steady state unidirectionally solidified, austenite reversion and determ. 77−25118
steel, martensitic, Cr-Ni deform., effect of phase composition and struct. *(Russian)* 77−25102
steel, martensitic, fatigue life, low-cycle, temp. and strain rate effects 80−85056
steel, martensitic, medium alloy, quenched state, deform. hardened, ageing effects *(Russian)* 77−21179
steel, martensitic, submicrostructure alterations in ageing and plastic deform. *(Ukrainian)* 79−79032
steel, martensitic transformation, lattice deform. 78−27511
steel, martensitic-aged, plastic deformation influence in type N17K12M5T steel on mech. props. *(Russian)* 80−76305
steel, medium and high C, deformation ageing, entropy, free energy, dislocations *(Russian)* 80−66581
steel, medium C, deform. hardening, plasticising action of Sn-Zn melts 80−55415
steel, medium C, deformed, H_2 enhanced load relaxation 79−61635
steel, medium C, difference between strain energy changes during repeated bending and rotatory bending fatigue tests *(Japanese)* 78−39894
steel, medium C, isothermally quenched, high-temp. deform. effects on struct. and props. *(Russian)* 80−25760
steel, medium C, low-cycle fatigue effect of mean plastic strain and stress factor 77−63766
steel, medium C, microflow and strain hardening under cyclic loading 80−104182
steel, medium Cr, B effects on struct. and toughness 77−21265
steel, microalloyed, hot-rolled, Nb(C,N) precip. and austenite recrystn. 80−97513
steel, microplastic deform. meas. in grains of polycryst. substances 77−77665
steel, mild, 1019 AISI, acoustic emission generated during deform. 80−60921
steel, mild, cantilever beams, structural response under random loading conditions, memory model 77−3784
steel, mild, cold rolled, texture and plastic anisotropy rel. to alloying and precipitation *(French)* 80−108475
steel, mild, conical rider on Cu surface, SEM exam. of plastic deformation and wear at friction junction 78−88542
steel, mild, cyclic plastic deform. effect on electrode reactions in aq. chloride soln. of varying pH 77−52548
steel, mild, cyclic strain enhanced dissolution in NH_4NO_3, corrosion fatigue props. 80−85083
steel, mild, deformation texture *(French)* 79−70082
steel, mild, dynamic plastic loading of frames 79−20117
steel, mild, etching method for revealing plastic deformation 78−72825
steel, mild, fatigue crack propagation, stress ratio effect 80−71733
steel, mild, large deform. of thin walled tubes under transverse loading 77−36567
steel, mild, orientation distribution function, representation of texture and slip directions 80−11665
steel, mild, plastic deform. and pitting corrosion in neutral media 79−52415
steel, mild, plastic deform. around fatigue cracks, X-ray microbeam and recrystn. studies 80−35258
steel, mild, plastic deform. during fatigue, detection by Barkhausen noise meas. 79−43524
steel, mild, plastic deform. energy const. 77−32658
steel, mild, plastically pretorsioned, dynamic props. 79−83267
steel, mild, stress/strain relation formulation for plastic deform. for strain trajectroy 78−52913
steel, mild, temperature monitoring system used during mech. deform., stress anal. appl. 79−12796

plastic deformation continued
steel, mild, tensile and cyclic loading effect in Barkhausen noise 80−40560
steel, mild, tensile deformation, behaviour under high pressure *(Japanese)* 80−16381
steel, mild, tubes between rigid plates, lateral compression, strain hardening effect 78−48422
steel, mild, with different sensitivities to strain ageing, cyclic plastic strain amplitude *(Japanese)* 77−8932
steel, mild and HSLA, mech. behaviour, deform. rapidity influence *(French)* 79−57056
steel, mild cylindrical shells, limit loading under loop bending moment 78−80581
steel, mild explosively welded, 0.1% C tube to 0.2% C plate, microstructure 77−70221
steel, Mn, Mn influence on martensitic transform in presence of strain *(Russian)* 80−20934
steel, Mn, plastic deformation, shape recovery during γ to and from ε, ε' transformations *(Russian)* 79−83196
steel, Mn (13.5 wt.%) hardening mechanism during friction 79−96152
steel, Mn-Cr-B (1.46, 1.03, 0.003 wt.%) 80−55422
steel, Mo and MoCr, X-ray elastic consts. as function of plastic strain *(German)* 78−31436
steel, N32, $\alpha \rightarrow \gamma$ transform., struct., texture conc. var. depend. on plastic deform. *(Russian)* 79−66050
steel, Nb,(V),(Al), hot-rolling, laboratory simulation, recrystn. of austenite 80−97512
steel, Nb-stabilised, orientation depend. of cell size and recrystallisation texture development 79−91682
steel, Ni(9 wt.%), isothermal bainitic transform., thermomechanical effects on mech. props. *(German)* 80−40383
steel, Ni (17 wt.%), martensitic deform. temp., cryst. struct. effect *(Russian)* 80−66576
steel, Ni (9 wt.%), tempered, mech. stability of retained austenite 79−24521
steel, Ni-(Cr)-Ti, thermomechanical and heat treatment effects on retained austenite *(Russian)* 77−66661
steel, Ni-Co-Mo (17.55, 8.02, 4.92 wt.%) maraging, lath martensite microstruct. and props., cold rolling effect 80−55422
steel, Ni-Cr, 36NKh, thermal expansion under stress at −253°C 78−22871
steel, Ni-Cr, case-hardened roller, rolling contact fatigue life, effect of changing rolling direction 77−77519
steel, Ni-Cr-Mo, quenched and tempered, nothced bar tensile tests *(German)* 80−35247
steel, Ni-Cr-Mo-V, corrosion fatigue crack growth in NaOH soln., cathodic pot. effect 80−89403
steel, Ni-Cr-Mo-V, temper embrittled, crack initiation strength *(Japanese)* 77−52474
steel, Ni-Cr-Ti, thin bands, cold working, props. and struct. of 36NKhTYu 79−78994
steel, Ni-Mn directional martensitic transform expt. 79−11613
steel, Ni-Mn-C, austenitic, proof stress change meas. by internal friction with martensitic transform. 78−56638
steel, Ni-Ti-Al, 36NTYu, heavily deformed, subgrain struct. due to discontinuous precipitation of γ' phase *(Russian)* 79−52218
steel, non-alloy, work hardening due to shearing *(French)* 78−15423
steel, nonpropagating fatigue cracks, in steel component strenthened by surface plastic deformation, anal. 78−88529
steel, pearlite, deform. and fracture mechanisms, HV SEM obs. 80−104243
steel, pearlitic, deform. microstruct. and cementite fracture, −196 to 700°C 78−27576
steel, pearlitic, heat-resist., secondary phase precipitation, deform., and fracture during creep *(Russian)* 80−50669
steel, pearlitic, strength, fracture, microstructure effect 77−40449
steel, pearlitic, struct. variations under plastic strain and subsequent heating, cementite decomp. *(Russian)* 80−84954
steel, pearlitic or spheroidal plastic deform. and fracture *(French)* 78−35448
steel, phase separation, effect of plastic deform. and heat treatment *(Polish)* 78−92295
steel, plastic anisotropy coeff., effect of strain rate 77−25097
steel, plastic deform., density changes *(German)* 80−60908
steel, plastic deform. effect on third-order elastic moduli, dislocation anharmonism *(Russian)* 80−50786
steel, plastic deform. resist., three-cam plastometer meas. 79−87792
steel, plastic deformation, C distrib. *(Ukrainian)* 80−50668
steel, plastic deformation and cryst. texture in equibiaxial expsn. 80−7653
steel, plastic deformation zone, caused by crack, extent determ. with microhardness, surface roughness, measurements *(French)* 80−7682
steel, plastic loosening and deform. defect healing during recovery annealing of 12Kh18N10T *(Russian)* 80−66530
steel, plastic props., room temp. to recrystallisation temp., stress-strain relations, computer program 77−1865
steel, plastic working of wires, high-density current appl. 79−57002
steel, plastically deformed, force and speed criteria interactions during hot rolling *(Russian)* 80−55463
steel, plasticity of grooved specimens at high temp., rel. to hot forming 78−23902
steel, powder, rotary forging, porosity and deform. 78−23646
steel, pressurised tubes under dynamic bending and torsional loading, inelastic deform. 77−77549
steel, problems of X-ray determ. of dislocation density from one diffraction line *(German)* 78−2129
steel, quasi-cleavage fracture *(Chinese)* 80−21060
steel, quench-hardened, exam. of anomalous plasticity when deformed *(Russian)* 79−11663
steel, quenched, martensite, tensile and compressive deform. resist. *(Russian)* 78−19819
steel, quenched and tempered 52100 bearing, plastic deform. in compression 77−40437
steel, reheat cracking in weld zone, method for evaluating sensitivity to cracking 78−72855
steel, relaxation of residual stress with fatigue loading 77−56051
steel, ShKh15, carbide particle size and pearlite grain size changes *(Russian)* 78−6946
steel, soft, explosive deform. and destruction of tubes 78−6995
steel, spheroidised AISI 1095, U-notched bend specimens, hydrogen effect on fracture 79−52363

plastic deformation continued
steel, spring, 60C2A, tempered under stess, influence of tempering conditions on mech. props. *(Russian)* 79−47724
steel, spring alloys, microplastic deform. and endurance limit 80−81197
steel, spring wire and springs, type 60S2A and 50KhFA, stress tempering effect on mech. props. 79−66085
steel, stainless, 0Kh12G14N4Yu2, effect of plastic deform. on biphase struct. 78−44176
steel, stainless, 20% cold worked type 316, creep deform. 77−66688
steel, stainless, 304, deformed in torsion, annealed, static recrystallization and restoration after hot deform. 79−47735
steel, stainless, 316, intergranular crack growth by diffusion 79−24608
steel, stainless, 316, nuclear fuel cladding, crack nucleation 78−72864
steel, stainless, 36NkhTYu, heavily deformed, subgrain struct. due to discontinuous precipitation of γ' phase *(Russian)* 79−52218
steel, stainless, $\alpha+\gamma$ phase, tensile deform. induced α' martensite, morphology 78−44122
steel, stainless, AISI 304, dislocation struct., carbides, deform. mech. map 77−16650
steel, stainless, AISI 304, dislocation substruct. around fatigue cracks, SEM obs. 78−15516
steel, stainless, annealed 310, deform. at erosion sites, TEM and SEM studies 78−64725
steel, stainless, austenite stability, deform. rel. to $\gamma \rightarrow \alpha$ transform. kinetics 79−24522
steel, stainless, austenitic, Cr-Ni-Mn-Si-Mo-C alloy, 13Khi8N10G3S2M2, elastic moduli exam. after thermomechanical treatment *(Russian)* 79−24558
steel, stainless, clad Al, sandwich sheet material, forming limits 80−3131
steel, stainless, cold plastic deform. effect on struct. and props. 80−29113
steel, stainless, cold worked, pitting corrosion in NaCl soln. 78−44257
steel, stainless, Cr-Mn (21, 14 wt.%), grain boundary precipitation and fracture *(Japanese)* 79−100149
steel, stainless, Cr-Ni, for cryogenic engineering, mech. props. 78−11240
steel, stainless, Cr-Ni, low temp. plastic deformation, in mag. field 79−83256
steel, stainless, Cr-Ni type, low temp. plasticity, effects of deform. rate and cooling conditions 77−70099
steel, stainless, creep test at elevated temps., based on state variable theory 79−61687
steel, stainless, deformation, rapid dynamic, at −196°C 80−104220
steel, stainless, deformation temp. determ. for high yield strength 78−44177
steel, stainless, diffusive crack growth under plastic deform. 79−20182
steel, stainless, EBR-II fuel pin cladding, obs. of in-reactor creep and swelling 80−13600
steel, stainless, failure analysis at elevated temperatures 80−55499
steel, stainless, fatigue, influence of ageing and plastic deformation *(Russian)* 79−15857
steel, stainless, FBR fuel pin cladding strain under transient testing 80−18425
steel, stainless, ferritic, 18%Cr, stress/strain curve, H_2 charging influence, room temp. *(Japanese)* 78−39884
steel, stainless, ferritic, anisotropic lamellar fracture mechanism 78−64639
steel, stainless, ferritic, roping phenomena and tensile strain direction 77−90406
steel, stainless, ferritic, roping phenomena and tensile strain direction 77−90407
steel, stainless, ferritic Ti stabilised, changes in structure and mech. props., after alkali bath etching *(Russian)* 79−29271
steel, stainless, fibre reinforced Al alloy, exam. of deformation, fracture and forging behaviour 80−11681
steel, stainless, fibre reinforced wustite, strength and toughness 78−27602
steel, stainless, fracture and crack tip plastic zones, in situ obs. 80−108686
steel, stainless, grain growth after deform. by rolling, C effects on kinetics *(French)* 77−28866
steel, stainless, high temp., smoothing for plastic pre-straining of material cut by turning *(Russian)* 80−60911
steel, stainless, hot rolling resist., multistage mode of deform. effects *(Russian)* 78−80583
steel, stainless, in-reactor deformation and fracture behaviour of EBR-II driver fuel cladding 80−42769
steel, stainless, in-situ obs. of deform. in HVEM 80−103338
steel, stainless, inelastic deformation, generalised strain rate dependent constitutive eqn., load relaxation tests 79−11655
steel, stainless, Kh18N10T, struct. and mechanical props., effect of previous deform. in rolling *(Russian)* 79−29099
steel, stainless, Kh18N10T, substructure after high-temp. thermomechanical treatment with high deformation rates *(Russian)* 78−76657
steel, stainless, Kh18N10T surface treatment by plastic deform. effect on gas evolution and H_2 permeability *(Russian)* 79−15853
steel, stainless, martensite nucleation and growth, expt. study 78−3125
steel, stainless, martensite nuclei obs., role of defects in nucleation 80−25693
steel, stainless, martensite to austenite transform. at various heating rates *(Russian)* 78−76649
steel, stainless, martensitic, ageing, strength/structural charact. relationship 77−90426
steel, stainless, metastable, determ. of strain-deform. martensite content 78−3282
steel, stainless, microduplex, austenite/ferrite, recrystallisation, annealing and cold work effects 79−47713
steel, stainless, phase instability effect on cladding deform. profile of LMFBR fuel elements 77−74921
steel, stainless, prestrained, heat treatment effect on fatigue strength *(Czech)* 78−60747
steel, stainless, recrystallisation of thin bands, heating time investig. 79−38848
steel, stainless, reversibility of plastic strain during fatigue with martensitic transform. 78−31526
steel, stainless, sensitised type 304, cyclic loading effect of SCC susceptibility in water 80−45428
steel, stainless, sheet, deformation charact. determ. test *(German)* 79−24569
steel, stainless, single crystals, shear cracks, electron microscope study 80−40522
steel, stainless, solution annealed 304L, in-reactor deform. 77−42076

plastic deformation continued
steel, stainless, spherical shell with reinforced holes, local stability 80−50686
steel, stainless, stress corrosion testing, slow strain rate, elevated temp. and high press. study 80−97615
steel, stainless, SUS 304, acoustic emission signals in plastic deform., amplitude distrib. *(Japanese)* 78−6978
steel, stainless, type 304, description of deformation induced plastic anisotropy 79−43268
steel, stainless, type 304, hydrogen assisted cracking, martensite formation on deformation effects 79−52362
steel, stainless, type 304, viscoplastic model, uniaxial, based on total strain and overstress 80−64387
steel, stainless, type 309, low-cycle fatigue, effects of notches on crack initiation 79−74249
steel, stainless, type 316, cold worked effect of prior neutron induced creep on burst strength 78−62599
steel, stainless, type 316, low cycle fatigue props. in vac., fracture mode 80−85021
steel, stainless, type Kh17N13M2T, strengthening by plastic deformation and cold working *(Russian)* 78−52839
steel, stainless 18KhNMA, microplastic deform. *(Russian)* 77−66681
steel, stainless 18N10T, electroplastic drawing, deformation zone current delivery schemes 79−91761
steel, stainless 304, explosive loading technique for uniform plastic expansion at high strain rates 80−81273
steel, stainless 304, recrystallisation, effect of dislocation structure 77−32595
steel, stainless 304, shock loading response, grain size effect 77−36601
steel, stainless 304L, plastic deform., accelerated evolution of H_2 77−36594
steel, stainless 316, carbide precipitation rel. to in-reactor deform. 79−8302
steel, stainless 316, cladding failure during thermal transients 79−8316
steel, stainless AISI 316, biaxial cyclic deformation behaviour 80−21057
steel, stainless brittle zone Al 3 component composites deform. and fracture 77−56104
steel, stainless electroplastic drawing 79−20142
steel, stainless SUS 304, fatigue crack propag. work coeff. 80−16422
steel, stainless type 03Kh13AG19, deformation temp. influence on dislocation struct *(Russian)* 80−11698
steel, stainless type 304 L, mech. behaviour under constant stress associated with cyclic strain 80−25767
steel, stainless type 316, in-situ HVEM studies under ion beam irradiation 80−103396
steel, stainless type 316, prediction of transient mech. response using equation of state approach 79−74207
steel, stainless/Al laminate, sandwich sheet material, plane strain compression and rolling 79−57062
steel, strain hardening, weakening factor 1273-1473K *(Russian)* 79−78990
steel, strengthened, high temp. deform. line charact. *(Russian)* 77−25099
steel, strengthened by surface plastic deform., tempering effect on physicomech. props. *(Russian)* 78−35409
steel, stress and strain intensity, determ. after plastic deform. using microhardness meas. 80−40641
steel, stress meas. device *(German)* 78−3261
steel, stress relaxation in cyclic deformation 80−3119
steel, stress/strain diagrams of structures 79−87703
steel, structural, effect of stressed state nature on ductility and failure 79−57078
steel, structural, exam. of mech. props. when under impulsive loading *(Czech)* 79−91742
steel, structural, influence of deform. heat on the mech. props. *(German)* 78−84904
steel, structural, strained in tension after tempering, compression effects on struct. changes *(Russian)* 80−66577
steel, structural, temp. increase during plastic deform. *(German)* 78−84903
steel, structural, wide plate tensile testing eval. *(German)* 80−100969
steel, structural changes after deformation and annealing, Mossbauer spectroscopic exam. *(Russian)* 78−35446
steel, tempered, high strength, internal stresses and mech. props. 80−3200
steel, tempered, notched, impact bending tests, cold brittleness curves 80−71758
steel, tempering effect on fatigue strength 80−60891
steel, thermally and thermomechanically treated, struct. and decomposition of martensite 78−19784
steel, thermomechanical treatment effect on mech. props. and microstruct. *(French, German)* 79−66090
steel, thread rolled, Moire fringe method for examining local deform. zones 80−21220
steel, transformations, influence of type of cold plastic strain *(Russian)* 79−52232
steel, transforms CC types M6 and M3N, elastoplastic bending, insulating coating influence on magnetic losses *(Russian)* 79−100284
steel, TRIP, fatigue strength 80−108552
steel, TRIP, strengthened by hydrostatic extrusion, struct. and mechanical props. *(Russian)* 78−76647
steel, two-phase austenitic-ferritic, plastic deformation under hot working conditions 77−48466
steel, type 1045, hydrogen enhanced nucleation of microvoid as function of local plastic strain 79−79053
steel, type 10G2SAF, yield strength, influence of deform. rate *(Bulgarian)* 80−89315
steel, type 12KhN4MDA, deformation and fracture props. on extension and twisting *(Russian)* 80−55504
steel, type 15Kh2NMFA, strain ageing effect on strength and toughness, susceptibility to strain hardening 79−57028
steel, type 1Kh17N2, white zone formation and props. during friction in vac. *(Russian)* 80−40542
steel, type 1Kh18N9T, stress state form influence on creep and plasticity charact. rel. to cyclic stress intensity change 79−87694
steel, type 20Kh deformed, austenite grain size, inheritance effect with quenching and tempering 80−60881
steel, type 4340, shear-band temp. meas. 80−48655
steel, type 4Kh5MFS, 5KhNM, 5KhNMFS, stress conc. effect on low-cycle fracture results 79−87697

plastic deformation continued
steel, type 55SM5FA, formation of hardened layer during burnishing 78−85046
steel, type AISI 4340, quenched and tempered, U-notched bend specimens, effect of H_2 on fracture 79−61716
steel, type KVK, deform. strengthening of bayanite phase *(Russian)* 80−100851
steel, type N18K9M5T, maraging, rate of movement change of fatigue cracks as result of ageing *(Russian)* 79−70149
steel, types 45 and U8, plastically deformed, magnetoelastic props. *(Russian)* 80−44893
steel, V containing dual-phase, yielding and strain ageing, early stages 80−25794
steel, V strengthened dual phase, deform. and fracture props. 78−48467
steel, W-Mo, high speed, hot deform. and heat treatment effect on props. 77−90372
steel, X-ray and microhardness meas. at high strain rates *(German)* 78−3184
steel, Zn coated, cold rolling influence on struct. and deform. of diffusional layer *(Russian)* 80−55465
steel, Zn coated strips, plastic deform. influence on struct. and quality *(Russian)* 80−40377
steel *(German)* 80−100869
steel 18 Gps, ductile fracture, rel. between plastic deform. in fracture zone and fracture charcts. *(Russian)* 77−52457
steel 20, deformability, H_2 absorption effects *(Russian)* 77−77561
steel 20, deformation process, stage-by-stage nature investigation using acoustic emission *(Russian)* 80−40434
steel 2Kh13, damping props., effect of plastic deform. by torsion 77−70095
steel 45, B-Al coated, creep and long term strength in NH_3 79−91854
steel 45, fractional fatigue, microcrack formation in surface layers 77−86193
steel A-106, yield point suppression by H_2 79−8368
steel austenite, recrystallisation diagrams, heating, plastic deform. rel. to struct. 79−20067
steel austenitic stainless, fatigue, low cycle, temp. and strain rate effects *(Japanese)* 79−29198
steel bar, in four point bending machine, measurement using holographic interferometry 79−34266
steel bar deformation meas. by holographic interferometry using four point bending machine 78−60721
steel bar with inhomogeneous props. of lagging creep, deform. 79−15731
steel beams, inelastic, mild, flexural behaviour and lateral buckling anal. under cyclic loads *(Japanese)* 78−87283
steel C60, machined, surface morphology, struct., SEM, topographic investigs. *(German)* 77−73372
steel C, fatigue life and cumulative fatigue damage under const. stress cycling, plastic strain range effect *(Japanese)* 77−8940
steel C, fatigued, strengthening by surface plastic deformation 78−88505
steel cold plastically deformed, exam. of structure of diffusion layers after borating *(Russian)* 79−34054
steel cylindrical bar loaded by longitudinal impact, dislocation struct. and plastic deform. *(Czech)* 78−60713
steel EI736, creep, viscosity, resist. to inelastic deform. 80−89309
steel fatigue in surface active media, adsorption facilitation mech. 80−55586
steel fibre reinforced Ag, exam. of recrystallisation behaviour *(German)* 78−84849
steel fibre reinforced epoxy composite, static tensile behaviour *(Japanese)* 78−15482
steel fibre reinforced Pb, fabrication, mech. props. *(Korean)* 77−12579
steel granular model material, equipment for shear deform. investigation *(German)* 80−35449
steel HF-1, acoustic emission during extension, frequency content variation 77−81301
steel ingot, state of viscoelasticoplastic stress deformation, in process of solidification *(Russian)* 80−45295
steel Kh, work hardening under nonisothermal loading 79−57005
steel low C, notched, fatigue strength, crack propagation, plastic torsional prework depend. *(Japanese)* 79−15744
steel M16C, low C, natural discrete microlamellar composite *(Russian)* 78−39810
steel mild, plastically deformed, X-ray meas. of stress and TEM 77−48496
steel moulds for die-casting Al alloys, thermal fatigue 79−24619
steel N22, crack movement rate during cyclic deform., internal microstress effects 78−3225
steel nitriding, distortion prediction, appl. 79−24663
steel notched rods in tension, 20-700°C, yield conditions *(Polish)* 78−80604
steel piping components, incremental collapse tests, structural behaviour 77−6526
steel reinforced concrete, local bond-stress/slip relationships under repeated loading 79−20123
steel spheroidised type AISI 1090, hot rolled H_2 promotion of plastic instability 78−60725
steel SS-41, plastic working with vibr., US hardness tester 78−53044
steel St3kp, deformability at 600 to 950°C 77−70117
steel stainless, plastic deform. of single crystal, contribution of $\gamma \rightarrow \varepsilon$ transform. 77−52394
steel strips, elec., grain-oriented, effect on stress-relief annealing treatments on permeability and ageing 78−23832
steel structural bars, subjected to plastic bending, random fatigue analysis *(Japanese)* 78−27619
steel structure in elec. furnace, distortion meas. by noninterferometric optical probe 77−74362
steel SW7M, low-cycle fatigue at high hardness levels *(Polish)* 80−89323
steel tearing rate determ. by elec. resist. meas. method *(German)* 78−15619
steel tubes, square section, collapse in bending 80−25792
steel welding, development and results of an instrumented restrained cracking (IRC) test *(German)* 78−85060
steel welds, bead-on-plate, H_2 diffusion and trapping 80−96697
steel wires, reinforced Pb, deformation behaviour and effect of volume fraction and surface treatments *(Japanese)* 79−66118
steel XC80 isothermal and pearlitic transform. mech. prop. meas. using dilatometer *(French)* 78−31598
steels, 110G13 and 40Kh10G10, hardening and structural transformations during friction *(Russian)* 77−52527

plastic deformation continued
steels, alloy, stress relax. data anal. using total strain-time parametric method *(Japanese)* 80−104198
steels, alloy, surface plastic deform., effect of heating conditions, types 45, 40 Kh 78−53033
steels, austenitic and type 316, neutron irradiation effect on tensile, creep-rupture, deform., fracture props. 79−65120
steels, austenitic stainless, crack propag. rates under high-temp. low cycle fatigue conditions 80−21088
steels, C, H_2 embrittlement after patenting and cold deform. *(Russian)* 79−29175
steels, heat-treated, nature of high sensitivity to stress raisers 80−21051
steels, hot forming property and struct. *(German)* 80−25730
steels, hot plastic strain, stress- strain-time dependences *(Russian)* 80−40430
steels, tool, cold hydrostatic extrusion rel. to struct., props. 79−20068
steels 20Kh and 38Kh2N2VA, tensile testing, deform. rate effect 79−70115
steels 2Kh13 and 20Kh1M1FTR, sulphide cracking resistance, strengthening method influence 80−55577
steels 4Kh4VMFSSh and 45Kh3V3MFSSh, grain size, hot deform. and austenitising effects 80−76286
steels 60, 18Kh2N4MA, 17GSND, and 12Kh21N5T structure after high-speed cold plastic deformation 80−76316
stell, austenitic stainless, deformation process, stage-by-stage nature investigation using acoustic emission *(Russian)* 80−40434
stiff constitutive models, numerical integration, inelastic deform. 80−96208
stiffened layered structs., dynamic large-deflection inelastic and thermal stress anal. 77−3752
stiffened thin shells, elastoplastic, buckling and stability *(Chinese)* 79−72824
stored energy, and increment in heat capacity due to plastic deform. 80−54302
stored energy determ., analytical method *(Russian)* 77−25096
strain and damage electrical measurement method *(French)* 80−71854
strain and failure relationship of stressed solids 78−9574
strain gradients and thermodynamics 77−75813
strain rate changes, transient functions 77−15480
strain state determination, automated method, dividing nets appl. 80−100982
strain trajectories of constant curvature for plastic deformation 80−48591
strain/stress analysis, metalworking process appl. 78−27586
straining experiments, in situ, strong frictional force, quantitative anal. 80−100244
strength parameter dispersion/inhomogeneity of microscopic damage relation 77−86122
stress and deform. conc. in plastic region during creep, approx. calc. 77−56045
stress concentrations in plastic range for struct. materials 77−31222
stress dip technique for effective stress determination in cyclic straining 80−2113
stress relaxation in crystals, review 79−73248
stress relaxation theory, for plastic deform. *(Hungarian)* 80−97661
stress-deformation diagram for materials without significant elastic section *(Russian)* 78−13923
stress-deformation relns. allowing for anisotropic material strengthening *(Russian)* 79−10503
stress-strain curve from continuous indentation test 77−90396
stress/strain relation, rate and temp. depend., analytic formulation 80−40466
stretched plate with noncircular hole, stability anal. *(Ukrainian)* 80−53661
strictly momentless shell with zero gauss curvature 79−90152
strip rolling, rigid-plastic anal. *(Russian)* 79−29085
structural changes in single crystal under single electric impulse discharge *(Russian)* 79−65086
structural deformation under dynamic loading, state variable description of material behaviour 80−85137
structural materials in complex stress state, criterion for strength at low temp. 78−71292
structural member, dynamic loading and plastic response, review 80−83756
structural phase transition induced refractive index changes in crysts. 80−16000
structural steel cracking, plastic deform. and fracture toughness obs. *(German)* 77−59936
structure during cutting, investigation by TEM *(Japanese)* 80−70086
structures, determ. of last plastic hinge 79−37197
structures, stochastically loaded, reliability estimate, kinematic approach 79−27546
structures under impulsive and dynamic press. loading 77−62169
Stussi-Kollbrunner paradox rel. to decohesive carrying capacity concept 77−7315
styrene-butadiene rubber, reinforcing effect of fillers, strain energy meas. *(Japanese)* 78−31468
styrene-methacrylic acid copolymer, glassy, intermol. interaction during inelastic deform., optical spectra obs. 77−59878
sulphide minerals, superstructure and modulated struct. 79−99146
superconducting transition, effect on jump-like deform. *(Russian)* 80−34538
superconductors, plastic deformation, Cooper pair scatt. model 80−39709
supersonic gas jet, penetration into the ground *(Russian)* 80−28544
surface, mech. and corrosion props. improvement using US energy *(Rumanian)* 79−15821
surface damage, plastic deformation cause in fatigue, wear, fretting and rolling fatigue 80−40537
surface deformation treatment, tool design for 78−13824
surface dislocation anal. of plastically bent cryst. 80−2019
surface irregularities, deformation under static loads 80−58985
surface plastic deformation, damping effect, vibration theory anal. 79−94511
surface roughness, mathematical models 79−82428
Taylor model description of plastic deform. in polycrystals 79−90720
Teflon, creep in shear, hydrostatic pressure effect 79−57065
TEM obs., conf., Clermont-Ferrand France (June 1976) *(French)* 77−44298
tensile device, const.-load, for UHV electron microscope, appls. to materials science 78−11462
tensile strain associated with mech. twinning, calcs. 77−31676
plastic deformation continued
tensile strain associated with mechanical twinning, calcs. 77−31675
tensile test, uniaxial, for plastic deform. *(Hungarian)* 80−97657
tensile test piece, profile of contracted part after the beginning of necking *(German)* 77−86269
tensile testing, low-temp., strain gauge for testpiece deform. meas. 78−7118
tension test, computer simulation, effect of testing conditions 80−7729
tension test with neck triaxiality reduction 78−7159
tension tests, analysis of misalignment 80−11864
tensors of anisotropic component of yield condition *(German)* 77−23901
tetraglycidyl 4,4′ diaminodiphenyl methane epoxy, diaminodiphenyl sulphone cured, struct., deform. mode, failure 79−29141
tetramethyl-p-silphenylenesiloxane-dimethylsiloxane block copolymer films, deformation 79−15739
texture, influence on mech. and phys. props. 79−83224
texture calc. according to Taylor model 79−87652
texture development and polycrystalline modelling 79−91671
texture evolution 79−90721
theoretical analysis, deform. coeff. and specific work input *(Russian)* 77−25098
theory of anisotropic materials 77−1166
thermal activation analysis, of plastic deformation and dislocation motion using stress and temp. jumps 80−74771
thermal stress distribution associated with elastoplastic deform. 77−19549
thermally activated dislocation transforms. in plastic deform. theory 77−20008
thermocyclic stress effects in corrosive-media, electrochem. polarization applic. *(Russian)* 78−11356
thermoelastic wave propag., critical thermal load 78−30228
thermoelastoplastic medium, variables for universal deform. representation 78−49666
thermoplastic, deform. at low cycle loading 77−70122
thermoplastic body at finite deformations, incompressible plastic deformation *(Russian)* 80−53651
thermoplastic layers, isothermal smoothing of surface deformation *(Russian)* 80−76394
thermoplastic polymer, linear viscoelasticity, rel. to orientation, recoverable strain and mech. props. 77−56041
thermoplastic record development, behaviour of charge and deforming load *(Russian)* 78−38216
thermoplastic recorder development, interaction of regular and chaotic deformation *(Russian)* 80−42291
thermoplastics, structural changes during deformation, rel. to impact resistance 80−25800
thermoviscoplastic struct., finite deformations anal., energy dissipation effects 77−3744
thermoviscoplasticity theory based on infinitesimal total strain 80−87719
thick laminar reinforced plastics, deformation fixing in polarisation optics *(Ukrainian)* 78−90802
thick walled tube, incremental collapse criterion, including yield point stress temp. depend. 79−98625
thick-walled cylinder subject to internal press. and bending, full plastic anal. at collapse stage 78−22275
thick-walled cylinders, unloading after plastic deformation 77−42728
thin film, internal friction meas. apparatus for 4.2-300K 79−5093
thin film, internal friction meas. during plastic deformation, 4.2 to 300K 79−71442
thin film bicrystals, dislocation interaction, with grain boundaries during plastic deform. electron microscopy technique 80−54281
thin hemispheres, deform. during making of circular welded joints, special features 79−90155
thin metal strip, effects of hardening and anisotropy on plane strain compression 77−80083
thin plate, behaviour of circular prismatic dislocation loops, using linear theory of elasticity *(Japanese)* 79−4302
thin plate, determ. using holographic interferometry *(German)* 77−77653
thin shells loaded by local normal force, plastic failure 77−39238
thin wallled tube, limiting deform. in creep deform. 79−41593
thin-wall tubing expansion, scale factor, limiting edge deform. 77−23900
α-Ti alloy, deformation and failure, microstructural, mechanism in biaxial stress state 79−66132
Timoshenko shells with curved openings elastic-plastic deformation under impulsive loading 80−33483
tip of blunt notch, plastic yielding during static and fatigue loading 79−77010
Tishomingo Fe meteorite, microstructural study rel. to shock deform. 79−16898
toluene sulphonate diacetylene polymer, vibr. modes, strain depend. using Raman spectra 80−20626
torsion, elongation due to Bauschinger effect and fibre rotation *(German)* 77−72184
torsional deformation testing for plastic deformation, fracture *(Hungarian)* 80−97659
torsionally loaded tube of anisotropic compressible material, length change *(German)* 77−23898
transformation laws for materials with elastic range 77−50918
transition metal, dislocation magnetism *(Russian)* 78−39379
transition metal alloys, deformation and solute-induced microstructural effects on superconductivity 79−7925
transition metal diborides, C32-type, phys., chem. props., appls., review, book contrib. 78−47308
transition metal-metalloid metallic glasses, deformed, mag. props., mag. screening 79−15287
transtropic bodies, simplified method for plastic anisotropy determ. 78−3270
transverse deformation theory, development to fourth stage *(Russian)* 77−56027
Tresca type plastic material, simple shear deform. with combined work hardening *(Japanese)* 80−35206
truss, pin-jointed, plastic wave propag. *(German)* 77−35069
tube, oval straight, plastic collapse under external pressure 79−10508
tube, thick-walled, axisymmetric deformation in presence of upper yield point *(Russian)* 80−74758
tubes, thin wall, model for collapse due to creep *(Spanish)* 78−87276
tubes between rigid plates, lateral compression, strain hardening effect 78−48422
tuff, deform. charact., expt. study *(Japanese)* 78−56704

plastic deformation continued
twinning, mech. result of deform. or martensitic transform. hypothesis 77−62550
two flat surfaces in contact, thermal conductance with applied load, variation, determination for plastic surface deformation 79−72782
two layered parallelepiped under large elastoplastic deformations, deformation instability 80−33499
two phase materials, plastic strain and meas. stress hardening rate 77−52449
two phase polycrystals, grain size stability and switching, dislocation climb and glide, computer model 78−75715
two-phase structures, high-temp. deform. 78−68738
Udimet 520, γ' distribution in slip plane, dislocation loop form. during creep *(Japanese)* 79−42075
ultimate load interaction surface 79−76989
uniaxial deformation of plastic body, model with account of microcrack form. and growth *(Russian)* 78−26051
uniaxially compressed crystal, exciton molecule radiation *(Russian)* 80−108264
unidirectionally reinforced composites, large deflection, plastic constitutive relations 80−43624
unidirectionally reinforced metal composite, complex torsional and tensile loading 79−61669
universal quasi-static deformation for an incompressible isotropic body with memory *(Russian)* 79−81735
unstable fracture criteria under large plastic deformation 78−67143
unsteady-flow processes, boundaries of area of plastic deform. determ. method 77−52401
vinylidene chloride copolymer, stretched free radical form., meas. using indirect scavenger method 79−61923
visco-elastoplastic medium mechanical birefringence in loading and unloading processes 78−59314
viscoelastic shell, thick-walled, deform. in post critical stage 77−58566
viscoelastic system, fracture mechanics 78−67145
viscoelastic-plastic tube, successive deformation under cyclic, temp. variation 80−92074
viscoelastoplastic deformation of isotropic body, tensor laws of behaviour *(French)* 77−62160
viscoplastic axisymm. deform. of thin shells *(Russian)* 77−80080
viscoplastic structs., impulsively loaded, perturbation solns. 79−50615
viscoplastic thin walled systems, stability *(Russian)* 80−1452
viscoplasticity, implicit functional theory for metallic materials 79−27549
viscoplasticity, thermodynamic yield criterion 79−27534
viscoplasticity problem, analytical soln. 77−84832
viscoplasticity theory based on infinitesimal total strain and nonlinear viscoelasticity 80−79164
von Mises and Coulomb materials, two dimens. deform., numerical appl. of limits anal. 77−54899
W, static deform., removal of surface layer effect on mech. props. in single crystal 79−43359
W fibre reinforced Nb, plastic deform. and fracture 77−40438
wear, delamination theory, review 78−3229
wedge-shaped crack plastic zone, superdislocation model 79−94557
welded joints, strain concentration zone detection by holographic interferometry 77−40512
welding, transient longitudinal strain changes meas. 80−16332
Westerly granite, dry, deform. behaviour 78−36153
white cast iron, plasticity in impact toughness, bending angle tests 77−56039
wire reinforced Al, stress-deformed state, elastic, strength props. *(Russian)* 80−76303
wood, vibratory cutting, behaviour of chip and effect on cutting force *(Japanese)* 77−77540
Woodroffe thrust, deform. and fold axes reorientation in ductile mylonite zone 78−32101
work hardening material indentation analysis 79−8308
work-hardened material, elastic-plastic stress distrib. near flat surfaced notch with cycloidal tip 77−35084
wrought metals, plastic deform. testing, X-ray line profile anal. *(Hungarian)* 80−97663
X-ray analysis methodology appl., wide-angle *(German)* 80−3283
X-ray scattering by deformed cryst., theory *(Russian)* 80−70077
X-ray study *(Japanese)* 79−66117
yield surface motion and loading surface 78−15449
yield surfaces, dislocation mech. study 77−14916
yield surfaces and loading surfaces, recommendations and expts. 79−90146
yielding, bounding theorems of stochastic limit anal. 77−89037
yielding of plates with hardening and large deformations 78−59311
zincblende-type crystals, sublattice displacement from elect. or mech. deform. 80−81123
Zircaloy, deformed, positron annihilation and electron microscopy 77−8898
Zircaloy cladding, effects of stress biaxiality on ballooning behaviour 79−30919
Zircaloy cladding, internally pressurized, effect of temp. nonuniformity on diametral expansion during transient heating in steam 79−30920
Zircaloy fuel sheathing, NIRVANA high temp. creep model 79−87704
Zircaloy LWR cladding, modeling of deform. and fracture in SPEAR code system 79−93729
Zircaloy PWR fuel cladding, balloon deformation during LOCA 80−659
Zircaloy PWR fuel cladding deformation tests under mainly convective cooling conditions 80−57862
Zircaloy reactor fuel cladding tubes, high temp. deformation model with nonlinear temps. 80−661
Zircaloy tubes, grain struct., texture, dislocation density effect on irradiation creep, X-ray diffr. and optical microscopy anal. 79−74208
Zircaloy tubing, I_2 stress corrosion cracking, pellet cladding interaction mechanism *(German)* 80−16565
Zircaloy-2, deformation and fracture behaviour, uniaxial tension test in I_2 environment 80−13580
Zircaloy-2, deformation instability and tensile elongation 77−32655
Zircaloy-2, iodine environment, plane strain tension test 80−22944
Zircaloy-2, neutron irrad., low temp. deform. studies 79−47757
Zircaloy-2, neutron irradiated, inhomogeneous deformation behaviour 80−50679
Zircaloy-2, recoverable plastic strain 77−63708
zircaloy-2 and 4, tubing, rel. between contractile strain ratio R and texture 79−61607
plastic deformation continued
Zircaloy-2 cladding tubes, heat treatment influence on texture and mech. anisotropy 79−91694
zircaloy-2 cladding tubes, post neutron irrad. ring-tensile props. prehydriding effect 77−42053
Zircaloy-2 fuel tubes, low cycle fatigue studies at room temp., 300 and 350°C 80−93637
Zircaloy-4, exam. of plastic props. at elevated temps. in air 77−4811
Zircaloy-4, fuel cladding, steady-state creep from 940 to 1873K 79−74206
Zircaloy-4, load relaxation and tensile tests 79−20093
Zircaloy-4, microstrain and particle size meas. by Warren-Averbach method 80−55420
Zircaloy-4, stress-relieved and cold-worked, stress relaxation in bending at 673K 80−93609
Zircaloy-4 cladding, creep transients, plastic hoop strain meas. 79−57068
Zircaloy-4 cladding deformation under LOCA transient heating conditions, analytical modelling 80−104236
Zircaloy-4 cold worked, strain ageing behaviour with varying O_2 content 77−48455
Zircaloy-4 fuel cladding axial deform. in PWR LOCA 80−13585
Zircaloy-4 fuel sheaths, ballooning behaviour at heating rate 0.5°C s^{-1} 79−24593
α-Zr, ω phase proportion during high press. deform. *(Russian)* 79−74147
AG, hardness, temp. depend. 77−40440
AL, laminate, free-free plates, predicted and expt. natural modes 79−10520
Ag, (211)[$\bar{1}$11] single crysts., shear band effects on rolling deformation 80−50651
Ag, deformed bars, cold rolled, exam. of microstruct. by thin foil TEM 78−88502
Ag, elec. resistivity increment due to low temp. plastic deform. *(Russian)* 77−31990
Ag, FCC, low stacking fault energy, nucleation phenomena 79−90681
Ag, FCC, polycrystalline, deformation-strain curve description using substruct. parameters *(Russian)* 79−87690
Ag, FCC crystal, stress-strain curve, stage I to stage II transition *(Japanese)* 78−19834
Ag FCC crystals, compressively activated slip, theoretical latent hardening 80−65128
Ag, fatigued single crystal, annealing of deform. struct. 78−3204
Ag, filament produced by glass coated melt spinning, mech. props. 77−86125
Ag, high purity, nucleation and twinning during recrystallization, TEM study 79−29082
Ag, microcrack propagation and plastic strain 80−81187
Ag, neutron irradiation, low temp. recovery, effect of plastic deform. 78−51588
Ag plastically deformed crystal, exam. of dislocation dynamics during strain rate changes 78−88506
Ag, plastically deformed crystals, exam. of dislocation dynamics during strain rate changes 78−88507
Ag, recrystallisation texture development after plain-strain deform. 78−48448
Ag single cryst., effects of impurities and prestraining on temp. depend. of yield stress *(Russian)* 77−47506
Ag single crystal, dislocation density decrease during reverse deform., obs. by etch-pit method 77−7725
Ag, stacking fault energy meas. by tensile deform. of polycrystalline samples 78−95060
Ag, tensile deformed, dynamic recrystn. *(German)* 80−84959
Ag, tensile deformed single crystal, recrystallisation texture 79−91685
Ag, tensile plastic deformation, energy storage efficiency 77−4807
Ag:He, implanted films, solid solutions radiation induced polymorphism 79−86810
$Ag/Na_2SO_4(WO_4)$, and $Ag/Ag_2SO_4(WO_4)$ solid cell systems interface form., intergrain contact growth 77−16827
Ag-Cu, directionally solidified, obs. of cutting deform. zone *(Japanese)* 78−15422
Ag-Cu (8 wt.%), deformed, free energy changes in process of discontinuous precipitation 80−3054
Ag-Cu (8 wt.%), plastic deform. effect on discontinuous precipitation 80−3053
Ag-Ni, two ductile phase, exam. of rolling deformation 78−72819
Ag-Ni (10 wt.%) wire, plastically deformed, fracture struct. *(German)* 80−71744
Ag-Sn, splat-quenched, X-ray diffr. study 80−81094
AgBr crystals, effect on positron lifetimes *(German)* 77−11589
AgBr:Sr, stress induced anomalies in internal friction, logarithmic decrement 79−66095
AgCl, temp. fields during plastic deform., cholesteric liq. cryst. technique 79−82278
AgCl, thermal fields generated during plastic deform. 78−35457
AgI solid electrolyte plastic deformation and thixotropy obs. 78−79660
AgMg, deform. at high temp., yield pts. 79−61674
Al, [111] single crystal, in situ deform., HVEM obs. 78−52886
Al, AE under plastic deform., appl. of spectral anal. energetic anal. of moving US source *(French)* 77−77543
Al, acoustic emission from moving dislocations during tensile tests 77−19964
Al, acoustic emission signals in plastic deform., amplitude distrib. *(Japanese)* 78−6978
Al, acoustic emission under plastic deform., spectral anal., dislocation mean free path 78−84934
Al alloy, acoustic emission power, strain rate depend. 77−4808
Al alloy, acoustic stress wave emission during plastic deform., dislocation motion explanation 77−36697
Al alloy, cast, forging and heat treatment effects on diamond planishing treatment 79−43237
Al alloy, D16, extruded rod, substruct. anisotropy and decomp. at subboundaries *(Russian)* 77−25095
Al alloy, deformation and fracture resistance due to low-cycle fatigue in plane bending 79−66166
Al alloy, deformation at large plastic strains, work hardening rate 79−20065
Al alloy, ductility effects during plastic deform., rel. to struct. changes and hot forming 78−23770
Al alloy, laws governing discontinuous yield under tensile strain in liquid He 77−63760

plastic deformation continued
Al alloy, particle strengthened, yield drop and creep minimum *(German)* 78−39881
Al alloy, plastic zone form. and fatigue crack growth 78−64702
Al alloy, precipitation hardening, creep deform. effect 77−16601
Al alloy, recrystallisation during hot deform. and after cold working 79−47715
Al alloy, two phase, strength contribution of particles and dislocations *(German)* 79−29080
Al alloy, type 7175 T 651 *(French)* 80−65145
Al alloy, type AK4-1T bar, verification of existence of thermal force surface of creep process 79−87695
Al alloy, types L73 and L88, fatigue crack propagation, stress ratio effect 80−71733
Al alloy, yield surface of material subjected to combined cyclic loadings 78−84905
Al alloy, yield surfaces, effect of preloading under combined axial load and torsion 77−25091
Al alloy 2024, relief of residual quenching stresses *(Korean)* 79−70091
Al alloy 2029-0, circular plates with work hardening, nonlinear behaviour, experimental deflection and strain data 79−38893
Al alloy 2036, thermomechanical treatment on struct. and props. 79−29109
Al alloy 2219-T87, sheet, fatigue tested, fracture surface rotation mechanism 80−11764
Al alloy 5056, under abruptly changing loading or strain paths 78−56700
Al alloy 5086, plastic deform., accelerated yielding of H_2 77−36594
Al alloy 6061, high-purity, precipitation hardening, prior strain and ageing effect 77−66651
Al alloy 6061, thermomechanically treated elev. temp. mech. props. 79−8310
Al alloy 7075, acoustic emission sources during plastic deform. 78−27573
Al alloy 7075-T6, acoustic emission response 79−87801
Al alloy AK4-1T1, endurance at elev. temp. of strip with loaded hole 77−86181
Al alloy AMg6, preliminary plastic deform., effect on stability of compressed rods 77−81305
Al alloy stress/strain curve, in reverse loading process *(Japanese)* 80−7622
Al alloys, age-hardening, resistivity charge by low temp. deform. *(Japanese)* 78−84831
Al alloys, creep deformation investig. using method of precision lattices 77−86250
Al alloys, cryogenic, AMg5 and AMg6, mech. props. at −196°C 77−63748
Al alloys, deformation processes in sheet materials, application of failure maps 78−56718
Al alloys, high strength, cyclic plastic strain damage eval. and summation 79−57060
Al alloys, inclusions, oriented distrib. metallography and effects on anisotropy *(Russian)* 78−80589
Al, alloys, limiting plastic props. *(Russian)* 78−88504
Al alloys, oxide-covered, characteristic emission of negatively charged particles during tensile deform. 78−92179
Al alloys, quenching rate rel. to mech. props., residual stresses, optimum quench coolings *(French)* 78−64562
Al alloys, types 2017A, 2014, 2618A, 7049A, 7050, 7075, low-cycle fatigue *(French)* 79−74250
Al alloys 2024-T4, 2219-T861, overaged 2219, fatigue crack propag., plastic work role 79−79070
Al alloys aged, local plastic strain distrib. by selected areas channelling patterns 77−44349
Al, alternating bending of single crysts., shear strain accumulation and microstrain distrib. *(Russian)* 78−60706
Al and Al alloys, influence of microstruct. on energy storage 78−84894
Al and Al-Mg (5.5 wt.%), instantaneous plastic strain associated with stress increments during steady state creep 78−48478
Al, annihilation spectrum, narrow component, Fermi impulse of electrons, plastic deform. recovery *(Czech)* 78−64591
Al anodic films, acoustic and electron-emission during deform. 80−80143
Al, anodised, photostimulated exoelectron emission, effect of oxide thickness 78−80461
Al, anodised surface, neutral particle emission during tensile deform. 79−78856
Al, bicrystal, ⟨100⟩ oriented, plastic deform. 78−19812
Al bicrystal, plastically deformed, slip heterogeneities 80−79858
Al bicrystal, tensile and creep deform. obs. by holographic interferometry *(Japanese)* 77−56197
Al bronze, BA 1032, deformation at high temp. *(Polish)* 79−79023
Al cell structures produced by cycling and monotonic creep 80−55452
Al, cold neutron small angle elastic scatt., microstruct. exam. 77−84736
Al, cold-worked, plastically deformed, internal friction spectrum, Hasiguti peaks associated with dislocations 80−7618
Al, commercial purity, density changes, void growth in biaxial stress fields, plastic deformation 80−71692
Al, commercially pure, stress-strain curves, cyclic loading initial stage *(Japanese)* 80−93617
Al, compressed, nucleation and recrystallisation study by electron microscopy and Kikuchi diffr. 79−52236
Al, creep behaviour, at high temp., influence of oxidation 80−97538
Al, crit. resolved shear stress, orientation depend. 80−21001
Al crystal, lattice rotation during tensile deform., X-ray diffr. meas. 80−49231
Al, cyclic torsional deformation, final texture 80−7595
Al, defect structure after plastic deformation, X-ray investigation 78−31467
Al, defects formed during cryst. growth or by plastic deform., X-ray transmission topography obs. *(Russian)* 80−25761
Al, deformation, internal friction, dynamic modulus and creep meas. 79−91727
Al, deformation enhanced photoemission meas. 77−32511
Al, deformation mechanism map 79−34109
Al, deformed, efficiency of dislocation as sink for vacancies, resist. obs. 77−36570
Al, deformed, nucleation and recrystallisation at second phase particles 78−6941
Al, deformed, resist. decay, meas. of initial stages, method and results 79−49256
plastic deformation continued
Al, deformed, struct. and recrystallisation transmission Kossel diffr. obs. 77−52340
Al, deformed in tension, elec. cond. changes at 78 and 283K, grain boundary effect *(Japanese)* 80−30029
Al, deformed in uniaxial and equibiaxial tension, dislocation arrangements 80−108516
Al, dislocation line movement at low temp., obs. by US meas. *(French)* 79−95025
Al, dislocation struct. change during cyclic straining at high temps. 78−44218
Al, dislocation substructure formation under hydrostatic extrusion 78−56696
Al, dynamic defect annealing during plastic deform. 78−88478
Al, dynamic strength and logarithmic modulus of plasticity 77−16655
Al, electron drag on mobile dislocations at low temps., strain rate, temp., and field depend. 80−19808
Al, elongated, deformation and recrystallisation, Rowland transform. model *(French)* 77−77498
Al, etching technique for revealing plastic zones 78−72955
Al, exoelectron emission under recrystallisation annealing 77−90412
Al, FCC, polycrystalline, deformation-strain curve description using substruct. parameters *(Russian)* 79−87690
Al, FCC, strain hardening and recovery by pure metal mode, high temp. deform. *(Japanese)* 78−52843
Al FCC crystals, compressively activated slip, theoretical latent hardening 80−65128
Al FCC single crystal, crystal rotation accompanying scratch deform. *(Japanese)* 79−15733
Al films, appl. of current noise technique for dislocation processes 80−35442
Al foil, α-particle irrad. under fusion reactor conditions, He bubble alignment during deform. 80−107345
Al foil, deformation, laser optical scanning obs. 80−100995
Al foil, internal friction changes during low temp. plastic deform. *(Russian)* 80−100304
Al foil, laser irrad., fracture props. *(Russian)* 80−108523
Al, fracture mechanism, plastic strain role 79−38977
Al, grain boundary sliding and deformation mechanism maps 80−3128
Al, He bubble behaviour during high plastic deform. 80−29087
Al, high purity, deformed at 573K, stress reductions effect on creep behaviour 79−74216
Al, high purity 6061, thermomechanical treatment 77−44277
Al, high-temp. internal friction peaks, deformation and annealing effects 77−32615
Al, influence on thermal conductivity maximum, 4.2 to 70K 78−76049
Al, initial stages of plastic deform. *(Japanese)* 80−93618
Al, internal friction due to dislocation-loop interaction *(French)* 79−79017
Al, isoaxial bicrystal, deformation behaviour, study by photoelastic coating and moire methods *(Japanese)* 78−11294
Al, large deform. of thin walled tubes under transverse loading 77−36567
Al, lattice resistance stress, Bordoni relax., microdeform. and US attenuation results 80−25747
Al, load relaxation, plastic deform. theory and plastic eqn. of state 78−27554
Al, magnetoplasic effect and eddy current heating *(Russian)* 77−43858
Al, mech. props., 20 to 300°C *(French)* 77−56018
Al membranes, circular, plastic deform. under impulsive loading by underwater wire explosion 79−100208
Al, microcrack propagation and plastic strain 80−81187
Al, non-elastic deformation, phenomenological model with solute strengthening effect incorporation 78−39832
Al notched bars, deform. behaviour and strength having biaxial state of stress at notch root *(Japanese)* 80−81116
Al, oxidation, influence on deformation map 80−40599
Al, oxide covered, tensile deform. in high vac., particle and photon emission 78−39672
Al, plastic deform. and prominent cross slip ⟨100⟩ oriented single crystal 78−19851
Al, plastic deform. build-up during low cycle fatigue *(Russian)* 77−25207
Al, plastic deform. effect on third-order elastic moduli, dislocation anharmonism *(Russian)* 80−50786
Al, plastic deform. of poly- and single-crystals, AE study 79−24579
Al, plastic deformation and prominent cross slip in ⟨100⟩ oriented single crysts. *(Japanese)* 77−8889
Al, plastic deformation meas. in normal and supercond. states, down to 0.4K *(Russian)* 79−11658
Al, plastic deformation thermal activation parameters from creep kinetics and stress relaxation 80−71717
Al, plastic props., room temp. to recrystallisation temp., stress/strain relations, computer program 77−1865
Al, plastic strain in tension, effect of strain rate 77−32654
Al, plastically deformed, positron annihilation momentum spectra, low temp depend. 79−19948
Al, plastically deformed, spreading of extrinsic grain boundary dislocations 78−43023
Al, plastically deformed by pulsed mag. field, mobility of Fe atoms, radiotracer profiles 79−28584
Al, plastically deformed single crystal, X-ray diffr. by defects 77−68976
Al, plastically deforming at high strain rates, distrib. of temp., strain rate and strain 79−19311
Al, plastically prestrained, dynamic props. 79−15743
Al, polycrystalline, deform. sub-struct., effect on tensile props. *(Japanese)* 78−11279
Al polycrystalline, exoelectron emission under tensile deform. and fracture *(Japanese)* 77−55870
Al, polycrystn., HVEM in-situ investigation of creep mechanism 80−104214
Al, positron annihilation radiation, ang. correl. shape, deform. effects 77−85831
Al, recrystallisation kinetics after small deform. and grain growth *(Czechoslovakian)* 77−32592
Al, recrystallisation nuclei form. and well defined deform. band struct. 79−20136
Al, resistivity decrement under torsional deform., impurity segregation at moving dislocations 77−4321
Al rings, deformation modes under static axial compression 80−25768

plastic deformation continued
Al rods, waveform variation of reflected acoustic shock pulse due to work hardening 77−21167
Al, rolled single crystal, annealing texture 79−91678
Al, rolled strip from granules, coeff. of deform. 77−90422
Al, secondary recrystallization *(Czech)* 79−70080
Al sheet, texture evolution, effect of rolling or tensile deform., rel. to strain ratio 79−91672
Al sheet alloy, type 2036-T4, in-plane deformation, correlation with Hill's theory 79−83260
Al sheet D16AT, plastic strain distrib. at crack tip by coordinate-grid method 80−16400
Al single crystals, ⟨100⟩ oriented, deform. temp. effect on stage IV deform. *(Japanese)* 80−66587
Al single crystals, relation between axial orientation rotating and deform. banding 80−104206
Al, strain rate sensitivity and ductility, trace element conc. effect 80−66597
Al, strained, localised corrosion on slip steps 79−20265
Al, struct. changes in single cryst. under influence of static and dynamic stresses *(Russian)* 78−92300
Al, tensile curve and specific value of anisotropy coefficient *(French)* 77−28867
Al, tensile plastic deformation, energy storage efficiency 77−4807
Al, thermoactivated creep and stress relax. 79−87692
Al, torque and length change during fracture in torsion test *(German)* 79−24611
Al, transient creep, effect of pre-torsional deform., dislocation glide and density 77−4147
Al, type 2014-T6, shear-band temp. meas. 80−48655
Al, vacuum condensate, struct. and mech. props. depend. on deposition conditons 80−15417
Al, wire, determ. of incomplete axial texture by X-ray diffr. 78−23720
Al wire, hot and cold deformation drawing strengthened, thermal EMF study *(Russian)* 80−54674
Al, yield surface motion and loading surface 78−15449
Al, yield surfaces from dislocation mechanics 77−14917
Al, Young's modulus changes after plastic deforms. at room and cryogenic temps. 78−23747
Al, zone refined, vacancy annihilation to dislocations, annealing profiles 77−80536
Al/Sn interface, effect of plastic deformation on structure and adhesion strength of interface *(Russian)* 79−28218
Al-(Mg)(Fe), pure (dilute), large wire drawing plastic deform. 80−108508
Al-Ag, nonhomogeneity of deform. 78−84888
Al-Ag (15 wt.%), precipitation hardenend cyclic stress-strain response 78−35412
Al-Ag (40 wt.%), deformed, free energy changes in process of discontinuous precipitation 80−3054
Al-Ag (40 wt.%), plastic deform. effect on discontinuous precipitation 80−3053
Al-Ag alloy precipitation and heat of evolution, microcalometric obs. *(Japanese)* 78−15406
Al-Al_2O_3 composite, brittle zone on fibre surface deform. and fracture 77−56104
Al-Al_3Ni, aligned, eutectic alloy, mech. behaviour at high strain rates 78−39855
Al-Al_3Ni, eutectic composite, directionally solidified, thermal cycling induced distortion 78−39899
Al-Al_3Ni eutectic composite, substructural matrix hardening *(Russian)* 77−21162
Al-Al_6Fe, fibre reinforced eutectic, deformation behaviour by rolling, TEM and SEM study 79−29129
Al-alloy, type 6351 and 6061, stress relaxation in cyclic deformation 80−3119
Al-alloy, type PA6, under complex cyclic loading, behaviour of stress strain diagrams 80−16372
Al-bronze, single crystal rod, energy dissipation, deformed by cyclic buckling in superelastic range 78−31479
Al-Cu, high strength, type 2024-T3, crack growth, fatigue induced surface deform., holographic detect. 80−85120
Al-Cu, precipitation hardened, hysteretic plastic work as failure criterion in Coffin-Manson type relation 77−32657
Al-Cu, type 2036-T4, plane-strain work hardening, meas. and anal. 80−81073
Al-Cu (4 wt.%), AE during deform., effect of ageing at 170°C 78−64597
Al-Cu (4 wt.%), interparticle spacing influence on cyclic deformation and fatigue crack propag. 79−61717
Al-Cu (4 wt.%), supersaturated and aged conditions, high strain deform. 80−60907
Al-Cu (4 wt.%) alloy, coherency loss of θ'-phase due to deform. 77−15424
Al-Cu (4 wt.%) alloy, high temp. cyclic deform., θ' particle dissolution obs. 80−108515
Al-Cu (4 wt.%) partially coherent precipitation hardened alloy, high temp. cyclic deform. 80−25710
Al-Cu alloy, Portevin-Le Chatelier effect, influence of specimen dimensions and machine stiffness 77−70128
Al-Cu alloy, press-forming under coexisting state of liquid and solid, mech. props. 77−81240
Al-Cu full coherent precipitation hardened alloy, high temp. cyclic deform. 80−25711
Al-Cu solid soln., supersaturated, plastic deform. effects *(French)* 79−91748
Al-Cu-Mg, acoustic emission during tensile testing 80−7632
Al-Cu-Mg, cold plastic deformation, stress/strain relations 79−56991
Al-Cu-Mg, tpye RR55, high strength, creep behaviour, effect rel. to anodic coatings, SEM study 80−97542
Al-Cu-Mg, tube drawing, tensile forces, plastic deformation *(French)* 79−70130
Al-Cu-Mg, type 2036, deformation at ageing temp., effect on struct. and props. 80−7605
Al-Cu-Mg alloy, influence of plastic deformation on fatigue limits, for prestrained components 78−68799
Al-Cu-Mg type 2036, thermomech. treatment, flow stress anal., effect in mech. props. 80−93584
Al-Cu-Mg-Mn(-Zn-Cr), low temp. deformed, ageing and mech. props. 79−1881

plastic deformation continued
Al-Cu-Ni, alloy RR 350, θ'-hardened, deform. induced microstructural instability, high temps. 80−16321
Al-Cu-Si-Mg, deform. simulation using torsional test, elastoplastic constitutive eqn. 80−93594
Al-Cu-Zr (6, 0.3 wt.%), superplastic, mech. anisotropy and deformation mechanisms 79−83254
Al-$CuAl_2$ eutectic, heat treatment and interlamellar spacing effect on tensile deformation 80−29979
Al-Cu(Mg), age-hardenable, US cavitation erosion mechanisms, effects of comp. and heat treatment 78−53002
Al-Cu(Mg), low freq. internal friction during plastic deform. *(Chinese)* 80−103420
Al-Cu(Mg)(Zn), cold working causing preprecipitation, thermoelec. power *(French)* 79−8306
Al-Cu(Si)(Mg) binary and ternary alloys, dimensional changes in heat treatment. 80−89271
Al-Cu(Zn-Mg), age hardening, conditions leading to localised plastic deform. and fracture in slip bands during fatigue 78−64670
Al-Cu(2.6 wt.%), sheets, effect of strain path changes on formability 79−43347
Al-Ge (2 wt.%), quenched and aged, deform. slip line obs. 78−51544
Al-Mg, acoustic emission during tensile testing 80−7632
Al-Mg, ageing process, effects of Ag additions and pressure *(Russian)* 80−45321
Al-Mg, cold plastic deformation, stress/strain relations 79−56991
Al-Mg, deformation, tension, torsion compression test exam. *(Russian)* 78−31455
Al-Mg, discontinuous deform. under various conditions 77−63716
Al-Mg, plastic deform., separation of internal friction components *(Russian)* 79−52282
Al-Mg (2 wt.%) subgrain formation at low stresses 78−84928
Al-Mg (4 wt.%), enhanced ductility at elevated temps. 77−63740
Al-Mg (5 wt.%) deformed bars, cold rolled, exam. of microstruct. by thin foil TEM 78−88502
Al-Mg alloy AMg6, deform. in plane stress at low temps. 78−39873
Al-Mg single crystal, fatigue deform. 79−91747
Al-Mg solid soln., AE during plastic deform. 78−64592
Al-Mg spherical shell with reinforced holes, local stability 80−50686
Al-Mg_2Si(1.42 wt.%), aged, dislocation structs. caused by plastic deformation 80−25786
Al-Mg-Cr, tube drawing, tensile forces, plastic deformation *(French)* 79−70130
Al-Mg-Si, DTA exam. after small and medium deform. 80−21002
Al-Mg-Si, deformed, orientation of recrystallisation nuclei 79−91681
Al-Mg-Si, thermomechanically treated, age-hardening 78−11236
Al-Mg-Si alloy, Mg_2Si dispersion hardened US waveguides, concentrators *(Polish)* 80−89237
Al-Mg-Si alloy, Mn additions, effect on deform. 77−8876
Al-Mg-Si alloys, effects of dispersoids upon micromechanism of crack propagation 79−83286
Al-Mg-Si rod, extruded and cold drawn, annealing *(German)* 78−39804
Al-Mg-Si-Cu, cold plastic deformation, stress/strain relations 79−56991
Al-Mg-Si-Cu, tube drawing, tensile forces, plastic deformation *(French)* 79−70130
Al-Mg(Si), acoustic emission signals in plastic deform., amplitude distrib. *(Japanese)* 78−6978
Al-Mn(Cu)-Zr, particle stabilized structures, hot deform. 79−47733
Al-Ni (6 wt.%), fine-grained, deform. in tension and torsion 80−85008
Al-rare earth alloys, granules, rolling to form foil, exam. 80−20825
Al-Si, deformed, local lattice rotations at second phase particles 80−25709
Al-Si eutectic, high temp. creep, two regimes of flow, modified Dorn eqn. anal. 79−74215
Al-Si(9.3, 12) with graphite particles seizure resistance study using Hohman wear tester 80−89360
Al-Sn dil. alloy, cube orientation texture development 79−96040
Al-Zn, nonhomogeneity of deform. 78−84888
Al-Zn, plastic deform. effect on struct. transform. at elev. temp. *(Czech)* 79−79044
Al-Zn (30 wt.%), precipitation ageing plastic deform. effects 77−66645
Al-Zn (3.9 wt.%), single crysts., fatigued age-hardenable, dislocation structure *(German)* 80−54247
Al-Zn (40(50)(65) wt.%), deformed, free energy changes in process of discontinuous precipitation 80−3054
Al-Zn (40(50)(65) wt.%), plastic deform. effect on discontinuous precipitation 80−3053
Al-Zn (6.5 at.%), fatigue props., effect of ageing and thermomech. treatment 78−27620
Al-Zn-Mg, fatigue crack propag., stage I 77−36653
Al-Zn-Mg, plastic deform. influence on structural transform. and mechanical props. *(Russian)* 80−7623
Al-Zn-Mg (3.6, 1.95 wt.%), ageing and plastic deform., effect on structure, electron microsc. and X-ray diffr. study *(Russian)* 80−81108
Al-Zn-Mg (6, 2.5 wt.%), fracture toughness-transgranular fracture relation 77−52447
Al-Zn-Mg (6,3 wt.%) high-strength alloy, dislocations distrib., corrosive environment influence *(Russian)* 79−52442
Al-Zn-Mg alloy, thermomech. treatment, precipitation and strengthening 79−24527
Al-Zn-Mg alloy 7075, unstable shear failure 77−48516
Al-Zn-Mg-Cu (6, 2.5, 1.5 wt.%), deform. simulation using torsional test, elastoplastic constitutive eqn. 80−93594
Al-Zn-Mg-Cu (6,2, xwt.%) type alloy, fatigue crack propag., Cu content and recryst. effect 80−60960
Al-Zn-Mg-(Zr), low cycle fatigue, grain refinement effect 77−44345
Al-Zn-Mg(3.2, 2.2 wt.%), deform. strengthened by Guinier Preston zones 77−52343
Al-Zn(11 wt.%), dynamic recovery during and after steady state deform. 77−1842
AlCu, electron microscope spot prep. of deform. bands 79−15922
Al_4Cu_9, rhombohedral γ-brass, direct imaging of struct. and structural defects 80−15115
AlCuMgPb, microstruct. and flow stress during deform. at 573K 77−81307
AlMg5, memory effect of plastically deformed alloy under complex loading 79−38891
Al_8Mn_5, rhombohedral γ-brass, direct imaging of struct. and structural defects 80−15115
Al_2O_3, creep and long term strength 78−23802
Al_2O_3, deform. curve and modulus-temp. relation *(Russian)* 78−35613

plastic deformation continued
Al_2O_3, deformation mechanism map 79−34109
Al_2O_3, dynamic deform., stress-wave response 80−21020
Al_2O_3, fine grained, basal slip and nonaccommodated grain boundary sliding 80−60916
Al_2O_3, fine grained, interface-controlled diffusional creep 80−60915
Al_2O_3, spray dried agglomerates, compaction response, fracture, deform. 79−43172
Al_2O_3-AlN, creep 77−21235
Al_2O_3-SiO_2 refractory, creep, viscosity, resist. to inelastic deform. 80−89309
Ar, solid, diffusion processes in plastic deform. *(Russian)* 80−92591
As-Se system glasses, opt. absorpt. edge shift on densification 77−77250
Au, deformed bars, cold rolled, exam. of microstruct. by thin foil TEM 78−88502
Au, hardness, temp. depend. 77−40440
Au, pure, electromigration and deform. 78−2286
Au/Ag couple, diffusion induced stresses and plastic deform. 78−26736
Au-Ag, plastic deformation, energy storage efficiency 77−4807
Au-Cu-Zn-Ni (13, 3.4, 8.5 wt.%), white gold, metallographic structure after cold rolling, effect of heat treatment, recrystallisation *(French)* 79−52238
Au-Ni-Cu-Zn, white gold, metallographic struct., heat treatment and plastic working effect 80−40403
B_2O_3, vitreous, torsional deform. above T_g under low stresses, temp. effect 80−21052
B_2O_3, vitreous, torsional deform. above Tg under low stresses 80−25804
$BaTiO_3$, cubic-tetragonal phase transition, birefringence meas., surface distortion effects 78−95564
Be bronze BrB2, quenched deformed, substruct. and props., effect of prerecrystallisation annealing *(Russian)* 78−60677
Be, creep mechanism 77−36586
Be crystal, failure on basal plane 78−15525
Be, deformation strengthening, microstruct. and impurity effects 77−4791
Be fibre reinforced Ti-Al-V (6.4 wt.%), synthesis and mech. props. 77−32544
Be, grain size effect on mech. props. *(Russian)* 79−47749
Be, plastic strain mech., effect of impurities *(Russian)* 79−34101
Be, polycryst. plasticity, cleavage strength, ductility transition temp. 80−44250
Be polycrystalline, metallographic observation of cleaved grains 78−72824
Be, ultra fine-grained, recrystn. after deform. 79−52239
Be, wire, elec. cond., heat treatment and strain effects *(Russian)* 80−24870
Be-bronze BrB2, struct. and phase transform. during mechano-thermal treatment *(Russian)* 80−11667
Bi, deformation calculations, band struct. variation, electron phase transitions due to deform. *(Russian)* 80−65137
Bi polycrystalline, plastic deform. and stored energy of cold work 79−43348
Bi, strain hardening curve correlation with slip band nucleation stress spectra 80−70217
Bi, texture of deformed polycryst. 77−59809
Bi, thermal cond. under plastic deform., phonon scatt. by dislocations and twin boundaries 77−11746
Bi, US propagation anomalies, under hydrostatic press. *(Russian)* 78−83884
$Bi_{1-x}Sb_x$, deformation calculations, band struct. variation, electron phase transitions due to deform. *(Russian)* 80−65137
n-$Bi_2(Te,Se)_3$ semiconducting solid solns., plastic deform. during hot extrusion 79−20143
Bi_2Te_3-Sb_2Te_3 composite billet, diffusion during plastic deformation *(Russian)* 79−23767
p-Bi_2Te_3-Sb_2Te_3 semiconducting solid solns., plastic deform. during hot extrusion 79−20143
Bi_2Te_3-Sb_2Te_3 solid solns., plastically deformed by hot extrusion, diffusion meas. using micro-X-ray spectrum anal. 79−14954
n-$Bi_2Te_{2.88}Se_{0.12}$, extrusion deformed, powder dispersion degree influence on thermal and elec. props. *(Russian)* 80−39366
C fibre reinforced composites, mech. props., rel. to aircraft appl. 77−81289
C fibre reinforced composites, kinking as structural degradation mode 78−52893
C fibre reinforced Cu, mech. props. *(Japanese)* 77−63723
C fibre reinforced Kinel, mech. props., 20 to 300°C *(French)* 77−56018
C fibre reinforced plastic multilayer laminate, strength and deform. *(Russian)* 80−30019
C fibre reinforced plastic, deform. and failure using AE method *(Russian)* 80−40630
C fibres, pitch and lignite based, exam. of microvoids by X-ray scatt., heat treatment and stretching effects 79−20091
C steel, type 45, inelasticity under cyclic strain in active media 78−80613
C steel, yield strength, anisotropy in relation to temp. of deformation 78−80612
$CaCO_3$, calcite, cryst. preferred orientation in marble, mag. susceptibility anisotropy development 78−56286
$CaCO_3$, plastic deformation in compression parallel to (111) 78−38709
CaF_2 antireflection coated, 3.8 μm CW laser damage threshold obs. 80−33053
CaF_2, plastic deform, work hardening regions, TEM obs. 80−3140
$Ca_5F(PO_4)_3$, colour centre accumulation deformation effects 77−84743
CaO-MgO-Al_2O_3-SiO_2, glass-ceramic prep. by hot pressing and crystallisation of powder 78−11192
Cd, Cottrell-Stokes law, 4.2 to 300K, forest dislocations and other obstacles 77−43269
Cd crystals, X-ray topographic examination of basal dislocation glide, generation and locking 80−88156
Cd, electronic properties depend. on $2^1/_2$-th order phase transition under high press. *(Russian)* 80−11128
Cd, electroplastic deform., stress relax. meas. *(Russian)* 79−38894
Cd, grain size effect on acoustic emission generated during plastic deformation 78−80609
Cd, loading and annealing, dislocation struct. control *(Russian)* 78−3142
Cd, single cryst. stress relax. depend. on elec. current, electron plastic effect 79−79021
Cd, single crysts., plasticity study during deformation by twisting *(Russian)* 80−93597

plastic deformation continued
Cd whisker, supercond. crit. temp., stress depend. 77−39989
Cd-Mg single crystals, exam. of critical resolved shear stress from 77 to 300K *(Czech)* 79−91741
Cd-Zn single crystals, crit. resolved shear stress at low temps. 80−3138
$Cd_xHg_{1-x}Te$, correlation between structural and chemical inhomogeneity *(Russian)* 80−49484
CdS, (10$\bar{1}$0) face, deformed zones around microimprints 78−23812
CdS, characts. of interaction of light with dislocations 78−2137
CdS, deformed, dislocation struct., TEM obs. 80−54250
CdS, dislocation motion, TEM obs. 80−79799
CdS, dislocation structural optical absorpt., plastic deformation *(Russian)* 80−34959
CdS, elec. cond., plastic deform. and annealing effects 77−55534
CdS, plastically deformed, optical and electronic transport anisotropies 77−8611
CdS, plastically deformed, photo-EMF rel. to cryst. polarity 77−55581
CdS, plastically deformed, electronic transport and optical props. 79−73508
CdS, plastically deformed cryst. with dislocation slip band, residual cond. 80−6839
CdS(Se)(Te), charged dislocations, flow of charge with plastic deform. 80−85010
CdSe, plastically deformed, luminescence line 0.96 eV 78−10950
CdSe, recombination mechanism at dislocations, photoluminescence 80−103993
n-CdTe, cathodoluminescence microscopy obs. of dislocations, compared with etch pit pattern 79−69105
n-CdTe, photolum., plastic deform. effects 79−15509
CdTe, photoplastic effect, influence of plastic deform., heat treatment and doping 79−82277
CdTe, plastic deformation activation anal. below room temp. 78−84935
CdTe, single crystals, plastic deformation and dislocation struct. 79−8321
$CeO_2La_2O_3$, ceramic, thermal stability, sintering, deform., effect of La_2O_3 79−11532
Co allotropic transformation, X-ray diffr., analysis exam. *(Russian)* 79−34027
Co, anomalous plasticity near martensitic transform. temp. *(Russian)* 78−6971
Co, deformed, microstruct. singularities in pre-transform. temp. range *(Russian)* 80−45347
Co, deformed and annealed, mechanism and kinetics of polymorphic transformations *(Russian)* 78−35381
Co, FCC, mag. props. of single-domain powders after plastic deform. *(Russian)* 78−6554
Co, flow stress, effect of mag. field 77−20673
Co, influence of FCC phase retained at room temp. on mech. props. 79−47677
Co, internal friction anomalies in spin reorientation temp. range *(Russian)* 80−49299
Co, particle formation by evap., electron microscopy obs. of interaction processes 80−104053
Co, recrystallisation kinetics, deform. degree effects *(Russian)* 78−6943
Co, single crystal, cavitation erosion, role of twinning 80−107272
Co-Al alloys, mag. props., positron annihilation *(Russian)* 77−85416
Co-CoAl, two phase, interaction between deform., fracture initiation and propag. 80−85006
Co-Cr-Ni-TaC, directionally solidified eutectic, mech. props. and sruct., thermal cycling effects *(Russian)* 78−92282
Co-Fe, internal friction anomalies in spin reorientation temp. range *(Russian)* 80−49299
Co-Fe alloy, plastic deform. effects on phase comp. *(Russian)* 78−19743
Co-Fe-Ti (12,6 wt.%), semihard permanent magnet, magnetic precipitation hardening 78−52830
Co-Ni, deformed and isochronally annealed, positron lifetimes, annihilation at dislocation trapped monovacancy 80−55221
Co-Ni (33 wt.%), FCC deform. twinning kinetics, relationship to stress-strain behaviour 78−52887
Co-Ni alloy, slip charact., and fatigue, FCC twinning and FCC to HCP martensite transform. effect 80−35182
Co-Ni-Cr-C, carbide precipitation 79−29065
Co-Ni-Cr-Mo, mech. props., effect of twinning and FCC to HCP transform. 77−4779
Co-Ni-Cr-Nb FCC alloy, electron microscope obs. of deform. twins 79−60380
Co-Ti-C, secondary precipitation and allotropic transform., TEM obs. 80−108453
Co-WC dispersion hardened alloy, tensile deform., volume fraction of second phase effect, simulation *(Japanese)* 79−70122
Co(Cr,Ni)-TaC fibrous eutectic, deformed, thermal stability of microstruct. *(Russian)* 79−1895
CoO, polycrystalline, high temp. deform. 78−3174
CoO single crystals, strain rate deform. characts., yield stresses and work hardening 77 to 1400K 80−60939
Cr, anomalous US damping under hydrostatic press. 79−14890
Cr bronze Sn, recrystn. props., hot rolling, annealing, polygonisation *(Russian)* 80−55419
Cr, diffusion coating strengthening by plastic deformation, controlling physical factors *(Russian)* 77−25187
Cr-Al alloy KH40NYu3, microplastic deform. *(Russian)* 77−66681
Cr-Co-Fe permanent magnet anisotropic alloys, plastic deform., ageing, particle alignment temp. 80−35254
Cr-Nb, dislocation cell growth kinetics by TEM during annealing *(Russian)* 79−65084
Cr-Nb-Mo alloy system, comp. and temp. depend. alterations in mech. props., phase diagram interpret. *(Russian)* 80−85045
Cr-Ni, fatigue, low cycle, test results, least square deviation method 77−63796
Cr-Ni compressor disk, surface plastic deform., optimal method 80−60924
Cr-Ni steel, strengthening by elastic deform. at −196°C 77−55987
Cr-Ni VKh-4 alloy, deformation and fracture mechanism investigation *(Russian)* 80−11738
Cr-Sm-Pr, Sm and Pr additions and plastic deform. effects on texture *(Russian)* 77−55983
CrO_2 semidry refractory, struct. and mech. props., surface-active agents effect 80−89304
CsCl, twin form. by compressive stress during phase transform. 80−49358

plastic deformation continued
CsI crystals, relation of struct. and bond type to slip geometry 80−88165
CsI, crysts., microplasticity mechanism 78−30696
CsI, exam. of kinking process, using cholesteric liquid crystals 80−7629
CsI, single cryst., plastic deform. at 4.2K, temp. rise 77−15481
CsI, thermal fields generated during plastic deform. 78−35457
Cu, ⟨100⟩ oriented single crystal plastic deform. and prominent cross slip 78−19852
Cu, acoustic emission signals in plastic deform., amplitude distrib. *(Japanese)* 78−6978
Cu, acoustic losses due to strong ultrasonic and static stress fields 80−79886
Cu, aftereffect deformation, creep duration effect on structure, rupture time 79−91766
Cu alloys, cryostat for thermal cond. meas. 78−81985
Cu alloys, flat spring, mechanical props. in bending, stress relax. test, 23 to 232°C 78−72806
Cu and Cu alloys, deformed, texture development 79−87653
Cu and Cu-Al (8 wt.%) single crystal, surface dissolution effect on fatigue damage and crack nucleation 78−39936
Cu and Cu-Cr (0.6 wt.%), electron microscope obs. of shear bands *(German)* 77−48454
Cu and Cu-Si, deformation and fracture under dynamic loading 78−35442
Cu, anisothermal annealing, effect on props. of MOOB bands 78−23719
Cu, annealed, cyclic plasticity under cyclic nonproportional strain histories, cyclic hardening, memory erasure, strain hardening 78−88510
Cu, annealed, plastic strain during non-proportional loading 80−89291
Cu, bicrystal, {110} ⟨112⟩, deform. *(German)* 77−48513
Cu bicrystals, effect of grain boundary on tensile deformation *(Japanese)* 78−88495
Cu, brazed butt joint, static torsional deform. 77−16657
Cu, cold neutron small angle elastic scatt., microstruct. exam. 77−84736
Cu, cold rolling, mechanical props., ageing, annealing, recrystallisation, plastic strain *(Russian)* 80−35202
Cu, cold worked, dislocation production 77−32597
Cu, cold worked, grain size effects on short-term strength *(Russian)* 78−56693
Cu, cold-drawn, low-cycle fatigue, effect of mean plastic strain and stress factor 77−63766
Cu, cold-rolled, microstruct. 79−83216
Cu, condensates of different thicknesses, polycrystalline, mech. props. 79−65350
Cu crystal, Cr-plated, const. strain rate tests, yield stress 79−83276
Cu, cyclic hardening and saturation behaviour of single crystals 78−64555
Cu, cyclic straining anal., discrete polycrystal model 77−47507
Cu, cyclic torsional deform. at high deform. amplitudes *(German)* 79−87701
Cu cyclic torsional deformation, final texture 80−7595
Cu, cyclic work hardening during frequency change fatigue tests *(German)* 79−34068
Cu, cyclically deformed, nucleation of persistent slip bands 78−72830
Cu, deform. instability and tensile elongation 77−32655
Cu, deform. of ⟨100⟩ single crystal *(Japanese)* 77−59864
Cu, deformation band, role in fatigue crack nucleation and propag. 79−24585
M-1Cu, deformation process, stage-by-stage nature investigation using acoustic emission *(Russian)* 80−40434
Cu, deformed, defects, thermal relaxation, positron experiments *(German)* 80−50455
Cu, deformed, temp. depend. of positron trapping 77−48270
Cu, deformed and annealed, positron lifetime investig. of recovery and recrystn. 77−70064
Cu, deformed by hydrostatic extrusion, drawing or drawing under press., dislocation struct. obs. *(Russian)* 77−21213
Cu, deformed by rolling and torsion, stored energy *(German)* 79−29160
Cu, dil. alloy, dislocation inertial effects in plastic deform., internal friction meas. 77−36609
Cu, dislocation content at large plastic strains 79−74224
Cu, dislocation damping strain amplitude depend. on 1 MeV electron irrad. and quenching 79−95023
Cu, dislocation increase by electron wind *(Russian)* 79−95024
Cu, dislocation mechanism of luminescence during fracture 79−24376
Cu, dislocation substructure formation under hydrostatic extrusion 78−56696
Cu, drawability, mech. props., effect of O impurities 79−83272
Cu, dynamic strength and logarithmic modulus of plasticity 77−16655
Cu, elastic modulus and internal friction during plastic deform., dislocation props. determ. 80−35244
Cu, electrical conductivity, effect of cyclic strains and work hardening at 4.2K 78−91655
Cu, electron drag on mobile dislocations at low temps., strain rate, temp., and field depend. 80−19808
Cu, electron irrad. at 100K, comparison of irrad. hardening with dislocation vel. 80−54284
Cu, electron-dislocation interaction, influence of mag. fields on flow stress meas. 77−31672
Cu, electroplastic drawing, deformation zone current delivery schemes 79−91761
Cu, explosive loading, depend. of struct. on deform. *(Russian)* 78−3177
Cu, extended single crystal wire, orientation of cross section ellipse 77−86115
Cu, FCC, polycrystalline, deformation-strain curve description using substruct. parameters *(Russian)* 79−87690
Cu FCC crystal, stress-strain curve, stage I to stage II transition *(Japanese)* 78−19834
Cu, FCC single crystal, crystal rotation accompanying scratch deform. *(Japanese)* 79−15733
Cu, fatigue crack propag., influence of specimen thickness *(German)* 80−66669
Cu, fatigue hardening and failure at intermediate life 77−48548
Cu, fatigue of single crystals and low const. plastic strain amplitude 79−20174
Cu, fatigued high-purity polycrystals, temp. depend. of flow stress 77−44316
Cu, fatigued polycrystals, impure, temp. depend. of flow stress 77−44317
Cu fatigued polycrystals, point defect cluster rel. with yield stress temp. depend. 78−6989

plastic deformation continued
Cu, fatigued single crysts., temp. depend. of saturation stress and dislocation substruct. 80−44211
Cu, fragmentation and dynamic recrystallisation after heavy and very heavy deform. *(Russian)* 78−39793
Cu, friction and prow form. in scratch process by diamond cone 78−11349
Cu, friction mechanism, HV TEM expts. 80−35341
Cu, grain size effect on acoustic emission generated during plastic deformation 78−80609
Cu, hardness, temp. depend. 77−40440
Cu, heavily drawn ETP wire, secondary recrystallisation 77−36537
Cu, high purity, creep cavitation topology, high temperature region *(Czech)* 80−65138
Cu high purity, grain boundaries as dislocation sources in premacroyield strain region 79−34096
Cu, high purity, identification of imperfections by thermal resistivity meas. 80−59951
Cu, high purity, low cycle fatigue, cumulative damage, absorbed plastic energy anal. 79−38932
Cu, high purity crystal, resistivity changes with deform., subsequent recovery 77−52397
Cu, high-purity, grain size and strain rate influence on mech. behaviour, precursors existence 80−85016
Cu, hot ductility and torsional deform. *(Japanese)* 79−57069
Cu, influence on thermal conductivity maximum, 4.2 to 70K 78−76049
Cu, internal stresses in plastically deformed crystals *(Russian)* 78−79615
Cu, layered cell structures and slip lines in deformed cryst., TEM obs. 79−99209
Cu, low temp., internal friction and microplastic strain 77−84839
Cu, M1E, yield stress decrease in compression, rel. to previous elongation *(Polish)* 80−50665
Cu, microcrack propagation and plastic strain 80−81187
Cu, microdeformation distrib., effect of form of stressed condition 77−63759
Cu, microplastic deform. and amplitude depend. of internal friction *(Russian)* 80−45349
Cu, neutron irrad. cryst., edge and screw dislocation groups, mean vel. 79−7607
Cu, OFHC effect of cold drawing under combined stress 80−60912
Cu pin, heavily deformed surface layer after dry sliding against steel ring, TEM obs. 77−60033
Cu, plane strain deformed, electron microscope obs. of morphology 78−31424
Cu, plastic deform. build-up during low cycle fatigue *(Russian)* 77−25207
Cu, plastic deform. micropattern under various loading conditions 77−44321
Cu, plastic deformation thermal activation parameters from creep kinetics and stress relaxation 80−71717
Cu, plastic props., room temp. to recrystallisation temp., stress/strain relations, computer program 77−1865
Cu, plastic rate calc. *(French)* 77−73303
Cu, plastic strain meas. due to sliding wear 78−64731
Cu, plastic working of wires, high-density current appl. 79−57002
Cu, plastically deformed, containing dislocation distribs., X-ray diffr. line broadening 77−43218
Cu, plastically deformed, lattice strain distrib. *(German)* 80−85012
Cu, plastically deformed, positron trapping rate temp. depend. 78−31276
Cu, plastically deformed, recovery, isochronal annealing, positron lifetime meas. 77−59807
Cu plastically deformed crystals, SEM exam. of light and dark etch pits, dislocation arrangements 78−87679
Cu, polycryst., low temp., plastic deform., structural defects, elec. resist. meas. *(Russian)* 78−39844
Cu, polycryst., surface layer hardening by multiple impact 80−108469
Cu, polycrystn., cold worked, calc. of dislocation density as function of plastic strain 79−38924
Cu, polycrystn., strain localisation during hot deform. 80−104195
Cu, polycrystn., stress relaxation in cyclic deformation 80−3119
Cu, positron trapping rate by dislocations in plastically deformed sample, 6 to 77K 77−11592
Cu powders, electron-positron annihilation charact. *(Russian)* 77−63485
Cu, recrystallisation kinetics after small deform. and grain growth *(Czechoslovakian)* 77−32592
Cu, recrystallisation textures, and deformation formed by dry sliding against steel 79−91698
Cu, recrystallised, inhomogeneous deform. due to texture changes *(German)* 79−29158
Cu, recrystallization annealing, grain growth, effect of type of deform. 80−100847
Cu, recrystallization diagram for fine grained metal in region of small deform. *(Czech)* 77−59811
Cu, rolling textures and texture inhomogeneities, exam. of development in single- and poly-crystals 79−11637
Cu, shear mode of ductile fracture 78−31525
Cu, single cryst., deform. process, effect of surface layer 79−8315
Cu single crystal, stored energy meas. by new deform. calorimetry method 78−39834
Cu single crystal, weakly deformed, elec. resist. recovery, annealing effect 77−81304
Cu, single crystals, absorbed H, strain anal., X-ray divergent beam method 78−15463
Cu, single crystals, amplitude and freq. response to 1-dimens., transient stress waves 78−14399
Cu, single crystals, deformed, extinction, γ-ray diffractometry and neutron struct. refinement 77−84588
Cu, single crystals, dislocation breakaway, etch pit study 78−6064
Cu single crystals, dispersion strengthened, low temp. recovery of work-hardening and creep 79−83211
Cu single crystals, neutron irradiated, secondary slip 80−88161
Cu, single crystals, neutron irradiated, stresses and secondary slip between overlapping and dislocation arrays 80−88162
Cu single crystals oriented along [100] and [111], exam. of slip line length 78−76664
Cu, single crysts., ⟨110⟩ oriented, tensile deformed, HVEM of recrystn., recrystallised state 80−89256
Cu, single crysts., cyclically and unidirectionally deform. X-ray diffr. study 80−89319

plastic deformation continued
Cu, single crysts., deformed in [001] and [111] axes, cell structs., TEM 80−70209
Cu single crysts., deformed, HVEM study of recrystn. texture 80−104179
Cu, single crysts., fatigued, random strain amplitude cycling 80−3146
Cu, single crysts., hysteresis behaviour implications rel. to fatigue, plastic strain cycling 80−3191
Cu, sintered, deform., temp. and loading rate effects 77−77548
Cu, sintered preform, porous, ductile fracture criterion, rel. to forging process 77−56105
Cu, steady state, transients due to strain rate changes 77−81302
Cu, stress-strain behaviour over large strain range 79−15745
Cu, strip, formed by high deform., mech. props. charact. *(Russian)* 78−27534
Cu, struct. changes in single cryst. under influence of static and dynamic stresses *(Russian)* 78−92300
Cu, tensile curve and specific value of anisotropy coefficient *(French)* 77−28867
Cu, tensile deformed ⟨110⟩ orientated single cryst., recrystn., high voltage electron microscopy study 80−84958
Cu, tensile plastic deformation, energy storage efficiency 77−4807
Cu, tension deformed single crystal, dynamic recrystallisation 79−47716
Cu, thermal conductivity, low temp., influence of plastic deform. 78−30899
Cu, thermoactivated creep and stress relax. 79−87692
Cu, torsion deformation texture *(French)* 79−70082
Cu, tough pitch wire, rel. between oxygen contents and cupping *(Japanese)* 79−79087
Cu tubes, anisotropic, plastic deformation in hydraulic bulging 79−61688
Cu, types MOb and M1, primary recrystallisation kinetics depend. on state of impurities *(Russian)* 79−66069
Cu, ultrasonic velocity response to stepwise change of stress *(Japanese)* 79−38905
Cu, vacuum condensate, struct. and mech. props. depend. on deposition conditons 80−15417
Cu, virgin surface, contact formation and cohesion, influence of multiple contacting *(Russian)* 80−40548
Cu, void growth and localisation of shear in plane strain tension 78−64613
Cu, whiskers, hardening during uniaxial extension, preliminary torsion deform. *(Russian)* 78−15420
Cu wire, drawn through diamond die, deformation zone EMF *(Russian)* 77−81327
Cu wire, mech. props. and struct. after high-speed recrystallisation *(Russian)* 79−47704
Cu, wire, recrystallisation *(German)* 77−86055
Cu wires, electrolytic, Young's modulus, working temp. effects 80−50667
Cu, X-ray and microhardness meas. at high strain rates *(German)* 78−3184
Cu-AL(Zn), effect of original grain size on struct. and props., after deformation and annealing 78−44178
Cu-Ag, deformed, recrystallization nucleation at second phase particles, electron microscope obs. 79−34059
Cu-Ag, solid soln., nonhomogeneity of deform. 78−84889
Cu-Ag (3 at.%), plastically deformed, lattice strain distrib. *(German)* 80−85012
Cu-Ag (8 wt.%), deformed, free energy changes in process of discontinuous precipitation 80−3054
Cu-Ag (8 wt.%), plastic deform. effect on discontinuous precipitation 80−3053
Cu-Ag solder composite, plastic deform. below worn surfaces 77−36670
Cu-Ag-P amorphous alloys, strain gauge factor and elec. props. *(Japanese)* 79−79130
α-Cu-Al, disordered by plastic deform. and ordered by heat treatment, effect of annealing on residual elec. resist. *(Russian)* 79−51547
Cu-Al, heavily deformed martensites, annealing 79−38873
Cu-Al, short range order and static distortion contribution to residual elec. resistivity *(Russian)* 80−70672
Cu-Al, single crystal, dislocation velocity meas. 78−3172
Cu-Al, single crysts., hysteresis behaviour implications rel. to fatigue, plastic strain cycling 80−3191
Cu-Al, vacuum condensate, struct. and mech. props. depend. on deposition conditons 80−15417
Cu-Al (10 at.%), single crystal, orientation depend. of work hardening near [111] axis 77−12646
Cu-Al (10 wt.%), deformed and tempered transform. during heat treatment of β′ martensite *(Rumanian)* 79−34031
Cu-Al (10.5 at.%), dislocation generation and displacement in single crystal in bending 79−60368
Cu-Al (13 wt.%), polycrystn. rod specimens effect of diameter on slip mode, optical microscopy obs. 79−79051
Cu-Al (15 at.%), single crystal, steady state deform. with ⟨001⟩ axis at high temp. *(Japanese)* 78−6980
Cu-Al (15 wt.%) single crystal, steady state deform. at high temps. *(Japanese)* 78−19833
Cu-Al (2.5 at.%), single crystal, steady state deform. at high temps. *(Japanese)* 77−52415
Cu-Al (5 wt.%), subjected to tension-compression fatigue, deform. and fracture strength *(Japanese)* 80−93644
Cu-Al (9 wt.%), deformed, fatigue crack propag. 78−27621
Cu-Al (9 wt.%) deformed, dispersed, ordered, microcalorimetry of plastic zones during fatigue crack propag. 79−47769
Cu-Al (<3 at.%), new type of discontinuous slip at low temps. 77−12676
Cu-Al alloy, low temp. deform., heating of dislocation sources 78−18660
Cu-Al_2O_3, sinterec, deform., temp. and loading rate effects 77−77548
Cu-$Al_2O_3(SiO_2)(TiO_2)$ alloys, internally oxidised, plastically deformed, influence of particle form on primary loop nature *(French)* 80−103344
Cu-Al-Fe, strength increase from intermediate annealing determ. of annealing temp. by recrystallisation 78−44136
Cu-Al-Ni, 2H to 6R lattice restructurization during deform., anomalous elasticity 78−19753
Cu-Al-Ni, long period martensite phases, X-ray diffr obs. 80−7571
Cu-Al-Ni, rubber like behaviour 77−86114
Cu-Al-Ni alloys, deformed, fine struct. of martensite *(Russian)* 78−6923
Cu-Al-Ni(Mn), duplex shape memory effect after nonuniform plastic deform. *(Russian)* 80−25759

plastic deformation continued
Cu-Al(8 at.%), single crystal, twinning deform. 77−21236
Cu-Au, (0.02-5 at.%), cold worked, internal friction peaks 79−11652
Cu-Au, cold worked solid solution, flow stress and activation volume 80−16393
Cu-Au, plastic deformation, energy storage efficiency 77−4807
Cu-Au (50 at.%), ordered, influence of elastic stresses on mech. props. *(Russian)* 78−92298
Cu-Au(Ni)(Zn), elastic modulus and internal friction during plastic deform., dislocation props. determ. 80−35244
Cu-Be (2 at.%), plastic deform. and dislocation substruct. 80−76307
Cu-Be (2 wt.%), plastic deformation influence on ageing, granular microhardness *(Russian)* 80−55474
Cu-Be-Ni-Ti-Mg bronze, alloying element influence on minimum thermo EMF, cold working *(Russian)* 80−34426
Cu-Bi (0.0115 wt.%), embrittled, transgranular fracture accompanied by plastic deformation 79−27998
Cu-Cd (0.03 at.%), single cryst., deformed, dislocation arrangement 79−10856
Cu-Cd (1.0 wt.%), yield stress and flow stress 80−97524
Cu-Co (2 wt.%), single crysts., fatigued age-hardenable, dislocation structure *(German)* 80−54247
Cu-Co-Fe, dil. alloy, low temp. resistivity maxima, deform. and ageing effects *(Russian)* 79−87091
Cu-Cr (0.75 wt.%), deformation characts., fully reversed cyclic strain with fatigue cracks and dislocation struct. 80−81148
Cu-Fe(2.5 wt.%), isothermally reacted austenite stability in very small particles 77−48432
Cu-Ga, high dislocation density alloys and oxide precipitated struct., NMR, spin echo 80−39892
Cu-Ge, primary coplanar slip, role in deform. of FCC crystals *(Japanese)* 77−52412
Cu-Ge (1 at.%), FCC crystal, stress-strain curve, stage I to stage II transition *(Japanese)* 78−19834
Cu-Ge (10-12 wt.%), intermediate ξ′-phase form. during deform. *(Russian)* 78−19747
Cu-Ge (2 wt.%), positron annihilation, photon ang. distrib. meas. effect of deformation, annealing temp. *(Russian)* 78−35220
Cu-Ge (8 wt.%), anelastic effect due to deform. twins *(Japanese)* 79−20095
Cu-Ge single cryst. containing heavily faulted regions, X-ray diffr. profiles 80−24462
Cu-H, rolled sheet, plastic anisotropy theory based on yield function of fourth order 78−31458
Cu-Nb multifilamentary composites, in situ formed, anomalous strength increase 79−43323
Cu-Nb-Sn, multifilamentary supercond. composite wires, fabrication on laboratory scale and mech. props. 80−29897
Cu-Ni, cold worked solid solution, flow stress and activation volume 80−16393
Cu-Ni, cyclically deformed, electrical resistance changes 79−57096
Cu-Ni, powder, sintered, effect of cold and hot dynamic pressing, upon structure and props. 79−33970
Cu-Ni (10 at.%), struct. changes during deform. *(Russian)* 78−19818
Cu-Ni (10 wt.%), deformed bars, cold rolled, exam. of microstruct. by thin foil TEM 78−88502
Cu-Ni alloy, dislocation density during deform., comparison of electron microscopy and X-ray diffr. *(Russian)* 79−5002
Cu-Ni diffusion couple, diffusion bonding process, fracture surface exam. *(German)* 77−35762
Cu-Ni-Al (5, 2.5 at.%), precip. hardening *(Japanese)* 80−71663
Cu-Ni-Fe alloy, quenched and aged, deformed, low-temp. elec. resist. meas. *(Russian)* 77−52514
Cu-Ni-Sn (10, 6 wt.%), temp. depend of yield stress and work hardening 80−21026
Cu-Ni-Sn (15, 8 wt.%), prior deform. effect on spinodal age hardening 80−108465
Cu-Si, high dislocation density alloys and oxide precipitated struct., NMR, spin echo 80−39892
Cu-Si, stacking fault energy meas. by tensile deform. of polycrystalline samples 78−95060
Cu-Si (6.5 at.%), plastic deformation, HVEM study *(French)* 80−66605
Cu-Si (6.5 at.%) alloy, easy glide deform., obs. and mechanism 77−8887
Cu-SiO_2, deformed, lattice rotations at second phase particles 80−25709
Cu-SiO_2, in-situ deform. in HVEM 80−103338
Cu-SiO_2, low-temp. recovery creep, Orowan loop accumulation 80−81126
Cu-SiO_2 systems, cavity nucleation, by plastic deform. 79−29127
A-Cu-Sn, cyclic work hardening during frequency change fatigue-tests *(German)* 79−34068
Cu-Sn industrial bronzes, Sn diffusion in deform. zone influence on wear resistance, friction *(Russian)* 80−108582
Cu-Sn solid soln. steady state deform. *(Japanese)* 78−19832
Cu-Sn-Al, deform at high temps. *(Polish)* 80−89284
Cu-steel and Cu-brass system, realisation of selective transport mode with friction, effects of normal stresses 79−87735
Cu-Ti, deform. effect on precipitation and recrystallisation, electron microscope study 77−70115
Cu-Ti (3.5 wt.%), internal friction in dissociating alloy following deform. by US *(Russian)* 78−35419
Cu-Ti (4 wt.%), combined recrystallization and precipitation 79−29072
Cu-Ti(Ag) alloys, activation vol. stress depend., single crysts. 77−48499
Cu-Ti(0.7 at.%), plastic deform. and precip. hardened, annealing time 78−48446
Cu-Zn, cold worked solid solution, flow stress and activation volume 80−16393
Cu-Zn, interface sliding of FCC and BCC boundaries 80−104240
β′Cu-Zn, martensite to martensite transformations 79−11615
Cu-Zn single crystal, pseudoelastic effects 79−47739
Cu-Zn-Al, reversible shape memory effect obtained by heating under constraint *(Japanese)* 79−43335
Cu-Zn-Al, reversible shape memory effect associated with $\beta_1 \rightleftarrows \beta_1' \rightleftarrows \alpha_1'$, transform. *(Japanese)* 79−43242
α-Cu-Zn-Al (18, 7 at.%), deform. and mech. props. 79−29159
β-Cu-Zn-Al (27.5, 4.0 wt.%), strain induced martensite, exam. of structure, microstructure 80−7648
Cu-Zn-Al martensite, the rubber effect 79−47684
Cu-Zn-Al martensites, model for rubber like behaviour 79−47685
Cu-Zn-Si, deform. close to martensitic transform. temp. 77−63714

plastic deformation continued
α-Cu-Zn(Al), solid soln., intermediate temp. embrittlement *(Japanese)* 79−20158
α-Cu-Zn(Al) fracture behaviour, effect of deform. temp. and alloying content *(Japanese)* 79−20159
(Cu-Au)-Co, single crysts., solid soln. and particle strengthening, superposition 80−97495
Cu_3Au, deformation twinning 77−63717
Cu_3Au, disordered [001]-orientated single crysts., plastic deform., TEM and slip line studies 80−97541
Cu_3Au, ordered and disordered, cavitation induced erosion 77−16743
$CuFeS_2$, explosive-shock deform. 78−95108
Cu_2MnAl, dislocation structure, antiphase boundary energies, deformation behaviour prediction *(Russian)* 79−65085
Cu_2MnAl, Heusler alloy, single crystal, plastic deform. 77−44308
Cu_2MnAl, plastically deformed, domain struct., X-ray diffr. and electron microscope obs. *(Russian)* 79−20110
β-(CuNi)Zn, anomalous strengthening 77−48503
Cu_2O, creep substruct. under compression, X-ray diffr. study 78−95785
Cu_2O, heterogeneous deform. during high temp. compression creep 78−48456
Cu_2O, thermal activation of plastic deform. *(French)* 80−16394
Dy, magnetoplastic deform., 70-90 kOe, 4.2K 77−8376
Dy, single crystal, plastic and magnetoplastic deform. 77−63713
Dy, substructural changes during plastic deform., stress-strain diagrams and microhardness meas. *(Russian)* 79−52296
$DyVO_4$ Jahn-Teller crystal, deform. induced transitions, elastic and dielectric characts. *(Russian)* 80−80726
Er, substructural changes during plastic deform., stress-strain diagrams and microhardness meas. *(Russian)* 79−52296
Fe, [110] and [410] single crysts., push-pull fatigue 79−74257
α-Fe, acoustic emission signals in plastic deform., amplitude distrib. *(Japanese)* 78−6978
Fe alloy granules in Cu binder, exam. of wear characteristics without lubrication 79−96154
Fe alloy MA-956E, oxide dispersion strengthened sheet, tensile and creep props. at 1365K 78−48470
Fe alloys, influence of plastic deform. on twinned martensite struct. *(Russian)* 78−88493
Fe, amorphous, tensile deform., three-dimens. computer simulation 79−43350
Fe and Fe alloys, strain amplitude depend. of US attenuation 77−1182
Fe and Fe_3Si, hardening and softening during adsorption fatigue in surface active medium, governing laws 77−86230
Fe, annealed, and deformed, exam. of immobile dislocation distrib. *(Russian)* 79−32995
Fe, anodic behaviour in 1M H_2SO_4, influence of straining 80−97612
Fe, Armco, cold-rolling cavity formation, TEM study 78−6947
Fe Armco, corrosion and mechanical behaviour in liquid Li 78−53036
Fe, Armco, cyclic deform. in presence of H_2 *(Russian)* 77−16728
Fe, Armco, fatigue crack propag., influence of specimen thickness *(German)* 80−66669
Fe, Armco, fatigue cracking under 23 kHz loading at 23°, 60° and 100°C 78−60763
Fe, Armco, flat-rolled and annealed, dislocation struct. and mech. props. *(Russian)* 79−20062
Fe, Armco, H_2 diffusion 0 to 300°C, effect on elongation tension *(Russian)* 77−66044
Fe, Armco, inelasticity when under cyclic strain, in active media 78−80613
Fe, Armco, microflow and strain hardening under cyclic loading 80−104182
Fe, Armco, microstruct., effect of strain rate on change, due to tension-compression 78−80614
Fe, Armco, microstructure in quasibrittle and plastic fracture 77−1863
Fe, Armco, plastic zone around fatigue crack, vac. effect 80−100914
Fe, Armco, surface dissolution effect 77−8883
Fe, Armco and carbonyl, kinetic singularities of plastic deform. during γ→α transform. *(Russian)* 78−92262
Fe, BCC, strain hardening and recovery by pure metal mode, high temp. deform. *(Japanese)* 78−52843
Fe, cast, contact deformation, reverse slipping effect *(Russian)* 80−97591
Fe, cast, mech. charact. in plane stressed state of type SCh15-32 79−57072
Fe, cast, spherical, mech. behaviour, continuous theory of dislocations appl. 78−67717
Fe, cast, US study of sections undergoing deform. or thermal cycling 80−104285
Fe, cast, white, graphitisation, effect of hot impact deform. 78−19780
Fe, cast, with uniaxial loading, changes in ultrasonic waves vel. and attenuation 79−15756
Fe, cast nodular, high strength, low cycle fatigue 79−57112
Fe cast with spheroidal graphite, fine cryst. struct. on tempering *(Russian)* 80−96476
α-Fe, cavitation and sliding distrib. changes during creep at 500°C 78−6991
Fe, cold rolled, struct., transmission Kossel patterns obs. 77−48451
Fe, commercial, deformability at 600 to 950°C 77−70117
Fe, compressed, recrystallisation, transmission Kossel study of struct. 78−19776
α-Fe, creep and fracture between 77 and 673K 79−7649
α-Fe, cyclically deformed, mag. props. 77−28412
Fe, damping during and after deformation 79−43344
Fe, deformation, influence of crystallographic lattice type *(Russian)* 79−34106
α-Fe, deformation induced intergranular creep cavitation 78−31473
Fe, deformed, deep trapping states for H_2 80−29045
Fe, deformed, defects, thermal relaxation, positron experiments *(German)* 80−50455
Fe, deformed single crystal, dislocation distrib. 77−59880
α-Fe, dislocation loops, equilib. shape under shear stress 79−7608
Fe, effect of plastic deform. and martensite transformation on Fe atom mobility *(Ukrainian)* 78−55974
Fe, electroplated with soft Fe coating, fatigue fracture, struct. characts. 80−55524
δ-Fe, ferritic, plastic deform. at intermediate strain rate 77−36592
α-Fe film, deform. in electron microscope, dislocation mechanism 79−82227
Fe, flow stress, effect of mag. field 77−20673

plastic deformation continued
α-Fe, Frenkel defect recombination zone, effect of uniaxial compression 78−6987
Fe, grade EA, plastically deformed, magnetoelastic props. *(Russian)* 80−44893
Fe, grain growth kinetics under 2 to 10% tensile deform. 77−40435
Fe, H_2 induced cracking, stress state effect 79−20147
Fe, high purity single crystals, dislocation density rel. to work hardening *(German)* 77−32590
Fe, high purity single crysts., thermally activated slip deformation between 4.2 and 300K 80−25801
α-Fe, high temp. deform. and substruct. *(Japanese)* 77−21226
Fe, inelastic deformation, mech. eqn. of state, stress relax. 77−56047
α-Fe, influence of C and ZrH_2 on static and cyclic creep behaviour 78−39856
Fe, internal friction in plastic deformation process *(Chinese)* 80−88259
α-Fe, internal friction peaks from dislocation relax. in plastically deformed and/or neutron irrad. sample 78−48438
Fe, isochronous annealing recovery, in cold rolled and explosively formed samples 79−100166
α-Fe, low cycle deform., strain rate and depressed temp. effect 79−61660
Fe, low temperature deform., strain-rate cycling and stress relaxation tests *(Japanese)* 78−52876
Fe, microcracks formed by H_2 precipitation, SEM and TEM obs. *(Japanese)* 79−70071
Fe microcrystals, dislocation struct. singularities in early deform. stage *(Russian)* 77−55284
Fe, model for Luders band formation and plastic instability related with strain softening due to Johnston-Gilman-Hahn theory 79−61676
Fe, particle formation by evap., electron microscopy obs. of interaction processes 80−104053
Fe, plastic deform. and fracture, H_2 effect, studied by electron microscopy and Auger spectrography *(French)* 77−77545
α-Fe, plastic deform. in neck leading to fracture 78−64655
Fe, plastic deform. of single crystal with shear tests in {110}⟨111⟩ and {112}⟨111⟩ slip system 77−48509
Fe plastic strain, thermoactivation anal. exam. of method *(Russian)* 79−57164
Fe, plastically deformed, dislocation arrangement exam. by ferromag. techniques 78−63774
Fe, plastically deformed, high field suscept. anisotropy and domain struct. 78−15002
α-Fe, plastically deformed and/or irrad., high purity, internal friction peaks due to dislocation relax. 77−86075
Fe, plastically deformed by pulsed mag. field, mobility of Fe atoms, radiotracer profiles 79−28584
Fe, point defect estimation from specific heat and volume in plastically deformed pure metals *(Russian)* 80−54223
Fe, polycrystalline, exam. of Luders deformation 78−84893
Fe, powder, consolidated, exam. of mech. and electrical props. 78−56599
Fe, pure, cathodic charging effect on creep and tensile deformation 80−76320
Fe, pure, deformed, internal friction, dislocation relax. and dislocation-defect interactions 79−29125
Fe, pure, grain growth, abnormal, kinetics 79−24537
Fe, pure, rolling texture *(German)* 77−86054
Fe, pure, tensile deform., sources of acoustic emission 78−19814
Fe, residual stress induced by uniaxial deform., magnetic meas. 77−73390
Fe, single crystals, absorbed H, strain anal., X-ray divergent beam method 78−15463
Fe single crystals, size effect on slip deformation ability at very low temps. 80−21049
Fe, sintered, fracture behaviour, microscopic obs. 79−47771
Fe, sintered, plastic deform., porosity effects 78−23801
Fe, sintered, strength and elongation, rel. to density 80−30047
Fe sintered powder, plastic deform., constitutive eqns. 79−61667
Fe static loading over wide deform. and temp. range, acoustic emission, plastic flow, fracture 77−90424
Fe, static loading over wide deform. and temp. range, acoustic emission, fracture, plastic flow 77−90425
α-Fe, strengthening kinetics due to deformation ageing, impurity atom sources *(Russian)* 80−55435
Fe, thermally activated slip deformation, 0.7 to 77K 79−91755
Fe thin layers, vacuum coated on PMMA, mag. behaviour during mech. stress cycles *(German)* 80−80581
Fe, US oscillatory stress superimposition effects on deformation 80−35287
Fe, var. in mag. moment of ferromags. during plastic deform. *(Russian)* 77−66401
Fe, varying purity, internal friction, H-dislocation interactions 77−52377
Fe, volume changes and defect healing due to plastic deform. *(Russian)* 80−81139
Fe, wear sliding track, deformation 77−12707
Fe, whisker, H_2 effect on deform. 78−68755
Fe whiskers, elastically and plastically deformed, mag. domain structs. 80−15752
α-Fe, yield point behaviour for extremely inhomogeneous deformation *(German)* 80−55453
α-Fe, yield point behaviour in homogeneous plastic deformation *(German)* 80−35248
Fe/Fe-Cu composites, microplastic deformation development 78−39877
Fe-Ag (50 vol.%), two-phase system, plastic deformation *(French)* 78−39831
Fe-Ag (50 wt.%), plastic behaviour in compression, deform. rate effect *(French)* 80−71711
Fe-Al, Al effect on softening in solid soln. *(French)* 79−52226
Fe-Al, deformed, low temp. recovery of elec. resist. *(Russian)* 80−7697
Fe-Al, single crystals, deform. at high temps. 80−81125
Fe-Al (0.069 and 0.158 wt.%), internally oxidised, low temp. deform. *(Japanese)* 78−52876
Fe-Al (4 wt.%) single crystals, rolling induced mag. anisotropy and its removal by annealing treatment *(Russian)* 79−61746
Fe-Al (40 at.%), ordered, plastically deformed, neutron irrad. damage and recovery, resist. meas. 77−19993
Fe-Al-(Nb), fatigue deform. 77−44350
Fe-Al(25 at.%), mag. anisotropy induced by plastic deform., dislocations, long-range order 77−4544
Fe-Co, prod. of point defects *(French)* 78−72829

plastic deformation continued
Fe-Co alloy, V addition effect on atomic order parameters, dislocation struct., mechanical props. 79−91762
Fe-Co-Cr, alloy K25Kh15, phase tranforms., nucl. gamma reson. and X-ray diffr. meas. *(Russian)* 77−44241
Fe-Co-Ni-W alloy, 45KKhVN, plastic deform., electron microscope obs. *(Russian)* 78−80584
Fe-Co-V, Vicalloy, $\alpha \rightarrow \gamma$ transform. under plastic deform., morphological singularities *(Russian)* 77−32576
Fe-Co-V (2%), prod. of point defects *(French)* 78−72829
Fe-Co(-V) alloys, neutron irradiated, influence of dislocation doping on recovery 79−46715
Fe-Cr-Al (12, 3 wt.%), internal friction and rigidity modulus, strain amplitude depend. *(Japanese)* 80−92606
Fe-Cr-C alloy, bainitic struct. morphological changes, due to external stress, plastic deform. 78−44120
Fe-Cr-Mo (26, 1 wt.%), single crysts. and polycrysts. strain rate influence on low cycle fatigue props. 80−3126
Fe-Cr-Ni, two phase ($\alpha+\gamma$) alloys, transformation-induced plasticity 77−63721
Fe-Cr-Ni, two-phase ($\alpha+\gamma$), and metastable austenitic, uniform elongation peak 77−77547
Fe-Cr-Ni (18,14 wt.%), γ to ε to α martensitic transform., external stress effect, double tensile deform. exam. 80−108438
Fe-Cr-Ni austenitic alloy, cold deformed, α-γ transition, calorimetric study *(Russian)* 80−55390
Fe-Cr-Ti-Mo, sintered, mech. props. *(French)* 79−91726
Fe-Cu-glass ternary multiphase composite, microstruct. and props. *(German)* 77−90314
Fe-Fe_2C, cavity nucleation, by plastic deform. 79−29127
Fe-H, internal friction 79−57041
Fe-Mn, γ to ε phase transform. induced by high press. and plastic deform. 78−68686
Fe-Mn, mechanical twinning of close-packed hexagonal ε-phase during plastic deform. *(Russian)* 80−60909
Fe-Mn (-C), Mn influence on martensitic transform in presence of strain *(Russian)* 80−20934
Fe-Mn (12% Mn), decomposition during plastic deform., Mossbauer parameters *(Russian)* 77−36166
Fe-Mn (15(24)(30)wt.%), high hydrostatic pressure influence on stress-strain curve 80−25805
Fe-Mn (32.5 and 38.3 wt.%), steel sheet, exam. of form limit diagrams and damage 78−48461
Fe-Mn-C, structural var. during warm deform. in $\gamma \rightarrow \varepsilon$ transform. region *(Russian)* 77−81293
Fe-Mn-C (0.7, 0.9 wt.%), pearlitic, deform. 77−86095
Fe-Mn-Cr-C, twinning and strain induced FCC to HCP transform. 77−44248
Fe-Mn-Cr-C (20, 4, 0.5 wt.%), hyperquenched and predeformed, mech. props. *(French)* 78−23786
Fe-Mn-Nb-V, high Mn, dispersion strengthening 77−16602
α-Fe-Mo (1.5 and 1.8 at.%), deform., testing mode effect at stages prior to steady states 77−66721
Fe-Mo (3 wt.%), substitutional solid soln. with cubic faced symmetry, Portevin-Le Chatelier effect *(French)* 78−23785
Fe-N, neutron irrad. effects on mech. props. 79−4338
Fe-N single crystals, plastic deform. in temp. range 4.2 to 300K 80−76321
Fe-Ni, hardening by plastic deform. during polymorphic transform., struct. mechanics for γ-phase form. *(Russian)* 77−90344
Fe-Ni, hardening by plastic deform. during polymorphic transform., mechanical props. *(Russian)* 77−90345
Fe-Ni, reverse martensitic transform., prior deform. effect 77−63668
Fe-Ni, secondary recrystallization *(Czech)* 79−70080
Fe-Ni (15, 25 at.%), longitudinal forces in the hot torsion test *(German)* 79−38889
Fe-Ni (23 wt.%), struct., composition changes during α to γ transform., martensite plastic deformation influence *(Russian)* 80−11642
Fe-Ni alloy, effect of electron irradiation and deform. on martensitic transform. 77−16581
Fe-Ni alloy, effect of plastic deform. and martensite transformation on Fe atom mobility *(Ukrainian)* 78−55974
Fe-Ni alloy, solid solution, vibr. analogue of Bain deform. and morphology of martensite in 78−2224
Fe-Ni alloys, influence of hydrostatic press. on γ to α' transform. during plastic deform. *(Russian)* 79−15663
Fe-Ni single crystal, lattice strain induced by anisotropic distrib. of M_2 *(Japanese)* 80−35262
Fe-Ni solid solution, deformation mechanism, softening phenomena, dislocation-solute atom interactions *(French)* 80−45344
Fe-Ni-Al-Co-Cu-Sn alloy YuNDK35T5, Sn addition effects on physicomechanical and magnetic props. and workability *(Russian)* 77−70101
Fe-Ni-Al-Co-Cu-Ti YuNDK type, S effect on mech. props. 80−60927
Fe-Ni-C, HVEM study of strain induced martensite 79−20047
Fe-Ni-C, martensite nucleation, tensile prestraining effect 77−8828
Fe-Ni-C, martensitic, deformed, stress induced C distrib. *(Czechoslovakian)* 77−32641
Fe-Ni-C, martensitic, mech. charact., effect of ageing and tempering *(Slovak)* 78−19791
Fe-Ni-C, martensitic, mech. and fracture charact., effect of starting austenite heterogeneity *(Slovak)* 78−19792
Fe-Ni-C, N31, martensitic point lowering by microplastic deform. and room temp. ageing *(Russian)* 77−25049
Fe-Ni-C, plastic deform. effect on austenite stabilisation *(Korean)* 80−21021
Fe-Ni-C, role of strain in deform. induced martensitic transform. *(Japanese)* 78−92263
Fe-Ni-C, single crystal, form. and strength of strain-induced martensite 79−100225
Fe-Ni-C (19.5, 0.73 wt.%), banded struct. formed by deform., TEM and optical obs. 78−39869
Fe-Ni-C (21, 0.6 wt.%), stress assited and strain induced martensite morphologies 78−3187
Fe-Ni-C (24, 0.45 wt.%), single crystal, plastic deform. effect on martensitic burst transform. 79−15695
Fe-Ni-C (25, 0.2 wt.%), strain-induced martensite *(Korean)* 80−71646
Fe-Ni-C (26.4, 0.24 wt.%), austenitic single crysts., effect of prior deformation on martensite burst transformation, SEM obs. 79−38823
Fe-Ni-C (30.59, 0.02 wt.%), effect of loading on transformation of retained austenite to martensite 79−47686
plastic deformation continued
Fe-Ni-C (31, 0.1 wt.%), kinetics of deform. induced martensite, shock loading and grain refinement effects 78−15395
Fe-Ni-C (31, 0.1 wt.%), metastable austenite, fractography 77−59919
Fe-Ni-C (31, 0.1 wt.%), pre-deformation and temp. effect on transformation-deformation behaviour 80−3127
Fe-Ni-C (31, 0.28 wt.%), crossings of thin plate martensites, TEM obs. 80−25756
Fe-Ni-C (31.24, 0.21 wt.%) effect of deformation and ageing after deformation, on martensitic transformation temp. 78−76650
Fe-Ni-C alloys, obs. of banded struct. formed by deformation 79−79050
Fe-Ni-C austenite, metastable, influence of prior deform. on yield stress 78−15461
Fe-Ni-C austenitic alloy, banded struct. formed by deform. 80−71713
Fe-Ni-C austenitic single crysts., deform. props., martensitic transformation, SEM study 79−29143
Fe-Ni-Cr (23, 5 wt.%), martensite orientation formed under uniaxial stress alloy [001] 77−77475
Fe-Ni-Cr based alloy, KhN35VTYu, temp. depend. of energy of fracture, influence of γ' phase *(Russian)* 80−81147
Fe-Ni-Mn, martensite, aged, grain boundary embrittlement 79−96144
Fe-Ni-Mo alloy, high-strength ferritic, for cryogenic service, mech. characteris. 77−70143
Fe-Ni-Ti (25.9, 2.15 wt.%), exam. of effect of inhomogeneous solid soln., on martensitic transformation *(Russian)* 79−34034
Fe-Ni-Ti (27.4, 2 to 3 wt.%), aged, stress induced martensitic transform., mech. props. *(Russian)* 79−87632
Fe-Ni-V-C alloy, reverse α to γ transformation, previous deformation influence on struct. and props. *(Russian)* 79−100139
Fe-Pt, plastic deform. effect on struct. singularities and mag. props. *(Russian)* 80−44892
Fe-Si, dynamically strained, temp. depend. of twinning charact. *(Russian)* 79−46673
Fe-Si, fatigue fracture fractography in broad strain-amplitude range, in air and vacuum 80−81186
Fe-Si, maze domains upon appl. of horizontal mag. field or mech. tension 80−11218
Fe-Si, microflow and strain hardening under cyclic loading 80−104182
Fe-Si, microplastic deform. and amplitude depend. of internal friction *(Russian)* 80−45349
Fe-Si, polycrystalline, exam. of stress-strain state of individual grains 78−80580
Fe-Si, stress and plastic deform. effect on Barkhausen effect, instrumentation 78−52313
Fe-Si, strips and rods, spatial extent of flux due to irreversible changes of mag. polarisation 79−33506
Fe-Si, synchrotron X-ray topography dynamic expts. 78−67621
Fe-Si, temp. depend. of twinning intensity, development of deform. *(Russian)* 79−51116
Fe-Si, twinned annealing, plastic deform., and recrystallisation *(Russian)* 77−28829
Fe-Si (3 at%), deformation and electron bombardment, influence on dislocation struct., 20-500°C *(Russian)* 80−92536
Fe-Si (3 at.%), acoustic emission response 79−87801
Fe-Si (3 wt.%), (110)[001] oriented single crystal, form. of rolling and annealing texture 77−16608
Fe-Si (3 wt.%), deform., effect of superimposed US oscillatory stress *(Japanese)* 78−31461
Fe-Si (3 wt.%), electron irradiated, yield strength and elongation 80−76325
Fe-Si (3 wt.%), exam. of plastic deformation, slip band dislocation, under hydrostatic pressure 78−56695
Fe-Si (3 wt.%), fatigue crack propag. work coeff. 80−16422
Fe-Si (3 wt.%), pulsed laser induced deform. 77−36605
Fe-Si (3 wt.%), recrystallisation along grain boundaries *(Russian)* 78−6942
Fe-Si (3 wt.%), single crystal, plastic deform., 473 to 1000K 77−73310
Fe-Si (3 wt.%), single crystals, cyclic deformation oriented for single glide 79−100224
Fe-Si (3 wt.%), single crysts. and polycrysts. strain rate influence on low cycle fatigue props. 80−3126
Fe-Si (3 wt.%), strain aged polycrystalline samples, AE study of deform. 77−63696
Fe-Si (3 wt.%), texture form., plastic strain effect, hot rolled 79−79002
Fe-Si (3 wt.%), US oscillatory stress superimposition effects on deformation 80−35287
Fe-Si (3 wt.%) locally deformed, EM loss depend. on cryst. struct. and orientation *(Russian)* 80−7694
Fe-Si (3 wt.%) struct. and texture changes during repeated deform.-recrystn. *(Russian)* 78−88474
Fe-Si (3.5 wt.%) plastic deform., slip initiation, X-ray topography study 79−47750
Fe-Si (3wt.%), hardening under dynamic load, grain boundary effect 77−12674
Fe-Si alloy, deformed by slip, polygonal boundary form. *(Russian)* 79−24534
Fe-Si-MnS-Al, Al effect on hot rolling struct., recrystallization, texture magnetic props. *(Chinese)* 78−11237
Fe-Si(3.25 wt.%), crack nucleation depend. on twins during intense slip *(Russian)* 79−100239
Fe-Ti (0.056 at.%) alloy, mobile dislocations during stress relax. 77−7729
Fe-Zn alloys, coercive force anisotropy after cold plastic deform. *(Bulgarian)* 80−75809
$Fe_{80}B_{20}$, amorphous, deform. and annealing effects on mag. and mech. props. 77−12717
Fe_2MnAl, dislocation structure, antiphase boundary energies, deformation behaviour prediction *(Russian)* 79−65085
Fe_2MnAl, plastically deformed, domain struct., X-ray diffr. and electron microscope obs. *(Russian)* 79−20110
$Fe_{32}Ni_{36}Cr_{14}P_{12}B_6$, shear band form. 78−68756
$Fe_{32}Ni_{36}Cr_{14}P_{12}B_6$ Metglas, bending deform., shear band form., high-speed cinematographic obs. 80−89322
$Fe_{40}Ni_{40}P_{14}B_6$, amorphous, deform. and annealing effects on mag. and mech. props. 77−12717
$Fe_{40}Ni_{40}P_{14}B_6$, amorphous, mag. polarisation in approach to ferromag. saturation 80−80560
Fe_xO_y-Fe, oxide scale fracture on substrate deform. 78−11407
Fe_3Pb, reversible shape memory effect, rel. to microstruct. memory and residual stresses 77−90419

plastic deformation continued
Fe_3Pt, plastically deformed, struct. inhomogeneities, positron annihilation meas. 79−33859
Fe_3Pt, stoichiometric composition, internal friction, microdeform. and memory effect, rel. to martensitic transform. *(French)* 77−52323
Fe_3Si, etching of slip produced antiphase domain boundaries 78−63769
GaAs, deep radiation centres from heat treatment, γ-irrad., deform., probability of nonradiative electronic transitions 80−50408
n-GaAs, deform. produced deep levels, DLTS meas. 80−54634
GaAs, dislocation density effect on polarisation and intensity of reflected $CuK_{\alpha 1}$ radiation 77−1131
GaAs, during deformation, acoustic emission rel. to cracks, dislocations 80−35441
n-GaAs, effect on elec. props. 77−28178
GaAs, luminescence emitted from deep centres, plastic deform. effect on internal quantum efficiency 80−60672
GaAs, plastically deform., photocond., spectral response and decay process 80−29435
GaAs, produced by thermocompression bonding 77−76807
GaAs pure and Se-doped, photoluminescence at dislocations, band gap electronic levels 79−99926
GaAs:Si, single crysts., asymmetric deform. 79−23616
GaAs-$Ga_{0.7}Al_{0.3}As$ (001), (211), threading dislocation in single layer heteroepitaxial struct., bowing 79−65341
GaP, birefringence observations of strain and plastic deform. 80−50678
GaP/Si heterostruct., differential thermal contraction, plastic deform., fracture 80−108494
GaSb crystals, uniaxial deform., effect on polarised luminesc. 78−10957
n-Ge, deformed, 0.1 eV optical transition, interpretation using electronic states theory for Si 77−20261
n-Ge, deformed, 1/f noise, resist., mobility, and carrier density 77−8161
Ge, dynamical recovery and self-diffusion 79−82379
Ge, high press. appl. by spherical diamond indentor, plastic deform. obs. method 78−35619
p-Ge, highly deformed, hole scattering 77−20309
Ge, low-temp. dislocation cond. mechanism in plastically-deformed pure samples 80−15527
Ge mobility of screw and 60° dislocation at low stresses 77−11554
Ge, nonequilibrium charge carrier-mag. field interaction electron-hole drops, recombination *(Russian)* 80−75511
n-Ge, plastic deformation, impurities and dislocations interaction, cond. *(Russian)* 79−47100
n-Ge, plastically deform., dislocation state spectrum, photocond., elec. cond., and Hall const. meas. *(Russian)* 80−2362
n-Ge, plastically deformed, elec. cond., magnetoresistance, Hall effect study *(Russian)* 79−99568
Ge, plastically deformed, photocond. and absorpt. spectra, dislocation levels 77−28219
Ge, plastically deformed, photocond. produced by polarised light 79−82641
Ge, plastically deformed low temp. cond. *(Russian)* 80−6831
Ge, plastically deformed under high temp. creep conditions, elec. props. 80−92915
Ge, point defect creation by plastic deform., Hall const. electrical conductivity 78−6053
Ge, self-diffusion, dynamical recovery 80−29215
Ge single crystals, brittle, deform. during static indentation 79−87714
Ge, stacking faults of dislocations, constrictions obs. using weak-beam electron microscopy 77−35576
Ge, stationary creep depend. on deform. stabilisation of material struct. *(Russian)* 80−100300
Ge, under laser irrad. rel. to diamond-type structure *(Russian)* 77−56023
Ge uniaxially deformed, cyclotron resonance of RF field heated hot holes, *(Russian)* 80−44925
n-Ge: Ga(P), uniaxial compression, 0.6-2.9 mm radn. absorpt. 79−82629
n-Ge:Bi,O, plastically deformed, dislocation scatt. anisotropy, effect of state of O in Cottrell atm. 78−19028
Ge_2N_2O, pressure induced tetrahedral tilting and deform. 80−24415
GeTe, stoichiometry deviations influence on mech. props., 25-500°C 80−103410
H_2, solid, 2-4.2K, o-H_2 content effects *(Russian)* 77−7787
n-H_2, solid, controlling mechanisms *(Russian)* 77−89493
^{4}He, HCP, free standing cryst., shear deform. 78−2333
^{4}He, plastic deform., athermal processes 79−56017
^{4}He, solid, charge mobility, plastic deform. effect *(Russian)* 79−60599
^{4}He, solid, pure and with ^{3}He admixtures, effect of plastic deform. and impurities on internal friction *(Russian)* 79−77860
^{4}He, solid BCC, plastic deform., stress-strain relations and US attenuation 78−38909
Ho, substructural changes during plastic deform., stress-strain diagrams and microhardness meas. *(Russian)* 79−52296
In, acoustic emission characts. of twinning, nondestructive testing evaluation 77−4873
In, and alloys, whisker samples, stress depend. of supercond. T_c 77−39988
In, stress depend. of supercond. parameters 77−12045
α-In-Sn, stress depend. of supercond. parameters 77−12045
InAs single crystals, brittle, deform. during static indentation 79−87714
InBi single crystal, deform. mode under dynamic indentation 80−88163
InP, photoluminescence at dislocations, band gap electronic levels 79−99926
InP, plastic deform. and scratch microhardness meas. 78−27583
InP single crystals, uniaxial compression deform. characts. 80−84991
InSb, asymmetrical behaviour of 60° dislocation glide 79−7611
InSb, electrical effects of dislocation, galvanomag. props. 78−23119
p-InSb, influence of plastic deform. on elec. props. 80−103711
InSb, photocond. under uniaxial deform. 79−82637
InSb, plastically bent single crysts., dislocation struct. obs. 78−59816
InSb, X-ray topographic evidence of asymmetrical pre-yield behaviour 80−75229
Invar alloys, plastically deformed, struct. inhomogeneities, positron annihilation meas. 79−33859
K, plastic deformation 78−30693
KBr crystal, cordlike defects and countermeasures 79−72636
KBr, point defect concs., effect of plastic deform. 77−1124
KBr-KCl, birefringence, annealing effects, photoelasticity 78−72483
KCl birefringence, annealing effects, photoelasticity 78−72483
KCl, γ-irrad., photoplastic effect and internal friction aftereffect 80−24529
KCl, microcrack propagation and plastic strain 80−81187

plastic deformation continued
KCl single crystals, piezobirefringence and plastic deform., stress-strain curves 77−69798
KCl, single crysts., deform. effects on US attenuation 77−1181
KCl, strain hardening during relax. of deforming stresses 77−7786
KCl, US plastic deform., dislocation struct. 80−19809
KCl:Cu,Ti, charge exchange of hole centres *(Russian)* 77−11876
KCl:Sr, mechanical props. as function of dopant conc., dislocations 77−69027
KCl:Sr^{2+}, polarisation-plastic effect 78−2794
KCl(Br)(I), single cryst., quenched, microstruct. around indentations 80−7628
$KD_{2x}H_{2(1-x)}PO_4$ crystals, plastic deform. and mech. props. 79−79035
KH_2PO_4 crystals, plastic deform. and mech. props. 79−79035
KH_2PO_4, optical props., plastic deform. effect 77−59552
Li-Na ferrite powders, props. rel. to Fe_2O_3 chem., thermal, mech. historical 79−11539
LiF bicrystal, high-angle tilt boundary and edge dislocation intersection effects 80−79836
LiF bicrystals, intergranular fracture due to single slip 78−34520
LiF, charged dislocations, comprehensive deform. effects on charge, elec. field 79−14815
LiF crystal, contact damage obs. by cathodoluminesc. 80−71728
LiF, crystal, electron emission under uniaxial compresssion 80−7483
LiF crystal, plastically deformed, elec. field distrib. on surface meas. 77−31716
LiF crystals, relation of struct. and bond type to slip geometry 80−88165
LiF, deform. mech. map. 77−81298
LiF, deformed, influence of surface on density of edge components of dislocations 77−31670
LiF, deformed by conc. loading, X-ray beam scattering *(Russian)* 78−35430
LiF, deformed in liquid He, penetration of He, dislocation effects 77−20131
LiF, dislocation distrib., after deform. *(Russian)* 78−22732
LiF, dislocation structure, influence of variable deform. temp. 80−70211
LiF, electrification by plastic deform. 79−33334
LiF, hardening under dynamic load, grain boundary effect 77−12674
LiF, irradiated and plastically deformed, thermoluminesc. defect centres 77−1740
LiF, irradiated at 20K, deformation under stress *(French)* 79−90715
LiF, kinetics analysis of stress relaxation 80−65136
LiF, microcrack propagation and plastic strain 80−81187
LiF, microindentation, dislocation rosette generation 77−27936
LiF, multiplication of screw dislocations during deform., yield stress depend. 77−24321
LiF, plasic deform., cleavage-crack propag., X-ray topography 77−39625
LiF, plastic strain accompanying local rise in surface temp., of natural shear *(Russian)* 80−6411
LiF, single cryst., impression creep 78−6986
LiF single crystals, dislocation motion and generation on plate impact 79−95011
LiF, strain hardening curve correlation with slip band nucleation stress spectra 80−70217
LiF TLD, plastic deform. effects on thermolum. sensitivity, rel. to handling technique 77−16988
LiF, thermocyclic stress effects in corrosive-media, electrochem. polarization applic. *(Russian)* 78−11356
LiF, US attenuation, 4.2 to 300K 77−47513
LiF:Co, flow stress changes during precipitation 80−92594
LiF:Mg^{2+}, deformed in ^{3}He and ^{4}He, dislocation struct. characteristics 79−69112
LiF:Ti, thermoluminesc., effect of plastic deform. 79−33853
α-$LiIO_3$, surface defect layer struct. due to mechanical working *(Russian)* 80−100238
$LiNbO_3$ single crystals, brittle, deform. during static indentation 79−87714
$LiNbO_3$, twinning systems produced by plastic compression 77−1135
Li_2SO_4 solid electrolyte plastic deformation and thixotropy obs. 78−79660
Mg alloys, strain rate effects during reverse torsional shear 77−4143
Mg alloys MA12, fatigue crack growth in air and vacuum 79−15792
Mg, extruded, continuum mech. anal. of flow curve anisotropy and plastic strain *(German)* 78−84947
Mg, internal friction spectrum after plastic deform. *(French)* 79−15737
Mg, plastic anisotropy of extruded bars *(German)* 77−86126
Mg, pure, Bordoni relax. behaviour after plastic deformation 80−20997
Mg-Mn-Ce, structural changes and deformation during superplastic flow 78−15472
$MgAl_2O_4$ spinel, deform., stacking fault energy 77−28853
$MgAl_2O_4$, spinel materials press forged, mech. props., IR appl. 78−39722
Mg_3Cd, effect on order, of compression deformation 78−52924
MgF_2, single cryst., tensile strength and yield point, temp. depend. 77−14785
MgO, crack propagation during in-situ deform., plastic zone formation 80−16468
MgO, cryst. preliminary processing rel. to deform. curve parameters, slip line struct. 77−52421
MgO crystal, contact damage obs. by cathodoluminesc. 80−71728
MgO, crystal, electron emission under uniaxial compresssion 80−7483
MgO crysts., plastic deform. activation parameters, rel. between macroscopic and in-situ HVEM expts. 80−103355
MgO crysts., radiation damage influence on deform. in HVEM 80−103391
MgO, deformation induced damage, effect on optical props. 77−77258
MgO, deformed, cathodlum. obs. by STEM 80−76088
MgO, filamentary crysts., mech. props. 77−52402
MgO, fracture and crack tip plastic zones, in situ obs. 80−108686
MgO, high temperature prestrain effect on plastic props., dislocation struct. 80−79866
MgO, hot-pressed, elasticity props. of polycrystals and single crystals 80−54301
MgO, lattice misorientation and displaced vol. for microhardness indentation 78−64617
MgO, local loss of stoichiometry caused by plastic deform., cathodoluminesc. spectra 78−35209
MgO, MgO-CaO (58 wt.%), comparison of high temp. creep and fracture 77−16658
MgO, photoluminesc. during mechanical deform. 80−60665

plastic deformation continued
MgO, plastically deformed, recovery of internal friction at room temp. *(French)* 78−80577
MgO polycrystals, hot-pressed, changes in residual strain on annealing 79−34073
MgO single cryst., impact wear characts. 80−76374
MgO single cryst., internal stresses and dislocation mobility, stress relaxation method 80−6413
MgO single crystal, absorbed fluid effect on rolling contact deform. 78−64719
MgO single crystal, dislocation struct. of slip lines, TEM 79−27990
MgO, single crystals, deform., dislocation motion and multiplication in HV electron microscope 77−84754
MgO, slip line struct. using replica electron microscope technique 79−7605
MgO:Li, mech. deformed crysts., imprinting of slip bands using Li impurities 80−59473
MgO:nAl_2O_3 spinel, plastic deformation at T<1000°C, slip systems 80−108505
MgO$(Al_2O_3)_n$ spinel, plastic deformation at 400°C 80−40453
MgO.1.1 Al_2O_3 spinel, high temp. deform., cryst. orientation effect 80−107263
Mg_2SiO_4, forsterite, decorated dislocations 80−54245
Mg_2SiO_4, microhardness variation, exam. using Vicker indentor 80−25849
$MgZn_2$ Laves phase, deformation-mechanism maps 79−29150
Mn-Cu (25 wt.%) alloy, critical shear stresses of twinning and glide 79−87693
Mn-Cu alloy, plastic deform. mechanism and shape-memory effect, mag. struct. obs. *(Russian)* 78−60705
Mn-Y-Zn-Cd alloy,phase equilibria, plastic deformation, microhardness *(Russian)* 80−40334
MnF_2, piezo-optical effect, birefringence variation on uniaxial compression *(Russian)* 80−34887
Mn_5Si_3, elastic moduli, phase transitions, ultrasonic velocity 80−92589
MnZn ferrite, spray dried agglomerates, compaction response, fracture, deform. 79−43172
MnZn ferrites, abrasive wear mechanism *(Japanese)* 78−39917
Mo alloy, ZrC dispersion hardened, thermally activated plastic deform. *(Russian)* 77−36612
Mo alloy MT, strain hardening depend. on temp. and structural state *(Russian)* 79−91664
Mo alloy TsMb, mech. props., effect of gaseous H_2 *(Russian)* 78−31508
Mo alloys, dispersion-strengthened, plastic deform. and hardness, temp. depend. 80−3087
Mo alloys, fractography of deformed samples *(Russian)* 78−19889
Mo, BCC lattice, texture form. by drawing and pulling through non-powered rolls *(Russian)* 77−25100
Mo, block boundary dislocation struct. singularities under high temp. steady state creep conditions *(Russian)* 79−90670
Mo, cast state, interaction nature between C, O_2 and N_2, influence on struct. and props. *(Russian)* 79−70114
Mo, cellular structure, initial stages of formation in rolled single crystals 79−23611
Mo cold worked, dislocation struct. change during postdeform. at 493K 79−43271
Mo, defect struct. in plane strain deformed single crystal 77−63751
Mo, deformation and fracture patterns under complex stress conditions 77−70134
Mo, deformed, dislocation-free channels prod. by heat pulses, electron microscope obs. and hardness meas. *(Russian)* 79−52251
Mo deformed single crysts., struct. state and dislocation splitting *(Russian)* 80−29029
Mo, dislocation (100) density variation, deformation effects, dislocation stability *(Russian)* 80−15108
Mo dislocation a ⟨100⟩ stability, plastic deform. at high-press. 78−43030
Mo, dislocation structure inhomogeneity in electromachining crater zone, rel. to plastic deform., dynamic recovery *(Russian)* 80−16326
Mo, dislocation structure of diffusional welding zone *(Russian)* 80−96531
Mo, fatigue of single crystals, dislocation struct. and strain localisation *(Russian)* 80−71741
Mo, Fermi surface, homogeneous strain response 78−34753
Mo fibre reinforced Cu, rule of mixtures of deform. parameters in stage III 80−97532
Mo fibre reinforced Cu with weak interfaces, stability of tensile deform. 80−97533
Mo film, deform. in electron microscope, dislocation mechanism 79−82227
Mo, fracture and crack tip plastic zones, in situ obs. 80−108686
Mo, fracture surface, effect of plastic deform. by rolling at 950°C *(Russian)* 77−59893
Mo, fragmented struct. formed during plastic deform., TEM investig., dislocation model *(Russian)* 77−32634
Mo, high purity single crystal doped with C, low temp. mech. props. 77−77544
Mo, irradiated with fission fragments, creep, 20-30K *(French)* 77−48493
Mo, macroscopic heterogeneity of plastic deform., metallographic examination *(Russian)* 79−100210
Mo, mech. props., influence of temp. on singularities of deform. *(Russian)* 78−6970
Mo, mechanical eqn. of state *(Japanese)* 78−91375
Mo, monocrystalline, density change during plastic deformation *(Russian)* 79−87689
Mo, orientation distrib. function depend. on deform. during cold rolling *(Russian)* 80−50647
Mo, plastic deform. by rolling at 293K, dislocation struct. *(Russian)* 77−48481
Mo, plastic deform. mechanism during hydrostatic extrusion *(Russian)* 77−8879
Mo, plastic deformation during rolling at 293K, crystallography of slip *(Russian)* 77−32588
Mo, plastically deformed single cryst., mag. susceptibility *(Russian)* 80−93074
Mo polycrystn., cyclically deformed, dislocation arrangements 80−108506
Mo, recrystallisation kinetics, deform. degree effects *(Russian)* 78−6943
plastic deformation continued
Mo, shock deformation twinning, shock press., pulse duration and grain size effects 79−5021
Mo, single crystal, subjected to plastic deform., substruct. using X-ray diffr. 79−70083
Mo single crystal, thermocyclic strength of high temps. of single crystal 77−16685
Mo single crystal dislocation interactions during parallel shear in (011) plane *(French)* 78−43029
Mo single crystals, simulating initial stage of deformation in fatigue loading 80−35328
Mo, single crysts., pressure masgnitude influence in hydroextrusion on plastic strain mechanism *(Russian)* 80−21009
Mo, single crysts., work hardening and softening in cyclic strain 80−20957
Mo, sintered, fusion reactor blanket struct. material, low cycle fatigue behaviour 80−30073
Mo, strength, temp. depend. 78−3193
Mo, strength and internal friction 77−63711
Mo, strengthening by vacuum-deposited W film *(Russian)* 77−66714
Mo, structural singularities of plastic deform. at localised flow stage, TEM obs. *(Russian)* 78−6968
Mo, surface machined, struct., electron diffr., TEM *(German)* 77−73371
Mo, US working effect on single cryst. during deform., strengthening effect, plasticity resource *(Russian)* 79−34107
Mo X-ray electron spectra, paramag. susceptibility, depend. on plastic deform. for single crystals 77−28683
Mo-B-Al-C, alloy TsM-10 rolled, recrystallised, deformed system, behaviour under cyclic loading 79−91795
Mo-C (0.07 wt.%), two-phase alloy, fracture and deform. characts., struct. depend. *(Russian)* 77−32635
Mo-Re, cold worked, strength 78−31426
Mo-Re, solid soln., dislocation internal friction *(Russian)* 78−23748
Mo-Re alloy MR47-VP, dislocation struct. and fatigue damage during room temp. deform. *(Russian)* 79−20111
Mo-Re(Os)(Ru), recovery after deform. and annealing, destrengthening mechanism *(Russian)* 80−97546
Mo-Ru-C, deformed, singularities of fragmented structs. *(Russian)* 77−44289
Mo-TiC lamellar eutectic composite, deformation and strength, room temp. to 2073K *(Japanese)* 80−71702
Mo-V-C, hot-worked, substructural hardening and high-temp. strength *(Russian)* 80−25731
Mo-Zr-B-C, dil. alloy, struct. changes under prolonged high temp. annealing *(Russian)* 78−6944
Mo-Zr-C, deformed, singularities of fragmented structs. *(Russian)* 77−44289
Mo-Zr-C (0.063, 0.06 wt.%) alloys, ageing, effect of cold deform. by hydrostatic extrusion 79−57001
Mo-Zr-Ti-C(0.1, 0.15, 0.004 wt.%), alloy TsM2A, cavitation failure mechanism 77−70169
β-$MoTe_2$, low-temperature structural phase transition, X-ray meas. 79−14928
NH_4Cl, order-disorder phase transform., effect of plastic deform. and electrooptic effect 79−33672
NH_4Cl, transitional plasticity, light scatt. study 79−77674
$NH_4H_2PO_4$ crystals, plastic deform. and mech. props. 79−79035
Na, plastic deformation 78−30693
NaCl, changes in internal friction and discharge following plastic deform. 79−99191
NaCl, cross slip of screw dislocations during deform. at room temp. 77−84758
NaCl, crystal, electron emission under uniaxial compresssion 80−7483
NaCl, damage process preceding semibrittle fracture, plastic strain depend. 77−32692
NaCl, deform. mech. map. 77−81298
NaCl, deform. process, exoemission and desorption meas. *(Russian)* 78−75708
NaCl, deformed, dislocation densities, TEM 77−43219
NaCl, deformed, influence of surface on density of edge components of dislocations 77−31670
NaCl, deformed by conc. loading, X-ray beam scattering *(Russian)* 78−35430
NaCl, dislocation density in monocrystal deformed under high hydrostatic press. 80−70216
NaCl, dislocation microplasticity, internal friction expts. 78−47388
NaCl, electric field induced by homogeneous stresses 80−11343
NaCl, γ-irrad., photoplastic effect and internal friction aftereffect 80−24529
NaCl, hydrostatically compressed crysts. in easy glide stage, plastic deformation 80−7630
NaCl, internal stresses and dislocation mobility 78−48440
NaCl, microcrack propagation and plastic strain 80−81187
NaCl, microindentation, dislocation rosette generation 77−27936
NaCl, monocrystalline, defect struct. and intrinsic ionic cond. relationship 79−95211
NaCl, moving dislocations, interaction with defects, elec. effects meas. in plastic deformation *(Hungarian)* 80−10572
NaCl, plastic deform., cleavage crack propag., X-ray topography 77−39625
NaCl, plastic deformation influence on shape recovery effects 80−6684
NaCl, plastically deformed [001] orientated single crystal, glide props. and X-ray topography 77−21228
NaCl, plastically deformed, recovery of work hardening *(German)* 77−35626
NaCl, plastically deformed [001] oriented single crystals, TEM 77−36579
NaCl, plastically deformed, containing dislocation distribs., X-ray diffr. broadening 77−43218
NaCl, plastically deformed, integrated X-ray reflection coeff. determ. 77−65981
NaCl, plastically deformed, glide on {111} planes 79−82234
NaCl, strain ageing exam. 78−56661
NaCl, temp. fields during plastic deform., cholesteric liq. cryst. technique 79−82278
NaCl, thermal fields generated during plastic deform. 78−35457
NaCl, US deformation, stress anal. by polarised light method *(Russian)* 77−11641
NaCl, uniform deformation and birefringence in nonuniform elec. field *(Russian)* 79−87396

plastic deformation continued
NaCl whiskers, plastically deformed, internal friction amplitude depend. 77−15727
NaCl whiskers, plastification in elec. field *(Russian)* 80−21010
NaCl:Cd^{2+}, dielectric loss following plastic deform. 80−84690
NaCl:Sr, mechanical props. as function of dopant conc., dislocations 77−69027
NaCl:Sr deformation control by thermally activated processes 195 to 300K 79−24570
NaCl. deform. in steel band, X-ray investig. *(Russian)* 78−68727
NaF, deformed, influence of surface on density of edge components of dislocations 77−31670
NaF, dislocation microplasticity, internal friction expts. 78−47388
Na_2O-CaO-SiO_2 glass, crack nucleation around plastic indents 78−92327
Na_2O-CaO-SiO_2 glass foils, HVEM in-situ straining expts. 80−104216
Na_2O-SiO_2(-B_2O_3) glass, torsional deform. above Tg under low stresses 80−25804
Nb and Nb alloys, cold plastic deform., oriented microdistortions *(Russian)* 78−39840
Nb and Nb-Zr (1 wt.%), fusion reactor blanket struct. material, low cycle fatigue behaviour 80−30073
Nb, changing lattice dynamics 78−67793
Nb, cold-rolled, deform. zone geometry and texture gradients 77−48452
Nb, deformation at 77-158K, slip and dislocation struct. 79−83277
Nb, deformed, α-peak, internal friction meas. between 90 and 300K 79−100205
Nb, deformed, α'-peak in internal friction spectra 80−16368
Nb, deformed polycryst., γ-peak obs. and interpret. in internal friction, 300-500K 80−81098
Nb, dislocation substruct. in deformed and recovered single crystal 77−8897
Nb, dislocation-free single crystal, deformed at 180K, X-ray topographic obs. 79−24587
Nb, effect of electron irradiation on low temp. deform., tensile stress-strain curves 79−55784
Nb, effect on positron annihilation and supercond. transition *(Russian)* 77−39993
Nb, elec. resist. changes with plastic deform. 77−89749
Nb, electron-coupled phonon spectrum, effects of strain 79−7943
Nb film, deform. in electron microscope, dislocation mechanism 79−82227
Nb, fusion reactor first wall material, cyclic deform. tests 80−30074
Nb, H_2 loaded, cold worked, plastic deformation, exam. of α internal friction peak 78−92307
Nb, high purity, dislocation relaxation by internal friction meas. over wide freq. range 79−38876
Nb, hydrogen embrittlement, deformation behaviour of Nb-H alloys 79−11687
Nb, local heating during abrupt strain, catastrophic slip band formation 80−7652
Nb, neutron irrad., yield stress and activation vol. 77−90418
Nb, plastic deformation effects on superconducting specific heat transition 80−20352
Nb, plastically deformed, flux density gradients and pinning forces, Faraday effect obs. 79−61010
Nb, plastically deformed, hydrostatic pressure effect on dislocation relaxation, US exam. 78−76696
Nb, Shubnikov phase penetration, Faraday effect obs. 79−82731
Nb, single crystal, low temp. thermal cond. 79−28336
Nb, single crysts., plastic relaxation of internal stresses during mech. twinning at 4.2K, optical and SEM study *(Russian)* 79−66108
Nb, strain profile of plastic zone in dislocation-free single cryst. by X-ray topography 79−14876
Nb, stress differential in surface oxide softening of single crystals 77−86116
Nb, supercond., field history effect of flux gradient 78−91828
Nb, supercond., influence of plastic deform. 77−85378
Nb, superconductor, deformational twinning, mag. props. *(Russian)* 79−95543
Nb, temp. effects on ageing, interstitial conc. depend. *(French)* 77−21182
Nb wire, neutron irrad., tensile props. 79−70077
Nb-H system, temp.-stimulated acoustic emission, hydride precip. 80−3044
Nb-Mo alloy, single crysts. slip geometry on straining in tension *(Russian)* 77−66678
Nb-N (0.3 to 300 at. ppm), deform. 77−48477
Nb-O, effect of neutron irradiation damage on low temp. deformation characts. TEM study 79−42117
Nb-Ti, metallurgical treatment, effects on props. 79−38846
Nb-Ti alloy, supercond., low-temp. plasticity 77−15992
Nb-V-O solid soln., thermodynamics of O_2 78−68673
Nb-W-Mo-Zr (5, 2, 1 wt.%), surface-layer struct. and mech. props., effect of O_2 diffusion saturation 79−5087
Nb-Zr, deformed, α-peak, internal friction meas. between 90 and 300K 79−100205
Nb-Zr, deformed strip, pinning force, widely varied j_c, temp. and mag. field variations *(Russian)* 79−7948
Nb-Zr-C, (1, 0.1 wt.%) alloy, mech. characts. structral sensitivity in strained state *(Russian)* 79−52301
Nb-Zr-C, structural depend. of elasticity limit fracture features *(Russian)* 79−29171
Nb-Zr-C (0.1, 0.01 wt.%) plastic deform. influence on electronic state of Nb atoms 80−40463
Nb-Zr-C alloys, dispersion-hardened with carbide phase, influence of hydrostatic extrusion on struct. and props. *(Russian)* 77−52338
Nb-Zr-C alloys, plastic deform. and annealing, dislocation struct. *(Russian)* 80−20951
Nb-Zr-N, deformed and annealed, internal friction, rel. to structural state *(Russian)* 78−6957
Nb-Zr-N biphase alloy, recrystallization annealing 80−104180
NbC, deformation behaviour during rubbing in wide temp. range 80−16486
NbC, high-temp. plastic deform. effects on elec. props. 77−44370
Nb_2C powders, plastic deform. characts. on vibratory milling 78−11183
Nb_3Ge, DC sputtered films, annealing and mech. deform. effects on struct. and supercond. props. 79−38217
Nb_3Sn, A15 compound, exam. of deformation processing, review 78−39864
plastic deformation continued
Nb_3Sn fatigue effects in unidirectional composites, computer simulated model 80−35289
Nb_3Sn, filamentary supercond., mech. props. and crit. current 77−24657
Nb_3Sn filamentary superconducting composites, mechanical property variations between composites 79−57054
Nb_3Sn, hot isostatically pressed, plastic deform. 80−108510
Nb_3Sn, lattice microstrain induced metastable phase, low temp. struct. and props. 77−8482
Nb_3Sn, martensitic transition, lattice anharmonicity 79−8300
NbTi, dynamic stress effects, supercond. magnet training problems 78−49870
NbTi, superconducting multifilamentary conductors, crit. current density, bending effects *(German)* 80−39727
Ni 200, C interstitial effect of yield point develop. during static strain ageing, model 78−88498
Ni, 200, high temp. cyclic deformation and hardening 80−21055
Ni alloy, recryst. after hot deform. *(German)* 80−25716
Ni alloy 718, creep crack growth 77−63776
Ni alloy EI617, cyclic temp. variation, loading parameter effect on laws governing distortion 77−16627
Ni alloy KhN56VMKYu, creep, viscosity, resist. to inelastic deform. 80−89309
Ni alloys, creep transients, friction stress and recovery, dislocation substruct. 80−60933
Ni alloys, heat resistant, creep resistant deform. 79−100234
Ni and Ni-Co, recovery of single crystal after varying amounts of cold work 79−100162
Ni base alloys, heat resistant, cyclic determ. at elev. temps. 79−66125
Ni, cold neutron small angle elastic scatt., microstruct. exam. 77−84736
Ni, cyclically deformed, polarisation stress field, dislocation shuttling, computer calcs. 79−96095
Ni, defect electronic struct., strength characteristics relation by positron annihilation 79−91526
Ni, deformed, coercivity and remanence anisotropy 78−31093
Ni, deformed, magnetic susceptibility anisotropic changes 78−27025
Ni, deformed, struct. form. during annealing, Ni_3Al type ordered phase precipitation *(Russian)* 80−45325
Ni, deformed, work-hardening, dislocation and mosaic struct., X-ray and electron microscopy 77−35625
Ni, deformed bars, cold rolled, exam. of microstruct. by thin foil TEM 78−88502
Ni, deformed by hydrostatic extrusion, drawing or drawing under press., dislocation struct. obs. *(Russian)* 77−21213
Ni, dislocation intersection and solution strengthening, effect of solute on obstacle profiles 80−7590
Ni, dislocation structure evolution after hydroextrusion *(Russian)* 80−96530
Ni, dislocation structure parameter determ. due to plastic deformation *(Russian)* 80−54242
Ni, dislocation substructure formation under hydrostatic extrusion 78−56696
Ni, dispersion strengthened, high-temp. cyclic deformation 80−21056
Ni, dynamic strength and logarithmic modulus of plasticity 77−16655
Ni, effect of plastic deform. and martensite transformation on Fe atom mobility *(Ukrainian)* 78−55974
Ni, electrical resistance in DC mag. field after ultrasonic deform. *(Russian)* 80−54671
Ni, FCC, polycrystalline, deformation-strain curve description using substruct. parameters *(Russian)* 79−87690
Ni, grain boundary ledge density, effect on flow stress 78−48465
Ni, grain boundary sliding and deformation mechanism maps 80−3128
Ni, high temperature cyclic deformation 80−16429
Ni, high-purity, softening of strained single crystals *(Russian)* 80−40499
Ni, mag. props. of single-domain powders after plastic deform. *(Russian)* 78−6554
Ni, magnetic aftereffect reactivation of single crystal by plastic deform. 79−65697
Ni, magnetic permeability, reversible, deform. and ion implantation effects 77−48013
Ni, magnetised mono- and polycryst., activation vol. var. during low temp. deform. *(Russian)* 78−3178
Ni, magnetoplastic effect and eddy current heating *(Russian)* 77−43858
Ni, microcrack propagation and plastic strain 80−81187
Ni monocrystals, struct., effect of stress applied during electrodeposition 78−26777
Ni, neutron irradiation, low temp. recovery, effect of plastic deform. 78−51588
Ni, oxidation, high temp., effect of C on cavity form., SEM study 80−97638
Ni, oxide covered, tensile deform. in high vac., particle and photon emission 78−39672
Ni, particle formation by evap., electron microscopy obs. of interaction processes 80−104053
Ni, plastic deform., accelerated, evolution of H_2 77−36594
Ni, plastic deform. build-up during low cycle fatigue *(Russian)* 77−25207
Ni, plastically deformed, dislocation struct., mag. small angle scatt. of neutrons *(German)* 78−22730
Ni, plastically deformed, positron trapping rate, temp. depend. 80−71507
Ni, plastically deformed, recovery stages III and IV investig. by positron annihilation 77−31715
Ni, plastically deformed, volume fraction of recrystallised material determ. from positron annihilation 77−1760
Ni plated Fe single crystal, deformed at 77K, surface obs. 78−19916
Ni, point defect estimation from specific heat and volume in plastically deformed pure metals *(Russian)* 80−54223
Ni, powder, subjected to vibratory milling, exam. of plastic deformation, recrystallisation, sintering 80−16234
Ni, pure and doped, mech., mag. relax. meas. dumb-bell self-interstitital reorientation *(German)* 78−52879
Ni, shock loaded, work softening 78−27537
Ni, shock-loaded, residual strengthening, effect of grain size, dislocation cell size and deform. twin spacing 79−91744
Ni, single cryst., cyclically deformed, HVEM in-situ deform. study 80−103339
Ni single crystal, stretched, electron microscope exam. of deformation cell structure during polygonization *(German)* 80−7651

plastic deformation continued
Ni single crystal foil, H_2 induced deform. during thinning, electron-optical obs. 79−57059
Ni, slip character, H effect 80−89287
Ni spring alloys, microplastic deform. and endurance limit 80−81197
Ni, strain amplitude-depend. damping and modulus *(Japanese)* 80−92606
Ni, structural singularities of plastic deform. at localised flow stage, TEM obs. *(Russian)* 78−6968
Ni, texture nonhomogeneity during rolling 79−91670
Ni, thermal softening, influence of alternating mag. field *(Russian)* 78−23312
Ni thin-walled cylinder, elongation upon torsion 80−64386
Ni, transport of H, effect of plastic deformation 80−21044
Ni, US deform., electron microscope exam. *(Russian)* 78−35447
Ni, US deformation at low temps. *(Russian)* 79−11656
Ni, volume changes and defect healing due to plastic deform. *(Russian)* 80−81139
Ni, wire bamboo struct., plastic deform. *(French)* 77−28877
Ni wire reinforced epoxy resin, and cement paste matrices, debonding and pull-out of wires 79−29142
Ni/Cr-Fe-C, Inconel, dislocation intersection and solution strengthening, effect of solute on obstacle profiles 80−7590
Ni/Ni_3Al-Ni_3Nb, directionally solidified lamellar eutectic alloy, deform. anisotropy and fracture 77−36604
Ni/Ni_3Al-Ni_3Nb eutectic, directionally solidified, plastic deformation *(Russian)* 78−39843
Ni-A-Ti (6,1 wt.%), γ' phase precip., deform. effects *(Russian)* 78−48404
Ni-Al (7.2 wt.%), fatigue crack propag., plastic work role 79−79070
Ni-Al-Cr alloy Ehi 826 77−86120
Ni-base alloy, age hardened, stress corrosion cracking resistance, plastic deform. and microstruct. relation 77−63829
Ni-base superalloy, ⟨111⟩ monocrystals under compression, inhomogeneous deformation 77−63736
Ni-base superalloy, microscopic inhomogeneity of plastic strain influence on fatigue cracks *(German)* 80−40470
Ni-based heat resisting alloys, strain resistance under complex loading program conditions 79−57073
Ni-Co, dislocation intersection and solution strengthening, effect of solute on obstacle profiles 80−7590
Ni-Co, mag. props. of single-domain powders after plastic deform. *(Russian)* 78−6554
Ni-Cr, (30 wt.%), collective dislocation movements, in situ study 80−100243
Ni-Cr, deformed, struct. form. during annealing, Ni_3Al type ordered phase precipitation *(Russian)* 80−45325
Ni-Cr (Mo), solid soln., US deform., electron microscope exam. *(Russian)* 78−35447
Ni-Cr (33 at.%), plastic deformation, HVEM study *(French)* 80−66605
Ni-Cr (33 at.%), US deform. effect on short range order form. *(Russian)* 78−39839
Ni-Cr (33.3 at.%) alloy, ordering after US deform., microhardness and elec. resist. meas. *(Russian)* 79−20113
Ni-Cr alloy, structural changes, during thermal stress cracking, X-ray and microhardness meas. *(Russian)* 78−35496
Ni-Cr alloy Ehi 617, equation of condition for creep, expt. checking 77−86120
Ni-Cr-Al-Ti alloy, KhN78TYu, heavily deformed, subgrain struct. due to discontinuous precipitation of γ' phase *(Russian)* 79−52218
Ni-Cr-Co-Ti-Mo-W-Al (14, 9.8, 5, 4, 3.9, 3 wt.%), low cycle fatigue, prior heat treatment effect 80−60962
Ni-Cr-ThO_2 (20, 2 wt.%), dispersion hardened, model for high temp. deform. based on struct. obs. 78−19809
Ni-Cr-ThO_2(20, 2 wt.%), dislocation struct. after high temp. deform. 77−52393
Ni-Ge (2 at.%), vacancy cluster form. during deform. positron lifetime meas. 79−56882
Ni-Ge (2 wt.%), positron annihilation, photon ang. distrib. meas. effect of deformation, annealing temp. *(Russian)* 78−35220
Ni-H, thermally charged, serrated yielding 80−85007
Ni-HfO_2 (3 wt.%), dispersion hardened alloy VDU-2, thermal and mech. treatment 77−90376
Ni-Mo (14.4 wt.%) single crystals, ordered phase precipitates influence on deformation character, mechanical props. *(Russian)* 79−74155
Ni-Nb-Al (21,2.5 wt.%), eutectic aligned alloy, mech. behaviour at high strain rates 78−39855
Ni-Ni_3Al-Ni_3Nb, directionally solidified, role of twinning in cyclic stress strain behaviour 78−80605
Ni-Ni_4Mo, strengthening by ordered precipitates 77−86041
Ni-Ni_4Mo system, deformation microstruct. 80−93591
Ni-P, struct. obs. by X-ray diffr., low temp. annealing and deform. effects 79−56995
Ni-Pd-P amorphous alloys, tensile deform. 77−32646
Ni-ThO_2, dispersion strengthened, high temperature cyclic deformation 80−16430
Ni-ThO_2 (2.51 wt.%), dispersion hardened, high temp.-strength, deform. method and annealing effects 79−1882
Ni-Ti (60 at.%) alloy, high stress effects on struct. and props. *(Russian)* 78−19838
Ni-Ti alloy, shape memory effect mechanism 77−28865
Ni-Ti/Cu composite, plastic deform. influence on internal friction *(Russian)* 80−100871
Ni-Ti(Fe), neutron irradiated, thermally activated deform. 80−6438
Ni-W surfaces in contact, deform. and adhesion at very low loads 80−39457
Ni-Zn ferrite, grain size depend. of grain boundary sliding *(Japanese)* 80−15120
Ni-Zn ferrites, polycrystalline, grain boundary slip *(Japanese)* 77−63764
Ni_3Al and Ni_3(Al,Ti), deformation charact., temp., strain rate and orientation depend. 77−44320
Ni_3Al, ductility, tensile and compressive tests *(Japanese)* 77−52414
Ni_3Al, ductility in poly- and single crystals, compressive and tensile tests 78−56715
Ni_3Al, overshooting while testing in tension 78−44189
Ni_3Al-Fe (10 at.%), activation anal. of plastic deform. 79−1900
Ni_3(Al,Ti), single crysts., flow and fracture behaviour tested in tension 79−79075
$Ni_3Al(\gamma')$-$Ni_3Nb(\delta)$, directionally solidified, deformation substruct. and slip systems 79−8326

plastic deformation continued
Ni_2Cr, fine-domain ordered alloy, early deform. stages, dislocation struct. and motion *(Russian)* 77−81291
NiCrAlY, mechanically alloyed, maintaining elongated grain struct. after deform. 77−36534
Ni_3Fe, dislocations, rate of piling up, rel. to average length of slip lines *(Russian)* 77−76416
Ni_3Fe, disordered single crysts., thermo-activated mechanism of plastic deform. *(Russian)* 78−84909
Ni_3Fe, domain struct. after tensile deform., dislocation effects 80−71083
Ni_3Fe, nondislocation origin friction stress in alloys, deformation hardening 80−21050
Ni_3Fe, polycrystalline alloy evolution of slip-line pattern during straining 80−107362
Ni_3Fe, superlattice dislocations, compression induced mag. anisotropy 77−85442
Ni_3Fe, superlattice dislocations, compression induced mag. anisotropy 77−85443
$Ni_{2/3}Fe_{7/3}O_4$, precipitation of α-Fe_2O_3, optical microscopy, SEM and TEM studies *(French)* 80−11650
Ni_3GA single crystals, anomalous temp. depend. of strength, dislocation struct., optical and TEM 79−74228
Ni_3Ga, form. mech. of superlattice intrinsic stacking faults 77−27897
Ni_3Ga, stacking fault form. in situ obs. by stretching thin foils in electron microscope 77−62547
Ni_3Ga, temp. depend. of mech. props. *(Russian)* 79−38895
Ni_3Ga, with $L1_2$ struct., dissociated struct. of superlattice dislocations 79−37706
Ni_3Ge single crystal, yield stress, temp. and orientation depend. 77−90432
Ni_3Ge, temp. depend. of mech. props. *(Russian)* 79−38895
Ni_4Mo, domain struct. on annealing, and dislocation struct. during deform. *(Russian)* 77−16640
NiO, doped and pure single crystals, plastic deform. 77−36578
NiO, polycrystalline, high temp. deform. 78−3174
NiPt, short-range order, effect of plastic deform., electron diffr. anal. *(Russian)* 80−24403
NiTi based alloys, plastic deform. mechanism 79−11676
Ni_3V, deform. propag., electron microscopy obs. 78−6070
α-Np, deform. modes around hardness indentations 77−20009
Pb, anomalous grain growth 77−8855
Pb, deformed by torsion, stored energy and recrystallization 79−34069
Pb, dil. alloy, dislocation inertial effects in plastic deform., internal friction meas. 77−36609
Pb, dislocation electron drag coeff. temp. depend., internal friction method, superconducting state 80−29031
Pb, electroplastic deform., stress relax. meas. *(Russian)* 79−38894
Pb film, thermal strain, strain relax. mech. 79−42427
Pb, model material, specimen size effect on plastic deform. around deep notches 79−70142
Pb, phonon thermal conductivity of deformed cryst. below 2K *(Russian)* 78−60244
Pb, plastic deform. rate rel. to supercond. transition, temp. depend. *(Russian)* 78−31015
Pb, plastic properties over wide range of strain rates 80−71693
Pb, plastically bent, effect of dislocations on electron relax. time, cyclotron reson. 79−24217
Pb, plastically deformed, annealed, positron trapping rate, 4-100K 78−31275
Pb, polycryst., plastic deform. at 4.2K temp. rise 77−15481
Pb, recrystallisation textures, and deformation formed by dry sliding against steel 79−91698
Pb, SO type, commercial purity, local deform. meas., using Moire method 80−21219
Pb, sample length effect on plasticity 78−44179
Pb, single cryst. stress relax. depend. on elec. current, electron plastic effect 79−79021
Pb, strength loss during upsetting 77−90430
Pb, superconducting transition curves, meas. during plastic deform. 79−60956
Pb, thermal conductivity, in normal and supercond. states, 0.6-7.5K *(Russian)* 80−6815
Pb thin films, thermal strain, multiple cycling to 4.2K effects 79−90918
Pb, virgin surface, contact formation and cohesion, influence of multiple contacting *(Russian)* 80−40548
Pb, work hardening, and recovery rates during steady state deformation, temp. and stress effect 80−45319
Pb-In, difference in stress for deform. between mixed and supercond. states 78−43514
Pb-In (5%), supercond. mobile dislocation density, instantaneous flux change meas. 80−15670
Pb-Sb, influence of quench deform. on precipitation *(German)* 77−86064
Pb-Sb (1 wt.%), highly averaged, fracture behaviour 79−8366
Pb-Sn, directionally solidified lamellar eutectic, deform. induced microstruct. instability 77−32623
Pb-Sn, eutectic alloy, plastic deform., work hardening *(German)* 78−92279
Pb-Sn eutectic alloy, high temp. deform. 77−16637
$Pb_{80}In_{20}$ foil, deformed, annealed, correlation between pinning strength and flux flow noise charges 77−43792
$PbMo_6S_6$, cold-worked core-wires, supercond. transition temp. and lattice instability 78−6469
PbS, crystals, relation of struct. and bond type to slip geometry 80−88165
PbS, plastic deform. on compression along ⟨100⟩ direction 79−28036
PbS single crystals, thermal activation anal., dislocation behaviour, point defect influences 79−65095
$Pb_{1-x}Sn_xTe$:In, tunnelling impurity self-localisation, anomalous props. nature *(Russian)* 80−59915
n-PbTe, cold hydroextrusion, plastic deform. rel. to thermoelec. props., struct. 77−11945
$Pb(Zr,Ti)O_3$, polarisation effect on deform. and strength, Curie pt. region 79−42902
Pd, annealed, cold worked, H_2 diffusion effect on mech. props. *(Japanese)* 78−10222
Pd-Fe, dil., plastically deformed, positron annihilation study of recovery of crystal, imperfections *(German)* 77−85835
Pd-H, dil. α-phase, influence of deform. on low-temp. sp. ht. 77−31783
Pd-H(D), elastic energy dissipation peak 80−60905

plastic deformation continued
Pd-Si, struct. obs. by X-ray diffr., low temp. annealing and deform. effects 79−56995
Pd-W, elect. resist., mag. susceptibility, Hall coeffs., in plastically deformed state and after annealing *(Russian)* 79−66174
$Pd_{1-x}Ag_xH_n$, positron annihilation examination of electronic structure *(German)* 77−69931
$Pd_{80}Si_{20}$ metallic glass, tensile deform., shear band form., high-speed cinematographic obs. 80−89322
$Pd_{80}Si_{20}$, shear band form. 78−68756
$Pd_{1-x}W_x$, calc. of short-range order parameters from X-ray scatt. data *(Russian)* 80−75367
polyoxymethylene, linear, plastic deform. behaviour 78−84910
Pt, diffusion of Au at low temp., deform. effect on penetration curve 78−30789
Pt, neutron irradiation, low temp. recovery, effect of plastic deform. 78−51588
Pt, self diffusion of ^{197}Pt at low temp., deform. effect on penetration curve 78−30789
Pt, tension-strained, thermostimulated exoelectron emission, excitation mechanism *(Russian)* 80−71581
Pt-W interface, contaminated, contact adhesion, deform. and interfacial energy 78−22306
$^{239}PuO_2$, stoichiometric, high-temp. deformation 80−81111
RbH_2PO_4 crystals, plastic deform. and mech. props. 79−79035
$RbMnCl_3$, twinning struct., cryst. domains, orientation mag. transition *(Russian)* 80−107275
Re, elec. resistivity temp. depend., plastic deform. effects *(Russian)* 77−35909
Re, metallo-ceramic, deform. and cold working by cold rolling *(Russian)* 78−56655
Re, plastic deform. rel. to low temp. sp. ht., supercond. *(Russian)* 78−31005
Re-Ir (1 wt.%), positron annihilation, photon ang. distrib. meas. effect of deformation, annealing temp. *(Russian)* 78−35220
$(SN)_x$, deform. and defects, lattice strain, fibrillation 80−3139
$(SN)_x$, kink bands, deform. and defects 79−52308
$(SN)_x$ single crystal, mech. props. 79−24580
$(SN)_x$, stress-induced phase change geometry 78−23776
Sb, deformed in compression, secondary slip system *(French)* 79−66120
Sb, dislocation internal friction depend. on high ampliutde US vibrations *(Russian)* 79−90727
Sb, electronic band struct. changes due to plane straining effects *(Russian)* 80−54602
Sb, texture of deformed polycryst. 77−59809
Sb-Bi (2%), medium-oriented, plastic deformation *(German)* 77−70109
$p\text{-}Sb_{1.48}Bi_{0.52}Te_3$, extrusion deformed, powder dispersion degree influence on thermal and elec. props. *(Russian)* 80−39366
Se, amorphous, US relaxation and retardation of deform. near T_g point 80−84256
Si, compressed, polycrystalline, deform. and recrystallisation texture 78−27538
Si, controlled dislocation formation, struct. density *(Russian)* 80−107244
Si crysts., deformed, strain distrib. characterisation, annealing response 77−70140
Si crysts., dynamic processes associated with stacking faults and deform. twins, HVEM in-situ obs. 80−103369
Si crysts., in-situ HVEM obs. of dislocation processes during high temp. deform. 80−103342
Si, deep centres associated with plastic deform. and quenching *(French)* 77−28145
p-Si, deformed, 1/f noise, resist., mobility, and carrier density 77−8161
Si, deformed, annealed and recrystallized, struct., implications for solar cells 80−60922
Si, deformed, defect states associated with dislocations, capacitance transient spectroscopy 79−42483
Si, deformed, ENDOR of dislocation centre 78−72434
Si, deformed, faulted dipole, TEM obs. 78−38712
Si, deformed, photo-EPR of dislocations 80−11267
Si, deformed, recomb. radiation from electron-hole drops and free excitons 77−8641
n-Si, deformed, thermal treatment effect on elec. cond. and dislocation mobility 80−107265
Si, deformed crystal, Czochralski and float zone growth, Luder's bands 79−79025
Si, dislocation dynamics during plastic deform., stress-strain characts. 79−27996
Si, dislocation dynamics in plastic deform., theoretical anal. 79−42077
Si, dislocation mobility and mech. behaviour 79−82208
Si, dynamical recovery and self-diffusion 79−82379
Si, EPR spectra of point defects, temp. depend. 77−90033
Si, elec. props., plastic deform. and annealing temp. depend., dislocation effects *(Russian)* 77−89765
Si, heat treated, spin-depend. recomb. at dislocations 79−47122
Si, high dislocation density crystals, photoelectret state investigation 80−97191
Si, high press. appl. by spherical diamond indentor, plastic deform. obs. method 78−35619
p-Si, highly deformed, hole scattering 77−20309
n-Si, influence of deform. on capture of electrons by divacancies 77−1449
Si, laser induced surface deforms. 79−82262
Si, low dislocation density, plastically deformed, electron mobility anisotropy anomaly *(Russian)* 77−80777
Si particle reinforced Al, internal stresses, X-ray diffr. meas. *(Russian)* 78−23765
Si, photoelectret effect, plastic strain induced dislocation relax. time enhancement *(Russian)* 79−15397
Si, plastic deformation, dislocation density in yield point area *(German)* 78−38720
Si, plastically deformed, dislocations reactions obs. by X-ray topography 78−75691
Si, plastically deformed, dislocation structure with different sample orientation 80−70207
Si, plastically deformed, spin-depend. charge transport 80−6895
Si, polycrystalline, recrystn. after plastic deform. and annealing 80−3145
Si, self-diffusion, dynamical recovery 80−29215
Si single crystals, brittle, deform. during static indentation 79−87714
Si single crystals, plastic deformation, dislocation gliding *(German)* 79−52316
plastic deformation continued
Si, stationary creep depend. on deform. stabilisation of material struct. *(Russian)* 80−100300
Si, stressed, at high mag. field, submillimeter cyclotron res. of electrons 77−81012
Si, two-step photoconductivity by dislocations 78−14761
n-Si, uniaxially deformed, intervalley scatt., 78-300K 77−20330
Si wafer creep testing using stress provided by deposited Si_3N_4 film 77−66000
Si wafers, process-induced in-plane distortion and wafer bowing 79−11048
Si wafers, scribing and subsequent fracture 80−11743
Si, X-ray topographical study *(German)* 78−59813
Si:B(Ga)(Sb), plastic deform. and formation of dislocation loops, effect of Au atoms 79−69184
Si:B(P), deformed, EPR fine struct. spectrum of dislocation 77−66422
Si:B(Sb), deform. coeff. due to impurity diffusion 78−18671
SiC (6H), slip systems and plastic deform. at high temp., Knoop hardness meas. 79−87683
SiC containing material, deform. props. investigation by pure bending 78−19823
α-SiC, effect of cryst. shape and size on plastic deform. to rupture and strength 77−56043
SiC, effect of crystallographic anisotropy on Knoop microhardness 80−66626
SiC, high-temp. creep interpretation by deform. mapping techniques 77−21230
SiC, influence of plastic deform. on struct. of photoluminesc. spectra 77−55824
α-SiC, plastic deform. 77−12673
SiC single crystals, friction, deform., and fracture, crystal orientation effect 79−96150
SiC, spray dried agglomerates, compaction response, fracture, deform. 79−43172
SiF_4, thermocyclic stress effects in corrosive-media, electrochem. polarization applic. *(Russian)* 78−11356
Si_3N_4, hot-pressed, creep and strain recovery 80−100874
Si_3N_4, reaction-bonded and hot pressed, deform. and fracture during creep 79−38916
SiO_2 fibres, plastic deformation and Young's modulus *(French)* 78−23746
SiO_2-Al_2O_3, refractory fibrous heat insulating material 78−6990
Sn, and alloys, whisker samples, stress depend. of supercond. T_c 77−39988
Sn, recrystallisation textures, and deformation formed by dry sliding against steel 79−91698
Sn, single cryst., 1.6-300K, hardening curves *(Russian)* 78−3179
Sn, single crystal, dislocation walls consisting of double arrays 79−46664
Sn, stress depend. of supercond. parameters 77−12045
Sn-Pb eutectic, struct. and plasticity, thermomech. treatment effects *(Russian)* 78−60686
SrF_2 antireflection coated, 3.8 μm CW laser damage threshold obs. 80−33053
$SrTiO_3$, defects grown by Verneuil method 77−51390
$SrTiO_3$ film, polycrystn., dielec. props. and struct. 77−81057
steel, C, annealed S45C, multiple repeated low cycle torsion fatigue under controlled strain *(Japanese)* 78−27610
steel, C, eutectic, YU8, effect of segregating structurally free ferrite *(Russian)* 79−15677
Steel, C, fibre reinforced Cu matrix, deformation parameters controlling dislocation motion, flow stress, activation volume 79−57055
steel, Nb, deform., recrystn. and precip. interaction 80−97515
Ta, deformed at 4.2K, electrical resistivity recovery spectrum, stage III 77−8895
Ta, effect on positron annihilation and supercond. transition *(Russian)* 77−39993
Ta, Ta-Re, Ta-Re-N, deformed at 77K, dislocation substruct. 77−32647
Ta-H, physical properties, plastic deformation, H ordering *(Ukrainian)* 80−71689
Ta-Ir (1 wt.%), positron annihilation, photon ang. distrib. meas. effect of deformation, annealing temp. *(Russian)* 78−35220
TaC-TaB_2, exam. of high temp. friction and wear, and deformation behaviour 79−34152
Tc, temp. depend. of hardness and hot plastic strain *(Russian)* 79−74202
Te, single crystals, expts. using device for pure shear deform. 77−81367
Ti, acoustic harmonic generation by long-range dislocation motion 79−42150
Ti alloy, deform. under biaxial stress at elevated temps. 77−12675
Ti alloy, deformation field investigation in danger zone of sheet 77−16654
Ti alloy, hot deform. *(French)* 77−52371
β-Ti alloy, rolling orientation pattern form. *(Russian)* 77−21161
Ti alloy, VT22, thermomechanical treatment, effects on struct. and props. *(Russian)* 78−19785
Ti alloy, yield, discontinuous, under tensile strain in liquid He, governing laws 77−63760
Ti alloy A-75, plastic instability in sheet deformed in uniaxial tension at 300 to 700K 79−47742
α and $\alpha+\beta$Ti alloy of different stability, exponential law use for anal. of strain hardening process 79−15697
Ti alloy sheet, plastic microstrain study during rolling under industrial conditions *(Russian)* 79−52263
Ti alloy TA6V, fatigue, low cycle, and microfractography *(French)* 77−70168
Ti alloy TA6ZrSD, low cycle fatigue at 450°C *(French)* 79−70169
Ti alloy VT20 and VT22, yield strength anisotropy and durability after cyclic loading *(Russian)* 78−27565
Ti alloy VT22, hardening during thermomechanical treatment, precipitate particle internal struct. *(Russian)* 79−91657
Ti alloy VT25, thermomechanical treatment effect on struct. and mech. props. 78−3152
Ti alloy VT5-1, annealed, plastic deform. nonuniformity depend. on stressed state and test temp. 79−57071
Ti alloys, fatigue crack propagation resistance, grain size effect, exam. 80−11765
Ti and Ti alloys, struct. sensitivity of mech. props., alloying influence *(Russian)* 79−47748
Ti and Ti-Al (4,6,9 wt.%), X-ray line profile anal. 77−47459
Ti and Ti-Nb, plastic deform. and thermal cond., 2.5 to 10K, dislocation pinning 77−35629

plastic deformation continued
Ti based alloy, type VT65 and VT5-1, describing cyclic-creep processes with parametric eqn. 79−57074
α-Ti based alloys, deform. twinning effect on mech. props. at low temps. *(Japanese)* 78−6979
Ti, commercial purity, stress relaxation expt. 77−48472
Ti commercially pure VTI-0, heterogeneity of strain field 80−35286
Ti, Cr coating effect on mech. props. *(Russian)* 77−44290
Ti, crystalline orientation distribution analysis of texture development 79−91669
Ti, deform. and H_2 inclusion effect on annihilation γ-ray ang. correl. curve shape 78−31273
Ti, deform. mech. map 77−77546
Ti, deformation, tension, torsion compression test exam. *(Russian)* 78−31455
Ti, diffusion of Fe, under plastic deformation *(Russian)* 79−28146
Ti, dynamic plastic loading of frames 79−20117
Ti, effects of strain rate, temp. interstitial contact on electroplastic effect 79−83279
Ti, extruded, continuum mech. anal. of flow curve anisotropy and plastic strain *(German)* 78−84947
Ti, fast neutron irrad., twinning deform. at room temp. 80−65061
Ti, fatigue damage, SEM, X-ray diffr. and surface trace anal. 80−85040
Ti, fracture mechanism at different temps. 77−63785
Ti, grain size effect on acoustic emission generated during plastic deformation 78−80609
Ti, grain size effect on yield stress and work hardening at 295 and 575K 78−64593
Ti, IMI-125, strain rate effect on mech. behaviour 80−3153
Ti, industrial grade structural changes during polygonization *(Russian)* 78−19779
α-Ti, initial stage of strain ageing *(Russian)* 77−81278
Ti, mech. props., 20 to 300°C *(French)* 77−56018
Ti, metal and alloys, compression at high strain rate, deformation anal. 80−25769
Ti metal-metal interface, adhesion energy, surface treatment and ion implantation effects 80−107660
Ti, neutron irrad., low temp. deform. studies 79−47757
Ti, plastic anisotropy of extruded bars *(German)* 77−86126
α-Ti, plastic deform., anharmonicity, and Gruneisen parameter 80−88246
Ti, plastic deform. dynamics, mech. characts. and phys. props., effect of O_2 *(French)* 80−45353
α-Ti, plastically deformed by rolling, optical and electron microscope obs. 79−91666
Ti, point defect estimation from specific heat and volume in plastically deformed pure metals *(Russian)* 80−54223
Ti, polycrystal, discontinuous electrical resistivity, low temp. active straining *(Russian)* 80−103666
Ti polycrystalline sheet, strain ratio prediction from the ODF, appl. of Taylor's model 79−91773
Ti polycrystalline wire, electroplastic effect 79−57067
Ti, pure plate, silver band formation in ductile fracture process *(Japanese)* 80−16445
Ti sheet, anisotropy and texture, effect of plastic deform., recovery and recrystallisation *(Russian)* 77−8850
Ti, tensile properties and creep behaviour at high temp. 78−23773
Ti, twinning deformation, neutron irradiation effects 80−75236
Ti, volume changes and defect healing due to plastic deform. *(Russian)* 80−81139
Ti-6Al-4V, stress distrib. for steady axisymmetric extrusion 80−3103
Ti-Al, age-hardened, deform., order effects in Ti_3Al and temp. effects 77−25111
Ti-Al (14 at.%), with precipitate free zones, tensile props., grain size effects 77−16690
Ti-Al-Cr-Mo-V, VT22 alloy, metastable β-phase decay under continuous heating, plastic strain effect *(Russian)* 80−71656
Ti-Al-Mo-Cr (4.5, 5, 1.5 wt.%), weld metal, α/β interace sliding 80−108512
Ti-Al-Mo-Sn alloy, elastically and plastically deformed, positron annihilation meas. of deformation 80−21038
Ti-Al-Mo-Zr, compressor disk, surface plastic deform., optimal method 80−60924
Ti-Al-Mo-Zr alloy VT9, Cu-Cr(Ni) coated, plastic deform. and diffusion annealing effect on props. *(Russian)* 78−35425
Ti-Al-Sn, alloy 6242, dynamic effects of flow and fracture during isothermal forging 80−76343
α-βTi-Al-Sn-Zr-Mo (6, 2, 4, 6 wt.%), deformation associated with surface cracks and α particles 79−79107
Ti-Al-Sn-Zr-Mo (6,2,45 wt.%), surface cracking under unidirectional loading 78−56753
Ti-Al-V (6, 4 wt.%), annealed and rolled plate, elevated temp. plastic anisotropy 79−61663
Ti-Al-V (6, 4 wt.%), deform. charact. under isothermal forging conditions 77−36600
Ti-Al-V (6, 4 wt.%), ring test, evaluation for strain rate sensitive materials 78−39991
Ti-Al-V (6, 4 wt.%), temp. distrib. for steady axisymmetric extrusion 80−11670
Ti-Al-V (6, 4 wt.%), temp. distrib. for steady axisymmetric extrusion numerical results 80−11671
Ti-Al-V (6,4 wt.%), age hardened, deform. charact. 77−36608
Ti-Al-V (6,4 wt.%), surface cracking under unidirectional loading 78−56753
Ti-Al-V(Sn) alloys, plastic deformation and fracture characts. at low temps. *(Russian)* 80−7624
Ti-alloy, VTZ-1 and VT8, decomposition of metastable phases, effect of plastic deform. *(Russian)* 78−39770
Ti-Cr, sintered, friction and wear, structural factors 78−60843
Ti-Cr-TiC, sintered, friction and wear, structural factors 78−60843
Ti-Er(Y), effects of Er and Y additives on deformation behaviour 80−81121
αTi-Fe, plastically deformed, α→ω transform. 78−3095
Ti-Fe (1.4 wt.%), polymorphic transform. due to plastic deform., positron annihilation 80−79939
Ti-Mn (0.4 and 12 wt.%), bonding between α-β interfaces, subsequent deform. 78−14517
β-Ti-Mo, alloy, struct. changes during deformation and ageing *(Russian)* 78−39791
Ti-Mo, fracture behaviour and tensile props. at elev. temp. 78−60822
Ti-Mo (15 wt.%) alloy, metastable β-phase, deform. characts. 78−6975
plastic deformation continued
Ti-Mo (16 at.%), effect of H impurities on lattice spacing, hardness, and plastic strain *(Russian)* 79−11664
β-Ti-Mo-Zr-Sn (10.2, 5.8, 4.7 wt.%) heat treated, tensile yield, fracture behaviour, primary deform. mode, exam. 78−60724
Ti-Mo-Zr-Sn (11.5, 6, 45 wt.%), plastically strained regions, decoration 77−28864
Ti-Mo-Zr-Sn (11.5, 6, 4.5 wt.%), metastable beta III phase, recrystallization and grain growth 80−3091
Ti-Mo-Zr-Sn (11.5, 6.0, 4.5 wt.%) alloy, struct. as affected by processing history 80−84972
Ti-Mo-Zr-Sn-Fe-C-Si alloy, β-III, cold deform. and annealing, effect on struct. and mech. props. *(Russian)* 79−24533
Ti-Mo(Nb)(Ta), BCC struct., tetragonal phase form. by cold deform. *(Russian)* 78−88462
Ti-Nb-Mo(V)(Ta)(Al)(Zr), BCC struct., tetragonal phase form. by cold deform. *(Russian)* 78−88462
Ti-Nb-Zr-Fe-Mo-V, cold worked, struct. and phase transform. during ageing 78−3153
Ti-Ni, effect of alloying on crit. points and martensitic transform. hysteresis 80−20935
Ti-Ni (51 at.%), plastic deform., two reversible form change effects *(Russian)* 77−8881
Ti-Ni-Co(Fe) alloys, shape memory temp., alloying effect 79−38912
Ti-Ni-Fe, plasticity, tensile stress-strain diagrams, ultimate tensile strength, elec. resist. depend. on temp. *(Russian)* 79−61652
Ti-Pd (0.15 wt.%), IMI-260, strain rate effect on mech. behaviour 80−3153
Ti-TiC system, sintered, friction and wear, structural factors 78−60843
β-Ti-V metastable alloys, fatigue crack propag. 80−60964
Ti-V-Si, Si effects on precipitation and strengthening 77−55970
Ti-Y(Er), dispersoid effect on deform. 79−24530
α-β TiAl-Sn-Zr-Mo (6,2,4,6 wt.%), age hardening 79−61604
Ti_3Al, cyclic deform., dislocation struct. 78−7003
TiC, deform. at high temps. 80−104239
TiC, deformation behaviour during rubbing in wide temp. range 80−16486
TiC, frictional characts. and contact-zone deform. in homogeneity range 80−66673
TiC layers, on steel and cemented carbides, load-bearing capacities 80−40606
TiC powder, plastic strain of particles under vibratory milling 77−90423
TiC single crystal, deformation behaviour, operative slip systems 79−100211
TiC-TiB_2, strength and antifriction props. over wider range of concs. 80−50673
TiNi-TiCu, exam. of shape memory effect, specific work 79−100216
TiO_2 rutile single crystals, stoichiometric, dynamic strain ageing 80−50661
TiO_{2-x} reduced, crystallographic shear planes, dislocation struct. 80−107175
(U, Pu)C, ceramic fuel, plastic deform. behaviour at stress changes 80−35261
α-U, mech. behaviour, strain rate influence, 300 to 550°C 79−38907
α-U, mech. props. at very high strain rates, double-notch shear test use 80−85131
α-U, polycrystalline, compressive deform. at low temps. 77−28856
α-U, strain rate effect on tensile flow and fracture 80−84992
U/(Zr-Cu-Mo alloy) welded joints, mech. characts. determ. 20 to 750°C 79−29113
U-Mo (1.5 wt.%) metallurgical study of forging *(French)* 78−21737
U-Mo(Nb) and U-Mo(Nb)-Zr alloys, shear martensitic transform. during quenching, plastic deform. and annealing 77−28815
U-Nb (14 at.%), exam. of shape memory effects 78−76694
UO_2, compressed, dislocation substructure obs. *(French)* 78−78461
UO_2-PuO_2, ceramic fuel, plastic deform. behaviour at stress changes 80−35261
U_3Si, reversible twinning, in-situ obs. 80−104241
V, and V-H, fusion reactor first wall material, cyclic deform. tests 80−30074
V, different grain sizes, room temp. microstrain *(German)* 77−36614
V, dynamic deformation, influence of previous static loading *(Russian)* 78−6972
V, effect on positron annihilation and supercond. transition *(Russian)* 77−39993
V, high purity, neutron irradiated effect, comparison of high purity with V-O 77−84805
V, internal friction α-peak origin 78−95773
V, neutron irrad., yield stress and activation vol. 77−90418
V, polycryst., struct. changes during deform. *(Russian)* 78−48447
V, purification and plastic props. 80−25810
V, radiation hardening and plastic instability *(Russian)* 78−39842
V, rolling textures, microstructure, micro orientation *(Russian)* 79−91663
V, slip geometry and dislocation struct., rel. to degree and temp. of deform. *(Russian)* 78−38717
V, supercond., influence of plastic deform. 77−85378
V, zone-refined, deform. behaviour, stress relax. and slip plane patterns 79−29163
V-O, neutron irradiated effects, comparison with high purity V 77−84805
V-Zr-C, radiation hardening and plastic instability *(Russian)* 78−39842
V_3Ga, A15 compound, exam. of deformation processing, review 78−39864
V_3Ga, cast, effect of hydrostatic extrusion on supercond. props. *(Russian)* 77−21215
V_3Si, A15 compound, exam. of deformation processing, review 78−39864
V_3Si, plastic deform. effect on supercond. props. 80−29500
V_3Si plastically deformed cryst., lattice transform., Kossel technique 78−95153
V_3Si single cryst., A-15 compound supercond., plastic deform., at high temp. 79−20104
V_3Si, supercond. structure and properties *(German)* 80−93631
W, (100) oriented cryst., plastic relax. effect on semi-brittle fracture 77−69036
W alloys, deformed, vacuum technology appl., mech. props. *(German)* 79−57046
W, block boundary dislocation struct. singularities under high temp. steady state creep conditions *(Russian)* 79−90670

plastic deformation continued
W, cast state, interaction nature between C, O_2 and N_2, influence in struct. and props. *(Russian)* 79−70114
W, deformed, surface layer struct. effect on polygonisation and recryst., X-ray diffr. anal. and metallographic exam. *(Russian)* 80−84948
W, doped wire, secondary recrystallisation temp., bubble parameter effects 77−32596
W, doped wire, textural aspects of recrystallization 78−11239
W, electroplastic drawing, deformation zone current delivery schemes 79−91761
W fibre reinforced epoxy composite, static tensile behaviour *(Japanese)* 78−15482
W fibres, dependence of fine struct., on processing parameters 79−34082
W, plastic working of wires, high-density current appl. 79−57002
W, plastically deformed single cryst., mag. susceptibility *(Russian)* 80−93074
W, polygonisation critical stage in single crystals deformed in compression 79−4979
W, powder, subjected to vibratory milling, exam. of plastic deformation, recrystallisation, sintering 80−16234
W strip production, flattening mill employing US and electroplastic effect 78−84941
W surface layer struct. during milling, plastic deform., failure *(Russian)* 80−40586
W, texture form. by drawing and pulling through nonpowered rolls, BCC lattice *(Russian)* 77−25100
W, twinning dislocation, math. model 77−59024
W, US working effect on single cryst. during deform., strengthening effect, plasticity resource *(Russian)* 79−34107
W wire reinforced Cu, exam. of thermal cycling induced deformation 79−5050
W-Cu, porous material, skeletal type, produced by liquid phase sintering, exam. of mech. strength, determ. resistance 80−16245
W-Ir (1 wt.%), positron annihilation, photon ang. distrib. meas. effect of deformation, annealing temp. *(Russian)* 78−35220
W-Ni compact, sintering behaviour and workability *(Japanese)* 80−20822
WC, cemented carbide, deformation, high temp., stress relaxation, and strain rate depend. 78−39854
WC, deformation behaviour during rubbing in wide temp. range 80−16486
WC-Co, cemented carbide, deformation, high temp., stress relaxation, and strain rate depend. 78−39854
WC-Co, elastic and plastic charact. 80−35280
WC-Co, exam. of effect of continuous carbide phase, on hardness, and deformation 78−52974
WC-Co (10 wt.%), elevated temp. bend deform. and fracture, effect of C 77−59877
WC-Co (6 to 20 wt.%), bend deform. and fracture up to 1000°C 77−48510
WC-Co and WC-Co-TaC-TiC-NbC cemented carbides, microstructure, high temp. deformation, uniaxial plastic compression 80−40451
WC-Co cemented carbides, irreversible deformation, yield stress, SEM study 79−70110
WC-Co sintered hard alloy, yield stress, internal thermal stress effect 79−100230
WC-Co-Ta(Ta-Ti-Nb), cemented carbide, deformation, high temp., stress relaxation, and strain rate depend. 78−39854
W_2C and WC, plastic deform. under bending, 800-2200°C *(French)* 80−55482
W_2C, slip systems, at ambient temp. *(French)* 78−84926
Y, polycrystn., plastic deform. at different deform. speeds, dislocation glide *(Russian)* 80−93598
$Y_3F_5O_{12}$, X-ray determ. of deformed surface layer thickness 78−53119
YH_x, mech. props. 77−44333
YIG, deformed at high temp., subgrain boundaries and dissociations of dislocations, TEM obs. 79−90658
YIG, electron and γ-irrad., photomagnetic effect 80−103877
YIG, plastic deform. and mag. props 77−40087
Y_2O_3, monocryst., HV electron microscopy obs. of dislocation config. *(French)* 79−55747
Y_2O_3, plastically deformed, dislocations obs. by TEM *(French)* 78−51545
Y_2O_3, plasticity, microhardness testing, indentation, plastic deform. temp. depend. *(French)* 78−56713
Y_2O_3-AlN, creep 77−21235
$(YSmCa)_3$ $(FeGe)_5O_{12}$ mag. bubble garnets, ion implantation induced stress influence on props. 79−91274
ZN, anomalous US damping under hydrostatic press. 79−14890
Zh, extruded, continuum mech. anal. of flow curve anisotropy and plastic strain *(German)* 78−84947
Zircaloy 2, mechanical equation of state, stress relax. meas. 78−52880
Zircaloy-4, deformation behaviour between 77 and 900K 80−71686
Zn alloys, deep drawing behaviour, exam. in binary and ternary alloys *(French)* 79−52325
Zn alloys, rolled and press. die-cast, creep and deformation behaviour *(German)* 80−66611
Zn, alternating bending of single crysts., shear strain accumulation and microstrain distrib. *(Russian)* 78−60706
Zn, basal slip, early stages in single crystal 77−72623
Zn bicrystals, grain boundary slip in deform. 80−34008
Zn, coating on steel strip, plastic deform. 77−90368
Zn, compatible bicrystal, plastic deform. *(Japanese)* 78−31460
Zn, Cottrell-Stokes law, 4.2 to 300K, forest dislocations and other obstacles 77−43269
Zn crystal, $\{11\bar{2}2\}\langle 11\bar{2}3\rangle$ slip system, deform. stress, dislocation density depend. *(Russian)* 80−103353
Zn crystals X-ray topographic examination of basal dislocations 80−88156
Zn, deep drawing behaviour *(French)* 79−52325
Zn, deform. twin form. kinetics, Rose channel form. and interactions, twin growth rate *(Russian)* 79−60378
Zn, deformed, internal friction meas. 77−86067
Zn, deforming stress under basal slip, contrib. of forest and primary dislocations 78−3186
Zn, density of basal dislocations, rel. to deforming stress, 1.5-300K *(Russian)* 80−29028
Zn, dislocation mechanism of Rose channel formation under impact loading conditions *(Russian)* 79−79073
Zn, electroplastic deform., stress relax. meas. *(Russian)* 79−38894
plastic deformation continued
Zn, hydrostatically compressed single crystal, work hardening studied by stress relax. method 79−20069
Zn, incompatible bicrystals, effect of grain boundaries on mech. props. *(Japanese)* 78−39798
Zn, loading and annealing, dislocation struct. control *(Russian)* 78−3142
Zn, low-temp. thermal fatigue, causing fracture and plastic deform. 77−28837
Zn, microcrack propagation and plastic strain 80−81187
Zn, nitrided, yield strength, influence of deform. rate *(Bulgarian)* 80−89315
Zn, oriented polycrystals, tensile behaviour under hydrostatic press. *(Japanese)* 77−52417
Zn particulate composite, mech. props., microstruct. correlation, at low and high temps. 77−32624
Zn, plastic anisotropy of extruded bars *(German)* 77−86126
Zn, plastic deform after pinch effect *(Russian)* 78−27563
Zn, plastic deform., effect of hydrostatic press. stress relax. meas. *(Russian)* 79−96102
Zn, plasticity under hot deform. conditions, temp. depend. *(Russian)* 79−29133
Zn polycryst., compressive strength, temp. and strain rate effects 80−16616
Zn polycrystals, deformation, grain sizes effect at room temp. *(Czech)* 80−45359
Zn, positron annihilation in plastically deformed sample, electric field effect 79−69899
Zn, single cryst., contribution of basal dislocations to residual elec. resist. *(Russian)* 80−75539
Zn single cryst., dislocation velocity and plastic deform. 80−64998
Zn, single cryst., in metal melt, plastic deform. and fracture obs. by acoustic emission *(Russian)* 78−56737
Zn, single cryst., plastic deform., 1.5-300K *(Russian)* 77−77533
Zn, single cryst. stress relax. depend. on elec. current, electron plastic effect 79−79021
Zn single crystals, temp. and strain rate effects on strength, slip and twinning 80−16373
Zn, stacking faults, plastic deformation, due to laser beam irrad. *(Russian)* 80−15121
Zn, strengthening by electroplastic strain, surfactant effect *(Russian)* 80−20953
Zn, thermal recovery and stress-strain relations 78−11266
Zn, twinning, influence of dislocation drag. mag. field effects 80−59472
Zn whisker, supercond. crit. temp., stress depend. 77−39989
Zn, work hardened crystal, jump-like plastic deform., dislocation struct. instability 79−96094
Zn-Al, near eutectoid alloy, deformation kinetics analysis 79−29161
Zn-Al (0.4 wt.%), grain size effect on acoustic emission generated during plastic deformation 78−80609
Zn-Al eutectoid alloy, straining at elev. temp., whisker crystal 79−29087
Zn-Al eutectoid alloy sheets, creep bulging 80−1439
ZnO(S)(Se)(Te), charged dislocations, flow of charge with plastic deform. 80−85010
ZnS, 4H and 6H polytypes, struct. changes on plastic deform. 77−43328
ZnS crystals, structural change under plastic deform., partial dislocation movement 80−79736
ZnS, glide plane of dislocations 79−46667
ZnS, interaction between charged dislocations and luminesc. centres *(Russian)* 79−56860
ZnS, plastic deform. induced luminesc., dislocations role *(Russian)* 78−10985
ZnS, plastically deformed, anisotropic cond. 78−56143
ZnS, polymorphic transition, $(\beta \rightarrow \alpha)$ effect of mech. deformation 79−1858
ZnS, sphalerite modification, polysynthetic cryst., struct. changes due to uniaxial compression 77−15482
ZnS, work done and heat evolved in plastic deform., stacking fault energy 77−80573
ZnSe cold pressing 77−52258
ZnSe, electric charge transport by dislocations 80−103709
ZnSe, mech. of electroplastic effect 79−28035
Zr, acoustic emission during deformation, expt. 77−73425
Zr, deformation texture during rolling in sequential passes 79−11674
Zr, deformed at 77K, effect of fast-neutron irradiation on deformation twinning, TEM and optical microscopy obs. 79−37741
Zr, low temp. deformed, O_2 effect on production and recovery of defects, elect. resist. meas. 79−47705
Zr, mag. susceptibility, plastic deform. effect *(Russian)* 80−65984
Zr, martensite, furnace cooled and water quenched, strength and deform. 79−20101
Zr, neutron irrad., low temp. deform. studies 79−47757
α-Zr, polycrystalline, cyclic deformation *(Japanese)* 78−68757
Zr polycrystalline, low-temp. alternating deformation and annealing, yield stress, elec. cond. variation *(Russian)* 79−74199
Zr, structural changes during plastic deform. *(Russian)* 77−8880
Zr, tensile deformation behaviour, neutron irrad. effects, dislocations, twinning inhibition 77−90393
Zr-base alloy as reactor core material, microstruct., deform. and fracture 78−4988
Zr-Cu, dil. martensites, struct. and strength 79−29077
Zr-Cu (1.6 wt.%), mechanical equation of state, stress relax. meas. 78−52880
Zr-Cu-Ti (2.5, 0.15 wt.%), indentation irregularity at elastic limit after heat treatment *(French)* 79−79004
Zr-Dy dil. alloys, plastically deformed, mech. props. and microstruct. *(Russian)* 79−20112
β-Zr-Mo-(Al)(Ti)(La), metastable, deform. induced transform. 78−52805
Zr-Nb (1 wt.%), static strain ageing between 295 to 773K, TEM obs. of plastic strain 79−38855
Zr-Nb (1 wt.%), tensile props., 295 to 773K 79−8318
Zr-O-N system, struct. and plastic deform. *(Russian)* 78−80588
Zr-Ti martensites, furnace cooled and water quenched, strengh and deform. 79−20101
Zr_3Al, deformed and irrad., lattice defects obs., superlattice dislocations and defect clusters 80−107261
Zr_3Al, neutron irrad. effect on tensile props. 80−3156
Zr_3Al, ordered polycrystals, ductile fracture 78−64641
Zr_3Al, tensile props., surface preparation depend. 80−3155
ZrC high-temp. plastic deform. effects on elec. props. 77−44370

plastic deformation continued
ZrC, high-temp. strength, affecting factors 77—63794
ZrC powder, plastic strain of particles under vibratory milling 77—90423
ZrC-ZrB_2, strength and antifriction props. over wider range of concs. 80—50673
$Zr_{50}Co_{50-x}Ni_x$, transform. and deform. studies 79—1864
$ZrH_{1.92}$, plasticity 77—36569
ZrH_x, mech. props. 77—44333
ZrN high-temp. plastic deform. effects on elec. props. 77—44370
ZrO_2, CaO stabilised, preferred slip system 80—66585
ZrO_2, spray dried agglomerates, compaction response, fracture, deform. 79—43172

plastic flow
see also ductility; Luder's bands; necking; rheology
abraded surfaces, topography rel. to contact area and abrasion mechanism 80—58986
adiabatic plastic deformation, shearing phenomena, review 80—50692
alloy, strengthening mechanism anal. by thermal activation theory 79—78987
anisotropic constitutive equations of continuous media *(French)* 79—25846
annealed OFHC Cu, plastic behaviour 80—59559
annular plates, minimum weight design *(Russian)* 79—10498
bars, rectangular, plastic flow during closed die cropping 79—37190
Bauschinger AE peak detection of back stress component in flow stress *(Japanese)* 78—6977
Bauschinger effect parameters and plastic flow rules 78—6984
bisphenol-A-diglycidyl ether epoxies, amine-cured, microscopic failure 77—90441
Bragg bubble glass, struct. and plastic flow 80—84091
α-brass, Bauschinger AE peak detection of back stress component in flow stress *(Japanese)* 78—6977
brass, cold rolling, inhomogeneous texture 80—89251
brass, crack opening displacement, rel. to flow stress 78—68810
brass, plastic flow, rate controlling mech. at high temps. 77—81308
brass, superplastic deform. rate rel. to flow stress, determ. methods 78—60709
$\beta'+\gamma$- brass, two-phase, acoustic emission from β' plastic flow and γ cracking 80—16452
β-brass, uniaxial tension and compression, cyclic stress-strain behaviour 80—97551
β-brass bicrystals, shear-incompatible, grain boundary contrib. to Bauschinger effect 80—97550
brittle materials, abrasion, size effect 79—34131
bulk moulding compound, flow state, closing speed effect *(Japanese)* 80—55469
complex system reliability under nonuniform random perturbation, asymptotic anal. *(Ukrainian)* 79—41589
composite medium, two-component residually stressed, elastoplastic crack model *(German)* 78—90790
compressible materials, flow behaviour 78—55573
compressible plastic solid, plane flow, operator method for variational principles *(Polish)* 77—54898
compression, high strain rate, 1023 steel 79—34099
compression, isentropic, optimal, reversed time numerical method, solid pellet implosion 78—79446
compression test, determ. of accurate flow props. 78—27718
consecutive energy barriers, props., and associated behaviour in plastic flow 78—75710
consecutive energy barriers system, reaction kinetics theory 80—106730
constitutive equations derivation from Clausius-Duhem inequality 80—46804
corner theories, time-independent incremental behaviour at corner of yield surface 80—64388
crack propagation, fracture viscosity and plastic flow calc. *(German)* 77—54934
crack tip plastic zone, thermal props. calcs. 80—7659
crack under friction and combined stress, plastic flow around tip 78—79280
creep, generalised variational principles, Lagrange multiplier method applied to flow theory *(Chinese)* 80—79171
cropping and blanking, plastic flow, fracture, crack propagation 80—74761
crystalline and amorphous solids, plastic behaviour in terms of defect motions 78—95104
crystalline material, flow during plastic deformation *(Russian)* 78—76705
cubic crystals, scratch hardness, anisotropy 79—96130
cup ironing process, two-dimens. plastic flow prod. by temp. field *(Polish)* 78—26053
cylinder, plastic flow rules and Bauschinger effect parameters 78—6984
cylindrical body, axisymmetrically deformed *(Russian)* 79—7300
cylindrical shell, thick-walled, effect of non-homogeneity on plastic flow, numerical calc. 80—19248
cylindrical shell under internal press. elastoplastic nonhomogeneity 79—37196
defects, influence on solid-state props., review 77—7709
deformation kinetics analysis of stress sensitivity 77—3737
deformation localisation in tension, determ. 79—87790
deformation localization into shear band, as instability of plastic flow and precursor to rupture 77—68458
discontinuous, acoustic wave spectrum resulting from interaction with unstable thermal mode 77—27937
dislocation distrib., fracture relation, plastic flow at crack tip, slip line theory 80—64482
dislocation motion, thermal activation through random point obstacles 79—1434
dislocation motion through random array of weak obstacles of finite width, digital computer simulation 78—30633
dislocations model, compatibility with transient and steady state creep *(Italian)* 80—33487
disperse systems, plastic, laminar flow in circular tubes 80—87798
dispersion strengthening, dislocation interaction treatment, digital simulation models 78—31419
dolomite, strain rate depend. and intracrystalline plastic flow 77—44977
Drucker postulate verification at high temp. 80—30025
ductile fracture, strain hardening and damage relationship 80—108564
ductile single crystals, exam. of strain localisation 78—52912
ductile-brittle transition, atomistic simulation by computer, exam. of thermal activation of crack tip plasticity 78—60801

plastic flow continued
Dugdale model validity limits for thin cracked plates under biaxial loading 80—43667
Duralumin 2017, superplasticity *(Korean)* 79—38902
dynamic variation principle taking into account geometric nonlinearity 79—23227
Earth upper mantle, micromechanisms of flow and fracture 78—69331
Earth upper mantle, plastic flow rel. to seismic anisotropy of subcrustal lithosphere 77—49039
easy glide, computers modelling, range of permissible parameters *(Russian)* 78—47375
elastic-plastic circular plates, biaxially stretched, necking calcs. 78—5666
elastic-plastic plates and shells, flow rule for lowering buckling stresses *(Japanese)* 80—99949
elasto-plastic flow in computer simulated, A533 steel 78—56720
elastoplastic circular plates, nonlinear behaviour equilibr. eqns. 79—14279
elastoplastic half-spaces interface, oblique refr. of plastic wave, self-similarity problem *(Russian)* 78—20974
elastoplasticity algorithm, finite difference and variational methods in flow theory models 77—871
enamel slips, control of rheological props. 79—29136
extrusion and forming of solids, plastic deform., nonNewtonian flow, numerical solns. 78—19824
fatigue, multi-stage nature, review 77—21269
FCC material, irradiation induced creep, climb induced glide model 80—89292
FCC polycrystals, plastic flow self-consistent scheme extension 79—64530
Fe, pure AISI, flow stress, temp. and strain rate sensitivities 77—90421
ferromagnet, flow stress, effect of magnon mechanism of dislocation drag 77—69662
fibre lightguide form., from tubular blank, optimisation 77—75719
fibre reinforced composite, notched, analytical method for predicting plastic flow 77—70114
finite elements method, convergence *(Russian)* 77—58569
finite strain work-hardening theory for rate independent elasto-plasticity 79—76983
flow curves determ. by method of representative viscosity *(German)* 77—68642
flow planes and flow laws for plastic mechanics *(German)* 79—86359
fluid saturated porous solid, fundamental solns., deformation, pore-fluid diffusion, soil mechs. 77—84160
force plane diagrams for plane strain slip-line fields 78—63314
forming limit curve for bending processes 80—7627
fracture and plasticity, lattice-statics approach, review 80—39212
gabbro, long-term creep, large and small specimen results obtained over 20 and 3 years respectively *(Japanese)* 78—56705
glacier, sliding on plane strewn with hemispherical obstacles *(French)* 79—8640
granite, long-term creep, large and small specimen results obtained over 20 and 3 years respectively *(Japanese)* 78—56705
granular material, plane plastic flow, expt. test 78—34027
granular materials, intergrain slip in flowable zone, stress distrib., internal friction 79—99261
granular materials, shear deformation, entropy model 80—84233
hardened irradiated metal, flow stress temp. depend., effect of interstitial atom clustering and embrittlement *(Russian)* 78—34538
hardening rigid-plastic bodies, deformation propagation, dynamic flow 79—86356
high strength materials, exam. of flow localisation and fracture toughness 78—60764
hole, circ., in infinite plate, dynamic expansion 78—55574
hot rolling, simplified load calcs. incorporating material strain rates 77—52359
hot rolling exam. of empirical relations for plastic flow strength 79—61630
hot strip rolling simulation, by hot torsion technique 80—29990
hyperbolic sine creep, flow potential function 79—32304
hypoelastic compressible rate-sensitive material flow, integrable generalized wave eqns. 78—38213
impact attenuation system using plastic deform., effect of strain-rate sensitivity 77—23890
Inco 718, fatigued specimens, plastic zone size 77—25150
Inconel 600, mechanisms of dynamic strain ageing and jerky flow 79—79024
inelastic membrane shells of revolution, large deformations in plastic flow theory 80—58917
inorganic solid, stress depend. of activation volumes in creep and stress relaxation 79—19312
instability in tension 78—67060
ionic crystal, point defect-dislocation interactions 78—63787
isotropic body, finite element method for volume integration 80—74770
isotropic material, modified stress deviator for plastic compressibility *(German)* 78—13914
isotropic polycrystalline plasticity, dislocation theory 79—14875
isotropic strain hardening theory *(Russian)* 80—38279
lamination, hydrodynamic analogy, utilisation of current function *(French)* 80—19292
laser optical component props. depend. on material flow props. *(Russian)* 80—38047
lecithin-water system, lamellar phase, rheology 80—89779
limestone, finegrained, superplastic flow 78—20398
loosening, plasticity theory with microstresses 77—89071
low-alloy steel, bending, effect of strain rate on dynamic stress factors 77—56046
metal, anisotropic, description of history dependent plastic flow behaviour 80—11732
metal, cold worked, grain size depend. of dislocation density 79—7614
metal, cyclic and damage constitutive laws, calculation methods *(French)* 79—43408
metal, ductile fracture mechanism, theoretical and expt. investigation *(German)* 77—70142
metal, flow during rolling *(Russian)* 78—27561
metal, flow stress, subgrain size and subgrain stability of elev. temps. 77—86094
metal, fracture toughness and temp.-rate sensitivity of plastic flow stress 78—35501
metal, hydroextrusion, effect of longitudinal US vibrs. 79—96046
metal, plastic flow, during extrusion, computer simulation 78—31491

plastic flow continued
metal, plastic flow, finite element approach to axisymmetric problems, METFLO 78−31490
metal, plastic flow rate during rolling under two dimensional strain *(Russian)* 79−52264
metal, radiation stimulated diffusional flow, neutron irrad. *(Russian)* 79−29132
metal, role of osmotic forces in low cycle fatigue, vacancy generation *(Russian)* 79−60430
metal deformability, flow curves mathematical description, thermal dependence *(German)* 78−15484
metal forming processes, finite element anal. appl. 79−50606
metal hydroextrusion process, boundary-value problem *(Russian)* 79−10505
metal plastic flow through ultrasonic vibrated die, mechanism *(Rumanian)* 77−70242
metallic glass analog, plastic flow in disordered bubble raft 79−91745
metallic glasses, entropy model 77−24345
metallic glasses, mats. props. review 77−4043
metallic thin film, polycryst., plastic flow, dislocation slip 79−82505
metals, athermal region of plastic flow at intermediate temps. 77−48497
metals, BCC and FCC, dislocation dynamics method appl. to plastic flow 79−47745
metals, cold forging, upset tests anal., stress-strain law determ. appl. *(French)* 79−20064
metals, deformation induced anisotropic plastic flow, constitutive model 79−59930
metals, longitudinal flow velocity distribution in rolling *(Russian)* 80−93575
metals, porous, plastic flows, microscopic frictional effects, J_2-flow potential and yield function 80−64384
metals, recrystallisation during hot deform. 78−68714
metals, rheological interpretation of planar deformed state in extremal friction regime *(Russian)* 80−64385
metals, rolling of complex sections, unified anal. function of surface of strain focus *(Russian)* 80−21017
metals under load, plastic deform. local instability *(Russian)* 77−76415
metastability effects on plastic flow 78−1579
mild, plastic flow under proportional and non-proportional straining at controlled rates 79−57084
muscle, glycerol-extracted fibrillar fibres, cross-bridge slippage induced by AMP-PNP and stretch 78−77075
naphthalene, cryst. plasticizing by surface active organic media, creep rate meas. 79−55813
naphthalene single crysts., surface active substances effect on plastic flow 80−44248
non-Newtonian fluids in circular pipes, laminar flow stability loss 78−79342
noncoaxial plastic soil, steady in-plane deformation, flow conditions 79−84279
nonlinear behaviour in 1- and 2-dimens., elastoplastic hysteresis, flow and relaxation *(French)* 79−46229
nonlinear monotonic functions with selectable intervals 79−46230
nonlocal thin elastic plates, impact by cylindrical projectile, shearing stress anal. 79−10467
olivine, creep mechanisms 78−69332
olivine, plastic flow of oriented single crystals, dislocation struct. interpretation 78−36156
olivine, plastic flow of oriented single crystals, mech. data 78−36155
olivine flow laws rel. to lithospheric stress 77−91121
oriented transversely isotropic solid, yielding and failure 78−13915
orthorhombic symmetry, yield surface characts. 80−64405
orthotropic plate, plastic flow, effect of shear stress and geometrical changes *(Russian)* 78−13925
plane plastic flow, hydrostatic press. influence on shear resistance *(Russian)* 77−58562
plane plastic flow of compressible solids 78−55575
plane symmetric rolling mill, vector field system soln. *(German)* 78−63333
plane-strain radial flow of plastic materials 79−64529
plastic wave theory, comparison of predictions with impact expts. 80−83742
plastomer, compressible plastic material, isotropic and anisotropic flow *(German)* 77−4817
plate, round, elastoplastic, plastic flow stability *(Russian)* 79−32293
PMMA, craze zones at crack tips, validity of Dugdale model, comment 80−108535
PMMA, craze zones at crack tips, validity of Dugdale model 80−108534
polyester dough moulding compounds, fibre orientation and mech. props. 77−25116
polyethylene, high density, hydrostatic extrusion behaviour 80−50649
polyethylene, high density, impact yielding, flow stress rel. to temp. 77−32653
polyethylene, high density, plastic behaviour determ. at const. true strain rate 79−39073
polyethylene, high-density, deform. resistance and flow curve 77−90405
polyethylene, melt, elongational flow, necking and ductile failure mechanisms 77−43267
polyethylene, polyethylene-D_4, migration and copolymerisation at high press. with shearing stress 78−51678
polyethylene, ultradrawing, effects of temp. and drawing rate *(Japanese)* 79−91760
polyethylene film, minimum running thickness, biaxial extensional flow study 80−100993
polyethylene pipe butt welding, tensile tests rel. to melt flow index 77−73389
polymer, flowing, relaxation of normal stresses 77−881
polymer melts, elongational flow, necking and ductile failure mechanisms 77−43267
polymers, glassy, initiation and growth of crazes 78−60767
polyolefins, plastic flow, yield limit rel. to press. *(Russian)* 80−7657
polypropylene, melts, elongational flow, necking and ductile failure mechanisms 77−43267
polystyrene, compressed, TEM obs. of coarse shear bands 79−70117
polytetramethylene terephthalate, injection-moulded, struct. depend. of fracture behaviour 77−8912
porous ductile media, rupture by void nucleation and growth, criteria and flow rules 77−52492
porous materials, deformation theory *(Russian)* 79−37189

plastic flow continued
Prandtl punch problem for case with eccentric forces *(Russian)* 80−23965
pressure sintering, inhomogeneous flow and effective press. 80−93512
punch identation with isolated slip line 78−79286
PVC, hard, flow zone effect on degradation, rigidity, deformation, under fatigue *(German)* 78−15471
PVC, plastic behaviour determ. at const. true strain rate 79−39073
PVC, rigid, tensile fracture morphology, rel. to mol. props. 77−59883
PVC, Sn stabilized, effect of paraffin and polyethylene lubricants on flow props 79−8325
quartz, ion bombardment, extrusion, evidence for radiation-induced stress relax. of silica network 77−24335
radial flow, approx. analytic soln. *(Ukrainian)* 79−76979
reinforced material, thin layer, compression between plane parallel plates *(Russian)* 80−87725
Rene 80, dislocation behaviour during plastic deform. *(Japanese)* 80−108504
rheological analysis of stress change experiments during high temperature creep 79−37193
rheological and metallurgical discussion of superplastic behaviour 78−30200
rigid-viscoplastic bodies, class of exact solns. of dynamical eqns. 77−68454
rigid/linear-hardening materials, axially symmetric radial flow 80−48604
rings, bearing capacity under compression 78−83256
rocks, faulting and flow during deform. expt. in transmitted light 77−86860
rocks, long-term creep tests, rel. to Earth crust rheology 79−79828
rocks, steady state flow rel. to lithospheric stress 77−91120
rod penetrating thick target, plastic deform.-jetting flow transition vel. 77−62163
sapphire, work hardening 77−16604
sheet metal forming, material behaviour 78−95787
sheet metal forming, strain hardening and strain rate sensitivity 78−7000
shell, fracture behaviour, forming severity and metal flow in deep drawing 79−38975
shells of revolution, thin, numerical anal. thermal stress relief 77−89041
singular wave surfaces in linear inelastic media 79−81799
sintering, initial phase kinetics, model with diffusion *(French)* 78−35328
slip line fields around elliptic holes, Riemann integral solns. 79−32303
soil, plastic flows, microscopic frictional effects, J_2-flow potential and yield function 80−64384
solid lubrications dynamics, obs. using Micro Contact Imager 78−85002
solid soln., flow stress, temp. plateau 79−14877
solid solution, activation energy for dislocation motion, from crit. resolved shear stress data 77−55289
solid solution hardening, dynamic simulation 79−11635
spatial problems, plane strain and axially symm., soln. appls. 78−51089
spatial problems, soln. 78−51088
spatial problems of rigid plastic equilib. 78−55569
spatial problems of rigid plastic equilib. 78−55570
stainless steel, bending, effect of strain rate on dynamic stress factors 77−56046
standing shear waves in hardening rigid-plastic bodies 77−84163
static flow stress, decrease, by superimposition of ultrasonics 79−7652
steady-state creep determ. eqns., microscopic stability restrictions *(Russian)* 79−10493
steel, acoustic emission, quantitative evaluation from plastic zone growth, book contrib. 79−100328
steel, alloy, Ni-Cr-Mo, exam. of transformation behaviour 78−76718
steel, alloy, tension test, computer simulation of deform. to fracture 79−11667
steel, austenitic, phase transform to pearlite and martensite, kinetics, stresses due to quenching, anal. *(Japanese)* 78−27508
steel, austenitic stainless, 304, solution annealed, tensile flow behaviour after exposure to flowing Na, in temp. range 550 to 700°C 78−35463
steel, austenitic stainless, flow cavitation erosion, initial part of incubation period 78−44224
steel, austenitic stainless, high temp. alternating torsion behaviour, saturation state phenomenology 79−70111
steel, Bauschinger effect minimization by dynamic strain ageing 78−48469
steel, C, crack opening displacement, rel. to flow stress 78−68810
steel, case hardened gas carbonitrided, holographic interferometry study of plastic flow *(German)* 77−77723
steel, cold deformation hardening, effect of C content and cementite shape 78−92277
steel, data reduction for samples under high ambient press. and axial tension 78−3181
steel, effect of H_2 on phys. and mech. props. 80−101657
steel, Fe-Cr-Ni (17.20, 7.34 wt.%), transform.-induced plasticity 78−23774
steel, free cutting, with MnS inclusions, tensile flow and fracture 78−11290
steel, H_2 effect on yield 78−15474
steel, high strength, sensitivity to stress concentration with various H content *(Russian)* 79−15724
steel, lattice hardening and anomalous softening caused by electrolytic H_2 charging *(Japanese)* 79−43398
steel, low C, flow stress variation after unloading, tensile load/strain diagrams *(Russian)* 78−76703
steel, low C, high temp. plastic flow under thermal cycling in superplasticity interval 77−70130
steel, low C, normalised, plastic deform., using microhardness and grain strain meas. 77−4810
steel, low C, surface layer struct. under sliding friction 79−52393
steel, microalloyed, recrystallisation, precipitation effect 79−47695
steel, mild, annealed, plastic flow under proportional and non-proportional straining 80−40465
steel, mild, plastic flow, photoelastic investigation of temp. and strain rate effects 77−86238
steel, mild, plastic flow localisation under dynamic torsional loading, crit. variables 80−85015
steel, mild, plate, effect of striking velocity on perforation energy 78−68818
steel, plastic flow area, determ. of relative elongation and rel. to yield point 78−23769

plastic flow continued
steel, S45C and SS41 types, dynamic yield condition under dynamic torsion and static tension 79−34214
steel, stainless, 304, isochronous relaxation curves after monotonic and cyclic strain 79−87676
steel, stainless, fibre reinforced Al alloy, tensile props., cryogenic cooling effect 79−61623
steel, stainless, Ti modified 316, uniaxial tensile behaviour, Na environment effect 78−52916
steel, stainless 304, cyclic deformation behaviour at elevated temps. 79−52322
steel, stainless SUS 304, Bauschinger AE peak detection of back stress component in flow stress *(Japanese)* 78−6977
steel, stainless/Al laminate, sandwich sheet materials, deform. in uniaxial tension 79−57061
steel, structural, sharp notched bending specimens, fracture stress, temp. depend. anal. 77−56062
steel, structural, St37-2, crack tip displacement and flow curves *(German)* 79−47747
steel, structural, St37-2, large plastic deform., fracture behaviour, COD concept validity *(German)* 79−47764
steel, type 4130, high strain rate compression, plastic flow 79−34099
steel 45-antifrictional alloys friction pairs, electrochem.-mech. investigation *(Russian)* 80−76367
steel mild, bar stress wave propagation, finite element analysis *(Japanese)* 79−79030
steel plate collapse, anal. by live energy minimisation 78−52910
steels, thermal hardening stress determ. by thermoplasticity theory 79−29076
Stouffer-Bodner constitutive model 80−92071
strain analysis in metalworking 78−27586
strain rate gradient development 79−46219
stress and configuration, elastic and plastic strain increments 80−87718
stress field, body subjected to limit load, cylindrical flow surfaces 79−76988
stress relaxation test, appl. to discerning frictional and internal stresses 77−63712
stress-rupture data correlation 77−44346
stretch zone width and striation spacing. The comparison of theories and experiments 80−85051
superalloy thin walled tubes, exam. of stress/strain relations in tube eversion 79−61689
superplastic deformation, grain rearrangements 78−83828
superpotential flow problems and application to metal forming processes with friction boundary conditions 79−66119
Ta, single crystals, microyielding, high amplitude damping 77−52396
tensile stability, effect of crack and cavitation generation 77−16659
thin cylindrical shell, compression dynamics, nonlinear evolution of Rayleigh-Taylor instability 78−79243
thin shells, relations of plastic flow theory *(Russian)* 77−14914
torispherical vessel heads, elastic-plastic internally pressurized, stresses and buckling 77−58574
trajectory determ. in geometrically similar plastic flows, expt. 78−64588
transition metal-metalloid glasses, struct. and plastic flow, review 80−84090
triaxial loading test, plastic flow and fracture 78−27701
trigonal monocrystals, classes 3 and $\bar{3}$, plastic potential and yield stress *(Russian)* 80−29109
tube, under adiabatic torsion 77−62161
Udimet 700, creep, rupture, grain size effects 77−21229
Udimet 700, Ni-Co-Cr-Al-Ti (18.8, 15.2, 4.5, 3.39 wt.%) exam. of high temp. creep, viscoplastic flow 79−61685
viscoplastic, coupling of dissipative mechanisms 78−38206
viscoplastic flow, appl. of Moire fringe method *(Russian)* 77−35102
viscoplastic flow, finite element method with added boundary terms 78−42543
viscoplastic material, mixing process, Bingham model, two-dimens. flow *(German)* 80−92076
viscoplastic materials, dynamic convergence theorem for strain and work hardening 80−96199
viscoplasticity with singular yield surfaces, side and corner flow rules, finite element applications 80−48594
viscous plastic lubricant, nonlinear effects on stability of bearing tenon movement *(Russian)* 79−32393
W, wire reinforced Cu 77−70114
yield, nonsteady-state mechanism 78−48481
Zircaloy, annealed, neutron irradiated, inhomogeneous deform. behaviour 80−85014
Zircaloy 4 tubing, cold-worked and annealed, stress relaxation behaviour 77−57717
Zircaloy-2, martensitic transform. contrib. to strength and work hardening, and martensite flow props. 78−84842
Ag, cold rolling, inhomogeneous texture 80−89251
Ag single crystal, dislocation dynamics during stress rate changes 78−19813
Ag-Al, plastic flow enhancement during massive transformations 78−48468
AgMg single crystals, orientation and temp. depend. of slip 78−87682
Al, 6061-T6, pressure shear impact in transverse displacement interferometer, plastic flow 80−81137
Al 7039 alloy, high strain rate compression 79−29137
Al alloy, slip deformation and low-cycle fatigue damage 77−73301
Al alloy 7075, stress-rupture data correlation 77−44346
Al alloy compacts, specific press. for extrusion 79−20070
Al alloy sheet, anisotropic, yield strsses and plastic strain rates, directionality correl. 78−23760
Al alloys, plastically anisotropic, non-associated flow law *(Polish)* 78−80603
Al alloys, stress-strain state after treatment by pressure, moire strip method appl. *(Russian)* 80−40648
Al and Al-Mg (5.7 at.%), test, appl. to discerning frictional and internal stresses 77−63712
Al and annealed alloy 5086, plain strain extrusion, photographic appl. 80−7626
Al, annealed, subjected to torsional impact loading strain-rate effects 78−92303
Al, Bauschinger AE peak detection of back stress component in flow stress *(Japanese)* 78−6977
Al, bicrystal having $\Sigma 7$ and $\Sigma 21$ coincidence tilt boundary, plastic deform. *(Japanese)* 79−66116
Al, cold rolling, inhomogeneous texture 80−89251
plastic flow continued
Al, cold rolling of 1100 plates, substruct. development 80−108476
Al, flow mechanism in cutting, crystal orientation effects in single crystal 79−100300
Al high strength alloy bar stress wave propagation, finite element analysis *(Japanese)* 79−79030
Al, numerical smoothing of flow patterns 80−7625
Al, oriented single crystal, plastic deform. *(Japanese)* 79−43336
Al, plastic deform., strain rate history and temp. effects depend. 79−11684
Al, polycrystalline, acoustic emission energy release, grain size and flow stress depend. 80−11722
Al, polycrystalline aggregate, various grain sizes, specimen thickness effect on mech props. 79−61645
Al, prestrained, isotropic hardening rule, rel. to stress/strain curve 78−23772
Al, role of osmotic forces in low cycle fatigue, vacancy generation *(Russian)* 79−60430
Al, single cryst., latent hardening *(Japanese)* 78−44135
Al single crystal, Bauschinger effect, orientation depend. 77−21237
Al, substruct. developed during recrystallisation, exam. *(Japanese)* 78−64566
Al, tensile flow stress at room temp., grain size and strain effect 77−77528
Al, thermoactivation parameters of plastic flow in torsional deform. *(Russian)* 79−38926
Al, use in design of composite superconductors in elasto-plastic region 77−28851
Al, work softening, microstruct. interpretation 77−32593
Al-Cu, flow stress, origin of high strain rate sensitivity 78−44186
Al-Cu (4 wt.%), with θ' precipitates, relation between elastic limit and hardness *(French)* 79−5018
Al-Cu-Zr (6, 0.4 wt.%), superplastic flow activation energy 80−11701
Al-$CuAl_2$ eutectic, deformed, thermal stability 77−52348
Al-Ge (2 wt.%), averaged, plastic flow mechanism 77−48507
Al-Mg, Mg effect on ductility, 25 to 250°C 79−100214
Al-Mg (1 wt.%), mechanisms of dynamic strain ageing and jerky flow 79−79024
Al-Mg (5 wt.%), recovered dislocation substruct. during plastic flow 79−83273
Al-Mg-Si (0.7, 0.4 at.%), effect of precipitation hardening on strain rate behaviour and yield behaviour 79−29075
Al-Zn, tension deformed superplastic specimens, instantaneous strain rate variation *(Russian)* 79−79033
Al-Zn (11 wt.%), stress depend. of strain rate at elev. temps. 78−23757
Al-Zn alloy, flow stress, Zn content effect 79−38913
Al-Zn-Mg-Mn, correlation of microscopic features, with macroscopic crack propagation 78−60800
Al_2O_3+TiC system, elastic and fracture charact. at elev. temp. *(German)* 79−43299
Au, flow stress during cutting 77−59881
Be, brittleness problems, elevated plasticity and superplasticity, temp. depend. *(Russian)* 79−15758
Be, polycryst., plasticity and cleavage, yield and flow stresses 80−44249
Be-Ni(Y)(Al), plastic deform., flow stresses, fracture *(Russian)* 80−108496
β-brass, nonisoaxial bicrystal, simultaneous hardening and softening 77−36606
C, pyrolytic, high-temp. deform. under mech. loads 77−16644
C steel, bending, effect of strain rate on dynamic stress factors 77−56046
$(CF_x)_n$ rubbed films applied to different finished surfaces, obs. 79−83332
CaF_2, impurity effects on strengthening 77−63682
Cd, single crysts., plasticity study during deformation by twisting *(Russian)* 80−93597
Cd-B(W) particulate composite, dispersion hardening, grain size and texture strengthening 77−8840
$Cd_xHg_{1-x}Te$, low temp. piezoresistance, Hall effect, elec. cond., plastic flow 80−6844
$Cd_xHg_{1-x}Te$, uniaxially compressed, deform. effects, elec. resist. 78−39114
Co based metallic glass, B and P glass former additions, elastic consts., flow behaviour correlations 78−44154
Cr/Cu/Cr layer composite, influence of phase boundary on flow stress 78−60717
Cr-Mo-Ni-Ti alloy A-286, stress-rupture data correlation 77−44346
CrO_2 semidry refractory, struct. and mech. props., surface-active agents effect 80−89304
CsI, yield point, obstacles to dislocation motion 77−43270
Cu alloy, superplastic, activation energy of plastic flow 78−64584
Cu and Cu-Al alloys, effect of grain size and specimen thickness 78−84945
Cu, Bauschinger AE peak detection of back stress component in flow stress *(Japanese)* 78−6977
Cu, deformation under mutual indentation in contact with Pb-Bi eutectic melt *(Russian)* 77−59853
Cu, flow stress during cutting 77−59881
Cu, flow stress of single crysts., strain rate sensitivity analysis 77−16645
Cu, grain refinement of dynamic recrystallisation during hot working *(Japanese)* 77−52345
Cu, high purity, recrystallisation kinetics *(Russian)* 78−11238
Cu, OFHC, strain rate variation effects on flow stress 79−43324
Cu, OFHC effect of cold drawing under combined stress 80−60912
Cu, polycrystalline aggregate, various grain sizes, specimen thickness effect on mech props. 79−61645
Cu, swaged, inhomogeneous work hardening *(German)* 80−76267
Cu, thermal and athermal plasticity *(Russian)* 79−11685
α-Cu-Al, stress-strain behaviour, effect of grain size and composition 77−56038
Cu-Al (10 at.%), single crystal, variation of flow stress after changes in strain rate 77−28879
Cu-Al (13 at.%), polycrystalline aggregate, various grain sizes, specimen thickness effect on mech props. 79−61645
Cu-$Al_2O_3(SiO_2)$ dispersion hardening single crystal, cyclic deform. *(French)* 79−1893
Cu-Al(Au)(Ga)(Ni)(Pd)(Rh)(Zn) (4 at.%), anneal hardening mechanism 80−60879
Cu-Au, cold worked solid solution, flow stress and activation volume 80−16393

plastic flow continued
Cu-Ga, plastic flow enhancement during massive transformations 78−48468
Cu-Ge, single cryst., dislocation motion obstacles, effective strength 80−15107
Cu-Ge(Zn), conc. single crystal, yield region investigation, flow stress and obstacle charact. 78−3173
Cu-Ni, cold worked solid solution, flow stress and activation volume 80−16393
Cu-Zn, cold worked solid solution, flow stress and activation volume 80−16393
CuAu-type superstructure, interaction of reacting dislocations *(Russian)* 78−83814
Cu_3Au, flow stress 77−21231
Cu_2O polycrystalline and single cryst. mech. behaviour 78−95777
FE, electrolytic, dissolved H precip., effect on flow stress *(Japanese)* 78−39848
Fe and Fe-Cr, flow stress, effect of cathodic, H_2 charging *(Japanese)* 79−52313
Fe based metallic glass, B and P glass former additions, elastic consts., flow behaviour correlations 78−44154
Fe, cast, ductile, strain rate and temp., influence on strength, elongation and deformation *(Japanese)* 80−45356
α-Fe, deformed, changes in dislocation density, mech. props., dependence on deformation temp. *(Russian)* 79−20130
Fe, flow stress during cutting 77−59881
Fe, H_2 charged, depend. of softening on specimen size, charging current density and strain rate 80−16455
Fe, H_2 effect on yield 78−15474
α-Fe, high temp. deform., Cottrell-Stokes law 79−83274
Fe, lattice hardening and anomalous softening caused by electrolytic H_2 charging *(Japanese)* 79−43398
Fe, quenched-in hydrogen, yield stress decrease of prestrained specimens 80−16454
Fe, relaxation process effect on initial stages of flow *(Russian)* 79−74189
Fe, single crysts., effect of hydrostatic pressure on plastic flow props., dislocation distribs. 79−38887
Fe, softening and hardening by H_2 charging during tensile deformation 80−16453
Fe static loading over wide deform. and temp. range, acoustic emission, plastic flow, fracture 77−90424
Fe, static loading over wide deform. and temp. range, acoustic emission, fracture, plastic flow 77−90425
Fe-Co(-V), plastic flow, order-disorder transform. effect on creep, traction and relaxation *(French)* 80−35180
Fe-Cr (2 at.%), plastic flow enhancement during massive transformations 78−48468
Fe-Ni-Al, correlation of microscopic features, with macroscopic crack propagation 78−60800
$Fe_{40}Ni_{40}P_{14}B_6$, amorphous, annealed and unannealed, temp. depend. of flow stress and ductility 79−29119
$Fe_{40}Ni_{40}P_{14}B_6$, metallic glass, acoustic emission generated during viscous flow 78−39853
$Fe_{40}Ni_{40}P_{14}B_6$, Metglas 2826, hot forming 80−84980
Ge, deformation, annealing charact., X-ray study 78−75713
$Ge_{30}Si_{70}$, hot press sintering 80−50572
He, solid, vacancies and dislocations *(Japanese)* 78−91507
^{3}He, BCC, plastic flow 79−46880
^{4}He, HCP, free standing cryst., shear deform. 78−2333
^{4}He, HCP, plastic flow 77−62702
Hf-O(N), solid soln. hardening, impurity cluster and interstitial mechanisms 77−36523
KCl, elec. field effect on flow stress, charged-dislocation model 77−27935
KCl:Eu, flow stress 77−36577
KCl:KOH, influence of anion impurities on mech. props. of alkali halide crystals 78−87736
KCl:S, influence of anion impurities on mech. props. of alkali halide crystals 78−87736
LiF single crystals, glide band sources, work hardening 80−34126
LiF, strained, mean mobile dislocation velocity 78−18657
Mg alloy, quenched-in defect behaviour, effect on flow stress 79−61625
Mg crystal basal slip, anal. of pairwise dislocation interactions and contrib. to flow stress 78−35440
Mg, extruded, continuum mech. anal. of flow curve anisotropy and plastic strain *(German)* 78−84947
Mg, flow stress during cutting 77−59881
Mg, pyramidal dislocation pair interactions contrib. to flow stress during slip 78−35441
Mg-Al cylindrical shells, loading history, effect on plastic buckling *(Russian)* 79−14288
Mg-alloy, superplastic deformation mechanism, deformation model 78−31477
Mg-Mn-Ce (1.5, 0.3 wt%), superplasticity role of diffusional creep *(Russian)* 80−97528
$MgAl_2O_4$ spinel, single cryst., fracture behaviour, temp. depend. 80−40503
MgF_2, hot pressing in vacuum, compaction kinetics, selective recryst. 77−16517
Mg_2GeO_4, geometric flow props. 78−57198
Mo, dislocation structure, temp. depend., at crack tip, of fractured single cryst. 79−29210
Mo single crystal, early stages of plastic flow 77−36584
Mo, strain induced damping, micro- and macro-, and dislocation structures in single crystals 78−19797
Mo-Ti-Zr, alloy TZM, polycrystalline, anal. of elastic anisotropy and microyielding 80−30050
Mo-Ti-Zr alloy TZM, fatigue and plastic flow, irradiation effects 77−52466
NaCl, high-temp. deformed, dislocation grain subboundaries *(Russian)* 80−96534
NaCl, strained in one glide system at 450°C, dislocation struct. 78−22728
NaCl:Ca, precipitate form., transform. after annealing, critical flow stress 78−38848
NaCl:Mn^{2+}), influence of elec. field on flow stress 79−51193
Na_2O-CaO glass, shear deform. under pyramidal indentations 80−84989
Na_2O-CaO-SiO_2, dynamic hardness testing, pendulum attenuation, yield stress obs. 79−24699
Na_2O-CaO-SiO_2 glass, hot erosion plastic flow and fracture 80−89354
plastic flow continued
Nb, anodic oxide coating effects on mechanical behaviour 77−32659
Nb, flow stress, depend. on magnetic fields 77−73311
Nb single cryst., slip localisation during discontinuous plastic flow at 4.2K *(Russian)* 77−69029
Nb, single crystal, surface oxide softening, TEM obs. 77−40462
Nb, surface oxide softening, anisotropy 78−60716
$(Ni,Co)_3Ge$, Co effect on temp. depend. of yield stress 78−31487
Ni, creep, mag. field effects, 30-250 Oe 77−16141
Ni, cyclic flow stress and microstructural changes during multiple step testing at elevated temperatures 79−91746
Ni, grain boundary ledge density, effect on flow stress 78−48465
Ni-Al-Cr-Co-Ti, Waspaloy, exam. of dislocation-precipitate interaction, cyclic stress-strain behaviour 78−84925
Ni-Cr complex alloy with good creep resistance, friction stress/flow stress relation 79−8337
Ni-TaC, eutectic alloy, fibre reinforced, directionally solidified, anisotropic yielding behaviour 79−11675
Ni_3(Al, Nb) single crystal, yield stress, orientation and temp. depend. 80−108511
Ni_3Al-Fe (10 at.%), activation anal. of plastic deform. 79−1900
Ni_3Fe, disordered single crysts., thermo-activated mechanism of plastic deform. *(Russian)* 78−84909
Ni_3Fe, ordered, monocrystals, thermally activated deform. processes 80−50684
$Ni_{49}Fe_{29}P_{14}B_6Si_2$ glass, flow and failure 80−40438
Ni_3Ge single crystals, orientation and temp. depend. of flow stress 79−5008
Ni_3Ge-Fe_3Ge solid soln., flow stress, transition from positive to negative temp. depend. 80−60906
NiO, stress relief and plastic flow in temp. range 1323-1473K 80−89302
Pb, crystal defect accumulation after plastic deform. in normal and supercond. state resist. meas. 77−85196
Pb single crystal, normal-superconducting transition and plastic flow 78−3166
Pb-Sn, with brass insert, tensile flow and fracture 78−11290
Pb-Sn microduplex eutectic, cavitation during superplastic flow due to hard particles 77−36575
Pd-Cu-Si glass, cold drawn, serrated plastic flow, optical and SEM study 79−79052
$Pd_{80}Si_{20}$, glass, deform. localisation, plastic instabilities and fracture 80−89320
$Pd_{80}Si_{20}$, plastic flow, fracture, slanted necking and elongation at high temps. 79−57057
$Pd_{82}Si_{18}$, stress/strain rate depend. of homogeneous flow 80−71687
Pt_2Mo-type superstructure, interaction of reacting dislocations *(Russian)* 78−83814
Si, deformation, annealing charact., X-ray study 78−75713
Si, initial stages obs. 78−64602
Si, single crystals, dynamical recovery and self-diffusion 78−87816
Sn-Pb-(Bi)(Ag)(Sb) (Cu), microduplex eutectic, cavitation during superplastic flow 78−48457
Ta, flow stress, temp. and strain rate depend. 77−77534
Ta, oxide coating effects on mechanical behaviour 77−32659
Ta, single crystal, microyielding microflow parameters 77−52395
α-Ti, determination of microflow parameters from compression tests 80−66584
Ti, extruded, continuum mech. anal. of flow curve anisotropy and plastic strain *(German)* 78−84947
Ti, flow stress during cutting 77−59881
Ti, fracture mechanism at different temps. 77−63785
Ti, high purity, flow stress relaxation *(French)* 77−86117
α-β Ti Widmanstatten alloy interfaces, elastic interact. stresses, effect on plastic flow onset 80−104218
Ti-Al-V (6, 4, wt.%), texture influence on fracture toughness and deformation 79−91801
Ti-Al-V (6,4 wt.%), plastic flow instability and multiple necking during superplastic flow 77−8896
Ti-Al(Sn) alloys, thermal and athermal solid solution strengthening 77−4787
β-Ti-V (40 at.%), BCC, flow stress asymmetry and cyclic stress-strain response 77−36583
α-U, strain rate effect on flow and fracture 80−100887
V and V-Fe (5.0 at.%), stress relaxation test, appl. to discerning frictional and internal stresses 77−63712
V-Nb, mech. props., −196-1000°C, comp. depend. 78−39847
W, strain induced damping, micro- and macro-, and dislocation structures in single crystals 78−19797
W wire reinforced Cu, microfield, flow stress 78−27575
WC-Co alloy, short-time creep rupture strength, C content effect 400° to 900°C *(Japanese)* 78−48487
Y, plastic deformation props., deformation ageing, plastic flow, dislocation-impurity interactions *(Russian)* 80−66582
Y, polycrystn., plastic deform. at different deform. speeds, dislocation glide *(Russian)* 80−93598
Zh, extruded, continuum mech. anal. of flow curve anisotropy and plastic strain *(German)* 78−84947
α-Zircaloy, strain ageing at 1000K 79−47725
Zn, flow stress during cutting 77−59881
Zn, pure single cryst., fracture stress 80−104269
Zn-Al (22 wt.%), meas. of plasticity parameters under superplastic flow 78−60710
Zn-Al (22 wt.%), superplastic deform. rate rel. to flow stress, determ. methods 78−60709
Zn-Al alloys, dislocations obs. in superplastic deformation 78−51549
α-Zr, strain ageing at 1000K 79−47725
Zr-Sn (1.5 wt.%), martensitic transform. contrib. to strength and work hardening, and martensite flow props. 78−84842
Zr_3Al, ordered polycrystals, hardness and flow stress relationship 77−44309
ZrO_2-CaO-SiO_2, relationship between texture parameters, and sintering, elec. cond. and mech. strength props. *(German)* 79−24474

plastic strain *see plastic deformation*

plastic theory *see plasticity*

plasticity
see also elastoplasticity; photoplasticity; superplasticity
adhesive materials 77−16638
alloys, brittle and plastic, energetic strength theories *(Bulgarian)* 80−38296
alumina, polycryst., compressive strength, microplasticity 77−36620

plasticity continued
anisotropic constitutive equations of continuous media *(French)* 79−25846
anisotropic hardening of initially orthotropic materials 80−33488
anisotropic materials, elastic and plastic pots. *(German)* 77−46926
anisotropic materials, invariant theory *(German)* 77−22417
anisotropically strain deformed materials, condition for transfer to plasticity *(Russian)* 77−46940
anisotropy, Bauschinger effect, general formulation, comparison with expt. yield curves *(German)* 77−20006
atomistic models, idealized, for inelastic processes 77−72193
automatic piecewise linear approximation of yield function in ideal plasticity 77−46929
axisymmetric bodies, semi-analytical finite element soln. 79−90149
axisymmetric sandwich plates for alternative loads, design 77−68446
bar, rectangular, necked, void growth, finite element anal. 80−64383
basic equations of perfect plasticity parametrised by general stress functions 77−58561
Bauschinger effect and plastic anisotropy, descriptive eqn. *(German)* 77−84154
beam, fibre reinforced rigid plastic, impulsive loading 79−3928
beam, impulsively loaded rigid plastic, additional support optimal location *(Polish)* 79−64498
beam, rigid plastic, stepped, impulsively loaded, optimal design for asymmetric mode motions 78−90723
beams, rigid plastic, quasimodel form solns. for dynamic response 79−90170
beams thin-walled, of open cross section, finite-element model 80−74767
biaxially stretched sheets, exam. of void growth and local necking 78−90735
binary, ternary oxides, dislocation motion and high temp. plasticity 80−59468
boundary element method appl. to plasticity 80−69680
boundary value problem in general theory *(Russian)* 80−28441
boundary value problems, stability evidence 77−84167
α-brass, thin sheet, plastic anisotropy 77−63683
brittle material, dynamic solid particle damage, elastic and elastic-plastic response regimes 77−8910
brittle solid, atomically sharp cracks, TEM study 80−71729
brittle-plastic phase transform. 77−11630
chemisorption modification of strength of solids 79−51423
circular cylinder, creep transition in torsion 79−59929
circumferentially notched tension specimens, stress distrib. and plastic strain 77−50919
clays and ceramics, plasticity determ. using drying process and shrinkage 79−20307
coating, free, of vert. surface, by viscoelastic (viscoplastic) fluid 78−42576
cold work in tension, strain rate effect on stored and dissipated energies 77−86111
compaction and lime stabilization effect on pore size distrib. *(Japanese)* 78−31365
composite material, mechanical behaviour, book 80−94935
composite with plate like inclusions, plastic props., sintered Al-Al_2O_3 results *(Russian)* 80−58923
compressible media, variational method 78−94602
compressible plastic solid, plane flow, operator method for variational principles *(Polish)* 77−54898
concrete, plasticity theory anal. of shear 78−83270
constitutive equations derivation from Clausius-Duhem inequality 80−46804
constitutive laws, analogy with energy criteria in rupture and fatigue *(French)* 78−90771
construction element, optimal design in case of impulsive loading 79−86382
Cosserat continuum, non-Reimannian geometrical theory of imperfections 80−53639
Cosserat theory of crystal plasticity, appl. to anal. of lattice rotations under constrained deform. *(Japanese)* 78−2189
couple-stress theory and plane boundary problem *(Russian)* 79−86358
coupling phenomena in thermoplasticity 80−87721
crack edge tip deformation, exact analytic soln. 80−69734
crack separation energy rates for the DBCS model under biaxial modes of loading 79−81814
crack tip integral for non-elastic materials 77−68528
crack tip plasticity, inclined strip yield superdislocation model 77−68526
crack tip plasticity in dynamic fracture mech. 79−41627
crack tips, yielding on inclined planes 80−33525
creep and plasticity, theory, microhomogeneity in plastic strain 79−14281
creep modelling incorporating initial strain and ageing 80−58939
crystal elastic and plastic anisotropy and dislocations *(Japanese)* 79−95069
crystal plasticity, analytical development review *(Japanese)* 79−60424
crystal plasticity, hardening law for slip systems 79−33030
crystal plasticity, surface effects, review 77−47505
crystalline and amorphous solids, plastic behaviour in terms of defect motions 78−95104
crystals, with diamond struct., vacancy formation energy rel. to plastic state transition temp. *(Russian)* 80−19795
4-cyano-4-n-cyanobiphenyl, smectic A mesophase, plasticity anal., defects motion, Grandjean wall form. 78−91227
4-cyano-4-n-octylbiphenyl, smectic A phase, focal conics motion and plasticity, stroboscope obs. 79−86692
cyclic, plastic internal variables formalism 77−54904
cyclic plasticity, creep recovery unified approach to interaction prediction 79−8329
cyclic thermoplasticity, finite element analysis by subvolume technique 77−42749
damage rupture, phenomenological approach to plasticity, creep and fatigue *(French)* 79−37245
defect dynamics, closure of governing eqns., plastic state theory 79−37702
deformation localisation in tension, determ. 79−87790
diamond, optically active centre effect on strength props. 80−40462
differentially nonlinear second order bifurcation 79−86362
discrete structures under dynamic loading, work hardening adaptation 80−74726
disperse systems, instrument for strength props. determ. 80−76426
Dugdale plastic zone sizes, for edge cracks 79−72853
dynamic plastic instabilities in stretching plates and shells 79−7302
dynamic plasticity, linear eqns., pulse loading, lumped-mass model, mode approx. technique 80−74769
dynamic plasticity experiments, review 80−35288
dynamical thermoplasticity, appl. of mathematical system theory 78−83271
edge problem of fracture mechanics, plasticity theory inadequacy 79−3978
elastic viscoplastic body, differential rheological eqn. *(Ukrainian)* 78−55617
elastic waves in viscoplastic-elastic media under complex strain *(French)* 79−27570
elastic-plastic body, weakened by double periodic slit system, antiplane strain 80−53657
elastic-plastic materials, dynamic behaviour *(German)* 79−14271
elastic-plastic struct. cyclic thermomech. loading 79−7299
elastic-plastic-creep-large strain analysis at elevated temperature by the finite element method 79−37185
elastic-viscoplastic boundary value problem, stress anal. variational method 77−35051
elastic-viscoplastic materials, hardening parameters 78−46895
elasto-viscoplastic analysis of large deform. problems, natural finite element formalism 78−83258
endochronic inelasticity and incremental plasticity, tangential linearisation, material instability 78−87277
endochronic plasticity, appl. to structural dynamic response of radioactive waste containers 80−16407
endochronic theory, simple wave solns. 79−40361
endochronic theory of viscoplasticity, steady waves in impacted plate, Al numerical calc. 78−83282
existence-uniqueness result for some models of thermoplasticity 80−92077
eye striated muscle, bovine, physico-chemical anal. of contractile proteins 77−90819
fatigue crack propag., plastic wake zone effect investigated with optical interference technique 80−55502
fatigue crack propag., plastic work 77−56068
fibre-reinforced rigid-plastic plates transverse impact anal. 78−38211
field theory, integral presentations of second-rank tensors 80−69690
fine ceramic masses, organic plasticizer, plasticity model and plastic behaviour meas. by cyclic shear test *(German)* 79−96080
finite element anal. with nonconforming plane element 78−38209
finite element analysis of problems of plasticity and viscoplasticity *(French)* 78−63334
finite element plasticity, slip model 79−32301
fission reactor materials, thermomechanical transient anal., strain-rate dependent plasticity 80−79864
flat rolling theory with spread, cross-section warping *(German)* 80−92064
floating plug, drawing speed influence on optimum shape, viscoplastic incompressible model 79−94508
flows in dissipative materials, a priori estimates 78−16643
formulation of plasticity theory in tension and expansion space *(German)* 80−106733
fraction model, numerical plasticity and creep anal. 77−3743
fracture, plasticity model, dislocation based, geometrically consistent 78−30242
fracture mechanics, K_{Ic} values determ. in elastic-plastic material behaviour range 80−45376
glass, viscoplastic, gas-vapour interlayer problem 80−49490
glass-fibre reinforced PET, order-disorder transitions during extrusion 80−50633
governing relationships in stress and strain spaces 79−88812
grain boundaries 80−65135
grain boundary theory is independent crystal imperfections, plastic rotation, boundary continuum *(Russian)* 79−82236
granular materials, invariants depend. models 78−34026
graphite/epoxy laminates, T300/5208, effect of curing stresses on first ply failure, thermoplastic props. 79−43329
with hardening, mixed finite element method appl., error estimate 78−9577
hardening of materials, plastic and viscous, steady and cyclic loading 77−4793
hardening rigid-plastic bodies, deformation propagation, dynamic flow 79−86356
hardness law for inelastic deformation, elastic-viscoplastic constitutive eqns. 78−46896
heat transfer problem in plastic injection moulding 80−38242
heat treatment, struct. and mech. props. 78−52864
heteroolastic beam, progressive creep under loading *(French)* 79−7290
heteroplastic material, memory function, stress/strain vel. relations *(French)* 79−10488
hexagonal polycrystals, creep and plasticity, rel. to single crystal slip 78−13920
high-strength alloy filamentary crystal prep. from brittle high-strength mats., mech. props. *(Russian)* 77−59712
high-temp. nucl. reactor components, elastic-plastic-creep response, computer program 77−3112
Hohenemser-Prager type material, constitutive inequalities for viscoplasticity 77−14926
hollow thick-walled cylinders, stress-deformation, limiting state anal. *(Russian)* 79−27538
HTR, inelastic structural anal. for component design 79−6734
hydrogen embrittlement, role of plastic fracture processes, exam. 78−60810
hyperbolic theory, plane strain and axial symm. problems 77−7317
impact end in longitudinal dynamic plastic wave propagation 79−14294
Incoloy 800, review of mech. props. up to 600°C 79−43368
incompressible anisotropic material, plastic material eqn. *(German)* 78−26057
incompressible isotropic homogeneous anelastic bodies, quasistatic controllable processes 79−68592
incremental theory, modified constitutive relation 77−50928
incremental theory, reassessment of constitutive eqn. 77−50930
inelastic rate problems, improved soln. methods 79−18733
inelastic structural behaviour, finite element computational aspects 78−42546
inhomogeneous problems, variational soln. *(Russian)* 77−23892
integral relations in stress and strain spaces, interrelationships 77−19548
internal struct. tensor 78−79227
ionic-covalent crystal transition to plastic state 79−90717

plasticity continued
isotropic and anisotropic raw materials, plastic pot. *(German)* 80−33474
isotropic material, criterion of rupture and plasticity *(Russian)* 78−13973
isotropic material in plane stress, piecewise linear theory, plasticity 80−43622
isotropic plastic behaviour, role of body rotation in mathematical models 80−28432
isotropic polycrystalline plasticity, dislocation theory 79−14875
kinematic hardening models, use in multi-axial cyclic plasticity 80−25717
L-plasticity, boundary value problems for plane strain or stress 80−58926
large deflections and creep problems, soln. strategy 77−42750
lattice-statics approach, review 80−39212
limit analysis with anisotropic parabolic yield function 77−91114
limit load theory of ideally plastic body, duality problems 80−19254
limiting lines theorem in perfectly plastic material 77−62159
loading, finite element anal. for materials with convex yield criterion *(French)* 79−10501
loading paths classification 79−98634
localisability of deformations theory, representation 80−10163
low cycle fatigue and plasticity testing, specimen verification 80−30202
lubricant, shear rheological behaviour at high press. 80−35342
materials with memory, intrinsic physical limits, viscoelasticity, viscoplasticity, hydromorphic materials 79−64523
materials with memory, thermodynamics 80−64356
medium with nonlinear uploading, plastic wave propag. 80−23913
metal, cutting rel. to plasticity theory 80−16610
metal, electroplastic deform. 78−3200
metal, FCC polycrystalline, work hardening, plastic deform *(Hungarian)* 77−77504
metal, plasticity, dynamic, governing relations, elastic energy 79−43328
metal, plasticity under hydrostatic pressure *(Russian)* 78−68726
metal, surface layer dissolution, effect of rate on softening during plastic strain 78−39957
metal, thermo-inertial mechanism of plasticity enhancements normal to superconducting transition *(Russian)* 79−47183
metal, viscoplastic constitutive eqns. for cyclic and anisotropic behaviour 77−62162
metal-liquid surface energy, effect of lubricants, plasticity during cold working stresses *(Russian)* 77−55419
metallic glasses, structure and properties, review 78−47245
metallic glasses manufacture, struct. and stability *(Norwegian)* 79−14687
metallic heteroplastic stable material beyond elastic limit, memory *(French)* 79−81733
metallic media, varying loads, elevated temp. inelastic anal. using state variable theories 78−83264
metallic structures, elastic/plastic bodies with work hardening, general shakedown theorem 77−3746
metallic system, thermodynamically unstable, produced by spark discharge *(Russian)* 78−19933
metals, brittle and plastic, energetic strength theories *(Bulgarian)* 80−38296
metals, crack resistance, high temp., during creep due to stress relaxation *(Russian)* 79−52348
metals, deformability, quantitative determ. in drawing 79−52229
metals, effect of hydrostatic pressure and stress on plasticity 78−52907
metals, effect of neutron irrad. on plasticity characts. 78−64607
metals, FCC, hardened, plasticity, review 79−11683
metals, plastic yield criteria, interpolation scheme 80−64400
metals, residual stress on drawing calcs. by stress state changes variational principle *(Russian)* 80−65125
metals, rheological interpretation of planar deformed state in extremal friction regime *(Russian)* 80−64385
metals, strain hardening, creep, stress relaxation correlation with high temp. processes *(Russian)* 79−34053
metals, theory extension to three dimens. and appl. to geophysics 80−104955
metals, transversely isotropic plastic props., yield charact. 78−60707
metals, viscoplastic behaviour anal. 80−6457
metals and alloys, fatigue behaviour, vacuum effect, review 80−35309
metals and alloys, strain rate history, endochronic theory of viscoplasticity 80−65122
metals in nuclear reactors, thermo-elasto-visco-plasticity and neutron irradiation 77−3111
microcrystalline alloys, metastable, rapidly quenched particulates, props. appl. and production 80−84887
micropolar plasticity theory, soil mechanics appl. 79−94504
Muller's entropy principle restrictions on constitutive eqns. *(Japanese)* 78−9578
multiple cracks, plasticity spread under tensile loading 77−46969
multiple-mode plastic straining, numerical anal. uniqueness 77−62166
nematic and smectic liq. cryst., viscous and plastic behaviours 79−86686
nitriding in glow discharges, influence on phase comp. and plasticity of diffusion layer *(Russian)* 80−76400
non-associated plasticity, dual extremum principles in rate boundary value problems 79−25845
non-linear uniaxial integral constitutive equation incorporating rate effects, creep and relaxation 80−28436
non-Newtonian fluid, free convection, heat and mass transfer 79−68765
non-Newtonian liquid, heat flux from nonisothermal surfaces to gradient flows *(Russian)* 79−68767
nonhomogeneous plastic polytropic medium, plane shock wave propagation, closed form soln. *(Polish)* 79−32350
nonisothermal theories, of plastic flow and theory of work hardening in creep 79−57077
nonlinear isotropic body, plasticity theory determinantal ratios *(Russian)* 79−14274
nonlinear model of anisotropically reinforced plane plastic medium based on slip concept *(Russian)* 77−35057
nonlinear stress wave propagation, in perfectly flexible string 78−5670
nonlinear viscoplastic materials, upper yield points 79−10490
nonlinear viscoplastic media, dispersion in circular tubes for laminar motion case 77−58626
nonlinearity viscoplastic liquid, convective dissipative heat exchange 80−87772
nonlinearly viscoplastic liquids, rheodynamics 78−83265
nuclear fuel compacts for HTR, irrad.-induced creep 78−44168
plasticity continued
nuclear reactor press. vessel and piping design, plasticity-related damage prevention 79−6735
oceanic lithosphere mechanical behaviour, implications of two earthquakes seaward of Tonga Trench 79−16405
one dimensional plastic materials with work hardening, acceleration waves 79−32339
one-dimensional plastic material with work hardening constitutive eqns., stress-strain relations 79−32296
operator equations solution by iterative methods using 'near' operators 79−58547
optimal plastic design, superposition principles and bounds on min. cost 78−42538
optimal plastic design of circular plates, linear programming appl. 78−42539
orthotropic dilatant bodies, plasticity theory, plane problems *(Russian)* 80−23910
orthotropic plastic plate, optimal design under in-plane loading 79−7303
orthotropic strip, stress intensity factors and crack opening displacements 80−53710
oxides, interaction between point defects and dislocations, cryst. plasticity 80−15149
perturbation of front of flat plastic wave 79−5980
planar shear specimen with V-notch, anal. of stress and strain conc. factor using finite element method *(Japanese)* 78−38212
planar stressed state, crack growth, influence of thermal stabilities 79−69190
plane bending-and-torque supporting grids, numerical plastic collapse anal. 79−68594
plane plasticity theory based on shear synthesis *(Russian)* 80−38281
plane strain of ideal rigid-plastic bodies allowing for the change of boundary *(Russian)* 79−68599
plane strain problem of hardening and softening plastic materials, theory 78−83869
plane stress crack problems, fully plastic soln. and large scale yielding estimates 77−19573
plastic design of complex machine parts 77−35048
plastic wave, two-dimensional, propagation in nonlinearly compressed half-plane 79−7325
plastic zones, monotonic and cyclic, eval. 77−72239
plastics and reinforced plastics, tabulated data as design guide 77−21087
plate, circular, viscoelastic response to impulsive loading, expt. tests 79−81825
plate, circular impulsively loaded, finite viscoplastic deflections by mode approx. technique 79−81738
plate, hole enlargement under plane stress conditions, viscoplastic rate sensitive constitutive eqns. 80−79163
plate, obliquely stiffened, subjected to uniform compression, buckling strength *(Japanese)* 78−67067
plate, rate sensitive plastic, circular hole, dynamic expansion 79−10509
plate, rectangular viscoplastic under pressure impulse, deflection determination *(Polish)* 79−64533
plate, simply supported circular, transverse shear and rot. inertia, dynamic plastic response 80−79175
plate with central hole, estimation of plastic zones from elastic stress field 77−19547
plates, simply supported, plastic buckling under edge thrusts 79−10510
plates design, circular, rigid-plastic, w.r.t. minimum-cost, variational formulation 77−68440
plug formation in plates, cylindrical projectile impact, nonlocal viscous fluid model 78−49653
polycrystal, HCP, microstress and starting boundary of plasticity *(Russian)* 78−30695
polycrystalline, based on dislocation processes, probabilistic approach 78−26621
polycrystalline, probabilistic approach, appl. 78−26622
polycrystalline solids, nonelastic behaviour 78−87280
polyethylene, high density, lamellar struct. and plasticity micromechanism 78−23791
polymer solutions, drag-reducing, in U-tube 79−1217
polymeric materials, inelasticity degrees estimation, hysteresis friction model appl. rel. to US testing 80−3136
polymers, crystalline, bulk, lamellar struct. and plasticity mechanisms 77−65957
porous bodies, plastic deform. anal. using plasticity theory 80−25802
porous materials, deformation theory of plasticity *(Russian)* 80−75291
porous media, extension to reinforced composite materials *(Russian)* 77−68443
porous media, plasticity as function of porosity *(Russian)* 80−75290
porous metals, plasticity, stress-strain curves, yield stresses, strain vectors 80−83738
porous metals, plasticity theory, stress-strain curves determ. 77−17812
porous powder solid 79−68604
porous rigid-plastic material containing rigid inclusions, yield function, plastic potential, void nucleation 78−64612
Prandtl punch problem, finite element model for plane-strain plasticity 80−58940
Prandtl-Reuss plastic material with scalar and tensor internal variables 79−68589
Prandtl-Reuss plastic materials, with general work hardening, constitutive equations *(Japanese)* 78−92276
prestrained plastic materials, rate-independent behaviour 79−68591
problem of calculating the variations occurring in the study of plasticity *(French)* 79−53978
problem soln. by symbolic computer processing of formulae 80−17803
projective geometry determination of plasticity and elasticity coefficients *(Spanish)* 79−50605
punch stretching, localised necking, finite element anal. 80−102971
PVC, antiplasticisation rel. to ageing and nonlinear viscoelasticity 78−52929
quartz, water saturated, plasticity, rel. to dislocation theory 79−34104
rapidly heated rigid plastic cantilever, expanding and contracting hinge concept 79−7293
rare earth oxides, microhardness anisotropy of single cryst. *(French)* 77−52489
rate type constitutive eqns., free energy of viscoelastic and viscoplastic materials 80−79168
rate type materials with general work hardening 78−42548
rate type plastic material with general work hardening, acceleration waves 79−37211

plasticity continued
rate-independ. theory for multimode plastic straining, unifying concepts 78−42545
rate-independent plasticity, axiomatic model 80−87717
rate-type material with scalar and tensor internal variables, work hardening 77−68449
reinforced concrete curved beam, expt. investigation of collapse 77−90404
rigid cylinder rolling on a rigid perfectly plastic half space 79−41629
rigid perfectly plastic strip, plane strain compression between parallel dies with slipping friction 80−48603
rigid plastic continua, adaption under dynamic loadings 79−27548
rigid plastic fibre reinforced plates, impulsive loading, dynamic deformations theory 79−23222
rigid viscoplastic spherical container, perturbation soln. 79−98626
rocks, plasticity rel. to Earth crust press.-temp. conditions modelling *(Russian)* 78−96207
rolling process, math. model based on plasticity theory *(Russian)* 80−16335
Saint Venant-von Mises materials, two-field variational methods *(French)* 77−17816
sandwich cores, superplastically formed, shear modulus 79−32286
shakedown analysis, numerical, circular plates subjected to press and temp. cycles 77−3749
shallow cylindrical shell, equiv. reinforcing of small circular opening *(Russian)* 78−13904
shear crack, discrete dislocation anal. 79−50659
sheet metals, ductile, shearing process 78−84841
shell, shallow, limit analysis and optimal design *(Russian)* 77−42752
shell, viscous plastic layers, viscous elastic filler, variable loading *(Russian)* 80−69695
shells, thin, torispherical and internally pressurised, plastic collapse 80−28440
shells, viscoplastic cylindrical, critical velocity for collapse without buckling 77−65673
shells of revolution, rigid perfectly plastic, limit anal. program, plasticity criterion *(French)* 79−37155
shells of revolution, rigid-plastic limit anal. under rotationally symmetric loading *(French)* 79−14276
sign-reversing loading *(Russian)* 79−23224
Silumin, AlSi10Mn, struct. and mech. props., Na modification effects 77−63786
singular yield conditions, thermodynamic study 77−84162
sintering, cold, under high pressures, correlation to plastic props. and diffusion 79−38757
slip concept, statistical approach *(Russian)* 78−18196
sludge, cohesive, dynamic props. *(Japanese)* 80−45580
smectic-A liquid crystal, layer rigidity, stress relax. 78−18545
soil, max. mol. moisture capacity correl. with plasticity 77−78267
soil, mechanical properties rel. to viscoplasticity under dynamic loads 78−96197
soil model, viscoplastic, eqns. and expt. determ. *(Russian)* 78−7619
solid body, unbroken continuity conditions, role in description of deformed state *(Russian)* 77−84159
spherical indentation of nonhomogeneous materials 79−46276
spheroplastic, spherical shells, supporting capacity 80−87723
stacked stress concentrations in elastic solid, spread of plasticity 77−31259
stacking faults, plasticity and transform. kinetics under high press. 78−51560
static rate theorem derivation from internal variable model 79−64531
statically admissible stress fields in plane plastic problems 80−58919
statically loaded structure design, limit load method *(German)* 79−50688
steel, 12KhN, plasticity, temp. and rate dependence for different rigidities of stressed state *(Russian)* 79−29139
steel, 12X2H4A, nonmetallic inclusion effect on plasticity and impact strength *(Ukrainian)* 78−92296
steel, 3Kh2V8F, brittleness depend. on high temp. deform. at high stress. temp. *(Russian)* 80−50698
steel, age hardened, dynamics of cyclic plasticity *(Czech)* 80−108464
steel, AISI 4340, sulphide inclusion behaviour during thermomechanical treatment 78−3151
steel, austenite, carbide strain hardened, strength and plasticity, effect of Mn content *(Russian)* 80−97500
steel, austenitic, high content of low melting additives, high temp. neutron irradiation embrittlement *(Russian)* 79−73218
steel, austenitic Mn-Ni ageing , alloying element influence on struct. and mechanical props. *(Russian)* 80−35256
steel, austenitic stainless, hot plasticity, Y additions effect 79−83270
steel, austenitic stainless, viscoplatic constitutive eqns. under hot working conditions 79−57024
steel, C, corrosion carcking by sulphide, effect on props. 80−55587
steel, C, fatigue failure in type 45, strength charact. 79−52373
steel, C and alloy, restricted durability, subject to pure bending with rotation 77−90431
steel, Ce, Nb, addition effects on hot plasticity *(Russian)* 77−66680
steel, Cr-Mn, annealing effect on mech. props. for cryogenic appl. *(Russian)* 78−19788
steel, fatigue and cyclic plasticity rel. to struct. inhomogeneity 80−81184
steel, high speed, plasticity depend. on plastic strain gradient *(Russian)* 79−57048
steel, high speed, props. after electroslag remelting 80−104139
steel, high strength, dislocation sweeping model for hydrogen assisted subcritical crack growth 80−97577
steel, high strength, press. depend. yield and plastic vol. change 78−19810
steel, high strength, subcritical crack growth, role of time delayed H_2 assisted plastic zone growth 80−97576
steel, high strength low alloy, plastic work during fatigue crack propag. 77−56068
steel, high-temp. isothermic combined heat treatment and mech. working influence on struct. and mech. props. of 60S2 *(Russian)* 80−20969
steel, hot rolled strip formability, mech. testing and mech. props. *(German)* 79−66089
steel, KhN77TYuR, deform. parameters effect on plasticity and resist. to deform. 77−63750
steel, killed ingots, freezing process, liq. core movement *(Russian)* 80−20921
steel, low C, containing P, Mg effect on annealing texture, mech. props. and plastic anisotropy 78−27536
plasticity continued
steel, low C, cyclic plasticity and low cycle fatigue life in variable amplitude loading 80−16433
steel, low C, fatigue crack plasticity, effect of water vapour 78−64678
steel, low C, microplasticity at high and low loading freq. *(Slovak)* 79−38910
steel, low C, P, plastic anisotropy and mech. prop. dynamic strain ageing effect 78−64608
steel, low C, plasticity role during low temp. fracture 78−39905
steel, low C, type 17G2SF, crack critical opening evaluation using plasticity diagram 80−45382
steel, low C hot rolled sheet, drawability improvement by Al addition *(Ukrainian)* 79−78996
steel, low-alloy, props. with nitride and Cu hardening at low temps. *(Russian)* 80−40372
steel, martensitic low C, development and props. *(Russian)* 80−20933
steel, mech. props., temp. effects *(French)* 77−56017
steel, mild, adiabatic viscoplastic deform. at high strain rate, negative strain hardening *(French)* 77−21212
steel, mild, precracked Charpy bars, plasticity spread 80−16415
steel, plastic, thermally strengthened, not prone to H_2 embrittlement, prod. *(Russian)* 79−52267
steel, plasticity, simplex planning method for temp. rate determination 77−56025
steel, plasticity depend. on hydrostatic press. in low-angle fatigue, Manson-Coffin coeff. *(Russian)* 79−61651
steel, plasticity indices in anisothermal extension *(Russian)* 80−16378
steel, plasticity of two-phase, coarse microstruct.-material *(German)* 77−59882
steel, quenched, reheating, to improve plasticity and notch toughness 77−63701
steel, rail, AE use for mech. tests 80−35467
steel, stainless, anelastic and nonlinear viscoplastic behaviour relations at low homologous temps. 77−63742
steel, stainless, C-Cr-Ni-Mn-V , non mag., aged, struct. and mech. props. *(Russian)* 78−56666
steel, stainless, fracture micromechanism when kept isothermally in sulphur pulp 80−76355
steel, stainless, porous sheet, mech. strength, bend and reverse bend tests *(Russian)* 80−93595
steel, stainless, proneness to intergranular corrosion, plasticity change tests 77−73366
steel, stainless, type 304, viscoplastic behaviour, strain rate sensitivity, creep, relaxation, tensile tests 80−66727
steel, stainless, type 304, viscoplastic model, uniaxial, based on total strain and overstress 80−64387
steel, stainless, wire, cold drawing 80−50650
steel, stainless 304, cyclic plasticity, exponential stress-strain law 77−25157
steel, stainless austenitic, low alloy 316, high temp. plasticity, B addition effects *(Russian)* 77−28852
steel, TRIP, strength and plasticity rel. to thermomech. treatments 77−44281
steel, TRIP, strengthened by hydrostatic extrusion, struct. and mechanical props. *(Russian)* 78−76647
steel, tubing, viscoplastic bending 78−35464
steel, type 1Kh18N9T, stress state form influence on creep and plasticity characts. rel. to cyclic stress intensity change 79−87694
steel, type Kh13N9D2MT martensitic aged, struct. and mech. props. *(Russian)* 80−93600
steel, ultra-high strength, H induced delayed plasticity and cracking 80−21100
steel bearing rings, optimisation of thermomechanical working parameters *(Russian)* 80−93579
steel boiler tubes, Cr-Ni-Mo, austenisation conditions effects obs. 80−3151
steel inclusions and plasticity, crystn. conditions influence *(Russian)* 80−20923
steel transformer, Mossbauer atomic struct. anal., decarburising annealing, cold rolling *(Russian)* 80−11294
steels, spring, 60S2A and 50KhFA, heat treatment and mech. working effect on mech. props. *(Russian)* 80−20962
strand with axial load, static plastic behaviour 80−69685
stress analysis of plastic zone during rolling under plane strain conditioner, Fourier calcs. *(Russian)* 78−80555
stress field, body subjected to limit load, cylindrical flow surfaces 79−76988
stress-strain relation anal. using anisotropic hardening plastic pot. 80−19250
stress-strain stiffness matrix calc. in inelastic material 78−34032
stress/strain distrib. meas. inside plastic zone of notched sheet, fatigue crack propag. *(Japanese)* 78−6981
structural anal., underlying concepts of finite element analysis 78−66337
structural analysis, assumptions, models and computational methods 79−32285
structural analysis, inelastic response, constitutive modelling 77−3093
structural plasticity problems, nonlinear finite element anal., mathematical programming 79−46224
structures, stochastically loaded, reliability estimate, kinematic approach 79−27546
subgrain imaging, in bulk specimens to study localised plasticity using SEM 80−66609
suspension, dielectric, convective heat transfer, rheodynamics, in horizontal coaxial cylindrical channel 78−59494
tension-torsion impact testing apparatus, instantaneous plastic property 79−52474
tetrafluoroethylene-vinylidene fluoride copolymer, exporide-diphenylolpropane resin filled, viscoelastic and strength parameters 79−91730
textured aggregates, theoretical plasticity, anisotropy and yield function 79−32298
theory, recent contributions 77−50925
theory and constitutive equations, review *(Japanese)* 78−83267
thermo-elastic-plastic transition in rotating disks with steady state temperature 79−64528
thermo-plastic materials, polarisable, constitutive eqns. *(Japanese)* 78−67062
thermo-plasticity of irradiated metals 77−4146
thermoelastoplasticity, doubly periodic, soln. 77−84165
thermomechanics, introduction, book 78−54187
thermoplastic body at finite deformations, incompressible plastic deformation *(Russian)* 80−53651

plasticity continued
thermoplasticity, time evolution under quasistatic conditions, existence theorems 80−74764
thermoplasticity using thermodynamics of materials with internal state variables 78−18189
thermoplastics as engineering materials 78−27581
thermoviscoplastic struct., finite deformations anal., energy dissipation effects 77−3744
thermoviscoplasticity theory based on infinitesimal total strain 80−87719
thick-walled tubes, compression by external pressure, expt. data, modified plasticity theory 78−59316
thin wafer method, analytical examination for rate independ. and rate depend. materials *(Japanese)* 79−59931
three-dimensional problem soln. *(Russian)* 78−75079
torsion pendulum, with anelastic solids of discrete relaxation spectra, resonant system 80−69687
trajectory of projectiles fired parallel and near free surface of plastic solid 78−83237
transverse isotropic inelastic work hardening constitutive model, numerical implementation 78−42547
Tresca yield condition usage in finite element plane strain anal. 78−83263
truss joints, elastic and plastic wave distrib. *(German)* 79−18769
tube, thin walled plastic, subject to ageing, cyclic loading *(Russian)* 79−68600
uncompressed viscous plastic lubricant, in bearing with temp. depend. viscosity, nonfixed motion *(Russian)* 79−50672
uniaxial stress/strain relations, generalisation 80−83739
unified theory of elasticity and plasticity using rate theory type constitutive eqns. 78−9571
unifying concepts in the theories of elasticity, plasticity, and dislocations 79−77599
unloading wave propagation in cylindrical, semi-infinite, elastic-plastic rod, asymptotic behaviour 80−69659
upper bound theorem for deformation of porous mats. *(Japanese)* 77−46937
variational inequalities and multilevel optimization techniques in the theory of plasticity 78−79224
variational Lagrangian irreversible thermodynamics of nonlinear thermorheology 77−27467
variational Lagrangian thermodynamics, nonisothermal finite strain mechanics of porous solids, thermomolecular diffusion 77−65668
variational principles for an incompressible, perfectly plastic material with non-associated flow law 78−67050
visceral smooth muscles in vertebrates, viscoelastic and plastic props. 78−73169
visco plastic torsion, prismatic bar, finite element solution 80−38282
visco-plastic anal. of axisymmetric bodies, semi-analytical finite element soln. 79−90149
visco-plastic steady-state flow finite element solns. 77−5670
visco-plasticity problem with hardening, finite element anal. *(French)* 79−46222
viscoelastic tube filled with viscoplastic media, unsteady motion 78−87366
viscoplastic and elastoplastic structures, partial shakedown under thermomechanical loading path *(French)* 80−74757
viscoplastic deformation, adiabatic, at high strain rate and very high strain *(French)* 77−21212
viscoplastic flow, finite element anal. *(Russian)* 78−18195
viscoplastic incompressible media, static and kinematic load limits 80−28430
viscoplastic kinematic hardening model, cyclic loading appl., yield surface 80−79162
viscoplastic large shape changes, calc. method *(German)* 79−90157
viscoplastic limit load problem, kinematic soln. method *(French)* 78−30195
viscoplastic liquid, steady filtration with variable initial gradient, exact solns. of two-dimensional problems 77−58786
viscoplastic liquid film, shaking off flat surface 79−14362
viscoplastic liquid film on vertical vibr. wall, with slip, shaking loose 78−59371
viscoplastic material, mixing process, Bingham model, two-dimens. flow *(German)* 80−92076
viscoplastic materials, dynamic convergence theorem for strain and work hardening 80−96199
viscoplastic media, flow in channels with varying cross section 79−94680
viscoplastic medium, asymmetric breakdown of thin layer between two sand surfaces 79−94503
viscoplastic medium, flow between two noncoaxial circular cylinders under pure shear 80−99938
viscoplastic medium, formation of contact with solid surface under pressure 79−69320
viscoplastic medium, optimum control of transient process under press. *(Russian)* 79−72821
viscoplastic medium, plane wave propag. and scatt., similarity condition 77−35072
viscoplastic medium, wave-barrier interaction 80−14609
viscoplastic round heated specimen, stability of extension *(Russian)* 79−68601
viscoplastic shock profile analysis 77−72203
viscoplastic structs., impulsively loaded, perturbation solns. 79−50615
viscoplastic thin walled systems, stability *(Russian)* 80−1452
viscoplastic wave propagation, inversions for const. vel. case 79−12614
viscoplasticity, constitutive inequalities 77−14926
viscoplasticity, implicit functional theory for metallic materials 79−27549
viscoplasticity, min. principle in stress field boundary-value problem 77−46927
viscoplasticity, thermodynamic yield criterion 79−27534
viscoplasticity, wave problems, appl. of methods of characteristics and perturbation 79−68614
viscoplasticity coefficient of stress concentration *(French)* 77−19541
viscoplasticity problem, analytical soln. 77−84832
viscoplasticity theory based on infinitesimal total strain and nonlinear viscoelasticity 80−79164
viscoplasticity with hardening, quasi-variational problems *(French)* 77−14913
viscoplasticity with singular yield surfaces, side and corner flow rules, finite element applications 80−48594
wave propagation speeds in isotropically work hardening materials 77−65711

plasticity continued
wedge-shaped crack plastic zone, superdislocation model 79−94557
work bounding function 77−17814
work hardening, plastic constitutive equations *(Japanese)* 80−25718
work-hardening model evaluation 77−77501
work-hardening of plastic materials, model evaluation 77−77500
X-ray diffr. study of plastic zone at tip of fatigue cracks 77−56058
Zircaloy-2, role of oxide plasticity in oxidation behaviour 77−36680
Ag-MgO, laws of plasticity of dispersion strengthened materials 78−84832
AgCl:Ba^{2+}, plasticity, impurity hardening effect 78−47466
AgCl:Li^{+}(Na^{+})(K^{+})(Rb^{+}), impurities effect on plasticity, brittleness 78−14398
Al alloy, 7050, plastic work during fatigue crack propag. 77−56068
Al alloy, adiabatic viscoplastic deform. at high strain rate, negative strain hardening *(French)* 77−21212
Al and Al alloy 5052 plastic anisotropy *(Japanese)* 79−34103
Al and alloys, plasticity variations rel. to heat treatment *(Russian)* 79−57050
Al bronze, plasticity of two-phase, coarse microstruct. material *(German)* 77−59882
Al, cast, strength and plasticity under hydrostatic pressure 78−56694
Al, electroplastic effect 80−7647
Al, plasticity, temp. and rate dependence for different rigidities of stressed state *(Russian)* 79−29139
Al, tension-torsion impact testing, instantaneous plastic property 79−52474
Al-Cu-Mn (1-5.2, 0-0.6 wt.%), N alloying and comp. effect on mech. props. *(Bulgarian)* 80−71719
Al-Mg sheet, artificial stress raiser effect on strength and local plasticity of weld joint 80−81130
Al-Mn sheet, artificial stress raiser effect on strength and local plasticity of weld joint 80−81130
Al-Si alloy, rod, tensile loaded, internal friction and Young's modulus measuring equipment, inelastic phenomena exam. *(Hungarian)* 79−52546
Al-Si-Mg (1, 0.6 wt.%), plasticity due to superimposed macrosonic and static strains 78−60719
Al-Zn eutectoid alloy, sensitivity analysis of torsion method in evaluating superplasticity indicators 77−56179
Al-Zn-Mg, plastic instability rel. to grain boundary failure at low temps. 78−56702
Al-Zn-Mg plasma sputtered, mech. props. rel. to heat treatment *(Russian)* 80−40387
Al-Zn-Mg-Cu-Co (6.5, 2.5, 1.5, 0.4 wt.%), fatigue crack propag. 80−55521
AlN powder, plasma-chem. and self-propag. high-temp. thermoplastic slips, synthesis 80−25633
Al_2O_3:Cr_2O_3(Ti_2O_3), dopant influence on struct. and mech. props. 80−24471
Au, rod, tensile loaded, internal friction and Young's modulus measuring equipment, inelastic phenomena exam. *(Hungarian)* 79−52546
Be-bronze BrB2, struct. and phase transform. during mechano-thermal treatment *(Russian)* 80−11667
Bi, low temp. effect on strain hardening, slip *(Russian)* 77−31713
C fibre reinforced plastic, nonlinear stress strain relations, under continuous static loading 77−59872
C polymeric chains, reduced from poly(tetrafluoroethylene), plasticity of C skeleton 80−89488
Cd-Zn single crystal, plasticity, 4 to 50K 79−43362
Co alloys, binary, and MAR-M322 type, influence of phase transform. on diffusion and mech. props. *(Russian)* 79−5000
Cr, and Cr alloys, cast, B additions effect on struct. and props. *(Russian)* 78−19891
Cr-Re(Ru)(Os)(Ta)(V)(Nb), Invar alloys, thermal expansion, plasticity *(Russian)* 79−55907
Cu, annealed, plastic strain during non-proportional loading 80−89291
Cu, plasticity, temp. and rate dependence for different rigidities of stressed state *(Russian)* 79−29139
Cu, rod, tensile loaded, internal friction and Young's modulus measuring equipment, inelastic phenomena exam. *(Hungarian)* 79−52546
Cu, tension-torsion impact testing, instantaneous plastic property 79−52474
Cu viscoplastic constitutive equations, for metal with strain rate history and temp. effects 79−61686
Cu-Al_2O_3, dispersion strengthened, plasticity qualities, fractographical analysis *(Czech)* 80−50680
Cu-Cr(-SiO_2), single crysts., yield and pre-yield behaviour rel. to aging time 80−81103
Cu-Ni tubing, viscoplastic bending 78−35464
Cu-SiO_2, dispersion hardened, surface plasticity effect 78−52832
Fe based dispersion strengthened thick condensates, struct., mech. props. 77−90361
Fe, cast strength and plasticity under hydrostatic pressure 78−56694
Fe, commercial, deformability, containing H_2 77−90411
α-Fe, plasticity, temp. and rate dependence for different rigidities of stressed state *(Russian)* 79−29139
Fe, pure, mech. props. at low temps. 78−44219
Fe-Ag (50 wt.%), plastic behaviour in compression, deform. rate effect *(French)* 80−71711
Fe-Cr-Ni, two phase (α+γ) alloys, transformation-induced plasticity 77−63721
Fe-Mn-C (11.5, 0.2 to 1.6 wt.%), water quenched, effect of C on phase composition, abrasion, plasticity *(Russian)* 78−35445
Fe-Ni-C alloy, austenitic, pre-deform. effects on TRIP *(Japanese)* 77−8890
Fe-Si (2.6 wt.%) single cryst., crack propag., controlled plastic crack tip opening rate 80−60943
Fe-Si (3 wt.%), effect of heating rate during primary recrystn. on props. after secondary recrystn. 78−84837
^{4}He, plastic props. *(Russian)* 77−62705
$MgAl_2O_4$, microplasticity at room temp., dislocations, TEM study 80−19805
MgO, compressive stress-strain behaviour at high temps. 80−25774
MgO, high temperature prestrain effect on plastic props., dislocation struct. 80−79866
MgO-$MgAl_2O_4$($FeCr_2O_4$), thermoplastic and thermophys. props. for steel vacuuming installations 80−35281
Mn-Cu-Al alloy under torsion, anomalous elasticity and transformation plasticity obs. *(Russian)* 78−75834

plasticity continued
Mo, fatigue charact., effect of Ni and Re surface doping on mech. props. *(Russian)* 80−7660
Mo, mechanical props. and dislocation struct., mag. field effect 80−54935
Mo, monocrystalline, exam. of microplasticity at ambient temps. *(French)* 78−52888
Mo single crystals, orientation and alloying effect on mech. props. *(Russian)* 80−71706
Mo-B, Mo-B-Fe(Ni), microalloying influence on mechanical props., cold rolling, plasticity *(Russian)* 80−40502
Mo-Hf (0.3 wt.%), strength, plasticity and microhardness, internal nitriding effect *(Russian)* 80−40433
Mo-Mn alloy, plasticity, fracture, strength depend. on C content *(Russian)* 80−35257
Mo-Nb-C, mech. props., effect of alloying and Mo cryst. orientation *(Russian)* 80−71706
Mo-Ti-La-C, influence of high pressure on mech. preps. after nitriding *(Russian)* 79−57137
NaCl single crystal, plasticity, effect of alternating electric field 78−15481
NaCl, single crystal, temp. anisotropy of plasticity and brittleness 78−3198
Na_2O-CaO-SiO_2, foil, exam. of surface plasticity, and cracks, by electron microscopy 78−68733
Nb, mechanical props. and dislocation struct., mag. field effect 80−54935
NbC, NbC-ArC, right-through sat. prep., strength and plasticity, temp. depend. 77−40432
Ni alloy, fatigue and cyclic plasticity rel. to struct. inhomogeneity 80−81184
Ni alloy, heat resistant, high temp. plasticity at different strain rates 77−21233
Ni alloys, plasticity, heat treatment effect 80−76277
Ni, hardness after-effect studied by anelastic relaxation 80−66570
Ni, high temp. plasticity, oxide inclusion effect 80−50681
Ni, rolling texture, athermal softening *(Russian)* 77−66655
Ni, sintered, pressed, plasticity as function of porosity *(Russian)* 80−75290
Ni-Al-Ti(Nb), heat-resisting dispersion-hardening alloys, props. and struct., γ'-phase comp. influence *(Russian)* 80−20943
Ni-base, heat resistant alloy KhN60MKBYuT, plasticity, precipitation 77−70120
Ni-base alloys, US vibration during crystallisation, effect on mech. props. *(Russian)* 78−19827
Ni-Cr alloy, Kh20N80, inclusions and plasticity, crystn. conditions influence *(Russian)* 80−20923
Ni-Cr-Ti(Al), effect of ultrasound on crystallisation, dendritic structure, and plasticity *(Russian)* 80−11637
β'-NiAl, ordered, hardness after-effect studied by anelastic relaxation 80−66570
NiO:Mn, microhardness, plasticity, ageing effects 79−43291
Pb, plastic properties over wide range of strain rates 80−71693
$Pd_{77.5}Cu_6Si_{16.5}$ metallic glass wire, cold drawing 80−50650
Sc, strength and plasticity 77−90429
Si crysts., deformed, strain distrib. characterisation, annealing response 77−70140
Si, failure in strong melt grown single crysts. 78−3205
Si, plastic properties, internal friction, dislocation motion *(Russian)* 80−54305
SiC, reaction-bonded, impact erosion by ang. Al_2O_3 particles 80−89362
Ti alloy β III, precipitation of α and ω phase, evolution of mech. props. *(French)* 77−16591
Ti alloy VT14, strength in uniaxial dynamic extension, influence of α-ω transform. *(Russian)* 79−52200
Ti alloys, plasticity, temp. and rate dependence for different rigidities of stressed state *(Russian)* 79−29139
Ti-Al-Mo-V (8, 1, 1 wt.%), Widmanstatten colonies, fracture toughness 80−85031
Ti-Al-V (6, 4 wt.%), textured, anisotropy of fracture toughness over various specimen orientations 79−8353
Ti-Zr-Mo-V, alloy VT20, exam. of plasticity in temp. range 20 to 1000°C 78−56712
TiN powder, plasma-chem. and self-propag. high-temp. thermoplastic slips, synthesis 80−25633
V, plasticity and strength change in temp. range 20 to 1000°C impurity effects 80−35235
V_3Si, supercond. structure and properties *(German)* 80−93631
W and alloys, wire, increasing plasticity, by electroplastic rolling *(Russian)* 79−29103
W, metal-ceramic, mech. props. and structural nonuniformity 79−15705
W surface layer struct. during milling, plastic deform., failure *(Russian)* 80−40586
W, with impurities, grain boundaries, effect on high temp. plasticity *(Russian)* 79−79057
W-Al fibrous heat treated composites, thermal stress anal. 77−46943
Y_2O_3, dislocation and plasticity dissociation 80−107247
Zn, cutting mechanism of large crystals *(Japanese)* 77−48523
Zn, internal friction anomalies in temp. initiated brittle-plastic transition *(Russian)* 80−96648
Zr alloys with Fe, Cu, Cr, Nb, role of oxide plasticity in oxidation behaviour 77−36680
Zr, ion-implanted polycryst., thermal oxidation 80−71786
ZrC, NbC-ZrC, right-through sat. prep., strength and plasticity, temp. depend. 77−40432
ZrN, microhardness and resist. to brittle fracture 79−87715

plastics
see also glass fibre reinforced plastics; polymers
ABS, glass-filled, deform. and fracture behaviour, 293-353K 77−56077
ABS mouldings, selective Cu plated in areas, effect on mech. props. 79−34182
ABS-2 plastic, etching rate rel. to electroless Cu adhesion *(Russian)* 78−35542
accelerated life testing, by thermal analysis 77−70261
acrylic, deform. of rigidly clamped specimens subject to one sided cyclic heating 77−59932
acrylic bone cement containing second phase dispersions, strength 77−81663
acrylic bone cement-stainless steel interface, shear strength 77−86706
acrylic moulding formulations, optical and mech. props. 80−106582
amorphous plastic injection moulding, frozen-in orientation, pressure loss during filling 79−77047
anisotropic reinforced, stress-strain state, theoretical principles of nonvisible exam. 78−68745
arc resistance test *(Japanese)* 78−27697
artificial ligaments and tendons, dynamic motion simulator for testing plastics *(German)* 78−81070
bending fatigue, exam. of new method of testing 78−53056
building components, material testing, for use as building component *(German)* 78−39984
carbon fibre reinforced plastic, fracture energy improvement by delamination promoters 77−8909
carbonmetalplastic, heating rate effect on thermal deform. in various atmos. 79−65226
cellulose acetate, neutron irrad., elec. conductivity, rel. to personnel dosimetry 77−40776
cellulose diacetate as solid state heavy ion track detector 78−17523
cellulose nitrate, etching behaviour, nuclear track detector 78−17485
cellulose nitrate, nuclear track detectors, etch induction time, particle identification parameter 78−17486
cellulose nitrate, proton, H_2^+ mol. ion, and heavy ion irrad., track prod., etching obs. 78−86757
cellulose nitrate CA8015, calibration for fast neutron dosimetry 79−49907
cellulose nitrate plastic detector technique in fast neutron radiography 79−76299
cellulose nitrate plastics, determ. of B in complex matrices from ^4He and ^7Li tracks 79−18080
cellulose nitrate plastics, heating and alpha track revelation charact. 79−49910
cellulose nitrate track detectors, detect. of efficiency and range meas. of alphas and protons 78−17524
chemical resistance for medical laboratory techniques 79−88926
coated optical glass fibres, liq. N_2 strengths 80−58707
coke, imbedded in epoxy, X-ray diffr. 79−90495
Columbia Resin, CR-39, fracture mirrors, static and impact tests 78−27601
composites, mechanical props. 79−29162
corrosion managing problems with plastics *(Japanese)* 78−92382
corrosion protection of metals 79−96211
CR-39, proton-sensitive, method of producing thin sheets for plastic track detectors 80−35155
CR-39 plastic, electrochem. etching, optimum conditions 80−95505
CR-39 polymeric nuclear track detector, props. and appls. 78−94170
CR-39 thermoset plastic nuclear track recorder, etching in hot NaOH 78−74535
crack growth stability anal. using catastrophe theory 80−74810
creep of metals and plastics under combined stresses. A review 80−59567
deformation speed in static tensile tests, machine rigidity effects *(German)* 78−48473
design guide 77−21087
Dewar vessels for liq. N_2, foam plastic, manufacture, heat insulation test *(Japanese)* 78−37023
diallyl phthalate methyl methacrylate, copolymerisation, two-step, prep. of light focusing plastic rods *(Japanese)* 79−37064
disperse systems, generalised flow theory with account of wall effect 78−87320
display plastic optical components and systems 78−25967
double-layer antireflection coatings for plastic lenses, evaporation coating process 80−14491
drying of thermolabile plastics, heat and mass exchange in vibro-rotational bed *(Russian)* 77−68377
Eccosorb HF-2050, AC resistivity meas., 100-320K, 500-2000 MHz, von Hippel's method 77−32314
elasticity, hardness, creep, and relaxation meas. with Vickers indenter by electroacoustic method *(German)* 78−48584
electrochemical etching studies of the CR-39 plastic solid state nuclear track detectors 80−91391
electrophotographic layer, electrostatic force calc. *(German)* 80−42285
electrophotographic recording media, high resolution, expt. charact. 78−70208
endurance testing machine 77−52580
epoxide resin, amine-cured, crack propag. 78−27596
epoxy C plastics, under tensile stress, effect of whiskerization of polymer matrix on creep resist. 79−87699
epoxy resin, plastic deform. mechanism 80−97534
epoxy resin DLS 351/$BF_3$400, C-fibre reinforced, thermal expansion, 90-500K, fibre vol. fraction effects 78−26703
epoxy-Al composite, thermal conductivity 77−76630
epoxy-Al composite, thermal conductivity model 77−76629
equilibrium glass-plastic pressure vessel of minimum mass with non-geodesic winding 77−50905
extrusion and heating of plastic layer under shock 78−34064
fatigue fracture props. correl. with viscoelastic damping 78−52993
fatigue limits, apparatus for comparison under shock and harmonic loading 77−63855
fatigue testing machine under axial load 77−66734
fibre, light focusing, heat drawing process prep. 77−14815
fibre reinforced, mech. props. stabilisation by PVA fibres modification 79−20022
fibre reinforced plastics, spread of strength rel. to stress conc. *(Japanese)* 79−24610
fibre reinforced polyurethane foam, with chopped fibres, morphology and fracture 77−36447
fibre-optic glass manufacture using polypropylene sump pumps 80−14410
fibreglass, classical reaction force density meas. in material media at LF 79−64141
film, self-supporting beam splitter, for far IR interferometers 78−275
film tear test, fracture mechanical analysis *(Japanese)* 77−81351
flameproof coating for PVC insulated cables, composition, tests *(Russian)* 78−68828
flexural fatigue props. *(Japanese)* 79−20171
fluid, charact. by torque rheometer 77−32751
fluoroplastics, mech. props., accumulation of submicrocracks, thermal treatment effects 77−4850
foam insulation, spray-on, crack inspection using dye solution or X-ray opaque solution 80−76440
foam layer beneath sheets, NDT *(German)* 77−1896

plastics continued
foam PS-4-40, microslip, effect of friction 77−77588
foamed, shock absorbing capacity determ. *(German)* 80−19877
focusing fibre for imaging appls., fabrication and charact. 77−62040
foil, Li ferrite clad, thermal deform. *(Polish)* 80−30002
foil prod. by extrusion blowing *(German)* 80−20786
foils for neutron dosimeters, electrochem. etching prep. techniques 79−76298
formvar-Al superconductive junction, Ginzburg's generalised jellium model 80−15663
glass plastic, fatigue strength, loading frequency effect 77−52484
glass plastic coating, thick-walled, compressive strength evaluation method 79−15897
glass plastics, strength criteria 80−10208
glass-plastic, engineering, nondestructive structural identification 78−92422
glass-plastic, Young's modulus, expt. study 77−52389
glass-plastic AG-4c, fatigue resistance under bending in H_2SO_4 *(Russian)* 79−34163
gradient index lens fabrication and image evaluation 80−14426
greenhouse solar distillation and cultivation materials 79−74496
high temperature, properties, brief review 77−25092
hip joint, wear of plastic material 77−21661
Homalite 100, dynamic fracture specimens, dynamic photoelastic analysis 77−44364
Homalite 100, stress intensity factor determ. from isochromatic fringe loops 78−34097
Homalite-100 plates, modified compact-tension specimens, dynamic anal. 80−97561
ideal plastic material, film flow along oscillating wall 79−81927
identification by simple qualitative test 79−5944
imaging plastic focusing fibre with parabolic refractive index distribution 77−19437
impact force vs. displacement curves, expt. determ. 78−83344
impact-torsion test machine *(German)* 77−52595
injection-moulded thermoplastics for demountable optical fibre connectors 80−53472
insulation of HV and MV cables, dielectric breakdown obs., distribution law parameters estimation *(French)* 77−24794
ion plating 80−16533
ion-plated metal film structure on plastic substrate 79−82501
Kaprolon, compressibility, elec. cond., sound vel. behind shock front 78−95105
laminate removal from metal using laser beam 78−7061
laser processing capacity using CO_2 laser 77−5820
leachability determ., radioactive tracer method 78−61135
lenses, aspherical-surface, for large screen TV, optical design and evaluation 80−78937
Lexan, etching rate temp. and conc. depend. 77−10533
Lexan, on polypropylene window of soft X-ray proportional counters, for eliminating UV sensitivity 79−74273
lexan, stress wave propagation 78−46910
lexan polycarbonate track detector, for U estimation in zircon *(French)* 77−64445
light guides development for high optical power transmission *(German)* 78−33913
linear thermal expansion coefficient, meas. technique 77−41598
load-bearing surfaces, secondary structures obs. by electron microscopy, specimen thinning method 79−52484
LR-115 plastic track detector, etching behaviour 80−99423
lucite, adhesive bonds, US attenuation effects 78−7141
Makrofol-E polycarbonate detectors, liq. N_2 enhancement of α-particle tracks 77−67946
materials testing, application-oriented test standardisation *(French)* 78−85061
mechanical strength and brittleness, effect of moisture and notches *(German)* 77−48543
Mersilene mesh, herniorrhaphic reinforcing prosthetic, mech. and struct. props., SEM study 79−74789
metal electroplated, durability and struct. 78−3242
metallographic methods application, advantages 77−60030
microballoon reinforced plastics, acoustic and mech. props. rel. to hydrophone applic. *(Japanese)* 77−7793
micropore filters, preparation by bombarding lavsan film with Ar ions 78−3305
mirror, large size lightweight, for airborne laser sensor system, fabrication 78−66891
modular solar energy collector with reticulated foam 80−16833
molecular electronics appl. 80−6355
Mossbauer radiation scatt. by condensed matter, review 79−78596
notched fibre reinforced composites, tensile fracture 78−52991
nuclear track detector, primary damage and secondary electron damage in heavy ion tracks 78−17514
nuclear track detectors, background holes and reduction methods *(Japanese)* 77−71721
optical, moulded, design advantages and appl. 78−87119
optical component specification 80−48362
optical components, moulding techniques for single, multi-element systems 78−63210
optical constant determ. of filled and reinforced plastics 78−19472
optical fibre clad with Teflonlike plastic coating, press. sensitivity 80−33149
optical fibres development materials *(French)* 79−55236
optical material, components 79−32010
optical material physical props., seminar, San Diego, CA, USA (Aug. 79) 80−105423
optical recording media, review 78−71172
optical storage materials and methods, conf., San Diego, USA (Aug. 1977) 78−71171
optical systems applications 79−32008
optical tolerance, glass and plastics comparison 79−59780
organic fibre reinforced plastics, failure 80−11774
penetration hardness testing, exam. of thermal effects *(German)* 78−76801
pentaplast, plasticised, thermal treatment effect on props. 80−40324
permittivity of coaxial samples, rapid determination using freq. variation *(German)* 79−26078
Perspex, adhesion of silicone rubber, surface topography effects 78−15644
Perspex, breakdown by treeing 78−84526
plastics continued
Perspex, dislocation dynamic props., investigation by impact loading *(Russian)* 78−85069
Perspex, positronium form. and decay, elec. field effect 80−97369
perspex confined arc, ablation-induced effects 80−70073
Perspex for astronomical telescope lens and mirror manufacture 78−36458
Perspex magneto-electret, equiv. elec. field calc. from thermally stimulated discharge current 80−7259
perspex prism, refr. index meas., crit. angle method, student expt. 80−12873
Perspex pyramid electret, thermally stimulated discharge currents 80−2688
perspex spheres, internal fractures due to stress wave focusing 78−18239
Perspex spheres, times to fracture due to point explosive loading 77−50989
phenol formaldehyde resin reinforced with chrysotile asbestos fibres, thermal expansion, specific heat 79−55908
phosphate bonded refractory plastics, hot modulus of rupture, 1500 to 2500°F 78−19855
photo-thermoplastics for fast optical recording *(German)* 79−72530
photocopolymerisation for light focusing rod prep. 77−11000
photothermoplastic devices, conventional and self-developing, sensitivity and development 79−44958
photothermoplastic devices, performance and limitations 77−38832
photothermoplastic layer, diffraction effectiveness, registration of discrete holograms *(Russian)* 79−7100
photothermoplastic layers, optical transmission function, charge carrier drift effects *(Russian)* 79−3661
photothermoplastic material recorded information visualisation by schlieren projector 80−87544
photothermoplastic recording material for holographic interferometry 77−7038
photothermoplastic recording with rapid switching 80−32941
pigmented, elec. cond. depend. on mech. stress *(German)* 80−20264
Pilot U scintillation response to neutrons, 50 to 120 MeV 77−54453
pipe, hardness testing *(Japanese)* 77−60017
plastic:Eu^{3+}, Faraday rotation sign oscill. in very strong mag. fields *(Russian)* 80−88973
plastic optical components, flexible rapid curing abrasion resistant coated film 78−66890
plasticised cellulose acetate sheet, post-yield fracture 80−25859
Plexiglas, fast cracks propag. and interaction 80−100905
plexiglas, shock compressed, vel. of sound meas. 78−10123
Plexiglas, spark energy balance 79−23474
Plexiglas, thin slab, microwave beam displacement upon transmission 80−1107
Plexiglas 80−66592
Plexiglas-Al(Cu), double layer barrier, deform. of electron spectra *(Russian)* 78−84292
plexiglass, red, gamma dose meas. by optical absorpt., elec. conductivity, and mechanical hardness 78−55045
plexiglass, scatt. of 150 MeV protons, mean-square transverse displacement 79−6808
plexiglass, shock loading, method for producing isentropic compression 77−44424
plexiglass composite, long term strength and durability 80−75294
plexiglass-Cu channel with parallel flat walls, ice growth in laminar flow 79−3908
PMMA, lens manufacture, mould punch surface radii calc. 77−799
PMMA fracture toughness, flame-retardant additive effect obs. 80−16470
poly(vinylidene fluoride) orientation, solid state deformation by coextrusion 80−40394
polyacetal, exam. of fatigue crack propag. 78−48497
polyamide thermoplastic, glass or C fibre reinforced, stiffness and strength 78−27600
polyamides 6 and 66, response function characterization of thermal state in dynamic testing 79−18680
polycarbonate, glassy, fatigue crack initiation in high strain fatigue tests 80−97564
polycarbonate, yield behaviour *(Japanese)* 80−93620
polycarbonate plastic, gamma-ray dosimeter at high exposures 79−63815
polycarbonate plastic film detectors for light and heavy element fission studies 79−72193
polycarbonate purification for medical use 78−84759
polycrystalline body, energy criterion for failure 77−4823
polyester thermoplastic, for electrical insulators 80−103685
polyethylene tube insert, for tritiated NMR sample handling 79−40546
polyimide, directional O ion beam etching, compared with reactive ion etching 80−71781
polymeric fibre-reinforced plastic, creep prediction from components props. 80−40448
polymethylmethacrylate, rheological meas. with new rotational rheometer *(German)* 77−51006
polyoxymethylene copolymers, response function characterization of thermal state in dynamic testing 79−18680
polyoxymethylene-copolyamide mixture melt, plasticiser effect on props. and fibre form. during flow 77−27500
polypropylene, (Moplen) influence of temp. and mol. wt. on high speed fracture mechanics 80−76341
polystyrene, (-Kraton G blend), rubber toughened, charact. by SEM 79−14697
polyurethane, void detection by neutron gauging 78−23910
polyurethane foam, press wave propag. and refl. charact. 77−35634
polyurethane foam plastics, sorbents for marine oil pollution 79−53011
polyvinyltoluene scintillators, energy transfer in organic systems 78−92127
Prandtl-Reuss plastic materials, with general work hardening, constitutive equations *(Japanese)* 78−92276
prestrain effect on dynamic modulus of elasticity and attenuation coeff. in nonconducting materials 80−29110
process computers for control and meas. of laboratory testing *(German)* 79−61821
projector having a thermoplastic target and operator's eye, charact. 80−96023
PVC, electroluminesc., constant electric field effects 77−81154
PVC, glassy, fatigue crack initiation in high strain fatigue tests 80−97564
PVC, orientation hardening 78−76662
PVC, plasticised, foam growth, thermomech. anal. 80−3416

plastics continued
PVC, plasticised film, defect form. study, turbidity and shrinkage meas. *(Russian)* 77−62490
PVC, plasticized, permeability *(Polish)* 79−52771
PVC, with stabiliser, dielec. and mech. charcts. under γ-irrad., plasticisers effects *(Korean)* 77−81054
PVC, yield behaviour *(Japanese)* 80−93620
PVC compositions, influence of formulation on the compounding and rheological props. 80−40321
PVC magnetoelectrets, mag. susceptibility 80−2687
PVC with lead-containing stabilisers, degradation obs. using X-ray diffr. *(German)* 79−34297
radio and light polarisation stress analysis 78−68857
reactive, structurisation kinetics, torsion cord method *(Russian)* 79−34304
reactor neutron detection, plastic with ^{65}Zn impurity used as nuclear track and activation detector 78−13346
recording media for holography at 10.6 μm 77−71952
reflectance, aluminised thermal screens for energy conservation in greenhouses 80−64351
reinforced, anisotropic, stress distrib., using mm region of EM waves 80−25968
reinforced, load-bearing capacity, effect of one-sided heating 80−81135
reinforced organic composite, graphite, or C-C, ablation, mathematical modelling 79−41564
replicated and plastic optics, conf., San Diego, USA (Aug. 1977) 78−66961
residual stresses in shells of revolution, cut-out element method glass-plastic composite, thermoelastic residual stresses in shells of revolution, cut-out element method 80−38271
resins, secondary coating of optical fibres, effect on transmission props. 80−58704
rheological characteristics of compact of plastic powders *(Japanese)* 78−95770
rubber toughened plastics, ABS- and AAS-resin, flow props., effect of heating and shearing hysteresis *(Japanese)* 79−94685
sample containers, for trace element samples, selection, cleaning methods 78−35745
scintillation granules, efficiency of α radiation recording 78−9028
scintillation material, plexiglas 1921, linear response and energy resolution results 78−78586
scintillator excited by ^{60}Co γ-rays, absolute radioluminesc. yield meas. 80−2829
scintillators, fluoresc. meas. 78−86747
scintillators, quenched, sub-nanosecond 77−54419
scintillators, study of light pulse shapes 77−54450
scintillators, sub-nanosecond time response studies using laser produced X-ray pulsed excitation 77−54434
scintillators, ultrafast, primary energy transfer process 78−90026
sealing materials, friction and wear tests *(German)* 79−38987
sheet blowing and extruding, process identification for automatic process control *(German)* 80−81023
shell, cylindrical, composite with viscoelastic filler, optimisation w.r.t. long-term stability 79−18760
shell, elastic cylindrical, optimisation with allowance for geometrically nonlinear factors 80−38270
shock compression at 30 kbar, expansion adiabats 80−66592
short-time testing using process computers *(German)* 79−61822
silica-plastic fibres, propag. charcts. and fabrication for short-medium distance appls. 78−66892
solar glazing hemispherical transmittance props. 79−52957
solid state nuclear track detectors, effect of etching conditions on energy resolution of phosphate glass and polycarbonate detectors 80−91390
static relaxation behaviour, test rig design *(German)* 79−39081
static strength determ. from elasticity and internal friction 77−70094
stress and deformation analysis, using pseudo-elastic method, validity in load-bearing appl. 78−39868
stress relaxation estimation for electric connectors, expts. 77−21206
stress relaxation testing method 77−52576
stress-cracking test 79−74311
stycast 2850FT, low temp. thermal cond. 79−23790
substrate, plasma polymerisation, mech., effect of substrate and substrate topography 78−88633
Teflon, creep under joint action of tension, hydrostatic pressure 78−68750
Teflon, dielec. in solid-plasma waveguide, effect on slow surface wave propag. 79−50862
Teflon, surface alteration by interaction with Ar^+ and Xe^+ beams 78−91347
Teflon FEP film, thermoelectret, TSC spectra 77−52012
Teflon foils, cryst. struct. and texture changes due to polarisation process *(Polish)* 80−35209
tensile and flexural testing device, incorporating an impacter *(German)* 80−3276
testing, automation 80−76443
testing *(German)* 78−27716
testing device, for prop. changes at high temps. *(German)* 80−66741
testing methods *(Japanese)* 78−39974
textolite glass, stress relax. calc. from creep curves 80−71709
thermal conductivity data, need and demand 77−72725
thermal properties identification using temp. heat flux data 77−26297
thermomechanical reliability, rel. to transmission media applic. 80−40666
thermoplastic, acrylic, hot stretched, aircraft cabin windows, exam. of anisotropic fracture 78−76763
thermoplastic, low-profile polyester moulding materials *(Polish)* 80−66523
thermoplastic, partially crystalline, microscopic methods of struct. anal. *(German, English)* 80−30198
thermoplastic based composites, mean stiffness 80−11693
thermoplastic beams, constant stress, design 80−38248
thermoplastic complex filter for optical pattern recognition 80−99656
thermoplastic film, photoconducting, double exposure holographic interferometry using memory effect *(Chinese)* 80−37967
thermoplastic film for holographic display and recording 79−50263
thermoplastic foil, US welded, IR detection for measuring temp. distrib. *(Polish)* 80−22362
thermoplastic holographic recording 78−78961
thermoplastic layers, isothermal smoothing of surface deformation *(Russian)* 80−76394
thermoplastic light modulators, status and prospects 78−79138
plastics continued
thermoplastic materials, flexure testing 77−86087
thermoplastic media for hologram recording *(Russian)* 78−58948
thermoplastic moulding quality assurance using holography and speckle photography 78−27720
thermoplastic photoconductor media, review *(Japanese)* 78−78956
thermoplastic photoconductor technology for optical recording and storage 78−71175
thermoplastic pipes, apparatus for time-to-failure determ. *(Polish)* 79−74328
thermoplastic plates, strength meas. when supported by annular ring 80−81257
thermoplastic recorder development, interaction of regular and chaotic deformation *(Russian)* 80−42291
thermoplastic recording, IR laser heating 78−71065
thermoplastic recording material, latent image and surface deformation *(German)* 80−42284
thermoplastic recording media for frozen-fringe holographic interferometry 78−90402
thermoplastic rectangular parallelepiped pressure vessel, photoelastic coating anal. 79−59950
thermoplastic rubber morphologies and applications 78−26457
thermoplastic sheet, deep drawing *(German)* 80−104114
thermoplastic spatial light modulator 80−102841
thermoplastic-photoconductor, holographic recording technique 78−9346
thermoplastic-photoconductor hologram recording media, frost suppression 78−17869
thermoplastic-photoconductor image transducer, input to coherent optical processor 78−83098
thermoplastic-photoconductor media, charge carrier behaviour, microscopic response 79−28370
thermoplastic-photoconductor tape for holographic recording, spatial filter prod. 78−90391
thermoplastics, effect of mol. orientation on fracture toughness 78−52992
thermoplastics, homogeneous, fracture under plane strain and plane stress conditions 78−52941
thermoplastics, internal stresses revealed by artefacts produced in SEM 78−35634
thermoplastics, mech. props., 4.2-300K 77−25160
thermoplastics, post manufacture high temp. heat treatment, controlled geometry loss technique 78−52853
thermoplastics, reinforced testing by dynamic mech. anal. 80−16626
thermoplastics, structural changes during deformation, rel. to impact resistance 80−25800
thermosetting, characterisation by thermal anal. 80−61204
thermosetting materials, formation and props., phase diagram and torsion pendulum anal. 80−55381
threaded plastic parts, load distrib., taking into account vibr. creep 79−83282
tissue-equivalent plastic A-150, density and composition uniformity 78−73252
torsional rigidity testing instrument, used with strength testing instrument *(German)* 77−52596
track detectors, treatment and application 77−46459
tubing, pulse echo US thickness gauging 77−73392
ultradrawing technique, solid state coextrusion 80−84979
urethane elastomer, thermoplastic, dilute soln., viscosity and sedimentation 80−103512
Valox 752m thermoplastic, for electrical insulators 80−103685
Vicat softening temp., meas. instrument *(German)* 77−63871
N-vinylcarbazole containing polymers, sensitization to Ar laser for single laser photothermoplastic devices 80−83651
viscoelastic anisotropic, creep 80−35249
viscoelastic plastics, fatigue testing, using hollow cylindrical specimens *(German)* 78−44292
viscoplastic material, mixing process, Bingham model, two-dimens. flow *(German)* 80−92076
waste, pyrolysis to produce organic raw materials *(German)* 80−3307
wear measurement, attachment to MI machine 79−87784
wear tests with plastic lubricants, friction machine attachment 78−3273
Al_2O_3 ceramics, with thermoplastic bond, prep. 80−45254
C fibre reinforced epoxy resin, thermal expansion, influence of fibre type and orient. 77−35722
Cu films, ion plated on polyethersulphone, structural and resistivity study 79−42411
^{210}Po contamination of surfaces, removal coeff. determ. 79−26769

plastics industry
adaptive control of molecular weight distribution in polymers 80−58434
computerised automatic tensile tester, ISO and ASTM standards 77−26284
extrusion cylinder and feed channel wall temp. and pressure meas. and control, US appl. 77−27448
extrusion process, viscosity control and meas. 77−27639
injection moulded GFRP distortion meas. by holographic interferometry 79−79020
injection-moulded article mech. props. rel. to process parameters 79−78929
instrumentation and control automation, conf., Brussels, Belgium (1976) 77−27638
methyl group meas., computer-infrared method 77−27073
multicomponent, multipoint infrared ambient air monitor, microcomputer-controlled 80−40945
polymer melt pressure meas., slit die rheometer appl. 77−27501
polyolefins, molten, basic rheological charcts., industrial appl. *(Polish)* 79−50689
temperature meas. by IR camera *(German)* 79−58685
thermoplastic sheet, extruded, thickness adjustment and cooling between calender rolls 79−68597
vinyl chloride suspension polymerisation monitoring by US attenuation and velocity 79−70328

plates (anodes) *see anodes*

plating (electroplating) *see electroplating*

platinum
see also nuclei with
5d band structure effects on line shapes and intensities of core electron excitations 78−92177
(111) surface, backscattering, channelling spectra, H adsorption, surface relaxation 80−71552
absorption of activated N_2 on Pt single cryst. faces 77−85070

platinum continued
acetylene adsorption, desorption and surface dissoc., (110) face 77−62749
adatom, on W (110), dipole moment, field emission meas. 77−47674
adsorbed benzene on (111) surface, vibr. loss spectra 79−23838
adsorbed C, determ. of monolayer coverage by AES 79−46916
adsorbed CO, adsorbate induced electron losses 79−46959
adsorbed CO oxidation, AC pulsing technique 79−100439
adsorbed Cs layer on (100) surface, struct. anal. by LEED 77−89654
adsorbed cyanogen on (100) surface, electron energy loss spectrum 78−14592
adsorbed H_2O on (100) surfaces, bonding, electron energy loss spectra 80−34311
adsorbed H on (111) surface, vibr. modes, EELS study 80−15377
adsorbed layers of H_2, energy loss spectra *(French)* 79−83069
adsorption, of CO, mol. internal optic modes, mol. dipole model 80−100395
adsorption, of $CO(C_2N_2)$(benzene)(ethylene), Auger spectra 79−52077
adsorption, of H_2, electrolyte environment and crystallite size effects 78−27774
adsorption, of H_2+D_2, on (111) or (332) surface exchange reaction, mol. beam obs. 79−66269
adsorption and catalytic reactions of H_2, CO, and O_2 80−81362
adsorption and decomp. of ethylene, 90 to 500K 79−46933
adsorption of acetic and propanoic acids on (111), LEED obs. 80−80073
adsorption of acetylene and ethylene on (111) surface, UPS meas. 77−52223
adsorption of acetylene or ethylene, intermolecular forces and kinetics of adsorption 78−75930
adsorption of Br, irreversible order-disorder transition 79−69361
adsorption of CO, adsorption site investigation by IR reflection spectra 78−14565
adsorption of CO, AES obs. 77−35818
adsorption of CO, binding states, desorption and adsorption kinetics 77−85065
adsorption of CO, effect of interactions on chemisorption bond 77−51598
adsorption of CO, electron energy loss 77−15688
adsorption of CO, electron energy loss spectral study of surface vibrs. 77−69160
adsorption of CO, electron energy loss spectroscopy and IR reflection spectroscopy 77−85729
adsorption of CO, IR reflection absorpt. spectra, 1875 cm^{-1} band 79−65852
adsorption of CO, low temp. vibr. mode, site occupation, electron energy loss spectra 80−29263
adsorption of CO, O_2, H_2, thermal desorpt. spectra 78−14607
adsorption of CO, O_2, H_2, UV photoemission spectra 78−14608
adsorption of CO, O_2, NH_3, surface composition, AES and temp. programmed desorption meas. 80−34313
adsorption of CO, on (111) surface, oxidation, reflection-adsorption IR study 78−76468
adsorption of CO and D_2, absolute coverage meas. using nucl. microanal. 80−54511
adsorption of CO on (111) surface, XPS, UPS, thermal desorption, and work function meas. 79−77905
adsorption of Cs, field-emission microscopy 78−51822
adsorption of Cu monolayer on (100), (110), and (111) surfaces, optical and electrochem. studies 79−99419
adsorption of cyanogen, UPS 77−36351
adsorption of cyclopropane, NMR and PMR obs., chem. shift 77−51591
adsorption of ethylene on (100) surface 78−18905
adsorption of H_2 and CO on (110) clean and oxidised surfaces 77−28078
adsorption of H_2 and D_2, on stepped surface, reaction probability, reactant ang. of incidence effects 77−47670
adsorption of H_2 and O_2 on (111) surface, and their interaction 77−55461
adsorption of H_2 on single crystal surfaces, recording contact pot. changes using diode 79−88982
adsorption of H_2S, intermolecular forces and kinetics of adsorption 78−75930
adsorption of H, (111) surface, role of at. steps 77−15690
adsorption of H, electrode surface, struct. and comp. exam. by LEED and AES 79−70342
adsorption of H, electrode surface exam. by LEED and AES 77−47665
adsorption of H, face specificity, field emission probe-hole microscope obs. 77−11783
adsorption of HI on (111) and (100) surfaces, superlattice form., LEED, AES, and thermal desorption studies 80−55715
adsorption of hydrocarbons, on (111) surface, LEED intensity obs. 77−51592
adsorption of K on Pt(111), UPS and XPS meas. 80−95675
adsorption of N_2, thermal desorption meas., α and β-states 77−15696
adsorption of N_2 and Xe, field emission meas. 77−24479
adsorption of NO, on surface (100), 40-400°C LEED, AES, XPS and UPS obs. 77−35820
adsorption of NO on (111) surface, anal. of adsorption processes and surface reactions, vibration spectroscopy 78−87868
adsorption of NO on (111) surface, EELS, thermal desorption, LEED, and AES study 80−80086
adsorption of O_2, AES, LEED and thermal desorption spectroscopy exam. 78−79891
adsorption of O_2, surface struct. depend., LEED, AES, and electron energy loss spectra 79−46934
adsorption of O_2, surface struct. effects on rate, data assessment 78−43251
adsorption of O_2 on (110) surface, Ar^+ bombardment effects on reactivity 80−89099
adsorption of O_2 on Pt(S)-[9(111)×(111)] face, flash desorpt., LEED and AES obs. 77−69182
adsorption of O, anal. by low energy ion scatt. *(French)* 77−59663
adsorption of O on (111) and (S)-12 (111)×(111) surfaces, thermal desorption, AES, XPS, and LEED study 80−70534
adsorption of S, LEED pattern interpretation model 77−69184
adsorption of S on Pt (100) 78−14606
adsorption of water, H_2 and reaction between H_2 and adsorbed O 80−49514
adsorption of water on (111) surface, thermal desorption, UPS, and XPS study 80−80088

platinum continued
adsorption sites of CO on Pt (111), surface vibr. modes, electron energy loss meas. 77−43422
adsorption state of acetylene on Pt (111), surface vibrs. meas. 77−76657
aluminization 78−31583
angle resolved XPS, temp. independence 79−19975
annealed, ultralow temp. transport anomalies 77−69297
anode, impedance behaviour study in β-ZnS suspension-electrolysis leaching in 1N H_2SO_4 soln. *(Japanese)* 79−24754
anode, oxide film growth in H_2SO_4 solns., temp. study 80−71802
atom, α-particle impact K-shell ionisation, 40 to 110 MeV 78−17752
atom, L-shell Auger and Coster-Kronig intensities from relativistic theory 79−93962
atom, L-shell internal excitation accompanying L-capture 80−95726
atom, L-subshell ionisation with high vel. positive ions 79−50122
atom ground state configurations, isotope shifts and fine struct. anal., visible and UV spectra 80−42987
atomic Compton cross sections 79−18152
Auger spectra, $N_{4,5}N_{6,7}N_{6,7}$ and $N_{4,5}N_{6,7}O_{4,5}$ 80−89094
automotive exhaust gas catalysts, radiometric determ. of Pt and Pd attrition 78−31740
band model, mag. susceptibility of exchange-enhanced paramagnet 78−2644
band-structure determ., angle-resolved photoemission 80−66398
black, form. from neutron α-irrad. PtO, adsorpt. props. 77−11796
black, sunlight absorber, struct. and thermal efficiency 77−125
black surface, solar radiation absorpt., comparison with Planckian black body *(German)* 77−35026
boiling water reactor, corrosion and oxidation potentials monitoring 79−20252
on C, crystallite behaviour on sintering 78−7235
with C adsorbed layer, effects on NaCl mol. beam condensation 77−66593
catalysis reaction studies on single cryst. surface in XHV system limitations 77−9126
catalyst, dispersed onto silica support, EXAFS meas. 78−48258
catalyst, interaction of CO, NO and H_2, NH_4OCN formation 78−73082
catalyst, MgO supported, H_2 adsorption, 300-873K *(French)* 78−38967
catalyst, on C electrode, surface area loss in H_3PO_4 80−101091
catalyst, oxidation kinetics of CO, determ. using ^{13}C tracer 79−29400
catalyst, stepped surface, H_2-D_2 exchange 77−1945
catalyst, surface reactions analysis by spectroscopy of surface vibrs. 78−15701
catalyst, Z-contrast, in STEM 79−46530
catalyst surface morphology, faceting induced by NH_3 and propane oxidation 77−52669
catalysts, supported, adsorbed CO, temp. programmed desorption 79−46915
catalysts, supported, characterisation, hydrogenation and H_2-D_1 equilib. 78−76910
catalytic activity of Pt implanted cryst. supports, toluene hydrogenation appl. 79−20462
catalytic gasification of graphite, small bimetallic particle identification by controlled atm. electron microscopy 79−83502
catalytic H_2 oxidation, OH radical form., laser diagnostics 80−5572
catalytic oxidation of CO, CO_2 product vel. and ang. distribs. 78−20065
catalytic oxidation of H_2 and D_2, matrix isolation and laser fluoresc. obs. of prods. 80−66865
cathode, porous, for implantable hybrid cells, recent improvements 77−40933
cathodic polarisation in alakaline earth metal salt solns., surface changes 79−61869
chemisorbed CO, orientation of CO from angle resolved photoemission 77−8721
chemisorbed CO layer, mag. phase transition obs. *(Russian)* 77−77083
chemisorbed CO on Pt {111} surface, IR spectra, evidence for strong absorbate coupling interactions 78−14604
chemisorbed water on (111) surface, EELS spectra, vibr. freqs. 80−80920
chemisorption, acetylene or ethylene on (111) surface, ethylidyne form. 79−57291
chemisorption, of benzene, on (111) surface LEED and Auger spectroscopy obs. 78−30823
chemisorption, of H, on electrode, entropy, temp. and press. effects 78−84059
chemisorption, of H(O), on electrode, volume of adsorbed species, temp. and press. effects 78−84060
chemisorption, of NO, effect of particle size of Pt supported on inorganic oxide carriers *(French)* 78−11552
chemisorption, of substituted hydrocarbon monolayers, on (100) surface, AES quantitative anal., calibration 78−31724
chemisorption, pot. energy function of two H atoms around Pt atom protruding from metallic Pt surface 80−10781
chemisorption bonding of H on surface (111), UPS obs. 77−76671
chemisorption of acetylene, characteristic loss spectrum and AES 77−55458
chemisorption of acetylene, on (111) surface, self-consistent EHT studies 79−61896
chemisorption of acetylene, reaction at room temp., form. of vinyl-like species 79−46939
chemisorption of acetylene and benzene, LEED, AES, HPS and temp. programmed dehydrogenation exam. 77−55456
chemisorption of acetylene on Pt (111) surface, EHT calcs. 77−62733
chemisorption of Cl_2 on (111) face, LEED, AES, thermal desorption, and work function meas. 80−75444
chemisorption of CO, C-O bond lengths, electronic struct. 78−6210
chemisorption of CO, comparison with XPS and UPS results for Ir (111) 78−38942
chemisorption of CO, photoemission meas. 77−63531
chemisorption of CO and O_2, SCF-Xα cluster calcs. 80−65365
chemisorption of CO on (111) surface 77−72781
chemisorption of CO on unreconstructed (100) surface 78−38962
chemisorption of cyclohexane, C-H stretch vibration, broadened and softened, dehydrogenation 78−47666
chemisorption of ethylene, IR refl. obs. 77−31903
chemisorption of ethylene, reaction at room temp., form. of vinyl-like species 79−46939
chemisorption of H_2 on Pt(111) plane and stepped surfaces, bond breaking, model pot. 80−108744
chemisorption of H, bond nature 80−34297
chemisorption of H, embedded cluster model 80−39427

platinum continued
chemisorption of H, model, comparison with UPS data 79−46932
chemisorption of H, O and CO on (001) surface, localised orbital approach 77−69166
chemisorption of H and O, (001) surface, localised orbital approach 78−14587
chemisorption of mol. O_2 on (111) surface, XPS, UPS, EELS, and work function meas. 80−76139
chemisorption of N_2, on Pt {111}, refl.-absorpt. IR spectroscopy 77−47676
chemisorption of NO on (100) surface, vibr. spectra, electron energy loss, LEED and Auger investig. 79−90866
chemisorption of O_2, adsorbate reaction with CO, transient kinetics obs. 78−7229
chemisorption of O_2, catalytic activity, SCF-Xα-SW calcs. 78−15711
chemisorption of O_2, thermomag. effect, temp. depend. *(Russian)* 78−60034
chemisorption of O_2 and H_2 on (100) surface, (1×1) and (5×20) configs. 77−51599
chemisorption of O_2 and H_2 on (100) surface, and their interaction, UPS 77−51600
chemisorption study, ethylene and halogen-substituted alkenes on Pt (100), Pt (111) substrates, photoelec. spectra 77−43429
cluster, catalytic, XPS obs. of electronic struct. 77−77345
cluster, conduction electron density oscills., NMR spin-echo meas., indirect exchange interaction 80−44954
clusters, at. struct. 79−19186
clusters, electronic struct. and mag. props., MO calc. 77−20219
clusters, supported on Y-zeolites, X-ray absorpt. spectrosc. obs. 79−24390
coadsorption of CO and H_2 77−59220
coating, electron beam deposition and ion plating 77−44166
coating on razor blades, surface roughness effects on the energy dispersion of backscattered protons 79−24403
coating on Ti, true surface area determ. by cathodic charging in H_2SO_4 79−61877
coatings on glass, quartz, ceramic or sitall, method 77−44376
collection mirrors for synchrotron radiation, Pt coated 78−62275
Compton cross-sections due to K-shell electrons, ang. variation 78−21883
concentration in deep sea Mn nodules from Pacific Ocean *(German)* 79−44169
contact to GaAs, effect on minority carrier diffusion length 78−72260
core level excitation effects, synchrotron radiation UPS study 80−40234
core-electron excitation edges 80−66345
crossed fibres, mol. attraction forces meas., depend. on air gap width 77−27216
crowdion conversion to dumbbell, two-interstitial model, thermal neutron irrad. 80−33992
crucible, glass melting power supply frequency convertors 79−72728
crucibles, surface changes rel. to Fe anal. 80−61192
crystallite morphology, surface struct., electron microscopy obs. 80−29257
damage production by high energy d-Be neutrons, elec. reist. meas. 77−62564
DC reactive sputtering, glow discharge mass spectrometry and X-ray diffr. 79−38701
Debye-Waller factor temperature parameters, vibr. depend. 79−99288
desorption, associative from mixed adlayers of O and N 80−54512
desorption of Ar, gas surface interactions, 3-D generalised Langevin model appl. 80−107637
desorption of cyanogen adsorbed on (100) surface 77−31884
desorption of Xe, gas surface interactions, 3-D generalised Langevin model appl. 80−107637
determination, by at. fluoresc. anal. with pulsed dye laser excitation *(Russian)* 78−35774
determination, in Italian chondritic meteorites, by destructive neutron activation anal. 78−12172
determination by computerised thermal neutron activation anal., interference correction 77−44544
deuteron irradiated, energy release and resist. recovery, self-interstitial-atom interaction energies 79−95002
dielectric screening and phonon frequencies using isotropic noninteracting s-d-band model 79−19343
diffusion and saturation solubility in Pb, melting curve, conc. profiles 80−88365
diffusion in Ag, 700-1000°C *(Russian)* 78−91484
diffusion of ^{199}Au at low temp., 78−30789
diffusion of ^{54}Mn radioactive tracer *(French)* 79−51306
diffusion of H, diffusivity and diffusion-elastic phenomenon 79−51310
diffusivity permeability and solubility of H_2 79−95170
discontinuous film, elec. cond. and current noise 78−72286
dispersed metal catalyst clusters, EXAFS obs. 79−91530
dissociative chemisorption of acetylene on (111) surface, EHT calcs. 79−39190
dissolution from automotive exhaust gas catalysts 79−100433
double beam photoemission study of electronic struct. 79−83098
electrical conduction, impurities on grain boundaries 79−87076
electrical resistance and H solubility at high press. *(Russian)* 79−91018
electrocatalysts for methanol oxidisation in acid electrolyte with improved steady state activity for fuel cell appls. 80−76629
electrochemical adsorption of H_2, adsorpt. states, tensiodynamic meas. 77−20196
electrochemical behaviour in nucl. reactor radiation field 77−52650
electrode adsorption of H, dynamic impedance meas. 79−74393
electrode, compact layer struct., absorpt., EHT calcs. 77−16828
electrode, elec. props., impedance meas. and time-domain anal. 78−40360
electrode, electrochemical behaviour in oxygenated $NaHCO_3$ soln. at elevated temps. 78−85026
electrode, evaporation rate from cathode spot in vac. arcs. 80−49024
electrode, in liq. NH_3, photoelectron emission 79−60868
electrode, in Na_2SO_4-NaCl melt, polarisation meas., reactions 78−68898
electrode, multilayer oxides, electrochem. reduction mechanism, kinetics 78−61019
electrode, rotating, appl. to fast reaction kinetics obs. 77−16821
electrode, spectrophotometry during electrolysis 79−74395
electrode, underpotential deposition of Ag or Cu, XPS 77−59672
electrode, unroughened, I_2, I_3^- adsorbed from H_2SO_4-KI, Raman spectra 78−31689
platinum continued
electrode (100), (111), polycryst. surfaces, comparison of electrochem. activity 78−61015
electrode O_2 reduction kinetics in conc. H_3PO_4, H_2SO_4 and $HClO_4$ 78−23952
electrode reactions with molten glass 80−85186
electrode stimulation of nervous system, electrochem. safety aspects 77−21659
electrode surface, oxide layers, anisotropy of optical props. 80−60534
electrode with adsorbed Cu, optical props., electronic struct. 77−69855
electrodeposited coating on Fe membrane, effect on H permeation, proposed catalytic mechanism 78−53252
electrodeposition, from chloride-sulphate soln., galvanostatic transients *(Russian)* 78−31655
electrodeposition, from molten chloride and cyanide 79−24640
electrodes, chemisorbed H, anion effects on multiple states, reflection spectra obs. 79−43634
electrodes, double layer capacity measurements 77−53933
electrodes, nonlinear AC and DC polarisation obs. 80−56247
electrodes, platinised, adsorpt. of Au in aq. HCl 78−56914
electrodes, polymer film coated, prep., characterisation, electrochem. stability 78−76866
electrodes, polymeric surface film form. by electrooxidation of phenolic cpds., ellipsometric study 80−104450
electrodes for elec. stimulation, exposed electrode area determ. 77−86704
electrodes for elec. stimulation, max. surface redox limits estimation 77−86705
electron and deuteron irrad., close Frenkel pair recomb. during annealing 78−87716
electron irradiated, interstitials activation vol. 79−51154
electron irradiated, selfinterstitial atomic defect interaction radii, recovery expts. and error sources 80−65049
electron loss spectra, scattering from (111) surface *(German)* 78−52605
electron wave interference in adsorbed CO film 79−33332
electronically driven phonon anomalies and phase transforms. 78−63834
electroplated film, Schottky barrier metallisation, Au diffusion, AES obs. 79−14968
EM isotope separation and in-beam electron spectroscopy, Pt target preparation 80−52812
emissivity, integral, meas., modulation technique 80−62672
emittance, calc. from spectral radiative and reflecting props. 77−35730
energy band structure, X-ray emission spectra, APW calc. 80−92811
epitaxial growth on (001)W and (001)Mo 79−99450
EXAFS amplitudes, many-body effects 80−97379
EXAFS Debye-Waller factors 80−45168
Fermi surface, de Haas van Alphen obs. 78−91601
Fermi surface 78−47693
fibres crossed in air, mol. attraction meas. as function of dist. 78−13566
field evaporation patterns, multilayer 77−59675
field ion emitter, calibration using energy distrib. of free space field ionisation 77−69971
field-emission microscopy from glass-coated-tips, Fowler-Nordheim emission regime and periodic current oscills. 79−95907
film, catalytic activity on effect of Ag interdiffusion in Ag_2S film reduction 78−14519
film, discontinuous, adsorption of alkali halide mols., effect on elec. cond. 80−2487
film, double layer with Ni on Si substrate, silicide formation 78−84010
film, evaporated, optical props. meas. in VUV, 220 to 150 Å 80−45159
film, growth on amorphous Si:H, AES and LEED study 80−88447
film, laser induced reactions with Si 79−70365
film, laser-induced reaction with Si, surface struct. obs. 79−19471
film, microporosity induced by nucleation and growth processes, TEM expts. 78−10303
film, on pyrex, surface roughness meas. by ellipsometry and TEM 77−20205
film, on sapphire epitaxial relations 79−60649
film, on Si, ion-induced intermixing 80−15420
film, on Si substrate, Pt-Si layer form. by laser irrad. 79−99438
film, polycrystalline, trapping of ^{3}He and ^{4}He ions at room temp. 80−84221
film, quantum size effect, and its temp., tunnelling obs. 79−91160
film, RF diode sputtered, thickness distrib., XPS determ. 77−39743
film, RF impedance temp. and freq. depend. 77−4453
film, RF sputtered, thickness distribution function 78−11083
film, spike effects of heavy ion sputtering 80−35034
film, triode sputtering, for beam lead metallisation, reduction of contamination 78−72721
film, ultrathin, elec. cond., amorphous Ge overlayer thickness depend. 78−72284
film, vacuum deposited, ethylene adsorption and reactivity with adsorbed H, surface pot. meas. 79−86995
film, work function changes upon water contamination 80−44705
film and foil, surface IR wave propag. distance 77−28641
film characterisation technique, APFIM, time-of-flight spectroscopy 80−75138
film coatings for Mo tips, film characterisation by atom probe FIM atomic clusters, voids 80−33863
film electrode, Ag electrodeposition, interface struct. 77−16512
film on Si, PtSi form. kinetics, AES, SIMS, EPMA 77−11800
film on Si substrate, ion-beam induced silicide form. 79−46718
film on W (110), field ion microscope exam. 78−34731
film presence effect on PtSi dissoc. 79−47892
film resistance temperature detection 78−49830
film resistance thermometer, fabrication, appls. 77−37890
films, high-purity, sputtered onto Si, PtSi and Pt_2Si form. 77−76676
films, optical props. and radiation stability 80−34999
foil, crystal struct. as function of substrate temp. during deposition 80−18742
foil, quenched, 1.2 MeV electron irrad., subthreshold irrad. effects 78−51585
force field 79−33051
freezing point determ. 77−26288
Frenkel defect migration and reactions, by subthreshold recoil events, exam. 78−47364
frequency spectra, and correlated spectral density between bulk atoms 79−19330
gasification by atomic F, high temp. kinetics 78−53019
generalised susceptibilities and phonon anomalies, band struct. calcs. 79−90953

platinum continued
heat capacity, 80 to 1000K, laser flash calorimetry 79−95179
high field de Haas van Alphen spectroscopy 79−73425
implantation on Cr-Ni Nb stabilized austenitic stainless steel surface, effect on oxidation behaviour 80−71791
interatomic pair potential, phonon spectra 80−33927
interatomic potentials from experimental phonon spectra 78−75621
International Practical Temp. Scale, instrument interpolation, from 630.74 to 1064.43°C 79−40564
interstitial thermal conversion study by elec. cond. meas. 80−15096
ion irradiation damage, temp. depend., electron microscopy obs. of defect kinetics 80−107339
ion plating on $\alpha+\beta$ Ti alloy Ti-6242, creep property improvement 80−16408
island film photoconductivity obs. 78−95392
isochronal recovery of high energy d-Be neutron damage 78−51592
Knight shift and spin-lattice relax., up to 1358K 78−72425
L_{III}-edge X-ray absorpt. reson., chem. environment effects 79−72256
L X-ray spectra and X-ray electron spectra, influence of chem. bonds 77−28656
lattice dynamics, ang. forces and normal vibrs. 78−22810
lattice dynamics, dispersion, spectrum, sp. ht., modified ang. force model 77−69054
lattice dynamics, phonon dispersion curves, θ-T curves 78−26642
lattice parameters, densities and atomic vols., tabulation for Pt metals 79−65033
liquid, multiple scatt. calcs. of resist. 78−76039
liquid, Percus-Yevick equation, perturbation theory calcs. 78−75515
liquid-forming agent in vapour-liq.-solid growth of Si 78−42935
liquid-forming agent in vapour-liq.-solid growth of Si 78−42936
low index surface, struct. sensitivity of O_2 reduction in acid electrolyte 79−70343
luminescence characteristics of pure surfaces acted on by flux of field emission electrons 80−100695
magnetic field induced conduction electron polarisation, magnetisation density, and neutron mag. form factor 78−18945
magnetic ground state props., simple one-electron theory 77−63063
many-body effects, role of density of states 77−15777
membranes, H_2 diffusion at high press. and temps. 78−55984
metallography 78−3289
microcell for polypeptide hormone microelectrolytic radioiodination 79−48340
microelectrode potentials and small-signal impedances 79−34716
microelectrodes for O_2 sensing, operation 79−84043
microvoid form., gaseous impurity atom effects, positron annihilation study 80−49275
MNMOS structure, with Pt interposed at Si_3N_4-SiO_2 interface, charge storage props. 77−51821
MOS structure Pt diffused, hysteresis and memory props. 80−96992
Mossbauer effect on ^{119}Sn and ^{197}Au meas. 78−15080
Mossbauer spectra, 2nd-order Doppler shift, 1-100K 79−91317
neutron damage, positron annihilation 80−65056
neutron irradiated, recovery spectrum, resist. obs., Au addition effect and defect conc. depend. 80−65057
neutron irradiation, low temp. recovery, effect of plastic deform. 78−51588
nuclear target preparation using EM isotope separators 78−70676
nucleate and film boiling in travelling wave regime 80−19231
optical constants 12 to 24 μm, anomalous skin effect region 77−20842
oxidation, Auger spectra 78−14600
oxidation, O Auger peak studies 77−1769
oxidation, XPS spectra study 80−3254
oxidative vaporisation, thermochemical analysis 78−11447
pair potentials calc., appl. to point defect props. 80−19798
paramagnetic, induced magnetic form factor, 73 kOe at 78K 79−33454
particles, nucleation centres in polyethylene terephthalate crystn. 79−15658
particles in dual SiO_2 interface, effect on charge storage props. 77−35992
particles supported on SiO_2 gel, reaction between adsorbed H_2 and O_2, low press. 77−52668
phonon density of states determ. from thermodynamic functions 80−96616
phonon density of states from thermodynamic functions *(Russian)* 79−35631
phonon dispersion, simplified Frielek model 78−79683
phonon dispersion calcs. on basis of Fielek model 79−19335
phonon dispersion curves calc. 77−20030
phonon dispersion relations, 5-parameter model calc. 78−75748
phonon dispersion spectra from 5-parameter lattice dynamical model 78−10136
phonon spectrum, Kohn anomaly 79−46766
photodecomposition over Pt/TiO_2 catalysts 80−81337
photodesorption, of acetone, photoion emission, quantum yield limit 78−79896
photoemission from CO absorbed on (111) surface, 40-150 eV 77−16465
photon absorption and photoelectric cross-sections calcs. 79−31486
plasma, laser produced, Ni-like X-ray spectrum 80−43983
point defect properties, damage curve anal. 78−47359
polycrystalline, He ion refl. *(Russian)* 80−35051
polycrystalline foils, methanation reaction, kinetic information 78−73081
polycrystalline wire, multilayer surface oxidation 78−88579
powder, NMR expts. on confined liq. ^{3}He 79−51371
powdered electrode, aggregation in disperse system 79−11830
quenched, deviations from Matthiessen's rule 77−69289
quenching, vacancy loss, random sink models 78−60698
radiation damage, recovery of elec. resist., interstitial migration and clustering 77−11604
radiation damage, self-interstitials migration modes and thermal conversion 79−65126
radiation damage recovery curves, evidence for two self-interstitial configs. 77−7773
radiation damage with radioactive probes, TDPAC meas. 77−24336
radiolytic product detection by Pt electrode rest potential 80−11973
reactive sputtering in Ar-O_2 mixtures, glow discharge mass spectrometric meas. 79−91552
reactor radiation-induced hardening, computer modelling *(Russian)* 79−37738
reconstructed surfaces, reorganisation of (100) 78−95214
recovery of thermal-neutron-irradiated samples 78−95081

platinum continued
resistance standard low-temp. thermometer checking methods 78−37006
resistance temperature probes, constructional types and state of technique *(German)* 80−52213
resistance thermometer, heat shock influence on elec. cond. and thermophysical props. *(Russian)* 80−52210
resistance thermometer, in-situ response-time testing for nuclear power station safety systems 79−93743
resistance thermometer, oxidation problems 80−52206
resistance thermometer, two-point calibration for 13.81 to 273.15K 79−206
resistance thermometer for high pressure vessels 79−21744
resistance thermometer response time testing in situ 79−13484
resistance thermometers, effect of Pt oxidation 80−101794
resistance thermometers, heat leaks effect anal. 80−57296
resistance thermometers, response time estimation by noise anal. technique 79−93742
resistance thermometers, temp. range influence on error due to non-linearity *(Russian)* 80−90841
resistance thermometers and I_{68} calibrations, intercomparison 79−40565
resistance thermometers for high temperatures *(Russian)* 78−57958
resistance thermometry, medium precision, A/D convertor appl. 80−86297
ribbon, melting temp. determ. from continual melting and freezing 77−51476
s-electron densities at nucleus, meas. using internal conversion of 31 keV M1 transition in $^{195}Pt^{m}$ 78−27140
secondary electron spectroscopy 77−85854
self-diffusion of ^{197}Pt at low temp. 78−30789
self-powered flux detectors, response characts. in CANDU reactors 78−82594
self-powered neutron flux detector response in mockup Bruce reactor core 78−58391
SEM exam., ultra-high vacuum, secondary electron emission dependence on electron beam dose, surface interactions from AES and ELS 80−61209
shadowing of freeze-fractured or freeze-etched specimens using electron beam gun 78−20329
silicide formation due to laser and electron beam annealing 80−84849
single crystal spheres, electrolytic deposition of Zn 80−104080
small particles, contraction and relax. of interatomic distances using EXAFS 79−47546
small particles, on graphite substrate, crystallographic struct., electron microscopy study 79−99465
small particles deposited on NaCl and mica substrates, struct. and orientation *(French)* 77−43458
solubility of H_2, temp. depend. 79−77756
solubility of H_2 at press. up to 67 kbar *(Russian)* 79−51260
specific heat, electron-phonon effects and anharmonic contrib. 79−90795
specific heat at const. vol., high temp., dilation correction 79−14940
specific heat meas., 0.4 to 30K, Debye temp. 78−55955
spectral emissivity in 1-10 μm range at 100 to 400 °C 77−11713
spectrophotometric methods of determination, review 78−61115
spherical inclusions in polymethyl methacrylate, thermochem. instability caused by CW laser beam 80−29689
spin fluctuation model interpretation of mag. susceptibility 80−80477
spin-density functional theory of temp. depend. spin susceptibility 79−56497
spin-orbit projected d density-of-states 78−38999
spin-polarised LEED from low-index surfaces 78−14556
sputtering yields for ions over 15-135 keV 79−56899
STEM, bright field single atom images with half plane detectors 78−66010
STEM, Pt on Γ-Al_2O_3, atomic number contrast, supported catalyst particles 80−79651
stepped surface, 6(111)×(1$\bar{1}$1), relax. and force const. 79−86973
stepped surface, adsorbed H, adsorption sites study by EELS 80−49521
stepped surface, adsorpt. and decomp. of NO and NH_3, LEED, AES, and thermal desorption expts. 78−38943
stepped surface, edge atom dipole moments 78−14791
stepped surface, high freq. vibr. modes, cluster recursion method calcs. 80−6615
stepped surface, localised surface phonons obs. 78−95223
subshell photoelectron branching ratio meas., synchrotron radiation 80−66397
superconducting transition temperature, ab initio calc. 80−25036
superconductivity, search for, at very low temps. 78−91799
supported metal catalysts, particle growth, obs. of Pt on alumina 77−8831
surface, (100), adsorption of acetylene and benzene 77−59216
surface, (100), LEED intensity spectra, double diffr. model 77−31858
surface, (100), phase transition and relax. by MeV ion backscatt. and channelling 79−86970
surface, (100), reconstruction, superstruct., model 80−103551
surface, (111), 400 eV H^+ ion scatt. obs. of surface relax. 78−43972
surface, (111), adsorbed Br, $M_{2,3}M_{4,5}V$ and $M_{4,5}VV$ Auger spectra 79−69926
surface, (111), adsorbed ethylene and benzene, electronic energy losses 79−46931
surface, (111), desorption, of H, preexponential factors 79−46918
surface, (111), identification of adsorbed OH species 80−49509
surface, (111), O_2, CO and C_2H_2 adsorption and cooxidation, AES *(German)* 78−14619
surface, (111), O_2 interactions, UPS, EELS and thermal desorption study 80−100409
surface, (111), overlayer covered systems, angle-resolved UPS, substrate effects 78−84694
surface, (111), surface diffusion of C, AES 78−71954
surface, (111), surface struct. and bonding of (2×2) acetylene overlayers, LEED analysis 77−85067
surface, (111), Xe direct inelastic scatt. with trapping-desorption scatt., vel. and ang. distribs. 80−16140
surface, (111) chemisorbed acetylene, complex form., UPS spectra 77−12826
surface, (111) stepped, adsorption of O_2, CO, C_2N_2 and ethylene 78−71992
surface, (III), electronic struct. of adsorbed Na 78−19117
surface, adsorbed C^+ layer removal, by 20-30 keV Ar^+ bombardment, in plasma 77−76103
surface, adsorbed CO, intermediate UPS/XPS synchrotron radiation study 78−52633

platinum continued
surface, adsorbed O_2, isotopic exchange and thermal desorption *(French)* 78−43249
surface, adsorption of H_2, rel. to electrocatalysis 78−38935
surface, anodically polarised, ^{147}Pm deposition 78−27424
surface, AR thermal accommodation coeffs., 300 to 1350K 80−30272
surface, atomic interplanar spacing determ. from simulation of channelling expts. 77−80563
surface, chemisorbed CO, IR refl.-absorpt. spectra, absorbate island struct. 80−84385
surface, chemisorbed O, reaction with CO, AES expts. 77−90639
surface, chemisorption of ethylene, vibr. anal. of C_2H_3 species 80−61150
surface, clean (001), electronic props. 77−72901
surface, clean and Cs covered, LEED intensity spectra, τ-matrix interpretation method 77−15673
surface, $CO(O_2)$ interactions, surface electronic struct. (surface chem.) using synchrotron radiation 78−53254
surface, CO chemisorpt., mol. cluster calc. 80−100407
surface, CO or C_2N_2 adsorpt. induced backscatt. enhancement 77−90227
surface, CO oscillatory oxidation, theory 80−85215
surface, CO oscillatory oxidation, theory 80−85216
surface, coverage and desorption of CO flash desorption spectrum 80−49493
surface, dissoc. sorption of CO, XPS obs. 77−16863
surface, electrochem. oxidation and reduction, XPS obs. 78−95653
surface, H_2-D_2 exchange, mol. beam scatt. data 77−24469
surface, kinetics of CO oxidation 79−61903
surface, kinetics of NH_3 decomposition 77−1948
surface, Lyman-α emission from proton bombard. 79−91503
surface, mean residence time and ionisation efficiency meas. of K 77−85874
surface, oscill. oxidation of CO 77−4926
surface, oscillator oxidation of CO 79−61905
surface, polycrystalline, reaction kinetics between NO and CO *(German)* 79−15989
surface, polycrystalline, reaction kinetics between NO and CO at low press. *(German)* 79−15988
surface, scattering of Ar and N_2 mol. beams 77−16449
surface, secondary electron current, $Hg(6^3P_2)$ impact, in $Hg(6^3P_1)$ stepwise electron excitation function meas. 79−858
surface, stability and struct. of high Miller index forces in vacuum and with adsorbed C and O 77−76651
surface, stepped or flat, H_2 chemisorption, calcs. 79−28208
surface, superstructure from LEED meas. 79−73259
surface, UV photoemission, from (111) and [6(111)×(100)] surfaces 79−91566
surface 6(111)×(100), clean and O_2-covered, UPS studies 80−76151
surface {111}, chemisorpt. of CO, refl.-absorpt. IR spectroscopy 77−1306
surface (110), reconstructed, LEED-AES study, O_2 treatment effect 80−39398
surface (110), two-dimens. diffusion of Pt adatom 79−28183
surface (111), adsorption and desorption of H_2, obs. by dynamic meas. of work function 79−77915
surface (111), adsorption of CO using XPS, UPS, TDS and dynamic meas. of work function 79−65322
surface (111), chemisorption of acetylene (ethylene), ethylidyne group form., LEED and ELS obs. 78−73075
surface (111), clean and oxidised, binding states and sticking coeffs. of CO and H_2 77−72787
surface (111), coadsorption of CO and hydrocarbons, C≡O bond weakening 79−90863
surface (111), H adsorption, inert model 80−50889
surface (111), LEED, quantitative anal. 80−44085
surface (111), relax. effects, and thermal vibrs., medium energy ion scatt. 79−28182
surface (111) and (100), surface struct. anal. by MeV ion backscatt. and channelling 78−71916
surface (997), partial facetting, He beam scatt. and LEED study 80−103547
surface (997), terrace bending obs. from He beam scatt. 80−40202
surface adsorpt. of water, D_2O+H, $D_2{}^{16}O$+^{18}O exchange reacts. 77−80695
surface and subsurface adsorbed O, low energy ion scatt. obs. 80−65372
surface area loss, on graphite support, in H_3PO_4 78−73076
surface diffusion energies for Pt, Ir, Au adatoms 79−77923
surface diffusion of single atoms of Pt, Ir and Au, FIM expts. and Morse potential calcs. 78−34717
surface dipole moment calc. 80−60060
surface electron density crimping, Ashcroft potential, density functional calcs. *(Russian)* 79−82653
surface electronic props. 78−95332
surface H-H interactions on Pt(111), heats of adsorption and desorption 78−18899
surface interaction with O_2 rel. to thermomag. effect in gas *(Russian)* 77−11302
surface props. rel. to adsorbed O_2, H_2O vapour, work function determ. 78−60187
surface reaction with acetylene, ethylene and H_2, EELS 78−71947
surface reconstruction, physical realisation of two-dimensional Ising and X-Y model 80−15351
surface reflection of He ions 79−87551
surface relaxation, (111), dynamical LEED calc. 77−59196
surface relaxation, temp. depend., He scatt. 79−19447
surface stress curves, electrocapillarity type curves 79−61866
surface struct. and electronic props., CO_2, O_2 and H_2 chemisorption, LEED, AES 77−1300
surfaces, adsorption and chemisorption of H, field emission study 77−24477
surfaces, clean and S covered, desorption of CO, binding energy meas. 79−46950
surfaces, oxidation by electrosorpt., of H_2, effect of soluble prods. *(German)* 80−55717
surfaces (100) (5×20) and (1×1), stability and reactivity, adsorption of H 80−75434
surfaces (111) and 6(111)×(111), CO adsorption, EELS and thermal desorption spectroscopy 78−91547
surfaces with variable kink concs., catalysed hydrocarbon reactions, surface O_2 effects 80−35576
target, O^+ low energy ions, interaction obs. 79−34352

platinum continued
TEM exam. of ion damage in FCC metals 78−87727
thermal and fission neutron produced defect configuration 78−47432
thermal expansion, 100-1000°C, as standard samples for dilatometry 78−26699
thermal expansion coeff. meas. using strain gauges and thermocouple 78−53059
thermoelectric power, 290-560K 79−42522
thermomodulation spectra of high-energy interband transitions 80−108226
thermostimulated exoelectron emission, excitation mechanism *(Russian)* 80−71581
thin surface overlayer, H uptake rate enhancement of bulk Nb(Ta) 79−82345
thread, pull-off force with respect to Au thread, in air, influence of elec. charge 79−11196
vacancy and divacancy diffusion 79−82377
valence bands, angle-resolved photoemission determ. 80−108323
vapour deposited coating, on Ir and W, defects and their effect on props. 80−39474
vapour-phase epitaxial growth *(Russian)* 77−59227
VPE, on Au, crit. thickness of pseudomorphic film growth, substrate size depend. *(Russian)* 80−29286
wear coefficients determ. using pin-on-cisc apparatus 80−76366
wetting and reactions of B_2O_3 containing glasses, effect of C and water 77−7951
wetting by molten silicate, applied polarization potential effect *(Japanese)* 79−51394
wire, cold worked, recovery of elec. resist. 77−12643
wire, O_2 covered, accommodation coeff. meas. of Ne(Kr), 400-1400K 77−63948
wire, single vacancy form., activation energy meas. 80−49212
wire, thermal cond., 900-1800K, elec. cond., 800-1800K 78−26845
wire temperature sensor, temp. fluctuation meas. in turbulent airflow 78−21135
work function, absolute value determ. 77−28697
X-ray absorption spectra, white line at L_3 edge 77−36313
X-ray cross sections, L-shell, proton induced, 1 to 3 MeV range 79−1799
XPS, 4f core threshold effects 79−83096
XPS, electronic struct. 80−7464
Young's modulus and shear modulus, temp. depend. 78−27553
AgCl:Pt^{2+}(Pt^{4+}), single crystal EPR, substitution effects on photochemistry 79−15348
AgCl(Br):Pt, photochemistry and role of Pt impurity ions 79−24783
Al-Pt catalyst, deep oxidation of benzene, kinetic model depend. of reaction rate 77−90583
Al-Pt film sandwich, interdiffusion and intermetallic form. 77−24448
Al_2O_3-Pt metal-ceramic reaction, micro/macro obs. 80−66467
As_2Se_3:Pt, impurity effects on elec. props. 80−103699
Au surface, atomic interplanar spacing determ. from simulation of channelling expts. 77−80563
Au/Pt interface, diffr. studies of conc. variations 79−42322
Au/Pt/Cr films, diffusion of Si, depth anal., optical and Rutherford backscatt. meas. 79−10981
Au-Pt composite coating for steel inner vac. liner of fusion reactor 77−30669
Au-Pt epitaxial film system, mismatch dislocations obs., electron microscopy 77−4268
(Au-Ge)-Pt film, for contacts to n-GaAs, metallurgical investigation using inert substrate 77−85313
C coating on Pt temp. depend. of $H_2{}^+$ sputtering 78−95634
C-coated, UF_6 mol. negative surface ionisation 78−56913
C+O^+ ion-molecule reaction, 15 eV energy O^+ production system 80−84817
CO oxidation, surface struct. effects on rate, data assessment 78−43251
CdTe/$SnCl_2$/Pt, solar cell photoelectric props. *(Spanish)* 80−85290
Cr-Pt thin film couple, diffusion, new Cr-Pt phases obs. 79−42319
Cr_2O_3/γ-Fe_2O_3/Pt electrode, two layer oxide surface film anal. by modulation spectroscopy *(Japanese)* 80−11491
D exchange reaction between H_2 and water a hydrophobic catalyst supporting Pt 80−30208
Fe-Pt, Invar alloy, magnetic excitation exam. by neutron diffr. 79−56521
GaAs-Pt interface states energy distrib. and relaxation time 79−33345
GaAs-Pt-air system, far IR propag. distances of surface EM waves 79−42616
Ge-Au-Pt trilayer film, interdiffusion obs., on annealing 78−2308
Ge-Au-Pt trilayered film, annealing, interdiffusion 78−22902
H_2+D_2, exchange on Pt stepped surface mol. beam incidence angle depend. 78−31686
^{166}Ho electrosorption on anodically polarised Pt surface 79−52684
KF/Pt thick layer/substrate system, thermal positive and negative ion emission, surface prop. non-uniformity effect 79−28882
Mg $(Fe,In)_2O_4$:Pb,Pt film, LPE 77−77436
MgO:Pt^{3+}, Jahn-Teller effect in EPR spectrum 80−7160
Mo-Mo_2C-La_2O_3-Pt cathode, Pt effect on work function *(German)* 79−74048
$NaCl_4$ on Pt and Ir surfaces, adsorption kinetics 80−84393
Ni/Pt/Si(111) Schottky diodes, current-voltage characts. and comp. profiles 80−84508
$Pb(Zr,Ti)O_3$, internally electroded with Pt, resonance behaviour 80−84701
Pd-Pt bilayers, on single cryst. Si, vacuum annealing, silicide form. 79−51444
Pr ion plating, on creep behaviour of α-Ti 79−66123
Pt, adsorption and desorption of O_2 on (110) surface, thermal desorpt., LEED/AES obs. 77−72788
Pt alloys, influence of Rh, Au, Mo, W, Zr, Hf alloying elements on creep activation energy at high temp. *(Chinese)* 80−66573
Pt cluster-H, electronic struct. calc., H-metal bonding 77−89823
Pt group, even atom config., parametric calcs. 78−82631
Pt I, radiative lifetimes, beam-sputtering technique meas. 79−18142
Pt, quenched, coprecipitation of vacancies and C atoms 79−78978
Pt thin-film temp. sensor *(Japanese)* 80−105645
Pt:^{181}Hf, interaction of implanted impurity with radiation induced lattice defects, TDPAC meas. 80−24494
Pt:^{181}Ta, lattice defect induced elec. field gradient, PAC meas. 79−42878
Pt:C, C layer formation on (111) surface, temp. depend., LEED, AES study 78−71911

platinum continued
Pt/Al_2O_3, electron accepting sites by pyridine absorpt. 80−71947
Pt/Cr/n-GaAs Schottky contact, barrier height change due to heat treatment 79−47165
Pt/polymer/metal capacitors, electroforming and elec. cond. 80−54800
Pt/Rh thermocouple, Type B, HI BX extension wire, EMF characteristics 78−49832
Pt/TiO_2 catalyst for photoassisted decomposition at room temp. of H_2O and ethylene 80−55703
Pt/Y_2O_3-ZrO_2/Pt cell, Faradaic reaction kinetics, impedance dispersion anal., electrode/electrolyte interface process 79−11798
Pt/ZrO_2 porous electrode/solid electrolyte system, interface polarisation effects 80−61114
Pt/ZrO_2-Y_2O_3 interface, electrode kinetics, complex impedance dispersion anal. 79−96325
Pt-(Re-Mo) bimetal sheet specimens, interdiffusion, 1500°C *(Russian)* 77−62683
Pt-Al_2O_3, composite solar selective absorbers optical props. 79−52037
Pt-Au, thick film, adherence meas. and evaluation 80−50813
Pt-Au bimetallic films, electron diffraction on networks of grain-boundary and interphase dislocations *(Russian)* 79−73168
Pt-Au film couple, diffusion of Au, depend. on annealing ambient, AES exam. 77−1261
Pt-C replicas, for rapid aimed replica prep. 80−61037
Pt-Cr(Si) interface, low-temp. diffusion, ambient effects 80−100355
Pt-Cu_2O-Cu double injection diodes, I-V characts. and photomemory effects 77−47900
Pt-Cu_2O-Cu single carrier space charge limited diodes, I-V characts. 77−47901
Pt-electrolyte interface, electron states, photoemission studies 78−85171
Pt-electrolyte interface laser speckle movements related to electrode pot., H_2 adsorb. 78−40052
Pt-GaAs contacts, sintered, eval. of W, Ti, Mo and Hf barrier metals 77−8193
Pt-graphite catalyst, H adsorption, ESR obs. 79−24818
Pt-Mn(III)-porphyrin electrode for possible wet solar cell 79−100529
Pt-Mo bimetal sheet specimens, interdiffusion, 1500°C *(Russian)* 77−62683
Pt-n-GaAs Schottky diode, microplasma breakdown 79−91140
Pt-Ni bilayers, on single cryst. Si, vacuum annealing, silicide form. 79−51444
Pt-O, preanodised or passivated, DTA 77−16733
Pt-polymer contacts, charge transfer and contact charge spectroscopy 79−56305
Pt-polymer-Au capacitor, electroforming, negative resist., electron emission 80−80406
Pt-Pt mechanical contact, FIM obs. of contact area 78−35527
Pt-Re bimetal sheet specimens, interdiffusion, 1500°C *(Russian)* 77−62683
Pt-Si, silicide layer struct. and elec. props., effect of processing conditions 77−62991
Pt-Si contact, annealed in H_2 ambient, elec. props. 78−64110
Pt-Si film struct., silicide form. He^+ back scatt. and X-ray diffr. obs. 79−51442
Pt-Si film system, silicide first phase form., reaction kinetics 78−79821
Pt-Si Schottky barriers on Si, laser formation and characts. 80−60079
Pt-Si:As, silicide form. during laser irrad., p-n junctions and ohmic contacts 80−84397
Pt-SiO_2 cermet films, struct. and props. 80−96956
Pt-SiO_2 granular sputtered film, size effects in electronic sp. ht. 77−43346
Pt-$SrTiO_3$ (100) interface, struct. and electronic props., AES, LEED, EELS, and UPS study 80−24986
Pt-$SrTiO_3$ (100) interface, Auger and photoemission studies, relax. and chem. shift effects 80−54749
Pt-W interface, contaminated, contact adhesion, deform. and interfacial energy 78−22306
Pt-WO_3, electrochromic cermet, optical and electrical props. 79−33674
Pt+H^+, L-subshell ionisation cross-sections, X-ray meas. 77−46520
Pt+H^+, L-subshell X-ray prod., cross-section meas. 77−46575
Pt+Kr^{n+}, K-L level matching, X-ray obs. 79−63948
Pt_2, ab initio relativistic core pot. studies of metal-metal bonding 80−106257
$Pt_{90}Rh_{10}$/Pt thermocouple, Inconel sheathed, MgO-insulated, decalibrations during 1200°C use, ion microprobe obs. 78−57957
$ScH_{1.9}$:Pt, Gd, effect of Pt on Gd^{2+} ESR lineshape 78−68371
Se:K, glassy, photolum. and optically induced ESR 80−50398
a-Si:H/Pt, Schottky diode, influence of prep. conditions on forward bias currents 79−78171
Si:Pt, deep level, exam. by thermally stimulated current and capacitance techniques 79−1579
Si:Pt, depth depend. of atomic mixing by ion beams 80−29837
Si:Pt, elec. props., deep-level transient spectroscopy and thermal emission meas. 79−82542
Si:Pt, electron and hole capture, DLTS obs. 80−49661
Si:Pt, heavily doped, gradual p^+-n junctions, trap levels *(French)* 80−34392
Si:Pt, hole capture cross-section at E_v+0.34 eV, capacitance meas. *(French)* 80−65493
Si:Pt, implant redistrib. and enhanced solubility following laser irrad. 79−69129
Si:Pt, implanted and laser annealed, segregation and increased dopant solubility 80−65016
Si:Pt, photoionisation cross-sections, photocurrent and photocapacitance meas. 78−10497
Si:Pt, photoionisation cross-sections and energy levels 79−87060
Si-Pt Schottky diode, type II localised interface states, Si surface prep. effects 78−39210
Ti-Pt link on Si_3N_4-SiO_2-Si substrate, laser vaporisation, interference effects 77−69941
W-Pt mechanical contact, FIM obs. of contact area 78−35527
^{90}Y electrosorption on anodically polarised Pt surface 79−52684
^{169,175}Yb electrosorption on anodically polarised Pt surface 79−52684
ZnS:Cu,Pt phosphors, photoluminesc., thermoluminesc. 78−43915
ZrB_2, etching method using H_3PO_4 and H_2SO_4, effect of Pt 78−44339

platinum alloys
see also platinum compounds
alkaline earth borides, $M_{0.67}Pt_3B_2$, cryst. struct. and supercond. props. 79−38231
blistering of ^{252}Cf-exposed surfaces 78−86601

platinum alloys continued
formamide oxidation at Pt alloy catalytic electrodes 79−57245
neutron activation determ. of microcomponents Pt, Pd, Ir, Rh, in noble metal alloys *(Russian)* 77−32858
Ni-Pt-P, metallic glass, electronic structure, pulsed NMR study 80−75869
ordered equiatomic, lattice specific heat meas., Debye temp. 80−54396
Pt-Au, chemisorption of H_2 and CO, effect of surface segregation 77−51601
rare earth alloys, R_2Pt (R=Gd, Tb, Dy, Ho, Er), magnetic susceptibility meas., mag. transition obs. 80−60222
rare earth alloys, RPt_2Si_2, struct. determ. 77−89407
rare earth alloys, RPt_2X_2 (X=Si,Ge), cryst. struct. 80−1964
rare earth intermetallics, RPt, (R=Gd, Tb, Dy, Ho, Er, Tm), structs. and mag. props. 80−50069
rare earth-Pt, cryst. struct. and lattice meas. determ. 77−55266
rare earth-Pt, RPt_5, low temp. mag. susceptibility 80−93075
Ag-Pt, dil., electric field gradient temp. depend., TDPAC meas. 78−39451
Ag-Pt, dil., electric field gradient meas. by TDPAC method 78−39452
Ag-Pt, dil., TDPAC exam. of radiation damage 78−39464
Ag-Pt, dil., virtual bound states, transport props. obs. 80−70667
Ag-Pt, sintering, limited solid solubility, peritectic diagram 77−28754
Ag-Pt film, optical absorption spectra meas. 77−85823
Al-$Al_{21}Pt_5$ eutectic alloys, unidirectionally solidified, struct. study 80−108394
Al-Ni(Pt)(Zn), rapidly solidified, twinned dendrites 80−70572
Al-Pt, rapid quenching, struct. and decomp. 80−76244
Al-Pt (2 at.%), splat cooled, $AlPt_2$ phase, electron diffr. obs. 79−15657
Al-Pt (2 wt.%), rapidly solidified alloy, metastable phase formation and decomposition 79−52194
Al-Pt_2Ni_{1-x}-n-Si system, Schottky-barrier height 80−34520
Al-$Pt_xNi_{1-x}Si$-Si system, diffusion, compound form., and microstructure 80−34253
$AmPt_5$, preparation and cryst. struct. *(French)* 78−42959
Au-Pd-Pt-Ag, composition-property diagrams, mathematical models for diagrams *(Russian)* 79−11554
Au-Pt, cold worked, impurity conc. rel. to internal friction Bordoni peak, solid soln. hardening mech. 80−16363
Au-Pt, dil., virtual bound states, transport props. obs. 80−70667
Au-Pt, elect. resistivity, temp. depend. between 1.6 and 4.2K *(German)* 79−28337
Au-Pt, surface composition determ. 79−69328
Au-Pt (60 at.%), solid soln. neutron small-angle scatt. study of phase decomp. 79−15646
Au-Pt-Pd-Ag-Cu, commercial dental alloy, age-hardening characts. 80−89235
$BaPtSn_3$, cryst. struct. rel. to $ThCr_2Si_2$ type *(German)* 78−51470
C/Pt-W (8 wt.%), desorption of K from C film surfaces 80−59784
Ce-Pt, paramag. suscept. 79−61047
$CeNi_2$-$CePt_2$ system, structural and mag. studies on valence behaviour of Ce 80−103809
$CePt_2$, ESR of Er^{3+} 79−87315
$CePt_3$, ^{195}Pt NMR and susceptibility meas. 77−63299
$CePt_5$, mag. susceptibility, 4.2 to 295K *(German)* 79−47233
Ce_3Pt_2, structure determ., rhombohedral Er_3Ni_2 type 77−80443
Co-Cr-Al-Y coating, Pt-modified, oxidation and hot corrosion resist. 78−11437
Co-Pt, amplitude depend. of internal friction *(Polish)* 79−95627
Co-Pt, atomic ordering props. and domain growth in strong pulsed mag. field *(Russian)* 80−54918
Co-Pt, films, electrolytic deposition conditions over large comp. range *(French)* 80−45242
Co-Pt, mag. annealing, form. of ordered phase, study using X-ray scatt. *(Russian)* 80−81052
Co-Pt, struct. and mag. props. rel. to degree of order 78−72368
Co-Pt ferromagnetic alloy, 6 T ultrasonic study of magnetoelastic coupling 80−93154
Co-Pt film, electrodeposited, saturation mag. induction, mag. anisotropy and coercive field meas. *(French)* 80−2610
Co-Pt films, mag. and magneto-optic props., appl. to holographic and bit-by-bit storage 79−33512
CoPt film, on Al_2O_3, quantitative electron microprobe analysis 77−9150
$CoPt_3$, electrolytic films, saturation mag. induction, coercive fields, thickness depend. *(French)* 80−44883
$CoPt_3$, meas. of ordering instability 79−38818
Cr-Pt, dil., effect of Pt on itinerant antiferromagnetism 78−64191
Cr-Pt alloy, mag. props., effect of atomic environment 78−23247
Cr-Pt alloys, neutron diffraction study, (100) magnetic peak, magnetic structure transitions 79−56506
CrPt film, on sapphire, epitaxial relations 79−60649
$Cr_{0.995}Pt_{0.005}$ alloy, mag. struct., neutron diffr. study 80−60198
Cu-Mn-Pt spin glasses, anisotropic exchange interactions, effect of non-mag. impurities 80−80534
Cu-Pt, dil., screening charge density round $\Delta Z=-1$ impurities, vacancies, NQR study 80−103897
Cu-Pt, disordered, shaft range order diffuse scatt., electron diffr., reinterpretation 77−84596
Cu-Pt, order-disorder transform, influence of strain energy 78−84796
Cu-Pt, quenched, microdomain model anal. of diffuse X-ray scatt. 79−52276
Cu-Pt, surface segregation, comparison of low-energy ion-scatt. results with theory 78−38923
Cu-Pt, temp.-press. phase diagram *(Russian)* 78−3100
Cu-Pt alloy, quenched, SRO, microdiffr. obs. 77−76360
Cu-Pt existence regions of FCC superstructs. *(Russian)* 78−52760
Cu-Pt system, phonon dispersion relations, force constant disorder effect 80−84263
Cu-Pt type alloys, theory of ordering *(Russian)* 77−1100
Cu-Pt-O alloys. dil., O-metal interactions, activity coeff. meas. at 1423K 80−93792
Cu_3Au-Cu_3Pt, quasibinary system, order-disorder transform., superlattice form. 80−2159
CuPb, coexistence of ordered and disordered phases, elec. resist. meas. 77−85992
CuPt alloy, equiatomic, ordering processes, anisothermal annealing exam. *(Japanese)* 78−39765
CuPt equiatomic alloy, effects of quenching temp. on ordering, study by elec. resistivity meas. *(Japanese)* 79−43285
CuPt, quenched, short-range order X-ray diffuse scatt., microdomain model anal. 79−96043

platinum alloys continued
CuPt, quenched, state of local order 79−47722
CuPt, specific heat, Debye temp. below 30K 78−55956
CuPt type alloys, static stress influence on ordering, theory *(Russian)* 77−59775
Cu_3Pt, antiphase domains morphology 80−108460
$(Cu_3Pt)_{1-c}Mn_c$, mag. suscept. and effect of atomic order and disorder 77−24669
Dy_5Pt_4, mag. props., 4.2 to 160K 79−78343
Dy_5Pt_4, isotypic with Pu_5Rh_4, X-ray cryst. struct. refinement anal. 79−4271
Er_5Pt_4, mag. props., 4.2 to 160K 79−78343
Er_5Pt_4, isotypic with Pu_5Rh_4, X-ray cryst. struct. refinement anal. 79−4271
Eu+t_{2g} high press. Mossbauer spectra, interconfig. charge fluctuations 77−63341
$Eu_{0.95}Ba_{0.05}Pt_2$, ^{151}Eu Mossbauer studies at high press. 80−39923
$EuPt_2$, ^{151}Eu Mossbauer studies at high press. 80−39923
$EuPt_2$, elec. field gradient, spin echo NMR meas. 80−20509
$EuPt_2$, indirect exchange, spin echo NMR meas. 80−15822
$EuPt_x$ compounds, partial valence change, ^{151}Eu Mossbauer and magnetisation obs. 80−70167
$EuRh_{2-x}Pt_x$, intermediate-valance state, XPS obs. 77−28687
Fe-Ni-Pt alloy, Invar behaviour 79−56531
Fe-Ni-Pt system, ordered phase fields of equilibrium diagram 78−48373
Fe-Pd-Pt alloy powders, coercive force and specific remanence *(Russian)* 79−47302
Fe-Pt, austenite ordering effect on mode of reverse transform 79−61588
Fe-Pt, crystallography and morphology studies, lenticular thin plate transition, thin plate morphology 79−1862
Fe-Pt, high mag. field phase transition 77−66301
Fe-Pt, Invar, magnetoelastic contribs. to US vel., elastic consts., and susceptibility 80−75829
Fe-Pt, Invar alloy, paramag. susceptibility 80−70940
Fe-Pt, Invar alloy, strong ferromagnetism, magnetostriction and thermal expansion 79−8037
Fe-Pt, Invar alloy, thermodynamic properties, effects of forced magnetostriction 79−11331
Fe-Pt, Invar type, charact. magnetovolume effects 79−82855
Fe-Pt, Invar type, strong ferromagnetism, mag. props. 78−64197
Fe-Pt, itinerant electron ferromagnet, magnetovolume effects 80−60397
Fe-Pt, magnetic struct. changes assoc. with crystallite thickness increase *(Russian)* 77−80913
Fe-Pt, Mossbauer exam. 79−56639
Fe-Pt, nearly thermoelastic, irreversible lattice defects formed by martensitic transform. cycles 78−60671
Fe-Pt, ordered, anisotropy of mag. props. *(Russian)* 78−60280
Fe-Pt, ordered single cryst., magnetisation in strong mag. field *(Russian)* 78−47954
Fe-Pt, plastic deform. effect on struct. singularities and mag. props. *(Russian)* 80−44892
Fe-Pt, solubility of H_2 at press. up to 67 kbar *(Russian)* 79−51260
Fe-Pt, X-ray exam. of dynamic characts. *(Russian)* 77−62608
Fe-Pt (22-24 at.%) austenite, long range order parameter, temp. depend. 80−40353
Fe-Pt (23,24,25 at.%), effect of austenite ordering on some thermoelastic transform. factors 78−88466
Fe-Pt (24 at.%), colour metallographic technique, for studying microstructural reproducibility, in martensitic transformations 78−72954
Fe-Pt alloy, diffusion of ^{197}Pt and ^{59}Fe *(Czech)* 79−77804
Fe-Pt films, mag. and magneto-optic props., appl. to holographic and bit-by-bit storage 79−33512
Fe-Pt Invar, elastic and mag. props., magnetoelastic interaction effects *(Russian)* 80−84631
Fe-Pt Invar, magnetovolume effects 79−56597
Fe-Pt Invar alloy, bulk modulus anomaly, mag. effect 79−91728
Fe-Pt Invar alloy, homogeneous strong ferromagnet, thermal expansion and mag. props 79−91278
Fe-Pt Invar alloy, magnetocryst. anisotropy energy, itinerant electron model 80−54884
Fe-Pt Invar alloys, magnetocrystalline anisotropy const. determ. 80−65861
Fe-Pt-Ir, Mossbauer effect of ^{193}Ir and ^{57}Fe, hyperfine field, isomer shift 78−15072
Fe-Pt-SiO_2 supported catalysts, Mossbauer spectra 80−11296
Fe_3 Pt, ordered ferromagnetic alloy, magnetic excitation obs. 80−70978
$Fe_xMn_{1-x}Pt_3$, ferro-antiferromag. transform. at 4.2K *(Russian)* 78−88117
Fe_3Pb, reversible shape memory effect, rel. to microstruct. memory and residual stresses 77−90419
$FePd_{1-x}$ Pt_x, permanent magnet, coercive force increased by Pt 79−24157
FePt epitaxial film, vacuum-deposited, for thermomag. recording, mag. and magneto-optical props. *(Russian)* 78−60319
FePt lattice, symmetry, state of order, vibration, temp. effects *(German)* 77−4067
$FePt_3$, metamagnetic transitions in external fields 80−60272
$FePt_3$, neutron scattering study of spin waves 78−91856
Fe_3Pt, atomic thermal vibr. anisotropy, martensitic transform. model *(French)* 80−70355
Fe_3Pt austenite, long range order parameter, temp. depend. discussion 80−97481
Fe_3Pt austenites, ordering kinetics 80−104155
Fe_3Pt austenitising conditions on M_s temp. 80−81088
Fe_3Pt, interface struct. of martensite 78−48400
Fe_3Pt Invar alloy, anomalous Curie const., susceptibility meas. 80−75731
Fe_3Pt, Invar alloy, elastically stressed, ^{57}Fe effective field, anomalous behaviour, Mossbauer obs. *(Russian)* 77−8485
Fe_3Pt Invar alloy, mag. props., martensitic transform. 79−78365
Fe_3Pt, Invar alloy, theory of elastic-anomalies 78−95505
Fe_3Pt Invar alloy, thermal expansion and spontaneous magnetisation, Invar anomalies, low spin model 80−71001
Fe_3Pt Invar alloys, elec. resist. anomalous crit. behaviour 79−78067
Fe_3Pt, martensite austenite interface, twin thickness in martensite 77−32579
Fe_3Pt, martensitic transform., change from nonthermoelastic to thermoelastic type 78−19755
Fe_3Pt, non-linear local environment effect, Mossbauer effect of ^{57}Fe and ^{195}Pt 80−39910

platinum alloys continued
Fe_3Pt, off stoichiometric, austenite ordering and martensite tetragonality 77−36501
Fe_3Pt, plastically deformed, struct. inhomogeneities, positron annihilation meas. 79−33859
Fe_3Pt, premartensitic phenomena *(French)* 79−8297
Fe_3Pt, quasi-localised spin system, neutron scatt. 78−68194
Fe_3Pt, stoichiometric composition, internal friction, microdeform. and memory effect, rel. to martensitic transform. *(French)* 77−52323
$Fe_{3-x}Pt_{1+x}$, ordered and disordered, mag. props. at low temp. 79−56517
$Fe_{72}Pt_{28}$, ferromagnetic Invar alloy, lattice vibrations 78−91403
$Fe_{72}Pt_{28}$ Invar alloy, low temp. thermal expsn. 79−65221
$Fe_{76}Pt_{24}$ Invar alloy, ferromag., fine-powdered, Mossbauer effect 79−56634
$GdPt_x$, $Gd_{1-x}A_xPt_2$ (A=Sc, La), Laves phase alloy, NMR, nonstoichiometry 77−63298
Gd_3Pt_4, mag. props., 4.2 to 160K 79−78343
$(Gd_{1-x}R_x)(Co_{1-y}Pt_y)_5$, origin of hyperfine fields acting on Gd, Mossbauer study 80−44967
$HfPt_3$, corrosion resist. and elec. cond., bulk and film samples 78−72285
Hg_2-Pt, ^{199}Hg Mossbauer meas., isomer shift and quadrupole splitting calcs. 80−28039
Ho_5Pt_4, mag. props., 4.2 to 160K 79−78343
Ho_5Pt_4, isotypic with Pu_5Rh_4, X-ray cryst. struct. refinement anal. 79−4271
$LaPt_2$, H_2 sorption props. 79−86980
$LaPt_2$:Nd^{3+}, ESR investigation 79−78514
$LaPt_3$, ^{195}Pt NMR and susceptibility meas. 77−63299
$LaPt_5$, cryst. field effects on transport props. 78−72133
La_3Pt_2, structure determ., rhombohedral Er_3Ni_2 type 77−80443
Li-Pt, phase diagram for comp. range 0-40 at.% Pt, mag. and elec. props. *(German)* 80−84912
Li_yPtH_x, production and cryst. props. *(German)* 77−43176
Lu_5Pt_4, isotypic with Pu_5Rh_4, X-ray cryst. struct. refinement anal. 79−4271
Mn-Pt, diffusion of ^{54}Mn, radioactive tracer study *(French)* 79−86915
Mn-Pt, Elinvar props., −150 to 500°C *(Japanese)* 77−52385
Mn-Pt, exam. of Elinvar props., from −150 to 500°C 78−76684
Mn-Pt, mag. struct., neutron diffr. study 79−91210
Mn-Pt (<29 at.%), eutectoid transform., antiferromag. struct. transform. *(French)* 78−92259
$Mn_{1-c}Fe_cPt_3$, noncollinear mag. structs., neutron diffr. anal. *(Russian)* 80−25087
MnPt, disordered film produced by RF sputtering, ferromag. behaviour 78−68310
Mo-Pt, electron beam melted, alloying addition effects on brittleness and ductility 79−61728
Nb-Ge-Pt, A15 cpds. prod. by liq. quenching, phase stability and supercond. props. 79−95538
Nb-Pt, A15 phase, comp. and order effects on supercond. props. 77−85372
Nb-Pt, A15- and δ-phases, Knight shift of ^{195}Pt meas. 78−19350
Nb-Pt alloy, superconducting parameters of A15- and σ-phases 78−39242
Nb-Pt-O system, phase equilibria, diagram, unit cell parameters, supercond. 80−55352
Nb-Si-Pt, A15 cpds. prod. by liq. quenching, phase stability and supercond. props. 79−95538
$Nb_{\sim 3}Au$, upper crit. field 79−82729
Nb_3Ga-Nb_3Pt, supercond. crit. temp., comp. depend. *(Russian)* 77−59347
Nb_3Pt, A-15 struct. ^{93}Nb NQR spectra 80−20496
Nb_3Pt, composition effects on T_c 77−76993
Nb_3Pt, neutron irrad. effects on supercond. props. 79−38224
Nb_3Pt, X-ray $M_{IV,V}$ emission bands *(Russian)* 80−45170
Nb_3Pt, XPS of valence electrons meas. 77−21003
Nd_3Pt_2, structure determ., rhombohedral Er_3Ni_2 type 77−80443
Nd_3Pt_4, mag. props., 4.2 to 160K 79−78343
Ni-Cr-AlPt, exam. of phase diagram 79−8276
Ni-Pd, mag. form. factor, polarised neutron diffr. meas. 80−29525
Ni-Pt, disordered, extension of Taylor's theory of lattice vibr. 79−4387
Ni-Pt, ferromag., influence of local ordering on spin wave stiffness const. 77−89937
Ni-Pt, ferromag., press. effect on Curie temp. 79−51781
Ni-Pt, itinerant ferromagnet. magneto-volume expts. 77−66404
Ni-Pt, local environment and mag. props. effect of disorders 77−63085
Ni-Pt, mag. props., average and local density of states, CPA calc. 77−59242
Ni-Pt, magnetic moment distrib., diffuse neutron scatt. meas. 80−34593
Ni-Pt, magnetovolume effects near crit. conc. for ferromag. 79−56591
Ni-Pt, renormalisation of spin wave stiffness 79−51764
Ni-Pt, short range order, many electron effects, pseudopotential method 78−79954
Ni-Pt, short-range order parameter calc. in pseudopot. approx. *(Russian)* 80−49183
Ni-Pt alloys, mag. props. under hydrostatic press. 78−6556
Ni-Pt alloys, magnetic-moment distrib. neutron study 80−97066
Ni-Pt alloys, thermal expansion, mag. contribs. 77−43355
Ni-Pt disordered alloy, off-diagonal, T-matrix itinerant electron ferromagnetism calcs. 80−25067
Ni-Pt spin susceptibility, temp. variation, band model calc. 77−28365
Ni-Pt-P, metallic glass, amorphous and electronic structs., NMR Knight shifts and linewidths meas. 78−68400
NiPt, quenched, ordering kinetics and domain struct. form. during isothermal tempering *(Russian)* 80−66502
NiPt, short-range order, effect of plastic deform., electron diffr. anal. *(Russian)* 80−24403
$Ni_{1-x}Pt_x$, disordered, phonon dispersion relations using neutron inelastic scatt. 79−69212
$Ni_{1-x}Pt_x$, disordered phonon dispersion relations, neutron inelastic scatt. 78−43085
$Ni_{1-x}Pt_x$, disordered system, phonon dispersion relations using pseudo unit cell model 79−28066
Ni_3Pt, change of H_2 diffusivity with order-disorder transformation 80−59729
Ni_xPt_{1-x} disordered alloy, itinerant system, induced magnetism 78−52191
$NiPt_NGe_{N'}$, cryst. struct. *(German)* 80−44171
$(Ni_xPt_{1-x})_{75}P_{25}$ metallic glass system, ^{31}P and ^{195}Pt NMR 77−12211
P+Nb, dil. alloy, NMR obs. of ^{93}Nb 80−71203

platinum alloys continued
Pd-Pt, adsorption, of CO(NO), on SiO_2-supported surface, IR spectrosc. obs. 80−92780
Pd-Pt, and other substitutional alloys with large mass disorder, phonon modes 78−95122
Pd-Pt, elect. resistivity, temp. depend. between 1.6 and 4.2K *(German)* 79−28337
Pd-Pt, local environment and mag. props. effect of disorders 77−63085
Pd-Pt, low temp. magnetoresistance up to 60 kG 78−91668
Pd-Pt, mag. props., average and local density of states, CPA calc. 77−59242
Pd-Pt, resonant modes, rel. to CPA predictions 78−75757
Pd-Pt, T diffusion, effect on freq. factor and activation energy 78−63880
Pd-Pt alloys, soln. of H_3, partial thermodynamic parameters determ. 77−66027
Pd-Pt surface, adsorbed Xe, 5p photoemission, local surface struct. influence 80−2920
Pd-Pt-Au alloys for low-temp. precision resistors 79−69490
Pd-Pt-H(D), elastic energy dissipation peak 80−60905
PdAu wires, sorption of H_2 78−43239
$(Pd_{99}Ni)_{1-x}Pt_x$, spin-fluctuation thermopower 79−60802
$(Pd_xPt_{1-x})_3Fe$ atomically ordered alloy, thermoelectric power, carrier energy spin shift, mag. props. 80−29394
$(Pd_xPt_{1-x})_3Fe$, magnetisation intensity and coercive force, antiferro- to ferromag. transition *(Russian)* 77−48008
$PrPt_2$, hyperfine sp. ht. and magnetisation meas. at 4.2K 80−75775
$PrPt_2$, sp. ht., differential susceptibility and elec. resist. meas., 1.4-40K 80−71063
$PrPt_3$, ^{195}Pt NMR and susceptibility meas. 77−63299
$PrPt_5$, cryst. field effects on transport props. 78−72133
Pr_3Pt_2, structure determ., rhombohedral Er_3Ni_2 type 77−80443
Pt/Au alloy surface chemistry, sample morphology effects 78−7233
Pt-^{95}Nb, nuclear orientation meas. 79−65644
Pt-actinide diatomic mol., calc. dissoc. energy 78−78832
Pt-Al, development, growth and adhesion of Al_2O_3 77−8994
Pt-Al (22 wt.%), elec. props. of growing alumina scales 79−20282
Pt-Al(In)(Sn) alloys, Fermi energy influence on thermodynamic props. *(German)* 80−24619
Pt-Au, amorphous struct. produced by Au implantation, spinodal decomp. TEM obs. 78−31379
Pt-Au, dil., recovery spectrum after thermal neutron irrad., Au effect and defect conc. depend. 80−65057
Pt-Au, electronegativity and core electron binding energy shifts of Au 77−15346
Pt-Au, ion-irradiated, self-interstitial migration in stage II recovery, FIM obs. 77−59140
Pt-Au, miscibility gap, thermodynamic anal. *(German)* 79−91629
Pt-Au, surface segregation using atom-probe FIM 79−77883
Pt-Au, surface segregation, comp. depth profiles meas. using atom-probe field ion microscope 80−100380
Pt-Au (100), chemisorption of H_2 and O_2 and their interaction, UPS investig. 77−51600
Pt-Au (4.0 at.%), ion irradiated, direct obs. of vacancy struct. of (220) platelet 78−51534
Pt-Au glass-bonded printed thick-film conductor, adherence fracture energy 77−9037
Pt-Au thick film conductor, glass bonded, adherence, fracture energy, Al_2O_3 substrate effects 77−56075
Pt-Au(Al)(In)(Sn)(Zr), solid soln., magnetic props. and lattice parameters *(German)* 79−87236
Pt-Au(Cr), grain boundary permeation 79−65253
Pt-Ba, elemental comp. and chem. state of surface during thermal activation, AES obs. 78−2345
Pt-Ba cathode, vaporisation expts., heat of adsorpt. and migration of Ba on Pt 78−10272
Pt-C, dil., C segregation to single cryst. surfaces 80−39301
Pt-C (graphite), adhesion and wettability of graphite *(Russian)* 80−20008
Pt-C film automatic thickness control in freeze etching and related techniques, resist. monitor 78−49810
Pt-Cd, thermodynamic props. 79−43207
Pt-Co, dil, magnetopower, magnetoresistivity 78−68016
Pt-Co, dil., skew scatt. Hall effect, magnetoresist. and mag. anisotropy, orbital magnetism of impurity 80−70678
Pt-Co, dil., thermopower and magnetothermopower 79−65456
Pt-Co, magnetically hard, struct. and morphology, electron microscope study 79−82171
Pt-Co, magnetostatic and exchange interactions in composite magnets 77−69536
Pt-Co alloys, crit. neutron scatt. in crit. conc. region for onset of ferromagnetism 78−72347
Pt-Co resistance thermometer, for low temp. appl. 78−73994
Pt-Co system, low temp. susceptibility 80−65920
Pt-Cr, (13-18 at.% Cr) resistivity and AC susceptibility, temp. 1.4−300K 78−2461
Pt-Cr, dil., appearance of mag. order for Cr impurities in exchange enhanced hosts 79−4690
Pt-Cr, dil., elec. resist., 7.4 to 300K, anomalous temp. depend. associated with cond. electron scatt. 79−73491
Pt-Cr, disordered, atomic order-disorder transform. effect on resist. min. 80−65911
Pt-Cr, elec. resist. meas. through percolation limit, mag. order onset 77−69298
Pt-Cr, shallow silicide contact 80−70819
Pt-Cr (0.3 and 0.5 at.%) anomalous resist. associated with conduction-electron scatt. from Cr impurities 79−99530
Pt-Cr(Fe)(Ni), dil., surface segregation, equilib. surface compositon, AES meas. 77−85039
Pt-Cr(Nb)(Re)(Rh)(V), dil. alloy, 0.5 at.%, ^{195}Pt NMR for local mag. susceptibility 78−84484
Pt-Cu, ESCA study 80−2923
Pt-Cu, surface composition, XPS *(Portuguese)* 80−24722
Pt-Cu, surface segregation, ion scatt. spectroscopy meas. 79−82423
Pt-Cu (49.37 at.%), coexistent phases in homogeneous ordering 79−29052
Pt-Cu alloy, asymmetry of XPS of shell electrons *(Russian)* 78−76579
Pt-Cu alloys, ESCA determ. of electronic struct. 80−34352
Pt-Fe, competing interactions in FCC alloys 78−95453
Pt-Fe, dil., breakdown of ferromag. order, magnetoresist. obs. 80−71046

platinum alloys continued
Pt-Fe, dil., skew scatt. Hall effect, magnetoresist. and mag. anisotropy, orbital magnetism of impurity 80−70678
Pt-Fe, supported, mag. prop. meas. in H_2 and O_2, 77 to 700K 79−91257
Pt-Fe, very dil., Mossbauer emission spectra, relax. effects 80−66084
Pt-Fe alloy, low field AC susceptibility 79−73698
Pt-Fe alloy, ordered, T-c phase diagram, antiferro- and ferromagnetism *(Russian)* 80−65871
Pt-Fe alloy foils prep. by electrodeposition of Fe 80−35113
Pt-Fe ordered alloy, multiply mag. phase transitions 80−60264
Pt-Fe(Co), dilute ferromagnets, press. effect on Curie temp. 80−65873
Pt-H solid solutions, thermodynamics 79−77756
Pt-In, cryst. struct. determ. *(German)* 78−26494
Pt-In, dil., damage induced quadrupole interactions, DPAC exam. 78−39465
Pt-In, dil., radiation damage heating, TDPAC exam. 78−39466
Pt-Ir, Au covered, spectral characts. of VLF noise, allowing for logarithmic creep *(Russian)* 77−85301
Pt-Ir, catalytic behaviour on graphite-O_2 reaction, small bimetallic particle identification by controlled atm. electron microscopy 79−83502
Pt-Ir, cleaning and polishing by low press. high frequency induction plasma *(Russian)* 78−35578
Pt-Ir, structural phase transform., ion field emission microscopy obs. *(Russian)* 80−50628
Pt-Ir alloys, surface composition 79−19433
Pt-Ir coated Ti anode, corrosion and passivation behaviour in Cu electrowinning appl. 80−55573
Pt-Ir coating electrodeposition, from molten chloride and cyanide 79−24640
Pt-Ir solid solutions, investigation of field-ion micropattern contrast, selective evaporation and ionisation models 79−69962
Pt-Mn, dil., low temp. susceptibility, spin glass and Kondo behaviour 77−66372
Pt-Mn, dil., nuclear orientation exam. 79−61171
Pt-Mn, dil., skew scatt. Hall effect, magnetoresist. and mag. anisotropy, orbital magnetism of impurity 80−70678
Pt-Mn, dil. alloy spin glass, mag. sp. ht. 78−14966
Pt-Mn dilute alloy, cubic foil, Mn spin behaviour, nuclear orientation technique 78−27044
Pt-Mn dilute alloys, spin glass, low temp. resist. meas., cluster model explanation 78−26851
Pt-Mn-Sn alloy, mag. hyperfine fields 79−1737
Pt-Ni, disordered, vol. paramagnetostriction calc. 77−80985
Pt-Ni, mag. inhomogeneity, low field DC susceptibility meas. 78−56301
Pt-Ni, XPS d bands and core levels 77−32498
Pt-Ni (42 wt.%) relationship between mag. saturation flux and tensile strength 79−15819
Pt-Ni alloys, onset of ferromag. 79−56533
Pt-Ni disordered alloy, Landau model for mag. props. 77−66276
Pt-Ni vacuum condensates on Si and SiO_2, thermally treated, X-ray anal. *(Russian)* 80−70559
Pt-Ni-P, metallic glass, viscous flow, alloying effect 78−79793
Pt-O, preanodised or passivated, DTA 77−16733
Pt-Pb fibre, CO adsorption and oxidation, AES and ESCA obs. 79−52469
Pt-Pd (Co)(Su)(Al)(Si) melts, surface tension and density *(Russian)* 80−39388
Pt-Pd alloy, surface composition determ. by AES 78−79869
Pt-Pd system, sorption of H_2 during cathodic charging, deflection technique meas. 79−51427
Pt-Pd(Au), surface comp. and catalysis, AES and thermal desorption meas. 79−46898
Pt-refractory metal/Si interactions, phase separation 80−65303
Pt-Rh, elec. cond., temp. influence *(Russian)* 80−39549
Pt-Rh, surface comp. determ. by ion scatt. spectroscopy 80−6602
Pt-Rh, surface composition using ion scatt. spectroscopy 79−82422
Pt-Rh alloy, on rock salt, epitaxial growth and struct. 77−20211
Pt-Rh alloys, low temp. resistivity 79−60787
Pt-Rh alloys, surface behaviour on heating in air, XPS and SIMS *(French)* 77−40327
Pt-Rh thermocouple, Ta-sheathed, Al_2O_3-insulated, large decalibrations above 1330°C 78−24790
Pt-Rh-W (30, 8 wt.%), intergranular embrittlement by Se vapour 80−3185
Pt-Rh-W alloy corrosion by radioisotopic power system insulating and thermoelec. materials 78−7094
Pt-Ru, surface segregation, appl. of quantification of atom-probe FIM data 78−62263
Pt-Sb, amorphous sputtered film, elec. props. 78−68006
Pt-Si, constitution 79−29054
Pt-Si, Cs ion-bombarded, surface Cs concs., AES meas. 79−83073
Pt-Si film system, silicide first phase form., reaction kinetics 78−79821
Pt-Si layers, form. by laser irrad. of Pt film on Si substrate 79−99438
Pt-Si system, formation of Si enriched metastable cpds. using ion bombardment and post annealing 79−69143
Pt-Si thermally degenerated Schottky diodes, resonant tunnelling 80−100503
Pt-Si:As, silicide form. during laser irrad., p-n junctions and ohmic contacts 80−84397
Pt-Sn/Al_2O_3 catalyst, Mossbauer effect, reactivity 80−11298
Pt-Ti, Matthiessen's rule breakdown 77−15823
Pt-Ti bielectrode use as insoluble anode in electroplating 77−44490
Pt-transition metal, dil., impurity resist. 80−92875
Pt-transition metal dil., mag. susceptibility and NMR meas. 78−39290
Pt-V, Matthiessen's rule breakdown 77−15823
Pt-W, substrate temp. influence on shallow contact formation on Si 80−96963
Pt-W, surface segregation, appl. of quantification of atom-probe FIM data 78−62263
Pt-W (92-8%), UF_6 mol. negative surface ionisation 78−56913
Pt-Zr alloy, activity coeffs. rel. to electronic props. *(German)* 77−20084
Pt-Zr(Hf), high temp. thermodynamic props. 77−63633
$Pt_{53}Al_{47}$, ordered BCC phases at high temp. 79−32948
Pt(Au), ion irradiated alloys, stage II recovery 78−47440
PtBi, XPS, electronic struct. 80−7464
$PtBi_2.h_3$, cryst. struct. *(German)* 80−107113
β_1-PtCd, structural parameters 79−27953
γ-$Pt_8Cd_{40(41)}$, X-ray cryst. struct. determ. 80−54172
PtCo, absolute thermopower meas., 4-300K 78−10421
PtCo, ferromag. domain wall, freq. const. for thermal activation 77−89976

platinum alloys continued
Pt_3Co, radiation damage profiles from low energy Ne^+, bombard. 80−70268
PtCr, AC susceptibility near percolation limit, ordered and disordered alloy 80−65900
Pt_3Cr, ferrimag., magnetisation density, polarised neutron diffr. meas. 80−60204
$Pt_{0.75}(Cr_{1-x}Mn_x)_{0.25}$, pseudobinary, magnon energy derivation 80−107996
$Pt_{0.72}Fe_{0.28}$, isomer shift and effective mag. field at ^{57}Fe, press. depend. 77−16232
Pt_3Fe, collision cascades, neutron induced superparamagnetism *(Russian)* 78−2166
Pt_3Fe, transport and mag. props. near Neel temp. 79−7976
$Pt_{50}Fe_{12.5}Co_{37.5}$, elec. resist., cond. electron scatt. and heterogeneities of spin system *(Russian)* 79−56189
$Pt_{13}In_9$, exam. of crystal structure, and phase diagrams *(German)* 78−83779
$Pt_{50}In_{50}$, ordered BCC phases at high temp. 79−32948
$Pt_3In(Sn)(Pb)(Ti)(Cr)(Al)(Ga)$, Ll_2 ordered alloy, positive temp. depend. on strength, phase destabilization 80−81203
$Pt_{90}Ir_5Au_5$, $Pt_{80}Ir_{10}Au_{10}$, low temp. sp. ht. 79−73320
PtMn, spin glass, nonlinear susceptibility and sp. ht. 80−60304
PtMn spin glass alloy, cooperative freezing, susceptibility meas. 79−91233
Pt_3Mn, cryst. dynamics at 80K 79−23688
Pt_3Mn, mag. excitation dispersion relation 80−25090
Pt_3Mn, obs. of magnon sp. ht. 77−63217
$Pt_3Mn_xCr_{1-x}$ alloys, mag. props. 80−2562
$Pt_3Mn_xCr_{1-x}$, electronic specific heat meas. comparison with band model calcs. 80−54400
PtMnSb, hyperfine mag. field at Cd impurity, TDPAC study 80−39906
PtMnSn, ^{197}Au and ^{119}Sn hyperfine fields, Mossbauer expt. 78−72439
PtMnSn(Sb), Cd impurities, hyperfine field meas. 78−15074
Pt_2Mo-type superstructure, interaction of reacting dislocations *(Russian)* 78−83814
$Pt_{0.7}Ni_{0.3}Fe$, magnetically hard, cryst. morphology and mag. domain struct. 77−69615
$Pt_{45}Ni_{30}P_{25}$, metallic glass, viscosity meas. from rates of thermal transformations 78−26713
$PtPb_{0.7}Bi_{1.3}$, crystal structure *(German)* 80−84139
$PtPb_3Bi$, cryst. struct. *(German)* 78−59783
Pt_4PbBi_7, cryst. struct. *(German)* 80−107113
$Pt_{37.5}Pd_{12.5}Co_{50}$, elec. resist., cond. electron scatt. and heterogeneities of spin system *(Russian)* 79−56189
$Pt_{12.5}Pd_{37.5}Fe_{50}$, elec. resist., cond. electron scatt. and heterogeneities of spin system *(Russian)* 79−56189
$Pt_{90}Rh_{10}$/Pt thermocouple, Inconel sheathed, MgO-insulated, decalibrations during 1200°C use, ion microprobe obs. 78−57957
$Pt_{86}Rh_9Au_5$, $Pt_{74}Rh_{17}Au_9$, low temp. sp. ht. 79−73320
PtRh5 alloy, phosphate glass addition effect on high temp. strength *(German)* 80−25807
Pt_4Sb, Ll_2 ordered alloy, positive temp. depend. on strength, phase destabilization 80−81203
PtSi, 10-160 keV Ar ion sputtering, Rutherford backscatt. obs. 79−15574
PtSi, Ar bubble formation after 20 to 160 keV sputtering, TEM and backscatt. spectrometry obs. 78−64435
PtSi, dissociation in presence of Pt film 79−47892
PtSi, epitaxial film, cryst. perfection and thermal stability, channelling and backscatt. meas. 79−99255
PtSi, epitaxial film on Si, ^4He ion channelling meas. and RHEED anal. 80−10834
PtSi film, on (001) Si, crystallography 78−75955
PtSi film formation by ion sputtering and annealing, form. and exam. problems 80−100782
PtSi films, on Si, stress obs. 80−80145
PtSi, form. kinetics, AES, SIMS, EPMA 77−11800
PtSi, growth rate for form. by Pt film deposition under ultrahigh vac. and controlled impurity atm. 80−65388
PtSi, partial sputtering yields 77−8696
PtSi, Schottky barrier, resistivity, elec. characts., barrier heights, solar cell use 78−14825
PtSi Schottky-barrier monolithic IRCCD focal plane 80−86427
PtSi, substrate ion implantation, channelled, through metal silicide film 80−70231
PtSi surface, and interface with Si, impurity effects 80−80037
PtSi thin film structures, preferential sputtering meas. Rutherford backscatt. 79−43087
PtSi-n-Si, photoelec. barrier height and elec. props. 79−33344
PtSi-Si:As(Sb), implanted dopant redistrib. after silicide form., appl. to ohmic contacts 79−37729
$PtSi_x$-Si contact, struct. and elec. props., sputtering etching and annealing ambient effects 77−62991
Pt_2Si film formation, AES exam. to characterise impurity effects 79−15054
Pt_2Si formation from Pt-Si sample, obs. by ^{31}Si tracer and Rutherford backscatt. methods 79−4431
Pt_2Si, growth rate for form. by Pt film deposition under ultrahigh vac. and controlled impurity atm. 80−65388
Pt_2Si-Si, and PtSi-Si interfaces, chemical state, AES expts. 78−91767
Pt_3Sn, electronic struct., calc. using linear-muffin-tin-orbitals method 77−24516
Pt_3Sn, Fermi surface, de Haas-van Alphen effect meas. 77−24514
PtV, dil. alloys, NMR obs. of ^{51}V 80−71203
β_1-PtZn, defect struct., lattice parameter meas. 78−43009
β-PtZn nonstoichiometric Ll_0 phase, thermodynamic activity of Zn 77−90320
Pu-Pt, exam. of phases and crystal structure 78−80518
Pu-Pt-Rh, exam. of phases and crystal structure 78−80518
Pu_2Pt, cryst. struct. determ. 78−79564
$Pu_{31}Pt_{20}$, crystal struct. determ. 77−80445
Rh-Pt, local environment and mag. props. effect of disorders 77−63085
Sc_2Pt, X-ray powder struct. anal., Debye-Waller factors 79−77553
$SmPt_2$, hyperfine field exam. by NMR spin echo 78−23365
Ta-Pt, electrospark alloying for obtaining stable effective electrodes for electrochemical processing *(Russian)* 79−39157
Tb_3Pt_4, mag. props., 4.2 to 160K 79−78343
Tb_5Pt_4, isotypic with Pu_5Rh_4, X-ray cryst. struct. refinement anal. 79−4271
ThPt, valence bands, XPS spectra 80−50520

platinum alloys continued
Ti-Pt, electrospark alloying for obtaining stable effective electrodes for electrochemical processing *(Russian)* 79−39157
Ti-Pt, eutectoid decomposition 79−24491
Ti-Pt-Au, nonalloyed ohmic contacts to n-GaAs by pulse-electron beam annealed Se implants 80−2466
Tm_3Pt_4, mag. props., 4.2 to 160K 79−78343
Tm_5Pt_4, isotypic with Pu_5Rh_4, X-ray cryst. struct. refinement anal. 79−4271
U-Pt, paramag. suscept. 79−61047
UPt, valence bands, XPS spectra 80−50520
UPt, weak ferromag., magnon heat capacity, magnetisation and mag. entropy 77−24685
V-Pt, dilute, inelastic neutron scatt. and quasilocal vibrs. *(Russian)* 77−80595
V-Pt, sp. ht. and mag. meas. in ordered and disordered phases 80−70422
V_3Ga-V_3Pt, supercond. crit. temp., comp. depend. *(Russian)* 77−59347
$V(Ir_{1-x}Pt_x)_3$, mag. props., ferromagnetism, comp. depend. 77−77039
$V(Ir_{1-x}Pt_x)_3$, NMR study of ferromag. 79−65760
$V_{0.76}Pt_{0.24}$, supercond., Knight shift contrib. to reson. line shift meas. 77−4467
$V_{1-x}Pt_x$, A-15 cpds., nucl. mag. relax. in normal and supercond. state 80−49993
$V_{1-x}Pt_x$, A-15 struct., Knight shift in normal state, upper crit. field curves *(French)* 78−43519
V_3Pt, supercond., Knight shift contrib. to reson. line shift meas. 77−4467
V_xPt_{1-x}, nuclear spin-lattice relax. time, electronic density of states 77−59354
$YPt_2:Nd^{3+}$, ESR investigation 79−78514
Y_5Pt_4, isotypic with Pu_5Rh_4, X-ray cryst. struct. refinement anal. 79−4271
YbPt-YbAu system, valency state, Yb behaviour *(French)* 80−45277
$ZrPt_3$, corrosion resist. and elec. cond., bulk and film samples 78−72285

platinum compounds
see also platinum alloys
chain compounds, one dimens. conductors, Fermi wavevector determ., X-ray scatt. obs. 80−44187
complex, coordinatively unsaturated, electronic struct. and catalytic activity 78−72228
complexes, INDO calcs. for predicting ground-state props., charge distributions and force const. determ. 80−83283
DC elec. cond. props. 79−51582
dichlorodiammineplatinum(II) binding to calf thymus DNA, X-ray absorpt. spectra 78−85291
double oxides, elec. cond. 80−34438
double oxides, exam. of elec. cond. 78−51990
intercalation, electron microscopy 80−84164
linear mixed valence compounds, lattice modes obs. 79−46763
linear mixed valence compounds, longit. modes 78−95119
mixed valence-mixed metal compounds, ionic crystals, longitudinal lattice modes, Raman spectroscopy 80−40099
phthalocyanine, energy band structs., carrier mobilities 77−72817
phthalocyanine, reson. Raman excitation profiles, solvent effects 80−102512
phthalocyanine, valence band studies, UPS meas. 77−52221
phthalocyanine single cryst., triplet state Zeeman effect, phosphoresc. 78−6747
rare earth tetracyanoplatinates, energy transfer from linear stacks of donors 78−68546
silicides, formation in double layers of Ni and Pt films on Si substrate 78−84010
tatrakis(ethyl isocyanide) platinum(II) tetracyanoplatinate(II), cryst. data, X-ray powder anal. 80−2003
tetracyanoplatinate conductors, IR and Raman spectra, cyanide stretching vibrs. 79−11415
Wolffram's red salt, mixed valence, reson. Raman calcs. using vibronic coupling model 80−97249
Am-Pt intermetallics, after-effects of ^{241}Am α-decay, ^{237}Np Mossbauer spectra obs. 79−61271
$Ba[Pt(CN)_4Br_2]4.5H_2O$, single crystal neutron diffr. struct. exam. 78−2082
$Ba[Pt(CN)_4].4H_2O$, cryst. struct., neutron diffr. 77−35521
$Ba[Pt(CN)_4].4H_2O$, polarised time-resolved emission spectra 79−33811
$Co_{0.83}(Pt(C_2O_4)_2).6H_2O$, cond., dielec. const., microwave obs. 80−44636
$Co_{0.83}[Pt(C_2O_4)_2].6H_2O$, quasi-one-dimens. conductor, Peierls distortion and superlattice, X-ray study 80−29397
$CrSi_2$ formation on Pd_2Si and PtSi, radioactive Si tracer obs. 78−60578
$Cs_2(Pt(CN)_4)Cl_{0.3}$, elec. cond., 300-40K, 3-dimens. ordering temp. 79−78087
$Cs_2Pt(CN)_4.H_2O$, cryst. struct., neutron diffr. meas. 77−47393
$Cs_2[Pt(CN)_4](FHF)_{0.39}$, cryst. struct., X-ray diffr. meas. 78−59789
$Cs_2[Pt(CN)_4].H_2O$, polarised emission, correlation to cryst. struct. 79−19917
$Cs_{1.75}[Pt(CN)_4].xH_2O$, one-dimensional, X-ray diffuse scatt. meas. 77−19937
Cu-Pt complex, $[Cu(C_2N_2H_8)_2][Pt(C_2O_4)_2]$, cryst. struct. determ. 77−4072
$Eu_2[Pt(CN)_4]_3.18H_2O$, nonradiative energy transfer from tunable donor states to Eu^{3+} 79−43018
$H_2Pt(OH)_6$, platinic acid, X-ray cryst. struct. determ. 80−28967
$KNa[Pt(CN)_4].3H_2O$, neutron diffr. cryst. struct. exam., refinement by least squares 78−2079
$K_{1.75}Pt(CN)_4 . 1.5H_2O$, quasi 1D metals, electric conductivity meas., semiconductor-metal transition 79−99538
$K_2Pt(CN)_4$, muonic X-ray radiation anisotropy *(German)* 80−69267
$K_2Pt(CN)_4$, Peierls transition temp. and 0K energy gap, mean field theory calc. 80−24782
$K_2Pt(CN)_4$, quasi-one-dimens. Peierls system, phonon dispersion and neutron scatt., calc. 80−24550
$K_2Pt(CN)_4Br_{0.3}2.6H_2O$ crystal, quasi-one-dimensional, optical consts. and dielec. permittivity dispersion 77−1695
$K_2Pt(CN)_4Br_{0.3}3H_2O$ incommensurate linear conductors correlation length in 77−80745
$K_2Pt(CN)_4Br_{0.3}3.2H_2O$, linear conductor, dynamical aspects of fluctuations 79−33715
$K_2Pt(CN)_4Br_{0.3}3.2H_2O$, linear cond., ^{195}Pt NMR evidence of low lying non-linear excitation 80−44933

platinum compounds continued
$K_2Pt(CN)_4Br_{0.3}\times3H_2O$, struct., neutron determ., Peierls distortion 79−46640
$K_2Pt(CN)_4Br_{0.3}\times3.2D_2O$, Kohn anomaly in longit. acoustic phonon 77−7812
$K_2Pt(CN)_4Br_{0.3}.2.7D_2O$, under hydrostatic press., compressibility, neutron diffr. 79−46742
$K_2Pt(CN)_4Br_{0.30}.3H_2O$, dynamic ^{195}Pt NMR meas. below metal-insulator transition 80−34810
$K_2Pt(CN)_4Br_{0.3}.3H_2O$, IR absorption peak theory 77−43991
$K_2Pt(CN)_4Br_{0.3}.3H_2O$, struct. rel. to quasi one-dimensional elec. props. 78−14716
$K_2Pt(CN)_4Br_{0.3}.3H_2O$, one-dimens. cond., review 78−60070
$K_2Pt(CN)_4Br_{0.3}.3H_2O$, one-dimens. cond. transition, spin suscept. and DC cond. temp. depends. 78−84198
$K_2Pt(CN)_4Br_{0.3}.3H_2O$, specific heat and ferroelastic behaviour 78−91447
$K_2Pt(CN)_4Br_{0.3}.3H_2O$, Krogmann salt, non-empirical localised orbital cal. of electronic struct. 78−91636
$K_2Pt(CN)_4Br_{0.3}.3H_2O$, spin-lattice model for elastic anomalies 80−15179
$K_2Pt(CN)_4Br_{0.3}.3H_2O$, quasi one-dimens. conductor, EPR linewidth 80−54938
$K_2Pt(CN_4)Br_{0.3}.3H_2O$, anisotropic radiation damage in electron microscopy, diffr. spot fading rate obs. 80−107329
$K_2Pt(CN)_4Br_{0.3}.3.2D_2O$, lattice dynamics, neutron scatt. expts. 78−14412
$K_2Pt(CN)_4Br_{0.3}.3.2D_2O$, dynamic struct. factor, inelastic neutron scatt. study 79−42185
$K_2Pt(CN)_4Br_{0.3}.3.2H_2O$, deuterated, coupling of charge density wave and water mode 77−4646
$K_2Pt(CN)_4Br_{0.3}.xH_2O$, conductivity and optical refl. depend. on water content 77−39828
$K_2Pt(CN)_4Br_{0.3}.xH_2O$, dynamical props. near Peierls instability, neutron scatt. 78−14436
$K_2Pt(CN)_4Cl_{0.3}(Br_{0.3}).3H_2O$, struct., single cryst. neutron diffr. expts. 78−14321
$K_{1.75}Pt(CN)_4 1.5H_2O$, anomalous elec. cond. 79−47088
$K_{1.75}Pt(CN)_4\times1.5H_2O$, struct., neutron determ., Peierls distortion 79−46640
$K_{1.75}Pt(CN)_4.1.5H_2O$, struct., single cryst. neutron diffr. expts. 78−14321
$K_{1.75}Pt(CN)_4.1.5H_2O$, Pt chain distortion, X-ray obs. 78−14322
$K_{1.75}Pt(CN)_4.1.5H_2O$, Raman scatt. and luminesc. studies 80−25394
$K_{1.6}Pt(C_2O_4)_2\times1.2H_2O$, struct., neutron determ. 79−46640
$K_{1.62}Pt(C_2O_4)_2.2H_2O$, plasma resonance absorpt. from small particles 77−24841
$K_xPt(C_2O_4)_2.nH_2O$, chem. analysis and elec. cond. meas. 78−76060
$K_2PtCl_6:Os^{4+}$, sharp line luminesc. band at 10K, vibr. assignment 78−95600
$K_{1.75}[Pt(CN)_4]1.5H_20$, elec. cond. studies, Peierls transition 80−24901
$K_2[Pt(CN)_4].3H_2O$, DC elec. cond. props. 79−51582
$K_{1.75}[Pt(CN_4)].xH_2O$, one-dimensional, X-ray diffuse scatt. meas. 77−19937
$Li_2O.2SiO_2$ glass, kinetics of crystal nucleation, effect of Pt and other impurities 78−88440
$Li_2[Pt(CN)_4].3H_2O$, DC elec. cond. props. 79−51582
$Mg_{0.82}Pt(C_2O_4)_2\times5.3H_2O$, struct., neutron determ. 79−46640
$Mg[Pt(CN)_4].7H_2O$, high press. tuning of optical transitions 79−28813
$Mg[Pt(CN)_4].7H_2O$, DC elec. cond. props. 79−51582
$(NH_4)_2[Pt(CN)_4]Cl_{0.42}.3H_2O$ quasi one dimensional conductor, physical props., cond. freq. depend. 79−95393
$(NH_4)_2[Pt(CN)_4].2H_2O$, DC elec. cond. props. 79−51582
$Na_2Pt(CN)_4Br_{2.}2H_2O$, cryst. struct., neutron diffr. determ. 77−24296
NaPtY zeolite, proton spin relax., adsorbed H_2O effect on Pt distrib. 78−88216
$Na_2[Pt(CN_4)].3H_2O$, cryst. struct. 77−58990
Ni compound, $[Ni_3(CO)_6]_n^{2-}$, n=1,2, one-electron states in polynuclear carbonyls 79−95358
Ni-Pt silicide Schottky diodes, current-voltage characts. and comp. profiles 80−84508
Pd and Pt mixed valance complex, $[Pd(ethylenediamine)_2Pt(ethylenediamine)_2Cl_2](ClO_4)_4$, Raman spectra 80−84734
Pt complex, 1,1,1-trifluoro-2,4-pentanedionate, struct., chem. ionisation mass spectra 78−61079
Pt complex, 1,2-benzoquinonedioximates, refl. spectra, 0.5-2.5 eV, Young's modulus and internal friction 78−39562
Pt complex, 2-hydroxy ethanethiolato-2, 2', 2''-terpyridine-Pt, DNA double helical fragment intercalator complex, molecular struct. 79−16140
Pt complex, $(C(NH_2)_3)_2Pt(CN)_4Br_{0.23}.H_2O$, pseudo-one-dimens. cpd., solitary wave excitations, and cryst. struct. 78−6307
Pt complex, $[C(NH_2)_3]_2[Pt(CV)_4]Br_{0.23}.H_2O$, one-dimensional, X-ray diffuse scatt. meas. 77−19937
Pt complex, $[Pt(dapn)_2][Pt(dapn)_2Br_2](ClO_4)_4$, (dapn=1,2-diaminopropane), optical absorpt. spectra of small particles 79−56812
Pt complex, $[Pt(en)_2][Pt(en)_2Cl_2](ClO_4)_4$, reson. Raman spectra 80−2760
Pt complex, [2, 2', 2''-terpyridine PtCl]$^+$, motion of Pt atoms, electron microscopy obs. 80−103314
Pt complex, bis [4-(n-butyl)-styryl dithiolato] Pt nematic complex with strong IR absorption 80−88305
Pt complex, bis(1,2-benzoquinonedioximato)platinum(II), intrinsic elec. cond. 78−6377
Pt complex, bis(1,2-benzoquinonedioximato)Pt(II), cryst. and mol. struct. 79−60327
Pt complex, chloro-bromo complexes of Pt (IV) and Pt (II), ^{195}NMR, cooperative shift effect 79−33547
Pt complex, cis-dichlorobis (cyclopentylamine) platinum II, potentiation of radiation effect 78−85345
Pt complex, DBCP, effect on cell survival, synergistic interaction with radiation 77−21565
Pt complex, dimethylglyoxymate film, prep. and physical props. 79−90923
Pt complex, KCP, periodic lattice distortions, charge density waves 79−82536
Pt complex, linear chain type, synthesis 78−6047
Pt complex, linear ionic mixed valence cpd., IR and resonance Raman spectra rel. to lattice modes 80−25393
Pt complex, $Mg_{0.82}Pt(C_2O_4)_2.xH_2O$, X-ray diffuse scatt., 1-D Peierls-Kohn anomaly and struct. transforms. 78−14680
Pt complex, $Pt^{II}(CNCH_3)_4(PF_6)_2$, $Pt_2^{I}(CNCH_3)_6(PF_6)_2$, and $Pt^{I}Pd^{I}(CNCH_3)_6(PF_6)_2$, vibr. spectra, M-M bonds. *(French)* 80−47997
platinum compounds continued
Pt complex, $PtCl_3$ (9-methyladeninium), laser Raman spectra 77−66499
Pt complex, $PtCl_4^-$, effective charge, from IR and Raman scatt. intensity obs. 78−62809
Pt complex, $PtCl_4^{2-}$, in chloride-sulphate soln., Pt electrodeposition, galvanostatic transients *(Russian)* 78−31655
Pt complex, Pt(II) diamine, ^{13}C NMR *(Japanese)* 79−6952
Pt complex, $Pt(NH_3)_4Cl_2.H_2O$, Raman spectrum *(French)* 79−19876
Pt complex, $Pt(S_2C_2(CN)_2)_2^{1-}$, elec. cond. 79−73505
Pt complex, tris[bis(1,2-diaminoethane)Pt(II)dichlorobis(1,2-diaminoethane)]Pt(IV)tetrakis[tetrachlorocuprate(I)], cryst. and mol. struct. 80−28964
Pt complex-TCNQ radical salt, $[Pt(dipy)_2]^{2+}[TCNQ]_3^{2-}$, cryst. struct. 78−63741
Pt complexes, chain cpds., orientational antiphase struct., X-ray scatt. determ. 80−24435
Pt complexes, cyano and cyanohalide hydrates, IR absorpt. spectra 77−6771
Pt complexes, dithiolato complexes, smectic C phase, synthesis, isobaric phase diagrams 78−94970
Pt complexes, one-dimensional conductivity, pressure effect obs. 77−35930
Pt complexes, $Pt(NH_3)_4Cl_2$, $Pt(ND_3)_4Cl_2$, Raman spectra in solid state and aq. soln. *(French)* 79−19876
Pt complexes, X-ray absorpt. spectra, mol. orbital interpretation 78−42097
Pt complexes, XY_4Z_2 type ions, vibr. anal., force consts. 78−70812
Pt compound, $[Pt_3(CO)_6]_n^{2-}$, n=1,2, one-electron states in polynuclear carbonyls 79−95358
Pt dithiene complexes, mesomorphic props. 80−88026
Pt-nucleoside complexes, Raman spectra, vibr. anal. 77−65473
Pt-S mixtures, binding of phases, two-correl. model 77−80438
Pt-Se mixtures, binding of phases, two-correl. model 77−80438
Pt-Si, amorphous thin films, laser irrad., metastable phases 80−96622
Pt-Te mixtures, binding of phases, two-correl. model 77−80438
Pt^{2+}-L-Cl$^-$, model fragment (L=Cl$^-$, F$^-$, OH$^-$, H_2O, NH_3), bond strengths, EHT calcs. 77−23434
PtAl, form. in hollow cathode discharge, emission spectrum obs. 78−27819
Pt_4B, Pt_2B, and other Pt_xB_y cpds., cryst. chem. 80−19769
$PtBi_{1.6}Pb_{0.4}O_{3.8-\delta}$, cpd. with unidirectional linear chains of metallic atoms *(French)* 77−19934
$PtBr_4^{2-}$-$PtBr_6^{2-}$ doped in Cs_2ZrBr_6, mixed valence, absorpt. spectra, vibronic struct. 80−97308
PtC, ground and first excited states, dissoc. energy and dissoc. curves., pot. energy curves 77−50555
$Pt(CO)_4$, valence orbital energies, pseudopot. calcs. 78−37546
$(Pt_3(CO)_6)_n^{2-}$, n=1,2, one-electron states in polynuclear carbonyls 79−95358
$PtCl_2$, PtCl, decomposition equilibria by simultaneous torque Knudsen technique 77−29035
$PtCl_4^{2-}$, electronic struct., SCF Xalpha ESCA spectrum assignment 80−23339
$PtCl_4^{2-}$, vibr. force consts. calc. 78−58655
$(PtCl_6)^{2-}$, quasi-relativistic SCF-MO-LCAO methods, CNDO and MWH appls. 78−41953
Pt_6Cl_{12}, Pt L X-ray spectra and X-ray electron spectra, influence of chem. bonds 77−28656
$PtCl_4^{2-}$(Br_4^{2-}), mean vibr. amplitudes and force field, Muller approx. 77−10659
$PtCl_n(H_2O)_{4-n}^{2-n}$, electronic absorpt. spectra, band assignments 78−50553
$PtCl_2(NH_3)_2$, cis- and trans-isomers, electronic struct., SCF-Xα study 80−18795
$PtCl_2Pt(NH_3)_4$, Magnus' Green Salt, extended localised holes charge distrib. 77−55496
PtD, form. in hollow cathode discharge, emission spectrum obs. 78−27819
PtF_6, electron affinities from collisional ionisation with alkali atoms 78−55226
PtF_6, ionis. energies, optical spectra, Dirac-Slater model 77−83488
PtGeSe, ferroelastic, cryst. struct. models 77−19927
PtH, ab initio effective core potential studies, relativistic effects 79−93933
PtH, ab initio relativistic core pot. studies of metal-H bonding 80−106257
PtH(D), pot. energy curves, r-centroids, Franck Condon factors, rot. depend. 80−28082
PtI_4, aerosol, X-ray fluoresc. anal., particle size correction method 78−48705
Pt(IV), reduction to Pt(II), X-ray irrad., Ar ion bombardment, XPS obs. 80−35573
cis-$Pt(NH_3)_2Cl_2$, torsions, metal-metal interactions, inelastic neutron scatt. study 79−46581
$Pt_6(NH_3)_{10}Cl_{10}(HSO_4)_4$, chain struct. and elec. cond. 78−2469
$Pt(NH_3)_4CuCl_4$, ferromag., antisymmetric and anisotropic exchange, EPR linewidth 78−10761
$Pt(NH_3)_4SO_4$, cryst., absorption spectrum *(French)* 79−28784
$(Pt(NH_3)_4)[PtCl_4]$, torsions, metal-metal interactions, inelastic neutron scatt. study 79−46581
PtO, existence 78−18923
PtO film, electrochemically formed, anisotropy of optical constants, reflection spectroscopy and Kramers-Kronig analysis 77−32456
PtO, form. in hollow cathode discharge, emission spectrum obs. 78−27819
PtO, ground and first excited states, dissoc. energy and dissoc. curves., pot. energy curves 77−50555
PtO, ground state, matrix isolation spectra 78−46352
PtO, ground state identification from 3800-7000 Å emission spectrum 78−21937
PtO, neutron, α-particle irrad., black form., adsorpt. props. 77−11796
Pt(O)-Pt(O) dimers, bounding in a d^{10}-d^{10} system 78−74579
PtO_2, finely divided, reduction 77−90643
PtO_2, sputtered film, optical props. under H_2 reduction 80−20728
PtO_x films, electronic struct., reduction processes, photoemission, optical absorpt. and resist. meas. 80−80931
PtO_x, thin film, sputtering deposition, XPS and X-ray diffr. chracterisation 79−78878
$Pt(PF_3)_4$, force fields, mean vibr. amplitude calcs. 77−54552
$Pt_{0.97}S_2$, optical props. at absorption edge 78−35140
$PtS_4C_4(CF_3)_4$.TTF, 1-dimens. mag. props. 77−66271

platinum compounds continued
$PtSb_2$, high field elec. props., impact ionisation 80−96892
Pt_5Se_4, cryst. struct. determ. *(German)* 77−89415
$Pt(SeC(NH_2)_2)_4Cl_2$, crystal and mol. struct. 78−59794
PtSi diode, sputtering-induced defects, elec. characts. 78−51941
PtSi formation on Si with Pt-W alloys, effect of substrate temp. 80−96963
PtSi, formation with high-purity Pt films 77−76676
PtSi, growth under protective layers on Pt covered Si substrates, X-ray diffr. and Rutherford backscattering anal. 78−22965
PtSi, parallel contacts, Schottky barrier height meas. 80−96965
Pt_2Si formation with high-purity Pt films 77−76676
PtTe, electronic struct., self-consistent and non-self-consistent band calcs. 80−44499
PtX_4^{n-}, X=Cl, Br, n=1, 2, force consts., bond polarizability 78−5201
Pt(diethylenetriamine)(guanosine)$(ClO_4)_2$, crystal and molecular struct. 79−73157
$Rb_{1.75}Pt(CN)_4$. $1.5H_2O$, quasi 1D metals, electric conductivity meas., semiconductor-metal transition 79−99538
Rb_2PtI_6, cryst., role of ordinary and harmonic Raman processes, ^{127}I nucl., spin-lattice relax., obs. 79−8063
$Rb_2[Pt(CN)_4Br_2]$, neutron diffr., cryst. struct. 77−35522
$Rb_2[Pt(CN)_4].3H_2O$, DC elec. cond. props. 79−51582
$Rb_{1.75}[Pt(CN)_4].xH_2O$, one-dimensional, X-ray diffuse scatt. meas. 77−19937
$Sr[Pt(CN)_4].5H_2O$, DC elec. cond. props. 79−51582
$Y_2[Pt(CN)_4]_3.21H_2O$, first order phase transform., spectroscopic and thermodynamic anal. 78−38829

pleochroism
see also dichroism
anthraquinone pleochroic dyes in liq. cryst. soln., photostability, appl. to liq. cryst. displays 80−88961
dyes, dissolved in nematic liq. crysts., guest-host interactions, appl. to electrooptic displays 80−44113
quartz, synthetic, Al centres conc. and anomalous pleochroism depend. on crystn. parameters 80−107311
p-$CdSnP_2$, photocond. meas., polarisation depend. 78−39157
GaSe, photosensitivity anisotropy in polarised light, pleochroism coeff., suitability as photoelec. analysers 79−60873
$HgGa_2Se_4$, anisotropic photocond., pleochroism, and band struct. 78−19094
InSe, photosensitivity anisotropy in polarised light, pleochroism coeff., sensitivity as photoelec. analysers 79−60873
$ZnGeP_2$ p-n homodiode, polarisation photosensitivity and photopleochroism spectra 80−107866

plexiglas *see plastics*

plotters
analytical, photogrammetric appl., development progress and advantages 78−40710
analytical, photogrammetric appl., future prospects 78−40708
analytical, props. and software aspects, photogrammetric appl. 78−40709
analytical stereoplotter, OMI AP/C4, photogrammetric appl., features 78−40715
analytical stereoplotter, TRASTER 77, photogrammetric appl., features 78−40712
analytical stereoplotting system, C-100 PLANICOMP, features 78−40711
Bruel and Kjaer acoustic level recorder type 2306, interfacing to a digital computer for a graphical output 80−53572
calligraphic projection display resolution and contrast photometer and X-Y plotter 80−86373
chart recorder, adaptor for converting single channel to multi-channel instrument 77−37874
chart recorder and plotter assimilation 79−93128
chart recorders, technology improvements 79−88933
chromatography, data processor with thermal printer-plotter for GC and LC *(Japanese)* 80−50920
close-range photogrammetry problems solved by analytical plotter 77−71397
colour plotter system for computer graphics output, appls. in geoscience 80−98467
coordinatograph, precision, 120×120, accuracy of applicability 80−52158
graphics calculator system using X-Y recorder and computer as digitiser 80−13046
graphics plotter using linear step motors 79−93127
hologrammetric plotter for three-dimensional meas. 79−7103
interface for serial computer terminals 80−98904
laser point transfer machine, TRANSMARK, performance testing 78−81438
microprocessor-controlled plotter/printer, HP-IB 7245A model 79−35689
minicomputer-controlled high-speed transient recording system *(Russian)* 77−9992
monocomparator use of digitised stereoscopic plotter 77−26420
pictorial electrographic printing, tone reproduction and screen design 80−62752
stereoplotter, orthoprinting system, TOPOMAT, appls., accuracy 78−81437
stereoplotter, TOPOCART B, accuracy and performance study 78−81436
stress-strain diagrams, tensile testing 80−3269
for tracing oscilloscope waveshapes under 1 MHz 78−70111
twin-pen chart recorder, differential thermal anal. result plotting appl. 79−12797
universal stereoplotter, US-1, photogrammetric appl., features 78−40713
X-ray spectrometry, quantitative, comparison of mathematical models 79−17587
X-Y recorder, interface for CRT oscilloscope *(French)* 77−53951
x-y recorder sweep generator, sweep speed dependent on four terminal network transfer charact. 80−62649
X-Y recorders, analogue, dynamic accuracy 79−88932
X-Y recorders, selection criteria *(French)* 77−53884

plugs (electric) *see electric connectors*

Pluto
1978 P 1, cosmogonical implications of satellite discovery *(Chinese)* 79−84744
1978 P 1, discovery of possible satellite, ephemeris 78−69744
1978 P 1, Pluto image elongation obs. 78−81586
1978 P 1, possible satellite, orbit and eclipses ephemeris 78−93152

Pluto continued
1978 P 1, satellite, of Pluto, obs. 78−85900
1978 P 1, speckle interferometric obs. (1980 June) 80−101553
1978 P 1, speckle obs. rel. to orbital radius and system mass and density 80−109394
appulse on 1980 April 6, no occultation from S.England 80−67650
astrometric posns. (1975 May-1978 May) 79−70993
astrometry (1973 to 1979) 80−85894
atmosphere, review 77−5470
basic props. 77−41354
Charon, account of discovery 80−12708
Charon, tidal evolution 80−26806
Charon (1978 P 1), occultation on 1980 April 6 probable 80−67651
Charon (1978 P 1), probable stellar occultation, 1980 April 6, min. dia. 80−62071
Charon (1978 P 1), satellite of Pluto, positions and dynamical parameters 80−62069
Charon (1978 P 1), stellar occultation obs., 1980 April 6, rel. to satellite dia. and struct. 80−94754
composition constraints and mass-radius relationships 80−82298
diameter meas. by speckle interferometry 80−41763
discovery and review of data (book) 80−82591
encounter possibility in extraplanetary mission 80−17466
formation, implications for solar system origin and transneptunian planets 79−8856
geocentric positions for the 1974-8 period 80−46478
image tube spectra, 6800-9000 Å, search for possible atm., methane upper limit 79−16880
IR spectrum, 1.5 to 2.5 μm obs. 80−56765
light variation, surface albedo distrib. 77−82160
methane frost, IR photometry obs. 77−22136
motion, long-term effects, semi-analytical theory 78−69741
observing in 1977, prospects 77−56874
no occultation of star on 1980 April 6, ephemeris 80−62070
opposition on 1979 April 8, satellite confirmation opportunity 79−44409
orbital motion, long term librational character 80−94753
orbital motion, theory and perturbations of giant planets *(French)* 80−26724
orbital motion solutions comparison 78−93151
origin, through Neptune encounter with massive body 79−84743
physical parameters and current research of Pluto and its satellite, review *(French)* 79−70994
properties and satellite Charon 79−30006
satellite observation *(Czech)* 80−31252
surface and atmosphere from 1.4-1.9 μm spectrum 80−46480
surface composition, IR photometry 79−53768

plutonium
see also nuclei with .....
see also fission of plutonium
accountability, computerised gamma spectrometer system for meas. isotopic and total Pu conc. in solns. 80−63363
accountability, nondestructive assay using neutron counting, calorimetry and gamma spectrometry 80−63266
accountability and control, field nondestructive assay measurements as applied to process inventories 80−63265
acute inhalation, early mortality and morbidity estimate 78−96079
advanced MX fuels, Pu depletion by vapour-phase transport in carbothermic reduction processes 80−815
aerosol, characterisation inside safety enclosures of mixed oxide fuel fabrication facility 79−13501
aerosols, charge distribution from mixed-oxide reactor fuel fabrication lab. 79−5181
air concs. near Rocky Flats, $^{239+240}Pu$ 78−16150
air monitor with background compensation system 80−27824
alpha-bearing wastes, operational techniques for minimisation, segregation and accounting 77−61567
alpha-energy and mass analyses, using single sample mount 78−15744
analysis, in fuel fabrication facility 79−16115
analysis in bone and tissue samples, appl. of liq. scintillation alpha counting and spectrometry 77−25617
anion-exchange refinement of Pu and Np separated during extraction refinement of spent fuel elements 78−70624
assay, low-background, using modified commercial liq. scintillation detector and sample changer 77−54474
assay and accountability using neutron correlation meas. tech. 80−69015
assay in radwaste using thermal neutron counter 79−85716
assay methods, in vivo, humans 79−20674
assay of large samples using portable neutron coincidence counter 80−69041
atom, isotope shifts rel. to $|\psi(0)|^2$ 78−17580
automated nondestructive assay system 77−61512
biologically important physicochemical props. and methods of human contamination *(French)* 80−98004
biota levels from E. Tennessee floodplain forest 78−85394
body burden estimation from urine data influenced by DTPA therapy 78−73259
borehole assay using delayed-neutron activation anal. 80−21419
breeder reactor fuel, remote fabrication program, France 80−13748
breeder reactor fuel, source and availability for breeder reactor programme 77−61625
burnup, alternative waste management techniques 79−59210
calorimetric nondestructive assay for in-field meas. 80−71874
CANDU, Pu-topped Th fuel cycle characts. 79−36322
CANDU reactor, Pu-topped Th cycle characts. 79−31101
chemical and isotopic anal. of U, Pu, and Th in nuclear fuel materials 79−81046
computerised inventory control system 79−36386
concrete and criticality 79−63788
conference, Baden-Baden, Germany (Sept. 1975) 77−19807
Conference, nuclear materials, safeguards and accountability meas., Williamsburg, USA (May 1978) 79−81045
contaminated soil, nondestructive anal. 79−11879
contamination at fuel facilities, waste management techniques 77−61568
creep of fine and coarse grained α-Pu, internal stresses 77−28880
decorporation, DTPA treatment schedules for ^{239}Pu decorporation from simulated wounds 77−64137
decorporation, influence of inhaled Ca-DTPA on long-term effects of $Pu(NO_3)_4$ 77−66861
denatured fuel cycles for international safeguards 79−41011

plutonium continued
detection and meas. of Pu in sealed container by passive neutron technique 77−67954
determination, by automated coulometric method, apparatus 79−16114
determination, in irrad. fuel dissolver soln. by isotope dilution alpha spectrometry 80−78428
determination, in soln., on-line γ-ray spectrometric meas. 79−11872
determination by volumetric and coulometric methods, effect of Am on accuracy 79−52826
determination in soln. using automatic controlled-potential coulometer 77−25335
determination system by passive neutron counting 79−40985
diffusion in pyrocarbon in HTGR 78−29578
diffusion in UO_2 79−7711
diffusion of Co in FCC and BCC phases, diffusion coeff. and mechanism 77−28046
distribution in $(U,Pu)O_2$, autoradiographic anals. 79−49811
dose to lung and bone from contaminated soils, statistical uncertainties 80−109028
dosimetry, calibration of whole-body counters 80−21547
dynamics in deciduous forest ecosystem, linear compartment donor-controlled model 78−85392
elastic constants at elevated temps., noncontact meas. tech. 80−104405
electrical resistance, self-radiation damage effect, Matthiessen's rule deviations 77−28170
electrolytic stabilisation for separation from nuclear reactor fuels *(German)* 79−3229
environmental contamination, review 80−101136
environmental impact of Pu-bearing materials, linear regression anal. 80−85308
extraction-spectrophotometric determination of Pu in spent fuel of first Czechoslovakian nuclear power station *(Czech)* 77−3105
fallout in alkaline, saline lakes 80−97826
fallout-derived ^{239}Pu and ^{240}Pu, concs. in drinking water and organic fertiliser 77−56488
fast breeder reaction, Pu utilisation in France 77−50279
FBR, Pu use in France 77−67859
FBR, use of Pu in UK 77−67860
FBR fuel, U-Pu extraction by equilibrium water systems with 0.15 to 1 M HNO_3 acidity 79−71940
FBR fuel remote fabrication development at PNC 80−13749
fissile material accountancy using controlled potential coulometry 80−63298
fissile material assay, cyclic method of neutron activation and delayed-neutron counting 77−34395
fissile materials, anal. by cyclic activation of delayed neutrons 78−53296
fission reactor fuel, general survey of possible use 77−34399
fracture toughness, plane strain, of α-Pu 77−25161
fuel, charging of VVER-440 water-cooled water-moderated reactor 77−50214
fuel, fabrication, use and handling anal. *(Japanese)* 77−349
fuel, unmoderated, criticality safety practices for handling in glove boxes 79−26669
fuel fabrication and reprocessing plant, radiation protection device based on neutron detection *(French)* 78−66362
fuel fabrication and reprocessing plants, Pu neutron emission checks *(French)* 79−26720
fuel reprocessing, spectrophotometric determ. of Pu 80−78433
fume aerosols, aerodynamic and dissolution behaviour of laser-ignited droplets 79−13438
glove boxes, Pu-contaminated, size reduction and waste packaging 80−18469
half-life determ., sample preparation 79−9936
hazards and nuclear fuel reprocessing 79−45387
human organ concentration meas. for Japanese 78−80980
hybrid fusion reactor, Tokamak type, with fissioning matter, blanket parameters 77−34446
hybrid fusion reactors, problems 77−38403
hybrid Tokamak reactor, for prod. of Pu fuel and elec. energy, preliminary design 79−76122
industrial effluent, behaviour and transport in Great Miami River, Ohio 78−16061
inhaled hot particle toxicity, recommendations of German Commission on Radiation Protection 78−69150
inventory verification at ANL, IAEA safeguards 78−821
ionisation potentials, 2nd-6th, thermochemical calcs. 79−98248
ions, electronic props., Dirac-Fock studies 78−60094
in Irish Sea, oxidation state 79−16516
in irradiated reactor fuel, microamounts meas. by radiometric method *(Czech)* 77−42111
isotope compositon, determ. using gamma spectrometry 80−66915
isotope ratios, γ-ray spectrometric determ. 77−6518
isotope separation, chemical treatment of irrad. targets *(French)* 77−26883
isotope separation and ratios, neutron irrad. of natural U in Japan Material Testing Reactor *(Japanese)* 80−52730
isotopes, in soil, determination using alpha-spectrometry 80−45601
isotopes, maximum permissible inhalation values 79−70640
isotopes in Antarctic snow layers, deposition and accumulation 79−70820
isotopic analysis by resin-bead mass spectrometry for materials safeguards 80−78392
isotopic composition, determ. using precise absolute gamma spectroscopic meas. 80−66916
isotopic composition, determ. using thermal ionisation spectrometry with automatic data eval. 80−66913
isotopic composition, nondestructive anal. using gamma spectrometry 80−63392
isotopic safeguards analysis to determ. Pu content in nuclear fuels 80−99210
isotopically denatured, diversion resistance 79−89385
K-absorption edge energy, accurate determ. using γ-attenuation 77−59642
laboratory stack monitoring, computerised system 79−3256
liquid, enthalpy and heat capacity meas. using neutron heating 77−20078
liquid, hard-sphere model, phys. prop. meas. interpret., adjacent solid phase implications 77−19866
long-term environmental behaviour, chemical approaches 79−93765
lung burden X-ray counting efficiency, from inhaled ^{103}Pd studies 78−85391
plutonium continued
lung burdens in Austrian residents 80−109042
lung Pu of pronghorn antelope near a nuclear fuel reprocessing plant 80−30906
LWR, Pu recycling experience 79−45391
LWR, Pu reprocessing and safeguards 77−67838
LWR, safety and use within Federal German Republic 77−67839
LWR fuel, partial partitioning of U and Pu by coprocessing solvent extraction 79−36382
LWR recycling in the European Communities 78−58394
LWR recycling of Pu in $(Th,Pu)O_2$ fuels, economic viability 80−18576
LWRs, commercial recycling assessment 79−71935
Manhattan project workers, 32-year medical follow-up 80−26379
measurement of microamounts for U fuel burnup estimation *(Czech)* 77−6521
minerals of U, Pu content, ore model calcs. comparison with expt. *(Spanish)* 77−70654
mixed oxide fuels, development status, Japan 79−31130
monitoring in gaseous CO_2 coolant by gamma spectrometry 79−89374
monitoring of PU holdup in glove-gox exhaust filter by gamma ray detection 80−78458
movement through food chain 78−61264
neutron analysis in solid waste 80−42840
nondescructive assay meas. using NaI(Tl) detectors during fabrication plant decommissioning 80−63495
nondestructive analysis, calibration by calorimetric assay 80−71878
nondestructive assay, gamma-spectrometric method 79−81068
nondestructive assay of large samples 80−71871
nondestructive assay of leached Zr-hulls in reprocessing plant 79−81070
nondestructive assay reference materials 79−49702
nondestructive element and isotope assay 80−71870
nondestructive rapid isotopic anal. gamma-ray spectrometric method 79−81069
nuclear fuel, burn-up, chemical separation, ion exchange 80−42746
nuclear fuel, power distrib. comparison of U and Pu in KWO PWR core 77−14224
nuclear fuel centre, fuel and waste facilities, safety, protection and socioeconomic aspects 78−58395
nuclear fuel decontamination, sorption and distillation methods, review *(Czech)* 78−82496
nuclear fuel recycling in LWRs and environmental impact 78−89969
nuclear fuel reprocessing, displacement re-extraction, math. simulation 77−61586
nuclear fuel reprocessing, re-extraction with weak acid, math. simulation 77−61587
nuclear fuel workers management 79−74763
nuclear fuels, elemental and isotopic conc. anal. using nondestructive assay 79−49691
nuclear materials safeguards, Pu accountancy by ceric oxidation, ferrous reduction and dichromate titration 80−63364
nuclear power use in United Kingdom 77−50280
nuclear reactor in the nineties, anal. *(German)* 78−8960
nuclear reactor use 77−67813
nuclear use, decision making 77−42168
oxidation, binding energies, Auger and X-ray photoelectron spectra study 80−76550
particulate biogeochemistry of coastal zone 79−29787
passive assay using Euratom variable dead-time neutron counter 80−69042
passive neutron assay of Pu contaminated solid waste streams 79−36373
phase transformation, $\beta \rightarrow \alpha$, after full and partial β phase form., kinetics 77−21139
phase transformation, $\beta \rightarrow \alpha$, after partial B phase form., kinetics 77−28809
phase transformation kinetics anal., β to α 77−70044
phase transformations, $\beta \rightarrow$Ga and $\gamma \rightarrow \alpha$, microstructures and kinetics 77−25048
pollution in stream near Argonne National Laboratory, ^{239}Pu and ^{240}Pu 77−45037
portal monitors for detecting and safeguarding special nuclear materials 80−63406
power reactor fuel and fuel elements *(Russian)* 79−30933
power reactor fuel cycles, Pu, Th and U evaluation 79−26706
power station use within German Federal Republic 77−54350
production by U_xS_y irrad. in reactor, chem. separation, yield 77−63986
production of pure α-phase 78−50252
proliferation and Pu recycling, effects of future nuclear power 79−18021
Purex process, concs. of U, Pu, HNO_3, fission products, in LMOM2 extractor, expt., graphical determ. 78−41843
Purex solvent extraction process for fuel recovery and recycling 79−36387
PWR, physics of U-Pu fuel cycle 77−50278
PWR, U-Pu, mixed oxide fuel, physical props. 77−67814
radiation monitor, Pu wound, sensitive simple instrument 79−8547
radiation protection and monitoring of personnel handling Pu reactor fuels 80−5389
radioactive effluent, Pu and Am inventory of ecosystem near a nuclear facility 80−97820
radioactive fallout in air and rain, results to end of 1977 78−82535
radioactive target preparation and characterisation 80−18734
radioactive waste, low conc. meas. in earth samples, appl. of Si(Li) X-ray detector 78−58505
radioactive waste, oxidation by radiation, effect on migration rate 80−13714
radioactive waste, Pu and trans-Pu element isotopes, accumulation and disposal 79−59187
radioactive waste, Pu contaminated incinerator facility, decontamination and decommissioning 80−13987
radioactive waste, transport, environmental impact 80−779
radioactive waste management, and plutonium, Swedish approach 79−31075
radioactive waste monitoring, anal. of enhanced variance and twin gate methods 80−5454
radioactive waste reprocessing for Pu extraction, methods and risks *(German)* 77−42157
radioactive wastes, leach behaviour of hydrofracture grout 77−10478
radiological implications of Pu recycling in HTGR fuels 80−68777
radionuclides decomposition in glaciers 80−40934
radwaste partitioning, separation of transplutonium and rare earth elements 79−97881

plutonium continued
reactivity enhancement in transportation and storage arrays from density reductions 77−57756
reactor fuel, input accountability in reprocessing plants, tracer tech. using Mg and Pb 80−73919
reactor fuel, production and availability, uses, reprocessing, fast reactor fuel cycles 80−68767
reactor fuel, safety training program 79−18053
reactor fuel extraction processing of nuclear fuel fluxes, effect of flux oscill. on Pu accumulation, math. simulation 80−63355
reclamation, precipitation-ion exchange scheme for actinide removal from salt waste soln. 79−49820
recovery by radioactive waste processing, volume reduction of organic alpha waste by pyrohydrolysis 80−95366
recycle, indecisiveness, impact on nuclear utilities 77−46384
recycle facilities in Foratom countries, status and prospects 79−31131
recycle fuel experience in LWR in West Germany 79−30932
recycle options in USA, benefit/cost anal. 79−31132
recycling, influence on US future nuclear power developments 79−36394
recycling in mixed oxide fuel for LWR 79−36385
release into estuarine-coastal sea ecosystem, assessment methodology 79−70471
reprocessing fast reactor fuel in Britain 78−89966
reprocessing programme in W.Germany *(German)* 78−8954
reprocessing waste pond Pu ecological export 78−53533
safe working, safety measures 79−41040
safeguarding, automated ion-exchange system for rapid Pu separation from impurities 80−78383
safeguarding, computer-assisted controlled potential coulometric determ. 80−78384
safeguarding, determ. of U and Pu content of fuels using isotope correl. tech. 80−68834
safeguarding, Pu content determ. in irradiated fuel assemblies 80−68806
safeguarding, tracer techniques for Pu input accountability in reprocessing plants 80−68827
safeguarding using resin bead mass spectroscopy 80−73984
safeguards, eval. of thermography 79−93719
safeguards, product soln. gamma-ray NDA using K-absorption edge densitometer 80−83162
safeguards accountability, NDA of crated waste by gamma-ray and neutron coincidence counting 80−83166
safeguards assay, isotopic meas. by gamma ray spectrometry using two-detector method 80−83161
safeguards verification methods for input-accountability meas. at reprocessing plant 80−95349
security, near-real-time accounting of strategic nuclear materials during reprocessing 79−85755
self diffusion of β-, γ-, δ-, δ'-, ε-phases, 393 to 886K 78−87811
separation, by column extraction chromatography 78−44421
separation, by MnO_2 coprecipitation from fresh and saline water 78−27814
skeletal level estimation based on DTPA induced excretion in faeces 78−85390
in soil, meas. in respirable dust using different size fractionation methods 79−66836
soil, remote contamination and total inventory from Rocky Flats, mass spectroscopic anal. 77−73739
soil distrib., Ohio, local and stratospheric sources 78−16015
soil distribution at Rocky Flats 78−73265
solar nebula, Th, U, Pu and Cm condensation and fractionation 79−35154
solvent extraction processing of mixed actinide residues, air sparge batch contactor 77−46369
sound velocity in α-Pu, meas. at press. to 50 kbar, elastic moduli 77−20015
specific heat, Debye temp. 80−15258
spent reactor fuel, burnup determ., isotopic comp. and conc. determ. by mass-spectrometric isotope dilution 79−89373
spent reactor fuel burnup determ. using anal. chem. [conf. Piestany, Czechoslovakia (Sept. 1978)] 79−89371
spontaneously fissioning material, assay using neutron correl. counting 79−85605
St. Severin chondrite, U and Pu distrib. 80−72889
steady state isotopic composition for nuclear power industry model 79−59166
storage, international scheme 79−67848
tensile properties of α-Pu and δ-stabilised Pu-Ga alloy, strain rate effect 77−21284
thermal reactors, reprocessing and recycle, economic and environmental benefits 77−46372
THTR fuel reprocessing Pu and Np separation from aqueous soln. *(German)* 77−83067
toxicity, cancer risk calc. 77−2025
toxicity hazards, cancer fatalities 77−66864
translocation from simulated wound sites in rat 78−77117
transport properties and sp. ht., role of optical and acoustic phonons 77−15821
transportation of irradiated fuels and Pu, regulations *(French)* 79−26777
utilisation in fast breeder and light water reactors, Italy 79−30931
utilisation in thermal and fast reactors in Japan 79−26534
utilization in reactors *(French)* 79−30930
vapour pressure, at high temp., pure Pu 79−55880
vapour pressure determ. 1724 to 2219K by Knudsen effusion technique 80−654
waste disposal, retention by rock 77−71679
waste produce of thermal, FBR reactors, comparison, nuclear power stations appl. 78−86641
water reactor Pu wire 77−50277
X-ray absorption spectra of α and δ phases, 5f states modification obs. 77−28649
X-ray emission, M-lines, for metallic state 78−15251
X-ray emission spectra of α-Pu, 5f electron distrib. analysis 77−28663
X-ray fluorescence anal. for solns. and slurries, feasibility study 79−81051
^{238} ^{239} ^{240}Pu, vertical distribution in Mediterranean Sea 79−84301
^{239,240}Pu(V) in alkaline freshwater pond, determ. by coprecipitation technique 80−71988
^{239}Pu sample irrad. in EBR-II, calc. and exptl. anal. 80−22947
^{241}Am(n,X), Japan Material Testing Reactor, separation of transuranium elements *(Japanese)* 80−52731

plutonium continued
fuels, relative occupational hazards 78−94101
LMFBR, U-Pu-Zr fuelled breeding potential assessment 79−9685
^{239,240}Pu, conc. in thermonuclear test debris, collected near Bikini Atoll 78−96103
^{238,239,240}Pu, concs. in arthropods at a nuclear facility 80−30905
Pu accidental release at Thule, Greenland, environmental behaviour 77−56656
Pu fallout detection using fission tracks prod. with neutron irrad. spectra 80−95479
Pu safeguards accountability, gamma-ray meas. of Pu and Am in molten salt residues 80−83165
Pu use, present status and prospects, use in fast and breeder reactors 79−26533
$^{239}Pu^{4+}$ diffusion in ion exchange membrane, autoradiographic obs. 77−90637
Pu/^{241}Am ratios, environmental meas. using X-ray spectrometry 77−60265
Pu-Am survey instrument, β-α-γ-X-ray scintillation detect. probe 78−33376
Pu-Be neutron source, for activation anal., β-ray meas. 78−73114
Pu-enriched LWR fuels, remote fabrication at Belgonucleaire 80−13754
Pu-O system, partial molar enthalpy of solution of O 77−47578
Pu(VI) in drinking water, max. permissible conc., chlorination effects 79−34448
^Pu, A=238,239,240, contents in coastal sediments 79−57974
^Pu, A=238 to 241, in-situ anal. of radioactive waste 79−85715
^pu, A=238-241, in English Channel, transfer into S.North Sea 79−48519
^Pu, A=239, 240, distrib. of fallout Pu in southern Finns 80−109045
^Pu, A=239,242, muonic atom lifetimes from muon induced fission 80−69269
^{236}Pu, ^{239}Pu, ^{242}Pu, ^{244}Pu, distrib. in mice after injection 79−12001
^{236}Pu conc., prediction for mixed-oxide fuel 77−42121
^{237}Pu, ^{239}Pu, citrate, early retention in mature beagles 78−96095
^{237}Pu, bioaccumulation in inland water and marine algae *(German)* 80−108820
^{237}Pu IV and VI oxidation states, relative uptake from water by bush beans 78−73266
^{237}Pu, intracardially injected in channel catfish, distrib. kinetics 79−20673
^{237}Pu, K-shell fluorescence yields from Auger electrons and X-rays, precision meas. 79−31462
^{238}Pu, ^{239}Pu, ^{240}Pu, content in deer from integrated nuclear fuel cycle facility 79−57778
^{238}Pu, alpha spectrometric determ. 80−81404
^{238}Pu, factors affecting particle mobility in rats 79−12003
^{238}Pu isotopic pacemakers, 2 to 4 years' follow-up 77−81695
^{238}Pu production from ^{237}Np, optimisation techniques 79−71936
^{238}Pu self diffusion, $(U_{0.8}Pu_{0.2})N$ mixed nitride fuel 78−82461
$^{238}Pu^{4+}$, $^{238}Pu^{6+}$, $^{239}Pu^{4+}$, $^{239}Pu^{6+}$, alga uptake rel. to isotope and oxidation state 80−30692
^{239}Pu, ^{240}Pu, Danish cereal grains, variation of direct contamination 79−5382
^{239}Pu, ^{240}Pu, concs. in fish and seawater from Kwajalein Atoll 80−26380
^{239}Pu, $(U,Pu)O_2$ fuels 80−71873
^{239}Pu aerosol, inhalation exposure of miniature swine 79−11976
^{239}Pu, aquatic microscosms, trophic transfer by Chironomoids 79−5383
^{239}Pu, atmospheric radioactivity data, applicability of Weibull distrib. function 77−2230
^{239}Pu, biological availability, influence of DTPA at soil-plant and plant-animal interfaces 78−73264
^{239}Pu, bone dosimetry model, surface and volume 79−8550
^{239}Pu, bone model for calc. of annual limits of intake in man 79−53252
^{239}Pu, cancer risk from $^{239}PuO_2$, max. permissible conc. in air 79−25108
^{239}Pu, carcinogenicity of inhaled dioxide, rat obs. 79−66492
^{239}Pu contamination in snakes inhabiting Rocky Flats plant site 77−81591
^{239}Pu, criticality of thin flat foils versus spherical shells, two-group diffusion anal. 79−26530
^{239}Pu deposition in bone, rel . to ^{59}Fe uptake in marrow, mouse 78−85395
^{239}Pu direct enrichment of LWR assemblies in a fusion hybrid 80−37604
^{239}Pu, distrib. and behaviour in Urazoko Bay sediment 80−97825
^{239}Pu, distribution in mouse skeleton 79−12002
^{239}Pu distribution in mouse testis, significance of interstitial tissue ultrastruct. 79−57610
^{239}Pu droplets burning in air, aerosol generation investig. rel. to inhalation hazards 79−67959
^{239}Pu, effect on mouse haemopoietic stem cells 80−51174
^{239}Pu, endosteal cell dose and relative distrib. factors compared to ^{226}Ra 78−96091
^{239}Pu, fissile fuel preparation by spallation of ^{238}U *(Russian)* 79−22441
^{239}Pu, gastrointestinal absorpt. in hamster 79−39520
^{239}Pu in aqueous soln., limiting critical conc. and thermal value of eta 79−63773
^{239}Pu in organic media, survey of criticality parameters 79−26670
^{239}Pu in plankton, upper limit calc. method for α-dose rates 79−2133
^{239}Pu, influence of administered mass of cross-placental transfer in mice 79−20672
^{239}Pu, isolation and characterisation of particles in atm. effluent 79−63757
^{239}Pu, lung burden, assessment of tissue substitutes for calibration purposes 79−16307
^{239}Pu, nanocurie amounts, lesions in CBA mice 80−81657
^{239}Pu, polymeric, effects on erythrocyte survival in mice 80−45973
^{239}Pu, radiation dose-response curves, hazard function method of resolution 79−66556
^{239}Pu, release from Institution of Nuclear Research meas. *(Czech)* 77−6568
^{239}Pu removal after inhalation of aerosol, bronchopulmonary lavage and chelation therapy 77−9270
^{239}Pu soil concs., in situ gamma anal. and sampling data comparison, Nevada 77−64143
^{239}Pu, study of non-uniform distrib. in mouse testis 79−39507
^{239}Pu, transuranic trace analysis using resonance ionisation spectroscopy of inert gases 80−93833
^{239}Pu uptake by pea plants 77−9282
^{239}Pu, use in weapons and energy prod., radiological hazards, security 77−10492

plutonium continued
^{239}Pu-^{241}Am monitor for in situ soil surface and pond bottom assay 77−9546
^{240}Pu, 42.9 keV γ transition, Mossbauer reson. obs. 79−36229
^{240}Pu content of commercial Pu, criticality of fast assemblies *(German)* 77−6564
^{240}Pu, effect on neutron lifetime in nuclear explosives 79−13531
^{241}Pu bone distribution, high resolution autoradiography 78−7399
^{241}Pu concentrations in Swedish reindeer lichens, radiochem. anal. 78−15912
^{241}Pu, concs. in sediments from coastal basins off California and Mexico 80−98303
^{241}Pu dosimetry, applicability of methods used for ^{239}Pu alphas 77−90906
^{241}Pu, environmental pollution, biophysical aspects 79−39530
^{241}Pu in ^{241}Am, determ. by γ spectrometry 79−52808
^{241}Pu, uptake and redistribution within the gonads, hamster, rabbit 79−12004
^{242}Pu preparation by EM isotope separation, for use as α-spectrometry and mass spectrometry tracer 78−9011
^{244}Pu standard reference material for nuclear materials safeguards appls. 80−78373
^{293}Pu, polymeric, effects on erythrocyte survival in mice 77−9227
U/Pu separation, use of carboxylic acids 77−38377
U-^{238}Pu-^{237}Np GCRF fuel cycle to produce isotopically denatured Pu for LWR 80−78427
U-Pu, isotope separation in HNO_3 by exchange resins 78−74782
U-Pu radial redistrib., effect of fuel rod parameters and fuel porosity *(German)* 79−49799
^{235}U-^{239}Pu, initial conversion, fast fission, and relative fission product activity ratios 78−58347

plutonium alloys
binary, enthalpy of form., atomic model approach, correl. with phase diagrams 77−21415
binary alloys, periodical depend. of equilibrium distrib. coeffs. of Pu admixtures on atomic number of admixture 80−18419
conference, Baden-Baden, Germany (Sept. 1975) 77−19807
crystal structure rel. to anomalous props. of δ-phase alloys 77−19910
metastable phases production by splat cooling 77−21134
Ag-Pu, metastable, high rate sputter deposition, annealing behaviour of deposits 77−21025
Ag-Pu (0.5 wt.%) deposited profiles, homogeneity, from hexagonal point source array 80−25559
Co-Pu, metastable, high rate sputter deposition, annealing behaviour of deposits 77−21025
Fe-Pu, dil., effective mag. fields, temp. depend. *(Russian)* 78−43587
Ni-Pu, dil., effective mag. fields, temp. depend. *(Russian)* 78−43587
Pu-Al-Ga system, phase diagram 77−21108
Pu-Ga, δ⟶α transform. kinetics 77−25047
Pu-Ga (1 wt.%), alloy powder, hydriding kinetics 80−76503
Pu-Ga (1 wt.%), single cryst. elastic consts. US wave vel. meas. 77−20005
Pu-Ga (1 wt.%) delta-stabilised, heat transport props., room temp. to 500°C 77−20294
Pu-Ga (1-8.56 at.%) alloys, enthalpy sp. ht. determ. at elevated temp. 78−78458
Pu-Ga (3.3 at.%), oxidation in air, 250-400°C 77−44401
Pu-Ga (3.4 at.%), δ-stabilised, strain rate effect on tensile props. 77−21284
Pu-Np, elec. resist., reson. scatt. from Np and local spin fluctuations 77−28170
Pu-Pt(Rh)(Pt-Rh), exam. of phases and crystal structure 78−80518
Pu-Zr, BCC, self-diffusion activation volumes, melting-diffusion correl. validity 77−20122
ζ-Pu-Zr, X-ray powder diffr. cryst. struct. determ. 79−19187
$PuAl_2$, low temp. sp. ht., spin fluctuation phenomena 77−28405
$PuAl_4$ clusters, band struct., variational Xα calc. 79−4508
$PuAl_4$ clusters, X_α calculations *(Japanese)* 79−82519
$PuFe_2$, ferromag. mag. cross section, form factors, saturation magnetisation values, polarized neutron study 79−47245
$PuFe_2$, high temp. mag. props., 300 to 1100K 79−51757
$PuFe_2$, Laves phase cpds., thermodynamic props. 77−20092
$PuFe_2$, magnetisation, neutron diffr. and Mossbauer expts. 77−63137
$PuFe_2$, Mossbauer diffr., combination type maxima, hyperfine interactions on nuclei 80−25263
Pu_5Ir_3, cryst. struct. 77−58975
Pu_5Ir_4, cryst. struct. 77−19909
PuO_{52}, Laves phase cpds. thermodynamic props. 77−20092
η-$Pu_{19}Os$, cryst. struct. 78−42954
ζ-$Pu_{19}Os$, X-ray cryst. struct. determ. 79−99117
Pu_2Pt, cryst. struct. determ. 78−79564
$Pu_{31}Pt_{20}$, crystal struct. determ. 77−80445
$PuRe_2$, mag. susceptibility 78−68182
$Pu_{31}Rh_{20}$, crystal struct. determ. 77−80445
Pu_5Rh_4, cryst. struct. 77−19909
Pu_5Rh_4, cryst. struct. 77−58974
Pu_5Rh_4, cryst. struct. determ. 77−55267
$PuRu_2$, intermetallic cpd., sublimation thermodynamics 80−96639
$PuRu_2$ Laves phase cpds., thermodynamic props. 77−20092
δ-PuSc (5, 12, 18 at.%), f.c.c., contraction by self irradiation at 4.2K *(French)* 77−4129
Pu_5Tr_4, cryst. struct. determ. 77−55267
Ta-Pu, metastable, high rate sputter deposition, annealing behaviour of deposits 77−21025
Th-Pu (20 wt.%) metal fuels, compatibility with cladding alloys for FBR appls. 80−102242
Th-Pu-U-Zr (20, 4, 8 wt.%) metal fuels, compatibility with cladding alloys for FBR appls. 80−102242
Th-U-Pu metal alloys, LMFBR appl. 77−83040
Th-U-Pu-C-O-N, kernel migration for HTGR fuel 77−38335
U-Pu carbides, advanced LMFBR fuels, equilib. thermodynamics 79−67862
U-Pu-Zr metal fuel remote alloying and casting 79−89477
U-Pu-Zr(-Th) LMFBR metal fuel elements, development and performance 80−57856

plutonium compounds
see also plutonium alloys
BWR island-design Pu recycle fuel assemblies, nuclear fuel performance meas. 79−30907

plutonium compounds continued
carbides, solvent for NaCl type monocarbide and sesquicarbide fission products, solubility rules 78−59953
ceramic fission reactor fuels, high temperature chemistry, nonstoichiometry, review 77−14238
conference, Baden-Baden, Germany (Sept. 1975) 77−19807
double orthovanadates and orthoarsenates, struct. evolution due to cationic and anionic substitutions 77−19938
in fused salts, redox and chem. props. 77−29038
mixed U-Pu oxide O_2 potential and O/M ratio determ. by solid-state galvanic cells 79−96324
mixed-oxide fuel fabrication in 1980s changes in process equipment and facilities 79−63797
nitrides, solvent for NaCl type mononitride fission products, solubility rules 78−59953
oxide fuels, irrad. behaviour, chemical process, densification, corrosion *(Japanese)* 77−83033
oxide fuels, recycling in thermal reactors and fast breeders 79−31129
oxides, matrix isolation studies with Fourier transform IR 78−45740
slab tanks for criticality control, neutron multiplication calc. 80−13606
swelling in mixed-oxide fuel pins 79−22393
thermal reactor fuel cycles, actinide wastes toxicity limitations *(German)* 80−99220
(U, Pu)O_2 fuel, remote fabrication experience in FRG 80−13753
HTGR 79−54583
β Na_4PuO_5 release from contaminated burning Na, LMFBR safety evaluation 77−23224
(Pu,U)O_2, <5 wt.% PuO_2, criticality data generated by SU-HAMMER 79−3198
(Pu,U)O_2, core materials development for water cooled reactor systems 77−46296
(Pu,U)O_2, criticality data generation using SU-HAMMER code 78−29581
(Pu,U)O_2, low-enriched fuel assemblies, profiles of activity ratios of ^{134}Cs, ^{137}Cs and ^{106}Ru fission products 77−57713
(Pu,U)O_2, oxidation rates 80−37557
Pu fuel research facility for advanced LMFBR fuel *(Japanese)* 78−29624
Pu IV citrate, monomeric, containing ^{237}Pu and ^{239}Pu, early retention in mice 78−80983
Pu-O system, partial molar enthalpy of solution of O 77−47578
Pu-O system, substoichiometric phase range obs., high temp. thermodynamic parameters 77−21125
Pu-Re-C and Pu-Tc-C systems, phase relationships 77−21127
Pu+U mixed oxide aqueous solns., limiting critical concs., multiplication factor 77−26859
(Pu-Th)O_2, FBR fuel pellet fabrication, control of O_2-to-metal ratio 80−13760
(Pu-U)O_2, fuel and fuel elements for fast and power reactors 79−616
Pu(C,N), lattice parameter variation, 50 to 300K 78−51709
Pu(C, N), lattice parameter variation at low temp., thermal expsn. 80−15046
PuC, lattice parameter variation at low temp., thermal expsn. 80−15046
PuC-TaC, solubility study 78−83956
PuC-ZrC, solubility study 78−83956
$PuC_{0.82(1.49)}$, high temp. enthalpies 80−49384
PuC_{1-x} and Pu_2C_3, sp. ht., 10 to 300K, mag. ordering 77−28403
PuC_x (x=0.8, 1.44, 1.67), low temp. sp. ht., mag. ordering obs. 80−49372
PuC(N), lattice parameter variation, 50 to 300K 78−51709
$PuC_{0.8}N_{0.2}$, self diffusion processes 78−50259
$Pu(C_2O_4)_2$ precipitator, dynamic process model for nuclear materials safeguards 80−83150
$PuCl_3$, vapour phase hydrolysis and ht. of formation of PuOCl 78−20062
PuF_4, reactor fuel reprocessing, separation of Ru compounds 79−31091
PuF_6, electronic struct. and transitions, SCF-Xα-SW calcs. 78−78627
PuF_6, energy levels and bonding, relativistic SCF Dirac-Slater calcs. 77−6691
PuF_6, near IR spectrum, isotope shifts, vibronically induced transitions 77−6773
PuGa, cryst. and powder diffr. data at room temp. 80−28982
PuH_x, mag. props., 4 to 700K 79−61075
Pu(IV) catalytic redox reactions, kinetics and mechanisms 77−29006
Pu(IV) oxide polymer, potential pollutant from fuel reprocessing, IR spectrum 78−76456
PuN, fabrication, high-temp. thermodynamic and transport props. 77−28774
PuN, heat capacity, at low temps. 79−24168
PuN, high-temperature enthalpy, heat capacity 79−24809
PuN, in Ar matrix, IR spectra, stretching freq. and isotope shifts 78−78690
PuN, lattice parameter variation at low temp., thermal expsn. 80−15046
PuN_2, in Ar matrix, IR spectra, stretching freq. and isotope shifts 78−78690
$Pu(NO_3)_4$ in light water, reactivity predictions using discrete ordinates transport theory 78−89957
$Pu(NO_3)_4$, long-term effects of inhalation, influence of inhaled Ca-DTPA 77−66861
$Pu(NO_3)_4$, particle fuel prep., wet chem. process, for LWR, FBR and HTR *(German, English)* 77−65314
$Pu(NO_3)_4$ solution concentrator equipment for criticality safety 80−18432
$Pu(NO_3)_4$-nitric acid soln., direct denitration in screw calciner 80−37567
PuO, and PuO_2, electronic struct. and chem. bonding and XPS line shape calcs. 79−33264
PuO, in Ar and Kr matrices, IR absorption spectra, normal coord. anal., assignments, force consts. 78−78681
PuO, nuclear oxide fuel anal., coulometry, emission anal., chromatography, X-ray anal. 80−18420
PuO, spectroscopic data rel. to thermodynamic functions 80−34208
PuO_2 aerosol, acute inhalation, predictive model of early mortality 80−36028
PuO_2 air transportable package PAT-1, dose rate and criticality calcs. 80−13938
PuO_2, alpha radiation damage, point defect ingrowth and annealing behaviour 77−27926
PuO_2 and (Pu,U)O_2 assemblies, fission and explosive energy releases 77−65295
PuO_2, conversion to $PuC_{0.88}$, thermodynamic assessment 77−70293

plutonium compounds continued
PuO_2, dissolution in HNO_3-HF soln., effects of metal ion impurities 77−70295
PuO_2 fuel, reproducible fabrication 77−77452
PuO_2 heat sources, ave. total decay power meas. using Bunsen ice calorimeter 77−6547
PuO_2, in Ar and Kr matrices, IR absorption spectra, normal coord. anal., assignments, force consts. 78−78681
PuO_2, LMBR fuel, burnup rate determ. using Nd isotope separation, anal. 77−44553
PuO_2, micro-heterogeneities in LWR mixed oxide fuels, safety aspects 79−49798
PuO_2, Mossbauer resonance 80−20554
PuO_2 multiple low level exposure, case study 78−80967
PuO_2 nuclear fuel, eqn. of state and thermodynamic props. 80−13592
PuO_2 particle behaviour, fuels 79−49684
PuO_2 pellets, control of microstructural damage caused by He release 79−67926
PuO_2, rare earth, Y impurities separation, at. emission anal. 77−52723
PuO_2, reactor grade, calorimetric assay 79−16116
PuO_2 refractory, dissolution in HNO_3-HF-H_2O at 100°C 77−18683
PuO_2, release from contaminated burning Na, LMFBR safety evaluation 77−23224
PuO_2, spectroscopic data rel. to thermodynamic functions 80−34208
$^{239}PuO_2$, stoichiometric, high-temp. deformation 80−81111
PuO_2, struct. changes under self- and reactor irrad. 77−27927
PuO_2, substoichiometric, unified model for defects, thermodynamic functions 77−20094
PuO_2, thermal and transport props., electronic contrib. 80−15432
PuO_2, XPS meas. 77−48314
PuO_2, XPS of 5f electrons 77−73216
$^{238,239}PuO_2$ inhalation toxicology in Syrian golden hamsters 77−86552
$^{238}PuO_2$, high-fired particles, inhalation carcinogenesis in rats 78−28009
$^{238}PuO_2$ particle inhalation, pulmonary tissue local dose computation 79−92385
$^{239}PuO_2$ alpha-particle freq. in lung cells 78−69151
$^{239}PuO_2$, fragmentation of respirable particles in water by alpha decay 77−56487
$^{239}PuO_2$, in vivo solubility in rat lung 78−28093
$^{239}PuO_2$ inhalation, rat pulmonary connective tissue modification by internal α-irrad. 79−92302
$^{239}PuO_2$, inhaled, biochem. effects on lung lipids 77−25510
PuO_2-Na_2O, biological solubility of aerosols in rats 78−96096
PuO_2-UO_2, actinide redistribution in the outer regions of mixed-oxide fuel 79−36321
PuO_2-UO_2 critical clusters in D_2O perturbation anal. of buckling 78−29573
PuO_2-UO_2 fuelled lattice, reactivity predictions using multigroup transport theory 78−89957
PuO_2-UO_2 mixed oxide fuel, plutonia particle behavior during sintering in Ar-H_2 (8%) atmosphere 79−8258
PuO_2-UO_2 possible Pu particle detection by neutron radiography, simulated fuel expts. 77−71637
PuO_2-UO_2-Na aerosol, from LMFBR HCDA conditions, characterisation 78−94104
$^{238}PuO_2$-ZrO_2, particle inhalation, hamster lung cell chromosome aberrations 77−56440
$PuO_2C_2O_4$, Mossbauer resonance 80−20554
PuOCl, heat of formation from vapour phase hydrolysis of $PuCl_3$ 78−20062
PuP, conduction electron polarisation, model density of states 79−37949
PuP, electronic ground state, neutron diffr. 77−15789
PuP, ferromag. mag. cross section, form factors, saturation magnetisation values, polarized neutron study 79−47245
PuP, lattice distortions in ferromag. phase, X-ray obs. 80−15774
$PuTe_3$, magnetis. meas. 77−20542
$(Pu_{0.2}U_{0.8})O_{1.96}$ LMFBR fuel aggregates, dynamic shape factors 79−67853
Pu(VI) reduction to Pu (IV) with NO_2 and NO gases 79−31108
Pu(VII) formation in molten salts 77−29039
$^{238}PuO_2$, uniformly dense aerosols prod. by gas phase neutralisation of acidic droplets 80−26427
$^{238}PuO_2$, uptake by plants in polluted soil 79−5381
^{239}Pu citrate, internally deposited, pot. genetic dose, influence of testicular microanatomy 80−36147
$^{239}PuO_2$, induced lung carcinogenesis in rats, high-fired oxides 78−96077
$^{239}PuO_2$, inhalation by mouse, effect on pulmonary clearance of S. aureus 80−36013
$^{239}PuO_2$, inhaled by baboons and dogs, comparison of early mortality 80−108977
$^{239}PuO_2$, inhaled particles, toxicity and translocation in baboons 79−2109
$^{239}PuO_2$, size characts., Rocky Flats soil, autoradiographic technique 78−96102
$^{239}PuO_2$ high-fired particles, inhalation carcinogenesis in rats 77−21576
$^{239}PuO_2$ inhaled by rhesus monkeys, cytogenetic and other biological effects 80−108968
^{242}Pu halflife from precise low-temp. heat capacity meas. on PuF_3, PuF_4, PuO_2 77−2952
(Th,Pu)O_2 nuclear fuels, economic viability of Pu recycling in LWR 80−18576
Th-PuO_2 kernels, effect of fuel particle size on power excursions, Doppler feedback mechanism 79−30911
Th-U(Pu) fast breeder fuels, chemical, thermodynamic and selected transport props. 79−54505
(U,Pn)O_2, LMFBR fuel pin lattices, calcs. of k_{eff} valves 80−13569
(U,Po)O_2, liq., v.p. meas. at 5000K 77−20077
(U, Pu) C, nuclear fuel, irradiation induced creep meas. 80−93605
(U,Pu) O_2, pore struct., characterisation for gas exchange anal. *(German)* 79−49687
(U,Pu)-oxide nuclear fuel, near and non-stoichiometric, O_2 potential, thermogravimetric and galvanic cell meas. comparison 79−63744
$(U,Pu)_{2+x}$, elec. cond., pure state and Mo addition influence, 350 to 750°C 77−20320
(U,Pu)(C,N) and (U,Pu)N, high burn-up simulated, Pu self diffusion 80−92712
(U,Pu)C FBR fuel pins, irrad. behaviour w.r.t. fission gas release, fuel/clad compatibility, Pu migration 80−57847
(U,Pu)C fuel, interaction with molten stainless-steel shroud 78−86592
(U, Pu)C, LMFBR carbide fuel cladding damage anal. at TREAT 80−13602
plutonium compounds continued
(U,Pu)C LMFBR fuel elements, transient overpower test results 77−46334
(U,Pu)C LMFBR fuel, Na-bonded, consequences of rapid Na loss on fuel behaviour 80−102238
(U,Pu)C, pellet and sphere-pac nuclear fuels, comparative irrad. tests 80−78367
(U,Pu)C, porosity in MX-type fuel and its stability 78−86629
(U,Pu)C possibility for GCFR fuel 77−18667
(U,Pu)C, self-diffusion meas. 80−6544
(U,Pu)C, sintering, role of Ni as sintering additive 80−84892
$(U,Pu)C_{1\pm x}$, evap. behaviour, 1500-2458°C 77−27994
(U,Pu)CN, porosity in MX-type fuel and its stability 78−86629
$(U,Pu)C_{1-x}N_x$ LMFBR MX-type fuels, fission gas release and microscopic swelling 80−73921
(U,Pu)CNO irradiated fuel, electron microprobe anal. 78−70601
(U,Pu)N, porosity in MX-type fuel and its stability 78−86629
(U,Pu)N, self-consistent normal fluid eqn. of state, press., density, and enthalpy of vaporisation calc. 78−8909
(U,Pu)N, self-diffusion meas. 80−6544
$(U,Pu)O_2$ 80−63252
$(U,Pu)O_2$ 316 stainless steel clad rods for GCFR high temp. fast flux irrad. tests 77−18666
$(U,Pu)O_2$ (30 wt.%), oxidation behaviour 79−66210
$(U,Pu)O_2$, anal. of densification in BWR 79−49685
$(U,Pu)O_2$, autoradiographic anal. of PU distrib. 79−49811
$(U,Pu)O_2$, build-up and decay of actinide nuclei in fuel cycle of BWR, PWR, HWR, HTGR and LMFBR 78−17314
$(U,Pu)O_2$, ceramographic exam. of Dounreay PFR fuels, data bank storage 79−49811
$(U,Pu)O_2$, close coupled O-to-metal ratio anal., rapid thermogravimetric method 79−11878
$(U,Pu)O_2$, determ. of H_2O, Hz content by hot extraction methods *(German)* 79−49808
$(U,Pu)O_2$ FBR fuel cycle, review 80−47682
$(U,Pu)O_2$, FBR fuel pellets, gel-supported precipitation conversion and prep. 80−813
$(U,Pu)O_2$, FBR fuel pellet fabrication, control of O_2-to-metal ratio 80−13760
$(U,Pu)O_2$ FBR fuel pin thermal design, effect of fuel stoichiometry 80−18570
$(U,Pu)O_2$, fission gas release and retention in irrad. nuclear fuels 80−57841
$(U,Pu)O_2$ fuel, criticality control, critical mass meas., fission rate distrib. by solid state dosimetry 80−13723
$(U,Pu)O_2$ fuel performance, effect of O_2-metal ratio 80−13762
$(U,Pu)O_2$ fuel pin behaviour during FFTF 3c/s reactivity insertion event, TREAT expt. anal. 80−102240
$(U,Pu)O_2$ fuel-cladding chemical interaction, effect of O_2-metal ratio 80−13763
$(U,Pu)O_2$ fuels, eqn. of state up to 5000K, high-temp. laser technique 77−27971
$(U,Pu)O_2$ GCFR fuel behaviour, effect of O_2-metal ratio 80−18569
$(U,Pu)O_2$, hyperstoichiometric, oxygen potentials determ., 1500-1850K 77−20095
(U, Pu)O_2, hypostoichiometric fuels for FBR, effect of O_2 pot. on fuel props. *(German)* 79−49800
$(U,Pu)O_2$, in pile creep 77−42060
$(U,Pu)O_2$, irradiated fuel, O_2 pot. meas. using galvanic cell 79−49689
$(U,Pu)O_2$ LWR high burnup fuels, remote fabrication and performances 80−13755
$(U,Pu)O_2$, lattice defects and irrad. damage, review 77−27873
$(U,Pu)O_2$, liq., v.p. up to 5000K 77−1239
$(U,Pu)O_2$, microsphere fabrication, hydrolysis process 77−23204
$(U,Pu)O_2$, mixed oxide fuel elements, lenticular pore movement 78−78460
$(U,Pu)O_2$, mixed oxide fuel elements, Pu redistribution 78−78463
$(U,Pu)O_2$ powder, FBR fuel prep. by Au/PuC coprecipitation process 80−814
$(U,Pu)O_2$, power reactor fuel manufacture, technological aspects 79−640
$(U,Pu)O_2$ rare earth, Y impurities separation, at. emission anal. 77−52723
$(U,Pu)O_2$, substoichiometric, unified model for defects, thermodynamic functions 77−20094
$(U,Pu)O_2$, thermal creep in 40 to 100 N/mm^2 stress range 77−28881
$(U,Pu)O_2$, vapour press. eqn. of state, VENUS-II code studies 78−8908
$(U,Pu)O_{2-x}$, chemical diffusion of O *(French)* 79−42300
$(U,Pu)O_{2-x}$, fuel, particle cavitation during reduction by H_2 78−8958
$(U,Pu)O_{2-x}$, mixed oxide fuel, final stage densification 79−49681
$(U,Pu)O_{2-x}$, O_2 thermomigration described by cluster model 78−22888
$(U,Pu)O_{2\pm x}$, cluster model approach to thermodynamic props. 77−20093
(U, Pu)$O_{2\pm x}$, gradient of U, Pu and O at surface 77−18665
(U, Pu)$O_{2\pm x}$, O chemical diffusion coeff. 79−10977
$(U,Pu)O_{2\pm x}$, solid state transport as mechanism of O thermomigration 79−19395
$(U,Pu)O_3$, prod., recycling for use in LWR *(Spanish)* 79−63786
U-Pu aqueous solutions of oxides and nitrates, criticality, effect of Gd, Gd-B neutron absorbers 77−34393
U-Pu mixed oxides, impurities, emission spectrometric anal., single carrier method 78−68944
U-Pu-C system, segregation and v.p. obs. 77−28793
U-Pu-C-N system, phase relationships and equil., effects of oxygen, review 77−21126
U-Pu-O system, substoichiometric phase range obs., high temp. thermodynamic parameters 77−21125
(U-Pu)C, new CRBRP reload core design 79−59155
(U-Pu)O_2 interaction with stainless steel cladding, corrosion products, electron microprobe anal. 79−26524
UC-PuC, carbothermal synthesis *(German)* 77−18661
UC-PuC, ceramic fission reactor fuels, fabrication and performance, review 78−58392
UC_n-PuCn, refabricated fuel for breeder reactor, C determ. 79−11877
UN-PuN, ceramic fission reactor fuels, fabrication and performance, review 78−58392
UO_2-P-uO_2 rods, isotopic anal., gamma-ray spectrometric meas. calibration appl. 77−81440
UO_2-PuO_2, ceramic fission reactor fuels, fabrication and performance, review 78−58392
UO_2-PuO_2, Cs interaction with UO_2 79−6743
UO_2-PuO_2, effects of stoichiometry on cladding attack 79−26523

plutonium compounds continued
UO_2-PuO_2, irradiated fuel pins with various initial stoichiometries, radial O_2 distrib. *(German)* 77−46285
UO_2-PuO_2, mixed oxide fast reactor-fuel pin, fission gas bubble distrib. 78−78459
UO_2-PuO_2, reaction with Zircaloy-2 79−17982
UO_2-PuO_2 fuel, O_2 diffusion at low temps. 78−8899
UO_2-PuO_2 fuel pin, hyperstoichiometric, post irradiation examination 80−63258
UO_2-PuO_2 powder compacts, homogenization kinetics study by X-ray diffr. technique 79−37883
$(U_{1-y}P_y)O_{2-x}$, thermodynamics 78−70594
$(U_{0.8}Pu_{0.2})C$, enthalpy, 1039 to 2421K 77−74920
$U_{0.8}Pu_{0.2}C_xN_{1-x}(0\leq X\leq 1)$, MX-type LMFBR fuels, TEM exam. of microscopic swelling 78−70596
$(UPu)O_{2-x}$, thermal expansion as a function of deviation from stoichiometry *(French)* 78−21645
$U_{0.77}Pu_{0.23}O_{2\pm x}$, oxygen potential in temp. range 1523 to 1822K 80−106113
$(U_1Pu)O_2+x$, O_2 chem. diffusion *(French)* 80−49427
$(U_{1-y}Pu_y)O_{2-x}$, thermodynamics 78−70593
$U_xPu_{1-x}O_2$, theoretical study of electronic thermodynamic and valence props. 79−37655

PMDR
anthraquinone, in Shpolskii matrices, triplet state spin-lattice relax. rates 78−21952
aromatics in stretched PVA films, ESR of phosphorescent triplet state 77−30908
benzene-d_0,-d_6, phosphoresc., Boltzmann population and spin-lattice relax., decay processes 78−31230
benzophenone L in dibromodiphenylether, benzophenone triplet state, nanosecond resolved ODMR, freq.-agile techniques appl. 80−34825
benzophenones, in host crysts., triplet state PMDR, phosphoresc. spectra, transitions mechanisms 77−46585
p-benzoquinone, mixed crysts., PMDR and thermal modulation spectroscopy, electron-phonon interaction 77−32297
2-benzoylpyridine crystals, lowest triplet state, optically detected EPR 80−15827
camphorquinone, cryst., PMDR and fluoresc., S_2 state, intersystem crossing 77−32296
4,4′-dibromodiphenylether:benzophenone-d_{10}, photoexcited triplet state near level anticrossing fields, ODMR at 1.4K meas. 78−80250
1,4-dibromonaphthalene, phosphorescence microwave photoexcitation spectrum (PMPS) 77−32294
4,4′-dichlorobenzophenone, cryst., X-traps, rel. populations, elec. field effect 77−12414
9,10-dichlorophenanthrene, intramol. heavy atom effect, PMDR obs. 79−13745
duraldehyde, S_1-T_1 nonradiative transition mechanism, double reson. obs. 77−30893
durene:quinoline-d_0,(-d_n), phosphorescent triplet spins, phase coherence, spectral diffusion effects 79−87334
molecular solids, substitutionally disordered, Anderson localisation of mol. excitons 77−89733
naphthalene in durene matrix, spin-lattice relax. of phosphoresc. triplet state, PMDR study 79−27012
naphthalene-d_8, metastable triplet states, spin-lattice relax. at high mag. fields, phosphoresc. meas. 78−15063
naphthalene-tetrachlorophthalic anhydride charge-transfer cryst., electronic states 77−32415
naphthalenes, heavy atom effects on phosphorescent triplet states 78−70858
phenanthrene-d_{10}, oriented in biphenyl, triplet zero-field splittings, conc. depend. 78−2773
phenazine, zero field studies of spin lattice relaxation in excited triplet states 79−18219
phosphorescent triplet spins, phase coherence, spectral diffusion effects 79−87334
polar molecule, Stark effect in electron spin transition in zero-field 77−27099
pyrazine, in pyrazine-d_4, p-dioxane, X-trap, p-xylene, benzene(-d_6), cryst., MIDP, PMDR, low temp., assignments 77−36154
pyrazine, PMDR due to single defect species, vibronic structs. 78−19535
pyrazine, zero field studies of spin lattice relaxation in excited triplet states 79−18219
pyrazine-d_4, in p-dioxane, p-xylene, benzene, cryst., MIDP, PMDR, low temp., assignments 77−36154
pyrimidine, zero field studies of spin lattice relaxation in excited triplet states 79−18219
quinolines, heavy atom effects on phosphorescent triplet states 78−70858
quinoxaline, zero field studies of spin lattice relaxation in excited triplet states 79−18219
reaction yield detected mag. reson. spectra, evolution, degenerate energy levels, triplet excitons 78−19378
1,2,4,5-tetrachlorobenzene, excited triplet state dimer, intermol. exchange integral, isotope effect 80−15826
tetrachlorobenzene, in durene, 1.6K, $S_1\sim\rightarrow T_1$ relax. mechanism, Zeeman phosphoresc. and PMDR obs. 77−30912
1,2,4,5-tetrachlorobenzene, in durene host, phosphoresc., cross-relax. between spin levels 78−9186
1,2,3,4-tetrachloronaphthalene, intramol. heavy-atom effect, PMDR obs. 79−13745
triphenylene, triplet state, MIDP and T-S excitation spectrosc. 79−81233
xanthone in host crysts., triplet state PMDR, phosphoresc. spectra, transition mechanisms 77−46585
CaO, F_A(Mo) centre, spin coherence zero-field double reson. 78−43689
CaO F-centre luminesc. and PMDR 79−95832
CaO, ODMR and spin coherences in phosphorescent state of exchange-coupled F^+-centre pairs 79−87336
CaO, random intrinsic strain effect on ODMR, PMDR, of F-centre in Jahn Teller states 78−84499
KCl:PO_2^-, phosphoresc. and PMDR spectra, electronic and vibr. states 79−65768
KCl:PO_2^-, photo-orientation, spectrosc. and ODMR obs. 80−29772
PO_2^-, in K halides, ODMR in zero and weak mag. fields 80−88894
SO_2 PMDR, CNDO CI calcs. 79−72342

PMPS *see PMDR*
p.m.r. *see proton magnetic resonance*
pneumatic control equipment
arterial pressure modulator for perfusion circuit of isolated organ *(French)* 78−81004
artificial heart operation and monitoring system *(German)* 79−8583
blood pressure cuff control unit, automatic multi-function device 78−36013
blood pump regulation electropneumatic servo operation *(German)* 79−8579
capacitor, as liquid-level sensor for process-control appls. 79−71438
counterpulsation operating mechanisms for assisted circulation 79−48371
fatigue testing unit, varying temp., automatic control 77−77667
flow-generated noise through pipe walls, transmission at acoustic pipe coincidence 80−53767
internal gas volume measurement, Boyle-Mariotte's rule *(Hungarian)* 79−49196
left ventricular assist device design and performance 79−96708
level detector, operational principles *(Polish)* 79−85114
microdensitometer precision focus control 79−58769
noise characteristics of control valves 80−53562
pneumoelectric automatic device for passing splices in cinefilm, still photography film *(Russian)* 79−2864
process composition transmitter experience 77−44524
process transmitter for chemical composition meas. 77−36854
prosthetic knee, adjustable pneumatic swing-phase control 79−74792
tank water flow control and meas. appl. 77−41569
testing device for plates under alternating flexure 78−7119
transducers with pneumatic output signals, testing with reference air, water multitube manometer 78−93717
He, gas-cooled power reactor core rod drive *(German)* 78−54837
pneumatic logic *see fluidic logic*
pneumodynamics
see also lung
aerobionic systems in flapping-wing flight *(Russian)* 77−64066
aerodynamic forced oscillation principles appl. to meas. of velopharyngeal orifice area 77−5017
aerosol, electrostatically charged, particle deposition in hollow cast of human larynx-tracheobronchial tree 79−43953
aerosol deposition, particle settling and diffusion 77−52678
aerosol sedimentation in closed finite tubes in random orientation 79−24841
air flowrate in the pneumatic transport of particulate solids in a dense bed *(Russian)* 79−74700
air mixing in model lung alveolus 79−62287
airflow measurement in speech using mask-type wire screen pneumotachograph 77−52808
airway, collapsible, fluid-dynamic flapping, sound generation and flow limitation 80−94258
airway changes induced by histamine or vagal stimulation, vol. history effects 80−67115
airway closure, importance in limiting max. expiration in normal man 80−104606
airway closure and closing volume 79−88102
airway geometry determ. by anal. of acoustic pulse response meas. 78−28026
airway network geometry inference, broadband relfection data 79−29560
airway resistance measurement in infants, heated rebreathing system 78−7471
airway smooth muscle, contracted, hysteresis, dog expts. 80−81634
airways aerosol deposition, two-component theory 79−34582
alveolar CO_2, technique for meas. in infants 79−66564
alveolar gas exchange, effect of altered gas diffusivity 80−97970
alveolar membrane, dog, role of bulk fluid flow in protein permeability 77−52814
alveolar surface tension in excised lungs 79−92257
alveoli albumin clearance, tissue permeation vs. airway displacement 78−27979
amplitude-frequency response of pulmonary air tract 79−20574
anatomic deadspace meas. in mechanically ventilated patients, using N_2 washout 79−96694
area under max. expiratory flow-vol. curve, meas. using analogue device 80−41284
artificial membrane lung, fluid vortices and mass transfer 77−52919
asthma-preventive cromolyn Na inhaler fluid mechanics 79−79587
basic eqns., for flow in human air passages 79−34594
biomedical transducers, information exchange and humanisation *(German)* 79−88204
breath by breath anal. of ventilation and pulmonary gas exchange, minicomputer system 79−62393
breath dispersion patterns, exptl. model study 80−51139
breath volume and time components, computer aided meas. using magnetometers 79−16332
breathing, effect of recirculating breath collection systems on exhalation rate in Ca meas. by ^{37}Ar method 78−40316
breathing, vars. in total respiratory impedance 77−52835
breathing control hierarchical goal-seeking model description 78−80899
breathing control hierarchical goal-seeking model performance 78−80900
breathing parameters, simple testing method *(Hungarian)* 78−31918
breathing pattern and ventilatory response to CO_2 in divers 80−45934
breathing process analogue model *(German)* 79−16228
breathing ratemeter for neonatal intensive care 80−41311
breathing responses to increased transrespiratory press., man and guinea pig obs. 80−30741
breathing work, effect of decreasing inspiratory phase time, analogue integrator meas. 78−85331
bronchial branches, time-dependent flow model 77−44701
bronchial collapsibility of excised dog lungs, effect of lung surface tension 80−67118
bronchial elasticity and air flow, mathematical anal. 80−45942
bronchial elasticity and ventilation mechanism inequalities, theoretical anal. *(French)* 79−48281
bronchial system model, pulsations, meas. by laser photon correlation 78−87420
bronchial tree, non-symmetrical, flow study, asynchronous ventilation appl. 79−70573
bronchial tree axial forces 77−90830
canine input impedance meas. by transient forced oscillations 79−16359
canopy ventilation monitor for quantitative meas. of ventilation during sleep 80−104792

pneumodynamics continued
cardiac effects of increased lung vol. and decreased pleural press., man 80−41073
cardiopulmonary function automated testing system 79−70673
cardiopulmonary readjustments in passive tilt 80−56084
cardiopulmonary stress test data acquisition and control systems 79−79673
cardiopulmonary stress testing in children 80−30911
cardiovascular effects of positive-pressure ventilation in normal subjects 80−41081
chest radiology, introduction to physiological aspects 79−25071
chronic obstructive pulmonary disease detection, airway resistance model 79−96603
coughing, fluid mech. expts. 79−11960
deformations of lung at minimal vol. 80−97977
deposition of inhaled particles, airway generations of normal subjects 80−67125
deposition of particles in model airways 80−72192
diffusing capacity at different lung vols., breath holding and rebreathing obs. 80−30739
diffusivity effects on pulmonary gas transport and mixing 80−108927
dispersion of inhaled particles in humans, model 78−11689
divers, large lungs, functional charact. 80−3680
dust clearance from lung, long-term, impaired by smoking 79−74713
dynamic compliance, freq. dependence, anal. from 1 breathing cycle 80−97967
elastic recoil, use of exponential function 80−8090
elastic recoil rel. to ageing healthy males and females 80−67117
electro-aerosols, precipitation in the airways, effect of electrostatic scatter 80−108929
electrophrenic respiration, feedback control of tidal vol. *(Japanese)* 80−41316
electrophrenic respirator, implantable, Hg battery powered, design, features *(Japanese)* 78−3675
endotracheal tube as factor in meas. of respiratory mechs. 77−21549
enforced smoothing techniques for recovering dV_A/dQ distribs. 79−43946
exercise body plethysmograph, head-out, for extrathoracic airways investigation 80−81754
exhalation in lung model, effect of ventilation and diffusion nonuniformity 80−104603
expiratory duration and abdominal muscle responses to elastic and resistive loading 79−100653
expiratory end pressure, positive, shifting of left ventricular diastolic press.-area curves 80−104604
expiratory flow, expt. test of wave-speed theory of flow limitation in elastic tubes 78−27981
expiratory flow, wave-speed limitation model 78−27980
expiratory flow and transpulmonary pressure maxima, hamster 79−88101
expiratory flow rate, influence on closing vol. meas. 80−35934
expiratory flow-volume curves, configuration variability for maximum expiration 80−3677
fibrous particle motion anal. by two-pulse Fraunhofer holography 80−58476
flow patterns during mech. ventilation of infants 79−57685
flow-volume curves and total pulmonary resistance, monkey 79−83828
flow-volume curves of excised right and left rabbit lungs 80−3673
flowmeter, hot-wire, evaluation for clinical appls. 80−72346
forced oscillatory impedance data, computation of respiratory parameters 79−83821
forced oscillatory parameters of the canine respiratory system with altered vagal tone 80−56082
forced perturbation of respiratory system, continuum mechs. anal. 79−100640
fossorial mammal ventilation, obs. in hypoxic and hypercapnic conditions 80−72195
frequency response measurement technique for press., vol. and flow transducers 80−41344
functional residual capacity, breath-by-breath variation obs. 80−45938
functional residual capacity meas. in neonates with endotracheal tubes 78−53556
functional residual capacity meas. instrumentation for neonates and small animals 78−53590
gas analyzer, response time, incorporation in gas exchange computations 80−72344
gas exchange in normal and abnormal lungs, effects of inspiratory flow pattern 80−45936
gas exchange kinetics determinants during exercise, dog expts. 80−45932
gas transport in human lungs, revised model 79−100643
gas transport models, boundary conditions and geometry 80−85426
gas trapping mechanism model in excised lungs 79−96604
human respiratory airways, diffusional deposition of airborne particles in curved tract 77−81519
hygroscopic particle size, air humidity depend., applic. to lung dynamics 77−90841
hyperthermia due to exercise, effects on breathing pattern 80−72196
hypobaric decompression, changes in lung vol., density and ventilation distrib. 79−100655
hypocapnia in normal subjects, pattern and mechanism of airway response 80−30738
inert gas a-A differences, direct reflection of dV/dQ distrib. 79−20567
inert gas dynamics in subcutaneous gas pockets 77−44707
inert gas elimination charact., computer model 79−20566
inert gas elimination studies without mixed venous partial pressures 80−26250
inert gas exchange, mathematical lung models, effects of common dead space 80−67126
inhaled particle deposition appl. of human lung airways models 80−89776
inspiration, graded inhibition, specific effects of flow rate 79−100647
inspiratory inhibition, sustained graded, phasic lung vol. changes, cat 80−101201
intensive care ventilator, microcomputer-controlled 80−51292
intraoral air pressure, production of /p/ and /b/, children, youths, adults 79−20560
intrathoracic airway models, impedance during low-freq. periodic flow 80−41077
intrathoracic airways mechanics in normal man, sex and age diffs. 80−3676
lobar atelectasis forces, intact dog obs. 80−97966

pneumodynamics continued
lung, analytic model, Green's function for convection-diffusion eqn. 78−11684
lung, apical and basal regions, asynchronism in non-sequential ventilation 78−48820
lung, functional residual capacity and ventilation interaction with occlusion press. 77−86521
lung, human, with uneven ventilation, gas transport *(Japanese)* 80−3700
lung, regional distrib. of tracer bolus inhaled from residual volume, using scintigraphy 77−12950
lung aerosol particle regional deposition 77−44579
lung airway, human cylindrical laminar channel flow model, electrostatic precipitation 78−83491
lung airways aerosol impaction model 77−90840
lung and vascular tree structs., optimisation of diameters and bifurcation angles 78−11683
lung compartmental models, steady state inert gas exchange 80−26249
lung compartmental models, transient inert gas exchange 80−26251
lung compliance loop recovery eliminating cardiac interference by digital filter 79−20570
lung dead space vol. meas. 80−35935
lung emptying patterns, multiple breath N_2 washout data 78−92666
lung function assess., ^{99m}Tc labelled aerosol particles rel. to ^{81M}Kr ventilation imaging 79−100716
lung function examination using ^{13}N *(French)* 77−70521
lung function meas. system, mobile, computer-aided *(German)* 78−3630
lung gas concentrations during air breathing, influence of gas exchange 77−12942
lung gas transport model, derived from human anatomical data 77−5020
lung interdependence and lung-chest wall interaction obs., pig 79−83825
lung isopressure-flow-volume curves, electronic device for automatic recording 78−40382
lung model, human, velocity distrib. and pressure drop. expt. 79−96602
lung numerical modelling, human 78−80911
lung parameter measurement, rebreathing technique for small lung vols. 77−36994
lung perfusion determination by dilution principle with expiration detection of indicator *(German)* 78−85326
lung perfusion determination using O isotopes and dilution principle *(German)* 78−85327
lung phantom, dynamic, use as educational tool 80−8757
lung pressure-volume charact., curve-fitting anal. using programmable calculator 77−48821
lung regional differences, effects of left heart failure 79−25076
lung regional ventilation and perfusion, dynamic meas. with ^{133}Xe 77−86595
lung response data area-distance inversion, consequences of wave dispersion and branching asymm. 78−27994
lung simulation model, simultaneous He and N_2 single-breath washout 79−16233
lung tissue volume and blood flow, rebreathing methods for determ. 79−20569
lung ventilation and perfusion scintigrams, computer aided diagnosis 79−88181
lung ventilation-perfusion imaging vs. angiography in dogs 78−65113
lung ventilation-perfusion ratio resolution of inert gas data 77−12943
lung volume, online calc. by digital computer 80−72351
lung volume change estimation from torso hemicircumferences using Whitney gauge transducers 78−65141
lung volume effects on collateral and airways resistance in man 79−88106
lung volume estimation method, constant inflation pressure 80−67306
lungs long-term forced ventilation control excitation 77−60296
lungs-airway system impedance during breathing in healthy man 77−90832
magnetometers, use to vol.-reference flow-vol. curves 80−104694
magnetopneumographic measurement of particle conc. and clearance in the lung 80−21514
mammalian lung airways, aerosol deposition in anatomical models, theoretical evaluation 80−81627
maximal flow in man, viscosity and density dependence 80−101202
maximum expiratory flow-volume curves, anal. of configuration 79−20565
maximum flow time dependence as index of nonuniform emptying 80−72197
mechanical response at high frequencies, input impedance computation method 79−16239
mechanics of the lung *(Japanese)* 80−41094
MEFV curves, smoothing by digital filtering 80−98157
microcomputer-based data acquisition and analysis system for CO_2 rebreathing studies 80−36161
microwave respiration monitor 79−96646
nasal deposition, theory 79−34581
nasal flowmeter for preterm infants, self-retaining 80−98158
nasal mucous velocity, effect of exercise in normal subjects 80−8088
nematode oesophagus pumping mechanism 78−69121
neonatal pulmonary assist membrane oxygenator 79−25159
neuromuscular blockade, effects on respiratory mechs. in conscious man 80−81632
neuromuscular mechanism maintaining extrathoracic airway patency 79−100656
nonhomogeneous ventilatory mechanics, analogue computer model 79−79575
nose aerodynamics, proposal for meas. method 79−83956
occluded airway pressure, difference with generated muscle press. 80−67101
occlusive sleep apnea, respiratory mechs. and timing 80−97973
oscillatory respiratory resistance in pregnancy and during lying-in 80−56081
particle deposition due to turbulent diffusion 79−66478
peribronchial fluid pressure rel. to vascular and airway press. and interstitial oedema 80−97971
peribronchial pressure in excised dog lungs 79−83823
peripheral asynchronous time constants, comparative study of techniques 80−26256
perivascular pressure measurements by wick-catheter technique in isolated dog lobes 80−35932
physiological compartment tracer flow modelling and digital imaging 80−101257
physiology and chest radiology 79−25072

pneumodynamics continued
physiology system models, breathing control example 80−41058
plethysmograph, body, vol.-displacement using large flowmeter without press. compensation 80−72345
plethysmograph for long-term ventilation meas. in unrestrained animals 79−62413
pleural pressure and lung vol. obs., anesthetised hamster 80−30749
pneumotachograph, for flow and vol. meas. in normal and dense atm. 77−5120
postural effects on lung vols. and asynchronous ventilation, anaesthetised horses 80−97968
precision meas. of anatomic dead space, theory 79−29536
pressure transducers, differential, air-filled, dynamic charact. 80−3879
pressure transducers, gas-filled, effects of gas density on freq. response 80−56249
pressure-volume curves inflection points, 3-balloon-catheter system obs. 80−72190
pressure-volume relationship of fetal rhesus monkey lung, effect of betamethasone 80−41079
prophylaxis for disturbances due to water immersion 77−52893
pulmonary air emboli, effect of ventilation with different gas mixtures 78−27991
pulmonary airway constriction localisation using gases of varying density and viscosity 77−12949
pulmonary airways, longitudinal mixing, impulse response of He, SF_6 79−20568
pulmonary airways, longitudinal mixing, inspiration rel. to expiration 79−100657
pulmonary and recirculation parameter identifiability following sequential bolus inputs of ^{133}Xe 78−44605
pulmonary blood flow meas. from pneumotachograph signals 79−70685
pulmonary conductance, elastic recoil, computerized meas. 79−16317
pulmonary contusion and flail chest, effects on perfusion and O_2 exchange 80−67119
pulmonary filtering capability measuring instrument 79−100729
pulmonary function, plethysmographic meas. method to assess X-irradiation damage in mouse 79−20721
pulmonary function, SI unit system 77−21541
pulmonary function analysis, parameter estimation, lumped-parameter model 77−44815
pulmonary function measurements, aid in diagnosis of suspicious pneumoconiosis 80−21567
pulmonary function parameter meas. system for small animals 80−8227
pulmonary function test automated apparatus for use on Space Shuttle 78−31912
pulmonary function testing, continuous distribution of specific ventilation from N_2 washout 78−92665
pulmonary function testing and monitoring using self-diagnosing microcomputer-based cart 78−31943
pulmonary gas exchange following irrad. of cervical, mediastinal, hilar and axillary nodes 77−73542
pulmonary gas exchange in man, effect of increased gas density 77−16947
pulmonary haemodynamic effects of lung inflation, graded hypoxia in conscious sheep 79−83824
pulmonary interdependence of gas transport 80−41076
pulmonary measurement system, HP model 47804A 80−36163
pulmonary mechanics and perfusion rel. to meas. gas concs. at mouth, simulation 78−31845
pulmonary mechanics computation algorithms on programmable calculator 78−7382
pulmonary mechanics parameters, meas. of breath-to-breath vars. 77−36990
pulmonary mechanics vector scope meas., error anal. 78−40358
pulmonary model for ventilation automatic control 77−21556
pulmonary physiology, pathology, and ventilation-perfusion studies 79−29613
pulmonary resistance, human, effect of freq. and gas physical props. 80−30744
pulmonary resistance, lower, effect of gas phys. props. and flow 77−12945
pulmonary resistance distribution, effects of gas density, viscosity and flow-rate 77−12948
pulmonary resistance measurement by forced oscill. technique 77−40877
pulmonary single-breath N_2 washout rel. to mech. function 77−36991
pulmonary vascular interdependence in isolated dog lobes, continuum mechs. anal. 80−3671
pulmonary vascular resistance, longitudinal distrib., and lung inflation in hypoxia 80−56086
pulmonary ventilation and perfusion distrib. during short weightlessness periods 79−83951
pulmonary volume calculator, automatic analogue device, performance in hospitals *(French)* 78−31930
pulsing elastic alveoles, gas transport, conc. depolarisation *(French)* 78−85328
radioactive tracer tidal breathing, lung ventilation model, radioactive tracer tidal breathing 80−56095
radioisotope cinepneumography, flow-vol. imaging of the respiratory cycle 80−94343
regional differences, effects of body position and respiration 79−25073
regional differences effects of smoking 79−25075
regional distrib. of (dV/dt)A/(dQ/dt) in man, at rest and with exercise, meas. with ^{81m}Kr 79−16232
regional electroaerosol deposition model 79−83842
regional ventilatory clearance, estimation by Xe scintigraphy 80−30854
respirable fraction definitions, matching air sampler penetration curves 77−90827
respirable fraction of airborne dust, performance charact. of samplers 78−53438
respiration, aerosol deposition/clearance, radioactive particle administration technique 77−60312
respiration, automated real-time whole-body plethysmographic anal. system 78−28112
respiration, choice of catheter system for intra-oesophageal press. meas. 77−90937
respiration, density depend. of max. expiratory flow 78−27993
respiration, external, anal. determ. of energy expenditure of man 78−69268
respiration, feature selection appl. to coal miner spirograms 78−40387
respiration, human, managment of artificially ventilated patients 79−70576
pneumodynamics continued
respiration, looped receiver impinging jets flowmeter with circular and rectangular jets 77−40878
respiration, lung parameter estimation by meas. of air press. and flow 77−21642
respiration, maximum expiratory flow changes induced by longit. tension on trachea in normal subjects 78−27982
respiration, planar fluidic flowmeter appl. 78−35993
respiration, two-stage ladder network model for detect. of small airway disease 78−31846
respiration dynamic model eqns., explicit solns. and periodic functions *(French)* 79−79574
respiration model eqns. soln. *(French)* 79−62283
respiration rate automatic meas. device *(German)* 79−2146
respiratory airflow pattern modelling by optimisation criteria 78−80898
respiratory apparatus effects on breathing pattern 80−104602
respiratory control in cats, interactions between central and vagal mechanisms 78−53436
respiratory control system, time series cluster anal. 78−56959
respiratory control system simulation, state-of-the-art 78−53441
respiratory data management subsystem 79−83980
respiratory data recording using XY recorder with data storage 78−7474
respiratory flow integrator with improved stability 79−16331
respiratory flow telemetering with mag. type flowmeter 77−86654
respiratory flow-volume integrator 77−48914
respiratory forced oscillation parameters in dogs following papain exposure 79−88105
respiratory function indices, microprocessor based analyser 79−25131
respiratory function telemetering by combined sensor 78−80995
respiratory function telemetering using combined receptor 77−86657
respiratory gas exchange by avian embryo 77−44708
respiratory gas flow meas., constant-temp. hot-wire anemometer evaluation 79−83967
respiratory gas monitoring instrument using microprocessor *(Japanese)* 80−72358
respiratory heat exchange analysis, during inspiration, under environmental conditions of deep diving 78−15856
respiratory impedance and derived parameters in young children by forced random noise 80−30745
respiratory impedance meas. system for small children 79−92277
respiratory impedance measurement, direct-display oscill. method 80−36174
respiratory impedance measurement instrumentation using forced oscills. 77−37079
respiratory measuring equipment, flow and vol. calibrator 79−96687
respiratory mechanical behaviour lumped parameter models evaluation using simplex algorithm 80−89783
respiratory mechanics, effect of breathing He-O_2 and SF_6-O_2 78−27992
respiratory mechanics and body plethysmography, model 77−90846
respiratory mechanics in normal bonnet and rhesus monkeys 79−83827
respiratory mechanics in recumbent dogs under general anesthesia 79−100651
respiratory monitors, instrumentation and maintenance, review 78−69236
respiratory oscillations, altitude effects disclosed by identification methods 80−97979
respiratory parameter interval estimation using least squares techniques 79−48277
respiratory period prediction, men exercising while wearing masks, comparative model study 80−94253
respiratory phase detector system, battery operated cct., air temp. change meas. 79−100770
respiratory plant dynamics under open control loop conditions 77−44705
respiratory rate and ventilation digital recorder 78−81005
respiratory rate monitor using microphone pickup 79−79617
respiratory resistance, central and peripheral, estimation using elec. analogue model 80−81636
respiratory resistance fractionation in young children, expt. obs. 80−56087
respiratory resistance freq. depend. in normal dogs 78−44542
respiratory resistance freq. dependence, health children 80−41075
respiratory resistance measurement, modified forced oscill. technique using computer 77−86692
respiratory response to exercise, computer-based anal. 78−7458
respiratory rhythm influence on fluid flow *(French)* 77−40702
respiratory system, freq. charact. determ. 77−5093
respiratory system, human, mechanics of regulation 80−41102
respiratory system, human, modelling and parameter estimation 80−12169
respiratory system, human, modelling and parameter identification 79−39444
respiratory system, role of the Van der Pol oscillator 78−65073
respiratory system forced perturbation, traditional model 79−83815
respiratory test performance indicator for subject motivation 79−57797
respiratory total compliance non-invasive meas. in free-breathing rabbits 78−28123
respiratory total resistance meas. in pre-school children using modification of forced oscill. technique 78−77129
respiratory tracer gas nonlinear computer anal., non-invasive meas. method 79−62395
respiratory tract, human, aerosol particle deposition during breathing, sampling apparatus 79−96719
respiratory ventilator model and design optimisation 79−20713
respirometric open systems, error anal. *(German)* 80−104782
respirometry with flow-through mask, meas. of VO_2, VCO_2 and evaporative water loss 77−48961
rhino-manometry measurements, theory of some systematic errors *(German)* 79−83957
rhino-rheo-manometer for dynamic and static nasal pressure meas. with capacitance probes 79−83961
rhinomanometer, new-type, and relating test experiences 79−100768
roentgenfilm densitometry and linear lung expansion relationship 79−25074
servo control of end-tidal CO_2 in paralysed animals 79−39607
specific airway resistance changes meas. technique 80−8228
spirogram, forced, transit-time anal., healthy children and adults 80−8082
spirometric data, automatic classification 79−57803
spirometric parameters, interactive on-line computerised computation 78−44656
switch valve, lightweight, remotely actuated, for rebreathing exercise studies 80−101278

pneumodynamics continued
thoracoabdominal mechanics during relaxed and forced vital capacity 80−30740
tidal ventilation, estimation of a distribs. central moments 79−88104
tidal volume, contrib. of rib cage and abdomen-diaphragm during CO_2 rebreathing 79−100650
trachea wave speed, dog 78−31841
tracheal direct phase velocity meas., distal branch reflection artifact model 79−92280
transthoracic impedance curve processing, patient-computer interface 79−34686
upper airway patency in the human infant, influence of airway press. and posture 80−97978
vagal blockade effects on lung mechs. in normal man 80−8081
ventilation, gated regional spirometry (GRS) 79−25097
ventilation, human, twin exponential model fitting process development 79−48284
ventilation, radionuclide studies, clinical comparison of ^{127}Xe and ^{133}Xe 77−86594
ventilation abnormalities detection using ^{133}Xe, washout rel. to single-breath imaging 80−41183
ventilation and regional vols. distribs. in excised canine lobes, gravitational deform. 80−30747
ventilation and ventilatory pattern maturation in normal sleeping infants 80−35933
ventilation by HF oscill., beagle expts. 80−104607
ventilation device for newborns, especially during incubation 79−100786
ventilation regional and whole, math. model for radioactive tracer studies 78−20249
ventilation regional measurement using ^{81m}Kr, math. lung model 77−86611
ventilation regional phase differences demonstration by breath sounds 80−8087
ventilation scintigraphy, comparative analysis of ^{81m}Kr and ^{133}Xe 78−85360
ventilation studies, ^{127}Xe distrib. in lungs 78−44606
ventilation studies test for free Br in carrier gas from $^{81}Kr^{m}$ generator 79−79642
ventilation-perfusion inequality, susceptibility of different gases, theoretical anal. 80−8089
ventilation-perfusion ratio, practical considerations of multiple inert gas elimination technique 77−56411
ventilation-perfusion ratio distrib. determ. from inert gas data with enforced smoothing algorithm 78−61208
ventilation-perfusion ratio distribs., graphical assessment from inert gas elimination data 77−52834
ventilation-perfusion ratio intraregional maldistribution simulation 78−31834
ventilation-perfusion ratio obtained by noninvasive freq. response technique 77−12952
ventilation-perfusion relationship in young healthy awake and anesthetised-paralysed man 80−67120
ventilators for animals, automatic sigh feature 80−98186
ventilatory function testing, appl. of versatile microcomputer 80−41291
ventilatory measurements in children, respiratory jacket for 79−62379
ventilatory monitoring in operating room, current techniques and future requirements 78−20307
ventilatory phonetics, analogic 80−51131
ventilatory phonetory conflict, investigation using glottiscope 80−51145
ventilatory response to added mech. loads, 1st breath, naive men 79−100654
ventilatory response to CO_2 obs., sprint swimmers *(Japanese)* 80−8077
ventilatory responses to elastic loading at constant Pa_{CO2} in hypercapnic hyperpnea 80−67121
vocal cord vibration, computer model of air vol. displacement 78−69111
volume of lung, reduction during behavioural active sleep in newborns 80−45935
volume shifts with partial submersion of isolated lung lobes 80−81631
washout, multibreath, modelling and moments 79−43940
washout curves using N_2, multiple-breath, new method for anal. 80−101199
CO, single breath diffusing capacity in man, meas. by rapid CO anal. 80−46115
CO uptake in respiration, computer aided measuring system *(German)* 80−3875
CO_2 pressure, end-tidal and arterial diff. obs. 80−72193
CO_2 pressures in dogs during acute hypercapnia, arterial-expired differences 80−72198
CO_2 responses of conscious rabbits at ambient temps. of 5, 20 and 35°C 80−56085
HeO_2, breathing, dogs, mechanisms of increased max. expiratory flow 80−56083
O_2 consumption meas. with flow-through system, accuracy assessment 78−65067
O_2 consumption rate determination, dynamic mode of N_2 storage in man 78−27997
O_2 stores during hypoxia in goats, freq.-domain anal. 79−100639

PNO calculations
chloromethane, mol., valence and core ionis. energy, RHF-SCF and PNO-CEPA calc. 79−85890
hydride ions, XH^+, X=first and second row elements, PNO-CI and CEPA studies of electron correlation effects 77−34561
second-row atoms, static dipole polarisabilities, finite perturbation calcs. 77−6690
ArH^+, $^1\Sigma^+$ ground state, molecular consts. calc. from pot. curves 80−9680
BO, spectroscopic properties, PNO-CI and CEPA calcs. 78−41961
C atom, ^3P state, valence shell correl. energy, IEPA-PNIdme IEPA-PNO method 77−10597
$C_2H_3^+ + HF$, interaction, struct. and stability, ab initio calcs. 80−58347
$C_2H_3O^+$ and $C_2H_3S^+$, stability, proton affinity, ab initio SCF, CEPA PNO, MINDO/3 and MNDO calcs. 79−59357
$Cl' + HCl \rightarrow Cl'H + Cl$, barrier height, PNO-CEPA calculation 77−16795
HF dimer, stabilisation energies, harmonic force constants, intermolecular vibrations, SCF and CEPA PNO calcs. 79−98177
HNB,(HNBH), spectroscopic properties, PNO-CI and CEPA calcs. 78−41961
HOB,(HBO), spectroscopic properties, PNO-CI and CEPA calcs. 78−41961

PNO calculations continued
H_3SiCl, mol., valence and core ionis. energy, RHF-SCF and PNO-CEPA calc. 79−85890
$H' + BrH \rightarrow H'Br + H$, collinear reaction, barrier height, PNO-CEPA cals. 78−3328
$H' + XH \rightarrow H'X + X$, X=H, F, Cl,CH_3, collinear pot. energy barriers, PNO-CEPA calcs. 77−32777
LiF oligomers, struct., stability SCF and CEPA-PNO calcs. 78−78640
LiH oligomers, struct., stability SCF and CEPA-PNO calcs. 78−78640
NaF oligomers, struct., stability SCF and CEPA-PNO calcs. 78−78640
NaH oligomers, struct., stability SCF and CEPA-PNO calcs. 78−78640
O_3, wave function calc. rel. to energy separation, cyclic and open isomers, CEPA-PNO method 79−93929
P_2H_4, conformation, ab initio, HF, PNO-CI and CEPA calcs. 77−46495
SiH_4, mol., valence and core ionis. energy, RHF-SCF and PNO-CEPA calc. 79−85890

Pockels effect
acousto-optical snapshot Pockels Readout Optical Modulator 77−19193
active pulse shaping in ps domain using fast Pockel cell and GaAs switch 80−28257
bistable optical systems based on Pockels cell 79−59827
cell, large aperture, variable pulse width generation for CO_2 lasers 78−46691
cell driver of fast rise time and high repetition rate using thyratron 80−69537
differential electro-optic shutter with ns pulse operation 78−74994
double Pockels shutter in ruby laser with active phasing of spectrum *(Russian)* 79−98419
electro-optic voltage dividers, capacitor type, current meas. appl. *(Italian)* 77−26339
insulator surface flashover in vacuum, electro-optical meas. 80−38823
IR pulsed radiation production using 2.25 cm^2 aperture Pockels cell system 80−5806
large-aperture Pockels cell design 77−19438
laser subnanosecond pulse production, of variable length, using Pockels cell 78−94405
light modulation, max. depth, Pockels cell modulator 80−102819
light modulator with small nonactive losses 80−78981
materials, and device applications *(Italian)* 77−42626
optical glasses, Brillouin scattering meas., sound vels., Pockels coeffs., phonon damping 79−95792
optical wave conjugation by three photon mixing, effect of strong wave front distrib. 80−5783
organic electrooptical materials for light modulators and deflectors, characts. *(Japanese)* 77−73128
Pockels readout optical modulator, current status and appls. 77−72085
polar phonons in crysts., Raman scatt. theory 79−47447
PROM, diffr. efficiency 80−14467
shutter for laser pulse shaping, Pockels cell with programmable transmission control 80−64162
space-time light modulator 80−69526
ultralinear bistable electro-optic polarization modulator based on Pockels cell 78−83077
uniaxial crystal, first-harmonic electromodulation 78−35116
Ar, single crystal, Pockel coeffs. and short-range-interaction parameters 79−73962
$Bi_{12}SiO_2$ Pockels readout optical modulator, X-ray response 79−64313
$Bi_{22}SiO_{20}$, Pockels readout modulation struct., information registration *(Russian)* 77−10990
CdS, transition metal centres, first-harmonic electromodulation spectra 78−35116
$CdS_{0.75}Se_{0.25}$, linear electro-optic effect meas., light modulator appl. 78−76434
CdTe crystal Pockels modulator, PCM of CO_2 TEA laser pulse 80−102742
GaAs, birefr. harmonics, permittivity dispersion 77−52044
GaAs, intracavity modulation of polarization direction of CO_2 radiation 80−102744
GaSe, Pockels effect 79−51933
$In_{1.9}Sn_{0.1}O_3$ laser-damage-resistant transparent conductive coatings, appl. in Pockels cells 79−50333
KD_2PO_4, cryst. high-freq. modulation in Pockels cell, acoustic phenomena 78−1336
KD_2PO_4 light valves for optical information processing 77−72080
KH_2PO_4, cryst. high-freq. modulation in Pockels cell, acoustic phenomena 78−1336
KH_2PO_4, Pockels effect in UV region 77−12398
KH_2PO_4, Pockels' const., linear electro-optic consts., sign of piezoelectric const. 78−60425
Kr, single crystal, Pockel coeffs. and short-range-interaction parameters 79−73962
$LiNbO_3$:Fe, optical damage depend. on temp., press., and applied elec. field *(Japanese)* 79−81498
N_2, TE laser, anal. of time variation of discharge channel voltage by Pockels effect 78−90412
$NH_4H_2PO_4$, Pockels effect in UV region 77−12398
Nd:glass, oscillator, short laser pulses *(Rumanian)* 79−7165
Nd:YAG laser, Q-switched, pulse stretching using Pockels cell 80−95927
Xe, single crystal, Pockel coeffs. and short-range-interaction parameters 79−73962

point contacts
1/f noise, theoretical analysis *(Polish)* 78−91737
alkali metals, point contacts, current-voltage characts. at liq. He temps. 80−39663
electrical transport, influence of mech. modulation 80−2481
far IR laser output detection by MOM point-contact diodes *(Japanese)* 79−21811
heating effects limit on intrinsic high-frequency performance, comparison with Josephson junctions, props. 79−28456
HF rectification at low temp. in point contacts between identical metals 80−105706
IR detector tunnelling and rectification characteristics, geometrical and multiple image interactions 80−57376
IR point-contact diode tunnelling and rectification rel. to electrode geometry 80−57378
Josephson contacts, three-dimens. assembly, crit. currents and penetration depth 80−84560
Josephson point contact junctions and microbridges, HF props. 79−28461
Josephson point-contact resonance responses 79−99658

point contacts continued
metal whisker diode, thermal field emission, nonlinearity, response time and polarity reversal 78−2579
metal whisker diode, with thermally enhanced field emission, elec. fields, calc. by antenna theory 77−47889
metal whisker point contact junctions, tunnelling and rectification charcts. 80−6955
metal-barrier-metal diodes, I-V charcts., nonlinear mechanism in low voltage region 80−88618
metal-metal, α^2F depend. of electrical impedance 78−47848
metal-metal, direct meas. of electron-phonon coupling 78−6433
metal-vacuum-metal point contact junction charcts., Green's function calc. 80−103744
metallic, elec. cond., spectroscopy of phonons, impurities *(Russian)* 78−38797
metallic, nonlinear resist. rel. to phonon emission and background effects 78−68074
metallic, small radius, voltage-current curves, electron-phonon interaction theory of results *(Dutch)* 77−62985
metallic point contact diodes, tunnelling props., geometrical asymmetry effects 78−10576
metals, ferromagnetic, point contact spectroscopy, electron-magnon interactions *(Russian)* 80−54766
metals, phonon point-contact spectroscopy 79−65152
metals, struct. of d^2J/dV^2 charcts. of point contacts 80−96975
microscopic point contact resistance, size depend. 79−69582
MIM diodes, freq. response, effect of d-electrons 77−47898
MIM diodes for harmonic generation and mixing 78−88044
MIM point-contact diode harmonic generators and mixers 80−60105
multiple flux quantum transitions, comparison with I-U charcts. using Nb-point contacts 80−60149
$n\text{-}n^+$ junction point contacts, I-V charcts. 77−1480
$n\text{-}n^+$ point contacts, current-voltage charcts. 78−26940
submillimetre mixing, high order, for heterodyne detect. 77−5910
submillimetre wave detection, sensitivity detn. 77−37984
subMM wave mixing in metal-metal and metal semiconductor point contact diodes 80−4769
superconducting, LF fluctuations, cond. and voltage *(Russian)* 77−20500
superconducting metal point contacts, struct. of current voltage charcts. 79−56441
superconducting microbbridges and point contacts, nonstationary Josephson effect 79−38256
superconducting point contact, excess current *(Russian)* 79−19702
superconducting point contact, in wide-band radiometer for short millimetre range wavelengths 79−62750
superconducting point contact microwave detector/receiver 77−79153
superconducting point contacts, Nb and Ta, 9 GHz complex impedance 77−28303
Ag_2Se, between metal electrodes, current-voltage charcts *(French)* 80−97005
Ag_2Se thin film, switching and Ag movement, point contact technique 80−60107
Bi-Sb alloys, metal-semimetal point contacts, volt-ampere characteristics *(Russian)* 80−65683
Cd point contacts, electron-phonon coupling, microcontact spectroscopy investig. *(Russian)* 78−38796
Cu, electron-phonon interaction anisotropy, microcontact spectroscopy *(Russian)* 78−43372
Cu, magnetic focusing of electrons 79−65540
Cu-Zn heterocontacts, microcontact spectra *(Russian)* 80−34502
Fe, electron-phonon coupling, point contact spectroscopy obs. *(Russian)* 80−70342
Fe, point contacts between ferromag. metals, singularities depend. in d^2V/dI^2, phonon spectra 79−60457
Gd, microcontact magnon spectra, electron-magnon interaction *(Russian)* 80−54768
$GdCu_2Si_2$/Mo, point contact spectroscopy of magnons 79−38312
Ge p-n junctions with hot carriers, current amplification, elec. domain form. 80−6966
Ho, microcontact magnon spectra, electron-magnon interaction *(Russian)* 80−54768
Nb, AC Josephson effect meas. at 604 GHz 77−80876
Nb, Josephson effects in far IR, high freq. behaviour 79−1643
Nb Josephson point-contact far IR detector props. 79−30543
Nb point contact, far IR freq. depend., of AC Josephson effect 79−33407
Nb, point contact Josephson junctions, thermally recyclable, as low-noise mixers 78−62224
Nb, point contacts as low-noise Josephson mixers, 115 GHz meas. 79−26123
Nb, supercond. point contacts, freq. and voltage depend. in noise background 79−58796
Nb, superconducting point contacts, cond. mechanism 79−56440
Nb superconducting point contact, high freq. props. in far IR 80−54840
Nb-Nb point contact junction, supercond. weak couplings, high-freq. props. 78−68122
Nb-Nb(Nb_3Sn) supercond. point contacts, crit. currents, effect of laser radiation *(Russian)* 79−28484
Nb_3Sn-Nb_3Sn supercond. point contacts, crit. currents, effect of laser radiation *(Russian)* 79−28484
Ni, electron-phonon coupling, point contact spectroscopy obs. *(Russian)* 80−70342
Ni, point contacts between ferromag. metals, singularities depend. in d^2V/dI^2, phonon spectra 79−60457
Pt-Pd discontinuous film MIM point-contact diode detector 77−5917
Si, n-type, noise meas. on ohmic point contact 77−4443
Si-W point diode, utilisation as radiation detector and mixer in sub MM band 79−89006
SiC, point contact, stable elec. oscill. generation by high field strength *(Russian)* 77−62989
Tb, microcontact magnon spectra, electron-magnon interaction *(Russian)* 80−54768
Tb/Mo, point contact spectroscopy of magnons 79−38312
V_2O_5-P_2O_5 glass, switching and memory behaviour, Pt point contact effects 77−11970
W-C, compared with TGS pyroelec. detector, appl. to temporal coherence meas. of HCN laser 80−31871
W-Ni, MBM diode, resist. depend. of detected signals 80−2482
W-Ni point contact diode, rectifying props. in CO_2 laser radiation 77−76942
point contacts continued
W-Ni point contact diode detectors at 10.6 μm, mech. and props. 78−24861
W-Ni point contact diode fast acting detector for modulated CO_2 laser beams 79−3730
W-Ni(Co) point-contact diodes as harmonic generators and mixers, DC bias dependence 80−75653
Zn, electron-phonon interaction anisotropy, microcontact spectroscopy *(Russian)* 78−43372
Zn, electron-phonon interaction anisotropy, microcontact spectroscopy *(Russian)* 79−37786
Zn point contacts, electron-phonon coupling, microcontact spectroscopy investig. *(Russian)* 78−38796

point defect scattering
used for carrier scattering by point defects
anthracene, cryst., cyclotron reson. and carrier scatt. 77−76746
degenerate semiconductors, longitudinal thermo-EMF in quantising mag. field, scatt. mechanism *(Russian)* 80−24960
elastic wave interaction defects of finite vol. and defect mutual interactions 78−32676
insulator, low temperature, role of point defect scatt. in lattice thermal cond. 77−76631
metal, resistomatic studies of lattice defects review *(Japanese)* 78−59799
metal, unstable vacancy-interstitial atom pair, scatt. of electrons 79−15129
metal, with closed orbits, high-field magnetoresistance of point defects 79−7819
metal thin wires, size effect correlation to longitudinal magnetoresistance 78−34824
metals, cubic, relationship between defect resist. and bulk resist. at melting temp. 78−6344
mixed crystal, disorder scatt. theory using model pseudopot. 77−15811
optical properties of band charge carriers, nonlinear, rel. to carrier scattering by lattice defects 80−29399
organic molecular crystal, temp.-independ. mobilities, elec. field and defect scatt. effects 80−10963
semiconductor, carrier scatt. and mobility transient processes, pulsed Hall photoeffect 80−15546
semiconductor, exact calc. of mobility due to point defect scatt. 78−19029
semiconductors, elec. cond. in elec. and mag. fields, carrier scatt. mechanisms 79−65467
semiconductors, free electron scattering and dynamical cond. 78−2476
Al, low-field galvanomag. props., Fermi surface and defect struct. effects 77−4323
Al, magnetoresist., linear growth in strong. mag. fields *(Russian)* 78−51972
Al-Ge(Mg)(Zn)(Ga), dil., electronic transport coeffs. for point defect scatt., 4-OPW calc. 79−42531
Au, magnetoresist of quenched and annealed metal, defect scatt. 79−4981
Au, pure, small resistivities, size correction 77−43742
Au, quenched and annealed, cond. electron scatt., de Haas-van Alphen Dingle temp. meas. 77−89688
Au, quenched and annealed, conduction electron scattering 78−47774
BP film, high temp. thermoelec. power, scattering processes 80−80305
CdSe, heat treatment effect on carrier mobility, role of defect centres 77−72861
CdTe, phonon conductivity, 2 to 300K, scatt. mechanisms 79−4436
Cu film, electron transport props., struct. defects role 77−40117
Fe-Al alloy, B_2-type, electrical resist. meas. 78−30917
$FeCl_2$, antiferromag., magnon-phonon interactions in thermal cond. 80−65315
Ge, charge carrier scatt. and compensation effect on Hall mobility of majority carriers *(Russian)* 77−32026
n-Ge, deform. induced point defects, Hall coeff. meas. 80−19800
Ge, irradiated and annealed, cyclotron reson. linewidth investig. of electron scatt. 77−55707
InSb, phonon conductivity, 2 to 300K, scatt. mechanisms 79−4436
Nb, elec. resist. changes with plastic deform. 77−89749
$Pb_{0.82}Sn_{0.18}Te$, Hall mobility, scatt. mechanisms, temp. and carrier conc. depend. 77−55548
$RbMgF_3$, irradiated, thermal conductivity 78−22909
Si:P, heavily doped, influence of impurities and crystalline defects on electron mobility 79−78095
V_3Si, channelling, at displacements and electron phonon/defect interactions 77−84815

point defects
see also colour centres; interstitials; point defect scattering; vacancies (crystal)
actinide carbides, lattice defects and rel. to phys. props., review 77−27874
ageing, influence of neutron irradiation *(Czech)* 78−84859
alkali halide, brittle fracture of single crysts. and active struct. of cleavage surfaces 79−28039
alkali halide, effect of lattice of point defects on activity and brittle fracture 79−15785
alkali halide, lattice relaxation around tetragonal and rhombic defects 79−95110
alkali halide crystals, heat of form. for high-conc. substitutional defects, model 78−10048
alkali halides, ^{14}N impurities, molecular point defects, EPR isotropic hyperfine triplets 80−2636
alkali halides, effect of ionisation of condensing flux on nucleation of metal films 80−107675
alkali halides, matter transport rel. to point defect parameters 80−107488
alkali metal halides, defect production in cation sublattice, mechanisms 80−96510
alkaline earth halide crystals, thermal transport of charged point defects 80−15293
alkaline earth oxides, point defect props., band struct., lattice simulation calc. 80−19797
alloy, production process strength *(Russian)* 77−21152
alloys, irradiated, effect of defect trapping and solute segregation, on defect recombination rates and void swelling 78−47369
alloys, rapidly quenched crystalline, struct., and heat treatment effects 80−76292

point defects continued
amorphous metals, struct. imperfections, review of expt. evidence 79−37630
anelasticity, general linear response, anal. 79−10895
anelasticity, influence of anisotropic point defects 78−14403
anisotropic continuum theory 79−73162
anisotropic cubic elastic Green's tensor function, elastic energy coeff., Algol 60 program, crystal point defects 77−11537
basis sets for study using Green's function methods 79−90994
bimolecular recombination controlled generation, theoret. approxs. eval. *(Russian)* 80−103323
binary, ternary oxides, dislocation motion and high temp. plasticity 80−59468
book 77−47442
book contribution 78−10044
Bragg reflections, ratio of integral intensities, determ. struct. perfection of single crystals 80−87987
chemisorption on defective surface, theory 78−2362
coatings, defects and their effect on props. 80−39474
collective dislocation motion, dynamic effects 78−79632
compressed crystals, dislocations and point defects *(Russian)* 78−75666
concentration monitoring during low-temp. irradiations and anneals 80−7741
consecutive energy barrier systems, deform. kinetics 79−77672
covalent semiconductors, electronic struct. of localised defects, review 80−44535
creep, diffusional, grain boundaries as point defect sources or sinks 79−37757
creep, irradiation induced, correlation of theory with expt. evidence 80−88255
creep, irradiation induced, dislocation glide enabled by preferred absorption of point defects 80−88250
crystal, subjected to high-energy, particle flux, change in mobility 79−7708
crystal melting, pre-melting near point defects 77−76524
crystal surface elastic props., surface tension tensor, volume stress *(Russian)* 80−100389
cubic crystal, close packed clusters of 5 substitutional point defects, configs. 78−59802
cubic crystal, non-Arrhenius diffusional behaviour and high-field nuclear spin relax. 77−47611
cubic crystal, relaxation effect around point defects 77−84740
cubic crystal edge and screw dislocation−point defect elastic interactions 80−15151
cubic lattices, ordered dispersal of point defects, appl. to fluorite related structs. 77−47447
dark-field electron micrographs, defocused, for point defect accumulations investigation 79−99036
deformation kinetics analysis of stress sensitivity 77−3737
density matrix formalism for anelastic relaxation 79−14880
derivation and classification 78−2111
diamond, defects and impurities 80−29017
diamond, effective ion interaction and force consts., model of Si point defect 80−65185
diamond, optical absorption and luminesc. spectra, review 80−2848
diamond lattice, point defect grasshopper effect 79−90830
1,5-dichloroanthracene, photodimerisation, orientational defects, lattice energy 78−80724
diffusion-controlled reactions, theory, rate equations 78−18677
dilatation centre periodic distrib. in anisotropic half space, deformation 79−46649
dilatation centres, elastic interaction with disclination dipole 77−68994
dilatation energy of extended defects of arbitrary shape and size near solid surfaces 78−34508
dilute alloys, point defect electric field gradient, anisotropic screening effect 79−56177
dislocation damping, unified theory, point defect dragging 80−88144
dislocation field effect, dislocation photoconduction spectrum *(Hungarian)* 80−51977
dislocation interaction with point obstacle in non-uniform stress field, localised force approx. 80−15150
dislocation percolation through absolute obstacles in impurity crystals *(Russian)* 80−70196
distribution in bounded media under irradiation 77−7712
Earth mantle, thermally activated point defects interpretation of low vel. zone 78−88806
elastic amorphous medium, relax. by defect diffusion 80−58925
elastic continuum point defect model, inhomogeneity correction 77−27878
elastic interaction of point defects and volume defects near interfaces 79−65115
elastic interaction with grain boundaries 80−59483
elastic interactions between defects and interfaces 80−39147
elastic interactions in semi-infinite medium 80−39146
elastic strain energy, stable configuration determ., computer calc. 78−30663
electrolytes, solid oxide, elec. props., study methods *(French)* 80−22386
electron accelerator cryogenic equipment for study *(French)* 77−132
electron displacement damage simulation in HVEM irrad. 80−107325
electron microscopy imaging, approx. for dynamical calcs. of microdiffr. patterns 78−26393
electronic structure, formation energies and diffusion parameters 80−2009
fast reactor materials, fast neutron damage 78−10093
fatigue crack, dislocation diffusion mech. of form. 78−60829
FCC crystal, elastic interaction of 60° and screw dislocations with point defects 78−63786
ferroelectric, polarisation switching influence of mobile point defects 78−31165
ferroelectric domain wall shift, mobile point defect interaction effects 77−32338
ferroelectrics, properties near phase transition point, influence of defects 79−42918
fission reactor materials, defect trapping and solute segregation in irradiated alloys 80−13603
fission reactor materials, point defect nucleation and growth, rate theory model for simultaneous clustering 80−13604
GaAs, dislocation-free, radiation damage 80−88141
n-GaAs, neutron irrad. and thermally induced defects, annealing stages 77−51409
garnet film, motion of mag. bubble domains near point defect 79−28575
point defects continued
graphite, pyrolytic, neutron irrad., Raman spectra, point defects 77−69834
graphite crystal, electron irrad., threshold energy for displacement damage 77−76461
harmonic lattice with point defects, exponential transformations for Hamiltonian 77−39638
heavy ion irradiated target, number of point defects in displacement cascade, computational code *(French)* 79−19300
homopolar crystals, imperfect, lattice dynamics 80−59601
homotopy groups of condensed matter physics 78−63752
ice, polarisation processes, in lattice, thermodynamics of irreversible processes, universal relation 79−38446
II-VI compounds, electron energy radiation damage threshold meas., EPR and luminesc. 77−84799
III-V compounds, point defects, internal friction meas. 78−71787
III-V crystals, thermally enhanced diffusion of point defects near dislocations during device operation 79−90820
III-V semiconductor, point defects and dislocation climb 79−82209
III-V semiconductors, piezoelectric induced polarization charge distribs. around point defects 79−56725
III-V semiconductors, point defects and deep traps, thermodynamic history, model 80−59908
III-V semiconductors, radiation-induced defects, review 77−80544
III-V semiconductors, stress-induced elec. props. of point defects, piezoresistance effect 79−56726
impure solids, laser pulsed, mechanism for point defect generation 78−47368
impure solids, pulsed irrad., point defect generation 77−1150
n-InSb, acceptor effect of plastic bending 80−6885
insulator, lattice thermal cond., point defect scatt. relax. rate role 80−70478
interaction energy, influence of solid surfaces 77−62520
interaction in nonlocal elasticity theory 77−860
interaction mechanism, long range forces, incompressible continuous media 80−54232
interaction with edge dislocation near solid surface 80−79834
interaction with inclusions near solid surface, energy *(Germany)* 78−38750
interface interaction of point defects and volume defects 79−14843
intrinsic point defect-impurity atom mobile complex form., influence on defect diffusive fluxes 80−2063
intrinsic properties, rel. to void growth 78−47315
ion axial channelling analytical model, point defect scatt. 80−39192
ion bombardment, electron microscopical anal. of surface effects and volume defects, review *(Rumanian)* 80−29093
ion polarisation and point defect resistivity in metals 80−103672
ionic crystal, continuum model for periodic incorporation of aliovalent impurities 79−33012
ionic crystal, FCC, point defects at surfaces 77−47443
ionic crystal, point defect-dislocation interactions 78−63787
ionic crystal defects, mag. reson. studies 80−108066
ionic crystal. interaction energies between point defects and dislocations, shell-model calc. 78−22759
ionic crystals, electronic and vibr. props. of point defects, book 80−51962
ionic crystals, statistical space charge waves 80−103321
ionic solids, lattice and defect props., modified electron gas approx. 79−42054
irradiated dilute alloys, kinetic model for solute redistrib. to sinks and void growth 79−78973
irradiated materials, point defect trapping and void growth 79−7626
irradiation creep, climb-enabled glide of dislocations resulting from preferred absorpt. of point defects 79−82280
irradiation creep and stress-induced interaction between point defects and dislocations 79−19313
irradiation creep due to stress induced preferred absorption of point defects, anisotropic dislocation struct. effects 79−42140
irradiation effects, void nucleation, swelling, creep, rate eqns. 80−49274
irradiation-induced swelling, and creep, effects of pt. defect trapping and solute segregation 79−79040
large unit cell semiempirical mol. orbital approach to props. of solids, general theory 79−87029
large unit cell semiempirical mol. orbital approach to props. of solids, Si and diamond appl. 79−87036
large unit cell semiempirical mol. orbital approach to props. of solids, LiF and KCl appl. 79−87037
lattice defects, characterisation 80−103320
LEED, surface defect struct. determ., book contrib. 77−62726
localised and resonant defect vibr. 77−1200
localised centres, inversion symmetry, Stark effect in wideband electronic-vibr. spectra 77−69864
magnetic domain boundary, interacting with localised defects, unidimensional flow of configs. *(Russian)* 80−65954
magnetic domain lattice motion in field of point defect *(Russian)* 78−39358
magnetic domains, cylindrical, stationary motion in field of point defect *(Russian)* 77−51916
magnets, randomly distributed point defects, critical exponents, renormalisation theory 80−60346
martensite ageing, influence of neutron irradiation *(Czech)* 78−84859
metal, anelastic study of intrinsic point defects, irradiation effects 78−47323
metal, creep, point defects 78−48462
metal, diffusion, radiation effects 78−47555
metal, electron irrad., elastic point defect-dislocation interactions, defect dragging model extension 80−65050
metal, fatigued, relationship between stress and point defect cluster density 80−10592
metal, interaction energies between point defects 78−47360
metal, nucleation, oriented island growth on point defects 78−87889
metal, plasma oscills. of cond. electrons localised near point defects, contrib. to charact. losses *(Russian)* 77−43525
metal, point defect clusters, TEM obs., review 78−26564
metal, point defects, theory, book 78−71730
metal, positron self-trapping conditions 78−47338
metal, resistomatic studies of lattice defects review *(Japanese)* 78−59799
metal, review 77−7709
metal, superconducting transition, effect of change of electrostatic interaction of defects 78−10610

point defects continued
metal colloids in ionic cryst., preparation, optical, mag. resonance, elec. props. 80−59459
metal condensation on alkali halide, nucleus saturation density and epitaxy 78−18928
metal foils, electron irrad., loss of pt. defects 79−73215
metal point defects, computer simulation of dark field electron micrographs 78−47219
metal surface, near point-defect, annealing, diffusion theory and Monte Carlo anal. 78−47646
metal swelling, max. point on temp. scale rel. to point defect generation *(Russian)* 78−38751
metal-ion point defects in solids, non-radiative relax. 78−6753
metals, dynamical props. of point defects, book contrib. 80−103317
metals, influence of a surface coating, on void formation 78−47416
metals, irradiated, validity of rate theory, point defect diffusion eqns. 79−55777
metals, point defect diffusion controlled reaction theory, book contrib. 80−103318
metals, point defect dynamic props. and diffusion controlled reactions, book 80−101674
metals, point defect solute interactions 78−47410
metamagnetic transition, nucleation of new phase, role of planar, linear and point defects 77−24695
microscopic derivation of theory of extended objects in crysts. 79−37704
migration energy in pure metals and dil. alloys 78−47572
migration in crystals, anharmonic model description 77−65976
migration into dislocation loops, finite difference calc. 80−54225
minority carrier recombination at surfaces, dislocations and microdefects, luminesc. evaluation 78−6769
molecular crystal with point and linear defects, Rayleigh scatt. 77−44011
molecular crystals, diffusion and point defect struct., review 79−82373
molecular crystals, semi-infinite, with surface point defect, exciton states 80−20271
MOS processing, influence of point like and extended defects 79−82679
motion-dependent Burgers vector in elastic continuum 77−51371
multiphonon effects on dispersion, Faraday rot., associated with point imperfections 78−43839
near-surface impurities, adiabatic potential 80−70786
Nimonic PE16, neutron irradiated after heat treatment, solute segregation to pt.-defect sinks 79−78976
non-stoichiometric compound with ionised punctual defects, Gibbs-Duhem eqn. 77−31786
non-stoichiometric solids, correl. between dielectric const. and defect struct. 77−85638
nuclear spin relax., motion induced, orientation depend., point defect self-diffusion mechanism 77−48078
olivine, point defect formation 78−85547
olivine, point-defect chemistry, effect of enstatite activity and O_2 partial pressure 78−40549
olivine with fixed cationic ratio, O_2 pressure effect on defect cores 78−85548
optical absorption, Urbach's rule 79−91474
orbit degenerate electron state localised at point defect, T-term multimode Jahn-Teller effect *(Russian)* 80−15490
orbitally degenerate interacting impurity thermodynamics, stress field depend. due to point defects, dislocations 79−69477
ordered alloys, analysis of annihilation kinetics and irradiation creep 78−75659
oxides, interaction between point defects and dislocations, cryst. plasticity 80−15149
oxides, point defects diffusion coeffs. calc. *(Japanese)* 80−15302
perovskite oxides, ferroelec., point defects and elec. props. 79−42533
phase transitions in migrating orientable lattice defects 2D systems 79−77719
plastically deformed crystal, lattice defects influence on axial shadow figure *(Russian)* 80−25508
point defect interactions due to static lattice displacements, continuum and lattice theory approach 80−39082
polar crystals, relaxation currents; point defects *(Russian)* 80−100486
polydiacetylene, fully conjugated bond-alternation and orbital-flip defects 77−4311
polymer, crystallising, defects and mech. relax. *(Russian)* 78−22789
polymethylene compounds, continuous diffuse electron scattering, oblique layer cryst. 78−95004
positive muons as probes of defect structure, feasibility 79−15389
positron trapping, lifetime calc. 78−48253
precipitation near grown-in dislocations during neutron irradiation 78−26600
precipitation of point defects into dislocation loops, diffusion-controlled 77−62529
precipitation stability under irradiation, point defect effects 77−21148
pulsed fusion reactor first wall, point defect kinetics 79−93827
quantum crystal, model of tunnelling point defect at finite temp. 78−38907
quantum crystal, one-dimensional, solitary defectons 78−2332
quantum crystal, theory of defectons *(Russian)* 78−60004
quantum field theory of crystals and extended objects, review 79−42164
quantum objects, point defects as possible model 77−22433
α-quartz:Al, γ-irrad., thermal cond. below 10K 79−51320
α-quartz, electron irrad., defect struct. and radiolysis 80−107321
quartz, point defects rel. to strain amplitude depend. of internal friction 77−27939
quartz fibre, ESR and IR obs. of microinhomogeneities 77−8401
radiation creep and void swelling, bias factors in reaction-rate-theory anal. 79−46700
radiation creep rate as function of point defect formation rate and temp. 79−69187
radiation damage to construction materials, math. modelling 79−90703
radiation defect accumulation in recovery stage II, unsaturable trap model 77−47481
radiation-induced solute redistribution and precipitation, model 79−19277
rare earth dihydrides, lattice thermal expansion and point defect form. energy 77−51524
rare earth metals, HCP, point defect production during electron irrad. at low temp. 80−49273
rate equations, transport theory formulation for fusion reactor materials 79−95050
point defects continued
relaxation of third-order elastic const. in crystal with point defects 77−8873
retardation of interstitial atom diffusion by point defects *(Russian)* 77−59143
review, book contrib. 78−10043
Schmid's law deviations, in uni-directional strain 78−71783
screening of fields of static distortions 80−6797
semiconductor, cryst. field coeff. of point defect 77−43537
semiconductor, electronic struct. of point defects, surfaces and interfaces, Green's function scatt. theoretic method 79−33258
semiconductor, localised defects, theory of SEM charge-collection imaging 79−1374
semiconductor, quenching of luminesc. by charged defects 78−23531
semiconductor, radiation dose for amorphisation, max. point defect conc. 77−55301
semiconductor, review 77−7709
semiconductor, tetrahedrally coordinated, models of dislocation struct. 79−82205
semiconductor defects, spectroscopic techniques to study of electronic props. 80−84446
semiconductor light source degradation, review of recent expts. 78−82970
semiconductor neutral point defect electronic struct., self consistent method 78−91641
semiconductors, electron states of point defects 80−39526
semiconductors, high energy radiation effects, new developments 77−19980
semiconductors, impurities and other point defects, electronic struct., review 79−7803
shielded point defect potential well calcs. using Poole-Frenkel effect 80−20122
shock wave formation of point defects *(Russian)* 80−6401
silicate minerals, lattice imaging 78−30522
simple ionic crystals, ion transport 78−63878
sink strength in irradiated materials 77−51368
solid surface, point defects, inclusion and separation zones, elastic energies determ. *(German)* 78−95054
steel, austenitic stainless, creep dependence on electron irrad., in type SS316 steel, dislocation motion *(Russian)* 80−108495
steel, microstructure of 0Kh16N15M3B after creep tests in BR-10 reactor, electron, microscope invest. *(Russian)* 80−92531
steel, stainless, ion irradiated, carbide precipitation *(French)* 77−16585
steel, stainless, neutron irrad., point defect cond. and void radius change, appl. of model for void growth 78−47436
steel, stainless, swelling, effect of free surface 78−10097
stress induced absorption, and emission by grain boundaries 80−39081
superconductor, dislocation-point defect interaction, rel. to internal friction *(Russian)* 77−36018
surface, point defects, inclusion and segregation zone, elastic energies *(German)* 78−95049
surfaces and interfaces, elastic energy of point defects and inclusions 80−73272
ternary compounds, defect chemistry 79−90648
ternary compounds, thermodynamic characterisation, case of extensive defect association 77−47445
TGS, interaction of γ-irrad., induced defect electron microscope expts. 79−10876
thin foil point defect profile rel. to dislocation loop growth during HV electron microscope irrad. 80−2018
transition metal alloy, dil., size effect 79−99508
transition metal carbides, solid-phase reacts., effect of nonstoichiometry, thermodynamic evaluation 78−60632
transition metal oxides, defect struct. review 79−42052
transition metal oxides, defects, coordination, topology, struct. 77−51367
transition metals, BCC, point defects chem. binding energy 79−82260
transparent optical materials, laser induced damage and lattice strain due to lattice defects 80−48315
trapping, effect on irradiation induced creep and swelling 78−71756
trapping by extended sinks, model of cloud random walk of lattice pts. 79−82199
unstable pairs 77−15409
US absorpt. near displacive phase transitions, anomalous temp. depend. 80−92612
vacuum condensation, kinetic model of oriented growth of nucleating curves *(Russian)* 79−74092
void nucleation, acquisition reaction rates calcs. 79−42051
void nucleation and growth, effect of point defect trapping on impurities 79−23637
void reactions, conc. depend. of rate const. for diffusion or reaction controlled reactions 79−7625
void swelling, role of bulk point-defect recombination 79−42105
Ag, elec. resistivity increment due to low temp. plastic deform. *(Russian)* 77−31990
Ag halides, matter transport rel. to point defect parameters 80−107488
Ag-Zn (24 at.% Zn), γ-irradiated, freely migrating defects, rate of production *(French)* 79−10877
Ag-Zn (30 at.%), electron irrad. exam. of defect supersaturation by elasticity, and creep meas. 78−47366
Ag-Zn (30 at.%), neutron irrad., at. mobility enhancement, Zener relax. meas. 77−1157
$AgGaS_2$, optical quality, grown from melt, EPR characterisation 78−64260
Ag_2S, α- to β-phase transform, phase boundaries effect 79−83179
Ag_2S, α-β transform., role of phase boundaries in heterogeneous solid state reactions 78−71849
Al, annealed and neutron irrad., exam. of positron lifetimes in voids and other defects 78−47426
Al, dislocation and point defect interactions, US study under quasistatic stress *(French)* 80−2061
Al, positron trapping, defect specific temp. depend. 78−47336
Al-Mg, dil., form of distortion field produced by Mg substitution, elastic neutron scatt. meas. *(German)* 79−42092
Al-Mg, dil., long-range solute-host interactions 78−95062
(AlGa)As DH, proton-striped, proton-induced defects, photoluminesc. study 80−48251
AlGaAs-GaAs double heterostructure laser lifetime, point defect generation model calcs. 80−32992
AlGaAs-GaAs remote junction heterostructure laser, recomb. enhanced annealing effect 79−98355

point defects continued
$Al_xGa_{1-x}As$ DH laser material, Ar laser induced catastrophic damage 79−86178
$Al_xGa_{1-x}As$, point defects, recomb. enhanced interactions with dislocation networks 79−60398
α-Al_2O_3, atomic disorder, dominant type 78−63757
β-Al_2O_3, defect props. and ionic transport 80−107486
α-Al_2O_3:Ti, defect struct., electronic and ionic cond., optical absorption meas. 78−30603
$Al_2O_3:Ti^{3+}$, corundum, point defect diffusion and interaction with impurity, Ti^{3+} to Ti^{4+} reaction 79−10985
$(Am,Cm)O_2$ solid soln., struct. changes under self- and reactor irrad. 77−27927
Ar, solid, X-ray induced point defects 80−59514
As-Se system glasses, point defects, positron lifetime spectra meas. 78−88380
Ba ferrites, lattice imaging 78−30522
BaF_2, ionic conductivity meas., computer anal. point defect parameters 80−54429
$BaF_2:K^+(La^{3+})$, nuclear spin relax. orientation depend., point defect self-diffusion mechanism 77−48078
$BaSO_4$, single cryst., neutron bombard. effect on struct. 78−63793
$BaTiO_3$, single crysts., electron microscope study of domain and defect structs. 79−15425
Bi_2Se_3:Hg point defects in crystal lattice, Hall coefficient and IR spectra determ. 80−55129
CaF_2, (n,γ) induced lattice defects, struct., polarised ^{20}F NMR 77−20724
CaF_2, (n,γ) induced lattice defect annealing, polarised ^{20}F NMR 77−20725
CaF_2, fluorite, electron irrad., {100} faceted anion voids 79−51153
$Ca_2LaFe_3O_{8+x}$, influence of O_2 partial pressure on nature of point defects, characterisation by elec. cond. meas. *(French)* 79−42055
CaS, polycryst., cathodoluminesc. of point defects 79−78759
Cd, recovery after 6.1 MeV α-particle irradiation at 4.2K 78−47441
Cd:^{116}Sn, quadrupole interaction, radiation damage effects 78−43752
Cd-Ag, polycryst. wire, cold worked, resistivity changes 78−68827
Cd-Zn, polycryst. wire, cold worked, resistivity changes 78−68827
$CdCr_2Se_4$ film, electron irradiated, struct. 79−15032
CdI_2 polytypic crystals, dielectric loss behaviour 80−66108
CdO, point defect props., band struct., lattice simulation calc. 80−19797
CdS film, chemically deposited, nonstoichiometry effect on cond., optical absorpt. *(Russian)* 77−8210
CdS, neutron and fast electron irrad., local centre form., TSC and photoluminesc. meas. 78−87719
CdS, surface charge and ledge dynamics, point defect annihilation during sublimation 79−90642
CdSe, recombination mechanism at dislocations, photoluminescence 80−103993
CdTe, defect struct., review 77−39581
CdTe, low temp. themal cond., growth parameter influence 80−92725
n-CdTe, photolum., plastic deform. effects 79−15509
CdTe, thermal cond. and X-ray topography investig. of cryst. defects 77−39706
CdTe, undoped and halogen-compensated, defect conc. calc. 77−39602
CdTe:Be, impurity modes and IR absorption 78−76506
CmO_2, struct. changes under self- and reactor irrad. 77−27927
Co, magnetic permeability, effect of ion implantation 77−28414
$CoAl_2O_4$, single crysts., pt. defects type determ. involved in reactions of form. and decomp. of inclusions 79−95003
CoO, defect struct. and self-diffusion 78−63759
CoO, total conc. of point defects and deviation from stoichiometry 77−15407
$Co_{1-x}O$, point defect struct., elec. cond. and Co tracer diffusion 79−10849
CsI, crysts., microplasticity mechanism 78−30696
Cu alloys, FCC, climb of extended dislocations due to irradiation in HVEM 80−103343
Cu, electron irrad., elastic point defect-dislocation interactions, defect dragging model extension 80−65050
Cu fatigued polycrystals, point defect cluster rel. with yield stress temp. depend. 78−6989
Cu foils, electron-irradiated, point defect agglomerates, HVEM invest. during in-situ annealing 80−84213
Cu, high purity, identification of imperfections by thermal resistivity meas. 80−59951
Cu, inhomogeneous clustering of radiation damage after neutron irradiation between 200 and 400°C 80−15161
Cu monocrystals, positron annihilation quanta ang. correl., point defect effects 77−76729
Cu, neutron irrad., replacement sequences, calcs. using ADDES and COMENT codes 79−46714
Cu, neutron irradiated, effect on internal friction 78−15445
Cu, neutron irradiation induced dislocation loops and point defects, temp. depend., 316 to 483K 77−51410
Cu, polycryst., low temp., plastic deform., structural defects, elec. resist. meas. *(Russian)* 78−39844
Cu, positron trapping, defect specific temp. depend. 78−47336
Cu-Al alloy, irrad. in HVEM, climb of dissociated dislocations and point defect absorpt. 80−107257
Cu-Fe, dil. alloy, anomalous thermoelec. power, sensitivity to defects, annealing effect 77−51728
Cu-Ni, Ni atom cluster break up, slip band formation, point defect motion 79−57096
$CuAl_2$, constitutional defect struct., from X-ray and density meas. proposed substitutional-vacancy model 79−37696
α-Fe, lattice defects relax. studies, computer simulation 78−79604
α-Fe, plastically deformed and/or irrad., high purity, internal friction peaks due to dislocation relax. 77−86075
Fe, radiation induced defects, annealing exam. using channelling tech. 78−47316
α-Fe, radiation induced displacement cascade, short term annealing, computer simulation 80−54282
Fe:Xe(Te), interaction of impurities with point defects, Mossbauer spectroscopy exam. 78−47414
Fe-Al (40 at.%) and Fe-Al (50.5 at.%) ordered alloys, 20K neutron irrad. effects, stoichiometry depend., resist. obs. *(French)* 80−84215
Fe-Co alloy, prod. of point defects by plastic deformation *(French)* 78−72829
Fe-Co-V, neutron irradiated, damage rates 79−77646
point defects continued
Fe-Co-V (2%), prod. of point defects by plastic deformation *(French)* 78−72829
Fe-Co(Al), B_2 superlattices, point defect investigations 78−47357
Fe-Ni, point defect form. at high temps. *(Russian)* 79−86787
Fe-Ni-Co, magnetic permeability, effect of ion implantation 77−28414
FeCo, neutron irradiated, damage rates 79−77646
$Fe_{1-x}O$, wustite, thermoelec. power coeff. rel. to O_2 press. at high temp. *(French)* 77−76850
$FeSb_2O_{4-y}$, defect struct. and mag. transition, elec. transport and Mossbauer expts. 78−59803
GaAlAs-GaAs heterostructures, electronic excitation effects on mobility of point defects and dislocations 78−2561
$Ga_{1-x}Al_xAs$ laser, DH, rel. to enhanced localised degradation and anomalous emission spectra 77−680
$Ga_{1-x}Al_xAs$, point defects and dislocation climb, interaction with deep level donor 79−82209
$Ga_xAl_{1-x}As$:Cu epitaxial layers, spatial distrib. of nonradiative defects, STEM imaging spectroscopic technique 77−89438
GaAs, electroluminescent study of irrad. induced struct. damage, athermal annealing 80−108280
GaAs, gamma-irrad., contrib. of inelastic nucl. reactions *(Russian)* 77−27905
GaAs, γ- and electron irradiation, influence on recomb. characts. near surface 80−71478
GaAs heterojunction laser, origin of dislocation climb during laser operation 77−51380
GaAs, homogeneity region calc. 80−92681
GaAs, impurity-point defect complexes 78−6097
GaAs, laser annealing of point defects 80−107224
GaAs, lattice thermal cond., point defect scatt. relax. rate role 80−70478
GaAs, point defect generation by electron-hole recombination at dislocations 79−37699
GaAs:Sn, doping characts. during LPE 79−10866
GaAs:Te, LPE, Te induced defects, rel. to growth conditions 78−6067
GaP epitaxial layer, crystal defects influence on lumines. obs. 79−87511
GaP, frozen-in pt. defects annihilation 79−99949
n-GaP, LPE, non-radiative recombination 78−19565
n-GaSb, stress-induced elec. props. of point defects, piezoresistance effect 79−56726
GaSe, fine struct. of exciton spectrum 78−39567
Ge, formation under electron or γ-irradiation, reliable and questionable hypotheses 77−80501
Ge, impurity modes due to point defects, comparison with IR and Raman meas. 79−4386
p-Ge, neutron irrad. quenched sample, lattice defects 79−19284
Ge, neutron irradiated, positron annihilation, ESR and resist. meas. 80−15160
Ge, point defect creation by plastic deform., Hall const. electrical conductivity 78−6053
Ge, review of point defect characts. *(Japanese)* 77−89428
Ge:As, thermally induced defects properties obs. 77−63692
Ge:O, elec. props., O interaction with point defects 79−11081
Ge:P(Sb)(Bi), γ-irrad., carrier trapping and recomb. at point radiation defects 80−107810
Ge:Sb, annealing stages of thermal defects, elec. meas. 77−55282
Ge:Si, impurity modes and IR absorption 78−76506
He, solid, diode properties 79−56021
He, solid, energy absorpt. and size effect, point defect diffusion *(Russian)* 77−4243
$Hg_{1-x}Cd_xTe$, ionized intrinsic pt. defects, effect on carrier density 77−47835
n-InAs, electron irrad., rel. to thermal and electrophysical props. *(Russian)* 80−39154
InAs:Sn, single crysts., defect formation 80−88606
InAs:Te(Se)(S), intrinsic pt. struct. defects 80−33998
InGaAsP-InP, double heterostructure laser lifetime, point defect generation model calcs. 80−32992
n-InP, γ-ray and electron irrad., annealing of radiation point defects, elec. cond. and Hall coeff. meas. 80−65051
InSb films, melt-grown, point defect effect on elec. props., 77-300K 80−2502
KBr, single crystal, preirradiation and radiation defects, electron microscopic estimation *(Russian)* 78−75695
KCl, point defect characterisation from energy and temp. depend. of defect enhanced dechannelling study 79−4365
KCl, single crystal, preirradiation and radiation defects, electron microscopic estimation *(Russian)* 78−75695
KCl:Ba^+ structural changes due to γ-irradiation *(Russian)* 77−76460
KCl:Li^+, press. tuning of motional behaviour in shallow off-centre pots. 79−78718
KCl:$Na^+(Rb^+)(Ag^+)$, entropy changes associated with point defect form. calc. 77−7741
KCl-KF:Pb^{2+}, point defects, ionic thermal currents and optical meas. 80−6403
β-Li-Al, lattice parameters, density, defect struct. 80−24440
LiF, electron irradiated, mech. characts. 78−26595
LiF, NMR exam. of point defects generated in (n,γ)-reaction *(Russian)* 78−60347
LiF, radiation induced voids, formation on dislocations 80−15159
LiF:Mg,Ti, (TLD-100), optical bleaching of defect centres 79−19911
LiF-MgF_2, ionic conductivity increase rel. to point defect cone 77−72717
α-$LiIO_3:Cr^{3+}(Mn^{2+})(Fe^{3+})$ and radn. induced defects, EPR spectra *(German)* 78−84480
Li_3N, defect props. and ionic transport 80−107486
Li_3N, superionic conductor, cryst. growth and struct., phys. props., book contrib. 79−42308
$LiNbO_3$, damping of LF elastic vibrs., internal friction meas. 79−28043
Li_2O, cation diffusion, NMR obs., MgO and LiF doping effects *(German)* 77−20112
Mg, electron irrad. damage, dislocation loop growth, in situ obs. 78−87715
Mg_3Cd, disordering under electron irrad. in electron microscope 78−83849
MgF_2 obs. of radiation induced point defects, cross-relaxation processes, polarised β-active nuclei 80−60431
MgO crysts., geometrical-statistical parameters of dislocation interactions with point obstacles 80−103341

point defects continued
MgO, electronic excitations and luminescence, review *(Russian)* 78−72575
MgO, intrinsic defects at (001) and (011) surfaces 77−47443
MgO solution in UO_{2+x}, shell model calcs. of enthalpy, computer program for formation energies 79−42251
MgO:Fe^{3+}, point defect complex-edge dislocation interaction energies, atomistic calc. 80−107314
$Mg_2Si_2O_6$, enstite, elec. cond. var. with O_2 partial press., obs. and theory 79−1609
Mn-Zn ferrite, oxidation-reduction equilib. and struct. defects 77−20189
$Mn_{1-x}Fe_{2+x}O_{4+\delta}$, ferrites, homogeneity region, cluster component model 78−35367
Mo, annealing in stage I, dose depend. and radiation doping defects 78−47422
Mo, electron irrad. in HVEM, anisotropy of damage prod. 80−107322
Mo, H penetration of Mo cathode in glow discharge, point defect depend. 79−41903
Mo, lattice defects, relax. studies, computer simulation 78−79604
Mo, monocrystalline, density change during plastic deformation *(Russian)* 79−87689
Mo, neutron bombard., radiation damage, electron microscopy obs. *(Russian)* 80−44235
Mo, point defect migration, stage III annealing 77−80548
NaBr:Cu^+, press. tuning of motional behaviour in shallow off-centre pots. 79−78718
NaCl, intrinsic defects at (001) and (011) surfaces 77−47443
NaCl, investigation of fast electrical processes, during cleavage 79−24045
NaCl, point defect interaction with dislocations, internal friction meas. 79−90662
NaCl preirradiation effect on proton channelling, thermoluminescence study 80−19860
NaCl-NaF:Pb^{2+}(Eu^{2+})(Zn^{2+})(Mn^{2+})(Sn^{2+}), point defect ionic thermal current and optical meas. 80−6403
NaF, lattice thermal conductivity, point defects effects at low temp. 79−90836
Na_2SO_4-$Y_2(SO_4)_3$, solid solution, effect of defect concentration on ionic conductivity 78−75870
Nb_3Ge, low temperature electron, neutron irrad. effects on critical temp. *(French)* 80−75669
Nb_3Ge(Sn) film, superconducting transition temp. var. under ^4He irrad. 77−8220
Nb_xO_y, lattice imaging 78−30522
Nb_3Sn, gap anisotropy, electron irrad. effect on transition temp. 78−10599
Nb_3Sn, supercond. props., effect of neutron irrad. 80−80463
Ni dilute alloys, implant profiles modification by radiation enhanced diffusion and segregation 80−88217
Ni dilute alloys, mechanisms of radiation induced segregation 79−77649
Ni, high purity, quenching expts. 78−48432
Ni, magnetic permeability, effect of ion implantation 77−28414
Ni model material, defect buildup and solute segregation, in alloys under pulsed irradiation 78−71757
Ni, point defect-dislocation loop interaction, effect on dislocation loop growth kinetics 78−47415
Ni, positron trapping, defect specific temp. depend. 78−47336
Ni, self-ion irradiated, defect clusters, annealing 78−18687
Ni:^{235}U (0.1 at.%), exam. of saturation defect conc. and elec. resistivity meas., for neutron irrad. at 7K 78−47435
Ni:Cr, He^+ radiation-enhanced diffusion and segregation effects of point-defect trapping 79−77824
Ni-Ag, thin-film, effect on elec. cond. 79−7911
Ni-Al (12.8 wt.%), Ni^+ ion irradiation, precipitate restructuring, mechanisms and kinetics 79−77650
Ni-Cr-Fe alloys, radiation enhanced precip. and dissolution of precipitates, point defect kinetics and dislocation obs. 80−108467
Ni-Si (12.7 wt.%), Ni^+ ion irradiation, precipitate restructuring, mechanisms and kinetics 79−77650
Ni-Si solid soln., radiation-induced solute redistribution and precipitation, model 79−19277
Ni-Si:Cr, He^+ radiation-enhanced diffusion and segregation effects of point-defect trapping 79−77824
β-NiAl, omega-like structural defects, diffuse X-ray scatt. obs. 79−95005
β-$Ni_{1\pm x}Al_{1\pm x}$, defect struct. and Debye Waller factors vs. composition 77−31658
Ni_3Al, substitutional soln. and defect hardening mechanisms 77−21155
Ni_3Al(Ga), off-stoichiometric alloy, inverse mag. susceptibility rel. to defect conc. 80−60216
Ni_2Cr, neutron irrad., point defect prod. and annealing 78−87718
NiGa, point defects, lattice parameter determ. 78−38695
Pb-Au, dil., solute resist. meas., multiple point defect form. 78−10433
Pb-Bi (4.1 at.%) solid soln., tetragonal distortion field for substitutional Bi atoms, neutron scatt. 78−51568
PbS, point defects and effect on decopperization of Pb with S 79−47918
PbS single crystals, plastic deform. thermal activation anal., dislocation behaviour, point defect influences 79−65095
Pd-Fe, dil., plastically deformed, positron annihilation study of recovery of crystal, imperfections *(German)* 77−85835
Pt, point defect properties, damage curve anal. 78−47359
PuO_2, alpha radiation damage, point defect ingrowth and annealing behaviour 77−27926
PuO_2, struct. changes under self- and reactor irrad. 77−27927
RbBr:Ag^+, press. tuning of motional behaviour in shallow off-centre pots. 79−78718
RbCl:Ag^+, press. tuning of motional behaviour in shallow off-centre pots. 79−78718
Sb, electron microscope irradiation effects, agglomeration of point defects, dislocation climb and loops *(French)* 80−59518
ScN_x, region of homogeneity, physicochem. props. 78−52018
Se, glassy, localised electronic states, photoluminesc. and ESR studies 80−65501
Si amorphisation dependence on low-energy irrad. conditions 79−60408
Si, dislocation generation, influence of film stress and thermal oxidation 79−23609
Si, dislocation-free crystal point defect condensation 78−6026
Si, float zone crystal, dislocation creation and elimination 80−107072
Si, impurities displacement by H^+ or He^+ irrad. 79−86824
Si, integrational etching composition and method 78−10055
n-Si, interaction of disordered regions with point defects 79−19296

point defects continued
Si, introduction of defects during growth and processing 79−95925
Si, ion bombardment induced buildup of disordered material, model 77−47496
Si, ion-implanted layers, residual defects after high temp. annealing 78−87695
Si, laser annealing of point defects 80−107224
Si, neutron irrad., point defects photopopulation and photoionis., IR spectra meas. 80−25423
Si, packing defects, change in size during heat treatment 80−39079
Si, point defects, H passivation 80−75515
Si, review of point defect charact. *(Japanese)* 77−89428
Si single crystal surface, He^+ bombardment, damage production, defect diffusion 80−39181
Si single crystals, nearly perfect, high resolution diffuse X-ray scattering study 79−32854
Si, small-diameter cryst. grown by pedestal technique, out-diffusion of point defects 79−55683
Si, substrates, review of defects 77−39597
Si with thermal defects, photocond., effect of annealing on elec. resist. 80−6837
Si, zone melting, swirl defects A-type as source of dislocation generation on macroscopic scale 80−25554
Si:Au, P-induced point defects influence on Au gettering mechanism 80−65030
Si:B, ESR at zero and small external stress, elastic strengths for point defects 79−19764
Si:B, lateral effect of oxidation on B diffusion 80−29217
Si:B ion implanted, strain profiles from X-ray rocking curves 80−107290
Si:P, ion implanted with small doses, defect annealing by nanosecond laser pulses 80−107297
SiC, radiation damage, review 77−80553
SiO_2, vitreous, exam. of electron excitations and intrinsic defects 78−87905
SiTe-ATe, A=Ga, In, Tl, solid solns., mag. suscept. meas., defects 78−43552
Ta:H, recovery after cold working at 4.2K, resist. meas. 79−4977
Te, deformed and annealed crystal,, effect on elec. props. 79−7847
Ti-O system, nonstoichiometry between Ti_3O_5 and TiO_2 comps. at high temps. 77−15594
Ti(Fe, Co), off-stoichiometric alloy, inverse mag. susceptibility rel. to defect conc. 80−60216
TiO_2 rutile single crystals, stoichiometric, dynamic strain ageing 80−50661
TiO_2, sputtering defects, associated surface electron states, UPS, XPS and AES obs. 80−60755
TiO_2:Nb, rutile, elec. cond., 1273-1623K, O_2 press. depend., charge compensation mechanism 77−85217
TiO_{2-x}, nonstoichiometric and Nb_2O_5 doped, defect struct. and thermodynamic props. 79−90650
TiO_{2-x}, rutile, O chem. diffusivity, near stoichiometric ratio 77−11731
UC_x, self-diffusion and nonstoichiometry, modified Monte Carlo method 77−69114
UO_2, alpha radiation damage, point defect ingrowth and annealing behaviour 77−27926
UO_2, effect of point defects on nonequilibrium bubble behaviour 79−93722
UO_2, neutron irradiated, thermal recovery of defects 79−45348
V, lattice defects, relax. studies, computer simulation 78−79604
V, structural changes in single crystal under single electric impulse discharge *(Russian)* 79−65086
V_2O_5 and lower oxides, electronic, optical, structural and surface props., review 80−88120
V_3Si, phase transition and transition temp., chemical comp. effects, defect struct. exam. 78−18651
V_3Si, plastic deform. effect on supercond. props. 80−29500
V_3Si, supercond. props., effect of neutron irrad. 80−80463
W, electron irrad., or ion irrad., stage II, point defect struct., FIM 77−80542
W, electron irradiated, or quenched, point-defect mechanism for Stage III recovery, field ion microscope study 79−60403
W, low-energy ion bombardment, depth of sputtering damage obs. by FIM 80−60734
W, neutron irrad., recovery of defects, isochronal and isothermal annealing 79−46712
W, threshold atomic displacement energy, temp. depend., computer simulation 77−1148
WO_3, nonstoichiometric, elec. investig. of correl. between defects and O chem. pot. *(French)* 77−47817
(Y,Eu,Tm,Ca)$_3$(Fe,Ge)$_5O_{12}$ garnet film coercivity, new annealing method 78−84459
(Y,Sm,Lu,Ca)$_3$(Fe,Ge)$_5O_{12}$ garnet film coercivity, new annealing method 78−84459
$Y_2(Co_{0.31}Fe_{0.69})_{19.2}$, statistical site occupancy deviations, neutron diffr. investig. 77−7717
Yb_2O_3, electronic cond. rel. to partial press. of O_2 of high temp. *(French)* 80−59979
Zn, recovery after 6.1 MeV α-particle irradiation at 4.2K 78−47441
ZnO (10$\bar{1}$0) prismatic surfaces, nonstationary sublimation, point defect conc. *(German)* 78−60035
$Zn_{1+x}O$, nonstoichiometry investig., 400 to 1200°C 77−11543
ZnS with Au film coating, calc. of defect conc. 78−95052
ZnS:Be, impurity modes and IR absorption 78−76506
ZnS-Cu, polycryst., influence of alternating elec. field and UV light on struct. defects, electrolum. expts. 79−43041
ZnSe, multiphonon ionisation of deep point centres in a charged dislocation field *(Russian)* 80−100281
ZnSe:Mn, single crysts., associated pt. defects, EPR method 77−48040
ZnSe-HgSe, solid soln., defect distrib., elec. props., Hagemark's theory 78−64040
ZnTe, refined, undoped, Cu acceptor, optical absorption and photoluminesc. meas. 80−34970
Zr alloys, factors affecting anisotropy of irradiation creep and growth, calcs. from crystallographic texture 79−83255
Zr base alloys, irradiation growth, dislocation model 78−51595
Zr, low temp. deformed, O_2 effect on production and recovery of defects, elect. resist. meas. 79−47705
Zr, point defect migration into dislocation loops, finite difference calc. 80−54225
Zr polycrystalline, low-temp. alternating deformation and annealing, yield stress, elec. cond. variation *(Russian)* 79−74199

point defects continued
Zr-base alloys, annealed specimens, irradiation growth 80−49276
$Zr(HPO_4)_2H_2O$, ^6Li loaded, α-radiation damage, X-ray Guinier powder reflection study *(German)* 78−47437
ZrO_2:Cu, point defects, electrochem. characterisation 80−35599
point groups *see crystal atomic structure*
point of sale systems
hologram scanner for POS bar code symbol reader 80−48182
rotating mirror deflector design cost/performance tradeoffs 77−58485
point to point radio links *see radio links*
Poiseuille flow
13 GK model, numerical results for Couette, Poiseuille and thermal creep flow between parallel plates 79−77057
aerosol, diffusion and sedimentation in Poiseuille tube flow 78−59463
aerosol, simultaneous diffusion and sedimentation in rectang. tube 77−11266
aerosol particle gravitational deposition from developing flow in horizontal circular tube 79−50776
aerosol particles, gravity settling in horizontal rectangular tube with diffusion 77−84310
aerosols, asymmetric deposition motion in circ. tube, anal. by Laplace transform methods *(Chinese)* 79−37379
bead-spring-type model in nonuniform vel. gradient, dil. soln. kinetic theory results 80−64628
boundary layer, thermal, thickness for Poiseuille flow past permeable bed 79−46299
boundary value problems, compound matrix method 80−57096
Brownian particle diffusion in shear induced convection, Poiseuille flow 80−33591
channel flow, finite amplitude, instability shear layer parallel flow, cellular motion 80−1601
channels with unequal wall temps., low Peclet no. heat transfer 77−42813
charged particle suspension, deposition in tube flow 79−37416
cholesteric liquid crystals, steady low shear rate flow normal to helical axis 80−96443
colloidal dispersions, microrheology, Brownian diffusion of doublets of spheres 77−4942
colloidal particles, Poiseuille flow, total particle conc. axial change 80−108752
complementary variational principles for Poiseuille flow 80−96310
convective instability and heat transfer in plane Poiseuille flow, viscous dissipation effects 77−31295
critical Reynolds number in pipe Poiseuille flow 78−94644
developing pipe flow, arbitrary curvature pipe, Navier-Stokes eqn. 78−79378
dispersion of contaminant mol. in laminar flow 77−39347
drop, deformable, motion in second-order fluid 79−64754
ducted flow, velocity and temperature development behind shock wave 78−34161
elastic liquids, stability of plane Poiseuille flow 78−9662
elastic tubes, stability to axisymm. disturbances 77−65796
energy stability limit for rot. modified flow 78−30268
energy stability of a natural convective flow in a horizontal annular space 79−68815
Fermi liquid viscosity in finite geometry 80−24702
finite amplitude stability, perturbative and iterative methods 78−38293
flat plate streaming potential investigations: hydroynamics and electrokinetic equivalency 80−106777
Hagen-Poiseuille, of microthermopolar fluids in circular pipe 80−24092
horizontal plane flow heated from below, axial heat cond. effects on thermal instability 77−42825
hydrodynamic stability including viscous dissipation, temp. fluctuation *(French)* 79−32466
inhomogeneous liquid, spin echo signal shape *(Russian)* 80−50225
instability in elliptic pipe flow 78−71397
internal separated flows at large Reynolds number, Poiseulle flow development in channel 80−53755
laminar flow in a channel variable cross-section with movable and porous walls *(Polish)* 79−64768
laminar to turbulent alternating transition, crit. Reynolds no. 78−46935
laminar to turbulent boundary layer shear flow, three-dimens., stability eqns. 78−38284
laminar to turbulent boundary layer transitions, numerical simulation 78−38286
laser speckle photography for fluid flow vel. meas. 78−14112
liquid crystal, nematic, Poiseuille flow, instabilities 77−1073
liquid crystal, nematic, Poiseuille flow, uniform instability 77−1074
local similarity solutions and their limitations 80−33675
longitudinal vibration effects on Poiseuille non-Newtonian flow in non-circular pipe 79−86514
magnetic fluid, motion in external mag. field, Couette and Poiseuille flow 79−14491
MHD Poiseuille flow in annular channel with radial mag. field, Hall effect 78−67276
MHD Poiseuille perturbed pipe flow in nonuniform axisymmetric mag. field, anal. 80−24104
MHD stability of flow with flexible boundaries 77−11277
molecular and transition flow in long rectangular channels 77−7418
monodimensional Poiseuille and thermal creep flows, rigorous constructive soln. 78−30319
Navier-Stokes equations, numerical integration, small disturbances as functions of time *(German)* 78−94633
nematic liquid crystals, book contrib. 78−59531
nematic liquid crystals, homogeneous instabilities 78−63674
nematics, Poiseuille flow instabilities 79−77499
non-Newtonian flow in oscillating pipe, peristaltic and Poiseuille flow phenomena 78−63463
non-Newtonian fluid, applicability of the theory of directed jets 79−60019
non-Newtonian fluid, influence of vibr. 79−81930
non-Newtonian fluid, Poiseuille flow, influence of vibrs. 79−7391
non-Newtonian Poiseuille flow in cooled channel, hydrodynamic stability 79−14441
nonlinear stability, subcrit. Re, finite axisymmetric disturbances 77−84224
nonlinear Tolmin-Schlichting waves, self-excited oscillation stability 79−90263
Orr-Sommerfeld problem, orthogonal expansions 77−58646
parallel flows, stability anal. by finite element anal. 79−81843
Poiseuille flow continued
parallel-plate channel, theory of capillary rise of liq. 80−28567
particle distribution in Poiseuille flow of suspension in micropolar fluid model 80−10314
pentyl-cyano-biphenyl, nematic, hydrodynamic parameters meas. with and without applied elec. field 80−100297
periodic flow in a curved tube 80−69920
periodic secondary motions in plane channel, num. soln. method 77−55092
pipe, bifurcation from infinity, nonlinear differential eqn. 79−98806
pipe flow, finite amplitude stability theory 78−63498
pipe flow, hydrodynamic stability *(French)* 78−18347
pipe flow linear instability 79−90223
pipe flow of incompressible second order fluid *(German)* 78−87395
pipe flow transitional behaviour, effect of inlet flow disturbances 79−90216
pipes, porous, complementary variational principles for steady and unsteady Poiseuille flow 80−92225
plane, instability caused by nonlinear, nonperiodic and three-dimensional disturbance 78−38291
plane, nonlinear stability by high order amplitude expansions 80−74975
plane, transition to turbulence and finite amplitude disturbances 80−33558
plane flow, direct optical meas. of vel. gradients 80−59132
plane flow, nonlinearity and non-periodicity of two-dimensional disturbance 77−62231
plane flow of second grade fluid through contraction 77−3870
plane parallel flow, free convection in Couette and Poiseuille flows, numerical simulation 80−99995
plane Poiseuille flow, at large Reynolds numbers, Navier-Stokes eqn. soln. *(Russian)* 78−59364
plane Poiseuille flow, stability numerical computation 79−10549
plane Poiseuille flow in channel, stability, orthogonal expansion method *(Russian)* 78−5730
plane turbulent Couette-Poiseuille flow, asymptotic anal. 80−33674
plane two-layer flows, effect of fluid microstructure on stability 79−77212
plane variable viscosity flow with unequal wall temps. 78−18344
polyethylene oxide, dilute aq. soln., laminar viscous tube flow, scale-depend. effect 79−7367
porous annular region, steady flow 78−75201
porous media, Knudsen to Poiseuille flow transition, capillary model 78−55689
pulmonary resistance, lower, effect of gas phys. props. and flow 77−12945
PVC rigid, flow and therm. stability 79−64618
rarefied flow, Poiseuille slip and thermal creep at boundary surface *(Russian)* 78−38371
rarefied gas, thermal creep and slip at boundary wall 79−68753
rarefied gas dynamics projection and variational methods 80−6189
rarefied gas mixture Poiseuille flow 79−14438
rectangular pipe with large aspect ratio, plane Poiseuille flow nonlinear instability 78−59492
rotating gas, Poiseuille-like flow 77−15043
secondary flow in plane channel *(Russian)* 78−87394
short-lived radioactive gases, long range transmission in tuned pipeline 79−53239
shpere between plane parallel boundaries, creeping parallel motion, strong interaction theory 80−103075
solute dispersion coefficients 79−60060
spherical particle, lateral migration in 2-dimens. shear flow 77−15100
spherical particle in circular tube flows, lateral migration 80−92221
stability, external forcing effect 78−22327
stability of channel flow 78−90835
stability of flow in elliptic pipe with large aspect ratio 78−1745
stability of plane horiz. rot. Poiseuille flow, effect of Coriolis force 78−67203
stationary flows in channels, Hagen-Poiseuille law generalisation, technical appls. 79−81980
steady laminar flow through channel with symmetrical constriction in step form 80−100036
stress near rigid boundaries 77−80200
sudden expansion, steady flow, mixed-interpolation finite elements comparison 78−45486
suspension, laminar Poiseuille flow, particle lateral migration, tubular pinch effect 79−98783
suspension, Poiseuille to plug flow transition in tubes 79−90316
suspension of slender fibres, Poiseuille flow stability 78−71388
suspensions of charged particles, laminar tube flow, entrance deposition 80−59100
thermal instability anal. for horizontal liq. layers with a density max. 78−67193
thermally stratified, linear differential eqn., asymptotic fundamental system construct. *(German)* 77−902
tube elasticity effect on flow stability 77−72278
tube flow, contaminant initial dispersion, snout smoothing 77−11261
tubular flow reactors with first-order kinetics 79−4088
turbulence theory, review 80−4536
turbulent shear flow, large eddy simulation 80−38390
turbulent velocity profiles from stability criteria 79−50717
two layer flow stability *(Russian)* 79−14380
vertical channel parallel flow modification associated with density extremum 78−79380
vertical cylindrical tube, theory of capillary rise of liq. 80−28567
vertical porous stratum, natural convection, modified Poiseuille flow distrib. 78−5794
viscoelastic converging pipe flow, vel. vectors and radial stresses, rheological model and laser anemometry 79−60028
viscoelastic fluid, Poiseuille flow and temp. distrib. 79−60039
viscoelastic fluid flow between eccentric cylinders 80−1652
viscoelastic liquids, Poiseuille flow, hole-press. meas., computer model 80−59080
viscous flow in curved tube of triangular cross-section 77−7458
viscous flow through cylindrical tube Poiseuille formula determ. *(Dutch)* 78−51238
viscous incompressible fluid flow between parallel porous flat plates, transpiration cooling 77−47082
water, 1st normal stress difference meas., rel. to polymer solns. 79−98829
water, flow through circular pipe, pulsed NMR study 80−28566

Poiseuille flow continued
^{3}He, solid, low temp. thermal cond., structural crystalline defects 80−2240
^{4}He, solid, boundary limited thermal cond., Poiseuille phonon flow 80−2241

Poisson ratio
alkali halides, Poisson ratio and Gruneisen parameter, vol. depend. anal. 80−96614
anisotropic materials, Poisson coefficients, allowable values 80−64370
Araldite CT200/HT907, 263 to 343K, mechanical, physical and optical props. 78−56682
blood vessels, medium sized, mech. characts. 80−41101
bones, long, struct. anal., appl. to human tibia 77−21551
brittle plate containing stochastically distributed rigid rod like inclusions, strength *(Russian)* 77−23917
celluloid, mech. props. under proportional load, time lapse, heating and isotropic props. effect *(Japanese)* 79−79043
Co-base metallic glasses, elastic const. 77−66671
coarse grained materials, dynamic technique for determ. 77−86244
composite, elastic props. meas., reliability establishment 77−52574
composite material, structural anisotropy in viscoelasticity 77−86073
consolidating soil indentation effect 78−83340
contacting bodies, roughness and Poisson's ratio effect on deform. 79−79122
couple stresses on infinite strip with periodic edge loads 77−72160
crack tip plastic zones and strain energy density factor 79−50654
creep modelling incorporating initial strain and ageing 80−58939
crystals, strain wave vels., Poisson ratios and elastic moduli 78−51609
cylindrical shell, circumferentially cracked, transverse shear effect 80−28472
cylindrical shell, stress and strain in elastically distinct layer 77−872
Earth crust, shear waves Poisson ratio rel. to Lithospheric Seismic Profile in Britain (LISPB) 78−73313
eddy current determination 80−65116
elastic constants determ. by resonant vibr. in thin disk, apparatus 77−56182
elastic cylinder, end resonance under axisymmetric vibr. *(Ukrainian)* 80−23932
elastomers, filled, unfilled, Poisson ratio, dilatometric method 79−11733
FCC cryst., theory of response to [110] uniaxial loading 79−19310
FCC crystal, existence of negative Poisson ratio 79−69178
fibre reinforced composites, thermal cycling, elastoplastic strain calc. under action of external stresses *(Russian)* 79−38896
fibrous composite materials, models for composites with different props. in tension and compression 78−35417
film on cylinder, calc. of moduli *(Russian)* 78−63304
glass, stress in working zone under biaxial compression, Moire-band method 77−81369
glass fibre reinforced composite, random short fibres, elastic props. 77−70090
glass fibre reinforced epoxy composite, mech. and photoelastic props. at high temps. 78−19799
hexagonal crystal, anisotropic behaviour of Poisson's ratio, Young's modulus, shear modulus 77−11622
high-temperature US apparatus for elasticity characts. and thermal cond. meas. of materials 78−5705
infinite medium containing periodic ribbon-like inclusions, local intensification of thermal stresses *(Japanese)* 80−96195
isoperimetric gradient bounds for Poisson and torsional creep problems 79−98639
isotropic materials, rod shaped, elastic moduli and Poisson ratio determ. method 80−55606
isotropic solid, viscoelastic characterisation using harmonic dispersion of longit. reson. 79−10538
laminate, anisotropic layers, fibre reinforced, effective moduli of elasticity 77−4802
laser window materials, optical suitability 77−58361
load carrying flat bar with hole, Poisson ratio influence on stress distrib. *(Polish)* 77−9032
magnetic fields, inhomogeneous medium, numerical calc. 79−72454
measurement, laser-target technique, for glass, over wide temp. range 77−27497
mechanical anisotropy of texture effect on X-ray stress measurement *(German)* 79−29091
metal, Gruneisen ratio, rel. to Poisson ratio press. depend. and shock data 77−11712
metal, press. depend. rel. to Gruneisen coeff. 77−47504
metals, radiation effects on elasticity and elastic moduli, yield stress 80−2078
methane, solid, thermodynamic props. from US velocity obs. 79−46753
Moire method appl. to classical plate flexure test 78−51137
Navier equations of elasticity, iterative solns., depend. on Poisson's ratio 79−1107
optical expt. method to determ. Poisson ratio/elastic modulus ratio 79−82273
optical method of exptl. determ. 79−43523
optical waveguide blanks, thermal and elastic stresses in a cylinder 80−14447
optically transparent materials, evaluation of elastic ratio by interferometry 78−90804
paper, in-plane elastic moduli depend. on basis weight *(Japanese)* 77−77523
piezoceramic planar Poisson ratio variation with poling conditions 79−11391
piezoceramic Poisson ratio rel. to electromech. coupling and energy trapping 78−43796
plane orthotropic elasticity, elastic const. 79−55328
plasma coatings, elastic properties, acoustic meas. *(Russian)* 80−97519
plastic, glass-reinforced bottoms with a filler, rigidity 80−15183
plastic plates, B-, organic-fibre, glass-fibre reinforced, optimization 80−20996
polycrystal, elastic deform., effect of Young's modulus, shear modulus, Poisson's ratio 77−24344
polycrystalline aggregates, Poisson's ratio, central-force interatomic pot. calcs. 77−15479
polycrystalline materials, effect of grain boundary sliding on anelasticity 80−96592
polyethylene, filled with glass particles, uniaxially drawn, elastic constants, filler addition effect *(Japanese)* 78−95780
polyethylene, Poisson's ratios, parallel lamellas morphology 78−84882

Poisson ratio continued
polyethylene, polypropylene, ultradrawn fibres, Poisson ratio from Michelson interferometry 78−80596
polyethylene terephthalate, sheet, mech. anisotropy meas. by optical technique 77−12662
polyethylene terephthalate, sheet, Poisson ratio compliance consts., interferometry 77−12663
polyhydroxyethyl methacrylate swollen network filled with polyhydroxyethyl methacrylate, viscoelastic and ultimate behaviour in rubbery region 79−83247
polymer, foamed, rigidity 78−95769
polymer, rigid, prefractured states study, elastic limit and strength 77−70092
polymer film, oriented, compliance constants meas. 78−38261
polymers, testing using Rayleigh surface waves 79−70249
polypropylene film, double-exposure speckle pattern obs. of tensile deform., displacement, Poisson's ratio and stress relax. 80−84795
polystyrene-polyethylene block copolymer, deformation ratios, Poisson ratio and adhesion, dilatometric obs. 80−60937
prosthesis block copolymers, non-thrombogenic, struct. and mech. props. 77−52925
pyroceramic, stress in working zone under biaxial compression, Moire-band method 77−81369
reinforced plastic, elastic orthotropic cylindrical shell, axisymmetric contact problems, shell interaction with tires 78−1569
rim of semi infinite plate, crack originating from triangular notch under transverse bending 79−77009
rock, mech. props. rel. to cooling *(Japanese)* 80−31036
rocks and minerals, Poisson number determ., discrepancies *(German)* 78−69324
sandstone, mech. props. rel. to water content *(Japanese)* 77−44980
silicate glasses, elastic moduli calc. 78−60696
slab, surface displacements for high speed rubs 80−83767
soft elastic block bonded to rigid end plates, plane strain rotation moduli 79−90135
soft elastic material bonded to rigid end plates, compression moduli 79−90134
softwoods, transverse Poisson's ratio and Young's modulus *(Japanese)* 80−2111
solids of revolution, stressed state 77−14910
steel, 300 grade maraging low temp. elastic props. 78−27555
steel, austenitic stainless, N-alloyed 80−108490
steel, Cr-Mn (13, 19 wt.%), elastic const. behaviour, anomalous, low temp. 80−97521
steel, elastic moduli, temp. depend. *(Japanese)* 77−59840
steel, sheet, cold-rolled, US inspection for mech. prop. anisotropy 78−23750
steel, stainless, Cr-Ni-Mn, N strengthened, low-temp. elastic props. 79−70109
steel, stainless type 304, elastic const. variability, US vel. meas. 80−55446
steel, type 20 and Kh18N10T, Poisson ratio, prestrain effects 79−70103
strip and plate, end resonance for materials of varying Poisson ratio 77−51438
tetragonal crystal, elastic moduli, anisotropic behaviour, cryst. symmetry effects 78−51604
transparent materials, low-modulus, mech. props. determ. method 78−5704
triangular finite elements compact representation 77−26176
trigonal crystal, elastic moduli, anisotropic behaviour, cryst. symmetry effects 78−51604
viscoelastic material, complex dynamic moduli and loss angles 77−68451
viscoelasticity, instantaneous moduli, determ. from long-term static test results 80−38286
viscoelasticity equations, numerical soln. via Poisson ratio-related operator 77−89042
volume dependence, Debye theory 78−22785
volume dependence of Poisson and Gruneisen ratios 77−43351
wood, stress distrib. in cell wall subject to tensile force in transverse direction *(Japanese)* 77−77539
Zircaloy-4, Poisson's ratio determ. at several temp. levels 78−52874
Al alloy, elastic moduli, temp. depend. *(Japanese)* 77−59840
Al alloy, precipitation hardened 2014 and 2219, temp. depend. of elastic constants 77−66673
Al_2Cu crystal, Young's modulus, Poisson ratio, elastic consts. determ. by extensometry and US meas., anisotropy discussion *(French)* 79−50683
Al_2O_3 refractories, fracture, J-integral meas. 80−108537
B fibre reinforced epoxy resin, anisotropic laminate, effective modulus of elasticity 77−4802
$BaO-P_2O_5$, glass, US velocity rel. to elastic props. 80−103425
C fibre reinforced plastic, laminate, non Hookean behaviour in fibre direction, effect of fibre waviness on tensile props. 78−19804
C fibre reinforced plastic, modulii meas. *(Russian)* 80−39199
$CaO-P_2O_5$, glass, US velocity rel. to elastic props. 80−103425
$CeH_{1.98}$, $CeH_{2.98}$, elastic props. at high press. 77−84825
Co based metallic glass, B and P glass former additions, elastic consts., flow behaviour correlations 78−44154
Cu alloy, precipitation hardened, anomalous elastic props. 77−86071
D_2, solid, melting curve, meas. of P, V, T and longitudinal sound velocity 79−37814
Fe alloys, elastic props., texture correction formulae *(German)* 78−15439
Fe based metallic glass, B and P glass former additions, elastic consts., flow behaviour correlations 78−44154
Fe-base metallic glasses, elastic const. 77−66671
Fe-Si, (3 wt.%), nonuniform elastic deform. in grains *(Russian)* 78−35415
$(FeCo)_{80}B_{20}$, glass, elastic consts. 79−83249
$(FeNi)_{80}B_{20}$, glass, elastic consts. 79−83249
GaS, elastic prop. anisotropy, Debye temp. *(Russian)* 80−88244
Ge-As-Se glasses, US vel. and reson. freq. meas. 78−23756
$K_2O-PbO-SiO_2$, glass, mech. and optical props. *(Russian)* 77−20860
$K_2O-SrO-SiO_2$, glass, elastic constants 77−16630
$LaH_{2.96}$, elastic props. at high press. 77−84825
$MgO-P_2O_5$, glass, US velocity rel. to elastic props. 80−103425
Ni-base metallic glasses, elastic const. 77−66671
Pb-Bi, elastic moduli, internal friction from US velocity meas. 79−15717
α-Pu, sound vel. meas., press. to 50 kbar 77−20015
Pu-Ga (1 wt.%) alloy, polycryst. consts. calc. from single cryst. data 77−20005

Poisson ratio continued
$SbGe_xSe_y$ glasses with const. Sb content, heat capacity, thermal expansion, US vel. and elastic moduli 77−76574
Se, vitreous, elastic coeffs. about glass transition temp. US study *(French)* 80−19865
Si_2N_2O, elastic props. 79−29122
$SrGa_2Si_2O_8$-$SrGa_2Ge_2O_8$, solid solution, exam. of elastic and electrical props. 79−96057
SrO-P_2O_5, glass, US velocity rel. to elastic props. 80−103425
Ti-Mo alloys, elasticity moduli, 80-300°C *(Russian)* 78−80574
TiC_xO_y, elastic characts. 77−80568

polar cap absorption *see ionospheric electromagnetic wave propagation*

polar cap flow *see airglow*

polar plots (control systems) *see Nyquist diagrams*

polar semiconductor materials *see polar semiconductors*

polar semiconductors
see also ferroelectric semiconductors; piezoelectric semiconductors
ambipolar semiconductors, thermoelectric redistribution of carriers 80−107830
amorphous semiconductor, mobility gap temp. derivative calc., polar contrib. 78−26861
biexcitons, variational wave functions 78−23031
bipolar, strong EM wave propagation, effect of generation-recombination processes *(Russian)* 79−78115
boundary with nonpolar semiconductor, weakly bound surface polaron 79−69576
carrier, mobility in mag. field, extreme quantum limit, iterative technique 78−2498
chemical shift of Zeeman masses 78−10338
chemisorption, charge transfer processes, expt. obs. method 77−89824
conduction states, pseudopot. and tight-binding calcs. 80−24785
conductivity in quantising mag. field, anharmonicity effect 80−2406
crystalline thin films, surface vibr. states, IR absorpt. spectra obs. *(Russian)* 80−60606
degenerate, asymptotic soln. to Boltzmann transport equation 77−4332
degenerate semiconductors, electron scattering interaction with coupled plasmon-polar-phonon modes 79−42536
effective exciton-exciton interaction 79−42465
effective Hamiltonian for few-particle systems 77−15776
electron momentum distribution for high elec. field 77−1428
electron-hole liquid, electron-phonon interactions 80−6739
electron-hole liquids, phase diagram 77−89706
electron-hole system, interaction with phonons 80−6738
electron-phonon and electron Raman scatt. in mag. field 79−91438
EM wave propag. in solid-state plasma, DC electric field effect 79−82620
exciton, energies, oscillator strengths, and phonon side bands 80−44512
exciton dispersion, influence of optical phonons, effective exciton mass. variational calc. 79−15091
exciton interaction potential, repulsive barrier, polaron effects 77−24523
exciton-dispersion, influence of optical phonons 80−6741
exciton-neutral donor and biexciton complexes 79−90968
exciton-phonon interactions, optical absorpt. spectra, theory 80−49614
excitons bound to ionised donors, binding energy calc. 77−28128
excitons in mag. field, exciton-phonon interaction 80−24806
free carrier absorption by photon-ionized-impurity-plasmon processes 79−4578
HF conductivity at low temperatures, anal. *(Russian)* 77−8128
HF mobility, in longitudinal quantising mag. field 79−51619
high field collision rates 78−30932
high field quantum magnetotransport theory 78−30941
highly excited, optical dielec. function of electron-hole plasma 80−92847
hot exciton scatt. accompanied by transitions to excited states, phonon interactions 80−44516
hot exciton transitions to excited states, interaction with acoustic phonons 80−96799
impurity levels, influence of electron-phonon coupling 78−64007
impurity pseudopotential screening 79−15121
interface between two polar semiconductors, phonon-plasmon-polariton mode propag. 79−60731
intraband magnetoabsorption theory for weakly polar semicond. 79−42949
light scattering, multiphonon cascade theory 78−19490
longwave secondary radiation *(Russian)* 78−80343
magneto-Seebeck coeff., electron spin depend. 78−80011
MIS device, polar-optical phonon interaction with two-dimens. electron gas 79−82434
n-type, doped, IR absorpt. in Drude tail, effect of finite electron densities 79−47449
n-type, hybrid mode instability 77−80800
nonlinear transport, field-dependent relaxation time 80−6866
optic-phonon-magnetoplasmons at interface between two polar semiconds. 78−23146
optical phonon-magnetoplasmon interface oscills. 78−43467
oscillatory electron drift rel. in non-ohmic regime at low temp. 79−33291
peak electron velocity, simple method for estimation 77−8129
photoexcited, carrier and optical phonon distrib. time evolution 80−34158
piezoelectric polar materials, appl. to SAW and other devices 80−66114
polariton propagation between semiconductor-metallic screen interface *(Spanish)* 80−84510
polaron mass of exciton 79−95344
quasi-monopolar semiconductors, I/V characts., effect of weak diffusion 80−70824
Raman spectra of coupled LO phonon plasmon mode, de Haas-Shubnikov like quantum oscills. 78−43863
resonance electron-phonon Raman scatt., cross-section oscills. 80−60598
resonant magneto-Raman scatt. 79−51958
resonant secondary radiation 78−31242
saturated, polar exciton model 79−82524
secondary cyclotron emission giant oscillations of intensity and line shape 80−66192
secondary emission, multiphonon cascade process *(Russian)* 78−2850
secondary radiation intensity oscills., effect of high mag. field 79−19880
strongly anisotropic, electron-hole liq. in mag. field 80−59890
surface, energy levels and geometry, theory 80−49481
surface biexciton in polar semicond., binding energy calc. 80−96796
surface inversion layers, energy loss of warm and hot carriers 77−11981

polar semiconductors continued
surface plasmon-phonon modes in quantizing mag. field, nonlocal shift 77−72908
p-Te, impact ionization rate of holes at 77K 80−10993
theory of excitons bound to neutral impurities 79−73441
TO phonon-helicon coupling 79−73539
transient high-field conductivity, theory 78−79998
two-phonon resonance Raman scattering 80−108204
Wannier excitons, effective Hamiltonians and binding energies 78−34777
AgBr, polar semiconductor, electron-hole liquid, electron-phonon interactions 80−6739
CdS, spin flip Raman scatt. linear k term 78−19475
CdS, transmission spectra, region of exciton reson., spatial dispersion effects 79−78704
CdS(Se), polar semiconductor, electron-hole liquid, electron-phonon interactions 80−6739
CdSe, collisions between hot excitons and hot electrons 80−7415
Cu_2O, polar semicond., effective exciton-exciton interaction 79−42465
α-GaAs, amorphous, mobility gap temp. derivative calc., polar contrib. 78−26861
GaAs, collisions between hot excitons and hot electrons 80−7415
GaAs, optical cond. of free carriers 78−19436
n-GaAs, Raman spectra of coupled LO phonon-plasmon mode, de Haas-Shubnikov like quantum oscills. 78−43863
GaAs, weakly excited, luminesc. from exciton polaritons, based on exciton-electron collisions 79−83020
GaP, electron-hole drops, self-consistent surface calculation 80−65464
GaP, electron-hole liquid props., luminescence at high excitation intensity 79−69882
GaP, polar semicond., radiative recomb., electron-phonon interaction effects, calc. 80−49631
GaP, polar semiconductor, electron-hole liquid, electron-phonon interactions 80−6739
GaSe, direct exciton excited state hot luminescence, band struct. props. 80−55183
InAs(Sb), IR reflectivity, longitudinal optical phonon-plasmon coupling 77−59578
InP, collisions between hot excitons and hot electrons 80−7415
InSb, impact ionisation in crossed elec. and mag. fields 79−28355
InSb, longit. magneto-Seebeck coeff. in quantising mag. field 79−56250
n-InSb, mobility in mag. field, extreme quantum limit, iterative technique 78−2498
InSb, polar semicond., resonant magneto-Raman scatt. 79−51958
n-InSb, TO phonon-helicon coupling, Doppler shifted cyclotron reson. region 79−73539
InSb, warm electron coeff. 78−10452
$La_{0.9}Ca_{0.7}CrO_3$ polar semiconductor, elec. props., slight reduction effect 80−20183
PbI_2 direct gap polar semicond., electron hole liquid phase diagram *(Russian)* 80−93314
n-PbS, natural galenite, optical and crystallographic props. 79−42975
n-PbSe, mag. field influence on high-freq. relaxation time 79−95438
SiC (15 R), polytype, many valleyed polar semicond., electron-hole-liquid, obs. from excitation and time delayed spectra 79−28289
SiC, cubic, electron-hole liq., luminesc. obs. 78−31239
SiC, cubic, electron-hole liq., ground state props. calc. 79−69429
SiC, polar semiconductor, electron-hole liquid, electron-phonon interactions 80−6739
Tl halides, polar semicond., binding energy of Wannier excitons 77−69232
ZnO, excitonic molecule transitions, M-band emission 79−78742
n-ZnO film, highly degenerate, IR absorption by free polarons 77−4697
ZnO, polar semiconductor, electron-hole liquid, electron-phonon interactions 80−6739
ZnO, polar surface, clean (O_2-H-exposed), reflection energy loss spectra, 2-30 eV 78−64434
ZnO, reflection spectra, exciton reflection at high excitation levels 77−69853
ZnO surface, adsorption of O_2 and CO, electron energy loss spectra meas. 78−14601
ZnSe, polar semicond., radiative recomb., electron-phonon interaction effects, calc. 80−49631

polarimeters
see also polarimetry
astronomical, and photon-counting magnetograph, for stellar circular polarisation obs. *(Russian)* 78−65500
astronomical, detector array and polarising optics 78−57453
astronomical, near IR, for solar corona emission line obs. 78−61740
astronomical, spectrum scanning Stokes, for solar research 78−61741
astronomical and atmospheric meas. appl. 78−61745
astronomical IR instrumentation on NASA airborne observatories 78−45224
astronomical polarimeter, attached to multi-channel spectrophotometer *(Japanese)* 78−89072
astronomical polarimeter, stellar photometric appl. for interstellar grain size meas. 80−12792
automated polarimeter for determ. of ellipsometric characts. of optical surfaces 80−101822
automatic polariscope interactive control system to evaluate stresses 80−19299
Babinet-Soleil modified compensator 77−74485
beam profile monitor, determ. of intensity and polarisation profiles 79−76251
calibration, illuminator with adjustable polarisation 77−57380
Cary 60 spectropolarimeter, conversion into fast circular dichroism instrum. for use with standard rapid reaction techniques 80−52296
commercial circular dichroism instruments, magnetic shielding problems 77−87807
Compton polarimeter, calc. of linear polarisation sensitivity 80−77839
Compton polarimeter for gamma rays 79−76317
conference, San Diego, CA, USA (Aug. 1977) 78−54437
deuteron tensor polarimeter using $^3He(d,p)^4He$ at 430 keV 77−3242
dichrograph calibration apparatus, 185 to 600 nm 77−5886
digital lock-in technique using electro-optic cryst. 78−273
Dollfus stellar polarimeter, modification for linear polarization meas. 79−53723
double focusing crossed field electron spin polarimeter, theory, construction, and operation 78−86761

polarimeters continued
electro-optical effect meas., appl. to ferroelec. crysts. *(Japanese)* 78−37045
electro-optical modulator-based instrument, for polarisation dependent light scatt. meas. 78−58010
electrooptic four-modulator photopolarimeter, for Mueller matrix meas. 80−73417
error quadratic mean value determ., statistical method *(Russian)* 77−41668
far IR polarimeter for balloon astronomy 79−35094
Faraday cell polarimeter magnetic potential difference calc. 77−82587
fluorescence polarimeter for flow cytometry 78−73191
fluorescence polarisation detector for polarisation degree calc. 79−219
Fourier photoellipsometers and photopolarimeters based on modulated optical rot. 78−54439
Fourier photopolarimeter, for Stokes parameters of light meas. 79−21805
Fourier photopolarimeter, optical rot. simulation of mech. rot. 78−65958
Fourier photopolarimeter with rot. polariser and analyser for meas. Jones and Mueller matrices 78−54435
gamma ray, 100 to 800 keV, high resolution 80−52839
glass, thermal stresses, temporary and residual, monitoring by semiautomatic heating polariscope-polarimeter 78−16833
hadron polarisation meas. at high energies 78−884
halfshade analyser using two polariser sheets 78−54434
High Altitude Observatory Coronagraph/Polarimeter on the Solar Maximum Mission 80−51662
high-speed scanning polarimeter for study of kinetics of polarisation processes 80−31845
holographic platform, optical path stabilisation with magnetooptic periodic grating 80−99678
ionospheric phase switched correlation polarimeter, appl. to D-region partial refl. expt. 77−87169
IR polarimeters for contactless meas. of semicond. free-carrier conc., Faraday effect 77−73135
IR video camera at 10 μm, using liq. cryst. thermooptical convertor and scanning polarimeter 79−94326
laser polarimeter for active spill detection 77−21938
laser polarimeter for e^+ e^- beam polarisation meas. in storage ring 80−14019
microscope polarisation adapter, for transparent material anisotropy and internal stresses meas. 80−31863
microspecular apparatus, for polarised specular reflectance spectra meas. 77−5926
microwave, for 8 mm (35 GHz) band, MnF_2 Cotton-Mouton-Voigt effect *(French)* 78−74040
modulated submillimetre-laser polarimeter for meas. of Faraday rotation in toroidal plasma 79−46474
modulators, photoelastic radiation polarisation, review 80−102846
Mossbauer 14.4 keV gamma-ray source, design, calibration and polarimeter 80−86535
Mott-Schwinger scatt. polarimeter for MeV neutrons 79−22571
multichannel polarimeter, data acquisition and control system *(Japanese)* 80−77842
multichannel polarimeter, description *(Japanese)* 80−77841
near IR polarimeter of Hatfield Polytechnic Observatory, design 79−2482
near IR transparent material, birefringence meas. polarimeter 79−44925
neutron, double scatt. fast, optimisation of geometrical factors 77−54478
neutron, meas. in (γ,n) reactions at threshold 77−30739
neutron depolarisation meas., exptl. set up and process program 80−18771
neutron polarimeter, 3-D, critical spin dynamics in ferromagnets meas. 79−18098
neutron polarimeter, 3-D calibration procedure 80−18770
neutron polarisation anal., separation of coherent and spin coherent scatt. from D_2O 77−6655
nucleon polarimeter for 100 to 500 MeV range 78−82599
opticophysical and physicochemical meas. instrum. 80−13121
oscillating compensator-analyser-polarimeter with AC optical rotators 78−29142
photoelastic coating, tests, construction of polariscope *(Polish)* 77−5887
photoelectric, construction and applics. 77−22589
photoelectric, effect on accuracy of light interference in biquartz modulator 80−62713
photoelectric, optical path determination birefringent plates, Senarmont compensation method *(German)* 77−10091
photoelectric mangetopolarimeter for studying inhomogeneous optically anisotropic media 78−77964
photoelectric polariscope quartet for induced birefringence meas. 78−21204
photographic double exposure for controlled density eval., replacement of quarter wave plates 77−87859
photometric, drift stabilization and photomultiplier linearization with feedback cct 78−54436
photometric system, photomultiplier linearisation and system stabilisation 78−54441
photopolarimeter, Mueller matrix meas., Fourier analysis of single detected signal 78−74048
Pioneer Venus Orbiter cloud photopolarimeter 78−57429
plasma electron density and mag. field meas. by far IR polarimeter-interferometer 79−32817
polariscope, for elliptical light polarisation meas. 79−2809
polarising radiometer, data reduction technique 77−78472
positron polarisation in ^{68}Ga decay, precision meas. using new polarimeter 77−46144
precision polarimeter, systematic errors, instrumental errors *(German)* 78−272
precision polarimeter, systematic errors, quartz plates standards *(German)* 78−16832
proton polarisation at high energy elastic scatt. meas. apparatus 77−30439
proton recoil polarimeter for zero gradient synchrotron 77−38511
proton spectrometer/polarimeter for photoreactions below 1 GeV 80−18751
radar polarimeter, for study of air flows in clouds 77−91243
radiopolarimeters, fully automatic, for solar patrol at microwave freqs. 79−101065
recoil deuteron polarimeter for polarised ^3He beam 77−34529
reflected and transmitted light, meas. instrument 77−74487
reflection polarisers and analysers in vac. UV, design criteria 78−55424
polarimeters continued
resonant cavity microwave polarimeter, meas. of Cotton-Mouton-Voigt effect *(French)* 78−89514
servo-polarimeter utilizing rotating plastic film, for birefringence determination 79−71509
slow proton beam spin polarisation meas. by Lamb shift 78−78031
small flow-through cryostat for polarization microscope 78−86327
Solar Maximum Mission UV polarimeter design, operation and calibration 79−80225
spectrophotometer universal cryostat attachment 80−31765
spectropolarimeter for analysis of scattering objects *(Russian)* 79−26110
spectrum scanning Stokes polarimeter for solar work 80−51663
spin-scan imaging photopolarimeter for Pioneer Jupiter missions 77−41303
Stern-Gerlach, for measuring polarisation of cold neutron beams 80−37679
stress and strain measurement methods, monograph 78−19988
student polarimeter, easily constructed 79−25812
submillimeter wave, for plasma diagnostics 78−91158
thin film thickness meas., automatic Brewster angle spectrophotometer 79−6078
three Ge(Li) Compton polarimeter with kinematic selection, for γ polarisation meas. 77−83456
two-channel polarimeter, for ionospheric Faraday effect meas. at 140 MHz, first results 80−61912
Ultraviolet Spectrometer and Polarimeter on Solar Maximum Mission 80−51661
universal interference and polarisation apparatus 78−19986
UR-10 and UR-12 IR spectrophotometers, disrupted total internal reflection polarising attachment 77−74528
Voyager photopolarimeter experiment 78−20616
X-ray, Bragg crystal, using position sensitive proportional counter 78−74117
X-ray, design and appls. 79−6251
X-ray, mosaic graphite, on OSO-8 satellite, design, preliminary results 79−25490
X-ray, Thomson-scatt., satellite-borne, for solar obs. 79−25491
X-ray astronomical polarimeter, for solar and extrasolar obs. 78−57454
X-ray astronomy, calibration of Bragg X-ray analyser crysts. 77−64664
γ-ray, linear systems, optimisation of geometrical factors 77−54478
Ar, liquid, scintillating target, fast neutron polarisation analyser 80−47833
C, plate polarimeter for recoil proton polarisation meas. in $\gamma p \rightarrow \pi^\circ p$ reaction 79−93898
C, proton analysing power, 300-560 MeV 80−23279
Ge(Li) planar detector, in γ-γ polarised directional correlations set-up 77−34530
H_2, liquid polarimeter for recoil proton polarisation meas. in $\gamma p \rightarrow \pi^\circ p$ reaction 79−93898
He polarimeter, low temp., 20 to 50 MeV proton polarisation analysing apparatus *(Russian)* 79−76318
$^3He(d,p)^4He$, polarimeter for deuteron beams 80−47834
Si, proton polarisation in nucl. reacts. meas. 79−31346

polarimetry
see also ellipsometry; polarimeters
acousto-optic polarisation modulator, use in dynamic ellipsometry, polarimetry *(Russian)* 80−14472
alignment using He-Ne laser/polarimeter system 77−37967
asteroids, radiometric and polarimetric sizes and albedos, review 77−60708
astronomical, new automatic technique for galaxy obs. 77−17692
astronomical radiosources, aperture synthesis obs. of circular polarisation, techniques and appl. 77−9670
atmospheric turbidity, skylight at South Pole station, Antarctica, polarising radiometer meas. 78−57320
birefringence modulator devices for sensitive polarisation determ. 78−8437
blood O_2 anal., for teaching 78−49622
calibration using d-10-camphorsulphonic acid ammonium salts 77−24816
charged particle polarisation, methods of meas. *(Rumanian)* 79−59321
circular dichroism in presence of birefr. and linear dichroism, meas. method 78−27178
circular ring, inner boundary shapes, optimised, diametral compression 80−38369
coherent light beam, azimuth of plane of polarisation determ. *(Russian)* 78−29143
condensed gases, solid phase transition, optical meas. in diamond-anvil cells 80−73381
conference, polarised light, San Diego, Calif., USA (Aug. 1976) 77−45881
conference, San Diego, CA, USA (Aug. 1977) 78−54437
correlation techniques, amplitude and intensity correls. meas. 77−154
crystal gyrotropy, meas. in IR region 80−88957
crystal optical activity meas. method, appl. to KH_2PO_4 78−52466
demonstrations with polarised light 77−45657
depolarisation degree and concentration relationship *(Russian)* 77−44561
EM noiselike radiation, noncoherent polarimetry anal. 80−1111
Faraday effect measurement in pulsed mag. field 80−80758
fluctuations in laser illumination, circuit for compensation, ms sensitivity 77−57379
fluorescence polarisation meas., T-format photon-counting polarisation photometer 78−54423
fluorescence polarisation meas. at high press. 78−66576
fluorescence polarisation measurements, correction for finite apertures 78−21224
fluorosilicate, Mossbauer polarimetry, double motion drive and effective thickness meas. 78−23379
glass, flat, horizontal annealing process, math. model 79−61615
graphical methods for determ. action of polariser-retarder system 77−155
gravitational radiation detection method, elastooptical antenna, photoelastic effect 80−46947
impulse response matrix formalism for polarised light, appl. to holography 78−63045
inhomogeneous optically anisotropic media, parameters by photoelec. polarimeter 77−74486
intraresonator high-sensitivity meas., using Nd:YAG laser with min. amplitude noise 79−63317

polarimetry continued
Jupiter clouds spectropolarimetry, lines equivalent widths information content 80−31215
Jupiter decametric radio bursts, colour representation of polarisation patterns 77−5490
linear dichroism measurement, appl. of polarisation scrambling using photoelastic modulator 78−4683
linear optical system, techniques for polarisation-altering props. meas. 78−54438
liquid light scatt. coeff. absolute determ. apparatus 78−86319
macromolecular rapid circular dichroism meas. with small gas lasers 77−37968
MCD and Faraday effect in chemistry and physics, optical instrumentation 78−54466
metal optical constants meas., simple polarimetric method *(French)* 77−45880
modulated-Mueller-matrix photopolarimetry [MMMP]: a technique for the study of elastic light scattering by depolarizing temporally modulated media and surfaces 80−90882
Mueller matrix photopolarimetric meas., Fourier analysis of single detected signal 78−74048
natural surface polarisation imagery, remote sensing appl. 78−61625
neutron polariser-analyser efficiency meas. by spin flip meas. 80−27911
noise suppression by polarization-plane rotation-angle amplification 80−68241
Norikura Observatory, use of coronagraph *(Japanese)* 80−82223
optical fibre signal polarisation statistical meas. 80−99877
optical fibres, glass-plastic, measurement using magneto-optic device employing silicone-clad fused silica fibre 79−50425
optical materials, piezo-optic coeff. determ. under static loading, interferometric and polarimetric techniques 79−4787
optical measurement technique using He-Ne stabilised transverse Zeeman laser 80−48272
optical phase difference meas., using polarisation technique 78−29141
optomechanical properties determ., polarisation device application, by compensation method 80−40643
orthorhombic crystal, birefr. and refr. index determ., refl. method 80−86380
partially polarised waves, accuracy 77−46666
periodic analysers for freq. mixing detect. of polarisation modulated light 77−45883
photocathode polarisation sensitivity, two-beam interferometer expts. 80−4772
photon counting approach to meas. polarisation of low level light flux 77−13795
planetary atmosphere, remote sensor, high resolution Fourier transform spectropolarimetry 78−57469
proton polarisation meas. for $^{12}C(p,p)$ at 40-75 MeV 80−52840
radio sources Faraday rotation measures, computation method 80−4263
ray optics, theory of light field, statistical optics, light meas., photometry, polarimetry 77−79748
Rayleigh atmosphere, polarisation meas. rel. to single scatt. albedo determ. 79−35117
reflected sunlight polarisation, meas. from high-altitude balloon 78−61561
remote sensing, polarimetry of particulate surfaces 78−58011
semiconductor, Faraday effect meas. using IR magneto-optic polarimeter 77−34014
semiconductor defect birefringence detection by polarisation IR microscopy 79−83405
single mode fibre polarisation stabilisation 80−58724
small angle, new expt. method 77−26383
soil moisture and component estimation from spectral polarisation 79−16678
Spacelab facility for X-ray source spectroscopy and polarimetry 78−32314
spectropolarimetry with an intensifier-dissector-scanner 80−109367
Stokes parameters, of light beam, polarisation modulation meas. 79−21803
Stokes parameters meas. 78−32854
Stokes parameters of light meas. using Fourier photopolarimeter 79−21805
Stokes vector of light automatic meas. 79−63292
stress measurement, polarisation device application, by compensation method 80−40643
structural components, photoelastic methods of stress distrib. anal. *(Polish)* 77−9031
submillimetre beams, meas. using mechanical polarisation modulator 77−37987
sugars, detect. in HPLC systems using polarimetry, refractometry and optical rot. 78−48734
sunlight polarisation by atmosphere measurement, ships compass adjustment appl. in fog 78−24831
survey of methods for polarisation state complete determ. 77−45882
thick laminar reinforced plastics, deformation fixing in polarisation optics *(Ukrainian)* 78−90802
tilted absorbing glass plate, polarisation response rel. to polarising radiometer calibration 78−55297
Tokamak, poloidal field meas. by far IR polarimetry 79−32794
Venus clouds spectropolarimetry, lines equivalent widths information content 80−31215
$Fe_{40}Ni_{40}P_{14}B_6$, amorphous, stress-induced mag. easy axis 79−33516
Ge, standard measures of magnetooptical rotation of plane of polarisation in IR region 80−60551
InSb, standards for magnetooptical rotation, charge carrier density determ. in semiconductors 80−60551
KCl, photoelastic consts. at 10.6 μm, interferometric and polarimetric meas. 78−25934
MnF_2, Cotton-Mouton Voigt effect using microwave polarimeter *(French)* 78−74040
Nb, BCC lattice, optical prop. in range $\lambda = 0.265-18$ μ, polarimetric meas. 79−15075
Si, surface, selectively roughened, polarimetry of specular and non-multiple scatt. EM radiation 79−13904
$SrF_2:Tm^{2+}$, modulation magnetooptic spectroscopy of cross-relaxation resonances using laser polarimeter 79−15381

polarisability
see also atomic polarisability; molecular polarisability
aliphatic unsaturated normal hydrocarbons, positron annihilation time spectra, polarisability depend. 78−6806

polarisability continued
alkali chalcogenides, electronic polarizabilities and ion sizes 80−59432
alkali halide, optoelectronic props. 80−25330
alkali halide, polarisability analysis using Narayan-Ramaseshan repulsive pot. 77−76353
alkali halide, strain polarisability parameter, evaluation 77−35617
alkali halides, exchange charge shell model analysis of strain derivatives of static polarisability, effective charge parameter 78−91296
alkali halides, photoelastic consts., short range polarisability effect 80−80748
alkali halides, static polarisability, vol. depend. 78−52428
alkali metal halide, electronic strain polarisability consts. 80−29677
alkaline earth chalcogenides, electronic polarisabilities and ionic radii of metal and chalcogenide ions in cryst. state 80−100198
alkaline earth chalcogenides, electronic polarizability of ions, effect of crystal potential 78−26490
alkaline earth halides, electronic polarizabilities and ion sizes 80−59432
bacteria, E.coli strains in aq. suspension, polarisability anisotropy and aminoglycoside antibiotic effects 80−85441
benzene binary liquid mixtures, polarisation rel. to mol. interactions, US study 77−15494
carbazole, birefr. meas., 20 to 190°C, crystal-to-crystal phase transform. 80−45031
cavity with cylindrical hole in wall of infinite thickness, elec. and mag. polarisabilities determ. 78−71004
colloid, dichroism in homogeneous elec. field 79−8122
colloid, electro-optical characterisation methods 77−24821
colloids, interfacial electric polarisability, and interactions 80−108751
colloids, macromolecules, particle size distribution, reduced electric dipole moments, polarisabilities using electric birefringence 78−95958
convergence properties of generalized inner projections to dynamic polarizabilities 79−5999
corrosion processes, polarisation resistances method of study 77−28930
crystal under hydrostatic press., electronic polarisability and ion size var. 78−26487
cubic ionic crystal, photoelastic shear consts. 79−86833
degenerate electron system, low-freq. polarisability, RPA calc. with temp. correction 79−95354
dielectric, nonpolar, temp.-depend. polarisability, anharmonic oscillator anal. 79−8087
Earth, polarisability time const. rel. to EM transients *(Russian)* 79−39644
electron gas, two-dimensional, in mag. field, polarisability 80−107888
electronic polarizabilities of ions in doubly refracting crystals 78−79551
fluid, dense, isotropic Raman polaris., correlation function, kinetic eqn. 77−28567
fluid, dense of polarisable dipolar hard spheres, Monte Carlo study 79−86665
graphite, Van der Waals interactions, in and between layers of atoms 77−84695
graphite surface, asymptotic interaction with He, H, and H_2 79−99429
hadron polarisabilities, quark models 77−82703
ice, hexagonal, i.r. polarisability 77−4639
II-VI and III-V, ion effective charge parameter, electronic polarisability 78−51463
ion, polarisable, Brownian motion in periodic pot., polarizability effect on cond. 79−4427
ionic crystal, electronic dielectric const. first and second electronic dielectric const., effective charge parameters 80−29669
ionic crystal, quadrupole antishielding factors and polarisabilities 77−51346
ionic crystals, evaluation of photoelastic consts. 80−50297
ions, electronic polarisabilities and refraction screening power 77−35504
ions in group III-V compounds, electronic polarisabilities 77−35505
linear aggregates, small, polarisability determ., CNDO method and analytical models *(French)* 80−29298
liquic crystals, orientational order parameter, optical birefr. meas., polarisation field problems 80−79688
liquid, simple, depolarised light scatt., double scatt. considerations 79−87410
Lorentz-Lorenz formula, microscopical derivation 78−92014
low energy proton Compton scattering, p polarisabilities 78−93886
macromolecular soln., electro-optical characterisation methods 77−24821
metallic grain polarisability, two -dimens. film subjected to elec. field 79−4859
molecular crystal with impurity, polarisability in exciton transition region 78−27268
molecular crystals, Stark splitting ang. depend. dipole moment and polarisability effects 77−51711
nematic liquid crystal, diamagnetic susceptibility, refractive index, density and polarisability 77−15315
nematic liquid crystal, optical anisotropy, determ. from NMR and birefringence data *(German)* 77−40205
orthosilicates, determ. of electronic polarisabilities of ions 79−7570
phosphosilicate glasses, photoelastic consts. and polarisability 79−65839
pion polarisability 78−456
polar fluids, Debye and far IR absorpt. theory 77−69829
polaritons, LT mixed mode, dispersion relation 80−65470
polymer film, small-angle light scatt., Debye-Bueche theory treatment of multiple scatt. 80−84794
quartz, $\alpha \rightarrow \beta$ transition obs. from nonlinear optics and bond polarisability model 77−15336
refractive index transients, laser-induced, low-temp. solns., excited triplet state polarisabilities role 79−87411
rutile-type compounds, crystal binding energies and electronic polarisabilities 80−75202
sapphire, shock compressed, refractive index, density, and polarisability behaviour 80−50295
semiconductor, electronic polarizability as function of Penn gap 80−49638
semiconductor, n-type, donor-polarizability enhancement as the insulator-metal transition is approached from the insulating side 80−80184
semiconductor, nonlinear optical props. 80−25333
semiconductor compounds, electronic polarisability rel. to energy gap 80−10524
sepiolite, clay mineral in suspension, elec. cond., depend. on length 79−38520
small particles, optical absorpt., sum rule for polarisability 77−28532
solute-solute-solvent interaction, dielec. behaviour problems, review 80−25298
solvated electrons, dipole polarisability, Compton profiles 78−27877

polarisability continued
sum-rule relating polarizabilities of proton and pion *(Russian)* 79−93420
suspension of rod-like molecular particles, anisotropy of interfacial elec. polarisability, length depend. 79−38520
transition metal oxides, electronic polarisability of ions 77−19901
γp high multipole polarisabilities from Compton scatt. amplitudes 79−85301
$\gamma\pi$ high multipole polarisabilities from Compton scatt. amplitudes 79−85301
n, electric polarisability, from photoabsorption cross-section 80−57597
n dipole polarisation, possible detection in U(n,n) small angle scatt. 77−22674
p, electric polarisability, from photoabsorption cross-section 80−57597
$p\bar{p}\rightarrow\gamma\gamma$ annihilation, influence on sum rule proton polarisability 80−18143
ρ EM polarisabilities difference contribs. from $N\bar{N}\rightarrow\pi\pi$ and $\pi\pi\rightarrow\gamma\gamma$ 79−3023
Ag halides, cryst. electronic polarisability and ion sizes 77−51341
AgBr, dielectric behaviour under hydrostatic press. 78−52420
AgCl, dielectric behaviour under hydrostatic press. 78−52420
AgCl(Br), electronic dielec. const., vol. depend., Clausius-Mossotti model 80−100630
AgCl(Br)(I), static polaris. and effective charge parameters, Born-Mayer pot. 77−31628
Ar, solid, vibr. and thermal props., effect of polarisability 78−71807
BaF_2, electronic polarizability and dielectric const., strain derivatives 78−19406
$BaO-K_2O-VO_2-SiO_2$, glass, elec. cond. rel. to ion polarisability, polarons 80−49729
$BaO-La_{0.6}O-VO_2-SiO_2$, glass, elec. cond. rel. to ion polarisability, polarons 80−49729
$CaCO_3$, point-dipole theory and optical birefringence 79−73896
CaF_2, electronic polarizability and dielectric const., strain derivatives 78−19406
CaF_2, fast ion transport, computer simulation 80−107485
Cd chalcogenides, electronic polarisabilities of ions 78−79559
ClO_3F, heat capacity, permittivity, thermodynamic props., 2.7 to 160K 77−35713
Cs_2NaRCl_6, R=Pr^{3+}, Eu^{3+}, Tb^{3+}, Tb^{3+}, crystal field, ligand polarisability contributions 80−39536
CuCl(Br), electronic dielec. const., vol. depend., Clausius-Mossotti model 80−100630
CuCl(Br)(I), electronic polarisability, strain derivative calc. 78−10868
CuCl(Br)(I), static polaris. and effect charge parameters, Born-Mayer pot. 77−31628
FeS_2, pyrite, semiconducting props., energy gap press. and lattice parameter depend., Mossbauer obs. 80−44494
$Gd_2(MoO_4)_3$, ferroic, linear and nonlinear optical susceptibility 78−22164
Ge, donor polarizability, multivalley effective mass calc. 80−96817
H_2, solid, from dielec. const. determ. 77−8488
^4He, polarisability, second and third virial coeffs. meas. 4.2 to 27.1K 80−43825
^4He, solid, from dieleec. const. determ. 77−8488
$Ho_{2x}Gd_{2(1-x)}(MoO_4)_3$, ferroic, linear and nonlinear optical susceptibility 78−22164
In_2ZnI_4 and In_4CdI_6 solid electrolytes, ion transport mechanism and polarisability role, comparison with Cu^+ and Ag^+ cond. 80−107531
KD_2PO_4, Rayleigh scatt. and narrow central component, depend. on scatt. wave vector direction 80−29747
$KTa_{1-x}Nb_xO_3$, local polarisability in quantum paraelec. and quantum ferroelec. phases 78−64325
Kr, solid, vibr. and thermal props., effect of polarisability 78−71807
$MgCO_3$, point-dipole theory and optical birefringence 79−73896
$MnCO_3$, point-dipole theory and optical birefringence 79−73896
MnO, dielec. behaviour, Dick and Overhauser shell model calcs. 80−45001
MoS_2 molybdenite band structural props. rel. to supercond. and semicond. 80−96781
NaCl-type crystals, ionic polarisabilities, pseudopot. calc. 80−88913
Na_2SbF_5, linear and nonlinear optical props., hyperpolarisability 78−30010
$Nd_{2x}Gd_{2(1-x)}(MoO_4)_3$, ferroic, linear and nonlinear optical susceptibility 78−22164
Ne, solid, from dielec. const. determ. 77−8488
NiO, dielec. behaviour, Dick and Overhauser shell model calcs. 80−45001
O^{2-} polarisability rel. to ferroelec. phase transitions 80−71326
Si, donor polarizability, multivalley effective mass calc. 80−96817
SiO_2, fused, shock compressed, refractive index, density, and polarisability behaviour 80−50295
$Sm_{2x}Gd_{2(1-x)}(MoO_4)_3$, ferroic, linear and nonlinear optical susceptibility 78−22164
$SnO_2(F_4)$, elec. field gradient at Sn^{4+} site, Mossbauer quadrupole splitting and anionic polarisability calc. *(French)* 79−15384
SrF_2, electronic polarizability and dielectric const., strain derivatives 78−19406
$Tb_{2x}Gd_{2(1-x)}(MoO_4)_3$, ferroic, linear and nonlinear optical susceptibility 78−22164
Tl, halides, cryst. electronic polarisability and ion sizes 77−51341
TlBr, dielectric behaviour under hydrostatic press. 78−52420
TlCl, dielectric behaviour under hydrostatic press. 78−52420
TlCl(Br)(I), static polaris. and effective charge parameters, Born-Mayer pot. 77−31628
$Tl_2ZnBr_4(I_4)$, solid electrolytes, ion transport mechanism and polarisability role, comparison with Cu^+ and Ag^+ cond. 80−107531
Zn chalcogenides, electronic polarisabilities of ions 78−79559

polarisation
see also beta-ray polarisation; deuteron polarisation; dielectric polarisation; electron spin polarisation; gamma-ray polarisation; light polarisation; neutron polarisation; nuclear polarisation; photon polarisation; polarisation in elementary particle interactions; polarisation in elementary particle scattering; polarisation in nuclear reactions and scattering; proton polarisation
30 GHz signals, thunderstorms 78−3854
ψ collapse and locality 80−372
Abell 2256, X-ray cluster of galaxies, radio emission linear polarisation 80−36726
Abell 401, X-ray galaxy cluster, radio emission polarisation 80−98731

polarisation continued
acoustic shear waves, polarisation meas. via optical method 77−35006
acoustic waves in quartz rod, electrodynamic meas. method *(Russian)* 77−75764
aerosol, thin flat, EM wave scatt. and absorpt. 80−91723
air, due to Compton electrons excited by γ-quanta pulse, radial electric fields 80−21805
Alfven waves in magnetosphere, polarisation relations rel. to auroral radiation 79−75051
alkali atom dimer polarisation transfer, atom-molecule-exchange reaction 78−13574
anisotropic solids with magnetic symm., unified dynamic theory 78−77713
AO 0235+164, radio polarisation, evidence for rot. in variable radio-source 79−48917
UX Arietis, binary star, radio emission polarisation obs. 77−64793
UX Arietis, RS Canum Venaticorum binary, two-freq. radio polarimetry 79−21335
astronomical OH 18 cm emission sources, fluxes and circular polarisation (1965-1972) 77−13441
asymptotic theorems and polarization phenomena 79−63334
atmospheric precipitation properties using radar polarisation techniques 80−61925
atomic fluorescence weak polarisation meas. using alternating magnetic field 78−1105
atomic muon repolarisation by polarised nuclei of arbitrary spin 79−94112
atomic systems, dynamic multipole polarisability 80−74252
austenitic stainless steel weld metal defect detection, shear-wave polarisation effect 78−44337
B2 1502+28, head-tail galaxy in Abell 2022, Westerbork obs. of spectral index and polarisation distrib. 80−36727
B 0844+31, extended radio galaxy, polarisation distrib. from multifreq. obs. 80−56963
beam polarisation in e^+e^- PETRA storage ring, backscattered Ar^+ laser meas. 79−63839
Bonn 2.5 GeV synchrotron, acceleration of polarised electrons, and subsequent depolarisation 79−68002
Bonn synchrotron, polarised electron accel., and possible depolarisation 79−63826
brass corrosion in HCl, HNO_3 and NaOH, p-thiocresol inhibitor effectiveness 79−57147
bremsstrahlung contrib. to $q\bar{q}$ sea polarisation 79−67507
4C+36.11, extragalactic source, Faraday rot. in S232 rel. to mag. field strength 80−51840
3C 105, radio source struct. and polarisation 79−35413
3C 120, radio galaxy, linear polarisation and flux density vars. 77−9805
3C 219, double radio galaxy, high-resolution polarisation obs. at 1.48 and 4.89 GHz 80−77500
3C 310, extended radio galaxy, multifreq. intensity and polarisation obs. 80−51890
3C 31, radio jets linearly polarised brightness distrib. rel. to mag. field struct. 80−82526
3C 326, very large radio galaxy, linear polarisation multifreq. obs. 78−28810
3C 382, 3C 386, radio galaxies, two freq. polarisation obs. 78−86031
3C 84, 3C 273, quasars, vars. in circular polarisation at 8 GHz 77−33673
Cassiopeia A, intensity and polarisation at 9 mm wavelength 80−36732
celestial masers physics, polarisation origin 79−21455
trans-1,4-chlorobromocyclohexane, liquid, crystalline and amorphous state, conformation and vibr. spectra, IR obs. 80−60568
trans-1,4-chloroiodocyclohexane, liquid, crystalline and amorphous state, conformation and vibr. spectra, IR obs. 80−60568
CIDEP, examples of S-$T_{\pm1}$ polarisation 78−86891
circular on satellite-Earth path from SIRIO 1 experimental satellite, propag. meas. 79−84334
circularly polarised radiation, absorpt. coeff. influence of ESR saturation 79−15442
circumterrestrial plasma faraday inverse effect *(Russian)* 80−4190
cold neutrons, 5 to 6 Å, polarised, prod. methods and existing systems 79−68120
colloidal spherical particle, nonlinear polarisation of diffusion part of thin double layer 77−25315
colloidal spherical particle, numerical method for electrophoretic mobility determ. allowing for polarisation 77−25269
colloidal spherical particle, zeta-pot. determ. from electrophoretic mobility, double-layer polarisation 77−29015
Coma galaxy cluster, halo radio source polarisation, influence of foreground galactic radiation 78−86027
complex representation of polarised signal rel. to ULF wave anal. 77−53236
conducting rectangular bar transmission gratings 78−62993
conference on few body systems and nuclear forces, Graz, Austria (Aug. 1978) 79−67567
conference on high energy phys. with polarised beam and target, Argonne, USA (Oct. 1978) 79−63526
converting linearly polarised incidence waves to circular polarisation 79−76551
cosmic microwave background radiation, polarisation in anisotropic universe 80−82552
cosmological models with anisotropic curvature, polarisation effects 80−94903
Coulomb-nuclear interference polarisation in high energy large momentum transfer hadron reactions 77−79282
covariant representation of microscopic charge and current densities in terms of polarisation and magnetisation fields 79−71
Crab Nebula, linear polarisation mapping at 2.7 GHz with 3.7×10 arcsec ang. resolution 79−40248
Crab Nebula, obs. of linear polarisation at 7.2 cm during occultation by solar corona 77−60837
Crab Nebula, polarimetry with OSO-8 X-ray polarimeter 78−12426
Crab nebula radioemission, polarisation vars. during occultation by solar corona *(Russian)* 78−77527
Crab pulsar, pulse polarisation rel. to high energy particles momentum distrib. 78−73727
cross-polarisation comparison with circular and linear polarisation at 11.6 GHz 79−16633
crystal acoustics, linear and nonlinear 80−5855
V1057 Cygni, OH line polarisation rel. to Zeeman splitting 80−36629
Cygnus X-1, polarimetry with OSO-8 X-ray polarimeter 78−12426

polarisation continued
Cygnus X-1, search for X-ray polarisation 78−4406
Cygnus X-1 (X-2, X-3), X-ray polarisation obs. from OSO 8 80−90571
Cygnus X-2, polarimetry with OSO-8 X-ray polarimeter 78−12426
dielectric and absorbing nonspherical particles, scatt. and polarisation props. 77−34823
differential attenuation and phase shift meas. for 36.5 GHz polarised waves rel. to raindrops 78−3856
diffractive dissociation kinematic polarisation of large-mass final states, helicity violation 77−82723
Dirac particle, polarisation in external EM field 78−58116
disperse hydrocarbon system electrokinetic and polarisation phenomena *(Russian)* 79−83514
double radio sources in directions of rich galaxy clusters, spectral indices and polarisation 78−57662
doubly rotated α-quartz plate vibration, polarising effect 79−14186
dual-polarisation radar for rain targets, rel. of diff. reflectivity to correl. 79−62556
Earth, E-polarisation rel. to boundary conditions for EM field above two-dimensional inhomogeneous struct. 80−85595
Earth, induced polarisation response of polarisable inhomogeneous sphere 79−44092
Earth crust, in situ induced polarisation meas. at Yerington mine, Nevada 80−51323
Earth crust, induced polarisation surveys for sulphide mineralisation in Rajasthan and Gujarat, India 79−39714
Earth crust, multifreq. induced polarisation meas. for mineral discrimination and inductive coupling removal 79−5448
Earth crust, resistivity and induced polarisation (IP) survey for delineating saline water and fresh water zones 80−104867
Earth EM sounding, induced polarisation data inversion 79−16695
Earth EM sounding, induced polarisation effect on near-field form. *(Russian)* 79−39641
Earth induced polarisation (IP) sounding, effects of EM coupling in electrode arrays over uniform half-space 80−101324
Earth induced polarisation sounding, freq. depend. of measured parameters *(Russian)* 79−74836
Earth induced polarisation soundings interpretation, freq.-effect transform function definition and appl. 80−56624
Earth-space paths, rel. between rain depolarisation and attenuation 78−3858
Earth-space radio signals, depolarisation rel. to ice particle orientation and alignment changes 80−17330
Earth-space signals, at 19 and 28 GHz, depolarisation by ice particles 78−73492
elastic charged particle scatt., polarisation anal. Coulomb interference term, transition matrix 79−67559
electrochemical, applic. to solids to control deform. and fracture *(Russian)* 78−11356
electrochemical electrode processes, kinetics from transitional sections of polarisation curves 77−25283
electrodialysis, rotating disc studies 79−47933
electron band structure, optically induced in external plane wave field 80−106432
electron beam polarisation in storage ring by laser beam interaction 79−93860
electron beams, production methods and current status of polarisation meas. 79−63836
electron polarisation by circularly polarised EM waves in storage ring 80−14020
electron storage ring, control of low-energy characteristics using wiggler magnets 77−6585
electron storage rings, depolarisation 77−3197
electron storage rings, SPEAR and PEP, estimate of spin polarisation 79−72093
electron-positron gas in external mag. field, polaris. tensor *(Russian)* 79−35982
EM radiation, low freq. spectrum and polarisation 79−44350
EM radiation, polarisation plane rot. induced by non-Minkowskian space-time 79−35115
EM radiation, polarisation transfer through rarefied magnetoactive plasma 79−92669
EM radiation, scattered, polarisation in presence of internal energy sources 80−67541
EM radiation in media with spatial dispersion, spatial coherence formation and polarisation increase 80−106442
EM scattering by corrugated periodic trapezoidal conducting surface, TE/TM polarisation 78−62994
EM wave, description by irreducible tensorial sets 77−68152
EM wave, forward scatter and crosspolarisation from ice spheroids 78−3853
EM wave, homogeneous, energy flux under conical refraction and induced gyrotropy 78−17861
EM wave polarisation transfer in inhomogeneous magnetised plasma, non-orthogonality props. inclusion 79−84662
EM wave propagation in inhomogeneous media, 'W'-shape transients, modified ray tracing technique appl. 80−48119
EM wave propagation in inhomogeneous media, polarisation rotation analysis by modified ray tracing 79−89831
EM wave traversing thick weakly anisotropic layer with random irregularities 77−10822
EM waves, polarisation coeffs. for incoherent backscatter from two-scale rough surface 78−71013
EM waves in inhomogeneous plasma, polarisation transfer eqn. 77−84436
extragalactic radio sources, polarisation props. 79−53920
extragalactic radiosources, mag. field orientation evidence 80−46690
far field diffraction by variable thickness semi-infinite plane, parallel polarisation 79−50194
field-induced molecular multipoles, local polarisation theory 80−74141
fluorescence apparatus, for simultaneous meas. of orientation and mobility in uniaxial media 78−86320
forward scatter and cross-polarisation from spheroidal ice particles 77−25733
G 21.5−0.9, supernova remnant, linear polarisation at 6 cm 77−5553
galactic 1 m radio emission, obs. of linearly polarised bright spot 77−17709
galactic radio background, linear polarisation between 408 and 1411 MHz, reductions 77−2500
galaxies, nearby, radio continuum polarisation obs. rel. to mag. fields *(German)* 80−109544
polarisation continued
geomagnetic Pi 2 pulsations, polarisation characts. and phase differences at conjugate stations 79−21107
GL 2591, protostellar source, 3 μm ice absorpt. band, linear polarisation obs. 80−105303
gravitational radiation, low freq. spectrum and polarisation 79−44350
gravitational radiation from neutron stars and white dwarfs, polarisation and intensity 78−65646
gravitational waves, circular polarisation rel. to scatt. from vac. black holes 78−65648
gravitational waves, polarisation in Yang's gravitational field *(Chinese)* 80−17850
gravitational waves, relativistic theories of gravitation, expt. testing using spacecraft-Doppler detection 78−77793
gyrotropic media, EM waves polarisation *(Russian)* 79−81333
gyrotropic medium, Green's function and field of moving charges 80−58445
H Lyman α in solar chromospheric flares, direct collisional excitation rel. to profile and polarisation 80−41780
hadron low |t| elastic scatt., polarisation effects and forward amp. in quark model *(Russian)* 77−258
hadron-hadron high-$p_\perp$ collisions, weak effects 77−30457
hadronic high momentum transfer scatt., spin meas. and polarisation review 79−63498
hadronic polarization in neutrino scattering 78−74245
heavy ion beams, polarisation monitors 80−27910
hectometric wavelength emissions of Jupiter, Voyager obs. 79−84732
AM Herculis (4U 1814+50), linear and cirular polarisation modulation with orbital period 80−105403
high P_T theory, use of polarised beams and targets, QCD tests 79−63409
homogeneous explosives, electrical polarisation with initiation of shock wave detonation 79−100378
HR 1099, binary star, radio emission polarisation obs. 77−64793
HR 1099, RS Canum Venaticorum binary, rapidly variable polarisation obs. at radio freqs. 79−21336
HR 1099, RS Canum Venaticorum binary, two-freq. radio polarimetry 79−21335
HR 1099, RS Canum Venaticorum binary, VLA radio obs. during 1977 international campaign 79−21334
W Hydrae, OH masers polarisation obs. and suspected Zeeman splitting 80−36632
internal conversion electron polarisation, parity violating nuclear forces 78−50125
interstellar H I absorpt. lines, Zeeman splitting rel. to mag. field determ. in dense clouds 79−5757
interstellar OH main line maser, circular polarisation and probable Zeeman pattern 80−56908
interstellar reflection nebulae, polarisation rel. to simplified scatt. models 78−96526
interstellar type I OH masers, positions, polarisation, nearby H_2O masers, radio and IR props. 79−25671
ion beam prod. from optically pumped electron spin polarised targets 80−27851
ion selective membrane, polarisation at high current densities, Nernst model 79−91962
ionosphere, Faraday effect meas at 140 MHz using two-channel polarimeter first results 80−61912
ionosphere high-latitude electrostatic turbulence, polarisation, freq. and wavelengths 78−88981
IRC+10420, stellar OH maser polarisation rel. to mag. field 79−25742
IRC+10420, supergiant star, new OH maser feature polarisation and spatial struct. 79−48946
Ising model, infinite metastable states 80−34577
Jupiter, 11 cm radiation Stokes parameters meas. 78−12141
Jupiter, circular polarisation of 1.4 GHz radio emission 77−64692
Jupiter, decametric radio bursts hyperfine polarisation struct. 77−33400
Jupiter, linear polarisation obs. at 6, 11 and 21 cm wavelengths 77−87313
Jupiter, linear polarisation study at 2.7 GHz with Cambridge 5 km telescope 80−82272
Jupiter decametric radio bursts, polarisation patterns in dynamic spectra 77−5490
Jupiter radio emission, Stokes parameters obs. at 11 and 18 cm wavelength 80−67637
Kerr metric effect on EM wave plane of polarization 80−94827
laser technology, parallel plate, hard seal technique 80−1225
latticed polarizer for high-pressures 78−21206
LEP storage ring, polarised $e^\pm$ beams, Siberian Snake scheme 79−63827
limiting polarization of electromagnetic waves escaping from a nonuniform layer of magnetoactive plasma 79−64875
line circular polarisation due to magnetic and vel. field inhomogeneities 79−5804
low energy positron beams, spin polarisation 80−9442
M1-92, bipolar nebula, unpolarised OH emission obs. 78−41016
M31, M51, M81, spiral galaxies, polarisation detect. at radio wavelengths 77−5575
M31, polarised radio emission detect. 78−86017
M31, polarised radio emission distrib. rel. to large-scale mag. field 80−41899
M87 radio emission, Faraday rot. in radio/X-ray halo 80−67844
magnetically ordered crysts., absorbent, EM waves polarisation 80−108189
magnetisable and polarisable media with microstructure, models 80−88708
magnetite electrochemical polarisation in surfactant solns. *(Russian)* 79−83465
magnetosphere high-latitude electrostatic turbulence, polarisation, freq. and wavelengths 78−88981
Majorana transitions, spin-flip probability, LZS model calc. 77−57959
Maxwell eqns., asymptotic soln. near caustic edge *(Russian)* 78−58882
metals, radiation flux polarised components 78−94566
methyl halides, mol. force fields, IR intensities, and vibr. props. 80−47879
microscopic charge and current densities in terms of polarisation and magnetisation fields 78−8251
microwave background radiation polarisation, anisotropic cosmological expansion 78−73778
microwave background radiation polarisation, IR survey 78−73779
microwave beams, meas. using mechanical polarisation modulator 77−37987

polarisation continued
microwave crosspolarization, effects of sizes of nonspherical raindrops 80−21790
microwave crosspolarization on satellite to Earth path, effect of rain 80−21789
microwave link, cross-polarisation on terrestrial path, wind, raindrop size and canting angle effects 79−66736
microwave satellite paths, crosspolarisation phase due to ice crysts. 78−7684
microwave signals cross-polarisation rel. to atm. elec. field strength 77−49132
microwaves, polarisation depend. of gravit. deflection, improved upper limits 77−2596
microwaves anomalous depolarisation on 19 and 12 GHz Earth-space paths 77−78354
Mira variables, polarisation variation detect. in absorption features 77−33496
molecular crystal, polarisation energy of localised charge, appl. to anthracene and naphthalene 80−15034
moving dielectric medium, Brewster angle for E-polarised wave 77−38776
muon repolarisation in muonic atoms with polarised nuclei 77−61878
muonic atoms, X-ray emission polarisation *(German)* 80−69268
muonic X-rays, circular polarisation *(German)* 80−69266
neutron, exact spin rotation by precession 80−32584
neutron beams, compact polarising Soller guides 78−54501
NGC 315, NGC 6251, very large radio galaxies, linear polarisation obs. at 11.1 cm 78−86014
NGC 315, radio jets linearly polarised brightness distrib. rel. to mag. field struct. 80−82526
NGC 7822 (W 1), supernova remnant, search for linear polarisation at 2.8 and 6 cm 78−4383
nonlinear dissipative media, circularly polarised EM waves 80−63891
NP 0532, Crab pulsar, search for X-ray polarisation 79−5851
ocean-coast model, EM response to E-polarisation induction 78−61321
OH 205.1−14.1, unusual OH maser, left circularly polarised 1667 MHz line obs. during flare 80−98734
Orion A, 22 GHz water line outburst linear polarisation 80−8703
U Orionis, stellar OH maser polarisation rel. to mag. field 79−25742
parallel conductors in external field 80−28136
particle polarisation meas., set of efficient estimators 80−27909
Pc3 magnetic pulsations at synchronous orbit, statistical study of ATS 6 obs. 77−45256
Pc 5 pulsations recorded in auroral regions, Earth induction effects on vertical polarisation 79−12355
periodic polarization variations in rotating astrophysical systems 79−88585
photoelectrons from ferromagnets, review 77−32505
photon propagation in mag. field, radiative correction to polarisation operator *(Russian)* 78−8567
photosynthetic membranes, functional processes, polarisation effects 80−67045
picosecond spectroscopy, anal. using polarisation method 80−13152
piezoceramic articles, microwave Kerr effect obs. of nonuniform polaris. 78−72969
pion magnetic polarisability using guage and relativistic invariance 78−4861
plane wave, motion and radiation of charge *(Russian)* 79−21986
plane waves, difference between polarisation and coherence 80−8805
plasma, moving cold magnetised, wave propag., polarisation relations and dispersion eqns. 80−64723
plasma, polarisation freq. depend. of electron cyclotron emission 80−33808
plasma, resonant charge exchange, polarisation effect 80−43859
polar material, PMMA-type, polaris. induced by shock waves *(French)* 77−62583
polyatomic gas, plane Couette flow in Knudsen regime, wall induced polarisation 80−19443
polymer, electret, vapour-induced depolarization currents 79−87379
pseudo Brewster angle, vertical polarization reflection coeffs., between two media 78−5403
PSR 0525+21, pulsar, radio polarisation rel. to assoc. with supernova remnant 78−85965
PSR 1133+16, polarisation of high freq. radio emission microstruct. 78−45348
PSR 2020+28, pulsar, orthogonal polarisation modes obs. 78−93291
pulsar microstructure, propag. effects in shearing field-free plasma 80−17483
pulsar radiation, Stokes parameters in polarised shot noise model 77−13374
pulsar radio emission, propagation effects on polarisation 79−75235
pulsar signal microstructure, periodicities, polarisation and pulsar magnetospheres probing 79−75232
pulsars, individual pulse-polarisation patterns and quasi-transverse propag. theory 80−46591
pulsars, polarisation angle swing rate rel. to relation between braking and beaming 79−92793
pulsars, polarisation characts. at 640 MHz for 43 southern pulsars objects 78−65642
pulsars, radio polarisation rel. to model of emission mechanism 78−12257
quark polarisation, transverse, quantum chromodynamics test 79−17741
quasar 3C 273, rapid fluctuations of radio flux and circular polarisation and optical linear polarisation 77−91663
quasars, radio intensity and polarisation distribs. at three freqs. 78−96560
radar anisotropy of sea ice due to horizontal c axes preferred azimuthal orientation 79−34836
radial field polariser for magnetising a moving liquid 78−250
radiation from relativistic charged particle in nonuniform mag. field *(Russian)* 78−78876
radiation transfer, polarised, in inhomogeneous medium 80−99607
radiative polarization at ultra-high energies for e^- and e^+ beams in storage rings 79−72127
radio beacon signals from ATS-6 satellite, ground refl. effects on polarization 78−40612
radio continuum obs. of supernova remnant CTA1 at 2695 MHz 79−62890
radio emission from 3C 31 radio galaxy, obs. at 2.7, 4.8 and 10.7 GHz 79−35375
radio polarization of quasars with optical absorption spectra 78−12405
polarisation continued
radio recombination lines from H II region NGC 2024, search for linear polarisation 80−41872
radio sources, compact, linear polarisation rel. to physical conditions 78−4384
radio sources, EM waves depolarisation turbulent cosmic plasma 77−17358
radio sources, extragalactic, intracluster Faraday rot. obs. 79−75285
radio sources, linear polarisation catalogue 80−51671
radio sources, superluminal, circular and linear polarisation in mag. dipole model 80−56959
radio sources circular polarisation, 1.4 GHz aperture synthesis obs. 77−29656
radio sources Faraday rotation measures, computation method 80−4263
radiosources, compact extragalactic, flux density and linear polarisation at 3.7 and 11.1 cm wavelength 77−49490
radiosources, extragalactic, polarisation data rel. to origin of rot. measures 77−5584
radiowave depolarisation due to snow at 11.6 GHz 78−57239
radiowave propag., scattering amplitudes and crosspolarisation of spheroidal ice particles, calc. 77−70740
radiowave propag. crosspolarisation and attenuation meas. at 11.6 GHz using theoretical rain model, canting angle distrib. 80−4070
radiowave propagation, raindrop canting angle as function of wind velocity 78−3855
radiowaves, scatt. props. of Pruppacher-Pitter form raindrops and cross polarisation due to rain 77−41129
raindrops, spreading of ellipsoidal raindrops orientation during intense rainfall, expt. results 79−16634
reaction matrix representation, no-go theorem for polarisation struct. 78−62120
relict radiation in anisotropic universe, polarisation and anisotropy 80−67917
resistance polarisation in electrochemical potentiostatic meas., automatic compensator 77−21393
resonance line polarisation, non-LTE, absence of magnetic fields, solar models 79−80293
Rhinegraben anomalous geomag. field and telluric field, perpendicular linear polarisation meas. 79−74832
role of polarisation in atomic and nuclear physics 80−63162
rotation of US plane of polarisation under ESR saturation conditions 80−29123
satellite communications wideband polarisation separation network with adaptive control 77−78394
satellite link, lightning crosspolarisation model 78−11961
satellite links, ionospheric wave disturbances effect on polarisation fading freq., simulation 78−69572
satellite links at 20 and 30 GHz, crosspolar phase variations on satellite-Earth path, meas. 77−81957
satellite retroreflector arrays 80−5778
Scorpius X-1, linear X-ray polarisation obs. 79−101221
Scorpius X-1, linear X-ray polarisation upper limit 77−49503
Scorpius X-1, linear X-ray polarisation upper limit 78−49557
Scorpius X-1, mag. field determ. via linear polarisation spectrum *(Russian)* 80−90344
seismic body waves in anisotropic media, polarisation prod. by refl. and refr. 77−49019
seismic body waves in anisotropic media, synthetic seismograms and polarisation 77−49021
seismic shear waves, polarisation anisotropy in Pacific Basin 77−49018
seismic surface waves, higher mode, polarisation rel. to anisotropy in Eurasia upper mantle 77−49015
seismic waves, ground displacement polarisation determ. rel. to three-component registrations interpretation *(German)* 78−32017
seismic waves, polarisation anomalies assoc. with anisotropic layering 77−49012
semiconductor, spin injection, carrier polarisation, luminesc. polarisation 77−15957
small-aperture diffraction polarisability coefficients rel. to wall thickness 79−68355
solar 6 cm radio emission, polarisation obs. of active region and burst sources 80−62096
solar 'spike' type radio bursts, morphological characts. and circular polarisation 78−65599
solar active regions radio emission, circular polarisation obs. with 6 arc seconds resolution 77−33444
solar flare, circular polarisation of transition region thermal radioemission *(Russian)* 79−48763
solar flares, microwave polarisation obs. by VLA, interpretation with optical X-ray data 79−44428
solar flares, polarisation and directivity of hard X-ray bremsstrahlung from thermal source 80−90374
solar hard X-rays, backscatter, anisotropy and polarisation 78−28594
solar impulsive microwave bursts, superimposed fast time structs. with slowly varying polarisation 79−40173
solar metre-wave radio emission, wave ducting rel. to polarisation and source positions 80−21978
solar microwave bursts, polarisation features interpretation 78−96468
solar microwave bursts fast structures, circular polarisation rel. to mag. field changes 79−2536
solar moving type IV radio burst, polarisation obs. 78−69776
solar moving type IV radio bursts, obs. and interpretation 79−40174
solar radio bursts, high-resolution 6 cm obs. and circular polarisation 78−53897
solar radio emission, polarised zebra struct. interpretation 78−96467
solar radio emission in inhomogeneous magnetic field of coronal plasma *(Russian)* 78−16385
solar radio radiation, spectral polarisation obs. of local sources during March (1970) 77−53535
solar thermal sources, microwave brightness temps. and polarisations derivation 77−22172
solar type III radio bursts, fundamental and harmonic, circular polarisation, 24-220 MHz *(Russian)* 78−16384
solar type III radio bursts, fundamental emission and polarisation 80−36603
solar type IIIb radio bursts, polarisation meas. 77−22161
solar type IV meter bursts, microstruct. modulation by whistlers wave-packets rel. to polarisation 77−78761
solar type U radio bursts, polarisation evolution 80−26834
solar wind MHD turbulence, Alfvenic and slow magnetosonic modes polarisation 80−61977

polarisation continued
solar X-ray flares, 1974 July 5 and 6, polarisation obs. 77−2397
statistical theory of asymmetry detection 79−26853
sulphide ores, disseminated, electrochemical model of induced-polarisation phenomena 79−92526
sunspots bipolar groups, circularly polarised radioemission obs. at 1.35 cm *(Russian)* 78−57532
SW radio waves, polarisation on slant path 78−73573
synchrotron, spin flip by adiabatic passage of depolarisation resonances 80−5415
synchrotron sources, boundary effects and circular polarisation 79−48668
Taurus A, intensity and polarisation at 9 mm wavelength 80−36732
terrestrial electricity, induced polarisation induced potentials and derivatives rel. to deep sounding *(German)* 80−56626
terrestrial electricity, source field polarisation 80−56356
thermal neutrons, 2 to 3 Å, polarised, prod. methods and existing systems 79−68120
thermal radiation polarisation, of permanent snow fields, from meas. obtained from the 'Meteor' satellite 78−88870
thermal radiation sources, polarisation theory *(Russian)* 77−91656
thermal radio emission from random layered media, appl. to Antarctic glaciers *(Russian)* 77−33106
thermal radio emission polarimetry, loss matrix 79−21069
thermorigid dielectrics, nonlinear thermodynamic theory 80−10149
thick crystals, X-ray diffr. process, layer model, reflectivity, polarisation *(German)* 77−51262
thick crystals, X-ray diffr. process, layer model, reflectivity, polarisation *(German)* 77−51263
transverse quark polarization in large P_T reactions and e^+e^- jets 79−63410
type II radio burst, 1973, May 3, 74 MHz polarisation and spectral fine struct. 78−24501
vacuum polarisation by ambient mag. field, effects on Compton scatt. by unmagnetised electrons 80−86631
vacuum polarisation by strong mag. field, effects of Thomson scatt. 80−86632
vegetation reflectivity, effect on atmospheric radiance and polarisation 78−40650
Vela pulsar radio emission, detect. of change in rot. measure 77−29867
Vela supernova remnant, rot. measure and turbulent struct. 80−51836
Vela X supernova remnant, radio polarisation maps 80−56909
VHF and UHF terrestrial propag., influence of polarisation on transmission quality *(German)* 78−61518
VHF/UHF measurement, radiowave irradiators with switching of polarisation *(Russian)* 77−22090
Virgo A (M87), 1.3 cm polarisation obs. 78−49550
Virgo A (M87), linear polarisation distrib. at 610 MHz, Westerbork map 80−62302
VLF signals, time-varying, determination of wave normal directions *(French)* 79−70927
wave packet polarisation, in X-ray monochromators, dynamic theory *(Russian)* 80−64826
wavy water surface thermal radioemission obs. at 3.5 and 14.5 MHz *(Russian)* 78−61425
whistlers, effect of Earth-ionosphere waveguide propag. on polarisation and arrival angles 79−100924
whistlers, effect of Earth-ionosphere waveguide propagation on polarisation and arrival angles 80−36457
whistlers polarisation and arrival direction meas. at low latit. 77−45240
white dwarfs, magnetic, circular polarisation prod. by cyclotron absorpt. 80−4351
X-radiation, cryst.-monochromated, polarisation factor, assessment of errors 80−100121
X-radiation, cryst.-monochromated, polarisation factor, weighted scheme for products 80−100122
X-ray beam, polarisation meas. 79−37588
X-ray binaries and pulsars, effect of vacuum birefringence on polarisation 78−4408
X-ray crystal monochromators, determ. of polarisation ratio 80−99018
X-ray dynamic diffraction, polarisation states in Laue case 80−28878
X-ray polarisation plane diffr. rot. *(Russian)* 77−27787
X-ray pulsars, vacuum polarisation effect rel. to radiative transfer and X-ray spectra 80−27015
X-ray radiation emitted near black holes, polarisation features 80−46700
X-rays, tuneable polarisers 80−315
X-rays from mag. neutron stars, vacuum birefringence effects 79−40209
zero cross-polarisation mode for orthogonally polarised signals in rain 77−81991
ed tensor polarisation and d wave function short range behaviour 79−67564
e^+e^- SPEAR storage rings, beam polarisation meas., backscattered laser method 79−63838
e^+e^- storage rings, expt. review of beam polarisation 79−63837
$\gamma p \rightarrow \pi^+ n$, 520 to 2250 MeV, meas. of Σ, T, and P polarisation parameters 79−75778
$K^+ n \rightarrow K^0 p$, 6,12 GeV/c polarised n, polarisation measurements 79−63521
$K^- p \rightarrow \Lambda X$, 4.2 GeV/c, polarisation and triple Regge framework 78−45948
$K^+ p \rightarrow K^+ p$, 6,12 GeV/c, polarised p, poalrisation measurements 79−63521
$\Lambda(\bar{\Lambda})$ in $K^\pm p \rightarrow \Lambda(\bar{\Lambda})X$ at 32 GeV/c 79−45122
Λ polarisation meas. in $K^- p \rightarrow \Lambda\pi^0$, $\Lambda\eta$, $\Lambda\eta'$ at 4.2 GeV/c 77−65176
Λ^0 polarisation in inclusive prod. by 24 GeV protons on Pt 77−67691
μ prod. at large transverse momenta, μ polarisation meas. 77−71542
μ^+ polarisation dynamics in mag. mirror field, neutrino emission asymmetry 77−61645
NN elastic scatt., spin struct. interpretation, polarising power 79−85342
NN two body systems, polarisation phenomena, 6 MeV/c to 150 GeV/c, QCD anal. 79−80840
np free elastic scatt., 220-495 MeV, Wolfenstein parameters and polarisation, I=0 phase shifts 79−67594
$\nu(\bar{\nu})p$ elastic scatt., final state polarisations, test for T-invariance and 2nd class currents 79−63466
$\bar{\nu}N$ in Fe, μ^+ polarisation in high energy charged current interactions 79−93399
$\nu p^+ \rightarrow \mu^- \Delta^{++} (\nu\Delta^{++})$, Δ polarisation, test of T-invariance of weak and charge currents, comment 79−67531
$\bar{\nu} p^+ \rightarrow \mu^+ \Delta^0$, Δ polarisation, test of T-invariance of weak and charge currents, comment 79−67531

polarisation continued
pn elastic scatt., 24 GeV/c, polarisation and anal. power 79−63528
$pN \rightarrow \Lambda^0 X$, Λ^0 polarisation and quark prod. mechanisms 79−63542
pp, elastic scatt., 150 GeV/c, $-t=0.2$-3.0 GeV^2, polarisation meas. 79−85343
pp bremsstrahlung with polarised p, soft photon approx. 79−67585
$pp \rightarrow d\pi^+$, deuteron polarisation, isobar model anal. 79−49535
pp elastic scatt., 10 MeV, A_{yy} component of spin correlation tensor 79−67592
$pp \rightarrow \Lambda^0 X$, 53 and 62 GeV, Λ^0 polarisation at CERN ISR 79−49550
$pp \rightarrow \Lambda^0 X$, high energies, semiclassical model for polarisation 79−89202
pp scatt., intermediate energy, polarised p, three body model 79−67590
pp scatt., polarisation measurement at 6.14 MeV 79−67591
pp small angle elastic scatt., 312, 392, 493 MeV, Wolfenstein and polarisation parameters 79−67593
$\pi^- p \rightarrow \pi^+ \pi^- n$, polarization measurements and a narrow ε(750) 79−63514
$\pi^+ p \rightarrow \pi^+ \pi^- \Delta^{++}$, polarization measurements and a narrow ε(750) 79−63514
T, polarised, charge asymmetry in lepton pair decay of polarised resonances 79−17716
Al, autoionisation reson. determ. from photoelectron polarisation meas. 80−58221
$Ba^+ + Kr$, quasimolecular states interference, degree of polaris. oscill. *(Russian)* 77−6917
CO_2, laser excitation by RF discharge with rot. elec. field, linear and circular polarisation 80−37991
CdTe, Cl compensated detectors, polarisation suppression methods 77−61661
Cygnus A, intensity and polarisation at 9 mm wavelength 80−36732
Fe XIII coronal emission line polarization from mag. sublevels statistical equilib. 77−53492
Ge-$Na_2S_2O_3$ interface anodic oxidation electron transfer 79−56304
H, $2^2S_{1/2}$ state F=1 hyperfine component, Majorana transitions, LZS model 77−57959
H^-, target polarisation rel. to free-free transitions 79−66917
H_2, synchrotron radiation scattering cross sections 78−55213
He, synchrotron radiation scattering cross sections 78−55213
^{4}He atomic Bose system, equilibrium superradiance 78−55994
^{180}Hf, polarisation of internal conversion electron calc. 78−50125
$K^- n \rightarrow \pi^- \Lambda$, 1750 to 2000 MeV, ang. distrib. and polarisation, comparison with PWA 79−75796
Kr gas discharge plasma, electron impact depolarization 80−43847
Li_2, circular polarisation of emission, influence of nucl. hyperfine interactions and elastic collisions 80−9635
Li_2, collisional depolarisation and rot. energy transfer, laser-induced fluoresc. obs. 80−9698
LiF, thermocyclic stress effects in corrosive-media, electrochem. polarization applic. *(Russian)* 78−11356
Na beam polarisation, optimal magnetic multipole 77−30684
Ne gas discharge plasma, electron impact depolarization 80−43847
Ni electrodeposition cathode polarisation, influence of unsaturated sulphates *(Russian)* 79−91963
Pb-PbO_2, bielectrodes, anodic polarisation 77−44483
Pt electrodes, nonlinear AC and DC polarisation obs. 80−56247
Si, with various dislocation densities, ang. depend. of X-ray polarisation of curve of 111 Bragg reflection 79−46509
Si-$NaNO_3$ aq. soln., anodic polarisation of semicond. electrode 77−11999
SiF_4, thermocyclic stress effects in corrosive-media, electrochem. polarization applic. *(Russian)* 78−11356
SiO 86.2 GHz maser, astronomical sources polarisation props. 80−4449
Tl, autoionisation reson. determ. from photoelectron polarisation meas. 80−58221
W, rot. of polarisation plane and ellipticity of US waves near doppleron-phonon reson. *(Russian)* 79−19325
ZrO_2/Pt solid electrolyte/porous electrode system, interface polarisation effects 80−61114

polarisation in elementary particle interactions
$\pi^- p \rightarrow \pi^0 n$, 617 to 2267 MeV, polarisation meas. 79−9401
Bethe-Heitler pair production, neutral current effects 78−33022
charged-lepton-nucleon scattering, neutral current effects 78−33071
charm photoprod. with linearly pol. photons, QCD calcs., gluons 80−68464
Coulomb interference term in polarization analysis 79−67559
deep inelastic scatt., parton transverse momenta role, struct. function, QCD evolution 80−78034
electron-hadron interactions, P-invariance, lepton, quark anapolar moments with pol. e *(Russian)* 80−52518
electroproduction, polarised, flavour singlet coefficient functions, QCD corrections, sum rules 80−47301
gluon fragmentation, polarised, in e^+e^-, $e^\pm q$ and hadron scattering 80−82988
hadron electroproduction, polarised coincidence scaling laws 77−49975
hadronic collisions at small momentum transfer, polarisation phenomena *(Russian)* 78−58196
hadronic interactions, review 80−52527
hadrons interacting, isospin-spin polarisations, dynamical characts. 80−32035
high energy lepton pair prod. with pol. hadrons, P and C violations 80−99068
inclusive interactions in triple Regge region 77−10294
interfacing theory and experiment in polarization studies 80−73837
isobar production by weak neutral current, polarisation effects *(Russian)* 77−18220
large transverse momentum interactions and hadron cumulative prod. *(Russian)* 78−74293
lepton + nucleon deep inelastic scatt., final state polarisation 78−458
lepton pair production, QCD and hard-scatt. model, spin-spin asymmetries 80−63014
meson photoproduction on polarized nucleon targets 77−34162
polarisation experiments, theoretical review 77−57564
polarization measurement from particle decays 77−22721
polarized photoproduction of single pions, even-wave harmonic-oscillator theory 79−40791
QCD structure function relation between deep inelastic ν reactions and polarised electroprod. 80−37221
spin dependence at very high energies 78−58164
spin-flip and inclusive processes, dynamics *(Russian)* 78−41589
target mass effects in polarized electroproduction 80−78072

polarisation in elementary particle interactions continued
ed, deep inelastic polarised scatt., Weinberg model test 79−22006
ed→epn, polarised deuteron disintegration, virtual nucleon density matrix formalism *(Russian)* 80−52519
$e^{\pm}d_{\uparrow}\rightarrow e^{\pm}np$, polarised, parity violating asymmetry 80−78080
$e^-e^+\rightarrow N^*\bar{N}^*$, weak neutral current effects for polarised e^+e^- pair 80−37287
$e^+e^-\rightarrow$ heavy lepton, longitudinal pol. beam, parity violation 77−38154
$e^+e^-\rightarrow$ jets, transversely polarised annihilation, charged gluon jets, Pati-Salam model 80−86739
$e^+e^-\rightarrow$ quark jets, charge polarisation 77−38183
$e^+e^-\rightarrow 2\gamma$, hadron prod., polarisation effects *(Russian)* 77−74702
e^+e^- annihilation, cross-sections and multiplicities 79−36111
e^+e^- annihilation, polarisation anal. 78−29339
e^+e^- annihilation, polarised hadron prod., neutral currents 78−50041
$e^+e^-\rightarrow\Delta X$, nucleon isobar polarisation vector *(Russian)* 79−22121
$e^+e^-\rightarrow\Delta X$, polarisation effects in nonperturbative parton model, scaling 80−105912
$e^+e^-\rightarrow e^+e^-X$, beam polarisation, effects on cross sections 77−61269
$e^+e^-\rightarrow F\bar{F}$, weak asymmetries 78−8636
$e^+e^-\rightarrow\gamma$, polarisation correlations 78−78158
$e^+e^-\rightarrow h_1h_2X$, polarised; electrons, structure functions, γ^* partial widths *(Russian)* 77−61308
$e^+e^-\rightarrow$hadron, longitudinal polarisation 77−30397
$e^+e^-\rightarrow$hadrons, polarised beams, neutral weak current effects 77−49987
$e^+e^-\rightarrow$heavy lepton, transversely polarised 77−18261
e^+e^- inclusive hadron prod., polarisation and p nonconservation asymmetries, π, $K^{\pm}$, $D^{\pm}$ prod. 80−78084
$e^+e^-\rightarrow l^+l^-$, neutral current effects around vector resonances, polarisation 80−105878
$e^+e^-\rightarrow\mu^+\mu^-$, polarised beams, weak neutral currents *(Russian)* 78−62383
$e^+e^-\rightarrow\mu^+\mu^-$, polarised beams, weak neutral currents *(Russian)* 78−62384
$e^+e^-\rightarrow\mu^+\mu^-$, ψ/J excitation models 79−13095
$e^+e^-\rightarrow\mu eX$, beam polarisation effects on anomalous events 77−6102
$e^+e^-\rightarrow\mu eX$, longit. polarised beam, asymm., heavy lepton props. 77−10238
$e^+e^-\rightarrow pX$, weak neutral current effects *(Russian)* 78−459
$e^+e^-\rightarrow p\bar{p}S_p$, asymmetry and polarisation 78−58195
$e^+e^-\rightarrow\pi^+\pi^-\pi^0$, neutral currents, interference effects with polarised beams 77−87990
$e^+e^-\rightarrow\pi X$, forward-backward asymm. 77−18308
$e^+e^-\rightarrow\psi(z)$, spin correlations, spin 0, 1/2, 3/2 pair prod. *(Russian)* 79−22117
$e^+e^-\rightarrow q\bar{q}g$, gluon bremsstrahlung, neutral current and beam polarisation effects 80−99106
$e^+e^-\rightarrow q\bar{q}g$, gluon fragmentation, polarised 80−82988
$e^+e^-\rightarrow q\bar{q}g$, long. polarised beams, beam-event asymmetry, massless QCD null result 80−91104
$e^+e^-\rightarrow$quark jet, transverse polarisation 79−63410
$e^+e^-\rightarrow$three jets, acoplanar angle relative to beam polarisation, vector/scalar gluons 80−63005
$e^+e^-\rightarrow\tau^+\tau^-$, neutral current effects, polarisation sensitivity 78−74239
$e^+e^-\rightarrow V^+V^-\rightarrow e^+\nu_e\mu^-\bar{\nu}\mu$, beam polarisation, anomalous events 77−74669
$e^+e^-\rightarrow VX$, parton model, polarisation effects *(Russian)* 80−63002
$e^+e^-\rightarrow VX$, polarisation states and differential cross sections for πA_1 and $\rho^+\rho^-$ *(Russian)* 80−102059
$e^+e^-\rightarrow VX$, vector meson polarisation states 78−25058
$e^+e^-\rightarrow W^+W^-$, polarisation amplitudes 80−42484
$e^+e^-\rightarrow ZZ$, polarisation amplitudes 80−42484
$e^+e^-\rightarrow\ell^+\ell^-$, near Z° pole, polarisation and radiative effects 79−22085
e^+e^- annihilation, weak neutral currents, longitudinal polarisation 77−26483
eN, deep inelastic polarised scatt. asymm., gauge theory predictions 79−22104
eN, deep inelastic scatt., nucleon polarisability 77−49966
eN, deep inelastic scatt., P-violation search 77−34156
eN, deep inelastic scatt., polarisation meas. 79−67566
eN, inealstic scatt., odd-parity asymmetry *(Russian)* 79−45093
eN, inelastic scatt., P-violation 79−63482
eN, parity violating asymmetries 78−89719
eN deep inelastic polarised scatt., QCD corrections 80−52517
en→enπ, pol. e, P-odd asymmetry and cross sections, SU(2)xU(1), SU(3)xU(1) calcs. *(Russian)* 80−62998
eN→epX, longitudinal-transverse separation 77−49977
eN→e$\pi^{+\text{or}-}$X, longitudinal-transverse separation 77−49977
eN→meson, spin effects 78−25053
eN→π, polarised production, vector like theories *(Russian)* 78−37221
eN→πeN, EM and weak processes *(Russian)* 78−45928
ep, deep inelastic asymmetry meas. 78−70376
ep, deep inelastic polarized scatt., Weinberg model test 79−22006
ep, deep inelastic scatt., cross section asymmetries 78−45926
ep, deep inelastic scatt., polarisation data 78−33073
ep, deep inelastic scatt. asymm. 77−6133
ep, deep inelastic scatt. expts. at SLAC 79−63483
ep deep inelastic scatt., pol. p and e, straton model, sum rule *(Chinese)* 80−42475
ep→eX, SLAC data anal., parton distrib. functions for polarised protons 77−82747
ep→epρ, cross section asymm. 77−6135
e p→e π^+n, transverse and longiltudinal polarisation 78−66126
eq→eqg, gluon fragmentation, polarised 80−82988
γd→np, 400-650 MeV, proton polarisation and possible dibaryon resonances 80−105908
γd→np, 400-700 MeV, p polarisation *(Russian)* 80−106046
γd→pn, 250 to 800 MeV, differential cross-section and proton polarisation, theoretical models 80−78081
γd→pn, 340 t0 700 MeV, proton polarisation meas. 78−82215
γd→pn, proton polarisation ang. depend. 79−58967
γd→π^0d, differential cross section asymmetry 77−30389
γd→π^0d, recoil deuteron polarisation 78−74348
γe→$\gamma\gamma$e, polarised photon splitting on unpolarised electron *(Russian)* 79−371
$\gamma\gamma\rightarrow\pi\pi$ scalar-isoscalar amplitude and p EM polarisability 77−82743
$\gamma\gamma$e, polarised γ fusion at unpolarised e *(Russian)* 77−79260
γn, n electric polarisability, from photoabsorption cross-section 80−57597
$\gamma N\rightarrow K^+\Sigma$, meas. of asymmetries and cross sections using 16 GeV linearly polarised photons 80−13318
polarisation in elementary particle interactions continued
$\gamma N\rightarrow l^+l^-$, in crystals by circularly polarised quanta 78−17005
$\gamma N\rightarrow l^+l^-X$, polarisation effects on P-violating asymmetry in Weinberg-Salam model 80−32055
$\gamma N\rightarrow$lepton pair, weak neutral currents 78−8670
$\gamma N\rightarrow N\pi$, spatial parity nonconservation *(Russian)* 77−61301
$\gamma N\rightarrow\pi$, double polarisation meas. up to 2.5 GeV 77−34163
$\gamma N\rightarrow\pi$, polarised target above 3GeV 77−34164
$\gamma N\rightarrow\pi$, target asymmetry in second resonance region 78−21438
$\gamma n\rightarrow\pi^-p$, 0.9-1.65 GeV, pol. γ, cross section asymmetry *(Russian)* 80−86728
$\gamma n\rightarrow\pi^-p$, 700 MeV, target asymm. meas. 77−13967
$\gamma n\rightarrow\pi^-p$, 700 to 1200 MeV, recoil proton polarisation 80−78075
$\gamma N\rightarrow\pi^-n$, meas. of asymmetries and cross sections using 16 GeV linearly polarised photons 80−13318
$\gamma N\rightarrow\pi\Delta$, meas. of asymmetries and cross sections using 16 GeV linearly polarised photons 80−13318
γp, p electric polarisability, from photoabsorption cross-section 80−57597
$\gamma p\rightarrow$ lepton pair, P violating asymmetry 80−105901
$\gamma p\rightarrow\eta^0p$, cross-section asymm. for 1.39 to 1.78 GeV polarised photons 77−79273
$\gamma p\rightarrow K^+\Lambda$, meas. of asymmetries and cross sections using 16 GeV linearly polarised photons 80−13318
$\gamma p\rightarrow K^+\Lambda^0$, 2.5 GeV, target asymmetry 78−66125
$\gamma p\rightarrow n\pi^+$, 250 to 790 MeV, polarisation effects 77−46055
$\gamma p\rightarrow n\pi^+$ section asymmetry, pion-proton twin birth contribution *(Russian)* 80−47308
$\gamma p\rightarrow n\pi^*$, 340 MeV, pol. p, first resonance region, π^+ photoprod., T-asymmetry *(Russian)* 80−62997
$\gamma p\rightarrow p\pi^0$, 1.0 to 1.1 GeV, forward prod. of polarised protons 77−74692
$\gamma p\rightarrow p\pi^0$, 500 MeV, double polarisation expt. *(Russian)* 77−74696
$\gamma p\rightarrow\pi^0p$, 400 to 1142 MeV, recoil proton polarisation 80−82981
$\gamma p\rightarrow\pi^0p$, 450 to 800 MeV, proton polarisation, Walker-type anal., $P_{11}(1470)$, $D_{13}(1470)$, $S_{11}(1535)$ resonances 80−73721
$\gamma p\rightarrow\pi^+n$, 1.35-1.65 GeV, pol. γ, resonance energy region, cross section asymmetry *(Russian)* 80−86727
$\gamma p\rightarrow\pi^+n$, 340 MeV, cross section asymmetry *(Russian)* 79−63487
$\gamma p\rightarrow\pi^+n$, 600-1875 MeV, pol.p and γ, G and H polarisation parameters 80−99105
$\gamma p\rightarrow\pi^+n$, below 1.02 GeV, polarised target asymm. 78−17029
$\gamma p\rightarrow\pi^+n$, formation asymmetry near πN resonance 78−66124
$\gamma p\rightarrow\pi^+n$, polarised target asymm. ang. distrib. 77−34165
$\gamma p\rightarrow\pi^+\pi^-p$, cross sections 78−17028
$\gamma p\rightarrow\pi^0$, 0.7 to 1.45 Gev, polarised target asymm. 77−46054
$\gamma p\rightarrow\pi^0$, 0.8 to 1.3 GeV, production asymm. *(Russian)* 78−17031
$\gamma p\rightarrow\pi^0n$, cross section asymmetry in πN resonance region 78−54636
$\gamma p\rightarrow\pi^0p$, 650 and 700 MeV, polarisation ang. depend. 78−78191
$\gamma p\rightarrow\pi^0p$, below 1 GeV, polarised target asymm. 78−62409
$\gamma p\rightarrow\pi^0p$, proton polarisation *(Russian)* 78−78192
$\gamma p\rightarrow\pi^0p$,360 to 500 MeV, polarisation meas. 78−54637
$\gamma p\rightarrow\rho$, 3 GeV, polarised beam 77−30390
$\gamma p\rightarrow\rho^0X$, 2.8 to 9.3 GeV, cross-section, multiplicity, energy depend. 77−61303
$h_1h_2\rightarrow l\bar{l}X$, massive lepton pair prod., polarisation and spin effects 80−105929
$K_L^0\rightarrow\pi^-\mu^+\nu_\mu$, transverse polarisation of μ, violation of time-reversal invariance 80−68448
$K_{-}^{\circ}p\rightarrow K_s^{\circ}p(\pi^+\Lambda)(\pi^+\Sigma^0)(\pi^+\pi^0\Lambda)$, 550 MeV, differential and polarisation cross sections 79−17757
KN, 360 to 1320 MeV, partial wave anal. 78−82235
$K^+n\rightarrow K^+p$, 6 and 12 GeV, polarisation meas. 79−22140
$K^+n\rightarrow K^+p$, 6 GeV, polarisation meas. 77−30426
$K^+N\rightarrow K^+p$, 6 and 12 GeV, polarisation meas. 79−63521
$Kp\rightarrow\Sigma^+\pi^-$, 500 MeV/c, meas. of polarised Σ^+ magnetic moment 80−22614
K^-p, 14.3 GeV, $O^-1/2^+$ and $O^-3/2^+$ final states, cross sections, polarisations 77−13989
K^-p, neutral channel cross sections 78−82237
$K^-p\rightarrow(\Lambda^\circ,\Sigma^\circ,\Sigma(1385))X$, 8.25 GeV 79−30749
$K^-p\rightarrow f(1514)\Lambda$, 4.15 GeV, cross sections, Λpol., density matrix elements 77−46077
$k^-p\rightarrow\lambda^0\sigma^0+$ vector mesons, 3.1 tp 3.6 GeV, exchange model 77−74718
$K^-p\rightarrow\Lambda X$, 10 and 16 GeV, polarised prod. 78−62466
$K^-p\rightarrow\Lambda X$, 42 GeV, polarisation cross sections 78−45948
$K^-p\rightarrow\Lambda\eta$, 6 GeV/c, baryon exchange reactions, ηNN coupling constant, Λ polarisation, nucleon-Regge exchange 80−78098
$K^-p\rightarrow\Lambda\eta_0$ cross section near threshold 77−82765
$K^-p\rightarrow\Lambda\pi^0$, 6 GeV/c, baryon exchange reactions, ηNN coupling constant, Λ polarisation, nucleon-Regge exchange 80−78098
$K^-p\rightarrow\Lambda\pi^0$, polarisation and differential cross sections in Regge pole model 77−54122
$K^-p\rightarrow M^0X$, 4.2 GeV, quark model relations 78−82233
$K^-p\rightarrow\pi^-\Sigma^+$, exchange degeneracy test 78−41581
$K^-p\rightarrow\pi^-\Sigma^+$, polarisation meas. 78−41573
$K^-p\rightarrow\pi^-\Sigma^+$ and $\pi^+p\rightarrow K^+\Sigma^+$, exchange degeneracy 80−57634
$K^-p\rightarrow\pi^-Y^+$, $Y^+=\Sigma^+$ or $Y^{*+}(1385)$, 7 GeV/c, hypercharge exchange in line-reversed π^+p and K^-p 80−82998
$K^-p\rightarrow\pi^-Y^*(1285)$, 11.5 GeV, exchange degeneracy 78−82247
$K^-p\rightarrow\pi^-\Sigma^+$, Σ^+ polarisation meas. 77−30431
$K^-p\rightarrow\rho^-Y^+$, $Y^+=\Sigma^+$ or $Y^{*+}(1385)$, 7 and 11.5 GeV/c, hyperon polarisation, vector meson decay angular distribs. 80−82997
$K^-p\rightarrow\Sigma^-X$, 4.2 GeV, prod. cross sections 78−4875
$K^-p\rightarrow\Sigma^+\pi^-$, polarisation parameter meas. 77−30432
K^+p, $\Delta(\bar{\Delta})$, 32 GeV, polarisation study 79−45122
lN, deep inelastic scattom P-odd asymmetries *(Russian)* 79−49527
lN→bX, polarisation transfer from initial to final state 77−82746
Λ hyperon polarisation, meas. by hybrid Monte Carlo tech. 80−99431
$\mu\rightarrow e\gamma$, decay ang. distrib. and pol. effects 77−41835
μN, deep inelastic scatt. as gauge theory test 78−62408
N+vector meson, polarised deep inelastic collisions in nuclei *(Russian)* 80−102209
NN, cross sections, polarisation meas. 78−62419
NN, spin depend. phenomena induced by EM interference 78−422
NN→direct muon, 1.9 GeV, longitudinal polarisation 79−9411
NN→direct muons, 1.9 GeV, longitudinal polarisation 79−3038
NN→μX, direct muon asymm. coeff. 77−6185
NN→NNπ, polarization analysis of reactions with four spin-1/2 particles 80−86745
NN→$\pi\pi$, p EM polarisabilities difference controls 79−3023

polarisation in elementary particle interactions continued
np charge exchange reaction, imaginary amplitude part, Regge behaviour 77−38145
np→d(πx)°, 800 MeV, deuteron spectrum 78−70384
np→dγ, circular polarisation, P-violating nuclear force 77−10333
np→dγ, photon circular polarisation 78−70390
np→dγ, photon circular polarisation, deuteron relativistic effect 78−93900
np→dγ, polarisation in Weinberg model 78−54644
np→γd, circular polarisation, relativistic calcs. 79−67582
np→γd, parity violating effects on gamma pol. 77−41851
$n^{\pm}p\rightarrow\pi^{-}(\pi^{\circ})X$, polarised target, beam fragmentation region, asymm. scatt. *(Russian)* 77−79292
$\nu(\bar{\nu})$N, pol.N, deep inelastic processes from valence straton distrib. functions *(Chinese)* 80−99095
$\nu_e\rightarrow\nu_\mu e$, weak and EM radiative corrections, sensitivity test 80−105880
νN, polarised deep inelastic sum rules 77−13952
νN, polarised sum rules 77−34144
$\nu N\rightarrow\Delta+$leptons, spin 3/2 polarisation density matrix determ. 77−87965
$\nu n\rightarrow\mu^{-}$ p, bounds on outgoing baryon transverse polarisation, T-odd effects 77−87966
$\nu n\rightarrow\mu^{-}$ p, Higgs boson exchange effects on second-class currents 80−91075
$\bar{\nu}p\rightarrow\mu^{+}\Lambda$, polarised strange particle prod. 78−82195
$\bar{\nu}p\rightarrow\mu^{+}$n, Higgs boson exchange effects on second-class currents 80−91075
$\nu p\rightarrow\mu\Delta$, Δ polarisation, T-invariance test 79−67531
$\nu p\rightarrow\nu p$, hadronic neutral current probe by proton polarisation 78−82200
pα, 1300 to 2300 MeV, π^{0} photoproduction, double polarisation parameters 80−13317
pd, polarised pn total cross sections 80−22633
$pd\rightarrow(\pi^{\pm},K^{\pm},p)X$, prod. asymm. at 11.75 GeV 79−22155
$pd\rightarrow V^{\circ}X$, 18 GeV, K°, γ Λ, Λ^{+} prod. 77−87993
pN, 400 GeV, prompt muon polarisation in D-meson prod. 78−70413
pN, dilepton production by pol. protons, parity violating, asymmetry, Weinberg-Salam calcs. 80−42488
$pN\rightarrow\Lambda^{0}X$, 28.5 GeV/c, Λ^{0} polarisation 80−32137
$pN\rightarrow\Lambda^{\circ}X$, Λ° polarisation 79−63542
$pN\rightarrow\Lambda(\bar{\Lambda})X$, 400 GeV, polarised production 78−82253
$pN\rightarrow\mu$, polarised prompt meon prod. 77−13991
$pN\rightarrow\mu X$, prompt μ polarisation at large transverse momenta 77−71542
pN→pX, 28.3 GeV, produced proton polarisation 78−93917
pp, 100, 200 GeV, elastic scatt., polarisation effects at large momentum transfer, quark model *(Russian)* 80−83005
pp, 28 GeV, in H, D, Be, inclusive Λ polarisation 80−47337
pp, 7.9 GeV, spin depend. 79−3056
pp, inelastic diffraction and charge exchange reactions 77−30399
pp, phase shift at 2 GeV, polarisation spin correl. cross sections 77−41852
p̄p, pp, pol. and unpol. beams, hadronic jets, vector bosons, QCD and weak interference 80−57648
pp, resonant structures in region 2.1 to 2.8 GeV 78−89745
pp, total cross section, Δ(1232) prod., spin depend. 78−62436
$\bar{p}p\rightarrow(\Lambda,K_{9}^{\circ},\bar{\Lambda})X$, 3.6 GeV, inclusive polarisation prod. 79−45095
$pp\rightarrow(\Pi^{\pm},K^{\pm},p)X$, prod. asymm. at 11.75 GeV 79−22155
$pp\rightarrow(p,\pi^{\pm})X$, spin depend. effects at 7.9 GeV 77−30413
$pp\rightarrow(\pi^{\pm},K^{\pm},p,d)X$, 6 to 11.8 GeV, left-right assym. 77−30455
p̄p annihilation, cross-sections and multiplicities 79−36111
pp→bremsstrahlung asymmetry studies 79−67585
$pp\rightarrow d\pi^{+}$, 1.03 GeV, analysing power 78−93901
$pp\rightarrow d\pi^{+}$, 305 to 425 Mev, d-wave pion prod. 79−36094
$pp\rightarrow d\pi^{+}$, deuteron polarisation calc. in isobar model 79−49535
$pp\rightarrow d\pi^{+}$, differential cross section and polarisation 78−8683
$pp\rightarrow d\pi^{+}$, differential cross section and polarisation 78−54648
$pp\rightarrow d\pi^{+}$, differential cross sections 79−9392
$\bar{p}p\rightarrow\gamma K_{s}^{\circ}\Lambda X$, polarisations, struct. functions 79−58983
pp inclusive scattering, 6 GeV/c, depolarisation parameter, dominance of natural parity exchange 80−78088
$\bar{p}p\rightarrow K^{\circ}(\Lambda^{\circ})$, differential cross sections, polarisation 78−58197
$pp\rightarrow K^{\circ}(\Lambda)(\delta^{++})X$, 6 GeV 77−30400
pp→lepton pair, Drell-Yan mechanism 78−8718
$\bar{p}p\rightarrow\Lambda^{\circ}X$, 12 GeV, polarisation depend. 78−4885
$pp\rightarrow\Lambda^{\circ}X$, polarisation meas. 79−49550
$pp\rightarrow\Lambda^{\circ}X$, polarised prod. by 24 GeV collisions on Pt 77−67691
$\bar{p}p\rightarrow\Lambda^{\circ}X$,100 GeV, inclusive prod. distrib. 77−38213
$\bar{p}p\rightarrow\bar{\Lambda}\Lambda$, 1.5 to 2.06 GeV, polarisation, cross sections 78−74271
$\bar{p}p\rightarrow\bar{\Lambda}\Lambda(\Sigma^{\circ})$, 6 GeV, cross sections 79−407
$pp\rightarrow\Lambda X$, 19 GeV, polarisation meas. 78−37246
$pp\rightarrow\Lambda X$, Λ polarisation in Mueller-Regge model 77−2876
$pp\rightarrow\Lambda X$, polarisation prediction in Mueller-Regge model 77−30454
$pp\rightarrow\Lambda X$, polarisation transverse momentum depend. 77−61327
$pp\rightarrow\Lambda(K^{0})X$, 12 GeV/c, beam polarisation induced asymmetries 80−42507
$pp\rightarrow\mu^{+}\mu^{-}X$, Drell-Yan parton model anal. 79−58981
$pp\rightarrow\mu^{+}\mu^{-}X$, parity violating effects 79−67613
$pp\rightarrow\mu^{+}\mu^{-}X$, polarised cross-section 79−63544
pp→NΔ resonance with T=1 and $J^{P}=2^{+}$end 78−17041
pp→pX, out going proton polarisation at 100-400 GeV 79−63543
pp→pX, polarised 6 GeV projectile, L-R asymm. 77−49995
pp→pX, polarised target, beam fragmentation region, spin correls. *(Russian)* 77−79292
$\bar{p}p\rightarrow\pi^{-}\pi^{+}$, amplitude anal., meson prod. in 2.02 to 2.58 GeV 77−41853
$\bar{p}p\rightarrow\pi^{-}\pi^{+}$, amplitude anal., meson prod. in 2.02 to 2.59 GeV 77−46075
$\bar{p}p\rightarrow\pi^{-}\pi^{+}$, asymmetry, proof of protons negative parity 77−2860
$\bar{p}p\rightarrow\pi^{-}\pi^{+}(K^{-}K^{+})$, 1 to 2.2 GeV, polarisation parameter meas. 77−74711
$\bar{p}p\rightarrow\pi^{-}\pi^{+}(K^{-}K^{+})$, polarisation parameter meas. 77−87995
$pp\rightarrow\pi^{0}X$, pol.p, 24 GeV/c, high $p_{T}\pi^{0}$ prod., spin. depend. 80−105935
$pp\rightarrow\pi^{+}d$, 515 and 575 MeV, spin depend. parameter meas. 80−73734
$pp\rightarrow\pi^{+}d$, differential cross sections from polarised beam 79−17748
$pp\rightarrow\pi^{+}d$, SIS, 578 MeV, pol. beam and target, spin depend. parameters 80−42651
$\bar{p}p\rightarrow\pi^{+}\pi^{-}$, polarised target, charge parity determ. 77−57567
$\bar{p}p\rightarrow\pi^{+}\pi^{-}(K^{+}K^{-})$, polarisation parameter meas. 77−30401
$pp\rightarrow\pi^{\circ}X$, asymmetry ub karge P_{T} interactions 78−12936
$pp\rightarrow\pi X$, large P_{T}, QCD predictions 79−49553
$pp\rightarrow\pi X$, large transverse momentum processes, QCD spin tests 79−63558
$pp\rightarrow\pi d$; π^{+} negative parity assignment 80−32117
pp spin observables 78−78224
pp total cross-sections, transverse spin depend 77−30409
polarisation in elementary particle interactions continued
pp→WX, parity violating asymmetries 79−63538
pp→X, inclusive cross sections, asymm. parameters 79−63559
pp→X, polarisation asymmetry 79−40819
$p_{0}p\rightarrow K^{\circ}\Lambda^{\circ}$, up to 1.334 GeV, differential cross sections 79−412
$\pi^{0},\pi^{\pm}$ EM polarisabilities, sum rules, coloured quark field theory 80−57561
$\pi^{+}\rightarrow K^{+}Y^{*}(1385)$, 11.5 GeV, exchange degeneracy 78−82247
πN→πX, sum rules induced by EM current 78−89718
$\pi n\rightarrow\rho\eta(\omega n)$, polarisation and Regge cuts 78−45947
$\pi p\rightarrow K^{+}\Lambda^{\circ}$, resonance region, Λ polarisation 78−66131
$\pi p\rightarrow K^{\circ}\Lambda^{\circ}$, up to 1334 MeV, polarisation, cross sections 78−70404
$\pi p\rightarrow\pi^{\circ}n$, polarisation parameter meas. 77−22773
π^{-}p, neutral strange particle prod. at 15 GeV 78−45981
$\pi^{-}p\rightarrow(\pi^{+}\pi^{-})\eta$, 17.2 GeV, A_{1} exchange role 77−61325
$\pi^{-}p\rightarrow(\rho^{\circ},\omega)\Delta^{++}$, polarisation effects 79−54355
π^{-}p charge exchange, polarisation meas. 77−30420
π^{-}p elastic scatt., 2.22-3.5 GeV/c, backward polarisation 80−82999
$\pi^{-}p\rightarrow\eta n$, tensor exchange amplitudes and polarisations 78−45962
$\pi^{-}p\rightarrow K^{\circ}\Lambda$, 3.5 GeV/c, Λ polarisation, high statistics meas. 80−57637
$\pi^{-}p\rightarrow K^{0}\Sigma^{0}$, 1395 to 2375 MeV/c, differential cross-section and polarisation meas. 80−9183
$\pi^{-}p\rightarrow K^{0}\Sigma^{0}$, 1395 to 2375 MeV/c, differential cross-section and polarisation 80−57635
$\pi^{-}p\rightarrow K^{+}\Sigma^{-}$, 3.5 GeV, backward scatt. polarisation meas. 78−41572
$\pi^{-}p\rightarrow K^{\circ}\Lambda^{\circ}$, 1400 to 2380 MeV, polarisations, differential cross sections 78−70405
$\pi^{-}p\rightarrow K^{\circ}\Sigma^{\circ}$, up to 1334 MeV, differential and polarisation cross sections 79−17755
$\pi^{-}p\rightarrow K^{\circ}\Sigma^{\circ}$, up to 1.334 GeV, polarisation and cross-sections 78−89733
$\pi^{-}p\rightarrow K^{*0}(890)\,\Lambda^{0}/\Sigma^{0}$, 10 GeV/c, K^{*0} polarisation meas. in hypercharge exchange reaction 80−63017
$\pi^{-}p\rightarrow\Lambda K^{\circ}$, 3 to 6 GeV, cross sections and polarisation 78−25074
$\pi^{-}p\rightarrow\Lambda K^{\circ}$ or $\Lambda K^{*}(890)$, 8 GeV, differential cross section, Λ polarisation 77−34175
$\pi^{-}p\rightarrow ne^{+}e^{-}$, vertical photon polarisation 78−12930
$\pi^{-}p(\omega)n$, 6 GeV, abnormal polarisation effect *(Russian)* 77−10282
$\pi^{-}p\rightarrow\pi^{-}\pi^{+}n$, polarisation meas. and narrow ε(750) 79−63514
$\pi^{-}p\rightarrow\pi^{+}\pi^{-}n$, 17.2 GeV, exchange amplitudes 77−30449
$\pi^{-}p\rightarrow\pi^{\circ}n$, 617 to 2267 MeV, polarisation meas. 78−82231
$\pi^{-}p\rightarrow\pi^{\circ}n$, 618 to 2724 MeV, polarisation parameter 77−6162
$\pi^{-}p\rightarrow\pi^{\circ}n$, charge exchange pol., Gribov Reggeon calculus 77−46076
$\pi^{-}p\rightarrow\rho^{\circ}(\omega^{\circ})X$, 15 GeV, polarisation props. 78−37251
$\pi^{-}p\rightarrow\Sigma^{\pm}X$, 4.35 to 4.85 GeV, cross sections and polarisations *(Russian)* 77−13977
π^{+}p, backward polarisation importance 77−30421
$\pi^{+}p\rightarrow K^{-}\Sigma^{+}$, 1.72 to 1.95 GeV, polarisation, cross sections 78−4872
$\pi^{+}p\rightarrow K^{-}\Sigma^{+}$, exchange degeneracy test 78−41581
$\pi^{+}p\rightarrow K^{+}\Sigma^{+}$, polarisation meas. 78−41573
$\pi^{+}p\rightarrow K^{-}\Sigma^{+}$ and $K^{-}p\rightarrow\pi^{-}\Sigma^{+}$, exchange degeneracy 80−57634
$\pi^{-}p\rightarrow K^{+}Y^{*}$, $Y^{*}=\Sigma^{+}$ or $Y^{*+}(1385)$, 7 GeV/c, hypercharge exchange in line-reversed $\pi^{+}p$ and $K^{-}p$ 80−82998
$\pi^{+}p\rightarrow K^{*+}(890)Y^{+}$, $Y^{+}=\Sigma^{+}$ or $Y^{*+}(1385)$, 7 and 11.5 GeV/c, hyperon polarisation, vector meson decay angular distribs. 80−82997
$\pi^{+}p\rightarrow\pi^{+}\pi^{-}\Delta^{++}$, polarisation meas. and narrow ε(750) 79−63514
$\pi^{+}p\rightarrow\rho^{\circ}\Delta^{++}$, ωΔ, ΔJ=1 rule test 77−30471
$\pi^{\pm}$p, 16 GeV, three (four) body final states, strange particle prod 78−475
$\pi^{\pm}p\rightarrow$ polarised mesons 78−41577
ππ→γγ, pion polarisabilities, analyticity bounds 79−13157
$\pi^{-}\rho^{\circ}$n, nucleon polarisation effect obs. 79−45106
ρ^{0}-electroproduction, parity violating effects 80−9178
W^{0} effects in $e^{+}e^{-}$ interactions on a⁻ resonances 80−42386

polarisation in elementary particle scattering
hadron scatt. mediated by qg→qg and gg→gg 80−82988
hadron scattering, 39-445 GeV, pol. and spin rotation meas. 77−30438
hadronic high momentum transfer scatt., spin meas. 79−63498
hadronic polarisation in neutrino scatt. 78−74245
hadrons, multipole polarisabilities from Compton scatt. amplitudes 80−13311
high energy polarisation data interpretation 77−30435
pp eN, polarised scattering as gauge model probe 78−45901
ZGS, polarised beam results, review 80−99361
e scattering, polarised on spin-zero and polarised spin-$^{1}/_{2}$ targets, covariant formulation 80−78069
e-p, scatt. and polarisation matrices *(German)* 80−27508
ed, P-odd correlations, neutral weak currents *(Russian)* 78−21434
ed, parity violation, polarisation asymmetry 79−40787
ed, parity violation asymmetry 79−36085
ed, polarisation effects in presence of weak neutral current *(Russian)* 77−61291
ed, recoil deuteron polarisation tensor 79−67564
ed, recoil deuteron vector polarisation 79−398
ed scatt., P-violation calc. in weak interaction theory 80−42469
$e^{-}e^{-}$, polarised cross sections 79−372
$e^{+}e^{-}$, polarised cross sections 79−372
$e^{+}e^{-}\rightarrow e^{+}e^{-}gg$, gluon jet polarisation in photon-photon scatt., QCD test 80−52550
eN, C and T invariance, polarisation phenomena *(Russian)* 77−10256
eN, form factors and P-odd asymmetry 79−71753
eN, P-odd asymm., unified model *(Russian)* 77−61300
eN, polarisation asymmetry in SU(2)xU(1) 79−40781
eN, unified gauge theories test 79−17732
eN elastic scatt., pol. e, nucleon form factors, P violating symmetry, Weinberg-Salam calcs. 80−68461
ep, high energy scattering 77−34157
ep, polarised scattering, asymmetries, gauge models 80−62991
ep, scatt. asymmetry 77−6131
ep scatt., longitudinal cross section and asymmetries for jets in leptoproduction 80−32106
γe, 6.0 to 9.7 MeV, Compton scatt. cross section 77−18260
γN, nucleon polarisability, Compton scatt. amplitudes 77−18289
γp, 450 to 950 MeV, Compton scatt. differential cross sections 78−93885
γp, <400MeV, proton polarisability coeff. *(Russian)* 77−49973
γp, Compton scatt., dispersion relation anal. 77−82744
γp, differential cross section 78−17025
γp, low and intermediate energies, dispersive anal. 79−396
γp, low energy Compton scatt. 78−93886
KN, charge exchange, Regge pole model anal, 77−74719

polarisation in elementary particle scattering continued
K^+n, 0.851 to 1.351 GeV, polarisation parameter meas. 80−42498
K^+n elastic scatt., 0.851-1.351 GeV/c, polarisation parameter 80−68478
K^-p, low energies, polarisation meas. 78−12932
K^-p elastic scatt., 0.955, 1.272 GeV/c, polarisation parameter meas. 80−37299
K^-p elastic scatt., 0.955-1.272 GeV/c, polarisation parameter 80−86753
K^+p, 6 and 12 GeV, asymmetry effects 79−49542
K^+p, polarisation and differential cross-section 77−6164
K^+p, polarisation parameter meas., 45 GeV *(Russian)* 77−34179
K^+p, up to 2 GeV, cross section, polarisation 79−17758
lh, high energy polarised scatt.m invariance principle tests 79−67560
Λp, 60 to 380 GeV, polarisation meas. 78−37234
Λp, spin depend. EM interference expts. 78−12923
μ scattering, polarised, on spin-zero and polarised spin-$^1/_2$ targets, covariant formulation 80−78069
μ^-p, final lepton polarisation *(Russian)* 77−26529
nd, parity nonconserving asymmetry 78−21449
NN, 11.8 GeV, polarisation parameter 78−66158
NN, 12 GeV, spin depend., quark exchange evidence 80−102074
NN, Coulomb-nuclear interference polarisation in large momentum transfer scatt. 77−79282
NN, elastic polarisation data, eikonal description 77−13948
NN, polarisation and spin correlation parameter 77−30404
NN, polarisations, eikonal description 77−30405
NN, polarising power, spin-correlation parameters 79−67568
NN, spin polarisation meas. implications 78−74272
NN, spin polarisation meas. implications 79−63505
NN, weak neutral current model test 78−41568
NN, ZGS to Fermilab energies, asymmetry meas. 78−62459
np, 14-17 MeV, analysing power precision meas. 78−70393
np, 220-495 MeV, Wolfenstein parameters, I=O phase shifts 79−67594
np, 325 MeV, phase shift anal., mixing parameters 77−79277
np, charge symmetry tests 78−89798
np, multiple scatt. effects in analysing power meas. 77−10572
np, spin correlation parameter at 50 MeV 77−49993
np, spin depend. EM interference expts. 78−12923
np→np, polarisation phenomena in close-to-forward scatt., intermediate energy region 80−78086
νd, polarised d, recoil d emission asymm. 77−79264
νe, polarisation effects on weak lepton streams 78−25039
νe, spin correlations, neutral and charged currents 78−12901
νe, weak neutral current space-time struct. 79−17715
$\nu e \rightarrow \nu e\gamma$, radiational scatt. polarisation effects *(Russian)* 77−46038
νN, final state polarisations 79−63466
νp, neutral currents, elastic scatt. in Weinberg model *(Russian)* 77−26507
νp, polarised proton, differential cross sections *(Russian)* 77−46042
νp, weak neutral currents space-time struct. 79−17715
pd, backward scatt., analysing power 78−93901
pn, 1.03 Gev, polarisation meas. 78−82245
pn, 24 GeV, analysing power 79−63528
pN, high energy polarised scatt. particle struct. studies, book 80−41952
pp, 0.35 to 1 MeV, ang. distrib. data 78−62423
pp, 0.97 GeV, polarisation parameters *(Russian)* 79−30745
pp, 100, 300 GeV/c, polarisation parameters and ang. distribs. for elastic scatt. 80−95287
pp, 100 and 300 GeV, polarisation and ang. distribs. 78−89738
pp, 100 and 300 GeV, polarisation meas. 79−63527
pp, 100 GeV, polarisation values 77−30440
pp, 11.75 GeV, pure initial spin states, polarisation meas. 77−30436
pp, 150 GeV, spin effects, evidence 78−66157
pp, 1.03 GeV, polarisation meas. 78−82245
pp, 1.2 to 6.0 GeV, total cross section difference in longitudinal spin states 78−62432
pp, 2 to 6 GeV, spin parameters 78−25078
pp, 20 to 200 GeV, recoil proton polarisation 78−50054
pp, 209 to 515 MeV, polarisation parameters 78−461
pp, 24 GeV, polarisation parameter meas. 77−30437
pp, 24 GeV, polarisation parameter meas. at 24 GeV 77−46081
pp, 2.1 GeV, polarisation meas. *(Russian)* 79−9377
pp, 3 and 6 GeV, total cross sections 78−4870
pp, 3-spin cross section at 6.0 GeV 77−30411
pp, 398 to 472 MeV, small angle scatt., amplitude anal. 77−30407
pp, 45 MeV, longitudinally pol. p, parity nonconservation in anal. powers 80−57626
pp, 4.5 to 5.1 GeV, spin depend. 79−3049
pp, 52.34 and 68.19 MeV, polarisation meas. 78−54641
pp, 550 to 630 MeV, correlation coeff. *(Russian)* 78−12929
pp, 6 GeV, differential cross sections 77−38189
pp, 6 GeV, observables from absorption model 77−2858
pp, 6 GeV, parity violation search 79−63500
pp, 6 GeV, polarisation parameter meas. 77−38188
pp, 6 GeV, polarised initial and final states 78−41568
pp, 6 GeV, spin-spin correlation parameter meas. 77−18327
pp, 610 MeV, polarisation correlation coeff. *(Russian)* 77−30419
pp, 610 MeV, spin correlation parameter meas. 77−30406
pp, $\Delta\sigma_T$ and A_{nn} meas in 1 to 3 GeV region 79−63504
pp, high energy polarisation data interpretation 79−3048
pp, high energy scatt., polarisation and rotation parameter 78−70341
pp, high energy scatt. polarisation meas. 77−30439
pp, high P_T^2 scatt. in pure initial spin states 78−8698
pp, intermediate energy polarised scatt. 79−67590
pp, large angle scatt., 79 GeV, polarisation parameter meas. 77−82759
pp, P-violation longitudinal asymmetry meas. 79−63499
pp, parity violation meas. at 45 MeV 80−78092
pp, polarisation, depolarisation, spin correlation studies 77−30434
pp, polarisation analysing power, 643, 787, 796 MeV 78−78207
pp, polarisation and spin correlation meas. in 400 to 600 MeV scatt. 79−63503
pp, polarisation meas. in 6.14 MeV scatt. 79−67591
pp, polarisation normalisation between 200 and 520 MeV 78−70397
pp, polarisation parameter meas., 45 GeV *(Russian)* 77−34179
pp, polarised 6 GeV scatt., spin depend. forces in eikonal model 80−37246
pp, polarised beams, Wolfenstein parameter meas. near 1 GeV *(Russian)* 77−49997
pp, pp high energy elastic scatt., cross section rise and polarisation, Regge model *(Russian)* 80−37301
pp, spin correlation meas. 78−54649
pp, spin correlation parameter meas. at 6 GeV 77−30410

polarisation in elementary particle scattering continued
pp, spin correlation parameter meas. in 10 MeV scatt. 79−67592
pp, spin correlation sealing, energy depend., polarisation parameters 77−34173
pp, spin correlative parameter at 643 and 796 MeV 79−63502
pp, spin-spin correlation parameters 78−62433
pp, spin-spin forces, energy depend. 78−45941
pp, spin-spin interactions at high $P\perp^2$ 77−88009
pp, Wolfenstein and polarisation parameters 79−67593
pp elastic scatt., 1-3 GeV/c, pol. p, spin parameters A and A_{nn} 80−95304
pp→pp, high-energy, polarisation and energy dependence 80−63030
pp→pp, polarisation phenomena in close-to-forward scatt., intermediate energy region 80−78086
pp→pp, polarisation structure and Pomeron flip, Regge pole model 80−102073
pp scatt., <300 MeV P-odd asymmetry for pol. ρ *(Russian)* 80−102063
pp scatt. amplitude, phase anal. ambiguities, cross sections and polarisation parameter *(Russian)* 80−86749
pp scattering, parity violation at 50 MeV *(German)* 80−68471
pp small angle scatt., 312-575 MeV, pol. p, Wolfenstein and polarisation parameters 80−57629
$p\pi^+$, 6 and 12 GeV, asymmetry effects 79−49542
πd, pion absorption and emission polarisation 79−17939
πd, polarisation observables 78−78210
πd elastic scatt., 142-256 MeV, dibaryon resonance interference with Faddeev amplitudes 80−32123
πN, 6-200 GeV, amplitude anal. in impact parameter representation, non-zero polarisation, shell struct. *(Russian)* 80−86752
πN, backward scatt. polarisation 77−2862
πN, Coulomb-nuclear interference polarisation in large momentum transfer scatt. 77−79282
πN, cross sections and polarisations *(Russian)* 78−8703
πN, elastic and charge exchange scatt., generalised reaction matrix *(Russian)* 77−50013
πN, one photon exchange polarisation meas. 78−93906
πN, scatt. amplitudes, isotopic invariance *(Russian)* 79−9404
π^-p, 1.18 to 1.36 GeV, polarisation parameter 77−61316
π^-p, backward angle polarisation meas. 77−2863
π^-p, backward scatt. polarisation parameter meas. 77−13974
π^-p elastic scatt., 450-560 MeV, polarisation parameter *(Russian)* 80−37295
π^-p elastic scatt. at 490 and 600 MeV, polarisation parameter meas. *(Russian)* 80−42496
π^+p, 291.4 and 310 MeV, polarisation parameter 78−41571
π^+p, polarisation parameter meas., 45 GeV *(Russian)* 77−34179
$\pi^\pm p$, 100 GeV, polarisation values 77−30440
$\pi^\pm p$, 100 GeV, polarisation meas. 79−63527
$\pi^\pm p$, 100 GeV/c, polarisation parameters and ang. distribs. for elastic scatt. 80−95287
$\pi^\pm p$, total and near forward differential cross sections 79−63529

polarisation in nuclear reactions and scattering
2s-1d shell nuclei, cluster struct. and inelastic scatt. of polarised protons 79−6557
^{116}Sn(d,d), polarised d, 8.22 MeV, anal. power 80−5114
^{16}O(p,p), spin orbital interaction and nucl. matter density distrib. *(Russian)* 79−22176
^{18}O(p,p), polarised p, elastic and inelastic, 6.1-16.6 MeV, ^{19}F resonance parameters and J^π values 79−45232
A=12, decay of T=1 isospin triplet, β-ray anisotropy 78−78322
A=12, recoil polarisation in muon capture, arbitrary nuclear spin, form factors 79−75978
A=70, heavy-ion induced fission-evaporation reactions, magnetic substrate distribs., nuclear alignment 80−73857
backward inclusive scattering of polarised protons from nuclei 78−17206
baryon+nucleus elastic scattering, polarisation phenomena in hadron collisions at small momentum transfer *(Russian)* 78−58196
bremsstrahlung, pair production, lepton and photon nuclear interactions *(Russian)* 77−88104
charge and slope polarisation of nuclei, liquid drop model anal. 79−9543
collective tube model of high energy proton scatt. on polarised nuclei 80−32273
conference on heavy ion reaction dynamical props., Johannesburg, S.Africa (Aug. 78) 80−17715
conference on nuclear spectroscopy and structure, Alma Ata, USSR, (Mar. 78) 79−75809
cool compound nucleus formation with oriented heavy ions, ^{258}104 and ^{260}106 prod. 80−99179
core polarisation in inelastic scatt., extension to include charge-exchange reactions 78−78359
crystal nuclei, e^+e^- and e^- bremsstrahlung photoprod. cross sections, longitudinal polarisations 79−75969
(d,τ) reactions, 52 MeV, analyzing powers, spins of proton hole states 78−25111
deep inelast. electron scatt., nucleon polarisabilities 77−82919
deep inelastic electro-creation by polarised vector mesons *(Russian)* 80−102209
deep inelastic heavy ion reactions, fast light particles and heavy ejectile ang. correlation 80−57791
deuteron elastic scatt. from ^{12}C, ^{29}Si, ^{40}Ca, ^{56}Fe, ^{58}Ni, ^{64}Zn, ^{90}Zr, ^{118,120}Sn, ^{208}Pb at 30 MeV 77−54228
deuteron-nucleus polarisation transfer in elastic scatt., tensor interaction 77−57647
differential polarisation coefficients for (γ,X) reactions 80−73838
diffraction scatt. of nucleons *(Russian)* 79−89285
direct reaction contrib. in fluctuating cross sections 77−50102
eikonal approx., electron-oriented nucleus scatt., polarisation of e^-, nuclei and emitted γ rays 78−37331
elastic and breakup polarisation, realistic nucleon-nucleon interactions, few nucleon systems 78−62526
elastic and quasi-elastic polarised heavy ion collision theory, semi-quantal description 80−18330
elastic nucleus scatt., below Coulomb barrier, effects of polarisability 77−88102
elastic scatt., semiclassical approx. 79−26417
elastic scattering, triangle graph decomposition, spin effects *(Russian)* 77−6331
Ericson fluctuations in polarised (p,p) reactions *(Rumanian)* 80−5113
excited nuclear levels, polarisation induced by at. orientation 80−91144

polarisation in nuclear reactions and scattering continued
few-body reactions, polarisation 77−22995
few-nucleon system investigation using polarised deuterons 77−18578
few-nucleon systems 77−18520
gamma reactions initiated by polarised particles, Legendre polynomial coeffs. 80−73107
Glauber calculations of p+nucleus elastic scatt. at 1 GeV 79−13260
hadron-nucleus scatt., corrections to circular polarisation of γ quanta *(Russian)* 78−41683
Hamburg polarised neutron facility, initial expts. 77−26946
heavy ion collision induced fission, fragment ang. distrib., reaction mech. 78−74412
heavy ion collision polarisation, damping mechanism approach via elementary excitation modes 80−18338
heavy ion collisions, dispersion around mean classical path, effect on polarization of fragments 79−17891
heavy ion elastic scattering, generalised Fresnel model, dynamic polarisation effects 78−74394
heavy ion quasielastic reactions, polarizations 78−37368
heavy ion reactions, deflection function, effect of nuclear vibr..mode and orientation 79−59080
heavy ion reactions, polarisation, Strutinsky model, asymptotic Clebsch-Gordan coeffs. 78−74391
heavy ion scattering, polarisation by Coulomb excitation in closed formalism, $^{184}W(^{18}O, ^{18}O)$ appl. 78−37376
heavy ion transfer reacts., nuclear wave function polarisability 78−54785
heavy-ion induced fusion-evaporation, phenomenological restrictions for spin alignment attenuation factors 77−57686
heavy-ion induced reactions, dynamically deformed rot. nucleus calcs. of polarisation effects 78−25222
heavy-ion scattering, dynamic polarisation pot. for Coulomb excitation effects 77−67765
high-energy physics with polarised beams and targets, conference 77−30470
interfacing theory and experiment in polarization studies 80−73837
knock-on reactions, absorpt. and polarisation effects *(Russian)* 77−79354
knock-out reactions, polarisation phenomena in the presence of strong absorption *(Russian)* 80−37360
lepton-nucleus scattering, bremsstrahlung and neutral currents 80−32268
light and intermediate nuclei, proton induced reactions, polarisation phenomena interpret. 78−13051
light ion direct reactions, polarisation expts., tensor polarised deuteron beams 78−54732
light nuclei, (p,π^+) reactions, π distortion effect on asymmetry 78−50176
longitudinal polarisation meas., β^+ decay 78−8781
low energy polarised beam expts., review, book contrib. 80−68642
maximum polarisation for spin-1 particles 77−79355
multichannel scattering chamber for polarisation anal., adapter for securing detectors 77−6654
multiple scatt. effects in fast neutron polarisation expts., Monte Carlo anal. 78−13052
N=50 isotones populated in heavy-ion beam reactions, mag. moments, proton core polarisation 78−21598
N=82 nuclei, elastic and inelastic polarised proton scatt., isobaric analogue states 77−74825
(n,n), polarised neutrons, 2.50 MeV, meas. of small angle scattering ($<1^d$) 80−99432
neutron and nuclear polarisation expts., spin depend. of neutron cross-sections, mag. moments, radiation capture of neutrons *(Russian)* 80−52654
neutron polarisation meas. and facilities for reactions between light nuclei 77−18764
nuclear clustering, polarisation and correlation probes, (^{6}Li,^{6}Li) scatt. 79−6437
nucleus matter current density and R parameter meas. 77−30544
nucleus-nucleus pot., static polarisation effects, nuclear shapes 80−5154
off-shell effects model-independent meas. via polarisation expts. 77−18515
optical model proton scatt. parameters at subcoulomb energies 79−93584
parity nonconservation, asymmetric α-emission in polarised nuclei decay 79−6379
photon-nucleus scatt., 5 to 30 MeV 77−79359
photonuclear reactions, differential polarisation coeffs. 78−4926
photonuclear reactions, S-matrix element transformation, particle polarisation 79−89293
polarimeter designs for high energy p and d beams, polarised beam spin anal. 78−58516
polarised beams, review of appl. 79−45243
polarised deuteron beam uses in nuclear structure studies 77−71612
polarised nucleus fission, parity nonconservation mechanism, rot. state mixing *(Russian)* 80−37408
proton polarisation meas. with Si polarimetry facility 79−31346
revew of recent advances in technique 79−30822
review of research at low energies *(Russian)* 78−33162
role of polarisation in atomic and nuclear physics 80−63162
s-wave level reson., tensor analysing power far light nuclei 77−82893
semileptonic weak and EM interactions, (e,e) P-vibrations and state abnormal P admixtures 79−75977
spectroscopy by continuation of polarisation observables into nonphysical region, nuclear struct. 78−78356
spherical tensor formalism, polaris. transfer and spin correlation reactions *(Russian)* 79−59047
spin $\pm 1/2$ polarised neutrons, differential scatt. by chiral systems, coupled oscill. model 80−102177
spin 1 particles, new states of maximum polarisation, anal. power values 79−36222
spin 1/2 particles, polaris. in nucl. scatt., diffr. model anal. *(Russian)* 79−89273
spin $^1/_2$ particles scattered from nuclei, beam polarisation and nucl. recoil effects 79−67738
spin polarisation analysing power in nuclear reactions, extreme values 78−37326
spin zero nuclei+polarised proton, Coulomb multiple scatt. anal. 79−22277
spin-1 nuclei or mesons, elastic scatt., relativistic spin-1 wave eqn. EM interaction 77−50104
spin-alignment attenuation factors in mass 61-67 nuclei populated by (α, n) and (α, p) reactions 79−26390
polarisation in nuclear reactions and scattering continued
spin-polarisation analysing powers in nuclear reactors, M-matrix conditions 78−8787
spin-rotation effects in elastic proton-nucleus scattering 79−26441
stopped muons, macroscopic polarisation (Hanle) signals 80−5130
sub Coulomb elastic scatt., adiabatic and dynamic polarisation effects 79−97698
vector analysing power and polarisation studies with low energy proton and deuteron beams 77−2970
(d,α) reactions, ang. momentum transfers, determ. using polarized beams 78−37354
(d,d), pol. d, 12 MeV, A=46-82, cross sections, anal. powers, global optical model anal. 80−47459
(d,d), pol. d, 56 MeV, A=16-208, cross sections, optical parameters, anal. powers 80−78270
(d,d), pol.d, 52 MeV, A=12-197, vector anal. power and optical parameters 80−57764
(d,d) 12 MeV, tensor polarised, differential cross section, vector and tensor analysing power 78−78357
(d,d) medium heavy nuclei, optical model anal., cross sections, anal. powers 80−73839
(d,^{3}He) on ^{12}C, ^{16}O, ^{24}Mg, ^{40}Ca, 29 MeV, polarised d, low lying analogue states, DWBA anal. 78−82285
(d,t) on ^{12}C, ^{16}O, ^{24}Mg, ^{40}C, 29 MeV, polarised d, low lying analogue states, DWBA anal. 78−82285
(γ,f), linear polarised photon on even-even nuclei 80−543
^{1}H(n,n)^{1}H at 16.9 MeV, analysing power meas. 78−4941
(n,α), polarised n, expt. determination of parity violation 79−59048
(N,α) knock on reactions, final nucleus polarisation, polarised N capture 78−74352
(n,γ), polarized space parity nonconservation, optical pot. and GDR parameters *(Russian)* 80−86803
(n,γ), spin assignments using polarised neutrons and oriented target nuclei 78−29724
(n,γ), spin assignments using polarised beams and gamma spectroscopy 80−37323
(n,n), cross section and polarisation, Lane model extension to light nuclei 79−85449
(n,n), pol. n, 16.1 MeV, differential cross section, optical model fit 80−32259
(n,n) compound scatt. and optical model polarisation 77−2971
(n,p) scatt. observables, R-matrix calc., 20-140 MeV 77−57668
np radiative capture, triplet state effect, γ-ray circular polarisation meas. *(Russian)* 77−23009
(p, 2p), pol. p, quasi-free scatt. on closed shell nuclei, effective polarisation 80−91173
(p,α), polarised p, anal. power, direct 3-nucleon transfer reactions, microscopic approach review 79−6545
(p,d), pol. p, 65 MeV, A=12-94, differential cross sections and anal. powers, pickup 80−91172
(p,γ_0), polarised p in giant dipole resonance region on ^{14}C, ^{30}Si, ^{54,56,58}Fe, ^{59}Co, ^{88}Sr 78−82346
(p,n) quasielastic reaction, cross section and polarisation, Lane model extension to light nuclei 79−85449
(p,n) quasielastic reactions with polarised 22.8 MeV protons, targets A=49-208 77−6382
(p, p), 1 GeV, polarisation data, Glauber anal. spin-orbit parameters, matter distribs. 80−52655
(p,p), 1 GeV, polarisation features, Glauber model calcs. 79−40915
(p,p), 600, 750 MeV, polarisation and cross section, Glauber model calc., NN matrix test 80−47485
(p,p), cross section and polarisation, Lane model extension to light nuclei 79−85449
(p,p), elastic, inelastic polarised and unpolarised, intermediate energy study review 80−42653
(p,p), pol. p, sd, fp shell nuclei, 65 MeV, effective two-body interaction range 80−32201
(p,p), polarisation in elastic scatt., multiple diffraction approx. 79−97696
(p,p), polarised p, 0.8 GeV, neutron isotopic density differences and RMS radii 79−67643
(p,p), summed scattering (elastic and inelastic with no meson production), 2.1 GeV/c, asymmetry meas. *(Russian)* 79−89313
(p,p) 1 GeV, Glauber theory of spin-orbit interactions 78−37336
(p,p) 800 MeV, polarised p, n density uncertainties from optical model anal. 79−22185
(p,p) elastic and inelastic on s-d shell nuclei, polarised p, nuclear matter distrib. 78−78297
(p,p) isotopic effects, cross sections and polarisation ang. distrib. *(Russian)* 79−36246
(p,p) quasifree scatt., polarised p, nuclear state information 79−75846
(p,p) scatt., polarised proton, 30 MeV, optical model anal. 78−597
(p,p) scatt., with polarised protons, ang. distribs. anal. 77−2973
(p,p′), light and intermediate nuclei, analysing capacity, 2^+ state excitation 79−6558
(p,p′), scatt. of 32 MeV polarised protons, spin-flip 77−71601
(p,p′) and (e,e′) scattering, core polarisation, microscopic models, transitions, cross sections, form factors 78−604
(p,p′) inelastic scattering, spin effects, diffractive minima 78−89875
(p,p′) on light nuclei, analysing power, primary factors 79−6559
(p,p′) on light nuclei, polarised protons, analyzing power ang. depend. 77−61411
(p,π), pion prod. in proton-nucleus collisions, expt. and theoretical results, book contrib. 79−75991
(p,π), polarised p, light nuclei, cross sections, ang. distribs. and anal. power 79−85460
(p,π^+), polarised p, 200 MeV, p distortion and asymmetries 79−22285
(p,π^-), 585 MeV, A=1-208, differential cross section and pol. parameter 80−106056
(p,π^-), 585 MeV, cross sections, polarisation parameter for H, D, Be, C, O, Al, Ni, Cu, Mo, Pb targets 80−73848
(p,t), pol. p, strong ground state transitions, anomalous anal. power, direct and sequential processes 80−5115
(p, X), A=12-209, pol.p, 65 MeV, continuum spectra anal. powers 80−102178
(p,X), experimental information review, polarisation phenomena 80−42655
p-nucleus reaction at 70 GeV, μ^+ longitudinal polarisation meas. 77−2995
p+A→p+X, 800 MeV polarised protons, inclusive cross sections, analysing power 78−70524

polarisation in nuclear reactions and scattering continued
pd, elastic scatt. analysing power meas. 78−93901
pp, low energy scatt., spin depend. EM force effects, Coulomb DWBA anal. 79−9568
(t,α) reaction, 17 MeV, proton hole states in ^{187,189,191}Re 77−88025
(t,t), A=40-208, 17 MeV, pol. t, cross sections and anal. powers, optical anal. 80−47462
^{12}C(p,p), 11.5-18 MeV polarised protons, ang. distribs. 77−3010
^{2}H(d,d), 5-45 MeV deuteron wave function asymptotic D- to S-state normalisation, anal. power 80−78304
^{208}(N,γ), pol. N, anal. power and giant multipole resonances, direct-semidirect model 80−18265
Ag, static mag. moments, spin, parity and excitation energy from nuclear orientation *(Dutch)* 79−80872
Ag+^{40}Ar deep inelastic reactions, γ-ray polarisation meas., neg. deflection angles 78−8845
Ag+^{40}Ar(^{86}Kr), γ-ray circular polarisation meas. 78−54788
^{107}Ag high spin states, J$^{\pi}$ assignments, polarisations and transitions from (^{7}Li,4nγ), (^{6}Li,3nγ) 80−27536
^{109}Ag(p,p'), pol.p, 6.06 MeV, anal. powers, large absorption pot., optical model 80−83092
^{27}Al, J$^{\pi}$=5/2 state, cross section and analysing power ang. distribs. 80−18296
^{27}Al+^{16}O, 100 MeV, fragment spin orientation meas. 77−30627
^{27}Al(d,^{3}He)^{26}Mg, 12.4 MeV, tensor analysing power, D-state component in ^{3}He wave function 78−54769
^{27}Al(d,^{3}He)^{26}Mg, 12.4 MeV polarised beam, $d_{5/2}$-$d_{3/2}$ admixing in pickup strength 77−6399
^{27}Al(d,α)^{25}Mg, analysing power calc., distorted wave method 77−6404
^{27}Al(n,γ), pol. Al and n, 0.017 eV, ^{28}Al levels, transitions and spin 80−78153
^{27}Al(p,α)^{24}Mg, finite-range cluster-model description, DWBA approach 80−52667
^{28}Al levels, spins and γ-rays, multipole mixing from ^{27}Al(n,γ), pol. thermal 80−47398
Al(p,p), 36.2 MeV, differential cross section, asymmetries, 0 to 7° scatt. 78−94002
^{38}Ar(α,nγ), ^{41}Ca, spin and parity from angular distrib. and linear polarisation of γ 80−63079
^{40}Ar(d,d), optical model parameter investigation using 9-12 MeV polarised d 78−94016
^{197}Au+^{136}Xe, 1064 MeV, fragment spin orientation from continuum γ-ray anisotropy meas. 80−22853
^{197}Au(^{86}Kr,X) 612 MeV, γ-ray circular polarisation 80−13453
^{197}Au(n,γ), ^{198}Au energy level spins 79−457
^{198}Au level spin assignments from γ ang. distrib. and circular polarisation from ^{197}Au(n,γ) 80−52570
^{10}B(d,p)^{11}B, 2.5 to 21.0 MeV, angular distrib., DWBA analysis 80−68675
^{10}B(n,α)^{7}Li, thermal polarised n capture, P-odd asymmetry meas. *(Russian)* 80−13452
^{11}B(α,n)^{14}N, n polarisation ang. distrib., R-matrix anal., ^{15}N excited states 78−4937
^{11}B(p,n)^{11}C, analogue reaction at 16.3 to 26.5 MeV, polarisation transfer meas. 77−26735
^{11}B(p,n)^{11}C, shell model anal. of polarisation-analysing power differences 80−22804
^{11}B(p,p), 1.9 to 3.0 MeV, polarisation map, R-matrix study, ^{12}C 17.77 and 18.36 MeV state struct. anal. 79−9435
^{11}B(p,p), polarisation effects for elastic scatt. near (p,n) reaction threshold 78−13075
^{12}B average polarisation, form factors and partial capture rate from ^{12}C(μ^{-},ν), polarised π^{-} 79−22263
^{12}B J-transfer determ. from ^{13}C(d,^{3}He), polarised d, 29 MeV 79−49579
^{12}B polarisation, quantum mechanical explanation for ^{100}Mo(^{14}N,^{12}B) 79−17890
^{138}Ba(p,p'), 10-11.7 Mev polarised protons scatt. at IAR 77−2991
^{9}Be (p,π^{+}), 200 MeV polarised protons, differential cross sections, analysing power 78−78382
^{9}Be(^{3}He,α)^{8}Be, j-depend. of analysing powers, ^{8}Be spectroscopic factor 77−328
^{9}Be(^{3}He,d)^{10}B, j-depend. of analysing powers, ^{10}B spectroscopic factors 77−328
^{9}Be(^{3}He,p), 14 MeV, proton polarisation, ang. distribs., differential cross section 77−82944
^{9}Be(d,n)^{10}B, polarised 4.5 MeV neutron source 77−57790
^{9}Be(d,p), 12 MeV polarised deuterons, analysing powers, j-mixing ratio 77−82937
^{9}Be(d,t), 12 MeV polarised deuterons, analysing powers, j-mixing ratio 77−82937
^{9}Be(γ,π), photoabsorption and sum rules, structure, RMS radius, polarisability and exchange parameters 80−22686
^{9}Be(n,n), 2-5 MeV polarised neutrons, analysing power, R-function and phase-shift anal. 77−23088
^{9}Be(n,n), cross sections and polarisation from Lane model anal., multichannel constraints 79−80914
^{9}Be(p,n), cross sections and polarisation from Lane model anal., multichannel constraints 79−80914
^{9}Be(p,p), 22-8 MeV, polarised protons, R-matrix theory 77−82921
^{9}Be(p,p), cross sections and polarisation from Lane model anal., multichannel constraints 79−80914
^{9}Be(p,p), polarisation effects for elastic scatt. near (p,n) reaction threshold 78−13075
^{9}Be(p,p) polarisation behaviour near (p,n) threshold, virtual scatt. mechanism feasibility 79−6592
^{9}Be(t,t)^{9}Be, 15, 17 MeV, polarised t, differential cross sections and optical model fits 78−41730
^{209}Bi(p,p'(d)X), pol. p, 65 MeV, anal. powers of continuum energy spectra 80−68637
Bi(n,n), 10 MeV, neutron polarisation meas. at small angles 77−3014
Bi(n,n), 10.4 MeV, polarised neutrons, analysing power 77−30545
Bi(n,n), 2.5 MeV, small angle scatt., cross section, asymm. 78−74361
C (π^{-},p) 1.5-5 GeV/c, cumulative proton polarisation *(Russian)* 80−86896
^{12}C J-transfer determ. and isospin mixing from ^{13}C(d,t) polarised d 79−49579
^{12}C mag. transition form factors, core polarisation and exchange current effects 79−75899
^{12}C μ capture rate, average nuclear polarisation, elementary particle approach 78−66246
^{12}C p_0 channel E2 strength from ^{11}B(p,γ) pol p. 80−22790
polarisation in nuclear reactions and scattering continued
^{12}C, quasielastic scatt. of polarised 635 MeV protons, depend. of left-right asymm. on nucl. momentum *(Russian)* 77−79384
^{12}C+^{6}Li(^{7}Li), 9 MeV, isotopic shape effects in elastic scatt. of aligned ions 78−89904
^{12}C(^{3}He,^{3}He), 20.5-33.0 MeV, energy depend. of analysing power optical model 78−17226
^{12}C(^{3}He,α)^{11}C, j-depend. of analysing powers, ^{11}C spectroscopic factors 77−328
^{12}C(^{3}He,d)^{13}N, j-depend. of analysing powers, ^{13}N spectroscopic factors 77−328
^{12}C(^{6}Li,α)^{14}N, E(^{6}Li)=20 MeV, using polarised ^{6}Li source, exact finite range DWBA anal. 78−58293
^{12}C(^{6}Li,d), ^{12}C(^{6}Li,α), 20 MeV, analysing powers 78−46098
^{12}C(^{6}Li,d)^{16}O, 20 MeV polarised ^{6}Li, DWBA calc. of analysing powers, 0^{+} g.s. and 2^{+} state of ^{16}O 79−6678
^{12}C(^{6}Li,d)^{16}O, 20 MeV polarised ^{6}Li, DWBA calc. of analysing powers for ^{14}N 1^{+} states 79−6679
^{12}C(d,α)^{10}B, 20.7 and 29 MeV, polarised deuterons 77−82938
^{12}C(d,n), 6-10 MeV polarised deuterons, differential cross-section, vector analysing power 77−6398
^{12}C(d,p_0)^{13}C, proton polarisation in stripping reaction, obs. and DWBA calc. 79−30816
^{12}C(e,e'), 12.71 MeV 0^{+} to 1^{+} transition, axial isoscalar neutral current, polarisation asymmetry 79−26425
^{12}C(μ^{-}, ν)^{12}B, polarisation studies, muon capture, weak interaction aspects 80−68655
^{12}C(μ^{-},ν)^{12}B*, average polarisation of recoil ^{12}B in direct capture 79−93602
^{12}C(μ^{-},ν)^{12}B(g.s.), qualitative meas. of longitudinal recoil polarisation 79−54429
^{12}C(n,n')C* 15.85 MeV polarised neutrons, analysing power meas. 77−2969
^{12}C(n,n), 15.85 MeV polarised neutrons, analysing power meas. 77−2969
^{12}C(n,n), spin-flip probability to first 2^{+} level 80−78288
^{12}C(n,n)^{12}C, polarised neutron scatt. 77−26734
^{12}C(p,γ)^{13}N, pol. p, 10-17 MeV, ^{13}N electric quadrupole strength semi-direct capture model calcs. 80−47370
^{12}C(p,p'), 0.8 GeV, polarised p, spin orbit deformation effects, DWBA anal. 79−30832
^{12}C(p,p'), 1 GeV, proton polarisation in natural parity level excitation *(Russian)* 80−42634
^{12}C(p,p'), 185 MeV, elastic and inelastic scatt., proton polarisation and ang. distribs. 79−59060
^{12}C(p,p'), 50, 65 MeV, isospin depend. on analysing powers 78−82343
^{12}C(p,p'), 64 MeV, direct reaction, model t-matrix test, cross section and anal. power 79−93594
^{12}C(p,p'), natural parity level excitation *(Russian)* 80−5144
^{12}C(p,p'), pol. p, 800 MeV, unnatural parity states excitation, anal. powers and isospin 80−68538
^{12}C(p,p'), spin flip excitation of 1^{+} T=0 state 78−8817
^{12}C(p,p')^{12}C*, pol. p., 19-23 MeV, giant resonances as doorway states, virtual excitation 80−5102
^{12}C(p,p')X, 316, 516 MeV, analysing powers at backward angles 78−46062
^{12}C(p,p'), 20-40 MeV, pol. p, anal. powers, imaginary spin-orbit pot., coupled channels anal. 80−102179
^{12}C(p,p'), polarised p, 20, 30, 40 MeV, anal. power and cross sections, spin-orbit deformation 79−75963
^{12}C(p,p), 0.8 GeV, polarised p, differential cross section, anal. power, nuclear matter densities 79−13299
^{12}C(p,p), 11.5 to 18 MeV polarised beam, ^{13}N level structure 77−315
^{12}C(p,p), 40-75 MeV, polarisation meas., differential cross sections 80−52840
^{12}C(p,p), 6-8 MeV polarised proton calib. standard 77−10573
^{12}C(p,p), elastic and inelastic scatt., 185 MeV, polarisation, diffraction model anal. 79−75943
^{12}C(p,p), pol. p, 14.23 MeV resonance broadening, nuclear recoil, atomic excitation effects 80−102165
^{12}C(p,p), pol. p, 450-600 keV, Mott-Schwinger interaction existence, anal. power 80−22805
^{12}C(p,p), spin rotation angle meas. appl. to phase shifts 77−3011
^{12}C(p,p) quasielastic scatt., 635 MeV polarised protons, asymm. meas. *(Russian)* 77−74852
^{12}C(p,p)^{12}C, 1 GeV, polarisation meas. 77−88103
^{12}C(p,pn), pol. nucleon quasi-elastic scatt., nuclear wave function and model tests 80−42656
^{12}C(p,π^{+}), 200 MeV polarised protons, differential cross sections, analysing power 78−78382
^{12}C(p,π^{+})^{13}C, polarised protons, π distortion effect on asymmetry 78−50176
^{12}C(t,t)^{12}C, 15, 17 MeV, polarised t, differential cross sections and optical model fits 78−41730
^{13}C+^{6}Li(^{7}Li), 9 MeV, isotopic shape effects in elastic scatt. of aligned ions 78−89904
^{13}C(d,X), 13 MeV, cross section, vector and power, optical model parameters, DWBA anal. 79−22301
^{13}C(p,α)^{10}B$_{g.s.}$, 65 MeV, pol. p, DWBA form factor 80−52559
^{13}C(p,γ), pol. p, 6.25-17.0 MeV, anal. power and cross section ang. distribs., E1, E2 amplitudes 80−47461
^{13}C(p,p), 9.1-18.4 MeV, polarised p, cross section phase-shift anal., ^{14}N possible resonances 79−6602
^{14}C(p,n)^{14}N, n polarisation ang. distrib., R-matrix anal., ^{15}N excited states 78−4937
^{16}C(p,π^{+})^{13}C, polarised protons π distortion effect on asymmetry 78−50176
^{A}Ca(p,p'), pol. p, A=40,48, 800 MeV, diff. cross sections, anal. powers, DWIA anals., high spin levels 80−83067
^{A}Ca(p,p), 800 MeV, polarised p, A=40, 42, 44, 48, differential cross sections and anal. powers 79−36244
^{40}Ca (p,2p), polarised p, 200 MeV, quasi-elastic scatt., asymmetry meas. 79−67755
^{40}Ca (p,p), elastic scatt., polarisation and spin-orbital amplitude parameters, 1 GeV *(Russian)* 78−17208
^{40}Ca+^{16}O, polarisation of single particle states, two centre shell model 77−30622
^{40}Ca(^{16}O,^{15}N)^{41}Sc, effect of polarisation of shell-model states 77−67768
^{40}Ca(^{16}O,^{15}N)^{41}Sc, DWBA anal. including nuclear wave function polarisation 78−629

polarisation in nuclear reactions and scattering continued
^{40}Ca(^{3}He, x), pol. ^{3}He, x=d or α, 33 MeV, anal. power and cross sections 80−42628
^{40}Ca(^{3}He,^{3}He), pol. ^{3}He, 33.3 MeV, differential cross section and anal. power, optical pots. 80−42627
^{40}Ca(d,α)^{38}K, 7.5, 7.75, 8.0 MeV, polarised d, J^{π} assignment 77−6401
^{40}Ca(d,p)^{41}Ca(J^{+}) 11.0 MeV, analysing powers, CCBA and DWBA anal. 77−6402
^{40}Ca(μ,nν_{μ}), neutron longitudinal polarisation anal. 77−30559
^{40}Ca(n,γ), 10 MeV polarised neutrons, ^{41}Ca giant dipole resonance 79−93620
^{40}Ca(p,2p) 200 MeV polarised p, spin-orbit effects 79−89222
^{40}Ca(p,α), polarised p, 22.0 MeV, analysing power J dependence 79−67740
^{40}Ca(p,p), 1.04 GeV elastic scatt., polarisation 78−21549
^{40}Ca(p,p), 20-50 MeV differential cross section, polarisation ang. distrib., optical model exchange terms 80−27638
^{40}Ca(p,p), elastic and inelastic scatt., 185 MeV, polarisation, diffraction model anal. 79−75943
^{41}Ca(d,p)^{42}Ca, 11 MeV, cross section, vector analysing power, spectroscopic strengths 78−74374
^{48}Ca(d,p), 11.9 MeV, analysing power, cross section, ^{49}Ca levels, spins, parities, spectroscopic factors 78−78391
^{48}Ca(d,t)^{47}Ca, 13.5 MeV, polarised deuterons, low-lying levels in ^{47}Ca 78−13114
^{112}Cd(p,α)^{109}Ag, 22 MeV, analysing power, J-depend., DWBA 78−70523
^{112}Cd(p,p'), 30 MeV polarised proton inelastic scatt., phonon states 77−2982
^{114}Cd(p,p'), 11 MeV, polarised p, differential cross sections, anal. powers, spin flip prob. 79−89284
^{114}Cd(p,p'), optical pot. deform. effect on analysing power and p-γ ang. correlations 79−17903
^{116}Cd(p,t), 22 MeV, polarised p, anal. power systematic nuclear struct. depend. 79−22265
^{37}Cl(d,d), 12.0 MeV, polarised deuterons, vector analysing power 77−14094
^{37}Cl(d,t)^{36}Cl, 12.0 MeV, polarised deuterons, vector analysing power 77−14094
C(n,n), total cross sections below 2 MeV, R-matrix fits to data 80−13466
^{59}Co, deformation effect of aligned target, fast-neutron transmission 80−47364
^{59}Co+n, 8-31 MeV, spin-spin depend. of total cross section 78−17172
^{59}Co(n,n), compound nucl. effects in spin-spin cross-sections 77−10402
^{59}Co(n,n), spin-spin cross-section for polarised neutron and target, 0.4 to 30 MeV 77−26656
^{59}Co(p,γ_0), polarised p, 5.8 to 16.5 MeV, cross section and analysing power ang. distrib., model comparison 78−70533
C(p,p), 36.2 MeV, differential cross section, asymmetries, 0 to 7° scatt. 78−94002
^{50}Cr(d,d), 12.3 MeV polarised deuterons, precision tensor analysing power meas. 77−3019
^{50}Cr(d,p), 12.3 MeV polarised deuterons, analysing powers, ^{51}Cr spin assignments 77−30608
^{52}Cr(d,p), polarised d, obs. of D-state and compound nucleus effects 77−34319
^{54}Cr(d_{pol},p), cross section and vector analysing power, ^{55}Cr deduced levels and spins 80−52684
^{63}Cu(α,p)^{66}Zn, proton polarisation calc., distorted wave method 77−6404
^{63}Cu(d,^{3}He), 9 MeV, polarised d, tensor anal. power and D-state effects 79−85446
Cu(n,n), 14.2 MeV, polarisation in forward angle scatt. 80−18282
Cu(n,n), 16.1 MeV, 2.9 MeV, differential cross section and polarisation meas. 77−3013
Cu(n,n), 16.1 MeV, polarisation meas., optical model anal. 79−22264
Cu(n,n) 2.9 MeV, elastic differential cross section and polarisation ang. depend., statistical anal. 79−45264
Cu(π^{-},p) 1.5-5 GeV/c, cumulative proton polarisation *(Russian)* 80−86896
(d,d), A=24-54, pol.d, 20 MeV, quadrupole transition amplitudes 80−99148
(d,p), A=88-106, pol. d, excitation curve isospin anomaly, neutron single particle resonances 80−27595
D(p,p), 630 MeV, asymmetry in scatt. polarised protons *(Russian)* 78−46064
^{A}Dy(α,xnγ), A=162,164, Er yrast levels, spin alignment 80−52557
^{152}Dy yrast continuum γ-ray multipolarity via polarisation meas. from ^{140}Ce(^{16}O,4n) 80−9264
^{152}Dy yrast line single particle nature at high ang. momentum from Sn(^{22,24}S, 4n) 79−71783
^{166}Er(t,α), 17 MeV polarised tritons, ^{165}Ho levels, analysing powers, spins 78−78390
^{17}F 14.174 MeV T=3/2 level, spin assignment from ^{16}O(p,p'), polarised p 79−67648
^{18}F 1.04 MeV state lifetime and γ-transition polarisation from ^{18}O(p,n) 80−106016
^{18}F (e,e'), polarised e, parity mixing and form factors from elementary particle theory anal. 79−89233
^{19}F, nuclear dealignment of multiply ionised 3 and 6 MeV atoms recoiling in gases 80−78267
^{19}F(d,α)^{17}O, 1.8 to 3.0 MeV, vector analysing ability using polarised deuterons *(Russian)* 80−32288
^{19}F(d,d), energy depend. of vector analyzing capacity, 1.8 to 3.0 MeV, 120 to 150° scatt. 79−9592
^{19}F(d,d)^{19}F, 1.8 to 3.0 MeV, vector analysing ability using polarised deuterons *(Russian)* 80−32288
^{19}F(p,p'), 5.5 MeV; time differential obs. of perturbed γ linear polarisation distrib., Hanle effect 78−78360
^{20}F cross sections and anal. power, compound nucleus contrib. Ericson fluctuations from ^{18}O(d,p), pol. d 80−22803
^{A}Fe(d_{pol},p), A=54,58, cross section and vector analysing power, ^{55,59}Fe deduced levels 80−52684
^{54}Fe(p,p'), pol. p, 800 MeV, diff. cross sections, anal. powers, DWIA anals. 80−83067
^{54}Fe(p,p), 800 MeV, polarised differential cross sections and anal. powers, n density 79−13297
^{56}Fe(t,p)^{58}Fe, 17 MeV, polarised triton, meas. and two-step calcs. 77−54204
^{57}Fe, γ-ray emission, test of time reversal invariance 78−29421
polarisation in nuclear reactions and scattering continued
^{58}Fe levels, J^{π}, anal. powers and cross sections from ^{56}Fe(t,p) pol.t 80−68539
Fe(n,n), 2.9 MeV, differential cross section and polarisation meas. 77−3013
Fe(n,n) 2.9 MeV, elastic differential cross section and polarisation ang. depend., statistical anal. 79−45264
Fe(p,p), 36.2 MeV, differential cross section, asymmetries, 0 to 7° scatt. 78−94002
Fe(p,p'), A=54,6, E=17.2, 20.4, 24.6 MeV polarised protons, optical model, DWBA anal. 78−13094
^{156}Gd(t,α), 17 MeV, pol. t., ^{155}Eu single proton states, spins and parity, rot. bands 79−30766
^{A}Ge(d,d) 16 MeV, A=70-74, polarised d, elastic and inelastic, levels and deformation 79−554
^{A}Ge(t,p), pol.t, A=70,72, octupole oscillations modes from anal. powers, 3_1^- octupole transition 80−102142
^{66}Ge states and decay scheme, polarisations J^{π} and ang. distribs. from ^{58}Ni(^{10}B,pnγ) 80−22692
^{70}Ge level spin and parity assignments from ^{56}Fe(^{16}O,2pγ), ^{67}Zn(α,nγ), ^{68}Zn(α,2nγ) 79−3081
^{70}Ge(d,t),(d,p), differential cross sections and vector analysing powers 78−17221
H(^{3}He,^{3}He), 33 MeV, ^{3}He polarisation anal. power meas. optical model anal. 77−38286
^{1}H+d, polarised projectile, parity nonconservation in low energy scatt. 78−66271
^{1}H(d,d), 2 GeV, polarised d, tensor and vector asymmetries 80−9285
^{1}H(d,d), 35, 45 MeV, d wave function D- to S-state ratio from anal. power and cross section 79−89314
^{1}H(d,d), 45.4 MeV, tensor anal. powers 79−85447
^{1}H(d,d), elastic backward scatt., GeV energies, tensor anal. power 79−80916
^{1}H(d,d), polarised d, 5-13 MeV, analysing powers 79−71833
^{1}H(d,d), polarised p and d, analysing power data 79−71830
^{1}H(d,d) 10, 20 MeV, 79−13304
^{1}H(d,pn), 45.4 MeV, tensor anal. powers 79−85447
^{1}H(γ,π^{0}), polarised γ, 0.76-1.3 GeV, asymmetry meas. in photoprod. cross section *(Russian)* 79−59051
^{1}H(n,γ), polarised neutrons, calc. of P-violating asymmetry 77−18565
^{1}H(n,γ), thermal calc. of γ-circular polarisation, p-nonconservation effects 77−18564
^{1}H(n,n), 14.2 MeV, polarised n, analysing powers 79−71832
^{1}H(n,n), 16.9 MeV, anal. power, F-wave contribs. 80−63158
^{1}H(n,n), pol. n, 13.5-16.9 MeV, anal. power and spin-orbit phase parameters 80−78269
^{1}H(n,n), pol. n, 50 MeV, anal. power 80−68639
^{1}H(n,n)^{1}H, 50 MeV polarised neutrons 77−26732
^{1}H(n,n)^{1}H, polarised neutron scatt. 77−26734
^{1}H(n,n)^{1}H analysing power, 14.5 MeV, Hamburg polarised neutron facility, initial expts. 77−26946
^{1}H(n,n)^{1}H, 14 MeV polarised neutrons, analysing powers 77−54210
^{1}H(n,p), pol. n and p, 220-495 MeV, free elastic scatt., D_t and P parameters 80−52674
^{1}H(n,p), pol. n and p, 220-495 MeV, free elastic scatt., Wolfenstein parameters R_t, A_t 80−52675
^{1}H(n,p)n, 50 MeV, polarisation parameter meas. 78−50148
^{1}H(n,p)n, pol. n,p, 50 MeV, spin correlation parameter $A_{yy}(\theta)$, phase shift anal. 80−68530
^{1}H(p,p), 1-3 GeV/c, pol. p, spin parameters A and A_{nn} 80−95304
^{1}H(p,p), 225, 327, 520 MeV, analysing powers 79−75961
^{1}H(p,p), 398-572 MeV, analysing power meas., EM-nuclear interf. 77−23008
^{1}H(p,p), 6.14 MeV, cross sections and anal. power for noncentral reaction 79−85444
^{1}H(p,p), 6.141 MeV, anal. power, Paris pot. predictions 80−63156
^{1}H(p,p), pol.p, 9.57 MeV, spin correlation parameter, phase shift anal. 80−102112
^{1}H(p,π^{+})^{2}H, pol. p, total cross section, ang. distribs. and asymmetry parameters 80−63182
^{1}H(p,π^{+})^{2}H, SIS, 578 MeV, pol. beam and target, spin depend. parameters 80−42651
^{1}H(p,π^{+})pn, polarised p, 305, 330 MeV, pion production differential cross section 79−67754
^{2}H, dynamic and static polarisability from Rayleigh scatt., two-photon disintegration 79−75867
^{2}H-N breakup calcs., separable interactions with P-waves and tensor forces, polarisation 77−50101
^{2}H+p, 50 MeV polarised p scatt., analysing power meas. 77−71608
^{2}H+p, polarised projectile, parity nonconservation in low energy scatt. 78−66271
^{2}H+p, polarised projectile, parity nonconservation in low energy scatt. 78−70522
^{2}H(^{3}He,^{4}He)^{1}H, 27 and 33 MeV, polarised ^{3}He beam analysing power and cross sections 79−89316
^{2}H(α,^{3}He(g.s.))p tensor polarisation ang. distribs. from sequential decay ^{2}H(α,p)^{3}He(α)n reaction 77−82899
^{2}H(α,^{6}Li)n, ^{6}Li tensor polarisation and cross sections 79−75967
^{2}H(α,n)αp, 100 MeV, differential cross-section and polarisation meas. 77−88157
^{2}H(α,np)^{4}He, differential cross section and polarisation, three body model 80−47460
^{2}H(d,n), 290, 460 keV, neutron polarisation, ang. depend. 80−42632
^{2}H(d,n), anal. power, comparison with mirror reaction (d,p) 79−75964
^{2}H(d,n), pol.d, anal. power and polarisations in R-matrix methodology, comparison with (d,p) 80−78273
^{2}H(d,n), polarised d, <5.5 MeV, comparison of analysing power with ^{2}H(d,p) 79−17911
^{2}H(d,n)^{3}He, 1.5-15.5 MeV, tensor anal. power, charge symmetry violation in mirror reaction 80−13368
^{2}H(d,n)^{3}He, 35-275 keV, neutron polarisation determ. 77−41942
^{2}H(d,n)^{3}He, neutron polarisation meas. with Mott-Schwinger scatt. polarimeter 79−22571
^{2}H(d,n)^{3}He and ^{2}H(d,p)^{3}H, comparison of analysing powers 2.5 to 11.5 MeV 79−6628
^{2}H(d,p), anal. power, comparison with mirror reaction (d,n) 79−75964
^{2}H(d,p), pol.d, anal. power and polarisations in R-matrix methodology, comparison with (d,n) 80−78273
^{2}H(d,p), polarised d, <5.5 MeV, comparison of analysing power with ^{2}H(d,n) 79−17911
^{2}H(d,p)^{3}H, ^{2}H(d,n)^{3}H, analysing power meas. 78−25204

polarisation in nuclear reactions and scattering continued
^{2}H(d,p)^{3}H, 13.4, 17 MeV, pol. d, anal. power direct reaction and isospin symmetries 80−515
^{2}H(d,p)^{3}H, 1.5-15.5 MeV, tensor anal. power, charge symmetry violation in mirror reaction 80−13368
^{2}H(e, e)pn, polarised e, neutral weak currents, right-left asymmetry 79−80787
^{2}H(e,e'), 19.4 GeV, polarized electrons, parity violation 79−13286
^{2}H(e,e), electric and mag. scatt., tensor polarisation, mesonic exchange current effects 79−85374
^{2}H(e,e), form factors, tensor pol., and two-nucleon force calcs. 80−106045
^{2}H(e,e), tensor polarisation and d wave function short range behaviour 79−40900
^{2}H(e,e), tensor polarisation and d wave function short range behaviour 79−67564
^{2}H(γ, π^-)2p, target asymmetry and effective neutron polarisation, polarised d 80−9286
^{2}H(γ,n), 20.3 MeV, linearly pol. γ, neutron yield and cross section 80−91171
^{2}H(γ,n)^{1}H, 400-700 MeV, p polarisation *(Russian)* 80−106046
^{2}H(γ,n)p, 375-650 MeV, proton polarisation energy depend. at CMS angle 90° *(Russian)* 80−63159
^{2}H(γ,n)p, cross section and polarisation with arbitrary number of EM multipoles 79−80923
^{2}H(γ,n)p, cross section asymmetry polarised photons 400 to 600 MeV, resonances *(Russian)* 79−89294
^{2}H(γ,n)p, differential cross section and proton polarisation using supersoft core pot. 79−89287
^{2}H(γ,np), 325-725 MeV, proton polarisation anomalous struct. 77−30551
^{2}H(γ,π^0)^{2}H, recoil deuteron polarisation statistical tensors anal. 78−74348
^{2}H(n,n')pn, polarised n, 14, 30 MeV, neutron analysing power 79−71835
^{2}H(n,n), 30 MeV, plarisation asymm., analysing power 78−62538
^{2}H(n,n), polarised n, anal. power predictions 79−85445
^{2}H(n,n) 14.2 MeV, polarised n, analysing powers 79−71832
^{2}H(n,n)^{2}H, 12 MeV, polarised neutrons, analysing power meas. 78−33193
^{2}H(n,n)^{2}H, 14 MeV polarised neutrons, analysing powers 77−54210
^{2}H(n,n)^{2}H, 2.45 MeV, polarised n, depolarisation factor ang. distrib., phase shifts 78−78358
^{2}H(n,n)^{2}H, 2.6 MeV polarised beam, ang. variation of polarisation 77−26733
^{2}H(n,n)^{2}H, 50 MeV polarised neutrons 77−26732
^{2}H(n,n)^{2}H, polarised n, 12 MeV, analysing power, similarity with (p,p) scatt. 78−70514
^{2}H(n,n)^{2}H, polarised neutron scatt. 77−26734
^{2}H(n,n)^{2}H analysing power, 14.5 MeV, Hamburg polarised neutron facility initial expts. 77−26946
^{2}H(p,2p)n, 15 MeV, polarised p, cross section in non-coplanar geometry 78−93997
^{2}H(p,2p)n, 22.7 MeV, proton analysing power 80−78302
^{2}H(p,γ), 7-15 MeV, polarised and unpolarised p, cross section and anal. power 79−40921
^{2}H(p,n)2p, pol. n and p, 10.6-15.1 MeV, transverse polarisation transfer at 0° 80−42630
^{2}H(p,p), 10 MeV, differential cross section, p and d analysing powers 78−46063
^{2}H(p,p), 600 MeV and 1 GeV, noneikonal theory 79−80930
^{2}H(p,p), 800 MeV, differential cross sections and anal. powers 80−83091
^{2}H(p,p), large angle scatt., cross section and anal. power 79−80917
^{2}H(p,p), pol.p, spin rot. and depolarisation, NN amplitude double spin flip part 80−78271
^{2}H(p,p), polarised p, 14.1 MeV, analysing power 79−71831
^{2}H(p,p), polarised p, 2.5-6.5 MeV, vector and tensor anal. powers 79−63653
^{2}H(p,p), polarised p, 316, 516 MeV, anal. powers in resonance region, backward angle scatt. 79−71834
^{2}H(p,p), polarised p, medium and high energies, polarisation phenomena 79−85448
^{2}H(p,p) 17, 20, 24 MeV, polarised p and d, analysing power data 79−71830
^{2}H(p,p)^{2}H, 316, 516 MeV, backscatt. anal. power meas. 78−74368
^{2}H(p,p)pn, polarised p, vector anal. power in final state interaction region 79−71836
^{2}H(p,pp)n, polarised p, polarisation effects in 3-body system 79−80946
^{2}H(p,π^-), 400-470 MeV, backward π differential cross sections and anal. power 80−86905
^{2}H(p,π^+), polarised p, 305, 330 MeV, pion production differential cross section 79−67754
^{2}H(π, π) 25-180 MeV, three body calc. up to (3,3) resonance, polarisations 79−40964
^{2}H(π,π), 140-260 MeV, (3,3) region, tensor force, cross sections, pol. parameters 80−68641
^{2}H(π,π), 142, 256 MeV, form factor−backward scatt. correlation, tensor polarisation 80−99189
^{2}H(π,π), effect of genuine π absorpt. and emission 79−17939
^{2}H(π,π), polarised d, dibaryon resonance signals in excitation functions 80−9181
^{2}H(π,π), relativistic description, πN waves, NN rescatt., ρ-exchange, π absorption and emission 80−9310
^{2}H(π,π)^{2}H, 142 MeV, elastic cross section and polarisation observables 79−75791
^{2}H(π^+,π^+), tensor polarisation and cross section at 180° 80−5116
^{2}H(t,n)^{4}He, 10.5 MeV polarised tritons, analysing power, polarisation function and transfer coeff. 77−10413
^{2}H(t,t)^{2}H, 10.5 MeV polarised tritons, analysing power meas. 77−10413
(^{3}H,^{3}H), polarised scatt., optical model parameters 78−70540
^{3}H(^{3}He,^{3}He), 20-33 MeV, analysing power, differential cross section meas. 78−17227
^{3}H(d,n), pol. d, below 6.75 MeV, tensor anal. power 80−42633
^{3}H(d,n)^{4}He, 700 keV, n polarisation meas., scintillation + TOF technique 78−86538
^{3}H(γ,π^0), polarisation effects 180 to 700 MeV, impulse approx. calcs. *(Russian)* 80−37368
^{3}H(γ,π^0)^{3}H, polarisation effects 180 to 700 MeV, impulse approx. calcs. *(Russian)* 80−37368
^{3}H(p,γ), 6 to 16 MeV polarised protons, ^{4}He excited states 77−18559
polarisation in nuclear reactions and scattering continued
^{3}H(p,n)^{3}He, R-matrix anal. of polarisation and analysing power 77−88142
^{3}H(p,p), 1.26-3.71 MeV polarised p, spin depend. N-N forces 79−6634
^{3}H(p,p), 5.8 and 6.8 MeV, phase shift anal. *(Russian)* 77−65225
^{3}H(p,p), 8 to 17.1 MeV, cf. neutron polarisation in ^{3}He(n,n) 78−25171
H(d,d), A=1, 2, E=52 MeV, polarised deuterons, vector analysing power 78−584
H(d,pp)n, polarised d, polarisation effects in 3-body system 79−80946
He+p, A=3,4, polarised projectile, parity nonconservation in low energy scatt. 78−66271
He+p, A=3,4, polarised projectile, parity nonconservation in low energy scatt. 78−70522
He(^{3}He,^{3}He), 33 MeV, ^{3}He polarisation anal. power meas. optical model anal. 77−38286
(^{3}He,^{3}He), 18-33 MeV polarised ^{3}He, ^{6}Be excitation 78−78400
(^{3}He,p), proton polarisation meas. with Si polarimetry facility 79−31346
(^{3}He, ^{3}He), coupled reaction channel effects on polarisation 79−85442
(^{3}He, ^{3}He), pol. ^{3}He, vector and tensor polarisation, closed form description 80−37363
(^{3}He, ^{3}He) scatt., polarisation effects, phenomenological ^{3}He pots. 79−97712
^{3}He(^{3}He,p)^{4}He, polarisation meas. in final state interactions 77−18589
^{3}He(^{3}He,p)^{5}Li, polarised protons, deuteron transfer obs. 77−329
^{3}He(α,α), 24.5 to 42.0 MeV, meas. of polarisation analysing power 77−3026
^{3}He(d,d), 0.32-5.0 MeV, anal. power, scatt. amps., ^{5}Li states, phase shift anal. 80−47382
^{3}He(d,d), polarised d, 10-17 MeV, cross sections, vector and tensor anal. powers 79−75966
^{3}He(d,d), polarised d, 1.5-11.5 MeV, differential cross sections and anal. powers 79−85443
^{3}He(d,p), 6.44 MeV polarised d, absolute standard of d vector analysing powers 77−34281
^{3}He(d,p), pol. d, below 6.75 MeV, tensor anal. power 80−42633
^{3}He(d,p), polarised d, 10-17 MeV, cross sections, vector and tensor anal. powers 79−75966
^{3}He(d,p)^{4}He, 8.5-10.5 MeV polarised deuterons, max. tensor analysing power 77−6397
^{3}He(γ,π^0), polarisation effects 180 to 700 MeV, impulse approx. calcs. *(Russian)* 80−37368
^{3}He(γ,π^0)^{3}He, polarisation effects 180 to 700 MeV, impulse approx. calcs. *(Russian)* 80−37368
^{3}He(n,n), 2.63 MeV polarised neutrons, asymmetry 77−26736
^{3}He(n,n), 3.7-15.3 MeV, polarised n, analysing power, A=4 system neutron channels 79−75965
^{3}He(n,n), 8 to 17.1 MeV, cf. proton polarisation in ^{3}H(p,p) 78−25171
^{3}He(p,p), 1.75 to 4.50 MeV polarised protons, analysing power meas. for ^{4}He T=1 level ordering 79−26438
^{3}He(p,p), 6.8 to 16.2 MeV, optical model pot. calcs. of cross section and polarisation data 79−63672
^{3}He(p,p), pol. p, 0.3-1.0 MeV, differential cross section, anal. power, and phase shifts 80−42629
^{3}He(p,p), polarised p, 6.8-10.7 MeV, polarisation transfer coeffs. 79−17889
^{3}He(p,p), polarised p, below 6 MeV, anal. power meas. for four nucleon system levels 79−71837
^{3}He(p,p)^{3}He, 2.3 to 8.8 MeV, ang. distribs. of analysing power 78−78375
^{3}He(p(polarised),p)^{3}He, nuclear force and T-violation effects 78−4797
^{3}He(t,d)^{4}He, 9-17 MeV, polarised tritons, analysing-power ang. distrib. meas. 78−29481
^{3}He(t_{pol},t)^{3}He, 9-17 MeV, analysing power, differential cross sections 77−74829
^{4}He (d,d), 17-45 MeV, differential cross section and tensor and power ang. distribs. 80−42631
^{4}He (d,d), pol. d, 20 MeV, optical pot. strong tensor term, anal. powers 80−37364
^{4}He (d,d) pol. d, 17-43 MeV, vector anal. power, highly excited six nucleon system 80−47458
^{4}He (p_i,p), high and intermediate energies, polarisation, research review 78−94010
^{4}He(^{3}He,^{3}He), 18-22 MeV, analysing power ang. distrib., differential cross sections, ^{7}Be excited state 78−46078
^{4}He(^{6}Li, ^{6}Li), 15.1-22.7 MeV, polarised Li, vector anal. power, spin-orbit pot. 79−67737
^{4}He(^{6}Li,γ)^{10}B, test of weak-interaction models 77−331
^{4}He(d,d), cross sections and polarisation parameters, three-body NNα model *(French)* 77−71598
^{4}He(d,d), noncentral forces, Pauli principle effects on d polarisation, orthogonality condition model 79−6614
^{4}He(d,d), pol. d, 12-17 MeV, differential cross sections, anal. powers, phast shift anal. 80−13449
^{4}He(d,d), polarised d, 20.2 MeV, elastic scatt. tensor anal. power 79−85450
^{4}He(d,d)^{4}He, 6-7 MeV, polarised d, ^{6}Li 1^+ reson., analysing powers 77−88095
^{4}He(d,n)αp, 50 MeV, differential cross-section and polarisation meas. 77−88157
^{4}He(d,p)^{4}He n, 15 MeV polarised deuterons, differential cross sections, vector analysing powers 78−89884
^{4}He(d,pn)^{4}He, differential cross section and polarisation, three body model 80−47460
^{4}He(γ,π^0), polarisation effects 180 to 700 MeV, impulse approx. calcs. *(Russian)* 80−37368
^{4}He(n,n), 2-5 MeV polarised neutrons, analysing powers, R-function and phase shift anal. 77−23088
^{4}He(p, p), 1.05 GeV, cross sections and polarisations, correlation effects calcs. 80−57774
^{4}He(p, p), 225, 327, 520 MeV, analysing powers 79−75961
^{4}He(p,2p), pol. nucleon quasi-elastic scatt., nuclear wave function and model tests 80−42656
^{4}He(p,p), 0.35-23.1 GeV, differential cross section and polarisation, Glauber theory *(Chinese)* 79−49628
^{4}He(p,p), 0.5-1.7 GeV, differential cross section and polarisation meas. 79−22295
^{4}He(p,p), 185 to 500 MeV, large angle cross section, analysing power 78−74363
^{4}He(p,p), 200-500 MeV, differential cross section and anal. power 80−68640

polarisation in nuclear reactions and scattering continued
^{4}He(p,p), 45, 52, 60, 65 Mev, cross sections and polarisation meas. 79−97706
^{4}He(p,p), medium energy, anal. power, relativistic optical model anal. 79−40925
^{4}He(p,p) elastic scatt., polarisation meas. 0.56 to 1.73 GeV, $0.006 \leq -t \leq 1.2$ (GeV/c)^{2} 77−57664
^{4}He(p,p')^{4}He elastic scatt., 11.93, 17.00 MeV, analysing power meas. 77−38269
^{4}He(t,n), 10-11 MeV, multichannel R-matrix anal. of polarisation effects 77−2968
^{4}He(t,t), 10-11 MeV, multichannel R-matrix anal. of polarisation effects 77−2968
^{6}He mass six supermultiplet system anal. power from ^{9}Be(t,^{6}Li), polarised t 79−45244
He(μ,μ), beam polarisation and nucl. recoil effects 79−67738
Hf, static mag. moments, spin, parity and excitation energy from nuclear orientation *(Dutch)* 79−80872
Hg(n,n), 2.5 MeV, small angle scatt., cross section, asymm. 78−74361
Hg(n,n) 2.9 MeV, elastic differential cross section and polarisation ang. depend., statistical anal. 79−45264
^Ho, A=167,169, energy levels from Er(t,α), polarised t 79−36155
^{165}Ho, electron-oriented nucleus scatt., eikonal approx. calc. 78−37331
^{165}Ho+n, polarised projectile and target, spin depend. of total cross section *(Russian)* 78−17211
^{165}Ho(^{165}Ho,X), deep inelastic, spin and transferred ang. momentum alignment 80−106043
^{165}Ho(e,e), polarised target, as possible test for charge density waves in finite nuclei 77−54144
^{165}Ho(n,n), 1 and 2 MeV, oriented nuclei, deformation effect meas., coupled-channel calc. 77−65218
^{165}Ho(n,n), polarised n and target 0.4-2.5 MeV, total cross section spin-spin effect 79−17899
^{165}Ho(π,π), aligned deformed nuclei, cross sections and diffractive minima from eikonal approx. 80−22860
Ho(n,n), 2.5 MeV, small angle scatt., cross section, asymm. 78−74361
I(n,n) 2.9 MeV, elastic differential cross section and polarisation ang. depend., statistical anal. 79−45264
In(n,n), 2.5 MeV, small angle scatt., cross section, asymm. 78−74361
^{46}K levels, J$^{\pi}$ and tensor anal. powers from ^{48}Ca(d,α), pol.d 80−102113
^{77}Kr, low lying state J$^{\pi}$ assignments, anal. powers from ^{78}Kr(d,t) 79−45153
^{5}Li (3/2^{-}) tensor polarisation from ^{2}H(α, αn)p 80−13450
(^{6}Li, ^{6}Li), 22.8 MeV, optical model test from vector anal. power data 79−97729
(^{6}Li, ^{6}Li) pol. ^{6}Li, vector and tensor polarisation, closed form description 80−37363
^{6}Li-n, R-matrix calc. of total elastic, (n,α) differential cross-sections and polarisation 77−57669
^{6}Li+n, spin depend. capture and scatt. of slow neutrons 78−46059
^{6}Li(^{3}He,p), 14 MeV, proton polarisation, ang. distribs., differential cross section 77−82944
^{6}Li(^{3}He,p)^{8}Be, 14 MeV, p-^{8}Be optical model parameters 78−25208
^{6}Li(^{3}He,p)$\alpha\alpha$, polarisation meas. in final state interactions 77−18589
^{6}Li(d, α), polarised d, 5-10 MeV, A_y=1 and A_{yy}=1 points search 79−36223
^{6}Li(d,α), extreme values of analysing power 77−3018
^{6}Li(d,α)^{4}He, 1.5-11.5 MeV, resonance behaviour, analysing powers 77−82935
^{6}Li(d,α)^{4}He, below 12 MeV, analysing powers, ^{8}Be reson. levels 77−82936
^{6}Li(d,n,)^{7}Be*, 0.6-1.0 MeV polarised deuterons, vector and tensor analysing powers 78−4925
^{6}Li(d,p$_0$)^{7}Li, 0.6-1.0 MeV polarised deuterons, vector and tensor analyzing powers 78−4925
^{6}Li(d,p$_1$)^{7}Li*, 0.6-1.0 MeV polarised deuterons, vector and tensor analyzing powers 78−4925
^{6}Li(n,^{3}H)^{4}He, polarised neutrons, 0.2-2.4 MeV, analysing power meas. 77−38268
^{6}Li(n,n), 2-5 MeV polarised neutrons, analysing powers, R-function and phase shift anal. 77−23088
^{6}Li(n,t)^{4}He, 0.2-1.4 MeV polarised neutrons, analysing powers meas. 77−23074
^{6}Li(n,t)^{4}He, thermal polarised n capture, P-odd asymmetry meas. *(Russian)* 80−13452
^{6}Li(p,p) quasielastic scatt., 635 MeV polarised protons, asymm. meas. *(Russian)* 77−74852
(^{7}Li, ^{7}Li), aligned Li ions, electric quadrupole moment of ^{7}Li 80−78141
^{7}Li system reactions, analyzing power meas. review 79−9582
^{7}Li(d,α), 1.5-11.5 MeV, meas. of differential cross section and analysing powers 77−3017
^{7}Li(p,γ)^{8}Be, polarised p, 380-960 keV, ^{8}Be level, J$^{\pi}$ 77−88131
^{7}Li(p,p), polarisation effects for elastic scatt. near (p,n) reaction threshold 78−13075
^Li(γ,π), A=6, 7 80−22686
^{2}M+hadron→proton+X, polarised d, S and D wave functions, nuclear core hypothesis 78−62417
^{24}Mg+d, 10 MeV vector polarised deuterons scatt., nuclear shape effects, optical pot., analysing power 78−54768
^{24}Mg(d,$\alpha\gamma$)^{22}Na, 7.75 MeV, ang. correl. meas. using tensor polarised deuterons 77−22934
^{24}Mg(d,p)^{25}Mg, 8-13 MeV, vector polarised deuterons, excitations function of cross sections 78−8826
^{24}Mg(p,p'), polarised p, 20.3 MeV, cross section and analysing power, DWBA and coupled channel anal. 78−82287
^{26}Mg(α,α_1), 15 MeV, anal. of α-γ angular correlations 77−74866
^{26}Mg(p, p'), pol.p, 5.5-17.5 MeV, cross sections and anal. powers, autocorrelations 80−106042
Mg(p,p), A=24, 26, 5-6 MeV, polarisation in elastic scatt., thick target method 78−13079
^{54}Mn low lying 2p-4h states, J$^{\pi}$ from tensor anal. powers of ^{56}Fe(d,α), pol.d 80−99124
^{55}Mn(n,γ), pol. Mn and n, 0.017 eV, ^{56}Mn levels, transitions and spins 80−78154
^{55}Mn(p,n)^{55}Fe, neutron polarisation at isobaric analogue resonances 78−54759
^Mo(p,p'), (A=92,94), 20 MeV, polarisation effects on nuclear excited states *(Russian)* 80−27645
^{92}Mo, elastic and inelastic scatt. of 30 MeV polarised protons 77−23004
^{96}Mo(t,p), pol.t, cross section and anal. powers, struct. depend., DWBA anal. 80−78272
polarisation in nuclear reactions and scattering continued
^{100}Mo(^{14}N, ^{12}B)^{102}Ru, 90 MeV, semiclassical analysis of ^{12}B spin polarisation 78−33212
^{100}Mo(^{14}N,^{12}B), 200 MeV, ^{12}B spin polarisation meas. 79−3168
^{100}Mo(^{14}N,^{12}B), 200 MeV, ^{12}B spin polarisation in deep inelastic collision 80−63160
^{100}Mo(^{14}N,^{12}B), 90 meV, spin alignment of products, semi-classical model calcs. 80−73859
^{100}Mo(^{14}N,^{12}B)^{102}Ru, 90 MeV, meas. of ^{12}B spin polarisation 77−71562
^{100}Mo(^{14}N,^{12}B)^{102}Ru, 90 and 125 MeV, spin polarisation of ^{12}B 78−50196
Mo(t,p), pol.t, 17 MeV, ^Mo, A=98,102, anal. powers, transitions, shape coexistence states, DWBA anal. 80−86895
^{13}N giant dipole resonance population amplitude and phase, E1 reaction amps. from ^{12}C(p,γ_0), pol. p 80−63145
^{14}N residual states, vector anal. power. optical pot. from ^{12}C(^{6}Li,α), pol. ^{6}Li 79−97697
^{14}N(^{3}He,p)^{16}O, 10 MeV proton polarisation ang. distrib. 79−71861
^{14}N(d, α), pol. d., vector anal. capacity energy and ang. depend. 80−18281
^{14}N(d, α), pol.d, 1.5-3 MeV, vector anal. capacity for two α-particle groups 80−78266
^{15}N 3/2^{-} state spin alignment and polarisation, 1/2-spin orbit interaction from ^{27}Al, ^{88}Sr(^{16}O,^{15}N) 80−27622
^{15}N giant resonance and cross sections from (γ,d) and (d,γ) pol. d 79−93587
^{15}N low lying states, cross sections and anal. power, transitions, spectroscopic factors from ^{14}N(d,p), pol. d 80−32183
^{15}N polarisation, spin alignment and excited state ang. distrib. from ^{88}Sr(^{16}O, ^{15}N) 79−67709
^{15}N(p,α)^{12}C, <1.25 MeV polarised protons, ang. distribs. 77−3009
^{15}N(p,γ)^{16}O, anal. of ^{16}O giant dipole reson. struct. 78−4942
^{23}Na(d,^{3}He)^{22}Ne, 12.4 MeV polarised beam, $d_{5/2}$-$d_{3/2}$ admixing in pickup strength 77−6399
^{24}Na^{m}, polarised, β-decay asymmetry and mag. moment from Na(n,γ) 80−91157
^{147}Nd, spin by vector analysing powers of ^{148}Nd(d,t)^{147}Nd 78−609
^{20}Ne 13482 keV level, parity violating effects in two resonance interference from ^{19}F(p,α) pol. p 80−83033
^{20}Ne E1 resonance from ^{19}F(p,γ) pol. p 80−22790
^{20}Ne giant E1 resonance intermediate struct. from ^{19}F(p,γ), pol. and unpol. 80−78251
^{20}Ne(d,α), 10.5 to 12.0 MeV, tensor analysing power meas., ^{18}F level spin, isospin and parity assignments 78−74305
^{20}Ne(d,d), pol. d, 10-12 MeV, cross section, coupled channel and fluctuations anal. 80−27617
^{20}Ne(d_{pol},p), 10 MeV, ^{21}Ne deduced spectroscopic factors, levels and anal. powers 80−83087
^{20}Ne(p,p), polarised protons, obs. of ^{21}Na levels near 5 MeV 77−2913
^{21}Ne states cross section, coupled channel and fluctuations anal. from ^{20}Ne(d,p) 80−27617
^Ni, A=60, 62, 66, levels, J$^{\pi}$, anal. powers and cross sections from Ni(t,p)pol.t 80−68539
^Ni, A=64, 58, level ang. momentum and spin values, DWBA anal. from (t,d) polarised t 79−36163
^Ni(p,α) A=60,62, polarised p, 22.0 MeV, analysing power J dependence 79−67740
^Ni(p,α)^3Co, A=60,62,22 MeV, analysing power meas. in L=0 transfer reactions 79−45268
^Ni(p_{pol}, α), A=58, 60, 62, 22 MeV, analysing power and cross sections, Co proton-hole states 80−68663
^{58}Ni (^{7}Li, ^{7}Li), 14.22 MeV, alignment axis orientation depend. of cross section, mass quadrupole moment alignment 80−68638
^{58}Ni+^{16}O, 100 MeV, γ-ray circular polarisation meas. 78−54788
^{58}Ni+^{23}Na, deformed aligned projectile ions, elastic scatt., fusion, polarisation effects 78−58303
^{58}Ni+^{6}Li(^{7}Li), 12.7 MeV, isotopic shape effects in elastic scatt. of aligned ions 78−89904
^{58}Ni(^{16}O,X), 100 MeV, deep inelastic, fragment spin polarisation and alignment, γ-rays 80−18284
^{58}Ni(^{3}He,^{3}He)^{58}Ni, 33.3 MeV, analysing power for polarised ^{3}He 77−67731
^{58}Ni(^{3}He,d)^{59}Cu, 33.3 MeV, analysing power for polarised ^{3}He 77−67731
^{58}Ni(^{6}Li,^{6}Li) scatt. of aligned spherical ^{6}Li ion c.f. strongly deformed ^{7}Li ions 79−6680
^{58}Ni(d_{pol},p), cross section and vector analysing power, ^{59}Ni deduced levels 80−52684
^{58}Ni(p,p'(d)X), pol. p, 65 MeV, anal. powers of continuum energy spectra 80−68637
^{58}Ni(p,p'), 15 MeV polarised protons, surface delta description of analysing power 77−61397
^{58}Ni(p,p'), 60 MeV, analysing power for excitation of giant resonance region of continuum 77−6387
^{58}Ni(p,p), 0.8 GeV, polarised p, differential cross section, anal. power, nuclear matter densities 79−13299
^{58}Ni(p,p), 178 MeV, ang. distribs., cross sections and polarisation, coupled channels calcs. 79−75984
^{58}Ni(p,p), 800 MeV, polarised differential cross sections and anal. powers, n density 79−13297
^{58}Ni(p,p), pol. p, 40 MeV, elastic and inelastic, asymmetries and differential cross sections *(Russian)* 80−27623
^{58}Ni(t,p)^{60}Ni, 17 MeV, polarised triton, meas. and two-step calcs. 77−54204
^{59}Ni levels, cross section and vector anal. power, ang. distribs. from ^{58}Ni(^{7}Li,^{6}Li), pol. ^{7}Li 80−106044
^{60}Ni high spin states, J$^{\pi}$, $T_{1/2}$, ang. distribs. and polarisations from ^{56}Fe(^{7}Li, p2nγ) 80−99116
^{60}Ni(d, d), 9, 12 MeV, polarised d, excitation functions, optical model parameters and spin-orbit pot. 79−67756
^{60}Ni(p,α)^{57}Co(3/2^{+}), anomalous analyzing power, DWBA calc. 80−86894
^{60}Ni(p,p'), 15 MeV polarised protons, surface delta description of analysing power 77−61397
^{62}Ni(p,p), 20 MeV, elastic and inelastic scatt., analysing powers *(Dutch)* 78−29464
^{64}Ni(p,p) 800 MeV, polarised differential cross sections and anal. powers, n density 79−13297
Ni(p,p), 36.2 MeV, differential cross section, asymmetries, 0 to 7° scatt. 78−94002

polarisation in nuclear reactions and scattering continued
Ni(p,p'), A=58,60,62, E=17.2, 20.4, 24.6 MeV polarised protons, optical model, DWBA anal. 78−13094
^{243}Np energy level spin assignments and anal. power from ^{244}Pu(t,α), polarised t 79−36165
^{16}O (p,2p) 200 MeV polarised protons, j-dependence obs. in quasifree scatt. 77−10401
^{16}O E1 and p_0 channel E2 strength from ^{15}N(p,γ) 80−22790
^{16}O mag. dipole strength, M1 resonances from ^{15}N(p,γ), polarised p 79−80898
^{16}O, quasielastic scatt. of polarised 635 MeV protons, depend. of left-right asymm. on nucl. momentum *(Russian)* 77−79384
^{16}O residual states, vector anal. power. optical pot. from ^{12}C(^{6}Li,d), polarised ^{6}Li 79−97697
^{16}O(^{16}O,^{12}C)^{20}Ne, angular distrib. of ^{20}Ne polarisation at 68 MeV 79−6681
^{16}O(^{16}O,^{12}C)^{20}Ne, reaction mechanism by polarisation meas. 80−9301
^{16}O(^{16}O,^{12}C)^{20}Ne*, strong polarisation of ^{20}Ne levels obs. 78−25213
^{16}O(^{3}He, ^{3}He), pol. ^{3}He, 33.3 MeV, differential cross section and anal. power, optical pots. 80−42627
^{16}O(^{3}He, x), pol. ^{3}He, x=d or α, 33 MeV, anal. power and cross sections 80−42628
^{16}O(d,X), X=d or N, elastic scatt. and stripping, three body calc. 80−91165
^{16}O(d,α_3), 6.84 MeV polarised d, absolute standard for d vector analysing powers 77−34281
^{16}O(d,d), <4 MeV, d polarisation, vector analysing power, level characts. of ^{18}F compound nucleus 77−61434
^{16}O(e,e'p), polarisation effect on quasi-free electron scatt. 77−71607
^{16}O(γ,n_0), 21.6-25.7 MeV, ground state photoneutron polarisation ang. distrib. 80−57765
^{16}O(μ,ν), recoil nucleus odd and even tensor orientations, general expressions 80−13451
^{16}O(n,n), 2-5 MeV polarised neutrons, analysing power, R-function and phase-shift anal. 77−23088
^{16}O(p,2p), 200 MeV polarised beam reaction, possible knockout polarisation 77−88099
^{16}O(p,2p), 320 MeV polarised protons, quasifree scatt., spin orbit coupling 78−66272
^{16}O(p,p'), 1 GeV, proton polarisation in natural parity level excitation *(Russian)* 80−42634
^{16}O(p,p'), 40 MeV, retarded isoscalar M2 strength obs. 78−93962
^{16}O(p,p'), proton polarisation and natural parity level excitations *(Russian)* 80−5144
^{16}O(p,p'), 20-40 MeV, pol. p, anal. powers, imaginary spin-orbit pot., coupled channels anal. 80−102179
^{16}O(p,p'), polarised p, 20, 30, 40 MeV, anal. power and cross sections, spin-orbit deformation 79−75963
^{16}O(p,p')^{16}O*, 42.5-49.3 MeV, octupole GR strength, polarised proton 77−57644
^{16}O(p,p), 20-50 MeV differential cross section, polarisation ang. distrib., optical model exchange terms 80−27638
^{16}O(p,p) polarised p, 800 MeV, differential cross section and anal. power, microscopic anal. 79−80915
^{16}O(p_{pol},2p), cross section, analysing power, energy sharing spectra, distorted wave impulse approx. 80−78291
^{17}O(e,e), mag scatt., form factors, HF calcs., core polarisation effects 80−42579
^{18}O, heavy ion excitation, single particle and core polarisation amplitude interference 80−5117
^{18}O(d,α), 8.5 to 11.3 MeV polarised deuterons, ^{16}N levels, spin parity assignments 78−89886
^{18}O(p,t), polarised p, 24.4 MeV, two-step reaction to unnatural parity state, anal. power 79−67739
(p,p), small-angle scatt. of polarised protons at 36.2 MeV 77−30603
^{31}P(p,p), 65 MeV polarised protons, asymm. in elastic and inelastic scatt. 78−54754
^{233}Pa anal. power for spin states from ^{234}U(t,α), polarised t 79−36165
^{206}Pb(p,p_0), polarised p, 13.6 MeV, analysing power near ^{207}Bi $3p_{1/2}$ isobaric analogue resonance 78−78346
^{207}Pb(e,e), magnetisation distrib. from elastic mag. form factors, core polarisation, exchange currents 80−47372
^{207}Pb(p,p_0), polarised p, 13.6 MeV, analysing power near ^{208}Bi $3p_{1/2}$ isobaric analogue resonance 78−78346
^{207}Pb(p,p), polarised p, 13.5-18 MeV, ^{208}Bi isobaric analogue resonances, spin assignments, decay amplitudes 79−75946
^{208}Pb (p,p), 1.04 GeV elastic scatt., polarisation 78−21549
^{208}Pb (p,p) elastic scatt., polarisation and spin-orbital amplitude parameters, 1 GeV *(Russian)* 78−17208
^{208}Pb(^{12}C,^{11}B)^{209}Bi, DWBA anal. including nuclear wave function polarisation 78−629
^{208}Pb(^{209}Pb, X), giant resonance polarisation pots. from nucleus-nucleus effective pot. 80−78248
^{208}Pb(d,p), polarised d, tensor anal. powers, sub-Coulomb stripping calc. corrections 79−80918
^{208}Pb(d,p), tensor analyzing power, deuteron wave functions 80−99137
^{208}Pb(d,p)^{209}Pb, 9.0 MeV, effects of d D state determ. 77−67752
^{208}Pb(d,t), 10 MeV, polarised d, tensor anal. power and D-state effects 79−85446
^{208}Pb(γ,γ), mean polarisation meas. of 4843 keV 78−29446
^{208}Pb(γ,n_0), 170-320 keV, search for collective M1 resonance 77−46103
^{208}Pb(γ,n_{pol}), evidence for M1 collective strength at 8-10 MeV 77−38255
^{208}Pb(γ,n) giant mag. dipole resonance location, photoneutron polarisation method 80−37357
^{208}Pb(p,P'), pol. p, 9, 10 MeV, vol. integrals for optical pots., real symmetry pot. 80−42659
^{208}Pb(p,p), 0.8 GeV, polarised p, differential cross section, anal. power, nuclear matter densities 79−13299
^{208}Pb(p,p), 20-50 MeV differential cross section, polarisation ang. distrib., optical model exchange terms 80−27638
^{208}Pb(p,p), elastic and inelastic scatt., 185 MeV, polarisation, diffraction model anal. 79−75943
^{208}Pb(p,t)^{206}Pb(3$^+$), pol. p, 22 MeV, anal. power and (p,d)(d,t) sequential transfer processes 80−5119
Pb(n,n), 10 MeV, neutron polarisation meas. at small angles 77−3014
Pb(n,n), 10.4 MeV, polarised neutrons, analysing power 77−30545
Pb(n,n), 14.0-17.4 MeV, neutron polarisation, ang. depend. diffraction struct. 80−18283
Pb(n,n), 14.2 MeV, polarisation in forward angle scatt. 80−18282
Pb(n,n), 16.1 MeV, polarisation meas., optical model anal. 79−22264
polarisation in nuclear reactions and scattering continued
Pb(n,n), 2.9 MeV, elastic differential cross section and polarisation ang. depend., statistical anal. 79−45264
Pb(π^-,p) 1.5-5 GeV/c, cumulative proton polarisation *(Russian)* 80−86896
Pb(t,α), polarised t, proton hole states in ^{203,205,207}Tl obs. 77−41978
^{A}Pd(p,t), A=104, 110, 22 MeV, polarised p, anal. power systematic nuclear struct. depend. 79−22265
^{106}Pd(t,p), pol.t, cross section and anal. powers, struct. depend., DWBA anal. 80−78272
^{110}Pd(p,t)^{108}Pd(2_1^+), analysing power difference from ^{110}Pd(p,t)^{108}Pd(2_1^+) 78−37341
^{149}Pm single proton states, spin assignments, spectroscopic factors from ^{150}Sm(t,α), pol.t 80−18170
^{153}Pm struct., spin and parity assignments, Nilsson model interpretation from ^{154}Sm(t,α) polarised t 79−469
^{141}Pr(n,γ), circular polarisation, ang. distrib. meas. 80−32285
^{239}Pu(n,f,) slow polarised neutrons, product separation asymmetry *(Russian)* 80−106088
Rh, static mag. moments, spin, parity and excitation energy from nuclear orientation *(Dutch)* 79−80872
^{100}Ru(p,t), 22 MeV, polarised p, anal. power systematic nuclear struct. depend. 79−22265
^{32}S (p,p), 5-6 MeV, polarisation in elastic scatt., thick target method 78−13079
^{37}S+d, 10 MeV vector polarised deuterons scatt., nuclear shape effects, optical pot., analysing power 78−54768
^{32}S(n,n), spin-flip probability to first 2^+ level 80−78288
^{34}S(d,α)^{32}P, 8.25-9.50 MeV, tensor-polarised deuterons, spin-parity assignments to ^{32}P levels 78−17219
^{34}S(d,d), elast. and inelast. scatt. of 11.8 MeV polarised deuterons 78−33191
^{34}S(d,p)^{35}S, 11.8 MeV vector polarised deuterons, optical pot. 77−88149
^{41}Sc 2p-1h intermediate struct. resonances, anal. powers, J^π from ^{40}Ca(p,p'γ) 80−86883
^{45}Sc(n_{pol},γ), ^{46}Sc energy levels, resonances, spin and parity 80−52673
^{46}Sc transition polarisation, levels and spin assignments from ^{45}Sc(n,γ), pol. n 80−52656
Se (d,p), 12.5 MeV, ^{77,79,81,83}Se level struct., spins, parities, cross section, vector analysing power 78−89885
^{A}Se(d_{pol},d), A=76,78,80,82, 12 MeV, two-step scatt. process via $J^\pi=2_1^+$ excited states 80−57781
Se(d,d), 12 MeV polarised deuterons, shell closure effects 77−38281
Se(d,d), polarised deuterons, vector analysing power, optical model calcs. 78−62550
^{28}Si+d, 10 MeV vector polarised deuterons scatt., nuclear shape effects, optical pot., analysing power 78−54768
^{28}Si(α,p)^{31}P, proton polarisation calcs., distorted wave method 77−6404
^{28}Si(d, p)^{29}$Si_{g.s.}$, 12.1 MeV, vector polarization transfer coeff., deuteron D-state effect 77−14135
^{28}Si(d,d'), 6 to 10.46 MeV polarised d, study of emission fluctuations 78−54735
^{28}Si(d,d') 6 to 10.46 MeV polarised d, study of Ericson fluctuations 78−54735
^{28}Si(d,d), 6-8 MeV, compound nuclear polarisation effects 77−3020
^{28}Si(d,di), 20 MeV, vector polarised deuteron scatt. from deformed nuclei 79−6629
^{28}Si(d,p), 6 to 10.46 MeV polarised d, study of Ericson fluctuations 78−54735
^{28}Si(d,p)^{29}Si, 1.8 to 3 MeV, energy behaviour of vector analysing power, intermediate resonances *(Russian)* 79−49617
^{28}Si(d_{pol},pγ), ^{29}Si, low lying energy level structure, multi-step reaction calcs. 80−68537
^{28}Si(n,n), spin-flip probability to first 2^+ level 80−78288
^{28}Si(p,p'(d)X), pol. p, 65 MeV, anal. powers of continuum energy spectra 80−68637
^{28}Si(p,p), 2.0-3.8 MeV polarised protons, analysing powers meas. 77−3012
^{28}Si(p,p), pol. p, 12-18 MeV, cross section, anal. power and states, ^{29}P resonance coherence widths 80−32258
^{30}Si(d,α)^{28}Al, 18 MeV, cross-section and vector analysing power ang. distribs. 78−41728
^{30}Si(d,α)^{28}Al, 8-12 MeV, polarised d, spin-parity assignments in Al 77−6222
^{30}Si(d,p), pol.d, 1.9-2.5 MeV, anal. power excitation function anomaly 80−5118
^{30}Si(p,α)^{27}Al, 17 MeV, polarised p, cross-section and analyzing power ang. distrib. 79−54427
^{30}Si(p,γ), pol.p, 6.4-15.0 MeV, cross section and anal. power ang. distribs. 80−99168
^{30}Si(p,p), polarised proton fluctuation expt., compound elastic enhancement factor determ. 79−519
Si(p,p), A=28, 29, 30, 65 MeV polarised protons, asymm. in elastic and inelastic scatt. 78−54754
Si(p_{pol},p_{pol}), giant multipole resonance region, optical model anal. 80−57779
^{A}Sm(^{20}Ne, ^{20}Ne), 70 MeV, A=148, 150, 152, Coulomb polarisation pot., coupled channel calcs. 80−22855
^{144}Sm(γ,γ), resonance fluorescence up to 5 MeV 78−66263
^{152}Sm(t,α) 17 MeV, polarised t, ^{151}Pm single proton states, rot. bands, level J^π assignments, spectroscopic strengths 79−67626
^{A}Sn(n,n), A=116,118,120,122,124, isovector deformation parameters and core polarization 79−67642
^{A}Sn(p,p'), A=116, 124, 0.8 GeV, polarised p, spin orbit deformation effects, DWBA anal. 79−30832
^{116}Sn(d,p), pol. d, 8.22 MeV, vector anal. power, p and d spin depend. effects 80−5114
^{116}Sn(p,α)^{113}In, 22 MeV, analysing power, J-depend., DWBA 78−70523
^{117}Sn(p,d), polarised p, 12.9 MeV, anal. power 80−5114
^{117}Sn(p,p), polarised p, 12.9 MeV, anal. power 80−5114
^{118}Sn(p,α)^{115}In, 20 MeV polarised protons, DWBA calcs. 78−41714
^{118}Sn(p,t), 22 MeV, polarised p, anal. power systematic nuclear struct. depend. 79−22265
^{118}Sn(d,t), 6 MeV, polarised d, tensor anal. power and D-state effects 79−85446
^{118}Sn(γ,n), giant mag. dipole resonance location, photoneutron polarisation method 80−37357
^{120}Sn(^{12}C,3n), 52 MeV, obs. of ^{129}Ba γ-ray linear polarisation 78−50121
^{122}Sn(d,d), 15 MeV, optical model calc. 78−41729
^{122}Sn(p,p), 20 MeV, elastic and inelastic scatt., analysing powers *(Dutch)* 78−29464

polarisation in nuclear reactions and scattering continued
^{124}Sn(n,n), pol. thermal, parity violation near resonance, DWBA calcs. 80−68528
^{124}Sn(p,p), 0.8 GeV polarised p, differential cross section and analysing power data anal. 78−70526
Sn(p,n), 4 to 10 MeV polarised protons, optical model parameters 77−2972
Sn(p,p), 8.8 MeV polarised protons, optical model parameters 77−2972
Sn(p,p$_0$), pol.p, 6.77-8.8 MeV, cross sections, optical parameters and nuclear radius A-depend. 80−57773
^{88}Sr(d,p)^{89}Sr, 12 MeV polarised d, ^{89}Sr level transitions and spin assignments 78−66286
^{88}Sr(p,p')^{88}Sr(2_1^+), 7-7.5 MeV polarised protons, scatt. at IAR 77−318
^{149}Tb, high spin states obs. 80−18158
^{159}Tb polarised target, transmission of polarised resonance neutrons, 20 eV to 100 keV, spins *(Russian)* 77−50138
^{159}Tb, transmission of polarised resonance neutrons through polarised target, 20-100 keV 77−26657
^Te(p,t) A=122, 128, 22 MeV, polarised p, anal. power systematic nuclear struct. depend. 79−22265
^{126}Te(t,p), pol.t, cross section and anal. powers, struct. depend., DWBA anal. 80−78272
^{232}Th(^{14}B,^{12}B), 129 MeV, ^{12}B spin polarisation 80−63161
^{46}Ti(d,d), 10 MeV, optical model calc. 78−41729
^{46}Ti(d,p), polarised d, obs. of D-state and compound nucleus effects 77−34319
^{175}Tm single proton states, rot. bands, J$^\pi$ assignments from ^{176}Yb(t,α), pol. t 80−452
U linear polarisation of elastically scatt. γ-rays of 279 and 662 keV 77−6344
^U(n,f), A=233,235, ejection fission products angular depend. on thermally polarised neutron capture *(Russian)* 80−86941
^{233}U fission by polarised neutrons, P odd asymmetry of emitted fragments *(Russian)* 80−18354
^{233}U(n,f), thermal polarised neutrons, neutron emission P-odd asymmetry *(Russian)* 80−78338
^{233}U(n,f) slow polarised neutrons, product separation asymmetry *(Russian)* 80−106088
^{235}U(n,f), 0.001-25 keV, polarised n, spin separated cross sections, resonance struct. 79−3126
^{235}U(n,f), spins of resonances below 150 eV 77−23147
^{235}U(n,f), thermal polarised n capture, P-odd asymmetry meas. *(Russian)* 80−13452
^{236}U(n,f), P-odd asymmetry in neutron emission *(Russian)* 79−89339
U(n,n), 2.5 MeV, small angle scatt., cross section, asymm. 78−74361
U(n,n) small-angle scatt., possible test of neutron electric polarisability 77−22674
^{51}V(n,γ), circular polarisation, ang. distrib. meas. 80−32285
^{51}V(p,n)^{51}C neutron polarisation at isobaric analogue resonances 78−54759
^{186}W(t,α), pol.t, 17 MeV, ^{185}Ta single proton states and rot. bands, J$^\pi$ 80−91130
^{86}Y(p,p), (p,p'γ), 4.5-8.0 MeV polarised protons, IAS spectroscopy of ^{87}Y 77−61396
^{89}Y(p,p), 185 MeV, ang. distribs., polarisation, cross section, optical pot. 78−89873
^{89}Y(p,p), 65 MeV polarised protons, asymm. in elastic and inelastic scatt. 78−54754
^{89}Yb(p,p), 20 MeV, elastic and inelastic scatt., analysing powers *(Dutch)* 78−29464
^Zn(p,p), A=66,68, 20-50 MeV differential cross section, polarisation ang. distrib., optical model exchange terms 80−27638
^{64}Zn (d,^{3}He), polarised d, 13 MeV, vector analysing power, ^{63}Cu levels deduced 77−88100
^{64}Zn(d,^{3}He)^{63}Cu, 13 MeV, polarised d, tensor analysing powers 77−88101
^{64}Zn(d,d), polarised d, 13 MeV, optical model parameters, vector analysing power 77−88100
^{64}Zn(d,t), polarised d, 13 MeV, vector analysing power, ^{63}Zn levels deduced 77−88100
^{64}Zn(d,t)^{63}Zn, 13 MeV, polarised d, tensor analysing powers 77−88101
^{64}Zn(p,p'), 15 MeV polarised protons, surface delta description of analysing power 77−61397
Zn(d,d), A=66, 67, 12.3 MeV polarised deuterons, precision tensor analysing power meas. 77−3019
Zr(^{16}O,xnγ)Cd, parity assignments of Cd with A=105 to 109 78−41630
^Zr, A=90, 92, elastic and inelastic scatt. of 30 MeV polarised protons 77−23004
^Zr(p,p'), (A=90,92), 20 MeV, polarisation effects on nuclear excited states *(Russian)* 80−27645
^Zr(p,p'), A=94,96, 11.2-13.4 MeV, anal. power and excitation function T$^<$ fluctuations 80−42626
^Zr(p,p) A=90, 92, elastic and inelastic, 40 MeV polarised protons, cross sections and anal. power 79−54428
^{90}Zr (p, p'), 57.5 MeV, polarised p, low lying level and giant resonance excitation 79−36157
^{90}Zr(d, d), 10, 11, 12 MeV, polarised d, excitation functions, optical model parameters and spin-orbit pot. 79−67756
^{90}Zr(d,d), 10 and 15 MeV, optical model calc. 78−41729
^{90}Zr(d,p)^{91}Zr, 5.5 MeV, effects of d D state determ. 77−67752
^{90}Zr(p,p'), polarised protons, compound nuclear contribs. to IAR inelastic decay 78−8813
^{90}Zr(p,p), 0.8 GeV, polarised p, differential cross section, anal. power, nuclear matter densities 79−13299
^{90}Zr(p,p), 4.5-9 MeV polarised protons, reaction cross-section near (p,n) threshold 77−3015
^{90}Zr(p,p), 65 MeV polarised protons, asymm. in elastic and inelastic scatt. 78−54754
^{90}Zr(p,p), elastic and inelastic scatt., 185 MeV, polarisation, diffraction model anal. 79−75943
^{90}Zr(p,p), spin orbital interaction and nucl. matter density distrib. *(Russian)* 79−22176
^{91}Zr(d,t), 6 MeV, polarised d, tensor anal. power and D-state effects 79−85446
^{92}Zr levels, J$^\pi$, cross sections, vector anal. power, optical parameters from ^{91}Zr+pol. d 80−78268
^{92}Zr(p,α), 35 MeV, polarised p, DWBA anal., anal. power, optical pot., J-depend. 79−3143
^{92}Zr(p,α)^{89}Y, 35 MeV, analysing power study *(French)* 79−75981
polarisation in nuclear reactions and scattering continued
^{92}Zr(p,p'), 40 MeV polarised protons, 2$^+$ states excitation 79−6600
^{92}Zr(p_{pol}, A)^{89}Y, finite-range cluster-model description, DWBA approach 80−52667

polariscopes *see polarimeters*

polaritons
acentric crystals, optical phonons, small oscillator strength meas. from frequency-angular polariton spectra 80−92629
ammonium bioxalate monohydrate spontaneous parametric scatt. spectra, polariton wave vector and Stokes lines analysis 78−43885
anisotropic continuum, with anisotropic surface layer, coeff. of attenuated total reflection 80−60535
anisotropic crystal films, surface polaritons 78−26822
anisotropic transition layer, surface polariton spectra in presence of resonance 80−88484
anthracene, cryst., polariton luminesc. 80−84775
anthracene, lifetimes of exciton-polariton luminesc. 79−33761
anthracene, mol. cryst., polariton fusion, two-photon excitation spectra 77−90139
anthracene, O-O exciton absorption bands, thermomodulation study 78−39563
anthracene, polariton effects in transmission and absorpt. spectra in thin crysts. 77−20886
anthracene, surface polaritons, attenuated total refl. 77−63423
anthracene crystals, photocond. by polaritons 77−69373
anthracene films, optical props., comparison between free and optical contact mounting 80−89079
antiferromagnet, uniaxial, mag. polaritons in spin-flop phase 78−23349
antiferromagnetic, dispersion relation and light scatt. 77−35871
antiferromagnetic polaritons, inelastic light scatt., theory 77−73144
barium formate, cryst., Raman scatt. 79−4804
biexcitons recombination, polariton effects 78−23033
bipolariton dispersion laws 77−51677
Bose condensation, polaritonic, effects of superfluidity 78−18976
bounded crystals, auxiliary boundary conditions in theory of additional light waves and excitons *(Russian)* 78−56080
Brillouin scattering of exciton polaritons and additional boundary conditions 79−95795
chalcopyrite type ternary crystals, IR dispersion *(Russian)* 78−76451
classical and quantum mechanical aspects *(French)* 80−103634
classical crystal optics, lattice dynamical background, review 80−97221
coherent optical pulse propag., polariton effects 77−42576
conference, luminescence, Paris (July 1978) 79−33755
coupled-mode excitations in cryst., relax. rates, theory 80−59881
cryst. with defects 78−60478
crystal luminescence, polariton mechanism, reabsorption, spatial dispersion effects, boundaries *(Russian)* 80−55186
CTIP, exciton surface polaritons at room temp. 79−47476
cyanine dye, crysts., extraordinary exciton polaritons in refl. spectra, macroscopic dielec. theory 77−89715
γ-cyclopropyl-bis (1,3,3-trimethylindolenine-2-yl)pentamethinium fluoroborate, exciton surface polaritons, reflecting faces obs. 80−65645
damped surface polaritons at a boundary between isotropic crystals 80−2346
damping and fluctuations due to interaction with lattice vibrs., theory 77−85156
degenerate semiconductor, with surface depletion layer, surface polaritons, hydrodynamical model 80−6752
degenerate valence band semiconductors, polariton effect 79−15102
p-dibromodiphenylether surface, normal and ultra-Brewster refl. spectra 80−25400
Dicke model, modification for long wave photons 80−1169
dielectric film, reflectivity, polariton standing-wave struct. as test of boundary conditions for spatial dispersion theories 79−4865
dielectric films, transition layer vibrs., resonance region auxiliary surface polaritons *(Russian)* 80−2347
dielectric half space, spatially dispersive exact microscopic theory of polaritons 77−4301
dielectric interface, surface polariton effects in spontaneous emission 77−20391
dielectric medium, steady propag. of coherent light pulse, dynamic behaviour of long pulse 79−98433
dielectric medium, steady propag. of coherent light pulse, effect of spatial dispersion 79−72480
dielectric surfaces, rough, interaction of EM waves 77−43688
dielectric-vacuum interface, spatial dispersion in optical props. 77−4613
dielectrics, nonlinear phonon-photon interactions, physical basis 77−61998
dispersion of dielectric axes in monoclinic and triclinic crystals related to lattice dynamics 78−87920
dye crystal, CTIP, exciton surface polaritons detect. by ATR spectra at 295K 79−4818
EM surface wave exam. by appl. of optical technique 77−76893
energy conversion radiation enhancement using surface polaritons 80−7941
exciton resonances, interacting, dielec. theory 78−14673
exciton spectroscopy, polariton dispersion 80−54613
exciton-photon interaction, exciton absorpt. lineshape, polariton and wave models 79−38564
excitonic molecules, Bose-condensed, emission spectrum, polariton effect 77−11856
far IR surface polariton obs. by attenuated total reflection 77−39790
Fermi reson. as detection of weakly polar vibrs. 79−7791
Fermi-resonance, EM wave dispersion 80−2344
ferrimagnet, polaritons, mag. susceptibility 80−7095
ferrimagnet, two sublattice, mag. polaritons 80−65845
ferroelectric bodies, deformable, coupled acousto-optic modes 80−96093
ferroelectric crystals, polariton light scatt. freq.-angle spectra, nonlinear susceptibility interference *(Russian)* 80−92834
ferroelectric H bonded crystals, linear response function for tunnelling systems in polariton region 78−43799
ferroelectrics of order-disorder type 80−10894
ferromagnetic polariton linewidths, theory 78−87918
ferromagnetic slab, asymmetrical guided mag. polaritons 80−88738
ferromagnetic slab, retarded EM modes 78−84405
film, light scatt. from interface, polaritons 79−8202
foil, surface guided modes, excitation by electrons 77−59310
form dichroism, theoretical treatment, determ. of macromol. shape 78−60417

polaritons continued
glass, IR total internal refl. spectrum, surface polaritons *(Russian)* 77−20861
guided wave polaritons in thin crystals, light scatt. spectra 79−15100
hemicylinder-air-quartz system, semi-infinite crystal, dispersion of surface phonon polaritons 78−71939
hybrid bulk-surface polaritons 80−49626
hybrid bulk-surface polaritons 80−49627
II-VI compounds, magnetoreflectance of exciton-polaritons 79−91410
interaction of light with phonon excitations in medium, coherent effects 79−15103
interface between two conducting or dielec. media, polariton modes, review 78−87922
ionic conductors, polaritonic spectra 79−23908
ionic crystal plate, line widths in spectrum of surface vibr. 79−33174
ionic crystals, optical generation of longit. phonon modes 77−43288
IR reflectivity and Raman scatt. expts. 77−40237
kinematical levels arising from Frenkel excitons interaction 79−56134
kinematical polariton levels resulting from excitons, interaction, optical absorption line broadening 80−10892
laminarly-nonuniform media, surface polaritons, spectrum, rel. to transition layer at each interface *(Russian)* 77−35982
laser action in dense exciton systems 77−75531
laser intraresonator forced Raman radiation with polariton excitation *(Russian)* 79−94286
layer systems, mag. polaritons 78−31060
layered structure, surface polaritons, dispersion relations, recursive soln. 77−69390
lecture on phonons and polaritons 78−26638
light hyper-Raman scatt. by polaritons, active spectroscopy *(Russian)* 80−60623
lithium formate, and deuterated, polaritons, spontaneous parametric light scatt. 77−90150
lithium formate, optical phonons, small oscillator strength meas. from frequency-angular polariton spectra 80−92629
localised electron nonequilibrium vibration interaction secondary radiation spectrum 80−2778
lossy media, nonlinear excitation of surface polaritons 79−90974
LT mixed mode, dispersion relation 80−65470
magneto-optic Raman scattering of Raman-inactive phonon polaritons 80−91843
magnon splitting, photon effects 78−64276
metal, struct. induced surface plasmon polariton modes using ATR, theory 79−60890
metal cavity, lifetime of trapped excited atom, broadening mech. for optical absorption line 79−38578
metal circular cylinders, inhomogeneous, non-radiative surface plasmon-polariton modes 80−29455
metal surface, light refl. from dye molecule monolayer 78−48246
metal-metal interface, EM wave propag., plasmon polaritons, computer simulation 78−84276
metals, SHG by surface polaritons, theory 78−9416
MIM tunnel junctions, roughened, photon emission, calc. 80−44738
molecular crystal, Raman scatt. by external vibrs. 77−85711
molecular crystal with point and linear defects, Rayleigh scatt. 77−44011
molecular crystalline slab, optical spectra 77−8534
molecular crystals, polariton spectra and lattice dynamics 80−49313
molecular crysts., extraordinary exciton polaritons in refl. spectra, macroscopic dielec. theory 77−89715
molecular solids, Raman, fluoresc. and nonlinear props. 79−33702
molecular thin plate, with near-surface polariton transition layer, reflection and transmission spectra *(Russian)* 78−14677
monoclinic materials, polariton dispersion and cryst. optics 78−79685
multi-component, reflectance spectrum, internal struct. of excitons, review, book contrib. 80−44518
multi-component, reflectance spectrum 78−87921
naphthalene, a-exciton lineshape, exciton-photon coupling 79−33243
naphthalene, a-exciton temp. depend. scatt., optical absorpt. profile 78−72088
naphthalene, mol. cryst., polariton fusion, two-photon excitation spectra 77−90139
neutron scattering from equilibrium and non-equilibrium phonons, excitons and polaritons 80−84032
noncentrosymmetric crystals, anti-Stokes stimulated Raman scatt. by polaritons 79−36962
nonlinear crystal, polariton parametric oscill. and stimulated Raman scatt. 78−30026
nonlinear optics, two-photon absorption and stimulated Raman effect 77−50729
nonlinear Raman active media, third-order light mixing at polariton reson. frequencies 77−19364
nonlinear spectroscopy of bulk and surface polaritons 77−50730
nonstationary Raman scattering, by polaritons, correlation spectroscopy *(Russian)* 78−23450
nonstationary Raman scattering, of light, by vibration and polariton excitations *(Russian)* 78−23449
one-dimensional two-band model, free electron-hole pairs and exciton-polariton 80−29331
optic mode-EM mode coupled systems, soliton relation to polaritons 79−77707
optical activity in crystals, lattice dynamical theory 80−34883
optical system, for polariton measurements 77−38018
organic crystals, exciton surface polaritons 79−4519
organic monolayer/metallic substrate, exciton-surface plasmon interaction 79−69569
organic solid state chemistry, conf., Waltham, USA (June 1978) 79−46990
parametric amplification, oscillation and interaction processes, induced scattering by polaritons 79−72629
parametric excitation of phonons in field of strong EM wave 80−2133
parametric interaction of travelling and pump accompanied waves, induced scattering by polaritons *(Russian)* 79−3739
phonon-polariton modes for freq. chirped optical pulse compression 78−46689
photon magnon bound states in ferromag. 78−47711
photon-matter system, polariton instability and thermodynamic phase transition 79−86150
piezoelectric cubic crystals, stimulated Raman effect 79−73927
piezoelectric cubic single crystal stimulated Raman effect, coupled waves dispersion *(German)* 79−36963
polaritons continued
plasmon surface polariton dispersion curve, optical obs., demonstration 80−101690
polar dielectric interface, phonon-polariton modes 77−24474
polar dielectrics interface, phonon-polariton damping 77−51587
polar semiconductors, phonon-plasmon-polariton mode propag. at interface 79−60731
polariton-exciton dispersion curve 79−33244
poly-2,4-hexadiyne-1,6-diol bis (p-toluene sulfonate), exciton surface polaritons, reflecting faces obs. 80−65645
poly-2,4-hexadiyne-1,6-diol bis (p-toluene sulphonate), cryst., exciton surface polaritons, reflectivity of (100) face, 295K 78−80372
polystyrene coated Ag holographic grating, Raman spectra enhancement by plasmon surface polaritons 80−80885
PTS, exciton surface polaritons at room temp. 79−47476
quantum field theory of solids, book 77−31922
quartz, amorphous and crystalline, surface polaritons and splitting of optical frequencies 78−72090
α-quartz, Au film coated, surface polariton dispersion, IR spectra obs. 78−48249
quartz, fused, IR total internal refl. spectrum, surface polaritons *(Russian)* 77−20861
Raman scattering, photoelec. recording method *(Russian)* 78−23468
Raman scattering, polariton and phonon scatterers, freq.-angle spectra 79−4805
Raman scattering, two-photon reson., by excitons via intermediate excitonic mol., polarisation and polariton effects 78−10880
Raman scattering by surface polaritons 77−12391
Raman scattering by surface polaritons and compensation effect 78−10374
Raman scattering investig. of polaritons in solids 77−40238
Raman scattering of light by polaritons, reviews 80−34928
Raman scattering on excitons, polaritons in crysts. *(Rumanian)* 77−48172
Raman spectra in band of many-particle states at polariton Fermi reson. 80−25374
rare earth systems, mag. field depend. 79−33246
renormalisation by biexciton virtual formation 79−99490
resonance Raman scattering, polariton theory, book 79−37966
resonance Raman scattering, polariton theory, book contrib. 79−38551
resonant Brillouin scattering via exciton-polaritons, theory 80−50353
reststrahlen bands, bulk phonon polariton dispersion 77−35647
sapphire-LiF film system, ATR, substrate surface polaritons reson. effect *(Russian)* 77−32384
self induced transparency, steady-state exciton-photon pulse dispersion law 78−30028
semi-infinite crystals, linear wave vector effects on optical props. 77−85721
semiconducting film, exciton oscillator strength, EM wave-polaritan propagation, reflective power *(Russian)* 79−99491
semiconducting films, exciton polariton attenuation, spatial dispersion effect 80−20097
semiconductor, direct band gap type, polariton theory of reson. electronic Raman scatt. on neutral donor levels 80−108194
semiconductor, direct band-gap, polariton emission spectrum, exciton kinetics influence 78−14676
semiconductor, direct-gap, polariton luminesc., under strong excitation conditions, exciton gas model 77−8650
semiconductor, EM properties, general lecture 78−27173
semiconductor, excitons and nonlocal optical props. 79−95345
semiconductor, luminesc. due to exciton-electron scatt., calc. 77−16379
semiconductor, magnetoplasmon-polariton surface modes, Voigt geometry 78−43451
semiconductor, polariton dispersion change by virtual biexciton form. under laser irrad. 79−38607
semiconductor, polariton structure of interband transitions 79−87048
semiconductor, resonant Brillouin scattering of exciton polaritons 80−93357
semiconductor, struct. induced surface plasmon polariton modes using ATR, theory 79−60890
semiconductor, two-phonon Brillouin scattering 80−20656
semiconductor, two-polariton decay of excitonic mols. at 2K 79−95339
semiconductor, Wannier excitons, fine structure, lineshape and dispersion, review 80−44520
semiconductor, wurtzite-type, emission lineshape of excitonic mols., polariton states 77−20918
semiconductor epitaxial layer, polariton wave packet propag. in exciton reson. 80−2345
semiconductor films, free exciton polaritons, energy dissipation 79−95870
semiconductor sandwich structure, magnetoplasmon-type surface polaritons at interface 77−85292
semiconductor surfaces, optical props., book contrib. 80−80737
semiconductor with dipole impurities, light absorption 79−28796
semiconductor with superlattice, optical phonon excitation by light absorpt., impurity photoionisation 80−44275
semiconductor-dielectric interface, surface polaritons of LO-phonon-plasmon coupled modes 79−7792
semiconductor-metal boundary, magnetoplasma polaritons at the interface 79−38163
semiconductor-metallic screen interface, polariton propag. *(Spanish)* 80−84510
semiconductors, mixed crystals, polaritons, dispersion relation 78−18977
semiconductors, resonant Raman scatt. from exciton-polaritons *(Japanese)* 80−50349
semiconductors with direct band gaps, exciton-polariton interactions, Green's function approach 80−92831
solid plasma slabs, hybrid bulk-surface polaritons 79−60904
spatially dispersive media, optics, energy theorem and boundary conditions 79−47408
spatially dispersive medium, surface effects 78−56081
spatially dispersive semi-infinite media, polariton Green's functions, refl. spectra 77−85154
stimulated Raman scatt. of surface polaritons, amplification coeff. *(Russian)* 77−38993
stimulated Raman scattering in transversely bounded layer 77−75621
superconductivity, exciton and polariton mechanisms 79−60959
superconductor, possibility of surface polaritons at interfaces 77−24639
surface, and Brewster waves, in exciton luminescence spectra *(Russian)* 79−43033
surface, effects of roughness on dynamical props. 78−75923

polaritons continued
surface, excitation by stimulated Raman scatt., theory 78−9413
surface, linear photon and two photon absorpt. 80−49863
surface, nonlinear optical spectroscopy, stationary and nonstationary, theory *(German)* 80−6922
surface, plasmon dispersion, appl. to INSb 77−1464
surface, spectrum, coupling to excited fluorescent molecule near surface 77−69395
surface exciton polaritons, attenuated total reflection spectra 77−24867
surface exciton polaritons, book contrib., review 80−49623
surface exciton-polariton *(Japanese)* 77−39910
surface magnetoplasmon-type polaritons, LF, existence criterion in Faraday config. 80−96961
surface phonon-polaritons, semi-infinite crysts., review 77−89827
surface polariton effects in spontaneous emission, effects of spatial dispersion 78−34879
surface polariton frequency shift, cryst. surface and dielec. function depend. 80−44522
surface polariton generation through grating couplers 77−85153
surface polariton interaction with periodic surface struct. 77−47879
surface polariton modes, correlation with attenuated total reflection minima, computational study 78−31265
surface polariton motion in thin surface layer, nonstationary phenomenological theory *(German)* 80−88608
surface polariton scatt. at order parameter fluctuations, phase transition investig. *(Russian)* 77−20179
surface polariton scatt. by order parameter fluctuations near phase transition 77−35981
surface polariton use in optical storage 80−48414
surface polaritons, effect of surface roughness 79−73451
surface polaritons, freq. depend. of associated functions 79−78020
surface polaritons, Raman scatt., active spectroscopy theory 77−59576
surface polaritons, theory and spectroscopy uses 80−92835
surface polaritons allowing for spatial dispersion *(Russian)* 78−14675
surface polaritons due to spatial dispersion 79−69438
surface polaritons in anisotropic crystals, crystal optics 78−87919
surface polaritons in semi-infinite crystals, review 78−72087
surface-exciton polaritons, dispersion theory 78−72089
systems with minimum group velocity, time-depend. optical spectrosc. obs. 78−80376
$TCNQ^0$, crysts., extraordinary exciton polaritons in refl. spectra, macroscopic dielec. theory 77−89715
TCNQ, exciton surface polaritons at room temp. 79−47476
TCNQ, metallic reflection band, vibronic struct. 78−19502
TCNQ, single crystal, exciton surface polaritons, attenuated total reflection spectra 79−91460
thermal optical rotation, temp. depend. 79−8111
triclinic crystals, phonon-polariton dispersion relation 78−79946
two-photon absorpt., obs. of surface polaritons 77−51676
ultrashort laser pulses, interaction with condensed matter *(German)* 79−27335
uniaxial crystal, dispersion of bulk phonon polaritons meas. by IR refl. 78−59902
Wannier exciton-polaritons, real space wave eqn. 80−39508
Wannier-Mott polaritons in mag. fields, review 78−2437
wurtzite-type crystals, magnetopolaritons 79−78019
Ag, surface polariton absorption and emission spectra, edge effects 78−10375
Ag:Al_2O_3:Al tunnel-junction struct., surface polariton mean free path, roughness 80−93008
Ag/organic dye, excited mol. decay near metal surface, energy transfer to plasmon surface polaritons 80−50440
β-AgI, polariton dispersion curves, Raman spectra 80−29338
α-Al_2O_3, single crystal transmission and reflectance IR phonon spectra, polariton dispersion 80−66170
AmO_2, IR spectra, values of transverse vibr. frequencies 77−28585
$Ba(NO_3)_2$, dynamical props., IR reflection spectra meas., 10-300K 77−1676
$Ba(NO_2)_2.H_2O$, nonlinear optical props. and polariton scatt. spectra 77−75616
$BaTiO_3$, coherent excitation of soft polariton mode 79−15464
$BaTiO_3$, polariton freq. meas. by Raman scattering and permittivity 78−76006
$BaTiO_3$, struct. phase transitions, light scatt. meas. 79−95774
$BaTiO_3$, tetragonal, over-damped soft E-polariton and dielec. dispersion 78−15111
$CaCO_3$, hyper Raman scatt. of light by optical phonons 79−69844
CdS, A-exciton-polariton, time depend. optical spectrosc. obs. 78−80376
CdS, additional waves and polariton dispersion, reflectivity, transmittivity spectra 80−71443
CdS, B exciton-polariton, reson. Brillouin scatt. 79−33717
CdS, Brillouin scatt. of forbidden polaritons 79−33722
CdS, emission lineshape of excitonic mols., polariton states 77−20918
CdS, exciton polaritons, optical response 77−69792
CdS, exciton polaritons, Brillouin scatt. efficiency, additional boundary conditions 79−73960
CdS, excitonic polariton reflectance, quantitative anal. in spectral range of A-exciton 79−15480
CdS, excitonic polariton reflectance, B-exciton and k-linear term 80−7369
CdS, group velocity of light and polaritons, refl. and luminesc. spectra 77−24863
CdS, laser action in dense exciton systems 77−75531
CdS, laser thresholds and stimulated emission, intrinsic recomb. processes 79−15489
CdS, Raman shift dispersion near exciton reson., two-phonon cascade processes 80−11405
CdS, reflectance, transmittance and luminesc. spectra, light group vel. near exciton reson. *(Russian)* 77−69857
CdS, reson. Brillouin scatt. near A exciton 77−69846
CdS, reson. Brillouin scatt., book contrib. 79−42983
CdS, reson. Brillouin scatt. of exciton polaritons 80−11418
CdS, reson. Raman scatt., temp. depend. polarisation, A-exciton 77−12386
CdS, reson. scatt. of exciton-polaritons second emission under monochromatic excitation 77−1717
CdS, reson. scatt. of exciton-polaritons by acoustic phonons 78−60482
CdS, resonance hyper-Raman light scatt. on optical photons *(Russian)* 80−14396
CdS, resonant scatt. of exciton polaritons by LO and acoustic phonons 79−95760
polaritons continued
CdS, second order polaritons associated with van Hove singularities, light scatt. expt. 77−90146
CdS, three-branch exciton-polariton dispersion, direct meas. by reson. Brillouin scatt. 80−60620
CdS, transmission spectra, region of exciton reson., spatial dispersion effects 79−78704
CdS, two-phonon resonant Brillouin scatt. 78−84597
CdS, two-photon Raman scatt. via biexcitons, angle- and polarisation depend. 79−87446
CdS, virtually excited biexcitons polaritons dispersion, two photon Raman scatt. 80−45067
CdS(Se), magnetopolaritons in wurtzite-type crystals 79−78019
CdSe, resonant Brillouin scatt. via free and bound excitons 79−24330
CdSe, resonant Faraday effect, optical orientation of excitonic polaritons 77−69821
CdTe, exciton magnetoreflectance spectra, multicomponent polaritons, Zeeman splitting 80−88974
CdTe, luminescence and reflect. investig. of excitons, polariton model 77−40281
CdTe, reson. Brillouin scatt., book contrib. 79−42983
CdTe, reson. Raman scatt. by excitonic polaritons 80−11396
$CeCl_3$, mag. field depend. 79−33246
CmO_2, IR spectra, values of transverse vibr. frequencies 77−28585
Cr_2O_3, optical generation of longit. phonon modes 77−43288
Cu halides, phonon anomalies for Cu^+ at off-centre sites, dynamical model and Raman meas. 80−10618
Cu, surface polariton absorption and emission spectra, edge effects 78−10375
Cu-halides, phonon anomalies, dynamical model 79−73272
CuBr, biexciton dispersion, two-photon absorpt. 80−76045
CuBr, dispersion of multicomponent exciton polaritons, hyper-Raman emission spectra 80−20096
CuBr, surface exciton polariton, ATR meas. 77−77236
CuBr(Cl)(I), polariton Raman spectra, oscillator strengths, temp. depend. 80−66197
CuCl, anomalous TO-doublet origin for light scatt. study 78−43872
CuCl, anomalously slow group velocity of upper branch polariton 80−10893
CuCl, dielectric function for semiconductors with high exciton conc. 80−84443
CuCl, exciton luminesc., reabsorpt. and polariton effects 80−50430
CuCl, excitonic mol., two-photon excitation via polariton state 80−54612
CuCl, excitonic polariton-polariton resonance scattering 79−24306
CuCl, excitonic polariton, picosecond time of flight meas. 80−29337
CuCl, fission of relaxed excitonic mols. into upper and lower branch polaritons induced by M_L emission 80−11380
CuCl, giant two-photon absorption into excitonic mol., anomalous dispersion of excitonic polariton 78−27211
CuCl, luminesc. from Bose-condensed state of biexcitons 79−23905
CuCl, polariton effects in resonant Raman scatt. 78−10881
CuCl, polariton vel. direct obs. 79−28297
CuCl, propagation process of polaritons *(Japanese)* 80−24809
CuCl, reson. Raman scatt. and luminesc. under two-photon excitation 79−95765
CuCl, reson. two-photon Raman scatt., excitonic polariton dispersion 78−72509
CuCl, surface exciton polariton, ATR meas. 77−77236
CuCl, third-order nonlinear optical spectroscopy 77−23713
CuCl, three-branch polariton dispersion curve, two-oscillator model 80−92832
CuCl, two-photon reson. Raman scatt. with recoiling excitonic polariton 77−36223
CuCl, two-photon reson. Raman scatt., recoil of upper-branch excitonic polariton 78−27212
CuCl, two-photon resonant Raman scatt. via biexcitons 78−43302
Cu_2O, sample thickness depend. of exciton polariton absorption coeff. 80−34941
Fe film bounded by dielec. layers, surface polariton in ATR angular spectra 79−15545
FeF_2:Mn, mag. polariton, impurity mode enhancement and superradiance effects 79−28622
Fe_3O_6, O_2 annealed, optical absorpt., spin struct., polaronic absorpt., cryst. field transitions 78−68493
$Ga_{1-x}Al_xAs$, surface phonon polaritons, frustrated total internal refl. expts. 78−47656
GaAs base laminated epitaxial struct., surface plasmon phonon polaritons *(Russian)* 80−59905
GaAs, epitaxial film on GaAs substrate, two-interface surface polariton modes 78−60180
GaAs, exchange interaction, analytical and nonanalytical parts, from polariton spectra in mag. fields 80−50367
GaAs, exciton motion under external electric field 79−56135
GaAs, exciton-polariton reflectance spectra, exciton impact ionization and illum. intensity effects 79−42943
GaAs, excitonic polariton reson. interaction with LA phonons 78−60481
GaAs, impact ionisation of excitons 79−38079
GaAs, intrinsic, on degenerate n-Ge, surface polaritons, hydrodynamical model 80−6752
GaAs, luminescence by laser excitation, photocarrier thermalisation and polariton kinetics 77−66533
n-GaAs, mechanical polishing damage effect on IR refl. and ATR spectra 77−20848
GaAs, polar modes, light scatt. intensities, wave vector depend. 77−77219
GaAs, polariton fluoresc., spatial and spectral features 79−33760
GaAs, polariton scattering, free carrier effects 78−34783
GaAs, reson. Brillouin scatt., book contrib. 79−42983
GaAs, reson. Brillouin scatt. of exciton polaritons 80−11418
GaAs, reson. polariton fluoresc. obs. 77−85785
GaAs, resonant Brillouin scatt. of excitonic polaritons 77−44010
GaAs, surface nonlinear interactions, Green's function theory 78−42379
GaAs, weakly excited, luminesc. from exciton polaritons, based on exciton-electron collisions 79−83020
$GaAs_xP_{1-x}$, surface phonon polaritons, total internal refl. *(Russian)* 79−38688
GaP, high-order Raman spectra, polariton scatt. 78−56483
GaP, light scatt. spectra of guided wave polaritons 79−15101
GaP, polariton dispersion, IR reflection spectroscopy 80−11415
GaP, polariton linewidth in k-space, anharmonicity and permittivity 77−85155

polaritons continued
GaP, Raman scatt. from surface polaritons, selection rules 77−52083
GaP, Raman scattering selection rules for surface polaritons 78−72091
GaP, surface polariton linear photon and two photon absorpt. 80−49863
GaP, surface polaritons, freq. depend. of associated functions 79−78020
GaP, surface polaritons, light scattering studies, effect of surface roughness 80−6753
GaP, two-particle states and polariton spectrum 77−59261
GaP, upper polariton branch obs. by ATR 78−68510
GaSe, exciton absorption spectrum, polariton effects 77−85747
GaSe films, optical props. at lattice vibr. freqs., IR and Raman spectra 80−60696
ε-GaSe films, optical props. in IR region, metal substrate effect 80−71502
GaTe, exciton polariton effect on absorpt. edge, absorpt. and refl. spectra, 4.2 to 300K 80−20664
GaTe, exciton polariton effect on absorpt. edge, thickness depend. of absorpt. 80−20665
Ge-type semiconductors, two-photon parametric excitation of phonons 80−29339
GeF_4, Raman spectra at 77K, scatt. angle, polaritons and space group 78−23439
HCN crystals, polarition spectra and lattice dynamics 80−49313
HIO_3, polariton Fermi-resonance and dissociated phonon states *(Russian)* 80−20634
HgI_2, red anisotropic polariton dispersion, reson. Brillouin scatt. 80−7366
InP, exchange interaction, analytical and nonanalytical parts, from polariton spectra in mag. fields 80−50367
InP, surface phonon polariton dispersion and damping, frustrated total internal refl. meas. 80−80792
InSb, depletion layer, plasma and vibr. plasma type guided polaritons *(Russian)* 80−96933
n-InSb, dispersion curves for surface polaritons 79−19646
n-InSb, surface polaritons, excited by microwave magnetoplasma 79−19530
$KB_5O_8.4H_2O$, polariton Fermi reson., spontaneous parametric light scatt. 78−87923
$KBrO_3$, near-forward Raman scatt. by polaritons 78−43842
$KD_{2x}H_{2(1-x)}PO_4$ crystals, $0<x<0.98$, light scatt. by polaritons 80−96802
KH_2AsO_4, ferroelec. modes, polariton lineshape calc. 77−8585
KH_2PO_4 crystals, polarisation of unbound many particle states, IR spectra *(Russian)* 78−84556
KH_2PO_4, ferroelectric phase transition exam. by spontaneous parametric light scatt. 78−19427
KH_2PO_4, paraelec., Raman scatt. spectra of B_2-polariton and B_2(LO) modes 79−28762
KH_2PO_4, paraelectric phase, forward and backward Raman scatt. 79−33681
KH_2PO_4, Raman scatt. for polaritons of mixed B_2-E symm. 79−56795
KH_2PO_4, struct. phase transitions, light scatt. meas. 79−95774
KI, electron irrad., polariton effects in reson. emission 79−33843
KI, polariton effects in resonant emission 78−76533
LiF, molten, polaritonic spectra 79−23908
LiH, LiD, single cryst., reson. zero-phonon exciton luminesc., polariton emission 78−52564
$LiIO_3$, active spectroscopy of polaritons, interf. of direct and cascade processes *(Russian)* 77−38982
α-$LiIO_3$, attenuated total reflection spectra of anisotropic surface polaritons 78−87919
$LiIO_3$ crystal, coherent antiStokes Raman scatt. by polaritons 79−36961
$LiIO_3$ crystal, noncollinear stimulated Raman scatt. using parallel pump beam 80−78912
α-$LiIO_3$, Fermi resonance in surface polariton spectra *(Russian)* 80−71423
$LiIO_3$, possible separation of direct and cascade processes in active combination scatt. Raman spectroscopy 78−13764
$LiIO_3$, Raman induced Kerr effect with elliptical polarisation 78−42392
$LiIO_3$, Stokes and antiStokes scatt. by LF polaritons 77−77202
$LiIO_3$, surface polariton spread length by modified DCIR method *(Russian)* 79−73566
α-$LiIO_3$, surface polariton spectroscopy, frustrated total reflection method *(Russian)* 80−49628
α-$LiIO_3$, temp. depend. studies of Raman spectra of polaritons in region of phase transition 78−76467
$LiNbO_3$, comparative frustrated total refl. and Raman scatt., fundamental mode freq. and phonon dispersion 77−28579
$LiNbO_3$, dispersion law of polaritons, refr. index in IR, and Raman spectra meas. 78−27232
$LiNbO_3$, dispersion law and temp. depend. of polariton damping constant 79−95779
$LiNbO_3$, inverse Raman scatt. by polaritons 78−23434
$LiNbO_3$, low freq. Raman scatt. spectra of polaritons, photographic recording 79−73952
$LiNbO_3$, nonstationary intracavity stimulated Raman scatt. by polaritons 79−18473
$LiNbO_3$, polariton excitation for tunable coherent far IR generation 79−31982
$LiNbO_3$, spontaneous parametric scatt. line profile, IR absorpt. coeffs. 80−25377
$LiNbO_3$, tunable parametric Raman laser utilizing polaritons 79−41418
$LiTaO_3$, anomalous polariton dispersion near Curie temp. 77−80743
$LiTaO_3$, low freq. Raman scatt. spectra of polaritons, photographic recording 79−73952
$LiTaO_3$, uniaxial ferroelec., polariton dispersion relations 77−20249
MnF_2, inelastic light scatt. from antiferromag. polaritons, theory 77−73144
NH_4Cl crystal, polariton light scattering spectra in zone of dissociated states 79−47029
NH_4Cl, obs. of Raman scatt. by Cu vapour laser 78−95586
NH_4Cl, polariton Raman spectra, bound and many particle states 77−32372
$NaBrO_3$, surface polariton spectroscopy, frustrated total reflection method *(Russian)* 80−49628
NaI, single cryst., reson. zero-phonon exciton luminesc., polariton emission 78−52564
NpO_2, IR spectra, values of transverse vibr. frequencies 77−28585
$Pb_5Ge_3O_{11}$, Raman spectrum factor group anal., external and librational modes 77−36240
PbI_2 (2H), multi-phonon scatt. near direct absorpt. edge, resonant Raman obs. 79−87448
PbI_2, photocond. induced by polaritons at band-edge 79−95450
PbI_2, photoexciton interaction, luminescence spectra, polariton dispersion diagram 80−93397
$Pb(NO_3)_2$, dynamical props., IR reflection spectra meas., 10-300K 77−1676
α-quartz, reflection and surface polariton spectra, ion implantation effect *(Russian)* 79−47451
RbI, electron irrad., polariton effects in reson. emission 79−33843
Sb_2S_3 layered biaxial cryst., surface phonon polaritons *(Russian)* 78−60021
Si film, polariton resonance obs. from reflectivity meas. 77−69251
n-Si, surface polaritons in DC current 80−34369
SiC, dielectric coating effect on surface polaritons, optical consts. *(Russian)* 80−88489
SiC with dielectric coating, surface polaritons, waveguide modes 80−80195
SiF_4, Raman spectra at 77K, scatt. angle, polaritons and space group 78−23439
SiO_2, amorphous and crystalline, surface polaritons and splitting of optical frequencies 78−72090
$Sr(NO_3)_2$, dynamical props., IR reflection spectra meas., 10-300K 77−1676
$SrTiO_3$, centrosymmetric crystal, phonon polariton hyper-Raman scatt. obs. 80−76028
$SrTiO_3$, hyper Raman scatt. on polaritons, polariton branches *(Russian)* 80−50334
TeO_2, paratellurite cryst., polariton Raman scatt. 78−25928
TiO_2-LiF film system, ATR, substrate surface polaritons reson. effect *(Russian)* 77−32384
Xe, crystalline, polariton effects, reflectivity, absorpt., and resonant luminesc. spectra calcs. 80−20095
YIG-LiF film system, ATR, substrate surface polaritons reson. effect *(Russian)* 77−32384
ZnO, ang. depend. of reflection spectra and directional dispersion of anisotropic exciton polaritons 78−31216
ZnO, E1 and A1 polaritons, spectra, optical meas. system 77−38018
ZnO, excitonic mol. transitions, optical gain and induced absorpt. spectra 80−11438
ZnO, excitonic molecule transitions, M-band emission 79−78742
ZnO, laser thresholds and stimulated emission, intrinsic recomb. processes 79−15489
ZnO, near-forward Raman scatt. intensity of E_1(TO) polariton mode 78−23462
ZnO, polariton dispersion, IR reflection spectroscopy 80−11415
ZnO, stimulated two-photon emission from excitonic molecules 79−28815
ZnO, surface exciton polariton, nonlinear optical excitation 77−59259
ZnO, surface exciton polaritons, ATR obs., book contrib. 79−42620
ZnO, surface exciton polaritons, nonlinear optical excitation and dispersion relation 79−82657
ZnS, Raman scatt. by phonon polaritons 80−103959
ZnS(Se), wavelength-modulated refl. spectra, 2.5 to 8 eV, excitonic polariton 77−20877
ZnSe, attenuated total refl. spectra of surface exciton polariton 77−36262
ZnSe film, surface polaritons, thermostimulated emission *(Russian)* 78−10904
ZnSe film, thermostimulated polariton emission 78−2436
ZnSe films, long wavelength IR polariton emission band thermal shift and broadening 80−92833
ZnSe, magnetoreflectance of exciton-polaritons, semiclassical treatment 79−99857
ZnSe, polaritons, reson. Brillouin scatt., heavy and light excitons 79−99898
ZnSe, relaxation processes in Raman scattering and exciton luminescence under resonant excitation 80−25386
ZnSe, resonance Raman scatt., exciton-polariton luminescence *(Russian)* 80−97287
ZnSe, single cryst. and film, long wave IR emission by lattice vibrs. 77−51528
ZnSe single crystal, exciton photolum. and refl. spectra, 4-90K *(Russian)* 77−66540
ZnTE, relaxation processes in Raman scattering and exciton luminescence under resonant excitation 80−25386
ZnTe crystals, polariton effects in luminesc. 80−103988
ZnTe, laser thresholds and stimulated emission, intrinsic recomb. processes 79−15489
ZnTe, luminescence spectra struct. surface and volume polaritons *(Russian)* 80−16089
ZnTe, Raman scatt. and exciton luminesc. under reson. excitation 79−38617
ZnTe, relax. processes at high excitation levels, Bose-Einstein condensation of excitons 78−48219
ZnTe, resonance Raman scatt. of excitonic polaritons by LO and acoustic phonons 79−65879
ZnTe, secondary emission, transient behaviour under band-to-band excitation 80−108266

polarization in elementary particle interactions *see polarisation in elementary particle interactions*

polarization in elementary particle scattering *see polarisation in elementary particle scattering*

polarographs *see polarography*

polarography
see also voltammetry (chemical analysis)
AC, effect of cell circuit resistance on peak height 77−29068
AC, use of nonlinear pot. time ramp to generate DC pot. 78−53292
adsorption at soln.-electrode interface, AC polarographic data anal., computer program 80−3400
alternating current electrode processes, review 80−61107
amalgam, film, with accumulation, appl. to micro-, macro-object anal., review 78−61098
amplifier, programmable- or auto-gain, for gas chromatograph, spectrometer or polarograph 79−43644
analyser, modifications 77−2679
arterial pO_2 intravascular monitoring using catheter-tip polarographic electrode *(German)* 78−85408

polarography continued
automatic controller for polarography, design, operational sequence 80−71968
auxiliary unit, for a.c. voltammetric meas. on conventional d.c. polarograph 77−4954
bacteriochlorophyll *b* and pheophytin pair redox potential obs. 79−39338
biomedical catheterisable sensors, PO_2 probes, press. transducer and photometers 80−46080
blood pO_2 meas. polarographic technique 79−100782
cell voltage step production methods 78−7282
chlorophyll, aq. solns. of detergents, polarographic obs. 79−57565
data acquisition, fast autoranging techniques 78−85233
DC, charging current compensation, in situ methods 77−25337
DC wave automatic anal., minicomputer appl. 77−25333
derivative neopolarograms, shapes, theory 78−53289
desensitising dye polarographic half-wave potential meas. 80−7802
development, review 78−35769
dextran aqueous solutions, microviscosity investig. by square-wave polarography 79−95200
difference polarography, review of method, instrumentation 80−26078
differential cathode ray polarograph, exam., determination of Cd, Zn 78−56930
differential polarographic waves, peak reading instrument, exam. 78−56931
differential pulse, improved signal to noise ratio 77−29072
differential pulse polarography, current-pot.-time relationships, theory 79−24844
differential pulse polarography of irreversible reactions, anal. appl. 79−79325
differential pulse type, digital simulation with incremental time change 77−90662
double tone polarography, optimisation, measuring, dropping freq. synchronisation 77−25340
electrochemical voltage indicators, production, voltage response, resist. 77−1936
electrolyte solution, streaming at neg. polarographic maximum 78−61020
Fournier and higher order harmonic polarograms; data anal. 77−63985
haemoglobin-O_2 equilibrium curve determ., semipermeable membrane transport model 79−92418
immunoassay, differential pulse polarography method 79−79709
intermodular AC phase-selective 77−29057
Kalousek, computerised 79−52792
liquid chromatography, use of electrochemical detection methods 80−50906
liquid film flow down inclined plane, polarographic velocity meas. method *(French)* 78−34214
liquid metal electrode, polarographic max. current theory, electrochem. and hydrodynamic instability 79−24750
liquid metal electrode, polarographic max. current theory, hydrodynamic instability 79−24749
low frequency AC small-size polarograph 79−70390
maximum suppression by substituted vinyl quinolones 79−57325
microprocessor controlled polarograph for determ. of species with overlapping waves 77−12844
natural water chem. anal., modulated polarographic, voltammetric techniques 77−37253
5-nitrobenzimidazole in photographic processing solns., AC polarography determ. 79−24861
OH 103 and OH 105 polarographs description *(Hungarian)* 77−40608
ohmic drop compensation, appl. to electrochem. impedance, pot. curve meas. *(French)* 77−52693
photographic colour developing agents in processing solns., polarographic determ. 78−4726
photographic processing solns., anal. by AC polarography 77−12861
polarographic detection for high performance liquid chromatography, conference, Carlsbad, Czechoslovakia (April 79) 80−73097
polyethylene capillary dropping mercury electrodes, for corrosive media appls., prep. 78−61090
polymers, paints, testing, modern analytical methods appl. *(Polish)* 78−85253
polyphenylquinoxaline-cellulose acetate, battery separator membrane, diffusion meas. 80−35574
potentiostat principles and construction *(Dutch)* 77−77856
pulse, chronoamperometric, chronocoulometric techniques, kinetic, mass transport effects 77−25334
pulse, polarographic current const. determ. using Cd^{2+}, Zn^{2+} ions in soln. 77−25338
pulse, time scanning, limiting current diagnostic differentiation technique 77−25339
pulse polarography, appl. *(Chinese)* 78−85245
pulse polarography, microcomputer-controlled polarograph appls. 80−66895
rapid scan alternate drop pulse polarographic methods 79−24845
regional myocardial perfusion determ. from H_2 washout curve 79−92459
respirometer, flowmeter-polarographic electrode sensor, for respiratory function telemetering 78−80995
reverse polar figure const. using linear eqn. system, appl. to cold worked Al 77−73488
reverse pulsed polarography, reversibility characterisation, electrode reaction product determ. 80−66889
reversible adsorption waves, origin 78−53288
semiautomated system, using modified Technicon sampler 77−70354
semidifferential electroanalysis, derivative neopolarogram peak shapes 78−7256
sensor with microwire indicator electrode, exam. of design 80−21340
signal components, meas. using multiplier circuitry 78−61119
thermal energy, electrochem. conversion using cells with reversal of pot. with temp. 80−26124
thin-layer continuous-flow and pulsating systems, anal. characts. 78−23980
transuranium cpds. in aq. soln., electrochem. 77−29040
$ZnCl_2$-KCl-NaCl, molten system, containing Ni^{2+} ions, appl. to electrorefining 80−66810
Cd, polarographic determination *(Japanese)* 77−77852
Cu alloys, determ. of Cu, Sb, inverse voltamperometry method 78−61099
Eu(III) complexes with gluconate ions, reduction, polarographic behaviour 78−92568
GaP:Te epitaxial layers, dopant distrib. obs. by amalgam polarography 77−39609
In, polarographic determination *(Japanese)* 77−77852
In(III) complexes with gluconate ions, reduction, polarographic behaviour 78−92568
N_2O, determ. in blood or gas by polarographic sensor 79−62412
Na_2O-B_2O_3-Na_2SO_4, glass, exam. of chemical differentiation, using Cu ion segregation 78−87625
O_2, determ. in blood or gas by polarographic sensor 79−62412
O_2 electrode, membrane-covered catheter-tip system, construction and performance 78−81003
O_2 partial pressure and bioelectric potential simultaneous meas. in living tissue *(German)* 78−85453
O_2 partial pressure measurement with thin-layer polarographic probe, intracortical appl. *(German)* 78−85410
O_2 partial pressure on blood sample meas., error reduction 78−7470
Te, polarographic prewave, photo-effect 77−36833
Te separation, determ. in inert gas, H_2 mixtures, oscillograph polarography method 78−61100
V, microconcs., polarographic determ. 79−16072
W-Re alloys, polarographic determ. of Re 79−16071
Zn^+, transport in cation-exchange membranes 78−96033
Zn(II) complexes with gluconate ions, reduction, polarographic behaviour 78−92568

polarons
see also small polaron conduction
acoustic deformation pot. polarons, linear energy-momentum relations 80−80196
acoustic deformation potential polaron 77−69254
acoustic mode, energy-momentum relations 78−51908
acoustic mode, frustrated linear energy-momentum relations 78−23034
alkali halide, excitonic mechanism of defect form. 77−47737
alkali halide, F-centres, vibronic problem in higher excited states 78−10931
alkali halide, rel. to optical breakdown, damage threshold calcs. 79−95708
alkali halide crystal, hole localisation at two halogenide ions, polaron theory *(Russian)* 77−69268
alkali halides, bound polarons, vibronic theory, appl. to F-centre excited states 78−84150
alkali halides, optical breakdown, 1.06 to 0.172 μm 78−35089
alkali metal halide, laser damage morphology simulation 80−35015
alkali metal halide optical breakdown, multiphoton carrier generation theory 79−19953
amorphous compound semiconductor, thermoelectric power and transport models 78−10482
antiferromagnetic semiconductor, ferron-polaron states of carriers 77−69257
benzophenone, charge carrier generation and mobility 78−84231
2-benzoylpyridine crystals, lowest triplet state, optically detected EPR 80−15827
Bessel function integral, asymptotic evaluation 78−56082
bound, excited states 77−69256
bound, ground state energy 78−87925
bound, non-perturbative variational method 80−88485
bound, shallow, energy levels 79−15104
bound, variational calc. of ground state energy 78−84152
bound polaron, excited states 79−78021
bound polaron, non-perturbative approach 79−69439
central peak in polaronic cryst. 78−47712
chalcogenide semiconductors, optical and elec. props., comparison with SiO_2 78−6721
conducting molecular crystals, atomic limit and polarons 80−39860
deep oxide acceptor, intra- versus inter-small-polaron transitions 78−30874
defect tunnelling, phonon assisted, in-band defect-induced phonon reson. modes effect 78−14419
deformation potential polaron, perturbation theory breakdown 80−84440
degenerate semiconductors, heavy hole-phonon bound states for valence band with degeneracy point *(Russian)* 80−15461
density of states of critical polarons near low. temp. ferroelec. transition 78−60065
dielectric and molecular polarons, comparison and new props. 79−28298
dielectric slab, polaron self-energy 79−56144
dispersion self-energy of an electron in a dielectric 79−42461
effective mass and optical absorpt. spectrum, f-sum rule 77−43520
electron radius of qyratron in polaron model 80−88486
electron-lattice systems, strongly bound, excited states, polaron model 78−84151
electron-phonon interactions, dressed electron construction, Brillouin-Wigner and Tamm-Dancoff approaches 80−49629
electron-phonon system, kinetic equation, chronological and antichronological T-products 80−70627
electronic localised state at edge dislocations, parabolic dispersion law *(Russian)* 80−65479
electronic polaron, excess electron transport, polarisation dynamical self consistency depend. 79−47030
electronic Raman scatt. in polaron gas 79−95753
electrons in surface phonon field 80−107885
energy bound to Coulomb potential 80−88487
energy eigenvalue, systematic calculation procedure 80−84439
exciton, polaron mass 79−95344
ferroelectrics and antiferroelectrics, polaron state of electron near structural instability 79−33245
ferromagnetic semiconductor, bound mag. polaron 79−90976
ferromagnetic semiconductor, energy and mobility of spin polarons 80−70982
ferromagnetic semiconductor, mag. polaron stability 80−96803
ferromagnets crystal, $S \geq 1$, ground state of mag. polaron *(Russian)* 77−63142
Feynman effective mass, Frohlich model, path integral method 79−69440
free, multiphoton absorpt. spectra, electron reson. coupling via longit. optical phonons 79−95347
free polaron spectrum and convergence radius in perturbation theory 80−70626
free-particle and mag. masses, equivalence 80−107718
Froelich Hamiltonian, perturbation theory calcs. 79−33247
Frohlich model, method of functional derivatives 78−51909
Frohlich polaron, mean field theory, phase transitions 80−34371
gas of interacting polarons, ground state energy 77−76758

polarons continued
generalised path integral formalism, ground state energy corrections 80−84438
glasses, low temp. props., two-electron excitons 77−15786
ground state energy and effective mass calc., arbitrary coupling force on mag. field 77−66128
homopolar crystal, self-trapping barrier in strong mag. field 77−20250
hopping, quantal occurrence probability treatment 78−43313
ice film, low-temp. diffusion of electrons, evidence for polaron bands 77−1380
II-VI compounds, doubly ionisable centre binding energy 79−65405
insulator to superconductor phase transition, possibility 79−47190
intermediate valence system, local polaron model 80−107717
ionic crystals, surface polaron 78−60020
ionic crystals, weakly bound surface polaron 79−69576
ionic crystals with intermediate polaron coupling, magneto-optical effects in shallow F-centres 80−20615
ionisation of polarons, temp. depend. dispersion self-energy approach 80−34370
kinetic equation for dynamic system *(Russian)* 80−54619
large polaron ground state, first order phase transition 78−87924
large polaron phase transition in strong coupling limit 79−73452
large radius polaron, bound-state spectrum 80−59894
large radius polaron model, soliton excitations 79−42470
lifetime of carriers and excitons before self trapping 77−85236
localised bipolarons in ionic crystals 78−67957
long-wave quasiparticle states localized at screw dislocation *(Russian)* 78−95126
magnetic semiconductor, self-trapped electrons 77−59262
magnetic semiconductor, spin polarons in s-d model with off-diagonal exchange 78−34784
magneto-optical response props. of cond. electron 77−52057
metal-semiconductor disordered interface, supercond. transition temp. enhancement by bipolaron interface centres 80−84528
mixed valence, stabilisation by polaronic effects 79−4520
mixed- and intermediate-valence compounds, polaronic effects 79−60732
mobility at low temperature, self-consistent equation-of-motion approach 79−56142
molecular crystal, charge carrier mobility temp. depend. 78−10376
molecular crystal, Frenkel excitons, effect on charge carrier transfer 78−79936
molecular polaron, dynamics and thermodynamics 78−14678
molecular polaron, first-order phase transition 79−90977
molecular system, electronic polarisation energy, quantum effects 78−67956
Mott insulators, excitonic spin polarons, appl. of Nagaoka's theorem for electron-Hole pair 80−107978
nonpolar fluid, excessive electrons near crit. points 80−92836
one dimension, electron-optical phonon interaction with strong coupling via deform. potential, vibr. excitations 78−51907
one-dimension, electron-acoustic phonon interaction via deform. potential 77−4302
one-dimension, lower bounds to self-energy 77−72827
one-dimensional, asymptotic spectrum of momentum eigenstates 79−56143
optical characts., bound polaron and phonon states *(Russian)* 78−39556
optical polaron, ground state and first internal excited state 77−89716
orbit degenerate electron state localised at point defect, T-term multimode Jahn-Teller effect *(Russian)* 80−15490
paraelastic tunnelling system dynamics, intermediate coupling regime 77−55489
paramagnet system, low-temp. diffusive transport for polarons and defectons 78−43174
particle-field interaction, classical version of polaron-like models 80−46834
Peierls-Frohlich state, electron excitation *(Russian)* 79−23909
periodic solutions of the classical polaron and bipolaron systems 80−100438
phonon-assisted defect tunnelling with quadratic defect-lattice coupling, small polaron theory 79−73274
photoferroelectric phenomena, physical models derivation for photoferropolaron 79−15407
piezoelectric crystal, surface polaron states, polaron-phonon interactions 80−70790
piezoelectric polaron lifetime, elimination of IR divergence 78−76007
piezoelectric semiconductor, optical absorpt. by free polaron 77−59547
piezoelectric semiconductor, polaron optical absorpt., external static elec. field depend. 77−85158
piezopolarons and condensons, temp. and screening effects on effective mass 77−43521
polar crystal, polaron effective mass temp. depend., electron interaction *(Chinese)* 80−84436
polar crystal with impurity atom, lattice energy change, optical vibrs. freq. shift 77−11652
polar crystals, exciton interaction pot., polaron effects 77−24523
polar dielectrics, triplet two electron states 80−24810
polar lattice coupling, effect of excitons 80−24811
polar liquid, additional electron delocalised state, optical excitation calcs. 80−54622
polar liquid, solvated electron optical props. and thermodynamic characts., polaron model 78−85170
polar semiconductor, exciton dispersion, influence of optical phonons, effective exciton mass, variational calc. 79−15091
polar semiconductor, exciton-dispersion 80−6741
polar semiconductors, chemical shift of Zeeman masses 78−10338
polar semiconductors, effective Hamiltonians and binding energies of Wannier excitons 78−34777
polyacetylene, intrinsic conformational defect states 80−65500
polyatomic crystal, isotropic polaron 77−85157
polydiacetylene, intrinsic conformational defect states 80−65500
quantum field theory of solids, book 77−31922
rare earth compounds electron-phonon interaction influence on electronic phase transitions *(Russian)* 78−47743
rate processes in condensed media, anharmonicity effects 79−19349
renormalizable interactions in two dimensions and sharp-time fields 78−81882
resonance Raman scattering in systems with localised carriers 80−7356
self-trapped acoustic polaron with site diagonal and off-diagonal electron-phonon interaction 80−2348
semiconducting crystal, phonons and localisation at impurities 80−24812

polarons continued
semiconductor, core excitons, binding energy in effective mass approx. 80−24808
semiconductor, ferromag., bound mag. polaron form., anomalous carrier density mag. field depend. 80−49774
semiconductor, ferromag., polaron solitary waves 80−70625
semiconductor, ferromag., spin polaron props., effect on carrier scatt. 80−60233
semiconductor, ground state energy of shallow impurity centres 77−4314
semiconductor, ionic., ionisation of doubly charged centres 79−11085
semiconductor, magnetophonon resonance oscills., peak shape, theory 80−107824
semiconductor, phonon spectrum in mag. field, renormalisation 79−28060
semiconductor, pinning struct. of cyclotron reson. lines 78−72414
semiconductor, polaron aspects of generalised Haynes' rules 78−18978
semiconductor, polaron mechanism of narrow band form. in quantising mag. field 77−76759
semiconductor, polaron transport in long phonon waves approx. 79−90975
semiconductor, polaronic hopping conduction at low temp. 78−51906
semiconductor, shallow donor states exam. by two photon spectroscopy 79−23925
semiconductor, weakly polar, IR absorption by optical polaron in mag. field 77−66127
semiconductor degenerate-band case, weak to intermediate hole-phonon coupling 77−66126
semiconductor physics in high mag. fields, review *(Japanese)* 80−50192
semiconductor thin film, polaron near-threshold spectrum 80−65471
semiconductor with degenerate valence band edge, hole polaron self energy 77−43519
semiconductors, binding energies of core excitons, effective mass approx. 79−73439
semiconductors, elementary excitations in disordered systems with localised electrons, polarons *(Russian)* 80−49632
semiconductors, excitonic polarons, Pollmann-Buttner variational method, donor and exciton binding energies 79−42469
semiconductors, IR absorpt. of light by polarons 79−56799
semiconductors, temp. depend. electronic cond. 80−59975
semiconductors, weakly polar, free polaron IR absorpt. effect of DC field 77−81132
semiconductors, weakly polar, intraband magnetoabsorption theory 79−42949
shallow impurity centres near Curie point, influence of dielec. nonlinearity on temp. depend. of ionisation energy 80−10916
shell-model crystal, electron-phonon interactions effect of F-centre on shell screening 77−72825
singularities of the small polaron effective mass 78−63989
small polaron theory, translational symm. breaking transform. 80−92838
small-polaronic glass, dynamics of optically induced props. 80−49630
spin polarons in narrow almost half-filled s-band, appl. to BCC ^{3}He 77−62703
strong coupling theory, variational approach 80−54621
surface, surface self-trapped states *(Japanese)* 80−2445
surface exciton energies and radii 80−92829
surface lattice vibrations, interaction with low-energy electrons 78−30820
surface polaron in mag. field 79−23912
TCNQ, electron- and phonon-polaron effects in valence and cond. bands 77−76757
TCNQ, optical IR antireson. absorption, characts. rel. to cryst. parameters 77−77183
tetrahedral semiconductors, Haben methods for single isotropic parabolic energy bands 79−56140
transport equation soln. in strong alternating elec. field 80−39596
tunnelling of small polarons, thermally assisted, computer anal. 80−2391
two-dimensional surface layer, ground state energy and effective mass of polaron 79−23910
two-level tunnelling system, phonon interaction theory 77−15525
two-polaron bound state, strong and weak coupling approx. 78−39039
Urbach's rule derived from thermal fluctuations in the band-gap energy 79−33729
water, solvated electron, polaron coupling const. from dipolar plasmon freq. 77−89720
weak coupling theory, energy spectrum, lifetimes 77−20251
AgBr, cyclotron reson. of polarons at high microwave fields 78−67958
AgBr, cyclotron reson. of polarons at high microwave fields 79−61228
AgBr, cyclotron reson. of polarons at high density excitation 80−75859
AgBr, localisation of polarons on (100) surface, rel. to photographic sensitivity *(Russian)* 77−35983
AgCl, cryst. luminesc. and photovoltaic effect kinetics 78−64391
AgCl(Br), crossed elec. and mag. fields, hot electrons, streaming motion, population inversion 80−44649
BaO, electronic struct. of V^- and related centres 80−2355
$BaTiO_3$, melt grown, drift mobility meas. 79−19596
CaO, electronic struct. of V^- and related centres 80−2355
n-CdS, piezoelectric polaron and polaron pinning 77−35872
CdS, polaron cyclotron resonance freq. shifts, halfwidths, cumulant expansion method calcs. *(Russian)* 80−88880
n-CdS, polaron effective mass, DC Hall effect meas. 78−39037
CdS, polaron IR cyclotron reson. 80−25347
CdSe, polaron IR cyclotron reson. 80−25347
CdTe, shallow donors, excited state transitions 78−6710
Cu_2O, pure and Fe doped, carrier cyclotron resonance impurity scattering effects, polar mass extrinsic origin 79−56614
$Cu_xV_2O_5$, nonmetallic bronze, low field sp. ht. and mag. suscept. 78−72357
Er_2O_3, mag. susceptibility, elec. cond. and dielectric const., hopping cond. 77−12083
Eu chalcogenides, mag. polaron stability 80−96803
Eu chalcogenides, multiphonon inelastic light scatt., hot recomb. 77−8559
EuO, anomalies in transport props. under hydrostatic press. due to bound mag. polaron 77−20372
EuO, hydrostatic press. effects on elec. resist. in temp. range 3 to 300K 79−23968
EuO, light-induced metal-insulator transition, mol. mag. polarons 77−4396
EuO, transmission and resistivity, stress modulation effect near Curie temperature 80−96874
EuO(Se), complex elec. cond. anomalies 80−107812

polarons continued
$Eu_2(WO_4)_3$, mag. susceptibility, elec. cond. and dielec. const. meas. 77−11916
Fe, μ^+SR, theory of spin depolarisation rate 78−80271
Fe_3O_4, neutron diffuse scatt. due to mol. polarons 80−15460
Fe_3O_4, neutron diffuse scatt. due to molecular polarons 80−88488
GE, microwave cyclotron resonance lineshape, magnetoplasma interference effect, reinterpretation of excitonic polaron 78−43287
GaAs MOS and Schottky systems, electromodulated reabsorption of luminesc. 79−15524
GaAs, shallow donors, excited state transitions 78−6710
GaAs, surface exciton energy 80−92829
GaAs-$Al_xGa_{1-x}As$, heterojunction and superlattice, magnetophonon reson., polaron mass 80−44715
GaSe, electron-phonon interaction and optical props. 80−34942
Gd_2O_3, B-type monoclinic, DC(AC) elec. cond., thermoelectric power, dielectric const., temp. depends. 80−59980
c-Gd_2O_3, electrical cond., dielectric const. mag. susceptibility, polymorphic transition 77−59505
Ge, cyclotron resonance peaks under high excitation 77−48056
Ge, electron interaction with many excitons 78−26823
^{3}He, BCC, spin polarons in narrow almost half-filled s-band 77−62703
^{3}He, FCC, vacancy induced spin polarons 80−59756
^{3}He, HCP, vacancy-induced transitions 80−88395
^{3}He, solid, as mag. semicond., analogy to Mott insulator 80−96720
^{3}He, solid, magnetic polarisation around vacancies, on two-dimens. lattice 79−51368
^{3}He solid, paramag., low-temp. diffusive transport for polarons and defectons 78−43174
^{3}He, solid, struct. of vacancy induced spin polarons 79−95244
^{3}He, solid BCC, contrib. of vacancy mag. polarons to sp. ht. 79−56032
$Hg_{0.72}Cd_{0.28}Te$ semiconductor, two-mode reson. polaron 79−15105
$Hg_{1-x}Cd_xTe$ mixed crysts., magneto-opt. obs., semicond. config., semimetal-semicond. transition 77−73131
InSb, impurity polarons at two LO-phonon region, magneto-optical anomalies 79−61227
InSb, magneto-optical anomalies of impurity electrons, two-LO-phonon region 78−72415
InSb, mobility from soln. of Boltzmann eqn. for electron-LO phonon scatt. 79−19586
InSe, exciton and polaron anisotropies, reson. Raman scatt. study 80−76033
KBr, transient infrared absorption of bound polarons 78−92071
KBr(Cl), positron ang. correl., cryst. orient. depend., positron states and ionic distortion 77−63484
$La_{1-x}Sr_xCrO_3$, x=0-0.2, AC and DC cond., 77-1300K, hopping of polarons 78−2477
$LiNbO_3$ crystals, polaron character of colour centres 80−2013
$LiNbO_3$, optical absorption of hole centres, polaron model 80−97314
$LiNbO_3$, two-photon and X-ray induced Nb^{4+} and O^- small polarons, ESR and optical absorpt. 78−76306
$LiNbO_3$:Fe, thermally activated trapping caused by small polaron formation 77−20259
$LiNbO_3$:Fe, X-ray and γ-ray irradiation effects on Fe charge state, Mossbauer study 80−40013
MgO:Li, $[Li]^0$ defect, stress induced optical dichroism 78−35179
MgO:Li, $[Li]^0$ defects, magneto-optical props. 77−12365
NH_3, solvated electron, polaron coupling const. from dipolar plasmon freq. 77−89720
NH_4Cl, Raman scatt. at polarons near intramol. vibrs. 77−44003
NaCl, positron ang. correl., cryst. orient. depend., positron states and ionic distortion 77−63484
NaCl, transient infrared absorption of bound polarons 78−91642
NaCl:Ag, irrad. with synchrotron radiation, thermolum. light-sum spectrum of L absorpt. edge of Cl^- 79−15540
$Na_xV_2O_5$, nonmetallic bronze, low field sp. ht. and mag. suscept. 78−72357
Nd_2O_3, A-type, thermoelectric power, AC cond. 78−68044
Ni complex, (1,4,5,8,9,12,13,16-octamethyltetradbenzporphinato nickel)$^{+\gamma}$ $(I_3^-)_\gamma$, atomic limit of Hubbard model and polarons 80−39860
NiO, dipole orientation from bound polaron hopping 80−84437
NiS, spin polarons exam. and metal-insulator transition 78−10377
PbI_2 (2H), electronic transport and cyclotron reson. 79−28369
$PbMoO_4$, optical absorption of hole centres, polaron model 80−97314
n-PbTe, far IR magnetotransmission and refl., dielec. function 77−52091
PbTe, magneto-optical pinning phenomena 79−82962
RbCl:Ag^-, off-centre system, quadratic-coupling phonon-assisted defect-tunnelling theory 79−55849
Si, inversion layer, polaron model for localisation 80−20280
Si, mag. props. of dislocations, spin polarons 79−82531
Si_xGe_{1-x}:H, amorphous, photoinduced optical absorption 79−82973
SiO_2, amorphous, optical and elec. props., comparison with chalcogenide semiconds. 78−6721
SiO_2, amorphous electron transport and breakdown at high elec. fields 79−78108
Sm_2O_3, B-type monoclinic, DC(AC) elec. cond., thermoelectric power, dielectric const., temp. depends. 80−59980
$Sm_{0.75}Y_{0.25}S$, mixed-valence, electron-lattice correlations, EXAFS studies 80−76103
SrO, electronic struct. of V^- and related centres 80−2355
Tb_2O_3, B-type monoclinic, DC(AC) elec. cond., thermoelectric power, dielectric const., temp. depends. 80−59980
Te, photoconductivity in strong mag. fields, doping effects, impurity levels 80−75602
TiO_2-SiO_2, semicond. glass, optical props. 78−60412
Ti_4O_7 and $(Ti_{1-x}V_x)_4O_7$, metal-insulator transitions, EPR, elec. and mag. props. 80−2336
Ti_4O_7, rel. to optical absorpt. and metal-insulator transitions 78−15165
$(Ti_{1-x}V_x)_4O_7$, elec. cond. and phase diagram near metal-insulator transition 80−11054
TlBr, resonant polaron coupling and excitons under mag. field 80−71383
TlBr(Cl), polaron-induced anomaly of exciton 79−60719
TlI, magnetoabsorption, exciton polaron pinning 77−28593
VO_2, metallic phase, electronic props., plasma freq., Hall coeff. 78−84195
V_2O_5 single crystals, contact-limited conduction 79−95493
$W_xM_{1-x}O_3$, reduction and temp. effect on electronic core levels, XPES 79−91564
WO_3 amorphous layers, electrochromic absorpt. depend. on crystallinity and electron localisation 77−59589
WO_3 electrochromic absorption dependence on crystallinity 77−77314
polarons continued
WO_3 electron density map of W^{5+} polarons, EPR and optical absorpt. obs. 80−44912
WO_3, light induced W^{5+} ESR 77−36126
WO_3, polar, electrochromic absorpt. bands, small polaron theory 78−39528
WO_3, reduction and temp. effect on electronic core levels, XPES 79−91564
YAG, colour centres conceived as bound polarons 78−63990
YAG, optical absorption of hole centres, polaron model 80−97314
Yb chalcogenides, multiphonon inelastic light scatt., hot recomb. 77−8559
n-ZnO film, highly degenerate, IR absorption by free polarons 77−4697
ZnS, radiation emission, stimulation by IR light, electron traps and polaron energy determ. *(Russian)* 77−66542
n-ZnSe crystals, electron scatt. mechanisms, high mobility 80−34433
n-ZnSe, purified by annealing in molten Zn, Hall mobility and polaron coupling 77−85243
p-ZnTe, cyclotron resonance from photoexcited electrons, polaron effective mass determ. 79−69723
ZnTe, valence band parameters and free exciton reduced mass, free exciton magnetoreflectance 80−45046
ZnTe, wavelength-modulated reflectance spectrum, electron-phonon and exciton-phonon interactions 79−11434

poles and towers
lightning stroke flashover calc. *(Russian)* 77−55180

poles and zeros
analytic extrapolations towards interior points from a cut, applic. to elementary particle scatt. theory 80−12952
atomic eigenfunctions, nodal structure 80−57122
Bessel functions, infinite system of eqns. characterising zeros 79−12570
Bessel functions, infinite systems of nonlinear equations containing zeros 80−46786
composite signal anal., by cepstral inverse filtering, biomedical appl. 78−69243
confluent hypergeometric functions, high order nonlinear eqns., sum rules, zeros 79−92923
confluent hypergeometric functions, nonlinear eqn. infinite system, zeros 79−92922
data reduction, approximate realisation, new techniques 79−70898
event location by recursive least squares prediction 80−96131
grand canonical partition function type polynomial, zeros 77−22498
heat exchangers, approx. of dynamics of method of weighted residuals *(Japanese)* 78−67024
Hermite polynomials, systems of nonlinear eqns. for zeros 78−69961
Hermite polynomials, zeros, asymptotic density, singular integral operator props., 79−17188
Jacobi polynomials, asymptotic behaviour of zeros as t tends to infinity 79−42
Jacobi polynomials, zeros, asymptotic density 79−17189
Laguerre polynomials, matrices and algebra related to zeros 79−92920
Laguerre polynomials, nonlinear enqs. systems and sum rules for zeros 78−69962
Laguerre polynomials, zero asymptotic behaviour, limiting formula for Hermite polynomial relation 78−93509
Laguerre polynomials, zeros, asymptotic density 79−17189
Laguerre polynomials, zeros satisfying nonlinear eqn. 79−97182
many particle systems with $1/r^2$ pot., Riccatti eqn. and completely integrable systems *(French)* 79−12711
neutron, charge form factor zeros 80−413
one dimensional function, resolution into sum of exponentials, roots of polynomial 80−77603
orthogonal polynomials, asymptotic density of zeros, many-body physics 79−30286
orthogonal polynomials, nonlinear eqns. for zeros 80−12888
particle scattering amplitude, analytic extrapolations, EMZERO 80−47221
plasma, collisionless drift modes, graphical method for finding complex roots of nonlinear eqn. 80−33762
polynomial satisfying linear second order partial differential equation, properties of zeros 80−12889
polynomials, zeros, sum rules 80−57521
polynomials, zeros, sum rules 80−62888
S-matrix poles, connection with resonances, local distortion technique 77−74609
speech processing, parameter estimation of noisy all-pole process using pole-zero modelling 79−64419
spherical ferromagnetic models, Yang-Lee edge singularity density in thermodynamic limit 79−30378
stream pollution controller design via pole assignment 77−60434
zeros of classical polynomials and Bessel functions, diophantine props., review 79−35530
zeta function of quartic oscillator 80−62532

police
crime countermeasures, physical techniques for detection 79−12920
holography appl., footprint obs. *(French)* 78−9347

police data processing
crime prevention measures, fingerprints, voice prints, and identikit presentations *(Italian)* 79−100465

polishing
see also electrolytic polishing
arsenides (Ti, V, Cr, Mn, Fe, Co, Ni, Cu, Zn, Ga, Ge), oxidation, hardness and electromechanical polishing response 80−71776
aspheric axisymmetric lens figuring, wear pattern prediction 77−27398
aspheric figuring, single-spindle, with flexible pads 77−84017
aspheric optics low scatter finishing, polishing of f/2 paraboloids 79−59855
aspherical lens, polishing technique with equal polishing rate distrib. 80−58818
aspherical optical surface low-scatter finishing 79−14125
aspherical surface polishing with ring polisher 79−41465
aspherical surface prod., review 77−7224
aspherics precision manufacture with programmed microelectronic control 80−1368
beamsplitter using ultrathin metal grids, polishing technique to improve reflectivity 78−55459
borides (Ti, V, Cr, Mn, Fe, Co, Ni), oxidation, hardness and electromechanical polishing response 80−71776
brass, magnetoabrasive machining, optimum conditions 80−30172

polishing continued
bronzes, ancient, chem. polishing and etching for metallographic exam. 78−356
carbides, sintered, sample prep. for metallographic structural anal. 80−13048
carbides (Ti, V, Cr, Mn, Fe), oxidation, hardness and electromechanical polishing response 80−71776
ceramic, flat parts containing Ti, efficiency increase in fine diamond polishing 79−20228
ceramic, polished section prep. using pedepin *(German)* 78−19983
ceramic, specimen prep., time saving methods *(German, English)* 80−35459
ceramic material specimens, prep. with Pedemax-Planopol automatic grinder and polisher 79−74333
ceramics, and metal-ceramic mixtures, metallographic method for polishing specimens 78−56850
ceramics, mounting and polishing technique, for microstruct. exam. 78−48580
computationally directed axisymmetric aspheric figuring 79−23105
computer-controlled polisher for small-tool fabrication of mirrors 80−14496
corundum, single crystal, dispersion medium for polishing 80−102870
cylindrical lens surface generation, grinding and polishing machinery design 80−79023
diamond surface, polished, RHEED pattern 80−65345
dielectric coating adhesion improvement of diamond turned mirrors, ion polishing surface prep. 79−23102
electro-optic material cutting and polishing, book 79−81583
epoxy, mica filled, polishing by abrasive papers and lapping cpds. 80−108620
fast aspheric mirror figure control by profile monitor, wire tester and null lens 80−14419
fibre optic elements, damaged layer struct. after diamond grinding and polishing 79−7220
fibre-optic component polished end degradation in storage 79−32064
glass, ancient, X-ray fluoresc. anal., importance of sample prep. 77−34064
glass, GLS, surface radiation strength, grinding and polishing press. effect 77−72104
glass, heat treated, thin foil prep. for TEM obs. 78−7154
glass, polished surfaces, environment sensitive, ellipsometric obs. 77−48559
glass, rare earth elements use as dopants *(Polish)* 80−97455
glass, surface treatment effect, on chemical polishing time of crystal products 78−92436
glass microbubbles, method for polishing bubbles into hemispheres 78−95869
glass polishing process acceleration with chem. reagents 78−90542
glass surface, polished and laser-annealed, characterisation by ellipsometry 80−103544
glass thermopolishing, by use of low temp. plasma radiation *(Russian)* 80−45406
goniometer, universally adjustable polishing device 79−2755
graphite, highly oriented, pyrolytic polished surface, optical anisotropy 79−15481
hard and brittle materials, microsection prep. technotron and polishing systems *(German, English)* 80−11859
III-V semiconductor, surface microhardness depend. on surface treatment method 78−15560
III-V semiconductor epitaxial ultra-thin layers, bevel cross sectioning 79−74275
ion polishing for diamond-turned mirror dielectric coating adhesion 80−1370
jet electropolishing, monitoring of transmission electron microscope foil thinning, PP-8 radiometer (USSR) 80−73525
Large optical component grinding and polishing condition selection 79−81579
laser mirrors, optical fabrication techniques 77−65600
lens, water soluble cryst., protective coating to aid polishing 80−33250
lens surface geometry model, high-speed generating, smoothing and polishing 78−50889
lenses surface, spectacle type, using automatic and semi-automatic machines *(French)* 80−58822
leucosapphire, unique polishing features of hard crystals 80−64225
lubricating and cooling liquids, breakdown and exhaustion during diamond abrasive polishing 79−96196
magnetic collimator mirrors, grinding and polishing processes *(German)* 79−71433
metal, frictional forces during polishing in vacuum 80−28365
metal, two-way polishing, thermal stresses and surface quality *(Russian)* 80−30151
metal polishing for optical appl. 78−5587
metal reflective optics, single-point diamond-turned, polishing 79−23104
metal surface electrochemical smoothing, roughness, diffusional pre-electrode layer *(Russian)* 80−76401
metal surfaces for laser mirrors, ion polishing and vac. annealing 78−5588
metallographic specimens, automatic machine and procedure for prep. 80−13050
metallographic specimens, grinding and polishing apparatus 78−23889
metallography, quantitative methodology *(French)* 80−30205
meteorites, diamond-containing, polished thin section preparation technique 78−65566
Metglas 2826 ribbons, ferromagnetic resonance and SEM obs. 80−15804
microchannel plate surface finishing using liquid 78−90544
microsection preparation by vibration polishing for metallography 79−87786
mirror, nonaxisymmetric, fabrication by stressed mirror polishing 80−99885
mirror, paraboloid, off-axis section, fabrication by stressed mirror polishing 80−99886
mirror, single point diamond-turned, polishing technique 79−14126
mirror, single-point diamond-turned, performance before and after polishing 80−74466
mirror fiducial system compatible with computer-controlled polishing facility 80−74539
mirror of lunar laser ranging receiving telescope, polishing and Foucault test *(Japanese)* 78−89065
mirror surface manufacture on pyroceramic blanks 77−62079
mischmetal-cobalt alloy, $MMCo_5$, polished, domain wall grooving, optical microscopy and SEM obs. 77−8334
polishing continued
monocrystal surface layer damage depend. on abrasive working parameters *(Russian)* 80−76368
off-axis parabolic mirror fabrication for laser function expt. 80−1374
opical element polishing simulation calc. and results *(German)* 80−87566
optical aspheric rotationally symm. surface generation, computer control 77−27395
optical blank grinding and polishing, for LAT primary mirror 78−90541
optical coating ion polishing 80−33261
optical coating removal by Al_2O_3 powder and NH_4HF_2 soln. 80−74521
optical component manufacturing of low stiffness plates 78−71236
optical component polishing process modelling *(German)* 80−87565
optical components, polishing defects obs. by etching 77−75724
optical components using diamond tool 77−72105
optical elements, high speed production line design 77−27397
optical fabrication using computer controlled polisher 78−75006
optical fibre, grinding and polishing productivity, diameter depend. 77−62067
optical flatware, annular lapping 77−27396
optical glass, K8, foam form. and suppression methods during polishing 80−28364
optical glass, kinematic relationships in automatic glass grinding and polishing machines *(Czech)* 79−32096
optical glass, polishing with ZrO_2-SiO_2 powder mixture 80−28367
optical glass, semiautomatic machines kinematics *(Czech)* 78−63208
optical glass, surface layer structure after grinding and polishing, Kr sorption meas. 77−31122
optical shop computer-controlled interferometry, in-process production tool 80−74531
optical surface, computer controlled polishing, optimisation 77−23787
optical surface, polishing efficiency obtained on standard machines, quantitative analysis 78−50959
optical surface shaping by successively corrected mask method 78−18076
optical workshop machines, kinematic relationships *(Czech)* 78−50953
pellet precision grinding and high-speed polishing using synthetic material 78−50958
pitch polisher profiling 79−7234
pitch-polymer polisher layer, durability 77−34969
plasma, low press. high frequency induction cleaning and polishing of glass and Pt-Ir substrates *(Russian)* 78−35578
Polirit, commercially produced, for optical surface polishing, phys., chem. and tech. props. 78−46848
Polirit, optical polisher powder, particle size distrib., dispersion analysis 77−9141
Polirit granules for polishing, evaluation of disintegration degree 77−11057
Polirit polishing ability and physicochemical props. 79−72730
Polirit suspension, factors reducing polishing ability 80−74543
polisher, computer controlled, efficiency 80−91938
Polytron polishing pad, method and applications 80−69567
porous materials, effects of different methods of prep. on reproducing surface 80−60995
prism, diamond polishing method, technology and automated equipment 77−34968
prism optical figuring, polishing technique 77−72094
pyroceramic plate surface quality obs. after mechanical polishing 79−72732
α-quartz, Raman FTIR spectra, surface layer and vol. spectra comparison 78−52491
quartz fused, refractive index distrib. normal to polished surface, ellipsometric meas. 79−86965
quartz surface, chemical polishing by etching 78−60858
rare earth polisher powders, comparative analysis 79−50453
refractory transition metal, abrasive polishing mechanism 77−12745
resin polishers, holders, and tools 80−33248
rocks used as aggregate in pavement surfaces, exam. of polishing charcts. 78−53057
ruby, single crystal surface disruption after polishing investigation by chemical etching *(Russian)* 79−38995
ruby, unique polishing features of hard crystals 80−64225
sapphire, absorbing microdefects effect on anisotropy of optical strength 78−2952
sapphire, polishing with colloidal SiO_2 78−39925
sapphire substrates, prep. for GaN epitaxy 78−39929
semiautomatic machines, kinematic ratios calc. *(Czech)* 78−79146
semiconductor TEM 90° cross-section and 1° angle-lap specimen prep. 80−71881
silicate glasses, polishing, surface charcts. using grazing X-ray reflection *(French)* 80−65353
small grinding and polishing tool control by computer 79−98516
small nonsymmetrical aspheric surface fabrication, using grinding or polishing minipad 79−64365
smoothness parameters meas. of polished surfaces, using spectral analysis optical system 80−86261
soft magnetic mat. prep. by precip. of insulating film on Fe powder in polishing bath 78−23637
steel, 40KhNMA, corrosion fatigue strength, effect of polishing and diamond smoothing *(Russian)* 78−31575
steel, C, nonmetallic inclusions, improved metallographic technique for examining 78−72956
steel, chemical polishing for opt. microscopy 77−9021
steel, low C, fatigue endurance limit, metallurgical technology and mech. treatment effect 80−55536
steel, stainless, Cr-Ni-Mo, surface, scraping, mech. (electrolytic) polishing, ion etching, effects on ESCA 78−53037
steel, stainless, smoothing for plastic pre-straining of material cut by turning *(Russian)* 80−60911
steel, surface state influence on etching effect 80−81235
steel 40Kh, surface working effects on crack resist. *(Russian)* 78−56734
sulphides (Fe, Co, Ni, Cu, Zn), oxidation, hardness and electromechanical polishing response 80−71776
superconducting Pb resonators, polishing procedure for high surface electric fields 77−83197
surface quality estimation after polishing, Kikuchi reflection obs. *(German)* 77−86208
surfaces, Beilby layer generation, plate distortion by heat *(German)* 77−73370

polishing continued
thin and polished section preparation status and trends *(German)* 80−28360
thin metal films, for electron microscopy, production by jet polishing apparatus 78−86247
thin-wall cylinder cold rolling method 80−66535
toroidal mirror optical polisher 80−5848
two-surface analysis, of polished sections in scanning electron microscope 80−77912
Twyman effect plane-parallel glass preparation and interpretation *(German)* 77−58401
vibratory polisher for semicond. single crystal, construction 78−80659
wear test specimen, metallographic technique 80−35496
weld, specimen prep. for TEM obs. 77−60029
Ag, effect on emissivity, 335-1100K 77−39682
AgCl, surface layer stress distrib. after mech. treatment, polarisation-optical obs. 78−18887
Al, effect on emissivity, 335-1100K 77−39682
Al, transfer etch control in chemical polishing 80−16599
Al-Cu-Mg, type D16T, thin-wall cylinder cold rolling method 80−66535
Al_2O_3, grinding and polishing, quantitative control and optimization *(German, English)* 80−35460
β-Al_2O_3.Na_2O cryst. or sintered disc, Au electrode interface impedance rel. to roughness 77−4437
Au-Er, dil., cold-worked, EPR expts. 80−39864
Au-Pd alloy, surface comp., polishing, cleaning and Ar sputtering effects 77−72763
$BaTiO_3$, cubic-tetragonal phase transition, birefringence meas., surface distortion effects 78−95564
Be polycrystalline, metallographic observation of cleaved grains 78−72824
CaF_2, polished crysts., rocking curve meas. *(German)* 78−2347
CaF_2, press-forged laser window, polishing, cleaning and grinding 79−59849
$Cd_xHg_{1-x}Te$, comp. in successive layers determ. by chem. polishing etching of surface 77−7868
$Cd_xHg_{1-x}Te$ single crystal, photoconductivity spectral distrib. rel. to surface condition 79−78136
$Cd_xHg_{1-x}Te$, surface microhardness depend. on surface treatment method 78−15560
CdS, cathodolum. in red and exciton regions, surface treatment influence 77−77303
CdS, chemical polish for Cd and S faces 77−73355
CdS, single cryst., surface treatment effects on photoluminesc., struct. and optical props. *(Russian)* 78−15224
CdS single crystal laser screen, photolum., determ. of layer depth disturbed by polishing 78−17977
n-CdTe, cathodoluminescence microscopy obs. of dislocations, compared with etch pit pattern 79−69105
Cu, effect on emissivity, 335-1100K 77−39682
Cu, heterogeneous, new polishing technique *(German, English)* 79−20322
Cu, metal surface cleaning, by electron cyclotron resonance plasma of hydrogen 79−47822
Cu mirror, surface defect layer form. on mech. polishing 80−33122
$ErCo_6$, domain wall grooving due to mech. polishing 79−70232
Er_2Co_{17}, domain wall grooving due to mech. polishing 79−70232
Fe, degree of charging of surfaces polished by TiC and synthetic diamond micropowders 78−60880
Fe, sintered, influence of metallographic treatment on pore analysis 80−76417
Fe, surface contamination due to polishing, determ. by luminescent-discharge spectrometry *(French)* 79−52839
Fe-Ni-Mn (20, 5 wt.%), surface martensite, crystallography and morphology 80−40354
Fe-TiC pseudofused composite magnetoabrasive powders, props. 80−100926
GaAs (110), comparison of LEED intensities for chemically polished and cleaved surfaces 78−18884
GaAs, etchant, universal, multipurpose 78−53008
n-GaAs, mechanical polishing damage effect on IR refl. and ATR spectra 77−20848
GaAs, peculiarities of plasma region reflection, effect of surface treatment methods *(Russian)* 79−69827
GaAs, substrate for epitaxial growth, backscatt. anal. of surface prep. and anodic oxidation 77−25175
GaAs, vapour phase etching and polishing with $AsCl_3$ 78−3243
n-GaAs-electrolyte interface, surface pretreatment rel. to photocurrent, spectral response 80−3204
$Ga_xIn_{1-x}P$ electrode, in aqueous electrolytes, impedance meas. *(French)* 79−87153
$GdCo_5$, domain wall grooving due to mech. polishing 79−70232
GdGa garnet single cryst. substrate surface quality *(Russian)* 77−44371
$Gd_3Ga_5O_{12}$, garnet substrate, surface polishing, damage, abrasion, brittle fracture model *(German)* 77−73357
$Gd_3Ga_5O_{12}$, garnet substrate surfaces, working damage, electron microscope investig. 77−77605
$Gd_3Ga_5O_{12}$ single crystals, comparison chemical, mechanical methods, magnetic bubble device appl. *(Japanese)* 79−5067
GeTe, machining effects on electrophys. props. 77−86199
$In_xGa_{1-x}P$, TEM foil preparation, using polishing set 'Elypovist' *(German)* 79−9264
InP (110) surfaces, cleaved and polished-sputtered-annealed, LEED and AES study 80−103550
InP substrates, HCl etching speed and polarity obs., with aid of laser beams *(Slovak)* 78−56575
InP substrates preparation, etching and polishing in Br-methyl alcohol solution *(Slovak)* 78−56576
InSb, optical constants and oxidation with various surface treatment *(Russian)* 80−88955
n-InSb, phonon-assisted cyclotron reson. strongly depend. on surface condition 80−70755
KBr, IR laser window appl., crystal growth, polishing and optical absorpt. 77−7102
KCl IR window material, polish layer effect, ellipsometric meas. 78−55419
KCl surface texture and optical props. after forging between polished dies 80−33102
KH_2PO_3, mechanically treated single crystal, depth and struct. of disturbed layer *(Russian)* 78−23839
polishing continued
KH_2PO_4, and other soft water-soluble crystals, two-step polishing process 79−64363
La-N-C system, metallographic investigation *(German, English)* 77−52600
LiF crystal, dislocation movement study with new chem. polish 78−15614
$LiNbO_3$:Ti in-diffused optical waveguide fabrication 79−76892
$LiTaO_3$ monocrystal lapping and precision machining characteristics *(Japanese)* 79−80593
Mg cast iron, microstruct. of spheroidal graphite, rel. to polishing and annealing treatments 77−56160
MgF_2, mech. props. anisotropy effect 77−797
MgO, anisotropy of grinding damage, chem. polishing and etching 79−47793
MgO, cryst. preliminary processing rel. to deform. curve parameters, slip line struct. 77−52421
MgO crystals, etching and polishing, inorganic or organic acids effect 80−40573
MgO single crystals, chem. polishes for {100}, {110} and {111} surfaces, spectrochem. anal. for impurity content 79−2924
Mn-Zn ferrite single crystals, mech. polishing effect on mag. props. *(Japanese)* 80−16569
Mo alloys (MChVP and TsM10VD), erosion, effect of ion bombardment dose and previous surface treatment 80−89419
Mo-Zr-Ti (0.5, 0.1%), adhesive wear polishing of 25 mm spheres 80−89397
$NH_4H_2PO_4$, surface effects on strength of whiskers and microcrysts. *(Russian)* 78−51864
NaCl, kinetics of defect formation *(Russian)* 78−95819
NaCl large window continuous polishing 80−74527
Nb, mono- and polycrystn., crystallographic orientation, etching technique determ. 80−71814
Nb-N(O)(C) system, specimen prep. for metallography *(German, English)* 80−89439
Ni:He, implanted, profile meas. technique 77−80524
NiO_2 single crystals, welding, optical and SEM study 79−65097
PLZT ceramic, thin wafer production polishing process 80−81214
PbO-SiO_2 glass, use of $Na_2S_2O_3$.$5H_2O$ in polishing 80−33258
$PbTiO_3$, spontaneous polaris. shielding destruction by polishing and scribing 79−15427
n-Si, exoelectron emission, effect of surface polishing rel. to defect distrib. in surface layer 80−40239
Si, local mechanical defects, annealing and effect on autoepitaxial growth *(Russian)* 80−7701
Si, optical reflectance rel. to surface damage 79−14985
Si, polished plate, internal friction *(Russian)* 78−15441
Si, reactivity with organic nitrogen compound, rel. to polishing *(Russian)* 79−70192
Si single cryst., chem.-mech. polishing of low-scatt. optical surface 80−96040
Si single crysts., mech. polishing with reagent, activation energy effects *(Japanese)* 80−89379
Si, slice double-sided free polishing 78−11380
p-Si wafer, self-interstitials form. during chemicomech. polishing *(German)* 79−34175
Si wafers, floating-zone, etch struct. on microdefects as affected by dopants and surface treatment 80−79773
SiO_2, fused silica optical surface, ion polishing rel. to laser damage thresholds 77−75717
SiO_2-Na_2O-CaO-MgO-Fe_2O_3-Al_2O_3-SO_3-Sn thermally polished, exam. of strength of surfaces 80−25887
$SmCo_5$, polished, domain wall grooving, optical microscopy and SEM obs. 77−8334
SmS, mechanical polishing, stabilisation mechanism for metallic phase on surface 78−60015
SrF_2, press-forged laser window, polishing, cleaning and grinding 79−59849
$SrTiO_3$ electro-optic crystals, mechanical grinding and polishing 80−48471
$SrTiO_3$, fabrication damage characterisation by internal and external meas. 80−102782
Ta-N(O)(C) system, specimen prep. for metallography *(German, English)* 80−89439
Ti, degree of charging of surfaces polished by TiC and synthetic diamond micropowders 78−60880
Ti-Al-Cr-Mo, type VTZ-1, machinability, using different abrasive materials *(Russian)* 80−97593
Ti-Al-Mo, type VT14, machinability, using different abrasive materials *(Russian)* 80−97593
Tl single crystals, growth and polishing procedure for (0001) face 79−78870
TlCl-TlBr, KRS-5, KRS-6 crystals, optical strength pulsed CO_2 laser radiation 79−27307
V-N(O)(C) system, specimen prep. for metallography *(German, English)* 80−89439
W, monocrystalline cylindrical component surface finish, electroerosion polishing *(Russian)* 79−15847
Y-Er, surface, high-freq. elec. cond. dispersion function, effects of polishing and annealing 78−19506
YAG brittleness anisotropy, microcrack formation due to surface treatment 80−40526
ZnO monocrystal and RF sputtered heteroepitaxial film, SAW attenuation comparison 79−56063
ZnO:Li_2O single crystal, triboelectric charge and photodischarge obs. 79−82663
ZrO_2, near-surface phase transforms., effect of grinding and polishing 78−15557

pollution
see also air pollution; pollution detection and control; water pollution; water treatment
actinide industrial dusts, lung clearance studies at NRPB 78−65137
alpha-emitting contaminants in environment, field monitoring using ZnS scintillator and phoswich detector 78−70646
biophysics of living organisms communities in natural state, pollution effect 77−73503
biosphere, radioactive contamination, influencing factors, 1962-76, Hungary *(Hungarian)* 78−92711
Birmingham, England, heat island synoptic climatology (1965-74) 80−85740

pollution continued
Chalk River Nuclear Laboratories research in radiation biology, environment and radiation protection 78−61222
chemical migration of radionuclides in soil 80−17144
cigarette smoke, alpha radioactivity per smoke particle 77−29181
citrinin distribution in tissues and serum protein, radioactive chem. anal. 79−53292
city lights obs. by Defense Meteorological Satellite Program 80−104494
coal, bituminous, subbituminous and lignite, gamma-ray activity 77−25684
conference, Osaka, Japan (Nov. 1979) 80−98756
decommissioning of commercial power reactors, environmental, economic and sociological effects 79−67901
decommissioning of commercial power reactors, technical feasibility, cost, environmental effects 79−67902
diffusion of contaminant cloud in incompressible turbulent flow 79−50774
disposition assessments for decontamination and decommissioning of inactive nuclear sites, data requirements 80−95474
dose-rate conversion factors for external exposure to photons and electrons, modifications to DOSFACTER code 80−104775
dosimetry, environmental radiation meas., instrument calibration 80−9426
dosimetry calculations due to radionuclides in aquatic food chains, NEPTUN interactive code in FORTRAN 80−109039
Earth albedo, anthropogenic changes and effects on climate 80−81893
ecosystem analysis methods for the assessment of inactive nuclear sites 80−95476
energy, environment and health, Failla Memorial Lecture, learning from nucl. experience 78−80982
enriched heavy minerals in sand grains, enhanced natural radiation exposure *(German)* 80−51018
environment, biophysical aspects of ^{241}Am, ^{241}Pu 79−39530
environment, resistance to technogenic action *(Russian)* 79−88044
environmental, X-ray fluorescence analysis 77−41161
environmental assessment, graph-matrix method 79−57502
environmental assessment, management system for local development project in Japan 79−57503
environmental impact of nuclear fuel cycle, monitoring and control 79−57504
environmental information consequences in information systems 79−57500
environmental modelling principles, radioactive effluent 79−79414
environmental pollution and monstrous variations of organisms and tumours *(Chinese)* 79−52961
environmental protection, radioactive waste from power plants in USSR 79−26601
environmental radioactive pollution by U industry, monitoring using analytical chemistry 80−95488
environmental radioactivity near a radioactive waste disposal site 80−98148
environmental radioassay, Italy, appl. of quality control procedures 79−25117
environmental radiological surveillance, relative importance of environmental media 79−66421
environmental research, bibliography of AECL publications 79−34444
environmental risks associated with radioactive waste management 79−26604
environmental system modelling, identification and control, conf., Ghent, Belgium (Aug.-Sept. 1977) 79−25250
fallout on Taiwan, 1971 to 1975 period 77−90918
Florida, ^{238}U and ^{226}Ra in phosphates 80−30615
fusion power stations, recirculating power, unit cost, thermal pollution 78−29643
fusion reactors hazards assessment *(Czech)* 78−86681
gamma sources in walls of dwelling rooms, exposure rate calc. 78−73260
gamma-emitting activation products, plant uptake of ^{59}Fe, ^{58}Co, ^{54}Mn and ^{65}Zn 80−30614
gamma-ray activity in coals, rel. to power station choice 78−11746
gamma-rays from extended sources, energy distrib. calc., rel. to remote spectroscopy 78−61586
geological medium interfered with by man, geophys. investigation methods 80−85323
geopressured geothermal energy production plant, environmental effects 80−97764
geothermal power developments and environmental pollution 80−61470
global problems soln., scientific and social approaches 77−74185
health physics conference, San Francisco, USA, June/July (1976) 77−16983
heat release effect on general circulation and climate 80−89694
hydrocarbons in Antarctic marine sediments 79−92096
industrial end pollution control capital costs 79−79413
Lakes Ontario and Erie, comparison of bluffs and sediments composition 77−5248
light, neutron skyshine from nucl. facilities *(Japanese)* 79−18054
light pollution, effect on astronomical obs. 78−3954
light pollution, effects of urban lighting on night sky brightness 77−73853
light pollution, Simkin effect and Hg I 4047 Å night sky contamination effect on galaxy redshift determ. 78−41032
light pollution at Sacramento Peak Observatory, effect on night sky brightness 80−12545
light pollution over Jena, night sky brightening at Karl-Schwarzschild Observatory 80−51533
low level radioactive waste disposal site, trench water study 79−52963
magnetosphere, contamination by spacecraft at geosynchronous orbit 80−72701
metal enrichment of sediments, partitioning of metals, Ranafjord N. Norway 79−83641
methyl mercury, in isolated estuarine sediments, growth and decay during storage 77−66937
methylmercury, equilib. concs. in Ottawa River sediments 78−11923
milk radioactive fallout monitoring in Britain 80−12283
modelling, numerical estimation of unknown parameters *(Japanese)* 80−89702
night sky zenithal brightness monitoring, light pollution rel. to astronomical observations 78−49141
noise, subjective annoyance by low level sound, sound character as a physical attribute 80−35902
non-proportionality between flux and reservoir content 80−46261
nuclear and fossil power plants effluent environmental impact comparison 78−96290
nuclear energy, environmental effects *(German)* 79−70468
nuclear facilities, forecasting of environmental impact *(French)* 78−8994
nuclear facilities, off-site radiological impact assessment real-time computer program CEPADAS 80−95475
nuclear power, effect on the environment, general radiation level and waste product disposal 79−18051
nuclear power, environmental impact 80−101143
nuclear power, Royal Commission Report, on Environmental Pollution, UK, overview 77−54267
nuclear power plant, environmental radioactivity and dosage models *(Spanish)* 80−32518
nuclear power reactor accidental release, isopleth method for population reaction 79−13533
nuclear reactor fission product release, evaluation of population hazards 77−14250
nuclear reactors, UK standards and procedures 79−81032
nuclear site decontamination, radiochemical anal. of environmental samples 80−95477
nuclear waste disposal, migration in geologic formations 78−4994
numerical modelling appls., conf., Southampton, England (July 1977) 78−77285
organic fertiliser, concs. of ^{239}Pu, ^{240}Pu and ^{241}Am 77−56488
photographic film development techniques, environmental pollution appl. *(German)* 80−7806
plant trace element anal. by X-ray fluoresc. for environmental pollution study 78−3690
polycyclic aromatic hydrocarbons in Gulf of Maine sediments and Nova Scotia soils 79−74555
polycyclic aromatic hydrocarbons in recent sediments, global distrib. 78−57192
population radiation exposure, radioactive effluent from nuclear facilities in West Germany 79−26781
potential radiation exposure, West German nuclear installations 79−26603
power stations, LWR and coal, effects on ambient media from mining to waste disposal *(Spanish)* 77−75005
power stations environmental effects, nuclear and thermal comparison 77−71706
radiation research, lab. contamination in the early period 80−42031
radioactice waste storage, interaction of actinides and humic acid 80−13715
radioactive actinides, man-made, health effects compared to natural radionuclides 80−61647
radioactive building materials, environmental radiation and gonad dose in Norway 77−44761
radioactive contamination of biosphere, explosion and power plant influence *(Hungarian)* 80−21548
radioactive fallout effects of Nagasaki atomic bomb 78−85393
radioactive high-level waste disposal in deep geologic formation, environmental aspects 79−49712
radioactive impact of nuclear facilities, preoperational evaluation 80−3534
radioactive material migration in soil, hydrologic transport model 80−16848
radioactive release into environment, limits, new derivation approaches 79−26773
radioactive waste, biochemical and chemical processes leading to radionuclide transport from low-level waste burial sites 80−101275
radioactive waste, geochemical aspects of radionuclide migration from waste repositories 80−13711
radioactive waste, geologic isolation repositories, long-term safety assessment 79−49714
radioactive waste, geological disposal, chemical factors controlling environmental actinide sorption 80−13713
radioactive waste, geological disposal, Netherlands programme 79−26609
radioactive waste, geological long-term disposal of high-level, Sweden 80−13712
radioactive waste, high-level, repository site selection, concerns of Michigan State 79−49716
radioactive waste, sorption of actinides in igneous rocks 80−95367
radioactive waste disposal in geological formations 79−31070
radioactive waste geologic disposal, geotoxicity hazard index 80−97822
radioactive waste repository in geologic primation 79−49713
radioactive waste repository siting, socioeconomic impacts, environmental decision making 79−49715
radioactive waste storage, Am sorption on major rock-forming minerals 80−13716
radioactive waste storage, migration of ^{137}Cs in Magenta dolomite by aquifer 80−13718
radioactive waste storage, mineral-contributed anion effects on the retention of trivalent actinides in the environment 80−13717
radioactive waste underground disposal, solutes movement through aqueous fissures in porous rocks 80−94553
radioactivity in W.Cumbria, Pu and ^{137}Cs conc. in environmental samples and possible maritime effect 80−108817
radioactivity of building materials and γ-radiation in dwellings 79−92095
radioactivity surveillance in Switzerland and descent of Kosmos 954 *(German)* 78−77119
radioiodine release from U_3O_8 in O_2 and inert gas atm., chem. identities 77−57712
radioisotope transport in terrestrial food chains, dynamic modelling using RAGTIME code 80−104776
radioisotopes, derived working limits for surface contamination calcs. 79−66562
radiological assessment of inactive nuclear sites, statistical design and anal. 80−95473
radiological assessment of inactive nuclear sites 80−95478
radiological impact of the Rhein-Maas region from nuclear facilities under normal operation 80−3535
radiological survey of inactive nuclear sites, quality assurance 80−95472
radionuclide absorption through damaged and undamaged skins of guinea pigs 80−26383
radionuclide conc. rel. to residence time in marine sediments near Maine Nuclear Power Reactor 78−49021
radionuclide concentrations in food products, FOOD II interactive code calc. 79−48348

pollution continued
radionuclide intake by man through terrestrial pathways, TERMOD II interactive code analysis 79−48349
radionuclide migration through soils 80−16849
radionuclide pathway anal., RAMM system of programs 77−13015
radionuclide transport through geologic media, one-dimens. model 80−786
radionuclides, movement through soil *(Japanese)* 77−81593
radionuclides, sediment-bound, absorpt. through digestive tract of marine demersal fish 79−92400
roadside soil and plants in Alexandria district, Egypt, contamination with Cd, Ni, Pb and Zn 78−81171
safety and environmental pollution *(German)* 80−63370
simulated, T content in organs, and DNA of rat liver cells, after doses of tritiated food, protein or water 80−56226
soil, Pb adsorption, Langmuir and Freundlich isotherms 77−33078
soil, specific Pb adsorption 77−33079
soil pollution elemental deposition downwind of coal-fired power plant 79−20838
soil pollution indication, Ca and NO_3-N loss from microcosms 78−16019
soil residual contamination levels and decommissioning nuclear facilities, radiological criteria 78−11747
soil-water system interfacial reactions and heavy metal adsorption 78−3832
soils of Everglades National Park and adjacent agricultural areas, polychlorinated biphenyls and chlorinated pesticides 79−92098
synthetic fuel production, environmental effects 80−21417
trace metals pollution, contents in Antarctic snows (1914 to 1974) 79−34867
transportation effects, public, future outlook 80−35621
transuranic elements in environment, recommendations for exposure of persons 79−93842
transuranic mobility in agricultural ecosystem 79−96668
transuranic transport from environment to man modelling 79−96669
transuranic wastes, interaction with soils 79−96488
transuranics, plant uptake, techniques for long term field studies 79−57821
transuranics biological availability, influence of DTPA at soil-plant and plant-animal interfaces 78−73264
transuranium elements, resuspension from contaminated surfaces 79−62376
transuranium elements in thermonuclear test debris, collected near Bikini Atoll 78−96103
transuranium radionuclides in the foodchains 79−74554
trench leachates, low-level radioactive waste disposal sites, organic carbon content 80−17145
tritium in rabbits after ingestion of freeze-dried tritiated food and tritiated water 80−21549
Ural disaster questioned, possible fallout from atmospheric test 80−76666
urban heat island convergence in calm periods, St. Louis USA 80−90169
urban light pollution, interference filters for nebulae observations 79−88599
^{241}Am, concs. in sediments from coastal basins off California and Mexico 80−98303
^{241}Am, gastrointestinal absorpt. in hamster 79−39520
^{241}Am sorption on USA subsoils from differing weathering intensity areas, ^{241}Am, ^{237}Np and ^{99}Tc 78−16014
Ba isotopes, uptake and retention of ^{133}Ba and ^{140}Ba-^{140}La in mouse tissues, eye and skeleton doses 77−9276
CO_2 cycling in environment, non-proportionality between flux and reservoir content 80−46261
$C0_2$ pollution, role of homogeneous buffer factor in $C0_2$ solution in ocean surface waters 80−21783
^{14}C fallout from nucl. weapons testing, human radiation burden 77−64091
^{14}C fallout from nucl. weapons testing, use as biological tracer 77−64162
^{14}C production by nuclear power industry 77−54367
^{14}C production in reactors and explosions, population dose, health impact 77−14274
^{144}Ce gastrointestinal absorpt. and distrib. in suckling pig 78−15942
^{144}Ce, intravenous injection, wound site absorption, comparison of metabolic behaviours in rats 79−8545
Co isotopes, whole-body retention of $^{60}CoCl_2$ and ^{58}Co-cyanocobalamin in rats 77−70559
^{60}Co, radioactive waste migration by complexing agent ethylenediaminetetraacetic acid 79−20687
^{60}Co retention in mouse, rat, monkey and dog, at tracer levels 77−9271
Cs, transport in soil, evaluation of combined sorption model 79−8554
^{137}Cs accumulation in fruitbodies of Basidiomycetes 78−80977
^{137}Cs body burden in Japanese from 1967 to 1975 77−9283
^{137}Cs, coyote scats, Hanford Reservation, radioactive waste distrib. 79−25120
^{137}Cs in alpine tundra habitats, effects of phys. habitat factors and plant morphology 77−37058
^{137}Cs in Straits of Malacca marine environment 79−12135
^{137}Cs, intake by Bikini Island residents, model using bioassay data 80−109043
^{137}Cs, K, model for turnover in pike 79−8553
^{137}Cs levels in soils and vegetation of W.Malaysia 78−73263
^{137}Cs transfer coefficient into cows milk rel. to level of milk prod. 78−80978
^{137}Cs whole-body content in a normal New Mexico population 1956-1977 80−26382
HTO incorporation in maize and barley 79−25107
HTO potential radiation dose to man, HT gas escape into forest ecosystem 78−96101
^{3}H biological half-life estimation in man, model 79−20689
^{3}H, environmental transport from atm. release of mol. ^{3}H 78−11987
^{3}H persistence in soil-plant system, compartmental model 77−90919
Hg, average content of oceans and European air, soil, and river sediments 79−8687
^{203}Hg-methyl mercury chloride retention in man after inhalation 77−9277
Hg, abundance in Greenland Ice Sheet 78−65349
^{129}I in man, cow and deer 78−80975
^{129}I measurement rel. to ^{131}I accumulation in thyroids of pasture animals *(German)* 77−52891
pollution continued
^{129}I, thyroidal burdens from dietary sources 77−44755
^{131}I accumulation in thyroids of pasture animals, rel. to ^{129}I meas. *(German)* 77−52891
^{131}I measurement in human thyroid gland, use of NaI(Tl) scintillation survey meter 78−80970
^{131}I, milk transfer coeff., review of meas. values 79−2141
^{131}I radionuclide pollution, protection of thyroid gland 79−66560
^{113m}In eluates from ^{113}Sn generator, monitoring Zr and ^{113}Sn breakthrough 77−5078
^{99}Mo-^{99m}Tc generators with (n,γ)-prod. ^{99}Mo, eluate contamination from ^{131}I, ^{103}Ru and ^{239}Np 77−5079
^{237}Np, sorption on USA subsoils from differing weathering intensity areas 78−16014
Pb, New Zealand, battery factory and smelter emissions compared with vehicle exhausts 78−85562
Pb, pollution in Christchurch, New Zealand 78−85561
^{210}Po activity in Indian tobacco, meas. and lung dose calc. 77−9224
^{210}Po and ^{210}Pb concs. in liver and kidneys of cattle 80−30904
^{210}Po in Bombay diet 77−81592
^{238,239,240}Pu, concs. in arthropods at a nuclear facility 80−30905
Pu distribution in Ohio soils, local and stratospheric sources 78−16015
Pu distribution in Rocky Flats soil 78−73265
Pu dynamics in deciduous forest ecosystem, linear compartment donor-controlled model 78−85392
Pu in biota from E. Tennessee floodplain forest 78−85394
Pu in lungs of pronghorn antelope near a nuclear fuel reprocessing plant 80−30906
Pu in soil, meas. in respirable dust using different size fractionation methods 79−66836
Pu, Manhattan project workers, 32-year medical follow-up 80−26379
Pu measurement in Japanese human organs 78−80980
Pu, prep. of ^{237}Pu gamma-emitting tracer by ^{238}U(^{3}He,4n) 77−34497
Pu radioactive waste, oxidation by radiation, effect on migration rate 80−13714
Pu radioactive waste, transport, environmental impact 80−779
Pu toxicity hazards, cancer fatalities 77−66864
Pu-bearing materials, environmental impact of transportation, linear regression anal. 80−85308
^Pu, A = 239, 240, distrib. of fallout Pu in southern Finns 80−109045
^{236}Pu, ^{239}Pu, ^{242}Pu, ^{244}Pu, distrib. in mice after injection 79−12001
^{238}Pu, ^{239}Pu, ^{240}Pu, content in deer from integrated nuclear fuel cycle facility 79−57778
$^{238}PuO_2$, uptake by plants in polluted soil 79−5381
^{239}Pu, ^{240}Pu, Danish cereal grains, variation of direct contamination 79−5382
^{239}Pu, aquatic microscosms, trophic transfer by Chironomoids 79−5383
^{239}Pu contamination in snakes inhabiting Rocky Flats plant site 77−81591
^{239}Pu, gastrointestinal absorpt. in hamster 79−39520
^{239}Pu uptake by pea plants 77−9282
$^{239}PuO_2$, size characts., Rocky Flats soil, autoradiographic technique 78−96102
^{241}Pu, concs. in sediments from coastal basins off California and Mexico 80−98303
^{226}Ra in Taiwan buffalo bone and environmental samples of N. Taiwan power reactor site 77−64142
^{226}Ra long-term retention in contaminated dial painters 77−90917
Rn, diffusion coefficient and exhalation rate from building materials, meas. technique 80−4694
^{220}Rn unattached decay products, diffusion coeff. depend. on ventilation and rel. humidity 77−9279
^{222}Rn releases associated with cultivation of agricultural land 80−16850
^{222}Rn short-lived daughter population exposure in Great Britain 78−35970
S, man-made sources influence on NE United States S cycle 80−26178
Sr isotope excretion in man, comparison of stable Sr, ^{85}Sr and ^{90}Sr 78−24153
^{90}Sr, coyote scats, Hanford Reservation, radioactive waste distrib. 79−25120
^{90}Sr in human bone, Yugoslavia 77−56490
^{99}Tc accumulation by plants 77−56489
^{99}Tc accumulation by tumbleweed and cheatgrass grown on arid soils 78−80974
^{99}Tc sorption on USA subsoils from differing weathering intensity areas 78−16014
^{99m}Tc contamination of laboratory personnel, its degree and routes 80−98147
U analysis in phosphate fertilisers and other materials using liq. scintillation spectrometry 78−53280
U environmental distribution and movement, agricultural product distrib., Japan 77−90921
U mill tailings generated between 1975 and 2030, environmental impact 79−85825
^{187}W, absorpt., distrib. and milk secretion by dairy cow 77−9281

pollution detection and control
see also air pollution detection and control; noise abatement; remote sensing; waste disposal; water pollution detection and control; water treatment
aerosol samples, X-ray diffraction compound analysis 77−49176
aircraft noise, practical abatement at general aviation airport 77−65653
asbestos fibres concentration meas., in air and liquid, analytical methods review 80−72120
asbestos fibres identification, electron microscope techniques comparison 78−66012
ashing methods, critical anal. possible appl. in low activity determ. *(Bulgarian)* 79−88043
atmospheric analysis, using laser, from orbiting satellite 77−9571
bioelectronics symposium, Ahmedabad, India, (Dec 1975) 77−40808
Caorso nuclear power station airborne and liquid radioactive release monitoring systems 79−13553
chart data processing equipment [pollution monitoring] *(Japanese)* 79−100555
chemical pollutants and radiation, comparative biological hazards 79−25035
coal power station fly-ash and slag, natural radioactivity meas. 78−17442
conductometric instruments metrological monitoring, for environmental contaminants control 80−55973
conference, Rochester, NY, USA (May 1979), polluted rain 80−82585

pollution detection and control continued
conference on analysis instrumentation, Charleston, West Virginia, USA (May 1977) 79−16100
corrosion protection for control equipment 78−77317
dose comparisons in the effects of radiation and of chemical pollutants 79−88115
emission spectrochemical analysis, use of quantitatively coupled plasma quantometer *(Japanese)* 78−83624
environment, global background pollution, ecological monitoring program 80−81518
environment monitoring ground radioactive burial site *(Japanese)* 80−67015
environmental, meas. by means of light scatt. characts. 79−21061
environmental, methodological approach problems 77−21899
environmental, problem-solving approach, book 77−41065
environmental analysis, recent advances, book 80−41961
environmental analytical chemistry developments 79−53006
environmental control technology R and D, environmental impact of energy storage technology development 80−61471
environmental monitoring and control 79−39328
environmental obs. from space based systems, present and future 79−5657
environmental problems, nuclear power stations prospects *(Hungarian)* 80−13742
environmental radioactivity, meas. of water, soil, and foodstuffs 79−5378
environmental radioactivity control, relevance to control of other environmental contaminants 79−9889
environmental radioactivity prior to the Kori nuclear power plant operation 79−6773
environmental release prediction digital simulation, time split finite element algorithm 78−92880
environmental remote sensing, molecular absorpt. methods 80−72651
environmental sample, anal. by anodic stripping voltammetry 79−11836
environmental samples, proton induced X-ray anal. method appl. 77−63990
environmental science, trace analysis *(Japanese)* 77−87116
environmental science and engineering advances, book 80−105448
environmental systems control, transient finite element and linear programming method 79−57497
environmental systems planning, design and control, conf. Kyoto, Japan, (Aug. 1977) 79−52962
equipment operation and maintenance 78−61615
estimation, meas. and sampling methods *(French)* 78−20506
field desorption mass spectrometry, appl. to biochemistry, medicine, and environmental science 80−35592
Fourier transform IR spectrometry, chem. and environmental anal. appls. 78−20100
French nuclear power plant gaseous and liquid effluent release monitoring *(French)* 79−13551
gamma dose intensity in dwelling places, dose conversion factors *(Hungarian)* 77−77990
gamma spectrometric mobile computerised analysis and data processing system 79−9959
gamma-ray airborne mapping and tracking system 77−38427
gamma-ray environmental measurements using standard Ge(Li) detectors 77−38568
gamma-ray spectrometer, remote computer-controlled, for nuclear power plant monitoring 79−9916
gamma-ray spectrometer systems, portable, in situ field meas. applications 79−9958
gas and fluid analysis, continuous and quasicontinuous methods *(German)* 78−44437
GC/MS/computer techniques for environmental anal. 79−57554
geological medium interfered with by man, geophys. investigation methods 80−85323
Gulf of Taganrog salinity, after restriction of exchange with Sea of Azov 80−36335
hair, human, PIXE analysis, correction factor, rel. to pollution monitoring 80−61743
highway traffic noise prediction, state of the art review 77−65651
hydrocarbons, detect. in water and sediment of wilderness lake, Canada 79−12155
industrial complex environmental impact, Whatcom County, Washinton, USA 79−57532
instrumentation for pollution control 78−24363
integrated optical devices and applications 79−14117
ion chromatography appl., on-stream, impact on energy conservation 80−55737
lake sediments, radionuclide geochronology and pollution history 78−61451
laser absorption techniques for air pollution 77−9570
lasers in air pollution detection, review 77−9569
lidar measurement problems in hazy visibility conditions 77−9572
liquid phase pollution monitoring by optoacoustic spectroscopy 79−58797
marine sediments, near drilling sites, Ba content, potential pollutant indicator 79−12144
marine sediments, radioactivity uptake, rel. to metal pollutants monitoring 79−12145
metal species, identification and determ. by chromatographic-at. spectrosc. method 78−68972
metallic pollutants, study of movement in environment and biological chains *(French)* 77−41162
MHD conversion, pollutant emissions and controls 80−30613
mineral particulates, identification by selected area electron diffraction 77−90970
mobile trace analytic laboratory, design, construction, operation *(German)* 79−70504
monitors, metrological support, pesticide control 79−21060
N-nitroso compounds, estimation in environmental samples at parts-per-billion level 79−74448
neutron activation analysis, cyclic activation and short-lived isotopes meas. 79−88217
nondestructive neutron activation analysis of environmental samples using low-energy photon spectrometry 78−3995
nuclear based techniques, conf., Vienna, Austria (Mar. 1976) 77−41148
nuclear fuel cycle environmental assessment methodology 78−94112
nuclear fuel disposal safety in Switzerland *(German)* 78−74455
nuclear power, environmental aspects *(Japanese)* 77−83112
nuclear power plant, radiation monitoring systems, review 78−33292
nuclear power station, contamination monitoring station *(Polish)* 80−74033

pollution detection and control continued
nuclear power station, environmental protection methods *(Hungarian)* 79−88008
nuclear power stations, contamination prevention methods *(Hungarian)* 79−88007
nuclear waste disposal, discussion 79−39528
nuclear waste disposal, social criteria 77−30652
nuclear waste management, technology assessment 79−89392
nucleation model, for nonuniform vapour, cluster diffusion effects 77−4206
oil, in marine sediments, rapid field detect. method 79−12143
organic residues, gas chromatogram quantitation, using algorithms for microprocessor based integrator 78−27839
particle counting and vol. determ. in suspensions, optical-electronic device 78−57894
particulates, quantitatives charact. by computerised high voltage, SEM 79−48036
passive and active environmental remote sensing techniques 77−21935
PCM telemetry systems *(German)* 78−93003
pesticide analysis in biological extracts, mass fragmentography with glass capillary columns 77−9312
pesticides at high conc., adsorpt. and movement in soils 79−92097
petroleum refinery, use of radioactive tracers 77−41163
petroleum samples, extinction coeff., refractive index meas., 0.25-25 microns 79−65818
pH instrument research, stability, buffering and electrode designs 77−81438
phosphate and related industries, need for radiation controls 77−56483
polychlorinated biphenyls, pollutants, radiation degradation in organic solvents, H_2O 80−30262
polynuclear aromatic compounds, second derivative UV absorption spectrosc. anal. 79−83526
problems and numerical data 80−3536
proton activation analysis of environmental and ecological pollution determ. 78−3994
radiation, environmental meas. made with integrating detectors, error anal. 77−38428
radiation and isotopes appl., development trends 78−55041
radiation measurements, low level, with plastic scintillation detector system 77−38567
radiation monitoring, gamma and beta meas. 77−38429
radiation protection legislation in West Germany, standards aspects *(German)* 78−5049
radioactive, nuclear power stations safety, Czechoslovak practices *(Slovak)* 80−13632
radioactive contaminant unplanned release meas. and countermeasures 78−89994
radioactive contamination detectors assessment, w.r.t. German 1977 protective measures *(German)* 78−86693
radioactive decontamination methods, effectiveness for different terrains 78−96104
radioactive effluent monitoring, symposium, Portoroz (1977) 78−89985
radioactive liquid waste from nuclear reprocessing, vitrification, durability 78−54852
radioactive material control on medical science campus 77−44759
radioactive waste, commercial burial site, radionuclide dynamics and health implications 77−61618
radioactive waste, geological disposal, Canadian program 77−3140
radioactive waste disposal into salt deposits, fault tree anal. appl. to safety assessment 78−55046
radioactive waste management, solidification, storage, dispersal control 77−10469
radioactive waste storage, in situ instrumentation for meas. of radionuclide migration 80−95485
radioactive waste storage, long term subsurface migration of radionuclides 80−95483
radioactive waste storage, radionuclide migration determ., adsorption of Cs(I), Sr(II), Eu(III), Co(II), and Cd(II) by Al_2O_3 80−99240
radioactive waste storage, Sr, Cs, Co sorption meas. on soil sediment 80−95482
radioactivity, environmental meas. and US regulatory responsibilities 77−38430
radioactivity, environmental standards, USA 77−38431
radioactivity, NBS gamma-ray standards for calibration of Ge(Li) detectors 77−38541
radioactivity, surface contamination monitoring, test surface method 78−50409
radiochemical and chemical trace analysis, reliability aspects 78−40106
radiochemical neutron activation anal. of environmental matrices for Hg and noble metals 80−16889
radioisotope applications in agriculture, hydrology, medicine industry etc., booklet 78−35947
radionuclide liquid contamination measurement using $CaSO_4$:Dy TLD 77−38574
radionuclide migration from buried radioactive waste 80−95484
radionuclide transfer to crops and agricultural products *(French)* 78−8996
Raman laser microprobe analysis appl. 80−57390
Raman spectroscopy, remote spontaneous, new trends in recording of signals 80−73485
Regional Activities Model for economic and environmental impact evaluation 77−37376
remote monitoring of all types of environmental pollution, promising trends 80−35811
remote sensing, appls. 77−5349
remote sensing technology developments and appl. *(Japanese)* 79−8701
river bottom sediments, in situ neutron activation anal. appl. 77−87115
room temperature phosphorimetry, anal. technique, review, methodology, instrumentation, appls. 78−95972
samples, X-ray anal., absolute sensitivity and detection limits 78−7261
satellite remote sensing appls. 77−25788
scale model flow testing 77−3901
science role in solving world problems 79−80413
sediment leachates, trace element anal., multielement-direct reading method 78−69514
sediment pollution by Hg and As, instrumental neutron activation and atomic abs. spectrometric anal. 80−16890
smoke plumes, meas. of effective stack height with lidar *(German)* 77−9490
soil, ^{89}Sr and ^{90}Sr determ. using total sample decomp. 80−35808

pollution detection and control continued
soil homogeneity evaluation by radionuclide tracer breakthrough curve interpretation for radwaste storage appls. 80−97821
space-borne remote sensing *(Italian)* 80−109333
standard reference materials, based on river sediment and urban particulate matter (SRM 1645 and SRM 1648) 80−21831
subterranean gamma-ray in situ spectroscopy, appl. to radioactive waste detect. 77−57806
surface β-activity caused by nuclear explosion products, depend. on isotope vertical migration 78−86700
surface treatment, ionic deposition and electron bombardment industrial equipment *(French)* 80−7699
toxic chemical wastes, incineration 79−57496
toxic substances identification using online computerised infrared system 77−90709
toxicity studies, TOXIPAC-300 data processing system *(Japanese)* 79−25172
trace analysis in gases by laser-induced schlieren technique 80−3436
trace element detection in hair, possible pollution indication method, Japanese survey 79−66435
trace element profile of a California Redwood tree for environmental monitoring 80−97850
traffic noise, cost and safety aspects of quiet tyres use 77−65652
tree rings, trace element distribs. using neutron activation 78−3939
tunable IR solid-state laser characteristics and principles 80−87406
United States Air Force infrared reconnaissance set 78−81458
water, organic compound isolation using liq. chromatography 77−1957
water, sensitive sampling method for radioactivity meas. 79−39768
wheat endosperm, radiometric determ. of Cd conc. following Cd addition to soil *(German)* 77−25631
X-ray analysis, appls., conf., Denver, USA (Aug 1975) 77−56307
X-ray diffraction chem. anal., historical review 77−70383
X-ray fluorescence analysis, energy dispersive, matrix correction method 77−70352
X-ray fluorescence analysis of environmental samples, book 77−41217
Am, low conc. meas. in earth samples, appl. of Si(Li) X-ray detector 78−58505
^{241}Am and Pu/^{241}Am ratios, environment meas. using X-ray spectrometry 77−60265
^{241}Am soil concs., in situ gamma anal. and sampling data comparison, Nevada 77−64143
As determination in rocks and soils by at. absorpt. 79−88475
^{14}C low level liq. scintillation counting using small vol. teflon-Cu vial 80−16887
Cd, oscilloscopic polarography determ. in environmental pollution anal. *(Chinese)* 79−53002
Cd sorption and accumulation in sediment of Tama River 79−74924
^{137}Cs fallout in arid watersheds, phys. and chem. parameters affecting transport 78−61461
Cu, oscilloscopic polarography determ. in environmental pollution anal. *(Chinese)* 79−53002
Hg determ. in environmental samples, neutron activation anal. methods, review 77−56284
Hg pollution of Mediterranean sediments around Alexandria, Egypt 80−3538
I, radioactive waste, solidification in conrete, leach rates 78−703
^{131}I determination in vegetation, ashing procedure 78−15930
^{131}I in milk, rapid method of detect. 80−46106
^{131}I, low level detection in milk rel. to population dose 78−31911
Pb determination in Earth materials by at. absorpt. 79−88035
Pu borehole assay using delayed-neutron activation anal. 80−21419
Pu contaminated soil, nondestructive anal. 79−11879
Pu, low conc. meas. in earth samples, appl. of Si(Li) X-ray detector 78−58505
Pu low-background assay using modified commercial liq. scintillation detector and sample changer 77−54474
Pu, remote contamination and total inventory from Rocky Flats, mass spectroscopic anal. 77−73739
Pu/^{241}Am ratios, environmental meas. using X-ray spectrometry 77−60265
^{239}Pu soil concs., in situ gamma anal. and sampling data comparison, Nevada 77−64143
^{239}Pu, use in weapons and energy prod., radiological hazards, security 77−10492
^{239}Pu-^{241}Am monitor for in situ soil surface and pond bottom assay 77−9546
^{226}Ra, determ. in environmental samples by ^{222}Rn separation, integral counting methods 77−63988
Rn detection, effect of humidity 77−6647
^{222}Rn diffusion through U mill tailings covers, coeff. meas., lab. techniques 80−95387
^{222}Rn flux measurement using charcoal canister 77−6646
SO_2, ground-level conc. calcs. near a nuclear facility 80−97823
SO_4^{2-}, spatio-temporal distrib. in Antarctic snow 79−20870
Sb determ. in biological and environmental samples by neutron activation anal. 79−53008
^{89}Sr and ^{90}Sr, radiochem. determ., error anal. comparison of methods 77−16873
^{90}Sr body content determination, ^{90}Sr body content determination, ^{90}Sr+^{90}Y bremsstrahlung efficiency for humans 77−2061
^{90}Sr bremsstrahlung radiation meas. for well logging using Ge spectrometer 80−94619
T release control and environmental monitoring *(Japanese)* 79−81078
T, release from CTR, radiological dose calc. 78−78511
U, in environmental samples, determ. by gamma spectroscopy of 1.0015 MeV radiation in ^{234}U 77−1954
U ores, dusts and mill tailings, simultaneous determ. of ^{238}U, ^{234}U, ^{230}Th, ^{226}Ra, and ^{210}Pb 78−15736
Zn, oscilloscopic polarography determ. in environmental pollution anal. *(Chinese)* 79−53002

polonium
see also nuclei with .....
chemical bonding in group V and VI elements and compounds with tetradymite structure 80−15036
collector in electrometer, reductive effect, determ. from leakage current 78−37036
contamination of surfaces, removal coeff. determ. 79−26769
determination in air, radiochem. separation and α-counting method 78−73113

polonium continued
groundwater in Grants Mineral Belt, New Mexico, effects of U mining and milling 77−56657
haloes in rocks, use in geochronology 80−56468
haloes of Po in Precambrian biotite and other old minerals 78−85556
metabolic model for Po, dosimetry appls. 79−79657
mica, Po anomalous haloes origin 79−44186
particulate biogeochemistry of coastal zone 79−29787
^{210}Bi→, ^{210}Po→^{206}Pb, decay chain, L-shell ionisation investig., X-ray emission during β, α decay 77−18891
^{208}Po, L-shell ionisation in α-decay 78−78324
^{210}Po, ^{211}Po, KLM- and KLN-Auger transitions 77−18884
^{210}Po, ^{226}Ra and ^{210}Pb disequilibria in western N.Pacific 77−5227
^{210}Po and ^{210}Pb concs. in liver and kidneys of cattle 80−30904
^{210}Po, concs., physico-chem. states and residence times in marine and estuarine waters 78−11913
^{210}Po, determ. in human urine by direct extraction by Ni foil 79−100707
^{210}Po distrib. in Pacific surface waters 77−5226
^{210}Po distrib. in S.Pacific water profiles 77−5225
^{210}Po, expt. lung cancer, Syrian hamster, effect of dose distrib. 79−16254
^{210}Po, from ^{222}Rn released by uranium tailings piles, potential population dose 79−85824
^{210}Po, galvanic deposition at rotating Ni disk electrode 80−55314
^{210}Po in Bombay diet 77−81592
^{210}Po, inner shell electron ejection in α-decay 77−79342
^{210}Po, nucl. alpha decay, electron inner shell vacancy creation, semi quantal approach 80−68607
^{210}Po/^{210}Pb atmospheric ratio, modification by volcanic emissions 80−41507
^{210}Po/^{210}Pb disequilibria in seawater and suspended particulate matter 77−5224
^{218}Po, ^{214}Po, dosimetry in Syrian golden hamster lung 79−16304
^{218}Po, airborne Rn daughter concs. in dwellings in Great Britain 78−77118
Ra A (^{218}Po) adsorption to monodispersed aerosol 80−32535

polonium compounds
No entries

polyelectrolytes *see electrolytes; polymers*

polymer films
see also dielectric thin films; insulating thin films
acrylate adhesive coating on glass substrate, mech. props. determ. using transfer functions of US oscillations *(Russian)* 79−87644
acrylic coating, surface tension effects 80−53487
acrylourethane coatings, radiation curable, tensile, elongation and modulus props. appl. techniques 80−66847
adhesion, structure-time analogy 79−70292
adhesion to metals and non-metals, principles and meas. methods *(Czech)* 78−80709
adhesive bonds breaking under high vacuum, light and electron emission, spectral comp. obs. 80−55190
adhesive joint contact layer, dried polymer dispersion intermol. interaction with substrate and filler *(German)* 79−8421
adhesive strength, determ. for thin laminates 79−57178
adsorbed layer, energy of interaction between two spherical particles 78−53271
adsorbed monolayer, rheological behaviour 79−95245
aliphatic unsaturated poly(1,3,4)-oxadiazole films, electrode and bulk limited currents 77−69436
amino acid block copolymers, morphology and mech. props. 78−91264
amylose, micromech. fracture anal. 78−68784
angular-dependent studies on some prototype vertically and laterally inhomogeneous samples 78−95655
antireflection coating of CdTe KO-6 optical ceramic components 79−27345
antireflection coatings of TlCl components 79−27346
antistatic polymer film surfaces, microammeter meas. method for elec. conductivity 80−98932
aromatic copolyesters, charge storage props., electret stability 80−7277
asymmetric dense polymeric membrane, gaseous mixture separation 78−9696
barrier plastics, high nitride polymers, liq. transport, temp. effects 78−76921
BBB polybisbenzimidazobenzophenanthroline-dione, films, dynamic mechanical investig. at high temps. 77−4800
benzene, polymerised, plasma polymerisation in glow discharge, thin film IR and free radical EPR obs. 80−2964
benzonitrile, anodic polymer growths during electrical breakdown conditions, TEM study *(French)* 78−75960
biophenol-A-polycarbonate, liquid induced crystallisation 80−30125
bisphenol-A-diglycidyl ether epoxies, amine-cured, microscopic failure 77−90441
Brillouin scattering at transitions 80−70312
bulk electric conduction parallel to film surface 79−87094
bulk electric conduction parallel to film surface 80−92889
carbonaceous surface contamination growth on ion bombard. 77−90229
carrier transport meas. 80−6874
cellulose, in metal coated, sandwich system, spontaneous elec. current induced by heating 80−40700
cellulose acetate fibre and film, stabilisation, post UV-irrad. mech. strength *(Russian)* 79−24778
cellulose acetate films, light scatt., tensile creep, desalination 80−16050
cellulose acetate membrane, thermoosmosis of H_2O 79−52768
cellulose acetate membranes, modified, tensile props., desalination performance 79−11818
cellulose film, meas. of shear modulus and damping in a torsion pendulum 79−4989
cellulose film, moisture effect on phys. and mech. props. 80−40450
cellulose hydrate, nondestructive control of mech. props. anisotropy, appl. of capacitance method 77−86277
cellulose hydrated film, orientational heterogeneity, IR spectra and dichroism obs. *(Russian)* 78−38990
cellulose membrane, methanol(formamide)-water soln. permeabilities 78−11557
cellulose membrane, nonstationary diffusion of glycerol trioctadecanoate soln. in toluene 79−52767
cellulose nitrate, effect of high γ-doses on etching characts., dosimetry appl. 79−31224
characterisation, by TEM 80−103270

polymer films continued
charge distrib. determ., thermal pulse technique, meas. accuracy 78−80287
chemiphoretic deposition without electric current onto metal 78−64763
circular dichroism of trigonal Se formed in chiral polymer matrix 77−85685
coated steel, Pt and glassy C electrodes, prep., charact., stability 78−76866
coating, creep determ. by impression of rigid sphere 78−85084
coating on glass, current leakage path form. by water diffusion 78−10535
coatings, wear resist. props. 78−72914
coatings for corrosion protection, electrochem. techniques for performance monitoring 80−3234
coatings on metal electrodes, through electroinitiated polymerisation 77−77632
conformational transitions, activation energy determ. *(Russian)* 78−48186
copolyimide glass based on benzophenone tetracarboxylic acid dianhydride 77−63720
copolymer thermoplastic layers, isothermal smoothing of surface deformation *(Russian)* 80−76394
crosslinked collagen membranes, transport props., physical props. effects 78−77028
crystallinity degree estimate by diffraction pattern anal. 78−75555
crystallisation induced by biaxial stretching during manufacture 79−82164
defects obs., Raman microprobe-microscope appl. 80−62737
dielectric constant meas. parallel to film surface 80−97183
dielectric electret effect, homo and heterocharge charge distribution 80−11317
dielectric film, glow polymerised, struct. and props. *(German)* 77−20799
dielectric film on cond., sliding spark development in air 79−86634
dielectric thin film, polymerisation on carrier foils in discharge plasma *(German)* 77−16508
diffusion coefficients of organic vapours calc. from sorption data 79−77831
diffusion of Au electrode into polymer film 79−77821
dimensional changes meas. using stroboscopic-disk tester 79−17386
3,4-dimethyl-1,2,5-thiadiazol plasma polymerised film for holographic recording 80−106490
dimethylpolysiloxane rubber reinforced film in membrane oxygenator 79−48373
dynamic loading influence on sliding friction 79−50675
elastic anisotropy based on thermal shrinkage strains 77−86245
elasticity of bulk and film from multipass Brillouin spectra 78−76485
elasto-plastic deformation calc. in re-drawing stretched film, finite element analysis appl. *(Japanese)* 80−7621
electret, absorpt. and relax. of charge 80−6942
electret, charge distrib., generalized model 80−6873
electret charge, relax. mechanism at high humidity *(Russian)* 77−63360
electret films, produced in HF discharge, props. *(Russian)* 80−20578
electret state and adsorption during injection 79−69770
electrets, charge distribution determ. *(German)* 80−75920
electrical properties, conf., Dublin, Eire (July 1977) 79−55012
electrification, frictional, temp. and friction speed dependence obs. 80−70798
electrochemically deposited on Pt, energy losses, secondary electron spectra, AES and EELS 79−99997
electrochromic materials, polymer-modified electrode characts. 80−66149
electron energy loss spectra 77−81188
electron inelastic mean free paths 79−33370
electron inelastic mean free paths 79−33369
electron irradiation controlled form., elec. props. 80−15635
electron spectroscopy for chemical anal., appls. to materials for electrophotography 78−92565
electronic conductivity, electro-, photoresponsive effects, review 79−56261
electrophoretic coating, effect of silicone additive on electrophys. props. *(Russian)* 79−15615
electropolymerisation, in aq. medium, book contrib. 80−50778
electropolymerisation, on electrodes, book contribs. 80−50854
epoxy acrylate coated silica fibres, tensile strength >500 ksi, km length prod. 77−11052
epoxy films, in polished metal mirrors, refl.-absorpt. IR spectrosc. and ellipsometry obs. 79−78765
epoxy phenolic lacquer, dissolved in Sn powder, applied to tinplate containers 78−80671
ESCA of films on Au, sample charging phenomena 80−20764
etching and cleaning by plasma treatment 80−1855
ethyl cellulose films, secondary ion injection 79−24094
ethylene-methacrylic acid copolymer, dielectric relax. and IR obs. 79−69772
ethylene-vinyl acetate copolymers, extrusion and heavy duty films, radiation crosslinking, struct. effect 80−66844
ethylene-vinyl alcohol laminated copolymer film, O_2 permeability *(Japanese)* 79−24824
ethylenic polymer films, highly fluorinated, exam. of wetting props. 78−60856
FEP foil, charge transport, injected carrier hopping model 78−19171
ferrocene films, plasma-polymerised, carrier trapping, elec. cond. meas., 300 to 525K 80−100543
film, directional effect of impulse breakdown strength 77−20796
film, multiple light scatt., light depolarisation effects 77−4696
fluorocarbon polymer, plasma-deposited thin films for lubrication of Au contact surfaces 80−89157
fluorocarbon polymer film, prep. by RF sputtering and plasma polymerisation, props. 77−55890
fluoroplastic coatings, fretting corrosion resistance, effect of fillers *(Russian)* 77−59972
foam-film solar energy reflector fabrication, physical and chemical processors 78−90530
formation, time-lapse IR spectroscopic obs. 79−74458
Fresnel lens film prep. by electron beam irradiated mould polymerisation 79−98515
frictional electrification, temp. depend. at various friction speeds 77−11985
gas solubility, gas chromatographic determ. *(Russian)* 79−65205
gelatin, internal stresses, 20-240°C *(Russian)* 79−87645
polymer films continued
glass fibre protective coatings, materials and techniques 80−33252
glassy and rubbery, isotope effect in H_2 and D_2 diffusion, T_g region behaviour 80−84327
glassy polymers, films and spheres, transport props., film thickness and sample history effects 78−76917
glow deposition rate obs. in DC discharges 78−68633
glow discharge polymerised, conditions for attaining perfect self-healing breakdown 80−20590
glow-discharge deposited dielectric thin films, time-dependent props. 77−63564
glow-discharge polymer surface blood compatibility, Lindholm coagulation tests 77−81658
graphite fibre electrodes, coating by electropolymerisation, adhesion to epoxy matrix 79−15644
growth by glow discharge polymerisation, temp. depend. 78−68632
growth in glow discharges *(German)* 78−35343
Gunn type steady oscillations in higher polymer films *(French)* 79−28351
hexamethylcyclotrisilazane film, glow-discharge-polymerized, in MIM and MIS structs., elec. cond. mechanism 79−42680
hexamethylcyclotrisilazane film, plasma-polymerised, TEM study 80−44456
hexamethyldisiloxane, polymer film, struct. determ., IR spectra, elemental anal. *(German)* 77−59224
n-hexatriacontane, vacuum deposited on alkali halide crystals, structure and heat treatment 80−103600
high-energy electron emission, in breaking adhesive contact 79−65981
holographic laser beam deflector performance characteristics 77−19287
integrated circuit, plasma-removal of polymeric layers 80−1851
IR spectroscopic examination and anal. using multipass cavity accessory 77−57414
isoprene-styrene copolymer latexes, film-forming properties 78−53266
laser stimulated active diffusion, appl. to isotope separation *(Russian)* 78−2302
latex film composite, glass transition temp. determ. using thermomech. curves 80−75342
latex films, surface struct., vulcanisation, radiothermoluminesc. obs., 100-230K 78−75575
lavsan film, Ar ions bombardment for micropore filters preparation 78−3305
Lawsonite end plates for working spaces of liq. H_2 targets, prep. technique 77−67926
light scattering, small-angle, Debye-Bueche theory treatment of multiple scatt. 80−84794
light scattering by pressed film, effect of birefringence *(Russian)* 77−44007
light scattering obs., automated apparatus 77−53969
light-scattering, low-angle apparatus, calibration 79−58803
liquid continuous flow squeeze film, load-bearing capacity 78−87306
liquid crystal alignment on plasma-synthesized polymer films 77−76308
malononitrile, plasma-polymerised, in Ag-polymer-Ag struct., SCL currents and carrier trapping 79−51687
Marlex bulk film, γ-irrad. induced allyl chain free radical, decay kinetics 78−76855
mechanical props. meas. using automated direct reading dynamic viscoelastometer, Rheovibron 79−3980
mechanochem. degradation, substrate effects 79−79134
melt grown, birefr. effect on polarised light scatt., phase limitation 78−10867
membrane gas permeation, pore size distrib. *(Japanese)* 78−79372
membranes, use of McInnes glass electrode for determ. of CO_2 diffusion coeffs. 78−20067
memorised mechanical birefringence *(French)* 80−43677
metal-containing plasma polymerised fluorocarbon films, deposition, struct., and polymerisation mechanism 79−78928
metal-polymer, electron irrad. controlled form., elec. props. 80−15635
metal-polymer contact, short-circuit current with temp. variation 77−32090
metal-polymer films formed by electron-beam polymerisation, cond. control 78−48331
metallized polyester film as a solar filter 80−51666
methacrylic polymer films, highly fluorinated, exam. of wetting props. 78−60856
N-methacryloil-ω-aminolauric acid cholesterol ester, liq. cryst. polymers, copolymers, structuring *(Russian)* 79−55665
micropores, localisation prior to electron microscopy 80−103271
molecular weight distrib. by gel-permeation chromatography *(German)* 78−85252
Mylar, wall material for wide-gap spark chamber 77−65394
Mylar, window material for optical spark chambers 77−65395
Nafion, densities and expansion coeffs. as function of various parameters 80−79711
nylon 6, frictional electrification between metal and polymer, depend. on temp. and friction speed, contrib. of mol. motion of polymer to electrification 80−6953
nylon 6, photoelectric emission and contact charging, surface states 79−33885
Nylon 6, prior high-press. treatment effects, weight swelling, density, IR crystallinity, X-ray and viscosity obs. 80−81025
Nylon 6 and 12 films, drawn, NMR, mol. orientation, motions *(Japanese)* 77−32268
nylon (N12), uniaxially oriented, anisotropy of elec. cond. 79−87095
Nylon-12, casting conditions effect on polymorphism 80−84903
optical fibres, plastic-coated fused silica, ageing and static fatigue 79−46067
optical fibres development, polymer clad, for communication use 80−69546
optical films for waveguides and dye laser, prep. and charact. *(Japanese)* 78−5551
optical interconnections in thin-film guided-wave optics 77−58487
optical polarisation data interpretation of aromatic hydrocarbons in stretched films, photoselection spectroscopy appl. 80−58302
optical properties meas., by integrated optical techniques 78−27342
optoacoustic signal, thickness effect on signal magnitude 80−11969
organo-tin polymer films, glow discharge prep., comp. determ. by XPS and AES 80−35109
orientation, uniaxial and biaxial, obs. and effect on mech. props. 78−80590
orientation evaluation of noncrystalline chain, with polarised fluorescence method *(Japanese)* 80−6368

polymer films continued
oriented, elastic constants meas. 78−38261
oriented polyethylene, deformation band studies 77−52420
PAN, spectroscopic analysis of electrically polarised films 78−68443
partial discharges, HNO_3 absorption, expt. *(German)* 77−77147
partially crystalline, electron microscope struct. anal., soln. and melt-grown films as model specimens 78−30523
parylene (vacuum deposited polymeric coating), appl. to electronics 80−108607
penetrant sorption kinetics, transverse differential swelling stresses 78−76923
pentaplast, plasticised, thermal treatment effect on props. 80−40324
permeability of O_2, determ. with Zircon gas analyser 79−39195
permeation, diffusional time lags determ. 80−65272
PET, biaxial orientation, refr. index meas. by Raman and IR spectrosc. 80−60583
PET, charge effects at Al electrodes obs. 80−75625
PET, crystallised by nonreactive liquids, exam. of mech. props. 79−43338
PET, dyed, local mech. stresses, IR spectrosc. determ. 80−65418
PET, in MIM struct., injection current enhancement at metal insulator interface, theory 80−49953
PET, interatomic bond determ. by IR transmission and reflection spectroscopy 77−65958
PET, metallized, reflecting surface, ageing under natural conditions, destructive factors identification 79−83340
PET, transverse constriction and stresses accompanying uniaxial orientation 78−48475
PET film, crystallised by nonreactive liquids and vapours, exam. of diffusion of liquids and vapours 79−42314
PET film, Cu vacuum condensate 77−77385
PET films, one-way drawn, constant strain effects, IR meas. 80−60584
photolytic, form. on semicond. surface, thickness modulation by p-n junction microfield 78−10561
photon and electron absorbed-dose detector 80−91379
photopolymer, biaxial stress-strain test 80−40417
photoresist, KTFR, thermally stimulated discharge current studies 80−75924
photoresistive film based on polymer-bisazide systems, photosensitivity *(Russian)* 77−48641
photoresists, cross-linking, photographic characteristic curve, sensitivity 77−10128
photoreticulation by UV irradiation 80−40717
photovoltaic properties, for solar cell appls. 80−60040
piezoelectric transducers using polar polymers 79−23162
piezoelectricity and pyroelectricity, review 77−8514
planar molecules in stretched polymer films, solute orientation, transition moment direction, dichroic spectra 78−58742
plasma deposited, adhesion to plastics 80−50745
plasma polymerisation, light propag. expt. *(Japanese)* 78−6846
plasma polymerisation on solid substrate in RF discharge 80−2963
plasma polymerized on metal substrates, adhesion and cohesion 78−3259
plasticised cellulose acetate sheet, post-yield fracture 80−25859
PMMA, diffusion-controlled penetration by monohydric normal alcohols 78−76918
PMMA, electron beam scattering, Monte Carlo simulation 80−100148
PMMA, molecular interaction in frictional-contact zone, absorpt. spectra 79−78688
PMMA, optical waveguide, direct writing of gratings by electron beam 79−46091
PMMA, photodielectric media for holographic recording, photochem. response 78−7219
PMMA, Plexiglas, penetration depth of 10.6 μm laser radiation, transmission, refl. and absorpt. meas. 79−74010
PMMA, sheets, in methanol, case II swelling and transport kinetics 78−76922
PMMA, solvent cast, surface characts., chromatographic study 80−20020
PMMA, struct. of boundary layers on solid substrate determ. by total internal reflection *(Russian)* 79−32922
PMMA, surface charge decay and TSC 80−11328
PMMA, threshold switching effects 78−84270
PMMA coatings, packing density investig. by mol. probe method *(Russian)* 77−44398
PMMA electron resists, molecular weight depend. of developed contours 79−87859
PMMA electron-resist films, energy loss calcs., Bethe and Spencer-Fano theories 78−87728
PMMA film, doped, time resolved absorpt. spectra, decay kinetics of exciplex state 80−84098
PMMA film, in Al-PMMA-Al struct. SCL currents and cond. mechanism 79−51686
PMMA film, Monte Carlo simulation of electron penetration 79−23659
PMMA film in small area lateral MIMS device, cond., switching 80−97003
PMMA sheet in methanol, pre-soak, dissolved gas content rel. to craze nucleation, creep 79−66185
PMMA-spirobenzopyran mixed monolayers, photoresponsive effects 79−66316
PMMA-spiropyran Langmuir monolayers, reversible photochemical strain 80−50867
polar, piezoelectricity and pyroelectricity 80−7267
polar polymer, piezoelectricity and pyroelectricity 80−7267
polarised polyvinylidene fluoride film, piezoelectric transducer 80−75993
poly(4-methyl-1-pentene), semicrystalline, bulk and film, surface effects using Brillouin scatt. 79−42982
poly(β-benzyl L-aspartate), conformational transitions 77−88613
poly(γ-benzyl L-glutamate), soln. and film, light scattering study 79−66374
poly(alkyl methacrylate) films, chemical characterisation from C Auger spectra, appl. of pattern recognition and factor anal. 79−79347
poly(chlorotrifluoroethylene) films, crystalline superstruct., mol. orientation, X-ray diffr., depolarised light scatt. 78−71685
poly(cis-isoprene), tagged, in untagged matrix, instantaneous shape, segmental density 78−62966
poly(ethyl vinyl ketone) film, reacted with phosphoryl chloride, elec. cond. 80−97599
poly(ethyl-methacrylate), surface charge decay and TSC 80−11328
poly(ethylene terephthalate)-polystyrene, two-phase polymer alloy, deformation of films 78−52904

polymer films continued
poly(glutamic acid)-poly(oxyethylene glycol), heterogeneous network film, polarising microscopic struct. obs. 78−9948
poly(L-glutamic acid), texture in conc. soln. and solid films *(Japanese)* 79−90534
poly(n-butyl-methacrylate), surface charge decay and TSC 80−11328
poly(N-vinylcarbazole), fluoresc. and phosphoresc., energy transfer mechanism 80−16112
poly(N-vinylcarbazole), hole photogeneration 78−80021
poly(N-vinylcarbazole) layers, supermol. struct. effect on elec. props. 80−44606
poly(n-vinylcarbazole)-trinitrofluorenone films, charge carrier trapping 78−14846
poly(oxyethylene glycol), texture in conc. soln. and solid films *(Japanese)* 79−90534
poly(p-xylylene), electron MFP as function of kinetic energy, XPS 78−52114
poly(p-xylylene), film, high field cond. 79−99647
poly(vinyl alcohol) porous film, polymerisation and porosity 80−107063
poly(vinyl alcohol)-Cu(II) complex, ESR study 79−61199
poly(vinyl bromide), surface charge decay and TSC 80−11328
poly(vinyl pyrrolidone)-Cu(II) complex, ESR study 79−61199
poly(vinylidene fluoride), phase-III, IR study 80−20624
poly(vinylidene fluoride), piezoelec. response depend. on phase I vol. fraction 80−20593
poly(vinylidene fluoride), poled, piezoelec. activity and field-induced cryst. struct. transitions 80−20592
β-poly(vinylidene fluoride), single cryst. orientation, piezoelec. 80−20591
poly(vinylidene fluoride), strong piezoelec. under high press. annealing 80−11344
poly(vinylidene fluoride), surface charge decay and TSC 80−11328
poly(vinylidene fluoride) film, pyroelectric coefficient determ. using dielectric heating 78−35096
poly 2,6-dimethyl-1,4-phenylene ether, liquid-induced crystallisation 78−30551
poly γ-methyl L-glutamate films, thermal motion of α-helical mols. 79−64133
poly (N-vinylcarbazole): trinitrofluorenone films photovoltaic properties for solar cell appls. 80−60040
poly-1,1-dihydropentadecafluorooctyl methacrylate barrier films, props. 79−51197
poly-2-vinylpyridine-iodine, semicond. film, elec. cond., depend. on I conc. and temp. 79−73606
poly-α-naphthol, SCL currents, obs. 77−47910
poly-α-naphthol, semicond., isothermal depolarisation currents, electron trap parameters 80−60492
poly-β-benzyl-L-aspartate films, circular dichroism, IR spectra, α, β, ω conforms. 77−48197
poly-β-benzyl-L-aspartate films, conformational stability, effect of organic solvents, IR spectra 78−70988
poly-γ-benzyl-L-glutamate, monolayers, struct. studies, IR, ATR, and TEM obs. 80−44396
poly-γ-benzyl-L-glutamate, soln., liq. film, diamagnetic susceptibility 78−74794
poly-γ-methyl-L-glutamate, uniaxially oriented, anisotropy of elec. cond. 79−87095
poly-(bisphenol) carbonate, photocond., of double layer polymer systems doped with charge transfer complexes 79−87124
poly-gamma-benzylglutamate, oriented films, piezoelectric relax. 77−24798
poly-N-vinyl carbazole by melt extrusion, orientation 78−67665
poly-N-vinylcarbazole, electrophotographic film, dark discharge 78−34864
poly-N-vinylcarbazole, in polymer film, excimer fluoresc., high press. effects 80−34966
poly-N-vinylcarbazole, thin films, impedance states switching 77−20461
poly-N-vinylcarbazole film, triplet-triplet energy transfer, chemiluminesc. 78−43944
poly-N-vinylcarbazole thin amorphous film, hole drift mobility, mol. mass. depend. 80−75663
poly-p-xylylene films, carrier traps, X-ray induced TSC, thermolum. and dielec. loss study 80−88570
poly-vinylidene fluoride-co-tetrafluoroethylene, dipolar theory applications to piezoelectric props. 79−78627
polyacetonitrile film, in Pt/polymer/metal capacitors, electroforming and elec. cond. 80−54800
polyacetylene: Br(Cl)(I)(AsF_5) electrical conductivity, metal-to-insulator transition 78−10525
cis-polyacetylene:AsF_5, conductivity meas., non-Ohmic effects 80−96891
polyacetylene:AsF_5, heavily doped, transport props., evidence for metallic state 79−87121
polyacetylene:AsF_5, soliton doping mechanism, mag. susceptibility meas. 80−107979
polyacetylene:SbF_5, elec. cond. meas. 80−60055
polyacetylene, $(CH)_x$, synthesis, struct. and elec. props., doped materials, review 80−15623
trans-polyacetylene, and AsF_5 doped, EPR 79−42835
polyacetylene, doped, transport props. 80−24913
polyacetylene, doped film, elec. cond. 80−24921
polyacetylene, ESR study, effects of O_2, No and halogens 80−25186
trans-polyacetylene, halogen doped, elec. cond. 79−19589
polyacetylene, halogen doped, mass spectrometric anal. 80−108771
polyacetylene, n- and p-type doping, and compensation, p-n junction formation 78−76070
polyacetylene, nascent morphology obs. 80−24379
polyacetylene, partially oriented, anisotropic elec. cond., quasi-one-dimens. behaviour of fully oriented doped material 80−11112
polyacetylene, semiconducting and metallic, thermoelec. props. 80−40884
cis-polyacetylene, unpaired electrons, isomerisation, EPR obs. 80−60405
polyacetylene, variable density, synthesis, elec. cond., thermopower 80−60016
polyacetylene and derivatives, chemically doped, elec., chem. and phys. props. 80−24912
polyacetylene film, anisotropy of dielec. const. 80−108146
polyacetylene film, heavily doped with AsF_5, conductivity and Hall effect meas. 79−28353
polyacetylene films, AsF_5 doped, photocond. and junction props. 80−70770
polyacetylene films, doping effect on elec. cond., chem. and optical props. 80−65572

polymer films continued
polyacetylene films, doping investigation, insulator-metal transition, optical transmission meas. 80−103729
polyacetylene films, electrical properties *(Japanese)* 80−96888
polyacetylene films, pure and Br and I doped, Raman scatt. 79−47457
polyacetylene films, pure and doped, cond., ESR 79−82859
polyacetylene films, stretch-aligned, prep. and morphology 80−66471
polyacetylene films, tensile props. and partial alignment 80−104210
polyacetylene films, undoped, nonlinear current-voltage charcts. 80−75574
polyacetylene pure and doped films, anisotropic optical properties 78−92137
polyacrylamide-CU(II) complex, ESR study 79−61199
polyacrylic acid film, structurisation and mech. props., EM obs. *(Russian)* 80−59406
polyacrylonitrile, film, dielectric polarisation 78−52431
polyacrylonitrile, film, IR attenuated spectra determ. of chem. origin of TSC 77−55746
polyacrylonitrile, plasma deposited, adhesion to plastics 80−50745
polyacrylonitrile, polaris., pyroelec., electret film, solar energy conversion *(Russian)* 78−39507
polyalkyl methacrylates, oriented stretched membrane, gas diffusion, entropy correl. theory 79−69291
polyamide 6 and 12 films, permeability to H_2O vap. *(Russian)* 78−53255
polyamide coating on steel roller, experimental exam. of contact parameters 78−68842
6-polyamide films, cond. and relax. under very high press. 77−35748
polyamide-polyurethane copolymer dispersions, structurisation and relax. props., coating from props. 80−76559
polyamidoimide film, thermomech. props. rel. to mol. struct. *(Russian)* 79−57029
polyarylate, F-2, film, rigid chain orientation in surface active medium *(Russian)* 78−88513
st-1,2-polybutadiene, oriented film, anisotropic C 1s XUV absorpt. spectra 80−55207
polybutene-1 film, deform. mechanism, rheo-optical meas. 80−21041
polybutene-1 film, tubular-extended, anal. of orientational and form birefringence 80−29712
polybutene-1 film, tubular-extruded, light scatt. from crystn. superstruct. 77−55796
polybutylene terephthalate, melt crystallised, solvent crystallised films and moulded bars, morpholigical obs. 80−84101
polybutylene terephthalate film, photoluminesc. exam. 78−48213
polycaproamide, molecular interaction in frictional-contact zone, absorpt. spectra 79−78688
polycaproamide, supermolecular structure and mech. stress distrib. among chem. bonds 78−75562
polycaprolactam, electric strength, temperature-time dependence *(Russian)* 78−76386
polycaprolactam film, subjected to 9 kV elec. discharge, X-ray obs. *(Russian)* 79−23536
polycarbonate: tri-p-tolylamine, chemical control of conductivity 80−59984
polycarbonate:tri-p-tolylamine amorphous film, elec. and mag. props 80−49959
polycarbonate, and charge-transfer complex modifications, isothermal dark currents 80−88559
polycarbonate, and charge-transfer complex modifications, TSC 80−88572
polycarbonate, oriented, US speed −180 to 160°C, orientation influence 79−19326
polycarbonate, struct. and mech. props. 79−19160
polycarbonate film, by aq. acetone solns., roughness form. mechanism *(Russian)* 78−48554
polycarbonate film, fission track etching charact., UV and ageing effects 79−76296
polycarbonate film dosimeter for high-level electron dose meas., optical density 77−25559
polycarbonate films, amorphous and crystalline, temp. depend. of US vel. 78−91575
polycarbonate films, effect of UV and visible mono- and polychromatic radiation, stability *(Russian)* 79−57268
polycarbonate films, high temp. relaxations 80−97187
polycarbonate foils, ^{239}Pu alpha particle tracks 79−76310
polycarbonate thin films, solution-grown, dielectric relaxations 80−55029
polychlorotrifluoroethylene, electret, TSC 80−7266
polychlorotrifluoroethylene on metal substrates, adhesion and cohesion 78−3259
polydiacetylenes substituted with urethane, solid and film, visible spectra, refl. and absorpt. 79−87460
polydimethyl siloxane-b-styrene-b-dimethyl siloxane block copolymer, morphology, mech. props. 80−64930
polydimethylsiloxane film, formed by RF discharge plasma polymerisation, optical props. 78−80479
polydimethylstyrene coatings, packing density investig. by mol. probe method *(Russian)* 77−44398
polyester, multilayer interf. film deposition by roll coating *(Japanese)* 79−81577
polyester film, cross-linked, low-mol. wt. substance sorption effect on struct. *(Russian)* 80−59405
polyester ultrathin films, photochemical props., transducer appl. 80−37020
polyester yellow in polyvinylacetate film, ablative optical recording 80−83555
polyester-hydrazide, aromatic, fibres and films, synthesis and props. *(Japanese)* 80−108387
polyethylene, 1/f noise, 10^{-4}-1 Hz, 20-80°C 79−51643
polyethylene, γ-irrad., electrolum., 77K 77−32442
polyethylene, γ-ray polymerised, cold compacted films, mech. relaxations, mechanism 77−16631
polyethylene, adhesive props. improvement by corona discharge appl. *(French)* 78−92438
polyethylene, C filled, ultrathin films, photochemical props., transducer appl. 80−37020
polyethylene, corona charged, surface potential decay 78−14795
polyethylene, cross-linked, thermal oxidation stability, influence of Cu 80−30128
polyethylene, cross-linked, topomorphism 77−43159
polyethylene, drawn, dielec. breakdown and morphological struct., dichroic ratio 80−25813
polymer films continued
polyethylene, elec. charge decay charact. 77−28238
polyethylene, elec. empulse breakdown strength, rel. to rate of drawing 80−15960
polyethylene, elec. props., effect of quenching 77−73114
polyethylene, electrets, polarisation obs. and influence of wax impurities, TSC obs. and analysis *(French)* 80−44999
polyethylene, elongated, γ-irrad., TSC meas. 80−11324
polyethylene, elongated, elec. impulse breakdown strength temp. depend., 20 to 80°C 77−73113
polyethylene, elongated, TSC, 20 to 60°C 78−10826
polyethylene, elongated low density film, TSC 79−47106
polyethylene, epitaxial crystallisation, IR investig., macromol. struct. changes 77−35493
polyethylene, high and low density, depolarisation thermocurrent study, relax. modes 80−7263
polyethylene, high density, carrier trapping, X-ray induced TSC 80−11005
polyethylene, high density, corona charged, thermally stimulated surface pot. 80−11327
polyethylene, high density, corona-charged, surface pot. decay 79−24254
polyethylene, high density, film, melt growth, cryst. superstruct., small angle light scatt. 77−31602
polyethylene, high moleculer weight, fibril structure induced by oriented crystallisation *(Japanese)* 79−90575
polyethylene, injection times for charging obs., with aid of computer 80−70796
polyethylene, lifetime under small loads 79−95301
polyethylene, lightly crosslinked, processed under mol. orient., transparent film prep. 80−38957
polyethylene, linear, films, elec. cond. rel. to drawing, annealing *(Japanese)* 79−15817
polyethylene, linear, irrad. crosslinking and chain scission in extended chain and bulk films 77−60095
polyethylene, linear, quenching of thin films to amorphous state 80−28929
polyethylene, low density, UV and heat treatment effects, DSC obs. 79−14915
polyethylene, low-density, crystallisation, automated light-scattering apparatus 77−53969
polyethylene, melt-cast, deform. in equatorial region of spherulites, electron diffr. 77−25115
polyethylene, mixed morphology and linear fractions, light scatt. obs. 78−2023
polyethylene, molecular interaction in frictional-contact zone, absorpt. spectra 79−78688
polyethylene, oxidised, energy of adhesion with polar and nonpolar liquids 77−55427
polyethylene, partial discharge degradation, effect of discharge products in air *(Japanese)* 77−69774
polyethylene, photoelectric emission and contact charging, surface states 79−33885
polyethylene, pristine and radiation-damaged film, electron energy loss spectra 79−81312
polyethylene, relation between electrostatic capacity and electronic space charges induced by high field 79−15154
polyethylene, soln.-cast, low energy electron scatt. obs. of band struct. 80−16131
polyethylene, stretched, containing anthracene, UV-visible and fluoresc. spectral shifts 78−62852
polyethylene, stretched, interpretation of polarised absorption and emission spectra of molecules 78−1012
polyethylene, stretched, linear dichroism of aromatic molecules 77−88480
polyethylene, surface pot. decay, drift mobility determ. 77−11979
polyethylene, ultra-oriented, prep. technique, extreme moduli 77−21086
polyethylene, uniaxially drawn low-density, pre-exponential factor in elec. cond. 77−21224
polyethylene coating used to increase strength of fused silica fibres 77−23768
polyethylene coatings, vac. deposited on Al and Cu, adhesion 79−61793
polyethylene crystal, preferred orientation relationship, epitaxy 78−67923
polyethylene film, chain rupture and tensile deform., viscosity-av. mol. wt. obs. 78−76714
polyethylene film, dielec. breakdown sites 80−50266
polyethylene film, directional effect of impulse breakdown strength 77−20796
polyethylene film, effect of corona generated excited molecules on surface pot. decay 80−6941
polyethylene film, gauche-trans transition, activation energy meas. by IR spectra 79−57220
polyethylene film, high density, anomalous transient currents around 50-70°C 79−33368
polyethylene film, minimum running thickness, biaxial extensional flow study 80−100993
polyethylene film, oriented, soln. growth 80−45244
polyethylene film, uniaxially drawn low-density, pre-exponential factor in elec. cond. 77−21224
polyethylene films, corona charged, charge trapping 80−88571
polyethylene films, electron beam irrad., carrier mobilities 79−1600
polyethylene films, hard elastic, deform. mechanism 77−32652
polyethylene films, internal lamellar struct. obs. by ion etching and SEM 79−73076
polyethylene films, low density, γ-irrad., elec. cond., effect of elongation 79−4564
polyethylene films, plasma surface treatment, ESR detect. of free radicals 79−15824
polyethylene films, preliminary treatment before corona discharge printing, technical parameter effects *(German)* 79−15838
polyethylene films, radiation initiated graft polymerisation of acrylonitrile, initiation rate rel. to props. *(Russian)* 80−7531
polyethylene films, stretched, molecular distrib., anthracene, naphthalene in film 78−27298
polyethylene films, surface pot. decay, appl. of Scher-Montroll method 79−7851
polyethylene films, two-layer, elongation, recovery rates meas., relaxational props. *(Russian)* 77−32663
polyethylene films, uniaxially and doubly oriented, crystallite size determ., microparacrystallite lamellar surface identification 78−48431
polyethylene films 4 to 100 μm, thickness meas. *(Japanese)* 80−52160

polymer films continued
polyethylene films modified by polyacrylonitrile grafting before, after orientating elongation, struct. *(Russian)* 77−32554
polyethylene oxide, peculiarities of struct. form. near below the melting point 80−54150
polyethylene oxide, thin layer melt, morphology of supermol. structs. 79−14705
polyethylene reinforced with graft polymers, molecular failure mechanism, IR spectra 77−16682
polyethylene resin coated paper formulation for photography 80−4794
polyethylene spherulites, thin melt-cast films, high density, deform. process in non-equatorial regions 80−81124
polyethylene stretched, film, effects of vapour phase application of compounds 77−90276
polyethylene terephthalate, 1/f noise, 10^{-4}-1 Hz, 20-80°C 79−51643
polyethylene terephthalate, corona charged, surface voltage decay mechanism, TSC meas. 80−11326
polyethylene terephthalate, deformation band studies 77−52420
polyethylene terephthalate, elec. cond., 120-180°C, anal. of results 79−47102
polyethylene terephthalate, elec. cond. and space charge accumulation 80−10998
polyethylene terephthalate, electret, TSC, due to injected charge 77−16242
polyethylene terephthalate, film, amorphous, Brillouin scatt. and splitting 77−24857
polyethylene terephthalate, film, optical consts., frustrated total internal refl. obs. 77−55763
polyethylene terephthalate, film, two-stage orientation in monoaxial extension *(Russian)* 77−62488
polyethylene terephthalate, films, deform., strength props., simultaneous meas. of several samples 79−15896
polyethylene terephthalate, induced crystn. on metallic nucleating particles 79−15658
polyethylene terephthalate, injection times for charging obs., with aid of computer 80−70796
polyethylene terephthalate, lateral motion of charge 78−43458
polyethylene terephthalate, mechanism of photocarrier generation 77−89798
polyethylene terephthalate, metallised coatings fracture under laser irrad. *(Russian)* 80−76333
polyethylene terephthalate, molecular interaction in frictional-contact zone, absorpt. spectra 79−78688
polyethylene terephthalate, Mylar C film, high field relaxation currents 79−11259
polyethylene terephthalate, nonlinear elec. cond. and space-charge effect 77−39980
polyethylene terephthalate, oriented, elastic constants meas. 78−38261
polyethylene terephthalate, preoriented sheet, plastic deform., anisotropic behaviour 79−8335
polyethylene terephthalate, space charge quantity meas. by Maxwell stress method 80−22389
polyethylene terephthalate, supermolecular structure and mech. stress distrib. among chem. bonds 78−75562
polyethylene terephthalate, surface modification by corona discharge, adsorption and wettability 77−86212
polyethylene terephthalate, TSC, depend. on heating rate 78−88249
polyethylene terephthalate, TSC spectrum from electron beam charging 77−77139
polyethylene terephthalate electrets, formed by electron injection, TSC meas., space charge drift 80−11321
polyethylene terephthalate electrets, TSC due to injected charges, electron trapping props. 79−4566
polyethylene terephthalate film, degree of crystallinity effect on particle tracks *(French)* 77−46471
polyethylene terephthalate film, gauche-trans transition, activation energy meas. by IR spectra 79−57220
polyethylene terephthalate film, photoluminesc. exam. 78−48213
polyethylene terephthalate film, X-ray diffr. exam. of morphology 78−18558
polyethylene terephthalate films, current peaks obs. with linearly increasing voltage 80−88654
polyethylene terephthalate films, gamma radiation induced cond. under high elec. field 78−47798
polyethylene terephthalate films, high-temp. elec. conduction 79−51588
polyethylene terephthalate sheeting, storage in aqueous media rel. to props. *(German)* 79−29250
polyethylene terephthalate thin films, electronic mobility 80−15634
polyethylene thin film, partial discharges energy content effect on breakdown *(German)* 77−81052
polyethylene ultrathin foil prep. by film casting 78−48340
polyethylene-paraffin wax, blends, rapid cooling processing techniques 80−84905
polyethylene-terephthalate, field-controlled photogeneration and carrier trapping 80−25285
polyethylene/polypropylene blends, surface growth of fibres and films 80−66470
polyethylenes, extrusion and heavy duty films struct. parameters influence on cross-linking by radiation 80−66844
polyethyleneterephthalate, crystallised from thin layer melts, temp. depend. of morphology 80−54149
polyethyleneterephthalate, foil, optical microscopy and low angle light scattering 80−55210
polyethyleneterephthalate, in Al-PET-Au system, short-circuit current with temp. variation 77−32090
polyethyleneterephthalate, props. of adhesive layer adsorbed on surface 79−56067
polyethyleneterephthalate film, in m.i.m. struct., short-circuit current induced by temp. change 77−4450
polyethyleneterephthalate influence of crystallisation on adhesive and cohesive props. 79−56100
polyethyleneterephthalate-polyethylene film, vapour permeability determ., gravimetric test method 79−39066
polyferrocene film, plasma polymerised, dielec. props., 40 kHz to 50 MHz, 30-400°C 78−52439
polyfluorocarbon, RF plasma deposition on glass or $In_{2-x}Sn_xO_{3-y}$, and liq. cryst. aligning props. 77−48350
polyhexamethyldisiloxane thin film form. in glow-discharge flow system 78−68631
polyhexamethylene adipamide, photocond. and dielectric props. 80−84489
polymer films continued
polyimide, heat treatment conditions effect on ultimate strength, expt. planning methods 78−6952
polyimide film, dielec. AC props., expt. 78−43783
polyimide film, dielectric breakdown in high-temperature region 78−84522
polyimide film, thermally stimulated depolarization anal. 79−69766
polyimide films, effect of atm. and temp. on wear, friction and transfer 78−85003
polyimide films, mol. relaxations, mol. orientation and friction charcts. 77−59939
polyimide films, transient current in time range 10^{-4} to 10 s at temps. 180 to 280°C 80−65729
polyimide substrate foils for nuclear targets 80−18739
polyimide thin film gasket seal fabrication for ultrahigh vac. 77−57334
polyimide thin film vacuum deposition 78−39695
polyimides, ultrathin films, photochemical props., transducer appl. 80−37020
polyisobutylene, impurity distrib. of tagged poly-cis-isoprene, individual and aggregate 79−68339
trans-1,4-polyisoprene, crystalline morphology in thin films 78−6019
trans-1,4-polyisoprene crystals, press. effect on growth rate 80−88064
polymalononitrile, plasma polymerized film, photoelec. props. 78−39158
polymer laminate, adhesive strength determ. 79−57178
polymer matrix composites, component interaction mass spectrometry investigation *(Russian)* 80−35511
polymer-bisazide system, light sensitivity of photoresisting films *(Russian)* 79−6214
polymethyl methacrylate, use of synchrotron radiation in X-ray lithography 80−62820
polymethyl-α-cyanoacrylate, photodielectric media for holographic recording, photochem. response 78−7219
polymethylsiloxane, in MIS struct., C-V charcts. and charge movements 77−85340
polymethylsiloxane-polyarylate block copolymer, soln., viscosity, rel. to film mech. props. and microstruct. *(Russian)* 79−23762
polymonochloroparaxylylene film, photoluminesc. exam. 78−48213
polynaphthalene films, plasma polymerised, photovoltaic and photocond. props. 80−34479
polynaphthol, semicond., trap depth and trapping cross section from TSC curves 79−51700
polyoxyethylene, epitaxial crystallisation, IR investig., macromol. struct. changes 77−35493
polyoxymethylene, epitaxial crystallisation from soln. 77−7984
polypentene-1, isotactic, polymorphism of form I 79−19159
polyphenylacetylene, phys. struct., AC and DC cond. 80−44750
polyphenylenesilsesquioxane, cast film, correlation between optical and mech. anisotropy 78−95000
polyproplylene, molecular interaction in frictional-contact zone, absorpt. spectra 79−78688
polypropylene, cold-drawn isotactic bars and thin films, microstruct. and annealing 78−95760
polypropylene, double-exposure speckle pattern obs. of tensile deform., displacement, Poisson's ratio and stress relax. 80−84795
polypropylene, drawn, rheo-optical studies 78−15440
polypropylene, effect of corona treatment on dielectric props. for capacitor appl. 79−33607
polypropylene, evaporated, elec. props. 78−84335
polypropylene, film, isotactic, ion injection, space-charge-limited currents 79−69775
polypropylene, film and fibre, chain rupture and tensile deform., viscosity-av. mol. wt. obs. 78−76714
polypropylene, low mol. wt., vapour phase epitaxial growth 78−67924
polypropylene, photoelectric emission and contact charging, surface states 79−33885
polypropylene, stretching flow for film prod., bubble blowing in solid phase 78−71303
polypropylene, stretching flow for film prod., stretching over canonical mandrel 78−71304
polypropylene, supermolecular structure and mech. stress distrib. among chem. bonds 78−75562
polypropylene, transparent film, strain anal. by scattered-light speckle photography 79−32399
polypropylene, ultrathin film prod. technique 77−41582
polypropylene, vacuum evaporated, electron trap depth, TSC meas. for MIM struct. 79−95535
polypropylene electrets corona charged at high temp., TSC study 80−7261
polypropylene fibers, and films, and their hard elastic precursor small-angle X-ray diffr. studies 79−10815
polypropylene fibrillated film reinforced cement, loading capacity, cracking 78−72759
polypropylene film, corona-charged, TSC and space charges 80−40041
polypropylene film, dielectric relaxation, β-mode investigation 80−93239
polypropylene film, effect of crystallinity on deformation mechanism of biaxial stretching 77−80426
polypropylene film, in MIM struct., electroforming 80−25019
polypropylene film and fibre, plasma etching 78−95871
polypropylene film electret, space charge injection induced pyroelectricity 77−12324
polypropylene films, hard elastic, gas permeability, extension effects 80−40412
polypropylene films, meas. of dielectric losses at cryogenic temps. 80−25301
polypropylene films, plasma surface treatment, ESR detect. of free radicals 79−15824
polypropylene isotactic film, cryst., dynamic mech. props., influence of struct. 79−4991
polypropylene reinforced with graft polymers, molecular failure mechanism, IR spectra 77−16682
polypropylene thin film conduction mechanism, expt. obs. 77−28271
polypropylene thin stretched foils, appl. as ionisation chamber windows 80−18764
polypyromellitimide, elec. cond., 120-180°C 80−60124
polypyromellitimide, low temperature relax., NMR, dielec. and mech. losses 78−71686
polypyromellitimide, thermal depolarisation current 78−52429
polypyrrole films, electrochemical prep., chem. and phys. characterisation 80−70708
polyquinoline carboxylic acid film, effective electron mass determ. from IV charcts. 77−85135

polymer films continued
polysiloxane plasma polymerised film growth on GaAs substrate, dry etching process 80−25575
polystyrene:I films, thermally stimulated discharge, I conc. and polarisation temp. depend. 80−107937
polystyrene, 1/f noise, 10^{-4}-1 Hz, 20-80°C 79−51643
polystyrene, γ-Fe_2O_3 powder filled, mag. films, packing and particle orientation *(Japanese)* 80−104115
polystyrene, craze and fracture surface morphology 77−12682
polystyrene, energy losses and straggling for H^+ and He^+ beams *(Russian)* 80−84226
polystyrene, energy straggling of H^+ and He^+ ions in 0.1 to 1.2 MeV range 77−80559
polystyrene, formed by RF electrodeless excitation, dielec. props. 77−24795
polystyrene, frictional electrification between metal and polymer, depend. on temp. and friction speed, contrib. of mol. motion of polymer to electrification 80−6953
polystyrene, glow discharge polymerised, conditions for attaining perfect self-healing breakdown 80−20590
polystyrene, isotactic gel film, Fourier transform IR spectrum 80−104465
polystyrene, n-heptane and methanol crazes, structure 77−12681
polystyrene, optical props. from near IR to X-ray, sum rules 77−48195
polystyrene, plasma deposited adhesion to plastics 80−50745
polystyrene, plasma produced, struct., NMR 77−25264
polystyrene, styrene plasma polymerisation in glow discharge, thin film IR and free radical EPR obs. 80−2964
polystyrene, TSC and dielectric props. *(Japanese)* 80−15632
polystyrene, uniaxially stretched atactic thin film, mol. orientation, polarized Raman study 80−103951
polystyrene amorphous film, cyclically fatigued, molecular behaviour 80−35310
polystyrene coated Ag holographic grating, Raman spectra enhancement by plasmon surface polaritons 80−80885
polystyrene coatings, packing density investig. by mol. probe method *(Russian)* 77−44398
polystyrene film, acrylic acid doped, elec. cond. and activation energy conc. depend. 80−15631
polystyrene film, craze growth and fracture 79−83319
polystyrene film, delayed luminesc. decay kinetics of 1,2-benzanthracene 80−43088
polystyrene film, Fourier-transformed IR photoacoustic spectra 80−34993
polystyrene film, graft, positive-ion emission in thermal destruction 80−66381
polystyrene film, in MIM struct., elec. conduction and free radicals 80−20340
polystyrene film, temp.-stress depend. of rupture life under hydrostatic pressure 80−16467
polystyrene film, thermally stimulated discharge currents 80−71300
polystyrene film, thermally stimulated discharge currents of polarised film 79−78609
polystyrene films, amorphous, X-ray small angle scatt. near glass transition, struct. *(Russian)* 77−31606
polystyrene films, soln. grown, elec. cond. meas. 80−97020
polystyrene films, UV irrad., struct. changes, gel permeation chromatogram computer manipulation, substraction 79−96387
polystyrene films on metal substrates, electrode effect on carrier injection, TSC, I-V characts. 80−34463
polystyrene thin film, glow discharge formed, dark current and photocurrent obs. *(Japanese)* 80−15633
polystyrene thin films, TSC and surface charge meas. 80−103769
polystyrene-collodion, tunable multilayer-film distributed-Bragg-reflector filter 79−76838
polystyrene-nylon 6, frictional electrification, temp. and friction speed depend. 78−60190
polystyrene-polycarbonate, frictional electrification, temp. and friction speed depend. 78−60190
polystyrene-polyvinyl alcohol, tunable multilayer-film distributed-Bragg-reflector filter 79−76838
polytetrahydrofuran, electrochemically prepared between metal electrodes, DC elec. props. 80−39695
polytetrahydrofuran, electrochemically prepared between Pt and Au electrodes, AC elec. props. 80−40062
polytetrahydrofuran film, in Pt/polymer/metal capacitors, electroforming and elec. cond. 80−54800
polythiourea, plasma polymerized film, photoelec. props. 78−39158
polyurethane: dye, photoinduced guided light stopping 77−23739
polyurethane:rhodamine 6G film, fluoresc. photoinduced disappearance and restoration 77−1727
polyurethane:rhodamine 6G film, laser, etched cavity 77−7140
polyurethane, TSD rel. to glass transition dipole relax. activation *(Russian)* 77−20793
polyurethane, variation of packing charact. near solid surface, IR obs. *(Russian)* 79−65349
polyurethanes, epitaxial crystallisation, IR investig., macromol. struct. changes 77−35493
polyvinyl acetate:Cu, and undoped, thermally stimulated currents exam. 78−35083
polyvinyl acetate, γ-Fe_2O_3 powder filled, mag. films, packing and particle orientation *(Japanese)* 80−104115
polyvinyl acetate, charge retention, adsorbed water vapour effects, TSC obs. 77−32321
polyvinyl acetate, thick film, pure and I_2 doped, electrical cond. 77−85234
polyvinyl alcohol film containing Cu^{2+} complexes, photoconductivity 80−107849
polyvinyl alcohol films, pure and doped, elec. cond. temp. depend. 78−88052
polyvinyl alcohol films activated, thermochromism *(Russian)* 79−91415
polyvinyl butyral, γ-Fe_2O_3 powder filled, mag. films, packing and particle orientation *(Japanese)* 80−104115
polyvinyl butyral film, charge storage mechanism, TSC expts. 80−25280
polyvinyl difluoride, γ-irrad., low-temp. TSD obs. 77−63358
polyvinyl fluoride, electret effects 77−90094
polyvinyl fluoride film, pure and vanadyl ion doped, elec. cond., annealing 78−26859
polyvinylacetate, in MIM struct., DC cond. phenomena 80−25020
polyvinylacetate film, dissolved polyester yellow, ablative optical recording 80−83555
polymer films continued
polyvinylacetate film, effect of electrode metals on depolarisation current characts. 78−76387
polyvinylacetate films, amorphous, X-ray small angle scatt. near glass transition, struct. *(Russian)* 77−31606
polyvinylbutyral, elec. and dielec. props., mol. wt. effect on charge storage 80−97192
polyvinylcarbazole, photocond., of double layer polymer systems doped with charge transfer complexes 79−87124
polyvinylcarbazole, Poole-Frenkel effect investigation by TSC 77−51755
polyvinylcarbazole xerographic film, discharge kinetics 77−13810
polyvinylidene fluoride, γ-phase containing films, thermocurrent spectra 79−42555
polyvinylidene fluoride, acoustic transducer-receiver appl., flexible configuration, activated by laser 80−83724
polyvinylidene fluoride, anisotropy and temp. depend. of piezoelec. consts. 77−1640
polyvinylidene fluoride, bending piezoelectricity 77−12319
polyvinylidene fluoride, biaxially stretched film, corona charging and piezoelec. effect 78−88256
polyvinylidene fluoride, birefr. change induced by elec. field 80−55065
polyvinylidene fluoride, chem. etching of fission tracks, growth of fine holes, TEM, SEM study 79−76297
polyvinylidene fluoride, corona-charged, surface effects 80−66102
polyvinylidene fluoride, dielectric relax. mechanism 80−55023
polyvinylidene fluoride, elastocalorific effect and thermal expansion *(French)* 79−46818
polyvinylidene fluoride, electro-optic and elasto- optic effects 80−80754
polyvinylidene fluoride, film, piezoelec., pyroelec., thermal expansion, elastic consts. 78−84529
polyvinylidene fluoride, film, piezoelec. relax. 79−87394
polyvinylidene fluoride, optimised target for IR vidicon camera tube 79−32050
polyvinylidene fluoride, plasma poling, piezoelec. and pyroelec. responses 80−71296
polyvinylidene fluoride, polarisation and depolarisation processes 80−11318
polyvinylidene fluoride, poled, short duration unipolar stress pulse detection, generation 80−106695
polyvinylidene fluoride, pyroelectric transient response 80−75956
polyvinylidene fluoride, stretched, struct. and elec. props. 79−90572
polyvinylidene fluoride, thermodynamic model and appl. 80−75955
polyvinylidene fluoride, uniaxially stretched, piezoelec. and pyroelec. 77−40181
polyvinylidene fluoride, uniaxially stretched and corona poled, piezoelec. meas. 80−25311
polyvinylidene fluoride, X-ray diffr. evidence for ferroelectricity 78−60399
polyvinylidene fluoride, X-ray induced TSC 80−75578
polyvinylidene fluoride film, biaxially oriented, charact. for transducer appl. 80−88931
polyvinylidene fluoride film, cryst. dipole orientation in elec. field 78−80286
polyvinylidene fluoride film, hysteresis and dipolar orientation 80−97217
polyvinylidene fluoride film, piezoelec., appl. in confocal pair of concave transducers 78−22241
polyvinylidene fluoride film, piezoelectricity, importance of metal-polymer interface 78−76391
polyvinylidene fluoride film, pyroelec. camera tube for IR imaging, thermal diffusivity of Bi-Bi_2O_3 black layer 80−57369
polyvinylidene fluoride film, shear props. by piezoelectric resonance 79−99824
polyvinylidene fluoride film, space charge, thermal expansion and pyroelectricity 77−4603
polyvinylidene fluoride film poling rates, 20 to 100°C 77−77138
polyvinylidene fluoride film polymer transducer, with US appl., durable lead attachment techniques 80−79094
polyvinylidene fluoride films, 200 ps laser pulse heating, pyroelectricity meas. 79−4768
polyvinylidene fluoride films, corona-charged, struct. changes, piezo- and pyroelec. props. 79−11389
polyvinylidene fluoride films, corona-poled, piezoelectricity *(Japanese)* 80−55040
polyvinylidene fluoride films, field depend. depolarisation behaviour 80−20580
polyvinylidene fluoride films, HF US absorpt. meas., 300 to 1500 MHz 80−74667
polyvinylidene fluoride films, pyroelectric current freq. depend., thermal diffusivity 79−78630
polyvinylidene fluoride films, SH and Lamb waves propag. 80−75948
polyvinylidene fluoride films, stretched and rolled, electrostriction and piezoelectric effects *(Japanese)* 80−55041
polyvinylidene fluoride films, uniaxially stretched, small-angle light scatt. 79−24377
polyvinylidene fluoride films for SAW transducers on Si substrates 80−74618
polyvinylidene fluoride foil, piezoelectric effect, 100 Hz acoustic and NMR meas. 78−60396
polyvinylidene fluoride foil appls. for electroacoustic transducers *(German)* 78−22243
polyvinylidene fluoride magnetoelectret, AF and RF charge and dielectric characts. 80−40038
polyvinylidene fluoride piezoelec. film for adaptive deformable mirror system 80−74455
polyvinylidene fluoride piezoelectric film, Lamb and SH wave attenuation *(French)* 80−79196
polyvinylidene fluoride SAW transducers, evaluation of performance 80−74617
polyvinylidene fluoride X-ray diffr. pattern changes due to corona charging 78−14285
powder layers, specific charge and thickness distribution meas., by electrostatic method *(Russian)* 77−10042
powdered polymer coatings, use on cine camera guide elements 78−78021
preparation for electronics appls. *(German)* 78−44011
PTFE, molecular interaction in frictional-contact zone, absorpt. spectra 79−78688
PTFE, on SiO surface, induced MBBA nematic liq. cryst. quasihomeotropic orientation 79−90525
PTFE, sliding charact., friction and wear *(Japanese)* 78−56778
PTFE electrets corona charged at high temp., TSC study 80−7261

polymer films continued
PTFE film, reactive sputtering in Ar-CF_4 mixture, MSCA 78−92191
PTFE film electret, optical spectra, band theory interpretation *(Russian)* 78−88376
PTFE films, plasma-polymerized, cond. mechanism, AC cond. and capacitance meas. 79−24093
PTFE films, sputtering conditions effect on comp. and optical props. 79−52115
PTFE grafted membranes, struct.-properties relationships, bifunctionality *(French)* 80−61137
PTFE grafted membranes, struct.-properties relationships *(French)* 80−61136
PTFE grafted membranes, struct.-properties relationships for poly-N-vinylpyrrolidone-containing membranes *(French)* 80−61138
PTFE on metal substrates, adhesion and cohesion 78−3259
PVA, matrix for Pr^{3+} spectra 80−7331
PVA, stretched, host for ESR of phosphorescent aromatics 77−30908
PVA-I_2, quantitative estimate of CO_2 laser radiation density 77−58368
PVC:Cu films, electron transport and dielec. props. 79−82700
PVC:Fe(Cu) film, struct. and optical props., soln. growth technique 78−51837
PVC, calendering, defects in calendered films and sheets 79−8267
PVC, effect of chlorinated polyethylene as impact modifier *(Polish)* 79−70037
PVC, electric strength, temperature-time dependence *(Russian)* 78−76386
PVC, film, uniaxially stretched, effect of mol. orientation on anisotropy of Young's modulus 77−86076
PVC, frictional electrification, contrib. of mol. motion of polymer 80−70798
PVC, metal doping effect on chain vibrs. 79−95868
PVC, plasticised film, defect form. study, turbidity and shrinkage meas. *(Russian)* 77−62490
PVC, rigid, viscoelastic props. rel. to thermal, mech. history 79−5016
PVC, solution-grown, between Al electrodes, AC elec. props. 80−15619
PVC, surface charge decay and TSC 80−11328
PVC, uniaxially stretched, mol. orientation, birefringence, effect of plasticizers, draw ratio 77−48500
PVC+Br_2(I_2), reaction in surface-modified film subject to thermal-radiative and photochem. action *(Russian)* 77−21385
PVC film, permeability to H_2O vap. *(Russian)* 78−53255
PVC film, testing device, for prop. changes at high temps. *(German)* 80−66741
PVC film, uniaxially stretched, mol. orientation, polarised fluoresc. investig., deform. mechanism 77−52440
PVC films, soln. grown, DC cond. mechanisms, field and temp. depend. 80−97021
PVC foil, piezoelectric effect, 100 Hz acoustic and NMR meas. 78−60396
PVC in metal sandwich struct., switching props., voltage- and current-controlled negative resist. 80−103767
PVC near-colourless transparent film, colorimetric determ. of colour 78−49884
PVC plastisol films, thermally hardened, struct. and props. *(German)* 79−70097
PVC thin films, pure and I doped, photoconductivity study 80−44646
PVC-polycarbonate, frictional electrification, temp. and friction speed depend. 78−60190
PVDF, film, polymorphism induced by poling and annealing 80−24372
PVDF dielectric, piezoelec. and pyroelectric props. rel. to crystalline forms 80−15982
PVDF pyroelectric IR detector *(Japanese)* 80−105714
PVF_2 bulk wave transducers for nondestructive evaluation 79−57199
PVF_2 film composite resonator for concave focusing US transducer 79−46155
PVF_2 pyroelectric coeff., depolarisation current meas. 79−56737
PVF_2 transducers for NDT 80−76476
pyroelectric coefficient determ. using dielectric heating 78−35096
pyroelectric polymer film for electron microscope sample preparation, rapid cooling effects *(German)* 80−13185
pyroelectric polymer IR detector *(Japanese)* 80−105713
radiochromic dyed plastic thin films, for absorbed dose and dose distrib. meas. 77−67906
Raman, spectroscopy of thin films, integrated optical techniques 80−22432
resin protective coating, UV cured, for optical fibre/cable 80−69547
resin-coated optical fibre, tensile strength tests *(German)* 78−33871
resonance method for meas. complex elastic moduli of polymer films 77−67426
RF discharge prep. using monomer organic semicond., elec. props. obs. 80−80432
rod-like superstruct., small-angle light scatt., vol. fraction, orient. effects 79−1795
rodlike morphology, small angle light scattering, multiple scattering 78−15241
rubber, friction against paper and polymer film surfaces, microroughness effect 80−71763
rubbery polymer film, on glass surface, interfacial dislocations spontaneously created by peeling 78−73011
sailcloth, optical transmission charact., telescope dome slit cover appl. 77−83936
semiconductor, in MSM struct., thermionic field emission from metal 79−1629
shear strength, for films between contacting surfaces, effect of contact pressure and temp. 78−60842
shear strength and friction 78−39913
silicone, film deposition, glow discharge polymerisation, elec. and thermal charact. 78−6467
silk fibroin, oriented, piezoelec. consts. temp. dispersions 80−11345
soil thawing under polar conditions using synthetic film covers, thermal balance meas. on polymeric film covered surfaces 77−78244
solar energy concentrators, metallised polymer films and Al coatings, spectral characteristics 79−96422
solar energy materials, transparent, optical charact. investigation 80−20724
solar-energy concentrator, foam-film parabolic-cylindrical, surface fabrication 80−21372
solvent cast, optical anisotropy origin 80−20610
sorption and diffusion, low-molecular ligs., instrument 79−100305
space charge, thermal expansion and pyroelectricity 77−4603

polymer films continued
stretched, impurity mol. orientation, proton intramolecular transfer, light absorpt. and emission, dichroism, polarised fluoresc. 80−87166
stretched, interpretation of polarised absorption and emission spectra of molecules 78−1012
stretched, orientation and transition moment directions of small planar molecules 78−1015
stretching, with suction and blowing, heat and mass transfer 78−34033
styrene film, plasma polymerised, in vacuo photocurrent meas. 77−89799
styrene films, glow discharge polymerized, self-healing breakdown 79−91374
styrene glow-polymer in MIM sandwich, tunnelling and interface barriers 77−63001
styrene-acrylic terpolymer surface tension rel. to temp., compatibility of external plasticiser 79−15834
styrene-acrylonitrile copolymer film, multiple relax. obs. using TSC 80−45000
styrene-butadiene triblock copolymer films, mech. props., effect of casting solvent 79−11651
superconducting magnet insulators, gamma-ray radiation effects 80−24495
supermolecular structure and mech. stress distrib. among chem. bonds 78−75562
surface film form. on Pt electrodes by electrooxidation of phenolic cpds. 80−104450
surface profile obs. and nature of contact by multiple beam interferometry 77−1878
swollen, diffusion-relax. cojpling, two-stage sorption correl. 79−94864
synthesis and characterisation, review 79−91584
synthetic, piezoelectric properties, acoustoelectric transducers appl. *(Italian)* 79−98577
tear resistance of semicrystalline networks 77−52488
Teflon, negatively corona charged, new model of isothermal charge transport 80−34536
Teflon, TSC studies of carrier trapping and mobility 80−7016
Teflon coatings for H maser, TFE 42, FEP 120, wall shift comparison 78−78984
Teflon FEP, annealed electret, charge stability 80−6943
Teflon FEP, electron beam charged film, charge centroid location 78−15095
Teflon FEP, electron-beam-charged, population and temp. shift of TSC peaks 79−82914
Teflon FEP-A, corona and electron beam charged, TSC peak identification and surface-voltage stability 79−78614
Teflon films, hole transit, trap modulated mobility and dispersive hopping discussion 79−69616
Teflon-FEP, film, plate-electret, construction and use in condenser type headphone 80−5907
terylene film, electret state prod. using electrochem. injection, adsorbed states, frozen field 79−91344
tetramethyl-p-silphenylenesiloxane-dimethylsiloxane block copolymer films, deformation 79−15739
tetramethyl-tetraphenyl-trisiloxane, in metal-polymer-Si and metal-polymer-metal structures 77−28256
thermoplastic film, photoconducting, double exposure holographic interferometry using memory effect *(Chinese)* 80−37967
thermoplastic films, high modulus, new method of prep. 79−100105
thickness determ. using profilograph-profilometer, on metal substrates 79−70244
thickness monitor, using differential electronic circuit 80−73315
threshold switching, statistical aspects 79−33315
transducer, piezoelec. and pyroelec. response rel. to dipole polarisation 80−7267
transparent, protective ability for optical surfaces 77−31135
tribopolymerised lubricants, mechanism of action, SEM expts. 79−29226
trinitrofluorenone: poly (N-vinylcarbazole) films photovoltaic properties for solar cell appls. 80−60040
TTF polymer thin film batteries 80−45709
tubular film blowing, flow instability, expt. 77−42804
vacuum deposition of thin film device 77−77384
vapour deposition process, in corona discharge, reverse corona influence obs. *(Russian)* 77−12526
vapour permeability determ., gravimetric test method 79−39066
vertical development, from gas phase, computer simulation *(German)* 77−27839
vesicular film sensitometry, review 78−16878
vinyl chloride:vinyl acetate copolymer film dipole continuous relax. spectrum 78−91700
vinyl chloride-vinyl acetate copolymer film, dielec. relax. and thermally stimulated depolarisation current meas. 80−11336
vinyl chloride-vinyl acetate copolymer film between metal electrodes, depolarisation current studies 80−2691
vinyl chloride-vinyl acetate copolymer organodispersions, film strengthening with n-paraffins *(Russian)* 79−52150
vinylidene fluoride-tetrafluoroethylene copolymer, two types of pyroelectricity 80−11346
vinylidene fluoride-trifluoroethylene film, cryst. phase transition 80−66120
vinylidene-fluoride-trifluoroethylene copolymer, piezoelectricity 80−88930
vinylidenechloride-vinylchloride latex copolymers grafted on to elastomers, film struct. and props. *(Russian)* 77−21090
vinylidenefluoride/tetrafluoroethylene copolymer, piezoelect. and pyroelect. response rel. to dipole polarisation 80−7267
vinyltrimethoxy silane, plasma polymerised, abrasion resist. antirefl. coating for polycarbonate 77−42635
viscoelastic props., capacitance change meas. *(Japanese)* 78−23752
X-ray detector window for ultrasoft X-rays *(Chinese)* 78−82083
p-xylene, plasma polymerised, as laser fusion target 78−88431
p-xylene, plasma polymerised films on glass, as laser fusion targets, deposition method 78−60860
xylene plasma-polymerised film, ESR 79−99750
ZnO-resin electrophotographic photosensitive layers, dark decay mechanism of corona charge *(Japanese)* 79−24002
Al particles, coating by polymer film *(Russian)* 77−86232
GaAs-$(SN)_x$, solar cell fabrication and efficiency 80−26143
PVF_2, film, origin of pyroelectricity 79−99828
PVF_2, film, static and dynamic pyroelectric coeffs. from 90-370K 79−99827
PVF_2 film US transducers, review *(Japanese)* 79−98579

polymer films continued
$(SN)_x$ polymer, elec. props. of amorphous thin film and single crystal, role of chain breaks *(Japanese)* 78−68104
Si-polymer interface states in MOS structure, capacitance and cond. meas. 77−20438

polymer melts
acrylonitrile-butadiene-styrene terpolymers Sb_2O_3 effect of melt viscosity *(German)* 78−18265
acrylonitrile-styrene copolymer melts, rheological behaviour *(German)* 77−51012
n-alkane mol. config. in melt and cyclohexane soln., small-angle neutron diffr. 78−55800
annular flow, secondary normal stress difference 80−106816
azobenzenes, p-acryloyl- and p-methacryloyl-oxy-p′-substituted, monomers and polymers, liq. cryst. props. 79−99065
azoxybenzenes, p-acryloyl- and p-methacryloyl-oxy-p′-substituted, monomers and polymers, liq. cryst. props. 79−99065
Barus effect, and normal stress effect in steady shear flow case 80−64589
blended polymer melts, flow indices *(Japanese)* 80−79360
blended resins, flow charact. *(Japanese)* 80−24059
blends, fluctuation dynamics, spinodal decomp. 80−79943
blends, interdiffusion, meas. method 79−69271
Brillouin scatt. and segmental motion, appl. to polypropylene glycol 78−91217
Brillouin scattering at transitions 80−70312
Brownian motion in equilib. state 79−41645
bubbles formation, non-coalescing bubbles theory appl. 78−42640
butadiene rubber, polymer melt, extrusion at constant deformation rate 78−68744
butadiene-styrene block copolymer, star shaped, rheological props. 77−68542
chain conformation and struct. determ. by diffr. 77−80429
chain conformation of melt inside small pores *(French)* 79−90516
channel flow stability, moving boundary, mould filling problem 77−58793
complex modulus, freq. depend. var. during extensional flow 79−55351
composite flow anal. in sandwich sheeting die 78−94637
converging and stretching flow 78−71374
cross-links effect on struct. 79−41928
crosslinking, capillary viscometer obs. 79−7431
crystallisation, deformation effects 80−10504
crystallisation, natural and artificial heterogeneous nucleation 78−51431
crystallisation from melt 80−84107
crystallisation from melt at large undercoolings, kinetics 80−28925
crystallisation models, Avrami eqn. extension 80−19723
crystallisation thermodynamics, various degrees of coiling 78−51445
defect fluctuations, reptation, Monte Carlo investig., NMR autocorrel. function 77−3499
deformation, loss of fluidity 77−89078
deformation, mol. motion under flow 79−41646
demixtion, crit. points 78−26419
drop wetting solid surface, spreading index for polymer surface props. *(Russian)* 78−51802
dynamics, kinetic theory, book 77−42795
dynamics, self-diffusion const., relax. time and viscosity 80−64874
elastic, uniform extension by const. force, rheology 80−43682
electric field dependence of the glass temperature 79−86875
elongational behaviour in const. elongation rate, tensile stress and tensile force expts. 80−38372
elongational flow, necking and ductile failure mechanisms 77−43267
elongational properties, microscopic stretch history 80−23981
entangled polymer liquid, phenomenological consequences of Doi-Edwards viscoelasticity theory 80−79250
EPDM-Viton A fluoroelastomer blends, melt viscosities 77−7781
equation of state analysis w.r.t. Ising fluid model 80−79907
ethylene methacrylic acid polymer and Na salt, ionic aggregation and melt rheology, H_2 bonding effect 78−67159
ethylene-propylene copolymer, melt struct., X-ray diffr. obs. *(Russian)* 79−23533
ethylene-vinyl-acetate copolymer melt, viscosity 79−33105
exit press. meas. from capillary or slit rheometer 77−72260
extensional rheometers for molten polymers 78−71302
extrusion melting, integral energy-balance model 77−46899
falling coaxial cylinder viscometer for wide range of shear rates 78−79393
fibre reinforced polymer, soaking, wetting and compounding of materials during production *(German)* 80−93535
flexible chain polymer, topomorphism and phase dualism 78−14265
flow, birefringence meas. of normal and tangential stresses 77−58625
flow, unsteady, in rotary devices 80−24061
flow analysis of the non-isothermal two-dimensional filling process in injection molding 79−77038
flow birefringence, in shear flow, rel. to time depend. rheological props. 77−36198
flow birefringence, vel. and temp. profiles calc. in cone and plate rheometer 77−54945
flow birefringence meas., influence of parasitic birefringences 80−88963
flow in channels of noncircular cross-section 77−7451
flow in cooled channels, dimensional anal. *(German)* 79−81833
flow of two-phase prepolymer, US flowmeter optimisation 77−31410
flow properties and stress relaxation anal., slit die rheometer appl. 77−27501
flow resistance through granular beds 78−87322
flow under const. and periodic deform. 78−47004
flow under const. and periodic deform. 78−64579
flow-induced crystallisation, conference, Midland, MI, USA (Aug. 1977) 80−82576
flow-induced orientation freezing-in by vitrification, appl. to processing 79−23531
flows, propag. of large amplitude low frequency vibration 77−65770
gas bubble pulsations and assoc. dissipation effects 80−59079
generalised polymer problems, Flory exponents 80−107039
harmonic distortions, under nonlinear periodic deform. 80−28482
heat transfer problem in plastic injection moulding 80−38242
heat transfer to polymer melt flowing through duct 80−103049
high mol. wt. polymer melts, viscoelastic props., relaxation and retardation spectra 80−19310
high polymers, molten, bundle model, appl. of continuum approach of physical line structures 78−81859

polymer melts continued
immiscible polymers, interface and surface props., thermodynamic theory *(German)* 78−26753
intermittent shear flow transient birefringence 78−63457
intermolecular interpenetration and entanglement, crit. concs. 79−27900
irreversibility assumption of network disentanglement, effects on elastic recoil predictions 80−6006
isothermal and non-isothermal stress relaxation following steady state shear flow *(German)* 79−77044
laminar and melt fracture flow through successive capillaries 80−59085
LDPE melt, nonlinear shear creep and constrained elastic recovery 78−87318
linear, viscoelastic props. under flow conditions, transition to highly elastic state *(Russian)* 79−50690
linear polyethylene, PMR spectrum 77−51979
long chains, in solns. or melts, statistics 79−31758
longitudinal flow of periodically deformed polymers 80−6008
LPDE melt, tensile stress overshoot in uniaxial extension, single integral constitutive eqn. 80−1507
mixtures, breakup of anisometric drops 77−40578
mixtures, molten, interface props. near consolute point 78−87792
mixtures, thermodynamically incompatible, flow, specific fibre formation mechanism 77−23926
molecular weight distribution correlations 77−84207
motion under unstable conditions and in channel terminals 79−77046
NBS polystyrene, memory-function determ., relax. tests 78−1619
network models, loss of junctions due to stretching of material planes 79−77043
network theory in nonlinear region *(German)* 79−77050
neutron scatt., quasielastic incoherent, Q^4-depend. broadening 77−47327
NMR relaxation, mol. motion, local defect component theory 77−55722
non-linear model, constitutive equation testing with free. vol. relax. spectrum 80−6011
non-Newtonian model for melting in single screw extruders 79−32589
non-steady two-phase stratified laminar flow in pipes 79−81832
nonisothermal spinning mechanics 77−51010
nonlinear network viscoelastic model 79−3985
normal stress measurement, modification to Weissenberg rheogoniometer unit 80−69750
Nylon 12, short-time adhesion, rel. to diffusion properties *(Japanese)* 79−70294
Nylon 12 melt, bulk diffusion coeff. and local diff. coeff. *(Japanese)* 79−46823
Nylon 12 melt, diffusion *(Japanese)* 79−95192
Nylon 12 melt, diffusion coeff. meas. by microspectrophotometry using dye-tagging *(Japanese)* 79−23756
orientable polymer fluid, Ericksen's anisotropic fluids theory extension 80−79359
oxidative stability determ. technique 80−45412
particulate mixing, fluid dynamics, rheological and energetic considerations 80−43686
perfluorinated polymer, Krytox 143-AB, viscous, viscoelastic and dielectric properties 80−70440
PET, P-V-T relationships 80−107400
PMMA, spreading of two-phase film of melt, heat and mass exchange, ignition and combustion *(Russian)* 78−76861
PMMA melt, stress relax. at large deformations 80−58994
poly(ethylene terephthalate), stress-induced crystn. from melt, optical studies 80−84113
poly(ethyleneterephthalate)-p-hydroxybenzoic acid copolyester, liquid crystalline, X-ray scatt. obs. 78−9949
poly(m-xylylene adipamide), molten, gel form. kinetics *(Japanese)* 80−108757
poly(S)-2-methylbutyl vinyl ether, conformation, IR spectra 78−1116
poly(S)-5-methyl-1-heptene, conformation, IR spectra 78−1116
poly(vinylcarbazole), stress-induced crystn. from melt, optical studies 80−84113
poly-1-butene, sheared melts, nucleation and crystal growth meas. 79−69027
poly-1-olefin melts, steady-state and dynamic rheology 79−59956
poly-1-olefin melts, viscous flow activation energy, melt struct. 77−7654
poly-4-chlorostyrene, undiluted, dielec. relax. spectrum above Tg 80−97194
poly-4-methylpentene-1, P-V-T relationships 80−107400
poly-ε-caprolactone, melt, crystallisation kinetics, shear effects 79−69021
poly-(p-alkoxy-phenyl-p-acryloylbenzoates), nematic polymer, struct. determ. 79−99064
poly-(phenyl-p-acryloyloxybenzoate), nematic polymer, struct. determ. 79−99064
poly-tetramethyl-p-silphenylene-dimethylsiloxane block copolymers, crystn., morphology, kinetics 79−14695
polyalkylene isophthalates, surface tension meas. by sessile bubble method *(Japanese)* 80−75405
polyarylate-arylenesulfone oxide block copolymer, glass transition, melt and soln. viscosity *(Russian)* 79−55915
polyarylate-polyethylene oxide block-copolymers and mixtures, phase separation, DSC obs. *(Russian)* 79−55895
polybutadiene, hydrogenated, linear and star branched, melt rheology 80−23978
1,4-polybutadiene, stress-induced crystn. from melt, optical studies 80−84113
polybutene-1, P-V-T relationships 80−107400
polycaproamide-polyethyleneterephthalate melts, two-phase blend, rheological props. *(Russian)* 80−58997
polycarbonate, secondary flow and stress birefringence patterns in pressure hole 80−64590
polydimethylsiloxane film, non-pure, dielec. behaviour 80−29672
polydimethylsiloxane oligomers, Brillouin scatt. obs. of hypersonic sound speed and loss, mol. wt. depend. 79−91457
polydimethylsiloxanes, rubbery and liq., hypersonic sound vel., Brillouin spectra meas. 80−75308
polydisperse polymers, viscoelasticity of melts 78−67160
polydispersion effects, crit. behaviour *(French)* 78−42879
polydispersity, estimation from rheological data 80−6535
polyesters, thermotropic, quiescent crystn. 80−38937
polyethyl siloxane, liqs., thermal cond. at high press., 20-200°C 78−79825
polyethylene, and general elastic liquids, stability of plane Poiseuille flow 78−9662
polyethylene, applicability of statistical rubber elasticity theory 78−42579

polymer melts continued
polyethylene, branched, P-V-T relationships 80−107400
polyethylene, chain conform. in solid and melt, low angle neutron scatt. 77−76329
polyethylene, elongational flow, constitutive anal. 78−71375
polyethylene, entanglement effects in NMR spin-spin relaxation 79−19795
polyethylene, foam growth, thermomech. anal. 80−3416
polyethylene, high and low density, secondary flow and stress birefringence patterns in pressure hole 80−64590
polyethylene, high density, filled with pearlite, melt rheology *(Japanese)* 77−54942
polyethylene, high mol. wt., inorganic filler, calendered sheet, flow props., crystalline texture *(Japanese)* 77−70111
polyethylene, high-density, polymer melt, shear stress at wall 80−19450
polyethylene, high-press. melt, spreading index on Cu, Al, glass, PTFE 79−37902
polyethylene, linear, melt props. correl. with chain length distribs. *(Russian)* 80−37920
polyethylene, linear, melt rheology 80−23976
polyethylene, liq., electron diffr. radial distrib. 77−4032
polyethylene, liq., very high mol. wt., pulsed NMR obs., entanglement, crosslinking, irrad. effects 78−66702
polyethylene, low and high density, normal stress and Barus effect 80−64589
polyethylene, low density, melt elongation, stress and recovery maxima 79−90209
polyethylene, low density, melt flow, mech. degradation *(Russian)* 79−50691
polyethylene, low density, N_2 and ethylene solubilities statistical thermodynamical method, sorption data 78−71859
polyethylene, low density, nonlinear viscoelastic model, creep and recoil rates 77−42794
polyethylene, low density, rheology and molecular struct. effect on viscoelasticity 77−62227
polyethylene, low density, temp. depend. of the elongational behaviour 80−6012
polyethylene, low- and high-density, melt, extensional flow 77−72259
polyethylene, low-density, critical deform. in rotary rheometer with active cone-plate pair 77−89080
polyethylene, low-density, viscosity and viscoelasticity, filler effect 80−10222
polyethylene, melt, elongational flow, necking and ductile failure mechanisms 77−43267
polyethylene, melt, low density, filler effect on viscosity and viscoelasticity 77−68546
polyethylene, melt, shear flow birefringence meas. using cone-and-plate apparatus 77−36197
polyethylene, melt struct., X-ray diffr. obs. *(Russian)* 79−23533
polyethylene, melts, stratified two-phase flow, interface deform. 77−11158
polyethylene, nonlinear shear response during periodic deformation 79−100202
polyethylene, origin of hole press. in slit die apparatus 78−63462
polyethylene, plastic flow, yield limit rel. to press. *(Russian)* 80−7657
polyethylene, pulsed NMR study of crystallization kinetics from melt and soln. 79−87624
polyethylene, rheology of filled polymer melts, appl. of parallel-plate plastometer 79−77036
polyethylene, solid liq., secondary electron emission spectroscopy 80−80916
polyethylene, structure formation, near and below melting point 79−65003
polyethylene, viscoelastic property measurement using improved design rheometer 79−37276
polyethylene extruded melt, elongational viscosity, tensile props. 78−67163
polyethylene extruded melts, force-strain relation 79−77049
polyethylene film-resin melts, rheological props., prep. method depend. 78−34099
polyethylene flow crystallisation, in extensional flow developed by convergent capillaries, props. 80−84111
polyethylene fractions, quasi-binary systems, solidification and crystn. 80−84108
polyethylene glycol, conformation in liq. state from flow birefringence 78−76423
polyethylene high density melts, anomalous flow behaviour *(German)* 79−77048
polyethylene melt, comparison of elongational behaviour at constant stress and constant strain rate 77−63753
polyethylene melt, cryst. kinetics during cooling, nucleation density effect 80−100181
polyethylene melt, drawing filaments, surface instabilities 78−71305
polyethylene melt, dynamics anal. by three components, proton relax. 79−65754
polyethylene melt, flow in profile channel of extrusion head 79−98780
polyethylene melt, flow with steady state and recurrent deform. 77−898
polyethylene melt, high density, oscillating flow during extrusion, model anal. 80−100016
polyethylene melt, lightly crosslinked, crystn. under uniaxial compression, stretching 80−38957
polyethylene melt, low density, filler effect on viscosity and viscoelasticity 78−46919
polyethylene melt, nonlinear shear behaviour, strain-dependent memory function 78−67161
polyethylene melt, oscillatory flow through capillary 80−103046
polyethylene melt, rheology and molecular struct., melt identification from mech. props. 77−11490
polyethylene melt, rheology and molecular struct., relaxation spectra, charact. relaxation time 77−72255
polyethylene melt, rheology in shearing and extensional flow 77−72256
polyethylene melt, vortices in die entry region and viscosity meas. 78−1700
polyethylene melt spinning, extensional flow induced crystallisation 78−55818
polyethylene oxide, melt, crystallisation kinetics, shear effects 79−69021
polyethylene oxide, NMR relaxation in melt, three component model 77−55723
polyethylene oxide fractions and blends, melt viscosity, thermal props. 78−83990
polyethylene oxide melts, viscoelasticity meas. 78−87324

polymer melts continued
polyethylene pipe butt welding, tensile tests rel. to melt flow index 77−73389
polyethylene ribbons, flow-induced crystn. from melt, in dies fed by single screw extruder 80−84110
polyethylene stabilized with home-made antioxidants, thermal resistance *(Polish)* 79−52328
polyethylene terephthalate, induced crystn. on metallic nucleating particles 79−15658
polyethylene terephthalate, solid and molten, press. effects on compressibility and crystn., thermodynamic interpret. 80−84102
polyethylene-paraffin wax, blends, rapid cooling processing techniques 80−84905
polyethylene-polyoxymethylene mixtures connection of melt thermodynamic props. with solid state struct. *(Russian)* 80−54152
polyethylenes, molten, Weissenberg effect 78−9616
polyethyleneterephthalate-polycaproamide melts, two-phase blend, rheological props. *(Russian)* 80−58997
polyisobutylene, extrusion at constant deformation rate 78−68744
polyisobutylene, low molecular weight, nonlinear shear response during periodic deformation 79−100202
polyisobutylene melt, thermodynamic constitutive eqns., adiabatic deform. expts. 78−1620
polyisobutylene melt, transient shear and elongational data 77−58631
polymer additive effects on wall slip and viscosity in flow through capillaries *(German)* 80−59086
polymeric fluids, entropy effects in viscoelasticity 78−9618
polymethyl siloxane liquids at high pressures 78−47609
polymethylmethacrylate, rheological meas. with new rotational rheometer *(German)* 77−51006
polymethylphenylsiloxane liquid, pumped, improved heat transfer near crit. press. 77−7421
polymethylsiloxane-2, liq., thermodynamic props. at high press., US propag. meas. *(Russian)* 80−65157
polyolefin, eqns. of state analysis w.r.t. Simha-Somcynsky hole theory 79−37807
polyolefine, liq., memory effect 80−103268
polyolefins, molten, basic rheological characts., industrial appl. *(Polish)* 79−50689
polyoxymethylene-copolyamide blend melt, viscoelastic peculiarities *(Russian)* 78−38263
polyoxymethylene-copolyamide melts, flow, fibrillation, mechanism 77−4765
polyoxymethylene-copolyamide mixture, plasticiser effect on props. and fibre form. during flow 77−27500
polyoxymethylene-copolyamide mixtures, melt rheological props., extrudate microstruct. *(Russian)* 80−7530
polyperfluorobutadiene, melts, solns., ^{19}F NMR, ^{13}C NMR spectra, microstruct., configurations 77−43894
polypropylene, flow-induced crystn. from melt, in dies fed by single screw extruder 80−84110
polypropylene, isotropic, molten and cryst., small-angle neutron scatt., chain-folding 78−63680
polypropylene, melt, extensional flow 77−72259
polypropylene, melt, velocity field rearrangement in stagnation flow leading to diverging radial flow between parallel plates 79−37360
polypropylene, melts, elongational flow, necking and ductile failure mechanisms 77−43267
polypropylene, normal stress and Barus effect 80−64589
polypropylene, P-V-T relationships 80−107400
polypropylene, plastic flow, yield limit rel. to press. *(Russian)* 80−7657
polypropylene, viscoelastic property measurement using improved design rheometer 79−37276
polypropylene glycol, liq., Brillouin scatt. and segmental motion 78−91217
polypropylene glycol, low freq., multiple relaxation behaviour, dielectric and dynamic Kerr-effect techniques 80−29682
polypropylene glycol melt, mol. motion, dielectric and Kerr effect relax. obs. 80−60498
polypropylene melt, flow in profile channel of extrusion head 79−98780
polypropylene melt, particle filled, blow moldability eval. by melt rheology *(Japanese)* 79−94578
polypropylene melt, zero-shear-rate viscosity, press. depend. meas. 78−43164
polypropylene oxide, isotactic, crystallisation, heterogeneous nucleation, interfacial energy effects 79−69023
polypropylene-polyethylene blends, capillary flow, rheology and morphology 80−59088
polypropylene-polyethylene blends, flow behaviour in capillaries 80−59087
polystyrene, isotactic, spherulite radial growth retardation by SiO_2 nucleation 80−107066
polystyrene, melt, extensional flow 77−72259
polystyrene, melts, stratified two-phase flow, interface deform. 77−11158
polystyrene, molecular weight effects in die swell and in shear rheology 79−94575
polystyrene, origin of hole press. in slit die apparatus 78−63462
polystyrene, rheological props. 79−37273
polystyrene, rheology of filled polymer melts, appl. of parallel-plate plastometer 79−77036
polystyrene, secondary flow and stress birefringence patterns in pressure hole 80−64590
polystyrene blend, melt, bulk local viscosity determ. 77−31796
polystyrene meas. of elongation props. with universal extensional rheometer 80−6004
polystyrene melt, carbon-black filled, rheological study 80−48665
polystyrene melt, linear viscoelastic props. influence of molecular wt. distrib. 80−19309
polystyrene melt, local viscosity determ. rel. to temp. *(Japanese)* 77−31795
polystyrene melt, normal and shear stress relax., Rheometrics mech. spectrometer transient response 78−42577
polystyrene melt, viscosity, thermodynamic props. *(Russian)* 79−51295
polystyrene melt, vortices in die entry region and viscosity meas. 78−1700
polystyrene melt dynamic viscoelastic props., mol. weight distrib. 78−63407
polystyrene melts, flame-retardant high-impact, shear viscosity-temp.-shear rate relationships 80−59691
polystyrene melts, low mol. mass, dynamic viscoelastic behaviour, alternating shear expts. 77−62226

polymer melts continued
polystyrene melts, wetting kinetics for spreading of viscous sessile drops 80−15338
polystyrene-fluorescent conjugates in melt, local diffusion *(Japanese)* 79−23757
polystyrene-mineral oil mixture, viscosity and normal stress coeff. 80−44349
polystyrenes, blends, molten, rheology, dynamic viscoelastic props. in terminal zone 77−31268
polysulphone, glass and melt, PVT props., glass transition 79−14911
polysulphone, P-V-T relationships 80−107400
polysytrene melts, stresses and birefringence in intermittent shear flows 80−19308
polytetrafluoroethylene copolymers and oligomers, melt and solid, Raman active longit. acoustic modes 78−19484
polythenes of high density, viscosity meas., entropy and compressibility *(German)* 78−67162
polytrifluorochloroethylene, rheological props. *(Russian)* 80−6015
polyvinylacetate melt, thermodynamic constitutive eqns., adiabatic deform. expts. 78−1620
polyvinylcyclohexane, plastic flow, yield limit rel. to press. *(Russian)* 80−7657
polyvinylidene fluoride, crystallisation, α-polymorph equilib. melting point, heat of fusion determ. 77−4054
PTFE, P-V-T relationships 80−107400
PVA, liq., mobilities at const. temp., vol. 78−95174
PVC, emulsion, melts, slip, visual observations 79−4047
PVC, flow behaviour, particulate and melting flow, rheology 79−3981
PVC, plasticised, foam growth, thermomech. anal. 80−3416
PVC, rheology, viscoelasticity, panel discussion 79−3984
PVC, suspensions, melts, rheological props. rel. to struct. 79−3983
PVC, viscoelastic property measurement using improved design rheometer 79−37276
PVC cpds., rigid, plasticised, capillary flow 79−4046
quasistatic bulk strength meas., specially built apparatus 80−7737
relaxation oscillators using unstable flow of polymer melts *(French)* 80−79361
reptation in entangled melts 78−22669
rheological constitutive eqn. 79−41647
rheological equations, review 79−86391
rheological properties at low shear stresses, meas. using sandwich type creep rheometer 80−59153
rheological props., effects of hydrostatic press. 80−48663
rheology, characterised by mol. int. distrib., review 80−1504
rheology, fluid mechanics, book 77−65772
rheology and mol. struct. 78−63405
rheology of filled polymer melts, appl. of parallel-plate plastometer 79−77036
row nucleation, phenomenological model 78−14301
rubber, liq., viscosity meas. using manual viscosimeter *(German)* 79−27729
saturated liquid polydielectrics, secondary electron emission and energy loss spectra 80−55239
SCF approximation, connection between Yvon-Born-Green and Kirkwood hierarchies 78−42882
segregation of two molten polymers of different lengths, critical props. 78−55801
self-diffusion, review 80−29193
shared polymer melt, birefringence build up and relax. Lodge's rubberlike liquid model 77−54946
shear stress over wide shear rate range, in falling coaxial cylinder, rheometer 79−7363
sol-gel transition, US attenuation meas. 80−101043
spike-strain test relevance for network connectivity destruction by deformation 80−6001
spinning mechanics, relaxation time spectrum 77−31267
stabilisation of foams *(French)* 80−21323
static bulk props., reptation Monte Carlo method, LJ pot. 80−64868
statistical thermodynamics using Midha-Nanda cryst. state theory 79−41979
steady shear flow, parallel superposition of oscillatory motion 79−18919
strain crystallised, electron microscope obs. of molecular struct. 78−26450
structure, review of expt. results 79−37636
styrene copolymer, props. rel to composition *(German)* 79−66291
styrene-butadiene-styrene block copolymer, melt rheology 80−87751
styrene-butadiene-styrene block copolymer, nature of melt rheological transition 78−75113
styrene-butadiene-styrene block copolymer, stress relax. following steady-state flow, residual shear stress development 80−83772
styrene-diene triblock copolymer, hexagonal struct., flow props. of melt and fracture 78−76729
styrene/acrylic terpolymers, viscoelastic props. 80−64509
surface tension theory 79−65296
suspension, plastic-viscoelastic constitutive eqn. 79−60014
suspension of interacting particles, cell model theory of shear viscosity 80−103048
temperature measurement, thermocouple probe heat loss correction 77−65034
thermal conductivity, statistical mech. calcs. 78−34661
thermoplastic, linear viscoelasticity, rel. to orientation, recoverable strain and mech. props. 77−56041
time constants from shear viscosity data 79−37275
time dependent nonlinear stresses, constitutive eqn. 77−35178
time dependent nonlinear stresses, memory function nonlinearity 77−35180
time dependent nonlinear stresses, shear and uniaxial elongation 77−35179
triblock copolymer, model for rheology 80−23979
trifluoropropylmethylsiloxane fluids, viscoelastic props., mechanical impedance, viscosity and density meas. 80−79249
uniaxial and biaxial stretching, viscoelastic model 77−68547
vinyl copolymers containing biphenyl units in backbone, thermal props. and soln. viscosity, synthesis *(Japanese)* 77−90316
viscoelastic, 2-dimens. nonisothermal processing between calender rolls, mathematical model 79−68670
viscoelastic, stratified two-phase flow, interface deform. 77−11158
viscoelasticity, rheological props., prep., transport and processing effects, tensile and shear flow *(German)* 78−13982
viscosity, determ. by extrapolation method *(German)* 79−99347
viscosity, normal stress coeffs. determ. method *(German)* 79−7360

polymer melts continued
viscosity meas., Brabender torque rheometer calibration and reading's interpretation 79−10620
viscosity of particle filled polymer melts 78−87319
viscosity under hydrostatic pressure, falling cylinder viscometer *(German)* 77−55115
vulcanisation process, crit. behaviour 78−11518
$CaCO_3$ filled polymer melts, viscous props. 80−19311

polymer solutions
θ-domain, tricrit. props. in poor solvent 80−103450
acrylamide, polymerisation, liq. phase radiation chem. 77−60091
acrylonitrile methallylsulphonate copolymers in DMF, polyelectrolyte behaviour 79−66351
acrylonitrile Na methallylsulphonate copolymer electrolytes in dimethylformamide, gel permeation chromatography appl. 80−21345
admixtures influence on origin of vortices in wake behind cylinder 77−58744
adsorption at plane surface, computer rel. to real expts. *(Russian)* 79−56077
adsorption of chain molecules with polar head, scaling description 78−3378
adsorption on small spheres, scaling approach 78−3377
air bubbles, production, pulsation and damping 80−69879
angular correlation ranges in flexible chains 77−34790
annular two-phase flow of non-Newtonian liqs. and gases, press. drop and gas vol. fraction 80−10286
apparent scaling laws for polymer dimensions in poor solvent, too high excluded volume exponents 80−28901
aqueous, meas. of thermal props. 77−51555
aqueous dilute, appl. of Hildebrand's fluidity model, apparent viscosity temp. depend. *(German)* 79−37366
aqueous polymer solns., shear stress and normal stress meas. using cone-and-plate rheogoniometer 80−1496
aromatic copolyamide solns., conformational energy and mesomorphic character *(French)* 79−99066
p-aromatic poly(amide hydrazide), dimethyl sulphoxide solvent, dynamic birefringence, conform., viscosity *(Russian)* 78−39525
aromatic polyamides, rigid and nonrigid, ultrahigh modulus fibres 79−95992
associating sedimentation equilib. distrib. anal. 77−14628
atactic matrix for benzene peroxide+dibenzylsulphide reaction, kinetics *(Russian)* 77−21362
athermal polymer in strong soln., size and eqn. of state, screened convolution approx. 79−60257
azo polyamide, solutions, spectra and viscosity 79−68340
azobenzenes, p-acryloyl- and p-methacryloyl-oxy-p′-substituted, monomers and polymers, liq. cryst. props. 79−99065
azoxybenzenes, p-acryloyl- and p-methacryloyl-oxy-p′-substituted, monomers and polymers, liq. cryst. props. 79−99065
BBB, polybisbenzimidazobenzophenanthroline-dione, solns., viscosity rel. to temp. 77−4137
bead suspension, time depend. viscoelastic behaviour polystyrene solution, glass 80−99982
bead/spring model, matrix algebra and eigenvalues 77−72543
binary polymeric mixtures, soln. viscosities meas. 80−54423
biopolymer, low angular scatt. of synchrotron radiation, use of proportional chambers 78−65155
biopolymer motions, nonsteady hydrodynamics, damping effects 77−36861
biopolymer soln. heat capacity, conformational props. temp. depend. 80−8009
biopolymers, conditions of liquid crystal formation 80−30642
biopolymers, N-acetyl-D-alloisoleucine, soln. struct., dynamics, proton relaxation mechanisms 80−76708
birefringence lines in elongational flow *(French)* 80−25337
bisphenol-A-epichlorohydrin copolymer, single cryst. aggregate growth 77−27842
block copolymer in soln., molecular motion study by high resolution PMR 78−55803
blood simulant, flow model, hydrodynamic study 79−25023
branched chains, chain length, mol. architecture rel. to second virial coeff. 78−94964
branched molecule systems, second virial coeff., chain length effects calcs. 78−37775
branched polymer solutions, interaction function, thermodynamics, decomposition *(German)* 78−18531
branched polymers near gelation threshold, field theory statistics 78−91220
Brownian motion, fluctuation-dissipation theorem 80−46980
Brownian motion in equilib. state 79−41645
bubble behaviour, Denn model 78−79343
bubble behaviour, second-order fluid model 78−79344
bubble behaviour in pulsating pressure, natural freqs. 80−64591
bubble collapse calcs. 77−933
bubble growth and collapse, dilute polymer soln. effects in unbounded and bounded flow 79−81956
bulk viscosity theory 78−22880
butadiene-acrylonitrile copolymer liquid, viscosity *(Japanese)* 80−39334
butyl rubber solution, shear flow, rel. to rheologic theory 77−55051
carbowax in benzene, evaporation, vapour press. determ. from gaseous diffusion coeff. 80−10654
carboxymethyl cellulose, aqueous soln., diffusion and mass transfer from rotating disc 80−83827
carboxymethylcellulose-$CaCO_3$(-SiO_2) suspension, filtration eqn. 78−55690
cavitation bubble in liquids with polymer additives, small pulsations 77−68647
cavitation onset on cylinder, effect of dil. aqueous polymer solns. 77−68645
cavitation suppression by dilute solutions 78−67233
cell type optical circuitry fabrication using photopolymer 77−42633
cellodextrin alditols, alkali solns., hydrodynamic props., frictional envelope form. 77−28031
cellulose, acoustic relax. mechanisms *(Russian)* 79−90733
cellulose, fibrous crystn., from flowing solns. 80−84106
cellulose acetate, conc., light scatt. studies 80−16050
cellulose acetate, solvent effect on lyotropic mesomorphicity 80−70121
cellulose acetate butyrate, in soln., hydrodynamic behaviour 80−64876
cellulose acetate solutions, US relaxation 77−35638

polymer solutions continued
cellulose trinitrate, in soln., gel-like aggregate form. rel. to configuration 77−31036
chain, θ-behaviour 77−84615
chain collapse, in poor solvent, small angle neutron scatt. obs. 78−91215
chain conformations in liq. and cryst. slates *(French)* 78−18552
chain molecule, excluded vol. theory based on fifth-power eqns. for unperturbed mol. dimens. 77−50578
chain molecule dynamics, intramolecular diffusion controlled reaction for pr. terminal reactive groups 78−9289
chain motions, electron-electron double reson. obs. 79−69753
chain statics and dynamics, Lennard-Jones interaction, calcs. 80−58425
chains, freely rotating, depolarised light scatt. spectrum calcs. 80−78731
chains, helical wormlike, statistical mechanics, anisotropic light scatt. near the rod limit 80−93346
chains in cubic lattice solvent, thermodynamic props., Monte Carlo method, computer simulation *(Russian)* 77−31787
chains with rigid bonds, local relax. times, mol. dynamics study *(Russian)* 80−59373
channel flow, drag reduction, viscous sublayer struct. 78−22385
channel flow, flow struct. determ. 78−59486
coil configuration, neutron scatt. under different constraints 79−10778
coil dimensions, Monte Carlo calc., computer simulation *(Polish)* 79−3606
collapsing polymers, numerical studies, phase transition 77−38755
colloid stability near repulsive wall 80−21326
colloid suspensions in a polymer solution *(French)* 79−87879
colloidal dispersions, interactions 78−11572
colloidal particles in polymer soln., depletion stabilisation and depletion flocculation, theory 80−89534
complex coacervation, virial expsn. method 79−77750
complex modulus, freq. depend. var. during extensional flow 79−55351
computer simulation techniques for mol. theory verification 78−13633
concentrated, computer-aided simulation of individual chain conforms. *(Russian)* 77−42454
concentrated, constitutive eqn. applic. to shear and elongational flow 79−90292
concentrated, viscous function, hyperelasticity and viscoelasticity 80−48662
concentrated macromolecular solution, sedimentation behaviour rel. to particle shape 77−81428
concentration-dependent collapse in presence of second polymer 78−56949
conference, drag reduction and turbulence struct., Washington, USA (June 1976) 78−22329
configuration on interaction with interface 78−47659
configurational props. of model lattice chains under varying solvent conditions 77−89364
conformation, IR spectra 78−1116
conformation, small angle neutron scattering studies, deuteration effects 79−50956
conformational mobility, fluorescence obs. 80−63877
conformational motions, comp. of neutron and light scatt. expts. 79−41938
conjugated, polymer two-photon dispersion, freq. depend., symmetry assignment and oscillator strengths 79−86094
constitutive eqn. derived from network theory 77−75947
constitutive eqn. with factorised memory function 80−70105
constitutive relns. determ. using stiffened Weissenberg rheogoniometer for uniaxial shear flow 77−80188
convection, forced, heat transfer in ultradeep boreholes 79−68762
converging and stretching flow 78−71374
converging radial flow, expt. for charact. time 78−90941
cooperative phase transitions 80−45850
copoly(ethylene terephthalate)-p-oxybenzoate solns., polymer mesophases, optical microscopy obs. 79−99067
copolymer micelles in solution, review 77−21424
copolymer solns., small-angle neutron scatt., molecular struct. determ. 77−19863
copolymer solution, small angle neutron scatt., excluded vol. effect *(French)* 79−60259
corrlations, scaling laws from renormalised field theory, rel. to mag. variables 77−47326
Couette cell for birefringent, viscous and dielectric props. meas. 78−37034
Couette flow stability *(German)* 77−47047
critical mixture, binary, dynamics 77−58943
cross-over, pair correlation function, small-angle neutron scatt. meas. 78−22626
crown ether-containing polymers, in alkali salt solns., complexation, viscosity obs. 80−64877
crystallisation, deformation effects 80−10504
crystallisation, natural and artificial heterogeneous nucleation 78−51431
crystallisation at low supercooling 79−10823
crystallisation from solution 80−84105
crystallisation kinetic data, status of anal. 80−84104
crystallisation thermodynamics, various degrees of coiling 78−51445
cyclodextrins, diffusion in aq. polymer solns., complex form. 78−91460
Debye-Brinkman equation, macroscopic derivation 77−10799
debye-Huckel theory of model polyelectrolytes 79−5162
trans-decahydronaphthalene-polystyrene system, press. and mol. wt. depend. of polymer solubility 79−23734
dectran hydrolyzates in soln., branching assessment using small-angle X-ray scatt. 79−41926
deformation, mol. motion under flow 79−41646
demixtion, crit. points 78−26419
dextran, aq. soln., conc., PMR *(Russian)* 80−71225
dextran aqueous solutions, microviscosity investig. by square-wave polarography 79−95200
dextran fractions, production, characterisation and solution properties 80−59368
dextrane, aq. solns., H_2O diffusion, PMR investig. *(Russian)* 79−51290
Dextrane in aqueous solution permittivity meas., dielec. relaxation study 77−77143
dextrans, branched, cross-section factor correction in small-angle X-ray scatt. data 80−84048
diagram of states of semiflexible macromol. soln. *(Russian)* 79−50977
diblock copolymer solution, second virial coeff., perturbation theory 80−29148
dielectric relaxation data interpret. by model for macromol. chain dynamics 77−52014

polymer solutions continued
dielectric relaxation time, diluent effects 78−10843
diffusion, viscosity and dynamic struct. factor, dynamic scaling theory 79−64977
diffusion and relaxation time 78−55964
diffusion and self-diffusion phenomena, review 80−15273
diffusion coefficients, limiting, of high mol. weight solutes 80−24626
diffusion coefficients estimation methods, review 79−90807
diffusion equation with hydrodynamic interaction, equiv. normal coord. 80−79966
diffusion of a chain, conc. effects 80−70103
diffusion of ionic species, meas. by diffusion controlled electrolysys 80−74920
diffusion of macromolecular solutions in the boundary layer 78−87368
diffusion of tagged interacting spherically symmetric polymers 79−81314
dilute, assoc. influence on reduced viscosity 79−90518
dilute, buoyancy-driven instabiliy 78−10206
dilute, chain mol. dynamics and transport processes 80−14989
dilute, coherent scattering law, continued fraction formalism 80−103234
dilute, coherent scattering law, two-component description 77−51296
dilute, depolarised light scatt., solvent effects 77−20862
dilute, depolarised light scatt. 79−99892
dilute, depolarized Rayleigh scatt. 78−35155
dilute, dynamical props. 78−38608
dilute, effect on dynamic modulus of linear viscoelastic fluid *(Russian)* 77−39316
dilute, elongational flow, meas. using tubeless siphon apparatus 77−7486
dilute, equilibrium theory *(German)* 80−33872
dilute, extensional and sink flow in channel 80−74925
dilute, finite deformability of chain with hindered internal rot., rel. to rheology 77−34793
dilute, flow microcalorimetry, heat of mixing 77−56247
dilute, Hartree self-consistent field analysis 80−5648
dilute, internal viscosities, frictional coeffs. calcs. 78−6171
dilute, intrachain dynamics and forward depolarised scatt. 78−68525
dilute, Kramers-Giesekus stress tensor 80−6105
dilute, mod. wt. depend. of partial specific vol. 80−99594
dilute, multiple internal light scatt. calcs. 77−77229
dilute, origin of internal viscosity *(French)* 78−91465
dilute, oscillating spherical bubble, natural freq., theoretical study 77−24017
dilute, regularly alternant, thermodynamic props. self avoiding random walk calcs. *(French)* 80−59369
dilute, rheological constitutive eqn. eval. 79−90208
dilute, rheological constitutive eqn. eval. 79−94577
dilute, rheology, role of rigidity constraints 79−81928
dilute, rotating Couette flow, elongational viscosity and stability 79−27669
dilute, turbulent boundary layers, turbulence simulation 79−98767
dilute, turbulent flow behaviour in annulus 80−33633
dilute, viscoelastic props. 78−94626
dilute branched polymers, statistics, field theory 80−22303
dilute incompatible, segregation effects, scaling laws appl. 79−60254
dilute polymer liquids, time-temperature superposition principle 80−6005
dilute polymer soln. heterogeneity, ageing and non-Newtonian characts. 79−60030
dilute polymer solns., flow activation energy *(German)* 79−77191
dilute polymer solution viscosity/pH meas. 79−68831
dilute solution, critical ratio limiting values using renormalisation group methods 78−83715
dilute solution, friction tensor, microscopic treatment 78−22314
disperse systems, polymer-modified, filtration coeffs. 78−67264
dissolution kinematics, numerical solution and expt. verification 78−26687
dissolution rates and polymer-solvent system phenomena *(German)* 80−13167
DNA, soln., quasielastic light scattering, in AC elec. field 79−62186
drag reducing additive for torque suppression in mech. stirred liqs. 77−3864
drag reducing agents, decreasing mass transfer rate for Cu corrosion inhibition in soln. 78−19920
drag reducing pipe flow, boundary turbulence 77−68578
drag reducing polymer solns., dynamical behaviour, mol. conformation and optical props., expt. and rheological model 79−60034
drag reduction, dilute polymer soln., wall roughness effective slip depend., turbulence model 78−26162
drag reduction, elec. field effects 77−72334
drag reduction, laminar to turbulent transition, rot. disc expt. 78−75173
drag reduction, parameters affecting onset 79−77189
drag reduction, Polyox coagulant effects on turbulent boundary layer 78−26165
drag reduction, turbulent energy dissipation model 78−79345
drag reduction and burst cycle mechanism, dil. polymer soln. 78−26164
drag reduction enhancement by mol. aggregates 78−26161
drag reduction in pipe flow, flow time scales 78−22386
drag reduction polymer additive in helicoidal flow, screw pump press. head 78−26166
drag-reducing, in U-tube 79−1217
drag-reducing aqueous solution, turbulent wall motion 77−55047
drag-reducing polymers aqueous solutions, turbulent bursts rel. to wall friction 78−63454
dumbbells, nearly-Hookean, dilute soln., rheological equation of state 80−100321
dynamic compressibility study via press. transient technique 77−86256
dynamic scaling theories at nonzero concs., tagged chain translational diffusion coeffs. 80−75143
dynamic storage and loss compliances determ. from creep data 80−5948
dynamical polymer coil overlap, NMR model 80−23583
dynamical props., critical indices, cross-over effects 79−27899
dynamical scaling, neutron spin echo obs. 80−14990
dynamics, generalised Fokker-Planck eqn. appl. 79−1386
dynamics, kinetic theory, book 77−42795
dynamics, model for dil. solns. 79−73086
dynamics and hydrodynamics, book contrib. 79−60261
dynamics including side group motion, free draining limit 80−48111
dynamics of polymer chains trapped in slit 78−2276
educational courses, integration with phys. chem. 78−77642
elastic, load bearing capaicty of squeeze film flow 80−103051
elastic, vel. meas. in die entry region of capillary rheometer 80−99988
elastic fluids, shear-thinning, Carreau viscosity eqn., creeping motion of spheres 80−87753

polymer solutions continued
elastic mixtures, stability criteria 78−18514
elastic moduli meas., rheological spectrophasemeter, with digital display 80−33547
electric field-induced optical rectification, rel. to electro-optic kerr effect 80−84726
electrical dispersion in different gaseous environments 78−88254
electrical phenomena, nature and appl., review 80−50254
electrically induced fluorescence polarised component change meas. 80−32863
elongational flow, wet spinning process for fibres 78−72760
elongational flow in non-Newtonian fluids, effects of rheology 77−23998
elongational flow through porous bed, drag increase 78−22419
elongational viscosity and secondary instability in laminar boundary layer 77−23997
entangled polymer chain solutions, dipolar spin coupling modulation effect obs. on NMR spectra 78−56381
entangled polymer fluids, relax. dynamics, viscoelastic response functions 77−31578
entanglement density, statistical theory 78−5381
entrance effect in capillary flow of dilute and semi-dilute polymer solutions 79−60033
epoxy resin Lekutherm X-30, entrance flow into a slit 79−64619
epoxy/graphite composite and cured epoxy resin, thermal expansion and swelling 80−92450
ethyl cellulose in benzene, shear-rate depend. of relative permitt. 77−8489
ethylene vinylacetate copolymers in paraffin, viscosity of conc. solns. 79−81835
(ethylene-co-vinyl alcohol)-g-ethylene oxide graft copolymers, sol. behaviour 80−19682
ethylene-maleic acid copolymer 78−84515
ethylene-polyethylene mixtures, phase behaviour under high-press., polymer mean mol. wt. influence 79−24745
ethylene-propylene copolymer, solution in hydrocarbon solvents, adiabatic compressibility 77−51425
ethylene-vinylacetate-copolymers charact. by gel chromatography, viscometry, osmotic meas. *(German)* 78−14496
excluded volume and intrinsic viscosity plots 77−89363
excluded volume parameters, light scatt. obs., graphical calcs. 80−89009
extruded polymer soln. through capillary, flow instability and electrostatic effects 79−60035
fibre masses, interconnected, precipitated from polymer solns. under sonic agitation 79−47655
fibre suspension, dil., mechanistic aspects of drag reduction in turbulent pipe flow 80−6102
filled, normal stresses and hyperelasticity under simple shear flow 80−1506
filled, structural strength 79−64973
finite difference numerical solns 78−9661
flexible chain, entanglement effects in segmental motion, dielec. obs. 80−40050
flexible chain molecules, mutual interpenetration, fluorescence obs. 80−63877
flexible macromolecules, flow-induced crystallisation, nonhomogeneous shear rates effect 80−38952
flexible molecules, dynamic intrinsic viscosity, hydrodynamic interaction 78−47548
flexible polymer chain in nematic solvent, phase diagram *(French)* 80−39253
flexible polymers, in soln., obs. of pair correlation function, temp. and conc. effects small neutron scatt. anal. 79−10780
flexible polymers in soln., hydrodynamic interactions in quasi-elastic light scatt. 79−37612
flexible ring polymer, intrinsic viscosity 80−103511
flexible rings, nondraining, intrinsic viscosity, translational friction coeff. 79−18855
flow, 1st normal stress difference meas., rel. to water 79−98829
flow, laminar, in capillary, excess press. drop 79−60038
flow anomalies, narrow slits between rotating and stationary discs *(Russian)* 80−19454
flow at high strain rates, data correlation 79−10596
flow behaviour in porous media *(German)* 78−55666
flow birefringence, analysis using U-shaped glass modulator 79−63293
flow birefringence, in time dependent field 80−7323
flow birefringence, local, in double roller mill *(French)* 78−80315
flow birefringence, localized, induced behind obstacles in polymer soln. *(French)* 80−93275
flow in exit region of tube, jet swell problem 80−38452
flow in porous media, oil extraction appl. 79−68802
flow singularities, polymer chain extension and hydrodynamic instabilities 78−71376
flow through sand filters, flow resistance 80−79395
flow under const. and periodic deform. 78−47004
flow under const. and periodic deform. 78−64579
flow visualization near rot. disc 79−72914
flow-induced crystallisation, conference, Midland, MI, USA (Aug. 1977) 80−82576
flowing viscoelastic fluid, bubble and solid particle separation through apertures *(German)* 79−37389
fluctuation-dissipation relations, viscosity, mol. wt. depend. 78−14266
Fourier transform IR spectroscopy, least squares curve fitting, appls. to polymer systems 78−15726
free energy of mixing, modelling, critical exponents 80−44106
free polymer+latex, dispersion flocculation, equilib. anal. 80−45574
free precipitation of spherical particles in centrifugal force field 77−11247
freely jointed polymer chain, with excluded vol. interaction, Monte Carlo studies 80−10475
frequency dependent energetics, Orwell-Stockmayer hopping model 80−24346
galactomannan aqn. soln., rheological props., role of molecular mass and conc. *(French)* 78−22312
gas bubble-water mixture with polymer additive, shock wave propag. 78−47021
gel, quasielastic laser light scatt. theory 79−82986
gel modes in solns. and networks at equilib. swollen state, inelastic light scatt. 78−1972
gel rods, elastic dilatational mode, light beam positional modulation 80−64167
gelatin, aq., crystn. and melting 79−61914
polymer solutions continued
gelation, crit. percolation probabilities, appl. to hard sphere packing expt. 78−61063
gelation process, field theory statistics 78−91220
gels, dynamic light scattering in poor solvent 78−88318
generalised polymer problems, Flory exponents 80−107039
glassy soln., fluoresc. yield, polarisation and decay., temp. depend. 80−89043
Hamaker consts. and principle of corresponding states 78−11543
heat of mixing and interfacial tension for cohesive energy density determ. 77−55431
heat transfer to pseudoplastic fluids in agitated vessel 77−35174
heparin, in soln., small angle X-ray scattering 80−14993
heteroatom-containing polymers, struct., ^{13}C NMR investigs., review 79−55013
heterocyclic polymer, rheological props. conc. soln. 79−68671
HPAM dilute polymer solutions, elongational flow 80−103047
HPAM solns., anomalous defect pressure in laminar orifice flows 80−48664
hyaluronate solns., cooperative phase transitions, review 80−45850
hydraulic resistance of channels calc. *(Russian)* 80−38451
hydrodynamic boundary conditions and polymer chain dynamics 77−11155
hydrodynamic interactions in polymer solns. and suspensions, Navier-Stokes eqn. calc. *(Russian)* 79−32652
hydrodynamics, mean field theory 78−67227
hydroxyethyl cellulose, polymer segments, fluoresc. depolarisation on conjugated spin lables 80−91711
hydroxylpropylmethyl cellulose, aq. solns., turbulent flow charact., friction-reducing props. 78−94649
hydroxypropyl cellulose-water, bubble elongation dynamics, modelling with viscoelastic constitutive relations 79−37388
hydroxypropyl cellulose/H_2O, rheo-optics of shear and elongational flow, quiescent and flow birefringent charact. 80−83773
hydroxypropylmethyl cellulose soln., drag reduction by centre line fibre injection 80−14749
impregnating soln. concentration meas. by transmission photometer *(Russian)* 77−73484
inhomogeneous flows of non-Newtonian fluids: generation of spatial concentration gradients, stress and diffusion effects 79−60032
intermolecular interaction phenomena *(Russian)* 77−21414
internal viscosity, in poor solvents, self-entanglements *(French)* 79−4229
internal viscosity, rel. to dynamic behaviour 77−55379
intrinsic stress, birefringence tensor, bead/spring model, freq. depend. 78−42574
intrinsic velocity meas. *(Polish)* 79−4097
intrinsic viscosity, individual bead contribution 77−84206
intrinsic viscosity, mol. wt. and temp. dependence 80−34222
intrinsic viscosity of dilute and moderately concentrated polymer solns. 80−48753
ionomer solutions, in water, gel form. and demixing transition 80−61172
isocyanate polymers, partitioning between isotropic and anisotropic phases 80−24343
isotropically swollen networks, vol. depend. of elastic eqn. of state 78−67832
IUPACA polyethylene melt, elongational behaviour, strain rate, stress depend. 79−32429
jet thrust technique for normal stresses 78−9669
Kramers chain, mol. dynamics calc., incorrectness of random walk description confirmed 77−561
laminar flow, effect of anisotropy on stress and strain-rate tensors *(Russian)* 78−22387
laminar flow, effect of capillary entrance *(French)* 78−87330
laminar flow on inclined plane, edge effects 80−19451
laminar flow through porous media *(French)* 79−46376
laminar-turbulent transition in boundary-layer flow 78−9663
latex, monodisperse, Kirkwood-Alder transition press. meas. 78−7239
latex spheres in H_2O, photon correlation spectroscopy, diffusion coeffs. determ. 80−93802
light scatt. curves, struct. model 79−4810
light scattering, by dil. soln., Perrin matrix construction, for small particles 77−77227
light scattering, dynamic, by flexible macromols. in fluctuating elec. field 80−84722
light scattering, dynamic behaviour obs. 80−55727
light scattering, macromol. charact. in Rayleigh-Gans-Debye region 77−42452
light scattering, Perrin matrix including mag. dipole and elec. quadrupole interactions 77−77228
light scattering, polydispersity and internal modes of motion 80−20651
light scattering, quasielastic, from rigid mols., theory 79−64127
light scattering anisotropy, statistical mechs. of helical worklike chains 79−99891
light scattering charact. of thermodynamic props., solvent and mol. wt. effect 80−16717
light scattering meas., apparatus 78−74058
linear, viscoelastic props. under flow conditions, transition to highly elastic state *(Russian)* 79−50690
linear block copolymers, hydrodynamics 79−69273
linear molecule systems, second virial coeff., chain length effects calcs. 78−37775
liquid physics, book 79−60245
liquid-crystalline solns., struct. 80−103235
long chain immersed in shorter chains, end-to-end dist. 79−1387
long chains, in solns. or melts, statistics 79−31758
long polymers in solution, props., direct renormalisation method for study 80−59370
low conc., complex coacervation occurrence condition 80−79944
low eddy friction polymer soln. hydrodynamics 80−53818
macromolecular, laminar ultrafiltration, limiting flux numerical calc., variable diffusion coeff. 78−40214
macromolecular dispersion in dilute solution flowing in circular tube, band broadening meas. 77−68632
macromolecular fluid, stress-induced diffusion 78−10205
macromolecular liquids, dynamic viscosity, for static-oscill. vel. gradients superposition 77−76279
macromolecular polydispersity by dynamic light scatt. and thermodiffusion 78−18816
macromolecular solns., stress and heat flux in dumbbell soln. 79−68999
macromolecular solutions, kinetic theory and rheology 77−7424
macromolecular system, critical branching, a statistical theory 80−3413

polymer solutions continued
macromolecule, charged, in external elec. field, spherical case 80−75145
macromolecules, volume interactions, coil-globule transition, statistical physics, review 80−78737
magnesium alginate, light scatt., wt.-average mol. wt., charge density 77−61882
maleic acid-styrene copolymer, aq. soln., conform. transition 78−75526
Markovian polymeric systems, Rayleigh scatt. and fluctuation correls. *(Russian)* 79−65890
mass transfer between solid surfaces and drag-reducing fluids 78−79339
mean molecular weight of polymer from US meas. *(German)* 77−54641
mechanical model flow, extensional viscosity 78−22378
mechanical properties, elastic dumbbell model 79−59957
medical polymers, chem. problems, conf., Prague, Czechoslovakia (Aug. 1977) 80−56996
metal fraction contents and properties, meas. by eddy current method *(Russian)* 80−76571
methacrylic acid-methyl methacrylate statistical copolymer suspension polymerisation, stabilisation effects, viscosity 78−85157
methacrylic acid-N,N'-ethylenedimethacrylamide crosslinked copolymer soln., 3-dimens. struct. peculiarities *(Russian)* 79−55678
N-methacryloil-ω-aminolauric acid cholesterol ester, liq. cryst. polymers, copolymers, structuring *(Russian)* 79−55665
methofas, degradation and viscosity meas., transition process 77−72258
methyl methacrylate copolymers, dielec. relax. 77−85644
microgel-containing, physico-chem. and rheological props., light scatt. obs., review *(Polish)* 78−50704
microhydrodynamics, characteristic effects, developments 77−68681
mixed solvents, preferential adsorpt. coeff. rel. to mol. dimens. 80−103237
mixing of polymers in common solvent, breakup of anisometric drops 77−40578
mixtures, perturbed hard chain theory, thermodynamic props., appl. in chem. technology 79−34343
mixtures, viscosity *(Russian)* 79−65236
models and viscometric props., book contrib. *(French)* 77−84284
molecular diffusion coefficient, meas. using impedance meas. technique 79−23328
molecular dynamics, review, book contrib. 77−39268
molecular end-to-end distance relax., Monte Carlo simulation, model depend. 78−22061
molecular weight, distrib. function type rel. to light scatt. *(German)* 79−1767
molecular weight changes during reactions, automatic recording capillary viscometer meas. 77−27631
molecular weight distrib. effect on drag reduction in turbulent stream 78−83437
molecular weight distribution correlations 77−84207
monodisperse, 2nd virial coeff., renormalisation group calc. 79−10777
monodisperse, thermodynamic fluctuations, light scattering 77−52107
monodisperse polystyrene solutions, at intermediate concs., small X-ray scatt. 79−10779
monodisperse solutions, macromol. length rel. to anisotropic light scatt. in elec. field 77−32391
Monsanto X-500 aromatic polyamide hydrazide soln., light scatt. study 80−76038
Monte Carlo study, scaling props., excluded vol. expansion 80−96435
motion under unstable conditions and in channel terminals 79−77046
motor oils, polymer-thickened, rapid extensional flow through small orifice 78−1709
multicomponent system, phase separation, thermodynamic perturbation theory, calculus 78−18778
nematic helix-coil transtition model 79−94870
net repulsive van der Waals forces between different particles, macromolecular, or biological cells in liqs., appls. 80−34274
network, small ang. neutron scatt. 79−90569
network in solution, free energy of deform. 80−38900
neutron quasielastic scattering from freely jointed chains 78−18534
neutron scattering, elastic, coherent small-angle neutron scattering 77−80428
neutron scattering observations, review 78−14245
Newtonian calibrating oil, stress transient data obtained from cone and plate flow 77−31407
NMR spectrum narrowing, dipolar spin coupling modulation 78−39413
non-ion-exchange, solubility of electrolytes *(Russian)* 80−54391
non-linear model, constitutive equation testing with free. vol. relax. spectrum 80−6011
non-Newtonian fluid, steady flow, numerical modelling 78−51205
non-Newtonian fluid flow through helical coils, studies 78−51204
nondraining coils, first order excluded volume effect on intrinsic viscosity 78−55968
nonisothermal laminar flow in pipes 77−58741
nonisothermal rheology, significance in polymer processing 79−90206
nonlinear network viscoelastic model 79−3985
nonlinear response to uniaxial shear flow histories 80−59084
nonlinear viscoelasticity, stress-temp. equiv. eqns. 77−80128
nonrigid polymer chains, theory of dynamic depolarised light scattering 79−3601
normal stress meas. using flight velocity 79−77039
normal stress measurement, modification to Weissenberg rheogoniometer unit 80−69750
normal stress measurement of dilute polymer solutions 80−83776
nylon 6.6 in 100% H_2SO_4, primary normal-stress difference coeff., dependence on molecular wt. 80−87752
nylon 6 fibre, melt spun crystallisation *(Chinese)* 79−14792
Nylon-6, shish-kebab struct., obtained from quiescent soln. by self seeding 80−15017
nylon-6 dilute soln., gelation and crystallisation, struct. determ. 79−37635
oligomeric liquid mixtures, transition to, polymer systems, thermodynamics 78−20048
one- and two-phase flow through porous media 78−42659
optically active stereoregular, conform. props., rel. to config. 78−33644
order, conf., Midland, USA, (Aug 1973) 79−10769
orientable polymer fluid, Ericksen's anisotropic fluids theory extension 80−79359
oscillatory flow in U-tube manometers, effect of drag reducing polymer additives 80−64584
osmotic compressibility from elastic neutron scatt., general formulation 79−90517
polymer solutions continued
osmotic pressure, correlation functions, in grand canonical formalism 80−100159
osmotic pressure, sedimentation and diffusion, scaling law for conc. depend. 79−70377
PAN in DMF, ultracentrifuged, effect of pressure on sedimentation *(Russian)* 79−34369
partially labelled chains, neutron scatt. obs. 80−38899
PBLG in dioxan, freq. and shear-rate depend. of relative permitt. 77−8489
PBLG solns., dielec. meas., using pseudorandom noise dielectric spectrometer 78−15084
PCP, oriented swollen soln., IR dichroism, short-range orient. order *(Russian)* 79−51941
PEO 301, dilute soln., pipe flow turbulence struct. drag reduction 78−26196
permeable polymer mol. in soln., intrinsic viscosity and friction coeff. 78−30353
phase diagrams, pulse-induced critical scatt. 79−1490
phase dualism, gas-, liq.-like, appl. to compression effects 79−1388
phase-equilibria of rod-like molecules in extensional flow field 78−26158
phenolic resins, average molecular weight and viscosity of acetone solns. *(Japanese)* 79−65234
phenomenological theory of polymer chain, renormalisation group approach 78−26418
phenyl methacrylate copolymers, photoluminescent behaviour 80−25432
photolysis, disentanglement of fractions 79−66314
photon correl. spectroscopy, macromolecular soln. dynamics, review 79−59603
pipe flow, drag reduction 78−42631
pipe flow, early turbulence 78−22380
pipe flow, fluid friction 78−5769
pipe flow, triggered laminar to turbulent transition, random coiling macromolecular soln. 78−26195
piperylene-acrylonitrile copolymers, polymerisation, monomer composition rel. to copolymer struct. *(Russian)* 80−5651
plane interface between two viscoelastic superposed cond. fluids, instability in mag. field 80−1694
plane polygonal, normal stress under oscill. shear flow 78−34420
PMMA, benzene soln., single chain dynamics by neutron scatt. 79−19136
PMMA, diffusion coeffs. and thermodynamic props., conc. depend. 80−15274
PMMA, in isopropylbenzene, mol. mass effect on mobility and interaction parameters *(Russian)* 79−31754
PMMA, isotactic, syndiotactic, ^{13}C spin-lattice relaxation times, chain config., dynamics 77−24760
PMMA, mol. motions in benzene soln., ^{13}C NMR and EPR 79−78551
PMMA, solns., shear flow, dielec. anisotropy 79−15393
PMMA, stereoregular, assoc. 79−11793
PMMA, stereoregular, assoc. in dilute soln., PMR obs. 78−76321
PMMA, syndiotactic, solns. in toluene, NMR obs. of struct. and dynamics of associates 80−75867
PMMA+diethyl phthalate, conc., viscoelasticity and glass transition, Adam-Gibbs theory 78−83353
PMMA aqueous colloid, coagulation kinetics, light scatt. determ. 79−39215
PMMA in benzene solution, ultrasonic irradiation, polymer chain scissions obs. by ESR spectra and spin-trapping techniques 80−84653
PMMA isotactic, syndiotactic stereocomplex formation in soln., composition, struct. 79−66292
PMMA soln. in toluene, diffusion, viscosity rel. to temp. *(German)* 79−42289
PMMA-aerosil, adsorption at plane surface, computer rel. to real expts. *(Russian)* 79−56077
poly(2,6-dimethyl phenylene oxide) enthalpy of mixing with polystyrene 78−14471
poly(2-vinyl pyridine), dil. solns., translational diffusion, chain conformation influence 80−103508
poly(α-methylstyrene)-cyclohexane, translational friction coeff. conc. depend., multiple scatt. formulation 77−20102
poly(γ-benzyl)-L-glutamate, viscosity behaviour in dioxane solvent, conc. depend., aggregation 79−82371
poly(γ-benzyl L-glutamate), soln. and film, light scattering study 79−66374
poly(γ-benzyl-L-glutamate), soln., rot. diffusion, ^{13}C NMR 77−75350
poly(aminiumphosphate)s, mol. wts., and cond. studies 80−14264
poly(butyl acrylate) solutions, dielec. relaxation 80−40045
poly(butyl methacrylate) solutions, dielec. relaxation 80−40045
poly(isobutyl methacrylate) solutions, dielec. relaxation 80−40045
poly(L-glutamic acid), texture in conc. soln. and solid films *(Japanese)* 79−90534
poly(methacrylic acid), aq. soln., gelation kinetics under shear stress 78−3387
poly(methacrylic acid)-D_2O soln., proton and deuteron relax. rates, temp. and freq. depends 77−88472
poly(oxyethylene glycol), texture in conc. soln. and solid films *(Japanese)* 79−90534
poly(S)-2-methylbutyl vinyl ether, conformation, IR spectra 78−1116
poly(sodium 10-undecenoate), form. by γ-ray induced polymerisation in aq. micelle solns. 80−61093
poly(vinyl acetate)+diethyl phthalate, viscoelasticity and glass transition, Adam-Gibbs theory 78−83353
poly(vinyl methyl ether)-polystyrene mixture, electric field depend. of cloud point temp., laser scatt. meas. 80−6519
poly (ar-methylstyrene)s, steric effects on excimer formation, fluorescence spectra exam. 80−25430
poly L-lysine, temp. induced conformation transition in solns., optical rotary meas. 78−46474
poly N,N-diallyldimethylammonium chloride, soln. props., struct. 79−94861
poly-1,4-phenylene terephthalamide, in H_2SO_4, dilute soln. viscosity 78−75524
poly-1-vinyl napthalene, excimer dissoc., time resolved fluoresc. spectra 78−33643
poly-1-vinylnaphthalene, time-resolved fluoresc. spectroscopy, excimer form. and dissoc. 79−38637
poly-2,4-dimethylstyrene, intermolecular interaction phenomena *(Russian)* 77−21414
poly-2,6-dimethyl-p-phenylene oxide solns., US and viscoelastic relax., conformational changes 77−31033

polymer solutions continued
poly-2,6-dimethylphenyleneoxide, fluoresc. correction in light scatt. meas. 79−1771
poly-2-vinylnaphthalene, soln., lowest triplet props., flash photolysis and radiolysis obs. 80−32861
poly-4,4′-diphenylphthaleinterephthalamide in DMF, ultracentrifuged, effect of pressure on sedimentation *(Russian)* 79−34369
poly-4-vinyl-pyridine, solns. in ethanol, spin label obs. of local density of monomer units and mol. dynamics 80−44099
poly-4-vinylpyridine, electro-optic study of conformational changes induced by heavy metal ions 80−84725
poly-4-vinylpyridine, intramol. mobility and local density in soln. spin mark method obs. *(Russian)* 80−70107
poly-4-vinylpyridine, mol. dynamics and local density in conc. soln., spin mark method obs. *(Russian)* 80−70108
poly-4-vinylpyridine N-oxide, aqueous, solns., IR spectra 80−2761
poly-9-vinyl carbazole, fluoresc. props. 78−84647
poly-α-methylstyrene, in cyclohexane, crit. opalescence *(Russian)* 77−62463
poly-α-methylstyrene, intermol. interactions *(Russian)* 77−21414
poly-α-methylstyrene, shear flow, transient stress effects, network rupture constitutive eqn. 77−11157
poly-β-benzyl-L-aspartate, soln., ^{13}C and ^{1}H NMR dynamic study 79−69737
poly-γ-benzyl-glutamate, conc. soln., rheology, liq. cryst. transition 79−94574
poly-γ-benzyl-L(D)-glutamate, soln., liq. cryst. and pretransitional regions, optical rot. 80−66145
poly-γ-benzyl-L-glutamate, γ-methyl-L-glutamate solns. in p-Cresol-$CDCl_3$ mixed solvent system, NMR 79−91303
poly-γ-benzyl-L-glutamate, lyotropic liq. cryst., crosslinking in mag. fields, aligned orientation form. 77−43137
poly-γ-benzyl-L-glutamate, soln., ^{13}C and ^{1}H NMR dynamic study 79−69737
poly-γ-benzyl-L-glutamate, soln., liquid crystal transitions anal. 80−65207
poly-γ-benzyl-L-glutamate, synthetic polypeptide, nonlinear dielectric effect in nonpolar medium 80−84682
poly-γ-benzyl-l-glutamate solns., mesomorphic re-entrance phenomena 79−99074
poly-γ-benzyl-L-glutamate solution orientation of liq. cryst. domains, IR spectroscopy *(Russian)* 77−62477
poly-γ-benzyl-L-glutamate-dichloroethane in conc. soln., mol. assoc., electro-opt. investig. 78−1973
poly-γ-benzyle-L-glutamate in dioxane solution, relax. mechanisms, light scatt. spectra 80−20659
poly-γ-methyl-L-glutamate, conformational props., viscosity, osmotic press. meas. 77−31032
poly-γ-methyl-L-glutamate solns. in p-Cresol-$CDCl_3$ mixed solvent system, NMR 79−91303
poly-ε-caprolactone in dioxane soln., low freq. dielec. response 77−40177
poly-(phenyl-p-acryloyloxybenzoate), nematic polymer, struct. determ. 79−99064
poly-L-alanine, soln., ^{13}C NMR dynamical study 79−69737
poly-L-glutamic acid-Na, cooperativity parameter determ. from viscometry 80−75147
poly-L-ornithine, ^{15}N NMR, coil-helix transition, solvent effects and pH depend. 80−74275
poly-m-phenylene isophthalamide, soln. and cryst., conform. props. calcs. *(Russian)* 79−65009
poly-m-phenylene-isophthalamide in dimethylacetamide, flow birefringence *(Russian)* 80−66148
poly-n-benzamide, lyotropic liq. cryst., structural orientation *(Russian)* 77−31593
poly-n-butyl methacrylate, θ-solns., temp. coeff. of unperturbed dimens. 78−9290
poly-n-phenyleneterephthalamide, conformational and structural props. *(Russian)* 77−61889
poly-N-vinyl carbazole, solns., shear flow, dielec. anisotropy 79−15393
poly-N-vinyl imidazole, light scatt. viscosity and dynamic birefringence, mol. wt. obs. *(Russian)* 79−33665
poly-N-vinylbenzocarbazole, soln., luminesc., effect of electronic excitation energy vibr. 80−55174
poly-N-vinylcarbazole, polymerisation, struct., props., elec. characts., review 79−41972
poly-N-vinylcarbazole, soln., picosecond time-resolved fluoresc. by pulse radiolysis 80−28122
poly-N-vinylcarbazole and N-isopropylcarbazole with p-dicyanobenzene in dimethylformide soln., laser photolysis 79−100360
poly-p-aminobenzhydride terephthalamide in dimethyl sulphoxide soln., rheological study 80−43683
poly-p-chlorophenyl glycidyl ether, struct., tacticity and addition isomerism, ^{13}C NMR 80−58427
poly-p-chlorostyrene-propylbenzene soln., excluded vol. effect and transitional phenomena 79−77795
poly-p-ethoxystyrene, solns., shear flow, dielec. anisotropy 79−15393
poly-p-phenylene terephthalamide/H_2SO_4 80−83773
poly-p-phenyleneterephthalamide, diffusion in conc. H_2SO_4 *(Russian)* 79−65232
poly-p-phenyleneterephthalamide solns., rheological props. comparison with nylon 6,6 soln. 80−6007
poly-p-tert-butylphenylmethacrylate, soln., viscometric behaviour 80−88016
polyacenaphthalene, glassy soln., fluoresc. yield, polarisation and decay., temp. depend. 80−89043
polyacids, unsaturated carboxylic, in organic solvents, hydrogan bonding, structurisation *(Russian)* 78−71666
polyacrylamide, additive to water supply, effect on cavitation and erosion in pipes 78−83441
polyacrylamide, aq. soln., thermodynamic props., light scatt. obs. *(Russian)* 80−71439
polyacrylamide, aq. soln, viscoelastic effect in flow through porous media 79−94684
polyacrylamide, aq. solns., conform. changes, intermol. interactions, optical mixing spectroscopy 79−10770
polyacrylamide, gels and single chains, phase transitions and crit. behaviour 80−40759
polyacrylamide, turbulent flow of water, effect of polymeric additives 79−1216
polyacrylamide, very dil. drag reducing soln., nonlinear viscoelastic props. 79−7355

polymer solutions continued
polyacrylamide aq. soln., supermol. struct. determ. from scattered light spectrum *(Russian)* 79−32880
polyacrylamide aqueous solution, ultrasonic investigation *(Chinese)* 80−107371
polyacrylamide gel and single chain in soln., laser light scatt. obs. near phase transitions 80−93808
polyacrylamide in glycerine-water dilute soln., rheological props. in extensional and shearing expts. 77−58630
polyacrylamide Separan MG200, aq. soln., rheological props. 80−64507
polyacrylamide single chain in acetone-water mixtures, coil-globule transition obs. 80−1098
polyacrylamide soln., films, hydrodynamics *(Russian)* 77−31338
polyacrylamide solns., anomalous effect in first normal stress difference meas. 77−80130
polyacrylamide solution, drag reducing, rheological props. meas. 79−37271
polyacrylamide solution, tube flow, friction and convective heat transfer, rheological changes effect 79−1220
polyacrylamide solutions, dil., static and dynamic breaking tensions 79−23346
polyacrylamide solutions, viscous behaviour 80−2185
polyacrylamide weak soln., wall turbulent flow 80−38450
polyacrylamide-fluorescein conjugates, fluoresc. polarisation, high press. obs. 80−20683
polyacrylamide-maltose, aq. soln., capillary flow, thermal noise, low freq. oscills. 80−48754
polyacrylamide-maltose syrup soln., meas. of viscoelastic flow props. 78−1622
polyacrylamide-water gel, translational and collective diffusion 79−52787
polyacrylamide-water-glycerine, bubble elongation dynamics, modelling with viscoelastic constitutive relations 79−37388
polyacrylamides-water-glycerol, streaming birefringence in extensional flow 80−6013
polyacrylic acid in aqueous systems, spin labelling using Woodward's reagent 79−96308
polyacrylonitrile, hydrolysed, cutting fluid, operational characteristics 80−89359
polyacrylonitrile-dimethylformamide soln., viscoelasticity and shear modulus meas. *(German)* 80−38374
polyadenilic acid, semi-dil. soln., slow modes 78−53319
polyamide, aromatic, persistence length, rel. to optical anisotropy of worm-like chain 77−50577
polyamide in isoamyl alcohol solutions, spin coating process modelling and rheology 78−27655
polyamide-hydrazide solns., rheology 79−64978
polyarylate-arylenesulfone oxide block copolymer, glass transition, melt and soln. viscosity *(Russian)* 79−55915
polyaspartamides, fluorescent labelling 80−58426
polyazomethines, dil. soln. props. 80−19972
polyazomethines in H_2SO_4, lyotropic nematic phase, threaded textures *(French)* 80−19691
polybut-1-ene and but-1-ene-polypropylene copolymers in solution, ^{13}C spin-lattice relax. and mol. motions 79−95670
1,2-polybutadiene, crosslinked in states of strain, entanglement networks, swelling anisotropy obs. 80−79666
polybutadiene, dil. soln., viscosity, temp. depend., solvent effects 80−59686
polybutadiene, elastic fracture, polymer chain entanglement criterion 78−79290
polybutadiene, low mol. wt., NMR study of terminal group struct. *(Russian)* 77−63912
cis-polybutadiene and butadiene-styrene copolymer mixture, effect of temp. on phase composition 79−96005
polybutadiene and butadiene-styrene in tetrahydrofuran, second virial coeffs. 80−65188
polybutadiene soln., rheological behaviour of flow patterns around agitators 77−31269
polybutadiene-cyclohexane-benzene system, vapour-liq. equilibria 79−95147
polybutadiene-n-hexane-n-heptane soln., Rayleigh scatt., diffusion coeff., viscosity 78−15179
polybutadiene-poly-α-methylstyrene copolymers, struct. obs., prep. *(French)* 80−59401
polybutane H-1900, entrance flow into a slit 79−64619
polycaproamide, US degradation in H_2SO_4 soln. 80−15191
polycaprolactam, and copolymers, optical anisotropy and rigidity 80−88959
polycyclohexanamide, and copolymers, optical anisotropy and rigidity 80−88959
polydiacetylene, urethane substituted, conjugated polymer soln. spectral shift on planar-nonplanar conformational transition 79−64129
polydiacetylene solutions, third-order nonlinear mixing (CARS) 79−10354
polydicarboxylic acids, electrophoretic and viscometric props. 80−66811
polydichlorophenylsiloxane, cyclolinear, flow birefringence and orientation angles in soln. *(Russian)* 79−65835
polydiethylsiloxane chains, dipole moments 78−78844
polydimethyl siloxane solns., limiting viscosity no.-mol. wt. relations 78−18267
polydimethyl siloxane solns., US attenuation meas. 80−107372
polydimethylsiloxane, benzene soln., single chain dynamics by neutron scatt. 79−19136
polydimethylsiloxane, intermol. interactions *(Russian)* 77−21414
polydimethylsiloxane chains, end-linked, swollen model networks, stress/strain isotherms and elastic modulus 80−79668
polydimethylsiloxane fluid, irradiated, NMR anal. of cross-linked and entangled networks 77−51980
polydimethylsiloxane-solvent system, NMR spectrum narrowing, dipolar spin coupling modulation 78−39413
polydimethysiloxane, conc. soln. in benzene, polarised Raman scattering 78−9286
polydisperse, hydrodynamic invariants *(Russian)* 77−19580
polydisperse systems, photon correlation spectroscopy, diffusion coeffs. determ. 80−93802
polydispersity anal. in photon correlation spectroscopy 78−27247
polydodecane amide soln., viscosity, mol. wt. *(Russian)* 79−51296
polyelectrolyte, 1-1 soln., excluded vol. theory, Khun statistical segment basis 78−83716
polyelectrolyte, non-Newtonian effects *(French)* 78−22311

polymer solutions continued
polyelectrolyte+physiologically active substance complexation, stability, kinetics *(Russian)* 80−8006
polyelectrolyte 'catalysis' of chem. reactions 79−57217
polyelectrolyte aqueous salt soln., inelastic light scatt. obs., conformational changes 78−60474
polyelectrolyte complexes, nonstoichiometric, solubility in water *(Russian)* 80−55674
polyelectrolyte complexes, nonstoichiometric water-soluble structure *(Russian)* 80−54112
polyelectrolyte conformation, electrostatic interaction effects at varying conc. 77−35461
polyelectrolyte in solution, variation of contrast, neutron forward scatt. calc. *(French)* 80−54104
polyelectrolyte soln., counterion condensate around line charge as δ-function, nonlinear Poisson-Boltzmann theory 80−85184
polyelectrolyte soln., small ion self-diffusion, Manning's limiting law derivation 80−54416
polyelectrolyte solution, neutron scatt. 79−77484
polyelectrolyte solution, polyion-polyion interaction effects, computer simulation 80−35817
polyelectrolyte solution, thermodynamic props. determ. from Donnon equil. obs. 80−7846
polyelectrolyte solutions, activity coeffs. and osmotic coeff., higher-order limiting laws 79−29387
polyelectrolyte solutions, apparent ionic charge 78−76875
polyelectrolyte solutions, colligative props., chain flexibility influence 78−94962
polyelectrolytes, appl. of Poisson-Boltzmann eqn. 79−77483
polyelectrolytes, saturation of induced dipole moment, orientation mechanism and electro-optical effects 80−84785
polyelectrolytes in soln., conform., small-angle neutron scatt. investigs., review 79−873
polyelectrolytes in soln., electrostatic persistence length rel. to unified theory 78−95932
polyester-organic solvent mixtures, phase diagrams, eutectic props., devitrification, crystn. *(French)* 80−3015
polyesterimides, solns., ultrasonic vel. and Rao formulism 80−103422
polyethersulphone dissolution in chloroform 80−21353
polyethylene, alcohol infused, loss peaks due to secondary groups 80−84688
polyethylene, flow-induced fibril form. from soln. 80−59402
polyethylene, linear, in theta solvents, Mark-Houwink eqn., chain dimensions 77−38764
polyethylene, molten, effect of hydrostatic press. on long-chain organic mol. diffusion 80−92697
polyethylene, pulsed NMR study of crystallization kinetics from melt and soln. 79−87624
polyethylene, standard reference material, limiting viscosity numbers 79−14952
polyethylene glycol, aqueous, solns., IR spectra 80−2761
polyethylene glycol, depolarised Rayleigh scatt., orientational motion, pure and soln. 77−44008
polyethylene glycol, liquid, Brillouin scatt. and segmented motion 79−37609
polyethylene glycol solns., US vel. meas. 77−72655
polyethylene glycols, aq. solns., volumetic props. 79−20460
polyethylene imine, oligomers, solns., linear struct., props. *(Russian)* 79−50177
polyethylene in organic fluids, swelling 79−60255
polyethylene oxide, aq., rot.-oscill. flow, rheological consts. determ. 78−30251
polyethylene oxide, aq. salt soln., meas.-based thermodynamic quantities 78−75525
polyethylene oxide, aq. soln., capillary flow, thermal noise, low freq. oscills. 80−48754
polyethylene oxide, aq. soln., dielec. relax., interferometric transmission obs. 78−52437
polyethylene oxide, aq. soln., mech. props. in parallel superposed flows, geometric effects 80−19448
polyethylene oxide, aq. soln., nonlinear dynamic viscoelasticity 79−94576
polyethylene oxide, dil. aqueous solns., dynamical shear characts. *(Russian)* 79−86393
polyethylene oxide, dil. soln., chain dipole moment, dielec. const. meas. 77−40169
polyethylene oxide, dil. soln., neutron scatt. mol. motion obs. 77−23593
polyethylene oxide, dilute aq. soln., laminar viscous tube flow, scale-depend. effect 79−7367
polyethylene oxide, dilute aqueous solution, effect of chemical additives on flow 80−83823
polyethylene oxide, dilute solns., mol. motion, EPR and NMR investigations 79−94863
polyethylene oxide, dilute solution, flow round circular cylinder 80−69882
polyethylene oxide, discharge coeff. from slot *(French)* 79−98766
polyethylene oxide, drag reduction of highest mol. wt. fractions 77−68636
polyethylene oxide, drag reduction props., Congo Red additive effects 79−64717
polyethylene oxide, molecular dynamics in conc. soln., quasi-elastic neutron scatt. meas. 78−29870
polyethylene oxide, polymer segments, fluoresc. depolarisation on conjugated spin lables 80−91711
polyethylene oxide, semidilute aq. soln., sedimentation of large colloidal particles 78−95965
polyethylene oxide, solns. in toluene and ethyl benzene, phase equilib., struct. and thermodynamic stability *(Russian)* 79−86871
polyethylene oxide aqueous solns., spectroscopic obs. of structural variability WRT turbulent resistance reduction 77−7356
polyethylene oxide in benzene solns., ^1H relaxation times, intermol. interactions 77−32281
polyethylene oxide soln., NMR meas. of dilute to semidilute regime crossover 79−11355
polyethylene oxide solution, turbulent flow in water, effect of polymeric additives 79−1216
polyethylene oxide-Co^{2+} solution, complex struct., PMR *(Russian)* 77−40140
polyethylene oxide-liquid crystal phase diagrams 79−23709
polyethylene single-crystal suspensions, small-angle X-ray scatt. lamellar thickness determ. 79−10784
polymer solutions continued
polyethylene soln., conc., laminar steady flow, expt. *(German)* 79−14443
polyethylene soln., light scatt. from shish-kebab structs. 78−76482
polyethylene solns., conc., viscosity, shear speed depend. *(German)* 79−27671
polyethylene solutions, conc., flow behavior in laminar steady flow field, mol. wt. numerical freq. distrib. *(German)* 79−68673
polyethylene-co-vinyl alcohol-g-ethylene oxide aq. soln., surface tension *(Japanese)* 80−24716
polyethyleneoxide dilute solns., flow birefringence at high rates 79−81834
polyethylenoxide, flow rate increase by electric field 78−75210
polyethylenoxide additive mixing, turbulent drag reduction, schlieren obs. 78−26163
polyfluorostyrene, para- and meta-, dil. soln., ^{19}F magnetic resonance 78−10792
polyglutamic acid molecular dynamics in soln., γ-ray perturbed angular correl. 78−94960
polyglycidyl methacrylate, soln., mol. dynamics, by spin mark method *(Russian)* 79−60260
PolyHall 295 polyacrylamide, aq. soln., cylinder oscillating in viscoelastic fluid, secondary flow 79−60037
polyhexamethylene oxide, dil. soln., chain dipole moment, dielec. const. meas. 77−40169
polyisobutene solns., X-ray scatt., Kratky cone collimation 80−19681
polyisobutylene, Aerosil-filled, solution, periodic and unidirectional deform. effects 77−42791
polyisobutylene, intermol. interactions *(Russian)* 77−21414
polyisobutylene, linear, interpretation of spin relax. in terms of specific motion 79−42857
polyisobutylene, memory-function determ., relax. tests 78−1619
polyisobutylene, soln., ^1H NMR relax. 77−24759
polyisobutylene, soln., stress deform., integral rheological relations 77−11159
polyisobutylene conc. solns., die-swell theory, analytical results 77−58624
polyisobutylene in cetane, hyperelasticity, filler effect 80−10223
polyisobutylene in tetralin, first and second normal stress differences in steady laminar shearing flows 79−46348
polyisobutylene in toluene solution, effect of capillary materials on drag reduction *(German)* 80−87785
polyisobutylene soln., NMR, chain segment motions 80−20475
polyisobutylene soln., start-up tests, relaxation meas. of shear and normal stress *(German)* 78−67166
polyisobutylene solns. in thermodynamically different solvents, conc. dependence of viscoelastic props. *(German)* 77−46980
polyisobutylene solutions, viscous behaviour 80−2185
polyisobutylene-oil, laminar plane stagnation flow kinematics, laser Doppler anemometry 78−38374
polyisobutylene-toluene solution, dynamic compressibility from press. transient technique 77−86256
polyisobutylenes, turbulent drag reduction, influence of mol. wt. and mol. conformation 77−80189
polyisocyanates, rigid backbone, ternary phase relationships obs. 80−59371
polyisocyanides, solns., struct. and acidification 80−19915
polyisoprene, in cyclohexane soln., conform. transition *(French)* 79−7542
polyisoprene-g-styrene, dil. soln., conformation, light scatt. obs. 78−91218
polymer additives diffusion in turbulent boundary layer 77−35176
polymer chain, long, in dilute soln., 2nd order phase transform. 79−13851
polymer rheology nonlinear singularly perturbed Volterra integrodifferential eqn. 79−23290
polymer solns., not infinitely dilute, second-order fluid coeffs., conc. depend. 80−106771
polymer solution, boundary layer having laminar, transitional and turbulent flow zones *(Russian)* 77−80185
polymer solution, drag reduction in turbulent flows, book contrib. 78−59432
polymer solution, intermolecular interpenetration and entanglement, crit. concs. 79−27900
polymer solution, short-range order and solvent crystallisation; spectroscopic and microcalorimetric, methods *(Russian)* 78−26416
polymer solution, short-range solvent orientational order, IR dichroism and photoelasticity obs. *(Russian)* 78−26415
polymer solutions, concentrated, transport properties, hydrodynamic mean field theory of voscisity of sphere suspension 79−4422
polymer-solvent interaction from gas-liquid chromatography, open tubular column expts. 78−35753
polymer-solvent systems with solvent crystn., state diagrams *(Russian)* 79−52185
polymeric cryoprotectants in preservation of biological ultrastruct., aq. soln. low temp. states 78−65157
polymeric cryoprotectants in preservation of biological ultrastructure, physiological effects 78−65158
polymeric cryoprotectants in preservation of biological ultrastructure, morphological aspects 78−65159
polymeric fluids, entropy effects in viscoelasticity 78−9618
polymers, self-consistent field approximation, BBGY and Kirkwood calcs. *(Russian)* 79−64981
polymers containing carbazole units, optically active, fluoresc. props. 78−84647
polymers in liquid stream, Toms effect mechanism, turbulent drag decrease 80−79270
polymethacrylamide copolymers, mobility of spin label bonded to chain end 80−63873
polymethacrylic acid, colloidal cylinders in solns., electrophoresis, random orient. in elec. field 79−1956
polymethacrylic acid, dye-tagged, electrically oriented solns., fluoresc. polaris. changes 78−76523
polymethacrylic acid, swollen networks, viscoelastic photoelastic behaviour 80−59366
polymethacrylic acid, syndiotactic deuterated, aq. solns., methylene deuteron relax., freq. and temp. depend. 77−90062
polymethacrylic acid aq. solns., PMR spectra 78−27099
polymethacrylic acid in water, ^{13}C nuclear Overhauser enhancement, reduced value rel. to ^1H spin-lattice relax. 77−46581
polymethacrylic acid semi dilute solutions, conformation and organisation, small-angle neutron scatt. 79−10782

polymer solutions continued
polymethine dye solution, optoacoustic response 80−6465
polymethylene coils in solution, dimension and shape, computer simulation *(Russian)* 80−54111
polymethylene in binary n-alkane solvents, lower critical soln. temp. 79−37841
polymethylene in n-alkanes, lower critical soln. temp. 79−37840
polymethylsiloxane-polyarylate block copolymer, soln., viscosity, rel. to film mech. props. and microstruct. *(Russian)* 79−23762
polymethylstyrene, mech. scission by US irradiation *(Japanese)* 78−59190
polynucleotide-protein mixture, aqueous, inverted turbidity versus conc. depend. 77−9165
Polyox, drag reduction meas. in square duct, anomalous effects due to polymer degradation 80−83824
Polyox 701, aq. soln., spectral effects in turbulent press. suppression 78−5771
Polyox dilute soln., elongational flow obs. 79−60029
polyox solution, turbulent flow in tube with large surface roughness 78−1651
polyox WSR-301, posterior rat extremity perfusion, hydrodynamic friction lowering 79−79586
Polyox-701 aq. soln., pipe flow, Newtonian and non-Newtonian LF turbulent press. similarity 78−5772
polyoxyethylene, dil. solns., laminar flow in tubes, scale effect 79−86472
polyoxyethylene, semidilute and dilute soln. behaviour crossover, UV spectrometry 78−80375
polyoxyethylene aq. soln., kinetics of soln. form. 78−64913
polypeptide in conc. soln., mol. assoc., electro-opt. investig. 78−1973
polypeptides, helical, conc. solns., rheological behaviour and liq. cryst. order 80−83771
polypeptides, helical, dielectric polarisability, side chain motions 78−76378
polyperfluorobutadiene, melts, solns., ^{19}F NMR, ^{13}C NMR spectra, microstruct., configurations 77−43894
polyphenyl ether in benzene, evaporation, vapour press. determ. from gaseous diffusion coeff. 80−10654
polyphenylene terephthalamide in H_2SO_4-H_2O system, phase equilib. 79−73314
polyphenylquinoxaline, soln., conform., equilib. rigidity *(Russian)* 79−55643
polypropylene oxide, solns., mol. relax., dielectric relax. and Brillouin scatt. obs. 77−23590
polypropylene solns., viscosity-mol. wt. relation 79−37867
polypropylene sulphide, atactic chains, dipole moments, dielec. const. meas. 80−23584
polypropylene sulphide in athermal solvent, viscosity-temp. coeffs. 80−39333
polypropylene-chloroform (chloromethane), χ-parameters, heat of mixing, vap. press. and microcalorimetric meas. 78−34626
polyribonucleotides, dye tagged, aqueous solns., elec. induced fluoresc. changes 80−85346
polystyrene, 7% in tricresyl phosphate and Arochlor, stress transient data obtained by cone and plate flow 77−31407
polystyrene, benzene soln., self-diffusion, test for scaling and reptation 79−77789
polystyrene, binary and ternary cluster integrals, small angle neutron scattering 79−50975
polystyrene, bridge method for meas. dielectric relaxation 80−82793
polystyrene, chain motions, electron-electron double reson. obs. 79−69753
polystyrene, conc. soln., friction const., Rayleigh scatt. 77−35737
polystyrene, conc. solns., diffusion and sedimentation, frictional coeff., crit. soln. temp. 79−95195
polystyrene, cyclohexane soln., coil-globule transition 80−54110
polystyrene, cyclohexane soln., temp. depend. of chain dimensions, small-angle neutron scatt. 78−50671
polystyrene, diethyl malonate soln., near-crit., osmotic compressibility, correlation length, scaled functions 80−11422
polystyrene, dil. soln., neutron scatt., quasielastic broadening 77−76286
polystyrene, dilute soln., ^1H mag. relax., selective inversion technique appl. 80−44957
polystyrene, elastic fracture, polymer chain entanglement criterion 78−79290
polystyrene, enthalpy of mixing with poly(2,6-dimethyl phenylene oxide) 78−14471
polystyrene, in butan-1-ol, colloidal particles, dispersion force interactions calcs. 79−24842
polystyrene, in cyclohexane soln., mol. wt. distrib., photon correl. obs. 79−10239
polystyrene, in mixed theta solvent, intramol. motion, photon-correlation spectra obs. 79−77480
polystyrene, in solns., intrinsic viscosity rel. to mol. wt., unperturbed dimensions 80−65268
polystyrene, in theta solvent, intramol. motion, photon correl. spectrosc. 78−90328
polystyrene, in toluene and cyclohexane, acoustic absorption and dynamic compressibility 77−55321
polystyrene, in trans-decalin soln. refr. index, temp. and conc. depend. 78−84547
polystyrene, intermolecular interaction phenomena *(Russian)* 77−21414
polystyrene, ion cyclohexane, mol. dimens. near theta point 80−54105
polystyrene, low mol. wt., conc. transdecalin soln., hydrodynamic and gel modes light scatt. obs. 79−73085
polystyrene, moderately conc. solns. in cyclohexane, polymer diffusion and dimensions 77−62462
polystyrene, ordered monodisperse latexes, viscoelasticity and flow props. 80−58992
polystyrene, polydisperse, quasielectric light scatt. obs., mol. wt. and polydispersity 79−96376
polystyrene, semidilute and dilute soln. behaviour crossover, UV spectrometry 78−80375
polystyrene, soln., laser light scatt. Rayleigh linewidths anal., intramol. motion 77−3500
polystyrene, soln., macromol. dynamics, us relax. 80−19882
polystyrene, soln. in trans.-decalin, viscosity and thermodynamic props., press. depend. 79−69275
polystyrene, solns., diffusion coeffs. meas., Fourier transform NMR, pulsed field gradient system 80−57353
polystyrene, solns., nonlinear viscoelasticity, stress development at start of shear flow 77−3800
polymer solutions continued
polystyrene, solns., sedimentation behaviour, branching effects determ. 80−66887
polystyrene, spin-labelled, EPR, end group mobility, temp. and solvent depend. 78−56368
polystyrene, star branched in cyclohexane, upper and lower critical soln. temp. 79−90789
polystyrene, suspension of monodisperse spherical colloidal particles, layered sedimentation 79−39217
polystyrene, swollen network in benzene, pendent chains, influence on thermodynamic and viscoelastic props. 80−28481
polystyrene, time-resolved fluoresc. spectroscopy, excimer form. and dissoc. 79−38637
polystyrene+dibutyl phthalate, conc., viscoelasticity and glass transition, Adam-Gibbs theory 78−83353
polystyrene and butadiene-styrene in tetrahydrofuran, second virial coeffs. 80−65188
polystyrene chain conformations, in conc. solns. and in bulk, small-angle X-ray scatt. 79−10781
polystyrene coils, benzene soln., internal modes by photon beat 78−10905
polystyrene conc. sols. in toluene, rheological behaviour *(German)* 78−55618
polystyrene in 1-chloroparaffins, perturbed chains, hydrodynamic interaction effects in intrinsic viscosity 79−99344
polystyrene in benzene and decalin, diffusion coeff., solvent effect 80−19971
polystyrene in benzene or cyclohexane, zero shear-rate intrinsic viscosities 80−75376
polystyrene in benzene solution, ultrasonic irradiation, polymer chain scissions obs. by ESR spectra and spin-trapping techniques 80−84653
polystyrene in chlorinated biphenyl, flow birefringence on appl. of step-shear strain 80−25335
polystyrene in cyclohexane, dil. theta soln., translational diffusion coeffs., conc. depend., Rayleigh scatt. meas. 79−90812
polystyrene in cyclohexanol, polydispersities from temp.-drop turbidimetry 77−25314
polystyrene in cyclopentane, sedimentation vel., conc. and temp. depend. 79−70385
polystyrene in dil. sol., solvent depend. of molecular motion, proton mag. relax. meas. 79−41932
polystyrene in mixed solvents, intrinsic viscosity 78−67843
polystyrene in solns., unperturbed dimensions rel. to temp., solvent composition 79−64132
polystyrene in tetrachloroxylene and tetrachlorobenzene, morphology of crystallized additives 79−99082
polystyrene in toluene, unstirred solns., transient diffusion through membrane 78−92508
polystyrene latex, colloidal crystal, grain boundary struct. and boundary diffusion obs. *(Japanese)* 78−15721
polystyrene latex aq. solns., monodisperse, exponential clipped photon autocorrel. spectra, data anal. 79−2837
polystyrene latex particles, swollen, aggregation studied by photon correlation spectrosc. 80−66886
polystyrene latex spheres, characterisation using light scattering spectrom. 80−95753
polystyrene mixture solutions, second virial coeff. light scatt. meas. 78−14438
polystyrene model molecule, 2,4-di-p-bromophenyl pentane, US relax., mol. dynamics 79−73258
polystyrene monomer, high purity, soln., rheological behaviour of flow patterns around agitators 77−31269
polystyrene networks swollen in cyclohexane, swelling equil. and light scatt. at theta conditions 80−107036
polystyrene soln., macromolecular chain dynamics, C^{13} and NMR 78−55267
polystyrene soln., monosubstituted, mol. chain dynamics, NMR meas. 78−56393
polystyrene soln., rheological behaviour of flow patterns around agitators 77−31269
polystyrene solns., correlations of network model parameters 80−106772
polystyrene solns., non-Newtonian flow curves, viscosity 30°C 78−83438
polystyrene solns. at theta conditions, Rayleigh scatt. determ. of conc. depend. of diffusion coeff. 79−77790
polystyrene solution, conc., diffusion and NMR relax. times 77−55725
polystyrene solution, constitutive models, exptl. tests based on birefringence data 80−100015
polystyrene solution, differential meas. of ultrasonic velocity *(French)* 80−75302
polystyrene solution, drag reduction, mean vel. profile 78−22384
polystyrene solution, flow birefringence, in time dependent field 80−7323
polystyrene solution, internal viscosity, model for Lamb-Matheson-Philippoff increment 77−62284
polystyrene solution in benzene, laser light scatt. meas. 79−91458
polystyrene solution in benzene, thermodyn. interaction coeff. determ. 78−3367
polystyrene solutions, light scatt., mol. parameters, computer anal. assessment 79−1766
polystyrene solutions, ordered and disordered, particle dynamics determ. from time depend. multiple light scatt. 78−33672
polystyrene solutions, translational diffusion coeff., light-scatt. meas. 78−52519
polystyrene solutions, US degradation obs. 78−95989
polystyrene solutions, viscous behaviour 80−2185
polystyrene solutions in decahydronaphthalene, viscoelastic props., time depend. *(German)* 79−77051
polystyrene suspension, laminar flow, augmentation of heat and mass transfer, correl. of data 80−53840
polystyrene-Aroclor 1254, streaming birefringence in extensional flow 80−6013
polystyrene-benzene, polymer excluded volume exponent, experimental verification of n vector model for n=O 80−70104
polystyrene-benzene, semidilute solns., viscosity and reptation time 79−99345
polystyrene-benzene-methanol system, preferential solvation 79−10772
polystyrene-co-divinylbenzene microgels in dimethylformamide, diffusion coeff., viscosity and mol. wt. meas. 80−30286
polystyrene-cyclohexane, polymer solns., coexistence curve 79−28101
polystyrene-cyclohexane, translational friction coeff. conc. depend., multiple scatt. formulation 77−20102

polymer solutions continued
polystyrene-cyclohexane mixture, Rayleigh and Brillouin scatt. and struct. relaxation 80−63640
polystyrene-cyclohexane soln., excluded vol. effect and transitional phenomena 79−77795
polystyrene-cyclohexane system, temp. depend. of hydrodynamic lengths 80−92449
polystyrene-cyclohexanone, thermal cond., appl. of spherically symmetric apparatus for liqs. and solns. *(French)* 79−94477
polystyrene-decalin solns., flow irregularity obs. in theta conditions 80−38453
polystyrene-diethyl malonate system, osmotic compressibility and correlation range near crit. point 78−6694
polystyrene-liquid crystal phase diagrams 79−23709
polystyrene-methylcyclohexane, coexistence curve, comparison obs. and free energy calc. 80−88323
polystyrene-methylcyclohexane, coexistence curves, range of simple scaling and critical exponents 80−88322
polystyrene-methylcyclohexane soln., excluded vol. effect and transitional phenomena 79−77795
polystyrene-PMMA-benzene, soln., polystyrene diffusion, photon correl. spectroscopy 80−34220
polystyrene-polydimethylsiloxane, block copolymer micelles, small angle X-ray scatt. 79−69003
polystyrene-polyethylene/propylene block copolymer, micelle form. in lubricating oil 80−61171
polystyrene-polyisobutylene, solns., incompatibility, binodal and spinodal calcs. 77−28005
polystyrene-polyisobutylene, solns., incompatibility, light scatt., conc. and angle depend. 77−24407
polystyrene-polyisobutylene, solns., incompatibility, light scatt., crit. opalescence 77−24408
polystyrene-polyisoprene two-block copolymer soln., conformation, small angle neutron scattering, X-ray diffraction, review *(Rumanian)* 80−6348
polystyrene-tetrachloroxylene(tetrachlorobenzene) glassy solns., additive morphology rel. to mech. props. 79−65007
polystyrene-tetrahydrofuran-water system, thermodynamic and hydrodynamic props. 79−96353
polystyrene-trans-decalin system, ^{13}C spin-lattice relax., solvent rot. diffusion 79−33556
polystyrene-tricresyl phosphate solns., viscoelastic props., conc. depend. 80−76299
polystyrenecobutadiene, vapour sorption isotherms for benzene and n-heptane 78−68912
polystyrenes, in toluene 79−1773
polystyrenes, solns., shear flow, dielec. anisotropy 79−15393
polystyrenes, toluene soln., diffusion through cellulose membrane, friction coeffs. 78−73085
polystyrenes, toluene soln., turbulent drag reduction, mol. wt. and struct. influence 79−7373
polystyrenesulphonates, in dioxane-water mixtures, heats of dilution meas. 80−59655
polystyrenesulphonic acid, in dioxane-water mixtures, heats of dilution meas. 80−59655
polysulphonamide solutions, mech. props. during gelling *(Russian)* 77−19579
polysytrene, benzene soln., characterisation using light scattering spectrom. 80−95753
polytetrahydrofuran, dil. soln., neutron scatt., quasielastic broadening 77−76286
polytetrahydrofurane in CS_2, dil. solns. neutron quasielast. scatt. study 79−41935
polytrimethylene oxide, soln., chain dipole moment, dielec. const. meas. 77−81043
polyurethane, branched soln., viscous reduction props. *(Russian)* 78−87807
polyurethanes, linear, in physiological soln., degradation by ester hydrolysis *(Russian)* 80−40690
polyurethanes, vapour press. of solvent above swollen crosslinked networks rel. to rubber elasticity theory 80−45536
polyvinyl acetate, and conc. solns., viscosity meas. 80−65269
polyvinyl acetate with iodine-iodide, reaction system, colour complex form., temp. effect 79−83457
polyvinyl acetate-vinyl acetate, partially polymerised, ^1H-, ^{13}C-spin lattice relax. time meas. *(German)* 79−28633
polyvinyl alcohol, atactic, thermoelasticity of networks swollen in water, polymer-diluent interactions 80−29102
polyvinyl alcohol, in water-ethanol mixture, processes of structure formation 80−10482
polyvinyl alcohol, viscosity raising additive for dye laser 77−10953
polyvinyl alcohol networks, swelling equil. with dil. salt solns., thermoelastic behaviour, hydroxyl group interact. 80−79667
polyvinyl alcohol/vinyl acetate copolymer, in water-ethanol mixture, processes of structure formation 80−10482
polyvinyl alkylates, surface tension *(Japanese)* 79−95247
polyvinyl imidazolium sulphobetaine, aq. soln. props. 79−32879
polyvinyl methyl ether, aq. soln., dielec. relax., interferometric transmission obs. 78−52437
polyvinylacetate, long-chain branching characterisation, molar masses 79−94122
polyvinylacetate in benzene solution ultrasonic irradiation, polymer chain scissions obs. by ESR spectra and spin-trapping techniques 80−84653
polyvinylalcohol, aqueous, solns., IR spectra 80−2761
polyvinylbenzocarbazole, weak solution, intramolecular energy transfer by singlet and triplet excitons 80−34971
polyvinylcarbazole, weak solutions, intramolecular energy transfer by singlet and triplet excitons 80−34971
polyvinylpyrrolidone, aqueous, solns., IR spectra 80−2761
poly[(R)-oxypropylene], opt. rot. dispersion and vac. UV circular dichroism 80−40084
poor solvent, loop expansion of irreducible diagrams 80−100160
pore-trapped, statistics 77−39524
porous media flow, polymer effect onset and saturation limit 78−26190
power laws of reduced turbulent friction for pipe flow 77−15068
PPT in 100% H_2SO_4, primary normal-stress difference coeff., dependence on molecular wt. 80−87752
protonated and deuterated mixtures, partial miscibility 80−107037
pseudo-turbulent flow, nonlinear dumbbell model for drag reduction 78−51206
polymer solutions continued
pseudoisocyanine bound by sulphated polysaccharides, dil. aq. soln., visible and circular dichroism spectra 80−45107
pseudoplastic fluid, upper and lower Newtonian fluid behaviour 77−15080
PTFE, in butan-1-ol, colloidal particles, dispersion force interactions calcs. 79−24842
pulsatile flow in tube, flow enhancement, Goddard-Miller model 78−30324
PVA, aq. soln., dielec. relax., interferometric transmission obs. 78−52437
PVA, aq. solns., US absorpt., acetate groups effects *(Russian)* 80−65162
PVA, semidilute and dilute soln. behaviour crossover, UV spectrometry 78−80375
PVA soln., flow in profile channel of extrusion head 79−98780
PVC, diffusion coeffs. and thermodynamic props., conc. depend. 80−15274
PVC, in chlorinated aromatic solvents, mol. wt. characteris., ref. materials, soln. props. 79−7045
PVC in DMF, THF solns., mol. wt., aggregation, light scatt. investig. *(Polish)* 77−28587
PVC plastisol, flow behaviour at high shear rate *(German)* 80−92186
PVC plastisol, steady shear rheological behaviour 79−37274
PVC-THF-H_2O, precipitation fractionation, influence of stereoregularity 79−7046
quartz fibres, possible role as templates for biopolymers 79−39345
quasi-elastic light scatt., slow modes 80−74271
quasimonomers, concept and appl. to polymer statistics 79−41931
quenching solution, ZSP-1 78−23739
radiation scattering, quasielasric, Rouse-Zimm model 80−84047
random coil, radial distrib. function calcs. 80−44101
random coil molecules, radial distrib. function 77−76289
random coil polymer, nonzero thickness, shear viscosity conc. depend. 79−10238
random coil polymers, intramol. fluctuations by photon correl. spectroscopy 77−48184
random copolymer solution, electrooptics of crystal-like mols. *(Russian)* 77−63396
randomly coiled polymer, models for spin relaxation 77−85607
Rayleigh light scattering photometry, low angle, soln. props. 78−35156
Rayleigh scattering, depolarised, time correlation function 78−2862
Rayleigh scattering, intermolecular correlations effect 80−75146
renormalised field theory, polydispersity 80−74270
resistance to aggressive liquid media, accelerated determ. using periodic-action method 79−52533
rheological constitutive eqn. 79−41647
rheological eqns. of state, macromol. elasticity and internal viscosity effects 77−80127
rheological equations, review 79−86391
rheological properties of concentrated soln., rod-like mol. model 78−75114
rheological props. in flow through porous media 80−53819
rheological relationships, concentrated solns. 77−75867
rheologically anomalous fluids, flow in porous media 80−53851
rheology, applications to polymer processing 77−23925
rheology, characterised by mol. int. distrib., review 80−1504
rheology, finitely extensible nonlinear elastic dumbbell theory 78−9617
rheology, fluid mechanics, book 77−65772
rheology, rel. to turbulent drag reduction 78−22315
rheology and kinetic theory, review 78−38611
rheology based on a finitely extensible bead-spring chain model 80−83775
rheology in laminar capillary tube flows 78−34170
rheology of polymeric systems, review 78−87317
rigid, modified Oseen tensor, superposition approximation appl. 80−92447
rigid aromatic polymer solution, exciton transport 79−69431
rigid chain polymer solns., flow birefringence rel. to mol. wt. and chain length *(Russian)* 79−33664
rigid macromolecule, in soln., depolarised Rayleigh spectroscopy 79−94119
rigid-chain, flow birefr., hydrodynamic and dynamic-optical props. 79−24286
rodlike, and flexible chain polyamide conc. solns., comparison of rheological props. 80−6007
rodlike particles, polydisperse soln., isotropic-nematic phase transition, Onsager theory 80−100324
rotating disc in polymer solutions under a turbulent regime 80−33634
Rouse-Zimm theory of hydrodynamic props., limiting viscosity 77−558
Rouse-Zimm theory of hydrodynamic props. 77−559
row nucleation, phenomenological model 78−14301
scaling theories for general interaction potentials 80−99592
scattering, small angle, curves calcs., of conc. polymer solns. 79−10783
SCF approximation, connection between Yvon-Born-Green and Kirkwood hierarchies 78−42882
second normal stress difference, meas. 80−43747
second-order fluid constants for freely jointed bead-rod chain suspensions 77−75948
sedimentation, expt. determ., errors due to diffusion *(Russian)* 78−76934
sedimentation field-flow fractionation in macromolecule characterization 80−66879
sedimentation rates for low mol. wt. materials in dilute region 80−108756
sedimentation velocity in ultracentrifugation, absolute mol. at. and mol. heterogeneity determ. *(German)* 80−14261
self-avoiding random walks, exact enumeration method and Monte Carlo sampling 79−67228
self-diffusion, review 80−29193
semi-dilute, field theoretic formalism 77−31575
semidilute, chain size 78−87607
semidilute, hydrodynamic interaction of two permeable spheres, method of reflections 78−71394
semiflexible macromolecule soln. liquid-crystalline ordering 78−94963
semirigid macromolecule, dynamo-optic const. *(Russian)* 77−20821
Separan, 1.5% in 50/50 glycerine water, stress transient data obtained by cone and plate flow 77−31407
Separan AP-30, aq. soln., cylinder oscillating in viscoelastic fluid, secondary flow 79−60037

polymer solutions continued
shear and normal stress behaviour in steady shear flow *(German)* 78−67165
shear flow, transient stress effects, network rupture constitutive eqn. 77−11157
shear thinning and shear thickening additives in reservoir flooding for oil recovery 80−72100
short range correlation between elements of long polymer in good solvent 80−59367
short-chain molecules, hydrodynamic behaviour, extended Rouse-Zimm theory 77−558
short-chain molecules, hydrodynamic behaviour, viscosity 77−559
simulation of macromol. dynamics, Monte-Carlo method, conc. depend. *(Polish)* 78−51404
simulation of polymer dynamics, general theory 78−91210
simulation of polymer dynamics, relax. rates and dynamic viscosity 78−91211
single chain, dynamical scaling exponent, renormalisation along the chain 79−10786
single chain dynamics, computer simulation 78−83718
single-relaxation-time constitutive model 77−11156
small angle neutron scatt., single chain form factors 80−107038
small peptide antibiotic and protein solns., US absorption 79−48286
small-angle scattering, of X-rays and neutrons, (fourth international conf., Gatlinburg, USA (Oct. 77)) 79−10745
Smoluchowski eqn., one-particle generalised, perturbation solution 77−27211
sodium alginate, light scatt., wt.-average mol. wt., charge density 77−61882
sodium copoly(ethyl acrylate-acrylic acid) copolymer, quasi-elastic light scatt. 78−35157
sodium polystyrene sulphonate, dye-tagged, electrically oriented solns., fluoresc. polaris. changes 78−76523
sodium polystyrene sulphonate, solns., infinite dilution viscoelastic props. 79−14363
sodium polystyrene sulphonate in aq. soln., quasi-elastic light scatt. 80−100661
solution, second virial coeff., segment cloud model, chain length and branching study 80−24559
solvation, preferential, effect on polymer dimensions 79−10771
solvent osmotic stresses, prediction of Case II transport kinetics 80−26049
spatial cross-over, obs. in small angle neutron scatt. 79−41937
specific heat, conform. effects 80−24607
spherical polymer, long time tail in diffusion 80−88018
spherical polymer molecule in compressible flow, Navier-Stokes eqn. 79−10595
spherically symmetric polymer, time depend. compressible flow, Faxen theorems 79−23345
spherically symmetric polymers, in soln., Faxen theorems 78−94342
spherically symmetric polymers, in soln., hydrodynamic interaction 78−94343
spirobenzopyran copolymer photochromic soln., photoviscosity effect 80−6536
squeeze-films, elastico-viscous, superimposed rotation 77−3850
squeezing flow between parallel plates 78−83434
stabilisation of foams *(French)* 80−21323
static bulk props., reptation Monte Carlo method, LJ pot. 80−64868
statistical theoretical methods 78−18535
statistical thermodynamics 78−18528
steady two-dimens. flow in rectangular hyperbolae contraction 78−63453
stiff polymer chain dynamics, local and global mode interaction, dil. soln. viscosity, dielectric relax. 78−37776
stiff polymer dilute solutions, non-Newtonian viscosity 77−35103
Stokes problem for a suspension of spheres at finite concentrations 78−55967
stress deformation, integral rheological relations 77−11159
stress effects 77−32867
structural characterisation, small-angle neutron, X-ray and light scattering, recent developments 79−10751
styrene isoprene multiblock copolymers, microstruct. and dil. soln. props. 78−42885
styrene-acrylonitrile copolymer, of azeotropic composition, Mark-Kuhn-Houwink relations *(Russian)* 79−50176
styrene-acrylonitrile copolymer in dimethyl formamide, methyl ethyl ketone and benzene, diffusion coeff., solvent effect 80−19971
styrene-butadiene block copolymers, in 1-chlorohexadecane, rheological props., viscoelasticity 79−23288
styrene-butadiene block copolymers, in dil. soln., extrapolation methods for intrinsic viscosity 80−24636
styrene-butadiene copolymer, soln., rheological behaviour of flow patterns around agitators 77−31269
styrene-butadiene-styrene copolymer, struct. investigation by diffusion anal. 78−42884
styrene-isoprene block copolymers, dilute soln., conform. obs. 79−10774
styrene-isoprene block copolymers, mol. wt. from frictional props. 78−90329
styrene-p-chlorostyrene triblock copolymer, dil. soln., conform. behaviour, comp. depend. 78−42886
styrene-p-chlorostyrene triblock copolymers in dil. soln., conform. behaviour, temp. depend. 79−90519
styrene-phenylacetylene copolymer, fluoresc. emission, energy redistrib. 78−39580
styrene-vinylpyrrolidone block copolymer soln., conform. props., light-, X-ray scatt. and viscometry obs. *(Russian)* 78−37779
submerged jets impinging on baffle, flow and mass transfer, polymer additive effects 80−92194
supermolecular struct. of dilute solns. determ. from scattered light spectrum *(Russian)* 79−32880
surface, atomic processes, book contrib. 79−60605
surface region, lattice model, orientation effects 79−1540
surface tension, theoretical estimation 80−44394
suspensions of spheres in viscoelastic media, alignment and aggregation effects, photographic obs. 77−80129
swollen, diffusion-relax. cojpling, two-stage sorption correl. 79−94864
swollen rubber network, stress-optical coeff. and amorphous order 77−77169
synthetic, solns., assoc., quantitative evaluation, review 79−10773
Taylor-Gortler vortices, elongational viscosity effects 78−22379
terephthalic acid polyester in solution, ^{13}C spin relaxation study 79−87327
polymer solutions continued
ternary, dilute, mutual selective exclusion at unlike mols., light scatt. investig. 77−4922
2,4,6,8-tetraphenylnonane soln., macromol. dynamics, us relax. 80−19882
thermodynamic properties, under high press., light scatt. obs. *(German)* 78−20049
thermodynamics, Flory-Huggins lattice theory appls. 77−40574
thermodynamics, review *(German)* 78−18530
thermodynamics, scaling theories 79−10775
time constants from shear viscosity data 79−37275
time dependent nonlinear stresses, constitutive eqn. 77−35178
time dependent nonlinear stresses, memory function nonlinearity 77−35180
time dependent nonlinear stresses, shear and uniaxial elongation 77−35179
toluene in polymers, drag reduction 79−32591
Toms effect, polymer struct. effect 79−81929
translational friction coeff. conc. depend., multiple scatt. formulation 77−20102
transport coeffs. and scaling laws in dil. regime *(French)* 79−82372
transport properties, conc. effects 80−64875
tricritical effects, small angle neutron scatt. studies 79−41939
tube flow, drag reducing additives and sudden enlargement of diam. 79−37397
turbidimetric titration, determ. using SPEKOL spectrocolorimeter 79−79301
turbulence, book contrib. 77−58775
turbulence, grid-generated, polymer additives effect 77−68638
turbulence near walls *(German)* 77−15109
turbulence structure, drag reduction 78−22381
turbulent, mass transfer rate, frictional force *(French)* 79−37357
turbulent boundary layer, drag reduction 78−22414
turbulent boundary layer flow, drag reducing additives, 2-D channels and circular pipes 78−26167
turbulent boundary layer in pipe flow of viscoelastic fluids 78−67256
turbulent boundary layers 78−18317
turbulent cloud spreading, polymer additive effects 78−22383
turbulent drag reduction, polymer additive mech. mixing 77−68637
turbulent drag reduction in pipe flow due to nonuniform polymer conc. 79−27672
turbulent flow, drag reduction 78−26159
turbulent flow investig. using laser Doppler velocimeter 77−58822
turbulent flow over plate, drag reduction 78−5768
turbulent flow through smooth and rough tubes, viscoelastic flow models *(German)* 77−11224
turbulent flow with polymeric additives, convective heat transfer 79−77098
turbulent fluctuations in viscous wall region 78−26160
turbulent friction reduction, rheological model 79−86408
turbulent friction resistance, logarithmic equations 77−51042
turbulent heat transfer in dilute surfactant or polymer solutions 79−77101
turbulent jet behaviour 78−1732
turbulent mass transfer to pipe flow 78−1695
turbulent shear flow without solid boundaries, effect of polymeric additives 79−77084
turbulent wall flow model 78−18316
unsaturated polyester resins, gelation, viscosity meas. *(Polish)* 80−59690
unstable flow, reservoir to capillary, jet instability onset and flow patterns, obs. 78−87364
urethane elastomer, thermoplastic, dilute soln., viscosity and sedimentation 80−103512
US absorpt., internal viscosity-normal mode description 79−10899
US atomisation efficiency and particle size distrib. rel. to supply volume rate 79−68468
US waves absorption in vinyl-series polymer solutions 80−15192
vapour bubble growth from gas nuclei, viscoelasticity effect 77−89172
vinyl alcohol-vinyl acetate copolymers, mol. architecture and physicochem. props. 80−44103
vinyl copolymers containing biphenyl units in backbone, thermal props. and soln. viscosity, synthesis *(Japanese)* 77−90316
vinyl polymer solutions, proton spin-lattice relax. and Overhauser enhancements 77−55721
vinylpyrrolidone-tert-butylphenyl methacrylate copolymers, prep., soln. props. 79−18854
virial coefficients and osmotic press. 79−90751
viscoelastic, in annular die entry, upstream flow characts., instability onset 79−60036
viscoelastic, tubular entry flow, vortex characts. in stable flow 79−32428
viscoelastic laminar flow round spherical obstacle, finite boundaries effect 77−15076
viscoelastic liquid, boundary layer anal. of oscillating cylinder flows 77−65771
viscoelastic liquid, radial flow, expt. 77−15072
viscoelastic polymers, surface wave calcs. 79−32593
viscoelastic properties, appl. to meas., at small constant shear stresses 79−54123
viscoelastic properties, direct meas. method using channel flow 79−37265
viscoelasticity, rheological props., prep., transport and processing effects, tensile and shear flow *(German)* 78−13982
viscoelasticity and glass transition, of conc. soln., Adam-Gibbs theory 78−83353
viscometric flow in capillary *(French)* 79−64711
viscoplastic liquid film on vertical vibr. wall, with slip, shaking loose 78−59371
viscosities of dilute polymer solutions in nematic liquids 80−29199
viscosity, determ. by extrapolation method *(German)* 79−99347
viscosity, eqn. for dilute to moderate concs. 79−69276
viscosity, generalized conc. depend. 77−62229
viscosity, intrinsic, friction coeff., porous sphere model 78−71301
viscosity, intrinsic 78−2281
viscosity, method for meas. of conc. solns. at high temps. 80−19535
viscosity data as function of mol. wt. 78−18266
viscosity data as function of mol. wt. 79−37866
viscosity data represented as function of mol. wt. 78−26716
viscosity measurement method at high press. 80−69955
viscosity of suspension of nonharmonic dumbell mols. 78−2282
viscosity rel. to mol. mass *(Russian)* 80−2190

polymer solutions continued
viscosity v. molecular weight, linear plot 78−67844
viscous drag of two-dimensional contours moving in a weak polymer solution 80−100014
viscous drag reduction by polymer injection at high Reynolds number *(Chinese)* 79−32582
viscous polyurethane, optical fibre cable filling, telephone trunk system appl. 79−72708
vortex inhibition, velocity profile meas. 77−19628
vortex pairs, neutral surroundings, turbulent mixing on motion 78−26127
vulcanisation process, field theory statistics 78−91220
wake behind cylindrical body, laminar flow 79−37355
water, turbulent flow, effect of polymeric additives 79−1216
water flow through orifice, polymer additives effect on cavitation and noise 79−98768
water jet, turbulence fine struct., polymer addition effects, high speed photography 78−26178
water-polystyrene spheres (highly charged), solid- and liq.-like phases, soft core liq. theory 77−63963
weak polymer solution in smooth pipes, turbulent wall motions 80−14823
weak polymer solutions, flow props. in narrow channel between rotating and stationary discs *(Russian)* 80−59089
weak polymer solutions, wall region turbulence models *(Russian)* 79−14440
weakly correlated, radial distrib. function 80−84050
xanthan gum, rheology 79−37272
xanthane, dilute solns., viscosity rel. to temp., shear rate *(French)* 80−39332
zero-component field theories, high order behaviour without $n \to 0$ limit 79−75438
zero-shear rate viscosity meas. 79−90293
zero-shear viscosity estimates from falling sphere data 80−19306
Al soap solutions, viscous behaviour 80−2185
^{13}C nuclear Overhauser enhancement, reduced value rel. to ^{1}H spin-lattice relax. 77−46581
polystyrene in CS_2, dil. solns., neutron quasielast. scatt. study 79−41935

polymerisation
A-copolymerisation, on basis of oligodienedihydrazides and diepoxides, cross-linked polymer charact. *(Russian)* 80−58431
acetylene, adsorption on Ni (111), identification of CH species by electron energy loss spectra 79−15022
acetylene, polymerisation, variable density polyacetylene prop., elec. props. 80−60016
acetylene adsorbed on Fe containing segregated C, hydrogenation, C-1s XPS spectra obs. 80−84366
acetylene derivatives, elec. cond. of cis- and trans- stereo isomers *(German)* 78−84221
acetylene polymerisation in RF discharge, discharge power effect 79−43581
acrylamide, laser-initiated polymerisation kinetics, holographic obs. 79−29383
acrylamide photopolymerisation, Fe^{3+} sensitised, holographic recording appl. 77−54677
acrylonitrile, radiation initiated graft polymerisation on polyethylene films, fibres, PVC fibres *(Russian)* 80−7531
acrylonitrile-vinylidene chloride copolymerisation, sequence distrib. determ. by ^{13}C-NMR 79−79247
adaptive control of molecular weight distribution 80−58434
aliphatic diallyl esters, radical polymerisation, rel. between vol. contraction and chem. changes *(German)* 78−61009
alkali metal polyphosphates, vitreous, mol. weight distrib. determ. by gel-chromatography 79−50173
alkali metal polyphosphates, vitreous IR spectra 80−16043
alkenyl polysulphide, oligomeric, synthesis and characterisation by NMR 79−79248
allyl methacrylates, anionic polymerisation and radical reactivity *(Japanese)* 78−61007
azetropic copolymerizations computer calc. *(Rumanian)* 78−23945
1-(2-N-aziridinoethyl)-4-vinylbenzene 79−39146
benzene, plasma polymerisation in glow discharge, thin film IR and free radical EPR obs. 80−2964
benzoin containing system, photosensitized free radical polymerisation 80−7825
benzophenone, sensitised crosslinking, polymerisation, UV curing, IR investig. 78−35709
benzophenone containing system, photosensitized free radical polymerisation 80−7825
biimidazole+leuco dye photochem. reaction, modulation by photopolymerisation 80−40714
biological polymers, form. from monomers rel. to origin of life 78−69461
1,6-bis(2,4-dinitrophenoxy)-2,4-hexadiyne, effect on apparent ferroelec. transition 80−66121
bis(p-toluene sulphonate)diacetylene, fully and partially polymerised, optical props. 77−1696
bis-(p-toluene-sulphonate) of 2,4 hexadiyne 1,6 diol, X-ray scattering obs. of polymerisation mechanism and phase transition *(French)* 80−70399
bis-acrylamide anilinefluorene polymerisation in thermostable card polyamide (polyimide) amorphous matrix *(Russian)* 79−57231
bromostyrene-crosslinked polyester, craze resistance 80−35421
butadiene, and synthetic rubber manuf., review 77−55938
butadiene, effect of redox initiation in emulsion polymerisation *(German)* 78−85158
butyl acrylate-vinyl acetate, two-stage emulsion polymerisation, forced compatibility *(Russian)* 80−44950
ε-caprolactam, after polymerisation under reduced press. *(Japanese)* 78−95929
carbonaceous surface contamination growth on ion bombard. 77−90229
carbonization, polymeric aspects 80−2972
catalysis by graphite intercalation compounds *(French)* 78−27822
catalysis significance by coordination complexes *(French)* 77−12797
cationic polymerisation promotion by free radicals 79−34301
cellulose, fibres, membranes and composites, polystyrene used for modification of props. 78−95727
chain size, struct., distribution control, review 77−40544
charged particle detection, graft-and-dye method 78−17520
coating of electrodes by polymer films, glow discharge polymerisation 78−76866

polymerisation continued
compartmentalised free radical polymerisation reactions 79−24748
conference, Terrigal, Australia (Nov. 1975) 77−48640
cooperative reaction between simple synethetic macromolecule, rel. to chain length *(Russian)* 77−63911
copolyesters, diol sequencing, NMR spectra 79−52657
copolymerisation, alternate random and block, role of temperature 78−76859
copolymerisation, bi-nuclear regulated, ladder struct. synthesis, bulk props. 77−32553
copolymers, alternating block, prep. by polycondensation, mol.-mass distrib. parameters *(Russian)* 78−73042
crosslinked compositions formation, structural kinetic method *(Russian)* 79−34303
curing, UV, photochem., liq. ink appl. 78−35709
deformation of viscoelastic solids, depth of polymerisation 80−40414
1,6-di-p-methoxybenzene sulphonyloxy-2,4-hexadiyne, thermal polymerization, Raman spectra 80−103952
diacetylene, low temp. photochemical polymenisation, decay kinetics, ESR spectra obs. 80−100616
diacetylene, photopolymerisation, optical absorpt. spectra, time depend., reaction kinetics 80−85174
diacetylene, single cryst., EPR of low-temp. photoproducts, photopolymerisation 78−85175
diacetylene, single cryst., photopolymerisation, intermediate states, struct. changes 80−30235
diacetylene (TSHD), low temp. photopolymerisation, short chain intermediates obs. 80−93754
diacetylene derivatives, solid-state polymerisation, isotope effects 80−66799
diacetylene mixed crystals, co-crystallisation, influence of crystal composition on struct., reactivity in solid state 80−81324
diacetylene monocarboxylic acids, multilayers, struct. phase transitions and polymerisability 80−80129
diacetylene single crystals, photopolymerisation, optical transmission spectroscopic exam. 78−27757
diacetylene-d_2, excited quintet states during photopolymerisation, ESR obs. 80−84635
diacetylenes, photopolymerisation, solid-state reaction, photoacoustic photocalorimetric obs. 80−61089
diacetylenes, solid state photopolymerisation, reaction products, electron spin resonance anal. 80−81338
diacetylenes, urethane substituted, polymer conversions in γ-ray polymerisation 80−26014
diallyl, thermally stable, as laminating resins for PCB material 79−52658
diallyl isophthalate-methyl methacrylate copolymer, light focusing rod prep. by copolymerisation, refractive index distrib. const. *(Japanese)* 79−46042
diallyl phthalate methyl methacrylate, copolymerisation, two-step, prep. of light focusing plastic rods *(Japanese)* 79−37064
diamagnetic solids cyrstallised from melt, mag. fluid effect on props. 79−37815
1,6-dicarbazolyl hexadiyne, solid-state polymerisation, monomer to polymer phase transformations 80−38948
dielectric thin film, polymerisation on carrier foils in discharge plasma *(German)* 77−16508
dielectric thin films deposited by glow discharge, time-dependent props. 77−63564
diepoxide-diamine network polymers, reaction mechanism investigation using gel permeation chromatography 80−40789
N,N-diethylacrylamide, cross-linked copolymer, improved mech. props. 80−61091
difluoroethylenes, plasma polymerisation, ESCA characterisation of polymers 80−21283
L-β-3,4-dihydroxyphenyl-α-alanine with L-glutamic acid, polymers and copolymers, synthesis and conform. 79−33996
3,4-dimethyl-1,2,5-thiadiazol plasma polymerised film for holographic recording 80−106490
diolefins, substituted, topochemically controlled solid-state polymerization 80−35532
4,7-dioxaoctanal, equilib. anionic polymerisation, −90 to −68°C, polar substituent effects 78−88631
DNA hypochromic effect, oscillator strength, perturbation theory calc. 79−96515
dynamic living polymers, thermodynamic enhancement of oligomers, end-group interactions 80−58423
electric phenomena, book 80−46746
electroinitiated, on electrodes, book contrib. 80−50854
electroinitiated, polymer film coating in aq. medium, book contrib. 80−50778
emulsion, kinetics in unsteady state 79−47923
emulsion polymerisation, ideal, first-stage kinetics calcs. *(Russian)* 79−66295
emulsion polymerisation, particle size calc., applicability of Gardon's eqns. 78−92479
emulsion polymerisation of polar monomers, model calc. *(Russian)* 79−34302
emulsion type, homogeneous nucleation 79−29354
endosseous implant material, radiation processed alumina-polyacrylic acid composite 77−60308
epithiopropyl methacrylate polymerisation and copolymerisation *(Japanese)* 78−56892
epoxide compound, polymerisation in non-uniform magnetic field, exam. of structural changes 80−7791
epoxy resin, curing investigation by polarisation current method 80−3345
1,2-epoxypropane, photopolymerisation by arenediazonium salts, obs. 79−24747
esters, long-chain, X- and Y-type multilayers, form. conditions and struct. characterisation 80−80127
ethylene, high pressure polymerisation investig. using near IR spectroscopy *(German)* 77−21384
ethylene, high-press. equipment design 79−24746
ethylene, high-press. polymerisation, autoclave process 79−24744
ethylene, polymerisation kinetics, heterogeneous Ziegler-Natta catalysts, polyethylene struct. and morphology 79−96307
ethylene imine derivates, cationic polymerisation, appl. in dentistry 79−83435
ethylene plasma polymerisation by magnetron discharge 79−33995

polymerisation continued
ethylene polymerisation and dissociation in high-freq. discharge 77−70299
ethylene propylene/polyolefin blends, radiation cross linking 80−66801
ethylene vinylacetate copolymers, prep., props. and appls. 80−35154
ethylene-polyethylene mixtures, phase behaviour under high-press., polymer mean mol. wt. influence 79−24745
feedstock projection for petrochemicals 80−2991
fibre optic sheet form. by selective photopolymerisation, appl. in image guiding equipment 78−42477
fibre optic sheets fabricated by selective photopolymerization 79−55235
fibre reinforced polymer, soaking, wetting and compounding of materials during production *(German)* 80−93535
fibres development, based on condensation (step-growth) process 79−83168
fibrin, modification by synthetic polymers 80−61090
finite polycondensing system, mean chain length distrib., probabilistic theory 79−70324
flexible polymer chain in nematic solvent, phase diagram *(French)* 80−39253
flow-through reactor, low-temp. polymerisation conditions 80−61092
fluorocarbon glow discharges, plasma polymerising and etching, mass spectrometric obs. 77−32790
fluorocarbon monomers, plasma polymerisation 78−35304
fluorocarbon polymer film, prep. by RF sputtering and plasma polymerisation, props. 77−55890
formaldehyde, polymer formation in interstellar space 77−78858
free radical copolymerisation, reactivity ratios, press. directional effect 79−100362
free radical copolymerisation kinetics, monomer reactivity ratios under high press. conditions, meas. methods 79−91950
Fresnel lens film prep. by electron beam irradiated mould polymerisation 79−98515
gelation process, field theory statistics 78−91220
glass fibre reinforced plastic cylindrical shells, temp. stresses developing during polymerisation 80−40326
glow discharge, polymer surfaces, appl. of ESCA to struct. and bonding 79−57344
glow discharge polymerisation double probe meas. and contamination effects 77−70300
glycerides, high mol. wt. species prod. after contact with lunar grains 78−3333
GMA-Quetol 523, ultraviolet polymerisation in embedding procedure for semithin sections prod. 78−92767
graft copolymerization by macrozwitterion mechanism 80−21285
graphite fibre electrodes, coating by electropolymerisation, adhesion to epoxy matrix 79−15644
heterodisperse polymers ease of fabrication, dependence on mol. wt. distribution 80−35530
2,4-hexadiine-1,6-diol-bis(p-toluene sulphonate), cryst., polymerisation, elastic consts., Brillouin scatt. 79−1950
2,4-hexadiyne-1,6-diol bis-(p-toluene sulphonate), dielec. const. during solid state polymerisation 79−51899
2,4-hexadiynyl-1,6-bis(p-toluenesulphonate), programmed temp. and DSC obs., cryst. forms and polymerisation kinetics 79−43583
hexamethyldisiloxane plasma polymerised thin film, charge trapping characts. 80−96895
hydrocarbons, in residual gas, polymerisation by electron bombard. *(German)* 77−40315
hydrocarbons, plasma polymerisation 78−88634
hydrogel pilocarpine release rate control by plasma polymerisation 77−60284
N-hydroxyethyl acrylamide-styrene(methyl methacrylate) copolymers, synthesis, anion active membrane transport appl. 80−61142
impact resistant styrene copolymers, control of morphology and props. *(Bulgarian)* 80−35153
inorganic polymers, viscoelastic materials, physical props. *(Japanese)* 77−72569
interstellar molecules and prebiological evolution, tunnelling mechanism 79−92842
ion exchange membranes, production by electron irrad., cross linking, graft polymerisation *(Japanese)* 77−81403
IR thin film plasma deposition processes 80−87466
isoprene-styrene copolymer latexes, film-forming properties 78−53266
isopropyl vinyl ether, chem. initiated soln. polymerisation and radiation-initiated bulk polymerisation 79−91952
kinetic relationship in free radical polymerization 79−70323
kinetics analogue simulation 77−36754
laser initiated polymerisation kinetics, mol. wt. distrib. of resultant polymer 78−15673
light scattering, macromol. characts. in Rayleigh-Gans-Debye region 77−42452
linear macromolecules, cryst. growth 78−30561
liquid vinyl monomers, ionic polymerisation and related props. at high dose rates 77−77758
lithium polyisoprene, struct. regularity and crystn. 80−103269
macromolecules, conf., Dublin, Eire (July 1977) 79−55012
medical polymers, chem. problems, conf., Prague, Czechoslovakia (Aug. 1977) 80−56996
metal-containing plasma polymerised fluorocarbon films, deposition, struct., and polymerisation mechanism 79−78928
metal-polymer films, electron-beam polymerisation, cond. control 78−48331
metals, passivation, using in situ polymerisation by microwave plasma discharge 78−64762
methacrylamide, by H transfer, catalyst sodium-naphthalene *(Japanese)* 78−95726
methacrylic acid-methyl methacrylate statistical copolymer suspension polymerisation, stabilisation effects, viscosity 78−85157
methacrylic acid-N,N'-ethylenedimethacrylamide crosslinked copolymer soln., 3-dimens. struct. peculiarities *(Russian)* 79−55678
methacrylic esters with vinyl benzoates, for light focusing plastic rod 77−11000
methyl methacrylate, free radical polymerisation, viscosity effects 77−81404
methyl methacrylate, polymerisation in toluene in presence of s-PMMA 78−76321
methyl methacrylate, stereospecific replica polymerisation 79−11793
methyl methacrylate+diallyl phthalate, two-step copolymerisation, light focusing plastic rod prep. *(Japanese)* 79−37064
methyl methacrylate-styrene copolymers, ^{13}C NMR 80−20473
polymerisation continued
methylmethacrylate soln., aqueous, polymerisation under pulse electronic accelerator irradiation 80−66802
α-methylstyrene, photoinduced ionic polymerisation 80−7828
α-methylvinyl alkyl ethers, polymerisation mechanism, ^{1}H-, ^{13}C-NMR 80−48112
molecular tunnelling in chemical reactions *(Russian)* 77−52615
monolithic glass, formation by chem. polymerisation 79−78926
monomer gas photopolymerisation, polymer film form. on semicond. 78−10561
Mossbauer spectroscopy 77−12798
multicomponent, differential and integral rate eqn. 78−23944
network formation, pre-gel intramol. reaction and gelation, shear moduli and glass transition 80−45501
network formation, relaxational props. variation 80−38961
network polymers, heterogeneous, from partially hydrolysed poly(methyl D-glutamate) and poly(oxyethylene glycol) *(Japanese)* 78−95002
β-nitrostyrene free anionic polymerisation during electron radiolysis, primary reactions 78−44378
nonequilibrium plasma chemical reaction kinetics 78−76863
nonisothermal, in spherical reactor, temp. distrib., and reaction kinetics 79−87844
octadecylacrylamide films, oriented ultrathin, radiation-induced solid state polymerisation 80−80128
n-octanal, equilib. anionic polymerisation, −90 to −68°C, polar substituent effects 78−88631
oligomeric liquid mixtures, transition to, polymer systems, thermodynamics 78−20048
optical reticle and scale fabrication, cyclohexadiene-1,3 pleinomer photoresist 79−27452
organic optical thin films, plasma polymerisation, light propag. expt. *(Japanese)* 78−6846
organic reactions in solid state 80−21309
organic solids, electron microscopic approach to struct. and reactivities 79−73077
organo tin polymers, glow discharge formed, interface composition and adhesion 79−82467
organo-tin polymer films, glow discharge prep., comp. determ. by XPS and AES 80−35109
perfluorocarbons, plasma polymerisation 78−88634
m-phenylene diacrylic acid, four-centre-type photopolymerisation in cryst. state, holographic appl. 78−37832
photoimaging system based on photopolymerisation in cryst. coatings 80−40716
photoinitiated cationic polymerization by photosensitization of onium salts 80−7822
photopolymer systems, conf., Washington, USA (Nov. 1978) 80−4799
photopolymerisation, 0_2 inhibition elimination 80−7821
photopolymerisation, dye-sensitized, activation by trialkylbenzylstannanes 80−7824
photoresistive film based on polymer-bisazide systems, photosensitivity *(Russian)* 77−48641
piperylene-acrylonitrile copolymers, polymerisation, monomer composition rel. to copolymer struct. *(Russian)* 80−5651
pivalolactone-α-methyl-α-propyl-β-propiolactone copolymers, struct., thermal and mech. props. 79−43582
plasma applic. 77−70198
plasma polymerisation, pulsed RF discharge 77−56227
plasma polymerisation by glow discharge method, formation mech. *(Japanese)* 80−61094
plasma polymerisation coating on glass shell, for laser fusion targets 78−60859
plasma polymerisation on solid substrates, thin film form in RF discharge 80−2963
plasma-initiated biradical polymerisation 80−3343
plastic scintillators, polymerisation of blocks with large dimensions 77−65400
plastic track detectors, processing 77−38560
PMMA, laser initiated polymerisation kinetics, mol. wt. distrib. of resultant polymer 78−15673
PMMA coated frit powder prep. corona-charging props. *(Japanese)* 80−25891
PMMA-metal oxide composite powder, prep. and props. *(Japanese)* 78−95708
PMMA-PVC mixtures, dielec. relax. and struct. rel. to formation *(Russian)* 77−20073
poly(m-xylylene adipamide), molten, gel form. kinetics *(Japanese)* 80−108757
poly(vinyl alcohol) porous film, polymerisation and porosity 80−107063
poly(vinyl alcohol)-based membranes for haemodialysis *(Japanese)* 78−96115
poly (N,N-dipropylacrylamide), 'feathered' polymer resin, prep. from suspension 80−35533
poly [2-(p-azidobenzoyloxy)ethyl methacrylate], MW distrib. effects on photosensitivity *(Japanese)* 78−94418
poly [nitrilo-bis(phenylamino)phosphoranetriyl]s, synthesis and characterisation *(Italian)* 77−66755
poly-1,6-di-N-carbazolyl-2,4-hexadiyne, synthesis, thermal expansion, photocond., optical transition 78−76858
poly-1,6-di-p-toluenesulphonyloxy-2,4-hexadiyne, thermal polymerisation, Raman spectra 80−35531
poly-β-substituted vinyl ethers, cationic polymeris., stereochem. 80−21284
poly-bis-phenyl glutarate diacetylene, cryst., solid-state synthesis, struct. 79−15638
poly-m-toluenylsilsesquioxane mesomorphic struct., form. during polymerisation *(Russian)* 80−61095
poly-N-vinyl carbazole, containing carbazylium cation radicals, synthesis and semicond. props. 77−85224
poly-N-vinylcarbazole, synthesis and photocond. props. 77−55563
poly-N-vinylcarbazole films, drift mobility of photocarriers, polymerisation method influence 77−76986
poly-thio-1-N,N-diethylaminomethylethylene, optically active samples, ^{13}C NMR spectra 80−28127
polyacetylene, polymerisation and Raman spectra on zeolite and alumina surfaces 79−13721
polyacetylene film synthesis, review 80−15623
trans-polyacetylene obtained by polymerisation on TiO_2, Raman spectrum *(Spanish)* 80−88988
polyacrylamide, high mol. wt., prep. by electron beam irrad. 80−76222

polymerisation continued
polyacrylamide, mech. degradation, polymerisation effect *(Japanese)* 78−11194
polyacrylonitrile, copolymerisation with poly-2-hydroxyethyl methacrylate rel. to crystallinity 80−38935
polyacrylonitrile, single cryst. formation, during soln. polymerisation, struct. determ. 80−38938
polyaromatics, synthesis, correl. with elec. cond. *(German)* 80−15514
polyarylbutadiene, microstructure, NMR and IR obs. *(Japanese)* 79−24488
1,2-polybutadiene, dynamic viscoelastic props. in curing process 80−76298
polybutadiene, low mol. wt., NMR study of terminal group struct. *(Russian)* 77−63912
polybutadiene-polystyrene block copolymer, anionic prep., random coupling struct. 79−64134
polycaprolactam, after polycondensation, falling film evaporator system *(Japanese)* 79−70325
polycaprolactam characteristics dependence, at equilibrium state, on polymerisation conditions, in closed system *(Japanese)* 78−95928
polychlorotrifluoroethylene, crystalline and amorphous peaks, dielectric props. 80−93237
polycondensation, equilib. and nonequilib. *(Russian)* 79−57230
polydiacetylene, extended-chain crysts., struct. and morphology 79−82165
polydiacetylene, single cryst., polymerisation under hydrostatic press. 79−20367
polydimethylsiloxane film, formed by RF discharge plasma polymerisation, optical props. 78−80479
polydimethylsiloxanes, equilibrated, living oligomer distrib., end-group interactions 80−58423
polydiphenylgermylene, crystn. from chem. transport reaction 80−104439
polyester resin, unsaturated, glass fibre reinforced, polymerisation by UV irrad. *(German)* 79−100367
polyesterification reactions, uncatalysed, kinetics, comments on Flory's work 79−96309
polyesters, continuous production plants, technical details, polycondensation reaction stage analysis 79−100361
polyether-urethane elastomers, crosslinked, three dimensional polymerisation, kinetics, gel. form., mech. props. *(Russian)* 80−7792
polyethylene, γ-ray polymerised, dielectric loss reduction 77−24783
polyethylene, nascent, electron microscope study 80−38940
polyethylene, obtained from heterogeneous Ziegler-Natta catalysts, cryst. morphology and growth 80−38941
polyethylene, polyethylene-D_4, migration and copolymerisation at high press. with shearing stress 78−51678
polyethylene, polymerisation kinetics math. model, mol. wt. evaluation *(Russian)* 79−52661
polyethylene, supermolecular structure, polymerisation at low pressure *(Russian)* 79−64126
polyethylene catalyst, $TiCl_4$-$MgCl_2$, struct. and mechanism 80−11951
polyethylene films modified by polyacrylonitrile grafting before, after orientating elongation, struct. *(Russian)* 77−32554
polyhexamethyldisiloxane thin film form. in glow-discharge flow system 78−68631
polyisobutylene, SiO_2 grafted, synthesis and characterization 80−97456
polymer, porous, prep., appl. as stationary phase in gas chromatography *(German)* 79−29434
polymer film coatings on metal electrodes, through electroinitiated polymerisation 77−77632
polymer science, conf., Pittsburgh, USA, (June, 1975) 77−38756
polymer thin film growth by glow discharge polymerisation, temp. depend. 78−68632
polymer thin films formed in RF discharge using monomer organic semicond., elec. props. obs. 80−80432
polymer-cement composites, polymerization of impregnated liquid monomer 79−70039
polymethacrylic acid, stereoregular, synthesis, ^{13}C NMR obs. 80−58422
polynaphthalene films, plasma polymerised, photovoltaic and photocond. props. 80−34479
polyorganosiloxane, thermogravimetric assessment of stability at high temps. 77−52704
polyoxymethylenes, determ. of crystalline fraction from X-ray diffraction 80−44150
polypentenamer, thermodynamics *(Russian)* 77−21386
polyphenylene sulphide, high mol. wt. soluble resin, prep., mech. props. 80−60828
polyphenylene terephthalamide, fibril form. from nascent spherulite formed during polymerisation in hexamethylphosphoric triamide *(Japanese)* 78−56893
polyphenylquinoxaline, synthesised in different media, mass-mol. distrib. *(Russian)* 79−61862
polypropylene coating, glow-discharge-polymerised, adhesion and hydrophilicity 79−15829
polypyrrole films, electrochemical prep., chem. and phys. characterisation 80−70708
polyquinazolones with N-phthalimide groups in side chain, prep., props. *(Japanese)* 79−15642
polysiloxane plasma polymerised film growth on GaAs substrate, dry etching process 80−25575
polystyrene, crazing, fracture, polymerisation route and internal lubricant effects 77−12683
polystyrene, graft polymerisation on alkali halide crystals *(German)* 79−100365
polystyrene, mechanical degradation, limiting degree of polymerisation 77−85985
polystyrene, rubber-modified, rubber particle morphology influence 79−94925
polystyrene-b-isoprene-b-styrene, struct. regularity and crystn. 80−103269
polystyrene-polybutadiene systems, phase separation obs. 79−94926
polytrivinyl benzene, thermal and mech. props. rel. to high-press. polymerisation conditions 79−70326
polyurethane, stress relax. meas., effect of cure temp. on network struct. 77−84674
polyvinyl cyclohexane, head-to-head, prep., characterisation 79−70036
polyvinylidene fluoride, heat to head chain imperfections, synthesis 77−52148
powder catalyst, catalytic and sorption processes, calorimetric and adsorpt. kinetic methods 79−43629
polymerisation continued
propergol, rheological props. during polymerisation *(French)* 78−23762
protective coating plasma polymerisation in vacuum chamber 79−70183
protein supramolecular structures, calorimetric and van't Hoff enthalpies of assembly comparison 77−90717
PTFE latex, emulsion polymerisation, radiation-induced *(Japanese)* 78−80747
PVC, long-chain branched with narrow mol. wt. distrib., precipitation polymerisation 77−90315
PVC, rigid, tensile fracture morphology, rel. to mol. props. 77−59883
PVC granule morphology during polymerisation, kinetic parameters influence *(German)* 80−85176
PVC particles, Raman spectra, conform. during polymerisation 79−33709
PVC plastisol films, thermally hardened, struct. and props. *(German)* 79−70097
radiation, control by dose rate regulation, expt. study 77−32787
radiation chemistry in liq. phase using ^{85}Kr source 77−60091
radiation processing, conf., Miami, FL, USA (Oct. 1978) 80−36772
radiation-induced, solid state, computer modelling 79−66294
radical, const. elec. field effects *(German)* 78−61008
radical, relation between vol. contraction and chem. changes *(German)* 78−61009
radioactive waste, medium-level and low-level, incorporation in polymer impregnated cement 77−61564
reactivity and gelation, intrinsic reactivity 79−100363
reactivity and gelation, substitution effect 79−100364
semiconductive conjugated polymers, synthesis and elec. props., review 80−15513
sickle cell anaemia sickling kinetics, multiangle laser scatt. spectrophotometer 79−79494
silicate triplex glass, produced by polymerisation, effect of monomer purity 79−24485
silicone elastomers, dental impression materials, dimens. stability, holographic and interferometric study 80−67204
silicone membrane progesterone release rate control by plasma polymerisation 77−60285
silicone rubber biomaterial, filler free, radiation chemical and physical evaluation 79−39608
silicone rubber with radiation-grafted methacrylate, for burn wound dressing 79−29657
sodium 10-undecanoate, γ-ray induced polymerisation in aq. micelle solns. 80−61093
sodium undecanoate/water system, lyotropic liq. cryst. struct. change due to polymerisation of amphiphilic component 80−59386
solid state mechanism 79−74381
solid-state, in macromol. epitaxial crystallisation, review 79−42409
solid-state reaction kinetics for single-phase polymerisation 78−61006
solidification front propagation, residual stress levels, polymerisation 80−59635
stomatologic polymeriser for dental prostheses 79−57812
styrene, bulk, thermally initiated, batchwise, optimal temperature policies determ. 79−87845
styrene, cationic polymerisation by $SnCl_4$ in presence of C black 78−68891
styrene, effect of redox initiation in emulsion polymerisation *(German)* 78−85158
styrene, photoinitiation by aliphatic azo cpds., EPR obs. 78−80746
styrene, plasma polymerisation, polymer struct., NMR 77−25264
styrene, plasma polymerisation in glow discharge, thin film IR and free radical EPR obs. 80−2964
styrene, thermal polymerization, PMR obs. 80−3342
styrene, thermal polymerization, Rayleigh-Brillouin light scatt. study 78−53206
styrene(-butadiene), polymer reactions, below glass transition, limting conversions 78−88632
styrene divinylbenzene, viscosity meas. during radical copolymerisation 80−3344
styrene polymerisation in RF discharge, discharge power effect 79−43581
styrene solutions, polymerisation initiation by intense pulsed electron beam 79−15997
styrene thermal polymerisation, kinetics, Rayleigh scatt. 79−57228
styrene-α-methylstyrene copolymers, prep., charact. by pyrolysis gas chromatography *(German)* 79−29355
styrene-acrylonitrile, plastomer and elastomer, styrene copolymer synthesis, props. rel. to composition *(German)* 79−66291
styrene-acrylonitrile copolymer, synthesis and props. for optical use 78−90466
styrene-butadiene block polymers, multiphase systems, struct., props. 77−31600
styrene-H_2O suspensions, particle size, surface tension, stabilizer conc. effects meas. *(German)* 79−24834
styrene-maleic anhydride copolymerisation, alternate random and block, role of temperature 78−76859
substrate, plasma polymerisation, mech., effect of substrate and substrate topography 78−88633
sulphosalt minerals, exam. of crystal chemistry and morphology 79−10838
surface properties of materials, Conf., Missouri, USA (August 1977) 78−87867
suspension polymerisation, particle size distrib. of obtained particles, eval. using Coulter Counter data 80−76564
synthetic polymer chemistry, developments 80−63875
TEM, appl. to organic solid-sate chemistry, review 79−60235
terephthalate liquid crystals, vibr. spectra, vol. struct. 78−18547
tetrahydrofuran-propylene oxide copolymers, prep., ^{13}C NMR, end group anal. 79−66293
tetraoxane, NMR obs. of mol. motion, rel. to polymerisation temp. effects on polytetraoxane texture 77−84663
textile industry, agitating type polymerizer, synthetic resins and fibres manufacturing process 80−3341
thermosetting materials, formation and props., phase diagram and torsion pendulum anal. 80−55381
toluene polymerisation in CC N_2 afterglow, chem. reactions rel. to plasma props 80−3346
bis p-toluene sulphonate diacetylene, low-temp. spectral line splitting 77−32397
toluene-sulphonate-diacetylene, thermal polymerisation, near IR absorpt. and low lying states obs. 80−71399

polymerisation continued
trifluoroethyl methacrylate vinyl chlorobenzoate copolymer light focusing rod, photocopolymerisation temp. effect *(Japanese)* 79−46043
trioxane, epitaxial crystn. of polyoxymethylene during 79−55676
trioxane, in nitrobenzene soln., polymerisation, polyoxymethylene morphology 80−59403
trioxane, NMR proton relax., mol. rot., rel. to polymerisation 79−73843
trithiane, NMR proton relax., mol. rot., rel. to polymerisation 79−73843
1,3,5-trivinyl benzene polymerisation, thermal and mech. props. rel. to high-press. polymerisation conditions 79−70326
two-phase polymer reactions, below glass transition, limiting conversions 78−88632
two-phase unpolymerised system, particle size, surface tension, stabilizer conc. effects meas. *(German)* 79−24834
unterminated reactions, kinetics of intermediates 79−91949
UPS polymerization technique, production of special polymers *(German)* 80−93533
vaccine production, use of ^{60}Co-γ-irradiation, polymerisation conditions 78−40320
vinyl acetate, partial polymerisation, ^{1}H-, ^{13}C-spin lattice relax. time meas. *(German)* 79−28633
n-vinyl carbazole, radiation induced polymerization ESH study 80−7817
n-vinyl carbazole-acrylamide, post radiation induced polymerisation 80−7818
n-vinyl carbazole-acrylamide, radiation induced polymerization, monomer crystallinity effects 80−7819
vinyl chloride, charge on nascent PVC particles in monomer 79−79249
vinyl chloride, electrophoresis of PVC dispersed in monomer 79−79250
vinyl chloride, two phase model *(German)* 79−15996
vinyl chloride, US monitoring of local phase transitions 80−33299
vinyl chloride in suspension, origin of charge on nascent PVC particles in monomer 79−79251
vinyl chloride suspension polymerisation monitoring by US attenuation and velocity 79−70328
vinyl methacrylates, anionic polymerisation and radical reactivity *(Japanese)* 78−61007
vinyl monomers, radical polymerisation, const. elec. field effects *(German)* 78−61008
vinylacetate-H_2O suspensions, particle size, surface tension, stabilizer conc. effects meas. *(German)* 79−24834
N-vinylcarbazole, polymerisation, polymer struct., props., elec. characts., review 79−41972
N-vinylcarbazole, polymerisation in presence of C black 79−20366
vinylidene chloride, radn. induced emulsion polymerisation 79−74383
vinylidenechloride-vinylchloride latex copolymers grafted on to elastomers, film struct. and props. *(Russian)* 77−21090
vinylpyrrolidone-tert-butylphenyl methacrylate copolymers, prep., soln. props. 79−18854
vinyltrimethoxy silane, plasma polymerised, abrasion resist. antirefl. coating for polycarbonate 77−42635
vulcanisation process, crit. behaviour 78−11518
vulcanisation process, field theory statistics 78−91220
waste waters of paper manufacture, radiative purification, polymer prod. *(Russian)* 78−61035
xylene, plasma polymerisation deposition and ESR of trapped free radicals 79−83455
p-xylene, plasma polymerised, as laser fusion target 78−88431
p-xylene, plasma polymerised films on glass, as laser fusion targets, deposition method 78−60860
xylene plasma-polymerised film, ESR 79−99750
As-S, amorphous, glass transition and specific heat, intermolecular bond saturation 80−15011
As_xS_{100-x} amorphous film, composition depend. of photo-induced refr. index changes 79−78644
$As_2S_3(Se_3)$ films, vitreous, photodecomp. and photostruct. changes 77−76318
C black-graft polymers crosslinked with epoxy resin, electrical props. *(Japanese)* 80−24920
CO_2, negative Van der Waals polymer mols., formed by nozzle expansion 78−90307
C_3O_2 polymer, preparation, spectra rel. to polymerisation temp. electron spin resonance 77−32239
CaO-SiO_2 melt, viscosity and polymerisation *(Russian)* 78−26712
1,6-di-(N-carbazolyl)-2,4 hexadiin, cryst. struct., luminesc., γ-ray polymerisation 78−18629
FeO-SiO_2 melt, viscosity and polymerisation *(Russian)* 78−26712
H_2O, Van der Waals polymer mols., negative ions formed in nozzle expansion 78−90296
^{181}Hf, decay, perturbed γγ directional correlations, complex chem. 77−36774
K_2O-Al_2O_3-P_2O_5-TiO_2, structural role of Ti, kinetic study of chem. destruction 80−88055
LiH_2PO_4, formation of low- and high-temp. forms of $(LiPO_3)_x.H_2O$ 79−19179
MnO-SiO_2 melt, viscosity and polymerisation *(Russian)* 78−26712
N_2O, negative Van der Waals polymer mols., formed by nozzle expansion 78−90307
Na_2O-SiO_2 melts, cryoscopic struct. study 80−14994
Ni complexes, solid-state polymerisation 79−74380
P-S, amorphous, glass transition and specific heat, intermolecular bond saturation 80−15011
S, liq., temp. depend. of absorption edge at polymerisation temp. 77−66515
S, liquid, conductivity meas. from melting point to 900°C 78−84209
S, liquid, polymerisation transition, anomalous light scatt. obs. 77−19861
S, single liq. droplet, optical transmission and elec. resist. changes on polymerisation 77−35460
S_2 polymerisation, kinetics obs. by pulsed field ionis. time-of-flight mass spectrometer 77−63890
S_8-1,2,-propylene sulphide, copolymer preparation method, anionic copolymerisation 78−64836
$(SN)_x$, phonon evolution during polymerisation of SN units 78−79711
$(SN)_x$, polymerisation, EPR obs. 79−73800
$(SN)_x$, struct. defects, nature and origin 77−24313
$(SN)_x$, synthesis and prep., TEM study 79−65004
S_2N_2, polymerisation, mol. struct., INDO calcs. 77−70301
S_2N_2, XPS, solid-state polymerisation 78−19630
$(SN)_n$* radicals polymerisation to $(SN)_x$ in thin films, optical spectra 80−16656
$Si_{1-x}H_x$, noncrystalline film, struct., interatomic distances, SRO 80−107053

polymerisation continued
SiO_2 fibres, freeze formed from polysilicic acid aq. soln. 80−71609
SiO_2 polymerisation and deposition from dil. solns., kinetics, 5-180°C 80−7790
SiO_2, small amorphous particles, prop. by vapour-phase hydrolysis of $SiCl_4$; high resolution TEM 79−82157
TiO_2-SiO_2 glass form. by low temp. chem. polymerisation 80−84899

polymers
see also elastomers; filled polymers; glass fibre reinforced plastics; glass transition; plastics; polymer films; polymer melts; polymer solutions; rubber
2,4-hexadiyne-1, 6-diol, bis(p-toluene sulphonate), dark-current meas. 80−15520
π-electron energies for linear conjugated polymers, polynomial matrix method 78−17830
A-150 plastic-equivalent gas for ionisation chambers, dosimetry appl. 80−81745
ABA poly(styrene-b-butadiene) copolymer, physical props., casting solvent effects 77−55935
abrasion mechanism rel. to groove sizes, shapes 79−20216
abrasive wear resistance rel. to physicomechanical props. 79−91804
ABS, fracture behaviour, rubber content effects 77−32676
ABS plastic, Cu film coating by ion plating *(Japanese)* 78−6858
ABS polymer, transparent, fracture of notched tensile specimens 77−63772
ABS polymers, deposited in internal magnet magnetron sputtering system, adhesion of Cu films 79−83121
ABS resin, craze growth and fracture 80−50705
ABS substrate, Sn autocatalytic deposition 80−100965
ABS-rubber modified, two-phase struct. influence on fracture toughness *(German)* 80−66666
absorbed dose for electron irradiation for polymeric part of electrical wire 79−46708
accelerated ageing data processing using linear regression analysis 78−39815
acetal copolymer, notches effect on fatigue strength 80−25857
acetal homopolymer, exam. of bending strength, using new method 78−53056
acetylene photopolymers, presence in Jupiter stratosphere 80−31244
acetylferrocene-furfural resins in glass like C matrix, Fe particles synthesis and props. 80−11229
acoustic props. appl. in US flaw detection 79−47857
acoustic vel. and absorpt. in liquids containing gas bubbles, effect of polymer additives 78−38779
acryl-melamine resin film, crosslinked, stress relaxation in hot water *(Japanese)* 78−60695
acrylamide gel, spinodal line and critical point, light scatt. meas. 79−79315
acrylamide-acrylic acid (acrylic acid salts) copolymers, composition determ., IR spectra *(Russian)* 80−7358
acrylic, denture base, tensile testing 80−16621
acrylic, ductile-brittle transition conditions 77−66001
acrylic, plastic optics, design patterns 79−32009
acrylic, Raman spectra using pulsed laser and gated detection 77−74529
acrylic, transparent, permanent antistatic, colourless, bending of organic silicone cpds. 79−1839
acrylic, wideband optical transmission meas. 79−76771
acrylic bone cement containing second phase dispersions, strength 77−81663
acrylic bone cement spinal fixation, mech. props. 78−81072
acrylic bone cement viscosity characterisation 79−79690
acrylic bone cement-stainless steel interface, shear strength 77−86706
acrylic copolymer adhesives, performance of polar and non-polar, relevance of glass transition temp. 79−39119
acrylic ester polymer networks, low temp. dielectric relaxation 77−36172
acrylic fibre, oxidative stabilisation, O_2 takeup and general model 79−38998
acrylic fibres, oxidative stabilisation dynamics 79−38999
acrylic gel, US observation of critical behaviour *(French)* 79−29414
acrylic phantom, absorbed dose calibration of high-energy X-rays 79−8548
acrylic plastic, stretched, fracture toughness 79−15778
acrylic polyester containing α-diketone camphorquinone, integrated optics medium 77−7215
acrylic resin wear and cutting surface against brass *(Japanese)* 78−56779
acrylic surgical bone cement fracture behaviour 80−56277
acrylic thermosetting powders, parameters 79−20003
acrylonitrile-butadiene-styrene copolymers, micromechanism of deform. and rupture *(German)* 80−35276
acrylonitrile-dimethylaminoethyl methacrylate copolymer structure and blood compatibility 77−81656
acrylonitrile-methylacrylate-acrylamide latexes graft copolymerised onto PVA,for haemodialysis membranes *(Japanese)* 80−12297
acrylonitrile-MMA copolymers, sequence distrib. determ. by NMR 77−14622
acrylonitrile-styrene copolymers, compositional heterogeneities, determ. by thin-layer chromatography 79−24847
acrylonitrile-vinylacetate(styrene) copolymer films, gas permeation, chem. struct. effects *(Japanese)* 78−31691
acrylonitrile-vinylidene chloride copolymers, sequence distrib. determ. by ^{13}C-NMR 79−79247
p'-acryloyloxyozoxybenzenes, substituted 79−1494
ACS blendmer and chlorine containing polymers, electrostatic property 80−54764
activation energy, dielectric relax. meas. method 77−24784
adaptive control of molecular weight distribution 80−58434
additives, effects on bubble motion and cavitation noise intensity in viscoelastic liquid 77−68648
adhesion ability enhancement by block copolymer incorporation *(Russian)* 80−61065
adhesion phenomena and influence of various factors, work of adhesion *(Polish)* 80−3292
adhesion strength 77−70278
adhesion to metal, temp.-depend. determ., rapid method 77−51610
adhesional strength, review *(Russian)* 79−52619
adhesive, pressure sensitive, radiation curing, literature review 77−86283
adhesive bonds with metals, shear resist., polymer crystn. effect 80−89462
adhesive layer, interlaminar stresses, direct determ. 77−86237

polymers continued
adhesive wear 78−56781
adhesives, thermosetting acrylic, electron beam curing 80−16634
adsorbed, conformation, excluded vol. effects 78−2372
adsorbed, excluded vol. effects, Monte Carlo investigation 79−95259
adsorbed chain structure, Monte-Carlo simulation *(Russian)* 77−19122
adsorbed layer, on particles in suspension, thickness meas. by mag. birefringence 80−42191
adsorbed layers, hydrodynamic thickness, Navier-Stokes eqn. calcs. 77−65726
adsorbed molecules, configurational behaviour, computerised dynamic display 79−874
adsorbed plasma proteins, Fourier transform IR spectrometry 80−16899
adsorbed polymer chains, surface restricted self avoiding walks span, mol. weight depend. 80−65360
adsorbent, for cryovacuum, highly-efficient, N_2 adsorption obs. 79−63249
adsorption, at liquid surface 77−20166
adsorption, of molecules, Green matrix local impurity SCF calcs. 80−92778
adsorption, onto inorganic substrate 79−69342
adsorption, scaling theory 77−35811
adsorption, self avoiding walk attached to a surface, tests of scaling theory 78−81927
adsorption at interface, self-avoiding random walk anal. 77−1085
adsorption in condensed phases, statistical mechanics 80−84365
adsorption into surface pores, computer simulation, phase transition *(Russian)* 78−51824
adsorption transition, excluded vol. effects, Monte Carlo and enumeration calcs. 78−67906
adsorption/adhesion, smooth surface, mech. stress effects *(Russian)* 78−50672
aged glasses, enthalpic state determ. by scanning calorimetry 80−6528
ageing and stabilisation, struct.-kinetic aspects *(Russian)* 79−52660
ageing through exposure to light, device *(French)* 80−30126
agglomerates, forces in dispersive mixing 77−29052
air permeability subject to high press., testing apparatus 78−27823
aliphatic polymer fibres, supermol. struct., X-ray diffr. and acoustic methods 78−75570
aliphatic-aromatic block copolyamides, synthesis, struct. and dynamic viscoelasticity, DTA and X-ray anal. *(Japanese)* 78−31377
alkali metal polyphosphates, vitreous, mol. weight distrib. determ. by gel-chromatography 79−50173
alkali polymethacrylates in alkali bromide soln., ion mobilities 79−96323
n-alkane, polymer, liq., mol. arrangement, computer model 80−92446
n-alkanes, oligomers, hydrodynamic behaviour, viscosity 77−559
alkenyl polysulphide, oligomeric, synthesis and characterisation by NMR 79−79248
alkoxyphosphazene polymer, elastic and thermoelastic props. 77−56014
α,ω-alkoxypolyethylene oxide, low mol. wt., crystallinity and fusion 78−51448
all-trans-polyene, ground state props., ab initio studies 79−47002
allyl ester polymerizates and copolymerizates, relaxation behaviour, 77 to 170K *(German)* 77−32614
allyl methacrylates, anionic polymerisation and radical reactivity *(Japanese)* 78−61007
alternating copolymer of styrene and N-substituted maleimides, NMR relax. studies of mol. motion 77−85608
amberlite XAD copolymers, packings for gravity flow, high press. liq. chromatography 77−77822
amino acid block copolymers, morphology and mech. props. 78−91264
aminoacidic side chain-liquid crystalline polymers, synthesis physicochem. props., struct., optical anisotropy *(Russian)* 79−23521
amorphous, acoustical props. and struct. 77−51446
amorphous, bulk, structure models and exptl. methods, review 78−22671
amorphous, conform. from simulation of filling diamond lattice with chains *(German)* 78−75595
amorphous, conform. from simulation of thermal motion *(German)* 78−75594
amorphous, diffusion of large penetrant molecules 80−15305
amorphous, domain struct. determ. by electron microscopy and electron diffr. 77−84667
amorphous, enthalpy relax. rel. to Tg 77−52278
amorphous, excess charges, band gap levels and elec. props. 78−23053
amorphous, influence of space network of linkages on acoustical props. 80−19194
amorphous, injection moulded, residual thermal stress calc. by FEM 79−55322
amorphous, localised low-energy excitations 79−73322
amorphous, molecular origin of relaxations 78−26058
amorphous, press. effect on thermal cond. *(German)* 79−95225
amorphous, segmental distrib., light-, neutron- and X-ray scatt., piezooptical and dielec. meas., review 78−51444
amorphous, semi-cryst., mech. motions, review 77−32616
amorphous, specific heat rel. to rate of heating *(Russian)* 77−85986
amorphous, stress-optical investig. of short-range order 78−22672
amorphous, struct. determ. by small-angle X-ray and neutron scatt. 77−84668
amorphous, struct. rel. to mech. props. 80−79713
amorphous, super-glass transition processes, damping process 80−24573
amorphous, thermal conductivity and thermal diffusivity, press. and temp. depend. 77−7915
amorphous, translational motion and lattice vibr. obs. by Raman scatt., T_g phenomena 78−23469
amorphous polymer, Rayleigh-Brillouin spectroscopy 79−38556
amorphous polymer, thermal transport at high temp., rel. to longitudinal phonon modes 77−62691
amorphous polymer matrix, stressed, thermodynamics of embedded crystallite deform. *(Polish)* 77−52424
amorphous polymer multiple dielectric relaxation, time-correlation function representation 80−15951
amorphous polymers, intrinsic time to fracture criterion 78−92320
amorphous polymers, segmental distrib., crystallisation and viscoelastic relax. meas. 78−51443
amorphous solids, time-temperature-pressure superposition phenomena, free volume theory 78−26059
amphiphilic-polymer liquid crystal, NaCl conc. influence on struct., X-ray diffr. study 80−44126
angular correlation ranges in flexible chains 77−34790
angular-dependent studies on some prototype vertically and laterally inhomogeneous samples 78−95655

polymers continued
anion exchange resins for Pu recovery from nitric acid waste 80−681
bis(9-anthryloxy)polyoxaalkanes,, intramolecular excimer form. and photodimerisation, kinetic anal., rate constants determ. 80−66800
antifriction, self-lubricating, behaviour at elevated temps. in friction process 77−86192
antithrombotic polymeric materials for artificial heart and devices for assisted blood circulation 78−36052
application of cross-polarisation ^{13}C NMR with magic angle spinning, solid material studies 80−77819
Araldite, dynamic crack propagation modelling, 1D anal. validation 79−72857
Araldite, high vacuum sealant at liq. N_2 temp. 80−57319
Araldite, neutron irradiation, elastic moduli effects, hardener conc. depend. 79−55804
Araldite AW106/Hardener HV953U epoxy resin, thermal props. at high press., glass transition 77−59160
Araldite B, crack arrest toughness determination 78−72867
Araldite B specimens, dynamic fracture toughness, influence on dynamic crack propag. 80−99966
Araldite CT200/Hardener HT907 cylinder, thermal stresses and photoelastic fringe order 77−62219
Araldite CT200/HT907, 263 to 343K, mechanical, physical and optical props. 78−56682
Araldite D cured with triethylenetetramine, fracture stability 80−30070
aramid/epoxy composite, tensile test 80−11778
aromatic polyamide fibre, sputter etching 80−21147
aromatic polyamide fibres, evidence of radial and tangential morphology 79−73107
aromatic polyamides, rigid and nonrigid, ultrahigh modulus fibres 79−95992
aromatic polyesters, broad-line NMR, dynamical mechanical behaviour 77−55718
aromatic polyesters, with S atoms, configurational props. 80−74269
aromatic polymer fibres, supermol. struct., X-ray diffr. and acoustic methods 78−75570
aryloxyphosphazene polymer, elastic and thermoelastic props. 77−56014
asymmetric skinned synthetic polymeric membranes struct. 79−29417
athermal model chains, pair distrib. function, Metropolitan Monte Carlo calcs. 78−17827
atmospheric resistance, distrib. function determ. and anal. *(German)* 80−81225
band structure calc. using symm. considerations and line groups 77−51636
benzene, polymerised, barrier in MIM tunnel junction, zero-bias anomalies 77−43739
(β-benzyl D- and L-aspartate) obtained by polymerisation of N-carboxylic anhydride IR spectra 77−55784
binary high molecular weight polymer systems, spinodal decomposition 79−70062
bioabsorbate, standards for in vitro and in vivo comparison and qualification 78−3677
biocompatibility evaluation by cell culture method *(Japanese)* 80−12301
biodeterioration in vitro and in vivo *(Japanese)* 77−66874
bioelectrets, electrets in biomaterials and biopolymers 80−80686
bioelectrets, occurrence of electret state and appl. in mol. biophysics and bioengineering 80−8007
bioelectrochemistry and bioenergetics (book) 80−8749
biological macromolecules, conformation studied by calorimetry, review 80−97870
biomaterials for blood-contacting appls., problems and new dimensions 78−85423
biomedical engineering textbook for undergraduates 80−8750
biomedical materials 79−83998
biopolymer, electronic transport mechanisms, asymmetry role 78−6370
biopolymer, electronic-conformation interactions 80−3588
biopolymer chain, uniform, elastic, possible conformational states 80−37913
biopolymer chains, intramol. reacts., enzyme catalysis appl., review 80−40953
biopolymer constituents, protonation, ab initio Hartree-Fock-Roothaan SCF calcs. 80−9503
biopolymer localised modes, due to impurities, FG-matrix technique 79−34474
biopolymer model compounds, calorimetric instrumentation used for studies 80−61746
biopolymer negative resistance, rel. to living cell props. 78−64923
biopolymer soln. heat capacity, conformational props. temp. depend. 80−8009
biopolymers, chromophone aggregates in Frenkel exciton model, dynamic perturbation effects on circular dichroism intensity 80−93273
biopolymers, circular dichroism, optical rotatory dispersion, conformational anal., review 77−3497
biopolymers, deform. under uniaxial stretching during UV irrad. 80−108935
biopolymers, dynamics of helix-coil transition 79−29499
biopolymers, electro-optical changes, chem. and rotational contribs. 80−85352
biopolymers, electronic struct. and possible chem. carcinogenesis mechanisms 79−22874
biopolymers, hydrophobic interactions 78−37777
biopolymers, primary structure determ. algorithms 79−48209
biopolymers, solid, apparatus for Seebeck coeff. meas. 78−21172
biopolymers, studied by circular dichroism and optical rot., review 78−44457
biopolymers, tautomeric forms protonation, ab initio HF Roothaan SCF calcs. 80−78534
biopolymers, X-ray struct. study using synchrotron radiation and multichannel detector 78−47210
B.I.P. An interactive graphic system for indexing energy bands of model polymers 79−59608
biphenyl glutarate polymer, resonant Raman spectra and fluoresc. 77−24830
bipolymer, charge carriers origin and mobility, adsorbed water effects 79−92461
birefringence, hereditary depend. of optical propag. difference on strain 78−48142
birefringence coeff., polarisation-spectral method *(Russian)* 78−52470
birefringent, stress intensity factor determ. 80−14633

polymers continued
bis(p-toluene sulfonate) diacetylene polymer cryst., second order phase transition 79−73922
bis(p-toluene sulphonate) diacetylene, partially polymerised, defect-induced absorpt. and fluoresc. 77−44030
bis(p-toluene sulphonate) diacetylene polymer, EPR, thermal history and temp. effects 78−52352
bis(p-toluene sulphonate) diacetylene polymer, spin conc., g-values of single cryst. from EPR study 78−48037
bis(p-toluene sulphonate)diacetylene, fully and partially polymerised, optical props. 77−1696
bis(p-toluene sulphonate)diacetylene, monomer and polymer, solid state phase transformation, far IR transmission spectra obs. 80−55077
bismaleimide resin, charact. by differential scanning calorimetry 80−71869
bispenol-A epoxy resin, glass transition temp., effect of absorbed water, PMR line width 79−90766
bisphenol A polycarbonate, end-cap ratio and mech. props. of block copolymer 78−91266
bisphenol A-phthallic anhydride epoxy resin, diglycidyl ether, Rayleigh scatt., Brillouin and IR spectra 80−66211
bisphenol-A polycarbonate, Brillouin scatt., hypersonic relax. 79−4811
bisphenol-A polycarbonate, plasticized, melting and equilib. melting temp. 78−2234
bisphenol-A-diglycidyl epoxy, light emission under high elec. field, compared with photolum. 80−25465
bisphenol-A-diglycidyl ether epoxies, struct., fracture and mech. response, cure and crystallisation conditions effects 79−15779
bisphenol-A-polycarbonate:N-isopropylcarbazole, hole photogeneration efficiency 79−56243
bisphenol-A-polycarbonate polymer, triphenylamine doped, photoinjection of holes from amorphous Se 78−72191
bisphenol-A-polycarbonate-triphenylamine solid soln., hole transport meas. 78−43438
bistable oscillator chain, Brownian dynamics of transitions 78−86983
bis[catena-poly(methylarsenic)], LF dielec. response 79−56719
blend, interphase phenomena, form., thermodynamic, colloidal and morphology props. *(Russian)* 78−40089
blends, interdiffusion, meas. method 79−69271
blends, morphology and compatibility, X-ray and optical obs. 79−69026
blends, selective staining method for TEM obs. of morphology 80−84103
blends, two-component, glass transition, calorimetric investig. *(Russian)* 80−39268
block copolymer chain conformations 80−69282
block copolymers, as ideal model system for a pseudo two phase solid texture, small-angle X-ray scatt. 79−14693
block copolymers, chromatographic separation on porous adsorbents *(Russian)* 79−66392
block copolymers, IR spectroscopy for struct.-props. relations 78−91268
block copolymers, microphase separation, thermodynamic treatment *(Chinese)* 80−79947
block copolymers, morphology rel. to stress/strain props., deform. hardening effect, birefringence meas. 77−48501
block-copolymer, mol. wt. distrib. and comp. determ., gel permeation chromatography method *(Russian)* 79−31755
blood contacting polymer surface, roughness effect on thrombus formation 79−48369
blood proteinpolymer interfacial behaviour, influence of hydrophilic-hydrophobic type of microphase separated struct. *(Japanese)* 80−12051
branched and crosslinked molecules, mol. description of dynamics 80−9767
branched polymers, mean end to end distance 79−86097
breakdown plasma analysis, mass-spectrometric installation 78−88670
breaking down of anharmonic chain, computer calc. 80−106410
Brillouin-Rayleigh scattering, local struct. in amorphous phase 77−81111
brittle, in vitreous state, resistance to brittleness and fracture kinetics *(German)* 77−32688
brittle fracture, principal stress distrib. meas. at running crack tip *(Japanese)* 77−42784
brittle photoelastic, use of gelatin gels in prep. for optical polarization stress study 80−40325
brittle point determ., new method 77−70260
bromostyrene-crosslinked polyester, craze resistance 80−35421
bubble rupture between two solid walls, effect of drag-reducing polymers on cavitation 80−106822
butadiene, effect of redox initiation in emulsion polymerisation *(German)* 78−85158
butadiene, styrene, 4-vinylpyridine terpolymer, cross-linked by coordination with Fe (III) chloride, ion clustering 78−83748
butadiene acrylonitrile copolymer, relaxation processes *(German)* 78−31439
butadiene copolymers, diffusion and solubility of solid low mol. wt. substs. rel. to structure *(Russian)* 79−33092
butadiene styrol rubber, effect of polyfunctional nitro-oligomers on relaxation *(German)* 78−31441
butadiene-acrylonitrile copolymer, electronic struct., reactivity, SCF CNDO calc. 77−50580
butadiene-isoprene copolymers, monomer unit distrib., ^{13}C NMR determ. 78−26456
butadiene-styrene block copolymer, containing free polybutadiene mols., viscoelastic behaviour 77−56015
butadiene-styrene block copolymer, oriented, isotropic, struct. changes during deformation *(Russian)* 78−88512
butadiene-styrene block copolymer, star shaped, rheological props. 77−68542
butadiene-styrene block copolymer, viscoelastic props. 79−8336
butadiene-styrene copolymer, pyrolysis, determ. of kinetic parameters *(German)* 78−85155
butadiene-styrene latexes, ageing *(Polish)* 79−70098
butadiene-styrene polymers, relaxation time spectra and mechanical losses *(Russian)* 78−76698
butadiene-styrene three-block copolymer, rheological props., 60-110°C *(Russian)* 79−23292
butanediol terephthalate-polytetramethylene oxide terephthalate copolymers, dielec. props. 78−95546
butodiene-styrene copolymer, viscoelastic props., crosslinkage in presence of active silica *(Polish)* 78−79231
n-butyl-4,5,7-trinitrofluorenone-2-carboxylate/Lexan polycarbonate, dielectric. relax. 77−4598
polymers continued
N-tert-butylacrylamide-styrene copolymers, struct., composition, IR, DTA investigs. *(Polish)* 79−31751
cable insulation, radiation modification using electron beams 80−66848
capacitors, injection charging 77−76902
ε-caprolactam, after polymerisation under reduced press. *(Japanese)* 78−95929
Ω-caprolactam-ε-caprolactam polymers, vitrification, fusion, crystallisation *(Russian)* 77−47561
ε-caprolactone-γ-(tert-butyl)-ε-caprolactone copolymers, dynamic mech. props., glass transitions 77−25086
carrier species determ. using galvanic cell 77−69384
carrier traps in polymeric insulating materials, investigation by X-ray induced thermally stimulated current and thermoluminescence methods 80−93240
cast-epoxy resins, AC breakdown-voltage charact. *(Japanese)* 80−88927
catheter materials, intravenous, tissue response 77−37065
cation-exchange membrane, Zn^{+} transport 78−96033
cellophane, UV spectrum comparison with interstellar medium spectra 78−61913
cellophane membrane, polarised, electret transport props., permeability coeff. 80−7860
cellophane membrane, transient diffusion of unstirred polystyrene solns. 78−92508
celluloid, mech. props. under proportional load, time lapse, heating and isotropic props. effect *(Japanese)* 79−79043
celluloid, nonlinear viscoelastic deform. under superimposed hydrostatic pressure 79−34116
cellulose, comparison of conclusions from small-angle X-ray scattering and electron microscope obs. 79−86717
cellulose, degradation by high voltage electrons 80−100283
cellulose, dielec. relax. studies, TSD meas. 80−88907
cellulose, fibres, membranes and composites, polystyrene used for modification of props. 78−95727
cellulose, fibres crystallised from hydrazine, texture by X-ray diffr. 79−69030
cellulose, in Valonia, pole figures and orientation functions 77−86439
cellulose, mech. relaxation at low temps. rel. to adsorbed H_2O 77−43277
cellulose, mechanochem. degradation 80−40371
cellulose, mobility of adsorbed water, NMR pulse obs. 80−108835
cellulose, mol. motions, role of water, temp. and morphology 77−89386
cellulose, New Zealand kauri, $^{13}C/^{12}C$ dating for last millennium 80−21819
cellulose, nitrated, strength, deform. and disintegration, influence of stable free nitroxyl radicals 80−11717
cellulose, phase transitions, kinetics of precipitation from diluted cadoxen solns. 80−7845
cellulose, shish kebab-like structures 77−62485
cellulose, struct. and conform. props. of cotton fibre grown from γ-irrad. seed 77−81539
cellulose, thermally stimulated discharge studies 80−11329
cellulose acetate, I_2 doping effect on elec. props. 80−49757
cellulose acetate, reverse osmosis membranes, ion mobility, diffusion coeff., elec. resist. obs. 80−45550
cellulose acetate, solubility of CO_2, 0-70°C, up to 45 atms. 78−83957
cellulose acetate fibre and film, stabilisation, post UV-irrad. mech. strength *(Russian)* 79−24778
cellulose acetate film, diffusion and permeation of gases 79−55934
cellulose acetate freeze-dried membrane, gas permeation rates 79−79295
cellulose acetate membrane, asymmetric, elec. and electroosmotic transport behaviour in dialysis-osmosis expts. 80−108745
cellulose acetate membrane, asymmetric, elec. and electroosmotic transport behaviour in hyperfiltration expts. 80−108746
cellulose acetate polymer-solution interface props. from liq. chromatographic data 79−16039
cellulose acetate porous membrane, inert gas separation appl. 77−36791
cellulose acetate-dimethylphthalate gel, mech. props., substitution effect *(Russian)* 79−23291
cellulose acetate-g-polyacrylamide membranes, radiation grafted, appl. in water desalination by reverse osmosis 80−45548
cellulose blotter/torsion pendulum technique, for relax. determ. 80−54357
cellulose char, O_2 chemisorpt. kinetics 80−96730
cellulose diacetate membrane, diffusive permeability 80−104460
cellulose diacetate membranes, press. depend. of permeabilities *(French)* 79−52756
cellulose diacetate membranes, unilayer, transport phenomena, hydration and dialysis coeffs. 80−76556
cellulose esters, plasticiser effects on mech. and dielec. relax. 80−40047
cellulose fibre, gamma-irrad., and storage effects on props. *(Russian)* 80−61121
cellulose fibre, moist, dielec. props. 78−76380
cellulose fibre formation in stirred dimethyl sulphoxide-paraformaldehyde soln. 80−104440
cellulose fibres, elec. anisotropy 80−97220
cellulose fibres, from jute, crystallinity percentage, estimation by X-ray methods 79−7553
cellulose fibres, surface aggregation of dispersed resin particles in elec. field 78−53262
cellulose fibres, with planar crimp, tensile deformation 80−84235
cellulose hydrate, pulsed laser irrad., struct. changes *(Russian)* 77−66560
cellulose II, paracrystalline lattice disorder, X-ray diffractograms 78−83751
cellulose II, preparation and crystal growth, electron diffr. obs. 78−91285
cellulose II, unit cell parameters, neutron diffr. 77−1086
cellulose nitrate, creep behaviour under superimposed tensile and hydrostatic loading 77−56029
cellulose nitrate, exam. of strength charact. 78−68748
cellulose nitrate, solid state track detector for neutron irradiated B quantitative anal. 78−56937
cellulose nitrate emulsion, sensitivity and efficiency for α-particle detection 78−13380
cellulose nitrate emulsion for α-particle track relocalisation 78−17480
cellulose nitrate plastic detector technique in fast neutron radiography 79−76299
cellulose triacetate, pulsed laser irrad., struct. changes *(Russian)* 77−66560
cellulose triacetate I, mol. and cryst. struct., parallel chains 78−30548

polymers continued
cellulose triglycerl ether hexanitrate, exam. of strength characts. 78−68748
cellulose tripentaerythrityl ether nonanitrate, exam. of strength characts. 78−68748
cellulose-PAN copolymer, luminesc., ageing effect 78−64401
cement mortar-epoxy resin mortar, durability of jointing of successive pours with epoxy resin adhesive *(Japanese)* 77−8793
cement-polymer composites, review 79−70039
ceramic filled with polymer, ZrO_2 stabilised, fracture mechanism *(Russian)* 80−100895
chain, adsorption on diamond lattice, span calc., self-avoiding walk model 77−15679
chain, collective excitations and optical absorpt. 79−47019
chain, config. statistics, in impenetrable barrier confinement systems 77−562
chain, heuristic approach to excluded-volume problem 77−14630
chain, irregular, lattice distortions, SCF perturbation calcs. 78−6018
chain, linked rigid body, Brownian dynamics 80−74267
chain, self-interacting, in three-dimens. continuum, config. props. 78−58876
chain, three-body intrachain collisions *(Japanese)* 77−42448
chain, two-particle probability, path integral approach 77−61886
chain, virial expansion, two parameter expansion 79−72450
chain, virial expansion 78−5383
chain, zero component field *(French)* 80−69280
chain configuration in amorphous state 77−80427
chain configurational characts., review 77−38758
chain conform., small-angle neutron scatt. obs. *(Polish)* 80−10511
chain conformation and struct. determ. by diffr. 77−80429
chain conformation in amorphous state, neutron scatt. 77−76328
chain conformations in liq. and cryst. slates *(French)* 78−18552
chain consisting of interacting chain units, mol. dynamics, relax. times *(Russian)* 79−31753
chain cyclisation, lattice embedded model, discrete scatt. series representation 80−48109
chain dynamics, ang. correl. function decay by multiple rot. pot. diffusion 80−3569
chain dynamics, Forsman's equations, graph theory appls. 78−55265
chain dynamics, in confined space 77−75351
chain dynamics, repulsive Lennard-Jones pot. mol. dynamics calc. 79−36805
chain dynamics, review 77−38759
chain folding, cross-sectional area 78−70989
chain in solution, mol. dynamics obs. 80−5643
chain length effect on excluded volume, generalised mol. architecture 79−59607
chain molecular amorphous solids, stat. thermodynamics and mol. theory 78−26442
chain mols., conformational transition kinetics 80−83339
chain moments, charact. function, distrib. function, numerical calc. 78−78843
chain partition function, equivalence of quantum many-body problem 80−57181
chain relaxation when trapped in suddenly deformed gel *(French)* 77−62483
chain statistics and universality 78−29869
chain subjected to elongation, conformational microstruct. variation *(Russian)* 79−31756
chain with rigid side branches, intramol. phase transition of 1st kind *(Russian)* 80−58432
chain-folded crystal, statistical mechs. in lattice model 78−47247
chainlike systems, Coulombic contributions, LCAO-SCF-CO method, Fourier representations 80−32862
chains, electronic correl., similarities with Mott insulators, AMO method *(French)* 80−24775
chains, statistics, dynamics and graph theory 77−14627
chains, with volume interaction, statistical physics problems, coils and globules, review 78−94347
chains containing planar cyclic groups, flexibility, stat. mech. model *(Russian)* 77−42453
characterisation by size exclusion chromatography 78−11580
charge absorption and transport in polymer wetted by insulating liquid subjected to electric field 80−6534
charge carrier species determ. using interfacial phenomena 80−24978
charge movement study using capacitance-voltage characts. of MIS struct. *(French)* 80−39575
chemical analysis, literature review, 1974-76 77−77815
chemically reacting, kinetic characts. of thermal effects determ. using Calve type microcalorimeter 77−57328
chitin (poly-N-acetyl-D-glucosamine), dynamic mech. behaviour, effect of water 80−97522
chitosan (poly-D-glucosamine), dynamic mech. behaviour, effect of water 80−97522
chlorinated polymer-vinyl monomer mixtures, high dose rate electron beam curing 77−59958
chlorine-containing, dose rate effect on degradation behaviour 79−99239
cholesterol-containing, struct. and liq. cryst. props. *(Russian)* 78−38622
cholesteryl acrylate, and monomer, liq. cryst. order 78−9942
cholesteryl methacryiate, and monomer, liq. cryst. order 78−9942
cholesteryl p-acryloyloxybenzoate, and monomer, liq. cryst. order 78−9942
cholesteryl vinyl succinate (fumarate), polymer+monomer systems, liq. cryst. phase states 79−1494
chondroitin-4-sulphate, adsorption on adsorbed collagen 79−79459
chopped glass fibre reinforced polyester resin, deformation and thermoset cure effect on heat cond. during molding 79−86325
chromium phosphinate polymer, one-dimensional antiferromagnet, spin-flop 80−50131
chromophore aggregates, optical absorpt. and circular dichroism spectra, degenerate ground state model 79−70523
circular craze analysis, simple membrane model 77−3779
classification, fabrication techniques and appl., historical development, 1979 status and future trends 80−93532
coating, vibration-damping, for constructions, theory 80−10178
coil configuration, in polymer, polyelectrolyte solns., and hot-stretched polymer samples, neutron scatt. 79−10778
coil-globule phase transition 77−19119
collagen, adsorption on solid surfaces 79−79459
colloid stabilisation by polymers, excluded volume effects 77−60129
polymers continued
colloidal plates, parallel, polymer adsorption, excluded volume effects, polymer-solvent interactions 80−45568
colloidal suspension, steady state shear flow coupled to conc. fluctuations 80−61170
comb-like, gels, dielec. polarisation *(Russian)* 77−48698
comb-like, with amide groups in side chains, stabilisation via H bonds *(Russian)* 77−46665
comb-like polymers of smectic liq. cryst. struct., synthesis and props. *(Russian)* 79−32904
complex dielectric const. determ. from polarisation current 77−66451
complex permittivity and compliance, algorithm for calc. freq. depend. 78−68442
composite, wear mechanisms at metal surfaces 79−87742
composite, wire-reinforced, dynamically loaded, crack propagation and arrest 80−97567
composite materials, fracture kinetics 80−11770
composite matrix materials, spacecraft, space radiation effects evaluation 80−70263
composite three dimensional model for photoelasticity 78−52871
composition coatings for rubbing mechanisms of optomech. instruments 78−29198
concrete, fracture toughness meas. 79−70168
concrete composite, short steel wire reinforced (polymer impregnated) concretes, cracking and toughening 78−80626
concrete cylinder, failed, compressive props. enhancement by polymer impregnation 77−77542
conducting materials, struct. and phys. props., symposium, San Jose, USA (March 1979) 80−62379
conductive, freq. depend. of elec. cond. and polarisation 77−11918
conductive filler-polymer composite conductivity theory *(Japanese)* 78−11351
conference, Dublin, Eire (July 1977) 79−55012
conference, Mainz, Germany (Sept. 1979) 80−58429
conference, nonmetallic materials and composites at low temps., Munich, Germany, July 1978 80−22139
conference, Pittsburgh, USA, (June, 1975) 77−38756
conference, Rothenburg, Germany (Mar. 1977) *(German)* 78−75583
conference, Shrivenham, England (Sept. 1977) 78−75576
conference, Terrigal, Australia (Nov. 1975) 77−48640
configuration, excluded volume effect, YBG and Kirkwood hierarchies 77−46661
configuration in amorphous and crystalline state, small-angle neutron scatt. *(German)* 77−85398
configurational properties of athermal self-avoiding polymer chains at intermediate to high concentrations 80−18950
configurational statistics of polymer confined to wedge of interior ang. α 79−45875
conformation, correlated walk model calc. 80−78733
conformation, IR spectra 78−1116
conformation of polymer chain residing in density gradient of segments 79−13853
conformation of polymer confined between two adsorbing surfaces 77−3501
conformational energy calcs., appl. to defect props. of polymer cryst. 80−54154
conformational sp. ht. determ. method 78−14474
conformational transitions, Brownian dynamics, simulation 79−45873
conformations of polymers attached to inert interface 79−94120
conjugated and saturated chain, electronic struct., review 80−59860
conjugated hydrocarbons, energy gap estimation, graph-theoretical approach 80−24789
conjugated polymers, effect of long-range coulombic repulsion of electrons on ground state 77−68147
conjugated polymers, one- and two-dimensional, band structs. and band gap sizes 79−47008
constitutive relations in photomechanics 80−43251
contact angle at solid-water interface 80−20010
contact electrification, extrinsic surface state contrib. 77−11984
contact electrification, meas. using computer-controlled apparatus 80−86341
contact electrification of dielectric solids, review 78−26934
contact potential and charge exchange meas., at Hg-polymer interface 80−75642
contract electrification, analogue model 79−51655
contractile polymeric structures, deformative props., artificial muscles 77−25595
contractile polymers (artificial muscle), use in chemical-mechanical energy conversion *(Russian)* 77−64167
cooled epoxy resin vacuum mould computational simulation of design *(German)* 80−81020
coordinated motion simulation of chains 79−86721
coorientation with low molecular organic substances *(Russian)* 77−21089
copoly(ethylene terephthalate/5-methoxyisophthalate), isothermal crystallisation, differential scanning calorimetry 78−30546
copoly(ethylene terephthalate/isophthalate), isothermal crystallisation, differential scanning calorimetry 78−30546
copolyazomethine, nematic mesophase, DSC study *(French)* 78−71672
copolyester, melting temperature changes due to heat treatment *(Japanese)* 79−70096
copolyesters, diol sequencing, NMR spectra 79−52657
copolyethylene terephthalate-p-oxybenzoate, nematic phase, thermodynamics 78−91427
copolymer, fluorine-based, plastic-clad silica fibre termination appl. 79−41466
copolymer, graft or block, multiphase composite systems, struct., colloidal behaviour *(Chinese)* 78−73088
copolymer, semicryst. random, characterisation by small angle neutron and X-ray scatt. 80−75189
copolymer cooperative reactions, sequential anal. 77−36752
copolymer cooperative reactions sequential anal., Markov chain structure 77−36753
copolymer globule model, orientationally-ordered liq. cryst. state *(Russian)* 80−59389
copolymer mesophases, scaling laws 79−94872
copolymer model with alternating spins, kinetics 80−9768
copolymers, cooperative reactions, sequential anal. of 2nd order Markovian chains 78−7204
copolymers, cooperative reactions, sequential anal. of binary copolymer with protecting monomer 78−7203

polymers continued
copolymers, molecular architecture determ. by small-angle neutron scatt. of solns. 77−19863
copolymers, self-replicating, temporal evolution, Monte Carlo calcs. 77−83773
copolymers grafted with oxirane, synthesis and charact. 79−69032
copolymers with interchanging struct. units, quasi-equilib. states 79−41975
core levels of simple homopolymers, ESCA methods 78−88673
corona charged polyethylene thermally stimulated current and surface potential decay obs. 80−15945
corona charged PVF_2 α_c relaxation obs. 80−15956
corrosion protection of metals 79−96211
crack extension micromechanisms, review 80−108561
crack growth kinetics in uniaxially extended specimen *(Russian)* 80−1483
crack propagation kinetic model *(Russian)* 78−63381
crack tip failure mechanism modelling 80−108565
craze mechanics, elastic model 77−48519
crazing, associated mech. behaviour, specimen size effects 77−73337
crazing limit in creep and stress relax. 79−34177
Crazing under applied compression 78−19875
creep, effect of temp. and humidity, field test results 78−23793
creep, energy considerations *(German)* 77−80081
creep curves, correl. between isothermal and thermomech. 78−64587
creep during scission reactions in polymer networks 79−15738
creep in tension under hydrostatic press. 77−70124
creep prediction during random changes in load, ambient temp. and humidity, computer calc. 77−70121
creep prediction during random load changes and random stationary temp.-humidity conditions 77−86104
creep tests for determining degree of cross-linking *(German)* 78−76822
creep under plane stress, nonlinear viscoelasticity models appl. 80−89308
cross linked, chem. struct. *(German)* 78−75584
cross-linked, mech. props. theory *(German)* 77−63752
cross-linked, with different degrees of hardening, bulk-creep prediction 80−104223
cross-linked polyethylene insulator breakdown by treeing *(Korean)* 79−91353
cross-linked polymer system, influence of chem. cross-link network on spin-spin relaxation *(Russian)* 77−32284
cross-sectional area per chain: a useful structural parameter for polymer characterization 78−86984
crosslinked, amorphous probabilistic theory of time to fracture 77−90448
crosslinked, probabilistic theory of structural and physical characteristics 80−5649
crosslinked, specific charact. *(German)* 78−75585
crosslinked compositions formation, structural kinetic method *(Russian)* 79−34303
crosslinked networks, stress-induced crystallisation, theory 77−24277
crosslinking, rel. to azide photooxidation in polymer matrix 80−66832
crosslinking in continuous flow stirred reactors 79−79246
crosslinking with X-ray irrad., active group and heavy atom effects 80−7829
crystal, electron-irradiated, free radical stabilisation, filler content effects *(Russian)* 77−56241
crystal, hydrostatic compressibility, H_2 bonding effect on anisotropy 80−25782
crystal and melt, stat. thermodynamics using Midha-Nanda cryst. state theory 79−41979
crystal density, X-ray diffr. determ. 78−91273
crystal growth, during annealing 78−14300
crystal in suspension, light scatt. in streaming system, dimens. characterization 79−69852
crystal orientation distributions, thermodynamically controlled 80−84112
crystalline, accordion-type laser-Raman oscills., elastic moduli 79−55854
crystalline, broadline PMR spectra, math. separation procedure 80−2647
crystalline, bulk, lamellar struct. and plasticity mechanisms 77−65957
crystalline, elastic modulus, strength, rel. to crystallite shape 80−45335
crystalline, hard-elastic fibres, morphology mech. props., mechanisms, review 77−32612
crystalline, in hydrostatic tension, plastic deform. of model 77−59870
crystalline, necking stress, thermodynamically derived equation *(Japanese)* 79−91758
crystalline, oriented, drawing, load elongation behaviour, fibre composite model 79−15691
crystalline, review, crystallisation, morphology rel. to props. 77−39546
crystalline, stress transmission 80−35240
crystalline, texture studies, review 79−83221
crystalline, vibr. spectra, theory *(Russian)* 78−13502
crystalline, with lattice defects, exam. of plastic deformation for 2-d models 78−68747
crystalline formations study, light refl. from untreated surface 77−28945
crystalline polymer, deform. and fracture, submicrocrack nucleation and supermod. struct. 78−52918
crystalline structure stability *(Russian)* 77−19880
crystallinity, characts., effect on props. 79−55673
crystallinity, Hermans-Weidinger X-ray diffraction determ. technique *(Russian)* 78−75582
crystallinity, kinetic and morphological aspects *(French)* 80−1942
crystallinity determ. by thermal method *(Russian)* 80−38966
crystallisation, chain folding, statistical mechanical calc. 78−2020
crystallisation, flow-induced, conf., Midland, Michigan, USA, Aug (1977) 79−82161
crystallisation, growth rates, nucleation, annealing and random copolymer crystallisation 78−51435
crystallisation, rate eqn., effect of vol. relax. of amorphous material 77−62482
crystallisation, review 80−64925
crystallisation, surface area estimation and secondary nucleation theory 77−89396
crystallisation, thermodynamic analysis of nucleation *(Russian)* 77−19881
crystallisation, under extreme temp. and press. gradient 79−82163
crystallisation, under mol. orientation, formation of stacked lamellar structs. 80−84109
crystallisation 79−82162
crystallisation and fusion, conf., Louvain-la-Neuve, Belgium (1976) 78−51429
polymers continued
crystallisation kinetics, rel. to light effect on $SSe_{22.5}$ amorphous-cryst. transition 79−99076
crystallisation rates from melt, universal relation 79−10816
crystallisation review 78−51430
crystallising, defects and mech. relax. *(Russian)* 78−22789
crystals, melting, intramol. and intermol. interactions effects 78−18745
cyanine dyes, J-aggregates, swirl-induced optical activity 78−72482
cyclic deformation amplitude, automatic meas., apparatus design 78−85082
cyclic paraffin, longitudinal acoustic mode freqs., general theory for composite perturbed elastic rod 78−14421
cyclic polyphenylacetylene, thermally excited paramag. props. 77−88614
cycloaliphatic polyimides, oriented, thermomech. props., synthesis *(Russian)* 80−55443
cyclopentadiene-butyl vinyl ether copolymer, oxidative degradation *(Japanese)* 80−108714
Dacron, arterial prosthetic material, props. 78−7537
damage accumulation problem *(Russian)* 80−21053
decamethylene polyester, epitaxial crystn. on aromatic hydrocarbon substrates 79−61521
decomposition by hydrolytic mechanism 79−55016
defect elementary movement orientation from acoustic expts. 79−94927
defect polymer, freq. branch calc. of n-paraffins, fatty acids, and glymes 79−31747
defect solids, local and resonance vibrations, appl. to deuterated polyethylene 79−99287
defocus transmission electron microscopy 80−28927
deformable solids, fracture and hardening kinetics 80−35210
deformation, device for testing under hydrostatic pressure and anisotropic conditions 79−87783
deformation, failure, kinetic model *(Russian)* 78−72832
deformation, ultimate regimes for flexible chains 78−19844
deformation mechanism, stress-induced phase transform. of $(SN)_x$ 78−23776
deformation mechanism, twinnign in polydiacetylene single crysts. 78−23777
deformation mechanisms of constrained chains, geometrically induced correlations of tie molecules 78−19835
deformation mechanisms of constrained chains deform. energetics of tie molecules 78−19836
deformation of interatomic bonds, IR spectral meas. 79−38918
deformation of polymer materials, review 78−68749
deformation of viscoelastic solids, depth of polymerisation 80−40414
deformation polarisation effect on interaction with liquid environment, fracture *(Russian)* 77−25166
deformation under combined action of shear stress and hydrostatic pressure, testing equipment 77−56184
degradation, mol. mechanisms *(German)* 78−76860
degration, reaction product volatility effect on thermogravimetric anal. 80−104316
dentistry, polymers and polymer science 79−83435
dentistry, problems with polymers 79−83434
denture base materials, multi-station machine for fatigue testing 80−108648
denture base polymers, fatigue test machine 80−66712
detector particle track diameter rel. to etching time *(French)* 80−9463
dextran, activation of acid hydrolysis by ultrasound, mech. stress effect on reactivity 79−74375
dextran structural modifications, I_2 sorption, porosity depend. *(Russian)* 79−23535
diacetate-nitrocellulose, long period struct., 180-265°C, X-ray diffr. obs. *(Russian)* 79−24556
diacetylene, low temp. photochemical polymenisation, decay kinetics, ESR spectra obs. 80−100616
diacetylene, photopolymerisation, optical absorpt. spectra, time depend., reaction kinetics 80−85174
diacetylene polymer, EPR exam. of partially crystalline polymer extracts 78−39400
diacetylene polymers, high freq. vibr. mode modelling 79−19346
diacetylene polymers, photoelectron valence band spectra 78−43979
diacetylenes, urethane substituted, polymer conversions in γ-ray polymerisation 80−26014
diallyl, thermally stable, as laminating resins for PCB material 79−52658
diallyl, thermally stable, laminating resins for PCB manufacture appl. *(Japanese)* 78−92232
diallyl isophthalate-methyl methacrylate copolymer, light focusing rod prep. by copolymerisation, refractive index distrib. const. *(Japanese)* 79−46042
1,6-dicarbazolyl hexadiyne, solid-state polymerisation, monomer to polymer phase transformations 80−38948
dichlorophosphazene polymer, resistivity 77−51735
dichromated PVA specific wavelength sensitisation for laser beam recording 78−5531
dicyano bisphenol polycarbonate, crazing, polar group incorporation 78−85017
dielectric anomalies at very low temps., acoustic anomalies analogy 78−31146
dielectric breakdown, DC trees caused by space charge accumulation, carrier injection and trapping effects 80−84695
dielectric breakdown theories, mol. and morphological features rel. to elec. strength, review *(Japanese)* 80−60501
dielectric conduction and breakdown, conf., Gainesville, FL, USA (Oct.-Nov. 1979) 80−82564
dielectric loss, multiple relax., comparison with small-mol. solids 78−19409
dielectric loss meas., on-line calculator based system 78−54397
dielectric loss measurement in solids using superconducting microwave resonators, 2.2 to 15K 79−67316
dielectric loss tangent, 0.1-10 GHz, 2.2-4.2K 77−24786
dielectric materials exposed to partial discharges, degradation product anal. 79−4765
dielectric nuclear track detector, particle stopping power depend. on preirrad. annealing 79−72185
dielectric properties, study by capacity method, strip electrodes capacity calc. 80−25327
dielectric relaxation, theory, appl. of derived dielec. loss formula 80−50262
dielectric relaxation and heating rate 77−66453
dielectric relaxation meas. using automatic dielcometer 77−45864

polymers continued
dielectric relaxation processes of polar molecules introduced into polymeric matrix *(Russian)* 79−87387
dielectric relaxation time distrib. function determ. 77−73111
dielectric to viscoelastic data conversion 78−48109
diepoxide-diamine network polymers, chem. props. and average mol. wt. 80−37915
diepoxide-polyepoxide, relax. props. of cross-linked system *(Russian)* 78−51450
N,N-diethylacrylamide, cross-linked copolymer, improved mech. props. 80−61091
diffraction line-broadening of soln.-grown cryst., bending contrib. 78−75574
diffuse boundary thicknesses, determ. by small angle X-ray scattering 80−38947
diffusion coeffs. of gases, sorption, permeation investigs., review 78−67868
diffusion of simple penetrants in polymers, statistical mechanical model 80−10704
diglycidyl ether of bisphenol A epoxy resin, rubber toughened, struct. and mech. props. 78−52901
L-β-3,4-dihydroxyphenyl-α-alanine with L-glutamic acid, polymers and copolymers, synthesis and conform. 79−33996
dimethacrylate resins dental composite, abrasion and wear props. 79−96710
dimethyl terephthalate in contact with Al(Mo)(Cu)(W), effect of elec. field on contact electrification 79−19660
dimethylaminoethyl methacrylate copolymers, modification for improved blood compatability 79−39609
α,ω-diphenyl-trans-polyenes, 1st excited singlet valence states, CI and extended CNDO/S calcs. 78−74807
all-trans-diphenyltetradecaheptaene, oriented, photochem. reaction production and monitoring, reson. Raman spectroscopy 77−29020
diphilic polyelectrolytes, aqueous solns., Wilhelm method 80−10745
direct renormalisation group procedure for polymer chain 80−91712
dissolution kinematics, model and its expt. verification 78−26687
distribution function for random walks without self-intersection 78−8350
DNA and other biopolymers, radiolysis 80−67163
dotriacontane polyester, epitaxial crystn. on aromatic hydrocarbon substrates 79−61521
double layer system, high field cond., xerographic characts. 79−95448
Dowex 50 W×8 cation exchange resin, sorption of Zn^{2+} from HCl soln., temp. depend. *(Bulgarian)* 79−87004
drawing properties, role of interfibrillar tie mols. 78−76706
dye concentration distributions, microdensitometric determ. *(German)* 77−37962
dye-polymer system, diffusion based direct marking process, laser induced, spectral thermal characteristics 79−76779
dyestuffs in polymers, conc. distrib., microdensitometric determ., stops effect *(German)* 78−11598
dynamic light scattering theory 78−60475
dynamic living polymers, thermodynamic enhancement of oligomers, end-group interactions 80−58423
dynamic mech. anal. 78−60697
dynamic storage and loss compliances determ. from creep data 80−5948
dynamics, neutron scatt. obs., book contrib. 77−89505
dynamics of polymer chain, hydrodynamic and excluded vol. interactions, critical exponent 78−50668
ebonite, nontransparent dielectric, laser emission reflection and destructive action *(Russian)* 79−74031
elastic and creep moduli meas. by contact methods 80−11852
elastic deform. meas., occurring under reversible slippage, friction method 77−52598
elastic moduli, press. depend. 78−52877
elastic modulus, precision meas. using reson. method *(German)* 78−76823
elastic modulus, temp. depend. 80−39202
elasticity, effect of geometric constraints on junctions 78−75711
elasticity of bulk and film from multipass Brillouin spectra 78−76485
elasticity of chains 80−3116
elasticity of polymer globule 77−70404
elastometric glasses and porous network polymers, review of future developments 78−22657
electret, charge dissipation, transport mechanisms 80−7268
electret, vapour-induced depolarization currents 79−87379
electrets, fundamental aspects of research, book 80−77552
electrets, piezo- and pyroelectric props. 80−80685
electrets and dielectrics, conf., Sao Carlos, Brazil, Sept. (1975) 80−7251
electric phenomena, book 80−46746
electric strength rel. to permittivity, loss-angle, and volume resistivity 78−6631
electrical conduction and polarisation phenomena at low fields 78−48113
electrical conductivity, self-consistent continued-fraction theory of cond. 79−69482
electrical phenomena, nature and appl., review 80−50254
electrical props., book 80−7257
electrification by metals, contact time effect obs. 80−70829
electrochemical mass transfer, drag-reducing polymers, effects, comparative study 80−76528
electrochemical mass transfer between rough surfaces and solutions containing drag-reducing polymers 80−19447
electrolytes, solid polymer, H_2O electrolysis, H_2 technology 80−67012
electron microscopy, LV, struct. obs. 79−6223
electron problems by SCF method, HF matrix 77−79718
electronic conductivity, bulk controlled mechanism 80−20182
electronic structure, fragmental calc. by nonempirical method 77−89684
electrophotographic developers, triboelec. two-step decay scheme 79−80711
emulsion particles containing epoxy groups, cleavage study of epoxy groups *(Japanese)* 77−90649
end-to-end distribution function, for most probable molecular weight distribution 78−13635
endoprosthetic joint, fatigue life 80−40521
energy bands of polymers with defects, ab initio SCF crystal orbital calcs. 78−30884
energy transfer, intra- and intermolecular nonradiative processes 77−34792
engineering materials, nature and props., book 78−72707
engineering materials, vibration damping and control, design and meas. 78−87185
engineering materials review 79−56918

polymers continued
entangled, ternary blends of monodisperse homopolymers, viscoelastic props. 80−19301
entangled, viscoelastic props., binary blends of monodisperse homopolymers 79−96062
entangled, viscoelastic props., interchain-intrachain entanglement model 78−42575
entangled monodisperse polymers kinetic network model for nonlinear viscoelastic flow props. 80−28538
entangled polymers, viscoelastic props., transient network model 78−13918
entanglement, topological theory, chain centre friction coeffs. 80−91709
environment effect on stability of cracking 79−100273
epichlorohydrin/bisphenol A epoxy polymer concrete, viscoelastic props. 80−45340
Epikote 828 cured with tetraethylenepentamine, fracture stability 80−30070
episulphide network polymers, mech. relaxation 79−96061
Epon 828, simple procedure for casting plates for 2D photoelastic models 79−39061
Epon 828 epoxy, composite three dimensional model for photoelasticity 78−52871
Epon 828-Z, acoustical determ. of shear relax. functions 78−76686
epoxide cellular, in vitreous state, creep 79−96092
epoxide network polymers, glass-transition and chem. struct. *(Russian)* 78−51653
epoxide resin, low temp. crack propag. 80−85020
epoxide resin, self-toughening mechanism on Al substrate 79−70293
epoxide resin, struct. and elastic moduli 77−85984
epoxide resin, tensile, compressive and shear yield strengths, pyramidal criteria 77−8884
epoxide resin cured with aliphatic dicarboxylic acids, fatigue behaviour *(Japanese)* 79−79092
epoxide resin with maleic anhydride hardened, edge effect of time, surrounding medium effect 77−86211
epoxide resins, amine-hardened, heat distortion, glass transition temps., chem. cure 80−44302
epoxides, dielectric relax. and deform props., cross-link density effect *(Russian)* 80−60942
epoxies, Ablefilm, Dupont, EPO-TEK and Eccobond, water vapour sorption 79−82454
epoxies, Epo-Tek H31 LV and H62, low temp. sp. ht. 78−43138
epoxies, mechanical characterisation at low temps. 78−64611
epoxies, stress-enhanced chemiluminesc. 80−40628
epoxy, clear, refr. index and extinction coeff. meas. 79−18492
epoxy, crosslinked, time-temp. superposition applied in creep with superimposed hydrostatic press. 77−70127
epoxy, curing composition, viscoelasticity in critical region 77−62228
epoxy, elastic and rubbery strain optic coeff., birefringence effect depend., room temp. 77−32348
epoxy, elastomer-modified, loading rate depend. fracture prop. 80−76342
epoxy, for interference filter, γ-radiation effects on transmission 79−64297
epoxy, mech. props., 20 to 300°C *(French)* 77−56018
epoxy, reinforced, outgassing rate in vacuum, control by pretreatment 79−40583
epoxy, Stycast 1266, very low temp. thermal conductivity and optical props. 78−55992
epoxy, thermomech. props., rel. to hardener type and conc. 79−1913
epoxy, three-component modified, development for dynamic photoelastic obs. of fracture 78−35474
epoxy (Araldite B), photothermoelasticity meas. by heating method 80−6000
epoxy acrylate coated fused silica fibres, dynamic and static fatigue 78−1385
epoxy acrylate coated optical fibre, long term strength, environmental effect 78−5582
epoxy acrylate coated optical glass fibre, strength and static fatigue 78−1386
epoxy acrylate coatings, UV cured, for optical fibres 78−1444
epoxy adhesive, ultrasonic curing time investigation 79−83430
epoxy adhesive layers, interlaminar stress distrib. in nonlinear range 79−39117
epoxy adhesive-Al system, open and edge-sliding fracture toughness 78−95805
epoxy Al bonded, adhesive joints under complex loading, development of failure criterion 78−92344
epoxy based structural adhesives, time-temp. cure behaviour, torsional braid anal. 80−55621
epoxy cement for $Pb(Zr,Ti)O_3$ fibre arrays, ferroelectric ceramic-plastic composites 80−81015
epoxy cure, autocatalytic reaction, kinetic parameter estimation 79−70327
epoxy EDT-10, rigid polymer, thermal stress isothermal relaxation 80−71683
epoxy impregnated superconducting composites, mech. props., strain effect at 4K 80−25822
epoxy materials, crack blunting mechanisms 80−66624
epoxy meas. of H_2O diffusion by radionuclides, corrosion effects *(Czech)* 77−48566
epoxy polymers, cured spin-spin and lattice relax., proton coupling, ^{13}C NMR obs. 80−34799
epoxy polymers, dense-network, elastic deform. rel. to props. *(Russian)* 80−40468
epoxy polymers, high temp./press. materials test for undersea environment 78−3213
epoxy polymers, unfilled and filled effect of specimen size on elec. strength expt. 77−8505
epoxy replication of optics 77−27401
epoxy resin, arc resistance tests in various gas insulators *(Japanese)* 80−81250
epoxy resin, Cl-containing, relation between static and dynamic deform. characts. 80−3137
epoxy resin, crack propagation, photoelasticity investig. 79−8341
epoxy resin, cure history effect on dynamic mech. props. 80−54356
epoxy resin, curing accelerator effect on props. and ingredients *(Japanese)* 78−27726
epoxy resin, curing investigation by polarisation current method 80−3345
epoxy resin, deform. rate depend. of mech. props. at cryogenic temps. 80−55456

polymers continued
epoxy resin, destruction by diffused water 78−48511
epoxy resin, E-glass fibre reinforced, flexural fatigue properties 79−66138
epoxy resin, effect of environment on stability of cracking 78−95887
epoxy resin, electron beam effect on struct. 77−69001
epoxy resin, exam. of shear stress-strain charact. 78−60691
epoxy resin, fracture energy under plane strain conditions 78−80624
epoxy resin, glass bead filled, elastic moduli, interfacial slippage effect anal. 78−76688
epoxy resin, glassy, thermoelastic effect, thermal expansion coeff. 79−14944
epoxy resin, hardening, mechanical and dielectric losses 78−48115
epoxy resin, heat generated by fatigue *(Spanish)* 80−11736
epoxy resin, interaction with SF_6 plasma, in glow discharge, emission spectrum 80−87960
epoxy resin, low temp. fatigue, tensile strength, Young's modulus *(German)* 78−76748
epoxy resin, low temp. irradiation effects on mechanical props., use in superconducting magnets 78−60737
epoxy resin, low temp. thermal props., phonon states and crosslinked struct. *(German)* 78−75846
epoxy resin, mag. susceptibility, constant mag. field effect 80−11154
epoxy resin, meas. of glass transition temp., linear viscoelasticity 80−29157
epoxy resin, mech. and thermal props., amine hardeners, added softeners and filter effects *(Polish)* 78−68741
epoxy resin, mobility of sorbed water, low resolution PMR method 80−11276
epoxy resin, nitroxide spin label doped, EPR study 79−78523
epoxy resin, outgassing and its reduction 77−71333
epoxy resin, parabolic mirror made by rotation method, fabrication and defects 79−76889
epoxy resin, partial discharge initiation phase, effects of field strength, temp. and internal mech. stresses *(German)* 78−72461
epoxy resin, partial discharge long-time tests obtained by automatic data acquisition and computation *(German)* 79−71432
epoxy resin, plastic deform. effect on crack propag. 80−97563
epoxy resin, plastic deform. mechanism 80−97534
epoxy resin, rubber modified, positron annihilation 80−29825
epoxy resin, shear strength determ., anal. of methods 77−86107
epoxy resin, sheet, stress intensity distrib. through plate thickness along crack front 79−43390
epoxy resin, stresses arising during high-speed droplet impact 80−71764
epoxy resin, thermoelastic stress creation and motion picture recording of interaction with dynamic crack 78−56697
epoxy resin, thermosetting, crosslinking kinetics and structure *(German)* 78−76624
epoxy resin, thermosetting, electrical props. during cure cycle 77−72864
epoxy resin, time-temp. superposition of creep data, linear viscoelastic props. 80−30045
epoxy resin adhesives, capillary flow and bond strength 80−71883
epoxy resin adhesives, crack propag. and mech. props. 78−68783
epoxy resin as coupling layer in acousto-optical charact., freq. charact. 77−62069
epoxy resin as pressure transmitting medium, appl. to compression expts. on Si, MgO, and $ZrSiO_4$ 77−89496
epoxy resin based tissue substitutes for radiography studies 78−7424
epoxy resin bond layer, prep. methods, ultimate thickness 80−71884
epoxy resin clad metal, corrosion charact. by electrical resist. and capacitance meas. *(German)* 80−30171
epoxy resin compositions, shrinking and thermal tension estimation using ferrite sensors *(Polish)* 80−35456
epoxy resin cross linked with aliphatic polyamines, struct. and dynamic mech. props. *(Japanese)* 80−38956
epoxy resin cured with composite curing agents, arc resistance *(Japanese)* 78−92371
epoxy resin curing, elastic moduli changes, US wave propagation monitoring technique 79−20305
epoxy resin DGEBA, cured with TETA, crack propag. and fractography 79−70154
epoxy resin ED-5, specific heat during solidification *(Russian)* 78−38816
epoxy resin EhDT-10, temp.-time rel. of strength 80−25798
epoxy resin fast fracture and crack arrest, finite difference anal. 78−1607
epoxy resin glued overlapped steel sheets, strength tests, nonuniform adhesive layer *(German)* 78−15647
epoxy resin hardened with maleic anhydride and PMMA, viscoelastic props. 77−25089
epoxy resin microcircuitry elements, thermoelastic phenomena *(Polish)* 80−93724
epoxy resin parabolic shells, exam. of viscoelastic creep 79−43307
epoxy resin Quetol 651, low viscosity, embedding biol. tissue for electron microscopy 78−20322
epoxy resin RDGE MPDA hardened with dispersed Al, light scatt., holographic correlometer study 80−74321
epoxy resin removal from tissue for SEM 79−5424
epoxy resin subjected to extensional creep, dynamic props. 80−71697
epoxy resin systems, synthesis review, phys. and mech. props. at low temps. 80−25650
epoxy resin use in noise and vibration control 77−50829
epoxy resin wear and cutting surface against brass *(Japanese)* 78−56779
epoxy resin with various fillers, filler effect on relaxation time spectra 77−52390
epoxy resin-Al alloy 5086, scarf joint test specimen, mixed mode adhesive fracture, bond angle effect 78−68768
epoxy resins, charact. by differential scanning calorimetry 80−71869
epoxy resins, correlation between valence energies and low temp. flexibility 80−25815
epoxy resins, crack propag. stability, effects of water, temp., specimen geometry, hardener 78−11324
epoxy resins, exam. of fracture energy above glass transition temps. 78−56743
epoxy resins, fracture props. study at cryogenic temps. 80−25869
epoxy resins, mech. and elec. low temp. props. 80−25814
epoxy resins, mech. props., alteration by reactive elastomers *(German)* 79−100106
epoxy resins, phenomena and mechanisms of tree inception 80−29687

polymers continued
epoxy resins, relationship between struct. and mech. props. *(Japanese)* 78−31438
epoxy resins, strain anal. by fluoresc. meas. *(French)* 79−47846
epoxy resins, struct. changes under mag. field action 80−40516
epoxy resins, VLF partial discharges meas. over freq. range 0.1 to 50 Hz 77−76227
epoxy resins analysis, cured, combination of pyrolysis, gas chromatography and conventional analytical techniques *(Japanese)* 79−87914
epoxy structural adhesives, tensile tests, stress/strain relations, stress relaxation 78−60702
epoxy system, rubber-modified and unmodified, sub-T_g annealing expts. 79−11643
epoxy systems, thermoreactive, elasticity modulus, change on curing *(Russian)* 79−64521
epoxy thermosetting powders, parameters 79−20003
epoxy treeing breakdown, slit model 80−15970
epoxy type adhesives, solidification temp. conditions rel. to strength *(Russian)* 79−56972
epoxy-Al composite, thermal conductivity 77−76630
epoxy-Al composite, thermal conductivity model 77−76629
epoxy-anhydride-polycaprolactone, cross-linked block copolymer, morphology and impact strength 78−91265
epoxy-based crosslinked polymers, deform. and strength charact., temp. effects *(Russian)* 79−65139
epoxy-metal joints, environmental fracture and effects of shrinkage stresses 80−16635
epoxy-Nb interface, Kapitza resist. in supercond. and normal states 77−66085
epoxy-paper, flashover behaviour at low temps. 80−25882
epoxy-resin join with Teflon-glass fabric double layer material, adhesion strength determ. method 77−77681
epoxy-resins, sp. ht. and thermal cond., 0.1 to 80K, phonon scatt. 79−65215
epoxy-rubber particulate composite, toughness and fracture mech. 80−71727
epoxy-steel system, friction and wear 78−44229
epoxy/metal joint under combined stress, expt. study of strength 79−74339
EPR of free radicals, spin-lattice relax. time meas. 78−19331
equation of state *(German)* 79−82309
ESCA, polymer primary struct., extended HMO density of states and band struct., chemical shifts 78−52630
ESCA, struct., bonding and reactivity 78−53299
ESCA investigation of struct., reactivity and bonding, O_2 (inert gas) surface modification 78−3438
ESCA investigations on selected systems, struct. and bonding obs. 78−14302
ESR spectroscopy in polymer research, book 78−91958
ester-inide varnishes, electroinsulating, thermal resist. *(Polish)* 78−84014
α,ω-ethoxy-poly(ethylene oxide), crystallisation 77−51329
ethyl acrylate ionomers, stress relax. 80−104200
ethylene copolymers, partially cryst. pseudoeutectoid, swelling, thermodynamics 80−39311
ethylene copolymers, partially crystallised, quasistatic moduli at small strains *(German)* 78−76700
ethylene copolymers with acrylic monomers, NMR investig *(Russian)* 80−54959
ethylene oxide-propylene oxide copolymers, composition dependence, sessile bubble method, surface tension measurements *(Japanese)* 79−69323
ethylene propylene diene terpolymer, crosslinked, AC elec. breakdown studies 78−43787
ethylene propylene rubber, effect of electrode profile on dielec. breakdown voltage, epoxy resin insulation system 80−60502
ethylene propylene terpolymer, insulating materials, dose rate effect on degradation behaviour 79−99239
ethylene propylene/polyolefin blends, radiation cross linking 80−66801
ethylene vinyl acetate copolymer, torsional rigidity testing *(German)* 77−52596
ethylene vinyl alcohol copolymer, prep., props. and appls. *(German)* 80−89194
ethylene vinylacetate copolymers, prep., props. and appls. 80−35154
ethylene-β-chloroethylacrylate, ^{13}C-NMR microstruct. investigation, substitution increments, sequence distrib. *(German)* 78−13636
ethylene-base ionomers, impact tensile props. *(Japanese)* 79−96120
ethylene-CO copolymer, dielec. absorpt. meas., permittivity *(French)* 80−103916
ethylene-CO copolymer, highly alternating, melting and internal motion 77−51474
ethylene-Co copolymers and -SO_2 copolymers prep. by catalysis and ^{60}Co γ-radiation, mech. props. 80−66841
ethylene-deuteroethylene copolymer, polymeric unit heterogeneity *(Russian)* 79−55017
ethylene-glycidylacrylate copolymer, ^{13}C-NMR microstruct. investigation, substitution increments sequence distrib. *(German)* 78−13636
ethylene-methyl acrylate, random copolymer, review 80−108330
ethylene-propylene copolymer, surface tension, composition and temp. depend. *(Japanese)* 78−79860
ethylene-propylene copolymers, mech., photoelastic props. rel. to chain microstruct. 77−48468
ethylene-propylene copolymers, thermoelastic effects 78−88491
ethylene-propylene terpolymers, vulcanized, cond. of props. with mol. weight distrib. function parameters *(Polish)* 79−50175
ethylene-tetrafluoroethylene copolymer, chem. etching of fission tracks 80−896
ethylene-vinyl acetate copolymer, powdered, prep. by emulsion polymerisation *(Japanese)* 80−104110
ethylene-vinyl acetate copolymer, X-ray irrad., trapped carriers, TSC 77−69338
ethylene-vinyl acetate-vinyl chloride graft copolymers, rel. between morphology and toughness *(German)* 80−66665
ethylene-vinyl alcohol (<36.3 mol.%) copolymer, elastic moduli of crystalline region *(Japanese)* 79−15715
ethylene-vinyl alcohol (>40 mol.%) copolymer, elastic moduli of crystalline region *(Japanese)* 79−15716
ethylene-vinyl alcohol copolymer, drawn samples, annealing effect around T_g temps. on shrinkage and mol. orientation 80−79712
ethylene-vinyl alcohol copolymer, O_2 permeability *(Japanese)* 78−31702
ethylene-vinyl alcohol copolymer membranes for haemodialysis, prep. conditions and props. *(Japanese)* 80−12299

polymers continued
ethylene-vinyl alcohol copolymers, H bonding study by near-IR spectra *(Japanese)* 80−78734
ethyleneterephthalate-ethylene glycol copolyester/15% polyglycol, semicryst. melting and glass transitions 80−49346
excluded vol. component, physical bound 78−66698
extruded, glass transition temp., melting pt., DTA 78−2235
extrusion, flow and heat transfer relationships, numerical anal. 79−77188
extrusion, solid phase, anal. of mechanics 80−39204
extrusion dynamics, visual study 78−94625
extrusion properties prediction using capillary rheometer 79−90204
F-10, flexible accumulator vessel H oscillator, wall-induced frequency shift measurement appl. 79−2749
fabrication, processing, production, book 78−48363
failure, book 78−92361
failure build-up on micro- and macro-level 77−70172
fatigue, fracture 79−43425
fatigue crack growth, model 78−15506
fatigue crack growth model 79−70160
fatigue crack growth model 79−70161
fatigue life, determ. from reheat temp. 79−61724
fatigue testing apparatus in plane stressed state 78−3300
fatigue testing machine under axial load 77−66734
ferrography of polymer form. under lubricated nibbing contact 77−21292
fibre, highly oriented, struct. and mech. props. 78−75563
fibre, lifetime under load, in presence of UV radiation, stress depend. 78−48535
fibre, lifetime under load, in presence of UV radiation stress depend. 78−48534
fibre-reinforced plastic, creep prediction from components props. 80−40448
fibres, cyclic tension endurance, Prevorsek-Lyons theory 78−52967
fibres, ultra high modulus, prep. by soln. and melt spinning, review 79−11544
fibres preparation, development and uses 79−83168
fibrillation during cold drawing *(Russian)* 77−63691
fibrils, formation by flow-induced crystallisation 80−33908
fibrin, modification by synthetic polymers 80−61090
fibrous, electron diffr., inelastic scatt. background correction 77−27782
fibrous crystallisation, chain extension and fibre form. 78−75573
fibrous material, drawing and annealing 78−15458
fibrous polymeric material, molecular model of fracture 78−60768
Fickian diffusion of a solvent, and organic penetrant in a polymer 79−42292
filled polymer, elastic moduli, effect of particle shape 78−15444
flammability, correlation with heat of combustion *(Polish)* 78−53246
flammability, heat transfer meas., moving wire technique 80−3347
flashover behaviour, of spacers at low temps. 80−25882
flexible chain collapse 78−87628
flexible macromolecules, flow-induced crystallisation, nonhomogeneous shear rates effect 80−38952
flexible structures, physical props. 79−19331
floating chain, config. statistics, impenetrable barrier confinement 77−58216
Flory formula for the polymer size exponent ν 78−70985
flowing, relaxation of normal stresses 77−881
fluid high polymer, ultimate strength in unixial extension 79−38920
fluid-permeable rod, longit. stability during creep 79−57066
fluorescence polarisation meas. at high press. 78−66576
fluorinated copolymers, mech. and elec. props., processing and appls. 78−84760
fluorinated ethylene-propylene copolymer, charge transfer by non wetting liquid contacts 77−4420
fluoro epoxy resins, surface props., appls., wear resistance and friction 78−64713
fluorocarbon ether bibenzoxazole polymers of low glass transition temp., preparation and characts. 79−51006
Fluorolon-3, utilisation factor determ. during electron beam sputtering *(Russian)* 79−66008
fluoroplastics, heavy charged particle detectors 79−26821
fluoroplastics, mech. props., accumulation of submicrocracks, thermal treatment effects 77−4850
fluoropolymer adhesive joints, fracture and surface anal. by SEM and ESCA 77−55434
fluoropolymer components, pulsed US quality control of heat treatment 78−60953
fluoropolymers, determ. of microstruct. by secondary emission mass spectrometry *(Russian)* 77−31604
fluoropolymers, ion beam sputtering 79−83353
fluoropolymers, ion-beam textured, adhesive bonding 79−87752
fluoropolymers, linear, valence electronic struct., LCAO cryst. orbital calcs., ESCA 78−5384
foamed, rigidity 78−95769
foams, cell cracking 79−11701
foil, electron irradiated, charge dynamics, computer simulation 79−82915
foil optical props. study by photoelasticity in const. and oscillating mech. fields *(German)* 78−31168
formaldehyde polymer formation mechanism in interstellar space 78−54032
formaldehyde resin, effect on metrological charact. of resistance wire strain gauge 77−120
Formvar, phonon spectrum from Al-Formvar-Pb junction electron tunnelling 77−59080
formylstyrene copolymers, luminesc. *(Russian)* 79−56861
Fourier anal. of X-ray diffr. patterns 80−15016
Fourier transform IR spectroscopy, use in polymer research as vibr. spectroscopy tool 80−55744
fraction exponential function use for viscoelastic behaviour *(Russian)* 80−53652
fracture, molecular interpretation 78−60769
fracture, time depend., mol. motions effect 79−15780
fracture and crazing under plain strain *(Japanese)* 80−25850
fracture and fatigue, review 78−68781
fracture energy spectrometer 79−57181
fracture kinetics, book 79−29222
fracture mechanism, surface crazing 77−90446
fracture mechanism of material with macrodefects *(Russian)* 78−35500
fracture of material with initial defects 80−38339
polymers continued
fracture time variability, endochronic prediction 78−76734
fracture toughness, mol. theory of low mol. wt. polymers 79−66140
framed particles, automatic selection of polymer shells for laser targets 77−80336
free radicals determ., on polymer surfaces, using spectroscopic method *(German)* 80−7892
free vol. theory 79−94919
freely jointed polymer chain with bond vectors of fixed lengths 79−3605
fretting on steel, polymer composition effect on metal surface wear 78−60848
Fretting-induced damage between contacting steel-polymer surfaces 78−15539
friction, calc. of coeff. for isotropic surface contact 78−64716
friction, changes in material performance 77−52509
friction 77−4859
friction and wear, role of mech. props. 78−52998
friction coefficient calc. for contact surfaces with nonspherical asperities 79−20200
friction of polymer-polymer pair, adhesive, interaction 78−3227
friction pair with metal, temp. calc. under severe friction 80−40550
frictional properties, crystn. effect 80−40551
frost deform. 77−50624
FSGO model, X-ray diffr. struct. factor calcs. 77−46660
furfuryl alcohol resins, PMR study of mol. motion 79−8062
fusion reactor materials, effects of radiation on electrical insulators 78−95082
gas chromatography meas. of struct. and interactions 77−90698
gas environment effects 77−4845
gas permeability measurement in high polymers, techniques and detectors 80−14854
Gaussian polymer molecule config., large mol. Kirchhoff matrix reduction 79−13850
Gaussian polymer molecule config., stars and random regular nets, distrib. functions 79−13849
gel, heterogeneous two-phase, permeability 80−76563
gel, magic angle rot. H NMR spectra meas. by variable temp. probe 80−31830
gel permeation chromatography, appl. to polymer characterisation 80−16740
gel permeation chromatography, data treatment 79−92037
gel permeation chromatography of polymers, using silicic sorbents *(Russian)* 79−52857
gelation, statistical mech. model, site-band correl. 79−34368
gelation site-bond percolation, low-density series anal. of uncorrelated limit 80−4657
gels, light scatt. intensity, network struct. effects 79−70381
gels, non-linear behaviour under strong deform. 78−7240
gels, thermodynamic props., review *(German)* 78−20073
gels, with liq. cryst. solvents, theory 80−11963
general composite perturbed elastic rod soln., longitudinal acoustic mode 78−18726
glass, fracture toughness determ. method *(Russian)* 78−11457
glass, isobaric vol. and enthalpy recovery, transparent multiparameter theory 80−24375
glass, isothermal struct. relax., in high elasticity transition region, mol. model *(Russian)* 78−87629
glass, specific heat discontinuity at glass transition 80−19954
glass, struct., review of expt. results 79−37636
glass, thermodynamics of densification process 78−95723
glass article, polymer bound, rapid kinematic corrosion test, method and apparatus 79−39063
glass bead-reinforced epoxy resin composite, bulk and shear elastic props. 78−6959
glass fibre reinforced plastic/polyurethane foam/Al sandwich, flexural props. *(Japanese)* 78−56707
glass temp., correl. to dilute soln. dielec. relax. rates 78−10175
glass temperature, rel. to cohesion energy and vacancy form. energy *(German)* 78−22670
glass transition, dynamic props., mol. model *(Russian)* 78−87777
glass transition, fluctuation theory and thermodynamics *(German)* 79−51242
glass transition, mol. wt. depend. 79−95144
glass transition, positron annihilation studies, review 78−95614
glass transition, temp., conform. effects 78−83925
glass transition due to plastic deform., high-molecular linear polymer of narrow molecular mass distrib. 79−96065
glass transition evaluation by entanglements 78−83926
glass transition kinetic nature, sp. ht. 79−10929
glass transition T_g rel. to ESR parameter T_{50G}, mol. interpretation 78−67817
glass transition temp., dilatometric and dielectric relaxation data 80−6497
glass transition temp., effect on various polymers *(German)* 78−30742
glass transition temperature, domain size dependence 77−89525
glass transition temperature, rel. to mol. wt. 80−34176
glass transition thermodynamics, fluctuation theory approach *(German)* 79−33078
glass transition under high-press., dielec. loss method obs. *(Russian)* 78−71841
glass-forming polymer, paramag. spin-lattice interactions 80−7149
glass-like, DSC obs. of mol. interaction variations *(Russian)* 79−32924
glass-transition point meas. apparatus using vibration meas. of immersed plate *(Russian)* 78−71842
glass-transition temps., mol. wt. effect, thermodynamic theory 80−19920
glass/Cu-polymer compound powders, prep. and corona charging props. *(Japanese)* 78−19679
glass/epoxy composite, tensile test 80−11778
glass/polymer interface, exam. using ion scattering spectroscopy and scattered ion mass spectrometry 78−60641
glass/polymer/glass plate in temp. field, failure 80−43674
glasses, enthalpy relax., scanning calorimetry technique 80−90851
glasses, mech. or elec. props., struct. recovery *(French)* 80−59393
glassy, ageing, scanning calorimeter meas., theoretical prediction 79−10810
glassy, craze surface displacements, model 80−93651
glassy, elastic moduli, calc. method from chem. struct. *(Russian)* 78−75707
glassy, elec. resist., corresponding states relationship 80−59704
glassy, flow behaviour 78−55573
glassy, gas sorption and transport, review 80−15360

polymers continued
glassy, generality of discontinuous fatigue crack growth 77−32677
glassy, generality of plastic fracture process 80−35321
glassy, Gruneisen const. calc. from thermoelastic meas. 79−14945
glassy, improvement of alignment in diffuse fibre diffr. patterns 77−55243
glassy, initiation and growth of crazes 78−60767
glassy, multi-phase Stefan problem describing swelling and dissolution 78−2263
glassy, power law relationship between yield stress and shear modulus 78−15467
glassy, sheets and spheres, gel diffusion with discontinuous swelling 80−44354
glassy, sorption of solvents, sample-dimension effects 79−52766
glassy, strength and safe calcs. for brittle state *(Russian)* 77−59898
glassy, stress analysis aspects of crazing 80−21148
glassy, structural acoustic relaxation 79−95088
glassy, tensile stress/strain curve description 78−67158
glassy, tricritical points 79−82320
glassy, viscoelastic relaxation processes role in macrodeformation 79−72825
glassy, yield stress, Robertson eqn. modification 77−36574
glassy and crystalline relax. process characterisation, ^{13}C NMR obs. 80−34802
glassy linear polymer, mol. model *(Russian)* 77−62610
glassy organic polymers, total fracture surface energy, theory 79−43406
glassy polymer, relationship between activation energy of creep and cohesive energy 79−69188
glassy polymers, HVEM in-situ deform. 80−104215
glassy polymers, non-elastic deformation, thermodynamic and kinetic anal. 78−64604
glassy polymers, powders, transport props., vapour sorption expts. 78−76919
glassy polymers double NMR, appl. of cross relaxation dynamics in modulated systems 80−71242
glassy state, ^{13}C NMR *(German)* 80−93188
globule formed by saturating bonds, spatial struct. *(Russian)* 77−10802
glow polymerisation, thin organic polymer coating technique *(German)* 77−12774
graft copolymers, normal vibrs., calc. method *(Russian)* 78−29871
granules, compression, stress state 80−10218
graphite-epoxy composites, moisture profile meas. using nucl. reaction anal. 80−55760
graphite-epoxy hybrid laminates, low level Charpy impact response 78−11333
graphite/epoxy laminate, T300/5208, proof testing under cyclic tension-tension fatigue 80−81249
graphite/epoxy laminates, statistical fatigue, high load effect 80−93642
graphite/polyimide laminates, effect of ply stacking sequence and orientation on residual stresses 77−52378
grinding technique, cryogenic 77−32555
group theory in polymer physics 77−19124
growth, stochastic models 77−72567
Gruneisen formulation of p-V equation of state, for solid and liq. 78−30733
gutta percha, partially hydrogenated, ^{13}C NMR 80−20472
haemolytic characteristics of polydimethylsiloxanes 77−60290
Hall effect extensometer for simple shear meas. in polymers 79−23286
hard disc necklaces, rigid and nonrigid models, mol. dynamics 80−43219
hardening of liquid photopolymer materials, mathematical modelling *(Russian)* 80−62784
heat transfer processes relax. 79−90122
heat treated, numerical simulation of AC elec. props. 78−43431
helical, optical activity, decorrel. approx. theory 77−63389
helical wormlike chain statistical mechanics, persistence vectors, comparison rot. isomeric state model 77−50573
helical wormlike chain statistical mechanics, scatt. function 77−54637
heterodisperse, molecular weight distribution rel. to ease of fabrication 80−35530
heteropolymer in random mag. field, Ising chains, statistical mechanics, free energy, numerical calcs. 78−77803
heteropolymers, melting theory, correlated chains 79−25996
heteropolymers, melting theory, random chains 79−25995
2,4-hexadiine-1,6-diol-bis(p-toluene sulphonate), cryst., polymerisation, elastic consts., Brillouin scatt. 79−1950
2,4-hexadiyne-1,6-diol bis-(p-toluene sulphonate), dielec. const. during solid state polymerisation 79−51899
2,4-hexadyne-1,6-diol-bis-p-toluene sulphonate, partially polymerised single crystal, fluoresc. 78−6756
hexafluoropropylene-tetrafluoroethylene copolymer, surface component of vacuum absorpt. and resorpt. currents, surface charge accumulation 80−60063
hexafluoropropylene-tetrafluoroethylene copolymer, surface component of vac. absorpt. and resorpt. currents, source of dielec. loss 80−70792
hexamethylene polyester, epitaxial crystn. on aromatic hydrocarbon substrates 79−61521
hexamethylolmelamine, doped, and condensation resin, room temp. phosphoresc., thermal transforms. 80−45132
HF density of states 80−6689
HF storage and loss moduli, determination using US immersion apparatus 80−74668
high, material behaviour under influence of stress and aggressive media *(German)* 79−39009
high field conduction and breakdown in solid dielectrics, review 80−84691
high molecular weight, glass transition temp. and crit. props. 80−39265
high molecular weight polyethylene for HV cables, characterisation using size exclusion chromatography 80−66897
high polymer physics, conf., Washington, USA (March 1978) 79−11633
high polymers, solid, mech. energy relax., linear response theory 77−89387
high-impact polymers, HVEM in-situ deform. 80−104215
high-modulus, behaviour in solid state, nonlinear irreversible thermodynamic approach 80−44154
high-polymer physics, conf., San Diego, California, USA (March 1977) 78−14292
high-polymer physics, conference, Atlanta, GA, USA (Mar.-Apr. 1976) 77−4051
highly elastic state, mechanical losses and relaxation processes *(Russian)* 78−76698
highly oriented, elastic wave dispersion relations 78−51618
polymers continued
highly oriented polymers, small-angle X-ray diffr., fibril struct. 78−75565
Hilhorst model, generalised, statistics of trees and branched polymers 79−3604
Holmalite-100, dynamic photoelastic and dynamic finite-element analyses of dynamic-tear-test specimens 79−55348
hologram recording by thermoplastic deform., book contrib. 78−25836
holomicroscopic investigation 79−17474
Homalite, specimen geometry effect on crack propag. and arrest 79−34148
Homalite, stress intensity factor measurement, dynamic fracture toughness determination from isopachics of a running crack [holographic interferometry] 79−34257
Homalite 100, dynamic fracture toughness 78−60740
Homalite-epoxy duplex specimens, crack arrest study via dynamic photoelasticity 78−31515
homologue mixtures, viscosity, conc. depend. *(Russian)* 79−23761
homopolymer, theory of 1D adsorpt. on to 80−51034
homopolymer chain adsorpt. on uniform surface 78−53316
homopolymer chain adsorption on homogeneous surface, theoretical model 77−70403
hopping transport, microscopic rate equations 80−39580
hydrocarbon resin, mol. wt., chem. constitution investigation by gel permeation chromatography *(German)* 78−64910
hydrodynamic boundary conditions and polymer chain dynamics 77−11155
hydrodynamic props., struct. depend. and Brownian motion 77−50575
hydrogel coatings, and impregnations in silastic, dacron and polyethylene 79−20719
hydrogels, two-component, elasticity theory and compress. meas. 80−44246
hydrogels on silicone rubber, radiation grafted, thrombogenicity meas. by vena cava ring test 79−44062
hydrophilic polyamides, sorption and permeation of water and water vapour *(Japanese)* 79−70376
hydrophilic polymers, ESCA evaluation of surface layer water structuring and protein adsorpt. 80−108758
hydrostatic extrusion, deform. of crystalline and amorphous and thermosetting resins 79−38875
hydrostatic extrusion effects on subsequent mechanical behaviour 77−90392
2-hydroxy, 3-allyl, 4,4′-dimethoxybenzophenone, methyl methacrylate copolymer, excitation singlet, internal H^+ transfer, visible spectra 80−32728
2-hydroxy-3-crotonyloxypropyl methacrylate, synthesis, copolymerisation with maleic anhydride, photocrosslinking *(Japanese)* 78−31376
N-hydroxyethyl acrylamide-styrene(methyl methacrylate) copolymers, synthesis, anion active membrane transport appl. 80−61142
hydroxyethyl cellulose, microviscosity, mobility profile 80−91710
2-hydroxyethyl methacrylate-methacrylonitrile or acrylonitrile copolymer network, mech. response 79−57031
hydroxyl-terminated prepolymers, functionality determ. 79−31746
Hypalon 40, chlorosulphonated polyethylene, mech. props., press. effects 77−32618
ill-condensed matter, summer school, Les Houches, France (July-Aug. 1978) 80−82561
impact resistant styrene copolymers, control of morphology and props. *(Bulgarian)* 80−35153
impact testing, elastic analysis of conventional test, reassessment of testing 78−60770
inelasticity, estimation using hysteresis friction model 80−7617
inelasticity degrees, estimation, hysteresis friction model appl. rel. to US testing 80−3136
infinite chain, trigonometric series evaluation 79−7041
infinite conjugated polymers, π-electron energy and energy gap, topological calcs. 80−91713
infinite helical, classical theory of circ. dichroism 77−65550
infinite polymers, long-range Coulombic interactions, LCAO-CO calcs. 79−7042
insulating materials, water treeing initiation and growth, effects on cable service life 80−84698
insulation, tree initiation mechanism 77−24791
insulators, controlled current DC meas. 78−57982
intercalation inorganic-organic layered complexes, effects of intercalation on elec. and mag. props. *(Japanese)* 79−8255
interfaces, visualisation by phase contrast electron microscopy 78−14295
at interfaces and interactions in colloidal dispersions 78−11572
interpenetrating polymer networks, and related materials, review 78−42923
interpenetrating polymer networks, synthesis and properties 78−76623
interrelations, raw materia 80−63876
interstellar molecules and prebiological evolution 79−92842
interstellar polymers, assoc. with grain clumps and prebiotic molecules 77−26042
interstructural filling, effect on props. 77−63622
intramolecular cross-linking reactions, Monte Carlo calcs. *(Russian)* 78−31636
intravenous catheters, comparative study of polymers in animals and man 78−7459
intrinsic viscosity meas. *(Polish)* 78−42687
ion etched surface microstructures 79−83362
ion exchange resins, macroporous rapid method of rating total void volume 80−21208
ion-exchange resin:phenoxyl, electron spin echo spectra, instantaneous and conventional spectral diffusion 79−15355
ionene polymers, counterions and absorbed water influence on mech. relax. 77−40430
ionene polymers, ion conc. effect on mech. relax. 77−44284
ionene polymers containing triethylenediammonium or 4,4′-bipyridilium ring, TCNQ salts, chem. struct. correl. with cond. 79−91032
ionic polymer, role of electrostatic forces in glass transition temp. 77−84908
ionised ethylene-acrylic acid copolymer, heterogeneous ionomer, dynamic mech. props. *(Japanese)* 77−59843
IR Fourier transform spectroscopy 78−58870
irradiated, crosslinking density effect on glass transition *(German)* 80−34175
irradiation by high energy electron beams, industrial applications 80−3210
Ising model equivalent 80−37914

polymers continued
isolated chain, molecular span and end to end probability distrib. 79−64137
isotactic polypropylene/butene-1 copolymers, soln. grown crystals, props. 77−55247
isotactic polystyrene gel, anomalous X-ray diffraction effects, rel. to chain conformation and isomeric homogeneity 77−50576
izod polystyrene, influence of dimensions in mech. props. *(German)* 80−21039
joist, bending calc. *(Rumanian)* 77−68396
jute, cement reinforcing fibre, alkali resist. 80−89377
Kapton, optical, elec. props., struct., ion textured surface 78−72904
kapton, positron source, temp. depend. 80−93426
Kapton, pyrolysed, cond. polymer, transport and mag. props. 80−96887
Kapton (polyimide), insulators for superconducting magnets, effect of low temp. irradiation 80−25817
Kapton H, aromatic, polyimide, conformational investig., X-ray method, pot. energy calcs. 77−3498
Kapton H, discharge area scaling and surface/subsurface damage due to electron beam irrad. 80−34853
Kapton laminate, substrate, electron beam evaporation of uniform Al film 78−11373
Kelzan dilute aqueous solns., flow in various geometries 79−41757
Kevlar 29 and 49, aramid fibres, microvoid obs. 80−38960
Kevlar 49, fibre, mech. props., environmental effects incl. sunlight, ionising rad. 77−36560
Kevlar 49 fibre, macromol. struct., electron diffr. and dark-field electron microscope obs. 78−34446
Kevlar 49 fibre, poly p-phenylene terephthalate, Raman spectroscopy, heat, stress, radiation effects 79−65871
Kevlar 49 high modulus polyaromatic fibre, supramolecular struct. 78−55819
Kevlar aramid fibre, regular fine bands obs. by polarization microscopy 80−107064
Kevlar fibres, effect of crystallinity and orientation on mech. props. *(Japanese)* 79−38952
Kevlar-29, flexural fatigue and surface abrasion 78−15504
Kevlar-49, chemical characterisation 78−95725
Kevler fibre, mech. props. in aq. H_2SO_4 soln. *(Japanese)* 79−47753
Kinel 5504, mech. props. 20 to 300°C *(French)* 77−56018
kinetic nature of strength 78−15524
kinetic study of random scission *(Japanese)* 77−66754
lambda tight cement, for low temp. techniques 79−35752
lamella growth, kink nucleation and propagation along steps of finite length, modelling 77−31669
lamella structure, crystallisation under high supercooling 79−69028
lamellar structures, effects of distortions, small angle scattering, finite cluster model 79−10814
lamellar two-phase systems, interface distrib. function determ., X-ray small angle scatt. 79−10812
laminar copolymers of collagen and synthetics, tissue compatibility 77−60289
laminates, C/epoxy, moisture distribution determination, low cost method 79−65252
large molecule, electronic struct., photoemission and optical absorpt. spectrum, CNDO/S3 model 80−53172
laser damage mechanism due to multiple pulse exposure 77−731
lateral grain boundaries in synthetic polymers 79−14700
latex, monodisperse, phase transition pressure determ. from sedimentation equil., Alder transition model 77−70344
latex, monodisperse, reflectivity obs. of phase separation into ordered and disordered phases 77−70345
latex colloidal crystal, melting, particle packing fraction depend. 77−73475
latex particles, surfactant adsorpt., electrokinetic investig. 80−3363
latex polymer, electrodeposition on metal 78−53015
latex solids, agglomerating and dewatering 80−104470
lattice model polymer chain Monte Carlo study, Rouse coord. distrib. and dimens. 79−89814
lattice polymer dynamics, relax. time Monte Carlo anal. 78−5380
lattices, particle size control 79−38785
lattices, purification 78−7243
Lennard Jones polymer, eqn. of state, collapse transition 77−19117
Lexan:triphenylamine, molecularly doped, hole transport by hopping 78−34831
Lexan:triphenylamine, photosensitisation using rhodamine B or thiapyrylium 78−34856
Lexan, optical and phys. parameters 79−32004
Lexan polycarbonate, N-isopropylcarbazole and triphenylamine doped, trap-controlled dispersive hopping transport 77−15850
Lexan polycarbonate, thermolum. radiation-induced EPR of free radicals and track etchability 79−76295
LF vibration spectrum, effect of dimensional quantisation *(Russian)* 79−1480
lifetime, hydrostatic press. effect 77−70170
lifetime, ultimate, at high loads 79−20184
lifetime reduction under cyclic loading 77−66695
light and Raman scattering obs. of high press. phases *(Japanese)* 80−2773
lightguide, light propag., nonlinearity, quasi-optical approx. 80−99837
lightguide attenuation coeffs. meas., data anal., accuracy 79−1005
linear, liq. cryst. state prediction using Flory's model of phase transitions *(Russian)* 77−43318
linear, slow relax. processes *(Russian)* 78−46475
linear, struct. disordered, electron localisation 80−29359
linear and ring, intrinsic viscosities, perturbation calc. 79−55914
linear chains, excluded vol. problem 80−5650
linear macromolecules, cryst. growth 78−30561
linear polymer excluded vol., SCF theories 78−70983
linear self interacting chains, configurational props. 80−23586
linear self interacting chains, internal distrib., radius of gyration 80−23587
linear viscoelastic model and dynamic behaviour elec. transmission line representation *(Spanish)* 77−72185
linear viscoleastic creep under arbitrary temp. variations 79−95075
liquid, entropic elasticity and time temp. superposition principle, thermodynamic eqn. of state 78−63406
liquid, flow, hydrodynamic eqns., centre of mass model, friction approx. 78−55664
liquid, Ising fluid equation of state 77−51469

polymers continued
liquid and solid state at 200 MPa, thermal variables meas. *(Russian)* 77−57327
liquid crystalline, struct. and morphology, theory 79−69025
liquid crystalline discotic phases, optical microscopy obs. 79−41951
liquid crystals structurally related to 4-alkoxyphenyl-4'-alkoxybenzoates, nematic phase 79−60267
liquid N_2 immersed short-term insulating characts. 79−85145
loaded, mech. of macrocrack generation and propag., photometric and X-ray meas. 77−4886
local plastic deform. mech., effect of lattice defect 77−28870
localised electron states in impure polymer, Koster-Slater method, convergence and interleaving theorem 78−23051
long-range Coulombic interaction, Fourier transform technique calcs. 79−31748
long-term durability prediction methods, review 79−20320
long-term strength prediction, review 80−104226
longitudinal acoustic mode, appl. of general theory to planar zigzag methylene chains 78−14421
longitudinal acoustic mode, perturbing forces 80−70348
longitudinal acoustic mode in 79−73277
longitudinal acoustic mode in polymer chain 77−7816
loss-loss, dielectric loss meas., automatic, high resolution, at 100 MHz to 300 MHz and 2°C to 40°C 80−68219
low-temperature materials, IR spectra rel. to heat shield prod. for changing mag. fields 77−74408
macromolecular configurations symmetry group construction 77−71898
macromolecule, microconformation by fast exchange NMR spectra 80−102593
macromolecule functional groups, reaction kinetics and statistics, review *(Russian)* 79−87825
macromolecules, molecular structure, conformation and properties 80−63874
magic angle rotation ^1H NMR, appls. 78−43649
magnet appl. based on moulding with ferromagnetic powder material *(Japanese)* 80−60829
magnetic, spin-spin correlation excluded volume effects 79−42781
magnetic, suscept. and neutron scatt. function 77−12099
magnetic field, nonuniform const., effect on props. during hardening 78−11235
magneto-optical props., MCD, Frenkel exciton model 78−10873
maleic anhydride-styrene copolymer, photochromic, recording material for holograph 79−72537
manipulator for placing ring shaped testpiece in cold chamber of tensile testing machine 77−63859
matrix, decreased stabilisation energy of excimers and exciplexes 80−25431
matrix effect on photochromism of spiropyrans 80−76537
mech. props., temp. dependence of polymers of different struct., 4.2 to 300K 78−68746
mechanical properties, rel. to struct., review 77−7301
mechanical properties, testing using Rayleigh surface waves 79−70249
mechanical properties at 4.2K, depend. on chemical struct. and physical struct. form. 77−28847
mechanical relaxation, nonlinear *(Russian)* 80−40467
mechanical retardation time spectrum, thermostimulated creep 79−5014
mechanics, atomistic models 77−72193
mechanics, use of statistical methods, review 78−67031
mechanics, Volterra eqns. approx. soln. 79−50614
mechanochemical degradation 80−40371
medical applications review, book contrib. 80−12307
melt crystallisation, intrachain trans double bonds influence 79−14701
melt-crystallised, one-dimensional characterisation of microstruct. 78−75588
melting, theoretical aspects 80−59633
melting, theory 77−76325
melting theory, phonon anharmonicity effects 78−67659
membrane, porous, gas permeability *(Japanese)* 79−24825
membrane, transport of organic liqs., review 80−16720
membranes, self-supporting, 2-3 μm, dip-coating technique, props., appls. 79−1838
metal, polymer coated, wear and friction 77−21328
metal polymer contact, charge transfer and contact charge spectroscopy 80−65680
metal polymer contact, charge transfer and contact charge spectroscopy 80−65681
metal polyphosphinates, bulk compressibility meas. to 30 kbar 80−76306
metal-filled polymers, thermal cond., var. calcs. of upper and lower bounds 78−9550
metal-polymer, ply-separation resist. polymer polarity effect *(Russian)* 80−61064
metal-polymer contacts, methods of decreasing wear 79−20209
metal-polymer deposit, simultaneous electrophoretic deposition and electrochemical precipitation 79−56938
metal-polymer sliding, wear eqn. in terms of fatigue and topography of sliding surfaces 80−108597
metal-polymer splices, adhesive bond destruction and strength w.r.t. electrochem. interaction 79−20339
methacrylamide, by H transfer, catalyst sodium-naphthalene *(Japanese)* 78−95726
methacrylate polymer, carbazolyl substituted, excimer and charge transfer complex trapping of excitons 80−34367
methacrylates, cross-linked, structure-transformation relations, properties *(German)* 79−55677
methacrylic acid-methyl methacrylate statistical copolymer suspension polymerisation, stabilisation effects, viscosity 78−85157
methacrylic heterocyclic ester polymers, electron beam irradiation 77−76466
methacrylic polymers, multiple dielectric relaxations, investigation by thermally stimulated current and creep methods 80−93238
methacryloyloxyethyleneoxycarbonyloxypropylene, NMR relaxation mechanism *(German)* 78−33527
α,ω-methoxy-poly(ethylene oxide) effect of swelling on longitudinal acoustic mode 80−29739
methyl α-n-alkylacrylate methyl methacrylate copolymer, friction and wear 77−63809
methyl methacrylate methacrylic acid copolymer, hydrogen bonding effect on mol. relax., IR obs. of dissoc. process 77−58959
methyl methacrylate natural rubber latex copolymer, electrochemical initiation 77−55936

polymers continued
methyl methacrylate-methacrylic acid copolymer, hydrogen bonding effect on dielec. relax., T_g region 77−59512
methyl methacrylate-p-chlorostyrene copolymer, side-group rot. and dielec. relax. 79−61303
methyl methacrylate-styrene copolymer, dielec. characts. change rel. to composition 80−25296
methyl methacrylate-styrene copolymer, side-group rot. and dielec. relax. 79−61303
methyl methacrylate-styrene copolymers, ^{13}C NMR 80−20473
methyl polymethacrylate, heat emission coeff. and cooling const., Angstrom periodic heat wave method 77−72706
α methyl styrene-acrylonitrile, molecular mass determ., solubility studies *(German)* 80−23590
3-methyl-3-buten-2-one copolymers with styrene and methyl methacrylate, photodegradation *(Japanese)* 80−108725
α-methylstyrene-butadiene copolymers, chem. composition determ. by gel permeation chromatography 79−70410
methylundecanhydride hardened phenol formaldehyde resin, hardening kinetics and mech. losses 80−66520
microcrack enlargement in heterogeneous materials, conc. criterion 80−11769
microfibils of oriented polymers, struct. of amorphous sections 78−18559
microinhomogeneous, elastic props. description rel. to crystallinity 79−19307
microparacrystallites, small angle X-ray scattering 79−10813
microporous, lubricant supply charact. 78−64711
microscopic images quantification *(Polish)* 79−49347
microstructure morphogenesis, book contrib. 78−83757
microtoming for structure analysis 80−40665
microvoids as pigments in polymeric materials, review 79−52617
mixed amorphous system, correlation of Tg, glass transition 80−24574
mixed heterogeneous homogeneous nucleation and nonintegral exponents of time 78−55820
mixing, heats 80−61132
mixtures, compatible, glass-transition temps. 79−46789
mixtures, heterophase, excess energy 78−53264
mixtures, IR difference spectra, dispersion effects 79−96379
mixtures, IR spectra, ratio method anal., computer simulation 77−71387
mixtures, thermodynamics, review 79−1506
mobility edge, classical solns. and crit. exponents 80−10936
model adhesives, peeling, morphology and rheology obs. 78−92439
model polymer, conformation theory, correlated walk model 80−74268
modelling with paraffins, mol. motion, thermal expansion and phase transitions 78−51436
molecular charge states, contact charge exchange 78−14822
molecular configuration, expansion of self-avoiding chains, studied by loop elimination 79−86100
molecular configurational packing statistics near surface 77−35491
molecular dynamics, Brownian dynamics model for backbone chain 79−86096
molecular dynamics, review of Brownian motion theory 80−23589
molecular dynamics simulation of polymer chains with excluded volume 78−78845
molecular dynamics simulation of struct. 80−28923
molecular mechanism of orientation 77−69033
molecular motion, fluctuational network of nodes *(Russian)* 79−51011
molecular motion, thermally stimulated creep 77−90402
molecular orientation, extensional effects, IR obs. 77−23591
molecular relaxation, comparison of TSD and dielec. loss meas. 78−10834
molecular relaxation kinetics, time-depend. Ising model 79−54066
molecular size distrib., high temp. ALC/GPC equip., Waters 150C, polyolefin exp. data 79−10806
molecular struct. rel. to bulk props. 77−32553
molecular ultraslow rot. obs. using D probe spin alignment tech. 80−88890
molecular weight, distrib. determ. by low angle laser light scatt. combined with gel permeation chromatography 78−92230
molecular weight correlation with physical and rheological props. 77−51011
molecular weight distrib., generalised exponential distrib. description 78−94346
molecular weight distribution of multi-functional polymers 80−83531
molecular weight meas., improved graphical method 79−36806
molecular weight measurement using recording thermistor cryoscope based on standard components 77−50572
molecular weight ratio, number-average: weight-average, polydispersity 80−74274
molecularly doped, carrier drift, percolation approach 80−2390
molecules, irreducible representations of symmetry groups 79−3603
Monte Carlo renormalisation group for polymers 80−42148
morphology and electrical properties, correlation, review 78−43786
morphology and lamellas in bulk and oriented linear high polymer 78−51434
Mossbauer spectroscopy 77−12798
multichain polymer system, simulating dynamic and equilib. props. 80−53179
multicomponent, props. and struct., review 78−44076
multicomponent inhomogeneous system, diffusion with moving boundaries and swelling at const. volume 80−44353
multicomponent polymer homopolymer blends, macroscopic phase separation 80−45289
multicomponent polymer system, liq.-liq. phase separation, thermodynamic aspects of polymer compatability 78−14469
multicomponent-multiphase polymers, bulk struct. by rheo-optical techniques 78−91267
multiphase polymer systems, conf., Ohio, USA (May 1976) 78−91262
multiphase polymers, morphology using electron microscopy 78−91271
multiphoton photodestruction, mechanism 79−39177
multiple dielectric relax. processes, mol. aspects, book contrib. 80−50264
multiple surface waves on viscoelastic half-space 78−79254
multipolymers, glass transition rel. to phase separation 78−91270
Mylar, discharge area scaling and surface/subsurface damage due to electron beam irrad. 80−34853
mylar, implantation of positrons from ^{22}Na 80−16118
mylar, positron source, temp. depend. 80−93426
Mylar, shells, conical and cylindrical, high speed photographic exam. of buckling 78−44184
Mylar, substrate for ^4He film growth, vap. press. meas. 80−70499
polymers continued
Mylar (polyester), insulators for superconducting magnets, effect of low temp. irradiation 80−25817
mylar caps for working cavities of liquid H_2 targets, fabrication 77−46441
Mylar film sliding against polyethylene and PVC , material transfer 78−64726
Mylar/adhesive/Al laminates, mech. interactions 80−81112
N-allyloxymethyl-poly(ε-caprolactam), electron crosslinkable, electron and photosensitivity *(Japanese)* 79−91951
n-octadecyl methacrylate methyl methacrylate copolymer 77−63809
Nafion, densities and expansion coeffs. as function of various parameters 80−79711
Nafion per fluorosulphonic acid ion exchange membranes, Mossbauer spectroscopy 80−80659
1-naphthyl methacrylate-9-vinylanthracene copolymer, time-resolved fluoresc. spectra 78−80401
Neoprene WB, polychloroprene rubber, mech. props., press. effects 77−32618
network, crosslinks and trapped entanglements, two-network model 80−38962
network, crystn. and form. through crystn., crystallinity influence on radiation induced form. 80−38964
network, permanently crosslinked, topological struct. and macroscopic behaviour 80−37919
network, Riemann's metric degeneration to graph metric demonstration, chain entanglement problems 80−38963
network, small ang. neutron scatt. 79−90569
network, small-angle neutron scatt. obs. of mol. behaviour 80−37918
network entanglement contribution to rubber elasticity 80−39203
network formation, pre-gel intramol. reaction and gelation, shear moduli and glass transition 80−45501
network formation, relaxational props. variation 80−38961
network formation, struct. and mech. props., computer simulation 80−38965
network junctions, elasticity, local constraints effects 78−2021
network polymers, cured, low freq. mol. mobility, quadratic electrochromism method *(Russian)* 78−71688
network polymers, heterogeneous, from partially hydrolysed poly(methyl D-glutamate) and poly(oxyethylene glycol) *(Japanese)* 78−95002
network systems, intramol. mobility, polarised luminesc. obs. *(Russian)* 77−42455
networks, deformation free energy, vol. depend. 80−40454
networks, diffusion mechanism and model, local conform. change 80−15288
networks, stochastic cross-linked, modulus of elasticity, functionality effects *(German)* 80−59555
networks, stress-strain behaviour, nonlocalised junction effects 77−59063
networks, stress-strain behaviour models, multiaxial tension *(German)* 79−69183
neutron scatt. studies of chain conform. and dynamics 78−83753
neutron scattering, elastic, coherent small-angle neutron scattering 77−80428
neutron scattering by molecules, polymers and absorbed species, review 79−41911
neutron scattering from strained polymer networks 78−78846
neutron scattering spectroscopy, recent advances, biology and chem. phys. appls. 77−35445
neutron scattering techniques in applied research, medium-flux research reactors 79−13514
nitrocellulose-nitroglycerine propellant, glass transition temp., thermomech. anal. meas. 79−14917
NMR, review 80−11277
NMR, review 80−88888
Nomex, fibre, mech. props., environmental effects, incl. sunlight and ionising rad. effs. 77−36560
Nomex (nylon paper), insulators for superconducting magnets, effect of low temp. irradiation 80−25817
noncrystalline, thermal cond. rel. to temp. *(German)* 79−28159
noncrystalline solid, preferred orientation from scatt. ang. distribs. 78−75560
nondestructive testing, rigidity and hardness from acoustic, thermal, optical and dielectric props. *(Russian)* 77−48601
nonlinear electric behaviour interpreted through free vol. changes 78−84226
nonlinear stress relaxation under tension and torsion 79−52290
nonlinear viscoelasticity and relaxation phenomena of polymer solids 77−68439
nonlinear viscoelasticity problem with geometric nonlinearity, variation principle 77−62176
nonoriented partially crystalline, elasticity and strength 77−52386
nonvinyl polymers, diffusion of simple penetrants, statistical mechanical model 80−6556
normal stress difference, estimation from shear stress data in polymer rheology 79−64506
novolac and novolac allyl ether electrets, thermal depolarisation, chem. struct. effect 80−71297
nuclear filters, prep. from polymers using Ar ions 78−86714
nucleation, bundle-like and longit. growth of fibrillar crystal from flowing soln. 78−51433
nylon, exam. of bending strength, using new method 78−53056
nylon, H-bridge interactions, far IR spectra study 80−11374
nylon, oriented, transverse compression 78−68728
nylon, partially crystn., temp. effects on fracture 77−63771
nylon, positronium form. and decay, elec. field effect 80−97369
nylon, Raman spectra using pulsed laser and gated detection 77−74529
nylon, steady-state deform. and its effect on struct. and morphology 78−15459
nylon, stress cracking induced by $ZnCl_2$ solns. 78−27594
nylon, thermal cond., near 100 mK, rel. to appl. in cryostat construction 77−82535
nylon 11, pyroelectricity and piezoelectricity 77−69780
nylon 12 membranes, permeation charact. *(Japanese)* 78−31692
nylon 66, annealed in glycerol, stepwise lamellar thickening 77−86059
nylon 66, doubly oriented, annealing of drawn and rolled samples, struct. 78−52859
nylon 66, fatigue crack propagation, effect of moisture 80−3166
nylon 66, filament, heat setting and thermomechanical behaviour 78−15435
nylon 66, polymorphism 79−14694

polymers continued
nylon 66, predominant carrier species determ. using galvanic cell 77−69384
nylon 66, stress-enhanced chemiluminesc. 80−40628
Nylon 66, stress-oriented NMR expt. using multiple impulses to achieve line narrowing *(German)* 77−28457
nylon 66 films, superstructural ordering 80−15344
nylon 6,6, drawn fibre, selective degradation, cryst. morphology 78−71683
nylon 6,6, selective degradation, morphological charact. 78−71682
Nylon 6,6, sliding behaviour against Cu or Al spheres at cryogenic temps. 80−66671
Nylon 6,6 fibres, birefringence determination, using backscattered light intensity distrib. 79−42939
nylon 6, α-form, crystal struct. and molecular packing 80−33905
nylon 6, drawn yarn, origin of double melting peaks 78−3118
nylon 6, effect of moisture content on glass transition temp. and Young's modulus 79−4401
nylon 6, evidence of electron transfer as mechanism of static charge generation, contact with Hg 79−47153
Nylon 6, fibre, crystallite dimensions, effect on struct., mech. and diffusive props. 78−11273
nylon 6, fibres, viscosity-average mol. wt. change during fracture 78−19882
nylon 6, influence of monomer and water diluents on mech. relax. 79−4993
Nylon 6, injection moulded, residual stresses 80−38950
Nylon 6, injection moulded, yield stress and fracture toughness 80−38951
nylon 6, microfibril dimensions, from small-angle X-ray scattering 79−37574
nylon 6, notched sheet, deform. mech., fracture, X-ray obs. *(Japanese)* 77−59863
Nylon 6, oriented, extensional deformation, and effects 80−7613
nylon 6, oriented glassy, mol. wt. influence on cryst. rate 80−44156
Nylon 6, plasticized with NH_3, deformation by solid-state extrusion 80−25736
Nylon 6, pressurized heat treatment effect on fatigue props. 79−87669
nylon 6, relationship between morphology and dynamic mech. props. 79−4992
Nylon 6, small-angle X-ray scatt. struct. changes w.r.t. thermal and mech. history 79−41976
Nylon 6, solution crystallization 79−86719
nylon 6, stress depend. of US velocity *(Japanese)* 78−26629
nylon 6, swelling by absorbed water, mol. orientation effect 78−11285
nylon 6, transient elec. conduction at high temp. 79−69513
nylon 6, vacuum-UV irrad. photoelec. emission and contact charging 79−52075
nylon 6, water effects on TSC 80−75925
nylon 6 (polycaproamide), salted, glass transition temp. and elastic modulus, moisture effect 80−103465
nylon 6 and 66, necking stress *(Japanese)* 77−56037
Nylon 6 fibre, shrinkage, influence of chain rupture during tensile deform. 79−34055
nylon 6 fibres, chain rupture during tensile deform. 79−15740
nylon 6 fibres, dynamic mech. props., interpretive nonlinear viscoelasticity 79−4994
nylon 6 fibres, highly oriented, fatigue process, struct. changes 77−90447
nylon 6 fibres, struct. changes due to strain annealing 79−15692
Nylon 6 gut yarn, fine struct. change in twisting, annealing and untwisting, microbeam X-ray obs. 80−81026
Nylon 6 gut yarn, fine struct. change in twisting, annealing and untwisting, X-ray and electron microscopy obs. 80−84904
Nylon 6 yarns, NMR, fibre struct. rel. to annealing, drawing *(Japanese)* 77−32269
nylon 6-inorganic salt mixtures, glass transition temp. 80−19921
nylon 6-LiCl mixtures, DC cond. and struct., Lill effects 80−44149
Nylon 7-7 and 11, dielectric const. and dielectric relax. 80−25294
nylon II, high-press. X-ray structural study 78−14296
1-nylon stress-strain curve 80−60938
nylon-11, folded-chain crystal, pressure-induced crystallisation from melt, annealing 77−84671
nylon-12, folded-chain crystal, pressure-induced crystallisation from melt, annealing 77−84672
Nylon-12, hydrostatic extrusion, struct. change *(Japanese)* 79−15693
nylon-12, roll-oriented, conduction anisotropy *(Japanese)* 80−54707
Nylon-1 polymers and copolymers, mech. props. rel. to glass transition 77−11625
nylon-6,6, creep meas. at const. temp., humidity 78−95883
nylon-6,6, creep prediction for different physical conditions, by superposition of creep curves 79−68603
nylon-6, chain extension mechanism during crystallisation under press. 77−56008
nylon-6, crystalline, atomic coords. calcs. 78−91272
Nylon-6, injection moulded, struct. and morphology 80−38949
nylon-6, ns breakdown voltage, polarity effect, mechanism 77−63367
nylon-6, pressure-crystallised, morphology and structure 77−84669
Nylon-6, viscoelastic props., meas. with modified torsion pendulum *(Spanish)* 77−31264
nylon-6 fibre, chain rupture and tensile deform. viscosity-av. mol. wt. obs. 78−76714
Nylon-6 fibre, crystal struct., WAXS obs. 80−15015
nylon-6 pressure-crystallised, annealing under pressure 77−84670
nylon-quartz fibre support for low temp. mag. suscept. meas. 78−65947
nylons, exam. of frictional behaviour *(Japanese)* 78−64714
Nylons, glass transition temp., thermal, mech. meas. 77−31758
Nylons, inorganic salt influence on fracture 80−30119
Nylons, morphology and crack propag. in inorganic salts 80−30118
Nylons 6, 66, 610, change in cryst. struct. with temp. 77−15324
off-lattice chains, Monte Carlo anal. of excluded vol. problem 80−5647
off-lattice polymer chains, Monte Carlo calcs. 78−5382
oil-polymer mixture, acoustic attenuation CW meas., tissue simulation appl. 80−35961
oligobutenes, anomalous behaviour of viscoelastic props. 77−63704
oligoesteracrylates, three dimensionally linked, dynamic mech. props. *(German)* 78−64577
oligoethylene glycol, crystallisation kinetics in presence of tetrachloromethane, NMR investig. *(Russian)* 80−54153
oligomeric model of excitable membrane, with asymm. behaviour of inner and outer sides *(Japanese)* 77−44611

polymers continued
oligomers, polymer-derived, mass spectral charact. 80−37916
oligourethaneacrylate photopolymerised layers, production of holograms *(Russian)* 79−7102
one dimensional, nonlinear optical props. 78−46708
one dimensional polymers, compositional disorder, approx. band struct., self consistent virtual crystal approx. 80−39486
one-dimensional chain, thermal fluctuation induced rupture, computer simulation 78−91378
one-dimensional semiconducting polymer, demonstration of high mobility 80−20212
one-dimensional systems, optical props. 77−43472
optical absorption spectra and symmetry of polymer chain 79−55011
optical components, moulding techniques for single, multi-element systems 78−63210
optical fibre, polymer clad SiO_2, ionising radiation effect 78−42405
optical fibre polymeric coatings, Bell Labs activities 78−1388
optical fibre waveguide, glass core/polymer cladding, high numerical aperture 80−96024
optical fibres, flexible, manufacture *(German)* 79−27393
optical microscopy, birefr. obs., high polymers 77−32733
optical microscopy exam. techniques, high polymers 77−32734
optical recording media, review 78−71172
optical storage materials and methods, conf., San Diego, USA (Aug. 1977) 78−71171
optical waveguide and appl. *(Japanese)* 78−90518
optically active cold-setting, for models of composite materials in thermal stresses investigation 80−40639
optically active stereoregular, conform. props., rel. to config. 78−33644
organo tin polymers, glow discharge formed, interface composition and adhesion 79−82467
organosilicon binders, kinetics of gasification in production of BN ceramics 78−60635
organosilicon ladder polymer, vel. meas. of longitudinal and shear US waves 78−95114
organosilicon ladder polymers, effect of γ-rays on props. *(Russian)* 78−76891
organosilicon ladder polymers, struct. and phys. props., book contrib. 79−65012
organosilicon polymer precursor for SiC fibre development 78−60627
organosilicon polymers, ladder-type, local conforms. *(Russian)* 77−19121
organotextolite, in plane state of stress, temp. depend. variant of strength 80−40449
orientation effects, conf., Budapest, Hungary (April 1976) 78−75557
orientation measurement and characterisation methods, using X-rays 78−75559
orientation measurement by spectroscopic techniques, mech. anisotropy 78−75558
orientation measurement methods, review 78−48589
orientation of plane of large cracks prod. by laser pulses 80−11753
orientational ordering rel. to mech. props. *(Russian)* 78−59766
oriented, amorphous-crystalline low ang. X-ray diagrams, supermol. struct. models, schematic representation *(Russian)* 78−87630
oriented, dynamic shear modulus determ. by acoustic method 78−23911
oriented, macroscopic yielding 77−90397
oriented, partly cryst., macromols. in amorphous regions, length, mobility 80−49132
oriented, polarized dielectric appl. *(French)* 79−51902
oriented, small-angle X-ray patterns, processing method *(Russian)* 78−71642
oriented, thermostable, relax. transitions, thermomech. and isometric heating obs. *(Russian)* 79−23538
oriented, under load, crystallite stability 77−70126
oriented block copolymers, single cryst. mesomorphic state 78−75572
p-n junction, rectification effects in dark and photocurrents 77−69407
PA-6, polymer fibre, orientation changes during stretching, IR spectra 78−75568
packing coefficient determ. from acoustical meas. data 80−38959
Pade approximant method, appl. to excluded vol. effect 79−94918
PAN fibre, pre-oxidised, IR absorpt. 77−28561
para-polyamide based fibres, struct. deform. props. 80−60928
paracrystal theory, thermodynamic stability, statistical mechanics 78−75592
paracrystal theory appl. to real systems *(German)* 78−75591
paracrystallinity, mosaic block concept 77−84673
n-paraffins, longitudinal acoustic mode freqs., general theory for composite perturbed elastic rod 78−14421
partial discharges, simulation and meas. *(German)* 77−77146
partially crystalline, comparative evaluation of various prep. techniques for morphology visualisation 80−13049
partially crystalline, sp. vol. press. depend. *(German)* 78−75852
partially labelled chains, neutron scatt. obs. 80−38899
particle pigment agglomerate display, optical microscopy method 79−85177
particle track detectors appl., for neutron dosimetry *(Czech)* 78−66425
particle-filled polyurethane resin, tensile strength, particle size effect 77−73305
particles, photomicrography of submicrometer birefringent contaminants in C black dispersions 80−62757
parylene, for chronically stable reproducible microelectrode insulation 77−40942
parylene polymers, synthesis, elec., phys., corrosion props. *(German)* 78−64521
path integrals with a periodic constraint: entangled strings 79−2651
PBI fibre, mech. props., environmental effects, incl. sunlight and ionising rad. effs. 77−36560
PC, foil, electrochem. track etching for charged particle detection 78−17521
PCA, dehydration effect on carbonisation process, high temp. resistant materials *(Russian)* 79−8269
PCA metal adhesive bonds, shear resist., polymer crystn. effect 80−89462
PCBM, thermal and sp. ht., temp. depend. anal. rel. to oligomer base 80−19721
PCDM, thermal and sp. ht., temp. depend. anal. rel. to oligomer base 80−19721
PCEM, thermal and sp. ht., temp. depend. anal. rel. to oligomer base 80−19721
PCGM, thermal and sp. ht., temp. depend. anal. rel. to oligomer base 80−19721

polymers continued
PCTFE, work to produce environmental crazing at low temps. 78−15553
penetrant diffusion, statistical mech. model 80−44351
pentaplast, crystn. effect on frictional props. 80−40551
perdeuteropolyethylene, IR and Raman intensities by electro-optical parameters, single chain 78−1115
perfluoro polyether, vacuum behaviour 79−63254
perfluoro polyether, vacuum use as pump fluid 80−52251
perfluorocarbocyclic ethers, NMR, microstruct. 79−51863
perfluoropolyether, appl. to vac. pump technology *(Japanese)* 78−229
perfluoropolyethers as vac. pump fluids 78−32828
Perspex, clear, effect of storage temp. on dosimeter calibration 77−60256
Perspex, dielec. breakdown and space charge, treeing 78−27160
perspex, electric conduction and isothermal dielectric relax. 80−80285
perspex spheres, internal fractures due to stress wave focusing 78−18239
perylene, organic soln., picosec. fluoresc. for rot. diffusion 79−56839
perylene crystallite, photophoretic force, action spectrum determ. 79−50841
PET, amorphous, intrinsic birefringence calc. from wide angle X-ray scatt. 80−108178
PET, crystallised in liquid environment, exam. of crystallisation kinetics and X-ray scattering 79−41980
PET, crystallization, lamellar growth kinetics and thickness 80−103266
PET, densification, cryst. perfection, mechanism 79−66082
PET, effect of liquid aliphatic compounds on mech. props. 80−55488
PET, fibre, crystallite dimensions, effect on struct., mech. and diffusive props. 78−11273
PET, filament form. from gels 78−80508
PET, foil, electrochem. track etching for charged particle detection 78−17521
PET, glassy polymer, local struct. determ. 80−33904
PET, intrinsic briefringence 80−29711
PET, ionic cond. current rel. to neutralisation at polymer-metal interface at elevated temps. 80−24664
PET, ionizing radiation effect on life *(German)* 80−19853
PET, IR, spectra of prefractured state 77−69032
PET, oriented, extensional deformation, and effects 80−7613
PET, penetrant diffusion, statistical mech. model 80−44352
PET, photoexcited, thermolum. and carrier detrapping mechanism 79−61445
PET, pyroelectric effects and depolarisation currents, illumination effects 80−34859
PET, rigid, unoriented, prefracture state study, forced high-elastic deform. 77−59931
PET, selective chem. etching using primary amines 79−57130
PET, stress induced crystallisation, X-ray and light scattering obs. 79−99083
PET, surface component of vacuum absorpt. and resorpt. currents, surface charge accumulation 80−60063
PET, surface component of vacuum absorpt. and resorpt. currents, origin and magnitude 80−70791
PET, thermodynamic equilib. melting parameters, effect of annealing 78−71837
PET, uniaxially drawn, comparison of polarised fluorescence, polarised Raman and IR dichroism measurements 79−99084
PET fibre, aminolyzed, dynamic viscoelasticity and thermal behaviour *(Japanese)* 79−38880
PET fibre, anisotropy of dielectric relaxation 80−25297
PET fibre, irrad., radical yields 79−96343
PET fibre, molecular orientation determ. by US propag. velocity 77−58961
PET fibres, adhesivity improvement by plasma surface treatment 79−15823
PET fibres, amorphous, exam. of birefringence 80−11360
PET fibres, orientation distrib. of crystallites 79−86722
PET film, relation between deform. and rotational isomerism 77−52438
PET-CdS photoreceptors, air space effects on electrophotographic props. *(Japanese)* 79−44962
PFFE, impact fracture toughness, rate effect 78−56741
PFTE wear, combined rotating and linear motion effects 80−3201
phenoformaldehyde thermosetting resin, computer stimulation of form *(Japanese)* 77−66619
phenol formaldehyde resin (Novolak), with and without feldspar filler, mech. and thermal props. determ. *(German)* 78−84828
phenol formaldehyde resin medium, protection methods for tensoresistors 79−54121
phenol resin (Resol), with and without feldspar filler, mech. and thermal props. determ. *(German)* 78−84828
phenol-formaldehyde resin, thermodynamic props. 78−91452
phenol-urethane composition based, properties and production methods *(German)* 79−56951
phenolformaldehyde resin, sp. ht. obs. *(German)* 78−75845
phenolic, two-stage cured, molecular struct. of Novolac effect on thermal stability *(Japanese)* 78−3092
phenolic novolac resin-rubber mixture, glass transition, mixing ratio effect *(German)* 79−77732
phenolic resin filled and unfilled, mech. relaxation behaviour, effects of temp. and time *(German)* 78−6963
phenylone, deformability in physiological salt soln. 80−12305
phonon density of states in linear disordered system, self-consistent continued-fraction method 77−69062
photo-oxidation 80−3380
photochemical probes 77−90626
photochemistry 80−3381
photochromic polymer, thermal effect in photomech. conversion 80−16706
photochromism in bulk polymers 80−5805
photodegradation, materials testing, problems *(Japanese)* 77−55245
photoelastic modelling, suitability of materials under γ-irradiation *(German)* 79−33666
photoelectric effects in insulating polymers and relation to cond. processes 77−43640
photoelectron escape depths determ. from X-ray photoelectron spectra 78−27368
photographic emulsion 78−16866
photopolymer for holographic recording, sensitised by redox system *(Japanese)* 77−7030
photopolymer imaging systems, for laser recording 78−71173
photopolymer in holographic real-time fluid flow measurement 80−6176
photopolymer laser recording materials development 77−54678

polymers continued
photopolymer latent imaging system, for vol. phase hologram recording 78−42298
photopolymer printing surfaces for gravure 79−35871
photopolymers, for holographic recording, using photopolymer material, redox sensitized 78−13674
photoradiative processes in free radical form. *(Russian)* 79−57269
photoresists, crosslinking efficiency, exptl. determ. 77−87862
photosensitisation processes in mol. doped polymers 79−2857
phthalocyanine polymer, dynamic mech. props. and fracture energy 80−100866
physical chemistry teaching, macromol. principles 78−77643
physical problem determ. problems, tensile strength, elastic moduli *(German)* 78−15470
physical structure, of amorphous state, conf., Atlantic City, USA (Sept. 1974) 77−76327
physically nonlinear, stress relaxation during stretching 78−23754
piezoelectric, transducer appls. 79−32169
piezoelectric polymer flexural disk hydrophone 78−63254
piezoelectric polymers, props. and appls. 78−80289
piezoelectricity and pyroelectricity, appl. *(Japanese)* 78−88257
piezoelectricity and pyroelectricity, review 77−8514
pigment-antioxidant interaction, numerical analysis 79−39136
pivalolactone-α-methyl-α-propyl-β-propiolactone copolymers, struct., thermal and mech. props. 79−43582
plane materials stress relax. and creep under biaxial loading, test procedure 78−3279
plasma polymerisation and surface treatment 77−70198
plasma polymerised ethane for laser window coatings 77−50737
plastic clad metal, corrosion charact. by electrical resist. and capacitance meas. *(German)* 80−30171
plastic deformation, TEM obs. 77−44305
plastic polycrystalline body, energy criterion for failure 77−4823
plastic powder coating, technique and appl. 79−38786
plasticized epoxy polymer rods, stress wave propag. 79−19322
plasticized triblock copolymers, thermodynamic theory 78−15377
plasticizer effect on polymer charact. *(German)* 80−92467
plastoelasticity theory 78−75712
plastomer, compressible plastic material, isotropic and anisotropic flow *(German)* 77−4817
plate, analysis subject to local loads 77−65687
platelet adhesion to solid surfaces, effects of plasma proteins and substrate wettability 78−35814
plates, freely supported orthotropic elliptical, deflection, interlayer shear effects 79−98622
plates and shells, construction elements, review of physical props. 78−67056
Plexiglas, rod, breakdown charact. by longitudinal stress waves 78−38773
plexiglas, strength in biaxial compression, testing machine 79−15899
Plexiglas 55, optical and phys. parameters 79−32004
plexiglas plates, static and dynamic stress intensity factor meas. by method of optical transmitted caustics 77−66740
PMA, phosphorescence depolarisation, segmental relax. time 78−95606
PMA interaction with glass bead, mica or TiO_2 fillers, glass transition *(Japanese)* 77−51479
PMMA:butlacrylate, breakdown threshold to ns IR laser pulses *(Russian)* 77−81179
PMMA:rhodamine 6G, luminesc. greenhouse solar collector 78−13789
PMMA, μs pulse tension loading, strength lifetime depend. on amplitude and temp. *(Russian)* 77−81303
PMMA, abrasion, SEM obs. 78−64742
PMMA, absorbing defect role in laser damage 80−108308
PMMA, acoustical determ. of shear relax. functions 78−76686
PMMA, activation energies of fracture and deform., comparison *(Russian)* 78−11303
PMMA, activation parameters of creep 79−38925
PMMA, ageing charact., sub-atm. pressure partial discharge obs. 80−1867
PMMA, amorphous, electron microscope and small angle X-ray studies 77−84666
PMMA, amorphous, LF Raman modes, strain and temp. effects 77−36219
PMMA, amorphous, reorientational relax., 6-165°C, polarised laser beam scatt. correlation 78−2864
PMMA, amorphous, structural cause of orientation modification, exam. 78−67664
PMMA, amorphous, thermophysical props. depend. on hydrostatic press. 78−47612
PMMA, amorphous, tunnelling models and thermal expansion below 4K 79−73326
PMMA, amorphous polymer, Rayleigh scattering of Mossbauer γ-rays 80−39926
PMMA, and related cpds., ionic charge carriers, dielec. studies 80−25291
PMMA, atactic, elastic strain detection by X-ray scatt. 80−25751
PMMA, atactic, FT IR spectrum, ^{18}O substitution effects 80−23581
PMMA, atactic and syndiotactic chains, statistical mechanics, operational method 77−560
PMMA, biaxially oriented, shrinking kinetics in transform. range 78−27588
PMMA, birefringence in elec. field 80−88962
PMMA, brittle fracture initiation charact., under biaxial loading, exam. 78−60803
PMMA, C-H stretching and bending vibrs. in Raman spectra 80−93300
PMMA, C-H stretching and bending vibs., IR spectra, selective deuteration 80−23582
PMMA, cathode initiated surface flashover, propag. vel. 78−14233
PMMA, coating on metal backing, thermophys. charact., expt. determ. technique 80−4707
PMMA, conformational energies calc. 78−25762
PMMA, constancy of composition obs., dosimetry appls. 79−60286
PMMA, correlations of craze profile with Dugdale's plastic zone profile 79−100272
PMMA, crack growth rate effect, fracture surface structure 80−16466
PMMA, crack jump determ. from specific failure and elastic energy 79−87712
PMMA, crack response to impact by caustics 78−56724
PMMA, crack size and effective specific work for failure determ. 80−85108

polymers continued
PMMA, crack velocity depend. on critical stress in fracture, static and dynamic loading 77−63768
PMMA, crack velocity meas. using US fractography 79−15772
PMMA, cracking kinetics, effect of small vibrs. 79−57108
PMMA, craze shape, fracture toughness, −30 to 45°C 77−48542
PMMA, craze shape and fracture, temp. depend. 77−52486
PMMA, craze zones at crack tips, validity of Dugdale model, comment 80−108535
PMMA, craze zones at crack tips, validity of Dugdale model 80−108534
PMMA, craze zones at crack tips at different temps., meas. correl. with Dugdale model 78−23826
PMMA, crazing, deform. kinetics 80−84990
PMMA, creep compliance calc. from short-term creep expts. 80−89303
PMMA, creep meas. in N_2 atmos., craze parameters 79−15734
PMMA, critical stress-intensity factor, determ. under mixed mode loading conditions by shadow optics 78−68868
PMMA, cross-linked positive electron resist, synthesis and props. 80−76221
PMMA, damage mechanism due to multiple laser pulse exposure 77−731
PMMA, defect build up in service, effect on notch sensitivity 77−66694
PMMA, destruction kinetics of intense ms loading, laser differential interferometry obs. 79−24623
PMMA, destruction of microsec. time scale, tensile stresses 79−70172
PMMA, destructive mech. cracks, electron microscope exam. of generation centres 78−68782
PMMA, dielec. relax. spectrum, thermodepolarisation and dilatometric meas. 77−32322
PMMA, discontinuous fatigue crack growth, generality of mechanism for glassy polymers 77−32677
PMMA, ductile glassy, notch brittleness under plane strain 80−100900
PMMA, durability over extensive time temp. range 77−90460
PMMA, effect of mol. orientation on fracture toughness 78−52992
PMMA, effect of surface finish on strength, and craze reistance 78−76724
PMMA, effect of temp. on freq. sensitivity of fatigue crack propag. 78−76762
PMMA, effects of notch shapes on Charpy impact values, tensile props., fracture surfaces *(Japanese)* 79−38951
PMMA, effects of permanent mag. field on macromolecules 77−25364
PMMA, electret, dielectric meas. at ultralow freq. by reheating 80−4741
PMMA, electric phenomena in process of deform. and failure, role in fracture mechanism 77−44344
PMMA, electron energy loss spectra, optical props. 79−10887
PMMA, EM shear stress gauge for large amplitude shear waves 78−70113
PMMA, EPR of NO radicals, rot. mobility 79−33539
PMMA, estimation of activation parameters in sclerometric tests 80−66625
PMMA, experimental separation of coherent component of X-ray scattering prior to RDF anal. 80−64838
PMMA, exposure for C K X-rays, diamond soft X-ray source for high-resolution lithography 79−21884
PMMA, expt. checking of ultimate equilibrium for crack in plane stress field 77−90462
PMMA, extruded, glass transition temp., melting pt., DTA 78−2235
PMMA, fabrication of surface relief struct. with linewidth below 2000 Å 78−42478
PMMA, fatigue crack growth, under biaxial stress 79−70144
PMMA, fatigue crack growth rate freq. depend. 79−74256
PMMA, fatigue life enhancement, prior crazing 80−89331
PMMA, filled amorphous polymer, heat capacity meas. *(Russian)* 79−65211
PMMA, flashover behaviour at low temps. 80−25882
PMMA, fluorescence from mols. embedded in small particles, angular distrib. 78−76926
PMMA, fracture morphology in notched tension, mol. wt. effects 77−52487
PMMA, fracture rib spacing, temp. effects 77−77564
PMMA, fracture stress 78−3216
PMMA, fracture surface parabola markings, temp. 78−52969
PMMA, fracture toughness for moving crack 77−44365
PMMA, fracture toughness testing, plane strain, simple meas. method 77−73381
PMMA, fracture toughness under biaxial stress 78−76760
PMMA, fracture under biaxial stresses, simple testing technique 77−73383
PMMA, glass-rubber transition, time-temp. superposition, shear creep compliance meas. 80−88309
PMMA, glassy, craze and crack growth *(Japanese)* 77−8970
PMMA, glassy, craze growth, expt. and model 78−15520
PMMA, glassy, in methanol, growth kinetics of solvent crazes, hydrodynamics 79−15836
PMMA, glassy, optical absorpt., visible region, determ. by laser calorimetry 80−66218
PMMA, glassy, photoelasticity 80−45034
PMMA, glassy, thermoelastic effect, thermal expansion coeff. 79−14944
PMMA, glassy atactic, thermodynamic analysis of plastic deform. modes, 150 to 330K 80−84999
PMMA, glassy rods, craze initiation, kerosene wetting effects 77−25172
PMMA, Gruneisen const. and thermal props., temp. depend., 4-300K, Brillouin scatt. obs. 80−100662
PMMA, helical structure 78−66699
PMMA, hydrostatic extrusion 80−108479
PMMA, immersion in high press. gaseous media, breakdown characts. for direct voltages with ripple 80−45009
PMMA, impact strength, exam. with pulsed drop impact loading 78−84944
PMMA, impact testing, elastic analysis of conventional test, reassessment of testing 78−60770
PMMA, in distilled water, influence of liquid environmental media on mech. behaviour 78−52902
PMMA, indentation fracture mechanics 78−35490
PMMA, influence of craze configuration on fracture 78−76758
PMMA, instantaneous crack resist. during stable crack propag. 80−85058
PMMA, isotactic and syndiotactic, chain distrib. function calcs. 77−75353
polymers continued
PMMA, isothermal and adiabatic effects assoc. with crack propag. 78−23827
PMMA, Kerr electro-optical effect, relative phase retardation meas. in elec. stressed samples 80−84716
PMMA, kinetic theory of quasi-brittle fracture *(German)* 78−84991
PMMA, large deforms. at tip of running crack, opt. interference obs. 80−85062
PMMA, laser damage mechanism rel. to viscoelastic props. 80−55233
PMMA, laser damage threshold, freq. and size depend. 80−104018
PMMA, laser damage threshold, microstructural defects effect 77−52205
PMMA, laser initiated polymerisation kinetics, mol. wt. distrib. of resultant polymer 78−15673
PMMA, lifetime reduction under cyclic loading 77−66695
PMMA, light absorption, laser crack development 78−68780
PMMA, liq. drop collisions, simulation of erosion in rainfield 77−56113
PMMA, low-energy excitations and hypersonic props., Brillouin scatt. meas., 1.7 to 15K 77−90160
PMMA, mech. degradation in presence of metals, effect of low mol. wt. environment generated during mech. working *(Russian)* 78−31422
PMMA, methanol crazes, grown from cracks, exam. of growth criteria 78−48551
PMMA, methanol crazes, mech. props., craze-strain profile 78−72844
PMMA, modified with dibutyl phthalate, mech. and optical props. *(Polish)* 77−52423
PMMA, molecular alignment 78−14299
PMMA, monolayers collapse mechanism, surface press. and ellipsometric obs. 78−43214
PMMA, multicomponent network, pulsed NMR study of mol. motions 77−55724
PMMA, neutron and gamma irradiation effects 80−66839
PMMA, neutron irradiation, radical distribution, ESR study *(Japanese)* 80−44920
PMMA, nondestructive acoustic elec. field probe meas. 80−47076
PMMA, nondirectional glow under laser irrad. 78−52575
PMMA, nonlinear dynamic mech. moduli 78−60693
PMMA, nonlinear viscoelastic behaviour in torsion 79−61640
PMMA, notched, sheet, deform. mech., fracture, X-ray obs. *(Japanese)* 77−59863
PMMA, ns breakdown voltage polarity effect, mechanism 77−63367
PMMA, optical damage threshold, alteration methods 80−99814
PMMA, optical interference meas. of critical crack tip displacements 78−84964
PMMA, optical strength rel. to surface defectiveness 77−28665
PMMA, oriented, hypersound propag., elastic props. 78−75737
PMMA, oriented, indentation fracture 78−35489
PMMA, oriented by extrusion, stress-optical study 78−47248
PMMA, overlapping skew-parallel crack dynamic propag. and arrest meas., method of caustics 78−84962
PMMA, partial draining of low-molecular weight polymers with flexible chains 80−23592
PMMA, phosphorescence depolarisation, segmental relax. time 78−95606
PMMA, piezobirefringence, optical and mech. relaxations, temp. depend. 80−34885
PMMA, plastic deform. by crazing *(Japanese)* 80−93619
PMMA, plate containing 'silver' cracks, arterial crack growth 77−86209
PMMA, porous, used as tooth replicas, phys. props. and biological acceptance 77−52926
PMMA, pulsed dielectric breakdown, mech. stress photoelasticity obs. *(Russian)* 78−2800
PMMA, radical form. in explosive loading, electron spin reson. obs. 80−63678
PMMA, rain erosion behaviour, exam. 78−53001
PMMA, Rayleigh scatt. of Mossbauer γ-rays 79−73864
PMMA, reactor irrad., growth of macroscopic radiolytic gas bubbles, diffusion model 80−65058
PMMA, rigid polymer, thermal stress isothermal relaxation 80−71683
PMMA, secondary loss peaks, effect of structural features 79−11649
PMMA, shear-wave Brillouin scatt. intensity from photoelastic consts. 79−91454
PMMA, shock induced polarisation, dielec. const., dipole lifetime rel. to particle velocity *(French)* 77−69776
PMMA, shock loaded, lateral compressive stresses meas. using Yb piezoresist. gauges 80−103007
PMMA, shock-loaded, shear meas. 77−11633
PMMA, shock-wave compressed, dielectric props. 78−80281
PMMA, slow to fast crack propag. transition 77−12687
PMMA, solid, mol. relax., photon correl. spectroscopy 77−90159
PMMA, solid, stress-strain behaviour, strain rate and temp. effects, cryogenic temps: *(Japanese)* 78−11315
PMMA, space radiation effects evaluation 80−70263
PMMA, specimen size effect on mech. behaviour associated with crazing 77−73337
PMMA, stability of cracking, effect of environment 78−95806
PMMA, stability of cracking, effect of environment 78−95807
PMMA, stimulated backscatt. under mech. stress 78−1304
PMMA, stopping power of valence electrons, Monte Carlo calcs. 79−10886
PMMA, strain rate effects on viscoelastic crack bifurcation 78−35473
PMMA, stress fields round indentations 77−28861
PMMA, stress relaxation during crazing, eqn. 79−61762
PMMA, stress wave propagation 78−46910
PMMA, struct.-prop. relationship between mol. wt. and fracture surface energy 78−80633
PMMA, submicroscopic cracking in dynamic extension, light scatt. meas. 79−70171
PMMA, surface energy anal., comparison of one- and two-liq.-contact-angle methods 77−59181
PMMA, thermochem. instability at Pt sphere inclusions caused by CW laser beam 80−29689
PMMA, thermoelectrets, γ-irrad., heterocharge stability, TSC spectra 78−72453
PMMA, thermophysical props. at high hydrostatic press. 78−2317
PMMA, thermorheologically simple material, thermostimulated depolarisation currents 77−90092
PMMA, time independent fracture criterion 79−83298
PMMA, transparent colourless cementing of milled surfaces 77−34970
PMMA, tubular magnetoelectrets, TSC obs. 78−88250

polymers continued
PMMA, ultrasonically modulated tensile stress produced fracture surface 79−91815
PMMA, uniaxial tension, fractographic anal. of crack growth kinetics 80−40519
PMMA, uniaxially drawn, shrinkage, continuum model *(German)* 78−76722
PMMA, unstable crack propagation in liq. environment, fractographic study 80−30155
PMMA, use in nanostructure fabrication, dense metal patterns 79−75657
PMMA, viscoelastic props. in plastic zone, cooling rate effect 80−40418
PMMA, visoelastic props., γ-irrad. influence *(Russian)* 78−88492
PMMA, water drops, effect of drop size on contact angle 80−2245
PMMA, water swollen membrane, permeability *(Japanese)* 78−31704
PMMA, work to produce environmental crazing at low temps. 78−15553
PMMA, X-ray absorption, shock wave compression meas. *(German)* 78−95618
PMMA, X-ray irrad., thermoluminescence emission, exam. of kinetic order 79−43046
PMMA, X-ray irradiated, thermolum. glow peaks 77−90204
PMMA and brittle materials, slow crack propagation anal. thermodynamic model 78−35488
PMMA bar, notched and perforated, fracture produced by longitudinal impact 79−43388
PMMA based composite (acrylic bone cement), effect of $BaSO_4$ and glass particle dispersions, on fracture behaviour 78−76753
PMMA based plastics, specific fracture energy depend. on crack growth rate., mol. struct. effect 80−66639
PMMA biaxially stressed plate, fracture trajectories 77−70152
PMMA bone cement, free radical EPR, feasibility study 80−94318
PMMA cement, rel. to wear mechanisms in total joint replacement 77−52929
PMMA cement in tibial plateau fixation, biomech. factors 77−56534
PMMA coated frit powder prep., corona-charging props. *(Japanese)* 80−25891
PMMA crosslinked by dimethacryloxymethylanthracene, radiothermoluminesc. *(Russian)* 78−73068
PMMA dental biomaterials, fracture toughness testing 80−50800
PMMA Doppler scatt. optical determ. of US radiation patterns 79−76930
PMMA femoral cement compactor for total hip replacement 79−79688
PMMA fracture toughness, flame-retardant additive effect obs. 80−16470
PMMA fuel, combustion and extinction in stagnation pt. boundary layer 79−29356
PMMA latex particles, laser light scatt. for visualisation in EHD 78−75236
PMMA modular matrix dye laser, pulse width influence on power output 80−28247
PMMA moist surface mech. strength reduced by electric charge *(Russian)* 80−60486
PMMA notched beam, fracture due to central impact 80−16426
PMMA organic glass, stress relax. calc. from creep curves 80−71709
PMMA organic glass shell, circular, cylindrical, under combined twisting moment/axial load buckling 79−100220
PMMA plano-cylindrical Fresnel lens, design and performance analysis as solar collector 80−53403
PMMA plate with angled elliptic notch in tension, exptl. investig. 78−38257
PMMA plates with flawed fastner holes, static fracture testing 80−97651
PMMA sheets, flame spread in laminar forced oxidising gas flow 80−35535
PMMA thermo-electrets, temp. and field effects 78−31148
PMMA with stress-raising flaw, deform. 80−25799
PMMA-d_8 ductile plastic optical fibre cables with improved visible and IR transmission 78−46834
PMMA-latex particles in benzene light scatt., appl. of liquid state theory 80−40750
PMMA-metal oxide composite powder, prep. and props. *(Japanese)* 78−95708
PMMA-mortar composite, thermocatalytically polymerised, fracture morphology and mech. props. 78−27595
PMMA-PVC mixtures, dielec. relax. and struct. rel. to formation *(Russian)* 77−20073
PMMA-steel pair, temp. calc. under severe friction 80−40550
PMMA-styrene acronitrile system, selective electron beam etching 78−45603
PMMA/PVC, cracking in layered composites 78−95808
PMMAF fatigue life in stepped and stationary nonisothermal cyclic loading 77−28905
bis cantena pol methylarsenide, energy gap depend. on As electron delocalization *(German)* 78−43296
polar material, PMMA-type, polaris. induced by shock waves *(French)* 77−62583
Polaroid K, oriented analogue of polyacetylene, reson. Raman spectroscopy 80−66208
polethylene-polypropylene blend, extruded, thermal swelling and mech. characterisation 80−81110
poleythylene, linear, butane diffusion coeff., VP depend. nulc. spin echo obs. 79−38404
Polimal 109 based H_2O emulsion, laminate prep. open pore density and content *(Polish)* 80−59665
poly(1,3,4-thiadiazole amide), from thermal cyclodehydration of polydiacylthiosemicarbazides *(Japanese)* 80−108388
poly(1,3 phenylene isophthalate), broad-line NMR, dynamical mechanical behaviour 77−55718
poly(1,3-dioepane), dipole moments, dielectric const. meas 80−66099
poly(1,4 phenylene terephthalate), broad-line NMR, dynamical mechanical behaviour 77−55718
poly(1-butene), melting and annealing behaviour; X-ray diffr. and DTA 79−28083
poly(2,6-dimethyl phenylene oxide) enthalpy of mixing with polystyrene 78−14471
poly(2,6-dimethyl-1,4-phenylene oxide)/poly(styrene-co-p-chlorostyrene) blends, tensile props. modelling 80−19868
poly(2-hydroxyethyl methacrylate), membrane, solute transport 79−43630
polymers continued
poly(2-vinyl pyridine), electronic struct., molecular-ion states and dielectric props. 79−37969
poly(2-vinylpyridine), isotactic, X-ray struct. determ. 77−84664
poly(3,3-dimethyl oxetane), conform. energies and random-coil config. meas. 80−99590
poly(4,4′ diphenylene 4,4′ biphenyl dicarboxylate), broad-line NMR, dynamical mechanical behaviour 77−55718
poly(4,4′ diphenylene isophthalate), broad-line NMR, dynamical mechanical behaviour 77−55718
poly(4,4′ diphenylene terephthalate), broad-line NMR, dynamical mechanical behaviour 77−55718
poly(4-chlorostyrene, 4-methylstyrene) copolymer, time-depend. ang. correls. 79−73881
poly(4-methyl pentene-1), US props., glass transition, Gruneisen parameters 80−54316
poly(4-methyl-1-pentene), semicrystalline, bulk and film, surface effects using Brillouin scatt. 79−42982
poly(4-methylpentene-1), isotactic, permanganic etchant for TEM obs. 80−21132
poly(5,7-dodecadiyne-1, 12-diol-bis phenylurethane), visible refl. spectra, photocond., excitons 77−81117
poly(9-vinyl anthracene), struct. *(German)* 79−98256
poly(α-ethuinyl naphthalene), elec. cond. of cis- and trans- stereo isomers *(German)* 78−84221
poly(α-methylstyrene), entangled, viscoelastic props., transient network model 78−13918
poly(α-methylvinyl alkyl ether)s, ^{1}H-, ^{13}C-NMR spectra, stereoregularity 80−48112
poly(β-ethinyl naphthalene), elec. cond. of cis- and trans- stereo isomers *(German)* 78−84221
poly(β-methylalanine), methacrylamide polymerisation by H transfer, catalyst sodium-napththalene *(Japanese)* 78−95726
poly(γ-benyl-D-glutamate) liquid crystal, orientation in magnetic field, NMR study *(Japanese)* 77−72550
poly(γ-methyl L-glutamate), electric conduction mechanism *(Japanese)* 80−54696
poly(γ-n-amyl L-glutamate), crystal transition, X-ray diffr. exam. of structure 80−24374
poly(γ-n-butyl L-glutamate), crystal transition, X-ray diffr. exam. of structure 80−24374
poly(γ-n-ethyl L-glutamata), crystal transition, X-ray diffr. exam. of structure 80−24374
poly(γ-n-propyl L-glutamate), crystal transition, X-ray diffr. exam. of structure 80−24374
poly(ε-caprolactone)-PVC system, Fourier transform infrared spectroscopic exam. 80−25361
poly(alkyl methacrylate), vitreous state, thermal cond., hole theory of liqs., press. 78−84013
poly(alkyl methacrylate)s, corona charged, decay of surface charge and TSC *(Japanese)* 80−54712
poly(alkyl methocrylates), US determ. of relax. 77−51449
poly(alkylene glycol), surface tension, sessile bubble method *(Japanese)* 78−79857
poly(alkylene glycol)-eicosane, interface tension, sessile bubble method *(Japanese)* 78−79857
poly(azomethines), thermotropic mesophases *(French)* 79−77507
poly(butyl acrylate), crosslinked, cholesteric liq. crystalline order 79−94893
poly(di-n-heptyl itaconate), alkyl side chain independent relax., double glass transition 80−59636
poly(diallyldimethylammonium) chloride, struct., ^{13}C NMR 77−565
poly(dihydroxypropyl methocrylate), surface charact., by contact angle methods 80−61140
poly(dimethyl siloxane), networks formed by gamma irradiation, crystallisation 77−51330
poly(dimethyl siloxane) diffusion of dichlorodifluoromethane, conc. and pressure dependence 77−55392
poly(dimethylsolixane), chains, angular correlation calcs. 79−45871
poly(ethylene oxide), partial draining of low-molecular weight polymers with flexible chains 80−23592
poly(ethylene oxide), spherulite growth rate determ. method 77−62493
poly(ethylene terephthalate), surface props. rel. to UV irrad. *(Japanese)* 78−79859
poly(ethylene-but-1-ene) copolymer, gelation and precipitation from solutions, NMR exam. 79−43641
poly(ethylene-oxide), isothermal growth, thickening, melting, bilayer crysts. and chain end effects 80−38939
poly(ethyleneterephthalate)-p-hydroxybenzoic acid copolyester, liquid crystalline, X-ray scatt. obs. 78−9949
poly(halo-N-vinylcarbazoles):2,4,7-trinitro-9-fluorenone charge transfer complexes, dark DC cond. 80−39626
poly(hydroxyethyl methacrylate), surface charact., by contact angle methods 80−61140
poly(L-alanine) fibres, mol. motion and fine struct., X-ray, thermal, mech., dynamic loss tangent meas. *(Japanese)* 78−59765
poly(L-histidine), molecular motions in solid state, NMR and dielec. meas. 80−11332
poly(m-methylene terephthalate) polymers, IR and Raman spectra 77−52088
poly(m-xylylene adipamide), crystallisation induced by water absorption *(Japanese)* 79−90573
poly(m-xylylene adipamide), crystallised by water absorption, morphology *(Japanese)* 80−24378
poly(m-xylylene adipamide), water induced crystallisation *(Japanese)* 79−90574
poly(methoxyethyl methacrylate), surface charact., by contact angle methods 80−61140
poly(methylmethacrylate), tactic chains, angular correlation calcs. 79−45871
poly(N-ethinyl carbazole), elec. cond. of cis- and trans- stereo isomers *(German)* 78−84221
poly(N-monosubstituted methacrylamides), relaxation 79−57033
poly(N-vinyl carbazole) sensitisation with Se, purification effect on electrophotographic characts. 80−49825
poly(N-vinylcarbazole), glass transition temp., mol. wt. relation 80−19922
poly(N-vinylcarbazole)-Se, double layer polymeric photoreceptor, potential discharge kinetics 78−72194
poly(N-vinylcarbazone), charge transport and struct., bromination effect 78−11516

polymers continued
poly(octadecyl ethylene), temp. depend. of 720 cm^{-1} IR band 80−97281
poly(octadecyl ethylene oxide), temp. depend. of 720 cm^{-1} IR band 80−97281
poly(oxycarbonylimino-1,4-phenylene), apparent sublimation: thermal decomposition+condensation repolymerisation 78−3332
poly(p-benzamide), highly oriented, ultimate mech. props. 79−91751
poly(p-chlorostyrene) electret, thermally stimulated discharge 77−4595
poly(p-phenylene), AsF_5 doped, highly cond. charge transfer complexes, elec. and optical props. 80−70778
poly(p-phenylene), electronic struct., one-electron band theory 80−65450
poly(p-phenylene terephthalamide), crystallised during polymerisation, morphology *(Japanese)* 77−51328
poly(p-phenylene terephthalamide), liq. cryst. phase transition *(Chinese)* 79−65175
poly(p-phenylene terephthalamide), quiescent and strain induced crystallization from H_2SO_4 soln. 79−90571
poly(p-phenylene terephthalamide) fibres, chain orientation distrib., and elastic props. 78−75566
poly(p-phenyleneterephthalamide), highly oriented, ultimate mech. props. 79−91751
poly(pyromellitimide), shock-induced electrical activity, mechanically induced bond scission model 80−50256
poly(S)-5-methyl-1-heptene, conformation, IR spectra 78−1116
poly(spiro[2,4]hepta-4,6-diene) molecular characterisation, glassy state props. 80−64928
poly(tetramethylene terephthalate), IR obs. of reversible stress induced crystal-crystal phase transition 80−20627
poly(tetramethylene terephthalate), struct., X-ray obs. 80−19725
poly(tetramethylene tetraphthalate), IR studies of α crystal phase 77−62486
poly(trans-1,4-butadiene), crystals in suspension, epoxidation kinetics 79−61861
poly(trioxane), γ-irrad. effects on melting behaviour 77−62620
poly(vinyl acetate), entangled, viscoelastic props., transient network model 78−13918
poly(vinyl alcohol), mol. wt. determ., high-speed aq. gel-permeation chromatography 79−61922
poly(vinyl alcohol)-acrylonitrile copolymer membrane, water permeability increase *(Japanese)* 79−70375
poly(vinyl cinnamate), excited state, low-energy EELS and INDO/S calcs. 80−106407
poly(vinyl pyrrolidone), mol. wt. determ., high-speed aq. gel-permeation chromatography 79−61922
poly(vinyl pyrrolidone), silicone grafted, for contact lenses, surface props. and stability of thin tear film 80−17194
poly(vinylcarbazole), photoelectret state 77−55745
poly(vinylidene fluoride), melting and crystn. temps., press. depend., DTA meas. 79−90568
poly(vinylidene fluoride) phase II, field induced phase transitions 80−96640
poly(vinylidene fluoride) piezoelectric film, Lamb and shear wave propagation *(French)* 80−44256
poly 2,3-dichlorobutadiene, struct., morphology, polymorphism 79−65008
poly (4-chlorosytrene, styrene), linear copolymers ang. correls., dipole moments and dielec. consts. 77−61884
poly (γ-methyl L-glutamate) film, oriented, conduction anisotropy meas. *(Japanese)* 80−54707
poly (alkyl cyano acrylate), sensitised with parabenzoquinone, holographic storage mechanism exam. 78−37850
poly (N^{ε},N^{ε}-terephthaloyl-L-lysine) membrane for artificial red blood cells, interaction with serum proteins *(Japanese)* 80−12061
poly (N,N-dipropylacrylamide), 'feathered' polymer resin, prep. from suspension 80−35533
poly (N-vinylcarbazole), hole photoinjection from Au 78−76144
poly (trioxane), melting behaviour, simultaneous thermogravimetric and differential scanning calorimetric meas. 77−76529
poly methylene oxide bulk sample, spherulite primary nucleation, determ. from spherulite shapes 80−70359
poly N-vinylcarbazole, soln., laser induced ionic photodissoc., transient polyelectrolyte form. 80−53068
poly vinylidene fluoride, injection process nature during poling, rel. to pyroelectricity 78−19422
poly [2-(p-azidobenzoyloxy)ethyl methacrylate], MW distrib. effects on photosensitivity *(Japanese)* 78−94418
poly [nitrilo-bis(phenylamino)phosphoranetriyl]s, synthesis and characterisation *(Italian)* 77−66755
poly-1,2-bis 4-isopropylcarbamoyloxy-n-butyl-1-buten-3-ynylene, cryst., UV refl. spectra, 25-160°C 79−82991
poly-1,3-pentadiene, microstruct., IR, NMR, X-ray determs. 79−37637
poly-1,6-di-N-carbazolyl-2,4-hexadiyne, synthesis, thermal expansion, photocond., optical transition 78−76858
poly-1,6-di-p-toluenesulphonyloxy-2,4-hexadiyne, thermal polymerisation, Raman spectra 80−35531
poly-1,6-dip-toluenesulphonyloxy-2,4-hexadiyne single cryst., twinning 80−33906
poly-1-butene, annealing and melting behaviour 79−38871
poly-1-naphthyl methacrylate, time-resolved fluoresc. spectra 78−80401
poly-2,4-hexadiyn-1,6-diol bis(p-toluene sulphonate), exciton theory of excited states 77−80733
poly-2,4-hexadiyne-1,6-diol bis (p-toluene sulphonate), cryst., exciton surface polaritons, reflectivity of (100) face, 295K 78−80372
poly-2-chloro-p-xylylene, photoinjection of holes from metal electrodes, barrier height 78−76145
poly-2-chloro-p-xylylene, photoinjection of holes using Au, Ag, Cu, Sn, Pb and Al electrodes 79−47161
poly-2-hydroxyethyl methacrylate, copolymerisation with polyacrylonitrile rel. to crystallinity 80−38935
poly-2-hydroxyethyl methacrylate, dielectric γ relaxation 80−34850
poly-2-hydroxyethyl methacrylate, glass transition temp., water content and tacticity effects 79−37817
poly-2-vinylpyridine, electron energy loss spectra, for optical and dielec. props. 79−15569
poly-4,4-diphenylphthaleinterephthalamide, mol. mass distrib., sedimentation and fractionation method meas. *(Russian)* 80−71957
poly-4-methyl pentene-1, long wave IR filters 77−75695
poly-4-methyl-1-hexene, optically active, ^{13}C NMR obs. of conform. 77−10801
poly-4-methylpent-1-ene, TPX, thermally stimulated conductivity 77−11905
polymers continued
poly-4-methylpentene-1, elastic parameters, US velocity meas. at 2.1-240K 80−40415
poly-4-vinyl pyridine-PMMA, codeposition with Cu, effects on morphology 79−74102
poly-4-vinylpyridene, protonated and deuterated vibr. spectra *(Russian)* 77−19120
poly-α-deuteroacrylonitrile, thermal degradation under reduced press., Fourier transform IR studies 79−87437
poly-α-methyl styrene, viscoelastic relaxation and methyl group tunnelling 79−57038
poly-α-methylstyrene, cross linked with polybutadiene, characterisation by gas pyrolysis chromatography *(German)* 79−57223
poly-β-ethynylnaphthalene, insoluble, reson. Raman spectrum, struct. models 78−70981
poly-γ-benzyl-L-glutamate, lyotropic liq. cryst., trifluoroacetic acid effect on viscoelasticity, susceptibility 77−84644
poly-γ-benzyl-L-glutamate, preliq. cryst. mol. alignment, space charge effect, electro-optical obs. 77−40206
poly-γ-ethyl-D-glutamate, pulsed photoconduction 80−24969
poly-γ-methyl-D-glutamate, α-helical form, annealing effect, morphology 79−14702
poly-ε-caprolactone-PVC blends, crystallisation kinetics 79−69020
poly-ε-caprolactone-PVC blends, morphology 79−69019
poly-ε-caprolactum, semicryst. melting and glass transitions 80−49346
poly-aryl-acetylene, elec. cond. of cis- and trans- stereo isomers *(German)* 78−84221
poly-aryl-vinyl, photon generated radical ions, photocond. *(German)* 79−52708
poly-arylate-dimethyl siloxane, polyblock copolymers, struct., thermodynamic stability *(Russian)* 80−64931
poly-bis-phenyl glutarate diacetylene, cryst., solid-state synthesis, struct. 79−15638
poly-ethylen-oxide, solubilisation in nematic phase, effect on twist viscosity 78−67642
poly-L-glutamic acid-poly-L-leucine block copolymers, association colloids 80−26064
poly-L-proline, TSC and dielec. study of multiple relaxations 77−55748
poly-m-phenylene, isophthalamide-b-dimethyl siloxane, morphology and tensile deform. 78−91263
poly-m-phenylene isophthalamide, precipitated from soln., morphology *(Japanese)* 79−14706
poly-m-phenylene isophthalamide, soln. and cryst., conform. props. calcs. *(Russian)* 79−65009
poly-m-phenylene isophthalamide-ε-caprolactam, complex polymer cryst. 78−9967
poly-m-phenylene isophthalamide-b-ethylene oxide, morphology and tensile deform. 78−91263
poly-m-phenyleneisophthalamide, sedimentation coeff. distrib. at 25°C *(Russian)* 77−63971
poly-m-toluenylsilsesquioxane mesomorphic struct., form. during polymerisation *(Russian)* 80−61095
poly-n-benzamide, mols. in soln., dynamic birefringence and rigidity *(Russian)* 77−32349
poly-n-butyl isocyanate, helical wormlike chain, dipole moment, elec. birefringence, elec. dichroism, statistical mech. calcs. 80−14262
poly-n-epoxypropilcarbazole electrophotographic layers, photogeneration and drift mobility 79−19631
poly-n-hexyl L-glutanate, sorption and permeation mechanism 80−26048
poly-N-n-alkylmaleimides, glass transition temp. 77−65956
poly-n-phenyleneterephthalamide, conformational and structural props. *(Russian)* 77−61889
poly-N-vinyl carbazole, and Br-substituted derivative, transient hole hopping transport, 150-500K 78−39108
poly-N-vinyl carbazole, containing carbazylium cation radicals, synthesis and semicond. props. 77−85224
poly-N-vinyl carbazole, hole hopping mobility, transit pulse dispersion 80−65565
poly-N-vinyl carbazole, pulsed laser excitation, time resolved fluoresc., 80−89041
poly-N-vinyl carbazole, trap-free lifetime, neutral traps, hopping systems 80−65566
poly-N-vinyl carbazole containing cation radicals, photocond. 78−68052
poly-n-vinyl carbazole-poly-9-vinyl anthracene double layer, high-field cond., xerographic characts. 79−95448
poly-N-vinylcarbazole, fluoresc. kinetics, stroboscopic meas. 79−11443
poly-n-vinylcarbazole, higher-lying singlet states, CNDO/S study 79−89815
poly-N-vinylcarbazole, in polymer film, excimer fluoresc., high press. effects 80−34966
poly-N-vinylcarbazole, interface with amorphous Se, photoinsulator-air gap-dielectric system, charges on surfaces 79−67407
poly-N-vinylcarbazole, polymerisation, struct., props., elec. characts., review 79−41972
poly-N-vinylcarbazole, struct. model, using NMR and diffr. data 78−83750
poly-N-vinylcarbazole, synthesis and photocond. props. 77−55563
poly-N-vinylcarbazole−metal electrode, photoemission of electrons, photocond. meas. 79−91142
poly-N-vinylcarbazole films, drift mobility of photocarriers, polymerisation method influence 77−76986
poly-N-vinylcarbazole-biacetyl, triplet exciton quenching, exciton trapping model 80−66267
poly-N-vinylcarbazole-polycarbonate mixture, hole drift mobility and photosensitivity 77−85260
poly-N-vinylpyrrolidone-containing nonionisable membranes, equilib. props. struct. *(French)* 80−61138
poly-N-vinylsuccinimide, dielec. and pulsed NMR relax. glass-rubber transition, mol. motions 77−48125
poly-p-benzamide fibre, supermol. struct., X-ray diffr. and acoustic methods 78−75570
poly-p-phenylene, charge transfer complexes, elec. cond. 79−91031
poly-p-phenylene sulphide, NMR relaxation for mol. motions *(German)* 80−11288
poly-p-phenylene terephthalate, high modulus fibre, struct. obs. 78−75564
poly-p-xylylene, α-β phase transition, electron microscopy study 79−69241
poly-propyleneoxide-ethyleneoxide-spirooxazolidine, proton nuclear mag. relaxation *(Rumanian)* 78−91977

polymers continued
poly-Schiff bases, thermotropic smectic B mesophase *(French)* 79−27911
poly-thio-1-N,N-diethylaminomethylethylene, optically active samples, ^{13}C NMR spectra 80−28127
poly-[1,2-bis-(p tolylsulphonyloxymethylene)-1-butene-3-inylene], defect imaging 77−15418
polyacene quinone radical copolymer, reversal of usual electric field effect and nomadic polarisation 77−12304
polyacene quinone radical polymers, elec. props. described by variable range hopping model 80−44588
polyacene quinone radical polymers, two-dimens. variable range hopping 79−51608
polyacenequinones, dielec. polarisation, role of conducting mol. chains *(Russian)* 79−65794
polyacetal, exam. of fatigue crack propag. 78−48497
polyacetal, stress-strain relations, effect of strain rate and static outer press. *(Japanese)* 77−52418
polyacetonitrile in MIM capacitor, electroforming, negative resist., electron emission 80−80406
polyacetylene: AsF_5 X-ray and UV photoemission spectra, Auger spectra 79−98150
polyacetylene:AsF_5, AES, XPS, UPS, and X-ray induced 80−66400
polyacetylene:AsF_5, Hall effect meas. 80−24955
polyacetylene:AsF_5, mag. susceptibility, Fermi surface density of states, semicond.-metal transition 79−95566
polyacetylene:AsF_5, thermal decomp. kinetics, elec. cond., ESCA and mass spectra 80−50830
polyacetylene:AsF_5, thermopower and transport props. 80−65611
polyacetylene:AsF_5, X-ray absorpt. meas. of mol. struct., orientation and charge transfer 80−25486
polyacetylene:$ASF_5(AsF_6)(SbF_6)(PF_6)$, metallic, band theory 80−49570
polyacetylene:AsF_5(I), pure and doped, electronic excitations, momentum depend., EELS study 80−76121
polyacetylene:Br(Pd), ion implantation effect on elec. props. 80−65026
polyacetylene:I, dc microwave cond., permittivity 80−107843
polyacetylene:I, electric props. in semicond. and metallic regions 80−29432
polyacetylene:I, electronic structure, XPS and UPS meas. 80−66385
polyacetylene:I, NMR investigation of struct. 80−39011
polyacetylene:I, NMR struct. investigation 80−108082
polyacetylene:I, pure and doped, reson. Raman spectroscopy 80−66208
polyacetylene:I, semiconductor-metal transition, thermoelec. power meas. 79−56271
polyacetylene:I charge transfer complex, struct. 79−74052
polyacetylene, AsF_5 doped, X-ray absorpt. meas., 5K to room temp. 80−71516
polyacetylene, band struct. 79−51477
polyacetylene, band struct. valence Hamiltonian minimal STO-3G basis calc., nonempirical model pot. 80−54596
polyacetylene, bond length alternation and energy gap, intermediate exciton formalism 80−29305
trans-polyacetylene, bulk crystallinity, small-angle X-ray diffr. study 80−103263
polyacetylene, continuum model for solitons 80−65472
polyacetylene, Coulomb repulsion, bond alternation, Peierls distortion, HF approx. 80−44524
cis-polyacetylene, cryst. struct. determ. 78−75556
polyacetylene, doped, elec. cond. and thermopower 80−96951
polyacetylene, doped, field theoretical model of insulator-metal transition 79−99483
polyacetylene, doped, fluctuation-induced tunnelling cond. in metallic regime 80−65516
polyacetylene, doped, p-n junction, elec. props., review *(Japanese)* 80−29410
polyacetylene, doping with AsF_5, mechanism, effect on elec. cond. and spectra 80−24473
polyacetylene, dynamic nuclear polarisation of protons *(French)* 80−43217
polyacetylene, electrical conducting, current status 80−44579
trans-polyacetylene, electronic energy band struct., extended Huckel and MNDO studies 80−20065
polyacetylene, electronic struct., one-electron band theory 80−65450
cis-polyacetylene, electronic struct. 79−47012
polyacetylene, intrinsic conformational defect states 80−65500
polyacetylene, lightly doped, charged π-phase kinks 79−56163
polyacetylene, lightly doped, donor and acceptor states, IR absorpt. obs. 79−73979
polyacetylene, lightly doped, phenomenological theory of soliton formation 80−103644
polyacetylene, mag. soliton defect ESR study 80−80590
polyacetylene, nascent morphology obs. 80−24379
polyacetylene, phototransport effects 80−44653
polyacetylene, polymerisation and Raman spectra on zeolite and alumina surfaces 79−13721
polyacetylene, pristine and doped, press. effects on resist. 80−103698
polyacetylene, pure and doped, electronic props. from one-dimens., tight-binding LCAO-SCF-MO calcs. 79−56123
polyacetylene, pure and doped, metal; and semicond.-semicond. junctions 79−95474
polyacetylene, pure and heavily doped, optical and IR studies, electronic struct. calcs. 80−7347
polyacetylene, soliton form. 79−76540
polyacetylene, soliton formation and cis trans isomerization 80−76505
cis-polyacetylene, static lattice calcs. for crysts. 80−10509
polyacetylene, trans- and cis-isomer, electronic struct. calcs. 80−24788
polyacetylene, undoped, thermally activated mobile defect, temp. EPR line broadening 80−43218
polyacetylene, variable density, synthesis, elec. cond., thermopower 80−60016
polyacetylene, vibr. excitations of charged solitons 80−108201
polyacetylene and polyacetylene: AsF_5, one-dimens. spin diffusion, NMR T_1 and dynamic nuclear polarisation meas. 80−44946
polyacetylene conductivity mechanism, Peierls phase one dimensional cond. *(Russian)* 80−88546
polyacetylene film, partially oriented, anisotropic elec. cond., quasi-one-dimens. behaviour of fully oriented doped material 80−11112
trans-polyacetylene obtained by polymerisation on TiO_2, Raman spectrum *(Spanish)* 80−88988
polyacetylene photoelectrochemical solar cell, fabrication and efficiency 80−50954
polymers continued
polyacetylene X-ray and UV photoemission spectra, Auger spectra 79−98150
polyacetylene-I_2, highly conducting, Raman, XPS and X-ray diffr. obs. 78−80454
polyacetylene-iodine derivatives, cryst. struct. determ. 78−75556
polyacetylenes, hologenated, quasi-one-dimensional, high-cond., prep. *(Czech)* 79−28340
polyacrylamide, conversion to poly-N-dimethylaminomethacrylate, Raman method meas. 79−74460
polyacrylamide, mech. degradation, polymerisation effect *(Japanese)* 78−11194
polyacrylamide, mol. wt. determ., high-speed aq. gel-permeation chromatography 79−61922
polyacrylamide dilute aqueous solns., flow in various geometries 79−41757
polyacrylamide gel, audiofrequency very slow propagating mode 79−74429
polyacrylamide gel, network density fluctuations, crit. behaviour 77−44518
polyacrylamide gel structure inhomogeneity from permeability and viscoelasticity 77−89384
polyacrylamide gel swelling kinetics 79−39214
polyacrylamide gels, structural collapse in solvent, crit. endpoint 78−48702
polyacrylamide-water gels, copolymerised with N,N-methylene bisacrylamide, dynamic light scatt. 78−60477
polyacrylic acid:Fe^{3+}, electron state of Fe^{3+}, Mossbauer and magnetisation obs. 79−73872
polyacrylic acid crosslinked with PVA, force rel. to elongation in swollen or contracted states 77−40434
polyacrylonitrile, AC conduction mechanism, freq. and temp. depend. *(Japanese)* 80−54706
polyacrylonitrile, copolymerisation with poly-2-hydroxyethyl methacrylate rel. to crystallinity 80−38935
polyacrylonitrile, elec. polarisation 80−7275
polyacrylonitrile, electronic struct., reactivity, SCF CNDO calcs. 77−50580
polyacrylonitrile, new model for structure, small-angle X-ray scattering and TEM study 79−77531
polyacrylonitrile, prep. of C fibres with large breaking strain 78−44077
polyacrylonitrile, pyrolized, pulsed photoconduction 80−24969
polyacrylonitrile, pyrolyzed, elec. cond. and dielec. const. in AC regime 78−60173
polyacrylonitrile, struct. of heat treated fibres, X-ray diffr. 78−83752
polyacrylonitrile, thermal degradation, Fourier transform IR obs. 78−92474
polyacrylonitrile and copolymers with polyisobutylene, specific heat and glass transition temp. meas. *(German)* 78−34603
polyacrylonitrile fibres, section cutting, technique *(Russian)* 80−7754
polyacrylonitrile glassy polymer, energetics of gas sorption 80−29270
polyacrylonitrile-$Mn(ClO_4)_2.6H_2O$, complex permitt. meas. by time-domain spectroscopy 77−49741
polyalkane imides, crystallisability, supermol. and crystalline structures 80−84100
polyalkaneimide, mech. and thermophys. props. at liq. He temps. 80−3117
polyalkanimide, US vel. and absorpt. at liquid He temps. 78−51619
polyalkenamers, longitudinal accordion mode, low frequency Raman spectroscopy 80−25369
polyalkylene tetephthalates, amorphous and cryst., durability under stretching *(Russian)* 78−88511
polyalkylmethacrylates, vitreous, thermal cond., press. and temp. depend. 78−2315
polyamide, aromatic, fibre, high modulus, mol. and supramol. struct. 80−79710
6-polyamide, dielec. relax. time, thermally stimulated current neas. 79−87381
6-polyamide, dielectric relax. time determ., piezostimulated current curves 78−92020
polyamide, directionally solidified, morphology 79−10808
polyamide, directionally solidified, X-ray diffr. 79−10809
polyamide, flashover behaviour at low temps. 80−25882
polyamide, hydrogen bonding rel. to mech. props. 77−4053
polyamide, PA 66, rel. strain meas. during creep in liq. environments 80−30046
polyamide, stress relaxation, eqn. and expt. *(German)* 77−28846
polyamide, test pipes, static tensile strength, equipment effect on tension-extension diagram *(German)* 78−35453
polyamide, torsional rigidity testing *(German)* 77−52596
polyamide, viscoelastic, linearity conservation 80−108492
polyamide, viscoelastic behaviour determ. from reln. between creep and relaxation *(German)* 77−62174
polyamide 6, alkaline, viscoelastic meas. *(German)* 77−84204
polyamide 6, fatigue under rotary bending *(German)* 79−15782
polyamide 6, reinforced and unreinforced, fatigue fracture types under circular flexural loading *(German)* 79−70170
polyamide 6 (polycaproamide), temp. depend. of complex permittivity rel. to moisture content 80−50251
p-polyamide based organic fibres, effect of temp. and deform. time, on deform. strength props. 80−11720
polyamide blends, formation by injection moulding, structs. *(Russian)* 80−44155
polyamide chain, conformational freedom above MP 77−55344
polyamide fibre, chain-segment orientation, US vel. meas., humidity effects *(German)* 78−75590
polyamide fibre, sputter etching 80−21147
polyamide fibres, crystallinity and crystallite size meas. 78−30549
polyamide fibres, differently matted, meas. of diffuse reflectance spectra, using SPEKOL spectrocolorimeter 80−77836
polyamide mixtures, thermodynamically incompatible, composition-prop. relationship *(Russian)* 80−7872
polyamide resin, computer approx. of families of curves of physically non-linear creep 77−66684
polyamide resin wear and cutting surface against brass *(Japanese)* 78−56779
polyamide single crysts., struct. *(Russian)* 77−43158
polyamide-12 plasticized with sulphonamides, relaxation props. *(Russian)* 80−55031
polyamide-6, fibrillar struct. and annealing, small-angle X-ray diffr. 78−75565

polymers continued
polyamide-6, surface defects and mech. strength, oriented polymer *(Russian)* 78−51451
polyamide-polyoxirane copolymers, mechanical properties evaluated 80−11700
polyamide-polyurethane, enamel lacquer, far IR transmission, encapsulation of optical devices 79−55194
polyamides, 1,3-cyclohexanebis(methylamine) based, thermal props. and glass transition temp. 80−39264
polyamides, carborane-containing, antifrictional props., chem. struct. effect *(Russian)* 79−57123
polyamides, extended chain aromatic, fibres, tensile strength and moduli 80−81021
polyamides, molecular breaking under load, hydrolysis 78−11519
polyamides, preoriented, method for increasing elastic moduli 77−80425
polyamides containing 1,3-cyclohexane rings, cryst. struct. 80−103262
polyanide, thermorheological and mech. props. 79−96067
polyaromatics, elec. cond. correl. with chem. struct. and synthesis, charge transfer complexes *(German)* 80−15514
polyarylate, F-2 influence of water on mech. props. *(Russian)* 78−88513
polyarylate, rupture mechanism 79−52372
polyarylate, solvent crazing *(Japanese)* 79−29246
polyarylate organosiloxane polyblock copolymer, struct., props., phase conversion *(Russian)* 79−65010
polyarylate-arylenesulfone oxide block copolymer, glass transition, melt and soln. viscosity *(Russian)* 79−55915
polyarylate-polyethylene oxide block-copolymers and mixtures, phase separation, DSC obs. *(Russian)* 79−55895
polyarylates, sorpt. kinetics of tetrahydrofuran, struct. transform *(Russian)* 79−51432
polyarylbutadiene, microstructure, NMR and IR obs. *(Japanese)* 79−24488
polyarylenealkyls, colour, EPR, electron density delocalisation degree determ. *(Russian)* 80−7152
polyaryleneimides, oriented, elastic props. 80−40416
polyaryloxyphosphazene copolymers, thermal, morphological and rheological props. 80−103265
polyazomethines, thermotropic nematic phase formation, role of molecular mass *(French)* 78−75547
polybenzoxazole, dielectric β relaxation, role of water molecules 77−90100
polybiphenylacrylate, atactic, crystalline character effect on dynamic mech. response 78−56686
polybis-p-toluene sulphate, single crysts., morphology 79−23594
polybisaminophosphazenes, elec. cond. 77−32016
polyborodiphenylsiloxane, binder for SiC and Si_3N_4 sintered bodies 77−40401
polyborodiphenylsiloxane, synthesis and thermal decomposition 77−40541
polybrene, catalysis of $Co(NH_3)_5Br^{2+}$ alkaline hydrolysis, high pressure, effect 80−55657
polybromoprene, crystn., morphology, kinetics *(Russian)* 79−4256
polybut-1-ene, cryst. forms I and II, far IR spectra 79−33708
polybutadiene, adhesive, uncured linear flexible-chain polymers of narrow molecular mass distrib., fracture in triaxial stress 79−43550
polybutadiene, adsorption behaviour, surface tension exam. *(Japanese)* 78−31690
polybutadiene, carboxyl-terminated, glass transition temp., thermomech. anal. meas. 79−14917
polybutadiene, complex modulus meas. using forced vibrations at ultralow frequency 77−70258
polybutadiene, cross linked with poly-α-methylstyrene, characterisation by gas pyrolysis chromatography *(German)* 79−57223
polybutadiene, dihydroxy-terminated, with unattached styrene-butadiene copolymer, stress relax. 80−104202
1,2-polybutadiene, dynamic viscoelastic props. in curing process 80−76298
polybutadiene, electronic struct., reactivity, SCF CNDO calcs. 77−50580
polybutadiene, entangled, viscoelastic props., transient network model 78−13918
1,4-polybutadiene, epoxidised, ^{13}C NMR, Overhauser effect 79−51872
polybutadiene, hexafluoro acetone substituted, H-NMR and ^{19}F-NMR spectroscopy *(German)* 80−103893
polybutadiene, high cis-1,4, orientation effects induced by shear rate in capillary rheometer 77−51014
polybutadiene, hydrogenation 80−26008
polybutadiene, linear and star branched, rheology 80−23977
polybutadiene, mol. motion in solid and soln., ^{13}C NMR relaxation meas. *(Japanese)* 80−2666
polybutadiene, molecular mobility, influence of S cross linkage, torsion pendulum meas. *(German)* 79−13856
polybutadiene, NMR line narrowing *(German)* 78−76341
high cis-,1,4-polybutadiene, orientation effects induced by shear rate in capillary extrusion 77−48389
1,4-polybutadiene, oxidation stabilisation by singlet O_2 quencher 4-(1-imidazolyl)-phenol 80−16677
cis-1,4-polybutadiene, partially hydrogenated, ^{13}C NMR 80−20472
polybutadiene, pyrolysis, determ. of kinetic parameters *(German)* 78−85155
1,4-cis-polybutadiene, stereoregular, recrystn. in partial melting temp. region *(Russian)* 80−6495
polybutadiene, transverse nuclear magnetisation decay rel. to slow mol. motions *(Russian)* 78−72423
cis-polybutadiene and butadiene-styrene copolymer mixture, effect of temp. on phase composition 79−96005
polybutadiene blend, viscoelasticity using Rheovibron, Massa correction for loss tangent meas. 78−83349
1,2-polybutadiene crosslinked in strain states; entanglement networks, stress-birefr. relations 80−66590
polybutadiene miscibility with butadiene/styrene copolymers, viscometric method *(Polish)* 79−42260
polybutadiene networks, cis-trans, thermoelastic obs. 79−74220
polybutadiene networks, cis-trans isomerisation, γ-ray induced 79−74374
polybutadiene-poly-α-methylstyrene copolymers, struct. obs., prep. *(French)* 80−59401
polybutadiene-polystyrene, ^{13}C NMR assignments, rel. to mol. configurations 77−54640
polybutadiene-polystyrene block copolymer, anionic prep., random coupling struct. 79−64134
polymers continued
polybutadienes, radiation chemically cross-linked, charact. by pyrolysis gas chromatography *(German)* 80−81348
polybutene-1, microstructure determ. by ^{13}C-^1H NMR 78−26455
polybutene-1 glass, Raman spectra, low temp. crystallisation *(French)* 79−99875
polybutylene terephthalate, hysteresis of stress-induced cryst. phase transition 78−31404
polybutylene terephthalate, melt crystallised, solvent crystallised films and moulded bars, morpholigical obs. 80−84101
polybutylene terephthalate, semicryst., mech. props., effect of annealing below glass temp. 77−25066
polybutyleneterephthalate, drawn annealed, struct. and props., X-ray scattering 79−7552
polycaproamide, addition to high-activity carburiser 80−76412
polycaproamide, crystn. effect on frictional props. 80−40551
polycaproamide, deformability props. in cyclic extension-compression 79−20183
polycaproamide, low-mol. wt. oligomers crystallisation kinetics from melt solid struct. *(Russian)* 79−69034
polycaproamide, metal adhesive bonds, shear resist., polymer crystn. effect 80−89462
polycaproamide, oriented, molecular rearrangements during deformation, IR spectra exam. 80−7644
polycaproamide, oriented filaments, mech. props. 80−66550
polycaprolactam, after polycondensation, falling film evaporator system *(Japanese)* 79−70325
polycaprolactam, crystallisation effect on adhesion to Al 77−66742
polycaprolactam, fibre, struct. change when used as resin reinforcement *(German)* 77−21091
polycaprolactam, pure and TiO_3 filled, radiation effects *(Bulgarian)* 79−33015
polycaprolactam, stretched sheets, electron emission 78−88411
polycaprolactam characteristics dependence, at equilibrium state, on polymerisation conditions, in closed system *(Japanese)* 78−95928
polycaprolactam fibre, lifetime under load, in presence of UV radiation, stress depend. 78−48535
polycaprolactam-finely divided Cu metallic polymer, determ. of impregnation depth in porous sintered Fe-graphite 79−70272
polycaprolactone, epitaxial crystn. on aromatic hydrocarbon substrates 79−61521
polycapromide, fracture, interatomic bonds deform. 79−57107
polycarbonate:triphenylamine, field-depend. UV photogeneration of holes, polymer composition depend. 78−76104
polycarbonate, γ-irradiated, dielec. behaviour and glass transition 80−97182
polycarbonate, amorphous, electron microscope and small angle X-ray studies 77−84666
polycarbonate, amorphous, thermophysical props. depend. on hydrostatic press. 78−47612
polycarbonate, amorphous, yield behaviour in oriented and unoriented condition, effect of temp. 80−97537
polycarbonate, amorphous morphology, from NMR obs. of swelling penetrant mol. motion 79−27929
polycarbonate, amorphous US vels. from Brillouin scatt., room temp. to 250°C 79−91454
polycarbonate, anelastic component of strain *(Japanese)* 77−8870
polycarbonate, bisphenol A, birefringent plates, cracks, stress intensity factors, refl. caustics method 80−93718
polycarbonate, bisphenol A, WAXS pattern, temp. effect and thermal history 80−93583
polycarbonate, bisphenol-A, mol. wt. determ. using gel permeation chromatography 80−58424
polycarbonate, brittle fracture of notched ductile polymers *(Japanese)* 80−16448
polycarbonate, coating by plasma polymerised abrasion resist. antirefl. layer 77−42635
polycarbonate, colour appearance during oxidation *(Russian)* 79−24643
polycarbonate, compressive recovery behaviour 79−38919
polycarbonate, crack instability under impulse loads, dynamic fracture toughness 77−48518
polycarbonate, craze morphology, 77 to 375K, gaseous environment effect 77−63819
polycarbonate, craze roles in fatigue 79−29183
polycarbonate, craze thickening mechanism during craze growth 79−91823
polycarbonate, crazes, statistical aspects optical microscopic obs. *(Japanese)* 79−29247
polycarbonate, creep deform. caused by crazing 80−21133
polycarbonate, criterion for craze nucleation 78−19881
polycarbonate, cyclic deformation and craze growth 78−76759
polycarbonate, decomposition by H_2SO_4 and grinding by ball mill, exam. of molecular chain scission *(Japanese)* 78−64827
polycarbonate, deform. and failure modes, surface craze characts. 79−91753
polycarbonate, degradation behaviour by vibratory ball mill *(Japanese)* 78−39732
polycarbonate, delayed yiedling under const. load 79−38906
polycarbonate, dielec. relax. and ductile brittle transition 78−52438
polycarbonate, discontinuous fatigue crack growth, generality of mechanism for glassy polymers 77−32677
polycarbonate, ductile, large strain cyclic deform. 80−85000
polycarbonate, ductile glassy, notch brittleness under plane strain 80−100900
polycarbonate, effect of mol. weight on craze shape and fracture toughness 80−25858
polycarbonate, effect of rolling on mech. props. 78−52837
polycarbonate, effect of temp. on freq. sensitivity of fatigue crack propag. 78−76762
polycarbonate, effect of thermal treatment on strength, TSC meas. 77−52368
polycarbonate, environmental stress crazing 78−68832
polycarbonate, exposed to ethanol, craze nucleation and growth 79−24639
polycarbonate, fatigue crack propag., mol. wt. depend. 80−50700
polycarbonate, flexure testing 77−86087
polycarbonate, fretting on steel influence of experimental conditions on wear 78−44228
polycarbonate, glassy, craze and crack growth *(Japanese)* 77−8970
polycarbonate, glassy, fatigue crack initiation in high strain fatigue tests 80−97564

polymers continued
polycarbonate, glassy, IR dichroism at small strains 78−56475
polycarbonate, glassy, rolled, craze initiation *(Japanese)* 77−8969
polycarbonate, glassy, temp. drop during deform. 78−15456
polycarbonate, glassy, thermoelastic effect, thermal expansion coeff. 79−14944
polycarbonate, glassy polymer, energetics of gas sorption 80−29270
polycarbonate, glassy state, enthalpy relax., thermal density fluctuations 80−59678
polycarbonate, glassy state, rel. between thermal pre-treatment and viscoelastic behaviour 79−79038
polycarbonate, highly hot-drawn, mechanical prop. and phys. struct. changes 78−14293
polycarbonate, impact behaviour, effects of thermal pre-treatment and mol. wt. 78−95798
polycarbonate, insulators for superconducting magnets, effect of low temp. irradiation 80−25817
polycarbonate, irrad., electron spin-lattice relax. at low temp. 78−68382
polycarbonate, magic-angle ^{13}C NMR, relax. times, motions 79−4739
polycarbonate, neck propag., rel. to dry craze growth mechanism 80−59563
polycarbonate, nonlinear dynamic mech. moduli 78−60693
polycarbonate, notched sheet, deform. mech., fracture, X-ray obs. *(Japanese)* 77−59863
polycarbonate, notched specimens, impact fracture behaviour 77−28888
polycarbonate, notched specimens deform. and fracture 78−11293
polycarbonate, particles, critical stress 77−28869
polycarbonate, photoconductivity, UV-IR light, absorpt. and photoluminescence. spectra *(Japanese)* 78−34857
polycarbonate, plane strain fracture energy instability and mixed mode crack propag. 78−68775
polycarbonate, plastic deform. by crazing 79−52310
polycarbonate, plastic insulation for cryogenic power cable, exam. of dielectric, tensile props. 80−25823
polycarbonate, shear-wave Brillouin scatt. intensity from photoelastic consts. 79−91454
polycarbonate, solvent crazing *(Japanese)* 79−29246
polycarbonate, sorption of water and its effect on dielec. behaviour 79−11383
polycarbonate, specimen size effect on mech. behaviour associated with crazing 77−73337
polycarbonate, stress crazing, liq. environment effects 78−84970
polycarbonate, stress relaxation during crazing, eqn. 79−61762
polycarbonate, stress-cracking test, rel. to part failure 79−74311
polycarbonate, stress-strain relations, effect of strain rate and static outer press. *(Japanese)* 77−52418
polycarbonate, struct. determ. by electron microscopy 79−55675
polycarbonate, struct. ordering changes after annealing 79−94921
polycarbonate, theoretical prediction of temp. rise at tip of running crack 80−2114
polycarbonate, thermal cond., 2-100K, crystallinity effect 77−20137
polycarbonate, thermal diffusivity meas., flash method 77−47632
polycarbonate, TSC anal. by activation energy spectra 80−20579
polycarbonate, turning yellow during oxidation, kinetic regularities *(Russian)* 79−24644
polycarbonate, viscoelastic behaviour determ. from reln. between creep and relaxation *(German)* 77−62174
polycarbonate, viscoelastic ductile, delayed yielding of plane stress viscoelastic Dugdale model 78−27569
polycarbonate, viscoelastic props. in plastic zone, cooling rate effect 80−40418
polycarbonate, wideband optical transmission meas. 79−76771
polycarbonate, X-ray orientation and texture meas., compared with polystyrene 78−75559
polycarbonate, yield behaviour *(Japanese)* 80−93620
polycarbonate, yielding and crazing behaviour in torsion under superimposed hydrostatic press. 78−52898
polycarbonate blends, yield and deform. behaviour, impact modification 77−36572
polycarbonate craze shape temp. depend. 78−48529
polycarbonate diflone, air permeability, subject to high press. 78−27823
polycarbonate fast neutron dosimeter, development and comparison with conventional emulsion dosimeter 80−86990
polycarbonate fibre, highly-oriented, drawing behaviour and mech. props. 78−76708
polycarbonate foils, detection of low energy ^{4}He, ^{12}C, ^{14}N, ^{16}O ions, etching props. 78−13391
polycarbonate membrane, porous, gas permeability *(Japanese)* 78−31698
polycarbonate notched beam, fracture due to central impact 80−16426
polycarbonate of bisphenol A, neck form. and propag., strain anal. 80−16376
polycarbonate of bisphenol bar, notched and perforated, fracture produced by longitudinal impact 79−43388
polycarbonate ophthalmic-prescription lens series 79−81501
polycarbonate plastic, gamma-ray dosimeter at high exposures 79−63815
polycarbonate plate, impulse surface flashover in vacuum, effect of normal elec. stress 79−4199
polycarbonate plates, modified compact-tension specimens, dynamic anal. 80−97561
polycarbonate porous membrane, pore size effect on gas permeability *(Japanese)* 78−31699
polycarbonate resin-steel pair, temp. calc. under severe friction 80−40550
polycarbonate structure foams, fracture toughness 78−15500
polycarbonate styrene-acrylonitrile copolymer mixture, determ. of phase structure, electron microscopy 80−103272
polycarbonate track detector, electrochemically etched, meas. of low neutron fluences 80−32577
polycarbonate-polymethylmethacrylate blends, kneading characts. *(Japanese)* 80−104112
polycarbonate-steel surfaces, changed in morphology induced by fretting 78−15538
polycarbonates, degradation products, chem. anal. by UV photoelectron spectroscopy 78−53300
polycarbonates, glass transition pt., calorimetric determ. *(Polish)* 79−51241
polycarbonates unstretched and stretched, orientation relationships, ^{13}C NMR meas. *(German)* 80−20474
polychloroprene, microstruct. determ. by ^{13}C NMR 79−33546

polymers continued
polychloroprene, polar dielectric, mech. polarisation *(Russian)* 77−40174
polychloroprene and polychloroprene vulcanizates, γ-radiation effects on struct., physicomech. props. 77−1840
polychloroprenes, microstruct., IR digital subtraction method, struct. irregularities effect on copolymer IR bands 79−38543
polychloroprenes, microstruct., IR digital subtraction method, struct. irregularities 79−42965
trans-1,4-polychloroprenes, prep. and struct., Raman spectra 77−66496
polychlorotrifluorethylene, cryst. and melt, stat. thermodynamics 79−41979
polychlorotrifluoroethylene, creep meas. in N_2 atmos., craze parameters 79−15734
polychlorotrifluoroethylene, crystalline and amorphous peaks, dielectric props. 80−93237
polychlorotrifluoroethylene, necking stress *(Japanese)* 77−56037
polychlorotrifluoroethylene, tensile deform. in He, N_2, Ar, O_2 and CO_2 gaseous environments 77−56040
polychlorotrifluoroethylene electrets, TSC profiles, poling conditions depend. 78−10835
polychlorotrifluoroethylene waxes, thermoxidative stability study, hybrid microcircuit appl. 79−100271
polycondensation copolymers, block length distribs. 79−31752
polyconjugate system, interrelation between physicochem. props. and microstruct. 78−55816
polycyclohexylphenyl acrylate, crystalline character effect on dynamic mech. response 78−56686
polydecamethylene-oxide, dynamic mechanical measurements using a dynamic viscoelastometer *(Spanish)* 79−61636
polydeoxyribonucleotides, poly(dA).poly(dT) and poly(dAT).poly(dAT), HF vibr. modes, Raman and IR spectra 80−32698
polydextran, γ-irrad. frozen gel, electron trapping, EPR and optical obs. 78−20030
polydiacetylene:carbene, zero field splitting parameter sign, ESR temp. depend. determination 78−27075
polydiacetylene, cryst., refl. spectra, Kramers-Kronig transforms 78−43889
polydiacetylene, crystalline and amorphous, γ-ray effects, gel form. and crosslinking 80−93777
polydiacetylene, extended chains with realistic model side groups, self-consistent electronic band structs. 77−39776
polydiacetylene, extended-chain crysts., struct. and morphology 79−82165
polydiacetylene, fully conjugated bond-alternation and orbital-flip defects 77−4311
polydiacetylene, intrinsic conformational defect states 80−65500
polydiacetylene, model chain, band struct. calcs. 77−8016
polydiacetylene, monocrystal, vibr. freq. stress depend., Raman obs. 77−50574
polydiacetylene, photoconduction in multilayer structs. and single cryst. 78−80024
polydiacetylene, reflection spectra, thermochromism, temp. hysteresis and phase transformation 78−19452
polydiacetylene, single cryst. piezomodulated and specular refl. spectra 77−20869
polydiacetylene, single crystal, electroreflectance and electroabsorption spectra, π-electron system and excitonic transitions 79−78653
polydiacetylene backbone sequence, electronic structs., unrestricted HF approach 78−63975
polydiacetylene bis-(toluenesulphonate), single cryst., charge carrier mobility and recomb. 77−8132
polydiacetylene cryst., electronic struct. change at phase transition, Raman spectra 78−2833
polydiacetylene crystals, electronic spectra and struct. 79−73923
polydiacetylene polymer crystals, one dimensional conjugated, optical props. 77−43993
polydiacetylene polymer crystals, optical nonlinearities, chain pairing effects, one dimens. band model 77−69851
polydiacetylene PTS crystal, Davydov splitting in spectra at 15000 to 19000 cm^{-1}, at low temp. 78−31212
polydiacetylene single crysts., twinning 78−23777
polydiacetylene-bis(toluenesulphonate), refl. spectra, 0-15 kbar, doublet press. shift 78−43891
polydiacetylene-bis(toluenesulphonate), single cryst., thermal expansion and optical band splitting 77−8594
polydiacetylene-bis(toluenesulphonate), XPS valence band obs., binding energies 77−77339
polydiacetylene-p-(toluenesulfonate), photocurrent transients, intensity depend. 78−52027
polydiacetylene-toluenesulphonate, photocond. meas., 0.62-3.1 eV 80−70757
polydiacetylenes, band struct., ab initio cryst. orbital method, and transport props. calc. 78−26811
polydiacetylenes, electronic struct., cyclic vs. linear models 80−54587
polydiacetylenes, electronic structure, bond length variations effect, Xα SCF calc. 78−5378
polydiacetylenes, excited singlet state electronic struct., band and excitonic models 78−91620
polydiacetylenes, optical props., and electronic struct., rel. to polyenes 77−23592
polydiacetylenes, photocond. action spectrum of single crysts., charge transport obs. 80−15557
polydiacetylenes, reversible creation of defects by laser pulses 78−23480
polydiacetylenes, visual conformational transitions, absorpt. and fluoresc. spectra, pH and electrolyte effect 80−102590
polydiacetylenes substituted with urethane, solid and film, visible spectra, refl. and absorpt. 79−87460
polydiacylthiosemicarbazides, synthesis and thermal cyclodehydration *(Japanese)* 80−108388
polydiethylene glycol terephthalate, relaxation, dielectric prop. 78−68447
polydiethylene terephthalate chains, dipole moment, config. props. 78−9288
polydiethylsiloxane, mol. motion, NMR spin relax. data re-interpret. 80−84664
polydifluoroacetylene, electronic struct., tight-binding LCAO-SCF-MO calcs., prep. 80−70591
polydimethyl siloxane, Brillouin scatt. and hypersonic relax. 77−55795
polydimethyl siloxanes, cyclic and linear, neutron scatt. meas. of dimensions 80−18952

polymers continued
polydimethylcarbosiloxane net-type, crystallisation, NMR obs. *(Russian)* 77−20744
polydimethylsiloxane, crosslinked, stress/strain relations from large compression to high elongation 80−66589
polydimethylsiloxane, crystalline and amorphous, characterised by DTA, polarised light microscopy, dielectric relax. 80−25295
polydimethylsiloxane, end-cap ratio and mech. props. of block copolymer 78−91266
polydimethylsiloxane, helical wormlike chain, dipole moment, elec. birefringence, elec. dichroism, statistical mech. calcs. 80−14262
polydimethylsiloxane, stress-strain props., cross link functionality 79−46575
polydimethylsiloxane chains, with known radiative side chain amounts, model elastomeric networks prep. by sel. crosslinking 79−73106
polydimethylsiloxane end-linked chains, nonGaussian effects 80−65127
polydimethylsiloxane membrane, permeability of triethylamine vapour *(Japanese)* 78−31697
polydimethylsiloxane networks, high freq. US absorpt. rel. to crosslink density, α-relaxation 79−95091
polydimethylsiloxane networks, stress-strain isotherms at high elongations to rupture point 77−40433
polydimethylsiloxane proton spin-lattice relax., chain motions 78−70987
polydimethylsiloxane-bisphenol-A polycarbonate block copolymer, PMR spin diffusion effects 77−66431
polydimethylsiloxanes, equilibrated, living oligomer distrib., end-group interactions 80−58423
polydimethylsiloxanes, linear, mol. wt. determ. from density and viscosity 79−81310
polydimethylsiloxanes, liq., proton spin relax., mol. motion, network form. 79−15369
polydimethylsiloxanes, partially cryst., spin diffusion rel. to nuclear spin-lattice relax. *(Russian)* 79−51878
polydimethylsiloxanes, rubbery and liq., hypersonic sound vel., Brillouin spectra meas. 80−75308
polydimethylsiloxne, end-linked chains, viscoelastic losses 78−46898
polydioxolan, crystallisation, morphology and melting props. 78−14297
polydioxolan, crystn. kinetics, dilatometric analysis and microscopy obs. 80−79706
polydiphenylgermylene, crystn. from chem. transport reaction 80−104439
polydiphenylsiloxane, thermodynamics of fusion 80−84280
polydisperse, anal. of mol. mass distrib. *(Russian)* 77−31038
polydisperse, mol. wt. distrib. correl. with props. *(Russian)* 80−69286
polydisperse homopolymers, glass transition temp., mol. mass depend. 80−92656
polydisperse randomly branched polymer, sedimentation coeff. 77−63966
polydisperse suspension, two-parameter size distribs. eval. using photon correl. data 79−92011
polyelectrolyte, plasticised, effect of ion placement and struct. on props. 79−7679
polyelectrolyte chain in D dimensions, conformation props. 77−31034
polyelectrolyte complexes, nonstoichiometric, solubility in water *(Russian)* 80−55674
polyelectrolyte ion binding, Poisson-Boltzmann eqn. 80−45511
polyelectrolyte soln., small ion self-diffusion coeffs., cell model 79−19385
polyelectrolyte-counterion affinity, theory of Coulombic reactions 77−48648
polyelectrolytes, potential chloroform precursors 77−78252
all-trans polyene, ab initio studies 80−43222
polyene, different orbitals for different spins 79−69392
trans-polyenes, 1st excited singlet valence states, CI and extended CNDO/S calcs. 78−74807
polyenes, highly branched, large networks, abnormal bond orders 79−59610
polyenes, long chain, electronic struct. in Peierls-PPP model 80−84423
polyenes, optical prop., and electronic struct., rel. to polydiacetylenes 77−23592
polyester, ion mobility from ionic injection current at strong diffusion 80−2210
polyester, linear aliphatic, mol. motions determ. by dielec. relax. and loss meas. 77−63364
polyester, plasma induced grafting of acrylic acid 79−15825
polyester, practical testing methods for sheet and bulk moulding compounds *(German)* 79−70262
polyester, stress-optic law, photoplasticity, RPE transition temp. 78−10120
polyester, temp. index, rapid determ. by dynamic thermogravimetry 80−85101
polyester, unsat., copolymers, crosslinking effect on viscoelastic props., free torsion oscill. study *(Russian)* 79−34093
polyester (Mylar), plastic insulation for cryogenic power cable, exam. of dielectric, tensile props. 80−25823
polyester copolymer, modified with polypropylene glycol, addition to propoxylated bisphenol A, effect on mech. props. *(Polish)* 80−60902
polyester fibre, sputter etching 80−21147
polyester fibres, crystallinity and crystallite size meas. 78−30549
polyester fibres, orientation in drawn fibres, birefringence meas. 78−35344
polyester fibres, plasma surface treatment, ESR detect. of free radicals 79−15824
polyester filaments, solvent-induced crystallisation 78−83754
polyester filmbase experience in motion picture industry, review 80−42278
polyester foil, static polarisation depend. on heat ageing 78−60688
polyester model material, optical response and yield behaviour 78−31453
polyester model material, strain rate effect 79−83245
polyester moulding compounds, cyclic loading and strength 77−81310
polyester moulding materials *(Polish)* 80−66523
polyester resin, arc resistance tests in various gas insulators *(Japanese)* 80−81250
polyester resin, creep, temp. and humidity effects under shear and tensile strains 77−86105
polyester resin, creep, uniaxial elongation under variable temperature humidity 77−52434
polyester resin, cross-linked unsaturated, synthesis and fracture toughness 80−93634
polyester resin, PN-3, creep, effect of temp. and moisture 77−4820
polyester resin, POLIMAL 190, influence of MgO, BeO and TiO_2 on dynamical mechanical props. *(Polish)* 79−96074
polymers continued
polyester resin, reinforced with glass chopped strand mat and woven roving fabric, fracture toughness and crack-growth meas. 79−83299
polyester resin, unsaturated, glass fibre reinforced, polymerisation by UV irrad. *(German)* 79−100367
polyester resin, water diff. meas. by radionuclides, corrosion effects *(Czech)* 77−48566
polyester resin concrete, effects of styrene-unsaturated polyester ratio on props. *(Japanese)* 80−89299
polyester resin mortar, degradation in boiling water *(Japanese)* 78−11280
polyester resins unsaturated, enhanced elasticity, chem. resist. tests *(Polish)* 80−60901
polyester tapes, dynamic wetting behaviour 77−39723
polyester thermosetting powders, parameters 79−20003
polyester varnishes, electroinsulating, thermal resist. *(Polish)* 78−84014
polyester-hydrazide, aromatic, fibres and films, synthesis and props. *(Japanese)* 80−108387
polyester-paper, flashover behaviour at low temps. 80−25882
polyester-polyurethane interpenetrating polymeric network glues, props. 80−16640
polyester-polyurethane semi-interpenetrating networks, mech. props., morphology 80−45362
polyesteramide 6NT6 crystals, lamellar thickness invariance with crystallisation temp. 80−24380
polyesteramides, glass transition temp. determ. by DTA 79−4402
polyesterimide polymers, quasicrystalline struct. 78−75571
polyesters, aromatic, structural variation rel. to low temp. relax. 79−66096
polyesters, continuous production plants, technical details, polycondensation reaction stage analysis 79−100361
polyesters, corrosion-resistant, based on TMPD glycol, prep., phys. and corrosion props. 80−21136
polyesters, epitaxial crystallisation, on organic and inorganic substrates 78−91565
polyesters, linear, H_2O absorption and electric loss factor *(German)* 80−34849
polyesters, linear aliphatic, chem. struct. rel. to viscoelastic props. 79−41977
polyesters, photoreactive, synthesis and struct.-prop. relations 80−7826
polyesters from bridged bicyclic lactones, struct. characterisation by NMR 80−20476
polyethelene tubes and sheets, light resistance investigation under natural climatic conditions 80−21127
polyether ester-PVC blends, annealed, dynamic mechanical and sonic velocity behaviour 80−25740
polyether sulphone, effect of rolling on mech. props. 78−52837
polyether sulphone, evidence for crystallinity 80−28928
polyether-alkali metal salt adducts, cond. investigation rel. to use as solid electrolytes 80−59708
polyether-amidourethane, segmented, polymer domain struct., IR spectra and optical microscope *(Russian)* 78−51453
polyethers, NMR, microstruct. 79−51863
polyethersulphone, dielectric γ losses 78−68449
polyetheylene, charge carrier trapping phenomena *(Korean)* 77−89773
polyethyl acrylate atactic networks, stress-strain isotherms at high elongations to rupture point 77−40433
polyethyl acrylate modified mortars, inner struct. and flexural props., suspension and emulsion studies *(Japanese)* 77−86092
polyethyl ethylene and deuterated derivatives, modification I, vibrational spectra and normal coordinate anal. 79−87434
polyethylacrylate, benzene penetrant diffusion, statistical mech. model 80−44352
polyethylene: (Dy_2O_3), mech. props. and transfer to steel surfaces 80−16496
polyethylene: octadecanol, contact charging and donor impurity conc. relationship 80−20286
polyethylene:alkyl, electron spin echo spectra, instantaneous and conventional spectral diffusion 79−15355
polyethylene:$Br_2(I_2)$, films, electron-beam induced carrier mobility and elec. breakdown 80−80429
polyethylene:NaCl, internal field strength, Raman spectra obs. 80−40061
polyethylene:polyene, electron spin echo spectra, instantaneous and conventional spectral diffusion 79−15355
polyethylene, ^{13}C NMR rotating frame relaxation 80−7182
polyethylene, ^{60}Co gamma rays effects obs., on loss tangent variation *(German)* 80−75266
polyethylene, γ-irrad., alkyl radicals ESR and hindered oscill. 78−85182
polyethylene, γ-irrad., asymmetric 002 X-ray line profiles, analysis 80−96567
polyethylene, γ-irrad. induced allyl chain free radical, decay kinetics, state depend. 78−76855
polyethylene, γ-irradiated, effect of elec. field on TSC 79−65790
polyethylene, γ-irradiated, investigation of traps by photostimulated detrapping current analysis 77−15894
polyethylene, γ-irradiated, luminesc. in warming and cooling 77−32450
polyethylene, γ-ray polymerised, dielectric loss reduction 77−24783
polyethylene, {110} twinning mode, X-ray obs. 77−35572
polyethylene, accumulated charge profile during fast electron irradiations 77−4600
polyethylene, adhesion to Cu, reactions of CuO with Cu or polymer 79−39118
polyethylene, adhesion to Cu, substrate topography effect 79−74340
polyethylene, ageing in extreme cold climate *(Russian)* 77−59897
polyethylene, ageing prediction by isothermal differential scanning calorimetry 78−11485
polyethylene, amorphised by γ-irrad., interchain ordering, X-ray obs. 78−30545
polyethylene, amorphised by γ-irradiation, radial distribution function anal. for degree of interchain ordering 79−23530
polyethylene, amorphous, glass temp. 77−66017
polyethylene, amorphous, struct. from NMR line shape analysis and MAR-NMR 80−28931
polyethylene, amorphous fraction determ., multiple pulse NMR 77−77107
polyethylene, amorphous linear, glass transition temp. by torsion braid anal. 79−73296
polyethylene, amorphous-cryst., highly oriented, plastic deform. rel. to supermol. struct. *(Russian)* 79−51010
polyethylene, anisotropic surface stress 78−14562

polymers continued
polyethylene, annealed, crystallinity effect on mech. props. *(German)* 80−35230
polyethylene, anomalous photodepolarisation, trapping 78−10838
polyethylene, artificial voids, partial discharge charact. *(German)* 78−92023
polyethylene, Au nucleation, ion bombard effects 78−75965
polyethylene, band struct. valence Hamiltonian minimal STO-3G basis calc., nonempirical model pot. 80−54596
polyethylene, band structure, linear combination of localised orbitals calc. 77−62808
polyethylene, branched, annealing effect on lattice consts. 79−14698
polyethylene, branched, frictional props., normal force/shear for relationship 79−47785
polyethylene, branched, frictional props., true area of contact 78−64735
polyethylene, brittle fracture of notched ductile polymers *(Japanese)* 80−16448
polyethylene, brominated, single cryst., IR analysis 80−25362
polyethylene, bulk-crystallised, linear, PMR, phase struct. 77−84665
polyethylene, C muonic X-ray spectra, H(D) isotope effects 77−75344
polyethylene, carrier mobility determ. by current oscillation method 79−28344
polyethylene, carrier transport, expts. using hexatriacontane single cryst. as model polymer 80−6849
polyethylene, carrier trap study by X-ray induced TSC and thermoluminescence *(Japanese)* 80−54713
polyethylene, carrier traps, photostimulated detrapping currents and TSC meas. 78−10458
polyethylene, CH_2 Raman scissor modes *(French)* 79−69825
polyethylene, chain conform. in solid and melt, low angle neutron scatt. 77−76329
polyethylene, chain defects influence on crystn., reference to cryst. size and perfection 80−38942
polyethylene, chain end fixing, NMR line shape calcs. *(German)* 78−76322
polyethylene, chain end fixing, spin-lattice relax. time *(German)* 78−76340
polyethylene, chain-extended, deform. of lamellar microstruct. on drawing five-fold 77−21220
polyethylene, chain-extended, oriented, microindentation hardness 78−76728
polyethylene, chain-folded cryst., statistical mechs. in lattice model 78−47247
polyethylene, chains extended struct. *(Chinese)* 79−51092
polyethylene, chlorinated, ^1H and ^{13}C NMR microstructural investigation *(German)* 77−55246
polyethylene, chlorinated, high resolution ^1H and ^{13}C NMR, group fractions *(German)* 77−65551
polyethylene, chlorinated, history depend. recovery, stress relaxation, creep 78−80607
polyethylene, chlorinated, microstructure, use of ethylene vinyl chloride and copolymers as macromolecular models *(German)* 77−27838
polyethylene, chlorinated, partial struct. anal. of methane component by ^{13}C nuclear magnetic resonance *(German)* 79−73110
polyethylene, chlorinated, semicryst. random, characterisation by small angle neutron and X-ray scatt. 80−75189
polyethylene, chlorination, rate const. determ. using NMR spectra of chain sequence *(German)* 79−100366
polyethylene, comonomer unit partitioning, crystn. conditions effect 80−38943
polyethylene, Compton defect 77−73183
polyethylene, conduction band struct., LEED, secondary electron emission and UPS study 80−70601
polyethylene, conduction mechanism, expt. determ. *(German)* 78−76086
polyethylene, conform. stability, 1-electron levels, long-range effects calcs. 80−28123
polyethylene, conformation, Monte Carlo simulation 77−10797
polyethylene, contact angle data with many liquids, interaction parameter calc. 77−55423
polyethylene, cooled moderator on pulsed neutron source 78−70666
polyethylene, corona charged, direct drift mobility meas. 78−10837
polyethylene, correlation between valence energies and low temp. flexibility 80−25815
polyethylene, creep during shear deform. with applied hydrostatic press. 80−76324
polyethylene, creep in plane stressed state under programmed loads 79−11680
polyethylene, cross linking by energy rich radiation, mech. and elec. props. *(German)* 78−20035
polyethylene, cross-linked, insulating materials, dose rate effect on degradation behaviour 79−99239
polyethylene, cross-linked and low-density, pseudo spherulite structures and elec. discharges 78−42920
polyethylene, cross-linked crysts., deform. mechanism 78−15469
polyethylene, crosslinked, from HV cables, high-pressure liquid chromatography and differential scanning calorimetry 79−100466
polyethylene, crosslinked, super-oriented crystallisation under const. stress *(Japanese)* 78−34443
polyethylene, crosslinked networks, stress-induced crystallisation, theory 77−24277
polyethylene, cryst., soln. grown, neutron scatt., mol. dimens. rel. to mol. wt. 79−41258
polyethylene, cryst., transverse deform. and transverse movement of defects 80−38958
polyethylene, cryst. and melt, stat. thermodynamics 79−41979
polyethylene, cryst. struct. struct., rel. to n-paraffins, surface effects on core 79−23593
polyethylene, crystal, dielectric α-relax., soliton as crystal defect 80−45004
polyethylene, crystal, elastic line energies and line tensions of dislocations 79−90656
polyethylene, crystal split fundamentals, resolution by Raman difference spectroscopy 79−95373
polyethylene, crystal structure at 4.5K 78−14288
polyethylene, crystalline, Mossbauer anisotropic elastic scatt. fraction 78−6616
polyethylene, crystalline, steric struct. modelling of end defects 80−6371
polyethylene, crystalline, twist disclination formation and longitudinal motion of defects 80−19810
polyethylene, crystalline linear produced by rapid cooling from melt, structure determ. 77−19879
polymers continued
polyethylene, crystalline struct. transitions 77−51496
polyethylene, crystallinity, Raman spectral investig. 79−14696
polyethylene, crystallisation, chain folding, statistical mechanical calc. 78−2020
polyethylene, crystallisation, spherulitic, nonexponential transformation equation 78−67662
polyethylene, crystallisation at high-pressure, obs. using new dilatometer *(Russian)* 77−17950
polyethylene, crystallisation kinetics, use of DSC, comparison with dilatometry 77−31601
polyethylene, crystallisation of thick film from glassy state by annealing 80−54151
polyethylene, crystallised from oriented melt, mech. and thermomech. props., framework struct. 77−63756
polyethylene, crystn. at high press., small-angle neutron scatt. 77−55248
polyethylene, crystn. under high pressure 80−38946
polyethylene, crysts., subject to fold-surface tensile stress, elastic deform. 78−76712
polyethylene, DC partial discharge and current 78−43790
polyethylene, DC treeing breakdown with space charge formation, expt. 77−24789
polyethylene, deformation, Hartree-Fock SCF calcs. 80−18949
polyethylene, deformed cryst., IR spectrum, C-H stretching, effect of polymorphism 79−15453
polyethylene, delayed electrical response obs. in positronium form. 77−20273
polyethylene, deuterated, microspheres for laser fusion targets 78−46173
polyethylene, dielec., cryogenic tunnelling losses at microwave frequencies 77−52016
polyethylene, dielec. loss, 4.2K 77−24787
polyethylene, dielec. loss below 4.2K arising from proton tunnelling 77−52015
polyethylene, dielec. loss meas. using supercond. microwave resonators in oscillator loop 77−10043
polyethylene, dielec. props. rel. to mol. struct. 80−29681
polyethylene, dielec. relax. mechanism, 1-80K *(German)* 78−76384
polyethylene, dielectric loss at very low temperatures *(Japanese)* 80−11331
polyethylene, dielectric props., investigation for morphology changes created by mechanical drawing and annealing 80−84697
polyethylene, diffusion of long chain molecules 79−23784
polyethylene, diffusion of long molecules, meas. and results 78−55987
polyethylene, diffusion of long molecules, topological constraints 78−55986
polyethylene, diffusion of long molecules 77−27213
polyethylene, direct ram extrusion, correl. between chain folding and tensile modulus 77−44209
polyethylene, disintegration and vaporisation by high power laser pulses 77−39443
polyethylene, displacement of electronic spectrum during stretching, LCAO calc. 80−5481
polyethylene, doubly oriented, low density, deformation and structure, exam. 80−11705
polyethylene, drawing-out effect on vibrational normal modes *(French)* 77−15527
polyethylene, drawn, ultrahigh modulus, linear, melting behaviour 80−19916
polyethylene, drawn low-density, mech. and transport props. 79−74210
polyethylene, drawn polymer, fibre composite model 78−76719
polyethylene, dynamic mech. behaviour, longitudinal cryst. thickness 78−76691
polyethylene, dynamic mechanical behaviour during creep to failure in uniaxial extension 78−15455
polyethylene, dynamic modulus under high press., nature of high press. phase *(Japanese)* 80−3120
polyethylene, effect of ketones, temp. depend., environmental stress relax. study 80−45336
polyethylene, effect of morphology on viscoelastic props. *(Polish)* 79−51008
polyethylene, effect of pressure and environment on fracture and yield 78−76757
polyethylene, effect of Se on electrical and mechanical strength, after mechanical and electrical ageing *(Russian)* 79−52396
polyethylene, effects of mol. rot. and crosslink on specific draw ratios *(Japanese)* 79−96099
polyethylene, elasticity for different vibr. modes, algorithm 78−66696
polyethylene, elec. cond. of high and low density samples, oxidation effects 80−107784
polyethylene, elec. field effect on positron annihilation 79−4868
polyethylene, elec. props. and oxidation after electron beam irradiation and heat treatment 79−87092
polyethylene, elec. trees free radical ESR study 78−60393
polyethylene, electric breakdown charact. *(Korean)* 78−2799
polyethylene, electric cables, anal. of breaking strength distrib. *(Japanese)* 78−84921
polyethylene, electric field enhanced conductivity 77−35951
polyethylene, electrical capacitance under high DC elec. field 80−54705
polyethylene, electrical tree growth anal. using simultaneous meas. of light intensity and partial discharges 80−45008
polyethylene, electron beam crosslinking process for high voltage power cable 80−66846
polyethylene, electron energy loss, Monte Carlo anal. 77−31703
polyethylene, electron microscopy using electrostatic field *(German)* 78−82081
polyethylene, electron microscopy with chlorosulphonation aid 77−89351
polyethylene, electronic band struct., tight-binding approx. with MNDO 77−89691
polyethylene, electronic density of states, new algorithm 78−18939
polyethylene, electronic energy states and charge density contours studied muffin tin orbitals technique 80−80164
polyethylene, elongation, conform. set change IR obs. *(Russian)* 78−37778
polyethylene, environmental stress cracking, liq. efficiency criteria 80−21134
polyethylene, environmental stress cracking, theory 79−34176
polyethylene, environmental stress cracking at high stress, liquid wetting props. effects 78−92383
polyethylene, environmental stress cracking correl. with liq. sorption for low-swelling liqs. 80−81165

polymers continued
polyethylene, environmental stress cracking due to liq. viscosity, kinetic effect 77−4863
polyethylene, EPR of NO radicals, rot. mobility 79−33539
polyethylene, equation of state for semicrystalline, crystalline polymers 80−65187
polyethylene, expanded, dynamic model rel. to drop impact 78−7160
polyethylene, extended chain, prep. and study of separated single crystals 78−42924
polyethylene, extended chain crystal, fine structure and nucleation mechanism 78−14287
polyethylene, extended-chain cryst., high-press. crystallisation and melting obs. 77−27985
polyethylene, extruded, thermal cond. 220 to 360K 78−67873
polyethylene, extruded semicryst., thermal cond. and specific heat, <1K 80−59742
polyethylene, fatigue, fractographic study 80−30101
polyethylene, fatigue crack growth charact. 80−30100
polyethylene, fibre, phase structure and molecular mobility, broad-line NMR spectroscopy 78−14290
polyethylene, fibrillar, high mol. wt., oriented crystallisation, heat treatment effect *(Japanese)* 80−25738
polyethylene, fibrous samples, struct. obs. by low-angle X-ray diffr. 78−34445
polyethylene, fine struct., prep., O_3 selective degradation, chromatographic obs. 78−92475
polyethylene, FIR absorpt. freqs. using proved semiempirical pot. function 77−52090
polyethylene, flashover behaviour at low temps. 80−25882
polyethylene, for dry insulation in power cables *(Spanish)* 80−81024
polyethylene, fracture energy determ. 77−62208
polyethylene, friction and wear with lubrication by thermooxidative destruction products 77−52504
polyethylene, from the melt, small-angle X-ray scatt. study of crystn. 79−14692
polyethylene, gamma radiation effects on dielect. parameters, expt. *(Hungarian)* 78−59836
polyethylene, glass filled solids, ultrasonic absorpt., scatt., velocity and attenuation 80−44262
polyethylene, H bonding effects on skeletal optical and longitudinal acoustical modes 80−34914
polyethylene, halogen-doped, carrier transport and breakdown characteristics *(Japanese)* 80−96889
polyethylene, hard elastic fibres, deform. and struct., −196 to 80°C 78−51437
polyethylene, hexagonal, high press. crystn., review 79−23529
polyethylene, high density, adhesion strength to St. 3 steel 78−23920
polyethylene, high density, biaxial tension, long-time strength 77−66696
polyethylene, high density, carrier transport 79−33288
polyethylene, high density, cold-drawn, IR spectroscopy and X-ray diffr. 77−4764
polyethylene, high density, creep, computer program calc. *(German)* 78−60715
polyethylene, high density, creep curves, exponential functions for description *(German)* 78−90732
polyethylene, high density, crystalline, creep under plane stress state with const. loading 79−1903
polyethylene, high density, crystalline, flat stressed state, yield point time-temp. factors 78−64601
polyethylene, high density, crystallisation struct. revealed by solvent extraction 78−42922
polyethylene, high density, ductile, large strain cyclic deform. 80−85000
polyethylene, high density, durability, in emulsifier soln., effect of mol. mass and polydispersity *(Russian)* 79−66191
polyethylene, high density, effect of strain rate on stress relaxation behaviour 78−72807
polyethylene, high density, effects of draw rate and temp. on necking stress *(Japanese)* 79−91757
polyethylene, high density, elongational flow induced extrusion *(Japanese)* 79−91614
polyethylene, high density, environmental stress cracking and morphology 78−68834
polyethylene, high density, fracture buildup due to prolonged loading, exam. 78−68779
polyethylene, high density, fracture fatigue kinetics, IR absorption spectra 78−11323
polyethylene, high density, friction and transfer 77−52512
polyethylene, high density, hydrostatic extrusion behaviour 80−50649
polyethylene, high density, impact yielding, flow stress rel. to temp. 77−32653
polyethylene, high density, influence of dimensions in mech. props. *(German)* 80−21039
polyethylene, high density, injection moulding effect on strength props. *(Russian)* 79−34072
polyethylene, high density, lamellar struct. and plasticity micromechanism 78−23791
polyethylene, high density, monodisperse system mol. wt. effect on dynamic elastic modulus 77−70093
polyethylene, high density, necking stress *(Japanese)* 77−56036
polyethylene, high density, oriented extended chain crystals, transparency *(Japanese)* 80−38955
polyethylene, high density, plastic behaviour determ. at const. true strain rate 79−39073
polyethylene, high density, plastic deform. during hydrostatic extrusion 77−63722
polyethylene, high density, self-reinforced thermoplastic, extrusion 79−15699
polyethylene, high density, solid state coextrusion, geometric factors effect 80−71704
polyethylene, high density, solid state coextrusion, technique for ultradrawing thermoplastics 80−84979
polyethylene, high density, solid-state extruded, pole figure anal. 78−18556
polyethylene, high density, strength props. *(German)* 79−100219
polyethylene, high density, stress relaxation under tension and torsion 79−52290
polyethylene, high density, subjected to biaxial tension, effect of loading cycle asymmetry on fatigue strength 78−44215
polyethylene, high density, temp. change associated with adiabatic compression 77−66685
polymers continued
polyethylene, high density, thermolum. and its oxidation effects 77−77305
polyethylene, high density, time depend. deform. resistance 79−5019
polyethylene, high density, trapped carriers, thermally stimulated currents, influence of oxidation 77−80792
polyethylene, high density, treated in high elec. field, TSC *(Korean)* 79−28673
polyethylene, high density, TSC field depend. 78−76090
polyethylene, high density, wear mechanism at steel surface, SEM, TEM and DTA 78−64727
polyethylene, high density corona charged, TSC, oxidation effect 78−26882
polyethylene, high density extruded fibres, morphology effect on physical and mech. props. 79−83235
polyethylene, high field cond. current and elec. breakdown 77−76835
polyethylene, high modulus filaments, form. from melt, cryst. nucleation effects 79−70034
polyethylene, high mol. wt., deformability in physiological salt soln. 80−12305
polyethylene, high mol. wt., porous, hot drawing 80−60894
polyethylene, high molecular weight, effect of density on properties 77−90403
polyethylene, high oriented, deformation mechanisms of constrained chains, geometrically induced correlations of tie molecules 78−19835
polyethylene, high press. phase, US, DTA, and X-ray diffr. study 80−75188
polyethylene, high- and low-density, crystallinity degree, comparative obs. *(Polish)* 80−1943
polyethylene, high-density, damage accumulation kinetics under creep during prolonged loading 80−40447
polyethylene, high-density, deform. resistance and flow curve 77−90405
polyethylene, high-density, dielec. loss, below 4.2K, antioxidant, annealing and drawing effects 78−84518
polyethylene, high-density, environmental stress crack growth 80−25895
polyethylene, high-density, gaseous environment effect on mech. relaxations, tensile and torsion tests 79−96068
polyethylene, high-density, impact fracture behaviour, adiabatic heating at crack tip 80−85142
polyethylene, high-density, lamellar sep. during deform. 78−23775
polyethylene, high-density, longevity prediction, effect of surface active media 77−12729
polyethylene, high-density, oriented, deform. mechanisms 78−44171
polyethylene, high-density, oriented crystalline, anisotropic thermal expansion 80−39324
polyethylene, high-density, semicryst., fold-surface morphology effect on deform. processes 78−34447
polyethylene, high-density, solid-state coextrusion, mol. wt. distrib. effect 80−104212
polyethylene, high-density, stress-strain curve shape 77−63754
polyethylene, high-density, submicroscopic cracks form. and residual strength, hydrostatic press. influence 79−20185
polyethylene, high-density, tensile necking, specimen size and loading conditions effects 79−61672
polyethylene, high-density, thin-wall tubes, deform. and fracture processes 79−100222
polyethylene, high-density, vacuum-UV irrad. photoelec. emission and contact charging 79−52075
polyethylene, high-density fibres, extrusion conditions influence on thermal props. and morphology 79−61617
polyethylene, high-density fibres, solid-state extruded, form. props. 79−70035
polyethylene, high-density oriented, lamellar struct. obs. 77−55244
polyethylene, high-density ultradrawn, extrusion ratio influence on tensile props. 79−61618
polyethylene, high-density unorientated, damage buildup kinetics under creep conditions, during prolonged loading 80−60932
polyethylene, high-press., solubility coeffs. of propane and propene *(German)* 79−33093
polyethylene, high-press., temp. depend. of free vol., positron annihilation meas. 77−16419
polyethylene, high-press. charact. by torsional vibration anal. *(German)* 77−59842
polyethylene, high-press. phase transforms., X-ray diffr. obs. 77−80617
polyethylene, highly oriented, fibre composite model 78−3183
polyethylene, highly oriented, thermal conductivity 78−47614
polyethylene, highly oriented fibre composite, self-hardening, tensile props. 77−55939
polyethylene, highly oriented fibres, 2-dimens. ^{13}C NMR 77−77114
polyethylene, hip joint prosthetic component deformation meas. by holographic interferometry *(German)* 80−12302
polyethylene, homopolymers, copolymers and model systems, ^{13}C NMR chem. shifts and relax. times 79−72449
polyethylene, hot drawn, low density, stress relaxation 79−29121
polyethylene, hot-stretched, small angle X-ray scatt., computer anal. 79−14699
polyethylene, hydrostatic extrusion, deform. of crystalline and amorphous, and thermosetting resins 79−38875
polyethylene, hydrostatically compensated, SRO in precrystallisation phase 79−69033
polyethylene, hydrostatically extruded, linear, thermal expansion behaviour 79−77776
polyethylene, impact fracture toughness, rate effect 78−56741
polyethylene, impurity gas diffusion expts., test of two-phase cond. theory 79−69288
polyethylene, in toluene, pressure crystallised, swelling behaviour, rel. to densities 80−2167
polyethylene, influence of Se on mechanical and electrical strength *(Russian)* 79−11662
polyethylene, injection moulded high density, internal stress measurement, chemical cross linking effects 79−57035
polyethylene, interaction with SF_6 plasma, in glow discharge, emission spectrum 80−87960
polyethylene, intermolecular force field and normal vibrs. 79−73265
polyethylene, intrinsic photocond. under vacuum UV irrad. 80−70759
polyethylene, inverse currents, applied voltage, electrode material depend. 78−84206
polyethylene, ionising radiation effects crosslinking with accelerated electrons, ageing, SCC *(Polish)* 79−52701
polyethylene, IR and Raman intensities by electro-optical parameters, single chain 78−1115

polymers continued
polyethylene, IR spectra, −180°C, two-phonon absorpt. bands 78−72495
polyethylene, irrad., thermophys. charact. of amorphous phase, effects on crystallinity 77−7870
polyethylene, irrad., trapping regions, allyl radical distrib. 78−91957
polyethylene, irradiated, far IR spectrum rel. to crystallinity 78−27216
polyethylene, irradiation, crystallinity and crosslinking efficiency 80−66843
polyethylene, Kerr electro-optical effect, relative phase retardation meas. in elec. stressed samples 80−84716
polyethylene, lamellar stacks, screw dislocations 80−19728
polyethylene, lamellar structs. nucleated onto fibrous substrates for high modulus 78−75578
polyethylene, laser irrad., mol. emission from unionised gas 78−42777
polyethylene, laser irrad. chem. and struct. modifications *(Russian)* 79−27931
polyethylene, laser-prod. plasma, space-resolved extreme UV emission 80−54015
polyethylene, laser-prod. plasma, time of flight spectroscopy of fast ions 77−76190
polyethylene, laser-produced plasma, momentum transfer and interaction phenomena of high power CO_2 laser 80−48921
polyethylene, linear, ^{13}C spin-lattice relaxation 80−25235
polyethylene, linear, γ-irrad., plastic deform. 79−56996
polyethylene, linear, γ-irradiated, crystallite size distrib. and lattice distortions 79−69157
polyethylene, linear, γ-loss band, stress relax. 77−21201
polyethylene, linear, bulk-crystallised, morphology study 79−32918
polyethylene, linear, cold-deformed, texture and molecular chain mobility 78−19805
polyethylene, linear, crystallised from melt, effect of crystallisation time on density, mech. props., X-ray scattering 80−25680
polyethylene, linear, draw temp. and mol. wt. effect on draw ratio and Young's modulus 80−84998
polyethylene, linear, effect of HNO_3 treatment on γ-loss band 77−36562
polyethylene, linear, effect of pressure on vol. and dielec. relax. 79−61302
polyethylene, linear, far IR absorpt. spectrum, temp. depend., 14K to melting pt. 79−1758
polyethylene, linear, glass transition temp. 80−15225
polyethylene, linear, glass transition temp. upper limit, ^{13}C Fourier transform NMR 79−14918
polyethylene, linear, injection moulded at high press. struct. 79−11640
polyethylene, linear, melt-crystallised sharp fraction, lamellar morphology, electron microscopy obs. 80−84099
polyethylene, linear, nuclear relaxation, mol. motion *(Russian)* 80−44949
polyethylene, linear, plastic deform. behaviour 78−84910
polyethylene, linear, plastoelasticity theory 78−75712
polyethylene, linear, single cryst., surface melting, X-ray diffr. 77−31755
polyethylene, linear, solution-crystallized, NMR anal. of phase struct. 78−71684
polyethylene, linear, strain rate effects on ratio of recoverable to nonrecoverable strain 78−27566
polyethylene, linear, struct. and relax. transitions, pulsed NMR and X-ray diffr. *(Russian)* 77−47357
polyethylene, linear role of recovery forces in deformation 78−48459
polyethylene, liq. diffusion coeffs. determ., G-L chromatography, modified Deemter eqn. 78−2277
polyethylene, longit. acoustic mode 77−7816
polyethylene, longitudinal acoustic mode freqs., general theory for composite perturbed elastic rod 78−14421
polyethylene, low and high density, tensile relaxation changes *(German)* 78−64599
polyethylene, low and high density, thermoelastic effects 78−88491
polyethylene, low density, α mech. dispersion in relation to spherulite deform. mech. 80−25781
polyethylene, low density, γ irrad. effect on elec. cond. and temp. characts. 77−85221
polyethylene, low density, γ-irrad., unixial elongation effect on elec. cond. 80−25812
polyethylene, low density, absorption currents exam. 78−43785
polyethylene, low density, deformed in tension, lamellar reorientations 78−84914
polyethylene, low density, dielec. behaviour, struct. props. influence *(German)* 78−92017
polyethylene, low density, highly deformable, fracture surface roughness 78−44197
polyethylene, low density, isotropic, extensional deformation, and effects 80−7613
polyethylene, low density, linear viscoelasticity, relaxation func. determ. 79−7359
polyethylene, low density, meas. of shear modulus and damping in a torsion pendulum 79−4989
polyethylene, low density, melting and crystallisation, DSC characterisation 80−64927
polyethylene, low density, mol. motion, thermally stimulated creep 77−90402
polyethylene, low density, morphology and props. 80−64926
polyethylene, low density, nonlinear variable temp. creep 79−38908
polyethylene, low density, SEM exam. of environmental stress cracking 78−53011
polyethylene, low density, shear and tensile creep at finite strains 78−52903
polyethylene, low density, water tree growth under DC voltage stress, expt. 77−77148
polyethylene, low density, with a single texture, oriented crystallisation of biphenyl 78−9966
polyethylene, low density foam, two-step heating process *(Japanese)* 77−52369
polyethylene, low density foam production, viscosity meas., comparison with polystyrene *(Japanese)* 77−52276
polyethylene, low temp. dielec. loss due to antioxidants 79−99822
polyethylene, low temp. thermal cond. 79−73351
polyethylene, low-density, α-irrad., thermolum. mechanism biphenyl anions influence 80−2880
polyethylene, low-density, γ-irrad., spin trapping reaction 80−39873
polyethylene, low-density, environmental stress cracking, surfactant soln. effect 80−89376

polymers continued
polyethylene, low-density, fatigue fracture surfaces produced by monatonic and cyclic loading 80−40510
polyethylene, low-density, in nonuniform AC fields, influence of temperature on breakdown obs. *(German)* 80−29685
polyethylene, low-density, mol. characterisation 79−52843
polyethylene, low-density, temp. changes in large period structure *(Russian)* 77−31603
polyethylene, low-density natural, permittivity and loss factor meas. at elevated temps. 80−97185
polyethylene, low-temp. relax., effects of chem.- and electron irrad.-crosslinking 79−4990
polyethylene, lubricant additive effect on operating performance of sintered materials 80−11785
polyethylene, mag. susceptibility, constant mag. field effect 80−11154
polyethylene, meas. of high chain extensions by gel permeation chromatography 77−88611
polyethylene, mech. and elec. low temp. props. 80−25814
polyethylene, mech. retardation time spectrum, thermostimulated creep 79−5014
polyethylene, medium density, impact testing, elastic analysis of conventional test, reassessment of testing 78−60770
polyethylene, melt crystallised, chain defects distrib. and microstruct. 79−10818
polyethylene, melt crystallized, amorphous phase, IR spectrum 78−76463
polyethylene, melt-crystallised fractions, surface and full-strand melting, small-angle X-ray scatt. obs. 80−84279
polyethylene, melting, equilib. temp., confomational modifications *(Russian)* 79−51240
polyethylene, melting against Al, XPS obs. 77−32700
polyethylene, melting on Al, XPS meas. 78−15556
polyethylene, melting point, heating rate depend. 79−99296
polyethylene, microfine powder prod. for dispersions *(German)* 80−29920
polyethylene, microstruct. obs., variation during drawing and annealing, electron microscopy *(German)* 80−38944
polyethylene, microwave dielec. losses variation rel. to different sample treatments 80−25881
polyethylene, microwave photon echo 80−66330
polyethylene, migration and solubility of antioxidants *(French)* 79−46839
polyethylene, MIM structure, TSC study 79−78201
polyethylene, mixing of high and low density, mixing ratio determ. by thermo-optical anal. *(German)* 78−53070
polyethylene, modelled by hexatriacontane, vac. UPS 77−66570
polyethylene, modified with phosphonate ester pendant side group, thermal and mech. props. 78−11195
polyethylene, mol. conformations after recrystallisation or annealing at high press. 77−88612
polyethylene, mol. morphology determ. by NMR 78−94341
polyethylene, mol. motions, α relax, chain transport 79−15398
polyethylene, mol. ultraslow rot. obs. using D probe spin alignment tech. 80−88890
polyethylene, mol. wt. averages determ. by temp. drop turbidimetry 79−39207
polyethylene, molecular chain mobility, UV irradiation effect 77−84792
polyethylene, molecular clustering in mixtures with polyethylene-d_n, small-angle neutron scatt. 78−26451
polyethylene, molecular motion and spin-lattice relaxation 78−48071
polyethylene, molecular motions, exam. by PMR line shape anal. 79−41982
polyethylene, MP, heat of fusion, degree of crystn. determ. by differential scanning calorimetry *(Russian)* 77−62489
polyethylene, nascent, electron microscope study 80−38940
polyethylene, necking stress *(Japanese)* 77−56037
polyethylene, neutron irradiation, radical distribution, ESR study *(Japanese)* 80−44920
polyethylene, NMR relaxation times, computer-assisted meas. method 77−22586
polyethylene, NMR with rotation through magic angle *(German)* 78−76341
polyethylene, non-isothermal currents and space charge build-up 80−39590
polyethylene, nonoriented partially cryst., kinetic damage accumulation cure 80−71753
polyethylene, notched sheet, deform. mech., fracture, X-ray obs. *(Japanese)* 77−59863
polyethylene, ns breakdown voltage, polarity effect, mechanism 77−63367
polyethylene, observation of deformation process with X-ray TV system 78−15610
polyethylene, obtained from heterogeneous Ziegler-Natta catalysts, cryst. morphology and growth 80−38941
polyethylene, obtained with heterogeneous Ziegler-Natta catalysts, nascent struct. and morphology 79−96307
polyethylene, of low density, determ. of avoiding of tensile cracks *(German)* 80−19874
polyethylene, one dimens. synthesis of SAXS pattern 78−75589
polyethylene, one-, three-dimensional, energy band struct., ab initio calcs. 79−95330
polyethylene, orientated, var. of yield stress with orientation, yield criteria exam. 78−52900
polyethylene, oriented, elastic stiffness constants, US meas. 78−76690
polyethylene, oriented, high temp. deform. X-ray diffr. expts. 77−56028
polyethylene, oriented, partially crystalline, amorphous component obs., X-ray diffr. *(Russian)* 79−23534
polyethylene, oriented, Raman active modes 78−23457
polyethylene, oriented, shear strain, effect on stuct., props. *(Russian)* 80−7656
polyethylene, oriented, stress-strain curve, analogy with van der Waals isotherm 77−59869
polyethylene, oriented, thermal expansion 77−7881
polyethylene, oriented chain-extended, Young's modulus, fracture and compression behavior 80−11747
polyethylene, orthorhombic and triclinic lattices, eqns. of state 79−28069
polyethylene, oxidation rel. to spherulitic crystn. *(Russian)* 78−71689
polyethylene, oxidised, charge carrier, transport phenomena 80−15515
polyethylene, oxidised, low-temp. dielectric spectrum 79−61304
polyethylene, oxidised, origin of high temp. anomalous luminesc. 77−85812

polymers continued
polyethylene, oxidised, paraelectricity, dielec. relax. obs. 77—48123
polyethylene, oxidised and chlorinated, dielec. ops. of mol. relax. 77—40179
polyethylene, oxidised and gamma-irradiated, carrier traps, thermally stimulated currents 78—19050
polyethylene, partial discharges degradation effects, expt. 77—7617
polyethylene, partial draining of low-molecular weight polymers with flexible chains 80—23592
polyethylene, partially crystalline, far IR absorption and thermal props. 79—33690
polyethylene, perdeuterated, skeletal vibr. spectrum 78—23445
polyethylene, permanganic etchant for TEM obs. 80—21132
polyethylene, phase characterisation, Raman spectra study *(French)* 80—93303
polyethylene, phase orientation by stretching, Raman study *(French)* 80—93304
polyethylene, phosphonate derivatives, dynamic mech. behaviour 79—15713
polyethylene, photodegradation mechanism, from yield strength, elongation and mol. wt. studies *(Japanese)* 80—76311
polyethylene, photodegradation study by Fourier transform IR spectroscopy *(Japanese)* 79—24772
polyethylene, plastic insulation for cryogenic power cable, exam. of dielectric, tensile props. 80—25823
polyethylene, Poisson's ratios, parallel lamellas morphology 78—84882
polyethylene, polarised Raman studies of crystalline and amorphous orientation 78—67660
polyethylene, polyethylene-D_4, migration and copolymerisation at high press. with shearing stress 78—51678
polyethylene, polymer life eqn. appl. to dielec. strength 80—25304
polyethylene, polymerisation kinetics math. model, mol. wt. evaluation *(Russian)* 79—52661
polyethylene, porous, tensile strength of interface with bone 80—30737
polyethylene, positron implantation profile, electric field depend. 79—11483
polyethylene, positronium form. and decay, elec. field effect 80—97369
polyethylene, pressure phase transition, function of pressure and temp. 79—77745
polyethylene, pretreated surface, nitrobenzene contact angle, H_2O environment *(Japanese)* 78—79858
polyethylene, production of large warm plasmas by staged laser heating 77—19733
polyethylene, protonated and deuterated, neutron scatt. at intermediate Q-values 79—10807
polyethylene, pulsed NMR obs., crystallinity effects 78—76342
polyethylene, pyramidal crysts., soln.-grown, collapse mechanics 78—76713
polyethylene, quenched melt, factors controlling lamellar thickness 77—62484
polyethylene, radiation effects on EPR and differential thermal anal. *(Bulgarian)* 79—46698
polyethylene, radiation heating effect on creep 80—35285
polyethylene, Raman spectra, drawing effect on longit. acoustic mode *(French)* 77—24828
polyethylene, Raman spectra obs. of longitudinal acoustic modes intensities 78—84584
polyethylene, rapid crystn. from melt rel. to struct. 80—44152
polyethylene, relax. phenomena, −30 to 200°C, premelting and glass transition 78—51440
polyethylene, resist. to stress corrosion cracking, ionising radiation effect *(German)* 80—81224
polyethylene, rheological behaviour at high shear strain rates *(French)* 80—66574
polyethylene, roll oriented, superstructural change during uniaxial extension *(Japanese)* 77—52422
polyethylene, rolled, neck draw *(Japanese)* 77—86090
polyethylene, second order Raman scatt. 78—72504
polyethylene, self-adhesion, surface polarity effect, meas. by Ca^{2+} adsorpt. 79—11759
polyethylene, SEM meas. of fine lamellar struct. 79—51007
polyethylene, semi-crystn., neutron scattering study 80—38936
polyethylene, semicrystallised chains, small-angle neutron scatt., mean dimension evaluation 80—43220
polyethylene, shish kebab structure, formation mechanism 78—14286
polyethylene, shish-kebab crystals, core struct. 80—38945
polyethylene, shock compressed, vel. of sound meas. 78—10123
polyethylene, short chain branching, ^{13}C NMR 79—33557
polyethylene, shrinkability, orient. 79—11660
polyethylene, single, polycryst., ^{60}Co-γ irrad., effect on melting behaviour 77—15548
polyethylene, single cryst. and spherulites, microstruct., deform. micromechanisms 78—83758
polyethylene, single crystal, electron microscopy study 80—103273
polyethylene, single crystal, estimation of fold surface densities using space filling models 80—10507
polyethylene, single crystal, fold domain boundaries, TEM 80—107065
polyethylene, single crystal, structural changes due to electron irrad. 80—29053
polyethylene, single crystal texture, polarised Raman spectra 77—61888
polyethylene, single crysts. chain end location, IR spectra 78—71687
polyethylene, solid, heterogeneity investigation by small angle neutron scattering 78—14298
polyethylene, solid, IR spectra, interference distortion of 73 cm^{-1} absorpt. line 80—11375
polyethylene, solid, multicomponent decay of nucl. magnetisation, in rot. coord. system, anal. *(Russian)* 78—27106
polyethylene, solid, nucl. spin-lattice relax. time, freq. depend. defect diffusion, 77-373K 78—72428
polyethylene, solid liq., secondary electron emission spectroscopy 80—80916
polyethylene, solid-state extruded, exam. of props. 80—11669
polyethylene, solution crystallized and melt crystallized small angle neutron scatt. 79—14691
polyethylene, sonic frequency vibration effect on stress relaxation 77—86072
polyethylene, sp. ht. after annealing at low temps. 77—39679
polyethylene, space charge effect on local electric breakdown 77—69773
polyethylene, space charge injected from electrode at low temps., luminesc. obs. 80—25464
polyethylene, space radiation effects evaluation 80—70263

polymers continued
polyethylene, space-charge storage under high DC voltage condition, TSC meas. *(German)* 80—75576
polyethylene, specific vol. under high press., appl. of novel dilatometer 77—37844
polyethylene, standard reference material, limiting viscosity numbers 79—14952
polyethylene, standard reference material, number average mol. wt. 79—13854
polyethylene, standard reference material, preparation 79—15641
polyethylene, standard reference material, weight average mol. wt. 79—13855
polyethylene, steady-state deform. and its effect on struct. and morphology 78—15459
polyethylene, stopping cross-sections using alpha particles in energy range 1.5 to 4.2 MeV 78—53510
polyethylene, straight chain segment length distrib., from Raman LAM-1 band 79—41981
polyethylene, stress cracking in aqueous detergent 77—12727
polyethylene, stress crystallised, melting behaviour 77—47554
polyethylene, stress rel. to draw ratio during ultra draw *(Japanese)* 79—91759
polyethylene, stressed, thermodynamics of embedded crystallite deform. *(Polish)* 77—52424
polyethylene, stresses at spherulite boundaries causing black lines 77—72568
polyethylene, stretched, birefringence rel. to struct. changes 80—84714
polyethylene, stretched sheets, electron emission 78—88411
polyethylene, struct. changes on hot-rolling 77—86051
polyethylene, struct. transform. under tension in liqs. *(Russian)* 77—51492
polyethylene, structural changes induced by high elec. field *(Japanese)* 79—23532
polyethylene, structural changes on hot-rolling 77—86052
polyethylene, structure change on uniaxial compression *(Russian)* 79—34119
polyethylene, supermolecular structure, polymerisation at low pressure *(Russian)* 79—64126
polyethylene, supermolecular structure study, IR spectroscopy *(Spanish)* 79—77532
polyethylene, surface activation by corona treatment *(Japanese)* 77—77604
polyethylene, surface charge release, crossover phenomenon, thermally stimulated discharge current study 80—50255
polyethylene, surface component of vacuum absorpt. and resorpt. currents, surface charge accumulation 80—60063
polyethylene, surface component of vacuum absorpt. and resorpt. currents, origin and magnitude 80—70791
polyethylene, surface fluorination effects, internal refl. spectroscopy obs. 78—86340
polyethylene, surface topography rel. to adhesion props. 79—96280
polyethylene, target impurity effect on laser produced expansion, ion spectrography 80—43945
polyethylene, temp. depend. of elec. cond., isothermal current peak 79—51595
polyethylene, terephthalate, amorphous, electron microscope and small angle X-ray studies 77—84666
polyethylene, theory of adhesion to alkali halide crystals, allowance for boundary dislocations 77—70280
polyethylene, thermally oxidised, low-temp. dielec. relax., dipolar tunnel states 78—2797
polyethylene, thermoluminesc. spectrum *(German)* 78—76538
polyethylene, torsional rigidity testing *(German)* 77—52596
polyethylene, transcrystalline, anisotropic thermal expansion 79—4420
polyethylene, tree initiation by DC and impulse voltage appl., expt. 77—24790
polyethylene, tree initiation under impulse voltage, effect of needle electrode materials 77—73112
polyethylene, treeing at 77K, expt. 77—24792
polyethylene, treeing inception voltage, effect of blending and crosslinking 78—43788
polyethylene, TSC due to trapped electrons, rate-determining process 77—59290
polyethylene, TSC study of deuteration 80—20581
polyethylene, tubular magneto-electret, surface charge characts., forming temp./mag. field depend. 77—32318
polyethylene, two phonon Raman spectrum, final state interactions 78—76457
polyethylene, ultra high mol. wt., knee prosthesis, in vivo wear props. 80—17204
polyethylene, ultra high mol. wt., sliding behaviour against Cu or Al spheres at cryogenic temps. 80—66671
polyethylene, ultra-high modulus, drawing behaviour, effect of drawing temp. 80—35232
polyethylene, ultra-high modulus, micromorphology 77—63621
polyethylene, ultra-high mol. wt., wear mechanisms in total joint replacement 77—52929
polyethylene, ultra-high molecular weight, linear, impact fatigue response 79—100242
polyethylene, ultra-high-strength filaments, soln. spun/drawn, mech. and thermal props. 80—40440
polyethylene, ultra-oriented, prep. technique, extreme moduli 77—21086
polyethylene, ultra-oriented high density, shrinkage as meas. of deformation efficiency 80—40398
polyethylene, ultradrawing, effects of temp. and drawing rate *(Japanese)* 79—91760
polyethylene, ultradrawn, electron microscope exam. of struct. after annealing 80—11662
polyethylene, ultradrawn linear, kink bands by compression, interfibrillar motion 79—24581
polyethylene, ultrahigh draw ratios, mol. wt. effects 79—74211
polyethylene, ultrahigh modulus, drawing temp. effect on void form. and modulus 80—35241
polyethylene, ultrahigh modulus linear, annealing effects on mech. stiffness and struct. 79—91717
polyethylene, ultrahigh mol. wt., appl. to artificial joints 79—84001
polyethylene, ultrahigh molecular weight, wear, rel. to replacement hip joints 77—17008
polyethylene, ultrahigh-modulus, thermal cond. in region 2 to 100K 77—62690
polyethylene, ultraoriented, ^{13}C-^{13}C dipolar satellites 77—28465

polymers continued
polyethylene, ultraoriented, fibrillar struct. 77−89389
polyethylene, ultraoriented, prep. comments 77−85983
polyethylene, ultraoriented high-density, annealing characts. 77−8852
polyethylene, ultraquenched, electron diffr., morphology and thermal anal. 79−15640
polyethylene, uncrosslinked amorphous matrix embedded cryst. orientation distrib., strain energy and hydrodynamic pot. effects 78−9968
polyethylene, uniaxial, deuterated, interchain forces effects on acoustic phonon branches, neutron scatt. study 79−51228
polyethylene, uniaxially oriented, relation between deform. and rotational isomerism 77−52438
polyethylene, uniaxially stretched, density fluctuations 78−75587
polyethylene, valence electronic struct., LCAO cryst. orbital calcs., ESCA 78−5384
polyethylene, vel. spectrometry of 3.5 GeV N ions 78−48896
polyethylene, vibr. data and force field consts., review 79−31750
polyethylene, vinyl group reactions during γ-irrad., crystallinity effect, absorbance obs. 80−81346
polyethylene, VLF partial discharges meas. over freq. range 0.1 to 50 Hz 77−76227
polyethylene, voltage-induced charge transfer and its effects on tree initiation 80−25307
polyethylene, wear against dry stainless steel in unidirectional motion 79−20212
polyethylene, welded, exam. of neutron irrad. effects on tensile characts. *(Japanese)* 78−84918
polyethylene, X-ray diffr. at press. up to 14000 kg cm^{-2}, 298K 77−35492
polyethylene, X-ray emission spectra of CO_2 laser-irrad. targets, nonlinear processes 80−33793
polyethylene, X-ray irrad., trapped carriers, TSC 77−69338
polyethylene, X-ray scatt., models for stacks of lamellae 79−37638
polyethylene, Young's modulus, crystallite thickness 78−76689
polyethylene,environmental stress cracking, interlamellar failure 77−90476
polyethylene(-d_4), vibr. freqs., MNDO semiempirical SCF calcs. 78−1114
polyethylene 2,6-naphthalate, AC conduction mechanism, freq. and temp. depend. *(Japanese)* 80−54706
polyethylene 50 Hz tree propagation between needle electrodes 80−15968
polyethylene (orthorhombic), intermol. pot. functions, force consts., vibr. assignments, thermodynamic props. 77−39639
polyethylene and ethylene-vinyl acetate copolymer dielectric breakdown 80−15966
polyethylene and ion-exchange resin composite for radioactive waste solidification, ^{137}Cs leaching 77−65275
polyethylene and polyvinylchloride, degradation mechanism analysis, by mass spectroscopy *(Dutch)* 79−87893
polyethylene and resin-coated photographic papers 80−86474
polyethylene azelate, epitaxial crystn. on aromatic hydrocarbon substrates 79−61521
polyethylene cable grade crosslinked, effect of electrode profile on dielec. breakdown voltage, epoxy resin insulation system 80−60502
polyethylene cables carrying DC current, TSC and space charge effects *(French)* 80−40042
polyethylene capillaries, for polarography in corrosive media, prep. 78−61090
polyethylene catalyst, $TiCl_4$-$MgCl_2$, struct. and mechanism 80−11951
polyethylene chain with single deuterised unit, local and reson. vibrs. 79−99287
polyethylene charge carrier injection, contactless electrode expt. 80−15540
polyethylene chips on Cu-Ni mesh, surface, obs. at very low accel. voltage (200 V-1 kV) by SEM 80−10764
polyethylene coating on galvanized steel, thermal oxidation affect on adhesion *(German)* 80−35419
polyethylene cocrystals, partially and fully deuterated, chain folding, ^1H NMR solid echo technique 80−20507
polyethylene cryst., unit cell variations with temp. and high press. 78−47250
polyethylene crystal, computer simulation of {110} twin boundary 78−30646
polyethylene crystal, highly gamma-irradiated, unit cell dimension meas. 77−76326
polyethylene crystal, longitudinal growth in flowing soln., melting of continuous fibrillar crystal 80−19917
polyethylene crystal, thermal creation of defects, dielec. evidence 80−44151
polyethylene crystals, plastic deformation, molecular mech., TEM obs. 80−21022
polyethylene crystals, soln. formed, low mol. weight, swelling 79−94920
polyethylene crystals in suspension, heat of fusion 79−87870
polyethylene disordered chains, electron localisation 78−87945
polyethylene electret, internal pot. topography, Raman and IR spectra 80−7362
polyethylene electrets, charge trapping mechanism, TSC, DTA and optical meas. 80−11322
polyethylene expanding plasma, high power CO_2 laser radiation interaction 78−47138
polyethylene extrudate, transverse compression 78−68728
polyethylene far IR absorption rel. to crystallinity 77−40242
polyethylene fibre, high-strength high-modulus, morphology and tensile prop. relations 80−103264
polyethylene fibre explosion, neutron and energetic ion emission 78−5927
polyethylene fibre growth from flowing solns., kinetics 79−47654
polyethylene fibre prod. by surface growth method, mech. props. 80−104108
polyethylene fibres, electron microscope investig. of internal struct. 80−28926
polyethylene fibres, high density, ultra oriented, physical, mech. props. 80−25649
polyethylene fibres, X-ray diffraction-profile Fourier analysis, determ. of microstruct. parameters 80−49042
polyethylene fibres radiation initiated graft polymerisation of acrylonitrile, initiation rate rel. to props. *(Russian)* 80−7531
polyethylene fibril, high mol. wt., high melting point crystal *(Japanese)* 80−38954
polymers continued
polyethylene filament, plasma prod. by staged laser heating, optical obs. 77−89321
polyethylene filaments, ultrahigh-strength, from soln. spinning and hot drawing 80−45268
polyethylene film sliding against PTFE, PVC, PP, PMMA, material transfer 78−64726
polyethylene films, oscillatory necking 79−72826
polyethylene films electrical conductivity under various conditions *(French)* 80−70869
polyethylene filtration of 30 and 40 MeV Be+p neutron beams 78−53494
polyethylene foils, deuterated, prep. technique 77−88313
polyethylene glycol, depolarised Rayleigh scatt., orientational motion, pure and soln. 77−44008
polyethylene glycol, mol. polarisability from Faraday effect 78−58726
polyethylene glycol, mol. wt. determ., high-speed aq. gel-permeation chromatography 79−61922
polyethylene glycol, transverse nuclear magnetisation decay rel. to slow mol. motions *(Russian)* 78−72423
polyethylene glycols, ^1H NMR in presence of shift reagent 79−99779
polyethylene glycols, size exclusion chromatography, response correction of differential refractometer 79−34375
polyethylene high press. phase, struct., phase diagram and compressibility 78−9961
polyethylene imine and its oligomers, linear struct., props. *(Russian)* 79−50177
polyethylene implant-bone composite interfacial strength, porous high density polyethylene 78−31979
polyethylene insulation of HV cables, water-treeing, environmental stress cracking phenomenon of elec. origin 80−40575
polyethylene interfaces, randomly spaced, transition radiation spectra from relativistic electrons 78−21805
polyethylene lattice, inclusion of chain defects, stat. approach 80−75190
polyethylene layered target, laser produced plasma, expsn., X-ray meas. 77−80326
polyethylene life test needle electrode selection 80−15969
polyethylene low density and high density, spherulite obs. in low density *(German)* 78−31398
polyethylene low density flame treatment of surface, XPES study 79−66179
polyethylene matrix, trapped free radicals, decay in single crystal and diffusion 77−52657
polyethylene medium, embedded Ge particles, extinction cross section 80−9807
polyethylene membrane, permeation of hydrocarbons 80−30281
polyethylene membrane (graphite charged) electrode, electron transfer *(French)* 78−27778
polyethylene microspheres, deuterated, variable density, laser fusion targets, prep. 78−74468
polyethylene mixtures as IR filters, transmission characts. 77−39020
polyethylene molecule, fractured, local electron level calc. 80−14263
polyethylene molecules, transportation along their axis, energetics of defect motion, point dislocation energy calc. 78−14294
polyethylene naphthalate, photoconductivity, UV-IR light, absorpt. and photoluminescence. spectra *(Japanese)* 78−34857
polyethylene oxide, block polymer, crystallisation 79−10817
polyethylene oxide, cryst., lowest laser Raman active accordion oscillations, elastic moduli effect 80−29734
polyethylene oxide, drag-reducing, as corrosion inhibitor in Al tube 80−45445
polyethylene oxide, elec. polarisation in suspension, Kerr effect 77−63359
polyethylene oxide, low mol. wt., effect of end-group on crystallinity and fusion 77−84897
polyethylene oxide, melt grown single crystal, isothermal growth, thickening and melting 78−51432
polyethylene oxide, mol. wt. averages and polydispersity determ. by temp. drop turbidimetry 77−63959
polyethylene oxide, nascent and annealed, X-ray study of crystal structure 80−64922
polyethylene oxide, Raman scatt. from longitudinal acoustic modes of crysts. swollen by oligomers 78−27226
polyethylene oxide, relax. phenomena, −30 to 200°C, premelting and glass transition 78−51440
polyethylene oxide, solid state relaxation, DSC study 78−9962
polyethylene oxide, solid-state relaxation, spin labelling technique 78−9963
polyethylene oxide 2000-200 mixtures, Raman scatt., small-angle X-ray scatt. 77−52089
polyethylene oxide additive to clays, effect on plastic strength after tempering 79−24568
polyethylene oxide blends, thermal and mechanical props. 79−11679
polyethylene oxide crysts., small-angle neutron scatt. 78−51447
polyethylene oxide dilute aqueous solns., flow in various geometries 79−41757
polyethylene oxide homo and copolymers, monomer link lengths determ., IR spectral method *(Russian)* 77−32383
polyethylene oxide ionic complexes, order-disorder transformations 78−47251
polyethylene oxide trioxane mixtures, eutectic crystallisation 78−56626
polyethylene oxide-polyarylate, block-copolymers and mixtures, phase separation, DSC obs. *(Russian)* 79−55895
polyethylene oxide-polystyrene-polyethylene oxide triblock copolymer, surface and full-strand melting, small-angle X-ray scatt. obs. 80−84279
β-polyethylene oxybenzoate, cryst. struct. and mol. conformation 79−55674
polyethylene pellets, for ^{252}Cf storage safe, transport vessel, portable shield 79−5380
polyethylene photochemical aerosol, absorbance rel. to presence in Titan atmosphere 80−31249
polyethylene phthalate-metal adhesive bonds, shear resist., polymer crystn. effect 80−89462
polyethylene pipe butt welding, tensile tests rel. to melt flow index 77−73389
polyethylene pipes, lifetime determ., crack growth in thermoplastics under various conditions 78−39981
polyethylene plate, appl. of new method for potential distrib. meas. in dielectrics 77−26336
polyethylene plate, corona charged, electrostatic potential distrib. meas. *(French)* 77−143

polymers continued
polyethylene process plants, low-density, high pressure compressor design 77−13764
polyethylene prostheses, radiation crosslinking improvement of shock- and abrasion-resistance 77−60307
polyethylene rod, high oriented, mech. behaviour 78−15446
polyethylene shell, CO_2 laser implosion into D-filled conical region, neutron prod. 78−87468
polyethylene single cryst., FT IR spectra, CH_2 rocking mode 78−2843
polyethylene single cryst., FT IR spectra, CH_2 wagging mode 78−2842
polyethylene single crystal in suspension, Fourier transform IR study 78−10877
polyethylene single crystals, fold domain boundaries, diffr. contrast 77−15428
polyethylene single crystals, STEM advantages over TEM, microarea diffraction patterns specimen radiation damage 79−55620
polyethylene single crysts., force elongation meas. 79−87700
polyethylene sorption properties, γ-ray effects in N_2O_4 medium *(Russian)* 77−72796
polyethylene spherulites, high density, microstruct. and mech. props. 78−42921
polyethylene spherulites, lamellar struct. obs. 78−30547
polyethylene spherulites, STEM and microdiffr. obs. of micromorphology 78−34444
polyethylene spherulites, thermal expansion 78−2268
polyethylene stabilized with home-made antioxidants, thermal resistance *(Polish)* 79−52328
polyethylene structural transformations under fast electron irradiation *(Russian)* 79−94987
polyethylene substrate, effect of glow discharge on nucleation charact. of Au 79−77963
polyethylene sulphide, cryst. struct. by electron diffr. 78−51441
polyethylene sulphide, thermal stability and stability against solvents *(Russian)* 78−51449
polyethylene surface field strength under DC stress 80−15967
polyethylene surface-growth fibres, hot drawing 80−97517
polyethylene terephtalate, photoconduction carrier generation mechanism at UV and IR light region 77−80803
polyethylene terephthalate, β relax., dynamic mech. and dielectric loss data 79−15399
polyethylene terephthalate, amorphous, thermally stimulated creep and TSC expts., retardation modes 79−69768
polyethylene terephthalate, amorphous material orientation determ. *(Polish)* 79−73111
polyethylene terephthalate, amorphous state change by heat treatment below glass transition temp. 78−30550
polyethylene terephthalate, anomalous photodepolarisation, trapping 78−10838
polyethylene terephthalate, between metal electrodes, electrochem. effects as source of EMF 78−72278
polyethylene terephthalate, between metal electrodes, electrochem. effects as source of EMF 79−87162
polyethylene terephthalate, between metal electrodes, electrochem. effects as source of EMF 79−87163
polyethylene terephthalate, birefringence of solid 79−69805
polyethylene terephthalate, chain rupture and tensile deform., viscosity-av. mol. wt. obs. 78−76714
polyethylene terephthalate, CO_2 permeability above and below glass transition 79−73340
polyethylene terephthalate, conform. statistics *(Russian)* 78−70993
polyethylene terephthalate, conformation rel. to orientation, pot. energy surfaces study 79−68338
polyethylene terephthalate, crazing and shear deformation on stretching in air and liquids *(Russian)* 78−88558
polyethylene terephthalate, crystallisation kinetics from glassy state 78−75579
polyethylene terephthalate, crystn. effect on frictional props. 80−40551
polyethylene terephthalate, differential scanning calorimetry of melting, mosaic block struct. of cryst. layers 78−26452
polyethylene terephthalate, effect of excess thermodynamic props. versus struct. form. on dynamic moduli 77−86053
polyethylene terephthalate, effects of preliminary ht. treatment on crystallisation *(German)* 78−75593
polyethylene terephthalate, elongation, conform. set change IR obs. *(Russian)* 78−37778
polyethylene terephthalate, exposed to aq. medium and γ-radiation, lifetime levels and fracture 80−40520
polyethylene terephthalate, extruded, elastic consts. meas., mech. anisotropy 78−44155
polyethylene terephthalate, fatigue failure under cyclic loading, overstress in chem. bonds 79−57106
polyethylene terephthalate, fibre, melting in crystn., intermediate and amorphous phases 77−84898
polyethylene terephthalate, filament, heat setting and thermomechanical behaviour 78−15435
polyethylene terephthalate, fracture, interatomic bonds deform. 79−57107
polyethylene terephthalate, glass conversion zone determ. from DTA *(German)* 77−20059
polyethylene terephthalate, glass-rubber transition determ., small-angle X-ray scatt. 78−95145
polyethylene terephthalate, glassy, energetics of CO_2 sorption 80−29270
polyethylene terephthalate, glassy and partially cryst., X-ray scatt., differential radial distrib. function 79−14704
polyethylene terephthalate, high field transient cond., 50 μs-1 ms 78−43402
polyethylene terephthalate, insulating material, photoinjection 77−47849
polyethylene terephthalate, IR spectra, trans-conformational band *(Russian)* 79−27122
polyethylene terephthalate, irradiated with radiations with linear energy losses, peculiarities in chemical etching 78−39934
polyethylene terephthalate, isotropic and oriented, refr. index meas. 40 to 300 cm^{-1} 78−52482
polyethylene terephthalate, joint prosthesis fragment dispersal meas. *(German)* 79−8566
polyethylene terephthalate, low temp. sp. ht., effect of cooling rate 80−100336
polyethylene terephthalate, mean mol. orientation factors, from IR spectra and acoustic method 80−70142
polyethylene terephthalate, mech. props., influence of cryst. arrangement and noncryst. region struct. 78−76707
polymers continued
polyethylene terephthalate, mol. wt. determ. by GPC *(Chinese)* 79−55009
polyethylene terephthalate, Mylar, thermoelectric power 78−80010
polyethylene terephthalate, NMR relax. and mol. mobility *(Russian)* 78−88219
polyethylene terephthalate, nonisothermal crystallisation kinetics 79−32920
polyethylene terephthalate, oriented, amorphous, stress-induced crystn., shrinkage meas. 80−92466
polyethylene terephthalate, oriented, directional anisotropy, of dielec. β-relaxation 77−16247
polyethylene terephthalate, oriented amorphous phase 78−95003
polyethylene terephthalate, photocarrier transport mechanism 78−10499
polyethylene terephthalate, photoconductivity, UV-IR light, absorpt. and photoluminescence. spectra *(Japanese)* 78−34857
polyethylene terephthalate, photoexcited, thermoluminescence field quenching 78−43942
polyethylene terephthalate, polymer life eqn. appl. to dielec. strength 80−25304
polyethylene terephthalate, semicryst., Fourier transform IR spectra 77−23589
polyethylene terephthalate, semicrystalline, model for thermal cond., orientation effects 77−85004
polyethylene terephthalate, shear compliances meas. of oriented sheet 80−104363
polyethylene terephthalate, sheet, extensional compliance normal to sheet 77−12664
polyethylene terephthalate, sheet, mech. anisotropy meas. by optical technique 77−12662
polyethylene terephthalate, sheet, Poisson ratio compliance consts., interferometry 77−12663
polyethylene terephthalate, simultaneous mech. loading, UV rad. effects on overstrained chem. bonds 79−52706
polyethylene terephthalate, solid, rheology, deform. 77−11140
polyethylene terephthalate, solid and molten, press. effects on compressibility and crystn., thermodynamic interpret. 80−84102
polyethylene terephthalate, stretching, heat effects, struct. transforms. 79−15735
polyethylene terephthalate, struct. determ. by electron microscopy 79−55675
polyethylene terephthalate, tensile drawing behaviour 80−35279
polyethylene terephthalate, thermal diffusivity, conductivity meas., crystallisation rel. to glass transition 77−47632
polyethylene terephthalate, thermally stimulated creep method for mol. motions investig. 78−22787
polyethylene terephthalate, TSC and thermally stimulated creep, dielec. and mech. retardation modes 79−78613
polyethylene terephthalate, TSC and thermolum. due to electron detrapping by local mol. motions 80−96898
polyethylene terephthalate, TSC due to mobile ions and ionic conduction *(Japanese)* 80−54432
polyethylene terephthalate, TSC in high temp. region 78−38872
polyethylene terephthalate, TSC meas., space charge and injected surface charge effects 80−11320
polyethylene terephthalate, uni- and biaxially drawn films, preferred planar orientation 78−80590
polyethylene terephthalate charge transfer from metallic electrodes 80−15605
polyethylene terephthalate fabric, surface struct., props. rel. to plasma surface treatment 78−95831
polyethylene terephthalate far IR absorption rel. to crystallinity 77−40242
polyethylene terephthalate fibre, lifetime under load, in presence of UV radiation, stress depend. 78−48535
polyethylene terephthalate fibre, radiation grafting 79−96342
polyethylene terephthalate fibres, chem. stress cracking after exposure to aq. methylamine 79−57131
polyethylene terephthalate fibres, elastic modulus 79−79019
polyethylene terephthalate fibres, high freq. US effects on physical and chem. structs. *(Polish)* 78−51446
polyethylene terephthalate fibres, interdependence between struct. and thermal contraction *(Rumanian)* 78−91259
polyethylene terephthalate monofilaments, friction and adhesion 79−52386
polyethylene terephthalate photoelectret, TSC and photostimulated detrapping current obs. 78−10459
polyethylene terephthalate polymer insulator, conduction and breakdown mechanism *(German)* 80−100469
polyethylene terephthalate under high elec. fields, γ-ray induced cond. 79−60840
polyethylene terephthalate yarns, NMR, fibre struct. rel. to annealing, drawing *(Japanese)* 77−32269
polyethylene terephthalate-co-isophthalate, gelation and crystallization 80−24377
polyethylene terephthalate-Cu composite foil, fracture surface exam. by XPS *(German)* 78−84992
polyethylene terephthalate-metal adhesive bonds, shear resist., polymer crystn. effect 80−89462
polyethylene terephthalate-p-oxybenzoate, nematic→isotropic transition loss 80−44300
polyethylene terephthate substrate, thickness determ. of Al coating using photometry 80−62626
polyethylene thick-walled vials in liq. scintillation counting of ^{14}C 78−857
polyethylene total joint replacement, props. improvement by C fibre reinforcement, SEM obs. 78−24183
polyethylene TSC resulting from trapped carriers 78−6393
polyethylene ultradrawn fibres, Poisson ratio from Michelson interferometry 78−80596
polyethylene waveguide, O-type, loss charact. at 337 μm 80−33175
polyethylene wax characterisation by gel chromatography, osmotic meas. and scattered light meas. *(German)* 77−86420
polyethylene wear debris from simulated service as total hip prosthesis, quantitative recovery 79−48378
polyethylene with rutile pigment-antioxidant, photo-oxidation 77−63816
polyethylene-2,6-naphthalate, pulsed photoconduction 80−24969
polyethylene-2,6-naphthalate fluorescence, transparency decay, possible appl. as polymer scintillators *(Chinese)* 79−93870
polyethylene-Au interface, algorithm for energy deposition of X-rays 77−28648

polymers continued
polyethylene-Fe, wear resistance on steel counterbody, exam. 78−68826
polyethylene-GaAs mixture, optical props., IR bandpass filter appls. *(Russian)* 78−90468
polyethylene-GaAs mixture, optical transmission spectra, IR filter prep. using computer appl. 80−2763
polyethylene-glass pair, contact interaction under elastic strain, friction and γ-ray effects 80−40549
polyethylene-isostatic polypropylene mixture, melting anal. 80−29150
polyethylene-metal contact charging, electron transfer mechanism, PES characts. 80−35055
polyethylene-paraffin mixtures, crystallisation kinetics 79−41985
polyethylene-polypropylene blend, size distribution determ. of spherical occlusions from photomicrographs *(Czech)* 80−89539
polyethylene-polystyrene blends, crystn. characts. 80−103261
polyethylene-propylene copolymers, branching effect on struct. and mech. props. *(Russian)* 79−52333
polyethylene-steel adhesive bond strength, rel. to ultrathin layer of polymer remaining on metal 77−70279
polyethylene-steel pair, temp. calc. under severe friction 80−40550
polyethylene-terephthalate track detector, electrochemically etched, meas. of low neutron fluences 80−32577
polyethylene/Cu(Zn) adhesion, role of surface topography 80−35500
polyethylene/ethylene vinyl acetate copolymer mixture, rel. between hypermol. struct. and stability *(German)* 80−64929
polyethylene/Pb(Zr,Ti)O_3 ceramic, composite systems, piezoelec. props. 79−99823
polyethylene/polypropylene blends, surface growth of fibres and films 80−66470
polyethylenenaphthalate, elec. cond., appl. of model 80−24940
polyethylenepolyamine hardened epoxy resin, hardening kinetics and mech. losses 80−66520
polyethylenes, dielec. losses, for use in AC superconducting power transmission lines 80−25302
polyethylenes, dielectric γ-dispersion, crystallinity effect *(Japanese)* 79−87384
polyethylenes, linear, ultra-high modulus, tensile creep, recovery 78−95784
polyethylenes, thermal diffusivity anisotropy 78−75894
polyethylenes, u.h. modulus linear, cryst. modulus 77−4799
polyethylenes, ultra-high modulus, manufacture by drawing through conical die 80−66583
polyethyleneterephthalate, ordering, thermal pretreatment at vitrifying temp. effect *(German)* 79−65006
polyethyleneterephthalate, thermal effects of necking during stretching *(Russian)* 77−32662
polyethyleneterephthallate, sorption of low MW solvents on struct. and mech. props. *(Russian)* 78−11358
polyethylmethacrylate, Rayleigh-Brillouin light scatt. study 79−11425
polyethymethylene, necking stress *(Japanese)* 77−56037
polyfluoroacetylene, electronic struct., tight-binding LCAO-SCF-MO calcs., prep. 80−70591
polyfluorocarbon, synthesis and opt. spectra 78−23657
polyfluoroethylene resin, porous, wetting angles with cyclohexanone and isopropyl alcohol meas., porosimetry method 77−1278
polyfluoroethylenepropylene, prepared for dosimetry, thermocurrents 77−52877
polyfluorvinylide, determ. of microstruct. by secondary emission mass spectrometry *(Russian)* 77−31604
polyfurfuryl alcohol, carbonised, water vapour absorption, porosity, and surface chem. 79−52753
polyfurfuryl alcohol charcoal, adsorpt. isotherms of organic vapours 80−96731
polyglucosan, soluble, single crystals from Acetobacter xylinum, internal structure resemblance to Cellulose Hydrate II *(Japanese)* 79−94121
polyglycine, band struct., ab initio SCF LCAO calcs. 79−22874
polyglycine, IR spectra calc. for helix and β configs. 80−45853
polyheteroarylene-epoxy resin, thermodynamic stability and compatibility *(Russian)* 79−65204
polyheteroarylenes, linear, conform. and struct., statistical calcs. *(Russian)* 80−69284
polyhexamethylene adipamide, calorimetric, X-ray and IR study 80−10512
polyhexamethylene adipamide, photocond. 80−103718
polyhexamethylene terephthalate/polyoxytetramethylene block copolymers, thermal and mech. props. 78−91260
polyhexamethylene terephthalate/polyoxytetramethylene block copolymers, supramolecular texture 78−91261
polyhydroxyethyl methacrylate, spincasting contact lens fabrication 77−795
polyimide, adsorption modification of surface of macroporous SiO_2 80−6624
polyimide, carbonized layer form., friction, wear *(Japanese)* 77−52502
polyimide, effect of loading time on contact area *(Japanese)* 78−6230
polyimide, influence of monomer and water diluents on mech. relax. 79−4993
polyimide adhesive strain gauge, effect of cyclic heat exchanges, 20 to 300°C 77−16775
polyimide fibre reinforced polyamide-12 80−11754
polyimide PMF1, macrochains packing in atom-atom approx. 79−41973
polyimide polymers, quasicrystalline struct. 78−75571
polyimide resin, charact. by differential scanning calorimetry 80−71869
polyimides, appl. of thin film thickness meas. technique 79−58672
polyimides, cryst. lattices elasticity and mech. props. 80−20995
polyimides, DFOPF and DFOB, X-diffr. exam. of structure and elasticity 80−6370
polyimides, effect of orientational stretching on thermal aging 80−11721
polyimides, glassy aromatic, plastic deform. 77−48494
polyimides, temp. index, rapid determ. by dynamic thermogravimetry 80−85101
polyisobutane, relax. times, self diffusion, devel. and appl. of NMR data acquisition system 80−34807
polyisobutylene:alkyl, electron spin echo spectra, instantaneous and conventional spectral diffusion 79−15355
polyisobutylene, ^{13}C spin-relaxation parameters rel. to effect, mol. wt., temp. 77−40146
polyisobutylene, amorphous, Brillouin scatt., hypersonic relax. 79−4811
polyisobutylene, Brillouin scatt. and hypersonic relax. 77−55795
polyisobutylene, EPR, correlation with glass transition 79−11348
polyisobutylene, impurity distrib. of tagged poly-cis-isoprene, individual and aggregate 79−68339
polymers continued
polyisobutylene, in simple extension, nonlinear stress relax., recovery after partial relax. 80−5949
polyisobutylene, relax. modes of short range fluctuation, n.m.r. meas. 77−3502
polyisobutylene, relax. of birefringence and stress, extension ratio depend. 77−43962
polyisobutylene, RQP method of inferring a mechanical relaxation spectrum 79−37195
polyisobutylene, SiO_2 grafted, synthesis and characterization 80−97456
polyisobutylene, transverse nuclear magnetisation decay rel. to slow mol. motions *(Russian)* 78−72423
polyisobutylene, undiluted, mol. wt. influence on creep behaviour 80−45370
polyisobutylene and copolymers with polyacrylonitrile, specific heat and glass transition temp. meas. *(German)* 78−34603
polyisobutylene fibres, stretched, crystn. kinetic study using synchrotron radiation 80−33909
polyisobutylenes, shear behaviour of Vistanex LMMH and L 100 80−1443
polyisocyanurate foams, strength, cellular struct. effect 80−40518
cis-polyisoprene, ^1H NMR, T_1 and T_2 meas., −50-170°C 79−69738
cis-polyisoprene, ^1H NMR of γ-induced cross-linked polymer 79−69739
polyisoprene, blend, viscoelasticity using Rheovibron, Massa correction for loss tangent meas. 78−83349
polyisoprene, electronic struct., reactivity, SCF CNDO calcs. 77−50580
1,4-polyisoprene, epoxidised, ^{13}C NMR, Overhauser effect 79−51872
polyisoprene, from guayule rubber, TEM exam. of crystallisation 80−10508
trans-1,4-polyisoprene, kinetics of thin film growth from melt 80−10505
polyisoprene, positron lifetime, phase and temp. depend. 79−83051
polyisoprene, rheological props., accelerator and temp. effects *(German)* 78−34101
polyisoprene, small angle neutron scatt., single chain form factors 80−107038
trans-1,4-polyisoprene crystals, press. effect on melting temp. and lamellar thickness, press. crystn. 80−88302
polyisoprene-polystyrene block copolymers, low mol. wt., glass transition temp., DSC investig. 77−7854
polyisoprenes, partly deuterated, ^1H-NMR spectra, struct. 80−50202
polyisopropylene, isotactic, two-phase spherulite, ht. conduction anisotropy 78−2316
polyleucine membrane, water and water vapour permeation and solute separation *(Japanese)* 78−31701
polymer, amorphous, under press., glass transition phenomena, model 79−23706
polymer, yield behaviour, interpret. w.r.t. correlated motion 78−6973
polymer between planes, crossover between dimensionalities, Monte-Carlo study 80−74272
polymer chain dynamic critical index calcs. by renormalisation method 80−87256
polymer complex dynamic Young's modulus measurement equipment 78−1615
polymer materials, hysteresis flow model applicability for degree of inelasticity 80−28422
polymer radiation chemistry, computer modelling 79−74382
polymer reactants in organic reactions, review 78−95923
polymer sedimentation coefficient, diffusive broadening of distrib. function, from single record using model functions *(Russian)* 77−63970
polymer-bisazide photoresist. layer, effect of thickness on photosensitivity *(Russian)* 77−70324
polymer-bridged metal complex, props. of model system, MO theory 79−90940
polymer-metal friction pairs, triboelec. effects 80−11784
polymer-semiconductor solar cells 80−16810
polymeric, vibration-damping, for constructions, theory 80−10178
polymeric glasses, kinetic theory of brittle fracture 78−48526
polymeric macromolecule containing mesogroups, phase diagrams *(Russian)* 80−58433
polymeric systems, supported on inert substrates, dynamic thermomech. study 80−55623
polymers, atuomatic device for measuring elec. direct current props. *(German)* 78−45647
polymers, pyrolysis-mol. wt. chromatography−vapour phase IR spectrophotometry, on-line system, reviews 80−55768
polymetal phosphinates, linear chain magnet, ^{31}P NMR, spin density 77−77108
polymetallomethacrylates, Mossbauer spectra, long-range ordering 79−65776
polymetaphenylene isophthalamide, mean mol. orientation factors, from IR spectra and acoustic method 80−70142
polymethacrylates (PMMA, PBMA, PMA and PMA AN), radiation-induced degradation obs. 78−27795
polymethacrylic acid: ^{23}Na, nuclear relax. correl. times and counterion behaviour 80−50212
polymethacrylic acid, benzene penetrant diffusion, statistical mech. model 80−44352
polymethacrylic acid, stereoregular, synthesis, ^{13}C NMR obs. 80−58422
polymethacrylic acid crosslinked with PVA, force rel. to elongation in swollen or contracted states 77−40434
polymethacrylic acid network systems, intramol. mobility, polarised luminesc. obs. *(Russian)* 77−42455
polymethacrylic acid stabilised aq. paraffin oil emulsion, mech. props. 79−39223
polymethacrylic acid-polyethylene oxide polymer complex, H bond form., thermal behaviour *(Japanese)* 79−15454
polymethine-cyanine molecular aggregate, band struct. 80−53174
polymethineimine, all-trans, ab initio cryst. orbital calcs. 79−77530
polymethineimine, cryst. orbital studies by HF methods 80−44148
polymethyacrylate, swollen, and methacrylate copolymers, secondary relaxation 79−57032
polymethyl α-cyanoacrylate, photodielectric, for phase hologram recording 77−34842
polymethyl acrylate, head-to-head, high-resolution PMR spectra 79−73834
polymethyl acrylate, multicomponent network, pulsed NMR study of mol. motions 77−55724
polymethyl acrylate, phosphorescence depolarisation studies of relaxation effects 78−56685
polymethyl cinnamate, head-to-head, high-resolution PMR spectra 79−73834

polymers continued
polymethyl crotonate, head-to-head, high-resolution PMR spectra 79−73834
polymethyl isopropenyl ketons, spectrally sensitized decomposition and Deep UV resists 80−40715
polymethyl methacrylate, direct obs. of zero field surface 80−16133
polymethyl methacrylate, mol. wt. determ. by activation anal. of Cl in end group 79−66377
polymethyl methacrylate, subthreshold luminesc. 80−93414
polymethyl methacrylate resist, electron depth distrib., expt. test of Bethe-Bloch model 80−16132
polymethylacrylate, tacticity from peak-eliminated Fourier transform NMR 77−563
polymethylene, chain moments, charact. function, distrib. function, numerical calc. 78−78843
polymethylene, chains, angular correlation calcs. 79−45871
polymethylene, continuous diffuse electron scatt., correl. chain motion 78−6020
polymethylene, intramol. scatt. function calc. 77−38761
polymethylene, melt transition, theory 77−76325
polymethylene, short chain mean reciprocal distances, Monte Carlo calc. 77−14626
polymethylene, short chains, rot. isomeric representation 80−87254
polymethylene, short-chain molecules, hydrodynamic behaviour, extended Rouse-Zimm theory 77−558
polymethylene chain, vibr. spectra, CH stretching region, struct. and assignments 78−70991
polymethylene chain model, lattice walk variance reduction, with Markov chain sampling 79−27121
polymethylene chain packing in cryst., structure calc. by atom-atomic potential functions *(Russian)* 78−75581
polymethylene compounds, continuous diffuse electron scattering, oblique layer cryst. 78−95004
polymethylene crystals, lattice vibrations 80−59607
polymethylene flexible biradicals ClDNP and chain dynamics, field depend. 77−88473
polymethylene sulphide, thermal stability and stability against solvents *(Russian)* 78−51449
polymethylene terephthalate, thermal cond., 2-100K, crystallinity effect 77−20137
polymethylene-polystyrene-(polymethylmethacrylate) blends, kneading characts. *(Japanese)* 80−104112
polymethylmethacrylate, denture base resin, residual monomer determ. 79−16077
polymethylmethacrylate, effect of accumulated charge on depth dose profile of electron beam 79−90700
polymethylmethacrylate, glass filled solids, ultrasonic absorpt., scatt., velocity and attenuation 80−44262
polymethylmethacrylate, numerical description of treeing for dielectric breakdown 80−100633
polymethylmethacrylate-polycarbonate blends, kneading characts. *(Japanese)* 80−104112
polymethylmethacrylate-polystyrene system, phase relationships and fracture surface morphology 79−61571
polymethylmethacrylate-polystyrene-polyethylene blends, kneading characts. *(Japanese)* 80−104112
polymethylpentene, isotactic, crystal struct. 78−67663
polymethylpentene, LF acoustic relaxation 78−38784
polymethylpentene, press. effects on melting 78−56625
polymethylpentene, visoelastic props., γ-irrad. influence *(Russian)* 78−88492
polymethylpentene, wideband optical transmission meas. 79−76771
polymethylphenylsiloxanes, thermal cond. at high press. and 20-200°C temp. range 77−59162
polymethylsilosane resin MSN-7 additions to BN ceramic for increased strength and oxidation resistance 80−20880
polymethylsiloxane liquids, complex shear modulus determ. from shear wavelength meas. 79−14871
polymethylsiloxane-toluene gels, light scatt., compression moduli, cooperative diffusion 78−23970
polymide, elasticity of crystal lattice 78−3164
polymonochloro-p-xylylene, γ-ray-induced cond., hole injection effects 80−34452
polymorphic transformations polyethylene crysts., atom-atomic potential functions calc. *(Russian)* 78−75581
polynucleotides, double-stranded conformation model 77−14631
polyolefin, amorphous, thermostimulated creep, 77-350K 79−69185
polyolefin, amorphous, thermostimulated creep and glass transition 79−69186
polyolefin, cross-linked, insulation system for wire and cable for locomotives 80−66851
polyolefin, cross-linked, irradiation appl. to provide improved insulation props. to wires and cables 80−66850
polyolefin film, corona discharge treatment 77−56129
polyolefine, cryogenic grinding technique 77−32555
polyolefine, deep drying, internal mass transfer 79−14239
polyolefins, amorphous, compensation temp., thermostimulated creep 79−14919
polyolefins, biological implant, ion beam sputter of surface morphology, SEM exam. 77−44836
polyolefins, creep 79−100221
polyolefins, isotropic semicryst., neutron scatt. obs. of struct., radius of gyration 79−94922
polyolefins, semi-crystn., neutron scattering study 80−38936
polyolefins, triboelectric charging, linear free energy relationships 78−6431
polyolefins, ultra-high modulus, production by tensile drawing and hydrostatic extrusion 80−81022
polyorganosilasane impregnated BN composite 80−7526
polyorganosiloxane, thermogravimetric assessment of stability at high temps. 77−52704
polyorganosiloxane impregnated BN composite 80−7526
polyorganosiloxane-asbestos composites, high-temp. transitions 79−38802
polyox dilute aqueous solns., flow resistance mechanisms in porous media 79−41747
Polyox WSR 301, effect of additions to NaCl aq. soln. pipe flow heat and mass transfer 79−46309
polyoxadiazoles, cyclochain, conform. parameters calc. 80−78732
polyoxide chains, config. partition functions, entropy, (CH_2)y-o- repeat unit 78−17829
polymers continued
polyoxyethylene dodecyl ether/water system, lamellar liq. cryst., solubilized hydrocarbon effect on struct. and dislocation pattern 79−94885
polyoxyethylene-glutaric acid eutectic, melting and crystn. 80−28924
polyoxymethylene, chains, angular correlation calcs. 79−45871
polyoxymethylene, dielec. relax., 90-300K, 400-10^4 Hz *(Russian)* 77−69770
polyoxymethylene, drawn, extra meridional reflections 80−24376
polyoxymethylene, effect of pressure and environment on fracture and yield 78−76757
polyoxymethylene, effects of hydrostatic press. on shear deform. 78−15457
polyoxymethylene, electron density calc. in cylindrical coordinates, Fourier method 79−13852
polyoxymethylene, epitaxial crystn. during trioxane polymerisation 79−55676
polyoxymethylene, epitaxial growth on KBr single crystal *(Japanese)* 78−56054
polyoxymethylene, irrad., thermoluminesc. above room temp. 80−2871
polyoxymethylene, kinetics of epitaxy and over-growth on needle-like single crystals 78−14291
polyoxymethylene, low temp. thermal conductivity 78−38886
polyoxymethylene, low-strain deform., transmission electron microscope exam. 79−5013
polyoxymethylene, melt-crystallised, longit. acoustic mode obs. 77−59572
polyoxymethylene, mol. struct., least squares refinement 79−86720
polyoxymethylene, nascent, morphology, optical and electron microscopic obs. 80−59403
polyoxymethylene, rapid crystn. from melt rel. to struct. 80−44153
polyoxymethylene, relax. phenomena, −30 to 200°C, premelting and glass transition 78−51440
polyoxymethylene, rolled, prediction of yielding behaviour 77−73306
polyoxymethylene, thermal cond., 2-100K, crystallinity effect 77−20137
polyoxymethylene, thermal diffusivity, and cond. meas., two-phase model 77−47632
polyoxymethylene, transitions and relaxation spectrograph 80−65204
polyoxymethylene, ultra-high modulus, prod. by high temp. tensile drawing 79−43352
polyoxymethylene, ultrahigh modulus oriented, exam. of true crystal modulus, from −150 to 20°C 80−11687
polyoxymethylene, wear mechanism at steel surface, SEM, TEM and DTA 78−64727
polyoxymethylene, yielding behaviour under complex triaxial stress conditions 77−56030
polyoxymethylene co-polymers on interstellar grains 77−87500
polyoxymethylene copolymers, solid, mol. motions, 4-315K, dynamic-mech. study 79−4258
polyoxymethylene diacetate, bulk cryst. and melting, polyoxyethylene additive effects 79−32921
polyoxymethylenes, determ. of crystalline fraction from X-ray diffraction 80−44150
polyoxymethylenes, dielec. relax. and IR spectra, 90 to 300K *(Russian)* 79−28678
polyoxymethylenes, dielectric property relaxation, unidentical relaxator system activation model *(Russian)* 80−80694
polyoxymethylenes, dielectric relaxation, molecular mechanism *(Russian)* 80−88923
polyparabenzamide, mean mol. orientation factors, from IR spectra and acoustic method 80−70142
polyparaphenylene:SbF_5, pure and doped, metallic, absence of Pauli paramagnetism, mag. susceptibility meas. and ESR obs. 80−97060
polyparaphenylene terephthalamide, mean mol. orientation factors, from IR spectra and acoustic method 80−70142
polyparaxylylene film, photoluminesc. exam. 78−48213
polyparaxylyrene, photoconductivity, UV-IR light, absorpt. and photoluminescence. spectra *(Japanese)* 78−34857
polypentamethylene terephthalate, oriented fibres, struct. anal. of two cryst. phases 79−73108
polypentenamer, thermodynamics *(Russian)* 77−21386
polypentenamers, phosphonylated, hydrogenated derivatives, dynamic mech. and dielectric props. 78−68448
polypeptide chains, helix-coil transitions, statistical mech. calcs. 77−560
polypeptide copolymer, trans-cis photoisomerisation 78−3331
polypeptides, helical sense characterisation by IR spectra 78−17831
polypeptides, synthetic, chiral, with aromatic side chains, conform. from circ. dichroism 79−55014
polyperdeuteroethylene, IR and Raman spectra, 77K and room temp., vibr. anal. 78−72517
polyperfluoropropylene oxide, mass spectroscopic reference standard appls. 78−89582
polyphenyl chinoxalines, dielectric relaxation *(German)* 77−59513
polyphenyl ester, viscosity and density determ. up to 150°C and 150000 psig 77−59940
polyphenyl ether, glass transition temp., press. depend. 80−49135
polyphenyl ether fluid operating in elastohydrodynamic contacts, IR emission spectra 79−91807
polyphenylacetylene, cryst., resonant Raman scatt., opt. absorpt. 77−4630
polyphenylacetylene, crystallizable, DC cond., annealing and defect effects 77−62923
polyphenylacetylene cis-trans isomers, rel. mol. wt. distrib., heating effect 80−106409
polyphenylene derivs., temp. hysteresis in elec. cond. *(Russian)* 77−47803
polyphenylene oxide, with and without impact resisting polystyrene, photo-oxidative ageing, Cu and Fe trace effects *(German)* 79−100191
polyphenylene oxide thin films, electrochem. prep., impurity effects on cond., electroforming 80−88655
polyphenylene oxide-polystyrene blends, spectroscope exam. of chain conform. and bonding 78−42925
polyphenylene oxides, high temp. ageing effect on struct. and props. *(Japanese)* 77−70078
polyphenylene sulphide, high mol. wt. soluble resin, prep., mech. props. 80−60828
polyphenylene terephthalamide, fibril form. from nascent spherulite formed during polymerisation in hexamethylphosphorictriamide *(Japanese)* 78−56893
polyphenylisobutylsilsesquioxane, dielectric investigation of molecular mobility 77−58960
polyphenylquinoxaline, synthesised in different media, mass-mol. distrib. *(Russian)* 79−61862

polymers continued
polyphenylquinoxaline-cellulose acetate, battery separator membrane, diffusion meas. 80−35574
p-polyphenyls, band struct., mol. struct. effects calcs. *(German)* 77−47722
polyphenylsilsesquioxane, dielectric investigation of molecular mobility 77−58960
polyphosphazenes, new polymers with inorganic backbone atoms 77−564
polyphthalocyanine, amorphous, linear polymer, Hall effect meas. 79−23989
polypropene-alt-1,4-butadiene and hydrogenated derivative, mol. relaxations in glassy state 80−53177
polypropyl ethylene and deuterated derivatives, modification I, vibrational spectra and normal coord. anal. 79−87435
polypropylene, agitating type polymerizer, synthetic resins and fibres manufacturing process 80−3341
polypropylene, amorphous, ^{13}C NMR spin-lattice relaxation times of isotactic, syndiotactic sequences 77−4572
polypropylene, atactic, Brillouin scatt., hypersonic relax. 79−4811
polypropylene, atactic, Brillouin scatt. and hypersonic relax. 77−55795
polypropylene, audio freq. shear and Young's modulus determ. from torsional vibr. of laminated bar 77−62218
polypropylene, change of crystn. forms during purification 77−55934
polypropylene, cold-drawn isotactic bars and thin films, microstruct. and annealing 78−95760
polypropylene, creep and failure under low frequency cyclic loading 77−1858
polypropylene, creep curves *(German)* 78−64599
polypropylene, crystalline, morphological aspects of crack growth 78−76761
polypropylene, crystalline, yield behaviour in oriented and unoriented condition, effect of temp. 80−97537
polypropylene, crystalline spherulitic, shear bands formed under compression at low temp. 80−40507
polypropylene, dielec. loss 4.2K 77−24787
polypropylene, drawn fibres, SEM and US study 78−47249
polypropylene, drawn polymer, fibre composite model 78−76719
polypropylene, ductile, large strain cyclic deform. 80−85000
polypropylene, dynamic material behaviour under nearly uniaxial strain conditions, modified Kolsky apparatus 78−85070
polypropylene, effect of pressure and environment on fracture and yield 78−76757
polypropylene, effects of hydrostatic press. on shear deform. 78−15457
polypropylene, effects of notch shapes on Charpy impact values, tensile props., fracture surfaces *(Japanese)* 79−38951
polypropylene, electret, trapped injected electrons, EPR obs. 78−27093
polypropylene, electron bombarded, radical formation, piezoelectric and pyroelectric effects, ESR study 80−7169
polypropylene, electron bombarded electret, trapped charges ESR study 80−7170
polypropylene, EPR of NO radicals, rot. mobility 79−33539
polypropylene, extruded, chain orientation, polarised Raman scatt. 79−1756
polypropylene, extruded, elastic consts. meas., mech. anisotropy 78−44155
polypropylene, flashover behaviour at low temps. 80−25882
polypropylene, flexure testing 77−86087
polypropylene, Fourier transform IR study of ordered and amorphous phases 78−27225
polypropylene, fracture, interatomic bonds deform. 79−57107
polypropylene, fracture exam. using microscopic obs. *(German, English)* 79−20186
polypropylene, fracture toughness eval. with surface crack specimens 79−15777
polypropylene, gamma-irradiated, active centres recombination kinetics, ESR study *(Rumanian)* 79−19778
polypropylene, glassy state, macrodeformation stresses, anelastic characteristics 79−52289
polypropylene, Halen and Daplen, semicryst. melting and glass transitions 80−49346
polypropylene, hard elastic fibres, stress relaxation 77−36564
polypropylene, helical syndiotactic, laser Raman spectrum 77−79719
polypropylene, homopolymer, effect of mol. orientation on fracture toughness 78−52992
polypropylene, impurities redistribution during crystn. 78−75577
polypropylene, impurity gas diffusion expts., test of two-phase cond. theory 79−69288
polypropylene, injection moulded, texture *(Japanese)* 80−25722
polypropylene, insulators for superconducting magnets, effect of low temp. irradiation 80−25817
polypropylene, IR emittance of fibrous materials 79−95189
polypropylene, isomeric, microconformation from slow exchange ^{13}C-NMR spectra of low mol. wt. cmpds. 80−102592
polypropylene, isotactic, air permeability, subject to high press. 78−27823
polypropylene, isotactic, conformational origin of peak struct. in XPS spectrum 79−89819
polypropylene, isotactic, diffusion const., increased hydrostatic press. effect 78−22898
polypropylene, isotactic, epitaxial crystn. on alkali halide surface 78−26787
polypropylene, isotactic, equation of state for semicrystalline, crystalline polymers 80−65187
polypropylene, isotactic, longit. acoustic mode 77−7816
polypropylene, isotactic, low temp. annealing, differential scanning calorimetry obs. 80−60895
polypropylene, isotactic, melt-crystallised, longit. acoustic mode obs. 77−59572
polypropylene, isotactic, permanganic etchant for TEM obs. 80−21132
polypropylene, isotactic, shear induced β-form crystallisation 78−18555
polypropylene, isotactic, thermal cond., 2-100K, crystallinity effect 77−20137
polypropylene, isothermal crystn., effect of contact with fibrous substrates 80−79708
polypropylene, isotropic, molten and cryst., small-angle neutron scatt., chain-folding 78−63680
polypropylene, linear viscoelastic region, creep prediction using temp. pulse technique 78−68732
polypropylene, low and high density, exam. in transmitted and reflected light *(German)* 78−31398
polymers continued
polypropylene, lubricant additive, effect on operating performance of sintered materials 80−11785
polypropylene, mag. polarisation, optical studies 80−55013
polypropylene, mech. behaviour rel. to combined press.-temp. effects 77−16648
polypropylene, microstruct. changes during large strain cyclic deform. 80−66627
polypropylene, molten and cryst., mol. conformation, small angle neutron scatt. study 79−51012
polypropylene, monofilaments, drawing behaviour, melt-induced orientation effects 78−84922
polypropylene, necking stress *(Japanese)* 77−56037
polypropylene, neutron irradiation effect on weldability and adhesion *(Japanese)* 79−60405
polypropylene, nonlinear viscoelastic effects 77−90401
polypropylene, notched sheet, deform. mech., fracture, X-ray obs. *(Japanese)* 77−59863
polypropylene, orientated, loose fitting tube for optical fibre packaging 78−1338
polypropylene, oriented, annealing, mol. mechanisms 77−12642
polypropylene, oriented, compressive elastic modulus and yield strength 80−16385
polypropylene, oriented, microcracks diagnostics by paramag. probe method 80−66736
polypropylene, oriented, stress relax. process charact., 20-100°C 79−20097
polypropylene, oriented, stress relaxation 77−44285
polypropylene, oriented, thermooxidative degradation kinetics, durability, influence of mech. initiated processes *(Russian)* 79−24591
polypropylene, oriented crystalline, anisotropic thermal expansion 80−39324
polypropylene, oriented fibre drawing *(Russian)* 77−21088
polypropylene, photooxidation, initiation process nature 77−52523
polypropylene, plasma induced grafting of acrylic acid 79−15825
polypropylene, plastic insulation for cryogenic power cable, exam. of dielectric, tensile props. 80−25823
polypropylene, preoriented isotactic sheet, mol. behaviour in uniaxial drawing *(Japanese)* 77−68928
polypropylene, quenched form, struct., X-ray obs. 78−67661
polypropylene, reasons for disintegration under tension 78−84940
polypropylene, semi-crystn., neutron scattering study 80−38936
polypropylene, shear and tensile creep at finite strains 78−52903
polypropylene, shear effect on crystallisation *(German)* 78−75586
polypropylene, shear stress/strain behaviour, press. effect 78−84936
polypropylene, spherol crystals, morphology and growth 78−18567
polypropylene, stability under radiation sterilisation 77−60245
polypropylene, stereochem. additions, sequence lengths, ^{13}C NMR 77−27212
polypropylene, stretching reduces electrical values *(German)* 79−43446
polypropylene, structure change on uniaxial compression *(Russian)* 79−34119
polypropylene, surface fluorination effects, internal refl. spectroscopy obs. 78−86340
polypropylene, thermoelastic effects 78−88491
polypropylene, thermoluminesc. spectrum *(German)* 78−76538
polypropylene, thermoplastic, supramolecular struct. and frictional props. of surface layers 77−70188
polypropylene, TSC meas. of relax. modes, apparent double glass transition 80−11323
polypropylene, ultradrawn fibres, Poisson ratio from Michelson interferometry 78−80596
polypropylene, ultrahigh modulus, tensile drawing, mol. wt. effect 80−104211
polypropylene, vacuum-UV irrad. photoelec. emission and contact charging 79−52075
polypropylene, window of proportional counter, Lexan coating for eliminating UV sensitivity 79−74273
polypropylene, yielding behaviour under complex triaxial stress conditions 77−56030
polypropylene chloride co-polymer powder, cold compaction, product strength, heat treatment effects 80−11621
polypropylene coating, glow-discharge-polymerised, adhesion and hydrophilicity 79−45829
polypropylene fibers, and films, and their hard elastic precursor small-angle X-ray diffr. studies 79−10815
polypropylene fibre, hard elastic, macroscopic deforms. in lamellae 79−96097
polypropylene fibre, melt-spun with twist, helical orientation and mech. props. 78−75569
polypropylene fibre, with helical internal texture, SEM obs. of surface morphology 80−39394
polypropylene fibres, γ-irrad., microstruct. changes in glassy-high elastic state transition *(Rumanian)* 80−49347
polypropylene fibres, EPR during glass transition, γ-irrad. 79−8445
polypropylene fibres, helically twisted, small-angle light scatt. 79−1765
polypropylene fibres, high strength, elastic 80−20992
polypropylene fibres, homologue mixtures, props. 78−76709
polypropylene fibrillated film reinforced cement matrix for low cost sheeting 80−80996
polypropylene film, corona-charged, bistable electret, use in construotion of transmission light gate 77−50750
polypropylene film and fibre, plasma etching 78−95871
polypropylene films, dielec. props., impurity effects 80−71304
polypropylene glycol, depolarised Rayleigh relax. times, backbone motion 77−566
polypropylene glycol, Rayleigh-Brillouin spectra calcs. 79−47465
polypropylene monofilaments, draw rate effect on long period 79−47726
polypropylene monofilaments, tensile props., orientation degree depend., IR dichroism obs. 78−3163
polypropylene nonfilaments, highly drawn, plastic deform. 78−44174
polypropylene on oxidised Cu, degradation, ion scatt. anal. 77−40463
polypropylene oxide, complex with metal salt, glass transition temp. 79−69234
polypropylene oxide, rubber and glassy states, conformational motion, neutron scatt. study 79−41259
polypropylene partially crystn., temp. effects on fracture 77−63771
polypropylene powder, cold compaction, product strength, heat treatment effects 80−11621
polypropylene rods, prep. by die-drawing 80−45327
polypropylene sheet, deep drawing *(German)* 80−104114

polymers continued
polypropylene spherulites, refl. acoustic microscopy obs. 80−28922
polypropylene substrate, Sn autocatalytic deposition 80−100965
polypropylene terephthalate prepolymer, PMR 79−38392
polypropylene-bitumen mixture, thermomech. investigation changes in viscosity, ductility, elasticity, mol. wt. effects *(German)* 78−35454
polypropylene-lignin system, X-ray diff., EPR exam. of interaction 78−68668
polypropylene-nylon 11 fibres, bimodal cryst. texture, X-ray diffr. and electron microscopy 78−75567
polypropylene-PMMA graft copolymer, X-ray meas. of crystallinity of component polymer *(Japanese)* 77−58962
polypropylene-polyurethane laminates, meas. of dielectric losses at cryogenic temps. 80−25301
polypropylenes, impact modified, testing by dynamic mech. anal. 80−16626
polypropylenes, iso- and syndio-tactic, Raman tacticity bands, vibr. spectrum 80−66193
polypyrimidines, with azomethine in main chain, decaying process of surface potential *(Japanese)* 79−24095
polypyromelliteimide, fracture, interaction bonds deform. 79−57107
polypyromellitimide, mean mol. orientation factors, from IR spectra and acoustic method 80−70142
polypyrrole, electronic struct., one-electron band theory 80−65450
polyquinazolones containing pendant imide groups, prep. and props. *(Japanese)* 80−104111
polyquinazolones with N-phthalimide groups in side chain, prep., props. *(Japanese)* 79−15642
polyquinones, ladder, partially-ladder, synthesis, struct., props., review *(Russian)* 80−7529
polyribonucleotide complexes, mag. field orientation of nematic liq. cryst. solns., light scatt. and birefr. meas. 79−82152
polyriboxanthylic acid, spatial struct., H bonding 80−53086
polysaccharide gel, anomalous behaviour of PMR line width of water *(Russian)* 80−11962
polysaccharide grain model for IR spectrum of interstellar maser OH 26.5+0.6 78−12342
polysaccharides, evidence in IR astronomical spectra 77−78857
polysaccharides, vibr., conformation, IR spectra, computer anal. *(Russian)* 78−13637
polysaccharides in Galaxy, origin and nature 78−24543
polysilicane gel on glass plate, elastic deformation in adhesion of solids 78−60010
polysiloxane dizwitterionomers, mech., dielec. relax., effect of H_2O sorpt., thermal history 80−50261
polysiloxane dizwitterionomers, mech. props., microstruct. 80−49131
polysiloxane dizwitterionomers, morphology, ionic aggregation 80−49130
polysiloxane dizwitterionomers, sorption of H_2O, mechanism 80−49506
polysiloxane homopolymers and random-block copolymers, surface degradation, with HF soln. 78−15554
polysiloxane oligomers, ^{29}Si NMR, chem. shift effects of end groups 79−33550
polysiloxane urethane as optical cement, transmission 0.2 to 6.2 μm 77−7163
polysiloxane-metal oxide interfaces, bonding mechanism, surface anal. by XPS and static SIMS 78−15643
polysiloxene, irrad., linear, IR and solubility obs. 80−93775
polystyre, irrad, thermoluminesc. 78−2931
polystyrene:$Br_2(I_2)$, films, electron-beam induced carrier mobility and elec. breakdown 80−80429
polystyrene:triphenylamine, field-depend. UV photogeneration of holes, polymer composition depend. 78−76104
polystyrene, γ-ray-induced cond., hole injection effects 80−34452
polystyrene, activation energies of fracture and deform., comparison *(Russian)* 78−11303
polystyrene, adhesive bonds, US attenuation effects 78−7141
polystyrene, amorphous, fracture mechanism 77−8949
polystyrene, amorphous, LF Raman modes, strain and temp. effects 77−36219
polystyrene, amorphous, low temp. sp. ht. calcs. 77−28014
polystyrene, amorphous, press. effect on glass transition and glassy state 78−26674
polystyrene, amorphous, structural cause of orientation modification, exam. 78−67664
polystyrene, amorphous, thermophysical props. depend. on hydrostatic press. 78−47612
polystyrene, and copolymers, optical fibre waveguides, spectral characts. 80−14461
polystyrene, angle of intersection of coarse shear bands, optical obs. 79−66110
polystyrene, anionic, kinetic parameters assoc. with glass transition temp., calc. 80−49345
polystyrene, annealed, enthalpic retardation times 80−19959
polystyrene, atactic, Brillouin scatt., hypersonic relax. 79−4811
polystyrene, atactic, bulk and surface elec. props., contact charging obs., dielec. const. 80−15615
polystyrene, atactic, chain length depend. of hypersonic relax., Brillouin spectra 77−55797
polystyrene, atactic, effect of excess thermodynamic props. versus struct. form. on dynamic moduli 77−86053
polystyrene, atactic, indentation recovery, defect struct. produced by deformation 79−43275
polystyrene, atactic, indentation recovery 80−84988
polystyrene, atactic, isothermal internal friction meas. of glass transition 79−74191
polystyrene, atactic, Rayleigh-Brillouin scatt. 77−4648
polystyrene, atactic, stereoregularity study using Fourier transform IR spectroscopy 79−59612
polystyrene, atactic, structure elucidation, model construction and X-ray methods *(German)* 80−103267
polystyrene, atactic, thermal behaviour above glass-rubber relax. temp. 77−39548
polystyrene, atactic, uniaxially oriented, Fourier transform IR spectroscopic exam. 80−25360
polystyrene, bimodal mol. wt. blends, recoverable compliance 80−66568
polystyrene, chain conform. in solid and melt, low-angle neutron scatt. 77−76329
polystyrene, charge injection during extrusion 78−60135
polystyrene, chem. shift, conformational struct. *(Russian)* 80−5652
polystyrene, coarse shear bands and fracture, SEM study, craze fracture surfaces 79−29191
polymers continued
polystyrene, colloidal dispersion in butanol, stability ratio 79−29413
polystyrene, compressed, TEM obs. of coarse shear bands 79−70117
polystyrene, conform. and near all-trans extended-chain model relevant in gels, X-ray diffr. patterns interpret. 80−79707
polystyrene, constancy of composition obs., dosimetry appls. 79−60286
polystyrene, core-level spectra of adsorbed Cr and Ni atoms 79−56911
polystyrene, craze density meas. by quantitative TEM 79−24701
polystyrene, craze initiation, in tension-torsion expts. 78−15519
polystyrene, crazed, orientation and struct., electron diffr. meas. 80−30122
polystyrene, crazed, orientation and struct., optical meas. 80−30121
polystyrene, crazing, fracture, polymerisation route and internal lubricant effects 77−12683
polystyrene, crosslined, swollen, surface energy, contact angles 79−73379
polystyrene, cryogenic foam insulators, low temp. props. 80−25818
polystyrene, cyclically deformed under shear, energy dissipation, static tensile-compressive stress effect 80−104225
polystyrene, degradation behaviour by vibratory ball mill *(Japanese)* 78−39732
polystyrene, depolaris. Rayleigh scatt., optical anisotropy 78−27245
polystyrene, depolarized Rayleigh scattering near glass-rubber relaxation 79−47464
polystyrene, discontinuous fatigue crack growth, generality of mechanism for glassy polymers 77−32677
polystyrene, disintegration and vaporisation by high power laser pulses 77−39443
polystyrene, dissolution kinematics, model and its expt. verification 78−26687
polystyrene, effect of doping on TSC 79−38085
polystyrene, effect of pressure and environment on fracture and yield 78−76757
polystyrene, electron energy loss spectra, for optical and dielec. props. 79−15569
polystyrene, electron trap depth distribs., thermolum. data 78−11002
polystyrene, electron-beam-induced conduction 80−2397
polystyrene, end group modified, chain dynamics studied by fluorescence depolarization 80−19724
polystyrene, enthalpy of mixing with poly(2,6-dimethyl phenylene oxide) 78−14471
polystyrene, epimerised isotactic, methylene C mag. resonance spectra 80−63878
polystyrene, EPR of NO radicals, rot. mobility 79−33539
polystyrene, expanded, dynamic compressibility 78−48476
polystyrene, fatigue behaviour, cyclically loaded, mean stress effect 78−52968
polystyrene, fatigue props., effect of environment and surface coatings 79−43455
polystyrene, filled amorphous polymer, heat capacity meas. *(Russian)* 79−65211
polystyrene, filled with wood particles reversible deformation of wood particles 78−48437
polystyrene, form. of Cu-O-polymer complex 78−92372
polystyrene, fracture toughness eval. with surface crack specimens 79−15777
polystyrene, gamma photon backscattering, energy dependence *(Rumanian)* 79−76316
polystyrene, glass bead-filled, elastic moduli, interfacial slippage effect anal. 78−76688
polystyrene, glass transition temp. meas. reproducibility using differential scanning calorimetry 77−15563
polystyrene, glass-like, intermol. interactions temp. depend., IR spectra *(Russian)* 79−51967
polystyrene, glass-rubber transition, time-temp. superposition, shear creep compliance meas. 80−88309
polystyrene, glass-transition temp., mol. wt. effect, thermodynamic theory 80−19920
polystyrene, glassy, craze growth, expt. and model 78−15520
polystyrene, glassy, crazing and brittle fracture on flat die indentation 80−60970
polystyrene, glassy, fracture surface, formation and struct. of striations 77−28892
polystyrene, glassy, in methanol, growth kinetics of solvent crazes, hydrodynamics 79−15836
polystyrene, glassy, intermol. interaction during inelastic deform., optical spectral obs. 77−59878
polystyrene, glassy, light scattering, quenching effect 80−20649
polystyrene, glassy, optical absorpt., visible region, determ. by laser calorimetry 80−66218
polystyrene, glassy, struct., X-ray scatt. and conformational analysis 78−26449
polystyrene, glassy, thermally activated deform. 79−20126
polystyrene, glassy, thermoelastic effect, thermal expansion coeff. 79−14944
polystyrene, glassy atactic, struct. anal. from small-angle X-ray scattering 79−73109
polystyrene, glassy state, macrodeformation stresses, anelastic characteristics 79−52289
polystyrene, glassy state, relax., free vol. fluctuations effect 80−19722
polystyrene, graft polymerisation on alkali halide crystals *(German)* 79−100365
polystyrene, halogen-doped, carrier transport and breakdown characteristics *(Japanese)* 80−96889
polystyrene, head-to-head, high-resolution PMR spectra 79−73833
polystyrene, high impact, etching in CrO_3-H_2SO_4 soln. *(Russian)* 80−81223
polystyrene, high impact, hard elastic behaviour 79−57036
polystyrene, high impact, particle size distrib. in discrete phase 77−56257
polystyrene, high impact, under press., mech. behaviour 79−52305
polystyrene, high-impact, improved Coulter counter method for particle size distrib. meas. 77−56258
polystyrene, high-impact type, deformation and microvoid form. 78−80602
polystyrene, impact resisting *(German)* 79−100219
polystyrene, impact-torsion testing *(German)* 77−52595
polystyrene, in butanol, electrophoretic mobility, charge origin 78−85211
polystyrene, inelastic interaction of electrons, mean free path, stopping power and CSDA ranges 79−23663
polystyrene, interaction with glass beads, mica or TiO_2 fillers, glass transition *(Japanese)* 77−51479

polymers continued
polystyrene, intermol. interaction, conform. *(Russian)* 79−23539
polystyrene, intermolecular relaxation in cyclohexane photon correlation spectroscopy obs. 79−41255
polystyrene, intersections of coarse shear bands 79−100212
polystyrene, isotactic, conformation in bulk crystallised state 80−43221
polystyrene, isotactic, crystalline core of row structures, nucleation and growth 79−86718
polystyrene, isotactic, isothermal crystn. using SiO_2 as nucleating agent 79−24807
polystyrene, isotactic, morphology and growth of chain struct. *(German)* 78−75597
polystyrene, isotactic, normal vibrational anal. 78−43869
polystyrene, isotactic, orientation of remaining amorphous chains during crystallisation 80−10506
polystyrene, isotactic, semicrystallised chains, small-angle neutron scatt., mean dimension evaluation 80−43220
polystyrene, isotactic and static cold-crystallised blends, thermal transitions 80−24381
polystyrene, isotactic crystals, plastic deformation, molecular mech., TEM obs. 80−21022
polystyrene, isothermal and adiabatic effects assoc. with crack propag. 78−23827
polystyrene, lamellar stacks, screw dislocations 80−19728
polystyrene, laser irrad. chem. and struct. modifications *(Russian)* 79−27931
polystyrene, mean excitation energy from dielec. function 79−78031
polystyrene, mean mol. orientation factors, from IR spectra and acoustic method 80−70142
polystyrene, measurement of dielectric relaxation using transformer ratio arm bridge, 10^2 to 10^6 Hz 79−80641
polystyrene, mech. degradation, mass spectroscopic investig. 77−16668
polystyrene, mechanical degradation, limiting degree of polymerisation 77−85985
polystyrene, melt, bulk diffusion, local diffusion *(Japanese)* 78−95170
polystyrene, methacrylic acid/(PSMA) ionomers, far IR studies of ion clustering 79−87436
polystyrene, Millar interpenetrating network, viscoelasticity and phase domain form. 78−83749
polystyrene, MIM structure, TSC study 79−78201
polystyrene, mol. conform., craze fracture 79−15835
polystyrene, mol. wt., distrib. rel. to glass transition temp., ESR spin-probe investig. 79−8041
polystyrene, molecular alignment 78−14299
polystyrene, momentum-depend. dielectric response 79−69160
polystyrene, monodisperse, entangled, viscoelastic props., transient network model 78−13918
polystyrene, monodisperse latex, shear US meas. 78−31711
polystyrene, monodispersed particles, angular distrib. of fluoresc. 78−76927
polystyrene, monosubstituted, US relaxation, dynamics of mol. chains 80−29124
polystyrene, n-heptane and methanol crazes, micromechanics 77−12680
polystyrene, n-heptane and methanol crazes, structure 77−12681
polystyrene, non-isothermal rheological response during elongational flow 78−38262
polystyrene, nonisothermal rheology 77−32619
polystyrene, ns breakdown voltage, polarity effect, mechanism 77−63367
polystyrene, O treated, interaction with vapour-deposited Cr and Ni atoms 80−3407
polystyrene, oblique laser diffr. and reflection from surface crazes 77−47508
polystyrene, oriented amorphous, supermol. structures rel. to mech. behaviour 78−22673
polystyrene, oriented high-molecular, physicocomech. props. *(Russian)* 79−33028
polystyrene, partial draining of low-molecular weight polymers with flexible chains 80−23592
polystyrene, particles, critical stress 77−28869
polystyrene, photoconductivity, UV-IR light, absorpt. and photoluminescence. spectra *(Japanese)* 78−34857
polystyrene, photon penetration, photon backscatt. incidence angle depend. 80−104008
polystyrene, photophysical process, solvent effect obs. *(Spanish)* 79−57267
polystyrene, plasma polymerised, free radicals, O_2 effects, EPR study 80−71179
polystyrene, plasma polymerised, free radicals, transient elec. current, EPR, heat treatment 80−71178
polystyrene, plastic fracture near T_g at low strain rate 77−86178
polystyrene, plastic optics, design patterns 79−32009
polystyrene, polarised Rayleigh scatt. near glass-rubber relax., photon correl. spectroscopy 80−40124
polystyrene, polyisoprene modified, impact strength improvement 78−84993
polystyrene, polymer chain, internal friction range, HF viscosity theory *(French)* 80−79968
polystyrene, polymerisation by glow discharge method, formation mech. *(Japanese)* 80−61094
polystyrene, porous gel, solute elution behaviour in high performance liq. chromatography 78−92524
polystyrene, positronium form. and decay, elec. field effect 80−97369
polystyrene, props. changes upon photooxidation 80−30123
polystyrene, pure and doped, metal contact effect on persistent internal polarisation 79−78617
polystyrene, pyrolysis, determ. of kinetic parameters *(German)* 78−85155
polystyrene, Rankine-Hugoniot relation for shock waves 78−83317
polystyrene, ref. std. material testing, evaluation, glass transition temps., instrumental effects 79−4404
polystyrene, refr. index at 5461 angstroms, 30 to 260K 77−55764
polystyrene, rubber modified, two-phase struct. influence on fracture toughness *(German)* 80−66666
polystyrene, rubber-modified, crazing and fracture, Dugdale model 77−8907
polystyrene, rubber-modified, fracture, temp.-effect −120-20°C 77−4838
polystyrene, rubber-modified, impact-strength analysis 79−38972
polystyrene, rubber-modified, rubber particle morphology influence 79−94925
polystyrene, rupture mechanism 79−52372
polymers continued
polystyrene, sedimentation coeff. distrib. at 25°C *(Russian)* 77−63971
polystyrene, shear bands, morphology and annealing behaviour 80−100873
polystyrene, shear-wave Brillouin scatt. intensity from photoelastic consts. 79−91454
polystyrene, sol, light scatt. data, Fourier inversion anal. 78−76932
polystyrene, solid, low freq. Raman scatt., vibr. density of states, 29-300K 78−72516
polystyrene, soln. grown isotactic crystals, degree and distrib. of crystallinity, thermal stability 78−9964
polystyrene, solubility of benzene vapour *(Japanese)* 80−59667
polystyrene, solution grown isotactic crystal, thermal change kinetics study by X-ray diffr. 78−9965
polystyrene, sorption of organic vapours, glassy-state relaxation induction and meas. 80−44415
polystyrene, sp. ht. determ. by differential scanning calorimetry 79−33101
polystyrene, sp. ht. meas. by differential scanning calorimetry 77−51515
polystyrene, specimen size effect on mech. behaviour associated with crazing 77−73337
polystyrene, spherical pellets, ablation rates in Q-pinch plasma 77−89265
polystyrene, spin-labelled, EPR, end group mobility, temp. and solvent depend. 78−56368
polystyrene, stereochem. additions, sequence lengths, ^{13}C NMR 77−27212
polystyrene, stereostruct. of samples obtained by extraction of isotactic polystyrene with butanone 79−73112
polystyrene, steric effects on excimer formation, fluorescence spectra exam. 80−25430
polystyrene, stopping power for 2.2 to 5.9 MeV protons 78−90040
polystyrene, stress birefringence under nonisothermal conditions 78−15468
polystyrene, stress cracking, pressure-induced, mechanism 80−35361
polystyrene, stress relaxation during crazing, eqn. 79−61762
polystyrene, struct. determ. by electron microscopy 79−55675
polystyrene, substituted, Raman, IR and neutron spectra of LF vibs. 78−2848
polystyrene, sulphonated, polyelectrolyte solution, correlations and dynamics 80−104446
polystyrene, surface component of vacuum absorpt. and resorpt. currents, surface charge accumulation 80−60063
polystyrene, surface component of vacuum absorpt. and resorpt. currents, origin and magnitude 80−70791
polystyrene, T_{1l} relax. above glass transition 79−4259
polystyrene, tactic chains, angular correlation calcs. 79−45871
polystyrene, temp. and environmental effects on fatigue fracture 79−79079
polystyrene, thermal degradation, kinetic study *(Japanese)* 79−39139
polystyrene, thermal polymerisation, kinetics, Rayleigh scatt. 79−57228
polystyrene, thermoluminescence glow curves, quenching and isothermal decay plots 77−48258
polystyrene, total reflection Raman spectroscopy study 80−80784
polystyrene, uniaxially oriented atactic, laser Raman scattering 79−73920
polystyrene, unmodified and rubber modified, craze initiation in n-alcohols, kinetics 80−25894
polystyrene, unusual core level spectra of Cu coated surfaces, XPS obs. 79−24415
polystyrene, US propag. at low temp. 79−55834
polystyrene, viscoelastic, linearity conservation 80−108492
polystyrene, wideband optical transmission meas. 79−76771
polystyrene, X-ray irrad., thermoluminescence emission, exam. of kinetic order 79−43046
polystyrene, X-ray orientation and texture meas., compared with polycarbonate 78−75559
polystyrene+poly(2,6,-dimethyl phenylene oxide), isotactic, crystallisation and melting 78−18554
polystyrene aerosols, monodisperse, attachment of ^{220}Rn and ^{222}Rn delay products 80−41256
polystyrene and model cpds., conformational struct. influence on normal modes of benzene ring, Raman study 80−14144
polystyrene and styrene copolymers, amorphous, intermolecular interaction and disintegration 79−86723
polystyrene atactic carrier transport and photogeneration 80−80318
polystyrene blends, isotactic and atactic, small-angle X-ray scattering 78−55817
polystyrene chain conformations, in conc. solns. and in bulk, small-angle X-ray scatt. 79−10781
polystyrene charged particles in water, quasielastic light scatt. 79−24835
polystyrene coated Al, laser produced plasma energy transport 77−11375
polystyrene composite with mica flakes, TDC meas., interfacial polarisation 78−64316
polystyrene dispersion, sterically-stabilised, reversible flocculation 78−44411
polystyrene electret, thermally stimulated discharge 77−4595
polystyrene fibre, ageing effects on elongation to fracture *(German)* 78−76750
polystyrene filament, melt spun, struct. and mech. props., effect of drawing, twisting, annealing, untwisting 80−45331
polystyrene foam, X-band microwave dielectric spectra 79−87376
polystyrene foils, breakdown-charged, surface charge densities and depths, TSC spectra 80−7260
polystyrene fracture surfaces prod. by monotonic and cyclic loading 79−47768
polystyrene glasses, transition temp. and thermodynamic state 78−75819
polystyrene hexylmethacrylate-Se, interface photocurrent studies, charge transfer mechanism 79−99627
polystyrene hollow microspheres form., kinetic regularities *(Russian)* 79−57307
polystyrene hydrophobic gel beads, gel permeation chromatography behaviour 79−66386
polystyrene interfacial colloidal crysts., microscopic obs. 80−97737
polystyrene latex, aerosols, collection on micro-porous plates 79−64760
polystyrene latex, doublet particles, response of Knollenberg light scatt. counters 80−37152
polystyrene latex, grain boundary struct. obs. and boundary diffusion 78−51552
polystyrene latex, ordered lattices, model simulation of photon energy band, low energy photon diffr. 79−78795

polymers continued
polystyrene latex, ordered monodisperse, lyotropic liq. cryst., mech. props. 79−98676
polystyrene latex, particle size determ. by electron microscopy 79−21698
polystyrene latex monodisperse and peptized, structure determ. by neutron diffr. and small angle scatt. 80−40748
polystyrene latex particle size by electron microscopy and light scattering 79−66365
polystyrene latex particles, mixed sterically-stabilised dispersions, equilib. aspects of heteroflocculation 80−45570
polystyrene latex particles, particle sizing by forward lobe scatt. intensity ratio 78−71031
polystyrene latex particles, suspension in CTAB (Na_2SO_4), gas bubble surface charge meas. 78−21100
polystyrene latex sphere beams, secondary electron emission 77−24914
polystyrene latexes, edge dislocations 79−96370
polystyrene latexes, monodisperse, model colloid systems 80−89545
polystyrene latexes, soft X-ray scatt., struct. determ. 78−51395
polystyrene latexes, viscosity meas. *(Japanese)* 79−55432
polystyrene lattice, emulsions-polymerised, particle size determ. by soap titration 80−40753
polystyrene lattice cleaning, dialysis, steam stripping and ion exchange effectiveness 80−3414
polystyrene melts, flame-retardant high-impact, shear viscosity-temp.-shear rate relationships 80−59691
polystyrene microspheres, dye impregnated, fluoresc. spectra struct. resonances 80−50914
polystyrene microspheres in theta-pinch, ablation rates 78−18436
polystyrene model-networks, structure 77−89385
polystyrene monodisperse ^{51}Cr tagged aerosol prod. using aerosol centrifuge 78−92519
polystyrene monodisperse latex, anomalous viscosity in disordered state 80−74822
polystyrene monofilaments, uniaxial extension, strengthening 79−8334
polystyrene networks, characterisation by small-angle neutron scatt. 77−38765
polystyrene networks, glass networks, glass transition temp., mol. wt. depend. 77−11680
polystyrene particle colloidal suspension in KCl(LiCl) aq. solns., dielectric loss 78−35728
polystyrene particles, monodisperse, dil. and conc. aqueous dispersions, elec. cond., surface cond. and double-layer polarisation 80−89533
polystyrene particles flocculation, light scatt. for close range struct. determ. 78−53273
polystyrene polybutadiene polystyrene triblock copolymers, extension of contour plotting method for representing linear viscoelastic loss 77−32620
polystyrene scintillators, extrusion prod. 80−37698
polystyrene slab, electron emission from Nd laser prod. plasma 79−98944
polystyrene sphere crystals, in aqueous suspensions, solid-like phase transiton 80−50893
polystyrene spheres, crystallised suspension, gravitational compression 78−23975
polystyrene spheres suspended in isodecane, field depend. of electrophoretic mobility 78−56919
polystyrene substrate, Cu vapour deposition, surface complex, XPS obs. 78−72026
polystyrene sulphonic acid, charged membrane, electroosmosis and streaming potential *(Japanese)* 78−31696
polystyrene-Ag powder mixture, hot-pressed, elec. resist. 77−32556
polystyrene-b-isoprene and hydrogenated derivative, mol. relaxations in glassy state 80−53177
polystyrene-chain-stabilised nonaqueous SiO_2 dispersions 79−39219
polystyrene-chloranil molecular complex, glass-rubber and liquid-liquid transitions 80−45002
polystyrene-diethylmalonate, strongly opalescent critical isochore, scattered light intensity 80−71436
polystyrene-ethylene propylene copolymer, strength and impact props. 78−52899
polystyrene-metal contact-charge-exchange expt., charge induced relaxation 77−4309
polystyrene-poly(styrene-b-butadiene-b-styrene) polyblends, electron micrographs for struct. 78−51442
polystyrene-poly(styrene-b-butadiene-b-styrene) polyblends, mech. props. 78−52919
polystyrene-polybutadiene block copolymer, oriented microlattice obs. 78−2025
polystyrene-polybutadiene systems, phase separation obs. 79−94926
polystyrene-polydivinylbenzene, interpenetrating network, IR, NMR and chromatographic anal. of intermediate regions 77−55711
polystyrene-polyethylene(ethylene-propylene) blends, copolymer modified, mech. props., morphology 79−57088
polystyrene-polyethylene blends, crystn. characts. 80−103261
polystyrene-polyethylene block copolymer, deformation ratios, Poisson ratio and adhesion, dilatometric obs. 80−60937
polystyrene-polyethylene oxide, cryst. multiblock copolymers, crystallisation 78−91269
polystyrene-polyethylene oxide copolymer, elec. polarisation in suspension, Kerr effect 77−63359
polystyrene-polyethylene sulphonated copolymer, ionic transport, counterion effects in membrane 77−24430
polystyrene-polyethylene-(polymethylmethacrylate) blends, kneading charcts. *(Japanese)* 80−104112
polystyrene-polyisoprene, block copolymers, association colloids 80−26064
polystyrene-polyisoprene block copolymers, low mol. wt., glass transition temp., DSC investig. 77−7854
polystyrene-polyisoprene copolymers, macromol. chain conform. in lamellar phase *(French)* 80−2720
polystyrene-polymer, contact electrification model arising from eigenvalue spectra 78−47846
polystyrene-polymethylmethacrylate system, phase relationships and fracture surface morphology 79−61571
polystyrene-polyolefin blends, mech. and swelling properties 79−57053
polystyrene-polypropylene(polyethylene) mixtures, elastic moduli, phase struct. effect *(Polish)* 79−70107
polystyrene-polyvinyl methyl ether blends, dynamic mech. and sonic vel. behaviour 79−34090
polystyrene-wood, polymer composite, dielec. props. at low temperature range *(Japanese)* 78−95541
polymers continued
polystyrene/polyethylene blend, particle dimension as function of melt viscosity added graft copolymer conc. 77−52279
polystyrenes, anionic, TSC obs. of T_g and T_{II} transitions 80−84686
polystyrenes, comparison of head-to-head, head-to-tail, by thermally stimulated discharge 79−15396
polystyrenes, monodisperse, static and dynamic props., mol. wt. effect 78−84938
polystyrenes, p-halogenated, optical anisotropies, Kerr consts. 78−27246
polystyrol, ionizing radiation effect on life *(German)* 80−19853
polystyrol, test pipes, static tensile strength, equipment effect on tension-extension diagram *(German)* 78−35453
polysulfonamide, optically active, synthesised by interfacial polycondensation, mol. wt. determ. 80−99595
polysulphone, aromatic, sulphonated, reverse osmosis membranes appl., expt. results 77−44508
polysulphone, craze appearance effect on mech. props. 80−21135
polysulphone, dielectric γ losses 78−68449
polysulphone, discontinuous fatigue crack growth, generality of mechanism for glassy polymers 77−32677
polysulphone, effect of rolling on mech. props. 78−52837
polysulphone, effect of temp. on freq. sensitivity of fatigue crack propag. 78−76762
polysulphone, elec. appl., dielec. props. meas. 77−55750
polysulphone, glass and melt, PVT props., glass transition 79−14911
polysulphone, plastic insulation for cryogenic power cable, exam. of dielectric, tensile props. 80−25823
polysulphone, solvent crazing *(Japanese)* 79−29246
polysulphone, wideband optical transmission meas. 79−76771
polysulphone evaluation for biomedical applications 79−29670
polysulphone membrane, prep. and performance for ultrafiltration *(Japanese)* 78−31695
polysulphone-polydimethylsiloxane, linear block copolymer, morphology and impact strength 78−91265
polysulphone/S-glass adhesive failure, ISS and SIMS obs. 80−55626
polysulphur nitride:Br mag. susceptibility, linear temp. depend. 80−25114
polysulphur nitride:bromine, struct. and phase transition 80−24382
polysulphur nitride, elec. cond. at microwave freq. 80−24922
polysulphur nitride, Kohn anomalies in phonon dispersion 80−24555
polysulphur nitride, low temp. thermal cond. 80−24689
polysulphur nitride, pure and brominated, electronic model for high cond. 80−24923
polysulphur nitride, temp. depend. and anisotropy of H_{c2} 80−25054
polysytene, neutron and gamma-irradiation effects 80−66839
polyterephthalate, necking stress *(Japanese)* 77−56037
polytetrafluorethylene dispersed in acetal resin, tissue reaction 78−40412
polytetrafluoroethylene:peroxide, electron spin echo spectra, instantaneous and conventional spectral diffusion 79−15355
polytetrafluoroethylene, degradation by electron or γ-ray bombardment in inert atmosphere *(German)* 80−19840
polytetrafluoroethylene copolymers and oligomers, melt and solid, Raman active longit. acoustic modes 78−19484
polytetrahydrofuran, H bonding effects on skeletal optical and longitudinal acoustical modes 80−34914
polytetrahydrofuran, line-broadness in X-ray diffr. 77−19878
polytetrahydrofuran in MIM capacitor, electroforming, negative resist., electron emission 80−80406
polytetrahydropyran 2,6 diyliminocarbonyl hydrophilic membrane, water permeation and solute rejection props. 79−74419
polytetramethyl-p-silphenylene siloxane, morphology and mech. behaviour 78−84885
polytetramethyl-p-silphenylenesiloxane, degree of crystallinity 78−26453
polytetramethylene glycol, short range order, amorphous and liquid, ideal peak method calcs. 80−28900
polytetramethylene oxide-polytetramethylene terephthalate, block copolymer, props. 78−51438
polytetramethylene terephthalate, comparison of crystn. structs. in relaxed and strained forms 77−84675
polytetramethylene terephthalate, injection-moulded, struct. depend. of fracture behaviour 77−8912
polytetramethylene terephthalate, monofilaments, chain conform. rel. to strain 77−4055
polytetraoxane, polymerisation temp. effects on texture, and NMR obs. of mol. motion in tetraoxane cryst. 77−84663
polythene, finite element anal. of crazing and cavitation by dil. aq. detergent 78−53006
polythene, laser-produced plasma, use of electrostatic ion energy analyser 78−91157
polythene, stretching reduces electrical values *(German)* 79−43446
polythene, ultraoriented, microhardness, extrusion conditions effect 80−50704
polythene, Z dependence of thick target β-ray backscattering 80−76118
polythene pellet evaporation by CO_2 laser, multiple-frame laser shadow photography 77−80359
polythene sheets, crystalline formations study, light refl. from untreated surface 77−28945
polythene-polystyrene blends, differential scanning calorimetry and swelling characterisation 79−57053
polythioethers, bis(methylthio)alkane model compds. vibr. spectra 80−58430
polythylene, and perdeuteropolyethylene, crysts., IR and Raman intensities, factor group splittings 79−65851
polytrifluorclorethylene, determ. of microstruct. by secondary emission mass spectrometry *(Russian)* 77−31604
polytrifluorochloroethylene, moulding press. effect on struct. and props. *(Russian)* 79−52295
polytrifluoroethylene, dielectric relax. processes above and below glass trans. *(Japanese)* 80−55028
polytrifluoroethylene and copolymer, γ-irrad., Ar diffusion and solubility *(Russian)* 79−51315
polytrimethylene terephthalate, struct. determ. 80−19727
polytrimethylene terephthalate single crystals, X-ray and electron diffr. obs. of cryst. struct., packing analysis 79−94924
polytrioxane, γ-irrad., layer-like void formation 78−22760
polytrivinyl benzene, thermal and mech. props. rel. to high-press. polymerisation conditions 79−70326
polyuranate gels, changes in pore structure during reduction and sintering 77−71685
polyurethane, adherence on glass 78−83336

polymers continued
polyurethane, biological implant, ion beam sputter of surface morphology, SEM exam. 77−44836
polyurethane, cryogenic foam insulators, low temp. props. 80−25818
polyurethane, deform. under sheet pressworking, math. model 79−61673
polyurethane, effect of morphology on blood coagulation 79−39610
polyurethane, elastic fibres, cross link density effect on mech. props. 77−70023
polyurethane, foam, for organic material sampling in ambient air 78−20080
polyurethane, foaming parameters determ. from US wave vel. 80−71885
polyurethane, glass ball rolling on adhesive viscoelastic material, contact area 79−52394
polyurethane, high temp./press. materials test for undersea environment 78−3213
polyurethane, interpenetrating network, IR, NMR and chromatographic anal. of intermediate regions 77−55711
polyurethane, materials eval. 77−56533
polyurethane, quick-hardening SKU-PFL, synthesis and props., use in endoprosthetics 78−6887
polyurethane, rate dependent criterion of crack growth 79−32376
polyurethane, segmented, domain struct., deform. effect 80−93623
polyurethane, segmented, time depend. struct. changes on annealing, X-ray meas. 77−4052
polyurethane, simultaneous determ. of temp.-depend. thermal cond., heat capacity 77−11120
polyurethane, stress plate in contact zone with solid indentor 78−1624
polyurethane, stress relax. meas., effect of cure temp. on network struct. 77−84674
polyurethane adhesive, interface reactions with Al surface after surface treatments 77−81384
polyurethane adhesives, modified, struct. *(German)* 79−100333
polyurethane artificial ventricle construction with seamless interior *(German)* 79−8581
polyurethane cement, viscosity and shear strength, components influence *(German)* 80−93729
polyurethane Cu compsoite coil, fracture surface exam. by XPS *(German)* 78−84992
polyurethane elastomers, dry entry of ultrasound appl., for glass-reinforced plastics testing 77−90563
polyurethane foam, cylindrical cryogenic containers 79−35750
polyurethane foam, fast-neutron gauging for void detection 78−7157
polyurethane foam, rigid, gaseous thermal decomposition products, IR anal. *(German)* 79−29348
polyurethane foam, rigid, thermal expansion behaviour, mech. differential dilatometer method *(German)* 79−37859
polyurethane foam, rigid integral, effect on flexural and compressive strength, due to tall oil oligoether 78−68743
polyurethane foam, X-ray exam. *(German)* 78−75596
polyurethane foam layers, open-cell, refl. characts. for ultrasound in air 78−83139
polyurethane foam plastics, sorbents for marine oil pollution 79−53011
polyurethane foam plate, response to acoustic noise impulse *(French)* 79−1033
polyurethane foam solar concentrator, thermal and thermohydrolytic ageing 78−92281
polyurethane foams, elastic, stability against organic solvents *(German)* 80−85074
polyurethane foams, strength, cellular struct. effect 80−40518
polyurethane network, structural inhomogeneity by light scattering *(Russian)* 77−31605
polyurethane optical solid cct., preferential doping of rhodamine 6G 77−62075
polyurethane rigid foam, fracture props. over range of densities 79−79106
polyurethane solid foams, creep laws *(German)* 80−65139
polyurethane supportive dressing, radiolucency and mechanical properties, medical appl. 77−73561
polyurethane thermosetting powders, parameters 79−20003
polyurethane-polyurethane acrylate network, microinhomogeneities and props. *(Russian)* 78−51452
polyurethanes, crosslinked, thermoelastic props. 80−20991
polyurethanes, domain struct. obs. by NMR 77−47355
polyurethanes, linear, in vivo, degradation by ester hydrolysis *(Russian)* 80−40690
polyurethanes, rigid foamed, cellular struct. effect on water absorpt. 80−39416
polyurethanes based on toluene di-isocyanate, struct.-prop. relns. 78−80509
polyurethanes under tension loads, spectral exam. *(Ukrainian)* 78−92058
polyurethaneurylenes, segmented, structural features *(Russian)* 77−47356
polyvinyl acetal, temp. index, rapid determ. by dynamic thermogravimetry 80−85101
polyvinyl acetal derivatives of 9-anthraldehyde, preparation and electrophotographic props. 78−29183
polyvinyl acetate, Brillouin scatt. and hypersonic relax. 77−55795
polyvinyl acetate, partial draining of low-molecular weight polymers with flexible chains 80−23592
polyvinyl acetate, struct. relax., enthalpy and elec. polarisation obs. 79−41978
polyvinyl acetate, torsional stress/strain meas., press. effect 78−84937
polyvinyl acetate-polybutyl acetate crosslinked compositions, proton mag. relax., forced compatibility *(Russian)* 80−44950
polyvinyl acoustal, enamel lacquer, far IR transmission, encapsulation of optical devices 79−55194
polyvinyl alcohol, γ-irrad., ESR of trapped free radicals 78−85183
polyvinyl alcohol, absorption of H_2O mols. from liq., Raman spectrosc. technique 79−42364
polyvinyl alcohol, bulk polarisation, thermally stimulated discharge current meas. 80−40039
polyvinyl alcohol, crystallisation from dil. soln. by stirring *(Japanese)* 77−89388
polyvinyl alcohol, dichromated, sensitisation to visible laser wavelengths 78−4716
polyvinyl alcohol, doubly orientated, polarized Raman spectra 79−65872
polyvinyl alcohol, hydrocarbon suspension, temp. depend. of electroviscous effect and dielectric parameters 79−79299
polyvinyl alcohol, ionic charge carriers, dielec. studies 80−25291
polymers continued
polyvinyl alcohol, laser irrad. chem. and struct. modifications *(Russian)* 79−27931
polyvinyl alcohol, mean mol. orientation factors, from IR spectra and acoustic method 80−70142
polyvinyl alcohol swollen in aqueous glycol, network thermoelasticity, interactions 80−104201
polyvinyl alcohol-Cu interface, XPS study 79−83093
polyvinyl alcohol-polyelectrolyte membranes, heterocharge electret form., divergence model 80−15943
polyvinyl alcohol/$Pb(Zr,Ti)O_3$ ceramic, composite systems, piezoelec. props. 79−99823
polyvinyl butyral:triphenylamine, field-depend. UV photogeneration of holes, polymer composition depend. 78−76104
polyvinyl butyral, activation parameters of creep 79−38925
polyvinyl carbazole, and ring chlorinated derivatives, dielectric and NMR relaxation 79−73883
polyvinyl carbazole doped with trinitrofluorenone, thermoplastic-photocond., device for holographic recording 80−5707
polyvinyl chloride, agitating type polymerizer, synthetic resins and fibres manufacturing process 80−3341
polyvinyl chloride, carbonised, water vapour adsorption, porosity, and surface chem. 79−52753
polyvinyl chloride, dielec. props. at ULF, superimposed direct voltage *(French)* 78−15138
polyvinyl chloride, struct. determ. by electron microscopy 79−55675
polyvinyl cinnamate, and photocrosslinked form, low freq. dielec. loss evaluation 79−82919
polyvinyl cyclohexane, head-to-head, prep., characterisation 79−70036
polyvinyl cyclohexane, head-to-head high-resolution PMR spectra 79−73833
polyvinyl dispersion, ageing *(Polish)* 79−70098
polyvinyl fluoride, dielectric support for glass transition 78−2239
polyvinyl fluoride, glass transitions, Ar permeability and diffusion obs. 79−32919
polyvinyl fluoride, pure and doped, thermally stimulated currents 78−64315
polyvinyl fluoride, relax. phenomena, −30 to 200°C, premelting and glass transitions 78−51439
polyvinyl nitrate, exam. of strength characts. 78−68748
polyvinyl-pyrrolidone/polyethylene glycol oligmers, elasticity theory, and compression meas. 80−44246
polyvinylacetate and polyvinylacetate−microgels, light scatt. 80−20652
polyvinylbutyral, high density, adhesion strength to St. 3 steel 78−23920
polyvinylbutyrals, rupture activation energy and structurally sensitive coeff. *(Russian)* 77−21282
polyvinylbutyrolactonecoacrylonitrile membrane, selective and counter transport of Na^+ and K^+ *(Japanese)* 78−31700
polyvinylcarbazole, amorphous, hopping transport, reinterpretation of mobility meas. 79−42563
polyvinylcarbazole, Coloumb trap controlled hopping mobility model tests, mobility and permittivity meas. 79−56226
polyvinylcarbazole, exciton migration, luminesc. and quenching *(Russian)* 77−36275
polyvinylcarbazole, fast hole transport 79−51628
polyvinylcarbazole, fluoresc., photooxide quenching, exciton migration effects 79−56830
polyvinylcarbazole layer, diffraction effectiveness, registration of discrete holograms *(Russian)* 79−7100
polyvinylcarbazole-Hg interface, contact electrification, internal photoemission study 78−60191
polyvinylcarbazole-TCNQ complex, elec. cond. meas. 80−34456
polyvinylcinnamate, crosslink form. by photoreaction 80−7823
polyvinylcinnamate light-sensitised, reciprocity law in 240 to 436 nm range *(Russian)* 77−34052
polyvinylethylal, durability over extensive time temp. range 77−90460
polyvinylidene, fluoride, amorphous, low temp. anomalies, piezoelec. phenomenon 78−30724
polyvinylidene bimorph cantilever vibrator, resonant type, air flow generation, theory 79−87391
polyvinylidene chars, heat treatment, EPR rel. to temp., A-centers 78−43639
polyvinylidene chars, heat treatment, EPR rel. to temp., spin centres 78−48036
polyvinylidene chloride, carbonised, water vapour adsorption, porosity, and surface chem. 79−52753
polyvinylidene chloride, crystalline, preferred chain conform., mol. models 80−79709
polyvinylidene chloride, normal vibr. analysis using conform. model 80−83529
polyvinylidene chloride, vibr. spectra, amorphous and cryst. state conforms. 79−27930
polyvinylidene chloride charcoal, adsorpt. isotherms of organic vapours 80−96731
polyvinylidene electrets, IR and Raman spectra 80−7359
polyvinylidene fluoride, γ-irradiated, low temp. internal friction 78−83874
polyvinylidene fluoride, γ-phase form. from α- and β-polymorphs 79−11610
polyvinylidene fluoride, γ-ray irradiation effect on mech. props., in presence of triallyl trimellitate *(Japanese)* 77−86091
polyvinylidene fluoride, bimorph vanes, use in large area electronically controllable light shutter array 80−58696
polyvinylidene fluoride, correlated mol. motion in dielec. props. 77−55749
polyvinylidene fluoride, cryst., struct. phase transition theory, free energy, uniaxial stress 80−64924
polyvinylidene fluoride, cryst. and melt, stat. thermodynamics 79−41979
polyvinylidene fluoride, cryst. form II, anisotropy of dielec. relax. 80−103915
polyvinylidene fluoride, crystallisation, α-polymorph equilib. melting point, heat of fusion determ. 77−4054
polyvinylidene fluoride, crystn. process and elec. cond., differential scanning calorimetry 79−24024
polyvinylidene fluoride, DC conduction characts. 78−2488
polyvinylidene fluoride, dielec. breakdown and elec. cond., room temp. to 150°C 80−60500
polyvinylidene fluoride, dielec. props. and phase transitions *(French)* 80−55008
polyvinylidene fluoride, direct obs. of cryst. transform. process under high press. 78−38630

polymers continued
polyvinylidene fluoride, elec. field induced phase changes 79−11387
polyvinylidene fluoride, electrocalorific effect *(French)* 79−47392
polyvinylidene fluoride, equation of state, compression ratios, theory 80−10634
polyvinylidene fluoride, glass transitions, Ar permeability and diffusion obs. 79−32919
polyvinylidene fluoride, heat capacity, 5 to 200K 79−86900
polyvinylidene fluoride, heat to head chain imperfections, synthesis 79−52148
polyvinylidene fluoride, high-press. melting and crystallisation 78−91422
polyvinylidene fluoride, hysteresis phenomena under high elec. field 80−66134
polyvinylidene fluoride, melt-solidified, crystn. and morphology 80−103461
polyvinylidene fluoride, piezoelec., nonlinear dynamic response 80−75946
polyvinylidene fluoride, piezoelec., pyroelec., and improper ferroelec. 80−7301
polyvinylidene fluoride, piezoelec. and pyroelec., rigid dipolar model *(French)* 79−8090
polyvinylidene fluoride, piezoelec. and pyroelec. props., struct. model 79−11386
polyvinylidene fluoride, piezoelec, consts. calc. 80−103918
polyvinylidene fluoride, piezoelec. parameters versus bias field strength 79−91376
polyvinylidene fluoride, piezoelec. props., polarisation and appls. 80−75947
polyvinylidene fluoride, piezoelectric effect formation due to injection process, TSC *(French)* 80−34856
polyvinylidene fluoride, poled, dielec. relax. spectra 80−80690
polyvinylidene fluoride, poling by corona charging, pyroelec. effect 78−19423
polyvinylidene fluoride, poling process, kink propag. model 80−80679
polyvinylidene fluoride, poling process, solitary wave propagation model 79−87398
polyvinylidene fluoride, poling process effect on fine struct. 80−7285
polyvinylidene fluoride, polycryst. ferroelec., microstruct., piezoelec. and pyroelec. props. 80−7303
polyvinylidene fluoride, pyroelectricity, low temp. behaviour, due to origin 80−88932
polyvinylidene fluoride, relax., influence of monomeric unit conform. and supermol. struct. *(Russian)* 79−23537
polyvinylidene fluoride, relax. phenomena, −30 to 200°C, premelting and glass transitions 78−51439
polyvinylidene fluoride, struct. study, piezoelec. and pyroelec. props. 80−7300
polyvinylidene fluoride, structural phase transitions, statistical mech. theory 79−82331
polyvinylidene fluoride, structure, and its electret, review *(Japanese)* 80−10510
polyvinylidene fluoride, suitability as underwater transducer material 78−1531
polyvinylidene fluoride, thermally stimulated currents, effect of ageing 77−1634
polyvinylidene fluoride, thermodynamical model, applications *(French)* 80−39315
polyvinylidene fluoride, TSC and thermoluminescence, reln. to molecular motion *(Japanese)* 80−55200
polyvinylidene fluoride, US transducers, dielec. and acoustic losses 80−48541
polyvinylidene fluoride, X-ray high press. study 80−6369
polyvinylidene fluoride and poly-1-vinyl-3-methylimidazolium iodide interpolymer ultrafiltration membranes 79−15639
polyvinylidene fluoride drift mobility meas., I_2 charge transfer from surface charge decay technique 80−49744
polyvinylidene fluoride fan, electromech. conversion efficency and high field dielec. loss 79−82926
polyvinylidene fluoride film, piezoelec. coupling factor meas. servo system 78−60397
polyvinylidene fluoride piezoelectric film, acoustic wave reson. meas. 77−81058
polyvinylidene fluoride piezoelectric thin films, US atten. at high freqs. 79−65798
polyvinylidene fluoride thermal diffusivity and cond. meas., two-phase model 77−47632
polyvinylidene fluoride transducers, underwater acoustic meas. 79−14184
polyvinylidene fluoride vinyl fluoride copolymer, epitaxial crystallization 79−65005
polyvinylidene fluoride-Pb(Zr,Ti)O_3 ceramic composite film, complex dielec. props. 78−64323
polyvinylidene fluoride-PMMA blends, dynamic mech. props. and sonic velocity, cryst. phase transitions 78−26454
polyvinylidene fluoride-PTFE, thermoelectret, IR spectra, struct. modifications and dielec. props. 77−55785
polyvinylidene fluoride-PTFE copolymer, local electrostatic field determ. *(French)* 77−12305
polyvinylidene fluoride-tetrafluoroethylene, ferroelectric props. 79−42929
polyvinylidene fluoride/Pb(Zr,Ti)O_3 ceramic, composite systems, piezoelec. props. 79−99823
polyvinylidenefluoride, melting and freezing, effect of structural factors *(German)* 78−15389
polyvinylimidazole.Cu(II) complex, ESR studies on dimer form. between copper ions 80−100613
polyvinylpyrrolidone, conformational states investig. by atom-atom function method *(Russian)* 80−53178
polyvinylquinazoline-I_2 complexes, absorpt. spectra and elect. cond. 80−92891
polyvinyltoluene latex, doublet particles, response of Knollenberg light scatt. counters 80−37152
polyvinyltoluene scintillators, energy transfer in organic systems 78−92127
polyvinyltrimethylsilane, diffusion, sorption, solubility, permeation of hydrocarbons, Xe *(Russian)* 80−6564
polyvinyltrimethylsilane, sorption, diffusion, solubility of hydrocarbons, Xe rel. to temp. *(Russian)* 80−6565
polyvynylpyridines, atactic, chem. shift, conformational struct. *(Russian)* 80−5652
polywax 1000, linear polyethylene, depolarised Rayleigh spectroscopy 79−4808
polyyne, linear infinite chain, ground-state props., ab initio studies 79−95306

polymers continued
poly[trityl methacrylate-co-(S)-α-methylbenzyl methacrylate], abnormal optical rot. 79−31749
POM, creep compliance calc. from short-term creep expts. 80−89303
porous, prep., appl. as stationary phase in gas chromatography *(German)* 79−29434
powder, pneumatic conveyance through metal pipes, charging tendency meas. 79−50186
powder coatings, water permeability eval. by radioactive tracers *(Czech)* 78−11362
powder compact with metal, cond. threshold, particle size ratio effect 80−80337
powders, corona-charging props. 80−6946
prebiotic polymers, possibilities in IR spectra of galactic sources 78−4336
prefluorinated polymer, DuPont Krytox 143-AB, viscoelastic and dielectric props. 80−1503
prepolymers, H-NMR and ^{19}F-NMR spectroscopy *(German)* 80−103893
processing, US effects casting appl. *(German)* 77−48388
processing technology, prod. of high chain extension 78−31378
propergol, rheological props. during polymerisation *(French)* 78−23762
properties of glass transition, conformational effects anal. 79−69231
property-molecular weight distribution relation, non uniqueness, blending expts. 77−36445
propylene, isotactic, crack propag. rel. to morphology *(German)* 78−76749
propylene copolymers, ethylene incorporation meas. by ^{13}C NMR and IR spectrosc. 79−39225
propylene-alkyl acrylates alternating copolymers characterisation 79−51950
propylene-butadiene, alternating copolymer, struct., fractional composition obs. *(Russian)* 79−65011
propylene-butene copolymers, PB centred tetrad ^{13}C NMR spectra assignment 80−58428
propylene-butene-1 copolymers, thermal and mech. props. 79−34091
propylene/butene-1 copolymers, coisotactic shift contribs. in ^{13}C NMR spectra 80−29635
prosthesis block copolymers, non-thrombogenic, struct. and mech. props. 77−52925
prosthetic joint replacements in orthopaedic surgery 79−83999
PTE, polymer fibre, orientation changes during stretching, IR spectra 78−75568
PTFE, γ-ray effects on 19 and 30°C phase transitions, Fourier transform IR spectroscopy 80−103387
PTFE, abrasion, SEM obs. 78−64742
PTFE, anisotropic electrochemical attack 79−39004
PTFE, annealing effect on melting and crystallisation *(Japanese)* 80−20980
PTFE, chemiluminescence, 25 to 172°C 77−55839
PTFE, colloidal, in butanol, electrophoretic mobility, charge origin 78−85211
PTFE, contact angle data with many liquids, interaction parameter calc. 77−55423
PTFE, creep and recovery under hydrostatic compression in programmed loading 80−100881
PTFE, crystalline, subject to simple plane loading, limiting resistant, time and temp. factors 78−23794
PTFE, degradation products, chem. anal. by UV photoelectron spectroscopy 78−53300
PTFE, effect of loading time on contact area *(Japanese)* 78−6230
PTFE, electronic energy states and charge density contours studied muffin tin orbitals technique 80−80164
PTFE, epitaxial crystallisation of crystalline polymers on surface 78−14626
PTFE, friction and transfer 77−52512
PTFE, graphite filled, carbon aspect ratio effect on friction and wear characts. 77−59945
PTFE, $H_2(D_2)$ solubility and diffusion, activation enthalpy 78−79775
PTFE, heat shrinkable tubing, crystallite orientation 77−4795
PTFE, impact testing, elastic analysis of conventional test, reassessment of testing 78−60770
PTFE, interaction with SF_6 plasma, in glow discharge, emission spectrum 80−87960
PTFE, matrix for ultrafine Fe_2O_3 particles, EPR and Mossbauer study 80−100625
PTFE, mech. and elec. props., processing and appls. 78−84760
PTFE, melt transition, theory 77−76325
PTFE, MIM structure, TSC study 79−78201
PTFE, Ne, Ar, Xe and He diffusion and solubility 80−6561
PTFE, necking stress *(Japanese)* 77−56037
PTFE, NMR and X-ray diffr. investig. of press. induced III-I transition and mol. motion 77−51969
PTFE, nonlinear creep, compression bulk modulus 80−66593
PTFE, ns breakdown voltage, polarity effect, mechanism 77−63367
PTFE, oriented fibre drawing *(Russian)* 77−21088
PTFE, partially crystalline, time-temp. superposition 77−4801
PTFE, partly crystalline, viscoelastic props., stressed state estimation 79−66099
PTFE, peroxy radical labelled, temp. dependent rots., EPR obs. 80−28125
PTFE, prepared for dosimetry, thermocurrents 77−52877
PTFE, processing parameter effect on thermal props. and crystal struct. *(German)* 78−63679
PTFE, pyrolysis surface layer ablation, analytical model 77−52637
PTFE, Raman spectra obs. of high press. phase conformal deform. 79−1757
PTFE, relaxational props. effect of temp. and hydrostatic press. *(Russian)* 77−44325
PTFE, rheological props. below m.p. with certain low molecular smectic states 79−87675
PTFE, shape change during 19°C phase transform. 78−76646
PTFE, shock compressed, vel. of sound meas. 78−10123
PTFE, specimen size effect on mech. behaviour associated with crazing 77−73337
PTFE, spreading of high-press. polyethylene melt, index 79−37902
PTFE, stress-time analogy under shear and hydrostatic pressure in creep regime 80−104227
PTFE, struct. effects in stress-strain relations at elev. temps. 78−31484
PTFE, surface component of vacuum absorpt. and resorpt. currents, surface charge accumulation 80−60063

polymers continued
PTFE, surface component of vacuum absorpt. and resorpt. currents, origin and magnitude 80−70791
PTFE, surface layer optical consts. in 1000-1300 cm^{-1} region 79−51957
PTFE, thermal cond., effect of material on working parameters of cryo-surgery instruments 78−36037
PTFE, thin-wall tubes, deform. and fracture processes 79−100222
PTFE, transfer layers produced by rubbing, apparatus for study 79−47861
PTFE, trapped peroxy chain radicals, reactivity and struct., EPR spectra 80−66783
PTFE, vib. assignment, far IR spectrum 77−48170
PTFE, vibrational assignment problem, far infrared spectrum 77−52087
PTFE, wear, sliding speed, contact press. and rubbing surface temp. 80−76372
PTFE, wear mechanism at steel surface, SEM, TEM and DTA 78−64727
PTFE+D, DF* prod., Fourier transform IR spectroscopy 80−87105
PTFE+metal, fluoride prod., DSC and XPS anal., rel. to polymer wear 80−11889
PTFE copolymer, melting point, cryst. struct., modification *(Russian)* 77−31607
PTFE fibres, US effects on structure *(Polish)* 78−68702
PTFE impregnated porous bronze, coeff. of friction, temp. effect 78−64737
PTFE latex, emulsion polymerisation, radiation-induced *(Japanese)* 78−80747
PTFE seal for superfluid He 78−4625
PTFE-C black composite form. monitoring by electrochem. method 77−36446
PTFE-metal interaction, X-ray photoelectron spectroscopy obs. 80−11788
PTFE-steel pair, temp. calc. under severe friction 80−40550
PTFE/graphite bond in H_3PO_4 environment, electrochemical exam. of joint failure 78−60979
PTFR, surface energy anal., comparison of one- and two-liq., contact-angle methods 77−59181
PTS, exciton surface polaritons at room temp. 79−47476
PTS polydiacetylene single cryst. reflection spectra, exciton site splitting 78−31211
pulsed NMR technique for meas. radiation effects in polymer 80−66051
pulsed photoconduction 80−24969
pure and applied chemistry, conf., Tokyo, Japan (Sept. 1977) 78−95906
PVA, atactic, Brillouin scatt., hypersonic relax. 79−4811
PVA, H_2O-swollen, sorption of $TiCl_4$ from benzene solns. *(Polish)* 79−4471
PVA, hollow fibre membrane for industrial scale dialyser *(Japanese)* 78−31693
PVA, interaction with glass bead, mica or TiO_2 fillers, glass transition *(Japanese)* 77−51479
PVA, photooxidation, kinetic eval. for carbonyl form. *(Japanese)* 79−39007
PVA, swollen crystallinity determ. by laser Raman spectroscopy 80−38953
PVA adsorbed on polystyrene latex particles, flocculation and stabilisation, concentration effects 80−45569
PVA carbonisation process and carbonised block props., high temp. resistant materials *(Russian)* 79−8268
PVA hydrophobic gel beads, gel permeation chromatography behaviour 79−66386
PVA laser target, spherical-shell, energy absorpt., expt. determ. 80−54016
PVAC dispersions, US method of determining plasticiser content *(German)* 80−21257
PVC, amorphous, orientation study by creep thermomechanical method, computer anal. 78−75561
PVC, amorphous-cryst., highly oriented, plastic deform. rel. to supermol. struct. *(Russian)* 79−51010
PVC, antiplasticisation rel. to ageing and nonlinear viscoelasticity 78−52929
PVC, asbestos reinforced, CIR/Palram process preparation, mechanical and thermal properties measurements 79−66106
PVC, biological media effect on. physiomech. props. 79−96168
PVC, book 77−25006
PVC, brittle fracture of notched ductile polymers *(Japanese)* 80−16448
PVC, calendering, prediction of stress and torque 79−8266
PVC, chlorinated, fibres, radiation initiated graft polymerisation of acrylonitrile, initiation rate rel. to props. *(Russian)* 80−7531
PVC, chlorinated, microstructure, use of ethylene vinyl chloride and copolymers as macromolecular models *(German)* 77−27838
PVC, chlorinated, X-ray photoelectron spectra investig. 80−3469
PVC, cold drawn, plastic fracture around cavities 79−56994
PVC, commercial tubes, photoviscoelastic investigation 79−34095
PVC, compatibility with polyacrylonitrile 79−4416
PVC, crazes, statistical aspects optical microscopic obs. *(Japanese)* 79−29247
PVC, crazing, deform. kinetics 80−84990
PVC, creep meas., use of computer in rational determination of material values *(German)* 78−31474
PVC, cross-linked, irradiation appl. to provide improved insulation props. to wires and cables 80−66850
PVC, crosslinked, mech. and thermal props. with plasticisers *(Japanese)* 79−15741
PVC, crystalline syndiotactic, exam. of chain folding, lattice energy 80−24373
PVC, Cu evaporated film, electron-induced metallochromic reaction for metal image formation 80−86476
PVC, deform. temp.-time depend. props., viscoelastic linear and nonlinear regions comparative anal. 78−64600
PVC, degradation products, chem. anal. by UV photoelectron spectroscopy 78−53300
PVC, dielectric props. in ultra-low freq. range *(French)* 78−23395
PVC, different stereoregularities, heat treatment effect on glass transition temp. and c_p changes 79−4985
PVC, discontinuous fatigue crack growth, generality of mechanism for glassy polymers 77−32677
PVC, ductile fracture, SEM investig. 77−44343
PVC, ductile glassy, notch brittleness under plane strain 80−100900
PVC, electrophoresis of particles dispersed in vinyl chloride monomer during polymerisation 79−79250
polymers continued
PVC, electrostatic charge on nascent particles during polymerisation 79−79249
PVC, enthalpy determ. of order 79−7556
PVC, EPR of NO radicals, rot. mobility 79−33539
PVC, exam. of microstructure, using X-ray and light scattering 79−41983
PVC, extended syndiotactic, modified Urey-Bradley force field calcs. 78−25500
PVC, fatigue crack growth rate, tensile cyclic tests 79−5043
PVC, fatigue life, influence of cyclic loading conditions 80−76350
PVC, filled with SiC particles, abrasion resistance *(Japanese)* 78−7055
PVC, flexure testing 77−86087
PVC, for dry insulation in power cables *(Spanish)* 80−81024
PVC, free induction decay in high-elastic state *(Russian)* 78−92294
PVC, gamma radiation effects on dielect. parameters, expt. *(Hungarian)* 78−59836
PVC, gaseous thermal decomposition products, IR anal. *(German)* 79−29348
PVC, glass-rubber transition, time-temp. superposition, shear creep compliance meas. 80−88309
PVC, glass-rubber transition determ., small-angle X-ray scatt. 78−95145
PVC, glassy, craze and crack growth *(Japanese)* 77−8970
PVC, glassy, fatigue crack initiation in high strain fatigue tests 80−97564
PVC, glassy rods, craze initiation, kerosene wetting effects 77−25172
PVC, glassy state, macrodeformation stresses, anelastic characteristics 79−52289
PVC, hard, flow zone effect on degradation, rigidity, deformation, under fatigue *(German)* 78−15471
PVC, heat capacity and thermodynamic props., 6 to 375K obs. 78−79779
PVC, high temp. creep 78−48453
PVC, highly deformable, fracture surface roughness 78−44197
PVC, highly syndiotactic, X-ray diffr. and IR studies of annealed material, crystallinity 78−2022
PVC, impact strength, exam. with pulsed drop impact loading 78−84944
PVC, influence of thermal history on physical props. 79−4984
PVC, injection moulded, compression moulded and drawn samples, X-ray diffr. 78−83755
PVC, kinetic nature of strength 78−15524
PVC, long-chain branched with narrow mol. wt. distrib., precipitation polymerisation 77−90315
PVC, magneto-electrets, refr. index, temp. and mag. field effects 78−6655
PVC, magnetoelectret form., RF thermomagnetic treatment, dielectric aftereffects 78−6625
PVC, mean mol. orientation factors, from IR spectra and acoustic method 80−70142
PVC, mech. behaviour in nonlinear viscoelasticity range 79−4996
PVC, mech. comminution in fine struct. changes in porosity, density, specific surface area *(German)* 78−35345
PVC, mechanochem. degradation 80−40371
PVC, mechanochemical degradation in primary struct., mech. vibration effects, IR spectra *(German)* 78−19769
PVC, MIM structure, TSC study 79−78201
PVC, ns breakdown voltage, polarity effect, mechanism 77−63367
PVC, nuclear mag. relax. dipole-quadrupole nuclei interaction, quasi-rigid and tumbling lattice 77−66434
PVC, optical interference meas. of critical crack tip displacements 78−84964
PVC, oriented mouldings, struct. order 80−60896
PVC, origin of charge on nascent particles in monomer during suspension polymerisation 79−79251
PVC, ozonized, decomposition of peroxides, chemilum. meas. 78−68893
PVC, plastic behaviour determ. at const. true strain rate 79−39073
PVC, plasticised, fatigue, fractographic study 80−30101
PVC, plasticised, fatigue crack growth charact. 80−30100
PVC, plasticised, fracture energy determ. 77−62208
PVC, plasticised, history-independent recovery, creep, stress relaxation 78−80607
PVC, plasticisers effect on behaviour under γ-irrad. *(Russian)* 79−87864
PVC, plasticized, humidity depend. of ion mobility, polarity reversal of applied voltage method 80−49408
PVC, plasticized, solubility of O_2, N_2 and CO_2 *(Polish)* 79−69252
PVC, positron lifetime, phase and temp. depend. 79−83051
PVC, proton spin-lattice relax. dispersion, quadrupolar dip 77−16197
PVC, pyrolysis, HCl anal. in off-gases using ion-selective electrode 77−60146
PVC, radiation destruction, automatic control *(Polish)* 77−29025
PVC, Raman spectrum, C-Cl stretching region 78−84583
PVC, reaction with maleic anhydride in heated roll mill *(Japanese)* 79−38856
PVC, reduced, dielec. props. rel. to mol. struct. 80−29681
PVC, rheology, viscoelasticity 79−3982
PVC, rigid, craze and yield zones in fracture 80−50701
PVC, rigid, fatigue crack growth, under biaxial stress 79−70144
PVC, rigid, internal struct. of diamond shaped cavities 80−66628
PVC, rigid, microdomains, small angle X-ray scattering study 80−28930
PVC, rigid, physical ageing effect on elec. props. 78−10836
PVC, rigid, tensile fracture morphology, rel. to mol. props. 77−59883
PVC, rigid, tertiary creep *(German)* 77−52433
PVC, rigid plate, notching method effect on Charpy impact values, fractographic considerations *(Japanese)* 80−108541
PVC, rigid plate, simultaneous diffusion and dechlorination in H_2SO_4 *(Japanese)* 77−52521
PVC, rigid resin, TEM studies of morphology, processing effects 80−108385
PVC, rolled, anisotropic, creep fracture *(Japanese)* 79−34132
PVC, rubbed, TSC meas. 80−55017
PVC, rubber-modified, stress whitening and yield mechanism 79−8324
PVC, sintered powder, elastic props. and porosity 77−63619
PVC, sintered powder, permeability and porous struct. 77−63620
PVC, Sn stabilized, effect of paraffin and polyethylene lubricants on flow props 79−8325
PVC, solid, stress-strain behaviour, strain rate and temp. effects, cryogenic temps. *(Japanese)* 78−11315
PVC, sorption of monomer vapour, effects of previous history, time and temp. 79−4470

polymers continued
PVC, sorption of organic vapours, glassy-state relaxation induction and meas. 80−44415
PVC, spontaneous current emission, various metal electrodes 78−43412
PVC, stress relaxation in macrodeformation range 80−16370
PVC, stretched at various elongation degrees, dichroic meas. of anthracene orientation 77−30867
PVC, struct. and performance of porous membranes prepared from soln. *(Japanese)* 79−24823
PVC, structural studies by Raman spectroscopy 79−7044
PVC, suggested morphology-characterisation terminology 79−7555
PVC, surface coating constituent mat., adsorpt. of Cs^+ 78−23843
PVC, surface component of vacuum absorpt. and resorpt. currents, surface charge accumulation 80−60063
PVC, surface component of vacuum absorpt. and resorpt. currents, origin and magnitude 80−70791
PVC, surface energy anal., comparison of one- and two-liq.-contact-angle methods 77−59181
PVC, technological obs. and methods 79−7349
PVC, tensile and indentation behaviour, durability tests, glass transition 79−5017
PVC, tensile test neck development theory 78−52897
PVC, tensile tests, post-yield phenomena 79−91752
PVC, tensile tests at low strain rate, secondary instability form. *(German)* 77−66727
PVC, test pipes, static tensile strength, equipment effect on tension-extension diagram *(German)* 78−35453
PVC, thermal and dynamic glass transition temp. relation *(German)* 78−14450
PVC, thermal cond., 2-100K, crystallinity effect 77−20137
PVC, thermal history and treatment effect on mech. props. 79−4986
PVC, thermal stabilisation by triazine dithiols *(Japanese)* 80−108386
PVC, thermally induced conformational changes, Fourier transform. IR spectroscopy 78−9287
PVC, thermodynamic props. *(German)* 77−28024
PVC, thermooxidative degradation, crosslinking and chain scission 80−71912
PVC, tubular magneto-electret, surface charge charact., forming temp./mag. field depend. 77−32318
PVC, uniaxial tension, deep drawing, rigidity *(German)* 78−64556
PVC, unplasticized, evaluation method for chemical resistance *(Japanese)* 80−25893
PVC, volume stress/strain state using new apparatus 78−23896
PVC, wear props. *(Japanese)* 79−96151
PVC, with stabiliser, dielec. and mech. charact. under γ-irrad., plasticisers effects *(Korean)* 77−81054
PVC, X-ray absorption, shock wave compression meas. *(German)* 78−95618
PVC, yield behaviour *(Japanese)* 80−93620
PVC block copolymers, physical props. and morphology 79−82166
PVC branching, origin, extent 79−7048
PVC cases for Pb-acid batteries, pneumatic shock test *(German)* 78−85093
PVC chain branching, CH_2Cl group production mechanism, IR data evaluation 79−7047
PVC charcoal, adsorpt. isotherms of organic vapours 80−96731
PVC chlorinated, mol. parameters determ. 79−41974
PVC composite, MBS type multifunctional impact modifier effect on mech. and rheological props. *(Polish)* 78−52751
PVC dispersion, rheology, particle size effects 79−92007
PVC elastic modulus and loss factor meas. at 10-90 kHz range 77−86235
PVC electret, thermally stimulated depolarisation 78−48112
PVC latex size determ. by TEM, vertical shadowing technique 77−53857
PVC membrane filters, collection of α-quartz for X-ray diffr. anal. 77−70392
PVC particles, Raman spectra, conform. during polymerisation 79−33709
PVC past theology, viscosity props. 79−86724
PVC pastes, rheological, surface props. rel. to density of prep. foams *(Polish)* 78−85212
PVC physics symposium, Lyon-Villeurbanne, France (July 1976) 79−7554
PVC pipe, subjected to torsion, demonstration of holographic-moire technique extended to 3D 79−35661
PVC plastisol pastes, dispersion and characteristic functions, review *(German)* 79−55015
PVC plastisols, high resin level, rheological behaviour, discontinuous viscosity 80−23980
PVC powder, cold compaction, product strength, heat treatment effects 80−11621
PVC powder, quinoline diffusion, microdiffusion technique 79−7713
PVC products, brittle fracture initiation by defects or flaws 79−5042
PVC products, quality control on basis of particle structure 79−8265
PVC rigid, flow and therm. stability 79−64618
PVC rigid plate specimens, Charpy impacted, SEM exam. of fracture surface *(Japanese)* 78−52953
PVC sheet, notched, yielding 78−56708
PVC surfaces, natural and stabilised, composition, ageing, oxidation and weathering, ESCA obs. *(French)* 80−61139
PVC suspension rheological props. *(German)* 79−94579
PVC thermal degradation, reinitiation mechanism of HCl catalysis 80−71944
PVC tubing acid release effects on SO_2 air pollution daily volumetric meas. 77−29449
PVC-C composite, transport props. 79−38073
PVC-chlorinated, piping for secondary criticality control of fissable solns. 80−13607
PVC-chlorinated polyethylene blend, optical characterisation methods 79−8408
PVC-chlorinated PVC mixtures, compatibility, mixing techniques, elastic modulus determ. 79−4943
PVC-Cu composite, annealing effects on elec. resist. 78−68060
PVC-Cu composites with chemically deposited ultrafine copper particles 80−93534
PVC-ethoxymethylmelamine blends, dynamic mech. props. *(Japanese)* 79−96063
PVC-g-butyl rubber grafted copolymer, tensile strength increased by S_2Cl_2 curing 79−95993
PVC-metal interface, ionic carriers behaviour 79−99622
polymers continued
PVC-poly-ε-caprolactone, interdiffusion, meas. method 79−69271
PVC-poly-ε-caprolactone blends, gas permeation and compatibility 79−4433
PVC-polyvinylidene chloride copolymer, dielectric loss at low-temp 78−95543
PVC-vinylchloride system, glass transition, vinylchloride influence *(German)* 80−79917
PVF_2, plastic film sensors 79−99826
PVF_2 charge injection from metallic electrode, obs. 80−15947
PVFD, electret, polarisation process 80−7273
PVK/PVK-TNF/TNF.PMG system, electrophotographic charact. 80−62759
PVTE, heat capacity, 5 to 200K 79−86900
Pyran copolymer containing 5-fluorouracil, synthesis and antitumor props. 79−91613
pyrolysis, high-temp., heat transfer processes at gas/solid surface *(Russian)* 80−61152
pyrolysis, light and Curie point, determ. of kinetic parameters *(German)* 78−85155
pyrolysis-IR analysis 78−3404
pyrolysis-mass spectroscopy inlet system design and appls. 77−36816
quality control method based on solid surface wetting 79−52534
quality testing using US vel. propagation meter 78−19976
quantitative analysis by pyrolysis gas chromatography 80−61180
quantum mechanical effects, due to orbital overlap 78−50670
p-quaterphenyl, mol., charge density and bond orders, polynomial matrix method 78−74808
radiation appls. *(Japanese)* 80−55413
radiation curing of selected structural adhesives, lap shear strength props. 80−66842
radiation resistance of cable insulating materials for nuclear power stations, expt. 78−59835
radiation stability of 'nuclear class' ion-exchange resins 79−43609
radical and unsaturated polymer interactions, MO calcs. 77−44481
radiofrequency spectroscopy, structural energy characteristics, rotational isomerism, mol. motion *(Russian)* 79−56602
Raman active longitudinal-acoustical mode spectra interpretation 80−103950
Raman spectra, cryst. morphology, longitudinal acoustic mode 78−43859
Raman spectra, longitudinal acoustic mode 78−43858
random coil polymer chain relax., lattice model with excluded vol., head movement rules 80−5642
random coil polymer chains, asphericity relax., Monte Carlo calcs. 77−75354
random flight chain, surface adsorbed, end-to-end mean value 78−22060
random-flight chain in restricted environment, Monte Carlo simulation 77−46663
Rayleigh wave excitation in corrugated surface polymers, modified wedge method 79−37261
reaction with metal formates in frictional contact zone 78−7057
reactive polymers, for enzyme immobilised enzymes 79−29398
reactivity and gelation, intrinsic reactivity 79−100363
reactivity and gelation, substitution effect 79−100364
reciprocating impact wear testing apparatus, results 78−15639
recrystallisation during drawing 78−76658
rectilinear on square lattice, series expansion 80−5646
refractive index meas. in sub-mm. wavelength 77−18074
reinforced and isotropic high polymers, rubberelastic domain, thermodynamics 80−14579
reinforcement, fracture mechanics 80−10207
relaxation, computer used to calculate mech. charact. 77−52388
relaxation in glassy state, free vol. fluctuation effects 79−69022
relaxation investigation *(German)* 78−31152
relaxation phenomena, conference, San Francisco, CA, USA (Aug. 1976) 79−4257
relaxation properties, photometric transducer method of meas. 80−3268
relaxation properties investigation method and instrument 78−39967
relaxation spectra determ. from electric discharge meas. with increasing temp. *(German)* 78−31151
relaxation time spectra calc. from stress relax. data *(Russian)* 77−44288
relaxation times and dynamical modulus, viscoelasticity theory *(Russian)* 79−52293
renormalisation transformation 79−89816
residual stress measuring equipment for polymer materials based on cured synthetic resins 77−77675
resin:Cu^{2+}, interaction with ligands, EPR meas. 78−10756
resin:VO^{2+}, interaction with ligands, EPR meas. 78−10756
resin, highly crosslinked, fracture, review 77−4846
resin beams with glass fibres, crack propag. expt. 78−15521
resin particles, dispersed, precipitation on cellulose fibre in elec. field 78−53262
resin slab, stress response, fluctuating external moisture (temp.) effects 78−55620
resin synthesis for affinity chromatography 78−11579
resins, prepregs and composites, charact. by differential scanning calorimetry 80−71869
review, plastic deformation during freeze-cleavage 78−14400
rheology of polymeric systems, review 78−87317
rigid, modified Oseen tensor, superposition approximation appl. 80−92447
rigid, prefractured states study, elastic limit and strength 77−70092
rigid chain, synthesis and props., conference, New Orleans, Louisiana, USA, (March 1977) 79−94118
rigid polymers, error estimation in viscoelastic problem soln., using method of approx. 80−19253
rigid-chain, unity of deform. and spontaneous elongation mechanism 79−20138
ring chain, distrib. function of square radius of gyration 77−61885
ring polymer model with excluded volume 79−94117
ring polymers, internal viscosity, statistical theory 77−88610
rings, topological constraints and critical indices 79−81313
rosin and carnauba wax mixtures, hetero- to homocharge transition, temp. depend. *(Japanese)* 78−35082
rosin and carnauba wax thermal electret, elec. charge studied by TSC 80−7286
rotational degrees of freedom affecting physical properties 79−69029
rotational isomeric state model, approx. anal. soln. 77−58214
rotational isomeric state model, monomer-monomer distrib. function 77−71897

polymers continued
rubber hydrochloride, meas. of shear modulus and damping in a torsion pendulum 79−4989
rubber-epoxy resins, heterogeneity analysis, light scatt. and statistical methods 78−2024
rubber-like networks, thermoelasticity, rel. to rubber elasticity theory 77−31219
rubber-like polymer, molecular relaxation process effect on strength *(German)* 78−31440
rubber-modified glassy polymers, thermal stresses 77−77567
rubber-resin mixtures, viscoelasticity 79−43303
rubber-toughened thermoplastics, behaviour, review of blends and composites 78−76626
rubbery state, correl. between strength and relaxation props. 77−28848
saturated hydrocarbon polymers, conform. stability, 1-electron levels, long-range effects calcs. 80−28123
scanning-transmission electron microscopy for polymer research 80−76460
scattering methods, conf., Prague, Czechoslovakia, (July 1976) 79−1764
secondary relaxation, TSC meas. 77−85643
self-avoiding walks on the hyper face-centred cubic lattice in four dimensions 79−17355
self-avoiding walks with span limitations, cubic lattice, mean square end-to-end distance 80−62568
self-consistent field approximation, BBGY and Kirkwood calcs. *(Russian)* 79−64981
self-diffusion detection, NMR matrix technique 80−15806
self-interacting chains, Legendre transformation 80−15018
self-replicating macromolecules, Monte Carlo computer models 78−46473
SEM specimen mounting epoxies, aerosols, and adhesive tapes 79−71580
semi-crystalline, diffusion mechanism and model, local conform. change 80−15288
semi-crystalline, dynamical mech. props., relaxation, amorphous phase *(French)* 77−72653
semiconducting biopolymers and their part in biochemical phenomena 80−12053
semiconductive conjugated polymers, synthesis and elec. props., review 80−15513
semiconductor, synthesis from Cu^{2+} chelate of PVA and iodine, optimum prep. conditions 79−91612
semicrystalline, model for thermal cond., orientation effects 77−85004
semicrystalline, mol. morphology 78−38631
semicrystalline, partially and fully deuterated, chain folding, ^1H NMR solid echo technique 80−20507
semicrystalline, small-angle neutron scatt. function computation 79−10811
semicrystalline, swelling by organic fluids 79−60255
semitransparent filled polymer coating, thermal radn. characts. 77−35731
shape measures, flexible mol. chain, review 78−17832
shear strength and friction 78−39913
shear-induced crystallisation, optical study 78−14289
shellac platina, elec. cond., temp. and thickness depends., mechanism 79−99645
shells, for laser fusion targets 78−8987
ship noise reduction using viscoelastic materials 78−22226
short fibre reinforced polymers, expressions governing stress-strain curves 78−80592
short polymer chains, end-to-end vector, distrib. function 80−87254
short range order, amorphous and liquid, ideal peak method calcs. 80−28900
short range order, radial distrib. functions from X-ray diffr. 77−76330
silane coupling agent deposited on E-glass fibre, hydrolysis and drying effect on siloxane bonds 80−85072
silicate, polymerised binary melts, activities and free energy of mixing 77−47596
silicone resin electret, thermally stimulated discharge meas. 79−87378
siloxane, temp. transitions, linear dilatometry and X-ray diffr. obs. *(Russian)* 80−59404
simple glass forming materials, universal nature of two relax. processes in region of glass transition 77−84907
simulation, by self-avoiding nonintersecting random chains, conc. effect 78−12639
simulation of Brownian motion of chains, chain dynamics 79−86099
simulation of Brownian motion of chains, local motions and chain conformations 79−86098
single crystal, mosaic model for electron diffr., bend distortion 80−44080
single polymer chain, renormalisation along chem. sequence 78−50669
single ring polymer, Lennard-Jones model, eqn. of state calcs. 78−5379
sliding wear test apparatus, design and statistical evaluation, polymeric restoratives evaluation 80−21237
small angle neutron scattering studies, deuteration effects 79−50956
small segment transformation with applications to hindered reaction in polythene 79−41256
small-angle scattering, of X-rays and neutrons, (fourth international conf., Gatlinburg, USA (Oct. 77)) 79−10745
sodium carboxymethylcellulose, N_2 bubble form. at single submerged orifice, model 79−32640
sodium polyethylene sulphonate, catalysis of $Co(NH_3)_5Br^{2+}$ alkaline hydrolysis, high pressure, effect 80−55657
sodium polyethylene sulphonate, catalysis of $Co(NH\%d3)_5Fr^{2+}$ aquation reactions, high pressure effect 80−55656
sodium polystyrene sulphonate, catalysis of $Co(NH\%d3)_5Fr^{2+}$ aquation reactions, high pressure effect 80−55656
soft, lossy, viscoelastic props. determ. from torsional vibr. of laminated bar 77−62218
soft polymer, isotropic, viscoelastic behaviour in moderately large deformation 77−54944
solar glazing hemispherical transmittance props. 79−52957
solar water heater appl., low-cost unit development *(Afrikaans)* 80−7925
solid, impact compression crushing at low temps. *(Japanese)* 78−7032
solid, mech. deform., model 79−20120
solid insulating materials, dielectric properties at cryogenic temps. 80−90867
solid polymer electrolyte H_2O electrolysis, appl. to H_2 prod. 80−61442
solid state nuclear track detectors, review 80−37696
solid-liquid state transitions, state before breakdown 78−63842
solidification, as dissipative process 80−65205
polymers continued
solidification front propagation, residual stress levels, polymerisation 80−59635
solidification of low level radioactive waste, Dow process 80−37502
solids, shock-induced electrical activity, mechanically induced bond scission model 80−50256
solute orientation in stretched polymer matrix, dichroism anal. 80−75998
solutes in stretched polymers, linear dichroism methods for analysis 80−63693
solvent-polymer system, liquid multi-phase separation 78−14468
space charge behaviour and luminescence at 77K 79−99947
spacecraft materials, electron and proton irrad. effects 80−70262
specific fracture surface energy, meas., review *(French)* 80−104275
specific heat, 223 to 383K 77−7871
specimen prep., vacuum dispersed carbon replicas, for fast electron wide-angle scatt. *(Russian)* 79−32923
specimen preparation, sections of min. thickness 5 μ, microtome based on MBR-1 microscope 77−71306
spectral sensitivity and photochem. stability using Xe high press. lamp *(German)* 80−61119
sphere radii moments, size distrib. 80−21329
spherulite, cryst. lattice strains, mech. behaviour, X-ray diffr. detect. 80−59558
spherulite primary nucleation kinetics determ. from truncation of spherulites 79−69031
spherulites, deformation mechanism, linear isothermal viscoelasticity theory 80−58924
spherulitic materials, light scatt. theory 77−23613
spin-lattice parameters, rotating frame, dipolar narrowed Carr-Purcell meas. 79−47347
spray coatings, struct. investig. by multiple-external-refl. method 78−6235
spray-on dopants, junction formation technique, cost effective, high throughput 80−94014
sputtering, choice of type of electrostatic sputter *(Russian)* 80−50553
square lattice, close packing of rectilinear polymers 80−48114
star-shaped molecules with branched nuclei, statistics 77−89383
statistical copolymers, normal vibrs., calc. method *(Russian)* 78−29871
statistical interpretation of temp. and stress shift factor 77−65999
steel, polymer coated, electrolyte permeation and elect. permittivity rel. to metal substrate corrosion 79−96175
steel, sheets bonded with low density polyethylene, static fatigue *(French)* 80−108522
steel-polymer wear mechanism during fretting corrosion 78−35522
stereochemical definitions, IUPAC nomenclature 80−23593
stereoregular polymers, electronic density of states, new algorithm 78−18939
stereoregularity distortions, local oscill. freqs., eqn. *(Russian)* 80−5653
sterically stabilised dispersions, critical flocculation temperature, effect of dipolar substituent groups 78−61061
stiff, optimised Rouse-Zimm theory 78−46472
stimulated resonance between electrical and shear fields by a colloid system 79−1971
stochastic model, Edwards' model 80−68140
strain crystallised, electron microscope obs. of molecular struct. 78−26450
strain measurement, between −60 and +50°C 78−19974
streamer breakdown in divergent field 80−25308
strength, activation energy eval. from temp.-rate depend. 77−86103
stress analysis of circular craze, extension of linear membrane model 78−75081
stress birefringent materials, transition temp. and assoc. mechanical props. determ., simple test method 78−56454
stress distribution after action of rough surface indenter 79−52471
stress meas., X-ray diffr. technique 78−5713
stress relaxation, pre-exponential factor 79−18748
stress relaxation time spectrum, construction of single spectrum for polymers 78−44160
stress wave propagation, nonlinear, in perfectly flexible string 78−5670
stress-relaxation apparatus, stress and vibration relaxation in sound frequency range 77−1905
stressed, config. free energy change due to partial crystn. of chains, distrib. of cryst. orientations 79−94923
structural characterisation, small-angle neutron, X-ray and light scattering, recent developments 79−10751
structurally inhomogeneous, light scatt. by strains, theory and expt. 80−28162
structure and mech. props., book 78−83756
structure and molecular dynamics, neutron scatt. meas. 79−51009
structure and optical behaviour 80−106583
structure classification, according to rel. between chain symmetry and space group *(French)* 79−51058
structure determination from elastoosmometric parameters 80−64923
structure regularity, description and design 80−23591
stycast 1266 epoxy, thermal contraction, 4-300K 80−4724
stycast 2850FT, low temp. thermal cond. 79−23790
styrene, effect of redox initiation in emulsion polymerisation *(German)* 78−85158
styrene, thermal polymerization, Rayleigh-Brillouin light scatt. study 78−53206
styrene acronitrile copolymer, glass transition temp. determ. by elec. meas. 78−47506
styrene alpha methylstyrene copolymer, microcrack development under atmospheric ageing 77−86210
styrene crosslinked polyester networks, low temp. γ' relaxation 78−44156
styrene crosslinked polyester networks, low temp. γ relaxation, water and chem. struct. effects 78−44157
styrene polymers, elastomer toughening, grafting techniques 78−35347
styrene vinyltoluene, latex, doublet particles, response of Knollenberg light scatt. counters 80−37152
styrene-α-methylstyrene copolymers, prep., charact. by pyrolysis gas chromatography *(German)* 79−29355
styrene-acrylic copolymer, wideband optical transmission meas. 79−76771
styrene-acrylonitrile copolymer, amorphous, rubbery state, nonequil. tensile deform., effects of temp. and strain 80−40442
styrene-acrylonitrile copolymer, crazing and brittle fracture on flat die indentation 80−60970
styrene-acrylonitrile copolymer, synthesis and props. for optical use 78−90466

polymers continued
styrene-acrylonitrile copolymer swelling, glass transition and crazing, polar group incorporation 78−85017
styrene-butadiene block polymers, multiphase systems, struct., props. 77−31600
styrene-butadiene copolymer, birefringence and stress relaxation 78−44158
styrene-butadiene copolymer, pyrolysis, determ. of kinetic parameters *(German)* 78−85155
styrene-butadiene copolymers, chem. composition determ. by gel permeation chromatography 79−70410
styrene-butadiene copolymers, elec. strength meas. 78−15096
styrene-butadiene copolymers, struct. study by pyrolytic capillary gas chromatography *(German)* 78−18557
styrene-butadiene-styrene triblock copolymer, US relax. 77−89502
styrene-butadiene-styrene triblock copolymers, dielec. props. 78−95545
styrene-butyl vinylpyridinium-TCNQ copolymer, dielectric const. *(Japanese)* 78−60375
styrene-diene block copolymers, pressure sensitive adhesives, morphology and viscoelastic behaviour 77−52419
styrene-diene triblock copolymer, hexagonal struct., flow props. of melt and fracture 78−76729
styrene-divinylbenzene copolymers, porosity variation and swelling 80−97493
styrene-divinylbenzene grafted copolymer, structure investigation by IR spectroscopy *(Russian)* 77−62487
styrene-isoprene triblock copolymer, mol. relax. in glassy state 80−53177
styrene-methacrylic acid copolymer, glass-like, intermol. interactions temp. depend., IR spectra *(Russian)* 79−51967
styrene-methacrylic acid copolymer, glassy, intermol. interaction during inelastic deform., optical spectra obs. 77−59878
styrene-methacrylic acid copolymer, intermol. interaction, conform., composition depend. *(Russian)* 79−23539
styrene-methacrylic acid copolymer, ionomer radiothermoluminesc. 79−95856
styrene-method methacrylate copolymer glassy soln., excimer form., energy migration, fluoresc. depolarisation meas. 78−70986
styrene-phenylacetylene copolymer, fluoresc. emission, energy redistrib. 78−39580
styrene-sodium methacrylate (9 mol.%) copolymer cond. relax. 78−38874
styrene-sodium methacrylate copolymers, linear expansion coeffs., ionic groups conc. depend 79−42284
styrene-sodium methacrylate copolymers, Raman spectra, ion clustering 80−71416
styrene/MMA copolymers, struct. and rheology 80−1444
styrene/n-butyl-2-vinylpyridinium-TCNQ copolymer, dielec. permittivity *(Japanese)* 78−56416
styrene/p-chlorostyrene copolymer electret, thermally stimulated discharge 77−4595
Styrofoam spheres, diameter determ., mol. monolayer experiment, teaching appl. 79−44678
styrol batadiene polymers, light scattering and Curie point pyrolysis, pyrolysis gas chromatography *(German)* 79−96393
p-substituted polystyrene, shake-up phenomena, ESCA studies 77−54638
substrate with metal film, adhesion determ., US test device 79−91865
substrates, amorphous Se vac. deposited, with dynamic coating device 80−100792
substrates, for a active anthraquinone dyes, phototropic transformations *(Russian)* 77−66762
4-sulphone diglycidyl ether, on Al alloy D16T alloy base, dynamic shear modulus determ., −80 to −180°C 78−60916
superconducting magnet epoxy fracture after low-temp. irradiation 79−34147
surface, flame propagation velocity rel. to thermal props. *(Russian)* 80−7797
surface, plasma treatment in O, ESCA and XPS obs. 78−72910
surface, struct., bonding and reactivity, ESCA meas. 79−52073
surface, supramol. struct. characterisation, use of C X-radiation 80−79705
surface and bulk electrical resistance, screened meas. cell 79−49251
surface charact., combined ion scattering spectrocopy, SIMS, SEM, energy dispersive X-ray techniques 79−43702
surface component of vacuum absorpt. and resorpt. currents, origin and magnitude 80−70791
surface component of vacuum absorpt. and resorpt. currents, surface charge accumulation 80−60063
surface electric charge, effect on interaction with liq. medium 79−56036
surface free energy determination *(Polish)* 80−84362
surface free energy estimation for amorphous material 77−55438
surface heating during vacuum metal deposition 78−48319
surface modification by RF plasma, difference ESCA spectra 77−63529
surface oxidation, LCAO-SCF calc. of core binding energies of O-containing organic mols. 79−76344
surface polarisation from sessile drop contact angle meas. 77−85365
surface properties, review 78−34886
surface topography, high-resolution polymer replication 78−10264
surface-attached molecule dynamics, bead and spring model 78−75931
surfaces, appl. of ESCA to struct. and bonding 79−57344
swollen semirigid polymer, short-range orientational order *(Russian)* 77−84662
symmetry adapted bases and selection rules for polymer mol. 79−55010
symmetry properties, classification using line groups 77−51327
symposium, Amherst, Mass., USA (May 1977) 79−69018
synthetic, dil. solns., NMR relax., review 79−89693
synthetic, electron beam damage in electron microscope exam. 78−34409
synthetic, radiative degradation, chem., phys., environmental, technological effects, review 80−40948
synthetic polymer chemistry, developments 80−63875
sytrene-tetrahydrofuran block copolymer, H_2O contact angle and surface struct. *(Japanese)* 78−79861
TCDU, polydiacetylene cryst., elec. struct. change, stress induced 78−70990
TCNQ, elastomeric complexes, doped with pure TCNQ, elec. conductivity 78−84220
TCNQ complex salt of polymer, carrier species determ. using galvanic cell 77−69384
TCNQ polycation salts, elec. cond. and chemical stability 79−83456
teflon, γ-irrad., low dose, positron lifetime obs. 78−76550
Teflon, aluminised, spacecraft, surface material performance modelling 78−4061
polymers continued
Teflon, creep in shear, hydrostatic pressure effect 79−57065
Teflon, creep under flat cyclic stress 78−23800
Teflon, diagnostic neutron spectra from deuterons 2.5, 3.0, 3.5 MeV 79−40933
teflon, elec. resist., meas. technique *(French)* 78−77929
Teflon, F content, determ. by instrumental neutron activation anal. 78−7262
Teflon, flashover behaviour at low temps. 80−25882
Teflon, gamma irradiated, free four-term analysis of positron lifetime spectra 80−76101
teflon, microslip, effect of friction 77−77588
Teflon, non-destructive charge release 80−24946
Teflon, nontransparent dielectric, laser emission reflection and destructive action *(Russian)* 79−74031
Teflon, optical, elec. props., struct., ion textured surface 78−72904
Teflon, powder pellets for near-IR spectra 78−3401
Teflon, seeding technique for laser velocimetry in untreated air shock 77−84348
teflon, sliding behaviour against Cu or Al spheres at cryogenic temps. 80−66671
Teflon, surface modification, contact angle meas. 77−51574
Teflon, viscoelastic behaviour prediction of low temp., creep curves exam. 79−20141
teflon covered Ge(Li) diodes for fast neutron detection 78−25384
Teflon FEP, discharge area scaling and surface/subsurface damage due to electron beam irrad. 80−34853
Teflon FEP, ethylene glycol, decane drops, effect of drop size on contact angle 80−2245
Teflon FEP, N implanted, TSC spectra 80−88912
Teflon FEP, negative streamer development, computational model for electron irrad. dielec. 80−34852
Teflon spheres-nigrosin black dye-water dispersion, turbid laser backscatt. 80−1129
Teflon superleaktight gasket seals for use at low temps. 78−16806
Teflon thick-walled vials in liq. scintillation counting of ^{14}C 78−857
Teflon vials in Cherenkov counting 78−858
Teflon-4, gamma irrad., wear resistance and antifriction props. 80−7691
Teflon-4, utilisation factor determ. during electron beam sputtering *(Russian)* 79−66008
telechelic, chain extension, qualitative aspects 80−95752
telechelic polybutadiene-methacrylate acid copolymers, X-ray study *(French)* 78−18553
temperature shear function and temp.-time analogy in linear thermoviscoelasticity region 79−18747
tensile strength and butt joint strength, rel. to cohesive energy density, surface tension 77−55431
tensile testing, in situ EPR apparatus 78−85086
terephthalate copolyester, heat treatment effect on melting point *(Japanese)* 80−40400
ternary polymer systems, diffusion controlled formation of porous structures 80−7539
test apparatus for chem. resist. and penetrability in corrosive medium under hydrostatic pressure 79−39065
testing, modern analytical methods appl. *(Polish)* 78−85253
testing, photoresistor dilatometer design, with high stability and sensitivity 80−81251
tetrafluorethylene-ethylene copolymer, determ. of microstruct. by secondary emission mass spectrometry *(Russian)* 77−31604
tetrafluoroethylene hexafluoropropylene copolymer, surface component of vacuum absorpt. and resorpt. currents, origin and magnitude 80−70791
tetrafluoroethylene-vinylidene fluoride mixture, in epoxide-diphenylene propane resin, exam. of temp. depend. of stress relaxation, viscoelasticity 80−11688
tetraglycidyl 4,4′ diaminodiphenyl methane, diaminodiphenyl sulphone cured, failure and tensile mech. props., moisture effect 80−50735
tetraglycidyl 4,4′ diaminodiphenyl methane epoxy, diaminodiphenyl sulphone cured, struct., deform. mode, failure 79−29141
tetrahydrofran-propylene oxide copolymer, surface tension, composition and temp. depend. *(Japanese)* 78−79860
tetrahydrofuran-propylene oxide copolymers, prep., ^{13}C NMR, end group anal. 79−66293
tetramethyl-p-silphenylene siloxane/dimethyl siloxane, block copolymer, morphology and mech. behaviour 78−84885
tetramethyl-p-silphenylenesiloxane-dimethyl siloxane copolymers, degree of crystallinity 78−26453
Textolite, mech. props. in elastic symmetry planes 77−21211
thermal anal. methods, appls. 78−68845
thermal conductivity, 2-100K, crystallinity effect 77−20137
thermal conductivity, temp. crystallinity and orientation depends., review 78−10234
thermal conductivity as function of temp. 77−89603
thermal conductivity data, need and demand 77−72725
thermal conductivity-pressure relationship *(German)* 77−20139
thermal diffusivity, Fourier theory 80−31456
thermal expansion coefficient, determ. using optical dilatometer 80−45454
thermal inspection by one side method 79−52604
thermal sampling technique for thermally stimulated discharge meas. 78−10831
thermally stimulated creep 78−11245
thermally stimulated discharge, thermal sampling technique 77−85645
thermodynamics and relaxation, memory and equilib. theory 78−76903
thermoluminescence, rel. to mol. relax. 78−11003
thermoluminescence data numerical anal., glass-rubber transition temp. spread 77−52189
thermomechanical and linear, dilatometric testing, automatic recording device 80−11858
thermomechanical curves, automatic unit for recording 77−25217
thermomechanical effect in viscoelasticity with bodies under nonisothermal strain 79−86355
thermomechanics in transition and rubber regions 78−59354
thermoplastic, deform. at low cycle loading 77−70122
thermoplastic elastomers, crosslinked by secondary valence interactions, elasticity and processing, crosslinking behaviour 80−40320
thermoplastic enamel lacquer, far IR transmission, encapsulation of optical devices 79−55194
thermoplastic polymers, dynamic mechanical analysis appl. to materials testing 79−15911
thermoplastic rubber, plastics-rubber industries interface 77−55937

polymers continued
thermoplastics, glassy, embrittlement mech. and inelastic deform. criterion for delayed failure 78−52940
thermoplastics as engineering materials 78−27581
thermoreactive, elasticity modulus, change on curing *(Russian)* 79−64521
thermoset and coating technology, torsional braid and thermal anal. 80−55622
thermosetting, sp. ht. obs. *(German)* 78−75845
thermosetting, viscoelasticity, linear hereditary theory appl. *(Bulgarian)* 79−86357
thermosetting materials, formation and props., phase diagram and torsion pendulum anal. 80−55381
thermosetting polymers, dynamic mechanical analysis appl. to materials testing 79−15911
thermosetting resin, estimation of diff. co-eff. distrib. and mol. wt. distrib. by computer *(Japanese)* 77−66042
thermostable oriented polymers, load effect on relax. transitions *(Russian)* 79−52294
thermotropic liquid crystals, mesogenic elements and flexible spaces in main chain 79−60269
thermotropic polymers, cholesteric with mesogenic moieties and flexible spacers in main chain, synthesis and light reflection 80−88028
thickness depend. of G_c for shear lip propag. from single crack propag. 78−11305
thin film, micrometeroid penetration expts. performed in laboratory 80−77292
thin film, tensile testing multiposition unit, for testing in vacuo and gaseous media 78−11478
thin-wall tubes, rupture time determ. 80−64473
thiourea formaldehyde polymer, pyroelectricity and dielec. props. 79−91379
three-dimensional cubic lattice, random walk of particle, polymer chain config. approach 80−22294
thremosetting resin quality control by dynamic mechanical analysis 79−74319
tie chain content of oriented partially crystalline polymer *(Russian)* 77−47358
tissue-equivalent plastic, A-150, thermal diffusivity, sp. ht., thermal cond. obs. 80−34258
toluene sulphonate diacetylene, strain dependence of dominant electronic excitation 78−80373
toluene sulphonate diacetylene polymer, electronic and vibr. excitations, press. and temp. depend. 78−31188
toluene sulphonate diacetylene polymer, vibr. modes, strain depend. using Raman spectra 80−20626
toluene-sulphonate-diacetylene, thermal polymerisation, near IR absorpt. and low lying states obs. 80−71399
topological entanglements, gauge description 80−99593
topomorphism of polymer crysts. 77−43159
torsion pendulum dynamic mechanical testing, review 80−55620
torsional braid analysis, conference, Anaheim, CA, USA, March 1978 80−51952
torsional shear testing using electromech. high-press. apparatus 77−51005
total integrated light scatt. intensity 80−45092
trans-polyacetylene, intrinsic, electron-phonon coupling 80−79901
transducer, viscoelastic, in-situ, Duomorph, appl. to polymeric materials 79−30463
transfer film form. mech. in wear 78−64729
transformation reactions, kinetics, statistics and mechanisms 79−43584
transient current nature 78−80278
transitions, domain size effects 79−69232
transparent, absorbing defect role in laser damage 80−108308
transparent, form. of linearly extended destruction zone by pulsed laser radiation 77−69942
transparent, high-temp. zone form. in laser induced mech. breakdown 77−56086
transparent, laser-induced optical breakdown, chem. reactions effects *(Russian)* 78−35676
transparent polymers for electronics *(German)* 77−62021
transparent polymers with various atomic composition and viscoelastic props., laser damage 80−104017
treeing and elec. breakdown, tutorial 78−84524
treeing in solid extruded electrical insulation, bibliography 77−24788
treeing resistance assessment 80−15971
triacetate-nitrocellulose, long period struct., 180-265°C, X-ray diffr. obs. *(Russian)* 79−24556
triblock copolymers, lamellar domain dimensions, prediction 77−39547
tribopolymerized solid lubricating coatings, formation and behaviour 78−35528
triethylamylose-solvent complexes, conform. and packing analysis 78−75654
trifluoroethyl methacrylate vinyl chlorobenzoate copolymer light focusing rod, photocopolymerisation temp. effect *(Japanese)* 79−46043
trinitrofluorenone, amorphous, hopping transport, reinterpretation of mobility meas. 79−42563
1,3,5-trioxane-1, 3-dioxolane copolymer, semicryst. random, characterisation by small angle neutron and X-ray scatt. 80−75189
Trogamid, wideband optical transmission meas. 79−76771
TSC, generation mechanism and charact. *(Japanese)* 80−60488
TSC, trap modulated electron and hole mobilities 78−10441
tube, stepwise heat treatment *(Russian)* 77−25082
tubes, liquid filled Al and PMMA longitudinal wave experiments, laminar flow 79−64604
two-dimensional model of polymer with an excluded volume *(Russian)* 78−42926
two-phase polymer morphology, electron microscopy methods for study and specimen prop. 78−75580
ultrahigh modulus prod. 77−52277
uniaxial, fluoresc. polarisation, orientation and mol. dynamics effects 78−76516
unperturbed dimensions of branched cahin, star and ring polymers 78−66701
urea phenolic resins, long term thermal stability *(German)* 79−91943
urea-formaldehyde charcoal, adsorpt. isotherms of organic vapours 80−96731
urea-formaldehyde resin, carbonised, water vapour adsorption porosity, and surface chem. 79−52753
urea-formaldehyde resins, ^{13}C Fourier transform NMR of chem. struct. 79−42849
polymers continued
urea-formaldehyde resins, appl. for radioactive waste solidification, technical evaluation 79−67875
urea-formaldehyde resins, book 80−73114
urethane elastomer, temp. strain relaxation investigation by opticomechanical method and IR spectroscopy 77−4805
urethane foams for noise abatement, physical and acoustical props. 79−18592
urethane prosthetic compound, dynamic mode determ. 79−48376
US testing, using fast longitudinal and shear wave techniques 80−50793
US velocity and damping coeff. meas. of polymers *(French)* 80−7723
UV curable, lamps for curing 78−88443
UV photoconduction expts. and electronic props. 80−15572
varnish resin based on diacid prepared from 4,4'-oxydibenzoic aldehyde and dihydroxymethyl propionic acid *(Polish)* 77−28776
VC-EVAC graft copolymer, mech. props., effect of heat treatment *(German)* 77−63702
Vespel SP-22 resin, thermal contraction, 4-300K 80−4724
vibrational anharmonicity, intensities of overtones and component freqs. 77−69052
vibrational spectra of chain, Green's function anal., Fourier method for perfect infinite chain 78−18725
vibrational spectra of chain, Green's function anal. 78−18724
vibrational thinning, viscoelasticity and strength 77−8795
vinyl, with flexible side chains, configurational statistics, dipole moments 77−38760
vinyl acetate, monomer and polymer, Raman and IR spectra, liq. and solid 78−58700
vinyl and related polymers, diffusion of simple penetrants, statistical mechanical model 80−10705
vinyl aromatic polymer series, dielec. relaxs. at 220°C, −50°C and ~120°C interpret. 77−43929
vinyl copolymers, containing fluorescent groups, optically active 80−102594
vinyl ester adhesive/Al lap shear specimens, electron beam curing 79−20337
vinyl fluoride based polymer stabilisers, thermal degradation, post UV-irrad. mech. strength *(Russian)* 79−24778
vinyl methacrylates, anionic polymerisation and radical reactivity *(Japanese)* 78−61007
vinyl polymer mixed monolayer behaviour 77−85020
vinyl polymers, precip. from solns., temp. determ. *(German)* 80−85208
vinyl polymers quenched with electron donor (acceptor) in soln., ionic photodissoc. 79−11800
vinylbenzyl gluconate acrylonitrile copolymer membrane for heavy metal ions separation 79−74418
N-vinylcarbazole containing polymers, cryst. violet doped, for single layer photothermoplastic devices, photo and dark cond. 77−69374
N-vinylcarbazole containing polymers, sensitization to Ar laser for single laser photothermoplastic devices 80−83651
N-vinylcarbazole-1-vinylnaphthalene copolymer, triplet-triplet annihilation carrier photocurrent, delay fluoresc. 78−2513
vinylidene chloride copolymer, stretched, free radical form., meas. using indirect scavenger method 79−61923
vinylidene fluoride copolymer electret, charge and polarisation distribs. meas. 78−35081
vinylidene fluoride trifluoroethylene copolymer, ferroelec. behaviour 80−50284
vinylidene fluoride-trifluorochloroethylene copolymers, ^{19}F NMR *(Russian)* 80−7181
vinylidenechloride-acrylonitrile copolymer, amorphous, pyroelectricity due to space charge mechanism 79−87400
2-vinylnaphthalene-methyl methacrylate copolymer glassy soln., excimer form., energy migration, fluoresc. depolarisation meas. 78−70986
4-vinylpyridine acrylonitrile copolymer membrane, reverse osmosis charact. *(Japanese)* 78−31694
N-vinylpyrrolidone-methyl methacrylate copolymer water swollen membrane, permeability *(Japanese)* 78−31704
viscoelastic, fatigue, fractographic study 80−30101
viscoelastic, fatigue crack growth charact. 80−30100
viscoelastic, microrelax. model for moment effects interpret. 79−20098
viscoelastic chain, local relax. props. anisotropy, internal friction influence *(Russian)* 78−37780
viscoelastic droplet break-up, in nonuniform shear flow 80−64588
viscoelastic ductile, delayed yielding of plane stress viscoelastic Dugdale model 78−27569
viscoelastic material, complex dynamic moduli and loss angles 77−68451
viscoelastic prop. determ. with VR-72 vibrorheometer 77−70259
viscoelastic prop. meas., method in fluid and highly elastic states using forced vibrations 77−70258
viscoelastic properties dynamic evaluation for use in cardiac prosthetics 78−40405
viscoelastic-plastic, birefr. relation 77−31266
viscoelasticity, calc. using relaxation and retardation spectra *(German)* 78−92290
viscoelasticity, longit. oscills. of polymer rod *(Russian)* 77−19546
viscoelasticity, temp. depend. under dynamic conditions, linear theory of thermoviscoelasticity 79−61642
viscoelasticity and strength characterisation, advanced light scatt. techniques 80−11857
viscoelasticity theory, unimolecular approx., linear polymers 79−50613
viscofluid, extensional vibrorheometer 77−70257
viscose, long period struct., 180-265°C, X-ray diffr. obs. *(Russian)* 79−24556
Viton B, vinylidene fluoride-hexafluoropropylene copolymer, press. effects on mech. props. 77−32618
vitreous, quasibrittle fracture 80−21094
volatile constituents anal. by thermal desorpt., gas chromatography and mass spectrometry 79−43664
volume compressibility of polymer materials, meas. equipment 77−77674
volume dilatometer design 78−5706
volume stress/strain state, new testing apparatus 78−23896
vulcanisation, critical percolation exponents 79−61557
water absorption, osmotic effects 80−65366
water-soluble, use for quenching of Al alloys 79−38862
wear in thermally stressed state 80−3202
wear limit, γ-irradiated and unirradiated *(Japanese)* 78−27649
wear mechanisms, review of polymer-polymer and metal-polymer sliding 79−70174
wear testing of bearing material, new sliding bearing test facility 78−95862

polymers continued
wear testing of polymers for artificial joints 78−31981
wet resin, glass transition model 77−84901
wetting and discharge inception in atmosphere of fog *(Japanese)* 79−4201
wood-PMMA composites, temp. depend. of viscoelastic behaviour *(Japanese)* 77−77541
X-ray diffraction, high press., calibration of diamond anvil cell, 0-15 kbar 77−41635
X-ray diffraction, high press., high temp. variation in diamond anvil cell 77−74418
X-ray scattering, expt. separation of coherent component prior to RDF anal. 80−64838
yield stress and elastic modulus power law relationship 79−47752
yield stress estimation at high strain rate using Taylor's impact technique 79−64605
yield stress estimation from relaxation data 78−64594
zigzag chain, second order Raman scatt., theory, appl. to polyethylene 78−72504
Al epoxy bonded joint, determ. and appl. of COD 80−30078
Al/polyethylene/Al sandwich construction, flexural fatigue props. *(Japanese)* 78−56751
Al-epoxy adhesive joints, cohesive-interfacial mixed-mode fracture 79−39110
Al-PMMA laminated composites, shock wave propag., flash radiographi obs. 79−4370
Al-polyacrylonitrile-Al films, current-voltage characteristics 80−11125
Al-polymer joint, meas. of temp. dependence of joint strength 80−50824
Al_2O_3-epoxy mechanical mixtures, stress-wave propag. model, dynamic response expts. 79−1477
Al_2O_3-polymethylsiloxane composite, thermoreactive compaction 80−20879
B fibre reinforced epoxy, dynamic Young's modulus and internal friction 80−25754
B-epoxy-Al sandwich laminate. influence of residual stresses on tensile strength 78−60703
$(BH_2)_n$, energy band structure 80−5478
$(BeH_2)_n$, energy band structure 80−5478
C black-graft polymers crosslinked with epoxy resin, electrical props. *(Japanese)* 80−24920
C fibre reinforced polymer, strength props., fibre surface treatment effects 78−27636
C polymeric chains, reduced from poly(tetrafluoroethylene), reactivity 80−89488
C-PVC composite, fluctuation induced tunnelling conduction 78−52044
$(CD)_x$, polymer, heavily doped, IR spectra, vibronic intensity enhancement 80−28124
$(CH)_x$, polymer, heavily doped, IR spectra, vibronic intensity enhancement 80−28124
C_3O_2 polymer, as source of UV absorpt. in Venus clouds 78−20665
C_3O_2 polymer, preparation, spectra rel. to polymerisation temp. electron spin resonance 77−32239
C_3O_2 polymers in primitive atmosphere rel. to living systems genetic code 79−83690
^{13}C NMR in copolymers, monomer unit distrib. *(Russian)* 77−46664
CrFeCN epoxy resin-based membrane studies, Ag sensitive electrode 80−16726
Fe-Cr (13 wt.%)+polycarbosilane, powder metallurgy, characts. 77−85962
H+HR→H_2+R, (HR=hydrocarbon), tunnelling reaction, classical S-matrix calc. 77−29007
LiH chains, long-range Coulombic contribution to direct space LCAO CO matrix elements 78−37774
PMMA, polymer chain, internal friction range, HF viscosity theory *(French)* 80−79968
PVF_2 polymer probe for mapping pressure field from arrays 80−74669
PVF_2 thin film SAW tranducers for 8 MHz delay line 80−58876
PZT-polymer flexible composite transducer 78−80291
polyoxymethylene, linear, plastic deform. behaviour 78−84910
$(SN)_x$, different orbitals for different spins 79−69392
$(SN)_x$, vapour phase species, mass spectra 77−61873
Se, amorphous, vac. deposition on polymer substrates, use of temp. gradient vac. coating device 80−35099
Se-Ni-Mylar multilayered struct., interfacial bonding effect on adhesion, ESCA obs. 79−95274
Ti corrosion, by hot perfluoropolyether type Krytox MLO-71-6 80−93684
TiO_2 composite, dielec. props. *(Japanese)* 78−95540
TiO_2-polycarbonate laminate, impulse surface flashover in vacuum, effect of normal elec. stress 79−4199
U nuclear fuel particle prep. by ion exchange resin loading *(German)* 78−82499

polymorphic transformations
see also displacive transformations; order-disorder transformations
2-chloronaphthalene, vibr. and calorimetric investigation of polymorphism 78−87641
2-fluoronaphthalene, vibr. and calorimetric investigation of polymorphism 78−87641
alkali halides, theoretical considerations of sudden transforms. 78−51666
alkali hydrides, structural transition from NaCl to CsCl type under high press. 80−96458
alkali metals, pressure influence on absolute zero isotherms, polymorphic transform., phonon spectra *(Russian)* 80−49363
alkali perchlorates, elec. transport during struct. transforms. 78−59971
alkaline earth feldspars, homogeneous and heterogeneous polymorphic transformations 79−15659
p-alkoxybenzylidene-p-n-alkylanilines, thermotropic mesophases, proton spin-lattice relax. 78−91968
alkylammonium cadmium tetrachloride, struct. phase transition, PMR, spin-lattice relax. time 77−35688
alkylene diammonium cadmium tetrachloride, struct. phase transition, PMR, spin-lattice relax. time 77−35688
alloy, role of phase boundaries in phase transformations 78−72772
alloy steel, martensite structural singularities during tempering, electron diffr. study *(Russian)* 79−100177
alloy steels N30 and N29T, press. effect on reverse martensitic transform. and mech. props. *(Russian)* 79−38824
alloys thermal expansion coefficient, and volume effect anomalies during transformations, review of differential dilatometric error sources *(Russian)* 79−34223

polymorphic transformations continued
Alnico alloy, Ç addition effects on struct. and mag. props. 78−23835
alumina, role of $\alpha \rightarrow \gamma$ polymorphic transform. in hot pressing 77−63612
anthracene, polymorphic forms, generation by repeated slip 78−34457
aragonite, polymorphic transition kinetics, differential thermal anal. meas. 79−14722
austenite, lattice stability loss near $\gamma \rightarrow \alpha$ and $\gamma \rightleftarrows \varepsilon$ transitions *(Russian)* 79−61584
barium oxalate, lacunary phase form., morphological and kinetic characts. 79−60299
BBOA, polymorphism, radiothermoluminescence and differential scanning calorimetric study 80−24570
Bi, polymorphic transition up to 30 kbar, neutron diffr. investigation 79−14723
brass, α-β phase transformation caused by friction 80−76378
brass, calorimetric investigation of thermodynamic props. 79−52172
brass, two-phase α/β bicrystal, diffusion induced twins in α-phase 79−46967
brass, two-phase α/β bicrystal, morphology and crystallographic relationships between phases 79−46966
t-butyl chloride-d_0 and -d_9, polymorphism, Raman spectra 80−20617
caesium propanoate, solid state transitions and melting process, diffr. and conductometric meas. 80−10670
carbon tetrachloride, dual melting curves and metastability 80−92647
carbon tetrachloride, in porous medium, allotropic and liq.-solid-solid transformations *(French)* 78−83944
carbon tetrachloride, polymorphism, solid-solid phase transformations 77−62499
carbonate branches, in system of polymorphic transitions of ABX_3 compound struct. types 79−90591
chloritoid, topotactical transformation, X-ray diffr. and TEM study 79−51057
2-chloronaphthalene, elastic props. exam. by Brillouin scatt., rel. to polymorphism 79−77669
cholesterol crystal, polymorphic transition 77−1229
cholesteryl acetate, phase transitions and solid polymorphs 78−2255
choline bromide, radiation sensitivity, cryst. struct. depend., calorimetric investig. 78−88647
choline chloride, radiation sensitivity, cryst. struct. depend., calorimetric investig. 78−88647
choline iodide, radiation sensitivity, cryst. struct. depend., calorimetric investig. 78−88647
coke, pressure effects on structure, polymorphic transitions X-ray diffr. anal. 79−1859
copper phthalocyanine, chlorinated, stacking disorder 78−34622
copper phthalocyanine α-β phase transform., heat of transform., DTA investig. *(German)* 78−30754
critical isomorphic $\gamma \rightleftarrows \alpha$ transition, phase equilibrium curve *(Russian)* 80−55397
crystal growth by solid state techniques review 77−85935
cubic-tetragonal transitions, symmetry anal. of deformable cryst. 80−10636
deformable solids, fracture and hardening kinetics 80−35210
detonation in thermodynamic system with first order phase-transformation 79−42147
dialkylammonium copper chlorides, mag. and struct. transitions, IR absorption 77−52097
diamond to graphite, enthalpy at 1320K, from enthalpy of soln. expts. 78−59945
diamond-type structures, second kind phase changes, table of space groups *(Russian)* 78−63692
p-dichlorobenzene, mol. dynamics, allotropy, solid-state phase transitions effects, Raman spectra *(French)* 77−42372
p-dichlorobenzene, Raman spectra, P-T diagram for α, β and γ-phases 78−68515
diethylammonium cadmium chloride, X-ray study of structural phase transition 78−2055
p-diiodobenzene, phase transition obs. using interferometry 78−34616
p-diiodobenzene, polymorphic phase transformation 79−46591
p-diiodobenzene, polymorphic transition hysteresis, optical path difference expt. 79−99312
dimethylammonium manganese chloride, neutron diffr., 188K, cryst. struct. 77−47434
dimethylammonium manganese chloride, neutron diffr., 404K, cryst. struct. 77−47435
dimethylammonium manganese tetrachloride, elastic props. 79−60418
1,8-dinitronaphthalene, orthorhombic struct. determ., 22 and 97°C, rel. to phase transition mechanism 78−6048
2,2-dinitropropane-d_0(-d_6), phase polymorphism, vibrational assignments, IR and Raman study 80−16031
1,2-dipalmitoylglyceride, DTA and X-ray diffr., polymorphism *(French)* 78−43008
disordered crystals, 2H to 6H solid state transformation, deformation mechanism, X-ray diffraction study 80−33921
disordered crystals, 2H to 6H solid state transformation, layer displacement, X-ray diffraction study 80−33920
DTA apparatus for use in martensitic transform. studies at low temp. 79−49237
Earth mantle viscosity-depth profile, polymorphic phase transition effects 78−48998
EBBA, polymorphism, radiothermoluminescence and differential scanning calorimetric study 80−24570
elemental polymorphic phase diagrams, as function of pressure exam. 79−8289
FCC to HCP transform., model and expt. evidence 77−44243
ferromagnet, nonlinear magnetoelastic effects and phase transforms. *(Russian)* 78−48015
films, polymorphic transforms. and phys. props. 77−43450
graphite, pressure effects on structure, polymorphic transitions, X-ray diffr. anal. 79−1859
graphite, shock compression, polymorphic transform. kinetics 79−86838
graphite-diamond equilibrium, thermodynamic stability 79−65184
hexachloroethane, phase II-III polymorphic transformation kinetics 79−42240
hexachloroethane, phase II-phase III polymorphic transformation rate 79−23728
hexamethylbenzene, mol. dynamics, allotropy, solid-state phase transitions effects, Raman spectra *(French)* 77−42372
highly dispersed systems, phase size effect 80−6488
ice VI, polymorphic transition at high-press., 123.1K, HF permittivity study 79−55883

polymorphic transformations continued
ice VI, shock compression expts. for Hugoniot function 80−84248
ice VII-ice VIII phase transition, second-order, Haus-Tanaka model 80−70385
interface kinetics 77−69084
ionic cryst., polymorphic transition due to disordering 79−14724
kinetics 79−73306
kinetics model, computer modelling *(Russian)* 80−97478
liquid crystalline compounds polymorphic props., impurity effects 79−10930
lonsdalite→graphite phase transform. mechanism, electron diffr. expts. 79−28099
martensite formation, and lattice props. rel. to elastic constants 80−50630
MBBA, solid phase polymorphism and phase transforms., IR spectra obs. 79−8128
mechanical hysteresis in polymorphic transition region 80−79942
mechanochemical reactions, phase transformation and synthesis, review 80−3024
metal, allotropic transform., anharmonicity, effects due to thermal expansion and Gruneisen parameters 79−52207
metal, atomic heat capacity change during polymorphic transformations 79−29055
metal, electrical resistivity changes during polymorphic transform. A1 to A2 and A3 to A2 77−48430
metal, HCP to BCC phase transition and melting 78−14463
metal-H, phase transitions 80−50631
metal-insulator transition, chemical mechanism, thermodynamics, vacancies 80−103626
metallic thin films, optical props., effect of quench condensation 79−78773
metals, close packed, relationship between cohesive energy, and allotropic transformation temp., exam. 78−52802
methane-d_4, solid, lattice parameters and thermal expansion for different phases 78−51526
methylchloroform, polymorphism, solid-solid phase transformations 77−62499
molecular dynamics, allotropy, solid-state phase transitions effects, Raman spectra *(French)* 77−42372
molecular mechanism 79−73305
morphotropic transitions, between AX compounds, system between struct. types 79−60304
nematic liquid crystal, Merck 389, polymorphism, radiothermoluminescence and differential scanning calorimetric study 80−24570
nonpolar crystal, struct. transition, macroscopic quadrupole moment meas. *(Russian)* 77−62642
nonstoichiometric compounds, polymorphic (chemipolymorphic) transitions 79−11603
n-octadecanol, growth of high temp. α-phase crystals in γ phase single crystals 78−71700
organic molecular crystal, phase transforms. obs. using TEM, electron beam damage 78−34621
organic solid state chemistry, conf., Waltham, USA (June 1978) 79−46990
PAA, cryst. phase transitions, intermolecular motion, Raman and inelastic neutron scatt. spectra 80−2164
PAA, liq. cryst., solid-state polymorphism obs. 77−4200
PAP, cryst. phase transitions, intermolecular motion, Raman and inelastic neutron scatt. spectra 80−2164
perovskite ABX_3 compounds, system of polymorphic transitions, generic interrel. 79−60303
phenanthrene birefr. changes due to thermal expansion 78−52468
phthalocyanine, metal-free, molecular imaging and phase transformations using electric microscopy 79−33198
phthalocyanine, metal-free, solid, fluoresc., lifetimes temp. depend., polymorphic modification 78−80388
poly(tetramethylene terephthalate), IR obs. of reversible stress induced crystal-crystal phase transition 80−20627
poly(vinylidene fluoride), melting and crystn. temps., press. depend., DTA meas. 79−90568
polyethylene, deformed cryst., IR spectrum, C-H stretching, effect of polymorphism 79−15453
polyethylene, high-press. phase transforms., X-ray diffr. obs. 77−80617
polyethylene oxide, thin layer melt, morphology of supermol. structs. 79−14705
polymorphism at high press. and temp., thortveitite struct. stability *(French)* 80−10657
polyvinylidene fluoride, γ-phase form. from α- and β-polymorphs 79−11610
polyvinylidene fluoride, cryst., struct. phase transition theory, free energy, uniaxial stress 80−64924
prevoskite, anisotropically-stressed, Lifshitz-point crit. and transcrit. behaviour 79−33061
pyrochlore related structures, phases of type AM_2X_6, acentricity and phase transitions, X-ray diffr., DSC and NMR study 79−27943
quartz:Fe^{3+}, EPR for phase transform., reduced signal above 670K 77−90016
quartz, α→β transition obs. from nonlinear optics and bond polarisability model 77−15336
quartz, α to β transform., X-ray obs. *(French)* 79−96234
quartz, α-β phase transition, lattice dynamical study 79−65168
quartz, α-β phase transition point, struct., light scatt. *(Russian)* 78−47521
quartz, coexistence states during first order transition, optical obs. 80−75350
quartz, electro-optical props. near phase transition 80−80756
quartz, Fourier transform Ir spectroscopy of vibr. states at high temp. 80−97256
quartz, natural and synthetic, α-β transition, impurities effect, refr. index meas. 80−20928
quartz, phase transformations and domain structures *(French)* 78−27509
quartz, possible incommensurable phase near $\alpha \rightleftarrows \beta$ transition *(Russian)* 78−79768
quartz, synthetic, Ge doped, refr. index and α-β phase transition 78−83945
quartz, synthetic Fe-doped prisms, refr. index study of α-β transition 77−1225
quartz, synthetic hydrolytically-weakened α-β phase transform. effects on creep props. 77−43274
polymorphic transformations continued
quartz, thermal expansion near α-β transition under uniaxial stresses 80−70429
quartz crystal, opalescence near α-β transition, static model rel. to domain wall form. 80−11420
quasi binary eutectic systems, with inclusive phases, hardness, transform., decomposition *(Russian)* 80−97572
rare earth alloy-hydrogen system, $R^1_xR^2_{1-x}H_2$-H_3, phase transitions 78−18767
rare earth silver tungstates, α,β and β' phases, cryst. struct. 77−31627
rare earth sulphides, polymorphic transforms. on impact compression 77−47575
rare-earth compounds, reaction processes in solid phase *(French)* 78−30756
rare-earth intermetallics, R_2Co_7, polymorphism of Ce subgroup alloys, eutectic decomposition *(Russian)* 80−66504
rhombic distortion of cryst. lattice at low temp. 78−2253
Rochelle salt, low temp. phase transition, dilatometric exam. 77−11691
rubidium propanoate, solid state transitions and melting process, diffr. and conductometric meas. 80−10670
second-order phase transitions, changes in structural symmetry crysts. of D_4 and C_{4h} classes 77−89399
semiconductive compounds, type $A_3{}^{II}B_2{}^{V}$, genetic rel. between cryst. structs. of polymorphic modifications 79−60302
semiconductor, homologous series, semicond.-metal transitions, homeomorphous, polymorphous and morphotropic transitions 79−37988
semiconductor-metal transition, struct. changes 80−34360
semiconductors, homologous series, structural transitions associated with morphotropy 77−39675
shock wave induced transitions, review 80−15188
shock wave propag. in solid undergoing phase transition 79−14331
short-term local phase and polymorphic transforms. and changes of inner states in solids 79−14913
silicate branches, in system of polymorphic transitions of ABX_3 compound struct. types 79−90591
silicate glasses, struct. and phase transform. 78−64538
simple order parameter, for reversible martensitic transformations 80−20932
sodium benzoylacetonate, unit cell dimensions, X-ray determ. 79−69097
steel, alloy, high-speed, struct. changes investigation by hot hardness and quench dilatometry *(French)* 80−76249
steel, and alloy, austenitic transformation, temp.-conc. range of product formation 79−100135
steel, austenitic, high-speed, austenite grain growth, W addition effects 79−20085
steel, austenitic, pearlitic and bainitic transforms., effect of austenitisation conditions *(Russian)* 79−38820
steel, austenitic, type En58B, martensite formation and reversion, effect on void swelling 80−11641
steel, austenitic, type M316, martensite formation and reversion, effect on void swelling 80−11641
steel, austenitic stainless, ferritic, single phase ferritic solidification in welds, exam. 80−7546
steel, austenitic stainless, structure phase transitions due to high energy electron irrad. *(Russian)* 80−7553
steel, C, pearlite grade ShKh15, struct. transformations, hot plastic strain influence *(Russian)* 80−20927
steel, C, transform. kinetics, heat cond. and elastic-plastic stresses during quenching *(Japanese)* 80−25688
steel, Cr with metastable austenite, wear resist., temp. effect 80−76370
steel, Cr-Mn, metastable constitution diagram and phase transforms. *(Russian)* 80−50590
steel, Cr-Mo, martensite to ferrite transform. by fatigue deform. *(French)* 79−66056
steel, Cr-Ni (18%, 12(8)%), martensite formation and reversion, effect on void swelling 80−11641
steel, Cr-Ni-(Mo), cast, intercritical heat treatment *(Czech)* 80−89268
steel, Cr-Ni-Cu (14, 5, 2 wt.%), phase transform. and props., preliminary heat treatment effect 79−79011
steel, eutectoid, partitioning of Si during pearlite growth, electron microscopy study 79−83201
steel, ferrite-austenite transition, diffusion const. of C and carburisation rate consts., thermopower meas. 80−89216
steel, hereditary transfer of lattice defects at γ-α-γ transform. 79−96020
steel, hypoeutectoid Widmanstatten struct. form., contrib. to the laws *(Slovenian)* 78−84817
steel, low C, alloy, structural transform. during deform. and annealing *(Russian)* 79−91707
steel, low C, ferrite grain nuclei form. during polymorphic transform. *(Russian)* 80−50626
steel, low C, V(C,N) precipitation and twinning in γ→α transform. *(Polish)* 78−52807
steel, low impurity, peritectic transformations, influence on initial struct., solidification, grain boundaries *(Russian)* 80−66621
steel, low-C-Si, LS1.2, LS1.5, phase transformation 80−45302
steel, maraging, ageing kinetics and struct. of N12K7M5TYu, effect of high temp. deform. of austenite *(Russian)* 80−84960
steel, maraging, effect of thermal cycling (γ to and from α) on props. 80−20986
steel, maraging, hardening mechanism of quenched samples, tempering *(Czech)* 79−78989
steel, maraging, heated to high temperatures, γ to δ transformations 80−20930
steel, medium C, isothermally quenched, high-temp. deform. effects on struct. and props. *(Russian)* 80−25760
steel, Mn-Sn(-Nb), extra low C, shear transformation struct. *(German)* 80−60873
steel, Ni and W, recrystallisation mech. during laser treatment 80−50658
steel, Ni-Cu-Mo-C, powdered, influence of cooling rate after sintering on preps. 79−95969
steel, phase conversion kinetics, exam. using ultrasonic method, apparatus design 80−21203
steel, rimming, shape change and pore form. during multiple polymorphic transform. *(Russian)* 77−25044
steel, Si, bainite transform. 79−100134
steel, stainless, 12Kh13 and 15Kh11MF, austenite transform. kinetics 79−87612
steel, stainless, δ-ferrite, isothermal decomposition and transform. of heating at 550 to 950°C *(Chinese)* 79−43239

polymorphic transformations continued
steel, stainless, ferritic, Ni-free, effect of V, Ti addition on ductility 79−79048
steel, stainless, ferritic, Ti stabilised, exam. of grain boundary structure *(Russian)* 79−15662
steel, stainless, metallographic technique for detection of ferromagnetic δ-ferrite to paramagnetic σ-phase 79−61816
steel, stainless, two phase, variation of tensile and impact strength with heat treatment 79−34085
steel, stainless, type 304L, neutron irradiated, TEM study of ferrite formation 79−42112
steel, stainless ferritic, drawability, mech. props., and grain boundaries in 08Kh16AMT and 08Kh18T1 80−35270
steel, tool, maraging, based on N12M10, exam. of hardening, crack resistance and wear *(Russian)* 79−34047
steel, type 12Kh2N4A, belt grinding, struct. transformations 80−30169
steel, type 37KhN3MF, austenite grain growth depend. on structural inheritance *(Russian)* 79−61582
steels, high strength stainless, types 1Kh15N5AM3 and 1Kh16N4AB, phase transformations 80−20931
superionic crystals, structural transition theory 79−23731
TCNQ anion radical salts, phase transitions, solid solns., thermodynamic props. 77−47571
TCNQ salt, HFTTF-TCNQ, phase transitions, calorimetry study 79−51253
ternary compounds, AB_2X_4, system of polymorphic transforms. 78−95010
ternary compounds, variation of coordination numbers under polymorphic transitions 79−86737
ternary semiconductors, review of developments 78−34737
tetrachloro-p-benzoquineone, IR and Raman spectra of phase transition *(French)* 78−60445
2,2,2,6-tetramethyl-piperidino-oxy, cryst. growth and polymorphism 80−96645
tetramethylsilane, thermodynamic props. of polymorphic phases 77−84943
thermal energy storage using plastic crystal phase transitions 79−57480
thiourea, polycryst., mol. dynamics under hydrostatic press., NMR study 80−80619
Ticonal, effect of rare earth metals on mag. props., struct., and phase transformations 79−99732
Ticonal strength, effect of thermal stresses and phase transforms. 79−87721
transform., struct., texture conc. var. depend. on plastic deform. *(Russian)* 79−66050
transition metal alloys, deformation and solute-induced microstructural effects on superconductivity 79−7925
s-triazine, transverse elastic mode softening at structural phase transition 79−46777
3,4,5-trichloroaniline, polymorphism, ^{35}Cl NQR 80−54163
tris(hydroxymethyl)aminomethane, crystalline and plastic structs. phase transforms. studied by X-ray diffr. 80−84130
TTF-TCNQ, microscopic model for three low temp. phases 79−73303
Van der Waals film adsorbed on graphite, two-dimensional phase transitions 80−107653
vanadyl phthalocyanine-copper phthalocyanine mixed crysts., α-β phase transform., heat of transform., DTA investig. *(German)* 78−30754
vaterite, polymorphic transition kinetics, differential thermal anal. meas. 79−14722
weld metal, Type 316, transformation of δ-ferrites, diffusion model 80−40347
XX Ce, γ-α phase transition, study by Compton scattering 80−59650
Zircaloy-4-O alloys, rapidly heated and quenched, transform. charact. 79−20041
$[Ni(NH_3)_6](ClO_4)_2$, X-ray powder diffr. exam. of enantiomorphic transitions 78−2054
$ABCl_3$ cpds., basic struct. types and polymorphisms 78−79583
ABX_2 compounds, system of polymorphic transitions 79−42003
Ag-Hg amalgam, lattice const., temp. depend., explained in terms of Hg evaporation 78−26704
$AgBiS(Se)_2$, polymorphism and defects, electron microscopy 78−2254
Ag_2CO_3, high press. phase relations, DTA 77−43329
AgF, polymorphic transition from NaCl to CsCl struct., thermodynamic anal. *(Russian)* 77−7860
AgF_2, high press. modification, cryst. and mag. props. 80−38988
$AgFeSe_2$, thermographic investigation of phase transitions *(Russian)* 80−10661
$AgFeTe_2$, thermographic investigation of phase transitions *(Russian)* 80−10661
Ag_8GeS_6, fundamental absorpt. edge changes due to polymorphic transitions 77−20240
$Ag_8GeS_6(Se_6)(Te_6)$, Ag_8SiSe_6, $Ag_8SnS_6(Se_6)$, absorpt. edge investigs. at phase transitions 78−35149
Ag_8GeSe_6, fundamental absorpt. edge changes due to polymorphic transitions 77−20240
Ag_8GeSe_6, polymorphic transition, absorpt. coeff. meas. 78−2257
Ag_8GeTe_6, optical props. and polymorphism 80−45082
AgI, lattice instability, XPS 79−11500
Ag_8MSe_6, (M=Si, Ge, Sn), forbidden energy gap changes under high press., polymorphic transitions 77−51649
$AgNO_2$, high-pressure phase behaviour, crystal chemistry of univalent nitrites 78−30749
$AgNO_3$, polymorphic structural relationships, X-ray diffr. and microscopy 77−19930
$Ag_5Rb(PO_4)_2$, struct., density and elec. cond. 80−33952
Ag_2S, α- to β-phase transform, phase boundaries effect 79−83179
Ag_2S, α-β transform., heterogeneous solid state reactions, role of phase boundaries, dynamic equilib. at interfaces 78−71848
Ag_2S, α-β transform., role of phase boundaries in heterogeneous solid state reactions 78−71849
Ag_2S, α⇌β transitions 78−22846
Ag_2S film, tetragonal to cubic phase transform. kinetics, kinematic electron diffr. 77−4269
α-Ag_2S whiskers, growth in VLS system, polymorphic transformations to β-phase 79−46989
$Ag_2S(Se)(Te)$, changes in elec. cond. and thermoelec. power at melting point 79−15147
β-$AgSbS_2$, phase transitions, electrophysical props. 80−44316
$AgSbS_2$, synthetic crystals, DTA and cryst. struct., phase transitions *(German)* 78−42943
polymorphic transformations continued
α-$AgSbS_2$, X-ray diffr. study of phase transitions in quenched samples 77−15577
Ag_2Se, polymorphic transition, DTA meas. 78−34620
Ag_8SnS_6, fundamental absorpt. edge changes due to polymorphic transitions 77−20240
Ag_8SnSe_6, cryst., Hall effect investigation of polymorphic transform. 80−39605
Ag_8SnSe_6, fundamental absorpt. edge changes due to polymorphic transitions 77−20240
p-Ag_2Te, effect on electrophys. props. 77−39842
Ag_2Te, polymorphic transition, DTA meas. 78−34620
AgZn, β′ to ζ0 and β to ζ0 phase transform. 79−34026
AgZn, β′→ζ transformation, effect of additional elements 80−66507
Al alloys, liquid, kinematic viscosity temp. depend., porosity, H solubility, supercooling *(Russian)* 80−54425
Al, kinematic viscosity temp. depend. porosity, H solubility, supercooling *(Russian)* 80−54425
Al, liquid, kinematic viscosity temp. depend., porosity, H solubility, supercooling *(Russian)* 80−54425
Al-Mg-Si, dil. alloy, Mn additions and heat treatment effect on β→α transformation 80−7566
α-AlH_3, prep., thermal decomposition, transform., struct. *(French)* 80−3326
$Al_{45}Mn_{55}$, pure and C doped, phase transforms. 79−96022
Al_2O_3, α to γ transformations, electric field effects, proton gradient meas. by SIMS 79−52209
Al_2O_3, derived from boehmite, phase transformations and microstruct. 80−60857
Al_2O_3, polymorphic transformations rel. to prep. under low-temp. plasma conditions 77−40419
Al_2O_3, polymorphic transitions during heat treatment at 900-1500°C 79−11607
Al_2O_3, sintering as function of phase comp. 80−66464
Al_2O_3-Nd_2O_3, phase diagram at high temps. *(Japanese)* 77−63649
Al_2O_3-ZrO_2, tetragonal to monoclinic transform. of ZrO_2 particles *(German)* 79−43240
AlPO cristobalite form, polymorphic transform. investig., X-ray diffr. and IR spectra 77−4199
$AlPO_4$:Fe^{3+}, EPR, α-β phase transition 77−90016
Al_2SiO_5, kyanite, sillimanite, mullitisation, effect of gaseous atm. 79−11604
Am metal, dilatometry and thermal anal., melting point, transformation regions 79−43241
Am, polymorphic transform. exam. by hot stage X-ray diffr. anal. *(Russian)* 79−24518
Am, polymorphic transforms. obs. *(Russian)* 78−6153
As, cryst. struct. calc., pseudopot. expansion method 77−27848
As, film A1-type supercond. vapour-quenched transition temp., A7-type phase transition 78−52145
As(I) (yellow arsenic), new endothermic phase transition discovery 79−99315
As_2O_5-$Rb_2O(Rb_2CO_3)$ system, phase diagram, polymorphic transform. 79−83181
Au, vacancy size effect, surface energy in small particles and bulk specimens 80−75223
AuBr, α, I, P and BCC forms, transitions 78−38836
$Au_{11}Mn_4$, electron diffraction and microscopy obs. 78−75512
Au_5Mn_2, phase transformations and domain structures *(French)* 78−27509
BN, conversion of wurtzite into cubic form, stress state effect 80−64943
BN, cubic, press. and temp. stability region in presence of ammonium borate 77−85922
BN cutter contact plates, struct. and phase changes on working steel *(Russian)* 80−108433
BN, degree of conversion from cubic to hexagonal, determ. method 79−15887
BN, polymorphic modifications form. under low and high press. 79−15597
BN powder, wurtzite sphalerite struct. phase transition, effect on substruct. 80−25690
BN, shock compression, polymorphic transform. kinetics 79−86838
BN, sphalerite to graphite-like transform. in the 1100-1700°C range *(Russian)* 77−16572
BN, sphalerite transform., simple direct mechanism *(Russian)* 77−21135
BN, structural changes occurring during shock compression in presence of H_2O 80−16301
BN, wurtzite type, phase and struct. changes at high temps. 77−12618
$BaAl_2Si_2O_8$-SiO_2, celsian solid solns., effects on polymorphic transform. kinetics 78−68677
$BaFe_2O_4$, $BaFe_{12}O_{19}$, formation, dilatometric investigs. 78−27459
β-$Ba_9Fe_4S_{15}$, and low temp. α polymorph., cryst. struct. 78−67690
$Ba_7KNb_5O_{15}$, Raman scatt. experiments in tetragonal tungsten bronze compounds 80−40113
$Ba_7NaNb_5O_{15}$, Raman scatt. experiments in tetragonal tungsten bronze compounds 80−40113
BaO-SiO_2 glass-ceramic, crystallisation mechanism 79−90559
$BaSi_2$, trimorphic, transform. of three-connected Si nets, press.-temp. phase diagram, 40 kbar and 1000°C 80−75198
$BaTiO_3$, cubic-tetragonal phase transition, birefringence meas., surface distortion effects 78−95564
$BaTiO_3$, periodic domain struct. and opalescence at tetragonal to orthorhombic transition 80−66131
$BaTiO_3$, polycrystalline, exam. of effect of freq., temp. and DC electric field strength, on elastic consts. 79−1890
$BaTiO_3$, powders, Bragg reflection integral intensities due to structural anomalies 80−107098
$BaTiO_3$, struct. changes due to cubic-tetragonal phase transition 78−60407
$BaVS_3$, elec. resist., mag. susceptibility, structural transition amd Mossbauer effect meas. 77−84923
$BaVS_3$, polycrystalline, elastic behaviour, 40 to 350K 79−60498
Be, transformation enthalpies for α-β and β-liquid transitions 77−35690
Bi, film A1-type supercond. vapour-quenched transition temp., A7-type phase transition 78−52145
Bi, shock loading and unloading effects, 293K 77−84840
Bi_2O_3, polymorphic transformation and elec. resistivity *(Japanese)* 80−93555
Bi_2O_3-$Mo(W)O_3$ system, elec. cond. and dielec. const. obs. 77−89816
BiP_5O_{14}, condensed, thermal behaviour and IR spectra 80−19912

polymorphic transformations continued
$Bi_2Sn_2O_7$, polymorphic phase transition, X-ray, DSC, SHG, dielec. and optical obs. 80−44163
$BiTaO_4$, X-ray and ESR study of phase changes 78−72476
C, diamond like, graphitisation, elec. resist. meas., 30-550°C *(Russian)* 77−39676
C foil, ion irrad., crystallographic transform. 79−55794
C, hard, heat-treated under pressure, characterisation of carbon phase by electron microscope 80−60855
C, polymorphic modifications form. under low and high press. 79−15597
C_3S, influence of polymorphic transform. on sinter stability *(Russian)* 80−66503
Ca, electrical resistivity and thermoelectric power 78−26846
$Ca_2Al_2SiO_7$, gehlenite, new high-press. phase, rel. to Earth interior 79−29753
$Ca_{0.2}Ba_{0.8}TiO_3$:Nb, conductive single cryst. growth by Verneuil method 77−85928
$CaCO_3$-$NaAlSiO_4$, micromechanism for phase formation during sintering *(Russian)* 80−16253
$CaCr_2O_4$, β to α transform. temp., effect of partial O_2 press. 80−84292
$CaLaGaO_4$:Eu^{3+},Bi^{3+}, luminesc. influenced by struct. transition 78−6773
$Ca_2Mg(Co)(Zn)(Mn)(Cd)(Ca)TeO_6$, optical SHG study of acentricity, ferroelec. of low temp. phases 80−71324
$Ca(NO_3)_2.2h_2O$, β- to α-phase orientational transform., struct. interpretation *(French)* 77−80448
$(CaO)_3SiO_2$, effects of polymorphism on hydration, X-ray and TEM obs. *(Japanese)* 79−20046
$Ca_5(PO_4)_3F$:Cr^{3+}, ESR, polymorphic transform., spin Hamiltonians 77−36117
$CaSi_2$, high press. transform. of three-connected Si nets 79−77744
$CaSi_2$, high-pressure phase transform., cryst. struct. 77−35693
$CaSiO_3$, wollastonite, exptly. deformed, polytype transforms. 79−65021
γ-Ca_2SiO_4, polymorphic transformation scheme 80−71642
Ca_2SiO_4, structurally related phases, high-temp. X-ray powder diffr. 80−81050
Ca_2SiO_4-BaO, conditions and mechanism in cryst.-chemical stabilisation of unstable phases 80−39302
Ca_2SiO_4-FeO, conditions and mechanism in cryst.-chemical stabilisation of unstable phases 80−39302
Ca_2SiO_4-MgO, conditions and mechanism in cryst.-chemical stabilisation of unstable phases 80−39302
$CaWO_4$ type compounds, system of polymorphic transitions 78−47268
CdI_2, 2H to 4H structural change, X-ray diffr. study 78−75614
CdI_2, 20 layered hexagonal polytypic crysts., struct., transform. 77−7689
CdI_2, 6H-based polytypes, transformation characteristics 77−19889
CdI_2, hexagonal to rhombohedral phase transform., SFE 79−91643
CdI_2, hexagonal-rhombohedral polytypic transformation, electron diffr. and X-ray diffr. obs. 80−49163
$Cd_2Mg(Co)(Zn)(Mn)(Cd)(Ca)TeO_6$, optical SHG study of acentricity, ferroelec. of low temp. phases 80−71324
$Cd(NO_3)_2$, phase transition, SHG, optical and dielec. meas. 80−71334
CdP_2, Cd_3P_2, polymorphic transitions 78−23699
$Cd_{14-x}P_4S_{24-2x}I_{2x}$, icosahedral structs., synthesis and charact. 77−1107
CdS, X-ray diffr. investig. of high-press. polymorphism 77−43324
$CdUO_4$, phase transforms., anomalous oxidation state change 80−54369
Ce, $\alpha \rightarrow \alpha'$ high press. transition, volumetric study 78−83940
Ce, Compton profile study of γ-α phase transition 80−11503
Ce, electronic structure, Compton profile meas. rel. to $\gamma \rightleftarrows \alpha$ transition 80−10867
Ce, new allotropic phase above 121 kbar, X-ray diffr. obs. 77−35509
Ce, phase boundary between α' and tetragonal polymorphs, resistance anomaly meas. 79−60500
Ce, polymorphic $\gamma \rightleftarrows \alpha$ transform. and volume anomalies under press. 80−34189
Ce, surface and volume props., flow props., surface layer thickness *(Russian)* 80−59760
Ce-Pr powder, DHCP$\rightleftarrows$FCC transition, X-ray, DTA and resistivity studies 80−50629
$Ce_{1-x}La_x$, dil., $\gamma \rightarrow \alpha$ transition temp. and press., elec. resist. meas. up to 10 kbar 80−59643
(Co,M)$SiF_6.6H_2O$, (M=Mg,Mn,Zn), phase transition at low temp., IR spectra 79−24302
Co allotropic transformation, X-ray diffr., analysis exam. *(Russian)* 79−34027
Co alloys, binary, and MAR-M322 type, influence of phase transform. on diffusion and mech. props. *(Russian)* 79−5000
Co, deformed and annealed, mechanism and kinetics of polymorphic transformations *(Russian)* 78−35381
Co, ferromagnetic, anomalies in thermal expansion and heat capacity 79−73744
Co, HCP to FCC transition, mag. domain nucleation 78−64218
Co, influence of FCC phase retained at room temp. on mech. props. 79−47677
Co, internal friction meas. during polymorphic transform. *(Russian)* 79−29049
Co, steady creep rate, stress depend., exam. at phase transformation at 390°C 78−52923
Co-Fe, transformation matrices, electron diffraction patterns 77−59779
Co-Fe (6.25 wt.) FCC to HCP transform., model and expt. evidence 77−44243
Co-Fe alloys, mag. anisotropy induced by mag. annealing through to double h.c.p. 77−1552
Co-Fe epitaxial films, singularities of $\gamma \rightarrow \alpha$ transform., X-ray diffr. obs. *(Russian)* 79−52198
Co-Ni-Cr-Mo, mech. props., effect of twinning and FCC to HCP transform. 77−4779
Co-Ni(Ti)(Cu)(Mn), cryst. struct. and stacking fault influence on mag. props. *(Russian)* 80−25164
Co-Ti-C, secondary precipitation and allotropic transform., TEM obs. 80−108453
$CoBr_2.6D_2O$, crystallographic and mag. struct. determ. 77−8278
$CoCl_2.6D_2O$, crystallographic and mag. struct. determ. 77−8278
$CoCl_2.6D_2O$, neutron diffr. study, cryst. and mag. struct. *(French)* 78−42946
Co_5Ge_3, phase and struct. charact. 77−36450
$Co_{50}Mn_xGa_{50-x}$, cryst. struct. transform. of B2 type *(German)* 79−91642
$CoMoO_4$, mag. susceptibility and electrical transport props. 79−56511
$Co_{0.65}Ni_{0.35}$, precursory phonon obs. of FCC to HCP transition 78−43082
polymorphic transformations continued
Cr and Cr alloys, structural changes during low-temp. phase transform. *(Russian)* 79−52202
Cr bronze Sn, recrystn. props., hot rolling, annealing, polygonisation *(Russian)* 80−55419
Cr, crystal structure below Neel temp., X-ray diffr. study 78−83772
Cr-Ge system, phase diagram, thermal anal., X-ray diffr., microhardness, and electron probe anal. *(French)* 80−97462
Cr_2O_3 X-ray diffr. studies, crystallite size, phase transformation 77−21138
Cs, absolute zero isotherms and polymorphic transition 79−73310
CsCl, electron beam excited luminesc., phase transition effects 77−85810
CsCl, transition mechanism between CsCl-type struct. and NaCl-type struct. 77−31768
$CsCrCl_3$, α-β phase transition, dynamical aspects and thermodynamic theory 80−70404
$CsCrCl_3$, Jahn-Teller induced phase transitions 80−70391
CsH_2AsO_4, high temp. phase transition 78−71856
CsH_2PO_4, single cryst. growth, struct. and elec. props. 78−71693
$Cs_2LiFe(CN)_6$, struct., phase transformations, temp. depend. Raman spectra 79−11416
$CsLiSO_4$, crystal structures of I and III phases, twins 80−70181
$Cs_2NaFe(CN)_6$, structural phase transformations 79−19178
CsO_2, low temp. phase study, crystallographic domains and unit cell dimens. 78−63728
$CsPbBr_3$, cubic-to-tetragonal phase transition, critical anomalies, phenomenological eqns. 80−39275
$CsPbCl_3$, cubic-to-tetragonal phase transition, critical anomalies, phenomenological eqns. 80−39275
$CsPbCl_3$, elastic constants and thermal expansion, near struct. transitions 78−59849
$CsPbCl_3$, lattice thermal expansion, X-ray powder technique 80−19965
$CsPbCl_3$, O_h^1-D^5_{4h} transition, US and thermodynamic props. 78−67826
$CsR(MoO_4)$ R=Dy, Ho, Er, permittivity temp. depend., polymorphic transition 80−92670
Cu-Ni-Al, review 80−7564
Cu-Zn-Al, memory alloy wire and ribbon reversible martensitic transformation, ageing effect, review 80−7564
Cu-Zn-Al, reversible shape memory effect obtained by heating under constraint *(Japanese)* 79−43335
Cu-Zn-Al, reversible shape memory effect associated with $\beta_1 \rightleftarrows \beta_1' \rightleftarrows \alpha_1'$, transform. *(Japanese)* 79−43242
Cu-Zn-Al, reversible shape memory effect *(Japanese)* 80−108500
$Cu_xAg_{1-x}I$ crystals, layer structs., X-ray diffr. studies 80−96457
$CuCr_2O_4$, heat capacity, entropy, polymorphic transition, 298-1000K 78−10196
$CuFe_2O_4$, Jahn-Teller type crystal distortions 80−103904
Cu_2S, $Cu_{1.8}S$, $\alpha \rightarrow \beta$ transition, thermographic investigation of heats, entropies and activation energies 80−88314
Cu_2S, HP-FCC polymorphic transition stages 80−33924
Cu_2S, polymorphic transition from hexagonal to FCC packing and struct. of 12H and 14H polytypes 79−55692
$Cu_{2-x}S$, digenite, X-ray determ. of structural transitions 80−92474
$Cu_{2-x}S$ film, evaporated, ordering process, electron diffr. study 80−39477
$Cu_{2-x}S$ films, vacuum deposited, electrical conduction and phase transitions 78−84332
Cu_xS-CdS solar cells, Cu_xS transform. behaviour rel. to topotaxial growth, cell efficiency 77−11814
Cu_2S(Te), microstructure, work hardening in polymorphic transform. and subsequent annealing effect 79−52199
Cu_3SbS_3, skinnerite, polymorphism, X-ray diffr. and NQR meas. 80−49165
Cu_2Se, kinetics of polymorphic $\alpha \rightleftarrows \beta$ transformation *(Russian)* 80−70152
Cu_2TE, annealing and deform. of defects induced by phase work hardening during thermal cycling 79−52230
Cu_2Te, HP-FCC polymorphic transition stages 80−33924
Cu_2Te, microstructure, work hardening in polymorphic transform. and subsequent annealing effect 79−52199
e-D_2, solid-liquid coexistence curve anomaly *(Russian)* 78−75824
DI, thermodynamic properties 78−47517
DX, X=Cl, Br, I, thermodynamic properties, phase transitions 78−47518
Eu, mag. and struct. transitions, X-ray K-line shift, 77-1000K *(Russian)* 77−4518
Eu_2O_3, C$\rightarrow$B transformation 77−11688
Eu_2O_3, cubic to monoclinic transform. 77−8815
Eu_2O_3, from reactive evaporation, struct. 79−51441
$EuSi_2$, high-pressure phase transform., cryst. struct. 77−35693
Fe alloy type G18, martensitic $\gamma \rightleftharpoons \varepsilon$ transformation, dislocation pile-ups, ε phase nucleation *(Russian)* 80−55396
Fe and Fe alloys, polymorphism effect on failure accompanying electrospark action *(Russian)* 79−74236
Fe, α-, γ-, crysts., twinning, martensitic transforms., correspondence matrices *(German)* 78−31406
Fe, α-γ transition, US velocity anomaly obs. 78−75830
Fe epitaxial growth on Cu(111), supersaturation and mode of growth, LEED and AES exam. 78−18929
Fe, fine particle dispersions, shock induced mag. effects 79−82832
Fe, γ to α transform. 79−29051
Fe, phase transition thermodynamics 78−18769
Fe, polycryst., influence of α-γ transform. on creep *(Russian)* 80−89289
Fe, powder, sintering, effect of repeated allotropic transform. 77−40406
α-Fe, struct. after polymorphic transform. under press. *(Russian)* 80−29946
Fe-C (0.11, 0.23, 0.42 wt.%), grain boundary ferrite allotriomorphs, growth kinetics 77−44244
Fe-C-Mn-V, austenite microstruct. memory *(German)* 80−84977
Fe-Co alloy, isothermal compression and BCC$\rightarrow$HCP phase transition, up to 300 kbar, at room temp. 77−90346
Fe-Cr alloys and Fe, lattice parameters, 293 to 1273K, α to γ phase transform., X-ray diffr. exam. *(Russian)* 80−50625
Fe-Cr-Ni austenitic alloy, cold deformed, α-γ transition, calorimetric study *(Russian)* 80−55390
Fe-Mn, FCC to HDP transform. 79−61581
Fe-Mn, Mossbauer spectroscopy of temp. hysteresis of phase transformations *(Czech)* 80−29949
Fe-Mn (2 to 8 wt.%) alloys, phase transformations, tempering influence *(Russian)* 80−25735

polymorphic transformations continued
Fe-Mn alloys, α, ε and γ, brittleness 80−35314
Fe-Mn-Cu-C, Cu effect on ε'-martensite, X-ray obs. of heating effects *(Russian)* 79−87667
Fe-MoS_2, exam. of props., using differential thermal analysis, and metallography *(Russian)* 79−15653
Fe-NbC, exam. of phase diagram, and mech. props. *(Russian)* 79−20028
Fe-Ni, alloy 20N24, martensitic, exam. of structure after laser treatment, and recrystallisation *(Russian)* 79−11608
Fe-Ni, α to γ transformation, changes in Young's modulus and electrophysical props. *(Russian)* 79−20042
Fe-Ni, hardening by plastic deform. during polymorphic transform., struct. mechanics for γ-phase form. *(Russian)* 77−90344
Fe-Ni, hardening by plastic deform. during polymorphic transform., mechanical props. *(Russian)* 77−90345
Fe-Ni, reversibility of crystal orientation in reverse martensitic transformation 79−83199
α-Fe-Ni, struct. after polymorphic transform. under press. *(Russian)* 80−29946
Fe-Ni (20 to 31 wt.%), exam. of martensitic transform. and reverse transform. using differential and thermomagnetic resistance analysis *(French)* 79−52214
Fe-Ni (23 wt.%), struct., composition changes during α to γ transform., martensite plastic deformation influence *(Russian)* 80−11642
Fe-Ni (23.1 wt.%), α to γ transformation, struct., conc, changes, heating rate, residual austenite influence *(Russian)* 79−83194
α-Fe-Ni (3-12 wt.%), structure and $\gamma \rightarrow \alpha$ polymorphic transform. kinetics 80−71645
Fe-Ni (32 wt.%), EMF appearance during $\gamma \rightarrow \alpha$ transform. *(Russian)* 80−89215
Fe-Ni alloy, α to γ slow transformation mechanism, Ni content influence *(Russian)* 80−7569
Fe-Ni alloy, $\alpha \rightarrow \gamma$ transform., role of grain boundary diffusion, Mossbauer obs., homogenisation effect *(Russian)* 79−52197
Fe-Ni alloy, reverse martensitic transform., shape deform. reversibility 80−66506
Fe-Ni austenite, precipitation hardened, transform. strengthening 79−24531
Fe-Ni-C alloy with single-component martensite texture, $\alpha \rightarrow \gamma$ transform., changes in shape *(Russian)* 80−104152
Fe-Ni-Co-Ti, coherent particles effect inherited by martensite on $\alpha \rightarrow \gamma$ transformation *(Russian)* 80−108443
Fe-Ni-Co-Ti, martensite cryst. lattice tetragonality, $\gamma \rightleftharpoons \alpha$ transform. *(Russian)* 79−61587
Fe-Ni-Cr-Mo superalloy, mech. props., η-phase form. effect *(Chinese)* 80−20925
Fe-Ni-Ti (30, 3 wt.%), reverse martensitic transform. and memory effect *(Russian)* 79−87627
Fe-Ni-Ti-Al-Nb, struct. mechanism for inverse $\alpha \rightarrow \gamma$ transform. *(Russian)* 80−40351
Fe-Ni-V-C alloy, reverse α to γ transformation, previous deformation influence on struct. and props. *(Russian)* 79−100139
Fe-Ni(-Mo), formation of austenite structure in relation to α to γ transformations 79−100142
Fe-Pd, anomalous elec. cond. near mag. phase transition point, α to γ phase transition 80−15722
Fe-Pt, austenite ordering effect on mode of reverse transform 79−61588
Fe-Si alloys, recrystn. while carburising, interphase boundaries movement 79−52208
γ-Fe_2O_3, vibro-milled, energy storage and liberation 78−83941
Fe_2O_3, X-ray diffr. studies, crystallite size, phase transformation 77−21138
Fe_2O_3-Cr_2O_3, crystalline size and phase transform. study by X-ray diffr. 77−21138
γ- Fe_2O_3-Fe_3O_4, lodestone, microstructure and mag. props., source of mag. hardening 79−82828
FeS_2, marcasite and pyrite phases sp. ht., thermodynamics of transform. 77−28016
β-$FeSO_4$, high-temp. polymorph, stability, mag. struct., mag. props. 77−43815
$Fe_{1-x}Se$, phase relation 79−14926
$FeSiF_6$, phase transform. and relax., EFG and quadrupole spectra 77−51995
$FeTiD_x$ ($0 \leq x \leq 1.9$), structural phase transitions, absorpt. and desorpt. isotherms 80−19948
$Fe_xV_{1-x}O_2$, X-ray diffr. obs. 77−27858
$FeZrF_6$, phase transition at 212.3K, Mossbauer, EPR study, quadrupole splitting, Jahn-Teller effect *(German)* 78−68430
Ga, polymorphism at high press. *(French)* 78−47279
$GaNbO_4$, polymorphic transition under high press. 80−100835
Ga_2O_3, α to β monotropic transition heat determ. 80−54370
Ga_2O_3, entropy of beta→alpha transformation 77−36489
n-GaP:S, elastic moduli and mode gammas 79−73242
GaSe, pressure-induced polytypic transforms. and edge absorpt., exciton lines 77−28595
$GaSe_{1-x}S_x$, polytypes, exciton gap energies, luminesc. study 80−54611
$GaSe_{1-x}S_x$, struct. transition, Raman scatt. obs. 79−99888
Gd compounds, NaCl type, exchange striction 78−84409
Gd film, vac. deposited and VPE, deposition parameters effects on struct., FCC to HCP transition 79−90912
GdF_3-RF_3, R = Tb, Ho, Er, Yb, stabilisation of rhombic β-YF_3 type struct. 78−67700
$Gd_3Ge_2O_7$, polymorphism under pressure *(French)* 78−95150
c-Gd_2O_3, electrical cond., dielectric const. mag. susceptibility, polymorphic transition 77−59505
GeTe, elec. cond. and microhardness, thermal cycling effect *(Russian)* 78−35485
GeTe, enthalpy and specific heat, 0 to 860°C, polymorphic transitions obs. 77−43350
GeTe, interpretation of polymorphic transformations 80−15032
γ-GeTe, investigation by elec. resist., latent heat of phase transform. and plasma refl. of light 79−99317
GeTe, quenched, phase transitions and electrophysical props. 79−51250
GeTe, region of homogeneity 77−47582
GeTe, thermal expansion meas. at phase transition 78−18771
GeTe-MnTe, heat treatment effect on struct., elec. props. 80−54725
GeTe-MnTe-SnTe system, compds., GeTe phase transition temp., elec. props., thermal cond. 79−43220
$Ge_{1-x}Te_x$, elec. cond., Hall effect in phase transition region 79−11113
HI, thermodynamic properties 78−47517
polymorphic transformations continued
HX, X = Cl, Br, I, thermodynamic properties, phase transitions 78−47518
^3He, BCC-HCP transition effect on spin diffusion *(Russian)* 77−35794
Hf electron field emitter, temp. drop meas., allotropic transform. temp. 80−2931
Hf, polymorphic transition, emission images obs. in temp. range 1800-2100°K 80−100836
HfO_2, ZrO_2-HfO_2, soft phonon modes cond. monoclinic-tetragonal phase transition 77−62638
HfO_2:Er_2O_3(Y_2O_3)(Eu_2O_3), elastic props., sonic reson. meas. 80−7612
HfO_2-CeO_2, solid solutions 77−16549
HfO_2-Sm_2O_3, X-ray diffr. obs. of phase relations 79−61566
Hg chalcogenides, electrical charact. of pressure-induced transition 77−84921
Hg_2Cl_2, calomel, press. depend. optical soft mode 79−55859
Hg_2Cl_2, low temp. phase transition, X-ray diffr., Raman spectra 78−22849
HgI_2, cryst. growth from soln., doping rel. to elec. cond., phase transitions 77−55880
HgSe, press. induced phase transitions, nucleation, resistance discontinuity 77−27996
HgTe, pressure-induced polymorphic transition 80−10667
In, vacancy size effect, surface energy in small particles and bulk specimens 80−75223
In-Cd, shape memory *(Japanese)* 79−43243
In-Sb, cryst. struct. after appl. of high press., supercond. transition temp. 80−70169
In-Sn alloy crystals, phase changes and shape memory effect *(Japanese)* 80−108502
In-Tl, single crystal containing Li, X-ray study of FCC⇄FCT transform. *(Japanese)* 80−108435
In_2O_3, entropy of transform. from rare-earth ot corundum struct. 78−91433
In_2S_3 destabilisation of stabilised γ-phase obs. 78−71853
InSb, polymorphism and cryst. struct. at high temp. and press. 78−95026
$InSbO_4$, monoclinic high-pressure modification, structural type 80−33925
$InSbSe_3$, incongruently melting cpd. in In_2Se_3-Sb_2Se_3 system 78−44090
InSe, $InSe_{1.2}$, In_2Se_3, molar heat capacity and enthalpy of transition, 129 to 920K range 77−29030
InSe, second order Raman spectrum and phase transition 79−38545
In_2Se_3, transitions of high temp. α form *(French)* 80−92473
In_2Se_3-Sb_2Se_3 system, polymorphic transition pattern of In_2Se_3 78−44090
In_2Te_3, in In_2Te_3-PbTe system, polymorphic transition 78−35361
K, absolute zero isotherms and polymorphic transition 79−73310
$KAsO_3$-K_3AsO_4, phase diag. 78−23681
$K_2Ba(NO_2)_4$, ferroelastic, Raman spectra and phase transition 79−56800
$K_2Ba(NO_2)_4$, new ferroelastic, phase transitions, optical and electrical props. 79−55887
KCN, elastic anomaly at 168K 78−27242
KCN, polymorphic transitions, lattice energies calc. 77−1092
K_2CO_3, study of elec. cond. and transition points 78−75873
$KCaCl_3$, phase transitions, optical and dilatometric meas. 79−61394
KCl, polymorphic transition press. at high temp., elec. resist. meas. 78−38837
KCl, press. induced low-temp. polymorphic transition, hysteresis 78−14467
$K_2Cr_2O_7$, depend. on thermal and prep. history 80−34184
$K_2Cr_2O_7$, thermal props. thermal anal. and X-ray diffr. obs. 78−30752
KD_2PO_4, high temp. phase transition, dielec. const., elec. cond. and IR refl. meas. 78−43118
KF, high press. B1 to B2 phase transition, X-ray diffr. obs. 79−23722
KF-YbF_3, KF-LuF_3, phase analysis 78−44101
KH_2AsO_4, high temp. phase transition, dielec. const., elec. cond. and IR refl. meas. 78−43118
KIO_3.HIO_3, structural modifications, NQR study 80−20487
$KMgCl_3$, successive phase transitions 79−100132
$KMnF_3$, cubic-to-tetragonal phase transition, critical anomalies, phenomenological eqns. 80−39275
$KMnF_3$, phonon scatt., thermal cond. meas. 77−7916
$K_2Mn_2(SO_4)_3$, phase transition press. effect, dielectric const. meas. 79−37834
KNO_2, high-pressure phase behaviour 78−30749
KNO_2, polymorphism, calorimetric investigation 78−75827
KNO_3, orientations and twinning in the struct. transform. aragonite-type to calcite-type 77−24284
$KNbO_3$, photoferroelectric effects 78−92029
$KNbO_3$, X-ray diffr. before and after high temp. phase transition 77−11694
KO_2, low temp. phase study, crystallographic domains and unit cell dimens. 78−63728
KPO_3-$Pb(PO_3)_2$, phase diagram of binary system 77−21114
K_2SO_4, thermal phase transition 80−19738
K_3SmF_6, pressure temp. phase diagram to 35 kbar and 900°C 77−15575
K_3YF_6, pressure-temp. phase diagram to 35 kbar and 900°C 77−15575
$K[Ag(CN)_2]$, Raman scatt., press.-induced phase transitions and phonons 79−33698
La, surface and volume props., flow props., surface layer thickness *(Russian)* 80−59760
$LaAlO_3$, Pm3m to R3c or R3c phase transitions, TEM method for domain identification 80−14980
$LaCrO_3$, sp. ht., enthalpy, entropy, 298-900K, polymorphic transition 77−69094
$LaMnO_3$, orthorhombic lattice distortions, mag. props. rel. to prep. conditions 77−20592
$LaNbO_4$, single cryst., monoclinic to tetragonal phase transform. with intermediate state 77−52247
La_2O_3, from reactive evaporation, struct. 79−51441
La_2O_3-Y_2O_3, phase diagram at high temps. *(Japanese)* 77−70038
LaOF-LaF_3, high pressure phase transitions 80−55368
La_2S, α-β transition, temp. and thermodynamic charact., role in thermal dissoc. 80−104457
$LaSi_2$, thin film, exam. of phase transitions during vacuum annealing 79−95281
La_5Si_3 thin film, exam. of phase transitions during vacuum annealing 79−95281

polymorphic transformations continued
$LiAlO_2$, matrix support material for molten carbonate fuel cell, thermal stability, effects of different environments 80−50952
$LiBO_2$-In_2O_3, phase composition, mag. props, elec. cond. 80−55365
$Li_4B_7O_{12}Cl$, cryst. struct. and ionic conductivity 77−84690
$Li_{0.5}Ga_{2.5}O_4$-$CuCr_2O_4$ system, phase diagrams, IR spectra, Cu^{2+} electronic spectra *(French)* 78−51461
LiH, electronic struct., equation of state, insulator-metal phase transition 79−33234
$Li_{1-x}H_xIO_3$, cryst. growth from soln. and phys. props. 77−31634
$LiIO_3$, phase transitions obs. by DTA, heat treatment, X-ray diffr. *(Chinese)* 78−2249
$LiIO_3$, Raman spectra and phase transitions 77−16316
Li_2MgSiO_4-Li_2ZnSiO_4, solid soln. formation, phase relns. *(Japanese)* 77−25037
Li_6NBr_3, $Li_{13}N_4Br$, ionic transport 79−73336
$LiNbO_3$, shock-wave compression, 2.4-44 GPa 80−34139
Li_2O-(Al_2O_3)-SiO_2 glass-ceramic, crystallisation mechanism 79−90559
$(LiPO_3)_x.H_2O$, existence of high- and low-temp. cryst. forms, X-ray diffr. data 79−19179
Li_2SO_4:$Na^+(K^+)(Mg^{2+})(Zn^{2+})(Cd^{2+})(Al^{3+})$, monoclinic-cubic transform., effect of impurities 79−52744
$Li_2W_2O_7$ 77−48407
Li_2ZnSiO_4, tetahedral struct., polymorphic α-β transform. kinetic obs. and method 79−90778
$Lu_2Si_2O_7$, polymorphism under press., cryst. struct. 77−35692
β-$(Mg, Fe)_2SiO_4$, high-press. spinel phase identification in Tenham chondritic meteorite 79−80284
$MgBr_2.2Et_2O$, NQR freqs. temp. dependence, phase transition 79−42867
Mg_2Ge, under high press., radiographic data 77−20068
$Mg(H_2O)_6SiF_6$:Mn^{2+}, phase transition effects in EPR spectrum 79−42831
$Mg(NH_3)_6(ClO_4)_2$, phase exam. by adiabatic calorimetry and X-ray diffr. methods 78−63854
Mg_2Si, under high press., radiographic data 77−20068
$MgSiF_6$, phase transform. and relax., EFG and quadrupole spectra 77−51995
$MgWO_4$ type compounds, system of polymorphic transitions 78−47268
Mn-Cu, alloying behaviour and high damping capacity 80−35160
Mn-Y-Zn-Cd alloy,phase equilibria, plastic deformation, microhardness *(Russian)* 80−40334
MnF_2, rutile type, polymorphism at high press., distorted fluorite phase 79−69050
MnF_2, X-ray diffr. investig. of high-press. polymorphism 77−43324
Mn_6N_5 film, cryst. struct. and phase transform. exam. by electron diffr. 78−10189
MnSb-Mn_2Sn alloy system, continuous series of solid solns., homogeneity and ferromagnetic props. 79−52159
$MnSiF_6$, phase transform. and relax., EFG and quadrupole spectra 77−51995
Mo_2C coatings, phase and struct. transformations on heating 79−96206
N_2, solid, lattice dynamical calcs., use of anisotropic at.-at. pot. functions, α-γ transition 78−71811
N_2, solid, mol. libration and α-γ phase transition, Kihara pot. calcs. 80−44312
N_2, solid, mol. libration in α and γ phases, core pot. calcs. 79−86849
$(ND_4)_3D(SO_4)_2$, press.-temp. phase diagram 78−38834
NH_4Br, β-γ phase transition, critical anomalies, phenomenological eqns. 80−39275
NH_4Br, cubic-tetragonal transition, macroscopic quadrupole moment meas. *(Russian)* 77−62642
NH_4Br, supercooled, polymorphic transform., struct. correspondences and mechanisms 80−107097
NH_4Br:Tl, and pure crystals, luminesc., VUV irradiated at 80K *(Russian)* 80−84763
NH_4CNS, kinetic-morphological types of polymorphic transform., relax. theory 78−9993
NH_4Cl, thermal conductivity, crystal transformation 78−2310
NH_4ClO_4, polymorphous phase transition mechanism 80−79737
$(NH_4)_3H(SO_4)_2$, phase transitions, sp. ht. meas. 80−2157
$(NH_4)_3H(SO_4)_2$, successive phase transitions, dilatometric and X-ray expts. 80−11348
NH_4LiSO_4, high press. phase, point group symmetry 79−51039
NH_4LiSO_4, NH_4IO_3, phase transitions, SHG obs. 78−76398
NH_4LiSO_4, point group symm. at high press. phase 80−70150
NH_4NO_3, elastic growth of cryst. during IV to x polymorphic transitions 79−46593
NH_4NO_3, Raman spectra of low temp. phases 78−92081
$(NH_4)_2PtBr_6$, cubic to tetragonal phase transitions 79−1500
NH_4SCN, polymorphous structural-kinetic transformations, phase orientational relation 79−90590
NO, adsorbed monolayer on graphite, melting and polymorphism 78−84063
NO, adsorbed on cleavage face of lamellar halides, polymorphic phase changes 77−31900
$(Na,K)NbO_3$ solid solns., struct. transitions, neutron powder diffr. 78−38649
$(Na,Li)NbO_3$, ceramics, electrophys. and struct. props. near morphotropic transition 78−2816
NaCN, cubic, KCN-type anomalous thermoelastic behaviour 77−84823
NaCN, polymorphic transitions, lattice energies calc. 77−1092
Na_2CO_3, phys. props. related to phase transitions 80−96643
Na_2CO_3, struct. changes at incommensurate phase transition 79−95158
$NaCaPO_4$-Ca_2SiO_4 partial system, phase diagram 78−35364
$NaCaPO_4$-Ca_3SiO_5 partial system, phase diagram 78−35365
$NaClO_3$, metastable-stable phase transition mechanism *(French)* 80−15031
$Na_3Cr_2(PO_4)_3$, crystallographic data, ionic conductivity *(French)* 80−88077
$Na(D_xH_{1-x})_3(SeO_3)_2$, Raman spectra and nature of phase transitions 78−80341
$Na_3Fe_2(PO_4)_3$, crystallographic data, ionic conductivity *(French)* 80−88077
$Na_3Fe_2(PO_4)_3$, polymorphism and ionic conduction *(French)* 78−67678
$NaFeTiO_4$, form. in Na_2O-M_2O_3-TiO_2 ternary systems X-ray anal. 79−51067
$NaH_3(SeO_3)_2$, dynamics of α-β transition, Brillouin scatt. meas. 77−8526
$Na_3La(AsO_4)_2$, allotropes, prep. and cryst. struct. *(French)* 78−63724
NaN_3, NMR, Na nuclear quadrupole moment, phase transition 77−73092
polymorphic transformations continued
$NaNO_2$, high-pressure phase behaviour 78−30749
$NaNbO_3$, birefr., temp. depend., behaviour at P⇄N struct. transition 78−64331
$Na_3Nd(AsO_4)_2$, allotropes, prep. and cryst. struct. *(French)* 78−63724
$Na_3Pr(AsO_4)_2$, allotropes, prep. and cryst. struct. *(French)* 78−63724
Na_2SO_4, high temp. phase, DTA and dielec. meas. 79−82333
Na_2SO_4, pure and K-doped, X-ray, DSC and elec. cond. obs. 79−33082
α-$NaSbS_2$, cryst. struct. and β→α phase transform. features 80−33961
$Na_{1+x}Si_xZr_2P_{3-x}O_{12}$; monoclinic to rhombohedral phase transformation 80−29950
Na_xWO_3, struct. transitions and lattice dynamics 78−79771
Na_xWO_3, transition sequence, lattice parameters meas. 78−22852
$Na_3Zr_2Si_2PO_{12}$, NASICON, phase transition, X-ray diffr., ionic cond. and sp. ht. meas. 80−19979
Nb, oxidation kinetics, abnormal, at high temp. 79−29289
Nb-Ge film, phase transformations due to annealing, electron diffr. study 80−54551
Nb-H (30 at.%), specific heat at ϵ→ζ→β phase transition 77−12616
Nb-Si diagram of state, melting temp., polymorphic transform. temp. *(Russian)* 80−50594
$Nb_xCr_{1-x}O_2$, (x≥0.5), cryst. growth by chem. transport and phase transitions 78−35281
NbD_x, x=0.55 to 0.88, deuteron and ^{93}Nb mag. resonance, β-α transitions 77−20721
$NbH_{0.3}$, α-α' phase transition, sp. ht. anomaly 78−39764
NbH_x, thermopower, role of phonon dynamics 79−33284
NbS_2, high pressure polymorphs 78−51459
$NbSe_2$, high pressure polymorphs 78−51459
$NbTe_2$, high pressure polymorphs 78−51459
$NbTe_2$, phase transformations and domain structures *(French)* 78−27509
Nd, surface and volume props., flow props., surface layer thickness *(Russian)* 80−59760
$NdAg_2$, high temp. modification, thermal effects 78−38665
$NdNbO_4$, single cryst. monoclinic to tetragonal phase transform. with intermediate state 77−52247
Nd_2O_3, from reactive evaporation, struct. 79−51441
NdP_5O_{14}, ferroelastic, Raman scatt. from soft phonons, 4.2-600K, monoclinic-orthorhombic transition temp. 79−51962
Ni complex, $[Ni(en)_2Cl]_2Cl_2$, heat capacity, X-ray diffraction and mag. meas., phase transition 78−47515
Ni, ferromagnetic, anomalies in thermal expansion and heat capacity 79−73744
Ni-C. exam. of metastable phase diagrams, at high temp. and pressure *(Russian)* 79−56955
Ni-Ti-Al, martensitic, coherent γ'-phase particles and influence on α→γ transformation *(Russian)* 79−29056
$(Ni_{1-x}Cu_x)Ti$, martensitic, shape memory effect kinetics and thermodynamics 80−3021
$Ni(NH_3)_6(BF_4)_2$, enantiomorphic transition, X-ray powder diffr. meas. 78−30574
$Ni(NH_3)_6(ClO_4)_2$, structural phase transition, X-ray diffr. obs. 79−65023
$Ni(NH_3)_6(ClO_4)_2$, thermal expsn., phase transitions 79−60525
NiS inclusions in glass, microcracking, fracture mech. description 80−89333
NiS, thermodynamic study of α⇄β transition *(French)* 80−60854
NiSe, thin film phases, struct. and resist. 78−39236
NiTi, martensitic, shape memory effect kinetics and thermodynamics 80−3021
$(Ni[NH_3]_6)(ClO_4)_2$, reorient. correlation times of NH_3 and ClO_4 groups, Raman obs. 79−28748
O_2, β-γ transition as ref. temp. for IPTS 77−103
O_2, mol. dynamics, solid-state phase transitions effects, Raman spectra *(French)* 77−42372
O_2, solid, transformation charact. and orientation relations 80−33917
P, red to black conversion in quasiisentropic compression 79−33036
Pa, preparation by Van Arkel method, cryst. struct. 78−39715
Pb compounds, perovskites, polymorphic transformations possibility, mag. anal. elec. ordering effects 80−55389
Pb, splat quench in vacuum 79−52268
PbF_2, polymorphic transition temps. under hydrostatic press., DTA study 80−2156
$Pb(Fe_{2/2}U_{1/3})O_3$-$PbZrO_3$ solid solns., phase transition 77−48138
PbI polytypes, phase transforms. and electrical behaviour 78−47839
PbI_2 crystal, gel-grown AgI impurity effects on struct. transformations during growth 77−76339
PbI_2, first-order 2H-4H polytype transition, exciton spectroscopic study 80−59647
PbI_2, hexagonal to rhombohedral phase transform., SFE 79−91643
PbI_2 laminar semicond., phase transition of first kind by exciton spectroscopy *(Russian)* 79−82334
PbI_2, polytypic change, 5 new polytypes, X-ray diffr. anal. 79−37648
PbO, reactively evaporated, photocond., H_2O induced phase transform. 80−60122
Pb_3O_4, tetragonal to orthorhombic transition, heat capacity meas. 80−20929
$Pb_3(PO_4)_2$, ferroelastic transition, X-ray diffr. and scatt. *(French)* 77−31769
$Pb_3(PO_4)_2$, ferroelastic transition, soft modes, inelastic neutron scatt. obs. 77−31772
PbS, phase transitions under action of high press., elec. cond. meas. 77−4196
$PbSnF_4$, allotropic transformations 80−84926
$Pb_{0.95}Sr_{0.05}(Ti_xZr_{1-x})O_3$, solid solns., parameters of Curie Weiss law, permittivity meas. 78−15129
$Pb_8V_2O_{13}$, monoclinic lattice determ. and phase transitions *(French)* 79−99102
$Pb(Zr,Ti)O_3$:Mn, crystal struct. and electrophysical props., piezotransformer props. 78−43806
Pd alloy-H system, α-β phase transformations, hysteresis of press., elec. resistance, review 80−60859
Pd alloys, controllable hydrogen phase naklep, hardening and phase-strengthening 80−16323
Pd-H, electronic states from de Haas-van Alphen measurements 79−7777
Pd-H alloy, 50K transition, internal friction, LF torsion pendulum meas. 77−15490
Pd-H alloy, 50K transition, sp. ht. and thermal relax. meas., diffusion effects 77−15596

polymorphic transformations continued
Pd-H system, α-β phase transformations, hysteresis of press., elec. resistance, review 80−60859
Pd_2AlCu-PdAl system, interactions and solid-state transforms *(Russian)* 80−16272
PdF_2, high press. modification, cryst. and mag. props. 80−38988
PdH_2 internally-charged electrode stability rel. to charging current density, α to β transition 79−57251
$PdS_2(Se_2)(Te_2)$, polymorphism at 75 kbars, 400-1350°C 79−82173
Pr, surface and volume props., flow props., surface layer thickness *(Russian)* 80−59760
$PrAg_2$, high temp. modification, thermal effects 78−38665
Pr_2O_3, from reactive evaporation, struct. 79−51441
Pu, $\beta\rightarrow\alpha$ and $\gamma\rightarrow\alpha$ transforms., microstructures and kinetics 77−25048
Pu, $\beta\rightarrow\alpha$ transform. after full and partial β phase form., kinetics 77−21139
Pu, $\beta\rightarrow\alpha$ transform. after partial β phase form., kinetics 77−28809
Pu-Ga alloys, $\delta\rightarrow\alpha$ transform. kinetics 77−25047
Rb, absolute zero isotherms and polymorphic transition 79−73310
Rb halides, polymorphic transitions, temp. depend. of transition press., thermodynamical data *(French)* 78−38843
$RbAg_4I_5$, depolarisation of light by crit. fluctuations 79−61333
$RbAg_4I_5$, low temp. phases, $\alpha\rightarrow\beta\rightarrow\gamma$ transitions 77−15586
Rb_3Bi, cubic and hexagonal structs., transition 78−26480
Rb_2CO_3, high press. phase relations, DTA 77−43329
$RbCaCl_3$, phase transitions, optical and dilatometric meas. 79−61394
$RbCaF_3$, phonon scatt., thermal cond. meas. 77−7916
$RbCdF_3$:Cr^{3+}, EPR meas. of phase transition 79−61206
$RbCrCl_3$, α-β phase transition, dynamical aspects and thermodynamic theory 80−70404
$RbCrCl_3$ crystals, $\beta\rightarrow\gamma$ structural phase transition, lattice dynamical anal. 80−84291
$RbCrCl_3$, Jahn-Teller induced phase transitions 80−70391
RbF, high press. B1 to B2 phase transition, X-ray diffr. obs. 79−23722
RbH_2PO_4, high temp. phase transition, dielec. const., elec. cond. and IR refl. meas. 78−43118
RbI, phase transition NaCl→CsCl type, preferred orientation of CsCl type 80−49160
RbI, press. depend. of I nucl. relax. press. induced polymorophic transform. study 79−1720
$RbIn(MoO_4)_2$:Fe^{3+} monocrystals, EPR spectrum in the phase transition neighbourhood 80−2624
$Rb_2LiMO_xF_{6-x}$, M=Nb or Mo, high press. transforms. *(German)* 77−89400
$RbLiSO_4$, successive struct. transitions, X-ray diffr. 80−10521
$RbNO_3$, cubic to rhombohedral transition, X-ray diffr. obs. 78−22681
$RbNO_3$, cubic to rhombohedral transition induced by orientation-shear strain coupling 78−22682
$RbNbWO_6$, pyrochlore struct., tetragonal to cubic phase transition 80−75355
RbO_2, low temp. phase study, crystallographic domains and unit cell dimens. 78−63728
Rb_2PtI_6, cubic to tetragonal phase transition 79−1500
S, amorphous and monoclinic transform. kinetics *(German)* 79−42239
S, mol. dynamics, solid-state phase transitions effects, Raman spectra *(French)* 77−42372
α-S, monoclinic allotrope, thermal behaviour 78−67813
$(SN)_x$, polymeric, shear transformation to orthorhombic phase 77−55257
Sb and Sb-Bi, X-ray diffr. investig. of high-press. polymorphism 77−43324
Sb, film, liquid and vapour quenched, metastable struct. 79−56974
Sb film A1-type supercond. vapour-quenched transition temp., A7-type phase transition 78−52145
Sb, polymorphism at high press., temp. hysteresis, DTA *(Russian)* 79−82328
$SbTaO_4$, X-ray and ESR study of phase changes 78−72476
Sc-Fe system phase diag. *(Ukrainian)* 78−84773
ScF_3, metastable high press. phases, X-ray diffr. and IR absorpt. expts. 77−11499
ScO(OH), ScOF, and $Sc(OH)_3$, metastable high press. phases, X-ray diffr. and IR absorpt. expts. 77−11499
$ScSbO_4$, polymorphism at high pressure, X-ray phase anal. 79−46804
$Sc_2Si_2O_7$, polymorphism at high press. and temp., thortveitite struct. stability *(French)* 80−10657
α-Se, monoclinic allotrope, thermal behaviour 78−67813
Se, monoclinic to trigonal conversion, thermodynamic stability and associated investigs. 80−24592
Si, polymorphism under high press. *(Russian)* 78−59947
SiC, 2H→6H transform. mechanism, X-ray diffr. theory 78−30575
SiC, $\beta\rightarrow\alpha$ transformation, interfacial energetics 79−8296
SiC, $\beta\rightarrow\alpha$ transformation, microstructural aspects 79−8295
SiC, cubic to hexagonal, obs. using high-resolution TEM 79−23621
SiC, engng. ceramic, lattice resolution studies 78−27510
SiC, epitaxial film, effect of impurities on polymorphism during growth 80−15414
SiC epitaxial layers, crystallographic orientation effects on polytype stabilization and transform. 79−42413
SiC, HVEM obs. of various polytypes 80−76248
SiC, polycryst., high resolution TEM study of $\beta\rightarrow\alpha$ transform. 80−84928
β-SiC, polytype stability, $\alpha\rightarrow\beta$ phase transformation during growth 78−6028
SiC, polytypic transform. during hot pressing 78−52739
SiC, polytypic transform., interface struct. exam. by TEM 80−15033
β-SiC powder compact, microstruct. changes and β to α transform., Si vapour influence 78−19738
SiC-Bn composite, polymorphic transforms. 77−81259
Si_3N_4, N ion implantation synthesis, struct. and resonance mechanism of α-β transition during annealing 80−33981
Si_3N_4-MgO, hot pressing and α-β phase transform. 78−27461
α-Si_3N_4-MgO (5 wt.%), hot-pressed, rel. to mech. strength development 78−44195
Si_3N_4-ZrO_2, tetragonal to monoclinic transform. of ZrO_2 particles *(German)* 79−43240
SiO_2, cristobalites and topologically related structures, cryst. struct., $\alpha\rightleftarrows\beta$ transform. 77−7688
SiO_2, synthesized tridymite, thermal changes, X-ray and optical studies 79−65020
SiO_{2-x}, vitreous, →β-cristobalite, polymorphic transformation with stoichiometry changes 77−43325
α-Sm, low temp. phase transition *(Russian)* 79−32937

polymorphic transformations continued
Sm, mag. and struct. transitions, X-ray K-line shift, 77-1000K *(Russian)* 77−4518
$Sm_{0.8}La_{0.2}AlO_3$, high temp. Raman spectra, phase transition 79−61367
Sm_2O_3, from reactive evaporation, struct. and polymorphic transform. 79−51441
Sn, $\alpha\rightarrow\beta$ transform., α-Sn nucleation and growth in β-Sn 78−38838
Sn, $\beta\rightarrow\alpha$ polymorphic transformation, mechanism of growth of cubic modification nuclei *(Russian)* 77−44239
β-Sn, equation of state under press. 79−33070
Sn polymorphic transformations ($\beta\rightarrow\alpha$), effect of impurities, exam. 80−7557
Sn-Bi, crystal struct. and superconductivity after appl. of high press. and quenching 80−10531
SnF_2, α and γ modifications, elec. cond., $\alpha\rightarrow\gamma$ phase transitions, structs. 78−75867
SnF_2, second order $\beta\rightleftarrows\gamma$ transition, neutron diffr. and NMR obs. 80−107095
SnTe, polymorphism, high press. and temp., X-ray diffr. study 80−54375
Sr, electrical resistivity and thermoelectric power 78−26846
$Sr_2KNb_5O_{15}$, Raman scatt. experiments in tetragonal tungsten bronze compounds 80−40113
$Sr_2Mg(Co)(Zn)(Mn)(Cd)(Ca)(Sr)TeO_6$, optical SHG study of acentricity, ferroelec. of low temp. phases 80−71324
$SrMnO_{3-x}$, O-deficiency induced polymorphs and elec. cond. 80−71643
$Sr_2NaNb_5O_{15}$, Raman scatt. experiments in tetragonal tungsten bronze compounds 80−40113
$SrSi_2$, dimorphic, transform. of three-dimens. three-connected Si nets 78−42944
$SrSi_2$, high-pressure phase transform., cryst. struct. 77−35693
$SrSi_2$, phase diagram, 10 to 40 kbar, 600 to 1200°C, polymorphic transform. 80−29165
$SrTiO_3$, struct. transition temp. from self-consistent phonon spectrum 77−89517
Sr_2TiO_4-Eu_2O_3, synthesis, luminesc. of materials 79−11534
$SrUO_4$, α to β transition, anomalous behaviour 78−10182
$SrZrO_3$, high temp. phases, struct. determ., soft mode transitions 78−42942
Ta film, planar-magnetron-sputtered, props., β-α transition upon N doping 79−82474
Ta-N, domain configurations of new phase *(French)* 78−56648
Ta-W-Hf, small-angle electron scattering in TEM from lattice strains accompanying precipitation 79−14658
TaN, cubic phase formation from hexagonal by plasma jet heating 78−84726
TaS_2, $1T_\beta$ to $1T_\alpha$ phase transform., cinematographical obs. 77−84925
1T-TaS_2, nearly commensurate phase stabilisation 77−15588
TaS_2, phase transformations and domain structures *(French)* 78−27509
TaS_2(1T) pure and doped, electrical, structural and mag. props. 79−78141
Tb, press. induced polymorphic transition, X-ray obs. 77−59113
TbP_5O_{14}, Raman scatt. at monoclinic to orthorhombic phase transition, soft mode behaviour 78−56486
$TbSi_2$, γ-γ ang. correl. obs. of polymorphic transition, 200-900°C 80−29653
β-Ti alloy, metastable, alloying element effects on phase equilib. 79−56975
Ti alloy VT14, strength in uniaxial dynamic extension, influence of α-ω transform. *(Russian)* 79−52200
Ti alloy VT25, thermomechanical treatment effect on struct. and mech. props. 78−3152
Ti alloys, reversibility of martensitic transformations *(Russian)* 80−108442
Ti, $\alpha\rightarrow\beta$ phase transformation, elec. resistivity 79−15661
Ti, diffusion of Be, temp. depend, radioactive tracer method *(Russian)* 80−10703
Ti, heat capacity near polymorphic transition, temp. depend., vacancy mechanism 79−86884
Ti:transition metal, linear expsn. temp. coeff., polymorphic transition temp. shift 78−6164
Ti-Al, structural and phase changes due to annealing *(Russian)* 80−55440
Ti-Al (40 wt.%), TiAl plate dissolution 79−66055
Ti-Al-Cr-Mo-V, alloy VT22M, exam. of ageing and phase transitions *(Russian)* 79−11641
Ti-Al-Cr-Mo-V alloy VT-22, effect of heating rate on phase recrystallisation *(Russian)* 79−34077
(α+β)-Ti-Al-Mo-Fe alloy VT-22, behaviour during creep testing, solid soln. dissoc. *(Russian)* 80−40346
Ti-Al-V (4.7, 2 wt.%) pseudo alpha alloy, laminar struct. singularities, β to α transformation *(Russian)* 80−7552
Ti-Al-V (6,4 wt.%), phase transformation after hydrogenation 80−7560
Ti-Cr, phase transformation, appl. of Philips STEM400 system 80−25689
Ti-Fe, magnetic susceptibility depend. on phase composition *(Russian)* 80−54875
Ti-Fe (1.4 wt.%), polymorphic transform. due to plastic deform., positron annihilation 80−79939
Ti-Mo, structure associated with BCC to omega transform. *(Russian)* 80−108432
Ti-Nb, phase transformation due to shock wave treatment *(Russian)* 79−91641
Ti-Nb-W, 20 to 1000°C, isothermal section, X-ray anal., microstruct., hardness, cond., transform. *(Russian)* 77−55947
Ti-Nb-Zr (35, 3 wt.%), martensitic τ phase, X-ray diffr. obs. 80−16300
Ti-S, two novel polytype structs. in the system, 16H and 18H *(French)* 79−7582
Ti-V (10 at.%), $\alpha\rightarrow\omega$ transformation, electron diffr. evidence of intermediate BCC phase 80−81051
Ti-Zr, equiatomic, allotropic transform., metal purity and N_2 effects *(French)* 77−59782
$TiC_{1-x}N_x$, lattice distortion of ordered phase *(Ukrainian)* 78−68680
TiI_4, thermal diffusivity, near FCC to BCC transition 80−59740
TiO_2, anatase-rutile transition, additives, mechanism of action *(Japanese)* 78−95744
TiO_2, anatase-rutile transform., inhibition by Nb_2O_5 addition 79−78948
TiO_2, polymorphic transitions rel. to $Sm_2Ti_2O_7$ form. 79−11606
TiO_2 polymorphs, transform. enthalpy 79−100131
TiO_2, rutile, Raman study at high press. 80−89002
TiO_2 type compounds, system of polymorphic transitions 78−47268

polymorphic transformations continued
TiO_2-V_2O_5, interfacial reactions, 565-615°C, anatase-rutile transform. 78−31688
Ti_2O_3, struct. changes at semicond.-metal transition 77−47397
$TiS_{1.7}$, hexagonal polytypes form. mechanism 78−9990
Tl, α and β-phase stability ranges and supercooling, electron diffr. obs. *(French)* 77−84924
Tl, phase diagram and high press. phase transforms., DTA study *(Russian)* 80−66474
Tl, time of flight neutron diffraction meas. of c/a ratio and vol. change at transition 77−15335
Tl-Bi system, phase transitions near Tl_3Bi, elec. props. meas. 80−35181
TlI, rel. to mechanism of growth in silica hydrogels at 25°C 78−35287
$TlMnCl_3$, cubic to tetragonal phase transition, latent heat meas. 79−7694
$TlR(MoO_4)_2$ (R=La to Ho), polymorphism, X-ray diffr., thermographic anal. 78−47269
$TlR(MoO_4)_2$ (where R=Er, Tm, Yb, Lu, Y), polymorphic transition charcts., temp. regions of stability 79−14785
Tl_2SO_4, elec. cond. rel. to thermodynamic props. in phase transitions 77−39690
$TlSbS_2$, phase transitions under action of high press., elec. cond. meas. 77−4196
$Tm_2Si_2O_7$, polymorphism under press., cryst. struct. 77−35692
U, field emission microscopy, emissive props. 78−88409
U-Nb (14 at.%), martensitic and polymorphic transformations 80−60861
U_3As_4, rhombohedral distortion of low temp. 77−7828
U_3O_8, λ-type heat capacity anomalies 77−20080
U_3O_{8-x}, phase transition to U_8O_{21+x}, study by elec. cond. meas. 80−100489
U_3O_{8-z}, thermal expansion, phase transforms. rel. to temp. 77−35721
U_3P_4, rhombohedral distortion of low temp. 77−7828
V:transition metal, linear expsn. temp. coeff., polymorphic transition temp. shift 78−6164
$V_{0.985}Al_{0.015}O_2$, struct. aspects of metal insulator transitions 78−18965
$V_{1-x}Ga_xO_2$, M1→T phase transition, X-ray and mag. meas. 77−11692
V_2O_3, low temp. crystallographic struct. domains 78−83765
VSi_3, cubic-tetragonal phase transition two-band (s-d) model 79−56193
WO_3, condensed phonon modes in successive phases 79−46765
WO_3, electronically induced lattice distortion, screening effect on vibrs. 80−75356
WO_3, struct. transforms. during crystallisation from P_2O_5-WO_3-CaO 77−40343
Xe, adsorbed on $NiCl_2$, phase transition identified as 2D polymorphic transform. 78−56040
Y, film, thickness dependent polymorphism rel. to resistivity 78−39232
YFe_2O_4, low temp. phase transitions and mag. props. 80−7106
YOF-YF_3, high pressure phase transitions 80−55368
$Yb_2Si_2O_7$, polymorphic transforms. and phase diagram under press. *(French)* 77−15573
$Yb_2Si_2O_7$, polymorphism under press., cryst. struct. 77−35692
Zn-Cl boracite, X-ray powder spectra of structure 79−37828
ZnF_2, X-ray diffr. investig. of high-press. polymorphism 77−43324
ZnO ceramics, heat treatment effect on cryst. phases, microstruct. and elec. props. 79−100268
α-ZnP_2, rel. to lattice parameters and thermal expansion, 80-320K, X-ray obs. 80−75373
$Zn_3(PO_4)_2.4H_2O$, thermal transitions, thermographic investig. 77−9063
ZnS, 4H and 6H polytypes, struct. changes on plastic deform. 77−43328
ZnS crystals, structural change under plastic deform., partial dislocation movement 80−79736
ZnS, dependence of hexagonal layer formation on dopant conc. 79−19265
ZnS, polymorphic transition, (β→α) effect of mech. deformation 79−1858
ZnS:Cu AC electroluminescent patterns and polytypic transformations 78−6784
ZnTe-CdSe, solid soln. formation and effects 78−27489
$ZnTiF_6.6H_2O$ and $ZnTiF_6.6D_2O$, ^{19}F NMR, phase transition 79−19790
Zr, allotropic transform. BCC⇆HCP 77−36496
Zr, BCC, lattice dynamics, 1400K, phase transform. 79−19337
Zr based alloys, β→α phase transformation, cooling rate effects 80−7565
Zr, β→α phase transformation, cooling rate effects 80−7565
Zr-C, exam. of metastable phase diagrams, at high temp. and pressure *(Russian)* 79−56955
Zr-Nb, structure associated with BCC to omega transform. *(Russian)* 80−108432
Zr-Nb (2.5 wt.%), seam welding tubing, microstruct. in weld region 79−61621
Zr-Rh(Ir)(Os), α⇄β transform. *(Russian)* 78−80540
Zr-Ru, alloy Zr rich, Ru solubility, eutectic decay, α⇄β transform., struct. *(Russian)* 80−65227
ZrO_2, destabilisation by phosphoric acid, cubic to monoclinic transition, effect of temp., grain size, chemical composition 79−20037
ZrO_2, enthalpy and heat capacity at 1100-2500K 80−103472
ZrO_2, MgO partially stabilized, microstruct. development during ageing 79−91710
ZrO_2, monoclinic, variation of lattice strains *(Japanese)* 77−72600
ZrO_2, near-surface phase transforms., effect of grinding and polishing 78−15557
ZrO_2, neutron irrad., monoclinic to cubic transform. 78−87720
ZrO_2, partially stabilized, transform. toughened, fracture toughness 79−91775
ZrO_2, polymorphism at high press., X-ray diffr. obs. 79−73311
ZrO_2, polymorphism rel. to stabilisation *(Rumanian)* 78−59946
ZrO_2, Raman spectra, temp. depend. 78−6668
ZrO_2, technical grade containing CaO, polymorphic transform. up to 1200°C 78−64539
ZrO_2, tetragonal to monoclinic phase transf. by ball-milling 80−25687
ZrO_2, ZrO_2-HfO_2, soft phonon modes and monoclinic-tetragonal phase transition 77−62638
ZrO_2-Sc_2O_3 system, high-temp. phase transitions, elec. cond., thermal props. 77−16573
ZrO_2+$BaCO_3$ react., mechanism, effect of polymorphic transitions 79−11605
Zr_2O_3 microcrystals, tetragonal struct. stabilisation, crystallite size effect 78−51670

polymorphism
see also crystal structure; isomorphism; polymorphic transformations
4-acetyl-4′-n-alkanoyloxy-azobenzenes, type A, B smectic, nematic phase, solid state polymorphism, preparation, melting behaviour 78−59745
2-(4-n-aklylphenyl)-5(4-nalkoxyphenyl)-pyrimidines, smectic polymorphism, miscibility meas. 79−86678
p-alcoxybenzilidene butylaniline, liq. cryst., mag. anisotropy and polymorphism *(French)* 77−76532
n-alkane, long chain, syntactic coalescences between monoclinic and orthorhombic polymorphs 80−10520
n-alkanes, even, long-chain, layer interaction energies for different twin and polytypic positions 77−65985
1-(4-alkoxy-benzoyloxy-phenyl)-2-(4′-pentylphenyl)-ethanes, synthesis and mesomorphic props. 79−90536
N-4-n-alkoxybenzylidene-4′-n-alkylanilines, classification of polymorphic smectic phases 79−55661
p-alkoxybenzylidene-p-alkylaniline, liq. crysts., ^2H NMR, aliphatic and chain conformation 79−14670
4-n-alkoxyphenyl 4-n-alkylcyclohexanecarboxylates, smectic polymorphism, miscibility meas. 79−86678
n-alkyl 4′-n-alkoxybiphenyl-4-carboxylates, smectic polymorphism, X-ray diffr. and miscibility meas. 79−27912
4-4-n-alkyloxybenzoyloxy-benzylidene-4′-cyanoanilines, reentrant nematic and smectic phases 80−88308
n-(4-n-alkyloxybenzylidene)-4-n-alkylanilines, smectic polymorphism, miscibility meas. 79−86678
N-4-n-alkyloxybenzylidene-4-n-alkylanilines, smectic polymorphism, calorimetric study 80−88307
2-4-n-alkylphenyl-5-(4-n-alkyloxyphenyl)-pyrimidines, smectic polymorphism, calorimetric study 80−88307
amorphous systems, origin of thermal anomalies, struct. model 78−91256
astrophyllite, electron diffr. characts. of polytypic forms 77−39573
astrophyllite, polytypic forms 77−39572
bis-(4,4′-n-alkoxybenzylidene)-1,4-phenylenediamines, smectic polymorphism up to 3 kbars, differential thermal anal. 79−55873
carbon tetrabromide, ordered, polymorphism 78−22700
carbon tetrabromide, ordered phases, polymorphism obs. 80−54217
carbon tetrachloride, ordered phases, polymorphism obs. 80−54217
carbon tetraiodide, ordered phases, polymorphism obs. 80−54217
cellulose II, unit cell parameters, neutron diffr. 77−1086
ceramic characteristics *(Japanese)* 80−15075
chloritoid intergrown polytype identification by electron multiple scatt. 80−70184
p-(N-chlorobenzylidene)-p-chloraniline, cryst., polymorphism, cryst. struct. rel. to mol. conform. 78−75611
cholesteryl myristate, polymorphism of blue phase, DTA and microscopy meas. 79−37819
cholesteryl nonanoate, polymorphism of blue phase, circular dichroism at high-press. 79−37821
cholesteryl nonanoate, polymorphism of blue phase, DTA and microscopy meas. 79−37819
cholesteryl nonanoate, polymorphism of blue phase, optical rot. and refl. 79−37820
β-choline chloride, X-ray diffr. 78−55861
chrysotile, cryst. struct. rel. to milling, X-ray diffr. 77−55278
close-packed crystals, elastic moduli of polytypic modifications 79−51187
complex polytypic structure, layer sequence analysis by method of structural models 77−19824
convergent beam electron microscopy for materials science 80−107028
COOB, solid state dimorphism and cryst.-smectic transition, Raman study 80−45063
copper (I)-butyrate, dimorphism, X-ray diffr. and fluoresc. *(German)* 79−51090
copper phthalocyanine, on graphite, epitaxial growth of new polymorph 77−80712
cyano biphenyl-substituted benzoates, exhibiting reentrant nematic behaviour, polymorphism and X-ray diffr. 79−94890
cyclohexanol, polymorphism, Raman spectroscopy 77−73138
4,4′-di(p,n-alcoxybenzylideneamino)diphenyls, X-ray diffr. study of smectic polymorphism *(French)* 77−76299
dialkyl ammonium manganese chloride, phases and structural phase transitions, DSC and X-ray diffr. meas. 77−47574
dianthronylidene ethane, luminescent excimer geometries, intermol. shift 78−27294
1,5-dichloro anthracene, cryst. struct. calc., use of at.-at. pots. 79−46646
p-dichlorobenzene, Cl-Cl interactions at 100K, isotropic pot. functions calcs. 78−18578
p-dichlorobenzene($-d_4$), mixed cryst. phases, mol. reorientations and intermol. interactions, Raman obs. 79−28751
2,2-dichloropropane, thermodynamic and structural studies of polymorphism 78−18571
DNA, polymorphism, X-ray diffr. and computerised model building study 78−27894
electrostatic lattice energies of ABX_3 polytypes with close-packed AX_3 layers 77−80440
enantiomorphously related space groups, identification by electron diffr. 77−19848
ethanol, polymorphic forms, mol. motion, NMR obs. 80−88885
ethyl-p-azoxybenzoate, far IR and Raman spectra, smectic polymorphism 80−76022
α-, β-, γ- glycine, thermal expansion tensor 79−95187
grain boundary allotriomorphs, stereology 77−44211
hexaphenylcarbodiphosphorane, cryst. struct., triboluminesc., polymorphism effects 79−61447
n-hexatriacontane, cryst., orthorhombic modification, vibr. spectra 80−50314
ice, thermal conductivity of nine solid phases 78−30801
4,5-iminophenanthrene, polymorphism, X-ray diffr. and photoluminesc. obs., 77 to 300K 77−63449
interaction of layers for polytypic crystal structs., appl. of self-consistent field method to statistical model 79−37639
layer 1st order interaction for polytypic crystals, statistical model 77−80436
layer distrib. of polytypic crystals, stochastic model 77−80435
liquid crystals, solid state polymorphism, differential scanning calorimetry and IR and Raman spectra obs. 80−55094
lysozyme effect of pH on dimorphic crystal growth 79−14728
mathematical model, SEG-1, for polytypic structures *(Russian)* 78−75613
MBBA, polymorphism, positron annihilation obs. 78−72632

polymorphism continued
MBBA, solid phase polymorphism, IR and Raman spectra study *(French)* 79−87438
metals, entropy of fusion and allotropic behaviour, exam. of correlation and modification of Richard's rule 78−71838
metals and alloys, use of dilatometric methods *(French)* 79−5100
methane-d_1($-d_2$,$-d_3$), solid, struct. of phase III from thermodynamic meas. 79−82193
methanol, C-O-H bending mode in α- and β-forms at 85K 77−8588
mica, layer deformation and cryst. energy, struct. models for 1M and $2M_1$ polytypes 79−19184
micas, synthetic, polytypism and faulting, lattice imaging obs. *(French)* 78−79587
molecular crystal, polymorphism and isomorphism, cryst. forces and mol. conform. relation 79−46592
molybdates (double), of mono- and tri-valent metals, polymorphism, X-ray diffr. obs. 78−87642
Monte Carlo simulation of polytypes 78−6024
p-nitro-p′-methylbenzylidene aniline, polymorphism 78−18633
nomenclature recommendations of International Mineralogical Assoc. and International Union of Crystallography 77−65927
noncrystalline solid element, polymorphic bonding and thermal stability 77−31597
nylon 66, polymorphism 79−14694
Nylon-12 film, casting conditions effect on polymorphism 80−84903
octacosane crystals, complex growth polytypism and periodic polysynthetic twins 77−47360
order-disorder groupoid family, parameters, stacking 80−38982
order-disorder structures, desymmetrisation 80−38986
order-disorder structures, layer stacking 80−38981
order-disorder structures, X-ray powder patterns features 80−38864
organic compounds, crystallographic pedigree 78−91287
organic molecular crystals, use of atom-atom pots. in interpreting behaviour, book contrib. 80−84136
organic solids, electron microscopic approach to struct. and reactivities 79−73077
PAA, liq. cryst., solid-state polymorphism obs. 77−4200
PAA, solid state polymorphism 78−42945
p-pentoxybenzilidene alkylaniline, liq. cryst., mag. anisotropy and polymorphism *(French)* 77−76532
phenol I and II, permittivity and molar polarisation at pressures between 140-2000 bar 77−77136
phospholipid monolayers, polymorphism 78−40120
poly(vinylidene fluoride) orientation, solid state deformation by coextrusion 80−40394
poly 2,3-dichlorobutadiene, struct., morphology, polymorphism 79−65008
polyethylene, orthorhombic and triclinic lattices, eqns. of state 79−28069
polypentene-1, isotactic, polymorphism of form I 79−19159
polytype relative stabilities, entropy contribs. 80−100197
polytypes, computer simulation 80−79734
polytypes, one-dimens. Kronig-Penney model and calcs. 80−75494
polytypes 12H and 14H, struct., polymorphic transition in Cu_2S 79−55692
polytypic structure, determ. method, applic. to 26H Ti-S polytype *(French)* 77−11509
potassium palmitate-water bilayer, lamellar liq. cryst. polymorphism, NMR and birefringence 79−60270
PVDF, film, polymorphism induced by poling and annealing 80−24372
PVDF dielectric, piezoelec. and pyroelectric props. rel. to crystalline forms 80−15982
pyrene, cryst. struct. calc., use of at.-at. pots. 79−46646
rare earth oxyorthotitanates, crystallochem. classification 80−107142
rare earth silver tungstates, α,β and β' phases 77−31627
rare earth trialuminides, long period polytypes, electron diffr., high resolution imaging 78−83781
rare-earth intermetallics, R_2Co_7, polymorphism of Ce subgroup alloys, eutectic decomposition *(Russian)* 80−66504
review, structural, phase and cryst. growth aspects 78−83764
semiconductive compounds, type $A_3^{II}B_2^{V}$, genetic rel. between cryst. structs. of polymorphic modifications 79−60302
semiconductor morphotropic and isomorphic series, cryst. struct. stability 77−51353
semiconductor with polytype layers, interface exciton states 78−26819
semiconductors, homologous series, structural transitions associated with morphotrophy 77−39675
serpentine minerals, milling rel. to cryst. struct., X-ray diffr. 77−55278
smectic liquid crystal, polymorphism, mol. struct. effects 77−47348
stearic acid, large single cryst. growth from organic soln. 78−31314
steel, hypoeutectoid Widmanstatten struct. form., contrib. to the laws *(Slovenian)* 78−84817
stilpnomelane, complex layer silicate, struct. of long-period polytypes 77−64266
TEM, appl. to organic solid-sate chemistry, review 79−60235
terephthalylidene-bis-(4-n-alkylanilines), smectic polymorphism, calorimetric study 80−88307
terephtylidene-bis-(4-nalkylanilines), smectic polymorphism, miscibility meas. 79−86678
transition metal chalcogenide layer compounds, convergent beam electron microscopy obs. 80−108689
transition metal dichalcogenides, deform. modulated superstruct., model explaining results for VSe_2 78−51515
1,1,1-trichloroethane, polymorphism under high pressure *(French)* 80−96644
1,1,1-trichloroethane, thermodynamic and structural studies of polymorphism 78−18571
triphenylene hexa-n-dodecanoate, mesomorphic polymorphism 79−41950
tungstates (double), of mono- and tri-valent metals, polymorphism, X-ray diffr. obs. 78−87642
water, random network model, liq. and ice polymorphs enthalpy and heat content 80−64869
X-ray powder patterns for polytypic struct. with stacking faults anal. 78−38577
Zhdanov notation, resolution of ambiguities, homometric structs. 77−31619
Zircaloy-4, polytype struct. of intermetallic precipitates, electron microscope obs. 79−43250
$ABCl_3$ cpds., basic struct. types and polymorphisms 78−79583
Ag:He, implanted films, solid solutions radiation induced polymorphism 79−86810
β-AgI, 2H and 4H polytypes, exciton refl. spectra at 4.2K 79−69860

polymorphism continued
AgI, elastic behaviour near phase transitions with negative dP/dT 78−83885
β-AgI, exciton luminesc. of 2H and 4H polytypes 77−85783
β-AgI, luminesc. of 2H- and 4H-polytypes 80−2843
AgI, mixed-polytype cryst. containing new 12H polytype 77−19911
Ag_2WO_4-$In_2(WO_4)_3$, cpd. formation and polymorphism 77−86009
Ag_2WO_4-$Sc_2(WO_4)_3$, cpd. formation and polymorphism 77−86009
As, solid state, new phase identification 79−99315
As_4S_4 polymorphs, Raman spectra, structural implications for As_2S_3 amorphous films 79−61385
B, and borides, cryst. chem., struct., book contrib. 78−47278
B, polymorphism rel. to CVD mechanics and deposit structs. 80−15403
B_4C, morphology and struct. of vap. grown crysts. 79−7562
BN, polymorphic modifications form. under low and high press. 79−15597
$BaCrO_3$, 27 layer polytype, struct. determ. 80−107162
δ-$BaFe_2O_4$ room-temp. formation and polymorphism *(German)* 80−44192
$BaMnO_{3-x}$, O_2 deficiency induced polymorphs 78−26531
$BaTiO_3$ polymorph, hexagonal, low temp. and surface CO_3 adsorption and desorption 80−80713
Be-Si-O-N polytypes, X-ray study 78−27496
Be-Si-O-N system, polytype periodicities, direct obs. 78−18662
Be_3N_2-$BeSiN_2$ system, crystallography and phase relationships, TEM and electron diffr. study 80−92502
$Bi_2Sn_2O_7$, polymorphic phase transition, X-ray, DSC, SHG, dielec. and optical obs. 80−44163
C allotropes, diamond, graphite, gas-solid interface, electronic struct. HFR calc. 80−54745
C, crystalline, intermediate form, CI lattice energy *(Russian)* 78−22693
C, high temperature behaviour, over 2600K, polymorphic carbyne forms 79−7575
C, nature of metastable phases 77−89404
C, polymorphic modifications form. under low and high press. 79−15597
C_8 crystalline diamond-like form, cryst. struct. *(Russian)* 79−99114
$(CO(NO)_2CL)_2$, order-disorder struct., X-ray data 80−39037
C_2S mineral, chem. and polymorphism 79−69051
Ca-Nb-O perovskites, struct. characterisation *(French)* 78−10021
$CaBSi_2O_6$, B=Mg, Fe^{3+}, Al, pyroxenes, order-disorder interpretation 80−38987
$CaNbF_7$, polymorphism, X-ray powder diffr. data *(French)* 80−19779
$ZCaO.SiO_2$-$2CaO.Na_2O.P_2O_5$ system, polymorphism and solid soln. 78−19731
Ca_3SiO_5, polymorphism, X-ray diffr. data *(French)* 79−94973
$Ca_6Si_6O_{17}(OH)_2$, xonotlite, polytype identification from electron diffr. patterns 80−72519
$CdBr_2$, polytype 12R, cryst. struct. determ. 80−33937
CdI_2 crystals, growth conditions effect on polytypism, X-ray diffr. study 80−28942
CdI_2, dielec. props. rel. to polytypically modulated structs. 79−94971
CdI_2, faulted 4H structure analysis 77−80447
CdI_2 polytypes, centrosymmetric space groups 77−31618
CdI_2 polytypes, crystal structure analysis, refinements for structure determination 78−91312
CdI_2 polytypes, crystal structures using new refinements for structure determination 78−91313
CdI_2 polytypes, defect struct., electron microscopy 79−14809
CdI_2, polytypes, dielec. const., periodicity and disorder depend. 77−28506
CdI_2 polytypes, vapour growth mechanism 80−84124
CdI_2 polytypic crystals, dielectric loss behaviour 80−66108
CdI_2, polytypism, review 77−11498
CdI_2, polytypism and luminesc. *(Russian)* 78−56520
CdI_2, soln. grown, rotation twinning, arcing and polytypism 78−51557
CdI_2, sublimed films, preparation, struct. 77−24491
$CdI_{2-x}Br_x$, vapour grown mixed cryst., growth and polytypism 79−69044
$CdIn_2Se_4$, high resolution electron microscopic study of polytypism 80−88119
CdS films, chem. deposited, growth kinetics and polymorphism 80−75463
CdS, polytype relative stabilities, entropy contribs. 80−100197
Ce_5Sn_3, low temp. modification with tetrogonal struct. 80−1963
Co-Al alloy, multilayer martensite phases, illustration of polytype structures 80−84932
$Co_3(AsO_4)_2$ polymorph, cryst. struct., closest packing 80−70174
$Co(NH_3)_6Cl_3$, proton second moment meas., 96 to 404K 79−95652
Cs, structural energies, pseudopotential formalism 80−39519
$CsNO_3$, high pressure phases III and IV, X-ray struct. determ. 80−28953
Cs_2SO_4, IR absorpt. spectra, polymorphism, site group approx. and SO_4 stretching mode 78−52510
CuF_2, high temp. polymorphism and thermal props. 80−75199
$CuFe_2S_3$, cubanite polymorph, synthesis above 200°C and 1 GPa, lattice constants 80−108367
$Cu_{2-x}S$, digenite, X-ray determ. of structural transitions 80−92474
$DyAl_3$, polytypism, high resolution microscopy and electron diffr. obs. *(French)* 77−11503
Fe allotropy, rel. to alloy systematics in the long periodic table 79−37649
Fe complex, iodobis(morpholyldithiocarbamate), allotropes, intermol. exchange interactions 77−8455
Fe-C (0.11, 0.23, 0.42 wt.%), grain boundary ferrite allotriomorphs, growth kinetics 77−44244
Fe-WO_3 system, struct. phase exam. by optical microscopy and X-ray diffr. 78−31389
$Fe^{2+}BSi_2O_6$, B=Mg, Fe^{3+}, Al, pyroxenes, order-disorder interpretation 80−38987
α-$FeGa_2S_4$, 1T polytype, cryst. struct. refinement *(French)* 80−103304
$Fe_2(MoO_4)_3$, polymorphism 77−84691
δ-FeO(OH) and its solid solns. synthesis, X-ray diffr. and TEM studies 80−29891
FeS polymorph formation, Fe corrosion in aq. H_2S 80−81231
Fe_9S_{10}, polytypism, Fe diffusion near antiferromag. to ferrimag. transition 80−44830
$FeSO_4$, anhydrous, γ, β and γ-phases, Mossbauer spectra 77−12287
$Fe_2(SO_4)_3$, Mossbauer isomer shift in rhombohedral and monoclinic forms 78−6609
Ga, cryst. struct., high press., X-ray diffr. obs. 78−42952
Ga, film, polymorphism, electron diffr. obs. *(French)* 78−18922

polymorphism continued
Ga metastable states, supercooling and polymorphism *(French)* 78−14325
Ga-Se system, phase diagram and cryst. struct. of phases *(French)* 80−93544
GaSe polytypes, tight binding study of electronic states 79−60705
$GdAl_3$ thin films, polytypism 79−99446
$GeSe_2$, single crysts., 3 polymorphic forms, DTA, photolum., IR and Raman sepctroscopy 80−33923
H bonded systems, IR spectra, theoretical interpretation 79−31519
HBO_2, cubic, monoclinic and orthorhombic forms, H bonding, IR and Raman spectra 80−76029
HfO_2, high pressure polymorphism 80−59429
$_xI_{1-x}$ mixtures, high-temp. solids and melts, struct., thermodynamic props., Raman spectra obs. 80−66174
InSb, polymorphism and cryst. struct. at high temp. and press. 78−95026
$InSbS_3(Se_3)$, prep., polymorphism, cryst. struct. 78−44002
$KAlSiO_4$ metastable polymorph, prep. by ion exchange with $RbAlSiO_4$, struct. 78−79585
KCN, polymorphism, high pressure, Raman spectra 78−88302
$K_2Cr_3O_{10}$, cryst. struct. determ. 79−23592
KNO_2 polymorphs, high press. Raman spectra 77−85725
$KNbW_2O_9$, crystallography, polymorphism and phys. props. 78−79599
K_2SO_4, IR absorpt. spectra, polymorphism, site group approx. and SO_4 stretching mode 78−52510
$KX(MoO_4)_2$, X=Sm, Eu, Gd, polymorphism investig. by X-ray diffr. and DTA 77−4091
$K_4Zn(WO_4)_3$, cryst. struct. and polymorphism 80−1996
$K[Ag(CN)_2]$, Raman scatt., press.-induced phase transitions and phonons 79−33698
La_5Sn_3, low temp. modification with tetrogonal struct. 80−1963
$LiAlO_2$, fuel cell electrolyte matrix, prep. and struct. characts. 78−80488
$LiR(WO_4)_2$, R=La-Sm, triclinic modification, cryst. struct. 80−33976
Li_2SO_4, IR absorpt. spectra, polymorphism, site group approx. and SO_4 stretching mode 78−52510
LiSiON, allotropes, powder diffr. obs. *(French)* 78−63726
$Li_2W_2O_7$ 77−48407
Li_2WO_4, type II polymorph. crys. struct. determ. 80−15073
$Lu_2Si_2O_7$, crystal struct. of X form, polymorphism under press. *(French)* 77−47430
$MgBSi_2O_6$, B=Mg, Fe^{3+}, Al, pyroxenes, order-disorder interpretation 80−38987
MgF_2, high temp. polymorphism and thermal props. 80−75199
$MgNbF_7$, polymorphism, X-ray powder diffr. data *(French)* 80−19779
$Mg(OH)_2$, and calcination product, relations between particle size, shape and surface area 78−48355
Mn allotropy, rel. to alloy systematics in the long periodic table 79−37649
MnF_2, high temp. polymorphism and thermal props. 80−75199
$MoS_2(Se_2)(Te_2)(2H)$ polytypes, Kramers-Kronig anal. of reflectivity spectra, 0-30 eV, band model 79−51976
$MoSe_2$, single cryst., growth, struct. obs. 79−90607
$NaBSi_2O_6$, B=Mg, Fe^{3+}, Al, pyroxenes, order-disorder interpretation 80−38987
Na_2CO_3, structural modulation, theory 77−35535
Na_2SO_4, IR absorpt. spectra, polymorphism, site group approx. and SO_4 stretching mode 78−52510
α-$NaBSbS_2$, cryst. struct. and $\beta \rightarrow \alpha$ phase transform. features 80−33961
Nb_3Au, BCC, density of states, comparison with A-15 78−80095
Nb_2O_5, cryst. growth and microstructure 79−95913
NbS_3, Peierls distortion, chain polytypism and dislocation coupling 78−79589
$NbS(Se)_2$, polymorphism at high press. and temps., T_c and band struct. 78−26528
$Nb_{0.87}V_{0.13}Se_2$(4Hb), stacking layer study, appl. of convergent beam electron diffr. 80−39116
NiF_2, high temp. polymorphism and thermal props. 80−75199
P allotropic modifications, muonic X-ray intensities, computer analysis 80−23577
P, black allotrope, orthorhombic bonding, up to 26.6 kbar, neutron diffr. obs. 79−99106
PbI_2, 24-layered hexagonal polytype, growth in U-tube by silica gel method, struct. 77−4722
PbI_2, elec. props. rel. to polytypically modulated structs. 79−94971
PbI_2, photoelectromagnetic investigation, expt. 79−24010
PbI_2 polytypes, centrosymmetric space groups 77−31618
PbI_2, Raman spectra, phonon dispersion curves, vibrational props., lattice parameters 79−69211
$PbSnF_4$, anionic conductor, thin films and ceramics 80−107556
PdS_2, at 75 kbars, 400-1350°C 79−82173
$PdSe_2$, at 75 kbars, 400-1350°C 79−82173
$PdTe_2$, at 75 kbars, 400-1350°C 79−82173
$Pr_{24}O_{44}$, beta phase, high resolution cryst. struct. images 78−42991
Pr_5Sn_3, low temp. modification with tetrogonal struct. 80−1963
$RbNO_3$, high pressure phase V, X-ray struct. determ. 80−28953
S, effect of high pressure system configuration 78−43104
S, irrad., allotropic modifications and activity distrib. 80−70255
α-S, under hydrostatic press., deformable mol. lattice statics 80−49175
α-S, zone-centre lattice vibrs., including hydrostatic press. effects 80−49314
Sb_5O_7I polytypes, cryst. growth, struct., ferroelastic and ferroelec. props. 78−31309
Sb_5O_7I, polytypes 2MC and 2MA, photoferroelastic phenomena 79−95447
Sc-Fe-Si system, phase obs. at 800°C *(Russian)* 78−23661
$ScSbO_4$, polymorphism at high pressure, X-ray phase anal. 79−46804
Se allotropic modifications, muonic X-ray intensities, computer analysis 80−23577
Si polymorphs, optical props., orthogonalized LCAO calc. 78−10345
Si-Al-O-N ceramic systems, layer struct. 80−6382
Si-Al-O-N polytypes, direct lattice resolution using high resolution electron microscopy 78−38682
Si-Al-O-N polytypes, hot-pressed, microstruct. 80−3023
SiC, 102R polytype struct, and localisation, by RHEED *(French)* 77−65966
SiC, 126R polytype, struct. determ., use of lattice imaging in electron microscope 78−26498
SiC $147R_{(b)}$ polytype, crystal structure by X-ray diffraction method *(Chinese)* 80−54206

polymorphism continued
SiC, determ. of size and conc. of crit. clusters in vapour phase in homogeneous nucleation process 79−94951
SiC, epitaxial layer polytypism 77−62781
SiC, epitaxial layer polytypism 77−62782
SiC, epitaxial layers, growth processes 77−85105
SiC, extremely large-period polytypes, X-ray diffr. and TEM 77−31636
SiC, further polytypes discovered using Laue diffraction *(Chinese)* 80−10535
SiC, HVEM obs. of various polytypes 80−76248
SiC, high period polytype at interface of two interacting spirals 80−20041
α-SiC, lattice absorpt. bands in IR spectra, surface treatment effects 77−52071
SiC, one dimensional disorder 78−51492
SiC, polymorphism, electron diffr. and optical simulation *(French)* 77−39519
SiC polymorphs, widths of first minibands and effective masses, resist. anisotropy 80−20071
SiC polytype 6H, space group 80−1956
SiC, polytype relative stabilities, entropy contribs. 80−100197
SiC, polytypes, birefr. meas. 77−43963
SiC polytypes, contribution of ionic bonding to thermal stability 80−28946
SiC polytypes, elastic moduli, effect of degree of hexagonality 77−59845
SiC polytypes, electrolum. in anodic oxidation, band model *(Russian)* 80−50429
SiC polytypes, free exciton luminesc. meas., phonon energies 80−80852
SiC polytypes, lattice imaging studies on intergrowth structs. 80−107025
SiC polytypes, localisation of cond. band minima in Brillouin zone 80−20082
SiC polytypes, quantitative calcs. from X-ray diffr. peak intensities 79−82174
SiC polytypes, stacking sequences by high resolution electron microscopy 80−15054
n-SiC, polytypes, temp. depend. of piezoresist. constants 79−11125
SiC polytypes deformed, resist. anisotropy in (0001) plane 80−20198
SiC, polytypic forms determ. from Kikuchi electron diffr. patterns 77−31566
SiC, polytypic transform., interface struct. exam. by TEM 80−15033
SiC, polytypism, effect of furnace temp. and contamination *(Polish)* 79−27969
SiC, polytypism, reflection electron diffr. 78−83694
SiC, reaction sintered transform. interface morphology 78−31364
SiC single crysts., polytypism obs. by high temp. oxidation expts. 78−59797
α-SiC, single crysts. phase struct. rel. to heat treatment, nucleation 80−38991
B SiC, sintered, effect of Al trace amounts on specimen props. 79−83289
SiC, spiral growth of polytype struct. from faulted matrix, 15R and 4H struct. 77−4778
SiC, VPE layers, growth kinetics, polytypism 77−11809
SiC:Tb(Sc), various polytypes photolum. meas., identification of 4H and 6H polytypes 77−63459
SiO_2 (silicalite), new hydrophobic crystalline silica mol. sieve 78−30598
SiO_2, chem. bond and rel. props. 77−43199
SiO_2 polymorphs, CNDO/2 MO calc. 80−6386
SiO_2, polymorphs (cristobalite and tridymite), vibr. normal modes, GVFF calcs. 78−51627
SiO_2, stishovite, single cryst. anal. of struct. 78−53648
Si_3O_7 layered stacks, polymorphism, cryst. chem. anal. 79−60301
SnS_2, 2H and 4H, effect of press. on optical absorpt. edge 77−77238
SnS_2, effect of powdering on polytypic cryst. struct. 80−1979
SnS_2 polytypes, electronic bandgap meas. 80−34358
SnS_2, polytypism, and cryst. struct. by X-ray methods 79−77542
SnS_2(2H and 4H), Raman scatt. and phonon frequencies 77−48159
Sr Nb_2O_6, crystallography, polymorphism and isomerism, X-ray diffr. and DTA study 80−100216
$SrAl_2Si_2O_8$, TEM obs. of feldspar aand hexacelsian polymorphs 78−83827
Ta-Ga, crystal struct. at high press. 80−88112
Ta_2O_5, ϵ-modification, cryst. struct. and microstruct. 79−51083
TaS_2, 1T-, 2H-, 6R- thin cryst. polymorphs, anomalous resistivity, 0-350K 77−11909
$TaSe_2$, 1T and 2H superstruct., cryst. struct. using X-ray diffr. 80−39044
$TaSe_2$, 4Hb polytype, CWD induced atomic shifts 80−39045
$TaSe_2$(6R), stacking layer study, appl. of convergent beam electron diffr. 80−39116
$TbAl_3$, polytypism occurrence 80−44164
$ThSiO_4$, huttonite and thorite polymorphs, cryst. struct. 78−51478
26H Ti-S polytype, struct. determ. *(French)* 77−11509
$TiCl_3$, vib. spectra 77−40231
$Ti_{1+x}S_2$, polytypic struct., Ti ordering, two-dimensional model 79−14776
$Tl_2B_4O_7$, polymorphism *(French)* 78−6035
TlBr, polymorphism, XPS obs. 80−97398
TlCl, polymorphism, XPS obs. 80−97398
$TlR(MoO_4)_2$ (R=La to Ho), polymorphism, X-ray diffr., thermographic anal. 78−47269
$Tm_2Si_2O_7$, crystal struct. of X form, polymorphism under press. *(French)* 77−47430
$V_{13}O_{24}$ long-period Magneli phase as product of V_6O_{11}-V_7O_{13} periodic microsyntactic intergrowth 80−50618
VSe_2 (1T), deform. modulated superstruct., electron diffr. expts. 78−51515
WO_3 polymorph, hexagonal, cryst. struct. imaging by high-resolution electron microscopy 80−103309
YSeF, crystal atomic struct. *(French)* 78−10001
YSeF, direct lattice imaging of polytypes 77−4087
YSeF, orthorhombic polytype 140, struct. study *(French)* 80−88102
YSeF, ten-layer polytype 10M, cryst. struct., X-ray diffr. meas. *(French)* 77−47409
$Yb_2Si_2O_7$, crystal struct. of X form, polymorphism under press. *(French)* 77−47430
$ZnCl_2$, Raman spectra 78−80332
ZnF_2, high temp. polymorphism and thermal props. 80−75199
$ZnIn_2S_4$, electronic props. of polytypic forms, pseudopot. calc. 80−38997
ZnS crystal, inhomogeneous, microscopic struct. investig. using synchrotron radiation 77−76424

polymorphism continued
ZnS, dependence of hexagonal layer formation on dopant conc. 79−19265
ZnS, elastic moduli of polytypic modifications 79−51187
ZnS, polytype relative stabilities, entropy contribs. 80−100197
ZnS, Zn(S,Se), large single crystals, vapour growth and defect characterisation 80−25540
ZnS:Cu^{2+}, Jahn-Teller effect, stacking faults and formation of polytypes, absorption and emission spectra 77−4660
ZnS:Mn_2 dopant conc. effect on stacking fault energy 80−2041
ZnS:Tm^{3+}, charge compensation and polytypism influences on fluorescence 80−89051
$ZnS_{1-x}Te_x$, polytype single cryst. grown from melt 79−14762
ZrO_2, high pressure polymorphism 80−59429

polynomials
see also splines (mathematics)
2-D polynomial matrices, factorisation and coprimeness 77−64915
Abel integral eqn. solution by orthogonal polynomials 78−67436
absorbing-scattering semitransparent planar layer, flat temp. waves 78−90683
algorithm for high order polynomial extrapolation 79−88798
analytic continuation of the Fourier Series on connected compact Lie groups 78−93511
anisotropic elastic half-space, polynomial solns. for ellipse 79−10480
Appell function F_1, generating functions 77−17777
arbitrary pseudo-Euclidean space, real and complex boosts 78−113
area-preserving polynomial mapping, instability 78−77463
associated Legendre polynomial $P_L^M(x)$, Chebyshev expansion 80−8774
atomic spectra, two-electron matrix elements in Hylleraas coords., ang. integrals, radial recurrence relations 79−3386
beam vibrations, bending and twisting motions 78−90751
Bernstein's polynomials, differentiation and integration 78−40
Bessel polynomials, associated integrals 77−74191
Bessel polynomials 77−22385
Boltzmann eqn., Krook-Wu model solutions, distribution function *(French)* 80−17898
Cauchy type singular integral eqns. with complex singularities, numerical soln., stress intensity factors 78−55611
Chebyshev, shifted, soln. of second kind operation eqns., convergence 78−62059
Chebyshev, use in algorithm computation in electron optics aberrations 79−27156
Chebyshev polynomial method for computing analytic solns. to eigenvalue problems, appl. to anharmonic oscillator 78−62058
Chebyshev polynomials, application to nonlinear analysis of circular plates 77−49597
circular plates subjected to transient loads, nonlinear dynamic response 78−16648
circulatory system polynomial model *(Japanese)* 77−70488
classical, dimensions of irreducible representations 80−18087
classical functions, expansion problems 77−22390
continuous descent functions for polynomial eqns. 77−13581
curved finite elements, forbidden nodes 79−88796
differential eqn. approx. for gravity wave diffraction *(Russian)* 79−77143
direct pot. method for plane elastostatics, polynomial approx. 77−72177
dispersion relations, analysis methods 79−67141
dual series eqns. involving Konhauser biorthogonal polynomials 78−4464
Earth surface topography, polynomial and Fourier trend surfaces computation 78−32245
education, linear differential eqns. with polynomial appl. Schrodinger eqns. 77−49522
elastic shells, two-dimensional eqn. system *(Ukrainian)* 78−89342
elasticity, appl. of orthogonal polynomials 80−36857
elasticity, mixed boundary-value problems, orthogonal polynomial solns. 78−54193
elasticity plane mixed boundary value problem, Legendre polynomials soln. 78−4487
elastoplastic shell constitutive eqns. 78−18188
enthalpy calc. using pocket calculator, data-base library formation 77−67391
error summation using piecewise-polynomial distribution functions 77−67246
exospheric temperature, representation by sum of series in Legendre polynomials 78−45063
extended anistropic body, equations of equilibrium, polynomial solutions *(Russian)* 80−42063
extended integrity bases of finite groups 79−40349
failure analysis of damage zone in laminates 80−85059
finite element anal., hierarchical approx. 77−71197
fluid dynamics, coarse mesh methods appl. *(German)* 77−88197
Fokker-Planck eqn., sonine polynomial soln. *(Japanese)* 77−45681
Fokker-Planck equation, numerical soln., Chebyshev polynomial approx., first passage time probability density functions 77−37744
Fokker-Planck equation, Sonine polynomial soln. 77−17794
FORTRAN function writer, FURI, polynomial expansion 78−16631
FORTRAN program for Fourier coeffs. of assoc. generalised Legendre polynomials of generalised spherical harmonics in texture analysis *(French)* 77−15279
frame corner plane stress distrib. and local buckling *(German)* 78−13940
freons in nitrogen, interdiffusion coefficient, calc. and obs. *(Russian)* 77−76017
fusion reactor eddy currents, 3-dimens., perturbation-polynomial expansion calcs. 78−66372
Gaussian-Laguerre, used for evaluation of Hankel transforms 79−84938
Gegenbauer, double angle sum formula 80−22
Gegenbauer polynomials, generating functions from Lie group viewpoint *(French)* 77−67193
Gel'fand lattice polynomials and irreducible representations of U(n) 78−49700
geomagnetic secular variation in Europe, analytical representation on basis of observatory data 80−101323
gradient stress fields, stress intensity factor determ., nuclear safety appl. 78−34089
grand canonical partition function type, zeros 77−22498
graph, matching polynomial zeros, rel. to topological reson. energy 79−81145
graph theory, of MO, symmetrical analysis and calc., eigenpolynomials 78−29729

polynomials continued
gravity profile inversion by method 78−69476
Hausdorff representation of positive polynomials and convex approx., aerodynamic shapes simulation 80−38430
heat conduction in adjacent regions, approx. analytic solns. *(Russian)* 78−83212
Hermite polynomials, matrix eigenvectors 79−49013
Hermite polynomials, systems of nonlinear eqns. for zeros 78−69961
Hermite polynomials, zeros, asymptotic density, singular integral operator props., 79−17188
Hermite polynomials, zeros 78−20938
Hermite polynomials, zeros and the algebra related matrices 79−49421
Hermite polynomials and one-dimensional restoration in radio astronomy 80−82217
Hermitian, solving plane elasticity problems 77−14902
high resolution spectrometers, online polynomial optimisation 79−89563
Hill-Wheeler integral for rotational energies, polynomial expansion 79−95
HMO characteristic polynomial construction, group-theoretical rules 77−23432
integral representation and generating functions for the polynomials $U_n^{(\alpha,\beta)}(x)$ 79−53957
irreducible tensors, generating functions 78−49633
irreducible tensors for point groups 79−2593
Ising model, low temp. expansions for 4-D simple hypercubic lattice 79−61025
isotopic molecules, reduced partition function ratio, generalised finite polynomial approx. 78−66529
Jacobi, asymptotic behaviour of zeros and limit relations with Hermite polynomials 79−42
Jacobi, augmented, sign, rel. to X-ray diffr. 78−22599
Jacobi, representing nonuniform load on circ. plate, large deflection anal. 79−37184
Jacobi polynomials, props. of zeros of polynomial combinations 78−57773
Jacobi polynomials, zeros, asymptotic density 79−17189
Jacoby, tops and d-functions in even spaces *(Russian)* 80−4508
king and domino polynomials for polyomino graphs, lattice dynamics appl. 77−71278
Koornwinder's polynomials and representations of the conformal group 79−63343
Korteweg-de Vries eqn., polynomials soln. 78−69991
Laguerre, consistent approx. scheme for Schwinger function 80−336
Laguerre polynomials, matrices and algebra related to zeros 79−92920
Laguerre polynomials, nonlinear enqs. systems and sum rules for zeros 78−69962
Laguerre polynomials, props. of zeros of polynomial combinations 78−57772
Laguerre polynomials, zero asymptotic behaviour, limiting formula for Hermite polynomial relation 78−93509
Laguerre polynomials, zeros, asymptotic density 79−17189
Laguerre polynomials, zeros for equilib. config. of dynamical systems 79−97182
Laguerre polynomials 77−22385
Laguerre polynomials generating functions, Lie group viewpoint *(French)* 77−71181
Lame polynomial solns., elliptic crack and punch problems 78−75069
large finite element method 77−78963
least squares analysis appl. to topside ionograms 77−78476
Legendre, for sinusoidal ring current EM wave diffr. by cond. cone 79−27140
Legendre function solution of Laplace eqn. for ink-jet printer droplet charging 79−50184
LF fields in linear media, two-dimensional finite element analysis 79−41297
Lie algebra of polynomials under Poisson bracket, automorphisms 77−5624
Lie algebras of inhomogeneous symplectic groups *(French)* 79−53962
Lie groups, nilpotent, smooth functions Fourier transforms 80−99067
many-sorted, algebras *(Rumanian)* 79−80416
meteorological fields approx. by polynomials 79−29831
MHD generator, refractory channel walls, ceramic elements, thermal stresses calc. 77−70075
molecule, heteroconjugated, LCAO MO graph-theoretical formulation 78−890
multidimensional interpolation by polynomial roots 80−18778
multisolitons, kinklike, in polynomial field theories 78−21014
neuron models Volterra representation 77−90754
neutron diffusion asymmetric weighted residual methods, high-order schemes 77−82985
neutron escape probability from absorbing body, polynomial expression 80−47523
neutron flux spatial approximation using coarse mesh methods QUABOX and CUBBOX, and higher order polynomials *(German)* 77−88192
neutron transport in critical and non-critical slabs, anisotropic scatt., struct. polynomial soln. of transport eqn. 78−70582
nonlinear evolution eqns., conserved densities 79−71256
nuclear reactor kinetics eqns., piecewise polynomial approx. 78−4981
nuclear reactor neutron-physical calc., FBR, multi-group diffusion equation solution *(Czech)* 78−66332
off-diagonal operator equivalents, closed polynomial formula in terms of two-dimensional harmonic oscilltor 79−67186
one dimensional function, resolution into sum of exponentials, roots of polynomial 80−77603
operator equivalents, polynomial formula, derivation in terms of ang. momentum operators 79−6014
operator polynomials, divisors, perturbation theory 80−36905
optimal polynomials in calcs. of complex glass's properties 78−68026
Ornstein-Zernike eqn., rel. to pair pots. calc. 77−1054
orthogonal, asymptotic density of zeros, many-body physics 79−30286
orthogonal polynomial solns. to crack and frictionless punch problems 77−75857
orthogonal polynomials, nonlinear eqns. for zeros 80−12888
orthogonal polynomials expansions, summation procedure 78−81805
oscillatory subsonic piecewise continuous kernel function method 78−5763
Pade approximants via continued fraction approach 78−61972
paired summation eqns. with legendre associated function kernels, effective solution 79−84968
patch test for nonconforming finite elements, conditions for piecewise polynomial functions 78−77697

polynomials continued
planar least squares inverse approximation, equivalence relation 79−30208
plates, rectangular thin, effect of different edge flexibility coeffs. on transverse vibrs. 78−83294
Pocklington integral eqn. basis function continuity requirements 77−74208
polyatomic molecules, isotopic reduced partition function ratio approx., by polynomial perturbation method 78−66530
potential theory, higher-order approximations for integral eqns. 79−22877
power law rel. to slender blunt bodies in hypersonic flow 77−35164
projections, reconstructions and orthogonal functions 77−41463
quadruple sequence equations involving orthogonal polynomials 79−35531
quasiharmonic, stationary EM fields analysis, by Trefftz's method *(German)* 79−27128
p-quaterphenyl, mol., charge density and bond orders, polynomial matrix method 78−74808
reactant distribution functions in fusion reactors, fast computing method using Legendre polynomials expansion 78−78491
restricted range adaptive curve fitting 79−30214
Rice's polynomial, integral eqn. soln. 77−22371
scattering theory and polynomials orthogonal on the unit circle 79−30294
Schrodinger equation, Darboux theory, appl. to construction of general soln. with Poshl-Teller potential *(Russian)* 78−12607
self inverse Sheffer sequences 77−22392
series conversion by five term recurrence formula 77−13594
singular integral operators with integral eigenvalues and polynomial eigenfunctions 79−62997
smoothing, averaging method 80−31
spectra differentiation, filtering props. of polynomial methods 80−66900
spin traces, nature of S-depend. 79−17331
steam pressure and temp. in relation to enthalpy and entropy, approximation formulae in binary polynomial form *(German)* 78−59532
strong topology on algebra of polynomials 77−45673
structural dynamics, polynomials and variational methods 77−68393
SU(2) Yang-Mills invariants, polynomial basis 79−17609
Szego's theorem for Hankel determinants 79−49106
tensorial differential eqns. for monoenergetic neutrons in slab and sphere geom. 78−50232
thermal process, transient, approx. polynomial representation *(Russian)* 78−83211
thermocouple reference tables, standard, polynomial representations, report 78−81973
third-order Hermite polynomials, appl. to reactor kinetics eqns. 78−46138
time-dependent linear systems transient response, approx. anal. using orthogonal polynomials 77−37745
time-dependent polynomial Hamiltonians, nonlinear transform. 79−40395
topological resonance energy, new graphic polynomial, appl. to benzene and cyclobutadiene 80−5462
tracking of high speed bodies, appl. of sub-tabulation 77−60915
triangular finite element universal matrices construction 78−36805
U(n) boson polynomials, appl. to physical problems 80−4890
uniformly heated fluid between vertical parallel plates, thermal convection 79−98727
viscous flow calcs., polynomial interpolation methods 77−65729
visual information processing, multi-input system representation, polynomial algorithm properties 80−101145
visual models using second degree polynomials for research and clinical use 77−48804
wave diffraction at axisymmetric inhomogeneity, polynomial approx. *(Russian)* 77−50968
Weyl's, random functions with time correlation 77−17788
Whitney polynomial, Ising cluster size and shape, Whitney polynomial 79−33080
Zernike, appl. to diffr. of uniform and Gaussian beams 77−61912
Zernike circle polynomials, appl. in optics 77−67182
Zernike moment invariants, image analysis via general theory of moments 80−102629
Zernike polynomial generalisation, optimum balanced wavefront aberrations for annular apertures 80−95805
Zernike polynomials computation in optical testing 77−50776
Zernike polynomials for optical wavefront interpretation 80−78776
Zernike-Tatian polynomials for interferogram reduction 80−37077
zeros, sum rules 80−57521
zeros, sum rules 80−62888
zeros of classical polynomials, theorems, conjectures 77−74187
zeros of classical polynomials and Bessel functions, diophantine props., review 79−35530
zeros of polynomial satisfying second order linear partial differential equation 80−12889
H atom, ground state props., polynomial perturbation problem 78−73878

polytypism *see polymorphism*

Pomeranchuk poles and trajectories
1/N dual unitarisation, triple bare pomeron parameters of Gribov's Lagrangian 78−74232
$\alpha_P(0)>1$ theory, description of data, consequences *(Russian)* 77−10227
ϕ^3 weak coupling model, s-channel cutting rules for 4-pomeron amplitude 77−38101
analytic bounds on Pomeron trajectory from dispersion inequalities 79−361
asymptotic vacuum cuts for inclusive cross-sections with weak coupling *(Russian)* 77−49928
bare Pomeron in four-dimensional quantum chromodynamics 79−336
boson propagator in Reggeon field theory 78−74138
closed Regge eikonal formula, inclusive 6-point function, multiple Reggeon/Pomeron exchange contribs. 79−362
cluster formulation in the dual topological unitarization scheme 80−13293
cross section rise in high energy strong interactions, multipomeron exchange, Mandelstam diagrams 78−41516
crossover phenomenon, interactions of Reggeons and Pomerons, Reggeon field theory 79−93317
cut reggeon field theory, 4-pomeron couplings 80−42366
cylinder term structure in the topological expansion 79−13093

Pomeranchuk poles and trajectories continued
cylindrical mixing phenomena in dual topological unitarisation, pomerons, reggeons and gluonic states 80−86696
diffractive dissociation in high-energy collisions, information about pomerons 77−71533
diffractive reactions, pomerons and reggeons *(Swedish)* 77−65146
diffractive resonance prod. and pomeron f-dominance 77−41830
diffractive scatt., pomeron and f exchange in elastic and inelastic scattering 79−36049
dipole pomeron model, rescatt. *(Russian)* 77−13947
disconnected quark diags., forbidden coupling and inhibited decay 77−22686
double pomeron exchange characteristics, inclusive hadron-hadron reactions, cross section 78−17003
dual absorptive model with peripheral pomeron, energy depend. of dip in pp elastic scatt. 77−79281
dual analytical model for pomeron *(Russian)* 77−13946
dual bootstrap models, solns. satisfying Lee-Veneziano relation 79−71729
dual massive relativistic strings theory, mass spectrum of pomeron sector 77−34134
dual multiperipheral model, Pomeron and Reggeon slopes 78−62379
dual Pomeranchuk amplitude contrib. to multi-Regge limit and pomeron sister absence 80−13237
dual pomeron contrib. to inclusive distrib., triple-Regge, fragmentation, pionisation, regions 78−41509
dual resonance models 77−10223
dual resonance Pomeron, intermediate mass distribution 78−25026
dual topological expansion, Reggeon and Pomeron slopes 80−102032
dual topological unitarization, glueball exchange effects, pomerons and reggeons 80−52482
dual two-loop graph double Pomeron region, particle prod. 79−75751
dual unified model and Pomeron-Reggeon amplitudes 77−57504
dual unitarisation, Reggeon, Pomeron and annihilation prod. processes 77−65143
dual unitarisation, renormalisation of pomeron trajectory 77−2806
dual unitarisation scheme, Pomeron and f Regge pole prod. 78−41512
dual unitarity scheme, non-planar corrections to pomeron and reggeons 77−230
dual unitarity scheme, single particle distrib., bootstrap eqn. 78−17002
dual unitarization scheme with several trajectories, diffractive scatt. predictions 79−89133
dual-resonance model, M-loop amplitudes for excited states 78−50019
eikonal Regge model, opacity and diffr.-dissociation cross section of grey disks 78−4845
eikonal theory, interacting Pomeron production by retaining Feynman graphs 78−8633
f-dominated pomeron anal. 77−49927
fermion Reggeization without parity doubling, Reggeized absorpt. 78−54622
flavour transfer in quark and gluon exchange, Pomeron models 77−49917
froissaron dynamics in high-energy physics 77−61218
Froissaron exchange, unitary problem *(Russian)* 78−21403
gauge theory, non-Abelian, Pomeranchuk singularity *(Russian)* 77−30342
geometrical pomeron, shielding cut mechanism 77−2807
geometrical pomeron 78−37188
Glauber approach and the triple-pomeron coupling 80−68435
glueball pomeron singularity cancellation 80−73687
gluonic resonances in hadronic spectrum, scalar mesons, pomerons 78−21394
hadron+deuteron elastic scatt., inelastic shadow correction, complex cut integral 78−70347
hadron+hadron elastic scatt., >100 GeV, asymptotic theorems review *(Czech)* 78−29357
hadron multiproduction on nuclei, nature of pomeron 77−87955
hadron scattering amplitudes, integral axiomatic restrictions *(Russian)* 77−82685
hadron total cross section, anal. of Pomeron-f complex 78−483
hadron total cross section, role of string junction 78−89676
hadron total cross sections, semiempirical formulae, three component model with SU(3) components 78−41600
hadron-hadron collisions, parton model of hard and soft processes in small p_T inclusive reactions 78−41599
hadron-hadron elastic scatt. systematics at high and intermediate energies 77−22717
hadron-hadron interactions, effective radius and total cross sections Pomeranchuk theorem confirmation *(Russian)* 78−89737
hadron-hadron total cross-sections to 300 GeV/c, phenomenological anal. 77−38206
hadron-nucleon total cross section 78−45888
hadron-nucleon total cross-section, regularities and systematics 77−38205
hadron-nucleus high energy reactions, triple pomeron in coherent processes 77−18534
hadronic amplitudes, diffractive contrib., Chew Rosenzweig pomeron soln. 78−62382
hadronic cross section strength, nonlinear unitarity eqn., internal symm. restriction 78−33042
hadronic matter, Pomeron and critical temp. 80−22566
heavy-quark channels and threshold prediction, pomeron hypothesis, sum rules relating NN, πN, KN cross sections 78−89755
helicity structure of Pomeron-nucleon-nucleon vertex using multiperipheral model 77−57511
high energy behaviour of a double discontinuity and the bare Pomeron 78−82179
high energy collisions of heavy nuclei, Glauber rescatt., Reggeon field theory 78−37369
high energy diffraction scatt., model with shielded pomeron, pp, πp, Kp investigation 78−17004
high energy low P_T hadronic reactions, Pomeron contrib., parton fragmentation framework 80−73688
high-energy behaviour of a double discontinuity and the bare Pomeron 79−17696
high-mass diffraction in the supercritical region 79−22081
inclusive multi-Pomeron corrections in the Regge-eikonal model, appl. to πp, Kp interactions 79−63557
inclusive single-particle hadron scatt., Pomeron factorisation expt. tests 77−14005

Pomeranchuk poles and trajectories continued
integral and local forms of Pomeranchuk's theorem *(Russian)* 79−97609
intercept of pomeron and inelastic binary collisions 77−67635
intermediate mass distribution of dual resonance pomeron, rel. to multiperipheral processes 78−50020
inverse Pomeranchuk theorem, proof for logarithmically rising total cross sections, 10-2000 GeV 78−86425
large transverse momentum hadron prod. on nuclei 77−30461
low mass diffractive dissociation in a simple t-depend. dual bootstrap model 79−13089
low mass diffractive dissociation in a simple t-dependent dual bootstrap model 79−36042
low multiplicity diffractive dissociation, 1/N dual unitarisation scheme 79−75753
low-energy Pomeron coupling to hadron energy-momentum tensor trace 77−18248
mesons, unnatural parity, in dual unitarization scheme 77−87951
multi-jet structure of hadronic final states and trajectory slope 78−93843
multi-Pomeron couplings to external particles in Reggeon field theory, renormalisable field theory 78−78111
multi-pomeron exchange theory, froissaron exchange theory 77−67632
multi-Regge model, charge exchange and pomerons 77−65144
multipomeron bootstrap and rising cross sections *(Russian)* 77−46029
Nambu string model, reggeon and pomeron interactions *(Russian)* 80−13294
negative renormalisation of pomeron intercept in Reggeon field theory on transverse lattice 78−93823
non-Abelian gauge theory, high energy behaviour, T_{n-m} in leading ln s approx., pomerons 79−49374
ordered phase in Reggeon field theory, Hamiltonian formulation, scatt. amplitude calc. 78−4807
P+f diffraction model, two component duality and flavouring, Regge fits and pomerons 80−95261
P+f model, flavour and baryon number renormalisation 80−78050
P-f identity hypothesis, resolution problems 79−75747
particle correlations in multiperipheral resonance prod. model, broken SU_3 symmetry 78−45891
particle multiple prod. cross section in model with pomeron intercept $\alpha_P>1$ *(Russian)* 80−82959
parton model of the pomeron with $\alpha(0)>1$ *(Russian)* 78−74235
partons in Regge theory and pomerons 77−79250
perturbative reggeon calculus, transverse correls., multiparticle prod. 77−2879
pion exchange at high energies, review 80−95259
Pomeranchuk's theorem at asymptotic and finite energies 79−26260
Pomeranchuk singularity in QCD *(Russian)* 79−22078
Pomeranchuk-Okun hypothesis, Pomeranchuk theorem and modifications *(German)* 80−91067
pomeron, clothed, physical, shielding cut mechanism 78−21401
pomeron, two component, hyperon- and antihyperon-nucleon total cross sections 77−82784
Pomeron and critical temp. 79−12982
pomeron and critical temperature 79−3003
pomeron avoidance-f identity through systematic treatment of cylinder overlap contribs. 79−71731
pomeron building mechanism, in fragmentation region 78−89687
Pomeron coupling diag. to order 1/N 80−47263
pomeron current model for diffraction dissociation 78−4843
Pomeron exchange, SU(3) props., dual unitarisation scheme 77−13945
Pomeron flavouring and cylinder renormalisation 79−67524
pomeron flavouring and rising total cross sections 77−38102
pomeron flavouring in reggeon field theory with thresholds 78−41437
pomeron flavouring Reggeon field theory with thresholds 78−29275
pomeron flip-non-flip interference term in elastic polarisation, s-channel helicity 78−50021
pomeron model, study of pp elastic scatt. in impact parameter space 77−10226
Pomeron nondiffractive renormalisation, flavour and baryon quantum nos. 78−82177
pomeron pole+cuts, power series formula 78−8631
Pomeron propagator representations 77−10199
pomeron relative coupling strengths with other particles, pomeron-quark coupling 77−65145
pomeron strong coupling theory instabilities *(Russian)* 77−34139
Pomeron t-depend. bootstrap eqn., cylinder discontinuity 79−85282
Pomeron two-gluon exchange model, quark counting, hadron-size effects for total cross sections 77−57495
pomeron-f identity 79−22077
pomeron-f identity hypothesis, test 78−45887
Pomeron-f identity scheme, vector meson prod. 78−12887
pomeron-photon analogy, vector-meson photoproduction 77−87984
pomeron/f coupling universality and topological expansion 77−232
production at large transverse momentum 77−26502
proton-emulsion nuclei interactions, 70 GeV/c, reggeon-pomeron exchange 78−54750
QCD, two-dimens., bare pomeron graph 78−4824
Reggeized absorpt. with clothed, physical Pomeron 77−57469
Reggeon field theory, critical Pomeron intercept with block-spin methods 79−71615
Reggeon field theory, Pomeron intercept anal. 77−6003
Reggeon field theory, tunnelling at zero transverse dimens., path integral formulation 79−12986
Reggeon quantum spin model, critical exponents 78−62338
Reggeon-Pomeranchukon cuts, Mandelstam diagram model 77−30341
renormalisation group calculations for Reggeon field theory on transverse lattice 77−18203
restored symmetries, quark system, Pomeron as Josephson current 77−61211
s-channel helicity conservation in multiparticle amplitudes, Pomeron exchange 77−87922
S-matrix, planar, building of cylinder correction in topological expansion or dual unitarisation 78−62321
scattering amplitudes satisfying geometrical scaling, low and high-energy props. 78−86447
Shapiro-Virasoro model, multi-Regge limit, pomeron sister trajectory 77−82720
shielded fixed pole pomeron at high energies, geometrical features 77−30340
shielding cut mechanism of Arnold and Barnett 77−2775

Pomeranchuk poles and trajectories continued
string model, geometrical interpretation of reggeon and pomeron intercepts 77−26499
strong exchange degeneracy analysed in Kp and πp reactions, pomeron behaviour 78−41515
SU(3) anal. of Pomeron at very high energies 77−34105
supercritical pomeron, parton model interpretation, appl. to scatt. off nuclei 78−41497
supercritical pomeron propagator, representation 77−74619
t-channel diffractive scatt., elastic peak and hadron size 79−45083
topological expansion, cylinder contrib. doubling, Pomeron-f identity 79−97539
topological expansion, Pomeron and f-trajectory 77−82721
total and elastic cross sections, Pomeranchuk-type theorems, asymptotic props. 79−21972
total and triple-Regge inclusive cross sections 78−400
trajectory in multiperipheral cluster emission model 77−54089
triple Regge region, higher order ε terms 78−16954
triple-Pomeron coupling, normalisation 78−4842
triple-Pomeron coupling and high-energy deuteron break-up 79−22153
triple-Pomeron couplings in dual models 79−358
triple-Regge limit, cut Reggeon field theory 78−8629
two component Pomeron, πN, kN, NN forward scatt. amplitudes 80−37245
two component pomeron, ratio of real to imaginary parts 80−91068
two-component Pomeron and hadron total cross-sections 79−17697
unitarity and crossing in high energy scatt., differential cross section in diffraction region *(Russian)* 79−80764
unitary corrections to short-range order, long range rapidity correlations 79−26315
universality of clothed physical pomeron, geometrical pomeron, importance of asymptotically high energies 78−33047
vector gluon exchange model of pomeron, diffraction scatt. 77−30345
vector-tensor-Pomeron couplings, nonet mass formulas 77−49883
$\gamma N \rightarrow \phi N$, pole-cut nature of Pomeron 77−6136
$\gamma N \rightarrow \phi N$, suitability of reaction for revealing pomerons pole-cut nature 79−13091
$\gamma\rho$-Pomeron-Regge vertex function, spin depend. calc., multiperipheral model 78−82223
K*(890) prod. at 13 GeV/c, Regge models 78−45961
$K^+p \rightarrow K^+X$, triple Pomeron coupling, Reggeon treatment 80−68488
$NK \rightarrow NK^*$, diffractive process, Pomeron current model 77−87958
NN, relativistic interacting system, eqn. of state using Regge-type interaction amplitude *(Russian)* 77−79032
NN potentials from Regge pole model, one boson exchange, coupling consts., masses 78−70346
np scattering, dipole pomeron model, 70 to 400 GeV/c 80−105927
$N\pi \rightarrow N\pi^*$, diffractive process, Pomeron current model 77−87958
pd scatt., intermediate inelastic states and triple-Regge couplings, Pomeron 80−4972
$pN \rightarrow NN\pi$, 6 to 1480 GeV, pomeron exchange 78−45964
$p\bar{p}N \rightarrow \bar{N}(N\pi)_{1=1/2}$, 5.7 GeV/c ρ exchange contrib., cross channel isospin amplitude anal. 78−45938
pp, dual model, vacuum exchanges, double pomeron poles with exotic Regge poles 78−89686
pp, elastic scatt., 12 to 24 GeV, leading effective trajectories; residues, anal. 79−421
pp, high energy elastic scatt. cross sections, pomeron-nucleon coupling vertex, pomeron residue *(Russian)* 80−42492
$pp \rightarrow (\pi^+ n)p$, π energy and transverse momentum distrib., DHD model with nucleon exchange *(Russian)* 80−13327
$pp \rightarrow cX$, $c\bar{c}$ exotic, triple-Regge formalism, Pomeron exchanges 80−63041
pp colliding beam experiments, double pomeron cross sections 77−14007
pp collisions, local compensation for transverse momentum, Pomeranchuk trajectory 77−18326
pp elastic scattering, high energy phenomenology of fixed pole pomeron 78−25080
pp large |t| scatt. and Regge cuts 78−41587
$pp \rightarrow pX$, associated multiplicity, and pomeron-pomeron cross section 79−17770
$pp \rightarrow pX$, Deck effect contribution 78−21471
$pp \rightarrow pX$, triple-Regge fits, duality struct. of inclusive diffr. dissoc. 78−8715
$pp \rightarrow ppX$, double pomeron exchange in high energy collisions 79−3057
$pp \rightarrow ppX$, two particle distrib. and Pomeron-Pomeron total cross section 77−22811
$pp \rightarrow pp\pi^+\pi^-$, $s^{1/2}=31$ GeV, double pomeron exchange, dipion mass 77−13993
$pp \rightarrow pp\pi^+\pi^-$, 23, 45 GeV, double-Pomeron exchange anal. 77−65180
$pp \rightarrow pp\pi^+\pi^-$, double Pomeron exchange, 23.4 to 63.4 GeV 79−3050
$pp \rightarrow pp\pi^+\pi^-$ or ppX, cross section, double pomeron exchange 77−18333
$\bar{p}p \rightarrow \pi^+\pi^-X$, 100 GeV/c, tests of factorisation in Pomeron and Reggeon exchange 77−74731
$pp \rightarrow \pi X$, Pomeron struct., effects on one particle inclusive cross sections 79−89210
pp total cross section rise, critical character of pomeron 77−50029
πN total cross section sum rule, reln. of sea quark distrib. and pomeron 79−63441
$\pi^- n \rightarrow \pi^- \pi^- p$, 15 GeV/c diffr. dissociation and N* prod. by pomeron exchange 77−41865
$\pi^\pm N \rightarrow \rho^\pm \gamma N$, bremsstrahlung in vector meson prod. at high energy *(Russian)* 79−80851
$\pi p \rightarrow (\rho\pi)p$, A_2 diffractive prod., Deck model and Pomerons 79−71733
$\pi^- p$, elastic scatt., 12 to 24 GeV, leading effective trajectories, residues, anal. 79−421
$\pi^- p \rightarrow \pi^- p$+anything, 40 GeV/c, two-pomeron interaction cross section *(Russian)* 77−6186
$\pi^- p \rightarrow \pi^0 n$, secondary trajectories propagators in Reggeon field theory, interacting Reggeons and Pomerons 79−40764
$\pi^+ p$, elastic scatt. 50 to 200 GeV peripheral Pomeron explanation 79−40803
C, K^0 regeneration, Regge behaviour and nuclear effects, ω-pomeron cut 79−13347

Pontryagin maximum principle *see maximum principle*

Poole-Frenkel effect
amorphous chalcogenides, Poole-Frenkel effect, charged dangling bonds model 80−59994
amorphous insulator film, high-field cond. 79−56320

Poole-Frenkel effect continued
amorphous semiconductor, screening effects in Poole-Frenkel cond. 77−43606
amorphous solids, Poole-Frenkel cond. for centres with screened Coulomb pot. 78−19044
β-carotene, hole mobility meas. by transient photocond., Poole-Frenkel effect 77−11957
centres with screened potential, normalised barrier lowering 77−69332
chalcogenide glass films nonlinear current voltage charcts., Poole-Frenkel effect 80−7007
coronene thin films, elec. cond. mechanism 77−28189
glass, high-field ionic and polaronic cond., dielec. relax., Poole-Frenkel theory 80−100351
glass, single- and mixed-alkali, high field cond. and ionic jump processes 78−38873
hexatriacontane single cryst., elec. cond. and dielec. breakdown 80−6849
MIS structure, localised states, Frenkel effect in strong elec. field, kinetics of nonequilib. processes 77−66206
MNOS memory device, charge retention by Frenkel-Poole detrapping 78−47874
MNOS structure, rel. to charged centroid, as function of charge injected 77−85328
[p-]quinquaphenyl film between metal electrodes, memory switching 80−2484
paraffin wax, elec. cond., 33-55°C and 1-2 kV cm^{-1} 79−99555
poly(N-vinylcarbazole) layers, supermol. struct. effect on elec. props. 80−44606
polyacetylene films, undoped, nonlinear current-voltage charcts. 80−75574
polyacrylonitrile, pyrolyzed, surface layer, anal. of elec. cond. mechanism by impedance diagram *(Japanese)* 78−23148
polyethylene, conduction mechanism, expt. determ. *(German)* 78−76086
polyethylene terephthalate, elec. cond., 120-180°C, anal. of results 79−47102
polystyrene films, soln. grown, elec. cond. meas. 80−97020
polystyrene thin film, glow discharge formed, dark current and photocurrent obs. *(Japanese)* 80−15633
polytetrahydrofuran films, electrochemically prepared between metal electrodes, DC elec. props. 80−39695
polyvinyl acetate, thick film, pure and I_2 doped, electrical cond. 77−85234
polyvinylcarbazole, Coloumb trap controlled hopping mobility model tests, mobility and permittivity meas. 79−56226
polyvinylcarbazole, TSC meas. 77−51755
PTFE films, plasma-polymerized, cond. mechanism, AC cond. and capacitance meas. 79−24093
with screened Coulomb potential, analytic expressions 77−39860
semiconductor, Poole-Frenkel effect, grain boundary barriers 79−11137
semiconductors, n-type, metal-insulator transition and negative resist. effects 79−24026
shellac, electrical cond. mechanisms, Schottky and Poole-Frenkel processes and work function 80−29402
shielded point defect potential well calcs. using Poole-Frenkel effect 80−20122
stearic acid film, DC cond. using unconventional electrode geometry, Poole-Frenkel effect 77−55631
p-terphenyl, polycrystalline thin film, elec. cond., temp., thickness and elec. field depend. 79−65572
p-terphenyl film, polycryst., charge carrier transport and DC cond. 80−70858
tetranitrophenothiazine-5, molecular complex, elec. cond. *(Rumanian)* 79−73518
thermal ionisation of an impurity in strong electric fields *(Russian)* 78−43410
thin sandwich film photovoltaic analyzer for wavelength meas. in 2000-7000 Å range *(French)* 79−95441
trap filling differential equation, tunnel hopping current in insulating layers 79−65555
TSC investigation 77−51755
TTT film, hopping cond. AC and DC meas. and EPR 80−11111
valve metal oxide-semicond. oxide, electron injection, interface reactions 77−76936
ALF_3, evaporated layers DC props. and α-particle scatt. 78−14845
Al-Al_2O_3-Dy thin junctions, Poole-Frenkel effect obs. and cause 80−80398
Al-CdS-Au structures, asymm. Poole-Frenkel effect *(French)* 77−76949
Al-CdSe-Ag dry air stabilised struct., elec. cond. mechanism, breakdown phenomena 80−34527
Al-GaAs-Al sandwich-type sputtered film, elec. props. 78−91780
Al_2O_3, elec. props. meas. in MIM struct 79−99646
Al_2O_3 film, rel. to stored charge volatility in MAOS memory element 78−52100
Al_2O_3 plasma anodised films, dielec. props. and high-field cond. *(Japanese)* 78−23185
As_2S_3, vapour-deposited, pure and doped, hole mobility 80−49728
B amorphous film, elec. cond. in strong elec. field 77−11928
Bi_2Se_3, amorphous thin film, charge transport at high fields *(Rumanian)* 79−60841
CoO film, Poole Frenkel effect and elec. breakdown props. 77−85364
GaAs oxidation saturation and MOS diode equivalent cct. 78−47875
n-GaAs surface barrier diodes for nuclear radiation detection, deep trapping centres 80−92849
GaAs-native oxide interface, electronic props. 79−73590
GaSe film, charge transport models *(Russian)* 78−60233
Ge_3N_4 CVD film prod. and Al-Ge-Ge_3N_4-Al structure V-I and V-C characteristics *(Russian)* 78−47893
GeS film, between Al(Zn)(Sn) electrodes, Schottky and Poole-Frenkel cond. mechanisms 80−54799
Ge_4Se_5Te, amorphous layer, Poole-Frenkel controlled charge carrier transport, model of charged dangling bonds 80−49750
Ge_4Se_5Te, amorphous layers, charge carrier transport mechanism 80−54708
Mo-chalcogenide glass-Mo-Al struct., strong elec. field effects 80−97004
Nb_2O_5, polycryst. film, switching processes, dielec. breakdown 77−39981
$Ru_xTi_{1-x}O_2$ films, percolation elec. cond. in strong electric fields *(Russian)* 80−84471
Se, amorphous, carrier lifetime and drift mobilities 78−87985
Si, amorphous film, in Ti-Si-Ti struct., elec. cond. processes and threshold switching 79−78207
Si:O, polycrystalline layer on Si p-n junction, charge transport and passivation 79−38206

Poole-Frenkel effect continued
Si-P MOS devices, time dependence of depletion region formation at cryogenic temp. 80−34522
Si_3N_4, amorphous insulator film, high-field cond. 79−56320
Si_3N_4, CVD film, elec. cond., film formation by pyrolysis of SiH_4-NH_3 79−91176
Si_3N_4 degradation due to high-temp. processing 78−6454
Si_3N_4, film, cond. mechanism, double injection, trap SCL current 77−32099
Si_3N_4 film, on W-coated Si, photocond., 1.31-3.10 eV, mechanism 79−19679
Si_3N_4 films grown by pyrolytic reaction between silane and ammonia, DC cond. 79−15243
Si_3N_4 layers, cond. process kinetics 77−76991
Si_3N_4-SiO_2, interface, electron and hole cond. at moderate elec. fields 78−95376
SiO_2 layers, DC current-voltage behaviour 77−85333
SiO_2 pyrolytic film, conduction process determ. 77−20479
SiO_2:Cs(B) film, implanted electronic cond. mechanism in MOS struct. 77−15983
SiO_2:Na film, RF sputtered, low elec. field Poole-Frenkel effects in MIM struct. 79−95536
SiO_2-layers, charge transport induced by electron beam, simulation *(German)* 79−51702
SiO_2-Si, P ion implantation, electrical transport props. 80−39130
SiO_x film, in MIM sandwich, elec. props. 77−72933
$Si_{12}Te_{48}As_{30}Ge_{10}$, amorphous film, elec. cond. mechanisms, temp. depend. *(Japanese)* 78−80078
$Si_{12}Te_{48}As_{30}Ge_{10}$ amorphous film, current-voltage charcts. 79−87104
$Si_{12}Te_{48}As_{30}Ge_{10}$ film, amorphous, Poole-Frenkel cond. for centres with screened Coulomb pot. 78−19044
$Si_{10}Te_{40}As_{30}P_{20}$, amorphous films, optically assisted mono-stable switching 77−11968
SnO_2, glaze, high field cond., 4.2-470K 78−23100
Ta-Ta_2O_5-ZnS:TbF_3-Au thin films, MIS struct., DC electrolum. obs., Poole-Frenkel effect 78−88038
Ta_2O_5 film, for MIS device, CVD and characterisation 77−4742
Ta_2O_5 films, Poole-Frenkel effect and cond., effect of heat treatment in oxygen and in vacuum 80−39693
TeO_2 thin film, Al-TeO_2-Al, field-assisted cond. mechanism 80−11105
Ti-anodic oxide-Au(Al), electronic cond. *(French)* 79−95512
TiO_2 film, ion plated, DC cond. study 80−100457
Tm_2O_3 film, between Al electrodes, prep. and elec. props. 80−60103
Tm_2O_3 film, electron beam deposition, elec. props., and struct. 79−87580
V_2O_5 single crystals, contact-limited conduction 79−95493
WO_3 powders, hopping mechanism and Poole-Frenkel effect, elec. props. determ. 80−49734
ZnS film, photovoltaic effects under illum. from above and below 78−52031
ZnS, photocell, transient photoelec. phenomena 79−82687
ZnS-metal interface in MIM struct., photoexcitation level assignment *(French)* 80−15622
ZnSe, dislocation motion, influence on cond. and photocurrent 79−15149
ZnSe-electrolyte junction, current photoresponse 79−82669
ZnTe, elec. field and impurity conc. effects on ionisation energy of impurities, appl. to acceptors 80−88514
ZnTe films, simple and modified Poole-Frenkel cond. 80−97017

popcorn noise *see random noise*

population inversion
see also laser theory; lasers; stimulated emission
active particles, Lorenz-Mie scatt. theory paradox 80−74324
alkali halides, coloured, light amplification at activator centres 80−2795
amplifier, degenerate, swept-gain, steady-state pulse behaviour 78−87033
amplifying medium with infinite energy store, quasistable state 77−75470
atom, reson. interaction with laser field, nonperturbative theory 77−442
atom, resonant ionisation under adiabatic level inversion conditions *(Russian)* 80−32691
atom+vibrationally excited molecule reactions, rel. to high power lasers 79−5155
atomic collision processes and X-ray and UV lasers 80−64787
atomic collisional gas-discharge laser feasibility 80−91779
atomic engines, efficiency of coherent amplification 78−33717
atomic excitation by self-induced resonance 80−28189
atomic transition, inverted, anomalous resonance-radiation press. 80−52946
atomic two-level system, excitation, adiabatic following, relax. effects 77−23475
atoms, inversion to ground state by optical pumping 79−45681
catalysis, heterogeneous, vibr. excitation, classical trajectory calcs. 80−26045
chemical laser, electronic phototransition, with thermal initiation by shock wave 80−53283
chemical laser, vibr.-rot. levels, amplification of harmonics 77−38878
chemically reacting flow heterogeneous mixing, energy level population inversion 80−78848
Cherenkov radiation at resonance frequency of amplifying medium 79−22926
chirped steady π-pulses of arbitrary duration in lossy, exactly resonant inverted medium 79−89947
coherent two-photon reson. and Doppler free population inversion, perturbation anal. 77−643
collective atomic system population inversion driven by classical field 80−63964
collective processes in slightly inverted and absorbing media 80−87367
collisional laser with energy exchange between excited levels of two systems 80−28188
confined plasma column, soft X-ray lasing action conditions 80−74346
degenerate system, two-photon lasing process 79−86156
DFB laser, limiting spectral charcts. 79−64197
diatomic molecules, N_2 and CO nuclear pumped lasers, electron impact cross section meas. 80−63985
disc amplifier, amplified spontaneous radiation 77−3594
dye laser multiple system, flashlamp pumped, energy transfer 77−88720
dye laser spectral props., hole-burning effects 80−102718
energy trapping in atomic systems metastable states, continuous rad. source 78−78669
expanding plasma, gain on transitions of hydrogenic ions 78−17918
finite volume, maximum achievable population inversion 78−50749

population inversion continued
fluorescent dye medium, short laser pulse superposition, numerical anal. 79−31891
fluoromethane laser diagnostics using two CO_2 laser pump pulses 79−31869
fluoromethane-^{13}C, pulsed far IR emission 80−69370
four level laser, Q-switched, dynamics and lifetime of terminal energy level *(Chinese)* 78−66832
free-electron laser as laser, population inversion existence 79−59665
Fresnel formulas and law of stimulated emission 80−58489
gas laser, electrically pumped, breakdown delay 77−27270
gas laser, high intensity, multimode standing-wave operation, matrix formalism 77−19229
gas laser, reson. vibr. excitation by electron impact, low energy, book contrib. 77−50662
gas laser three-level gain medium, semiclassical theory, population pulsations and interf. effects 80−95863
gas laser with wide-band optical pumping, review 79−31885
gas stream, thermally nonequilibrated flow through supersonic nozzle, cooling, population inversion *(Russian)* 77−7412
gas waveguide laser, mode comp. of radiation 80−28192
gasdynamic laser with partial population inversion 79−55125
glass disc amplifier output stages, energy characts. for silicate and phosphate glasses 79−64237
Gunn diodes, impact ionisation 77−77251
homogeneously broadened three level atoms, intense standing wave saturated, spatial inhomogeneity, mode competition 80−23646
homonuclear selective population inversion in AB system 80−75865
inert gas molecule in high press. short discharge 77−71974
inert gas nuclear pumped lasers, electron impact cross section meas. 80−63985
injection laser, bias quenching of relaxation oscillations 79−72570
interaction process between radiation modes and laser atoms 77−38853
interstellar H II/OH masers, inversion and heating by ion streams 80−56912
interstellar masers, Λ-doublet population inversion in OH, OD, CH, CD and NH^+ collisions 80−22065
intracavity Raman laser theory 79−27296
intracavity spectroscopy, laser output spectrum, lineshape 79−55155
ion kinetics in high-pressure laser plasmas 80−64002
laser, high-intensity, multimode, dynamics theory 79−41363
laser glass inversion density, direct meas. 79−13969
laser limiting characteristics in self-limiting transition 80−14311
laser operation physical principles *(German)* 79−59664
lasers, kinetic processes 80−28190
low-temperature plasma atomic level population density computation 78−71461
methanol far IR laser emission spectroscopy 80−58524
molecular beam, population inversion induced by irradiation field varying in space *(French)* 78−17727
molecular laser, optical excitation by photodissoc. wave propag. in dense gas 80−74352
molecular spontaneous symmetry breaking, induced representations 80−5464
molecular vibronic states population inversion during chemiluminesc. 80−3351
molecule, reson. interaction with laser field, nonperturbative theory 77−442
molecules, inversion to ground state by optical pumping 79−45681
moving active medium, light production *(Russian)* 79−27237
moving striations, conditions for self-excitation 80−69358
multicomponent laser plasma, soft X-ray population inversion by resonant photoexcitation 79−10680
multiply charged laser plasma, rapid cooling, possible short-wavelength radiation generation 79−41852
N two-level atoms, interaction with radiation field in restricted rotating wave approx. 80−5713
N-level atom, mol., coherent dynamics, periodic anal. 79−94200
N-level atoms, coherent dynamics, anal. solns. 78−22105
N-level molecules, coherent dynamics, anal. solns. 78−22105
N-two level atoms, interaction with radiation field in restricted rotating wave approx., numerical anal. 80−5714
NMR, progressive-saturation selective population inversion technique, sensitivity gain 78−17692
NNR population inversion using composite sandwich 79−93197
nozzle flows with boundary layer, CO_2-N_2-He, gain coefficients 80−14312
nuclear inversion coherent excitation by relativistic electron beam *(Russian)* 80−48206
organic solution spatially inhomogeneous gain saturation due to amplified spontaneous emission 77−42534
phosphate laser glass inversion density, direct meas. 79−13969
photodissociation, switched, for inversion of atomic and molecular species 80−74206
photorecombination laser, shock wave triggered, waveguide mode optical gain 80−5730
photorecombination laser theory thermally induced behind a shock wavefront 79−76682
photorecombination lasers, thermal pumping *(Russian)* 77−19242
plasma, soft X-ray transitions, population inversion of H-like ions 77−62346
plasma, soft X-ray transitions in cooling plasma 78−87437
plasma containing H-like ions, CR model 79−10647
plasma expansion into ambient gas, electron cooling 80−96363
plasma flow, spontaneous superradiance of at. and mol. ions 77−3470
plasma lasers in molecular medium, thermal ionisation and recomb. *(Russian)* 78−22118
pulse duration increase in self-limiting transitions *(Russian)* 78−33719
pyromellitic dianhydride-phenanthrene, single cryst., charge-transfer triplet excitons, spin polaris. 79−11069
radiofrequency pulse sequences which compensate their own imperfections, appln. to population inversion 80−77827
recombination lasers using elemental vap., stimulated emission conditions 78−17922
resonant two-level medium, ultrashort light pulse propag. 78−50849
ring laser, intensity fluctuations taking spatial population-inversion grating into account 80−14364
ruby, optically induced two-phonon processes connecting ^2E states 80−25443
ruby, spin level population inversion, coherent phonon amplification and generation *(Russian)* 77−24364
population inversion continued
ruby laser rod, absorption coeff., loss coeff. and population inversion *(Japanese)* 78−37888
semiconductor, complex energy band under optical excitation, high-frequency negative cond. and population inversion 80−107858
semiconductors, population inverted, resonant Brillouin scatt., photoelastic consts. 80−89015
semiconductors with Zn blende struct., resonant Brillouin scattering 80−76042
single mode laser, interaction with two-level atoms, gain without population inversion 78−17895
soft apertures, method of controlling inversion profile in amplifier 79−98427
soft X-ray population inversion in laser plasmas, reson. photoexcitation, photon-assisted processes 80−87378
solid-state lasers, influence of inversion depletion on ultrashort pulse evolution, mode-locking behaviour 80−5736
statistical and dynamical models, appl. for chem. lasers, book contrib. 77−10910
superfluorescence, quantum beats 77−42275
superfluorescence, two-level atoms system, quantum theory, incl. propag. effects 80−58491
superlattice, one-dimensional, band structure instability under strong population inversion 77−43470
superluminescent laser theory for dye soln. *(Russian)* 79−951
supersonic flow of inverted population gas flow round blunt bodies, amplification factor 78−5828
TE glow discharge, influence of fluid-dynamic phenomena 78−71619
thermally excited quantum oscillators and second law of thermodynamics 77−34863
three-level laser, rate equations 80−69356
trifluoroiodomethane nuclear pumped lasers, electron impact cross section meas. 80−63985
triple optical resonance, N-level system, N-1 photon reson., steady state level population calcs. 78−17888
two level atom, coherent and Raman scatt. spectra, secondary emissions 80−69449
two level atom, with freq. chirping, pulse shape depend. 78−17886
two level system, homogeneously broadened, saturable absorpt., coherence effects 80−95958
two level system, wide band pump field 77−644
two-level molecular systems, optically pumped, increased inversion efficiency 80−23657
two-level system, adiabatic rapid passage, narrow IR saturation resons., book contrib. 78−9419
two-level system, crossing of optical resonances by chirped pulses 80−87084
two-level systems, nonadiabatic population inversion by laser frequency switching 78−94381
unstable telescopic resonator laser, energy parameters calc. 77−75577
vector model, inversion by near-resonant sequential optical pulses 78−42312
wide-gap semiconductors, distant donor-acceptor pairs, electroluminesc. effects 79−99944
X-ray and extreme UV lasers, basic physical concepts, review 79−31850
X-ray laser plasma population inversion evidence 78−74893
X-ray laser pumping and charge transfer, book contrib. 79−31852
X-ray lasers, plasma, production, optical transitions of multiply charged ions, population inversion, review 77−19227
zinc porphin in n-octane, population hole-burning using triplet reservoir 79−87491
AR, population inversion, intershell transitions, photoionisation, from UV irradiation *(Russian)* 78−70803
AgCl(Br), crossed elec. and mag. fields, hot electrons, streaming motion, population inversion 80−44649
AgCl(Br), hot electron population inversion, in crossed elec.-mag. fields, 4.2K 79−38128
Al, laser-produced plasma, population inversion between Al^{11+} levels, X-ray lines obs. 78−38539
Al XII, multiple photoexcitation in optically thick Si-Al plasma, lasing at 44 Å 79−3684
Ar-He ion laser, population inversion radial distrib. and output characts., mag. field depend 80−19019
BaO, ground state vibr. pop. distribs. from photoluminesc. in Ba+O_2 and Ba+N_2O 77−34731
Bi pulsed laser, stimulated emission mechanism at 472.2 nm 80−19022
C VI, n=3 and n=2 levels population inversion, possible extreme UV laser 77−7073
C VI, XUV gain in expanding cylindrical plasma 77−15170
C VI laser produced plasma, transient population inversion at 18.2 nm 79−41876
$C^{5+,6+}$+C reson. charge transfer, population inversion, in laser-generated plasma 77−50526
CH+p-H_2(He), collisional pumping of Λ-doublet transitions, pot. energy surface 80−23516
CO CW gasdynamic laser, gain and population inversion 77−27278
CO, solid, CO laser excited, strong vibr. population inversion 80−58547
CO-N_2-Ar mixture, supersonic expansion, CO vibr. level populations, gasdynamic laser appl. *(French)* 77−23659
CO_2 gasdynamic laser, population inversion, press. effect 80−102692
CO_2, gasdynamic laser, simplified model for cavity flow, population inversion calc. 78−46567
CO_2 gasdynamic laser with gas mixing, excitation efficiency 79−22934
CO_2 gasdynamic laser with partial inversion at 16 μm, gain calcs. 80−78833
CO_2, inversion transitions in aerodynamic cooling region *(Russian)* 77−34869
CO_2, inverted, on-resonant phase-conjugate refl. and amplification at 10.6 μm 79−64275
CO_2, inverted, wavefront reversal, high efficiency 80−74436
CO_2 laser cavity and Ge phase-conjugate 10 μm reflection expts. 80−78894
CO_2 laser light pulse amplification calc. Fortran program PULSAMP 77−58312
CO_2 laser with partial population inversion, 16 μm steady state action 79−36873
CO_2, upper laser level population, active medium gain in waveguide discharge channel 79−86158
CO_2, waveguide laser, population and gain, kinetic eqn. soln. 79−64200
CO_2^-, dissoc., $^2\Sigma_g^+$ state, Wall Porter pot. surface, autodetachment and vibr. level population inversion 80−21275

population inversion continued
CO_2-Br_2-He mixture, possible gas lasers with solar excitation 80−99695
CO_2-N_2-He (H_2O) gas mixture, method for obtaining vibrational population inversion 79−94210
CO_2-N_2-He flowing gas mixture, glow discharge produced population inversion 78−78992
CO_2-N_2-He mixture in gas-dynamic system with independent thermal excitation, population inversion in two-step mixing 79−89888
CO_2-N_2-He mixture supersonic adiabatic expansion, population inversion and gain 80−19017
CQ* prod. from Ar*+CO_2, use in laser systems 80−63824
$C(^3P)+O_2(^3\Sigma_g^-)\rightarrow CO(^3\Sigma^+)+O(^1D)$, pot. energy surface, vibr. population inversion, classical dynamics 77−52630
CS_2+O_2, vibr. relax., effect of atomic O 79−66300
Cd+N_2, vap., creation of inverse population of atomic Cd 6^3S and 5^3P_2 levels 80−58219
CdS, submillimetre laser emission due to transitions between free exciton level 79−27261
Cs plasma, decay in presence of N_2, population inversion 79−55455
Cs, superfluorescence quantum beats 77−42275
Cs-N_2 plasma, excited atomic state inversion obs. 78−71460
Cs_2, fluoresc. spectra, kinetics, laser candidate 79−64027
Cu, atom, electron impact cross section, elastic and ^2P and ^2D states, inversion ratios 78−9256
Cu vapour laser, discharge-heated 79−7149
Cu vapour laser, population inversion kinetics, modified hook method meas. 80−53275
Cu+N_2, Cu states population inversion by preferential energy transfer 80−43152
Cu+oxidant, chemiluminescence spectra and photon yields, population inversion 79−79255
dye solution output conversion of Cu vapour laser to 5782 Å 80−48241
Eu, visible Dicke superradiant transitions *(French)* 79−45690
Eu, visible Dicke-superradiant transitions 79−45692
F+$I_2\rightarrow$IF+I, energy partitioning, vibr. populations and rot. temp., population inversion 80−50832
Fe^{3+}:TiO_2, low noise travelling wave maser, noise temp. 80−32945
GAs, population inverted semicond., resonant Brillouin scatt., photoelastic consts. 80−89016
GaAs Gunn diodes, population inversion condition 77−77251
Ge, far IR radiation amplification on hot hole population inversion *(Russian)* 80−16060
GeO, population inversion of electronic levels by oxidation, visible emission 78−13697
H, inverted, optical gain at Lyman-α spectral line 80−95880
H levels, population inversion, in supersonic H-Ar plasma jet 79−3417
H, obs. in FM-1 spherator 77−7048
H plasma, freely expanding, population inversion obs. 80−95877
H plasma, recombining, weakly ionised, population inversion 80−87849
H, recombining atomic plasmas, population inversion 80−32679
H, recombining plasma, population inversion using collisional-radiative model 79−46423
H^- affinity radiation, theoretical study of negative absorption 80−38001
H-like ions, Lyman α self absorption, effect in quantum 2 and 3 states in recombining plasmas 78−37605
H-like plasmas for short-wavelength lasers, population inversion 78−34277
HCl laser, using H_2-ClF chain reaction, CW, performance 78−46593
H_2O cosmic masers, influence of dust on collisional pumping 78−54030
H_2O-H_2 cooling in supersonic nozzle, submillimetre wave generation 80−48229
H_2O-H_2 mixtures, vibr. energy transfer in shock waves, population inversion 80−37996
He II, obs. in FM-1 spherator 77−7048
He II, stationary population inversion between low lying levels of He^+ in recombining plasma 77−84494
He, plasma, stationary recombining, population inversion inferred from intensity meas. 78−9836
He plasma expansion, supersonic, population inversion 79−27755
He-Ne gas mixture plasma, role of charge exchange in form. of optical props. 80−28600
He-Ne laser, perturbation spectroscopy, *(Rumanian)* 78−50752
He-Ne laser, population inversion radial distrib. in active element, excitation conditions effect 78−71079
He-Ne lasers levels, modulation spectroscopy 78−46572
He+Ne, 2^1s_0-level excitation, rate const., temp. depend. 80−87218
He^{2+}+Li, electron capture, ionis. cross section, low-vel. $He^+(3l)$ production, X-ray production 79−22822
^{3}He-Ar nuclear pumped laser, first order model, lasing action depend. on Ar conc. 79−76668
^{3}He-Ar(Xe)(Kr)(Cl), direct nuclear pumped lasers using $^3He(n,p)^3H$ reaction 79−31863
^{3}He-Ar(Xe)(Kr)(Cl), nucl. lasing, population inversion mechanism 80−63980
Hg-N_2, optically pumped pulsed 546.1 nm laser emission 79−13952
Hg(6^3P_0)+Na, energy transfer, rate consts. *(Russian)* 79−54952
I amplifier pumped by open high-current discharge radiation, physical parameters 79−89904
I, chemical generation of population inversion between spin-orbit states 78−17767
I flashlamp pumped photodissociation laser characts., local optical inhomogeneities 80−53284
I, recomb. laser, possible use of alkali metals to obtain population inversion 79−94221
I short-pulse laser, preamplifier stages characts. 79−94227
InP Gunn diodes, population inversion condition 77−77251
Kr, population inversion, intershell transitions, photoionisation, from UV irradiation *(Russian)* 78−70803
$La_2Mg_3(NO_3)_{12}.24H_2O$:$Co^{2+}$, Ce^{3+}, relax. and ESR in magnetically cooled systems 78−88225
Li, low-temperature plasma atomic level population density computation 78−71461
Li plasma dynamic laser, using supersonic nozzle, population inversion, excitation cross section 78−50760
N, recombining atomic plasmas, population inversion 80−32679
N_2 pulsed laser, construction and theoretical explanation *(Slovak)* 80−95874
N_2-He plasma, laser produced, high press. amplified stimulated emission 80−78843
NH_3, excited state population decay time meas., press. depend. 77−75489
population inversion continued
NH_3, population inversion by adiabatic rapid passage 80−19073
NH_3, two-photon population inversion, adiabatic rapid passage 78−78763
N_2O, gasdynamic laser, population inversion mechanism, kinetics 77−7074
N_2O-N_2-He, population inversion of N_2O vibr. levels behind shock wave front 79−31886
$N_2(^1\Sigma_g^+)$, exact collinear calcs. of $N_2O(X^1\Sigma^+)$ photodissociation 77−30937
Na-seeded flame, H_2-O_2-Ar, population inversion, two-photon laser excitation 79−34307
Nd:glass, laser material, luminesc., population inversion depend. on pump pulses 77−23679
Nd:glass amplifier, pump radiation pulse shape influence on stored energy 79−64235
Nd:YAG giant pulse lasers, energy characts., superradiance effects 80−64031
Ne, atomic deexcitation effects of X-rays, X-ray preionisation in TEA lasers 79−793
Ne like ions, gain estimate for 40 to 80 nm range transitions 77−75482
Ne, population inversion mechanism between 4p→3d, laser generation conditions 80−1185
Ne, population of $5s'[1/2]_1^0$, $4p'[3/2]_2$ levels interacting with laser radiation 80−23670
Ne, radial profiles of upper and lower level emission 77−31088
Ne-like multicharged ions, vacuum UV lasing action 78−1213
Ni:glass, amplifier module inversion investigation, active element with rectangular cross section 79−27264
O I 6300 Å in type A aurora rays, emission intensification 80−4163
O, recombining atomic plasmas, population inversion 80−32679
OH interstellar masers, 18 cm lines pumping by H+OH collisions 79−48892
OH main lines, IR pumping 80−46632
OH maser sources, interstellar, radiative transport effects on inversion 80−17681
OH/IR stars, OH main lines masers inversion 78−28664
OH-CH rotationally inelastic collisions, maser action 79−94068
OH+p-H_2(He), collisional pumping of Λ-doublet transitions, pot. energy surface 80−23516
$OH(^2\Pi_{3/2}, v=1)$, population inversion of Λ doublets in microwave spectrum 80−974
Pb^+, electron collisional laser populated by recomb., excitation and decay mechanisms 79−18405
Pb^+ high-gain laser populated by direct electron excitation, 1.159 μm transition 80−37997
Rb+Xe, interatomic spectrum, theoret. and exptl. obs. 78−9112
Rb_2, mol. spectra, population inversion, high-power laser appls. 77−3406
^{85}Rb unperturbed hyperfine transition frequency determ. 77−7047
Si:Cr^+ EPR spectra and spin state population inversion with unpolarised optical lighting *(Russian)* 80−44909
SnO, population inversion of electronic levels by oxidation, visible emission 78−13697
Sr^+, inversion and lasing on optically pumped reson. line 78−70798
TbY ferrite garnet, Tb^{3+} energy level inversion, Faraday effect *(Russian)* 79−47418
Tl, $6^2P_{3/2}$-$6^2P_{1/2}$ transition, population inversion 80−950
Tl, green line superradiance, selective optical excitation and inversions via excimer channel using Tl-Hg and Tl-Cd-Ar systems 79−50281
Tl, inverted atomic populations, obs. of stimulated level shifting 80−58218
UF_6 nuclear pumped lasers, electron impact cross section meas. 80−63985
Xe, population inversion, intershell transitions, photoionisation, from UV irradiation *(Russian)* 78−70803
XeO*, mol. laser emitting at green wavelengths, population inversion kinetics 77−23661
Zn II, beam excited levels, population inversion 79−18161
ZnS:Mn, electroluminescent film, stimulated emission *(Russian)* 77−19255
ZnS:Mn electroluminescent films, amplification factor during electric field excitation *(Russian)* 79−78757

porosity
see also porous materials
adsorption data analysis, pore size and size distribution determ., review 78−63939
adsorption isotherm analysis, determ. of porous texture of solids 79−77897
agglomerate characterisation methods, review *(German)* 79−100443
alloy, hard, powder mixtures, porosity and hardness during pressing, u.s. vibration effects 77−1821
amalgam, dental, corrosion, immersion conditions 79−12037
anodic film, behaviour of emulsion particles during electrodeposition 80−104357
aquifer mineralisation field dynamics simulation, optimisation 77−56664
benzene adsorbent mesopores, capillary evaporation and struct. 80−107614
blind meas. method 77−90545
bone compact substance porosity determ., TAS Leitz 2D image analysis system *(German)* 78−92753
borides, metallic, sintering, review, book contrib. 78−48359
borosilicate glass, powder, sintering, foaming by chemical reactions 80−81017
brittle materials, influence of structural parameters on fracture toughness 79−96133
bronze powder, granulated, effects on sintering kinetics 77−63599
capillary condensation calorimetry method, determ. of pore struct. *(French)* 77−25245
capillary phenomena in cylindrical pores, appl. to pore size anal. 80−15340
carbide fuel pins, mixed, radial distrib. of Xe bonded fission gas, electron probe anal. 79−36318
carbides, brittle materials, swelling, blistering, p, d, and He ion irrads. porosity effects 77−35603
cemented carbide, porosity 77−59722
ceramic, creep, porosity depend. 80−97530
ceramic, electrical conductivity, porosity effects, 20 to 1000°C *(Polish)* 78−6385
ceramic, ferrimag. or ferroelec., microstructure and physical props. 78−72756

porosity continued
ceramic, mechanical failure, porosity effects *(Polish)* 77−59934
ceramic nuclear fuel, porosity characterization, optical and electron microscope exam. 78−44302
ceramic sherds, macroporosity determ. by replica techniques 77−34065
ceramics, crack extension micromechanisms, review 80−108567
ceramics, effects on room temperature fracture energy, elastic property-porosity data 78−88533
ceramics, elastic moduli, effect of inhomogeneous porosity distrib. 79−87674
ceramics, polycrystn., porosity, twinning and grain-size depend. on spontaneous cracking 80−44253
ceramics, porosity, exam. using image analyser and optical microscopy *(French)* 79−15880
ceramics, US investigation, porosity, mech. and dielectric strengths *(Polish)* 79−52565
ceramics acid-resistant, based on Artemov clay and obsidian 80−20852
chondrites, porosity estimation by image anal. of polished sections *(French)* 79−71009
clay, highly plastic, compaction and lime stabilization effect on pore size distrib. *(Japanese)* 78−31365
coalescence of gas-filled pores *(Russian)* 78−18679
coalescence of pores by dislocation mechanism, shape effect on charact. 77−73242
coatings, porosity determination by hydrostatic weighing 80−66714
coke, metallurgical, strength and struct. relationship 80−84997
cokes, metallurgical, struct. and strength 80−93610
compressibility rel. to material porosity, analytical expression 79−100069
concrete, porosity determ. from combined US and gamma absorption meas., mech. props. 79−29295
continuous ingots, two phase zone critical parameters during casting *(Russian)* 80−93549
crystal growth, cylindrical pores growth, numerical calcs. 80−92471
desorption isotherms, and pore size distrib., adsorbate flow method meas. 77−80693
diamond, synthetic powder, thermal cond. 80−96702
dielectric coatings, optical charact., effect of electric field during film condensation 80−69539
dielectric constant calculation by measuring porosity change using radio wave phase method 79−39096
dielectric film, electron beam produced pore form. mechanism, statistical model *(Russian)* 80−6667
dislocation configuraiton form. on pore healing under press. *(Russian)* 78−10050
dislocation mechanism of pore growth and healing under load, barrier influence *(Russian)* 78−18634
electrochemical cells with porous electrode, electrochem. and capillary charact. 79−91967
electrode, porous, capillary equil. and percolation theory 79−91971
electrodes, effect of porosity 80−66815
electrodes in Pb-acid battery, structure obs. 79−100516
electrographic porosity test, reclassification as nondestructive method *(German)* 80−97652
electrolytic foils, porosity meas. by electrochemical reaction 78−3265
endosseous implant material, radiation processed alumina-polyacrylic acid composite 77−60308
FBR fuel pin failure, fuel porosity and crack effects on transient overpower analysis 80−71760
ferrite, coprecipitated, hot pressed, for appl. to mag. heads 77−85968
ferromagnetic resonance linewidth, effect of pores *(Russian)* 78−6581
fibre reinforced composites densification in free forging, exam. of specific work and kinetics 80−16218
film, microporosity described in terms of vacancies and voids 80−24769
film, microporosity induced by nucleation and growth processes, TEM expt. 78−10303
fine dispersed solids, pore struct. anal., appl. to active C 77−32763
fission oxide fuels, in-pile densification of intergranular porosity, model 79−73345
Floc density, porosity and void ratio in colloidal systems and aerosols 78−3383
fluid saturated porous solid, fundamental solns., deformation, pore-fluid diffusion, soil mechs. 77−84160
fluidised beds, porosity measurement device, exam. 78−60911
fluoride film, rel. to contamination by 1 MeV proton bombardment, backscatt. obs. 77−11811
glass, swelling, blistering, 140 keV p, d and He ion irrads., porosity effects 77−35603
glass sintered powder porous bodies, liq. penetration mechanism *(Japanese)* 80−53853
grain growth, discontinuous, pore drag 77−44203
granular material, uniformly distributed, 1-dimens. shock waves, porosity discontinuity 78−83285
granular media modelling by steel spheres, packing density coeff. 78−84916
granular medium, compressibility and force transmission, discrete probabilistic model 78−15448
graphite, failure energy of polycrystalline sample considered as heterogeneous medium, porosity effect 79−96138
graphite, fusion reactor applications, mechanical constitutive laws for irradiation behaviour 80−32448
graphite, neutron irrad., microporosity, elec. resist., length, struct. changes 78−43051
graphite, neutron irrad., porosity changes, neutron small angle scatt. investig. 78−34544
graphite, nucl. grade, neutron small angle scatt., thermal and radiolytic oxidation effect, porosity size distrib. 79−17977
graphite, permeable, 0.6, 3.5 MeV He^+ irrad., surface erosion, porosity effects 77−35602
graphite, polygranular, flexural strength after heat treatment porosity correl. 80−84996
graphite, porosity effect on strength variation 78−31369
graphite, reactor-grade, permeability, effect of neutron irradiation 79−71900
graphite, thermal conductivity, effect of porosity 80−65314
graphitic reactor materials, determ. of macro and mesoporosity by stereometric anal. *(German)* 79−3205
haematite, degree of reduction, potential relaxation due to cracks *(Russian)* 80−66770
haematite reduction to magnetite, stress development mechanism *(Russian)* 80−93553
porosity continued
high alumina cement pastes, accelerated conversion, acoustic emission 77−36726
high pressure Hg intrusion porosimetry 79−24697
ion bombarded surface, microporosity, rel. to spectral refl. changes 77−55308
Knudsen flow, through periodically constricted pores *(Japanese)* 79−72911
kyanite-sillimanite concentration, mullitisation and sintering, props. of refractory products 80−20867
lunar fines, etching by adsorbed water, effect of annealing temp. 77−60632
LWR controlled porosity fuels, short term irradiation behaviour 79−49686
magnesite artifacts, roasted, props., filler porosity effect 80−104099
magnesite refractories, spinel bindal, with reduced thermal cond. 79−83162
magnesite refractories, unfired, by resin phosphate binding 80−104101
marine sands, resistivity-porosity-particle shape relationships 79−53339
measurement by combinational method 79−29303
measurement of plate porosity, by measuring pneumatic conductivity *(Polish)* 80−92097
measurement using soln. of luminescent material flowing around sorbent granules 80−53850
membrane selectivity, influence of particle/pore size ratio 80−11946
metal, porous, stresses in deform. region during cold rolling 78−11241
metal, sintered, ductility, porosity effect 77−59875
metal, sintered compacts, residual pore effect on grain size distrib. 77−85961
metal, welded joints, pore formation mechanism evaluation, rel. to solidification 80−3017
metal, work-hardening, plastic, sintered, porous, irreversible deform. 78−35459
metal extraction kinetics, from deep-sea Mn nodules, pore diffusion controlling case 77−28984
metal extraction kinetics, from deep-sea Mn nodules, pore diffusion with chemical reaction 77−28985
metal fiber permeable materials, struct. charact. 79−24464
metal parts, sintered, corrosion and protection 78−44278
metallic fibre knitted gauze permeable materials, mech. props. 80−66607
meteorites, matrix textures and porosity in unequilibrated ordinary chondrites 77−87340
mineral, swelling examination method 77−53232
Nb-O, effect of O_2 on penetration of Li at 400°C 79−11719
nonswelling porous body, moisture-retaining capacity and struct. 77−12773
nuclear fuel, gas release and swelling, operational model, grain boundary gas 80−95346
nuclear fuel element, cylindrical analytical soln. to mass transport eqn. 78−21643
nuclear fuel structure characterisation methods, review 79−49802
nuclear tracks, etched, statistical distrib. of quadratic holes on planar surface, computer simulation 80−37705
olivine and enstatite of meteoritic and terrestrial origin, porosity determ. *(Russian)* 77−9725
oxide coating, pore size distrib. and permeability 79−24641
oxide coating, thermal sprayed, AE study of porosity 80−25927
oxide thermal-sprayed coating on steel, acoustic emission 80−21247
oxides, brittle materials, swelling, blistering, p, d and He ion irrads. porosity effects 77−35603
particle porosimetry by inverse gel permeation chromatography 77−90659
particulate mixtures 79−61600
percolation probability for lattices of bonds and sites 77−63956
plasma sprayed coating, ultramicrostructure and porosity 79−82500
plasma sprayed materials, control of mech. props. 80−11560
plasticity as function of porosity *(Russian)* 80−75290
plugs, porous, in He II space cooling systems, charact. 78−49842
Polimal 109, polymer resin laminate, density porosity, water vapour diffusion sorption and permeation *(Polish)* 80−59665
poly(vinyl alcohol) porous film, polymerisation and porosity 80−107063
polycarbonate porous membrane, pore size effect on gas permeability *(Japanese)* 78−31699
polycrystals, models for constrained cavity growth 80−44251
polymer carbons, water vapour adsorption, porosity, and surface chem. 79−52753
polyvinylidene fluoride and poly-1-vinyl-3-methylimidazolium iodide interpolymer ultrafiltration membranes 79−15639
polyvinyltrimethylsilane, sorption, diffusion, solubility of hydrocarbons, Xe rel. to temp. *(Russian)* 80−6565
porcelain, elec., high-strength, development from ceramic raw materials, mech., elec. props. 79−24630
pore size determ. from charged particle energy loss meas. 77−71730
pore size determ. of powder and wire gauge filter materials 77−12776
pore size distribution curve quantitative evaluation, Fortran program *(Czech)* 78−80795
pore size measurement, comparison of methods 80−62622
poro-elasticity, disturbance due to expanding ring and disc load 78−79250
porosimeter, continuous scan mercury type, pore pot. contrib. to hysteresis 80−77928
porosimeter−volumetric apparatus *(Hungarian)* 79−40531
porosimetry technique for up to 6 kbar, Hg porosimeters design 79−21761
porous glass:In, effect of press. on transition temp. 80−97027
Portland cement-fly ash, physico-mech. props., SEM and X-ray diffr. anal. 79−74239
pottery, pore struct. rel. to characterisation 78−351
powder, effect on thermal conductivity *(Japanese)* 78−6191
powder, two component mixture, compact growth in liquid phase sintering 80−20835
powder materials, densification laws 79−66021
powder metallurgy, fatigue strength significance *(German)* 80−60946
powdered mixture, compaction, optimum porosity and particle sizes 77−85971
pressure sintering, inhomogeneous flow and effective press. 80−93512
PVA carbonisation process and carbonised block props., high temp. resistant materials *(Russian)* 79−8268
PVC, mech. comminution in fine struct. changes in porosity, density, specific surface area *(German)* 78−35345
PVC, sintered powder, elastic props. and porosity 77−63619

porosity continued
PVC, sintered powder, permeability and porous struct. 77−63620
pyrocarbon, low temp., isotropic, permeability study *(French)* 79−7549
quartz ceramic, physicomech. props., influence of surfactant incorporated during synthesis 80−20856
quartz ceramic, SiO_2-Cr_2O_3-TiO_2, creep and porosity, for ceramics with different structures 80−21011
quartz sand, press. soln. expt. 77−60370
radiation-induced porosity of Ni, effect of 2 MeV Xe^+ ion irradiation on pore distribution and size 79−71898
random bed, area porosity profiles, stratified model 80−19495
random bed, porosity estimation based on Lichtenstein Liapunov expansion functional 78−14078
refractories, multichamotte, sintering additives effect on props. 80−35147
reinforced magnetically hard material, fibre-reinforced, porosity and impact strength 77−55916
rock pore aspect ratio spectrum determ., seismic velocities inversion 80−51387
rocks, fractures effect on compressibility, anal. using new model 80−8300
rocks, igneous, initial crack porosity rel. to thermal cycling cracks 79−29759
rocks, nature of porosity rel. to transport phenomena in hydrothermal systems 78−36205
sandstone, porosity destruction through press. soln. 77−91110
sapphire, shaped single crystals, porosity, microstruct. 78−2125
silica gel, polymer adsorption into surface pores, computer simulation, phase transition *(Russian)* 78−51824
silica gel, pore struct., effect of washing with aq. solns. containing Mg^{2+}, Ca^{2+} ions 79−52786
Silumin, AlSi10Mn, struct. and mech. props., Na modification effects 77−63786
sintered material, porosity effect on temp. generated during grinding 78−35530
sintering, final stage, steady state diffusion models, testing of models by numerical simulation 79−4428
sintering and random structures, volume diffusion and creep effects 80−35125
sintering of porous solid, effect of gases, healing of isolated pore accompanied by internal oxidation 77−90286
solid gas layer, appl. to cryosorption pump *(Japanese)* 80−20031
solid-gas catalysed reacts., effect of nonuniform activity distribs. 79−96362
steel, 1Kh12V2MF, pore formation in creep, precip. hardening 77−63747
steel, austenitic Kh18N9T, porous fibres, oriented struct., strength props. 78−3199
steel, C, autectic, sintered, isothermal transformation behaviour, porosity effects 80−3031
steel, C, pore formation in surface layers, during As diffusion redistrib. 80−49421
steel, Cr-Mo, cast and forged, difference in mech. props. 77−48465
steel, low alloy, sintered, isothermal transformations, porosity effects 80−3032
steel, Ni, sintered, physical and mech. props. rel. to homogeneity 79−38762
steel, powder, rotary forging, porosity and deform. 78−23646
steel, powder forged, fatigue, surface treatment effect 80−85048
steel, rimming, shape change and pore form. during multiple polymorphic transform. *(Russian)* 77−25044
steel, stainless, from nonspherical powder, mean pore size of sheet material 77−28757
steel, stainless, fuel cluster sheath of LMFBR, steel-coolant interaction effect on porosity development 77−71651
steel, stainless, porous sheet, pore dimensions, filtration and permeability *(Russian)* 80−76480
steel, stainless 316, controlled-porosity, mech. props. 79−96083
styrene-divinylbenzene copolymers, porosity variation and swelling 80−97493
suspensions, degree of agglomeration assessment 77−70343
system with excess vacancies extraneous inclusion role in nucleation *(Russian)* 79−73164
ternary polymer systems, diffusion controlled formation of porous structures 80−7539
Terra Sigillata from La Peniche, Switzerland, chem. comp., mineralogy and porosity 79−26198
thermal stress resistance, effect of spatially varying porosity during steady-state heat flow 80−1488
thin films, microporosity and absorptivity in vacuo meas. apparatus 80−9053
transition metal nitrides of group IV-V, laser irrad. action, erosion strength *(Russian)* 77−56112
unhealed porosities and crystalline steps in flakes *(Chinese)* 79−74179
vacuum deposited film, relative porosity eqn. 78−56057
vitrinite, in bituminous coal, microporosity and micromineralogy, small-angle X-ray scatt. study 79−12117
zeolites, synthetic, effect of sintering on elec. cond., porosity and microstruct. 79−29009
zircon, rate of dissolution in molten Fe_3O_4, porosity effects *(Japanese)* 77−11699
$ZrC_{0.98}$, porosity influence on high temp. creep. *(Russian)* 80−25764
Ag overlayer on Cu laser mirror, microstruct. and 10.6 μm reflectivity 77−42543
Al alloy, forgings, unhealed porosities and crystalline steps *(Chinese)* 79−74178
Al alloys, laser surface melted, porosity form. 78−44279
Al alloys, liquid, kinematic viscosity temp. depend., porosity, H solubility, supercooling *(Russian)* 80−54425
Al, anodic film, formed in H_2SO_4, electron microscopy 78−68843
Al, anodic oxide film, porosity determ. by pore filling method 79−47848
Al, cast and directionally solidified, porosity 79−74145
Al coated steel, porosity evaluation, micro X-ray spectral anal. *(Russian)* 80−35389
Al coating, plasma sprayed on steel substrate, microstructural investigation and oxidation effects 78−11426
Al, constitutive equation for porous materials with strength, press. effects 80−79875
Al foils, high strength, vapour deposited on curved surfaces, quantitative characterisation 80−80144
Al, porosity determ. in ingot, US signal integration technique 77−44430
porosity continued
Al, secondary H porosity, development and pore growth *(Russian)* 80−19946
Al sputtered coating development, porosity, durability temp. depend., electric arc metallisation regime *(Russian)* 80−39402
Al, vacuum deposited, structural singularities and porosity *(Russian)* 78−75950
Al-Cu, cast and directionally solidified, porosity 79−74145
Al-Li-Mg-Be alloys, phase composition of surface films, oxidation protection mechanism *(Russian)* 80−65417
Al-Mg alloys, overheating effects on microstruct. and props. 77−63698
Al-Mg(Cu)(Si), (5.0(4.5)(11.8) wt.%), ingots, vibr. effect during solidification on porosity formation 80−108426
AlB_{12}, powder, production of nitride materials by nitriding 77−12560
AlGe (4 wt.%), struct. peculiarities of superplastic behaviour due to porosity 79−34111
Al_2O_3 and Al_2O_3-Y_2O_3, plasma spraying, microstruct., porosity and adhesion 77−32710
Al_2O_3 bioceramic synthesis, for orthopedic purposes, props. *(Polish)* 80−66465
Al_2O_3 cutting tool, performance relationships, porosity determ. 78−11169
Al_2O_3, detonation coating, porosity, electrical strength, phase anal. *(Russian)* 77−69204
Al_2O_3 detonation deposited coatings, porosity and adhesion, processing parameters effects 79−70227
γ-Al_2O_3, heat treatment rel. to texture 78−72789
Al_2O_3, insulator, electrical puncture strength at high temps. *(German)* 79−70175
Al_2O_3 plasma-sprayed, struct. and thermal diffusivity 79−86932
Al_2O_3, pure and SiO_2 coated, surface props., catalytic activity 79−79287
Al_2O_3, sintering in reducing atmosphere, Na effect on density and strength 77−63613
Al_2O_3, sintering response with const. rate of heating, depend. on processing related pore distrib. 79−28992
Al_2O_3, spray dried agglomerates, compaction response, fracture, deform. 79−43172
Al_2O_3, transparent hot-pressed, transparent and translucent properties 80−60533
Al_2O_3-glass mixture, microstructural changes and shrinkage during sintering 80−25640
Al_2O_3-polymethylsiloxane composite, thermoreactive compaction 80−20879
Au film, ion plated, defect growth structs., SEM obs. 80−24768
B-B_4C materials, hot-pressed, elastic modulus and flexural strength rel. to grain size and porosity 79−79018
$BaTiO_3$ ceramic, semiconductive sintering 77−36430
Be, neutron irradiated, gas porosity, Brownian motion 79−73222
C, dense hard-type solids prep. from petroleum coke powder by grinding 79−20002
C, determ. from isotherm eqns. 79−51419
C fibres, PAN-based, surface charact., active surface area, microporosity 78−35536
C, glassy, prep. from liq. phenolformaldehyde resin, TEM obs. 79−83145
C, micropore analysis 78−14570
C, micropore volumes from isotherm eqn. 78−14569
C, polygranular, flexural strength after heat treatment porosity correl. 80−84996
C, pyrolytic, 0.6 to 3.5 MeV He^+ irrad., surface erosion, porosity effects 77−35602
C, swelling, blistering, 140 keV p, d and the ion irrads., porosity effects 77−35603
C-C composite material, syntactic-foam type properties 78−44169
Ca aluminophosphate foam glasses, for prosthetic appl., porosity and mech. props. 79−74128
$CaAl_2O_4$ cement bond phases, corrosion in steam-CO at 199°C 79−29234
$CaCo_2(PO_4)_2$, growth by Bridgman method, crystn. speed depend. 77−59684
$CaHPO_4$, powder and granules with starch mucilage binder, surface topography variation under compression 80−80998
$Ca_{10}(PO_4)_6(OH)_2$, synthesis and characterisation in dense polycryst. form 77−4749
$CaSO_4 \cdot 1/2H_2O$, (α and β-phase), surface chem. and porosity 78−85200
$CaTiO_3$-TiO_2, ceramic, phys. props. 78−43784
$CaTiO_4$, perovskite, sintering during synthesis 77−36422
CdS, prepared by ceramic Technol., physical props. 79−60837
Ce_2O_3, hydrated, sorption props. rel. to dehydration conditions 79−66345
Co complex, (4-methylpyridine)$_4$Ni(NCS)$_2$, porosity 77−76364
Co-Cu-Fe-Ce alloys, sintered permanent magnets, mag. charact. 77−43855
Cr_2O_3, sintering in air and under reducing atmos., effect of oxide additions 77−59729
Cr_2O_3, vacuum vaporisation, porosity and thermodynamic treatment effects *(Japanese)* 77−43436
Cr_2O_3-Mo_2O_3, catalyst, effect of Al_2O_3 additives on catalytic activity, in oxidation of methanol to formaldehyde *(Russian)* 79−66346
Cu electrodeposit, US agitation effect on hardness, porosity and grain size, work-hardening 77−60075
Cu film, ion-plated, on stainless steel, porosity depend. on process parameters 78−84720
Cu, foils and powder compacts, pulsed action of laser radiation, dimens. effect *(Russian)* 77−16437
Cu, high purity, small-angle neutron scatt. from pores in high temp. fatigue 79−14795
Cu, ion plated, defect growth structs., SEM obs. 80−24768
Cu platings on C steel filaments porosity determ. 79−70239
Cu, powder, sprayed, effect of start props. in struct, and porosity of sintered products *(Czech)* 77−85960
Cu, sintering, cold working, recrystn. annealing, mech. props. and microstruct., porosity 78−76660
Cu tripolyphosphate complexes, electrolyte development for direct deposition of Cu 80−45246
Cu vacuum coating on steel substrate, influence of precipitation conditions on porosity *(Russian)* 80−54578
α-Cu-Ni-Zn-Pb, fire cracking, effect of pores and impurities 79−29207
CuCoNi ferrite magnetoacoustic oscills. rel. to microstruct. 77−85536
Dy_2O_3-based ceramic, preparation, mech. props. 77−24998
Fe, Armco, exam. of pore formation mechanism 78−85120

porosity continued
Fe atomised powder, sintering effect on recrystn., mech. props. 80−40292
Fe, electrode, porous, discharge capacity, importance of physical struct. 80−26123
Fe powder, density distrib. in rolling deformation region 80−40288
Fe powder, sponge and atomized types, steam oxidation, pore closure and surface hardness 80−45441
Fe, sintered, fracture mechanics *(German)* 77−8948
Fe, sintered, influence of metallographic treatment on pore analysis 80−76417
Fe, sintered, metallographic meas. of pore size, effect on mech. props. 78−19685
Fe, sintered, plastic deform., porosity effects 78−23801
Fe, sintered, porosity estimation by screen image of brittle fracture 77−52585
Fe, sintered, steam oxidation effect on porosity 77−59997
Fe, sintered and pressed, props., effect of atomised Fe powder particle size distrib. 80−11601
Fe-B_4C sintered material, mech. props. and struct. charcts. 79−100084
Fe-Ni-C (0.15, 0.05 wt.%) pore formation kinetics during crystallisation, FORTRAN study *(Russian)* 80−54158
Fe_3O_4, effect of Al ion on formation and structure *(Japanese)* 77−59727
$Fe(OH)_3$-Cr_2O_3 catalysts, for water-gas shift react., porous struct. 79−29407
β-FeOOH, lattice imaging and pore struct., high resolution electron microscopy obs. 80−103310
γ-FeOOH-Cr_2O_3 catalysts, for water-gas shift react., porous struct. 79−29407
Ge-Si alloys, hot-pressed, fine-grained, boundary scatt. of phonons, lattice thermal cond. 80−107583
HFO_2, polycrystalline, monoclinic, elastic props. at room temp. 78−27548
HfO_2, stabilised comps., elastic props. rel. to porosity and temp. 80−81096
KCl, annealed in KBr vapour, crack and pore formation, diffusionally induced stress relaxation *(Russian)* 80−40388
KCl, cryst. isolated pore healing under press., dislocation struct. evolution *(Russian)* 80−100245
K_2O-Ga_2O_3-Al_2O_3, solid solns., K ionic cond. 77−35747
Li_2O, porosity, dependence on thermal diffusivity and thermal conductivity, 200-900°C 80−92726
$Li_2O.2SiO_2$ ceramics unidirectionally solidified, porosity *(Japanese)* 79−38816
$Li_2O.2SiO_2$, directionally solidified, thermal and mech. props. *(Japanese)* 80−16295
$100(Li_2O.2SiO_2).3B_2O_3(3Na_2O)(3MgO)(3Al_2O_3)(3SiO_2)(3P_2O_5)$, directionally solidified, thermal and mech. props. *(Japanese)* 80−16295
Mg film, influence of isothermal and thermal cycling on porosity vacuum deposited coatings *(Russian)* 78−87884
$MgAl_2O_4$, composition rel. to ceramic microstruct. form., light transmission 79−43188
$MgCO_3$ powder, high speed method of porosity determ. 77−90543
MgO polycrystals, hot-pressed, change in porosity on annealing 79−34073
MgO, pore distrib. and grain size in intermediated sintering stage *(Japanese)* 79−74124
MgO-C in melts, corrosion resist., rel to oxidation, porosity, content 80−40578
MnZn ferrite, spray dried agglomerates, compaction response, fracture, deform. 79−43172
MnZn soft ferrites, commercial grade, microstruct. rel. to mag. props. 80−34009
Mo crystals, joined by compression during heating, structural changes *(Russian)* 80−108513
Mo, void lattice and depend. of vacancy porosity on irradiation dose *(Russian)* 79−27972
Mo-Zr-B, porosity and mech. props. after neutron bombard., 780-1080°C *(Russian)* 80−24502
Mo-Zr-B alloy, neutron irrad. at 780-1080°C, porosity, hardening and embrittlement *(Russian)* 80−29062
N_2 adsorbent mesopores, capillary evaporation and struct. 80−107614
NH_4Cl, submicron particles, density, morphology 80−61166
$(Na,Li)NbO_3$ ceramic, optimum prep. conditions and characterisation 78−3079
$NaNbO_3$-$SrNb_2O_6$, phase diagram, props. meas. 79−11576
NbC, elastic modulus, porosity factor 77−21207
Nb_2O_5, hydrated gel, prep. conditions on pore struct., adsorpt. meas. 78−3068
Nb_3Sn, powder metallurgically produced, microstruct. charcts. 80−89233
Ni alloy ZhS6U, US method of porosity detection 80−71828
Ni complex, (4-methylpyridine)$_4$Ni(NCS)$_2$, porosity 77−76364
Ni film, ion bombarded, porosity 77−66099
Ni, porosity depth distrib. of annealed samples following bombardment by 1 MeV Ar^+ ions 80−5333
Ni powder, nonspherical, mean pore size of sheet material 77−28757
Ni powders, stereological appl. in study of compacting process, elec. and mech. props. *(French)* 80−40286
Ni, temp. effect on porosity of Ni irradiated with Ni ions 78−2173
Ni, volume-strained sintered porous, physicomech. props., u.s. vibration propag. velocity 77−1823
Ni-Cd sealed battery electrode performance meas. 80−66962
Ni-Co-Cr-Al-Ti-Mo superalloy IN738, casking porosity removal using hydrostatic press. sintering 80−55322
Ni-Cr (20wt.%), powder, nonspherical, mean pore size of sheet material 77−28757
Ni-Zn ferrites, comp., lattice imperfections, sintering 78−3080
$Ni_{0.5-x}Co_xZn_{0.5}Fe_2O_4$ ferrospinal solid solutions, cryst. lattice defects and props. 80−19796
NiO, prepared by thermal decomp. of $Ni(OH)_2$, microporosity and irreversible water vapour adsorption 80−80060
NiZn ferrite, magnetic props., porosity and grain size effects 77−36095
NiZn ferrite, ZrO_2 additions influence on sintering and physicochem. props. 80−108369
Pb, positron annihilation, evidence for microporosity and dislocations 79−78786
Pb-Bi, splat quenched, solubility limit, vacancy conc. and supercond. transition temp. 77−12046
Pb-Cd(Tl) alloys, positron annihilation, evidence for microporosity and dislocations 79−78786
PbS films, polycryst. and epitaxial, small-angle X-ray scatt. and electron density inhomogeneities 80−96758
$Pb(Zr,TiNb)O_3$ ceramics, effect of porosity on piezoelec. planar coupling coeff. 79−11388
$Pb(Zr, Ti)O_3$ internal struct., prep. effect, ionic shadowing obs. *(Polish)* 80−11612
$Pb(Zr,Ti)O_3$, porosity-permittivity relations, depolarising factors determ. and pore effects *(Japanese)* 80−97189
Sc_2O_3, polycrystalline, elastic props., porosity and temp. depend. 77−52384
Si and Si:H amorphous films, porosity and oxidation of evap., sputtered and plasma-deposited films 80−10838
Si, powder compact, Ar-sintering, microstruct. changes 77−90306
Si-SiO_2 system, structural defect formation rel. to thermal oxidation kinetics *(Russian)* 78−43478
SiC, 0.6, 3.5 MeV He^+ irrad., surface erosion, porosity effects 77−35602
SiC coatings, CVD on microspheres in fluidised bed, parametric investig. 77−40457
SiC, spray dried agglomerates, compaction response, fracture, deform. 79−43172
Si_3N_4, reaction bonded, pore size and distrib. effect on strength 79−29165
Si_3N_4, reaction sintered, microstruct. charact. 80−35145
Si_3N_4, reaction-bonded, pore struct. variations 79−24480
Si_3N_4, swelling, blistering, 140 keV p, d and He ion irrads., porosity effects 77−35603
Si_3N_4, synthesis and props. of shapes 79−47650
Si_2N_2O, sintered with MgO or BeO additives, effect on oxidation *(French)* 79−20233
SiO_2, adsorption of albumin 80−10777
SiO_2 film, IR spectra and elec. props., influence of prep. conditions 79−87176
SiO_2 film, thermally grown, pore size influence of punch-through voltage 78−6632
SiO_2 films, vac. thermal evaporation, parameter stabilisation 80−87571
SiO_2 glass, monolithic, low temp. synthesis 80−40318
SiO_2, vacuum deposited, 7-10 μ, microhardness and structure 78−19669
SiO_2:Na^+, heat treated, heat of immersion in H_2O, organic compds. 80−3396
SiO_2-base cores, for superalloys, high temp. characterisation 80−10640
SiO_2-ZrO_2 adsorbents, coprecipitated, porous struct. rel. to form. conditions 78−53263
SnO_2, adsorption anomaly of water, effects of cryst. growth of solid 80−10779
$SrTiO_3$, sintering kinetics rel. to added SrF_2, ZrO_2 78−44037
ThO_2 ceramics, CaO and Y_2O_3 stabilised density, elec. cond., permittivity 78−47838
ThO_2 compacts, thermal conductivity, dependence on porosity, mathematical anal. 79−4437
$(Ti,Cr)B_2$, sintering kinetics and props. 80−100811
Ti 78−60602
Ti ion planted coating on steel 77−70217
Ti powder, nonspherical, mean pore size of sheet material 77−28757
Ti-Al system, compact growth in liquid phase sintering 80−20835
TiB_2, electrode, hot pressed, erosion resistance, struct. and porosity effects 78−3228
TiB_2, hardness of sintered material 78−60636
TiB_2, swelling, blistering, 140 keV p, d and He ion irrads., porosity effects 77−35603
TiO_2, porosity-permittivity relations, depolarising factors determ. and pore effects *(Japanese)* 80−97189
TiO_2, sintered ceramic, props. rel. to additives, impurities 78−35329
Tm_2O_3, polycrystalline, elastic props., porosity depend. 77−52384
$(U,Pu)O_2$, pore struct., characterisation for gas exchange anal. *(German)* 79−49687
(U,Pu)C, nuclear fuel, porosity and stability obs. 78−86629
(U,Pu)CN, nuclear fuel, porosity and stability obs. 78−86629
(U,Pu)N, nuclear fuel, porosity and stability obs. 78−86629
$(U,Pu)O_2$, ceramographic exam. of Dounreay PFR fuels, data bank storage 79−49811
U core fuel elements, of A-1 reactor, volume growth *(Czech)* 80−27745
U-Pu radial redistrib., effect of fuel rod parameters and fuel porosity *(German)* 79−49799
UC, effect of porosity on fission-gas-induced swelling 78−8959
UO_2, controlled porosity reactor fuel 77−23205
UO_2, interconnected grain edge porosity 79−17979
UO_2 irradiated, grain edge porosity growth 79−19285
UO_2 nuclear fuel element, lenticular pore movement 78−21644
UO_2 pellet fuel, radiation induced densification 77−6519
UO_2, resolution of fission gas from grain edge bubbles, porosity effect 79−85607
UO_2-20CeO_2 mixed powder, X-ray and microprobe exam. of homogenisation 80−25609
UO_2-PuO_2 fuel pellets, porosity meas. methods *(German)* 80−73915
U_3O_{8-z}, depend. of therm. cond. on porosity, phonon mean free path calcs., Debye temps. 79−37886
V_2O_5-$In(Tl)_2O_3$, ceramic, elec. resist., dielec. props., porosity 77−8093
W fibre reinforced Cu, interface porosity formation, on thermal cycling 80−30092
W, porous, variation of open and closed porosity during sintering 78−15342
W-Cu powder, liquid phase sintering, stabilisation of porous structure and control of volume changes 79−95974
W-Cu-Ni powder, liquid phase sintering, stabilisation of porous structure and control of volume changes 79−95974
W-Ni system, grain growth and densification during liquid phase sintering 79−38760
W-Ni-Fe (5(2), 5(2) wt.%) pore formation, effect on mech. props. 80−45396
W_2B_5, sintering rel. to prod. by boron carbide process 78−11184
WC-Ni hard alloy composite, sintered, void healing 80−60821
WSe_2, lubricant, prep. by self-propagating high-temp. synthesis, technological charcts. 78−35338
Yb_2O_3-based ceramic, preparation, mech. props. 77−24998
$Zn_{1-x}Ni_xFe_2O_4$, heat treatment and sintering effect on porosity 80−25610
ZrC, elastic modulus, porosity factor 77−21207

porosity continued
ZrC, high-temp. strength, affecting factors 77−63794
ZrO_2 coatings, prod. by low-temp. oxidation, props. 78−23856
ZrO_2 film, electron beam deposition, refr. index and microporosity 78−90467
ZrO_2, partially stabilized, processing defects 80−97558
ZrO_2, plasma deposited, porosity, gas permeability and dielectric strength 79−52125
ZrO_2 refractories, high-temp. induced porosity increase 80−35146
ZrO_2, sintering response with const. rate of heating, depend. on processing related pore distrib. 79−28992
ZrO_2, spray dried agglomerates, compaction response, fracture, deform. 79−43172
ZrO_2-$CaO(Y_2O_3)$ ceramics with grainy structure, props., effect of heating to 2000°C 80−104194
ZrO_2-Y_2O_3, solid solns., density meas. rel. to O vacancy model 78−2113
$ZrSiO_4$, natural zircon, nucl. radiation effect on elastic moduli 77−11616

porous materials
see also flow through porous media
acoustic absorption characteristics *(Spanish)* 78−14405
acoustic absorption coeff. in different media *(Japanese)* 77−84033
acoustic impedance, meas. rel. to damping in reson. absorbers *(German)* 77−14825
acoustic propag. and decay 79−7248
acrylic bone cement improvement by addition of fillers 77−37109
adsorbed layer below its freezing point, isothermal adsorption and dimensional changes obs. 78−75925
airborne particulate detection by metal-coated Nuclepore filters 77−37463
amberlite XAD copolymers, packings for gravity flow, high press. liq. chromatography 77−77822
anisotropic magnets, approach to mag. saturation 80−93146
anodic films on Al, nucleation and growth 78−44273
artificial kidney microporous membrane plasma filtration efficiency 78−48926
atom-atom interaction law *(Russian)* 80−19861
barrier fabrication for U isotope separation, powder metallurgy problems *(Italian)* 78−88439
bearings, linearised turbulent lubrication eqn. hydrodynamically rough permeable boundary 79−87741
Berea sandstone, effects of pore fluids on bulk and shear attenuation 80−51386
bicrystals, diffusion growth of pores under creep conditions 77−15404
biporous media, influence of double layer on dynamics of ion adsorption 79−11827
body of simple shape, internal stress distrib., expt. and calc. *(Russian)* 79−68569
bone mechanical model with appl. to human upper tibia, porous material, deform. *(Japanese)* 78−88724
borosilicate glass, porous, surface area change with acid treatment, adsorption of N_2 and H_2O *(Japanese)* 78−44244
borosilicate glasses, IR spectroscopic obs. of coordination state of B atoms 77−24268
brittle, US fractography appl., expts. on glass 77−44336
brittle model mats., porous and nonporous, strength and struct. 77−4849
brittle porous materials, critical stress and crack size evaluation *(Russian)* 78−35494
bronze powders preparation by electrodeposition, porous components fabrication appl. 78−20026
Brunauer-Emmett-Teller surface areas, automatic low-cost determ. 77−55441
capillary porous body, drying kinetics, infinite plate calcs. 77−46890
capillary rise, role of contact angle 77−24467
capillary rise, secondary phenomena 77−24466
capillary rise problem 77−24465
capillary rise rates in porous media with nonuniform pores, model 77−72747
carbons, active, micropore filling and adsorption of simple gases, Dubinin theory 77−47661
catalyst pellet, transient diffusion-react. eqns., approximation using Galerkin technique 79−96357
cathodes, flow-through, performance eval. for Cu electrodeposition 77−16514
cellulose acetate freeze-dried membrane, gas permeation rates 79−79295
cellulose acetate porous membrane, inert gas separation appl. 77−36791
ceramic implant/bone interface, tensile strength and bone form., effect of elec. stimulation 77−5108
ceramics, eval. of frost resistance by holography *(Japanese)* 78−19987
ceramics, frost action under one dimens. heat flow *(Japanese)* 79−79140
ceramics, frost resistance under 1-d cooling, pore size distrib. effect *(Japanese)* 78−44069
ceramics, granular, electrophysical props. depend. on porosity, temp., solid-phase props. 77−69764
ceramics, longitudinal US wave velocity 77−55323
ceramics with non-spherical holes, US wave vel. and elastic moduli evaluation 77−60031
circular viscoelastic porous shell, dispersion of longitudinal waves *(Russian)* 78−42556
clay layer, non-homogeneous, consolidation estimation via pore water press. Fourier anal. 79−58110
coated implant removal by ultrasound 79−79618
coke, chamber and formed *(German)* 80−100356
coke, metallurgical, microstruct., using refl. light microscopy and image anal. 80−66732
colloidal capillary-porous body, mass transfer parameters, adsorpt., osmotic moisture 78−11563
composite, of PTFE and C black, electrochem. method for monitoring form. 77−36446
compressibility 79−100069
consolidation in compressible mixtures 79−46271
contact stresses in hot rolling 77−77515
controlled pore glass, pore struct., determ. by electron microscopy and Hg penetration 78−43165
convective heat exchange in fibrous materials, at elevated press. in gaseous medium 80−19217
crack scattering in polycrystalline media 78−75089
creep at high-temp. and after-effect *(Russian)* 78−39835

porous materials continued
cryogens, solid, gradientless heat transfer, cryogenic liq. crystn. 79−59903
cryogens, solid, gradientless heat transfer, metallic thermal cond. theory 79−59902
crystalline, dislocation interaction between pores while being healed by external pressure *(Russian)* 77−19963
cylinder, permeable, in viscous fluid, friction coeff. 79−46385
deep evaporation characterisation, of water *(French)* 78−59468
deformation anal. using upper bound theory *(Japanese)* 77−46937
deformation diagram based on theory of plasticity *(Russian)* 78−88494
densification during gasostatic hot pressing 77−12567
densification kinetics in hot pressing, under quasi-isostatic conditions 80−11585
densification kinetics in hot pressing under quasi-isostatic conditions 80−25592
densification of porous body during hot extrusion, theoretical analysis 77−44189
densification of porous solids in hot rolling 77−63583
density determination of briquets, hydrostatic weighing method with preheating 79−49203
density variation during plastic shaping 80−84873
dextran structural modifications, I_2 sorption, porosity depend. *(Russian)* 79−23535
die filling and densification in hot extrusion forging of porous preforms 78−23645
diffusion of gases in porous solids, Monte Carlo simulation 80−65299
directionally dependent lineal porosity materials, continuum theory from isothermal elasticity 80−48588
displacements in porous elastic half-space prod. by impulsive line load, non-dissipative case 77−23908
drying, evaporation characteristics determ. *(Russian)* 79−37134
drying, internal mass transfer coeffs. calc. 78−67011
drying, theory and expt. verification 78−59278
drying intensification, thermolabile porous material in contact with sorbent, in vac. 77−89641
ductile media, rupture by void nucleation and growth, yield criteria and flow rules 77−52492
dynamic hot densification of porous blanks, degree of deformation 77−63585
E-glass fibre, pore size distrib. anal. method 79−87805
Earth interior, pore fluids and Q rel. to earthquakes brittle fracture model 79−39671
elastic deformation of porous body in rigid sheath, energy expenditure in the densification 80−16216
elastic media, boundary-layer analysis of propagating mode II cracks 78−5696
elastic properties determ. methods, review 77−42746
elastic soil, finite consolidation theory 77−46916
elastic wave propagation, influence of random porosity 78−90552
elastic-diffusion interaction of closely situated pores *(Russian)* 77−76592
elasticity theory, self-consistent imbedding approx. 77−33066
elasto-viscoplastic-viscous theories of granular and porous media, soil mechanics appl. 79−76982
electrical conductivity of porous bodies, exam. 79−4543
electrode, porous, contained electrolyte elec. cond. meas. 77−63927
electrode, wetproofed, pore filling degree with electrolyte and liq. reactant 80−40702
electrode sensors for using porous electrode sensors 77−17261
electrodes, flow-through, math. modelling 77−16832
electrolytic preparation of porous sintered materials 79−52530
evaporative cooling of porous wall, thermal state of vapour zone *(Russian)* 79−64763
excess pure pressure measurement with liq. manometers 77−52566
felt sound absorption rel. to airflow resistance, obs. 77−58506
ferromagnet, with Bloch walls and self-consistent magnetisation, energy and coercive field 80−15760
fibre, permeable, quantitative charact. of porous struct. 78−19683
fibre reinforced porous composite anal. by US wave velocity meas. of fibre vol. and matrix porosity 78−95902
fibre reinforced porous matrix materials, densification kinetics in free hot pressing 80−25618
fluid effects on mechanical props. 80−23883
fluid saturated porous solid, eqns. of motion 78−79208
fluid saturated porous solid, fundamental solns., deformation, pore-fluid diffusion, soil mechs. 77−84160
fluid-filled, transient waves refr. and refl. 77−49604
fluid-filled porous media, response to transient input 77−31244
fluid-infiltrated elastic materials, deformation of cavities and inclusions 78−51073
fracture behaviour estimation using simulation model and finite element method 77−42777
freezing dispersed medium, origin of water aspiration 77−60130
gas behaviour in closed porosity body, exam. 80−24642
gas diffusion technique for pore struct. investigation 80−30185
gas-bearing water-saturated sediment, sound vel. as function of bubble distrib. 79−39703
gas-saturated porous media, deform. theory *(Russian)* 77−41483
gel, electrical double layer on surface 80−11955
generalised p-α model, eqn. of state, sound vel. 80−65154
generalised thermorheologically simple porous materials, thermomechanical theory of viscoelasticity 80−33479
glass, dissoc. adsorption of ethanol, IR obs. 79−23830
glass, irradiated, accumulation and decay of paramagnetic centres *(Russian)* 77−85570
glass applications, review 78−3306
glass bead sintered pellets, pore struct. and diffusibility *(Japanese)* 78−14509
glass optimisation for immobilised enzyme systems 77−12891
glass porous, struct. and texture rel. to heat treatment effects *(German)* 78−44140
glass preform optical waveguide props. 79−94375
glass sintered powder porous bodies, liq. penetration mechanism *(Japanese)* 80−53853
Gorskii effect *(Russian)* 79−65109
gradient index lens fabrication by molecular stuffing 80−14499
granular material, simultaneous moisture content/thermal cond. meas. apparatus 78−53064
granular porous media, resisto-capacitive model of gaseous exchange *(Polish)* 77−12831

porous materials continued
granular solid, one-dimens., small amplitude wave behaviour 78−59339
graphite, heating in air atmosphere, spectral emissivity 80−19969
graphite, pyrolytic C coating within pores 79−41035
graphite foam, thermal props. 77−48689
graphite ionisation chamber, ionisation error due to porosity 80−52829
graphitic carbons, particle emission rel. to morphological changes during sublimation 77−47566
gravel, sedimentary deposit, NaCl mass transfer to stationary water region *(Japanese)* 77−25700
gravimetric measurement of sorption isotherms, errors 78−67905
ground surface, acoustic refr. index rel. to atmospheric sound propag. 77−50805
haematite-magnetite two-phase system, internal stresses *(Russian)* 80−16319
hailstones, foreign material obs. and derivation 78−96260
heat and mass transfer, boundary layer method 77−2625
heat and mass transfer, two-dimensional isoparametric finite element method 77−42708
heat conduction, thermodynamics of non-equilibrium processes *(Hungarian)* 80−178
heat transfer, environment effects *(Polish)* 79−18674
heat-pulse moisture meter for capillary-porous materials 77−82499
heterogeneous micropore systems, filling, generalisation of Dubinin-Radushkevich eqn. 77−47664
hot rolling, rheology, stressed state determ. 79−100194
hydrodynamic calculations, porous struct. parameters, theory 79−98797
hydromagnetic squeeze film between porous circular disks with velocity slip 80−74997
hydrophilic uniform branched porous media, capillary equilib., with correl., anal. 78−18877
hydrostatic loading and unloading relation for porous materials with various fluid contents 78−28222
inhomogeneous porous media, analytical theory for water flow 77−62301
interstellar porous grains, free-space equilib. temps. calc., rel. to optical props. 80−62223
interstellar porous graphite grains, rel. to 2200 Å extinction hump 80−62228
Kayenta sandstone, influence of pore press. on mechanical props. 78−81150
laser reflectors, cooling, prospects for use of porous materials 80−91809
leaching from model porous bodies by reflection spectroscopy 80−100031
linear thermoconsolidation, porous elastic solid containing compressible fluid 79−23186
liquid distribution across porous bodies 79−69326
liquid-saturated porous media theory with account of simultaneous deform. of structure and liq. *(Russian)* 77−41482
low angle X-ray diffr., pore or particle size distrib. calc. 77−39512
LWR controlled porosity fuels, short term irradiation behaviour 79−49686
macromolecular solutions trapped in small pores, statistics 77−39524
marine sediments, nature and reactions of dissolved organic matter in interstitial waters 78−49039
medullary implants with porous coating, stress distrib. 78−69256
melt infiltration, math. model 79−100089
meniscus, three-dimens. numerical simulation by finite elements 77−59183
metal, plastic, work hardening, sintered, porous, irreversible deform. 78−19849
metal, pore form. mech. investigation by directional solidification 77−28800
metal, porous, densification during volume plastic deform. without work hardening 77−40402
metal, shock compression calcs. using approx. eqn. of state 77−35657
metal, shock speed meas., continuous recording 78−5708
metal, sintering of solids containing several dissolved gases 80−20836
metal, stresses in deform. region during cold rolling 78−11241
metal, thermal conductivity meas. 78−18150
metal, yield stress variation during cold deformation 80−16395
metal couple, porous homogeneous vacancy migration and void form. 77−55401
metal fiber permeable materials, struct. characts. 79−24464
metal fibre materials, permeable, obliteration phenomenon 79−98799
metal fibre materials, permeable porous struct. parameters 79−100083
metal fibre materials, thermal and elec. conductivities 78−10419
metal fibre mats., struct., hydraulic characts.; liq. permeability 78−67848
metal gauze, struct. and hydraulic characts. 80−11729
metal gauze reinforced porous permeable mats. with prearranged struct., prep. 78−68652
metal porous strip, metal pressure in cold rolling in elastic aftereffect zone 80−40421
metal strip, elastic aftereffect in cold rolling 80−11689
metal wick, sintered, effective thermal cond. meas. 78−94582
metallurgical coke, mech. behaviour charact. *(French)* 80−104371
metals, plasticity, stress-strain curves, yield stresses, strain vectors 80−83738
metals porous, mean principal stress in rolling without lateral expansion 80−25803
micropore filters, preparation by bombarding lavsan film with Ar ions 78−3305
microporous adsorbents, experimental adsorption isotherms of characteris. of absorbents 77−69163
microporous alloy hip prosthesis clinical trials 79−79687
mixture theory, formulation of incompressible porous media models 80−96184
moist material, external heat transfer, calc. methods, drying kinetics 78−59467
moist materials, drying kinetics calc. method, heat (moisture) transfer 78−55555
moist porous solid, thermal cond., struct. model and computation method 78−2312
moistened, permittivity 79−95304
moisture transfer due to small temp. gradients in unsaturated porous media *(French)* 78−150
molecular sieves, bi-porous, sorption kinetics, expt. and theory comparison for batch systems 79−87873
molecular sieves, bi-porous sorption kinetics, math. models for systems with rectangular equil. isotherm 79−87872
porous materials continued
multi-layer soils, state vector approach to one dimens. consolidation 78−3757
multicomponent medium, heat radiation attenuation factor calc. model 79−94472
Ni powder 2JJ, porous, effect of sintering conditions in struct. and strength 80−20823
Ni-Cr alloy Kh20N80, sintered sheet material, stopping power and pore size relationship 78−19693
Nichrome, Kh20N80, varying porosity, effective thermal cond., 373-1400K, meas. method 78−75053
Nichrome wire, porous, strength charact. 78−6997
Nichrome/steel, porous metal-thread sheet materials, filteration, permeability and strength props. *(Russian)* 79−78915
non-steady flow problem in two-layer porous medium 78−81260
nonisothermal finite strain mechanics of porous solids, thermomolecular diffusion, variational Lagrangian thermodynamics 77−65668
nonisothermal mass transport, thermal energy flux and radiation pressure theory 78−76916
nonlinear theory of elastic materials with voids 80−53623
nonswelling porous body, moisture-retaining capacity and struct. 77−12773
nuclear fuel structure characterisation methods, review 79−49802
nuclear fuels, fission gas precipitation into intra- and intergranular porosity, theory 80−57849
Nucleopore membrane, pore struct., determ. by electron microscopy and Hg penetration 78−43165
outgassing, area/vol. config. influence 80−84371
oxide, porous transparent films as antirefl. coatings for glass surfaces, low refr. index 80−74448
oxide coating, pore size distrib. and permeability 79−24641
particle porosimetry by inverse gel permeation chromatography 77−90659
permeability of conical shells deep drawn from porous sheet 80−11728
planetary surface layers, validity of radiative-conductivity, theory 77−17354
plastic deformation, anal. using plasticity theory 80−25802
plastic deformation, constitutive eqns. 79−61667
plasticity, deformation theory *(Russian)* 79−37189
plasticity, deformation theory *(Russian)* 80−75291
plasticity as function of porosity *(Russian)* 80−75290
plasticity of porous powder solid 79−68604
plasticity theory, extension to reinforced composite materials *(Russian)* 77−68443
plasticity theory for porous metals, stress-strain curves 77−17812
PMMA, used as tooth replicas, phys. props. and biological acceptance 77−52926
poly(vinyl alcohol) porous film, polymerisation and porosity 80−107063
polyethylene implant-bone composite interfacial strength, porous high density polyethylene 78−31979
polyethylene-bone composites, fracture toughness 77−37108
polyfluoroethylene resin, porous, wetting angles with cyclohexanone and isopropyl alcohol meas., porosimetry method 77−1278
polymer, microporous, lubricant supply charact. 78−64711
polymer, porous, prep., appl. as stationary phase in gas chromatography *(German)* 79−29434
polymer charcoal, adsorpt. isotherms of organic vapours 80−96731
polymer filled ceramic, ZrO_2 stabilised, fracture mechanism *(Russian)* 80−100895
polymer films, micropore localisation, electron microscopy 80−103271
polymeric membrane, porous, gas permeability *(Japanese)* 79−24825
polyuranate gels, changes in pore structure during reduction and sintering 77−71685
polyurethane foam, press. wave propag. and refl. characts. 77−35634
poroelastic cone, inhomogeneous, forced torsional vibrs. 79−32338
poroelastic discs or slabs, dynamic response to harmonic loading 79−41578
poroelastic hollow cylinders, torsional vibrs. 79−64557
poroelastic material dynamic characterisation, complex, modulus meas. 80−14640
poroelastic medium, semi-infinite, disturbance produced by surface load 77−19533
porosity and pore size measurement using soln. of luminescent material flowing around sorbent granules 80−53850
porous moist body, contact heating moulding, temp. distrib. heat/mass transfer 77−75784
porous rigid-plastic material containing rigid inclusions, yield function, plastic potential, void nucleation 78−64612
porous surfaces, wind tunnel for evap. rate from soil samples *(French)* 77−80684
pressure generation during the drying of a porous half-space 79−23187
pressure solution thermodynamics, chem. and mech. forces interaction 77−60369
pressure waves, long wavelength, and transient regimes *(French)* 77−62193
production method using stainless steel gauzes, exam. of hydraulic characteristics 80−16243
PVC, struct. and performance of porous membranes prepared from soln. *(Japanese)* 79−24823
quartz, ceramic, elastic property changes on sintering 77−90301
quartz, Hugoniot synthesis at high pressures 79−95080
randomly-packed spherical particle bed, coord.-no. distrib., effective thermal cond., stat. thermodynamic theory 78−75028
Rankine-Hugoniot relation for shock waves 78−83317
reaction with mixed gases 78−44404
recrystallisation and grain growth, survey 78−76660
refractories, thermal cond. rel. to gas phase mass transfer in pores and microcracks 79−73352
rocks, dry and water-saturated, plane shock wave studies 80−21714
rocks, pore collapse rel. to deform., expt. in transmitted light 77−86860
rocks, saturated, effective stress law for anisotropic elastic deform. 80−51385
rocks, saturated with low cond. fluid, thermal cond. meas., systematic errors 77−86871
rocks, seismic wave vels. rel. to saturation 77−2114
rocks, self-consistent imbedding and ellipsoidal model 80−26503
rocks, texture heterogeneity study via dielectric const. and elec. resistance *(Russian)* 78−96195
rocks, US absorpt. from wave attenuation and scattering on random inhomogeneities *(Hungarian)* 77−86791
salt solutions in porous media, dielectric meas. *(French)* 79−52677

porous materials continued
sand, sedimentary deposit, NaCl mass transfer to stationary water region *(Japanese)* 77−25700
sandstone, determination of Biot parameters using static tests 79−20299
seismic wave propagation, dynamic poroelasticity fundamental soln. 79−74847
semiconductor probe point characterisation by footprint in porous Si 79−96243
semiinfinite porous media, heat cond., phase transitions effects 78−94523
shear stress enhancement of void compaction 79−69182
shock wave compression of porous samples, expt. and model 78−63807
shock-compressed porous solids, sound velocity *(Russian)* 78−71788
shrinkage kinetics in spontaneous compression, boundary slip and superplasticity 77−36611
silica gels, pore size meas. using reson. ion beam backscatt. 79−2747
simultaneous heat and mass transfer governing eqns., soil heating appl. 78−94562
sintered, mech. testing device for hydrostatic pressure conditions 80−40645
sintered battery material *(German)* 80−21394
sintered porous materials, effective thermal conductivities 80−19998
sintering, behaviour of pore filled with const. amount of gas 80−66450
sintering, gases influence, behaviour of assembly of pores filled with gas 80−84877
sintering, mechanism hindering boundary sliding 79−95962
sintering, rheological and microscopical models, relationship 79−95963
sintering, role of gas in healing of isolated pore by volume vacancy diffusion 78−15330
sintering kinetics, superplasticity of polycryst. materials 79−100072
snow, volumetric constitutive law based on neck growth model 80−48595
softwoods, transverse Poisson's ratio and Young's modulus *(Japanese)* 80−2111
soil, cohesionless, strength, influence of high pore-water press. 77−25678
soil, consolidation due to shear loads distributed over rectangular area 79−57936
soil, elastic, drained and undrained behaviour, anal. 77−3720
soil, Martian, fine-grained component model based on Viking lander data 78−85882
soil, pore water characts., modelling, similarity hypothesis 78−11941
soil, pore water expulsion rel. to sub-pingo water lenses, Northwest Territories 79−20873
soil, two phase with viscoelastic skeleton, finite element anal. of consolidation 77−11138
soil, water infiltration into uniformly packed soil 77−2152
soils, non-linear seismic response and liquefaction 79−57862
solar air heaters, use of porous flat plate solar collectors 80−35748
solid-fluid mixtures, thermostatics 77−856
solid-fuel mixture, incompressible, equilibrium theory 77−857
sorbent, biporous, internal diffusion 80−44414
sorption dynamics, nonisothermal multicomponent, with widely differing mass-transfer coeffs. 77−65793
sorption dynamics for nonlinear isotherm 77−39734
sorption kinetics in porous granules, integration of nonlinear eqns. 77−7967
sound attenuation in porous elastic solid containing compressible viscous fluid *(French)* 80−38149
sound porous material, stress anal. during stretching *(Russian)* 79−76980
sound pulse absorption, Fourier transform anal. 80−38170
specific surface, determ. using Hg porosimetry 80−29896
spherical wave reflection at fluid plane interface with porous medium 78−42484
steel, austenitic stainless, porous fibre, sintered and compacted, mech. props. 79−15623
steel, chemicothermal treatment, diffusional basis 80−104343
steel, Cr-Ni, rolled and sintered, to produce capillary structured filter material, exam. of mech. props., and production 80−16235
steel, high speed, atomised powder, defects in parts produced by hot isotactic pressing 78−60612
steel, permeability, deform. effects 79−100229
steel, sintered, fracture of residual pores 80−76352
steel, stainless, porous sheet, mech. strength, bend and reverse bend tests *(Russian)* 80−93595
steel, stainless, porous sheet, pore dimensions, filtration and permeability *(Russian)* 80−76480
steel, stainless, sintered sheet material, stopping power and pore size relationship 78−19693
steel fibre reinforced porous mat. prod., mat. props. 77−59723
stratified horizontal porous layer, onset of natural convection *(French)* 77−89002
strength, elastic modulus exponential porosity depend. 77−36563
stress determ. by X-rays *(German)* 77−44436
stresses induced by drying, elastoviscoplastic model, finite element anal. 80−23904
surface coating, influence on boiling of dielectric fluid *(Russian)* 79−72788
surface diffusion of adsorbable gases 77−80694
surface preparation, effect of different methods on porosity 80−60995
tensile strength, pore geometry effects 80−30048
thermal cond., diffusivity and water content meas., thermal shock transient *(French)* 78−94583
thermal cond. of gas and solid, separate determ. *(Polish)* 79−64486
thermal conductivity, corrections for porosity entrainment using analytical temp. solns. 79−59173
thermal conductivity, effect of decrease in thermal resistance of pores and microcracks 78−75892
thermal conductivity, theoretical models *(German)* 77−27462
thermal diffusion based on electrokinetic effect, coefficient determ., calc. and obs. *(Russian)* 78−90641
thermomechanics, mixture theory 78−63315
toughness-porosity phenomena 78−72874
transverse cutting of moving porous strip 77−55901
two-phase porous cooling system, hydrodynamic and thermal characteristics 77−10012
two-phase system, effective thermal cond. 79−30396
unconsolidated porous sand reservoirs, elastic props. 78−61400
US bulk compressional wave obs. 80−64235
vibrating porous material surface sound radiation *(Japanese)* 79−68474

porous materials continued
Volume changes experienced by porous solids during nonisothermal liquid-phase sintering and self-propagating high-temperature synthesis 78−15328
Vycor glass, porous, adsorbed NH_3 Raman scatt. 80−11948
Vycor glass, positronium-surface interaction in pores 78−27347
Vycor porous glass, adsorption of carbonium ions, reson. Raman spectra 78−84571
water content determ., rapid thermal method 77−86258
water-saturated struct. of sintered glass beads, elastic wave speeds, Biot's theory confirmation 80−103418
wave propagation in fluid saturation porous medium *(French)* 78−86165
web structures between cavities, stress anal., appl. to struct. materials with microcavities 77−874
wedge indentation hardness, slip line field theory 77−86128
X-zeolites, dielectric relax. anal. 80−108153
Al, 78% dense porous, dynamic compaction 78−63315
Al and its alloys, dynamic determ. of Gruneisen coeff. 77−24418
Al anodic films, cell walls anal. by STEM and energy dispersive X-ray anal. 79−19476
Al anodising, porous films formed in chromic acid 80−100966
Al, constitutive equation for porous materials with strength, press. effects 80−79875
Al, Hugoniot synthesis at high pressures 79−95080
Al-Si (8 wt.%), threshold H_2 for pore form. during solidification 78−52794
Al-SiC cermet elasticity, porosity meas. by US means 80−81101
Al_2O_3 based catalysts, porous pellets, thermal cond. 79−86936
Al_2O_3 film pore size distribution meas., adsorpt.-desorpt. vs. TEM methods 77−74357
Al_2O_3, porous, anodic, growth, physical model 78−48662
Al_2O_3, porous, anodic, growth, ionic cond. 78−48663
Al_2O_3 porous refractories, production 80−35149
Al_2O_3 porous transparent films as antirefl. coatings for glass surfaces, low refr. index 80−74448
α-Al_2O_3, sintered or hot-pressed, porosity effect on positron mean lifetime 78−27463
Al_2O_3, validity of high pressure Hg intrusion porosimetry 79−24697
Al_2O_3:Fe, pore form. during oxidative annealing, grain growth slowing 80−100856
Al_2O_3-bone composites, fracture toughness 77−37108
Al_2O_3-SiO_2-TiO_2-B_2O_3-Fe_2O_3, exam. of porous structure, using a combinational method 79−29303
Ar, solid, contact heat transfer in sublimation 77−31767
Au thin films, with nm-sized pores, prep. from Au-Ge eutectic films by etching 80−16227
BaO, CO_2 transport kinetics following $BaCO_3$ decomp. 79−23780
Be, porous, shrinkage during sintering, kinetics, photographic method 79−15622
C, activated, adsorpt. of I_2, pure struct. 77−31870
C, activated, surface oxidised, adsorpt. of organic vapour rel. to paramag. props. 77−32238
C black with pyrocarbon coating, surface props. *(French)* 78−68921
C molecular sieve prep. by pore blocking 78−15324
C, porous particle, internal combustion, model 78−92481
CaO, CO_2 transport kinetics following $CaCO_3$ decomp. 79−23780
$CaSiO_3$, hydrated in Ca_3SiO_3 pore struct. 77−56213
CdS, porous, dynamic phase transition at high press. 79−23723
Cs halide, porous layers, electron bombardment induced cond. 78−56550
Cu, electrolytic powder, sintering, gas effects, finite size bodies 77−77447
Cu, shock compression calcs. using approx. eqn. of state 77−35657
Cu, sintered preform, porous, ductile fracture criterion, rel. to forging process 77−56105
Cu, surface coating, influence on boiling of dielectric fluid *(Russian)* 79−72788
Cu-Ga porous solid formed by shock compression 80−29905
D-D fusion reactor, neutronics aspects of a porous blanket 80−83217
Fe, carbonyl pore struct. orientation, shrinkage anisotropy effect 80−20845
Fe compacts, porous, dynamic hot pressing, press. rel. to density, time 78−60599
Fe fibre, props. 79−98798
Fe ore pellet, meas. of gas permeability of individual pellets 78−80711
Fe, porous, density, elec. cond., Young's modulus, toughness 78−64645
Fe, porous, volume strained, correlation between strength and acoustic props. 77−16770
Fe powder, sintered and hot pressed, effect of porosity, grain size on magnetic props. 79−96159
Fe powder based sintered porous permeable materials, diffusion chromising 80−100958
Fe-based powder PZh2K, porous struct., effect of diffusion chromising with sintering 79−66219
Fe-Cu-C sintered porous materials, machinability 80−66457
Fe-glass porous material, wear resist. under dry friction 80−25876
Fe-graphite porous sintered, determ. of impregnation depth with polycaprolactam-finely divided Cu metallic polymer 79−70272
Fe-Ni, sintered, porosity determ. by US attenuation and sound vel. meas. *(German)* 80−76437
Fe_3O_4 briquettes, porous, struct. changes during reduction 77−21064
Fe_xO_y, sintered metallised compacts, pore struct. by Hg porosimetry 80−40280
In_2O_3, polycrystalline, electron conc. and mobility, 25 to 700°C, O_2 partial press. depend. 77−76811
KCl film, porous, injection mechanism for transmission secondary electron emission 78−19643
KCl single crystal, healing of isolated pore under pressure due to isostatic compression 77−21046
KCl-KBr-KCl, layered system, diffusion zone, pore form. and movement *(Russian)* 79−69282
LaB_6, porous, field emitter cathode sputtering and surface damage 79−11492
Li ferrites, porous, porosity effect on saturation of magnetisation 80−108036
Li-Si alloys eval. as negative electrodes for Li-FeS_2 cells, thermodynamic props. 77−16547
LiF, ceramic, characts. on pressing in vacuum and in air 78−52734
LiF compact, particle size rel. to pore characts. 78−60631
Mg, heating by shock compression, vap. form. *(Russian)* 78−2195

porous materials continued
$MgCr_2O_4$, chemisorption of CO_2, surface flow of CO_2 determ. 77−47083
$MgCr_2O_4$-TiO_2, porous ceramics, humidity-sensitive electrical conduction 80−107782
$MgCr_2O_4$-TiO_2 porous ceramic humidity sensors 80−86325
MgO, polycrystalline, ductile, porous, model 79−47653
MgO, polycrystalline, grain growth and grain boundary migration, pore effects *(Japanese)* 78−19701
Mo, permeability, deform. effects 79−100229
Mo, porous, high temp. props. 77−11894
N_2, solid, contact heat transfer in sublimation 77−31767
NaF powder, porous, of skeleton struct., grain size effect on strength *(Russian)* 77−24991
Na_2O-Al_2O_3-SiO_2 glass, crack shape, US fractography obs. 77−44336
Na_2O-CaO glass phlogopite mica powders, composite fabrication, cellular struct. 80−84902
Na_2O-P_2O_5-SiO_2 glass, substitution of Li^+, Mg^{2+}, Sr^{2+}, Ba^{2+}, Zn^{2+} for Na^+ 80−100332
Ni carbonyl powder, sheet filtration materials with metallic gauze backing layers, bending strength and ductility 78−60613
Ni coating, electron beam evaporated, ductility and struct. 78−11439
Ni, electrolytic and carbonyl grades, sintered sheet material, stopping power and pore size relationship 78−19693
Ni, fibre, porous, permeable material production 77−12580
Ni, porous, internal friction and effective elasticity modulus, temp. depend. *(Russian)* 79−29118
Ni porous layer, on Cu surface, accel. heat transfer, to boiling n-octane 77−85056
Ni powder, porous, relationships between mech., physical, and microstructural characts. 80−20846
Ni powder, sintered, use of extruded porous materials as fuel cell electrodes 80−40853
Ni sintered permeable materials with bidisperse structure, pore-forming additions effect 80−84885
$Ni(OH)_2$, electrolytic precipitation into porous sintered plaques for Ni-Cd batteries *(Chinese)* 79−57237
Pb electrode, oxidation in H_2SO_4 solutions obs. 79−100514
Pb porous electrode oxidation in H_2SO_4, potential step expts. 79−96438
PbN_3, pressed, lag time of breakdown and dielec. strength 77−36174
$Pb(Zr,Ti)O_3$ ceramics with ladder type struct., prep. and props. 80−75945
$Pb(Zr,Ti)O_3$, effect of spherical pores on strength 77−70103
$Pb(Zr,Ti)O_3$, porosity-permittivity relations, depolarising factors determ. and pore effects *(Japanese)* 80−97189
Pt/ZrO_2 porous electrode/solid electrolyte system, interface polarisation effects 80−61114
Re, sintered, preparation, thermal cond., linear expansion up to 1000K 79−61533
Si film, form. and oxidation by anodic reaction 79−28966
Si film, form. by anodic reaction in HF soln., struct. props. 77−24971
Si, formation during anodic treatment in HF aq. soln., growth kinetics and density 80−20059
Si, porous, form. during anodic treatment in aq. HF 80−35369
Si, porous layer, struct. and heat-treatment effect 79−1557
Si/surface porous oxide film, impurity distrib. during P diffusion 77−39944
Si_3N_4, reaction-bonded, internal oxidation processes role in high-temp. mech. props. 79−38915
SiO_2 based glass, high SiO_2 radioactive waste fixation 79−49708
SiO_2 films, dehydroxylation, sintering, IR investig. *(Russian)* 78−75967
SiO_2 films, microporous, sintering effects, IR ATR, transmission investigs. 79−66031
SiO_2 gel, macroporous, modification of surface by adsorption of thin layer of polymer 80−6624
SiO_2 gel, meso-porous, SCI/IUPAC/NPL surface area standard, pore meas. 77−4941
SiO_2 gel, $SiO_2Al_2O_3$, SiO_2MgO, pore structure influence on X-ray intensity in EPMA *(Japanese)* 80−26046
SiO_2 gels, heats of immersion, effects of pore narrowing 79−11833
SiO_2 glass, porous, adsorption of inorganic cations, in distilled water medium 79−24814
SiO_2, P-doped amorphous, porous and hydrophilic, water adsorpt. and IR spectra obs. 80−80061
SiO_2-Al_2O_3 porous catalysts, EPMA quantitative anal., new correction calc. method, modified ZAF method *(Japanese)* 80−93822
SiO_2-MgO porous catalysts, EPMA quantitative anal., new correction calc. method, modified ZAF method *(Japanese)* 80−93822
Ta_2O_5, hydrated, heat treatment effect on physicochem. props. 80−20966
Ta_2O_5-H_2O_n, influence of preparation on pore structure and ion exchange props. 79−1970
Ti, anodic oxidation under high voltage, porous layers *(French)* 80−54574
Ti, electrolytic powder, rolling of porous sheets 77−63578
Ti, porous structure, change in presence of liq. phase *(Russian)* 80−16223
Ti, sintered, fatigue strength, oxidation effect 79−96137
Ti, sintered sheet material, stopping power and pore size relationship 78−19693
Ti-Al (Sn), porous, effect of Al and Sn on sintering 80−20830
TiO_2, porosity-permittivity relations, depolarising factors determ. and pore effects *(Japanese)* 80−97189
(U,Pu) O_2, pore struct., characterisation for gas exchange anal. *(German)* 79−49687
U-Pu radial redistrib., effect of fuel rod parameters and fuel porosity *(German)* 79−49799
UO_2, SiC coated, small surface area determ. by Kr adsorption 80−44429
W, chromising 80−100959
W, porous, high temp. props. 77−11894
W, porous, physicomechanical props. sintering effects 77−12575
W, porous, variation of open and closed porosity during sintering 78−15342
W, room temp. shock compression expts., Hugoniot states, 0.6-7.6 GPa 77−84842
W, sintered, porous struct. rel. to powder props. 79−61540
W, thick-plate technique for measuring ejecta from shocked surfaces 79−37760
W-Cu, porous material, skeletal type, produced by liquid phase sintering, exam. of mech. strength, determ. resistance 80−16245
porous materials continued
W-Cu permeable materials, development 77−28755
W-Cu pseudoalloy, porous, chromising 80−100959
W-Re alloys, sintered, preparation, thermal cond., linear expansion up to 1000K 79−61533
Y ferrite-garnet, porous polycrystal, law of approach to saturation *(Russian)* 78−47956
Zn electrode, concentration changes during cycling 80−35666
ZrO_2, porous, sintered stabilised microspheres, strength and fracture studies 80−85019
ZrO_2, stabilized porous refractory, mech. strength 80−35322

porous media *see porous materials*

porphyrins *see organic compounds*

Portevin-Le Chatelier effect *see serrated yielding*

posistors
anemometer using posistor sensing element *(Russian)* 77−15139

position control
see also attitude control
32.5 cm IR airborne telescope, pointing system 78−28523
above knee prosthesis, feasibility of active control scheme 78−81081
Anglo-Australian 3.9 m telescope, computer-controlled slewing, setting and tracking 77−17371
autoguiders for optical telescopes 79−75109
automatic centring system for bubble chamber film measuring and premeasuring tables 77−83455
biological cell deposition system for deposition at predefined locations on microscopic slide 80−76876
C-CD based control system for Si cryst. growth 78−68623
capacitance-based micropositioning system for X-ray rocking curve measurements 80−205
concentrator solar cell with tracking control information 79−29470
deflection system, X-Y beam, accuracy and repeatability improvement 77−58480
depth control of towed submersibles by variable body forces 77−91315
differential games, stable position control 80−68024
displacement of mechanical guides in meas. systems, using speckle interferometry *(Czech)* 80−31852
elastic object in central force field, programmed motion control 80−17481
electron probe analysis, electron beam positioning, computer automated 79−43704
endoscopic carrier, directional control using magnetic clutches 77−2066
Fourier transform spectrometer, high resolution ruggedized 80−95152
hand prosthesis myoelectric aid *(Spanish)* 79−84011
hydraulic materials-testing system with 10-nm positional accuracy 78−85065
IR laser interferometer, length measuring, alignment using laser feedback 80−37075
JT-60 large Tokamak device, position and cross-section control 78−50366
laser automated alignment, CO_2 10 kJ laser for fusion research 79−76703
laser beam deflection, scanner complementary control 77−83982
lens, optical axis designation method 80−102798
linear accelerator microwave beam position monitors, at SLAC 77−38488
linear and angular microdisplacement instrument *(Japanese)* 79−21728
magnetic sensor appl., differential, built with magnetic resistances *(Italian)* 79−85155
manipulator attachment, high-vacuum, for azimuthal sample rotation with elec. readout 79−210
mass spectrometer solid specimens, movement in vacuum chamber by small-scale device 78−315
master-slave manipulator power-assisted grip system 79−9212
Michelson interferometer, active noise compensation *(Russian)* 78−12751
micropositioning, piezoelectric transducer appl. *(German)* 80−8967
microscope, single line CCD camera 78−41347
mirror positioner, tip/tilt, high performance 79−59795
mirror positioning in Michelson interferometer by means of capacitor probes 78−21119
mirrors, plane, spatially separated, adjustment to coplanarity, interferometric technique 80−95974
Multiple Mirror Telescope guide alignment system 79−75107
NC diamond turning system evolution 80−1369
neutron spectrometer, angular-displacement precision control with fast error-signal transducer 78−186
optical fibre coupling alignment by fully automatic system 77−79949
optical gauging instrument for measuring hole misalignment in flat plates, control aspects 78−57895
optical memory beam positioning and focusing system combination *(Russian)* 79−7194
optical ultramicrometer technique using composite diffr. grating 78−4589
optically levitated particles, feedback stabilisation 77−27290
patient position monitoring during radiation treatment using transmitted X-ray beam 77−40894
pendulum-gyroscopic platform stabilised in inertial space, autonomous determ. of coords. *(Ukrainian)* 78−65760
photogrammetric automaton 'Zenit' positioning, electromechanical system *(Russian)* 78−21101
photogrammetric system 'Zenit', read-out procedures design, for images with convex boundaries *(Russian)* 78−21105
plasma column, position control system, stability 80−106982
plasma control by feedforward-feedback system with digital computer 80−75093
plasma equilibrium feedback control in ORMAK 77−3976
precison measuring table with hollow rotor asynchronous motor, digital control system 80−105607
proton accelerator, target and collimator precision position control and monitoring via CAMAC 77−67927
radiation therapy, computer control 79−25099
recorder pen type, vertical, with improved performance and long life, using DC servo system 79−40552
repetitive photoelec. scanning system for high resolution optical spectra accumulation 78−54456
scanning microscope stage for microdensitometry, computer-controlled 79−26117
SEM multisample stage, viewing via rotary control 78−4738

position control continued
single crystal surfaces, goniometer control for precise grinding and electropolishing 78−4604
slit alignment procedure, appl. to X-ray tube focus 77−26448
Soviet 6 metre reflecting telescope, position control via computer *(Norwegian)* 78−36456
sphere, laser interferometric system for positioning of sphere and meas. roundness 79−97416
stepping motor microprocessor controller for 100 kJ CO_2 laser beam alignment system 77−54035
stereoscopic imaging synthesis allowing for real positioning of operator's head *(Russian)* 79−64391
stick insect leg, feedback mechanism open loop analysis 77−36907
target position checking by light beam using automatic two-coord. system 78−5564
TFTR, plasma position control, linear feedback optimal method 78−50365
Tokamak experimental power reactor, plasma position control and sensor requirements 78−62628
Tokamak power reactor, position control and sensor requirements 78−5035
tongue placement task performance of articulate and inarticulate children 79−57670
tow system with depth control, hydrographic and current meas. 80−17403
translation motors for position with micron precision *(German)* 80−86271
two-axes sample positioning mechanism 77−61076
US rail-inspection transducers lateral position automatic control for railway track 79−57200
C gases, position regulator for high-frequency heating 79−80612
CO_2 laser Helios fusion target positioning with orthogonal telescopes 80−74421

position finding *see navigation*

position measurement
see also astrometry
accelerator ion beam position monitor 79−89040
acoustic source passive location with symmetric line array, variance bounds 78−9480
acoustic systems for drill ship positioning 78−45057
Air Droppable Random Access Measurement System buoy sea ice tracking 77−5363
analogue interpolation system for incremental transducers *(German)* 80−17929
artificial heart valve closing element, kinematics photoelectric recorder 79−48370
astrometric horizontal meridian circle, mirror azimuth determ. technique 77−53405
astronomical photographs reduction by method of dependences 80−4237
ATS-5 location by L-band trilateration 77−9652
attitude determ. of uncontrolled satellite, correlated meas. error effect 78−16262
automated comparator-microphotometer for photographic plate spectral line position meas. 78−77962
bearing estimation bias resulting from source motion 78−29084
bolides topocentric coordinates determination, use of photography 78−61818
capacitive indicators, linear and angular *(German)* 80−57256
computerised tomographic scan edge position uncertainty reduction by density derivative processing 80−109017
contactless metrology with image dissector tube and computer *(French)* 77−33975
coordinate information processing, integer method 77−22518
coordinate meas. uncertainty computation program *(German)* 80−86256
crystal face orientation error rel. to axis, shear wave meas. 77−35006
deep ocean navigation, acoustic beacon-aided 79−32166
depth measuring apparatus for borehole logging 79−5643
double diffraction phenomenon as position monitoring technique 79−17389
drift chamber system, Dubna synchrophasotron, charact., on line operation 77−6627
electron beams, meas. by beam-position pickup 77−65392
electronic micropositioning with ferroelastic-ferroelectrics 79−17392
EM micrometers, noncontacting position transducer dynamic charact. 78−41277
equatorial coordinates derivation from astronomical photographs, Palomar Sky Survey appl. 78−32324
eye position measurement, method for implantation of mag. search coils 80−85548
eye position measurement from surface-recorded ERG 80−26400
film photopot detector characteristics for adaptive optical systems 79−59741
foetal head position in late pregnancy, B-scan estimation 77−77952
geodetic positioning convergence with navigation systems 79−25186
geosynchronous satellite orbit determination using VLBI and computer program *(Japanese)* 80−21925
Global Positioning System NAVSTAR connection to World geodetic system of DOD 79−25378
graphic materials digitisation, accuracy improvement via aided-track cursor 79−29899
gyroinstruments testing under operating conditions using system with astrocorrections 79−71413
hole positions, in small components, optoelectronic alignment technique 78−93650
hydrophones, towed, location system 79−2401
identifiable sound source location from time differences of arrival 80−91951
image dissector tube with minicomputer control suitable for IC mask inspection 79−55065
inaccessible target, meas. via noninterferometric optical probe 77−74362
interference fringe position determ. accuracy improvement by photodetector signal conversion 78−58015
jaw movement meas. using linear position transducer with improved linearity 77−44765
laser pulse, position determ. using ordinary paper 80−33046
laser pulse tracking position-sensitive photodetector characteristics 77−18098
light spot location photocathode of quantum detect. accuracy estimation 78−77832

position measurement continued
luminous pointlike object, three-dimensional trajectory recording 78−12671
machine tool position feedback by laser interferometer 80−73438
magnetic suspension densimeter, differential capacitance sensor as position detector 80−196
magnetoacoustic rod position monitoring transducer system for nuclear power plant 78−33262
magnetoelastic ribbon position sensor 79−80603
mechanical component features comparative metrology, misalignment meas. using photocell 80−31716
meteorological pilot balloon position meas., error anal. of double-theodolite data 79−21051
microdensitometer with computer-controlled scanning table *(Russian)* 79−6197
microspot CRT, non-deflected spot position stability testing device 77−82500
Mini Range III positioning system, meas. range improvements, technical details and charact. *(Italian)* 80−56611
nanosecond hydrodynamic diagnostics, streaking camera, fibre optic probes 78−37096
navigation and position location, conf., San Diego, CA, USA, Nov. (1978) 79−25374
NAVSTAR Global Positioning System, sea trials results 80−12645
noncontact optoelectronic position transducers 79−50406
object spatial location, TV meas. system accuracy 79−49200
ocean dumping surveillance and data recording system 77−5247
ocean mining, position location system 78−45046
oceanographic free-fall instruments, position determ. using acoustic navigation system 77−29490
offshore shoal positioning using LANDSAT imagery 77−73883
offshore surveys, accurate positioning at distances to 400 km 80−12328
optical gauging instrument for measuring hole misalignment in flat plates, control aspects 78−57895
optical instrument, target position meas., statistical model 80−101778
optical scanning system for 3D objects identification and spatial position meas. *(German)* 79−71405
optical sensor array systems for astronomic longitude determ. 77−82023
out of plane tilts measurement, Fourier speckle technique 77−13735
photodetectors with high linearity, position sensitive, appl. 77−79057
photoelectronic position sensor, light sensitive head and elec. circuit 77−54806
photogram meas. system using optoelectronic convertor of linear coordinates 80−17917
plasma column, position detector using segmented photodiode 78−1901
position sensitive light detectors with high linearity 78−89538
precision comparator, Zeiss PK-1, accuracy, appls. *(German)* 79−97359
precision comparator, Zeiss PK-1, astrometric plate meas. appl. *(German)* 79−97360
proton beam position monitor, based on detection of wall currents 79−58675
PWR, digital rod position indicator system for control rod drive line dynamic charact. study 78−33265
PWR control rod digital position indicating system *(Japanese)* 80−63314
quantum optical radiation, angular coords. determ. from a point source 77−65050
radio astrometry, review 77−25952
satellite location by tone-code trilateration 77−9653
satellite surveyor MX 1502, microprocessor controlled ground based system 79−25377
scanistor, luminous line coord. meas. 80−96019
semiconductor position detector analogue division cct. 77−54470
sonobuoy position meas., sound speed adaptive estimation 79−72773
spacecraft position determination on planetary surface, optimal navigation meas. 77−29621
speech production process, articulatory characteristics of tongue and jaw point movements in connected sounds of Japanese 80−26243
surveying underwater transducers by acoustic method, computer simulation model 79−32165
tachygraph, appls. to flow velocity and positional meas. 79−72977
terrestrial longit. determ., without time, from obs. of lunar altitude 78−85836
three dimensional computerised monitoring of human motion by optoelectronic means 77−48886
undersea platform location by acoustic signature processing 80−43519
vidicon appl. to low intensities meas., with Si-intensified target *(German)* 80−98545
VLBI, general considerations of international systems *(Japanese)* 80−17501
VLBI, Japanese domestic system, general aspects *(Japanese)* 80−17502
VLBI, Japanese domestic system, receiver and local oscillator *(Japanese)* 80−21923
VLBI, Japanese domestic system, recording signal generator *(Japanese)* 80−21924
VLBI, Japanese domestic system, selection of radio sources and experimental procedure *(Japanese)* 80−21922
VLBI, principles of measurement *(Japanese)* 80−21921
VLBI, results of observations of radio source QSO 3C273 *(Japanese)* 80−17503
X-ray stereography, method of precision position determ. 80−56314
Si photodiode as position sensing detectors for precision measurement and control 79−86273

position sensitive particle detectors
140 keV γ position-sensitive multiwire proportional chamber characteristics 79−54749
ΔE-E range detector of Heidelberg Q3D mag. spectrograph 79−45566
ΔE-E telescope 77−30726
alpha, position-sensitive, use of the SnO_2-Si heterotransition 80−91375
amplifier-shaper for drift chambers 80−69033
analog wire chambers for beam tuning 79−3267
angle-resolved photoelectron spectroscopy with cylindrical mirror analyzer, detection of azimuthal angles 80−57426
angular distrib. meas. with positron sensitive detector 80−27899
applications in high-energy physics and other fields 78−9035
astronomy, Lixiscope, X-ray and gamma-ray telescope system 80−62020
atomic physics applications and possible detector constructions based on microchannel plates 80−63472
avalanche 2-D parallel plate transmission counter 78−90023
avalanche azimuthal spread around anode wire 79−45532

position sensitive particle detectors continued
avalanche counter, fast, parallel-plate, bidimensional, position sensitive 78−37487
avalanche detector, position sensitive parallel plate with 2-D readout 78−55102
avalanche parallel plate detector for heavy-ion X-ray coincidence meas. 77−30719
avalanche square meter position sensitive parallel plate detector for heavy ions 79−93879
backscattered electron detector, multi-purpose 80−102404
beam-position pickup 77−65392
$Bi_4Ge_3O_{12}$, potential scintillation detector in positron cameras 78−3586
bi-dimensional drift chambers with flexible PC balanced delay lines 79−3300
binary encoded position-sensitive scintillation hodoscope with reduced photomultiplier, pion detection 78−17506
Brookhaven multiparticle spectrometer drift chamber system 80−58044
Buechner magnet/PSD system, mass spectrom. of unslowed fission products, feasibility 78−29702
calorimeter, segmented, hadron shower struct. meas. 79−63870
CAMAC/NIM system for data acquisition and monitoring of drift chambers 77−88338
centroid of charge determ. 80−58064
charge division mechanism on resistive electrode 79−45538
charge transfer device for particle detection 79−93883
charged particle detector system for high rate expts., drift-proportional chambers, operating parameters 78−33379
Cherenkov, spot focusing detector 80−5440
Cherenkov photographic detector appl. to search for Dirac monopole 78−70700
chevron microchannel plate photomultiplier tube with 400 anodes for high energy appl. 79−45545
compact detector electronics for blocking experiments *(German)* 77−38551
Compton telescope, appl. of Anger camera principle, for gamma-ray astronomy 79−80223
computed tomographic reconstruction noise, effect on detectability 78−40296
computer assisted ringdetector positron camera system for reconstruction tomography of the brain 78−40306
conference on nuclear power systems, Washington, USA (1978) 79−41045
curved crystal X-ray spectrometer, for HEAO-B satellite 78−49331
cylindrical drift chambers with delay line readout, resolution 78−33380
cylindrical wire proportional chambers, electrostatic field formulae, distrib. and asymmetry 80−78493
data acquisition, CAMAC I/O module 80−47835
delay line for position readout in wire chambers 80−18757
detector for heavy atomic particles in the keV energy range 77−10548
digital drift chamber digitizer system 79−45602
digital processor for position sensitive detectors 77−26941
digital scattering angle pre-processors 80−23268
directional drift chambers system, design, construction, testing 78−33378
discrete struct. influence on accuracy of coordinates determination 80−58076
drift, time projection chamber, performance 79−68148
drift chamber, 2-D 77−30703
drift chamber, 2-D 77−30708
drift chamber, 2-D 77−54422
drift chamber, cylindrical, used in superconducting solenoid 79−3311
drift chamber, delay line readout 79−3317
drift chamber, electroluminescent 79−22545
drift chamber, for use as time projection chamber trigger at LBL 79−41067
drift chamber, large cylindrical, for Mk.II detector at SPEAR 79−45561
drift chamber, liquid Xe, device description and spatial resolution using α-particles 79−41062
drift chamber, particle jet detection from e^+e^- reactions 79−3312
drift chamber, teaching information 77−18745
drift chamber, transition radiation detection 79−22546
drift chamber ($1.5m^2$), characteristics 78−5096
drift chamber and pulse height readout systems using analog multiplexing 77−54490
drift chamber based detector for X-ray scatt. expts. 80−58045
drift chamber counter, missed counts and registration efficiency calc. 78−78594
drift chamber data acquisition, microprocessor based system 80−58066
drift chamber detector, performance figures, γ-ray astronomy appl. 79−48674
drift chamber detector for high energy gamma-ray astronomy 77−9660
drift chamber electronics for time and pulse height meas. 79−3326
drift chamber for multitrack particle identification 79−3276
drift chamber gas mixtures, electron drift velocity meas. 79−41079
drift chamber in strong mag. field, electron drift angle meas. 79−3299
drift chamber large area with copper strip cathodes planes 77−83458
drift chamber performance in supercond. mag. field, electron drift angle meas. 78−37485
drift chamber system for BNL mag. spectrometer expt., design constraints, readout electronics 78−33382
drift chamber system for FNAL μ-beam high rate expt. 79−41065
drift chamber system for use in a high rate environment 79−41064
drift chamber telescope for gamma-ray astronomy 79−21185
drift chamber vertex detector for intersecting storage rings 79−3310
drift chamber with printed-board cathodes and flat solevoidal delay lines 80−74088
drift chambers, μ detection, construction of insensitive regions 79−3305
drift chambers, Ar-ethylene mixtures investigation 78−25391
drift chambers, B-depend. of space-drift time relation and space resolution 79−3309
drift chambers, construction and test of insensitive regions 79−3304
drift chambers, cylindrical, with two-dimensional read-out 79−3308
drift chambers, decay electron trajectory meas., MSR at CERN 78−82593
drift chambers, efficiency and losses of electronics 77−88347
drift chambers, ipherical 77−54423
drift chambers, large planar 77−30716
drift chambers, method of selecting true coordinates 79−13606
drift chambers, second coord. readout by charge division, optimised preamplifier system 78−33381
drift chambers, soln. to right-left ambiguity 78−58545

position sensitive particle detectors continued
drift chambers, space resolution study as function of gas press. 78−78583
drift chambers at the Dubna Synchrophasotron 77−6627
drift chambers for experiments on elastic scattering of pions and kaons by electrons 78−859
drift chambers in high-energy gamma-ray telescope 80−41726
drift chambers spherical 77−30721
drift chambers used in Fermilab experiment 77−10537
drift chambers with PC cathodes, design and props. 79−3303
drift identifier prototype at Fermilab 79−41072
drift tubes, quadratic and triangular, drift time and amplitude meas. 79−3314
electron drift velocities as function of elec. and mag. variables in several gas mixtures 78−71424
electron spectrometer using new multidetector based on charge-coupled imaging device 80−86502
electron transport coeff. in gases used in proportional and drift chambers 78−58541
electronically collimated gamma camera for single gamma emission computed tomography 78−44603
electronics for proportional drift tubes 80−106241
electrostatic electron emission into a gaseous medium from alpha-particle tracks in liquid isooctane 79−54747
EM delay lines readout in spark, proportional, and drift chamber appl. 78−74547
fast X-ray diffractometer based on a spherical drift multiwire proportional chamber with digital position encoder 80−90969
fission detector, avalanche, parallel plate, particle induced fission coincidence measurements 80−63485
flash chambers for neutrino detection, construction and performance 80−58026
flat helical delay lines for position readout along the anode wire in MWPC and drift chambers 77−54426
flexible geometry hodoscope using proportional chamber cathode read-out 79−3297
focal plane, large hybrid detectors, electric field uniformity improvements 80−37684
focal plane detector for both light and heavy ions 79−18077
focal plane proportional counters 79−68159
gamma camera, multidetector Ge 79−49353
gamma camera image intensifier with Si strip detector 77−81565
gamma cameras, performance comparison 78−44595
gamma ray detection system, 3-D, fabrication and efficiency 80−63483
gamma ray detectors using resistive charge division readout 77−54420
gamma ray shower detector of low press. flash tubes 78−70697
gamma-ray high energy detector 77−83445
gamma-ray imaging in fourier space 79−17588
gas flow detector, back-scatter-type, conversion electron Mossbauer spectrometry 80−37680
gas proportional neutron detectors, microprocessor testing method 78−70692
gas proportional scintillation counter for use in large area detector systems without photomultipliers 79−59302
gas scintillation proportional counter for X-ray astronomy 80−58053
gas scintillation proportional counter using a photomultiplier tube array 79−76294
gaseous detectors, evolutional steps 80−58041
graded-density cathode method for position determ. in multiwire proportional counters 80−87017
hard X-ray camera for study of gamma ray burst sources 79−25502
Harwell Buechner magnet/PSD system as a mass spectrometer for unslowed fission products 77−23360
heavy ion detection, using two dimens. gas-scintillation drift chamber 78−86730
heavy ion detection system, drift chamber with parallel plate avalanche counter 78−29709
helical cathode position sensitive proportional counter system for use in a broad range spectrograph 78−82578
helical delay line position sensitive proportional counters for mag. spectrometers 79−68160
high density projection chamber 80−58027
high density proportional counter, low energy neutral particle imaging 79−5399
high pressure proportional counters operating in pure hydrogen 79−3296
high resolution imaging X-ray detector, for astronomical meas. 78−49333
high spatial resolution particle physics detectors 79−76276
hodoscopic spectrometer, gamma-quanta coordinate meas. in NITsE scintillation spectrometer 78−78549
hybrid focal plane detectors for heavy ions 79−68163
hybrid MWPC gamma ray detecting system for applications in nuclear medicine 79−5397
hybrid scanner, design of detector and collimators 78−7423
imaging chamber, liquid Ar, drift distances, energy resolution, materials and readout scheme 79−41066
imaging Cherenkov detector using gas-filled MWPC, photoionisation of triethylamine 80−91400
imaging gas scintillation counter for X-ray astronomy 80−98551
induction wire proportional counter with sub-mm positron resolution 80−91399
inert gas scintillation counters for energetic heavy ion detection 79−45550
ionisation chamber, liquid, pulse shape anal. of recoil electron signals 80−52823
ionisation chamber telescopes for fission fragment position and nucl. charge identification 79−36478
ionisation fission chamber 79−26819
ISIS 1, full aperture, multiparticle identification 79−76258
jet chamber system, pictorial drift chamber for experiments at PETRA 79−41069
large area gas detectors 79−72202
large drift chamber system for use in an iron spectrometer 80−58046
LEED instrum. using pulse-counting electron detector 80−37133
limiting accuracies in multiwire proportional and drift chambers 79−3298
linear position sensitive proportional line scanner for β-emitters 79−31330
liquid Ar calorimeters, props. of EM and hadronic showers 79−45599
liquid xenon proportional scintillation counter, detection of ^{207}Bi conversion electrons 79−45563

position sensitive particle detectors continued
low level activity meas. of ^{3}H and ^{14}C using multielement and cylindrical proportional counters, comparison *(Czech)* 80−52818
magnetic spectrom. with position- and cutting angle-sensitive detectors, ang. distrib. reconstruction 78−70687
magnetic spectrometer, reconstitution of heavy ion trajectories 78−70684
microchannel plate detectors 79−72200
microchannel plate PSD, nonlinearity and resolution in charge sharing mode 79−22537
microchannel plates, low distortion resistive anodes 80−886
modular drift-chamber vertex detector at the CERN ISR 79−3302
molecular biology, contracting muscle, dynamic structure, X-ray scatt., time resolved, rapid data collection systems 80−61740
multianode cylindrical proportional counter for position sensing at high count rate 80−5446
multielement proportional counters, electrostatic problems 79−93877
multigap proportional wire chamber system for multiparticle spectrometer 79−3271
multiparameter focal plane detector, development of capacitively coupled distributed parameter delay lines 80−78491
multistep avalanche chamber, new family of fast high rate particle detectors 79−49904
multistrip β semicond. detectors for magnetic spectrometers 78−78545
multitrack pulse height electronics 79−3325
multiwire and drift chambers for the Omicron spectrometer 79−3277
multiwire and drift proportional chambers, design, operation, appls. 79−743
multiwire and drift proportional chambers 80−47826
multiwire drift chambers, left-right assignment 78−58544
multiwire drift chambers, left/right ambiguity and double track resolution 79−3307
multiwire drift chambers for the CERN intersecting storage rings 79−3301
multiwire proportional chamber, shift register read out system 78−86736
multiwire proportional chamber, small design, construct., performance, electronics 78−17507
multiwire proportional chamber with analogue data plotting 78−78566
multiwire proportional counter for microdosimetric studies 78−20286
multiwire proportional gamma camera for imaging $^{99}Tc^{m}$ radionuclide distribs. 78−53493
multiwire proportional quantameters, performance predictions by Monte Carlo methods 79−3294
muscle contraction, time-resolved X-ray diffr., data-collection system *(Japanese)* 80−46108
MWPC, γ-image blurring reduction by delay line readout 78−37492
MWPC, angular localisation of proportional chamber avalanche 78−78584
MWPC, anode modulation effects of X-ray beam positions 79−76282
MWPC, appl. as energy loss detector for the ISR 79−3331
MWPC, appl. to radiation localisation problems in medicine and biology, review 79−5432
MWPC, avalanche ang. localisation 78−50434
MWPC, Bellcord−a multilevel fast preprocessor for 1024 ECL channels 79−45577
MWPC, compact low mass system of four cylindrical chambers 80−14046
MWPC, correcting codes for information registration 78−94176
MWPC, counting gas props. at low pressure 79−85864
MWPC, cylindrical, soft X-ray detection in $p\bar{p}$ spectroscopy 79−3279
MWPC, drift chambers and time projection chambers, development, operation and appl. *(Italian)* 80−879
MWPC, drift time meas. electronics 79−3327
MWPC, external muon identifiers at CERN 78−37488
MWPC, fast, data encoding system for proton tomography 79−92337
MWPC, fast analogue logic 79−13605
MWPC, fast delay line readout 78−37490
MWPC, flat area detector data acquisition system for X-ray crystallography 80−91381
MWPC, for cosmic drift X-ray imaging 79−41063
MWPC, gas amplification factors and detection efficiencies 80−74079
MWPC, gas ionisation by double photon absorption using pulsed lasers 80−99414
MWPC, heavy ion timing at very low pressure 79−93884
MWPC, high accuracy chambers, progress 78−33391
MWPC, high press., for X-ray astronomy 79−5748
MWPC, high-flux fast readout system based on new monolithic integrated ccts. 78−37491
MWPC, improvement of position resolution from delay line readout 78−74543
MWPC, induced charges calc. at individual anode wire at the cathode 78−78585
MWPC, interwoven grid wires for second coordinate readout 80−27897
MWPC, large area, high-background rejection 78−93108
MWPC, large cylindrical dual coordinate 80−18759
MWPC, lateral distrib. of cathode charge 79−36470
MWPC, localisation of minimum ionising particles using cathode induced charge centre of gravity readout 80−32576
MWPC, localisation of X-ray quanta 78−62678
MWPC, low-level ^{14}C and ^{3}H meas. 79−6800
MWPC, medical image formation 77−86618
MWPC, missing data reconstruction in principal component anal. 78−17537
MWPC, modulation of anode signal in soft X-ray detection 79−18081
MWPC, multi-delay line cathode readout 79−45573
MWPC, nondestructive readout system 79−3315
MWPC, operation principles 77−83465
MWPC, optimum geom. for strip cathodes or grids for avalanche localisation along anode wires 79−76274
MWPC, position determ. method using graded density cathodes 80−102396
MWPC, position sensitive, pulse shape from cathode RC Lines, zero-cross time meas. 80−58038
MWPC, pressurised, for neutron imaging, gas density, cathode biasing, effects on resolution 78−37518
MWPC, programmable track selector 79−3316
MWPC, remote readout system, pulse-width modulation circuit 79−26847
MWPC, review of operating principles and functions 79−3293
MWPC, secondary beam profile monitor 79−6783
MWPC, spherical drift chamber area detector for X-ray crystallography 79−41073
position sensitive particle detectors continued
MWPC, teaching information 77−18745
MWPC and drift chambers, properties 79−72195
MWPC appl. as focal plane detection system for mag. spectrograph 79−3295
MWPC appl. high count rate X-ray detection 79−3292
MWPC appl. in multiparticle spectrometer, description and performance 79−3275
MWPC appl. in recoil spectrometer 79−3274
MWPC appl. to energy loss meas. 79−3330
MWPC appl. to molecular biology 79−5433
MWPC avalanche initial angular width determ. 79−31327
MWPC compact chambers and electronics for crystal ball detector 79−45534
MWPC construction for large aperture spectrometer 80−102381
MWPC delay line readout, position accuracy 77−54425
MWPC focal plane detector system with digital readout 79−68158
MWPC for beam definition in precision total cross section meas. 79−3268
MWPC for Fermilab single arm spectrometer 78−82585
MWPC for fission fragments with large solid angle 77−34517
MWPC gridded drift chamber for X-ray detection 78−70694
MWPC high resolution system for inclined tracks 77−30722
MWPC in big mag. spectrom. as counter hodoscope for fast majority discrimination 78−33392
MWPC in synchrotron beam spectrometer, performance under very high fluxes 79−3272
MWPC on cube lattice 79−93875
MWPC operation as drift chamber 77−54455
MWPC positron camera, two detector, appl. medical imaging 79−5398
MWPC read out, fast clustering processor 79−76304
MWPC readout system 78−17505
MWPC rotated, drift time relations and their advantages 79−3306
MWPC using charge division readout 77−38556
MWPC with analogue read-out, high energy e^{-}/γ detection 79−13593
MWPC with cathode read-out for separation of EM and hadronic showers 79−3273
MWPC with EM delay lines, localisation of charged particle passage 77−88349
MWPC with high spatial resolution, construction and efficiency meas. *(Italian)* 80−9452
MWPC with wire plane cathodes, extension of standard formulae for elec. fields 80−99413
neutron beam charged particle spectrometers, appl. of drift chambers 79−3278
neutron data acquisition system, low angle, for molecular biology 79−12053
neutron detection systems and electronics for ILL expts. 79−45571
neutron detector, position sensitive, high precision position readout 80−58063
neutron detector for thermal and epithermal spectra 77−38566
neutron detector using (n,γ) on ^{157}Gd, ^{177}Hf foils, proportional chamber detection of conversion electrons 78−37517
neutron time of flight single crystal diffractometer using a position sensitive detector 80−99404
orthogonal strip gamma ray detector employing resistive charge division, noise anal. and optimum filtering 77−10538
parallel grid imaging proportional counter optimized for detection of low brightness stellar XUV-sources 80−58049
parallel plate avalanche counters, simple accurate method for bidimens. position readout 78−21822
parallel plate avalanche detector for fission fragments 78−29710
parallel plate electron multipliers, multidetector array 79−31334
parallel plate imaging proportional counter and its performance with different gas mixtures 79−45533
photo-ionization and Cherenkov ring imaging 77−54448
photon position determination using microchannel plates, X-ray imaging for HEAO-B 79−45555
photon position monitors for CHESS synchrotron source, using split photoelectron detectors and ionisation chamber 80−91336
pictorial drift chambers, recent developments and particle identification 79−3307
planar positron cameras, 3-D reconstruction using Fourier deconvolution of generalised tomograms 78−40295
plasma neutron diagnostic techniques with good spatial and energy resolution 79−46478
position readout by charge division in large 2-D detectors 77−54421
positive ion effects in large-volume drift chambers 79−22541
positron camera, 3-dimens., for nucl. medicine 78−73225
positron camera proportional chamber, Fourier deconvolution technique 78−40297
positron cameras, 3-D iterative reconstruction method 78−40302
positron emission transverse tomograph, PETT IV 78−40299
positron imaging, Anger-type bar cameras, positron imaging 80−61687
positron imaging system, production model design and performance characteristics 78−40303
proportional and drift chambers in applied research, review 79−26824
proportional chamber, positive charge centroid direct meas., avalanche mechanism clarification 78−37486
proportional chamber with a draft gap for ionization measurements 77−14311
proportional chamber X-ray detection 78−86739
proportional chambers, μ detection, construction of insensitive regions 79−3305
proportional counter, delay line termination and timing signal extraction 77−402
proportional counter, direct position and time digitizer 80−58090
proportional counter, for thermal and epithermal neutrons 78−25390
proportional counter, for X-ray residual stress meas. *(Japanese)* 80−11853
proportional counter, resistive wire, multi-anode, focal plane detector 80−63464
proportional counter data acquisition providing max. spatial resolution at high rates 79−45572
proportional counter for the position detection of heavy ions *(French)* 77−34516
proportional counters, γ ray angular correl. meas. 79−4869
proportional counters, RC-line encoded, using low-resistance, metal wire anode and active load capacitance 79−54745
proportional counters, RC-line encoded position-sensitive, recent improvements 79−9963

position sensitive particle detectors continued
proportional delay line chambers for Fermilab external muon identifiers 78−37489
proportional detector construction *(Spanish)* 77−46464
proportional drift tube for large calorimeter ν detector 79−13592
proportional multidetector, for functional study of lungs *(French)* 77−37035
proportional RC line encoded counters 79−45537
proportional single 1 m wire counter for low ionisation particles 80−5441
proportional tube with helical delay line 79−3313
proportional wire chambers in high-intensity particle beams 78−9025
proportonal counter for neutrons 80−63459
prototype CCD system for the time projection chamber 79−45575
quadrant position sensitive photomultiplier with high detection efficiency 79−45546
radioisotopic cameras *(Spanish)* 78−7428
readout system for MWPC of focusing spectrometer 79−3280
resistive unidimensional detectors employing rise time readout method, position resolution and linearity 80−14048
resonance neutron radiography using a position-sensitive proportional counter, appl. to meas. of nuclear fuel 80−13597
scintigraphic systems and their computer assessment 78−57063
scintillation, large field gamma camera 78−7441
scintillation camera, high-speed, using plastic phosphors 79−93888
scintillation cameras with large field of view 78−44596
scintillation counter, energy resolution optimisation at high energies 80−37697
scintillation counter, light signal propag. speed. for spatial resolution determ. 80−69028
scintillation counter hodoscope for low energy light ions 77−38555
scintillation counters, neutron transit time and interaction coord. determ. 79−26807
scintillation gamma camera, anal. of basic charact. 78−57059
scintillation hodoscope, track correlator as a fast trigger in the detection of π-μ Coulomb bound states 79−45574
scintillation hodoscope counter for beam meas. in CERN SPS 79−36472
scintillation image intensifier cameras 77−40732
sealed position sensitive hard X-ray detector having large drift region for all sky camera with high angular resolution 79−48675
secondary emission chamber at Brookhaven AGS 79−72187
secondary emission monitors at the Bevatron-BEVALAC 79−72186
secondary emission multiwire chamber for GANIL cyclotron beam tuning 79−54733
segmented cathode drift chamber, expt. study of signals 79−41074
self-powered gamma-ray detector with directional discrimination 79−30895
self-quenching streamer discharge in a wire chamber 79−63869
self-scanning photodiode array for fast ion detection 80−87018
self-triggered liquid xenon drift chamber by the use of proportional ionization or proportional scintillation 79−45562
semiconductor, ion-doped, coordinate detector for charged particles 79−26825
semiconductor, spontaneous fission source size and uniformity determ. 78−86711
semiconductor counters, principles of operation, performance, and appl. 79−68155
semiconductor detector, analog division cct. 77−54470
semiconductor detector, analog meter for signal ratio 79−97943
semiconductor radiation detector, development 79−68153
SF5 lead glass Cherenkov counter, high energy photon position determ. 80−58032
small angle neutron scatt. with azimuthal symmetry 78−46212
solid state micro-detectors for high energy experiments 77−30705
sonic location spark counter system for mag. spectrometers 79−68162
spark chamber, plasma memory and read-out *(French)* 78−46223
spark chamber, wide gap for gamma ray astronomy 78−17503
spark chamber digitisation using CCD 80−27902
spark chamber gas monitor, used in Rutherford multiparticle spectrometer 79−3318
spectrometers for particles from 5 GeV π-He reacts. 78−90011
superconducting detector of ionizing particles 80−63460
superconducting mag. spectrom. for cosmic ray flux meas. 78−25383
superheated supercond. colloid neutron detector, detection and background rejection tests 78−78580
surface barrier, pseudostructures in spectra caused by digital data acquisition 79−76320
surface barrier detector for detection of He-Ne laser beams 79−36485
tapped delay line focal plane detectors for mag. spectrometers 79−68161
thermal neutrons, position sensitive detectors, review *(Japanese)* 78−78589
time detector, channel plate, for heavy ions 80−63466
time expansion chamber, and single ionisation cluster meas. 79−41068
time of flight scintillation system, coordinate sensitive, in large area gamma-ray telescope 79−84676
time of flight telescope for high energy gamma-ray astronomy 80−31210
time projection chamber, design, operation, appls. 79−745
time projection chamber multichannel ADC and readout system 79−45590
time-resolved X-ray diffraction counter and data acquisition system 78−45758
transmission drift chamber, 20 cm 100percent, with thin foil cathodes 77−83463
TREAT, fast neutron hodoscope perform. tests on 91-pin fuel bundle 79−41005
TREAT fast-neutron hodoscope, time and mass resolution of fuel motion, data acquisition system 79−41003
variable sampling-time technique for improving count rate performance of scintillation detectors 79−22565
vidicon systems, time digitiser in CAMAC format 80−14062
whole body-imaging methods, comparison 78−44597
wide-gap spark chamber used as a vertex detector in a high energy neutrino experiment 79−45569
wire chamber conf., Vienna, Austria, 1978 79−3291
wire chambers, review and forecast 77−14307
X- and γ-ray detectors and read out systems *(Japanese)* 78−33397
X-ray and neutron small-angle scattering instrumentation and data analysis 79−10750
X-ray astronomy appls. 79−25496
X-ray detector, position sensitive, inductance-capacitance line encoding 78−12800
position sensitive particle detectors continued
X-ray detectors, linear, circular, two-dimens. 78−62281
X-ray diffraction data acquisition using position-sensitive counter *(Japanese)* 78−88774
X-ray imaging gas scintillating proportional counters, performance in medical appl. 79−2153
X-ray kinetic diffr., position sensitive counter 78−62283
X-ray position sensitive detector, curved, for crystallography appl. 78−63635
X-ray position-sensitive scintillation detector for portable stress analyser 80−13190
X-ray spectrometer for low-intensity imaging 80−86539
X-ray streak camera electrode design using a plasma simulation code 79−30632
X-ray stress anal. using position-sensitive proportional counter 80−1498
zero-degree tagging system used for photon-photon experiments at DCI 80−102394
β-ray spectrom., proportional counter 78−86732
Ar, liquid, calorimeter, electron and proton response 80−47832
Ar/Fe liquid hadron calorimeter 78−37503
Ar-ethane gas mixture, XX 80−63467
Ge camera, 2-detector, 512 element high purity prototype 78−40301
Ge, Compton scatter, spatial spread meas., imaging with position-sensitive detectors 78−46214
Ge detectors, high purity, event timing, compared to Ge(Li) detectors 80−69018
Ge(Li) detectors, coaxial, zero cross-over timing 80−69017
H scintillating gaseous drift chamber for use as positron sensitive target 80−9457
^{3}He detector design for transuranic waste assay, low-level, Monte Carl calcs. 79−54542
^{6}Li(n,α)^{3}H reaction, as standard in neutron flux meas., instruments review 79−9969
MgO scintillator prep. for viewing accelerator beam spots 79−6803
NaI detectors, lung counter system, improvements to overcome interference from neighbouring compartments 79−2132
NaI position sensitive detector, test results 79−76288
NaI(Tl) single-crystal scintillation camera, image artifacts at high photon fluence rates 78−85364
Pb scintillator target counter for photons above 50 MeV 79−76285
Pb single convertor photon detection efficiency below 500 MeV, semi-empirical formula 80−27866
Pb-liquid large area shower detector with high spatial and energy resolution 79−742
Pb-scintillator calorimeter, electron energy and positron measurement 79−76273
Si 2-D position sensitive orthogonal electrode surface barrier detectors 78−50437
Si detectors and Pb absorber plate, telescope structure, high energy muon flux measurement 80−58061
Si microelectronic p-n junction photon detector 79−26815
Si photodiode array, position-sensitive photon detector for the UV or X-ray range 80−90970
Si, production using ion implantation methods 80−23247
Si(Li), 2D position sensitive detector with 100 μm resolution 79−45544
Si(Li)-emulsion shower counter for cosmic ray electron obs. 80−58033
Xe curved wire proportional chamber for powder X-ray crystallography 79−4210
Xe-ethane gas mixture, electron drift velocity and other transport coeffs. 80−63467
Xe-filled MWPC for hard X-ray imaging with sub-mm spatial resolution 80−99418

positioning *see position control*

positive column
see also glow discharges
AF glow discharge positive column, stratification obs. 78−67509
air, impulse breakdown processes at low press. 80−44021
air flow glow discharge, voltage, current oscills. 79−55585
alkali metal vapour discharge, low-press., energy balance eqns. 80−87969
arc, helical in stabilising channel in mag. field 79−60206
arc in channel bearing turbulent gas flow, arc parameters calc. 80−6298
autocompression, influence of external mag. axial field, review *(Rumanian)* 80−24148
axial electric field, in transverse mag. field 78−18472
axial electric field of column in transverse mag. field 78−30506
axial particle drift in the positive column of a discharge 80−100113
constriction in cryogenic discharge, ambipolar wall diffusion 78−18468
contracted positive column head oscillations 78−67516
corona to glow discharge transition mechanism, morphologic discussion 79−99014
correlation measurements of turbulent ionization and ion-acoustic waves 80−59329
deflection of radiation intensity by transverse mag. field 80−28866
density oscillations due to negative ions, metastable atom model 78−1799
diffuse discharge, HV, anode drop meas. in transverse air flow 77−39483
diffusion controlled circular positive column with one and two step ionisation, charact. eqn. 80−44033
diffusion controlled gas discharge, charact. rel. to diffusion and ionisation coeffs. 80−33833
diffusion recombination regime, theory 77−76241
electron drift velocities, wave determination 77−76052
electron energy distrib. function, Coulomb collision effects, in Xe plasma 80−38532
electron energy distribution 78−67465
electron relaxation to Maxwellian energy distribution, in low-press. Hg discharge 79−64949
electron temp. in medium press. flowing positive column with vol. recomb. 78−87561
electron temperature characteristics, unified, with vol. recomb. 77−84401
electron temperature characteristics, unified theory including ionisation of metastable atoms 77−11419
electron temperature with two- and three-body vol. recomb. 80−19645
electron-atom-bremsstrahlung standard radiometric source improvement 78−67484
electronegative gas, transverse stability, effect of dissoc. attachment 79−23475
electronegative gas discharge, spontaneous oscills. 80−87977

positive column continued
equivalent electrical circuit *(German)* 77−58909
excitation and ionisation mechanisms *(Japanese)* 79−4105
finite positive column moving striations, excitation and asynchronous quenching 78−67515
gas discharge with external ionisation, voltage-current characts. 80−96408
gas-discharge column with allowance for metastable atom effect, excitation of strata 80−96410
glow discharge, ionisation waves, half subharmonic excitation 80−44006
glow discharge of electronegative gas, molecular excitation and ionisation by electron collisions 80−49031
helical instability in magnetised positive column 77−35344
high-pressure metal-vapour/inert-gas mixture discharge peculiarities 78−71620
highly-ionised free-fall positive column, differential eqn. system 78−67489
highly-ionised positive column under free-fall and ambipolar diffusion conditions 78−67490
hollow cathode arc, model of positive column in mag. field 79−90494
hollow cathode arc positive column, in mag. field, discharge parameters 79−90493
hollow cathode discharge, large size, positive column expts. 77−62431
hydrodynamic contraction due to longitudinal turbulent flow 78−67510
inert gas, low-press. discharge, electron energy distrib., elec. field and electron wall loss effects 80−24294
inert gas 78−51379
inert gas discharge, electrophoresis anal. using plasma kinetic eqns. 77−43100
inert gas discharge, moderate press., visible and UV radiation spectrum 77−31533
inert gas glow discharge, origin of visible continuum radiation, bremsstrahlung theory 77−62421
inert gas positive discharge column, at. temp., interferometric meas. 77−35427
inert gases, atomic alignment *(Russian)* 80−87981
inhomogeneous magnetic field effect on particle distrib. *(Russian)* 77−72513
instability, of ionic component, amplification factor, dispersion eqn. 78−14232
ion motion, radial pot. distrib., in low-density and press. discharge 79−55599
ion-acoustic dispersion eqn. solution for positive column 78−75307
ion-acoustic instability in positive column of DC discharge 78−67335
ion-acoustic plasma turbulence, two-dimensional electron density spectra 78−75479
ionisation waves, excited in axial mag. field 78−59704
ionisation waves, in positive column, wave packet propag. 80−96356
ionisation waves excitation, in low-temperature plasma 78−1832
ionisation waves in axial mag. field, crit. current 78−42848
ionisation waves in plasma columns, microwave detect. 78−79461
irregular ionisation wave electron density rel. to light intensity variations 78−67520
isotope separation in rot. plasma column of hollow cathode discharge 78−75454
limiting current in steady state diffusion-recombination discharge 78−67466
long plasma column production, by efficient surface wave launcher 79−32836
magnetoplasma column in waveguide, wave packet bifurcation 77−7556
metastable atom radial transport, effect of wall boundary conditions 78−67493
metastable atom radial transport at various electron distribs., atom+atom collision effects 80−44037
metastable atom transport, excitation rate radial variation, flux to wall calc. 80−44038
mixed ion plasma general ambipolar diffusion theory 78−94897
molecular gas, discharge compression, thermal balance *(Russian)* 77−7615
moving striations, conditions for self-excitation 80−69358
multichord corpuscular diagnosis *(Russian)* 79−4190
neutral gas, ionisation and temp. effect on charged particle profile and density 80−79596
nonstationary arc in channel with gas discharge *(Russian)* 80−14950
nonstationary plasma column, Schottky's diffusion theory 78−91174
plasma, in high voltage diffuse discharge, nonstationary processes 80−64802
plasma parameter in transverse mag. field 78−9880
positive glow corona along a cylindrical rod between two parallel plates 80−38768
pulsed Hg-Ar discharge, electron energy distrib. calcs. 79−64919
pulsed low-pressure Hg discharge, radial distributions 79−64920
pumping of induced arc, pressure distribution meas. *(French)* 77−27763
RF medium pressure flowing positive column plasma, electron temp. 78−59549
scattering amplitude due to elec. current ring surrounding plasma column in semiconductor plasma 79−37457
space-charge double layers, anal. using fluid theory 80−75062
standing striation excitation conditions 78−67514
striation dynamics, velocity/amplitude correlation 78−67517
subnormal column, ion and electron radial distrib., theoretical description 80−79598
turbulent arc in channel with distributed gas flow, positive column anal. *(Russian)* 80−14949
two-step ionisation, var. calcs. 80−70056
unconstricted, of high-vel. gas flow 77−35426
volume recombination coeff. meas. method, in Ne positive column, ionis. role 77−51252
water vapour, electron energy distrib. function, electron sink and plasma resist. effect *(Russian)* 80−106987
Ar, arc positive column, atom-atom collisions effect on thermal equilib., model 79−1360
Ar, contracted, balance equations anal. 80−6312
Ar, contracted, electron density, temp., elec. field, line emission 80−6311
Ar, dissoc. recombination coeffs. 78−26367
Ar glow discharge, line radiation of plasma in early afterglow 80−38745
Ar, in transverse mag. field, plasma parameter diagnostics 79−19103
Ar low voltage arc, positive column ionisation waves, hydrodynamic model 78−79481
Ar, low-press. glow discharge, elec. characts. of positive column 80−100112

positive column continued
Ar, medium press., model calc. 79−50912
Ar, population processes of 4p levels, perturbation influence 80−38565
Ar, positive column, 4S and 4P levels populations, rel. theory with recomb. 77−10766
Ar, positive column, axial electric field in transverse mag. field 78−55766
Ar, positive column, local transverse mag. field, striation freq. spectra, microwave probe 78−87562
Ar, positive column, moving striations in longitudinal homogeneous mag. field 78−67523
Ar-Br_2, positive column at. state densities 80−44007
Ar-CO, glow discharge, ion cluster in positive column, ion mass spectra diagnostics 80−38752
Ar-CO glow discharges, positive ion spectra, ion clusters obs. 80−64807
Ar-hexamethyldisiloxane, glow discharge positive column ion mass spectra identification 80−38834
Ar-Ne, mixture, cataphoretic segregation, spectroscopic meas. 79−79261
CO loss in glow discharges in CO, CO-He and CO-N_2-He mixtures 77−19788
CO-He(-O_2), glow discharge ion cluster in positive column, ion mass spectra diagnostics 80−38752
CO_2 laser discharge, positive ion processes, mass spectrometric obs. 77−89337
CO_2+H+Xe plasma, elec. parameters, Xe effects *(Russian)* 77−84507
Cd II laser, positive column He-Cd discharge, excitation mechanism 78−58983
Cs plasma discharge, positive column constriction, ion conversion effect 80−44020
F glow discharge, positive column elec. props. 79−50916
H_2 discharge plasma, laser-induced transient striations obs. 79−27785
H_2 glow discharge with variable degrees of dissoc., diffusion theory of positive column 80−44018
H_2-H mixture positive column, static electric charact. 78−67500
H_2-$H_2O(Cl_2)$, diffusion in stratified positive column, impurity effects 77−11320
H_2-N_2 glow discharge, positive column, electron energy-distrib. spatial variation 77−47294
He, composition at intermediate press. 80−19646
He, fast electron energy distrib. in positive column and negative glow 80−38764
He flow discharge, intermediate press., positive column conc. of ions and metastables 80−44017
He, gas discharge flow, contracted strata rel. to turbulence 78−1923
He glow discharge, low press., excitation transfer and quenching of n=3 excited states 80−38743
He glow discharge plasma, ionis. waves in positive column 80−1876
He I, low-press., quenching of singlet states by N_2 80−49030
He, in transverse mag. field, plasma parameter diagnostics 79−19103
He low-current discharge, metastable atoms, radial density distrib. obs. and calc. 78−67495
He, magnetised, temps. of charged particles, nonlinear effect of ionis. waves 80−44023
He, magnetised positive column, exptl. study on moving striations 78−83634
He, medium press., contraction mechanism, inhomogeneous heating 80−44024
He modulated positive column, elec. and optical props. 77−27765
He plasma collisional-radiative model, appl. to positive column 79−64836
He, positive column, axial electric field in transverse mag. field 78−55766
He, positive column, moving striations in longitudinal homogeneous mag. field 78−67523
He, positive column, with diffusion loss to wall, axial elec. field effects *(Japanese)* 78−47196
He positive column discharge, IR optogalvanic spectrosc. using F-centre laser 80−78563
He, positive column ion-acoustic waves, obs. 78−75312
He positive column ionisation waves, influence of longitudinal mag. field 78−67522
He, positive column plasmas, metastable atom density meas. by improved self absorpt. method 80−87968
He-CO glow discharges, positive ion spectra, ion clusters obs. 80−64807
He-Cd discharge, principal Cd ionis. mechanism, radial profiles meas. 77−27758
He-Cd positive column laser power, effect of I_2 additive *(Japanese)* 79−7121
He-Cd positive-column laser discharge, excitation mechanisms from radial profiles 77−68205
He-Cd vapour excitation in hollow cathode discharge 80−64815
He-Cd^+, positive column laser, Cd II 441.6 nm line, effect of I_2 77−54697
He-Cd^+ laser, population densities of He excited states in positive column discharge 78−58989
He-Cd^+ laser, upper and lower laser states population densities, simultaneous determ. 78−87042
He-Cd^+ laser discharge, positive column, non-Maxwellian electron energy distrib., electron density determ. 77−84493
He-Cs mixture discharge, B-invariant transformation theory 78−67503
He-I^+ laser discharge, particle densities 80−103215
He-Na mixture, low-pressure discharge, radial cataphoresis obs. 78−67507
He-Ne gas discharge, positive column striations characts. 80−49032
He-Ne modulated positive column, elec. and optical props. 77−27765
He-Ne waveguide laser, discharge plasma theory, max. output intensity depend. on discharge tube radius 79−55110
He-Ne waveguide lasers, HF discharge stability 79−18401
He-Zn laser, negative glow and positive column discharges comparison 78−1217
Hg, alignment of Hg levels 78−83639
Hg discharge, positive column, elec. probe for diagnostics, teaching appl. 79−62979
Hg low-pressure arc, positive column, heat flow processes 80−24135
Hg, optically pumped positive column, E-I characts. 80−44035
Hg positive column, electron energy distrib., numerical soln. of Boltzmann eqn. 80−87982
Hg positive column, high press., excimer densities and destruction mechanisms 78−5967
Hg vapour, optically pumped positive columm, collisional processes 78−87499

positive column continued
Hg-A discharge, scaling towards display cells 77—84565
Hg-Ar, low press. discharge positive column ionisation processes 78—75445
K discharge plasma, neg. ion prod. 78—59712
K, ion distrib. function for each species using probe 78—55752
Kr afterglow plasma, electron energy distrib. funtion 80—38748
Kr, DC glow discharge excited atoms, radial conc. distrib. obs. 78—67494
Kr, low-press. glow discharge, elec. characts. of positive column 80—100112
Kr plasma, of positive column, at. alignment, radiative lifetimes, collision cross sections 79—4203
Kr-Cl_2 mixture, glow discharge positive column, electron energy distrib. and rates of inelastic processes, negative Cl ions form. 80—19632
N cooled discharge plasma electron energy distrib. function 78—63633
N-O mixtures, positive glow corona in quasi-uniform fields 80—100104
N_2, $B^3\pi_g$ state excitation and deactivation in positive column 77—3482
N_2, DC low press. positive column, electron distrib. function superelastic electron collision depend. 79—46498
N_2 dissociation role in plasma positive column Mg nitridation 78—63628
N_2, flowing, visible spectrum obs. 80—49026
N_2, gas temp., interferometric diagnostics, heat cond. calc. 79—32834
N_2, ionic comp., mass spectra meas. *(Russian)* 78—22571
N_2, low pressure discharge, gas temp., laser interferometric meas. *(German)* 79—68951
N_2, low-pressure DC discharge positive column, vibration temp. radial distrib. 78—67499
N_2 molecular plasmas, electron kinetics *(German)* 78—91171
N_2, superelastic collisions and electron distrib. function 80—1858
N_2-Ne, positive column, electron vel. distrib. function *(German)* 78—1885
N_2-O_2 mixture, impulse breakdown processes at low press. 80—44021
Na-Ne, low press. discharge positive column, multistep ionisation 78—75446
Na-Ne-Ar AC discharge, field strength, electron props., radiated power 77—39487
Na-Ne-Ar discharge low-press., instability 78—9868
Na-Xe_2 excimer lasers, high-power discharges, models 80—69373
Ne, $2p^53s^3P_2$ to ground state, electron collisions of the second kind, rate consts. 79—27090
Ne, axial elec. field decrease 79—77439
Ne discharge, wavenumber spectra of turbulent ionisation waves 78—71541
Ne discharge in high press. narrow tube, Kadomtsev-Nedospasov instability 80—107004
Ne discharge positive column in longitudinal mag. field, metastable atom radial density distrib. obs. 78—67496
Ne, electron temp. depend. on transverse mag. field 78—1932
Ne, in magnetised positive column fluoresc. obs., 4s and 3d levels props. 77—68006
Ne, in transverse mag. field, plasma parameter diagnostics 79—19103
Ne, low press. discharge positive column, multistep ionisation 78—75446
Ne, low-press., atom densities of first excited state 80—38750
Ne, luminesc. discharge, loss mechanisms *(French)* 78—9877
Ne, medium press., model calc. 79—50912
Ne, mol. ion conc. determ. 77—58913
Ne positive column, 3S and 3P level populations, rel. theory with recomb. 77—10766
Ne, positive column, axial electric field in transverse mag. field 78—55766
Ne, positive column, excited level decay at high electron temp. 77—23442
Ne positive column, high-press., optical and probe diagnostics 78—51383
Ne, positive column, moving striations in longitudinal homogeneous mag. field 78—67523
Ne, positive column, with diffusion loss to wall, axial elec. field effects *(Japanese)* 78—47196
Ne, positive column contraction under diffusion-recombination conditions 80—24293
Ne positive column plasmas, metastable atom density meas. by improved self absorpt. method 80—87968
Ne, radial distrib. of excited atoms *(French)* 78—14237
Ne, reson.-absorpt. plasma of glow discharge positive column, Ne superradiation pulse variation 78—71489
Ne superradiation propagation through reson.-absorbing positive column plasma, pulse shape change 79—4117
Ne, wall loss in transverse mag. field 78—55767
Ne-H-H_2 mixture, positive column characts. and comparison with approx. diffusion theory 80—44025
O low-pressure discharge, plasma atomic species, mass spectrometric obs. 78—67502
O_2, dissociation in discharge plasma 79—100356
O_2, electron energy distrib. function, electron sink and plasma resist. effect *(Russian)* 80—106987
SF_6 plasma column, in Maecker type arc, diagnostics and model *(French)* 80—19652
Tl-Xe, electric discharge excitation of Tl in high-press. Xe 80—49025
Zn^+-He, positive column laser discharge, upper and lower state densities, Penning collision 80—32964
ZnF_2-He positive column discharge cataphoretic distrib. of Zn and F atoms 77—68886
positive feedback *see feedback*
positive ray sources *see ion sources*
positive rays *see ion beams*
positive temperature coefficient thermistors *see thermistors*
positons *see positrons*
positron annihilation *see electron positron interactions*
positron annihilation in liquids and solids
absorption coefficients and profiles of positrons implanted from radioactive sources 79—55781
adamantane, cryst., vacancy formation energy, positron annihilation study 80—60706
aliphatic unsaturated normal hydrocarbons, positron annihilation time spectra, polarisability depend. 78—6806
alkali chlorides, positron-trapping colour centre dynamics, positron annihilation study 80—108294
alkali halide, coloured crystal, possibility of Auger effect as result of positron capture 78—14381
alkali halide, gamma irradiated, positron annihilation 79—23643
positron annihilation in liquids and solids continued
alkali halide crystals, binding energy of F_{e^+}', M_{e^+}' and R_{e^+}' centres, positron trapping 79—69460
alkali halide crystals, capture and annihilation of positrons at M- and R-centres *(Russian)* 77—85829
alkali halides, cryst., positron lifetime and Doppler broadening spectra 79—8208
alkali halides, Doppler broadening meas. of positron annihilation 78—26806
alkali halides, positron annihilation, expt. techniques, positron states, book contrib. 80—2894
alkali silicate glasses, struct. and thermal props. 80—84075
alloy, Fermi surface meas. using high resolution high intensity apparatus 78—23008
alloys, CPA calc. for spatial and momentum distrib. 77—80720
alloys, positron annihilation technique in Fermiology 79—69902
alloys, simple, positron annihilation and charge transfer 78—31274
amino acids, positron annihilation in D and L isomers 77—12887
amorphous metals, struct. imperfections, review of expt. evidence 79—37630
angular correlation meas. device for 2γ-positron annihilation radiation *(German)* 78—86726
angular correlation meas. of annihilation radiation, automatic installation 77—6648
annealing in cold worked state, review 79—100163
annihilation radiation from point isotropic photon sources, numerical calc. 79—85096
applications *(Chinese)* 80—66322
aromatics, halogen substituted, as positronium inhibitor 80—93783
benzene molecules, bound positrons, time spectrum of positron annihilation 78—42248
benzene solutions, liq. and solid, positron and positronium annihilation 77—1152
beta flux absorption, beam unfolding calc. in segment model 77—69004
biomembrane phase transition studied by positron annihilation energy spectrometry 80—35854
brass, α and $\alpha+\beta$ type, short-range order, clustering and lattice defects influence 79—29107
α-brass, dezincified specimen, effect of voids on positron annihilation 79—15553
α-brass, electronic momentum densities by two-dimensional angular correlation of annihilation radiation 78—91605
$\alpha+\beta$ brass, plastic deform., recovery and recrystn., positron annihilation 79—57003
brass, recovery and recrystallisation of plastically deformed α-phase, comparison of positron annihilation, elec. resist. and microhardness 79—52240
β-brass, vacancy form., ordering effect, positron annihilation obs. 80—93427
brass, vacancy form. enthalpy, determ. from threshold temp. for positron trapping in vacancies 78—80433
brass, vacancy formation energies in mixed $\alpha+\beta'$ phase 80—59456
brass, vacancy formation enthalpy, composition depend., position annihilation obs. in Cu rich phase 79—95872
1-bromoadamantane, orientationally disordered, γ-irrad. free radical defects, positron probe obs. 79—23647
bulk lifetime, temp. depend. 78—47337
carbon tetrachloride in benzene, positronium inhibition by Cl 77—8678
charge transfer complexes, solid, positron annihilation and ang. correl. meas. 79—87521
chemical structure studies with positrons and mesons, review 79—79277
chlorobenzenes in benzene, positronium inhibition by Cl 77—8678
cholesterol, solid-solid phase transitions, positron annihilation study 80—84289
cholesteryl oleate, solid-solid phase transitions, positron annihilation study 80—84289
COC, cholesteric liq. cryst., positron lifetimes and phase transitions 80—59383
core and valence electron enhancement factors from positron annihilation-correlation curves 80—25479
core annihilation enhancement in solid 80—2892
correlation energy in homogeneous electron gas 78—92142
cyclodextrin, α and β, positronium decay, test of freq. vol. model 78—19592
α-cyclodextrin, positron annihilation, effects of adsorbed gases 79—65952
cyclohexane-chlorobenzene, soln., positronium formation inhibited by chlorobenzene 79—50170
d-orbital participation in bonding, positron ang. correlation 79—97979
diamond, positron implantation profile and mobility, elec. field effects 77—48273
dielectric materials, phase composition determ. *(Russian)* 79—91527
dielectric solids, quasiequivalence of annihilative e^+e^- and ionisative e^-e^- interactions 78—72633
diffusion heating and cooling in constrained media 79—87523
diffusion of positrons to surfaces 80—71506
disordered alloy, positron annihilation, Fermi surface study, review 80—44480
Doppler broadened 2-D technique in positron annihilation 78—70722
Doppler broadened radiation line shape, data tables 79—19947
dual-parameter time and energy spectrometry for positron annihilation studies 77—34505
education, positron annihilation in solids, high temp. vacuum chamber for source protection, crystal defect obs. 79—9068
n-eicosane-n-docosane binary mixture, solid-solid phase transform. rate, positron annihilation meas. 77—20066
n-eicosane-n-docosane mixtures, lifetime spectra obtained as function of temp. for various solid mixtures 78—18768
elastomers, vulcanised, positron annihilation and positronium destruction 78—35221
electron gas, ang. correl. in positron annihilation 80—24821
electron gas, screening of positron, contribs. of different partial waves 77—11878
electron liquid, collective description, positron annihilation 80—4632
enhancement in solid with tightly bound electrons, Coulomb correl. effect 77—73184
epoxy resin, rubber modified, temp. depend. of o-positronium lifetime 80—29825
ethylenediamine-H_2O mixtures, inhibition of Ps form. by NO_3^- ions 78—95988
fast diffusion meas., nondestructive, using positron emitter as tracer 78—54519

positron annihilation in liquids and solids continued
Fermi surface topology by two dimens. angular correlation of annihilation radiation, appl. to Cu 79−65359
fusion reactor metals and alloys, microvoid form., gaseous impurity atom effects, positron annihilation study 80−49275
n-GaAs:Te, interaction of positrons with dislocations 79−99974
gamma ray Doppler broadening spectra, parameters 78−72630
gamma ray energy broadening demonstration 78−73814
gamma-ray Doppler broadened spectra, deconvolution, using solid state detector 78−72631
gamma-ray lineshape parameters, statistical props. and sensitivity to positron trapping 77−69929
graphite, momentum density of electrons, two-gamma positron annihilation determ. 77−69211
halide, RX_2-type, positron annihilation ang. correl., bondind depend. 77−20951
N-p-hexyloxybenzylidene-p′-toluidene, positron lifetime meas. in solid and liq. cryst. phases 79−61460
III-V semiconductor, single crystal, positron annihilation 78−72636
imperfect solids, positron-defect interaction and annihilation characts., book contrib. 79−99978
implantation profile effects, transport and annihilation props., solids of varying density 77−48273
Inconel X750, positron annihilation study of ageing and creep 80−29824
ionic crystal, positron annihilation decay kinetics *(Russian)* 78−6805
ionic crystals, imperfect, positron stabilisation 80−40182
ionic crystals, positron annihilation review *(Hungarian)* 78−27350
ionic crystals, positronic atom scatt. on optical phonons, positron thermalisation 80−50457
ionic crystals with defects, separation of positron and positronium states 78−27351
iterative unfolding method for positron annihilation radiation spectra measured with Ge(Li) detectors 80−97373
kapton, temperature dependence of positron source 80−93426
lattice defects study by lifetime meas. 79−28857
lifetime calculations, approx. method for positrons trapped by lattice defects 78−48253
lifetime spectra, analysis by computer program 78−88379
lifetime spectra, analysis method 77−90217
line shape Doppler broadening, lifetime spectroscopy, formation inhibition by solvated electron precursor scavenging 80−93784
liquid, positronium pick-off annihilation, improved bubble model 80−93424
liquid alloys, positron annihilation due to vacancy trapping, simplified model *(Russian)* 80−71511
longitudinal polarisation, of e,e^+ and γ-rays in e^+e^- annihilation in crystal 79−11482
lunar regolith fine fraction, Luna-24 slow positron probe 80−26762
MBBA, polymorphism, positron annihilation obs. 78−72632
metal, annihilation line broadening, Ge detector 77−16418
metal, BCC, high temp. positron annihilation 78−47421
metal, defect annealing study by positron annihilation, and elec. resistivity meas. 78−51584
metal, dislocation density, positron annihilation method 77−85834
metal, electron momentum distrib., reconstruction from point-geometry positron-annihilation data 79−56883
metal, formation of positronium in 'metallic' pores 78−35222
metal, NDT appl. 78−3293
metal, NDT appl. 78−3294
metal, nonlinear electron density distribution around point defects, applications 79−19549
metal, positron annihilation, ang. correl. data analysis 78−52592
metal, positron annihilation study of neutron damage, review 78−71769
metal, positron density distribution, temp. effects 78−47739
metal, positron lifetime spectra, anal. errors 78−19591
metal, positron lifetimes, phenomenological interpretation 77−73186
metal, positron self-trapping conditions 78−47338
metal, positron thermalisation by non-equilibrium statistical operator method 79−15551
metal, positron trapping at defects, positron-phonon scatt. effect 77−89736
metal, positron-phonon scatt. effect on positron trapping at monovacancies 78−26829
metal, positron-vacancy interactions, equilib. temp. depend. of positron annihilation 78−76547
metal, radiation defects, localized deformation of electronic state *(Russian)* 79−87061
metal, ultrafine particles, positron annihilation exam. 78−56542
metal surface, positron-electron correlations, RPA calc. 80−40181
metal vacancy conc. studies using positron annihilation spectroscopy 77−11544
metal-metal contacts, positron diffusion, ang. distrib. of annihilation photons meas. 79−8207
metallic glasses, aged, atomic clustering exam. using positron annihilation methods 77−84655
metallic glasses, mats. props. review 77−4043
metallic surface, surface traps and vacancy trapping, slow positron obs. 79−87522
metals, cryst. defects, positron annihilation method, review *(German)* 77−44082
metals, Doppler broadening of position annihilation line 79−43057
metals, effect of vacancy migration upon annihilation of trapped positrons 77−48271
metals, electronic structure, positron annihilation studies *(Japanese)* 78−18951
metals, lattice defects, positron annihilation study, book contrib. 79−99977
metals, mag. field effects on positron annihilation 77−62803
metals, positron annihilation, localised probe of lattice defects 80−55224
metals, positron annihilation, real-space approach 79−95874
metals, positron annihilation expts., electronic struct. and Fermi surface studies 80−54594
metals, positron annihilation technique in Fermiology 79−69902
metals, positron response to thermal expansion 80−84306
metals, positron trapping at dislocations 78−10091
metals, positron trapping by defects influence of positron-phonon and electron-phonon interactions *(Russian)* 80−93425
metals, slow positron studies 80−55223
metals, vacancy form. vol. from positron annihilation meas. 78−47339
metals and alloys, electron momentum density, positron interactions, book contrib. 79−99976

positron annihilation in liquids and solids continued
metals and alloys, NDT using positron meas. 80−55222
metals and alloys, positron annihilation, theoretical and expt. techniques, book 79−99975
molecular crystals, impurity effects on positronium formation 77−66554
molecular solids, existence of positronium, meas. on solid hydrocarbons 77−59638
molecular substances, positron annihilation and phase transitions, review 78−95614
momentum density measurements, multicounter two-dimensional angular correlation of annihilation radiation apparatus 78−10331
momentum distribution, use of running integrated difference curves 79−56881
Mossbauer effect and positron annihilation, review of appls. *(French)* 80−80899
mylar, implantation of positrons from ^{22}Na 80−16118
mylar, temperature dependence of positron source 80−93426
negative ions, positronium formation, Doppler broadened positron annihilation line shapes 80−45164
neopentane, soln., positronium form. inhibition by organic iodide addition, momentum distrib. 77−90631
nitrobenzene, quenching and inhibition of orthopositronium 80−35002
nitrobenzene molecules, bound positrons, time spectrum of positron annihilation 78−42248
noble metals, annihilation data anal. by Mijnarends' method 77−20223
nonmetallic solid, angular correlation curve 79−47537
nonmonolithic systems, positron diffusion effect on annihilation photon ang. distrib. 79−83053
nonpolar liquids, enhancement of positronium form. caused by scavenging of highly mobile positive holes 80−69265
nonpolar solvent, o-Ps yield in chlorinated ethanes, ethenes and cyclohexanes 79−70357
nonsolvated electron reactions, positron annihilation method 77−81417
nuclear medicine imaging, 3-dimens. positron camera 78−73225
organic crysts., γ-irrad., positron lifetime rel. to free radical conc. 78−72635
organic liquid mixtures, positronium form., spur process 78−1113
organic molecular liquid, orthopositronium pick-off annihilation lifetime calc. 78−56541
oxide powders, muonium and positronium form. 79−56679
p-(p-ethoxybenzylidene) amino benzonitrile, positron annihilation exam. 79−19149
p-terphenyl, positronium and thermal defects 80−24496
phospholipid vesicle phase transition probed by positron annihilation lifetime technique 79−88061
photon energy spectroscopy, stability problems 80−29821
photon linear polarisation, quantum mech. test 77−69932
photon lineshape measurement, simple correction technique 77−63482
plastically deformed metal, positron annihilation examination of recrystallisation *(German)* 77−70252
polybutadiene, C black filled, positron annihilation and positronium form. 79−28856
polycrystalline metal, ang. correl. curves parametrization *(German)* 77−90214
polyethylene, elec. field effect on positron annihilation 79−4868
polyethylene, high-press., temp. depend. of free vol., positron annihilation meas. 77−16419
polyethylene, positron implantation profile, electric field depend. 79−11483
polyisoprene, positron lifetime, phase and temp. depend. 79−83051
polymers, positronium form. and decay, elec. field effect 80−97369
POSITRON, evaluating system for positron annihilation R-40 computer meas. 79−78787
positron annihilation radiation, ang. correl. shape, deform. effects 77−85831
positron basic props., annihilation line shape, positronium formation, book contrib. 80−2893
positron lifetime spectra, lifetimes and intensities 79−33858
positron trapping, temp. depend., vacancy form. energy 77−90215
positron trapping rate into vacancy clusters in metals 80−2890
positronium determination in matter, Compton profile comparison to γ-annihilation radiation ang. correlation *(Russian)* 77−55845
positronium formation, in mixtures of competitive electron acceptors 80−28120
positronium oxidation react. in aq. soln., positron hydration energy 78−61039
prethermalisation trapping model 77−43541
PVC, positron lifetime, phase and temp. depend. 79−83051
pyrene, positronium and thermal defects 80−24496
quartz, fused, positronium form. and decay, elec. field effect 80−97369
quartz, phase composition determ. *(Russian)* 79−91527
radioactive source holder, fraction of positrons annihilating 78−70667
recrystallised material, volume fraction determ. from positron annihilation 77−1760
relativistic channelled positrons, EM energy emission spectra *(Russian)* 79−78785
ribonuclease, positron annihilation, temp. depend. meas. 79−66448
Rochelle salt, positron lifetime meas. during phase transitions 78−6644
semiconductor, causes of single short positron lifetime 79−28861
semiconductor, momentum distrib. of electrons, anisotropy, positron annihilation *(Russian)* 78−84676
semiconductor crystal, positron annihilation with electrons bound in edge dislocations 79−47539
sodium dodecylsulfate, micellar solution, critical micelle concentraion for thermalized positronium formation 79−96345
steel, AISI 4340, positron lifetime and X-ray particle size meas. during high cycle fatigue 79−5053
steel, Cr-Ni, martensite defect identification by positron annihilation 78−39867
steel, influence of a cyclic stress, ang. distrib. and lifetime obs. 78−76551
steel, positron meas., for trapping mechanism detection 80−84798
steel, quenched, exam. of phenomena taking place during tempering by positron annihilation *(Russian)* 79−24543
steel, reactor pressure vessels, positron annihilation as nondestructive monitor of radiation damage 77−4130
steel, type 4340, deformation study, positron lifetime and hardness correlation 79−87649
succinonitrile, defects in plastic phase, positron annihilation obs. 80−11504

positron annihilation in liquids and solids continued
sulphides, d-orbital participation in bonding, positron ang. correlation 79−97979
sulphones, d-orbital participitation in bonding, positron ang. correlation 79−97979
teflon, γ-irrad., low dose, positron lifetime obs. 78−76550
Teflon, gamma irradiated, free four-term analysis of positron lifetime spectra 80−76101
p-terphenyl:anthracene, impurity effects on positron lifetime spectrum 78−43954
p-terphenyl, cyclic hydrocarbon admixtures, positronium lifetimes meas. 78−19595
p-terphenyl, positronium form. at elevated temps. 77−89473
TGS, ferroelec., positron lifetime meas. during phase transitions 78−6644
TGS, positron annihilation and ferroelectric transition 78−19594
thermalised positron annihilation, photon emission and spectator electron recoil, short range electron correl. determ. 80−50456
transition metal, d-series, distance separating dislocation, determ. by positron-electron annihilation method 79−14811
transition metals, itinerant and localised d-electrons, positron annihilation data 80−93428
2,2,4-trimethylpentane-chlorobenzene, soln., positronium formation inhibited by chlorobenzene 79−50170
two-photon annihilation studies, positron wavefunction 77−36311
vacancies in cryst. materials., determ. of conc. using positron annihilation *(French)* 79−69901
1-vinyl-o-carborane, orientationally disordered, γ-irrad. free radical defects, positron probe obs. 79−23647
Vycor glass, positronium-surface interaction in pores 78−27347
water-dioxan mixtures, positron annihilation, o-positronium pick-off quenching 79−24386
windowed ang. correl. method for positron annihilation params. meas. 77−34528
Zircaloy, deformed, positron annihilation and electron microscopy 77−8898
γγ angular correlation measurement, design and construction of liquid He cryostat 79−93148
Ag, electron beam irradiation, 2.3 MeV, positron annihilation exam. of radiation defects *(Russian)* 78−34542
Ag, Fermi surface anisotropy meas. 77−20222
Ag, positron annihilation characteristics, effect of temp. 78−64427
Ag, positron annihilation spectra, Doppler-broadened, temp. depend., 9 to 1098K 80−71510
Ag, positron trapping, temp. depend., vacancy form. energy 77−90215
Ag, positron trapping by vacancies using ^{19}Ne source 78−47341
Ag series metals, positron annihilation rates, electron-electron and electron-positron correl. effects 78−76548
Ag surface, positronium emission 80−80897
Ag, ultrafine particle, sintering effect, study by positron annihilation 78−95615
AgBr crystals, positron lifetime *(German)* 78−19593
AgBr deformed crystals, mean lifetimes *(German)* 77−11589
Al alloys, precipitation hardening, positron annihilation investig. by γ-ray Doppler broadening 77−81174
Al, annealed and neutron irrad., exam. of positron lifetimes in voids and other defects 78−47426
Al, annihilation spectrum, narrow component, Fermi impulse of electrons, plastic deform. recovery *(Czech)* 78−64591
Al, CC vacancy, electron and positron densities and temp. depend. of positron lifetime 78−19001
Al, effect of microvoid size on positron annihilation and residual resist. 77−48272
Al, electron and neutron irrad., Doppler broadened positron annihilation meas. *(German)* 77−62563
Al, electron beam irradiation, 2.3 MeV, positron annihilation exam. of radiation defects *(Russian)* 78−34542
Al, electronic momentum densities by two-dimensional angular correlation of annihilation radiation 78−91605
Al, Fermi surface determ. by γ-ray angular correl. meas. 79−4869
Al, gamma-ray impact, absolute pair production cross-section meas. 78−43958
Al, He injected, tracing bubble evolution by positron annihilation 77−19992
Al, neutron damage, positron annihilation 80−65056
Al, positron annihilation, ang. correl. meas., electronic momentum density calcs. 77−4284
Al, positron annihilation, detection of N impurities 79−65777
Al, positron annihilation, effects of quenching, annealing and neutron irrad. 80−20732
Al, positron annihilation, angular distrib., Umklapp effects *(French)* 80−50454
Al, positron annihilation ang. correl., trapping by mono- and multivacancies 77−32466
Al, positron annihilation and vacancy formation, Doppler broadening study 80−60708
Al, positron annihilation characteristics, effect of temp. 78−64427
Al, positron annihilation in small voids, self consistent calc. 77−20952
Al, positron annihilation momentum profiles, core contrib. and independent particle model 77−24908
Al, positron annihilation momentum spectra, low temp depend. 79−19948
Al, positron annihilation radiation, ang. correl. shape, deform. effects 77−85831
Al, positron annihilation studies using high-density proportional chambers 80−25478
Al, positron annihilation with high-momentum core electrons, vacancies study 80−25481
Al, positron trapping, defect specific temp. depend. 78−47336
Al, positron trapping at voids, temp. depend. 79−61464
Al, positrons around vacancies 77−40297
Al, quenched, muon$^+$ trapping at vacancies, compared with positron annihilation 80−15937
Al, quenched, positron annihilation study, vacancy clustering 78−27348
Al, recovery features, TEM and positron lifetime meas. examination 78−80611
Al, subjected to thermocyclic treatment 79−52040
Al surface, positronium emission 80−80897
Al, surface fatigued single crystal, inhomogeneous positron trapping 77−90216
Al, vacancy form. energy from positron annihilation meas. 78−47340
positron annihilation in liquids and solids continued
Al, vacancy form. enthalpy, simultaneous positron lifetime and momentum meas. 78−47335
Al, vacancy formation enthalpy, positron annihilation spectroscopy 78−67707
Al-Co(Ni)(Ru)(Rh)(Pd)(Ir), composite, paramagnetic resonance and electron-positron annihilation *(Russian)* 79−87314
Al-Cu (4% wt.), single crystals, positron trapping at precipitates 78−76554
Al-Cu alloys, Cu precipitate detect. by positron annihilation, GP zone development 80−3051
Al-Cu samples (0.5, 2.0 and 4.0 wt.%) polycryst., precipitation, positron annihilation and TEM 80−50639
Al-Cu-Mg-Mn alloys, shot peened, positron annihilation meas. 77−63833
Al-Mg, dil., ang. correlation of annihilation radiation from impurity trapped positrons 80−104010
Al-Mg (0.1 at.%), neutron damage, positron annihilation 80−65056
Al-Zn, age hardenable precipitation and dissolution, positron annihilation and X-ray scatt. 80−16314
Al-Zn-Mf-Cu-Cr alloys, shot peened, positron annihilation meas. 77−63833
Al-Zn-Mg, age-hardenable, precipitation and dissoluton processes, positron annihilation and X-ray small-angle scattering comparison 80−89238
$Al_xGa_{1-x}As$:Si, charge state of impurity atoms, positron annihilation meas. 78−39062
AlH_3, covalent nature of chem. binding, positron annihilation obs. 78−18581
γ-Al_2O_3, magnetically quenchable positronium-like systems 79−87065
α-Al_2O_3, sintered or hot-pressed, porosity effect on positron mean lifetime 78−27463
Al(111), oxide layer amorphous to cryst. surface transition, slow positron obs. 80−75417
As-Se system glasses, point defects, positron lifetime spectra meas. 78−88380
As-Se(S), glassy and crystalline, point defect exam. by positron annihilation 78−72637
Au, electron and neutron irrad., quenched, Doppler broadened positron annihilation meas. *(German)* 77−62563
Au, Fermi surface anisotropy meas. 77−20222
Au, monovacancy and divacancy parameters, positron annihilation meas. 77−35550
Au, positron annihilation, 4.2-500K, Doppler broadening meas. 78−43957
Au, positron annihilation characteristics, effect of temp. 78−64427
Au, positron annihilation characteristics, 27 to 592K 79−91523
Au, positron lifetime and annihilation lineshape from 4.2K to MP 77−20272
Au series metals, positron annihilation rates, electron-electron and electron-positron correl. effects 78−76548
Au_xGe_{1-x}, liq., ang. distrib. of positron annihilation 77−55848
B, electron structure study by positron annihilation 80−16117
BN, dislocation struct., single crystals, positron annihilation study 78−11016
$BaTiO_3$, Doppler-broadened positron annihilation 78−64428
$BaTiO_3$:Gd, positron lifetime spectra meas. 78−43956
BeH_2, ionic nature of chem. binding, positron annihilation obs. 78−18581
Bi solid and liquid, positron annihilation temp. depend. 80−108296
Bi, temp. depend. of positron annihilation parameters 78−76553
α-brass, defect removal, obs. by positron annihilation 78−84677
C black, positron annihilation and positronium form. 79−28856
C structures, differentiation between graphite and diamond structs. 79−28860
$CaCO_3$ single crysts., positron annihilation, two photon angular correlation 80−108295
CaF_2, positron annihilation polarisation effects, electron momentum distribution 80−55225
CaF_2:Sm, charge transitions, positron annihilation exam. 78−92143
CaF_2:Sm, positron annihilation polarisation effects, electron momentum distribution 80−55225
CaF_2:Sm(Eu), capture of thermalised positrons by activator impurities 77−40299
Cd, anisotropy of free-electrons momenta distribution, positron annihilation meas. 77−36309
Cd, annihilation data anal. by Mijnarends' method 77−20223
Cd, positron annihilation, temp. depend. 77−69930
Cd, positron annihilation, 4.2-500K, Doppler broadening meas. 78−43957
Cd, positron annihilation lifetime spectra, low temp. trapping 80−29822
Cd, positron lifetime, investigation of temp. effect 78−2940
Cd, positron lifetime and annihilation lineshape from 4.2K to MP 77−20272
Cd, positron trapping at low temp. lifetime spectra 80−84799
Cd-Mg alloys, positron annihilation meas. of Fermi surface 79−56113
CdS(Se)(Te), positron annihilation study 80−60713
Ce, vacancy formation enthalpy in γ phase, positron annihilation meas. 79−99182
Co, HCP, positron annihilation meas. of electronic struct. 77−20224
Co, phase transformations and vacancy form. by positron annihilation 80−2155
Co, positron trapping, monovacancy form energy 79−74016
Co, positronium form. in two-photon positron annihilation 79−61462
Co-Al, positron lifetime and angular correl. curves 79−47538
Co-Al alloys, deformed, superparamag. inclusions *(Russian)* 77−85416
Co-Ni, deformed and isochronally annealed, positron lifetimes, annihilation at dislocation trapped monovacancy 80−55221
$Co_{92}Fe_8$, FCC, electronic struct., ang. correlation of positron annihilation γ-quanta, meas. 80−10864
Cr, band struct. and Fermi surface, angular correl. of positron annihilation radiation 78−6260
Cr, self-diffusion activation energies, positron trapping meas. 79−74015
Cr-Fe, electronic struct., Mossbauer and positron annihilation study 79−82518
Cu alloys, liq. and solid, positron trapping 78−48255
Cu, annealed, positron lifetime changes during cyclic fatigue 79−43060
Cu, conduction band, high momentum components determ. from annihilation radn. ang. correlation 79−19508
Cu, defect removal, obs. by positron annihilation 78−84677
Cu, defects at thermal equilib. and melting, positron annihilation meas. 77−76391

positron annihilation in liquids and solids continued
Cu, deformed, defects, thermal relaxation, positron experiments *(German)* 80−50455
Cu, deformed, positron lifetimes, trapping model 77−15451
Cu, deformed, temp. depend. of positron trapping 77−48270
Cu, deformed and annealed, positron lifetime investig. of recovery and recrystn. 77−70064
Cu, dlectron irrad. at 130K, positron lifetime investig. of stage III recovery mechanism 77−47484
Cu, electron and neutron irrad., Doppler broadened positron annihilation meas. *(German)* 77−62563
Cu, electron irrad., positron lifetime exam. of annealing recovery 78−47354
Cu, Fermi surface determ. by γ-ray angular correl. meas. 79−4869
Cu, Fermi surface studies by the positron annihilation technique 79−82515
Cu, Fermi surface topology by two dimens. angular correlation of annihilation radiation 79−65359
Cu, gamma-ray impact, absolute pair production cross-section meas. 78−43958
Cu, high current densities, ang. distrib. of annihilation quanta *(German)* 77−12462
Cu monocrystals, positron annihilation quanta ang. correl., point defect effects 77−76729
Cu, monovacancy and divacancy parameters, positron annihilation meas. 77−35550
Cu, plastically deformed, positron trapping rate temp. depend. 78−31276
Cu, plastically deformed, recovery, isochronal annealing, positron lifetime meas. 77−59807
Cu, point-geometry ang. correl. curves, enhancement in positron annihilation 79−95873
Cu, positron annihilation ang. correl., trapping by mono- and multivacancies 77−32466
Cu, positron annihilation characteristics, effect of temp. 78−64427
Cu, positron annihilation radiation, ang. correlation, APW calc. 80−7435
Cu, positron annihilation studies using high-density proportional chambers 80−25478
Cu, positron annihilation with high-momentum core electrons, vacancies study 80−25481
Cu, positron implantation profiles in mono- and polycryst. samples, channelling 77−48273
Cu, positron lifetime, Doppler broadening of annihilation spectrum, temp. effect 78−2941
Cu, positron lifetime as a function of grain size 77−15427
Cu, positron trapping, defect specific temp. depend. 78−47336
Cu, positron trapping by vacancies using ^{19}Ne source 78−47341
Cu, positron-lifetime study of 4.5-25 MeV proton irrad. effects 79−33021
Cu, positronium form. in two-photon positron annihilation 79−61462
Cu powders, electron-positron annihilation charact. *(Russian)* 77−63485
Cu, prevacancy temperature depend. of positron annihilation, Doppler broadening lineshape parameters 80−60709
Cu, reson. scatt. of annihilation quanta by ^{106}Pd *(Russian)* 77−26651
Cu single crystals, positron trapping by edge dislocations, produced by bending 78−80606
Cu, source effects 78−31272
Cu surface, positronium emission 80−80897
Cu, trapping rate by dislocations in plastically deformed sample, 6 to 77K 77−11592
Cu, umklapp annihilation of positrons, rot.-specimen method 78−2410
Cu, vacancy annealing exam. by positron annihilation 79−14801
Cu, vacancy form. enthalpy, positron annihilation meas. 80−97371
Cu:H, interaction of H and vacancies, positron annihilation, Doppler broadening 78−80434
Cu-Al-Ni, positron annihilation study of vacancies before and after martensitic transform. 79−99971
Cu-Al(23.5 at.% and 25.3 at.%), martensitic transform., positron annihilation meas. 77−16578
Cu-Co (1.5 and 4 wt.%) alloy, coherent Co-rich separations obs. by positron annihilation *(Russian)* 80−89082
α-Cu-Ge, Fermi surface, high resolution positron annihilation study 78−6261
Cu-Ge (2 wt.%), positron annihilation, photon ang. distrib. meas. effect of deformation, annealing temp. *(Russian)* 78−35220
Cu-Mn, positrons as probe of phase transforms. 78−31401
Cu-Pd, Fermi surface comp. depend. by positron annihilation ang. correl. 77−76727
Cu-Zn(30 at.%), electron irrad., positron annihilation, defect recovery 79−74018
α-$Cu_{0.7}$ $Zn_{0.3}$, point-geometry ang. correl. curves, enhancement in positron annihilation 79−95873
CuO film, positron annihilation meas. 77−40300
Cu_2O film, positron annihilation meas. 77−40300
Cu_xZn_{1-x}, positron annihilation and Mossbauer effect exam. 79−65775
Fe, appl. of KUR LINAC to radiation damage studies 78−71760
Fe, deformed, defects, thermal relaxation, positron experiments *(German)* 80−50455
Fe, Doppler broadened positron annihilation lineshapes, prevacancy lattice expansion 78−27349
α-Fe, electron irradiated, vacancy annealing 79−55785
Fe, electron-irradiated, positron lifetime meas. 80−93431
Fe, electronic structure, positron annihilation meas. 79−91524
Fe, gamma-ray impact, absolute pair production cross-section meas. 78−43958
α-Fe, laser irrad., Mossbauer effect and positron annihilation *(Russian)* 78−19390
Fe, phase transformations and vacancy form. by positron annihilation 80−2155
Fe, positron annihilation, temp. depend. 78−56540
Fe, positronium form. in two-photon positron annihilation 79−61462
Fe, pure and doped, electron irrad., mag. aftereffect 80−88838
Fe, spin dependent momentum distrib., APW calc. 78−2416
Fe vacancy form. by positron annihilation in thermal equilibrium 78−10041
Fe, vacancy formation energy by positron annihilation 78−51531
α-Fe:C, electron irrad., vacancy-C interaction, positron lifetime meas. 80−75264
Fe-Al, positron lifetime and angular correl. curves 79−47538
Fe-C, electron-irradiated, positron lifetime meas. 80−93431
positron annihilation in liquids and solids continued
Fe-Ni alloy, positron lifetime 80−2891
Fe-Ni(29.5at%) alloy, martensitic transform., position lifetime spectra meas. 77−36498
$Fe_{80}B_{20}$, metallic glass, Doppler broadening of positron annihilation γ-radiation and elec. resist. 80−66321
Fe_xGe_{1-x}, liq., ang. distrib. of positron annihilation 77−55848
$Fe_{78}Mo_2B_{20}$, metallic glass, Doppler broadening of positron annihilation γ-radiation and elec. resist. 80−66321
$Fe_{32}Ni_{36}Cr_{14}P_{12}B_6$, metallic glass, Doppler broadening of positron annihilation γ-radiation and elec. resist. 80−66321
$Fe_{40}Ni_{40}P_{14}B_6$ glass, positron lifetimes in as-received, cold-rolled, embrittled and crystallized samples 79−74177
Fe_3Pt, plastically deformed, struct. inhomogeneities, positron annihilation meas. 79−33859
Ga, positron annihilation lineshape factors, effect of thermal expansion 77−44084
Ga positron lifetime meas., comparison with theory 77−63483
Ga solid and liquid, positron annihilation temp. depend. 80−108296
$Ga_{1-x}Al_xAs$-GaAs:Si, momentum distrib. of valence electrons, positron annihilation meas. 79−51530
GaAs, electron-irrad., deep-level defect anal. using 2γ positron annihilation and IR absorption spectra 80−16120
GaAs, epitaxial film, positron annihilation, impurity centre study 79−15554
GaAs, mag. field effect, positronium states 77−16417
GaAs, native vacancies study using positron lifetime technique 79−83052
GaAs, positron annihilation depend. on doping 80−60710
GaAs, positronium-like states, low temp., ang. correl. of annihilation photons 78−76549
GaAs:Si, charge state of impurity atoms, positron annihilation meas. 78−39062
GaAs:Si, momentum distrib. of valence electrons, positron annihilation meas. 79−51530
GaAs:Si, positron lifetime temp. depend. 80−29826
GaP, positron annihilation, deep acceptor level props. 79−11485
GaP:Ti(Co)(Ni), positron annihilation meas. rel. to deep levels study 80−60712
Ge, electron beam irradiation, 2.3 MeV, positron annihilation exam. of radiation defects *(Russian)* 78−34542
Ge, neutron irradiated, capture of positrons by radiation defects 78−38756
Ge, neutron irradiated, positron annihilation, ESR and resist. meas. 80−15160
Ge, neutron-irradiated, positron lifetime 80−97374
Ge, positron annihilation, effect of vacancies 79−24385
Ge:Be(Mg)(Ca)(Ba), positron annihilation ang. distrib 80−45165
H-like atom in super-strong mag. field, photoeffect and relativistic positron annihilation *(Russian)* 77−75112
$H_2O(D_2O)$, positronium formation, isotope effects 80−93432
He, condensing on positron, Monte Carlo lifetime spectra, temp. and elec. field effects 78−55263
He, microscopic gas-liquid like phase transition around positron 77−43322
He, orthopositronium decay, liq. and solid phases, press. up to 140 atm. 77−39713
He, positron decay rate nonlinear density depend. 80−71509
^{4}He, positron self-trapping 77−62697
Hg-In, liq., positron annihilation meas. 78−43955
Hg-In alloys, liq., positron studies, trapping at solute-vacancy complexes 78−31271
Hg-Tl, liq., positron annihilation meas. 78−43955
Hg-Tl alloys, compositional depend. of positron annihilation 79−99973
In, Fermi momentum and core electron contribution 77−81173
In, positron annihilation, 4.2-500K, Doppler broadening meas. 78−43957
In, positron annihilation lineshape meas., 74 to 430K 77−36308
In, positron annihilation line Doppler broadening, self-trapping and vacancy form. 77−40298
In, vacancy form. vol. 78−15245
Invar alloys, plastically deformed, struct. inhomogeneities, positron annihilation meas. 79−33859
KBr, proton irrad., divacancies, positron capture, ionic cond. and TSC study 80−54289
KBr, single cryst., positron lifetimes, temp. depend. 78−48254
KBr(Cl), positron ang. correl., cryst. orient. depend., positron states and ionic distortion 77−63484
KCl, and KCl-AgCl, surface positron and positronium states, positron annihilation expts. *(Russian)* 78−39623
KCl crystals, positron annihilation, Doppler broadening 80−40180
KCl, delocalised positronium, 4.2K, direct obs. γ-spectra 78−88235
KCl, electron-irrad., positron-capture centres, thermal annealing kinetics 79−95875
KCl, positronium states near defects in cationic sublattice 80−16121
KCl, trapping by positive-ion vacancies, impurities and defect complexes, temp. depend. 77−27908
KCl:Ag positron annihilation and impurity states 80−97375
KCl:AgCl, positron annihilation charact., positronium state form., X-irrad. effects 77−4700
KCl:Sr, positron annihilation and trapping in A-centres 80−84802
KCl-KBr mixed crystal, containing defects, mag. quenching of positronium states 77−8680
KCl(Br), coloured, irrad. damage during positron bombardment 78−63791
KH_2PO_4, ferroelec., positron lifetime meas. during phase transitions 78−6644
Li-Mg, positron annihilation and charge transfer 78−31274
LiF, γ-irrad. induced defects, positron capture and annealing obs. 80−60707
α-$LiIO_3$, angular correlation curves of annihilation photons 78−19597
Li_2O-Al_2O_3-SiO_2, glass ceramic form. obs. using positron annihilation 77−776
Li_2O-SiO_2 glass, crystn. and phase separation, positron lifetime and annihilation lineshape meas. 78−23550
Li_2O-SiO_2 glass, crystallisation and phase separation 79−10803
Li_2O-SiO_2 glass, crystallisation study 79−90567
Mg, anisotropy of free-electrons momenta distribution, positron annihilation meas. 77−36309
Mg, annihilation data anal. by Mijnarends' method 77−20223
MgO, powder, positronium fine struct. interval meas. by Zeeman transitions 78−95616

positron annihilation in liquids and solids continued
$MgO:Al^{3+}$, positron annihilation meas. 77−8681
Mn, positronium form. in two-photon positron annihilation 79−61462
Mo (100) clean surface electron struct., positron annihilation study 80−24988
Mo, band struct. and Fermi surface angular correl. of positron annihilation radiation 78−6260
Mo, correlation of positron lifetime and pair momentum in radiation-induced voids 77−8679
Mo, deformed, ^{57}Fe doped, positron annihilation exam. 79−15556
Mo deformed single crysts., struct. state and dislocation splitting *(Russian)* 80−29029
Mo, effect of microvoid size on positron annihilation and residual resistivity 77−48272
Mo, electron irrad., positron trapping in vacancies and vacancy clusters 79−52039
Mo, gamma irradiated defects, interaction with positrons *(Russian)* 80−97372
Mo, gamma-ray irrad. positron annihilation during radiation defect annealing *(Russian)* 79−99970
Mo, high-temp. neutron irradiated, annealing study by positron lifetime 77−51413
Mo, neutron irradiated, relationship between void size and positron lifetime 77−15454
Mo, neutron-irradiated, high-temp., positron annihilation characts. meas. 77−89480
Mo, neutron-irradiated, positron lifetime study 79−23654
Mo, point defect migration, stage III annealing 77−80548
Mo, positron annihilation and vacancy formation 80−16119
Mo, positron lifetime meas. of neutron irrad. induced voids 77−7766
Mo, void containing, positron annihilation characts. 80−80898
Mo, voids, effect of impurities on positron lifetime 77−15453
$NH_4H_2PO_4$, antiferroelec., positron lifetime meas. during phase transitions 78−6644
Na, momentum density of electrons, two-gamma positron annihilation determ. 77−69211
NaCl, γ-irrad., C-centres, position ang. correl. obs. 78−22712
NaCl, positron ang. correl., cryst. orient. depend., positron states and ionic distortion 77−63484
NaCl, positron trapping by X-ray produced defects, A-centre form. 77−48273
NaCl, positronic atom scatt. on optical phonons, positron thermalisation 80−50457
NaCl, positronium-like states, ang. correlation of photons from positron annihilation 77−36310
NaCl, temperature dependence of positron source 80−93426
NaCl:Ag, positron annihilation and impurity states 80−97375
NaCl:AgCl, positron annihilation characts., positronium state form., X-irrad. effects 77−4700
NaCl:Sr, positron annihilation and trapping in A-centres 80−84802
NaF, delocalised positronium existence at room temp. 78−76546
NaF, positronium-like states, ang. correlation of photons from positron annihilation 77−36310
$NaNO_2$, positron lifetimes, ferro-paraelectric transition 79−74017
Nb, defect annealing in 7 MeV-irrad. samples, positron annihilation obs. 80−24497
Nb, electron beam irradiation, 2.3 MeV, positron annihilation exam. of radiation defects *(Russian)* 78−34542
Nb, neutron irrad., microvoid form., ang. correl. and yield strength meas., TEM obs. 78−88381
Nb, neutron-irradiated, positron annihilation ang. correl. meas. 80−93430
Nb, plastic deform. effect on positron annihilation and supercond. transition *(Russian)* 77−39993
Nb, positron annihilation and vacancy formation 80−16119
Nb, positron trapping and annihilation at vacancies 80−29823
Nb-Zr (3 wt.%), neutron-irradiated, positron annihilation ang. correl. meas. 80−93430
$NbSe_2$ pure and intercalated with ethylenediamine, positron annihilation study 80−84801
Ni, cathodic charging of H_2, positron annihilation Doppler broadening obs. 79−83055
Ni, cold rolled, influence of impurities on recovery and recrystallisation, positron annihilation meas. 79−15696
Ni, cold-worked, impurity-induced vacancy clustering 79−99972
Ni, defect electronic struct., strength characteristics relation by positron annihilation 79−91526
Ni, defect removal, obs. by positron annihilation 78−84677
Ni, defects at thermal equilib., positron annihilation meas. 77−76391
Ni, Doppler broadened positron annihilation lineshapes, prevacancy lattice expansion 78−27349
Ni, electron irradiated, temp. depend. positron trapping 78−91360
Ni fine particles, ang. correl. curves 79−61461
Ni, phase transformations and vacancy form. by positron annihilation 80−2155
Ni, plastically deformed, positron trapping rate, temp. depend. 80−71507
Ni, plastically deformed, recovery stages III and IV investig. by positron annihilation 77−31715
Ni, plastically deformed, volume fraction of recrystallised material determ. from positron annihilation 77−1760
Ni, positron annihilation ang. correl., trapping by mono- and multi-vacancies 77−32466
Ni, positron capture by dislocations, vacancies, rel. to temp. *(German)* 78−30606
Ni, positron lifetime meas., 4.2 to 1700K, monovacancy form. enthalpy 80−97370
Ni, positron trapping, defect specific temp. depend. 78−47336
Ni, positron trapping by vacancies using ^{19}Ne source 78−47341
Ni, positronium form. in two-photon positron annihilation 79−61462
Ni powders, interaction with defects in grain and pores *(Russian)* 77−16520
Ni surface, positronium emission 80−80897
Ni, transformed into hydride and decomposed, dislocation density and dislocation profile depth, positron annihilation and X-ray estimation 78−38711
Ni-Cr-Fe (75, 35, 12 wt.%), electron and α-particle irrad., positron annihilation and elec. resist. meas. 79−83054
Ni-Ge (2 at.%), vacancy cluster form. during deform. positron lifetime meas. 79−56882

positron annihilation in liquids and solids continued
Ni-Ge (2 wt.%), positron annihilation, photon ang. distrib. meas. effect of deformation, annealing temp. *(Russian)* 78−35220
Ni-P amorphous alloy, positron annihilation exam. of crystallisation 79−43061
Ni-Sb, dil., vacancy-impurity binding enthalpy, positron annihilation 79−91525
Ni_5Ge_{1-x}, liq., ang. distrib. of positron annihilation 77−55848
NiSb, dilute alloy, impurity-induced vacancy clustering 79−99972
Pb, Doppler broadening, 4.2 to 600K 79−47540
Pb, energy of form. of monovacancies, positron annihilation obs. *(German)* 78−71721
Pb, gamma-ray impact, absolute pair production cross-section meas. 78−43958
Pb, plastically deformed, annealed, positron trapping rate, 4-100K 78−31275
Pb, positron annihilation, evidence for microporosity and dislocations 79−78786
Pb, positron trapping by vacancies, high resolution lifetime meas. 77−1759
Pb-Cd(Tl) alloys, positron annihilation, evidence for microporosity and dislocations 79−78786
Pb-In, CPA interpretation of positron annihilation *(Russian)* 80−11507
Pb-Ni-Si, metallic glass, electron irrad., positron annihilation radiation, angular correlation study 78−84678
Pb-Tl, vacancies, positron capture, function of Tl concentration *(German)* 80−49213
Pb-Tl alloys, positron trapping in vacancies, varying concentration effects *(German)* 80−25477
Pd and Pd-Ag(Cd)(In)(H), electronic struct. from annihilation quanta ang. distribs. 77−66107
Pd, influence of adsorbed H on positron lifetime spectra 80−25480
Pd-Ag, influence of adsorbed H on positron lifetime spectra 80−25480
Pd-Ag(Cu) systems, positron annihilation, absorbed H_2 effect *(Russian)* 79−91528
Pd-Cu, influence of adsorbed H on positron lifetime spectra 80−25480
Pd-Fe, dil., plastically deformed, positron annihilation study of recovery of crystal, imperfections *(German)* 77−85835
Pd-H, degree of positron localisation on components 77−85833
Pd-Si amorphous alloy, positron annihilation exam. of crystallisation 79−43061
$Pd_{1-x}Ag_xH_n$, positron annihilation examination of electronic structure *(German)* 77−69931
PdH_x, positron localisation *(Russian)* 77−66555
Pt, neutron damage, positron annihilation 80−65056
Pu, liq., hard-sphere model, phys. prop. meas. interpret., adjacent solid phase implications 77−19866
RbBr crystals, positron annihilation, Doppler broadening 80−40180
Re-Ir (1 wt.%), positron annihilation, photon ang. distrib. meas. effect of deformation, annealing temp. *(Russian)* 78−35220
ReO_3, positron annihilation, Fermi surface shape 79−46997
SF_6 electron scavenging in positron spur in nonpolar liqs. 79−100421
SF_6, liq., positronium bubble states, temp. depend. 80−108293
Sb, positron lifetime meas., comparison with theory 77−63483
Se, amorphous, trigonal and α-monoclinic, positron lifetime and angular correl. curves 79−11484
Se, positron lifetime meas., comparison with theory 77−63483
Se, trigonal and amorphous, positron lifetimes, positronium form. 80−60711
Si, anomalous passage of positrons, expt. 79−95052
Si, anomalous positron passage mechanism *(Russian)* 77−85836
Si, electron beam irradiation, 2.3 MeV, positron annihilation exam. of radiation defects *(Russian)* 78−34542
Si, electron irrad., influence of high temp. annealing 78−76552
Si, electron irradiated, positron annihilation 78−87713
Si, electron-irradiated, annihilation of positrons 77−55847
Si, electron-irradiated, positron annihilation 78−48256
Si, electron-irradiated crystals, positron trapping, temp. depend. 80−104009
Si epitaxial film, containing struct. defects formed during growth, positron annihilation 80−93433
Si, laser irradiated, positron annihilation crystal struct. imperfection monitoring 80−11506
Si, mag. field effect, positronium states 77−16417
Si, mobility of positrons, drift vel. meas. 78−6808
Si, neutron irradiated, influence of defects and temp. on positron annihilation 77−4699
p-Si, positron annihilation, effects of applied elec. field *(German)* 78−72634
Si, positron annihilation, effect of doping 79−24385
Si, positron implantation profile and mobility, elec. field effects 77−48273
Si, three-dimensional electron-positron pair momentum density from positron annihilation meas. 79−43059
n-Si:Ar(P), single cryst., positron annihilation parameters, energy-band struct. on surface in free-electron approx. 79−15555
n-Si:B, ion-implanted damage, positron annihilation and sheet resist. meas. 80−35003
Si:B(P), positron annihilation in 100 and 111 orientation 77−44083
Si:P, ion implantation doped, positron annihilation meas. 78−14380
SiO_2 glass, crystallinity positron annihilation study 78−72629
SiO_2 glass, heat treatment study by positron annihilation 78−55812
SiO_2 powder, positron annihilation quanta ang. distrib. 77−28642
SiO_2, powder, positronium fine struct. interval meas. by Zeeman transitions 78−95616
α-SiO_2, quartz, positron annihilation, positronium effective mass and annihilation probability 79−28858
α-SiO_2, quartz, positron annihilation, positronium quasiparticle damping effect on momentum distrib. 79−28859
SiO_2 samples with high specific surface areas, positron lifetime meas. 78−92141
$Sm_{0.8}Gd_{0.2}S$, valence transition, positron annihilation study 80−15454
SmS, valence transition, positron annihilation study 80−15454
Sn, (100) surface, clean and O_2 exposed, slow positron studies, positronium formation 80−93429
Sn, Fermi momentum and core electron contribution 77−81173
β-Sn, Fermi surface, electronic momentum densities, positron annihilation obs. 80−6696
Sn, gamma-ray impact, absolute pair production cross-section meas. 78−43958

positron annihilation in liquids and solids continued
Sn, positron annihilation in fine particles, surface trapped states 80−84800
Sn, positron annihilation parameters, temp. depend. 77−85832
Sn, thermally induced vacancies, positron trapping 80−89083
Ta, plastic deform. effect on positron annihilation and supercond. transition *(Russian)* 77−39993
Ta, positron annihilation and vacancy formation 80−16119
Ta, positron trapping and annihilation at vacancies 80−29823
Ta, vacancy formation and migration energies, positron annihilation meas. 77−84739
Ta-H, degree of positron localisation on components 77−85833
Ta-Ir (1 wt.%), positron annihilation, photon ang. distrib. meas. effect of deformation, annealing temp. *(Russian)* 78−35220
TaH_x, positron localisation *(Russian)* 77−66555
TeO_2-Fe_2O_3 system, glass structure 79−90562
Th_3As_4, positron annihilation, mean ionic radius calc. 79−15550
Ti, deform. and H_2 inclusion effect on annihilation γ-ray ang. correl. curve shape 78−31273
Ti, pure (0.9998), positron annihilation study of defects 80−3281
Ti-Al-Mo-Sn alloy, elastically and plastically deformed, Doppler broadening meas. of positron annihilation 80−21038
Ti-Fe (1.4 wt.%), polymorphic transform. due to plastic deform., positron annihilation 80−79939
TiC, calcs. of 2γ-ang. correlations and Compton profiles 78−39624
$TiH_x(D_x)$, comp. effects *(Russian)* 78−6807
$TiH_x(D_x)$, electron-positron annihilation and X-ray K-spectra *(Russian)* 77−1761
TiO_3, semicond.-metal transition, positron annihilation study 78−15246
Tl, positron lifetime meas., comparison with theory 77−63483
U, liq., hard-sphere model, phys. prop. meas. interpret., adjacent solid phase implications 77−19866
U, vacancy formation and phase transformation by positron annihilation 80−49215
UAs_2, and U_3As_4, positron annihilation, mean ionic radius calc. 79−15550
UAsS(Se)(Te), positron annihilation ang. distrib., valence electrons and Fermi surface 77−28093
UAs(Se)(Te), positron annihilation, mean ionic radius calc. 79−15550
UP_2, positron annihilation, mean ionic radius calc. 79−15550
$UP_2(Sb_2)(As_2)$, positron annihilation ang. distrib., valence electrons and Fermi surface 77−28093
USb_4, positron annihilation, mean ionic radius calc. 79−15550
V, Doppler broadened positron annihilation lineshapes, prevacancy lattice expansion 78−27349
V, electron irradiated, positron study 78−76555
V, electron-irradiated, positron annihilation study 80−70259
V, electronic density of states, effective mass, electron-phonon interaction, Coulomb pseudopot. *(Russian)* 78−26804
V, plastic deform. effect on positron annihilation and supercond. transition *(Russian)* 77−39993
V, positron annihilation, temp. depend. 78−56540
V, positron annihilation and vacancy formation 80−16119
V, single cryst., surface investigation by positron annihilation 79−15552
V-D alloys, positron annihilation radn. angular correlation, electronic struct. study 79−43058
VH_x, positron annihil. lineshape Doppler broadening, H conc. and temp. depend., 20-500K 79−61463
VO_2 single crystal, positron annihilation, metal-insulator transition obs. 77−85830
V_3Si, Fermi surface, positron annihilation meas. 79−87039
V_3Si, Fermi surface determ. by γ-ray angular correl. meas. 79−4869
V_3Si, Fermi surface determ. by positron annihilation 80−2326
V_3Si, Fermi surface studies by the positron annihilation technique 79−82515
V_3Si, Fermi surface topology, positron annihilation meas. 79−56117
V_3Si, positron annihilation lifetime meas. 79−19946
V_3Si, press. depend. of positron lifetimes 78−11015
V_3Si, quasi-one-dimens. band struct. 78−19596
^{48}V positron source prep. for annihilation radiation lineshapes, positron lifetimes meas. 80−876
W, positron annihilation and vacancy formation 80−16119
W, positron lifetime meas., comparison with theory 77−63483
W, positron trapping and annihilation at vacancies 80−29823
W-Ir (1 wt.%), positron annihilation, photon ang. distrib. meas. effect of deformation, annealing temp. *(Russian)* 78−35220
W-Mo alloys, positron interactions with component atoms *(Russian)* 77−63486
Xe, ortho-positron quenching rate critical slowing down near gas-liquid transition 77−24907
Y-H, degree of positron localisation on components 77−85833
YH_x, positron localisation *(Russian)* 77−66555
Zn, anisotropy of free-electrons momenta distribution, positron annihilation meas. 77−36309
Zn, electron momentum distrib., neutron-induced defects, positron annihilation study, for single cryst. 80−71508
Zn, external electric field effect on ang. distribs. 77−77317
Zn, HCP struct., selection rule, electron momentum distrib. rel. to positron annihilation 80−39495
Zn, high current densities, ang. distrib. of annihilation quanta *(German)* 77−12462
Zn, positron annihilation, 4.2-500K, Doppler broadening meas. 78−43957
Zn, positron annihilation in plastically deformed sample, electric field effect 79−69899
Zn, positron-electron annihilation spectra, Doppler broadened 79−65953
Zn, single crystals, positron trapping by edge dislocations, produced by bending 78−80606
Zn-Al (22 wt.%), positron diffusion and trapping at grain boundaries 80−39157
Zn-Fe alloys, dil., positron-electron annihilation spectra, Doppler broadened 79−65953
ZnSe, positron annihilation study 80−60713
α-Zr 77−68999
Zr, elastically deformed, positron annihilation, Doppler broadening study 79−69900
α-Zr, vacancy recovery following 1.5 MeV electron irrad., positron annihilation meas. 77−47485

positron scattering *see electron impact*

positron states
alkali halide, binding energies of positron to F and F′ colour centres 78−87667
alkali halide, positron localisation at negatively charged centres 77−8055
alkali halides, positron annihilation, expt. techniques, positron states, book contrib. 80−2894
benzene molecules, bound positrons, time spectrum of positron annihilation 78−42248
density functional approach to electron and positron states 79−56107
electron gas, screening of positron, contribs. of different partial waves 77−11878
electron-positron correl. effects, positron annihilation in solid with tightly bound electrons 77−73184
elemental semiconductor, positron thermalisation, theory *(Russian)* 78−84170
imperfect solids, positron-defect interaction and annihilation charact., book contrib. 79−99978
inelastic positron scatt. in electron gas, plasmon excitation 80−92843
ionic cryst. positron-containing M-centre, struct. 80−49220
ionic crystals with defects, separation of positron and positronium states 78−27351
metal, plasmon model for image-potential-induced surface state, appl. to positron surface states 79−19559
metal, positron density distribution, temp. effects 78−47739
metal, positron self-trapping conditions 78−47338
metal, positron thermalisation by non-equilibrium statistical operator method 79−15551
metal, positron trapping at defects, positron-phonon scatt. effect 77−89736
metal, positron-phonon scatt. effect on positron trapping at monovacancies 78−26829
metal, strength of positron-phonon interaction 77−15796
metal surface, image-potential-induced states, plasmon model 79−78147
metal-metal contacts, positron diffusion, ang. distrib. of annihilation photons meas. 79−8207
metallic alloys, ordered and disordered, positron localisation 78−79962
metals, lattice defects, positron annihilation study, book contrib. 79−99977
metals, positron thermalisation on cond. electrons *(Russian)* 79−19558
metals, positron-phonon interaction through cond. electrons *(Russian)* 80−29126
metals and alloys, electron momentum density, positron annihilation meas., book contrib. 79−99976
metals and alloys, positron annihilation, theoretical and expt. techniques, book 79−99975
negative ions, positronium formation, Doppler broadened positron annihilation line shapes 80−45164
nitrobenzene molecules, bound positrons, time spectrum of positron annihilation 78−42248
polybutadiene, C black filled, positron annihilation and positronium form. 79−28856
polyethylene, delayed electrical response obs. in positronium form. 77−20273
polyethylene, elec. field effect on positron annihilation 79−4868
prethermalisation trapping model, appl. to Pb 77−43541
semiconductors, defective surface layer, surface positron states 80−75526
surface, positron-electron correlations, RPA calc. 80−40181
surface, thermal activation meas. of positron binding energies 79−95371
surface positron states, emission of positrons, positronium 80−54655
Ag (100) and (111) surfaces, positronium form. due to slow positron trapping 80−107748
Ag, positronium formation at (100) surface 79−82654
Al, CC vacancy, electron and positron densities and temp. depend. of positron lifetime 78−19001
$Al_xGa_{1-x}As$:Si, charge state of impurity atoms, positron annihilation meas. 78−39062
γ-Al_2O_3, magnetically quenchable positronium-like systems 79−87065
Au, positron lifetime and annihilation lineshape from 4.2K to MP 77−20272
B, electron structure study by positron annihilation 80−16117
C black, positron annihilation and positronium form. 79−28856
CaF_2, positron annihilation polarisation effects, electron momentum distribution 80−55225
CaF_2:Sm, positron annihilation polarisation effects, electron momentum distribution 80−55225
Cd, positron lifetime and annihilation lineshape from 4.2K to MP 77−20272
Cu (111) surface, negatively biased, positron impact, positronium form 80−35024
Cu (111) surface, positronium form. due to slow positron trapping 80−107748
$Ga_{1-x}Al_xAs$-GaAs:Si, momentum distrib. of valence electrons, positron annihilation meas. 79−51530
GaAs, positron annihilation, mag. field effect, positronium states 77−16417
GaAs:Si, charge state of impurity atoms, positron annihilation meas. 78−39062
GaAs:Si, momentum distrib. of valence electrons, positron annihilation meas. 79−51530
KBr(Cl), positron ang. correl., cryst. orient. depend., positron states and ionic distortion 77−63484
KCl, and KCl-AgCl, surface positron and positronium states, positron annihilation expts. *(Russian)* 78−39623
KCl, positronium states near defects in cationic sublattice 80−16121
KCl:Ag positron annihilation and impurity states 80−97375
KCl:AgCl, positron annihilation charact., positronium state form., X-irrad. effects 77−4700
KCl-KBr mixed crystal, containing defects, mag. quenching of positronium states 77−8680
Mg positron trapping and bound states 80−2367
Mo, positronium-like states *(Russian)* 77−89737
NaCl, positron ang. correl., cryst. orient. depend., positron states and ionic distortion 77−63484
NaCl, positronium-like states, ang. correlation of photons from positron annihilation 77−36310
NaCl:Ag, positron annihilation and impurity states 80−97375
NaCl:AgCl, positron annihilation charact., positronium state form., X-irrad. effects 77−4700

positron states continued
NaF, positronium-like states, ang. correlation of photons from positron annihilation 77−36310
Nb, positron trapping and annihilation at vacancies 80−29823
Pb, plastically deformed, annealed, positron trapping rate, 4-100K 78−31275
Se, amorphous, trigonal and α-monoclinic, positron annihilation 79−11484
Se, trigonal and amorphous, positron lifetimes, positronium form. 80−60711
Si, electron-irradiated, annihilation of positrons 77−55847
Si, positron annihilation, mag. field effect, positronium states 77−16417
Sn, (100) surface, clean and O_2 exposed, slow positron studies, positronium formation 80−93429
Ta, positron trapping and annihilation at vacancies 80−29823
TiC, positron wavefunction calc. 79−99512
W, positron trapping and annihilation at vacancies 80−29823

positronium
see also electron pairs
alkali halides, cryst., positron lifetime and Doppler broadening spectra 79−8208
annihilation in field of plane EM wave *(Russian)* 80−14259
annihilation in strong EM field *(Russian)* 77−83769
annihilation in strong magnetic fields of neutron star 79−17007
annihilation line shape Doppler broadening, lifetime spectroscopy, formation inhibition by solvated electron precursor scavenging 80−93784
Bethe-Salpeter equation, Coulomb like kernel 78−93831
biexcitons, symmetric trial function 77−68142
bound state formalism, modified functional formalism, self-energy and renormalisation effects 77−26463
bound-state solutions in relativistic two-body formalism 78−13443
break-up of relativistic positronium in atomic field *(Russian)* 77−46659
bubbles in liq. He, density profiles 79−55952
carbon tetrachloride in benzene, positronium inhibition by Cl 77−8678
chemical structure studies with positrons and mesons; review 79−79277
chemistry, in soln., form., inhibition and reactivity 77−44499
chemistry, inhibition in aq. solns. 78−40070
chlorobenzenes in benzene, positronium inhibition by Cl 77−8678
crystallography, vacancies in cryst. materials, determ. of conc. using positron annihilation *(French)* 79−69901
cyclodextrin, α and β, positronium decay, test of freq. vol. model 78−19592
cyclohexane-chlorobenzene, soln., positronium formation inhibited by chlorobenzene 79−50170
decay, asymmetrical, two- and threefold polarisation correlation of photons 80−57536
decay, in strong mag. fields, 10^{12} Gauss 79−88578
decay, theory and relativistic wave function corrections 77−10791
decay rate, $O(\alpha)$ corrections, graph theory 77−31029
decay rate in vacuum 79−13844
determination in matter, Compton profile comparison to γ-annihilation radiation ang. correlation *(Russian)* 77−55845
dielectric solids, quasiequivalence of annihilative e^+e^- and ionisative e^-e^- interactions 78−72633
$e^+e^-e^+$, three-body Coulomb interaction, adiabatic representation 79−31640
elastomers, vulcanised, positron annihilation and positronium destruction 78−35221
electrons and positrons as quantum rotators 79−35981
electrons and positrons in dense gases, review 80−103106
energy interval measurement by obs. Zeeman transition in microwave spectra 80−69274
energy levels, radiative corrections 80−32100
epoxy resin, rubber modified, positron annihilation 80−29825
ethylenediamine-H_2O mixtures, inhibition of Ps form. by NO_3^- ions 78−95988
exotic atoms, conf., Erice, Sicily, (1979) 80−67939
fermion-antifermion eqn., static interaction limit Breit eqn. 78−62963
formation, by positron scatt. from Ne, (Ar) atoms 78−9283
formation, e^+ + H charge exchange collision, two state approx. 77−79710
formation, in liq. hydrocarbons, mechanism, rel. to electron solvation 78−70980
formation, in mixtures of competitive electron acceptors 80−28120
formation, quenching and inhibition in Ag and Cd salt solns. 78−15690
formation and quenching in Ar-O_2 mixtures, orthopositronium quenching cross section determ. 80−74261
formation at metal surfaces 79−13845
formation at surfaces 79−95371
formation cross sections in He, diluent gas effect 80−5640
formation in organic liq. mixtures, spur process 78−1113
formation in polar liquids, unsolvated electron effects 78−17826
formation in positron+alkali metal atom collisions, first Born approx. 80−83525
formation in positron+alkali metal atom collisions, pseudopot. calcs. 80−83524
formation in positron scattering by H, He atoms 79−89772
formation inhibition by Br substituted benzenes 80−93783
ground state, fine struct. interval, collisional density shifts 77−34788
ground state, fine struct. interval, NMR meas. 77−34787
ground state, hyperfine struct. due to exchange and virtual photons 79−36804
ground state hyperfine splitting, logarithmic contributions *(Russian)* 79−94114
ground state splitting, appl. of new relativistic two-body formalism 79−2933
ground state splitting, more $\alpha^6 \ln\alpha$ terms 77−14621
$H(1s)+e^+ \rightarrow (e^+e^-)(nlm)+H^+$, highly excited states rearrangement collisions 79−59564
halobenzenes, benzene solns., positronium form., additive effects 79−43610
halocarbons, benzene solns., positronium form., additive effects 79−43610
hyperfine interval, α^2 corrections, three-photon virtual annihilation contrib., QED calc. 78−41451
hyperfine press. shift in buffer gas, calc. 77−557
hyperfine quadratic shift in electric field, pressure dependence 78−13442
hyperfine splitting, anomaloous contribs., radiation gauge 77−83771
hyperfine splitting, contrib. of ground state quasipot. approach 79−59606

positronium continued
hyperfine splitting 78−74806
hyperfine splitting and decay rates, contrib. from annihilation kernels 79−89812
hyperfine struct., three photon virtual annihilation 77−68143
hyperfine structure, order-$\alpha^4 R_\infty$ contribs., radiative corrections calcs. 79−76538
inert gases, dense, positronium annihilation rate 78−55258
inhibition processes of positronium formation, role of solvation properties of solvents 80−93786
ionic crystals, anomalous props. of positronium atom, exciton state 78−2433
ionic crystals with defects, separation of positron and positronium states 78−27351
lifetime in benzene solns. of Fe and Gd dipivaloylmethanates 77−38570
lifetimes in He-SiO_2(MgO) mixtures 78−42247
liquid, positronium pick-off annihilation, improved bubble model 80−93424
magnetic quenching of substates, positronium capture model 80−1090
metal, formation of positronium in 'metallic' pores 78−35222
metallic surface, surface traps and vacancy trapping, slow positron obs. 79−87522
metals, surface positronium formation, stopping distance, positron-phonon interactions 80−96582
methane, gas density fluctuations, orthopositronium annihilation rate depend. 78−37773
mixed molecular crystals, formation 78−91647
molecular crystals, impurity effects on positronium formation 77−66554
molecular solids, existence of positronium, meas. on solid hydrocarbons 77−59638
molecular substances, positron annihilation and phase transitions, review 78−95614
molecule complex, approx. MO theory 77−23583
negative ion, autoionisation states, complex rotation method 79−81307
neutron-irrad., void annealing, positron annihilation obs. 77−76469
nitrobenzene, quenching and inhibition of orthopositronium 80−35002
nonpolar liquids, enhancement of positronium form. caused by scavenging of highly mobile positive holes 80−69265
nonpolar solvent, o-Ps yield in chlorinated ethanes, ethenes and cyclohexanes 79−70357
nonsolvated electron reactions, positron annihilation method 77−81417
nylon, positronium form. and decay, elec. field effect 80−97369
optically stimulated electron-positron annihilation 77−57519
ortho-positronium self-trapping in dense fluid He 77−10793
orthopositronium, decay rate, prod. by slow positrons 78−42249
orthopositronium, mean lifetime in vacuum 77−83770
orthopositronium, vac. polarisation corrections in muonic molecules 78−78841
orthopositronium, vacuum decay rate, formed in MgO-lined cavity 79−18320
orthopositronium, vacuum decay rate 78−46468
orthopositronium annihilation, photon ang. correl. *(Russian)* 78−22059
orthopositronium decay into axions 78−78125
orthopositronium decay rate, double-vertex contribution improved error estimate 77−6964
orthopositronium decay ray meas. by Michigan apparatus 80−69274
orthopositronium quenching by O_3, meas. by two-photon coincidence rate difference technique 80−74262
orthopositronium three photon decay rate, vertex angle and electron self-energy radiation corrections *(Chinese)* 77−75342
oxidation in aq. soln., positron hydration energy 78−61039
oxide powders, muonium and positronium form. 79−56679
para- and orthopositronium prod. by electron accelerators *(Russian)* 79−13846
Perspex, positronium form. and decay, elec. field effect 80−97369
photoproduction of relativistic parapositronium, and muonium perturbation expansion *(Chinese)* 79−49432
polarisation effects in tripositronium decay into electron and photon *(Russian)* 80−58421
polyethylene, positron implantation profile, electric field depend. 79−11483
polyethylene, positronium form. and decay, elec. field effect 80−97369
polystyrene, positronium form. and decay, elec. field effect 80−97369
positron annihilation, positron basic props., annihilation line shape, positronium formation, book contrib. 80−2893
positron two-photon annihilation coincidence technique, difference mode 78−54516
positronium halides, [X^-; e^+], electronic struct., annihilation characts., HF calc. 77−50567
positronium halides, [X^-; e^+], electronic struct., annihilation characts., HF calc. 77−50568
positronium hyperfine struct., $m\alpha^6$ contribs. from two photon virtual annihilation 78−89642
positronium nitrate, [NO_3^-;e^+], existence, Hartree-Fock-Roothaan calcs. 80−83254
positronium nitrite, [NO_2^-;e^+], existence, Hartree-Fock-Roothaan calcs. 80−83254
production in nuc. monopole transitions 77−54635
QED predictions rel. to expts. 77−58213
quartz, fused, positronium form. and decay, elec. field effect 80−97369
relativistic beam intensity determ. by Monte Carlo method *(Russian)* 77−388
relativistic electron pair model of nucl. particles 79−45042
relativistic positronium atom stimulated form. in high-intensity opposite EM wave 80−9766
relativistic two-fermion equations with instantaneous potential 80−101918
semiconductor, anomalous props. of positronium atom, exciton state 78−2433
sodium dodecylsulfate, micellar solution, critical micelle concentraion for thermalized positronium formation 79−96345
solar flares, 0.51 MeV gamma-ray line prod. by positronium form. and decay 77−13292
spin conversion by phosphorescent impurities in gases 77−31030
succinonitrile, defects in plastic phase, positron annihilation obs. 80−11504
superpositronium, form factor corrections, short-dist. mag. moment behaviour of electron 77−83772
surface positron states, emission of positrons, positronium 80−54655
p-terphenyl, cyclic hydrocarbon admixtures, positronium lifetimes meas. 78−19595

positronium continued
p-terphenyl, positronium form. at elevated temps. 77−89473
2,2,4-trimethylpentane-chlorobenzene, soln., positronium formation inhibited by chlorobenzene 79−50170
tripositronium, probability of decomposition into an electron and a photon *(Russian)* 79−22866
tripositronium decay into electron and two photons *(Russian)* 78−62960
tripositronium ion splitting into electron and two photons, polarisation effect *(Russian)* 79−72448
vacuum polarisation, accurate fourth order computation by VAC4 subroutine 78−89639
Vycor glass, positronium-surface interaction in pores 78−27347
water-dioxan mixtures, positron annihilation, o-positronium pick-off quenching 79−24386
$e^+ + e^- + e^-$ binding energy 77−27137
e^+A^-, positron-containing ground-state negative ions, self-consistent Fock field 80−47888
(e^+e^-) atom, Coulomb disintegration, cross sections and energy spectra *(Chinese)* 80−102589
$e^+e^-e^-$, two-electron at., three-body problem, binding energy 79−3372
$\bar{p}p$ atoms, quasiatomic and very energetic γ-rays 80−42574
$\pi^0 \rightarrow \gamma$Ps, Ps=orthopositronium, π^0 lifetime, O(α) EM correction *(Russian)* 79−45089
Ag (100) and (111) surfaces, positronium form. due to slow positron trapping 80−107748
Ag, positronium formation at (100) surface 79−82654
$Al_xGa_{1-x}As$:Si, charge state of impurity atoms, positron annihilation meas. 78−39062
γ-Al_2O_3, magnetically quenchable positronium-like systems 79−87065
Ar, positron scatt., positronium form. cross-section calcs. 78−9283
$CN^-.e^+$, positron energy levels, rel. to Rydberg levels of Na, NO 79−86089
Cl^- soln. inhibition of o-Ps formation 80−1089
Co, positronium form. in two-photon positron annihilation 79−61462
Cu (111) surface, negatively biased, positron impact, positronium form 80−35024
Cu (111) surface, positronium form. due to slow positron trapping 80−107748
Cu, positronium form. in two-photon positron annihilation 79−61462
Fe, positronium form. in two-photon positron annihilation 79−61462
FeTi, positronium form. after hydrogenation-dehydrogenation cycling and annealing 80−18947
GaAs, positronium-like states, low temp., ang. correl. of annihilation photons 78−76549
GaAs:Si, charge state of impurity atoms, positron annihilation meas. 78−39062
H, positron elastic scattering, S-wave phase shifts calc., least squares method 80−106374
H, positron P-wave scatt., elastic and positronium form. cross sections 77−3468
H+positron, charge exchange, excited positronium states form. 78−58873
H+positronium elastic scatt., electronic S=1 state 77−512
H+positronium$\rightarrow H^+$+positronium$^-$, low energy, field theoretic approach 77−10790
$H_2O(D_2O)$, positronium formation, isotope effects 80−93432
$H(1s)+e^+ \rightarrow (e^+e^-)1s+H^+$, first-order approx. 79−55006
He, electron and positron total scatt. cross sections, positronium form. 78−62916
He, fluid, positronium and electron bubbles, density-functional theory 80−80016
He, gas, positron and positronium decay rates at high densities 77−54636
He, orthopositronium decay, in gas, liq. and solid phase 77−39713
KCl, and KCl-AgCl, surface positron and positronium states, positron annihilation expts. *(Russian)* 78−39623
KCl, delocalised positronium, 4.2K, direct obs. γ-spectra 78−88235
KCl, positronium states near defects in cationic sublattice 80−16121
Li+positron, positronium formation in highly excited states, first Born approx. 80−58420
MgO, powder, positronium fine struct. interval meas. by Zeeman transitions 78−95616
Mn, positronium form. in two-photon positron annihilation 79−61462
N_2, gaseous, positronium yields at 77K 79−98254
N_2-Ne mixture, gaseous, positronium yields at 77K 79−98254
NaF, delocalised positronium existence at room temp. 78−76546
Ne, electron and positron total scatt. cross sections, positronium form. 78−62916
Ne, positron scatt., positronium form. cross-section calcs. 78−9283
Ni, positronium form. in two-photon positron annihilation 79−61462
No_3 -Cl^- soln., inhibition of o-Ps formation 80−1089
PsH autodissociating Rydberg states 79−76539
PsH, positronium hydride, resonant and ground states 78−62964
PsO, stability and dissoc. energy, restricted HF and correlation correction calcs. 77−54634
PsS, stability and dissoc. energy, restricted HF and correlation correction calcs. 77−54634
SF_6 electron scavenging in positron spur in nonpolar liqs. 79−100421
SF_6, liq., positronium bubble states, temp. depend. 80−108293
Se, trigonal and amorphous, positron lifetimes, positronium form. 80−60711
Si, electron-irradiated, positron annihilation 78−48256
SiO_2, powder, positronium fine struct. interval meas. by Zeeman transitions 78−95616
α-SiO_2, quartz, positron annihilation, positronium quasiparticle damping effect on momentum distrib. 79−28859
α-SiO_2, quartz, positron annihilation, positronium effective mass and annihilation probability 79−28858
Sn, (100) surface, clean and O_2 exposed, slow positron studies, positronium formation 80−93429
V, single cryst., surface investigation by positron annihilation 79−15552
Xe, positronium formation in Xe gas near crit. pt. 79−86091

positrons
see also electron pairs; electrons
atomic anions positron complexes, ground and excited states theoretical studies 80−42934
beam, relativistic, collimation in single cryst. 79−23669
beam generation at low energy 80−5422
Bragg reflection from Al and Cu surfaces obs. 80−103221
bremsstrahlung, anomalous reduction in single cryst. 80−7433

positrons continued
classical Lagrangian theory with radiative reaction, monopoles and positrons in Rohrlich formalism 79−72
coherent radiation 77−76476
compact extragalactic radio sources, electron-positron pair prod. rel. to Faraday rot. 78−73770
cosmic ray positrons, galactic, primary source, prod. rate, and escape probability 80−109319
electron-positron storage ring, elementary particle physics *(Polish)* 79−76218
emission in Pb+Pb(U) collisions, evidence for strong field QED processes 78−93833
energy spectra and ang. distrib., 0.2-2 GeV electron conversion on W targets 78−86713
formation, in superheavy ion+atom collision 78−62873
galactic cosmic ray positrons, annihilation and gamma radiation spectrum 79−44309
gases, molecular, total scatt. cross sections for intermediate-energy positrons 80−91692
heavy ion collisions, positron prod. 78−50198
heavy ion collisions, positron prod. meas. 78−50197
heavy-ion collisions, critical distance for spontaneous positron prod. 77−14159
imaging instrumentation for physiological functions 78−24196
lifetime spectra, anal. using DBLCON version of POSITRONFIT with nonGaussian prompt 78−33359
magnetic moments of e^- and e^+ compared 77−18365
metal surface, slow-positron emission 78−95079
mobility edge in gaseous He 80−83880
mobility in uniform elec. field 80−9793
molecule complex, approx. MO theory 77−23583
momentum distribution in electron gas 79−56146
planar channelled, Compton scatt. anal. 79−7639
polarised positron, electron production by colliding photon beams in storage ring 80−5426
positron+H(He), second-order nonadiabatic polaris. pot. for elastic scatt. 79−22836
production in heavy-ion collisions at high-energies 77−27137
radiation therapy using π^-, in vivo beam localisation by positron activation 80−72316
radiative damping effect for ultrarelativistic channelled particles 78−67758
relativistic, EM energy emission spectra *(Russian)* 79−78785
relativistic positron channelling, radiation intensity and spectrum calcs. 80−2098
slow, time bunching for annihilation lifetime and pulsed laser photon absorpt. expts. 80−95492
slow beam production, using MgO-coated moderator 79−17557
slow positron form. in MgO-coated moderators 80−62796
slow positrons, narrow beam emission from negative electron affinity surfaces 80−89091
source, Au moderator surface preparation for increased yield 80−61011
source, for positron annihilation lifetime expts., using Na^{22} ion-implantation in Cu 79−45489
superheavy collision system, radiative processes, search for positron emission 80−63752
superheavy collision systems, positron prod., internal conversion 80−5168
superheavy ion-atom collisions, quasiats., K-vacancy form., positron emission 80−63753
total collision cross sections, for electron- or positron-atom scatt. in curved axial mag. field, transmission meas. 78−1082
ultrarelativistic collimated beam, emission spectra in Si 80−7434
e^+A^-, positron-containing ground-state negative ions, self-consistent Fock field 80−47888
e^+Br^-, positron-containing ground-state negative ions, self-consistent Fock field 80−47888
$e\bar{e}\nu_e\bar{\nu}_e$ mixture, covariant transport eqns., collision terms from Weinberg Salam theory 77−74315
e^+I^-, positron-containing ground-state negative ion, self-consistent Fock field 80−47888
μ^-e^+ pair production in ν_μN interaction *(Russian)* 80−91076
Ag, electron (positron), impact, K- and L-shell ionisation, Kα and L X-rays meas. 80−99575
$(CN^-.e^+)$ complex, ab initio LCAO SCF calc., positron affinity and excitation energy 79−49945
$(F^-.e^+)$ complex, ab initio LCAO SCF calc., positron affinity and excitation energy 79−49945
H+positron, charge exchange, excited positronium states form. 78−58873
$^{208}Pb+^{208}Pb$, 14 GeV, nonnuclear positrons creation 79−30847
$^{238}U+^{208}Pb$, 14 GeV, nonnuclear positrons creation 79−30847
$^{238}U+^{238}U$, 14 GeV, nonnuclear positrons creation 79−30847
W crystal, EM showers produced by electrons, positron spectral distribution *(Russian)* 80−55218
^{122}Xe-^{122}I short-lived positron emitter generator 79−100740

postal services
automated TLD processing and dose record keeping service 80−12267

potassium
see also nuclei with .....:
absolute zero isotherms and polymorphic transition 79−73310
abundance in Archaean granites from NE.Minnesota 78−61356
adion-surface interaction energy, density formalism calcs. for Al and W surfaces 78−68069
adlayer effect on CO and H_2 adsorption and desorption on Fe(100) 80−71573
adsorbed film on Ni (100), plasmon losses in electron energy loss spectra 79−61480
adsorbed layers on W (112) planes, flicker noise field emission obs. 78−26774
adsorbed on Pt(111), UPS and XPS meas. 80−95675
adsorbed on W, field emission flicker noise power 80−59795
adsorbed on W(112) planes, temp. depend. of noise spectral density functions 78−2992
adsorption, on Re, work function changes, FEM obs. 77−72772
adsorption, on Re(10$\bar{1}$0) surface, electron-adsorption props. 79−33192
adsorption, on transition metal carbides, adsorpt. energy, thermionic emission 77−7978
adsorption of K on Fe(110), UPS and XPS meas. 80−95675
adsorption of W, average work function change 79−28190

potassium continued
adsorption on Fe(100), adsorbate coverage determ. by LEED, AES and XPS 80−103566
adsorption on Fe (110), LEED, AES, UPS and XPS meas. 79−77919
adsorption on Ge (111), effect on surface elec. props. 79−90880
adsorption on Mo (100) and oxidised Ta (112), effect on emission props. and work function 78−11060
adsorption on Ta and Mo, work function depend. on surface coverage 77−11788
adsorption on W, field emission flicker noise, coverage depend. 78−35262
adsorption on ZnO (000$\bar{1}$) of alkali metals, anomalous behaviour of Na 78−79883
analytical determ. of K content of single bubbles in annealed W wire 78−64909
anharmonic lattice dynamics 78−18720
arc lamp, vapour, as optical pump source in ND:YAG space communications laser 79−86261
Ashcroft pseudopotential, unified study of props. 80−39239
atmosphere aerosols over tropica N.Atlantic Ocean, water-soluble K, Ca and Mg contents 80−72598
atmospheric aerosol, K-rich, emission by tropical forest *(French)* 79−100551
atom, 1st reson. level, effective electron-ionis. cross sections, plasma discharge method 78−13603
atom, $4^2P_{1/2}$ resonance substate, disorientation cross-section, Zeeman scanning obs. 80−42988
atom, ^2P fine struct. splittings, Hartree-Fock calcs. 77−10606
atom, absolute optical electron-impact excitation functions 80−18933
atom, associative ionis. from resonance levels 77−30978
atom, collisional depopulation of high-lying P state 77−3447
atom, cross section depend. of many-photon ionisation on light polarisation 77−42294
atom, D Rydberg state emission oscill. strength minima 80−32662
atom, damping const. in acetylene-air flame, Lorentz collisions, mag. field effects 80−66805
atom, diamag. Zeeman shift of S,D Rydberg states, two-photon absorpt. 77−23461
atom, elastic electron scatt., momentum-transfer cross sections 79−25777
atom, electron affinity, model pot. CI and SCF calcs. 77−38609
atom, electron collision cross sections determ. from plasma DC conductivity 77−3469
atom, electron elastic and inelastic scatt., 54.4-217.7 eV, 2-145° 80−1067
atom, electron excitation cross sections for six autoion. config., Born approx. calc. 78−25713
atom, electron impact excitation, combined classical theory and free fall model 79−98229
atom, electron impact excitation, identification of low energy autoionising levels 79−31703
atom, electron impact excitation and elastic scatt., cross-sections at 6.7, 16 and 60 eV 77−68117
atom, electron impact excitation cross sections, Vainshtein approx. 78−25721
atom, electron impact excitation velocity consts. for reson. levels, meas. *(Russian)* 78−1086
atom, electron impact reson. transition excitation, unitarised distorted-wave polarised-orbit model 78−25710
atom, electronic excitation cross-section determ. method 77−540
atom, emission and absorpt. spectra in inert gas matrix 79−54800
atom, excited np states, fine struct., core electrons effect 77−18807
atom, excited state lifetime var. along isoelectronic series, HF cal. *(French)* 77−46538
atom, excited states field ionis., p states spin-orbit interaction 79−59592
atom, fine struct. splittings of 5d and 6d states, energy level crossing expts. 79−76396
atom, fine-struct. intervals, polarisabilities, highly excited d states 79−27100
atom, first excited D-level, hyperfine struct. meas. by cascade, fluoresc. spectrosc. 80−69101
atom, formation of electronically excited molecules by photorecomb. of 4P and 4S states *(Russian)* 79−3531
atom, generalised quantum defect, energy and radius depend. 80−14067
atom, hyperfine struct. density and temp. shift coeffs., at high buffer gas densities 79−18138
atom, inner core neutral binding energies, relaxed orbital relativistic Hartree-Fock-Slater calc. 78−13433
atom, isolated in Ar matrix, optical absorpt. spectra 77−10619
atom, isotope shifts of individual nS and nD levels 80−102489
atom, K$\alpha\alpha^n$ emission, method for L-shell config. calc. 77−42269
atom, multiphoton excitation, Rydberg transitions, ionisation detection 77−42304
atom, $O^{2+,3+,4+,5+}$ induced K-shell X-ray production cross section, 7 to 24 MeV 77−61850
atom, optical reson. line electron impact excitation cross sections, polaris. 78−55244
atom, outer-shell photoelectron ang. distrib. 80−37797
atom, photosensitized assoc. ionisation, excited from reson. levels 77−83710
atom, polarised, ionis. by polarised electrons in crossed beam expt. 78−50645
atom, reson. line polarisation, 2-photon excitation 77−54546
atom, reson. three photon ionisation, saturation effects 78−90137
atom, resonance doublet excitation cross sections in collisions with alkali ions 77−27167
atom, resonance lines broadening and shift by noble gases 79−10070
atom, resonance spectral lines, Stark broadening and shift 77−75097
atom, resonantly excited in cylindrical discharge plasma, effective lifetimes 78−79413
atom, Rydberg autoionisation state lifetime calc. 77−444
atom, Rydberg state optical excitation, collision ionisation processes 80−102561
atom, Rydberg state quantum defects, semiclassical calc. 77−38621
atom, Rydberg states, two photon absorption, decay fluoresc. 77−71787
atom, s and d state radiative lifetimes, time and wavelength resolved fluoresc. spectra 80−14104
atom, scattering at high-energies, intermol. potential determ. 77−46609
atom, spin magnetic moment densities, spin density functional method calcs. 77−67969
atom, state determ. following photodissoc. of KI, time of flight meas. 79−18105
potassium continued
atom, stimulated electronic Raman light scatt. by mag. sublevels 78−50492
atom, stimulated multipole Raman scatt. between opposite-parity states 79−76753
atom, two photon excitation by opposing light beams, reson. lines polarisation studies 78−82705
atom, two-step photoionisation, triple crossed beam obs. 78−66616
atom, valence p-shell HeIIα photoelectron spectra, final state CI effects 80−14121
atom, XPS, free atom core binding energy 78−74699
atom+bromomethane (iodomethane), product translational energy calcs., energy depend. 79−70314
atom+inert gas, quenching cross sections of alkali n^2P states, 5-100 eV 79−76505
atom+O ion collisions, A=16, 18, K-X-ray production 77−23554
atom beam, impact on W surface, mean residence time of K^+ and ionisation efficiency 77−73208
atom beam impact on gas-covered W surface, K^+ ion current peculiar decay 79−74045
atomic beam form. by charge transfer for ion-pair form. expts. 79−59555
atomic electron collision cross sections 77−42410
atomic energy level ordering, in excited states 79−81162
atomic excited states photorecomb., mol. ions form. *(Russian)* 79−89779
atomic spectra, 5^2P to 4^2S resonance line, rare gas perturbations, constant calcs. 78−9126
atomic vapour, resonant interaction with laser, Vavilov-Cherenkov effect *(Russian)* 80−106573
atomic vapour, stimulated four-photon parametric scatt. *(Russian)* 78−71145
atomic vapour quantum counter, Stark tuning 80−53242
atoms, addition to MHD generator, automatic system for conc. meas. 79−50892
atrium, bullfrog, mechanisms for positive inotropism of low-K Ringer soln. 77−77884
axonal K conductance anal., squid giant axons 79−96543
axonal membrane of mammals (myelinated fibres), K channel conduction 80−61538
axons, giant, squid, interaction of Ba^{2+} with K^+ channels 80−85379
band structure and Fermi surface, MAPW calcs. 77−1359
BCC, modified tensor force model for lattice dynamics 77−35644
BCC crystal, elastic constants, thermal expansion and bulk modulus 80−6452
binding energy and equilib. struct., pseudopot. calc. *(Russian)* 79−47037
biomembrane, electrogenesis in model of boundary transfer with Na pump 77−25401
biotransport model, refractoriness accumulation and secondary range firing in spinal motoneurones 77−1985
blood cells, red, Ca stimulated increase in K permeability, dog 79−62218
body burden rel. to ^{137}Cs levels in low-teens in areas of different fallout level in Japan 77−90922
boiling, expt. study of outflow from accelerating two-phase nozzle 78−1721
boiling, in tubes, superheat and instability 77−35136
bound spin-helicon wave excitation, reson. refl. coeff. 79−95435
brain K^+ dynamics during cerebral angiography, rel. to contrast agent neurotoxicity 78−35954
brine, routine anal. by X-ray fluoresc. spectrometry applying matrix corrections 78−88690
bubble motion and growth in incandescent W wires *(Hungarian)* 77−48460
calc-alkaline rocks from the East Carpathians, K, Rb and Sr distrib. 78−85555
catalytic synthesis of NH_3 on Fe, promoter action of K 79−29390
cathode, liq., Ar arc, cathode erosion rate estimation *(French)* 80−44056
CDW, detection attempt by neutron diffr. 80−49634
CDW vector orientation, positive ion lattice distortion 80−6759
CESR linewidth and g-shift in presence of spin-orbit perturbation, spin-phonon scatt. 77−63285
channel flow, incipient boiling superheats 80−74709
cluster beam Stern-Gerlach mag. deflection 78−54504
coadsorption of K and O_2 on Ge (111) rel. to work function 78−79874
coadsorption with O_2 on Fe (110), XPS, UPS, AES, and LEED study 80−80084
conduction-electron spin flip by phonons, expt. data anal. 79−61219
content in natural samples, γ spectrometric determ. *(Russian)* 78−92562
core thresholds, inelastic electron scatt. spectra meas. 79−95359
crustacean neuromuscular junctions, synaptic facilitation obs. 79−39412
crystal, elec. cond., temp. depend. calcs. 77−59276
crystal struct., van der Waals and repulsive interaction 80−84137
crystal structure, effect of Van der Waals forces 79−99111
cyclotron wave dispersion and obs. of many body effects 77−28097
cyclotron wave excitation, surface electron scatt. effects 78−6429
cyclotron waves, intermediate-wavelength, Fermi-liq. effects 79−77986
de Haas-van Alphen effect, accurate meas. of Dingle temp. changes 77−51638
de Haas-van Alphen freq. and Fermi surface anisotropy, press. depend. 80−59856
determination in minerals, electron probe analysis with low temperature sample holder *(French)* 80−85248
determination in seawater using selective membrane electrode 79−53368
determination in small samples of healthy and burnt skin 79−5343
discharge plasma, anomalous bright 5730 Å band excitation mechanism 78−67475
discharge plasma, K_2 excited mols. form. by K(4P) collisions 80−44013
distiller for purification, construction, operation 78−80490
doped NH_3 frosts, reflectance spectra and implications for Io surface 78−84561
drop, in He atmosphere, diffusional evap. in EM radiation field 78−43112
dynamical structure factor S(Q, ω), molecular dynamics simulation 77−7806
Earth core, K content rel. to heat source and thermal model 78−15982
Earth mantle content, inferred from heat loss argument 80−76943
elastic constants, appl. of model pseudopot. to elastic consts. 80−59845

potassium continued
elastic constants, cryst. equilib. and electronic contrib. 79−73243
elastic scaling parameters, press. variation of yield stress., meas. device 78−53047
elastic scattering amplitudes, for high energy electron scattering, by ionised atoms, numerical calcs. 80−49057
electrical and thermal resistivity determ. from first principles 79−69493
electrical conductivity, Toya's theory 78−51965
electrical resistivity, data tables, 1-2000K 79−78072
electrical resistivity, effect of energy depend. of electron relax. time 77−69296
electrical resistivity, low temp., non validity of empirical expression from 1-2K 79−23945
electrical resistivity, low-temp., electron-electron contrib., sample depend. 80−24875
electrical resistivity, of ideally pure K, anisotropy correction 77−4317
electrical resistivity, temp. depend., anharmonic effects 78−76045
electrical resistivity, temp. depend., free energy approx., anisotropic continuum dispersive model 77−43557
electrical resistivity, temp. depend., low temp. limit 77−11892
electrical resistivity at low temp., phonon-dislocation scatt. 79−60820
electrical resistivity below 2K, temp. depend. 78−51969
electron density redistribution on passing from atom to cryst. *(Russian)* 77−66103
electron mean free path, stopping and straggling 78−91367
electron-dislocation scatt. anisotropy effect on electron-electron scatt. contrib. to elec. resist. 80−29398
electron-electron scattering, elec. resistivity, thermal cond., thermoelec. power and Lorenz function 79−95382
electron-phonon coupling const., calc., compared with expt. 79−99286
electronic structure, optical absorption 79−38566
elemental abundances of S, K and P in aerosols from S.American rain forests 79−100910
emission and fixation during pressurised fluidised bed combustion of coal 80−30352
Fermi surface distortion 80−2325
Fermi surface pressure dependence meas. by de Haas-van Alphen effect 78−26807
field desorption from W (001), (011) and (112) planes 78−34715
field emission from individual planes of single crysts. on W tips 78−27385
film, splitting of surface plasmon emission spectra 79−99954
fixation effect on physicochemical and engineering props., of montmorillonite *(Japanese)* 78−31366
frozen solution in HMPA, Wannier-Mott impurity ground state, EPR 77−8054
gamma ray analysis of K, U and Th for dose-rate estimation in thermoluminescent dating 79−79333
giant axon of the squid, gating current and K channels obs. 80−56012
ground state alkali molecules, mag. shielding and spin-rot. interaction 80−87186
ground state of solids, spin density functional method, binding energy, compressibility 80−65477
Gruneisen parameter, press. depend. 80−65184
Gruneisen parameter temp. var. for BCC struct. 78−6137
Hall coeff., 4.2 to 16K 80−44570
Hall effect, temp. depend. 78−64029
heat capacity, ultra-low temp., anomalies due to CDWs 79−42271
heat exchanger based on heat pipe principle for nucl. reactor 77−46210
heat pipe, heat transport characteristics, transverse mag. field effects 79−37127
heat pipes, for thermionic convertors using Li and K working fluids 79−48153
helicon-phonon interaction, numerical study 79−46758
helicon-phonon interaction 79−4379
helicon-phonon interaction for oblique propagation, dispersion relation 80−49315
helicon-phonon interaction for parallel wave propagation 78−64054
hexamethylphosphoramide-K(Cs)(Rb), low temp. glass, EPR of solvated ats. 78−91927
high field Righi Leduc effect and lattice thermal conductivity, comment 80−10948
high field Righi-Leduc effect and lattice thermal conductivity, reply to comment 80−10949
high field thermomagnetic coeffs., 1.5-4.5K, lattice thermal cond. calc. 79−60800
high pressure effect on supercond. and high temp. resist. 77−47917
high-field Righi-Leduc effect lattice thermal cond. 78−34825
ileum epithelial cells and intercellular spaces, microprobe meas. of Na, K and Cl conc. profiles, rabbit 78−35819
inert gas+K, photon emission polarisation anal., coincidence studies 80−5614
interatomic function from phonon-dispersion curves and Heine-Abarenkov-Shaw optimised model pot. 79−19185
interatomic potentials from experimental phonon spectra 78−75621
interatomic potentials from phonon spectra 80−19744
intercalated in graphite, electronic band struct. calc. 78−6255
intercalates with graphite, staging classical model variations, EXAFS results 80−45166
intercalation compounds with graphite, ^{13}C NMR spectra 80−66048
intercalation compounds with graphite, interlayer screening and mag. susceptibility 80−44794
intercalation compounds with graphite, low temp. sp. ht. 78−71868
intercalation-desorpt. cycle with partially graphitised C, stacking faults investig. 78−47396
in interstellar grains, isotopic anomalies 78−28761
interstellar K I, 4044 Å line obs. 78−24533
interstellar K I, quadratic depend. of column density on N_H 78−20872
iodomethane+K, mol. rearrangement, optical pot. calcs. 77−81399
ion diffusion in glass, plane optical waveguide form. 79−90043
ion exchange, of Na^+ in $\beta.Al_2O_3$ by Ag^+ and K^+ ions from the molten nitrates 79−24737
ion implantation in Fe, perturbed ang. distrib. 78−12969
ion implantation in LiF, migration, segregation, effect on optical props. 80−100269
ion mobility in SiO_2, triangular voltage sweep technique 79−95206
ionic exchange selectivity in PMMA gels 78−35719
ionisation efficiency and mean residence time meas. on Pt surface 77−85874
ions, adsorbed on porous SiO_2 glass in distilled water medium, determ. 79−24814
ions, passage through nerve membranes, protein channels 77−4994
IR spectra, Mayer-El Naby optical absorption anomaly 77−4643
isoelectronic series, hard-core pseudopotentials and struct. maps 80−44168
isotope separation, plasma ion cyclotron reson. 77−10787
isotope separation, using cylindrical RF mass analyser 79−80718
isotope separation in solution by thermal diffusion 80−87236
isotopic comps. of magnetic spherules in marine sediments 79−44423
K activation associated with intraneuronal free Ca 79−8494
Larmor wave spectrum 79−69397
laser, atomic Rydberg state 16 μm output 77−54696
laser, tunable subMM, using atomic K Rydberg states 80−69378
lattice dynamics, modified Bhatia model 77−51455
lattice dynamics, phenomenological model 77−20017
lattice parameter determ. by neutron scatt. 79−7576
lattice sp. ht. and thermal vibrs. 78−30768
lipid-protein interaction in membrane bound Na^+, K^+-ATPase, spin label anal. 79−11902
liquid, density, 1640-2030K, 36.1-100.2 atm 78−91369
liquid, density, at near critical temp. 80−103407
liquid, density meas. up to 1800K and up to 100 atm. 77−43264
liquid, elec. resistivity calcs. 78−79974
liquid, electrical resistivity, effect of inter-electron interactions *(Russian)* 77−24546
liquid, equation of state, press. and entropy along melting curve 77−47540
liquid, equation of state, vol. and compressibility meas. up to 22 kbar 77−47541
liquid, interionic interaction theory, pseudopotential calcs. *(Russian)* 80−79675
liquid, isothermal compressibility calc. at 400 to 1800K from density data 78−2186
liquid, mean spherical approx. and effective pair pots. 80−70099
liquid, nuclear reactor appl., high-temperature experimental plants *(German)* 77−10461
liquid, O_2 pot. and O_2 distrib. coeffs. between alkali and struct. metals 80−65231
liquid, pair correl. function and ion-ion pot. 79−50982
liquid, paracrystalline BCC lattice evidence 79−41942
liquid, radial distribution function, Monte Carlo calcs. 77−55230
liquid, reaction with Cu_2O and CuO 79−66277
liquid, resist. and thermo-electric power using corrected parameters of Shaw model 79−19566
liquid, shear waves, molecular dynamics 80−44096
liquid, short-wavelength density fluctuations 79−46550
liquid, stagnant, mag. field influence on boiling 77−47096
liquid, struct. factors, X-ray transmission diffr. expt. 77−47337
liquid, T_c, P_c, V_c, from eqn. of state 78−2228
liquid, thermal expsn. coeff. for high temp. 78−75853
liquid, thermoelectric power, optimised model pot. calcs. 80−29391
liquid cathode arc, cathode sheath model, liquid K in Ar *(French)* 77−1032
liquid cathode arc in Ar atm., plasma prod. and parameters, cathode sheath model 77−4003
liquid metal, incipient boiling press. signal and evaporation coeff. meas. 79−77734
liquid metal vapour, laminar film condensation under effect of electromotive force 79−1258
liquids, optimised cluster expansion, struct. function evaluation 80−49085
low temperature lattice cond., phonon drag thermopower 79−60789
low-temperature plasma atomic level population density computation 78−71461
magnetic hyperfine field in Fe, TDPAD meas. 78−52389
magnetic property volume depend., Knight shifts, electron spin response 80−88729
magnetoresistance anomalies due to inhomogeneities, examination 78−56130
magnetoresistance in terms of inhomogeneity models of current jetting and channelling 78−56131
magnetoresistivities, longitudinal elec. and thermal, meas. 80−88541
magnetoresistivity, elec. and thermal, quadratic field depend. 79−95388
marine chemistry, basalt weathering as oceanic K sink 77−81886
Mars, ^{40}K content rel. to ^{40}Ar in atmosphere 77−64687
Matthiessen's rule, low temp. deviations 78−14724
mechanical ideal strength, pseudopot. model calcs. 79−77670
melting at high pressures, thermodynamics 78−91426
melting thermodynamics *(Russian)* 78−71840
mesosphere Na and K abundances, simultaneous nighttime lidar meas. 78−36239
metal impurity effect on residual elec. resistance *(Russian)* 80−84457
metallic compressibilities, general pseudopotential approach 80−54631
methyl iodide+K(Rb), reaction cross sections 78−40043
microwave transmission modes at cryogenic temps. 79−42473
mode Gruneisen parameters, calc. 77−4180
mode Gruneisen parameters, neutron scatt. obs., 4.5K, 0.001-4.1 kbar 77−4179
model pseudopotential, form factors, binding energy and compressibility calcs. 78−26486
molecular beam, isotope selective two-step photoionisation study 80−74203
molecular ground state thermalisation speed, collision cross-sections meas. *(Russian)* 80−78723
molecular laser, optically pumped, review 80−58519
molecule, absorpt. and relax. const. determ. by optical laser pumping method 80−102550
molecule, IR absorption spectrum 77−34625
MOS capacitor, filament-metallised, effect of K contamination of W 79−51679
muonic K-shell X-ray transitions, nuclear charge radius 78−66195
muscle, skeletal, Na:K rel. to Na:Na exchange by Na pump 77−66807
nerve fibres, myelinated, diffusion of ions 79−24965
nerve impulse electro-diffusion model 79−53078
nerves, K ion noise currents and inactivation in voltage-clamped node of Ranvier 77−16924
nervous tissues, Ca dependent K activation, book contrib. 79−5266
neuroblastoma cultured cells, membrane currents under volt. clamp 77−60193
neuron adaptation model allowing for Ca influence on membrane K permeability 79−79508

potassium continued
oocytes, salamander, free and bound intracellular solutes, reference phase anal. 79−24967
oocytes, salamander, free and bound intracellular solutes, reference phase anal. 79−24966
optical filter, ultrahigh-Q isotropically sensitive, using at. reson. transitions 79−55216
ores, effective γ-ray attenuation coeffs. 77−25680
oxidation, adsorbate-induced structs., UPS obs. 79−47828
oxidation at low pressure, 77 and 295K 78−76792
pair potentials calcs. elastic props. calc. 80−49176
Pauli susceptibility and Knight shift meas., electron wave functions 80−44937
phasons, transverse, freq. dispersion relation in CDW state 80−96804
phonon dispersion, calc. using electron fluid model 78−75738
phonon dispersion, modified de Launay model 78−34573
phonon dispersion curve crossing in (ζ00) direction 78−38795
phonon frequencies, coherent inelastic neutron scatt. meas. 77−47525
phonon frequencies, normal mode Gruneisen parameters, pseudopot. calcs. 79−42184
phonon spectral density, pseudopotential calcs. 80−39234
phonon spectrum calc., microscopic theory of force constants 78−26647
phonon-dislocation scatt. and phonon equilibration at low temp. 79−51561
phonon-phonon scattering, Peierls condition 77−62910
phonon-phonon scattering relax. times, rel. to elec. resist. 77−39813
pike, model for turnover of ^{137}Cs, K 79−8553
PIXE anal. method 77−63973
plant motor organ K, Ca distrib., ion microscope obs. 79−66466
plasma, dense, in arc, elec. and heat conds., two-probe diagnostics 80−38560
plasma, magnetic-mirror-trapped, heating with array of hot W wires 80−33789
plasma in arc and capillary devices, optical props. 80−24244
plastic deformation 78−30693
point contacts, current-voltage characts. at liq. He temps. 80−39663
polycrystalline, transverse and longitudinal thermal magnetoresist., 3 to 9K 79−95385
positive column, ion distrib. function for each species using probe 78−55752
positive column discharge plasma, neg. ion prod. 78−59712
positronium, formation in positron+alkali metal atom collisions, first Born approx. 80−83525
positronium formation in positron+alkali metal atom collisions, pseudopot. calcs. 80−83524
power station ashes, Th, U, and K conc. meas., dose rates in Poland 79−100754
pseudopotential, energy-depend., for Fermi surface distortion and phonon dispersion calc. 77−15737
pseudopotential wavefunctions calc. 77−43542
purification by vacuum distillation 77−66599
radiometric determ. in NPK and GVH fertilisers *(Czech)* 80−22427
residual resistivity anomaly, theory 77−80765
residual-resistivity anisotropy using several impurity scatt. potentials 79−19571
resistivity, anomalous temp. depend. below 1.6K 79−78074
resistivity and thermoelec. ratio, electron-electron scatt. contrib. 80−70670
RF size effect, effect of modulation 78−91716
Righi-Leduc and Hall coeffs. meas., ^4He temp. range 77−66156
screw dislocation−vacancy interaction energy 77−15415
screw dislocations, ⟨111⟩, in BCC metals, displacements of atoms 77−15414
selective and counter transport through polyvinylbutyrolactonecoacrylonitrile membrane *(Japanese)* 78−31700
self-diffusion, high temp. bulk modulus determ. 80−79976
sensory fibres, amphibian, spike freq. adaptation due to slow K channels 79−2025
serum automated electroanal. using ion-selective disc electrodes with neutral cation-carriers *(German)* 78−73269
sinatorial node of rabbit heart, vagal stimulation, K^+ permeability and extracellular transients 78−92608
skeletal muscle of frog, displacement currents, K cond. channel contrib. 79−39409
smoke particles, optical props. 480 to 620 nm, rel. light scatt. cross sections meas. 80−97293
soft X-ray emission and absorpt. edges, self-absorpt. studies 80−40183
soft X-ray emission edge, temp. depend. 80−89090
Soft X-ray emission edge self absorption and effect of exciting voltage 77−90220
soft X-ray outer-shell absorption and emission, one-electron calc. 79−69904
solubility in Fe-S liq., silicate-K-(Fe-S liq.) equilibria and planetary implications 78−11843
spallogenic isotopes in Fe meteorites, radial distrib. 80−67488
spin susceptibility and volume dependence 79−95569
structural energies, pseudopotential formalism 80−39519
structure factor determination, by X-ray and neutron diffr. 79−51046
surface, clean and O_2-exposed, X-ray and UV photoelectron spectra 78−52636
surface (001), electronic struct. by density matrix method 79−60900
surface electron states and optical props. in IR spectral range *(French)* 80−54757
surface energy, barrier height and work function, jellium model calc. rel. to fracture model 77−72907
surface energy, self-consistent calc. including ion pot. perturbation effect 77−8166
surface layer on W, stimulated ionisation by superthermal Na, Cs beams, energy depend 78−31292
surfaces, Van der Waals forces computation 79−15204
thermal conductivity, electronic contrib., 1 to 330K 77−20291
thermal expansion calc. 77−11711
thermal magnetoresistance, high-field, 2.5 to 8K 78−23072
thermal resistivity, ideal, free-electron approx. 77−51724
thermionic emission of K ions from W *(Hungarian)* 77−48300
thermodynamic props. at high press. *(Russian)* 78−47536
thermoelectric power, high-temp., first-principles calc. 78−91672
thermomagnetic and thermoelectric properties, phonon scatt. processes 80−29390
thermopower, high temp., first principles calc. 79−65447
potassium continued
thermopower and elec. cond., relationship at low temps. *(Russian)* 80−92882
transport calculations, usefulness of theroretical form factor 79−23946
trapping and desorption on clean and O_2 covered W (110) surface 77−11786
ultrasonic attenuation at low temp., spherical Fermi surface model 80−84255
US cyclotron resonance, anisotropy effects 79−73816
US generation by EM radiation, surface scatt. effects 80−24973
UV absorpt. spectra 80−2780
UV absorption spectra, threshold singularities of p-shell absorpt. in XUV region 77−36261
vacancies and elec. resist. 79−82575
vacancy form. energy, math. model 77−51369
vacancy formation energies calc. 79−82197
vacancy formation energy calcs., electron density functional method 80−19801
vacancy superlattice 77−7713
vapour, 16 μm and 8.5 μm generated via stimulated Raman process 77−19361
vapour, absorpt. spectra 79−21509
vapour, mag. props. changes under laser irrad., induced EMF obs. 80−100059
vapour, mag. sublevels, stimulated electron Raman scatt. *(Russian)* 78−50861
vapour, thermal cond., 800-1050K 80−19546
vapour, tunable picosecond UV pulse generator 79−36956
vapour, two-photon resonant parametric generation, 2 to 20 μm 77−42563
vapour generator, heat transfer with drop motion in tube in supercrit. region 80−23880
Venus surface rock, radioactive element concs., Venera 9 and 10 meas. 77−78691
wire, low temp. elec. resist., size and temp. depend. 77−76958
wires, size effect and temp. depend. of resist. 79−51691
wires, size effect and temp. depend. of resist. 79−51692
X-ray emission, incomplete phonon relax. calc. 77−52202
X-ray spectra, temp. broadening 77−69936
AgCl:K^+, impurity effect on plasticity 78−14398
Ar loaded K heat pipe performance characteristics 78−89934
Ar:K seeded plasma, temperature diagnostics 78−67427
Ar+K^+, inelastic collisions, emission cross sections, quasimol. state interference 77−61848
$Ar_{N-1}K^+$, ionic clusters, thermodynamic props., struct. 77−88615
$BaBr_2$:K^+, X-irradiated, perturbed F-centre, EPR and optical absorption 77−68966
BaF_2:K^+, cryst., thermal depolarisation 79−82912
BaF_2:K^+, nuclear spin relax. orientation depend., point defect self-diffusion mechanism 77−48078
BaF_2:K^+ ionic conductivity meas., computer analysis, point defect parameters 80−54429
C/Pt-W (8 wt.%), desorption of K from C film surfaces 80−59784
CaF_2:Gd^{3+}, K^+, elec. field gradient at nuclei on orthorhombic sites, vs. elec. zero-field splitting 79−87070
Cl+K_2→KCl+K*, chemiluminesc., electronic emission intensity 78−35689
CsBr:K^+, impurity induced IR absorpt. spectrum, breathing-shell model 77−77256
CsBr(Cl)(I):K, optical absorpt. investig. of F_A-centres 77−44029
CsI:K^+, cryst., influence of impurities on yield stress 79−15748
CsI:K^+, luminesc. processes 80−103989
H plasma, K impurities, optical props. 80−103119
H^--K^+ exchange and cell enlargement in maize coleoptile segments treated with auxin and fusicoccin 77−86469
H^++Cs(Rb)(K)(Na), charge exchange, H(2s) form. 79−64101
Hg+Ne(Na)(K)(Rb), elastic scatt., interatomic pots. 77−58122
I_2:K, doping effect on elec. cond., semicond. props. 80−49732
K I, fine struct. splittings in some highly ionized n=3 doublets 80−43200
K I, in interstellar clouds, non-linear relationships between N(Ca II), N(K I) and N(H) 79−92832
K I, inner shell absorpt. spectrum, 3d wavefunction collapse 77−23455
K I, K II, ejected electrons from autoionis. levels excited by electron impact 77−88572
K I, lifetime meas. of lowest ^2D-states, elec. quadrupole excitation 78−42004
K I 7699 Å, emission line profiles in α Orionis (Betelgeuse) circumstellar shell 77−22210
K I 7699 Å line meas. of solar sidereal equatorial rotation rate 79−44441
K I 769.9 nm line obs. of solar 5-min. oscills. 80−26838
K I isoelectronic series, transition probabilities, oscill. strengths, lifetimes, branching ratios 78−33470
K I isolectronic sequence, transition probabilities, cancellations 80−91503
K I to K XIX, energy levels, tabulated data 80−51966
K II, isoelectronic series, photoionisation, multichannel CI calcs. 79−93931
K IX, wavelengths and energy levels, spectral obs. 77−428
K, Na, superthermal neutral beams impact on W surface, stimulated chemical reaction 77−9123
K solution, in KBr, conc. fluctuations, neutron small-angle scatt. study in electrolyte-metal transition range 79−14668
K^- and K_2^- form. and decay in discharge plasma *(Russian)* 79−90374
K^-, electron affinity, model pot. CI and SCF calcs. 77−38609
K^-, multichannel photodetachment 78−42027
K^-, photodetachment and at. polarisability 80−91522
K^-, photodetachment cross-sections and multipole polarisabilities, extended asymptotic model 78−42028
K^+, activity-dependent extracellular fluctuations in canine Purkinje fibres 80−89733
K^+, Ca^{2+}, blood concs. in rat, technique for continuous vivo meas. *(German)* 79−39533
K^+ channel of fragmented sarcoplasmic reticulum, voltage-dependent Cs^+ blockage 79−96524
K^+ channel response to time-dependent clamping functions, squid axon 79−62229
K^+ channels in squid giant axon, response to time-dependent clamping functions 79−39382

potassium continued
K^+ channels of myelinated nerve, conditioning hyperpolarisation-induced delays 79−88066
K^+ circulation across plasma membrane, role in bacterial growth 77−90751
K^+ concentration effect on muscle Na^+ efflux rate 79−79495
K^+ conductance absence in central myelinated axons 80−108871
K^+ conductance in bullfrog, $[Ca^{2+}]_i$-linked, oscill. obs. 80−35867
K^+, coupled transport in a liposome suspension 79−53069
K^+ currents in squid axons, single channel recordings 80−76721
K^+, dielectronic recomb., in crossed beams, UV emission obs. *(Russian)* 79−10212
K^+, direct excitation of levels, transition probs. and cross sections 80−37890
K^+, effect on extracellularly-recorded photoreceptor pots. of cephalopod retina 79−62245
K^+, electrogenic transport obs. in rat soleus muscle 80−21456
K^+, electron impact excitation of reson. levels *(Russian)* 79−45852
K^+ external conc., starfish egg cell membranes, inward rectification blocking model 80−61523
K^+, flow through ion channels in nerve cell membrane 79−74644
K^+, free-ion polarisabilities, empirical values 77−20792
K^+, H_2O affinity, ab initio SCF calcs. 80−58125
K^+ in frog blood cells, X-ray absorpt. edge fine struct. 79−66459
K^+ in Kr(Xe) gas, XX 79−10625
K^+ in molecular complexes, K-edge absorpt. spectra, Z+1 analogy, theory-expt. comparison 80−47935
K^+, in vivo continuous monitoring using ISFET probes 80−85512
K^+ ion flux through membrane channels, nerve impulses, random walk anal. 78−77045
K^+ ion increased conc. effect on particle motion in neurosecretory structs. 78−77046
K^+ ions occlusion in unphosphorylated Na^+ pump 79−88065
K^+ mobilities in gases *(Japanese)* 79−60101
K^+, mobility and clustering in Ar gas 77−84389
K^+ permeability of pancreatic islet cells, effect of Ca^{2+}, glucose 79−74615
K^+, red blood cell permeability repair after X-ray, fast-neutron damage 79−57615
K^+, reson. line regularities in plasma Stark widths and shifts 80−43881
K^+ selective channels, in apical membrane of toad gallbladder 79−2018
K^+ selective glass microelectrodes, electrochemical props. 79−91957
K^+, thermal and athermal effects on erythrocytes by microwave irradiation 79−70581
K^+ transport modification by 2,4-dichlorophenoxyacetic acid in lipid bilayer membranes 79−83709
K^+ transport of squid axon membrane, internal pH effects 79−62221
K^+, X-ray microanal. of cultured skeletal muscle cells, calibration 79−100798
K^{2+}, photoionisation cross sections calc., R-matrix theory 77−18865
K^{2+}, photoionisation cross-section, R-matrix theory 78−82702
^{40}K, isotope relati[illegible] abundance, radioactivity expt. for schools 79−21511
K:F^-(Ne), ground states and core hole states, self-consistent soln. using density functional formalism 79−69467
K/Na ratios in dew drops rel. to atmospheric aerosol comp. 77−91190
K-Ar dating of ore mineralisations in Erma River Area, Bulgaria 78−81115
K-ethylamine-ethylenediamine, soln., ion-pairing and EPR 79−78502
K-H plasma, low temp. discharge, ion constitution mass spectra *(Russian)* 77−4000
K-He(Ne)(Ar)(Kr)(Xe), oscill. strengths, for induced dipole transitions, pot. energy curves 77−75100
K-Kr, afterglow of laser plasma, fluoresc. spectra 79−19085
K-NaCl adhesion 78−18914
K-Rb arc lamp development for space laser communications 78−46646
K-rich globules in Luna 20 soil, SEM obs. 80−67591
K^+-$(H_2O)_n$, complex struct., coord. numbers 79−7049
K^+-affinities of methylamine, ab initio SCF calculations 80−102443
K+alkyl halide potentially reactive collisions, electronic excitation 80−74239
K+alkyl iodide, collisional electronic excitation, time-of-flight obs. 79−86049
K+Br, harpooning mechanism interactions, semiclassical optical model 79−89755
K+Br_2, inelastic scatt., total cross-sections, trajectory surface hopping calcs. 78−46420
K+Br_2, nonreactive differential scatt., 0-10 eV, scatt. angle 78−42156
K+Br_2 (Cl_2), electron transfer crossed beam reaction, energy and ang. differential cross section 79−20358
K+Br_2(BrI)(I_2), stripping reactions at hyperthermal energies 77−16815
K+Br^-, differential cross-section, small angle scatt. 79−98186
K+$CF_3I \rightarrow KI+CF_3$, products translational distrib., crossed beam reaction 78−31629
K+$CH_3I \rightarrow KI+CH_3$, products translational distrib., crossed beam reaction 78−31629
K+CO, bulge effect, in rot. inelastic scatt., isotope shift 79−86047
K+CO, rotational inelastic scatt., uniform semiclassical sudden approx. 80−99544
K+Cd(+N_2), optical excitation, rate consts., collisional energy transfer kinetics 80−32801
K+Cl_2(Br_2)(I_2)(ICl)(IBr), negative ion prod. cross sections 77−531
K+$Cl_2 \rightarrow K^+(Cl+Cl^-)$, 5.5−14.0 eV, energy loss, spectrum maxima, mechanism 77−75286
K+Cl^-, differential cross-section, small angle scatt. 79−98186
K+Cl⇄K^++Cl^-, KCl+M⇄K^++Cl^-+M, rate consts. in at. press. flames 77−60036
K+Cl⇌K^++Cl^-, chemi-ionis. and recomb. cross sections 78−33583
K+CsF collision complex, reactive decay branching ratio, rot. energy effect 77−66752
K+CsF(RbF), complex form., decay. branching fraction and cross-sections, translational energy depend. 77−21374
K+$D_2O \rightarrow OD^-+K^++D$, 100-200 eV, D_2O^-($^2A_1$), state 78−17770
K+F^-, differential cross-section, small angle scatt. 79−98186
K+F(Cl), quasiclassical charge transfer cross section, rel. vel. depend. 77−19073
K+H, covalent and ionic states interaction, config. mixing 78−50613
K+H_2O(D_2O), ionising collisions in crossed-beam systems 78−48641
K+H_2S(DS), collisional ionisation, positive and negative ion energy spectra obs. 80−63775
K+H^+, 4 MeV beam-foil X-ray production cross-section 79−7003
K+H^+, electron capture cross sections 79−86061
K+H^+(H), single-electron capture total cross sections 80−91656
K+H^+(He^+), excited state form. by inelastic processes, energy partitioning 78−82833
K+HCl, ion pair form., energy loss spectra 79−34286
K+HCl, ion pair form. reaction, energy loss spectra meas. 79−61849
K+HCl, mol. beam reaction, rot. state depend. 79−74365
K+halogen molecule (methyl halide), ion pair form., vibr. energy depend. 79−34287
K+halogenated methane, negative ion form., electron affinities, bond dissoc. energies 78−82827
K+He, 4^2P state $j_1m_1 \rightarrow j_2m_2$ Zeeman transition, total cross section energy depend. 80−83475
K+He, 93 eV, excitation of K atom, photon-scatt.-atom coincidence study 78−82829
K+He, fine struct. transitions, energy depend. crossed beam determ. 79−86035
K+He^+, 5-100 keV, electron capture form. of fast metastable He 78−74760
K+He^+, single-electron capture cross-sections 78−37737
K+He(Ar)(Ne)(Xe), K 5^2P level broadening and collisional relax., quantal, semiclassical and expt. comparison 80−18903
K+He(Ne)(Ar), 0.7-80 keV, K excitation, reson.-line emission and polaris. 80−18911
K+He(Ne)(Ar), K collision-induced alignment, reson.-line emission polaris. obs. 80−18912
K+He(2^3S_1), Penning ionis. in stationary afterglow 78−42184
K+Hg, 15-1400 eV, electronic excitation, integral cross sections 80−43159
K+Hg, electronic excitation, integral cross-section, 50-1500 eV 78−62888
K+$HgBr_2$, laser irrad., HgBr form., chemiluminescence 80−55658
K+I chemi-ionisation, integral cross section calc. for two state model 79−18282
K+I chemiionis. differential cross-section calc. for two-state model 79−18283
K+I_2, ion-pair form., differential cross sections, I_2 internal energy effects 77−61840
K+I_2, ion-pair form. cross section, 15-120 eV, mol. props. depend. 77−28996
K+I_2, ion-pair formation, energy transfer and differential scatt. 77−75272
K+I_2, ionising collision, trajectory surface hopping calc. 77−50509
K+I_2(IBr)(Br_2)(ICl)(Cl_2), ion-pair form., bond stretching effect on cross sections 78−1064
K+inert gas atom, ground-state pots. from elastic cross sections 77−75258
K+inert gas atom, resonance levels relax. 77−83684
K+K^+ collisions, charge exchange cross section 80−58374
K+K(Na), excitation in slow collisions 78−70918
K+methyl bromide→KBr+CH_3, yields, crossed mol. beam study 79−34293
K+methyl cyanide, collisional ionisation obs. 80−95716
K+Mg^+, charge exchange and excitation processes 78−17772
K+N_2 (CO) atom electronic excitation, vibr. to electronic energy transfer, seeded mol. beam studies 80−47919
K+N_2 collision, electronic excitation and energy transfer, time of flight spectra 80−43151
K+N_2^+, 50-1000 eV, crossed beams, electron transfer and excitation 80−14226
K+N_2(CO), anisotropy of the repulsive intermolecular potential from rotationally inelastic scattering 79−41226
K+N_2(CO), rot. inelastic scatt., quantum effects, simple model surfaces 80−48064
K+N_2(H_2)(O_2), excited atom quenching, semi-empirical model 78−1065
K+NH_3, rot. inelastic, time-of-flight spectra 78−5325
K+NO_2, charge transfer reactions, energy and ang. differential cross-sections meas. 80−53125
K+NO_2, ion pair form. reaction, energy loss spectra obs. 79−91921
K+NaCl, three dimens. collision, exponentiating trajectories and statistical behaviour 80−5595
K+NaCl(NaD), prior statistical distribs., collinear reactions 78−35670
K+NaK reactive collisions studied using circularly polarised laser fluorescence 80−69215
K+O_2, collisional ionisation, energy spectra of forward and backward directed positive and negative ions 80−87200
K+O_2 mol. target internal motion 80−78697
K+$O_2 \rightarrow K^+ + O_2^-$, electron transfer kinematics 77−6903
K+SF_6, ion-pair form. reaction, energy loss spectra 80−55630
K+trifluoroiodomethane→KI+trifluoromethane, molecular beam reactive scattering, angular distribution study 79−98198
K+UF_6, ionisation reactions, absolute cross sections 80−99565
K+UF_6(WF_6)(MoF_6)(TeF_6)(SeF_6), crossed beams, reaction cross section 77−77740
K^++Ar(Kr)(Xe), differential elastic cross-section meas. *(German)* 77−58130
K^++Cu crystal, elastic scatt., ang. and energy relationships, 1-3 keV *(Russian)* 79−78802
K^++H_2, dissociative collision, H_α, H_β emission prod. 77−75093
K^++H_2O, supermolecule calcs. with additive procedure, intermolecular interactions and binding energy 80−52880
K^++inert gas atom potential, determ. from total cross section meas. 77−68091
K^++molecule, total cross section anal. method, mol. quadrupole moment determ. 77−50495
K^++Na, differential scatt. cross section, electronic excitation via rot. coupling in NaK^+ 78−13579
K^++Ng(6^3P_1), excitation, optical polarisation fractions and mag. sublevels obs. 78−50619
K_2, $B^1\Pi_u$ state lifetimes, Hanle effect 78−90218
K_2, $B^1\pi_u$ state radiative lifetime, quenching cross section, fluoresc., single photon counting 77−75202
K_2, beam, multiphoton ionisation mass selective laser spectroscopy, vibronic, gyrovibronic states, clusters 78−21985
K_2, electron impact, vibr.-rot. excitation by slow electrons, multiple scatt. calcs. 78−13617
K_2, formed by K atoms photorecombination, luminesc. spectrum *(Russian)* 79−3531
K_2, in discharge plasma, anomalous 5725 Å band, photorecomb. mechanism 79−50088
K_2, laser-induced photodisintegration *(Russian)* 79−89719

potassium continued
K_2, optically aligned ground state, Hanle effect obs. 79−36707
K_2, optically pumped, relax. in at. collisions 78−17765
K_2, optically pumped CW dimer lasers 80−14322
K_2, photodissoc. products of $C^1\Pi_g$ and $C^1\Sigma_u^+$ states 79−98171
K_2, vapour, IR absorpt. bands obs. 79−31527
K_2^+, $^2\Sigma$ and $^2\Pi$ state pot. energy curves, two-centre model 79−26906
K_2^+, adiabatic pot. curves, ground and excited state, Hellmann-type model pots. 78−78647
K_2^+, core-core interaction potential calc. 78−25645
K_2^+, form. by electron impact in elec. discharge, low-press. vap. 79−10738
K_2^+ ion formation in low press. K discharge plasma 80−43862
K_2^+, pot. energy curve, pseudopot. calc. 77−6703
K_2^+, Simons-type pseudopots. calcs. 78−5120
$K_2+Br_2(Cl_2)$, collisional ionisation reactions 77−50508
$K_2+Cl(Br)\rightarrow KCl(KBr)+K^*$ product electronic state distrib., chemiluminesc. 77−40529
K_2+halogen mol., thermal energy mol. beam chemi-ionisation 77−9065
K_2+halogens$(SnCl_4)(MoF_4)(UF_6)$, ionisation reactions, absolute cross sections 80−99565
$K_2+Li_2(Na_2)\rightarrow 2KLi(2KNa)$, equilib. const., enthalpy change 78−25750
K_n^+, ion formation in elec. discharge, n=2-6, 10^{-3}−1 torr. *(Russian)* 79−77448
KCl, cryst., two-layer colloidal K and Cu colour centre light absorption 77−12408
K_2CrO_4, domain structure, ferroelastic 78−18702
$K_2Cr_2O_7$-K_2CrO_4-$K_2B_4O_7$ melt, decomposition to grow Cr_2O_3 crystals 79−100037
^{39}K, ground-state g-factor, rel. to ^{87}Rb, spin-exchange optical pumping meas. 77−34596
^{39}K pulsed NMR obs. of whole body live and dead newborn mice 80−40964
^{39}K, weakly excited, hyperfine struct. transitions obs., neoclassical theory 77−6737
$^{39}K/^{40}K$ ratio for inclusions in Allende meteorite, normality confirmed 80−26820
^{40}K, conc. in New Zealand soils 77−53057
^{40}K, contents in fish flesh 79−79718
^{40}K, decay consts. for use in geochronology and cosmochronology 78−28189
^{40}K, exposure rates from gamma sources in dwelling room walls, Monte Carlo calc. 78−73260
^{40}K Mossbauer isomer shifts, book contrib. 79−87363
^{40}K, natural content and internal radiation burden of Hungarian adult population 80−26355
^{40}K natural gamma photon fluxes in long-distance runners 79−96729
^{40}K, pressure-induced changes in electron-capture decay const., theory 80−22771
^{40}K, terrestrial beta radiation field in natural environment, numerical evaluation 78−81161
$^{40}K/^{41}K$ in deep-sea sediments magnetic spherules, poss. meteorite origin 78−11874
^{41}K in Allende meteorite, search for anomaly prod. by proton-associated alpha-irradiation 78−49398
^{41}K vapour, optically pumped, RF shift for one quantum transitions 79−26930
^{42}K calibration technique, whole-body counters for estimation of whole-body K content 79−25086
^{42}K, whole-body content, sex-dependent calibration factor of NaI scintillation counter 79−29593
^{43}K, prod. by V target bombard. with medium energy protons, separation, medical appls. 77−81572
^{43}K radioisotope preparation at variable energy cyclotron of Frederic Joliot Hospital Service *(French)* 77−65361
K^*+molecule, assoc. ionisation, mass spectra *(Russian)* 77−42393
$K(4^2P)$+He(Ne)(Ar)(Kr)(Xe), collisional excitation, differential cross-sections 78−66643
$K(4^2S)+CO\rightarrow K(4^2P)+CO$, differential cross section meas. by atom-photon coincidence techniques 79−31673
$K(4^2S)+N_2\rightarrow K(4^2P)+N_2$, differential cross section meas. by atom-photon coincidence techniques 79−31673
K(4p)+He, fine struct. transitions, vel. depend., interatomic pots. 77−42388
K^+affinities of NH_3, ab initio SCF calculations 80−102443
Li^++K, differential scatt. cross section, electronic excitation via. rot. coupling in LiK^+ 78−13579
Li^++K, rot. coupling, Fraunhofer diffraction effects 77−65526
Li_2SO_4:K^+, monoclinic-cubic transform., effect of impurities 79−52744
MgO:K, implanted K aggregates, TEM and optical spectra obs. 78−83838
$Mg(^3P)+K(Ca)$, energy transfer and excimer form. in flowing afterglow 77−60049
Na^+/K^+ intracellular ratio, rel. to protein synthesis control and cataract form. 78−11646
Na-K, rotationally stabilized liquid liner implosion for fusion plasma production 77−23274
$Na+H^+$, configuration interaction potentials and rainbow angle scatt. cross section 80−37745
Na^++K, differential scatt. cross section, electronic excitation via rot. coupling in NaK^+ 78−13579
Na_2+Na(K), electron energy transfer from optically excited mols. 77−34742
NaF:K^+, substitutional impurities, defect props. of (001) and (011) surfaces 77−47443
Na_2SO_4:K, phase transforms., X-ray, DSC and elec. cond. obs. 79−33082
Ni:K^+ ion implantation, effect on inelastic refl. and energy losses of fast primary electrons 78−55900
Ni(100), with adsorbed K^+, He^+ impact, Auger deexcitation spectrosc. 79−100010
O_2+Na(K)(Cs), negative ion pair form., total cross sections 79−3550
RbF+K collision complex, rot. energy effect on branching fraction for reactive decay 78−73023
Se:O(Cl)(K) amorphous, elec. cond. increase on impurity addition 77−11920
Si:K, amorphous, implantation effects on elec. props. 80−49716
Si:K, amorphous, ion implanted, control of cond. 79−60835
Si:K, bound exciton luminescence in mag. field *(Russian)* 80−108278
Si:K, ion implanted, influence of doping and annealing on carriers 78−38742

potassium continued
Si-SiO_2:K^+, physics, electron and ion motion *(Dutch)* 80−60093
Si-SiO_2-KCl_{aq}, interface, capacitance meas. 78−80051
SiO_2:K, ion trapping and mobility, energy levels 80−92985
SiO_2:K, MOS gate insulator, mobile K ions 77−47623
$SrCl_2$:K^+, X-irradiated, recomb. luminesc. between trapped electron and self trapped holes 77−73162
SrF_2:Gd^{3+}, K^+, EPR of orthorhombic Gd^{3+}-univalent metal ion complexes 80−11262
TaS_2-K intercalation compound, CDW's and superlattice patterns 77−47746
TiO_2, K^+ implantation, extended defects and precipitates 80−49251
W:K-Al-Si, state of bonding, distribution of impurities 78−92212
WF_6+Na(K) electron transfer, WF_6^- form., dissoc. energies, electron affinity 77−19071
ZnTe:K, fluorescence spectra meas. 78−10949

potassium alloys
dilute binary alloy, residual resistivity 77−1406
Fe-K, dil., mag. hyperfine field, TDPAC meas. 78−43699
FePC molten and amorphous alloys, struct. factors 80−79674
Hg-K, liquid, structure factors, X-ray scatt. *(Japanese)* 80−54122
K-Cs, extreme UV absorpt. spectra 80−97294
K-Cs, thermal conductivity determ. 80−107760
K-Cs alloys, elec. resist., minima for K_2Cs, K_7Cs_6 concs. *(German)* 78−14708
K-Cs solution, activity and saturated vapour press. of Cs, reson. line absorpt. obs. 77−51509
K-Cs(Na) liquid alloys as coolants, sp. ht. 79−86902
K-Na, dil., dynamical props. of quasiparticle excitations, de Haas-van Alphen effect meas. 78−84128
K-Na(Cs), thermodynamic props. at high temps. 80−15262
K-Rb, dil., calc. of press. depend. of low-temp. transport props. 78−30905
K-Rb, extreme UV absorpt. spectra 80−97294
K-Rb, internal energy, heat of mixing, entropy, dielectric function 80−88340
K-Rb, liq., elec. resistivity, temp. depend. 78−39084
K-Rb, liq., form factors and transport coeffs., pseudopot. perturb. theory 80−44561
K-Rb, liquid, resistivity calc. using general method pseudopot. 77−55506
K-Rb(Cs)(Na), solute atom-grain boundary interaction energy, electron-statistical calcs. *(Russian)* 79−73175
K-Rb(Na), dil., anisotropy of electron-impurity scatt. in K, de Haas-van Alphen effect meas. 78−18943
K-Rb(Na), dil., anisotropic scatt. of conduction electrons by impurities 78−18944
K-Tl, liq., elec. resist. meas. 77−51717
K_2Cs and K_7Cs_6, OPW calc. of struct., bonding and stability 77−43169
K_2Cs, Laves phase, chemical bonding, electronic charge density distrib. pseudopotential calcs. 79−77549
K_7Cs_6, μ-phase variant, chemical bonding, electronic charge density distrib. pseudopotential calcs. 79−77549
K_3Ga_{13}, X-ray cryst. struct. determ. 80−92479
KLi, appearance pot., dissoc. energy, ionis. pot., mass spectra obs. 78−25750
K_2Li^+, equilib. geom. and dissoc. energy, pseudopot. calc. 78−94329
KNa_2, binding energy and lattice const., nonparametric calc. *(Russian)* 78−51462
K_2Na^+, equilib. geom. and dissoc. energy, pseudopot. calc. 78−94329
K_cRb_{1-c}-alloys, lattice dynamics of substitutional alloys, force constant disorder 78−75786
Li_2K^+, equilib. geom. and dissoc. energy, pseudopot. calc. 78−94329
Na-K, internal energy, heat of mixing, entropy, dielectric function 80−88340
Na-K, liq., dynamical struct. factor calc. 78−22634
Na-K, liq., form factors and transport coeffs., pseudopot. perturb. theory 80−44561
Na-K, liq., static struct. factors 78−63664
Na-K, liq., third-order partial struct. factors 77−47339
Na-K, liq. alloy, electronic correl. functions calcs. 78−63663
Na-K, liq. alloys, electromigration driving force expression 78−51714
Na-K, liq. calc. of electromigration forces and resist. 79−82572
Na-K, liquid, collective excitations, mol. dynamics calc. 80−28895
Na-K, liquid, electron theory of chemical potential and activity *(Japanese)* 77−72702
Na-K, liquid, resistivity calc. using general model pseudopot. 77−55506
Na-K, liquid alloy energy of soln. pseudopotential calcs. *(Russian)* 79−66330
Na-K, partial structure factors, square well pot. calcs. 77−51300
Na-K, surface tension theory for liquid mixtures 80−88404
Na-K alloys, liq., thermal conductivity, NaK_2 formation 78−10416
Na-K liq. alloy, Moelwyn-Hughes parameter calc. from US data 80−59375
Na-K liquid alloy, self and mutual diffusion coeff. 78−22877
Na-K liquid alloy, small angle X-ray scatt. study, conc.-fluctuation structure factors 80−54120
Na-K liquid alloys, struct., X-ray and neutron diffr. meas. 80−107041
Na-K liquid alloys, triplet correlation functions and thermodynamics, solute partial structure factor 80−64881
Na-K-Cs alloys, liquid contact material, phase diagram calcs. 78−6145
Na-K-H system, H influence on component interactions *(Russian)* 80−54383
NaK, liq., engineering handbook, purification, heaters, coolers, radiators 80−27045
Na_2K, OPW calc. of struct., bonding and stability 77−43169
Na_2K+, equilib. geom. and dissoc. energy, pseudopot. calc. 78−94329
Na_xK_{1-x}, solid-liquid transition 78−6144
Nb-K melts, thermodynamic characts., elec. resistivity, single parameter rigid sphere calcs. *(Russian)* 80−34410
NiNaK, mol., intersection of pot. energy surfaces, ab initio calcs. 79−36557
Rb-K, dil., dynamical props. of quasiparticle excitations, de Haas-van Alphen effect meas. 78−84128
Rb-K, lattice vibrs. in CPA, comparison to neutron scatt. meas. 79−42165
Rb-K alloys, localised phonon modes, classical mol. dynamics compuer simulation 78−10147
$Rb_{1-c}K_c$, local mode exam. by neutron diffr. 79−37781
$Rb_{1-c}K_c$, phonon spectra, single site CPA 78−10142

potassium alloys continued
$Rb_{1-x}K_x$, influence of many electrons exchange and correlation effects on vibr. props. 79−69443
$Rb_{71}K_{29}$, lattice dynamics, molecular dynamics study 79−37782
W-K-Si-Al doped wires, heavily drawn, fibre struct., annealed 79−56993

potassium compounds
see also potassium alloys; Rochelle salt
acetylacetonate, polycryst., elec. cond., pyroelectricity, phase transition, UV spectrum 78−76392
acid oscalate, neutron inelastic scatt. spectra in 2200-200 cm^{-1} range 80−70327
acid phthalate curved crystal spectrograph, diffraction efficiency calc. method 80−79630
alkanoates, phase relationships and thermal behaviour branching effects 78−43111
n-alkanoates, phase transitions, differential scanning calorimetry 77−43319
alunite-jarosite, spcae group refinement by means of vibr. spectroscopy 79−94981
anion exchange, in tablet pressure for IR spectroscopy *(Russian)* 78−95927
antimonyl tartrate, neutral aq. soln., gamma radiolysis 80−101030
Auger spectra, shake-up satellites 78−27369
1,1-cyclobutane dicarboxylic acids and K salts, IR and Raman vibr. spectra *(French)* 80−2758
diffusion traps for divalent ions, dielectric loss and ionic thermocurrent techniques 80−6566
dipotassium tartrate single crystal, SHG 78−13757
feldspar, pulsed RF radiation produced by scratching *(Russian)* 78−19607
fluophlogopite, substrate for metal film epitaxial growth, orientation rels. *(Russian)* 77−31910
fluorides, $KM^{II}M^{III}F_6$, (M=1st row transition metal, Zn, or Mg), divalent and trivalent ion distribs., Mossbauer obs. 78−2777
germanate crystals and glasses, struct. and stability, IR spectra meas. 80−64911
graphite intercalation compound, $C_{8.8}K$, mag. susceptibility fluctuations near supercond. transition temp. 79−78259
graphite intercalation compound, polarised refl. spectra 78−31213
graphite intercalation compounds, C_nK, electronic struct. and elec. props. 80−44471
graphite intercalation cpds., C_nK, de Haas-van Alphen effect, cyclotron reson., and transport props. 80−44479
graphite-K compounds, intercalates IR active lattice mode obs. 80−45072
graphite-K inclusion compounds, paramagnetism after treatment by π or n donors *(French)* 78−10749
graphite-K intercalation compound, dielec. function, EELS study 80−45183
graphite-K intercalation compound, effect of H addition on superconducting transition temp. 80−70872
graphite-K intercalation compounds, Fermi surface, transport and supercond. props. 79−65367
graphite-K lamellar cpd., reversible intercalation of tetrahydrofuran 80−16211
halide solids, lattice dynamics, three body force shell model studies 79−55841
halides, absorpt., emission and lifetime data, temp. depend. 77−4671
halides, elastic constants, temp. derivatives at constant volume 80−59549
halides, F-centres, optical pumping, spin-orbit and hyperfine coupling 77−16359
halides, F-centres, optical pumping, spin-orbit and hyperfine coupling 77−16360
halides, He II photoelectron spectra, ionisation energy 77−18977
halides, lattice dynamics, bond-bending force model 80−54322
halides, lattice dynamics in five parameter model 80−107382
halides, photoelectric yield spectra, 10 to 40 eV photon energy 79−28887
halides, spin lattice relaxation meas. of O_2^- centres 80−88863
halides, surface lattice dynamics, by Green's function method 78−71936
hexahalogeno compounds: $ReCl_6^{2-}$ ($ReBr_6^{2-}$), low symm. splittings in vibronic spectrum due to phase transitions 80−55161
hollandite, matrix method appl.for calc. of diffuse scattering 79−99023
hollandite, one dimensional ionic and solitary wave conduction 79−23954
Hollandite, one-dimens. ionic conductor, modulation and incommensurability 80−19980
hollandites, ionic cond., impedance, struct. 78−67856
hydroxymethanesulphonate, X-ray cryst. and mol. struct. determ. 79−32983
Hygroscopicity of double-condensed sodium potassium phosphates 77−84939
intercalated donor cpds. of graphite, Raman scatt. 78−10890
intercalation compound with graphite, resistivity anomalies and phase transform. 78−26839
intercalation compounds with graphite, electronic props., de Haas-van Alphen effects and Fermi surfaces 80−75498
intercalation compounds with graphite, electronic props., resistivity, Hall effect and magnetoresistance 80−75585
intercalation compounds with graphite, phase transitions, resistive anomalies, electronic props. 79−95405
intercalation lamellar graphite derivatives, $KC_{24}(tetrahydrofuran)_m$, (m=1 and 2), ^1H NMR study 80−44932
K-TCNQ, high and low temp. phases, dielec. const. 80−34844
$KAlF_4$, single cryst., prep. and struct. *(French)* 80−79762
KBr, γ-irradiated and additively coloured, chemiluminescence origin *(Russian)* 77−32453
KBr, thermally processed cryst., optical absorption bands *(Russian)* 78−76513
$KCl-BaCl_2$ system, solid solns., phase diagram, enthalpy of soln., vibr. entropy. 78−39751
KCN, relax. times of F-centres meas. at 83K phase transition 77−59458
KD_2PO_4, high efficiency freq. doubling of Nd:YAG laser light 78−79071
$KFeF_4$, reflections of new type in Mossbauer diffraction pattern 79−78594
KI, linear dichroism spectra, stress-induced, reorientation of O_2^- and NO_2^- impurity ions *(Russian)* 80−45127
$KNbO_3$, near IR noncritically phase-matched SHG 79−72620
KOH solutions, effect on corrosion and electrochem. props. of Mo_2C 80−11813

potassium compounds continued
$KZnF_3$:Er excitation of 650 GHz phonons in spin-lattice relax. 78−27089
laurate-1-decanol-water mixtures, biaxial nematic phase obs. 80−107409
lithium potassium tartrate monohydrate: Mn^{2+}, isomorphism with lithium ammonium tartrate monohydrate, EPR obs. 80−29607
micaceous-crystalline material, cast, prep. and props. 77−12591
milarite-leucospherite-tuhualite, struct. series derived from α-celsian 79−19223
muscovite, substrate for metal film epitaxial growth, orientation rels. *(Russian)* 77−31910
nepheline-kalsilite system, subsolidus phase relations at 0.5, 2.0, and 5.0 kbar 79−66041
oxalate, EPR of Mn^{2+} and VO^{2+} 80−39858
oxalate monohydrate:Cu^{2+}, ESR and isomorphism of Cu^{2+} 77−32252
oxalate monohydrate:VO^{2+}, IR absorpt. study 80−55134
oxide, mass spectrometric investigation 78−64873
porcelain, crack propag. data applicability to failure prediction 80−81154
potassium acetate, thermal expansion 79−51280
potassium bis(oxalato)beryllate, cryst. struct. *(French)* 78−34499
potassium formate, X-ray cryst. struct. determ. 80−107194
potassium hydrogen malonate, deuterate, NQR data (I=1) from ENDOR expts. 80−54994
potassium hydrogen malonate, room-temperature ENDOR spectra obs. 80−106339
potassium hydrogen malonate single cryst., IR and Raman spectra 78−60444
potassium hydrogen oxalate, oriented single cryst., Raman spectra with very strong H-bonding 80−25359
potassium iron tri(hydrazoformate), Debye-Waller factor, Mossbauer spectra obs. 79−56627
potassium oxalate, anhydrous, phase II, vibr. spectra and cryst. struct. 80−34901
potassium oxyacid salts, aq. electrolytes, apparent molar heat capacities and vols. 79−23744
potassium palmitate-water bilayer, lamellar liq. cryst. polymorphism, NMR and birefringence 79−60270
potassium tetramethylborate, vibr. spectra and force constants *(German)* 79−26981
potassium zirconium oxalate, X-ray K-absorpt. spectra 78−76558
proton bombardments, spectral refl. change and luminesc. with implications for Io 79−96950
γ-quartz, reaction, with NaCl-KCl melt, exam. of struct., IR absorption spectra 80−55706
rare earth double sulphates, $K_{6+3n}R_{4-n}(SO_4)_9$, ($n\approx0.4$), cryst. struct. 80−28985
rare earth potassium molybdates, flux growth of $RKMo_2O_8$, R_2MoO_6 and R_6MnO_{12} in R_2O_3-K_2O-MoO_3 system 78−35289
sheet phases $K_x(L_xM_{1-x})O_2$, (L=In,Sc; M=Ti,Zr,Hf,Sn), ionic cond., influence of K^+ environment *(French)* 79−65244
silicates, entropy estimates at 298K from molar vols. 77−1243
soaps, heterogeneity of chain lengths, factor in lyotropic polymorphism 78−59746
sodalites, aluminogermanate- and aluminate-, IR spectra rel. to T-O bond length and T-O-T ang. 79−91445
TCNQ salt, K-TCNQ, ^{14}N NQR temp. depend. rel. to Peierls transition 79−82892
TCNQ salt, K-TCNQ, cryst. struct. *(French)* 78−43006
TCNQ salt, K-TCNQ, energy gap, electron-phonon interaction, IR spectrum 78−15167
TCNQ salt, K-TCNQ, EPR linewidth, ang. and freq. depend. 80−80591
TCNQ salt, K-TCNQ, spin-Peierls system, paramag. susceptibility, Heisenberg chains 79−38299
TCNQ-K, dielectric function of 1-dimens. Hubbard model 79−60740
TCNQ-K, X-ray exam. of phase transitions 78−55933
ternary chlorides, $ABCl_3$ type, optical props. 78−35111
tetracyanoplatinate conductors, IR and Raman spectra, cyanide stretching vibrs. 79−11415
triple orthoarsenates, $KM^{II}Cr_2(AsO_4)_3$, prep. by high temp. synthesis, and cryst. struct. 79−66028
trisoxalatoferrate complexes, Mossbauer studies of electronic relax. phenomena 80−44973
zeolite, faujasite type, intermed. state of enhanced mobility of adsorbed H_2O mol. 78−60027
$33K_2O.7Al_2O_3.60P_2O_5$, high expansion glass, chemical durability improvement by ion exchange 79−66180
AgCl-KCl, solns., activity coeffs., surface tensions, 860 to 1000K 78−76897
$AgNO_3$-KF in ice matrix, γ-irrad., Ag at. form., solution, ESR 77−59454
β-Al_2O_3-$(K,Li)_2O$ and β-Al_2O_3-$(K,Sn)_2O$, ionic cond. and Raman spectra 80−107509
β-Al_2O_3-$(Na,K)_2O$, equil. distrib. of ionic species 80−107511
β-Al_2O_3-$(Na,K)_2O$, model calcs. of cond. anomalies, pot. energies of cation arrangements 80−107510
β-Al_2O_3-K_2O, ESR of paramag. defects in cond. planes 80−29617
β-Al_2O_3-K_2O, far IR absorption and ionic cond. 78−72512
β''-Al_2O_3-K_2O, ionic cond. at room temp. 80−107513
β-Al_2O_3-K_2O, K-content determ., ave. backscatt. spectra anal., rot. sample technique 79−5208
β-Al_2O_3-K_2O, low temp. dielec. susceptibility meas. 79−82911
β-Al_2O_3-K_2O, low-energy excitation spectra, localised modes 80−59606
β''-Al_2O_3-K_2O, single cryst. Raman scatt., cond. mechanism and cryst. struct. 80−66209
β-Al_2O_3-K_2O, sp. ht., 0.1-1 K, evidence for localised low-energy excitations 78−34632
β-Al_2O_3-K_2O, thermal cond. below 300K 77−24454
β-Al_2O_3-K_2O, with mobile ion species, dielec. relax. 79−91351
β-Al_2O_3-K_2O, X-ray diffuse scatt. 78−71725
β''-Al_2O_3-K_2O 80−11394
β-Al_2O_3-K_2O/K ferrite, interfaces and solid soln., thermal expansion and lattice parameter variations 78−55959
β-Al_2O_3-K_2O-MgO, cryst. struct., nonstoichiometry, ion-ion correlations 80−88129
β-Al_2O_3-Na_2O-K_2O, cation interstitial pair modes in vibr. spectra 79−37788
β-Al_2O_3.$(K_xNa_{1-x})_2O$, anomalous behaviour in ionic cond. obs. 78−87818
β-Al_2O_3.K_2O, low temp. sp. ht., tunnelling states and diffusion theory 77−43345

potassium compounds continued
$Al_2(SO_4)_3$ $K_2SO_4.24H_2O$, formation, survival and growth of nuclei from secondary nucleation 80−50540
$Al_2(SO_4)_3$-$K_2SO_4.2PH_2O$, rel. between etch pits or growth hillocks and dislocations on (111) faces 79−77602
$Al_2(SO_4)_3.K_2SO_4.24H_2O$, spirals, growth and dissolution from liq. state 80−15027
Au condensation kinetics, on KCl 80−88453
B_2O_3-K_2O, thermal cond. of melt in region 900 to 1100°C, effect of convection 78−2309
B_2O_3-K_2O glass 79−24337
B_2O_3-K_2O-Na_2O-Rb_2O-Cs_2O glass, small angle X-ray scatt. exam. of struct. 80−38922
B_2O_3-NaKO glass, dielectric relaxation at low temp. 79−11384
$Ba_2KNb_5O_{15}$, Raman scatt. experiments in tetragonal tungsten bronze compounds 80−40113
$BaKP_3O_9.H_2O$, cryst. struct. *(French)* 78−51480
BaO-K_2O-Na_2O-ZnO-SiO_2, corrosion and microhardness, effect of detergents 80−16518
BaO-K_2O-VO_2-SiO_2, glass, elec. cond. rel. to ion polarisability, polarons 80−49729
BeF_2-KF-CaF_2-AlF_3:Nd^{3+} (Er^{3+}) glass, multiphonon relax., fluoresc. obs. 78−15219
BeF_2-KF-CaF_2-AlF_3-EuF_3 fluoroberyllate glass, Eu^{3+} fluoresc. linewidth 80−66285
BeO-P_2O_5-K_2O glass, gamma irrad., cation modifier effect on radiation centre formation 80−40720
α-Bi_2O_3+KCl, quantitative anal. of multocomponent powders, full-profile refinement of Guinier-Hagg X-ray film data 79−39249
$C_{12n}K$, graphite intercalated, two-dimens. structurally disordered phases, X-ray diffr. profiles 80−44181
C_8K, graphite intercalated, phonon dispersion relations and Raman spectra 80−44272
C_8K, intercalation compound, superconductivity 78−91827
C_8K, intercalation cpd. with graphite, supercond. props. 80−44755
C_xK intercalation compound with graphite, low temp. specific heat meas. and XPS 78−26693
$CaCl_2$-KCl, binary melt, viscosity *(Japanese)* 78−10209
$CaK_2As_2O_7$, cryst. struct., bond lengths 77−31639
$CdCl_2$-KCl-H_2O, water activity, 0 and 50°C, conc. depend. *(Russian)* 78−31679
$CdCl_2$-NaCl, KCl molten salt mixtures, US velocity and adiabatic compressibility obs. 78−75730
CdF_2-KF, liquid mixture, enthalpy of mixing 78−48684
$CdK_2(Cr_2O_7)_2.2H_2O$, X-ray cryst. struct. determ. using MULTAN *(French)* 79−69082
$CdK_2P_2O_7$, cryst. struct., bond lengths 77−31639
$CdK_4(P_3O_9)_2.2H_2O$, cryst. chemistry and cryst. struct. determ. *(French)* 78−26505
CeKFe$(CN)_6.4H_2O$, struct., X-ray diffr. obs. 79−51065
$CoCl_2$-KCl-NaCl system, melting diagram investigation by thermographic anal. *(Russian)* 78−3111
$CoK_4(P_3O_9)_2.7H_2O$, cryst. data *(French)* 78−79568
CsCl+KCl mixtures, osmotic coeffs. at 298.15K 78−92509
Cs_2KPrF_6, Raman spectrum and cryst. field *(German)* 79−51940
$Cs_2KTmBr_6(Cl_6)(F_6)$, mag. behaviour 2.9 to 251.3K, cryst. field levels, ang. overlap model *(German)* 80−29520
Cs_2KYbF_6, mag. behaviour, 3.5-251.3K *(German)* 80−50041
Cs_2O-SiO_2 glass, low temp. heat capacity 80−49373
$CuK_2Cl_4.2H_2O$, Heisenberg ferromag., mag. props. at high press. 77−69512
$CuK_2Cl_4.2H_2O$, Heisenberg ferromag., mag. field effect on susceptibility near crit. point 80−39758
$CuK_2Cl_4.2H_2O$, proton spin-lattice relax. and exchange interactions, temp. depend. 79−95663
$CuK_2H_2(PCrO_7)_2$, cryst. struct. determ. 80−28989
$CuK_2(SO_4)_2.6H_2O$-liquid ^{3}He interface, thermal boundary resist. from 8.5 to 110 mK 79−56001
Dy_2O_3-K_2O-MoO_3, melt, viscosity meas. 79−99346
F_2SnBr_6, cryst. struct. determ. at room temp. 79−19202
$Fe_{10.92}K_{1.55}O_{17}$, ferrite, cryst. struct., nonstoichiometry, ion-ion correlations 80−88130
Fe_2SiO_4-$KAlSi_2O_6$-SiO_2, phase relations at 1 atm., and low temp. liq. immiscibility 79−47664
n-GaAs/K_2Se-K_2Se_2-KOH/C solar cell, Ru (III) chemisorption on photoanode, effect on performance 80−3516
β-Ga_2O_3-K_2O/K ferrite, interfaces and solid soln., thermal expansion and lattice parameter variations 78−55959
β- and β''-Ga_2O_3-Na_2O-K_2O, fast ion conductor, Na^+ self diffusion and Na-K exchange 79−28133
β''-Ga_2O_3-Na_2O-K_2O mixed crystals, cond. anomaly 79−46838
GeO_2-K_2O, glass, Raman spectra, struct. and crystn. 80−92463
GeO_2-K_2O, glass composition effect on solubility in H_2O 80−39303
HCl-KCl-H_2O mixed electrolyte solns., elec. transport 80−3355
HgI$_2$:KI, cryst. growth from soln., doping rel. to elect. cond., phase transitions 77−55880
$Hg_4PO_4NO_3.H_2O$, cryst. struct. *(French)* 78−42992
(K,Na) $(AlSi_3O_8)$, feldspar, N^{2-} ESR spectrum parameters *(Ukrainian)* 79−38366
(K,Na)NbO_3 ceramic, hot pressed, dielec. props. 79−87375
K hollandite, one-dimens. ionic and solitary wave conduct. theory 79−86924
K salt of β-ketoaldehyde, configurations of anions in solutions studied by IR spectroscopy, H-bond form. 80−87117
K-β-Al_2O_3, far IR absorpt., Beevers-Ross sites, interstitials 80−66240
K-Cs, liquid, resistivity calc. using general method pseudopot. 77−55506
K-Cs silicate glass, thermal expansion 77−4186
K-intercalated graphite (stage-1), electron energy loss expts. and band struct. theory 79−100001
K-La-NH_3 system, cpd. formation, phase analytical and X-ray expts. *(German)* 79−66043
K-Rb silicate glass, thermal expansion 77−4186
K-TCNQ, low temp. relf. spectra 80−25353
K-U-O system, cryst. chem. 77−39568
$KALF_4$, dissoc. enthalpies, mass spectrometric determ., heat of form. 80−97720
KAg_4I_5, ionic conductivity and heat capacity near T_c 78−47584
KAg_4I_5, phase transitions and dynamics 78−59924
KAg_4I_5, solid electrolyte, Raman spectra 79−73934
KAg_4I_5, superionic cond., pressure effect on phase transitions 80−70405
KAg_4I_5, superionic film, elec. ionic cond. and electron spectra 80−6543
potassium compounds continued
KAg_4I_5, superionic phase transition, dynamical and crit. pt. props. 80−107535
KAg_4I_5, superionic solid films, preparation and elec. cond. 79−82380
K_3AgO_2, determ. of cryst. struct. X-ray diffr. *(French)* 78−95029
$K_2Ag_4Se_3$, crystal struct., X-ray study *(German)* 78−83795
KAl_2Br_7, ^{81}Br NQR and ^{27}Al NMR 78−6597
KAl_2Br_7, intramolecular configs., nucl. quadrupole double reson. obs. 80−34821
KAl_2Br_7, NQR double-reson., $Al_2Br_7^-$ ion in cryst. 78−91993
$KAlCl_4$, cryst., Raman spectra, orthorhombic space group, Cl splitting of $AlCl_4$ 77−85700
$KAlCl_4$, cryst. struct. 78−51487
$KAl(CrO_4)_2.2H_2O$, cryst. struct. *(French)* 77−80478
$KAlF_4$, hydrothermal growth method in presence of hydrofluorhydric acid *(French)* 80−25543
$KAlO_2$, phase diagram and thermodynamic props. 79−91985
$KAl(SO_4)_2.12H_2O$, single cryst., Raman spectra, temp. depend., SO_4^{2-} site dynamic disorder 77−40219
$KAl(SO_4)_2.12H_2O$, occlusion formation during dendritic crystal growth, expt. 78−38993
$KAl(SO_4)_2.12H_2O$, third order elastic consts. from stress shifted reson. freqs. 78−55905
$KAl(SO_4)_2.12H_2O$, secondary nucleation, origin, nuclei size distrib. 79−94933
$KAl(SO_4)_2.12H_2O$:Cr^{3+}, ESR high-order transitions 79−11338
$KAl(SO_4)_2.12H_2O$:MnO_4^-, visible and UV absorpt. spectra interpretation 80−45116
$K_2Al_2(SO_4)_4.24H_2O$, temp. depend. curves of quadrupole interaction parameter for $^{27}Al^{3+}$ 77−55727
$K_2Al_2(SO_4)_4.24H_2O$, growing in aqueous solution, observation of secondary nuclei production 78−68613
$KAlSiO_4$ metastable polymorph, prep. by ion exchange with $RbAlSiO_4$, struct. 78−79585
$KAlSiO_4$, phase diagram and thermodynamic props. 79−91985
$KAlSi_2O_6$, elec. cond. meas. 78−47787
$KAlSi_2O_6$-$Ca_2MgSi_2O_7$-$CaMgSi_2O_6$, phase diagram of ternary eutectic system 78−80529
$KAlSi_3O_8$, ball mill grinding, wet, dry, rate constant determination *(Japanese)* 78−95827
$KAlSi_3O_8$, ball mill grinding, rate constant determination *(Japanese)* 78−95828
$KAlSi_3O_8$, feldspar, fission fragment track registration development efficiencies, etchant (etching conditions) depend. 78−66454
$KAlSi_3O_8$, feldspar microwedge, melting by CO_2 laser, deform. of IR absorpt. spectra 77−19984
$KAlSi_3O_8$, orthoclase, impact structs., peak shock press., X-ray diffr. investig., lunar rock bombard. appls. 78−7002
$KAlSi_3O_8$:rare earth ion, glass, nonradiative energy transfer and fluoresc. quenching 77−20905
$KAlSi_3O_8$-$BaAl_2Si_2O_8$ hyalophane, natural and heat treated, cryst. struct. refinement 78−2072
$K_xAl_xTi_{8-x}O_{16}$, $1.6 \leq x \leq 2.0$, dielec. response in freq. range 10^{-3} to 10^6 Hz 79−65785
$K_xAl_xTi_{8-x}O_{16}$, ionic cond., K mobility rel. to struct. and bonding *(French)* 77−76594
$K_xAl_xTi_{8-x}O_{16}$, ionic cond., rel. to struct. and chemical bonding *(French)* 78−18824
$KAl[Fe^{(V)}(CN)_6]$, isomer shift of Mossbauer spectra 80−29662
$K_3As^{III}_xAs^{V}_{4-x}O_{11.5-x}$, solid-state synthesis, crystalline phase *(French)* 80−15079
$KAsO_3$-K_3AsO_4, phase diag. 78−23681
K_3AsO_4, aq. solns., isomorphous salts viscosity investig. 78−95173
K_3AsO_4-$KAsO_3$, glass and cryst., Raman and IR spectra 79−99862
$K_4As_2O_7$, solid-state synthesis, X-ray powder data *(French)* 80−15079
$K_5As_3O_{10}$, X-ray single-cryst. struct. determ., Patterson method 80−96484
KB_6, prep., cryst. struct., thermal stability, phys. and chem. props., book contrib. 78−47304
KB_3H_8, NMR study of proton and boron dynamics 80−71210
$K_2B_{12}H_{12}$, cryst. growth from soln. and morphology 77−44145
$K_2B_{12}H_{12}$-KBr, cryst. growth from soln. and morphology 77−44145
KBO_2, vapour over heated solid, XPS, obs. 80−87171
KB_5O_8, coherent CW radiation generation by mixing, tunable 211 to 216 nm 78−83029
KB_5O_8, sum freq. mixing, tunable coherent radiation source below 217 nm 77−19359
KB_5O_8, tunable coherent radiation generation, 201-212 nm 77−83921
KB_5O_8, tunable coherent vac. UV generation by sum freq. mixing 78−55404
$KB_5O_8(D_xH_{1-x})_2O$, isotope exchange during crystallisation from aqueous solns. 78−18569
$KBO_2.4/3H_2O$, unusual hydrogen bonding 78−2058
$KB_5O_8.4D_2O$, SHG and sum freq. mixing 78−55407
$KB_5O_8.4H_2O$, efficient UV generation, 2073 to 2174 Å 77−62003
$KB_5O_8.4H_2O$, freq. doubling, angle tuning, mol. appl. 77−3632
$KB_5O_8.4H_2O$, phase matched 2314 Å generation 77−7155
$KB_5O_8.4H_2O$, phase matched 2120Å generation, Nd:YAG fifth harmonic 77−14777
$KB_5O_8.4H_2O$, polariton Fermi reson., spontaneous parametric light scatt. 78−87923
$KB_5O_8.4H_2O$, tunable UV generation at 1966 Å 77−68238
K_2BRCl_6, B=Li,Ag,Na, systematic structs., X-ray Guinier-Simon method *(German)* 80−44186
$K(B_xW_{3-x})O_9$ (B=Na, Ca, Co, Ni, Cd, Ga, Bi, Nb, Ta) cryst. struct., temp. dielec. anomalies 80−1998
$K_2BaCu(NO_2)_6$, antiferromagnetic Heisenberg spin 1/2 simple quadratic lattice, mag. and caloric meas. 79−78397
$K_{6-2x}Ba_xM_6Si_4O_{26}$, M=Nb,Ta, IR spectra, appl. to nonstoichiometry in cpds. with $(M_6X_4O_{26})$ layers (X=Si,Ge) *(French)* 79−11418
$K_2Ba(NO_2)_2$, elastic props. 80−96588
$K_2Ba(NO_2)_4$, ferroelastic, Raman spectra and phase transition 79−56800
$K_2Ba(NO_2)_4$, new ferroelastic, phase transitions, optical and electrical props. 79−55887
$(K_{0.01}Ba_{0.24}Sr_{0.71})_2Al_{4.1}Si_{11.9}O_{32}.nH_2O$, brewsterite cryst. struct. refinement 77−80471
$K_{6-2x}Ba_xTa_6Si_4O_{26}$, struct. determ. *(French)* 77−27866
$K_{2-2x}Ba_{3x}Ti_{6-x}O_{13}$, $0<x<0.2$, struct. evolution, tunnel struct. 79−65049
K_2BeF_4, aq. solns., isomorphous salts viscosity investig. 78−95173

potassium compounds continued
$K_2Be_2Si_6O_{15}$, synthetic, epididymite group, X-ray diffr. struct. anal. 77−43204
$K_{1.14}Bi^{III}_{0.64}Bi^{V}_{1.73}O_{5.85}(H_2O)_{0.97}$, cryst. struct. *(French)* 77−72596
$KBiF_4$, anionic conductivity exam. *(French)* 77−35952
$KBiF_4$, fast ionic conduction of F^- ions 79−99360
$KBiF_4$, new solid electrolytes, conductivities and activation energies 79−28137
$K_2BiNb_5O_{15}$ substrate for $K_3Li_2Nb_5O_{15}$ film for optical waveguide, cryst. struct., dielectric props. 80−79016
$K_5Bi_{1-x}Nd_x(MoO_4)_4$ solid soln., growth, spectroscopic and laser props. 78−2901
$(K_{3/4}Bi_{1/4})(Zn_{1/6}Nb_{5/6})O_3$, cation disordered perovskite, elastic consts. and thermal expansion 80−96587
KBr, absorption coeff. determ. in 10.6 μm region, laser calorimetry method 79−7186
KBr, activation coefficients and solvation numbers in mixed methanol solvents 80−81334
KBr, additively coloured crystal, depend. of bleaching kinetics on F-light intensities, holographic storage *(Russian)* 79−27351
KBr, additively coloured crystal, amplitude-phase holograms *(Russian)* 79−59654
KBr, additively coloured, self-enhancement of amplitude hologram *(Russian)* 80−9828
KBr, additively dyed, amplitude-phase holograms *(Russian)* 80−1152
KBr, adsorbed CO_2 film, density fluctuations 79−42391
KBr, adsorption pot. energies of Ar and Kr calc. 78−71993
KBr, alkali halide crystals, defect state change during electrolysis 78−95057
KBr, amplitude and phase spectra, 80 to 280 cm^{-1}, Fourier spectroscopy technique 77−45903
KBr and KBr:Sr X-irradiated, optical investig. of Br_3^- centres 77−16348
KBr, aq. solns. hypersonic sound vel. and absorpt. meas. 78−30699
KBr, avalanche type crystal formation *(Hungarian)* 80−11552
KBr, barrier instability in strong elec. fields 79−69522
KBr bicrystal, Ag^+ injection transport and grain boundary mobility, electrodecoration obs. 80−2214
KBr bicrystal, grown from melt, interfacial substructure, impurity effects 77−4263
KBr, binding energy of F_{e+}', M_{e+}' and R_{e+}' centres, positron trapping 79−69460
KBr, Bragg diffraction, anharmonic contributions, Mossbauer study 78−76359
KBr, change of state of F-centres due to electrostatic field *(Russian)* 79−58827
KBr, chem. laser window material 77−46769
KBr cleavage plane, mobility of small Au crystallites 79−23857
KBr, cohesive properties, analysis using density functional formalism 79−90592
KBr, colour centre form. under polarised UV irrad., dichroism in absorption spectra 80−107232
KBr, colour centres isothermal decay 79−51975
KBr, Compton profile, 59.54 keV γ-rays 78−64426
KBr, cryst. growth physical vapour transport method for low dislocation density crysts. 78−43992
KBr crystal, cordlike defects and countermeasures 79−72636
KBr crystals, binding forces and eqns. of state, inner electron contrib., calc. 80−64950
KBr, crystals, X-ray irradiated, luminescence during release of pressure 79−65939
KBr, current oscills. in elec. fields of $\sim 10^6$ Vm^{-1} *(Russian)* 77−20334
KBr, Debye-Waller factors at 4.2 and 295K 79−7667
KBr, decay and time resolved emission spectra from σ-excitons produced by heavy-ion irradiation 80−89071
KBr, defect accumulation under electron irrad. at 4K 80−107233
KBr, defect modes due to H^--D^- pair impurities 80−59602
KBr, defect modes due to substitutional anion-pair and cation-pair impurities in ionic crystals 80−92540
KBr, diffusion of Br_2, 375 to 600°C, obs. using OH^- centre decomp. 77−43378
KBr, diffusion-controlled defect recombination, quasi-steady radius, tunnelling and elastic interaction *(Russian)* 80−10908
KBr, dislocation interaction with radiation-induced single halogen interstitials 78−34536
KBr, dislocation internal friction, orientation depend. 78−48439
KBr, doped with F-centres, Raman spectra meas. excitation in F and K bands 80−16027
KBr, dynamic equilib. between F and F_2 centres at room temp. 79−51103
KBr, ENDOR of F_A(Li) centre meas., 4.2 and 1.8K 77−63320
KBr, effect of addition on corrosion of Cu in seawater 78−80670
KBr, efficiency of creation of X_3^- centres in X-rayed alkali halides *(Russian)* 78−71731
KBr, efficiency of V_k- and Ag^0-centres generation *(Russian)* 80−39080
KBr, elastic moduli, quadratic fit against temp. 78−14397
KBr, electrolytic coloration effect on dislocation density 77−4106
KBr, electrolytically coloured single cryst., ionic SCL transient and steady elec. currents 77−62937
KBr, electron irrad., F-centre formation kinetics, interstitial stabilisation mechanism 79−69103
KBr, electron irrad. at 4K, role of V_K centres in equilib. among centres 78−67712
KBr, electron irradiated, defect accumulation kinetics of low temps. 80−10577
KBr, electron-spin memory and magnetic-circular-dichroic effects in F-centre luminesc. 80−29794
KBr, electronic states at (100) surface, accounting for spin-orbit interaction *(Russian)* 78−91750
KBr, electronic struct. of self-trapped excitons calc. 77−39784
KBr, emission spectra of O_2^- and NO_2^- centres at high hydrostatic press. 78−10943
KBr, energy of form. of Schottky defects 77−7714
KBr, enthalpies of soln. in water 80−50880
KBr, excitation of thermolum. near liq. He temp. 80−40171
KBr, exciton mechanisms of electron sputtering 77−55857
KBr, exposed to US waves, dislocation multiplication in original stage 78−47383
KBr extrinsic absorpt. near 9.6 μ, using CO_2 laser calorimetry 77−16341
KBr, F_A(Li)-centre spin-lattice relax. at 4.2K 78−91950

potassium compounds continued
KBr, F_2 centres triplet state, radiative and nonradiative decay 79−11438
KBr, F^--centres, thermal and photolytic decay processes 78−95053
KBr, F-centre emission, mag. circular polarisation 80−108251
KBr, F-centre lifetime, perturbation effects, luminesc. meas. 80−108252
KBr, F-centre luminesc., MCD effects 78−39598
KBr, F-centre radiative lifetime meas. near 65K 80−25439
KBr, F-centre spin-lattice relax., theory and MCD meas., phonon-modulated HFS 77−43883
KBr, F-centre trapping of conduction electrons, photocond. study 78−56179
KBr, far IR complex refr. indices, dispersive Fourier transform 78−80322
KBr, fast Li^+ ion stopping, chem. bonding effects 77−27929
KBr film, field enhanced secondary emission, energy spectrum obs. 77−1771
KBr film, oblique incidence transmission spectra for polarised extreme UV radiation 78−39614
KBr, gamma and additively coloured, dissolving in pure water, lyoluminesc. mechanism 80−100693
KBr, gamma-irrad., hologram recording by F-centre bleaching 80−78814
KBr, Gruneisen parameter, high press. phase transitions 79−60467
KBr, H-centre struct., hyperfine interactions 78−79611
KBr, heavy ion irrad., σ and π exciton emission spectra, 4.2K 78−76534
KBr, heavy metal ion implantation, mol. unit form. 80−100267
KBr, IR laser window appl., crystal growth, polishing and optical absorpt. 77−7102
KBr IR window refractive index var. with temp., −180° to +200°C obs. 79−14052
KBr in contact with KCl, mutual diffusion, development of relief on contact surfaces 78−22964
KBr, in K soln., conc., fluctuations, neutron small-angle scatt. study in electrolyte-metal transition range 79−14668
KBr, interaction between F- and α-centres, luminesc. meas. 79−73988
KBr, intra impurity local oscill. composition tone absorpt. band anharmonic temp. broadening *(Russian)* 80−60642
KBr, irrad., colour centres and thermolum. 77−85815
KBr, irradiated at room temp., thermolum. and F-centre thermal stability 78−84669
KBr, irradiated at room temp., stored energy 80−79839
KBr, K^+3p core excitons, refl. spectra study, low temp. 80−29759
KBr, kinetics eqns. of formation of F-centres and V_4-centres 78−67713
KBr, linear dichroism spectra, stress-induced, reorientation of O_2^- and NO_2^- impurity ions *(Russian)* 80−45127
KBr, liquid inelastic neutron scatt. obs. from short wavelength charge fluctuations 78−47487
KBr, luminesc. induced by ion impact, −160 to 200°C 77−8654
KBr, M-centre, lifetime data for excited state 78−35193
KBr, m-crocryst. powders coloured in electrodeless discharge, reflectance spectra, thermolum. 78−15238
KBr, mode Gruneisen parameters, acoustic phonon dispersion relations 79−42201
KBr, mol. dissoc. energy by photofragmentation spectroscopic method 79−76527
KBr, molten, charge fluctuations, neutron diffr. anal. 79−42198
KBr, molten, solutions of K, conc. fluctuations, small angle neutron scatt. study 80−92448
KBr, NO_3^- centre form. by γ-bombardment in air *(Russian)* 78−31668
KBr, optical conversion, luminesc. and colour centre formation 79−24354
KBr, optical damage threshold anisotropy, polarised laser radiation 77−16433
KBr, orbital g-factor and spin-orbit splitting of F-centre excited state, magnetoabsorpt. and MCD 78−2886
KBr, oscillatory and diffusive regime, above and below melting point, IR thermal emission spectra 78−83985
KBr pellet, appl. to IR spectroscopy of inorganic species 80−22455
KBr pellet spectroscopy, H_2SO_4 effect 79−88034
KBr, pellets, appls. in inorganic electronic spectroscopy 77−40597
KBr photochromic materials, F→M transform., electrostatic field control of optical information recording *(Russian)* 80−48370
KBr, photoluminescence under pulsed UV laser excitation 77−77289
KBr, photostimulated recomb., electron spin polarisation 80−60673
KBr, plate, distortions due to 10.6 μm laser irrad., interferometric obs. 78−46697
KBr, point defect concs., effect of plastic deform. 77−1124
KBr, porous insulator films, field enhanced emission, energy spectrum 77−20969
KBr, positron ang. correl., cryst. orient. depend., positron states and ionic distortion 77−63484
KBr, prep., 5-30 μ thick single cryst. for channellography appl. 78−80658
KBr, prep. of crysts. containing impurities of specified amounts *(Russian)* 80−66424
KBr, proton irrad., divacancies, positron capture, ionic cond. and TSC study 80−54289
KBr, pulse radiolysis of metastable interstitial centre of high temp. 80−20658
KBr, pulsed-laser-induced damage, role of avalanche multiplication and multiphoton absorpt. 80−48316
KBr, pure and Sr^{2+} doped, X-irrad., hole Br_3^- centre creation and destruction 77−15411
KBr purification for laser components, selective ion filter design and construction 79−14051
KBr, quench hardening of single crystals 79−43261
KBr, quench hardening related to dislocation density and slip 78−52855
KBr, quenched, absorpt. spectra, role of Schottky defects 77−59599
KBr, quenched single cryst., hardness var. with load 80−76337
KBr, radiation-induced F-centre accumulation efficiency *(Russian)* 79−69102
KBr, recomb. in ionic crysts., defect interaction 80−84206
KBr, recomb. in ionic crysts., defect interactions 80−84207
KBr, residual birefr., 3000-7000 Å, rel. to intrinsic piezooptical behaviour 78−60416
KBr, rot. of vacuum thermal etch pits 78−87674
KBr, S centres, luminesc. and photochemistry *(German)* 77−44055
KBr, second relaxed excited state of F-centre, optically detected EPR 79−87335
KBr, self-trapped exciton and F-centre form. 79−73443

potassium compounds continued
KBr, self-trapped exciton and F-centre form. by picosecond laser pulses 80−10546
KBr, self-trapped exciton form. via thermally induced defect reactions 80−60687
KBr, shock adiabatic, nonparametric equation of state 78−10121
KBr, single cryst., high-temp. creep, rel. to pipe diffusion, dislocation climb 77−11626
KBr, single cryst., lattice structure distortion on freshly formed surface, electrification 77−51582
KBr, single cryst., positron lifetimes, temp. depend. 78−48254
KBr, single cryst.; quenched, microstruct. around indentations 80−7628
KBr single crystal, epitaxial growth of polyoxymethylene *(Japanese)* 78−56054
KBr, single crystal, preirradiation and radiation defects, electron microscopic estimation *(Russian)* 78−75695
KBr solution, EPR of O_2^- luminesc. centres, 4.2K *(Russian)* 79−15339
KBr, spectral distrib. of triplet to singlet luminesc. of F_2 centre 77−59601
KBr, spin-lattice relaxation time of relaxed excited state of F-centre, MCD meas. 79−61350
KBr, spin-orbit interaction of relaxed excited state of F-centres 77−15808
KBr, Stark effect in F-centre emission 77−63434
KBr, stored energy after X-irrad. at low temp., 10-50K 77−76459
KBr substrate, electron irrad., epitaxial growth and surface coverage of Te films 80−10825
KBr, substrate, with colloidal centre vacuum deposition of Au particles *(Rumanian)* 78−60579
KBr, surface lattice dynamics, Green function method 78−34693
KBr, thermally stimulated luminesc. accompanying recomb. of V_F And F centres 80−55201
KBr, thermolum. and reactions of freed interstitial and trapped hole centres 78−23538
KBr, transient infrared absorption of bound polarons 78−92071
KBr, transparent, plasma form. at surface due to CO_2 laser irrad. 78−60534
KBr, transverse optic mode self-energy at 100 and 300K, expt. determ. 80−84265
KBr, triplet state lifetime of F_2 centre, mag. field effect 78−35177
KBr, two photon absorpt., 2p excitons relax., F-centre 79−91462
KBr, U_2 and U_1 centres, optical excitations 80−2803
KBr, UV two-photon absorpt. relative to known Raman cross section 79−81487
KBr, V- and X-centres accumulation *(Russian)* 80−54228
KBr, vacuum UV absorption spectra, exciton splitting rel. to exchange interaction 78−23494
KBr whisker, X-irrad., defect form., thermolum. and ionic cond. obs. *(Russian)* 78−84666
KBr whiskers, electric breakdown mechanism 79−28679
KBr, whiskers, F-centre accummulation and track effects due to X-ray irrad. 80−39484
KBr, with alkali and halogen impurities, colour centre deformation induced nonradiative decay 80−7387
KBr, with F-centres, vol. holograms diffr. efficiency 77−19205
KBr, with Frenkel cation defects, EPR and thermolum. of V_F, V_2-centres 78−10769
KBr, X-irrad., F-centre role in thermoluminescence 80−20720
KBr, X-irrad. crysts., halogen aggregation, absorpt. spectra obs. *(Russian)* 80−66234
KBr, X-irradiated, at 80K, interstitial K ions associated with interstitial Br ions *(Russian)* 78−75655
KBr, X-irradiated cryst., luminesc. during press. release 80−20722
KBr, X-ray irrad., tunnelling recomb. luminesc. 80−2873
KBr, X-ray struct. study using synchrotron radiation and multichannel detector 78−47210
KBr, XPS, satellite of Br 4s line 78−56556
KBr:$(CrO_4^{2-})(MoO_4^{2-})(MnO_4^-)(ReO_4^-)$, absorption spectra 78−10924
KBr:Ag, formation of electron centres and self-localised holes, ESR exam. 78−91947
KBr:Ag, mag. field effect on luminesc. of paired Ag^- ions 78−27313
KBr:Ag, optical absorpt. spectra interpretation mol. orbital scheme 80−20671
KBr:Au^-, optical absorpt. bands and MCD, electron-lattice interaction 80−108236
KBr:BeF_4^{2-}, IR absorption spectra of impurity anions *(Russian)* 80−2807
KBr:Br_2^-, triplet luminesc. kinetics, 0.4-4.2K 79−87482
KBr:CN^-, neutron scatt. studies of $(CN)^-$ defects 80−92620
KBr:CN^- 80−49316
KBr:CN^- tunnelling motion of dipolar impurities, absorption spectra 80−66239
KBr:Ca, F→Z_1 colour centre conversion, hologram recording appls. 78−17877
KBr:Ca, X-ray re-irradiation effects on Z_1 centres 78−75664
KBr:$CaSO_4$, SO_4^{2-} vibr. spectra, press.-scanned Fermi reson. spectroscopy appl. 79−73937
KBr:Cl^-, diffusion traps for divalent ions, dielectric loss and ionic thermocurrent techniques 80−6566
KBr:Co, coloured and uncoloured, Mossbauer effect, inhomogeneous hyperfine fields 77−32307
KBr:divalent cations, minimum work-hardening rates in compression and shear 79−74175
KBr:Eu, Z_2-centre investig. by EPR and optical absorpt. 77−16177
KBr:Eu^{2+}, single cryst. optical absorpt. spectra 80−45117
KBr:Eu^{2+}, spin Hamiltonian cryst. field consts. calcs. 79−38035
KBr:Eu(Yb), electron-irrad., photostimulated luminesc., ionic processes 78−52561
KBr:Ga^+, Jahn-Teller effect in orbital triplet, optically detected EPR meas. 77−66441
KBr:Ga^+, luminescence decay times, fluorescence kinetics, 1.6-300K 79−33825
KBr:Ga^+, polarisation of Ga^+ centre A_T emission, temp. depend. 80−80842
KBr:H^-, U-centre absorpt. band shape, piezodichroism dispersion curve and electron-phonon interaction 77−24873
KBr:$H^+(H_2^+)$, absorption bands, V_4- and M-centres 77−48204
KBr:$HS^-(HF_2^-)$, anharmonic interaction of impurity intramol. vibrs. with cryst. phonons 77−77217
potassium compounds continued
KBr:I, energy transfer due to excitons and holes under host sensitization 79−15526
KBr:I, luminesc., exciton and hole migration to I^- sites 79−38626
KBr:I^-, OH^-, luminesc. of interstitial atomic H 80−89062
KBr:In, A-luminescence spectra and polarisation, Jahn-Teller minima 77−20914
KBr:In, type A long-wave luminesc., polarisation obs. 78−10944
KBr:In^+, B-band, optical absorpt. and mag. circular dichroism calcs. 80−29765
KBr:In^+, Jahn-Teller split luminesc., high press. expt. 78−52565
KBr:In^+, luminescence spectra, emission lifetimes, temperature dependence 79−78745
KBr:In^+, mag. circular dichroism spectra line shape, lattice mode calcs. 79−82957
KBr:In^+, optical absorption and MCD spectra, Gaussian quadrature calc. 80−7367
KBr:$In^+(Ga^+)$, mag. circular dichroism meas. 79−42988
KBr:KI, microcrystalline powder, isothermal decay of colour centres 79−42995
KBr:Li, low temp. radiation hardening mechanism, dislocation-halogen interstitial interaction 79−23635
KBr:Li, paraelectric reson. meas. 77−36190
KBr:Li, radiative recomb. of localised excitons 78−72605
KBr:$Li^+(Na^+)$, electronic struct. of $(V_K e)_A$ 78−95269
KBr:Li^+, localised impurity modes, static lattice distortion effect 77−47530
KBr:Li(Na), F_A centres, optical detection of ESR 79−99793
KBr:Li(Na), low temp. radiation hardening mechanism, single halogen interstitials as hardening agent, Ha annealing 79−23634
KBr:Mg^{2+}, dopant aggregation and precipitation 80−107306
KBr:$Mg^{2+}(Ca^{2+})(Sr^{2+})(Ba^{2+})$, defect struct., Mott-Littleton technique study 80−59487
KBr:MnO_4^-, many-phonon impurity reson. Raman scatt. 80−60603
KBr:MnO_4^-, model system, reson. Raman spectra, general behaviour obs. 80−60592
KBr:MnO_4^-, vibronic spectra interpretation 79−37770
KBr:MnO_4^- (MnO_4^{2-}) Raman scatt. spectra, freq. and type of symm. of internal vibr. of impurity centres 79−15466
KBr:NO_2, Na effect of Na^+ impurity on self-trapped hole *(Japanese)* 78−67982
KBr:NO_2, X-irrad., paramag. and nonparamag. hole centres 77−16176
KBr:Na, exciton-like state disturbance in radioluminesc. *(Russian)* 77−85805
KBr:Na, U-centres, HFS and g-factor, EPR spectra 80−39869
KBr:Na, X-irrad., luminesc. from self-trapped excitons 77−28614
KBr:Na(Rb)(Cs), microcrystalline powders, isothermal decay of colour centres 80−2804
KBr:No_2^-, effects of Mg, Ca, Sr, Ba, Pb impurities on vibrational constants of NO_2^- ion 77−20035
KBr:OH^-, cc U_2 to H_2O^- defects conversion after UV photodecomp. 80−107230
KBr:$OH^-(OD^-)$, rotational barrier height for impurity, librational modes 77−11491
KBr:P, colour centre fine struct., ODMR 78−6604
KBr:PO_2^-, ODMR in zero and weak mag. fields 80−88894
KBr:PO_2^-, phosphorescence, triplet state sublevels, mixing 80−25446
KBr:PO_2^-, spin-lattice relax. in triplet state of PO_2^- centres, pulsed photoexcitation 79−95644
KBr:PO_2^-, vibr. spectra and struct. of PO_2^- impurity ions 77−16354
KBr:Pb, luminesc. spectra obs. 78−95604
KBr:PbI_2, single crysts. grown from aq. soln., growth striations obs. 77−1089
KBr:Pb; A-luminesc ., 8-80K 80−2836
KBr:Rb, H-centre interaction with Rb^+ ion 78−75662
KBr:Rb, U-centre modes, Green's function method calc. 77−24372
KBr:Rb^+, elastic interaction of H-centre with impurity, dynamic effects 77−76396
KBr:S^-, Jahn-Teller model of S^- ion centre 79−82567
KBr:SO_4^{2-}, $Ba^{2+}(Ca^{2+})$, IR absorpt. band parameters, temp. depend. *(Russian)* 78−31226
KBr:SO_4^{2-}, IR absorpt. spectra, cation impurity influence *(Russian)* 78−10901
KBr:Se^{2-} single cryst., dielec. relax. of impurity-vacancy dipoles, ITC meas. 79−91349
KBr:$SeO_4^{2-}(WO_4^{2-})$, IR absorpt. spectra, vibr. splitting *(Russian)* 79−51995
KBr:Sr, X-irradiated, first-stage F-centre production 77−76395
KBr:Sr^{2+},Cu^+, thermolum. response, extension of two-step reaction model 80−89075
KBr:TeO_3^{2-}, IR absorpt. of impurity complexes *(Russian)* 79−33746
KBr:Tl, 480K thermal glow peak, Tl^+ centres 80−108284
KBr:Tl, A-band absorpt., sruct. high resolution spectroscopy 77−20896
KBr:Tl, A-emission, line shapes and relative efficiencies 79−83011
KBr:Tl, electroluminescence, spectra and quantum yield activator conc. depend., cond. changes 80−89070
KBr:Tl, emission spectra, press. effects 78−23509
KBr:Tl, impurity-induced first-order Raman scatt., critical-point and critical-line anal. 79−19884
KBr:Tl, Jahn-Teller system, negative mag. circular polarisation in emission spectrum 80−20694
KBr:Tl, luminesc., decay model for A_T and A_X emissions 80−93379
KBr:Tl, nonradiative transitions in colour centres, WKB approximation 77−85803
KBr:Tl, thermoluminesc. excited by UV radn. and X-rays 79−87513
KBr:Tl, visible emission, temp. depend. 78−60511
KBr:Tl excitation in fund. absorpt. region, luminesc. and thermolum. 80−50433
KBr:Tl^+, Jahn-Teller split luminesc., high press. study 78−52565
KBr:Tl^+, quadratic Jahn-Teller effect, totally symm. vibr. mode effect, ang. overlap model 80−49680
KBr:Tl^+, recomb. luminesc. kinetics 77−16366
KBr:Tl^+, thermally induced absorpt. transfer between impurity bands, electron-lattice interactions 77−77257
KBr:Tl^{2+}, relation between bonding and g-shift 80−39492
KBr:V, covalency effects EPR meas. 77−85557
KBr:Yb^{2+}, X-ray and intracentre luminesc. 78−6737
KBr:Zn^+, optical absorpt. bands rel. to charge transfer 80−66245
KBr-Al_2Br_6 soln. in toluene, conduction mechanism 80−6870
KBr-$CaSO_4$:Dy thermolum. phosphor, thermal neutron detect. by activation 80−32581

potassium compounds continued
KBr-$KBrO_3$-H_2SO_4-Mn^{2+} system, chem. automat with three steady states 80−7769
KBr-KCl, birefringence, annealing effects, photoelasticity 78−72483
KBr-KF-LiBr-LiF, fused, miscibility gaps 79−82348
KBr-KI, mixed crysts., microhardness, theory 80−75298
KBr-KI mixed crystals, ionic cond., 100-450°C 79−14961
KBr-KI:Tl, spectral, polarisational and kinetic characts. 78−80385
KBr-LiBr, liq. mixture, struct. and diffusion 80−24344
KBr-$MgBr_2$ system, thermochem. and struct. investigation *(German)* 79−1423
KBr-OH^-, electron irrad., F_2^+ centre stabilisation 80−54231
$KBr_{1-x}(CN)_x$, mixed mol. cryst., coupled rot. and translational modes 80−84267
KBr(Cl), electron irradiated, electrotransport 79−69526
KBr(Cl):Li^+, far IR props. of lattice resonant modes, hydrostatic press. effects 77−28574
KBr(Cl)(I):O_2^- centres, luminesc., polarisation temp. depend. 78−87943
KBr(I), absolute cross sections of second order Raman scatt. 78−39548
KBr(I), sputtering, depend. on beam energy and target temp. 79−1804
KBr(I): O^{2-}(S^{2-})(Se^{2-})(Te^{2-}), low temperature photochemistry on chalcogen vacancy centres 78−18641
$KBrO_3$, ^{17}O NQR, spin echo double reson. method, electronegativity 80−54970
$KBrO_3$, hexagonal modification, temp. depend. of NQR freq., interpretation of long-wave spectra 80−25243
$KBrO_3$, in dioxane-water mixtures, ion-solvent interaction and conductance 79−34315
$KBrO_3$, near-forward Raman scatt. by polaritons 78−43842
$KBrO_3$, polarised IR reflection spectra, surface damage effects 79−19872
$KBrO_3$, trigonal, elastic, thermoelastic and dynamic piezoelec. props., US vel. meas. 77−32328
$KBrO_3$, uniaxial cryst., oblique phonon ang. dispersion 77−84861
$KBrO_3$-H_2SO_4-KBr-Mn^{2+} system, chem. automat with three steady states 80−7769
$KBrO_3$-H_2SO_4-Mn^{2+}-oxalacetic acid, chaos type reactions anal. 80−85165
$KBrO_4$, UV- and X-irrad., ESR spectra of trapped O_2 78−84474
$KBrO_2F_2$, struct. data, vibr. spectra 77−39563
KBr^*+Ar, inelastic collision, classical trajectory anal., vibr. excitation effects 77−34737
KBr^*+Ne(Ar)(CO)(N_2)(CO_2), information theoretic anal. 77−521
KC_{24}, intercalated graphite cpd., anisotropic mag. susceptibility and phase transitions 79−19370
KC_{24}, intercalated graphite, struct. phase transitions, X-ray diffr. 79−65189
KC_{24} intercalation compound, prep. by reduction of aromatic compounds 80−3306
KC_{24}, press. induced staging transition 80−79938
KC_{24}-tetrahydrofuran, physical props. *(French)* 78−26692
KC_8, graphite intercalation compound, band structure calc., charge transfer effect 80−6692
KC_8, intercalated graphite, electronic and cryst. struct. 80−44472
KC_8, intercalation compounds, development as reagents in organic synthesis 78−27444
KC_8 intercalation compound, H_2 chemisorption *(French)* 79−43624
KC_8 intercalation cpd., selective chemisorption of protium and deuterium *(French)* 77−32830
KC_x, lamellar cpds. with graphite, EPR studies 80−44902
KC_x, lamellar cpds. with graphite, ^{13}C NMR studies 80−44936
$KC_8H_{2/3}$, H_2 chemisorption *(French)* 78−27432
$KC_8H_{2/3}$, struct., X-ray anal. *(French)* 78−26538
KCL, crysts., X-ray irradiated, luminescence during release of pressure 79−65939
KCL:Pb^{3+}, interpretation of optical absorption spectra 79−51993
KCN, anomalous thermoelastic behaviour and orientational transition 77−76334
KCN, antiferroelectric phase, 83K phase transition based on model Hamiltonian 79−15418
KCN, Brillouin line width of phonons 78−80370
KCN, cryst., Debye characteristic temp. calcs. 79−37796
KCN, cryst., struct., phase transition, 6-300K, neutron diffr. obs. 77−76347
KCN, cryst. phases at press. up to 55 kbar, Raman spectra obs. 79−82975
KCN, crystal props., log potential model calc. 78−63829
KCN, cubic, third-order elastic consts., nonlinear behaviour 79−28026
KCN, cubic NaCl-type cryst., Debye temp. 80−54333
KCN, determination in seawater *(Chinese)* 79−52966
KCN, dipolar impurity tunnelling model, elastic interaction and const. 78−71826
KCN, disordered ordinary and metastable phases, light scatt., press. depend. 78−95151
KCN, dynamics of CN^- ions near phase transitions at 83K 80−80717
KCN, elastic anomaly at 168K 78−27242
KCN, elastic functions meas. by US pulse-echo method and Brillouin scatt. 77−84829
KCN, F-centre emission spectrum 77−12420
KCN, F-centres, optical props. 78−2892
KCN, He I photoelectron spectra 79−64046
KCN, inelastic neutron scatt. by coupled rot. and translational modes 80−79895
KCN, ionic mol. cryst., exciton struct. 78−79935
KCN, lattice dynamics and order-disorder transitions, neutron scatt. expts. 78−14434
KCN, lattice dynamics in disordered cubic phase 78−38794
KCN, lattice dynamics calc. 79−77705
KCN, librational and phonon sidebands of IR CN^- stretching mode 79−15457
KCN, liq., mol. dynamics computer simulation 78−38609
KCN, multidomain birefr. solid, light scatt. and IR transmission spike 80−60587
KCN, optical F centres and phase transitions 78−56504
KCN, order-disorder transition, light scatt., Raman obs. 77−1672
KCN, order-disorder transition, high-press. Brillouin scatt. exam. 77−44009
KCN, order-disorder transition, press. and temp. depend. of soft elastic const. 78−79769
KCN, phase transition at 168K, neutron inelastic scatt. line shapes for phonons obs. 78−38840
potassium compounds continued
KCN, phonon freq. distrib., cubic and monoclinic phases 78−22800
KCN, plastic phase, Raman scatt. spectra *(French)* 80−11379
KCN, polymorphic transitions, lattice energies calc. 77−1092
KCN, polymorphism, high pressure, Raman spectra 78−88302
KCN, Raman diffusion spectra, IR absorpt. in phases II and III *(French)* 80−84741
KCN, single cryst., orientationally disordered, Brillouin scatt., elastic consts. 77−85732
$K^{14}CN$, rat metabolism and internal dose 77−44754
KCN:H^-, U-centre, local mode meas. 77−1199
KCN:HCN^-, structural props. using ESR 80−25205
KCN-KCl mixed crystals, F-centre optical absorpt. half width 77−81134
KCN-KCl mixed system, order-disorder transition, dielec. props. meas. 78−15112
KCN-KCl mixed system, order-disorder transition, Raman spectra obs. 78−15113
KCN_x-KCl_{1-x}, finite-freq. local field catastrophe with appl. to spectra 79−51491
$K(CN)_{1-x}Cl_x$, elastic functions meas. by US pulse-echo method and Brillouin scatt. 77−84829
KCN_xCl_{1-x}, finite field local field catastrophe phenomena in spectra 80−92830
$K^+CN_x^-Cl^-_{1-x}$, influence of structural disorder on exciton spectra 80−108224
$(KCN)_{0.25}(KBr)_{0.75}$, rot.-translation interactions, neutron scatt., 0-300K 78−67783
$(KCN)_{0.5}(KBr)_{0.5}$, lattice dynamics neutron scatt. obs., glass phase formation 80−15207
$(KCN)_x(KBr)_{1-x}$, Brillouin scatt. of elastic anomaly 79−28779
KCN_xKCl_{1-x}, phase transition and OCN^- vibr. spectrum 78−43093
KCNS, librational modes in phase transition, Raman spectra obs. 79−55885
KCNS, single cryst., IR and Raman multiphonon bands, factor group anal. 77−4644
K_2CO_3 based reagent for NO_x removal, from highly polluted air *(Japanese)* 79−52976
β-K_2CO_3, cryst. struct. of high temp. monoclinic modification 77−11513
K_2CO_3, ionic equil., mass spectra obs., heats of reaction and form. of ions 79−87867
K_2CO_3 melt in combustion prods. medium, vaporisation of drops 79−57290
K_2CO_3, molten, IR emission spectra *(Japanese)* 78−19469
K_2CO_3, solid, low energy photoelectron spectra 78−95656
K_2CO_3 soln. droplet, solvent evaporation in hot gas 77−68673
K_2CO_3, study of elec. cond. and transition points 78−75873
K_2CO_3-D_2O, glass, 4.2K, trapped electron photocond. and optical spectra following radiolysis 79−29378
K_2CO_3-D_2O, glassy matrix, absorpt. spectra after X-irrad., solvated electrons 79−65903
K_2CO_3-SiO_2 glass forming batch, Raman spectroscopy 78−64519
K_2CO_3-SiO_2-As_2O_3, laser Raman spectrosc. study of ions in quenched reaction mixtures 80−25357
$K_2C_2O_4(SbF_3)_2$, growth from soln. and X-ray diffr. study *(French)* 77−80481
$KCaCl_3$, form. of equilib. pseudocubic phase from supersaturated solid soln. based on NaCl *(Russian)* 77−63681
$KCaCl_3$ impurity in NaCl cryst., precipitation and dissolution 79−42259
$KCaCl_3$, phase transitions, optical and dilatometric meas. 79−61394
$KCaF_3$, IR refl. spectra, vibr. modes, optical vibr. freq., Kramers Kronig anal. 80−66190
$KCaF_3$, struct. phase transitions, DSC, birefr., and neutron powder diffr. obs. 80−70149
$K_{2(1-x)}Ca_xSO_4$:Tl^+ phosphor, thermolum. characts. 77−90203
$K_2Ca(SO_4)_2.H_2O$, syngenite, space group refinement by vibr. spectroscopy methods 78−79507
$K_2Ca(SO_4)_2.H_2O$, single cryst., X-ray cryst. struct. refinement 79−14781
$K_2Ca(SO_4)_2.H_2O$, syngenite, thermal dehydration under nonisothermal conditions 80−3324
$K_2Ca(SO_4)_2.H_2O$, thermal dehydration, isothermal kinetics 79−15982
$K_2Ca[B_4O_5(OH)_4]_2.8H_2O$, synthetic, X-ray cryst. struct. study, H bond geometry 80−92509
$K_2(Cd(CN)_4)$, vibr. spectra, isotope substitutions, force consts. determ. *(German)* 77−61750
KCdCl$_3$:Co^{2+}, Zeeman Raman scatt. and Zeeman IR absorpt. spectra 79−56782
K_4CdCl_6:Co^{2+}, ground-state g-value, EPR meas. 77−16159
$KCdF_3$, IR refl. spectra, vibr. modes, optical vibr. freq., Kramers Kronig anal. 80−66190
$KCdF_3$, structural phase transitions, X-ray diffr. and differential type thermal analysis 77−80620
$KCdF_3$, structural phase transitions using linear birefringence studies 78−76424
$KCdF_3$:Cr^{3+}, EPR, successive phase transitions 79−65717
$KCdF_3$:Gd^{3+}, EPR, spin Hamiltonian parameters 79−65725
$KCdF_3$:Mn^{2+}, evidence for F distortion, ligand ^{19}F ENDOR meas. 78−23369
$K_2Cd_2(SO_4)_3$, ferroelastic phase transition, X-ray diffr. and dielec. temp. depend. meas. 79−55882
$K_2Cd_2(SO_4)_3$, langbeinite type cryst., search for ferroelec. phase transition 77−59535
$K_2Cd_2(SO_4)_3$, melt growth and ferroelastic transition, and K_2SO_4-$CdSO_4$ phase diagram 78−31335
$K_2Cd_2(SO_4)_3$, piezoelec. langbeinite-type, cryst. struct. and ferroelastic transform. 78−6036
$K_2Cd_2(SO_4)_3$, piezoelectric, cryst. struct., near ferroelastic transition 78−42984
$KCd_4(VO_4)_3$, cryst. struct., Patterson and Fourier calcs. 77−19916
$(K_{16}Ce(P_2W_{17}O_{61})_2).nH_2O$ (n=50), X-ray cryst. struct. determ. 79−94984
$K_2CeSi_6O_{15}$, cryst. struct., X-ray diffr. meas. 78−18619
$K_2CeSi_6O_{15}$, synthesis and X-ray structural anal. 78−2096
KCl, ^{14}N impurities, molecular point defects, EPR isotropic hyperfine triplets 80−2636
KCl, 10.6 microns absorption, calorimeter round robin meas. 79−35748
KCl (Br) aqueous solutions, IR absorpt. ν_1 (CN) band parameter temp., conc. study *(Russian)* 80−80801
KCl (001), water covered cold surface, H atom diffr. 77−66565
KCl (100), adsorption of H_2O ordered monolayer, SIMS 77−76660
KCl (100), elec.-mech. coupling of dislocations 78−75676

potassium compounds continued
KCl, (100) face, mol. dynamics computer simulation of surface props. 78−18880
KCl (100) surface, Au nuclei interactions 77−89670
KCl, absence of energy transfer between F- and M-centres 79−99935
KCl, absorpt. coeff. meas., using pulsed CO_2 laser, calorimetric method 78−18028
KCl absorption and emission of F_A(Li) centres under hydrostatic pressure 78−92117
KCl, absorption spectra of F-aggregate centres, 2K 77−48207
KCl, absorption spectra exam. of H-bearing complexes 79−8167
KCl, acoustic non-linearity parameter in cubic crysts. 77−51444
KCl, activation coefficients and solvation numbers in mixed methanol solvents 80−81334
KCl, additively coloured, colloid size distrib., replica microscopy, absorpt. spectra 77−47449
KCl, additively coloured, colloid nucleation and growth, TEM 77−62526
KCl, additively coloured photochromic crystals, spectral sensitivity *(Russian)* 80−91871
KCl, adsorbed on GaAS (110), adsorpt.-desorpt. processes and phase transitions 78−2361
KCl, adsorption-desorption behaviour on W (110) and W (111) surfaces 80−75442
KCl, agglomeration of crystals from aqu. soln. 79−90580
KCl, alkali halide crystals, defect state change during electrolysis 78−95057
KCl, amplitude and phase reflection spectra measured using Michelson interferometer and liquid He cryostat, 7 to 300K 79−54135
KCl, amplitude-phase holograms, optical parameter dispersion 80−58481
KCl, and KCl:$Ca^{2+}(Sr^{2+})(SO_4^{2-})$, conductivity, self-diffusion coeffs., lattice defect props. 77−4216
KCl and KCl:KBr, colour centres isothermal decay 79−51975
KCl and KCl:NO_2, X-irrad. crysts., Cl_3^- centres photodissoc., optical anisotropy and creation mechanisms *(Russian)* 80−66235
KCl and KCl:S, change of state of F-centres due to electrostatic field *(Russian)* 79−58827
KCl, and KCl-AgCl, surface positron and positronium states, positron annihilation expts. *(Russian)* 78−39623
KCl, annealed in KBr vapour, crack and pore formation, diffusionally induced stress relaxation *(Russian)* 80−40388
KCl aq. soln., lanoline emulsion, dielec. relax., 1 MHz to 70 GHz 77−77144
KCl, aq. soln., zero-angle X-ray scatt., 25°C, conc. depend. 78−83713
KCl, aq. solns. hypersonic sound vel. and absorpt. meas. 78−30699
KCl, aqueous film on Hg, secondary electrocapillary effects, interfacial tension and entropy 77−55420
KCl aqueous solution emulsions, complex permittivity meas., dielec. relax. 78−72459
KCl, axial shift of self-trapped exciton, semiempirical calc. 80−2339
KCl, Ba^{2+} diffusion, light scatt. meas., dipole mechanism *(Russian)* 78−22900
KCl, band struct. and charge densities, intersecting spheres model 80−49591
KCl, band struct. calc. by mixed LCAO and OPW method 77−8019
KCl, beam, surface ionisation on W ribbon, mass spectra 77−27173
KCl bicrystals, grain boundary migration kinetics, effect of solutes 78−43185
KCl, binding energy of F_{e+}', M_{e+}' and R_{e+}' centres, positron trapping 79−69460
KCl birefringence, annealing effects, photoelasticity 78−72483
KCl, Born-Mayer parameters of He and Ar, interstitial interaction with neighbouring ions 80−100228
KCl, Bragg diffraction, anharmonic contributions, Mossbauer study 78−76359
KCl, brittle fracture on electron bombardment, probability distrib. functions 79−86820
KCl, bulk and surface absorpt. of CO_2 laser radiation, calorimetric data analysis 78−25904
KCl, bulk and surface absorpt., 2 to 10 μm, calorimetric meas. 78−71160
KCl, bulk and surface absorpt. in 9.2-10.8 μm region 79−95808
KCl, bulk and surface absorption comparison, 9.2 to 10.85 μm 80−33051
KCl, calc. of third- and fourth-order elastic constants 79−10891
KCl, cation defects creation mechanism 80−75224
KCl, cation motion energy parameters, dielectric relax. meas. 78−30784
KCl, channelling of MeV H^+ and He^+, zero dose meas. 78−18689
KCl, charge transfer and pair polarisability anisotropy 80−43173
KCl, cluster expansion of density matrix and crystal energy 78−87952
KCl, colloidal suspension, radiowave dielec. dispersion 80−11311
KCl, colour centres laser spectra, induced F' band absorpt. 80−2779
KCl, coloured, trap-controlled photoelectron mobility, transit-time expts. 77−72880
KCl coloured crystal, susceptibility variation calculations 80−55055
KCl, Compton profile, 59.54 keV γ-rays 78−64426
KCl, Compton profile anisotropies, charge and momentum distrib., LCAO-SCF-MO calc. 79−3500
KCl, cryst., colour centres, ionic cond., X-ray effects, thermoluminesc. *(Russian)* 78−6056
KCl, cryst., etch hillocks on (100) cleavage planes 77−4109
KCl, cryst., gas-liquid inclusions movement in temp. field gradient 79−55942
KCl, cryst., optical breakdown plasma effects 77−66558
KCl, cryst., plasma prod. by laser impact, effect on surface 78−1866
KCl cryst., Sr and Na impurities radial distrib., influence of form of crystn. front 80−107312
KCl, cryst., two-layer colloidal K and Cu colour centre light absorption 77−12408
KCl, cryst. growth, physical vapour transport method for low dislocation density crysts. 78−43992
KCl, cryst. γ-irrad., holographic information recording appls. *(Russian)* 79−27218
KCl, cryst. isolated pore healing under press., dislocation struct. evolution *(Russian)* 80−100245
KCl, cryst. laser irrad. effects, electron microscopic obs. 77−73192
KCl crystal, F-H centre formation by opt. conversion of self-trapped excitons 78−91335
KCl crystal, refr. index, 10.6 μm ellipsometric meas. 78−24847
KCl crystal, surface elementary steps interaction with Au particles 80−39400
potassium compounds continued
KCl crystal, use of photoelectrons to investigate surface charges 80−2444
KCl crystal active element for colour-centre laser, thermal strain anal. 80−91804
KCl crystal growth in fluidised bed, comparison to dissoln. *(French)* 80−16167
KCl, crystal growth rate in cooling soln., nucleation and supersaturation 77−76337
KCl crystallites, nucleation, oriented growth on amorphous SiO_2 using square-wave surface relief grating 78−47672
KCl crystals, Eu^{2+} concentration effect on lattice parameter and density of crystals 80−88169
KCl, crystals, grown by Czochralski method, effect of growth rate on defect generation 79−51032
KCl crystals, positron annihilation, Doppler broadening 80−40180
KCl crystals with NaF surface absorpt. regions, photoacoustic detect. 79−87466
KCl, Czochralski-grown, creep and struct. changes, 77-300K *(German)* 77−28862
KCl, Czochralski-grown, dislocation subboundary characts. 78−67718
KCl, dechannelling of H^+, temperature and energy dependence calculation 77−89490
KCl, defect modes due to H^--D^- pair impurities 80−59602
KCl, defect modes due to substitutional anion-pair and cation-pair impurities in ionic crystals 80−92540
KCl, delocalised positronium, 4.2K, direct obs. γ-spectra 78−88235
KCl diamond turned window surfaces, 10.6 μm pulsed laser damage 77−50704
KCl, diffr. by M-centres, thick plane wave hologram recording 77−7021
KCl, diffusion of radioactive and stable Tl^+, transmutation effect 77−89589
KCl, dilute metal solutions in molten salts, optical absorption, F-centre model for bound state 80−89023
KCl, dislocation dynamic props., investigation by impact loading *(Russian)* 78−85069
KCl, dislocation etchant 77−4103
KCl, dislocation internal friction, orientation depend. 78−48439
KCl, dislocation motion in micro-plastic region 78−91341
KCl, distant F-centre pairs, ODNMR 78−68414
KCl, doped, elec. conductivity and optical absorpt., quenching from 750°C 78−2289
KCl, doped, grain boundary diffusion, space-charge contrib. 77−55386
KCl, doped, saturable absorber for CO_2 laser 79−10363
KCl, doped with alkaline earth ions, Z_1-centres form. under X-ray irrad. 79−24338
KCl, ENDOR line splitting by UHF field *(Russian)* 78−43678
KCl, ENDOR of F-centres, sign of ^{41}K elec. quadrupole moment 80−34820
KCl, efficiency of creation of X_3^- centres in X-rayed alkali halides *(Russian)* 78−71731
KCl, elastic moduli, quadratic fit against temp. 78−14397
KCl, elec. field effect on flow stress, charged-dislocation model 77−27935
KCl, electrolytic coloration effect on dislocation density 77−4106
KCl, electrolytically coloured single cryst., ionic SCL transient and steady elec. current 77−62937
KCl, electron impact, colour centre distrib., channelling 79−14866
KCl, electron injection, F-centre formation efficiency 78−63790
KCl, electron irrad., F-centre absorpt., ellipsometric obs. 78−23501
KCl, electron irrad., secondary electrons and radiation defects 79−55782
KCl, electron irradiation, energies greater than 1 MeV, defect form. and secondary electron emission *(Russian)* 77−55304
KCl, electron range-energy relation, thermally created lattice vacancies effect 80−92574
KCl, electron trapping by alkali ion impurities 78−47809
KCl, electron-irrad., positron-capture centres, thermal annealing kinetics 79−95875
KCl, electron-irrad. induced fracture, Monte Carlo modelling compared with expt. 77−69038
KCl, electron-spin memory and magnetic-circular-dichroic effects in F-centre luminesc. 80−29794
KCl, electronic states at (100) surface, accounting for spin-orbit interaction *(Russian)* 78−91750
KCl, electronic struct. of self-trapped excitons calc. 77−39784
KCl, emission spectra of O_2^- and NO_2^- centres at high hydrostatic press. 78−10943
KCl, energy of form. of Schottky defects 77−7714
KCl, entropy change associated with substitutional anion defects calc. 78−79782
KCl, entropy changes associated with formation of defects, Schottky defects 77−62552
KCl, etching, double poison role 80−54240
KCl, evaluation of proton dechannelling in ⟨100⟩ channel, temp. and incident energy depend. 79−4365
KCl, exp. valence charge density calc., accuracy of one-term Gaussian representation 80−28952
KCl, exposed to US waves, dislocation multiplication in original stage 78−47383
KCl extrinsic absorpt. near 9.6 μ, using CO_2 laser calorimetry 77−16341
KCl, F centre, EPR in relaxed excited state, via mag. circular polarisation of emission 79−24232
KCl, F centre pairs, ODMR, close and distant pairs 78−43691
KCl, F_A(Li)-centre spin-lattice relax. at 4.2K 78−91950
KCl, F_2-centre triplet-triplet transition at 685 nm, MCD obs. *(French)* 77−63433
KCl, F_3-centre quartet state, IR emission spectra 78−43930
KCl, F- and H-centre production by nonradiative decay of self-trapped exciton 78−23042
KCl, F-F' conversion at room temp. 78−51539
KCl, F-center pairs, light excitation, mag. field and resonance effects on absorption bands 78−92094
KCl, F-centre, wave functions and spin densities, pseudopot. calc. 79−4533
KCl, F-centre emission, mag. circular polarisation 80−108251
KCl, F-centre first excited state radiationless decay, cluster model 77−52158
KCl, F-centre first order reson. Raman spectra, line shape freq. depend. 77−32370
KCl, F-centre form. and dissociation under pulsed electron irrad. 78−18643

potassium compounds continued
KCl, F-centre form. by electron irrad., efficiency penetration depth 77−51370
KCl, F-centre formation, short-pulse optical exam. of exciton relax. 79−42061
KCl, F-centre formation efficiency, dependence on lattice vacancy concentration 79−82203
KCl, F-centre formation at highly excited triplet states of self-trapped excitons 80−76066
KCl, F-centre hyperfine interaction parameters, press. shifts 77−8043
KCl, F-centre luminesc., MCD effects 78−39598
KCl, F-centre optical absorpt., estimate using symmetry-adapted wave functions 80−11448
KCl, F-centre phonon many-mode interaction, absorption band shape 78−2883
KCl, F-centre relaxation kinetics, temp. depend. following electron irrad. 80−92527
KCl, F-centre trapping of conduction electrons, photocond. study 78−56179
KCl, F-centres, relaxed excited states, vibronic model of stress effects 78−95118
KCl far IR complex permittivity meas. by dispersive Fourier transform spectroscopy, 7 to 300K 80−15940
KCl, far IR complex refr. indices, dispersive Fourier transform 78−80322
KCl film, field enhanced secondary emission, energy spectrum obs. 77−1771
KCl film, oblique incidence transmission spectra for polarised extreme UV radiation 78−39614
KCl film, porous, injection mechanism for transmission secondary electron emission 78−19643
KCl, fine structure of X-ray absorption spectra 80−71514
KCl, fused, excess free energy of mixing, conformal ionic soln. theory 77−1230
KCl, gamma and additively coloured, dissolving in pure water, lyoluminesc. mechanism 80−100693
KCl, gamma irrad. relationship between thermolum. and deform. luminesc. 79−19942
KCl, gamma-irradiated crystal, interrelation between V_2 and V_3 centres *(Russian)* 79−69862
KCl, growth, supersaturation rel. to cryst. characts. 79−52101
KCl, γ-irrad., F-centre absorpt., flash-stimulated changes 80−92524
KCl, γ-irrad., photoplastic effect and internal friction aftereffect 80−24529
KCl, γ-irrad. and doped, lattice relax., cold neutron scatt. obs. 77−7715
KCl, γ-irradiated, photo- and thermoluminesc., F-centre interstitial recomb. 77−44036
KCl, γ-irradiation effect on dielectric const. *(Japanese)* 79−51896
KCl, γ-radiation effect on 10.6 μ absorpt. coeff. assoc. with F-aggregate centres 77−4661
KCl, H_2O-related centres 78−67711
KCl, H-centre struct., hyperfine interactions 78−79611
KCl, hardness increase mode, effect on dislocation mobility 79−51114
KCl, heavy metal ion implantation, mol. unit form. 80−100267
KCl, hologram recording by photodichroic F_A centres at room temp. 77−34846
KCl, IR absorpt. calcs. in rectangular crystallites 78−95583
KCl, IR transparent materials, bulk and surface absorpt., calorimetric meas. method 79−27347
KCl IR window material, polish layer effect, ellipsometric meas. 78−55419
KCl IR window refractive index var. with temp., −180° to +200°C obs. 79−14052
KCl, impurities, divalent, existence of charged aggregates 77−84790
KCl, influence of collisions on cryst. growth and secondary nucleation under conditions of meas. crystn. 80−50544
KCl, influence of elec. field on proton channelling 78−26614
KCl, internal damage threshold for CO_2 laser pulses rel. to absorption 77−75594
KCl, ion bombard., damage profiles, track effect anal. 77−15465
KCl, ion processes in $F \rightarrow Z_1$ transition, photocond. meas. 77−15412
KCl, ionic cond., defect parameters, diffusion coeffs. 80−79978
KCl, irrad., V_3-band in absorpt. spectra, model *(Russian)* 79−56821
KCl, irrad. with intense nanosecond electron beam, super-Rayleigh vel. of brittle fracture front 80−6458
KCl, irradiated, determ. of molar extinction coeff. and oscillator strength of V_2-centre *(Russian)* 78−80384
KCl, irradiated at room temp., stored energy 80−79839
KCl, irradiated crystal, determ. of oscillator strength of V_3-centre *(Russian)* 78−92095
KCl, isopiestic studies of aqueous solns., 382 to 474K 79−24815
KCl, isothermal compressibility calc., 0-1000K 77−7784
KCl, isothermal diffusion of ^{85}Sr 77−47625
KCl, K^+ 3p core excitons, refl. spectra study, low temp. 80−29759
KCl, Knoop microhardness anomaly on (001) planes 79−38942
KCl, LEED-AES study of oriented adsorption of TCNE 77−62737
KCl, large unit cell semiempirical mol. orbital approach to props. of solids 79−87037
KCl, laser produced shocks rel. to material damage 78−31285
KCl, laser window, thermal lensing 77−72021
KCl laser window, thermal lensing, effective optical distortion parameter 77−83916
KCl laser window, with chalcogenide glass two-layer low-absorpt. antirefl. coating 78−37927
KCl, laser window material, absorpt. at CO wavelengths, calorimetric meas. 78−25911
KCl laser windows at 10.6 μm, optical distortion parameter 78−79036
KCl laser-induced breakdown fields rel. to wavelength and focal spot radius 80−35019
KCl layers, minimum ionising particle detection by secondary electron emission 77−54475
KCl, linear dichroism spectra, stress-induced, reorientation of O_2^- and NO_2^- impurity ions *(Russian)* 80−45127
KCl, linear thermal expansion coeffs. meas., room temp. to 250°C 78−55416
KCl, liq., Brillouin scatt. determination of hypersonic vel. 79−82288
KCl, liq., elec. cond., mol. dynamics study 79−28116
KCl, liq. inclusion motion due to dislocation density gradient 77−89569
KCl, liquid inclusions, thermal migration, dislocation drag 77−7911
KCl long rod sample, calorimetric absorpt. coeff. meas. using pulsed CO_2 lasers 80−9918
potassium compounds continued
KCl, low temp. space charge polarisation 78−43789
KCl low-loss laser window material, surface absorpt. meas. at 2.8 and 3.8 μm 79−94267
KCl, luminesc. excitation spectra of F-aggregate centres, 400-900 nm. *(Russian)* 78−10980
KCl, luminesc. induced by ion impact, −160 to 200°C 77−8654
KCl, luminesc. of Z_4 centres 79−24355
KCl, luminesc. under 10.6 μm laser pulse irrad. *(Russian)* 77−16381
KCl, luminescence induced by tunnelling recombination between neutral Ag atoms and V_k centres 79−61442
KCl, M-centres, F-centre sensitised luminesc. 77−4681
KCl, m-crocryst. powders coloured in electrodeless discharge, reflectance spectra, thermolum. 78−15238
KCl, MCD, magneto-optical parameters of R-centre in H_3-mol. model 77−77253
KCl, MCD of R_1 band 77−8551
KCl, mag. circular dichroism of R-center, point-ion lattice model 79−69814
KCl, measurement of dielectric constant using transformer ratio arm bridge, 10^2 to 10^6 Hz 79−80641
KCl, mechanical props. meas., appl. of piezoelec. method, for small sandwich specimen 77−54939
KCl melt, effect of cooling rate upon glass transition, X-ray analysis 79−27920
KCl, melt, mol. dynamics simulation 80−54097
KCl, melt-grown, spiral growth, screw dislocation mechanism, phase-contrast microscopy obs. 78−87637
KCl, microcrack propagation and plastic strain 80−81187
KCl microcrystal, computer simulation of melting and glass form. 79−65173
KCl microcrystal boundary influence on IR spectrum 77−40243
KCl, migration of brine inclusion, nonequilib. morphology 78−38882
KCl, molten, diffusion of Li^+ ion *(Japanese)* 78−14489
KCl, molten, pair and triplet distrib. functions by mol. dynamics simulation 79−90520
KCl, molten, rot. ordered ion distrib., mol. dynamics simulation 78−22630
KCl, molten, vapour-liq. interface, mol. dynamics model 80−54362
KCl molten salt, thermodynamic function, Brillouin spectroscopy, hypersonic vel. *(French)* 78−35161
KCl, monatomic surface step effect on Au nuclei 77−15719
KCl, mosaic struct. 77−7740
KCl, motion of dislocation half-loops, influence of prestart loading and ensemble nature 78−71745
KCl, NO_3^- centre form. by γ-bombardment in air *(Russian)* 78−31668
KCl, negative muon capture, rel. probability meas. 77−50550
KCl, neutron diffraction examination, white beam technique 77−31565
KCl, optical breakdown, γ-irrad. effects, rel. to appl. in high power lasers 77−8507
KCl, optical breakdown from 0.53-10.6 μm 80−7292
KCl, optical breakdown threshold, illuminated spot dimension effects 78−68582
KCl, optical material, thermal expansion, 60-300K 78−33791
KCl, perturbed M-centre triplet state, M-F centre exchange mechanisms 79−69884
KCl, phonon dispersion curves calc. 77−39648
KCl, phonon scattering on small radius colloids 78−38798
KCl, phonon-phonon scatt. strength, thermal cond. in low- and high-temp. regions 77−43296
KCl, photo-induced F-centres, hologram recording 80−28174
KCl, photoconductivity during $F \rightarrow X$ transition *(Russian)* 77−43663
KCl, photodichroic, as optical processing elements 78−83056
KCl, photoelastic consts. at 10.6 μm, interferometric and polarimetric meas. 78−25934
KCl, photoelec. effect produced by far UV light, memory effect 79−24008
KCl, photoelectric emission in photon energy region 1.0 to 6.0 eV 80−108321
KCl, photofragment spectra, bond energies and excited state symmetries 80−87190
KCl, photoplastic effect *(Japanese)* 79−82279
KCl plate, distortions due to 10.6 μm laser irrad., interferometric obs. 78−46697
KCl, polarisability, near-Hartree-Fock limit SCF MO calc., bond length 78−42239
KCl, polymorphic transition press. at high temp., elec. resist. meas. 78−38837
KCl, porous insulator films, field enhanced emission, energy spectrum 77−20969
KCl, positive colour centres, long-lived excited states and spontaneous tunnel transitions 79−82552
KCl, positron ang. correl., cryst. orient. depend., positron states and ionic distortion 77−63484
KCl, positron annihilation by positive-ion vacancies, impurities and defect complexes 77−27908
KCl, positron annihilation in colour centres 77−73185
KCl, positron-trapping colour centre dynamics, positron annihilation study 80−108294
KCl, positronium states near defects in cationic sublattice 80−16121
KCl, powder diffr. using synchrotron radiation, energy-dispersive technique 77−24245
KCl, premelting due to thermal form. of dislocations 77−11671
KCl, premelting elec. cond., heat capacity 78−91445
KCl, prep. of crysts. containing impurities of specified amounts *(Russian)* 80−66424
KCl, press. induced low-temp. polymorphic transition, hysteresis 78−14467
KCl, press. shifts of F-centre hyperfine interaction parameters 78−79957
KCl, protective layer for III-V semicond. surface 77−89628
KCl, pulsed RF radiation produced by scratching *(Russian)* 78−19607
KCl, pulsed-laser-induced damage, role of avalanche multiplication and multiphoton absorpt. 80−48316
KCl, pure and Ba doped, symm. of elastic fields due to defect displacements, diffuse X-ray scatt. 80−70256
KCl, pure and Ba-doped, γ-irrad. effects on intensity distrib. of diffuse X-ray scatt. 77−24329
KCl, pure and Ba-doped, γ-irrad., point defect form. and interaction, X-ray and optical studies 79−65078
KCl, pure and Pb^{2+}-doped, X-irrad., quenching effects on thermal glow curves 78−27333

potassium compounds continued
KCl, pure and Sr doped crystals, strengthening effects rel. to IV-dipoles and aggregates 78−55907
KCl, pure cryst., thermal cond. meas., 50 mK to 50K 77−62692
KCl, quadrupole coupling, vibr. and rot. effects, Morse oscill. calcs. 77−6805
KCl, quench hardening behaviour and quenching temp. 78−64550
KCl, radiation damaged, proton and $^4He^+$ channelling, F-centre production, optical absorpt. meas. 78−79656
KCl, radiative tunnel transitions in negatively charged colour centre systems 80−49655
KCl, Raman spectra and vibrational modes of V_K centre meas. 78−80338
KCl, room temp. X-irrad., first stage F-centre form. 78−67709
KCl, S centres, luminesc. and photochemistry *(German)* 77−44055
KCl, second relaxed excited state of F-centre, optically detected EPR 79−87335
KCl, self trapped exciton, optical detection of spin relax. processes 78−60358
KCl, self trapped exciton, off-centre configuration 79−42455
KCl, self-trapped exciton luminesc. 77−48225
KCl, self-trapped exciton, ENDOR 79−15377
KCl, single cryst., electron beam irrad. optically simulated exoelectron study 79−95908
KCl, single cryst., laser window material, IR thermooptic coeff. meas. 77−36208
KCl, single cryst., liq. inclusion movement in stress gradient field 80−44370
KCl, single cryst., quenched, microstruct. around indentations 80−7628
KCl single cryst., stress birefr. 80−60542
KCl single crystal, dislocation velocity stress exponent estimation by stress relaxation and creep tests *(Japanese)* 78−55875
KCl single crystal, healing of isolated pore under pressure due to isostatic compression 77−21046
KCl, single crystal, preirradiation and radiation defects, electron microscopic estimation *(Russian)* 78−75695
KCl single crystals, F-band absorpt. and thermolum. under DC field and X-ray irrad. 79−65910
KCl single crystals, piezobirefringence and plastic deform., stress-strain curves 77−69798
KCl single crysts., thermal stability of neutron induced damage 78−79634
KCl, solid monodisperse aerosols, in He jet system, for unstable nuclide transportation 79−22507
KCl, soln., elec. cond., dielec. relax., kinetic characts. 78−34641
KCl, solution, apparent molar heat capacity and volume, at 298.15K 80−29179
KCl solution, EPR of O_2^- luminesc. centres, 4.2K *(Russian)* 79−15339
KCl solution, elec. cond. obs. for seawater salinity scale 80−72646
KCl solution, in Ag-AgCl/KCl/AgCl-Ag thermocell, thermal liq. junction pot. at high temps. 80−16819
KCl solution, streaming current and cross-coeff. meas. in electrokinetic processes 80−76531
KCl solution, thermodynamic driving force, for crystallisation at 298K 79−37643
KCl solution, viscosity of nonfreezing thin interlayer between ice column and quartz capillary 80−54475
KCl, solution of $ZnCl_2$, solubility of Co_2 79−90785
KCl solutions, weak electric field influence obs. for soln.-solid system *(Russian)* 78−11522
KCl, sp. ht., thermal cond. and thermal diffusivity, meas. by pulse method, influence of press. 79−7701
KCl, spark channel in solid, plasma light absorpt. coeffs. 79−7501
KCl, spectral distrib. of triplet to singlet luminesc. of F_2 centre 77−59601
KCl, spectral interference in at. absorption spectroscopy in C tube atomiser and flames *(Japanese)* 79−48019
KCl, spin-orbit interaction of relaxed excited state of F-centres 77−15808
KCl, spirals, growth and dissolution from liq. state 80−15027
KCl, spontaneous cleavage, step line propag., macroscopic defects 78−87662
KCl, sputtering by Ar ion bombardment, temp. depend. of sputtering rate *(Japanese)* 78−88389
KCl, standard for soln. calorimetry, enthalpy of soln. in H_2O determ. 77−73462
KCl, static and dynamic props. 77−7798
KCl, stepwise motion of edge and screw dislocations *(Russian)* 77−84748
KCl, strain hardening during relax. of deforming stresses 77−7786
KCl, strained single crysts., US attenuation 77−1181
KCl, stress distrib., meas. by scattered light photoelasticity *(Russian)* 80−7326
KCl, sublimation on (100) surfaces in elec. field 79−77739
KCl, sublimation struct., back force effect 77−15571
KCl substrate, epitaxial growth of Sn thin films 79−99441
KCl, substrate, with colloidal centre vacuum deposition of Au particles *(Rumanian)* 78−60579
KCl surface, electron bombard., F-centre absorpt. investigated by use of lateral light waves 78−4707
KCl surface, sublimation kinetics, elec. field influence, terrace-ledge-kink model 80−84287
KCl surface, TlI/KCl/TlI low absorpt. antireflection coatings 80−38078
KCl surface, VUV irrad., colour centre layer, angle-of-incidence derivative ellipsometry and reflectometry 80−73420
KCl surface, vacuum UV radiation damage, spectroscopic study 78−71758
KCl, surface and bulk absorpt. at 10 μm, temp. depend. 77−28576
KCl surface irregularity statistics for laser component materials 79−14057
KCl, surface lattice dynamics, Green function method 78−34693
KCl, surface radiative absorption meas., acoustic technique 77−3596
KCl, surface self-diffusion consts. from growth or evaporation spiral evolution kinetics 79−65301
KCl surface states, detection by photocharging spectroscopy 77−66193
KCl surface texture and optical props. after forging between polished dies 80−33102
KCl, TEA-CO_2 laser irradiated, damage struct. optical microscopy obs. 77−19983
KCl, TSM study of lattice statics and dynamics 79−82292

potassium compounds continued
KCl, temp. depend. of dislocation charge, piezoelec. defect technique 78−22733
KCl, temp. depend. of F-colouring efficiency 80−44204
KCl, thermal and photothermal conversion of colour centres, after high-dose electronic interaction *(Russian)* 80−39156
KCl, thermal annealing of F, V_2-, V_3-centres *(Russian)* 80−54229
KCl, thermal cond. press. depend. 77−15641
KCl, thermal cond. under press. meas. 78−30802
KCl, thermal conductivity at high temperature 79−55857
KCl, thermal expansion, rapid increase near melting point 77−51521
KCl, thermal expansion, compressibility and melting calcs. 79−33069
KCl, thermal expansion coefficients temp. depend., anharmonic effects 79−99290
KCl, thermal hysteresis in ionic cond., dielec. loss meas. 78−34652
KCl thermally stimulated luminesc. accompanying recomb. of V_F and F centres 80−55201
KCl, thermodynamic activity in Dead Sea brine 78−31673
KCl, thermodynamic props., lattice-dynamical calc. 77−35715
KCl, thermoluminesc., halogen and alkali impurity effects 80−97352
KCl, thermotransport of ^{85}Sr and ^{54}Mn, Soret effect meas. 77−47624
KCl, thin film, crystal-vacuum (100) surface, mol. dynamics computer simulation 80−34288
KCl, transverse optic mode self energy, freq. and temp. depend. 77−80589
KCl, triplet state lifetime of F_2 centre, mag. field effect 78−35177
KCl, two-dimens. nucleation and hole nucleation, mol. beam method *(German)* 80−93499
KCl, two-dimens. nucleation rate on the (100) surfaces, mol. beam method, 289-343°C *(German)* 80−93500
KCl, U_2 and U_1 centres, optical excitations 80−2803
KCl, U-centre electronic struct., expanded unit cell model 78−72109
KCl, US plastic deform., dislocation struct. 80−19809
KCl, UV visible absorpt. by laser calorimetry, wavelength modulation spectroscopy 78−66876
KCl, ultralow loss optical fibre material, loss mechanism 80−78920
KCl, undoped, or In- or Eu-doped, injection electrolum., fields up to 10^4 V cm^{-1} 77−12445
KCl, undoped and Pb- or NO_3^--doped, colloid centre formation, absorpt. spectra, 300-1000 nm 79−78710
KCl, V- and X-centres accumulation *(Russian)* 80−54228
KCl, vacancy comaplex formation and binding energies in zeroth approx. 80−24441
KCl, vacuum condensation of Au, spatial distribution of nuclei 78−18931
KCl, vacuum UV absorption spectra, exciton splitting rel. to exchange interaction 78−23494
KCl, water solution calorimeter, determination of energy equivalent 78−23961
KCl, whiskers, F-centre accummulation and track effects due to X-ray irrad. 80−39484
KCl window with antirefl. coating, laser damage at 10.6 μm 77−61992
KCl with adsorbed metal, photoexcited ions and electron emission *(Russian)* 77−40324
KCl with Al_2O_3 disperse spheres, dislocation mechanism for stress relaxation in cooling crystal *(Russian)* 80−54347
KCl, with alkali and halogen impurities, colour centre deformation induced nonradiative decay 80−7387
KCl, with colour centres, laser stimulated luminesc. 78−6749
KCl, with divalent impurity, reorientation of impurity-vacancy complexes, thermally stimulated depolarisation 77−65977
KCl, with F-centres, vol. holograms diffr. efficiency 77−19205
KCl, with Frenkel cation defects, EPR and thermolum. of V_F, V_2-centres 78−10769
KCl, X-centres thermal decay process, activation energy *(Russian)* 79−90651
KCl, X-irrad. induced deform. effects, glow curves *(Russian)* 79−52022
KCl, X-irradiated, formation of cation defects 78−91359
KCl, X-irradiated, release of stored energy 78−38753
KCl, X-ray integrated intensities in Bragg and Laue geometries 77−31553
KCl, X-ray irrad., thermoluminescence, TSC and thermal stability 79−95859
KCl, X-ray irrad., tunnelling recomb. luminesc. 80−2873
KCl, X-ray irradiated, first-stage F-centre prod. 80−107231
KCl, X-ray irradiated, vacancy conc. determ., thermal expansion meas. 80−79782
KCl, Z_2 centres in triplet state, EPR study 80−108068
KCl, zone refined single crystal growth for high power CO_2 laser optics 78−22181
KCl:$(CrO_4^{2-})(MoO_4^{2-})(MnO_4^-)(ReO_4^-)$, vibronic absorption spectra 78−10924
KCl:Ag, Br, EPR spectra of $Ag^0(Br_1)$ paramag. centres *(French)* 79−11346
KCl:Ag, formation of Ag atoms and self-localised holes by illumination, EPR meas. 78−31108
KCl:Ag, hole capture radius, scintillation luminesc. obs. *(Russian)* 78−39582
KCl:Ag, optical absorpt. spectra interpretation mol. orbital scheme 80−20671
KCl:Ag, thermoluminesc. meas. using high impedance DC amplifier 79−99955
KCl:Ag, X-irrad., thermoluminesc. study of Ag centres 80−80874
KCl:Ag,Tl, cryst. high-press. energy transfer, sensitised luminesc. 77−36281
KCl:Ag positron annihilation and impurity states 80−97375
KCl:AgCl, positron annihilation characts., positronium state form., X-irrad. effects 77−4700
KCl:AgCl, tunnelling-recombination luminesc. 78−88354
KCl:Ag(Cu), strong IR luminescence obs. of Ag_F^0 centres 78−6736
KCl:Ag(In)(Tl), excitation in fund. absorpt. region, luminesc. and thermolum. 80−50433
KCl:Ag(Tl), formation of electron centres and self-localised holes, ESR exam. 78−91947
KCl:Au, EPR and optical absorpt. 78−39397
KCl:Au^-, absorption bands and MCD, electron-lattice interaction 77−55808
KCl:Au^-, absorption band shape in D-mode model 79−47485
KCl:Au^-, fluorescence, stress and mag. field depend., Jahn-Teller effect and relax. processes 77−48220
KCl:Au^-, Jahn-Teller effect 78−64015

potassium compounds continued
KCl:Ba, defect struct., dark-field microscopy, anal. of decoration patterns 79−23506
KCl:Ba, γ-irradiation, defect struct., X-ray and chemical etching exam. 77−84793
KCl:Ba, negative photoplastic effect, photodestruction of Z-centres 77−43272
KCl:Ba, structural changes due to γ-irradiation *(Russian)* 77−76460
KCl:Ba (0.005 at.%), spatial diffuse X-ray scatt. intensity distrib. 77−7757
KCl:Ba solid solution decomposition, elastic ordered structure formation 79−86896
KCl:Ba^{2+}, localised stress relaxation in excess vacancy system, prismatic loops *(Russian)* 80−88160
KCl:Ba^{2+}, precipitation kinetics, supersaturation effects, geometry of formed heterophase struct. *(Russian)* 78−84824
KCl:Ba(Ca)(Sr), microstruct. and hardness, impurity distrib. effects 79−24529
KCl:Ba(Sr), Z-centre, luminesc. and absorpt. spectra obs. 80−49221
KCl:BeF_4^{2-}, IR absorption spectra of impurity anions *(Russian)* 80−2807
KCl:$BiCl_3$, electrical cond. as a function of temp., charge transport mechanism 78−83996
KCl:$Br^-(I^-)$, interstitial atomic H centres, formation kinetics and struct. MO calc. and EPR studies 80−75854
KCl:Br^{2+}, solid solution periodic precipitation in inhomogeneous conc. field 80−103485
KCl:CN, reson. scatt. of phonons in thermal cond. 79−14972
KCl:CN^-, paraelectric reson. study, tunnelling parameters and elec. dipole moment 80−25326
KCl:CN^-, phonon-defect interaction, Brillouin scatt. obs. 80−34935
KCl:CN^-, phonon-internal mode hybridisation, neutron scatt. 78−2217
KCl:CN^-, Raman scatt. from tunnelling and hindered rotational sites 77−66507
KCl:CN^-, coherent admixtures of phonons with impurity libronic excitations, neutron scatt. study 80−49316
KCl:Ca, additively coloured, spectral and temp. depend. of initial yield of Z_3-centre form. 79−78716
KCl:Ca, F→Z_1 colour centre conversion, hologram recording appls. 78−17877
KCl:Ca, optical studies of Z_4 centres 79−24336
KCl:Ca, thermolum. and optical absorpt. spectra of Z_1 centres 79−52029
KCl:Ca, vol. holographic grating, modulation characts. 79−94197
KCl:Ca, Z_2-centres, optical absorpt. and ESR spectra 79−91480
KCl:Ca, Z_4 centres, thermal and optical bleaching 80−19802
KCl:Ca,H, ENDOR studies of localised vibrations of substitutional atomic H 78−80248
KCl:Ca^{2+}, $Cl^-(Br^-)$, diffusion traps for divalent ions, dielectric loss and ionic thermocurrent techniques 80−6566
KCl:Ca^{2+}, cryst., hydrolysed, IR absorpt. bands 77−32404
KCl:Ca^{2+}, Z_3-centre thermolum. 80−80879
KCl:$Ca^{2+}(Sr^{2+})$, impurity precip., flotation density obs. 78−51690
KCl:$CaCl_2$, KOH, complex form., U-centre influence, optical absorpt. bands 77−80502
KCl:Ca(Ba), effect of doping on dislocation distrib., in melt grown cryst. 80−6410
KCl:Ca(Ba)(Mg)(Sr), microcrystalline powders, role of Z-centres in stabilizing coloration 80−54227
KCl:Ca(Pb)(Sr), structural state of impurities, hydrostatic press. effect, thermostimulated depolarisation exam. 77−39614
KCl:Ca(Yb), Z_2 and Z_2^+ centres, excited state, magnetooptical spectra 80−108233
KCl:Cd, EPR of anisotropic Cd_F^+ centres, similarity to Z-centres 77−77101
KCl:$CdCl_2$, elec. cond., role of electrode material, surface precipitation effects 80−59985
KCl:Co_3^{2-}, $Sr^{2+}(Ba^{2+})$, shift and broadening of local vibr. bands, temp. depend. 78−87755
KCl:CrO_4^{2-}, reorientation of dipolar complexes, ionic thermo currents meas. 77−80642
KCl:$Cs^+(I^-)$, low-temp. heat capacity enhancement due to impurities 80−107442
KCl:Cu, additively-coloured crysts., for hologram recording plates *(Russian)* 78−29914
KCl:Cu, EPR, optical absorpt. and luminesc. investig. of anisotropic Cu_F^0 centres 77−20893
KCl:Cu,Tl, plastic deform., charge exchange of hole centres *(Russian)* 77−11876
KCl:Cu^-, absorpt. and emission spectra, $3d^{10}4s^2 \rightarrow 3d^94s^24p$ bands 79−24343
KCl:Cu^-, excitation and absorpt. spectra 80−108255
KCl:Cu^+, exciton bands, optical absorpt. and MCD spectra 80−80821
KCl:Cu^+ US attenuation meas., 80-300K 77−43285
KCl:Eu, additively coloured, ESR obs. of $^{2+}$ complex 77−16170
KCl:Eu, flow stress 77−36577
KCl:Eu, impurity conc. determ. by optical absorpt. meas. 77−32409
KCl:Eu, luminescence and absorption of color centres in RbCl:Cu and KCl:Eu crystals 78−92118
KCl:Eu, OH^-, EPR meas. on Eu^{2+} complex 78−10773
KCl:Eu, Z_3-centre investig. by EPR and optical absorpt. 77−16177
KCl:Eu crystallophosphores, aggregation of $Eu^{2+}v_c^-$ centres *(Russian)* 78−43909
KCl:Eu IR laser window lattice equilibrium obs. 79−14055
KCl:Eu^{2+}, cation impurity-vacancy pairs, effect of X-rays 79−55778
KCl:Eu^{2+}, γ-irrad., photostimulated low temp. recomb. luminesc. 80−11435
KCl:Eu^{2+}, lattice defect equilib. optical absorpt. and cond. studies 80−29767
KCl:Eu^{2+}, optical absorpt. meas. for Eu^{2+} conc. determ. 79−51137
KCl:Eu^{2+}, radiationless transitions, photoacoustic spectra 77−32405
KCl:Eu^{2+}, radiationless processes, spectroscopic analysis 78−80391
KCl:Eu^{2+}, single cryst. optical absorpt. spectra 80−45117
KCl:Eu^{2+}, spin Hamiltonian cryst. field consts. calcs. 79−38035
KCl:Eu^{2+}, zero phonon lines, time-resolved fluoresc. spectra 77−77269
KCl:Eu^{2+} crystals, photostimulated afterglow investigation at room temp. 80−108259
KCl:$F^-(Br^-)(I^-)$, anion impurities substitution, energies of soln., association and migration 78−83831
KCl:$F^-(Br^-)(I^-)$, U-centres, local defect modes, Green's functions calcs. 80−44280
potassium compounds continued
KCl:$Fe(CN)_6^{4-}$, electron irrad., Mossbauer and ESR study 80−7238
KCl:Ga, optically detected EPR in relaxed excited states of Ga^+ 78−72437
KCl:Ga^+, polarisation of Ga^+ centre A_T emission, temp. depend. 80−80842
KCl:Ga(Tl,Pb), X-irradiated, EPR spectra 79−28613
KCl:H, dichroic H- and U-centres by polarised bleaching of interstitial H 80−29766
KCl:H, dynamical superhyperfine interaction 80−2663
KCl:H, ENDOR and ESR study of anion sites 80−108118
KCl:H, migration and stabilisation of H atoms, ESR and thermolum. study 79−1430
KCl:H^-, defect pairs of F-centres and U-centres, Raman meas. 79−7599
KCl:Hg^+, X-irradiated, ESR meas. 77−1588
KCl:I, luminesc. at low temp. 80−2818
KCl:I crystals, V-band development using X-rays 78−88337
KCl:I^-, H, fluorescence of interstitial H-centres 79−73987
KCl:I(Br), colouration under two-photon excitation, absorption spectra 78−84618
KCl:In^+, Jahn-Teller split luminesc., high press. expt. 78−52565
KCl:$In^+(Tl^+)$, HF calc. for ground and excited states of impurity centre 77−72835
KCl:In(Ga), ESR of impurity centres, impurity optical absorpt. bands 80−29618
KCl:K, F-centre coloured, for highly efficient holographic storage 78−37833
KCl:$K_4Os^{II}(CN)_6$, electron irrad., EPR, ligand hyperfine struct. 78−60335
KCl:K^+ crystal, highly efficient phase holograms 78−33707
KCl:KBr(KI), enhancement in sp. ht. due to anion impurities 79−51274
KCl:$KNO_2(KNO_3)$, anion exchange during tablet pressing, IR spectroscopy appl. 80−2764
KCl:KOH, influence of anion impurities on mech. props. of alkali halide crystals 78−87736
KCl:$KReO_4$, CO_2 pulse generation by free induction decay 80−53388
KCl:$KReO_4$ free induction decay generation of ultrashort CO_2 pulses 80−74444
KCl:Li, 9.4 GHz pulse paraelec. reson. at zero elec. field 77−81076
KCl:Li, $(F_2^+)_A$ centres, optical props. 80−89026
KCl:Li, ⟨111⟩ off centre Li^+ under biaxial stress, bistable tunnelling 78−15090
KCl:Li, additively coloured, luminesc. material for IR region *(Russian)* 78−15209
KCl:Li, F_A-centre optical absorpt., estimate using symmetry-adapted wave functions 80−11448
KCl:Li, M_A-centre, decay 77−77278
KCl:Li, microwave modulation by paraelec. reson. *(Russian)* 77−20809
KCl:Li, self-induced resonant optical rotation 79−65831
KCl:Li, tunable CW IR lasers using F-centres 77−88725
KCl:Li, X-irrad., F_A centres, thermolum. studies 80−80878
KCl:Li,H optical and EPR exam. of H centre, $(LiH)^+$ absorpt. spectra 79−99920
KCl:Li $(F_2^+)_A$ centres, tunable CW laser action 80−87399
KCl:Li F_A(II) centre laser, pumped by flashlamp-pumped dye laser 80−102737
KCl:Li^+, coherent excitation by EM and acoustic waves, induction and echo signal study 78−67773
KCl:Li^+, defect induced tunnelling states, depend. on strain, pot. model calcs. 79−69865
KCl:Li^+, localised impurity modes, static lattice distortion effect 77−47530
KCl:Li^+, off to on centre defect transitions under hydrostatic press. 78−15199
KCl:Li^+, phonon generation by EM excitation, mechanism 80−2129
KCl:Li^+, press. tuning of motional behaviour in shallow off-centre pots. 79−78718
KCl:Li^+, restricted interstitial motion of $H_A(Li^+)$ centre, ESR and uniaxial stress expts. 77−48053
KCl:Li^+, shape of pot. energy well of impurity 79−23692
KCl:Li^+, single-pulse excitation of paraelectric induction and echo signals 80−80732
KCl:Li^+,Na^+, F_A(II) to F_B(II) centre crystals, CW laser oscill. with extended tuning range 80−32997
KCl:Li^+ F_A (II) colour-centre laser, mode locking and tunable picosecond IR pulse generation 80−43364
KCl:LiCl photodichroic crystals as adaptive spatial filters 79−72713
KCl:Li(Na), tunable IR lasers with F_A(II) and F_B(II) colour centres 78−90420
KCl:Mg^{2+}, dopant aggregation and precipitation 80−107306
KCl:$Mg^{2+}(Ca^{2+})(Sr^{2+})(Ba^{2+})$, defect struct., Mott-Littleton technique study 80−59487
KCl:MnO_4^{2-}, Raman scatt. spectra, bands due to ν_1, vibr. of MnO_4^{2-} 79−15466
KCl:NCO^-, shift and broadening of local vibr. bands, temp. depend. 78−87755
KCl:NH_4Cl, PMR, NH_4^+ ion proton spin-lattice relax. time temp. depend. 78−27104
KCl:$NO_2^-(O_2^-)$, Stokes' losses on cryst. vibrs. in luminesc. spectra of mol. centres *(Russian)* 77−55827
KCl:Na, absorption from relaxed excited state by F_A and F_B centres 77−44031
KCl:Na, electron trapping from α_A^- and F_A-centres, low temp. depend. 80−11444
KCl:Na, F_A reorientation and $F_A \leftrightarrows F'_A$ conversions, laser induced, kinetic studies 80−10547
KCl:Na, F_B centre energy levels 80−107738
KCl:Na, F_B centres, optical detection of ESR 79−99793
KCl:Na, M_A-centre, decay 77−77278
KCl:Na, photodichroic holographic recording, polarisation sensitivity 78−29911
KCl:Na, photoinduced reorientation of A-centres near room temp. 78−64344
KCl:Na, thermoluminescence peaks cleaning using optical bleaching 77−81162
KCl:Na,Br, EPR of interstitial and diinterstitial $BrCl_2^{2-}$ centres 77−81007
KCl:Na and pure, hologram recording through F→X conversion 80−48190

potassium compounds continued
KCl:Na^+, CW laser action of $(F_2^+)_A$-centres, tunable from 1.62 to 1.91 μm 80−32998
KCl:Na^+, F_B(II) colour centres, tunable CW laser action obs. 77−83877
KCl:Na^+, lattice relaxation around tetragonal and rhombic defects 79−95110
KCl:Na^+, OH^-, IR absorpt. spectra, Na^+ ions rel. to OH^- stretching vibr. 79−47442
KCl:Na^+, R-centre exam., uniaxial stress effects on zero-phonon lines 78−47371
KCl:Na^+, self trapped excitons, optical absorption and emission 77−43503
KCl:$Na^+(Rb^+)(Ag^+)$, entropy changes associated with point defect form. calc. 77−7741
KCl:Na(Ag), UV irrad. anionic H and D atoms, ESR and optical absorpt. expts. 79−99187
KCl:Na(Li) 78−76016
KCl:OH, absorpt. in high-transparency region 80−89037
KCl:OH, low temp. spectrophotometry, impurity absorpt. band *(Russian)* 79−40635
KCl:OH, mag. field-independent capacitance thermometers 78−4623
KCl:OH^-, cc U_2 to H_2O^- defects conversion after UV photodecomp. 80−107230
KCl:OH^-, image effect in previously electrolytically coloured crystals 78−22714
KCl:OH^-, paraelec. system, acoustic susceptibility in strong phonon-coupling approx. 78−71801
KCl:OH^- type dipole-phonon system, superradiative phase transition *(Russian)* 78−71806
KCl:OH^- type paraelec. systems, phonon superradiant phase transition *(Russian)* 79−69206
KCl:$OH^-(CN^-)(Li^+)$, mag. moment due to orientational tunnelling calc. 77−68931
KCl:$OH^-(OD^-)$, rotational barrier height for impurity, librational modes 77−11491
KCl:P, colour centre fine struct., ODMR 78−6604
KCl:PO_2^-, ODMR in zero and weak mag. fields 80−88894
KCl:PO_2^-, ODMR spectra at 2K, HFS tensor of P 79−87333
KCl:PO_2^-, phosphoresc. and PMDR spectra, electronic and vibr. states 79−65768
KCl:PO_2^-, photo-orientation, spectrosc. and ODMR obs. 80−29772
KCl:PO_2^-, spin-lattice relax. in triplet state of PO_2^- centres, pulsed photoexcitation 79−95644
KCl:PO_2^-, triplet state pseudonuclear Zeeman effect, optical detections *(Russian)* 79−78571
KCl:PO_2^-, triplet state, level anticrossing and pseudonuclear Zeeman effect, microwave ODIMR 80−39896
KCl:PO_2^-, vibr. spectra and struct. of PO_2^- impurity ions 77−16354
KCl:Pb, 420 nm A-emission band *(Russian)* 79−56852
KCl:Pb, additive coloration 77−68967
KCl:Pb, colouring, room temp., influence of conc. and aggregation state of Pb 78−14339
KCl:Pb, geometrical parameters of impurity centres by scattered-light method 80−2043
KCl:Pb, impurity distrib., light scatt. and microhardness study, heat treatment 80−96562
KCl:Pb, impurity valence, heat treatment influence, absorpt. spectra obs. 79−38574
KCl:Pb, ionic electret behaviour, ionic thermoconductivity technique 80−7274
KCl:Pb, lead aggregation effect on yield stress, incoherent precipitates, solubility determ. method 80−50645
KCl:Pb, light induced ionic polarisation 80−7264
KCl:Pb, luminesc. spectra obs. 78−95604
KCl:Pb, photolum. in A band region, spectral and time decay anal. 79−33823
KCl:Pb, photoluminesc. induced by Suzuki-like occlusions, ionic thermocond. 79−33808
KCl:Pb, solid solution, electron microscope exam. of decomposition, of naturally aged specimens 79−96030
KCl:Pb, thermoluminesc. meas. using high impedance DC amplifier 79−99955
KCl:Pb, vibr. struct. of absorption band 79−33735
KCl:Pb crystal surfaces, Au decoration, electron microscope study 80−15144
KCl:Pb crystals, development of mechanical stresses during growth 80−19735
KCl:Pb exam. of simultaneous effect of heat treatment, Pb concentration on state, phase diagram construction 79−96008
KCl:Pb^{2+}, decay of luminescence emission 78−39593
KCl:Pb^{2+}, γ-irrad., rel. to props. 78−31262
KCl:Pb^{2+}, highly doped, state of dispersion of Pb^{2+} 77−1144
KCl:Pb^{2+}, inner-centre luminesc., 8 to 80K *(Russian)* 78−92112
KCl:Pb^{2+}, ion energetic parameters comparison with alkaline earth fluoride crystals 80−66243
KCl:Pb^{2+}, low temp. sp. ht. 80−2178
KCl:Pb^{2+}, origin of 420 nm emission band 77−40279
KCl:Pb^{2+}, pure and doped, electrolytically coloured, elec. cond. and optical absorpt. meas. 80−100668
KCl:Pb^{2+}, X-ray irrad., electron-trapped centres, Pb^+ and Pb^0, optical absorpt. spectra 80−71461
KCl:Pb^{2+} crystals, precipitation, density changes, nucleation mode, lattice relaxation, heat treatment 79−66066
KCl:$Pb^{2+}(Cu^+)$ 80−34890
KCl:Pb^{2+}(0.005% Pb), A band fine structure, electron-phonon interaction 78−60491
KCl:$PbCl_2$, tablet, 272 nm absorpt. band 78−84612
KCl:$Pr^{3+}(Sm^{3+})$, absorption spectra at 4.2 K, anal. 80−7378
KCl:RbCl, $SrCl_2$, IR window material, cryst. growth and props. 78−31333
KCl:RbCl, $SrCl_2$, laser window material, prep., grain boundary stability 77−46774
KCl:ReO_4, resonantly enhanced phase conjugation through degenerate four-wave mixing 80−58635
KCl:ReO_4^- nonlinear absorption for CO_2 laser pulse compression and mode locking 80−74443
KCl:Ru, optical absorption bands, complex form. 77−1705
KCl:S, influence of anion impurities on mech. props. of alkali halide crystals 78−87736
KCl:S^-, Jahn-Teller model of S^- ion centre 79−82567

potassium compounds continued
KCl:SO_4^{2-}, $Ba^{2+}(Ca^{2+})$, IR absorpt. band parameters, temp. depend. *(Russian)* 78−31226
KCl:SO_4^{2-}, ionic cond., defect parameters, diffusion coeffs. 80−79978
KCl:SeO_2^{2-} (WO_4^{2-}), IR absorpt. spectra, vibr. splitting *(Russian)* 79−51995
KCl:Sm^{2+}, spectra, ^5D states, Lauer-Fong formula and SCC model 79−15513
KCl:Sn, pure and doped, thermoluminesc. and luminesc. decay 79−83041
KCl:Sn^{2+}, EPR exam. of struct. and prod. of $Sn^-(5p^3,4S)$ defects 79−61215
KCl:Sn^{2+}, thermally stimulated space charge decay 78−48111
KCl:$SnCl_2$, action of ionising radiation on Sn aggregation processes 78−34543
KCl:$SnCl_2$, electronic struct. of Sn^+ centres, model 77−43530
KCl:$SnCl_2$, photostimulated hole recombination luminesc. *(Russian)* 80−80833
KCl:$SnCl_2$, Sn^+ centres, polarised luminesc. and EPR 79−65076
KCl:$SnCl_2$, X-ray irrad., polarised luminesc. and EPR study of Sn^{3+} centres 80−39868
KCl:Sr, Ca, simultaneous diffusion, coefficients meas. 78−79813
KCl:Sr, M-centre photoluminesc. *(Russian)* 78−84649
KCl:Sr, mechanical props. as function of dopant conc., dislocations 77−69027
KCl:Sr, positron annihilation and trapping in A-centres 80−84802
KCl:Sr, single crystal, thermally stimulated topochemical reactions 79−28011
KCl:Sr, thermally pre-treated, glow curves 80−25470
KCl:Sr, triplet state of F_2-centres, ESR spectra 80−29616
KCl:Sr crystal, Z_4 colour centre, luminesc. study 80−64993
KCl:Sr^{2+}, ionic cond., defect parameters, diffusion coeffs. 80−79978
KCl:Sr^{2+}, polarisation-plastic effect 78−2794
KCl:Sr^{2+}, X-irrad., thermolum., impurity aggregation, trapping centre form. 78−88367
KCl:Sr^{2+}, X-irradiated, thermolum. decay, effect of impurity aggregation 77−85814
KCl:Sr^{2+},Cu^+, thermolum. response, extension of two-step reaction model 80−89075
KCl:$Sr^{2+}(SO_4^{2-})$, defect parameters, self-consistent set, ionic cond. meas. 80−107487
KCl:$SrCl_2$, effect of impurity on thermoelec. power 78−76098
KCl:$SrCl_2$, H_{Na} annealing, X-ray irrad., H centre capture by IV dipoles 78−10927
KCl:$SrCl_2$, thermal depolarisation 77−28514
KCl:$SrCl_2$, Z_1-centres, dipolar relax., ITC meas. 78−75660
KCl:Sr(Ca), thermoluminescence and colour centre thermal stability in irradiated sample 78−43941
KCl:Tl, 375 nm emission band 79−95834
KCl:Tl, 475 nm emission, attributed to Tl^+ dimer 78−39611
KCl:Tl, ESR of trapped electron and hole centres 79−78516
KCl:Tl, effective cross sections ratio of charged and neutral centres for holes and electrons *(Russian)* 79−28319
KCl:Tl, electroluminescence, spectra and quantum yield activator conc. depend., cond. changes 80−89070
KCl:Tl, emission spectra, press. effects 78−23509
KCl:Tl, energy level scheme, mol. orbital model 80−10912
KCl:Tl, F-centre formation efficiency 79−82203
KCl:Tl, hole capture kinetics, influence of autolocalised and zone holes *(Russian)* 80−54714
KCl:Tl, impurity-induced first-order Raman scatt., critical-point and critical-line anal. 79−19884
KCl:Tl, Jahn-Teller system, negative mag. circular polarisation in emission spectrum 80−20694
KCl:Tl, low-temp. ionisation of activator, photoexcitation, in region of interzone transitions *(Russian)* 79−28320
KCl:Tl, mixed phosphor, dimer absorption bands, 200-300 nm 79−73976
KCl:Tl, neutron scattering from localised electronic excitation, theory 79−4539
KCl:Tl, temp. depend. of cathodolum. *(Russian)* 80−80868
KCl:Tl, thermal glow of trapped electron and hole centres 79−78762
KCl:Tl, thermoemission of positive ions in simple gas atoms *(Russian)* 77−28676
KCl:Tl, visible emission, temp. depend. 78−60511
KCl:Tl (0.003 to 0.27 mol.%), electrolum. 80−71490
KCl:Tl and KCl, F-centre production by positive ions and X-rays 78−38760
KCl:Tl F-centre form. by electron irrad., efficiency penetration depth 77−51370
KCl:Tl phosphors, heavily doped, luminesc. obs. 77−32427
KCl:Tl^+, absorpt. spectra, electrolytic coloration, migration in electric field, heat treatment 78−23504
KCl:Tl^+, cryst., electron transfer, optical and thermal excitation 79−4833
KCl:Tl^+, decay modes of 3000 Å emission band 77−73168
KCl:Tl^+, optical absorpt. spectra following X-irrad., F- and V-centres 79−99912
KCl:Tl^+, quadratic Jahn-Teller effect, totally symm. vibr. mode effect, ang. overlap model 80−49680
KCl:Tl^+, recomb. luminesc. kinetics 77−16366
KCl:Tl^+ cryst., A band, mag. field effect 80−34897
KCl:Tl^{2+}, hole mechanisms of H- can F-centre production, thermolum. obs. 77−16407
KCl:Tl^{2+}, Na, X-irrad., activator-impurity association *(Russian)* 77−85761
KCl:Tl^{2+}, optical absorpt. spectra interpretation mol. orbital scheme 80−20671
KCl:Ti^{2+}, relation between bonding and g-shift 80−39492
KCl:TlCl, lattice defects, X-ray line profile obs. 80−24455
KCl:V^{2+}, EPR spectrum temp. depend., crystal field theory 77−16163
KCl:V^{2+}, EPR spectra above 300K 80−34765
KCl:V^{2+}, phonon induced zero field splitting 78−39073
KCl:V^{2+}, spin-lattice relaxation 78−91941
KCl:Yb, Z_2-centres, optical absorpt. and ESR spectra 79−91481
KCl:Yb^{2+}, X-ray and intracentre luminesc. 78−6737
KCl:Zn^+, optical absorpt. bands rel. to charge transfer 80−66245
KCl-Al composite, optical and IR reflectance 78−56465
KCl-$AlCl_3$, molten mixture, vap. pres. meas. 78−87779
KCl-Al(Pd) composite, far IR absorption 78−56466
KCl-Ba, X-ray irrad. cryst., thermoluminescence spectra 80−20719

potassium compounds continued
KCl-$BaCl_2$ supersaturated solid soln., deformed, $BaCl_2$ precipitation kinetics, metastable region *(Russian)* 78−60673
KCl-$BaTiO_3$, composite cryst., F-centres, thermoluminesc., DC field and X-irrad. effects 78−2926
KCl-$CaCl_2$-NaCl, ternary phase diagrams, interactive computer program 80−71629
KCl-CsCl solid soln., SIMS, clustering distance critical to metal dimer form. 79−72379
KCl-CuCl eutectic fused salt, potential as intermediate temp. solar heat transfer and storage medium 80−101135
KCl-CuCl solid solution supersaturated, precipitation, impurity aggregation 80−29174
KCl-$CuCl_2$ solution, optical absorption of complex ions *(Russian)* 77−28592
KCl-doped phenol-water mixture, electrical conductivity near crit. pt. 77−15612
KCl-KBr, dislocation rosettes, diffusion origin 78−83820
KCl-KBr, mechanism of aggregation of divalent impurities, dielectric loss meas. *(Japanese)* 79−60394
KCl-KBr, mixed cryst., radiation hardening 79−99238
KCl-KBr, mixed crysts., microhardness, theory 80−75298
KCl-KBr, solid soln., negative muon capture ratios 80−55007
KCl-KBr, solution hardening and softening at low temp. 78−31414
KCl-KBr, solution hardening and softening at low temp. 80−108462
KCl-KBr, with equimol. conc., piezo-optic birefringence theory 80−100643
KCl-KBr conc. solid soln., edge dislocation motion in stress field *(Japanese)* 78−2138
KCl-KBr fused mixtures, electrocapillary phenomena on liq. Bi 77−40554
KCl-KBr mixed crystal, containing defects, mag. quenching of positronium states 77−8680
KCl-KBr mixed crystal, elastic consts. press. derivative 77−11619
KCl-KBr mixed crystal, piezo-optic birefringence 78−31169
KCl-KBr mixed crystals, microhardness studies, nonlinear depend. on composition 78−83872
KCl-KBr mixed crystals, sign reversal of piezo-optic birefringence 79−99849
KCl-KBr mixed crystals, thermolum. studies 80−11486
KCl-KBr mixed system, Gruneisen coefficient evaluation 80−39240
KCl-KBr single crysts., yield strength and dislocation mobility, solid soln. hardening model 77−72649
KCl-KBr solid soln., highly conc., computer simulation of dislocation motion *(Japanese)* 77−68972
KCl-KBr solid solution, yielding model on plateau stress 78−27568
KCl-KBr solid solution thermally activated edge dislocation motion computer simulation 79−19249
KCl-KBr:Mn mixed cryst. system for thermoluminescence dosimetry, glow curves, dose response 78−24150
KCl-KBr:Ti^+, cryst., luminesc. and excitation spectra 77−66535
KCl-KBr-KCl, layered system, diffusion zone, pore form. and movement *(Russian)* 79−69282
KCl-KF:Pb^{2+}, point defects, ionic thermal currents and optical meas. 80−6403
KCl-KF-K_3VF_6, phase diagram 77−21123
KCl-KH, F- and U-centre redistrib. at end of proton tracks, microspectrophotometric anal. 80−10583
KCl-KH cryst. stimulated by X-radiation, spatial redistribution of F and U centers 79−14804
KCl-KI:Tl, spectral, polarisational and kinetic characts. 78−80385
KCl-KNO_3-H_2O, apparent and partial molal volumes in mixed salt solns. 77−9114
KCl-LiCl:Cu^+, fused eutectic, diffusion and surface effects, chronopotentiometry *(French)* 78−11524
KCl-Mg, thermolum. of Z-centre, optical absorpt. 80−55203
KCl-Mg, X-irrad. and F-bleached, optical and ESR spectra 77−48052
KCl-Na, F_A, F_B and F_C-centres, wave functions and energy level of bound states 77−8049
KCl-NaCl, aq. solns., isopiestic studies, 383 to 474K 80−21320
KCl-NaCl, dislocation rosettes, diffusion origin 78−83820
KCl-NaCl, fused binary mixtures, electrocapillary phenomena on liq. Bi 77−40553
KCl-NaCl electrolyte mixtures, in aq. soln., viscosity, individual electrolyte effects *(German)* 78−22881
KCl-NaCl mixed crystals, contact angles and free energies at solid/melt interface 80−64937
KCl-NaCl solid solns., equilib. decay curve *(Russian)* 79−90760
KCl-NaCl-$FeCl_3$ system, shape eutectics line calc. *(Russian)* 79−96016
KCl-NaCl-K_2NaVF_6, phase diagram 77−48416
KCl-NaCl-NaF-K_2NaVF_6 system, phase diagram 79−66049
KCl-OH^-, electron irrad., F_2^+ centre stabilisation and tuneable laser operation 80−54231
KCl-RbCl(CsCl) fused binary mixtures, electrocapillary phenomena on liq. Bi 77−40553
KCl-$SrCl_2$, photoluminescence of Z_4-centre and associated Z type colour centre *(Russian)* 79−4851
KCl-Tl^+,Ca^{2+}(Sr^{2+}), electrolytic colouring, colour centre form., optical absorpt. spectra 79−15497
KCl-$ZnCl_2$, molten, US velocity, thermodynamic quantities and struct. *(Japanese)* 80−88270
KCl-$ZnCl_2$, molten, US absorption coeffs. and bulk viscosity coeffs. *(Japanese)* 80−88271
KCl+M⇄K^++Cl^-+M, rate consts. in at. press. flames 77−60036
KCl(:LiF), radiative Q-centres, opt. absorpt. and thermal conductivity 77−47450
KCl(Br), (100) surface, potential energy of isolated Au atom above surface 77−89650
KCl(Br), CESR of dendritic metal phase precip. 77−24744
KCl(Br), coloured, irrad. damage during positron bombardment 78−63791
KCl(Br) substrate, epitaxial crystn. of isotactic polypropylene 78−26787
KCl(Br):Eu, Eu^{2+} ESR meas. 78−80209
KCl(Br):Eu^{2+}, spin Hamiltonian, cryst. field const. calcs. 79−51537
$KCl_{0.5}Br_{0.5}$:Ca, X-ray irrad., Z_1-centres, thermoluminesc. and optical absorpt. meas. 80−16108
$KCl_{1-c}Br_c$, impurity centre local vibrs., comp. depend. of spectral parameters 80−79898
$KCl_{1-x}Br_x$, bulk modulus, room temp. to 400°C 80−92588
$KCl_{1-x}Br_x$, lattice dynamics 78−75761
potassium compounds continued
$KCl_{1-x}Br_x$:NCO^-, absorpt. band defect broadening *(Russian)* 78−72526
KCl_xBr_{1-x}, dielectric const. determ. 80−108145
KCl_xBr_{1-x}, mixed crystals, thermolum. and optical absorption studies 80−104000
KCl_xBr_{1-x}:Sr^{2+}, dielec. loss 77−85646
KCl(Br)(I), Czochralski growth, dynamical aspects, use of optical diameter controller 78−31332
KCl(Br)(I), electron beam excited, luminesc. and cond. of nonideal degenerate electron-hole plasma 78−10488
KCl(Br)(I), stress-induced birefringence meas., 1-12 μm 77−24818
KCl(Br)(I):Ag film, EPR and optical exam. of Ag impurity centres 77−85562
$KCl_{1-x}CN_x$, dipolar impurity tunnelling model, elastic interaction and const. 78−71826
$KCl_{1-x}I_x$:NCO^-, absorpt. band defect broadening *(Russian)* 78−72526
KClIn, absolute quantum output of low-inertial energy transmission *(Russian)* 77−32429
$KClO_3$, ^{17}O NQR, spin echo double reson. method, electronegativity 80−54970
$KClO_3$, ^{35}Cl NQR, Stark splitting *(French)* 79−47352
$KClO_3$, ^{35}Cl NQR appl. in thermometry below 77K 80−66067
$KClO_3$, Γ-irrad. defects, ^{35}Cl NQR, 77 and 300K 78−91981
$KClO_3$, NQR freq. of ^{35}Cl, temp. depend., mol. dynamics 77−12227
$KClO_3$, NQR frequency, appl. in pulsed NQR thermometer 77−13749
$KClO_3$, NQR press. depend. 77−12225
$KClO_3$, NQR spectroscopy, parametric superregenerator with phase quantisation application 80−22398
$KClO_3$ NQR spin generator 77−10077
$KClO_3$, NQR temp. depend., torsional mol. oscill. in solid 79−4743
$KClO_3$, quadrupole spin echo envelope EFG tensor axisymmetry in mag. field 80−20497
$KClO_3$, refinement of cryst. struct. 78−55850
$KClO_3$, with adsorbed film of soln., NMR investig. 77−8426
$K^{35}ClO_3$ NQR absorption precision thermometer 77−5841
$KClO_3$-$CsClO_3$, NQR, mag. susceptibility meas. 78−35059
$KClO_4$, AC electrical conductivity meas., mechanism 79−99367
$KClO_4$, AC electrical conductivity meas. between temp. range 25-325°C, automated technique 80−59699
$KClO_4$, ClO_3^- detection by EPR of ClO_3 radicals created by X-irrad. 78−76311
$KClO_4$, cryst. growth from gelatin gels, exam. of growth and morphology 80−7488
$KClO_4$, cryst. struct. determ. 77−80472
$KClO_4$ crystal growth and nucleation in SiO_2 gels 78−48299
$KClO_4$, electrical conductivity, frequency dependence 80−65288
$KClO_4$, single cryst. growth in silica gel 77−63549
$KClO_4$ single crystals, gel growth, temp. effects etching 79−78862
$KClO_4$, single crysts., growth by modified gel technique 78−72711
$KClO_4$, single ion props. by lattice energy minimisation 78−83769
$KClO_4$ soln. in liq. ammonia, conductance at −62.37°C 78−91459
$KClO_4$, spectral interference in at. absorption spectroscopy in C tube atomiser and flames *(Japanese)* 79−48019
$KClO_4$, X-irrad., ESR spectra of O_3^- and ClO_3 exchange-coupled to O_2 78−64856
$KClO_4$, X-irrad. induced paramag. defects, ESR study 80−24493
$KClO_4$:MnO_4^-, reson. Raman excitation profiles for totally symmetric mode, vibronic struct. 80−50309
$KClO_4$-$LiClO_4$, binary melt, Raman spectra, polarised line width, temp. depend. 78−84578
KCl:Na, F_A-centre optical absorpt., estimate using symmetry-adapted wave functions 80−11448
KCl.Pb^{2+}, relation between bonding and g-shift 80−39492
KCl(aq.)-pyrex systems, electrokinetic coeff. determ. from sedimentation pot. 80−3365
$K_3Co(CN)_6$, quadrupolar spin-lattice relax. in solids 78−39429
$K_3Co(CN)_6$, ^{59}Co quadrupole coupling const., temp. depend. 80−44557
$K_3(Co(CN)_6)$, excited state geometry calcs. 77−27047
$K_3Co(CN)_6$, NMR spin lattice relax. of ^{59}Co rel. to $Co(CN)_6$ octahedra vibr. modes 80−39885
$K_3Co(CN)_6$, Raman scatt. and electronically-induced phase transition at 130K 77−90142
$K_3Co(CN)_6$, spin 7/2 system, quadrupolar relax. parameters 78−56392
K_2CoCl_4, cryst. structs. of orthorhombic and monoclinic modifications 77−15358
$KCoCr_2(VO_4)_3$, synthesis and cryst. struct. 80−88114
$KCoF_3$, antiferromag., obs. of domains by X-ray topography 78−14981
$KCoF_3$, antiferromag., ^{59}Co NMR exam.. 78−76332
$KCoF_3$, antiferromag., with residual orbital moment, nucl. mag. relax. 80−71215
$KCoF_3$, antiferromag. domains obs. by cryogenic X-ray topography 77−39507
$KCoF_3$, antiferromag. domain wall motion under external stress 80−80583
$KCoF_3$, Co^{2+} spin-lattice relax. narrowing of ^{19}F NMR 77−85611
$KCoF_3$, crystal growth from flux, degree of perfection and dislocation density 77−77359
$KCoF_3$, flux-grown cryst., direction of dislocations, X-ray topography obs. 77−35565
$KCoF_3$, IR refl. spectra, vibr. modes, optical vibr. freq., Kramers Kronig anal. 80−66190
$KCoF_3$, lattice parameter temp. depend., phase transitions and thermal expansion coeff. 80−1988
$KCoF_3$, mag. form factor calc. for Co^{2+} 77−20555
$KCoF_3$, mag. suscept. and Neel temp. determ. 77−77044
$KCoF_3$, magnon-phonon interaction mechanism 77−20019
$KCoF_3$, multiplet struct. in XPS spectra of 3p and 3s subshells 78−43981
$KCoF_3$, NMR, magnon-phonon interaction contribution to nuclear spin-lattice relax. 78−88207
$KCoF_3$, reflectivity, 8-60 eV, excitonic struct. 77−20871
$KCoF_3$, single crystal, mag. susceptibility, ^{19}F NMR and static measurements 79−11301
$KCoF_3$, strain sensitive props., Mossbauer spectra obs. 77−20765
$KCoF_3$, XPS of band struct. 77−11851
K_2CoF_4, 2-dimens. Ising antiferromag., mag. excitons, Raman scatt. obs. 80−66181
K_2CoF_4, neutron scatt. obs. of mag. behaviour 77−66254
K_2CoF_4, pseudo Ising antiferromag., inelastic light scatt. by mag. excitons 80−11377

potassium compounds continued
K_2CoF_4, specific heat capacity, critical amplitude, cross-over from 2-D Ising to Heisenberg behaviour 80−39791
K_2CoF_4, two-dimens. Ising antiferromag., nearest neighbour correl. function, birefr. expts. 80−71386
K_2CoF_4, two-dimensional Ising-like antiferromag. birefringence, short-range order effect 77−81081
K_2CoF_4, two-dimensional antiferromag., one- and two-magnon Raman scatt. 79−51945
$K_2CoF_4:Mn^{2+}$, impurity induced mag. excitations, magnon gap mode, far IR spectra obs. 80−44821
K_2CoO_3:^{57}Co Mossbauer source 77−6592
$K_2Co_2(SO_4)_3$, cubic langbeinite struct., low temp. mag. susceptibility 78−56299
$K_2Co_2(SO_4)_3$ polycryst., growth and phase transitions 79−33918
$K_2Co_3(SO_4)_2$, phase transitions, dielec. props. obs. 78−6643
$K_2Co(SO_4)_2.6H_2O:Gd^{3+}$, EPR, low-symmetry effects 77−48043
KCr alum, relaxation behaviour, EPR study, environmental effects 80−66021
$K_2Cr_2O_7$, Cr $^7P_0$ state, radiative lifetime in matrices, meas. using laser ablation and selective excitation 80−71959
$KCr_xAl_{1-x}(SO_4)_2.12H_2O$, EPR of single crystals, zero-field splitting of Cr^{3+} 80−66015
K_2CrCl_4, ionic ferromag., temp. depend. intensity in optical absorption 77−12399
$KCrF_3$, mag. struct. and cooperative ordering or orbitals 79−99687
$K_2Cr_5F_{17}$, monocrystal, cryst. field and mag. props., EPR and optical absorpt. spectra 79−19773
$K_xCr(Mn)(Co)O_2$, layer struct., elec. cond. behaviour *(French)* 78−26542
$KCrO_2$, two-dimens. mag. order, neutron powder diffr. obs. 80−44805
$KCrO_2$, two-dimens. mag. props. rel. to cryst. struct. 80−75776
$KCrO_2$, two-dimensional antiferromag., mag. props. *(French)* 78−23251
K_2CrO_4 aq. solns., isomorphous salts viscosity investig. 78−95173
K_2CrO_4, corrosion inhibitor of mild steel 78−95839
K_2CrO_4, ice, γ-irrad., electron trap depth, ESR 79−66317
K_2CrO_4, $KCrO_3Cl$, γ-irrad. single crysts., identification of paramag. centres 78−67994
K_2CrO_4, $K\beta_{1,3}$ X-ray emission spectra, low energy plasmon $K\beta'$ satellite 79−74020
α-K_2CrO_4, single crysts. electron density distrib. 79−7584
K_2CrO_4, solid and solution, diffuse reflectance spectra 78−88326
K_2CrO_4, X-ray Lα emission spectra, excited states calcs. 79−59488
$K_2CrO_4:SO_4^{2-}$, IR absorpt. spectra, local symmetry of impurity ions *(Russian)* 78−2893
K_2CrO_4-$CaCrO_4$, phase diagram determ., struct. of double salt 77−15543
$K_2CrO_4+La_2(NoO_4)_3$, $(Nd_2(NoO_4)_3)$, X-ray phase analysis, IR absorption spectra, and thermogravimetric anal. 79−1944
$K_2Cr_2O_7$, acidic soln., UV absorbance standard verification 78−21092
$K_2Cr_2O_7$ acidic solns. as UV absorbance standards 77−53990
$K_2Cr_2O_7$, closed-shell tetroxo-complex triplet levels, luminesc. meas. 79−69874
$K_2Cr_2O_7$, growth and growth dispersion 80−49148
$K_2Cr_2O_7$ in perchloric acid soln., UV absorbance standards 78−32851
$K_2Cr_2O_7$, $K\beta_{1,3}$ X-ray emission spectra, low energy plasmon $K\beta'$ satellite 79−74020
$K_2Cr_2O_7$, luminesc., vibr. anal. 79−38620
$K_2Cr_2O_7$ melt, decomposition leading to growth of Cr_2O_3 crysts. 79−43131
$K_2Cr_2O_7$, polymorphic behavior, depend. on thermal and prep. history 80−34184
$K_2Cr_2O_7$, role of metastable β-phase in cryst. growth 79−32931
$K_2Cr_2O_7$ single crystals, X-irrad., EPR spectra 80−2638
$K_2Cr_2O_7$ soln. in H_2SO_4, standard for UV spectrophotometry 77−77819
α-$K_2Cr_2O_7$, symmetry centres exam. by morphological methods 78−59796
$K_2Cr_2O_7$, thermal props. thermal anal. and X-ray diffr. obs. 78−30752
$K_2Cr_2O_7+H_2SO_4$, in spectrophotometric determ. of reducing agents 79−39234
$K_2Cr_3O_{10}$, cryst. struct. determ. 79−23592
$K_2Cr_3O_{10}$, X-ray powder cryst. struct. determ. *(French)* 79−32960
K_3CrO_4, enthalpy of form. 78−53236
$K_2CrO_4.MoO_4$-Cr_2O_3 system, phase diag. 77−86007
$KCr(SO_4)_2.12H_2O$, phase transition associated fluctuations, Cr^{3+} EPR obs. 77−32247
$KCr(SO_4)_2.12H_2O$, spin lattice relaxation, in liquid He and in vacuum 78−39434
$KCr(SO_4)_2.12H_2O$, ESR, spin-lattice relax., ambient gas atm. thermal cond. effect 79−8046
$K_2CrTi(PO_4)_3$, cryst. data 77−39564
KCs^+, adiabatic pot. curves, ground and excited state, Hellmann-type model pots. 78−78647
$K_xCs_{(1-x)}Al(SO_4)_2$, solid soln., Raman and IR spectrum study *(French)* 79−47453
K_2CsSb, evaluation as photocathode material 78−11072
K_2CsSb photocathodes, prep. and props. 78−84693
K_2CsSb, semitransparent photocathodes, UV response 77−167
$K(Cu(CN)_2)$, NQR spectrum of $^{63,65}Cu$ 77−12235
$K_3Cu(CN)_4$, isotopic mixed crystal with ^{12}C and ^{13}C, Raman scattering 78−76476
$K_2CuCl_4.2D_2O$, quadrupolar interaction, 4-300K, reorientation 79−73848
$K_2CuCl_4.2H_2O$, and isomorphous cpds., mag. interactions of H and D nuclei, NMR obs. 79−87251
$K_2CuCl_4.2H_2O$, Bloch-wall NMR, anisotropic hyperfine interaction 79−51864
$K_2CuCl_4.2H_2O$, ferromag., hyperfine and exchange interactions, NMR study 80−50208
$K_2CuCl_4.2H_2O$, hyperfine and super-exchange interactions 80−103654
$K_2CuCl_4.2H_2O$, paramag. single cryst., PMR temp. depend., hyperfine const. and exchange interaction *(Korean)* 80−29630
$K_2CuCl_4.2H_2O$, proton NMR *(Korean)* 78−19342
$K_2CuCl_4.2H_2O$ structure compounds, 3-dimens. ferromag., exchange anisotropy by NMR 77−55714
$K_2CuCl_4.2H_2O$ structures, BCC Heisenberg ferromags., transferred hyperfine interactions of ^1H, ^2D and ^{17}O 77−69725
$K_2CuCl_4.2H_2O$, thermal effects in mag. exchange interaction 77−16067
$KCuCr_2(VO_4)_3$, synthesis and cryst. struct. 80−88114
$KCuF_3$, linear chain Heisenberg antiferromag., nearest neighbour correl. function, birefr. expts. 80−71386
potassium compounds continued
$KCuF_3$, ^{63}Cu NQR meas. 80−50219
$KCuF_3$, chain-like antiferromag., sublattice magnetisation temp. depend. 77−51892
$KCuF_3$, chain-like antiferromag., parallel susceptibility 78−80137
$KCuF_3$ crystals, with Jahn-Teller distortion, electron density distrib. X-ray diffractometry 79−69061
$KCuF_3$, Cu-Cu exchange interactions 77−69529
$KCuF_3$, hyperfine interactions of ^{19}F nuclei, n.m.r. meas. 77−12209
$KCuF_3$, mag. struct. and cooperative ordering or orbitals 79−99687
$KCuF_3$, multiplet struct. in XPS spectra of 3p and 3s subshells 78−43981
$KCuF_3$, nearly 1-D spin-$^1/_2$ antiferromagnet, spin wave energy dispersion 80−2551
$KCuF_3$, one-dimens. antiferromag., spin waves, neutron scatt. study 80−65848
$KCuF_3$, one-dimensional S=1/2 Heisenberg antiferromag., mag. energy, optical birefringence meas. 78−52467
$KCuF_3$, XPS of band struct. 77−11851
K_2CuF_4, 2-D ferromagnet, optical and magneto-optical props. 77−52062
K_2CuF_4, 2-dimens. ferromagnet, low-temp. mag. struct. *(Japanese)* 79−33461
K_2CuF_4, Brillouin scatt. and US meas. of phonons, elastic moduli and Debye temp. calc. 79−87454
K_2CuF_4, Cu-Cu exchange interactions 77−69529
K_2CuF_4, Curie temp. XY-like anisotropy effect, inter-layer exchange 77−59406
K_2CuF_4, ferromag., orbital ordering, review *(Japanese)* 78−76224
K_2CuF_4, hyperfine interactions of ^{19}F nuclei, n.m.r. meas. 77−12209
K_2CuF_4, layered, mag. sp. ht., two-dimens. S-$^1/_2$ Heisenberg ferromag. behaviour 77−32206
K_2CuF_4, layered spin system, planar rotator symmetry, phase transition 80−65951
K_2CuF_4, magnon condensation 79−91220
K_2CuF_4, magnon condensation obs. in quasi-2D planar ferromag. phase 80−60232
K_2CuF_4, microwave excitation, optical detection of ferromagnetic reson. 80−50197
K_2CuF_4, nearly two-dimens. Heisenberg ferromag., renormalised spin wave theory 77−66285
K_2CuF_4, nearly two-dimensional ferromag. nucl. transverse relax. rates meas. 77−81024
K_2CuF_4, obs. of magnon density of states by subthreshold steady-state absorption 77−12107
K_2CuF_4, optical absorption spectra, correl. with g-shifts, reduced spin-orbit coeff. determ. 78−23485
K_2CuF_4, quasi two-dimens. Heisenberg ferromag., spin wave spectrum lineshape, neutron scatt. obs. 77−66286
K_2CuF_4, single crysts., cryst. growth by Brigman-Stockbarger technique 79−52107
K_2CuF_4, spin relax., crit. behaviour, high freq. susceptibility meas. 80−65936
K_2CuF_4, spin wave meas. in low energy range, inelastic neutron scatt. 78−88105
K_2CuF_4, spin-wave relaxation, parallel pumping expt. 79−4729
K_2CuF_4, structural anal., X-ray diffraction meas. 79−86762
K_2CuF_4, two-dimens. ferromagnet, nuclear spin-spin-relax. *(Japanese)* 77−48082
K_2CuF_4, two-dimens. ferromagnet, half-field EPR line 79−19765
K_2CuF_4, two-dimens. ferromag., magneto-optical props., absorpt., MCD and MLD 79−87419
K_2CuF_4, two-dimens. ferromag., saturation of parallel-pumped magnons 80−97147
K_2CuF_4, two-dimensional ferromag., spin-wave lineshape, neutron scatt. data 77−16065
K_2CuF_4, two-dimensional planar ferromagnet, giant fluctuation of spins *(Japanese)* 80−54894
$K_2Cu_xFe_{1-x}F_4$, random ordered phase in site model, statistical theory 79−47218
$K_2Cu(H_2O)_6(SO_4)_2$, IR and Raman vibr. spectra 79−28743
$K_2Cu(H_2O)_6(SeO_4)_2$, IR and Raman vibr. spectra 79−28743
$K_2Cu_{1-x}Mn_xF_4$, Cu-Mn exchange interaction, optical determ. 78−72551
$K_2Cu_{1-x}Mn_xF_4$ system, (0≤x≤0.2), prep., cryst. chem., and ferromag. props., X-ray and neutron diffr. study 79−24162
$K_2Cu_{1-x}Zn_xF_4$, two-dimens., ferromag., spin wave excitations 78−80140
$K_2Cu_cZn_{1-c}F_4$, EPR, spin correlation decay rate 79−19772
$K_2Cu_xZn_{1-x}F_4$, Curie temp., Cu conc. depend. 80−60255
$K_2Cu_xZn_{1-x}F_4$, two-dimens. ferromag., spin correls. near percolation limit 80−44840
KD_2PO_4, polarisation echo, near ferroelec. transition 78−88266
KD_2AsO_4, AC conduction 79−55926
KD_2AsO_4, Cr^{3+} EPR, line shape and elec. field effect 79−11336
KD_2AsO_4, ferroelec., phase transition and Raman scattering 78−84540
KD_2AsO_4, ferroelec., high temp. phase transition, Raman spectra 80−71338
KD_2AsO_4, ferroelect. phase transition, NMR study *(Chinese)* 79−33644
KD_2AsO_4, ferroelectrics, Raman spectra, coupled tunnel-phonon modes and isotope effect 79−69205
KD_2AsO_4, ferroelectric, high temp. phase transitions, proton dynamics 80−76023
KD_2AsO_4, LF dielectric dispersion near phase transition 77−59530
KDF_2, deuteron mag. reson., quadrupole coupling consts., F-D distance 77−63313
$K(D_xH_{1-x})PO_4$, ferroelectric, photovoltaic and photorefractive effects 78−72187
$KD_{2x}H_{2(1-x)}PO_4$, 90° synchronism, second harmonic doubling of Nd laser *(Russian)* 77−58386
$KD_{2x}H_{2(1-x)}PO_4$ crystals, plastic deform. and mech. props. 79−79035
$KD_{2x}H_{2(1-x)}PO_4$ crystals, 0<x<0.98, light scatt. by polaritons 80−96802
$KD_{2X}H_{2(1-x)}PO_4$, deuteration effect on refr. index 77−59550
$K(D_xH_{1-x})_2PO_4$, D distrib. during crystallisation from aq. soln. 77−11496
$K(D_xH_{1-x})_2PO_4$ ferroelec., dielec. props., four-cluster approx. 80−97202
$K(D_xH_{1-x})_2PO_4$, isotope exchange during crystallisation from aqueous solns. 78−18569
$K(D_xH_{1-x})_2PO_4$, monoclinic and tetragonal forms, existence in aq. soln. 78−47262
$K(D_xH_{1-x})_3(SeO_3)_2$, ferroelastic, anelastic and elastic infra-low freq. props. 80−70304
KDP crystal, third-order moduli of elasticity 79−46737

potassium compounds continued
KDP, growth in soln., nucleation rate, supersaturation and temp. depend. 77−4728
KDP monocrystal, expansion and contraction coeffs., tricritical point, Landau theory explanation *(Russian)* 80−44340
KDP type crystals, ferroelec. phase transition, Greens function theory *(Chinese)* 79−56740
KDP-type cryst., Raman scattering and phase transitions, deuteration effects 78−76400
KDP-type crystals, electrooptic effect in ultraviolet region 78−76431
KDP-type crystals, polarisation, dielec. const. thermodyn. props. 77−59527
KDP-type crystals, phase transitions, quadratic electrooptical coeff., electrostriction 78−76430
KD_2P_4, nonlinear electrooptic effects 80−29721
KD_2PO_4, AC conduction 79−55926
KD_2PO_4, acoustic phonon dispersion, elastic stiffness, light scatt. obs. 80−103966
KD_2PO_4, attenuation const. meas. by SHF dielec. resonance 79−47406
KD_2PO_4, Brillouin spectrum and broad central component, depend. on scatt. wave vector direction 80−34931
KD_2PO_4, central mode, spin lattice relaxation dispersion 78−15108
KD_2PO_4, coexistence states during first order transition, optical obs. 80−75350
KD_2PO_4, cryst. high-freq. modulation in Pockels cell, acoustic phenomena 78−1336
KD_2PO_4 crystal, electro-optical extraction of Nd:YAG laser pulses *(German)* 80−87416
KD_2PO_4 crystal, photoresponse under laser irrad. 80−100479
KD_2PO_4 crystal electron-beam spatial light modulator, resolution 80−74503
KD_2PO_4 crystals in D_2O, two phase stable zone *(Chinese)* 79−82937
KD_2PO_4, deuteron tunnelling, barrier height and energy level calc. 80−6482
KD_2PO_4, domain structure obs. using SEM 77−1647
KD_2PO_4 doubler, KH_2PO_4 mixer and $LiIO_3$ doubler crysts., mW 213 nm source based on Nd:YAG laser 79−55178
KD_2PO_4, electron beam addressed light valve, optical processing appl. 78−83099
KD_2PO_4, electronic struct., UV reflection spectra 79−38558
KD_2PO_4 electrooptic modulator, field of view extension 78−94429
KD_2PO_4, ferroelec., tetragonal⇄monoclinic transition, neutron powder diffr. meas. 77−7693
KD_2PO_4, ferroelec. transition, ^{31}P chemical shift tensor meas. 77−28527
KD_2PO_4, ferroelec. transition, ^{31}P chem. shift obs. 78−76414
KD_2PO_4, ferroelec. domain struct. obs. using TOF neutron diffractometer 79−51923
KD_2PO_4, ferroelect. phase transition, NMR study *(Chinese)* 79−33644
KD_2PO_4, ferroelectric transition obs. by ^{31}P chemical shift 77−59531
KD_2PO_4, ferroelectric, longit. and transverse props., Monte Carlo study 79−51912
KD_2PO_4, ferroelectrics, Raman spectra, coupled tunnel-phonon modes and isotope effect 79−69205
KD_2PO_4 filled strip transmission line, for electro-optic beam deflection 79−46045
KD_2PO_4, H-bonded phase transitions, SCF approach 78−92030
KD_2PO_4, high efficiency SHG of Nd:YAG laser radiation 78−59088
KD_2PO_4, high press. phase diagram 78−52457
KD_2PO_4, high temp. phase transition, dielec. const., elec. cond. and IR refl. meas. 78−43118
KD_2PO_4, IR and Raman polarised spectra, rel. to crystal struct. 78−56489
KD_2PO_4 light valves for optical information processing 77−72080
KD_2PO_4 light valves 77−83992
KD_2PO_4, magnetoelectric susceptibilities, phenomenological rules for computation 80−55068
KD_2PO_4, microwave spectra, temp. depend. mode rel. to proton subsystem 80−24548
KD_2PO_4 monocrystal, electrooptical props. in paraelectric phase *(Polish)* 80−11368
KD_2PO_4, Nd:YAG laser radiation freq. doubling 77−88776
KD_2PO_4, Nd:YAG laser radiation freq. doubling 78−46615
KD_2PO_4, neutron scattering from coupled polar-elastic waves 80−92623
KD_2PO_4, noncentrosymmetric monocrystals, quadratic electro-optic coeffs. 79−28718
KD_2PO_4, nonlinear electrooptic coeffs. near Curie temp. 80−11366
KD_2PO_4, optical activity in paraelec. phase 80−60539
KD_2PO_4 optical parametric amplifier, gain limitations 79−55177
KD_2PO_4, optical parametric amplifier 79−81481
KD_2PO_4, optically addressed light valve, optical processing appl. 78−83101
KD_2PO_4, order-disorder type ferroelec., HF dynamics 77−39657
KD_2PO_4, para- and ferroelec. phases spatial distrib. during first order phase transitions 79−42923
KD_2PO_4 parametric amplifier, rhodamine laser light shifting into blue-green 79−18471
KD_2PO_4, phase transitions study, role of cryst. struct. determ. 80−75197
KD_2PO_4 photo-spatial light modulator, optical data processing appl. 80−9988
KD_2PO_4 photo-spatial light modulator, optical data processing 80−102839
KD_2PO_4, polarisation fluctuations, wavevector depend. 80−71295
KD_2PO_4, proton spin-lattice relaxation rate, temp. depend., field depend. 78−88208
KD_2PO_4 f_{63} laser modulator *(Chinese)* 80−28260
KD_2PO_4, Rayleigh scatt. and narrow central component, depend. on scatt. wave vector direction 80−29747
KD_2PO_4, SHG efficiency, 532 to 266 nm 77−23710
KD_2PO_4, soft ferroelec. mode anisotropy 78−14430
KD_2PO_4, struct. at high press. in rel. to effect of press. on T_c 79−42915
KD_2PO_4, transparent dielec., thermal analysis of laser-induced damage 80−66336
KD_2PO_4, transverse dynamics, short-range interaction effects 78−14408
KD_2PO_4, two photon absorption at 266.1 nm 77−88844
KD_2PO_4 type ferroelecs., distrib. functions and thermodynamic props. 78−76409
KD_2PO_4, ultrafast electro-optical modulator design and application 77−19432
KD_2PO_4, wideband light modulator in cylindrical waveguide, parameter optimisation *(Russian)* 79−94344
KD_2PO_4, X-irradiated, hysteresis effects obs. by ESR 80−103928

potassium compounds continued
KD_2PO_4, X-ray topography of single crysts. grown on KDP seeds 78−23594
KD_2PO_4:AsO_4^{4-}(SeO_4^{3-}), ferroelec., low freq. fluctuations, isotope effects, EPR, ENDOR, ESCA 77−73118
KD_2PO_4:$Cr_2O_7^{2-}$, optical absorpt. spectra, mol. orbital calcs. 79−15491
KD_2PO_4:Fe^{3+}, ESR, anomalous temp. depend. of D tensor 79−61205
KD_2PO_4:Tl^{2+}, EPR of ferroelec. and paraelec. phases 80−66012
KD_2PO_4-type crysts., photorefractive and photovolt. effects 79−15189
KD_2PO_4-type crysts., relax. processes in order-disorder transitions under short range correl. conditions 79−73889
KD_2PO_4-type ferroelectrics, parametric tunnelling-like reson. 80−66119
KD_2PO4 transmission line Pockels cells, optical rise time meas. 78−46778
$K_3D(SO_4)_2$, dielec. props. and phase transitions 80−60482
$KD_3(SeO_3)_2$, acoustic phonon softening and spontaneous strains 78−26652
$KD_3(SeO_3)_2$, central peak, soft acoustic shear mode, light scatt. study, isotope effects 78−52518
$KD_3(SeO_3)_2$, D NMR above and below ferroelec. transition, H-bond behaviour 78−52460
$KD_3(SeO_3)_2$, deuteron mag. reson. in ordered and disordered phase 78−39414
$KD_3(SeO_3)_2$, ferroelastic transition, EPR 80−7148
$KD_3(SeO_3)_2$, ferroelastic phase transition, mech. stress effect 80−70394
$KD_3(SeO_3)_2$, optical and dielec. props. near ferroelastic phase transition 79−38518
$KD_3(SeO_3)_2$, phase transition, neutron diffr. 80−2158
$KD_3(SeO_3)_2$, phase transition, neutron scatt. study 80−75351
$KD_3(SeO_3)_2$, second-order ferroelastic phase transitions, piezo-opt. props. obs. 78−95558
$KDy(MoO_4)_2$, polarised IR and Raman struct., $^{92}Mo/^{100}Mo$ isotope effect 80−108198
$KDy(WO_4)_2$, Jahn-Teller transition, permittivity behaviour 80−55012
$KDy(WO_4)_2$, low temp. phase transitions *(Russian)* 78−87787
$KDy(WO_4)_2$, phase transition mechanism, absorpt. spectra, symmetry props. *(Russian)* 80−55130
β-KEr_2F_7, crystal struct. *(French)* 80−107164
β-KEr_3F_{10}, cryst. struct. *(French)* 78−51500
$K_2Er(NO_3)_5$, cryst. struct. by X-ray diffr., cryst. binding 78−42988
$KEr(WO_4)_2$, crystallisation cond., stimulated emission in 2.8 μm band 80−53301
$KEuHP_3O_{10}$ acid, exam. of thermal decomposition 80−55638
$KEuHP_3O_{10}$, synthesis of K_2CO_3, Eu_2O_3 and phosphoric acid, exam. of structure 79−1837
$KEu(MoO_4)_2$, polymorphism investig. by X-ray diffr. and DTA 77−4091
$K_5Eu(MoO_4)_4$, electric dipole transition cross section and effective site symmetry of Eu^{3+} 78−52556
$K_{0.5}Eu_{0.5}Nb_2O_6$, ^{93}Nb NQR spectra, 77 to 450K 79−38401
$KEu(PO_3)_4$, synthesis of K_2CO_3, Eu_2O_3 and phosphoric acid, exam. of structure 79−1837
α-$KEu(PO_3)_4$, vibr. spectra 80−34905
$K_3Eu(PO_4)_2$, synthesis and IR spectra 80−16019
KF, ab initio SCF MO energy, dipole moment and polarisability 80−1085
KF, Compton profile, 59.54 keV γ-rays 78−64426
KF, Compton profiles, anisotropies 80−20730
KF, correlation between experimental and theoretical diffusion coeffs. 77−24421
KF, deformation coloration 77−76397
KF, diffusion in K, new NMR technique for slow diffusion exam. 77−51970
KF F_2^+-centre laser, picosecond pulse generation 1.24 to 1.45 μm, mode locking 79−89925
KF, F_2+-centre excited-state absorption spectrum, rel. to H_2^+ model 80−16066
KF, F-centre optical absorpt., estimate using symmetry-adapted wave functions 80−11448
KF, high press. B1 to B2 phase transition, X-ray diffr. obs. 79−23722
KF, IR absorpt. spectra from relaxed excited states of F-centres 77−69868
KF, K^+3p core excitons, refl. spectra study, low temp. 80−29759
KF, KCl and KI, monomers and dimers, Ar matrix-isolated, IR spectra, vibr. assignments and calcs. 79−45718
KF, one electron props., SCF-Xalpha scattered wave method 80−83279
KF, orbital g-factor and spin-orbit splitting of F-centre excited state, magnetoabsorpt. and MCD 78−2886
KF, photodichroic, as optical processing elements 78−83056
KF, piezo-birefringence, piezo-optical properties, temperature dependence 78−92050
KF, quadrupole coupling, vibr. and rot. effects, Morse oscill. calcs. 77−6805
KF, self-trapped exciton, ODMR spectra 79−28286
KF, spin-orbit interaction of relaxed excited state of F-centres 77−15808
KF, static SIMS, mol. rearrangement, cluster formation 78−64440
KF, surface lattice dynamics, Green function method 78−34693
KF, thermal expansion, higher-order anharmonic contrib. at high temps. 79−28113
KF, thermal positive ion emission from thick layers, effect of substrate metal 78−19627
KF, tunable CW lasers using F_2^+ centres for 1.26-1.48 and 0.82-1.07 μm bands 78−79023
KF^2, F_2^- mag. reson. absorpt. spectrum 77−73079
KF:Hg^{2+}, electrolytic colouration 78−75665
KF:Li, F_A-centre optical absorpt., estimate using symmetry-adapted wave functions 80−11448
KF:Li^+(Na^+)(K^+), shape of pot. energy well of impurity 79−23692
KF:LiF, photodichroic, real time recording medium, for optical spectrum analyzer 78−71174
KF:LiF, photodichroic real-time recording medium, for optical spectrum analyser 78−66878
KF:LiF photodichroic crystals as adaptive spatial filters 79−72713
KF:LiF photodichroic spatial light modulator for joint Fourier transform correlation 80−106617
KF:Pd^{2+}, pure and doped, two-step photoionisation, laser-active F_2^+ centre form. 79−963
KF:U, X- and γ-irrad., EPR of U^{5+} centre charge compensation mechanism 77−90030
KF:U^{5+} EPR of U^{5+} centre meas. 77−20684
KF/Pt thick layer/substrate system, thermal positive and negative ion emission, surface prop. non-uniformity effect 79−28882

potassium compounds continued
KF-AlF_3, ion-molecule equilibria studied by mass spectrometric method, heats of dissoc. and form. calc. 80−104479
KF-BeF_2, and BaO-SiO_2 systems complex ionic liquids, corresponding-state principle *(Japanese)* 77−56245
KF-BeF_2, molten, corresponding state principle with BaO-SiO_2 and appl. 79−11589
KF-BeF_2-DyF_3, crystalline and vitreous phases of cross sections 78−44096
KF-BeF_2-DyF_3, phase diagrams, intensification region 78−44097
KF-BeF_2-DyF_3 system, KBe_2F_5-DyF_3 cross section phase diagram, vitreous phases struct. 77−24383
KF-ErF_3, phase diagram 80−92645
KF-EuF_3 system, composition of phases determ. by DTA and X-ray crystallography *(French)* 77−68945
KF-H_2O, diffusion coeffs., diaphragm cell expts. *(German)* 78−83986
KF-LnF_3 (Ln=Y, La, Yb) binary liquid mixtures, thermochemistry 80−45538
KF-NaF-K_2NaVF_6, phase diagram 77−48416
KF-PbO-SiO_2 glass shear wave velocity and its temp. depend. *(Japanese)* 78−30702
KF-TbF_3 system crysts., X-ray struct. investig. 77−43187
KF-UF_4, ion-molecule equilibria, heat of form. and dissoc. and electron affinities determ. 80−104480
KF-UF_4, molten binary mixtures, viscosity meas. 80−65270
KF-YbF_3, KF-LuF_3, phase analysis 78−44101
KF+Eu^{2+}, cryst., hyperfine splitting, EPR 78−2733
KF_2-$3K_2O.2SiO_2$ freezing point depression meas., effect of silica compound additions 77−28797
$(KF)_n$-FeF_3, antiferromagnetic systems, dimensionality and spin reduction effects, Mossbauer study 80−39947
KF(Cl)(Br), mag. props. of relaxed excited state of F-centre, vibronic theory 78−60502
KF(Cl)(Br)(I), emission band of F-centre 80−76071
$KF(HF)_n$, (n=2,3,4), cryst., anion struct., H bonding, IR spectra 77−54560
$KF.2H_2O_2$, cryst. struct., X-ray and neutron diffr. meas. 77−39569
$K_3Fe(CN)_6$, automated electrodic potentiometry of solns. 78−35736
$K_3Fe(CN)_6$, electronic and mag. struct., semiempirical MO cluster calcs. 78−62733
$K_3Fe(CN)_6$, electronic struct., electron density, elec. field gradient, mag. susceptibility and g-tensor 79−91006
$K_3Fe(CN)_6$, electronic struct., elec. field gradient tensor 80−15483
$K_3Fe(CN_6)$ ice, trapped electrons, photostimulated decay, time-depend. rate const. 79−52692
$K_3Fe(CN)_6$, L_l and L_η X-ray emission spectra 78−39631
$K_3Fe(CN)_6$, mag. ordering and spin struct., Mossbauer obs. 77−40038
$K_3Fe(CN)_6$, paramag. relax., phonon bottleneck effects 78−23322
$K_3Fe(CN)_6$, pressure induced reduction, Raman spectra 80−66776
$K_3Fe(CN)_6$, Raman scatt. and electronically-induced phase transition at 130K 77−90142
$K_3(Fe(CN)_6)$ with NaCl, in aq. soln., electrolyte for porosity determ. of Cu platings on C steel filaments 79−70239
$K_3Fe(CN)_6$-KCl, press. induced reduction, IR spectra after pressurization 80−66776
$K_4Fe(CN)_6.3H_2O$, crit. dynamics, NMR data compared with dielec. data 78−76415
$K_4Fe(CN)_6.3H_2O$, C-N vibrs., Raman study 80−40106
$K_4Fe(CN)_6.3H_2O$, dynamic disorder and ferroelec. transition, Raman spectra obs. 77−81069
$K_4Fe(CN)_6.3H_2O$, effect of ordering on OH Raman bands 79−51959
$K_4Fe(CN)_6.3H_2O$ ferroelectric cryst., vibrational spectrum of $[Fe(CN)_6]^{4-}$ anion 77−69839
$K_4Fe(CN)_6.3H_2O$, ferroelec., sp.ht. and spontaneous polarisation, −65 to 0 degrees C, mol. field model 78−64333
$K_4Fe(CN)_6.3H_2O$, ferroelec. and paraelec. phases, dielec. props. meas. 80−60494
$K_4Fe(CN)_6.3H_2O$, internal field and ferroelec. ordering 78−76406
$K_4Fe(CN)_6.3H_2O$, Lamb-Mossbauer factor for crystalline lattice 79−78592
$K_4Fe(CN)_6.3H_2O$, nature of phase transition 79−38470
$K_4Fe(CN)_6.3H_2O$, Raman spectrum and dielec. relax. 78−19476
$KFeCl_3$, linear chain ferromag., optical absorpt. and dichroism in mag. field 77−77237
$K_2FeCl_5(H_2O)$, antiferromag., press. depend. on spin-flop transition 80−80505
$K_2FeCl_5(H_2O)$, phase diagram, antiferromag., paramag. and spin flop phases 80−44831
$K_3Fe(Cn)_6$, mag. and thermodynamic props. below 0.4K in mag. fields 79−56542
$KFe(CrO_4)_2$, cryst. struct., structural filiation with $KFe(CrO_4)_2.nH_2O$ series *(French)* 77−27855
$KFeF_3$, crystal growth from flux, degree of perfection and dislocation density 77−77359
$KFeF_3$, magnetisation density of Fe^{2+} 79−78313
$KFeF_3$, multiplet struct. in XPS spectra of 3p and 3s subshells 78−43981
$KFeF_3$, strain sensitive props., Mossbauer spectra obs. 77−20765
$KFeF_3$, XPS of band struct. 77−11851
$KFeF_4$, amorphous, mag. props. and Mossbauer spectra, speromagnetism and mictomagnetism 80−75778
$KFeF_4$, amorphous, Mossbauer study 80−39970
$KFeF_4$, struct. phase transitions obs. by dielec. const. and X-ray diffr. studies 79−95161
$KFeF_5$, one dimensional antiferromagnets, field depend. spin reduction temp. variation, spin flopping 79−78586
KFe_2F_6, flux growth of crystal 79−78861
K_2FeF_4, antiferromag., Mossbauer study of mag. ordering 79−28655
K_2FeF_4, antiferromagnet, two-dimensional, mag. excitations 80−80492
K_2FeF_4, charge transport and polarisation 80−80681
K_2FeF_4, Raman scatt. in two dimens. antiferromagnet 78−19488
K_2FeF_4, two dimensional planar antiferromag., mag. excitations, Raman and far IR spectra obs. 78−72343
K_2FeF_4, two dimensional easy plane antiferromag., neutron scatt. expts. 80−65838
K_2FeF_4, two-dimensional antiferromag., with easy-plane anisotropy, mag. excitations and two-magnon Raman scatt. 80−65839
K_2FeF_4, two-dimensional antiferromag., cryst. field effects, Mossbauer spectroscopy 80−71254
K_2FeF_5, crystal atomic struct., single crystal diffr. 78−10002
K_2FeF_5, mag. struct. and one-dimens. antiferromagnetism 80−60209

potassium compounds continued
K_2FeF_5, Mossbauer spectra, 1D antiferromag. 80−15886
K_2FeF_5, one dimens. antiferromag., zero point spin reduction 77−85456
K_2FeF_5, one dimensional antiferromagnet, Mossbauer effect, mag. and electric field gradient axes 79−78587
K_2FeF_5, one-dimens. antiferromag., single cryst. Mossbauer spectra 78−23376
K_2FeF_5, one-dimensional antiferromag., neutron diffr. and mag. meas. *(French)* 79−47241
K_2FeF_5, one-dimensional antiferromag. systems, Mossbauer studies 80−71266
$K_3Fe_2F_7$, two-dimensional antiferromag., cryst. field effects, Mossbauer spectroscopy 80−71254
$K_{1+x}Fe_7Ga_{11-y}O_{17}$, electron hopping and excitation at room temp., ^{51}Fe Mossbauer spectra 80−25257
$K(Fe_{1.5}Mg_{0.5}Si_4O_{10})(OH)_2$, cryst. struct. refinement 78−26545
$KFe(MoO_4)_2$, ferroelastic domain struct. *(Russian)* 79−90719
$KFe(MoO_4)_2$, phase transitions at 312 and 139K 80−70396
$KFeO_2$, cryst. and mag. struct., neutron and X-ray powder diffr., and Mossbauer effect meas. 77−84722
$KFeO_2$, overlap contribution to $^{57}Fe^{3+}$ isomer shifts, nuclear size change 80−39903
KFe_2O_3, β'' phase, mag. props., hyperfine interactions, Mossbauer study 80−20524
$K_{1+x}Fe_{11}O_{17}$, ionic cond. and chemical diffusion 77−47618
K_2FeO_4, antiferromag., critical fluctuations obs. using Mossbauer spectroscopy 80−39955
K_2FeO_4, crit. slowing down of spin fluctuations, Mossbauer spectra and relax. theory 80−65882
K_2FeO_4, XPS of hexavalent iron binding energies calcs. 80−43013
$K_{10}(Fe_3O(SO_4)_6(H_2O)_3)_2.12H_2O$, mag. exchange interaction of trinucl. Fe^{3+} complex *(German)* 78−14947
β-$K_5Fe_3O(SO_4)_6.10H_2O$, monoclinic struct. *(German)* 78−34473
$KFe(PO_4)F$, crystal struct., interatomic distances, X-ray phase anal. 80−39053
$KFeS_2$, cathodes for nonaqueous Li batteries 80−3506
$KFeS_2$, cryst. struct. by X-ray diffr., isolated from colloid 79−43635
$KFeS_2$, cryst. struct. and mag. ordering, neutron diffr. and mag. susceptibility meas. 80−54867
$KFeS_2$, crystal ligand field theory, band assignment, absorpt. spectra study 80−20657
$KFeS_2$, magnetic reson. meas. 78−95524
$KFeS_2$, quadrupolar hyperfine anisotropy, Mossbauer spectra meas. 78−19393
$KFeS_2$, spin analogue of active sites of ferrodoxins, mag. struct., neutron diffr. exam. 79−73688
$KFeS_2$+Li, electrochemical reaction, in situ Mossbauer spectra study 79−100397
$KFeS_3$, quadrupolar and mag. hyperfine anisotropy, Mossbauer meas. 78−56408
$K_2Fe_{48}Si_{70}Al_2O_{150}(OH)_{48}$, stilpnomelane, long-period polytypes struct. by electron diffr. and microscopy 77−64266
$KFeSi_2O_6$, elec. cond. meas. 78−47787
$KGaF_3$, new coating materials for IR laser optical components 79−65821
$KGaF_4$ coating materials for IR laser components 80−33105
$KGaHP_3O_{10}$, crystn. from reaction of Ga_2O_3 with H_3PO_4 and K_2O 79−52642
$KGa(PO_3)_4$, crystn. from reaction of Ga_2O_3 with H_3PO_4 and K_2O 79−52642
$K_2Ga_2P_8O_{24}$, cryst. struct., atomic coordinates, anisotropic temp. corrections 80−33974
$KGd(MoO_4)_2$, polymorphism investig. by X-ray diffr. and DTA 77−4091
$KGd(WO_4)_2$:Er^{3+}(Ho^{3+}), stimulated emission by subsidiary transitions of Ho^{3+} and Er^{3+} 79−3696
$KGd(WO_4)_2$:Ho^{3+}, stimulated emission at low temps. 80−106526
$KGd(WO_4)_2$:R^{3+}, stimulated emission 78−23496
K_2GeF_6, A=Si, Ge, Sn, IR absorpt. spectra, integrated intensity 79−73944
K_2GeF_6, IR absorpt. spectra, integrated intensity, 100-300K, phase transition 79−73945
$K(H,D)_2PO_4$ crystals, effect of isotopic replacement on growth kinetics 78−95006
KH II states and KH^+ ground state, pot. energy curves calc. 80−18812
KH, structural transition from NaCl to CsCl type under high press. 80−96458
KH, variational time-dependent H-F calcs. in pseudopot. framework 77−10588
KH^+, Σ state pot. energy, Hellman pseudopot. calcs. 78−70764
KH-H_2 crystal-gas system, with D impurity, thermodynamic equilib. 78−59954
K_2H^+, equilib. geom. and dissoc. energy, pseudopot. calc. 78−94329
KH_2AsO_4, AC conduction 79−55926
KH_2AsO_4, above T_c, ^{75}As NMR spectrum, correl. effects 78−76324
KH_2AsO_4, and deuterated isomorph, E-mode splitting in ferroelec. phase, Raman scatt. meas. 77−16296
KH_2AsO_4, and deuterated isomorph, ferroelectric mode and molecular vibr. press. depend. 78−19424
KH_2AsO_4, and KD_2AsO_4, IC spectra and phase transitions, under pressure 78−31180
KH_2AsO_4, dielec. polarisation and dielec. const. 77−59527
KH_2AsO_4, dielec. props. and birefr., simultaneous obs. 78−15130
KH_2AsO_4, domain struct. formation, opt. polarisation obs. 77−63381
KH_2AsO_4, electronic struct., UV reflection spectra 79−38558
KH_2AsO_4, fast and slow dynamic reorientation 78−80306
KH_2AsO_4, ferroelec. modes, polariton lineshape calc. 77−8585
KH_2AsO_4, ferroelec., phase transition and Raman scattering 78−84540
KH_2AsO_4, ferroelec., temp. broadening of hard mode Raman lines near Tc 78−88296
KH_2AsO_4, ferroelec., RF dielec. relax., loss mech. 79−38448
KH_2AsO_4, ferroelec. phase transition under hydrostatic press., NQR spectra obs. 79−69785
KH_2AsO_4, ferroelec., electronic struct. study *(Japanese)* 79−87463
KH_2AsO_4, ferroelec. phase, ^{75}As NQR, press. and temp. depend. 80−71227
KH_2AsO_4, ferroelec., high temp. phase transition, Raman spectra 80−71338
KH_2AsO_4, ferroelec., dielec. props., four-cluster approx. 80−97202
KH_2AsO_4, ferroelectrics, Raman spectra, coupled tunnel-phonon modes and isotope effect 79−69205

potassium compounds continued
KH_2AsO_4, ferroelectric phase transition under high hydrostatic press., mol. dynamics, NQR study 80−75880
KH_2AsO_4, ferroelectric, high temp. phase transitions, proton dynamics 80−76023
KH_2AsO_4, γ-irradiated, free radicals, EPR and ENDOR study of consequences of ferroelec. transition *(French)* 80−93209
KH_2AsO_4, high temp. phase transition, dielec. const., elec. cond. and IR refl. meas. 78−43118
KH_2AsO_4, irrad. ferroelec., AsO_3H^- free radical localised near impurity, ENDOR 77−24762
KH_2AsO_4, KD_2AsO_4, slow dynamics from Cr^{5+} EPR 78−15126
KH_2AsO_4, LF dielectric dispersion near phase transition 77−59530
KH_2AsO_4, magnetoelectric susceptibilities, phenomenological rules for computation 80−55068
KH_2AsO_4, microhardness, expt. determ. 79−24603
KH_2AsO_4, pres. depend., LF dielec. response, ferroelec. props. 78−15120
KH_2AsO_4, proton modes, dielec. spectroscopy 80−75915
KH_2AsO_4, Raman linewidth, isotope effect 77−8565
KH_2AsO_4, soft shear mode, Brillouin scatt. obs. 78−15176
KH_2AsO_4, thermal cond., anomalous temp. behaviour near structural phase transition *(Russian)* 80−75394
KH_2AsO_4, transverse elec. susceptibilities 80−50273
KH_2AsO_4:Cr^{5+}, ferroelec. phase transition, EPR intensity and linewidth meas. 79−4721
KH_2AsO_4:Cr^{5+}, lateral proton config., ENDOR spectra 77−59483
KH_2AsO_4-KH_2PO_4, AsO_4^{4-} centre, EPR central peak dynamics 79−33523
$KHCO_3$, $^1H/^2H$ quadrupole reson. freqs. detected by double reson. with level crossing 78−84497
$KHCO_3$, inelastic neutron scatt. spectra, H bonds bending vibrs. 79−14893
$KHCO_3$, PMR, proton shielding tensor proton ionis. in H-bond 77−1606
$K_2HCr_2AsO_{10}$, X-ray cryst. struct. determ. *(French)* 79−14756
$K_2HCr_2PO_{10}$, cryst. struct. data *(French)* 79−14756
$K(H_{1-x}D_x)_2PO_4$, for IR response exam. by asymmetric Fourier spectroscopy 77−28570
$K(H_{1-x}D_x)_1P_4$, polarised impurity cluster effects in light scatt. expts. 80−71431
$K(H_{1-n}D_n)_2PO_4$, degree of deuteration, depend. of Landau kinetic coeff. 77−85670
$K(H_{1-x}D_x)_2PO_4$, ferroelec., complex dielec. const., mm wave meas. 77−1633
$K(H_{1-x}D_x)_2PO_4$, ferroelec., dielec. susceptibility, pseudo-spin model 77−52024
$K(H_{1-x}D_x)_2PO_4$, polar mode softening and elastic anomaly temps. 79−28067
$K(H_{1-x}D_x)_2PO_4$ polarised impurity cluster effects in light scatt. expts. 80−29716
$K(H_{1-x}D_x)_2PO_4$, polarisation relaxation time and Landau kinetic coeff. rel. to degree of deuteration 80−84251
$K(H_{1-x}D_x)_2PO_4$, single cryst., 77K, γ-radiation damage centres, and EPR obs. 78−68379
$K(H_{1-x}D_x)_2PO_4$, static dielec. props., and Curie temp., press. depend. 79−87405
$KH_{2(1-x)}D_{2x}PO_4$, photoelasticity and electrooptic effects at forbidden deform. *(Russian)* 78−35117
$KH_{2(1-x)}D_{2x}PO_4$, proton modes, dielec. spectroscopy 80−75915
$KH_{2(1-x)}D_{2x}PO_4$, Raman spectra, effects of deuteration on proton tunnelling modes and coupled optic modes 77−59570
$KH_{2(1-x)}D_{2x}PO_4$, Raman spectra of overdamped mode 79−91427
$KH_{2(1-x)}D_{2x}PO_4$, X-ray topographic study of growth strains in single crystal 78−91279
$KH_{2x}D_{2(1-x)}PO_4$, domain struct. influence on switching processes 80−11355
$K(H_{1-x}D_x)_3(SeO_3)_2$, Brillouin spectrum central peak, soft acoustic mode 80−2777
KHF_2, IR refl. spectra 78−80324
KHF_2, nucl. spin-lattice relax. and anomalous thermal expansion meas. 77−8441
KHF_2, vibr. spectra, mol. interaction and Davydov splitting 79−8147
$KH_3(Ge_7O_{16}).3H_2O$, cryst. struct. determ. 79−90628
$K_3H(H_2P_3O_7)_2$, single cryst., X-ray cryst. struct. determ., direct methods *(French)* 79−14742
$KH(IO_3)_2$, cryst. struct. of new modification 77−80466
$K_4(H_2I_2O_{10}).8H_2O$, cryst. struct., bond lengths 77−68956
$K_x(H_2O)_yNbS_2$, cryst. struct. determ. 77−89416
$K_x(H_2O)_yTaS_2$, cryst. struct. determ. 77−89416
KH_2PO_3, mechanically treated single crystal, depth and struct. of disturbed layer *(Russian)* 78−23839
KH_2PO_4, ^{39}K spin-lattice relax. time doublé NMR meas. 79−47358
KH_2PO_4, 1.06 μm stable conversion into fourth harmonic, using composite medium master oscillator 78−46724
KH_2PO_4, AC conduction 79−55926
KH_2PO_4, amplitude depend. of permittivity and losses 79−99842
KH_2PO_4 and deuterated derivative, attenuation of LF elastic oscills. 77−7791
KH_2PO_4, and isomorphs, phase transition 77−20807
KH_2PO_4, and isomorphs, dielec. props. and birefr., simultaneous obs. 78−15130
KH_2PO_4, and isomorphs, ruby SHG 78−50856
KH_2PO_4, and isomorphs, ferroelectric transition and Curie temp., soft mode effect, Green's function anal. 79−24269
KH_2PO_4, and KD_2PO_4, IC spectra and phase transitions, under pressure 78−31180
KH_2PO_4 and KD_2PO_4, thermal cond., anomalous temp. behaviour near structural phase transition *(Russian)* 80−75394
KH_2PO_4 and $K(H_xD_{1-x})_2PO_4$, acoustooptical and photoelastic props. 78−27181
KH_2PO_4, and other soft water-soluble crystals, two-step polishing process 79−64363
KH_2PO_4 and related substances, electronic structures study *(Japanese)* 79−87463
KH_2PO_4, anharmonic phonons and central peaks at struct. phase transitions 79−95775
KH_2PO_4, appl. of γ-ray diffractometry to twinned crystals study 79−68987
KH_2PO_4, aq. soln., elec. cond. and Raman spectra at high-press., 25°C 79−56220
KH_2PO_4, aq. soln., elec. conductance in saturation region, effect of light *(Polish)* 80−10983

potassium compounds continued
KH_2PO_4, attenuation const. meas. by SHF dielec. resonance 79−47406
KH_2PO_4, Bloch equations 78−64324
KH_2PO_4, Brillouin-Rayleigh scatt. studies near ferroelec. transition temp. 80−76036
KH_2PO_4, Burgers vector sign determ. for nearly screw dislocations, X-ray obs. 80−59467
KH_2PO_4, central components in ferroelec. phase 78−56436
KH_2PO_4, central peak light scatt., scatt. centre props. 77−52108
KH_2PO_4, central peak susceptibility and US propag. near T_c 78−15125
KH_2PO_4, crit. behaviour near tricritical point, phenomenological interpretation 80−70389
KH_2PO_4, crit. behaviour, dilatometric study 80−92689
KH_2PO_4, critical and tricritical phenomena, susceptibility, exponents 80−75976
KH_2PO_4, cryst., cascade UV generation, by harmonic generation, temp. stabilisation calcs. 78−66868
KH_2PO_4, cryst. growth, splitting due to colloidal inclusions 77−7681
KH_2PO_4, cryst. high-freq. modulation in Pockels cell, acoustic phenomena 78−1336
KH_2PO_4, cryst. laser irrad. damage threshold, surface finish and defects effects *(German)* 78−59058
KH_2PO_4, cryst. regeneration of z-cut plates, effect of impurities 79−43120
KH_2PO_4 crystal, and deuterated cpd., optical meas. of phase transition point by domain obs. 77−40187
KH_2PO_4 crystal, laser freq. conversion to produce UV coherent pulse, 45 GW, for laser fusion 80−69450
KH_2PO_4 crystal, optical activity 80−71373
KH_2PO_4 crystal, photoresponse under laser irrad. 80−100479
KH_2PO_4 crystal electro-optic reflection deflector 79−76861
KH_2PO_4, crystal nonequilibrium thermodynamics, quasielastic light scatt., systematic anal. 79−61391
KH_2PO_4, crystal-solution interfacial tension, from crystn. meas. 79−69045
KH_2PO_4 crystals, mechanism of growth in presence of impurities 79−1403
KH_2PO_4 crystals, polarisation of unbound many particle states, IR spectra *(Russian)* 78−84556
KH_2PO_4 crystals, plastic deform. and mech. props. 79−79035
KH_2PO_4 crystals, rel. between selective and total soln. 80−39103
KH_2PO_4, D_2-impurities effect on Rayleigh central peak 77−81068
KH_2PO_4, damping of transverse acoustic and ferroelec. modes 78−14413
KH_2PO_4, dendritic growth in silica gel 80−35072
KH_2PO_4, depolarised light scatt., dynamic central peak 78−10858
KH_2PO_4, dielec. functions above and below ferroelec. transition 79−33588
KH_2PO_4, dielectric const. and polarisation, fluctuations, catastrophes 77−8491
KH_2PO_4, dielectric const. at ultra low freq., domain wall relax. effects 77−12348
KH_2PO_4, differential γ-ray diffractometry, exam. of ferroelectric-ferroelastic cryst. in cyclic fields 79−38511
KH_2PO_4, dislocation strain decoration and static central peak 79−99263
KH_2PO_4, dispersion of permittivity, 6 to 12 cm^{-1} 79−33616
KH_2PO_4, domain wall mobility, model 77−63385
KH_2PO_4, dynamic central peak in ferroelectric phase 78−84538
KH_2PO_4, E-mode splitting in ferroelec. phase, Raman scatt. meas. 77−16296
KH_2PO_4, E-symmetry Raman spectra 79−38535
KH_2PO_4, efficient high-energy SHG of triaxial flashlamp-pumped dye laser 80−38061
KH_2PO_4, efficient SHG by YAG:Nd^{3+} laser pumping 79−18481
KH_2PO_4, elec. cond. and diffusion, Co dopant effects 77−72716
KH_2PO_4, electro-optic props. near ferroelec. transition 78−19445
KH_2PO_4, electro-optic modulators, transient acoustic waves 79−59809
KH_2PO_4 electro-optic modulator crysts., pizoelec. induced acoustic transients 80−70316
KH_2PO_4, electrogyration near transition pt. in nonenantiomorphic cryst. 79−61339
KH_2PO_4, electronic struct., UV reflection spectra and XPS 79−38558
KH_2PO_4, electrophotoluminescence obs. 79−47521
KH_2PO_4 family of crystals, proton modes, dielec. spectroscopy 80−75915
KH_2PO_4, far IR c-axis transmission spectrum obs. 77−8571
KH_2PO_4, far IR dispersive reflection spectra 77−36213
KH_2PO_4 far IR dispersive reflection obs. with asymmetric polarising interferometer 77−40249
KH_2PO_4, ferroelastic cryst., appl. of γ-ray diffractometry 77−8533
KH_2PO_4, ferroelec., tetragonal cryst. struct. determ., neutron diffr. meas. 77−7693
KH_2PO_4, ferroelec., Raman internal-mode line broadening by proton jumps 77−43981
KH_2PO_4, ferroelec., positron lifetime meas. during phase transitions 78−6644
KH_2PO_4, ferroelec., temp. broadening of hard mode Raman lines near Tc 78−88296
KH_2PO_4, ferroelec., RF dielec. relax., loss mech. 79−38448
KH_2PO_4, ferroelec., change of sign in pyroelec. coeff. 79−82929
KH_2PO_4, ferroelec. transition temp., transverse Ising model 77−90110
KH_2PO_4, ferroelec. cryst., internal friction, torsion pendulum obs. 78−72474
KH_2PO_4, ferroelec. thin crysts., struct. investig. 79−27962
KH_2PO_4, ferroelec. phase transition, soft phonons, Raman scatt. obs. *(Japanese)* 79−65880
KH_2PO_4, ferroelectric phase transition exam. by spontaneous parametric light scatt. 78−19427
KH_2PO_4, ferroelectric-ferroelastic phase transition, γ-ray diffr. 78−43819
KH_2PO_4, ferroelectric, crystal growth in silica gel, effect of pH and gel ageing 78−48301
KH_2PO_4, ferroelectric, photovoltaic and photorefractive effects 78−72187
KH_2PO_4, ferroelectric transition, press. induced tricrit. point 78−80301
KH_2PO_4, ferroelectrics, Raman spectra, coupled tunnel-phonon modes and isotope effect 79−69205
KH_2PO_4, ferroelectric transition, neutron diffr. obs. 80−25324
KH_2PO_4, ferroelectric-elastic phase transition, theoretical model and expt. *(Russian)* 80−75961
KH_2PO_4, ferroelectric transition, order-disorder character of hydrogen bond 80−93251

potassium compounds continued
KH_2PO_4, filiform crystals at low temp., tensile strength determ. 80−100877
KH_2PO_4, Green's function theory of ferroelec. phase transition 77−85669
KH_2PO_4, growth and dissolution kinetics, temp. and pH effect 80−88070
KH_2PO_4, growth from gel and aqueous soln., oriented inclusions 80−15023
KH_2PO_4, H-bonded phase transitions, SCF approach 78−92030
KH_2PO_4, high-power picosecond pulse generation 218 to 316 nm 80−64106
KH_2PO_4, high. press. tricrit. point rel. to zero press crit. point 78−15117
KH_2PO_4, IR overtone spectra and temp. depend. 79−47456
KH_2PO_4, improved automatically tunable SHG of dye laser 79−985
KH_2PO_4, initial dielec. const. in ferroelec. phase by thermal noise method 77−16267
KH_2PO_4, KD_2PO_4 crystals used for laser control, acoustic vibr. suppression 78−1363
KH_2PO_4, KD_2PO_4, slow dynamics from Cr^{5+} EPR 78−15126
KH_2PO_4, KD_2PO_4, high-press. struct. rel. to dynamical models 78−80307
KH_2PO_4, $K(D_xH_{1-x})_2PO_4$, dielec. polarisation and dielec. const. 77−59527
KH_2PO_4, kinetics of crystn. from soln., activities, interfacial energy and solubility 77−76340
KH_2PO_4, kinetics of growth from aqueous soln. 78−6838
KH_2PO_4, Landau-Devonshire coeffs. 78−15116
KH_2PO_4, laser accessory for freq. doubling 78−46725
KH_2PO_4, laser light scatt. spectroscopy 78−10156
KH_2PO_4, light modulation in microwave light-range finder *(Russian)* 79−46041
KH_2PO_4, light scatt on light. phase synchronism *(Russian)* 77−38992
KH_2PO_4, light scatt. in elec. field, ferroelec.-paraelec. transition 80−2707
KH_2PO_4, linear response function for tunnelling systems in polariton region 78−43799
KH_2PO_4, liq. inclusion formation during large cryst. growth 78−64455
KH_2PO_4, liquid inclusion form., hydrodynamics and supersaturation role 78−30559
KH_2PO_4, longit. sound attenuation, strain depend. pseudo spin coupling mechanism 77−85666
KH_2PO_4, low impurity content, magnetic anisotropy *(Russian)* 78−6506
KH_2PO_4, low temp. transition, thermal hysteresis, Cr impurity effect on transition temp. 80−2705
KH_2PO_4, magnetoelectric susceptibilities, phenomenological rules for computation 80−55068
KH_2PO_4, microhardness, expt. determ. 79−24603
KH_2PO_4 mixer and KD_2PO_4, $LiIO_3$ doubler crysts., mW 213 nm source based on Nd:YAG laser 79−55178
KH_2PO_4, NMR spin echoes, indirectly induced 80−71239
KH_2PO_4, near IR absorpt., influence of deuteration 78−27237
KH_2PO_4, neutron critical scatt. in struct. transition due to homogeneous crystal deform. 79−42922
KH_2PO_4, noncentrosymmetric monocrystals, quadratic electro-optic coeffs. 79−28718
KH_2PO_4, nonlinear crystals, interference of optical harmonics 80−64102
KH_2PO_4, nonlinear electrooptic effects 80−29721
KH_2PO_4, nonlinear optical coeffs., interf. method for relative magnitude accurate determ. 77−31115
KH_2PO_4, one-dimensional Slater model, with random impurities due to partial deuteration 77−59537
KH_2PO_4, optical activity meas. 78−52466
KH_2PO_4, optical activity, gyration tensor determ. near Curie point 79−33660
KH_2PO_4, optical activity *(Japanese)* 79−65832
KH_2PO_4, optical material, thermal expansion, 60-300K 78−33791
KH_2PO_4, optical modulator efficiency in thermal mode *(Russian)* 79−94345
KH_2PO_4, optical props., plastic deform. effect 77−59552
KH_2PO_4, paraelec., Raman scatt. spectra of B_2-polariton and B_2(LO) modes 79−28762
KH_2PO_4, paraelectric phase, forward and backward Raman scatt. 79−33681
KH_2PO_4, paraelectric, dynamic central peak depend. on deuterium content 79−65752
KH_2PO_4 paraelectric phase, solns. of Bloch-type eqns. 80−7304
KH_2PO_4, parametric amplification suppression for improved SHG efficiency 77−50725
KH_2PO_4, parametric excitation of continuously tunable visible picosecond pulses 79−18482
KH_2PO_4, parametric superluminesc., picosec. spectroscopy 79−55187
KH_2PO_4, parametric generation of picosecond light pulses with an energy conversion greater than 50% 80−53377
KH_2PO_4, phase transition, pseudospin analysis 78−10157
KH_2PO_4, phase transitions study, role of cryst. struct. determ. 80−75197
KH_2PO_4, phonon echos in SiO_2, ADP, KDP, and Rochelle salt *(Japanese)* 79−51213
KH_2PO_4, photoelastic const. behaviour new ferroelectric transition 78−19441
KH_2PO_4, photoelectric phenomena, nonlinear optical rectification *(Russian)* 79−19628
KH_2PO_4, picosecond laser induced breakdown at 5321 and 3547 Å, freq. depend. 77−63495
KH_2PO_4, Pockels effect in UV region 77−12398
KH_2PO_4, Pockels' const., linear electro-optic consts., sign of piezoelectric const. 78−60425
KH_2PO_4 polarisation switches for digital light deflector 77−39049
KH_2PO_4, polarisation switching, influence of mobile point defects 78−31165
KH_2PO_4, polarisation effect in piezoelectric executing longitudinal vibs. 79−1741
KH_2PO_4, polarisation echo in ferroelec. phase transition region 79−42920
KH_2PO_4, polycrystalline materials; pyroelec. temp. anal. as method for studying ferroelec. transitions 79−38502
KH_2PO_4 powder, dynamic polarisation echoes 79−4773
KH_2PO_4, powder sample, pyrocharge temp. depend. near phase transition 79−87399

potassium compounds continued
KH_2PO_4, press. and deuteration effects on static ferroelec. props., four-particle cluster approx. 80−34861
KH_2PO_4, pressure effect on ferroelec. transitions *(Japanese)* 79−65814
KH_2PO_4, prism faces microtopographical study 79−42346
KH_2PO_4, proton spin-lattice relaxation rate, temp. depend., field depend. 78−88208
KH_2PO_4, proton tunnelling, barrier height and energy level calc. 80−6482
KH_2PO_4, pyroelectric investig. in ferroelec. phase 77−12321
KH_2PO_4, pyroelectric coeff., 1.8-300K, dynamic method *(French)* 79−19844
KH_2PO_4, RF dielec. response close to transition temp. 77−90099
KH_2PO_4, Raman scatt. near T_c, search for soft modes 78−15114
KH_2PO_4, Raman scatt. for polaritons of mixed B_2-E symm. 79−56795
KH_2PO_4, Rayleigh wave propag. near Curie temp. 77−89630
KH_2PO_4, real structure influence on optical strength 79−7187
KH_2PO_4, SHG of ps pulses, freq. tuning 77−50724
KH_2PO_4, SHG of rhodamine 6G laser, tunable UV source 77−42565
KH_2PO_4, servo tuning and stabilization of nonlinear optical crystals 79−55180
KH_2PO_4, shear angle and order parameter of ferroelec. transition by neutron diffr. 77−12339
KH_2PO_4, single cryst., thermal depolarisation current 79−51303
KH_2PO_4 single crystal evidence for spiral growth on pyramidal faces 80−84120
KH_2PO_4, single crystal neutron diffraction study at high pressure 80−92497
KH_2PO_4, soft branch Brillouin specta, quasielastic central peak suppression by annealing 78−95588
KH_2PO_4, soft mode behaviour, dispersive Fourier transform spectroscopy 77−7823
KH_2PO_4, soft mode spectroscopy, digital control system for Raman spectrometer 78−86345
KH_2PO_4, spectral phase-matching props. for SHG 77−83922
KH_2PO_4, spirals, growth and dissolution from liq. state 80−15027
KH_2PO_4, spontaneous electrooptic effect in far IR 79−95734
KH_2PO_4, spontaneous polarisation, low temp. meas. 80−75921
KH_2PO_4, strong coupling of proton-phonon system 77−7822
KH_2PO_4, struct. at high press. in rel. to effect of press. on T_c 79−42915
KH_2PO_4, struct. memory effects in low temp. changes 79−28700
KH_2PO_4, struct. phase transitions, light scatt. meas. 79−95774
KH_2PO_4, struct. transitions, optical SHG and γ-ray diffr. results 78−14459
KH_2PO_4, sum freq. mixing, 212.8 nm pulse burst generation of Nd:YAG laser 78−74934
KH_2PO_4, supersaturated solution, nucleation rates meas. from induction period 79−23549
KH_2PO_4, third order nonlinear optical difference frequency generation 78−22176
KH_2PO_4, transverse elec. susceptibilities 80−50273
KH_2PO_4, tricrit. point, γ-ray and neutron diffr. 78−39516
KH_2PO_4, tricrit. point, neutron diffr. study under high press. 79−33624
KH_2PO_4, tricritical point and tricritical exponent 79−33623
KH_2PO_4, tunable CW UV radiation generation, 257 to 320 nm 77−88860
KH_2PO_4, tunable coherent radiation generation below 250 nm at MW power levels 78−59080
KH_2PO_4, tunable parametric single-pulse picosecond light source with 50% efficiency 79−59765
KH_2PO_4, two doublet model for ferroelec. phase transition 78−39510
KH_2PO_4 type crystals, coupling between protonic E-mode and lattice vibrs. 77−7821
KH_2PO_4 type crystals, low lying ferroelec. modes, cluster dynamical theory 78−80305
KH_2PO_4 type crystal, H-bonded partially deuterated ferroelectrics, order parameter fluctuation spectra, central peak calcs. 79−61316
KH_2PO_4 type crysts., evidence of non-linear behaviour of soft modes, Raman spectra 79−33639
KH_2PO_4 type ferroelectrics, isotopically disordered, collective modes, CPA 77−7825
KH_2PO_4 type ferroelectric, phase transition to spontaneous coherent state, theory *(Russian)* 78−6647
KH_2PO_4 type ferroelectrics above T_c, soft mode and central-peak dynamics 78−87763
KH_2PO_4 type ferroelectrics, Green's function theory of phase transitions with pseudo-spin-lattice coupled mode model 80−71354
KH_2PO_4, type I and II phase matching, spectral backgrounds 77−27316
KH_2PO_4, types I and II optical mixing with ps laser pulses 77−72032
KH_2PO_4, UV radiation prod., freq. doubling of N_2 laser pumped dye laser output 77−743
KH_2PO_4, ultrashort light pulse parametric transform. under optimum interaction conditions 80−99791
KH_2PO_4, under electrostatic field, mechanism of enhancement of neutron diffr. *(Chinese)* 79−51907
KH_2PO_4, vac. UV transmission 77−73150
KH_2PO_4, vacuum UV spectra and electro-optical prop. *(Japanese)* 79−65900
KH_2PO_4, variational treatment of proton-photon system 78−88261
KH_2PO_4, wideband light modulator in cylindrical waveguide, parameter optimisation *(Russian)* 79−94344
KH_2PO_4, with and without inversion centres, nonlinear susceptibilities *(Russian)* 78−13750
KH_2PO_4, X-irradiated, hysteresis effects obs. by ESR 80−103928
$KH_2PO_4^-$ (KDP) type crystals, irradiated or doped, behaviour of ESR probes 77−48035
$K^2H_2PO_4$ electro-optic shutter natural birefringence compensation by β-$LiIO_3$ monocrystal 79−55247
KH_2PO_4:AsO_4^{4-}, ESR, paraelectric phase, proton dynamics 77−81011
KH_2PO_4:AsO_4^{4-}(SeO_4^{4-}), ferroelec., low freq. fluctuations, isotope effects, EPR, ENDOR, ESCA 77−73118
KH_2PO_4:cation impurities, growth domains 79−99224
KH_2PO_4:CrO_4^{2-}($Cr_2O_7^{2-}$), electrical cond., thermal depolarisation studies 79−95212
KH_2PO_4:Fe^{3+}, ESR, anomalous temp. depend. of D tensor 79−61205
KH_2PO_4:KH_2AsO_4, X-irrad., EPR 77−32257
KH_2PO_4:$NH_4H_2PO_4$, EPR of arsenic and phosphorus oxyradicals 77−77102
KH_2PO_4:SeO_4^{3-}, slowing down of fluctuations near T_c, EPR obs. 78−60403

potassium compounds continued
KH_2PO_4:Tl, 5.76 eV absorpt. band, temp. effects on doublet struct. 79−78713
KH_2PO_4:Ti^{2+}, EPR of ferroelec. and paraelec. phases 80−66012
KH_2PO_4:VO^{2+}, EPR spectra, Hamiltonian parameters, ferroelec. transition 78−39387
KH_2PO_4-KD_2PO_4 mixed cryst., dielec. polarisation, Green's function anal. 77−52011
KH_2PO_4-KD_2PO_4 mixed crystals, static and dynamic props., proton-lattice coupled mode model 78−64328
KH_2PO_4-type cpds., collective vibr. of protons, cluster approx. 79−51210
KH_2PO_4-type crystal, domain wall mobility, two-dimens. ordering effect 78−48137
KH_2PO_4-type crystals, H bond in ferroelectricity, role of high pressure research 79−15414
KH_2PO_4-type crystal, LF dynamics 80−10602
KH_2PO_4-type crysts., photorefractive and photovolt. effects 79−15189
KH_2PO_4-type ferroelectrics, pseudospin-phonon models, consistency with expt. results 77−59523
KH_2PO_4-type ferroelectrics, inelastic neutron scatt. theory 78−48122
KH_2PO_4-type ferroelectrics, IR and Raman spectral interpretation of ferroelectric phases 79−24312
KH_2PO_4-type ferroelectrics, tunnelling integral 80−70156
KH_2PO_4-type ferroelectrics, dielec. props., four-cluster approx. 80−97202
KH_2PO_4:Tl, UV absorption bands obs. 78−27266
$KHSO_4$, $^1H/^2H$ quadrupole reson. freqs. detected by double reson. with level crossing 78−84497
$KHSO_4$, DC electrical cond. 79−37874
$KHSO_4$, PMR, proton shielding tensor, proton ionis. in H-bond 77−1606
$KHSO_4$, phase diagram of 3.2 GPa, 450°C 80−76237
$KHSO_4$, pure ionic cond., proton mobility, irreversible phase transition 77−59141
$KHSO_4$:Co^{2+}, conduction and ^3H diffusion 77−15622
$KHSO_4$:Co^{2+}(Fe^{3+}), impurity effect on growth habit from saturated soln. 77−4059
$KHSO_4$:Co(II), DC conductance, extrinsic and intrinsic regions 77−59141
$KHSO_4$:Cu, DC electrical cond. 79−37874
$KHSO_4$:Fe^{3+}, DC cond. meas., mechanism 80−65285
$KHSO_4$:SO_3^-, X-irradiated, ESR saturation 78−80220
$K_3H(SO_4)_2$, dielec. props. and phase transitions 80−60482
$KHSO_4$.KH_2PO_4, cryst. struct. 80−75211
$KHSeO_3$, and deuterated analog, vibr. spectra 79−24311
$KH_3(SeO_3)_2$, acoustic phonon softening, US vel. meas. 78−14429
$KH_3(SeO_3)_2$, and $KD_3(SeO_3)_2$, anharmonic phonons and central peaks at struct. phase transitions 79−95775
$KH_3(SeO_3)_2$, central peak obs. by light scatt. 77−32390
$KH_3(SeO_3)_2$, dislocation strain decoration and static central peak 79−99263
$KH_3(SeO_3)_2$, ferroelastic, low-frequency elastic props., −190 to 50°C 79−37759
$KH_3(SeO_3)_2$, ferroelastic, lattice consts. and thermal expansion tensors, X-ray diffr. meas. 79−37856
$KH_3(SeO_3)_2$, ferroelastic transition under uniaxial press., EPR study 80−59562
$KH_3(SeO_3)_2$, ferroelastic phase transition, mech. stress effect 80−70394
$KH_3(SeO_3)_2$, high-resolution PMR 78−35053
$KH_3(SeO_3)_2$, optical and dielec. props. near ferroelastic phase transition 79−38518
$KH_3(SeO_3)_2$, phase transition, acoustic phonon softening 77−27997
$KH_3(SeO_3)_2$, phase transitions *(Japanese)* 79−65812
$KH_3(SeO_3)_2$, proton NMR study about paraelastic-ferroelastic transition 78−23363
$KH_3(SeO_3)_2$, second-order ferroelastic phase transitions, piezo-opt. props. obs. 78−95558
$KH_3(SeO_3)_2$, slightly deuterated, central peak obs. in Brillouin spectra 78−64374
$KH_3(SeO_3)_2$, thermal anomalies rel. to acoustic phonon instability 77−76545
$KH_3(SeO_3)_2$:Cr^{3+}, EPR, ferroelectric phase transition 79−65716
$KH_3(SeO_3)_2$:Cr^{3+}, ferroelastic material, EPR, 77-300K 78−60331
$KH_3(SeO_3)_2$:Mn^{2+}, single crystal, EPR 78−72396
$KH_3(SeO_3)_2$:VO^{2+}, electron spin reson. obs. 78−80196
$KHSi_2O_5$, cryst. struct., Patterson function anal., valency balance, hydrogen bonds 80−39051
$K_4Hf(C_2O_4)_4.nH_2O$, electric field gradient at metal site, γ-ray perturbed ang. correlation meas. 78−52380
K_3HfF_7:^{181}Ta, elec. quad. interac., DPAC 77−32299
$K_8Hf(MoO_4)_6$, X-ray structural investigation 78−79597
$KHgC_4$, and $KHgC_8$, intercalation cpds., synthesis and struct. 80−44183
$K_2Hg(CN)_4$, third order elastic consts. 80−84231
$K_2HgCl_4.H_2O$, cryst., IR spectra, water mol. struct., H-bonding 77−81089
$K_2HgCl_4.H_2O$ proton spin-lattice relax., 180° flips and diffusion of water mol. 77−15327
$KHgI_3.H_2O$, NQR spectra of ^{127}I and cryst. struct. 77−12230
KI, ^{14}N impurities, molecular point defects, EPR isotropic hyperfine triplets 80−2636
KI, binding energy of F_{c+}', M_{c+}' and R_{c+}' centres, positron trapping 79−69460
KI, containing F-centres, Raman scatt. calc. 77−16306
KI crystals, containing excess of halogen, V-centres *(Japanese)* 77−59596
KI, crysts., X-ray irradiated, luminescence during release of pressure 79−65939
KI, defect modes due to substitutional anion-pair and cation-pair impurities in ionic crystals 80−92540
KI, diamag. ion solvation in methanol soln., NMR relax. obs. 78−56389
KI, dispersion of phonons calc. 78−26646
KI, dissoc. energy by photofragmentation spectroscopic method 79−76527
KI, doped substrate for vac. deposition of Ag oriented films 80−2303
KI doped with F-centres, mag. vibr. Raman scatt. 77−4636
KI, edge emission of excitons 77−59606
KI, edge luminesc. under UV excitation 77−77273
KI, effect of addition on corrosion of Cu in seawater 78−80670
KI, efficiency of creation of X_3^- centres in X-rayed alkali halides *(Russian)* 78−71731
KI, electrolytically coloured single cryst., ionic SCL transient and steady elec. current 77−62937

potassium compounds continued
KI, electron impact, elastic scatt., model, static and static exchange calcs. 78−94321
KI, electron irrad., polariton effects in reson. emission 79−33843
KI, electron range-energy relation, thermally created lattice vacancies effect 80−92574
KI, electron-spin memory and magnetic-circular-dichroic effects in F-centre luminesc. 80−29794
KI, electronic states at (100) surface, accounting for spin-orbit interaction *(Russian)* 78−91750
KI, electronic struct. of self-trapped excitons calc. 77−39784
KI, enthalpies of soln. in water 80−50880
KI evaporated coating, photodetector sensitivity enhancement in VUV 79−85180
KI, exciton diffusion, luminesc. quenching, meas. 4 to 77K 77−32433
KI, exciton mechanisms of electron sputtering 77−55857
KI, F^--centres, thermal and photolytic decay processes 78−95053
KI, F-centre effect on particularities in vac. evaporated Cr film growth 79−82496
KI, F-centre luminesc., MCD effects 78−39598
KI, F-centre trapping of conduction electrons, photocond. study 78−56179
KI, far IR, quartic damping, and quasiselection rule for gap compounds 78−31195
KI, far IR complex refr. indices, dispersive Fourier transform 78−80322
KI, free exciton reson. luminesc. lines 77−77272
KI, free exciton-F^- centres interaction, electron excited emission 79−83036
KI, gap modes due to impurity pairs 77−62602
KI, gapmode calc. using Green's function technique, effect of uncertainty in eigendata 78−79708
KI, growth time of π emission in picosecond range 80−76067
KI in acetone, press. effects on Walden products, ion-solvent interactions 80−3398
KI, inelastic light scattering of localised vibration of interstitial H atom in alkali halides 80−88998
KI, intrinsic luminesc. quenching, by X-ray induced coloration 78−19539
KI, irradiated at room temp., thermolum. and F-centre thermal stability 78−84669
KI, irradiated at room temp., stored energy 80−79839
KI, isothermal compressibility calc., 0-1000K 77−7784
KI, K^+3p core excitons, refl. spectra study, low temp. 80−29759
KI, load relaxation studies 79−79016
KI, luminesc. due to free excitons, line shapes 79−33803
KI, luminesc. lines due to n=2 free exciton state of Wannier series 80−29776
KI, luminesc. polarisation for free and bound excitons 78−10942
KI, MCD of α and β bands 78−27192
KI, mag. circular dichroism in luminesc. of F-centres 77−20919
KI, mean free paths of 200-1500 eV electrons, XPS determ., model calc. 79−38715
KI microcrystals, UV spectra by diffuse reflectance technique, surface electronic transitions obs. 80−75614
KI, near UV photodissoc., at state determ. 79−18105
KI, optical bleaching of V_2 and V_3 bands 79−33739
KI, oscillator strengths of defects, Smakula eqn. generalisation 80−108232
KI, oscillatory and diffusive regime, above and below melting point, IR thermal emission spectra 78−83985
KI, perturbed by Jahn-Teller centres, lattice dynamics 80−107394
KI, photostimulated recomb., electron spin polarisation 80−60673
KI, piezo-optical study of excitons 80−16055
KI, polariton effects in resonant emission 78−76533
KI, quench hardening behaviour and quenching temp. 78−64550
KI, quenched, absorpt. and emission spectra, α-centres 80−11442
KI, recomb. luminesc. of H-centre and F-centre electrons *(Russian)* 78−80402
KI, relationship between fourth moments in molten state and phonon freq. in solid phase 80−10477
KI, rot. excitation by electron impact, calc. cross sections 78−66670
KI, secondary electron spectra, primary electron energies up to 30 eV 77−12473
KI, self trapped exciton form. time at $^1\Sigma_u^+$ state under pulsed electron beam in ps range 80−97347
KI, self-trapped excitons and F-centres, picosec. range form., absorpt. bands 78−19515
KI, self-trapped exciton and F-centre form. by picosecond laser pulses 80−10546
KI, self-trapped exciton form. via thermally induced defect reactions 80−60687
KI, single cryst., quenched, microstruct. around indentations 80−7628
KI, soln. in organic solvents, elec. cond., shock compression effects 79−46822
KI, solutions, preferential solvation, NMR obs. 78−95919
KI, spectral distrib. of triplet to singlet luminesc. of F_2 centre 77−59601
KI, spin-lattice relaxation time of relaxed excited state of F-centre, MCD meas. 79−61350
KI, Stark effect in F-centre emission 77−63434
KI, surface, 420 nm band laser-stimulated emission, V_2 centres 78−84633
KI, surface, laser induced ionic desorption, mechanism 77−15686
KI, surface lattice dynamics, Green function method 78−34693
KI, thermal cond. press. depend. 77−15641
KI, thermal cond. under press. meas. 78−30802
KI, U_2 and U_1 centres, optical excitations 80−2803
KI, UV two-photon absorpt. relative to known Raman cross section 79−81487
KI, V-centres, optical and thermal bleaching of V_2 and V_3 bands 77−85751
KI, with alkali and halogen impurities, colour centre deformation induced nonradiative decay 80−7387
KI, X-irrad., V-centres, Raman spectra 79−91429
KI, X-irradiated cryst., luminesc. during press. release 80−20722
KI, zero phonon and LO phonon assisted luminesc. of free excitons 79−28799
KI:Ag^+, far IR props. of lattice resonant modes, hydrostatic press. effects 77−28574
KI:BH_4^-, far IR absorption in phonon gap 77−12406
KI:$CaSO_4$, SO_4^{2-} vibr. spectra, press.-scanned Fermi reson. spectroscopy appl. 79−73937

potassium compounds continued
KI:Cl, dielec. relax. of impurity-vacancy complexes, ionic thermal current meas. 77−48124
KI:$Cl^-(Br^-)(Na^+)(Rb^+)$, lattice relaxation around tetragonal and rhombic defects 79−95110
KI:Co, coloured and uncoloured, Mossbauer effect, inhomogeneous hyperfine fields 77−32307
KI:Cu^-, absorpt. and emission spectra, $3d^{10}4s^2 \rightarrow 3d^9 4s^2 4p$ bands 79−24343
KI:Cu^+, exciton bands, optical absorpt. and MCD spectra 80−80821
KI:Eu, electron-irrad., photostimulated luminesc., ionic processes 78−52561
KI:Eu^{2+}, single cryst. optical absorpt. spectra 80−45117
KI:$Eu^{2+}(Sr^{2+})(Mn^{2+})$, elec. field effect on mech. of recomb. 78−80397
KI:Ga, optically detected EPR in relaxed excited states of Ga^+ 78−72437
KI:Ga^+, polarisation of Ga^+ centre A_T emission, temp. depend. 80−80842
KI:$Ga^+(In^+)(Sn^+)$, magnetic circular dichroism of A- and B-absorption band region 77−12412
KI:H^-, U-centres, force consts. using Green's functions 79−46775
KI:I_2^-, triplet luminesc. kinetics, 0.4-4.2K 79−87482
KI:In^+, Jahn-Teller split luminesc., high press. expt. 78−52565
KI:In^+, luminesc. decay, excited state symm. and g-value 79−99922
KI:$In^+(Tl^+)(Ga^+)$, mag. circular dichroism meas. 79−42988
KI:In(Tl), type A long-wave luminesc., polarisation obs. 78−10944
KI:NCO^-, shift and broadening of local vibr. bands, temp. depend. 78−87755
KI:NO_2^-, first-order Raman scatt. meas. 77−52085
KI:NO_2^-, Raman spectra, high press., low temp. effects 78−52479
KI:OH^-, HF phonon studies under uniaxial stress 79−83002
KI:OH^-, paraelec. reson. at 1.5 and 4.2K from 12 to 150 GHz 79−38512
KI:$OH^-(OD^-)$, rotational barrier height for impurity, librational modes 77−11491
KI:PO_2^-, ODMR in zero and weak mag. fields 80−88894
KI:PO_2^-, vibr. spectra and struct. of PO_2^- impurity ions 77−16354
KI:Pb_2 absorpt. spectra of Pb^{++} centres 80−76058
KI:Pb^{2+}, absorpt., excitation and luminesc. spectra 78−19519
KI:Pb^{2+}, UV absorpt. and mag. circular dichroism spectra 80−25418
KI:S_2, Raman spectra, orientational dynamics 78−56482
KI:S_2^-, spin-lattice relax. rate, 1.5 to 2.2K 77−20686
KI:S_2^-, Stokes' losses on cryst. vibrs. in luminesc. spectra of mol. centres *(Russian)* 77−55827
KI:S_2^- centres, luminesc., polarisation temp. depend. 78−87943
KI:S^{2-}, impurity-vacancy dipole UV absorpt. and ionic thermocurrent, F-centre form. 77−36271
KI:S^{2-}, photochemical reaction, F-centre production 78−64861
KI:S^{2-}, photoinduced polarisation and depolarisation 79−33738
KI:S^{2-}, vacancy dipoles, photo-induced polarisation and depolarisation 80−2690
KI:Se_2^-, reson. secondary emission, total spectrum *(Russian)* 78−19551
KI:Sn^{2+}, luminesc. 79−33817
KI:Sn^{2+}, red emission, mag. field effect on radiative decay time 79−33818
KI:Sn^{2+} luminesc. decay, excited state symm. and g-value 79−99922
KI:Tl, activated crystal, induced recombination emission *(Russian)* 78−48214
KI:Tl^+, A_T emission, mag. circular polarisation, WKB approx. for non-radiative transition rate 80−55180
KI:Tl, $(Tl^+)_2$ centre luminesc. 78−84632
KI:Tl, A_T emission, linear polarisation, appl. of semi-classical WKB formalism 80−45134
KI:Tl, cryst., induced recomb. emission 79−4845
KI:Tl, crystallisation from melt by various methods, impurity distrib. 77−4733
KI:Tl, decay of fast component of impurity luminesc. excitation in A-absorption band *(Russian)* 80−84767
KI:Tl, electron-hole and V_k-Tl recomb., TSC and thermolum. study *(French)* 80−34461
KI:Tl, emission and excitation spectra, press. effects 79−83028
KI:Tl, emission bands, press. effect 79−33789
KI:Tl, emission spectra, press. effects 78−23509
KI:Tl, nonradiative transitions in colour centres, WKB approximation 77−85803
KI:Tl, phosphor, press. effect on emission spectra at low temps. 77−85771
KI:Tl, polarised luminesc. of $(Tl^+)_2$ centres 80−71473
KI:Tl, triple decay-time in low-energy emission 78−43929
KI:Tl, X-ray phosphor, influence of different factors on emission intensity 79−8171
KI:Tl^+, luminesc., time depend. polaris. 79−33810
KI:Tl^+, phosphor, anomalous stress-induced dichroism 79−4828
KI:Tl^+, pre-resonant enhancement of Raman scatt. 80−7354
KI:Tl^+, recomb. luminesc. kinetics 77−16366
KI:Tl^+ type phosphor, press. effects on triplet relaxed excited states, quadratic Jahn-Teller interaction 78−23510
KI:Tl(In), A-luminescence spectra and polarisation, Jahn-Teller minima 77−20914
KI:Yb^{2+}, X-ray and intracentre luminesc. 78−6737
KI:Zn^+, optical absorpt. bands rel. to charge transfer 80−66245
KI-CsI, binary molten mixture, surface tension meas. 79−65294
KI-CuI, AC elec. cond. rel. to phase diagram 77−72712
KI-Hg interface, specific adsorption of I ions, electrical double layer, interface excess activity coeff. 80−49523
KI-KCl:Cu^+ mixed cryst., off-centre Cu^+ 79−65112
KI-KCl(CsI) melts, X-ray diffr. struct. determ. 79−41925
KI-NaI, binary molten mixture, surface tension meas. 79−65294
KI-Tl, Jahn-Teller system, negative mag. circular polarisation in emission spectrum 80−20694
KI+TlCl, solid state displacement reaction, kinetics and mechanism 79−11788
KI(Br)(Cl), fundamental luminescence at high ionisation levels *(Russian)* 80−103985
KIO_3, and KIO_4, enthalpies of soln. in water 80−50880
KIO_3, cryst. struct. 79−19234
KIO_3, in dioxane-water mixtures, ion-solvent interaction and conductance 79−34315
KIO_3, propan-1,3-dioic acid, H_2O_2, $MnSO_4$, $HClO_4$, I_2, periodic chem. reactions, bi- and tristability, rel. to biological mech. *(French)* 78−80726
potassium compounds continued
KIO_3, temp. depend. Raman spectra and phase transitions *(Russian)* 78−15171
α-$KIO_3.HIO_3$, ^{127}I NQR study of ferroelec. phase transition 79−38400
$KIO_3.HIO_3$, cryst. struct. 79−19230
$KIO_3.HIO_3$, I atom electronic struct. in X-ray-neutron difference synthesis 79−90595
$KIO_3.HIO_3$, new orthorhombic modification, X-ray cryst. struct. determ. 79−55723
$KIO_3.HIO_3$, structural modifications, NQR study 80−20487
$KIO_3.KNO_3.2HIO_3$, cryst. struct. determ. 79−23591
$K_2InCl_5.H_2O$, crystal structure and H-bonding 80−64978
KIn_2F_7, cryst. struct. *(French)* 78−18590
$KInO_2$-MO_2, M=Zr, Hf, Sn, Pb, ionic cond., lamellar struct. *(French)* 77−1257
$KIn(SO_4)_2.4H_2O$, cryst. struct. 80−15082
$KIn(WO_4)_2$, ferroelastic domain struct. *(Russian)* 79−90719
K_2IrCl_6, mag. susceptibility in ordered and paramag. phases 79−73759
K_2IrCl_6, radiation-induced lattice defects and solid-state reactions *(German)* 79−42101
K_2IrCl_6, sp. ht. meas. at low temp. 80−7119
K_2IrCl_6, thermal expansion meas. near antiferromag. transition 77−20610
K_2IrF_6, hyperfine spectra of mag. ordered state at very low temp., Mossbauer meas. 77−69744
$K_x(L_{x/2}Sn_{1-x/2})O_2$ (L=Mg, Ca, Zn; x<1), new family of cationic conductors *(French)* 79−60546
$(K_{0.5}La_{0.5})_xBa_{1-x}TiO_3$, cryst. struct., dielec. and IR spectral meas. 79−46614
$KLa(MoO_4)_2$, solubility in aq. K_2MoO_4 solns., hydrothermal conditions 80−96651
$KLa(PO_3)_4$ (α and β forms), vibr. spectra 80−34905
$K_5La(WO_4)_4$, formation possibility 77−36392
$KLi_3Ca_7Ti_2(Si_6O_{18})_2F_2$, baratovite, cryst. struct. determ. by X-ray diffr. 77−76382
$K_6LiFe_{24}S_{26}Cl$, Mossbauer spectra and lattice parameters 79−78584
$K_{2.89}Li_{1.55}Nb_{5.11}O_{15}$, elastic and piezoelec. props. 79−15403
$K_3Li_2Nb_5O_{15}$ films for optical waveguides epitaxial growth and characterisation 80−79016
$K_3Li_2Nb_5O_{15}$ optical waveguides fabricated on sapphire by RF sputtering 79−98488
$K_xLi_{1-x}NbO$ films, epitaxial growth by melting on $K_{1.5}Bi_{1.0}Nb_{5.1}O_{15}$ substrate 79−33204
$K_xLi_{1-x}NbO_3$, epitaxial growth of single-cryst. films on $K_2BiNb_5O_{15}$ substrate by RF sputtering 79−15041
$KLi(Pt(CN)_4).2H_2O$, cryst. struct., polarised emission obs. 78−52538
$KLiSO_4$, ^7Li NMR, spin-lattice relax. *(Chinese)* 80−39884
$KLiSO_4$, phase transition, lattice parameter variation with temp. 78−79767
$KLiSO_4$:(Cr), uniaxial crysts., circular dichroism and optical activity 80−45029
$KLiSO_4$:Cr; optical activity characts. cryst.-chem. exam. 78−95569
$K_{0.75}Li_{0.25}TaO_3$, press. depend. of impurity soft modes, low energy Raman scatt. meas. 78−2852
$KLi[Pt(CN)_4].2H_2O$, energy band calcs. 77−39780
KLu_3F_{10}:Eu^{3+}, crystal field and spin-orbit parameters 78−30892
$KLu(WO_4)_2$:Er^{3+}, room temp. stimulated emission obs. 80−106527
KMF_3:Mn^{2+}, (M=Mg,Zn,Mn,Cd), zero-field splitting of Mn^{2+}, superposition model *(French)* 79−15267
$KMgF_3$, bond energy, equilib. distances and compressibility calcs. 80−70159
$KMgF_3$:Fe^{2+}, US relax. absorpt., acoustic wave-impurity coupling, spin-orbit splitting 79−4375
K_2MF_4:Mn^{2+}, (M=Mg,Zn,Mn), zero-field splitting of Mn^{2+}, superposition model *(French)* 79−15267
$KM_nxMg_{1-x}F_3$, randomly diluted Heisenberg paramag. nucl. relax. 80−60444
$K_2M(MoO_4)_3$, M=Zr, Hf, synthesis and struct. 77−36386
$K^+M^{III}(SO_4)_2$, M=Al^{3+}, Cr^{3+}, Fe^{3+}, Raman and IR spectrum study *(French)* 79−47453
$K_x(M_yTi_{2-y})O_4$, (M=Mg,Zn,Ni,Cu,Fe^{III},Mn^{III}), ($0.7 \leq x \leq 0.9$), new layer struct. *(French)* 80−84149
K_2MX_6 (M=Sn, Re, Os, Ir, Pt; X=Cl, Br), heavy metal ion implantation, mol. unit form. 80−100267
$KMeF_3$(Me=Cr, Mn, Fe, Co, Ni, Cu), discrete variational Xα cluster calcs. 80−15444
KMg, laser induced fluoresc. spectra 78−74692
$KMg_2(AlSi_3O_{10})F_2$-$KMg_{2.5}Si_4O_{10}F_2$, solid soln., melting and crystn., quenching and DTA study 80−39263
$KMg_3AlSi_3O_{10}F_2$, dislocations, subgrain boundaries, X-ray diffr. topography study *(Chinese)* 80−88149
$KMgCl_3$, successive phase transitions 79−100132
$KMgCl(ClO_4)_2.nH_2O$, IR spectra and struct. features 79−15452
$KMgCl_3.nH_2O$, IR spectra and struct. features 79−15452
$KMgCr_2(VO_4)_3$, synthesis and cryst. struct. 80−88114
$KMgF_3$, elastic moduli, press. and temp. depend., US technique 80−6453
$KMgF_3$, extreme UV spectra, 9-30 eV 78−23486
$KMgF_3$, F-centre, superhyperfine interaction, g-factor, symmetry, ENDOR obs. 80−39893
$KMgF_3$, F-centre ENDOR study 80−108117
$KMgF_3$, laser window material, surface and bulk absorpt., photoacoustic meas. 78−25912
$KMgF_3$, reflectivity, 8-60 eV, excitonic struct. 77−20871
$KMgF_3$ residual IR absorption, freq. and temp. dependence obs. 79−15468
$KMgF_3$, spin Hamiltonian parameters for Fe^{3+} ions, superposition model anal. 80−108053
$KMgF_3$, struct. of H-centre, low-temp. EPR meas. 77−12202
$KMgF_3$:Co^{2+} $^4T_1$-$^4T_2$ transition, zero-phonon lines intensities 80−75529
$KMgF_3$:Co^{2+}, γ-irrad. single cryst., visible and IR absorption, MCD, annealing data 78−10926
$KMgF_3$:Co^{2+}, MCD and linear dichroism, 3d→4s transitions 79−56768
$KMgF_3$:$Co^{2+}(Fe^{2+})(Mn^{2+})(Ni^{2+})$, high energy absorption spectra interpretation 78−6716
$KMgF_3$:Cr^{2+}, dynamic Jahn-Teller effect 77−66416
$KMgF_3$:Cr^{2+}, HF phonon spectroscopy using supercond. tunnel junctions 80−65178
$KMgF_3$:Cr^{3+}, EPR spectrum, effect of external elec. field 78−68368
$KMgF_3$:Cr^{3+}, trigonal centres, EPR lines, pseudo-Stark splitting 78−68367

potassium compounds continued
$KMgF_3$:Er^{3+}, Orbach-Aminor paramag. relax. processes, phonon bottleneck 79−28610
$KMgF_3$:Eu^{2+}, f-f transition, cryst. field parameters calc. 77−15805
$KMgF_3$:Eu^{2+}, Zeeman absorpt. and luminesc. spectra *(Russian)* 77−69872
$KMgF_3$:Fe, EPR temp. depend. 78−80202
$KMgF_3$:Fe^{2+}, anomalous acoustic relax. absorpt. and APR 80−88864
$KMgF_3$:Fe^{2+}, Jahn-Teller quenched spin-orbit, splitting of $^5T_{2g}$ state 77−63442
$KMgF_3$:Fe^{2+}, octahedral symm., vibronic effects from Zeeman field induced Mossbauer spectra 77−8477
$KMgF_3$:Fe^{2+}, super hyperfine struct., Zeeman splitting and dynamic Jahn-Teller effect 77−85555
$KMgF_3$:Fe^{2+}, transferred hyperfine interactions, EPR exam. 78−31105
$KMgF_3$:Fe^{3+}, superposition-model anal. of second- and fourth-order spin Hamiltonian parameters, EPR study 79−87311
$KMgF_3$:Mn^{2+}, crystl. field theory, superposition model 77−28149
$KMgF_3$:Mn^{2+}, exchange and spin-orbit interactions, optical spectra study 79−95817
$KMgF_3$:Mn^{2+}, MCD and linear dichroism, 3d→4s transitions 79−56768
$KMgF_3$:Ni, Co, emission from Ni-Ni and Ni-Co pairs, exchange coupling const. 79−33788
$KMgF_3$:Ni, Ni-Ni pair optical spectra 80−45042
$KMgF_3$:Ni^{2+}, absorpt., MCD and emission spectra 79−51953
$KMgF_3$:Ni^{2+}, acoustic Faraday and Cotton-Mouton effects, theory 80−65987
$KMgF_3$:Ni^{2+}, EPR meas., g-factor, spin-orbit coupling const. and mag. moment determ. 77−80999
$KMgF_3$:Sm^{2+}, absorpt. spectra and Zeeman effect, 3000-12000 Å, 4.2-295K 79−24341
$KMgF_3$:Sm^{2+}, luminesc. spectra 4.2, 77 and 295K and Zeeman spectra, 4.2K 77−81146
$KMgF_3$:Ti^{3+}, ESR and ENDOR spectra 77−40121
$KMgF_3$:V^{2+}, ^{51}V ENDOR meas., spin Hamiltonian parameters 79−28638
$KMgF_3$:V^{2+}, combined spin-orbit and Jahn-Teller coupling, method of soln. 79−60773
$KMgF_3$:V^{2+}, dynamical Jahn-Teller effect on spin orbit multiplets, intensity quenching 79−95374
$KMgF_3$:V^{2+}, first and second order Jahn-Teller coupling const. calc. 79−65906
$KMgF_3$:V^{2+}, MCD and linear dichroism, 3d→4s transitions 79−56768
$KMgF_3$:V^{2+}, zero-phonon line splitting in $T\times\varepsilon_g$ Jahn-Teller problem 78−19006
$KMgF_3$:V^{2+}(Cr^{2+})(Fe^{2+}) 3d→4d absorpt. band exam. 77−63435
$KMgF_3$:Yb^{3+}, ^{19}F hyperfine interaction, anisotropic Fermi and isotropic dipolar interactions 79−78056
$KMgF_3$:Yb^{3+}, cryst. field parameters, optical, EPR spectra, spin-lattice relax. time 77−51950
$KMgF_3$:Yb^{3+}, perovskite type cryst., ENDOR meas. 80−80638
$KMgF_3$:Yb^{3+}, transferred hyperfine interaction of Yb^{3+}, ENDOR meas. 78−19375
$K_3Mg_4LiSi_{12}O_{30}$, cryst. struct., X-ray diffr. and IR spectra *(French)* 80−107158
$KMg_2LiSi_4O_{10}F_2$-$NaMg_2LiSi_4O_{10}F_2$, solid soln., solid solubility and swelling characts. 80−59660
$K_2Mg_3M_2Si_{12}O_{30}$ (M=Cu, Fe, Zn, Mg), cryst. struct., X-ray diffr. and IR spectra *(French)* 80−107158
$KM_{1-x}Mn_xF_3$, disordered paramagnet, ^{19}F NMR study 80−71216
$K_2Mg_4Mo_4O_{16}(OH)_2(H_2O)_2$ study of non-stoichiometry *(French)* 78−30604
$K_2Mg_4Mo_4O_{16}.(OH)_2(H_2O)_2$, dehydration processes rel. to stoichiometry *(French)* 79−24734
$K_2Mg_2(SO_4)_3$, langbeinite type cryst., search for ferroelec. phase transition 77−59535
$K_2Mg_2(SO_4)_3$, langbeinites, structural phase transitions 78−83938
$K_2Mg(S_2O_3)_2.6H_2O$, isolation, struct., decomposition *(French)* 78−52506
$K_{1.54}Mg_{0.77}Ti_{7.23}O_{16}$, hollandite, cationic short range order, ion-ion interaction 77−11729
$K_{1.54}Mg_{0.77}Ti_{7.23}O_{16}$, hollandite, one-dimensional ionic conductor, site-occupancy correlation and effective interionic pot. 77−62663
$K_{1.54}Mg_{0.77}Ti_{7.23}O_{16}$, one-dimens. superionic cond., ionic order, defect cond. 78−87815
$K_{1.54}Mg_{0.77}Ti_{7.23}O_{16}$, hollandite, one-dimens. superionic cond., transport model 80−107529
$K_{1.6}Mg_{0.8}Ti_{7.2}O_{16}$, solid electrolyte, dielec. response, 5.2-77K 79−56709
$K_2Mg_xTi_{8-x}O_{16}$, stochastic Langevin dynamics study of correlated ionic motion in 1-D solid electrolytes 80−65279
$K_xMg_{x/2}Ti_{8-x/2}O_{16}$ $1.6\leq x\leq 2.0$, dielec. response in freq. range 10^{-3} to 10^6 Hz 79−65785
$K_xMg_{x/2}Ti_{8-x/2}O_{16}$, ionic cond., K mobility rel. to struct. and bonding *(French)* 77−76594
$K_xMg_{x/2}Ti_{8-x/2}O_{16}$, ionic cond., rel. to struct. and chemical bonding *(French)* 78−18824
$KMg_3[AlSi_3O_{10}].F_2$ with excess Al, synthetic fluorphlogopite, radiation-induced paramag. O^- centres 80−60417
$K_{0.54}(Mn,Fe)F_3$, room temp., X-ray single cryst. struct. anal. and refinement 79−19195
$K_3Mn(CN)_6$, low-spin mag. studies 79−95582
$KMnCl_3$, magnetic spiral struct., neutron diffr. study 80−39748
$KMnCl_3$, rare earth doped, energy transfer, emission spectra obs. 80−20684
$KMnCl_3.2H_2O$, antiferromagnet, symm. of field-induced phases, mag. space groups 77−32166
$KMn_{1-x}Co_xF_3$, Raman scatt. by mag. excitations 77−55775
$K_2Mn_{1-x}CoF_4$, mag. and neutron scatt. exam. 79−33466
$K_2Mn_{1-x}Cu_xF_4$, dynamic Jahn-Teller effect, NMR *(Japanese)* 78−19347
$KMnF_3$, 185K structural transition, wavevector reversed ultrasound study 80−75306
$KMnF_3$, acoustic nucl. spin echo *(Russian)* 77−48088
$KMnF_3$, antiferromag., multi-magnon luminesc. sidebands 78−76525
$KMnF_3$, antiferromag. cryst., luminesc. enhancement in mag. field, exciton model *(Russian)* 77−48214
$KMnF_3$, antiferromagnetic resonance in strong mag. field *(Russian)* 79−8054
$KMnF_3$, birefr. and opt. rot. near structural phase transition points 78−75823
$KMnF_3$, critical dynamics of sound 80−103424
potassium compounds continued
$KMnF_3$, cubic-to-tetragonal phase transition, critical anomalies, phenomenological eqns. 80−39275
$KMnF_3$, dynamic scaling and US attenuation at structural phase transition 80−44260
$KMnF_3$, EPR antiferromag. reson. linewidths near Neel point, exchange interactions *(Russian)* 77−8386
$KMnF_3$, exchange integral in Mn^{2+}-Mn^{2+} pair calc. 78−34974
$KMnF_3$, exchange interaction of excited Mn^{2+}($^4A_1$) ions, Anderson model 80−25124
$KMnF_3$, exciton and exciton-magnon emission 79−33779
$KMnF_3$, exciton dynamics by time resolved emission spectroscopy 80−54615
$KMnF_3$, exciton line and magnon satellite in UV spectrum at high press. *(Russian)* 79−4517
$KMnF_3$, Faraday effect mechanism in paramag. phase 80−60552
$KMnF_3$ film, photoelec. yield spectra, rel. to band struct. 78−43980
$KMnF_3$, flux growth of crystal 79−78861
$KMnF_3$, IR refl. spectra, vibr. modes, optical vibr. freq., Kramers Kronig anal. 80−66190
$KMnF_3$, IR-active phonons in tetragonal phases 80−2748
$KMnF_3$, lattice dynamics, rigid-ion model calc. 77−15512
$KMnF_3$, lattice parameter temp. depend., phase transitions and thermal expansion coeff. 80−1988
$KMnF_3$, luminesc., emission from localised traps 79−33777
$KMnF_3$, mag. props. and struct. transitions, antiferromag. reson. meas. 79−8052
$KMnF_3$, Mossbauer effect in ^{57}Fe, struct. and mag. transition investig. 77−20779
$KMnF_3$, Mossbauer gamma quanta scattering near 186K transition 80−108126
$KMnF_3$, multiplet struct. in XPS spectra of 3p and 3s subshells 78−43981
$KMnF_3$, optically detected antiferromag. reson. 78−15029
$KMnF_3$, perovskite with space group I4/mcm, determ. by cryst. struct. 78−75643
$KMnF_3$, phonon scatt., thermal cond. meas. 77−7916
$KMnF_3$, precursor order and Raman scatt. near displacive phase transitions 80−45061
$KMnF_3$, reflectivity, 8-60 eV, excitonic struct. 77−20871
$KMnF_3$, second-order displacive transition region, static and dynamic characts. determ. 80−70409
$KMnF_3$, soft phonons and mag. phase transitions 80−54889
$KMnF_3$, solid and molten paramag., high-temp. e.p.r. linewidth meas. 77−4548
$KMnF_3$, specific heat near Neel temp. *(Russian)* 80−100340
$KMnF_3$, spin density parameters at ^{19}F nuclei 78−68001
$KMnF_3$, stress-induced phase transition, optical props. meas. 77−20067
$KMnF_3$, temp. depend. of NMR linewidth of ^{19}F in paramag. region 78−60346
$KMnF_3$, width of central peak in crit. scatt. of γ-rays 77−1623
$KMnF_3$, XPS of band struct. 77−11851
$KMnF_3$:Rb, phase transition and atomic motions, NMR study 80−75872
K_2MnF_4, 2-dimens. antiferromagnet, with dipolar broadening, spin diffusion, EPR obs. 79−38371
K_2MnF_4, antiferromag. reson. relax., multimagnon processes 77−4564
K_2MnF_4, antiferromagnet, magnon renormalisation, two-magnon Raman scatt., kinematic interaction 78−23228
K_2MnF_4, EPR g-shift and anisotropic mag. susceptibility 77−85546
K_2MnF_4, Heisenberg antiferromag., magnon renormalisation 78−23259
K_2MnF_4, IR active modes, interlayer and intralayer forces 77−59575
K_2MnF_4, low-dimensional system, obs. of sidebands on EPR lines 77−80993
K_2MnF_4, nucl. spin-magnon relax. time, temp. depend., NMR study 80−25117
K_2MnF_4, ordered quadratic-layer Heisenberg antiferromag., nucl. spin-magnon relax. 80−71217
K_2MnF_4, perovskite type layer struct., far IR reflectivity and Raman spectra 77−15511
K_2MnF_4, perovskite type layer struct., lattice dynamics, rigid-ion model calc. 77−15512
K_2MnF_4, quadratic layer antiferromag., intrinsic emission obs. 77−20906
K_2MnF_4, quadratic layer antiferromag., field induced two magnon nuclear spin-lattice relax. 79−61258
K_2MnF_4, specific heat capacity, critical amplitude, cross-over from 2-D Ising to Heisenberg behaviour 80−39791
K_2MnF_4, spin waves *(Dutch)* 79−1663
K_2MnF_4, two dimens. Heisenberg system, shift of half-field EPR line 78−23325
K_2MnF_4, two-dimens. antiferromag., two-magnon Raman scatt. linewidth, finite temp. 77−66508
K_2MnF_4, two-dimens. antiferromag., diffusion-controlled mode coupling, EPR linewidth 79−51844
K_2MnF_4, two-dimens. Heisenberg antiferromag., field and temp. depend. of magnetic 77−66272
K_2MnF_4, two-dimensional antiferromag., NMR, magnetisation field-depend., spin-wave theory 77−63294
K_2MnF_4, two-dimensional antiferromag., crit. behaviour, quasielastic neutron scatt. 77−85468
K_2MnF_4:Co^{2+}, Raman spectra meas. 77−12389
K_2MnF_4:Ni^{2+}, and undoped, magnon spectra, Raman and far IR spectra meas. 77−20573
K_2MnF_4:Zn(Mg)(Ni), mag. effects of impurities 80−65869
K_2MnF_4:Zn(Mg)(Ni), local magnetisation, NMR and Green's function study 80−65870
$K_3Mn_2F_7$, antiferromagnet, two magnon Raman scatt. 78−15164
$K_3Mn_2F_7$, crit. EPR line broadening near Neel temp. 80−71165
$K_3Mn_2F_7$, double layer antiferromagnet, susceptibility 77−16061
$K_3Mn_2F_7$, double-layer antiferromag., mag. prop. meas. and calc. 77−55666
$K_3Mn_2F_7$, double-layer antiferromag., mag. ordering, neutron scatt. meas. 79−61062
$K_3Mn_2F_7$, quadratic double-layer antiferromag., NMR, spin-wave anal. of sublattice magnetisation 77−63293
$K_3Mn_2F_7$, quadratic double-layer Heisenberg antiferromagnet, sublattice magnetis., NMR obs. 77−66270
$K_3Mn_2F_7$, quadratic double layer antiferromag., two-magnon Raman scatt. 80−66183
$K_3Mn_2F_7$, two magnon Raman scatt., magnon dispersion, susceptibility, Green's function methods 80−50340

potassium compounds continued
$K_3Mn_3F_7$, Heisenberg double-layer antiferromag., neutron scatt. 79−61065
$K_2Mn_{0.987}Fe_{0.022}F_4$, antiferromag., mag. field induced transitions, neutron scatt. meas. 79−82782
$K_2Mn_{1-x}Fe_xF_4$, anisotropy on two and three dimens. mag. order 77−66259
$K_2Mn_{1-x}Fe_xF_4$, layered antiferromag., anisotropy effects on mag. ordering, neutron diffr. study 79−47254
$K_2Mn_{1-x}Fe_xF_4$, mag. and neutron scatt. exam. 79−33466
$K_2Mn_{1-x}Fe_xF_4$, mag. ordering, neutron scatt. expt. 79−42789
$K_2Mn_{1-x}Fe_xF_4$, tetracrit. line in x-H-T phase diagram, neutron scatt. exam. 78−47977
$K_2Mn_{1-x}Fe_xF_4$, vs. transition temperature, phase diagram, critical lines crossing tetracritical point, discussion 78−39326
$KM_{0.9}M_{0.1}F_3$, (M=Co,Ni), lattice parameter temp. depend., phase transitions and thermal expansion coeff. 80−1988
$K_2Mn_xM_{1-x}F_4$, (M=Mg,Zn,Cd), 2-dimens. antiferromag., sidebands on EPR lines 78−56370
$KMn_{1-x}Me_xF_3$ (Me=Mg^{2+}, Fe^{2+}, Co^{2+} and Ni^{2+}) Bridgman growth, 80−60764
$K_2Mn_cMg_{1-c}F_4$, EPR spectra 78−76298
$K_2Mn_cMg_{1-c}F_4$, impurities effect on EPR spectra 79−91283
$K_2Mn_xMg_{1-x}F_4$, impure two-dimensional system, ESR line reson. shift due to low symmetric spin distrib. 80−93162
$K_2Mn_xMg_{1-x}F_4$, two-dimensional antiferromag., ESR meas. 77−36121
$KM_{1-x}Ni_xF_3$, antiferromag. crit. props., neutron scatt. obs. 80−88749
$K_2M_{1-x}Ni_xF_4$, antiferromagnets, impurity associated and host magnetizations, NMR exam. 78−10800
$KMnO_4$, ^{55}Mn NMR second-order quadrupole splitting, asymmetry parameter 77−63312
$KMnO_4$, cryst., bond lengths and coordination numbers, EXAFS meas. 79−51043
$KMnO_4$, thermal decomp., $K_3(MnO_4)_2$ intermediate phase 77−44479
$KMnO_4$, X-ray emission spectra, plasmon satellites 79−99985
$KMnO_4$+muonium in aq. soln., rate const. 77−38752
$K_2Mn_2(SO_4)_3$, cubic langbeinite struct., low temp. mag. susceptibility 78−56299
$K_2Mn_2(SO_4)_3$, elastic props. using piezoelec. reson. and US vel. meas. 80−15180
$K_2Mn_2(SO_4)_3$, langbeinite type cryst., ferroelec., phase transitions, dielec., elastic and pyroelec. meas. 77−59535
$K_2Mn_2(SO_4)_3$, optical and dielectric props. 79−11403
$K_2Mn_2(SO_4)_3$, phase transition, X-ray diffr. study of high and low temp. phases 78−38832
$K_2Mn_2(SO_4)_3$, phase transition press. effect, dielectric const. meas. 79−37834
$K_2Mn_2(SO_4)_3$, structural phase transition, phenomenological theory 79−7693
$KMn_{0.1}Zn_{0.9}F_3$, exchange interaction determ. by neutron scatt. 79−47274
$KMn_{0.18}Zn_{0.82}F_3$, excitation of Mn^+ clusters, neutron scatt. 78−68200
$KMn_xZn_{1-x}F_4$, three dimens. Heisenberg antiferromag., fluctuations near percolation threshold 79−78390
$K_2Mn_5[Si_{12}O_{30}].H_2O$, synthetic Mn milarite, cryst. struct. 78−18618
$K_4(MoCl_4)_2$+acetic acid, reaction kinetics and mechanism 77−86305
$K_{0.3}MoO_3$, thermochemistry 77−77801
K_2MoO_4, aq. soln., solubility of $KLa(MoO_4)_2$ 80−96651
K_2MoO_4, hysteresis of phase transitions and modulated structures 80−29169
$K_2Mo_3O_{10}$ melt volatility, solubility of $YAl_3(BO_3)_4$ 80−65211
K_2MoOCl_5, mol. and cryst. struct. from X-ray diffr. obs. 78−6046
$K_3MoO_3F_3$, ferroelec. and order-disorder phase transitions 78−92037
$K_3MoO_3F_3$, ferroelec., transition obs. 80−75989
$K_3(MoO_4)(ReO_4)$, cryst. struct. *(French)* 78−47295
K_2MoO_3S, aq. soln., Raman spectrum, MoO_3S^{2-} force consts. 78−74668
$K_2Mo_2O_7.H_2O$, cryst. and mol. struct. 77−76373
$K_2Mo_{15}S_{19}$, superconducting chalcogenides containing Mo_6 and Mo_9 clusters 80−103804
$K_2Mo_9S_{11}$, prep. and struct., Mo_{12} cluster in $Mo_{12}S_{14}$ unit 80−107168
$K_3Mo(SCN)_6$, electronic struct., XPS and X-ray emission spectra 77−42336
$K_2Mo_{15}Se_{19}$, superconducting chalcogenides containing Mo_6 and Mo_9 clusters 80−103804
$K_8Mo_4V_8O_{36}.12H_2O$, single cryst. X-ray cryst. and mol. struct. 79−99131
$K_7Mo_8V_5O_{40}.\sim 8H_2O$, containing structurally new K-coordinated octamolybdopentavanadata anion, cryst. struct. 80−96479
KN_3, ab initio calcs. of elec. props. of N_4^- 79−95363
KN_3, dynamic electron density distribution, calc. from static mol. wave functions 77−27776
KN_3, ESR undergraduate expt. 80−105471
KN_3, electron density distrib. by high-resolution X-ray diffr. 77−62505
KN_3, exptl. electron density distribs. cf. theoret. density distribs. of N_3^- 77−46489
KN_3, fluoresc. spectrum, 30K, vibronic and vibr. assignments 79−27023
KN_3, heat capacity from 5 to 350K 79−55901
KN_3, IR refl. spectra, fundamental lattice modes, azide ion dipole derivatives 78−48166
KN_3, migration of K^+ and N^0 interstitials, activation energies 79−77813
KN_3, mono- and polycrysts., IR active lattice vibr., optical consts. 77−77185
KN_3, Raman spectra, weaker features obs. 77−68045
KN_3, X-irradiated, N defect, EPR obs. 79−82870
KNCO, fused, soln. mechanism of Fe and Cr 79−39271
KNCO, polycryst., IR and Raman spectra, lattice and internal modes 77−32369
KNCS, long-wave lattice modes 78−59881
KNCSe, IR and Raman spectra, internal and external modes 77−16312
KND_2, neutron diffr. anal. of librations of amide ion *(German)* 77−27788
KND_2, neutron diffr. exam. 31K *(German)* 77−62506
$K^+(NH_3)_n$, gas phase clusters, relative bond strengths, thermodynamic props. 78−35649
$K_2NH(SO_3)_2$, X-ray cryst. struct. refinement 79−69062
KNO_2, high-pressure phase behaviour 78−30749
KNO_2, melting pressure curves up to 5 kbar 77−15547
KNO_2, molten, electrolytic cond. at pressures up to 6 kbar 77−15609
KNO_2, NQR spectrum of ^{14}N at low temp., poss. ferroelec. transition 77−12223
potassium compounds continued
KNO_2, polymorphism, calorimetric investigation 78−75827
KNO_2 polymorphs, high press. Raman spectra 77−85725
KNO_2-$NaNO_2$-Na-NO_3 eutectic salt, use in indirect heating systems *(German)* 80−38233
KNO_3, activation coefficients and solvation numbers in mixed methanol solvents 80−81334
KNO_3, and KNO_2, fused, electrolum. 79−99945
KNO_3, antiferroelec., press. induced II to IV phase transition, Raman scatt. 78−15161
KNO_3, aq. soln., At^- $(AtO_3^-)(AtO_4^-)$ ion velocities, carrier free 79−34318
KNO_3, aq. soln., heat capacity at 298.15K 78−3364
KNO_3, aq. solns., laser induced breakdown 79−87530
KNO_3 calcite-type crystals, topotaxial decomp. TEM obs. 80−108710
KNO_3, cryst. growth rates, random processes theory to study fluctuations 79−55689
KNO_3, far IR study of dielec. function by asymmetric Fourier spectroscopy 79−51947
KNO_3, ferroelec. thin crysts., struct. investig. 79−27962
KNO_3 in alkali halides tablets, phase transition and ion exchange, IR spectra 80−79937
KNO_3 infrared spectroscopic study of structural transformations, electronic structure characteristic features 79−47436
KNO_3, LF Raman spectrum, effect of cryst. size *(Russian)* 77−28581
α-KNO_3, lattice dynamics, inelastic neutron scatt. 79−4383
KNO_3, melt, NO_3^- ion struct., pulsed neutron diffr. obs. 78−22631
KNO_3, melt, Tl^+ high dilution diffusion, interferometry 78−47546
KNO_3 melts, ion exchange reaction with Na silicate glasses 80−16673
KNO_3, molten, thermomagnetoelec. effect *(French)* 77−76849
KNO_3, molten, X-ray diffr. structural anal. 78−42887
KNO_3, neutron diffraction examination, white beam technique 77−31565
KNO_3, orientations and twinning in the struct. transform. aragonite-type to calcite-type 77−24284
KNO_3, paraelec., precision lattice parameters, thermal expansion 77−11517
KNO_3 pellet, dissolution in KNO_3 soln., mass transfer coeff. in crossed electric and mag. fields 78−48741
KNO_3, phase II, lattice dynamics, coherent neutron inelastic scatt. 78−59897
KNO_3, Raman and IR spectra and lattice vibrs. 80−60565
KNO_3, Raman spectroscopic study of NO_3^- component with temp. 78−76458
KNO_3 soln., Raman spectral studies of NO_3^- motion and interaction 78−92067
KNO_3, solns. coagulation of amphoteric latex sols, reversibility and specific ion effects 80−45567
KNO_3, solution, apparent molar heat capacity and volume, at 298.15K 80−29179
KNO_3, spectral interference in at. absorption spectroscopy in C tube atomiser and flames *(Japanese)* 79−48019
KNO_3, vibrations of isotopic impurities, IR reflection and Raman spectra meas. 77−51465
KNO_3, with adsorbed film of soln., NMR investig. 77−8426
KNO_3-$Ca(NO_3)_2$ glasses, radiation products and recombination 79−57261
KNO_3-$Cd(NO_3)_2$ molten mixtures, eleetrical conductance, non-Arrhenian behaviour 78−43158
KNO_3-$Cd(NO_3)_2$ molten mixtures, elec. cond. 79−90813
KNO_3-$K_2Cr_2O_7$ 77−44232
KNO_3-$LiClO_3$, binary melt, Raman spectra, polarised line width, temp. depend. 78−84578
KNO_3-$LiNO_3$ (urea), solid eutectic mixtures, Raman, IR spectra, line shifts, widths 77−55793
KNO_3-$Pb(NO_3)_2$ molten mixture, elec. cond., Tobolsky parameter *(German)* 80−15282
KNO_3-$RbNO_3$, liq., electromigration cation and mobility and isotope effect 80−10691
KNO_3-$Sr(NO_3)_2$ molten mixtures, electrical conductance 78−43159
KNO_3-TlBr, fused mixture, coexistence curve and elec. cond. 77−20071
$KNbO_3$, single domain crystal growth, SHG with Nd:YAG laser 78−74954
KNO_3(II), Raman spectral study of struct. props., disordered groups 77−66486
$3KNO_3-2Ca(NO_3)_2$, glass form. from liq., struct. transform., Raman spectrum obs. 80−64916
$3KNO_3-2ZnCl_2$, glass form. from liq., struct. transform., Raman spectrum obs. 80−64916
$K_3N(SO_3)_2.H_2O$, X-ray cryst. struct. determ. 79−69062
$K_3N(SO_3)_3.2H_2O$ and ^{15}N derivative, Raman and IR spectra, $N(SO_3)_3^{3-}$ normal coord. anal. 79−91433
$K_3N(SO_3)_3.2H_2O$, cryst. binding of H_2O, IR spectra 78−75620
$(K_xNa_{1-x})_2$ 0.58 Ga_2O_3, anomalous behaviour in ionic cond. obs. 78−87818
$K_2NaAlF_6:Cr^{3+}$, ^2E_g-$^4A_{2g}$ phosphoresc. spectrum, vibr. struct. 79−47494
$K_4Na_4(Al_8Si_8O_{32}).10H_2O$, amacite, cryst. struct. determ. 80−28961
$K_{1-c}Na_cCl$, impurity centre local vibrs., comp. depend. of spectral parameters 80−79898
K_2NaCrF_6, Cr^{3+} optical spectrum open shell SCF MO cluster CI calc. 78−19501
$K_6Na(Fe,Cu,Ni)_{24\pm}S_{26}Cl$, jerfisherite, X-ray cryst. struct. determ. 80−92512
$K_2NaGaF_6:Cr^{3+}$, mag. circular dichroism and absorption spectra 77−77254
$K_2NaGaF_6:Cr^{3+}$, magneto-optical study of $^2T_{1g}$, $^4T_{2g}$, ^2E_g-$^4A_{2g}$ transitions 80−71384
$(KNa)NbO_3$ ceramic, piezoelectric effect due to polarisation, expt. *(Polish)* 77−77151
$(K_xNa_{1-x})NbO_3$ single crystals, growth and phase transitions 79−33915
$K_3NaP_2O_7.4H_2O$, cryst. struct. *(French)* 78−42961
$KNaSO_4$, sulphate ion optical and spectroscopic props., cryst. environment effect 77−40224
$KNaSO_4$, X-ray cryst. struct. determ. 80−64963
$(K_{1-x}Na_x)_2SO_4:Tl^+$ phosphor, thermolum. characts. 77−90203
$K_3Na(SO_4)_2$, X-ray cryst. struct. determ. 80−64963
$K_{1-x}Na_xTaO_3$, quantum ferroelec., elastic compliance, impurity effects 79−99835
$K_{1-x}Na_xTaO_3$ quantum ferroelectric, dielec. susceptibility 80−103922
$K_xNa_{1-x}TaO_3$, press. depend. of impurity soft modes, low energy Raman scatt. meas. 78−2852

potassium compounds continued
$KNa_3[AlSiO_4]_4$, nepheline, continuous laser emission effects on surface, spectroscopic obs. 79−94271
$K_2Na[Co(NO4d2)_6]$, single cryst., X-ray deffrs. determ. of electron density distrib. 79−14746
$KNa[Pt(CN)_4].3H_2O$, neutron diffr. cryst. struct. exam., refinement by least squares 78−2079
$KNa[Pt(CN)_4].3H_2O$, energy band calcs. 77−39780
$K_3Nb_3B_2O_{12}$, pentagonal tunnel struct. *(French)* 77−58985
$KNbF_6$, NMR, quadrupole effects and struct. distortion 80−15809
$K_6Nb_6Ge_xSi_{4-x}O_{26}$ ($0 \leq x \leq 4$), synthesis, structs. *(French)* 78−51519
$KNbO_3$, acoustic modes near orthorhombic-tetragonal phase transition, temp. depend. 79−28058
$KNbO_3$, anomalous scatt. and asymmetrical line shape in Raman spectra 77−20853
$KNbO_3$ catalysts, ferroelectric, for reactions involving CO and NO , and adsorption of NO 80−30282
$KNbO_3$, complex electronic dielectric const. from tight binding energy bands 78−60054
$KNbO_3$ crystals, growth from melt 79−100041
$KNbO_3$ crystals, reduced, hologram recording and erasure sensitivity *(Russian)* 80−78795
$KNbO_3$, cubic, temp. depend. of intensity of X-ray interference 80−59613
$KNbO_3$, dielec. and optical props. using shell model 79−33654
$KNbO_3$, dielec. spectrum rel. to polarisation effects 80−15984
$KNbO_3$, displacive ferroelectric, effective charge determ. 80−97212
$KNbO_3$, domain struct. at transitions from twinned phase, appl. to tetragonal-orthorhombic transition 80−71360
$KNbO_3$, dopant effect on domain struct., etching study 79−56749
$KNbO_3$, elec. and thermoelec. singularities due to small polaron hopping motion cond. transition 79−42565
$KNbO_3$, elec. and thermoelec. props., influence of O defects 80−29401
$KNbO_3$, electronic props., SCF-MS-Xα calc. 80−54607
$KNbO_3$, electronic struct., XPS and band struct. calc. 79−38708
$KNbO_3$, ferroelec., nonlinear optical susceptibility calc. 78−9409
$KNbO_3$, ferroelec. cryst., IR and Raman spectra, mode coupling 80−66194
$KNbO_3$, ferroelec. phase, phonon dispersion relations and lattice dynamics calcs., comparison with expt. 80−49319
$KNbO_3$, ferroelectric soft modes and order-disorder transition 77−47534
$KNbO_3$, ferroelectric transition, neutron diffr. obs. 80−25324
$KNbO_3$ glass, quenched, ionic cond., appl. as solid electrolyte 79−1522
$KNbO_3$, growth from soln. in melt and characterisation of optical quality cryst. 77−8741
$KNbO_3$ half-wave voltage, electro-optic and polarisation-optic coefficients 77−40211
$KNbO_3$, high-efficiency SHG at 4250 to 4680 Å 79−81479
$KNbO_3$, ionic grouping theory of electro-optical and nonlinear optical effects of crystals *(Chinese)* 78−27183
$KNbO_3$, layer growth, optical and electron microscopy 77−59021
$KNbO_3$ monocrystals, low freq. oscills. of elec. current 79−91053
$KNbO_3$, one-dimens. ferroelectric, phonon dispersion surfaces 79−42180
$KNbO_3$, orthorhombic, anharmonic effects 78−79721
$KNbO_3$, perovskite structure, semiconductor props. *(Polish)* 78−56437
$KNbO_3$, photoconductivity and TSC 78−2520
$KNbO_3$, photoferroelectric effects 78−92029
$KNbO_3$, photovoltaic current, temp. and spectral depend. 78−47828
$KNbO_3$, photovoltaic effect lux ampere characts., photoconductivity 80−15561
$KNbO_3$, piezoelec. and electrostrictive coeffs. 77−85653
$KNbO_3$ powder synthesis, unit cell determ. 78−11168
$KNbO_3$, pseudo-ionic model applic. to dynamics 77−59077
$KNbO_3$, reduced, diffr. efficiency and energy transfer during hologram form. 79−72528
$KNbO_3$, reduced, phase hologram recording, energy transfer and sensitivity 80−69338
$KNbO_3$ reduced, phase hologram recording sensitivity, energy transfer, photovoltaic effects 80−78799
$KNbO_3$, SHG with $Ga_{1-x}Al_xAs$ lasers 80−5785
$KNbO_3$, SHG with $Ga_{1-x}Al_xAs$ laser 80−74431
$KNbO_3$, single cryst., dielec. breakdown and electroluminesc. 78−2917
$KNbO_3$ single crystals, preparation of pure, Fe doped, and reduced crystals 78−60564
$KNbO_3$, spontaneous polarisation and pyroelec. effect meas. 77−90107
$KNbO_3$, tetragonal phase, inelastic neutron scatt. 80−19676
$KNbO_3$, thermoelec. effect and phase transitions 78−48123
$KNbO_3$ thick crystals, vol. nucleation of domains by impurities 77−73120
$KNbO_3$, X-ray diffr. before and after high temp. phase transition 77−11694
$KNbO_3$, XPS, band struct., density of states, photoionisation cross sections 78−52629
$KNbO_3$:Al^{3+}, dopant effect on domain struct., etching study 79−56749
$KNbO_3$:Ba^{2+}, dopant effect on domain struct., etching study 79−56749
$KNbO_3$:Fe, ferroelec. semiconductor, anomalously high photovoltage 77−69378
$KNbO_3$:Fe, ferroelec., anomalous photovoltaic effect and photocond. 78−52449
$KNbO_3$:Fe, large single domain cryst., growth and prep. for optical storage 77−1799
$KNbO_3$:Fe, optically induced refractive index changes 77−4612
$KNbO_3$:Fe, orthorhombic, EPR of Fe^{3+} 80−39861
$KNbO_3$:Fe, photorefr. effects and photocurrents 78−43434
$KNbO_3$:Fe, photovoltages, photocurrents and photorefractive effects 79−42580
$KNbO_3$:Fe, thermal and spectral variations in the photovoltaic current in ferroelectrics 78−91719
$KNbO_3$:Fe photorefraction and photocurrent effects *(Russian)* 79−7091
$KNbO_3$-$BaTiO_3$, ferroelec. Curie temp., theory 80−7313
$KNbO_3$-$PbTiO_3$, ferroelec. Curie temp., theory 80−7313
$K_{12}Nb_{15.5}O_{35.5}F_{18.5}$, cryst. struct. determ. *(French)* 80−96489
$K_6Nb_{6.5}O_{14.5}F_{9.5}$, cryst. struct. determ. *(French)* 80−96489
$K_{10}(Nb_6O_{21})_2.Nb_6X_4O_{26}$, X=Si, Ge, cryst. struct. *(French)* 77−76378
$K_{0.5}NbS_2$, supercond. props., alkali cation and topotactic solvation influences 79−87180
$K_6Nb_6Si_4O_{26}$, luminesc. bands, Stokes shift, rel. to crystal struct., stacking faults 80−34974
$K_8Nb_{14}Si_4O_{47}$, luminesc. bands, Stokes shift, rel. to crystal struct., stacking faults 80−34974
$K_8Nb_{14}Si_4O_{47}$, struct. determ. *(French)* 77−27866
$KNbW_2O_9$, crystallography, polymorphism and phys. props. 78−79599
$K_3Nb_{8-x}X_xO_{21}$ (X=Nb, Ti, Cr, Fe, Ni, Mg, Zn), X-ray diffr., layer struct. *(French)* 77−15368
$K_5NdLi_2F_{10}$ (KNLF), spectroscopy and lasing 80−5737
$K_5NdLi_2F_{10}$, high yield luminesc. 79−1784
$K_5NdLi_2F_{10}$, X-ray cryst. struct. determ. and refinement 79−42030
$K_3Nd(MoO_4)_4$, Ar^+ laser pumped, quasi-CW laser action 79−18421
$K_3Nd(MoO_4)_4$, dielec. and optical props. 79−33590
$K_3Nd(MoO_4)_4$, spectral and struct. props. *(Russian)* 79−52020
β-$KNd(PO_3)_4$, vibr. spectra 80−34905
$KNdP_4O_{12}$, CW laser oscill., near 1.32 μm 77−61957
$KNdP_4O_{12}$, determ. of fluoresc. quantum efficiency and laser emission cross sections 80−48264
$KNdP_4O_{12}$ epitaxially grown waveguide, laser operation at 1.051 μm 79−18423
$KNdP_4O_{12}$, laser emission cross sections, fluorescence spectra, radiative lifetimes, quantum efficiency 80−23694
$KNdP_4O_{12}$, laser waveguide, fabrication by LPE 79−36925
$KNdP_4O_{12}$ laser waveguide, epitaxial growth 79−91597
$K_3Nd(PO_4)_2$, synthesis and IR spectra 80−16019
$K_3NdSi_6O_{15}$, cryst. struct. determ. 78−34493
$KNd_9(SiO_4)_6O_2$, cryst. struct. determ. 79−90624
$K(Ni(CN)_2HN_2S_2)$, cryst. struct. determ. 78−63715
$KNiCl_3$, disorder as observed by electron diffr. 80−75213
$KNiCl_3$, X-ray cryst. struct. determ. at room temp. 80−33938
$KNiCr_2(VO_4)_3$, synthesis and cryst. struct. 80−88114
$KNiF_3$, ^{19}F spin-lattice relaxation 80−93211
$KNiF_3$ and K_2NiF_4, MCD and stress linear dichroism on double excitonic transitions 77−52051
$KNiF_3$, and K_2NiF_4, double-excitonic optical transition intensity, exchange and dimensionality effects 77−69591
$KNiF_3$, antiferromag., nonlinear optical effects, spin wave contrib. 77−10987
$KNiF_3$, antiferromag., two-exciton transition 77−32398
$KNiF_3$, antiferromag., obs. of domains by X-ray topography 78−14981
$KNiF_3$, antiferromag. domains obs. by cryogenic X-ray topography 77−39507
$KNiF_3$, antiferromag. domain behaviour 77−69607
$KNiF_3$, antiferromag. domain wall motion obs. by X-ray synchrotron topography 78−88139
$KNiF_3$, cryst. field theory, superposition model 77−28149
$KNiF_3$, crystal growth from flux, degree of perfection and dislocation density 77−77359
$KNiF_3$, electronic struct. and spectrum of NiF_6^{4-} complexes, scattered wave method calc. 77−15807
$KNiF_3$, electronic UV laser excited Raman, scatt. by mag. excitons 78−68492
$KNiF_3$, flux-grown cryst., direction of dislocations, X-ray topography obs. 77−35565
$KNiF_3$, isotropic antiferromag., phase diagrams, US meas. 78−68350
$KNiF_3$, isotropic antiferromag., crossover behaviour of mag. phase boundaries 79−78370
$KNiF_3$, lattice parameter temp. depend., phase transitions and thermal expansion coeff. 80−1988
$KNiF_3$, low anisotropy antiferromag., phase boundary crossover behaviour 79−38324
$KNiF_3$, mag. form factor calc. for Ni^{2+} 77−20555
$KNiF_3$, magnetostriction, X-ray diffractometry and strain gauge meas. 80−65997
$KNiF_3$, multiplet struct. in XPS spectra of 3p and 3s subshells 78−43981
$KNiF_3$, reflectivity, 8-60 eV, excitonic struct. 77−20871
$KNiF_3$, refr. index, isotropic exchange contrib. 77−69808
$KNiF_3$, spin density parameters at ^{19}F nuclei 78−68001
$KNiF_3$, spin-lattice relax. exam. 79−73838
$KNiF_3$, XPS of band struct. 77−11851
$KNiF_3$:^{111}Cd, antiferromag., spin deviations and hyperfine fields, PAC meas. 77−48104
$KNiF_3$:Mn^{2+}, isotropic Heisenberg ferromagnet, localised spin-wave modes, biquadratic exchange effects 77−51896
K_2NiF_4, 2D antiferromag., volume depend. of superexchange, US velocity meas. of T_N 78−19237
K_2NiF_4, antiferromag., two-exciton transition 77−32398
K_2NiF_4, antiferromag., one-magnon light scatt. from spin-flop and paramag. regions, effect of anisotropy 79−33677
K_2NiF_4, antiferromag., one-magnon light scatt., effect of anisotropy 79−33676
K_2NiF_4, electronic UV laser excited Raman, scatt. by mag. excitons 78−68492
K_2NiF_4, neutron scatt. obs. of mag. behaviour 77−66254
K_2NiF_4, nucl. spin-magnon relax. time, temp. depend., NMR study 80−25117
K_2NiF_4, obs. of short range order by optical birefringence 79−11318
K_2NiF_4, ordered quadratic-layer Heisenberg antiferromag., nucl. spin-magnon relax. 80−71217
K_2NiF_4, quadratic layer antiferromag., optical spectra obs. 77−16326
K_2NiF_4, quadratic layer antiferromag., field induced two magnon nuclear spin-lattice relax. 79−61258
K_2NiF_4, specific heat capacity, critical amplitude, cross-over from 2-D Ising to Heisenberg behaviour 80−39791
K_2NiF_4, spin waves *(Dutch)* 79−1663
K_2NiF_4 structure, study by method of invariants, appl. to A_2BO_4 oxides *(French)* 80−33959
K_2NiF_4, two-dimens. antiferromag., two-magnon Raman scatt. linewidth, finite temp. 77−66508
K_2NiF_4, two-dimensional antiferromagnet, fine struct. obs., 4.2K *(Russian)* 77−59587
K_2NiF_4, two-dimensional antiferromag., crit. behaviour, quasielastic neutron scatt. 77−85468
K_2NiF_4:^{111}Cd, antiferromag., spin deviations and hyperfine fields, PAC meas. 77−48104
K_2NiF_4-type compounds, cationic radius ratio and formation 80−28992
$K_3Ni_2F_7$, quadratic double layer antiferromag., two-magnon Raman scatt. 80−66183
$KNi_xMn_{1-x}F_3$, mixed antiferromagnet, light scatt. meas. 80−16025
$KNi_xMn_{1-x}F_3$, two-magnon Raman scatt. 77−66509
$K_2Ni(MoO_4)_2$, paramag. props., 90-800K *(French)* 80−39734
$K_2Ni(MoO_4)_2$, X-ray cryst. struct. determ. 79−14782
$K_2Ni_3(P_2O_7)_2.10H_2O$, formation from $Ni_2P_2O_7$-$K_4P_2O_7$-H_2O system 80−54381

potassium compounds continued
$K_2NiP_2O_7.4H_2O$ formation from $Ni_2P_2O_7$-$K_4P_2O_7$-H_2 system 80−54381
$K_2Ni_3(P_2O_7)_2.nH_2O$, thermal dehydration 80−35513
$K_2Ni_2(SO_4)_3$, cubic langbeinite struct., low temp. mag. susceptibility 78−56299
$K_2Ni(SO_4)_2.6H_2O$:Gd^{3+}, EPR, low-symmetry effects 77−48043
$K_4NpO_2(CO_3)_3$, structure and bonding study 77−27868
$KO_{0.5}$-$AlO_{1.5}$-SiO_2 system, activities calc. from vapour press. meas. and known data 79−91985
$KO_{0.5}$-$NaO_{0.5}$-SiO_2 liquid, heat capacity of mixing at 1000K 79−77765
$KO_{0.5}$-SiO_2 liquid, anal. expressions for heat capacities 79−77765
KO_2, low temp. phases, mag. order, EPR and antiferromag. reson. 79−95630
KO_2, non-isothermal decomp. kinetics 80−16649
KO_2, thermal decomp. macrokinetics, differential thermal anal. 80−16650
KO_2, X-ray low temp. phase study, crystallographic domains and unit cell dimens. 78−63728
$KO_3+NH_3 \rightarrow KOH+NH_2O_2$, photolytic reaction 77−16838
K_2O, additive in ZnO sintering 78−80497
K_2O, determination of enthalpy of solution in PbO-B_2O_3 mixture 79−95166
K_2O, effect on props. of PbO containing cryst. glass 80−24637
K_2O glasses, partially leached, dehydrated surface reaction with water 80−3406
K_2O high temp. X-ray anal. using special cell for reactive substances *(French)* 79−68978
K_2O, in porcelain raw material, determ. by ion exchange chromatography 78−7272
K_2O melt, corrosion of CaO, SEM obs. 77−44383
K_2O, reaction with Cu_2O and CuO 79−66277
K_2O reaction with Ga_2O_3 and H_3PO_4, $KGaHP_3O_{10}$, $KGa(PO_3)_4$ and $Ga(PO_3)_3$ crystn. 79−52642
K_2O, under vacuum, exam. of thermal behaviour *(French)* 79−19365
β-K_2O-Al O_3, cation distrib. 77−80487
β-K_2O-Al_2O_3, synthesis 77−81238
K_2O-Al_2O_3 system, high temp. thermodynamics and phase equilibria 78−80521
K_2O-Al_2O_3-B_2O_3, subsolidus compatibility relations determ. *(Japanese)* 79−4957
K_2O-Al_2O_3-B_2O_3:Fe_2O_3, glasses, liq.-liq. phase separation, Fe^{3+} ions rel. to mag., optical props. 77−15322
K_2O-Al_2O_3-B_2O_3-SiO_2, glass, ESR exam. of paramagnetic centres formed during mech. destruction by grinding 78−88188
K_2O-Al_2O_3-P_2O_5 glass, low-temp. viscosity 80−39198
K_2O-Al_2O_3-P_2O_5-Nb_2O_5 glasses, struct. singularities, IR spectra *(Russian)* 78−2861
K_2O-Al_2O_3-P_2O_5-TiO_2, structural role of Ti, kinetic study of chem. destruction 80−88055
K_2O-Al_2O_3-SiO_2 system, crystallisation of glasses in primary phase field of leucite 78−67658
K_2O-Al_2O_3-$2SiO_2$-BaO plasma emitter 80−96368
K_2O-AlF_3-B_2O_3 glass, Al atom bonding mode, optical absorption of VO^{2+} and AlK_α spectrum *(Japanese)* 78−11023
K_2O-B_2O_3 glass, γ- and UV- irrad., thermodecolorisation and thermolum. 80−20721
K_2O-B_2O_3 glass, laser decolorisation of colour centres 79−43008
K_2O-B_2O_3 glass, PbO-activated, luminesc. and excitation spectra *(Russian)* 78−10979
K_2O-B_2O_3:Cu II, glass, O basicity, ESR study 78−80199
K_2O-B_2O_3:Mn^{2+} glass, fine struct. parameter distribs., EPR meas. 80−11256
K_2O-B_2O_3-Fe_2O_3, γ-irrad., Mossbauer spectroscopic study 80−108132
K_2O-B_2O_3-Fe_2O_3 glass, Mossbauer expts., 85-500K 78−80260
K_2O-B_2O_3-Fe_2O_3 glasses, nonbridging O formation, Mossbauer spectroscopy 80−55001
K_2O-B_2O_3-SiO_2, glass, crystallisation range *(German)* 80−38934
K_2O-B_2O_3-SiO_2 system glasses, hypersound propag., 77 to 300K, Brillouin scatt. obs. 77−84850
K_2O-BaO-B_2O_3 glasses, ESR detection of immiscibility rel. to Cu II ions 80−20916
K_2O-BaO-CaO-SiO_2 glass-Nichrome-CaF_2 multicomponent self-lubricating coating, prep. by plasma spraying, and props. 80−40604
K_2O-BaO-GeO_2:Bi^{3+}, Nd^{3+}, absorpt. and excitation spectra, fluoresc. 77−90183
K_2O-BaO-SiO_2 glass, rare earth ion activated, spectral intensity, effect of number of 4f electrons 78−84602
K_2O-BaO-SiO_2:Nd^{3+} glasses, absorption and fluoresc. spectra, density 80−53417
K_2O-BaO-SiO_2-Ti(Ce)O_2 laser glasses, TiO_2 and CeO_2 antisolarisation additive effects 79−94309
K_2O-CaO-Al_2O_3-SiO_2 glass, exam. of liquid phase separation phenomena 79−4417
K_2O-CaO-B_2O_3:CuII, immiscibility, ESR detect. 78−80200
K_2O-CaO-BaO-B_2O_3, glass, refraction, refractive index from 0.365 to 2.50 μm 80−88953
K_2O-CaO-BaO-SiO_2 (B_2O_3) (GeO_2), calc. of network refraction and exam. of glass structure 79−4783
K_2O-CaO-SiO_2 glass, composition-density relationship 77−90326
K_2O-CaO-SiO_2 glasses, Auger analysis, alkali signal decrease 80−61189
K_2O-Fe_2O_3-SiO_2, subsolidus sector of phase diagram, X-ray obs. 80−40335
K_2O-FeO-Al_2O_3-SiO_2 system, liquid immiscibility in silicate magmas 77−13076
K_2O-Ga_2O_3-Al_2O_3, solid solns., K ionic cond. 77−35747
K_2O-Ga_2O_3-P_2O_5-H_2O, reactions, 150-500°C 80−35514
K_2O-GeO_2, and Na_2O-K_2O-GeO_2 glasses, He permeability, diffusivity and solubility 79−51308
K_2O-GeO_2 glass, struct., Raman scatt. obs. 80−1936
K_2O-GeO_2:Tb^{3+}, Yb^{3+} glass, luminesc, cooperative sensitization correlated with Rayleigh scatt. intensity 78−52573
K_2O-GeO_2-SiO_2, refractive index and density 79−51926
K_2O-Li_2O(Na_2O)-SiO_2 glass heat of mixing *(Japanese)* 78−10195
K_2O-MgO-Al_2O_3, ionic cond. 80−107480
K_2O-MgO-B_2O_3:Cu^{2+}, micro-inhomogeneities, EPR and Raman study 80−84080
K_2O-MgO-SiO_2 glass, crystalline phase precipitation during crystallisation early stages, DTA *(Japanese)* 78−42919
K_2O-Na_2O-Al_2O_3-SiO_2 glass, ion exchange kinetics and interdiffusion mechanisms 80−80003

potassium compounds continued
K_2O-Na_2O-BaO-SiO_2 glass, corrosion kinetics in aqn. KOH, transition metal oxide addition effects 77−56125
K_2O-PbO-PbF_2-SiO_2 glass shear wave velocity and its temp. depend. *(Japanese)* 78−30702
K_2O-PbO-SiO_2, glass, mech. and optical props. *(Russian)* 77−20860
K_2O-PbO-SiO_2, glass, effect of DC on corrosion of SnO_2 electrodes 80−85075
K_2O-PbO-SiO_2, structural units, Raman spectroscopy 77−20847
K_2O-PbO-SiO_2 glass powders, ion exchange during leaching in HNO_3 79−100358
K_2O-PbO-ZnO-B_2O_3-SiO_2, corrosion and microhardness, effect of detergents 80−16518
K_2O-SiO_2, glass, influence of electric charge phenomena on AES *(French)* 80−50478
K_2O-SiO_2, vap. press., thermodynamic props. and phase diagram at high temps. 78−83932
K_2O-SiO_2 glass, AES obs. of K^+ electromigration to surface under electron bombardment *(French)* 79−33869
K_2O-SiO_2 glass, diffusion-controlled crystal growth 77−19876
K_2O-SiO_2 glass, effect of high-dose X-rays and reactor radiation 80−19838
K_2O-SiO_2 glass, IR reflection spectra change due to moisture corrosion *(Japanese)* 78−19914
K_2O-SiO_2 glass, Raman scattering of dissolved CO_3^{2-} ions 78−27848
K_2O-SiO_2 glass 80−33897
K_2O-SiO_2 glasses, Auger analysis, alkali signal decrease 80−61189
K_2O-SiO_2 glasses, IR reflection spectra, computer resolution *(Japanese)* 77−69832
K_2O-SiO_2 system glasses, ionic cond. correl. with chem. pot. 77−89581
K_2O-SiO_2-GeO_2 digermanosilicate glass, Raman study of structure 79−77524
K_2O-SiO_2-GeO_2 metagermanosilicate glass, Raman study of structure 79−77523
K_2O-SiO_2(-GeO_2) system glasses, X-ray diffr. anal., electron radial distrib. curves 78−87622
K_2O-SiO_2glass, structural analysis, using fluorescence excitation *(German)* 80−38923
K_2O-SrO-Nb_2O_5 system, selective delineation of dislocations by etching 77−72617
K_2O-SrO-SiO_2, glass, elastic constants 77−16630
K_2O-SrO-SiO_2, O_2 self diffusion exam. by proton activation anal. 79−65241
K_2O-SrO-SiO_2, solid glass, influence of composition on electrical conductivity 77−11723
K_2O-Ta_2O_5 mixed oxides, cryst. struct., electron microscopy study 78−91309
K_2O-Ta_2O_5 mixed oxides, cryst. struct., electron microscopy study 78−91310
K_2O-TeO_2 glass, radiational EPR centres, struct. model *(Russian)* 77−28426
K_2O-TeO_2 glass, struct. and props. *(Japanese)* 79−32917
K_2O-TiO_2-SiO_2 glass, Si-O bonding, Si$K\beta$ X-ray fluorescence and IR spectra 80−10500
K_2O-TiO_2-SiO_2 system, vitreous, struct. obs. using neutron scatt. 78−22667
K_2O-V_2O_5-Al_2O_3 melts, soln. of Al_2O_3 single crystals 80−20910
K_2O-ZnO-P_2O_5, exam. of chemical durability, glass transformation temp. 79−20221
K_xO_y, thermodynamic props. 80−29184
$K_2O_xCl_6$, soft rotary mode near phase transition, inelastic neutron scatt. obs. 79−60472
$K_2O_xCl_6$, sp. ht. meas. at low temp. 80−7119
KOD, mm wave spectrum, rot. transitions in excited vibr. states 77−3351
$K_2O_{5-x}Ga_2O_3.xFe_2O_3$, K ion cond. 78−83998
KOH, amorphous and aqueous soln., depolarised Rayleigh scatt., phonon-like excitations 77−81109
KOH, aq. soln., $H_5O_2^+$ and $H_3O_2^-$ IR vibr. freq. assignments 79−73916
KOH, aq. solns., laser induced breakdown 79−87530
KOH, aqueous solution, transport parameters for cation exchange membrane 78−64883
KOH, beam, formed at 300-800°C, electron elastic scatt. obs., species identification 80−14231
KOH, dissolution of Si, orientation effect 77−36674
KOH, electrolyte, using Mo disc electrode, anodic solution kinetics *(Russian)* 78−11523
KOH, electron collisions, integrated and momentum transfer cross sections, cond. integrals 79−41238
KOH gas-crystal system, isotopic equilibrium near phase transition points *(Russian)* 80−91697
KOH glass: tryptophan (tyrosine), γ-irrad., electron traps, stimulated luminesc. 78−11536
KOH, MHD plasma mol., pot. energy curves and dipole moment, bond lengths 78−71462
KOH, melt, preferential dissolution of Mg_2SiO_4, etching obs. 78−34513
KOH, mm wave spectrum, rot. transitions in excited vibr. states 77−3351
KOH, quadrupole hyperfine struct., Δ-level splitting, microwave spectra 77−88446
KOH solution, cleaning of epitaxial growth chamber appl. 78−64478
KOH, spectral interference in at. absorption spectroscopy in C tube atomiser and flames *(Japanese)* 79−48019
KOH-KO_2, phase diagram *(French)* 80−107177
KOH-O_2-N_2O-t-butane pulse radiolysis, kinetics of transient O compound form. meas. from Cherenkov emission 77−70321
KOH.xH_2O, pulse radiolysis, absorpt. spectra of electrons 79−16013
KO(K_2O)-TiO_2-P_2O_5, electrical resistivity *(Japanese)* 77−12719
K_2O−Na_2O-B_2O_3-SiO_2, glass character of elec. cond. 80−103516
$(K_2O)_x(SiO_2)_{1-x}$ glass, pure and with As_2O_3, Raman study of As 80−84733
$K_2O(WO_3)_n$, oxidation from K_2WO_3 bronze, struct. changes 78−68925
$K_2O.SiO_2$ glass, X-ray diffr. *(Japanese)* 80−19720
$(K_2O)_xTiO_2$ fibres, flux growth reactions 80−16171
$2K_2O.11TiO_2.3H_2O$ fibre+$Ba(OH)_2$ hydrothermal reaction to form $BaTiO_3$ fibres *(Japanese)* 80−93527
$K_2O.2GeO_2$, powder Raman spectra, compared with digermanosilicate glass 79−77524
$K_2O.2WO_3$ glasses, X-ray diffr. study of struct. *(Japanese)* 77−11489
$K_2O.4SiO_2$, glass, behaviour of VO^{2+} as spectroscopic probe 79−78510

potassium compounds continued
$K_2O.4TiO_2$, new fibrous phase 80−20917
$K_2O.5Ga_2O_3$, formation and ionic conductivity 77−4351
$K_2O.6Fe_2O_3$: divalent metal oxide, electronic and ionic cond. 79−87135
$K_2O.nB_2O_3$ (n=6, 4, 3), heat of soln. *(Japanese)* 77−77802
$K_2O.nWO_3$, n=4-20, X-ray diffr. 77−84726
K_2OsCl_6, Cl NQR spectra by Fourier transform methods 80−75879
K_2OsCl_6, displacive phase transition, thermal expansion meas. 78−10188
K_2OsCl_6, ferrorotative transition, neutron scatt. expt., consistency with displacive and order-disorder models 78−51673
K_2OsCl_6, impurity H^+ ion motion, ^{35}Cl NQR obs., 77 and 298K 80−60451
K_2OsCl_6, low temp. sp. ht. and thermodynamic props. near phase transition 77−39655
K_2OsCl_6 powder, spin-lattice relax., dynamic clustering near struct. transition 77−48079
K_2OsCl_6, radiation-induced lattice defects and solid-state reactions *(German)* 79−42101
K_2OsCl_6, single cryst. with H^+ interstitials, protonic cond. from dielec. meas. 80−107515
$KOsO_3N$, interatomic distances of statistically oriented OsO_3N^- by radial distrib. analysis 77−15365
KPF_6, γ-irrad., trapped free radicals EPR obs. 80−63683
KPF_6, static SIMS, mol. rearrangement, cluster formation 78−64440
KPF_6, temp. depend. hyperfine interactions of trapped pyramidal radicals 80−44918
KPF_6:AsF_6^-, γ-radiolysis, AsF_5^- form., ESR spectrum 77−16845
KPO_2, vitreous, microhardness 80−25864
KPO_3 crystal, P K-band X-ray emission spectra, state anal. 80−40190
KPO_3, He(I) photoelectron spectra, UTARC calc., assignments 79−72357
KPO_3, heat of melting and activities using cryoscopic data 77−40573
KPO_3-Fe_2O_3 glasses, γ-irrad., ESR 80−50182
KPO_3-$Pb(PO_3)_2$, phase diagram of binary system 77−21114
K_3PO_4 aq. solns., isomorphous salts viscosity investig. 78−95173
K_3PO_4 crystal, P K-band X-ray emission spectra, state anal. 80−40190
K_3PO_4, spectral interference in at. absorption spectroscopy in C tube atomiser and flames *(Japanese)* 79−48019
K_3PO_4-$M_3(PO_4)_2$, M=Ca, Sr, Ba, Zn, Cd, high temp. stabilisation of phases *(French)* 77−44235
$K_4P_2O_7$ crystal, P K-band X-ray emission spectra, state anal. 80−40190
KPO_3F, cryst. struct. *(French)* 80−19762
$K_2P_2O_5F_2$, cryst. struct. *(French)* 78−51501
$KPO_3.Al(PO_3)_3$:U, vibronic excitation, absorption and emission spectra 78−52524
$K_2PbCu(NO_2)_6$, antiferromagnetic Heisenberg linear spin 1/2 chain, mag. and caloric meas. 79−78397
$K_2PbCu(NO_2)_6$, effect of hydrostatic press. on successive Jahn-Teller phase transitions 78−43120
$K_2PbCu(NO_2)_6$, incommensurate Jahn-Teller transition, neutron scatt. meas. 77−69065
$K_2PbCu(NO_2)_6$, incommensurate Jahn-Teller phase transition 78−79730
$K_2PbCu(NO_2)_6$, incommensurate Jahn Teller phase transitions 79−95156
$K_2PbCu(NO_2)_6$, incommensurate Jahn-Teller transition, Hüang scatt. 80−70401
$K_2PbCu(NO_2)_6$, Jahn-Teller phase transitions, order-disorder model 78−79762
$K_2PbCu(NO_2)_6$ Jahn-Teller phase transitions, X-ray and neutron measurements 78−91438
$K_2PbCu(NO_2)_6$, phase transitions induced by Jahn-Teller effect, uniaxial stress effects 80−6512
$K_2PbCu(NO_2)_6$, phase transition obs., commensurate and incommensurate structural phase transitions in Jahn-Teller system 80−70403
$K_2PbCu(NO_2)_6$, US vel. near cooperative Jahn-Teller phase transitions 79−23680
$K_2PbCu(NO_2)_6$, uniaxial stress, EPR meas. 80−20455
$KPbI_3.2H_2O$, X-ray cryst. struct. determ. 80−64958
$K_2Pb(MoO_4)_2$, and isomorphs, domain struct. and phase transition *(Russian)* 78−6159
$K_2PbX(NO_2)_6$, (X=Cu, Ni), single cryst. growth in gel *(German)* 79−74076
$K_2Pb[Co(NO_2)_6]$, X-ray cryst. struct. determ. 80−88106
$K_2PdBr_4.2H_2O$, visible and UV absorpt. spectra, 10-295K 79−38572
K_2PdCl_4, visible and UV absorpt. spectra, 10-295K 79−38572
K_2PdCl_4:Cu^{2+}, meas. of covalency in tetragonal complexes 77−47781
$K_2Pd(SCN)_4$, visible and UV absorpt. spectra, 10-295K 79−38572
$K_5PrLi_2F_{10}$:Pr^{3+}, emission spectroscopy, ionic interaction 79−83015
$KPr(SO_4)_2$, X-ray cryst. struct. determ., least squares refinement 79−55725
K_2PtBr_4, visible and UV absorpt. spectra, 10-295K 79−38572
$K_{1.75}Pt(CN)_4 . 1.5H_2O$, quasi 1D metals, electric conductivity meas., semiconductor-metal transition 79−99538
$K_2Pt(CN)_4$, Peierls transition temp. and 0K energy gap, mean field theory calc. 80−24782
$K_2Pt(CN)_4$, quasi-one-dimens. Peierls system, phonon dispersion and neutron scatt., calc. 80−24550
$K_2Pt(CN)_4Br_{0.3}2.6H_2O$ crystal, quasi-one-dimensional, optical consts. and dielec. permittivity dispersion 77−1695
$K_2Pt(CN)_4Br_{0.3}3H_2O$ incommensurate linear conductors correlation length in 77−80745
$K_2Pt(CN)_4Br_{0.3}3.2H_2O$, linear conductor, dynamical aspects of fluctuations 79−33715
$K_2Pt(CN)_4Br_{0.3}3.2H_2O$, linear cond., ^{195}Pt NMR evidence of low lying non-linear excitation 80−44933
$K_2Pt(CN)_4Br_{0.3}×3H_2O$, struct., neutron determ., Peierls distortion 79−46640
$K_2Pt(CN)_4Br_{0.3}×3.2D_2O$, Kohn anomaly in longit. acoustic phonon 77−7812
$K_2Pt(CN)_4Br_{0.3}.2.7D_2O$, under hydrostatic press., compressibility, neutron diffr. 79−46742
$K_2Pt(CN)_4Br_{0.30}.3H_2O$, dynamic ^{195}Pt NMR meas. below metal-insulator transition 80−34810
$K_2Pt(CN)_4Br_{0.3}.3H_2O$, IR absorption peak theory 77−43991
$K_2Pt(CN)_4Br_{0.3}.3H_2O$, lattice softening, temp. depend. of elastic consts., US meas. 78−14432
$K_2Pt(CN)_4Br_{0.3}.3H_2O$, struct. rel. to quasi one-dimensional elec. props. 78−14716
$K_2Pt(CN)_4Br_{0.3}.3H_2O$, one-dimensional cond., phys. props. *(Japanese)* 78−30916
$K_2Pt(CN)_4Br_{0.3}.3H_2O$, one-dimens. cond., review 78−60070

potassium compounds continued
$K_2Pt(CN)_4Br_{0.3}.3H_2O$, one-dimens. cond. transition, spin suscept. and DC cond. temp. depends. 78−84198
$K_2Pt(CN)_4Br_{0.3}.3H_2O$, specific heat, 0.75 to 25.7K 78−87795
$K_2Pt(CN)_4Br_{0.3}.3H_2O$, specific heat and ferroelastic behaviour 78−91447
$K_2Pt(CN)_4Br_{0.3}.3H_2O$, Krogmann salt, non-empirical localised orbital cal. of electronic struct. 78−91636
$K_2Pt(CN)_4Br_{0.3}.3H_2O$, quasi-one-dimens. conductor, Br^- distrib. long-range Coulomb interaction, effect on structure and CDW 79−7591
$K_2Pt(CN)_4Br_{0.3}.3H_2O$, spin-lattice model for elastic anomalies 80−15179
$K_2Pt(CN)_4Br_{0.3}.3H_2O$, quasi one-dimens. conductor, EPR linewidth 80−54938
$K_2Pt(CN)_4Br_{0.3}.3H_2O$, CDW system, nonlinear amplitude-phase interaction 80−88490
$K_2Pt(CN_4)Br_{0.3}.3H_2O$, anisotropic radiation damage in electron microscopy, diffr. spot fading rate obs. 80−107329
$K_2Pt(CN)_4Br_{0.3}.3.2D_2O$ neutron→$_{0.3}.3.2D_2O$, neutronD_2O neutron scattering 78−10133
$K_2Pt(CN)_4Br_{0.3}.3.2D_2O$, lattice dynamics, neutron scatt. expts. 78−14412
$K_2Pt(CN)_4Br_{0.3}.3.2D_2O$, dynamic struct. factor, inelastic neutron scatt. study 79−42185
$K_2Pt(CN)_4Br_{0.3}.3.2H_2O$, deuterated, coupling of charge density wave and water mode 77−4646
$K_2Pt(CN)_4Br_{0.3}.3.2H_2O$, motion of Br^- ions, NMR 77−90051
$K_2Pt(CN)_4Br_{0.3}.xH_2O$, conductivity and optical refl. depend. on water content 77−39828
$K_2Pt(CN)_4Br_{0.3}.xH_2O$, one-dimensional cond., effects of dehydration on mag. props. 77−85549
$K_2Pt(CN)_4Br_{0.3}.xH_2O$, dynamical props. near Peierls instability, neutron scatt. 78−14436
$K_2Pt(CN)_4Cl_{0.3}(Br_{0.3}).3H_2O$, struct., single cryst. neutron diffr. expts. 78−14321
$K_2(Pt(CN_4))(FHF)_{0.3}.3H_2O$, struct. determ., X-ray diffr. exam. 78−63711
$K_2Pt(CN)_4X_{0.3}$, X=Cl,Br, electrochem. growth of highly conducting inorganic complexes 77−8739
$K_{1.75}Pt(CN)_4×1.5H_2O$, struct., neutron determ., Peierls distortion 79−46640
$K_{1.75}Pt(CN)_4.1.5H_2O$, electrochem. growth of highly conducting inorganic complexes 77−8739
$K_{1.75}(Pt(CN)_4).1.5H_2O$, 1-D cond., IR spectra 77−85703
$K_{1.75}Pt(CN)_4.1.5H_2O$, struct., single cryst. neutron diffr. expts. 78−14321
$K_{1.75}Pt(CN)_4.1.5H_2O$, Pt chain distortion, X-ray obs. 78−14322
$K_{1.75}Pt(CN)_4.1.5H_2O$, Raman scatt. and luminesc. studies 80−25394
$K_{1.6}Pt(C_2O_4)_2×1.2H_2O$, sinusoidally modulated structure 77−84730
$K_{1.6}Pt(C_2O_4)_2×1.2H_2O$, struct., neutron determ. 79−46640
$K_{1.62}Pt(C_2O_4)_2.2H_2O$, plasma resonance absorpt. from small particles 77−24841
K_2PtCl_4, far IR reflection spectra, assignments, effective ionic charges, force consts. 77−66488
K_2PtCl_4, visible and UV absorpt. spectra, 10-295K 79−38572
K_2PtCl_6, diamag. sp. ht. meas. at low temp. 80−7119
K_2PtCl_6, K_2ReCl_6, K_2SnCl_6, solid state phase transitions, lattice vibr., NMR and NQR obs. 80−34814
K_2PtCl_6, physical properties, application as lens or laser window materials 79−98450
K_2PtCl_6, radiation-induced lattice defects and solid-state reactions *(German)* 79−42101
K_2PtCl_6:Os^{4+}, multiple state luminesc. 78−72584
K_2PtCl_6:Os^{4+}, sharp line luminesc. band at 10K, vibr. assignment 78−95600
K_2PtCl_6:$ReBr_6^{2-}$, luminesc. spectra and relax. processes 78−68552
K_2PtCl_6:$ReCl_6^{2-}$, luminesc. and absorpt. spectra, relax. processes 77−85779
K_2PtI_5, synthesis and cryst. struct. *(German)* 78−79588
$K_{1.64}Pt(O_2C_2O_2)_2.2H_2O$, electrochem. growth of highly conducting inorganic complexes 77−8739
$K_2Pt(SCN)_4$, visible and UV absorpt. spectra, 10-295K 79−38572
$KR(PO_3)_4$, R=Ho, Nd, Bi, Sm, Dy, Eu, cryst. struct. 77−43188
$KR(SO_4)_2$, R=La to Tb, unit cell parameters, thermal stability and decomposition 78−18613
KRb^+, adiabatic pot. curves, ground and excited state, Hellmann-type model pots. 78−78647
$K_{1-x}Rb_xBr$, lattice dynamics on pseudo-crystal model 78−75762
$K_{1-c}Rb_cCl$, impurity centre local vibrs., comp. depend. of spectral parameters 80−79898
$K_{1-x}Rb_xCl$:HF_2^-, dynamic inhomogeneous broadening of bands of local vibr. 78−92102
$K_xRb_{1-x}Cl$:HF_2^-,SO_4^{2-}, nonuniform broadening of IR vibr. absorpt. bands of impurities *(Russian)* 77−16357
$K_xRb_{1-x}Cl_yBr_{1-y}$, far IR absorption spectra 79−33695
$K_xRb_{1-x}Cl_yBr_{1-y}$, IR reflection spectra 78−76474
$K_xRb_{1-x}HF_2$, nuclear spin-lattice relax. and internal motion mechanism 79−99787
$K_{0.5}Rb_{0.5}I$, mixed cryst., phonons, neutron scatt. 77−1192
$K_xRb_{1-x}I$, Debye temp. conc. depend. 79−90746
$K_xRb_{1-x}TiOPO_4$, new nonlinear optical material 77−14784
K_2ReBr_6, radiation-induced lattice defects and solid-state reactions *(German)* 79−42101
K_2ReCl_5, sp. ht. meas. at low temp. 80−7119
K_2ReCl_6, displacive phase transition, thermal expansion meas. 78−10188
K_2ReCl_6, elastic constants, softening of acoustic modes, obs. by Brillouin scattering 80−71440
K_2ReCl_6, low temp. sp. ht. and thermodynamic props. near phase transition 77−39655
K_2ReCl_6, radiation-induced lattice defects and solid-state reactions *(German)* 79−42101
K_2ReCl_6, struct. props. and lattice dynamics, mag. struct. 80−44268
K_2ReCl_6, structural phase transition, soft rotary mode, obs. by triple-axis neutron scatt. 79−1483
K_2ReCl_6, thermal expansion meas. near antiferromag. transition 77−20610
K_2ReCl_6, thermodynamic relations at solid state phase transitions 80−29164
K_2ReCl_6-K_2ReBr_2 solid soln., mixed ligand complexes 77−72585
K_2ReF_6, cryst. struct. 78−42971
$KReO_4$, heat capacity and thermodynamic props., 8 to 304K 80−100335
$KReO_4$, matrix isolated, IR spectra 80−28012

potassium compounds continued
$KReO_4$, NQR and thermal expansion 77−20745
$KReO_4$, nuclear electric hexadecapole interactions 80−65513
$KReO_4$, of ^{187}Re 79−1722
$KReO_4$, quadrupole coupling, cation electric field gradients 78−35060
$KReO_4$, quadrupole spin echo with two-frequency action, amplification and modulation 80−108116
$KReO_4$, vibr. spectrum, Raman and IR spectra obs. 80−55104
$K_2(RuCl_4NO)$, polarised Raman and IR spectra, vibr. anal. 77−69819
K_2S-Al_2S_3, prep., phase props. and elec. cond. 79−96010
KSCN, diamag. ion solvation in methanol soln., NMR relax. obs. 78−56389
KSCN, molten, precipitation reaction of UO_2^{++} 80−26040
K_2SO_3-Ag_2SO_4 mixtures, surface comp., AES and XPS obs. 80−81386
K_2SO_4, anhydrous, struct. relationships w.r.t. fast ion cond. 80−107188
K_2SO_4 aq. solns., isomorphous salts viscosity investig. 78−95173
K_2SO_4 aqueous solutions, differential diffusion coeffs. determ. diaphragm cell method 79−95193
K_2SO_4, α-β phase transition, Raman scatt. study *(French)* 80−55096
K_2SO_4, continuous multi-particle crystal growth in vertical cone 77−69978
K_2SO_4 crystals, surface nucleation, method for determining kinetic parameters 79−46980
K_2SO_4, D_{2h}^{16} and C_{2v}^{9} phases, internal and external vibrs., Raman spectra obs. 79−47446
K_2SO_4, displacive solid-state transformations meas., DTA method 80−218
K_2SO_4, effusion studies of vaporisation/decomposition 79−95153
K_2SO_4, electrostatic lattice energy, optimisation of convergence of Ewald series 79−7569
K_2SO_4, growth rate characts. in fluidised bed crystalliser 79−19164
K_2SO_4, hexagonal-orthorhombic phase transition, ferroelasticity 78−2251
K_2SO_4, high temp. form, X-ray struct. redeterm. 80−54179
K_2SO_4, IR absorpt. spectra, polymorphism, site group approx. and SO_4 stretching mode 78−52510
K_2SO_4, IR and Raman spectra of vap. over heated matrices 78−25525
K_2SO_4, in dioxane-water mixtures, ion-solvent interaction and conductance 79−34315
K_2SO_4, ionic equil., mass spectra obs., heats of reaction and form. of ions 79−87867
K_2SO_4, kinetics of crystn. from soln., activities, interfacial energy and solubility 77−76340
K_2SO_4, longitudinal-acoustic soft mode in phase transition 80−75326
K_2SO_4, mass spectrum obs. of vaporisation, vapour comp. and press., transition and form. heats 80−19933
K_2SO_4 molecules isolated in inert gas matrices, low freq. IR spectra 78−50547
K_2SO_4, molten, struct. analysis using X-ray scatt., correl. with cryst. struct. 80−10486
K_2SO_4, molten, treated MgO, effect on phys. and chem. props. *(Japanese)* 79−57133
K_2SO_4, phase transform., mech. of thermal hysteresis, DTA, dilatometry and dielec. meas. 80−75353
K_2SO_4 powder, IR photothermal radiometry absorption spectra, 295-942K 80−26088
K_2SO_4, solid-state detector for potentiometric determ. of SO_2 in air 78−16151
K_2SO_4 solid-state detector for potentiometric determ. of SO_2 in O_2-variable gases 78−20505
K_2SO_4, solution, dielectric relaxation studies 78−84519
K_2SO_4 solution, thermodynamic driving force, for crystallisation at 298K 79−37643
α-K_2SO_4, space group and cryst. struct., X-ray powder anal. 79−4275
K_2SO_4, sulphate ion optical and spectroscopic props., cryst. environment effect 77−40224
K_2SO_4, thermal phase transition 80−19738
β-K_2SO_4 type crystals, structural transitions 80−75349
K_2SO_4, vaporisation thermodynamics, MHD generation appls. 77−9112
K_2SO_4, X-ray L-emission spectra of S *(Japanese)* 78−15254
K_2SO_4:$(NH_4)SO_4$, X-irrad., EPR of NH_3^+ 80−11272
K_2SO_4:MnO_4^{2-}, electronic struct. by ESR 80−44906
β-K_2SO_4:Tl^{2+}, ESR spectra theory 78−23323
K_2SO_4:VO^{2+} polycryst., struct., EPR 78−15014
K_2SO_4:XO_4^{2-}, X=Cr, Se, Mo, W, lattice-impurity interactions, IR spectra 78−19522
K_2SO_4-Ag_2S mixtures, surface comp., AES and XPS obs. 80−81386
K_2SO_4-Cs_2SO_4-MoO_3 system, fusibility diagram 79−87619
K_2SO_4-$ZnSO_4$ glass, transition metal ion doped, visible spectra 79−51990
K_2SO_4-$ZnSO_4$ system, glass formation and phase diagram study, physical props. 78−27500
K_2SO_4-$ZnSO_4$:Cu II, glass, O basicity, ESR study 78−80199
$K_2S_2O_7$ as flux material for transition metal oxide cryst. growth 80−71582
$K_2S_2O_8$, thermal transitions, catalytic effects of CuO and ZnO 79−15983
$K_2S_3O_6$, X-ray cryst. struct. redeterm. 79−99126
$K_2S_4O_6$, X-ray cryst. struct. determ. 79−99127
KSO_3F, disordered cryst., IR and Raman spectra, internal modes assignment, space group *(French)* 79−95742
$K_2SO_4.Al_2(SO_4)_3.24H_2O$, stirring effect on crystalline quality of soln. grown crystals 78−91281
$K_2SO_4.Al_2(SO_4)_3.24H_2O$:$Cr_2O_7^{2-}$, optical absorpt. spectra, mol. orbital calcs. 79−15491
K_2Sb photocathodes, prep. and props. 78−84693
K_3Sb, and Na_2KSb, photocathode materials, band struct., empirical pseudopotential calc. 78−10346
K_3Sb, optical and dielectric props., energy spectra, density of states calcs. 80−20083
$K_2SbNb_5O_{15}$, dielec. and pyroelec. props. 79−99841
$KSbO_3$, cubic, K^+ ion ordering, electron microscopy 78−79550
$K_4Sb_2O_7$, solid state synthesis *(French)* 80−104438
$KSbO_3$.1/6KF, dielec. spectroscopy study, 100 Hz to 10 MHz, 238 to 417K *(German)* 80−108144
$K_{0.51}Sb_{0.67}^{III}Sb_2^{V}O_{6.26}$, pyrochlore, cryst. struct. *(French)* 78−34470
$KSbSe_2$, cryst. struct. 77−43184
$KSc(MoO_4)_2$, quadrupole interaction const., influence of phase transition, NMR meas. 77−16206
$KSc(MoO_4)_2$, soft modes and Raman spectrum at ferroelastic phase transitions 79−47450
$KSc(MoO_4)_2$:Gd^{3+}, hyperfine struct. of ESR spectrum 77−8399

potassium compounds continued
$KScO_2$-MO_2, M=Zr, Hf, Sn, Pb, ionic cond., lamellar struct. *(French)* 77−1257
$K_4Sc_2(OH)_2Si_4O_{12}$, crystal struct., X-ray diffr. study 80−79763
K_2SeBr_6, rotational phase transitions, cryst. struct., X-ray diffr. study 80−70400
K_2SeO_4, 1D displacive modulation, struct. using superspace-group concept 80−79726
K_2SeO_4, anharmonic phonons and central peaks at struct. phase transitions 79−95775
K_2SeO_4, aq. solns., isomorphous salts viscosity investig. 78−95173
K_2SeO_4, Brillouin scatt. at paraelectric-incommensurate phase transition, hypersonic waves 79−78690
K_2SeO_4, cryst. with modulated struct., neutron scatt. obs. 79−95713
K_2SeO_4, dielec. dispersion, 5-900 MHz, near incommensurate-commensurate transition 80−60522
K_2SeO_4, elastic compliance anomalies 80−45010
K_2SeO_4, elastic props. at commensurate-incommensurate transition, Brillouin scatt. and US study 80−93248
K_2SeO_4, ferrielectricity, triple 60 Hz D-E hysteresis loops 80−71364
K_2SeO_4, ferroelec., incommensurate struct., dynamic props. *(Russian)* 80−11373
K_2SeO_4, hexagonal-orthorhombic phase transition, ferroelasticity 78−2251
K_2SeO_4, hexagonal-orthorhombic transition, Brillouin scatt. study 80−97208
K_2SeO_4, improper ferroelec., struct., phase transform. and lattice instability neutron scatt. meas. 77−63379
K_2SeO_4, improved Raman spectra at room temp. 78−56487
K_2SeO_4, incommensurate modulation along axis perpendicular to x-axis 78−6154
K_2SeO_4, incommensurate phase transition, stress depend. of T_c 79−4391
K_2SeO_4, incommensurate phase transitions under existence of Lifshitz invariant 79−15416
K_2SeO_4, incommensurate structure, IR and Raman activity of soft mode 79−28738
K_2SeO_4, incommensurate lattice instability, ferroelec. transition, neutron scatt. study 79−42210
K_2SeO_4, incommensurate and ferroelec., far IR and mm dielectric response 79−73955
K_2SeO_4, incommensurate phase transition, Raman scatt. 79−95739
K_2SeO_4, incommensurate to ferroelec. transition, hydrostatic press. effects, neutron scatt. study 80−108166
K_2SeO_4, induction of incommensurate condensations of hard modes by incommensurate condensation of soft modes 78−55931
K_2SeO_4, lattice dynamics, displacive phase transform. 80−39248
K_2SeO_4, lower freq. soft-mode in ferroelec. phase 77−81065
K_2SeO_4, non-zero wave vector incommensurate soft mode, light scatt. study 80−29754
K_2SeO_4, phase mode in incommensurate phase, Raman scatt. obs. 80−80766
K_2SeO_4, phenomenological theory of transition sequence 77−76546
K_2SeO_4, Raman scatt. and dielec. props. 80−11313
K_2SeO_4, Raman scattering spectra and discovery of soft mode 78−76442
K_2SeO_4, Raman spectra, 77-300K *(Japanese)* 77−43988
K_2SeO_4, Raman spectra, effects of temp., substitutional cations, and stress 80−71405
K_2SeO_4, SHG, hexagonal phase centrosymmetry 79−37684
K_2SeO_4, single cryst., orthorhombic, Raman spectra 77−73140
K_2SeO_4, soft modes below incommensurate transition Raman and Brillouin scatt. meas. 79−91387
K_2SeO_4, structural transition, polarised Raman spectra 80−75349
K_2SeO_4, symmetry determ. of commensurate and incommensurate phases by EPR of γ-irrad. crysts. 79−78525
K_2SeO_4, thermal expansion, phase transitions, 77-190K 77−16263
K_2SeO_4, ultrasonic study in temp. range of incommensurate phase transform. 80−88276
K_2SeO_4, unpolarised-noncommensurate-polarised phase transition, phenomenological theory 79−15422
K_2SiF_6, A=Si, Ge, Sn, IR absorpt. spectra, integrated intensity 79−73944
K_2SiO_3 aqueous soln., ^{29}Si NMR expts. 78−15051
$K_2Si_4O_9$, phase diagram and thermodynamic props. 79−91985
K_3SmF_6 pressure-temp. phase diagram to 35 kbar and 900°C 77−15575
$KSm(MoO_4)_2$, polymorphism investig. by X-ray diffr. and DTA 77−4091
$KSnBr_6$:$ReBr_6^{2-}$, vibronic transition $\Gamma_7(^2T_{2g})\rightarrow\Gamma_8(^4A_{2g})$, intensity distrib. 80−45142
K_2SnBr_6, radiation-induced lattice defects and solid-state reactions *(German)* 79−42101
K_2SnBr_6, transform. dynamics probed by Raman scatt. and microscopy 78−63832
$KSnCl_6$:$ReBr_6^{2-}$, vibronic transition $\Gamma_7(^2T_{2g})\rightarrow\Gamma_8(^4A_{2g})$, intensity distrib. 80−45142
K_2SnCl_6, elastic consts., inelastic neutron scatt. and US meas. 80−59553
K_2SnCl_6, elastic constants, softening of acoustic modes, obs. by Brillouin scattering 80−71440
K_2SnCl_6, high-tem=. phase, X-ray investigation 80−24409
K_2SnCl_6, phase instabilities and mode softening X-ray and neutron diffr. 77−7830
K_2SnCl_6, phase-transition-induced dipolar relax. 80−66107
K_2SnCl_6, photoacoustic detection of phase transitions 78−75810
K_2SnCl_6, radiation-induced lattice defects and solid-state reactions *(German)* 79−42101
K_2SnCl_6, structural phase transitions, Raman spectra 77−73143
K_2SnCl_6, structural phase transition exam. by neutron powder diffr. 78−55940
K_2SnCl_6:$ReBr_6^{2-}$, luminesc. spectra and relax. processes 78−68552
K_2SnCl_6:$ReCl_6^{2-}$, luminesc. and absorpt. spectra, relax. processes 77−85779
$K_2SnCl_6(Br_6)$, low temp. vibr. spectra, lattice dynamics and phase transitions 79−73917
K_2SnF_6, A=Si, Ge, Sn, IR absorpt. spectra, integrated intensity 79−73944
K_2SnF_6, Group IV hexafluoride anion radical γ-irrad., EPR spectra 78−72411
$K_2SnF_6.H_2O$, cryst. struct., Fedorov space group 77−89422
$K_2SnF_6.H_2O$, crystallographic characts. *(French)* 78−10011
$K_2SnF_6.4HF$, cryst., H bond geometry, NMR obs. 79−42844
$K_2SnF_6.4HF$, molecular diffusion, spatial symmetry, HF molecule arrangement 79−42313

potassium compounds continued
$K_2Sn(NH_2)_6$, cryst. struct. determ. *(French)* 77−47384
$K_2Sr(CO_3)_2$, phase diagrams, evidence of new compound *(French)* 78−95033
$KSr(NH_2)_3$, cryst. struct. and cryst. chemistry *(German)* 79−51080
K(TCNQ), electronic absorpt. spectra, vibronic struct., charge transfer bands 79−24331
K(TCNQ), Raman spectra from 30 to 2300 cm^{-1} 80−11392
K^+TCNQ^-, cryst. struct. above and below 122°C transition 77−35541
K^+TCNQ^-, optical absorpt. spectra of small particles 78−19505
K^+TCNQ^-, spin polarised band struct., effective Coulomb repulsion 77−15734
$K(Ta,Nb)O_3$ ceramic, prep. and electro-optical props. 80−25620
$K_{10}(Ta_8.O_{21})_2.Ta_8X_4O_{26}$, X=Si, Ge, cryst. struct. *(French)* 77−76378
$K_3Ta_3B_2O_{12}$, pentagonal tunnel struct. *(French)* 77−58985
$K_{12}Ta_{15.5}F_{18.5}O_{35.5}$, X-ray cryst. struct. determ. 80−15059
$K_2Ta_4F_4O_9$, single cryst. X-ray struct. determ. *(French)* 79−99129
$K_3Ta_4F_7O_8$, X-ray cryst. struct. determ. 80−39018
$KTa_{0.65}Nb_{0.35}O_3$, ferroelectric devices for optical systems 78−90473
$KTa_{0.7}Nb_{0.3}O_3$, pressure-induced resistance and colour change obs. 80−75608
$KTa_{0.9}Nb_{0.1}O_3$, ferroelec. , dipolar behaviour, crit. exponent of dielec. const. 77−4604
$KTa_{1-x}Nb_xO_3$ film, RF sputtering, structural and electrical properties obs. 78−88426
$KTa_{1-x}Nb_xO_3$, holographic storage using photorefractive effect, dielectric const. 80−78800
$KTa_{1-x}Nb_xO_3$, local polarisability in quantum paraelec. and quantum ferroelec. phases 78−64325
$KTa_{1-x}Nb_xO_3$, paraelectric phase, defect induced fluctuations, Raman meas. 79−15423
$KTa_{1-x}Nb_xO_3$, quantum limit of ferroelec. transitions, dielec. and elastic consts. meas. 78−15128
$KTa_{1-x}Nb_xO_3$ quantum ferroelectric, dielec. susceptibility 80−103922
$KTa_{1-x}Nb_xO_3:Fe^{3+}$ ($0 \leq x \leq 0.16$), ferroelec., EPR meas. *(French)* 79−11337
$KTa_{1-y}Nb_yO_3$, quantum ferroelec., elastic compliance, impurity effects 79−99835
$KTa_xNb_{1-x}O_3$, ferroelectric transition, US attenuation, elastic consts., soft modes 78−23411
$KTaO_2$, electronic density of states calc. for perovskite struct. cryst. 77−76720
N-$KTaO_2$, light and heavy cond. electrons at zone centre 79−73426
$KTaO_3$, complex electronic dielectric const. from tight binding energy bands 78−60054
$KTaO_3$, complex refr. index meas. in far IR, by dispersive Fourier transform spectroscopy 78−92042
$KTaO_3$, crit. dielec. and optical props. and storage, 4K 77−24805
$KTaO_3$ crystals, nonlinear optical phenomena, expt. *(Japanese)* 77−38990
$KTaO_3$, defect struct. and elec. props. 78−91695
$KTaO_3$, depletion region and donor levels determ., appl. in surface barrier volume wave transducer 80−33403
$KTaO_3$, dielec. nonlinearity and parametric interactions at low temps. 79−38430
$KTaO_3$, dielec. response temp. depend. meas., dispersive Fourier transform spectroscopy 79−15449
$KTaO_3$, electrocaloric effect for refrigeration at cryogenic temp. 80−77789
$KTaO_3$, electromech. props. and electron tunnelling 78−23403
$KTaO_3$, electronic props., SCF-MS-Xα calc. 80−54607
$KTaO_3$, electronic struct., XPS and band struct. calc. 79−38708
$KTaO_3$, ferroelec., local field determ., phase transition study by EPR 79−38471
$KTaO_3$, field depend. sp. ht. and soft modes at low temps. 79−8105
$KTaO_3$, freq. depend. of soft mode self-energy, for IR dielec. response meas. 79−33632
$KTaO_3$ glass, quenched, ionic cond., appl. as solid electrolyte 79−1522
$KTaO_3$, incipient ferroelectric, mode-mode coupling 78−79717
$KTaO_3$, light-sensitive surface-barrier generation of acoustic vol. waves 78−63252
$KTaO_3$, mode anharmonic self energies, freq. depend. 78−59908
$KTaO_3$, nonpiezoelec. dielec., light-sensitive Rayleigh wave generation by surface piezoelectricity 78−43228
$KTaO_3$, photoconducting, negative differential conductivity 79−65515
$KTaO_3$, photoconduction in ferroelectrics 78−91720
$KTaO_3$, polarisation, dielectric. const., relax. effects, electret state 77−12302
$KTaO_3$ pseudodisplacive ferroelec., temp.-dependent dielectric response obs. 77−40247
$KTaO_3$, pure and Gd_2O_3 doped, elec. cond. and sp. ht. 79−78097
$KTaO_3$, quantum magnetoresist. results, using pulsed fields up to 35 T 79−73528
$KTaO_3$, Raman scatt. and ferroelec. soft modes 77−16300
$KTaO_3$, Rayleigh wave generation by surface piezoelectricity 78−71925
$KTaO_3$, SHG and quadratic electrooptic effect 78−76429
$KTaO_3$, second harmonic generation, bond charge theory 78−76395
$KTaO_3$, Shubnikov-de Haas effect, cond. band struct. 80−10875
$KTaO_3$, single crystal, for electrocaloric refrigeration, 4 to 15K 79−80624
$KTaO_3$, sp. ht. and electrocaloric props. at low temps. 77−84945
$KTaO_3$, stress-induced ferroelectricity, Raman scatt. obs. 77−40190
$KTaO_3:Fe^{3+}$, EPR, elec. field effect, local fields *(Russian)* 79−8048
$KTaO_3:Fe^{3+}$ local phase transition, EPR line temp. broadening *(Russian)* 80−54944
$KTaO_3$:Gd semicond., temp. depend. of thermal diffusivity and Seebeck coeff. 78−10481
$KTaO_3:Gd^+$, influence of external elec. field on EPR 78−15020
$KTaO_3$:Li, ferroelec. transition and atomic motions, ^7Li NMR study 80−75872
$KTaO_3$:Li, polarised cluster stabilisation by Li defects, polar glass form. 79−91342
$KTaO_3$:Li, susceptibility extrinsic peak, dielectric const. meas. 79−11394
$KTaO_3$:Li(Na)(Nb), microscopic distortions in paraelec. phase 78−75793
$KTaO_3:OH^-(OD^-)(OT^-)$, IR spectra, spectrosc. consts. 80−100671
$KTaO_3:Ti^{3+}$, EPR meas. 78−35028
$KTaO_3$-metal contact, surface barrier Rayleigh wave transducer 79−98578
KTa_5O_{13} structure, relationship to α-PbO_2 struct., crystallography data 78−42996
potassium compounds continued
$K_{4+5x}Ta_{16-x}O_{42}$, (x=0.3), cryst. struct. 79−90611
$K_6Ta_{10.8}O_{30}$, cryst. struct., X-ray diffr. and electron microprobe meas. 78−34489
$K_2Ta_2O_3F_6$, Marignac's salt, X-ray diffr. study of cryst. struct. 77−89417
$K_2Ta_4O_9F_4$, NMR meas. on ^{19}F, localisation of F^- ions *(French)* 79−77579
$K_6Ta_{6.5}O_{14.5}F_{9.5}$, X-ray cryst. struct. determ. and refinement 79−42029
$K_{0.33}TaS_2$, supercond. props., alkali cation and topotactic solvation influences 79−87180
$K_8Ta_{14}Si_4O_{47}$, struct. determ. *(French)* 77−27866
$K_{1+x}Ta_{1+x}W_{1-x}O_6$ pyrochlore system, comp. depend. of ionic cond. 80−107517
$KTaWO_6.H_2O$, pyrochlore struct. and its relatives 79−14773
$K_{1-x}Ta_{1-x}W_{1-x}O_6.nH_2O$, composition, struct. and ionic conductivity 80−49410
KTb_3F_{10}, cubic packing of $[Tb_3F_{32}]^{14-}$ polyanions, X-ray diffr. obs. 78−10023
KTb_3F_{10}, Faraday rotation, optical absorpt. spectra and refr. index 78−72542
KTb_3F_{10}, mag., optical, magneto-optical behaviour 78−68484
$K_2(TeBr_6)$, far IR and Raman spectra and phase transitions 80−11376
K_2TeCl_6, cryst. data from Guinier powder diagrams *(German)* 80−79751
$K_2(TeCl_6)$, IR and Raman spectra, lattice and internal modes, phase transition 78−6659
$K_2TeCl_6(Br_6)$, low temp. vibr. spectra, lattice dynamics and phase transitions 79−73917
K_2TeO_3, D_2O soln., $^{123,125}Te$ Fourier transform NMR 78−15046
$K_2TeO_3.3H_2O$, X-ray cryst. struct. determ. 78−95017
$K_2Te^{IV}Te^{VI}O_{12}$, cryst. struct., Te IV pentacoordination by O 78−63704
$K_2Te^{IV}Te_3^{VI}O_{12}$, mixed tellurate, cryst. chem. and elec. cond. *(French)* 80−107150
$KTh_2(VO_4)_3$, X-ray cryst. struct. determ., Fourier and Patterson method 80−19757
$KTiF_4$, struct. phase transitions obs. by dielec. const. and X-ray diffr. studies 79−95161
$KTiF_4$, X-ray cryst. struct. determ. and refinement *(French)* 79−69068
K_2TiF_6, anion motion and phase transition, NMR spectra 79−99788
K_2TiF_6, in LiCl-KCl eutectic mixture, analysis of reduction waves of Ti ion in chronopotentiometry *(Japanese)* 78−20025
$K_{1-x}(Ti_{1-x}M_{1+x})O_5$, M=Nb, Ta, layer compound, cryst. struct., nonstoichiometry 80−64972
$KTiMO_5$(M=Ta, Nb), ion exchange props., synthesis and crystallographic props. *(French)* 80−28997
K_2TiO_3 fibres, use for anatase fibres synthesis, hydrothermal leaching *(Japanese)* 79−56949
$K_2Ti_3O_7$ fibres, synthesis by kneading, drying, calcination process *(Japanese)* 79−38779
$K_2Ti_4O_9$, preparation, cryst. struct. determ. 78−75646
$K_2Ti_6O_{13}$, crystallographic study 77−72601
$K_2Ti_6O_{13}$ fibre synthesis from melt reaction of TiO_2 and K_2CO_3 *(Japanese)* 78−44070
$K_2Ti_6O_{13}$ fibres, synthesis by the hydrothermal dehydration method 79−43121
$KTiOPO_4$, freq. doubling material for Nd lasers 78−71173
$KTiOPO_4$, nonlinear optical props., freq. doubling of 1.06 μm laser radiation 78−42386
KTi_3SbO_9, X-ray cryst. struct. determ. *(French)* 80−107178
K_xTiSe_2, intercalation cpd., struct. and phase limits *(French)* 77−35536
$KTi_2Ta_5O_{17}$, chemically twinned rutile struct., X-ray study 80−107149
$K_{2.64}Tl_{2.36}Fe_3O(SO_4)_6.5H_2O$, X-ray cryst. struct. determ. 80−92483
$KTl(SeO_4)_2$, $K_3Tl(SeO_4)_3$, and $K_5Tl(SeO_4)_4$, cryst. struct. *(French)* 80−84148
$KTl[Fe(CN)_6]$, isomer shift of Mossbauer spectra 80−29662
$K_{0.5}Tm_{0.5}Nb_2O_6$, ^{93}Nb NQR spectra, 77 to 450K 79−38401
K_2UF_6, X-ray photoelectron spectra 77−32491
KUO_3, EPR and mag. susceptibility, temp. depend. 79−33451
$K_3UO_2Br_4$, force consts., IR spectra 78−5216
$K_2UO_2Cl_4$, fluoresc. decay rate of pure and impure cryst. 79−47487
$K_2UO_2Cl_4$ melts and mixtures, thermogravimetric determ. of uranyl cation state 80−101050
$K_3UO_2F_5$, normal coordinate anal. 79−22596
$K_5(UO_2)F_9$, optical spectra, vibr. freqs. calcs. *(Russian)* 78−31205
$K_3(UO_2)_2F_7.2H_2O$, single cryst., polarised Raman spectra, vibr. modes assignment *(French)* 80−29728
$K_2(UO_2)_3F_8.4H_2O$ and $K_3(UO_2)_2F_7.2H_2O$, IR and Raman vibr. spectra *(French)* 79−51937
$K_2UO_2(HPO_3)_2$, synthesis and comp. 80−35516
$KUO_2(NO_3)_3$, fluoresc. decay rates, temp. depend. 80−25429
$K_2UO_2(NO_3)_4$, fluoresc. decay rates, temp. depend. 80−25429
$K_2(UO_2)_4O_2(OH)_2Br_4(H_2O)_6$, cryst. data 77−76366
$K_2(UO_2)_4O_2(OH)_2Cl_4(H_2O)_6$, cryst. data 77−76366
$K_2(UO_2)_4O_2(OH)_2Cl_4(H_2O)_6$, tetranuclear complex, struct. determ. *(French)* 77−80451
$K_6(V_2,Mo_{10})VO_{40}.13H_2O$, X-ray cryst. struct., electron spin resonance spectrum 80−88096
KVF_3, antiferromag. ordering points, thermal anal. and X-ray diffr. meas. *(French)* 78−84421
KVF_4, struct. phase transitions obs. by dielec. const. and X-ray diffr. studies 79−95161
$K_2V_3F_{14}$, ferrimagnetic props., ordering temp. and anisotropy *(French)* 77−47990
K_xVF_3 (x=0.25,0.19), cryst. struct. examination by electron diffr. using TEM 79−23583
K_xVF_3 (x=0.45 to 0.56), non-stoichiometric, struct. depend. on composition 79−99152
α-K_xVF_3, mag. props. *(French)* 77−80933
KVO_3, cryst. struct. 78−6043
$KVO_3:Cr^{3+}$, study of ESR spectra 80−80601
β-$K_{0.27}V_2O_5$, heat of form. and sp. ht., 450 to 900K 80−61129
$K_{1.8}V_8O_{16}$, hollandite-type struct., synthesis and cryst. struct. 80−29003
$K_2V_8O_{16}$, Hollandite type compound, synthesis, struct. and magnetic props. 79−11543
$K_2V_8O_{16}$, hollandite-type struct., synthesis and cryst. struct. 80−29003
$K_xV_{12}O_{30}$, oxygen bronze synthesis and thermal props. of single crysts. 77−84717
$K_{0.26}WO_3$, single cryst. X-ray and powder neutron diffr. studies 80−29001
$K_{0.27}WO_{(3+y)}$, struct. analysis 77−11510

potassium compounds continued
$K_{0.33}WO_3$, hexagonal, phonon dispersion curves, neutron scatt. obs. 78−14411
$K_{0.33}WO_3$, supercond. and special phonons, neutron scatt. obs. 80−15643
K_2WO_4, hysteresis of phase transitions and modulated structures 80−29169
K_2WO_4, liq. mixture, mixing enthalpy with WO_3 at 950°C 79−10949
$K_2W_3O_{10}$, thermal expansion, X-ray diffr. obs. 77−43353
$K_2W_4O_{13}$, twinned crystal, X-ray cryst. struct. determ. 79−7588
K_xWO_3, atom motion 78−75874
K_2WO_3, x=0.20 and 0.32, hexagonal W bronzes, X-ray cryst. struct. refinement 79−77577
$K_xWO_{(3+y)}$, direct imaging of ordering 77−11511
$K_3WO_3F_3$, ferroelec., transition obs. 80−75989
$K_3WO_3F_3$, ferroelec. and order-disorder phase transitions 78−92037
K_2WS_4, electronic struct., XPS and X-ray emission spectra 77−42336
KX, (X=F, Cl, Br), photoelectron spectra using Zr $M\zeta$, Al $K\alpha$ and other X-ray lines, photoionis. cross sections ratios 77−90246
$KX:SO_4^{2-}$, X=Cl,Br, impurity ion IR spectra analysis *(Russian)* 77−85762
$KX:Tl^{2+}$, (X=Br, Cl, I), F-centres energy levels change 79−65075
KXe, dye laser induced emission, excimer bands and uses 80−9650
KXe, fluoresc. excitation and emission spectrum 79−6947
KXe_n exciplexes (n=1-4), visible emission bands 78−78746
KYF_4, KY_2F_7, KY_3F_{10}, Er^{3+} and Yb^{3+} doped, IR excitation curves for visible luminesc. 79−33795
$KY_3F_{10}:Eu^{2+}$, luminescence 79−78746
$KY_3F_{10}:Eu^{3+}$, cryst. field parameters and intensity parameters, J-mixing effects 80−59932
$KY_3F_{10}:Eu^{3+}$, crystal field and spin-orbit parameters 78−30892
$KY_3F_{10}:Eu^{3+}$, fluoresc. intensity, 77 to 4K, cryst. field parameters of Eu^{3+} 78−72580
$KY_3F_{10}:Eu^{3+}$, fluoresc. decay, radiative and nonradiative transition probabilities 78−72581
K_1YF_6, pressure-temp. phase diagram to 35 kbar and 900°C 77−15575
$KY(WO_4)_2:Er^{3+}$, stimulated emission at 300K 80−34951
$KY(WO_4)_2:Ho^{3+}$, 3 μ stimulated emission at 300K 80−20667
$KY(WO_4)_2:Ho^{3+}$, stimulated emission at low temps. 80−106526
$KY(WO_4)_2:R^{3+}$, stimulated emission 78−23496
β-KYb_3F_{10}, cryst. struct. *(French)* 77−15350
$KYbHP_3O_{10}$, thermal decomp., thermogravimetric and X-ray obs. 80−101013
$K_3Yb(SO_4)_3$, X-ray cryst. struct. determ. 79−65058
K(Zn,Mn,Co)F_3, crysts., Mn, Co distrib., as function of cryst. region *(German)* 78−14375
$K_2Zn_3Be_2(SiO_4)(Si_2O_7)$, cryst. struct. determ. 80−88121
$K_2Zn(CN)_4$, third order elastic consts. 80−84231
$K_2(Zn(CN)_4)$, vibr. spectra, isotope substitutions, force consts. determ. *(German)* 77−61750
K_2ZnCl_4, ^{35}Cl NQR study of incommensurate phase transition 80−60450
K_2ZnCl_4, cryst. with modulated struct., neutron scatt. obs. 79−95713
K_2ZnCl_4, ferrielectricity, triple 60 Hz D-E hysteresis loops 80−71365
K_2ZnCl_4, ferroelec. props. 79−4772
K_2ZnCl_4, incommensurate phases, neutron scatt. 79−38501
K_2ZnCl_4, incommensurate phase transitions, ^{35}Cl NQR study 80−75968
K_2ZnCl_4, modulated struct. in ferroelec. phase, X-ray obs. 80−64970
K_2ZnCl_4, X-ray cryst. struct. refinement 79−55705
$KZnF_3$, cryst., ^{20}F elec. quadrupole interaction, NMR meas. 77−12253
$KZnF_3$, Cu^{2+} and Mn^{2+} exchange interactions, luminesc. line temp. depend. 79−69480
$KZnF_3$, exchange interactions of transition metal ions in orbitally degenerated excited states 80−65512
$KZnF_3$ film, photoelec. yield spectra, rel. to band struct. 78−43980
$KZnF_3$, multiplet struct. in XPS spectra of 3p and 3s subshells 78−43981
$KZnF_3$ single crystal growth, Czochralski method 80−97421
$KZnF_3$, spin Hamiltonian parameters for Fe^{3+} ions, superposition model anal. 80−108053
$KZnF_3$, XPS of band struct. 77−11851
$KZnF_3:(Fe^{3+}\text{-}O^{2-})$, overlap and covalency contrib. to zero field splitting, LCAO-MO calc. 80−24850
$KZnF_3:(Fe^{3+}\text{-}V(K)^+)$, overlap and covalency contrib. to zero field splitting, LCAO-MO calc. 80−24850
$KZnF_3:Cr^{2+}$, ESR spectra of tetragonal Cr^{3+} centres, in external elec. field, 77K 77−24738
$KZnF_3:Er^{3+}$, ESR spectrum, higher order Zeeman effects 79−99766
$KZnF_3:Eu^{2+}$ f-f transition, cryst. field parameters calc. 77−15805
$KZnF_3:Gd^{3+}$, EPR, spin Hamiltonian parameters 79−65725
$KZnF_3:Mn^{2+}$, Cu^{2+}, exchange coupled, luminesc. props. 79−33781
$KZnF_3:Mn^{2+}$, exchange and spin-orbit interactions, optical spectra study 79−95817
$KZnF_3:Ni^{2+}$, absorpt., MCD and emission spectra 79−51953
$KZnF_3:Ni^{2+}$, mechanism of conc. quenching of fluoresc. from T_{2g} of Ni^{2+} 77−59605
$KZnF_3:Ni^{2+}$, Mn^{2+}, interference transition electric dipole mechanism 80−34896
$KZnF_3:Ni^{2+}$, temp. depend. of luminesc. 79−83016
$KZnF_3:V^{2+}$, ^{51}V ENDOR meas., spin Hamiltonian parameters 79−28638
$KZnF_3:V^{2+}$, calc. of t_{2g} antibonding mol. orbital in $|VF_6|^4$, rel. to ESR 80−50174
$KZnF_3:Yb^{3+}$, cryst. field parameters, optical, EPR spectra, spin-lattice relax. time 77−51950
$KZnF_3:Yb^{3+}$, perovskite type cryst., ENDOR meas. 80−80638
K_2ZnF_4, charge transport and polarisation 80−80681
$K_2Zn(H_2O)_6(SO_4)_2$, IR and Raman vibr. spectra 79−28743
$K_2Zn(H_2O)_6(SeO_4)_2$, IR and Raman vibr. spectra 79−28743
$KZn_2H(PO_4)_2$, X-ray cryst. struct. determ. *(French)* 79−69080
$K_4Zn(MoO_4)_3$, cryst. struct., cohesion 77−31641
$K_4Zn(MoO_4)_3$, domain struct. and phase transition, ferroelastic behaviour 77−62581
$K_2Zn(NH_2)_4$, cryst. struct. determ. *(French)* 78−79590
$KZn_4(PO_4)_3$, X-ray cryst. struct. determ. *(French)* 79−19205
$K_2Zn_2(SO_4)_3$, langbeinite type cryst., ferroelec., phase transitions, dielec., elastic and pyroelec. meas. 77−59535
$K_xZn_{x/2}Ti_{8-x/2}O_{16}$, ionic cond., K mobility rel. to struct. and bonding *(French)* 77−76594
$K_xZn_{x/2}Ti_{8-x/2}O_{16}$, ionic cond., rel. to struct. and chemical bonding *(French)* 78−18824
$K_4Zn(WO_4)_3$, cryst. struct. and polymorphism 80−1996

potassium compounds continued
$K_2Zn(ZrF_6)_2.6H_2O$, EPR of Cu^{2+}, temp. depend. 78−80201
$K_2Zn(ZrF_6)_2.6H_2O:CO^{2+}$, anisotropic exchange interactions between Co^{2+} ions, ESR spectra 79−95637
$K_2Zn_3[Fe(CN)_6]_2.xH_2O$, X-ray cryst. struct. determ. and refinement *(French)* 80−28955
$K_8Zr(MoO_4)_6$, X-ray structural investigation 78−79597
$K_4Zr_5O_{12}$, cryst. struct., X-ray study 80−33957
$K_3Zr_2(O_2)_2F_7.2H_2O$, photodecomp. 80−108724
K_xZrS_2, intercalation cpd., X-ray K absorption edges 78−39627
K_2ZrSe_2, intercalation cpd., struct. and phase limits *(French)* 77−35536
$K_2ZrSi_2O_7$, second monoclinic modification, struct. determ. 77−84734
$K_2Zr[Si_3O_9]$, wadeite, cryst. struct. refinement, X-ray diffr. meas. 78−2091
^{40}K Mossbauer isomer shifts, book contrib. 79−87363
K(5S)Xe, K(5S)Kr, excimer, visible emission band, exptl. results relative to theory 78−82779
$K[Ag(CN)_2]$, Raman scatt., press.-induced phase transitions and phonons 79−33698
$K[AlSi_3O_8]$, microcline, continuous laser emission effects on surface, spectroscopic obs. 79−94271
$K_2[B_{12}D_{12}]$, in aqueous soln., laser Raman spectra 78−15158
$K_2[B_{12}H_{12}]$, in aqueous soln., laser Raman spectra 78−15158
$K[B(SO_3Cl)_4]$, cryst. struct. 78−63701
$K[B(SO_3Cl)_4]$, space group 80−33913
$K_4[Bi_2Br_{10}].4H_2O$, cryst. struct. 77−58988
$K_3[Co(CN_6)]$, X-ray Co K absorpt. edge struct. meas. 77−20956
$K_{0.4}[(Cu_{0.9}HCO_3)_2(OH)_2]1.66H_2O$, Cu(II) carbonato complex, crystal struct. *(French)* 77−1111
$K_2[Fe(CN)_6]$ ice, γ-irrad., electron trap depth, ESR 79−66317
$K_3[Fe(CN)_6]$ X-ray Fe K absorption edge struct. of $[Fe(CN)_6]^{3-}$ meas. 78−43959
$K_4[Fe(CN)_6].3H_2O$, X-ray Fe K absorption edge struct. of $[Fe(CN)_6]^{4-}$ meas 78−43959
$K_3[Fe(SCN)_6].4H_2O$, optical reflection spectrum, mag. suscept., permittivity dehydration temp. 79−56809
$K[Fe_4S_3(NO_7)]$, valence levels, X-ray photoelectron and X-ray spectra 77−88500
$K_5[IMo_6O_{24}].5H_2O$, X-ray cryst. struct. determ. 80−54183
$K[InBr_4(H_2O)_2]$, X-ray cryst. struct. determ. 80−54186
$K_2[M(H_2O)_6](YO_4)_2$, Tutton's salts, M=Cu, Ni, Zn, Y=S, Se stereochem., neutron struct. determ. 78−18609
$K_2[M^{II}(H_2O)_6][(UO_2)_2Fe_8]$, M^{II}=Mn, Co, Ni, Cu, Zn or Cd, structural type, IR spectra 77−35525
$K_6[MnMo_9O_{32}].6H_2O$, cryst. struct. 77−76374
$K_2[MoO_{1-x}(OH)_{2x}(H_2O)_{1-x}O(MoO_4)_2].2H_2O$, proton NMR for chem. comp. at −195°C 78−38651
$K[(OH)_{0.42}(O_2)_{0.50}]$, cubic solid soln., structural and mag. study *(French)* 80−107177
$K[OsNBr_4H_2O]H_2O$, mol. and cryst. struct. from X-ray diffr. obs. 78−6046
$K_2[Pd(SO_3)_2].H_2O$, X-ray cryst. struct. determ. and refinement, connexion modes 79−46608
$K_2[Pt(CN)_4]Br_{0.3}.3H_2O$, high press. structs. and phase transitions 80−107423
$K_2[Pt(CN)_4]X_{0.3}.3H_2O$, X=Br, Cl, X-ray and neutron diffr., 31K-room temp. 78−42964
$K_{1.75}[Pt(CN)_4]1.5H_20$, elec. cond. studies, Peierls transition 80−24901
$K_2[Pt(CN)_4].3H_2O$, DC elec. cond. props. 79−51582
$K_2[Pt(CN)_4].3H_2O$, energy band calcs. 77−39780
$K_2[Pt(CN)_4].3.2H_20$, energy band calcs. 77−39780
$K_{1.75}[Pt(CN_4)].xH_2O$, one-dimensional, X-ray diffuse scatt. meas. 77−19937
$K_4[Ru_2Cl_{10}O]$, X-ray cryst. struct. determ. and refinement *(French)* 79−37670
$K_2[RuCl_6]$, X-ray cryst. struct. determ. and refinement *(French)* 79−37670
$K_3[SO_3ON(SO_3)_2].3/2H_2O$, struct. determ., X-ray and neutron diffr. 79−42038
$K_6[Si_2Te_6]$, cryst. struct. *(German)* 78−79569
$K_2[SnCl_6]$, defects determ., dipole relax. in phase transform. *(German)* 78−22711
$K_2[UF_2O_2(SO_4)].H_2O$, X-ray cryst. struct. determ. 80−54194
$K_2[(UO_2)_3F_8\text{-}H_2O].3H_2O$, cryst. struct. *(French)* 80−49193
$K_4[V(CN)_6(NO)].1/2KOH.1/2H_2O$, cryst. and molecular struct. 77−80469
KbR, inelastic light scattering of localised vibration of interstitial H atom in alkali halides 80−88998
Kbr ^{14}N impurities, molecular point defects, EPR isotropic hyperfine triplets 80−2636
Kbr surface, residence times of Au atoms, time-of-flight meas. 80−10788
$K_4(\beta_1\text{-}SiMoW_{11}O_{40}).9H_2O$, X-ray cryst. struct. determ. and refinement 80−28973
Kcl, aqueous soln., high precision viscosity meas. 80−10695
$kH_{2(1-x)}D_{2x}PO_4$, monoclinic, electro-optical props. 79−82951
$Khu_3F_{10}:Eu^{3+}$, site occupancy from excitation and emission spectra *(French)* 77−81145
Kl:Tl, excitation in fund. absorpt. region, luminesc. and thermolum. 80−50433
$Kl:Tl^+$, X-irrad., absorpt. spectra investig. of Tl_2^+ centres 77−20887
$KliFeS_2$, end product of Li+$KFeS_2$ electrochemical reaction, cryst. struct. 79−100397
$KnBO_3$:Fe, anomalous bulk photovoltage effect, Jahn-Teller mechanism 77−28218
$KniF_3$, antiferromagnetic, field-induced domain reorientation, NMR obs. 79−82816
KrF, excimer, electron impact deexcitation, low energy cross-sections and rate consts. 80−1071
KrF*, electron beam pumped laser, pulse shape and laser-energy extraction, model and expt. comparison 79−98345
$LaKFe(CN)_6.4H_2O$, cryst. struct. determ. 78−55844
(Li,Na,K) (Nb,Ta)O_3, pseudo-binary and ternary systems quenched metastable glassy and cryst. phases 80−29935
Li,K/PO_3,F system, low melting point comp., solvent for InP electrodeposition 79−28079
Li,K/PO_3,F system, low melting-point comps. for electrodeposition appl. 79−43662
(Li-K)NO_3, molten, $K^+(Rb^+)(Cs^+)(Tl^+)$ diffusion, wavefront shearing interferometric obs. 79−60535
$LiBeF_4$-KBF_4, phase diagram 77−21119

potassium compounds continued
LiCl-KCl, analysis of reduction waves of Ti ion in chronopotentiometry of K_2TiF_6 *(Japanese)* 78−20025
LiCl-KCl, molten mixture, struct., diffusion, cond., mol. dynamics calc. 80−64871
LiCl-KCl eutectic, anodic corrosion rate of candidate current collector metals for Li-FeS_2 battery 79−100512
LiCl-KCl eutectic melt, impedance meas. of Ni/Ni(II) electrode reaction *(Japanese)* 79−100392
LiCl-KCl eutectic mixture, purification, effect of impurity ions *(Japanese)* 78−40108
LiCl-KCl molten eutectic mixture, PbS solubility product and Li_2S solubility 80−54387
LiCl-KCl:Ln^{n+}, fused eutectic, electrolytic behaviour *(Japanese)* 79−16009
LiCl-KCl:Th^{n+}, fused eutectic, electrolytic behaviour *(Japanese)* 79−16009
Li_2CrO_4-K_2CrO_4, phase diagram determination by DTA and X-ray diffr. 78−31391
LiF-KF, densities of binary molten salts *(Japanese)* 79−7644
LiF-KF binary molten salt, elec. cond. *(Japanese)* 77−76588
LiF-NaF-KF molten mixture, diffusivity and solubility of H_2 78−34640
LiF-NaF-KF-K_2GeF_6-GeO_2 fused mixture, for electrodeposition of Ge powder 80−2979
$Li_{1-x}K_xI$, intrinsic optical absorpt. spectra 78−23500
$Li_2K(IO_3)$ in $LiIO_3$-KIO_3 system, lattice parameter, equilib. and metastable phase diagram *(Chinese)* 80−7538
$LiKSO_4$, sulphate ion optical and spectroscopic props., cryst. environment effect 77−40224
$LiKSO_4$, thermal and dielec. props. 80−34860
$LiKSO_4$, uniaxial crystal, pyroelectric, thermal expansion, phase transition 80−19966
$LiTaO_3$-$NaTaO_3$-$KTaO_3$, quenched metastable glassy and crystalline phases 79−61568
$MNbO_3$, orthorhombic, electronic struct., SCF-MS-Xα calc. 80−70600
$MNbO_3$, tetragonal, electronic struct., optical anisotropy 80−70599
$MgCl_2$-KCl, binary melt, viscosity *(Japanese)* 78−10209
$MgKPO_4.6H_2O$, struvite analogue, X-ray single cryst. struct. determ. 79−19190
$MgK_2(SeO_4)_2.6H_2O$:Mn^{2+}, EPR, crystal field and hexahydrate distortion 78−91938
$Mg(NO_3)_2$-RNO_3 (R=Li, Na, K), thermogravimetric anal. of dehydration processes *(Japanese)* 80−66791
$Mg_{0.7}Na_{0.9}K_{2.0}Ca_{2.4}Al_{9.1}Si_{26.9}O_{72}.xH_2O$, erionite, cryst. struct. exam., stacking faults 78−2083
MgO-KCl, solution under hydrothermal conditions, exam. of phase equilibria 79−8292
$Mg_2S_2O_3$-$K_2S_2O_3$-H_2O system, 20°C isotherms *(French)* 78−52506
$MnCl_2$-KCl system, molten, EPR spectra, linewidth study 78−88173
$(NH_4)_2HPO_4$:KH_2AsO_4, EPR of arsenic and phosphorus oxyradicals 77−77102
$((NH_4)_{1-x}K_x)_2CuCl_4.2H_2O$, Raman scatt. spectra 79−15459
$(NH_4)_{0.16}K_{0.84}I$, $(NH_4)_{0.16}K_{0.84}Br$, reorientation motion of NH_4^+ 78−79542
$((NH_4)_xK_{1-x})_2SO_4$, NH_4^+ dynamics, neutron scatt. study 79−42167
$((NH_4)_xK_{1-x})_2SnCl_6$, mixed cryst., spectroscopic study 79−33712
$((NH_4)_xK_{1-x})_2SnCl_6$, mixed cryst., NQR relax. and reson. 80−54990
$(NH_4)_2SO_4$-K_2SO_4 mixed crystal, cryst. struct., X-ray diffr. meas. 77−80484
$(NH_4)_2SO_4$-K_2SO_4 mixed crystal, ESR study of NH_3^+ radicals 79−38367
$(Na,K)NbO_3$ solid solns., struct. transitions, neutron powder diffr. 78−38649
$(Na,K)(V,P)O_3$ system, cation substitutions, crystallographic studies 78−79581
Na,K/PO_3F system, low melting-point comps. for electrodeposition appl. 79−43662
Na-K silicaalumo gels, crystn. and characts. of A-type zeolites 79−52780
Na-K silicate glass, thermal expansion 77−4186
Na^+-K^+-F^--SO_4^{2-}, asymmetrical reciprocal molten salt system, excess enthalpies 80−30268
$NaBF_4$-KF, phase diagram 77−21119
NaBr, cation defects creation mechanism 80−75224
NaCN, cubic, KCN-type anomalous thermoelastic behaviour 77−84823
NaCl:K_3IrCl_6 electron irrad., ligand field anal., EPR obs. 80−29612
NaCl-KCl, interdiffusion and demixing, electron microprobe anal. *(French)* 80−54444
NaCl-KCl, molten, alkaline earth oxides solubility products, potentiometric determ. 80−76488
NaCl-kCl melt, reaction with LiO_2-$2SiO_2$ X-ray, IR exam. 80−55706
NaCl-KCl melt, X-ray diffr. struct. determ. 79−41925
NaCl-KCl mixed aq. solns., viscosity meas. 79−82370
NaCl-KCl mixed crystal, growth, X-ray exam. and microstruct. 78−44001
NaCl-KCl mixture, electrical, electromag., and acoustic props. *(Russian)* 78−30759
NaCl-KCl novel encapsulant for LEC growth of GaSb single crystals 80−93475
NaCl-KCl system, interdiffusion, miscibility, Kirkendall effect 80−107568
NaCl-KCl-$CaCl_2$, solid soln., X-ray examination of final decomp. stage *(Russian)* 77−63681
NaCl-KCl-CuCl system diagram investig. *(Russian)* 79−96015
NaCl-KCl-H_2O, ionic diffusion theory, use of activity coeffs. in transition-state models 78−57224
NaCl-KCl-H_2O mixed electrolyte solns., elec. transport 80−3355
NaCl-KCl-$NiCl_2$ system diagram investig. *(Russian)* 79−96014
NaCl+KF→NaF+KCl, solid state reaction mechanism 79−61857
$Na_2HPO_4.7H_2O$:KH_2AsO_4, EPR of arsenic and phosphorus oxyradicals 77−77102
NaK, $C^1\Pi$ state, spectroscopic consts., vibr.-rot. struct., K fluoresc. obs. 77−18901
NaK, mol. transition dipole moment, from laser-induced fluoresc. spectra 79−94034
$Na_{1-x}K_xNbO_3$, solid soln., crystal lattice parameters, conc. depend. calc. 78−95041
Na_2KSb, evaluation as photocathode material 78−11072
Na_2KSb photocathodes, prep. and props. 78−84693
$Na_2KSb(Cs)$, photocathode, optical props. 79−78827
$Na_{0.5}K_{3.5}(Te_2O_6(OH)_4).6H_2O$, cryst. struct. determ. 78−26520
$NaMo_6O_{17}$, thermochemistry 77−77801
$NaNO_3$-KNO_3-$Ca(NO_3)_2.4.09H_2O$ melt, mixed alkali effect 80−34219
Na_2O-K_2O-Al_2O_3-SiO_2 glasses, effect of Al_2O_3 on elec. cond. 77−8104
Na_2O-K_2O-Al_2O_3-SiO_2 glass, mixed alkali effect, nonbridging O content effects 78−18827
Na_2O-K_2O-Al_2O_3-SiO_2, structure of modified surface layer, internal friction method 80−103258
Na_2O-K_2O-$Al_2O_3SiO_2$-H_2O system A-type zeolites, crystn. from Na-K silicaalumo gels, and characts. 79−52780
Na_2O-K_2O-CaO-SiO_2 glasses, chemical durability, mixed alkali effect 79−8377
Na_2O-K_2O-SiO_2, Na diffusion 78−26724
Na_2O-K_2O-SiO_2 based glasses, high field cond. and ionic jump processes 78−38873
Na_2O-K_2O-SiO_2 glasses, optical absorption of Ni (II) complex, complex co-ordination change, annealing effects 79−69870
Na_2O-K_2O-SiO_2 glass melt, interdiffusion coeffs. of Na^{2+}, K^{2+}, temp. depend. 80−44348
Na_2O-K_2O-SiO_2 melts, Na^+ and K^+ diffusion and interdiffusion processes 80−34221
NaOH-KOH eutectic molten mixture, elec. cond. and sp. mass 79−82365
Na_2SiO_3-K_2SiO_3, molten, thermodynamics of mixing at 1100°C, CaO addition effects 77−47581
$NaVO_3$-KVO_3-Al_2O_3, melts soln. of Al_2O_3 single crystals 80−20910
Na_2WO_4-K_2WO_4-WO_3 ternary system, phase diagram investig. 77−12608
$NiK_4(P_3O_9)_2.7H_2O$, cryst. struct. determ. *(French)* 78−79568
$Ni_2P_2O_7$-$K_4P_2O_7$-H_2O solubility at 25 degrees C, double phosphates formation 80−54381
P_2O_5-K_2O-CdO-Na_2O glass:Nd^{3+}, highly doped, spectroscopic props. and CW laser action *(French)* 79−41385
PbI_2:KI, trapped exciton states, absorption spectra 80−50383
PbI_2:KI alloys, fundamental abs. edge, potential as solar convertor 80−101128
$Pb_2KNb_5O_5$, SAW props., rel. to device appl. 78−71923
$Pb_2KNb_5O_{15}$, strong electromechanical coupling of SAW 78−63919
$PbK_2(PO_3)_4$, cryst. struct. 77−31638
$Pb_{0.9}K_{0.1}(Zn_{1/3}Nb_{2/3})O_{2.95}$-$PbZrO_3$-$PbTiO_3$, morphotropic tetragonal-rhombohedral phase boundary 78−48129
PbO-B_2O_3-K_2O melt, activity of PbO 77−11708
PbO-K_2O-SiO_2, O tracer diffusion above transform. temp. 79−28120
PbO-K_2O-SiO_2-(Al_2O_3) glass, corrosion in acid, leaching kinetics 78−92378
phase transition in transverse field with deform. depend., phonon anomaly separation KH_2PO_4 80−39258
RbBr, Stark effect in F-centre emission 77−63434
RbCl/KCl interface, diffr. studies of conc. variations 79−42322
RbCl-KCl powder blends, diffusional homogenisation, X-ray diffr. exam. 78−18847
RbCl-KCl(H_2SO_4)-H_2O, water activity, 0 and 50°C, conc. depend. *(Russian)* 78−31679
RbIn(MoO_4)$_2$:Gd^{3+}, hyperfine struct. of ESR spectrum 77−8399
$Rb_xK_{1-x}MnF_3$, struct. transitions, NMR and birefr. expts., 60-300K 77−47577
$(Rb_xK_{1-x})AgI_3$, cryst. struct. 77−51360
$(Rb_xK_{1-x})Ag_4I_5$, cryst. struct. 77−51360
$Rb_xK_{1-x}H_2PO_4$, 90° phase matching in freq. doubling, appl. to lasers 80−33088
$Rb_xK_{1-x}[GaSi_2O_6]$, partially ordered leucite-type struct. *(German)* 79−51088
$RbMnP_2O_7.3H_2O$, physicochem. characts. 77−39562
Sb_2O_4-$KSbO_3$, phase equilibria and crystal growth 77−70035
Sb_2O_4-$NaSbO_3$($KSbO_3$)-NaF, phase equilibria and crystal growth 77−70035
Sc_2O_3-GeO_2-KF-H_2O system, scandium germanates crystallisation in high temp. aq. solns. 77−24942
SiO_2-Al_2O_3-B_2O_3-CaO-Na_2O-K_2O system glasses, relax. of struct. stresses rel. to forming process 79−34088
SiO_2-Al_2O_3-CaO-BaO-SrO-ZnO-Na_2O-K_2O-B_2O_3, glaze effect of P_2O_5 additions 80−60824
SiO_2-Al_2O_3-CaO-K_2O system glass, phase separation and crystn., F catalytic effect 79−60280
SiO_2-Al_2O_3-CaO-MgO-NaO-K_2O-B_2O_3-ZrO_2, glaze, exam. of zircon crystallisation 79−19155
SiO_2-Al_2O_3-CaO-MgO-Na_2O-K_2O effect of partial substitution of Na_2O by K_2O, on crystallisation 80−10499
SiO_2-Al_2O_3-Fe_2O_3-K_2O, form. of Al-Fe leucite, inversion temp. *(Japanese)* 77−62481
SiO_2-Al_2O_3-Fe_2O_3-Na_2O-K_2O-CaO-MgO glasses, Mossbauer spectra study 80−39967
SiO_2-Al_2O_3-K_2O glass ceramic interaction with Pb borosilicate glaze 80−84398
SiO_2-Al_2O_3-K_2O-Na_2O, exam. of leucite crystal growth 79−19496
SiO_2-Al_2O_3-MgO-K_2O-F, glass ceramic, crystn., microstructures rel. to conditions 80−11638
SiO_2-B_2O_3-Al_2O_3-k_2O, Ag interdiffusion, optical and NMR studies 80−24683
SiO_2-B_2O_3-Na_2O-K_2O system glass, phase separated, loss of oxides during acid leaching, atomic absorpt. anal. 79−11716
SiO_2-K_2O, thermodynamic approach to ionic conds., statistical model of chem. potential 79−46833
SiO_2-K_2O-Na_2O-BaO-SrO-ZnO system glass, props. optimisation 79−91611
SiO_2-Li_2O-Al_2O_3-K_2O:Ag_2O(-CeO_4) (-Sb_2O_3), surface resist. meas. 80−44700
SiO_2-Li_2O-K_2O-ZnO-P_2O_5, glass ceramic, phase changes and crystn. processes 80−7562
SiO_2-Li_2O-K_2O-ZnO glass ceramic, prep., phase transformations and physical props. 80−45299
SiO_2-M_2O (M=Na,K) glasses, temp. depend. of elastic modulus 80−40410
SiO_2-Na_2O-K_2O water glass with polyethylene filler, thermogravimetric and thermomechanical anal. 79−20020
SiO_2-Na_2O-K_2O-CaO-MgO-Al_2O_3 glass melt, anodic dissolution of Ti 80−19949
SiO_2-NaO-K_2O-CaO-MgO-Al_2O_3 melt, anodic dissolution of Co and Ni in melt 78−88582
SiO_2-PbO-B_2O_3-Al_2O_3-CaO-Na_2O-K_2-O glaze, interaction with aluminosilicate glass-ceramics 80−84398

potassium compounds continued
SiO_2-ZrO_2-Al_2O_3-CaO-Na_2O-K_2O-Li_2O, chemical resistant glass for glass fibres 80−21128
$SiO_2B_2O_3$-K_2O-Al_2O_3-As_2O_3 glass fibres containing metallic granules, tensile strength, Young's modulus, DC conductivity 80−30023
Sn-KCl granular superconductors, far IR absorpt. 80−84548
$SrCl_2$:KCl, polycryst., ionic cond. 78−2292
$Sr_2KNb_5O_{15}$, Raman scatt. experiments in tetragonal tungsten bronze compounds 80−40113
TeO_2-V_2O_5-K_2O, glass, IR spectra of crystalline phases 79−38536
$Th(NO_3)_4$-K_2HPO_3-H_2O, mixed phosphites formation and characterisation 77−52304
TiO_2, solubility in KF aq. solns. 80−34197
TiS_2-Na_2S(K_2S) systems, synthesis of Na_2TiS_3, K_2TiS_3, K_4TiS_3 and K_8TiS_6 *(French)* 79−52636
$TlNO_3$-$LiNO_3$(KNO_3) mixtures, molten, surface tension, regular solution theory 78−71903
V_2O_5-BaO-K_2O-ZnO glasses, elect. props. and struct. 80−15547
$ZnCl_2$-KCl, melt, viscosity meas. by oscillating cylinder method *(Japanese)* 80−10696
$ZnCl_2$-KCl, molten, density meas. *(Japanese)* 79−19383
$ZnCl_2$-KCl, molten, viscosity, 260 to 560°C *(Japanese)* 77−51537
$ZnCl_2$-KCl-NaCl, molten system, containing Ni^{2+} ions, appl. to electrorefining, polarographic study 80−66810
$ZnK_4(P_3O_9)_2.4H_2O$, cryst. struct. determ. *(French)* 78−26503
ZnS-Na_2O-K_2O-SiO_2, form. using electric furnace, furnace design 80−11620

potential dividers *see voltage dividers*

potential energy curves and surfaces of molecules
for Morse curves see Morse potential
see also molecular vibration
ab initio Cl pot. curves, mol. wavefunctions and vibr. freqs. comparison of methods 80−27956
ab initio effective core pot. method appl. to F_2, Cl_2 and LiCl 80−32625
acetaldehyde radical cation, fragmentation, MO calc. 79−18109
acetylene, core ionised, core-excited and shake-up states, ab initio MRD-CI methods 80−42950
acetylene, force consts. of asymmetric stretch motions, accurate ab initio calcs. 77−83567
acetylene, vibr. fine struct. accompanying core ionis., STO calcs. 78−62844
adiabatic nuclear group transfer processes in condensed media, electronic energy hypersurfaces 80−25982
adiabatic potential, correlation with Raman scatt. and vibronic coupling 77−71804
alkali halide molecules, interaction potential 78−58612
alkali halides, geometries, force consts., charge distribs., FSGO model pot. calcs. 77−88379
alkali halides, improved interaction pot., spectroscopic consts. calc. 79−86024
alkali hydrides, ionic-covalent config. mixing, pot. curves 77−34576
alkali metal diatomics, pot. curves, selected valence electron SCF MO calc. 79−10053
alkali metal dimers, photodecomp. 79−27049
alkali trimers, LEPS pot. energy surfaces, equilib. geometries, vibr. force consts. 79−22624
alkali trimers, London pot. energy surfaces 79−6893
alkali trimers, semiempirical pot. energy surfaces calcs. 78−25649
amide group molecules empirical pot. model EPEN/2, development, parameter testing 79−54935
2-aminopyrimidine($-d_1$), amino inversion vibr., planarity, far IR obs. 79−31515
analytical expressions from constrained optimisation 77−6698
anomalous energy minimum, MINDO/3 calc. 77−34559
9,10-anthraquinone, Shpolskii quasi-line phosphoresc. spectra, electronic-vibrational interactions 78−55196
Ar_3^+, visible photoabsorpt., pot. energy surface 79−98112
atomic clusters, main group elements, pot. energy surfaces 78−46477
autonitryl, electronic struct. and geometry, open-shell SCF calcs. 79−18106
avoided surface crossing, energy level transitions, Born-Oppenheimer approx. 77−71763
7-azaindole dimers, photoautomerisation by double proton transfer, double-well excited-state pot. surface 80−11880
azomethane, trans-cis isomerisation, INDO-SCF and CI calc. 78−25440
bacteriorhodopsin, excited state energy surface to explain photochemistry 79−48218
band system transition moment ab initio SCF and CI calcs. 79−13770
benzaldehyde, and deuterated forms, in p-xylene, 4.2K, $n\pi^*$ phosphoresc. assignments 78−9197
benzene, and deuterated forms local mode oscill. strengths 79−27039
benzene, noncrossing and degeneracy in Hubbard models 80−14096
1,3-benzodioxole, far IR spectrum anal., pot. function 79−76427
p-benzoquinones, chlorinated, transferable force field for in-plane vibrs. 80−964
Born-Oppenheimer adiabatic pot. energy hypersurface gradient, exact formula 79−9992
n-butane, conformational hypersurface, anal. 79−41252
n-butane, LF vibr. spectrum, methyl torsional pot. function, internal rot. 79−89670
charge stabilization mechanism in the visual and purple membrane pigments 79−34500
chloroacetic acid, acid salts, NQR obs. of H-bond pot. energy curves 77−18941
p-chlorobenzene, and deuterated forms, in p-dibromobenzene and p-dimethoxybenzene, 4.2K, $\pi\pi^*$ phosphoresc. assignments 78−9197
chloromethyl formate, conformation potential energy surfaces, ab initio calcs. 80−69065
CI description, partitioning theory 77−38616
CI wavefunction, terms selection for pot. energy surface 77−88401
classical harmonic oscillators, microcanonical ensemble, Monte Carlo sampling 80−102459
classical many-body collision model incorporating Heisenberg and Pauli principles 80−63511
constrained molecule, atomic motion on polydimensional pot. energy surface 79−59378
crossing of potential energy curves, Teller's conditions 78−13407
curve crossing systems, two-state, non-adiabatic transitions, semi classical Magnus approx. 80−37756

potential energy curves and surfaces of molecules continued
cyanocyclopentane, microwave spectral study of axial and equatorial conformers 80−95604
cyclic tetrapeptides, potential energy minima 79−59527
cycloalkanones, carbonyl charact. freqs., kinematic and pot. energy effects 80−95578
cyclobutadiene, noncrossing and degeneracy in Hubbard models 80−14096
2-cyclohexene-1-one, planarity barrier, from LF Raman spectrum 79−54859
1,2-cyclooctadiene, conformational energy surface, Boyd's iterative force field investig. 80−95737
cyclopentadienyl radical, pot. surface and vibronic states, ab initio CI calcs. 80−47897
cyclopropenyl radical and anion, planar, E state pot. surfaces, CI and SCF calcs. 78−5155
diacetylene radical cation, and deuterated forms, electronic spectrum in solid inert gases 79−94026
diatomic bound molecules with zero bond order, excited biexcitons 78−9049
diatomic homonuclear molecule, of 1st row, canonical exchange energy modulation parameters, MTXα calc. 79−97997
diatomic homopolar molecules, light scatt. *(Hungarian)* 77−50442
diatomic hydrides of first and second row elements, PNO-CI and CEPA calc. 79−768
diatomic long-range molecules, highly vibr. excited state 78−29768
diatomic molecule, force const., Morse function in pot. curve *(Russian)* 79−49968
diatomic molecule, Franck Condon factors, vibr. rot. interaction effect 80−74198
diatomic molecule, overtone intensities in reson. Raman scatt. 80−48001
diatomic molecule, predissoc. at intermediate coupling strengths, semiclassical theory 78−50601
diatomic molecule, trigonometric pots., refinement 80−9676
diatomic molecule+diatomic molecule, collinear collision, anharmonicity effects 79−31656
diatomic molecule vibr. pots., representations accuracy 78−66531
diatomic molecules, bound, hybrid potential function 80−69209
diatomic molecules, electronic and vibr. functions of non-adiabatic wavefunction 79−22621
diatomic molecules, empirical pot. curves, Pade approximant calcs. 80−14184
diatomic molecules, Franck-Condon factors for Morse pots. 79−72365
diatomic molecules, pot. energy functions, virial theorem calcs. 77−88519
diatomic molecules, potential energy functions, spectroscopic consts., correls. 79−18253
diatomic molecules, predissoc., simplified model 79−6892
diatomic mols., pot. energy curves representation 80−87061
diatomic mols., spurious avoided crossing detection 80−87057
diatomics-in-molecules, generalised theory for surface, valence bond theory 79−97970
diatomics-in-molecules, VB method 79−85919
difference electrostatic mol. pot. contour maps, basis set superposition effect 80−102462
differential cross sections, rainbow and diffr. oscills. damping, anisotropic pots. 78−50608
difluorodiazine, cis-trans isomerisation, mechanism and kinetics, CNDO/2 study 77−90589
dihydrophenazine derivatives, in 3-methylpentane-(ethanol) (PMMA), radiationless processes, temp. depend. 80−43087
dihydroxycarbene, singlet and triplet state rot. pot. surfaces 80−32627
1,4-dimethoxy-2,6-dimethylbenzene, methyl reorientations, NMR relax. and inelastic neutron scatt. obs. 79−61253
dimethyl sulphide dimerisation, S lone pair nonbonded contacts, EH, MINDO/3, CNDO/2 calcs. 79−773
dissociation, nonadiabatic interactions, conical and Jahn-Teller intersections, classical trajectory method 80−25997
B-DNA helix, sugar-phosphate backbone, molecular electrostatic pots. calc. 80−9679
double minimum vibr. pot., FORMAC program 77−23444
Dunham coeffs., high-order contribs. 78−46285
electron correlation theories, coupled cluster and 4th-order perturbation theory 79−39125
electronic degrees of freedom, classical models 80−63507
electronic spin orbit interaction, molecular Aharonov-Bohm effect 80−83303
electrostatic isopotential maps for large biomolecules, STO transferable bond calc. 80−3571
electrostatic potential, using overlap-multipole-expansion 79−63931
empirical potential model EPEN/2 for conform., intermol., solvation studies 79−50102
ethane, two-channel dissoc., dynamical effects, classical trajectory study 78−40042
ethane, unimol. decomp., mode localised excitation, trajectory studies 78−64815
ethyl cation, rearrangement pseudorotation modes, reaction mechanisms, permutation theoretic anal. 78−44369
ethyl radical decomposition, mol. dynamics, trajectory studies 80−7780
ethylene, core ionised, core-excited and shake-up states, ab initio MRD-CI methods 80−42950
ethylene, pot. energy and dipole moment surfaces, polarisation effect, ab initio CI calcs. 80−106272
ethylene, S_0,S_1-states, twisting vibrs., pot. curve calcs., absorpt. spectra 77−83576
ethylene as singlet methylene dimer, nonempirical double zeta calculations, zwitterionic singlet excited states 80−83258
ethynyl radical, emission spectra and pot. energy surface, ab initio MRD CI calc. 79−41099
exchange reactions, light atom, quantum dynamics 80−101011
excimer laser, electronic structure, pot. energy curves, radiative transition probabilities, quantum mech. calcs. 79−10284
excited molecular systems, relax. processes, nanosecond time-resolved spectra 77−26992
excited states time evolution in presence of nonadiabatic interactions 79−3379
first derivative of potential energy, open-shell restricted HF and MC SCF calcs. 79−98004
fluoroethyl radical, unimol. dissoc., pot. energy charact. and energy partitioning calcs. 80−45488

potential energy curves and surfaces of molecules continued
2-fluoroethyl to ethylene fluoronium ion interconversion, pot. energy surface, MNDO calc. 79−34296
fluoroformaldehyde, pot. energy surface characts., substitution effect 80−89505
fluoromethyl formate, conformation potential energy surfaces, ab initio calcs. 80−69065
formaldehyde$^+$, excited state dissoc., nonadiabatic interactions, conical and Jahn-Teller intersections, classical trajectory method 80−25997
formaldehyde, adiabatic CI pot. surface LCAO calc., gradient determ., mol. dynamics 80−48056
formaldehyde, core ionisation, valence orbital relax. calcs. 78−5135
formaldehyde, ground state, potential energy surface 80−42967
formic acid, and dimer, ab initio MO calcs., ground and excited states 77−83492
formyl radical, electronic struct., dissoc. energy and pot. energy surface many body perturbation theory and couple cluster doubles calc. 80−23296
formyl radical, lower electronic states, ab initio calc. of pot. energy surface, hydrocarbon flame band 79−68287
Fues potential, vibr.-rot. spectra, Schrodinger eqn. soln., pot. energy curves *(Spanish)* 78−36784
geometry optimisation, Newton-Raphson method algorithm 77−10612
geometry optimisation, self consistent, semiempirical force field method 77−83760
geometry optimisation with explicit inclusion of electron correl. 80−37748
ground state props., coupled cluster and MBPT methods appl. 80−47881
group IV A monosulphides, dissoc. energy calcs. 78−29733
Group VIA photolytic laser systems, for fusion research 78−59002
H_3 dynamics, on accurate H_3 pot. surface 79−5139
2-haloethanols, torsional interaction, IR spectra, ab initio calcs., 2-dimens. model 80−74160
halogen molecule negative ion, Cl_2^-, Br_2^-, I_2^-, $ClBr^-$, ClI^-, pot. curve calc. 77−10596
harmonic and Morse oscillator freq. change influence on Franck-Condon factors 80−106312
harmonic oscillator model in predissoc., level widths, shifts and curve crossing 78−90239
homonuclear molecular ions, adiabatic pot. curves 80−929
homotetrahedryl cation, rearrangement pseudorotation modes, reaction mechanisms, permutation theoretic anal. 78−44369
hydrocarbons, unsaturated, empirical potential model EPEN/2 parameterisation, testing 79−50103
icosahedral molecules and complexes, Jahn-Teller effect, pot. surface 78−78642
inert gas complexes spectroscopic data, geometry, pot. energy curve, dissoc. energy, equilib. internuclear distance, determ. 80−53018
inert gas dimer ions, electronic struct., chem. binding 79−31376
inert gas oxides, low-lying electronic states, ab initio CI calcs. 77−57888
inorganic molecules with polytopic bonds, motion of nuclei 79−41125
intermolecular exchange potentials, Bonham series representation Born-Oppenheimer calcs. 79−10169
intramolecular energy transfer, quantum effects 79−18134
intramolecular energy transfer, stochastic, crit. point anal. of Hamiltonian system instabilities 79−98005
intramolecular energy transfer, stochastic theory 79−22618
intramolecular H-bonds, H, D and T NMR, isotope effects and pot. energy surfaces 79−76447
isopropyl radical, pot. energy surfaces, ab initio UHF calcs. 80−106258
large internuclear separations, discrete mol. energies calcs. 80−91472
large molecular systems, local pot. surface and charges, parametrisation scheme for quantum mechanical computation *(German)* 80−18793
laser induced molecular predissociation, by stimulated emission or absorpt. of IR photons 79−54925
Linnett potential, generalisation 79−18252
long range mol., electronic and vibr. levels 78−94301
methane, $1B_1(1T_2)$ state, photodissoc., extended basis calcs. 78−9093
methane, pot. energy curves, Monte Carlo and SCF LCAO MO calcs. 80−63526
methane, pot. energy surface of excited singlet state, appl. to photodissoc. 79−83440
methane, vibration-rotation energies of harmonic and combination levels 80−47962
methane-d_3, activation, dissoc., internal energy distrib., trajectory calcs. 77−4899
methyl cation-He interaction energy, nonempirical calc. 78−86799
methyl chloride-d_3, activation, dissoc., internal energy distrib., trajectory calcs. 77−4899
methyl cyanides and isocyanides, isomerisation, ab initio (STO-3G) geometry optimised calc. 78−46265
methylene, vibronic anal., ab initio CI pot. curves calcs. 78−50479
methylene anion, vibronic anal., ab initio CI pot. curves calcs. 78−50479
methylene ion, pot. energy surfaces of excited states, ab initio GTO SCF CI calcs. 78−58602
methylene peroxide, multiconfig. SCF CI calcs. 80−18803
methylenimine, photoisomerisation, SCF MO pot. surfaces 79−11772
methylphosphorous pentafluoride, CH_3PF_4, pseudorotation, quantum dynamics 77−34570
methylsilylene, isomerisation, lowest triplet state reaction surface studies 79−15963
minimum energy reaction paths, reactive domains of energy hypersurfaces and stability 80−71893
molecular complex, pot. energy curves, INDO calc. 79−54784
molecule+ion collision system pot. curves at low collision energies, beam studies 80−61088
trans,trans-muconodinitrile, mol. reorientation, unequal well pot. energy calcs. 78−26461
multidimensional surface intersection problem and classical surface hopping 77−14512
nitromethane, torsional barriers, electronic spectrum 79−59424
nitrosomethane, ground state and nonvertical n-π^* excitation energy calcs. 80−18804
non non-crossing in mol. pot. energy curves, comment 78−78770
nonadiabatic transitions, comparison of surface hopping and complex-valued time calcs. 77−9049
nonbonded interactions, pot. energy curves, CNDO/2, INDO and extended Huckel calcs. 77−27140
noncrossing rule for electronic pot. energy surfaces, role of time reversal invariance 79−54929
potential energy curves and surfaces of molecules continued
nonequilibrium config., Politzer and Ruedenberg type energy relations 79−18135
nonlinear polyatomic molecules, centrifugal distortion, phenomenological consts. 77−75120
nonradiative transitions, single and double minima pot. energy surfaces 79−50067
nuclei acid phosphate group, analytical atom-pair pot., SCF-LCAO calc. 79−70516
nucleic acids, electronic absorpt. and emission spectra 80−55989
nucleotide bases, electronic absorpt. and emission spectra 80−55989
one-electron methods, pot. curves, spin-projected EHF methods 79−10054
organic carbonyl compounds, empirical pot. model EPEN/2, development, parameter testing 79−54934
organic molecules, saturated, empirical potential model EPEN/2, parameterisation testing 79−54933
oxirane cation, struct. rearrangement following vertical ionisation, ab initio CI calc. 80−58191
peptide architectural units, ab initio SCF MO calcs. 78−96004
phenol-phenyl complex, electrostatic mol. pot. contour maps, MODPOT and VRDDO calcs. 80−102463
photochemical reactions, isomerisation, complexing, proton transfer, initiation of internal conversion processes 80−40713
polar anion, ab initio ground state pot. energy surfaces, electron affinity 79−49958
polar mol. anion ab initio ground state pot. energy surfaces calc. 80−47923
polyacenes, planar vibrs. classification using potential energy distrib. anal. 79−98065
polyatomic molecules, atomic pot. energy distrib., Kyong calcs., parameter for mol. vibr. studies 78−58762
polyatomic molecules, force consts. and geometry, pot. energy surface calcs. 77−14379
polyatomic molecules, small, analytical functions for pot. energy surfaces 80−102457
polyatomic system, pot. energy surfaces, semiempirical calcs. 78−41974
polyatomic van der Waals molecules, struct. and dynamics calcs. 79−41097
polyenes, twisting force consts., CNDO theory potential energy surface 78−50474
polyethylene terephthalate, conformation rel. to orientation, pot. energy surfaces study 79−68338
porphin, ground-state energies, force consts. and vibr. freqs., CNDO/2 calc. 79−18118
porphin, hypersurface of adiabatic pot. calc. by CNDO/2 method, vibr. freqs., absorpt. spectra calc. 80−95543
potentials, anisotropic, from rotationally inelastic and elastic cross sections, direct inversion method 80−69090
potentials with Coulomb tails, eigenenergy calc. 79−58560
predissociation, unimolecular, type I, level widths and shifts, quantum-mech. method 79−31629
propion-aldehyde ion, field dissociation, pot. surface 77−65544
propion-aldehyde ion, fragment/mol. ion current ratio, field ionis. mass spectrum, CNDO/BW calc. 77−65544
protein architectural units, ab initio SCF MO calcs. 78−96004
pyridine-N-oxides, substituted, absolute energy levels in gas and condensed media, ionis. energy, electron affinity 77−67995
rainbow maxima, pot. well depth determ. method 77−14527
resonant states, potential surfaces, complex coord. calcs. in adiabatic approx. 80−102464
resonant states, potential surfaces, complex coord. calcs. using stationarity condition 80−102465
RHF molecular potential eqns., interactions of open-shell systems 77−30949
rhodopsin, excited state energy surface to explain photochemistry 79−48218
scattering amplitude calculations, role of radiative crossings between potentials of dressed mol. 80−63642
selenocyclopentane, interconversion barrier, spectra and struct. 79−10115
semiclassical eigenvalues for nonseparable bound states from classical trajectories 77−14514
serine proteases, enzymatic reaction mechanism, CNDO/2 mol. orbital calcs. 78−27751
1-silabicyclo 2,2,2 octane, double-min. skeletal torsion, microwave spectroscopy 80−47972
silacyclopentane, Raman spectra, pot. energy surface, barrier to interconversion 78−25541
silaethylene, isomerisation, lowest triplet state reaction surface studies 79−15963
silylcarbene, isomerisation, lowest triplet state reaction surface studies 79−15963
simple mol. charge distrib., empirical method, electrostatic pots. and struct. 78−82652
spectroscopic data analysis, phenomenological and theoretical 80−52963
spurious avoided crossings, noncrossing rule calcs. 77−6661
Stockmayer-type polarisable mols., N-particle dynamics 77−68089
strongly coupled systems, one dimens. barriers, transfer rate 80−63735
subtilisin charge-relay system, electrostatic pot. map, STO transferable bond calc. 80−3571
symmetrical molecules 80−102458
tetrafluoromethane, pot. consts., IR spectra 78−82808
tetramethyls, of IVA metals, pseudo-exact force consts., force fields 77−31022
tetramethylurea-d_0-d_{12}, IR spectra, normal coord. anal. 78−978
s-tetrazine, pot. surface of low-freq. out-of-plane modes 78−62741
thiourea, ground and first excited triplet state configs., ab initio SCF calcs. 79−89597
transition metal nitrosyls, appl. of HF and CI calcs. 80−9513
transition state determination and characterisation ab initio calcs. 77−28975
triatomic linear molecule, photodissoc., products rot. distrib. 79−66309
triatomic molecular systems, unimol. decomp., exit-channel coupling effects 80−25984
triatomic molecule, large amplitude vibr. model, appl. to H_2O 79−41150
triatomic molecules, motion, regular and irregular spectra, theory 80−9590
triatomic mols., bound state. mol. Aharonov-Bohm effect 80−83302
triatomic negative ion fragmentation, energy partitioning isotope effects, Monte-Carlo calcs. 77−27126

potential energy curves and surfaces of molecules continued
triatomic negative ions, dissoc. product kinetic energy, classical trajectory method 78−64809
triatomic potential surfaces, global topology 77−50381
triatomic surface defined over orthogonal bond order coordinates 80−5492
1,2,4-trichlorobenzene liq., mol. reorientation, translation and vibr. relax., Rayleigh and Raman spectra 80−95632
trichlorofluoromethane, dissoc. electron attachment, pot. curves calcs. 79−98231
trichlorofluoromethane anion, dissoc. electron attachment, pot. curves calcs. 79−98231
trifluoromethyl cyanides and isocyanides, isomerisation, ab initio (STO-3G) geometry optimised calc. 78−46265
trimeric molecular complex, excitation localisation and transfer, monomeric internal vibr. effect 78−17581
trimethylene diradical, generalised Hartree-Fock natural orbital config. interaction approach 77−75062
trioxolane, methyl substituted, stability, pseudorotation, electronic effects in final ozonide 79−45654
trioxolanes, methyl substituted, stability, pseudorotation, electronic effects in primary ozonide 79−49961
trioxolanes, pseudorotation surface, mol. struct. and conform. 79−45653
tunnelling in asymmetric double-min. pots. 77−6660
tunnelling in double-well potentials, symmetric and asymmetric, periodic orbit theory 80−23488
unimolecular decay, nonadiabatic interactions, transition probability as function of Massey parameter 80−35503
valence-nonbonded H atoms interaction and two-centre contrib. to total energy of mol. 80−32624
van der Waals dimers, intramolecular vibr. dynamics, vibr. predissociation 80−28083
van der Waals T-shaped mol., perpendicular vibr. predissoc., vibr. relax., Morse pots. 78−82659
vibrational levels inversion splitting, generalised WKB method 80−9585
vibrational predissociation in hydrogen bonded complexes 80−61078
virial relations, for mols. in applied elec. field 80−53087
XY_4 molecules, tetrahedral, vibration-rotation energies of harmonic and combination levels 80−47962
A_2B, analytical pot. functions, several surface minima 78−5158
Ag_2, Harris-Pohl selected valence electron split-shell MO calcs. 80−91439
AgCl, bond dissoc. energy, electronegativity pot. function, pot energy curves 77−10784
AgH, bond dissoc. energy, electronegativity pot. function pot. energy curves 77−10784
Al_2, repulsive region ground state pot. curves, SCF with STO basis set calc. 80−14188
Al_2^{6+}, repulsive region ground state pot. curves, SCF with STO basis set calc. 80−14188
AlH, SCF pot. curves, 0.1-10 Bohr, ground and excited states 78−58610
AlH, valence excited states, pot. curves 78−41973
AlH^+, SCF pot. curves, 0.1-10 Bohr, ground and excited states 78−58610
Al_2H_6, electron density distrib., reaction channels and bonding characts., electrostatic mol. pot. CNDO/2 calc. 80−23309
AlN, (^{2}P)Al-(^{4}S)N, (^{2}P)Al-(^{2}D)N, nonempirical pseudopotential, configuration interaction calcs. 79−93930
AlO, ground state, pot. energy curve, dissoc. energy 78−46286
AlO radical, ground state dissoc. energy 80−53159
AlO, spectra, vibr. consts., pot. curves, Franck-Condon factors and r-centroids 78−42243
AlOH→HAlO system, intramol. rearrangement, ab initio calc. of pot. surfaces and min. energy paths, geom. parameters 80−32623
Ar-HBr, intermol. pot. energy surfaces calcs. 80−91625
Ar^{++}+He, $X^2\Sigma$ and $A^2\Pi$ states, CI pots. 78−74727
Ar_2, excited state pot. curves, ab initio CI calc. 78−78643
Ar_2, VUV emission spectrum, rot. anal. 79−98119
Ar_2 van der Waals dimer, intermol. pot., SCF CI ab initio calcs. 80−106274
Ar_2^+, bound-free absorpt. cross section for Π and Σ states 78−5140
Ar_2^+, electronic states, pot. curves, with/without spin-orbit interaction 78−33443
Ar_2^+, electronic struct., pot. energy curves, spectroscopic consts. 79−18114
Ar_2^+, photodissoc., pot. curves and photofragment spectra 77−88514
ArBr, emission spectrum and chemiluminesc. 80−45508
ArBr, pot. curves, population distribs. and chemiluminesc. for B(1/2) and C(3/2) electronic states 80−45509
ArC^+, pot. energy curves calcs. 79−45651
ArCl, neutral and negative ion states SCF pot. energy curves 78−62745
ArF_2, ab initio diatomics in mols. pot. surface, spin-orbit coupling 79−3519
ArH, excited states, theoretical pot. curves 80−95548
ArH, neutral and negative ion states SCF pot. energy curves 78−62745
ArH^+, $^1\Sigma^+$ ground state, molecular consts. calc. from pot. curves 80−9680
ArH^+, transition moments, perturbation calcs. 80−102542
ArHCl, pot. energy surface of Van der Waals complex 78−94299
$Ar_{N-1}K^+$ clusters, equilib. configs. and binding energies 80−48115
$ArKr^+$, absorpt. spectra, ab initio calc. of potential energy curves 78−74568
ArO^+, $X^4\Sigma^-$ state, pot. energy curves and correl. effects, elastic scatt. cross sections 80−23502
Ar.HBr(DBr), van der Waals complexes, rot. spectra and struct. 80−48055
Ar.HCl, Van der Waals mols., SCF energies and dispersion forces 80−74279
Ar.HF, Van der Waals mols., SCF energies and dispersion forces 80−74279
Ar.H_2O, Van der Waals mols., SCF energies and dispersion forces 80−74279
AsF, pot. energy curves and dissoc. energy, Hulbert-Hirschfelder calc. 80−30210
AsO, dissoc. energy calcs. 77−3486
Au, ground and excited states, pot. energy curves, relativistic effects calcs. 79−31416
Au_2, ground state, ab initio effective core pots., relativistic effects calcs. 79−31377
Au_2, Harris-Pohl selected valence electron split-shell MO calcs. 80−91439
potential energy curves and surfaces of molecules continued
BF_3, dissoc. pathways and mol. vibr., compliance consts. and min. energy coords. 78−35661
BH, CI wavefunction, terms selection for pot. energy surface 77−88401
BH, PE curve, spectroscopic consts., perturbation theory appl. 80−23341
BH, pot. curve, one-config. Hartree-Fock-Roothaam calc. for force consts. 78−82627
BH_2, potential energy surface, DIM method 79−18110
BH_4, pot. energy surfaces and mol. deform. induced by external cation 80−106285
BOH→HBO system, heterovalent isomerism, ab initio calc. of pot. surfaces and min. energy paths, geom. parameters 80−32622
Ba_2^{2+}, very long lived vibr. states, lifetimes, WKB calc. 80−78560
Be^{2+}+H_2O, mol. complex struct. and interaction energy, CI calc. 79−18133
Be_2, pot. curve, coupled-pair many electron theory, quadrupole excitation 79−36538
Be_2, pot. curve of ground-state, many-body perturbation theory and SCF-CI method 79−36563
BeH_2, pot. energy curve, minimal basis ab initio VB calcs. 78−50477
BeH_2, potential energy surface, DIM method 79−18110
$BeHHe^+$, from BeHT β-decay potential energy curves 78−56910
BeO, $X^1\Sigma^+$ state pot. energy curve, ground state dissoc. energy 78−41977
$Be_2(^1\Sigma_g^+)$, binding energy, ab initio pot. curves, interacting correlated fragments method 80−63557
BiBr, $A^3(0^+)$ and X^3Sigma$^-(0^+)$ states, pot. energy functions comparison 80−43133
BiBr, empirical pot. energy curves for $A^3\pi(0^+)$ and $X^3\Sigma^-(0^+)$ states 79−22617
BiO, dissoc. energy calcs. 77−3486
Br_2, $B^2\Pi(O_u^+)$ predissoc. rates, analytical interpretation 80−91617
Br_2, pot. curves, asymptotic calcs. 77−6881
Br_2+Li, bond stretching effect on charge transfer reaction cross section 78−11507
$BrCl_2^-$, photodissoc. and photodetachment, pot. curves. 79−64060
BrHe, pot. energy curve in Br^-+He electron detachment, SCF calc. 80−23503
$BrHe^-$, pot. energy curve, in Br^-+He SCF calc. 80−23503
C_2, ground state potential energy, non-muffin tin MS Xα calcs. 77−14355
C_2, pot. curves, binding and ionisation energies and config. variational cellular method 80−32597
C_2, Swan band system, vibr.-rot. interaction on pot. energy curves 80−27965
C_2, valence states, CI calcs. 79−45642
C_3, electron spectrum, ab initio MRD CI calcs. 78−90089
C_3, ground and excited states, vibr., pot. curves, CI calcs. 77−83509
C_3, ground state pot. surfaces, analytical functions 80−83304
$C_3(C_2^-)$ pot. energy curves calc. using SCF, MCSCF and CI methods, dissoc. energies, bond lengths, electron affinity 80−95523
CH, $B^2\Sigma^-$ state predissoc., calcs. and time resolved spectrosc. 80−23576
CH^+, $^1\pi-{}^1\Sigma$ band systems, vibr.-rot. interaction on pot. energy curves 80−27965
CH^+, $a^2\Pi$-$b^3\Sigma^-$ transition moment, ab initio calcs. 80−87047
CH^+, excited states, pot. curves and transition moments determ. by ab initio CI methods 80−106286
CH_2^+, unimol. decay, nonadiabatic interaction, selection and propensity rules 78−23932
$(C_2H_5)_2Fe^+$ complexes, vibrational electronic (Franck-Condon) Raman transitions 78−42070
CHNO isomers, interconversion pot. energy surfaces, geometries, electronic structs. 78−35660
CN^-, ground state pot. curve, CI and coupled pair method calcs. 79−68197
CN^+, ab initio full CI calcs. 78−50480
CN_2^+, ground state, identity, ab initio CI calcs. 80−5468
CN^+, ground state, SCF pot. energy curves calcs. 79−13782
CN^+, lower states, pot. energy curves, equilib. distances SCF CI calcs. 80−27957
CN^+, lowest $^1\Sigma^+$ and $^3\Pi$ states, ab initio CI pot. curves calcs. 79−85905
CO, electric field depend. 78−13424
CO, ground state potential energy, non-muffin tin MS Xα calcs. 77−14355
CO, inner-shell ionisation, vibr. struct., sudden approx. calcs. 79−50002
CO, isotopic mols., Dunham pot. energy coeffs. 78−41979
CO, pot. curve by variational cellular method, electronic struct. calcs. 80−54591
CO, pot. curves, binding and ionisation energies and config. variational cellular method 80−32597
CO, pot. energy functions, virial theorem calcs. 77−88519
CO, $X^1\Sigma^+$ state, diagrammatic many-body perturbation theory, pot. curves 79−10014
CO^+, ab initio pot. energy curves, full valence CI with minimal STO 79−72361
CO^+, dissoc. energy determ. from pot. energy curve 79−13837
CO+N_2, electronically inelastic collision, distorted wave calc. and pot. energy curve 80−9709
CO_2, ab initio SCF calcs., force consts., vibrs., pot. energy surface 78−5209
CO_2, anomalous energy minima surfaces 78−86791
CO_2, Dunham coeffs., high-order contribs. 78−46285
CO_2, spectra, Fermi reson. and classical motion 80−28000
CO_2, stretch-stretch interaction force const., electron correlation influence, ab initio CI study 80−58161
CO_2^-, complex symmetric stretch pot., from CO_2 reson. electron impact data 78−25726
CO_2^-, dissoc., $^2\Sigma_g^+$ state, Wall Porter pot. surface, autodetachment and vibr. level population inversion 80−21275
CO_3, and isotopic forms, struct., normal coord. anal. 78−965
C_3O_2, bending pot. function, vibr. depend. 80−48058
COS, mole. potential surface, evaluation from spectroscopic observations 80−43207
Ca_2, $A^1\Sigma_u^+$-$X\Sigma_g^+$ system, laser induced fluoresc., pot. energy curve and mol. consts. 80−58307
Ca_2, ground state, multiple scatt. Xα calcs. 80−58149
Ca_2^+, pot. energies in Ca^+ and Rydberg Ca** collisions with Ca 79−27055
CaCl, $B^2\Sigma$−$X^2\Sigma$ transitions, rot. anal. by laser spectroscopy 80−91536
CaCl, $X^2\Sigma$ pot. energy curves, polarisability and dissoc. 80−91629

potential energy curves and surfaces of molecules continued
CaH, low lying electronic states, ab initio SCF-CI calcs. 80−52893
Cd_2, pot. energy curve of low-lying states, MO theory 79−89624
CeO, dissoc. energy, rel. band strengths of a_2-X_2 and b_2-X_2 systems 80−99495
Cl_2, pot. curves, asymptotic calcs. 77−6881
Cl_2, photodissoc. and photodetachment, pot. curves. 79−64060
Cl_2^-, pot. energy curves, from Cl_2 dissoc. electron attachment, 0−11.5 eV 77−75312
Cl_2+Li, bond stretching effect on charge transfer reaction cross section 78−11507
Cl_2+muonium (H)(D), pot. energy surfaces, inversion calcs. 80−93734
Cl_3^- energy surface, comparison of CNDO and ab initio results 77−23445
Cl_3^-, photodissoc. and photodetachment, pot. curves. 79−64060
ClO^-, photodissoc. and photodetachment, pot. curves. 79−64060
ClO_2, analytical pot. functions, several surface minima 78−5158
ClO_2, ground state pot. calc. using orthogonal internal coords. definition 79−76479
$CrCl_4$, ligand field states, multiple scatt. Xalpha calcs. 80−47891
CrO molecule, $B^3\pi$ and $X^3\pi$ states, potential energy curves 80−42962
Cs_2, 6^2S-7^2P doublet, mol. satellites 79−85956
Cs_2, ground state consts., pot. curve, laser spectroscopy 79−98247
Cs_2^+, $^2\Sigma$ and $^2\Pi$ state pot. energy curves, two-centre model 79−26906
Cs_2^-, adiabatic pot. curves, ground and excited state, Hellmann-type model pots. 78−78647
$Cs_{2_2}^+$ pot. energy curve, pseudopot. calc. 77−6703
Cs_2^-, low-lying states, MC SCF+CI 80−69053
CsH, $X^1\Sigma^+$ and $A^1\Sigma^+$ states, pot. energy curves, Rydberg-Klein-Rees methods 78−50486
CsH^+, Σ state pot. energy, Hellman pseudopot. calcs. 78−70764
CsH^-CsH^+(CsH), ab initio ground-state pot. energy curves, electron affinities 78−41946
Cs_2MX_6(M=Se, Te, X=Cl, Br), $\Gamma_4^-(^3T_{1u})$ state, Jahn-Teller effect, luminesc. obs. 80−60650
Cu_2, Harris-Pohl selected valence electron split-shell MO calcs. 80−91439
$^6Cu_2$, $B^1\Sigma_u^+$-$X^1\Sigma_g^+$ transition, Franck-Condon factors, r-centroids and pot. curves 80−43114
D+H_2 reaction, transition state theory calculations, kinetic isotope effect explanation 80−66784
$D_2^+(DT^+)$, IR transition freqs. calcs. 77−88452
D_2, $^1\Sigma_g^+$ states, adiabatic calc. of vibronic states 78−5198
D_2, c, I and i states, pot. energy curves and vibr. levels, Born-Oppenheimer approx. 78−931
D_2, G, K double-minimum excited state, vibr. eigenvalues 78−33442
D_{2_u} semiempirical nonadiabatic pot. energy curves calcs. 78−17744
D_2^+, semiempirical nonadiabatic pot. energy curves calcs. 78−17744
D_3^+, ab initio vibr. intervals and vibr. freq. refinement 80−47968
DCN, electronic spectra, vibr. struct., ab initio calc. 78−9166
F_2, PE curve, spectroscopic consts., perturbation theory appl. 80−23341
F_2, pot. curves, binding and ionisation energies and config. variational cellular method 80−32597
F_2, pot. curves and electronic phototransitions 79−63935
F_2CS, pot. surfaces, X^1A_1, a^3A_2 and $a^3A_2(b_1)$ states, ab initio SCF calcs. 78−86795
FH_2, pot. energy surface, valence states, VB diatomics-in-mols. method 79−85920
FHF^-, H bonds, vibr. dynamics calcs. 80−23397
FHe^+, fragmentation and potential energy curves from FT β-decay 78−56910
GaI, $A0^+$-$X0^+$ and B1-$X0^+$ transitions, isotope shifts, UV and visible spectra obs. 80−53005
GaKr, low-lying electronic states, PE curves, transition moments, emission coeffs. 79−6894
GaO, B-X band system, electronic spectrum, struct. and anal. 79−45732
GeO, RKRV Franck-Condon factors and r-centroids, ($A^1\Pi$-$X^1\Sigma^+$) transition, pot. energy curves 78−29817
H bonded species, IR line broadening, kinematic and electronic coupling mechanisms 77−68043
H bonds, linear triatomic model, adiabatic approx., freqs. and isotope effects 77−65448
H-like clusters, DIM pot. energy hypersurfaces, stationary points 78−25763
H+D_2 reaction, transition state theory calculations, kinetic isotope effect explanation 80−66784
H+H_2, least squares fit to ab initio pot. energy function 78−56883
H+HCl, semi-empirical pot. energy surfaces calc. by diatomics-in-molecules method 80−95556
H^++H_2→H_3, nonadiabatic transitions, comparison of surface hopping and complex-valued time calcs. 77−9049
H_2, excitation energy, pot. curves, oscill. strength, Hartree-Fock calcs. 77−6685
H_2, excited $G+K^1\Sigma_g^+$ double minimum state, Born-Oppenheimer pot. energy curve 77−30847
H_2, G, K double-minimum excited state, vibr. eigenvalues 78−33442
H_2, ground state, pot. curves, MTXα_R method 80−5482
H_2, ground state potential energy, non-muffin tin MS Xα 77−14355
H_2, HD, $^1\Sigma_g^+$ states, adiabatic calc. of vibronic states 78−5198
H_2, HD, c, I and i states, pot. energy curves and vibr. levels, Born-Oppenheimer approx. 78−931
H_2, ionic-covalent config. mixing, pot. curves 77−34576
H_2, lowest singlet and triplet states, interactions, electronic force calcs. 80−63742
H_2, photoionisation, resonant, dissociative 79−68272
H_2, pot. curves, binding and ionisation energies and config. variational cellular method 80−32597
H_2, pot. energy functions, virial theorem calcs. 77−88519
H_2, semiempirical nonadiabatic pot. energy curves calcs. 78−17744
H_2, solid, equation of state, intramol. zero pt. energy contrib., total sublimation energy 78−71829
H_2, tempered orbital energies and pot. curve 79−89584
H_2, triplet state, pot. curve van der Waals region, MS-MA calcs. 77−79551
H_2^-, variational calcs. of resonant states 79−3571
H_2^+, ground state, pot. energy curves, 1/R expansion coeff. calcs. 80−91472
H_2^+, nonexponential wavefunctions for $1s\sigma_g$ and $2p\sigma_u$ states 77−415
H_2^+, nonexponential wavefunctions for $2p\pi_u$, $3d\pi_g$ and $3d\delta g$, $4f\delta_u$ states 77−416
H_2^+, semiempirical nonadiabatic pot. energy curves calcs. 78−17744
potential energy curves and surfaces of molecules continued
H_2-H_2 intermol. pair pot., ab initio SCF-CI surface 80−91457
H_2-inert gas, bound complex form., anisotropic intermol. pot., IR spectra anal. 78−37634
H_2+H^+, low energy rot. excitation, ab initio differential inelastic cross section calcs. 77−88542
H_2+He, vibr. relax. cross section 80−99494
H_2^++H^-→H_2*+H recombination react., calcs. *(Russian)* 80−55659
H_3, bent, spline-fitted pot. surface 77−57851
H_3, CI calc. of three dimens. pot. energy surface 78−56882
H_3, diatomic state mixing parameter 80−74139
H_3, H_4, pot. energy hypersurfaces, diatomics-in-molecules method extension 77−30780
H_3, LEPS pot., from force field data 79−63934
H_3, pot. energy surfaces, semiempirical calcs. 78−41974
H_3, three atom ab initio energy surface calc. 78−82663
H_3^-, dissociating states, lowest singlet and triplet PE surfaces, HF calcs. 79−81160
H_3^+, ab initio calcs. of vibr. spectrum 77−6753
H_3^+, ab initio vibr. intervals and vibr. freq. refinement 80−47968
H_3^+, pot. surface, GTO config. expansion 79−26907
H_3^+, uncoupled symmetric stretching freq. calcs. 78−66532
H_4, excited potential energy hypersurfaces, trapezoidal geometry, rel. to photochem. 2s+2s processes 77−30797
H_4, FGSO open-shell calcs., pot. energy surface of configurations 79−10025
H_4, pot. energy surfaces, valence bond calcs. 80−74129
HBr, Dunham pot. energy coeffs. 78−41979
HC_2, ground state energy surface, ab initio SCF calc. 78−33446
HC_2^-, ground state energy surface, ab initio SCF calc. 78−33446
HCC→H+C=C dissoc., trajectory calcs., random vibr. excitation 80−45491
HCN and HNC, analytic functions from pot. energy surfaces 78−62743
HCN, electronic spectra, vibr. struct., ab initio calc. 78−9166
HCN, ground state pot. surfaces, analytical functions 80−83304
HCN, H-CN dissoc. curves, SCF CI calc. 79−100405
HCN, SCF ab initio ground state pot. energy surface, geometry, rel. to HCN^- 78−78646
HCN, vibr. fine struct. accompanying core ionis., STO calcs. 78−62844
HCN^-, SCF ab initio ground state pot. energy surface, geometry, rel. to HCN 78−78646
HCN^+, A and $B\ ^2\Sigma^+$ states, pot. surfaces, ab initio SCF calcs. 80−27959
HCN^+, photoelectron spectra of third electronic state, ab initio calc. of pot. energy surface 78−70871
HCO and HNO, pot. energy functions for ground state surfaces 79−89620
H_2CO^+ ion, unimolecular decay paths of electronically excited species 79−3359
HCOH, prediction, potential energy surface for ground state of formaldehyde 80−42967
HCS^+-CSH^+ system, pot. surface for H abstraction, internuclear bending for ground and excited states 78−29744
HCl^-, resonance states, CI calcs., pot. energy curves 78−29755
HD, G, K double-minimum excited state, vibr. eigenvalues 78−33442
HD, nonadiabatic effects in the B, C and E, F states, rot. line strengths 78−5148
HF, low lying states, GVB and CI calcs. 77−14362
HF, polarisation model representation for chem. reactions 79−39131
HF, pot. curve, one-config. Hartree-Fock-Roothaam calc. for force consts. 78−82627
HF, pot. curves, diagrammatic perturbation theory, spectrosc. consts. 78−25458
HF, pot. energy curve, minimal basis ab initio VB calcs. 78−50477
HF, pot. energy functions, virial theorem calcs. 77−88519
HF, potential curve calc. using angular momentum depend. of pseudopot. 77−30804
HF-HCl, SCF energy hypersurface, stationary points, thermodynamics of form. 80−102436
HF+H^-, reaction, ab initio pot. energy surface calcs. 79−39127
$(HF)_2$, intermol. force model, rel. to liq. struct. 78−78773
$(HF)_2$, polarisation model representation for chem. reactions 79−39131
$H_2^+(HD^{++})$, $1s\sigma_g$ state, pot. energy curves, relativistic corrections 77−57892
$H_2(HD)(D_2)$, ab initio pot. energy curves and vibr. levels, B″, B̄, B′ states 77−6754
$H_2^+(HD^+)(HT^+)$, IR transition freqs. calcs. 77−88452
HI, dipole moment function, multiconfiguration SCF calc. 77−75330
HI, Dunham pot. energy coeffs. 78−41979
HNC→HCN, transition state determination and characterisation ab initio calcs. 77−28975
HNO, CI-SCF-MO basis function calc. 77−42246
HNO, low-lying states, pot. energy curves 80−9533
HNO, low-lying states, pot. energy surfaces calcs. 80−102460
HNO, vibr. freqs. from anharmonic ab initio/empirical PE functions 79−76406
HNO^+, ab initio pot. surface, and isomerisation barrier of lowest states 79−22622
HNSi, and HSiN, electronically excited states, MRD CI calc. 79−49947
HO_2, analytical pot. functions, several surface minima 78−5158
H_2O, ab initio SCF CI calcs., ground state energy, config. and force consts. 77−18782
H_2O, and D_2O, local model vibrs. 79−76414
(H_2O), electron affinity, ab initio SCF calcs. 79−76343
H_2O, electronic ground state, SCF HF and CI calcs, pot. energy hypersurface, spectroscopic consts. 78−50473
H_2O, empirical potential model EPEN/2, parameterisation testing 79−54933
H_2O, energy levels, triat. large amplitude vibrs. model appl. 80−23392
H_2O, excited states, pot. energy curves w.r.t. bond ang., one-centre expansion approx. 79−6886
H_2O, modified LEPS surface, ground state 78−17584
H_2O, mol., quartic force field, many-body methods using STO 79−85921
H_2O, molecule, shape as function of O-H separation 80−43203
H_2O, pot. energy surface by MS Xα method 79−13656
H_2O, quantum mech. pot. surface, power series expansions 77−34577
H_2O, theoretical IR transition matrix elements 79−85953
H_2O, vibr. anal., normal coord. calcs., nucl. corrections to mol. props. 77−88441

potential energy curves and surfaces of molecules continued
H_2O, vibr. freqs. from anharmonic ab initio/empirical PE functions 79−76406
H_2O^+, pot. energy surface, linear approach 78−41978
H_2O^+, X^2B_1 and B^2B_2 states, pot. surfaces, SCF and CI calcs. 77−3338
H_2O-ethylene (H_2O) nonbonded interactions, pot. energy curves, CNDO/2, INDO and extended Huckel calcs. 77−27140
$(H_2O)_2$, difference electrostatic mol. pot. contour maps, basis set superposition effect 80−102462
$(H_2O)_2$, electrostatic mol. pot. curves, proton transfer and bridging pot., CNDO/2 calc. 79−94054
H_3O radical, stability, ab initio UHF-CI calcs. 78−5137
HOBr, analytical pot. energy functions and surfaces 79−68203
HOCl, analytical pot. energy functions and surfaces 79−68203
HOCl, photodissoc., ab intio SCF CI calcs. 78−50604
HOCl, vibr. freqs. from anharmonic ab initio/empirical PE functions 79−76406
HOF, analytical pot. energy functions and surfaces 79−68203
HOF, ground state pot. calc. using orthogonal internal coords. definition 79−76479
HOF, vibr. freqs. from anharmonic ab initio/empirical PE functions 79−76406
HOI, analytical pot. energy functions and surfaces 79−68203
HOO radical, lowest doublet electronic states, rel. to photodissoc. 79−93914
H_2PNH_2, inversion-rot. mechanism, basis set and geometry optimisation effects 80−83273
HPO, 4-const. valence force pot., from IR(UV) matrix isolation spectra 80−47985
H_2S^+, $^2B_1$, $^2A_1$ and $^2B_2$ electronic states, pot. energy curves, CI calcs. 80−87048
$(H_2S)_2$, hydrogen bond, proton transfer, pot. energy surface 77−67977
HSiN and HNSi, analytic functions from pot. energy surfaces 78−62743
$H_2(X^1\Sigma_g^+)$, semiempirical Morse pot. extension, fitting procedure appl. 79−36560
H_2*, energy and occupation curves, wave functions, natural spin orbital anal. 77−83493
He-Ar(Kr)(Xe), 208 and 707K, intermol. forces, virial, diffusion, and viscosity coeffs. 77−75256
He-He, potential energy curves, dispersion damping functions, Hartree Fock interaction energy 79−98176
$He+H_2$, pot. energy surface, analytical expressions from constrained optimisation 77−6698
He_2, 600 Å emission continuum struct., in 700-900 Å region in glow discharge 80−95641
He_2 excimer potentials, long range, from He+He differential cross-sections 79−81167
He_2, ground state, interaction energy, many-body perturbation theory calcs. 80−69210
He_2 high press. afterglows, reviews 80−64823
He_2, pot. curve using CEPA-PNO correl. wavefunction 79−63932
He_2^{2+}, autoionising states, adiabatic pot. energy curves calcs. 78−42140
He_2^{2+}, bound excited states, potential energy curves and rovibronic energy, dissociation 80−23327
He_2^{2+}, electronic energies, James-Coolidge method calcs. 78−17564
HeH, neutral and negative ion states SCF pot. energy curves 78−62745
HeH^+, excitation energy, pot. curves, oscill. strength, Hartree-Fock calcs. 77−6685
HeH^+, $X^1\Sigma^+$ electronic ground state, pot. curve, rovibronic and dissoc. energies 79−72254
HeH^{2+}, pot. energy curves for 2pπ and 3dδ excited states 78−29756
HeH_2^+, electronic struct. 79−31414
$HeHe_2^+$, doublet, ab initio pot. energy surface calcs. for ground and lower excited state 79−63898
$He_2(He_2^+)$, variational electronic struct. calcs. using Hylleraas type wavefunctions 77−88375
HeI_2, Van der Waals mol. vibr. predissoc. anharmonicity effects 80−52971
$HeLi^{4+}$, pot. energy curves for 2pπ and 3dδ excited states 78−29756
$HeNe^+$, collisional form., excitation, pot. energy curves calcs. 77−6697
$He_2^+X^2\Sigma_u^+$ state, ab initio CI calc., pot. energy curve, vibr. and rot. levels 77−3263
^{4}He trimer and tetramer, ATMS appl., bounding and ground state energies 79−86026
Hg_2, emission bands, pot. energy surface calcs. 77−10601
Hg_2, fluoresc. and absorpt. spectra anal., pot. energy curves 78−999
Hg_2, model calc. of electronic struct. and spectroscopy 79−3352
Hg_2^+, electronic struct. and photoabsorpt. calcs. 80−27932
HgH, ab initio studies using relativistic effective core pots. 78−86767
HgXe, fluoresc. spectra, pot. curves and binding energy 78−66581
I_2, A-X system 79−63995
IBr, $B^3\Pi(0^+)$ states, Franck-Condon factors, RKR turning pts. 77−34681
IBr, photodissoc., curve crossing of $Br(^2P_{3/2})$ and $Br(^2P_{1/2})$ 78−62859
ICN, photodissoc., product rot. distribs. 79−66310
ICl, $B^3\Pi(0^+)$ states, Franck-Condon factors, RKR turning pts. 77−34681
$I^{35}Cl$, predissociations in $B^3\Pi_{0+}$ state 80−1033
$I^{37}Cl$, predissociations in $B^3\Pi_{0+}$ state 80−1033
IF, $B^3\Pi(0^+)$ states, Franck-Condon factors, RKR turning pts. 77−34681
$I_2(I_2^+)(I_2^-)$, HF and SCF calcs., pot. curves, electron affinity and quadrupole moment determ. 80−95527
K+H, covalent and ionic states interaction, config. mixing 78−50613
K_2^+, $^2\Sigma$ and $^4\Pi$ state pot. energy curves, two-centre model 79−26906
K_2^+, adiabatic pot. curves, ground and excited state, Hellmann-type model pots. 78−78647
K_2^+, pot. energy curve, pseudopot. calc. 77−6703
KCs^+, adiabatic pot. curves, ground and excited state, Hellmann-type model pots. 78−78647
KF, ab initio SCF MO energy, dipole moment and polarisability 80−1085
KH^+, Σ state pot. energy, Hellman pseudopot. calcs. 78−70764
KOH, MHD plasma mol., pot. energy curves and dipole moment, bond lengths 78−71462
KRb^+, adiabatic pot. curves, ground and excited state, Hellmann-type model pots. 78−78647
KXe, fluoresc. excitation and emission spectrum 79−6947
K(5S)Xe, K(5S)Kr, excimer, visible emission band, exptl. results relative to theory 78−82779
Kr-HCl, intermol. pot. energy surfaces calcs. 80−91625

potential energy curves and surfaces of molecules continued
Kr_2^+, electronic states, pot. curves, with/without spin-orbit interaction 78−33443
Kr_2^+, electronic struct., pot. energy curves, spectroscopic consts. 79−18114
Kr_2^+, photofragment energy spectra, pot. energy curves 78−55207
$Kr_2Cl(F)$, ab initio diatomics in mols. pot. surface, spin-orbit coupling 79−3519
KrF, A state pot. in $Kr+F_2(NF_3)(CF_3OF)$, emission spectra calc. 80−7799
KrF, electronic states, ab initio CI calcs., spin-orbit coupling, pot. curves, dissoc. energy, dipole moments 77−38619
KrF, fluoresc. spectrum, theoretical modelling using electronic potential curves 78−63086
KrF*, bound-free emission spectra, simulation 78−29806
KrO^+, $X^4\Sigma^-$ state, pot. energy curves and correl. effects, elastic scatt. cross sections 80−23502
LaO molecule, potential energy curves, Rapid method by Morse function 77−26998
Li clusters, DIM pot. energy hypersurfaces, stationary points 78−25763
Li-He, oscill. strength, for induced dipole transitions, pot. energy curves 77−75100
Li_2, $A^1\Sigma_u^+$ state, vibr. energy levels calcs. 77−83566
Li_2, $B^1\Pi_u$, pot. energy curve, MC SCF approx. calcs. 77−38618
Li_2, core-excited states, UV photoabsorpt. and ejected electron spectra 78−37655
Li_2, pot. energy curves, bound states 77−88409
Li_2, pot. energy surface, half-projected HF model 79−36564
Li_2, potential curve calc. using MTXα_R method 77−10593
Li_2, $X^1\Sigma_g^+$ and $A^1\Sigma_u^+$ states, electronic struct. and spectra 79−89615
Li_2^+, $^2\Sigma$ and $^2\Pi$ state pot. energy curves, two-centre model 79−26906
Li_2^+ exchange and ion-multipole interactions, vibrational energy levels 79−98175
Li_2^+, $X^2\Sigma_g^+$, $^2\Sigma_u^+$, $A^2\Pi_u$ and $^2\Pi_g$ states, electronic struct. vibr. spectra, ab initio calcs. 79−36507
Li_3, BO hypersurface and vibronic states, coupled electron pair approx. 78−94203
Li_3, potential energy surface and config., RHF CI calc. 77−34562
$LiAlF_4$, struct. pot. energy surface, Li^+ migration, ab initio LCAO SCF calcs. 80−23305
$LiAlH_4$, $LiBH_4$, ab initio calc. of geom. struct., charge distrib., bonding and pot. energy surfaces 80−18796
$LiBF_4$, nonrigid mol. struct. and stability, ab initio calcs. 80−83259
$LiBH_4$, non-rigid complex molecule, ab initio calcs. of pot. energy surface and geometric struct. 77−6678
$LiBH_4$, pot. surface and geometry, ab initio calcs. 78−86771
$LiBH_4$, struct., pot. surface, ab initio calcs. 79−41092
$LiBeF_3$, pot. energy surface, struct., stability and internuclear distances, ab initio calc. 80−58147
$LiBeH_3$, ab initio calc. of pot. surfaces and geometry 79−10024
$LiBeH_3$, pot. surface, struct., ab initio calcs. 77−88385
LiCN, vibr.-rot. spectra, model with two large-amplitude coords. 78−5196
LiCa, laser chemiluminesc. 80−93759
LiF, ab initio SCF MO energy, dipole moment and polarisability 80−1085
LiF, ground state, pot. curve, determination and use of molecular α values in MS$X\alpha$ calcs., MTXα_R meth. 79−10032
LiF, pot. curve, one-config. Hartree-Fock-Roothaam calc. for force consts. 78−82627
LiH, correlated potential energy curve, correlation hole concept, restricted Hartree-Fock solutions *(Spanish)* 80−14081
LiH, ground state, pot. curves, MTXα_R method 80−5482
LiH, half-projected HF scheme, stability conditions 77−61676
LiH, isotopic species, $A^1\Sigma^+ \rightarrow X^1\Sigma^+$ bands 78−42091
LiH, LiH^-, pot. energy curves, electron affinity, spectroscopic consts. 78−5129
LiH, $LiHe^+$ and $LiHe_2^+$ systems, ab initio SCF LCAO calcs. of stability and spectroscopic consts. 77−71748
LiH, pot. curve, one-config. Hartree-Fock-Roothaam calc. for force consts. 78−82627
LiH, $X^1\Sigma^+$ and $A^1\Sigma^+$ states, hybrid pot. energy curves, dissoc. limits 77−79669
LiH^{3+}, pot. energy curves for 2pπ and 3dδ excited states 78−29756
^{7}LiH, $A^1\Sigma^+$-$X^1\Sigma^+$ bands, radiative transition probabilities calcs. 78−66603
^{7}LiH, radiative transition probability, from pot. curves, $B^1\Pi$ curve calc. 78−78752
$(LiH)^+$ + meson system, ground and 1st excited state pot. surfaces, quantum mech. calc. 78−5377
LiH_2, quantum mech. pot. surface, power series expansions 77−34577
$(LiH)_3$ complex, SCF interaction energy nonadditivity 80−91437
LiHH system, pot. surfaces, nonempirical GO calcs. 77−42374
$LiH_2(LiD_2)(LiT_2)$, pot. surfaces, fundamental freqs. and thermodynamic functions 80−69205
$Li_2H(Li_2D)(Li_2T)$, pot. surfaces, fundamental freqs. and thermodynamic functions 80−69205
$LiH^-(LiH)$, ab initio ground-state pot. energy curves, electron affinities 78−41946
$LiHe^+$, from LiT β-decay, pot. energy curves 78−56910
LiI UV photodissoc. cross section, reson. ionis. Li detection 80−63719
LiNC, metal atom motion, WKB calcs. 78−82623
LiNC, struct. vibr. states and pot. energy calcs. 78−86776
LiNa, ground and excited states, model pseudopot. calcs. 77−75069
LiOH, $^1A'$ pot. energy surface, diatomics-in-mols. method calcs. 79−36566
LiOH, fundamental vibr. freqs. 79−98068
LiOH, potential energy surface, diatomics-in-molecule method 79−63929
$^7Li_2$ $A^1\Sigma_u^+$-$X^1\Sigma_g^+$ band system anal. 77−83565
$LuCl_3$, pyramidal struct. and force field coeffs., electron diffr. obs. 78−9250
Mg_2, empirical pot. curves, Pade approximant calcs. 80−14184
Mg_2, ground state, multiple scatt. Xα calcs. 80−58149
Mg_2, Mg_2^+, electronic struct., pot. energy curves, multiconfig. SCF calcs. 78−5124
Mg_2, pot. energy curve for $X^1\Sigma_g^+$ state, many-body perturbation calcs. 78−55216
Mg_2, $X^1\Sigma_g^+$ state, pot. curve, coupled pair many electron theory calc. 79−89621
Mg_2Cl_4, equilib. config., pot. energy curves, ion model 77−65540

potential energy curves and surfaces of molecules continued
MgD, emission spectra, 600 to 850 nm, rot. anal., dissoc. energies 78−62815
MgH, emission spectra, 600 to 850 nm, rot. anal., dissoc. energies 78−62815
MgH, Morse and Lippincott pots., r-centroids, dissociation energy 78−13446
MgH^+, CI pot. curves and cross sections for lowest singlet states 80−23343
MgO, dissociation energy from RKRV potential energy curve 78−37768
Mn-C_2H_2 and Mn-C_2H_4, π-bonded, pot. energy curves, SCF calc. 78−5136
N_2, core photoelectron line shape, localisation role 79−59512
N_2, electron impact dissoc., EELS, N^- autoionisation 80−106397
N_2, ground state potential energy, non-muffin tin MS Xα calcs. 77−14355
N_2, multi-config. SCF super-CI calc., density matrix formulation 80−78547
N_2, PE curve, spectroscopic consts., perturbation theory appl. 80−23341
N_2, pot. curves, binding and ionisation energies and config. variational cellular method 80−32597
$^{14,15}N_2$, Fourier spectrometry and IR emission spectra 80−83368
N_2^{2+}, low-lying electronic states, pot. energy curves calcs. by SCF technique, vibr. and ionisation consts. 80−69091
N_2^{2+}, recomb. energy determ. from pot. curves 80−58335
N_2^{n+}, Coulomb explosion following heavy ion impact, ab initio SCF calc. 79−18277
NCNO⇌NC+NO, ground state pot. energy surface, ab initio calcs. 77−90593
NCO^+, CI-SCF-MO basis function calc. 77−42246
NCO^+, partial pot. energy surfaces, ab initio SCF CI calcs. 78−37554
NF, pot. energy curves and dissoc. energy, Hulbert-Hirschfelder calc. 80−30210
NH^+, pot. curves, ab initio CI calcs., equilib. distances 78−17579
NH^{3+}, pot. energy curves, model pot. method, orbiting and reson. effects 80−63815
NH_2, pot. energy curves of X^2B_1, A^2A_1, $^2B_2$ valence-shell and $\pi_u{}^2$3s-type Rydberg states calc. by CI 80−74138
NH_2^-, photodetachment energy calcs. 77−27123
NH_2^+, low lying states, ab initio MRD-CI pot. surface calcs. 79−89611
NH_2^+, quintet states, pot. energy surfaces, ab initio SCF MO calc. 78−25419
NH_2^+, triplet state ab inito CI pot. energy surfaces 78−74729
NH_3, ab initio SCF calcs., force consts., vibrs., pot. energy surface 78−5209
NH_3, double min. vibr. pot., FORMAC program 77−23444
NH_3, first triplet state, photodissoc. and Rydbergisation investig. 80−53067
NH_3, pot. energy surface by MS Xα method 79−13656
NH_3, predissociation of A''_2 state from UHF calcs. of potential energy surface 80−1034
NH_3-CO_2 complex, matrix isolation IR spectrum, struct., ab initio SCF calcs. 78−5209
N_3H_3 radical, lowest two electronic states 80−925
NH_4Cl, gas $^1A_1$ ground state, pot. surface 80−32626
NO, core photoelectron line shape, localisation role 79−59512
NO, photoionis. resonant processes, pot. energy curves 77−65516
NO^+, pot. energy curves, dissoc. energy 79−22623
NO^+, pot. energy curves calcs. 80−5602
NO_2, ground state pot. surface, ab initio LCAO MO SCF calcs. 80−102461
N_2O, and isotopic forms, pot. energy function determ. from vibr. data 77−18812
N_2O^-, ground state potential energy surfaces 77−27175
N_2O^-, N_2O, ground state calcs., and expts. 77−27175
N_2O^+, pot. energy hypersurface charact. calc. in $O^+ + N_2 \rightarrow N + NO^+$ react. 78−60996
NOH^+, ab initio pot. surface, and isomerisation barrier of lowest states 79−22622
Na-He model pot. calcs., fluoresc. line profile 79−36723
Na+H, covalent and ionic states interaction, config. mixing 78−50613
Na+O_2, semiempirical pot. surfaces, dynamical considerations 79−11766
Na_2 $A^1\Sigma_u^+ \rightarrow X^1\Sigma_g^+$ system, transition moments and radiative lifetimes calcs. 77−34697
Na_2, $B^2\Pi_u$ state, pot. energy curve, shape determ. 79−31432
Na_2, ground state, pot. curves, MTXα$_R$ method 77−71762
Na_2, long range mol., electronic and vibr. levels 78−94301
Na_2^+, $^2\Sigma$ and $^2\Pi$ state pot. energy curves, two-centre model 79−26906
Na_2^+, adiabatic pot. curves, ground and excited state, Hellmann-type model pots. 78−78647
Na_2^+, pot. energy curve, pseudopot. calc. 77−6703
Na_3, electronic struct., pot. energy surface, ab initio CI study 78−70996
$NaAlH_4$, $NaBH_4$, ab initio calc. of geom. struct., charge distrib., bonding and pot. energy surfaces 80−18796
NaAr, ground and excited state pot. curves, dispersed fluoresc. spectrum 79−98140
$NaBH_4$, struct., pot. surface, ab initio calcs. 79−41092
$NaCs^+$, adiabatic pot. curves, ground and excited state, Hellmann-type model pots. 78−78647
NaH, $A^1\Sigma^+$-$X^1\Sigma^+$ electronic transition, spectroscopic anal. and potential energy curves 80−48102
NaH, ground state, pot. curves, MTXα$_R$ method 80−5482
NaH Π states and NaH^+ ground state, pot. energy curves calc. 80−18812
NaH^+, Σ state pot. energy, Hellman pseudopot. calcs. 78−70764
NaH^-(NaH), ab initio ground-state pot. energy curves, electron affinities 78−41946
NaK, ab initio and pseudopot. energy curves 78−90068
NaK, laser-induced fluoresc. in supersonic nozzle beams 78−25593
NaK^+, adiabatic pot. curves, ground and excited state, Hellmann-type model pots. 78−78647
NaLi, ground state, pot. curves, MTXα$_R$ method 77−71762
NaNe, laser spectroscopy, interat. pot. curves 78−86871
NaNe, van der Waals mol., form., laser spectroscopy 78−29797
NaNe, $X^2\Sigma$, $A^2\Pi$ and $B^2\Sigma$ states, model pot. calcs. 78−78776
$NaRb^+$, adiabatic pot. curves, ground and excited state, Hellmann-type model pots. 78−78647
Na(4S)Xe, Na(4S)Kr, excimer, visible emission band, exptl. results relative to theory 78−82779

potential energy curves and surfaces of molecules continued
Ne_2^+, electronic struct., pot. energy curves, spectroscopic consts. 79−18114
Ne_2F, ab initio diatomics in mols. pot. surface, spin-orbit coupling 79−3519
Ne_2F, energy surfaces, application of molecular electronic struct. theory 78−25452
NeH_2^+, ab initio potential surfaces, frozen orbital approximation calcs. 78−41927
Ne_2* excimer, transient absorption spectra assignment 79−41115
Ni, chemisorptive binding of O, CNDO calc. of potential energy curves *(German)* 80−44431
Ni_n clusters, Ar matrix, UV-visible spectra, pot. energy curves 77−65552
NiH, pot. energy curves, Hartree-Fock and valence bond methods 78−41958
NiH_2, pot. energy curves, Hartree-Fock and valence bond methods 78−41958
NiNaK, mol., intersection of pot. energy surfaces, ab initio calcs. 79−36557
O^{n-} (n=0 to 2), core binding energy shifts, ΔSCF calcs. 80−95558
O_2, $^3\Pi_g$ diabatic Rydberg states, ab initio CI calcs. 80−95554
O_2, $^3\Sigma_g^-$ ground state, pot. energy curve, direct CI method appl. 80−58165
O_2, adsorbed on graphite, pot. energy curves of dissoc., CNDO/2 calcs. 79−28206
O_2, core photoelectron line shape, localisation role 79−59512
O_2, excited state geometries and energies, ab initio pot. energy surfaces 78−5151
O_2, ground state, ab initio pot. curve calcs. 77−83510
O_2, harmonic oscillator model in predissoc., level widths, shifts and curve crossing 78−90239
O_2, microwave spectrum, press. broadening 80−23412
O_2, valence states, ab initio config. interaction calcs. 78−25448
O_2^-, $A^2\Pi_u$ state pot. energy curve, MCSCF calcs. 80−63565
O_2^-, ab initio pot. curves of $X^2\Pi_g$, $A^2\Pi_u$, $a^4\Sigma_u^-$, $^2\Sigma_u^-$ states 78−66483
OCS, motion, regular and irregular spectra, theory 80−9590
OCS, rot.-vibr. levels and semiclassical energy levels 80−37804
OH, Dunham pot. energy coeffs. 78−41979
$OH^- + CO_2 \rightarrow HCO_3^-$ react., MO-LCAO-SCF calcs., energy barrier 78−76846
$(OH)_2^{2-}$, electrostatic mol. pot. curves, proton transfer and bridging pot., CNDO/2 calc. 79−94054
ONCl, vibr. freq., anharmonic ab initio/empirical pot. energy functions 80−99457
$Os_5O_3F_2$, normal coordinate anal. in Urey-Bradley force field 79−49966
P_2^+, electronic states pot. energy curves, dissoc. energy, ionisation pot., curve fitting 80−32796
PF, (PF^+), pot. energy curves and dissoc. energy, Hulbert-Hirschfelder calc. 80−30210
PF_4, MS Xα calcs., pot. energy surface, electronic struct. 77−57877
PH_2 radial, pot. energy curves. config., ab initio SCF-MO calcs. 77−50419
PH_5, rearrangements, CI calcs. in large at. orbital basis 79−94106
Pb_2, low-lying states, energy curves, bonding 79−76367
PtC, ground and first excited states, dissoc. energy and dissoc. curves, pot. energy curves 77−50555
PtH(D), pot. energy curves, r-centroids, Franck Condon factors, rot. depend. 80−28082
PtO, ground and first excited states, dissoc. energy and dissoc. curves, pot. energy curves 77−50555
Rb_2, $X^1\Sigma_g^+$ state, Raman spectra, fluoresc., vibr. energy 78−46345
Rb_2^+, $^2\Sigma$ and $^2\Pi$ state pot. energy curves, two-centre model 79−26906
Rb_2^+, adiabatic pot. curves, ground and excited state, Hellmann-type model pots. 78−78647
Rb_2^+, pot. energy curve, pseudopot. calc. 77−6703
$RbCs^+$, adiabatic pot. curves, ground and excited state, Hellmann-type model pots. 78−78647
RbH^+, Σ state pot. energy, Hellman pseudopot. calcs. 78−70764
S (S-He) discharges, stability, emission spectra 80−107003
SCl_2, microwave spectrum, quadratic pot. function, average struct. 77−65456
SF_6, multiphoton absorpt., energy transfer, dissoc. probability, laser field interaction, classical trajectory approx. 80−37730
SF_6, photon-enhanced dissociative electron attachment, isotope selectivity 80−18939
SO, pot. energy curves, pseudopot. multi-struct. valence bond calcs. 78−9094
SO, pot. energy curves, dissoc. energies 78−50485
SO_2, analytical pot. functions, several surface minima 78−5158
SO_3, dissoc. pathways and mol. vibr., compliance consts. and min. energy coords. 78−35661
SO_4, and isotopic forms, struct., normal coord. anal. 78−965
$S^{16}O_2(S^{18}O_2)$, $^1B_2('A')$ state, force field for large amplitude motions 80−43023
SSF_2, FSSF, and ^{34}S isotropic forms, matrix IR and Raman spectra *(German)* 79−89674
SbF, pot. energy curves and dissoc. energy, Hulbert-Hirschfelder calc. 80−30210
SbO, dissoc. energy calcs. 77−3486
ScF_3, pyramidal struct. and force field coeffs., electron diffr. obs. 78−9250
ScO, pot. energy curves and dissoc. energy of $X^2\Sigma$ state 80−69203
SeO, IR bands of 10296 and 10491 Å, rot. struct. 78−5224
SeO, pot. energy curves, dissoc. energies 78−50485
SiH^+, mol. consts., pot. curves and dissoc. energy determ. from time resolved precision spectroscopy 80−58272
SiH_4, $1B_1(1T_2)$ pot. energy surface calcs. 80−53085
SiO molecule, true potential energy curves, dissoc. energy, ionisation potential 77−6704
SiO, $X^1\Sigma^+$, $A^1\Pi$, $C^1\Sigma^-$ and $E^1\Sigma^+$ states, SCF CI calcs. 79−45641
SiO(g), enthalpy of formation and dissociation energy, time-of-flight mass spectra 77−16859
SiS molecule, true potential energy curves for various states, dissoc. energies 77−6704
Sn_2, low-lying states, energy curves, bonding 79−76367
TeO, pot. energy curves, dissoc. energies 78−50485
TiO, potential energy curves and dissociation energy 78−50531
XY_3, XY_4 mols., harmonic force field calcs., average pot. energy criterion 77−57903

potential energy curves and surfaces of molecules continued
Xe_2, dispersion damping functions and interaction energy calcs. 80−78673
Xe_2^+, bound ground state, pot.energy curves 78−66599
Xe_2^+, electronic states, pot. curves, with/without spin-orbit interaction 78−33443
Xe_2^+, electronic struct., pot. energy curves, spectroscopic consts. 79−18114
XeCl, B-X and D-X band systems, vibr. anal. 79−59482
XeCl* spectra, for $Xe(6s,^3P_2)$+RCl vibr. energy disposal assignment 79−100345
XeF, in Ar and Ne matrices, reson. fluoresc., ground $X^2\Sigma^+$ state pot. well 77−14482
XeF, $X^2\Sigma^+$, energy curve calcs. 77−10719
XeF_2, photodissoc. yield in solid Xe and Kr, time-resolved photolum. excitation obs. 80−3372
XeF_2, pseudopotential SCF-MO studies, equilib. struct., stretch-stretch interaction force const. 80−95525
XeF_4, pseudopotential SCF-MO studies, equilib. struct., stretch-stretch interaction force const. 80−95525
XeF_5^+, pseudopot. SCF MO studies, steric aspects of struct. and force fields, Jahn-Teller effect 80−99444
XeF_6, pseudopot. SCF MO studies, steric aspects of struct. and force fields, Jahn-Teller effect 80−99444
XeF_6, UV absorpt. band shape 78−5289
XeH^+, pot. energy curves, VB calcs. 77−61688
XeO, $d^1\Sigma^+ \rightarrow a^1\Sigma^+$ ($b^2\Pi$), green band emission spectroscopic anal., RKR pot. curves, bond lengths and dissoc. energies 79−41181
XeO^+, $X^4\Sigma^-$ state, pot. energy curves and correl. effects, elastic scatt. cross sections 80−23502
Xe_2^*, Xe_2^+, Xe_2, pot. energy curves, relativistic ab initio effective core pots. 78−86800
Zn_2, ab initio SCF LCAO MO calcs., contracted basis set effects 77−83495
Zn_2, electronic states, CI calcs., rel. to Hg_2 77−10601
Zn_2, pot. energy curve of low-lying states, MO theory 79−89624

potential energy functions
see also Lennard-Jones potential; molecular vibration; Morse potential; muffin-tin potential
^{4}He, superfluid, one phonon excitation spectrum and interaction pot. 80−54455
AB_2, bent molecule, ab initio force fields, appl. of Simons-Parr-Finlan expansions 79−41218
acetamide, IR spectra, amino group inversion transitions and pot. functions 80−43041
acetonitrile, quadratic force fields, MOCIC pot. functions calcs. 80−5475
acetylene, quartic anharmonic pot. energy function 78−58662
activated state of multidimensional planes of pot. energy of chem. reactions 77−90585
adiabatic potential energy, perturbation expansions *(Japanese)* 77−69205
adsorbed monolayer, effective two particle potential 79−11012
adsorption, selective, correlation of intensity features with at.-surface pot. Fourier components 79−15013
DL-alanine-α,β-d_4, Raman spectra, intermol. pot. 79−91432
alkali atom+H, long-range interaction, S-state alkali atom 79−76480
alkali atom+inert gas, long-range interaction, S-state alkali atom 79−76480
alkali chlorides, thin film, crystal-vacuum (100) surfaces, mol. dynamics computer simulation 80−34288
alkali diatomic molecular ions, core-core interaction pots. 79−18251
alkali halide, hydride and deuteride, cryst. binding energy formula, halogen, H, D electron affinity 77−35501
alkali halide, overlap repulsion and pot. energy function for Bohr-like atoms 77−15344
alkali halide, polarisability analysis using Narayan-Ramaseshan repulsive pot. 77−76353
alkali halide crystal, Gruneisen parameter, vol. depend. anal. 80−2135
alkali halide crystal, second-neighbour interaction potential 78−91298
alkali halide mols., electronic polarisability, ionic radii and repulsive pot. parameters, mol. consts. 80−87242
alkali halide solutions in DMSO, modelling of interactions 79−77469
alkali halides, cryst., force consts., IR absorpt. freq., logarithmic pot. function calcs. 78−2832
alkali halides, cryst., pot. parameters, Hellman function calcs. 80−2181
alkali halides, improved interaction pot., spectroscopic consts. calc. 79−86024
alkali halides, interaction pot. 79−36720
alkali hydride molecules, pot. energy function, rot. const., vibr. const., and binding energy 80−99532
alkali hydrides, crystal binding anal. interatomic force model, cohesive energy, compressibility, Debye temp. 79−65030
alkali hydrides, lattice props. from interacton pot. energy function 80−100199
alkali hydrides, Woodcock pot. calcs. 80−43136
alkali metal, oscillator strengths, nonlocal Simons pot. anal. 80−32795
alkali metal+alkali metal, pseudopotential method 79−68294
alkali metal+inert gas, line profiles, width, shift and asymmetry, square well pot. approx. 80−52936
alkali metal diatomic ions, core-core interaction potential calc. 78−25645
alkali metal halides, crystal properties, cohesive energy, bulk modulus and press. depend., interionic force model 80−15035
alkali-inert gas system, mol. band profiles of induced dipole transitions 78−42135
alloys, ordered, thermal and static displacements effect on axial shadow pattern width and shape *(Russian)* 80−107024
amide group molecules empirical pot. model EPEN/2, development, parameter testing 79−54935
aminopyrazine, far IR spectra, barrier to planarity, pot. function and energy levels 80−69137
amorphous solids, diffusion of nonspherical particles, correl. effects 80−39337
anisotropic molecule-atom interactions, glory scatt. calc. in sudden approx. 78−25654
aromatic hydrocarbons, excited state vibr. freqs. 79−85947
atom+diatom collinear collision, refined Born approx. 78−74724
atom+electron scatt., distorted wave expansion with off diagonal pots., local approx. 79−31694
atom+molecule collision, reactivity band origin 77−32774
potential energy functions continued
atom+triatom collisional energy transfer, ergodicity in mol. vibr., Henon-Heiles pot. 80−18906
atom interaction in reson. light field *(Russian)* 79−54936
atom-diatom collinear collision, first order nonlinear matrix differential eqn. 80−37853
atom-diatom collinear reaction, potential classical transition collinear state theory 79−98191
atom-surface 3-9 interaction, bound state vibr. spectrum 78−14615
atomic, optimum pot. model used to generate numerical pot., energies and electron affinities determ. 80−99534
atomic collisions, rotationally induced transitions in two-state model 80−47945
atomic collisions in solids, interatomic pot. 79−51173
atomic local pot., density functional formalism, linear response theory, appl. polarisability 80−42924
atomic long-range forces, contrib. to phaseshift in electron scatt. 78−5344
atomic particles, equilib. const. and parameters of interaction pot. 78−1045
atomic Rydberg states, Coulomb and Yukawa pot., wave functions and quantum defects, Schwinger's var. principle 80−63549
atomic vapours, three-level system, collisional effects in saturation spectroscopy, appl. to Na 80−78579
atoms, electron densities and electrostatic pot. calc. 80−102430
atoms, electrostatic pot. at nuclei, mathematical formulations 80−106369
atoms in optical reson. field, bound states, interaction potential 79−93958
azabenzene dimers, C, N, H atom-atom parameters, dispersion energy calcs. 80−23489
azastilbenes, fluoresc., excitation energy anomaly, pot. energy model. 77−50466
B-DNA helix, guanine-cytosine base pair, electrostatic pot. 80−8003
benzene, single crystals by Brillouin spectra examination 79−42977
benzene derivatives, mol. electrostatic pot., approx. evaluation 80−58337
benzenoid hydrocarbons, normal coord. calcs., simplified valence force field models 78−94229
Bohr potential, applicability to 20 MeV ion+at. (mol.) electron loss data anal. 79−27082
Born-Oppenheimer nuclear motion wave function determ., incl. conical intersections and identical nuclei 79−54932
boron trihalides, quadratic potential functions, Coriolis consts. calcs. 79−72239
butane, adsorbed on graphite, struct. and dynamics, empirical interatomic pots. 79−99417
cis-2-butene, Raman and IR spectra, torsional mode pot. function 79−89676
t-butyl cyanide-HF, hydrogen bonded heterodimer, spectroscopic consts. from IR and microwave spectra 80−43039
carboxylic acids, crystals, empirical interatomic potential functions 79−7567
chain of coupled nonlinear oscillators, large amplitude motion, numerical study 79−25993
channelling calculations, interatomic pot., simplicity considerations 79−82267
charge exchange, differential cross-sections, static Brinkman-Kramers approx. 77−83723
chemisorbed atoms on transition metal surface, interaction energy calc. 80−54507
chemisorption, pot. energy function of two H atoms around Pt atom protruding from metallic Pt surface 80−10781
chloro(ethyl)silanes and its C derivatives, Raman spectra, mol. vibr. and rot. isomerism 80−87134
chloroaromatics, mol. crysts. Cl atom pot. energy calcs. 78−42948
p-(N-chlorobenzylidene)-p-chloraniline, cryst., polymorphism, cryst. struct. rel. to mol. conform. 78−75611
closed shell atom+ion interaction, electron gas model, polarisation inclusion 78−37699
complex atom*+inert gas atom, model pot. curves, including CI 78−42154
complex energy eigenvalues of a zero-range atom in a uniform electric field 79−72227
complex potential energy surface systems, nonradiative processes, WKB calcs. 80−45133
composite interatomic potential, validity over large atomic separation 80−84225
computer modelling of matter, conf., Anaheim, USA (March 1978) 80−51954
condensed matter, SCF theory, orbital and pot. functions calc., eq. of state 80−44463
confining pot., eigenvalue problem for Schrodinger operator 80−27154
correlation energy, modified bielectronic potential method calcs. 79−59365
Coulomb Hamiltonian, one-dimensional, spectral props. 80−47859
Coulomb potentials, screened, energy approximants and perturbation theory 80−106368
crystal, elastic moduli, calc. from interatomic forces 79−95071
crystal orbital calculations, deformation density method, transferable integrals 80−38992
crystal orbital calculations, deformation density method, transferable integrals, neutral atom pots. 80−38993
crystal-liquid phase boundary, pair distrib. functions and free energy functionals 80−24734
crystalline state properties, pot. energy parameters calcs. 79−73124
cyanomethane-HF, hydrogen bonded heterodimer, spectroscopic consts. from microwave spectrum 80−43038
cyclic voltammograms at spherical electrodes, switching pot., drop size effects, digital simulation technique 80−40766
cycloheptanone, vibr. spectra, pot. functions and conformers 77−83569
cyclooctanone, vibr., rot. spectra and conformations, pot. function 78−78707
cyclopentene, mol., pot. functions of bending modes 80−9753
d transition metal, interaction between partial dislocation cores, representation by oscillatory pot. 79−14811
dense gases, vel. autocorrelation function, memory function 80−59154
dense gases and liqs., three-body nonadditive interactions, thermodynamics props., mol. dynamics simulation 79−7435
determination from gas transport coeff. data inversion 77−35293
diatomic mol. pot. energy function, rot. consts. and Sutherland parameter 79−54931

potential energy functions continued
diatomic mol. scatt., Schrodinger eqn. phase shift differences for some trigonometrical potentials 80−43132
diatomic mol. scatt., Tietz phase shift differences, semi-empirical relations, Varshni and Hulbert-Hirschfelder pots. 80−9673
diatomic molecular scattering, phase shift difference, trigonometric pots., radial Schrodinger eqn. 79−22787
diatomic molecule, analytic model potentials, extended accuracy 79−64066
diatomic molecule, bound-states, new trigonometric pots. 79−72383
diatomic molecule, electronic states calc. using five-parameter pot. function *(Russian)* 77−3270
diatomic molecule, new potential function 79−3384
diatomic molecule, pot. and spectroscopic consts. 79−94053
diatomic molecule, pots. superposition, rel. to lattice dynamics, mol. consts. calcs. 80−5598
diatomic molecule, trigonometric pots., refinement 80−9676
diatomic molecule, vibr. potential representations 79−68219
diatomic molecule, vibr.-rot. states, high accuracy wave functions and energies 80−74159
diatomic molecules, bound, hybrid potential function 80−69209
diatomic molecules, dispersion energy, nonexpanded multipoles 78−9215
diatomic molecules, dissoc. energy determ., Simmons-Parr-Finlan pot. calcs. 80−58128
diatomic molecules, homonuclear, molecular dynamics, translation-rotation coupling 80−44094
diatomic molecules, modified pot. energy functions from normalised kinetic field functions 79−838
diatomic molecules, pot. energy functions, virial theorem calcs. 77−88519
diatomic molecules, potential energy functions, spectroscopic consts., correls. 79−18253
diatomic molecules, soluble potential 78−21996
diatomic potential, modified Morse function fitting procedure, appl. to $H_2(X^1\Sigma_g^+)$ 79−36560
p-dichlorobenzene, bicentric expansion of potential function of mol. interaction 79−94056
p-dichlorobenzene, Cl-Cl interactions at 100K, isotropic pot. functions calcs. 78−18578
differential scattering cross-section, Brinkman pot. calcs. 80−106373
2,5-dihydrofuran, mol., pot. functions of bending modes 80−9753
dilute aqueous solutions, Monte Carlo studies of struct., review 80−54101
dilute gases, transport props., softness expansion for inverse power pot. 80−28589
dimethyl aluminium hydride dimer, electron density distrib., electrostatic mol. pot. anal. 80−52885
dimethyl sulphide dimerisation, S lone pair nonbonded contacts, EH, MINDO/3, CNDO/2 calcs. 79−773
2,3-dimethylbuta-1,3-diene, IR, Raman spectra, torsional pot. function, thermodynamic function 80−43046
trans-dimethyldiazene-1, 1, 1-d_3, IR and Raman spectra, vibr. assignments and pot. functions 78−33507
trans-dimethyldiazene-d_0,d_6, IR and Raman spectra, vibr. assignments and pot. functions 78−33507
dimethylsulphide-d_3, two interacting C_{3v} rotor system, mol. coupling parameters, Raman spectra 78−42074
1,4-dioxadiene, mol., pot. functions of bending modes 80−9753
distorted wave matrix elements for inverse power pots., approx. analytic evaluation 80−83442
DNA, improved definition of A and B forms, atom-atom potential functions method 78−96000
droplet evaporation, diff. coeffs., vap. press. and Lennard-Jones pot. function determ. 77−80262
education, composite potential well, energy level determ. using Green's function factorisation theorem 79−97148
education, Maxwell fish-eye pot. and Coulomb pot. from mechanics 78−49585
effective pair potentials, first order derivation of differential equations 80−1041
electron+molecule, scatt., polarisation pot. determ. 80−17721
electrostatic molecular potential from completely transferable group contribs. 77−88408
electrostatic pot. energy of atoms in mols., electronegativity, charge transfer and polarisation 79−63885
empirical diatomic pot. functions comparison, BiBr $A^3\pi(0^+)$ and X^3Sigma$^-(0^+)$ states calc. 80−43133
empirical potential model EPEN/2 for conform., intermol., solvation studies 79−50102
ethane, adsorbed on graphite, struct. and dynamics, empirical interatomic pots. 79−99417
ethane, force consts., model potential function vs. mol. orbitals calcs. 78−29829
ethane, gas, second virial coeffs., intermol. pot. at low temp. 79−46416
ethyl alcohol-d_0(-d_1)(-d_1)(-d_2), internal rot. and microwave rot. spectra 80−69128
ethyl methyl sulphide, low freq. vibr. spectra, methyl torsional pot. functions and internal rot. 80−5543
ethylene, dimer interaction, lattice energy, multipole expsn., at.-at. pots. 78−9218
ethylene, gas, second virial coeffs., intermol. pot. at low temp. 79−46416
ethylmethylamine, low freq., vibr. spectra, methyl torsional pot. functions, mol. struct. 80−43045
ethylmethylether(-d_3), low freq. vibr. spectra, methyl torsional pot. functions, internal rot. 79−26978
exchange interactions of atoms in paired orbital approx. 77−88521
exponential cosine screened Coulomb pot., s-states, Ecker-Weizel approx. calcs. 80−101732
flexible double minimum potential, modified Gauss perturbed harmonic oscillator 80−1042
fluid, hard dumbbell mols., reference pot., perturbation theories, spherical reference systems 80−28898
fluid with nearly spherically symmetric molecules, thermodynamic perturbation theory 80−14985
fluids, hard core, distrib. functions and equation of state, zero-separation theorem 80−44089
fluoroform, quadratic force fields, MOCIC pot. functions calcs. 80−5475
fluoromethanal, visible spectrum, rot., vibr. and vibronic anal., double min. pot. 79−41182
fluorometh.HF, H-bonded complex, ab initio calcs. *(French)* 80−52866
formaldehyde-d_2, vac. UV Rydberg spectra, pot. function 77−61763
formaldehyde-water, heuristic intermol. pot. function, ab initio MO calcs. 78−33566
formamide, IR spectra, amino group inversion transitions and pot. functions 80−43041
formyl-triglycyl amide-H_2O, analytical pot., ab initio calc. 79−48206
Fues potential, vibr.-rot. spectra, Schrodinger eqn. soln., pot. energy curves *(Spanish)* 78−36784
fulminic acid, semirigid bender Hamiltonian, rot.-vibr. level separations, config., bending pot. 79−41152
gas, thermophysical props. inversion, anisotropic pot. energy function generation 80−99531
gas transport coeff. data inversion iterative procedure, pot. energy function determ. 78−91051
general-purpose molecular mechanics program construction principles 78−13411
glass, vibrational modes, conjecture effect of small anharmonicity 79−95112
α-glycine-C-d_2, Raman spectra, intermol. pot. 79−91432
Gordon-Kim interatomic pot. theory variants, appl. to inert gases and Hg_2 79−76478
grain boundary segregation, computer simulation using Mie type interatomic pot. 80−54259
graphite surface interaction with He atom 80−34316
graphite/inert gas adsorption, modified Buckingham pot., virial coeff. anal. 79−65312
group IIB elements, interatomic potentials, relativistic effects 79−3516
group IV A monosulphides, dissoc. energy calcs. 78−29733
Hamiltonians, effective, appl. to atomic pot. transferability in hydrocarbons 80−42933
hard-sphere fluid, Yukawa tail pot. for eqn. of state 79−42211
hard-sphere liquid, pair pot. softness effect on liq., struct. factor 80−88012
HCP lattice, Ewald potential calc. 80−64948
heavy metal diatomic halides, Wasastjerna pot. function, force consts. internulcear separations and binding energies 80−14187
high temperature electron diffraction, review 80−52237
higher order modified pot. for effective phase integral approx. 79−44779
homonuclear diatomics, equilib. geometries, Gaussian-based model pot. calcs. 78−94183
hot matter, conductive opacities and free-free Gaunt factors 80−3361
hydrides, first row, bending pot. calc. using MINDO approx., force const., equilib. geometry 80−95544
hydrocarbons, conformational anal., modified Urey-Bradley force field, gauche-H_2 interactions 77−6749
hydrocarbons, unsaturated, empirical potential model EPEN/2 parameterisation, testing 79−50103
hydrogen bonded systems, electrostatic molecular potentials 79−3356
hydrophobic solutions molecular properties, one dimensional soluble models 79−46536
ice, D_2O, H_2O, intramolecular potential from overtone spectrum anal., H-bonding dependence 79−93972
inert gas atom+degenerate atoms, pairwise additivity, DIM calc. 79−89728
inert gas atoms, pot. energy curves analysis 80−53083
inert gas crystal, correlation forces *(Russian)* 78−22686
inert gas diatomic molecule, excited state pots., fast calc. 80−9490
inert gas dimer ions, photofragment spectroscopy using fast ion beams 80−9755
inert gas systems, absolute total cross-section data anal. 80−53093
inert gases, interatomic potentials, relativistic effects 79−3516
inert gases, second virial coeffs., intermol. pot. at low temp. 79−46416
interacting particle systems, configuration with min. pot. energy per particle 80−4517
interacting systems, general theory of natural states, use for calc. of intermol. forces 78−82807
interacting systems, natural states in the asymptotic 1/R expansion, use for calc. of intermol. forces 78−86930
interaction potential, direct determ. from gas viscosity meas. 78−37702
interatomic force calcs., zeroth-order exchange energy for optimised atomic basis set 80−43131
interatomic potential between two equal ions 78−94300
interatomic potential for atomic pairs, Thomas Fermi model with quantum corrections 80−32797
interatomic potentials, Regge poles positions and residues, inverse power pots. 80−83439
interionic force pot. in ideal dipolar gas 80−96330
intermolecular interactions, gaussian overlap model potentials 77−75251
intermolecular pair pot. energy function from gaseous transport coeffs. 78−62870
intermolecular pair pot. energy function from gaseous transport coeffs., unlike monatomic interactions 78−62871
intermolecular potentials, vibr. coupling behaviour 78−25668
intermolecular site-site potential, spherical harmonic expansion 79−41217
inverted triangle potential, non-symm., appl. to photodissoc. continua 79−74400
ion+atom, long-range interaction, anal. Born-Oppenheimer pot. energy function calcs. 78−1048
ion+polar molecule collision freq., thermodynamic model 80−43145
ion clusters, 3-body pots., SCF energy partitioning calcs. 80−18953
ion-surface impact, interatomic pot. screening function correction factor for computer simulation 78−23574
ionic crystal, thermodynamic props. calc., pot. energy function approach 80−54407
ionic crystals, defects, computer modelling, review 80−107205
ionic type function ν(XH), non-monotonic freq. variations, effect on Hammett freq. factors *(French)* 79−22690
isobutene-d_0, -d_6, torsional pot. functions, spectra anal. 78−25528
isolated molecules, vibration relax. theory, adiabatic approx. 80−58237
JWKB phase integrals, higher order, evaluation 80−87195
Kratzer molecular and general pot. superposed 80−9674
lattices, two-dimensional, detonation, shock propagation, computer simulation 79−64554
Lennard-Jones and Stockmayer pot. parameters, crit. evaluation, correl. methods 78−1966
Lenz-Jensen pot. calc. using third order approx. 78−95099
Lenz-Jensen potential, applicability to 20 MeV ion+at. (mol.) electron loss data anal. 79−27082
light atoms (up to Ni), contact term, use of local spin density functional method 80−58158

potential energy functions continued
lipid hydrocarbon chain, biomembrane, rot. motion and fluidity 80−76714
liquid crystal ordering and theory of mol. dispersion forces and pair pots. 80−64886
local scaled Schrodinger relations and the virial theorem, kinetic energy operator 80−78527
long range atomic potentials in Thomas-Fermi theory 79−50101
long-range potentials, vac. fluctuations and retardation effects 79−3522
metallic compounds, cohesive props., augmented-spherical-wave calcs. 79−94952
metallic glasses, structure and formation, thermodynamic props., cluster relaxation approx. 80−54143
metals, Gruneisen parameters, interatomic forces, pseudopot. calc. 80−44165
metals, interatomic potentials of Na, K, Al, Cu, Fe from phonon spectra 80−19744
methane, gas, second virial coeffs., intermol. pot. at low temp. 79−46416
methane, intermol. pair pot. energy function 77−10721
methane+methane, intermol. pot., electron gas approx. calc. 78−9214
methane+Ne ion, nuclear stopping power and interatomic potentials 78−74549
methane $+H_2O$, pairwise interaction pot. function, ab initio SCF MO calc. 79−22786
methane-d_2, rotation-vibration constants, C−H bond length 79−94055
methanol (d_3), OH stretch fund., torsion-rot. levels, IR spectra obs. 80−32711
methyl groups in solids, tunnelling freq. for internal rotation in pot. function 80−49134
N-methylacetamide, and isotopic forms, low-freq. Raman spectra, internal torsional mode 79−26992
methylacetylene, quadratic force fields, MOCIC pot. functions calcs. 80−5475
trans-methyldiazene, pot. function 78−33507
methylene fluoride, anharmonic pot. function and equilib. struct. 78−78774
methylphosphinosilane, IR and Raman spectra, vibr. assignment and asymmetric potential function 79−85962
microphysics to macrochemistry, discrete simulations, review 80−54102
molecular crystals, Cl atom pot. energy calcs. 78−42948
molecular crystals, optimum packing in atom-atom approx., algorithm and computer program 80−1960
molecular electrostatic potentials influence of polarisation functions 79−839
molecular fluid perturbation theory, Pople expansion third order term, anisotropic pot. 78−79510
molecular fluids, coupling of rotation and translation 80−38892
molecular fluids, ref. system selection and average Mayer-function perturbation theory 80−38891
molecular force fields, virial theorem appls., zero virial reaction coords. and diatomic pots. 79−31433
molecular homeomorphism, structural, between nuclear pot. and electronic charge density 80−42968
molecular interaction, bicentric expansion of potential function 79−94056
molecular interaction pot., extended law of corresponding states 79−81251
molecular liquid, mol. dynamics simulation, multiple time step methods and improved potential function 80−54098
molecular quadratic potential functions, calc. MO constraint of interaction coordinates 78−74631
molecular systems, saddle points and min. energy paths, constrained simplex optimisation procedure 80−42943
molecular vibrational energy transfer, potential well depths 80−43156
molecule, quartic potential function with finite BE, props. 79−26913
molecules, electron densities and electrostatic pot. calc. 80−102430
molecules, electrostatic pot. at nuclei, mathematical formulations 80−106369
molecules, interacting, rigid, HF, self-consistent nonorthogonal group function approx. 79−31430
molecules, spherically symmetric, repulsive energy determ. 78−42153
molecules at equilibrium, nuclear-nuclear potential energy regularities 80−32793
molecules at short internuclear distances, adiabatic pot. energy calc. 79−27056
molecules containing 1st row atoms, K-shell binding energy shifts, NDDO MO calcs. 80−58413
n(R)-6 potential model, modification 77−75254
n-body potential energy functions, for teachers 79−40318
naphthalene, phosphorescence spectra in rare gas matrices, multiplet struct. and pot. energy functions 80−106341
naphthalene in Ar matrix, geometry changes and multiplet struct., mol. fluoresc. and phosphoresc. obs. 80−95663
non-bonded potential functions, Morse curve, exp-6 and 12-6 pots. comparison 79−10166
non-spherical molecule ensemble, background correl. in statistical thermodynamic calcs. 80−36958
non-surface scattering, interatomic pot. functions *(Japanese)* 80−45192
nonadiabatic reactions, rate const. temp. depend., influence of charact. features of elastic scatt. 80−37852
nonpolar molecules, intermol. interactions in intense radiation field 80−78679
nuclear matter, variational techniques, review 80−22748
nucleic acid bases, protonated, anion binding, electrostatic mol. pots. 79−1999
octahedral mols., anharmonic force field, decoupled rigid bender model 79−41153
one centre pot. energy functions and two electron integrals for STO's 80−14070
one-dimensional particle-in-the-box problem, perturbation theory illustration using champagne bottle situation 80−36816
one-dimensional polaron, electron-acoustic phonon interaction through deform. pot. 79−56143
one-electron density functions, many-centred finite multipole expansions 78−71624
open-shell systems, FSGO calcs. with model pots. 78−33413
organic carbonyl compounds, empirical pot. model EPEN/2, development, parameter testing 79−54934
organic compounds, low freq. anharmonic vibr., pot. function determ., Raman and IR spectra obs. 80−52997
potential energy functions continued
organic molecules, saturated, empirical potential model EPEN/2, parameterisation testing 79−54933
ovalene, isolated ultra cold mol., intermediate level structure of S_2 state 80−28048
oxalyl chloride (fluoride), centrifugal distortion consts. and thermodynamic functions, pot. energy calc. 79−22619
palmitic acid-choleic acid complex, cryst. struct. and van der Waals energy 80−64983
partial at. charges calc. from ab initio mol. electrostatic pots., appls. 78−70739
pentaphenylantimony, Coulombic interactions in anomalous structure 77−24285
perchlorohydrocarbons, crystn., intermol. potential-function models 80−49168
periodic potential functions, with sine and cosine terms, matrix elements for level calcs. 77−57904
phospholipid inter-and intra-molecular interactions, PCILOCC and pot. function calc. 80−3570
polar molecule clusters, 3-body pots., SCF energy partitioning calcs. 80−18953
polar molecules interaction, Wooley pot., 2nd virial coeff. 77−65831
poly(spiro[2,4]hepta-4,6-diene) molecular characterisation, glassy state props. 80−64928
polyatomic mol. force consts. and heat of atomisation, approx. separable pot. function 80−78675
polyatomic molecule, intramolecular coord. relax., generalised classical theory 80−78589
polyatomic molecule, quartic anharmonic pot. energy function 78−58662
polyatomic molecules, pot. energy functions 79−89726
polyatomic mols., anharmonic pot., determ. of zeroth approx. 77−75255
polyatomic mols., multiple photon IR processes, reviews 80−43125
polyatomic mols., nuclear charge model and valence force consts. prediction 80−43022
polyatomic mols. in liqs., vibr. energy relax. 80−63611
polynucleotides, double helical, conformation, pairwise pot. function calcs. 80−53173
polytypes, computer simulation 80−79734
porphins, reson. Raman spectra, selection rules, normal coord. treatment 80−53175
porphyrin in n-octane Shpolskii matrix, defect props., Monte Carlo obs. 80−63533
Poschl-Teller, symmetric, position-momentum uncertainty products for exactly solvable potentials 80−12939
propane, adsorbed on graphite, struct. and dynamics, empirical interatomic pots. 79−99417
isopropyl chloride, torsional pot. function, far IR and Raman obs. 80−28022
pyrazine, dimer interaction, lattice energy, multipole expsn., at.-at. pots. 78−9218
quasi-linear molecules, low frequency anharmonic vibrations, pot. function determ., Raman and IR spectra obs. 80−52997
Raman spectra, correlation with vibronic coupling and adiabatic potential 77−71804
rare gas solids, Debye Waller factors from unpaired elastic force model 80−19896
real fluids, short range repulsions and long range attractions, simple pair pot. model 80−64850
resonance Raman scattering from small molecule, vibronic theory 79−94004
RHF molecular potential eqns., interactions of open-shell systems 77−30949
Rosen-Morse, symmetric, position-momentum uncertainty products for exactly solvable potentials 80−12939
rotational isomerism, torsional pot. anal., from spectrosc. data 78−62787
RX^-, radical anion stability conditions, pot. energy diagrams 80−85161
second virial coefficient data, complete iterative inversion method calcs. 80−83448
semiconductor, impurity ion pot., screening charge density expansion convergence 79−7799
simple fluid, mol. dynamics simulation, including three-body interactions 80−54100
slow atomic particle collisions, quasiresonant processes 79−41216
solvated electrons, optical spectra and model potentials 80−30318
spherical potentials, energies and widths of quasibound levels (orbiting resons.) 79−10168
spline interpolation method, for potential energy data 78−46412
spurious avoided crossings of pot. energy curves, eigenvectors and representation space 79−68286
square well fluid, viscosity, transport processes 79−98847
square-well liquids, equation of state, acoustic properties 79−99270
Stockmayer and Lennard-Jones pot. parameters, crit. evaluation, correl. methods 78−1966
Stockmayer fluid, mol. dynamics and thermodynamic perturbation theory, mol. polarisability effects 78−71419
symmetric double minimum potentials, functional representation 79−13781
symmetric double-well potential, semiclassical inversion 80−83447
test charge bounded by solid state plasma, analytic expression for pot. energy 78−84154
meso-tetraphenylporphine, potential parameters of H migration tunnel rates calcs. 80−5600
s-tetrazine, mol., pot. functions of bending modes 80−9753
thioacetamide, IR spectra, amino group inversion transitions and pot. functions 80−43041
third row element mols., general harmonic force field, SCF-MO-MNDO and freq. calc., MOCIC pot. 80−27948
third-row oxyanions, tetrahedral, kinetic and pot. consts. calcs. 77−30951
Thomas-Fermi potential, applicability to 20 MeV ion+at. (mol.) electron loss data anal. 79−27082
transition metal oxyanions, tetrahedral, kinetic and pot. consts. calcs. 77−30951
transition metals, adatom surface diffusion charact., pair potential calcs. 80−39446
triatomic molecule, internal coords. choice for pot. surfaces with more than one minima 79−76479
triatomic molecules, angle deformation, force constant of angle deformation derivation 79−98239
triatomic van der Waals complex, vibr. predissoc. and photodissoc. lifetimes 80−9661

potential energy functions continued
two body T matrices derived from strong potentials 80−63732
two-centre systems, pot. energy functions approx. 79−6984
valence-nonbonded H atoms interaction and two-centre contrib. to total energy of mol. 80−32624
Varshni V and Lennard-Jones pots., 3rd order WKBJ eigenvalues 79−6982
virial coefficient data inversion for potential function, second coeff. 79−72381
water, liq., Monte Carlo studies of struct., review 80−54101
water, Monte Carlo simulation 80−54113
water, pot. energy function appl. to ice lattice energy 79−73125
Wigner-Seitz potential, binding energy of diatomic mols. and diamond 79−50160
XY_6 molecules, octahedral, cubic and quartic anharmonic pot. energy functions 79−98185
Yukawa potential function, determ. of phase shifts 78−58237
zero-radius potential, regularised model for multicomponent systems 79−27052
Ag, thin film deposited on Si, work function *(French)* 80−80353
AgCl, bond dissoc. energy, electronegativity pot. function, pot energy curves 77−10784
AgH, bond dissoc. energy, electronegativity pot. function pot. energy curves 77−10784
Al, thin film deposited on Si, work function *(French)* 80−80353
Al+Al, repulsive region ground state pot. curves, SCF with STO basis set calc. 80−14188
$Al^{3+}+Al^{3+}$, repulsive region ground state pot. curves, SCF with STO basis set calc. 80−14188
β-Al_2O_3-$(Na,K)_2O$, model calcs. of cond. anomalies, pot. energies of cation arrangements 80−107510
AlOH⇌HAlO system, intramol. rearrangement, ab initio calc. of pot. surfaces and min. energy paths, geom. parameters 80−32623
Ar, aqueous soln., dil., energy and struct., pair pot. energy function, Monte Carlo calc. 80−54107
Ar, atomic props., calculation from optimised potential model 79−6895
Ar, from viscosity results and Ar_2 data 78−29830
Ar, interatomic pot. and transport props. 77−14519
Ar, liquid, diffusion coefficient for model potentials through means square displacement 80−70098
Ar, liquid, velocity autocorrelation from memory function, hard-sphere and square well pots. 80−28893
Ar, monolayer, two-dimensional compressibility on graphite, calc. using empirical Ar-Ar pot. 79−65316
Ar-Ar pot. parameters, from CO in Ar matrix, empirical evaluation 80−48057
Ar-Kr, glory structure in total cross section, crossed supersonic atomic beam, n(x)-6 potential 80−48060
Ar-Kr, internal pot. function calcs. 79−68292
Ar-Ne(Kr) systems, pot. parameters from binary diffusion coeffs. 78−37700
Ar+Br_2, effective vibr. pot. of Br_2 in Ar gas, Monte Carlo simulation 79−59526
Ar+Kr, elastic collision total cross-section, low energy 80−5603
Ar_2, excited state pots., fast calc. 80−9490
Ar_2, interatomic potential single parameter 80−48059
Ar_2+, weakly bound excited states, dissoc. energies 78−78748
As, elastic moduli, calc. from interatomic forces 79−95071
As_4O_6, IR and Raman spectra vibr. spectra, valence force field calc., pot. function *(French)* 78−50549
As_2S_3, chalcogenide glass, effect of press. on elastic props. 80−10590
BCl_2NCO, soln., force fields and normal modes, vibr. spectra, IR and Raman obs. *(French)* 80−58266
BOH⇌HBO system, heterovalent isomerism, ab initio calc. of pot. surfaces and min. energy paths, geom. parameters 80−32622
$BX_2{}^{14}NCS$ (X=Cl, Br, I), soln., force fields and normal modes, vibr. spectra, IR and Raman obs. *(French)* 80−58266
Ba+Xe, spectral line contour meas. determ. of potentials 78−25477
$BaO:Mn^{2+}$, impurity pot. well shape calcs. 78−87950
$BeAr^+$, long range pot., pot. inversion method 78−21992
Bi, elastic moduli, calc. from interatomic forces 79−95071
Bi, spheres, mean inner pot., elec. biprism and interf. electron microscopy 80−49063
BiBr, empirical pot. energy curves for $A^3\pi(0^+)$ and $X^3\Sigma^-(0^+)$ states 79−22617
Br_2 in liq. Ar, effective intramol. pot. 80−69208
Br_2, model potential SCF calcs. 80−95528
C-Ar pot. parameters, from CO in Ar matrix, empirical evaluation 80−48057
CO, ground states, anal. pot. function calcs. 78−78775
CO in Ar matrix, vibr. freq. shift and interaction pot., force-field calcs. 80−47958
CO, intermolecular pot. parameters from WCA perturbation calc. 79−90770
CO, mol. potential energy functions, extended accuracy 79−64066
CO, pot. energy functions, virial theorem calcs. 77−88519
CO+e, momentum transfer cross-sections, effect of nonspherical short range interactions 80−9745
CO_2, anharmonic pot., determ. of zeroth approx. 77−75255
CO_2, gas, second virial coeffs., intermol. pot. at low temp. 79−46416
CO_2, low energy electron (positron) collisions, ab initio adiabatic polarisation pots. 80−14240
CO_2, VV processes, estimation of almost resonant molecular energy transfer due to multipolar pot. 80−91642
CO_2+e, momentum transfer cross-sections, effect of nonspherical short range interactions 80−9745
CO_2+H_e, collinear atom-triatom transition probabilities for anharmonic triatom pots., quantum mech. calcs. 80−83455
CO_2+Kr, collinear atom-triatom transition probabilities for anharmonic triatom pots., quantum mech. calcs. 80−83455
C_3O_2, mol., pot. functions of bending modes 80−9753
C_3O_2, semirigid bender, rot.-vibr. energy level separations obs., struct. and pot. functions determ. 80−83446
Ca, vibr.-rot. states, high accuracy wave functions and energies 80−74159
$CaO:Mn^{2+}$, impurity pot. well shape calcs. 78−87950
Ce, isostructural solid-solid phase transitions, core collapse, cell theory 80−59620
Cl+Xe, elastic scatt. for interaction pot., $Cl(^2P)+Xe(^1S)$ 79−27059
Cl_2, model potential SCF calcs. 80−95528
Cs^+-Ar(Kr)(Xe), ion mobility and interaction pot., drift tube meas. at 300K 78−59537
Cs+Xe, broadened Cs principal series lines, absorption meas., Cs-Xe pots. 77−79584
Cs+Xe (neopentane), Cs line shape broadening, satellite data inversion, interaction pot. 78−74608
Cs^++Ar(Kr)(Xe), elastic beam scatt., repulsive pots. 79−98184
CsF+Ar, 87.7 meV, reorientation effects by approx. quantum methods 77−79680
Cu, pair potentials calcs., elastic props. calc. 80−49176
D_2O, energy levels and mol. vibr., internal coord. model 79−799
D_2S, energy levels and mol. vibr., internal coord. model 79−799
D_3SiNCO, low freq. bending mode, pot. function 78−82728
$^nD_2$, compressed fluid, vibrational population relaxation time obs. 80−69219
F_2, gas, second virial coeffs., intermol. pot. at low temp. 79−46416
$F^-(H_2O)_2$, 3-body pots., SCF energy partitioning calcs. 80−18953
F_2O, absorpt. band freq. and intensities, electro-optical parameters, pot. energy, IR spectra 80−37812
Fe close-packed phases, intermolecular pots. and eqns. of state 79−20780
Ga trihalides, vibr. anal., pot. const. determ., mol., compliance and Coriolis coupling const. calc. 80−95579
$GeO_4{}^{4-}$ compounds, vibr. pot. function, force consts., isotopic shifts, mean vibr. amplitudes 80−23395
H bonded ν_{X-H} band, dynamic theories survey 80−52983
H, hyperfine shift and interatomic pots. in inert buffer gas 80−5491
H+HCl(HBr)(HI), elastic scatt., <50 meV, Van der Waals pot. 79−54937
H+He, elastic scatt. cross-section, using model pot. 79−13786
H+He, long and intermediate range interaction, model pot. calc. 79−22789
H_2, diatomic transition operators, L^2 basis expansions, $^1\Sigma$ and $^3\Sigma$ state pots. 80−63519
H_2 electron scatt., equivalent exchange pots., algebraic variational method, 2p-2p and 2s-2p transitions 80−18931
H_2, electronic chemical pot., natural orbitals occupation numbers and electronegativity 80−63509
p-H_2, FCC, equation of state and lattice dynamics, temp. depend. 77−76521
H_2 interaction at jellium surface, adsorption curves, independent atom effective pot. study 80−29259
H_2, pot. energy functions, virial theorem calcs. 77−88519
H_2^+, intramol. interaction energy, convergence of perturbation expansions 78−17745
H_2-Ar(Kr)(Xe) mixtures, intermol. forces 78−62867
o-H_2+Ar, relax. and kinetic cross sections, DWBA calc. 78−25655
H_2+Fe(001), gas-surface reactions, semiempirical generalised LEPS pot. 78−68923
H_2+$H_2(D_2)$ potentials, isotropic part 78−5311
o-H_2+He, relax. and kinetic cross sections, DWBA calc. 78−25655
H_2+inert gas, intermol. pot. anisotropy determ. from total collision cross sections, expt. 78−21988
H_2+inert gas, intermol. pot. anisotropy determ. from total collision cross sections, theory 78−21989
HBr, Dunham pot. coeffs., nonlinear least squares fit calcs. *(French)* 78−13561
HBr-nN_2 aggregates, near IR spectra in monatomic matrix 78−21921
HCN, anharmonic pot., determ. of zeroth approx. 77−75255
HCN...HF, hydrogen bonded heterodimer, spectroscopic consts. from microwave spectrum 80−43037
HCl-nN_2 aggregates, near IR spectra in monatomic matrix 78−21921
HCl+Ar, pure rot. line shift, density depend. 77−79652
HCl+Ar, rot. linewidth calcs., using different pots. 78−66602
HCl+HCl(HF)(HI)(HBr), supersonic-thermal beam collision, rot. energy transfer, classical trajectory calc. 79−68302
HF, liquid, struct. and props., intermol. pot. function calcs., basis set depend. 79−82134
HF, nucl. mag. shielding and susceptibility, elec. field depend., SCF-Hartree Fock method 80−18791
HF, pot. energy functions, virial theorem calcs. 77−88519
$(HF)_2$, intermol. force model, rel. to liq. struct. 78−78773
$(HF)_2$, intermol. pot. function, ab initio 6-31G calc. 79−18254
$(HF)_3$, 3-body pots., SCF energy partitioning calcs. 80−18953
H_2O, anharmonic pot., determ. of zeroth approx. 77−75255
H_2O, complete quartic force field calc., algorithm 80−37736
H_2O dimer, intermolecular pot. functions from ab initio calcs. 80−5473
H_2O, empirical potential model EPEN/2, parameterisation testing 79−54933
H_2O, energy levels and mol. vibr., internal coord. model 79−799
H_2O, ST2, discrepancy between Monte Carlo and mol. dynamics calc. using truncated pot. anal., internal energy determ. 80−95702
H_2O+H_2O, pair pot. near H bonded equilib. config., amorphous and crystalline solid and liq. 80−64946
$(H_2O)_2$, accurate atom-atom potential 78−21990
$(H_2O)_2$ dimer intermolecular pot., liq. struct. mol. dynamics simulation 78−71657
H_2O_2, internal rot., pot. energy calcs. 79−3521
HOBr, analytical pot. energy functions and surfaces 79−68203
HOCl, analytical pot. energy functions and surfaces 79−68203
HOF, analytical pot. energy functions and surfaces 79−68203
HOI, analytical pot. energy functions and surfaces 79−68203
H_2S, complete quartic force field calc., algorithm complete quartic force field calc., algorithm 80−37736
H_2S, energy levels and mol. vibr., internal coord. model 79−799
H_2Se, complete quartic force field calc., algorithm 80−37736
H_3SiNCO, low freq. bending mode, pot. function 78−82728
H.HF, H-bonded complex, ab initio calcs. *(French)* 80−52866
He beams, scattering by crossed at. and mol. beams, elastic differential cross section 79−10171
He, isoelectronic series, charge densities and 2-electron intracule functions calcs. 77−88382
He, two body potential, theory 79−69305
^{4}He, FCC quantum cryst., lattice dynamics 79−77859
He-He, Born-Oppenheimer pot. using Hylleraas-type electronic wave functions 79−31438
He-He, energy and interaction potential of two ground-state atoms 80−63740
He+Ar, interatomic pot. well depth, SPFD pot., diffusion, viscosity and second virial coeff. 80−5599

potential energy functions continued
He+Ar, scatt. pot., He in (2^3S) state, 0.02-0.12 eV 79−54938
He+Cs(Rb), interatomic pots., hyperfine shifts, diffusion coeffs., perturbation exchange theory 79−41220
He+H_2, collinear collision, first order nonlinear matrix differential eqn. 80−37853
He+H_2^+(H^+)(H_3^+) interaction pots., comparison with values from ion mobility data 77−14518
He+He, interatomic force calcs., zeroth-order exchange energy for optimised atomic basis set 80−43131
He+methane (NH_3)(H_2O)(SF_6), differential scatt. cross-section, intermol. pot. 79−36728
He_2, pot. surface well depth calc. 77−79667
He_2 potentials, configuration interaction calculations, superposition corrections 79−72382
$^4He_2$, bound state at small and large separations, variational calcs. 78−50609
$He_2(A,C^1\Sigma_{u_g}^+)$, long-range excimer pot. determ., high resolution at. beam expt. 77−42371
HeH^+, spectroscopic characts. in ground and first excited triplet states, Dunham pot. approach 77−42234
$^3He_2^4He$, ground state binding energy, Faddeev-UPE method 79−72377
$^3He_3$, ground state binding energy, Faddeev-UPE method 79−72377
$^4He_2^3He$, ground state binding energy, Faddeev-UPE method 79−72377
He^*+D_2(Ar)(Kr) interaction pots. 77−83674
Hg vapour, absorpt. spectrum, 1849 Å line, self-broadening, interatomic interaction *(French)* 80−32661
Hg-Hg potential, relativistic effects on interactions 77−75252
Hg+Ar, spectral line broadening of Hg in UV, interaction pot. 79−26937
Hg+Xe, pressure broadened absorption profiles *(French)* 79−98033
$HgBr_2$, electronic struct. and photodissoc., effective core pots. and POL(1) CI wave function 80−63560
$HgCl_2$, electronic struct. and photodissoc., effective core pots. and POL(1) CI wave function 80−63560
HgI_2, mol. struct. and vibr. pot. function, gas-phase electron diffr. obs. 79−31689
I_2, dissociative mol. pot. functions from continuum reson. Raman spectra 77−38673
I_2, in CCl_4 and cyclohexane solns., higher vibr. levels, dephasing lifetimes, from reson. Raman spectrum 78−42068
I_2, model potential SCF calcs. 80−95528
IBr, $B^3\Pi(0^+)$ states, Franck-Condon factors, RKR turning pts. 77−34681
ICl, $B^3\Pi(0^+)$ states, Franck-Condon factors, RKR turning pts. 77−34681
IF, $B^3\Pi(0^+)$ states, Franck-Condon factors, RKR turning pts. 77−34681
In trihalides, vibr. anal., pot. const. determ., mol., compliance and Coriolis coupling const. calc. 80−95579
In+Hg, spectral-line contours in high-press. arcs 79−3412
K, pair potentials calcs., elastic props. calc. 80−49176
K+inert gas atom, ground-state pots. from elastic cross sections 77−75258
KCl:Li^+, shape of pot. energy well of impurity 79−23692
KF, thermal expansion, higher-order anharmonic contrib. at high temps. 79−28113
KF:Li^+(Na^+)(K^+), shape of pot. energy well of impurity 79−23692
KI:Tl, A_T emission, linear polarisation, appl. of semi-classical WKB formalism 80−45134
Kr, gas structure by neutron diffr., three-body pot. contrib. 79−90358
Kr, interatomic pot. and transport props. 77−14519
Kr interatomic potential functions 79−68293
Kr-Kr(Ar)(Xe), glory structure in total cross section, crossed supersonic atomic beam, n(x)-6 potential 80−48060
Kr_2^+, weakly bound excited states, dissoc. energies 78−78748
$KrAr^+$, quasimolecule Auger spectra 79−68269
Li^+ mobility in He 300K, interaction pot., drift tube meas. 77−76026
Li^++Ar, interaction pot. of $X^1\Sigma$ state, CI calc. 79−50100
LiBr, pair pot., dipole moment, polarisability tensor, bond length depend., finite field SCF calcs. 80−58127
LiH, $X^1\Sigma^+$ ground state, spectroscopic and pot. functions, method for combining spectroscopic data 79−45782
^{6,7}LiH(D), cryst., cohesive energy, force const., lattice freq., Debye temp., Gruneisen parameters, calc. 78−91293
$LiNO_3$, mol. struct. ab initio calcs. 79−26884
$Li^+(OH_2)_2$, 3-body pots., SCF energy partitioning calcs. 80−18953
Mo, interatomic pot. from phonon spectrum 78−67784
Mo, pair potentials calcs., elastic props. calc. 80−49176
Mo surface, clean and gas covered, He^* impact, deexcitation, pot. energy transfer mechanism 80−60743
N_2, electron scattering, local-exchange approx. for intermediate-energy-differential cross sections 80−48094
N_2, gas, second virial coeffs., intermol. pot. at low temp. 79−46416
N_2 gas, structure factor 80−43137
N_2, inner shell $(1s)^{-1}(\pi 2p)^1\Pi$ state, energy, vibr. struct., electron impact investig. 78−13611
N_2, liquid, mol. correl. functions, effective pair pot. evaluation 80−10476
N_2, low energy electron (positron) collisions, ab initio adiabatic polarisation pots. 80−14240
N_2, N_3, spectra, review 77−38680
N_2, neutron diffraction patterns at room temp., correls. and struct. factor 78−82810
N_2, thermodynamic and transport props., consistent correlation using Lennard-Jones (12-6) and Buckingham (exp-6) pots. 78−91045
$^{14}N_2$+CO, vibr.-vibr. energy transfer, long and short range pot. effect 80−99556
$^{15}N_2$+CO, vibr.-vibr. energy transfer, long and short range pot. effect 80−99556
NBr, mol. pot., r-centroids, $A^1\Sigma^+$-$X^3\Sigma^-$ band system 77−3373
NH_3, anharmonic pot., determ. of zeroth approx. 77−75255
NH_3, ground state, analytical pot. function 78−1050
NH_3, inversion-vibration interactions, pot. energy function calcs., isotope effects 78−33567
NH_3,HF, H-bonded complex, ab initio calcs. *(French)* 80−52866
$^{14}N^{15}N$+CO, vibr.-vibr. energy transfer, long and short range pot. effect 80−99556
NO+Ne(AR)(Kr)(Xe), angle depend. intermolecular pot., crossed beams study 80−9682
NO_2, complete quartic force field calc., algorithm 80−37736
NO_2^- hydrate clusters, ground-state HF pot., Monte Carlo simulation, energy surfaces and rot. barriers 80−106412
N_2O, and isotopic forms, pot. energy function determ. from vibr. data 77−18812
Na, equilibrium struct. and phys. props., pseudopot. method 80−96778
Na isoelectronic series, wave functions and effective pots. of valence electron 80−47873
Na, Liq., dynamic struct. factor, two body interaction pot. sensitivity 78−67638
Na, liquid, diffusion coefficient for model potentials through mean square displacement 80−70098
Na, velocity autocorrelation from memory function, hard-sphere and square well pots. 80−28893
Na+Ar, differential cross-section at thermal energy, Na-Ar ground state pot. 78−58769
Na+Ar, scatt. cross-section, thermal energy, interaction pot. for Na(3^2P) 79−27060
Na+methyl iodide, anisotropic interactions from double rainbow struct., interaction pot. meas. 80−99540
$Na+SiCl_4(C(CH_3)_4)(Si(CH_3)_4)(Sn(CH_3)_4)$, rainbow scatt. at thermal energy, anisotropic pot. 78−29837
Na+t-butyl bromide, anisotropic interactions from double rainbow struct., interaction pot. meas. 80−99540
Na+t-butyl chloride, anisotropic interactions from double rainbow struct., interaction pot. meas. 80−99540
Na+t-butyl iodide, anisotropic interactions from double rainbow struct., interaction pot. meas. 80−99540
Na^++ether(thioether)(amide) interaction, pair pots., ab initio SCF LCAO MO calc. 79−36721
Na_2 molecular electronic struct. for lowest $^3\Sigma_u^+$, $^1\Sigma_u^+$, $^3\Sigma_g^+$, $^1\Pi_u$, $^1\Pi_g$, $^3\Pi_u$ and $^3\Pi_g$ states 80−63738
NaAr, intramol. pot. functions of ground and excited state 79−54785
NaNe, intramol. pot. functions of first excited state 79−54785
Na(3^2P_J)+Na($3^2S_{1/2}$), collisional excitation transfer, pot. symm. rules and cond. function 80−9690
Ne, adatom on Xe-plated graphite 78−18904
Ne, exponential-six pot., new parameters 78−55217
Ne, interatomic pot. and transport props. 77−14519
Ne, liquid, effective pair pot. from perturbation approach 77−68908
Ne+D_2, anisotropic inversion pot., rot. inelastic cross sections 80−78696
Ne+Ne, pot. curve derived from gas and solid scatt. data, ESMSV pot. 80−1040
Ne+Ne, total cross-section, 0.5-1.4 km s^{-1}, long range pot. 79−13787
Ne_2, excited state pots., fast calc. 80−9490
Ni, (001) surface, local density of states, asphericity of pot. and charge transfer, ab initio self-consistent calcs. 79−15064
O-Ar pot. parameters, from CO in Ar matrix, empirical evaluation 80−48057
O_2, gas, second virial coeffs., intermol. pot. at low temp. 79−46416
O_2, liquid, mol. correl. functions, effective pair pot. evaluation 80−10476
O_2, photoionisation cross section and asymmetry parameters calc. in UV region using static pot. 80−95692
O_2+Ar, gas, intermol. pot. for spectral props. and rot. energy transfer 79−68224
O_2+O_2, gas, intermol. pot. for rot. energy transfer and spectral props. 79−68224
O_3, analytical potentials from spectroscopic data, vibr., bond length, dissoc. 77−10613
O_3, isotope effects, complete quartic force field calc., algorithm 80−37736
OH-HF, H-bonded complex, ab initio calcs. *(French)* 80−52866
OH+H_2, interaction pot. energy rel. to OH rot. excitation at interstellar temps. 80−62232
$O^-(O_2^-)$, optimum pot. model used to generate numerical pot., energies and electron affinities determ. 80−99534
P_4O_6, IR and Raman spectra vibr. spectra, valence force field calc., pot. function *(French)* 78−50549
Pd adsorbed on W (110), long range interatomic interactions with coadsorbed Re, W 80−59789
Pd-Zn, $L1_0$ type intermetallic phase, X-ray diffr. study of lattic compression 80−49182
Pd_2, ab initio relativistic core pot. studies of metal-metal bonding 80−106257
PdH, ab initio relativistic core pot. studies of metal-H bonding 80−106257
photoionisation cross section and asymmetry parameters calc. in UV region using static pot. 80−95692
Pt_2, ab initio relativistic core pot. studies of metal-metal bonding 80−106257
PtH, ab initio relativistic core pot. studies of metal-H bonding 80−106257
Rb, Rydberg levels, Stark patterns, expt. and central pot. calc., positions and intensities 79−93953
Rb^+, ionic mobility in Ar, Kr and Xe, interaction pot. determ. 79−18991
Rb+inert gas atom, ground-state pots. from elastic cross sections 77−75258
Rb^++Ar(Kr)(Xe), elastic beam scatt., repulsive pots. 79−98184
Re adsorbed on W (110), long range interatomic interactions with coadsorbed Pd 80−59789
SF_2, microwave spectrum inertia defects, ν_1, ν_3, ν_2, equilibrium structure, vibration rotation constants, anharmonic potential functions 79−93988
SF_6, gas, thermodynamical and spectral props., effect of angle-dependent part of dispersion forces 80−43138
SO_2, complete quartic force field calc., algorithm 80−37736
$S^{16}O_2(S^{18}O_2)$, $^1B_2(^1A')$ state, force field for large amplitude motions 80−43023
Sb, elastic moduli, calc. from interatomic forces 79−95071
Sb_4O_6, IR and Raman spectra vibr. spectra, valence force field calc., pot. function *(French)* 78−50549
Se, molecular cryst., Se-Se nonbonded pot. parameters derivation from heat of sublimation 79−27945
Si+C ion, nuclear stopping power and interatomic potentials 78−74549
SiO_4^{4-} compounds, vibr. pot. function, force consts., isotopic shifts, mean vibr. amplitudes 80−23395
SrCl:Mn^{2+}, shape of potential well, calc. 78−87951
SrO:Mn^{2+}, impurity pot. well shape calcs. 78−87950
TTF stacks, intermolecular energy and struct. from atom-atom potentials 80−79738
Tl+Hg, spectral-line contours in high-press. arcs 79−3412
W adsorbed on W (110), long range interatomic interactions with coadsorbed Pd 80−59789

potential energy functions continued
Xe, thermal conductivity calc., law of corresponding states and interatomic pots. 79−7437
Xe-Xe(Kr), glory structure in total cross section, crossed supersonic atomic beam, n(x)-6 potential 80−48060
^{129}Xe+nonspherical molecule, interaction pots., effect on mag. shielding, NMR meas. 77−71816

potential energy surfaces for collision processes
A+BC→AB+C, vibr. excitation, centrifugal effects calcs. 77−16791
acetic acid, ionised, pot. energy profiles for unimol. reactions 80−43210
acetic acid-pyridine, H-bonding, proton transfer, isolated system, solvent effect, MO calc. 80−55629
activated state of multidimensional planes of pot. energy of chem. reactions 77−90585
alkali + inert gas molecule, far wing line broadening, quasistatic theory 79−22762
alkali atom+halogen mol., ion pair form., trajectory model 77−16800
alkali atom+inert gas, three-body interaction, secondary satellites of alkali line 77−83683
alkali atom (ion)+inert gas, collision studies of quasi-one-electron systems 80−63750
alkali metal+HX (X=F,Cl,Br,I), reaction, semiempirical pot. surfaces calcs. 79−74362
alkali metal atoms, resonance interaction, resonance lines self-broadening, adiabatic pot. curves 77−83676
alkane+He, scattering at high velocities, short-range pot. determ. 77−27143
alkane+He, scattering at high velocities, short-range pots. determ. 77−27142
analytical expressions from constrained optimisation 77−6698
atom+atom, small angle differential cross section, semiclassical description 80−28086
atom+diatom, 3-dimens. electronic nonadiabatic reactive collision theory, electronuclear basis 78−3321
atom+diatom, ab initio pot. hypersurface anal. fit 79−13785
atom+diatom, collinear exchange reaction rates and probabilities, threshold behaviour 78−27738
atom+diatom, complex formation in collinear collision, trajectory study using pot. surface 79−87821
atom+diatom, long-lived trajectories near reactivity band boundary 78−29836
atom+diatom, prior statistical distribs., collinear reactions, theory review 78−35670
atom+diatom, reaction products ang. distribs., Franck-Condon theory 79−87835
atom+diatom, rot. infinite-order sudden-approximation, low energy appls. 78−1052
atom+diatom, transition states, trapped trajectories and classical bound states in continuum 78−88630
atom+diatomic molecule, collinear collision, light absorption 79−76486
atom+ion, electron capture, non relativistic theory and Coulomb pot. anal. 80−32804
atom+ion collision system pot. curves at low collision energies, beam studies 80−61088
atom+molecular inelastic collisions, statistical decoupling 77−517
atom+molecule, reactivity bands, collinear SSMK surface calcs. on X+HX 77−36738
atom+molecule, rotational rainbow maxima: a time dependent study 80−58353
atom+molecule collision, reactivity band origin 77−32774
atom+molecule reaction dynamics, translational energy effect, review 80−76489
atom+negative ion, term parameters, electron spectra and scatt. cross sections 77−27148
atom pair recombination, on solid surface, dynamics pot. calcs. 78−7197
atom-diatom collision, vibrationally inelastic scattering attractive well of variable depth 77−46624
atom-molecule collision, electron contact, model system *(Dutch)* 79−50111
atoms, chemical ionisation, classical description, complex interaction pot., exponential representation 80−99570
avoided surface crossing, multidimensional problem 79−89619
benzene-Dewar benzene, lower excited states pot. energy surfaces for isomerisation 80−104429
bimolecular diffusion-controlled reversible reactions, detailed equilib. principle 80−7770
bimolecular reactions, complex and direct reaction mechanisms, unified statistical model 77−1914
bimolecular reactive system, pot. surface, incorporation of electronic nonadiabatic effects 77−40536
binary collisions, time correlation functions, influence of bounded trajectories 80−43143
bound state systems, kinetic energy and path curvature 78−19998
CA(s)+B^{+++}→A^{++}+B^{+}(p), charge exchange, at term pseudointersection, level degeneracy effect 79−27084
chemical kinetics, eigenvalue and eigenfunction anal. of Kramer's theory 79−29330
chemical laser, classical dynamics of bimol. reactions, book contrib. 77−10909
chemical reaction, energy barrier position between initial and final states 78−76831
chemical reaction, multidimens. pot. surface, topological stochastic approach 77−48638
chemical reaction rate constants, in solution, short-range caging effects 79−96286
chemical reactions, quantum chemical methods appls. 80−93752
chemical reactions, tree construction by algorithm, using tabular pot. functions 77−70286
chemical reactions rate constants, in solution, escape probability and time-depend. reactivity 79−96287
chemical reacts. in condensed phase at low temps., at.-mol. transforms. 77−25253
chemically reacting systems, differential geometrical analysis 79−31434
classical small-angle anisotropic potential scattering, comparison with Li^{+}+N$_2$(CO) results 80−1043
classical trajectories, use of perturbation theory in asymptotic region, appl. to HF+HF 79−98199
collinear collisions, classical transition state theory exactness test 77−61819

potential energy surfaces for collision processes continued
collinear collisions, vibr. energy transfer, exact classical and quantal calcs. 77−19014
collinear reaction prob. and thermal rate constant for pot. energy surface with middle barrier, classical dynamics. theory 79−91916
collinear reaction prob. and thermal rate constant for pot.-energy surface with early barrier, classical dynamics theory 79−91917
collisional processes, nonreson. laser field effects 77−60093
complex atom*+inert gas atom, model pot. curves, including CI 78−42154
complex potential surfaces for molecular dynamics 79−72374
concerted reaction, rate depend. on degrees of freedom in transition 77−70285
curve crossing collisions, transition probabilities 80−32631
deflection functions for curve-crossing collisions 79−94051
diabatic molecular states, definition basis set calcs. 79−97969
diatom, phase shift difference, trigonometric pots. in radial Schrodinger eqn. 79−22787
diatom-atom gas mixture, infrared line shape, rotational lines, influence of collision duration 80−43110
diatomic isovalent systems, pot. curves, ab initio MRD-CI method 80−83293
differential cross section, simple classical method of curve fitting 77−58118
dissociative charge transfer collisions, vibr. enhancement 78−33597
double potential wells, tunnelling and over-barrier decay rates, method of beats calcs. 78−44363
double well potential, transfer and tunnelling rates, density matrix calcs. 80−30209
doublet and quartet states, abstraction reactions, pot. energy surfaces calcs. 78−31627
electron+molecule, scatt., polarisation pot. determ. 80−17721
electron correlation theories 79−39125
electron transfer reactions, semiempirical pot. energy surfaces calcs. 78−73022
electronic-vibrational energy transfer and quenching, modified model 77−14534
electrostatic molecular potential from completely transferable group contribs. 77−88408
endothermic reactions, extreme mass combinations LH+H→L+HH and HH+L→H+HL 79−43570
energy barrier, transitions due to pot. energy surfaces crossing, non-Arrhenius behaviour 79−13653
energy barrier location, sudden and gradual late barriers, classical trajectory method 78−92454
ethylene+F(CH$_3$), transition state, ab initio calc. 78−48640
fluoroiodomethane, vibr. excited, dissociation, trajectory calcs. using pot. energy surface parameters 80−76508
formaldehyde, photodissoc., pot. energy surface features 79−79271
formaldehyde+formaldehyde, medium distance interaction, SCF LCAO MO, supermol., perturbation and MCF calc. 79−837
formaldehyde decomposing to H$_2$+CO, reaction path Hamiltonian 80−45486
formamide+formamide, medium distance interaction, SCF LCAO MO, supermol., perturbation and MCF calc. 79−837
formyl-triglycyl amide-H$_2$O, analytical pot., ab initio calc. 79−48206
Franck-Condon factors in reactive collision dynamics, general theory and applic. 77−36741
Franck-Condon factors in reactive collision dynamics, vibr.-rot. distribs. in atom-diatom reactions 77−36742
gas phase chemical reactions in IR laser field, collision-induced absorpt. spectra 80−76499
gas-solid energy transfer, internal vibr. energy effects 78−35234
gaseous relax. phenomena, few-level approx. validity 80−53097
halogen atom (^{2}P)+inert gas atom (^{1}S), coupled channel study, rel. to elastic approx. 79−81255
heavy ion fusion and deep-inelastic reactions 77−330
heavy ion reactions *(Rumanian)* 78−86547
Hulthen repulsive pot., atom-atom pots., Hilbert Schmidt expansion, transition operators 78−66621
hypersurfaces, transition state location, energy minimisation method 80−52904
inert gas atom+atom, excited state-ground state interactions 79−18259
intermolecular force, scaled electron gas approximation 79−98181
intermolecular forces, generalised electron gas-Drude model 79−98182
intermolecular interaction theory, modern state, rel. to large mols. 80−14186
intermolecular interactions and potential energy wave calcs., review 80−43140
intermolecular potential well depth estimation method 79−86034
intermolecular potential well depth role in collision-induced state changes 79−81257
internuclear parameters measurement method using total scatt. of fast electrons 80−32857
intrinsic reaction coordinate, ab initio SCF calc. method 77−48626
iodomethane+K, mol. rearrangement, optical pot. calcs. 77−81399
ion+molecule, induced dipole-induced dipole potential, capture rate const. 79−13783
ion+permanent dipole, capture rate consts., transition state theory, summary of theories 80−28091
ion+polar molecule collision freq., thermodynamic model 80−43145
ion-Rydberg atom collision cross sections, classical trajectory Monte Carlo calcs. 80−43174
IR laser single photon absorption reaction chemistry, solid state 79−66308
ketocarbene-ketene rearrangement, reaction path, ab initio calc. 78−20008
large mol. reaction with intermediate complex, vibr., translational distrib., pot. hypersurface calc. 77−52612
laser collision induced chemical reactions, collinear exchange model 79−66313
laser field linewidth effect on mol. collisions 79−6980
laser-controlled unimolecular and bimolecular processes, field-depend. rate const. 80−11906
linear rigid rotors, scattering calcs., ab initio intermol. pots. fitting 77−83680
methane, dissoc. chemisorption on Rh (111) surface, vibr. activation 79−57292
methane, pot. energy surface of excited singlet state, appl. to photodissoc. 79−83440

potential energy surfaces for collision processes continued
methyl isocyanate, isomerisation RRKM theory using effective strong collision freq. 78−44365
methyl radical+ethylene(acetylene)(propene)(allene), reaction pot. surfaces, MINDO/3 calcs. 79−22601
minicomputer appl. 77−25246
minimum energy reaction paths, reactive domains of energy hypersurfaces and stability 80−71893
minimum energy reaction paths, virial theory implications 80−97686
model potential, phase shifts 80−927
mol. target internal motion 80−78697
molecular collision processes in presence of picosecond laser pulses, radiative transitions 80−23479
molecular force fields, virial theorem appls., zero virial reaction coords. and diatomic pots. 79−31433
molecular spectral line broadening, semiclassical straight line vs. curved trajectories 79−45765
molecular systems, saddle points and min. energy paths, constrained simplex optimisation procedure 80−42943
molecule+ion collision system pot. curves at low collision energies, beam studies 80−61088
molecules, chemical ionisation, classical description, complex interaction pot., exponential representation 80−99570
monothioformate anion, protonation site, ab initio SCF calc. 79−47894
multicharged ion thermal charge exchange reaction, rel. to astrophysics 80−63815
multidimensional surface intersection problem and classical surface hopping 77−14512
multiphoton IR photodissoc., pot. energy surface classical trajectory calcs. 78−11532
multiply charged collision systems, slightly asymm., curve crossings, constraints, MO theory 78−74734
multiply charged ion+atom, autoionisation, electron and photon emission 80−63813
non-adiabatic transitions induced by rotational coupling 80−106385
nonadiabatic cage reactions, relaxation hindrance 80−93740
nonadiabatic coupling, rel. to complex intersection of two surfaces, avoided crossings 77−77736
nonadiabatic transitions, comparison of surface hopping and complex-valued time calcs. 77−9049
nonadiabatic transitions, linear curve crossing problem, generalised Stueckelberg method 80−28085
noncrossing interactions, Rosen-Zener model, differential cross-section calcs. 77−46621
noncrossing interactions, Rosen-Zener model, total cross-section calcs. 77−50497
nonempirical calculation methods, review 80−35505
organic ions, pot. energy profiles for unimol. reactions 80−43210
photochemical reaction, avoided crossings in excited states potential energy surfaces 78−76881
polyatomic molecule, dissoc., natural collision coords. 78−44373
polyatomic mols., dissoc. reaction path Hamiltonian 80−45486
polyenes, photoisomerisation, triplet pot. energy surfaces and normal mode anal. 80−108700
potential energy surface and collective spectra 78−86464
predissociation, multichannel, and inelastic scatt., uniform WKB theory 79−72404
proton-transfer reactions, potential energy curves and Bronsted exponents 77−32784
qualitative potential energy surfaces, from linear comb. of fragment configs. 78−44349
rainbow maxima, pot. well depth determ. method 77−14527
reaction barrier from overlap repulsion scheme 77−36734
reaction coordinate generation by Pauling relation 77−25251
reactive and charge transfer collisions, between ions and molecules 78−62914
reactivity band boundaries, trapped trajectories, theory 78−29836
serine proteases, enzymatic reaction mech. mol. orbital studies 77−60183
slow atoms, inverse scatt., semiclassical approx. calcs. 78−17747
slow heavy ion scattering, screened Coulomb pot. 77−14522
stilbene, diphenylpolyenes, photoisomerisation, 'phantom' photochem. singlet state, PPP SCF CI calcs. 78−73058
surface, mol. chemisorption, self-consistent calc. 79−95260
symposium contrib., Florida, USA (March 1979) 80−51946
tetrahedral and octahedral complexes, mol. vibrs. and reaction pathways, min. energy coords. and compliance consts. 77−57966
thermal chemistry as an exercise in photochem. 80−3379
thermal rate constants, quasiclassical trajectory calcs., detailed balance 79−87822
transition probability between two electronic states, curve crossing 77−3445
transition state characterisation by struct.-reactivity coeffs. 78−40026
transition state determination by the X-method 77−90580
transition state theory, absolute rate theory and variational formulations, Porter Karplus pot. surface 80−16642
transition state theory, energy limit determ. 79−13654
two-state curve-crossing collision, total cross-sections interatomic attraction effects 79−68297
unimolecular reactions, in one dimension, theory 78−44364
unimolecular reactions, pot. energy surfaces, SCF perturbation theory 79−91918
unimolecular reactions, RRKM theory using effective strong collision freq. 78−44365
vibrational excitation calcs. by sudden approx., pot. energy surface choice 77−27158
XH-Y complexes, IR absorpt. spectra, intramol. coupling influence, pot. energy surfaces derivation 80−91624
Ar-N_2 interaction, electron gas pot. calc., Gordon-Kim model, ang. orientation depend. 78−70893
Ar+CO_2, rot. inelastic wide angle scatt., differential cross sections 77−14536
Ar+CO_2, rot. transitions, classical trajectory calcs. 77−50501
Ar+$CO_2(N_2)$, repulsive pot. energy surface, approx. calc. and differential scatt. expt., comparison 79−22788
Ar+H_2, dissoc., recombination and inelastic scatt. pot. energy surface and cross section Monte Carlo calc. 77−27162
Ar+H_2, vibr. and rot. transfer enhancement of dissoc. cross section 77−34732
Ar+H_2, vibr. transition rates, thermally averaged, Monte Carlo trajectory calcs. 80−23519
potential energy surfaces for collision processes continued
Ar+HCl, differential cross section, quasiclassical close coupling approx. 80−63743
Ar+HHe^+, ab initio pot. energy data, SCF-LCAO calcs. 80−63530
Ar+N_2, polarisation in elastic scatt., close-coupling calcs. 78−25650
Ar+N_2, rot. inelastic collision, orientation depend., close coupling calcs. 78−9232
Ar+N_2, rot. inelastic cross section, classical trajectory calc. surprisal anal., pot. energy surface depend. 77−14542
Ar+$NO(X^2\pi)$, intermol. pot. surfaces, electron gas model calcs. 77−34721
Ar+SF_6(tetrafluoromethane), differential scatt. cross-sections, intermol. pots. calcs. 79−89742
Ar^++H_2, collinear reactions, electronic nonadiabatic transitions 78−7180
Ar^++$H_2(v_i=0)\rightarrow ArH^+$+H, electronic nonadiabatic transitions, two-state model calc. 78−73035
$Ar(Ar^+)+H_2^+(H_2)\rightarrow ArH^+$+H, electronic transitions, collinear reaction, curve crossing model, DIMZO surface 79−74373
ArF, Ar_2F, electronic struct., pot. energy curves, radiative transition probability calcs. 77−57879
ArN_2, interaction potential, modified electron gas model potential 79−72385
$Ar^*(^3P)+CO_2(X^1\Sigma_g^+)$, differential elastic and quenching cross-sections 78−58773
B+He(Ne)(Ar), ground and excited states interaction, B spectral line breadth 77−68092
B^{3+}+H, charge transfer cross sections, ab initio potential energy curves 78−37741
B^{3+}+He, charge-exchange total cross-sections 77−79691
BaCl+Ar(He)(N_2), intermultiplet energy transfer 79−27063
Be^{2+}, ion compexes with HF, H_2O, and NH_3 solvent molecules, structural and electronic props. calc. 77−57873
Be+FH→BeF+H, collinear, pot. energy surface study 79−11782
Be^++He(Ne)(Ar), Be II 2^2P excitation, alignment and orientation 80−91647
Bi+NF, near-resonant electronic energy transfer, surface-hopping model 79−86030
Br+Br_2, atom-exchange, rate and activation energy, trajectory model and pot. energy surface 78−64811
C^++H, fine struct. excitation cross section 77−38724
C^++H_2, C^+ fine-struct. excitation, interstellar cloud cooling 78−25675
C^{4+}+H, charge transfer cross sections, ab initio potential energy curves 78−37741
C^{4+}+He, charge-exchange total cross-sections 77−79691
CH+p-H_2(He), collisional pumping of Λ-doublet transitions, pot. energy surface 80−23516
CO+Ar(He)(Ne)(Kr)(Xe), intermol. pot. energy surfaces from electron gas model, ang., distance, and vibr. depend. 79−3520
CO+H_2, pot. energy surface anisotropy in nonreactive region, ab initio calcs. 78−29832
CO+H_2, thermal energy collision, ab initio pot. energy surface 79−45788
CO+N_2, electronically inelastic collision, distorted wave calc. and pot. energy curve 80−9709
$CO_2\rightarrow$CO+O, dissoc. pathways, pot. energy surface and vibr. anal. of IR and Raman spectra 78−64826
CO_2, electron impact spectra, 35 keV electrons, Bethe surface and Compton profile 79−27091
CO_2+H_2, rot. transfer, ab initio intermol. pot. energy surface 80−58354
CO_2+$H_2(D_2)$, ab initio LCAO-MO-SCF intermolecular pot. energy surface, V→T transfer 77−50489
CO_2+He, rot. inelastic collision, ab initio SCF, electron gas and pot. energy surfaces 80−83468
CO_2+He(Ar), rot. relax. rates and cross sections 79−848
CO_2+inert gas, vibr. and rot. energy transfer, quasiclassical trajectory study 78−33578
$C(^3P)+O_2(^3\Sigma_g^-)\rightarrow CO(^3\Sigma^+)+O(^1D)$, pot. energy surface, vibr. population inversion, classical dynamics 77−52630
$C(2^1S_0)+H_2(O_2)$(ethylene) 80−74241
Ca+He(Ne), press. broadening, line shifts 78−5290
Ca*+He(Ne), model pot. curves, including CI 78−42154
$Cd(^3P_J)(^1P_1)+H_2(HD)(D_2)$ reacts., CdH(CdD) yields, quenching cross sections 79−1948
Cl+$D_2\rightarrow$DCl+Cl, LEPS pot. energy surface, rate consts., isotope effect, quasiclassical trajectory calc. 78−56887
Cl+HI→HCl+I, Monte Carlo quasiclassical trajectory anal., product distribs. 77−16783
Cl_2, rot. relax. classical trajectory computation, using Lennard-Jones pot. 78−62880
Cl_2+F, reaction kinetics, pot. energy surface and Franck-Condon integrals 79−61855
Cl_2+H(D), uni- and bimodal product energy distribs. 79−57207
ClO+O→Cl+O_2, rate consts. calc. 220-1000K 79−79233
Cs inert gas, pot. energy curves, collision induced oscillator strengths 79−22659
Cs+I_2, ionising collision, trajectory surface hopping calc. 77−50509
Cs+Xe, Cs spectral line profile and absorpt. transitions 80−47944
Cs^++benzyl chloride, beam reactions for 5.8 eV collision energy, mechanism 80−66777
$CsCl(Cs_2Cl_2)$+Ar(Kr)(Xe), collision-induced ion-pair form., absolute cross sections 78−73029
CsF+Ar, elastic and rot. inelastic scatt., quantum mech. calcs. 77−14525
$Cs(5D_{5/2,m=1/2})$+inert gas, dipole-induced transitions, pot. curves, oscillator strength 80−32816
$Cs(8^2P)$+He(Ar)(Xe), fine-struct. transition cross sections, semiclassical calcs. 77−30972
D+Cl_2, reaction probabilities, information theoretic anal. 77−16799
D+F_2, DF initial vibr. energy distrib., IR chemiluminesc. obs. 80−45497
D+FD(FH), low barrier quantum models vibrational deactivation 80−69216
D+H_2, pot. surface, isotropic part determ. 79−36729
D+H_2 reaction, transition state theory calculations, kinetic isotope effect explanation 80−66784
D+H_2 rearrangement collision, vibr. excitation effects 80−71910
D+$He(2^1S)(2^3S)$, associative and Penning ionisation, autoionisation, calcs. 78−25674
D_2+F, reaction kinetics, pot. energy surface and Franck-Condon integrals 79−61855

potential energy surfaces for collision processes continued
D_2+HD(Ne)(Ar), state-resolved $\Delta j=2$ rot. transitions 80−63772
D_2^++O(^{3}P)→OD^++D, reaction dynamics, cross-section at. quadrupole moment effects 78−3324
F ($^2P_{1/2}$)+H_2, quenching, classical path calcs. 79−22800
F+D_2, electronic-to-rot. energy transfer cross sections 78−86935
F+H_2, 3-dimens. electronic nonadiabatic reactive collision theory, electronuclear basis 78−3321
F+H_2, collinear quasiclassical trajectory study 78−80718
F+H_2, electronic-to-rotational energy transfer 77−3431
F+H_2, Franck-Condon factors in reactive collision dynamics 77−36741
F+H_2, Franck-Condon factors in reactive collisions dynamics, vibr.-rot. distribs. 77−36742
F+H_2, reaction probabilities, information theoretic anal. 77−16799
F+H_2, reaction quantum dynamics, reson. model, transition state props. 79−11781
F+H_2, reactive collision, semiclassical dynamics on multiple electronic surfaces, 3-dimens. calcs. 78−27746
F+H_2, reactivity, multiple electronic surface effects 77−21363
F+H_2, two electronic pot. energy surfaces, collinear quantum calcs. 80−16646
F+H_2 nonadiabatic effects, scatt. theory, coupled-channel calcs. 78−22010
F+H_2→FH+H, collinear probability, quantum calc. using pot. energy surface 78−64829
F+HCl(DCl)→HF(DF)+Cl, dynamical props., pot. energy hypersurface computer anal. 77−77735
F+Ne(Ar)(Kr), thermal energy interaction pots., crossed beam study 79−68288
F+Xe, differential scatt. cross sections, crossed beam study, interaction pot. 79−3517
F^-+fluoromethane, S_N2 reaction, ab initio LCAO SCF calcs. 77−81402
F^++H_2, empirical and ab initio correlation diagrams, pot. energy surfaces 78−40041
F_2+Mu (H)(D)(T), exchange reaction, quasiclassical dynamics calcs. 79−91942
F_2+X→XF+F (X=Mu,H,D,T), isotope effects, quantum mech. and information theoretic calcs. 78−44360
FH_2^+, reactive processes, ab initio MCSCF-CI and diatomics in mols. calc. 78−56881
H adsorpt. on Cu, potential energy curves, pairwise additive model calcs. 78−73087
H exchange reactions, low temp., tunnelling dynamics 79−29340
H^--H_2 system, pot. energy surfaces 80−74215
H+ adsorbed H, W(001) surface, pot. model 77−10726
H+alkali metal atom, interaction potentials 80−63736
H+Br_2, H+HBr, reaction props. dimensionality depend. 77−9050
H+Br_2→HBr+Br, pot. energy surface, ab initio generalised valence bond calc. 78−73026
H+C^{2+}(C^{3+})(N^{2+}), radiative charge transfer, rate coeffs., pot. energy curves 77−88554
H+Cl_2, Franck-Condon factors for reactive collision processes 77−36741
H+Cl_2→HCl+Cl, quantum mech. reaction coords., point transformation calcs. 77−36730
H+D_2, pot. curve, thermal energy absolute integral cross-sections meas. 80−53096
H+D_2 reaction, transition state theory calculations, kinetic isotope effect explanation 80−66784
H+ethylene⇌ethyl radical, pot. energy surface, analytic function 79−11779
H+F_2(Cl_2), reaction probability, information theoretic anal. 77−16799
H+F_2→HF+F, vibr. adiabatic and static distorted wave Born approx. calcs. 80−7768
H+FH(FD), low barrier quantum model, vibrational deactivation 80−69216
H+H_2, ang. momentum decoupling approx., quantum mech. reactive and nonreactive scatt. 77−12780
H+H_2, CI calc. of three dimens. pot. energy surface 78−56882
H+H_2, collinear, collision-induced dissoc., quantum mech. probabilities calcs. 79−20359
H+H_2, collinear classical dynamics, chemically accurate pot. energy surface 77−48620
H+H_2, collinear reaction, Delves radial coord. S-matrix propag. calcs. 80−108695
H+H_2, collinear reactive scatt., Magnus approx. 77−16801
H+H_2, Franck-Condon factors in reactive collision dynamics, vibr.-rot. distribs. 77−36742
H+H_2, least squares fit to ab initio pot. energy function 78−56883
H+H_2, reaction, quasi-classical trajectory calcs. using new pot. energy surface 80−7767
H+H_2, reaction probability, max. entropy derivation, statistical theories 80−66781
H+H_2, reactions and collisions in IR laser field, collision-induced absorpt. spectra 80−76499
H+H_2, reactive scatt., sudden approx. calcs. 78−68878
H+H_2, sudden rot. reactive scatt., 3-dimens., approx. quantum mech. calcs. 80−76498
H+H_2, three dimens. reaction, Porter-Karplus pot. energy surface, rot. distribs., rate consts. 77−21378
H+H_2 reaction, classical trajectories on spline-generated pot. energy surfaces 77−60047
H+H_2(D_2)(T_2) reactions, accurate pot. energy surface, isotope effects, quasiclassical trajectory study 80−97698
H+H_2(0,0)→H+H_2, quasiclassical cross sections, pot. surfaces comparison 79−74364
H+H^- low energy, quantum theory, integrated cross sections, phase shifts 77−30957
H+HCO→H_2+CO, classical trajectory study 80−93750
H+HR→H_2+R, (HR=hydrocarbon), tunnelling reaction, classical S-matrix calc. 77−29007
H+He, D+He, low energy elastic scatt., pot. well depth determ. 77−6884
H+He (2^3S), pot. energy surfaces and autoionisation lifetimes calcs. 77−34740
H+He(Ne)(Ar)(Kr)(Xe), low energy elastic scatt. cross section MCSCF calc., van der Waals forces 78−70897
H+He(2^1S)(2^3S), associative and Penning ionisation, autoionisation, calcs. 78−25674
H+inert gas atom, interaction pot. from electron gas model 79−31637

potential energy surfaces for collision processes continued
H+Li_2, collinear reactions, SCF correl. diagram for Li_2H form. 77−70292
H+methane, abstraction and exchange reactions, energy barriers, UHF-CI calcs. 78−11512
H+methane, abstraction and exchange reaction, barrier height calc. using POL-CI wave functions 80−81304
H+N^{3+}, charge exchange, assoc. reaction, rel. to interstellar gas 80−7763
H+Ne(Ar)(Kr)(Xe), free electron production, integral cross-sections determ. 79−89754
H+O_2+Ar, HO_2 free radical prod., rate const. calc. 80−101026
H+O_2→OH+O, combustion, quasiclassical trajectory calcs. 78−53201
H+O^{q+}(N^{n+})(C^{n+})(B^{n+}), charge transfer cross sections, oscillatory behaviour in low-energy collisions 80−63806
H+Zn^{2+}(Cd^{2+})(B^{2+})(Mg^{2+})(C^{6+}), electron capture by slow ions, pseudo-crossing 80−43176
H^-+CH_4⇌CH_4+H^- intrinsic reaction coord., ab initio SCF calc. method 77−48626
H^-+H^+→H(1S)+H, level degeneracy effect on charge exchange at term pseudointersection 79−27084
H^-+methane→methane+H^-, nucleophilic substitution, ab initio pot. energy classical trajectory anal. 78−68886
H^++CO ($^1\Sigma$), ground state pot. energy surface, ab initio SCF calc., protonated equilib. geometry 80−83301
H^++CO($^1\Sigma$), vibr. excitation calc., close coupling and sudden approx. 80−78561
H^++Cs(6s), elastic scatt., pot. determ. from differential cross-sections meas. 78−78778
H^++D_2, collisional complex form. 80−58339
H^++H_2, coupled states calcs. of inelastic collisions at 3.7 eV 77−14538
H^++H_2, elastic of rot. excitation, semiclassical treatment 79−31657
H^++H_2, rot. and vibr. excitation, energy loss obs. 80−63773
H^++H_2, vibr. excitation, ab initio CI pot. energy surface calcs. 80−74228
H^++H_2, vibr.-rot excitation, ab initio CI pot. energy surface calcs. 80−74229
H^++H_2(CO_2), vibr. excitation, 10-30 meV 80−58358
H^++H_2→H_3, nonadiabatic transitions, comparison of surface hopping and complex-valued time calcs. 77−9049
H^++Kr, mol. orbit approach, spin-orbit interaction, adiabatic pot. and projected valence band treatments 77−533
H^-+metal ion, pot. curve, for exchange, Landau-Rosen and Rosen-Zinner model *(Russian)* 77−75287
H_2, accurate determ. 77−46503
H_2, chemiionisation by He(2^3S) and He(2^1S), pot. surfaces, autoionisation widths, cross sections 77−36739
H_2 elastic electron scatt. at 1 keV, Glauber model 80−43178
H_2, semiempirical model for polarisation of s-type AOs, pot. curve and surfaces determ. 77−88400
H_2^+, semiempirical model for polarisation of s-type AOs, pot. curve and surfaces determ. 77−88400
H_2-H_2, intermol. pot. surface, ang. depend., nonorthogonal CI calc. 77−46613
p-H_2+^{4}He, vibr. relax., 50-2000K, coupled channel, coupled states and effective pot. methods comparison 79−6995
H_2+Ar, Arrhenius dissoc. activation energy, vibr. depend., trajectory calc., 4500K 78−35662
H_2+Ar, vibr. energy transfer rate, ab initio calcs. 78−82821
H_2+C(O)(N), pot. surfaces, HF calc. 80−16669
H_2+Cl^-, 4-11 eV, inelastic scatt. 79−98202
H_2+Cl(Br)(I)(F), gas phase H-atom transfer reactions, struct.-reactivity correl., pot. energy surfaces 80−104433
H_2+D_2, reactive and inelastic scatt. using repulsive model pot. energy surface 78−66620
H_2+D_2, reactive and inelastic scatt., semiempirical pot. energy surfaces calcs. 80−74140
H_2+D→HD+H, three dimens. ab initio pot. energy surface 80−55646
H_2+F, reaction kinetics, pot. energy surface and Franck-Condon integrals 79−61855
H_2+H, reactive scatt., 3-dimensional quantum mechanical calcs. 77−30802
H_2+H_2^+→H_3^++H, ab initio calcs. of vibr. spectrum of H_3^+ 77−6753
H_2+H_2(He), anisotropic intermol. repulsion, pot. energy models 77−46610
(H_2+H^+, H_2^++H) collinear system, electronically nonadiabatic effects 78−1063
H_2+H(D)(T) reactions, accurate pot. energy surface, isotope effects, quasiclassical trajectory study 80−97698
H_2+H(F), minimum energy reaction path, reference coord. approach 78−40025
H_2+He, inelastic collisions, statistical decoupling 77−517
H_2+He, rot. relax. time, <300K, classical trajectory method invalidity 77−10739
H_2+He, vibr. relax., pot. surface depend. 77−75266
H_2+He potential surfaces, SCF and MRD-CI calcs. 79−10172
H_2+He*, Penning ionisation, singlet interaction pot. anomalous struct. 77−75274
H_2+He(2^3S), pot. energy surfaces and autoionisation lifetimes calcs. 77−34740
H_2+I→HI+H, collinear reaction, reson. effects, quantum mech. calcs. 77−52625
H_2+I→H+Hi, quasiclassical tragectory vs. quantum calcs., vibr. state depend., kinetics 78−80733
H_2+Kr, differential cross-sections, diffraction undulations, anisotropic pot. calcs. 78−9223
H_2+N^+→NH^++H, classical trajectory calc. 79−100337
H_2+Ne, collision-induced dissociation, Monte Carlo quasiclassical trajectory calcs. 79−74357
H_2+O→OH+H, vibr. energy effects, classical trajectory calcs. 77−63904
H_2+Pt(111) surfaces, interactions, bond breaking activity, model pot. 80−108744
H_2^++CO excited products dissoc., proton transfer dynamics, correl. diagram anal., corssed beam obs. 80−48079
H_2^++H_2, pot. energy surface and nonadiabatic regions, charge exchange and reaction, VB calc. 78−40027
H_2^++He→H+HeH^+, total cross sections, quasiclassical trajectory results compared with mol. beam data 77−60051
H_3, bent, spline-fitted pot. surface 77−57851
H_3, form. and dissoc., kinetics, historical review, book contrib. 77−40527

potential energy surfaces for collision processes continued
H_3, semiempirical model for polarisation of s-type AOs, pot. curve and surfaces determ. 77−88400
$H_3^+ + H_2 \rightarrow H_5^+ \rightarrow H_2 + H_3^+$, ab initio GO pot. surface, C_{2V} symmetry 77−25252
H_4, excited potential energy hypersurfaces, trapezoidal geometry, rel. to photochem. 2s+2s processes 77−30797
H_4^+, ground and excited state pot. energy surfaces and geom. struct., SCF and CI calcs. 78−78769
HCN(DCN), photodissoc. dynamics, rot. (vibr.) energy disposal 78−48672
$H_2CN^+H_2 \rightarrow HCN^+H + H_2$, ab initio GO SCF pot. energy surface, saddle point, reaction path 77−50379
HCl+Ar, rot. linewidth calcs., using different pots. 78−66602
HCl+Ar(He), rot. energy transfer, quasiclassical trajectory calcs. 78−42173
HCl+Ar(Xe), infrared line shape, rotational lines, influence of collision duration 80−43110
HCl+HCl(Ar), pure rot. Raman lines, press. broadening cross sections 78−74702
HCl+Kr(Ar), pot. energy surface determ. from rot. line broadening data 79−13784
HCl(v=1,2)+O(^3P_g), reaction and deactivation, laser-induced fluoresc. obs. 78−35669
HD^+, radiative recombination rates 78−37708
H(D)+Ar, differential collision cross sections, diffraction oscills., data anal. 79−22783
HD+He, relax. and kinetic cross-sections, DWBA calcs. 79−41782
HD($^1\Sigma_u^+$)+He, fluoresc. quenching and energy transfer processes 79−86032
HF, polarisation model representation for chem. reactions 79−39131
HF+H_2O(methanol)(ether), mol. electrostatic pot., H-bonds, CNDO/2 calc. 77−61822
HF+HF, ab initio pot. surface, ang. depend. fit calcs. 77−19006
HF+HF, medium distance interaction, SCF LCAO MO, supermol., perturbation and MCF calc. 79−837
HF+HF, rot. inelastic collisions, partial opacities, integral cross sections, pot. surface 77−38716
HF+HF, vibr. relax., temp. depend. calcs. 78−70906
HF+Li→LiF+H, pot. energy surface, SCF and CI calcs. 80−71904
$(HF)_2$, polarisation model representation for chem. reactions 79−39131
HF($^1\Sigma^+$)+Xe($^1S_0$), expt. and computational study, 0.044 and 0.153 eV 79−89748
HN_3+F, strong interactions in gas-phase reactions, arrested relax. IR chemilum. obs. 80−7773
HNC⇌HCN, intrinsic reaction coord., ab initio SCF calc. method 77−48626
HO_2, pot. energy surface for $H+O_2 \rightarrow HO_2^* \rightarrow OH+O$ reaction, MC SCF CI method 79−74353
H_2O, bond dissociation, MCSCF LMO calcs. 77−57886
H_2O^+, ab initio potential energy surface study by CI techniques, equilibrium conform. determ., mol. dissoc. pathways 80−78550
H_2O^+, spin and rot. fine struct., orbital angular momentum 80−83247
H_2O^+, vibr. and rot. struct., intensity factors and orbital angular momentum 80−83246
H_2O+Ar, collisional energy transfer in unimol. reaction, classical trajectory calcs. 78−62882
H_2O+H_2O, medium distance interaction, SCF LCAO MO, supermol., perturbation and MCF calc. 79−837
H′+XH→H′X+X, X=H, F, Cl,CH_3, collinear pot. energy barriers, PNO-CEPA calcs. 77−32777
Hbr+Cl_2(BrCl), four-centre reaction, quasiclassical trajectory study 79−57213
He-H_2^+, classical trajectories, on 3D cardinal spline fitted surfaces 77−90584
He-LiH, rot. inelastic collisions, ab initio pot. energy surface calcs. 80−87208
He+ArH^+, ab initio pot. energy data, SCF-LCAO calcs. 80−63530
He+$Br^-(Cl^-)(I^-)(Sb^-)$, term parameters, electron spectra-scatt. cross sections 77−27148
He+CO_2, repulsive pot. energy surface, approx. calc. and differential scatt. expt., comparison 79−22788
He+CO_2, translational-vibrational energy transfer, quantum dynamical study 80−63746
He+$CO(N_2)$, differential scatt. 0 to 5×10^{-2} rad. detector angle, 800 eV He *(Russian)* 77−79674
He+H, associative and Penning ionis. cross-sections, pot. energy curve study 79−87836
He+H_2, CI pot. energy surface, small distances 77−38708
He+H_2, pot. energy surface, analytical expressions from constrained optimisation 77−6698
He+H_2, pot. energy surface, ab initio calcs., van der Waals const. determ. 80−106372
He+H_2, simultaneous rot. and vibr. transitions, cross-sections calc. 77−68098
He+H_2^+, endothermic reactive and vibr. inelastic collisions, pot. well effects 79−8430
He+H_2^+, reactive and dissociative scatt., crossed-beam and trajectory obs. 78−64833
He+$H_2^+ \rightarrow HeH^+ + H$, diatomics-in-mols. and spline fitted ab initio surface, vibr. effects 78−20010
He+$H_2^+ \rightarrow HeH^+ + H$, spline-fitted ab initio surface, quantum mech. scatt. calcs. 77−63898
He+$H_2(D_2)$, vibr. deexcitation, cross sections, rate consts., vibr. rot. model 78−62879
He+$H_2(\mu H)$, interaction pots. and rot. scatt. calcs. 80−43158
He+H^+, differential scatt., 1-12 eV, high resolution beam meas. 80−58348
He+$H^+(H_2^+)(H_3^+)$, interaction pots. from ion mobility data 77−14518
He+HCN, translational-vibrational energy transfer, quantum dynamical study 80−63746
He+HCl(HF)(DCl)(DF), slow collisions, rot. excitation cross-sections, quantum mech. calcs. 77−12795
He+LiH, rot. inelastic collisions, dynamics 80−87209
He+LiH, rot. inelastic collisions, state-to-state cross sections determ. 80−87210
He+NH_3, rot. excitation rate consts., semiclassical method 79−3538
He+Na_2, elastic scatt. and rot. excitation, model pot. energy surface 77−6895
He+Ne pot., differential cross section, quantum mechanical inversion 78−70896
potential energy surfaces for collision processes continued
He+O_2, vibr. energy transfer, exact classical and quantal calcs. 77−19014
He+OCS, translational-vibrational energy transfer, quantum dynamical study 80−63746
He^++Ca(Ba), 2-1000 eV, spontaneous ionis. mechanisms 79−64090
$He^+ + H_2$, DIM approx. pot. energy surfaces and nonadiabatic coupling 80−23330
$He^+ + H_2$, dissoc. charge transfer, vibr. enhancement 78−33597
He^++He, He_2^+ mol. collision complex, pot. energy curve spectrum 77−19008
He^++He, multicurve-crossing problem, numerical test of semiclassical approx. 78−13590
He^{2+}+He, radiative single charge transfer cross section 79−7011
He^{2+}+He, two-electron excitation of quasimol. states 79−18274
He_2, $^1\Sigma_g^+$ states, pot. curves, ab initio multiconfig. SCF calcs. 77−46632
HeH^+, radiative recombination rates 78−37708
He_2H^+, ground state pot. energy surface for form. by collinear collision, DIM calcs. 79−97996
$(HeLi)^{2+}$, ab initio PE curves, coupling matrix elements, for He^{2+}+Li 79−22822
He*+D, Penning and assoc. ionis. with metastable He, 0.01 to 10 eV beams 79−27074
He*+He, collisional ionisation, cross-section meas. 77−46631
He*+He, collisional ionisation, He_2 $^1\Sigma_g^+$ state pot. curve calcs. 77−46632
He*(2^1P)+Ar→He+$Ar^+ + e^-$, anisotropic interaction potential, impact parameter method 77−68102
He(2^1S, 2^3S)+Ne(e^-), transition probs., pots. 80−58371
He($2s^1$S,2^3S)+Ne(Ar)(Kr)(Xe), Van der Waals forces, one-electron model pot. calcs. 80−14094
Hg, slow atoms, inverse scatt., semiclassical approx. calcs. 78−17747
Hg+I_2 reaction, adiabatic pot. energy surface 78−15666
Hg+I_2→HgI+I, endoergic reaction, prod. ang. distrib. 78−15665
Hg*+Ar(Ne), 6^3P_0 and 6^3P_2 metastable states, interaction pot. parameters 77−79670
Hg(6^3P_1)+$Li^+(Na^+)(K^+)$, excitation, optical polarisation fractions and mag. sublevels obs. 78−50619
I+HCl, quenching of I($5^2P_{1/2}$), temp. depend., time resolved at. absorpt. spectrophotometry 80−32655
I+O_2, near-resonant electronic energy transfer, surface-hopping model 79−86030
I_2 collision-induced predissoc., Landau-Zener model, method of analytic continuation 77−83687
I_2+Na(K)(Cs), ion-pair form. cross section, 15-120 eV, mol. props. depend. 77−28996
I_2+Na(K)(Cs), ion-pair form., differential cross sections, I_2 internal energy effects 77−61840
I_2+Na(K)(Cs), ion-pair form., energy transfer and differential scatt. 77−75272
K+$Cl_2 \rightarrow K^+(Cl+Cl^-)$, 5.5−14.0 eV, energy loss, spectrum maxima, mechanism 77−75286
K+I_2, ionising collision, trajectory surface hopping calc. 77−50509
K+I_2(IBr)(Br_2)(ICl)(Cl_2), ion-pair form., bond stretching effect on cross sections 78−1064
K+N_2(CO), rot. inelastic scatt., quantum effects, simple model surfaces 80−48064
K+O_2, mol. target internal motion 80−78697
$K+O_2 \rightarrow K^+ + O_2^-$, electron transfer kinematics 77−6903
KBr*+Ar, inelastic collision, classical trajectory anal., vibr. excitation effects 77−34737
Li^+ ion complexes with HF, H_2O, and NH_3 solvent molecules, structural and electronic props. calc. 77−57873
Li+H_2, inelastic collision, ab initio pot. energy surface 79−10055
Li+H_2, rot. and vibr. transitions, close-coupling calcs. 77−58136
Li+He, press. broadening, line shifts 78−5290
Li+inert gas atom, low energy, excitation, emission cross sections and polarisation fractions 80−37867
Li+LiH, collinear reactions, SCF correl. diagram for Li_2H 77−70292
Li^++Ar, interaction pot. of $X^1\Sigma$ state, CI calc. 79−50100
Li^++CO, differential cross-sections, ab initio CI vibrotor pot. energy surface calcs. 78−46421
Li^++CO, pot. energy surface, equilib. distance, SCF calcs., correl. effects 77−3430
Li^++CO, rot. excitation, ab initio CI pot. energy surface, classical mech. and coupled states calcs. 78−25665
$Li^+ + CO_2$, collisional excitation, quasiclassical trajectory calcs. 80−83467
Li^++$CO(N_2)$, differential cross-sections, classical trajectory calcs. 78−29841
Li^++ether(thioether)(amide), pair pots., ab initio LCAO SCF MO calcs. 80−58184
$Li^+ + N_2$, rot-vibr. transitions, semiclassical calc. of cross sections 79−22798
$Li^+ + N_2$, rot. and vibr. inelastic collisions, trajectory calcs. rel. to previous data 78−62878
Li^++Na, charge exchange, generalised Rosen-Zener model 77−50497
Li^++Na, direct and charge exchange scatt., differential scatt. cross-sections meas. 78−42158
Li_2, MCSF accurate pot. energy curves for $^3\Sigma_u^+$ and $b^3\Sigma_g^+$ states, level crossing 77−50369
LiF, low-energy electron impact rot. excitation, close-coupling calc. 77−58187
LiH+Ar, rot. transition cross-section, 0.8 eV 79−36742
LiH+HCl(DCl), rot. inelastic collisions, sudden theories 79−98201
LiH+H→Li+H_2, Li+H_2→LiH+H, LiHH pot. function calcs. 77−6699
LiH+H→Li+H_2, linear LiH_2 pot. energy surface, MCSCF functions optimisation 77−67960
LiH+He, rot. inelastic collisions, rigid shell models 80−99545
Li^+H_2, elastic of rot. excitation, semiclassical treatment 79−31657
Li_2H, natural orbital contour diagrams and occupation nos. for form. and dissoc. 79−18107
Li*+He(Ar), Li principal series line broadening and shift, interat. pot. consts. 78−42165
Li*(2^2P_J)+$H_2(D_2)$, collision induced quenching and fine struct. transition rate coefficients meas. 80−74221
Li(2p)+$H_2(N_2)$, Li(2p) excitation, alignment and orientation obs. 80−63794
Mg*+He(Ne), model pot. curves, including CI 78−42154

potential energy surfaces for collision processes continued
N+O, endoergic chemiionisation, semiclassical theory 79−98208
$N^+ + H_2$, triplet state ab inito CI pot. energy surfaces 78−74729
N_2, rot. relax. classical trajectory computation, using Lennard-Jones pot. 78−62880
N_2+Ar, total differential cross section, diffr. oscills. quenching 78−66625
N_2+Li, vibr.-rot. relax., optical pot. method 78−62886
N_2^++He, vibronic excitation, curve-crossing trajectories 80−23520
N_2^++Li(Na)(K), 50-1000 eV, crossed beams, electron transfer and excitation 80−14226
$N_2(A^3\Sigma_u^+, \nu_i) + N(^4S) \rightarrow N(^2P \text{ or } ^2D) + N_2(X^1\Sigma_g^+, \nu_f)$, energy partitioning 78−66636
NCNO⇌NC+NO, ground state pot. energy surface, ab initio calcs. 77−90593
NH_2, spin and rot. fine struct., orbital angular momentum 80−83247
NH_2, vibr. and rot. struct., intensity factors and orbital angular momentum 80−83246
NH_3 bond dissociation, MCSCF LMO calcs. 77−57886
NH_3+He, interaction potentials, ghost orbital SCF and Gordon-Kim calcs. 79−94057
N_2O^+, pot. energy hypersurface characts. calc. in $O^+ + N_2 \rightarrow N + NO^+$ react. 78−60996
$N^{2+}(^2P^0)$+H, charge transfer, ab initio CI pot. curves and coupling-matrix elements 80−37878
$N^{3+}(^1S)$+H, charge transfer, ab initio CI pot. curves and coupling-matrix elements 80−37878
$N(^4S) + N^+(^3P) \rightleftharpoons N^+(^3P) + N(^4S)$, gerade-ungerade splitting of N_2^+ pots., cross sections 77−30987
$N(^4S) + O_2(^3\Sigma_g^-) \rightarrow NO(^3\pi_u) + O(^3P)$ doublet surface minimum energy path calcs. 78−7194
Na, slow atoms, inverse scatt., semiclassical approx. calcs. 78−17747
Na^+ ion complexes with HF, H_2O, and NH_3 solvent molecules, structural and electronic props. calc. 77−57873
Na+H_2, electronic to vibr. energy transfer, close coupling calcs. 79−98203
Na+I_2, ionising collision, trajectory surface hopping calc. 77−50509
Na+Na, electronic-field pot. curves determ. for large interatomic distances, excitation cross sections calc. 80−95704
Na+Na, excited atoms, coupling terms, asymptotic pot., excitation energy transfer 80−23530
Na+Ne, differential cross section at thermal energy, expt. and theoretical results comparison 80−37851
Na+Ne, interaction model potential calcs. 79−86036
Na+Ne, Na(3p) excitation 80−1056
Na+Ne, potential curves from a model potential *(French)* 80−78685
Na+O_2, semiempirical pot. surfaces, dynamical considerations 79−11766
Na+Xe, nonreson. two-photon absorpt., 4s excited states and pot. energy curves, close coupled eqns. 80−48068
Na^++He (Kr) thermal, two trajectory model from meas. cross-sections 77−75257
Na^++Li, direct and charge exchange scatt., differential scatt. cross-sections meas. 78−42158
Na^++Ne, excitation and charge transfer, 0.2-12 keV collision 79−68314
Na^*H_2, potential energy surfaces 80−74215
Ne+H_2^+, reaction pot. energy surface, LCAO-MO-SCF energies 77−1917
Ne+HD, j=0 to 1 rot. excitation, differential cross sections, time of flight obs. 80−48104
$Ne + He_2^+ \rightarrow$ He+products, surface-hopping trajectory calc. 79−52637
$Ne + HeH^+$, collinear reaction, pot. energy surface SCF-LCAO-MO and DIM calc. 78−92467
$Ne^- + Na^+(K^+)(Li^+)$, electron gas model pots. and collision integrals *(French)* 78−42169
Ne^++Ba, 2-1000 eV, spontaneous ionis. mechanisms 79−64090
Ne_2^++He, pot. energy surface, reaction cross sections, ab initio calcs. 80−11881
NeH^{2+}, rel. to Ne^{2+}+H charge transfer reaction, astrophys. appl. 79−59550
NeH_2^+, ab initio potential surfaces, frozen orbital approximation calcs. 78−41927
$NeHe_2^+$, electronic structure calcs., extended valence bond diatomic calcs., applications to method of diatomics-in-molecules 79−45635
Ne^*+H_2O, pot. energy surfaces, MO and CI calcs., Penning ionisation electron spectra 80−106376
Ne^*+Ne, differential elastic scatt., rainbow max., mol. states 77−38710
O+H_2, classical trajectory calcs., ab initio surface, singlet state, rate consts. 80−66786
O+H_2, pot. energy surfaces and reaction rates, ab initio calcs. 80−63531
O+H_2, trajectory calcs., fitted ab initio pot. energy surface 79−74358
O+N_2, quenching of $O(^1D)$ state, at 300K, semiclassical study 79−45823
O+saturated hydrocarbon, reaction dynamics, model pot. surfaces, quasi-classical trajectory calcs. 80−97696
O+saturated hydrocarbon→OH+alkyl radical, reaction dynamics, mol. beam-laser induced fluoresc. obs. 80−97695
O^++H_2, linear approach, pot. energy surface for H_2O^+ 80−47922
O^++inert gas, potential energy curves from elastic scatt. cross sections 80−23502
O^++Ne, pot. energy curves, nonadiabatic coupling matrix elements 80−53110
O_2^+, electron impact dissoc. recomb., pot. energy curves calcs. 80−53150
O_3, pot. energy surface analytical function, atmospheric reactions 78−7174
O_3+He(Ar)(Xe), collisional energy transfer in unimol. reaction, classical trajectory calcs. 78−62882
$O(^1D)$+Ar(Kr)(Xe), inelastic collisions, spin-orbit coupling 80−5605
$O(^1D)$+N_2, electronic quenching resons., collinear collision, quantum mech. calcs. 77−60050
OH^{2+}, rel. to O^{2+}+H charge transfer reaction, astrophys.appl. 79−59550
OH-CH rotationally inelastic collisions, maser action 79−94068
OH+H_2, pot. energy surface, barrier heights and transition state geometry, POL-CI calc. 80−55649
$OH + H_2 \rightarrow H_2O + H$, reaction product vibr. distribs, quasiclassical trajectory, calcs. 80−85162

potential energy surfaces for collision processes continued
OH+p-H_2(He), collisional pumping of Λ-doublet transitions, pot. energy surface 80−23516
OH^-+inert gas, collision-induced dissociation 78−29834
OH_n, ab initio LCAO SCF calcs. of ionisation pot., electron, proton, H and hydride affinities 77−88387
$O(^3P,^1D) + H_2(^1\Sigma_g^+) \rightarrow H_2O$, potential energy surfaces, extended basis first-order CI study 80−7776
$O(^3P) + CO(X^1\Sigma^+)$, effective adiabatic pot. surface, Monte Carlo calc., vibr. deactivation and atom exchange 77−48627
$O(^3P) + CS_2 \rightarrow CS + SO$, reaction rate enhancement, triat. mol. symmetric vs. asymmetric stretch excitation 79−91927
$O(^3P) + H_2 \rightarrow OH + H$, potential energy surface, theory 80−45492
$O^+(^4S) + N_2(X^1\Sigma_g^+) \rightarrow NO^+(X^1\Sigma^+) + N(^4S)$, MCSCF potential energy surface for collinear $^4\Sigma$ pathway 80−63540
Rb^*+He(Xe), thermal, $5p\ ^2P_{1/2}$ state depolarisation cross-sections 77−71852
$Rb(6^2P)$+He(Ar)(Xe), fine-struct. transition cross sections, semiclassical calcs. 77−30972
$Si + H_2(O_2)(He)(SiCl_4)$, $3p^2(^1D_2)$ state behaviour, at. absorpt. spectra 78−29846
Sr+He(Xe), Sr reson. line width, 4607 Å, press. effects, pot. well depths 79−89643
U+U, K-shell ionis., classical relativistic trajectory method appl., 1, 10 GeV/n 80−43129
$U^+ + U(U^+)(U^{2+})$, elastic scatt. in plasma, interaction pots. and momentum transfer 80−38534
Xe_2, photoelectron spectra, $X^1\Sigma^+_{(1/2)g}$ ground state pot. 78−5280

potential scattering
1/N perturbation theory, large orders by inverse scatt. in 1-dimens., anharmonic oscillators 80−22214
3 wave bound state in spherically symmetric potential, inequality with correct coupling constant depend. 77−82405
δ-functions global operators, identities for scatt. states including spin 79−92985
absorbing boundary method, Golden Rule generalisation 79−97226
adiabatic oscillator and related pots., spectral and scatt. theory 79−58568
an inhomogeneous Schrodinger equation and its solutions in scattering theory 79−63073
analytical continuation of bound state, scatt. wave function construction 77−74258
anharmonic potential models, exactly soluble, const. and soln. 78−54221
anisotropic, classical, small-ang., theory, comparision with $Li^+ + N_2(CO)$ results 80−1043
anisotropic, in classical mechanics *(Russian)* 80−27183
anisotropic potential scattering in classical mechanics *(Russian)* 80−62541
anisotropic potentials, rainbow scatt. 77−82407
applied inverse problems, book 79−49017
asymptotic behaviour of quasipot. scatt. amplitude in plane of a complex orbital momentum *(Russian)* 79−75701
asymptotic completeness, geometrical and spectral transformation approaches 79−80459
asymptotic completeness for quantum mechanical potential scattering. I. Short range potentials 78−81869
asymptotic completeness of wave operators 77−74259
asymptotic expansions in motion of two electrons in nuclear field 78−66459
atom, neutral, scatt. by exponential corrugated pot. 80−25512
atom+atom(ion), total cross section, explicit bounds by geometric method 80−43130
atom-surface, elastic scatt. effective potential theory 79−43084
atomic electron resonant potential scattering in a low-frequency laser field 80−23545
atomic resonances, S-wave pot. scatt., coord. rot. method 80−28104
atomic scattering amplitudes, two-cluster, partial-wave, analytic continuation 80−52045
attractive potential, $r^{-(s+2)}$ type, SL(2,R) acting on quaternions 80−57125
Azzarelli Collas representation for scatt. amplitude, generalisation 78−8261
backscattering and Fresnel diffraction 77−13895
backward potential scatt., approx. methods comparison 79−17262
backward potential scattering at high energies *(Chinese)* 79−9143
backward scattering, Chen-Hoock formula, modulating operator formalism 79−35971
baryon-antibaryon harmonic oscill. pot. model, orbital matrix elements and selection rules 77−49930
beam multiple scatt. displacement by parallel mag. field 79−81110
Birman trace theorem, generalisation 78−57815
black hole, Reissner-Nordstrom, coupled gravitational and EM perturbs., scatt. matrix, energy conversion, quasi-normal modes 80−67775
book, scatt. theory in quantum mechanics 78−49573
Born approximation, error bounds 77−57217
Born series rearrangement, convergence improvement, orthogonal projections basis 77−60974
Born series rearrangement in model space, resolvent operator expansion 80−13422
boson, negative interactions with positive particles via Coulomb forces, $N^{5/3}$ law 79−44792
boson field in external potential, instability, Klein paradox, particle creation 77−6017
boson system, 1-D, with δ-function interactions, time-depend. Hartree approx. 79−9184
boson system, bound state scatt., interaction via δ-function potentials 78−16728
bound states, sufficient condition for existence, potential without spherical symmetry 80−68070
bound states for higher angular momenta, scatt. length 80−22209
bound states for r^{-2}-like potentials in one and three dimensions 79−2645
bound states for the symmetric shifted Coulomb potential 79−6007
bound states in continuum, local pot. and normalisable wavefunction construction 77−49632
bound states in weak pot. fields depend. on free particle density of states *(Russian)* 78−62091
bound states of weakly coupled long-range one-dimens. quantum Hamiltonian 77−87656

potential scattering continued
bound-state effective pot. formulation of dynamical symm. breaking 78−8554
boundary condition model, two and three nucleon problems *(Russian)* 78−86491
boundedness of total cross-sections in potential scattering 80−79
bounds on number of eigenvalues of Schrodinger operator 78−49693
bremsstrahlung, stimulated, high intensity, convergence of approx. 78−16687
canonical formulation for Lagrangian of two interacting relativistic particles 79−21973
central force field, arbitrary, fermion scatt. *(Russian)* 77−22668
charged particle, pot. scatt. in low-freq. laser field 79−41311
charged particle pot. scatt. in laser field, eikonal theory, quasi-static approx. 80−77647
charged particle potential scattering in laser field, eikonal theory 79−81249
charged particle scatt. in quantising mag. field 80−46853
charged particle scattering in homogeneous mag. field, transition amplitude 79−10218
charmed mesons, props. determ. from two-step pot. model 77−74682
classical and quantum transport theories 78−16603
collective phenomena in high energy scattering, 1-dimens. 3-particle model 79−80455
combined variable-phase-off-shell scattering theory 79−67190
complex coord. method, error bounds 78−49705
complex nuclei collisions, scatt. by schematic pot. landscape 77−26782
complex poles residues of outgoing Green function, eigenfunction expansion involving resonant states 77−82885
complex pot. barrier scatt. in semiclassical theory 77−9915
composite Coulomb scatt., eikonal approx., short range interactions 80−31534
composite particles, form factors in terms of inelastic Jost functions 77−2831
confining pot., Regge poles, coupled Schrodinger eqns. 77−61219
confining potentials, order of levels theorem, two body nonrelativistic interacting system 77−49634
conformal pot. in N dimens. (N>1) 77−74271
construction of L^2 dependent potentials 80−86129
coordinate asymptotic behavior of (3→3) wave functions for a system of three charged particles 79−21980
correspondence principle, rel. to potential step scattering, theory 80−46761
correspondence principle for potential x^{2N} 80−42088
Coulomb+rational separable pots., T-matrix, effective range functions 77−57221
Coulomb amplitude, integral representations 78−78118
Coulomb and Coulomb-like off-shell Jost functions 79−75388
Coulomb and Yamaguchi pot. scatt., bound states 77−57222
Coulomb coupling, strong, group SO(2,1), Klein Gordon eqn. 77−17837
Coulomb effects in N-particle scattering processes, channel distortion approx. 79−45222
Coulomb electron atom scatt. in laser field, asymptotic dynamics 79−94084
Coulomb interaction effects on calc. of scatt. characts. 79−9529
Coulomb off shell two body amplitudes, numerical computation 80−46858
Coulomb off-shell Jost functions, simple analytic expressions 78−62121
Coulomb phase shift, of quantum theory, for teachers 79−97135
Coulomb problem, zero-energy 78−62097
Coulomb scatt. in N dimensions, algebraic approach 79−75386
Coulomb scattering, Green's functions, integral eqns. soln. 77−37789
Coulomb scattering, N-particle, cluster props. 80−73192
Coulomb scattering as the limit of scattering off smoothly screened Coulomb potentials 80−94986
Coulomb spheroidal functions, integral eqns. and relations 78−409
Coulomb T-matrix, modified integral eqn. using Green's functions 79−35976
Coulomb-nuclear Lippmann-Schwinger eqns., constraints on pot. 77−2552
coupled channel Coulomb excitation, asymptotic soln. 77−46146
critical screening length for static screened Coulomb pot. 78−49706
cross sections and scatt. amplitudes 78−42152
cross-sections, total, boundedness 80−77639
curve crossing collisions, transition probabilities 80−32631
cut-off paths and forms extensions 77−33898
DC electron scattering, by spherical macroscopic pot. including screening 77−51739
deflection function, particle in central field, for teachers 79−24
degenerate electron gas, with elastic scatt., form of memory function 80−101753
dilute gases, transport props., softness expansion for inverse power pot. 80−28589
Dirac distributions, perturb. of self-adjoint Hamiltonians, Green's functions and wavefunctions, scattering theories 80−62514
Dirac eqn. with linear confining pot., asymmetric model 79−363
Dirac eqn. with linear confining pot. symmetric model 79−364
Dirac eqn. with oscillating pot., scatt. problem *(Russian)* 77−79225
Dirac equation with one-dimens. step potentials 77−49642
Dirac operator with highly singular potentials 78−21359
Dirac particles, high energy scatt. by arbitrary pot. 77−57508
direct reactions, semiclassical theory, complex paths and uniform approximations 77−71244
discrete inverse scatt. theory, Schrodinger eqn., difference approxs. 78−32724
distorted wave formalism, Pade approximants to K-matrix 77−10374
distorted wave series convergence, Lippmann-Schwinger eqn. 79−75942
education, Rutherford's scattering formula via the Runge-Lenz vector 80−73141
education, Rutherford scatt., electron deflection, inverse 1st, 2nd and 3rd power field, program 77−87594
education, Schrodinger eqn. solns. using approximate nucleon-nucleon and Λ-nucleon pots. 80−62429
effective potential calculation to order ħ using functional Schrodinger Rayleigh-Ritz approach 77−74257
eikonal, Rytov high-energy approx. 77−53802
eikonal approx., backward and transverse effects 77−10205
eikonal approximation, analytic props. 80−32038
eikonal theory of high-energy pot. scatt. 78−16675
eikonal type approximations for potential scattering 78−89635
eikonal-type expansions, projectile scatt. by local pot. 78−41195
potential scattering continued
elastic scatt., variationally optimised T matrices 78−74
elastic scattering by central field, unified semiclassical description 80−31575
elastic scattering large-ang., approx. classical theory, for teaching 79−25801
elastic three-body linear collision, inverse scatt. problem, for teaching 79−35468
electron+atom potential scatt. in low freq. laser field, perturbation theory 80−43191
electron conductivity in random pot., diffusive mode existence 79−65421
electron scatt. by any electrostatic multipole field, Born partial wave amplitude 80−53128
electron scattering by Coulomb potential in Born approx., bremsstrahlung statistics 80−5665
electron scattering from two-centre potential, phase shifts, semiclassical calcs. 79−25887
electron scattering in LF laser field, sum rule and classical limit 80−18978
electron-photon cascade simulation by Monte Carlo programs 79−54330
energy eigenvalues of Coulomb and oscillator potentials, connections 79−12637
extended Levinson's theorem for two-particle scatt. 77−45729
Faddeev eqn. soln. in adiabatic approx. with separable pots. *(Russian)* 80−52437
Faddeev equations, two-potential formula, three-body scattering 80−4893
Fadeev integral eqns. for 3 particles in boundary condition model, wave function determ. 78−54248
fast particle scattering on exponential type singular potential 78−37157
Fermi problem for rigid rotor, 2-dimens. case *(Russian)* 80−86153
few-body quantum mechanical system, sum of two-body potential operators 80−62516
finite range potentials, inverse problem 79−49097
finite volume statistical mechanics for highly singular two body pots., many particle interactions 77−5752
finite-rank potential that reproduces the Pade approximant 80−42106
fitting technique approach in pot. scatt. theory 77−79000
five-body equation, wave function treatment for binary partitions 78−16686
fixed scatterers, integral eqns. in wave mech. 77−78996
forward scattering amplitude analyticity for 3 particles in neighbourhood of physical region 79−40415
four charged particle system, two-body Coulomb singularities *(Russian)* 79−30291
four-body problem, appl. of hyperspherical functions 79−21981
Fredholm equations solns., error bounds, appls. to pot. scatt. and bound state problems 77−71234
Fredholm integral eqn., soln. by collocation variational method 77−71229
free particle Green's function, Gaussian matrix elements 79−2667
functional integral for scatt. amplitude in presence of long range interaction 80−101734
Gauss quadrature generated by diagonalization of H in finite L^2 bases 79−6016
Gell-Mann-Goldberger formula for long-range pot. scatt. 77−6040
global wavefunctions, appl. to scatt. theory 78−41179
Green's functions in quantum theory, book 79−65147
ground state properties, energy level lower bounds, particle in mag. field and external pot. 78−8260
hadronic matter, string junction model and spectrum energy density of string 80−57556
hadronic potentials, field theoretical interpretation, Poincare invariance, causal solns. 79−26266
half off-shell phase eqns. for non-local interactions 78−70019
half off-shell t-matrix elements for class of equivalent pots., ΔN scatt. 77−2562
hard core potential scattering, semiclassical phase shifts, WKB calcs. 78−86178
heavy particle elastic collisions, quantum effects *(Japanese)* 78−21015
heavy particle scatt. in solids, classical deflection ang. using Brinkman pot., numerical calc. 80−11525
heavy-ion potential scattering, single reflection approx. 77−10422
Heisenberg-Ising spin chain quantum inverse scatt. method, Jordan-Wigner transformation 80−93068
high energy, model pot., large angle scatt. amplitude 79−88821
high energy behaviour of scatt. amplitude in presence of confined channels 78−8268
high-momentum transfers and completeness of the Mandelstam program in potential scattering 80−82668
higher-order Levinson's theorems and the high-temperature expansion of the partition function 80−4558
impulse approx., neglect of binding 79−112
infinite gradient systems, asymptotic behaviour 79−40386
infrared radiation in potential scattering 80−42098
instability of a three-body system in one dimension 79−35542
integrable nonlinear evolution eqns. with saturation effects, inverse scatt. 79−92995
integrable system, finite dimens., scatt. behaviour 77−82415
integral bounds for N-body total cross sections 79−75405
integral equations for three particles with Coulomb long-range interaction 79−40407
integral equations of scattering theory, close coupling method *(Russian)* 77−74268
interacting electron system, orthogonality catastrophe 80−6757
intermediate system lifetime in quantum mech. collisions 78−45521
invariance principle in scatt. theory, proof 79−75378
inverse power singular pot. with complex coupling const., phase shift 78−41176
inverse problem, radial Schrodinger eqn. solns., analytic investigation *(Russian)* 79−87
inverse problem at fixed energy 78−41203
inverse problem for pot. scatt. at fixed energy, Newton Sabatier numerical method appl. 77−67593
inverse problem for radial Schrodinger eqn., incorrect nature 80−86139
inverse problem formal solns. 77−2555
inverse problems in quantum scatt. theory 78−54587
inverse scatt., generalised problem prolongation structs., soliton solns. 77−3833
inverse scatt., Newton's method modification at fixed energy 80−73207
inverse scatt. method, N-dimens. resolvent of linear problem, soliton theory 79−12643

potential scattering continued
inverse scatt. method generalisation, generalised nonlinear Schrodinger eqn. eigenfunction 79−92994
inverse scatt. problem, explicit expressions for Newton's soln. 77−57216
inverse scatt. problem, quantum mech. systems with discrete spectra 77−78995
inverse scatt. problem, spin-orbit and central pot. 78−32714
inverse scatt. problem for nonlinear Schrodinger eqn. 77−33890
inverse scatt. problem for scalar wave eqn., nonlinear approach 79−44778
inverse scatt. problem in 3-dimens., Marchenko eqn. analogue 79−88835
inverse scatt. problem method generalisation 77−60905
inverse scattering, one-dimens. Schrodinger eqn. pot. from S-matrix 80−57127
inverse scattering at fixed energy, oscillating tail phenomenon 79−30295
inverse scattering formalism, self induced transparency, physical interpretation 79−85005
inverse scattering in three dimens. 80−86130
inverse scattering method for solving nonlinear evolution equations 79−49096
inverse scattering problem, nonuniqueness 78−65820
inverse scattering problem for semi-infinite crystals 79−12651
inverse scattering problem for single-speed transport equation 79−88895
inverse scattering problem in the eikonal approximation *(Russian)* 80−57522
inverse scattering problem method, connection to pseudopotentials 79−71293
inverse scattering problem soln. in finite difference approx. 79−75414
inverse scattering transform, cylindrical Korteweg-de Vries eqn. and similarity solns. 79−75408
inverse scattering transform for potentials of compact support 79−97
inverse scattering transform solvable nonlinear evolution eqns., existence, Lax's method extension 78−32711
inverse square law potential, algebraic eqn., for teachers 78−81749
inversion-like integral equations, construction and appl. 79−49095
ion+electron collision, resonant electron bremsstrahlung *(Russian)* 80−102580
ion-ion scattering, momentum dependence, in microscopic theory 78−41752
Jost function, off-shell, for Coulomb, Hulthen and Eckart pots., limiting relations 78−81875
Jost function and S-matrix for pot. of general form., Schrodinger eqn. soln. in hypergeometrical functions *(Russian)* 78−81870
Jost functions, S-matrix of massive Thirring model, relativistic field theoretic model 78−54552
Jost Pais theorem, off energy shell generalisation, reply to comments 79−9142
Jost-Pais theorem, off-energy-shell generalisation, comments 79−9141
K-harmonics in one dimension 79−2584
K-matrix, off-shell 2-body scatt. with Woods-Saxon pot. 78−21002
K-matrix in distorted wave theory 77−22439
kinematics-free ang. momentum trajectories, Yukawa pot. numerical examples 79−89135
Kohn-Hulthen var. method for bound-state problems 78−62109
Kondo problem, Wilson's numerical technique 78−79972
Korteweg-de Vries eqn. solns., existence and regularity 79−71265
Kratzer molecular and general pot. superposed 80−9674
large-angle potential scattering in variable phase approach 78−91
laser field, generalised LF scatt. approx. 79−58590
Legendre Pade approximants, and appl. to pot. scatt. 78−28982
Legendre Pade approximants, convergence, to Coulomb and other scatt. amplitudes 78−28983
Legendre Pade approximants to scatt. amplitudes, convergent sequences 79−85014
Levinson's theorem for nonlocal interactions, phase shifts, continuum bound states 77−26195
Levinsons theorem, generalisation to abstract scatt. systems, appl. to pot. scatt. systems 78−62090
linear potential, energy eigenvalue eqn. 79−2646
linear scattering problem for finite depth eqn., Miura maps 80−105534
linearised inverse problems, variational approach 79−71259
Lippman-Schwinger eqn. for non-central pots., appl. of Fredholm theory 77−71232
Lippmann-Schwinger approach to elastic scatt. by semiinfinite crystals 78−47687
Lippmann-Schwinger eqn. constraints on Born approx. applicability 79−6527
liquid metal, integrated density of states, expression in Roth's effective-medium approx., generalisation of Friedel formula 79−99467
local two-body interactions, general off-shell phase eqns. 78−36880
long range atomic potentials in Thomas-Fermi theory 79−50101
long range oscillating pots., scatt. theory and dispersion relations 80−22213
long range potentials, EM polarisabilities, interacting systems, neutral, spinless, with mag. moment 77−6058
long-range, existence of wave operators 77−74244
long-range potentials, vac. fluctuations and retardation effects 79−3522
Lorentz process, convergence to random flight process 78−73941
low-energy scatt. by velocity depend. potls. 77−49631
low-energy scattering by long-range pot. 78−74723
low-frequency approximation for scattering in a laser field 79−92996
magnetic and laser fields simultaneously influencing potential scattering 79−81248
magnetic monopole-electric charge scatt., rotationally invariant approx. 78−54225
many channel Marchenko transform. operator, upper bounds 79−63091
many-body problem, vertex function and crossing symmetry 80−62515
many-channel pot. scatt., formal series meth. *(Russian)* 77−74821
many-photon ionization, resonance scattering on a nonstationary potential, and complex poles of the S-matrix 79−22677
massive quark pot. scatt., cancellation of infrared divergences 79−71707
master kinetic equation for a particle in the field of randomly varying scatterers 79−58634
matrix Pade approximants, applics. in pot. theory 79−78
matrix Pade approximants, variational bounds 77−65120
Matrix variational Pade approximants and multi-step square-well potentials 79−71283
metal foils, low energy heavy ion multiple scatt. in finite range potential 80−70283
mixed boundary value problem in three dimens. 77−71184
modified Coulomb potentials, bounds for phase-shifts 80−57112

potential scattering continued
modified wave operators for long range simple pot. scatt., two types 79−17266
Moeller operators and Birmann-Kato invariance principle, classical analogues, Pearson example 79−75390
Moller wave operators for pot. scatt. 78−45495
momentum transfer cross section, ave. force and force correlation formulas 79−92
monopole pot., wave function for electron motion *(Chinese)* 78−77768
monopole-charge scatt., analytic struct. of quantum amplitude 78−54226
monotone dependence in scattering theory, proof from S-matrix explicit formula 78−74163
Morse function off-shell K-matrix, computation method 78−74164
multi-instanton solutions of the duality equation and the inverse-scattering problem *(Russian)* 79−21591
multichannel, time-depend., nonrelativistic quantum scatt. theory for identical particles 79−44798
multichannel potential scattering theory with permanently confined channels, quark model appls. 77−13634
multichannel scatt. theory for temp. depend. Hamiltonians, charge transfer problem 80−90695
multichannel scattering, optimised Kohn method 79−49108
multichannel wave eqns., explicit perturbative solns. 80−31577
multiple diffraction exact and approx. calcs. 77−41831
multiple pot. scatt., soln. by finite iteration 78−28993
multiple scatt. series, eikonal approx. 78−21358
multiple scattering approximations in 3-body problems, comparison 79−84
muon single and multiple scatt. in continuous media with focusing mag. field 77−24328
Muskhelishvili Omnes integral equation, soln. procedure 77−13577
Muskhelishvili-Omnes equation and final state interactions 79−67196
N nonrelativistic pairwise interacting particle scatt., ($N \geq 4$), soln. uniqueness 79−75379
n-body quantum system, time depend. scatt. theory for infinite delta function pots. 78−49704
N-body scatt. systems, explicit bounds for total scatt. cross section 79−80462
N-boson problem, nonlocal interactions 79−71296
N-particle scatt. ionisation T matrix 79−44777
n-particle scatt. theory, asymptotic completeness 79−75413
natural modes, completeness for quantum mech. pot. scatt. 79−30283
neutral fermion scatt. by force centre *(Russian)* 79−5998
neutron coherent scatt., parity-violating pots., weak interaction probe 77−71599
neutron scatt. from parity violating pot. 78−25167
neutron scattering theory, parity violating interaction 78−25166
noble metals, TEP calc. 77−24549
non-local potential problems, Perey effect, WKB method 80−68077
non-relativistic scattering on cylinders and spheres 79−17251
noncentral transition pot. scatt., exact soln. 77−9918
nonlinear, inverse scatt. method generalisation, Schrodinger equation 79−75381
nonlinear evolution eqns., inverse scatt. method, conservation laws *(Russian)* 80−105804
nonlinear evolution eqns. in one space dimens., inverse scatt. soln. 79−97222
nonlinear Hamiltonian systems, integrability by inverse scatt. method 80−46864
nonlinear Schrodinger eqn., inverse scatt. problem method 80−4577
nonlocal continuous potentials, theory of integral operators and eigenvalue anal. 78−8274
nonlocal pot. model, energy independent, bound and scattering states 77−18504
nonlocal pot. scatt., off energy shell results 79−49104
nonlocal pot. scatt., off energy shell results 79−49105
nonlocal potential scatt., phase shift and extra nodes 77−74265
nonrelativistic, Hilbert-Schmidt type commentators and scatt. cross section 79−75375
nonrelativistic bound s-states in linear central potential 80−82936
nonrelativistic models for inelasticities in N/D eqns. many channel scatt. problems 77−49879
nonrelativistic multichannel potential scattering model, confined channels, Hamiltonians 77−5684
nonrelativistic particle in spherical space, dynamical symmetries 79−26255
nonsingular potential, scatt. length by iterative-perturbation method 80−27160
nonvanishing potentials, eigenvalue problem 77−74270
nuclear inelastic scatt. interactions from realistic pots. 77−67727
nuclear scatt., local-pot. models, appl. to α-α, ^{3}He-α and ^{16}O-^{16}O 77−34270
nuclear spherical pot., heavy charged particle scatt., Debye expansion and JWKB approx. 77−53803
nucleon-nucleon hard-core system, bound states and scatt., for teaching 78−41115
off energy two body t-matrix in the R-matrix theory *(Russian)* 80−22780
off shell scattering amplitude, S-matrix, pot. scatt., Mittag-Leffler expansions of Green's function, convergence 78−73874
off-energy-shell generalisation of nonrelativistic pot. scatt. 77−37780
off-shell continuation of scattering amplitude in quantum mech., inverse method 79−49423
off-shell p-p T matrix for Graz separable interactions 79−40795
off-shell scattering by Coulomb-like potentials 80−31560
on shell S-matrix relations for pot. scatt. variable phase method eqns. 79−9149
on-shell three-body multiple scatering eqns. 78−28988
one dimensional infinite particle systems with hard core interaction, nonequilibrium dynamics 77−82443
one dimensional Schrodinger eqn. with energy dependent potential, inverse problem, pt.I 77−26186
one dimensional Schrodinger eqn. with energy dependent potential, inverse problem pt.II 77−26187
one dimensional wave function for the effective Hamiltonian of non-local potential 80−46847
one-dimensional scatt. theory, stability of direct and inverse problems 78−4523
one-dimensional Schrodinger eqn. scatt. pot., reflection coeff. rescaling effects 79−71291
optical anal. of resonances in velocity depend. square well pot. 78−62098

potential scattering continued
orthogonal projection method, pseudopotentials 78−49688
oscillating potentials, scatt. matrix 80−57126
oscillating potentials, spectral and scatt. theory 80−52072
oscillation-free transformations, periodic potential 78−16636
oscillatory pots. of slow decay, moller wave operators and S operator unitarity 80−4559
Pade approx. and low-energy Lagrangian field theory 77−61220
Pade approx. in scatt. and effective range theory 79−30271
pair potentials, equilib. configuration of one-dimens. many-body problems 78−49692
parameter dependent potentials, inversion formalism, appl. of differential eqns. satisfied by Fredholm determinants 77−22437
partial wave expansion summations in scatt. by long range pots. 78−49707
partial wave expansions summation in scatt. by short range pots. 80−31570
partial waves with nonzero ang. momentum, zero range pot. method *(Russian)* 78−29006
partial-wave Schrodinger differential and integral eqns., comparison of numerical solns. 78−16671
partial-wave two-cluster atomic scattering amplitudes 79−44763
particle beam, potential scatt. into cone 79−97234
particle in box problem, path integral soln. 79−71279
particle interactions with infinite and semi-infinite periodic potentials 78−28991
particle scattering, low-energy, two-pot. formulation with r^{-4} interaction 80−31552
path integral formulation, central scattering potentials 80−82906
path integral representation for inelastic scatt. amplitude quasiclassical approx. 78−36888
path integral representation of pot. scatt. amplitudes 80−17820
penetration through and reflection on two thin potential barriers 78−65793
peratisation technique, iteration approach 80−86100
peratization technique, new approach 79−12646
perturbation methods for local and nonlocal pots. 78−16696
phase eqns., new class 77−37783
phase shifts, high energy behaviour for Coulomb-like potentials 80−98814
phase shifts, stability in spherically symmetric pot., Coulomb-strong interference 77−74237
phase shifts produced by repulsive, strongly singular, inverse power pots., high-energy behaviour 79−97233
phase shifts using recurrence relations for spherical Bessel functions 78−89364
phase space packets, time depend., differential cross sections obtained by superoperator methods 80−105544
phase-amplitude method for complex pot., generalised approach 77−53800
phase-equiv. non-local potentials 78−66224
phaseshift variational calc., s-wave scattering, non-zero energy 79−88822
polarised spin-1 nuclei or mesons, elastic scatt., relativistic spin and wave eqn. EM interaction 77−50104
pole structure of the off-shell T-matrix in pot. scatt. 79−25890
potential scattering, JWKB phase shifts, using Gauss-Mehler quadrature formulas 78−46411
principal value collision integrals, reduction scheme 77−57234
product represenation in effective range theory 78−78273
prolongation structures, nonlinear evolution eqns., general class of eqns. 79−25885
propagation properties, bound and scatt. states 80−73204
propagators, approximate representations in external field *(French)* 79−44782
pseudo Coulomb problem, group O(2,1), irreducible representation 80−73209
quantal Coulomb excitation calcs., error anal. of code AROSA 77−2550
quantum decay models, complex energy eigenstates for pot. scatt. 79−6011
quantum oscillating pots., no. of bound states, inequalities 77−45717
quantum scatt. theory, gauge transform. for variational method 77−65
quantum scatt. theory, variational principles and virial theorem 78−54231
quantum scatt. with δ-function pot. 77−17849
quantum scattering by external metrics and Yang-Mills potentials 80−31535
quantum scattering theory, quasi-classical limit 80−4562
quantum wave, linear pot. hill, Schrodinger eqn. soln. for teachers 78−12492
quantum-mechanical virial theorem, for central field scatt. 79−80469
quasiclassical asymptotic behaviour, quantum correction, potential scatt., amplitude, 78−62325
quasiclassical scattering amplitude, first correction (of order ħ) 79−40410
quasipotential eqns., Levinson theorem violation, S-matrix 78−54576
R-matrix theories 78−58760
ray representation of scattering amplitude in the presence of resonances 79−21587
reaction matrix theory, phase equivalent pots., general case 78−58131
recoil effect, light particle scatt. by two heavy particles *(Russian)* 78−82129
refined Born approximation 80−77
Regge amplitude construction through soln. of S-matrix equations 79−49413
Regge pole calc. by formal series 77−6056
relativistic electron Coulomb scatt., approx. to cos γ 78−28962
relativistic electron scatt. from 2-centre pot., approx. soln. 77−18187
relativistic electron scattering from a two-centre potential 78−66058
relativistic equation derivation and associated potentials from field theory 79−12954
relativistic generalisation of linearly rising pot. 78−4768
relativistic two body Schrodinger equation, generalisations of quasipot. eqn. for scalar interactions 77−13871
relativistic two-body t matrix, separable expansions to local potentials in a quasipotential approach 79−63641
resonance calculations for arbitrary potentials 79−22779
resonance theory of potential scatt., phase shift parameters 78−16685
resonant states in pot. scatt. theory, wave packet description 79−40391
Riemann solution in one-dimen. inverse problem 78−28979
rotated Hamiltonian resolvent, approx. in scatt. region 77−71233
potential scattering continued
Rutherford scattering, positively charged particles interaction calc. 77−27468
Rutherford scattering formula, small-angle end, for teachers 78−16608
S-matrix, Debye expansion convergence 79−40679
S-matrix theory, determinant and its relation to number of eigenvalues due to perturbation 78−58132
s-state, probability density calc. 78−57812
s-wave resonances with square well pots. 77−9914
s-wave scattering by Eckart, Woods-Saxon and optical potentials 77−49639
Saito pot., zero energy continuum bound state 79−9151
Saito potential, off-energy-shell unitarity 80−18207
scattering amplitude, high energy asymptotic behaviour 79−75409
scattering amplitude, punctual Pade approx. as regularisation procedure for partial wave expansions 79−17639
scattering amplitude for low energy, two sided estimates 80−46873
scattering by hard corrugated wall potential, Schrodinger eqn. exact soln. 79−40404
scattering by singular potentials of the general type at high energies 80−63141
scattering lengths, variational calcs. 77−57218
scattering on δ-function potentials in two dimensions 79−17250
scattering phase shifts, first order error estimates in approx. calcs. 79−58573
Schrodinger and Dirac eqns. with short range pot., exact scatt. soln. 79−17268
Schrodinger eqn., 1-D, oscillatory integral approach, semiclassical, linear and parabolic potentials 80−57124
Schrodinger eqn. eigenvalues for particle in monotonic pot. 79−40412
Schrodinger equation for two body problem with nonlocal separable central and tensor interaction, exact soln. 78−69997
Schrodinger equation solutions with time depend. pots. and associated scatt. theory 79−17263
Schrodinger operator, scatt. and local absorpt. 78−93546
Schrodinger operator, scattering theory and continuous spectra for class of strongly oscillating potentials 80−77638
Schwinger's variational principle in the nuclear two-body problem and in multichannel theory 79−75868
Schwinger variational principle for bound states and scatt. problems 78−16932
screened Coulomb scatt., eikonal approx. by h transforms 77−82413
screened Coulomb scattering, Martin Newton condition on amplitude phase 78−70006
screened Coulomb T-matrices, absolute values 78−66059
semiclassical off-shell T-matrix elements, repulsive local pots. 77−17845
semiclassical path integral methods, at finite temp., double well pot. problems 79−97256
semiclassical scattering theory, spurious excitation 80−73142
semiconductors, electron-electron collision effect on current voltage characts. in quantising mag. field 80−103705
separable optical potential theory, Schwinger variational principle *(Russian)* 79−3122
separable potentials, building of 'dual' amplitudes *(Russian)* 77−5702
separable potentials 80−90708
short range local interactions, radial wave functions and scatt. phase shift calc. program 79−84976
$(\sin\phi)_2$ interaction in box, soliton soln. fermionisation 79−88840
single channel scattering, optimised Kohn method 79−49107
single channel Schrodinger eqn. for e-scatt. off static pot., de Vogelaere's method 79−63062
single-barrier penetration of electrons, Eckart pot. 79−44788
singular continuous measures in scattering theory, examples of potentials and physical interpretation 78−57802
singular interaction potentials in classical statistical mechanics 79−71354
singular pot., variable phase eqn., formal series method 77−67330
singular potentials, bound states, WKB approx. 77−82402
singular potentials, Gel'fand-Levitan theory of the inverse problem 79−49098
singular potentials, short wavelength phase shift, turning point approx. 79−44797
singular potentials in the non-relativistic quantum theory *(Russian)* 79−63063
singular quasipotential eqn. for bound states, soln. 77−60973
spectral and scatt. theory, Schrodinger operator with singular attractive potential 80−86151
spectral function methods, non-relativistic two-body off-shell amplitudes 77−26643
spin-orbit potentials, quantum scattering theory inverse problem, fixed energy Jost functions *(Russian)* 80−68082
spinless elastic scatt., phase-shift ambiguities 77−9905
spinless particle scattering by central pots., soln. 80−27156
square well potential, separable representation 80−82922
square-well potential, integral eqns. and scatt. solns. 80−31451
square-well potential, scatt. states, wave eqn. numerical solns. 77−33877
Stark effect, spectral and scatt. theory of Schrodinger operators 77−22435
static inhomogeneities, elastic low angle multiple scatt. *(Russian)* 80−46874
stationary theory, spectral forms 77−45714
statistical mechanics, quantum and classical, unified treatment of scatt. and dynamics 78−45522
stochastic Liouville equation for quantum-mechanical scatt. for particle in field of variable scatterers 78−140
Sturm-Liouville equation, convergence, rel. to nucleon-nucleus pot. 79−6534
Sturm-Liouville equation, math. aspects rel. to nucleon-nucleus pot. 79−6533
summation of partial wave expansions in scatt. by long range pots. 79−41239
systems with different spatial asymptotics on left and right 79−12633
T matrix from bound states and resons. with separable pot. 77−30036
T-matrix eikonal expansion, higher order terms 80−86149
term entry into continuum in presence of Coulomb field 79−21583
three body systems, spectral and scatt. theory of Schrodinger eqn. 77−45715
three particle reactions, S-matrix theory kinematic props. 78−54578
three particle systems with Coulomb interaction, modified Faddeev eqns. 79−54284
three-body Amado-Lovelace eqn. at positive energies, anal. soln. 78−16938

potential scattering continued
three-body problem, bound state and scatt. problems 78−16684
three-particle scattering, subtraction techniques 78−24694
three-particle system, orthogonal projection 78−90
time delay in N-body scattering 79−75389
Todorov equation, Coulomb interaction between two spinless particles, infinite-multiplet spectrum 79−45039
total cross section, semiclassical limit, fast oscills. 77−83672
total scatt. cross section, time depend. approach 79−84992
total scattering cross sections for optical pots., quasiclassical calcs. 78−8270
transit time measures in scattering theory, time depend. Schrodinger eqn. 80−73194
transmission coeff. for 1-D potential barrier, discretisation of Schrodinger eqn. 80−57123
transparent pots. in classical approx. 77−50872
transport theory integral eqn. soln. in Green's function formalism, scatt. amplitudes 80−4566
two body scatt., non-relativistic, variational matrix Pade approximants *(German)* 78−54247
two cluster scattering amplitudes, dilation anal. reson. rel. to scatt. reson. 79−40389
two space scatt. theory, Cook-Kuroda theory 79−67194
two-body, off-shell wave matrix 80−82681
two-body scattering, T-matrix elements, on and off energy shell 79−67177
two-body transition matrix and UPA model, convergence props. of generalised separable expansion 78−16939
two-centre problem for Dirac eqn. 77−67328
two-centre problem with realistic potentials, single particle energies, wave functions 77−82887
two-centre scattering amplitudes, var. determ. 77−78998
two-cluster scattering of N-charged particles 79−40387
two-particle scattering, use of Coulomb wavefunctions in momentum space 79−84996
two-potential formulae for rearrangement scattering 78−4512
two-space scattering theory, with applications to many-body problems 79−17264
ultracold neutron reflection from one-dimens. pot. barrier, reson. struct. *(Russian)* 78−37393
unified formalism for quantum and classical scattering theories 80−100
variable amplitude nonlinear eqns. for one-dimens. scatt. 77−22431
variable phase method for scatt. on non-local spheroidal pot. 80−95
variational methods calcs., comparison of convergence 80−52043
variational scattering calculations, error estimation 79−111
variational [1/1] matrix Pade approx. in pot. scatt., exact solns. 77−22447
velocity-dependent pot., Regge trajectories, S-matrix singularities 77−57468
wave functions, variation-iteration principle, bound and scatt. states 78−54227
wave operator asymptotic completeness for singular and long-range potentials 79−71264
wave operator completeness breakdown 79−40388
wave operator completeness in two Hilbert spaces 79−75376
wave operators for momentum depend. long range potential 77−64953
wave packet scattering 77−74248
wave reflexion by real potentials, phase integral treatment 79−49084
Wigner transform and the eikonal approximation for nonlocal potentials 80−13423
WKB approx. for potential reconstruction by differential scatt. cross section *(Russian)* 78−45818
Yukawa pot., s-wave off shell T and K matrices by Ecker-Weizel approx. 79−63074
Yukawa pot. scatt., separable expansion method, off-shell T matrix 78−93564
Yukawa potential, scatt. amplitude, nonperturbative var. approx. calcs. 78−24981
Yukawa potential function, determ. of phase shifts 78−58237
Yukawa scatt. and impact parameter amplitudes using Legendre Pade approximants 80−22227
zero energy scattering quantities, bounds 78−49686
zero-range pot., stripping and rearrangement anal. 77−67331
α-α and α-nucleus calcs. using effective pot. interaction, ^{8}Be rot. levels. 77−22915
α-nucleus large-angle scatt. 77−71614
ΔN, Δ well depth with class of equiv. pots., nuclear matter appl. 77−26605
n, ultracold, transmission through moving pot. barrier 78−8867
N scattering from two fixed potentials, exact multiple scatt. calc., Fresnel approx. comparison 78−66054
N-N soft photon bremsstrahlung in pot. model 77−6381
nd scatt., at d breakup energy, boundary condition method 79−22127
np system, dispersion approach to the inverse scattering problem *(Russian)* 79−22128
p+H atom, low energy, quantum theory, integrated cross sections, phase shifts 77−30957
p+^{4}He, interaction potential from inverse scatt. problem method *(Russian)* 78−46068
pd potential scattering, total cross section calcs., 200-1000 MeV, Glauber model 77−61309
pp scatt. in $^{3}P_0$ and $^{3}P_1$ states 77−38186
π absorpt. and prod., relativistic scatt. models, equivalence theorem 77−74884
πA, multiple scatt. theory *(Russian)* 79−49640
πN elastic interactions, potential determination using Newton-Sabatier method, inverse scatt. problem 78−89731
πN scatt., separable interactions for three-body problems 78−78113
πN-interaction, linear wave eqn. with energy-depend. pot. 77−18317
$\pi\pi\rightarrow\pi\pi$, p-resonance production, quasipotential approach, linear σ-model 80−86755
$\pi\pi$ scatt., separable interactions for three-body problems 78−78113
Ar, electron pot. scatt., 100 and 500 eV, extended Glauber approx. calcs. 77−54610
^{A}C, A=12,13, large angle scatt. of ^{9}Be, optical model and DWBA anal. 79−36259
^{13}C(π^{+},π^{0})^{13}N, charge-exchange transition vertex, optical pot. 77−6461
Ce(n,n′) 1.8 meV to 1.8 eV, total neutron cross-section meas. using TOF spectrometry 79−85466
H, positron elastic scatt. lengths and phase shifts, variable phase method 79−22838
potential scattering continued
H+e^{-}(e^{+}), elastic scatt., asymptotic effective pot. 80−14233
H_2, electron impact low energy rot. and vibr.-rot. excitation cross sections, static exchange approx. 79−89799
He+Ar(Kr)(Xe), He*(2^{1}S) scatt., low energy repulsion systematic struct. 78−22000
^{4}He+π^{-} second-order optical pot., multiple scatt. theory 77−82966
^{4}He(α,α), nuclear separable plus Coulomb interaction 80−83106
^{4}He(α,α), size change of α effect on phase shift, generator coordinate and variational methods *(Chinese)* 80−68683
Kr, electron pot. scatt., 100 and 500 eV, extended Glauber approx. calcs. 77−54610
N_2, electron scatt., adiabatic polaris. pots. 79−10203
Tm(n,n′) 1.8 meV to 1.8 eV, total neutron cross-section meas. using TOF spectrometry 79−85466
potential transformers
600 kV repetitive stacked line transformer pulse generator 78−77935
coupled Marx-Tesla circuit for production of intense relativistic electron beams 79−17558
HV instrument transformer calibration system based on LV inductive voltage divider 77−82567
MV, constructional principles and production technology *(Hungarian)* 80−100118
MV, optimum rating nomogram *(Bulgarian)* 77−60916
oil immersed transformers, dissolved gas causes and phenomena, anal. *(German)* 80−76570
Tesla transformer accelerator, electron beam prod. 78−326
potentials (bioelectric) *see bioelectric potentials*
potentials (electric) *see electric potential*
potentiometers
see also voltage measurement
AC, features and ccts. *(Polish)* 78−29128
AC, self-balancing, nonlinear servomechanism design *(Russian)* 78−70156
automatic, microprocessor-controlled for nanovolt meas. 79−21771
automatic crack growth recording using PSR-1-19 potentiometer 78−39971
automatic potentiometric monitoring station, for examining industrial wastewater 78−56932
bipotentiostat of simplified design 80−35589
cardiac system pressure pulse LF wave synthesizers, mammalian cardiac system 77−9301
computer interfaceable potentiostat 78−57976
DC galvanometer internal resistance meas. by potentiometer 77−13777
DC meas., in 100 mV-10 nV range *(Polish)* 78−41332
decade, method for linearised readings 79−21765
electronic potentiometer, attachment for measuring deform. 77−17974
functional photopotentiometers, synthesizing method, calc. examples and expt. test results 79−6151
joint motion meas. by triaxial electrogoniometer, for human prosthesis design 78−11781
level indicator for electrically conducting substances 79−77312
linear rotary type, nonlinearities compensation 78−45646
low resistance differential type for standard cells testing *(Polish)* 78−29127
magnetic potentiometer, appl. to testing and anal. of mag. devices 78−62210
microprocessor-controlled, for nanovolt meas. 78−89502
multifunctional chronopotentiometer for electrochemical studies 77−81413
PDK potentiostat for electrochemical investigations 79−70345
potentialograph, electrical circuit 78−4638
potentiostat, electrochemical, with automatic resist. polarisation compensator 77−21393
potentiostat, P-04, for electrochem. meas. 80−61185
recorder, Servogor, features, appls. *(German)* 78−12681
resistive and potentiometric transducer connection line checking *(Bulgarian)* 79−93120
self-balancing nanovolt potentiometric system for thermometry and calorimetry 77−53903
selfcalibrating AC potentiometer, theory 77−82570
semiautomatic, webermeter testing appl. 77−74464
standard cell calibration against Josephson voltage reference 77−5874
strip chart recorder calibrator/performance evaluator 77−87752
temperature measuring bridge cct., thermistor appl. 78−207
twenty-turn dial for multiturn potentiometer 77−45866
two-coordinate, component quantity determination in solutions, automatic method 78−93657
two-coordinate recording (PDS-021), method for accomplishing time scanning 77−61080
unit power standard for 53.57 to 78.33 GHz 80−90808
voltmeter calibration appl., digital, errors analysis 77−10059
CdSe linear photopotentiometers, output characts. 77−1453
powder diffraction cameras *see cameras; X-ray crystallography apparatus*
powder metallurgy
active shrinkage theory and mechanism 77−63579
agglomerate structure parameters of powders in the incoherent zone in rolling 80−84876
alloys, two component, sintering 80−20847
alloy, binary, vol. changes during sintering, inter-ion interaction influence 79−28982
alloy, hard, powder mixtures, porosity and hardness during pressing, u.s. vibration effects 77−1821
alloy, rapidly solidified powder, nucleation, undercooling and homogeneous struct. 79−11598
alloy manufacture for vacuum deposited resistive foils of low surface resistivity *(Polish)* 80−35124
alloy powders, production using electrodeposition and heating in reducing atm. 79−100079
applications, history and development 80−68014
atomisation of melt, charact. of metal powder 78−19688
atomisation units, gasdynamic and acoustic props. 80−66451
atomised powder, new alloy production 77−21054
atomised-Fe powder, friction of compaction process *(Japanese)* 77−59716
atomization of melts with water, process parameter effect on powder props. 78−19689
boronising, physicochem. characts. 80−61024
borsic fibre reinforced Al, hot pressed forged, plasma sputtered *(Russian)* 78−35330

powder metallurgy continued
bronze, Al, electrode strip, short-time sintering 77−1824
bronze, Al and Ti, sintered frictional material, wear resistance, effect of matrix struct. 77−28911
bronze, spherical powder, negative magnetic resistance changes 77−1410
bronze, spheroidal, equivalent sphere diameter calc., Saltykov method 78−31362
bronze powder preparation by electrodeposition, porous components fabrication appl. 78−20026
bronze powders, electric-pressure sintering onto cylindrical parts in fluidised bed 80−100960
coating of refractory metals with silicide, local heating 77−81335
cold rolling, deform. region stresses 79−61609
compact, elec. resistivity 78−64028
compact growth in liquid phase sintering 80−20835
compaction, by impact of projectiles launched by compressed air 80−2973
compaction, stereoscopic SEM micrographs, quantitative anal. 80−57433
compaction equations, best description of expt. data 80−2974
composite, metals and materials, powder metallurgical parts, development, and manufacture of semifinished products 80−50578
composite materials *(German)* 80−20849
conference on powder metallurgy, Bowness-on-Windermere, England (Oct.-Nov. (1978)) 80−17713
consolidation by pulsed magnetic fields *(German)* 77−8783
continuous extrusion of metal powders for electrical industry appl. 79−95968
contribution of vacuum techniques 78−84736
crystalline particles at sphere-plane contact, nondiffusional deform. under capillary forces 78−15329
deformation, boundary conditions on sliding surfaces 80−60978
densification, electrohydraulic effect appl. 80−60798
densification during isostatic compression 80−66449
densification of porous solid during volume plastic deform. without work hardening 77−40402
densification on heating under high pressure, to 80 kbar 80−25602
diamond tool, metallic binder, microstruct. charact. by electron probe anal., SEM obs. *(Rumanian)* 79−74114
diamond-metal strip, strength props. 79−61678
die filling and densification in hot extrusion forging of porous preforms 78−23645
die steels for cold plastic working, powder metallurgy, charcts. 78−68649
dilatometric method for study of dimensional anomalies in metallic materials rel. to crystal struct. *(French)* 79−52563
direct resistance sintering, electric circuit components, breakdown voltage *(Ukrainian)* 77−70018
dispersion hardened metallic matrix composite, powder metallurgically produced effective interparticle distance effects *(German)* 78−52727
dynamic hot pressing, process parameters for parts of varying complexity 80−100799
electric discharge sintering, metal powder+punch electrode reactions 78−11148
electric discharge sintering of binary powder mixtures 77−63594
electric discharge sintering of metal powders, effect of diffusion coatings on steel electrode 77−63598
electric sintering *(German)* 80−25598
electrical contacts based on powder metallurgy and powder composites 80−29902
electrical discharge powder compaction 80−35135
electronic industry appl. 80−29903
explosive compaction 78−64501
explosive pressing, shock compression parameters *(Russian)* 77−52260
fatigue strength significance *(German)* 80−60946
FCC metal, hot pressing diagram 79−70027
Fe sintered material, operating performance, effect of polymer and graphite lubricant additives 80−11785
forging, review 79−43166
granular materials, hot isostatic pressing in sheaths, process parameters calc. 80−84874
granular materials, rolling, granule kinematics 80−84875
granule rolling process, energy and force parameters determ. 77−63577
granules, form. mechanism study during centrifugal atomisation of rotating blank 80−100798
hard alloy coatings, detonation deposition from fine powder mixtures 79−100078
hard metal powders, electric-pressure sintering onto cylindrical parts in fluidised bed 80−100960
hard-alloy powder mixtures, compressibility in hydrostatic working 78−68645
hardened metal, sintered, CVD of C rel. to atmosphere *(German)* 79−95966
high strain rate processes, review 80−84864
hot pressing effect on formation of struct. and props. during sintering 79−100088
hot swaging test method for tensile testing 77−25235
Inconel 718, grain growth during sintering 80−97449
information service, Soviet 78−8181
magnetic materials technology developments, high-energy *(Italian)* 80−54914
manufacture by CaH method, $Ca(OH)_2$ separation 80−84878
manufacturing appl., state of art and developments until (1990) *(Bulgarian)* 78−52714
mathematical-physical considerations rel. to metal powder prod. 80−11595
mean normal contact stress in rolling 77−12571
melt atomising unit, gasdynamic parameters 77−63576
melt infiltration of porous materials, math. model 79−100089
metal, liquid, jet disintegration by electric pulse, powder and granule prod. 79−33968
metal, sintered compacts, residual pore effect on grain size distrib. 77−85961
metal, work-hardening, plastic, sintered, porous, irreversible deform. 78−35459
metal couple, porous homogeneous vacancy migration and void form. 77−55401
metal powder density meas. by US velocity 77−32760
metal powder production, interactions between N_2 jets and liq. Pb and Sn streams 79−43170
metal powders, strip densification in forward slip zone in rolling 79−95972
powder metallurgy continued
metal submicron particle heating in hot gas, plasma metallurgy 80−81092
metallic glasses props., development and appl. 80−19710
metallic sputtered powder, struct. and phase composition, cooling rate effect *(Russian)* 79−56941
microcrystalline alloys, metastable, rapidly quenched particulates, props. appl. and production 80−84887
micropowder, cyclic classification, using variable electric field, device design 80−36982
milling conditions effect on densification during pressing and sintering 78−11149
mischmetal-Co-Cu-Fe-Mg, mag. props. 80−35353
mischmetal-Co-Cu-Mg, mag. props. 80−35353
mixture with decomposing oxide, growth kinetics of surface film during annealing 79−96216
Ni powder 2JJ, porous, effect of sintering conditions in struct. and strength 80−20823
Ni-Cr alloy Kh20N80, sintered sheet material, stopping power and pore size relationship 78−19693
Nichrome wire, porous, strength charact. 78−6997
Nichrome/steel, porous metal-thread sheet materials, filteration, permeability and strength props. *(Russian)* 79−78915
oxidized metal powder electric discharge sintering 77−59719
packed powder, induction heating mechanism *(Japanese)* 79−59615
particle deformation during cold isostatic pressing 78−44052
particle shape analysis, review 77−1820
particle size distribution determ. appl. of pulse conductivity 77−10157
particles produced by gas evaporation, form., growth and interaction 80−16220
Permalloy, pressing velocity effect on quality of compacts 80−20834
Permalloy 51N, powder metallurgy product. and props. 78−60603
Permalloy powders, electric pulse shaping and sintering 80−25605
plasma appl., low-temperature *(Bulgarian)* 78−52715
plasma arc spraying, effect of thermal power of jet on heating and deposition on substrate 77−59959
plasma industrial utilisation, synthesis, powder, metallurgical and surface treatments, review *(French)* 80−96398
plasma-sprayed coating, process instability, effect on struct. and mech. props. of coatings 77−56131
porous barrier fabrication for U isotope separation, powder metallurgy problems *(Italian)* 78−88439
porous materials, production method using stainless steel gauzes, exam. of hydraulic characteristics 80−16243
porous strip, moving, transverse cutting criteria 77−55901
powder additions to impregnating mixture, effects on rate of diffusion processes 77−28044
prealloyed powder blending, composite materials fatigue and tensile props. *(French)* 80−20850
preforming using high-voltage electrical discharge 80−84872
pressing dies, dimensions of hard-alloy inserts calc. 78−60593
pressing-ejection unit, industrial, for long filter element prod. 77−63595
rare earth-Co alloys, powdered, fine grinding in gastight attrition mill 79−33967
rare earth-iron intermetallic, O-stabilised, $R_{12}Fe_{32}O_2$, prep., struct. and mag. props. 77−8956
recent developments, book contrib. 79−66026
recent developments, Sweden 80−93514
refractory group VI metal, activated sintering mechanism 79−91605
refractory metal, generalised model for prediction of periodic trends in sintering activation 78−64498
refractory metals and alloys, processing by powder and vacuum melting techniques 79−33966
review of instruments for particle and powder charact. 77−66735
rolling, contact stresses distrib. 79−66083
rolling, overall strain co-eff. 77−24984
saturation of Ti alloys with A and Cr, powder method 77−21052
sheet filtration materials with metallic gauze backing layers 78−60613
sinter-forging process, powder charact. effects 77−59714
sintered composite materials, form of C present *(German)* 79−95978
sintered materials, operating performance, effect of polymer and graphite lubricant additives 80−11785
sintered metal, cold forming with self aligning dies 78−11158
sintered metal, ductility, porosity effect 77−59875
sintered metal parts and powders standardisation of quality control methods 79−96266
sintering, activated 80−25611
sintering, application of stereological charact. of interface interaction 77−63589
sintering, rel. to definition powder metallurgy 80−20841
sintering, solid state, models for kinetics 79−78912
sintering, surface oxide layer effects, oxide dissolution process, anal. 80−11588
sintering, with intense energy release of interparticle contacts 78−60615
sintering at 1 to 10 MPa, melting mechanism *(German)* 80−35122
sintering of solids containing several dissolved gases 80−20836
solid state sintering, compact length change 80−11593
spark alloying powder particle interaction obs. *(Russian)* 79−83146
spark erosion prep. of powders 78−27452
steel, 10R6M5 and 10R6M5K5, atomised powders *(Russian)* 80−97446
steel, alloy hot forging for differential pinion gear 78−15337
steel, austenitic Kh18N9T, porous fibres, oriented struct., strength props. 78−3199
steel, austenitic stainless, porous fibre, sintered and compacted, mech. props. 79−15623
steel, austenitic stainless, powder, sintering behaviour 78−44051
steel, boriding in powdered mixture with high activity 80−30164
steel, Cr (13 wt.%), sintered, organometallic complex addition effects on mech. props. 80−25595
steel, Cr-Mn, powder forged, fracture processes and fracture toughness 78−72870
steel, Cr-W-Mo-Co, high-speed, from atomised powders, mech. and cutting props. 80−66556
steel, Cu-Mn-Zn, Zn addition effects in powder forgings produced by liquid solid alloying 78−11157
steel, Cu-Ni-Mo (2, 2, 0.25 wt.%), sintering, kinetic charcts. 80−60805
steel, high speed, atomised powder, defects in parts produced by hot isotactic pressing 78−60612
steel, high speed, powder, cold isostatic compaction effect on thermophysical props. 78−52717

powder metallurgy continued
steel, high speed, W-Mo-Co-Cr-V, production from atomized powder 80−20837
steel, high speed, W-Mo-Cr-V, production by powder metallurgy 77−12574
steel, high speed R6M5K5, excess carbide size and distrib. effect on grain size 77−90356
steel, high V-W-Mo, high speed, phase composition and struct. of atomized powders 77−90323
steel, high-speed, atomised powders and sintered blanks, particle size effects 77−44188
steel, high-speed, fracture toughness of powder metallurgy vs. conventionally produced steels 78−64647
steel, high-speed, powder, atomised, microdefects in particles 77−28753
steel, high-speed, sintered, refractory carbide additions effect on hardness and cutting performance 77−66608
steel, high-speed tool, properties, powder metallurgy prep. method *(Czech)* 80−60800
steel, high-speed tool, splat quenching, props. and struct. 80−76294
steel, low-C, bond form. between powder layer and dense basis during hot pressing 79−24669
steel, maraging, 250-grade, ductility and toughness of hot isostatically pressed powder 78−52925
steel, maraging 350, produced by powder metallurgy, mech. props. 78−15334
steel, mixed alloy, sintering, reaction kinetics of Fe and graphite powders 77−55907
steel, Mn, sintered, production, effect of initial Fe powder struct. on mech. props. 80−104095
steel, Mn-Cr-Mo, Mn-V-Mo, high-strength heat-treatable sintered 80−50575
steel, Ni, sintered, physical and mech. props. rel. to homogeneity 79−38762
steel, Ni, sintered, relation between microstruct., microchemistry and mech. props. 78−64504
steel, Ni-Cu and Ca, shrinkage kinetics of sintering and dependence on carbon content 79−100087
steel, Ni-Cu-Mo-C, powdered, influence of cooling rate after sintering on preps. 79−95969
steel, Ni-Mo, powder forged, as-forged props., effect of process variables 77−59715
steel, Ni-Mo, powder forged, fracture processes and fracture toughness 78−72870
steel, Ni-Mo-C (2.0, 0.2, 0.4 wt.%) sintered, struct. transforms. and mech. props. after quenching 80−66557
steel, Ni-Mo-C (5, 0.5, 0.5 wt.%), sintered, effects of powder and sintering variables on props. 80−104093
steel, powder, prealloyed, struct. formed by atomisation, props. *(French)* 77−70020
steel, powder, rotary forging, porosity and deform. 78−23646
steel, powder forged, fatigue, surface treatment effect 80−85048
steel, powder forged, impact strength and fatigue strength, slag inclusion effects 77−21271
steel, powder forged for carburizing appl., core props., mech. props. 78−15339
steel, powder-forged, fracture toughness 79−66155
steel, sintered, Cr-Mo, CaF addition effects on struct. heterogeneity 78−60611
steel, sintered, diffusion chromising 77−66607
steel, sintered, diffusion treatment with B, Si, Cr and C, corrosion and wear improvement 77−77642
steel, sintered, fracture of residual pores 80−76352
steel, sintered, high speed, with Ti(C,N) additions 78−11160
steel, stainless, 20Kh13, prep. by diffusion impregnation 80−60803
steel, stainless, atomised powder, effect of ultasonic refining on processing preps. 79−33972
steel, stainless, atomized 0Kh18N9 powder, activated sintering, US treatment 77−90291
steel, stainless, fibre reinforced porous coating, isostatically compressed for bone ingrowth 80−35134
steel, stainless, from nonspherical powder, mean pore size of sheet material 77−28757
steel, stainless, medium hardness, densification of particulate materials, general law 78−19692
steel, stainless, porous boronising sintering in BC packing material 78−60594
steel, stainless, sintered, prod. methods and props. for machine components, review 79−100082
steel, stainless, sintered sheet material, stopping power and pore size relationship 78−19693
steel, stainless 304L, sintering, effect of grain growth and boundaries on shrinkage rate 77−36419
steel, TRIP, powder processing, tensile strength, ductility 78−64499
steel, W-Mo-V-Cr(6,5,2,4 wt.%), 56-5-2, microstruct. produced by melting and powder metallurgy *(German, English)* 77−63591
steel (alloy)-TiC (70, 30 wt.%) composite, sintered, wear resist. 80−100815
steel base composite, sintering, mech. props. 77−21061
steel casting surface alloying feasibility trials 79−83395
steel fibre reinforced porous mat. prod., mat. props. 77−59723
steel powder, high speed, S and O reduction in a H_2 gas stream 80−61015
steel W-Mo-V-TiC, powder, TiC effect on milling, pressing and sintering 78−60607
steel-Al bimetallic wire for overhead lines, manufacturing methods 80−16247
superalloy, hot consolidation of rapidly solidified powders, review 79−33965
superalloy, wrought, phase relations and microstruct., C and Hf conc. effect 77−44218
superalloy appl., aircraft engine production techniques 78−3073
surface area meas. apparatus using falling press. permeameter 79−38765
surface diffusion effect on sintering 79−74117
technology innovations, 1978 status 79−47646
β-III Ti alloy, powder compacted by hot swaging, tensile and toughness prop. 79−38764
transverse pressing 79−100081
US applic. to refining atomised metal powders 77−44187
vacuum treatment, method of calc. evacuation time and permeability 80−20827

powder metallurgy continued
Volume changes experienced by porous solids during nonisothermal liquid-phase sintering and self-propagating high-temperature synthesis 78−15328
water atomisation production of metal powder 78−64506
Ag, fine particles, adhesion and sintering, TEM exam. 78−44053
Ag, loosely packed powder, sintering SEM and dilatometry obs. 80−20843
Ag, powder, sulphide coated, Fritt effect on appl. of DC voltage *(German)* 80−25599
Ag powder, ultrafine, sintering, coalescence growth stage 80−89174
Ag, sintering of spherical powder, intermediate stage 78−52713
Ag, solid state sintering, compact length change 80−11593
Ag, spherical powder, sintering, study of initial stage 79−20004
Ag, spherical powder, struct. of sintering necks in compacts 80−11594
Ag, ultrafine powder, role of evap. during sintering 78−64505
Ag-Ni alloy, composite powder mixtures, compressibility and sinterability 77−63592
Ag-Pt, sintering, limited solid solubility, peritectic diagram 77−28754
Ag-Sb (1.16 wt.%), Sb effect on sintering kinetics in early stages 79−52137
AgCdO, powder metallurgy production, for switchgear in power engineering 80−104094
Ag_3Sn-Hg, metallic powder-liquid system, correlation between hardness and evolution and sintering states 80−25614
Al, 78% dense porous, dynamic compaction 78−63315
Al alloy, powder, erosion resist. to hot propellant gases 77−56165
Al alloy, sintering of powder metallurgy parts, metallographic exam. and hardness testing 77−4752
Al alloy AK5M2 granules, rolling speed effects 78−60604
Al alloy granules, rolling, temp. and speed effects 79−70015
Al alloy melts, centrifugally atomised, granule size distribution 79−100080
Al and Al alloy granules, hot rolling, angle parameters and forward slip 80−25601
Al, atomized powder, metallic contact for hot rolling in air 77−73294
Al, dispersion hardened with refractory carbides, sintering 79−74118
Al, powder, fission under weightlessness conditions *(Russian)* 78−31357
Al, powder, liquid phase sintering, solid-state solubility effect on vol. change 78−35332
Al, powder, nonuniformity of stress and strain distrib. over width of rolled powder strip 77−12577
Al powder, resist.-sintability *(Japanese)* 80−16228
Al powder thin foil, prep. for TEM study 80−42310
Al powders, electric-pressure sintering onto cylindrical parts in fluidised bed 80−100960
Al, powders, grain size determ. by sedimentation, automatic recording system 78−60897
Al, rolled strip from granules, coeff. of deform. 77−90422
Al, sintered powder, heat resistance increase method 77−90292
Al, sintering, activated, under thermal cycling 77−21053
Al sintering, low temp., form. of interparticle metallic contacts 80−20844
Al, sintering mechanism and sintered body anodization 79−95964
Al-C, dispersion hardened, effect of processing parameters on mech. props. 80−20826
Al-C alloys, dispersion hardened exam. of production method using pressed powders 80−16244
Al-Cu, electric discharge sintering of powder mixtures 78−60605
Al-Cu(0-10 wt.%) sintered compacts, mech. props. rel. to sintering 80−76210
Al-Ni-Si sintered SAS-1 alloy, struct. *(Russian)* 79−52135
Al-powder based composite, hydrostatic pressing 77−63593
Al-rare earth alloys, granules, rolling to form foil, exam. 80−20825
Al-Si, thermal control of interphase microstresses and mech. props. 77−12654
Al-Si-Cu, granules, energy conditions of rolling 77−12578
Al-steel mixture, wear resistant, produced by compaction by discrete shock waves 80−84882
Al-Zn-Mg-Cu-Co (6.5, 2.5, 1.5, 0.4 wt.%), fatigue crack propag. 80−55521
Al_2O_3 targets manufacture, for vacuum thin film deposition *(German)* 80−11586
Au, fine particles, adhesion and sintering, TEM exam. 78−44053
Au plated Ni powder for electroplating conductive pastes 79−95957
Au powder, ultrafine, sintering, coalescence growth stage 80−89174
B fibre reinforced Al, prep. by reaction sintering 79−38769
B fibre reinforced H, hot pressed forged, plasma sputtered *(Russian)* 78−35330
Be fibre reinforced Ti-Al-V (6.4 wt.%), synthesis and mech. props. 77−32544
Be, low oxide, isostatically pressed block, factors affecting tensile strength, elongation, impact resistance 77−16610
Be, plasma spray/sinter technique, Ar, satellite support structures, appls. 78−7079
Be, porous, shrinkage during sintering, kinetics, photographic method 79−15622
Be, sintered, physicomech. props. anisotropy, BeO inclusions effect 80−60804
CC TaC based hard metal, non-stoichiometric sintering, mech. props. 80−25616
CU-Zr-(Cr), powder metallurgical alloys, thermomech. treatment effect on props. 80−50660
Cd-Ag-Zn (96, 3, 1 wt.%.) soldering alloy powder, atomised, prod. and appl. 79−100073
Cd-Fe powders, predetermined comp., electrodeposition 79−70014
$CeRh_{3-x}Pd_x$, powdered alloys, catalytic behaviour correlation with electronic struct., lattice struct. and surface comp. 79−82181
Co, fine powder, magnetic props., effects of electrolysis conditions in prep. 77−40091
Co, powder, hot pressing on steel substrate, densification kinetics 80−40290
Co-Ce Mischmetal powder, sintering 77−21055
Co-Cu-Fe-Ce, mag. characteristics of sintered permanent magnets 78−60312
Co-Cu-Fe-Ce alloys, sintered permanent magnets, mag. characts. 77−43855
Co-Mo, sintering, limited solid solubility, peritectic diagram 77−28754
Co-Ni-Cr (20,20 wt.%), internal oxidation, improvement of mech. props. *(French)* 77−16521
Co-WC, levitation quenching 77−59711

powder metallurgy continued
Cr, powder, plasma deposition for production of contact portions of cermet electric heating element 78−11364
Cr powder, thermogravimetric exam. of nitridation rate *(Japanese)* 79−20292
Cr, powder comminution method effect on props. of TiC-steel+Cr composite 78−15341
Cr-Fe (30 wt.%) alloys, refined fine comminution 78−60598
CrC-Ni alloys, exam. of activated sintering 80−16241
CrC-Ni-(P), hard alloys, sintered, fracture props., P addition effects 78−60610
Cr_3C_2-(WC)-Ni, sintered, cavitation erosion resistance *(Japanese)* 77−52500
Cr_3C_2-Ni alloys, electrophoretic deposition from conc. suspensions for P/M prep. of hard alloys 77−63575
Cu compact, exam. of anisotropic shrinkage as function of pressure 79−8257
Cu, compacted powder, thermal agglomeration, green strength 77−36417
Cu, densification of particulate materials, general law 78−19692
Cu, dislocation form. during sintering *(German)* 78−31361
Cu, electrolytic powder, sintering, gas effects, finite size bodies 77−77447
Cu, equivalent sphere diameter calc., Saltykov method 78−31362
Cu, flowability, apparent density and comp., effect of Na, Mg and Al additions 79−28986
Cu formation by constant and pulsating overpotential electrolysis, experimental study 77−81234
Cu, hot forged powder compact 77−24981
Cu, initial sintering, method for obtaining surface diffusion coeffs., appl. to shrinkage data 78−95713
Cu, loosely packed powder, sintering SEM and dilatometry obs. 80−20843
Cu, powder, electric discharge sintering, struct. changes 77−77446
Cu powder, electrodeposition prep. conditions, statistical anal. 80−20828
Cu powder, electrodeposition, mathematical model for current efficiency and electric power consumption 80−20831
Cu, powder, exam. of consolidation process based on electronic structure of solid 80−20842
Cu, powder, hot pressing on steel substrate, densification kinetics 80−40290
Cu, powder, sprayed, effect of start props. in struct, and porosity of sintered products *(Czech)* 77−85960
Cu powder, two layered medium dynamic compaction 80−35138
Cu powder compacts sintering, depend. of neck form. on particle size and sintering temp. 79−28988
Cu powder props. and sintered samples with Al_2O_3 77−55909
Cu powder under press., elec. cond. *(German)* 79−69485
Cu powders, electroless tinning 80−25607
Cu, pressing pressure effect on consolidation 79−74116
Cu, sintered, appl. of stereological charact. of interface interaction 77−63589
Cu, sintered, residual voids, quantitative anal. of morphological changes by metallography 79−47854
Cu, sintered strip, external friction of rolling 77−1845
Cu, solid state sintering, compact length change 80−11593
Cu spheres, Shewmon rotation mechanism, selected area channelling patterns obs. in SEM 79−38759
Cu-Al, fission under weightlessness conditions *(Russian)* 78−31357
Cu-Al-Ni (14, 8 wt.%), γ'-martensitic, sintered high damping 80−50577
Cu-BN composite electromachining tools, dynamic hot pressing 80−84889
Cu-C bushings, powder metallurgically prepared, exam. of friction and wear charact. 79−15813
Cu-Fe, metastable solid solutions, production by explosive plasma compressor *(Russian)* 77−90289
Cu-MgO, dispersion hardened, prep. by milling Cu and Mg oxidising atmos. *(German)* 78−64509
Cu-Nb filamentary composites, powder metallurgy prod., supercond. props. 79−56477
Cu-Nb-Sn, multifilamentary supercond. composite wires, fabrication on laboratory scale and mech. props. 80−29897
Cu-Nb-Sn composites, cold-powder-metallurgy processed, supercond. critical currents 79−78279
Cu-Nb(Nb_3-Sn) composite wires, powder metallurgy prod., supercond. props. and annealing 79−33428
Cu-Ni, diffusional homogenisation in compacted powder blends, X-ray diffr. line profile analysis 78−80491
Cu-Ni, powder, sintered, effect of cold and hot dynamic pressing, upon structure and props. 79−33970
Cu-Ni, powder mixture electric discharge sintering, struct. changes 77−77446
Cu-Ni, powder mixtures, form. using electric discharge sintering 77−12563
Cu-Ni, sintered, props. and degree of nonhomogeneity 80−20848
Cu-Ni, sintering, Kirkendall effect 80−93518
Cu-Ni alloy prep. by sulphide-oxide reactions 77−48366
Cu-Ni composite formation by electric discharge sintering 77−63594
Cu-Sn warm pressed compact prep. 80−35136
Cu-Ti, liquid phase sintering, metallographic electron beam microanalytical investigation 78−95888
Cu-TiC precipitation hardened composite, struct. effect on friction 78−11337
Cu-W, powder, prod. by controlled reduction in H_2O/H_2 mixture of $CuWO_4$ 79−24458
Cu-W composite powder, prod. by H_2 reduction of $CuWO_4$ 79−20006
Cu-W sintered materials, porous, mech. and X-ray elastic const. *(German)* 77−81288
Cu(Sn)/Nb(Al), composite superconductor fabrication and charact. 77−81242
$Cu_{60}Zr_{40}$, amorphous powder, production using gas-water atomisation unit 80−7518
EuB_6, synthesis and hot pressing fabrication for appl. to neutron absorbing core control material 78−8904
Fe, air-atomised, manufacture with predetermined charact. 80−100808
Fe alloy, oxide dispersed, mech. alloying, microstruct. 77−25063
Fe alloy electrodes, rolled from powders, sintering problems 80−25608
Fe alloy porous powder metallurgical components, gamma nitriding 79−20088
Fe and Fe-C, (0.8 wt.%), sintered, hot forging ahd chemicothermal treatment, effect on wear resistance 80−25606

powder metallurgy continued
Fe atomised powder, sintering effect on recrystn., mech. props. 80−40292
Fe, atomised powder compacts for mag. cores, oxidation, compressibility, heat treatment *(Japanese)* 78−72752
Fe, atomized powder compacts for mag. cores, mag. props., green densities *(Japanese)* 78−72751
Fe base composite, sintering, damping props. 77−21061
Fe based sintered porous permeable materials, diffusion chromising 80−100958
Fe, carbonyl pore struct. orientation, shrinkage anisotropy effect 80−20845
Fe, carbonyl powder, mangetic material 77−12160
Fe, carbonyl powder, particle size distrib. anal. by microscopy with statistical anal. of results 78−19691
Fe, cast, air-atomized powder, effect of particle size on C and O contents 78−15340
Fe, cast, atomised powder, reduction and decarburisation annealing in converted gas 79−24463
Fe, cast, atomised powder, reduction-decarburisation annealing with converted gas, optimum conditions 79−24465
Fe, cast, atomised powders, particle size effect on purification in US pickling 79−28985
Fe, cast, P, powder, H annealing 79−66025
Fe, cast powder, exam. of reaction between C and O, before and after annealing in converted gas 79−33973
Fe, cold-pressed, props., effect of air 80−100810
Fe, compact, form. and growth of metal bridges during short sintering periods 77−1827
Fe, dynamic hot densification, degree of deformation 77−63585
Fe effect of repressing and double sintering on impact strength *(Japanese)* 78−92217
Fe, electrolytic Ag plating 79−66017
Fe, exam. of graphite and cast Fe dissolution during sintering 79−33969
Fe, high dispersion ferromagnet, magnetic powder defectoscopy material 80−35137
Fe, medium hardness, densification of particulate materials, general law 78−19692
Fe, metallised pellet, factors influencing crushing strength after H_2 reduction 79−11531
Fe, ore, wet sieving in fine grain range *(German)* 80−93515
Fe, oxidised powder in prod. of soft mag. mat. 77−63813
Fe, porous, density, elec. cond., Young's modulus, toughness 78−64645
Fe, powder, atomised, processing props., particle size distrib. effect, with and without Zn stearate additions 79−100077
Fe powder, carbonyl, R10 and R20, manufacturing effects on magnetic permeability 78−35009
Fe, powder, consolidated, exam. of mech. and electrical props. 78−56599
Fe powder, density distrib. in rolling deformation region 80−40288
Fe powder, electroless Ni plating 80−61026
Fe, powder, exam. of consolidation process based on electronic structure of solid 80−20842
Fe powder, final reduction annealing in vibrating bed 80−84883
Fe, powder, hot pressing on steel substrate, densification kinetics 80−40290
Fe, powder, reduction annealing, thermodynamic anal. 78−60597
Fe powder, reduction annealing, comminution of sintered cakes 80−66456
Fe Powder, resist.-sintability *(Japanese)* 80−16228
Fe powder, sintered and hot pressed, effect of porosity, grain size on magnetic props. 79−96159
Fe, powder, sintering, effect of repeated allotropic transform. 77−40406
Fe powder, sponge and atomized types, steam oxidation, pore closure and surface hardness 80−45441
Fe, powder, vibratory densification in vibratory press 77−12576
Fe powder, ZhGr1.0, optimisation of heat treatment in salt bath 77−28756
Fe, powder compaction, elect. cond. changes 79−66175
Fe powder compacts, pressed under static or vibr. load, shrinkage anisotropy during sintering 80−50574
Fe, powder forged, impact and fatigue strengths, slag inclusion effects 77−21271
Fe powder layers, sinter-bonded, hot-pressed, on steel, struct. and props 79−95976
Fe, powder preforms., hot consolidated rolled strip, mech. props. 78−15338
Fe powder production, water jet atomisation of Fe-C melts 79−100090
Fe powder sintered compacts, mech. props. effect of powder type and processing conditions *(Czech)* 77−59830
Fe, powder-forged, elastic consts., density depend. 80−84987
Fe, powdered compacts and Armco, electrolytic boriding 79−39044
Fe powders, Co- or Cu-plated, prep. by rad. and chem. plating, mag. props. 80−44867
Fe powders, exam. of production, props., and testing methods *(German)* 79−4927
Fe powders from Fe-C melts, atomisation, props. 79−70013
Fe, recryst. annealing effect on struct. and technological props. *(Czech)* 80−89250
Fe reduced powder manufacture, collision speed effect 80−84884
Fe, single component, powder, compressibility and elec. resistivity in cold pressing under low press. 77−77444
Fe, sintered, austenitic nitriding and bainitic hardening 80−85084
Fe, sintered, fracture behaviour, microscopic obs. 79−47771
Fe, sintered, fracture mechanics *(German)* 77−8948
Fe, sintered, plastic deformation, constitutive eqns. 79−61667
Fe, sintered, porosity estimation by screen image of brittle fracture 77−52585
Fe, sintered, porous, yield point *(Czechoslovakian)* 77−28748
Fe, sintered, produced by dynamic hot pressing, recrystn. diagram 79−70017
Fe, sintered and pressed, props., effect of atomised Fe powder particle size distrib. 80−11601
Fe sintered compact, shrinkage and mech. props., admixed zinc stearate lubricant effect 80−45402
Fe, sintered parts, densification in burnishing process by rocking die method 78−35331
Fe, sintered parts, struct. stabilisation with C potential control of protective atmosphere 78−60614
Fe, supersonic vibration effect on pressing *(German)* 78−64500
Fe/Fe-Cr composite powder, X-ray diffr. exam. of densification during rolling 80−40289

powder metallurgy continued
Fe-(Cr)-C alloys, sintered, successive impregnation with C and Cr 79−95979
Fe-(Cu)-C, sintered parts, struct. stabilisation with C potential control of protective atmosphere 78−60614
Fe-Al alloys, powdered composites, metastable gamma-phase decomp. *(Russian)* 77−59741
Fe-Al powder composite, phase composition, produced in low-temp. plasma 77−90295
Fe-Al powder cpds., prep. in low-temp. plasma, struct. props. 77−44192
Fe-B, for infiltration of Fe compacts 80−60806
Fe-B_4C sintered material, mech. props. and struct. charcts. 79−100084
Fe-C (1.0 wt.%), mixed powder compact, sintering, C diffusion meas. 77−90293
Fe-C (2. wt.%), sintering shrinkage kinetics 80−20829
Fe-C-Cr-Mn-Si-Ni (4.6, 38.7, 1.1, 2.0, 1.58 wt.%) alloy US-25, powder, compressibility and elec. resistivity in cold pressing under low press. 77−77444
Fe-C-Mn (0.5, 0.6 wt.%), powder forged, mech. props. 80−21096
Fe-C-Ni-Cr(Cu), dynamically hot pressed, mech. props., additives effect 78−60620
Fe-C-Pb, sintered, antifriction props., Pb introduction effect 79−96155
Fe-Co heterogeneous alloys, fabrication by powder metallurgy, tensile strength 77−63600
Fe-Cr, single and two component, powder, compressibility and elec. resistivity in cold pressing under low press. 77−77444
Fe-Cr (13 wt.%)+polycarbosilane, powder metallurgy, charcts. 77−85962
Fe-Cr-SiC-B_4C powder mixture, compressibility and elec. cond. in cold pressing under low press. 78−60609
Fe-Cu, liquid phase sintering 80−16232
Fe-Cu-C, mixed powder compact, sintering mechanism 78−15343
Fe-Cu-C alloy, sintered with added S, thermophys. props. 79−61541
Fe-Cu-C-O(-Ni) powder, atomized, reduction and decarburizing annealing parameters 80−25603
Fe-Cu(2, 4 and 6 wt.%), sintered, precipitation hardening 77−66653
Fe-graphite porous sintered, determ. of impregnation depth with polycaprolactam-finely divided Cu metallic polymer 79−70272
Fe-Mn powders, reactions with NH_4Cl and $(NH_4)_2CO_3$ 80−11597
Fe-Mo-(C)-(Ni), sintering 78−35333
Fe-Ni (25%), solidification of powder or large ingot, heat losses 77−12612
Fe-Ni heterogeneous alloys, ferrite, martensite and austenite phase distrib., effect on mech. props. 80−45363
Fe-Ni powder, Ni clad Fe grains, exam. of electrochemical formation process 79−33974
Fe-Ni system, Ni addition effects on activated sintering of Fe powder compacts 77−4756
Fe-Ni-C, atomized, O/C ratio effect, particle size on annealing kinetics, physicotechnological props. 80−20832
Fe-Ni(Co), powder mixture, effect of granulometric distrib. on importance of Kirkendall effect during calcination *(French)* 77−11721
Fe-P(S) sintered materials, antifriction props. 79−24626
Fe-Pd (47 at.%) alloy, powders and powder compacts, mag. props. rel. to heat treatment *(Russian)* 79−15816
Fe-S-C (1,3 wt.%), sulphidised Fe-graphite bearing materials, sintering, struct. form. 78−60601
Fe-Si (3 to 5 wt.%) sinters, mag. props., Si and Fe-Si additions effect 80−71104
Fe-Si-B amorphous powder, production by spark erosion, and mag. props. 77−90290
Fe-Si-B magnetic powder, amorphous, prep. by atomisation technique 78−92213
Fe-Si-C mixed powder, cast Fe powder sintering study *(Japanese)* 80−108373
Fe-Si(Mn)(C), atomisation of melt, charact. of metal powder 78−19688
Fe-VC-WC(TiC), sintering, densification 80−25615
Fe-WC-VC(TiC), sintering, densification 80−25615
Fe_3O_4 powder, used for prod. of Fe, Fe alloy sintered compacts *(Slovak)* 79−15626
$Ge_{10}Si_{70}$, hot press sintering 80−50572
Mg-Al (25 wt.%) powder, reaction with high press. H_2, MgH_2 form. and decomposition *(Korean)* 78−11554
Mg-noble metal alloy, sintered, supercorroding for heat and H_2 gas generation, seawater reaction 78−15607
MgO (:CaO) powder compacts, sintering studies, SEM obs. 79−78918
MgO, rate of reduction by C 77−28743
Mn-V-Mo-C master alloys, development for low alloyed PM steel 80−50576
Mo electronics industry applications, prep. processing and props. 80−89171
Mo, powder, cold isostatic compaction effect on thermophysical props. 78−52717
Mo, powder, defective structure and activated sintering, exam. 80−16240
Mo powder, influence of powder reduction processes on props. 80−89175
Mo powder, struct. changes under action of high-powder pulses 79−70018
Mo, powder sintering, transition metal activators, 1000-1350°C, heterodiffusion model 78−44044
Mo, prep. by powder metallurgy technique, appl. in lighting industry 80−29904
Mo, sintered, gas evolution and degassing 80−100814
Mo, sintering, effect of Ni activator grain size 77−63590
Mo-Cr, powder mixture, activating effect of Group VIII metals on alloy form. during sintering 77−59728
Mo-Cr powder mixture, electric discharge sintering, struct. changes 77−77446
Mo-Fe alloy powders, densification and alloy formation on sintering 77−63597
Mo-Hf-C, superior powder metallurgy die alloys for isothermal forging mech. props. 79−74201
Mo-Mn powder mixture, X-ray diffr. exam. of reaction between Mo and Mn, during sintering 80−16242
Mo-Ni powder mixtures, form. using electric discharge sintering 77−12563
Mo-Ti-Zr alloys TZM and TZC, superior powder metallurgy die alloys for isothermal forging mech. props. 79−74201
Mo-W solid soln., joint solubility of C and Zr 77−25025
$MoSi_2$, high temp. material, coatings, powder metallurgy, review *(German)* 79−74295

powder metallurgy continued
Mu-Cr-Mo-C master alloys, development for low alloyed PM steel 80−50576
Nb_3Al, prep. by reduction of Nb_2O_5 and Al_2O_3 by CaH_2, thermodynamic calc. 80−100809
Nb_3Sn, composite supercond., powder metallurgical prep. 80−2981
Nb_3Sn filamentary wires, fabricated by infiltration method, supercond. props. 77−28761
Nb_3Sn, high-current A-15 microcomposite material 80−44781
Nb_3Sn, multifilamentary supercond., prod. by ECN powder metallurgy method and props. 77−28762
Nb_3Sn, multifilamentary superconductor preparation by 'in situ' and cold powder methods, review 80−93522
Nb_3Sn, powder metallurgically produced, microstruct. charcts. 80−89233
Nb_3Sn-Cu, high-current A-15 microcomposite material 80−44781
Nb_3Sn-Cu superconducting composites, produced by cold extrusion of fine powders 79−38767
Ni alloy, KhN55VMTFKYu, produced by powder metallurgy, hot worked, short- and long-time strength 77−28752
Ni alloy IN-738, Y_2O_3 (1.5 wt.%) addition, mechanical alloying 77−40427
Ni alloy powders hot hydrostatic pressing of disk, capsule design 80−20839
Ni alloy ZhS6U, US method of porosity detection 80−71828
Ni base alloy IN792, carbide morphology 77−36508
Ni base alloys, mathematical-physical considerations rel. to metal powder prod. 80−11595
Ni base alloys, production methods, review of powder metallurgy methods, mathematical-physical considerations 79−95970
Ni base superalloys, rapid solidification, use in gas turbine engines 80−84888
Ni based powders, determination of entrapped Ar content, using vacuum fusion tech. 79−5193
Ni, carbonyl powder, dislocation density sintering 80−108372
Ni coatings, detonation powder spray deposition 80−61028
Ni, ductile, electrolytic, densification of particulate materials, general law 78−19692
Ni, electrolytic and carbonyl grades, sintered sheet material, stopping power and pore size relationship 78−19693
Ni plated WC powder, detonation spray deposited hard alloy coating, electrical conductivity 77−12025
Ni powder, atomisation of melt, charact. of metal powder 78−19688
Ni, powder, correlation between specific surface area and technological props. 78−64503
Ni, powder, hot pressing on steel substrate, densification kinetics 80−40290
Ni, powder, magnetic resistance changes 77−1411
Ni powder, nonspherical, mean pore size of sheet material 77−28757
Ni powder, porous, relationships between mech., physical, and microstructural charcts. 80−20846
Ni, powder, recrystallisation, effect of sintering atmosphere 77−12573
Ni powder, resist.-sintability *(Japanese)* 80−16228
Ni powder, sintered, use of extruded porous materials as fuel cell electrodes 80−40853
Ni, powder, subjected to vibratory milling, exam. of plastic deformation, recrystallisation, sintering 80−16234
Ni, powder charact. effects on sintering 77−1828
Ni sintered permeable materials with bidisperse structure, pore-forming additions effect 80−84885
Ni, sintering kinetics, metallographic study 80−93519
Ni superalloy powder, thinning technique for microstruct. obs. using analytical electron microscopy 78−48587
Ni, surface diffusion effect on sintering 79−74117
Ni, volume strained, sintered, porous, physicomechanical props., electrical resistivity 77−12572
Ni, volume-strained sintered porous, physicomech. props., u.s. vibration propag. velocity 77−1823
Ni-Al-Cr alloy IN 100 powder, rapidly solidified, effect of high melt superheat on microstructure 79−52195
Ni-base superalloy, conventional and powder metallurgical, σ-phase precipitation 80−11646
Ni-base superalloys, powder metallurgical, creep-rupture at intermediate temps. 80−97568
Ni-Co-Cr-Mo-Al, Astroloy, extruded powder metallurgy superalloy, recrystallisation study 79−4976
Ni-Cr, dispersion strengthening, prep. from powder, mech. props. 79−91658
Ni-Cr (2 wt.%), role of hydrostatic pressure on sintering of creep cavities 79−28980
Ni-Cr (20 wt.%), powdered, prod. of Mo fibre reinforced composite by hot pressing exam. of strength 78−56710
Ni-Cr (20wt.%), powder, nonspherical, mean pore size of sheet material 77−28757
Ni-Cr alloy, dispersion-hardened, prod. by mech. alloying 78−15345
Ni-Cr powder mixture, dispersion hardened, homogenisation 77−12638
Ni-Cr-Al sintered alloy, hot vac. pressure, fracture and mech. charcts. 80−66667
Ni-Cr-Co base superalloy APK1, hot isostatically pressed, heat treatment, fracture props. 77−73251
Ni-Cr-Co-Mo-Ti-Al, powders, HCl surface treatment to prevent TiC precipitation, fracture props. 79−8397
Ni-Cr-Co-Ti, superalloy sintering thermochemical surface treatment 80−25617
Ni-Cr-Ti rapidly solidified superalloys, surface segregation 80−76263
Ni-Cr-Ti-Co-W-Al-Mo alloys AF-115 and AF2 1DA, superalloy powder compacts, fatigue origins 78−48521
Ni-Cr-W-Co granules type ZhS6U, EP741, hot hydrostatic pressing 80−60796
Ni-Fe alloy, Ni base cathodes, powder metallurgy technique 80−29903
Ni-Fe powder, effect of vibration and current pulses on shaping 79−95973
Ni-ferrite powders, form. in presence of Li_2SO_4-Na_2SO_4 molten salts, prep. and charcts. 80−84869
Ni-Mo, powder mixture, electric discharge sintering, struct. changes 77−77446
Ni-Mo, sintering limited solid solubility, peritectic diagram 77−28754
Ni-Re, sintering, limited solid solubility, peritectic diagrams 77−28754
Ni-Ti (10 wt.%), X-ray study of ageing of plate and powder 77−1847
Ni-ZrB_2 powders, densification by hot pressing 80−25604

powder metallurgy continued
Ni_3Al-Ti(Cr)(Fe)(Zr)(Mo)(W), powder, X-ray spectral analysis exam. 80−16239
NiCr-AlY sintered fibre metal struct. abradable seal material, friction and wear 78−56785
NiCr-MoAl-ThO_2 (13,3 wt.%), powder, mech. alloying 78−84744
NiCrAlY, mechanically alloyed, maintaining elongated grain struct. after deform. 77−36534
Pb powder, automatic image analysis for charact. of size and shape distrib. 78−11473
Pb powder prod. by electrolysis of fused salts 78−19690
Pb powder size and shape distribution via image anal. 80−16221
Pb, sintering, surface oxide layer effect 79−66024
Pb-Bi alloy, fine powder electrodeposition and X-ray struct. obs. 78−11163
Π, electrolytic powder, rolling of porous sheets 77−63578
Re, sintered, preparation, thermal cond., linear expansion up to 1000K 79−61533
Re, thin film preparation, by laser melting *(Japanese)* 79−78909
SiC fibre reinforced Al, plasma-formed semifinished products, props. 80−84890
Sm-Co, alloy powders and sintered magnets, effect of chem. treatment on mag. props. 78−60311
$SmCo_5$ magnets, sintering time effect on props. 79−95977
$Sm_{1-u}Ce_u(Co_{1-x-y-w}Fe_xCu_yCr_w)_z$, permanent mag., improved mech. props. 79−87593
$SmCo_5$ alloy powders, orientability and texture, milling time effect 79−100168
$SmCo_5$, mag. props., effect of phase and struct. transforms. during liq.-phase sintering 79−100086
$SmCo_5$, powder, comminution temp. effect on mag. props. 80−39819
$SmCo_5$, powder, exam. of protective preps. of organic media against oxidation 79−96220
$SmCo_5$ powder alloy, densification by cold working 77−4753
$SmCo_5$, powder prod. by electroerosion mag. props. 77−59718
$SmCo_5$ sintered magnets, struct. and magnetic charact., sintering temp. influence *(Russian)* 79−52397
$SmCo_5$, sintered permanent magnet manufacture 80−20838
Sm_2M_{17}, sintered magnet, hard mag. props. optimisation 77−8340
Sn bronze, air atomised, densification and pressure requirements during extrusion 77−59713
Sn bronze, extruded atomized powders, struct. and props. 79−38763
α-Sn, compact prep., from β-Sn containing 0.1 at.% Ge 80−55320
Sn fine powders, electrodeposition, effect of cathodic current density on structure 80−16238
Ta, particle shape effect on parameter of vol.-porous anodes of elecrolytic capacitors 79−61539
Ta powder, cathodic electrodeposit, effect of electrolyte composition and process parameters, on particle size distribution 80−16233
Ta, powdered, N_2 determ. by vacuum hot extraction with graphite addition *(Japanese)* 77−48683
Ta(C,N)-Ni-HfC(HfN)(Mo_2C)(VC), sintering, prod. of hard metals 78−11155
TaC-NiC, powder for plasma arc spray coating appl. 78−15591
$(Ti,Cr)B_2$, sintering kinetics and props. 80−100811
Ti base alloys, mathematical-physical considerations rel. to metal powder prod. 80−11595
Ti base composite sintered bearing materials, metallic solid lubricant infiltrated, antifriction props. 80−60981
Ti, beta III powder compact, fatigue origins 77−44351
Ti, infiltration by liq. Mg, kinetics 78−60595
Ti, porous structure, change in presence of liq. phase *(Russian)* 80−16223
Ti powder, exam. of mechanicochemical comminution, in the presence of epoxy resin or polysulphide rubber 80−16236
Ti powder, nonspherical, mean pore size of sheet material 77−28757
Ti powder, resist.-sintability *(Japanese)* 80−16228
Ti, powder, vibratory densification in vibratory press 77−12576
Ti powder metallurgy, developments 80−100801
Ti, production methods, review of powder metallurgy methods, mathematical-physical considerations 79−95970
Ti, sintered, fatigue strength, oxidation effect 79−96137
Ti sintered, struct. stability, effect of dispersed refractory compound inclusions 77−28825
Ti, sintered sheet material, stopping power and pore size relationship 78−19693
Ti, strip prod. by powder rolling 78−80493
Ti-Al (Sn), porous, effect of Al and Sn on sintering 80−20830
Ti-Al (14.7 wt.%), sintered, mech. props., effect of alloying and dispersed ZrO_2 phase 77−12636
Ti-Al (4 wt.%), sintered, long-time strength 80−40529
Ti-Al system, compact growth in liquid phase sintering 80−20835
Ti-Cr, sintered, friction and wear, structural factors 78−60843
Ti-Mg-ZrC(HfC)(TiC)(TiB_2) sintered, friction and wear props. 79−70019
Ti-TiO_2-ZrO_2-Mo, sintered struct. and mech. props. 78−60618
TiAl, manufacture by extrusion of blended elemental powders 77−28750
TiB_2, low temp. radiation damage, calorimetric investigation 77−27916
TiB_2-(Ni) (20 wt.%), initial stage sintering under high press., lattice strain 77−55905
TiC-(Mo-Cr-Ni-Mn) steel alloy, optimum comp. and manufacture conditions, Mn effect 80−84896
TiC-Fe-Cr powder mixture, exam. of milling condition effects 80−16237
TiC-Kh6V3M steel alloy, reaction during sintering and heat treatment 78−60617
TiC-Ni powder compact, wetting problems in sintering 80−11596
TiC-Ni-Co-Cr, sintered, mech. props. effect of processing factors 78−11159
TiC-steel alloys, structure formation during sintering 77−59732
TiC-steel cermet with Cu additions, precip. hardening and ht. treatment temp. 77−40414
TiC-steel compact prod. by sintering in vacuum and in Ar or H_2 atmos. 77−63616
TiC-steel composite, effect of method of Cr additions on props. 78−15341
TiN-Ni mixed powder compact, phase relations and denitrification during sintering *(Japanese)* 79−43167
TiN-Ni powder compacts, sintering, gas atm. and vac., shrinkage, solid solubility *(Japanese)* 78−72750
U_3O_8-Al cermet fuel for research reactors 79−9835
V_3Ga, high-current A-15 microcomposite material 80−44781

powder metallurgy continued
V_3Ga, multifilamentary supercond., prod. by ECN powder metallurgy method, and props. 77−28762
V_3Ga-Cu, high-current A-15 microcomposite material 80−44781
W, activated sintering, diffusion mech. *(Korean)* 77−73248
W alloys, recrystallisation alloying effects of ThO_2, Mo-Re, HfC, NbC 77−70083
W and W-Re alloy, prep., appl. in lighting industry 80−29904
W, brittle spiral fibre, densification of particulate materials, general law 78−19692
W, chemically activated sintering 77−1826
W, chemically driven grain growth during sintering in liquid Ni 79−61532
W, enhanced low temp. sintering, temp. sensitivity causes 77−36418
W fibre reinforced, Co powder alloys, reactions and recryst. 80−11603
W fibre reinforced Ni composite, prep. by hot isotactic pressing, mech. props. *(Slovak)* 78−19694
W fibre reinforced Ni-Cr (20 wt.%), hot pressing kinetics 78−35334
W fibre reinforced Ni-Cu composite, liquid phase sintering under press. 78−19695
W, fibre reinforced powder metal and alloy based composites, high temp. strength of W wire 79−70021
W, from $WO_{2.96}$ reduction 77−28744
W, porous, physicomechanical props. sintering effects 77−12575
W, powder, cold isostatic compaction effect on thermophysical props. 78−52717
W powder, effect of prep. temp. on fine structure, X-ray diffr. anal. 79−33971
W powder, hydrostatic pressing 78−11161
W powder, pressing with dispersed strengthening phase additions using flexible bags 79−70016
W, powder, produced by plasma regeneration *(Russian)* 78−31360
W, powder, subjected to vibratory milling, exam. of plastic deformation, recrystallisation, sintering 80−16234
W, powders, defective structure and activated sintering, exam. 80−16240
W production, H reduction of WO_3, starting specific surface effect on kinetics 80−11599
W, sintered, porous struct. rel. to powder props. 79−61540
W sintered rods, hot rolling with four roll passes, effect on struct. and mech. props. 79−100195
W, sintering, Ni activated, grain boundary diffusion mechanism 79−91606
W/Cu powder with varying W particle size, burning behaviour and crack form. tests *(German)* 78−7005
W-Co mixed powder, carburizing *(Japanese)* 79−52454
W-Cr powder alloys, sintering in presence of Cu-Ni liq. phase 80−16246
W-Cu, porous material, skeletal type, produced by liquid phase sintering, exam. of mech. strength, determ. resistance 80−16245
W-Cu contact materials with Ni and Co dopants, sintering 77−55908
W-Cu permeable materials, development 77−28755
W-Cu powder, liquid phase sintering, stabilisation of porous structure and control of volume changes 79−95974
W-Cu sintered alloy, produced from coreduced powders, densification 78−11154
W-Cu-Ni powder, liquid phase sintering, stabilisation of porous structure and control of volume changes 79−95974
W-Cu-Ni(6), contact materials, activated sintering, Ni and Co effects 79−95967
W-Mo, powder mixture, electric discharge sintering, struct. changes 77−77446
W-Mo powder mixture, activated sintering 77−21058
W-Mo powder mixtures, form. using electric discharge sintering 77−12563
W-Ni, liquid phase sintering, microstruct. meas. 78−44054
W-Ni, liquid phase sintering 80−16232
W-Ni, liquid phase sintering 80−25613
W-Ni liquid alloys, sintered, coarsening of W grains, exam. 78−56598
W-Ni powder compacts and wires, recrystallisation, influence of omnidirectional press. *(Russian)* 77−8849
W-Ni system, grain growth and densification during liquid phase sintering 79−38760
W-Ni-Fe (5(2), 5(2) wt.%) pore formation, effect on mech. props. 80−45396
W-Ni-Fe system, reduction kinetics and alloy form. 80−60801
W-Ni-Fe(Cu), liquid phase sintered, interfacial embrittlement 79−57101
W-Re(Mo)(Cr), powder mixture, activating effect of Group VIII metals on alloy form. during sintering 77−59728
W-ThO_2, sintering for fabrication of ionisers for electric propulsion *(French)* 79−56946
WC powder, chemical plating with Co and Co-P 80−25593
WC powder, effect of prep. temp. on fine structure, X-ray diffr. anal. 79−33971
WC-Co, precursor derived powder, prep. 77−32541
WC-Co, prep. temp. effect on fine struct. of WC phase, X-ray obs. 79−33971
WC-Co, sintered, obs. of spinel particles by TEM 78−95714
WC-Co, sintered hard alloy, mechanism of penetration of liquid metals 78−60619
WC-Co (12 wt.%), sintering with various binding phases *(German)* 79−28984
WC-Co (15 wt.%), detonation spray deposited hard alloy coating, electrical conductivity 77−12025
WC-Co compacts and sintered alloy, fine struct. of carbide phases, preforms re-pressing under high press. effect 79−28987
WC-Co from directionally carburized WO_3-C-Co_3O_4 mixtures, sinking *(Japanese)* 80−11589
WC-Co mixed powder prod. by rotary kiln, new continuous process 78−64502
WC-Co powder, prep. by direct carburisation of WO_3 in presence of Co_3O_4 80−50573
WC-Co powder form. from Wo_3 and Co_3O_4 carburization, C behaviour *(Japanese)* 80−7517
WC-Co sintered carbide tips, microscopic stress anal. 78−5663
WC-Ni detonation sprayed coating, wear resistant 78−35594
WC-Ni hard alloy composite, sintered, void healing 80−60821
WC-TiC, powder for plasma arc spray coating appl. 78−15591
WC-TiC-Co, powder for plasma arc sprayed coating 78−15591
WC-TiC-TaC, powder for plasma arc spray coating appl. 78−15591
$W_{50}Fe_{50}$ glassy alloy, refractory, triode sputtered 80−75185
Zn, die pressed powder, green strength 77−59876
Zn, fine powder, electrodeposition 80−60802

powder metallurgy continued
Zn-Ag-Cu alloy powder, brazing solder, production using electrodeposition and heating in reducing atm. 79−100079
ZrB_2-Nb, reactions between components 80−100812
$ZrRh_{3-x}Pd_x$, powdered alloys, catalytic behaviour correlation with electronic struct., lattice struct. and surface comp. 79−82181

powder sprayed coatings
adhesion, ASTM test 80−50812
comparison with other non-polluting electrostatic coating systems 78−68829
detonation deposition, conducting powder temp. meas. 80−11559
detonation spraying, powder velocity, methods of meas. 80−16530
electrostatic, particles velocity meas. by laser anemometer 78−18364
epoxy thermosetting powders, parameters 79−20003
hard alloy coatings, detonation deposition from fine powder mixtures 79−100078
plasma deposited materials, control of mech. props. 80−11560
polyester thermosetting powders, parameters 79−20003
polymer powder layers, specific charge and thickness distribution meas., by electrostatic method *(Russian)* 77−10042
polyurethane thermosetting powders, parameters 79−20003
powder materials, applications, characteristics, review 78−56577
thermosetting powders, parameters 79−20003
Al_2O_3 detonation deposited coatings, porosity and adhesion, processing parameters effects 79−70227
Al_2O_3(-TiO_2) coatings, detonation deposited on steel, prep., wear resist., antifriction props. 78−60877
Cr_3C_2 (Cr_7C_3) based coatings, detonation deposited, wear resist., 20-1000°C 80−11843
Fe-Si gas-flame spray deposited protective coating, for C steel heat exchanger 80−61025
Mo powder properties for plasma-sprayed coatings 78−48548
Ni coatings, detonation powder spray deposition 80−61028
Ni plated WC powder, detonation spray deposited hard alloy coating, electrical conductivity 77−12025
Ni-Al spraying powders, alumina and aluminide formation 80−25920
WC-Co (15 wt.%), alloy VK15 coating on Ti-Al, detonation sprayed, antifriction props. 80−21188
WC-Co (15 wt.%), detonation spray deposited hard alloy coating, electrical conductivity 77−12025
ZnO-Cs, fabrication, UPS meas. 78−15279
ZrO_2, plasma sprayed coatings, elec. cond. and gas permeability 79−82478

powder spraying
asthma-preventive cromolyn Na inhaler fluid mechanics 79−79587
back discharge effects in electrostatic powder coating *(Japanese)* 77−52516
comparison with other non-polluting electrostatic coating techniques 78−68829
detonation deposition, of coatings, conducting powder temp. meas. 80−11559
detonation deposition of coatings, monitoring method 80−60780
detonation spray deposition, metering devices 80−40256
detonation spray depositon, powder introduction methods 79−70195
detonation spraying, powder velocity, methods of meas. 80−16530
detonation spraying, pulse charact. 77−77607
electrostatic paint and powder spray coating developments 79−83363
electrostatic powder coating, parametric study, charging, transport, deposition props. 78−80662
enamelling by electrostatic frit powder spraying 80−97428
frictional charged electrostatic spray guns, exam. 78−80708
polymer powder layer, in corona discharge *(Russian)* 77−12526
powder metal sprayed coatings, bond strength, influence of surface preparation 78−11150
preferred orientation minimization by spray drying 80−3098
YIG, hot spraying to give fine, free flowing, sinterable powder 80−20865
ZrO_2 powders, stabilised, for plasma spray-coatings 80−20869
Al_2O_3 coating on Ti, detonation deposition, impact interaction parameters 80−40602
Cr-Al_2O_3 powder targets for plasma-ion spray deposition of resistance films 80−84897
Cr_2O_3-ZrO_2 granules, from spray drying of suspensions 80−104100
MnZn, pressing powders, spray dried, pressing behaviour and props. 80−11617
Ni-Cr-Al_2O_3 powder targets for plasma-ion spray deposition of resistance films 80−84897
SiC fibre reinforced Al, plasma-formed semifinished products, props. 80−84890
WC-Co (15 wt.%) detonation spraying on to Cr-Ni steel with automatic powder feed 80−25558
Y_2O_3, ceramic structs., thin-walled fabrication, plasma spraying technique 79−33978

powder techniques *see powder technology*

powder technology
see also densification; hot pressing; powder metallurgy; powder spraying; sintering
agglomeration techniques in powder technology, review 78−39713
AGR fuel element design improvement 80−23112
air-jet sifter for determining granulometric composition 79−75671
alkali halide pelleting technique for solid sampling in IR spectroscopy 78−87171
atomization review 78−23642
automated sintering and hot pressing system 79−33961
axisymmetric compacts from pressing in rigid discs, pressure and density distribs. 79−66022
ball mill grinding rate constant, under size increase feed rate effect *(Japanese)* 79−28974
binary powders, inhomogeneous mixture, procedure for determining specific volume 78−48345
blending, irregularly shaped particles 77−77441
ceramic, compaction during liq. phase sintering 80−55335
ceramic compact, morphological investigations significance 79−33988
ceramic compounds, lyophilisation parameters, freeze-drying synthesis 80−97453
ceramic powder pressing review 79−47652
ceramic powder suspensions, sputter drying *(Russian)* 80−55324
ceramic powder synthesis from laser-heated gas phase reactants 80−93525
powder technology continued
ceramics, rate constants of wet and dry ball mill grinding *(Japanese)* 80−29895
coatings, in metal finishing, review 80−104330
comminution in vibratory mill, prod. of small amounts of finely divided unoxidised mat. 78−68646
compacting, two-layer 79−47647
compaction, of metal powders 80−40279
concrete masonry units, use and production of pelletised slag, mech. props. 78−52707
condensation powder, production by plasma jets, math. model *(Russian)* 80−7513
consolidation by pulsed magnetic fields *(German)* 77−8783
contact of spherical particle with a droplet, approx. eqn. 79−60604
corundum ceramic, high-temp. treatment, powder medium effect on microstruct., comp., strength and dielec. props. 79−33984
cryochemical techniques, prod. ultrafine ceramic powders 80−55336
deforming powders, self-diffusion coeffs. in failure zones and percolation 80−76209
diamond, synthesis and characterisation 80−50580
diamond powder, consolidation by thermal decomposition of methane and benzene 80−66448
diamond powders, Mo coated, X-ray diffr. study 80−100936
die compaction 79−61528
disintegration of powder particle agglomerates under the action of an alternating electric field 78−68642
disperser for powder, suspension and emulsion production 78−23636
dolomite, powders sintering, decarbonisation cycle effect 80−104102
dry ball milling, breakage parameters variation with ball and powder loading 80−80999
dustiness, determ. method 80−45455
electrophotographic dry powder toner concentration control *(Japanese)* 78−24878
electrostatic coating, charging charact. of some powders, deposition efficiency 80−50780
ethylene-vinyl acetate copolymer, powdered, prep. by emulsion polymerisation *(Japanese)* 80−104110
ferrite, hard, fast firing in kilns with jet burners 78−64496
ferrite core, strength improvement method, SiO_2 and Bi_2O_3 additions, mag. charact. 79−24484
ferrites, hard and soft, conference on powder metallurgy, Bowness-on-Windermere, England (Oct.-Nov. (1978)) 80−17713
ferrites, manufacture, modified technology development *(German)* 77−21073
ferrites, soft, spray firing for presintered powder prep. 80−89181
ferrites of divalent metals, prep. by double decomp. reaction, mag. charact. *(French)* 79−33463
fine particle mixtures, morphological anal. 80−104087
flame spraying process, of powders, intercrystn. corrosion of base material *(Czech)* 80−30158
flow measurement by gravimetric method *(Polish)* 78−9740
fluid bed forming in vacuum under vibratory action model 78−11147
freeze drying, prod. ultrafine ceramic powders 80−55336
gas-water atomisation process unit, for producing amorphous powders 80−7518
glass, rate constants of wet and dry ball mill grinding *(Japanese)* 80−29895
grain size determination by transient low press. air transmission 78−32965
grinding, fracture and deform. mech., SEM obs. *(Japanese)* 79−15620
high-speed shaping of free-flowing materials, computer investigation 80−25591
hot pressing powder layer on steel backing plate, joint form. kinetics 80−100961
interparticle percolation, lateral and axial diffusion coeffs., shear cell appl. 79−61666
laser applications in materials processing, seminar, San Diego, CA, USA (Aug. 79) 80−90609
liquid phase sintering, elementary mechanisms, soln.-reprecipitation 80−50571
magnesite, powders sintering, decarbonisation cycle effect 80−104102
metal-glass mats. alloyed with Cu, powder prep. and props. 78−72912
metallic oxide powders and mixtures, hydrostatic pressing, density and hardness variation 79−70029
minerals, industrial, finest grinding methods *(German)* 79−8256
mixes, ordered, characterisation using X-ray microanal. 80−16215
mixing, mechanistic kinetic model data appl. from conventional batch solid mixers 77−77442
mixing indices for multicomp. solid mixtures 80−39300
mixing of solids, appl. of multivariate statistical anal. 79−61529
multichannel ceramic blanks, produced from a refractory material 79−83163
NASICON solid electrolyte, processing and phys. props. 80−60820
non-isothermal, powder compact densification charact. 79−28976
nonconducting powder, temp. determ. in detonation deposition 80−226
nonsinusoidal periodic current meas. using standard DC shunt with magnetic powder monitoring, frequency errors 80−104398
one sided die compaction, internal stresses 78−23641
ordered mixtures production, humidity effect 80−76208
oxide reactor fuel pellets, ammonium polyuranate precipitation, continuous, particle size distrib. and agglomeration control 79−93804
particle electrification by impact on metal plates 79−50180
particle motion and segregation by density difference in V-type mixer 80−45250
particle size analysis by automatic sieves 80−52380
particle size analysis by chord method 77−4890
particle size distribution, automation of real-time optical meas. of small structures 79−85115
particles, small, impossibility of comminution by compression 78−52709
particles in dilute suspension in general flow, mass flow and density meas. 80−101784
particles in nonisothermal plasma jet, trajectory and temp. calcs. *(Russian)* 80−7514
particulate materials, quantitative three-dimens. characters. using polished sections and computer-controlled SEM system 77−2714
perlite, low temp., processes occurring during firing 80−11607
permanent magnet alloys manufacture, Co-mishmetal alloys *(Polish)* 80−35132
permanent magnet ferrites, forming 78−64495
pharmaceutical, surface area determ., new instrument 77−26280
plasmochemical synthesis, powder dispersion control 80−55332

powder technology continued
plasmochemical synthesis, powdered infusible compounds, props. 80−55330
plastic powder coating, technique and appl. 79−38786
polymer powder, pneumatic conveyance through metal pipes, charging tendency meas. 79−50186
polymers and elastomers, cryogenic grinding technique 77−32555
polynary complex powder mixture compaction, new equation 77−21045
polypropylene powder, cold compaction, product strength, heat treatment effects 80−11621
polyvinylidene chloride co-polymer powder, cold compaction, product strength, heat treatment effects 80−11621
pore size determ. of powder and wire gauge filter materials 77−12776
porous materials, approx. solns. of problems of plastic working 78−68643
powders, rapidly solidified, nucleation, undercooling and homogeneous structs. 78−52708
pressing, role in producing zero defect parts *(French)* 80−40380
pressing dies, dimensions of hard-alloy inserts calc. 78−60593
pressing in vacuum with adsorbed layers, boundary surface adhesion *(German)* 77−32540
pressure sintering, inhomogeneous flow and effective press. 80−93512
PVC powder, cold compaction, product strength, heat treatment effects 80−11621
PVC-Cu composites with chemically deposited ultrafine copper particles 80−93534
pyrocarbon deposition in fluidised bed, qualitative model, investigation with Stromungsrohr 78−56595
quartz sand, high-conc. suspension, prod. principles 80−66463
refractory metal dichalcogenides and Ga alloys, mixing powders using US treatment 79−24454
refractory powders, wet decompaction and compaction 80−35150
refractory production by gas flame deposition from high melting oxides and compounds 77−21076
ring gap sizer, characterisation of particle shape in sieve range 78−84732
rolled powder strip, effect of densification zone shape on density distrib. 79−95960
rolling, critical speeds 79−70011
rolling, particle size effect on conditions of strip shaping process 77−12565
SAP 930 and Al, 300 keV He irrad., blistering, flaking, gas re-emission 77−35601
semi-automatic grain size separation apparatus 78−54351
semiconducting α-Fe_2O_3 ceramics preparation, gas sensor for city gas appl. *(Japanese)* 80−61498
sheared particulate beds, mass transport kinetics in, Markov chains appl. 79−60057
shrinkage measurement during hot pressing strain gauge device 78−11146
Si_3N_4-Ce_2O_3-SiO_2 materials: phase relations and strength 80−97465
Sialon, prep. and charact. of ultrafine powders 80−11604
single crystals under large loads, theoretical elastic behaviour, review and appl. 80−71681
sintering, particle size effects *(German)* 79−91602
sintering, study of phase contacts formation in porous disperse structs. *(Russian)* 80−20811
sintering, surface redistribution by grain boundary diffusion 80−84871
size analysis, irregular shape particles, from acoustic emissions 79−61825
solution techniques, prod. ultrafine ceramic powders 80−55336
spherical particles production, equal-sized, controlled disintegration of free jets 80−7515
spherical powder, particle deform. and sliding during compaction, metallographic study 79−66020
spray drying, prod. ultrafine ceramic powders 80−55336
steatite ceramic, sintering and crystn., depend. on original powder state 79−61527
stereological application, in study of compacting process, elec. and mech. props. *(French)* 80−40286
strength characteristics, unit for meas. 77−25216
strip shaping device, deform. zone configuration effects 77−24979
surface area determ., simple continuous flow apparatus 77−16777
suspensions, dielectric separation of solid particles 80−16213
sylvite, compression in smooth faced rolling presses, preferred orientation *(German)* 79−33959
ultrafine particles, VEROS prep. method and superparamag. props. *(Japanese)* 77−85954
uniaxially reinforced powder, densification by dynamic hot pressing in rigid sheath 77−12568
US pulse echoes and suppression 77−28520
vacuum hot pressing, continuous, of transparent ceramics, press design criteria 78−23643
vibrated bed electrostatic separation 80−16641
vibrovacuum compaction of fine powders and its influence on isostatic molding 79−83149
Zircon, fine ground, mechanised method of cleaning with acid 79−83357
Zircon ceramic, exam. of development and fabrication 80−11608
$3Y_2O_3.5Al_2O_3$, garnet, synthesis by firing mixed oxides 79−61545
Al-Cu alloy prod., Cu interdiffusion with sintered Al powder, struct. effect at high press. 78−60606
Al-Cu(0-10 wt.%) sintered compacts, mech. props. rel. to sintering 80−76210
Al-Si-N-O system, comps. corresponding to β'-sialon phase reaction hot-pressing 80−84891
AlB_{12}, production of nitride materials by nitriding 77−12560
AlN, plasmochemical synthesis, powder dispersion control 80−55332
AlN powder, plasma-chem. and self-propag. high-temp. thermoplastic slips, synthesis 80−25633
AlN powder, production using Al powder in N plasma with electric discharge 79−33990
AlN, prep. and charact. of ultrafine powders 80−2983
AlN, synthesis and impurities 80−55329
AlN, synthesis in low-temp. plasma 80−16257
Al_2O_3 ceramics, with thermoplastic bond, prep. 80−45254
Al_2O_3, grinding material, grain shape optimization *(Polish)* 80−29916
Al_2O_3, powder, phase composition, sintering, effect of explosive treatment 77−21079
Al_2O_3, sintering response with const. rate of heating, depend. on processing related pore distrib. 79−28992
powder technology continued
Al_2O_3 suspensions, grinding method influence on rheology and suitability for high-density sintering 79−29001
Al_2O_3/Al clad powder prep. and physicomech. props. 79−29010
Al_2O_3-AlN phase diagram and reaction sintering of transparent cubic ALON spinel 80−25669
β''-Al_2O_3-Na_2O solid electrolyte, tube fabrication from cast ceramic tape 80−60819
β''-Al_2O_3-Na_2O solid electrolyte, processing and phys. props. 80−60820
β''- Al_2O_3-Na_2O-Li_2O (8.85, 0.75 wt.%) pressing powders, prep. by spray drying 80−40294
Al_2O_3-Y_2O_3 ceramics, corrosion protective W coating 80−35367
Al_2O_3-$ZrSiO_4$, granular corundum-zircon refractory, development 80−66462
$3Al_2O_3.2SiO_2$, mullite, synthesis by freeze drying 80−16252
$Al_4Si_2C_5$, synthesis, X-ray diffraction pattern, lattice constants 80−50581
B C powders, effect of C on sintering 80−40312
B pellets preparation from powder, for X-ray materials testing under pressure 80−50569
BC, fine powder prod. *(German)* 77−32549
BN, contact reactions with Ti and WC-Co at high pressures 80−61029
BN, high-temp. plasmochem. synthesis, control of props. 80−55333
$BaFe_{12}O_{19}$ powder, chemical plating with Co, Co-P, Ni-P and Cu 80−25593
$BaFe_{12}O_{19}$ powders, fast reaction presintering 80−97445
$Ba(V_{1-x}Ti_x)S_3$, synthesis and struct. phase transitions 80−107415
C, dense hard-type solids prep. from petroleum coke powder by grinding 79−20002
CaO, produced from $CaCO_3$ powder decomp. in vac. and in CO_2 80−45255
$Ca_{10}(PO_4)_6(OH)_{2-2x}O_x\square_x$ polycryst. sintered bodies, prep. and thermal props. 80−25624
Co powder, isostatic compression, elec. cond., densification models *(French)* 80−55321
Co-powder, isostatic compaction *(French)* 80−40285
Co_xO_y (x=1, 2 or 3, Y=1, 3, 4), conducting oxide prod. by amorphous citrate process 79−95985
Cr_2O_3-Al_2O_3 solid soln., Vickers micro-hardness 80−66629
Cu PM parts, improving cond. by pretreatment of green compact 80−20824
Cu-Ni-Co, alloy pre-form prep. through reduction of sintered oxides 80−40284
Cu-Ni-Fe, alloy pre-form prep. through reduction of sintered oxides 80−40284
Cu-Ni-Fe, spinodally decomposable, densification using four different powder methods 80−40283
$Cu_{1-y}Ag_yInS_{2-x}Se_{2x}$, for solar photovoltaic cells 80−10982
Eu_2O_3 ceramic powder, in situ deposition of metal coating, cermet form. 77−32713
Fe ore super-concentrate, deep drawing props. by integrated powder technology route 80−100806
Fe, water atomized powder, compaction, bending strength *(French)* 80−40287
Fe-C (graphite, 0.3 wt.%), powder-forged, elastic consts., density depend. 80−84987
Fe-Cu: graphite-$BaSO_4$-$CuSO_4$, friction material, solid state sintering kinetics 80−104096
Fe-SiO_2-Al_2O_3 Lisakovskii concentrate mixture, sintering process, temp. thermal treatment *(Russian)* 80−55317
Fe_2O_3, powder, compression in moulds, meas. apparatus *(Dutch)* 77−44205
Fe_xO_y, sintered metallised compacts, pore struct. by Hg porosimetry 80−40280
Ge powder electrodeposition, from molten fluoride mixtures 80−60797
$LaCoO_3$, conducting oxide powder prod. by freeze drying 79−95984
$LaCoO_3$, conducting oxide prod. by amorphous citrate process 79−95985
$LaCr(Co)O_3$, conducting oxide prod. by amorphous citrate process 79−95985
$La_{0.5}Sr_{0.5}CoO_3$, conducting oxide powder prod. by freeze drying 79−95984
$La_{0.5}Sr_{0.5}CoO_3$, conducting oxide prod. by amorphous citrate process 79−95985
(Li,Na,Cu,Zn) ferrites, nonceramic synthesis, electrochem. investig. 78−35339
Mg-Mn ferrite, finely divided, synthesis 77−28773
$MgAl_2O_4$-Al_2O_3 powder prep., for plasma arc spraying, coating props. 77−66612
α-$Mg(IO_3)_2$, cryst. struct. using X-ray powder method *(Chinese)* 79−51059
$Mg_{0.8}Mn_{0.2}Fe_{1.8}Al_{0.2}O_4$, grade 6SChl ferrite, milling conditions effect on fine cryst. struct. and activity 79−24483
MgO briquets, prep. by shock compaction and characteris. 79−43178
MgO powders, hot pressing, mechanisms 80−40300
MgO-NaCl refractory clinkers, Cr containing, densification, thermal treatment and phase composition effect *(French)* 80−76219
$Mg(OH)_2$, and calcination product, relations between particle size, shape and surface area 78−48355
Mn-Zn ferrite powder, spray dried calcination 77−12558
MnO-MgO-ZnO-Fe_2O_3, grade 1.3 VT ferrite formation from hydroxides 77−90302
MnZn ferrite, microstructure and initial permeability, presintering process effect 80−89367
MnZn ferrite powder prep., wet method 80−89180
MnZn ferrite powders, reactive, mag. materials obtained by compaction 80−89182
MnZn ferrites, post sinter-cooling rates effects 80−89369
$Mo+H_2S \rightarrow MoS_2$ 78−3078
Mo_2C powder form. by CVD 77−12590
Mo_2C powders, prop. from vapour phase reaction of $MoCl_4$-methane-H_2 system 79−100068
MoS_2, self-propag. high-temp. synthesis, wear props. 80−2975
$MoSi_2$, ceramic additives effect on sintering, recrystallisation 80−40306
NaCl, in thermal induction plasma, vel. meas. via new opto-electronic method 77−39462
6NaCl.$CdCl_2$, 60 wt.% powders, Suzuki phases prep. and stability 80−35123
Na_2O-Ca glass powders, mixed with CO_3 compounds, cellular-struct. glass fabrication 80−108382
NbB_2, hot pressing 80−25635

powder technology continued
$Nb_{40}Fe_{40}P_{14}B_6$, metallic glass, explosive compaction, mech. props. 80−89176
Ni superalloy powders, removal of interstitial contaminants 78−84735
Ni-Al_2O_3 cermet, fabrication and mech. charact. 79−38781
Ni-Fe, alloy pre-form prep. through reduction of sintered oxides 80−40284
Ni-Zn-Co ferrites, synthesis from solid solns. of schoenite-type salts 80−93511
$0.5Ni(NO_3)_2 \times 1.5Ni(OH)_2$ form., X-ray parameters 77−16519
Ni_3S_2, heazlewoodite, dissolution in acidic ferric chloride soln. at 25°C 79−95172
$NiTiO_3$, synthesis from products of soln. spray drying, kinetics 77−16519
PLZT powder preparation, hyrolysis ball mixing 80−81006
$PbMo_{5.1}S_6$, supercond. wire prep. by powder technique 78−52705
$PbMo_6S_8$ wire, powder processed, crit. current density and field 80−80466
Pd sponge powder, sintering shrinkage kinetics 80−29900
Si-Al-O-N sintered ceramic, microstruct., phase composition and transformation mech., mech. props. 80−40309
Si-SiO_2-Mg-Cu powder compact, nitridation to form Si_2ON_2 whiskers *(Japanese)* 80−93674
SiAlON powder, prod. by reaction clay+C+N_2 80−40295
SiAlON, prepared from siliceous sand and Al powder, hot pressing, steatite contamination effects *(Japanese)* 80−93528
SiC, form. by vapour phase method 80−25623
SiC, grinding material, grain shape optimization *(Polish)* 80−29916
SiC, pressureless-sintered, high temp. strength *(Japanese)* 80−104299
SiC-AlB_2 (0.61 to 1.2 wt.%), hot pressed, microstruct. 80−93563
SiC-Si composite, bulk resist. of technical SiC powders 79−28350
Si_2N_4 powders, synthesis, charact. 79−33977
Si_3N_4, high-speed rolling bearings, fatigue strength 80−93655
Si_3N_4, hot pressing, starting powder requirements, review 79−33987
Si_3N_4, prep. and charact. of ultrafine powders 80−2983
Si_3N_4, reaction sintered, microstruct. charact. 80−35145
Si_3N_4, reaction-bonded, pore struct. variations 79−24480
Si_3N_4, sintering in powder bed with addition of MgO sintering aid 80−29910
Si_3N_4, slip casting from aqueous suspension, reactions with HCl and NaOH 80−16259
Si_3N_4, synthesis and props. of shapes 79−47650
Si_3N_4/Al_2O_3, powder compact, electron microprobe investigation of reactions *(French)* 80−26009
Si_3N_4-CeO_2 additive, hot-pressing and oxidation behaviour 80−71618
Si_3N_4-MgO (2-5 wt.%) hot pressed, tensile creep testing 80−40423
Si_3N_4-$Y_2O_3(CeO_2)$, hot pressed, sintered, microstruct., flexural strength and fractographic anal. 80−40293
Si_2N_2O-Al_2O_3, solid soln., prep., effect of Si_3N_4 powder reactivity 80−45256
SiO_2 particles, movement and heating in air plasma jet *(Russian)* 80−7522
SiO_2-Al_2O_3 (36.6 wt.%) plasma prep. powder, metastable immiscibility and microstruct. during sintering 80−35143
$SrCoO_3$, conducting oxide prod. by amorphous citrate process 79−95985
$SrFe_{12}O_{19}$, powder, chemical plating with Co, Co-P, Ni-P and Cu 80−25593
$Sr_x(Na_{0.5}Bi_{0.5})_{1-x}TiO_3$ ferroelec. ceramic, hot pressing, numerical simulation *(French)* 80−76220
SrO.nFe_2O_3 isotropic ferrite magnets, manuf. process and mag. props. *(Japanese)* 80−29915
TaC and Ta_2C, self-propag. high-temp. synthesis 80−60815
Ti-Al-V (6,4 wt.%), porous compacts, determ. of effective stress in hot pressing 80−100807
Ti-Cr_3C_2 composite, TiC and struct. form. during sintering 79−29011
Ti-Si_3N_4 system, reactions under heating and plasma conditions 79−95988
TiC, sintering and grain growth, metallographic anal. 80−25642
$TiC_{1-x}N_x$ formation in high temp. N flow, ultra disperse powder, thermodynamic anal. *(Russian)* 80−55325
TiN, from high-temp. reaction of NH_3 and $TiCl_4$, physicochem. props. 80−55334
TiN powder, plasma-chem. and self-propag. high-temp. thermoplastic slips, synthesis 80−25633
TiO, oxidation 77−90472
TiO_2-ZrO_2, submicron powders, vapour phase production from $TiCl_4$-$ZrCl_4$-O_2 system 80−40301
TiP_2, synthesis and charact. 77−85953
TiS_2 synthesis 80−35141
$(U,Pu)O_2$ powder, FBR fuel prep. by Au/PuC coprecipitation process 80−814
UI_6-alkali metal halide system, prep. 80−50568
UO_2 fuel fabrication by the AUC powder process 80−13744
UO_2 powder compaction, force transmission and friction 80−71620
UO_2-20CeO_2 mixed powder, X-ray and microprobe exam. of homogenisation 80−25609
V-Mn-O system, phase comp. during oxide prep. 78−27447
W powders, influence of geometrical props. on compaction *(Russian)* 80−20818
W/Cu powders, liq. phase sintering, particle rearrangement 80−45253
WC, powder prod. by vapour phase reaction in WCl_6-CH_4-H_2 system 78−60626
WS_2, self-propag. high-temp. synthesis, wear props. 80−2975
YAG, production of densely sintered ceramic, exam. of recrystallisation during sintering 80−11609
$Y_{3-x}Bi_xFe_5O_{12}$, ferrite-garnet formation 78−52737
YIG, open die hot pressing, spin wave and FMR line width 80−89170
ZnS-CdS system, solid soln. form. mechanism 79−43177
ZnSe, commercial feasibility for optical ceramic manufacture 79−87598
ZrB_2, synthesis and impurities 80−55329
ZrC powders produced by various methods, impurities 80−11615
ZrC, synthesis and impurities 80−55329
ZrN, plasma-formed, ESCA and supercond. transition temp. 78−19697
ZrO_2 ceramic, dense nonstabilized, fabrication by hydrothermal reaction sintering 80−97451
ZrO_2, partially stabilised ceramics, strengthening, post-sintering heat treatment 80−97518
ZrO_2, partially stabilized, processing defects 80−97558
ZrO_2, sintering response with const. rate of heating, depend. on processing related pore distrib. 79−28992
ZrO_2, stabilized porous refractory, mech. strength 80−35322

powder technology continued
ZrO_2, wet vibro-grinding with surfactants, superhigh density sintering suitability 79−33989
ZrO_2/Al clad powder prep. and physicomech. props. 79−29010
ZrO_2-Y_2O_3 ceramic powder, in situ deposition of metal coating, cermet form. 77−32713
ZrO_2-Y_2O_3 powder, prep. for plasma spheroidisation, sputter drying *(Russian)* 80−55324
ZrS_3 synthesis 80−35142
$ZrSiO_4$, mechanochemical effect by mechanical grinding *(Japanese)* 78−84754
$ZrSiO_4$-Al_2O_3 system, particle rearrangement kinetics due to densification 80−25626

powders
see also densification; granular structure; particle size; powder sprayed coatings; powder spraying; sintering
aerosol, ultradisperse condensational, formation by plasma-jet powder evaporation *(Russian)* 80−55721
agglomeration, computer simulation *(Japanese)* 78−95706
agglomeration, Monte Carlo simulation *(Japanese)* 78−95707
alkali halides, microcryst. powders, colour centres, refl. spectra 78−23493
alumina powder, particle size analysis, using centrifugal sedimentation *(German)* 78−57890
alumina synthesis rel. to prod. of transparent ceramic 77−52270
analysis by photoacoustic and photothermal spectroscopy 79−61929
anisotropic grains, effective thermal and elec. cond. 77−89601
atom-surface reaction, EPR anal. via ultrahigh vacuum/flow system 78−7232
autohesive strength, meas. installation 80−40644
ball mill grinding, effect of Vickers hardness and rate const. of spec. surface increase *(Japanese)* 77−52259
binary, inhomogeneity-packing density relations 78−92211
borosilicate glass, powder, sintering, foaming by chemical reactions 80−81017
brittle, shock wave disintegration test method 80−66744
bronze, preparation by electrodeposition from normal salt baths of Cu, Sn, porous components fabrication appl. 78−20026
bulk solids, strength and flow props., vibrations effect 79−37237
calculation, effect of granulometric distrib. on importance of Kirkendall effect *(French)* 77−11721
carbide micropowders, abrasive lapping of refractory metals 77−44391
carbon tetrafluoride+methyl trichlorosilane, reaction, metastable C phase prod. 79−29341
carbon tetrafluoride+SiC(Si), reaction, metastable C phase prod. 79−29393
ceramic, fine powder, compaction during pressing and green strength, absorbed layer effect *(German)* 77−77450
ceramic, specific surface area meas. by gas adsorption 78−11144
ceramic, ultrafine, prod. by cryochemical, freeze drying, spray drying or soln. techniques 80−55336
ceramic powder, thermal stresses during spheroidisation process *(Russian)* 80−40386
ceramic powders, electron microscope determination of particulate sizes *(German)* 78−57891
ceramic powders, equipment for sublimation drying, exam. 80−25733
ceramic processing before firing, book 78−56608
ceramic-metal composite using metal-coated alumina powder 77−21081
characterisation, survey of instruments and methods 77−55900
characterisation, survey of instruments and methods 78−11474
classification in electric field of plane capacitor 77−12775
cohesive strength and internal friction determination for small quantities of material 77−40495
compacted, stress relaxation pattern, moisture effect 80−20994
compacts, intermediate stage sintering, surface area reduction kinetics, anal. 78−76614
component particle size analyser, using X-ray fluorescence *(Japanese)* 78−15615
composition, meas. by 60 keV γ backscatt. from ^{241}Am 77−52695
composition of finely dispersed powders, electrostatic device for determ., exam. 80−25588
compressed powder mixture electrical conductivity calc. *(German)* 80−10940
consolidation process, exam. of quasimelt in pressing, sintering stages 80−20816
consolidation study by absolute thermoelectromotor force 77−73246
cyclic simple shear testing apparatus for granular materials 77−90578
cytidine, cryst. powder, absorption spectrum, unusual narrow line FIR modes, cryogenic temps. 79−69824
Debye parameter, powders characterization *(Japanese)* 78−95705
dendritic particle characterisation of automatic methods 80−25590
densification, under uniform directional loading 78−68644
densification laws 79−66021
densification of porous solids in hot rolling 77−63583
density measurement by pycnometry 80−69903
detonation wave front, heating of contained particles, residual cryst. defects anal. *(Russian)* 79−68749
diamond, powders, oxidised surfaces, thermal desorpt. spectra 78−47661
diamond, synthetic, thermal cond. 80−96702
diamond, synthetic micropowder, degree of charging of polished Ti and Fe surfaces 78−60880
diamond, ultradisperse, ESR, particle size and lattice microdistortions 80−97140
diamond particles, finely dispersed, in active C shock wave produced powder, electron diffr. identification 80−1903
diamond powder, explosion synthesized, impurity distrib. and thermal stability 80−15147
diamond powder, rapid oxidation development, kinetic model *(French)* 78−68917
diamond powders, EPR of defect centres 77−66423
dimension and shape evaluation by SEM 80−40278
discoidal agglomerate, stress pattern, distributed loading effect during diametral compression test 80−60934
discs of powdered samples, Raman versus Rayleigh light scatt. 79−91437
disordered solids, nonresonant paramagnetic absorption, quantum theory 79−69712
disordered systems, mode softened unified theory 79−55637
divalent Sr, Ba, Ca, Zn, Cd iodates, complex salts, phase transitions, cryst. struct. *(Chinese)* 80−70171

powders continued
dry, flow over inclined surfaces, expt. study 78−63488
dust content of gas meas. by laser *(French)* 77−64486
dynamic compaction, review 78−3071
dynamic flow rates, meas. apparatus 80−14860
electrostatic behaviour, methods for study 80−52266
electrostatic spark hazard identification and control, during collection in container 80−69291
feldspars, initial sintering, theoretical treatments and exp. procedure 78−44067
ferrite, grain size meas. by electron microscopy, sample prep. *(German)* 78−56833
ferrite, hot pressed, powders, influence of CoO and CuO alloying on physicomechanical charcts. *(Russian)* 77−66600
ferrite, mag. props., explosive shock treatment effects 79−52395
ferrite formation during calcining of sulphate mixture 77−63608
ferrite powders with high specific surface, manufacture using freeze-dry method *(German)* 77−63603
ferrites, M type anisotropic, powder prep. and, sintered, effect of powder and pressing technology on alignment *(German)* 79−24472
ferroelectric powders, origin of memory in echo-phenomena 79−38440
ferroelectrics, electroacoustic echoes and long-time storage 79−38454
fibre reinforced powder, densification during hot pressing 77−12566
fine, electrogravitation classification by particle mass 79−61531
fine particle profile, ruggedness and texture specification by fractal dimension 79−40535
fine particle shape characterisation by decision matrix design and cybernetic mode operation 78−11143
fine particles materials technology, fabrication and appls. *(Japanese)* 77−70016
flow, gravity-induced particle, stochastic theories 80−14798
flow measurement by gravimetric method *(Polish)* 78−9740
fluidisation, bubbling behaviour rel. to particle size 77−31362
fractal dimension characterisation, textured and structured particle profiles, dilation logic appl. 79−58673
glass ceramic prep. by hot pressing and crystallisation of glass powder, mech. props. 78−15351
glass powder, light scatt., close particle packing 78−1161
glass sintered powder porous bodies, liq. penetration mechanism *(Japanese)* 80−53853
glass theoretical aspect of sintering 80−20883
glass/Cu-polymer compound powders, prep. and corona charging props. *(Japanese)* 78−19679
grains, melting, in plasma flame 79−60200
granular material, particle crushing under high triaxial stresses *(Japanese)* 78−15466
graphite, model for testing liq. cryst. method for detection of small objects in optical microscopy 80−9034
graphite powder compacts, diffusion of H_2 and N_2, time-lag analysis 78−2301
graphite-Si powder mixture, reaction hot pressing 78−60592
graphitisation kinetics within first min. of heat treatment 77−66596
green bodies, isostatically pressed, extruded and slip cast, binder distrib. 78−27448
gypsum, powder Jeener-Broekaert three-pulse sequence, inhomogeneous lineshapes, second rank spin interactions 80−39891
Hall effect and mobility, mixing ruler, in compressed powder combinations *(German)* 78−84234
high speed rot., spin diffusion, NMR spin lattice relax. obs. of D 80−66056
high-pressure triaxial testing cell 79−74329
homogenization by dynamic hot pressing 77−73244
hot pressing, dynamic, laboratory unit 79−100071
hydrophobic powder, wetting props. 79−33162
III-V nitride, preparation technology *(Czech)* 78−3037
impurity segregation on sintering of technical purity powders 77−63586
Knudsen diffusion, gas diffusion relationship of Knudsen flow permeametry 77−55087
Knudsen diffusion, pore size distrib. effect on surface areas obtained by diffusion meas. and Hg porosimetry 77−55088
laboratory techniques for powder handling 80−45475
lactose powder coated with fatty acids, tensile strength 77−21304
lattice defect effect on mixing 79−73313
light scattering, close particle packing 78−1161
magnesian-spinel materials form. using heat treatment 79−38773
magnesite-chromite powder, exam. of rheological charcts., compaction 78−60628
magnetic particle inspection oxides, evaluation 80−40657
magnetic properties of ferromag. and ferrimag. powders, conc. charcts. determ. 77−73052
metal, on piezoelec. substrate, dynamic SAW reflecting struct. 80−74565
metal, thermally activated hopping, carrier-carrier interaction 77−15972
metal oxide, quantitative surface meas., XPS method and appl. 78−40104
metal oxide-C mixtures, mathematical analysis of reactions 77−73469
metal powder, method for TEM study 80−84038
metal powder suspension in air, spontaneous ignition temperature *(Russian)* 78−47027
metal powders, cold sintering under high pressures, correlation to plastic props. and diffusion 79−38757
metal powders, packed, complex mag. permeability calcs. 80−29583
metallic, thermal diffusivity meas., constantrate heating method *(Japanese)* 80−6572
metallic fine particles, theory of melting in the Percus-Yevick limit, appl. to particles on SiO_2 and C substrates 80−20060
metallic particles, spectrum fluctuations in two-dimens. model, specific heat calc. 77−82447
microscopic quantitative analysis 80−22475
minerals, adsorbed films influence on cohesion and angle of internal friction 77−25084
mixing, laboratory device 79−61828
mixing/segregation behaviour, 2 powders of different density, quantit. anal. 78−84733
mixture electric-discharge sintering mass transfer and homogenization 80−20817
mixtures, diffuse reflectance, quantitative anal. 80−87308
model laws, especially for silo models 78−38383
moist, granulation on vibrated chute *(Japanese)* 78−95710
monolithic materials for creating high pressures, anvil device with lune toroid 80−73377
powders continued
morphological anal. of fine particles 80−20813
Mossbauer spectra analysis, ambiguity problem *(Japanese)* 77−66449
narrow gap semiconductors, electrical properties, microwave study 79−95437
near IR diffuse reflectance analysis anomalies 80−86383
nonconducting powder, temp. determ. in detonation deposition 80−226
nonequiaxed orientation effect on pulse amplitude in pulse conductometric particle size anal. 79−100070
nonisothermal devitrification kinetics 80−92465
nonisothermal method for sintering kinetics of materials controlled by two mechanisms 77−63580
nonisothermal sintering, densification of powder compacts 78−60596
nonlinear mechanism leading to polarisation echoes 78−87739
nucl. echo signals, cryst. anisotropy *(Russian)* 79−99790
oxide powders, muonium and positronium form. 79−56679
particle classification calc. by geometry 78−23640
particle nonequiaxiality effect on size distrib. meas. in pulse conductometeric anal. 80−20833
particle profile charact. rel. to profile Fourier coeff. 78−11142
particle profiles, morphological characterisation derived from Walsh coeffs. 80−50816
particle shape charact. 79−74109
particle shapes determ., device 78−60899
particle size and size distrib. determ. from acoustic emissions 77−53861
particle size distrib. anal., photoelectric device 77−74379
particle size distrib. anal. by light blockage principle 79−6089
particle size distribution measurement apparatus, rel. time 79−17390
particle size measurement by monoparticulate film method *(Japanese)* 78−95874
particles, collecting, handling and mounting for SEM characterisation 79−21867
particulate analysis, aspects of specimen prep. and a limitations of precision by SEM and TEM 79−17574
particulate materials, cohesionless, mixing and segregation, microscopic mechanisms 79−37848
particulate materials, cohesionless, mixing and segregation, failure zone form. 79−42261
particulate solid, reactions, viscous flow and Knudsen diffusion 77−4937
particulate systems, coarse and fine, ordered powder mixing 79−61530
peizoelectric, polarisation echo and surface props. theory, *(Russian)* 77−48122
phonon electroacoustic echoes, storage mechanisms 80−75606
photochemistry of powder, conc. and radiation intensity reaction time and depth depend. 77−29023
piezoelectric, phonon echoes and long-time storage *(Japanese)* 80−70330
piezoelectric, polarisation echo for system of anharmonic oscillators *(Russian)* 77−81062
piezoelectric, RF dynamic polarisation echo obs. 77−16254
piezoelectric powder, mech. of long-time phase memory 79−42899
piezoelectrics, electroacoustic echoes and long-time storage 79−38454
piled bed, deform. character, two-dimens. model calcs. *(Japanese)* 79−34115
plasticity of porous powder solid 79−68604
PMMA coated frit powder prep., corona-charging props. *(Japanese)* 80−25891
PMR spectra of powders with spin 1/2 nuclei arranged in isosceles triangular mag. config., shape function 80−2648
Polirit, optical polisher powder, particle size distrib., dispersion analysis 77−9141
Polirit polishing ability and physicochemical props. 79−72730
polycarbonate, particles, critical stress 77−28869
polydisperse, heating and vaporisation in plasma stream *(Russian)* 77−59707
polyethylene, microfine powder prod. for dispersions *(German)* 80−29920
polymer filled ceramic, ZrO_2 stabilised, fracture mechanism *(Russian)* 80−100895
polymer materials, chem. reacting, kinetic charcts. of thermal effects determ. using Calve type microcalorimeter 77−57328
polymers, corona-charging props. 80−6946
polystyrene, particles, critical stress 77−28869
polystyrene, sorption of organic vapours, glassy-state relaxation induction and meas. 80−44415
powder, particle size distrib. meas. by spectral transparency method 78−49876
powder-cushion gripping to promote good alignment in tensile testing 78−92418
powder-water-oil system, cohesion of powder particles with water, rheological prop. *(Japanese)* 80−14647
pressed powder bed, determ. of side pressure distrib. 78−84734
purification of US cleaning and pickling, effectiveness of working liq. comp. 77−63587
purine, γ-irrad., dose-response curves 78−7215
PVC, mech. comminution in fine struct. changes in porosity, density, specific surface area *(German)* 78−35345
PVC, sorption of organic vapours, glassy-state relaxation induction and meas. 80−44415
PVC powder, quinoline diffusion, microdiffusion technique 79−7713
pyrimidine, powder, dose-response curves 78−7215
pyrimidine powder, γ-irrad., dose-response curves 78−7215
pyrolusite powder, thermal noise *(German)* 78−64075
quadrupole distorted NMR powder patterns, simulation, Fortran program 77−77105
quartz, decrepitation recording for gas-liquid inclusions, temp. meas. method 77−71325
quartz, heat treatment of dense moving layer, heat exchange development 79−20075
quartz, on piezoelec. substrate, dynamic SAW reflecting struct. 80−74565
quartz, powders, CaO soln. chemisorpt. rel. to lattice parameters, work function 79−37918
quartz, resonant, stimulated phonon echo, ang. and powder depend. 79−8093
quartz powdered, thermal effects of Fe contamination, adsorbed H_2O, annealing on DTA 79−100161
Raman laser spectroscopy, laser excitation, optimum conditions *(Russian)* 77−28580
random packing of spheres, computer simulation 80−77705
rare earth hexaborides, powders, evaporation 77−89535

powders continued
rare earth luminescence from intensity meas. on powdered phosphor screens self-concentration quenching mech. determ. 79−69880
rare earth polisher powders, comparative analysis 79−50453
rare earth selenides of yttrium subgroup, powder prep. conditions and energy of optical transitions 77−63581
rare earth-cobalt intermetallic, RCo_2 79−19725
refractive index measurement 77−156
refractory metal carbides, abrasive props. of micropowders for lapping 77−63821
resistive alloy foils, manufacture and props. of multicomponent alloys *(Polish)* 80−35131
review of instruments for particle and powder charact. 77−66735
rheological characteristics of compact of plastic powders *(Japanese)* 78−95770
ring gap sizer, characterisation of particle shape in sieve range 78−84732
rolling bottle device, for measuring flow of liqs. and powders 80−6174
rubber, finely dispersed, sedimentometric anal. 80−66883
rubber, prod. and processing, powder preblend mixes 79−52149
sample prep. for spectral anal. 78−23884
SAW interactions, for various directions of propagation 80−49486
science review *(Japanese)* 78−15326
second harmonic generation in powder mixtures 77−62009
segregation of solid mixture in rotating vessel, cascading angle of particles effect *(Japanese)* 78−15327
semiconducting, exam. of freeze drying rate in cryochemical prep. method 78−52706
semiconducting powders, band-gap energies, photoacoustic meas. 80−70579
semiconductor, prep., freeze drying of solid solutions, solvent choice 80−11583
semiconductors and semimetals, EPR, effect of mag. field depend. of elec. parameters 79−99749
shape indices, particle morphology 79−74110
β'-sialon compositions, reaction sintering obs. 80−55337
sieving of fine powders by sonic oscillating air column *(Japanese)* 78−95712
silica, colloidal, liquid imbibition characteristics *(Japanese)* 78−95963
sintered bodies and powders, particle size distributions from chord and area distributions *(German, English)* 80−35126
sintering, consolidation theory appl. 77−73243
sintering, electrical resistance, apparatus 80−16217
sintering, final stage, steady state diffusion models, testing of models by numerical simulation 79−4428
sintering and random structures, volume diffusion and creep effects 80−35125
sintering kinetics, powder kinetics, variation of mechanism dependent exponent, with coordination number and neck size 80−20815
sintering kinetics, superplasticity of polycryst. materials 79−100072
soft magnetic mat. prep. by precip. of insulating film on Fe powder in polishing bath 78−23637
specific heat, meas. apparatus for 4.3-300K 80−227
specific surface, determ. using Hg porosimetry 80−29896
specific surface, X-ray determ. method 80−47012
specific surface measurement, chromatographic method 77−77859
spectrochemical analysis, spark elutriation of powder into plasma *(German)* 78−68959
spherical particles, nonoverlap model for dispersion 77−36416
spherical powder sintering by surface diffusion, computer simulation 78−48344
steatite, dielectric ceramic 77−32546
stream mean flow rate meas. by Doppler scatt. null enumeration *(Russian)* 78−47071
strength characteristics, unit for meas. 77−25216
submicron, sintering, surface area reduction kinetics, model 78−44039
superconductor MM range receiver for radio astronomy 80−21919
surface area, meas. by Monosorb surface-area analyser using Brunauer-Emmett-Teller eqn., reproducibility 80−36979
surface area determination, calorimetric method, modified Harkins and Jura procedure 79−35667
surface area meas., chemical planimetry method, appl. to silicates, oxides *(German)* 79−88915
surface area measurement using Knudsen diffusional flow of gas 79−40536
systems with anisotropic g-tensor, EPR spectra, extra absorpt. peaks 79−51839
temperature effect on flow and tensile strength 79−61668
tensile strength data and failure loci from Jenike shear cell tests 78−31476
tensile testing, modification of split plate tester 77−70255
testing, nondestructive, using electron spectroscopy 78−3430
tetragonal powders, X-ray intensity corrections for preferred orientation 80−1880
TGS powder, complex dielectric const. temp. depend. 79−47379
thermal conductivity, particle size and porosity effects *(Japanese)* 78−6191
thermosetting, hot stage microscopic technique for examining curing 79−28979
trace element determ., atomic absorption spectrometry appl. *(Russian)* 77−66783
triaxial test procedure and num. calc. method for flow props. 77−60028
triboelectric charging, incremental charge-mass characterisation 78−17833
TTF-TCNQ, phase transition at 49K 77−89539
turbulent flat plate boundary layer, particle cloud concentration profile 77−24016
ultra fine, prod. by rotating friction mill, mechanism in initial wear region *(Japanese)* 80−25589
ultrafine, surface roughness effect on formation by rotating friction mill *(Japanese)* 78−95709
US pulse echoes and suppression 77−28520
vacuum-powder insulation, radiative heat transfer determ. by IR spectroscopy 77−13759
vibrating, motion from elec. cond. obs. *(Japanese)* 78−95711
wet particulate systems, pendular band strength between unequal-sized spherical particles 80−104418
work index estimation during grinding *(Japanese)* 78−19680
X-ray fluoresc. anal., of powdered samples, additivity of effective coeffs. for X-ray absorpt. 79−24856
X-ray phase analysis by external standard method 79−68976

powders continued
X-ray powder patterns for tetragonal and hexagonal polycrystalline materials, improved indexing method 80−24312
YAG powder, X-ray K_α doublet diffr. peak position rel. to lattice const. precision 77−68891
Ag-polystyrene powder mixture, hot-pressed, elec. resist. 77−32556
$Ag_2S+Ln_2S_3$, reaction rate, production of ionic semiconductors 80−93741
$Ag_3SbS_3(AsS_3)$, electroacoustic echo, ultrasonic wave attenuation *(Russian)* 80−88280
Al alloy, powder, erosion resist. to hot propellant gases 77−56165
Al, annealed and powder sintered (SAP 895), sputtering under D^+ and $^4He^+$ bombardment, microstruct. effects study 80−84821
Al powder, liq.-solid phase transforms. *(French)* 80−45294
Al sintered powder, 100 keV He ion irrad., surface erosion due to blistering 77−35600
Al-Fe_3O_4 binary thermite powder mixture, compaction 79−74125
AlN powder, effect of O impurity on sintering and thermal cond. *(Japanese)* 79−20017
AlN powder, plasma synthesized, sintering behaviour, props. and struct. 79−100097
AlN synthesis, temp. distrib. in plasma-chemical reactor 77−59730
AlN, ultradispersed powder, IR spectra 80−50312
AlN-Al_2O_3, hot pressing, crystalline phase obs. 78−95720
Al_2O_3, crystallite size and lattice distortion, determination using X-ray line broadening analysis, appl. to ceramic powders 79−8261
Al_2O_3, explosively compacted powder, struct. and annealing 77−55926
Al_2O_3, fine powder, prep. by evaporative decomposition of solns. 78−39725
Al_2O_3, injected into induction plasma, particle temp. and trajectory 78−59607
Al_2O_3, powder grains, melting, in plasma flame 79−60200
Al_2O_3, powder sintering, isochronal temp. depend. data interpreation 77−77453
Al_2O_3, sintering behaviour and props. of 24 aluminas *(German)* 79−4932
Al_2O_3, support for MnO_2 catalyst, N adsorption obs. of dispersion modes 80−81363
Al_2O_3, tensile and compressive strengths of fine powder bed *(Japanese)* 80−25780
Al_2O_3, transparent ceramic manuf., charact. of powder and process 77−48383
β-Al_2O_3-Na_2O, vacuum hot pressed, densification kinetics 78−72758
Al_2O_3-SiO_2, mullite, powder, synthesis using silicic acid, clay and $AlCl_3$ *(German)* 79−4933
Al_2O_3-SiO_2, plasma-prepared, glass form. and phase transforms 77−44208
Al_2O_3-SiO_2 glass powder, mullite crystallisation during hot pressing 78−60639
Al_2O_3-SiO_2-MgO, cordierite, powder, synthesis using silicic acid, clay and $AlCl_3$ *(German)* 79−4933
Al_2O_3-TiO_2 powder, plasma-prepared, morphology and phase constitution 80−100833
Al_2O_3-ZrO_2, microstructure effect on friability 78−64515
Al_2SiO_5, solid state reaction with $Ca_2P_2O_4$ *(Japanese)* 78−19702
B, appl. in abrasive pastes 80−21114
B dispersed fractionated powder, struct. obs. 80−19703
BN, O content depend. on heat treatment temp., neutron activation analysis 80−16356
BN powder, wurtzite sphalerite struct. phase transition, effect on substruct. 80−25690
BN powder particles coated by Ti or Mn, thermal stresses generated in vac. deposition 77−40455
Ba ferrite powder, effect of lattice defects on coercivity *(German)* 79−24194
BaB_6 powder, surface struct. effects on thermionic emission charact. and vapour pressure *(Japanese)* 80−50506
$BaFe_{12}O_{19}$, powder, milled and annealed, phase composition, lattice conts. and crystallite size 80−71677
$BaFe_{12}O_{19}$ powders, fast reaction presintering 80−97445
$Ba_2NaNb_5O_{15}$, X-ray powder diffraction data determ. *(Chinese)* 80−70170
$BaTiO_3$ powder, dispersion effect on meas. in electrical sensing zone particle size counter 79−17383
$BaTiO_3$, powders, Bragg reflection integral intensities due to structural anomalies 80−107098
$BaTiO_3$:$BaTi_3O_7$, dielec. props. and microstruct. 80−60481
Be, gas evolution during heating from 20-700°C 79−61796
Be sintered powder, 100 keV He ion irrad., surface erosion due to blistering 77−35600
BeO powder, sinterable and unsinterable, sintering processes, electron microscope exam. 79−33986
Bi, fine, precipitation on passivated electrodes 80−2977
Bi, powdered mag. resistance *(German)* 79−28358
α-Bi_2O_3+KCl, quantitative anal. of multocomponent powders, full-profile refinement of Guinier-Hagg X-ray film data 79−39249
Bi_2Te_3-Sb_2Te_3 solid solns., powders, particle shapes determ., device 78−60899
n-$Bi_2Te_{2.88}Se_{0.12}$, extrusion deformed, powder dispersion degree influence on thermal and elec. props. *(Russian)* 80−39366
C, binary muxtures, bulk density, charact. curves interpret. 77−63574
C black with pyrocarbon coating, surface props. *(French)* 78−68921
C blacks, powders, resistivity rel. to compression *(French)* 80−35349
C mixes, extruded, preoxidation treatment effect on transverse breaking strength 77−63767
$CaAl_2O_4$, fine powder, prep. by evaporative decomposition of solns. 78−39725
$CaAl_2O_5$, form. by solid state reaction of CaO and Al_2O_3, electric field effects 79−28997
$CaF_2+SiO_2+Mg(OH)_2$ matrix, quantitative anal. of multocomponent powders, full-profile refinement of Guinier-Hagg X-ray film data 79−39249
$CaHPO_4$, powder and granules with starch mucilage binder, surface topography variation under compression 80−80998
CaO-MgO-Al_2O_3-SiO_2, glass-ceramic prep. by hot pressing and crystallisation of powder 78−11192
CaO-MgO-Al_2O_3-SiO_2, glass ceramic, prep. by hot pressing and crystallisation, mech. props. 78−15351
$Ca_5OH(PO_4)_5$, powder, precise study of electron diffr. patterns, diffr. interpretation at high tension *(French)* 79−37594
β-Ca_2SiO_4, very reactive powder, prep. 77−55924

powders continued
CdS powder layers, surface pot. dark decay, moisture sorption and heat treatment effects 80−18038
CdS:Cu, IR photolum. at 10K 79−28824
Co, ferromagnetic micropowder, cryst. struct., coercivity, remanence, saturation 80−65967
Co powder, isostatic compression, elec. cond., densification models *(French)* 80−55321
Co-powder, isostatic compaction, mech. and elec. props. *(French)* 80−40285
Co_2NiO_4, powder prep. by freeze drying of solid solutions, solvent choice 80−11583
$(Co_yNi_{1-y})_{1-x}O$ and O_2 prep. props., and reactions 77−12569
Cr powders (60 to 70%), spectral determination of Al and Fe 77−90679
Cr, ultrafine particles, coatings for selective absorpt. of solar energy, efficiency 78−18060
Cr-Fe-C (28.4, 9.1 wt.%) prep. from $FeCr_2O_4$ chromite 80−100804
CrO, reduction by powdered graphite, mechanism 77−4748
CrO_2 and CrO(OH), fine particle obs. of cryst. morphology and topotaxy 80−65969
CrO_2 powder, thermal-magnetic props. 79−51821
Cr_2O_3, effect of oxide additions on sintering in air and reducing atm. 77−59729
Cr_2O_3 polycrystalline powder, crystallite sizes and surface areas 77−66086
CsI based powdered phosphors and screens possible appl. in X-ray radiography and fluorography 79−6245
Cu compact, pulsed action of laser radiation, dimens. effect *(Russian)* 77−16437
Cu complex with adenine, physical properties obs. *(Japanese)* 77−43878
Cu, compressed powder, elec. cond. −30 to +30°C *(German)* 79−28335
Cu, compressed powder, thermoelectric effects 80−20155
Cu, compressed powder, thermal cond. meas. *(German)* 80−70669
Cu, compressed spherical powder, electrical conductivity *(German)* 78−6343
Cu, electrolytic, particle profiles, morphological . characts. derived from Walsh coeffs. 80−50816
Cu, positron annihilation *(Russian)* 77−63485
Cu, powder, compression and stress relaxation *(Japanese)* 79−96060
Cu powder, corrosion protection during manufacture and storage 77−25200
Cu powder compacts, yield curve comparison, different loading paths *(Japanese)* 80−93621
Cu powder with homogeneous dispersion of Al_2O_3 particles 78−84743
Cu, powders, prep. of spherical starting particles, for suspension electrolysis 78−60689
Cu-Al powder compacts, elec. resist., temp. depend. 80−49690
Cu-Pb, gas-atomised, particle profiles, morphological characts. derived from Walsh coeffs. 80−50816
CuCl powder compacts, DC voltage depend. resist. under press. 80−80334
$CuF_2.2H_2O$ powder, EPR and Cotton-Mouton Voigt effect in Q-band *(French)* 79−8045
CuO powder, surface area determ. by adsorpt. of stearic acid and pyridine 80−107636
Cu_2O and CuO powders, contact resistance, temp. and pressure dependence, obs. *(German)* 79−4555
$Cu_2S+Ln_2S_3$, reaction rate, production of ionic semiconductors 80−93741
$DyFe_2$, mag. and hysteresis props. *(Russian)* 79−42800
$Dy_2Ti_2O_7$, pressed powder, low temp. thermal cond., mag. field depend. 79−23789
$ErFe_2$, mag. and hysteresis props. *(Russian)* 79−42800
F-Co-Ni alloy, video recording appl. *(Russian)* 77−55910
Fe aerosol powders, oxidised, nucl. gamma reson. study *(Russian)* 79−1725
Fe, atomised powder, props. 80−25600
Fe, BH_4 reduced, coercive force and remanence ang. variation 80−44879
Fe, carbonyl powder, kinetics of phosphatizing reaction 79−96218
Fe, carbonyl powder, specific elec. conductivity, 5 to 200 MPa *(German)* 80−70664
Fe, electrolytic, particle profiles, morphological characts. derived from Walsh coeffs. 80−50816
Fe, ferromagnetic micropowder, cryst. struct., coercivity, remanence, saturation 80−65967
Fe, passivating oxide layer comp. 78−31558
Fe powder, Mossbauer spectra parameter calc. with aid of computer *(Russian)* 78−76361
Fe, powder, oxidation magnetically soft material form., elec., mag. props. 77−8778
Fe powder, sponge and atomized types, steam oxidation, pore closure and surface hardness 80−45441
Fe powder compact, apparent density, mixing, and friction, zinc stearate lubricant effect 80−45403
Fe, prep. by reducing iron phthalate in mag. field, mag. props. 77−40090
Fe, prepared by BH_4 process, comp. and stability 80−44878
Fe pyrophoric powders, stabilising layer form. during passivation, saturation moment meas. 80−44865
Fe small, particle motion effect on Mossbauer spectra 80−84671
Fe, sponge, particle profiles, morphological characts. derived from Walsh coeffs. 80−50816
Fe, water atomized powder, compaction, bending strength *(French)* 80−40287
Fe-based PZh2K, porous struct., effect of diffusion chromising with sintering 79−66219
Fe-Co, ferromagnetic micropowder, cryst. struct., coercivity, remanence, saturation 80−65967
Fe-Co-Ni-O, mag. powder prod. by reduction of oxalates 77−63582
Fe-Ni mixed powders, effect of Ni particle size and unequal interdiffusion, on sintering process *(Japanese)* 78−84728
Fe-Ni-Cr-Ti, superalloy A286, powder, exam. of microstruct. and mech. properties 78−52979
Fe-TiC pseudofused composite magnetoabrasive powders, props. 80−100926
FeO compacted powder, effect of wall groove orientation and wall lubricants, on WC wall friction 78−23831
$Fe_{1-x}O$, wustite, AES study, ion and electron bombard. effects 80−76114
powders continued
Fe_2O_3 based catalysts for NH_3 synthesis, sintering of powders 79−61551
α-Fe_2O_3, hematite, AES study, ion and electron bombard. effects 80−76114
Fe_2O_3 powder, heat of adsorpt. of stearic acid, surface area meas., flow microcalorimetry 78−81974
Fe_2O_3, powder, preparation conditions rel. to morphology 77−8777
γ-Fe_2O_3 powders, mag. props., effect of Co plating 79−69699
γ-Fe_2O_3, small particles, vacancy sintering 77−65975
γ- Fe_2O_3:Co, increased coercivity by epitaxial doping 79−82833
Fe_3O_4 briquettes, porous, struct. changes during reduction 77−21064
Fe_3O_4, low temp. sintering 78−92221
Fe_3O_4, magnetite, AES study, ion and electron bombard. effects 80−76114
n-GaAs, strain sensitivity of specimens obtained from pressed powders 77−36177
GaAs:Te, quadrupole interactions in NMR spectra 79−51880
GaP, powder, electroluminesc. excitation by SAW, nonlinear effects 80−16104
$Gd_2(SO_4)_3.8H_2O$, pressed powder and single crystal, low temp. thermal cond., mag. field depend. 79−23789
Ge, elec. cond., temp. and press. depend. 77−8090
Ge, electrodeposition from fused salts 80−2979
Ge powder, diamag., strong mag. particle form., mag. props., EPR *(Russian)* 80−54863
Ge powder/Au electrode contact pot. difference, grain size depend. 80−44723
GeO_2 glass, nonisothermal devitrification kinetics 80−92465
$GeSe_2$, glassy, powdered and bulk, fatigue of photolum. 80−80855
$GeSe_2$ powdered crystalline, photoluminescence intensity under continuous excitation 80−71480
HFO_2, powder, preparation technique for highly sinterable powder 78−39714
In powders, uncoated and Cu-coated, fluctuation diamag. susceptibility above T_c 79−78309
InAs:Mn, quadrupole interactions in NMR spectra 79−51880
In_2O_3-SnO_2, X-ray and optical meas. of solubilities 79−55894
InP:Te, quadrupole interactions in NMR spectra 79−51880
n-InSb, microwave propag., 90-300K, magnetoplasma and helicon wave excitations 78−72183
InSb:Mn, quadrupole interactions in NMR spectra 79−51880
KBr, m-crocryst. powders coloured in electrodeless discharge, reflectance spectra, thermolum. 78−15238
KBr:KI, microcrystalline powder, isothermal decay of colour centres 79−42995
KCl, m-crocryst. powders coloured in electrodeless discharge, reflectance spectra, thermolum. 78−15238
KCl:TlCl, lattice defects, X-ray line profile obs. 80−24455
KCl(Br)(I) with alkali and halogen impurities, colour centre deformation induced nonradiative decay 80−7387
KH_2PO_4 powder, dynamic polarisation echoes 79−4773
$K_2M(MoO_4)_3$, M=Zr, Hf, synthesis and struct. 77−36386
$KNbO_3$ powder synthesis, unit cell determ. 78−11168
K_2O-PbO-SiO_2 glass, ion exchange during leaching in HNO_3 79−100358
K_2SO_4 powder, IR photothermal radiometry absorption spectra, 295-942K 80−26088
LaB_6, US comminution of refractory compound powders 78−23656
Li-Al-FeS, high temp. battery, ceramic powder, as electrode separators 79−61966
Li-Na ferrite powders, props. rel. to Fe_2O_3 chem., thermal, mech. historical 79−11539
$LiAlO_2$, fuel cell electrolyte matrix, prep. and struct. characts. 78−80488
LiF compact, particle size rel. to pore characts. 78−60631
LiF, energy distrib. of TSEE 77−12504
^{6}LiF, nonluminous, and $CaSO_4$:Tm powders mixture thermoluminesc. response to thermal neutrons 77−73588
$LiNbO_3$, powder, polarisation echo, repetitive read out effect 79−82913
$LiNbO_3$ powder, RF field depend. of memory echoes 79−8095
$MgAl_2O_4$, active spinel, prep. and crystallite growth mech. 78−27465
$MgAl_2O_4$, powder effect of precursory sulphate solution anion on sintering 78−56605
$MgCO_3$ powder, high speed method of porosity determ. 77−90543
$MgFe_2O_4$ ferrite form. mechanism in mixture of metallic oxide powders 77−63609
$MgFe_2O_4+ZnO$, powders, cation mutual diffusion coeffs. calc. 77−15635
α-$Mg(IO_3)_2$, cryst. struct. using X-ray powder method *(Chinese)* 79−51059
MgO, decomp. of chemisorbed ethanol, propanol and acetic acid 78−92502
MgO powder, surface area determ. by adsorpt. of stearic acid and pyridine 80−107636
MgO, powder activation during grinding 77−90300
MgO, technical powder purity, of technical purity powders 77−63586
MgO, tensile and compressive strengths of fine powder bed *(Japanese)* 80−25780
MgO-NiO, solid soln. formation, initial stage obs. 77−81243
MgO_2 powder exam. of packing behaviour *(Japanese)* 79−20016
(MgO-Fe_2O_3-Cr_2O_3-TiO_2):Na_2O, powder, prep., heat treatment, Na_2O impurity effect on props. 77−16528
MnO_2, battery grade, highly hydrated, electrical characts. obs. 79−100501
β-MnO_2, Hall carrier mobility mixing rule *(German)* 78−52008
MnO_2 porous powders, Al_2O_3 and SiO_2 coated, changes in surface free energy for N adsorption 80−84363
Mn_2SiO_3, effect of vibration during sintering, on electrical resistivity 80−16258
Mo powder, influence of powder reduction processes on props. 80−89175
Mo, powder specimens, fatigue and threshold behaviour under high cycle fatigue 80−40487
Mo, properties for plasma-sprayed coatings 78−48548
Mo-W alloy, fatigue and threshold behaviour under high cycle fatigue 80−40487
$(NH_4)_2BeF_4$, effect of surface layer on spontaneous polarisation 79−38445
$(NH_4)_2BeF_4$, powder, IR spectra, assignments, mol. libration, in paraelec. and ferroelec. phases 78−88299
NH_4HSO_4, ferroelectric powder dielectric behaviour particle size depend. 80−55046

powders continued
$NH_4[TcO_4]$, powder, Raman spectrum 80−39016
$Na_6Al_6(Si_{0.99}Ge_{0.01})_6O_{24}.2NaBr$, Ge-doped sodalite powders, UV absorpt. band 80−71452
NaBr powder coloured in electrodeless discharge, reflectance spectra, thermoluminescence props. 78−6796
NaCl, m-crocryst. powders coloured in electrodeless discharge, reflectance spectra, thermolum. 78−15238
NaCl, microcryst. powder, isothermal stability of colour centres, thermolum. glow curve 79−15535
NaF powder, porous, of skeleton struct., grain size effect on strength *(Russian)* 77−24991
$NaNO_2$, compressed powder, dielec. props., surface layer effects 78−76413
$NaNO_2$ powder, surface layer effects on dielec. props. 77−1631
Na_2O-B_2O_3-SiO_2 glass-Ni compact, indented, strength and fracture toughness 80−93636
Na_2O-Ca glass powders, mixed with CO_3 compounds, cellular-struct. glass fabrication 80−108382
$NaReO_4$, EPR spectra of paramag. centres and free radicals 80−108072
Nb_3Al core wires and pressed powder compacts, supercond. transition 80−34541
NbC micropowder surface finishing of metals, surface struct. 80−11842
NbC, refractory micropowder, geometric parameters of grains 77−16529
NbC, ultrafine powders and sintered compacts, prep. and supercond. props. 77−40015
NbC_X powders, nonstoichiometric, sintering kinetics 79−100099
Nb_2C powders, plastic deform. characts. on vibratory milling 78−11183
NbN, ultrafine powders and sintered compacts, prep. and supercond. props. 77−40015
δ-$NbN_{0.9}$ powder, oxidation obeying pressure independent sigmoidal kinetics *(French)* 79−66184
$NbSbS_3$, synthesis and single cryst. growth and struct. 77−52234
Ni alloy powder, crystallised by supercooling methods, struct. props. *(Russian)* 80−54483
Ni, positron annihilation, interaction with defects in grain and pores *(Russian)* 77−16520
Ni powder, light scatt., close particle packing 78−1161
Ni powder, neutron diffr. study of Debye-Waller factor using reverse Fourier time-of-flight method 80−49050
Ni, powders, prep. of spherical starting particles, for suspension electrolysis 78−60689
Ni powders, stereological appl. in study of compacting process, elec. and mech. props. *(French)* 80−40286
Ni superalloy powders, removal of interstitial contaminants 78−84735
Ni-Al thermally reactive powder, particle heating dynamics during plasma deposition 80−16179
Ni-Fe_2O_3 powders, obtained in presence of fused salts prep. and characts. 80−84869
Ni-W sintered powder pressings, intermetallic phases *(Russian)* 80−55349
Ni-Zn-Co ferrites, synthesis from solid solns. of schoenite-type salts 80−93511
NiCr-MoAl-ThO_2 (13,3 wt.%), powder, mech. alloying 78−84744
NiF_2, powder, preferred orientation, X-ray intensity corrections 80−1880
$NiFe_2O_4$ ferrite form. mechanism in mixture of metallic oxide powders 77−63609
$NiFe_2O_4$+ZnO, powders, cation mutual diffusion coeffs. calc. 77−15635
NiO, bulklike powder, sp. ht., 14-280K 79−69260
NiO powder, IR active modes in large clusters of spheres 79−42964
NiO-Al_2O_3 powders, coprecipitated particle-size distrib. meas. 78−39726
$NiSO_4$:Li (10 at.%), powder, semiconducting, exam. of freeze drying rate in cryochemical prep. method 78−52706
$^{237}NpO_2$ powder, oxalate based, prep. and charact. 78−11166
PLZT powders, chemical prep. and hot pressing 78−44059
PLZT, pure and doped solid soln. powders, synthetic process prep. 79−78920
Pb, powders, prep. of spherical starting particles, for suspension electrolysis 78−60689
Pb, prod., interaction between N_2 jet and liq. Pb stream 79−43170
Pb-Bi alloy, fine powder electrodeposition and X-ray struct. obs. 78−11163
PbO powder layers, adsorbed rhodamine B dye, charge storage and photocond. 78−64056
PbO, stoichiometric deviations on heating in vacuum 77−25035
PbO_2 and pyrolusite compressed powder mixtures, mixing rules concerning Hall effect and Hall mobility *(German)* 78−84234
PbO_2, compressed powder, electric conductivity obs. 77−32013
PbO_2 compressed powder magnetoresistance and apparent carrier mobility 80−35669
β-PbO_2, Hall carrier mobility mixing rule *(German)* 78−52008
PbO_2 pressed powder, Hall voltage and change of cond. in transverse mag. fields 79−4567
$Pb_{1-x}Sn_xTe$, polycryst. powder, low temp. prep. in PbI_2 flux 79−61524
Pd, confined geometry, p-wave supercond. or itinerant ferromag. 80−11129
$PrNi_5$, in contact with liq. ^3He, thermal relaxation and heat capacity, mag. susceptibility 79−44909
Pt electrode, aggregation in disperse system 79−11830
PuN, fabrication and high thermodynamic and transport props. 77−28774
RbH_2PO_4 powder, phase transition in paraelectric (upper) phase by measuring damping const. and amplitude of phonon echoes 79−19855
$RbHSO_4$, compressed powder, dielectric const. and particle size, 77-335K 78−76371
Rh_2ReO_6, preparation, X-ray powder diffractograms 78−76615
Ru, oxidation resistance in Ar and air 77−25201
RuP_2, oxidation resistance in Ar and air 77−25201
Sb, prod. by β-Sb_2O_3 reduction,, atomic H effect 80−2978
p-$Sb_{1.48}Bi_{0.52}Te_3$, extrusion deformed, powder dispersion degree influence on thermal and elec. props. *(Russian)* 80−39366
$^{121}Sb_2O_3$ powder, transverse chemical shift and quadrupole interaction strength 77−28479
Se powder compacts, sintered, electrical cond. 80−70693
Si, Ar-sintering, microstruct. changes 77−90306
Si, heap, thermal cond., effect of temp., press., and atmospheric composition, sintering appls. 78−80487
Si, microwave propagation, Rayleigh limit 79−78126
Si, nitridation, effect of Fe_2O_3 addition *(Japanese)* 77−60123
Si, nitriding, effects of Fe and $FeSi_2$ 79−33985

powders continued
Si, powder, nitridation to Si_3N_4, factors affecting α- and β-phase formation 78−52738
Si, powder, reaction with HF and HF+H_2SO_4 mixture 79−11821
Si powder, X-ray K_α doublet diffr. peak position rel. to lattice const. precision 77−68891
Si, powder compact, nitriding, growth of α and β phases 78−95717
Si, powdered, microwave propag. 78−56175
Si powders, laser synthesis using SiH_4 79−74119
Si-SiO_2, nitridation, formation and growth rate of Si_2ON_2 *(Japanese)* 79−91574
α-SiC monocrystalline grains, mech. props. and grain separation *(Polish)* 80−40554
β-SiC, powder, synthesis by chemical vapour phase reaction from methylsilane, exam. of props. *(German)* 79−4938
SiC, power, electroluminesc. excitation by SAW, nonlinear effects 80−16104
α-SiC, sintered, influence of B, C additives on microstructure, SEM exam. 79−8262
SiC, sintered with three dimensional crosslinked polycarbosilane 78−56601
β-SiC, submicron powder, prep. by siliconization of C black, props. *(Japanese)* 79−66192
SiC, US comminution of refractory compound powders 78−23656
SiN powder formation, in high-temp. N flow *(Russian)* 80−100818
Si_3N_4, hot pressed, effect of powder composition and sintering temp., on phase transformation kinetics, microstructure and mech. strength *(German)* 79−4939
Si_3N_4 powder, high press. hot pressing 79−38772
Si_3N_4 powders, laser synthesis using NH_3-SiH_4 gas mixtures 79−74119
Si_3N_4 reaction bonded, iron impurity influences 79−56947
Si_3N_4 with Y_2O_3 and Al_2O_3 additions, hot pressed, exam. of mech. props., grain boundary crystallization 79−20009
Si_3N_4, Zr-based hot pressing aids effect on oxidation resist. 77−8971
Si_3N_4-ZrO_2, sintered and hot pressed, exam. of mech. props. 78−48509
α,β-Si_3N_4+C, powders, high temp. reactions *(Japanese)* 77−48685
SiO_2 fused powder, difference between white and black silica, devitrification rates 80−28918
SiO_2 powder, positron annihilation quanta ang. distrib. 77−28642
SiO_2, support for MnO_2 catalyst, N adsorption obs. of dispersion modes 80−81363
SiO_2, tensile and compressive strengths of fine powder bed *(Japanese)* 80−25780
SiO_2:Al_2O_3, ultrafine and ultrapure powder prep., SEM study 79−70025
β-SiO_2-MgO reaction, diffusion controlled 78−6882
SiO_x, powder and vac. deposited, amorphous struct., X-ray diffr. meas. 80−1931
Si_3ON_2 needle crystal growth by nitriding Si-SiO_2 system in powder compacts *(Japanese)* 78−68609
$SmFe_2$, mag. and hysteresis props. *(Russian)* 79−42800
$Sm_{0.6}R_{0.4-x}M_xCo_5$ (R=Gd, Dy, M=Pr, Nd), temp. coeff. of magnetisation 80−34688
Sn, fine, electrodeposition from chloride-fluoride electrolytes 80−11598
Sn, incorporated into lacquers, applied to tinplate containers 78−80671
Sn, positron annihilation in fine particles, surface trapped states 80−84800
Sn, prod., interaction between N_2 jet and liq. Sn stream 79−43170
Sn-Bi fine alloy powder, electrodeposition, electrolyte comp. effect 80−7519
SnO_2, finely dispersed, Lamb-Mossbauer factor 80−39930
SnO_2 powders, specific area, granulation and sintering *(Polish)* 79−52146
$SrBaNaNb_5O_{12}$, X-ray powder diffraction data determ. *(Chinese)* 80−70170
$Sr_2(Co_{1-x}M_x)_{17}$, M=Mn, Ti, Zr, powders, influence of substitutes on mag. props. 80−100601
$SrFe_{12}O_{19}$, mag. props., effect of Sr dissolution by milling in water 77−25000
$SrFe_{12}O_{19}$ micropowder, high coercivity, obtained by extended wet milling, prep. and mag. props. 77−8776
$SrFe_{12}O_{19}$, prep. by fluidized bed technique, ceramic and magnetic props. 79−43445
$Sr_{2.05}Na_{0.90}Nb_5O_{15}$, X-ray powder diffraction data determ. *(Chinese)* 80−70170
SrO.HfO_2(ZrO_2), US comminution of refractory compound powders 78−23656
SrO.$6Fe_2O_3$, ultrafine, microstruct. development during sintering, mag. props. 79−70022
TZM powder alloys, fatigue and threshold behaviour under high cycle fatigue 80−40487
Ta powder, extraction of N_2 by vacuum hot extraction method, effect of graphite *(Japanese)* 78−84729
TaC, ultrafine grain, high pressure hot pressing 79−70024
TaC, ultrafine powder prep. in HF plasma 77−12562
$TbFe_2$, mag. and hysteresis props. *(Russian)* 79−42800
Ti, heap, thermal cond., effect of temp., press., and atmospheric composition, sintering appls. 78−80487
Ti powder, physical props., effect of prep. methods *(Russian)* 77−66603
Ti_2AlN, prep. and props. 77−28745
TiB form., kinetics investig., X-ray diffr. anal. using internal standard, dilution methods 77−70393
TiB_2, electrode, hot pressed, erosion resistance, struct. and porosity effects 78−3228
TiC, fine powder form. by vapour phase reaction *(Japanese)* 79−70030
TiC, micropowder, degree of charging of polished Ti and Fe surfaces 78−60880
TiC micropowder surface finishing of metals, surface struct. 80−11842
TiC powder, plastic strain of particles under vibratory milling 77−90423
TiC, pseudofused powder, abrasive props. 77−77589
TiC, refractory micropowder, geometric parameters of grains 77−16529
TiC, ultrafine powder prep. by plasma jet *(Japanese)* 77−52273
TiC-Cr_3C_2(Cr_3C_2-WC), powder mixture, steel bonded, exam. of sintering behaviour 78−52712
TiC-steel alloy, struct. form. during sintering, strength, rel. to heat treatments 77−59717
TiC-VC(NbC)(TaC), prod. and props. 77−28772
$TiC_{0.93}$-$TiN_{0.818}$, structural parameters, and X-ray and pycnometric densities in homogeneity range 77−90311
$TiC_{1-x}N_x$ formation in high temp. N flow, ultra disperse powder, thermodynamic anal. *(Russian)* 80−55325

powders continued
TiC_xN_y, powder preparation, physical, chemical props. *(Russian)* 80−76212
TiN, powder defect struct., thermal and elec. props. 77−59286
TiN, ultra-fine powder prep. by reaction in N_2 plasma jet *(Japanese)* 78−72757
TiN-Al_2O_3, exam. of sintering and densification kinetics, and physical props. 79−95986
TiN-VN refractory powder composite, resistors, produced in low temp. 78−11182
TiO, powder solubility of H_2 77−11698
TiO_2 powder, radiation induced defects 77−62562
TiO_2, thickness meas. of SiO_2 and Al_2O_3 coatings, XPS and ion sputtering 79−88913
TiO_2-SiO_2, anatase-rutile transition, mechanism investigation *(Japanese)* 78−95746
$TiSi_2$, crystal atomic struct., X-ray diffr. exam., lattice parameters and integrated intensities 78−75647
TlCl powder, Debye-Waller parameter by neutron diffr. 80−29140
U, hydriding kinetics, 13.3 and 26.6 kPa, 50-250°C 80−16725
$UO_{2\ and\ 2.11}$, temperature factor determ. by powder elastic neutron diffraction 78−10152
UO_2 pellets, sinterability, particle size effect 80−104098
UO_2 powder, precompaction effect on compressibility 78−41846
UO_2 powder, sintering charact. 78−35341
UO_2, powder, sintering effect of compaction 80−20874
UO_2 powder, temp. depend. of atomic thermal displacements, Rietveld profile-refinement procedure 80−49190
UO_2 powder compaction, friction between particles and die walls 80−71620
UO_2 powder prep., effect of ammonium uranate props. 78−66363
UO_2 powders, cond. between sintering and agglomeration phenomena 79−9830
UO_2 powders, sintering characterisation 79−43189
UO_2-PuO_2 powder compacts, homogenization kinetics study by X-ray diffr. technique 79−37883
V_3Si, powdered, Debye-Waller factors and lattice consts., 25-1000K, X-ray diffr. obs. *(German)* 79−33060
W, powder, gas adsorption and desorption *(Russian)* 80−75429
W powder, hydrostatic pressing 78−11161
W, powder preparation by WO_3 reduction in H plasma jet *(Russian)* 80−76211
W:Ni compacts, optimum conc. of Ni for activated sintering, optical microscopy obs. 79−38758
WC, crystallite size distrib. of powder, SEM method *(German)* 78−47218
WC, fine powder prod. from WO_3+C+Co_3O_4 *(Japanese)* 78−92226
WC, hexagonal, meas. of mean square shift of atoms in micron powders *(German)* 78−47313
WC micropowder surface finishing of metals, surface struct. 80−11842
WC, powder form. from WO_3-Co_3O_4-C powder mixture *(Japanese)* 78−92227
WC powder production from vapour phase 77−21077
WC, refractory micropowder, geometric parameters of grains 77−16529
WC-Co(TiC-Co), powder compacts, effect of additional pressing at hydrostatic pressures on props. 78−56596
WO_3 powders, hopping mechanism and Poole-Frenkel effect, elec. props. determ. 80−49734
WO_x, powders, coarseness meas. using powder surface reflectance 79−96246
Y_2O_3, hot cast ceramic, prod., used as dielectric 78−11181
Y_2O_3, translucent ceramic, prep. effect on struct. and props. 79−87601
Y_2O_3, US comminution of refractory compound powders 78−23656
Y_2O_3-Sc_2O_3 fused powders, production of ceramics of good thermal strength 77−63607
Y_3Se_4 powder, prep. and optical props. 77−28771
Zn ferrite, production by mechanochemical reactions by grinding in ball mill 79−20014
Zn-Cd liquid/Fe-Ni-Al mag. powder, effective viscosity of composites *(Russian)* 80−54424
$ZnAl_2O_4$ spinel powder prod. 77−52271
n-ZnCdS-PTA, photosensitive powder mixed with electrochromic material, photoinduced coloration and electrochem. bleaching 77−81082
$Zn_{0.2}Co(Ni)_{0.8}O$. $1.1Al_2O_3$ powders, ZnO vaporisation from 80−16675
ZnF_2 powder, preferred orientation, X-ray intensity corrections 80−1880
$ZnFe_2O_4$+NiO_2(MgO) powders, cation mutual diffusion coeffs. calc. 77−15635
ZnMn ferrites, prepared by wet chemical and ceramic methods, comparison of struct. and mag. props. *(German)* 79−24470
ZnO, ground powder, X-ray Fourier anal. *(Japanese)* 78−39727
ZnO, Hall effect, O_2 partial press. and illumination effects 79−51607
ZnO, of H_2O vapour, annealing and grinding effects 78−68656
ZnO, piezoelec. powder, dynamic polarisation echoes 78−52443
ZnO powder, adsorption of O_2, H_2, light effects *(Japanese)* 78−95230
ZnO powder, effect of dry grinding in EPR and catalytic activity *(Japanese)* 80−84640
ZnO, powder layers, conductivity, O_2 chemisorpt. and photodesorpt. effects 78−43441
ZnO powder layers, dyed, surface potential and photovoltage obs. dependence on adsorbed dye amount *(Japanese)* 79−24003
ZnO powders, direct meas. of intrinsic cond., using emulsion 79−99595
ZnO powders, electron-beam-induced desorption, phase-sensitive detection 80−54502
ZnO, segregation of Li_2O at grain boundaries 78−64513
ZnO, surface cond., effects of O_2 chemisorption and CO_2 photodesorption 77−11980
ZnO, UV luminesc. spectral distrib., comparison with single crysts., excitons role 80−55167
ZnO-ZnS powder mixtures, elec. cond. and Hall effect meas., percolation effects 79−7828
ZnO-ZnS powder mixtures, Hall effect and elec. cond. 79−51607
ZnS:Cu crystal, powder, epitaxial film, luminescence anomalous thermal 80−76077
ZnS:Cu powder exam. of dielectric constant anomaly, in terms of polarisation catastrophe phenomena 79−51897
ZnSe cold pressing 77−52258
Zr, heap, thermal cond., effect of temp., press., and atmospheric composition, sintering appls. 78−80487
ZrC powder, plastic strain of particles under vibratory milling 77−90423
ZrC powder, struct. after vibratory milling 77−28840
ZrC, US comminution of refractory compound powders 78−23656

powders continued
ZrN-Al_2O_3, effect of N on sintering 79−33991
ZrN-Al_2O_3, exam. of sintering and densification kinetics, and physical props. 79−95986
Zr_3N_4, powder, form. by vapour phase reaction of $ZrCl_4$-NH_3-H_2-N_2 system *(Japanese)* 77−73247
ZrO_2 crystalline particles, TEM and electron diffr. meas. 77−21350
ZrO_2, powder, preparation technique for highly sinterable powder 78−39714
ZrO_2 powders, vapour phase reaction production 78−68660
ZrO_2 shock wave treatment of powders *(Russian)* 77−44186
ZrO_2 stabilised with Nd_2O_3, refractories prod. and long-term high-temp. behaviour 77−59725
ZrO_2, Y_2O_3 stabilised, hydrothermal growth 78−15302
ZrO_2-SiO_2 powder mixture for optical glass polishing 80−28367
ZrO_2-Y_2O_3 powder, prep. for plasma spheroidisation, sputter drying *(Russian)* 80−55324
ZrO_2-Zr cermet composite, hot pressed, fracture toughness 78−27604
ZrO_2.SiO_2-αAl_2O_3 mixed powders, solid state reactions 80−40337

power amplifiers
accelerating resonator of ion synchrotron, tuned power amplifier 79−68063
Antares, for HEGLF fusion reactor, design 78−54958
Antares CO_2 laser power amplifier, design 80−69423
coupling cct. for four resonators and one buncher 79−68052
RF, 3 kW solid-state amplifier for pulsed NMR, 1 to 22 MHz 79−54162
RF, high power, accelerator appls., recent advances 79−68082
stochastic beam cooling expts., low-noise wide-band power amplifier system 80−58011

power apparatus
see also electric machines; power conversion; switchgear; transformers
electric apparatus and power lines, temp. rise meas. by infrared radiometer *(Russian)* 78−89537
industrial macrosonics apparatus, appl. to US soldering 77−58499
low inductance circuit apparatus, raised frequency current inflammability *(Russian)* 79−86626
superconductivity, research study *(Japanese)* 78−19192

power cables
see also gas pressure cables; power overhead lines; superconducting cables; underground cables
dry insulation, materials used and characteristics *(Spanish)* 80−81024
fusion reactor, TFTR, power line, variable freq. AC harmonic content 80−99293
harmonic radiation effects on weekend increase in geomagnetic activity 79−79738
HV, high molecular weight polyethylene insulation characterisation using size exclusion chromatography 80−66897
HV, XLPE samples high-pressure liquid chromatography and differential scanning calorimetry 79−100466
HV cable, PE-insulated, electron beam crosslinking process development 80−66846
lapped paper and plastic insulated, butt gap distribution and spliced joints study using X-ray method 77−77726
nuclear reactor power and control cable tests to IEEE standards 80−57884
ocean thermal energy conversion, OTEC system development, Conf. Houston, TX, USA (Nov. 1978) 79−83611
pipe-type, low-cycle fatigue tests 80−7731
PWR crosslinked polyethylene insulated low noise triaxial cable *(Japanese)* 78−670
three-phase pipe type, laminar flow friction factor prediction 77−75880

power control
see also load regulation
Calvert Cliffs power manoeuvring control strategy 79−9863
CW laser radiation power stabilisation by external control element 80−91832
electro-optic modulator, servo controlled, for CW laser power stabilisation and control 80−19060
electron microscope stabilisers, Hg-Zn battery as reference voltage source 79−9262
injection laser automatic level control by optoelectronic feedback *(German)* 78−33883
magnetically stored energy, fast switching into external load, for pellet fusion 78−13339
microwave enzyme inactivation system, electronic control to reduce dose variability 78−40285
multichannel analyser, versatile programmable power supply 77−42218
neutral beam filament supply, 15 V 10^3 A, programmable, regulated, for fusion reactor 78−70630
neutral beam power supply, series switch/regulator system, 40 kV, 80 A, 10 ms, for fusion reactor 78−66366
nuclear reactor, IRT-M, automatic control using in-core detector system 77−50264
PWR power plant, power control problems *(Russian)* 79−31158
rechargeable fuel cell battery output power stabilisation theory 80−35674
telemetry, totally implantable, integrated power controllers and RF data transmitters 80−67295
Tokamak superconducting coils, active energy transfer rate control using inductor-convertor bridges 78−13338
Veritron AC power controllers, thermal equipment, automated manufacturing processes *(German)* 79−80598
Ar laser power supply for discharge current and output power control 77−38912
Cs-Ba triode arc switch, high-current, low-voltage, pulsed control 78−71551
GaAlAs laser power control loop, optical path electronic simulator *(German)* 78−82987
InGaAsP InP DH lasers, optical power and wavelength stabilisation 80−38036

power conversion
see also direct energy conversion
energy fluctuations power conversion, in diode circuit, thermodynamics 80−17911
fusion reactor, JET, high voltage network to load AC/DC pulse power conversion 78−58497
high power restrictions imposed by physical laws 77−5616
plasma valve design with liq. metal cathodes, high-power conversion/switching appls. 78−9865

power conversion continued
solar cell arrays, DC to AC power conversion and utility interfacing, technqiues, requirements and components used 80−45703
solar power satellite, appl. of solid state microwave technology 80−40870
solar power satellite, microwave power transmission technology 80−40868
superconducting magnet for magnetic flux compression, compression generator, PULSAR, design optimisation 80−68957
voltage, AC measuring equipment calibration technique 77−53942
wind, diffuser augmented wind turbine concept 79−83556
wind power, vortex augmentor concept 79−83554
CO_2 fundamental condensation cycles in steam and nucl. power plants, performance characts. 80−63368

power convertors
600 MW pulsed energy convertors for toroidal field coil, design philosophy 78−58496
amorphous magnetic alloys, review, engineering magnetic props. and potential applications 80−71078
heart assist appl., using fluid controls logic 79−53286
HVDC, liquid trifluorotrichloroethane as insulating material and coolant, dielectric strength *(German)* 77−76218
semiconductor heterostructures, elec. and optical phenomena, discrete devices, review 78−72250
superconducting coil energy storage power supply 79−34442
switched-mode mains supplies for charging NiCd accumulators *(German)* 80−66961
variable speed wind power generator, control strategy for 3-phase output *(French)* 80−76591
GaAs antenna mounted FET for DC-RF conversion in solar power satellite 80−40870

power distribution networks *see distribution networks*

power factor
see also reactive power
Al-Al_2O_3-metal capacitor, capacitance and power factor rel. to voltage and temp. changes 80−54802
$La_4(TiO_4)_3$, electrical props., effect of initially used La_2O_3 *(Polish)* 77−59508
Na MHD generators, optimisation for maximum power factor *(Rumanian)* 80−64793

power factor correction
capacitor dielectric fluid test and anal., quality assurance 78−80272

power factor measurement
automatic single-channel power factor meters 77−79116
non-sinusoidal voltage and current, operation *(Polish)* 79−75555

power factor meters *see power factor measurement*

power factor Q *see Q-factor*

power generation, electric *see electric power generation*

power generators, electric *see electric generators*

power inductors
fusion reactor, use of homopolar generator for inductive energy storage 78−54948
fusion reactor inductive storage technology, new applications, review 78−55019
high power pulse production appl. *(German)* 78−50293

power lines *see power cables*

power measurement
see also wattmeters
AC, 60 Hz, current comparator bridge 77−18040
AC, at 120 V, 5 A 60 Hz, international comparison 78−93735
AC, differential thermal wattmeter, for AC/DC transfer of power 77−18041
AC, precision direct meas. facility 78−49863
AC, thermal meas., comparison with electrodynamic method 77−18034
AC power, voltage, current, frequency, digital panel meters, self-powering, COUNTERBALANCE A/D conversion technique 77−37909
AC power in coaxial channels at HF, comparisons of standards among COMECON countries 79−93166
antenna power density, conversion equations for meas. 77−26332
apparent, using analogue simulation *(Czech)* 77−5859
artificial satellites, effective isotropic radiated power, error anal. using calibrated radio star 78−93070
broadband mm-wave calorimeter, design and calibration 79−26084
calorimeters, high temperature, automatic measurement of electrical energy 79−71451
cardiac defibrillator, DC delivered energy measurement, electronic, oscillographic methods 78−61281
cholesteric liquid crystal visualisation of microwave fields 78−58031
coaxial power meter, based on Hall effect in semicondcutors 78−238
CW CO_2 laser power meter, thin film bolometer, NaCl monocrystal divider, 0 to 500 W range, digital output *(Russian)* 77−37992
defibrillator energy meters, traceable calibration methods 80−30928
digital, errors sources and suppression *(Rumanian)* 80−47078
dry calorimeter for power meas. at mm wavelengths 79−26085
electricity/fuel substitution coefficients, energy units and balance sheets *(French, English)* 79−92053
electrocutaneous stimulation, energy threshold meas. and channel capacity estimation *(Japanese)* 78−53573
electrostatic wattmeter with automatic voltage feedback for torque balance 77−82569
EM near field power density meas. *(Polish)* 79−21721
EM wave ponderomotive effect, props. with diffraction 78−71014
emission power fluctuation statistical meas. system 77−79881
far IR and near MM wave power energy meter calibration 80−57373
far IR laser, optically pumped, power meter 77−54725
fast-pulsed electron beam energy meas. using bremsstrahlung absorption spectroscopy 78−49940
FIR laser, optically pumped, nearly transparent power monitors 80−5773
galvanomagnetic semiconductor voltage and current transducers, Gauss effect compensation 78−77892
hand-arm energy dissipation using vibratory tools and accel. levels 78−96116
heat receivers with moving heat carrier, freq. characts. 80−4733
high energy deposition from pulsed electron beams 78−54500
lamp, calorimetric meas. of radiant energy, student expt. 78−8191
laser, far IR optically pumped, monitoring by piezoelec. transducers 80−102729
laser beam, CW, radiated power meas. *(German)* 78−79053

power measurement continued
laser beam energy distribution reconstruction using data from grid of bolometers 80−53350
laser calorimetry development at NBS and Calorimetrics Inc. 78−22161
laser energy, by optical calorimetry, hollow graphite cone appl., absorption characts. determ. *(Slovak)* 79−40572
laser energy, pulsed, measurement system and calibration facility 79−27301
laser energy meter *(French)* 80−102790
laser energy meters for calibrations at most principal laser wavelengths 80−99741
laser energy standards inequivalence simplification 77−79876
laser high power CW output meas. from temp. rise of Al slab power meter 79−59739
laser mass production and radiated power meas. improvements 78−37064
laser power, thermoelectric meas. 78−63124
laser power and energy meters, calorimeter system for calibration 80−38024
laser power meas., radiometric and calorimetric scales' equivalence 77−7115
laser power meas., scale comparison for calorimeter and radiometer systems 79−76729
laser power meter calibration for the range 5-1000 W using electrically calibrated calorimeters and beam splitters 78−1241
laser pulse energy, optical calorimeter design *(Polish)* 78−29998
laser pulse energy, picosecond order meas. *(French)* 80−74412
laser pulse energy measurement by liquid calorimeter *(Russian)* 78−22163
laser pulse energy monitor 78−66839
laser pulse power meter 79−86202
laser radiation, pulsed, measurement of energy using multichannel instrum. 79−76731
laser radiation energy, spectral and time range meas., instruments 79−35687
laser radiation pulse, liquid absorption cell technique, digital readers *(Russian)* 78−18000
laser sensing system for elec. and mag. fields in power transmission 77−45870
light beam, high-sensitivity optical power meter with tuning fork optical chopper 79−80661
living tissue stimulation energy threshold meas. using analogue instrument 79−57745
logarithmic electrometer, for pulse-reactor expts. 78−86291
loudspeakers, monitor for meas. of acoustic power response 80−87674
LWR, power distrib. monitoring using gamma thermometers 79−45368
microtransducer using fibre optics *(French)* 77−61084
microwave, calorimetric method, using Ge vane loads 77−82562
microwave, ponderomotive power meter, frequency range 8.5 to 12 GHz, power range 0.5 to 100 W, VSWR up to 1.1 *(Russian)* 77−37939
microwave, self-balancing DC-substitution RF power meter 77−18012
microwave diathermy equipment and power indicator 77−40901
microwave freq. power meas., conf., London England, (Jan 1979) 79−26082
microwave power meter using contact between metallic probe and Ge crystal 77−37986
microwave using absorption spectrum of $^{14}NH_3$ gas 77−18013
multiplier unit for acoustic and electronic wattmeters 77−79118
optical fibre absolute power meas. thermistor sensor 78−65971
optical fibres, power distrib. measurement method without need for scanning 79−50437
optical power meters for laser photometry 78−65953
optoacoustic power monitors for laser radiation 79−41404
plane-wave microwave power density of hazard probe, precise calibration techniques 77−71341
power and energy units reproduction for optical, elec. and mech. quantities 77−71287
precision AF power meas. methods and equipment 78−77939
production unit machinery, industrial method *(Polish)* 78−93727
radiation balance for US power meas. 79−83863
random signal mean power meas. error *(Polish)* 78−89425
RC network, bolometer, RF power, energy measurement, digital output *(Russian)* 77−37940
reactive, three-phase two wattmeters, meas. errors *(Croatian)* 80−105677
reactive power meter for periodical signals in range 50 Hz to 5 kHz *(Spanish)* 80−86339
RF, linear feedback method for twin load calorimetric RF power meters 78−77938
RF, method using sampling oscilloscope and LF multiplier, up to 1 GHz 80−37055
RF power, Measurement Standards Laboratory, capability improvement 78−54332
RF power absorption in biological specimens, meas., 10-100 MHz 77−90916
SI units fundamentals *(French)* 80−95059
solar cell maximum power output determ. 79−74527
solar cells, photoelectrochem. and p-n junction, power conversion efficiency monitoring 80−50989
standards for power meas. in mm. wave region 79−26083
stress-wave emission signals anal. to determ. relative energy released by materials under stress 79−86297
table top pulsed solar simulator, design and construction, for testing solar cell arrays powering artificial satellites 80−45696
thermoelectric, sample holder for rod-shape specimen 77−57309
thermoelectric, thin film and bulk samples 77−79092
thermoelectric power, absolute scale 77−71288
thermoelectric power of solids meas., up to 10 GPa 78−89495
thermopower and thermal conductivity, simultaneous meas., method and apparatus 77−72854
three phase AC circuits using two-wattmeter method *(German)* 77−74458
three-phase two-element VAr meter inaccuracies 77−13774
transient electric discharge power and energy meas. using wideband ICs 78−87520
unit power standard for 53.57 to 78.33 GHz 80−90808
US beam power meas. using calorimetric comparator 77−39181
VHF power measurements using Hall effect *(Polish)* 80−95112
VHF resonator radiant energy meas. *(Russian)* 78−77944
watt determination by elect. and calorimetric methods, wattmeter accuracy 79−167

power measurement continued
wattmeter, static, for use in educational establishments 78−45656
wattmeter, with IC multiplier, use in model power system 77−53930
wattmeter calibration, (3+3)-phase voltage and current source of high stability 77−18038
wattmeter calibration, at zero power factor using digital sinewave generator 77−18039
waveguide wattmeters, ponderomotive and bolometric types, standard, comparison 77−71345
wheelchair locomotion, power output requirements for manual operation 80−94416
wind, energy pattern factor meas., analogue technique appl. 77−81964
CO_2 high power laser beam monitor 78−74943
CO_2 laser, using thermoelectric detector *(French)* 77−58365
n-InSb Corbino disc power meter for 3 cm wavelengths 79−71428

power overhead lines
see also overhead line conductors; power cables; power transmission
60 Hz electric field effect on plant growth and development 77−81534
60 Hz electric field effects on small birds and mammals 77−86538
audible corona noise, assessment of human response using acoustic menu 80−19149
cooling by corona wind of heated cylinder in still air, expt. 80−84023
corona discharge from water drops, expt. 80−33851
current carrying capacity, determ. 77−84126
deflection of cables under complex loading, incremental algorithm 78−9558
EHV and UHV, 60 Hz, electric field impact on animal and plant growth 77−77933
electric apparatus and power lines, temp. rise meas. by infrared radiometer *(Russian)* 78−89537
electrification of objects under DC transmission lines, charge simulation calcs. 78−78853
EM field, rel. to suicide 80−94287
ground gradient simulation for biological effect exam. 77−86731
HV, electrostatic field effects on human body *(French)* 77−21562
lightning protection, overvoltage calc., pseudo-random number generator appl. *(Polish)* 77−24234
multi-conductor, flutter boundaries calc., aerodynamic force model appl. 77−62270
radiation power of lines, spectrophotometric appl. *(Japanese)* 78−8453
radio and TV interference control of AC lines 77−75745
VLF chorus, evidence for excitation by electrical power transmission lines 77−78572
VLF noise, effect on magnetosphere and chorus 79−101028

power overhead transmission lines *see power overhead lines*

power packs *see power supplies to apparatus*

power plants
see also solar power; space vehicle power plants; wind power plants
10 MWe pilot plant, collector field design 77−23779
100 MWe commercial power plant, technical feasibility and economics 77−23778
air pollution, plume dispersion modelling for inversion breakup at power plant 78−3933
American Power Conference, Chicago, Ill., USA, April 1976 77−46201
brine solns. as energy resource, reverse electrodialysis cells 80−85271
coal-fired, electrostatic precipitation technology development, stack gas ionisation by electron beams 78−57346
coal-fired, trace element anal. of radiological effluents 80−21426
coastal, breaking wave effects on power plant intakes *(Italian)* 80−109148
combined cycle, ash agglomeration coal gasification process appl. 79−48065
condensing, with four 200 MW blocks, noise level due to electric machines assessment *(Czech)* 79−57548
cryogenic, current lead thermodynamic optimisation using indefinite Lagrange multipliers 77−87768
district heating in Stockholm, nuclear power and oil-fired plant comparison 78−37458
district heating systems, combined generation by fossil fired and nuclear power plants 78−37457
emissions detection, microscopic samples molecular analysis, using Raman microprobe 80−57391
environmental effect and protection measures *(German)* 80−26574
fatigue, power engineering problems 77−86157
fuel cell, economics 79−57424
fuel cell power plant development and commercialisation program 80−16797
fuel cell power plants for utility applications 80−66967
fusion-MHD power plant, exhaust plasma pulsed accel. 78−62644
gas system entropy waves dissipation 80−19395
high-temperature, efficiency enhancement using coolant with particle suspension *(Russian)* 79−68549
Labadie Power Plant plume, lidar obs. of particulate density distrib. and behavior 80−55956
large-scale elec. energy storage, review 80−89676
machinery, shaft breakage, US detection 77−77716
MHD, 40 MWe, pilot 79−52945
MHD, commercialisation in United States, 1978 potential 79−52944
MHD, environmental assessment of a coal-fired open-cycle MHD power plant 80−35795
MHD, regenerative heat exchangers 79−1353
MHD, working fluid, seeded combustion products of petroleum-acetylene-O_2 mixtures 78−34256
MHD baseload power plant for intermediate and peaking duty 80−35702
molten carbonate fuel cell power plant, eng. development 80−66969
noise control, procedures and equipment 77−35002
noise control design objectives 77−75739
nuclear power plant, impact and fate of released Cu on aquatic environments 78−7665
ocean thermal energy conversion (OTEC), emerging programme of significance to marine community 78−44875
ocean thermal energy conversion plant design, oceanographic data interpretation, ERDA program 78−44874
ocean thermal gradients, power plant design 78−16059
operational danger levels, mathematical model determ. *(German)* 80−13633
osmo-hydro power system, using aqueous saline solutions, technical and economic feasibility 79−52916
osmotic power plants, closed-cycle 80−67000

power plants continued
OTEC, expt., 10 to 20 MWe, ocean engineering aspects 79−83616
pipelines under creep conditions, allowable thermal stresses *(Russian)* 78−13930
public health hazards, nuclear and fossil-burning plants 77−44880
reversed field pinch reactor, choice of parameters for 600 MW net electrical output 78−58471
site zone evaluation using computer-aided methods 80−861
soil warming, simultaneous heat and mass transfer governing eqns., waste heat utilisation 78−94562
solar, flux density distribution on central tower receivers anal. 77−46786
solar, tower type, configuration, solar energy concentrator efficiency 77−19379
solar sea power plants, site limitations 77−53074
thermal, cooling system design, optimal system synthesis, tower, pond 77−14260
thermal plant siting, regional policy and ecological aspect of landscape 80−862
thermionic, design point selection, economic impact 79−48155
total energy systems, energy cascading principles *(French)* 80−76621
waste heat recovery, from ceramic tunnel kilns, using tetra-chloroethylene Rankine cycle 79−52955
wet cooling system for power plants, atm. impact of plumes and fogging 78−7761
wet/dry surface for cooling towers 79−32199
H_3PO_4 fuel cells, commercial prototype plant for dispersed electric power generation 80−66968
ZnCl hydrate battery system, design fabrication and testing of 5 MWh system at BEST Facility 80−35763

power station computer control
BWR nuclear plant nonlinear digital simulator, optimal digital control methods appl. 79−9826
BWR power plant appl. of computer based systems 77−88264
CANDU, digital computer control 77−54324
CANDU distributed computer control systems 79−76105
CANDU nuclear plant DDC, dual redundant minicomputer system max. utilisation 79−36375
CANDU power plants, automated anal. system for control of secondary coolant chemistry 80−18446
control room and desk design, alarm system, information displays 79−89462
data processing system of Dungeness 'B' power station 77−67831
direct digital control of the WWR-SM research reactor 80−696
distributed microcomputer-based control system for a large scale solar total energy system 80−30396
electronic system of power-station control with modules and distributed software based on controbloc elements *(French)* 79−76110
Hinkley Point B AGR station computer control system, performance review 79−89457
industrial management program for energy conservation 80−40849
LMFBR data multiplexing system 79−76102
MWR feedwater and recirculation flow, minicomputer-based digital control 80−23027
neutron instrumentation for protection and control of nuclear reactors *(French)* 80−32407
nuclear, computer control systems for data acquisition and process control 79−22426
nuclear and fossil-fired stations, control room and desk design, alarm system, information displays 79−89464
nuclear control guidelines 80−106119
nuclear power plant control and instrumentation. [conf. Cannes, France (Apr. 1978)] 79−76096
nuclear power plant diagnostic instrumentation experience 79−3218
nuclear power plant operational diagnostics and control computerisation 79−3233
nuclear power station, reactor power control, 305 computer system at Stade 77−353
nuclear power stations, computerised monitoring and control system at Trawsfynydd 80−86965
nuclear reactor, point-model, heuristic approach to reinforcement learning control 78−46144
nuclear reactor control and safety, development of a reliable single-channel direct-digital reactor-control system 79−89458
nuclear reactor protection systems, reliability anal. using Markov methods 80−91229
nuclear reactors, online, computer applications, information processing, control, monitoring, data acquisition and evaluation 80−47595
on-power measurements of reactor parameters using dynamic meas. methods, computer system description 79−89467
PWR nuclear, comparison cost effectiveness of remote, centralised microprocessor based multiplexing control system 78−89971
reactor protection computer systems, statistical verification of reliability 80−32417
reactor protection system, development of integrated numerical protection system *(French)* 79−76097
reactor protection systems, treatment, analysis and presentation of information on component faults and [nuclear power] plant disturbances 79−76098
reactor trip system, design of internal architecture for Westinghouse microprocessor-based [nuclear reactor] integrated protection system 79−76100
remote multiplexing control and safety systems evaluation 79−76109
solar total energy system, Fort Hood, control system 80−30397
Super-Phenix FBR control system evaluation *(French)* 79−76106
He cooled reactor turbine control experiences Fort St. Vrain HTGR *(German)* 80−57927

power station control
see also power station computer control
Biblis core protection and German safety regulations 77−88260
BWR, automatic protection system *(German)* 78−4989
BWR, design, construction and organisation of Caorso nuclear power station, Italy *(Italian)* 79−26471
BWR power plant, direct cycle, low sensitivity optimal controller study 78−8947
decentralized instrumentation and control system with bus transmission in nuclear power plants 79−97847
fusion power plant, vacuum outer containment, safety, T control and monitoring 78−74498
HTR 77−14262
LMFBR, control rel. to operational safety aspects 77−14251

power station control continued
LWR plant control, linear quadratic theory appls. 77−88265
MHD/steam combined-cycle plant, combustion air temperature variations reduction, computer simulation appl. 79−52943
neutron flux optimum control during nuclear station load following 79−9761
noise emission controls for USA 77−23811
nuclear, B&W integrated control system improvement 78−8946
nuclear, modal control 77−14252
nuclear, operating and startup experience with control, instrumentation and electrical systems 77−65283
nuclear plant, multivariable control system theory appl. 77−67832
nuclear plant control problems survey 77−88258
nuclear plant system future trends justification 77−88263
nuclear power plant licensing procedures in the UK 80−27708
nuclear power station advanced control concept, computer-based system design 77−67909
nuclear power station model validation and automatic control 77−88261
nuclear reactor monitoring system for energy liberation fields of Beloyarsk power station reactors 77−23232
power station, Three Mile Island, operating experience with control, instrumentation and electrical system 77−65285
PWR, transient state studies 77−14263
PWR power plant modelling and simulation 79−9828
PWR power plant self-tuning control and simulation 79−9827
solar central receiver plant, dynamic simulation of thermal-hydraulic characts. of Na-cooled plant 80−30400
wind turbine generator, control and stabilisation of DOE/NASA Mod-1 80−30370

power station load
nuclear power stations, load factors and availability achieved with light water and heavy water reactors *(Slovenian)* 80−68843

power stations
see also energy resources; gas turbine power stations; geothermal power stations; hydroelectric power stations; nuclear power stations; power plants; solar power stations; steam power stations; tidal power stations
290 MW compressed air storage power station, construction and commissioning 80−16842
500 MW, noise level meas. methods *(German)* 78−55517
atmospheric heat releases, effects 80−40942
atmospheric radioactivity, radiological impact from model coal-fired power plants and from nuclear systems 80−3557
coal, mitigating community impacts of energy development 79−61938
coal conversion technologies, health and environmental effects 80−81493
coal fired power stations, review of conventional and advanced systems 80−35625
coal-fired, fly-ash and slag natural radioactivity meas. 78−17442
coal-fired MHD flow facility, development and operation 80−66982
dust-laden gas flow meas. cylindrical hot-wire anemometer appl. 77−27632
Earth satellite power stations (Powersats), economic assessment 77−91404
environment protection when siting power station, temp. and humidity meas. methods *(French)* 79−12318
environmental effects, nuclear and thermal power stations comparison 77−71706
environmental noise, coal-fired power stations 80−76683
estuary and river sited power plants, water discharge and chlorination, simulation 78−96250
estuary thermal impact of multiple power plant operations 78−96232
fibre-optic system installation 79−37028
flue gas analysis, in 200 MW plant, trial operation with Westinghouse O_2 probe *(Czech)* 80−89562
fly-ash radioactivity meas., environmental protection *(Polish)* 77−14318
fossil fuels for use in MHD power stations 80−72074
fossil plant maintainability, human factors engineering review of design, c.f. nuclear plant 80−22913
fossil-fired, control room and desk design, alarm system, information displays 79−89464
fossil-fuelled, air pollution detection and control, opacity monitoring 79−100557
fuel cell, 4.8 MW DC 80−89608
game for physics teaching appl. 79−62949
heat rejection, regional climatic effects 77−25768
heat treatment, post weld, during construction and maintenance 80−93574
industrial utilisation of energy, book 80−61222
ionisation in power station plumes, effect on natural lightning 78−88909
MHD power systems, coal-fired, retrofitting to existing non-coal power stations 80−66983
molten carbonate fuel cell based, coal fired power plants for electric power generation 80−30471
noise control costs 78−33958
ocean thermal energy conversion, open cycle approach, plant design 80−30506
ocean thermal energy conversion, technology development program 80−30504
oil-fired, SO_x critical conc. calc. *(Dutch)* 78−61547
pipelines under creep conditions, allowable thermal stresses *(Russian)* 78−13930
plants steam venting noise characts. 79−7257
pollutant trapping by local circulation, obs. 77−37397
power plant dynamics and control, conf. Hyderabad, India (Feb. 1979) 80−91215
radiation hazards from emissions of thermal and nuclear power stations, comparative study 79−34460
satellite power station, ionospheric heating by radio waves 78−77403
satellite solar power stations, preliminary cost benefit anal. 77−87231
site zone evaluation using computer-aided methods 80−861
stack emission monitoring systems, for air pollution detection and control 79−100558
steam-gas combined, based on natural gas resources from North Sea, economics and possibilities *(Norwegian)* 80−101073
thermal, thermomagnetic gas analysers improvement *(Russian)* 80−3445
thermal, water effluents effects on rivers and water basins, power engineering and water conservation viewpoints *(Czech)* 79−57505
thermal energy plants, NO_x emission, review of preventive measures *(Croatian)* 78−3935
thermal energy storage in industry and power stations 80−67002

power stations continued
thermal plant siting, regional policy and ecological aspect of landscape 80−862
Tokamak power plants, impact of technology and maintainability on economic aspects 80−27807
waste heat use for electrolysis of water as basis of future H_2 based economy *(German)* 79−79410
waste heat utilisation for energy conservation 80−35655
waste heat utilisation for fish farming and agriculture *(German)* 80−101080
wood-waste fired power plants, economic feasibility anal. 80−66923
worldwide energy prospects, synthesis of studies published in 1976 and 1977 *(French)* 79−29443
NO_2 and SO_2 pollution near industrial area, meas. and remote sensing equipment *(French)* 79−74928
SO_2 pollution electricity generation, policy options for control 80−51022

power supplies to apparatus
see also cells (electric); constant current sources; power plants; power supply circuits; prosthetic power supplies
5V reference supply, linear thermometer appl. *(French)* 79−197
28 kV for IR visual micropyrometer 28 kV power source features *(Russian)* 78−12701
34MW 120MJ pulsed DC supply for Divertor & Injection Tokamak Expt. 79−31214
200 kV Blumlein transmission line for Tokamak plasma heating, calc. and obs. 79−55521
220 W series-regulated supply, programmable, 0-50 V range 77−82543
475 MVA pulsed motor generators for TFTR 78−58498
500 V homopolar generator for Tokamak device 78−5957
1024-channel particle spectrometer power supply 79−68169
2000 V and 2×200 V, current-carrying, for ion source *(Czech)* 77−5963
accelerating resonator of ion synchrotron, tuned power amplifier 79−68063
accelerator magnet systems, piggy back power supplies advantages 77−83365
analytical graphite furnace power supply control to allow interruption of analytical cycle 77−21432
arc lamps, for UV spectrometry, highly regulated power source 79−40629
arc quenching system for transient and statistical flashover, fusion reactor systems 78−75455
artificial heart blood heat exchangers with radioisotopic power supplies 80−85532
atomic absorption spectrophotometry, W filaments as electrothermal atomisers 78−44433
batteries, primary, alkaline, button-type, for electronic appliances *(Japanese)* 79−83582
batteries development, Li-MnO_2, Sanyo with high energy densities 80−85272
betatron electromagnet pulsed power supply 78−82546
biomedical implantable power sources, radioisotope thermoelectric generators appl., high reliability contacts using local heat pulses 79−52952
bolometer amplifier, IR spectrometer for Meteor artificial satellites *(German)* 78−28484
CAMAC diagnostic module for on-line monitoring of CAMAC integrity 80−5459
camera battery, alkaline, effect of discharge resistance obs. *(Polish)* 79−57420
cardiac stimulator, isotopic generators appl. *(Spanish)* 78−15922
cardiac stimulator power supply battery selection 77−48931
CERN's 28 GeV proton synchrotron, RF power supply system, control equipment 77−79488
CERN SPS, 148 MW pulsed power supply, mains voltage stabilization and filtering 79−76207
CESR magnet power supply system 79−76210
Chalk River superconducting heavy-ion cyclotron RF struct. 77−88297
Cherenkov counter spectrometric channels, optimum supply conditions of 58AVP photomultipliers 78−9031
clearing electrode control system for CERN ISR 77−38514
communications repeater stations, photovoltaic solar cells appl. 79−29450
cryogenic fuelled power packs for operating pneumatic tools 79−58715
CTR neutral beam source, SCR series switch and impulse crowbar 78−66395
current-supply stabiliser, adjustable, for magnetic lens β spectrometers 78−74528
cyclotron, motor generator current control and stabilisation, semicond. device appl. 78−21790
DC checking calibrators, output voltage filtering methods 77−53940
D.C.I. storage rings, double frequency RF system 77−88299
diagnostic X-ray equipment power supply design 77−21608
discharge lamp, cold-cathode, current-regulated power supply design 77−57409
discharge lamps, metal halide, for film lighting, luminance fluctuations assessment 80−4796
DORIS current supplies, equipment design and performance *(German)* 78−21797
dynamic power supplies for TEA lasers 79−7136
EHV synchronous generation for US pulse-echo systems 77−78011
electrochemical measuring apparatus integrated triangular voltage generator appl. *(German)* 77−52724
electrolysis, power rectifier circuit description *(Dutch)* 77−63925
electromagnet power supplies for intersecting storage rings, types 77−42197
electron accelerator, high-current, high pulse, inductive energy storage 78−46189
electron and ion beam generation at high power, review 80−13988
electron e/m ratio measurement apparatus, power supply 77−60873
electron microscope, EM-300, power supply system for column 79−12888
electron microscope, power supply instability, theory and expt. estimate 79−6230
electron microscope stabilisers, Hg-Zn battery as reference voltage source 79−9262
electron synchrotron storage ring RF power supply *(German)* 78−17453
electron-optical corrector *(German)* 80−42308
electronic circuits implanted in freely moving animals, wireless power supply 79−29682
electrostatic accelerator delay line voltage multiplier 78−33326

power supplies to apparatus continued
Fermilab capacitor tree 77−83242
Fermilab main accelerator quadrupole transistorised regulators 77−83243
Fermilab main ring magnet supplies, bipolar operation 79−76206
Fermilab main ring power supply, minicomputers control system 77−83303
Fermilab neutrino focusing horn, 10 msec. 150 kA pulsed power supply 79−68092
Fermilab neutrino focusing horn, pulse stretching in high current power supplies 77−83367
Fermilab phase controlled pulsed power supplies, charact. of inversion operation 77−83223
Fermilab Tevatron He liquefier power supply 79−68044
ferroresonant power supply for sputter-ion pumps 79−97400
flash X-ray machine, distributed pulse power system anal. using SCEPTRE circuit code techniques 80−68336
flux pump supply, using inductive current transfer 78−12704
flywheel energy storage system for JT-60 toroidal field coil 78−62662
furnace power supply, transformerless 77−65035
fusion, reactor, MFTF, neutral beam accel power supply protection 80−102380
fusion reactor, Doublet III, plasma shape control, 1.5 Megawatt DC chopper power supply 80−102333
fusion reactor, Doublet-III, frequency generator-rectifier system performance 80−102326
fusion reactor, FTR, equilib. field coils, electrical supply system, optimisation and computer aided performance anal. 80−91288
fusion reactor, Heliotron E, neutral beam injector ion source power supply 80−99333
fusion reactors, ISX-B, neutral beam power system 80−91283
fusion reactor, JET, high voltage network to load AC/DC pulse power conversion 78−58497
fusion reactor, MFTF, power supply system, digital simulation using EMTP code 80−91286
fusion reactor, MFTF, start up neutral beam power supply system 80−91281
fusion reactor, MFTF, sustaining neutral beam power supply, cct. anal. using ASTAP and EMTP codes 80−91284
fusion reactor, MFTF, sustaining neutral beam power supply, shunt preconditioner, IBM-ASTAP anal. 80−102332
fusion reactor, neutral beam ion source, core snubber network design, fabrication and testing 80−102378
fusion reactor, passive notch filter for pulsed-off compression fields 77−23266
fusion reactor, PDX, neutral beam elec. power system, ion source supply upgrade 80−102330
fusion reactor, PHIBEX, poloidal field power supply for ignition, computer based cct. anal. 80−102329
fusion reactor, TEXT, motor-generator power supply system 80−99292
fusion reactor, TEXT, poloidal field power systems, design and anal. 80−102328
fusion reactor, TEXT, pulsed homopolar generator power supply, engineering and design 78−55016
fusion reactor, TEXT, toroidal field coil power supply, thyristor controlled 80−91289
fusion reactor, TEXTOR, poloidal coil system power distrib. system 80−102327
fusion reactor, TFTR, neutral beam power system 80−91282
fusion reactor, TFTR, power line, variable freq. AC harmonic content 80−99293
fusion reactor, TMX, mag. control system 80−95442
fusion reactor, Tokamak, commercial, plasma driving system requirements 78−54954
fusion reactor 150 kV negative ion test stand, electronics system 78−54934
fusion reactor auxiliaries, power distrib. system 78−54962
fusion reactor neutral beam injection, comparison of series and shunt regulation for power supply 77−23271
fusion reactor pulse power supplies development 78−8990
fusion reactor using air powered fibre optic coupled pulser 78−13342
fusion reactors, JT-60, poloidal field power supply system, AC voltage behaviour, simulation 80−91287
fusion reactors, MFTF, sustaining neutral beam power supply system, modelling with ASTAP code 80−91285
fusion reactors, PDX, shaping field-equilib. field power supply rectifier upgrade study 80−91290
fusion reactors, Wendelstein VII and ASDEX, neutral beam injectors, HV power supply system, thyristor control 80−99332
fusion reactors 80−102325
gamma spectrometer protection and operation simplification, by relay-device attachment 80−57447
GANIL cyclotron resonator RF systems, main parameters 79−72118
glow discharge electrolysis, power supply unit, current regulator 77−39489
harmonic current AC filters at KEK accelerator 78−33333
heavy ion linear accelerator, Munich, 50 kW transmitter, power stage design 77−83175
Helitron E, power supply and control systems 80−13897
High Density Z-pinch pulse power supply 79−14603
high field magnet laboratory of Grenoble, facilities and utilisation 79−71495
high voltage pulsed system, designed for small labs. 78−86079
high-density Z-pinch experiment pulse power supply, design and operation 80−70028
hot-filament device, electron current to anode stabilisation cct. 77−26341
HV AC supply for apparatus to perform electrochemical etching of particle tracks in plastic foils 77−10541
HV electron gun power supply protection 79−44989
HV power supplies for Tokamak neutral beam injectors 79−22456
HV stabilised supplies for 25 kV SEM *(Czech)* 79−21858
HV supply to EMIS isotope separator 77−14268
HV supply to MEIRA isotope separator 77−13778
HV switch tube development, for Tokamak fusion test reactor 78−66385
HV testing techniques 77−74422
inductive load, plasma coupled, crowbar system design for ZT-40 fusion reactor 78−55033
internal resistance of energy source meas., student expt. 79−30176
ion beam accelerator, multimegawatt, high-voltage power system, design philosophy, for fusion reactor 78−62613

power supplies to apparatus continued
ion source for fusion reactor, 1000-kVa arc power supply 80−99396
ion source with electron bombardment, power-supply block 78−8467
ISABELLE, superconducting magnet power supply and quench protection 79−76209
ISABELLE half-cell control system 77−88303
ISABELLE half-cell prototype, magnet power supply system 77−83244
JET additional heating power supply and protection 78−66391
JIPP T-II injector 78−29689
KEK 12 GeV proton synchrotron, computer control system of main ring magnet power supply 79−72071
KEK proton synchrotron, power supply 77−83245
large toroidal fusion expts., power supply situation 80−18635
laser 10kV/1.5kV power supply 79−36906
laser fusion, eight-beam system, high-voltage engineering 78−58492
laser isotope separation pulse power requirements 79−13972
laser power supply, high efficiency and high stability *(Rumanian)* 79−64248
laser primary regulated dual power supply 79−98396
linac, low cost RF struct. 77−88293
low-noise power supply for electrical transient meas. 80−52273
magnet power supply, current-regulated, for mag. reson. and susceptibility meas. 77−22587
magnetic lens, wide-angle focusing device for low energy π collection 78−70664
magnetic lens stabilized current supply, drift reduction 77−45867
magnetocumulative generator for pulsed air cored betatron 77−67924
mass spectrometer, programmable magnet power supply to allow rapid scanning with min. reset time 80−37121
mass spectrometer AEI MS702, transistorised unit 79−12881
mass spectrometer ion source, voltage polarity changing cct. 77−45914
microwave power source for electrodeless discharge lamps 79−36969
multipulse HV supply for filmless spark chambers 78−78565
MW impulse generator system, for ion cyclotron heating, fusion reactor 78−70635
neutral atomic beam source, power supply system 78−66393
neutral beam, pulsed, arc (arc filament) power supplies, for fusion reactor 78−70637
neutral beam filament supply, 15 V 10^3 A, programmable, regulated, for fusion reactor 78−70630
neutral beam injection system power supply, 80 to 150 kV, development program 78−13367
neutral beam injector, 150 kV, 80 A solid state power supply 80−13888
neutral beam power supply, 40 kV, 25 ms, for fusion reactor 78−62610
neutral beam power supply, series switch/regulator system, 40 kV, 80 A, 10 ms, for fusion reactor 78−66366
neutral beam power system, for Princeton TFTR fusion reactor 78−70639
neutral injection power supply system, for Princeton large torus fusion reactor 78−70638
NMR spectrometer, electromagnet current stabiliser 77−87800
nuclear fuel rod sealing by capacitor bank 78−8910
nuclear struct. facility tandem at Daresbury, elec. power provision 77−83153
optical fibre system, transmission design analysis *(Spanish)* 79−94349
optical glass melting in Pt crucibles, power supply freq. convertors 79−72728
optical glass melting in Pt crucibles, thyristor freq. convertor-fed power supply 77−50780
ORIC RF system, preparation by HHIRF 77−88300
particle, accelerator automatic klystron power supply system transient behaviour theory *(German)* 78−5077
PEP chopper magnet power supply system 79−76208
PEP magnet power supply systems 77−83216
PEP storage ring, RF system 77−88298
PETRA storage ring, RF power supply and cooling systems 79−68054
photomultiplier assemblies and associated electronics for high energy physics large counter expts. 77−83469
photomultiplier power supply using HF transmission 77−41651
photomultiplier tube base cct. for high pulsed anode currents 77−54472
phototube high-rate base 77−54469
photovoltaic, self-contained, cost minimisation 79−48098
plasmatron for gas heating, design and power supply *(Czech)* 79−68958
Pockels cell driver of fast rise time and high repetition rate using thyratron 80−69537
portable easy-operation long-period seismometer, peripheral device with DC power source 78−65399
portable voltage source, ultrastable 79−67351
Princeton large torus, ion temp. diagnostics system design and operation 78−54942
pulse forming network 34 kA rapid cycling supply for driving injection magnets 79−67974
pulsed power conversion with inductive storage, for particle accel. in fusion device 78−13340
pulser, high average power, for Cu halide laser systems 78−5497
quadrupole mass spectrometer with elliptical electrodes, 3-dim. 80−31931
R&D instrumentation, selection of power supply 78−246
radioisotope thermoelectric generators appl., terrestrial and undersea 79−48150
RF charged-particle separator power recovery, for synchrotron 78−66440
RF powered cage system for implanted biotelemetry 79−20737
ring magnet power supply, for 500 MeV synchrotron 79−18068
RISK 5 m magnetic spectrometer streamer chamber, bipolar nanosec. pulse shaper 79−68166
RISK 5 m magnetic spectrometer streamer chamber, bipolar voltage pulse generator 79−68131
rotating-anode X-ray tube apparatus 78−58100
SCR-type magnet power supplies, subharmonic ripple reduction 79−68094
Shiva pulse power conditioning, isolation and control system 78−54935
solar cells appl., Si, to electronic equipment and appliances *(Japanese)* 79−83599
solar powered microwave telecommunication links, Papua New Guinea, research 79−29449
solid-state laser miniature power pack 78−59015
spark chamber, multigap, HV supply cct. for parallel feeding 80−63456
sputtering methods status *(Czech)* 79−69979
streamer chamber, pulse transformer-based HV system 78−5095
streamer chambers, HV circuit for two-pulse supply 77−6619

power supplies to apparatus continued
superconducting coil energy storage power supply 79−34442
synchrotron beam continuous transfer elements for modulated fast bump 77−83240
Synchrotron Radiation Source booster magnet power supply 79−31272
telecommunication remote sites, solar cell power supply 80−26133
telescope drive, controlled 300 Hz freq. supply 78−61746
Texas fusion plasma research Tokamak, power supply system 77−23258
TFTR neutral beam source, power supply system 78−66394
thermoelectric power sources, militarised, technology improvements and 100 W and 500 W sources characts. 79−48151
Thornton's electronics modules for physics courses, evaluation 77−57133
three-phase system, computer aided cct. design 78−54959
thyristor thermostabiliser for at. absorpt., spectroscopy with non-flame atomisation, power supply *(Russian)* 78−76977
Tokamak, Texas exptl., homopolar generator, eddy currents, EM forces (torques), due to misalignment 78−54953
Tokamak device by homopolar generator 78−5958
Tokamak devices for nuclear fusion *(Dutch)* 78−741
Tokamak equilibrium field coils, thyristor-based pulsed supply 79−14622
Tokamak ohmic heating pulsed power supply digital simulation 78−8991
Tokamak toroidal field coil system, homopolar generator 77−23257
transformer-rectifier flux pump power supplies performance anal. 78−12703
transformer-rectifier flux pump using inductive current transfer and thermally controlled Nb_3Sn cryotrons 80−4727
transistorised potentiostat, for long-term melt electrolysis 77−86326
triode and diode ion sputtering pumps, power supply, press. control *(Spanish)* 77−37902
US flaw detector, portable, voltage stabilisation 77−90573
water decomposition plant for H_2 production, very high temp. nuclear reactor appl. 77−23247
wire chamber powering, current-limiting technique 77−54424
X-ray electron spectrometer appls. 78−21307
X-ray electron spectrometer reference voltage supply 78−21307
X-ray equipment, low power high-voltage devices 78−21309
X-ray pulse generator giving bell-shaped pulses with thyristor based power supply 80−57446
X-ray tube, HV and filament power, constant potential supplies and portable tubeheads 77−38068
zone refiner, electron beam, regulated DC power supply and emission current control 78−6844
Ar laser power supply for discharge current and output power control 77−38912
CdTe detector, Cl doped, for reentry vehicle appl., development electronics 77−45288
Cu, electrolytic refining using high-current-rectifier 77−9089
He-Ne laser tube LGR 7621 using coaxial glass technology 77−3567
Li batteries developments and appl. survey 80−50949
Li cells appl., in medicine, watches, photgraphy and military equipment, 1979 state of art *(Spanish)* 79−96432
Ne flash tubes, appl. of alternate polarity HT fields 77−10539

power supply, emergency *see emergency power supply*

power supply circuits
see also constant current sources; power supplies to apparatus
for amateur radiotelescope 79−21189
analytical graphite furnace power supply control to allow interruption of analytical cycle 77−21432
capacitor charging circuit selection for pulsed laser 77−79838
coils for RF powered implant telemetry, design 78−31926
constant current magnet, polarity reversing with triangular waveform, semiconductor electrical properties examination appl. 79−12827
controlled, for electrolytic enrichment of T in environmental samples 78−21173
crystal heater supply using controlled electron bombardment 78−181
current regulated sweep unit for supercond. solenoid 78−4659
EHT inverter for Geiger-Muller tubes, cct. 79−81120
EHT supply automatic cut-out unit for photomultiplier tubes 77−82544
electronics for the physicist with applications, book 80−62403
flash tubes, electronic, power supply with volt. and capacitance control 77−67518
GaAs laser diode power supply control cct. *(German)* 80−78852
guarded double insulation, reduction of shock hazard of grounded elec. systems in hospitals 77−56497
inductor-convertor bridges, for Tokamak supercond. coils active energy transfer rate control 78−13338
laser power supply, N_2 laser discharge dynamic characts. 79−18446
LF HV, ferroelectric material properties study applic. *(French)* 77−41647
photomultiplier active bias chain, cct. 79−71481
photomultiplier power supply using HF transmission 77−41651
programmable power supply, for use with multichannel analyser 77−42218
proton beam for neutrino experiments, focusing, pulsed power supply 79−9974
for proton storage ring guiding-field magnet, current stabilisation 77−65363
radiant energy source, highly stable, circuit design and evaluation 79−7190
rectified current supply modules, parallel ferroresonance circuit anal. *(Russian)* 77−55708
superconducting synchrotron, power supply and quench protection scheme 79−36445

power supply industry *see electricity supply industry*

power supply systems *see power systems*

power system analysis computing
see also power system computer control
electric field automatic computation, three methods, comparative study *(French)* 79−68346
fission reactor safety, fault tree anal. using Monte Carlo and anal. methods *(Spanish)* 80−57870
fusion reactor, FTR, equilib. field coils, electrical supply system, optimisation and computer aided performance anal. 80−91288
fusion reactors, MFTF, sustaining neutral beam power supply system, modelling with ASTAP code 80−91285
geothermal steam pipeline network, numerical simulation 80−40822
nuclear power plant, PWR, dynamic testing for model validation 77−3087
ocean thermal energy conversion, OTEC power modules optimisation, w.r.t. economics 79−83615

power system analysis computing continued
photovoltaic generator operation and cost simulation 79−61975
photovoltaic system analysis computer program; SOLCEL-II 80−94058
solar energy systems, Conf., San Francisco, CA, USA, (Dec. 1978) 79−83635
solar power satellite, computer modelling of power transmission system 80−40866
solar thermal power plants, dispersed, performance and economic risk evaluation, by computer Monte Carlo simulation 79−52902

power system CAD
see also power system computer control
fusion reactor, MFTF, sustaining neutral beam power supply, cct. anal. using ASTAP and EMTP codes 80−91284
fusion reactor, MFTF, sustaining neutral beam power supply, shunt preconditioner, IBM-ASTAP anal. 80−102332
solar heating and cooling systems, computer program validation methodology 80−35742
three-phase system, computer aided cct. design 78−54959
TRNSYS, solar energy systems design, computer simulation 80−35679

power system computer aided analysis *see power system analysis computing*

power system computer aided design *see power system CAD*

power system computer control
see also power station computer control; power system analysis computing; power system CAD
fusion reactor, MFTF, electrical systems, overview 80−91278
fusion reactor, TMX, mag. control system 80−95442
KEK 12 GeV proton synchrotron, computer control system of main ring magnet power supply 79−72071
solar collectors, design and data rate requirements of computer-based sun following system 79−83573
Tokamak Fusion Test Reactor, conceptual digital computer control systems 77−23281
toroidal fusion reactor, common problems in control system software design 77−23282

power system control
see also load regulation; power station control; power system computer control
6.3 Mb/s optical fibre communication for power system protection and control 78−1423
475 MVA pulsed motor generators for TFTR 78−58498
600 MW pulsed energy convertors for toroidal field coil, design philosophy 78−58496
environmental dispatch simulation and emission dispersion modelling 78−32221
fusion reactor, Tandem Mirror Reactor startup and shutdown, simulation and control 80−99277
fusion reactor, Tandem Mirror Reactor steady state, simulation and control 80−99278
fusion reactor inductive storage technology, new applications, review 78−55019
fusion reactor laser, Shiva pulse power, isolation and control system 78−54935
International Solar Energy Congress, New Delhi (1978) 79−57357
ion source light link control system 79−68093
JET pulse power supply system 78−25327
ohmic heating system for TFTR Tokamak 78−55017
photovoltaic transient analysis program for electrical and thermal anal. 80−94061
power system that includes wind energy generators, model based regulation 80−61256
pulsed MHD convertor, threshold energy characts. for elec. power production with resistive load 78−1908
Shiva laser, 25 MJ energy storage and delivery system 78−55015
variable speed wind power generator, control strategy for 3-phase output *(French)* 80−76591
wind energy conversion system, horizontal axis, performance in turbulent wind environment 79−48069

power system interconnection
wind generator oscillation modes in large power systems 79−29446

power system protection
see also lightning protection; overcurrent protection; overvoltage protection; relay protection; transformer protection
6.3 Mb/s optical fibre communication for power system protection and control 78−1423
AC, protective relaying, TFTR pulsed loads 80−63387
design of internal architecture for Westinghouse microprocessor-based [nuclear reactor] integrated protection system 79−76100
flashover voltage calc. of uniform-field gaps under steep-front impulse voltages *(Japanese)* 79−64932
fusion, reactor, MFTF, neutral beam accel power supply protection 80−102380
ion beam accelerators, high voltage protection, using floating deck modulators 78−66392
JET additional heating power supply and protection 78−66391
lightning incidence prediction and effects in electrical systems, obs. 79−39789
MW impulse generator system, for ion cyclotron heating, fusion reactor 78−70635
nuclear power plant, class 1E auxiliary power systems, degraded or loss of voltage protection 79−45363
nuclear power stations, IAEA nuclear safety standards program for protection, electric, instrumentation systems 79−45365
nuclear reactor core protection and surveillance system 79−9811
photovoltaic terrestrial systems, protection from lightning effects 80−89648
power overhead lines, overvoltage calc., pseudo-random number generator appl. *(Polish)* 77−24234
superconducting beam line magnets, fast energy dump 79−68091
three-phase system, computer aided cct. design 78−54959

power systems
see also distribution networks; power apparatus; total energy systems; transmission networks
25 kW solar photovoltaic flat panel power supply for electrodialysis water desalination unit 80−89643
communications conf., EUROCON, Venice, 1977, May 78−53552
consumer electricity supply demands fulfilment and ensuring full employment *(German)* 80−36831
economic assessment of energy technologies, based on renewable resources 79−48045

power systems continued
energy storage in power systems, reviews 79−24913
fibre-optic communication systems for electric power companies 78−1422
fusion reactor, TFTR, electrical power blanket module, conceptual design 80−102339
high-temperature materials for space power systems, mech. props. 79−57045
hospital engineering, conf., Lisbon Portugal (May, June 1978) 79−79667
integrated energy systems, environment impacts 78−73506
ion beam accelerator, multimegawatt, high-voltage power system, design philosophy, for fusion reactor 78−62613
ion pump, design, to accelerator specifications 79−63256
large-scale elec. energy storage, review 80−89676
magnetic storm disruption effects, research progress report 79−101021
military space power program, development of 10 to 50 KWe solar power systems 80−30415
MV overhead line conductor cross-section optimum choice, nomogram *(Bulgarian)* 77−60917
NASA space power technology program, power system distrib. and management 80−30494
neutral beam power system, for Princeton TFTR fusion reactor 78−70639
nuclear plant safety system redundancy, cable routine inspection 78−735
nuclear power station electrical supply system performance, reliability of protection and control systems 80−52761
photovoltaic energy generation integrations into electric grid systems, general methodology 80−45647
photovoltaic power conditioning system for professional services office building 80−89646
photovoltaic powered 20-hp DC/AC irrigation system and 3-kW N generator 80−89645
photovoltaic space power systems, 25 kW power module evolution 80−30495
power plant dynamics and control, conf. Hyderabad, India (Feb. 1979) 80−91215
reliability, NATO Advanced Study Institute, Liverpool, England (Jul. 1973) 77−38396
resource management, conf., Alamogordo, NM, USA, 1978 78−69541
solar electrical system comprising DC separately excited motor and mechanical load driven by solar cell array, performance analysis 80−16801
solar photovoltaic power system, design and performance charact. 80−89644
solar power systems, review 77−73798
solar thermal electric, line focus collectors, comparison 77−23775
stabilisation of electric power systems using superconducting mag. energy storage 80−30611
Tokamak fusion reactor power supply requirements 80−837
unloading charging voltages calc. using related maximum field strengths *(German)* 80−28130
wave power complexes, connection to Public Electricity Supply System, problems assessment 79−48082
wind power plants, integration into existing power systems, implications 80−61258
wind-driven generators integration 79−48077
work-capability anal. using Boolean algebra *(Russian)* 77−49550
Yugoslavia, system efficiency in the S.R. Croatia *(Croatian)* 80−3473

power transformers
see also autotransformers
acoustic noise prediction, control 79−18648
core vibration calc. method 77−74219
crowbar transformer, low leakage and high current for ZT-40 toroidal pinch power supply 80−102322
electro-medical equipment, leakage current source, safety measures *(German)* 78−3625
electromagnetic testing of partial discharges for failure and breakdown prevention *(Russian)* 80−97743
fault diagnosis, dissolved gas analysis of insulating oils 80−26097
leakage flux calc., use of integral transforms with non-standard kernals, teaching appl. 80−31466
magnetism conference, Freudenstadt and Bad Nauheim, Germany (March and April 1978) 79−24121
noise reduction, recent techniques, Fuji product appl. 77−72113
oil immersed transformers, dissolved gas causes and phenomena, anal. *(German)* 80−76570
oil-cooled transformer, heat exchange anal., network method *(Russian)* 78−83399
operating state determination by chromatography anal. of gases *(Czech)* 79−87894
transformer rectifier flux pump power supply using inductive current transfer 78−12704
transformer-rectifier flux pump power supplies performance anal. 78−12703
$Co_{57}Fe_5Ni_{10}(Si,B)_{28}$, amorphous, soft mag. props., switched-mode power supply appls. 80−88850
$(Fe,Ni)_{83}B_{15}C_2$ amorphous alloy core, mag. props. 79−28558
$(Fe,Ni)_{80}P_{14}B_6$ amorphous alloy core, mag. props. 79−28558
Fe-B-C amorphous alloys for use in power transformers 80−88808
Fe-Si (3 wt.%) cores with insulative coatings, morphological and struct. SEM characteris. 78−23881
$Fe_{40}Ni_{40}(Mo,Si,B)_{20}$, amorphous, soft mag. props., switched-mode power supply appls. 80−88850

power transistors
semiconductor heterostructures, elec. and optical phenomena, discrete devices, review 78−72250
V-groove multichannel power MOST, non-pinched off regime, elec. props. *(French)* 78−23174
VHF, UHF and microwave radiation effect on human body 80−8101
GaAs, MBE prep., device props. 77−77417
GaAs MESFET fabrication using dual-bubbler CVD system 78−6856
n-GaAs:Sn, nonalloyed and in situ Ohmic contacts for FETs 79−56307
Si, power transistor and solar cell epitaxy from SiH_2Cl_2 source 77−77402

power transmission
see also d.c. power transmission; distribution networks; transmission networks
cryogenics role *(Rumanian)* 80−7933
electric connectors, Al/Cu bimetal, galvanic corrosion elimination 80−35387

power transmission continued
ground-to-satellite power transfer by laser beam 79−62724
microwave, from solar power satellite, environmental aspects 79−52896
microwave, system design for space satellite power 79−52893
microwave transmission from Powersats, economic assessment 77−91404
OTEC (ocean thermal energy conversion) plants, alternative forms of energy transmission assessment 79−61958
satellite to Earth, induced ionospheric thermal instability 77−25826
solar, from satellite to Earth-based utility, efficiency analysis 79−48093
solar power satellite, computer modelling of power transmission system 80−40866
solar power satellite, microwave power transmission technology 80−40868
solar power satellites microwave power transmission system rectennas, Yagi-Uda receiving elements design, characteristics and economics 80−66938
space power satellite, 5 GW, power distribution design tradeoffs 79−52894
wave power complexes, connection to Public Electricity Supply System, problems assessment 79−48082

power transmission lines
200 kV Blumlein transmission line for Tokamak plasma heating, calc. and obs. 79−55521
AC, electromagnetic fields, health effects regulation 80−94286
biological effects of ELF electric fields: some US research results 80−94278
cap-and pin-type insulators, resistance to high current arcing for 110 and 400 kV power transmission lines *(Polish)* 80−70049
corona discharges from water drops, obs. 80−33851
DC transmission conductors, corona discharge and elec. charge on water drops, obs. 79−82114
EHV, biological/psychological effects 77−81535
EHV, ground level gradient, small plants and animals biological studies 78−31856
EHV, vibrations damper description 77−5660
EHV transmission cable, in backfill, heat and mass transfer, physical props. effects 78−94543
electric currents induced by auroral activity, meas. 79−62640
electric field effect on communication line maintenance personnel 78−40353
electrification of objects under DC transmission lines, charge simulation calcs. 78−78853
ELF radiation, from New Zealand power system, in Earth-ionosphere waveguide 79−48609
EM radiation, rel. to magnetospheric VLF wave activity Sunday decreases 79−66883
flashover of insulator surface in vacuum mag. inhibition 77−11411
ground gradient simulation for biological effect exam. 77−86731
harmonic radiation, effects on Earth's radiation belts 79−80098
harmonic radiation, satellite obs. of discrete VLF line radiation in magnetosphere 78−96360
health risks of high-Btu gas pipeline and electric power transmission systems 80−104520
high electric field biological effects on human nervous systems 80−89739
high-voltage transmission lines, depend. of instantaneous rainfall rate 80−98471
HV, electrostatic field effects on human body *(French)* 77−21562
HV field induced in humans, determ. using moment method 77−86535
HV lines to 800 kV, elec. and mag. field effects on human beings *(French, English)* 80−72209
HV transmission line elec. and mag. field exposure effects and hazards 78−77083
induced telluric current and power harmonic radiation enhancement during sudden storm commencement 79−2184
magnetically insulated vacuum power transmission lines, pulse propag. 79−85765
multi-conductor, flutter boundaries calc., aerodynamic force model appl. 77−62270
power line equipment, field work investigating corrosive effects *(Norwegian)* 80−97631
pulse transformer design for pulse forming transmission line charging appls. 80−63419
pulsed HV measurement in vacuum using 2 MV resistive voltage divider 80−31803
radiation effects in magnetosphere, transmitter simulation 79−12348
self-magnetically insulated triplate transmission line, power transport expts. 79−90471
superconducting, He refrigerators optimisation, w.r.t. cost and reliability 78−24802
UHV, biological effects obs., on plants and animals 80−17003
voltage wave propagation in mag. insulated line 80−5667
He unit requirements, for superconductive energy appl. in USA 78−89999
Nb_3Sn multilayered supercond. power line conductors, elec. props. and growth morphology 77−28325

power transmission networks *see transmission networks*

power utilisation
see also domestic appliances; drives; environmental engineering; heating; metering; refrigeration; transportation
advanced electric power utilisation technology, review 79−24884
buildings, residential and commercial, energy demand and conservation in USA, National Energy Plan impact 80−26121
chemical industry, electrolytic hydrogen production, raw material of the future *(French)* 79−96328
demand and technology forecasting, up to year 2000 *(French)* 79−92048
district heating from Kaiseraugst nuclear power station 78−37462
district heating in Stockholm, nuclear power and oil-fired plant comparison 78−37458
duplex chemical system for storage and transport of heat from LWR, district heating 78−37460
energy policy, climatic effects 78−61538
energy transfer by electric power generation and utilisation, economic case 80−16777
evaporation/crystallisation industry, using geothermal power, feasibility assessment 79−48086
heat recovery from nuclear plants for agriculture and pisciculture 78−37464
heat supply from nuclear reactors and coal combustion, appl. study 78−37455

power utilisation continued
high-temperature power-technological industrial processes use of nuclear power, reviews 79−26729
Iceland, geothermal energy exploitation 78−57181
KS-7F solar kitchen, economic effects on economy 80−89590
low temp. heat extraction from nuclear power plants for district heating 78−37456
low-temperature thermal solar motor 79−96480
nuclear energy for combined electricity and district heating prod. 78−37459
nuclear plants, heat extraction from steam generators 78−37465
nuclear power, nonelectrical energy production, review 79−26728
nuclear power appl. to centralised heat supply and central heating 79−26730
nuclear power appl. to district heating systems 78−37454
oil shale extraction in situ retort utilising fusion reactor 80−108780
PWR nuclear steam supply system for district heating and elec. prod. 78−37466
residences, energy conservation and noise control measures comparison 80−35807
soil warming, waste heat from nuclear power station 78−37463
solar distiller, multistage-inclined type, solar energy distribution determination 79−96423
solar energy utilisation, participation of meteorology *(Czech)* 79−83567
solar water heaters, aluminium alloy rolled-welded heating panels production and use 79−96421
space heating, energy utilisation improvements using new types of construction *(German)* 80−40903
space heating using solar heating installation, technical and operational details *(Dutch)* 80−72013
world distribution of commercial energy consumption (1950 to 1975) 80−26120
worldwide energy prospects, synthesis of studies published in 1976 and 1977 *(French)* 79−29443

PPP calculations
acetophenone, PPP limited CT calcs. 79−31406
acetophenones, spectrosc. characts. using PPP SCF CI calcs. 80−102448
[4N+2]annulenes, MCD spectra, B terms, semiempirical models 77−6814
anthracene, excited states calc., unrestricted HF theory in PPP approx . 77−50377
anthracene, singlet exciton transitions, energies and oscillator strengths, boson theory with PPP wavefunctions 80−92820
anthracene, spectra, PPP approx., CI clacs. *(German)* 79−36602
aromatic heterocycles, MC-SCF and CI calcs. in PPP framework 79−26892
1-arylbutadienes, lowest excited singlet states, photochemical implications 77−30795
benzaldehyde, PPP limited CI calcs. 79−31406
benzene, correl. problem, open-shell coupled-cluster approach, PPP calc. 79−81157
benzene, mol. semiempirical RPA calc. using PPP Hamiltonian, triplet instability 79−26893
benzene, p-disubstituted, MCD and absorpt. spectra, PPP calcs. 78−66574
benzene, X-ray photoelectron spectra, C 1s shake-up struct., PPP CI calc. 78−42126
benzenediazonium compounds, structure-property relationships, quantum chemical calcs. 79−22605
benzonitrile, excited single state B_1, electron-vibr. spectra and electronic struct. 79−26904
p-benzoquinone, hydroxy substitutions effect on $^1B_{1g}$←^1A_g transition 79−18200
bipyridines, torsional isomerisation of biologically active bicyclic molecules 80−27996
bispyrrol-indigo, π-electronic struct., PPP-type calc. and config. anal. 78−21855
1,3,-butadiene, π-electron struct., generator coord. method 79−26880
trans-butadiene, correl. problem, open-shell coupled-cluster approach, PPP calc. 79−81157
trans-butadiene, mol. semiempirical RPA calc. using PPP Hamiltonian, triplet instability 79−26893
trans-butadiene, polarisability, nonlinear elec. susceptibility, SCF calcs. 80−95547
carbonyls, electric polarisability, in excited singlet and triplet states *(Bulgarian)* 80−52897
carotenoid pigments, radical ions, radiolysis generation, absorpt. spectra, MO calcs. 77−65488
conjugated molecules, linear and mag. cir. dichroism interpretation 78−62835
cyclopenta[h]cycl[4.2.2]azine, electronic struct., photoelectron data 78−5286
cytochrome P-450-CO complex, absorpt. spectrum, electronic transitions, PPP calcs. 77−71811
diamino-quinone, π-electronic struct., PPP-type calc. and config. anal. 78−21855
dye laser materials, ground and excited states, triplet yields and efficiency 80−37743
ethylene, π-electron system, self-consistent many-body theory 78−25432
ethylene, Green's function electronic struct. calc., improving Σ perturbation approach 79−13642
ethylene, mol. semiempirical RPA calc. using PPP Hamiltonian, triplet instability 79−26893
ethylene, polarisability, nonlinear elec. susceptibility, SCF calcs. 80−95547
ethylene mol. Green's function Σ perturbation method for mol. calcs. 78−55123
fluorene conjugate bases, chem. shift, ring-current and excess-charge effects, semi-empirical calc. 78−33523
fulvene, correl. problem, open-shell coupled-cluster approach, PPP calc. 79−81157
haemoglobin-CO complex, absorpt. spectrum, electronic transitions, PPP calcs. 77−71811
heteronuclear molecules, alternant mol. orbitals energies, generalised formula 79−6867
1,3,5,-hexatriene, π-electron struct., generator coord. method 79−26880
trans-hexatriene, correl. problem, open-shell coupled-cluster approach, PPP calc. 79−81157
hexatriene, mol. semiempirical RPA calc. using PPP Hamiltonian, triplet instability 79−26893

PPP calculations continued
hexatriene, polarisability, nonlinear elec. susceptibility, SCF calcs. 80−95547
hydrocarbons, 6-π electron conjugated, orbital pair correlation energy calc. method 77−88374
hydrocarbons, conjugated, effect of semi-empirical parameters on simple RPA calcs. 79−10037
hydrocarbons, electric polarisability, in excited singlet and triplet states *(Bulgarian)* 80−52897
hydrocarbons, ionisation pots. calc., PPP method 78−58592
metal porphin, triplet state, spin density and zero-field splitting, PPP-SCF-CI calc. 79−68200
molecular electronic absorption spectra, intramolecular hydrogen bond 80−42949
multiconfigurational HF calculations, quadratically convergent reference state optimisation procedure 79−97966
naphthacene, excited states calc., unrestricted HF theory in PPP approx. 77−50377
naphthalene, excited states calc., unrestricted HF theory in PPP approx. 77−50377
naphthalene, singlet exciton transitions, energies and oscillator strengths, boson theory with PPP wavefunctions 80−92820
naphthalene, spectra, PPP approx., CI clacs. *(German)* 79−36602
nicotinamide, and related compounds, dipole moments, electronic transitions, chemical and biological activity 78−90086
nicotinic acid, and related compounds, dipole moments, electronic transitions, chemical and biological activity 78−90086
nucleic acids bases, excited state dipole moments and geometries 80−95738
1,3,5,7-octatetraene, π-electron struct., generator coord. method 79−26880
organic dyes, fluoresc. spectra calcs., β-variation method *(German)* 80−69182
organic molecules, quadrupole moments, dipole quadrupole A and C polarisabilities, perturbation theory anal. 80−27934
organic solids, one-dimens. conductor, dimer level splitting, hopping integral calc. using PPP Hamiltonian 80−24890
pentacene, excited states calc., unrestricted HF theory in PPP approx. 77−50377
pentacene, singlet exciton transitions, energies and oscillator strengths, boson theory with PPP wavefunctions 80−92820
perturbation theory, many-body, arbitrary point group symmetry, wave operator matrix elements 80−23311
phenylacetylene, excited single state B_1, electron-vibr. spectra and electronic struct. 79−26904
photochemistry, sudden polarisation effect 79−34328
polarisability of conjugated hydrocarbons and aromatics, linear and dynamic polarisability 79−98242
polyacenes, electronic transition bands, Franck-Condon factors, PPP SCF MO/CI calc. 78−33430
polyacenes, linear, open-shell ground state wave functions 79−762
polyacenes, spectra, correlation effects 79−81199
polycyclic aromatic hydrocarbons, diamagnetic susceptibility NCHF (SCF-PPP) calcs. 77−6686
polyenes, 2^1A_g-1^1B_u energy gap, extended CI study 79−81159
polyenes, highly branched, large networks, abnormal bond orders 79−59610
polyenes, linear, π-electron system, appl. of extended RPA excitation operators 79−97993
polyenes, linear, two-photon absorptivities, SCF-PPP-CI calcs. 79−31631
porphin, electron spectra, PPDP/S approx. calc. *(Russian)* 78−13435
porphin, MCD, LCAO MO SCR π-electron calcs., PPP approx. 78−9178
porphyrin, dication and dianion, spectra, quantum chem. calcs. 79−36597
porphyrin a, MCD, LCAO MO SCR π-electron calcs., PPP approx. 78−9178
protoporphyrin, MCD, LCAO MO SCR π-electron calcs., PPP approx. 78−9178
quantum chemistry, spin-free, particle-hole and pairing symmetries 79−6812
quinones, spectral solvent shifts, electrostatic model and semi-empirical PPP calcs. 77−83507
radical ions, conjugated, solvent effect in π-approx. calcs. of electronic transitions and spin densities 77−38623
radical ions and mols., solvent effect in π(PPP-like) and CNDO calcs. 77−38622
stilbene, cis- and trans-, picosecond flash photolysis, intramol. charge-reson. transition obs. 80−7810
stilbene, diphenylpolyenes, photoisomerisation, 'phantom' photochem. singlet state, PPP SCF CI calcs. 78−73058
stilbenes, substituted, dipole moment calcs., in excited singlet state *(German)* 77−50367
TCNE-stilbene complexes, and analogs, charge transfer energy calc. isomer prediction 78−21854
TCNQ derivatives, intramol. charge transfer, electronic absorpt. spectra obs., electron density calcs. 77−65490
tetracene, singlet exciton transitions, energies and oscillator strengths, boson theory with PPP wavefunctions 80−92820
1,3,6,8-tetraphenyl-pyrene, UV absorpt. spectra, SCF CI method 79−59479
transition from collective motion model of π-electrons to semiempirical Pariser-Parr-Pople theory *(Russian)* 78−5146
tribenzo [12] annulene, monovalent anion, MCD and absorpt. spectra 78−70859
sym-tribenzotridehydro [12] annulene, electronic spectra in Shpolskii type hydrocarbon matrices, electronic struct. and fluoresc. 78−66589
triphenylene positive ion, MCD spectra, test of pairing theorem 79−31565
TTT_2I_3, charge transfer salt, Coulomb effects, Madelung energy calcs. 80−19747
umbelliferone, excited states, in ethanol-water soln., absorption and emission spectra 79−13763
visual chromophores, two-photon absorptivities, SCF-PPP-CI calcs. 79−31631
π-electron systems, self-consistent many-body theory 78−25432
H_2, Green's function electronic struct. calc., improving Σ perturbation approach 79−13642

praseodymium
see also nuclei with .....
addition to Ni-Cr austenitic stainless steel, effect on heat resist. and comp. of non-metallic inclusions 80−76315
adsorption and absorption of $H_2(D_2)$ 77−4257
antiferromagnetic ordering 80−15709
atom, metastable, F=7⇌6 hfs, laser-RF double reson. spectroscopy 80−58170
atom, Sternheimer shielding functions calcs. 79−76352
atom, X-ray spectra, double K-hole creation in 145 keV internal conversion of ^{141}Pr 77−18823
calibo glass:Eu, Br, quantum efficiency of non-radiative energy transfer 79−33832
o-chlorobenzoic acid:Pr^{3+}, solid, vibrational spectra 80−84758
de Haas-van Alphen effect, Fermi surface 80−15435
de Haas-van Alphen freq. determ. 79−11054
determination by X-ray fluorescence 78−61127
DHCP, cryst. field effect in thermal expansion 80−49390
DHPC single cryst., Kondo-like resist. between 15 mK and 5K 79−60816
doped La-Al(Ag)(Sn)(Pb) superconductors, cryst. field transitions linewidths 80−24854
elastic constants, magnetic effects 78−68355
elastic constants, second and third order, calc. 79−51189
electrical resistance increase due to nucl. cooperative anomaly at low temp. 79−15133
film, vapour-quenched, unsuccessful search for supercond. above 0.3K 77−12053
fluoride:Pr^{3+}, photon-cascade emission quantum yield calc. 77−4669
fluoride, MF_2:Pr^{3+}, (M=Ba,Ca,Cd), far IR Stark and Zeeman splitting 77−48190
glass:Pr^{3+}, polarised luminesc. 78−48224
impurity in metallic host, exchange interaction, electrical resistivity 80−84453
ion, $4f^2$ config., semiempirical eqns. for deciphering spectrum 77−24874
lanthanum ethyl sulphate:Pr, phase transition under pressure, absorpt. spectra *(Russian)* 80−92667
lanthanum ethyl sulphate nonahydrate:Pr^{3+}, absorpt. spectrum, 400-700 nm, 78K, 22 kbar press. effects 77−81133
liquid, struct., neutron diffr. meas. 77−51305
localised 4f shell breakdown under press. 80−70411
magnetic excitation line shape, calc. compared with expt. 77−69482
magnetic excitations, exchange, crystal field and magnetoelastic interactions 80−2563
magnetic form factors, polarised neutron diffr. meas. 80−50057
magnetic ordering, possible mech. 79−47265
magnetic ordering, stress induced 80−15776
magnetic ordering due uniaxial stress, mag. excitons by neutron scatt. 78−84467
magnetic scattering, effects of cryst. field levels 77−62904
magnetisation and magnetostriction in pulse fields from 3-78K 79−99747
magnetoelastic effects, zero field single cryst. elastic consts. meas. 77−66403
magnetoresistance, longit., at low temps. and up to 80 kG 77−55515
mechanical properties from 78 to 525K 77−21165
normal spectral emittance above 1000K 77−28028
orthovanadate:Pr^{3+}, spectroscopic props 77−16363
quasielastic mode damping, dynamic susceptibility 80−15705
rare earth oxysulphide, R_2O_2S:Pr^{3+}, branching ratios for fluoresc. 79−33807
resistance anomalies under pressure up to 40 kbar 79−65430
single crystal prep. by solid state electrotransport 78−84709
soft mode excitation behaviour under press., long range order 80−39838
soft modes and central peaks, quasi-elastic mag. scatt. obs. 77−66377
specific heat anomaly at 700K *(Russian)* 77−28017
surface and volume props., flow props., surface layer thickness *(Russian)* 80−59760
thermal conductivity at low temps. *(Russian)* 79−11100
transport properties, low temp., effect of mag. field 80−70679
transport properties at high temp., scatt. mechanisms 77−15825
X-ray production by 9.5 to 41.8 MeV Fl ions, total L-shell cross-sections 77−85847
BaF_2:Pr^{3+}, wavelength and temp.-modulated UV absorpt. 80−2799
$BaY_4Si_5O_{17}$:Pr^{3+}, luminesc. props. 80−93376
BeF_2:Pr^{3+}, glass, optical homogeneous linewidths 80−7395
CaF_2:Pr, V_k-centre recomb. kinetics, phosphoresc. 77−55817
CaF_2:Pr^{2+}, EPR data interpretation for octahedral Γ_8 state in cubic cryst. field 80−2634
CaF_2:Pr^{3+}, laser selective excitation and energy transfer 79−38612
CaF_2:Pr^{3+}, multisite system, laser selective excitation and energy transfer 78−84634
CaF_2:Pr^{3+}, wavelength and temp.-modulated UV absorpt. 80−2799
CeF_3:Pr^{3+}, absorpt. spectrum, 400-700 nm, 78K, 22 kbar press. effects 77−81133
$^{144}Ce/^{144}Pr$ miniature radioisotope generator 79−49885
CsBr:Pr, absorpt. and fluoresc. spectra, crystal field 78−2885
GaP:Pr epitaxial films, photoluminesc. spectra 80−66294
GeO_2:Pr^{3+}, glass, optical homogeneous linewidths 80−7395
H, and He, stopping powers meas. 80−42904
HfO_2:Pr^{n+}, impurity valence transitions 77−51694
La-Pr/AlO_x/Al tunnel junctions, cond. meas., cryst. field effects 80−88694
$La_2Be_2O_5$:Pr^{3+} crystal, absorption and luminescence spectra studies, crystal-field splitting scheme of Pr^{3+} ion manifolds determ. 80−80853
$LaBr_3$:Pr, continuous wave and pulsed laser pumped Pr IR quantum counters 79−93219
$LaBr_3$:Pr^{3+}, laser-induced fluoresc. line-narrowing, hyperfine struct. and Zeeman effect 77−85789
LaCl-Pr, mech. for X-ray luminesc. and thermolum. 79−8170
$LaCl_3$:Pr, continuous wave and pulsed laser pumped Pr IR quantum counters 79−93219
$LaCl_3$:Pr_1 optical absorpt. and Zeeman spectra, zero mag. field splitting 79−91482
$LaCl_3$:Pr^{3+}, coherent transients by optical phase switching 80−95962
$LaCl_3$:Pr^{3+}, crystal field parameters using multiple-scatt.-X_α method 78−95271
$LaCl_3$:Pr^{3+}, dipole transition probabilities between states, electron correl. effects 80−23364
$LaCl_3$:Pr^{3+}, hyperfine Zeeman effects, fluorescence line-narrowing technique 77−62881

praseodymium continued
$LaCl_3$:Pr^{3+}, hyperfine struct. of 6011 Å line, laser-induced absorpt. line narrowing 78−15196
$LaCl_3$:Pr^{3+}, Nd^{3+}, single cryst., optical double reson. excitation, energy transfer and transform. 77−69891
$LaCl_3$:Pr^{3+}, satellite lines in optical absorpt. spectra, Zeeman effect 79−65911
$LaCl_3$:Pr^{3+}, second order Zeeman hyperfine effect *(French)* 77−52162
$LaCl_3$:Pr^{3+}, Zeeman second-order effects, fluoresc. line narrowing technique 80−16103
$LaCl_3(Br_3)$:Pr^{3+}, IR absorption, energy values for Stark manifolds 80−34955
LaF_2:Pr^{3+}, ultraslow optical dephasing for $^3H_2$-$^1D_2$ transition 79−64290
LaF_3:Pr, cryst. field anal. of triply ionised ion spectra 80−2796
LaF_3:Pr^{3+}, $^1D_2$ metastable state, hyperfine splittings, enhanced and saturated absorpt. spectra 78−43694
LaF_3:Pr^{3+}, 2K, optically detected coherent transients in nuclear hyperfine levels 79−19806
LaF_3:Pr^{3+}, anomalous luminesc. decay, phonon reson. trapping and bottlenecking 79−43023
LaF_3:Pr^{3+}, fluoresc., time resolved excitation technique 79−95820
LaF_3:Pr^{3+}, hyperfine splitting of $^1D_2$ metastable state, RF optical double reson. 78−35067
LaF_3:Pr^{3+}, laser-induced fluoresc. line narrowing 77−40280
LaF_3:Pr^{3+}, Nd^{3+}, fluorescence linewidth and energy transfer 77−8635
LaF_3:Pr^{3+}, nuclear hyperfine interactions, photon echo relax. obs. 79−59771
LaF_3:Pr^{3+}, nuclear quadrupole interaction, optical-RF double reson. meas. of ground electronic state 77−48092
LaF_3:Pr^{3+}, optical coherence storage in spin states, echo lifetime 80−58649
LaF_3:Pr^{3+}, optical free induction decay exam. of dephasing time 77−3637
LaF_3:Pr^{3+}, optical free induction decay meas. of low temp. dephasing 79−46009
LaF_3:Pr^{3+}, optical line narrowing by nuclear spin decoupling, photon echo meas. 80−48353
LaF_3:Pr^{3+}, optical meas. of spin-lattice relaxation of dilute nuclei 80−93212
LaF_3:Pr^{3+}, optical transition, spin decoupling and magic angle line narrowing 80−28286
LaF_3:Pr^{3+}, photon echo lifetimes, conc. independ. 78−74951
LaF_3:Pr^{3+}, photon echo decay as modulation process 78−79078
LaF_3:Pr^{3+}, photon-echo quantum beats in $^3P_0$-$^3H_4$ transition 79−86219
LaF_3:Pr^{3+}, pseudo-Stark effect meas. using population hole burning and optical free-induction decay 79−24292
LaF_3:Pr^{3+}, spectroscopic and relaxation character of $^3P_0$-$^3H_4$ transition, photon echo 80−39897
LaF_3:Pr^{3+}, ultrahigh resolution photon echo spectroscopy 80−28285
LaF_3:Pr^{3+}, ultraslow optical dephasing 80−58648
LaF_3:Pr^{3+}, ultraslow opt. dephasing at 2K 80−91864
$LiYF_4$:Pr, NMR meas. of hyperfine const. of Pr^{3+} excited state 80−88895
$LiYF_4$:Pr^{3+}, electron-irrad. induced defects, optical and EPR study 80−66238
$LiYF_4$:Pr^{3+}, mag.-dipole transitions obs. in fluoresc. 80−11451
$LiYF_4$:Pr^{3+}, polarized absorpt. and fluoresc. spectra, 10 to 300K, energy levels and live intensities 79−95836
$LiYF_4$:Pr^{3+}, spectroscopic determ. of ground config. energy levels 80−34969
$NaLaO_2$:Pr^{3+}, obs. of efficient luminesc., UV excitation 78−43922
$POCl_3$:Pr^{3+}, fluoresc. and lifetimes of excited states 80−71466
Pr based, IR quantum counter imaging system, resolution, sensitivity 79−81541
Pr IV, 3d and 4f energy level parametrisation, Slater parameters and correl. corrections 80−87041
Pr lines in photospheric spectrum, solar Pr abundance 79−44443
Pr, XIII, UV spectra, 60-600 Å reson. lines 78−33455
Pr^{3+}, anomalous hypersensitive $^3H_4$↔$^3P_2$ transition 80−106296
Pr^{3+}, aquo ion spectra, MCD of $^3P_0$←$^3H_4$ transition 80−7331
Pr^{3+}, change of spectra under free state to cryst. transition 79−33271
Pr^{3+}, configuration interaction contrib. to correlation cryst. field 78−56111
Pr^{3+}, correlation contributions to nuclear antiscreening factor, many-body calc. 79−56153
Pr^{3+}, elec. multipole polarisabilities, discrete basis set calcs. 80−91456
Pr^{3+}, fluoresc. quenching of organic excited singlet states, rate meas., mechanism 77−38685
Pr^{3+}, non-radiative energy transfer from Eu^{3+} in dimethylsulphoxide 79−47510
Pr^{3+}, nuclear quadrupole screening parameter, many-body perturbation theory calcs. 78−47751
Pr^{3+}, Sternheimer valence shielding antishielding factor including exchange 77−85182
Pr^{3+}:$LiYF_4$ laser, blue light emission, room temp. operation 77−38899
Pr^{3+}:NaCl(KCl), absorption spectra at 4.2 K, anal. 80−7378
Pr^{3+}:oxide glass, intensity parameters and laser transitions 79−50300
Pr^{3+}-based IR quantum counters, photon avalanche 79−97431
Pr_2NiO_4, elec. props., 300 to 1000°C 78−91694
$PrCr_{2.3}Ti_{2.3}O_9$, flux growth and chem. characts. 78−23595
PrIV, change of spectra under free state to cryst. transition 79−33271
PrP_5O_{14}, chemical synthesis and crystal growth of laser quality 78−92184
^{141}Pr, internal conversion decay, double K-hole creation 77−18887
^{143}Pr, anodic deposition on Pt anode, electrochem. separation 79−91958
^{144}Pr, effect of maximum β energy on colour quenching of Cherenkov radiation *(Spanish)* 79−76268
$SeOCl_2$:Pr^{3+}, $SbCl_5$ acidified, Racah and Judd-Ofelt parameters in laser liqs. 80−106516
Si:Pr, photoconductivity anomalies due to mag. impurities *(Russian)* 80−103722
SrF_2:Pr, far IR spectra 79−33736
SrF_2:Pr, V_k-centre recomb. kinetics, phosphoresc. 77−55817
SrF_2:Pr^{3+}, wavelength and temp.-modulated UV absorpt. 80−2799
$Tb_{55}Pr_{45}$, mag. struct. and ordered moments, neutron diffr. data 77−66252
ThO_2:Pr^{3+}, luminesc., calcination temp. and excitation process depend. 79−33749
$YAlO_3$:Pr, hyperfine interaction in lowest levels of $^3H_4$ and $^1D_2$ states 79−78065
$YAlO_3$:Pr^{3+}, ultrahigh resolution photon echo spectroscopy 80−28285

praseodymium continued
YIG:Pr^{3+} influence of Pr^{3+} ions on spin-wave damping 79−28625
$Y_2O_2S:Pr^{3+}$, enhancement of cathodolum. efficiency 79−69891
ZnO:Pr, electro- and photoluminesc. 79−83024
ZnO:Pr, electrolum. brightness, field strength and freq. depend. 80−100696
ZnO:Pr, phosphor, photoluminesc. and electroluminesc. spectra 79−11457

praseodymium alloys
hyperfine enhanced nuclear magnetic cooling 79−1674
mischmetall-Co system, phase relations, microstruct., mag. props. 80−104118
steel, austenitic, Cr-Ni-Pr(Ce,La,Na), nonmetallic inclusions modification using rare earth metals *(Russian)* 80−40369
Ag-Pr, cryst. struct. *(German)* 78−51472
Al-Pr (16 wt.%), resist. depend. on temp. and hot rolling *(Polish)* 80−39555
$Bi_{1-x}Pr_x$-Al oxide-Al tunnel junction, cryst. field struct. obs. in conductance 78−84358
Ce-Pr powder, DHCP⇄FCC transition, X-ray, DTA and resistivity studies 80−50629
$Ce_{1-x}Pr_xAl_2$, mag. struct., comp. depend., neutron diffr. and mag. susceptibility meas. 80−50054
$Ce_{1-x}Pr_xAl_2$, mixed mag. phase at low temp. 78−68228
Co-Pr, dilute, magnetic annealing effect, induced anisotropy 77−73054
CoPr, coercive force variation as function of annealing temp. *(Japanese)* 79−47787
Cr-Sm-Pr, Sm and Pr additions and plastic deform. effects on texture *(Russian)* 77−55983
$Dy_{50}Pr_{50}$, mag. struct. and ordered moments, neutron diffr. data 77−66252
$Ho_{40}Pr_{60}$, mag. struct. and ordered moments, neutron diffr. data 77−66252
La alloys, supercond., Pr-doped, crystal field effects, tunnelling within mK range 80−70907
La-Pr, superconductive tunnelling, cryst. field effects 78−88085
$La_{1-x}Pr_xSn_3$, Kondo effect from excited cryst. field levels, elec. resist. 78−14723
$La_{80-x}Pr_xAu_{20}$, amorphous, mag. and supercond. props. 80−75713
$(LaPr)Sn_3$, supercond., free energy and thermodynamical crit. field 77−32127
$La_{1-x}Pr_xSn_3$, singlet ground-state system, mag. susceptibility 78−19215
$La_{1-x}Pr_xSn_3$, supercond., 0.6 meV cryst. field transitions, neutron spectroscopy 78−67991
$La_{1-y}Pr_xSn_3$, neutron spectroscopy of 0.6 meV cryst. field transitions 78−30894
$(La_{1-x}Pr_x)_3Tl$, mag. props., simple phenomenological model 77−16041
Nd-Pr, Kaufman approach to calc. of intra-rare earth phase diagrams 80−25657
$Nd_xPr_ySm_zCo_5$ permanent magnets, coercive force, low-temp. annealing influence *(Russian)* 80−39812
$Pd_{1-x}Pr_x$ (x=0.02 and 0.03), dil. alloy, min. resist. around 20K 79−19583
Pr-Al liquid alloys, atomic interactions, thermodynamic props. *(Russian)* 80−39307
Pr-Ce, mag. order onset, elec. resistivity 80−20416
Pr-Cu-Al system, X-ray and microscopic anal. *(Ukrainian)* 78−84774
Pr-Dy, HCP struct., mag. props. 77−63177
Pr-Eu, dil., magnetisation, Mossbauer spectra 80−15928
Pr-Ga (0 to 50 at.%), phase diagram and cryst. structs. of intermetallic cryst. 80−3002
Pr-Ho, HCP struct., mag. props. 77−63177
Pr-In system, phase diagram determ. and intermediate phases characterisation 79−91621
Pr-Nd, elec. resist. and magnetisation 77−66367
Pr-Nd (5 at.%), paramag. excitation spectrum, CPA calc. 80−50043
Pr-Nd (5%), impurity modes and mag. ordering 78−84422
Pr-Ni, amorphous, thermal stability, crystn., DSC and elec. resist. study 80−107060
Pr-Ni-Al system, Pr (0 to 33.3 at.%), isothermal section at 800°C *(Ukrainian)* 79−34002
Pr-rare earth dilute alloy, low field magnetic props. 78−84443
Pr-Tb, elec. resist. and magnetisation, spin glass behaviour 77−66367
Pr-Tb, elec. resist. temp. depend. 78−2462
Pr-Tb, HCP struct., mag. props. 77−63177
Pr-Tm, mag. order onset, elec. resistivity 80−20416
$PrAg_2$, high temp. modification, thermal effects 78−38665
$PrAg_x$, low temp. mag. meas. 80−107989
$Pr_{21}Ag_{79}$, amorphous, sp. ht. at low temp. 80−75780
$Pr_{21}Ag_{79}$, $Pr_{50}Ag_{50}$, and $Pr_{10}Lu_{40}Ag_{50}$, amorphous, mag. props. 80−60182
PrAl, annealed, mag. props. and mag. struct. 78−6517
$PrAl_2$, cryst. field interpretations of inelastic neutron scatt. meas. and mag. props. 79−56174
$PrAl_2$, cryst. field splitting of Pr^{3+}, inelastic neutron scatt. exam. 77−20275
$PrAl_2$, cryst. field volume magnetostriction calc. 79−8029
$PrAl_2$, crystal field splitting, inelastic neutron scatt. study 79−47067
$PrAl_2$, elastic constants, 4.2K to 280K, crystal field effects 77−11615
$PrAl_2$, ferromagnetic, extraordinary Hall effect 80−39560
$PrAl_3$, crystal-field effects, inelastic neutron scatt. meas. 77−8268
Pr_3Al, crystal field splitting, inelastic neutron scatt. study 79−47067
$PrAl_{2-x}Ag_x$, cryst. field and exchange interactions 77−63076
$PrAl_2Ga_2$, synthesis, NMR and X-ray absorpt. studies 80−108083
$PrAu_{3.6}$, ordering temps. and effective moments 78−60283
Pr_2Au, mag. props., 4.2-300K 79−7972
$PrBe_{13}$, hyperfine enhanced nuclear mag. cooling 79−63216
$PrBe_{13}$:Gd, Van Vleck paramagnet, exchange parameters, ESR determ. 77−4557
$Pr_{1-x}Ca_xAl_2$, mag. props. and phase relations 80−107991
$PrCo_2$, magnetocryst. anisotropy props. by ^{57}Fe Mossbauer spectroscopy 77−63328
$PrCo_2$, strongly exchange-enhanced paramagnetism, susceptibility 80−60179
$PrCo_2$, sublattice magnetisation, powder neutron diffr. meas. 79−19725
$PrCo_3$-H_2, phase equilibria, from dissociation isotherms 80−50591
$PrCo_5$, EXAFS and shape of K absorption discontinuity of Co 77−20955
$PrCo_5$, mag. moment orientation, anisotropic mol. field model 77−89950

praseodymium alloys continued
$PrCo_5$, uniaxial ferromag. cryst., irreversible rotation processes 80−39768
$PrCo_{5\pm s}$, high field first order transitions, role of K_3 anisotropy const. 80−65879
$PrCo_x$, sorption at press. up to 1500 atm. 80−97819
Pr_2Co_7, mag. saturation and anisotropy, density, lattice parameters 77−85426
Pr_2Co_7, polymorphism of Ce subgroup alloys, eutectic decomposition *(Russian)* 80−66504
PrCoAl, mag. props. 78−2659
$PrCoAl_4$, X-ray anal. of crystal struct. *(Russian)* 77−55263
$Pr(Co_{0.7}Cu_{0.3})_5$, anomalous magnetisation curves 80−15757
$Pr(Co_{1-x}Cu_x)_5$, coercive force temp. depend. 79−82823
$Pr(Co_{1-x}Cu_x)_5$, magnetocrystalline anisotropy exam. 78−39315
$Pr(Co_{1-x}Cu_x)_5$, saturation magnetisation anisotropy 78−47960
$Pr_2(Co_{1-x}Fe_x)_{17}$, hard direction magnetisation, 5-300K, and anisotropy field 77−12114
Pr_3Co_3Ga, crystal struct., X-ray determ. *(Russian)* 79−27951
$PrCu_2$, cryst. field transitions near cooperative Jahn-Teller transition 78−84178
$PrCu_2$, Jahn-Teller transition, susceptibility, elec. resist., thermal expansion and acoustic meas. 77−20276
$PrCu_2$, mag. excitations and cooperative Jahn-Teller transition 79−65196
$PrCu_4$, Knight shift, mag. susceptibility, 80-800K 79−95570
$PrCu_5$, Knight shift, mag. susceptibility, 140-400K 79−95570
$PrCu_5$, nuclear induced ferromagnetism 79−61069
$PrCu_6$, coolant for two stage nuclear demagnetisation refrigerator *(Japanese)* 80−47063
$PrCu_6$, nucl. mag. ordering, heat capacity and magnetisation obs. 79−87272
$PrCu_2Ge_2$, magnetic props. 77−32180
$PrCu_5(Pt_5)$, cryst. field effects on transport props. 78−72133
PrEu(Gd), magnetic interactions, Mossbauer spectra quadrupole splitting, crystal field parameters 80−39907
$PrFe_2$, Curie temp., elec. quadrupole couplings, Mossbauer study 80−39949
$PrFe_2$, high field Mossbauer study 80−75893
$PrFe_2$, Laves phase, mag. props., Mossbauer spectra, crystalline field mag. anisotropy 80−65851
$PrFe_2$, preparation and mag. props. 80−25259
$PrFe_4Al_8$, mag. props. 78−52250
$PrFe_2Ge_2$, magnetisation, 4.2-273K, and Neel temp 77−8310
PrGa, ferromag., mag. props., 4.2 to 350K 77−63230
$PrGa_2$, mag susceptibility, 1.5-300K and Neel temp. 78−68184
$Pr_{11}Hg_{45}$, cryst. struct. determ. 79−77555
$PrIn_3$, crystalline elec. field parameters, exchange and Coulomb contrib. 77−20278
$PrIn_3$, nucl. orientation of ^{144}Pm in singlet ground state, exchange interaction and cryst. field splitting obs. 80−71275
$PrIn_3$, two stage nuclear demagnetization experiments 79−65644
$PrIn_3$:Gd, EPR relax. of impurity in Van Vleck paramag., host ion fluctuation spectra 77−48049
$PrIr_2$, sp. ht., differential susceptibility and elec. resist. meas., 1.4-40K 80−71063
Pr_5Ir_2, cryst. struct. 80−96473
$PrIr_2(Pt_2)(Rh_2)(Ru_2)$, hyperfine sp. ht. and magnetisation meas. at 4.2K 80−75775
$Pr_{1-c}La_cAl_2$, mag. props. 79−65658
$Pr_xLa_{1-x}Al_3$, cryst. elec. field 80−24856
$Pr_xLa_{80-x}Au_{20}$, amorphous, low temp. excitations, specific heat 80−100337
$(Pr_xLa_{1-x})_2In$, mag. props. 80−108009
$Pr_{0.25}La_{0.75}Mg$, cryst. field, neutron diffr. meas. 78−34810
$Pr_xLa_{1-x}Sn_3$, anomalous resistivity maxima in metallic magnetic system 78−79977
$Pr_{0.25}La_{0.75}Zn$, cryst. field, neutron diffr. meas. 78−34810
$PrMg_3$, cryst. field study, inelastic neutron scatt. and sp. ht. meas. 80−59939
$PrNi_5$, crystal field investigation from inelastic slow neutron scatt. expts. 80−39538
$PrNi_5$, crystal-field effects, comparison of calcs. with expts. 79−87071
$PrNi_5$, hexagonal, cryst. field effect in thermal expansion 80−49390
$PrNi_5$, LF dynamics and ^{141}Pr thermal relax., coupling parameter and RKKY exchange mechanism 80−103812
$PrNi_5$, metallic Van Vleck paramag., nucl. interactions, NMR meas. 80−44953
$PrNi_5$, nucl. cooling agent, relax. and exchange, EPR and NMR study 80−25237
$PrNi_5$, nucl. demagnetization, end temps., nucl. entropy 79−19718
$PrNi_5$, nuclear demagnetisation, cooling of ^3He to 1 mK 77−65037
$PrNi_5$, powder, in contact with liq. ^3He, mag. susceptibility, thermal relaxation and heat capacity 79−44909
$PrNi_5$, two stage nuclear demagnetization experiments 79−65644
$PrNi_5$-Gd, dil., single crystal, ESR study 80−75850
$PrNi_x$, sorption at press. up to 1500 atm. 80−97819
$Pr_{69}Ni_{31}$, amorphous, Curie temp., mag. susceptibility and coercive force, 4.2 to 300K 80−93092
Pr_3Os, cryst. struct. 80−96474
$PrPb_3$, crystalline elec. field parameters, exchange and Coulomb contrib. 77−20278
$PrPd_3$, crystalline elec. field parameters 77−20278
$PrPd_3$, heat capacity at low temps. 79−28547
$PrPt_2$, sp. ht., differential susceptibility and elec. resist. meas., 1.4-40K 80−71063
$PrPt_3$, ^{195}Pt NMR and susceptibility meas. 77−63299
$PrPt_5$, low temp. mag. susceptibility 80−93075
Pr_3Pt_2, structure determ., rhombohedral Er_3Ni_2 type 77−80443
$PrRh_2$, sp. ht., differential susceptibility and elec. resist. meas., 1.4-40K 80−71063
$PrRh_x$, Sny, crystallography X-ray powder diffr. study 80−100217
Pr_3Rh_2, structure determ., rhombohedral Er_3Ni_2 type 77−80443
$PrRu_2$, sp. ht., differential susceptibility and elec. resist. meas., 1.4-40K 80−71063
PrSb, lattice dynamics 79−37783
PrSb, neutron scatt., press. induced antiferromag. 80−15699
PrSi, mag. struct. and mag. moments, neutron diffr. meas. 77−85424
$Pr_{0.75}Sm_{0.25}Co_5$ magnets, struct. and props. sintering temp. depend. *(Russian)* 79−82819
$Pr_xSm_{1-x}Co_5$, magnetisation and magnetocryst. anisotropy 78−68215
$Pr_{1-x}Sm_xCo_2Ni_3$, giant intrinsic magnetic hardness 78−56347

praseodymium alloys continued
- $PrSn_3$, crystalline elec. field parameters, exchange and Coulomb contrib. 77−20278
- $PrSn_3$, inelastic neutron scatt. spectra, cryst. elec. field effects 78−43336
- $PrSn_3$, magnetoresistance 80−24877
- $PrSn_3$, Neel temp., hydrostatic press. depend. 80−29549
- $PrSn_3$, thermal expansion and transverse elastic const. near mag. phase transition 80−60394
- Pr_5Sn_3, low temp. modification with tetrogonal struct. 80−1963
- Pr_3Tl, critical fluctuations temp. depend. 80−25160
- Pr_3Tl, exchange-coupled singlet-groundstate system, central model 77−77060
- Pr_3Tl, hyperfine interactions, sp. ht. and magnetisation meas. 79−28531
- Pr_3Tl, induced ferromag., mag. props. under hydrostatic press. 78−56315
- Pr_3Tl, linewidth of cryst. field excitations 78−67988
- Pr_3Tl, magnetic low-frequency modes 78−88087
- Pr_3Tl, microwave resist. meas., rel. to singlet ground state paramag. systems 77−20353
- Pr_3Tl, resistivity and sp. ht. near threshold 79−78399
- Pr_3Tl, thermal expansion and transverse elastic const. near mag. phase transition 80−60394
- Pr_3Tl, transition temp. and magnetisation 80−25161
- Sm-Pr-Co, added Fe_2Sn, permanent magnets, demagnetisation curves, X-ray obs. 78−91900
- Sm-Pr-Co, mag. props. and struct., comp. depend. *(Russian)* 80−20430
- Sm-Pr-Co, sintered, cryst. phases *(Russian)* 80−39004
- $Sm_{0.5}Pr_{0.5}Co_5$, sintered alloy permanent magnets, temp. depend. of domain struct. *(Russian)* 77−66380
- $Sm_{0.5}Pr_{0.5}Co_5$ sintered magnets, periodic struct. and coercive force *(Russian)* 79−28554
- $Sm_{1-x}Pr_xCo_5$ single crystals, magnetocryst. anisotropy and stepwise mag. reversals *(Russian)* 77−66291
- $Sm_{0.6}R_{0.4-x}M_xCo_5$ (R=Gd, Dy, M=Pr, Nd), temp. coeff. of magnetisation 80−34688
- Tb-Pr, antiferromag. state, decrease in stability 77−20556

praseodymium compounds
- *see also praseodymium alloys*
- crystal field effects on EPR and NMR *(Japanese)* 77−43879
- ethyl sulphate, cooperative Jahn-Teller antiferroelec. ordering 77−66144
- ethyl sulphate, one-dimensional X-Y model, hyperfine contrib. to specific heat 79−1678
- ethylsulphate:Sm, one-dimens. X-Y system, spin dynamics, electron spin echo meas. 80−66031
- ferrite aluminates, prep. 77−85970
- field emission patterns and emission charact. *(Japanese)* 77−85900
- intermetallic compounds, singlet ground state magnetism, hyperfine enhnaced nuclear cooling *(Japanese)* 79−51744
- mixed valence compounds, charge dominated fluctuation props. comparison, mag. moments and ordering 80−54659
- neutron scatt. cross-section, mag. inelastic, rel. to cryst. field splitting 77−55659
- pnictides and chalcogenides, press. depend. of cryst. field splitting 78−68392
- praseodymium β-ketoesters, Pr^{3+}, visible spectrum, interaction, intensity and bonding parameters 80−993
- praseodymium ethyl sulphate, phase transition under pressure, absorpt. spectra *(Russian)* 80−92667
- praseodymium ethyl sulphate, specific heat, electric suscept. and thermal cone., one-dimens. electric dipolar XY system 77−32148
- praseodymium ethylsulphate:Sm, XY system, mag. relax. and spin dynamics 79−61211
- prep. by electron beam evaporation, and optical and elec. props. 80−20793
- Van Vleck paramagnets, mag. props., anisotropy from NMR anal. 80−54862
- Al_2O_3-Pr_2O_3, phase diagram at high temps. 77−63648
- Al_2O_3-Pr_2O_3, phase diagram at high temps. *(Japanese)* 78−88449
- CaF_2:PrF_3, EPR of cubic Pr^{3+} 79−28607
- $Ca_{0.5}Pr_{0.5}H_n$, H_2 dissociation press., phase behaviour and struct. 78−2260
- CdF_2:PrF_3 films, electroluminesc. meas. *(French)* 79−11471
- CeO_2-PrO_x system, mixed cryst. phase characterisation 79−14936
- $Cs_2NaPrCl_6$, struct. transitions, polarisation optical expts. 79−99318
- $CsPr(MoO_4)_2$, energy levels and mag. props. of Pr^{3+} ion *(Russian)* 79−7810
- $CsPr(PO_3)_4$, cryst. struct. 79−42022
- Eu-Pr-Fe-O system, solid solns. of ferrogarnet and ferroperovskite type 78−27488
- $(GdPrBi)_3(FeGaIn)_5O_{12}$, pure and In^{3+} doped, near IR absorpt. and Faraday rot. 78−95580
- HfO_2-PrO_x, phase equilibria and physicochem. props. in range 1000 to 1800°C 79−100117
- $K_5PrLi_2F_{10}$:Pr^{3+}, emission spectroscopy, ionic interaction 79−83015
- $(La_{1-x-y}Pr_xA_y)Cl_3$ (A=Ce, Gd, Y), satellite lines in optical absorpt. spectra, Zeeman effect 79−65912
- $La_{1-x}Pr_xP_5O_{14}$:Pr^{3+}, fluorescence spectrum 79−83014
- $La_{1-x}Pr_3(Sn_3)$, superconducting, cryst. field excitations, inelastic neutron scatt. obs. 80−15653
- $Li_3Pr_2(BO_3)_3$, cryst. struct. 78−87655
- $LiPr(SO_4)_2$, X-ray diffr. cryst. struct. determ. 79−14786
- Na_2O-SiO_2-Pr_2O_3 glass, magneto-optical props. 79−65894
- $Na_3Pr(AsO_4)_2$, allotropes, prep. and cryst. struct. *(French)* 78−63724
- $Na_3Pr(C_4H_4O_5)_3.2NaClO_4.6H_2O$, single cryst., forbidden $A_1 \rightarrow A_1$ transition, mag. field induced intensification 80−50302
- $Na_3Pr(C_4H_4O_5)_3.2NaClO_4.6H_2O$, absorpt., circular dichroism, and mag. circular dichroism spectra 80−97243
- $NaPrSi_6O_{14}$, cryst. struct., X-ray diffr. meas. 77−15385
- $Na_2PrSiO_4(OH)$, cryst. struct. 77−65970
- Pr $(NO_3)_3.6H_20$, Van Vleck paramag., Orbach processes and nucl. relax. 77−8439
- Pr complex, with ortho-phenanthroline and $\alpha\alpha'$-dipyridyl tris-trifluoroacetate, absorption spectra 79−98113
- Pr $H_{2.8}$, optical vibr. spectra of H, inelastic neutron scatt. study 80−107391
- Pr tinted glasses, transparency, dichroism and colour effects *(Polish)* 80−71371
- Pr^{3+} hexa-antipyrene triiodide, single cryst., polarised absorpt. spectra 77−77234
- Pr-Cr-B system, phase equil. at 800°C, boride lattice parameters *(Russian)* 78−31388

praseodymium compounds continued
- Pr-H, inelastic neutron scatt. exam. of lattice dynamics 80−29128
- Pr-H(D), lattice parameters 80−64982
- Pr_2ASe_5, A=Ge, Sn, diffuse refl. spectra and band gaps 79−51963
- $PrAl_3$, crystal field splitting of Pr^{3+}, inelastic thermal neutron scattering 78−67996
- $PrAlO_3$, ^{27}Al NMR, electronic spin dynamics at Jahn-Teller phase transition 78−68403
- $PrAlO_3$, mechanism of 118.5K phase transition 77−47532
- $PrAlO_3$, tetragonal, mag. props. 77−90052
- $PrAl_3[BO_3]_4$, thermal stability, X-ray struct. anal., refractive indices 79−4297
- PrAs, crystal field press. depend., negative point charge model representation 79−42502
- PrAs, room temp. compressibility 77−85595
- PrAs:Dy^{3+}, singlet-ground-state paramagnet, EPR meas. 77−20695
- PrAs:Gd, EPR relax. of impurity in Van Vleck paramag., host ion fluctuation spectra 77−48049
- $PrAsO_4$, ferroelectricity, dielec. meas. 80−60515
- PrB_4, ferromag. props. *(French)* 77−20566
- PrB_4, mag. and elec. props. 80−20386
- PrB_6, metallic, elec. resist., aspherical Coulomb and exchange scatt. of cond. electrons 77−51725
- PrB_6, plasma light reflection by free charge carriers 80−11403
- $Pr(BH_4)_3$, synthesis from chloride salts and $NaBH_4$ in tetrahydrofuran 80−30222
- $Pr(BO_2)_3$, single cryst., IR absorpt. spectra 80−34903
- $PrBe_{13}$, nuclear demagnetisation, prod. of μK temps. 77−17987
- PrBi, crystal field press. depend., negative point charge model representation 79−42502
- PrBi, Gd ESR, Gd-Pr exchange, conduction electron effects 79−69719
- PrBi, thermal expansion, 20-800°C 79−14942
- PrBi:Er, ESR of non S-state ions 77−43881
- PrBi:Gd, EPR relax. of impurity in Van Vleck paramag., host ion fluctuation spectra 77−48049
- $PrBr_3$, cooperative Jahn-Teller antiferroelec. ordering, struct. phase transition 77−66144
- Pr_2C_3, cryst. struct., mag. struct. and props., 1.6 to 300K 79−11296
- $Pr_{0.9}Ca_{0.1}MnO_3$, mag. struct. neutron diffr. and magnetisation study 79−61061
- $Pr_{1-x}Ca_xMnO_3$, struct. and magnetisation study 80−65804
- $PrCl_3$, anhydrous, Nd^{3+} absorption spectra and quantum states *(Chinese)* 80−89032
- $PrCl_3$, aq. soln., H_2O coordination of metal ion, X-ray diffr. 79−69000
- $PrCl_3$, cooperative Jahn-Teller antiferroelec. ordering, struct. phase transition 77−66144
- $PrCl_3$, cooperative Jahn-Teller ordering of elec. dipoles in non-Kramers doublets 78−15115
- $PrCl_3$, one and three dimensional antiferroelec. ordering 77−4607
- $PrCl_3$, one-dimensional X-Y system, far IR absorpt. spectra, cooperative spin excitations 78−95584
- $PrCl_3$, rare earth ion overlap in crystal field theory, configuration interaction 80−44552
- $PrCl_3$, Schottky anomalies, ht. capacity meas., 5-350K 77−31784
- $PrCl_3$, spectral energy transfer 78−19550
- $PrCl_3$, sublimation press. and thermodynamics, mass loss effusion meas. 79−99307
- $Pr(ClO_4)_3$, osmotic coeffs. 80−45556
- $PrCl_3.6H_2O$-$TbCl_3.6H_2O$, in DMSO soln., $Tb^{3+} \rightarrow Pr^{3+}$ energy transfer mechanism 80−5498
- $PrCo_5$, heat treated, coercive force exam. 78−68298
- $PrCo_2Ge_2$, cryst. and mag. struct., neutron diffr. study 79−69059
- $PrCo_2Ge_2$, crystal and magnetic structure obs. 80−64976
- $PrCoO_3$, ^{59}Co NMR, quadrupolar and hyperfine interactions 79−15366
- $PrCrOS_2$, single cryst. X-ray diffr. struct. determ. *(French)* 79−23581
- Pr_2CuO_4, catalytic props., mag. and elec. props. 79−66350
- $Pr_2Cu_2O_4$, magnetic properties obs. 80−70937
- $PrCu_3Ru_4O_{12}$, synthesis, cryst. struct., mag. and elec. props. *(French)* 80−107151
- PrD_2, neutron scatt. and cryst. fields 78−79970
- $PrD_{2.5}$, neutron scatt. and cryst. fields 78−79970
- PrF_3, ^{19}F spin-lattice relax. and mag. couplings 79−65753
- PrF_3, bomb calorimetric determ. of enthalpy of formation 80−50879
- PrF_3, coating materials for IR laser components 80−33105
- PrF_3, crystal field split levels, inelastic neutron scatt. study 79−47065
- PrF_3 crystals, shift tensors and F-diffusion, ion interactions, F^- NMR study 80−20471
- PrF_3, gamma-ray induced coloration 77−35586
- PrF_3, heat capacity from 5 to 350K, entropy enthalpy, Planck function 79−46811
- PrF_3, ionisation energies, satellite struct., photoelectron spectra, MS Xα calcs. 78−13425
- PrF_3, laser action of Pr^{3+} 80−95901
- PrF_3, new coating materials for IR laser optical components 79−65821
- PrF_3, orbital valency force consts. and mean square amplitudes 78−74627
- PrF_3, Pr^{3+} mag. form factor meas. by inelastic neutron scatt. 78−52221
- PrF_3, spectral energy transfer 78−19550
- PrF_3, van Vleck paramagnetic, nuclear acoustic resonance of ^{141}Pr using US *(Russian)* 79−78539
- $PrFe_4As_{12}$, synthesis and cryst. struct. 80−84154
- $PrFeO_3$, crystal field splitting, inelastic neutron scatt. study 79−47067
- $PrFeO_3$, elec. props., 300 to 1000°C 78−91694
- $PrFeO_3$, magnetic struct., time of flight neutron diffr. method 77−8280
- $PrFeO_3$, thermodynamic study of form. 78−48685
- $PrFe_4Sb_{12}$, prep. and cryst. struct. 80−100211
- $PrGaO_3$, crystal field splitting, inelastic neutron scatt. study 79−47067
- $Pr_3Ga_5O_{12}$, sp. ht. meas., 0.4-90K 77−55680
- Pr_2GeSe_5, elec. props., 300 to 1100K 79−51585
- $PrH_{2.2-2.65}$, low-temp. sp. ht., mag., elec., and cryst. field splitting effects 80−49379
- $PrH_{2.65}$, sp. ht., 2 to 260K, second-order phase transitions and cryst. field splitting 79−82355
- $PrIn_3$:Gd, indirect nuclear exchange interactions, ESR-linewidth meas., sp. ht. determ. 80−103825
- $Pr_{0.2}La_{0.8}F_3$, fluorescent line narrowing, time depend. effects 78−31244
- $Pr_xLa_{1-x}P_5O_{14}$, laser emissions, fluoresc. 79−72572
- $Pr_2Mg_3(NO_3)_{12}$, sp. ht. and elec. susceptibility 77−85642
- $Pr_2Mg_3(NO_3)_{12}.24H_2O$:$Mn^{2+}$, X-band EPR 77−66418
- $Pr_2Mg_3(NO_3)_{12}.24H_2O$:$Gd^{3+}$, EPR X-band, fine struct., low field lines 79−15351

praseodymium compounds continued
$Pr_2(MoO_4)_3$-$Pr_2(SO_4)_3$, system, sulphatomolybdates and isomorphous substitution 80−19763
Pr_2MoO_5, cryst. struct., IR spectra, elec. and mag. props. 80−33954
Pr_2MoO_6, flux growth 79−83113
$Pr_xMo_6Se_8$, supercond., mag. props., 0.7 to 295K 77−32113
PrN, compressibility, mag. susceptibility and NMR freq. shift meas. 77−85595
PrN, m.p. N_2 press. depend., Pirani-Alterthum meas. 78−43103
PrN, miscibility with UC *(German)* 80−96654
$PrNH_4P_4O_{12}$, cryst. struct. determ. *(French)* 77−24301
$Pr(NbO_3)_3$ form. mechanism, struct., dielec. props. 77−16235
$PrNbO_4$-$CaWO_4$, phase transitions of fergusonite-scheelite *(French)* 80−19942
$PrNiC_2$, struct. determ. using X-ray diffraction *(Ukrainian)* 80−33949
Pr_2NiO_4, magnetic properties obs. 80−70937
$Pr_6Ni_6P_{17}$, synthesis and cryst. struct. 78−75634
PrO, 0-0 band in XVII system, hyperfine splitting, visible excitation spectra 80−28028
PrO, D_0^0-state struct., dissoc. energy, mass spectrometric obs., 79−10228
PrO, high press. synthesis, struct. and lattice consts. *(French)* 80−29913
PrO, hyperfine structure, rotation, electronic spectrum obs. 79−98061
PrO, mag. props., lattice consts., and X-ray absorpt. spectra 80−44798
PrO, visible spectra, 7500-8500 Å, VII and X systems, rot. anal. *(French)* 78−46355
$PrO_{1.714}$, oxidation, kinetic study 80−108707
Pr_2O_3, and Pr_6O_{11}, reaction with liq. Li and liq. Li-N 79−66276
Pr_2O_3, atomic interaction effects in X-ray emission spectra *(Russian)* 79−69905
Pr_2O_3, from reactive evaporation, struct. and polymorphic transform. 79−51441
Pr_2O_3, microhardness anisotropy of single cryst. *(French)* 77−52489
Pr_2O_3, Raman spectra, lattice vibrs. 79−87440
Pr_2O_3:Gd^{3+}, EPR, zero-field splitting 79−51850
$Pr_{24}O_{44}$, beta phase, high resolution cryst. struct. images 78−42991
$Pr_{40}O_{72}$, ε-phase, defect cryst. struct. 79−90645
Pr_6O_{11}, mag. and transport props., multiphonon hopping conduction 78−19211
Pr_7O_{12}, n-beam struct. images, expt. observations and computer calc. 78−38593
Pr_9O_{16}, ζ-phase, defect cryst. struct. 79−90645
$Pr(OH)_3$, cryst. struct. 80−24424
$Pr(OH)_3$, electronic heat capacity, 0.45 to 4.2K, phase transition at 1.21K 80−59673
$Pr(OH)_3$, Jahn-Teller antiferroelectric ordering 78−10859
$Pr(OH)_3$, low temp. heat capacity, thermophys. props. optical spectra, anal. of Schottky contributions, review 80−24611
$Pr(OH)_3$, mol., XPES, satellite phenomena 79−27035
$Pr(OH)_3$, thermal decomposition, exam. 80−55640
$Pr(OH)_2Br$, hydrothermal phase equilib., cryst. struct. 78−35372
$Pr_7(OH)_{18}Br_3(I_3)$, hydrothermal phase equilib., cryst. struct. 78−35372
$Pr(OH)_2NO_3$, cryst. struct., X-ray diffr. meas. 77−4068
PrOI, X-ray diffr. coord. parameter determ. 78−87656
Pr_2O_2S-Ga_2S_3, exam. of preparation and props. *(French)* 78−80504
$Pr_2O_2S_2$, cryst. struct. determ. 79−51087
$Pr_2O_3.Si_3N_4$, prep. by sintering and X-ray diffr. data 79−77570
$3Pr_2O_3.2WO_3$, X-ray charact. and thermal props. 77−43194
$PrOs_4As_{12}$, synthesis and cryst. struct. 80−84154
$PrOs_4Sb_{12}$, prep. and cryst. struct. 80−100211
PrP, nonstoichiometric, with singlet ground state, induced van Vleck ferromag. spin glass 77−66378
PrP, sp. ht., 20-300K, cryst. field effects contrib. 77−16092
PrP:Dy^{3+} singlet-ground-state paramagnet, EPR meas. 77−20695
PrP:Gd, EPR relax. of impurity in Van Vleck paramag., host ion fluctuation spectra 77−48049
PrP-I, heterogeneous equilib. 77−36777
PrP_3O_9, X-ray powder data 79−51079
PrP_5O_{14}, laser emissions, fluoresc. 79−72572
PrP_5O_{14}, sp. hts. near ferroelastic phase transitions 78−63863
PrP(Sb)(Bi), singlet ground state paramag. system, microwave resist. meas. 77−20353
$Pr_xPb_{1\pm x}Mo_{6+n}S_8$, sputtered supercond. props. 80−50019
$Pr(ReO_4)_3.4H_2O$, Van Vleck paramag., Orbach processes and nucl. relax. 77−8439
$PrRh_4B_4$, ferromag. Curie temp. 77−89893
$PrRu_4As_{12}$, synthesis and cryst. struct. 80−84154
$PrRu_4Sb_{12}$, prep. and cryst. struct. 80−100211
PrS, heat carrier scatt., thermal and elec. cond. from 5-400K 79−14974
PrS, hydrostatic press. depend. of mag. suscept. 78−80122
PrS, isothermal compressibility 79−99262
PrS, nucl. demagnetization, end temps., nucl. entropy 79−19718
PrS, plasma light reflection by free charge carriers 80−11403
Pr_2S_3-1.8 Ga_2S_3 glass, vibr. spectra, electronic transitions, short range order 77−69820
$Pr_2(SO_4)_3.8H_2O$, ^{141}Pr spin-lattice relax. time meas. 77−28478
$Pr_2(SO_4)_3.8H_2O$, crystal struct. refinement 77−15369
$Pr_2(SO_4)_3.8H_20$, Van Vleck paramag., Orbach processes and nucl. relax. 77−8439
PrSb, compressibility and NMR freq. shift 77−85595
PrSb, crystal field effect in thermal expansion 78−19305
PrSb, crystal field press. depend., negative point charge model representation 79−42502
PrSb, forbidden band gap and electrotransfer parameters 80−39497
PrSb, Gd ESR, Gd-Pr exchange, conduction electron effects 79−69719
PrSb, mag. excitations, press. depend., inelastic neutron scatt. meas. 78−10699
PrSb, magnetic to nonmagnetic transition, press. or stress induced, neutron scatt. obs. 80−65880
PrSb, plasma light reflection by free charge carriers 80−11403
PrSb, pressure-induced antiferromag., neutron scatt. study 80−39750
PrSb:Dy^{3+}, singlet-ground-state paramagnet, EPR meas. 77−20695
PrSb:Dy(Yb), ESR of non S-state ions 77−43881
PrSb:Gd, EPR relax. of impurity in Van Vleck paramag., host ion fluctuation spectra 77−48049
PrSb:Gd, ESR study, relaxation narrowing 79−99765
$PrSbO_3$, single crysts., hydrothermal synthesis and crystallographic characteristics 79−95916
PrSe, crystal field press. depend., negative point charge model representation 79−42502
PrSe, isothermal compressibility 79−99262
PrSe, plasma light reflection by free charge carriers 80−11403
Pr_3Se_4, induced ferromagnet, effect of press. on magnetisation 78−95422
$Pr_3Se_4(S_4)$, induced ferromagnet, mag. props. under hydrostatic press. 80−60395
$Pr_4Si_2O_7N_2$, lattice consts., X-ray diffr. anal. 80−28986
$Pr_ySn_xMo_6S_8$, supercond. props. 80−97023
$Pr_{1-x}Sr_xCoO_3$, Anderson transition, elec. cond. meas. 77−51786
$Pr_{1-x}Sr_xCoO_3$, electronic and mag. props., itinerant ferromagnetism obs. 78−10660
PrT_2, ^3He detrapping and release after ^3H decay, strain model 77−60101
PrTe, crystal field press. depend., negative point charge model representation 79−42502
$PrTe_{1.44}$, high-temp. thermal cond., 80 to 750K, lattice and photon components 79−33126
Pr_3Te_4, paramagnet, rotational invariance and magnetoelastic phenomena 77−48027
Pr_3Te_4-Pr_2Te_3 system, characts. of thermal cond. 77−7917
$Pr_2Ti_2O_7$, ferroelec., layer type struct., cryst. growth 80−108348
$Pr_2Ti_2O_7$, ferroelec., temp. depend. of SHG intensity 79−24267
$Pr_2Ti_2O_7$, layered ferroelectric, anomalous photovoltaic effect, photovoltaic current 80−75603
Pr_3Tl, singlet-ground state system, central mode, in ferromag. transition, neutron scatt. obs. 77−66317
$PrVO_3$, neutron diffr. exam. of first order mag. transition 78−2685
$PrVO_4$, energy levels, opt. and NMR measurements 78−80226
$PrVO_4$, monazite struct., IR and NMR spectra 79−78534
$PrVO_4$, NMR of ^{141}Pr and ^{51}V 77−77110
$Pr_2(WO_4)_3$, mag. susceptibility, paramag. Curie temp., 300-900K 79−82753
Pr_2WO_6, growth from soln. in melt 77−1806
$Pr_xY_{3-x}Fe_{5-y}O_{12}$ film, IR absorpt. and Faraday rot. spectra 77−52093
$Pr_xY_{1-x}P_5O_{14}$, laser emissions, fluoresc. 79−72572
$Pr_2Zn_3(NO_3)_{12}.24H_2O$ single crysts., EPR of Mn^{2+} and Gd^{3+} 78−64270
$Pr_2Zr_2O_7$, synthesis from carbonates 77−85974
$SrCl_2$-$PrCl_3$, prep. and purification 78−88420
$SrPrFeO_4$, Mossbauer spectra 80−15880
U-Pr-C FBR nuclear fuels, phase anal., 1400°C 80−66486
UP-PrP systems, mag. phase diagrams 78−84424
$U_{1-x}Pr_xS$, mag. phase diagram 80−71027
$YO_{1.5}$-PrO_x, phase relns. and electrophys. props. of solid solutions 78−23686
$Y_{2.5}Pr_{0.5-x}Ca_xFe_5O_{12}$, magnetic aftereffect exam. 78−23304
$Y_{2.8}Pr_{0.2}Fe_5O_{12}$, magneto-optical props. 78−72489
YbPrBiIG, wave props. of domain wall 78−48011
ZrF_4-BaF_2-PrF_3 F^- ion cond. glasses, cond. process 80−107477

preamplifiers
1.5 Mb/s bipolar signal coding and decoding optical fibre link 77−27343
AC, non-blocking, biological appl. 77−90971
analogue differential preamplifier for mechanical recording 78−40447
avalanche Si photodiode receiver, for fibre-optic transmission systems 77−19455
biological, 24-channel, head-mounted, using low-noise operational amplifier 77−40807
bridge RF spectrometer, high freq. preamplifier 80−22380
charge sensitive preamplifier, fast low power, loop phase shift and delays 80−58089
charge sensitive preamplifiers, signal and noise response 78−33404
charge-sensitive, universal, using FET, cct. 78−77932
chopper, strain gauge blood pressure transducer appl. 78−3659
cooled low-noise bolometer preamplifier 78−4698
delay line readout for drift chambers 79−3317
ECIL preamplifier, modified for high counting rate Mossbauer studies 78−74546
EEG preamplifier for surgical appls. 77−40916
electrometers, high-speed general-purpose, features 77−74448
EMG, miniature skin-mounted preamplifier for surface meas. 78−35990
extracellular action potential recording, interference suppression 78−61294
far IR receiver optical preamplifier 77−39068
femtoamp current preamp for microprocessor controlled isotope calibrator 79−45586
FET, drain feedback, X-ray spectrometer appl. 77−38074
FET pre-amp., use with HgI_2 as low energy X-ray spectrom. 78−37479
hybrid p-i-n photodiode-FET preamplifier design for digital optical receivers *(German)* 78−33878
IC four-channel EEG amplifier 79−39535
integrating preamplifier, for InSb IR detectors 80−90337
IR detector-preamplifier for cryogenic spectrometer, optimization 80−95164
IR detector/preamplifier systems at cryogenic temp. 78−45710
isolated, electrophysiology appl., cct. 78−31922
leading-edge spectrometer for current signals from semiconductor detectors 77−6607
liquid He-cooled MOSFET preamplifier, for use with astronomical bolometer 77−61123
low noise, photoconductive detector interfacing appl. 77−61124
low noise amp. for nuclear radiation detectors and Johnson thermometry 79−76307
low noise preamplifier, for gravit. research 78−243
low noise preamplifier with continuous drain negative feedback for X-ray spectrometer 79−26072
low noise preamplifier with pulsed drain negative feedback for X-ray spectrometer 79−26071
low-noise universal preamplifier for particle spectrometers 77−14315
low-noise voltage-sensitive preamplifier output stabilisation by pole-zero cancellation 77−61088
low-temperature UHF detector, with low noise preamplifier based on n-type InSb 80−68230
MESFET preamplifier in p-i-n/FET hybrid optical receiver for communication systems 80−33158
microphone, line powered 77−7274
microwave, for ESR/ENDOR spectrometer sensitivity enhancement 78−82014
MOSFET, bioelectric measurements including intracellular potentials 77−40855

preamplifiers continued
Mossbauer systems, synchronous digital triangle generator and servo loop pre-amp 77−88351
multiwire proportional counter, linear read out electronics, hybrid preamplifier realisation 80−58091
muscle spindle afferents identification during in vivo recordings in man 80−98155
NMR probe and preamplifier for low freqs., fast recovery and high sensitivity 79−35806
NMR pulsed spectrometer wideband preamplifier 79−71502
nucleonic dual charge sensitive preamplifier 78−55110
photoconduction decays, fast, measurement, DC-10 MHz low noise amplifier system 80−57326
pulsed feedback preamplifiers, energy depend. loss anal. 79−45581
RF, tunable, low-dissipation, for low temp. NMR appls. 79−17458
semiconductor detector to cold resistance preamplifier, signal coupling through cable or delay-line transformer 78−33401
solid-state detector spectrometer system, energy resolution, electronic aspects 78−46231
spectrometer, high voltage power module and charge amplifier design 78−40826
spectrometric installation preamplifier modernisation by input FET operating regime control 80−32579
timing props. of detector-preamplifier system using laser pulser 77−54443
wideband low-noise charge pre-amp., spectroscopy with Si surface barrier detectors 77−54467
X-ray preamplifier with pulsed drain feedback 79−6249
X-ray semiconductor radiation detector, cooled preamplifier systems *(Slovak)* 78−21813
X-ray spectrometer, Si(Li) detector, preamplifier with drain feedback 78−66448
GaAs FET, cooled (4.2K), for use in UHF SQUID magnetometer 80−52282
GaAs, low-noise, FET preamplifier for low-temp. NMR and SQUIDs 78−4672
HgI_2 thin sections with Peltier-cooled preamplification for X-ray spectrosc. 80−324
InSb photodiode, in Fourier spectrometer, noise compensation using integrator in feedback loop 80−73474

precipitation
microstructural process and features only
see also Guinier-Preston zones; segregation; Widmanstatten structure
aerosol precipitation from laminar gas stream, free convection effect 78−83459
ageing metals, new particle phase spatial distributions, computer calcs. *(Russian)* 79−83202
Al alloys, influence of solid soln. elements and precipitation as correlation of formability parameters with texture 79−91696
Al-Cu(4wt.%), θ' precipitation, effect on Young's modulus, electron microscope obs. *(French)* 79−47689
alkali halide, CESR of dendritic metal phase precip. 77−24744
alloy, coarsening by temp. cycling 79−29111
alloy, cubic, computer simulation of formation of tweed and modulated structs. 79−96029
alloy, internally oxidised, orientational relationships of precip. oxide phase 77−4783
alloy, precip. dimensions, annealing temp. depend. *(Russian)* 78−15399
alloy, role of phase boundaries in phase transformations 78−72772
alloy, two phase, deform. 77−8893
alloy with dispersion precipitate of ordered phase, yield limit theory surmountable pair mech. *(Russian)* 77−1855
alloys, creep cavitation control, intergranular precipitates role 80−66664
alloys, dilute, radiation induced solute segregation and precipitation study by means of Johnson-Lam kinetic model 79−43252
alloys, intergranular precipitate effect on diffusion growth of creep voids 79−34041
alloys, phase transition premonitory phenomena, exam. by electron diffr. and microscopy *(French)* 80−59651
alloys, precipitated phases, size, shape, distrib., diffusion controlled changes 80−3072
alloys, substitutional, electrical resist., long and short range orders effect 80−107761
alloys, with second phase precipitates, transient sputtering characteristics, glow discharge optical spectroscopy meas. 77−44156
Alnico 8, permanent magnetic alloy, topography of precipitate phase *(Chinese)* 80−66512
Alnico alloy, C addition effects on struct. and mag. props. 78−23835
anisotropic media, elastic strain energy of precipitates, and periodic distrib. inclusions 78−84810
array model, stability concept 80−55411
array model, stability criteria, reply 80−55412
array of precipitates, stability 79−60509
austenite solid soln., decomposition, effect of struct. of initial state *(Russian)* 77−48442
austenitic stainless steel, 18 Cr-11 Ni, directly aged, nucleation of $M_{23}C_6$ carbides *(Polish)* 78−52806
austenitic steel, VN_x spherical misfitting particle precip. along dislocations, diffr. contrast 77−16595
binary alloy, morphological stability, discrete lattice theory, appl. to interfacial zones 78−3133
binary alloys, generalised coarsening theory 78−39778
binary metals, morphological stability study 78−11231
brass, surface microstruct. changes on immersion in $CuSO_4+H_2SO_4+HI$ soln. 78−19945
brass, Widmanstatten α-precipitates, edgewise growth 77−77481
β_1 brass containing α-precipitates, reversible shape memory effect *(Japanese)* 78−60711
brass LMtsSKA 58-2-2-1-1, heat treatment, struct. and props. 79−83239
ceramics, fracture toughness, exam. of methods of enhancing, merits and limitations 78−60771
ceramics, TEM study of precipitation 79−87637
chemically stabilised, sensitisation and corrosion resist., heat treatment depend., precipitation steel, stainless, Cr-Ni 79−38827
coarsening kinetics by ledge mechansism 79−46805
composites, planar, dissolution of precipitate plates, one-phase diffusion controlled 80−15244
conference, phase transformations in metallurgy, York, England (Apr. 1979) 80−2994
convergent beam electron microscopy for materials science 80−107028

precipitation continued
Coulter counter technique, new method to follow cryst. growth rate in precipitating systems 79−52100
creep and growth, irradiation induced, solute effects on defect precip. rate 80−88252
crystalline solid, secondary phase inception, Volmer-Weber-Becker-Doring theory *(Hungarian)* 79−10954
cuboidal precipitate in anisotropic matrix, elastic strain field calc. 78−48416
defects, influence on solid-state props., review 77−7709
deformation field of misfitting inclusion 77−73276
deformation field of misfitting inclusion 77−77488
diamond, natural, defect struct., recent obs. by new methods 78−30628
dielectric, dipolar point defects, studied by ITC 80−6405
diffusional crystal growth mechanisms 80−3059
discontinuous precipitation in binary metallic systems, review 80−3060
dislocation, inertia, influence on movement near precipitates *(Russian)* 78−14346
dislocation decoration, coherent precip. 79−95016
dislocation glide plane with precipitates, work hardening and softening 78−83815
dislocation loop growth during intrinsic point defect-impurity atom mobile complex formation *(Russian)* 79−90653
disordered and spinodally decomposed alloy, residual elec. resist. 79−19569
Dispersalloy, Sn-Hg amalgam, γ_2 precip. suppression and gettering kinetics 80−71651
elastic strain energy, coherent ellipsoidal precipitates in anisotropic crystalline solids 77−86034
elastic strain energy and interactions of thin square plates which have undergone simple shear 77−73277
electron microscopy, effect of diffuse scatt. on dark-field contrast of precipitates 78−67627
ellipsoidal morphology volume fraction estimation method using Young's modulus data 78−39781
equilibrium shape of disc-shaped precipitate, kinetics approach 77−90357
extended growth defect characterisation, review 78−30649
FBR fuel cladding alloys, phase instabilities and swelling behaviour 79−54500
FCC solid solutions, deformed, discontinuous precipitation 80−3053
Fe-Cr-C (10.6, 0.22 wt.%), fibrous precipitation 80−16303
ferrite, transform. kinetics, grain size, alloying element effect, carbide precip. 80−93560
FIM techniques, appl. to metallurgical problems, review 78−35620
glass, decomposition, phase separation processes, diffusion coeffs. determ. *(Germany)* 78−39736
glass ceramic, nucleation and growth studies by small angle neutron scatt. 79−32913
grain boundary cohesion, segregation effects 78−15411
grain boundary segregation, two dimensional compd. form. and precipitation 78−15408
grain growth, discontinuous, pore drag 77−44203
growth kinetics of plate shaped precipitates 78−6934
growth kinetics of plate-like precipitates, vol. diffusion controlled growth 78−6935
Hastelloy N, Si additions, comp. of eta carbide after ageing 78−52816
homogeneous precipitation of supersaturated soln., phenomenological theory, in liquid and solid soln. 78−67833
impurity precipitation on dislocations, and competitive diffusion sinks 77−76455
inclusions, misfitting, precipitated close together on dislocation, electron diffr. contrast 77−27886
incoherent ellipsoidal precipitate, re-exam. of elastic strain energy 78−51676
Incoloy, 800 intergranular precipitation, predicted behaviour 79−100148
Incoloy, alloy 800, $M_{23}C_6$/austenite phase boundary defect struct. resolution by weak beam microscopy 80−3046
Incoloy 800, exam. of mech. and microstructural props. 79−5022
Incoloy 800, mechanical props., heat treatment and appl., conf., Petten, Netherlands (March 1978) 79−43296
Incoloy 800, microstruct. effect on mech. props. 79−43367
Incoloy 800, review of mech. props. up to 600°C 79−43368
Incoloy 800, review of structural charact., heat treatment and comp. effects 79−43297
Incoloy 901, foil prep. for TEM exam. 80−88001
Inconel, type 706, precipitation and creep rupture behaviour, optical and TEM study 79−74158
Inconel, X-750 and 700, NDT turbine blades by small angle neutron scattering 79−20055
Inconel 600, carbide precipitation at grain boundaries, electron microscope study *(Japanese)* 79−79158
Inconel 600, S penetration leading to sulphide form. *(French)* 79−74306
Inconel 600, thermal treatment, grain boundary microstruct. and SCC resistance 80−71675
Inconel 617, creep, morphological changes of carbides, affect on creep props. 80−108509
Inconel 738, SEM and electron beam analyser study *(German)* 79−20056
Inconel alloy 600, precipitation effect on corrosion 77−25180
intercrystallic failure, quantitative methods *(Czech)* 78−60672
interface composition during diffusion controlled precipitate growth, model for ternary systems 77−36513
interface-controlled to diffusion-controlled coarsening kinetics, particle size distrib. 80−7579
interphase boundary, phase penetration during nucleation and nucleation on ledges and rises 78−52815
interphase boundary structure in solids, investig. 80−15112
irradiation induced precipitation, thermodynamic approach 79−78975
Kh20N40 alloys, phase composition after quenching, tempering 78−60650
kinetics, effect of particle solubility and inhomogeneities 78−27530
liquid phase sintering, elementary mechanisms, soln.-reprecipitation 80−50571
liquid phase sintering, role of grain and phase boundaries 78−72747
Magnico alloy, with Si, Nb, Ti effect of Ub on mag. props. and grindability 77−63811
materials interactions, stability, phase transformations, thermodynamics and corrosion 78−88444

precipitation continued
metal, radiation damage effects, neutrons and heavy ions, rel. to reactor technology, review 77−43255
metal-H, coherent, surface spinodal decomposition and quasiperiodic β-precip. 77−73257
metal-NH_3 solid solutions, phase comp., dissoc. *(Russian)* 77−35665
metallic alloys, supersaturated solid solution decomposition, model *(Russian)* 79−47656
metals, diffusion alloying conditions, deep chemical-heat treatment *(Russian)* 80−40393
metals, radiation effects, ion beam study, review 79−10883
metals and alloys, irradiated, solute segregation and precipitation effects on void swelling 78−67741
Meyrick criterion, for incidence of discontinuous precipitation, and maximum solute solubilities 79−78983
migration in applied field by vol. diffusion 78−64545
misfitting inclusion deformation field 77−36505
Mossbauer line broadening, drift-induced, in elastic field of second phase particle *(Russian)* 78−19382
mullite, crystallisation from SiO_2-Al_2O_3 melts 78−47243
multicomponent multiphase systems, phase coalescence regions by coexistence, internal sources of components *(Russian)* 77−8834
multiphase alloy deposits, microstruct. effects 79−28254
neutron irradiated, 573 to 923K, damage struct. 79−99247
Nimonic, IN100, γ' precipitates, casting conditions effect on morphology 80−7548
Nimonic 80A, rapidly solidified, struct. and initial precipitation, field-ion and TEM study 79−78982
Nimonic 80A, struct., fracture charact. 80−3071
Nimonic PE16, grain boundary carbide precipitation kinetics 77−52332
Nimonic PE16, neutron irradiated after heat treatment, solute segregation to pt.-defect sinks 79−78976
Nimonic PE16, precipitation and growth kinetics of γ' 78−64546
Nimonic type, elastic interphase strains on ageing effects on extinction *(Russian)* 77−66646
non-oriented elec., internal oxidation and nitridation effects on mag. props. 79−83336
nucleation, heterogeneous theory, appl. to precipitate nucleation at Guinier-Preston zones 77−36509
nucleation, orientation relationship generation 77−73275
nucleation, orientation relationship generation 77−77487
nucleation of second phase on screw dislocation 78−51540
ordered alloys with periodic struct., decomp. invest. *(Russian)* 80−93558
Orowan loop storage capacity, system containing ellipsoidal particles 77−76402
Ostwald ripening, effect of precipitate vol. fraction 80−40356
Ostwald ripening and its application to precipitates and colloids in ionic crystals and glasses [Review] 78−80548
oxide reactor fuel pellets, ammonium polyuranate precipitation, continuous, particle size distrib. and agglomeration control 79−93804
p-n junction, thermally associated field emission near precipitates 78−14801
p-n junctions, thermally assisted field emission near precipitates 78−14809
parallel plates, one-dimens. diffusion-controlled growth 80−55410
particle size distribution, continuity eqn. 80−55406
particle size distribution influence on exta-resist. of coherent precips. 80−49689
peritectic structure formation criteria *(Ukrainian)* 80−11636
peritectic systems with separate crystallisation of phases, number of phase constituents, calc. *(Ukrainian)* 80−25702
phase stability under irradiation, review 79−77722
pigeonite, inverted, from SW Norway, precipitation temp. estimation 80−72500
plate shaped growth kinetics 79−15680
platelet growth and stereological characterization of plates 80−55404
pores in system with excess vacancies extraneous inclusion role in nucleation *(Russian)* 79−73164
precipitate and dislocation loop strain and stress field calcs. using affine transformations 80−106722
quartz, defects growth, study by X-ray diffr. topography *(French)* 80−39095
quartz, synthetic influence of hydrostatic pressure on precip. of structure-bound water in microinclusions 78−75838
radiation induced segregation of impurities to voids, kinetic model 77−43245
radiation-induced solute redistribution and precipitation, model 79−19277
rare earth-iron alloy amorphous film, crystn., TEM obs. 79−87019
re-solution in low dose irradiations 80−93559
refractory fusion reactor materials, neutron irrad., microstruct., voids, nucleation TEM study 80−29065
repeated precipitation on edge dislocations, micromechanisms 78−95752
semiconducting binary alloy, cond. band edge shift near precip. point, order fluctuations 77−24517
semiconductor, electron scattering by layer struct., geometrical resonances, plasmon and free carrier freq. 79−56212
Si, single cryst. characteris. by SEM using Schottky barrier charge collection microscopy 77−4444
Si, X-ray step scanning section topography, lattice imperfection characterisation, automatic Bragg angle control 79−60221
solid, two-phase dispersion by volume diffusion 79−100146
solid solution, binary, radiation-induced instability, contrib. of dissipative processes 80−65039
solid solution, supersaturated, cellular precip. features, review *(Russian)* 80−84937
solid solution, supersaturated, isomorphic decomp., elastic interaction of dilating particles *(Russian)* 79−47691
solution, heterophase fluctuations 78−91444
solution reprecipitation during liq. phase sintering, grain growth, computer simulation 80−55427
spherical precipitate, diffusion-limited growth, linearised gradient approx. 80−55400
spherical precipitate isotropic diffusion controlled growth 80−100344
spherical precipitates in anisotropic matrix, elastic interaction energy 80−3049
spheroidal precipitate motion in temp. gradient by vol. diffusion 78−64544
stability under irradiation, point defect effects 77−21148

precipitation continued
stainless steel, 36NKhTYu, highly deformed, discontinuous γ'-phase precipitates cell boundaries, formation during ageing 79−87641
stainless steel, type 316, irradiated cladding, second-phase precipitation 79−54501
steel; low alloy, high strength, hot compression dynamic precip. and coarsening of Nb(CN) 80−97514
steel, 12% W, eutectic carbides struct. and comp. during heating 80−76283
steel, 30KhG and 30KhN, carbide formation, Mo alloying effects *(Russian)* 78−48402
steel, 36NKhTYu, ageing to produce ultrafine grains, discontinuous precipitation *(Russian)* 77−81277
steel, Al, quenched, tempered, orientation of precipitated Fe_xC particles, X-ray obs. *(Russian)* 79−29063
steel, Al killed, cold rolled and recrystallised grain shape anisotropy 79−34064
steel, alloy, ageing characts., precipitation and coarsening of VC, TiC, and V-Ti-C in ferrite 78−84874
steel, alloy, forgings, H precipitation kinetics, diffusion to voids, effect on shattercrack formation 80−16344
steel, alloy, type HSLA, exam. of NbCN precipitation by elec. resistivity meas. 78−84822
steel, alloy, type ST.5, structural and phase changes after high temp. heating *(Russian)* 80−55439
steel, alloy 40Kh, sulphide cracking resistance, strengthening method influence 80−55577
steel, alloy type, photoemission electron microscope obs. of high temp. precip. behaviour 80−108456
steel, austenite, carbide strain hardened, strength and plasticity, effect of Mn content *(Russian)* 80−97500
steel, austenite/ferrite interface, struct. and diffr. effects, TEM exam. 80−16308
steel, austenitic, Al-C, microstruct., Mossbauer obs. *(Russian)* 80−29655
steel, austenitic, alloyed with N, decomposition of solid solution 78−23712
steel, austenitic, cold worked 10Kh11N23T3MR, structural transformations, aging effect, electron microscope obs. 80−40402
steel, austenitic, Cr-Ni (18,12 wt.%), containing coarse grain boundary precipitates, thermomechanical treatment 78−27545
steel, austenitic, Cr-Ni-Mn (21, 4, 9 wt.%), heat resistant, grain boundary reaction, effect of alloying elements *(Japanese)* 77−52331
steel, austenitic, Cr-Ni-Mn-V, X-ray anal. of carbide phases formed during ageing *(Russian)* 80−20936
steel, austenitic, Cr-Ni-Mo (25, 28, 20 wt.%), containing N_2, electron microscope obs. of Cr_2N precipitates *(Japanese)* 78−15404
steel, austenitic, CrNi, high Mo, corrosion, effect of struct. *(German)* 77−90481
steel, austenitic, friction in vacuum of type U8 steel under microshock loading *(Russian)* 80−108583
steel, austenitic, Kh12N20T3R, ageing, submicroscopic struct. role in dispersion hardening *(Russian)* 78−64549
steel, austenitic, Mn-V-C, discontinuous precipitation, grain boundary struct. effect 79−29068
steel, austenitic, Nb modified, HSLA, interaction between recrystallisation and precipitation during high temp. determ. 79−100187
steel, austenitic, nitrided, creep, effect of N_2 and Ti and prior deform. 78−23789
steel, austenitic, type FV548, irradiated, Ni and Si rich phase, energy dispersive X-ray anal. 79−66063
steel, austenitic, type of Kh15N27T3MR, exam. of elasticity props. 78−56687
steel, austenitic 316, grain boundary sliding, creep strain and stress depend. 77−25109
steel, austenitic and duplex 308 stainless, mech. of intergranular corrosion and pitting corrosion 79−91846
steel, austenitic Cr-Mn, $M_{23}C_6$ carbide precipitates comp., heat and thermomech. treatment influence *(Russian)* 80−40361
steel, austenitic Cr-Ni (18,12 wt.%), containing coarse irregular carbide precipitates along grain boundaries, ductility 78−60718
steel, austenitic Fe-Mn-V-C, ageing characts., discontinuous precip. nature 80−84940
steel, austenitic stainless, 08Kh18N10T, hot-worked precipitation kinetics and struct. of dispersed phases, Ti effect 80−29964
steel, austenitic stainless, 12Kh18N10T, deformed, phase comp. and props. after prolonged heating 80−30040
steel, austenitic stainless, aged and deformed, growth and dissolution of NbC particles 78−39782
steel, austenitic stainless, Cr-Ni-Nb, intergranular precipitation, predicted behaviour 79−100148
steel, austenitic stainless, Cr-Ni-Ti, creep deform. effects on intergranular TiC dispersion stability 78−84912
steel, austenitic stainless, extrinsic grain boundary dislocations, effect on $M_{23}C_6$ precipitate nucleation 79−51118
steel, austenitic stainless, fatigue crack propag., stable and unstable, role of precipitation 80−40534
steel, austenitic stainless, He implanted 1.4970, high temp. fracture 77−86186
steel, austenitic stainless, interaction of grain boundary dislocations with precipitates during high temperature creep 80−16384
steel, austenitic stainless, matrix precipitation of Cr_2N, due to P addition, TEM exam. 79−4973
steel, austenitic stainless, MC precipitate comp., APFIM study 80−104161
steel, austenitic stainless, NbC precipitate particle size distrib., TEM study of grain to grain variations 79−29066
steel, austenitic stainless, Ni-alloyed, Cr_2N precipitation, interface struct. and morphology 80−11644
steel, austenitic stainless, phosphide analysis using nonaqueous electrolyte potentiostatic etching method *(Japanese)* 80−89221
steel, austenitic stainless, plastically deformed, TEM obs. *(French)* 77−44302
steel, austenitic stainless, precipitates and grain orientation by non aqueous electrolyte potentiostatic etching method *(Japanese)* 80−15102
steel, austenitic stainless, precipitation of $M_{23}C_6$ carbide by ageing *(French)* 79−52216
steel, austenitic stainless, stabilized, creep improvement, effect of B precipitation and hyperquenching *(French)* 78−23784

precipitation continued
steel, austenitic stainless, steam generator tubing, stress corrosion cracking in NaOH soln. 78−60866
steel, austenitic stainless, structure phase transitions due to high energy electron irrad. *(Russian)* 80−7553
steel, austenitic stainless, supersaturated, recrystallisation 77−77506
steel, austenitic stainless, type 800, grain boundary precipitation 79−38885
steel, austenitic stainless, type FV 548, 20% cold worked irradiated with 22 MeV C^{2+} ions or 46 MeV Ni^{6+} ions, study of void swelling 79−37744
steel, austenitic stainless, V alloyed, creep mechanism 77−36591
steel, austenitic stainless, V alloyed, creep mechanism 77−48514
steel, austenitic stainless AISI 304, dislocation substruct., carbide precipitation and deform. mech. map 77−70116
steel, austenitic stainless FV548, neutron irradiated, Si-rich phase occurrence of M_6C phase 80−15156
steel, austenitic stainless type 316, σ phase precipitation during long term high temp. creep, fracture 79−74157
steel, austenitic type EI-69, carbide transformations on precipitation of C from austenite *(Russian)* 80−97487
steel, C, hydrogen embrittlement, elastic interaction of H_2 with precipitates 78−92340
steel, C, isoforming and warm rolling, effect of mech. props. 80−11673
steel, C, phosphide analysis using nonaqueous electrolyte potentiostatic etching method *(Japanese)* 80−89221
steel, C, type S15CK, tufftrided, fatigue strength at elevated temp., under reversed axial strength *(Japanese)* 78−84980
steel, C type U10A, X-ray diffr. investig. of carbide residues after deform. and tempering *(Russian)* 77−81275
steel, C-Mn-Nb, Nb microalloying, weldable, structural, recrystallization and precipitation induced by high temp. deform. *(French)* 79−61632
steel, carbide form. depend. on Mn, Cr, V additions, cementite stabilisation, microstruct. *(Russian)* 80−55399
steel, carbide phases formation during annealing, of lower bainite *(Russian)* 78−6930
steel, cast, high speed, solidification, $(Fe,Mo)_6C$ form., struct. 79−24514
steel, CC Cr-Mo-V (1,1,.25 wt.%), Mo_2C-V_4C_3 precipitation, creep rupture test *(Japanese)* 79−70070
steel, cementite precipitation from binary alloys, hardness and Mossbauer effects 77−70054
steel, cold-formed, low pearlite, Nb alloyed, Nb effects, precipitation, recrystallisation *(German)* 77−8832
steel, complex alloy, ε-carbide precip. in bainite *(Russian)* 77−66647
steel, complex alloy, carbonitride comp. and solubility calcs. *(Russian)* 77−70052
steel, Cr, exam. of surface layer after electrochemical treatment, effect on mech. props. *(Russian)* 80−7727
steel, Cr, high C, in situ transform. of cementite to M_7C_3 and internal defects of M_7C_3 by tempering 78−31412
steel, Cr, lower bainite transform., significance of carbide precip. 80−97476
steel, Cr (4 wt.%), Cr_7C_3 precipitate growth during tempering, effect of Cr diffusion *(Russian)* 79−52219
steel, Cr bearing, carbide phase precipitation during tempering, Mossbauer, X-ray diffr. studies *(Russian)* 79−87636
steel, Cr maraging, internal friction, 120 to 700K *(Polish)* 79−96075
steel, Cr-Mn-W(Mo), W and Mo addition effect on carbide form. in type 30 KhG *(Russian)* 79−87638
steel, Cr-Mo, annealed, interaction solid soln. hardening, precipitation effects on creep 79−4974
steel, Cr-Mo, creep resistant, creep, effect of carbide precipitation *(German)* 77−52398
steel, Cr-Mo, Mn and Si effect on temper embrittlement, comp. and carbide precip. effects 80−85037
steel, Cr-Mo, toughness of heat treated steels of equal tensile strength *(German)* 80−25727
steel, Cr-Mo (2.25, 1.0 wt.%), temper embrittlement, effect of P, Sn, comp. and carbide precip. 80−85036
steel, Cr-Mo (2.25, 1 wt.%), annealed, heat treatment effect on tensile props. 78−11243
steel, Cr-Mo (2.25, 1 wt.%), decarburization, carbide effects in high temp. Na *(Japanese)* 78−15403
steel, Cr-Mo (9, 1 wt.%) appl. of electron energy loss spectrometry to precipitate morphology 78−48414
steel, Cr-Mo-Ni-WV (6, 4, 3, 2 wt.%), tempering and secondary hardening, TEM obs. *(Chinese)* 80−104245
steel, Cr-Mo-V (0.5, 0.5, 0.25 wt.%), creep crack growth in notched bend test, microstruct. effect 77−21261
steel, Cr-Mo-W-V, long term creep rupture props., turbine blade *(Japanese)* 77−59909
steel, Cr-MoV, isothermal decomp. of austenite and carbide precip. 79−38832
steel, Cr-Mu-W, carbide form., W effect 80−76259
steel, Cr-Ni-(Mo) (25, 28, 2 wt.%), lattice dilation by N_2 77−16592
steel, Cr-Ni-C (3, 1, 0.6 wt.%), grain boundary sulphide precip. and hot ductility *(Japanese)* 80−71654
steel, Cr-Ni-Mo-Cu, ε phase particle precipitation from martensite, local internal stress relaxation *(Russian)* 79−78969
steel, Cr-Ni-W(Mo), W and Mo addition effect on carbide form., X-ray obs. *(Russian)* 79−87639
steel, cratered overheating facets 77−52482
steel, CrMo and CrMoV, creep resistant, ductile-brittle transition temp., precipitation effects *(German)* 78−19856
steel, CrMoV, carbide phases precipitation *(Czech)* 80−29961
steel, Cu, precipitation hardening, struct. and fracture *(German)* 79−61696
steel, Cu precipitation hardening, struct. and fracture *(German)* 79−61696
steel, Cu-Mo, tempered, cementite precipitation along twin boundaries 80−45309
steel, deep drawing, texture control as affected by processing variables 79−91689
steel, deoxidised, AlN and V carbonitrides precip. effect on mech. props. *(French)* 80−45311
steel, effect of ε-Cu precipitates on H discharging phenomena *(Japanese)* 80−7583
steel, En 24, Cr, V, deform. effect on decomp. of austenite, carbide precipitation 80−84938
steel, eutectoid, Si partitioning during pearlite transform., analytical electron microscopy applic. 80−108458
steel, Fe-Mo-C low-alloy, photoelectron microscopy of diffusional transformations 77−44242
steel, ferritic, FeC form. kinetics, Monte-Carlo simulation *(German)* 78−39779
steel, ferritic, with interstitial N, continuous precipitation and clustering 80−7585
steel, ferritic Cr-Mo type, microanalysis of precipitates using TEM 80−108688
steel, ferritic stainless, phosphide analysis using nonaqueous electrolyte potentiostatic etching method *(Japanese)* 80−89221
steel, Hadfield, containing Ni, carbide precipitation, heat and cold work effects *(Korean)* 77−77484
steel, heat resistant, explosive loading effects on struct. and mech. props. *(Russian)* 78−39787
steel, heating effect on phase composition, microstruct. and mech. props. 80−100859
steel, high C, high Cr, rapidly quenched, in situ carbide reactions during tempering *(Japanese)* 78−84862
steel, high C, investigation of transformations during tempering by nuclear gamma resonance method *(Russian)* 80−76256
steel, high speed, microstruct. effect of splat cooling 79−61624
steel, high speed, props. after electroslag remelting 80−104139
steel, high speed, R18 and R6M5, rolled and annealed carbide phase investigation 77−90374
steel, high speed R6M5K5, excess carbide size and distrib. effect on grain size 77−90356
steel, high strength, low alloy, splitting of tensile and impact specimens 77−63777
steel, high strength, Nb(C, N) precipitation in austenite, effect on mech. props. *(Japanese)* 77−21186
steel, high strength, sulphide stress cracking props., density and distrib. of intergranular sulphide effects 79−74291
steel, high strength weld metal, fractography, microstructure and reheated zone toughness effects *(Japanese)* 80−108543
steel, high-C, type U12, U15, U17, cementite precipitation cryst. geometry singularities during decomposition of martensite *(Russian)* 80−7577
steel, high-speed, shiny nonfusion rings in friction welding, origin 78−23872
steel, HSLA, V and N effect on recovery and recrystn. during and after hot working 80−84973
steel, hypereutectoid, austenite dissociation depend. on strain at intercritical temps., pearlite transform. *(Russian)* 80−40362
steel, hypereutectoid, thermomech. treatment, Fe_3C distrib. and yield point *(German)* 79−52243
steel, KhVG, deformation ht. treatment on carbide precip. in KhVG 77−63700
steel, lath martensite, elastic interaction of H_2 with precipitates 78−3129
steel, low alloy, C-Ni-Cr-Mo (0.36 wt.%), impact toughness rel. to microstruct. *(Korean)* 77−21188
steel, low alloy, cleavage fracture, fine scale precipitation dispersion effect, TEM obs. 78−60788
steel, low alloy, coarsening at high temp. of small carbide particles dispersed in ferrite 77−52335
steel, low alloy, cold resistance, effect of nitrides, carbonitrides, carbides, Cu precipitates 77−16594
steel, low alloy, exam. of microstructure, in type PZhK-1000 soldered joint by metallography 79−52257
steel, low alloy, low C grain boundary proeutectoid ferrite formation, direct obs. method 80−3074
steel, low alloy, toughness, effect of packet size and lath width 77−16677
steel, low alloy creep resisting, causes of weldment cracking 78−56760
steel, low alloy ferritic, sub-micron cavity nucleation, SEM obs. 78−95753
steel, low C, Al-stabilized, AlN_2 precipitation 79−87659
steel, low C, cold rolled, graphite precip. and S segregation, AES investigation *(Japanese)* 80−89222
steel, low C, cold rolled and recrystallised, containing Nb(CN) dispersion, struct. and textural aspect of deform. 79−47712
steel, low C, cold rolled sheet, Cu effect on recrystallization texture *(Chinese)* 79−74173
steel, low C, deep-drawing, mechanism of recrystn. texture formation 79−87658
steel, low C, deformed, comp. of precipitated carbonitrides, X-ray diffr. anal. *(Russian)* 79−20051
steel, low C, Mn effect on recrystallisation and texture *(French)* 80−3110
steel, low C, Mn-Nb, quenched and tempered, microstruct. and props. 77−36549
steel, low C, precipitation of Nb and V, critical temperature identification by meas. electric resistance *(Slovak)* 77−4781
steel, low C, quenched, interphase precipitates obs. *(Russian)* 80−29957
steel, low C, rolling deform., effect on NbC particle size distrib. 79−47717
steel, low C, Ti-stabilized, recrystn. texture development 79−83231
steel, low C, V(C,N) precipitation and twinning in $\gamma \rightarrow \alpha$ transform. *(Polish)* 78−52807
steel, low C and alloy, serrated flow and thermomechanical treatment *(Korean)* 80−30026
steel, low C Mn-V, VC effects on strength and brittleness 77−70055
steel, low S, ESR, overheating effect on toughness 78−52860
steel, low S, ESR and electric arc, notch toughness, interaction between overheating and tempering temp. effects 78−52970
steel, low S, overheating 77−21185
steel, low-C, coherent precip. of VC 78−35392
steel, low-C, structural, with Zr impurities, grain boundaries, AES 79−24524
steel, low-C, with Nb-B addition, transform. characts. and mech. props. *(French)* 79−43253
steel, maraging, ageing study by internal friction meas. 77−12660
steel, maraging, intermetallic phases precip. study by electron microscopy *(Polish)* 80−89217
steel, maraging, Ni (18 wt.%), grain boundary precipitation, scanning Auger electron obs. 78−3132
steel, maraging, Ni-Co-Mo (18,10,5 wt.%) precipitation *(Japanese)* 78−15402
steel, maraging, precipitation hardening, struct. and fracture *(German)* 79−61696
steel, maraging, solubility of Fe-Mo-Co (10, 0 to 20 wt.%) Laves phase, depend. on Co *(Russian)* 79−100145

precipitation continued
steel, maraging, thermally embrittled, TiC precipitation 77−25055
steel, maraging alloy, intermetallic compound solubility, thermodyanmic calcs. *(Russian)* 80−40363
steel, maraging Ni-Co-Mo, precipitation, elec. resist. meas. *(Japanese)* 78−11228
steel, medium C, 40MnB, dissoln. and precipitation of $M_{23}(C,B)_6$ *(Chinese)* 80−66511
steel, Mg effect on precipitation of C and or N, and mech. props., during strain ageing *(German)* 78−35387
steel, microalloy V-Nb, V, Nb effects on strength and formability of cold rolled sheets 77−55979
steel, microalloyed, alloy carbide precipitation during isothermal ageing 80−3077
steel, microalloyed, hot-rolled, Nb(C,N) precip. and austenite recrystn. 80−97513
steel, microalloyed, precipitation effect on microstruct. and mech. props. *(French)* 80−25708
steel, microalloyed, recrystallisation, precipitation effect 79−47695
steel, microalloyed, types V1599, V1600, V1286, NbCN precipitation in undeformed austenite 80−89230
steel, mild, annealed, fatigue crack init., microstructure and strain ageing effect 77−86162
steel, mild, cold rolled, texture and plastic anisotropy rel. to alloying and precipitation *(French)* 80−108475
steel, mild, sheet, with low Al content, annealing, AlN recrystn., precipitation kinetics *(French)* 79−20083
steel, mild, yield strength and fracture toughness, microstruct. effect, heat treatment 78−27615
steel, Mn-C, formation of filamentary V(C,N) precipitates during diffusional $\gamma \rightarrow \alpha$ transform *(Russian)* 79−1865
steel, multicomponent duplex stainless, high temp. precipitation of α' 80−20939
steel, Nb,(V),(Al), hot-rolling, laboratory simulation, recrystn. of austenite 80−97512
steel, Ni, maraging, H_2 diffusion, diffusivity and solubility *(Japanese)* 79−42311
steel, Ni-B, B effect on temperability and microstructure 79−15710
steel, Ni-Co-Mo-Ti, hot formed, recrystallization and grain boundary precipitation effect on mech. props. *(German)* 79−66073
steel, Ni-Co-Mo-Ti, microfractographical features, embrittlement and grain size influence on fracture behaviour *(German)* 80−30053
steel, Ni-Cr, temper embrittled, electron microscope and X-ray microstruct. obs. 79−38870
steel, Ni-Mn-Al-V, nonmagnetic, ageing, dispersion hardening, microstruct., phase comp., mech. props. *(Russian)* 79−34046
steel, Ni-S-(Mn), ferrite to austenite transform. effect on sulphide precipitation 77−86025
steel, Ni-Ti-Al, 36NTYu, heavily deformed, subgrain struct. due to discontinuous precipitation of γ' phase *(Russian)* 79−52218
steel, pearlitic, heat-resist., secondary phase precipitation, deform., and fracture during creep *(Russian)* 80−50669
steel, plain C, quench ageing avoidance, critical cooling rate *(German)* 79−52244
steel, precipitation of AlN *(French)* 78−23711
steel, process induced matrix inclusion separation 77−28818
steel, quench ageing effect of Mn content on C and N precipitation and mech. props. *(German)* 78−31409
steel, second phases, appl. of DTA-evolved gas anal. 77−55971
steel, Si, grain-oriented, high permeability, dissoln. and precip. of AlN and MnS 80−89223
steel, Si, lower bainite morphology *(Czech)* 79−78959
steel, Si, metallography of bainitic transform., carbide precipitation 78−27527
steel, Si, textured, alloying addition inhibition effects on grain orientation and growth *(Japanese)* 79−43270
steel, stainless, 304, weld decay, precip. of $M_{23}C_6$ during thermal cycles *(Japanese)* 79−52468
steel, stainless, 316, creep and rupture, 525 to 900°C, rupture and ductility 79−8327
steel, stainless, 316, creep and rupture, 525 to 900°C 79−8328
steel, stainless, 36NkhTYu, heavily deformed, subgrain struct. due to discontinuous precipitation of γ' phase *(Russian)* 79−52218
steel, stainless, α-irradiated, He cavitation, rel. to TiC precipitation 80−45399
steel, stainless, carbide and intermetallic phases, quantitative anal. by X-ray diffr. 80−66514
steel, stainless, cladding, irradiation enhanced creep 77−42074
steel, stainless, Cr (17 wt.%), recrystallisation texture, effect of N *(Japanese)* 79−4978
steel, stainless, Cr-Cu (17, 0.6 to 1.1 wt.%), texture 80−84957
steel, stainless, Cr-Mn (21, 14 wt.%), grain boundary precipitation and fracture *(Japanese)* 79−100149
steel, stainless, Cr-Ni-Mo, phase anal. of carbide phases after isothermal annealing *(Czech)* 80−89224
steel, stainless, duplex, lattice-imaging technique 79−64965
steel, stainless, fatigue, influence of ageing and plastic deformation *(Russian)* 79−15857
steel, stainless, fatigue crack morphology of type 304 cycled at const. stress amplitude at elev. temps. 78−64671
steel, stainless, ferrite to austenite decomposition 80−3073
steel, stainless, ferritic, 430, precipitate study using ion microprobe mass analyser 79−15678
steel, stainless, ferritic, Cr-Mo-Ni (29,4,2 wt.%) 77−44276
steel, stainless, ferritic and duplex, Mossbauer effect study of 475°C embrittlement 78−52933
steel, stainless, high-strength 0Kh11N10M2T, phase transform. 77−70046
steel, stainless, intercrystalline corrosion, effect of alloying elements, thermodynamic anal. 77−90504
steel, stainless, ion irradiated, carbide precipitation *(French)* 77−16585
steel, stainless, maraging, type 03Kh11N10M2T, exam. of thermal brittleness 78−88526
steel, stainless, massive particle form. during creep, precipitation 77−63679
steel, stainless, nitride phase determination method 78−7276
steel, stainless, phase instability effect on cladding deform. profile of LMFBR fuel elements 77−74921
steel, stainless, precip. obs using convergent beam electron microscopy 80−108689
precipitation continued
steel, stainless, precipitate crystallography using electron microscopy 78−83698
steel, stainless, stabilised, knife line attack phenomenon, dissoln. of carbides in thermal cycles *(Japanese)* 78−68701
steel, stainless, two phase, variation of tensile and impact strength with heat treatment 79−34085
steel, stainless, type 304L, neutron irradiated, in-reactor precipitation and ferritic transformation 79−77644
steel, stainless, type 316, cast, precipitation kinetics of χ phase and $M_{23}C_6$ carbide 78−88469
steel, stainless, type 316, cold worked, precipitation response to neutron irrad. 80−34073
steel, stainless, type 316, electron beam heating effect on extracted intermetallic precipitate 78−35394
steel, stainless 316, carbide precipitation rel. to in-reactor deform. 79−8302
steel, stainless 316, soln. annealed, cavity alignment and precipitation during dual ion bombardment 80−70273
steel, stainless AISI 316, Si and Ti effect in phase stability and swelling behaviour 79−78972
steel, stainless austenitic, low alloy 316, high temp. plasticity, B addition effects *(Russian)* 77−28852
steel, stainless austenitic, neutron irrad., swelling due to gamma prime and $M_{23}(C,Si)_6$ form. 78−51590
steel, stainless M316, neutron irradiated, occurrence of ordered FCC phase 77−51411
steel, stainless precipitate phasee in type 321 after ageing 17 years at 600°C 78−27525
steel, stainless stabilised, knife line attack phenomenon, dissoln. of carbide during isothermal heat treatment *(Japanese)* 78−72784
steel, stainless SUS 316, creep fracture at elevated temps. vacuum environment effect *(Japanese)* 77−8942
steel, stainless type 304, AES of stoichiometric Cr carbides and carbide precipitates at grain boundaries 80−3055
steel, stainless type 304, $M_{23}C_6$ precipitation for various cooling cycles 80−60887
steel, stainless type 316, $M_{23}C_6$ carbide precipitation, intermetallic phases, X-ray diffr. study 80−7586
steel, stainless type 316, neutron irradiated, or themally aged diamond-cubic η phase formation, TEM study 79−99249
steel, stainless/Nb interaction in vacuum percussion welding, Ni interlayer effect 79−29061
steel, structural, austenite decomposition, 500 to 450°C 77−16593
steel, structural, CrN-modified, tempering and quenching effects on struct. and props. 77−59835
steel, structural, second phase particle effects on impact strength 80−108581
steel, structural, unalloyed, brittle fracture, grain size and precipitate thickness effect 78−60786
steel, tempered, kinetics of solution of Mn in precipitated cementite *(Russian)* 78−6891
steel, thermomechanical treatment effect on mech. props. and microstruct. *(French, German)* 79−66090
steel, Ti microalloyed structural, precipitation hardening, struct. and fracture *(German)* 79−61696
steel, Ti-V, Ti and V effects on precipitation, hardness and annealing *(German)* 77−55968
steel, tool, M2, laser surface melted, heat treatment effects on struct. 79−70086
steel, tool, type M2, laser melting and heat treatment, microstruct. charact. 79−100188
steel, type 08Kh15N5D2T, high temp. embrittlement *(Russian)* 79−70153
steel, types 10G2 and 18G2F, formation of transform. microtwins in ferrite *(Russian)* 79−1866
steel, V alloyed austenitic stainless, creep inhibition at grain boundaries, VN precipitation 79−43346
steel, V- or Cr- or Mn-, tempering, initial stages of carbide form., electron diffr. *(Russian)* 78−19760
steel, VN precipitation after heat treatment 79−29067
steel, W-Co-Mo-Cr-V-C (8.5, 8.1, 4.5, 3.5, 2.2, 1.02 wt.%), phase composition, struct. and props. 80−104163
steel, weld metal, contrib. to mechanism of Nb(C,N) precip. *(Slovenian)* 78−84816
steel, Zi, high permeability grain-oriented, AlN precip. study 79−83337
steel 30Kh2NMFA, microstructure of cup and cone fracture surface, effect of size of disperse phase particles *(Russian)* 78−68762
steel alloys, low and medium C content, relaxation phenomena in volume changes during tempering *(Russian)* 79−100176
steel austenitic Cr-Ni-Be, cellular precipitation *(Japanese)* 78−11229
steel austenitic stainless, fatigue, low cycle, temp. and strain rate effects *(Japanese)* 79−29198
steel austenitic stainless 316, grain boundary sliding, temp. depend. 77−25110
steel foil, microanalysis by energy dispersive X-ray spectrometry *(French)* 80−85250
steel VNS-2, damping capacity, magnetomechanical, phase transform. effects 78−31445
steelmaking, thermodynamics of rare earths 77−4782
steels, ferritic and martensitic, C and N migration at low temps., monograph 80−22149
steels, hypereutectoid, 120G4 and U15 type, with initially pearlitic struct., mechanism of structural inheritance *(Russian)* 77−52329
steels 2Kh13 and 20Kh1M1FTR, sulphide cracking resistance, strengthening method influence 80−55577
stereological counting measurements, use in testing growth rate theories 80−16311
strain energy and elastic strains *(Korean)* 79−65201
strain energy interactions, T_0 concept, sympathetic nucleation 77−73278
subscales, precipitate distrib. in dilute alloys 79−38834
superconductor, elementary interaction force between flux-line lattice and precipitates 78−10623
superconductors, flux pinning by precipitates 77−47948
supersaturated solid solution, diffusive decomposition 78−76653
supported metal catalysts, particle growth, models 77−8830
supported metal catalysts, particle growth, obs. of Pt on alumina 77−8831
thermally induced structural changes, specimen surface influence 80−103559
thermomechanical treatment on struct. and props. 79−29109

precipitation continued
thin films, precipitation and nuclei form. in presence of condensation centres, thermodynamic model 80−103594
thin films, segregation effects at surfaces and interfaces 80−39475
vacancy adsorption on internal boundaries, rel. to recrystalln. and precip. 78−10084
void swelling, rel. to in-pile precipitation 78−70595
water, mag. treatment affecting props., proposed mechanism 78−84827
weak-beam contrast calculation for spherical coherent precipitates *(French)* 77−35450
Zircalloy in thermal gradient, calc. of supercharging effect of H_2 and hydride distrib. 78−21639
Zircaloy-2, hydride precipitation and growth at crack tips, electron optical obs. 80−108449
Zircaloy-2, TEM study on intermetallics in Zr alloys 79−11622
Zircaloy-4, polytype struct. of intermetallic precipitates, electron microscope obs. 79−43250
Zircaloy-4-O alloys, rapidly heated and quenched, transform. charact. 79−20041
Zircaloy-4/stainless steel, diffusion bonding in presence of Fe intermediate layer 79−10987
Ag, compact, on H_2 permeated backing, precipitation *(Russian)* 78−27520
Ag growth in Ag-Bi and Ag-Pb melts, transition from round to face forms *(Russian)* 79−28906
Ag halides, light scatt. ang. depend. and depolarisation, precip. defects. 77−48141
Ag halogenide, grain form. and growth in metastable soln. *(Russian)* 77−34048
Ag, periodic precipitation, conc. depend. of diffusion coeffs. *(Russian)* 77−16584
β'-Ag-Cd (45 at.%), growth kinetics of bainite plates and Widmanstatten needles 77−36551
Ag-Cd peritectic system, separate crystallisation of phases *(Russian)* 80−66497
Ag-CdO cermets, coprecipitated carbonates and hydroxides, physicomech. props. 80−25706
Ag-Cu, metastable solubility lines on Ag side 78−39737
Ag-Cu (6.2 at.%), tricrystalline specimen, discontinuous precipitation, specific grain boundary energy *(German)* 77−86039
Ag-Cu (6.2 at.%), tricrystalline specimens, fine lamellar discontinuous precipitation *(German)* 78−52822
Ag-Cu (6.2 at.%), tricrystalline specimen, discontinuous precipitation, thermodynamics *(German)* 79−34043
Ag-Cu (6.2 at.%), with discontinuous precipitates, quantitative struct. anal. using SEM 79−43527
Ag-Cu (8 wt.%), deformed, free energy changes in process of discontinuous precipitation 80−3054
Ag-Cu (8 wt.%), plastic deform. effect on discontinuous precipitation 80−3053
Ag-Hg-Sn dental amalgams, non-γ_2 phase, transmission electron metallography 79−74162
Ag-In-Sn, internal oxidation, precipitation behaviour of oxide *(Japanese)* 80−66515
Ag-Pd-Cu-Au dental alloy, age-hardening charact. 79−87646
Al alloy, calorimetric studies on 700 series, matrix precipitate charact. of 7075 77−86036
Al alloy, calorimetric studies of 7000 series, comparison of 7075, 7050 and RX720 77−86037
Al alloy, FIM and microanalysis, developments 80−100155
Al alloy 7075, acoustic emission sources during plastic deform. 78−27573
Al alloy 7075, serrated flow and thermomechanical treatment *(Korean)* 80−30026
Al alloy AL22, influence of ultrasonics application on creep during multistage ageing *(Russian)* 79−91708
Al alloys, continuous precipitation, nucleation, spinodal decomposition 80−3061
Al alloys, neutron irradiation effects, on microstruct., mech. props. and swelling 79−65121
Al alloys, plate shaped precipitates, growth kinetics 80−3065
Al film, vacuum evaporation growth, impurity presence, effects *(Hungarian)* 80−7495
Al, fracture mechanism 80−100903
Al steel, austenite, martensite cryst. struct. changes on γ irrad. 79−90699
Al, superpure, anomalous primary creep behaviour, precipitate form. 80−7646
Al:Sb(Zn), ion implanted electron beam annealing, ion backscatt. and TEM meas. 80−59500
Al-Ag, discontinuous decomposition *(Polish)* 78−52808
Al-Ag, precipitation kinetics and coarsening, effect of interfacial props. 79−91651
Al-Ag (15 wt.%), precipitate growth kinetics 77−28817
Al-Ag (40 wt.%), deformed, free energy changes in process of discontinuous precipitation 80−3054
Al-Ag (40 wt.%), plastic deform. effect on discontinuous precipitation 80−3053
Al-Ag(Au)(Cu), growth kinetics of plate precipitates 77−66649
Al-Al_2Cu, aligned eutectic, precipitation, TEM and microhardness meas. 78−27529
Al-Au (0.2 wt.%), precipitation mechanism and creep behaviour 80−3058
Al-Au(Cu), growth kinetics of plate shaped precipitates 78−6932
Al-Au(Cu), growth kinetics of plate shaped precipitates 78−6933
Al-Au(Cu), growth kinetics of plate-shape precipitates 78−6934
Al-Au(Cu), growth kinetics of plate-like precipitates, vol. diffusion controlled growth 78−6935
Al-Ce (0.06 at.%) alloy, rapidly quenched from melt, vacancy loops and precipitates, TEM 77−59769
Al-Cr, rapidly solidified, crystalline and amorphous structures 77−44274
Al-Cr (0.1 wt.%), exam. of pre precip. behaviour, by elec. resistivity meas. and TEM exam. 78−48406
Al-Cr(Mn), cold-worked and homogenised, precip. kinetics, impurity resist. and TEM meas. 77−16596
Al-Cr(Zr), simultaneous recrystallisation and precipitation *(French)* 80−16313
Al-Cu, intergranular morphology of θ' precipitates, angle between grain boundary/precipitate plane 78−48413
Al-Cu, splat-quenched, microstruct. thickness and comp. depend., TEM 77−8863
precipitation continued
Al-Cu (Ag)(Au), precipitate plate growth kinetics 79−15679
Al-Cu (Mg)(Zn), corrosion of chill zone, solidification microstruct. effect 77−36687
Al-Cu (0.5 to 4.6 wt.%), cathode foil for electrolytic capacitors, relationship between comp., struct., and etchability 79−74314
Al-Cu (2-5 wt.%), precipitation total surface influence on resistivity *(French)* 80−71650
Al-Cu (2.12 at.%), irradiated by 8J CO_2 laser pulses, metastable precipitate and amorphous phase *(French)* 78−80552
Al-Cu (3.5 wt.%), precip. on stationary and non-stationary grain boundaries 78−84820
Al-Cu (3.93 wt.%), planar defects within theta precipitates 77−16583
Al-Cu (4 wt.%), effect of semicoherent precipitation on void swelling, when neutron irradiated 79−42115
Al-Cu (4 wt.%), elastic accommodation of semicoherent θ' 78−64543
Al-Cu (4 wt.%), non IPS geometric surface relief effects associated with diffusional phase transform. 77−32575
Al-Cu (4 wt.%), θ' phase coalescence 79−56985
Al-Cu (4 wt.%), θ'-phase precipitation, characterisation of stages 79−56984
Al-Cu (4 wt.%), with θ' precipitates, relation between elastic limit and hardness *(French)* 79−5018
Al-Cu (4 wt.%) alloy, coherency loss of θ'-phase due to deform. 77−15424
Al-Cu (4 wt.%) alloy, neutron irrad., weak-beam dark-field obs. of dislocations near θ' precipitates 80−107333
Al-Cu (4 wt.%) alloy, θ' precipitate growth kinetics, electron microscope obs. *(French)* 77−44253
Al-Cu (4.2 wt.%), precipitation strengthened, solute depletion at fatigue facets, AES study 79−38973
Al-Cu (4.5 wt.%), cast alloy, ductile intergranular fracture 77−28908
Al-Cu (4wt.%), elastic limit, precipitation effects *(French)* 79−47738
Al-Cu (5 wt.%), ageing, extinction effects *(Russian)* 77−81283
Al-Cu (5 wt.%), fatigue strength, coarse precipitation effect *(German)* 79−91660
Al-Cu alloy bicrystals, neutron irrad. effects on grain boundaries, intergranular fracture and precip. 77−48520
Al-Cu alloy precipitation and heat of evolution, microcalometric obs. *(Japanese)* 78−15406
Al-Cu solid soln., supersaturated, plastic deform. effects *(French)* 79−91748
Al-Cu-Mg (2.0, 1.1 wt.%), Ostwald ripening of S′ precipitates *(Korean)* 79−38831
Al-Cu-Mg (2.6, 0.4 wt.%), Fe, Si, Mn and Ti addition effects on age-precipitation *(Japanese)* 80−20937
Al-Cu-Mg-Si-Fe-Mn-Ti, Si, Fe, Mn and Ti effect on precipitation in solid soln. *(Korean)* 79−66064
Al-Cu-Mn-Zr-Fe-Si (6,0.3,0.18,0.3,0.1 wt.%) experimental evidence of Mn enrichment in Al_2Cu precipitates by EDS in TEM 78−15415
Al-$CuAl_2$, directionally solidified eutectic alloy, effect of heat treatment 77−55977
Al-Cu(Mg)(Zn), cold working causing preprecipitation, thermoelec. power *(French)* 79−8306
Al-Cu(Zn, Ag, Mg_2Si), intermediate precipitates, stability, X-ray, elec. resist. and hardness study 80−3063
Al-Fe, cast, influence of Zr on precipitation, solidification and grain size *(Rumanian)* 78−84813
Al-Ge alloy, Ge particle size, determ. by small- and wide-angle X-ray scatt. 78−19966
Al-Ge alloy, Ge precip., ion irrad., dose rate and temp. depend. 78−79642
Al-Li, ageing mechanism, metastable δ' phase and stable δ phase precip. *(Russian)* 77−8858
Al-Li, alloy, ageing, δ'-phase precip., effect of quenching conditions *(Russian)* 78−19761
Al-Li, diffusion coeff. determ. during hydriding *(German)* 79−29288
Al-Li (10 at.%), struct. changes on annealing, 25-500°C, Li atoms role 80−35183
Al-Li (1.3 wt.%), prismatic dislocation loop rows due to precipitation *(Japanese)* 79−52220
Al-Li alloy, thermal anal. of precipitation 78−15417
Al-Li alloys, precipitating, annealing spectrum 78−31429
Al-Li solid soln., decomposition exam. by secondary ion ion emission *(Russian)* 78−68696
Al-Li-Mn (2.8, 0.3 wt.%), recrystallised sheet, fracture behaviour, SEM and TEM study 80−97566
Al-Mg, Si alloy, void form. under different precip. conditions, after Al ion irrad. 80−59529
Al-Mg (2 wt.%), hardening and fracture charact., β-phase dissolution role 80−81178
Al-Mg (2 wt.%), steady creep charact., precip. effect 80−35189
Al-Mg (5.7 wt.%) alloy, pre-precipitation, elec. resist. investig. 77−32601
Al-Mg alloy, disperse β-phase, kinetic laws of coagulation *(Russian)* 78−27518
Al-Mg_2Si, ageing sequence study by electron microdiffr. 80−81068
Al-Mg_2Si (0.95 wt.%), excess Si effect on ductility 78−27580
Al-Mg_2Si (1 wt.%), precipitation reactions 80−11652
Al-Mg_2Si (1 wt.%) secondary recrystallisation by grain boundary unsewing 79−1886
Al-Mg_2Si alloy, STEM microdiffr. obs. of precip. struct. 80−104167
Al-Mg-Mn alloy, disperse β-phase, kinetic laws of coagulation *(Russian)* 78−27519
Al-Mg-Si, DTA exam. after small and medium deform. 80−21002
Al-Mg-Si, heterogeneous precipitation studies using differential scanning calorimetry 80−3062
Al-Mg-Si, nucleation and precipitation growth on dislocations, electron microscope studies 80−3064
Al-Mg-Si, precipitation of cube-shaped phases, electron diffr. study using TEM *(Japanese)* 79−43251
Al-Mg-Si, under ion irradiated, modification of precipitate interface and effect of precipitates stability 79−77651
Al-Mg-Si alloys, DTA meas. of struct. changes in zones after quenching and isothermal heat treatment 79−52248
Al-Mg-Si alloys, ductile intergranular fracture mechanisms, void formation and nucleation 80−108578
Al-Mg-Si rod, extruded and cold drawn, annealing *(German)* 78−39804
Al-Mg-Ti(Zr), struct. and factors determining brittle intermediate compound form. 78−52817

precipitation continued
Al-Mg(-Zn)(-Zn-Cu), exam. of precipitation struct. by neutron scattering 78−92270
Al-Mn, direct chill-cast, struct. changes during heat treating *(German)* 80−40408
Al-Mn (1 wt.%), commercial, recrystallisation 79−47710
Al-Mn (1 wt.%), single crysts., rolled to (123)[41$\bar{2}$], recrystn. textures 80−104183
Al-Mn (1.8 wt.%), cold-rolled, precipitation and recrystallisation 78−27540
Al-Mn alloys, study of solidification by rapid cooling *(Japanese)* 78−88459
Al-Mn-Si, recrystallisation and precipitation 78−52824
Al-Mn(Cu)-Zr, particle stabilized structures, hot deform. 79−47733
Al-Ni (2 at.%) alloy, rapidly quenched from melt, vacancy loops and precipitates, TEM 77−59769
Al-Ni (3.6 at.%) alloy, quenched from melt, distortion of matrix caused by coherent precipitates, electron diffr. meas. 77−59791
Al-Ni (6 wt.%) alloy, misorientation between subgrains, second-phase particles role, STEM microdiffr. obs. 80−104415
Al-Pd, rapidly solidified, new ordered phase, electron microscope obs. 79−11645
Al-Sb, ion-implanted, precipitation form. and evolution TEM obs. 79−55766
Al-Si, dilute, anomalous primary creep behaviour, precipitate form. 80−7646
Al-Si, hypereutectic Ostwald ripening of Si crystals during solidification *(Japanese)* 79−4962
Al-Si, internal friction and Si precipitate nucleation 78−60690
Al-Si, neutron small angle scatt. study 79−43255
Al-Si (0.57 at.%), Si precipitate dissolution kinetics 80−84935
Al-Si alloy, effect of irrad. on the nucleation of incoherent precipitates 79−8303
Al-Si alloys, neutron irrad., precip. processes, neutron small-angle scatt. obs. 77−4131
Al-Si(Cu)(Zn-Mg-Cu), extraction and phase anal. 79−15673
Al-Zn, comparison between very-slow-neutron transmission and small-angle neutron scatt. expts. 80−19677
Al-Zn, discontinuous decomposition *(Polish)* 78−52808
Al-Zn, grain boundary reaction sites, determ. of struct. aspects, by electron microscopy 80−103359
Al-Zn, isothermal preprecipitation, small angle X-ray scatt. expts. 80−35186
Al-Zn, plastic deform. effect on struct. transform. at elev. temp. *(Czech)* 79−79044
Al-Zn, precipitation struct. and phys. props. effect of miscibility gap *(German)* 78−92265
Al-Zn (11.8 at.%), growth and dissolution of metastable precipitates, neutron scatt. study 79−15671
Al-Zn (12.5 wt.%) alloy, retardation of precip. reaction by DC stress 77−55969
Al-Zn (15 at.%), supersaturated alloy, growth and decomposition kinetics 80−29965
Al-Zn (1.9 at.%), 1 MeV electron irradiated, induced homogeneous precipitation 79−77638
Al-Zn (21.8 at.%), elec. conductivity and α'-precipitates, 276-302°C 77−80758
Al-Zn (30 wt.%), precipitation ageing plastic deform. effects 77−66645
Al-Zn (38 at.%), TEM study of precipitation processes or different microstructures during ageing 80−93561
Al-Zn (40(50)(65) wt.%), deformed, free energy changes in process of discontinuous precipitation 80−3054
Al-Zn (40(50)(65) wt.%), plastic deform. effect on discontinuous precipitation 80−3053
Al-Zn (6.8 at.%), neutron small angle scatt., interparticle interference 77−77514
Al-Zn (6.8 at.%) alloy, elec. resist. temp. depend. rel. to ageing processes 77−77486
Al-Zn (7 at.%), liquid quenched, early stage phase separation, exam. 78−68698
Al-Zn (70, 30 wt.%), decomp. study, 25-160°C *(Czech)* 80−89225
Al-Zn alloy, resist. and X-ray small angle scatt. during GP zone form., theory *(French)* 79−29070
Al-Zn alloy, small-angle neutron scatt. in crit. point regions, 324-435°C *(German)* 77−85993
Al-Zn alloys, preprecipitation, elec. resist., microhardness meas., dislocation-growth distortion interactions *(Japanese)* 77−25053
Al-Zn alloys, room temp. decomp. of metastable phases precipitated at 200°C 78−84814
Al-Zn-Fe-Si, Fe and Si effects on precip., TEM and X-ray diffr. obs., ageing at 90°C 77−48439
Al-Zn-Mg, grain boundary surfaces, plasmon loss satellites in Auger spectra 78−15261
Al-Zn-Mg, oriented growth of precipitates on dislocations, model 80−108448
Al-Zn-Mg, precipitation mechanism, effect of Mg additions *(French)* 77−52330
Al-Zn-Mg, precipitation of η' phase, heat treatment, electron microscope obs. 78−68699
Al-Zn-Mg, stress corrosion cracking, grain boundary precipitate size and distrib. electron microscopy study *(Japanese)* 79−79159
Al-Zn-Mg (3.2, 2.2 wt.%) alloy, GP zone reversion, η' of formation, quant. investig. 77−4784
Al-Zn-Mg (3.6, 1.95 wt.%), ageing and plastic deform., effect on structure, electron microsc. and X-ray diffr. study *(Russian)* 80−81108
Al-Zn-Mg (3.87, 1.79 wt.%) TEM exam. of early stage precipitation, on dislocation lines 79−4972
Al-Zn-Mg (3.87, 1.79 wt.%), oriented growth of precipitates on dislocations, TEM obs. 80−108447
Al-Zn-Mg (4.5, 2 to 3 at.%) solid state reactions by interrupted continuous heating. 80−25737
Al-Zn-Mg (5,1 wt.%), decomp. process, TEM study 80−71660
Al-Zn-Mg (5,2 wt.%), TEM of early stages of precipitation 77−40423
Al-Zn-Mg (5.9, 2.9 wt.%), ageing effects on microstruct. 80−16306
Al-Zn-Mg alloy, elec. resist. of η' precipitates 77−48441
Al-Zn-Mg alloy, TEM characteris. of precipitates 80−104166
Al-Zn-Mg alloy, thermomechanically treated, precip. behaviour 78−84856
Al-Zn-Mg alloy, thermomech. treatment, precipitation and strengthening 79−24527
precipitation continued
Al-Zn-Mg(Mg-Ti), TEM exam. of early stage ageing behaviour, exam. of precip. kinetics 78−56645
Al-Zn(Ag)-Mg, metastable T′ phase 77−21151
Al-Zr, cast, precipitation and solidification *(German)* 77−36519
Al-Zr, interphases, formed during precipitation and solidification *(German)* 79−29062
Al-Zr, solidification and precipitation, Zr effect on cast struct. *(German)* 77−36518
Al-Zr (0.22 wt.%), hardness and struct. changes during prolonged ageing at 350, 400 450°C *(Japanese)* 79−52281
Al-Zr solid soln., discontinuous precipitation of metastable Al_3Zr 78−3130
AlCuMgPb, microstruct. and flow stress during deform. at 573K 77−81307
Al_2O_3 hydrated gel synthesis by homogeneous precip. method using $NaAlO_2$, phase change by heating *(Japanese)* 78−68937
α-Al_2O_3, radiation damage in HVEM, at high temp. and high dose 79−46707
Al_2O_3, sintered, containing $MgAl_2O_4$ precipitates, Mg distribution at grain boundaries 78−80498
Al_2O_3, sintered, TEM ons. of K containing β'' precipitates 78−27522
α-Al_2O_3:Fe, ferrimagnetic resonance exam. precipitate nature and size determ. 78−48405
Al_2O_3:Fe, pore form. during oxidative annealing, grain growth slowing 80−100856
Al_2O_3-ZrO_2 cast refractories, nucleation processes reconstruction by SEM, TEM and STEM 78−35380
Al_3Ti, precipitate shape, and distribution in chill-cast Al-14 wt.% Ti alloy 80−16310
Au, Co-hardened, characterisation by Mossbauer spectroscopy, Co precip. formation 80−80108
Au electrodeposited coating properties obs., Cu diffusion under high temperature *(Czech)* 78−91486
Au-Co electrodeposits, heating effect on microstruct. and surface topography 77−43456
Au-Cr alloy pressure gauges, annealing effects 78−49854
Au-Cu-Ni(Ag), phase precipitation on domain boundaries *(Russian)* 78−39777
Au-Fe, polygonisation, recrystallisation, precipitation microstruct. without external plastic deform. 79−43276
Au-Fe (40 at.%), discontinuous precipitation reaction at grain boundaries 79−87642
Au-Ge contacts on GaAs, SEM and TEM obs. of struct. 80−100522
B-Mg-N system, precipitation mech. of BN 79−70068
B-transition metal, amorphous thin film, crystallisation, TEM obs. 79−19483
BN, cubic, growth pressure-temp. region in system BN-Mg 79−66053
B_2O_3-Li_2O-Fe_2O_3, prep. by quenching methods, exam. of microcrystalline precipitates of Li_2O-Fe_2O_3 *(French)* 79−20019
BaF_2, formation and growth of oxidation centres result of O^{2-} diffusion 80−7706
Be ingot, high-purity, TEM obs. of BeO dispersion 80−104165
Be, phase struct. *(Russian)* 78−15401
Be-bronze BrB2, struct. and phase transform. during mechano-thermal treatment *(Russian)* 80−11667
$Bi_{95.6}Mn_{4.4}$, magnetisation of ferromag. precipitates, effect of ultrasonic pulses 80−2121
CC Al-Zn-Mg (4.5,1(2)(3) at.%), decomposition during ageing, preageing and cooling rate influence 80−20938
$Ca_2(Al,Fe,Cr)O_5$ solid soln., planar interfaces, TEM obs. 80−65008
CaF_2:CaO, optical scatt., absorpt. at 205 nm 80−20669
Ca_2TiO_3-La_3AlO_3, synthesis of solid solution by coprecipitation 79−1836
Cd-Zn alloys, splat-quenched, X-ray diffr., SEM and TEM study of struct. 79−66077
$CdBr_2(I_2)$, vapour growth crystals, decomposition, electron microscope study 78−92268
CdF_2:Eu, role of solution and precipitation phenomena on ITC spectra 80−7265
$Cd_xHg_{1-x}Te$, precip. 77−90352
CdSe, X-ray topography 77−89441
CdTe, low temp. themal cond., growth parameter influence 80−92725
CdTe, thermal cond. and X-ray topography investig. of cryst. defects 77−39706
CdTe:Cl, LPE from $CdCl_2$ soln., elec. props., defects 80−39689
CdTe:Cu films, impurity behaviour, Hall mobility and hole density meas. 80−80420
CdTe:In precipitation and out-diffusion of solute during cooling 80−100840
CdTe:P, annealing induced lattice defects, TEM obs. 80−2010
CdTe:Tl, growth by travelling heater method, elec. and optical characterisation 77−40356
$CeCo_{5-x}Cu_x$, $0 \leq x \leq$ internal oxidation kinetics, oxide struct., X-ray study 80−104329
Co, compact, on H_2 permeated backing, precipitation *(Russian)* 78−27520
Co-Al solid soln., lamellar spacing in discontinuous precipitation, expt. proof of Gaussian distrib. *(German)* 77−36517
Co-Cr-C alloys, $M_{23}C_6$ precip. mechanism 78−44130
Co-Cr-Ni superalloy Mar-M509 standard and Mo modified, phase anal. 77−63675
Co-Cr-Nr-TaC eutectic alloys, fatigue, microstructure effects 78−23803
Co-Fe-Nb (12, 3 wt.%), semihard magnetic alloy, relationship between precipitation and coercivity 77−8839
Co-Fe-Nb alloys, effect of cold working on mag. props., and precipitation morphology 78−39803
Co-Ni-Cr superalloys, γ'-precipitation-strengthened, yielding 77−8894
Co-Ni-Cr-C, carbide precipitation 79−29065
Co-Ni-Cr-Nb, effect of Fe addition on precipitation behaviour 80−29962
Co-Ti-C, secondary precipitation and allotropic transform., TEM obs. 80−108453
Co-W alloy electrolytic coatings, heat treatment effects on coercivity, hysteresis and structure *(Russian)* 80−60381
Co_4CuCe, cryst. struct., mag. characts., ageing and decomposition *(Russian)* 79−4272
$Co_2Ga_{2-x}Cu_x$, mag. and struct. phases from magnetisation, neutron, X-ray diffr. techniques 78−52253
$Co_2Ga_{2-x}Ni_x$, mag. and struct. phases from magnetisation, neutron, X-ray diffr. techniques 78−52253
Co_5Sm crystals, microstruct., homogeneous precip. and nucleation 80−104160

precipitation continued
Co_5Sm, magnetic domains, nucleation and pinning, magneto-optical Kerr effect 80−39811
Cr condensates, lattice const., internal stresses *(Russian)* 80−107141
Cr-C, binary alloy formation of nonequilib. Cr_3C in alloys quenched rapidly from melt 80−7581
CsI:Na, crystal, kinetics of decay of surface solid soln. 79−23810
CsI:Tl, precipitation of Tl solid solns. 80−70419
Cu alloy, creep fracture prediction, intergranular damage meas. 77−21268
Cu alloys, continuous precipitation, nucleation, spinodal decomposition 80−3061
Cu, cementation, electrochem. nucleation and growth on Fe and Al, TEM 80−104451
Cu, cementation, on Fe, deposit struct., reaction rates, SEM 80−104421
Cu, compact, on H_2 permeated backing, precipitation *(Russian)* 78−27520
Cu matrix, small oxide precipitates, two-phase system, sputtering and secondary ion emission 78−39650
Cu vacuum coating on steel substrate, influence of precipitation conditions on porosity *(Russian)* 80−54578
Cu:Co precipitates, mag. anisotropy, precipitate shape, coercive force 80−80500
Cu-Ag (8 wt.%), deformed, free energy changes in process of discontinuous precipitation 80−3054
Cu-Ag (8 wt.%), plastic deform. effect on discontinuous precipitation 80−3053
Cu-Al martensite, low temp. hardening, formation of clusters and stacking faults 79−43260
Cu-Al-Fe (11, 2 and 1 wt.%), Fe effects on microstruct. and mech. props. *(Korean)* 77−28807
Cu-Al-Fe-Mn, phase transform. during continuous cooling *(German, English)* 79−70044
Cu-Al-Ni-Fe, (10, 5; 5 wt.%), cast microstruct. 78−80535
Cu-Al-Ti, formation of modulated structure rel. to barrier nucleation of new phase *(Russian)* 77−32580
Cu-Al-Ti-Zr, internally oxidized, morphology of precipitates and dispersion hardening *(Russian)* 79−52217
Cu-Au-Fe, ferromag. ordering in FCC γ-Fe precipitates, Mossbauer study 80−71267
Cu-Be, quasiperiod struct. form. mechanism in eutectoid dissoc. 77−44257
Cu-Be (1.8 wt.%) alloy, discontinuous precip. form. and growth, TEM obs. 80−104169
Cu-Be (2 at.%), plastic deform. and dislocation substruct. 80−76307
Cu-Be (2 wt.%), alloying addition effects on grain boundary reaction *(Japanese)* 80−49236
Cu-Be (2.1 wt.%), discontinuous precipitation *(Japanese)* 78−19766
Cu-Be (6.2, 9.3, 13.4 at.%), cell growth of discontinuous precipitation *(Japanese)* 79−24525
Cu-Be alloys, CuBe precipitation 80−29966
Cu-Be alloys, relationship between discontinuous precipitation and continuous precipitation 79−100144
Cu-Be-Co, cuboid (Co, Cu, Ni, Fe)Be inclusions, metallography, ageing effects 80−11645
Cu-Be-Co, discontinuous reaction, analytical TEM 80−100842
Cu-Be-Co (1.8, 0.2 wt.%), TEM obs. of precipitates, ageing charact. *(Korean)* 77−66648
Cu-Be-Ni (1.9, 0.32 wt.%) solution treated alloy, age induced vol. changes in structural transformations *(Russian)* 79−100179
Cu-Be(25 wt.%), discontinuous precipitation *(Japanese)* 80−55402
Cu-Be(30 at.%), eutectoid decomp., elastic interaction between precip. phase particles *(Russian)* 77−8833
Cu-Cd(2.7 wt.%), cellular precipitation kinetics and dissolution *(German)* 80−11651
Cu-Co, thermoelectric power, precipitation effects *(German)* 77−85200
Cu-Co alloy, ageing and reversion phenomena 79−91718
Cu-Cr, age hardened, fine precipitates struct., TEM study 80−3066
Cu-Cr (0.55 wt.%), crystallography of precipitates, strain field study 80−25699
Cu-Fe, dil., diffusion and ageing processes, Mossbauer study 80−7245
Cu-Fe, dilute, low temp. heat capacity in mag. field, superparamagnetism 80−39804
Cu-Fe, growth kinetics and interfacial energy of coherent γ-Fe particles *(Japanese)* 78−19765
Cu-Fe, Mossbauer studies of ageing and precip. 79−38415
Cu-Fe, precipitation kinetics study by thermoelectric power measurement *(French)* 79−20050
Cu-Fe, precipitation processes during aging, TEM, resistivity, hardness study *(Japanese)* 80−35221
Cu-Fe, thermal treatment effect on thermoelec. power *(French)* 77−32000
Cu-Fe (0.2 at.%), clustering, precipitation, and oxidation, 298 to 919K, Mossbauer study 80−7242
Cu-Fe (1.5 wt.%), precipitation-effect on void formation during electron irradiation 80−84211
Cu-Fe (<4 wt.%), solubility determ. by thermoelectric power meas. *(French)* 77−62644
Cu-Fe system, ageing and reversion phenomena study 80−89274
Cu-Fe(2.5 wt.%), isothermally reacted austenite stability in very small particles 77−48432
Cu-Ga, high dislocation density alloys and oxide precipitated struct., NMR, spin echo 80−39892
Cu-In, thermally cycled, effect on mech. props. and microstruct. 79−4987
Cu-In(Sb), growth kinetics, of discontinuous precipitation, third element effects 77−36511
Cu-Mg(Sn) precipitating phase nuclei, diffuse X-ray scattering intensity determ. *(Russian)* 77−86031
Cu-Mn, positrons as probe of phase transforms. 78−31401
Cu-Mn (38 to 58 wt.%), age hardened, exam. of precipitation and strengthing 78−72782
Cu-Mn-Al, constricted hysteresis loop rel. to microstruct. 78−19273
Cu-Nb (0,4 at.%), splat quenched, aged, superconductivity *(Japanese)* 77−63018
Cu-Nb-Sn dil. alloys containing Nb_3Sn precipitates, superconductivity 78−43507
Cu-Ni alloys, artefacts in thin foil images 80−3056
Cu-Ni film, (001), in situ oxidation, TEM obs. 78−23874
Cu-Ni-Al, ageing charact., optical TEM, X-ray, hardness obs. 79−29079

precipitation continued
Cu-Ni-Be-(Al) (30,0.5,(0.2-2) wt.%), Al addition effect on grain boundary reaction *(Japanese)* 80−54254
Cu-Ni-Cr (28, 2.8 wt.%), spinodal alloy, microstruct. and tensile props. 78−39858
Cu-Ni-Fe, age hardened, yield strength correlation with internal coherency strains 77−44254
Cu-Ni-Fe solid solution, after precip., susceptibility of interacting superparamag. grains 79−99733
Cu-Ni-Nb (30,1 wt.%), precipitation 77−86035
Cu-Ni-Nb-Al, correlation of γ′ and γ″ precipitates phase stability 80−25704
Cu-Ni-Nb-Al, formation of γ′ and γ″ precipitates 78−76655
Cu-Sb solid soln., finely lamellar discontinuous precipitation, ternary addition effects 77−36510
Cu-Si, high dislocation density alloys and oxide precipitated struct., NMR, spin echo 80−39892
Cu-Sn (25 wt.%), struct. changes with ageing *(Russian)* 77−40421
Cu-Sn-Mg, precipitation, effect of thermomechanical treatment *(Japanese)* 79−4970
Cu-Ti, ageing effect on internal friction and elastic props. *(Russian)* 77−28842
Cu-Ti, deform. effect on precipitation and recrystallisation, electron microscope study 77−70115
Cu-Ti, dil. alloy, cellular precipitates, nucleation, TEM study 80−3069
β-Cu-Ti, dil. alloy, growth phenomena associated with precipitation, TEM study 80−3070
Cu-Ti, internally oxidised, morphology, struct., particle precipitation singularities *(Russian)* 79−70067
Cu-Ti, Zr effects on cellular precipitation 77−16587
Cu-Ti (1.07 wt.%), containing coherent precipitation, observations of flow and fracture 78−80643
Cu-Ti (4 wt.%), combined recrystallization and precipitation 79−29072
Cu-Ti-Cr(Fe), internally oxidised, morphology, struct., particle precipitation singularities *(Russian)* 79−70067
Cu-V-Ga dil. alloys with V_3Ga particles, supercond. props. and microstruct. 78−39278
$CuAl_2$, topological evolution during soln. heat treatment 77−32607
Cu_3Au-Co, single crystal, overaging mechanism 79−20081
CuCoNi ferrite magnetoacoustic oscills. rel. to microstruct. 77−85536
$CuFeO_2$-Fe_2O_3, decomposition kinetics and mechanism of spinel solid soln., composition and precipitation effects *(Japanese)* 77−77489
$CuGaSe_2$ crystals, electron probe microanal., correction procedure 80−2171
$CuInSe_2$ crystals, electron probe microanal., correction procedure 80−2171
CuMn, acceleration of coarsening by temp. changes, study by resistivity meas. 79−47718
$Cu_{2+x}Mn_{1-x}Al$, omega phase, roles of electron microscopy and electron diffraction *(French)* 78−27524
Cu_2O foils, electron microscope exam., Cu precipitates and CuO form. 79−1462
Cu_2S, molten, oxidation, exam. of product phase composition by X-ray anal. *(Russian)* 79−34166
η-Cu_3Si precipitates in Si, cryst. struct. 78−91304
CuZn, omega phase, roles of electron microscopy and electron diffraction *(French)* 78−27524
ErZn, preferred mag. domain orientation, and microstructural defects, magnetostriction meas. 79−73769
FE, electrolytic, dissolved H precip., effect on flow stress *(Japanese)* 78−39848
Fe, (100) surface, S segregation and 2D compounds precipitation *(Japanese)* 80−35188
Fe alloys, anisotropic precipitation struct. in external mag. field *(German)* 78−72785
Fe and Fe-Cr, flow stress, effect of cathodic, H_2 charging *(Japanese)* 79−52313
Fe, Armco, inter- and intragranular sulphidation 80−55570
Fe, cast, interdendritic dispersed graphite, dissolution kinetics on heating, excess time *(Russian)* 77−52360
Fe, cast, pearlitic, nodular graphite type, struct. evolution *(French)* 80−93551
Fe, cast, with Mn, high S, exam. of sulphide phases, cocrystallisation during solidification 78−56646
Fe, compact, on H_2 permeated backing, precipitation *(Russian)* 78−27520
Fe, diffusion and solid solubility of Sb, 773-873K, ion backscatt. anal., rel. to intergranular embrittlement 78−71880
Fe, gray, Mg bearing, high strength, eutectic grain determ. by Si reverse liquation 79−15886
α-Fe, irradiation induced void swelling, Cr additions effect 80−55408
Fe, microcracks formed by H_2 precipitation, SEM and TEM obs. *(Japanese)* 79−70071
α-Fe, nitrided, aging at room temp. 80−71679
Fe, pure, hydrogen-charged, initial cracking obs. 80−108580
Fe, reaction with methane at 750 C micro Auger anal. 80−104020
Fe-Al, liquid, N solubility, AlN precipitation 79−11630
Fe-Al-C, low C, precip. of carbides and cementite after quenching and ageing 78−52814
Fe-Al-N alloy, precipitation and coarsening of AlN *(Korean)* 79−91652
Fe-B, eutectic, crystallisation *(Russian)* 79−70087
Fe-B amorphous alloy, annealed, microstruct. and mag. domain changes 80−75790
Fe-Be, formation of quasi-periodic distrib. of precipitates during ageing *(Russian)* 78−56642
Fe-C, proeutectoid ferrite nucleation kinetics at austenite grain boundaries 80−55405
Fe-C (30 at.%), production of Fe_7C_3 at high press., morphology and microstruct. *(Russian)* 79−38828
Fe-CR (26 wt.%), role of C and N in brittle fracture 80−16456
Fe-C(0.47 wt.%) austenite, obs. of morphology and crystallography of proeutectoid ferrite 77−8837
Fe-Co-Cr, magnetic, phase transform. obs. *(French)* 79−47676
Fe-Co-Ta for semipermanent magnets *(French)* 79−47675
Fe-Co-V (2 wt.%), gamma phase 77−36514
Fe-Co-V(-Ni), annealing effect on microstruct. rel. to mag. and mech. props. 80−89267
Fe-Co-W-C steel, M_6C carbide behaviour during ht. treatment *(Russian)* 77−66658
Fe-Cr, decomposition Mossbauer study *(French)* 77−63678

precipitation continued
Fe-Cr, grain-boundary segregation of carbon, electrochemical study 79−100147
Fe-Cr, irradiation induced void swelling, Cr additions effect 80−55408
Fe-Cr-Al (7, 5 wt.%), expt. stainless alloys, phys. and mech. props. 80−97637
Fe-Cr-C, austenite to ferrite+precipitate reaction, TEM/STEM study 80−3075
Fe-Cr-C, isothermal transformations 80−16302
Fe-Cr-C (10,0.2 wt.%), isothermally transformed, precipitate orientations 80−50640
Fe-Cr-C (10,0.2 wt.%) isothermally transformed, carbide distrib., microstruct. development 80−3076
Fe-Cr-Co, mechanism of coercive force 80−34674
Fe-Cr-Co-Mo, microstruct., hardness, mag. props., influence of isothermal tempering and heat treatment 79−79129
Fe-Cr-N (5.9, 0.5 wt.%), martensitic, tempered, fine struct. 77−25079
Fe-Cr-Nb-C, X-ray microanal. of carbide phases rel. to Nb conc. *(Russian)* 78−88467
Fe-Cr-Ni, α-particle induced precip. and phase instability 79−1470
Fe-Cr-Ni alloy 800, sensitization times for intergranular corrosion 77−16746
Fe-Cr-Ni liquid alloy, N_2 soln. and TiN precipitation 78−6931
Fe-Cr-Ni melts, S solubility and solid soln. precipitation *(Russian)* 80−15251
Fe-Cr-Ni-Nb-C, austenitic, splat quenching 78−72798
Fe-Cr-V-C, X-ray microanal. of carbide phases rel. to V conc. *(Russian)* 78−88467
Fe-Cr-(Co), decomposition of solid soln. in mag. field, neutron and X-ray diffr. study *(Russian)* 78−68694
Fe-Cu (1.2 wt.%) effect of precipitation on recrystallisation, texture 78−88476
Fe-Cu alloy, effect of ε-Cu phase on strain ageing *(Japanese)* 80−7582
Fe-Cu alloy, vapour-deposited, struct. and thermal stability 78−43265
Fe-Cu alloys, transform. substruct., lath microstructure after quenching 80−16298
Fe-Cu-Ni, austenite to ferrite+precipitate reaction, TEM/STEM study 80−3075
Fe-Cu-Ni, Ni effect on austenite decomposition 80−3048
Fe-Cu-Ni (2, 5 wt.%), interphase precipitation obs. in assoc. with Widmanstatten ferrite lateral growth 80−40365
Fe-Cu-Ni (2,2 wt.%), isothermally transformed, precipitate orientations 80−50640
Fe-Ga (25 at.%), precipitation *(French)* 77−70057
Fe-Ge (10 to 50 at.%), phase diagram rel. to heat treatment, supercooling diagram *(German)* 78−92240
Fe-Mn (1 at.%), strain age hardening 80−108472
Fe-Mn-Ni-V-C (0.5, 3.0, 1.0, 0.2 wt.%), austenite decomp., isothermal transform. characts. 80−97477
Fe-Mn-S, thermodynamics, solubility of S and Mn in γ-Fe, 1100 to 1300°C 79−47662
Fe-Mn-V-C (0.5, 1.0, 0.2 wt.%), austenite decomp., isothermal transform. characts. 80−97477
Fe-Mn-V-C austenitic steel, discontinuous precipitation, morphological changes 80−3078
Fe-Mo (3at.%), internally nitrided, precipitate, morphology and chemistry 78−44128
Fe-Mo-Au, orienting of precipitating Au particles by external elastic stress 77−73279
Fe-Mo-C alloy, splat cooling, microstruct. changes 78−84855
Fe-N, neutron irrad. effects on mech. props. 79−4338
Fe-N, nucleation and precipitation growth on dislocations, electron microscope studies 80−3064
Fe-N, precipitated $Fe_{16}N_2$ nitride distrib. during isothermal ageing 77−21143
α-Fe-N, supersaturated solid solns., N atom precip. kinetics, resist. meas. 80−60864
Fe-N (0.022 wt.%), quenched, N precipitation during isothermal ageing 77−28820
Fe-N (0.03 at.%), single cryst., precipitation distrib. around spherical inclusion, TEM study 79−34038
Fe-N alloys, secondary ion emission, phase transforms. effect *(Russian)* 80−66347
Fe-N single crystals, solid soln. stress assisted nucleation of α″ precipitates 78−52810
α-Fe-N solid soln., N precipitation kinetics, defects effect 77−59789
Fe-N(C), solid soln., metastable and stable, interstitial atom config. 77−36512
Fe-N(0.013 wt.%), effect of electron irradiation on precipitation 79−52221
Fe-Nb creep resistant alloy, precipitate free zones elimination 80−16312
Fe-Ni, austenite formed from martensite during annealing in (α+γ) region, crystallographic study 78−19782
Fe-Ni austenite, precipitation hardened, transform. strengthening 79−24531
Fe-Ni-Al, liq. alloys, N solubility and AlN precipitation 80−11648
Fe-Ni-Al, magnetic anisotropy form. and struct. changes by annealing, Mossbauer obs. 80−39994
Fe-Ni-Al-Ti alloy, N27Yu2T2, aged austenite, diffuse electron scatt. distrib. during martensitic deform. *(Russian)* 78−60669
Fe-Ni-C, Fe rich portion of phase diagram determ. 79−24497
Fe-Ni-C, model alloy, intercrystalline brittleness caused by segregation and precipitation in austenite *(Slovak)* 79−70073
Fe-Ni-C, quenched martensite, annealing during cathodic hydrogenation, 200°C *(French)* 80−93573
Fe-Ni-C martensite, autoradiographic evidence of C clustering 79−83203
Fe-Ni-Co, diffusion controlled phase growth 78−30782
Fe-Ni-Cr, austenitic, creep strength and ductility, effect of γ′ precipitation 77−36597
Fe-Ni-Cr, Elinvar, struct. and mag. props., singularities during tempering *(Russian)* 80−50627
Fe-Ni-Cr (40, 15.8 wt.%), precipitation and creep rupture behaviour, optical and TEM study 79−74158
Fe-Ni-Cr alloy, carbide form. by C diffusion, precip. distrib. and morphology 80−104164
Fe-Ni-Cr alloy 800, creep ductility decline 77−48502
Fe-Ni-Cr alloy 800, minor alloying element effect on creep, ageing microstruct. 78−27572
Fe-Ni-Cr-Ti-Al, ausaging alloy, cellular precipitate indentification *(Chinese)* 78−11225
precipitation continued
Fe-Ni-Mo, small angle X-ray scatt. study, pre-precipitation phenomenon obs. *(French)* 78−19757
Fe-Ni-P, interface composition during diffusion controlled precipitate growth 77−36513
Fe-Ni-Ti (30, 6 wt.%), austenitic, discontinuous coarsening of lamellar cellular precipitates, morphology 79−78967
Fe-Ni-Ti (30, 6 wt.%), austenitic, discontinuous coarsening of lamellar cellular precipitates, growth kinetics 79−78968
Fe-Ni-Ti alloy, ageing mechanism, neutron diffr. expts. *(Russian)* 78−48403
Fe-Ni-Ti martensitic alloy, γ′ particle effect on crystallisation struct. *(Russian)* 78−44129
Fe-Ni-Ti-C (31, 4, 0-18 wt.%), coherent precipitates in austenite, effect on martensite substruct. 77−52327
Fe-Ni-V, nitrided austenitic alloys, modulated substitutional interstitial solute atom clustering 79−74160
Fe-Ni-V alloy, ageing of martensite *(Russian)* 78−39808
Fe-Ni(Si), precipitation of AlN *(French)* 78−23711
Fe-O-Ca-Al system, inclusion precipitation diagram 80−108415
Fe-P-C, amorphous alloy, crystallisation 79−100112
Fe-Sb-Ti(V)(Cr)(Mn)(Co)(Ni), dil., interactions and precip., Mossbauer study 80−39997
Fe-Si (3 wt.%), AlN-inhibited, Se effect on primary grain recrystallisation 77−12715
Fe-Si (3 wt.%), chemical comp. and hot rolling effect on brittleness *(Czech)* 80−50712
Fe-Si (3 wt.%), grain oriented, MnS-AlN-inhibited, precipitate morphology 77−12648
Fe-Si (3 wt.%), grain oriented, MnS precipitate distribution, electron microscope observation *(Chinese)* 78−95751
Fe-Si (3wt.%), grain-oriented, secondary recryst., grain growth inhibition 80−89245
Fe-Si-Al (5,10 wt.%) struct. anal. by electron microscopy and electron diffr. *(Chinese)* 79−11618
α-Fe-Ti, ion implanted, microstruct., ion beam anal. and TEM study 80−107294
α-Fe-Ti, ion implanted, with C impurity, microstruct. of TiC precips. 80−66513
α-Fe-Ti, ion-implanted and annealed, microstruct. evolution 80−15132
Fe-Ti-C, rapidly quenched by splat-cooling 80−84923
Fe-V (1 wt.%), nitrided and annealed, struct. 77−8998
Fe-V-C, austenite to ferrite+precipitate reaction, TEM/STEM study 80−3075
Fe-V-C (0.3, 0.05 wt.%), interphase precipitation obs. in assoc. with Widmanstatten ferrite lateral growth 80−40365
Fe-V(Nb)-N, precipitation study, 550 to 600°C *(German)* 77−90350
Fe-W-C, eta carbides at 1250°C 77−36506
Fe-W-C-Cr, eta carbides at 1250°C 77−32581
Fe-W-Cr-Mo-Co with austenitic phase, magnetic and mech. props., cold working and ageing effects *(Japanese)* 78−60678
Fe-Zn, physical-chemical metallurgy *(German)* 80−108390
$Fe_{36}Cr_{12}Ti_7Mo_3$, high temp. precipitation kinetics, internal friction study 79−43254
FeN alloy, coercive force, effect of $Fe_{16}N_2$, anisotropic model 77−85501
$(Fe_yNi_{1-y})_{80}B_{20}$, mag. anneal anisotropy in amorphous alloys 77−16069
$Fe_{1-x}O$, precipitation of Fe_3O_4 during decomposition 78−84823
$Fe_{1-x}O$, wustite decomposition, coherent magnetite precipitation, electron diffraction study *(Russian)* 80−16318
Fe_3O_4, precipitation in YIG 78−84815
Fo-Fe-Nb, cold-worked and aged, mag. props. and microstruct. 80−34690
Ga-Cu-Sn solders, exam. of structural transformations due to hardening, heat treatment *(Russian)* 80−7578
Ga-In-Sb system, precipitation of solid phase from liq. phase, thermodynamical formulation *(French)* 77−28003
$Ga_{1-x}Al_xAs$ DH injection laser diode, long-term-degraded, TEM obs. 78−71102
GaAs epitaxial layers, non-doped, from Ga-$AsCl_3$-H_2 system, TEM and RHEED study of micromorphology and defects 79−65340
GaAs, etched, saucer-pit defect identification 78−43021
GaAs, laser annealed, Ga precipitation, Rutherford backscattering and TEM study 79−79127
GaAs:Li diffused, lattice imperfections, TEM 77−80521
GaAs:Si defect density before and after Zn diffusion, SEM and TEM obs. 80−96529
GaAs:Te, LPE, Te induced defects, rel. to growth conditions 78−6067
GaAs:Te, preferential precipitation on dislocation loops 79−7612
GaAs:Zn(Cr), As precipitation at dislocations, TEM study 80−79820
$GaAs-Ga_xAl_{1-x}As$ laser, degradation, TEM obs. 77−51625
GaP crystal, structure defect formation due to annealing and stress, dendrites, slip, dislocations 80−29026
GaP:S, defect struct. and tetrahedral precipitates, TEM study 80−107246
GaP:S LEC grown crystals, HVEM investig. of defects 79−60376
GaP:Te, defects formed due to precipitation of Te, metallography and TEM exam. 77−84769
GaP:Zn, light attenuation by impurity precipitates 79−11441
$Gd_3Ga_5O_{12}$, decorated dislocations, large interstitial climb loops round precip. particles 77−19960
$Gd_3Ga_5O_{12}$, precipitates assoc. with dislocation climb trails *(German)* 77−35567
$Gd_3Ga_5O_{12}$, single cryst., helical dislocation obs. by etching 77−11558
Ge, amorphous thin films, fast crystn. and void precipitation in laser pulse annealing, TEM exam. 79−56086
Ge, As impurity precipitation from solid soln., neutron irrad. effect 80−29177
Ge:As, containing dislocation loops, dynamic scatt. of X-rays, extinction effect 78−47384
Ge-As, supersaturated solid soln., dislocation form. during thermocyclic treatment *(Russian)* 80−3057
Ge-Si alloys, n-type, phosphorous doped, precipitation effects due to heat treatment 80−107833
H_2 in Al-Zn-Mg at grain boundaries after water vapour embrittlement 78−15564
Hf-Nb (30 to 50 at.%) exam. of beta phase decomposition processes 78−76674
$HfAl_3$, anomalous growth in thin films, AES, TEM and He backscatt. meas. 77−43462
$Hf_{0.65}Nb_{0.35}$, superconducting alloy, transition temp. and flux line pinning 77−43772

precipitation continued
$(Hf_xZr_{1-x})_{80}Nb_{20}$, influence of Hf additions to ω-phase precip. kinetics 79−8304
$HgCr_2Se_4$:Cd, precipitations during growth by chem. transport method 80−55409
$Hg_{1-x}Fe_xTe$, struct. invest. using X-ray diffr. and electron microscopy 80−75365
In film, vacuum evaporation growth, impurity presence, effects *(Hungarian)* 80−7495
In surface, impurity precipitation and resolution at melting point 78−14553
InP:Fe, precipitate mixture 77−77485
InSb:Se, exam. of defects in crystal 80−6423
InSb-Sb alloy, form of growth of Sb crysts., precip. temp. effects *(Russian)* 77−21144
KBr(Cl):Mg^{2+}, dopant aggregation and precipitation 80−107306
$KCaCl_3$, form. of equilib. pseudocubic phase from supersaturated solid soln. based on NaCl *(Russian)* 77−63681
$KCaCl_3$ impurity in NaCl cryst., precipitation and dissolution 79−42259
KCl, pure and Ba-doped, rel. to γ-irrad. effects on intensity distrib. of diffuse X-ray scatt. 77−24329
KCl:Ba (0.005 at.%), spatial diffuse X-ray scatt. intensity distrib. 77−7757
KCl:Ba^{2+}, localised stress relaxation in excess vacancy system, prismatic loops *(Russian)* 80−88160
KCl:Ba^{2+}, precipitation kinetics, supersaturation effects, geometry of formed heterophase struct. *(Russian)* 78−84824
KCl:Ba(Ca)(Sr), microstruct. and hardness, impurity distrib. effects 79−24529
KCl:Br^{2+}, solid solution periodic precipitation in inhomogeneous conc. field 80−103485
KCl:Ca^{2+}(Sr^{2+}), impurity precip., flotation density obs. 78−51690
KCl:$CdCl_2$, elec. cond., role of electrode material, surface precipitation effects 80−59985
KCl:Pb, impurity distrib., light scatt. and microhardness study, heat treatment 80−96562
KCl:Pb^{2+}, highly doped, state of dispersion of Pb^{2+} 77−1144
KCl:Pb^{2+} crystals, density changes, nucleation mode, lattice relaxation 79−66066
KCl:Sn^{2+}, thermally stimulated space charge decay 78−48111
KCl-$BaCl_2$ supersaturated solid soln., deformed, $BaCl_2$ precipitation kinetics, metastable region *(Russian)* 78−60673
KCl-CuCl solid solution supersaturated, precipitation, impurity aggregation 80−29174
K_2O-MgO-SiO_2 glass, crystalline phase precipitation during crystallisation early stages, DTA *(Japanese)* 78−42919
$LaNi_5$, self restoring of active surface, photoemission, mag. susceptibility study 78−48280
LiF:Co, flow stress changes during precipitation 80−92594
LiF:Co^{2+}, solid soln. decomp., precip. of new phase, electron microscope expt. 79−11619
LiF:Co^{2+}, X-ray and electron microscope obs. of CoF_2 precip. morphology 77−31777
LiF:Fe, Mossbauer study of Fe precipitates 79−91327
LiF:Mg^{2+}, TLD-100, precipitation reactions and ionic cond. 77−56479
LiF:Mg^{2+}, TLD-100, solution treatment temp. and ageing effects 77−56480
$LiFe_5O_8$, hysteresis and other mag. props. rel. to microstruct., TEM investig. 77−20636
Li_4GeO_4-Zn_4GeO_4, solid electrolyte system, phase diagram 80−66489
Li_2O-Al_2O_3-SiO_2 glass, crystn. aggregation and migration of ion-implanted Ag 77−55240
Mg alloys, neutron irradiation effects, on microstruct., mech. props. and swelling 79−65121
Mg-Al (5, 7, 9 and 11 at.%,) discontinuous precipitation growth kinetics 77−63677
Mg-Al (9 wt.%), ageing via cellular reaction, microanal., cell boundary vel. meas. 78−11230
Mg-Al-Zn (94.3, 3.9, 1.8 wt.%), pricip. on dislocations, weak-beam TEM 80−76264
Mg-Al-Zn (9wt.%Al), sand cast, preferred orientation and mechanical props. *(Japanese)* 80−20979
Mg-Ce, diffusion coeff. determ. during hydriding *(German)* 79−29288
Mg-Ce, workability, aging characts. and tensile strength 80−55416
Mg-Ga (6 wt.%), precipitation, lattice const., ageing effects *(Chinese)* 79−43279
Mg-La, workability, aging characts. and tensile strength 80−55416
Mg-Li-Al (31, 1 at.%), heat treated, precipitation 80−40364
Mg-$MgNi_2$-Zn, diagram of state, Zn solubility, initial phase precipitation *(Russian)* 80−66478
Mg-Mn-Ce (1.5, 0.3 wt%), superplasticity role of diffusional creep *(Russian)* 80−97528
Mg-Nd-Zn dilute alloy, metallography and precip. kinetics 80−71655
Mg-Zn (5 wt.%), age hardening, X-ray diffr. anal. *(Chinese)* 80−104173
Mg-Zn alloy, aged, one dimensional transition phase β'_2, crystallographic obs. *(Chinese)* 80−60865
$Mg_xFe_{3-x}O_{4-y}$ precipitates, g-factor, ferrimag. reson. meas. 78−60337
MgO, Li precipitates orientation and struct. *(French)* 79−86888
MgO, melt-grown cryst., direct evidence for brucite precip. 77−28712
MgO, orientation relationship and struct. of Li precipitates 79−82342
MgO, precipitate morphology, strain energy effects 80−40358
MgO, precipitation on dislocations, ultramicroscopy and chem. etching 78−67720
MgO, technical powder purity, of technical purity powders 77−63586
MgO:Li, TEM studies 79−29069
MgO:Li^+(Na^+), precipitation rel. to dislocations *(French)* 79−51163
MgO:Ni, heavily doped, defect characterisation, rel. to use as laser material 80−65000
$MgO.3.5Al_2O_3$, precipitation during creep experiments 79−47694
$Mg_{74}Zn_{26}$, glass, exam. of crystallisation 78−71681
γ-Mn-Cu, metastable, structural aspects of decomposition 79−1871
Mn-Si (62.5 to 63.8 wt.%), phase anal. and cryst. struct. *(Japanese)* 80−15049
MnCu, neutron scatt. near crit. comp., effects of stress and ageing 79−19722
MnSi-Si system, striations and cryst. struct. of matrix 80−103292
$MnSi_{\sim 1.73}$ crystal growth and characterisation 80−93474
Mo alloy, finely dispersed precipitate distrib. change due to homogenisation annealing 77−70056
Mo, C doped sheet, electron beam welded, low temp. ductility 79−87685

precipitation continued
Mo, cast and low alloy, C distrib. between solid soln. and precipitate *(German, English)* 79−20059
Mo, compact, on H_2 permeated backing, precipitation *(Russian)* 78−27520
Mo form MoF_6 by H_2 reduction, 500 to 1200°C *(Russian)* 80−7516
Mo, TEM exam. of Mo_2C precipitates, exam. of crystallographic relationships 78−52811
Mo:C (110) surface, segregation, precip. and desorpt. of C, AES and LEED study *(French)* 80−103480
Mo-Hf-C-Ni, electrochemical phase composition anal., precip. of HfC phase *(Russian)* 80−20901
Mo-Ti, internally nitrided, lattice expansion by precipitation 78−68700
Mo-Ti (up to 5.48 wt.%), internal nitriding, hardness, nitride type, precipitation *(Japanese)* 79−79157
Mo-Zr, heavy ion irradiated, void swelling, phase instability 80−29084
Mo-Zr, nucleation conditions, effect on formation of oxide phase during internal oxidation *(Russian)* 80−81064
Mo-Zr alloys, TsM-6, Zr segregation at grain boundaries, carbide precipitation, X-ray spectral anal. *(Russian)* 79−74154
Mo-Zr-C alloys, carburising and annealing effects *(Russian)* 77−59828
$(Mo_{0.6}Ru_{0.4})_{80}Si_{10}B_{10}$, amorphous supercond. matrix, flux pinning by MoRu precips. 80−65756
$N_2O_4 \rightleftarrows 2NO_2 \rightleftarrows 2NO + O_2$, precipitation of corrosion products in a fractionating column *(Russian)* 80−25707
Na precipitation at Si-SiO_2 boundary, expt. *(Russian)* 80−49368
NaCl, impurity precipitation and grain boundary diffusion 80−107567
NaCl:Ba, Ba precipitation at dislocations, kinetics, ionic cond. meas. 79−60510
NaCl:$BaCl_2$, oriented growth of $BaCl_2$ phases, platelet-matrix interface structure and energy 78−87793
NaCl:Ca, precipitate form., transform. after annealing, critical flow stress 78−38848
NaCl:Ca crystals, surface recrystn., moisture effect 80−84950
NaCl:Eu^{2+}, oriented growth and cryst. struct. of precipitated phases 80−24303
NaCl:Mg^{2+}(Ba^{2+}), dopant aggregation and precipitation 80−107306
NaCl:$MnCl_2$, Suzuki phase precip. obs. by TEM, misfit dislocations 77−31776
NaCl:Ni^{2+}, kinetics of impurity precipitation 77−69090
NaCl:Pb_3 precipitation of Pb impurity 78−48415
NaCl:Sn^{2+}, thermally stimulated space charge decay 78−48111
NaCl-$BaCl_2$ 1%, oriented growth of $BaCl_2$ phases, morphology 77−80627
NaF:Fe, Mossbauer study of Fe precipitates 79−91327
$NaNO_3$(2), precipitation from mixed aq. solns. 80−100191
Na_2SiF_6, precipitation from H_2SiF_6 soln., mechanism, kinetics, habit 77−44142
Nb alloy SVMTs, high-temp. ageing, struct. and morphology of hardening phases *(Russian)* 80−40390
Nb alloys, non-metallic inclusion form. during quenching from liquid state 78−95766
Nb, H_2 embrittlement, microscopic obs. at low temps. 77−32666
Nb, low temp. annealing effect, precip. of Nb_2O_5 *(Russian)* 77−52456
Nb oxidation in H_2 atmospheres, TEM exam. of precipitated phase morphology and struct. 78−76790
Nb, resistivity studies of interstitial He mobility 79−14800
Nb, single crysts., fluxoid pinning by small nitride precips. 80−70913
Nb-Al (20 at.%), diffuse scatt. before Nb_3Al phase form., unstable phase *(Russian)* 78−3131
Nb-C alloys, alloyed with Mo, Ti, and Zr, phase comp. and precip. after heat treatment 79−57020
Nb-Cu (0.02 wt.%), Cu electron Nb_5Si, $NbSi_2$ and NbB_2 form. *(Russian)* 78−15400
Nb-Ge, compounds with A15 structure, films, TEM study *(French)* 80−80135
Nb-Ge-Si, compounds with A15 structure, films, TEM study *(French)* 80−80135
Nb-H, $\alpha+\alpha'$ region, precipitation morphology investigation by gamma ray diffr. 77−52333
Nb-H, coherent, surface spinodal decomposition and quasiperiodic β-precip. 77−73257
Nb-H single crysts., critical current and flux pinning *(Russian)* 77−47946
Nb-H system, accommodation effects during hydride precipitation, TEM 80−89218
Nb-H system, temp.-stimulated acoustic emission, hydride precip. 80−3044
Nb-Hf (38 at.%) superconductor, peak effect, summation problem, mag. history flux pinning force 80−20362
Nb-NbO system, single- and two-phase, sputtering yield, SEM and scanning Auger microprobe obs. 79−87545
Nb-Si, compounds with A15 structure, films, TEM study *(French)* 80−80135
Nb-Ti (60 at.%), aged, TEM exam. of precipitation process *(Japanese)* 78−48409
Nb-Ti superconducting alloy, critical current density, heat treatment effects *(Japanese)* 78−14909
Nb-Ti-Zr, superconducting, critical current density and microstruct. correlation *(Japanese)* 79−61748
Nb-Zr-C alloy, long term loading at high temps. effect on struct. and morphology of carbide phase 79−15754
Nb-Zr-C alloy, struct. changes during stressed and unstressed ageing at 900, 1100°C *(Russian)* 79−29064
Nb_3Al superconductors, sputter deposited, BCC to A15 transition, microstruct. investig. 78−27512
Nb_3Ge, CVD, hysteretic losses, precipitates and deposition temp. effects 77−28319
$NbH_x(D_x)$, H conc. detect. by neutron interferometry, precipitation effects 78−67735
Nb_3Sn film formation, solubility, precipitating processes *(Russian)* 80−92792
Nb_3Sn, high-rate sputter-deposited, effect of oxygen on microstruct. 80−20343
Nb_3Sn, vap. deposited supercond. film, effect of N_2 and tape heating 78−34939
NbZr, energy anal. of diffuse ω-reflections, Mossbauer, X-ray scatt. 78−60369
NbZr(Hf)-C(N) alloys, phase comp. after casting and annealing, precip. 79−56983

precipitation continued
Ni (111), C monolayer phase condensation, LEED and AES obs. 79−46960
Ni alloy, STEM microanalytical techniques comparison for precip. comp. determ. 78−35790
Ni alloy 718, intermetallic second phase obs. using electrolytic extraction and SEM 79−34074
Ni alloy Mar M200, directionally solidified Hf additions, effect of vol.% γ' on creep rupture 78−27526
Ni base alloy, precipitation identification by electron probe microanalysis *(German, English)* 77−77857
Ni base alloy IN792, carbide morphology 77−36508
Ni base superalloy, directionally solidified, struct. and props. *(Chinese)* 80−20918
Ni base superalloy, γ' precipitate size determ. technique 79−34221
Ni base superalloy, γ'-precipitation influence on recrystallisation 80−29955
Ni base superalloy, single crystal, apparent and effective creep parameters, incubation period 77−63715
Ni base superalloy IN-738, γ' precipitate coarsening during ageing and creep 79−52271
Ni base superalloys, recrystallisation 77−16616
Ni base superalloys, SIGMA-SAFE, phase diagram approach to sigma phase problem 78−64547
Ni, β-phase form., H enriched, at surface and grain boundaries, during H_2 absorption *(Russian)* 78−31410
Ni, C precipitation 80−29958
Ni, compact, on H_2 permeated backing, precipitation *(Russian)* 78−27520
Ni, deformed, struct. form. during annealing, Ni_3Al type ordered phase precipitation *(Russian)* 80−45325
Ni, electrolessly deposited, structural comparison with electroplated films 79−23869
Ni heat resistant alloys, orientational correspondence between γ solid solution, and $\gamma+\gamma'$ eutectic precipitation *(Russian)* 79−11621
Ni, integranular precipitation after annealing, ion imaging microanalysis *(French)* 79−61594
Ni, NMR study of metal precipitated onto a cathode *(Russian)* 80−93185
Ni, Ni-Fe, X-ray study of occluded H_2 77−16586
Ni, polycryst., bulk-to-surface precip. and surface diffusion of C, AES data interpretation 78−34713
Ni precipitates, isothermal annealing influence on structural state, X-ray diffr. anal. *(Russian)* 80−100849
Ni superalloy, cast, microstruct. and microanalysis 78−35393
Ni superalloy, STEM microanal. of precipitates and their nuclei 80−81067
Ni:C, bulk-to-surface precip. and surface diffusion, AES meas. 77−11784
Ni-A-Ti (6,1 wt.%), γ' phase precip., deform. effects *(Russian)* 78−48404
Ni-Al, (2 and 6 wt.%), oxidation, α-Al_2O_3 growth, microstruct., precip. 80−108626
β'-Ni-Al, precipitation studies 80−3067
Ni-Al (12.8 at.%), irradiation enhanced coarsening 79−66060
Ni-Al (12.8 wt.%), Ni^+ ion irradiation, precipitate restructuring, mechanisms and kinetics 79−77650
Ni-Al (14 at.%), two stage ageing effect on spatial distrib. of γ'-phase particles *(Russian)* 78−39805
Ni-Al (15 wt.%) single crystals, morphological changes of γ' precipitates during uniaxial stress-annealing 79−83236
Ni-Al (6.05 wt.%), prediction and meas. of precipitate number density 78−19756
Ni-Al (6.35 wt.%) foil, radiation-induced precipitate redistrib. 78−30681
Ni-Al (6.35 wt.%) precipitate coarsening, redistribution and renucleation during ion irradiation 78−23709
Ni-Al alloys, effects of electron irradiation in precipitation, nucleation and dislocation loop growth, TEM study 79−42106
γ,γ'-Ni-Al alloys, irrad. effects on precip. 77−8829
Ni-Al solid solutions, Ni-rich, phase transforms. during quenching 77−32577
Ni-Al-Cr, IN-100, growth geometry of carbides in dendritic monocrystals, solidification effects 79−11597
Ni-Al-Cr-Co-Ti, Waspaloy, exam. of dislocation-precipitate interaction, cyclic stress-strain behaviour 78−84925
Ni-Al-Mo (12.7, 21.6 wt.%), directionally solidified eutectic composite, precipitation 80−108454
γ-αNi-Al-Mo eutectic, γ' precipitation 77−12629
Ni-Al-Ta, solvus surface determ. using precipitation method 79−15674
Ni-Al-Ti ferromagnetic non-homogeneous alloy, composition determination by Curie temp. meas. 80−11196
Ni-Al-Ti-Cr superalloys, estimation of conjugate γ and γ' compositions 79−8282
Ni-Al(Si) foils, ion irrad., surface effects on precip. morphology 80−104168
Ni-Al(Ti)(Mo)(Si), effect of solute misfit and temp. on irradiation induced segregation 78−72779
Ni-base, heat resistant alloy KhN60MKBYuT, plasticity, precipitation 77−70120
Ni-base alloys, under ion irradiated, modification of precipitate interface and effect of precipitates stability 79−77651
Ni-base binary alloys, solute segregation and precip. under heavy-ion bombard. 79−11623
Ni-base superalloy, conventional and powder metallurgical, σ-phase precipitation 80−11646
Ni-base superalloy, effects of grain boundary carbides on creep and back stress 80−3130
Ni-base superalloy, STEM microanalysis of precipitates 80−104492
Ni-based superalloys, TEM obs. of cellular transformation products 80−3045
Ni-Be alloy, precip. sequence 78−80549
Ni-Be alloys, struct. and phase stability in neutron bombardment field *(Russian)* 77−76467
Ni-Be system, radiation induced solute segregation and precipitation study by means of Johnson-Lam kinetic model 79−43252
Ni-C, quenched, struct. of graphite precipitates, TEM obs. *(Russian)* 78−68695
Ni-C (1.8 at.%), precipitation of graphite and NiC TEM obs. 77−52334
Ni-Co-Al alloys, continuous precip., SEM, TEM, X-ray diffr. study 80−89220
precipitation continued
Ni-Co-C solid solution, C precipitation, Ni_3Co ordering, Ni-Co lattice parameter meas. *(Czech)* 80−60867
Ni-Co-Cr superalloy, powder produced, necklace struct. development 80−40395
Ni-Co-Cr-Mb-W-Ta, Cr, Mb, W, Ta effects on σ phase occurrence 77−36507
Ni-Co-Cr-Mo-Al, Astroloy, extruded powder metallurgy superalloy, recrystallisation study 79−4976
Ni-Cr, deformed, struct. form. during annealing, Ni_3Al type ordered phase precipitation *(Russian)* 80−45325
Ni-Cr, Ni rich, discontinuous precipitation *(German)* 79−91653
Ni-Cr, ordering in the vicinity of Ni_2Cr 79−38819
Ni-Cr alloy, structural changes, during thermal stress cracking, X-ray and microhardness meas. *(Russian)* 78−35496
Ni-Cr alloy KhN70VMTYu, heat resistant, explosive loading effect on struct. and mech. props. *(Russian)* 78−39787
Ni-Cr base alloy, strain relaxation, effect of grain size, particle size, γ' vol. fraction 79−47741
Ni-Cr-Al, shape of γ'-precipitates on surface after sublimation *(German)* 77−81266
Ni-Cr-Al-Cr-Hf-Zr-C, directionally solidified eutectic with (Hf,Zr)C reinforcement, precipitation, and thermal cycling 78−44057
Ni-Cr-Al-Ti alloy, KhN78TYu, heavily deformed, subgrain struct. due to discontinuous precipitation of γ' phase *(Russian)* 79−52218
Ni-Cr-Al-Ti-Mo, low temp. mech. behaviour, precipitation 78−39860
Ni-Cr-Co, Nimocast alloy 738, γ'' precipitate morphology and creep rupture, thermal stress crack effect 78−11318
Ni-Cr-Co based alloy, IN-738 turbine blades, hot isostatically pressed investment castings, effect of heat treatment on grain boundary struct. 80−89270
Ni-Cr-Co superalloy, combined TEM, FIM, atom probe microanalysis of precipitates and carbide phase comp. 80−100844
Ni-Cr-Co-Mo-Ti-Al, powders, HCl surface treatment to prevent TiC precipitation, fracture props. 79−8397
Ni-Cr-Fe alloys, radiation enhanced precip. and dissolution of precipitates, point defect kinetics and dislocation obs. 80−108467
Ni-Cr-Fe-Mo-Co (21.41, 19.28, 8.64, 2.16 wt.%), Hastelloy alloy X, exam. of thermal stability 78−84865
Ni-Cr-Mo-Fe-Mn, Kh12M23, intermetallic phases exam. *(Russian)* 78−39740
Ni-Cr-Ti (19.51, 4.2 wt.%), quench-ageing and fracture *(German)* 77−70088
Ni-Cr-Ti-Al alloys, precipitation of γ' phase during single and combined ageing treatment *(Russian)* 77−52328
Ni-Cr-W, oxidation behaviour in air at 1000-1250°C 80−89407
Ni-Cr-W-Mo-Al-Ti (15,6,3,2,2, wt.%), wrought, Si effect on transition brittleness *(Chinese)* 80−55491
Ni-Fe-Nb (Mo), magnetic alloy, TEM and X-ray obs. *(Chinese)* 80−24401
Ni-Ge , defect-solute interactions and radiation-induced segregation 80−25705
Ni-In, FCC, cellular precipitation kinetics 78−52823
Ni-In, FCC crystals, exam. of volume transform. kinetics of cellular precipitation 79−11625
α-Ni-In, solid solution, lamellar microstructure, influence of grain boundaries on thermal stability 78−72795
Ni-maraging weld metal, increasing fracture toughness by heat treatment 78−72871
Ni-Mo, and Ni-Mo-V alloys, struct. changes on annealing *(Russian)* 77−21145
Ni-Mo, discontinuous precipitation as internal sulphidation mode 77−8835
Ni-Mo (14.4 wt.%) single crystals, ordered phase precipitates influence on deformation character, mechanical props. *(Russian)* 79−74155
Ni-Mo (17.5 at.%), discontinuous precipitation reaction *(German)* 79−87643
Ni-Mo-Al and Ni-Mo-Al-V, high-resist., struct. transforms., TEM *(Russian)* 78−19762
γ/γ'-δ-Ni-Nb-Cr-Al (20, 6, 2.5 wt.%), growth kinetics of γ' precipitates 77−40424
Ni-Si, defect-solute interactions and radiation-induced segregation 80−25705
Ni-Si, ion beam irradiation induced Ni_3Si surface film segregation 78−38761
Ni-Si, proton irrad., γ' precipitation, early stages 80−34096
Ni-Si (12.7 at.%), heterogeneous precipitation at internal and external surfaces during Ni ion irradiation 79−77647
Ni-Si (12.7 wt.%) Ni^+ ion irradiation, precipitate restructuring, mechanisms and kinetics 79−77650
Ni-Si solid soln., radiation, induced precipitation dose rate effects 78−6936
Ni-Si solid soln., radiation-induced solute redistribution and precipitation, model 79−19277
Ni-Si solid solution alloys, γ phase precipitation under irrad. 77−1839
Ni-Ta-Al-Fe, Al and Fe effect on precipitation kinetics 79−20054
Ni-Ti (3 wt.%), C precipitation 80−29958
Ni-Ti (8 and 10 wt.%) alloy, aged, precipitation behaviour at 550 to 950°C, X-ray and electron microscopy exam. 78−39785
Ni-W-B, superalloy, M_5B_3 type boride 78−44131
α-Ni-Zn, continuous precipitation kinetics *(Russian)* 78−76652
Ni-Zn, physical-chemical metallurgy *(German)* 80−108390
Ni-Zn solid soln., lamellar spacing in discontinuous precipitation, expt. proof of Gaussian distrib. *(German)* 77−36517
NiAl martensite, Ni-rich, precip. of Ni_3Al, mechanism 77−86033
$Ni_{1-x}Au_x$-Co, dil., hyperfine field and isomer shift, precip. process, Mossbauer expts. 80−25267
$NiFe_2O_4$ precipitation process from silicate glass, ESR study, effective g value, transition temp. 80−25194
$NiFe_2O_4$ precipitation from silicate glass, Mossbauer study 80−54998
$Ni_{2/3}Fe_{7/3}O_4$, precipitation of α-Fe_2O_3, optical microscopy, SEM and TEM studies *(French)* 80−11650
βNiH, decomposing, α-phase precipitate detection by Bitter powder pattern 79−28104
$Ni(H_2V)_2(H_2O)_2$, synthesis and characterisation *(French)* 80−45225
NiO, undoped and Al doped, Ni self-diffusion, vacancy-impurity complex effects 80−107493
NiO, with spinel-type defect struct., ferromagnetic reson. meas. 78−43647
NiO:Fe, exchange anisotropy of Ni-ferrite precipitates 79−28520
NiO-Al_2O_3 powders, coprecipitated particle-size distrib. meas. 78−39726

precipitation continued
Pb glasses, Cu containing, crystallisation 78−47241
Pb-Ag, Ag precipitation kinetics 78−19758
Pb-Ag (0.068 wt.%), Ag precipitation kinetics and activation energy 80−66517
Pb-As (~0.01 wt.%), enhanced precip. phenomena, invest. of mechanism by elec. resist. meas. 80−104162
Pb-Au, interstitial and substitutional distrib. 80−84204
Pb-Bi, temp. regime of crystn. on rapid cooling *(Russian)* 80−66495
Pb-Ca-Sn, effect of Sn additions on precipitation behaviour, of Pb-Ca alloys *(German)* 78−52821
Pb-Cd (1.5 wt.%) discontinuous precipitation, metallographic study *(Japanese)* 77−48440
Pb-Na alloy, with Pb_3Na precips., flux pinning, crit. currents obs. *(German)* 78−14907
Pb-Sb, influence of quench deform. on precipitation *(German)* 77−86064
Pb-Sb (1 wt.%), highly averaged, fracture behaviour 79−8366
Pb-Sb alloy, form of growth of Sb crysts., precip. temp. effects *(Russian)* 77−21144
Pb-Sb-As (1.1-1.8, ~0.01 wt.%), enhanced precip. phenomena, invest. of mechanism by elec. resist. meas. 80−104162
$PbCO_3$-$BaCO_3$($SrCO_3$)($CaCO_3$), solid soln. form., regions of existence 79−11581
$Pb_{1-x}Cd_xS$ metastable epitaxial films, growth and physical props. 78−27417
PbNa, type-II superconductor, regularly ordered precipitates, peak effect, crit. current meas. *(German)* 78−19196
PbO/TeO_2 system, central region of phase diagram, X-ray and thermal anal. 79−70046
$Pb_{0.6}Sn_{0.4}Te$, supercond., hysteresis in flux flow charact., normal metal precipitates 78−80107
Pd-Ag-Cu (35,25 at.%), determ. of ageing transformations by resist. meas., metallography, TEM and X-ray diffr. 79−4967
Pd-Cu-Si, metallic glass, miscibility limits, computer study 79−65198
Pd-H alloys, in situ electron microscope obs. of precipitation 79−61589
Pd-$_x$Cu$_y$Si$_{1-x-y}$, ternary miscibility gap, simulation, dispersed phase composite form. 80−54379
Pt, quenched, coprecipitation of vacancies and C atoms 79−78978
Pt:C, C layer formation on (111) surface, temp. depend., LEED, AES study 78−71911
RbCl:$CoCl_2$ system, precipitate form., ionic cond. meas. 80−96653
Sb_2O_5 hydrated, preseparation stage in dehydration, phase transformation 80−35524
Si, ambient effect of O precipitation, self interstitial mechanisms, IR spectra, TEM study 80−66510
Si amorphous evaporated film, doping 79−51127
Si, annealed crystal, oxide precipitates identification by electron loss spectra 78−83952
Si, crucible grown, virgin and implanted, laser irradiation effects on surface structure 80−92768
Si crystal, Czochralski grown, enhanced Borrmann effect 80−70191
Si, crystal defects and impurities interaction obs. by electron microscopic methods 80−65003
Si, crystal defects in integrated circuits, review 78−88547
Si crystals, annealed, oxide precipitates identification, TEM, EELS 80−100723
Si, Czochralski grown, inhomogeneous O precip. and stacking fault form. 79−14820
Si, Czochralski grown, oxide precip. homogeneous nucleation 80−65221
Si, Czochralski grown, oxide precipitates, diffusion-limited growth 80−97484
Si, Czochralski grown crystal, O precip., nucleation behaviour and dislocation loop form. *(Japanese)* 80−59664
Si Czochralski wafer intrinsic gettering by oxide precipitate induced dislocations 78−6092
Si Czochralski wafer oxide precipitate-dislocation complex characterisation 78−14357
Si, Czochralski wafers, oxidation induced stacking fault sources 77−7737
Si, Czochralski-grown, oxide precip. form. process 80−49364
Si, Czochralski-grown crysts., thermally induced microdefects, annealing temp. and starting material effects 80−49141
Si, dislocation free, O_2 precipitation, stacking fault form. 78−38731
Si, dislocation-free, O_2 precip., IR and TEM obs. 80−29173
Si dislocation-free crystal O precipitation obs. 78−6095
Si, dislocation-free single crystals, growth microdefects, etching and X-ray expts. 78−47385
Si, dissolved O_2 precipitation, homogeneous nucleation 77−11695
Si, doped with metal impurities contact angle, water adhesion energy *(Russian)* 77−89620
Si, effect of SiO_2 precip. on generation currents in MOS capacitor 79−78088
Si, floating zone structural perfection changes by high temp. treatment, dendrites, dislocation interactions 80−29049
Si, heat-treated dislocation-free, elec. props. of stacking faults and precipitates 77−39796
Si, ion-implanted, defect struct., SEM, TEM and X-ray topography expts. 77−51399
Si MOS device, electron optical identification of precipitations 80−16309
Si, matrix O_2 precipitation and stacking fault formation 77−76427
Si n$^+$-p solar cells, degradation mechanisms associated with Ti impurities 80−81465
Si, nucleation of stacking faults at oxide precipi tate-dislocation complexes, TEM 77−19967
Si, O impurity precipitation from solid soln., neutron irrad. effect 80−29177
Si, precipitation of Au, supersaturated soln., Hall effect meas. 77−89465
Si, precipitation of O, 1000°C TEM, IR absorpt. and X-ray studies 80−34194
Si, precipitation of O, 650°C, IR absorpt. and X-ray diffr. 80−76258
Si, precipitation of O, annealing, IR spectra meas. 80−24606
Si, ring shaped stacking faults induced by oxide precipitates 78−67723
Si, substrates, review of defects 77−39597
Si, thermal donor generation in temp. range 600-800°C 79−11121
Si wafer, Czochralski grown, precipitation during high temp. oxidation 78−16381
Si wafers, Czochralski, gettering of surface and bulk impurities 78−64456
Si:Co^{57}Fe, Mossbauer spectra, deep level Co impurity study 80−29266
precipitation continued
Si:Au, precipitation of solid soln., effect of gamma irradiation 80−59515
Si:B, implanted, oxidation induced precipitate defects, TEM 78−31556
Si:B, implanted, shrinkage of rod shaped defects 78−6061
Si:B, ion implanted, laser and thermal annealing compared, TEM obs. 78−75681
Si:B, ion-implanted, dislocation climb, TEM obs. 78−6062
Si:B, solubility and precip., and supersat. resulting by thermal predeposition 78−11232
Si:B(P), diffusion induced imperfections, laser annealing, rel. to junction charact. 78−75678
Si:Bi, ion-implanted, solid phase epitaxial growth during annealing, supersaturated solid soln. form. 80−103384
Si:Co, substitutional Co and Co precipitates, identification by Mossbauer spectroscopy 79−11631
p-Si:Cu, Cu precipitation effects, for solar cells appl. 79−69249
Si:Cu, interaction between vacancy emitting absorbing precipitates and dislocations, TEM obs. 78−71755
Si:Cu, precipitate morphology, IR microscopy study *(Chinese)* 80−103539
Si:Cu extinction of X-ray topographic images of Cu precipitates 80−45310
Si:Fe, implanted, annealing and stripping, Mossbauer expts. 80−39141
Si:Fe, ion implanted, laser annealing studies using Mossbauer spectroscopy 80−79827
Si:Fe(Cu), impurity segregation and microstructural changes by pulsed laser irrad. 79−82254
Si:In, clustering and precipitation, time-dependent perturbed ang. correlation meas. 80−65234
Si:Ir, precipitation of solid soln., photocapacitance, electrical resistivity meas. 78−47833
Si:Li, precipitation centres, elec. cond., Hall effect meas. 78−48417
Si:Ni, low temp. annealing effect on behaviour of Ni 79−10862
Si:O, annealed, minority carrier lifetime 79−23985
Si:O, annealed, precipitates, dislocation and stacking fault loops, TEM characterisation 77−4111
Si:O, cryst., annealed, struct. defects 78−75673
Si:O, effect of interstitial O on elec. props. 77−76846
Si:O wafer, annealed, surface- and inner-microdefects, TEM obs. 80−54236
Si:P, SiP precipitation concomitant with P predeposition 77−24326
Si:P, stacking fault and dislocation growth induced by P predeposition 77−59023
Si:P polycrystalline layer, role in lattice defect reduction assoc. with P predeposition 80−70229
Si:P(As)(B), nonequilibrium solid solutions obtained by heavy ion implantation and laser annealing 80−92544
Si-Au, solid soln., influence of precip. on relax. of ^{29}Si nucleus 80−11287
Si-Ge, heavily doped, reversal of precip. 80−2409
Si_3N_4, hot pressing with Y_2O_3 and Li_2O additives 78−92220
SiO_2-Al_2O_3 mixture, depend. of phase comp. on nuclei available 79−11584
Si(111):Pb ion implanted amorphous layers, recrystallisation, impurity out-diffusion model *(Chinese)* 80−88363
Sm-Co, decomp. kinetics when aged, X-ray mag. props. and metallography study *(Russian)* 78−56644
Sm-Co-Cu, with Sm_2Co_{17} struct., aged, TEM high coercivity material, TEM obs. of microstruct. 77−77073
Sm-Pr-Co alloys, mag. props. and struct., comp. depend. *(Russian)* 80−20430
$SmCo_5$ based alloys, dissociation process *(Russian)* 78−27542
$SmCo_5$ based solid soln., X-ray diffr. obs. of decomp. *(Russian)* 77−81264
$SmCo_5$, nucleation of reversed domains at Co_7Sm_2 precips. 80−75791
$SmCo_5$, sintered, high coercivity, microstruct. and mag. props. 77−69629
$SmCo_5$ sintered magnets, eutectoid decomp. 80−89219
$SmCo_5$, sprayed magnet, microstruct. and mag. props. between 650°c and 800°C 79−82829
$Sm(Co_{1-x}Cu_x)_{7.8}$ alloys, coercive fields, domain wall energies, mag. and metallographic exam. 78−91897
Sn-Bi(Pb)(Ga), temp. regime of crystn. on rapid cooling *(Russian)* 80−66495
Sn-Ni electrodeposit, metastable, transform. kinetics, X-ray and SEM meas. 78−38979
Sn-Sb (10 wt.%), decomposition of supersaturated solid soln. 80−29960
stainless, carbide precipitation during post heat treatment, knife line attack phenomena 79−20288
steel, austenitic stainless, 18 Cr-11 Ni, effect of boron on nucleation of $M_{23}C_6$ carbides *(Polish)* 78−84808
steel, Cr-Ni, ferrite precip. *(Japanese)* 80−35187
steel, Nb, deform., recrystn. and precip. interaction 80−97515
Ta, acoustic emission induced by hydride formation 80−76257
Ta-Cr (15 wt.%), solid soln., discontinuous precipitation *(German)* 80−45314
Ta-H, N interstitial trapping of H, hydride precip., resist. meas. 77−20293
Ta-H, physical properties, plastic deformation, H ordering *(Ukrainian)* 80−71689
Ta-N (0.6 to 6.5 at.%), supersaturated solid soln., precipitation 79−96028
Ta-N (4 at.%), TEM obs. of ordering 79−96021
Ta-O solid soln., interstitial ordering and precipitation at 100 to 270°C, exam. 78−52813
Ta-W-Hf, small-angle electron scattering in TEM from lattice strains accompanying precipitation 79−14658
Te-Pb (20 at.%) alloy, amorphous, obtained by rapid cooling from liq. state, crystn. behaviour 78−26445
β-Ti alloy, metastable, alloying element effects on phase equilib. 79−56975
Ti alloy, type VTZ-1, two phase, mechanism and kinetics of metastable β and α^s phases dissociation *(Russian)* 79−74152
Ti alloy, type VT8, two phase, mechanism and kinetics of metastable β and α^s phases dissociation *(Russian)* 79−74152
Ti alloy, X-ray diffr. anal. of hydrides 77−12628
Ti alloy β III, precipitation of α and ω phase, evolution of mech. props. *(French)* 77−16591
Ti alloy VT22, hardening during thermomechanical treatment, precipitate particle internal struct. *(Russian)* 79−91657
α+β-Ti alloys, interfacial precipitation 80−3068

precipitation continued
Ti alloys, metallurgical characterisation using thermoelec. power meas. *(French)* 80−45462
Ti alloys, precipitate vol. fraction estimation from elastic modulus data 79−61595
β IIITi alloys solution treated and aged, estimation of precipitate volume fraction using Young's modulus 78−39781
Ti, and alloys, intergranular precipitation after annealing, ion imaging microanalysis *(French)* 79−61594
Ti β III alloy, elastic and anelastic phenomena associated with α and ω phase isothermal precipitation *(French)* 79−52288
α-Ti, hydride precipitation, resistometric investigation, isothermal ageing effects *(Japanese)* 77−81265
α-Ti, recrystallised commercial purity, Fe-rich precipitates obs. *(French)* 80−50637
Ti-Al (14 at.%), with precipitate free zones, tensile props., grain size effects 77−16690
Ti-Al (14.4 at.%), void form. and solute segregation under Ni ion irradiation 79−42122
Ti-Al alloy system, quenched from β-region, struct. obs. *(Russian)* 77−21146
Ti-Al alloys, α_2 phase obs. using microscopy and X-ray diffr. 79−52497
Ti-Al-Cr-Mo-V, VT22 alloy, metastable β-phase decay under continuous heating, plastic strain effect *(Russian)* 80−71656
Ti-Al-Sn (5, 2.5 wt.%), electron microscope and X-ray diffr. exam., of basal and near basal hydrides 78−80550
Ti-Al-V, (6,4 wt.%), single and dual ion irrad., microstruct. studies 80−29077
Ti-Al-V (4.7, 2 wt.%) pseudo alpha alloy, laminar struct. singularities, β to α transformation *(Russian)* 80−7552
Ti-Al-V (6,4 wt.%), heavy ion irrad. effect on microstructure 79−10884
Ti-Al-V (6,4 wt.%), ion irradiated, microstruct. study using TEM 80−96572
Ti-Al-V (6,4 wt.%), quenched, struct. and age hardening rel. to treatment temp. 80−11657
Ti-Cr (15 at.%), aged omega phase, electron microscope exam. 78−72783
Ti-Cr(Mo), alpha precipitation kinetics 78−68697
Ti-Fe, H storage material, Mossbauer surface studies, Fe clusters 80−97167
Ti-Mn (0.4 and 12 wt.%), bonding between α-β interfaces, subsequent deform. 78−14517
Ti-Mo, martensitic alloy, decomposition by nucleation and growth and spinodal mechanisms 79−61590
β-Ti-Mo alloys, thinning transformation 77−44438
Ti-Mo-Zr-Sn (11.5, 6, 4.5 wt.%), β III, mech. props. rel. to heat treatment 80−84961
Ti-Mo-Zr-Sn (11.5, 6.0, 4.5 wt.%) alloy, struct. as affected by processing history 80−84972
Ti-Mo-Zr(-Al) (15, 5 (3) wt.%), quenched and aged metastable β-phase, crystallography, morphology and decomposition 80−76262
Ti-N_2, condensate formed by plasma flow precipitation in vacuum, cryst. and surface props. *(Russian)* 80−100788
Ti-Nb, cold strained, exam. of ω and α phases, precipitated during ageing *(Russian)* 79−11620
Ti-Nb-Ge foils, β phase decomposition, electron microscopy struct. investigation *(Russian)* 79−83172
Ti-Nb-Si, amorphous alloy, supercond. props. and crystn. behaviour, TEM and DTA study *(Japanese)* 80−84536
Ti-Nb-V(25 wt.%, 15 wt.%), precipitation of β and ω phases during ageing at 350°C 77−8838
Ti-Nb-Zr-Ta, superconducting props. comp. depend., stress effects and precipitation behaviour, X-ray scatt. 80−93059
Ti-Si amorphous alloy, melt-quenched, transform. studies and mech. props. 80−100838
Ti-V (19 at.%), aged ω-phase precipitation, incomplete proximity effect 78−60252
Ti-V-Si, Si effects on precipitation and strengthening 77−55970
βTi-V-Si (40, 1 at.%), Si effect of precipitation and age hardening 77−63676
α_m-Ti-X (X=Ag, Au, Si), precipitation mechanisms and Meyrick theory of cellular reaction initiation 79−74163
α-β TiAl-Sn-Zr-Mo (6,2,4,6 wt.%), age hardening 79−61604
TiC-base alloys, anomalous phase flaky precipitation *(Japanese)* 78−48401
$Ti_{70}Co_{20}B_{10}$, amorphous alloys, crystn. behaviour, TEM study *(Japanese)* 80−84087
TiD_2, nucleation and growth in D_3^+ implanted Ti, TEM study 80−97717
$Ti_{70}Fe_{20}B_{10}$, amorphous alloys, crystn. behaviour, TEM study *(Japanese)* 80−84087
TiN, precipitation of ordered δ'-phase *(Russian)* 78−6929
$Ti_{70}Ni_{20}B_{10}$, amorphous alloys, crystn. behaviour, TEM study *(Japanese)* 80−84087
TiO_2, iron bearing, exsolution of Fe_2O_3 79−61597
TiO_2, K^+ implantation, extended defects and precipitates 80−49251
$Ti_xZr_{1-x70}Nb_{30}$, ω phase precipitation 79−34042
U-Al, transform. and struct. changes, cooling, cooling rate effect *(Korean)* 77−63660
U-Al (0.78 at.%), behaviour of metastable phases under neutron irrad., application of model 78−48408
U-V (0.2 wt.%), mech. and struct. props., effect of internal H *(French)* 77−21253
UC+UC_2, neutron irradiation, U_2C_3 deposition 78−33253
V and V-Mo, mechanical properties, O, N_2 and C addition effects 79−52356
V, dehydrogenation by annealing with Zr foils, internal friction meas. 80−96736
V wire, deformed in torsion, internal friction, H effect 80−76300
V/Cu-Ga, composite superconductor, V_3Ga phase form., TEM obs. *(Russian)* 80−84933
V-C alloys, low carbides struct. rel. to ht. treatment 77−48458
V-D alloys, low frequency internal friction study 78−48444
V-H rods, twisting effect, anelastic deviations on thermal cycling 80−21043
V-H single crysts., critical current and flux pinning *(Russian)* 77−47946
V-H system, crystallography of βVH precipitation 77−52326
V-N system, phase formation *(Russian)* 78−39739
V-N system, TEM of V-$V_{16}N$ precipitates 77−16590
precipitation continued
V-O alloy, temp., dose and conc. depend. of void form. following V^+ ion beam irradiation 78−10105
V-Ti-C, elemental anal. of second phase carbides using electron loss spectroscopy 79−20500
V-Ti-C, high temp. carbide form., electron microscopy study 80−89228
V-Zr-C-Y alloy weld metal, hardening phase precipitates examination, TEM appl. 80−7576
VC, precipitation in ferrite and pearlite, during C steel transformation, TEM exam. 78−52812
V_3Ga, supercond. A15 phase, prep. by controlled precip. 80−81000
β-VH, precipitation crystallography, TEM obs. 77−77480
$VH_x(D_x)$, H conc. detect. by neutron interferometry, precipitation effects 78−67735
$V_4O(\beta$-phase), X-ray study of precipitated phase *(Ukrainian)* 78−6928
V_3Si, dislocations, obs. by TEM 77−59012
V_3Si formation by bronze process 77−86032
W wire, AKS-doped, second phase particle obs. by TEM, SEM and atom probe microanalysis 80−108457
W-Cr solid solution, precipitation behaviour, reaction front motion, lattice parameters *(German)* 80−55401
W-Ni, liquid phase sintering 80−25613
W-Ni-Fe(Cu), liquid phase sintered, interfacial embrittlement 79−57101
WC-Co (5wt.%) hardmetal, η-phase precipitation effect on struct. and mech. props. 79−47696
WC-Co molten Zn reaction, lamellar struct. form. 79−33964
$Y_3Al_5O_{12}$, laser cryst., struct. inhomogeneity obs. by vac. decoration 77−35701
$Y_3Al_5O_{12}$, layer structuresrevealed by decoration method and electron microscopy 77−27902
zircalloy-2, annealed, neutron irradiated, 573 to 923K, damage struct. 79−99247
Zn single cryst., dislocation velocity and plastic deform. 80−64998
Zn-Ga, temp. regime of crystn. on rapid cooling *(Russian)* 80−66495
ZnO-Al_2O_3-SiO_2 glass, crystalline phase precipitation, crystallisation *(Japanese)* 79−32916
ZnS-O, single cryst., fast neutron irrad., optical props. 78−27331
ZnS-ZnO, solid solns., edge emission and exciton spectra *(Russian)* 77−24899
ZnSe:Ga, defect struct., Hall effect and resist. meas. 79−1428
ZnTe, TEM obs. of precipitates, shape of Te solidus line 80−25703
ZnTe:Ag, dislocation loops creation in region of interface 79−82210
ZnTe:Cu, precipitates, electron microscopic investigation 80−45312
ZnTe:Cu, voltage depend. on precip. contrast 79−1433
Zr, 10 keV deuteron irradiated, retention and precipitation 80−34099
Zr, annealed, neutron irradiated, 573 to 923K, damage struct. 79−99247
Zr base alloys, formation of phases precipitated from β solid solutions *(Russian)* 79−1869
Zr, crept single crystal, nature of γ-hydride 77−21147
Zr, hydride precipitation and growth at crack tips, electron optical obs. 80−108449
Zr-Al (14 at.%), martensitic, discontinuous precipitation, TEM obs. 79−34040
Zr-Al (14 wt.%), transformation sequence from Zr-Al martensite to Zr_3Al phase 80−3027
Zr-Al (4.6 wt.%) martensite, precipitation of Zr_3Al_2, TEM study 79−74156
Zr-B (1.3 wt.%), investigation of swelling due to neutron irrad. *(Russian)* 79−60404
Zr-Cr (1.9 wt.%), β-quenched and tempered, Ω-precipitation 79−66061
Zr-Cr (1.9 wt.%), β-quenched and tempered, $ZrCr_2$ precipitation, TEM study 79−66062
Zr-Cr-Fe, irradiation damage, metallurgical struct. effect 77−51412
Zr-Cu, dil. martensites, struct. and strength 79−29077
Zr-H alloy, precip. of γ-ZrH, shear mechanism 80−104170
Zr-N_2, condensate formed by plasma flow precipitation in vacuum, cryst. and surface props. *(Russian)* 80−100788
Zr-Nb (2.3 and 5.5wt.%) martensite, precipitation 77−8836
Zr-Nb (2.5 wt.%), effect of irradiation on stability of precipitates 77−69007
Zr-Nb (2.5 wt.%), hydride precipitation and growth at crack tips, electron optical obs. 80−108449
Zr-Nb (2.5 wt.%), memory effect in hydride precipitation 78−11227
Zr-Nb-V-Al (Fe) alloys, decomp. of β solid soln., metastable and equilib. phases 79−11632
Zr-Ta (5 wt.%), β-precipitation in martensitic struct., tempering temp. effect 79−34045
Zr-Ta (5 wt.%), martensitic transform. by rapid cooling, non-equilib. precipitation 79−34075
Zr-Ta (5 wt.%) martensite, β_1 precipitation, thermodynamics 79−74164
Zr-Y (15 wt.%) solid solution, decomp., during heating and cooling cycles *(Russian)* 78−92267
γ-ZrH, precipitation in Zr, exam. of precipitation mechanism due to shears, electron microscope exam. 78−84809
ZrO_2 ceramics, microstruct. and props., monoclinic to tetragonal transition 80−3035
ZrO_2, MgO partially stabilized, microstruct. development during ageing 79−91710
ZrO_2, partially stabilised ceramics, strengthening, post-sintering heat treatment 80−97518
ZrO_2, partially stabilized, precipitation hardening effect on fracture mode 77−90353
ZrO_2, partially stabilized, precipitation effects on fracture mode 77−90354
ZrO_2-CaO (15 mol.%), precipitation and ordering 80−100837
ZrO_2-CaO(MgO)($YO_{1.5}$), partially stabilised, growth morphology of tetragonal phase 79−4968
ZrO_2-P_2O_5, hydrated, heat treatment and coprecipitation, phase transitions 77−90335
ZrO_2-Y_2O_3 (9 mol.%), precipitation and ordering 80−100837

precipitation, electrostatic *see electrostatic precipitators; precipitation (physical chemistry)*

precipitation (atmospheric) *see atmospheric precipitation*

precipitation (meteorology) *see atmospheric precipitation*

precipitation (physical chemistry)
for precipitation within solid systems (microstructural changes) see precipitation
see also coagulation; crystal growth from solution; flocculation
acoustic particle agglomeration due to hydrodynamic collision between monodisperse aerosols 80−26191

precipitation continued
acoustic particle agglomeration of aerosols under standing-wave condition 80−30627
actinide lanthanide separation from high-level wastes by oxalate precipitation 79−49720
aerosol, multicomponent, coagulation eqn., with/without particle growth 78−35727
aerosol particle size distrib., dynamic behaviour, coagulation, condensation, nucleation and removal 78−35726
alkaline earth precious metal hexahydroxides, prep. and characterisation 79−90610
alkaline earth salts, supersaturated solutions, precipitation induction errors, a method for determ. 79−5175
alumina gel, hydrated, prep. by homogeneous precipitation method, phase change by heating *(Japanese)* 77−25046
calcite and aragonite precipitation, seed crystal effects 77−33054
cellulose, phase transitions, kinetics of precipitation from diluted cadoxen solns. 80−7845
cellulose acetate butyrate, in soln., hydrodynamic behaviour 80−64876
cellulose fibre formation in stirred dimethyl sulphoxide-paraformaldehyde soln. 80−104440
cellulose trinitrate, in soln., gel-like aggregate form. rel. to configuration 77−31036
chalcopyrite, aq. oxidation in hydrochloric acid 79−61764
colloids, hydrophobic, coagulation mechanism 78−40085
counterdiffusion of two substances, stationary boundary and precipitate form. 79−1933
electrolyte, binary, cryst. growth kinetics during precipitation 80−49149
electrostatic image force charged particle deposition in rectangular and cylindrical channels with laminar flow 78−83491
fibre masses, interconnected, precipitated from polymer solns. under sonic agitation 79−47655
formaldehyde, solid soln. in Xe, precipitation, IR spectra obs. 80−45059
III-V semiconductor-metal surface barrier structures, chem. precipitation and props. *(Russian)* 78−84298
ionic crystals, precipitation from aq. solns., induction period 80−50882
kinetic instabilities in 1st order transitions, ageing stage 78−87765
kinetics simulation 79−20347
leisegang rings, calcs., nonlinear partial differential eqns. appls. 80−4510
Liesegang rings demonstration of transient state pot. flow 78−63408
macromolecular multicomponent system, phase separation, thermodynamic perturbation theory, calculus 78−18778
metal surface, newly generated, occurrence of salt films during repassivation 79−15860
micro co-precipitation technique for X-ray fluorescence anal. of trace elements 79−57339
nitrate solutions, highly active, precipitation of Mo compounds during evaporation 78−37426
Ostwald ripening, reaction-controlled, of precipitates in steady state, general kinetics 78−35715
Ostwald ripening of precipitates, general kinetics 78−27808
oxalate precipitation for separation of Am, Cm, and trivalent lanthanides 80−83202
particle size analysis, of precipitation processes 80−50883
photosensitive glass, full-colour polychromatic, subcolloidal Ag precipitation 79−47953
poly(ethylene-but-1-ene) copolymer, gelation and precipitation from solutions, NMR exam. 79−43641
poly-m-phenylene isophthalamide, precipitated from soln., morphology *(Japanese)* 79−14706
polyethylene oxide, mol. wt. averages and polydispersity determ. by temp. drop turbidimetry 77−63959
polymer solution, free precipitation of spherical particles in centrifugal force field 77−11247
polypropylene, change of crystn. forms during purification 77−55934
polystyrene in cyclohexanol, polydispersities from temp.-drop turbidimetry 77−25314
preconcentration, for trace anal. of water using X-ray fluoresc. 77−12864
PVC-THF-H_2O, precipitation fractionation, influence of stereoregularity 79−7046
resin particles, dispersed, precipitation on cellulose fibre in elec. field 78−53262
rubber, blooming by waxes 80−104109
scale prevention, by annular flow of immiscible liquid along heated tube walls 79−1090
silicate gardens, growth morphology, mechanisms 80−100765
silver thioamides, precip., electron microscope and potentiometric studies, growth of photosensitive crysts. 80−33107
sodium aluminium tartrate, β-particle effects on crystallisation from aq. solns. 77−36387
soil, ^{89}Sr and ^{90}Sr determ. using total sample decomp. 80−35808
solute hydrophobic interaction, mol. aggregation, free energy, entropy and enthalpy, scaled particle theory 77−84609
spontaneous pattern formation, symmetry breaking instabilities 78−80792
transition metal precious metal hexahydroxides, prep. and characterisation 79−90610
vinyl polymers, precip. from solns., temp. determ. *(German)* 80−85208
$^{239,240}Pu(V)$ in alkaline freshwater pond, determ. by coprecipitation technique 80−71988
Ag cluster growth on AgBr microcrystals after X-ray and low-temp. light exposure 79−83485
Ag halides in thioamides, precip., electron microscope and potentiometric studies, growth of photosensitive crysts. 80−33107
AgBr cryst. growth mechanism in gelatin solns. 77−54004
AgBr, crystal growth behaviour, influence of Gibbs-Thomson effect 78−24883
AgBr(Cl) precipitates, phase boundary processes, quantum mech. law in mass transfer processes *(German)* 79−27937
AgCl-AgBr, microcryst., halide comp. profiles, XPS 77−12850
$Ag_xHg_ySI_z$, prep. of mixed sulphide iodides, photochromism 77−36385
Al chalcogenate and chalcogenite double salts, form. laws and acid-base props. 80−101070
$Al(OH)_3$, precip. from solns. containing Li ions, X-ray diffr. patterns and comp. determ. 80−76502
$BaCO_3$-BaF_2-$TiO(OH)_2$, coprecipitated, use in prep. of polycryst. $BaTiO_3$ 77−24996
$BaSO_4$, $BaCrO_4$ powders, precip. from aq. solns. with slow supersat. development 77−28707
$BaTiO_3$, chemically precipitated, exam. of sintering behaviour by isothermal shrinkage *(German)* 79−4935
$BaTiO_3$ formation from coprecip. products 77−24997
Bi powders, fine, precipitation on passivated electrodes 80−2977
BiOCl, exam. of crystal structure and morphology, as function of growth conditions, using electron microscopy 79−52103
$6Bi_2O_3.SiO_2$, stable γ-phase cryst. form. from supercooled melt, metastable δ-phase precip., surface contamination role 79−91635
C precipitates with preferred orientation [100], from dissoc. of n-xylene *(Russian)* 80−45484
$CaCO_3$, nucleation mechanism accompanying Ostwald ripening 80−50641
$CaCO_3$, precipitation from Mg^{2+} containing soln. *(French)* 77−85915
$CaCO_3.H_2O$, formation of aragonite 78−27427
CaO, single cryst. growth from molten $CaCl_2$ in wet atmosphere, habits 80−55287
β-$Ca_2(PO_4)_2$ whitlockite ceramic fabrication for prosthetic applications 79−78924
$CaSO_3.1/2H_2O$-$CaSO_4$ solid solution, prepared by coprecipitation from solns., exam. 79−20034
Cd, metallic precipitates, crystallography dendritic origin of hexagonal prisms 79−66366
$Cd(OH)_2$, highly dispersed precipitate, microstruct. and exchange props. 77−36793
CdS, chemically precipitated film, optical spectra, annealing effects *(Russian)* 79−11424
CdS precipitates from acetate solns., crystal structure and photocond. obs. *(Japanese)* 78−10502
CdS_xSe_{1-x} thin-film position-sensitive photoresistor prod. and props. *(Russian)* 78−43503
$Co(UO_2AsO_4)_2.8H_2O$, prep. cryst. struct. characterisation 78−30589
Cs-D_2, vap., oscill. production of particulates, by CW laser beam 77−77794
CsH, crystallisation in Cs+H_2 gas mixture, laser snow effect 80−40712
Cu, cementation, characterisation of nucleation and growth from aq. soln., TEM and SEM study 79−28972
Cu-Al_2O_3, composite coatings, prep. by precip., props. 78−23841
Cu-rare earth oxide-Y composite coatings, oxide and Y effect on coating precipitation 80−55554
$CuMn_2O_4$, formation in phase transition during ht. treatment of $Cu(OH)_2$-$\alpha Mn(OH)_2$ 78−23659
Fe_3O_4, magnetite, precip. with urea, prep. and props. 80−20854
$Fe(OH)_2$, gel, coprecipitation of divalent metal ions in soln. *(Japanese)* 78−31714
$Fe(OH)_3$, coprecipitation with Cu, Ag, Au; Ge, Sn, Pb; Mn and Ca 79−70415
FeOOH, crystal growth in $FeSO_4$ solution with NaOH or NH_4OH as precipitant, phase diagrams *(Chinese)* 80−44158
$Fe_2(SO_4)_3$ soln., precipitation of Fe as Jarosite *(Korean)* 79−87842
Ga chalcogenate and chalcogenite double salts, form. laws and acid-base props. 80−101070
Ge_2S_3, glass form. and characterisation *(German)* 80−64913
Ge_2Se_3, glass form. and characterisation *(German)* 80−64913
In chalcogenate and chalcogenite double salts, form. laws and acid-base props. 80−101070
$MgMn_2O_4$, formation in phase transition during ht. treatment of $Mg(OH)_2$-α-$Mn(OH)_2$ 78−23659
(MgO-Fe_2O_3-Cr_2O_3-TiO_2):Na_2O, powder, prep., heat treatment, Na_2O impurity effect on props. 77−16528
$Mg(OH)_2$, precip. 78−68615
^{99}Mo separation from neutron irradiated ^{235}U, HNO_3 soln., S collector 77−42161
Na coolant in EBR II, purification by cold trapping, effectiveness 77−14225
$Na_3M_2^{3+}Li_3F_{12}$ garnets, M=Al,Cr,Fe, synthesis from aq. soln., props. 77−44184
Nb, precipitation from gaseous phase, during H_2 reduction of $NbCl_5$ and $TaCl_5$, Ta behaviour *(Russian)* 78−44017
Nb_2O_5, hydrated gel, prep. conditions on pore struct., adsorpt. meas. 78−3068
$Ni(NH_4)_2(SO_4)_2.6H_2O$, precipitation from equimolar aqueous solns., kinetics study 80−7848
$Ni(OH_2)$-α-$Mn(OH_2)$ system, precip. and ht. treatment 77−85916
$Ni(UO_2AsO_4)_2.8H_2O$, prep. cryst. struct. characterisation 78−30589
^{231}Pa recovery and purification procedure 79−15977
^{233}Pa removal from ^{237}Np by coprecipitation with MnO_2 or sorption on silica gel 79−52733
$PbCrO_4$, cryst. growth kinetics and particle size in precipitating K_2CrO_4-$Pb(NO_3)_2$ mixed soln. 78−26472
PbS photosensitive deposit precipitation, alkali and acetate conc. effects 79−76781
PbS, thin film comp. and struct. rel. to precip. by allyl thiourea 77−48356
Pu reclamation, precipitation-ion exchange scheme for actinide removal from salt waste soln. 79−49820
Pu, separation, by MnO_2 coprecipitation from fresh and saline water 78−27814
Sb_2S_2O, kermesite, synthesis, controlled precipitation and crystn. 77−48332
SiO_2-ZrO_2 adsorbents, coprecipitated, porous struct. rel. to form. conditions 78−53263
SnO_2:Eu powder phosphor, prep., low energy electron excitation 78−39608
$SrSO_4$, mass transfer in precip. from mixed solvents *(German)* 78−67674
$SrTiO_3$, Sr_2TiO_4, $Sr_3Ti_2O_7$, prep. from coprecipitates of Sr and Ti 77−48374
Ta, purification from Nb during precipitation from gaseous phase, during H_2 reduction of $NbCl_5$ and $TaCl_5$ *(Russian)* 78−44017
Ta_2O_5-H_2O_n, influence of preparation on pore structure and ion exchange props. 79−1970
$Tb(NO_3)_3$-$Fe(NO_3)_3$-$(NH_4)_2CO_3$-H_2O system, cpd. form., comp. and props. 80−100832
Tb_2O_3-H_3PO_4-H_2O system, cpd. form., comp. and props. 80−100832
Th sulphito complex ion precipitation with hexammine Co(III) chloride cation 78−92495
ThO_4, prep., IR spectra and thermal exam. 77−89402
Ti^{4+} hydroxide, coagulation struct. effects on particle size of TiO_2 78−52732
TiO_2-Sb_2O_3 system, phase comp. of roasted coprecipitates 78−23651

precipitation continued
- $(U,Pu)O_2$, FBR fuel pellets, gel-supported precipitation conversion and prep. 80−813
- $(U,Pu)O_2$ powder, FBR fuel prep. by Au/PuC coprecipitation process 80−814
- UO_2^{++}, precipitation reaction in KSCN 80−26040
- U(VI) peroxo complex ion precipitation with Co(III) complex cation 78−80728
- U(VI) sulphito complex ion precipitation with hexammine Co(III) chloride cation 78−92495
- WC-Co cemented carbides, effect of Co form and distrib. in prep. starting mixture 78−44072
- $Y_{3-x}Bi_xFe_5O_{12}$, ferrite-garnet formation 78−52737
- $Y_2Ti_2O_7$, precipitation from oxalates, carbonates, exam. 80−55641
- Zn, metallic precipitates, crystallography dendritic origin of hexagonal prisms 79−66366
- $ZnC_2O_4.2H_2O$, crystn. kinetics by precipitation 80−50884
- $Zn(UO_2AsO_4)_2.8H_2O$, prep. cryst. struct. characterisation 78−30589
- ZrO_2 gels, calcination 80−11964
- ZrO_2, obtained by coprecipitation with different oxides, props. 78−64514
- ZrO_2-Y_2O_3-$Nd_2O_3(CeO_2)$, solid solns., form. by coprecipitation, struct., X-ray, electron diffr. anal. 77−12583
- $ZrTiO_4$, form. mechanism from spray drying of solns., precip., of hydroxides and reactions of hydrates and solns. 79−43182

precipitation ageing *see precipitation hardening*

precipitation annealing *see precipitation hardening*

precipitation hardening
- age temperature shifting rel. to phenomenological theory of annealing and precipitation hardening 78−15428
- ageing alloys, single cryst., deform. and hardening 78−23716
- alloy, heat-resistant, alloying and heat treatment effects on struct. and strength 78−95758
- alloy, high temperature, mechanical, thermal and corrosion props. 78−95763
- alloy, precipitation hardened, containing narrow soft zones at grain boundaries, fracture toughness 77−77553
- alloy, spinodally decomposed, interfacial energy effect on mech. strength, theoretical estimation 79−38790
- alloy, strengthening mechanism anal. by thermal activation theory 79−78987
- alloys, Co effect on martensite ageing at 300-600°C *(Russian)* 80−20972
- alloys, precipitation hardened, dislocation struct. *(Hungarian)* 79−55746
- alloys, precipitation hardening, yield stress *(Russian)* 79−56990
- alloys, radiation effects on ageing and precipitation, review 80−29956
- analogies in ferromagnetism and superconductivity, unified approach 77−77490
- austenitic steel, hardened by thermomechanical treatment with ageing, influence of stabilisation on mech. props. *(Russian)* 77−52356
- Corson alloys, AE during tensile deform. *(Japanese)* 79−61654
- dislocation physics research of F.R.N. Nabarro 80−62441
- Elinvar, γ to γ' transformation and γ' phase form. kinetics, lattice consts. 80−35191
- glass, chemically strengthened, ion exchange temp. and time influence on stress profiles and strengths 78−31417
- glass, diffusion strengthening technique 78−31418
- Incoloy 800, creep crack growth, age hardening effect 79−43436
- Incoloy 800, mechanical props., heat treatment and appl., conf., Petten, Netherlands (March 1978) 79−43296
- Incoloy 800, use up to 550°C, creep ductility 79−43369
- Incoloy 903, microstruct. and effect of H_2 charging 77−86143
- Inconel X, X-ray study of stress meas., elastic const. *(Japanese)* 79−66092
- Lagneborg particle by-passing model, creep rate stress exponents and friction stress 80−55481
- metal, diffusional relaxation of stress conc. at second phase particles 79−1889
- misfitting particles, precip. hardening, comparison with expts. 80−3086
- Nimonic 80A, order hardening, comparison between revised theory and expt. 80−93565
- Nimonic 90, creep rate stress exponents and friction stress, comparison with Lagneborg particle by-passing model 80−55481
- Nimonic 90, dispersion hardened, friction stress rel. to initial and secondary creep 80−11711
- Nimonic alloy, effect of annealing on hardness, carbide phase strengthening *(Russian)* 79−34137
- precipitate hardened material, intergranular cavity growth inhibition 80−50677
- rubber-epoxy resins, heterogeneity analysis, light scatt. and statistical methods 78−2024
- sapphire:Ti^{4+}, plastically deformed, precipitation hardening, TEM study 80−7592
- sapphire :Ti^{4+}, deformation history effects on precipitation hardening 79−83209
- stainless cast high-strength steel, fracture toughness 77−56109
- stainless steel aged by discontinuous precipitation mechanism ultrafine grain and mech. props. *(Russian)* 77−70053
- steel, 12KhN3A, case-hardened, friction austenite, electron diffr. obs. *(Russian)* 77−21286
- steel, 1Kh12V2MF, pore formation in creep, precip. hardening 77−63747
- steel, 37Kh12N8G8MFT, hardenss meas. and electron microscope exam. *(Russian)* 79−38843
- steel, age hardened, dynamics of cyclic plasticity *(Czech)* 80−108464
- steel, age-hardenable, relation between fatigue S-N and P-N charact., definite fatigue limit *(Japanese)* 77−8938
- steel, Al-Ti-(Mo), Al-Ti-V-(Mo), Al-Ti-Nb-(Mo) and Al-V-(Mo) low-alloy, toughness improvement through Ti additions 80−66525
- steel, alloy, cyclic strength after strain hardening and tempering, precip. hardened 40FT and 40 78−52988
- steel, austenitic, 33N25Yu3F, hardening, effect of quenching and ageing temps. *(Russian)* 77−81267
- steel, austenitic, age-hardening kinetics, study by resistivity, Young's modulus and internal friction *(Czech)* 80−29970
- steel, austenitic, aged, stress induced martensitic transform., mech. props. *(Russian)* 79−87632
- steel, austenitic, corrosion-resistant, strengthening by alloying with N_2 78−95757
- steel, austenitic, Cr-Ni, anomalous stress-depend. of creep rate 80−11712
- steel, austenitic, Ni-Cr, precipitation strengthened, anelasticity, plastic creep limit, 823K 79−1899
- steel, austenitic, precipitation hardenable, friction and wear under abrasive conditions *(German)* 77−59951
- steel, austenitic, precipitation hardened, ductility of grain boundaries and crack propag. *(German)* 78−52834
- steel, austenitic, precipitation hardening, effect on fatigue strength 78−84829
- steel, austenitic, precipitation of $Cr_{23}C_6$ at grain boundaries 78−84846
- steel, austenitic, type of Kh15N27T3MR, exam. of elasticity props. 78−56687
- steel, austenitic Fe-Mn-V-C, ageing charact., discontinuous precip. nature 80−84940
- steel, austenitic stainless, ageing at high temp., effect on creep props. SEM 80−97516
- steel, austenitic stainless, Cr-Ni-Mo-Mn, Mo, Mn and ageing effects 78−35413
- steel, austenitic stainless, precipitation of $M_{23}C_6$ type carbide on twin boundaries 80−89226
- steel, C-Mn-V-Cb-N, high strength low alloy, controlled-rolled 80−100803
- steel, CC Ti-C, threshold fatigue behaviour, effect of grain size and yield strength 79−91790
- steel, Co-Cr-Mo, maraging, age hardening, Mossbauer study 80−40002
- steel, Co-Cr-Ni-Mo-Mn (39.65, 20.25, 15.33, 7.08, 1.9 wt.%) carbide formation during tempering after plastic deformation 80−16330
- steel, Co-W-Mo-V-Ti-C (25.3, 12.8, 6.2, 0.5, 0.5, 0.05 wt.%), martensitically aged, structural transformation, and strengthening mech. *(Russian)* 79−15676
- steel, cold rolled, high strength, mech. props. 77−36527
- steel, cold strained, defects interaction with carbide strengthening phases, carbide decomp. degree *(Russian)* 80−84955
- steel, Cr-Mn(Ni), Mn and Ni additions, effect on corrosion resistance and hardness 80−104342
- steel, Cr-Mo-Mn-Si-W (3, 1.95, 1.55, 1.45, 0.95 wt.%), struct. and props. 80−104175
- steel, Cr-Mo-Ni-Nb, Nb effect on mech. props. *(German)* 80−30012
- steel, Cr-Mo-V, creep, effect of microstruct., heat treatment, transform. temp. 78−11248
- steel, Cr-Ni-Mo-Cu-Nb, corrosion resistant, heat treatment, structure and props. 79−74169
- steel, Cr-Ni-Nb, containing controlled particle dispersions, creep strength 77−52425
- steel, Cu, precipitation hardening, strength and struct. *(German)* 79−47701
- steel, Cu, struct. and fracture *(German)* 79−61696
- steel, ferritic, Cr-Mo (18, 2 wt.%), cold work effect on 885°F embrittlement 77−77499
- steel, ferritic, strengthened by VC interphase precipitation, cleavage 79−74171
- steel, high Mn, heat resistant, alloying additions, effect on mech. props. *(Korean)* 77−12631
- steel, high-speed, N effects on struct. and props. 77−59799
- steel, low alloy, tempered martensite embrittlement mechanisms 79−8351
- steel, low C, high strength, thermomech. treatment, strengthening mech. 79−57014
- steel, low C, weldable, precipitation hardening rel. to low cycle fatigue *(Czech)* 79−15686
- steel, low-C, with Nb-B addition, transform. charact. and mech. props. *(French)* 79−43253
- steel, maraging, 18% Ni content, exam. of age hardening-grain size relationships 78−84833
- steel, maraging, 18 Ni, welded joints ageing props. obs. *(Japanese)* 80−40401
- steel, maraging, Cr-Ni-Ti, effect of Ti addition on hardness and energy scatt. 79−15687
- steel, maraging, DI52, low cycle fatigue in gaseous H_2 *(Russian)* 78−35478
- steel, maraging, Fe-Cr-Co-Mo, phase transforms. during high temp. austenitisation and solid soln. decomp. *(Russian)* 80−66524
- steel, maraging, hardening mechanism of quenched samples, tempering *(Czech)* 79−78989
- steel, maraging, investigation with lower Ni and Co contents *(Chinese)* 78−84812
- steel, maraging, Ni-Co-Mo, ageing and evolution peak at 470°C, calorimetric anal. *(Japanese)* 79−100156
- steel, maraging, precipitation hardening, strength and struct. *(German)* 79−47701
- steel, maraging, solubility of Fe-Mo-Co (10, 0 to 20 wt.%) Laves phase, depend. on Co *(Russian)* 79−100145
- steel, maraging, steady state unidirectionally solidified, austenite reversion and determ. 77−25118
- steel, maraging, struct. and fracture *(German)* 79−61696
- steel, maraging Ni-Co-Mo, strengthening by repeated strain ageing *(Japanese)* 79−100157
- steel, martensitic, ageing of 05kh3N2MD2, hardness depend. on tempering temp. *(Russian)* 79−24544
- steel, martensitic, Cr-Ni-Co-Mo-Ti, Kh12N8K5M3TYu, ageing of C free martensite *(Russian)* 79−1884
- steel, martensitic, submicrostructure alterations in ageing and plastic deform. *(Ukrainian)* 79−79032
- steel, medium C, fatigue behaviour of NiAl precipitation hardening 78−84983
- steel, microalloyed structural, precipitation hardening, strength and struct. *(German)* 79−47701
- steel, Mn-Ni-Al, nonmagnetic, carbide-intermetallic strengthening 79−83208
- steel, Mn-V reinforcing type, strain ageing charact. rel. to mech. props. 80−84969
- steel, Nb-V, cold rolled, HSLA, prod. by precipitation hardening, annealing 78−88471
- steel, Ni-Co-Mo-Ti, maraging, electron diffr. obs. of second phase *(Chinese)* 80−11655
- steel, Ni-Cr-Ti, thin bands, cold working, props. and struct. of 36NKhTYu 79−78994
- steel, Ni-Ti, high-alloy, precipitation hardening, fatigue strength 79−79103
- steel, nitriding, diffusion layer hardening calc. 79−52456

precipitation hardening continued
steel, Si (3 wt.%), textured, secondary recrystn., precip. annealing effect *(Japanese)* 80−71662
steel, spring alloy, microstruct. and props. at low temps. 77−44286
steel, stainless, austenitic, CC Ni-Al, γ-phase, fracture mechanical aspects of abrasive friction, wear, chip formation 78−72865
steel, stainless, austenitic, N_2 effects obs. *(Rumanian)* 77−55973
steel, stainless, Cr-Ni-Co (13, 4.5, 0 to 13.8 wt.%), Co effect on martensite ageing *(Russian)* 77−66660
steel, stainless, ferritic, electron microscope obs. of precipitation hardening *(French)* 79−34049
steel, stainless, maraging high strength, embrittlement on low temp. ageing *(Japanese)* 79−100155
steel, stainless 304 sol. of annealed and thermally-aged, high-cycle fatigue behaviour 80−100923
steel, stainless Kh15N9Yu, elastic limit, effect of microstruct. and heat treatment 79−83251
steel, structural martensitic, corrosion resist. under stress effect of strain ageing with hydroextrusion *(Russian)* 79−38853
steel, Ti (0.1 to 0.55 wt.%), strengthening by carbide precipitation 77−25062
steel, Ti microalloyed structural, struct. and fracture *(German)* 79−61696
steel, tool, type M2, laser melting and heat treatment, microstruct. charact. 79−100188
steel, type 55SM5FA, formation of hardened layer during burnishing 78−85046
steel nitride phase hardening, precipitation and solution kinetics after heat treatment 78−95756
steel wire, drawn, mechanical and electrical props. relationship obs. 80−50662
steels, low alloy, particle coarsening reactions, effect of cold deform. 80−71664
steels, martensitic-ferritic, microdefect accumulation during creep, effects of heat treatment, hardening 79−24550
superalloy, microstructure resulting from alloying and heat treatment, effect on creep, fatigue, fracture strength 78−11246
texture influence on stress/strain curves, prestrain, solid soln. and particle hardening effect on inhomogeneous deform. *(German)* 80−30014
thermophysical property research, metallurgical applications 80−97457
β-Ti-Mo (15wt.%) metastable alloy, strength enhancement 77−66650
two phase alloy hardening by second phase particle coalescence 80−7591
two-phase decomposition and coarsening 78−88472
Udimet 520, γ′ distribution in slip plane, dislocation loop form. during creep *(Japanese)* 79−42075
Udimet 520, precipitation hardening *(Japanese)* 79−43259
Ag-Pd-Cu alloys, contact-spring props. and age hardening 78−88473
Ag-Pd-Cu-Au dental alloy, age-hardening charact. 79−87646
Al age-hardenable alloys, dissolution processes, positron annihilation and X-ray small-angle scattering comparison 80−89238
Al alloy, precipitation hardening, creep deform. effect 77−16601
Al alloy, precipitation hardened 2014 and 2219, temp. depend. of elastic constants 77−66673
Al alloy 2036, thermomechanical treatment on struct. and props. 79−29109
Al alloy 6061, high-purity, precipitation hardening, prior strain and ageing effect 77−66651
Al alloy AZ5G, age hardening heat treatment effect on mech. props. microstruct. *(French)* 77−52370
Al alloys, age-hardening, resistivity charge by low temp. deform. *(Japanese)* 78−84831
Al alloys, precipitation hardening, positron annihilation investig. by γ-ray Doppler broadening 77−81174
Al-2024-T351 alloy, precipitation hardening, thermal cond. 78−91661
Al-Ag (15 wt.%), precipitation hardenend cyclic stress-strain response 78−35412
Al-Ag(Cu)(Zn), electrical resist. of Guinier-Preston zones during age-hardening 77−72848
Al-alloys, precipitation hardening, effect on dynamic strain ageing and jerky flow 80−20945
Al-Cu, age hardened, coherency stresses, composition and dislocation interactions for θ″ precipitates 77−36525
Al-Cu, crack advance during fatigue, effect of cyclic hardening and COD 77−16675
Al-Cu, precipitation hardened, hysteretic plastic work as failure criterion in Coffin-Manson type relation 77−32657
Al-Cu (4 wt.%), precipitation hardened and fatigued alloys, solute loss at fracture surface, EPMA exam. 78−39893
Al-Cu (4 wt.%) alloy, high temp. cyclic deform., θ′ particle dissolution obs. 80−108515
Al-Cu (4 wt.%) alloy, precipitation hardened, single crystal, directional plastic behaviour, exam. 78−39788
Al-Cu (4 wt.%) alloy, reversion charact. *(Japanese)* 79−56989
Al-Cu (4 wt.%) partially coherent precipitation hardened alloy, high temp. cyclic deform. 80−25710
Al-Cu (5 wt.%), fatigue strength, coarse precipitation effect *(German)* 79−91660
Al-Cu full coherent precipitation hardened alloy, high temp. cyclic deform. 80−25711
Al-Cu single cryst., hardening due to oriented GP zones 80−55414
Al-Cu-Mg, dil. alloys, ageing response *(Korean)* 77−28832
Al-Cu-Mg (2.0, 1.1 wt.%), Ostwald ripening of S′ precipitates *(Korean)* 79−38831
Al-Cu-Mg-Ag casting alloy, precipitation hardening in artificially aged condition 79−1874
Al-Cu-Mg(:Fe,Si) alloys, double-ageing, resist., hardness meas. 77−28822
Al-Cu-Mn-Zr, type 2219, particle, coarsening of disk shaped Θ′ particles 80−45315
Al-Cu-Ni, alloy RR 350, θ′-hardened, deform. induced microstructural instability, high temps. 80−16321
Al-Cu-Si-Mg (4, 0.8, 0.8 wt.%) alloy, GPB zone formation during room temp. ageing 77−44263
Al-Cu-(Mg), precipitation strengthened, Bauschinger effect 77−36585
Al-Cu(Mg), age-hardenable, US cavitation erosion mechanisms, effects of comp. and heat treatment 78−53002
Al-Cu(Zn-Mg), age hardening, conditions leading to localised plastic deform. and fracture in slip bands during fatigue 78−64670
Al-Cu(4 wt.%), alloy AU4, θ′ precipitation, apparent hardening maxima *(French)* 77−16598
precipitation hardening continued
Al-Li (2.8 wt.%), ageing in US field, precip. hardening *(Russian)* 80−29968
Al-Li-Mn (2.8, 0.3 wt.%), recrystallised sheet, fracture behaviour, SEM and TEM study 80−97566
Al-Mg alloys, effect of Ag addition on ageing and related props. 77−36522
Al-Mg_2Si alloy, STEM microdiffr. obs. of precip. struct. 80−104167
Al-Mg-Ag, age effect on age hardening *(Japanese)* 78−52831
Al-Mg-Si, Guinier-Preston zones, inception and effect on ageing, review *(Hungarian)* 79−11627
Al-Mg-Si, Portevin-Le Chatelier effect, effect of precipitation hardening 77−32585
Al-Mg-Si, thermomechanically treated, age-hardening 78−11236
Al-Mg-Si (0.7, 0.4 at.%), effect of precipitation hardening on strain rate behaviour and yield behaviour 79−29075
Al-Mg-Si alloys, cast, precip.-rich zones on grain boundaries, soln. heat treatment conditions effect on mech. props. 80−104176
Al-Mg-Ti(Zr), struct. and factors determining brittle intermediate compound form. 78−52817
Al-Mn alloys, study of solidification by rapid cooling *(Japanese)* 78−88459
Al-Si (9 wt.%), precipitation hardening during isothermal ageing 80−29969
Al-Si-Cn-Mg, alloy AL32, ageing of castings produced by pressure die castings 78−56650
Al-Zn, age hardenable precipitation and dissolution, positron annihilation and X-ray scatt. 80−16314
Al-Zn, metastable solvus curve, struct. changes 77−55950
Al-Zn, resistivity calc. for age-hardened alloy 77−73284
Al-Zn-Mg, precipitation strengthened, Bauschinger effect 77−36585
Al-Zn-Mg (2.2, 4.7 at.%), precipitate free zones, X-ray microanal. 80−108768
Al-Zn-Mg (3,1.5 wt.%), precipitation hardened and fatigued alloys, solute loss at fracture surface, EPMA exam. 78−39893
Al-Zn-Mg alloy, TEM characteris. of precipitates 80−104166
Al-Zn-Mg alloy, thermomech. treatment, precipitation and strengthening 79−24527
Al-Zn-Mg alloy V95, two-stage ageing kinetics, mech. props. effects 79−83238
Al-Zn-Mg and Al alloy 7050, age hardenable, microstruct., effect of monotonic and cyclic straining 77−36633
Al-Zn-Mg-Cu-Co (6.5, 2.5, 1.5, 0.4 wt.%), fatigue crack propag. 80−55521
Al-Zn-(Mg), age hardenable single crystal, fatigue and fatigue cracks *(German)* 77−16689
Al-Zr, cast, precipitation and solidification *(German)* 77−36519
Al-Zr, interphases, formed during precipitation and solidification *(German)* 79−29062
Al-Zr (1-13 wt.%), rapidly quenched, extended solid solubility, grain refinement and age-hardening 80−76266
(Al-Mg-Si)-Al_2O_3, SAP type, ageing 79−96055
AlCu-NiCo (5 at.%), Θ′ hardened, creep mechanism 80−85013
AlZnMg alloy, precipitation hardened, strength 78−39786
Au-Cu-Ag dental alloy, age-hardened, struct. and morphology 78−92272
Au-Cu-Ag-Pd (35.4, 17.8, 9.7 at.%), dental alloy, age-hardenable, TEM obs. 77−21156
Be-Cu alloy, effects and appl. *(Italian)* 79−83207
Be-Cu high-strength alloy characteristics for electrical components 78−48547
Be-Cu mill-hardened strip stress relaxation obs. 78−48485
CU-Zr-(Cr), powder metallurgical alloys, thermomech. treatment effect on props. 80−50660
Cd-Zn (up to 1.57 at.%), single cryst., precip. hardening, 77-300K 78−60675
Co-Fe-Nb alloy, mag. precipitation-hardening and Bloch wall pinning 78−80173
Co-Fe-Nb semihard mag. alloy, mag. precip. hardening 77−8960
Co-Fe-Ti (12,6 wt.%), semihard permanent magnet, magnetic precipitation hardening 78−52830
Co-Mo-Cr-Si, plasma and detonation coatings, Laves- and carbide-strengthened, comparative props. 78−15562
Co-Ni-Cr (20,20 wt.%), internal oxidation, improvement of mech. props. *(French)* 77−16521
Co-Ni-Cr superalloys, γ′-precipitation-strengthened, yielding 77−8894
Co-Ni-Cr-Nb (40, 18, 1.8 wt.%), precipitation behaviour of NbC, effect of ageing temp. on morphology 80−89227
CsI, annealing effects on mech. and microstruct. props. 77−66686
Cu alloy, precipitation hardened, anomalous elastic props. 77−86071
Cu alloy, precipitation strengthened compositions with oxide particles, condensed, struct. criteria and thin layer possibilities *(Russian)* 80−89236
Cu based materials, sputter deposited at high rate, microstruct. and props. 78−22988
Cu-Be, dynamic strain age hardening 77−52375
Cu-Be, electrical resist. of Guinier-Preston zones during age-hardening 77−72848
Cu-Be (1.8 wt.%) alloy, discontinuous precip. form. and growth, TEM obs. 80−104169
Cu-Be (2.1 wt.%), discontinuous precipitation *(Japanese)* 78−19766
Cu-Be alloy *(Japanese)* 78−35398
Cu-Cd-Cr, precipitation hardened, low temp. elastic props. 77−73299
Cu-Co, age hardenable single crystal., fatigue and fatigue cracks *(German)* 77−16689
Cu-Co (2 at.%), age hardened, stage I fatigue crack propag. 78−3203
Cu-Co single cryst., precip. hardening *(German)* 80−84946
Cu-Cr, age hardened, fine precipitates struct., TEM study 80−3066
Cu-Cr, precipitation hardened, wear 78−3234
Cu-Cr-SiO_2 system, age and dispersion strengthened, dislocation struct. around SiO_2 particles 80−108468
Cu-Cr(-SiO_2), single crysts., yield and pre-yield behaviour rel. to aging time 80−81103
Cu-Fe, single crystal with coherent γ-Fe particles, precipitation hardening 78−31416
Cu-Fe (1.5 wt.%) alloy, void form. during irrad. in HVEM, reactor irrad. simulation and ageing effects 80−107327
Cu-Ni-Al, ageing charact., optical TEM, X-ray, hardness obs. 79−29079
Cu-Ni-Al, grain boundary reaction under isothermal ageing at 623 to 973K *(Japanese)* 79−70090
Cu-Ni-Al (5, 2.5 at.%), precip. hardening *(Japanese)* 80−71663
Cu-Ni-Be (30, 0.5 wt.%), grain boundary reaction after ageing and quenching, obs. *(Japanese)* 79−70089

precipitation hardening continued
Cu-Ni-Cr, microstruct. behaviour and mechanical hardening 78−47281
Cu-Ni-Fe, age hardenable, dislocation interactions with internal coherency stresses 77−36528
Cu-Ni-Nb (30, 0.9 at.%), precipitate free zones, X-ray microanal. 80−108768
Cu-Ni-Nb (30,1 wt.%), precipitation 77−86035
Cu-Ni-P, precipitation hardening 77−12633
Cu-Ni-Sn (15, 8 wt.%), prior deform. effect on spinodal age hardening 80−108465
Cu-Ni-Sn (15, 9 wt.%), age hardening accompanying phase transition 78−64551
Cu-Ni-Ti, ordering within precipitates, TEM obs. 80−108461
Cu-Ni-Zn-Mn fine grained precipitation-hardenable alloy, high strength and ductility 80−100805
Cu-Ti, strengthened by modulated structs., anomalous age hardening effects 80−97497
Cu-Ti (0.9 at.%), age hardening effect on critical resolved shear stress 79−61603
Cu-Ti (3.5%), coherent precipitates, US irrad. effect on struct. and hardness *(Russian)* 77−48446
Cu-Ti alloys (0.5 to 4.0 wt%) ageing charact. determ. 79−20089
Cu-TiC precipitation hardened composite, struct. effect on friction 78−11337
Cu-Ti(Ag) alloys, activation vol. stress depend., single crysts. 77−48499
Cu-Ti(0.7 at.%), plastic deform. and precip. hardened, annealing time 78−48446
Cu-Zn-Be, precipitation hardening 77−16599
(Cu-Au)-Co, single crysts., solid soln. and particle strengthening, superposition 80−97495
Cu_3Au-Co, underaged, ordered and disordered single crystal, hardening mechanisms 78−3134
Cu_3Au-Co single cryst., precip. hardening *(German)* 80−84946
γ-Fe alloy, supersat. solid soln., recrystn. inhibition by cold rolling 77−73286
Fe, cast, increase in yield strength, after phase transformations 78−44125
Fe-Be, formation of quasi-periodic distrib. of precipitates during ageing *(Russian)* 78−56642
Fe-C, ageing late stages, diffusional coalescence of precip. along dislocation lines *(Russian)* 77−25060
Fe-Co-Cr-W-Ni-C, alloy KKhVN, transforms. during annealing and nature of hardening *(Russian)* 78−56653
Fe-Cr, decomposition Mossbauer study *(French)* 77−63678
Fe-Cr-Mo-Ti (13, 1.5, 3.5 wt.%), equilibrium studies on chi-phase strengthening 79−24496
Fe-Cr-Ni, solid soln. strengthened and precipitation hardened, in-reactor creep 79−43327
Fe-Cu, precipitation hardening of α-Fe containing weak and strong particles 80−20946
Fe-Cu-C, fatigue behaviour for tempering at 500°C, precip. hardening 77−40442
Fe-Cu(2, 4 and 6 wt.%), sintered, precipitation hardening 77−66653
Fe-Mn, struct. and props., effect of Nb, C and Si alloying *(Russian)* 77−90360
Fe-Mn-Al-C, hardening during ageing, 450-750°C *(Russian)* 78−3135
Fe-Mn-Ni, age hardenable, struct. and strength 77−52339
Fe-Mn-Ni base maraging alloys, age hardening 79−74170
Fe-Mn-Ni-C, age hardenable, struct. and strength 77−8844
Fe-Mn-Ti alloys, austenitic, precipitation strengthened 80−25714
Fe-Mo (13-20 at.%) binary alloys, spinodal decomp. on ageing, TEM and X-ray diffr. study 80−97503
Fe-Mo-CaF_2 sintered composite, struct. and mech. props., heat treatment effect 80−66526
Fe-Mo-Ta, ternary Laves phase strengthening 80−108466
Fe-Nb-C (0.04, 0.02 wt.%), strengthening, hot rolling *(Chinese)* 79−100154
Fe-Ni (3 wt.%), low temp. softening *(German)* 79−29081
Fe-Ni austenite, precipitation hardened, transform. strengthening 79−24531
Fe-Ni austenitic, effect of Al and Ti on relaxation resist. 80−20993
Fe-Ni martensitic alloys, age hardening 79−47736
Fe-Ni system, constant modulus alloys for mech. oscillators 79−61641
Fe-Ni-Al-(Cu) (12, 0.5, 0.5 to 3 wt.%), Cu addition strengthening at 77K, mech. props. 80−60875
Fe-Ni-Al(2.5, 7.5 at.%), fracture surface morphology, ageing temp. effects 77−16600
Fe-Ni-Co-W(Mo) (18.65, 8.99, 4.87 wt.%), ageing charact., 380-530°C 80−60876
Fe-Ni-Cr (25, 15 wt.%), high temp. creep, dispersed γ'-Ni_3(Al, Ti) effects *(Czech)* 78−64590
Fe-Ni-Cr alloy, carbide form. by C diffusion, precip. distrib. and morphology 80−104164
Fe-Ni-Cr-Si alloy 800, Si effect on creep and age hardening 77−48444
Fe-Ni-Cr-Ti-Mn-Mo, (25.8, 14.04, 2.17, 1.27, 1.30 wt.%), superalloy A-286, precipitation hardening, exam. of fracture toughness and mech. props. 78−92355
Fe-Ni-Mn, martensite, aged, grain boundary embrittlement 79−96144
Fe-Ni-Mn martensitic alloy, precipitation 77−12630
Fe-Ni-Ti (27.4, 2 to 3 wt.%), aged, stress induced martensitic transform., mech. props. *(Russian)* 79−87632
Fe-Ni-Ti-(Cu) (12, 0.25, 2 wt.%), Cu addition strengthening at 77K, mech. props. 80−60875
Fe-Ni-V-Co, Co influence on age hardening *(Russian)* 78−68703
Fe-Ni-V-(Cu) (12, 2, 2 wt.%), Cu addition strengthening at 77K, mech. props. 80−60875
Fe-Ni-(Cu) (12, 0.5 to 3 wt.%), Cu addition strengthening at 77K, mech. props. 80−60875
Fe-Ti, precipitation hardening of α-Fe containing weak and strong particles 80−20946
FeNiCrAlLi alloy, γ' hardened, noncellular mech. for form of lamellar η phase morphology 77−28824
GeTe, elec. cond. and microhardness, thermal cycling effect *(Russian)* 78−35485
KCl:Pb, lead aggregation effect on yield stress, incoherent precipitates, solubility determ. method 80−50645
Mg alloy, quenched-in defect behaviour, effect on flow stress 79−61625
Mg-Al(-Zn), solute-vacancy binding energies from hardness meas. 78−39789
Mg-Ce, workability, aging characts. and tensile strength 80−55416
Mg-La, workability, aging characts. and tensile strength 80−55416
precipitation hardening continued
Mg-Sm, phase diagram and mech. props. *(Russian)* 80−20892
Mg-Zn (5 wt.%), age hardening, X-ray diffr. anal. *(Chinese)* 80−104173
MgO, mag. anisotropy, ionic distrib. and composition of magnesioferrite precipitates, ferrimag. reson. study 77−69699
MgO, single cryst., order hardening by large precipitated vol. fraction of spinel particles 80−3085
Mo alloys, yield stress in tension and compression, SD-effect *(Ukrainian)* 77−56021
Mo-Zr-Nb-C and Mo-Zr-C, carbide precip. hardening kinetics, ageing singularities *(Russian)* 77−25059
NaCl, with dispersed Au particles, age hardening of surface, double decoration obs. 79−11634
NaCl:Ca, aggregation and precip. hardening in impurity vacancy, dipole decay 80−16322
NaCl+Pb, Pb aggregation effect on yield stress, incoherent precipitates, solubility determ. method 80−50645
Nb-Ti-Al alloy, effect of heat treatment on strength and elastic props. 77−55976
Nb-Zr-C, strengthening phase struct. and morphology after prolonged high temp. stress in vacuum *(Russian)* 77−25065
Nb-Zr-C alloy, long term strength rel. to carbide precipitate geometry *(Ukrainian)* 78−92266
Ni alloy, precipitation strengthened compositions with oxide particles, condensed, struct. criteria and thin layer possibilities *(Russian)* 80−89236
Ni alloys, welding crack resist. during welding, heating, stress reduction by hardening 79−24618
Ni base superalloy IN-738, γ' precipitate coarsening during ageing and creep 79−52271
Ni-Al, order hardening, comparison between revised theory and expt. 80−93565
Ni-Al, with large volume fraction of γ', precipitation hardening 77−36524
Ni-Al-Cr, precipitation-strengthened, mechanical props. 78−84968
Ni-Al-Ti ferromagnetic non-homogeneous alloy, composition determination by Curie temp. meas. 80−11196
Ni-alloys, precipitation hardening, effect on dynamic strain ageing and jerky flow 80−20945
Ni-base, heat resistant alloy KhN60MKBYuT, plasticity, precipitation 77−70120
Ni-base superalloy, IN-738, microstruct. changes during isochronal heat treatment, 773-1467K 78−27531
Ni-base wrought superalloy, creep and stress rupture behaviour in air and vacuum 80−60918
Ni-Be alloy, annealed under load, spatial distrib. of precips., electron microscopy *(Russian)* 77−59790
Ni-Cr alloy, heat-resistant, conc. of hardening γ'-phase, effect on electrochem. shaping *(Russian)* 77−8979
Ni-Cr-Al (40, 4 wt.%), γ' and α-Cr duplex precipitation, TEM *(Japanese)* 77−25061
Ni-Cr-Co superalloy, combined TEM, FIM, atom probe microanalysis of precipitates and carbide phase comp. 80−100844
Ni-Cr-Fe alloys, radiation enhanced precip. and dissolution of precipitates, point defect kinetics and dislocation obs. 80−108467
Ni-Cr-Fe-Mo-Co (21.41, 19.28, 8.64, 2.16 wt.%), Hastelloy alloy X, exam. of thermal stability 78−84865
Ni-Cr-Ta alloy, precipitation hardening, 650 to 800°C 77−59798
Ni-Fe solid soln., precip. hardened, paramag.-ferromag. transition on ageing 78−52255
Ni-Fe-Cr superalloy 718, heat treatment effect on room temp. and elevated temp. fracture toughness response 80−100922
Ni-Mo-Cr-Si, plasma and detonation coatings, Laves- and carbide-strengthened, comparative props. 78−15562
Ni-Nb(-Cu)-C, NbC dispersed supercond. tapes, fabrication and characts. 78−19773
Ni-Ni_4Mo, strengthening by ordered precipitates 77−86041
Ni-P (8 wt.%), protective coating for wear and corrosion resistance of steel 77−21329
Pb-Sn-Ca alloy sheet, continuously cast, for battery grids, ageing behaviour 77−16603
Pd-Cu-Ga, cold work and annealing-induced hardening, X-ray diffr. anal. and metallographic exam. *(Russian)* 79−38844
$Sm(Co,Cu)_z$, precip.-hardened, mag. and metallographic props. 77−8339
$Sm_{1-w}MM_w(Co_{1-x-y}Cu_xFe)_z$, (MM-mischmetal), mag. meas. and metallographic exam. 77−56119
steel, 36NKhTYu, aged, rate of discontinuous precipitation of γ'-phase, short high-temp. treatments *(Russian)* 78−11226
Ta-N (0.6 to 6.5 at.%), supersaturated solid soln., precipitation 79−96028
Ta-O supersaturated solid solution, precipitation processes, hardness change meas. 80−25712
Ti alloy, hardening heat treatment, alloying element effects development trends 78−95759
Ti alloy, microstructure resulting from heat treatment, alloying, effect on creep, fatigue, fracture strength 78−11246
Ti alloy VT22, hardening during thermomechanical treatment, precipitate particle internal struct. *(Russian)* 79−91657
Ti-Al, age-hardened, deform., order effects in Ti_3Al and temp. effects 77−25111
Ti-Al-Mo-Cr alloy weldment containing orthorhombic martensite, autotempering behaviour and alpha precip. strengthening 80−84976
Ti-Al-V (6,4 wt.%), age hardened, deform. charact. 77−36608
Ti-Al-V (6,4 wt.%), quenched, struct. and age hardening rel. to treatment temp. 80−11657
Ti-Al-V-Cr-Mo-Zr (3,8,6,4,4 wt.%), beta-C, microstruct. effect on mech. props. 78−27577
Ti-M-V-Cr-Mo, RMI 38644, shock loaded, age hardening 79−29112
Ti-Mo, martensitic alloy, decomposition by nucleation and growth and spinodal mechanisms 79−61590
Ti-Mo-Zr-Sn (11.5, 6, 45 wt.%), plastically strained regions, decoration 77−28864
β-Ti-Mo-Zr-Sn(11.5, 6, 4.5 wt.%), metastable phase III, microstruct. and age hardening response 80−84945
Ti-V (27 and 30 wt.%), fatigue crack propag., in single and poly. crystals 79−5048
βTi-V-Si (40, 1 at.%), Si effect of precipitation and age hardening 77−63676
α-β TiAl-Sn-Zr-Mo (6,2,4,6 wt.%), age hardening 79−61604
Ti_3Al-Mo (0.5 at.%), ordering, Mo effect 77−28841

precipitation hardening continued
TiC-steel cermet with Cu additions, precip. hardening and ht. treatment temp. 77−40414
U-Mo-Nb-Zr-Ti (0.75, 0.75, 0.75, 0.5 wt.%), heat treatment effect on microstruct. and mech. props. 78−23729
Zn-Al-Cu-Mg (22, 0.5, 0.01 wt.%), superplastic alloy, strengthening mechanism *(Japanese)* 77−55975
Zr-Nb alloy, isothermal decomposition at elevated temp. 78−27470
ZrO_2, partially stabilized, precipitation hardening effect on fracture mode 77−90353
ZrO_2, partially stabilized, precipitation effects on fracture mode 77−90354

prediction theory *see filtering and prediction theory*

predictive control
BWR, control rod sequence exchanges utilizing an off-line predictive code 78−21725
EMG control enhancement using predictor feedback technology 77−48952
nuclear reactor core 78−54860
photochemical smog, minicomputer based prediction system for reducing acute damage 79−57541

predictor-corrector methods
see also Runge-Kutta methods
bubble chamber track following 78−90044
celestial mechanics, numerical determ. of asymmetric periodic solns. 77−49270
coupled thermomechanical phenomena, nonlinear transient anal. 79−32181
elastic-plastic models, integration algorithms 80−5959
flow modelling, boundary layer, vortex, atmospheric, two-eqn. turbulence model soln. 77−91237
helix method for cosmic ray tracing 79−62692
hyperbolic eqns. in one space dimens., finite-difference approx., method of lines 77−2525
isoparametric surface contouring algorithm 79−30215
molecular dynamics simulation of rigid polyatomics, singularity free algorithm 77−76277
pollutant dispersion in shallow sea, model 77−29324
sea pollution simulation, higher accuracy predictor-corrector method 79−66431
shock tube flows, unsteady non-equilibrium, discretisation of boundary layer terms 80−14742
supersonic trailing edge flow, numerical soln. of 2D laminar and turbulent flows 79−77172
supersonic two-phase flow, nonequilib. condensation, boundary condition numerical anal. 80−64565
temperate lakes, finite element analysis of one dimensional thermocline problem 78−49042

predissociation of molecules *see molecular predissociation*

prerotation *see rotation*

presentation, technical *see technical presentation*

presentation methods, radar *see radar displays*

presintering *see sintering*

pressing, hot *see hot pressing*

pressure
see also atmospheric pressure and density; high-pressure phenomena and effects; radiation pressure; vapour pressure
aerodynamics, pressures on a slender body at high angle of attack in a very low turbulence level air stream 79−77164
air, as function of internal energy and density, algorithm *(Russian)* 77−58829
anisotropic thin evolving shell stability loss *(Ukrainian)* 78−89340
composite cylindrical shells, reinforced, stability loss under isotropic external pressure 78−42554
cooled gas transport by pipelines, temp. and pressure distrib. determ. 79−23326
dew point temp. change with pressure, calc., nomogram 80−77607
Earth crust press.-temp. conditions modelling, appl. of rocks elastic props. experimental studies *(Russian)* 78−96207
elastic linear, material of hexagonal symm., half-space, indentation by circular punch 78−34020
flow metering nozzle, press. losses, anal. and reduction method 77−51144
fluctuations in heat transfer channels with surface boiling *(Russian)* 78−14088
Freon electrohydrodynamic flow, jet dynamic pressure obs. *(Russian)* 80−59117
W.Gulf of Maine, current and press. obs. rel. to winter circulation 80−51430
injection-moulded article mech. props. rel. to process parameters 79−78929
interstellar gas, press. effect in stellar line accretion theory 78−32525
Kayenta sandstone, influence of pore press. on mechanical props. 78−81150
lattice gas model, press. by Monte Carlo computer simulation 78−4564
Lennard-Jones fluid, 6-12 pot., press. calcs., using integral eqn. and perturbation theory 79−4224
liquid, Laplace molecular pressure and internal pressure, rel. to capillary theory formulas 77−25303
macromolecular liquids, normal press. coeff., for static-oscill. vel. gradients superposition 77−76279
Mars atmosphere pressure, annual cycle meas. by Viking landers 1 and 2 80−72812
matter under very high pressure *(French)* 80−90811
micelles, Laplace pressure 80−7865
non-Newtonian lubricant hydrodynamic theory *(German)* 78−79341
polymer solution, bubble behaviour, Denn model 78−79343
polymer solution, bubble behaviour, second-order fluid model 78−79344
pore fluid pressure in rocks, rel. to effective stress law for anisotropic elastic deform. 80−51385
proteoglycans, swelling pressures at the concs. found in cartilaginous tissues 80−67327
pump pipeline, pressure surges calc., method of characteristics appl. *(Spanish)* 79−23364
PWR power plant flow pressure fluctuations as vibration source, relationships *(Hungarian)* 80−47685
SF_6 compressed, breakdown threshold, effects 78−75449
sintering, inhomogeneous flow and effective press. 80−93512

pressure continued
skin temperature measurements using a disc sensor, effect of press. 80−56259
solar atmosphere, gas pressure rel. to nonequilib. mag. field states and preflare stage 80−105213
solar transition zone, energy balance and press. for network and active region features 80−21957
steady plane isochoric flows, acceleration and pressures 78−81845
thin films, role of disjoining pressure in equilib. and flow 79−14984
transformer oil electrohydrodynamic flow, jet dynamic pressure obs. *(Russian)* 80−59117
triple correlation of the pressure in subsonic circular jets and nonlinear interaction of instability waves 80−69893
turbulent flow noise generation, role of tornado-like vortices 80−69811
unit, optimum metric, for thermodynamic standard state 80−8950
wall-pressure spectrum in turbulent boundary layer, rel. to noise generation by boundary layer-surface interactions 80−69810
water purification, granular charge inhomogeneity effect on head losses 77−75976
wave generation and propagation by spark discharges in liquids *(Japanese)* 80−70060
N_2-H_2O mixtures, two-phase pressure drops in the low flowrate region 80−19480

pressure, atmospheric *see atmospheric pressure and density*

pressure control
see also vacuum control
absolute thermodynamic manometer for ultralow pressure control 79−35766
arterial pressure modulator for perfusion circuit of isolated organ *(French)* 78−81004
automated variable pressure controller design and error analysis 77−57315
blood flow/pressure relationships, when to meas. flow or hold flow const. 77−77926
blood pressure control, mechanical-chemical balloon implant 79−20712
blood pressure control in hypertensive crisis, closed loop control of sodium nitroprusside infusion 78−44688
blood pressure control system dynamic behaviour identification 79−2097
blood pressure or flow control system for unanaesthetised animal 77−48983
blood pump, experiences with miniaturised press.-controlled servo *(German)* 78−88762
blood pump pressure servovalve control, moving coil system *(German)* 78−24182
breathing gas supply regulator, for continuous positive airway pressure breathing *(German)* 79−2164
breeder reactor liquid Na cooling, differential recorder appl. *(German)* 77−88270
bubble chamber, monitoring of 25 valve expansion system 77−6617
cardiac synchronised augmented pulsation pressure concept, prototype 77−78058
cardiovascular modelling of pressure regulation effects, hypertension 77−73539
coronary perfusion pressure programmable control circuit 79−92278
cryogenic pressure regulator 78−57963
evaporator design for gas phase electron diffraction 80−57424
hydrostatic bearing, pressure regulator device, behaviour anal. 78−93668
instruments review 79−2781
intracranial pressure regulation, nonlinear parametric feedback model 79−96599
isobaric contraction system for left ventricular performance analysis *(Japanese)* 79−29677
liquid He transfer controller, semiautomatic 79−17428
manostat, stable automatic pressure controller, use of thin polyester film 79−35700
multidimensional gas chromatography, pressure balancing techniques 80−89576
nuclear power stations containment structures testing, for pressure tightness *(Spanish)* 80−13775
perfusion fixation of animals for electron microscopy 77−44866
plastic, extrusion cylinder and feed channel wall, US appl. 77−27448
plethysmograph with servo-control of hydrostatic press. 77−5118
pneumatic amplifier pump, for supercritical fluid chromatography, control and programming 78−88665
profiling pressure pulse by rarified gas layer 77−68631
proportional counters, thin-window, rocket-borne, gas press. control system 78−17512
proportional regulation of two gas pressures, anaesthetic appl. 78−53560
respirator, servo-controlled, constructed from positive-press. ventilator 77−13041
RF sputtering gas flow regulation with vacuum press. controller 77−28720
self-contained regulators, selecting and sizing 80−82759
vacuum system backing pressure automatic regulation device 79−49241
vapour pressure control, liq. ^4He applic. 78−16900
viscometer, capillary type with a feedback system, stabilization of press. difference 79−14502
X-ray telescope, gas control system for counter expts. 78−40827
H_2 bubble chamber, temp. and press. control 79−85860
He, liquid, manostat of vapour pressure 79−35757
Pu fuel research facility for advanced LMFBR fuel *(Japanese)* 78−29624

pressure measurement
see also vacuum measurement; vapour pressure measurement
absolute temperature stabilizer, below lambda point, the adritron 79−21757
absorption spectrum, press., temp., quantity and spectral resolution retrieval, appl. to N_2O 79−100462
aerospace instrumentation, conference, Las Vegas, Nev., USA, (May 1977) 78−12075
air intakes, instrument for unsteady meas. in wind tunnel *(French)* 79−72963
alpha particle pressure gauge, exptl. accuracy *(Japanese)* 78−58537
aortic blood pressure, harmonic signal anal. by computer 77−52899
arc column, pumping of induced arc *(French)* 77−27763
arterial blood pressure, indirect noninvasive automatic meas. device 77−44771
arterial blood pressure noninvasive monitoring by US imaging and phono cuff-sphygmomanometry 80−36180

pressure measurement continued
arterial elasticity determ. and transcutaneous continuous pressure monitoring analysis 79−53179
arterial pressure automatic determ., using microprocessor based instrument, Dinamap 78−96108
arterial system, forward and backward wave calc. 79−57697
arterial systolic blood pressure monitoring, circulation model 77−60224
atmosphere, use of NS LX1600A press. transducer as short-range altimeter 78−28344
atmosphere remote sensing from satellite using MM wave radar system 80−67443
atmospheric pressure meas. with syringe, student expt. 77−57122
atmospheric pressure sensing by solar occultation using wideband CO_2 absorption 79−80037
automated electromanometer, appl. for nuclear materials safeguarding 80−99211
balance, improved floating-element spinning mechanism 80−86331
balances, effective area at low press. 80−86332
beat-to-beat stroke volume estimation from pulmonary arterial pressure contour 79−53178
biological pressure meter, up to 40 kPa and 4 kPa, temperature and time stability 79−84059
biomedical, pressure inside hollow organs, recording through tubes, nomograms for calc. of system parameters 80−3836
biomedical noninvasive pressure meas., based on Doppler effect 79−5384
biotelemetry system using capacity-type transducer 77−86671
bladder pressure noninvasive determ. from micturition cinecystourethrogram 79−92370
blood, digital sphygmomanometer *(Spanish)* 77−40846
blood, mean arterial pressure, noninvasive automatic determ. 79−57796
blood, partial pressure of gases meas., in vitro electrochemical sensors 80−67303
blood and body fluid pressure meas., Medicor electromanometry 77−90943
blood flow/pressure relationships, when to meas. flow or hold flow const. 77−77926
blood pressure, automatic indirect sphygmomanometry methods, equipment 77−81616
blood pressure, cuff method errors, Korotkov and impedance plethysmography techniques 77−40886
blood pressure, human, noninvasive meas. *(Japanese)* 80−94395
blood pressure, indirect meas., meaning of max. oscills. point in cuff press. 80−94396
blood pressure, indirect meas. method, review 80−94383
blood pressure automatic monitoring, long-term, minicomputer system 80−101276
blood pressure cuff control unit, automatic multi-function device 78−36013
blood pressure direct measurement for intensive care and operations, computerised correction system 78−44635
blood pressure for extracorporeal circulations, elec. sensor *(German)* 78−92721
blood pressure in brachial artery, monitoring by modified phonosphygmomanometry procedure 77−2065
blood pressure in rats using modified non-invasive method 79−96722
blood pressure indirect meas., occluding cuff design criteria 77−64146
blood pressure instruments, direct systolic/diastolic meas., review 78−69234
blood pressure instruments, noninvasive arterial meas. using US Doppler effect 78−69167
blood pressure measurement, new air release valve design for sphygmomanometers 77−60266
blood pressure measurement, noninvasive techniques 80−41298
blood pressure measurement in baboons, direct vs. indirect methods 77−29233
blood pressure measurement with portable systems using Korotkov sounds, meas. accuracy 80−76855
blood pressure of neonate, noninvasive technique 77−48916
blood pressure recording, simple method for fidelity improvement, Korotkoff sounds 80−76811
blood pressure waves, forward and backward, total-occlusion method for anal. 80−56257
boundary layer turbulence, press. fluctuation meas. by optical interferometry 78−26222
Bourdon tubes, stainless, design and production *(Hungarian)* 79−85134
calibration of instruments, automatic procedures 77−53880
calibration pressure generation, fundamental methods *(French)* 79−58670
calibration system improvement using ruby R_1 fluorescence 80−98928
capacitive transmitter, features *(Polish)* 79−26066
cardiac, by US resonant scatt. from bubbles 77−37029
cardiac output estimation from aortic pressure curves, simulation model 79−53177
cardiac pressure noninvasive US measurement, scatt. from encapsulated bubbles 80−36048
cardiology, central venous-, pulmonary artery end-diastolic- and pulmonary capillary wedge-pressure meas. 77−90955
cardiovascular changes associated with age, US obs. in dogs 77−25504
carotid artery pressure, noise-resistant trigger cct. 77−48889
carotid back pressures in conjunction with cerebral angiography 80−98119
catheter, multi-transducer, for intraluminal press. recording in vivo 80−89879
catheter pressure meas., transducer smearing correction using microprocessor based discrete deconvolution 80−67275
catheter systems for respiratory intra-oesophageal pressure meas., selection, testing 77−90937
catheters, resist. rel. to applied volt., elec. shock risk 77−40818
cerebral blood flow, tissue pO_2 and pCO_2, continuous and simultaneous meas. 79−57829
cerebrospinal fluid pressure meas. and controlled withdrawal 79−39538
cerebrospinal fluid pressure meas. by passive telemetry, improved instrument 78−31927
compensated pressure derivative measuring transducers, electrical differentiating devices appl. 78−93716
constant pressure manometer with frequency read out, electrocapillary element appl. 80−73380
corrosive atm. pressure or vacuum meas. isolation chamber 77−30174
critical light reflection at a plastic/glass interface and appl. to foot press. meas. 80−81681
crusher method, dynamic error calc. 78−57974
cryogenic fluid, transducer suitability 77−30130
dead weight piston gauge, theory 78−49851
decrepitation recording for gas-liquid inclusions in quartz powder, temp. from press. rise 77−71325
deep sea temp. and pressure sensor for tidal meas. 77−37424
deep sea tide gauge, qualification of quartz pressure sensor *(German)* 79−74980
dial pressure gauges, reliability tests and failure mechanisms *(Rumanian)* 79−40557
diamond anvil cell for high pressure measurement, with uniform internal stresses at 200 kbar 79−67334
diamond anvil cell up to 50 kilobars, press meas. via ruby fluoresc. 77−31560
diamond anvil press, press. distrib. meas. from ruby fluoresc. line shift 78−12710
diaphragm pressure sensors using wire strain gauges *(German)* 79−80569
differential, digital technique 78−38424
differential integrated pressure sensor, using microprocessor cct. given *(French)* 79−54149
differential pressure recorder for breeder reactor liquid Na cooling pressure monitoring *(German)* 77−88270
differential pressure transducer, optimum use for high precision measurement 78−162
digital, bellow-type transducer appl. *(Polish)* 78−93719
digital automatic blood pressure recorder *(Japanese)* 78−24168
digital pressure indicator construction and application 78−21112
dilatometer for PVT meas. of liquids and plastic crystals at low temperature 80−68208
drag reduction spike, fluctuating pressure wind-tunnel meas. 78−30310
dynamic expansion method for press. scale realisation in 10^{-3} to 10^{-8} torr range, uncertainty analysis *(German)* 78−37025
Earth, upper mantle, peridotite equilibration press. from geochemical parameters 77−2130
education, gas pressure gauge for student expt., mol. weight determ. by law of atm. 79−25795
elastomagnetic pressductor, design, theoretical and operating charact. *(Czech)* 80−68205
electric field meas. using pressure sensitive elements and fibre optical transmission technique 79−97367
electrical sensors, seven types *(German)* 80−77772
electro-mechanical sensors, mechanical compensation methods influence on error charcts. *(German)* 78−16786
electrodynamic percussion unit, mode selection method 79−30448
electronic pressure difference transducer type 41103/41105, operational principles *(Polish)* 79−2782
enclosure fire, static pressure meas. 78−90871
epidural intracranial press. monitoring with press.-sensitive on-off type switch sensor 78−44626
EPR in isostructural ferroelectrics, for hydrostatic pressure meas. 79−38375
equipment development, design and appls. 80−13091
excess pure pressure measurement with liq. manometers 77−52566
ferrite sensors development, hydrostatic pressure effect on ferrite props. of pressure sensors *(Polish)* 80−31707
ferrofluid, pressure measurement using nonmag. manometer *(Russian)* 78−24785
fibre optic Mach-Zehnder interferometer, sensing of press. and temp. 79−72671
fibre optic sensors appl. *(Norwegian)* 79−93121
fibre optical interferometers for length, temp., pressure and force meas. 80−98971
finger instantaneous arterial press. meas. method 80−56245
fixed points for pressure calibration above 10 GPa 77−13765
fluid pressures, up to 2700 MPa, equipment for generation and measurement 79−21763
FM pressure transducer resonant diaphragm pressure-freq. charcts. derivation 78−41295
foot pressure distributions, technique for display 80−85508
free-piston gauges, effect of rotation speed and fluid viscosity on accuracy of high press. meas. 79−88973
fuel rod gas pressure meas. during LOFT, sensor description 80−57876
fundamentals and techniques, book 78−81941
gas, low density determ. using electronic flowmeter 79−37427
gas lubricated manometer, effective area calculation for free-piston 78−93714
gas parameter determ. using total internal reflection 77−58839
gas pressure transients due to weak shock waves, measurement using reflectivity of glass/gas interface 79−63297
gas sample, IR spectra, nonlinear least squares method 78−15738
gas thermometry by method of two containers 77−5838
gas-operated pressure balance, rotational freq. dependence 79−54151
gauge for ±12 to 20 kPa meas. low-temperature equipment development *(Czech)* 77−61069
gauge pressure meas. up to 1 kPa, NPL primary standard instruments 79−63265
geobarometer for plagioclase and spinel lherzolite using enstatite Al_2O_3 content 77−2142
geobarometry, appl. of plagioclase-garnet-Al_2SiO_5-quartz assemblage 77−2147
geobarometry, metamorphic bathozones and bathograds rel. to post-metamorphic regional scale uplift 78−81113
geobarometry, subsolidus phase relations of pyroxenes in CaO-MgO-Al_2O_3-SiO_2 system 79−16440
geobarometry and geothermometry, conf., University Park, Pennsylvania (October 1975) 77−2123
geobarometry and geothermometry 77−2254
heart valve prosthesis mean press. gradient meas. under in vitro pulsatile flow 77−56531
high dynamic, review of practical techniques 80−47070
high pressures, calibration via ruby fluoresc. R-lines at ambient and low temps. 77−18106
high pressures up to ~20000 bars using Au-Cr gauge 77−49740
high-pressure calibration scale based on Au, Ag and Cu melting curves, revision 80−39260
high-pressure chamber calibration using ruby R_1 luminescence line shift, 80 to 550K 78−86284
human hip prosthesis pressure radiotelemetering, design features 78−3671

pressure measurement continued
hydrophone, interferometric fibre optic, static press. sensitivity amplification 80−38094
hydrophone, multimode fibre optic, frustrated total internal reflection, testing 80−38096
IC pressure transducers, barometer and blood-pressure meter 79−35709
instruments review 79−2781
intra-ocular pressure measurement using sonics and coherent optics 77−81548
intracardiac pressure measurement, using fibre optic catheter tip press. transducer 79−2150
intracellular pressure measurement system 80−109084
intracranial pressure, remote meas. by passive reson. cct. detector *(French)* 77−37074
intracranial pressure and its epidural meas. 80−101282
intracranial pressure and temp. two-channel telemetry system 77−81619
intracranial pressure estimation, use of visually evoked pots. 80−26398
intracranial pressure measurement, some considerations 80−17155
intracranial pressure monitoring, implantable two-channel telemetry system 78−3637
intracranial pressure monitoring by passive radiosonde 79−57798
intracranial pressure monitoring in neurotraumatology 80−17156
intracranial pressure noninvasive monitor for infants, fontogram 78−40373
intracranial pressure telemetering, in vivo and in vitro, with capacitance transducer 78−7457
intracranial pressure telemetric meas. *(German)* 78−85403
intraocular pressure, importance of tonometry in glaucoma diagnosis and therapy 78−40383
intraocular pressure, telemetry monitoring 78−3632
intraocular pressure measurement, for glaucoma, comparison of Schiotz standard tonometer and applanation tonometer 78−48915
intrauterine pressure measurement during labour, limitations 77−56504
ionisation gauge, extension of upper limit of gauge *(Chinese)* 79−75542
Langmuir film balance meas. system 80−62659
laser pulsed pressure on targets, optical pressure-sensing element based on interferometer 79−35771
linear displacement transducer using vibrating string *(German)* 79−71441
linearly varying pressure rate meas., instrument design 78−8395
liquid filled manometers and U-tubes, advantages 78−49792
low and differential pressure meas. by pressure divider 80−90862
lung model, human, velocity distrib. and pressure drop. expt. 79−96602
manometer diaphragm pressure sensitive characts. plotting by tabular analytical method *(Russian)* 78−8397
McLeod gauge, capillary depression phenomena, Hg vapour drag effect 80−98923
megabar pressure cell, anal. of diamond strength, calibrated expts. 79−91888
membrane hydrophone for 0.5 to 15 MHz range, press. meas. in US fields 80−108987
membrane pressure convertors, errors arising due to differential heating 80−62680
membrane pressure gauge with displacement sensor *(Hungarian)* 80−31733
membranes nonlinear characts. calc. *(Czech)* 79−26021
MHD generator chamber *(Polish)* 77−7602
microcomputer-based blood-pressure recorder *(Japanese)* 80−67139
micromanometer, interferometric oil, as primary vacuum standard 79−88970
micromanometers, type-MMN, simplified processing of results 79−35692
microvascular, using micropipet, capacitive modulation of impedance 77−37080
multiple, technique using single transducer with several pressure switches 77−5800
nuclear reactor, press. and temp. loads on LWR containment after LOCA, scale model expts. 77−3134
nuclear reactor, pressure and temp. sensors, reactor time const. determ. by dynamic data system method 79−93750
nuclear reactor liquid cooling pipe, recorder characts. *(German)* 77−88218
nuclear reactor pressuriser, multiple surges pressure transients 77−26836
nuclear reactor thermal mixer temp. fluctuation and pressure loss, scale model tests 79−9673
ocular tonometry through sonic excitation and laser Doppler velocimetry 80−56152
oesophageal manometry, low-compliance perfusion pump 79−53272
oesophageal manometry by liquid-filled catheters 80−85514
oesophageal-balloon catheter, use in meas. of chest-wall compliance with biofeedback 77−52905
optoelectronic method for coloured or turbid mixtures, press. and phase equilib. study 78−70152
oscillating vane pressure gauge, electronic stabilization system 79−35775
piezoelectric press. bar transducer, dynamic transmitting props. *(Chinese)* 78−4605
piezoelectric sensor element for press. meas. in soil pores *(Polish)* 79−25363
piezoelectric transducer appl., for variable pressures up to 6×10^8 N/m^2 80−31785
piezoresistive C gauge for low shock pressure meas. 79−1278
pipeline, pressure-switch for multipoint meas., computer data acquisition system 80−62679
piston-cylinder gauge, effective area and accuracy up to 10 MPa 77−41632
plastic extrusion cylinder and feed channel wall, US appl. 77−27448
pneumatic/elec. transducer with miniaturised Si sensor *(German)* 78−185
polymer melts, slit die rheometer appl. 77−27501
pore pressure in Kayenta sandstone, meas. technique rel. to influence on mechanical props. 78−81150
pressed powder bed, bottom pressure distrib., meas. by scattered light photoelasticity *(Japanese)* 79−75543
pressure balance standard for the pascal SI unit 77−87725
pressure balance standards, international comparison over 1 to 10 MPa range 80−105671
pressure cells with strain gauge transducers operating ranges and principles *(Hungarian)* 78−54335
pressure changes in interconnected chambers, mathematical model 80−108678
pressure reducer, piston type, for continuous pressure meas. up to 1 MPa 78−4602
pressure transducer selection 78−49811
probe, omnidirectional, for wind meas. *(French)* 79−25349
probe for static pressure sensing in 2D flow, wind effect on buildings 79−71403
probe-tube microphone, press. fluctuation meas. in flowing combustion plasma 78−18443
pulmonary arterial hypertension meas., Bubble Ultrasonic Resonance Pressure method 79−92313
pulmonary artery blood press. anal. algorithm 78−40376
pulmonary artery press. estimation using pulse wave velocity 80−12203
pulmonary venous pressure estimation from routine chest radiographs using hybrid optical-electronic system 78−44657
pulsatile air flow, time-averaged stagnation pressure probe design 78−14116
pulse-pressure generator, quasistatic method for stepped pressure, transducer testing 80−62678
pulsed, using piezoelectric pick-up 80−31778
PWR, 450 MWe, noise obs., analysis and interpretation 78−94072
PWR power plant, vibr. and press. signals, information for online vibr. monitoring system 77−18674
radioisotope pressure transducer with linear conversion charact. from 100 to 1000 torr 79−35704
Raman cell, press. determ. at 42K 78−49850
re-entry vehicle flight tests, boundary layer acoustic meas. 78−16275
resistance bridge with linear charact., appl. to press. meas. using electroresistive gauges or extensometric transducers *(Polish)* 80−73385
RF telemetry for pressure monitoring of free swimming freshwater fish 77−90965
ruby, fluoresc. spectrum, appl. to glass transit fluid press. determs. 77−26321
ruby R_1 fluoresc. press. gauge, calibration, 0.06-1 Mbar, specific vol. meas. for Cu, Mo, Pd, Ag 78−70150
scale representation by ASMW, Germany *(German)* 77−74348
sea-floor pressure recorder 77−73864
seawater conductivity/temperature/pressure profiler errors 77−5377
secondary standard gauges for measurement up to 1 GPa 80−27289
semiconductor pressure transducers with reduced brittleness *(German)* 78−81964
SI units fundamentals *(French)* 80−95059
soil, using capacitive sensor with polyurethane foam dielectrics *(Slovak)* 80−86281
solid-lubricant interface, strain and deform. meas. techniques with diaphragms, comparison *(French)* 79−30453
special state standard and All Union test scheme, absolute press. meas. in 2.7×10^{-2}-4000×10^2 Pa 78−73962
Speer carbon resistors as pressure gauges 80−95108
sphalerite geobarometer, experimental extension to 10 kbar 78−85703
sphalerite geobarometry, regionally metamorphosed terrain appls. 77−2257
sphygmomanometer, random-zero design with variable height reservoir 78−35986
spreading pressure of adsorbed film, direct reading strain gauge 77−15692
standards, pressure balance, of NPL and PTB, intercomparison expts. 79−21764
standards comparison, primary, mercury barometer vs. gas-operated pressure balance 80−13090
standards for oil-operated pressure balances, intercomparison between NPL and LNE 80−98877
static omnidirectional atm. press. probe 77−53238
static or dynamic, interferometric techniques, transducer calibration 78−21159
static pressure probe, laminar limiting boundary layer *(French)* 77−31402
static pressure probe, yaw insensitive, development and testing 78−94869
steam, wet, supersonic flow, total- and static-press. probe characts. 77−84353
strain gauges for industrial pressure measurement *(Hungarian)* 80−86278
subatmospheric and small excess fluid pressure, tubular spring manometers performance improvement 78−81940
surface balance, monolayer parameters meas. in radiation field 78−82092
surface friction in turbulent boundary layer, meas. using plane Pitot tube 80−79284
surfaces, sliding, lubricated *(German)* 80−14643
techniques available at National Bureau Standards, USA 78−36964
three-dimensional flow field, novel arrangement for press. meas. 77−72378
tissue O_2 tension by multi-channel telemetry 77−56506
tissue pressure, continuous monitoring instrument 79−100762
tonometer, applanation, for intraocular pressure meas. 80−30833
transdiaphragmatic pressure measurement using a single gastric-oesophageal probe 80−56248
transducer elastic diaphragm creep metrological characts. anal. *(Russian)* 78−8396
transducers, freq. charact. meas., review of meas. apparatuses 80−62650
transducers, sensitivity to temp. gradients and transient environments 79−35716
transducers survey 78−86249
transonic flow with pressure gradients static pressure hole meas. errors 79−94645
TTF-chloranil visual pressure or temperature indicator 80−87443
tube outlet section gas flow at supercritical pressure differentials 80−28569
turbulent and high frequency fluctuating flow, mean static pressure measurement 78−57889
turbulent boundary layer, wall interference effects of static pressure probes 78−1762
turbulent boundary layers, freq.-wave-vector spectrum determ. using acoustic transducer 78−38430
turbulent structure determ. using thermoprobe unit in fluid stream *(Bulgarian)* 80−28584
two phase flow pressure drop measurement variations, analysis *(German)* 78−59445
U-shaped Hg manometer, 1300-2300 torr range 80−31784
ultra-high pressure estimation using β-decay rates of radioactive nuclei 78−77927
ultrahigh pressure devices, calibration via acoustic vels. ratio in NaCl 77−27945

pressure measurement continued
units for pressure, definitions and areas of use 80−77745
unsteady pressure coefficients digital measuring unit for wind tunnel tests *(French)* 80−68169
unsteady pressure measurement, large signal/noise technique 79−94743
ureteral catheterisation manometry and urodynamics *(Slovene)* 78−44668
US system for blood press. anal. during treadmill stress testing 80−81674
uterine activity monitoring, internal and external methods 78−35973
variable pressure manometer, electrocapillary element appls. and properties 80−73379
venous system visualisation combined with press. meas., technique and equipment 80−36094
walking, synchronisation of optical press. distrib. and 3-dimens. force meas. under sole human foot *(German)* 78−35975
wall pressure meas. using rectangular membrane as spatial filter 77−72107
water vapour, partial press. meas., student expt. 79−44685
wavy gas-liquid interface, gas pressure method 79−68837
wind pressure data acquisition system, microprocessor based 79−70888
X-ray diffraction study, high temp.-high press., appl. to press. calibration above 100 kbar *(Japanese)* 78−24809
zeranin resistance gauges for secondary meas. of high press., expt. *(Polish)* 77−65042
Ar, compressed gas, PVT meas. at high press. 80−98927
Au-Cr alloy pressure gauges, annealing effects 78−49854
CO_2 partial pressure in seawater, shipboard meas. 77−2263
Ge:Au film strain gauges *(Japanese)* 80−105631
Hg-melting pressure scale determ. at temp. below 0°C 79−12813
K arrested left ventricle finite deformation anal. in canine hearts *(Japanese)* 78−3543
N6d2-Ne discharge lamp, meas. method for partial H_2 press., selective gettering action 77−87775
Ni-Cr thin-film resistor pressure transducer for quickly varying pressure, expt. *(Polish)* 77−65041
O^{2-} low partial press., thermogalvanic meas. using O^{2-} ion conductors 80−73389
O_2 partial pressure, absolute meas. using impedance dispersion analysis on PdO form. 80−108728
O_2 partial pressure on blood sample, polarographic method, error reduction 78−7470
Pb, melting curve, use for press. determ. in girdle apparatus 77−65043
SF_6 partial press. meas. in mixtures with N, using separation by freezing 79−71478
T gas nuclear bombardment targets, pressure monitoring system 80−99370
TaN film, press. depend. of elec. props. appl. to press. meas. 79−78241
UF_6, negative surface ionisation investigation using sensitive detector and pressure gauge 80−31781

pressure sintering *see sintering*

pressure transducers
32.768 kHz X-Y flexure watch crystal as pressure-force transducer 78−57934
air jet/piston dynamical interaction pressure transducer errors 77−80245
airflow measurement in speech using mask-type wire screen pneumotachograph 77−52808
ambulatory blood pressure recording in man, transducer and perfusion system 79−53271
artificial heart, electronic pressure control with fast variable aperture valve *(French)* 77−40928
automatic blood pressure meas., device for linear press. change in cuff 77−48902
automatic calibration procedures 77−53880
automatic loading piston transducers for setting absolute and gauge pressures 79−67286
automatic pressure recording method, 5 to 10^{-2} torr 79−85148
biomedical catheterisable sensors, PO_2 probes, press. transducer and photometers 80−46080
biomedical semiconductor pressure transducer *(Japanese)* 80−94394
biomedical transducer for intraluminal press. recording 80−17152
biomedical transducers, information exchange and humanisation *(German)* 79−88204
blood, strain gauge transducer, chopper preamplifier cct. 78−3659
blood pO_2 meas. polarographic technique 79−100782
blood pressure, technical testing standard 79−44002
blood pressure electric sensor for extracorporeal circulations *(German)* 78−92721
blood pressure instruments, direct systolic/diastolic meas., review 78−69234
blood pressure monitoring systems simulator 79−83963
blood pressure recording, arterial and venous 79−34708
blood pressure transducer for student use, using hybrid IC 78−8186
blood pressure transistor device, high sensitivity, quasi-digital 79−79675
blood pump pressure servovalve control, moving coil system *(German)* 78−24182
calibration, interferometric techniques 78−21159
Camkometer, in situ soil testing pressuremeter 79−8717
capacitive sensor appl., charact. linear approximation, in vicinity of working point *(Slovak)* 79−40547
capacitive stress transducer optimum dielectric selection 77−73428
capacitive transmitter, features *(Polish)* 79−26066
capacity type, for biotelemetry system, features 77−86671
catheter pressure meas., transducer smearing correction using microprocessor based discrete deconvolution 80−67275
catheter-tip, with on-chip compensation and signal processing 77−44818
cerebrospinal fluid pressure meas. by passive telemetry, improved instrument 78−31927
clinical pressure measurements 79−96692
compensated pressure derivative measuring transducers, electrical differentiating devices appl. 78−93716
computer peripheral pressure transducer calibration and metrological servicing 77−57314
constant pressure manometer with frequency read out, electrocapillary element appl. 80−73380
cryogenic, high-resolution, operating at liquid He temps. 79−58735
cryogenic fluid, suitability discussion 77−30130
cylindrical tensoresistive pressure transducer 80−8978
design, CAI for biomedical instrumentation students 77−45656
design for nuclear reactor environment 78−823

pressure transducers continued
differential, air-filled transducers, dynamic charact. 80−3879
differential digital type, operations 78−38424
differential pressure transducer, optimum use for high precision measurement 78−162
differential pressure transmitter, electronic, design and appls. 79−17435
diffused Si pressure transducer, stress conc. at transverse gauges 78−12711
dynamometric transducers based on granular conducting material contact resistances 79−35706
eddy current pressure transducer elastic elements charact. optimisation *(Russian)* 78−77890
elastic diaphragm creep metrological charact. anal. using thin shell dynamics method *(Russian)* 78−8396
electrical transducers for skin pressure meas., accuracy obs. 79−83959
electrodynamic percussion unit, mode selection method 79−30448
electromechanical, using acoustical resonance, advantages and disadvantages 78−77897
electronic pressure difference transducer type 41103/41105, operational principles *(Polish)* 79−2782
epidural intracranial pressure meas. by piezoresist. transducer *(German)* 78−85404
epidural intracranial-pressure transducer with reduced tissue stress interference 80−41290
equipment development, design and appls. 80−13091
excess pure pressure measurement with liq. manometers 77−52566
falling-weight equipment pressure pulse parameter calc. 77−67425
ferrite pot core pressure transducer development and compensation 79−75519
fibre optic, catheter transducer, side hole type, for intracardiac press. meas. *(Japanese)* 78−73272
fibre optic catheter tip, for intracardiac press. meas. 79−2150
fibre optic catheter-tip micromanometer as intracardiac press. transducer *(Japanese)* 78−73270
fission reactor safety-related sensor, response verification 78−13253
force measuring, EM, design and appl. *(Russian)* 78−16784
force transducers, strain-gauge, normalization of AC charact. 79−35705
frequency response measurement technique for press., vol. and flow transducers 80−41344
gait trainer for hemiplegic patients with lower limb sensory loss 78−48940
gapped pot core and Permalloy foil pressure transducer 79−75520
gas flow control, automated, transducer 78−59508
gas-filled, effects of gas density on freq. response, medical appls. 80−56249
gastrointestinal pressure measurement using electronic transducer system, diagnosis appl. 77−86695
high resolution quartz transducer, high temperature electronics for geothermal energy 80−11997
high-pressure clamp cell for elec. conductivity measurements, 8 GPa, 77K 80−37047
high-temperature high response fluctuating pressure meas. probe 78−13855
hydrostatic pressure cells producing anisotropic strain, calibration 79−17410
IC, barometer and blod-pressure meter 79−35709
implantable biomedical pressure transducer 77−73606
implantable SAW pressure transducer/transmitter 79−29575
integrating transducer for oesophageal manometry 79−88208
intracranial pressure and temp. two-channel telemetry system 77−81619
intracranial pressure meas. in newborns, new non-invasive technique 80−67272
intracranial pressure noninvasive monitor for infants, fontogram 78−40373
intracranial pressure telemetering, in vivo and in vitro, with capacitance transducer 78−7457
ionisation manometric transducer, PMI-2, cathode protection 77−74416
jet-displacement transducer with sectional calibration, wide-band 80−4698
LC cct., epidural brain pressure measurement 77−32962
leg-load alarm system for partial-weight-bearing walking exercise *(Japanese)* 79−29658
linear unbalanced DC bridge 77−79123
LMFBR fuel pin plenum press. transducer 78−8884
long-term performance characterisation programme 78−12712
low-impedance microphone calibrator 78−59212
magnetic discharge manometric convertor 80−31779
magnetoelastic, Fe-cored, choke-type, compressive force meas. *(Polish)* 78−12684
magnetoelastic pressure gauges with monolithic cores *(Polish)* 78−24810
manganin pressure gauges, effects of shock compression and relief *(Russian)* 78−70149
manganin resistance gauge for high pressure meas. 77−10036
manganin thin film microtransducers for elastohydrodynamic lubrication studies 80−37048
measurement of frequency characteristics, review of meas. apparatuses 80−62650
medical monitoring device design, infection control considerations 77−21641
miniature implantable, biomedical appl. IC fabrication techniques 80−76849
miniature pressure-frequency convertor with pulse output 78−57926
minicomputerised pressure transducer data logging system *(Russian)* 79−6102
monolithic capacitive press. transducers for deep-body biomedical appls., pulse-period output 80−67274
monolithic capacitive pressure sensor with pulse-period output electronics on same chip 80−81752
MOS structure, p-channel, effect of isotropic stress on Si valence band struct., press. transducer appl. 80−25011
MOSFET, piezoresistivity effects and use as press. transducers 80−4695
non-invasive, for continuous meas. of arterial blood press. 77−44817
NS LX1600A pressure transducer, use as short-range altimeter 78−28344
oesophageal motility study in humans, circumferentially-sensitive miniature press. sensor 78−77131
one-piece sensitive element type, design 78−1617
operating temperture range extension using semicond. tensoresistors 78−4608
optical fibre, high-linearity multimode optical fibre sensor 79−68429

pressure transducers continued
optical pressure-sensing element based on interferometer, for meas. pressure of laser pulses on targets 79−35771
opticomechanical pressure transducers, designing and testing 80−105662
partial weight-bearing walk, limb load alarm system 79−29661
pathological gait assessment, foot force meas. device 79−20701
physiological miniature strain-gauge pressure transducers 79−100778
physiological pressure transducer design with negative feedback 77−48910
pick-up with Si column strain-gauge convertor 80−31732
piezoelectric, local press. meas. in cadaveric human hip joint 78−40445
piezoelectric double-diffused MOS transducer, detection of acoustic waves 77−80043
piezoelectric modulation transducers for alternating pressures 78−77891
piezoelectric press. bar transducer, dynamic transmitting props. *(Chinese)* 78−4605
piezoelectric pressure sensor 80−105670
piezojunction tunnel transducers for hydrostatic pressure *(Polish)* 78−89470
piezometer ring design 77−15142
piezoresistive, on IC *(German)* 77−49717
piezoresistive C gauge for low shock pressure meas. 79−1278
planary distributed transducers, artificial skin, to give tactile perception 77−81661
pneumatic amplifier pump, for supercritical fluid chromatography, control and programming 78−88665
pneumatic force transducer 78−21128
pneumatic output signals, precision, testing with reference air/water multitube manometer 78−93717
pneumatic press. transducer for corrosive media, error and sensitivity 80−22345
pneumatic/elec. with miniaturised Si sensor *(German)* 78−185
polarisation and piezoelectric, high dynamic pressure measurements in solids 80−47070
pressure cells with strain gauge transducers operating ranges and principles *(Hungarian)* 78−54335
pressure measurement, elastomagnetic pressductor, design, theoretical and operating charact. *(Czech)* 80−68205
pressure transducer measurements, thermal transient effects 80−31700
primary measuring transducers for fast-response gas analyzers, dynamic characts. 80−4697
primary pressure transducer dynamic charact. meas., automatic system 79−80589
protection, parylene (vacuum deposited polymeric coating) appl. 80−108607
pulse sensors, calibration, indirect piezoelectric effect *(Czech)* 77−5857
quartz piezosensor, construction and performance 79−88939
quartz pressure sensor, qualification as deep sea gauge *(German)* 79−74980
radioisotope pressure transducer with linear conversion charact. from 100 to 1000 torr 79−35704
resonant diaphragm pressure-freq. characts. derivation 78−41295
SAW resonator, freq./stress sensitivity 77−2645
SAW resonator 77−23850
SAW transmitting hydrophone development and performance 79−53586
secondary standard gauges for measurement up to 1 GPa 80−27289
selection 78−49811
semiconductor fluid filled triple membrane cell for differential pressure meas. *(German)* 78−81964
semiconductor mass balanced cell for absolute pressure meas. *(German)* 78−81964
semiconductor pressure sensors, thin Si diaphragm form., piezoresistive and capacitive structs. 80−13065
semiconductor pressure transducers, temp. compensation, strain gauge appls. *(Polish)* 80−31726
semiconductor sensors, props. and appls. *(German)* 78−36991
semiconductor strain gauge, method to improve temp. stability 80−87826
sensitivity to temp. gradients and transient environments 79−35716
solid-state pressure transducers and transmitters 77−30175
sputter-deposited thin-film pressure transducers 77−30139
sputtered thin films for strain gauge sensors 77−49719
strain gauge, signal simulator, for physiological monitoring applic. 77−40804
strain gauge semicond. transducers, Sapfir, development and appls. 80−13059
strain-gauge transducer sensitivity to directional thermal gradient error 77−74382
string transducer auto-oscillator cct., using ICs *(Russian)* 77−13741
survey 78−86249
telemetry system, implantable, multichannel, IC, for animal physiological data recording 77−86661
telemetry system, implantable, single-freq., for blood pressure monitoring 77−86688
temperature coefficient sensitivity, compensated using positive feedback 80−17928
testing, pulse-pressure generator, quasistatic method for stepped pressure 80−62678
thermal transients effect reduction, protective coatings eval. 78−54358
thick-film strain gauges and pressure transducers 80−57285
tooth mobility measuring instrum. employing 24 V transducers 80−36187
total artificial hearts, pneumatic powered, telemetric monitoring system, in calves 77−90956
two-conductor, pressure-to-current, using semiconductor pressure sensor *(Czech)* 79−97374
types reviews 79−2781
unsteady pressure measurement, large signal/noise technique 79−94743
US pressure gauge, using single-transducer sing-around system 77−13742
vacuum piezoceramic transducer for 760 to 10^{-5} torr 78−86283
variable pressure manometer, electrocapillary element appls. and properties 80−73379
velocimeter for fluctuating temp. and vel. meas. in combustion field 80−14856
zeranin resistance gauges for secondary meas. of high press., expt. *(Polish)* 77−65042
zero offset change rel. to transducer performance 80−56255
$Al_xGa_{1-x}As$, resistor pressure sensors 79−2756
$Al_xGa_{1-x}As$, temp. coeff. of resistance of pressure sensors 79−6108
Au-Cr pressure gauge, technological processing 77−49740
Bi foil element, determ. normal stress components in solid state high pressure test cell 80−73378
Cu-Mn-Ni alloy, Manganin, elec. resist. under static pressures up to 110 kbar, pressure gauge appl. 79−1594
Cu-Ni/Au-Ni multilayer films deposited on membrane, use as strain gauge 80−65713
GaAs and GaSb p-n junctions appl. *(Polish)* 77−67424
GaAs epitaxial tunnel diode pressure sensors 78−57975
GaAs, p-n junction pressure transducer characteristics *(Polish)* 77−89832
GaSb, p-n junction pressure transducer characteristics *(Polish)* 77−89832
NaCl primary press. gauge, failure of central force model 77−15492
Ni-Cr thin-film resistors for quickly varying pressure, expt. *(Polish)* 77−65041
O_2 analysis, gaseous and dissolved, direct readout instrument 77−40606
$Pb_{0.82}Sn_{0.18}Te$, film, effect of hydrostatic pressure on props. 80−70862
Si diaphragm pressure sensor, integrated signal conditioning 80−76859
Si, miniature, features, biomedical appl. 77−86666
Si miniature biomedical piezoresistive pressure transducer *(German)* 80−37016
Si p-channel MOS structure, direct parametric press. transducer props. 80−100526
Si, p-n junction pressure transducer characteristics *(Polish)* 77−89832

pressure vessels
acoustic emission inspection, during water-pressure testing, NDT 77−1901
advances in reactor pressure vessel design 77−71640
AE during fatigue crack expansion 80−108675
AGR pressure vessel, safeguards for man-access 80−27790
AGR pressure vessels, radiation protection for shutdown man-access 80−5374
alternative containment designs, value/impact comparison, containment failure and safety aspects 79−13464
ampoule for NMR meas. of self-diffusion coeffs. of liquid molecules under pressure 79−35773
automatic, US in-service inspection for reactor pressure vessels *(German)* 77−90538
axisymmetric, with structural discontinuities, computer aided elastic stress analysis *(Japanese)* 80−38265
axisymmetric vessels, shearing stress minimisation by automated design optimisation 78−17289
Babcock & Wilcox steam supply system, operating experience 78−21752
bimetallic, composite geometry reactor pressure vessel, subjected to thermal shock, temp. decay, 2-D soln. 77−88209
blowdown, fluid behaviour in pressure vessel *(Japanese)* 79−17999
brittle fracture criteria for nuclear reactor press. vessel steels, neutron effects *(German)* 77−34389
brittle fracture probability using reactor surveillance capsule data 78−80641
BWR, boilers and pressure vessels, in-service inspection, General Electric's code 77−3152
BWR, KRB reactor press vessel, fast neutron fluence evaluation, operational consequences *(German)* 77−34369
BWR, surface inspection methods, in-service inspection of reactor pressure vessel 80−27759
BWR, vacuum relief valve sizing in condensing steam situations, analytical model 79−54545
BWR LOCA, containment dynamic loadings 80−763
BWR LOCA, some considerations in small-scale pool swell simulations 79−49740
BWR LOCA, vent clearing, downward forces effects 79−49741
BWR passive containment system, LOCA safety features 79−13466
BWR plant, SOPRE 1, press. suppression containment system 77−38342
BWR vent clearing hydrodynamics, numerical simulation using SOLA-VOF code 79−49659
CANDU power reactor, pressure tubes, design and development 79−36372
Caorso plant, dynamic tests and seismic records of RHR building 78−41872
cell design for hydrostatic pressure up to 25 kbar 80−52260
cell with temp. uniformity monitoring 78−230
cladding, cracks under stainless steel cladding of pressure vessel, detection, causes, danger 80−52760
Clinch River Breeder Reactor Plant containment concept 79−13401
components reliability, conf. Vienna, Austria, 1977 79−17986
composite pressure vessel, holographic exam. 77−28957
composite spherical pressure vessels with hardening metal liners 80−7655
concrete, endochronic model for nonlinear triaxial behaviour 78−51095
concrete, finite element creep anal. 78−41813
concrete, fission reactor containment material, development of different types to overcome various problems 80−52738
concrete, pressure vessels, multicavity PCRV, design and anal. for ultimate strength calc. 78−44182
concrete, uniaxial compressive strength, 450-1033K 78−44299
concrete reactor vessels, behaviour of perforated slabs under temp. and external load 79−30917
concrete reinforced walls, local behaviour under missile impact *(French)* 78−44180
concrete reinforced walls, local response to missile impact 78−44181
conference, Berlin, Germany (Aug. 1979) 80−77539
container for volatile inorganic hydrides of specially high purity 80−47043
containment accident analysis using CONTEMPT4/MOD2 compared with experimental data 79−49738
containment analysis by ALICE code after HCDA 79−49736
containment liner seismic reliability under statistical uncertainty, cracking 78−89948
containment response to accidents, comparison of CONTEMPT-LT calculations with Marviken experiments 79−49737
containment subcompartment flow, film entrainment determ. 79−49657
corrosion protective coatings for reliable operation 78−11424
corrosion testing apparatus for high temps. 77−12754
crack detection by magnetic crack detection and dye-penetrant inspection 80−100994
crack in pressure vessel nozzles, stress intensity factors, photoelastic meas. 77−44360
crack propagation and arrest, exam. 78−56770

pressure vessels continued
cracks in press. vessel nozzles, stress intensity factors, photoelastic anal. 77−80125
creep bounds and brittle damage estimates 80−23908
cylinder, internally pressurised, stress intensity factors of inner and outer cracks 77−58610
cylindrical, thin torispherical ends, expts. on buckling under internal pressure 78−90736
cylindrical containers, crack propagation and arrest 77−58611
cylindrical shell under internal pressure, ductile growth of longitudinal flow 79−10530
cylindrical steel pressure vessels for hydrostatic pressures to 50 kilobars 78−70151
defect detection, strain evaluation, laser holographic and speckle photography methods 77−81365
diamond anvil cell, CO_2 and D_2 compression, 34.0 and 44.7 kbar respectively 78−74017
dynamic response to fluid pressure pulses 78−26077
dynamic response to impulsive loading in nonlinear range 77−3191
elastic continuum penetrated by elastic tube, biaxial stress field, computer program 77−46921
elastic creep fatigue rules fo ASME B&PV code case 1592 78−44211
elastic stress analysis of press. vessel with hemispherical head, homogeneous eigenfunction method 77−23884
elasto-plastic analysis, computer programs and appls. *(Japanese)* 79−21555
electrophysiological measurement, high-press. chamber 80−98185
end-loading ring in rigid cavity, elementary catastrophe theory modelling 79−68585
fatigue design curves using modified Langer eqn. for pressure vessel alloys 80−30107
fission reactor, blowdown two-phase level swell calc. using drift flux correl. 79−89428
fission reactor, failure risk due to manufacturing defect 79−22432
fission reactor, Oconee nuclear station, surveillance capsule results 79−18019
fission reactor, safeguarding containment *(German)* 79−13433
fission reactor, safety anal. of cooling pipes 80−32370
fission reactor, ultrasonic inspection reliability 79−24713
fission reactor Inconel, pressure vessel bottom, subcritical crack growth in ligament between instrumentation rods 79−22428
fission reactor pressure vessel and circuit development, conf. report 80−47541
fission reactor pressure vessel reliability and sfaety, in-service inspection, surveillance specimens 79−18020
fission reactor pressure vessel safety and reliability evaluation, two-criteria approach 79−18016
fission reactor pressure vessel supports, fracture-safe design in neutron environment 79−93700
fission reactor pressure vessel surveillance capsule exam., appl. of ASTM standards 79−22436
fission reactor steel pressure vessel, reliability aspects 79−22430
for fission reactors, high temp. design system *(Japanese)* 78−673
flaw nondetection, estimate of probability 78−78479
fluid pressure generation and measurement equipment, up to 2700 MPa 79−21763
gas cloud explosion pressure loading for reactor secondary containment 79−49789
gas-cooled fast reactor safety 79−26654
GCFR, development of PCRV steam generator cavity closure 78−41849
glass enclosed Pt resistance thermometer for high pressure vessels 78−70125
glass-plastic equilibrium pressure vessel of minimum mass with non-geodesic winding 77−50905
gradient stress fields, stress intensity factor determ., nuclear safety appl. 78−34089
heads, internally pressurized ellipsoidal and torispherical elastic plastic, nonsymmetric buckling 77−58575
hermetic metallic thick-walled vessel, cooling by nitrine coolant *(Russian)* 79−59158
HTGR prestressed concrete pressure vessels, design of removable closures for large cavities 80−78356
HTGR primary coolant system depressurisation accident, expt. and numerical anal. 80−775
HTGR steam generator, construction and development *(German)* 77−369
HTR plants components development and testing *(German)* 77−10482
HTR-PRCV development of a removable closure for large cavities 80−5221
HWR, pressure tube reactor safety 77−67842
hydraulic testing, leak detection using acoustic equipment *(French)* 80−789
hydrostatic testing of optical glass windows at high press. 79−90016
hydrotest, acoustic emission monitoring 77−46206
Incoloy 800, 600 and 718, press. vessel, fatigue design criteria 78−60758
inspection, ultrasonic testing techniques review 77−74899
intersections, review of lower-bound limit anal. 78−34008
IR investigations of gases, pressure cell 80−83522
K-band high-pressure cell for EPR-ENDOR studies 79−67336
KS-150 reactor, radial shielding model, neutron and γ-ray spectra meas. *(Slovak)* 78−21624
layered cylindrical pressure vessels, shell theory, comparison with uniformly valid theory 79−64516
life-expired LWR, neutron activation product density and dose rate calc. 79−9908
liquid cooled fast reactor HCDA, fluid filled vessel response to internal explosions 79−49771
LMFBR, pool-type, dried hot concrete vessel design 78−50248
LMFBR, reactor closure assembly, rotating plug size 80−5227
LMFBR, US testing of austenitic steel welds 77−1903
LMFBR concrete containment struct., exptl. anal. of dynamic loading 78−41867
LMFBR containment, anal. of nonlinear fluid-struct. interaction, improved ICECO code 78−70615
LMFBR containment response anal., Eulerian computer code MICE for multifield fluids 78−70616
LMFBR containment response to postulated Na spills and fires, computer anal. 79−54480
LMFBR core disassemblies, damage potential sensitivity in prompt critical excursion 79−49766
pressure vessels continued
LMFBR HCDA, containment response anal. to PAHR failure 79−49672
LMFBR HCDA, damage potential of core disassembly, sensitivity study 79−54531
LMFBR HCDA, wave propagation ICECO code predictions in rigid 2-dimens. vessel 79−49770
LMFBR head closures, dynamic struct. response to HCDA 78−70617
LMFBR prestressed concrete reactor vessels, analytical model and code applications 78−74448
LMFBR reactor closure assembly, seals for rotating plugs 80−5226
LMFBR safety, comparison of ICECO code with flexible vessel expts. 78−70619
LMFBR vessel cavity and cell liners, elastic/plastic design 80−52728
load bearing segmental walls, stress state anal. 79−64514
LWR, manufacuring trends, Sweden 77−71688
LWR, press. vessel and piping design, plasticity-related damage prevention 79−6735
LWR, radiation embrittlement, role of ASTM 79−22435
LWR, risk-sensitive Markovian policies for detection and maintenance of fatigue cracks in pressure vessels 79−54534
LWR, ultrasonics materials testing 78−17339
LWR accidents, containment venting and filtration approaches 79−13465
LWR pressure vessel, unstable fracture *(Japanese)* 79−9767
LWR primary circuit component production, metallurgical aspects 79−36330
LWR steel pressure vessel, neutron radiation effects on material props., review *(German)* 77−34382
LWRs, brittle fracture initiation, propagation and arrest, investigation 79−22422
materials considerations, radiation embrittlement, current regulation assessment 78−52966
metallic structures, elastic/plastic bodies with work hardening, general shakedown theorem 77−3746
multicavity PCRV, review of design and anal. 78−44182
neutron exposure of reactor press. vessel steel, safety limitations *(German)* 77−34405
neutron noise analysis in PWR and BWR power reactors 80−86964
NMR probe for high-pressure and high-temp. expts. 80−22403
nonlinear creep problems in symm. press. vessels, uniqueness of integral eqns. positive solns. 77−65694
nozzle-to-cylinder structures subjected to internal pressure, finite plate method 78−34007
nuclear, HCDA, REXCO code, comparison with flexible vessel expts. 78−70618
nuclear plant pressurized systems reliability, influence of codes, standards and practices 79−22433
nuclear power conf., Chicago, United States, July 1979 80−794
nuclear power plant cost reduction by containment elimination 79−13467
nuclear power reactor, austenitic stainless steel, appl. 77−3102
nuclear power station, exam. for compliance with safety regulations 78−89954
nuclear power station pressure component manufacture, new materials, technologies and equipment development 78−74436
nuclear pressure vessel steels, transient finite element crack propag. model 77−3106
nuclear pressure vessel surveillance capsule remote dismantling and testing 79−9817
nuclear reactor, in-service inspection and automatic US testing equipment 77−1892
nuclear reactor, remote controlled US pre-service and in-service inspections 78−89955
nuclear reactor containment designs, value-impact assessment 80−797
nuclear reactor containment structure design and service loads 80−106138
nuclear reactor containment structures, design and construction, ACI-ASME code of practice impact 80−798
nuclear reactor Pilgrim I nozzle-to-press. vessel weld discontinuities, fracture mechs. anal. 77−80110
nuclear reactor pressure components, common cause failures 79−18012
nuclear reactor pressure vessel steel irradiation, neutron flux densities neutron spectra and temp. fields in large specimens 77−74924
nuclear reactor pressure vessel steels, neutron irrad. embrittlement, temp. effects, annealing *(German)* 77−34384
nuclear reactor pressure vessels, strain measurements 80−79865
nuclear reactor pressure vessels, stress analysis program, STANSAS *(Japanese)* 80−22969
nuclear reactor prestressed concrete model pressure vessel, gas press. testing *(Dutch)* 79−13436
nuclear reactor vessel cracks and elastic fracture mechanics 77−67843
nuclear reactor vessel safety technology accident analysis 77−67840
nuclear reactor vessels, radiation embrittlement, allowable crack size, unstable fracture 77−10465
oceanographic pressure vessel for trapping deep-sea animals, simply actuated closure 78−3821
optical cell for Raman scattering at low temps. 79−49247
optimum shape design for pressure vessel and nozzle junction 78−89941
overpressure conditions in isolated piping section 77−74955
PCRV, embedment strain gauges 78−41873
PCRV, stress anal. considering concrete cracking 78−44213
PCRV integrity during HTGR core heatup, thermal anal. model 79−49735
pipe, axial crack, elastic-plastic dynamic finite element anal. 77−3795
piping for PWR, Aquitaine 1 loop for studies of crack growth rate and propagation 77−3796
plastic response of orthotropic spherical shells under blast loading 80−33477
polycrystalline cubic BN plunger chamber for high-pressure Mossbauer meas. 80−31786
prestressed concrete, historical review 79−601
prestressed concrete pressure vessels design, finite element anal., computer programs 77−23183
prestressed concrete reactor vessel, 3-D nonlinear failure anal. 77−50268
prestressed concrete reactor vessel for GCFR, development programmes 77−18648
prestressed concrete reactor vessel for GCFR, safety features 77−14244
prestressed concrete reactor vessels, construction movements, finite element anal. 79−621

pressure vessels continued
prestressed concrete reactor vessels, perforated plate ligaments, time varying stress 79−49679
prestressed concrete vessels, transient anal. for HCDA loads 79−85666
prestressed pressure vessel, calc. of principal stresses 78−13206
proof testing, British standard 79−70269
pump-induced acoustic pressure distribution in an annular cavity bounded by rigid walls [pressurised water reactor] 79−72848
PWR, availability of pressure vessel after small LOCA 79−30967
PWR, control and effects of pressure vessel failure in steam-water cycle 80−770
PWR, design *(German)* 77−42180
PWR, integrity assessment in Britain 77−71704
PWR, Obrigheim nuclear power plant, inservice inspection, nondestructive testing, primary components *(German)* 77−34406
PWR, pressure vessel steel, RT_{NDT} shift of ductile-temp. curve, correl. with neutron dose *(German)* 77−34388
PWR, superheated containment atmosphere heat/mass transfer to passive heat sinks, analytical model 79−49658
PWR, thermohydraulic processes in high press. water loop, constructional details of loop *(Hungarian)* 78−82431
PWR acoustic monitoring instrumentation 78−17309
PWR containment vessel optimisation 80−106137
PWR LOCA, pressure vessel hydrodynamic loads, effect of subcooled critical flow discharge model 79−49733
PWR LOCA reflood, effect of low containment press. on peak cladding temp. 80−57897
PWR power stations, operating record and reliability, reviews 79−22404
PWR pressure components reliability and residual life evaluation and precipitation 79−20191
PWR pressure vessel, novel design, advantages 77−79471
PWR pressure vessel availability after small LOCA 79−31055
PWR pressure vessel failure probability from pressure transients, OCTAVIA computer code 79−18011
PWR pressure vessel nozzle, comparison of 3-D and axisymm. finite element anal. 79−13423
PWR pressure vessel reliability, failure anal. 77−74962
PWR pressure vessel reliability, simplified model extension and appl. 80−27786
PWR pressure vessel vibration excitation, noise correlation and modelling 79−13442
PWR reactor pressure tubes cracking, Pickering power station experience 78−82472
PWRs in Framatome plants, manufacturing phases, quality assurance 77−38323
radiation induced embrittlement of nuclear reactor steel, slow neutron small angle scatt. study *(German)* 77−34390
radiographic testing, sensitivity using 10 MeV microtron 78−70603
reactor, stress intensities for nozzle cracks 78−70583
reactor flexible dual-containment approach design and licensing 79−13400
reactor press. vessel nozzle under internal press. safety against bursting *(German)* 78−17326
reactor pressure vessels, thick steel sections, inspection by US nondestructive examination 80−102258
reactor vessel design-basis-accident presure-pulse prediction using SPIRT code 79−89361
reactors, 1100 MWe, MARK-II type, primary containment vessel design and fabrication 77−18659
reactors, brittle fracture safeguards, American and German ductility requirements *(German)* 79−41017
rectangular fibre reinforced plastic pressure vessel *(Japanese)* 78−11197
reinforced concrete containment model behaviour under thermal gradients and internal pressure 80−42837
reinforced concrete structs., initial stress approach to nonlinear dynamic anal. 77−83036
reliability, sensitivity to material and other factors 79−18018
relief valves, maximum isentropic flow of dry saturated steam 79−81978
return to atm. press., desorption rate of H_2O and H_2 *(French)* 80−42233
safety and reliability of prestressed concrete reactor vessels 79−22412
secondary creep problem, lower bound approx. soln. sequence 79−14284
seismic anal., Bell ring. vibr. of vessels with attached masses 77−3181
shell, cylindrical, effect of material orthotropy on stress state around circular hole 78−34023
shells of resolution under asymmetrical loading, creep deformation anal. 77−3751
skirt-supported pressure vessel free vibrations, finite element analysis 79−68632
small PWR containment complex and coolant system 79−13402
spherical cavity surrounded by infinite elasto-plastic medium, upper bound on asymptotic pressure 78−38214
split-octahedron type, for X-ray diffraction studies at high pressure 79−49246
stability of thin-walled pressure vessels of elastic-plastic linear hardening material 80−92075
steam generator tube failures at water cooled nuclear plants, world experience in 1975 77−38394
steam supply system, German licensing conditions 77−46340
steel, A302B, neutron damage, ductile-brittle transition temp. 77−3109
steel, A516-60, press. vessels, fatigue crack growth rate 77−77585
steel, A533B alloy, fatigue crack growth of irradiated pressure vessel steels in simulated, reactor-grade water environment 80−97582
steel, AISI 1010, low-cycle fatigue at temps. up to 1200°F 78−35516
steel, alloy A533B1, neutron irrad., flow growth characts. by acoustic monitoring 80−100918
steel, austenitic, ASTM A533B and A542, H_2 embrittlement behavior of unirrad. steels for nuclear reactor press. vessels 79−8340
steel, CC Cr-Mo-V press. vessel, crack growth under creep 78−60827
steel, Cr-Mo, high-temp. props. and constitutive equations 79−34146
steel, Cr-Mo, Mn-V, V, fracture toughness, pressure vessel appl. *(Czech)* 79−79094
steel, Cu, fission reactor vessels, neutron embrittled, exam. of technique for in situ thermal annealing 79−29114
steel, failure and radiation damage *(Czech)* 80−619
steel, fatigue design criteria 78−60758
steel, ferritic nuclear pressure vessel, methodology for fracture props. variability evaluation 78−33257
steel, flow size meas. using V—US method *(French)* 77−68347
steel, fracture toughness of nuclear pressure vessels 80−81172
steel, heavy section, rupture tests 78−44212
pressure vessels continued
steel, internal pulsed loads, effect of scale, geometry and filler on strength 78−21659
steel, low alloy, reactor pressure vessel, effect of Mn and C content on irrad. response 79−20196
steel, maraging, with defects, failure anal. 77−44361
steel, mild, biaxial fatigue, data compilation and anal. 77−4856
steel, Mn (1.10 to 1.55 wt.%), reactor vessel material, assessment of weld heat affected zone mech. props. 79−29217
steel, Mn-Mo-Ni (A533 B), ductile-brittle transition, material fracture temp. depend., Gauss distrib. function 80−97574
steel, Mn-Ni-Mo, PWR pressure vessel, irrad. induced embrittlement, chemical composition effect *(French)* 79−20195
steel, neutron irradiated press. vessel material, small angle neutron scatt. meas. 79−13428
steel, notched, acoustic emission meas. during pressurisation 78−21638
steel, nuclear, fracture toughness at elevated temps. 79−20193
steel, pressure vessel, acoustic emission during loading by pulsating internal press. *(German)* 78−19973
steel, pressure vessel for light water reactors, corrosion fatigue, data review 79−79169
steel, prestrained pressure vessel, correl. between dynamical toughness characteristics 78−68816
steel, prestressed cast, mech. and nuclear realisation for HTGR *(German)* 79−3196
steel, PWR pressure components, mechanical factors affecting reliability *(French)* 79−20198
steel, testing by pendulum impact machines, energy meas. using optical system 80−69746
steel, type A508 C1 2, microcrack formation during stress-relief annealing of a weldment 78−80629
steel A533A, review of data in reln. to fracture toughness at upper shelf temp. 79−15797
steel C-Mn-V and Cr-Mo-V, fracture toughness and fatigue characts. 79−20192
steel for nuclear reactor pressure vessels, irrad. and post-irrad. examination equip. and techniques *(German)* 77−36696
steel plate for nuclear reactor containment, brittle fracture meas. 77−3115
steel plates for reactor pressure vessels prod. by basic oxygen process 77−74944
steel pressure vessel, multilayer, without longitudinal seam, model investigation *(German)* 79−34276
steels, dynamic material props. for FBR safety anal., testing devices 78−60966
steels, irradiated pressure vessel, reference fracture toughness curves 80−100921
steels, nuclear reactor pressure vessel steels, optimum chem. comp. rel. to props. 80−93517
steels for PWR vessels, props. and development 77−38336
stiffened layered structs., dynamic large-deflection inelastic and thermal stress anal. 77−3752
strength analysis, by thermal shock 78−68819
stress analysis of cylindircal shell with rigid circular inclusion 79−14267
stress concentrations around multiple windows, in high press. vessel, photoelastic anal., strain gauge tests 77−72254
stress cracking, note on two cases in chem. plants 78−85027
stress intensity factor determ. 80−37455
stress intensity factors for internal multiple cracks in thick-walled cylinders stressed by internal pressure using load relief factors 79−46261
stress intensity factors for reactor vessel nozzle cracks 79−15796
stressed state in reactor pressure vessels, model studies by polarised optics 78−78454
structural analysis, inelastic response, constitutive modelling 77−3093
structural materials, pressure testing *(Spanish)* 80−52735
structural mechanics, conf. 78−41874
structural representation in stress anal. 80−27703
structures anal. under creep conditions, acoustic emission method 77−25237
stud bolt, high temp. strain meas. *(German)* 79−30937
Super Phenix nuclear reactor containment vessel, stress anal. *(French)* 79−41023
Super Phenix reactor vessel research and development *(French)* 79−30947
surface cracks in thick-walled pressure vessels, 3D finite element anal. 79−10535
surveillance capsules, remote disassembly and examination 79−45463
tensile testing in high-pressure gases at high temps. 78−44303
testing, strain gauges performance in pressurised water at 50°C 79−35713
thermoplastic rectangular parallelepiped pressure vessel, photoelastic coating anal. 79−59950
thin walled, containing surface flaws, fracture mechanics and acoustic emission exam. of failure 78−84981
torispherical heads, elastic instability anal. with triangular thin shell finite elements 77−58576
torispherical vessel heads, elastic-plastic internally pressurized, stresses and buckling 77−58574
toroidal reactor primary containment vessels, consistent mass matrix anal. of hydrodynamic effects 79−76066
transient temperature distribution in the reactor vessel wall after cooling system failure 79−54473
Trino PWR pressure vessel in service inspection, planning and organisation *(Italian)* 79−17993
two-phase unsteady flow, meas. problems 77−27633
UMFBR molten core debris and core containment material interactions 79−13469
US inspection, of PWR reactor *(Czech)* 78−29658
vent clearing analysis of a mark III pressure suppression containment 80−32371
vibrations, free, engineering appl. of Timoshenko beam theory 78−83299
VVER anal. of relative motion between pressure vessel and its internals 79−67882
warm prestressing effects, fracture mechanics during severe thermal shock 79−22411
water cooled reactors, technology for accident anal. and consequences mitigation, pressure vessel types 77−34414
water pressure testing, test method and anal. *(German)* 78−25260
wave propagation effects on dynamic loading 77−3090
weld metal, submerged arc irradiated, reference fracture toughness curves 80−100921

pressure vessels continued
weld quality assessment, NDT methods and equipment 78−56871
welded joints, low cycle fatigue anal. 77−3789
welded pressure vessels, residual stresses determination 78−40014
Westinghouse steam generators, operations update 78−21751
Zircaloy-2, pressure tube, fragmentation on failure 78−72863
ZR-6M rupture test using scaled simulation *(Hungarian)* 78−89964
Al alloy, 5083-0, pressure vessel material, delay effects 78−35515
C-fibre reinforced plastics, acoustic emission detection, immersion techniques 77−1902
Cr-Mo steel types JIS SCMV 2, SCMV 3 and SCMV 4, high-temp. high-cycle fatigue props., press. vessel appls. *(Japanese)* 80−93650
Pt resistance thermometer for in situ meas. 79−21744
Ti-Al-Mo alloy VT-14, spherical pressure vessel, correlation between fracture stresses and mech. laboratory charcts. 80−25838
WC-Co, evidence for H embrittlement 78−48530
Zr-Nb, pressure tube alloy, initiation COD as fracture criterion 78−72862
Zr-Nb (2.5 wt.%), cold worked, press. tubes, secondary cracking obs. 78−80630
ZrNb, pressure tube, fragmentation on failure 78−72863

primary cells
alkaline, for camera appl., effect of discharge resistance obs. *(Polish)* 79−57420
alkaline batteries, button-type, for electronic appliances *(Japanese)* 79−83582
batteries, combinatorial rules, for teaching 79−62962
biogalvanic, pacemaker power supply, dog implants 77−52935
biogalvanic and biofuel cells, animal expts. 77−81657
camera expendable batteries, survey 79−71545
cardiac pacemaker, neutron radiography investigation of electrolyte, USA National Bureau of Standards 80−56179
cardiac pacemaker long-life battery test results 77−81735
cardiac pacemaker reliability technology workshop, Gaithersburg, USA (Oct. 1977) 80−27038
cardiac stimulator power supply battery selection 77−48931
comparison of available primary batteries and accumulators *(German)* 79−70444
cupric oxalate cathodes for seawater cells 79−92067
developments in electrochemical energy sources *(German)* 80−97770
dry air battery charcts., using $ZnCl_2$ electrolyte *(Japanese)* 79−83581
dry batteries development, $ZnCl_2$, 'NEO Hi-Top', discharge charcts. obs. *(Japanese)* 79−87986
dry battery with geometric shape chosen to suit appl. *(German)* 79−100503
dry cells, performance and life charcts. 79−100508
dry cells, use to power TTL ICs, teaching 77−17745
electrochemical cells without liq. junction, use of central connectors 78−8199
electrode resistance, effect on current density and electrode pot., rel. to cell design 77−60070
electrolytes, for high energy cells *(German)* 78−80751
galvanic cells using fluoride-conducting solid electrolytes 80−3501
graphite fluorides, $(CF)_n$ and $(C_2F)_n$, prep., struct., discharge charcts., electrode props. 80−89502
implantable hybrid cells, porous cathodes, recent improvements 77−40933
Leclanche cell, impedance spectrum of an undischarged cell 80−89604
Li-I hermetically-sealed cells, long life expectancy, pacemaker power source 80−40850
Li-metallic oxysalt organic electrolyte batteries 80−3502
Li-V_2O_5 reserve cells, characterisation of V_2O_5 cathode, microstruct. optical reflectance, elec. cond. meas., chem. anal., SEM obs. 79−43752
metal-polyethylene terephthalate metal system, electrochem. effects as source of EMF 79−87163
metal-polyethylene terephthalate-metal, electrochem. effects as source of EMF 78−72278
metal-polyethylene terephthalate-metal system, electrochem. effects as source of EMF 79−87162
mixed U-Pu oxide O_2 potential and O/M ratio determ. by solid-state galvanic cells 79−96324
pacemaker, battery longevity estimation using statistical methods 78−57131
pacemaker batteries, characterisation of internal power losses by calorimetry 78−92747
pacemaker battery characteristic meas. microcalorimeter 80−30936
pacemaker battery internal loss characterisation calorimeter 80−30934
pacemaker battery microcalorimetric testing 80−30933
performance limits, technical and economic factors 80−45657
polarity reversal, appl. of Evans' diagram 80−35664
self-discharge process assessment by microcalorimetry 80−30935
small-sized batteries development, Japanese industry and market trends 80−81429
solid electrolyte with Cu ion conductors, charcts. 77−77775
space power systems, 1979 state of art and development trends 79−100506
standard, saturated, use of air thermostat 77−10058
standard, testing using low resistance differential potentiometer *(Polish)* 78−29127
standard cell, calibration using supercond. junction device 77−18029
standard cell, combination type, composite amalgam electrodes, low temp. coeff. 77−18026
standard cell, temp. controlled enclosure with 25 μK stability 77−18027
standard cell EMF stability testing, thin-film tunnel Josephson function method 77−67468
standardisation and IEC activities *(Japanese)* 79−83580
superionic conduction in solids, high energy density batteries appls. 79−70445
temperature-stabilised enclosure for 54 standard cells 77−5872
tetramethylammonium silver iodide superionic film, electrocodeposition, electrochem. cells 80−107478
thermal battery, anode-electrolyte interface study 79−61965
thermal battery, using Ca anode, electrolyte composition improvement *(Japanese)* 79−83584
thermal battery cells using molten nitrates as electrolyte and oxidiser 80−76624
transition metal chalcogenides, reversible electrodes appls. 80−61112
unit voltage standard comparison with working standards, Josephson effect 77−53941
volt dissemination method and standard cell enclosure design 80−98876

primary cells continued
voltage, standard cell group enclosure monitored by AC Josephson effect 79−26076
voltage delay in lithium non-aqueous battery systems 80−35662
Weston cells, NPL voltage standard, computer control meas. 77−82572
$Ag/Ag_7I_4PO_4/I_2$ cell, cell voltage meas. 80−55315
Ag/AgI/Te thin film galvanic cell, shelf life determ. 78−35702
Ag-AgCl film aqueous soln., charge transfer mechanism 78−11527
Ag-Zn, failure-analysis program, test methods evaluation 79−48105
Ag-Zn batteries, miniature, fabrication and charcts. *(Polish)* 80−93866
AgI-Ag oxysalt electrolytes appl., investigation 77−4909
AgI-based solid electrolyte cell discharge mechanism 80−35663
Au/solid electrolyte/Au, charge storage with various electrolytes 80−89605
Cd-Sn-Pb composite amalgam electrode standard cells and combinations 77−5871
CdS(Se)-based photoelectrochem. cells, charcts. 77−25287
Hg-Zn battery as reference voltage source in electron microscope stabilisers 79−9262
Hg_2O_3-Zn and Li based pacemaker power sources compared 77−52920
Li, 1979 state of art, appl. in medicine, watches, photography and military equipment *(Spanish)* 79−96432
Li batteries, large energy content and long shelf life *(Danish)* 80−16794
Li batteries with voltage compatibility with conventional systems 80−97777
Li battery, button type, using CuO as cathode 80−97779
Li battery charcts. *(German)* 79−66404
Li, developments and appl. survey 80−50949
Li, for pacemakers, selection criteria *(German)* 78−3670
Li, future uses, production, and advantages 80−35659
Li metal for battery industry, sources and preparation 80−97781
Li nonaqueous battery iron sulphides preparation, charcts. and appls. 80−97778
Li organic electrolyte battery, using poly-carbonmonofluoride cathode *(Japanese)* 79−83583
Li pacemaker battery similarities and differences 77−81737
Li, Pb compounds as cathode materials, evaluation 78−11525
Li power sources, with Ag_2SeO_4 and Ag_2TeO_4 as cathodes, performance determination 79−52918
Li primary batteries, development trends. 80−101083
Li/SO_2 battery, charcts. and appls. 80−97774
Li/SO_2 cells, DTA, safety studies 80−81428
Li/SO_2 cells, explosion causing mixtures, differential scanning calorimetry studies 79−52919
$Li/SOCl_2$, cyclic voltammetric and coulometric obs. of $SOCl_2$ reduction 80−30440
$Li/SOCl_2$ cells, abuse tests 80−97776
$Li/SOCl_2$ cells, high rate discharge charcts. 80−72021
$Li/SOCl_2$ D cells, optimisation with respect to energy density, storability and safety 80−97775
$Li/SOCl_2$ hermetic primary cells, effect of type of C on performance 80−35661
$Li/SOCl_2$ primary cells, $SOCl_2$ reduction mech. in supporting electrolyte 80−108792
Li/TiS_2 cell with solvate melt, discharge charcts. and lack of rechargeability 80−72022
Li-$(CF)_n$ high energy density battery, cathode materials evaluation 80−97780
Li-$AgCrO_4$ pacemaker cell construction 77−81739
Li-I cell solid state, cardiac pacemaker power source, testing 79−66584
Li-I_2, self-discharge rates using microcalorimeter 79−61963
Li-I_2 batteries for cardiac pacemakers, capacity rating system 80−97773
Li-I_2 battery, construction, performance and reliability 80−97771
Li-I_2 cell for commercial and medical appls. 80−97772
Li-I_2 pacemaker battery electrolyte exam. by neutron radiography 80−30940
Li-I_2 pacemaker cell end-of-life characteristic approximation 80−30937
Li-I_2 power cell accelerated discharge test for battery longevity model 80−30938
Li-MnO_2 batteries development, Sanyo, with high energy densities 80−85272
Li-$SOCl_2$, discharge reaction mechanisms 79−100504
Li-$SOCl_2$ battery, nonaqueous, power sources appl., reviews 79−100505
Li-$SOCl_2$ battery for implantable cardiac pacemakers 80−30939
Li-$SOCl_2$ hermetic D cells, effect of $Li_2B_{10}Cl_{10}$ and $Li_2B_{12}Cl_{12}$ on performance 80−12000
LiAl-$NaAlCl_4$-$MoCl_5$ thermal battery test results 79−29459
LiAl-$NaAlCl_4$-$MoCl_5$ thermal battery evaluation and optimisation 79−29458
LiI complexes, ionic cond., electrochem. props. 77−60072
LiI hybrid IC pacemaker, reliability, experience 77−81736
LiI powered pacemaker types evaluated 77−81738
$LiSOCl_2$ battery undersea applications 80−45658
Li_xTiS_2, intercalation cpd., Li ordering, electrochem. obs. 78−59795
Li_xTiS_2, Li ordering in intercalation battery, theory 79−77580
Mg-AgCl seawater battery, performance and EMF at great ocean depths 80−76623
Mg-MnO_2, short-circuited cell, use as portable heater 79−61964
Mg-MnO_2 dry batteries, impedance parameters and state-of-charge 80−21390
MnO_2 batteries, type LR9, cathode composition, quality effects *(Polish)* 79−52920
MnO_2 battery-grade, resistivity rel. to water content *(German)* 79−96431
MnO_2, doped, dry cell depolariser, hydrazine reduction kinetics 80−89603
MnO_2, preparation and characterisation of doped samples for appl. as dry battery depolarisers 80−89602
$NH_4Ag_4I_5$, thin film solid state battery 78−76876
NaCl-$AlCl_3$-$CrCl_3$, molten, electrochemical exam. of Cr 78−56939
Ni electrode, appl. in rotating multipolar wiper-blade cell 79−43751
Zn electrode development, dispersed, electric vehicles appl. *(French)* 80−72023
Zn-Ag_2O, cation exchange membrane, transport parameters for KOH aqueous solution 78−64883
Zn-AgO cell, Zn electrode slurry-paste fabrication optimisation 79−96430
Zn-air, comparison with conventional Leclanche cells 80−35660
Zn-air, cylindrical, R-20 size, design and electrical charcts. 79−100507

primary cells continued
Zn-HgO, self-discharge rates using microcalorimeter 79−61963
Zn-MnO_2, dry batteries, impedance parameters and state-of-charge 80−21390
Zn-pore electrodes and cells, operation 80−26126
$ZnCl_2$ energy systems for public utility and automotive appls. 80−101082

primary cosmic radiation *see primary cosmic rays*

primary cosmic rays
acceleration processes in young supernova remnants 77−33613
angular distribution at heliosphere boundary, results from muon intensity vars. 79−80116
anisotropy, 10^{11} to 10^{20} eV 79−66892
antiparticles and collisions in interstellar medium 80−77241
antiprotons and antihelium, relative abundance in primary cosmic radiation 78−73594
atmospheric measurements determ. of primary spectrum 10^{12} eV and 10^{15} eV 79−66895
black holes, possible existence in cosmic rays *(Russian)* 77−29875
charge spectrum of high energy nuclei *(Korean)* 79−48633
chemical composition of primary cosmic rays, calcs. using sea-level muon spectrum 77−64555
composition, air shower cores, energetic hadron, $>10^{13}$ eV, arrival time distrib. 79−44321
composition, anal. of number of nucl. cascade avalanches in ionisation calorimeter 78−12064
composition, influence on atmospheric hadron families characts. 79−80160
composition and interactions for particles of energy 10^{14}-10^{16} eV, Tien-Shan data 79−80149
composition from hadron time distribs. near air shower cores 79−62697
difference coupling coefficients, method for cosmic rays 78−28461
discrete galactic sources, statistical theory of propag. 79−44312
EAS, violation of scale invariance in hadron interactions, 10^{15} to 10^{17} eV 78−7849
EAS age parameters, elementary act parameters, primary cosmic ray spectrum 77−64567
EAS data on primary particle spectrum at 10^{8}-10^{10} GeV 77−64568
EAS detectors pulse profiles, studies rel. to primary particles props. 79−25421
EAS radioemission, freq. spectrum, lateral distrib., primary cosmic rays comp. 77−87219
EAS research, primary cosmic ray energy $>10^{17}$ eV, equipment system parameters, capabilities 77−64569
electron component in galactic disc, estimate from gamma-ray emission obs. 80−82540
electron intensity and energy spectrum 77−45270
electrons, detect. by synchrotron radiation in geomag. and interstellar mag. fields 78−57412
electrons, high energy, spectrum obs. by emulsion chamber *(Japanese)* 79−80153
electrons in stratosphere, spectrum above 3 GeV 77−53374
energy spectrum, 10^{13} to 10^{16} eV, from EAS data 77−67014
energy spectrum, reassessment of Sydney EAS data 77−2315
energy spectrum above 10^{17} eV 77−64554
equatorial modulation and north-south asymm. due to interplanetary mag. field 78−16253
fluctuations of 10^{14} eV rays, Musala Peak obs. 78−49254
flux in atmosphere, primary and splash albedo components, polar orbiting satellite meas. 79−25415
flux measurements by supercond. mag. spectrom. 78−25383
galactic cosmic ray electrons, 30-1000 GeV, emulsion chamber obs. 80−85827
galactic cosmic rays, age distrib. of interacting and decaying particles 77−5401
hadron energy spectra produced by primary cosmic ray particles, $E>10^{14}$ eV 80−21880
heavy nuclei, charge and energy spectra 79−25418
heavy nuclei diffusion in atmosphere, spectra and comp. 80−41680
high energy, identification with intergalactic suprathermal dust grains 79−48911
isotope abundances, Cr to Ni 79−70937
low energy cosmic rays, Skylab meas. of heavy ions 80−56689
mass composition from μ multiplicity meas. using Homestake neutrino detector 79−66903
multiply charged nuclei, charge depend. of solar modulation 77−5403
muon-electron ratio and particle mass for primary cosmic rays of 10^{15}-10^{16} eV energy 79−80150
National Cosmic Ray Facility, for high energy physics and primary comp. studies, 10^{14} to 10^{18} eV 79−62704
neutrinos, high-energy prod. spectra and diffuse fluxes 79−44327
neutron-proton ratio determ. 77−70961
nuclear primary air showers, phenomenological model 77−22028
nuclei, charge comp. and energy spectra, energies $\geq$5 GeV per nucleon 78−16259
nuclei, high-energy gamma-quantum and hadron families prod., Monte Carlo studies 79−80158
nuclei composition effect on cosmic ray muons response function 80−41683
nuclei from 3000 MeV to 50 GeV per nucleon, charge comp. and energy spectra 78−93059
nucleon spectra from atmospheric γ-ray and muon data 79−44320
nucleon spectrum, Cocconi-Koester-Perkins model rel. to sea level muon spectrum 79−84612
nucleon spectrum and derived muon energy at sea-level, Cocconi-Koester-Perkins model 79−48634
nucleon spectrum calc. of atmospheric neutron/proton ratio and sea level neutron spectrum 80−8499
nucleon spectrum meas. at GSFC, vertical sea-level meson-neutrino spectrum determ. 78−85782
origin, appl. of galactic models with halo to proton nucleon component 80−61971
origin, energy spectrum, composition, general review 79−80117
origin, intergalactic suprathermal grains, accel. mechanisms 79−25412
photoemulsion nuclei interactions using satellite Intercosmos-6 *(Russian)* 78−93063
proton spectrum, 10^{12}-10^{14} eV 77−91389
relative abundances of nuclei with $Z\geq7$ from plastic detectors 78−16260
satellite and balloon research projects, problems 79−8785

primary cosmic rays continued
sidereal variation of 10^{11} eV particles and interplanetary mag. fields 80−17452
spatial diffusion coefficients, computation using nonlinear particle trajectories 77−45262
super-high energy cosmic rays, anisotropy in galactic disc direction *(Russian)* 78−57410
superheavy primary cosmic ray nuclei, obs. with solid-state track detectors and X-ray films *(Japanese)* 78−61688
supernova remnants, cosmic rays in dense shell 77−33599
ultraheavy nuclei, errors due to geomagnetically forbidden light nuclei 77−37489
underground observations, spectrographic method, medium to high energy range 78−32307
X-rays diffuse component, separation method using growth curves 79−25512
γ-rays in range 3.5 to 100 MeV, system for meas. ang. and energy distribs. 77−50324
B, isotopic composition meas. in nuclear emulsions 79−80155
^{7}Be, cosmic ray accel. probe 78−81512
C, isotopic composition meas. in nuclear emulsions 79−80155
He and heavy nuclei fluxes at Fort Churchill 77−70959
He isotopic composition from 123 to 279 MeV per nucleon, meas. and anal. 78−49251
He nuclei isotopic comp. meas. 79−80145
N and O, isotopic comp. with consequences for source models 79−84609
Ne to Fe nuclei, 200 to 650 MeV/nucleon, relative abundances 80−77246

printed circuits
14th Annual Reliability Physics Symposium, Las Vegas (1976) 77−40514
data acquisition, micro-based, low cost, system, developed in Vienna 79−44905
DC current measurement, in-circuit 77−18009
drift chambers with PC cathodes, design and props. 79−3303
fabrication, detrimental effect of aged Sn-Pb surfaces 80−108625
glass fibre reinforced epoxy, multilayer circuit board, holographic interferometry appl. to real-time studies of heat effects 79−91873
hot spots, identification using holographic interferometry 77−71950
inspection using optical microscope 77−41679
PCB construction using thermally stable diallyl polymers as laminating resins 79−52658
PCB contacts, additive-free hard Au appls. 80−108718
photosensitive material for PC forming, photolysis investig. of silver salts of org. acids 77−44496
protection, parylene (vacuum deposited polymeric coating) appl. 80−108607
PWB holes counting, wide-aperture telecentric laser scanning system design 80−1264
regular polygonal clamped plates carrying concentrated masses, free transverse vibration 78−42559
solar cells automated production, with wraparound contacts 80−76635
space-quality solder joints, resistance to thermal fatigue 80−25831
thermally stable diallyl polymers as laminating resins, multilayer PCB appl. *(Japanese)* 78−92232
Au, Cu diffusion, 75-150°C, AES, device appls. 77−1262
Au, Ni and Cu diffusion, relative rates 77−80652
Au, plating assessment for printed circuits 79−43163
Ni-Fe microelectrode array probe for electrophysiology 79−84049
Sn-Pb composition anal. of PCBs using beta-backscatter gauge 80−16631

printers
auxiliary information recording with B3-15 digital printers 79−26044
chromatography, data processor with thermal printer-plotter for GC and LC *(Japanese)* 80−50920
colour film, rapid-acting light-setting mechanism *(Russian)* 79−35878
data averager/printer, 7-channel, for cardiovascular and other physiological signals 78−40366
data logging digital system 77−22538
ECG recorder and printer with fixed writing heads 80−3854
electronic imaging hard copy methods and printing systems 80−47134
electronic ink system protection, parylene (vacuum deposited polymeric coating) appl. 80−108607
high-speed non-impact printer, design and principles 78−21247
high-speed non-impact printer, optical character generation requirements 78−21246
ink jet drop formation, scale model 77−75952
ink jet nozzle flow, 100:1 scaled-up model 77−75957
jet printer nozzle or convertor electrohydrodynamic output parameter exact solns. *(Russian)* 78−75230
laser alphanumeric character generator for line printer and COM 80−33067
laser beam printer scanning system with f-θ lens 80−78942
laser printer *(Japanese)* 78−90446
laser printers and scanners, fractional picture element registration clock generation 77−58486
line printer displayed binary hologram generation by phase reference method 78−9344
liquid jet air wake boundary layer eqns. 77−75954
liquid jet satellite droplet formation 77−75953
matrix, for digital LANDSAT colour image data display 78−12024
matrix, wire, high speed, wear resistivity obs. *(Japanese)* 80−55540
medical diagnostics problems of computer applications *(German)* 79−20696
metrological balance automatic recorder and printer 77−22530
microprocessor-controlled plotter/printer, HP-IB 7245A model 79−35689
modular contact printer for high speed automatic additive colour cinefilm printing 80−42276
photofinishing printer response customisation 80−4793
pictorial electrographic printing, tone reproduction and screen design 80−62752
stereoplotter, orthoprinting system, TOPOMAT, appls., accuracy 78−81437
time code, automatic print out, EEG paper, 10 sec. intervals 77−29219
GaAs laser facsimile printer 80−30207

printing
see also computer-controlled typesetting
additive photographic film printers, programmed control of light metering valves *(Russian)* 80−95174

printing continued
albumen paper, manufacture and use 79−35515
alphanumeric/graphic print photo-embossing for tactile reading 79−80710
Colour printer quality and productivity improvements 79−93245
contact printing method utilising heated photoresist adhesive prop. for hologram copying 80−5704
electronic imaging hard copy methods and printing systems 80−47134
electrostatic ink jet drop formation characteristics *(Japanese)* 78−25766
gravure and embossed papers, printability prediction by time series anal. 80−15345
halftone or line printing, Yule-Nielsen curve fitting parameter 79−13906
high-speed scanning colour printer 79−93246
holographic printing of discrete stereograms of group portraiture *(Russian)* 80−23644
image coloration psychophysics 78−65025
images, scanning laser beam direct picture printers on photographic paper, appl. in life sciences *(French)* 80−72119
impulse drive jet used in character printing, model for fluid ejection and refill 77−68656
ink jet droplet charging, math. model 79−50184
ink jet printer, leq. jet breakup, 3rd perturbation Cosserat soln. 79−32615
ink transfer analysis 79−17516
kinematic-optical projection for high-density optical information transmission *(German)* 79−72678
laser facsimile printing comprising real-time diffr.-limited reading, transmission and printing of large images 77−42559
laser printing, dry Ag material technology 80−13179
laser transfer printing of volatile dyes 77−53998
liquid jet breakup, second perturbation soln. for one-dimensional Cosserat theory 79−86478
magnetographic printing, ferrofluid droplet dynamics 79−50772
microfilm laser transfer printing 77−18121
motion picture printing using new colour attenuation system 79−2859
motion-picture films, wet, using variable speed step-optical printer 77−79175
paper, surface characterisation and printability criteria, stochastic approach 78−18878
paper membrane sound generation by impulsive tension 78−90581
photographic print timer, using ring of LEDs 80−77899
photopolymer printing surfaces for gravure 79−35871
polyolefin film, corona discharge treatment 77−56129
precision circular scale manufacture by contact photographic printing 79−75638
random nucleated halftone screen 78−62192
stroboscopes appl. 78−55453
subtractive colour photographic printing, exposure parameter calc. 79−26167
tonal reproduction via unscreened positive printing plates 79−17517
waterless planographic plate development 80−105729
wet printing systems development and future 79−21826

printing industry
see also printing
laser printing, seminar, Los Angeles, USA (Jan. 1979) 80−12852
quality control, appl. of microdensitometry *(Czech)* 79−30524

prismatic dislocations
electron microscope image calc. and Burgers vector sign determ. 77−59017
mean strain in crysts. containing prismatic dislocation loops 77−7720
metal, thermodynamics of electrons, dislocation dipole and prismatic dislocation loop effects *(Russian)* 79−56161
CdS, dislocation emission, photoluminesc. spectra 80−16084
$Ga_{1-x}Al_xAs$ DH injection laser diode, long-term-degraded, TEM obs. 78−71102
GaAs:Si, faulted and prismatic loops, TEM obs. 77−51386
GaAs:Te, heavily-doped, annealing-induced prismatic dislocation loops and elec. changes 78−51546
$Gd_3Ga_5O_{12}$, optical birefringence images of edge dislocations 77−1129
KCl:Ba^{2+}, localised stress relaxation in excess vacancy system, prismatic loops *(Russian)* 80−88160
$NdGa_5O_{12}$ wafer, dislocations, etch pits and birefr. obs. 78−83818
Si, Czochralski grown, intrinsic gettering by oxide precipitate induced dislocations 77−27903
n-Si, dislocation free, memory effect associated with appearance of prismatic dislocation loops 77−1130
Si, dislocation-free single crystals, microdefect type by anomalous X-ray transmission 79−95019
Si, oxidation-induced stacking faults, nucleation mechanism 80−15122
Si:O wafer, annealed, surface- and inner-microdefects, TEM obs. 80−54236
Si:P^+, misfit dislocation net propagation due to osmotic forces 79−65108
Ti, single crysts., recrystallised, X-ray topography obs. 78−10054
Zn, basal dislocation−prismatic dislocation ring interactions by method of moments *(Russian)* 80−10550
ZnO, dislocation loop nucleation on prismatic faults in high voltage electron microscope 77−72620
ZnO, irradiation in high voltage electron microscope dislocation loops study 80−88157

prisms (optical) *see optical prisms*

privacy of data *see security of data*

probabilistic logic
fault conditions diagnosis based on tree logic and probabilistic importance, appl. to nuclear power plant 77−6549
multivariate and conventional ECG analysis programs compared 78−7492

probability
see also game theory; Monte Carlo methods; queueing theory; random processes; statistics
20 GHz multi relay links, simultaneous probability of rain attenuation 78−3898
accidents at nuclear power stations *(Portuguese)* 80−68844
accidents during work, mapping of reasons using error beams by function sensed computations of admission probabilities *(German)* 80−68027
additive and cancellative interacting particle systems, book 80−41960
algebraic models for probability measures assoc. with solns. of random eqns. 77−67236
amplitude distributions, appl. in practical data assessment problems 80−27107

probability continued
atmopsheric precipitation probability forecasts, nonparametric technique based on pattern recognition algorithm 78−44946
atmosphere, speckle propagation through turbulence 78−66758
atmosphere, turbulent, conditional fading statistics of scintillation 78−66757
atmospheric surface layer temperature extremes, probability determ. method 78−45020
atomic collisions, quasiclassical theory, transition between spatially degenerate levels 80−43150
Bayesian prediction model for fire occurrences in nuclear power plants 80−18527
bibliography, probabilistic ideas in field theory and statistical mechanics 78−8230
binary stars formation by three-body encounters, probability and effects on cluster evolution 77−13396
Boltzmann-Gibbs-Shannon generalised entropy, unique characterisation 77−5747
book, Brownian motion, Hardy spaces and bounded mean oscillation 77−67180
Brownian motion, stochastic calculus, derivation from path integral expansion of conditional probability density 79−67227
cardiac electric field probabilistic model 79−39387
carrier-molecule complexes, probability description of electron transport processes 78−53314
cause-consequence chart to assess the availability of the containment spray system in a nuclear reactor 80−52756
cell motility and adhesion measures, Markov chain model 77−66804
cell proliferation transition-probability theory, cell cycle kinematics 78−24039
chance and origin of life 78−69269
chemical reactions, reversible, asymptotic expectation and variance of stationary probability distribution 79−11789
clinical diagnostic method effectiveness, decision probability calc. *(Hungarian)* 78−65146
coarse riverbed material, probability density function of biased samples 80−12445
colloidal dispersion, particle size distrib. change kinetics, statistical approach 78−7241
colloidal systems, dynamical props., correlation and response functions 80−22286
comets, discovery probability and reality of concentration of perihelia of concentration of perihelia 80−67660
complete computer program in FORTRAN, for analysis of variance and means 80−98792
complex compounds, calc. of probability of electronic excitation energy transfer 79−69478
composite materials, cylindrical shells, probability anal. of stability, mass minimisation 78−42553
computer programs for high-school expts. 78−86094
converse of dominated ergodic theorem 79−71349
cooperative stereo algorithm anal. 78−53413
Cos θ similarity coefficient, approximate levels of significance, sedimentology appl. 77−86877
course-graining, statistical inference from partial meas. 77−26148
critical point behaviour, probability theory 79−44889
crystallography, determinantal inequalities, invariant joint probability distrib., heuristic derivation 79−32927
defective material, with strength, anisotropy induced by pretreatment, limiting state probability calc. 77−86123
density function representation for three-dimensional rotational discrete time system 77−17782
deterministic dynamics, relationship to probabilistic description 80−4646
deterministic dynamics to probabilistic descriptions 80−68029
diffusion process Lagrangian, probabilistic anal. 78−62170
digital frequency meter jamming, distribution function determ. *(Russian)* 77−41575
digital system for measuring probabilistic and statistical characteristics of infralow-frequency processes 79−71431
discharge, ions energy distribution function, in homogenous medium *(French)* 77−19796
discharge, luminescent, in He, electrons energy distribution function evaluation, by Monte-Carlo type simulation *(French)* 77−19795
discrete stochastic electric double layer, electrostatic props. 79−96318
dynamic renormalization group, phenomenological fitting 79−75471
earthquake prediction, probabilistic significance 77−56589
earthquake response spectrum amplitudes, probabilistic computation 79−8610
ECG diagnosis, variation in probability levels 78−44664
elastic neutron scattering, probability density function approach 80−13480
electrical components, mathematical simulation of life *(Spanish)* 79−21532
elementary particle theory, fundamentalness of probability concept 77−49882
entropy, information and statistical, and law of large numbers, opacity of statistics *(French)* 80−73288
equilibrium statistical mechanics models random fields investigation, book 77−22485
ergodic measures, equivalence singularity dichotomies 77−53754
ergodic properties of an operator obtained from a continuous representation 78−89305
examination marks, reliability, in electronic engineering educational courses 79−75305
exponential distribution MTBF confidence limits determ. using Epstein and Harters methods 80−98790
exponential random variables sum, probability density function 78−12537
failure, high temp., life fraction rule and probabilistic approach 80−93608
fatigue probability diagram plotting for wires 79−52490
fibre bundle time-dependent failure, probabilistic model 77−3798
fibrous materials, chain of bundles probability model for strength, numerical study of convergence 78−88496
fission, supercritical multiplying systems, extinction problem, point model approx., models for neutron multiplicity 80−22883
fission reactor, criticality safety, fault tree logic anal. of violations 79−22445
fission reactor Pu fuel facility damage from high winds, risk anal. 80−63356

probability continued
fission reactor system reliability prediction, appl. of Bayes eqn. 77−67797
fission reactors, BWR decay heat removal systems, probabilistic risk assessment, fault and event tree anal. 80−63333
fission reactors, failure probability distrib. from observed failure data, beta distrib. 80−63335
fission reactors, operator reliability, Weibull distrib. model 80−63336
flashover probability dependence and Weibull distribution *(Czech)* 78−67449
flood frequency analysis, log Pearson type 3 distrib., max. likelihood theory 78−61470
Fokker-Planck equation with spatial coordinate-dependent moments, path integral soln. 80−77688
fracture model, time dependent probabilistic, for strength of glass fibre reinforced plastics 80−40477
fracture statistics for polyaxial tension, approx. treatment 77−58602
frozen precipitation forecasting, regression estimation of event probabilities method *(German)* 79−66770
fundamental concepts with essential analysis, book 77−37740
fuzzy spin spaces, probability theory, spectral densities 77−37811
galaxy groups, nearby, quantitative membership probabilities from three-dimensional method 79−62919
Gaussian cylinder set measures and abstract Wiener spaces mixtures as models for detection 78−89306
generalised (non-Markovian) Langevin eqns., correl. functions and master equations 79−21653
generalised Gram-Charlier series with application to the sum of log-normal variates 77−37736
generalised theory, conditional expectations 77−60911
genetic systems, dynamics of neutral mutation 78−86220
geophysical interpretation problems, soln., correl. theory of homogeneous random fields appl. 79−100986
geophysics, mineralized zones, probability and uncertain number theory appls. *(Rumanian)* 77−29509
geophysics, probabilistic model for oil and gas forms.. pre-drilling prediction *(Russian)* 79−39970
glacier friction law, shadowing function of Gaussian probability curve *(French)* 79−8641
glass fibres, fatigue failure probability 79−32045
Hilbert space formalism for probability theory 77−60955
hydrology, discharge probabilities, empirical formulae 80−26559
Image mensuration by maximum a posteriori probability estimation 78−63015
independent choice ordering, probabilities 79−75325
indeterminism, and epistemic relativisation 77−78947
inductive statistical explanations, Hempel's high probability requirement 77−78946
information theoretical aspects of gravit. field, space-time fluctuations 77−57266
instrumentation representation 78−49788
integral geometry and geometric probability, book 77−60910
interplanetary magnetic fields, probability distrib. functions of microscale fluctuations during quiet conditions 78−4053
Jeu de Rencontre, critical elaboration of de Moivre's resolution *(Italian)* 80−4499
Jeu de Rencontre, work by Euler 1751 *(Italian)* 80−4500
Jeu du Treize, demonstration of Nicolas Bernoulli's formula *(Italian)* 80−4498
Karl-Hauptman matrix, joint probability distrib. of struct. factors in space group P1 79−23480
Karle-Hauptman matrix, conditional phase probability distributions of struct. factors 79−19120
laser scattered light intensity, recurrence rate correl. 78−66760
lightning points, frequency of impact calculations, for selected and arbitrary objects *(German)* 79−79923
LMFBR accident consequences, probabilistic anal. by response surface techniques 78−29595
long elastic wave scatt., inverse problem 79−55819
LWR nuclear reactor sabotage risk modelling 80−23001
magnetic hysteresis, probabilistic mathematical models *(Polish)* 77−80960
magnetosheath, microscale mag. fluctuations during quiet conditions, probability distrib. functions 78−4053
master equations, discrete, continued fraction solns. not obeying detailed balance 80−101758
master equations steady state soln., chem. react., two-photon laser appls. 77−9945
maximum entropy histograms 77−78961
measurement errors, distribution function determ. feasibility for various sample sizes 80−90806
metallic structures initial fatigue quality characterisation using equivalent-initial-flaw-size distribution 80−58978
meteor observing probability determ. from apparent luminosity function 79−21231
meteorology 79−16621
micromechanics of discrete systems forming macroscopic body, stochastic deformations 77−40
microsystems, nondistributivity, empirical correctness 78−28989
minor planets, orbital elements probability distribs. 80−46461
mixing and entropy 79−71348
mixing distance of set theory 78−77662
mixing flow and Palm measures *(French)* 78−89307
multiparticle production processes, cluster formation model, math. formulation 78−478
multiple comparisons for Poisson rates 80−98789
neutron transport, probability table method extension 79−584
noise and vibration control systems, probabilistic evaluation and appl. to single-wall *(Japanese)* 79−18582
non-Gaussian stochastic processes, operators method of anal. *(Russian)* 78−16627
non-Markovian probability density function, itinerant oscillator model of mol. fluid 78−47222
nondecay probability, small-time behaviour and Zeno's paradox 79−97241
nonequilibrium critical phenomena, probability density functions, fluctuations 78−54327
nonlinear diffusion-process, appl. of Onsager-Machlup function 79−44888
nonlinear statistical theories, fluctuation effects, truncation schemes of cumulant hierarchies 80−68133

probability continued
nuclear engineering, probabilistic systems reliability analysis for students 77−37698
nuclear fuel cycle strategy in Korea, probabilistic anal. 77−57726
nuclear fuel pin gaps, probabilistic distrib. within wire-spaced fuel subassembly 78−78448
nuclear plant specific risk studies, data specialisation, Bayes' theorem 80−47601
nuclear power plant fire frequency and core damage probability estimation 79−13461
nuclear power plant siting evaluation, environmental impact probabilistic assessment model 79−79412
nuclear power plant structure probable risk assessment, improved safety system research plan 80−797
nuclear power stations, probabilistic methods, safety assessment, Fed. Rep. Germany 80−106124
nuclear power stations, probabilistic methods in safety analysis and regulations in France 80−106123
nuclear power stations, structural reliability, conference, Berlin, Germany (Aug. 1979) 80−105422
nuclear reactor accidents and failure, reliability technique appl. 77−30653
nuclear reactor emergency core cooling system motor operated valves, failure criteria 78−70592
nuclear reactor safety, probabilistic anal., 1978 American Nuclear Society meeting, overview 78−82468
nuclear reactor safety analysis, systems engineering appl. 77−38359
nuclear safety analysis, methodology and appls. of probabilistic risk assessment 80−63352
nuclear safety evaluation *(French)* 77−18677
nuclear steam supply, emergency core cooling system motor operated valves, failure mode anal. 78−54866
nuclear vessels, probabilistic model for assessment of collision likelihood 78−5063
objective decentring modulus, probability density distrib. calc. 79−76798
optical propagation phenomena, higher-order skewness probability distribution excess coeffs. 79−50224
optimal stopping times, existence and characterisation results *(French)* 77−13586
patient safety design, probabilistic approach by appl. of Markov chains to n-element environments 77−37106
peak-detection probability for line spectra, stochastic model 78−78597
periodic inspection of meas. facilities, probabilistic confidence characteristic selection 78−77839
photon counting with dead time, inversion problem 80−99682
planetary doublet craters expected frequency 78−61777
planetesimals in primitive solar system, statistical behaviour 78−93130
plasticity, polycrystalline, based on dislocation processes 78−26621
Poisson processes subset selection procedures, binomial and multinomial problem appls. 78−36802
Polya probability distrib. and measure relative information 77−5640
polymer, crosslinked, probabilistic theory of structural and physical characteristics 80−5649
polymer, long, short range correlations in solution 80−59367
power reactor, off-site power loss probability estimation 79−13460
precipitator, electrostatic, particle separation prediction reliability analysis *(German)* 79−4072
pressure vessels, brittle fracture probability using reactor surveillance capsule data 78−80641
pressure vessels, probability of flaw nondetection 78−78479
probabilistic vector model for identification of intervocalic stop consonants 78−69114
probability foundations, modal frequency interpretation 80−12885
propensity theory, hidden variables, coin tossing appl. 80−42040
PWR, probabilistic anal. of interfacing system in LOCA 78−21678
PWR, selection of events for probabilistic safety assesssment 80−742
PWR LOCA, fuel rod behaviour, probabilistic anal. using response surface method 80−663
PWR pressure vessel reliability, failure anal. 77−74962
PWR steam generator tube rupture, probability distrib. for releases of ^{131}I and ^{133}Xe 80−13668
PWR steam line break, pipe rupture probability 80−18526
PWR vessel and primary circuits estimation of reliability, probabilities and adaptive models 80−106125
quantitative risk evaluation, risk projection and human factors as related to nuclear systems 80−13722
quantum and classical theories, probabilistic descriptions 80−36899
quantum field theory, review of probabilistic concepts 77−5975
quantum logics and ideal measurement 78−54237
quantum mech. foundations, conditional probability of a generalised probability theory 80−12949
quantum mechanical one-system formalism, locality and joint probabilities 78−54238
quantum mechanics, Lagrangian and Hamiltonian eqns. 77−26191
quantum mechanics, zero probability problems, teaching approach 77−41499
quantum observables, joint probability distrib. 79−12650
quantum probability calculus 78−54236
quantum probability in logical space 80−31579
quantum theory, conditional probabilities and statistical independence 78−77757
quantum theory, probabilistic formulation, hidden variables theory 80−62508
quantum theory and probability theory 79−97223
quartet theory, probabilistic approach 77−19808
radiation stochastic effects after partial body irrad. in radiography 78−69152
radiative transfer in supersonic flows, probabilistic approach 79−53712
radioactive isotopes, probability determ. of number of atoms at end of production 79−63637
radioactive materials, risk anal. of transport using Monte Carlo and probability methods *(Norwegian)* 79−13437
radioactivity and quantum mechanics unification, probabilistic conceptions 80−12946
radioimmunoassay, hypergeometric theory of competitive binding 77−77980
radiotherapy treatment planning, FORTRAN program for optimisation using complication probability factor 80−81686
rainfall intensities probability distrib. 79−25318
Rand-condition form generalisation in theory of chaotic movements, appl. reverberation 77−26147

probability continued
random noise and vibratory system, multivariate state probability expression using unified statistical treatment *(Japanese)* 79−18584
random variables sums, independent, Gram-Charlier-Edgeworth expansion 77−41461
random variables sums, independently and identically distributed, Gram-Charlier-Edgeworth expansion 77−41460
random walks, spatial structure and stability 79−49169
Rayleigh probability distribution, use of quantiles for construction of correls. 77−91291
reaction of continuous dynamic systems with complex form under time-space random fields 78−65767
reactor core melt frequency, probabilistic model using prob. of rare events 79−54526
reactor fuel enrichment, random-walk model of holdup time of gas mols. in separation process 79−22481
reactor large-bundle LOCA expts., fuel rod ballooning probabilistic analysis 79−13462
remote sensing, max. likelihood estimation of signature transformation algorithm 77−78497
renewal theory appl. to linear chain molecules, asymptotic form of partition functions 77−53835
risk analysis methods, practical applications 80−12894
risk analysis of nuclear systems, anal. of human performance 80−18475
river basin water resource, Pareto region, stochastic multicriterial problem in control 80−4055
S-matrix in boson theory, probability struct. in Euclidean domain 79−89071
sample sizes for comparing two proportions 80−98791
sand grain size distrib. functions 77−29999
scaling theory of transient phenomena near instability point 77−33945
schlieren interferometer, 3-D vol., radiation transfer, probability model 77−87818
seismic risk analysis of lifeline networks 78−65192
seismic risk evaluation for Upper Rhine graben 79−25207
severe local storms, automated 12 to 36 hour probability forecasts 80−77062
soil-structure systems, probabilistic frequency variations 77−3176
solar systems modelling, for space and water heating 79−57459
solid laser, passively mode locked, intensity maxima probability distrib. 77−34891
speckle, noncircular Gaussian patterns, statistical distrib. of phase 78−66761
speckle image digital processing 78−71053
speckle patterns, partially developed correlated, statistical props. 79−3629
speech waveforms, probability density functions 78−80890
statistical mechanics, foundations 80−22271
statistical theory of the calculus of probability, wave mechanics 78−54301
statistical time interval analyser with visual display 77−37850
statistical treatment of experimental data, book 78−77834
steady-state process, probability charact. error calcs. 80−42145
steel, alloy, Cr-Mo-V, fatigue, failure probability based on residual strength 78−68797
stochastic and ordinary differential eqns., connections *(French)* 77−37734
stochastic cellular systems, model *(German)* 80−90661
stochastic integro-differential operator, optimal non-anticipative policy *(French)* 77−17786
stochastic point process with continuous probability measure, non-parametric test *(French)* 80−57184
stream-pollution model with random deoxygenation and reaeration coefficients 79−70472
streamflow data, empirical, fitting of multivariate gamma distribution 79−34878
submicroscopic processes, dice games illustrating reactor neutron flux and radioactivity, teaching 78−12515
teaching of probability and statistics, rel. to tennis 80−41997
theoretical structure, measuring techniques, ensemble concept 77−9868
theory, conf., Tashkent, USSR, (Aug. 1975) 77−26150
thunderstorms, automated 12 to 36 hour probability forecasts 80−77062
transducer precision model, angle-digital quantities conversion error evaluation 77−82498
truncated Kullback statistic, objective function for fitting partially known probability vectors 77−37737
turbulence field mixing and decay analysis, use of significant dynamic length scales 79−86404
turbulent irradiance probability distrib. in saturation regime 79−76588
two-body reactions, rigorous formulae for statistical errors on zeros and partial waves 78−4527
two-phase flows, particle interaction, obs. and calc. 79−72875
unstable systems, repeated measurements effects, primary decay law in spark chamber 77−41562
unstable systems, repeated measurements effects, theory 77−22517
upward lightning stroke parameters *(German)* 78−57237
US testing by digital scanning, adjustable step technique 77−90574
vibratory system, nonstationary, nonlinear, with arbit. random input, effect of feedback operation on probability distrib. 79−14316
vision, contrast thresholds of random patterns 78−65020
von Neumann algebra, conditional expectations 78−45459
wave-packet, position probability, classical and quantum spreading, for teaching 78−24606
weather event at two locations, joint probability estimation 79−53480
weather forecasts, nonexistence of ordinal relationships between measures of accuracy and value 78−61503
weather prediction, normalised variance anal. for meteorological time series, F-distribution *(Chinese)* 80−67388
weather prediction, probabilistic model 79−39835
Weibull wind speed distrib. parameters, estimation using Weibull prob. paper and percentile estimators 80−50931
white noise direct product, noncausal stochastic integral *(French)* 79−44858
wind magnitude and persistence models 79−5583
wind speeds, probabilities calc. from parameters of truncated distrib. curve *(Russian)* 77−53157
zero probability of scientific laws 77−33820
ZPR, noise analyses, determination of kinetic parameters *(Rumanian)* 78−46139
H II regions density and ionisation, joint probability density function 80−77468

probes
see also electron probes; muon probes; plasma probes
3-dimensional probes, meas. errors *(German)* 79−80574
100 kHz to 300 MHz radiation hazard probe requirements 77−44760
acoustic ringing effects in pulsed nuclear magnetic resonance probes 78−86313
anemometer, calibration device, operational principle *(Polish)* 77−72391
aspirating choked-nozzle probe for gas density meas., time response 77−84351
automated rail flaw detection, US wheel probe variation problems 79−47862
axially symmetric expts., data reduction from line, differential and surface probes 78−89464
biological electric-field probes, effect of material interface on probing internal field 79−53204
brain cell, parylene (vacuum deposited polymeric coating) appl. 80−108607
bubble size, correction for wall effect in point probe meas. 78−9681
calorimeter probes for measuring high thermal flux 80−13080
cardiac output meas. by US transoesophageal probe 79−92315
cardiac output thermodilution meas., thermistor probe construction for use in small animals 77−64161
cholestric crystal microprobes, non-perturbing, for meas. in EM fields 78−16791
combustion, gas phase, probe sampling rate effect on sample composition 77−52691
conductivity, for dynamic measurements on non-metallic catalyst during adsorption and catalysis 80−13096
conductivity probe design for use with bridge instrument, wide range of test solns. 80−95110
conductometric, field disturbances in conducting fluid modelling *(Russian)* 78−231
crossed slotted tube resonator, double resonance NMR probehead 78−265
cryogenic technique in treatment of neoplasms of oral cavity and pharynx 77−78030
cryogenic temp. sensors, for use in EM fields 77−2655
cryogenic treatment device for (sub)atrophic rhinitis and pharyngitis 77−78028
cryosurgical probe, Stefan-like problem in biological tissue analysis 77−17005
current rpobe, noninductive, construction 78−4663
diagnostic probe, for intense electron beams 78−12787
dielectric microthermometer, non-perturbing, for meas. in EM fields 78−16791
direction-sensing water wave probe design 77−58819
dosimeter, evaluation of implantable elec. field probe within finite simulated tissues 78−40345
drag sphere velocity probe, miniature, development and testing 78−55705
echoencephaloscope, two-probe three-mode design 78−44567
eddy current, thickness measurement of plating layers *(German)* 79−85112
eddy current imaging flaw detection system 80−89426
eddy-current, rotary, for defects scanning and detection 77−90557
electric field meas., in presence of space charge, static probe 79−17448
electric field meas. probes, widebandedness, influence of parasitic resonances *(Polish)* 79−2783
electric field probe, dielec. insulated, for field meas. in finite heterogeneous biological bodies 79−2170
electric field probe, miniature 60 Hz 78−77930
electrical conductivity probe, for meas. in stratified NaCl solns. 77−52718
electro-optical, for liquids refraction index sensing *(German)* 77−5889
electrodeless conductivity probe for high-temperature and pressure measurements 80−52272
electrodynamic earphone, mag. field probe 79−34690
electrolytic cell resistance meas., differential recorder 78−86297
electron beam evaporation source with integrated rate control *(Hungarian)* 80−20798
electroplethysmograph for regional lung function evaluation 77−21647
electrostatic probe for absolute measurement of SAW amplitude 79−50543
EM, fibre optic telemetric linked, 0.2 to 12 GHz range 78−15859
EM field of surface magnetostatic wave meas. 77−41658
EM field probe, implantable design for finite biological body 77−21670
EM field probe, miniaturised antenna 79−26136
EM field strength meas., broadband antenna probes *(Polish)* 79−21722
EM flowmeter, sensitivity 79−68853
EM radiation probes, implantable, design factors 78−73258
even harmonic ferrite probes with axial rectangular pulse excitation, anal. 77−77704
expendable bathythermograph digital recording and display system 80−46318
fast breeder reactor boiler tubes, eddy current probe insertion for in service inspection, method development *(Japanese)* 80−822
feeler probes for surface roughness meas., error source 78−169
ferromagnetic, with square cross section, numerical computation of eddy current phenomena *(German)* 78−77951
ferromagnetic probe coercimeter, NDT of mech. props. 79−11749
ferromagnetic probe inspection unit for automatic inspection of welded tubing 78−56860
ferromagnetic probe magnetometer with synchronous detector, operational analysis *(Russian)* 79−44921
ferromagnetic probe unit, MD-10F, automatic 78−56861
ferroprobes characteristics alteration, by using composite cores 77−87796
FET probes for inproving CRO meas. 78−93667
fibre optic acoustical detector probe 80−91916
fibre optic probe for thermal profiling of liquids during crystal growth 79−68443
fibre optic temperature probe 78−208
fibre-optic, bifurcated, used in photo-optic measuring system 79−81569
film probes, flush-mounting, effect of probe-body temp. changes on stability 77−7482
fission reactor, void fraction measurement, RF local probe development 80−568
five-hole, for complex flow field meas. calibration and appl. 80−69951
fixed hygrometer probe for very dry gases *(French)* 79−54145
flame, flow patterns at probe sampling pt. *(Russian)* 78−35687

probes continued
flow, four-wire, with output signal digital processing, appl. to cylinder wake characts. 80−19541
flow direction probes for turbomachine technology 80−87824
flow meas., two-dimensional nonsteady, X-hot wire probe method *(Japanese)* 80−59134
flow measurement, hot wire and hot film temperature compensating circuits, temp. probe appl. 78−59510
flow measurement, novel arrangement for vel. vector meas. 77−72378
foam insulation material thermal conductivity meas., unsteady probe method *(German)* 80−31740
free molecular flow, impact pressure probe 79−41716
freely sinking probe horizontal velocity meas. interpretation 80−46321
Fresnel region mag. field intensity meas. accuracy 77−79132
gas binary mixtures, flowing, probe for conc. meas. 79−4098
gas flow dust content, temp. and speed meas. method 78−34216
gas flows, particle-bearing, probe measurement of electrostatic fields 79−75552
gaseous insulating materials, elec. pot. meas. by corona probe 80−82790
gradiometer, ferromagnetic probe, fault detection optimisation 78−53096
Hall, differential configuration for small mag. field detection, temp. matching 79−40592
Hall, induction meas. in small dimension magnetic loops *(Hungarian)* 78−4665
Hall effect, linearity improvement of type TLMK Hall probes *(Slovak)* 80−82795
hazard probes, plane-wave microwave power density precise calibration techniques 77−71341
heat flux meas., nonstationary method using probe 77−42942
HF SAW phase/amplitude meas. using phase sensitive laser probe 79−14171
hot wire 45° slant probe for Reynolds stresses and turbulence intensities 79−72967
hot wire tachometric, calibration instrument features *(Italian)* 79−72966
hot-film, calibration in liquids 79−27723
hot-film, heat transfer to substrate *(French)* 79−23381
hot-film wall shear probes, miniature, for biomedical appls., method for alignment 79−53262
hot-film wall-shear probes in liquids, calibration device 79−50823
hot-wire, flow reversal detection in unsteady flow 80−10333
hot-wire, submerging, wind generated wave flow meas. 77−7483
hot-wire, triple, for measurement of air vel., response and transformation eqns. 79−27718
hot-wire, used in subsonic airflow measurement, interpretation of signals 80−14857
hot-wire for measurements of turbulent shear flow, effects of orientation 79−27722
hot-wire probe measurements on flow field, effects of cooling law and probe adjustment 79−27721
hot-wire probes in low speed flow 79−82010
hyperaldosteronism screening test with rectal potential difference probe *(German)* 79−16323
imaging atom probe, using single time-gated channel plate 78−21276
impedance probe calibration, for vacuum meas. in single component two-phase mixture *(Italian)* 80−62677
in vivo probe for meas. of living tissue dielec. props., 10 MHz to 6 GHz 77−78071
in vivo probe measurement technique for determining dielectric properties at VHF through microwave frequencies 80−85542
ion sensitive FET's development review, biological applications *(French)* 77−70578
ion temperature, for ionosphere sounding by rockets, system designs *(Japanese)* 80−85838
IR gas analyser, non-dispersive, for industrial processes and environment protection *(Hungarian)* 80−55735
irradiated fuel rod NDT using encircling and probe eddy-current systems 79−9751
jet type noncontact probe for halide leak detector 77−87750
Kelvin probe for surface potential meas. in high vac. 77−71343
Kerr magneto-optic probe, small region meas. of Permalloy I-bars 78−68328
Kulite 2-probe synchronized sampling technique for measuring flows behind rotors, calibration 80−14865
laser Doppler anemometer measurement, effect of finite-size probe vol. 77−24036
leak detector pickups, halide, optimal flow rate determ. 80−48825
light probe for bubble detection in fluidised bed 78−30376
linear dichroism probes for internal electric field study 77−86325
liquid N_2 level detector for storage Dewar, teaching labs. 78−41125
lunar and planetary, Soviet achievements survey *(German)* 77−41283
machined surface layer structure determ. using Barkhousen noise probe *(German)* 79−24710
magneto-modulation sensor, even-harmonic type, performance study *(Russian)* 77−53958
magnetometric, calib. by supercond. solenoid using NMR *(Czech)* 78−29130
magnetostrictive US probes using extensional, torsional and flexural waves 79−50562
Microprobe Mole/plasma chromatograph system, for anal. of compounds on micron scale 80−101049
microwave ferromagnetic resonance probe, for eddy current detection of surface flames in metals 79−34254
microwave magnetic-field distribution meas. using new resonant scatterer 79−49211
microwave probe for subsurface soil moisture profiling 78−65939
miniature probe microphone using optical fibre 80−48534
murine malignant tumours, in vivo probe dielectric meas. 78−11761
myocardial transmural heat gradient instantaneous meas. 78−44661
near-surface defects, US detection and analysis *(German)* 80−93728
neurological, parylene (vacuum deposited polymeric coating) appl. 80−108607
NMR probe, for combined homonuclear multiple pulse decoupling and magic angle spinning 78−12735
NMR probe and preamplifier for low freqs., fast recovery and high sensitivity 79−35806
NMR probe using single IC for HF head for magnetic field meas. 80−62697
NMR probes, design 77−53967
NMR Varian XL-100-15 spectrometer, multinucl. 18 mm probe construction 77−57376
probes continued
nondestructive acoustic elec. field probe 80−47076
nuclear microprobe as analytical tool, review 79−87913
nuclear power station heat exchangers, eddy current probe for nondestructive testing of transfer tubes *(Japanese)* 80−81246
nucleonic probe ccts with noise rejection, low-level activity meas. 80−52833
oblique entry probes for examining pipe welds, determination of optimal inclination angles for piezoelectric plates 78−76808
oesophageal multiprobe for temp., ECG and heart and lung sound meas. 78−77146
open-ended waveguide probe/applicator combination *(French)* 80−3820
optical, for absolute meas. of SAW amplitude 79−28185
optical, for two-phase flow local void fraction and interface vel. meas. 78−83505
optical array probes evaluation for cloud particle size distrib. meas. 77−41220
optical fibre, use in remote inelastic light scatt. probe 80−58769
optical waveguide probe for Langmuir film props. meas. 77−40294
optoacoustic material probing and imaging, far IR 80−83559
oscillating conductivity probe, density and density gradient meas., hysteresis effect 78−32796
otpical probe for fluidised bed meas. 79−82000
oxide thickness monitor, mild steel nuclear reactor structures 77−67806
oxygen monitoring in process gas streams, sensor 80−52181
PC implant, Ni-Fe microelectrode array probe for electrophysiology 79−84049
phase distribution in two-phase steam flows, effects of probe position 80−87799
photoresistor contactless temperature indicator *(Russian)* 77−10023
piezoelectric probe, conversion ratios 80−69624
plasma impurity flux and differential wall changes, in Alcator-A Tokamak, surface probes 80−38664
pneumatic purge probes for tank depletion flow meas. 77−80236
potentiometric level indicator for electrically conducting substances 79−77312
pulsatile air flow, time-averaged stagnation pressure probe design 78−14116
pulsed NMR, anal. of homogeneous RF field delay line probe 77−49758
quartz tube orifice leaks for local, fast-response gas sampling to mass spectrometers 80−35609
quick sample change probe for magic-angle-spinning NMR in a superconducting magnet 80−31834
radiant heat flux portable direct reading measuring device, CERL flux-probe features 78−45633
rail joint, thermit-welded, US flaw detection probe 78−56852
resistance meter, based on spreading resistance probes *(Polish)* 79−88981
reverse flow sensing hot-wire probe 79−98838
RF, for bubble size and vel. measurements 80−6177
'Scalar' oceanographic probe, information exchange with 'Minsk-22' computer *(Russian)* 78−77363
semiconductor domain instability and resistivity profile meas., universal capacitive probe 80−31796
semiconductor probe point characterisation by footprint in porous Si 79−96243
semiconductor temperature testing probes, accuracy and thermal characts. 80−52201
single coil double resonance NMR probe for solid state studies 78−264
single crystal NMR probe and circuitry *(Chinese)* 79−35807
single-coil triple-tuned NMR probe for simultaneous stimulation of ^{1}H, ^{2}H and ^{13}C resonances 80−86364
sound separation probe for jet engine flowing duct noise meas. 78−13878
spectrophotometer dip probe bubble formation prevention 80−13154
spherical Pitot, for flow meas., construction and calibration *(Italian)* 80−69957
stagnation temp. meas. in hypersonic flow using fine W wire probe 77−79095
static pressure probe, incompressible turbulent boundary layer, wall interference effects 78−1762
static pressure sensing in 2D flow, wind effect on buildings 79−71403
superconducting, fast-response thin-film, for detection of second-sound shock waves in superfluid He 79−63237
superconducting thin film probe, for detection of second-sound shock waves in superfluid He 79−73355
surface geometry meas., signal processing and analysing device, Herbert-Sigma *(French)* 80−57254
surface potential probe for 77K operation and with nanosecond-response 78−12726
surfacing probe for ocean surface layer elec. cond. meas. 79−2392
temperature probe, for use with digital multimeter, −10 to 100°C range 79−6125
temperature probes used in microwave dosimetry, thermographic comparison 79−96521
thermal, for gas high stationary temperature meas. 80−95101
thermal cond. meas. cylindrical probe improvement 80−92033
thermal conductivity measurement of soil by probe method, minimisation of errors 77−17259
thermal props. of lubricants, joint meas., relative probe method 77−41600
thermistor, for biomaterial thermal conductivity and thermal diffusivity simultaneous meas. technique 78−57098
thermistor, heat transfer intensification effect in nonuniform elec. fields 77−57354
thermocouple probe, spherical heated, for perfusion meas. 79−92456
thermoelastic expansion flexible acoustic probe 80−16618
thickness gauge EM probe output signal linearisation 78−56862
thickness mode piezoelec. US probe design factors 79−68540
thin film growth measurement using galvanically separated quartz monitor probe *(German)* 80−11576
three parallel wire type, characts. flow meas. appl. 77−62314
thyristor p-n-p-n structure turnon parameter meas. by optical probe 77−57358
triple hot-wire type, air velocity meas. appl. 77−62315
triple-sensor, for turbulent flow-field investigations 80−100043
tubing, ferromagnetic probe coercive force meter, different heads 78−60943
tunnel location by cross-borehole EM probing 77−78545

probes continued
turbulent and high frequency fluctuating flow, mean static pressure measurement, hot wire anemometer and Pitot tube combined appl. 78−57889
two-dimensional space isothermal and nonisothermal turbulent flow *(German)* 80−28505
ultra-high vacuum compatible, thin film supercond. meas. appl. 78−49867
ultrasonic, calibration procedure, practical appls. *(German)* 79−81677
US, multielement, for immersion inspection of contact butt welds 77−90569
US, rocking-beam, radiation pattern, NDT appl. 77−90572
US bulk wave electromagnetoacoustic excitation 79−57195
US device for inspection of welded joints of tube headers 79−11746
US flaw detection, focusing probes 80−104383
US materials testing, imperfect coupling between probe and test piece, effects *(German)* 80−85122
US transmission line of probe for hot metal inspection, spurious signals 80−66754
US wideband spherically concave transducers, for wideband probes, exam. of basic characts. 78−72979
vascular occlusion treatment by cryothrombectomy and cryovenectomy 77−78026
velocity probes for non-uniform gas flow in large ducts 80−48829
VHF waveguide dielectric scatt. model for pulse-probe data interpretation *(Russian)* 80−62682
vibrating capacitor probe for surface and adsorption studies 78−10274
vibrating viscometer probe for measurement of viscosity of slurries, assessment 80−28586
voltage, nanosecond, transmission line model 77−26331
voltage probe, with subnanosecond rise time, for oscilloscopes 77−10061
water-wave height probe with calibration stabilized for changes in water conductivity 80−57280
xerographic cascade flow, carrier bead velocity distribution meas. probe 80−47136
Au ball probe, nondestructive meas. of C-V characts. of m.o.s. capacitor 77−1491
H high-temp. probe for proton magnetic resonance expts. 79−49234
^{3}H meter for Na coolant systems 79−9690
HgI_2 miniature probes for in-vivo medical appls., fabrication, spectroscopic evaluation 78−40308
Ni-NiCr thermojunction for multichip component temp. meas. *(German)* 78−202
O_2 molecule reduction flow probe for cerebrospinal fluid 79−100777
O_2 probe, applic. to steelmaking 77−21050
PVF_2 polymer probe for mapping pressure field from arrays 80−74669
Pt resistance temperature probes, constructional types and state of technique *(German)* 80−52213
S probe, coal gasification systems appl. 78−76947
Xe, for radiation contamination monitoring 80−27826

problem oriented languages
see also LISP
FORMAC73 for formula manipulation 77−41522
formula manipulation with FORMAC73 language 77−41522
geology, PLATO CAI system, TUTOR language 77−20
Interactive Simulation Language application to nerve cell kinetics 77−21507
MAUS, for coordinate measurement *(German)* 78−89432
MULTELMT for neutron activation anal. 78−85241
nerve cell kinetics simulation using Interactive Simulation Language 77−21507
nuclear event analysis program using EVAL language 79−89561
QAL: a language for nuclear physics data acquisition 79−89552
QAL, data acquisition language 79−89551
synchrotron control with NODAL 79−9987
TEDDY2 for partial differential equatn. solutn. 79−2613
TUTOR, geology CAI, PLATO system 77−20
VEGA 1 interpreter language for meas. evaluation in nuclear physics 77−65413

procedure oriented languages
see also BASIC; FORTRAN; list processing
CAMAL language for algebra, appl. to electron optics 77−38798
minicomputer high-level languages and real-time operating systems for scientific instrumentation 79−12778

process computer control
astronomical optical surface shaping automation methods 79−84675
BWR nuclear power plant reactor operation and management using minicomputer 79−81042
chalcogenide glass semiconductor film kinoform production *(Russian)* 77−14670
Colour printer quality and productivity improvements 79−93245
digital computer applications, conference, The Hague (1977) 78−49808
distillation column, analogue recursive computer appl. 77−43321
electron beam evaporation rate automation by ion current meas. *(Hungarian)* 80−16198
electron test accelerator, Chalk River, control computer 78−90004
glass melting, automatic control, adaptive subsystem 79−61553
high-speed scanning colour printer 79−93246
IC manufacture, automatic high vacuum coater, using minicomputer or microprocessor 78−48317
image analysis by LEITZ-TAS with process computer 80−68773
kraft mill effluents control in Finland 79−52988
kraft process black pulping liquor appl. 77−29085
large laser control system, evolution from Shiva to Nova 80−9894
liquid-liquid extraction column online control by modal control techniques 78−54865
machine tool computerised control for diamond-turned surface finish 79−98517
machine tool for diamond-turned surface accuracy improvement 80−1367
Macsym One, automated measurement and control system based on 'real world' signals 79−17402
metallurgical industry, mathematical models appl. 77−70276
metrological support to computer-aided process control, design and upgrading 80−185
microprocessor triac interface, used to control kiln temperature 78−45632
microprocessor-based experiment controller/interface 79−80590
mirror fiducial system compatible with computer-controlled polishing facility 80−74539
multibeam microwave therapy with computer control 80−3766
multisource deposition rate control using mass spectrometer as sensing element 78−72730
nuclear materials safeguards, microscopic process monitoring [for nuclear materials safeguards] of fuel reprocessing facilities to prevent material diversion 80−83153
nuclear materials safeguards in Th-U fuel reprocessing facility, computerised analytical process control system 80−78429
nuclear power stations, computer control systems for data acquisition and process control 79−22426
nuclear reactors, process monitoring and parameter estimation, multivariate signal analysis algorithms 80−47585
optical multilayer coating production with continuous thickness reoptimisation 79−76890
photofinishing printer response customisation 80−4793
plasma control by feedforward-feedback system with digital computer 80−75093
plastic materials, process computers for control and meas. of laboratory testing *(German)* 79−61821
polisher for small-tool fabrication of mirrors 80−14496
quartz crystal manufacture, Z-plate, Japanese technology 79−91575
small grinding and polishing tool control 79−98516
spray cooling, characts. and minicomputer control *(French)* 79−3889
steel industry heat treatment digital process control systems *(German)* 79−74166
steel mill, basic oxygen furnace, process monitoring, use of X-ray spectrometer 79−17586
TLD reader, microcomputer controlled 80−69044
torsional oscillation test instrument *(German)* 77−21344
VPE impurity profile computer-aided control 80−2962
whole-body hyperthermia with oesophageal temp. feedback control 79−92423

process computers
atomic particles physics anal., advantages *(German)* 77−65025
BWR plant diagnosis system, on line appl. 78−46146
Josephson, superconductive logic and memory devices and refrigeration requirements 79−58726
multiaxis neutron diffractometer automation 80−102417

process control
see also process computer control
arc spraying, frequency analyses application 79−83359
automatic measurement systems, meas. of characts., compound and element-by-element methods 80−62612
automatic smoke gas purification system *(Russian)* 77−52712
benzene production, using process chromatographs, monitoring procedure for pure product 78−92583
chromatograph appl., gas, high-precision, on-stream 78−53283
cold light production by high vacuum deposition of multilayer interference coatings *(German)* 80−53486
crystal growth from solution in multisection continuous crystalliser 80−2935
crystallisation process, controlled, from binary melt *(Polish)* 79−14708
distillation process equipment influence 77−39671
electro-optical system manufacture, test and process control changes 80−96044
electronics in nuclear science and technology 80−9347
electroplated coatings testing and control *(German)* 80−2967
fibre drawing process, control of diameter 79−50468
gas and fluid analysis, continuous and quasicontinuous methods *(German)* 78−44437
gas chromatograph, on-stream, high-precision 79−16111
genetic and physiological process control by magnetic methods *(Russian)* 79−2088
glass raw materials and batch prep., review 78−3085
glow discharge etching and sputter deposition, optical spectroscopy for diagnostics and process control 79−15606
grinding, laser-based noncontact gauging systems appl. 79−2745
heat exchanger, mathematical models of processes *(Dutch)* 79−75525
levitation melting process control *(Russian)* 78−80531
liquid level sensor utilizing pneumatic capacitor 79−71438
modular instrumentation system for nuclear industry 77−67780
nuclear fuel reprocessing, on-line control *(Russian)* 78−74460
nuclear reactor fuel element manufacture, process control analysis of ^{235}U in U-Al alloy components, neutron absorpt. method 79−85720
on-line wet chemical colorimetric analysis 80−81378
optical fibre drawing process control, optimisation theory appl. 79−90039
optical fibre fabrication and drawing processes 78−90532
ore dressing X-ray spectrometric analysis centre 80−86541
pellet fuels, γ-active, remotely operated plant for fabrication 80−32340
plastics sheet blowing and extruding, process identification for automatic process control *(German)* 80−81023
pneumatic process composition transmitter experience 77−44524
polymer melts, temperature measurement, thermocouple probe heat loss correction 77−65034
polyurethane foam, processing machines and systems, motor car components appl. *(German)* 80−71955
production processes, nonstationary Doppler effect, freq.-phase methods of investig., control 80−45464
pumping, automatic ionisation vacuometers, with cold or hot cathodes *(Czech)* 80−73376
radiation treatment of waste water. process control techniques appl. 79−96489
radioisotope industrial gauging applications, cross section needs 77−23312
recycle reactors for catalyst evaluation 80−3402
refractometer, REMAT 20, for chemical process monitoring 77−45885
refractory metal refining, at. absorpt. spectroscopy for continuous process control *(Russian)* 77−56302
rotary tube photographic processor design 80−4795
semiconductor processing, ellipsometry for dielec. layers meas. 78−49887
sintering uranium oxide, resistance furnace appl. and characteristics *(Italian)* 77−81239
steel industry, furnace control, UNITROL Σ series using microcomputer, Japan 77−53877
sugar industry, measuring transducers for automation *(Polish)* 80−42212
Tevatron Central Helium Liquefier, Fermilab, process control system 79−72012

process control continued
thermal analysis applications in electrical and electronics industries 79−75531
ultrasonic flowmeters 79−50832
wastewater treatment, activated sludge, model 77−17154
processors (program) *see program processors*
Procopiu effect
cylindrical empty sample, theory 77−20675
EMF in ferromag. material under torsion *(Rumanian)* 78−86986
ferrofluid, Procopiu effect 79−33519
ferrofluids, Procopiu effect with different vol. conc. *(French)* 77−43845
ferromagnetic film, thickness deposition control using transverse Procopiu effect 78−23306
ferromagnetic sample, harmonics generated by Procopiu effect 77−24729
Permalloy cylindrical film, magnetisation in crossed steady/alternating fields, easy axis dispersion influence 79−8024
Ni, hydrostatic press. effect on magnetisation Procopiu effect and hysteresis meas. 77−48023
product control *see quality control*
production
this heading is restricted to industrial production
see also assembling; manufacture; quality control; reliability
artificial hand with sensory feedback 80−36191
battery, alkaline, for camera appl., effect of discharge resistance obs. *(Polish)* 79−57420
Bourdon tubes, stainless, design and production *(Hungarian)* 79−85134
electron beam processing, dosimetry and quality control 79−49871
electronic speckle pattern interferometry of surface shapes 78−94380
laser mass production and radiated power meas. improvements 78−37064
medical equipment production efficiency and quality improvement 80−3830
optical factory, pilot prod., struct. and technological prep. 78−18079
optical fibres, Si, drawn at high temperatures preform method *(Italian)* 77−3646
photovoltaic cells, current production and future prospects *(French)* 79−100531
SAW device production and test programme progress report 78−59206
water-moderated-water-cooled reactor VVER-1000, power plant technology 78−82501
Ag-Zn batteries, miniature, fabrication and charact. *(Polish)* 80−93866
C fibres, engineering applications, production requirements and mech. props. 80−89168
Cd electrodes plastic bonded, for Ni-Cd accumulators, production methods 80−45659
Li metal for battery industry, sources and preparation 80−97781
Li-FeS_2 battery development, for electric vehicles and stationary energy storage devices ANL program with industrial participation 79−48113
production control
see also process control; quality control
chemical analysis of solution components, automatic photometric method for determining and controlling concs. 79−79350
monitored parameters for quality control in instrument production 80−186
optical instrument, precision, microcomputer-aided manufacture *(German)* 80−95116
optical projectors, MSP-4 objectives, photoelectric distortion meas. *(German)* 80−95976
pipes, hot-rolled, automatic mag. quality control on prod. line 80−108661
vacuum deposition and sputtering plants, automation and programming *(Hungarian)* 77−4736
P in PSG protective film for ICs, X-ray fluoresc. technique for rapid determ. 77−40612
Si substrates during sputtering and sputter etching, thermal history of substrates 80−25562
production schedules *see production control*
production testing
acoustic methods, review 79−43504
beam splitters, multilayer polarised light, laboratory and factory testing 79−27428
capacitance meters, direct reading using auto-ranging 78−32835
ceramic, automatic US defect detection for tile grading and packing processes 78−23885
cylindrical ceramics-metal laminated components, X-radiography 79−5123
defect-marking system, position-delay, pulse signals of scanning defectoscope conversion 77−90566
diamond turned surface production, interferometric test repeatability 80−74538
diffraction pattern sampling, industrial appls. 80−9015
electron beam welds, defect detection by acoustic emission *(German)* 77−56193
electronic component hermetic package water content anal. by mass spectroscopy 78−21263
fission reactor pressure vessel, safeguarding containment *(German)* 79−13433
laser interferometer application to length meas. in production *(German)* 80−18007
Loviisa Nuclear Power Station, in Finland, guarantee testing for output and efficiency *(Russian)* 80−102291
medical instruments, quality control of mass production *(Hungarian)* 79−48354
method of indirect comparison of luminous fluxes *(Polish)* 79−93200
microdensitometers for highly accurate metrology, industrial use 80−9017
nematic liquid crystal material analysis in production quantities 77−76309
nondestructive test methods, impact of electronics *(French)* 77−44425
objective lens of amateur camera, production quality, MYF test freq. selection 79−81581
objectives, quality testing by semiautomatic modulation transfer coeff. meas. 79−14124
optical couplers, reliability *(Swedish)* 77−776
optical gauging, noncontact, by remote image tracking 80−8961
optical glass fibres proof-tester 80−53412
p-n junction, volt-farad charact. meas. with semiautomatic installation 77−41643
production testing continued
precision measurement, image analysis of precison components *(German)* 80−42193
pressure vessels, C-fibre reinforced plastics, acoustic emission detection, immersion technique 77−1902
semiconductor manufacturing, interferometric method for surface deform. meas. 78−32793
steel, low alloy, welded joints, cracking during heat treatment, simple detection method 80−7724
thermometers, resistance, transformer bridge cct. 77−53906
universal optical string for surface coaxiality and linearity meas. 77−26269
US, automatic noise-blanking, pulse-timing discriminator 80−76472
vibration, multiple shaker considerations 80−79047
weld quality testing, US, in spiral-welded gas pipes 77−90550
P in PSG protective film for ICs, X-ray fluoresc. technique for rapid determ. 77−40612
professional aspects
air pollution instrumentation, evidence of electronic malpractice 77−37453
astronomer on Space Shuttle, payload specialist experience 77−64588
bioengineer's role in modern medicine 77−86673
biomedical engineering, Spanish and foreign professional and educative trends *(Spanish)* 79−83964
cancer management, potential impact of particle radiation therapy 79−20620
clinical engineers' acceptability to hospital administrators 77−21640
engineering, educational courses, for professional engineers, economic costs and course contents considerations 79−80414
field mobility in Czech physics-related institute and facilities 78−89292
frontiers in education, conference, Urbana-Champaign (1977) 78−81779
industrial meteorologists, trade assoc. and National Council 77−53193
industrial meteorology policy of American Meteorological Society 77−53195
instructional technology, malpractice suits problem 79−92907
International Union of Crystallography, early history 77−17738
Mathematical Association of America, activities relevant for physicists 78−41107
meteorologists with Ph.D., training and distrib. 77−67179
nondestructive testing qualifications, redefinition 79−9048
nuclear engineering programme, eval. for accreditation, design component role 77−41430
occupational exposure, otolaryngologist's role in hearing conservation 77−64055
radiation therapy technology manpower needs, problems and potential in United States 77−86701
scientific paper writing, component parts 77−53718
sediment research, society's needs and professional opportunities 77−64342
social responsibility of physicist 77−9846
program and system documentation
pacemaker automated test system developments 80−30944
TELEMED system user support organisation and program library 78−7491
program assemblers
microcircuit system software 79−89573
program compilers
AKAIHOSHI flexible real time software system for radio astronomy obs. 80−82214
program correctness proving *see programming theory*
program interpreters
FOCAL interpreter for curve fitting program on KIM-1 79−35693
holographic store automated test using BASIC M-400 interpreter *(Russian)* 79−94180
VEGA 1 interpreter language for meas. evaluation in nuclear physics 77−65413
program processors
see also program assemblers; program compilers; program interpreters
hierarchical computer networks for processing data base generated by X-ray CT scanner 80−81732
point to line data reduction, computer links and hardware processor test 79−45613
pre- and post-processing techniques for complex analysis 80−94965
program testing
ECG analysis programs, diagnostic statement reproducibility 78−7495
Minnesota code ECG program validation 78−7507
reactor protection computer systems, statistical verification of reliability 80−32417
program translators *see program interpreters*
programmed control
see also process control; production control
additive photographic film printers, programmed control of light metering valves *(Russian)* 80−95174
artificial pancreas programmed control technology *(German)* 79−16346
aspherics precision manufacture with programmed microelectronic control 80−1368
astronomical optical surface shaping automation methods 79−84675
automated sintering and hot pressing system 79−33961
automatic acoustic emission analysis system *(Russian)* 78−46866
automatic test equipment for inorganic material internal friction meas. 77−90541
camera exposure setting accuracy 79−75639
cardiovascular system contractility characterisation by programmed premature contractions 79−88113
coronary perfusion pressure programmable control circuit 79−92278
diamond turning precision machine tool system 80−69568
digital stepping motor control system for repetitive scanning of a monochromator 78−54355
evoked potential multi-channel data acquisition system, microprocessor controlled 78−11750
fatigue testing machine 77−1906
Fresnel lens manufacture digital control *(Russian)* 78−50884
high performance liquid chromatography with programmed runs 78−11583
image analyser control, diode matrix replacement by PROMs 77−22539
insect optical cells anal. using microcomputer *(German)* 77−86724
insulin release, electronically controlled piezoelec. pump and valves 78−53565

programmed control continued
insulin/glucose transfer regulation for diabetics, user programmable system *(French)* 79−39614
laser interferometry coordinate control system, for photogrammetric automaton 'Zenit' *(Russian)* 78−21103
lingual tactile sensory system, automated instrumentation for research 80−8205
materials testing, programmed loading unit for test machines 78−23900
meter for photosensors time characts., using programmed strobing of anal. zone 78−283
microphotometer, automated, SAMB, for morphometric and densitometric analysis *(French)* 77−10085
multichannel analyser, versatile programmable power supply 77−42218
neuromuscular motor structures, programmed multichannel electrostimulation apparatus 77−25585
NMR spectrometer, programming device for control of frequency synthesizers 80−22400
nondispersive IR analysers, programmable switching device for semiautomated multichannel gas analysers 77−77830
NQR spectrometer, digitally programmed bidirectional square-wave freq. mdoulation 78−21189
NQR spectrometer, programming device for a spin-echo installation 80−17972
observatory scanning spectrophotometer *(French)* 78−20638
optical surface programmed aspherisation accuracy rel. to tool size 79−72727
particle counter, programmable command data acquisition equipment *(French)* 77−54464
photographic duplicator microprocessor control system *(Spanish)* 79−17529
pulsed light source, programmed command unit 77−79163
resistance furnace programmed temperature regulator 78−86256
sequence controller for Harwell 6000 series modular instrumentation 78−24784
spectrometer automatic control unit for discrete recording 78−58049
stimulator, programming unit for prolonged cyclic stimulation 78−3685
stomatologic polymeriser for dental prostheses 79−57812
tachycardia suppression by programmed premature stimulation 77−81650
tetraplegics' jointed manipulator with joystick control 78−53581
thermal loading automatic control system, quick-acting 77−48609
thermoelectric thermometer checking unit 77−22548
I_2 laser, with programmed mag. field 78−33750
Nd:glass laser with numerical programmed control *(Russian)* 80−91811

programmer training *see training*

programming
see also analogue computer programming; computer software; interactive programming; program and system documentation; program testing; structured programming; systems analysis
education, university science course for talented secondary-school students 78−89282
heat transfer calc. appl. 77−7289
heat transfer calc. appl. 77−7292
human factor studies, conf., San Francisco, USA (Oct. 1977) 78−48742
microprocessor-based, programmable laboratory equipment controller and data acquisition system 79−6104
optical design education program, desktop computer appl. 79−84922

programming, geometric *see geometric programming*

programming, interactive *see interactive programming*

programming, mathematical *see mathematical programming*

programming, structured *see structured programming*

programming theory
algorithm design, computational complexing 77−17959

programs (computer listings) *see complete computer programs*

project engineering
see also design engineering; electromagnetic compatibility; quality control; reliability; scheduling; systems engineering
Appalachian Education Satellite Project activities and outcomes 78−12450
CERN 400 GeV proton accelerator 78−70651
EHV transmission line ground level gradient, small plants and animals biological studies 78−31856
European Space Agency projects (Dec. 1977) 78−61703
International Sun-Earth Explorer B minimum-model project 78−61702
International Sun-Earth Explorer mission 78−61701
magnetic containment testing for JET 78−54870
Maneri Bhali Hydel hydroelec. scheme, stage I, model, India 77−9452
METEOR project 79−8695
nuclear plant, FUGEN project, Japan, construction and start-up 78−86675
nuclear power, CANDU type reactor implementation in Pakistan 77−61596
nuclear power plants, construction and engineering problems, layout aspects 78−86702
nuclear power station construction, experience, Yugoslavia 77−65354
Taipower, completion of first power plant, construction experience, testing and start-up 78−86674
vacuum system engineering, integrated approach 79−67320

project evaluation review techniques *see PERT*

projectiles
see also ballistics; missiles; rockets; weapons
acceleration meas. using stroboscopic picture, teaching demonstration 78−36779
artillery projectile inspection by noncontact EM transducers 79−47872
artillery shell, experimental determination of mass-property/trajectory-drift relationship 80−8779
artillery shells, radiographic inspection algorithm speedup by array processor 80−108659
axisymmetrically rotating, stability of nonstationary motions *(Russian)* 78−24659
continuous-wave transmitting, passive array tracking 80−94955
fragmentation and momentum, teaching 77−45654
gas-gun projectile vel. meas., magnetoflyer method 78−49805
high-speed cineradiography 78−41395
javelin dynamics including body interaction 78−38184
multiple interior impacts on Pb target, hard target high vel. impact simulation 77−72145
penetration into targets, mechanics 78−18159
penetration mechanics, theoretical and experimental study 78−30173

projectiles continued
projectile motion, teaching to sixth-form level 77−60862
ricochet of dumb-bell shaped projectiles off sand 78−30172
ricochet of spherical projectile off water and sand 77−17804
ricochet of spherical projectiles off sand 78−26025
rotation meas., Brenneke slugs 78−45744
spherical and other shapes, forces developed during ricochet 78−59289
spinning spheres and cylinders, ricochet from water surface 77−11122
steel, liquid bath, shooting methods for projecting buoyant alloy additions, expt. and mathematical eval. 77−21047
teaching, range formula for above ground level launch 78−8190
teaching, symmetry and geometrical arguments 79−35463
thick target penetration model based on pressure bar force meas. 78−30174
trajectory of projectiles fired parallel and near free surface of plastic solid 78−83237
Ti-Al-V (6, 4 wt.%), targets, metallographic features after ballistic tests 79−79046

projectors (optical) *see optical projectors*

promethium
see also nuclei with .....
nuclear battery, characts. of luminophores and photoelements *(Bulgarian)* 80−72084
Pm^{3+} in molten $LiNO_3$-KNO_3, transition probabilities in absorpt. and fluoresc. spectra 79−50085
Pm^{3+}, intermediate coupling props., relativistic average of config. wavefunctions applicability 78−17574
Pm^{3+}:$POCl_3$-D_2O soln., visible and IR spectra, fluoresc. assignments *(French)* 77−66514
Pm^{3+} + UO_2^{2+} solution, nuclear pumped liq. lasers, LASL program 80−64011
^{144}Pm, in $PrIn_3$, impurity behaviour obs. using oriented nuclei γ-ray anisotropy meas. 80−71275
^{147}Pm fuelled betavoltaic pacemaker system status 77−81733
^{147}Pm, sealed sources for phosphor light sources *(Hungarian)* 80−91348

promethium alloys
No entries

promethium compounds
see also promethium alloys
No entries

prominences (solar) *see solar prominences*

propagation, wave *see wave propagation*

proportional + derivative control *see two-term control*

proportional + integral + differential control *see three-term control*

proportional + integral control *see two-term control*

proportional control
3.39 μm He-Ne laser frequency stabilisation without FM 79−55152
astronomical proportional control autoguidance system using photosil detector 77−49296
autoguiders for optical telescopes 79−75109
hand opening by proportionally controlled electrical stimulator *(Croatian)* 78−44693
incubators, portable, improvements 78−81055
laboratory temperature regulation cct. 77−45836
master-slave manipulator power-assisted grip system 79−9212
solar battery, charging networks and stepping motors, microcomputer mechanical proportional control 80−50987
temperature regulator for heating units and cryostats 77−37880

proportional counters
see also position sensitive particle detectors
$4\pi\beta$-γ coincidence method for radioactive source standardisation *(Rumanian)* 77−46472
4π proportional counters, spurious Malter pulses 77−54452
$^{10}BF_3$-paraffin neutron counter calibrated with six neutron sources 79−36474
alpha recoil gas proportional counter, neutron spectra meas. 78−5089
analog wire chambers for beam tuning 79−3267
applications in high-energy physics and other fields 78−9035
avalanche azimuthal spread around anode wire 79−45532
avalanche localisation and effects 78−46217
avalanche multistep chamber 79−9965
avalanche parallel plate detector, appl. to photofission expts. 79−76263
avalanche spatial distrib. 78−58543
avalanche square meter position sensitive parallel plate detector for heavy ions 79−93879
background determ. by hard cosmic radiation 80−69027
barometric effect on low level counting 78−33374
beam meas. of proportional wire shower counter and hadron calorimeter modules 78−37499
Benjamin detectors, on-line, real-time neutron spectrum unfolding 79−59297
Bevalac, computed tomographic radiotherapy beam profile reconstruction with multiwire proportional chamber 79−79631
chamber with signal-wire spacing of 10 mm 79−97939
chambers, accuracy of spatial arrangement and tension of wire electrodes 79−97938
charged particle detector system for high rate expts., drift-proportional chambers, operating parameters 78−33379
composite amplifier-discriminator cct., RMS noise meas. 77−54473
conference on nuclear power systems, Washington, USA (1978) 79−41045
corona counter, determ. of U content in solid waste mats. by α-detection *(Russian)* 80−27904
cosmic gamma-ray telescope in 10-30 MeV range 78−73638
cosmic ray air shower observation, counter prod. characts. and lifetime determ. 80−98526
cosmic X-radiation recording, 2 to 25 keV, optimal characts. 77−23375
counter telescope for neutron induced charged particle reactions, finite geom. correction 77−57815
counting rate depend. gain shift and space charge 78−74536
Crystal Ball data acquisition system 79−89531
curved crystal X-ray spectrometer, for HEAO-B satellite 78−49331
cylindrical, gas multiplication factor dependence on anode wire attachment 78−78560
cylindrical, methane filled, optimisation of energy resolution 79−13603
cylindrical, operation at pressures up to 100 atm 80−23249
cylindrical wall-less counter, characteristics 77−3224
cylindrical wire proportional chambers, electrostatic field formulae, distrib. and asymmetry 80−78493

proportional counters continued
data acquisition providing max. spatial resolution at high rates 79−45572
data acquisition system 80−42913
delay line chambers for Fermilab external muon identifiers 78−37489
delay line for position readout in wire chambers 80−18757
DePangher precision long counter and neutron dose-rate meters, calibration 80−47822
design principles and characts. of 3×1.5 m proportional chamber 80−69024
detector, for gas chromatograph-mass spectrometer system 77−36815
diamond-anvil press. cell for X-ray diffr. obs. with solid-state or proportional counter 80−75119
digital drift chamber digitizer system 79−45602
digitisers of time and pulse height, monolithic flash A/D convertor 80−63475
double proportional counter for measurement of radioisotope Auger electrons and X-rays 79−81129
drift, time projection chamber, performance 79−68148
drift chamber, bidimensional 77−30703
drift chamber, large cylindrical, for Mk.II detector at SPEAR 79−45561
drift chamber, parallel wire with variable field shaping wire voltages 77−394
drift chamber counter, missed counts and registration efficiency calc. 78−78594
drift chamber detector for high resolution gamma-ray astronomy 77−9660
drift chamber development 80−27879
drift chamber system for K+e elastic scatt. expt. at Fermilab, efficiency, accuracy 77−57809
drift chamber telescope for gamma-ray astronomy 79−21185
drift chamber with thin foil cathodes 77−83463
drift chambers, Ar-ethylene mixtures investigation 78−25391
drift chambers, losses and recording efficiency of electronic cct. 77−88347
drift chambers, soln. to right-left ambiguity 78−58545
drift chambers, space resolution study as function of gas press. 78−78583
drift chambers, spherical large aperture X-ray imaging chamber 77−30721
drift chambers for eπ and eK scatt. meas. 78−859
drift tube for large calorimeter ν detector 79−13592
dual proportional counter for recording transition radiation 80−63458
dual registration channel cct. based on hybrid IC 80−23266
ECIL preamplifier, modified for high counting rate Mossbauer studies 78−74546
electron avalanches, generated by thermionic electrons, pulse-height distrib. 79−6796
electron drift velocities as function of elec. and mag. variables in several gas mixtures 78−71424
electron scattering experiments, detection system, Saclay linear accelerator facility 80−52809
electron transport coeff. in gases used in proportional and drift chambers 78−58541
electronic device for registering signals, K405KhP1 IC (USSR) 80−91376
electronic discrimination of effective thickness 77−54440
electronics for proportional drift tubes 80−106241
EM delay lines readout in spark, proportional, and drift chamber appl. 78−74547
energy dispersive X-ray spectrometry using proportional counters, resolution 77−34504
fast electron f(z) meas. using short accelerator pulses 80−12275
fast neutron dosimetry techniques 79−20677
fast X-ray diffractometer based on a spherical drift multiwire proportional chamber with digital position encoder 80−90969
filmless chambers in high energy physics, review *(Russian)* 77−67938
flexible geometry hodoscope using proportional chamber cathode read-out 79−3297
focusing gas scintillation proportional counter 77−83461
gas, energy loss of relativistic electrons and its fluctuation 78−94171
gas, for X-ray analysis, atomic K-lines *(Czech)* 79−31323
gas counters of slow neutrons, edge effect 78−33384
gas filled, fast gas mixtures 79−76279
gas proportional detectors, relativistic charged particle energy loss 77−88362
gas proportional scintillation counter, performance and applications evaluation 79−3289
gas proportional scintillation counter for use in large area detector systems without photomultipliers 79−59302
gas proportional scintillation detectors with uniform electric fields, secondary scintillation model 80−74087
gas quality test 77−10550
gas scintillation, large-area focusing, for X-ray astronomy 79−25494
gas scintillation counter, for high count rate X-ray detection 80−14052
gas scintillation counter X-ray spectrometer performance figures astronomy appl. 79−48673
gas scintillation proportional counter, burst length discrimination system 78−21824
gas scintillation proportional counter, gas fillings, preliminary studies 80−58054
gas scintillation proportional counter, review 77−57826
gas scintillation proportional counter coupling to photoionisation detectors 78−82581
gas scintillation proportional counter for first Spacelab mission 79−25488
gas scintillation proportional counter for X-ray astronomy 77−71004
gas scintillation proportional counter of large area for X-ray astronomy 79−80222
gas scintillation proportional counter using a photomultiplier tube array 79−[illegible]94
gas scintillation proportional counters, large vacuum photodiode imaging appl. 80−58050
gas scintillation proportional counters, props. in soft X-ray detection 79−13600
gas scintillation proportional large area counter, X-ray astronomy appl. 79−45556
gas-filled, low-background, with Si cathodes 77−65406
gas-filled electroluminescent detector for soft X-rays; constr. and characts. 80−32569
proportional counters continued
gas-filled photon counter, for mirror X-ray telescope on Salyut-4 78−86746
gas-scintillation proportional counters, high resolution, for X-ray astronomy, developments 77−54439
graded-density cathode method for position determ. in multiwire proportional counters 80−87017
hard X-ray imaging instrument, for solar and cosmic sources 78−49332
HEAO-B, imaging proportional X-ray counter 78−40823
HEAO-B monitor proportional counter instrument 78−40822
HEAO-B X-ray telescope, gas control system 78−40827
heavy particle with single positive charge, search in H_2, D_2 *(Chinese)* 78−876
helical cathode position sensitive proportional counter system for use in a broad range spectrograph 78−82578
helical delay line position sensitive proportional counters for mag. spectrometers 79−68160
high density, low energy neutral particle imaging 79−5399
high pressure proportional counters operating in pure hydrogen 79−3296
high resolution gas scintillation proportional counter for studying low energy cosmic X-ray sources 80−58052
high-energy particles detection by electronic method, principles of spark, streamer, proportional, drift and hybrid chambers *(Czech)* 77−42213
high-pressure proportional counter at low temperatures 80−23250
hybrid focal plane detectors for heavy ions 79−68163
hybrid MWPC gamma ray detecting system for applications in nuclear medicine 79−5397
hybrid spark chamber for radioisotope distrib. meas. 78−46227
imaging Cherenkov detector using gas-filled MWPC, photoionisation of triethylamine 80−91400
imaging gas scintillation counter for X-ray astronomy 80−98551
induction wire proportional counter with sub-mm positron resolution 80−91399
inert gas and mixtures, detection gas suitability for proportional scintillation counter *(German)* 78−41901
inert gas mixtures for proportional counters, Penning ionisation effect on resolution 77−26936
large load characts. of 3×1.5 m proportional chamber 80−69025
large multiwire proportional chambers for experiment NA3 at the CERN SPS 80−102388
large-area gas-scintillation proportional counters for in-vivo measurement of plutonium and americium 80−58086
large-volume proportional gas counter for measuring low concentrations of tritium 79−26822
Lass spectrom., performance of PWC cluster logic trigger 79−76262
limiting accuracies in multiwire proportional and drift chambers 79−3298
linear position sensitive, tests on X-ray diffr. goniometer *(French)* 77−31557
linear position sensitive proportional line scanner for β-emitters 79−31330
liquid H chamber Lyudmila, electronic apparatus for expanded diagnostic system 80−23265
liquid scintillation counting, quench monitoring, H Number concept 78−82576
liquid xenon proportional scintillation counter, detection of ^{207}Bi conversion electrons 79−45563
low level activity meas. of ^{3}H and ^{14}C using multielement and cylindrical proportional counters, comparison *(Czech)* 80−52818
low-background detection system for neutron reaction expts. 77−54395
low-pressure chamber with high space resolution 78−870
low-temp. counter for Mossbauer spectra meas. 77−10542
magnetic large acceptance spectrom. using wire chambers 78−46207
magnetic spectrometer, reconstitution of heavy ion trajectories 78−70684
magnetic spectrometer, SPES II, use with multiwire props. counters of three-body nuclear reaction study *(French)* 79−708
magnetosphere proportional counter, with thin mica windows, for low-energy particles 80−109260
MEA, magnetic detector at Adone 78−33367
methane, proportional counter gas, primary ion pairs distrib. prod. by $C\text{-}K_\alpha$ source 78−29704
methane filled, influence of electron avalanche KE on gas amplification factor 78−50439
methane filled telescopes for fast neutron spectrometry 80−37683
microdosimetric results from ionisation chamber and proportional counter compared 80−9429
microdosimetric studies with low LET radiation using cylindrical walled and wall-less proportional counters 80−36140
microdosimetry, interpretation of instrument lines of ionisation pulse spectrometer 77−73595
Mossbauer conversion electron spectroscopy at high temp., proportional 80−27886
Mossbauer spectroscopy, conversion electron, cryogenic proportional He counter 80−69010
Mossbauer spectroscopy, cryostat and proportional counter design 79−54238
multianode counters, wire cathodes 77−34521
multianode cylindrical proportional counter for position sensing at high count rate 80−5446
multichannel, appl. to thin layer radiochromatogram anal. 78−77174
multielement, anticoincidence techniques for measuring low T activities 80−27874
multielement proportional counters, electrostatic problems 79−93877
multielement proportional counters for low-level ^{3}H and ^{14}C counting 79−76287
multigap proportional wire chamber system for multiparticle spectrometer 79−3271
multilayer gas proportional counter system, CM CERN external particle identifier 79−45530
multilayer large scale detector, performance and relativistic rise meas. in 20-110 GeV/c range 78−82577
multiwire, flat helical lines for position readout along anode wire 77−54426
multiwire, for lung function study *(French)* 77−37035
multiwire, operation principles and appls. 77−18745
multiwire, Xe-filled, use as detector in bone mass meas. 78−15884
multiwire and drift chambers for the Omicron spectrometer 79−3277
multiwire and drift proportional chambers, design, operation, appls. 79−743
multiwire and drift proportional chambers 80−47826

proportional counters continued
multiwire chamber, frameless, cylindrically shaped, using charge division readout 77−38556
multiwire chambers, photoionisation process in gases, Cherenkov ring imaging 77−54448
multiwire cylindrical, two concentric series, electric field config. 77−6614
multiwire drift chambers, left-right assignment 78−58544
multiwire gas counter for VUV region coordinated meas. 79−67384
multiwire gas counters, photoelectric polling 79−68141
multiwire proportional chamber, corona discharge region effects *(Chinese)* 79−93887
multiwire proportional chamber, low mass, self triggering, cathode coupled coaxial-cable delay-time readout 77−57813
multiwire proportional chamber, shift register read out system 78−86736
multiwire proportional chamber, small design, construct., performance, electronics 78−17507
multiwire proportional chamber charact. using matrix cathode 79−81136
multiwire proportional chamber for identification of relativistic particles 80−23256
multiwire proportional chamber readout system, CAMAC test 78−17510
multiwire proportional chamber with analogue data plotting 78−78566
multiwire proportional chamber with anode wire winding pitch of 1 mm 80−23257
multiwire proportional chamber with short resolution time, high accuracy bidimensional readout 77−57810
multiwire proportional chambers, adaptions and appls. in medicine 77−86618
multiwire proportional chambers and drift chambers, charact. and appls. 77−14307
multiwire proportional chambers with delay line readout, factor contributing to position resolution 77−54425
multiwire proportional counter, electron capture ratios, calc. of corrections 78−29703
multiwire proportional counter for microdosimetric studies 78−20286
multiwire proportional gamma camera for imaging $^{99}Tc^{m}$ radionuclide distribs. 78−53493
multiwire proportional quantameters, performance predictions by Monte Carlo methods 79−3294
muon identifier, external, for Fermilab 15 ft bubble chamber, design, performance 77−6629
muscle contraction, time-resolved X-ray diffr., data-collection system *(Japanese)* 80−46108
MUTRON, cosmic ray mag. spectrometer, MWPC trigger system 78−55081
MWPC, γ-image blurring reduction by delay line readout 78−37492
MWPC, angular localisation of proportional chamber avalanche 78−78584
MWPC, anode modulation effects of X-ray beam positions 79−76282
MWPC, appl. as energy loss detector for the ISR 79−3331
MWPC, appl. of large-scale electronics 80−106235
MWPC, appl. to radiation localisation problems in medicine and biology, review 79−5432
MWPC, avalanche ang. localisation 78−50434
MWPC, Bellcord−a multilevel fast preprocessor for 1024 ECL channels 79−45577
MWPC, beta-ray imaging device for radiochromatography 80−102387
MWPC, CAMAC readout system 78−46248
MWPC, CERN Omega Spectrometer, modular trigger basic techniques 80−58104
MWPC, clinical, low energy radionuclide distrib. 80−61679
MWPC, compact low mass system of four cylindrical chambers 80−14046
MWPC, correcting codes for information registration 78−94176
MWPC, counting gas props. at low pressure 79−85864
MWPC, cylindrical, event triggers, correlation of wire addresses 80−58092
MWPC, cylindrical, soft X-ray detection in pp̄ spectroscopy 79−3279
MWPC, delay line readout of anode wires 77−38571
MWPC, delay time distrib. meas. *(Chinese)* 80−23261
MWPC, design and construction, for high count rate, Mossbauer spectroscopy 79−13580
MWPC, drift chambers and time projection chambers, development, operation and appl. *(Italian)* 80−879
MWPC, drift time meas. electronics 79−3327
MWPC, external muon identifiers at CERN 78−37488
MWPC, fast, data encoding system for proton tomography 79−92337
MWPC, fast analogue logic 79−13605
MWPC, flat area detector data acquisition system for X-ray crystallography 80−91381
MWPC, for cosmic drift X-ray imaging 79−41063
MWPC, gas amplification factors and detection efficiencies 80−74079
MWPC, gas gain and Diethorn eqn. *(Chinese)* 79−76301
MWPC, gas ionisation by double photon absorption using pulsed lasers 80−99414
MWPC, heavy ion detectors, book contrib. 79−31335
MWPC, heavy ion timing at very low pressure 79−93884
MWPC, high accuracy chambers, progress 78−33391
MWPC, high press., for X-ray astronomy 79−5748
MWPC, high-flux fast readout system based on new monolithic integrated ccts. 78−37491
MWPC, IC tapped delay line readout 80−5455
MWPC, improvement of position resolution from delay line readout 78−74543
MWPC, in external muon identifier for BEBC performance and data handling 79−730
MWPC, induced charges calc. at individual anode wire at the cathode 78−78585
MWPC, interwoven grid wires for second coordinate readout 80−27897
MWPC, large, tension control device 78−70703
MWPC, large area, high-background rejection 78−93108
MWPC, large cylindrical dual coordinate 80−18759
MWPC, large system for photon beam expt. 78−94162
MWPC, lateral distrib. of cathode charge 79−36470
MWPC, linear read out electronics, hybrid preamplifier realisation 80−58091
MWPC, localisation of minimum ionising particles using cathode induced charge centre of gravity readout 80−32576
MWPC, localisation of X-ray quanta 78−62678
MWPC, low-level ^{14}C and ^{3}H meas. 79−6800
proportional counters continued
MWPC, low-pressure, subnanosecond counter for heavily ionising particles 77−34519
MWPC, missing data reconstruction in principal component anal. 78−17537
MWPC, modulation of anode signal in soft X-ray detection 79−18081
MWPC, multi-delay line cathode readout 79−45573
MWPC, nondestructive readout system 79−3315
MWPC, operation as drift chamber 77−54455
MWPC, optimum geom. for strip cathodes or grids for avalanche localisation along anode wires 79−76274
MWPC, position determ. method using graded density cathodes 80−102396
MWPC, position sensitive, fast delay line readout 78−37490
MWPC, position sensitive, pulse shape from cathode RC Lines, zero-cross time meas. 80−58038
MWPC, position sensitive for fission fragments with large solid angle 77−34517
MWPC, position sensitive system with digital read-out for Munich Q3D-spectrograph 77−10549
MWPC, pressurised, for electron detection 77−14312
MWPC, pressurised, for neutron imaging, gas density, cathode biasing, effects on resolution 78−37518
MWPC, programmable track selector 79−3316
MWPC, rectangular electrode frame prestressing and deformation 78−29708
MWPC, remote readout system, pulse-width modulation circuit 79−26847
MWPC, review of operating principles and functions 79−3293
MWPC, secondary beam profile monitor 79−6783
MWPC, spherical drift chamber area detector for X-ray crystallography 79−41073
MWPC, very low press. operational props. 80−58043
MWPC, Xe filled X-ray imaging, counter, spatial resolution improvement by pulse height selection 77−18744
MWPC and drift chambers, operation principles 77−83465
MWPC and drift chambers, properties 79−72195
MWPC appl. as focal plane detection system for mag. spectrograph 79−3295
MWPC appl. high count rate X-ray detection 79−3292
MWPC appl. in multiparticle spectrometer, description and performance 79−3275
MWPC appl. in recoil spectrometer 79−3274
MWPC appl. to energy loss meas. 79−3330
MWPC appl. to molecular biology 79−5433
MWPC as area detector for protein crystallography 78−65166
MWPC at LAMPF, neutron physics programme 77−26951
MWPC avalanche initial angular width determ. 79−31327
MWPC compact chambers and electronics for crystal ball detector 79−45534
MWPC construction for large aperture spectrometer 80−102381
MWPC focal plane detector system with digital readout 79−68158
MWPC for beam definition in precision total cross section meas. 79−3268
MWPC for Fermilab single arm spectrometer 78−82585
MWPC gridded drift chamber for X-ray detection 78−70694
MWPC high resolution system for inclined tracks, focal plane instrumentation 77−30722
MWPC in big mag. spectrom. as counter hodoscope for fast majority discrimination 78−33392
MWPC in synchrotron beam spectrometer, performance under very high fluxes 79−3272
MWPC instrumentation for CERN SPS secondary beams 78−46206
MWPC on cube lattice 79−93875
MWPC positron camera, 3-D iterative reconstruction method 78−40302
MWPC positron camera, two detector, appl. medical imaging 79−5398
MWPC read out, fast clustering processor 79−76304
MWPC readout system 78−17505
MWPC rotated, drift time relations and their advantages 79−3306
MWPC to defect vac. UV photons from Cherenkov radiation 79−18078
MWPC using EM delay lines, read-out system *(French)* 77−88349
MWPC wire tension control system 80−102397
MWPC wire tension meas. by non-contact method 80−74081
MWPC with analogue read-out, high energy e⁻/γ detection 79−13593
MWPC with cathode read-out for separation of EM and hadronic showers 79−3273
MWPC with drift gap for ionisation meas. 77−14311
MWPC with high spatial resolution, construction and efficiency meas. *(Italian)* 80−9452
MWPC with wire plane cathodes, extension of standard formulae for elec. fields 80−99413
MWPC X-ray drift chamber for soft X-ray detection 79−18071
neutron counter development, electron drift vel. simulation 80−48843
neutron detector, position sensitive, high precision position readout 80−58063
neutron detectors, self-powered, sensitivity determ. on neutron flux density 80−52817
neutron dose and quality factor meas. by tissue equivalent proportional counters 80−58079
neutron gas proportional α-recoil spectrum 80−5433
neutron primary beam and shielding radiation quality and absorbed dose obs. 80−12281
neutron sensitive instruments, calibration using novel source emitting neutrons around 0.5 keV 77−6615
neutron spectrometry by means of the stilbene spectrometer and hydrogen-filled proportional counters 79−63860
neutron supermonitor 4-NM-64 with control of long term stability of meas. 78−21808
neutrons, thermal, energy depend. detection efficiency of cylindrical counter, wall effect, calc. 77−57803
nuclear ship streaming neutron meas. by two-detector method 77−46408
nucleon polarimeter for 100 to 500 MeV range 78−82599
one-coordinate detector for rapid multisnap recording on X-ray pictures 78−62282
optical gas-discharge chambers in mode of pulsed proportional amplification 79−726
optimisation for long term counting 79−76286
pair spectrum, high resolution for medium energy photons 79−31312
parallel grid imaging proportional counter optimized for detection of low brightness stellar XUV-sources 80−58049

proportional counters continued
parallel plate imaging proportional counter and its performance with different gas mixtures 79−45533
peak shifts and space charge effects 78−74537
photon counter, meas. of energy albedo of backscattered photons 80−99408
photon counter with proportional response 80−87021
planar symmetric multiwire proportional chamber, 500×500 mm^2, construction and charact. 79−97951
position sensitive, charge division mechanism on resistive electrode 79−45538
position sensitive, digital processor 77−26941
position sensitive, for X-ray residual stress meas. *(Japanese)* 80−11853
position sensitive, X-ray detectors, linear, circular, two-dimens. 78−62281
position sensitive 1.4 m ΔE-E range detector of Heidelberg Q3D mag. spectrograph 79−45566
position sensitive detector, construction *(Spanish)* 77−46464
position sensitive detector for thermal and epithermal neutrons 78−25390
position sensitive gas proportional neutron detectors, microprocessor testing method 78−70692
position sensitive gas scintillation proportional counter for X-ray astronomy 80−58053
position sensitive neutron detector using (n,γ) on ^{157}Gd, ^{177}Hf foils, proportional chamber detection of conversion electrons 78−37517
position sensitive proportional counter, resistive wire, multi-anode, focal plane detector 80−63464
position sensitive proportional counter for a β-ray spectrom. 78−86732
position sensitive proportional counters as focal plane detectors 79−68159
position sensitive proportional detector system for focal planes of multigap mag. spectrograph 77−54454
position sensitive RC line encoded counters 79−45537
position sensitive wire counter, heavy-ion appl. *(French)* 77−34516
position-sensitive, delay-line termination, timing-signals extraction 77−402
position-sensitive, RC-line encoded, using low-resistance, metal wire anode and active load capacitance 79−54745
position-sensitive, RC-line encoded proportional counters, recent improvements 79−9963
position-sensitive counter for neutrons 80−63459
position-sensitive proportional counter, direct position and time digitizer 80−58090
positive charge centroid direct meas., avalanche mechanism clarification 78−37486
positive ion effects in large-volume drift chambers 79−22541
positive ion mobility in gas mixtures 77−27646
positron annihilation studies using high-density proportional chambers 80−25478
positron camera proportional chamber, Fourier deconvolution technique 78−40297
positron image reconstruction in nuclear medicine, three-dimens., fast iterative method 78−7443
positron sensitive neutron detector 77−38566
pressurised Xe-filled multiwire proportional chamber for radionuclide imaging 78−48871
propane, ionisation loss meas. in region of relativistic rise 79−54743
proportional and drift chambers in applied research, review 79−26824
proportional tube with helical delay line 79−3313
proton counter telescope, efficiency for 89-466 MeV protons 77−57843
proton recoil, fast monoenergetic neutron fluxes meas. procedure anal. 78−17478
proton recoil proportional counter tests at TREAT 80−58072
proton spectrometer/polarimeter for photoreactions below 1 GeV 80−18751
proton-recoil counter technique for measurement of fast neutron spectrum 80−9447
prototype CCD system for the time projection chamber 79−45575
pulse height fluctuations, resonant ionisation studies 78−90025
pulse shape discrimination technique in a proportional counter *(Chinese)* 79−93867
PWC electronics system for high rate situations 79−26844
radiation loading effects on charact. of counters filled with pure Xe 77−23374
radiographic installation based on proportional chamber 79−67449
radioisotope imaging with Xe-filled multiwire chamber 79−49901
readout system for MWPC of focusing spectrometer 79−3280
recoil and fast particle spectrometers for 5 GeV π+^{4}He study 78−82569
recoil spectrometer for 5 GeV pion-He interactions 78−90011
relativistic charged particle identification by ionisation energy loss with delta ray suppression 79−85863
Relativistic charged particle identification by ionisation loss counters 78−70696
relativistic electron energy loss distribs. in thin gas layers of proportional counters 80−99429
relativistic electron ionisation loss, transition radiation effect 78−25389
resonance neutron radiography using a position-sensitive proportional counter, appl. to meas. of nuclear fuel 80−13597
RNB-76 monitor for low energy beta-emitter contamination 79−36486
Rossi counter equivalent dose meas. in high-energy radiation fields 80−94376
scintillating imaging proportional counter as X-ray to light image convertor 77−65063
scintillation, built-in K getter 78−29707
scintillation in Ar, Kr, and Xe 79−81131
scintillation large area gas counter for X-ray astronomy 78−49321
scintillation large area gas counter for X-ray astronomy 78−49322
sealed position sensitive hard X-ray detector having large drift region for all sky camera with high angular resolution 79−48675
secondary emission multiwire chamber for GANIL cyclotron beam tuning 79−54733
sectional flow, high background, γ-ray detection for Mossbauer spectroscopy 79−727
segmented cathode drift chamber, expt. study of signals 79−41074
self-triggered liquid xenon drift chamber by the use of proportional ionization or proportional scintillation 79−45562
shaper amplifier for proportional chambers, logical microcircuits and high time resolution 78−5103
simultaneous determ. of three elements by X-ray fluorescence 80−40786
proportional counters continued
single 1 m wire position sensitive counters for low ionisation particles 80−5441
single atom detection in particle tracks 80−9475
single wire proportional counter, heavy ion detectors, book contrib. 79−31335
small low-background counter for X-ray astronomy 78−29705
SNM-57 neutron counter, intrinsic background meas. 77−65399
soft X-ray sealed gas electroluminesc. detector, design and charact. 79−733
solid-state integrated cct. micro-detectors for high energy experiments 77−30705
SPEAR Mark II shower counter system 80−58031
spherical counter with isotropic sensitivity for soft γ-radiation 78−61732
standard long counter side-on response to fast neutrons 79−22548
stop detector for low energy particles *(Chinese)* 78−86740
superconducting mag. spectrom. for cosmic ray flux meas. 78−25383
tapped delay line focal plane detectors for mag. spectrometers 79−68161
thin-window, rocket-borne, gas press. control system 78−17512
time projection chamber multichannel ADC and readout system 79−45590
time-dependent properties of proportional counters SRPO-304 used with scintillation detectors 80−42894
time-resolved X-ray diffraction counter and data acquisition system 78−45758
tissue equivalent, meas. of photon dose fraction in neutron radiotherapy beam 78−3605
toroidal, Mossbauer spectroscopy appl. 78−33364
tritium counting sensitivity increase using completely labelled ethane as internal gas sample 79−54741
tritium detection in gases and liquids, state of art *(Czech)* 77−86403
two-coord. X-ray detector 78−62284
ultrasoft X-rays, detection with variable geom. proportional counter fitted to TEM for microanalysis 77−48712
UV photoionisation detector, operation with Cherenkov counter 79−26835
wall-less tissue equivalent counters, performance evaluation in microdosimetric work 79−13599
walled and wall-less proportional counter characteristics and microdosimetry 80−26371
walled tissue equivalent counters, performance evaluation in microdosimetric work 79−13599
wire chamber, high current mode of performance 78−70701
wire chamber conf., Vienna, Austria, 1978 79−3291
wire chamber powering, current-limiting technique 77−54424
wire chambers, sense wire damage 78−70699
wire chambers system for particle coords. meas. in π$^-$ beam 78−9025
wire devices with resistive cathodes, detection of induced pulses 78−70691
X-ray, position sensitive counter, appl. for time-resolved diffr. 77−13831
X-ray, soft Lexan coating on polypropylene window to eliminate UV sensitivity 79−74273
X-ray and neutron small angle scatt. recent developments 79−10750
X-ray detection by a proportional chamber 78−86739
X-ray detection for fluorescence anal., proportional counter with slight pulse amplitude shift *(German)* 78−46213
X-ray detector, position sensitive, for steel residual stress meas. 77−56211
X-ray detector, wall effect elimination, method 78−4753
X-ray emission meas., on Salyut-4, extraterrestrial sources 78−28521
X-ray fluorescence, spectrom. for Viking Lander 78−40792
X-ray gaseous discharge counters, ageing mechanism 78−78574
X-ray imaging gas scintillating proportional counters, performance in medical appl. 79−2153
X-ray low energy calibration sources for proportional counters using radionuclides 79−705
X-ray polarimeter, Bragg crystal, using position sensitive proportional counter 78−74117
X-ray position sensitive detector, curved, for crystallography appl. 78−63635
X-ray position-sensitive detector, employed in diffractometer, geometrical problems, stress measurement use 79−85205
X-ray powder diffractometer proportional counter detector system, digital read-out 78−4751
X-ray proportional counter background reduction by leading-edge discriminator 78−78561
X-ray scanning modulation collimator instrument for HEAO-A satellite 77−71003
X-ray spectrometer, proportional counter as input for meas. chain electronics 78−40826
X-ray spectrometer appl. 79−18088
X-ray spectrometry, proportional counters and counting electronics *(French)* 77−74564
X-ray stress anal. using position-sensitive proportional counter 80−1498
X-ray stress meas. of C steels, appl. of position sensitive proportional counter *(Japanese)* 78−64791
X-ray telescope for Aryabhata satellite project 79−84638
XTR-detector, Monte-Carlo simulation, 0.5-5 TeV cosmic ray hadron interactions *(Russian)* 79−49564
γ ray angular correl. meas. from e$^+$ annihilation in solids 79−4869
μ detection, construction of insensitive regions 79−3305
Ar, ionisation loss meas. in region of relativistic rise 79−54743
Ar, liquid, calorimeter, electron and proton response 80−47832
Ar-CH_4 proportional counter, light emission obs. 80−78488
Ar-N_2 gas scintillation MWPC for high-intensity 5-10 keV X-rays 78−82575
BF_3 in polyethylene sphere, secondary standard for total neutron prod. cross sections 77−23381
BF_3 proportional counter, high press. *(Japanese)* 78−66453
BF_3, response functions of spherically moderated neutron detectors 80−37687
^{10}B, neutron cross section standards, detection techniques 79−9970
CH_4 filled, geom. effects on proton recoil spectra 80−14050
CO_2 filled, continuous examination of counting efficiency during ^{14}C meas. 78−58548
^{14}C counter system using proportional counters of plastic scintillator 77−60491
^{14}C counters, for small samples dating 80−82102
^{14}C, high accuracy meas. by gas proportional and liq., scintillation counting 78−74544

proportional counters continued
^{109}Cd nuclear transformation rate meas. using 4π proportional counter 78−21826
D-D neutron meas. on 40 kV, 60 A neutral beam test facility 80−37710
^{57}Fe conversion electron Mossbauer spectroscopy at low temps. 77−10542
H_2 filled, neutron flux monitor for cross section meas. 77−23379
^{3}H meter for Na coolant systems 79−9690
^{3}H proportional counter for fast reactor neutron field spectral charact. *(Japanese)* 78−46222
He cryogenic counter 78−70693
^{3}He cylindrical counters, empirical expressions for gas multiplication 78−90028
^{3}He detector design for transuranic waste assay, low-level, Monte Carl calcs. 79−54542
^{3}He neutron portable detector, calc. and measured efficiency 77−65390
^{3}He proportional counter, neutron dose equivalent meas. from thermal energy to 10 keV 79−63875
^{3}He proportional counters, thermal neutron detection performance, temp. depend. 80−58071
^{3}He-filled proportional counter, for sensitive dose or dose equivalent meter 79−45427
^{125}I surface contamination meas., sensitivity comparison with other detectors *(Czech)* 79−34673
Kr filled counter for efficient backscatt. Mossbauer spectroscopy 79−76289
Kr photo-ionization proportional scintillation chamber 80−58056
^{222}Rn very low conc. meas. with proportional counter 80−27907
T, sampling and meas. in environmental samples using gas-filled proportional counters 78−86699
Xe curved wire proportional chamber for powder X-ray crystallography 79−4210
Xe filled, on International Sun-Earth Explorer C spacecraft, for solar flares and cosmic γ-ray obs. 78−85787
Xe filled gas scintillation proportional counter in space environment, background radiation rejection efficiency 78−21819
Xe filled proportional scintillation detector for charged particles 80−32572
Xe gas hard X-ray detector, risetime discrimination 78−90031
Xe gas proportional counter for astronomical hard X-rays detect., risetime discrimination appl. *(Japanese)* 79−80219
Xe gas scintillation proportional counter, UV emission spectrum, prod. mech. 77−26935
Xe high pressure proportional, scintillation camera for X-and γ-ray imaging 80−99412
Xe, ionisation loss meas. in region of relativistic rise 79−54743
Xe probe for radiation contamination monitoring 80−27826
Xe proportional scintillation detector, energies and angles of emission of ^{252}Cf fission fragments 80−63488
Xe uniform field gas proportional scintillation counter, secondary scintillation output 77−54428
Xe-filled MWPC for hard X-ray imaging with sub-mm spatial resolution 80−99418
Xe-Kr mixtures for gas proportional scintillation counters 77−83464

propulsion
see also aerospace propulsion; electric propulsion
explosive propulsion of bodies in plane and cylindrical symm. 77−58544
flagellar propulsion, hydrodynamic anal. 79−53072
flapping wing propulsive efficiency for plane parallel flow (bionics) *(Russian)* 77−32919
flexible slender propulsor, large-amplitude unsteady motion 79−53172
laser propulsion system, fluid mech. model, real gas effects 79−60089
nonuniform flow through nozzle 78−94796
nuclear, gaseous core reactor based on U plasma core, present research 78−33244
nuclear, gaseous core reactor with U-fuelling, preliminary expts. 78−33243
nuclear, ships, report on 1977 IAEA conference *(Dutch)* 77−83069
nuclear gaseous core reactor, UF_6 technology 78−33254
ship, fission reactor appl. *(German)* 78−29638
ship propeller induced underwater acoustic disturbance obs. 79−68463
slender body propulsion by boundary layer deform. in viscous fluid *(French)* 77−42798
small nuclear reactors for power production and ship propulsion appl., prospects 77−10485
solid propellant motor, industrial TV radioscopy applic. *(French)* 77−38072

prospecting (geophysical) *see geophysical prospecting*

prosthetic power supplies
battery self-discharge process assessment by microcalorimetry 80−30935
biofuel cells, implant in dogs, expt. results, pacemaker appl. 77−52935
biogalvanic and biofuel cells, animal expts. 77−81657
biogalvanic cells, implant in dogs, expt. results, pacemaker appl. 77−52935
biogalvanic implanted pacemaker performance 77−81732
blood pump, biventricular, brushless DC motor powered, development and in vivo evaluation 79−53285
cardiac pacemaker batteries, neutron radiography investigation of electrolyte, USA National Bureau of Standards 80−56179
cardiac pacemaker long-life battery test results 77−81735
demand pacemaker, with adjustable-pulse-width, clinical experience 77−81697
development progress 78−15917
fuel cell, implantable, effect of O_2 on Pt black anode 77−60309
heart, elec. powered totally implantable total artificial heart 78−40434
heart, impelling pump, energy source 77−78043
heart, implantable, definition of technological problems 77−44839
heart, miniature Stirling engine performance 79−53287
heart, nuclear powered, using modified Stirling engine *(Croatian)* 78−44695
heart assist energy convertors, using fluid controls logic 79−53286
heart hydraulic power and control modules, implantable 78−31978
implantable cardiac pacemakers, non-polarizable stimulating electrode development 79−92428
implantable hybrid cells, porous cathodes, recent improvements 77−40933
implantable piezoelec. drive invertor for left ventricular assist device 78−15927
left ventricular assist system microprocessor controlled electromechanical convertor 78−15928

prosthetic power supplies continued
long-term implantable devices energy sources 80−98175
pacemaker, battery longevity estimation using statistical methods 78−57131
pacemaker base rate follow-up reliability for long-term pacing 77−81694
pacemaker battery internal loss characterisation calorimeter 80−30934
pacemaker battery microcalorimetric testing 80−30933
pacemaker energy sources, clinical use 77−81731
pacemaker pulse generator replacement and other problems 77−81705
pacemaker pulse generator replacement indicator 77−81692
pacemakers, comparison of Hg_2O_3-Zn and Li based power sources 77−52920
pacemakers, Li-I hermetically-sealed cells, long life expectancy 80−40850
pacemakers and batteries, microcalorimetric study 78−57130
pacing impedance determination in man from resist. meas. 78−40417
percutaneous energy transmission system development 79−92433
radioisotope-powered cardiac pacemaker 77−81734
requirements for disabled person rehabilitation equipment 78−15929
Hg-Zn secondary cells for rechargeable pacemaker 77−40925
Li batteries for pacemakers, selection criteria *(German)* 78−3670
Li battery long use cardiac pacemaker choice, technical considerations *(German)* 78−88765
Li pacemaker battery similarities and differences 77−81737
Li-$AgCrO_4$ pacemaker cell construction 77−81739
Li-I cell solid state, cardiac pacemaker power source, testing 79−66584
Li-I_2 pacemaker battery electrolyte exam. by neutron radiography 80−30940
Li-I_2 pacemaker cell end-of-life characteristic approximation 80−30937
Li-I_2 power cell accelerated discharge test for battery longevity model 80−30938
Li-$SOCl_2$ battery for implantable cardiac pacemakers 80−30939
LiI hybrid IC pacemaker, reliability, experience 77−81736
LiI powered pacemaker types evaluated 77−81738
^{147}Pm fuelled betavoltaic pacemaker system status 77−81733
^{238}Pu isotopic pacemakers, 2 to 4 years' follow-up 77−81695
^{238}Pu power units for artificial hearts and auxiliary circulation systems 77−78052

prosthetics
see also artificial limbs; artificial organs; orthotics; sensory aids
above-knee sockets, total surface bearing, self suspending 80−51294
acoustic diagnostic technique for prosthetic fixation evaluation 80−21510
acrylic bone cement, cartilage/bone plugs, impact stress/strain data 79−43950
acrylic bone cement containing second phase dispersions, strength 77−81663
acrylic bone cement improvement by addition of fillers 77−37109
acrylic bone cement viscosity characterisation 79−79690
acrylic bone cement-stainless steel interface, shear strength 77−86706
acrylic cement, porous, sucrose filled, femoral tissue ingrowth in dogs 79−39611
acrylonitrile-dimethylaminoethyl methacrylate copolymer structure and blood compatibility 77−81656
afferent elec. nerve stimulation with ref. to prosthesis sensory feedback 77−90962
albuminated Dacron prostheses as improved blood vessel substitutes 79−29669
alignment, using visual presentation of centre of press. 77−56535
alumina ceramic artificial hip joint wear tests *(German)* 79−8567
alumina-acrylic composite bone cement 79−79689
amalgam, dental, corrosion, immersion conditions 79−12037
amalgam, dental, corrosion behaviour, market survey 79−12038
ambulation, energy expenditure in disabled subjects vs. normals 77−44712
animal model selection haematological and biochemical comparison of species 77−56540
antithrombotic prosthetic surfaces development, bioelectrochemical approach 78−40414
aortic, blood vel. meas. in vicinity of prostheses 79−74706
aortic and mitral valve prostheses, in vitro flow visualisation 77−86703
aortic concave-convex pivoting disc valve prosthesis, hydrodynamic evaluation 79−84027
aortic heart valve dysfunction computer-assisted detection 77−40922
aortic heart valves, blood pressure drop across, steady and pulsatile flow 79−74707
aortic heart valves, wall shear stress meas. in near vicinity 79−83829
aortic leaflet valve prosthesis, optimal design and longevity anal. 77−90958
aortic valve, Bjork-Shiley, steady flow in vitro vel. 78−44735
aortic valve, expansible nature of base, rel. to prosthetic design 78−40232
aortic valve, finite element stress anal., human data 77−44699
aortic valve, Reul-Ghista optimal tri-leaflet Avcothane design performance 78−44736
aortic valve, trileaflet, optimum design and in vitro testing 77−56541
aortic valve leaflets, stress anal. with smoothed geometrical data 77−52815
aortic valve mechanics, apparatus for in vitro study 79−44054
aortic valve opening, haemodynamics 78−20208
aortic valve prostheses, hydrodynamic losses eval. 80−72378
aortic valve prosthesis, Hancock porcine xenograft, comparison of models 242 and 250 77−56532
aortic valve prosthesis, Reul-Ghista optimal tri-leaflet, in vitro performance tests 79−92432
aortic valve prosthesis, wall shear stress in Bjork-Shiley and Starr-Edwards types in vitro *(German)* 78−81067
aortic valve prosthesis water hammer pulse effect *(Japanese)* 78−3676
aortic valve replacement with subcoronary ball valve, early expts. 77−56524
aortic valve stress analysis using finite element computer program 78−48930
aortic valves, press. drops under steady and pulsatile flow, in vitro meas. 78−44731
appendages, manipulators and robotics prospects 78−53582
aramid fibre reinforced acrylic bone cement, tensile strength and fracture toughness, SEM study 79−29667
arterial grafts, in vivo mech. props., biological vs. synthetic grafts 77−37002
arterial grafts, synthetic, mech. props. 80−17192
arterial prosthetic material, Dacron, props. 78−7537

prosthetics continued
arterial thrombosis, in vivo method for evaluation of effects of materials 78−81071
arterial vein grafts, acute and chronic studies of vel. profiles 77−52832
arteriograft, fracture phenomena, of bovine, swine 78−92746
artificial heart material *(Japanese)* 78−11773
artificial joints, appl. of ultrahigh mol. wt. polyethylene 79−84001
below knee amputee energy expenditure rel. to optimum prosthesis alignment 77−48939
below-knee modular prostheses, load rel. to walking velocity and walking surfaces *(German)* 77−56515
bicondylar knee joint, redesigned Gunston concept, simple operative procedure 77−60292
bioceramics in orthopaedic surgery, internal struct. of inorganic parts in bones *(Polish)* 79−20714
biocompatibility testing, cell culture and animal test correlation 77−81655
biocompatible implants, developed for bone fracture prevention, development research criteria 78−77155
bioengineering, international conf., Cape Town, S.Africa (April 1977) 79−20695
bioengineering advances conference, San Francisco, USA (Dec. 1978) 79−92416
bioengineering and medical instrumentation, symposium, Laramie, USA, (May '76) 77−25571
biomaterial compatibility for cardiovascular appls., biological evaluation 78−36056
biomaterial evaluation considering species-related haematological differences 77−60291
biomaterial observation using rabbit ear chamber as in vivo model 77−81755
biomaterials, radiation processing appls. to biomedical engineering 77−70542
biomaterials in dentistry and medicine, conf., Los Angeles, USA (Dec. 1978) 80−27028
biomechanics, engineering and medical, conf., Riga, USSR (Oct. 1975) 77−25481
biomechanics, foundations and appls. *(French)* 80−89778
biomechanics conference, Ann Arbor, USA (Oct. 1978) 80−31408
biomedical system control sensors 79−48380
Bjork-Shiley aortic prosthesis, in vitro vel. meas. using laser-Doppler anemometer 80−17196
Bjork-Shiley tilting disc heart valve 77−56525
blood circulation assist devices, antithrombotic polymeric materials 78−36052
blood compatibility of isolated veins and synthetic biomaterials, surface props. 77−56522
blood substitutes, surface energetics anal. 80−41321
blood synthetic substitutes, review 79−62405
blood vessel partial replacement, blood flow model 77−64082
bone, stress distrib. in long bone due to prosthesis positioning 77−36984
bone bioceramic implants, surface structure *(German)* 79−44057
bone cement used to grout hip prosthesis, stress distrib. obs. 80−104816
bone cements, PMMA, mech. props. 77−60298
bone fracture callus mech. props., intramedullary nailing rel. to plating 80−85438
bone implants, porous, O_2 supply anal. 79−70707
bone substitute materials, sintered hydroxylapatite as bioceramic 79−12036
bone-cement interface bond enhancement technique 78−31980
bone-pin connections, mech. behaviour 78−44698
bone-prosthetic material composites, fracture toughness 77−37108
breast, silicone, dose obs. 80−98144
cardiac, haemodynamic problems *(French)* 79−34590
cardiac assist system, implantable pulsed solenoid device 77−44848
cardiac disc mitral valve in left ventricle, computer model of motion 80−8214
cardiac valve, concave-convex pivoting disc, two-dimensional 79−84028
cardiac valves, role in artificial heart performance 80−21575
cardiac ventricle and valve evaluation, flow visualisation data anal. 78−40425
cardiovascular flow visualisation methods for in vitro studies 77−56409
cardiovascular prostheses, corrosion and thrombogenesis 77−9300
ceramic artificial hip joint, wear and friction tests *(German)* 79−8568
ceramic bone implants, material science of $Ca_3(PO_4)_2$, $Ca_4P_2O_9$, $Ca_5(PO_4)_3OH$ 80−93523
ceramic endoprostheses (total hips), mech. and tribological props. *(German)* 79−84005
ceramic implant/bone interface, tensile strength and bone form., effect of elec. stimulation 77−5108
ceramics for bone replacement *(Polish)* 78−20316
circulation apparatus, hydrodynamics of abdominal cavity organs in presence of extracorporeal perfusion 77−29172
circulatory device fluid mechanics and haemolysis, review 80−46101
communication prothetics, adaptive, microprocessor-based, for persons with severe motor handicaps 78−48941
conference, London, England (Mar. 1980) 80−94926
Cooley-Cutter heart valve prosthesis 77−56526
corrosion bending fatigue testing machine, multispecimen 79−39060
corrosion fatigue, props. of surgical implant materials 79−39604
corrosion of cast and forged implants for artificial joints 77−56520
Dacron, vascular substitute, exam. of tensile fracture behaviour 78−77157
Dacron vascular substitute, tensile mech. behaviour comparison with Tetron *(Japanese)* 78−11774
deformation measurements using holographic interferometry *(German)* 78−35911
dental alloys and amalgams, etching techniques for Au-containing Ag_3Sn 78−3291
dental amalgam, Ag_2Hg_3, grain-boundary and volume diffusion coeffs. of Hg 77−55385
dental amalgam, corrosion rates in Ringer solns. and artificial saliva 79−87758
dental amalgam, exam. of fracture toughness and critical strain energy release rate 78−48933
dental amalgam, simultaneous description of transient- and steady-state creep 79−83266
dental amalgams, Cu-rich, SEM and energy dispersive X-ray analysis 78−24184
dental amalgams, small additions of Au in Ag_3Sn, struct. and corrosion study 79−20718
prosthetics continued
dental composite paste, rapid setting non-Newtonian viscosity eval. with parallel-plate plastometer 79−27610
dental implant fixation, electrically mediated process, interfacial strength 79−16348
dental implant fixation by elec. mediated process, tissue ingrowth 80−8115
dental implants, stress anal; effect of elastic parameters and geometry 80−30930
dental implants, stress anal., effect of root-length and pseudo periodontal ligament incorporation 80−30931
dental material transparency meas. device 78−31975
dental moulding volumetric variation meas. holographic interferometry 79−88214
dental porcelains, determ. of U content and dose to oral mucosa 80−89830
dental restorations, in situ ion etching in SEM 79−30629
dental restorative materials, empirical eqn. including fracture toughness for friction 78−61283
dental stones, effect of particle size on hardness and scratch resistance 79−79077
dentistry, adhesion 79−20715
dentistry, methods and appls. for holographic interferometry 80−67203
dentistry, polymers and polymer science 79−83435
dentistry, problems with polymers 79−83434
denture base acrylic tensile testing 80−16621
denture base materials, multi-station machine for fatigue testing 80−108648
dentures, EM vibrator 80−104716
dentures, porcelain, rapid U anal. by delayed fission neutron method 78−15907
diacrylate fissure sealants, film charact., dentistry appl. 80−12306
digital EMG processor and three-state myoelectric control design 79−53283
dimethacrylate resins dental composite, abrasion and wear props. 79−96710
disk valves, max. opening rel. to aortic blood flow charact. 80−108941
dowel-retained prostheses cementation, new hydrostatic pressure change recording apparatus 80−67287
elbow flexion-extension and forearm pronation-supination for elbow endoprosthesis design 80−3682
elbow joint forces derivation and rel. to prosthesis design 79−96591
electrocutaneous sensory aid based on two-point discrimination thresholds 77−81652
electrode stimulation of nervous system, electrochem. safety aspects 77−21659
electronic eye for blind people, implementation through the optical nerve *(Croatian)* 80−109060
EMG control enhancement using predictor feedback technology 77−48952
EMG digital processor design and performance 79−96712
endosseous implant material, radiation processed alumina-polyacrylic acid composite 77−60308
engineering in medicine and biology, conf. Atlanta, USA (Oct. 1978) 79−39332
equipment and functional training *(Japanese)* 78−44701
extracorporeal blood circulation apparatus, tabulated data 77−78045
extracorporeal circulation equipment, automatic control 80−3865
femoral cement-free implant, mechanical strength tests *(German)* 79−8570
femoral head replacement prosthetic, transmission of load actions 80−56284
femoral implant, numerical simulation of acrylic grout curing 80−40968
femoral stem size and design effects on cement extrusion pressure, hip replacement 79−79692
femoro-popliteal by-pass graft, flow in idealised models 79−39429
femur, human, with implanted Charnley prosthesis, stress anal. 78−20314
femur, loaded, intact and with prostheses, strain gauge meas. 77−60228
femur with proximal prosthesis, 3-dimens. anisotropic stress anal. and failure prediction 78−40424
fibre reinforced composites, flexural strength, denture base appl. *(Japanese)* 78−40409
finger prosthesis, elastomeric bearing as internal joint 79−92429
finite element analysis as an aid to implant design 80−30932
fracture fixation, oblique, mechs. using finite element model 77−52922
fractured femur fixation device, optimum design using finite element anal. 78−36050
glass-ceramic implants, loaded, expt. studies on anchoring in the femur *(German)* 80−81624
glass-ceramic/bone histological and mechanical bonding *(German)* 79−8569
glow-discharge polymer surface blood compatibility, Lindholm coagulation tests 77−81658
haemodynamic design considerations 78−40428
haemofoil mitral valve, results of flow visualisation expts. 80−104632
handicapped persons technical aids, R&D in Sweden *(Japanese)* 78−48934
health care expansion aided by integrated electronics 78−11751
heart values, hydrodynamics rel. to vol. flow rate 77−25597
heart valve, disc-type, in vitro meas. of fluid stresses 77−52833
heart valve, disk-type, numerical soln. for steady axisymmetric flow 80−35952
heart valve, Edinburgh, butterfly type with occluder, canine exp. results 77−81665
heart valve, numerical anal. of blood flow 78−15854
heart valve, prosthesis, leaflet type, calc. of cusp stresses 77−25598
heart valve, tilting-disc, thrombogenic sites computer prediction 77−44834
heart valve, trileaflet, design, fabrication and evaluation 80−94415
heart valve bioprosthesis, devel. from xenograft (1965-77) 77−56528
heart valve bioprosthesis, porcine 77−56529
heart valve closing element, kinematics photoelectric recorder 79−48370
heart valve closing element surface pressure distrib. 79−57811
heart valve design flow evaluation using finite difference transforms 78−44733
heart valve flow pattern visualisation by laser technique 78−44734
heart valve models, effect of channel diffusion, cut-off element on hydrodynamic resistance *(Russian)* 79−44053
heart valve prostheses, fluid shear stress 77−90833
heart valve prostheses, past and future 77−52924

prosthetics continued
heart valve prostheses development 77−56523
heart valve prosthesis, mech. props. of SnO_2 coated bioceramics *(German)* 79−12028
heart valve prosthesis, theoretical limit to flow design 77−60302
heart valve prosthesis design, role of simulation studies 79−12033
heart valve prosthesis mean press. gradient meas. under in vitro pulsatile flow 77−56531
heart valve prosthesis testing 77−56530
heart valve resistance to flow measurement, 77−48830
heart valve testing, mock circulation system 77−52932
heart valve with convex closing body *(German)* 78−81066
heart valves, appraisal of power loads on elements 80−104811
heart valves, disc, ball and tilting disc types, fluid stresses in vitro 78−81078
heart valves, dynamics 80−72379
heart valves, elastomeric materials eval. 77−56533
heart valves, implanted, cause of thrombus form. 77−78047
heart valves, insufficiency, pressure loss and energy loss obs. *(German)* 79−83818
heart valves, insufficiency and pressure loss in mitral position 79−20717
heart valves, laser Doppler anemometer for velocity meas. 79−57814
heart valves, mechanical haemolysis fluid dynamics 80−97999
heart valves, pressure-flow relationship and dynamic behaviour 79−25158
heart valves, simple stress estimation method 80−8210
heart valves, vel. profiles under steady flow conditions 77−56410
heat valve, hydraulic design limits 77−60293
herniorrhaphic reinforcing materials, mech. and struct. props. 79−74789
hinged knee, influence of dynamic loading on mech. loosening 78−48938
hip, analytical approaches to femoral stem stresses 77−44849
hip, total prosthesis, 3D stress anal. of femoral stem 80−98176
hip endoprostheses, ceramic, fatigue strength investigation *(German)* 77−56514
hip joint, lubrication effects 78−40413
hip joint, noncemented, with bone development stimulator *(German)* 79−8575
hip joint, wear of plastic material 77−21661
hip joint biomechanical test procedures *(German)* 79−8577
hip joint construction compatible with femoral natural stress distrib. *(German)* 79−8576
hip joint prosthesis, internal strain meas. by built-in gauge calibration and error sources *(French)* 78−44705
hip joint prosthesis reliability 78−11777
hip joint prosthetic component deformation meas. by holographic interferometry *(German)* 80−12302
hip joint replacements, ^{99m}Tc-diphosphonate scanning in infection diagnosis 77−73558
hip joints, fatigue strength of Co base alloys 79−48375
hip prostheses, Charnley, expt. anal. of surface stresses 80−17191
hip prostheses, expt. study of friction and lubrication 80−17189
hip prostheses femoral component biomechanics, bone cement stress 80−56285
hip prosthesis design, femoral stem 78−36058
hip prosthesis stem loosening in human femur, biomechanical causes investigation 80−85435
hip prosthesis-porous coating-trabecular bone interface, mechanical behaviour 79−39436
hip replacements, total, causes of failure 77−81662
hip total replacements, welds in stems of cast Co-Cr femoral components 78−44697
hip-prosthesis stem, flexural coupling to femur, theoretical anal. method 79−39428
human hip joint, pressure radiotelemetering, design features 78−3671
hydrogel coatings, and impregnations in silastic, dacron and polyethylene 79−20719
hydroxylapatite, biological implant material, fatigue and fracture strength from diametral tests, after various treatments 80−60953
hydroxylapatite, sintered bioceramic, prep. and props. 79−43174
implantable prostheses, review 80−101292
implanted prostheses applics. of C fibre reinforced C 77−64150
implanted prosthesis failure analysis techniques and results 80−89906
implants, ion beam sputter modification of surface morphology 77−44836
internal fixation plate, effect on long bone remodelling 77−48935
internal fixation plates, evaluation of 1-, 2- and 3-dimens. finite element and exptl. models 77−48934
internal strain meas. by built-in gauges *(French)* 78−32806
intra-articular implant of filamentous C fibre, rabbit 79−44061
intramedullary implants pre-coated with bone study, fixation study 80−7587
joint endoprostheses, long-term stability of metallic materials 78−36059
joint function restoration, biomech. operating principles 78−69257
joint instantaneous centre and angle of rotation, minimum error optimisation 79−96605
joint materials, wear meas., test machine design 79−20716
joint motion meas. by triaxial electrogoniometer, for human prosthesis design 78−11781
joint replacement, design trends to reduce failures 78−31973
joint replacement, development and features 77−90960
joint replacement, present practice and results 78−11776
joint replacement in upper limb 78−3674
joint replacement using UHMWPE, wear mechanisms rel. to PMMA cement 77−52929
joint replacements, mech. factors 80−56286
joint wear in humans, ferrography appl. 79−34694
joints, techniques and materials *(German)* 78−77154
joints, wear testing of polymers 78−31981
knee, control by biofeedback training 79−34700
knee, hinged, influence of cyclic loading on loosening of cement bone interface 79−44056
knee, total joints, tribological investigation *(German)* 79−84004
knee joint, surgical replacement, design, materials and methods 78−53572
knee joint design, assessment using electrogoniometric recording 80−56288
knee joint design using human joint biomechs. *(German)* 77−56516
knee joint replacement, lubrication mechanism model 79−74790
knee joint replacement, mech. causes of loosening 77−90959
knee joint simulator, development 80−17190
knee locking, sensor-controlled external system, exptl. study 78−40406
prosthetics continued
knee prosthesis, sliding meniscus, design concepts, biomechanical techniques for movement study 80−41315
knee prosthesis tibial component fixations compared 79−92431
knee replacements, non-hinged, rot. characts. 77−44853
laminar copolymers of collagen and synthetics, tissue compatibility 77−60289
laryngeal prosthesis, internally worn, design and construction 80−41318
laryngeal prosthesis for fistula speech after laryngectomy 77−78056
left ventricular apex outlet-abdominal aorta valved composite conduit for outflow obstructions 77−56542
leg, electronic storage system for axial load meas. *(German)* 79−84006
manufacturing and selling problems *(Japanese)* 78−44702
material mech. props., effects of physiological environment, cardiovascular appls. 80−8212
materials for human implantation 79−96709
materials for orthopaedic implants, review 80−76862
mechanical efficacy determ. by holographic strain meas. *(German)* 79−8573
mechanical testing of implants and materials 78−36057
medial collateral ligament substitute specification and design 78−36060
medullary implants with porous coating, stress distrib. 78−69256
medullary pin, induced internal bone remodeling 79−29552
medullary pin causing surface bone remodeling 80−3683
medullary shaft implant, finite element anal. 77−44850
metacarpophalangeal joint compressive strength rel. to subchondral bone density, prosthetic development 79−92286
metals for long-term implants, corrosion resistance meas. *(German)* 79−8565
microporous alloy hip prosthesis clinical trials 79−79687
mitral valve, hydromechanical simulation facility 79−20708
mitral valve, pressure drop and flow pattern obs. 79−92430
mitral valve prosthesis in vitro tester, unique design 78−40426
mitral valve prosthesis with flexible fabric leaflets 77−78057
mitral valve replacement, prediction of postoperative systolic left ventricular wall stress 78−40427
mitral valves, insufficiency, press. and work losses *(German)* 78−88764
morphognostic coil design for implanted nerve stimulator 79−84014
Muller screws, fractured femoral necks fixation, mech. investigation 80−72377
multifunction powered device, multistate myoelectric channel, signal processing 77−44837
muscle, load meas. in animals 77−44852
muscles, deformative props. of contractile polymeric structs. 77−25595
musculo-skeletal system, materials engineering study of bone *(Japanese)* 77−25479
myocardium, functional left ventricular wall replacement 77−52931
myocardium prosthetic, haemodynamic results 79−84019
myoelectric control, S/N ratio of filtered EMG in isometric muscle contraction *(German)* 77−81490
myoelectric multistate control systems, operator error 78−81076
myoelectric processor and human operator dynamic error performance 79−96714
myoelectric processor sampling rate selection 79−96713
myoelectrically controlled systems, five-state, error rate obs. 80−72376
myofeedback control system, design 80−51296
myofeedback control system trainer 80−51297
myringoplasty, comparison of implant materials after tympanic membrane perforation in rat 79−39597
NDT by holographic interferometry and optical correl. 80−40659
neural prostheses, review 80−21576
non-thrombogenic material, block copolymers, struct. and mech. props. 77−52925
orthopaedic implants, fixation by acrylic cements 79−84000
orthopaedic implants, replication techniques eval. for SEM 79−34707
orthopaedic implants, SEM study of wear 78−15926
orthopaedics, exptl., quantitative eval. of holographic deform. investigations 80−67197
orthotic-prosthetic and manipulator system uses of microprocessors *(Croatian)* 78−44694
osteosynthesis, strength of bone preserved by freezing 77−25488
paralysed upper extremities rehabilitation systems, control signals *(Slovenian)* 80−81772
patellar tendon bearing prosthesis, simplified model for short-below-knee stump 78−27986
percutaneous implant devices, problems, experience 77−86702
phonetic defects caused by facial gaps, correction using prosthetics *(French)* 80−51298
physically handicapped persons' apparatus, recent status of R&D *(Japanese)* 78−44703
physically handicapped persons' apparatus standardisation *(Japanese)* 78−44699
pivoting disc heart valve prosthesis, clinical results and new all-C model 77−52923
plastic ligaments and tendons, dynamic motion simulator for testing *(German)* 78−81070
PMMA bone cement, free radical EPR, feasibility study 80−94318
PMMA dental biomaterials, fracture toughness testing 80−50800
PMMA femoral cement compactor for total hip replacement 79−79688
poly (N^{ε},N^{ε}-terephthaloyl-L-lysine) membrane for artificial red blood cells, interaction with serum proteins *(Japanese)* 80−12061
polydimethylsiloxanes, haemolytic characts. 77−60290
polyethylene, C fibre reinforced ultra-high mol. wt. 78−31969
polyethylene, porous, tensile strength of interface with bone 80−30737
polyethylene, ultra high mol. wt., knee prosthesis, in vivo wear props. 80−17204
polyethylene, ultrahigh molecular weight, wear, rel. to replacement hip joints 77−17008
polyethylene implant-bone composite interfacial strength, porous high density polyethylene 78−31979
polyethylene prostheses, radiation crosslinking improvement of shock- and abrasion-resistance 77−60307
polyethylene terephthalate, joint prosthesis fragment dispersal meas. *(German)* 79−8566
polyethylene total joint replacement, props. improvement by C fibre reinforcement, SEM obs. 78−24183
polyethylene wear debris from simulated service as total hip prosthesis, quantitative recovery 79−48378
polylactic acid polymer-filamentous carbon tissue scaffold, for ligament and tendon replacement 79−92434

prosthetics continued
polymer, bioabsorbable, standards for in vitro and in vivo comparison and qualification 78−3677
polymer biocompatibility evaluation by cell culture method *(Japanese)* 80−12301
polymer endoprosthetic joint, fatigue life 80−40521
polymer surface contacting blood, roughness effect on thrombus form. 79−48369
polymeric biomaterials for blood-contacting appls., problems and new dimensions 78−85423
polymeric biomedical materials 79−83998
polymeric joint replacements 79−83999
polymers, adsorpt. of plasma proteins, Fourier transform IR spectrometry 80−16899
polymers, biodeterioration in vitro and in vivo *(Japanese)* 77−66874
polymers, radiation grafted, blood thrombogenicity meas. by vena cava ring test 79−44062
polymers in medicine, review, book contrib. 80−12307
polymethylmethacrylate, denture base resin, residual monomer determ. 79−16077
polysulphone evaluation for biomedical applications 79−29670
polyurethane, effect of morphology on blood coagulation 79−39610
polyurethane, quick-hardening SKU-PFL, synthesis and props., use in endoprosthetics 78−6887
porous coated implant removal by ultrasound 79−79618
prosthetic, heart valves, load cell for meas. of dynamic forces 80−104815
prosthetic heart valves, rigid leaflet and caged-ball types, diastolic ventricular mechs. 78−81079
pulsatile blood pump, vortex diode used as outflow valve 78−44724
PVC, biological media effect on. physiomech. props. 79−96168
quality health care and cost containment, conf., Washington, USA (Mar.-Apr. 1978) 79−39333
regulation of surgical implant devices 79−92917
rehabilitation engineering *(Japanese)* 80−12304
respiratory, future developments *(French)* 77−13033
robots and manipulators, symposium, Warsaw (Sept., 1976) 78−53574
rubber, silicone, biomed. eval. for passive prosthetic devices 79−29666
scala tympani electrode for auditory prostheses, 8 channel 80−36194
sensory and neural, development *(French)* 80−89905
sensory feedback, human tracking performance with afferent elec. nerve stimulation 80−17195
sensory feedback, recommended electrocutaneous codes 78−44715
sensory feedback system for above knee prosthesis *(Japanese)* 80−72372
sheet metal, deep-drawn, for implant device encapsulation, mech. and metallographic props. *(German)* 79−8564
shunt for cerebrospinal fluid, press. data from dogs for anal. and design 77−56412
signal processing for multistate myoelectric channel, prosthesis control 78−88768
silicone elastomers, for teeth impressions, holographic interferometric meas. of dimens. variations 79−94195
silicone rubber, vulcanizing, possible substitute for damaged/diseased parts of eye 79−74788
silicone rubber vulcanisates, as alloprosthetic material 77−25596
skin, to give tactile perception, planary distributed transducers 77−81661
Smeloff-Cutter heart valve prosthesis 77−56527
speech and language prostheses evaluation 80−76864
speech prosthesis, computer driven, personal, portable and intelligent 78−92745
spinal fixation using acrylic bone cement, mech. props. 78−81072
standardisation of technical terms *(Japanese)* 78−44700
steel, austenitic stainless, 316, surgical implant ion beam textured, stress/strain relations, fatigue characts. 78−73297
steel, austenitic stainless, electrochemical behaviour in Ringer's soln., composition effects, SCC 77−90485
steel, austenitic stainless, fretting corrosion of orthopaedic implant materials by bone cement 80−104813
steel, austenitic stainless, stress corrosion cracking, mixed mode, fractographic evidence in surgical implant 80−30156
steel, austenitic stainless, TRIP, fretting corrosion of surgical implant material, electrochemical investigation 79−66197
steel, stainless, 316L, fretting corrosion of surgical implant material, electrochemical investigation 79−66197
steel, stainless, bone implant, stress corrosion cracking 77−56519
steel, stainless, fibre reinforced porous coating, isostatically compressed for bone ingrowth 80−35134
steel, stainless, Harrington rod implant failure analysis 79−79686
steel, stainless, orthopaedic, type En58J, Mo ion-plating, corrosion fatigue 80−66694
steel, stainless, orthopaedic fixation devices, failure, SEM exam. of fatigue crack surfaces and microstructure 78−77156
steel, stainless, surgical implant, SCC and corrosion fatigue in Tyrode's soln. 79−29263
steel, stainless, surgical implants, corrosion 79−70706
steel, stainless, TRIP and 316L, orthopaedic implant material, metallurgical cond. effect on pitting resistance 79−70704
stem, stress estimation, analytical 79−92250
stomatologic polymeriser for dental prostheses 79−57812
strain measurement in bone and prosthetic materials *(French)* 79−34695
surgical implant materials, corrosion props. 79−39605
surgical implants, corrosion fatigue behaviour of Ti-Al-V 79−39027
surgical implants, in human body, failure anal. 79−62407
synovial fluid boundary lubrication model, structuring of boundary water 80−35950
synovial joints, appl. of generalised Reynolds eqn. for porous boundaries 80−87803
synovial joints, rheology of synovial fluid, synthetic lubricants for degenerate joints 79−11955
tachographic data analysis, time interval and acceleration anal. for gait abnormality detect. 77−48938
tetraplegics manipulator, microcomputer control 80−41314
Tetron, vascular substitute, exam. of tensile fracture behaviour 78−77157
Tetron vascular substitutes, tensile mech. behaviour comparison with Dacron *(Japanese)* 78−11774
thermoplastics, appl., deformability in physiological salt soln. 80−12305
thromboresistance of biomaterial, influence of implantation techniques *(German)* 80−3861
prosthetics continued
tibial bone reaction to hydromech. implant dynamic loading *(German)* 79−8574
tibial fracture fixation, anal. of forces in screws 77−60300
tibial plateau fixation, biomech. factors 77−56534
tissue reaction to polytetrafluorethylene dispersed in acetal resin 78−40412
tooth, artificial-denture base joint, adhesion, fracture mech. 79−16350
tooth replicas, phys. props. and biological acceptance of porous PMMA implanted in baboon bones 77−52926
transapical left ventricular bypass, prolonged use in sheep and man 78−40435
urethane prosthetic compound, dynamic mode determ. 79−48376
urethral occlusive techniques for restoration of urinary continence, development 78−7543
veins, appl. of plastic tubular magneto-electrets 77−32318
visual prosthetic device, bioengineering and biomedical aspects of focal surface model 78−48942
visual prosthetic implant, cortical electrical phosphene props. 80−12112
Vitallium, surgical implant, SCC and corrosion fatigue in Tyrode's soln. 79−29263
Vitallium alloy, fretting corrosion of surgical implant material, electrochemical investigation 79−66197
wear, holographic studies using optical contouring 80−67288
wear of articulating surfaces in protheses, holographic interferometry exam. 78−40415
wrist kinematic and kinetic analysis rel. to implant design 80−16999
Ag-Hg-Sn dental amalgams, non-γ_2 phase, transmission electron metallography 79−74162
Ag-Sn alloys and amalgams, electrochem. considerations, corrosion in physiological soln. 80−93760
Ag_3Sn, dental alloy, prod. by melt extraction technique, exam. of mech. props. 78−48349
Al_2O_3 bioceramic synthesis, for orthopedic purposes, props. *(Polish)* 80−66465
Al_2O_3 ceramics in surgery for artificial limb-joints *(German)* 77−25593
Au dental fillings, cause of dose perturbation in radiation therapy 80−12265
Au-Pd-Pt-Ag, comp.-prop. diagram, possible use in dental prosthesis *(Russian)* 79−11554
C cardiovascular prosthetic devices and dental implants, review 77−44835
C fibre reinforced plastics, use in orthopaedic implants, exam. of mech. props. 79−20706
C films, vacuum-vapour-deposited for prosthetic coatings, wear behaviour 79−43440
C, isotropic pyrolytic, for biomedical devices, mech. props. 78−65150
C vacuum deposited coatings for prosthetic devices 77−40374
Ca aluminophosphate foam glasses, for prosthetic appl., porosity and mech. props. 79−74128
β-$Ca_3(PO_4)_2$ whitlockite ceramic fabrication 79−78924
β-$Ca_3(PO_4)_2$, synthesis and fabrication, prosthetic appl. 79−24479
Co-Cr orthopedic implants, surface oxide layer investigations using ESCA technique 79−25157
Co-Cr-Mo alloy shoulder prosthesis, wear and fatigue tests 80−26415
Co-Ni-Cr-Mo, hip joint anchorage stem, superior fatigue strength, high corrosion resist. 79−29671
Co-W-Cr (15,20 wt.%), surgical implant ion beam textured, stress/strain relations, fatigue characts. 78−73297
Ni-Cr, corrosion resistance of dental casting alloys 78−31561
Ti, for implant surgery appls., phys. props. 77−73615
Ti for implantation, biological props. and appls. 78−3678
Ti, integral composite joints, finite element and expt. eval. 79−11670
Ti-Al-V (6, 4 wt.%), fretting corrosion of orthopaedic implant materials by bone cement 80−104813
Ti-Al-V (6,4 wt.%), surgical implant ion beam textured, stress/strain relations, fatigue characts. 78−73297
Vitallium, orthopaedic implant material, metallurgical cond. effect on pitting resistance 79−70704

protactinium
see also nuclei with .....
body-centred tetragonal metal, enthalpy of soln. 78−48686
electrical resistivity meas., 0.90 to 300K 77−35915
lattice parameter variation at low temp., thermal expsn. 80−15046
Mossbauer resonance, elec. field gradient 80−15927
preparation by Van Arkel method, cryst. struct. 78−39715
recovery and purification procedure for ^{231}Pa 79−15977
superconductivity, transition temp. and upper critical mag. field 80−44756
^{231}Pa dating of fossil corals and shells 80−12434
^{231}Pa, determ. in coastal sediments and seawater, activity ratios, disequilib. 78−27851
^{231}Pa Mossbauer resonance, elec. field grad. 80−7207
^{233}Pa importance in neutron economy Th-fuelled CANDU reactor 80−22980
^{233}Pa removal from ^{237}Np by coprecipitation with MnO_2 or sorption on silica gel 79−52733
^{147}Pm, deposition on anodically polarised Pt surface 78−27424

protactinium compounds
Pa complex, protactinium tropolonate, synthesis, cryst. struct. parameters 80−33945
$PaAs_2$, Pa_3As_4, and PaAs, cryst. growth by chem. vapour transport, cryst. struct. 80−35066
PaN, prep. by heating Pa, cryst. struct. 78−39715
$PaSb_2$ and Pa_3Sb_4, cryst. structs., mag. susceptibility *(French)* 79−65641

protection
see also alarm systems; corrosion protection; machine protection; power system protection; protective coatings; radiation protection; safety
BWR, automatic protection system *(German)* 78−4989
contaminated live steam release into turbine hall at Brunsbuttel *(German)* 79−89388
cryogenic sorption trap for high-vacuum system protection 79−88963
electric shock, safety curves as function of ambient conditions *(French)* 77−17012
emergency protection drive, optimum ratio between operational component times 78−82474
fibre splicing, arc fusion 80−69565
fusion reactor, Doublet III, neutral beam interlock system using IR detector 80−106228

protection continued
fusion reactors switching and regulating elements, high-power tetrodes appl. 79−54592
hearing protector attenuation: a perspective view 79−81619
hearing protectors, meas. of real-ear attenuation by standardised test methods 78−1508
hearing protectors, performance estimation 78−40192
hearing protectors, rating method 77−7271
industrial ear protectors, standardisation of testing, current developments 78−22225
industrial noise and hearing conservation 78−22223
industrial noise induced deafness and protective measures 78−22224
ionisation manometric transducer, PMI-2, cathode protection 77−74416
magneto-inductive flowmeters, installation, earthing, isolation, protection against explosion *(German)* 80−64662
neutral beam accelerator electrodes, spark discharge protection, for fusion reactor 78−62609
nuclear facilities, tamper-indicating seal program development and implementation 79−85689
nuclear facilities, vital area identification, fault tree analysis appl. 79−85691
nuclear facilities in West Germany, physical protection program review 79−89450
nuclear facility physical protection system, role of barriers 79−85686
nuclear materials management, Conf., Cincinnati, OH., USA, (June 1978) 79−85672
nuclear materials safeguards, use of US identified seals 79−85677
nuclear power station, qualification requirements for class 1E equipment 77−67822
nuclear power station protection against earthquakes, design *(French)* 77−54332
operating room airborne contamination protection using electrostatic particle repulsion system 78−28125
overheating thermal sensors, appls. and types *(Japanese)* 77−71318
photomultiplier gain-changing protection circuit, scintillation neutron detector 80−74074
photomultiplier protection against optical overloads, electromagnetic shutter control 80−23255
plasma chromatograph/mass spectrometer sample overload protection 79−39237
smoke retardation, Mo-containing formulations 77−77761
solar access, perspectives and law 79−87979
strain gauge, sealants suitability determ. 78−4610
Swiss emergency organisation for nucl. and chem. accidents 78−57078
vacuum system protection for synchrotron radiation storage ring, acoustic delay line efficiency 79−88965
vacuum systems, 80−105666
X-ray tubes, rotary anode, HV insulation, discharges due to back scattered electrons elimination *(German)* 80−105758

protection of software, legal *see industrial property*

protective coatings
see also corrosion protective coatings; wear resistant coatings
acrylic coating for optical fibres, surface tension effects 80−53487
adsorption of Cs ions on constituent materials 78−23843
alkali-halide crystals, plastic deformation, effect of solid film coatings *(Russian)* 77−25167
aluminide coatings on superalloys, improvement by sputtering *(French)* 79−29278
aluminisation in Al packs, for protective coating form., kinetic diffusion theory 77−32727
antihygroscope thin film coating for optical elements, laser deposited 79−28926
arc spraying, frequency analyses application 79−83359
bearing capacity, testing under external and internal pressure 79−70254
boride coatings, reaction with Mo substrate 77−32716
boride coatings, under elec. heating conditions, hydroabrasion wear resist. on Armco, Fe and steel 80−55543
boride coatings on C and alloy steel, spectroscopic thickness determ. 80−85099
boride coatings on Ni alloy, thermal stability, exam. of coating 78−44271
boride coatings on steel effect of Cu impurities in reaction mixture on brittleness, acoustic emission meas. 80−16581
boride diffusion coatings on steel, fractographic exam. of struct. 78−44270
boride on W and Mo 80−21165
borides, lightweight ceramic armour appls., ballistic tests, computer simulation, book contrib. 78−48556
borozirconia glazes, low-melting, struct. and liq.-phase separation 79−60282
cadmium arachidate monolayers, bonding on oxidised In, Rh, Si, Sn, surfaces, XPS 79−15011
ceramic self-cleaning catalyst for ovens and grills *(Japanese)* 80−55557
ceramics, glazing with gaseous P_2O_5 80−108609
chromising porous W and W-Cu pseudoalloys 80−100959
coated cement stone heat and mass transfer obs. *(Russian)* 79−14219
composite protective coating effect on fibre-matrix bond strength fibre 77−44195
contact fatigue limit testing machine, for metals, alloys under vibrating load 80−55617
corrosion theory, rel. to protective coatings 78−19918
Cr on Kh25N20S2 steel; structural transformations, oxidation effect 79−57154
CrMoV, surface coating to prevent oxidation during high temp. AE 80−16539
double-layer coating with double cone nozzle in-line with optical fibre drawing 80−53488
electrical resistance alloys, oxidation *(Polish)* 79−79143
emissivity, monochromatic in 2-25 μ range at 100 to 400°C 77−71714
epoxy acrylate coated fused silica fibres, dynamic and static fatigue 78−1385
epoxy acrylate coated optical fibre, long term strength, environmental effect 78−5582
epoxy acrylate coated optical glass fibre; strength and static fatigue 78−1386
epoxy acrylate coatings, UV cured, for optical fibres 78−1444
epoxy primer, evaluation of corrosion protection of system Zn/$ZnSO_4$/Zn, using laser interferometry 79−35815
fibre pressure sensitivity meas. and limitation, using silicon rubber coating 80−106605

protective coatings continued
flameproof coating for PVC insulated cables, composition, tests *(Russian)* 78−68828
flamespraying process for aircraft 79−83115
fusion reactor, ORMAK, inner vac. liner coating materials 77−30669
fusion reactor, Tokamak, first wall coating materials and techniques 78−8974
fusion reactor environment, development of coatings 80−18618
galvanic coating thickness gauges using phase angle meas. 77−79114
gas turbine airfoils, protective coatings, degradation characts. and methods of application 79−24670
glass ceramic protective coatings for Ti, synthesis and props. 80−25900
glass fibre protective coatings, using polymers, materials and techniques 80−33252
glass-enamel coating on C steel tubes, prod. by induction fusion method, heating rate of steel effect 80−11825
glass-enamel coatings, effect of firing method on adhesion 79−24647
graphite body, heating, surface erosion, by high-temp. gas flow 79−37318
graphite fibre epoxy composites, eutectic coating moisture barriers 80−81228
hard overcoats in replicated optics 78−66968
heat pipes for radioisotope thermoelectric generator, Cu/H_2O, axially-grooved 79−48144
heat radiation screening from hypersonic shock layer in boundary layer *(Russian)* 79−32497
hydrophilic, on glass 78−85019
ion plating process features and surface film props. 79−83361
IR thin film plasma deposition processes 80−87466
laminated cermet coating on Cu, thermal shock performance 78−7081
large optical component antireflection and protective coatings 79−72660
laser CVD, film physical props. and applications 80−93493
laser damage protective coating, electric field interference 80−33062
latex polymer, electrodeposition on metal 78−53015
lens, water soluble cryst., protective coating to aid polishing 80−33250
metal, thickness meas. methods and apparatus *(Bulgarian)* 79−88906
metal and metal oxide spacecraft thermal control materials, low-energy proton effects 80−70288
metal coated optical fibres, high-strength advances in reduction in microbending loss 79−46066
metal coating of optical fibres, for strengthening and surface protection 78−30103
metal spraying methods and appls. 79−66202
metallic coatings, nondestructive testing, holographic interferometry appl. *(German)* 79−79186
mirror, interference filters for improved solar radiation resistance 77−39015
mirror coatings, protected and unprotected specular reflectance 79−76792
multicomponent thin film formation on K8 glass 79−72726
nuclear facilities, surface protection materials, tests on 900 commercial products *(German)* 80−35356
optical components mode of chem. unstable glass, protection from biological overgrowths 78−59107
optical element, film effect on mech. strength 78−1318
optical fibre coatings centering by monitoring forward scattering patterns 80−64146
optical fibre polymeric coatings, Bell Labs activities 78−1388
optical fibre primary coat using modified silicone, transmission characts 80−38098
optical fibres, Al coated, empirical formula for induced excess loss 79−46074
optical fibres, coated, strain-induced excess loss 79−50418
optical fibres, high strength hermetically sealed metal coated fibres, expt. 78−66929
optical waveguide fibre coating technology, overview 80−58828
oxide, in situ form. on heat exchanger materials, inhibiting effect on H_2 permeability 78−8895
paint, non-magnetic, non-destructive measurement of thickness 79−52557
paints and varnishes, stress anal. during drying 79−34183
parylene (vacuum deposited polymeric coating), appl. to electronics 80−108607
PET film, metallized reflecting surface, ageing under natural conditions, destructive factors identification 79−83340
phosphosilicate glass protective film for ICs, X-ray fluoresc. technique for rapid P determ. 77−40612
piezoelectric transducer emitting surface, for US testing of glass-reinforced plastics 77−90563
pipes, thickness gauge meas., of polymer protective coating 78−76818
plasma polymerisation in vacuum chamber 79−70183
plasma polymerized on metal substrates, adhesion and cohesion 78−3259
plasma sprayed coating, ultramicrostructure and porosity 79−82500
plastic coated optical glass fibres, liq. N_2 strengths 80−58707
plastic coating of Na_2O-B_2O_3-SiO_2 glass fibres, influence on strength 80−58697
plastic primary coating materials for optical fibres *(Japanese)* 79−59818
plastic resin coated optical fibres, effect of secondary coating technique on transmission loss 80−58704
polyamide-polyurethane copolymer dispersions, structurisation and relax. props., coating from props. 80−76559
polyethylene resin coated paper formulation for photography 80−4794
polymer coated glass, current leakage path form. by water diffusion 78−10535
polymer coated metal spheres, flow, degradation mechanism 77−9036
polymer film coating, electropolymerisation in aq. medium book contrib. 80−50778
polymer test apparatus for chem. resist. and penetrability in corrosive medium under hydrostatic pressure 79−39065
porcelain-on-aluminium, low-absorptance 80−76393
pressure transducers thermal transients effect reduction, protective coatings eval. 78−54358
PTFE, heat shrinkable tubing, crystallite orientation 77−4795
radioactive decontamination test procedures 77−34475
refractory ceramic coatings, for high temp. use, current status *(Japanese)* 80−71619
on refractory fibres, effect on high-temp. strength of refractory coatings *(Russian)* 77−52536
resin, UV cured, for optical fibre/cable 80−69547
silazane on radiation concentrators, UV exposure, ageing tests 78−79092

protective coatings continued
sitall coatings in Li_2O-Na_2O-CaO-SiO_2 system, heat treatment effects on tech. charact. 78−84853
soft metallic films, role in reducing friction between metal surfaces 80−55592
solar cells, degradation processes of electrophysical charact. during long-term operation 80−89617
solar cells, for space appl., coverglass development 79−48133
solar energy concentrators, metallised polymer films and Al coatings, spectral characteristics 79−96422
solar energy concentrators, optical coatings, accelerated tests, using reliability principle 79−96419
space-shuttle thermal-protection coating, testing techniques at 870°C 78−35604
spacecraft thermal control coatings, electron and proton irrad. effects 80−70262
stainless steel, ferritic SUS 410 type, coated with organometallic complexes and Ti alkoxides 80−34078
steel, alloy 08kp, sheet material with laminar coating, damping capacity improvement 79−66098
steel, boriding with B_4C based paste 80−16583
steel, C, wear of Cr, Zn protective coatings, exam. using nuclear radiation excited X-ray fluorescence 80−21206
steel, chromoaluminosiliconising with electroheating, for oxidation resistant coatings 79−52457
steel, Cr-Mn, high temp. oxidation, sub-cinder layer formation, protective coating role *(Russian)* 80−93686
steel, Kh17N2, endurance limit, effect of residual stresses caused by Cr plating and cyaniding 77−86184
steel, microalloyed, fine grained, mech. props., effect of hot dip galvanising *(German)* 77−36679
steel, nitride coated, brittleness eval. by AE *(Chinese)* 78−11453
steel, stainless, highly protective film development by surface treatment 80−66699
steel, type 08sp, vitreous enamel coatings effect on mech. props. of surface layers 80−35424
steel, U8, diffusion coating protection for H_2 embrittlement, SCC and tensile tests *(Russian)* 78−31513
steel 20, diffusion coating for protection against H_2 effect on mech. props. 78−31589
steel substrate, US testing 78−23908
surface coating technology, conference, London (1978) 79−83358
Teflon, aluminised, spacecraft, surface material performance modelling 78−4061
thermal barrier coating, two layer, for high temp. components 78−56789
thermally sprayed coating adhesive strength testing method 79−83432
thermally sprayed nonfused coating, adhesive bond strength NDT 79−83433
thermodiffusional, form. kinetics and struct. on iron, steel, and cast iron 77−56158
thermoelectric materials vaporisation suppression, p-type $(Cu,Ag)_2Se$ 79−48149
thickness meas. using radioisotope method 77−90520
tinplate surfaces, Auger depth profiling and anal. 80−59768
vibration-absorbing coatings, constrained, optimality 77−823
Ag film vacuum deposition and ion plating, effects on surface topography 79−82427
Al, bulk and plasma-sprayed coating, D_3^+ trapping meas. 80−20754
Al, coating thickness determ. H_2 generating method *(German)* 79−35660
Al mirrors, on metal substrates, resistance to heat and radiation 79−94319
Al, on Cr-Mo steel 79−70231
Al on Kh25N20S2 steel, structural transformations, oxidation effect 79−57154
Al plasma sprayed coating adhesion to mild steel, substrate pretreatment effect 79−83391
Al powder, protective coatings of Ni, Cu, Al and their alloys *(Russian)* 78−60881
Al rich surface layer, barrier to chemical attack of float glass by water *(French)* 80−89378
Al-Zn alloys on mild steel interface struct. 79−52466
AlN, reactively sputtered, on GaAs, $Ga_{1-x}Al_xAs$ and $GaAs_{1-x}P_x$ *(French)* 78−23849
Al_2O_3 barrier layer, for good high-temp. stability, BN in contact with W 79−70194
Al_2O_3 based cermet, protective coating for blast furnace tuyeres *(German)* 79−66193
Al_2O_3 coated Al mirrors, highly efficient refl. type polarisers for 10.6 μm laser radiation 78−71177
Al_2O_3 coating, protective, on SiC fibres in Ni-Cr alloy based composites, IR investigation 78−60623
Al_2O_3, coating on Cu, thermal shock performance 78−7081
Al_2O_3, glass resistant, plasma coating props. 79−34164
Al_2O_3, on Al mirror, refl. depend. on angle of incidence, 8 to 12 μm 78−37960
α-Al_2O_3 protective scale, influence of Pt 77−16749
Au-Pt composite coating for steel inner vac. liner of fusion reactor 77−30669
B and B-rich borides, protective coatings, in situ prep. for controlled nuclear fusion devices 79−3238
B coatings on graphite, fusion reactor appl. 80−23147
B_4C, first-wall coating for Tokamak, H retention and release 80−18620
Be coated limiters, first wall protection 80−32483
Be, plasma-sprayed coatings on Cu and stainless steel, fusion reactor appl. 80−18619
C coatings for fusion applications 80−23146
C fibre coated with Si or ZrC, mech. props. 77−70197
C fibre reinforced polyphenylsiloxane composites, long-time strength, and influence of protective coatings 80−3133
CaF_2, protection from biological overgrowths 78−18034
CeF_3, protective overcoating material for inhomogeneous interface laser mirror coatings 80−1252
Co-Cr-Al, protective coating, exam. of interdiffusion kinetics, development of analysing procedure 79−5085
Co-Cr-Al-Y coated turbine airfoils, effect of electron beam deposition rate on struct. 79−23870
Cr, diffusion coating, an Fe powder based sintered porour permeable materials 80−100958
Cr, diffusion saturation of commercial iron and steel in closed reaction space kinetics and mechanism 79−52458
protective coatings continued
Cr_3C_2, on Cr, mechanism of high-temp. oxidation, 1050 to 1100°C *(Russian)* 79−20226
Cu, electrodeposited, Ni alloy protection against hydrogen embrittlement, aerospace engine appl. 80−76416
Cu-Al_2O_3, composite-coatings, prep. by precip., props. 78−23841
Cu-benzotriazole (benzimidazole) thin films, ellipsometric study 80−35114
Fe, cast, grey, carbide-free Cr diffusion coating 79−96205
Fe powder layers, sinter-bonded, hot-pressed, on steel, struct. and props 79−95976
Fe-Cr alloys, in acid and neutral solns., thickness and optical constants of passive and transpassive films 80−66698
Fe-graphite, sintered, diffusion layer form. 79−100299
Fe-Si gas-flame spray deposited protective coating, for C steel heat exchanger 80−61025
$Fe_4(C,N)$, obtained by ion bombardment thermochemical treatment of Armco Fe *(French)* 77−86229
$FePO_4$ coating on Armco Fe, Fourier transform IR absorpt.-reflection spectra 80−71500
$Ga_{1-x}Al_xAs$ DH laser, LPE surface protective coating 78−35320
GaAs laser reliability, protective facet coatings 79−81452
$Gd_{0.85}Sr_{0.15}(Ca_{0.15})CrO_3$ self formed Gd coating, vaporisation protection 79−5069
Ge, on Sn superconducting thin films, effect on excess elec. cond. 80−65741
HfO_2 protected Al mirror, high refl. 8 to 12 μm, normal to high incident angles 78−79090
InSb, covered with thin oxide protective film, intrinsic photocond. 77−55578
KCl, on III-V semicond., LEED and Auger spectroscopy obs. 77−89628
LiF_2, protection from biological overgrowths 78−18034
$LiNbO_3$-InSb amplifier production, role of protective films 78−95220
MgF_2 overcoating on Al mirrors, reflective scatt. and reflectance meas. in vac. UV, moisture and oil vapour influence *(German)* 79−86227
MnZn ferrites, hot pressed, mechanism of protective action of Zn0 coating *(Russian)* 79−15822
Mo, carbonyl coating, deposition and props. 77−28725
Mo, ionic siliciding, diffusion layer prod. 78−23855
Mo, siliconised, adhesive interaction with Nb and unprotected Mo 77−48569
Mo-Zr, interaction with $MoSi_2$ diffusion coating, at elevated temps. *(Russian)* 79−28150
$Mo_5(B,Si)_3$, stability of heatproof coating 77−86201
MoS_2 on Mo, sulphate coating growth kinetics and mechanism 77−86220
$MoSi_2$ coating for SiC heating elements 80−21137
$MoSi_2$ on Mo, coating by local heating 77−81335
$MoSi_3$, high temp. material, coatings, powder metallurgy, review *(German)* 79−74295
Na_2O-CaO-Al_2O_3-SiO_2-F-B_2O_3-ZrO_2 glaze, crystallisation, MgO, ZnO, BaO and SrO effects 79−60279
Nb, protective coating form. by reaction with Sn-Al melt *(Russian)* 79−70221
$Nb_5(B,Si)_3$, stability of heatproof coating 77−86201
NbC coating on C steel and Armco Fe, deposition, struct. and props. 79−52462
Ni, pack aluminisation kinetics 77−32727
Ni-Al-Cr_3C_2, eutectic, Al_2O_3 coatings for oxidation resist. 80−50776
Ni-Al-Ti protective coating, on Ni-Al alloy IN 100, Ti content influence, oxidation behaviour *(French)* 78−3258
Ni-Cr-Al, protective coating, exam. of interdiffusion kinetics, development of analysing procedure 79−5085
NiCr, austenitic, oxidation *(Polish)* 79−79143
NiF_2 film preparation and characterisation 80−59815
Pb-Sn-Cd coating on stainless steel and Ti alloy, fracture toughness improvement 79−43416
Pd, on stainless steel, interdiffusion at reactor wall temps., Rutherford backscatt. obs. 80−39361
Si-containing deposit layers on Ni alloys, appl. methods *(German)* 78−85025
SiC coating on Mo, CVD and stability under thermal cycle conditions 80−7500
SiC coatings for first-wall candidate materials by RF sputtering 80−25563
$Si_{1-x}C_x$ protective coating for GaAs laser 80−5753
Si_3N_4 coated fibres for high-strength and improved fatigue 79−50470
Si_3N_4 films on Si wafers, O determ. by ^3He activation anal. 80−71981
SiO_2, on n-GaAs, Ga content after annealing at 730-940°C neutron activation anal. 78−43255
SiO_2, vacuum deposited, 7-10 μ, microhardness and structure 78−19669
SiO_x protected Al mirror, far UV refl., UV irrad. effect 79−7191
$SrZrO_3$ coatings, plasma-sprayed, spectral emittance *(French)* 78−26709
Ta_2O_5 thin film protection of unstable OF-type glass components 79−14079
Ti spongy metallic protective gettered coating for thermonuclear reactor walls *(Russian)* 80−106154
Ti(B,N), CVD coating on cutting tool 79−61802
TiB_2 coated limiters, first wall protection 80−32483
TiB_2 coating on graphite by CVD 80−21131
TiB_2, first-wall coating for Tokamak, H retention and release 80−18620
TiB_2, plasma-sprayed coatings on Cu and stainless steel, fusion reactor appl. 80−18619
TiB_2 thick film on low C steel substrate, CVD in US field, crystallite size 80−84854
TiB_2, TiB_2-ZrB_2, refractory compounds, direct evaporation deposition, struct. and props. 77−44392
TiC coated limiters, first wall protection 80−32483
TiC coatings, on cemented carbides, struct. and hardness 80−59771
TiC coatings on steels and hard alloys 80−76414
TiC, plasma-sprayed coatings on Cu and stainless steel, fusion reactor appl. 80−18619
TiC-coated C fibres in Ni, diffusion barrier effectiveness 78−60624
TiN, influence on interaction between SiC fibres, reinforced complex alloy *(Russian)* 78−95820
TiO_2 layers, activated reactive evaporation and absorpt. indices 80−97363
TiP, form. by high temp. reaction of Ti with P 78−44260
VBe_{12}, coated limiters, first wall protection 80−32483

protective coatings continued
VBe_{12}, plasma-sprayed coatings on Cu and stainless steel, fusion reactor appl. 80−18619
VC-TiC, high rate deposition by activated reactive evaporation, and characterisation 78−11372
W, CVD hardfacing of coal gasification unit components 77−40472
W, diffusion barrier between Ni-Cr-Al coatings and Ni eutectic alloys in gas turbines 79−24673
W fibre reinforced Ni-Cr steel, TiN coated fibre, protective props. *(Russian)* 79−66201
$W_5(B,Si)_3$, stability of heatproof coating 77−86201
WC_x formation during pyrolysis of WCl_6 and toluene, coating props. 77−36682
WSi_2 on W, coating by local heating 77−81335
Y_2O_3 barrier layer, for good high-temp. stability, BN in contact with W 79−70194
Y_2O_3 coated Ag mirror for the 0.5 to 14 μm region 80−87456
Y_2O_3, on fibres of W fibre reinforced Cr alloy composites, reactivity 79−100297
Y_2O_3 protected Al mirror, high refl. 8 to 12 μm, normal to high incident angles 78−79090
Zn coating on continuous galvanising line, mass meas. and control 78−19960
Zn, coating on steel strip, plastic deform. 77−90368
Zn hot galvanisation coatings, production components, installation and power supply *(French)* 80−66686
ZnO, spacecraft thermal control material, low-energy proton effects 80−70288
ZrB_2, on rapid steel, surface modification 79−66203
ZrB_2, refractory compounds, direct evaporation deposition, struct. and props. 77−44392
Zr(C,N), coating on Zr substrate, oxidation by water vap., kinetics, 0.2-20 torr, 500-600°C *(French)* 78−44266
ZrC, ZrC-ZrB_2, refractory compounds, direct evaporation deposition, struct. and props. 77−44392
ZrN, coating on Zr substrate, oxidation by water vap., kinetics, 0.2-20 torr, 550-700°C *(French)* 78−44266
ZrN-coated C fibres in Ni, diffusion barrier effectiveness 78−60624
ZrO_2, coating on Cu, thermal shock performance 78−7081
ZrO_2 coatings, prod. by low-temp. oxidation, props. 78−23856
ZrO_2, stabilised, coating for turbine components, degradation due to internal stresses 79−24671
ZrO_2, stabilized, protective coating for blast furnace tuyeres *(German)* 79−66193
ZrO_2, stabilized, thermal barrier coating system, spectral emission and absorpt., 300 to 1590K 79−24672

protective relays *see relay protection*

proteins
see also gelatin
α-helical, bioenergetics, solitons, muscle contraction mechanism 79−96508
α-helical, possible role in membrane charge transfer processes 80−81524
α-helix dipole rel. to props. 78−61140
β-pleated sheet topology rel. to relatedness 77−77866
acetylcholine receptor from Torpedo Californica, struct. anal., low-angle neutron scatt. obs. 80−30651
acetylcholine receptor protein, binding kinetics and Ca ions, rel. to membrane cond. changes of acetylcholine 77−40649
acetylcholine receptor protein structure 80−85339
acetylcholinesterase, membrane bound, activity rel. to struct. changes induced by cAMP 80−30674
acetylcholinesterase activity in visual centres after habituation due to colour flashes 77−12918
acetylcholinesterase increase on exposure of dark-reared rats to light 78−24069
acid phosphatase activity following hyperthermia of mouse spleen, rel. to heat potentiation of X-ray damage 78−48842
acid phosphatase of glial smooth endoplasmic reticulum, transport into damaged axons, role of microtubules 80−85381
actin, binding of myosin mol. to two actin filaments 78−27884
actin, microcrystals and tubes formed in the presence of Gd ions 79−16143
actin, mol. basis for chemomechanical energy transduction in muscle 80−72143
F-actin, muscle, quasi-elastic light scatt. 77−64010
actin, myosin subfragment-1 attachment, effect on equatorial X-ray refls. 78−27880
F-actin, struct. changes in living muscle fibres, polarised UV fluoresc. microscopy 80−67037
actin in the inner ear, struct. of the stereocilium 80−108918
F-actin subunit structural non-equiv., tension development in skeletal muscle 78−64959
actin-myosin, muscle contraction cross-bridge model 78−44475
actin-myosin binding, muscle mechanics thermodynamic model 78−80908
actin-myosin filament overlap rel. to number of Ca binding sites on glycerinated muscle fibres 78−44465
actin-myosin interaction, depend. of skeletal muscle energy transduction on time in tension 77−52754
actin-myosin interaction in skeletal muscle, quantitative model 77−52753
acto-myosin, cross-bridge slippage induced by AMP-PNP and stretch in fibrillar muscle fibres 78−77075
actomyosin, head rot. and dissoc., muscle exponential rate processes rel. to MgATP conc. 78−44468
actomyosin, heavy water effects 79−62220
actomyosin, thick filament linked Ca^{2+} regulation in vertebrate striated muscle 78−69020
actomyosin from a non-muscle system, tension generation 80−76781
actomyosin kinetic anal., review 80−21441
actomyosin-ATP system kinetics, energy transform. anal. 77−81476
adenylate cyclase regulation, depend. on sugar transport system, review 78−69031
adenylyl cyclases, stimulation by hormones and regulation by nucleotides, review 78−15760
adsorbed, use of Si-SiO_2 as electrode for elec. and ellipsometric meas. 80−15366
adsorbed at interfaces, fluoresc. spectroscopy study 80−12315
adsorbed layers on field-emitted tips, removal by UV radiation 80−104836
adsorbed on polymer surfaces, structural changes 80−89712

proteins continued
adsorption and immunological reactions at liq./solid interface, kinetics obs. by ellipsometry 77−52948
adsorption at liq.-solid interface, ellipsometric estimation of film thickness 78−44740
adsorption of homopolymer chain on homogeneous surface, theoretical model 77−70403
adsorption of non-paramag. compounds, spin probe investigation 78−65153
adsorption on glass, in detergent soln. 78−44401
adsorption on surface of hydrophilic polymers, water structuring, ESCA evaluation 80−108758
aequorin, Ca^{2+}-induced luminesc., inhibition by anaesthetics 78−76985
aequorin luminescence, light emission rel. to Ca^{2+} conc., Ca-independ. component 77−48750
aequorin-injected frog cardica muscle, Ca transients 78−61149
aggregates exposed to UV radiation, limiting conc. of paramag. centres 78−24029
aggregation in membranes, fluctuation-induced interactions in liquid crystals 77−90732
albumin, ^{99m}Tc labelling for lung imaging, quality control 78−28069
albumin, adsorbed layers on polystyrene, contact angle meas. 80−61508
albumin, adsorption on SiO_2 80−10777
albumin, bovine sercem, PMR spectra line narrowing, convolution and pulse methods 78−78729
albumin, bovine serum, charged macromol. translational diffusion coeff. 79−70510
albumin, bovine serum, diffusion, hydration and soln. environment effects 77−19116
albumin, bovine serum, diffusion, hydration effects, finite conc. 77−19115
albumin, bovine serum, diffusion, hydration effects 77−19114
albumin, bovine serum, hydrated, dielectric props. at 9.9 GHz 78−15758
albumin, bovine serum, in soln., five-component dielec. dispersion 78−15759
albumin, bovine serum, kinetics of binding with fatty acids, fluoresc. probe method 77−25365
albumin, bovine serum, laminar ultrafiltration, limiting flux numerical calc., variable diffusion coeff. 78−40214
albumin, bovine serum, macroion soln. viscosity and diffusion, quasielastic light scatt., electrostatic interaction 79−70508
albumin, bovine serum, solutions, fluctuation transport theory 78−70057
albumin, bovine serum, use of high heating rates in study of thermal denaturation 77−81470
^{125}I-albumin, convective and diffusive transport through rabbit aortic tissue 78−44482
albumin, human, labelling of microspheres with ^{197}Hg 80−51251
albumin, human serum, adsorption studies, feasibility of radiolabelling 78−85359
albumin, human serum, AsF_3^- NMR probe for anion binding sites 78−48748
albumin, human serum, assoc. solns., excited state deactivation, flash photolysis obs. 79−54895
albumin, human serum, elec. cond. and dielec. const., 1 to 15 MHz 78−53315
albumin, human serum, interaction with luminol. chemilum. and fluoresc. 77−21471
albumin, human serum, kinetics of eosin-sensitised photochemilum. of solns. 78−68991
albumin, pulsed laser study of adsorbed aromatic mol. excited states 77−86448
albumin, Reanal serum, mag. field effect on photoinduced reactions 79−92154
albumin adsorption and immunological reactions at liq./solid interface, kinetics obs. by ellipsometry 77−52948
albumin and albumin microspheres, ^{68}Ga labeling 80−17137
albumin clearance from alveoli, tissue permeation vs. airway displacement 78−27979
albumin denaturation, investigation by PMR 80−3582
albumin flux, differential permeability of endothelial and epithelial barriers, sheep expts. 80−81553
albumin macroaggregates labelled with radioisotopes for clot detect. 78−7438
albumin permeability of dog lung alveolar membrane, role of bulk fluid flow 77−52814
albumin transendothelial transport in steady state pipe flow at high shear rates 77−32939
albumin transport across aortic wall during acute angiotensin induced hypertension 77−44619
albumin-acceptor+chlorophyll lamellar system, steady photocond. 78−53328
albumin-fatty acid complexing rel. to struct. lability of biomembranes, using fluoresc. probes 77−25381
albumin-unsaturated fatty acid binding kinetics, fluoresc. anal., rel. to struct. lability of biomembranes 78−15755
alcohol dehydrogenase, horse liver, tryptophan residue room-temp. phosphoresc., temp. and enzymic complex form. effects 80−61512
alcohol dehydrogenases, yeast and horse-liver, radiation chem. evidence for differences in amino acid composition 78−40116
alkaline endonuclease activity in thymus and spleen of irrad. mice 78−28004
alkaline phosphatases in serum, as indicators of radiation damage in rats 77−86556
amide unit electron organisation, mol. orbital theory 79−2000
amino acid composition determ. by chromatography 79−44070
amino acid linear sequence form., cryo-sublimation of frozen aqueous solns. 78−95993
amino acid neighbourhood relationships, breakdown into overlapping doublets, triplets, and quadruplets 80−67035
D-amino acid oxidase, crit. residues, pulse radiolysis and inactivation study 78−27897
amino acid residues in globular proteins, hydrophobic character 79−2001
amino acid sequence determination of proteins labeled in tritium gas by microwave discharge 79−12057
amino acid sequence threadlike cryst. growth, light irrad., polycondensation 78−96009
amino acid side chains, NMR relax. due to multiple internal rots. 78−94340
amino acids, aromatic, solid, NMR, detection of individual C resonances, appls. 80−51042

proteins continued
L-amino oxidase, solvent effects on phosphoresc. props. of flavins 77−12885
amphiphilic-polymer liquid crystal, NaCl conc. influence on struct., X-ray diffr. study 80−44126
α-amylase transport across pancreatic acinar cell basolateral membrane 78−44481
Anacystis nidulans, unstable protein mediated UV light resist. 77−86536
analysis using $^{14}N(p,n)^{14}O$ reaction 77−81769
antibodies, conformation in presence and absence of antigen, small angle X-ray studies 79−11890
antibodies directed by Ca^{2+}-binding glycoprotein, inhibition of mitochondrial Ca^{2+} transport 77−4990
aortic wall stress-strain characts. after sequential enzymolysis 78−3530
apomyoglobin, nsec decay study of fluoresc. probe binding 77−29091
apomyoglobin reconstituted with ^{111}In(III)mesoprotoporphyrin IX, rot. correl. time determ. 80−76698
apoprotein of Folch-Lees lipoprotein, viscoelastic monolayer, dynamic surface potentials 80−3603
aqueous polynucleotide-protein mixture, inverted turbidity versus conc. depend. 77−9165
architectural units, ab initio SCF MO calcs. 78−96004
artificial liver support, protein-bound metabolite adsorbent equilibrium props. 79−20709
artificial liver support, protein-bound substance removal kinetics 79−20710
aspartate transcarbamylase, solid, enzyme activity and allosteric characts. after gamma irrad. 78−53341
aspartate transcarbamylase, solid, sedimentation and subunit interactions, after gamma irrad. 78−53342
aspartate-transaminase, phys. state in cryst., heating curves 77−70409
astatine labelling, prep. using electrophilic reaction 79−29627
ATPase, Ca^{2+}-activated, of sarcoplasmic reticulum, rot. motion and evidence for oligomeric structs. 80−72124
ATPase, Ca^{2+}-depend., struct. rearrangements during function 80−81527
ATPase, Ca^{2+}-depend. activity in bovine receptor cell outer segment 77−29147
Na^+, K^+-ATPase, identification of membrane-embedded segment of large polypeptide chain 78−3447
ATPase, ion-activated, role in biomembrane, active transport, review 78−15814
Na^+, K^+-ATPase, latent form, Lubrol activation, in retinal rod outer segments 77−12920
ATPase, localisation of Na^+, K^P-ATPase and Ca^{2+}-activated Mg^{2+}-depend. ATPase in retinal rods 77−44652
Na^+,K^+-ATPase, membrane, as digitalis receptor binding model 78−40111
ATPase, mitochondria, rat liver, vitamin E deficient, effect of X-irradiation 79−34511
ATPase, myofibrillar, chemo-mech. coupling in oscillatory contraction-relax. cycles 77−48829
Ca^{2+},Mg^{2+}-ATPase, of sarcoplasmic reticulum, transient kinetics obs. by fluoresc. 78−61156
ATPase, quantitative model of actin-myosin interaction in skeletal muscle 77−52753
ATPase cytochemical localisation in developing retina of teleost 77−70454
Na^+,K^+-ATPase generation of pot. jump at octane-water interface 77−81484
ATPase in membranes, role in loading of sucrose into plane sieve tubes 77−52757
ATPase kinetics in E. coli cells, ^{31}P NMR meas. 78−77022
Na, K-ATPase membrane prep. struct. characts. studied by paramag. probes 78−64930
ATPase of A-laidlawii membrane, Arrhenius plot artifacts due to temp. depend. of substrate-binding affinity 78−64949
ATPase of chloroplast, proton transfer from water to octane coupled with ATP hydrolysis 77−36876
Na^+,K^+-ATPase preparations, tryptophan fluoresc. 77−21477
autocatalysis in stoichiometric model of energy metabolism 77−36860
autoradiography and soft laser scanning in radioisotope work, appl. to metabolic studies 78−3576
axoplasmic transport of proteins, review 80−21464
Azotobacter ferredoxin, struct. of Fe-S clusters at 4.0 Å resolution 79−57575
bacterial bioluminescence protein, isolation and props. 78−92599
bacterial catalase, ^{57}Fe enriched, active centre, Mossbauer spectra meas. 80−8024
bacterial proteins, quantitation of electrophoretic profiles 79−70331
bacterio-opsin, changes in protonation state during reconstitution of bacteriorhodopsin 80−89707
bacteriochlorophyll electronic transition moment directions 79−100572
bacteriochlorophyll radicals, role in primary charge separation of Rhodopseudomonas viridis 80−63688
bacteriophage, gamma-ray induced cross linkage of DNA and protein 77−21485
bacteriophage DNA and protein cross-linkage by ^{60}Co gamma-rays 78−77002
bacteriopheophytin b radicals, role in primary charge separation of Rhodopseudomonas viridis 80−63688
bacteriorhodopsin, 13-cis and trans isomers, photochem. and dark equilib. 77−90798
bacteriorhodopsin, anomalous amide I IR absorpt. rel. to alpha helices distorted struct. 80−12058
bacteriorhodopsin, asymm. struct. of purple membrane, X-ray diffr. data anal. 77−73512
bacteriorhodopsin, charge stabilization mechanism in the visual and purple membrane pigments 79−34500
bacteriorhodopsin, dark-adapted, photocycle and light adaptation 77−73508
bacteriorhodopsin, dynamics, of pH-induced spectral changes 79−57587
bacteriorhodopsin, effect of high press. on absorpt. spectrum and isomeric composition 80−67041
bacteriorhodopsin, elec. response of a back photoreaction 80−98008
bacteriorhodopsin, emission lifetime meas. 78−96012
bacteriorhodopsin, enthalpy changes during photochemical cycle 79−34602
bacteriorhodopsin, excited state energy surface to explain photochemistry 79−48218
proteins continued
bacteriorhodopsin, in purple membrane, radial autocorrelation function, significance in X-ray diffr. patterns 80−51048
bacteriorhodopsin, kinetic isotope effects in photochem. cycle 77−44592
bacteriorhodopsin, new intermediates in photochem. conversions 78−96010
bacteriorhodopsin, photoelec. conversion in charged synthetic membranes 80−108954
bacteriorhodopsin, photoreactions, purple membrane light energy transduction 77−90726
bacteriorhodopsin, photosensory mechanism for Halobacterium, rel. to visual photoreception 77−90738
bacteriorhodopsin, photosynthetic cycle, time-resolved Raman spectra 78−85294
bacteriorhodopsin, primary intermediates in photochem. cycle 78−96011
bacteriorhodopsin, ps flash-photolysis obs., room and low temps. 79−57581
bacteriorhodopsin, purple membrane of H.halobium, effect of 560⇄570 transition and blue light on photochem. 80−30673
bacteriorhodopsin, purple membrane struct., Halobacterium halobium 78−15782
bacteriorhodopsin, reson. CARS spectrosc. 80−8014
bacteriorhodopsin, reson. Raman evidence for secondary protein-Schiff base interactions, primary excitation mechanism 80−55981
bacteriorhodopsin, reson. Raman kinetic spectroscopy on μsec time scale 78−20320
bacteriorhodopsin, subpicosecond spectroscopy, photochemical formation of bathobacteriorhodopsin 79−16156
bacteriorhodopsin, time-resolved resonance Raman characterisation 79−83705
bacteriorhodopsin, time-resolved resonance Raman spectroscopy 77−29103
bacteriorhodopsin 580 nm ultrafast transient, psec kinetics 78−44455
bacteriorhodopsin Br570, bathochromic shift of absorpt. band in external elec. field 80−35838
bacteriorhodopsin chromophore, bleaching by ^{60}Co γ-rays 80−30784
bacteriorhodopsin chromophore, light-induced isomerisation 80−108956
bacteriorhodopsin chromophore photoisomerisation rel. to purple membrane proton pump 78−35804
bacteriorhodopsin generated photocurrents on planar bilayer membranes 80−51050
bacteriorhodopsin in model membranes, new component of displacement photocurrent 79−43827
bacteriorhodopsin in planar membranes, elec. response to light 78−35806
bacteriorhodopsin in purple membrane, chromophore mobility 77−25366
bacteriorhodopsin in purple membrane, orthorhombic 2D crystal form 80−85362
bacteriorhodopsin in purple membrane fragments, proteolysis and flash photolysis obs. 79−62185
bacteriorhodopsin in purple membrane of H. halobium, chromophore excitonic interaction 77−21497
bacteriorhodopsin isomers, dark equilib. and photochem. 78−15771
bacteriorhodopsin membrane preps. associated with lipid-water interface, form. of elec. pot. diff. 80−81551
bacteriorhodopsin of purple membrane, quantum efficiency for photochem. conversion 77−29099
bacteriorhodopsin of purple membrane of H.halobium cells, luminesc. 77−36890
bacteriorhodopsin orientation in Halobacterium halobium, selective proteolysis investig. 78−77010
bacteriorhodopsin photoconversion products, EPR and low temp. spectrophotometry 78−15769
bacteriorhodopsin photocycle hydration effects, in thin purple membrane layers 78−7320
bacteriorhodopsin photocycle quantum efficiency 77−29098
bacteriorhodopsin phototransients, circular dichroism meas., comment 78−21954
bacteriorhodopsin reorientation due to elec. field 77−66789
bacteriorhodopsin Schiff base deprotonation dynamics using kintic reson. Raman spectroscopy 77−48981
bacteriorhodopsin-containing membrane fragments, quantum yield of flash-induced proton release 79−34601
basic pancreatic trypsin inhibitor, methyl group PMR, 360 MHz 78−27887
bathoproducts of rhodopsin, isorhodopsin I, and isorhodopsin II 80−51088
Bence-Jones Rhe protein (1.9 Å), phase extension and refinement 79−99168
beta sheet structures, anal. and prediction by combinatorial approach 80−76710
bimolecular rate constant ionic strength dependence, effect of a molecular dipole 80−55977
biological macromolecules, conformation studied by calorimetry, review 80−97870
biomembrane, high protein concentration 79−83714
biomembrane, phase changes and determination methods *(Czech)* 80−3599
biomembrane asymmetry, review 77−48768
biomembrane structural constitution and function *(German)* 79−5256
biomembrane systems, dynamical mechanical spectroscopy, mol. interactions 77−29109
biomembranes, intrinsic electric fields and proton diffusion 79−24964
biomembranes, lipid-protein interactions, flexoelectric effects 78−92600
biomembranes, proton transport, mol. mechanisms 78−96035
biomolecules+chloranil, charge transfer interaction, equilib. const., enthalpy and entropy determ., mol. polarisability 80−89708
Biophysical Society, 23rd annual meeting, conf., Atlanta, USA (Feb. 1979) 79−34468
biopolymer, electronic-conformation interactions 80−3588
biopolymer soln. heat capacity, conformational props. temp. depend. 80−8009
biopolymers, primary structure determ. algorithms 79−48209
biopolymers, reversible unfolding, mol. field theory 79−34479
biosynthesis, role of guanine nucleotides 78−68982
blood proteinpolymer interfacial behaviour, influence of hydrophilic-hydrophobic type of microphase separated struct. *(Japanese)* 80−12051
blue proteins, activation of electron transfer reactions 78−44446
bovine carbonic anhydrase, γ-ray perturbed directional correl. obs. of conform. change, active site ^{111}In ions 79−83700

proteins continued
bovine pancreatic trypsin inhibitor, struct. refinement by simultaneous minimisation of energy and R factor 79−7517
bovine plasma albumin, high conc. soln., quasielastic light scatt. line breadth meas., diffusion coeffs. 77−1976
bovine serum, adsorpt. meas. at interfaces by drop volume technique 78−60009
bovine trypsinogen, low-temp. study, effect on flexibility, temp. factor, mosaic spread, extinction and diffuse scattering 80−54214
brain, microtubule solns., calf, dynamic laser light scattering 79−16150
C1q of human complement, neutron scatt. obs., conformational calcs. 80−81537
C-reactive protein, interaction with artificial phosphatidylcholine bilayers 80−3579
calmodulin, stimulation of Ca^{2+} transport across red blood cell plasma membrane 80−12066
carbonmonoxyhemoglobin, spectroscopic meas. after pulsed optical excitation 79−92150
carbonmonoxymyoglobin, forzen soln., recoilless fraction, Mossbauer spectra meas. 80−8025
carboxyhaemoglobin, aq. soln., photolysis using nanosec. pulse, transient effects 79−79453
carboxyhaemoglobin, carp, variability of mag. moment 80−94159
carboxyhaemoglobin, redox investig. using reson. Raman, visible absorption and electrochem. methods 78−76832
cartenoprotein, lobster shell, photoacoustic spectroscopy obs. 79−62192
β-casein, adsorpt. isotherm, at air-water and air-oil interfaces 79−79461
β-casein, adsorption kinetics, surface denaturation 79−79460
β-casein, molecular structure of adsorbed film 79−79462
casein-methylglyoxal complex, electronic props. 77−52736
κ-caseins of cow and sheep, secondary structures 78−96001
catalase, from the fungus penicillium vitale pidopl. et bilai, preliminary crystallographic investigation and props. 79−66444
catalase, glucose embedded, measurement and reduction of radiation damage in frozen hydrated crystalline specimens 80−89810
catalase, phys. state in cryst., heating curves 77−70409
catalase, solid state, electron microscopy radiation damage, amino acid composition 77−25377
catalase crystal lattice stability 77−25380
catalase crystals and solns., calorimetric investigation 79−70526
catalysis of reversible flow reaction by oligomeric enzyme 77−36859
cataract formation in vitro, rel. to protein synthesis control and intracellular Na^+/K^+ ratio 78−11646
cell energy metabolism, ATP effect on initiator stage enzyme activity and conc. 78−64950
cell movement, molecular basis rel. to proteins 79−100586
cellular metabolism depend. of split-dose and liq.-holding recovery after X-irrad., yeast 77−86547
cellular protein two-dimensional analytical electrophoresis 79−96528
cereal, proton-induced X-ray emission and nuclear reactions for determ. of protein quality 78−20321
ceruloplasmin, human, calc. of rotation function for tetragonal. cryst. at 10 Å resoln. 80−108843
ceruloplasmin, human, mol. wt. determ. by hydrodynamic methods and low-angle X-ray scatt. 78−15761
chain reversal regions conservation 79−83699
chemical analysis using PIXE 80−61691
chemical reactions, rate coeffs., viscosity effects 80−71890
chloroperoxidase, ferric form, X-ray absorpt. fine struct., Fe-N and Fe-S lengths 79−48213
chloroplast fragments, fine struct. of fluoresc. spectra, derivative spectroscopy method *(Russian)* 79−34502
chloroquine-biopolymer binding interactions, PMR effects 80−55982
cholinesterase, microwave radiation interaction studies 79−39363
chondromucoprotein, effects of ^{60}Co γ-irrad. 78−7400
chorionic gonadotropin, human, α-subunit, cDNA isolation, cloning and sequence anal. 80−3587
chromatin, DNA-protein complexes, electron microscope visualisation, book contrib. 79−5434
chromatin, neutron scatt. rel. to higher order struct. 79−11894
chromatin, nucleosomal arrangement DNA, histones and non-histones, review 79−79464
chromatin from cultured mammalian cells, radiolysis, DNA-protein cross-links formation 80−81655
chromatin protein, increase kinetics for heated cells, possible role in cell killing 80−40980
chromatin structure and thermal denaturation profiles 77−12881
chromatin subunits, in glycerol/sucrose solns. containing various D_2O/H_2O mixtures, neutron scatt. study 79−11893
chromophores, fluoresc. props., use in macromol. equilib. struct. mobility investigs. 79−64130
chromosomal proteins and DNA syntheses in rat thymus after whole-body X-irradiation 79−34492
chromosomal proteins from Yoshida ascites tumour chromatin, γ-irradiation effects 79−96626
chymotrypsin, charge relay system, H-bond models, IR spectra 78−64935
α-chymotrypsin, Fourier phase refinement and dimeric struct. extension at 1.8 Å resolution by density modification 79−90634
chymotrypsin, inactivation role of tryptophanyls singlet and triplet states 79−57564
chymotrypsin, study by pulse radiolysis 79−8480
chymotrypsin hydrolysis of N-succinyl-L-phenylalanine-p-nitroanilide, enzymatic reactions 78−95992
chymotrypsin-like proteins, γ-irrad. rel. to UV irrad., unfolding obs. 80−35984
chymotrypsin-like proteins, gamma irrad. induced struct. changes 77−44594
chymotrypsin-like proteins, gamma-irrad., inactivation rel. to struct. changes 77−56341
Cl Mn II complex with protein, EPR spectra and zero field splitting interaction 78−35793
coiling and topology of the antiparallel β-struct. 80−40956
coiling and topology of the parallel β-struct. 80−40957
collagen, 3_1 helix-coil transition in polypeptides, circular dichroism obs. 78−35795
collagen, 3-dimens. struct., rel. to props. of connective tissue 80−67038
collagen, axial arrangement of α-chains, intramolecular polar and apolar interactions 78−27891
collagen, corrugated fibril mechs. in arteries 77−48823
proteins continued
collagen, enzyme- and alkaline-soluble, optical rot. dispersion and circular dichroism 77−70411
collagen, helical and coiled, thermodynamic values, 4 to 300K 77−25379
collagen, hydration and intramolecular fusion, NMR and calorimetry obs., dynamic model 79−79451
collagen, interpretation of small-angle X-ray diffr. using α1 chain primary struct. 77−66792
collagen, native, phasic transition, PMR 77−25363
collagen, optical SHG 79−53046
collagen, polarisation, contribution of permanent and induced dipole moments, elec. birefringence 80−85351
collagen, reconstituted, mech. props., drug release support appl. 78−3666
collagen, role in elastic props. of calcified tissue 78−3539
collagen, tendinous, highly ordered maromolecular composite, mech. props.-ultrastruct. relation 77−52826
collagen, X-ray and neutron small-angle scattering 79−11889
collagen and muscle elastic moduli rel. to phonons, Brillouin sectra 77−52824
collagen content rel. to US attenuation in myocardial tissue 79−43973
collagen effect on US propagation in tissue 78−61212
collagen fibre studies with SEM, bone prep. techniques 78−57150
collagen fibres, of dermis, structural and mech. charact. and natural interweaving 78−48824
collagen fibril, ^2H NMR of mol. motion 80−67034
collagen fibril, mol. cryst. model as basis for struct. 77−48751
collagen fibril, probabilistic aspects of struct. 78−27886
collagen fibril cross-striation, thermodeform., electron microscopy and X-ray diffr. 77−86438
collagen fibrils, in connective tissue, preferred orientation and orientation distrib. function determ., high-angle X-ray diffr. patterns 79−62177
collagen fibrils, ultrastruct. elements of muscle-tendon junction strength 77−25485
collagen fibrils as examples of smectic A biological fibres 77−90721
collagen film, dynamic mech. props., β-galactosidase impregnation effects 79−11885
collagen in skin, selection of radiation for X-ray diffr. 78−81087
collagen membrane H^+ diffusion-limited binding electromechanics 79−79489
collagen models, interchain interactions rel. to triple-helical coiled-coil conform. in poly(glycyl-prolyl-prolyl) 77−38762
collagen molecular organisation and connective tissues props. 80−97858
collagen piezoelectricity, rel. to stress generated pots. in bone 77−32932
collagen structure in cartilage of intervertebral disc 78−56951
collagen threads, mammalian, US meas. using scanning laser acoustic microscope 79−43972
collagen triple helical struct. study using Fourier transform 78−7318
collagen type supramolecular structs., 2 possible mechs. of formation 80−76702
collagen-mineral axial relationship in calcified turkey leg tendon, X-ray and neutron diffr. 77−32872
collagen-water system, phasic transition invesitgation by calorimetry and NMR 79−62167
collagen/synthetic polymer laminar copolymers, tissue compatibility 77−60289
collagne fibrils, rat tail tendon, quasi-hexagonal mol. packing model 80−30660
competitive protein binding assay, automatic treatment of data 77−13037
concanavalin A receptor, of human erythrocytes, receptor function in lipid bilayers 78−48764
concanavalin A-carbohydrate interactions, implication of protein aromatic amino acids, radiolysis 78−40110
conference, Dublin, Eire (July 1977) 79−55012
conformation, ^{13}C NMR investigs., review 79−55013
conformation, statistical mechanical theory, appl. to homopolymers 78−64931
conformation, statistical mechanical theory, folding pathway 78−64932
conformational analysis, algorithms and data structs. for array processing 80−83530
conformational analysis, empirical pot. energy algorithm 79−50174
conformational changes in aqueous soln. and in mixed solvents, IR absorpt. spectra 78−15762
conformational studies in presence of side chain chromophores, circular dichroism 79−55014
conformational transitions, temp.-depend. using fluoresc. probes 77−70410
conformations, quantitative approach 80−30652
crosslinking and affinity labeling, use of photoreagents 79−96517
crystal structural analysis by electron diffr., single scatt. approx., domains of validity 80−101150
γ-crystallin, calf-lens protein, single cryst., X-ray diffr. low resolution struct. anal. 79−16130
βs-crystallin, lens protein, prep. 80−16921
α-crystallin, of calf eye lens, small angle X-ray scattering study 79−11891
α-crystallin, organisation of lens proteins in fibre cell 77−90766
α-crystallin in study of mol. processes using vertebrate eye lens 77−90770
crystallisation, effect of protein conc. and solubility on nucleation rate 78−87632
crystallography, in mol. biophysics course 77−33720
crystallography, min.-variance Fourier coeffs. from isomorphous replacement method by least squares anal. 77−52938
crystallography, MWPC as area detector 78−65166
cyst liquid of human breast, US absorption obs. 79−62319
cytochrome, 3-D coordinates from stereodiagrams 80−64824
cytochrome b_5, cryst. struct., analysis by electron diffr., single scatt. approx., domains of validity 80−101150
cytochrome b_5 rotational diffusion in lipid bilayers, influence of lipid physical state 79−83693
cytochrome c_3, anhydrous film, elec. cond., temp. and ambient press. depend. 80−85327
cytochrome c_3, haeme-haeme mag. interaction, Mossbauer obs. 80−108836
cytochrome c_3−hydrogenase, reduction kinetics, Mossbauer spectra 80−67031
cytochrome c_3 film, anhydrous, elec. cond. 79−66439
cytochrome c, dilute soln., reson. Raman spectra, pulsed laser excitation; optical multichannel detection 78−76999

proteins continued
cytochrome c, effects of UV and temp. on optical props. and enzymatic activity 80−81648
cytochrome c, electron reactions in ethylene glycol/water glass at −196°C 79−62194
cytochrome c, electron tunnelling to cytochrome c peroxidase 79−20507
cytochrome c, fast Raman spectroscopy using dye laser intracavity reson. Raman amplification 77−66794
cytochrome c, ferric- and ferro-, reson. Raman excitation profile, Soret excited 79−92147
cytochrome C, immobilised, investigs. using magnetic micromixer attachment for SPECORD UV VIS spectrophotometer 80−56302
cytochrome c, low freq. modes and excitation profiles, reson. Raman spectra 80−94428
cytochrome c, metal substitution effect on mol. struct. and functional props. 79−53037
cytochrome c, PMR, eight-ring current model heme ring, conformation depend. shifts 80−74185
cytochrome c, protein influence on haeme, Raman difference spectroscopy 80−72125
cytochrome c, redox investig. using reson. Raman, visible absorption and electrochem. methods 78−76832
cytochrome c, trifluoroacetylated, electron transfer reactions 79−20505
cytochrome c, X-ray absorpt. edge fine struct. of active site haem 79−24945
cytochrome c adsorbed on different carriers, conformation study 79−53029
cytochrome c and related metalloproteins, fast electron transfer processes 79−8478
cytochrome c anhydrous film, electrical conductivity 77−44879
cytochrome c conformationally-nonequilibrium state reactivity obs. by pulse radiolysis 79−43816
cytochrome c interaction with bilayer phospholipid membranes 78−69001
cytochrome c interaction with phospholipid membranes 77−25384
cytochrome c oxidase, coupled to proton pump in mitochondria 77−25406
cytochrome c oxidase, Cu ENDOR 80−94170
cytochrome c oxidase, macromolecular struct., electron microscopy and image anal. 80−89716
cytochrome c oxidase, mitochondria, rat liver, vitamin E deficient, effect of X-irradiation 79−34511
cytochrome c oxidase, oxidised and reduced, X-ray absorpt., edges, using synchrotron radiation 78−48758
cytochrome c oxidase, struct. of cytochrome a_3-Cu_{a_3} couple, NO binding studies 80−67039
cytochrome c-bacteriochlorophyll, low-temp. electron transfer in bacterial photosynthesis 78−44470
cytochrome c-$Fe(CN)_6$ electron transfer, verification of vibronically coupled electron tunnelling 78−48750
cytochrome c-$Fe(CN)_6$ electron transfer, vibronically coupled tunnelling description 77−52737
cytochrome c-serotonin soln., UV effect on optical props. 80−30663
cytochrome f function in photosynthetic electron transport 79−62206
cytochrome oxidase as electron-proton generator of membrane potential, role of protons 79−43807
cytochrome oxidase reaction, semiconduction as mechanism 80−55983
cytochrome P-450_{cam}, Fe^{3+} zero-field splitting, Orbach relax. rates 77−21483
cytochrome P-450, anomalous T^7 temp. depend. of Raman spin-lattice relax. 77−21482
cytochrome P-450, ferric form, X-ray absorpt. fine struct., Fe-N and Fe-S lengths 79−48213
cytochrome P-450, non-equilib. states formed by low-temp-reduction, absorpt. spectra 80−35837
cytochrome P-450-CO complex, absorpt. spectrum, electronic transitions, PPP calcs. 77−71811
cytochrome-c, hydrated, dielectric props. at 9.9 GHz 78−15758
cytophotometry, multiparametric pulse technique for cell and radiation research *(German)* 77−78060
cytoskeletal proteins of human erythrocyte, in vitro complex formation 79−96514
dehydration of protein crystal, conformational changes with hydrostatic compression *(Russian)* 77−43339
denaturation, rel. to hyperthermia response of rat tail 77−73509
deoxy ferrous haemoglobin Fe atom distortion, pseudo-Jahn-Teller effect 80−55984
deoxyhaeme model, semiempirical calcs., EM props. rel. to electronic config. and Fe-plane distance 78−53324
deoxyhaemoglobin, complex with rhombic distortion, spectroscopic props. of high spin Fe^{2+} 77−51861
deoxyhaemoglobin, Fe(II)-N_ε(His-F8) stretching freq. rel. to quaternary struct. 80−94160
deoxyhaemoglobin, ferrous heme of high-spin type, MCD spectra in Soret, visible and near IR regions 80−94156
deoxyhaemoglobin, high mag. field Mossbauer spectra, electronic states 80−35845
deoxyhaemoglobin, vibronic coupling, mag. susceptibility and Mossbauer data interpretation 78−70984
deoxyhaemoglobin high spin ferrous ion, low lying electronic states, far IR mag. reson. 80−48110
deoxymyoglobin, forzen soln., recoilless fraction, Mossbauer spectra meas. 80−8025
deoxymyoglobin, high mag. field Mossbauer spectra, electronic states 80−35845
deoxymyoglobin, low temp. PMR, low-lying Fe^{2+} states model 78−68997
deoxymyoglobin, single cryst., paramag. anisotropy meas. 77−21469
deoxymyoglobin, vibronic coupling, mag. susceptibility and Mossbauer data interpretation 78−70984
deoxymyoglobin high spin ferrous ion, low lying electronic states, far IR mag. reson. 80−48110
deoxymyoglobin single crysts., Mossbauer study with polarised γ-rays 80−40962
deoxyribonucleoprotein, gamma-ray protein damage 78−53338
detection in implanted cardiac pacemaker epoxy housing 79−25156
diagmagnetic anisotropy, struct. origins 79−92136
diamine oxidase solutions, proton mag. relax. dispersion obs. 80−51136
diffusion coefficient of plant protein using quasielastic light scatt. apparatus *(German)* 80−12314

proteins continued
dihydrofolate reductase activity of mouse spleen, whole body irrad. effect 77−37013
dimensions, shape, conformational transitions, use of dielectric relaxation method 79−11888
DIP-trypsin, difference Fourier refinement using minicomputer, to 1.5 Å 77−58924
dipalmitoylphosphatidylcholine/glucagon (cardiolipin/insulin) systems, Raman spectra study 80−16903
dipeptidase activity of kidney after gamma irrad. 77−12976
dipeptide, struct. and bonding, ab initio calcs. 79−53039
dipeptides, reactions with hydrated electrons, EPR and spin-trapping studies 79−16124
diploid fibroblasts, human, nondividing, effect on RNA and protein synthesis 79−92291
disaccharidase activity of kidney after gamma irrad. 77−12976
dispersions, viscoelastic effects, shear viscosity and primary normal stress difference 80−87754
DNA, molecular motions, investigated by ^{31}P and ^{13}C NMR relaxation 80−63657
DNA helix destabilising protein cryst., electron microscopy 80−85338
DNA polymerase kinetics, gamma-ray response of leucoagglutinin stimulated lymphocytes 78−57041
DNA-protein cross linking mediated by X-rays 78−27898
DNA-protein interaction, biostereochem. modelling, interactive computer graphics 78−88693
DNA-protein interaction, effect of cooperativeness on recognition of specific sites 77−81463
dopamine, thermal blooming spectroscopy 80−86441
drug-matabolising enzymes in liver rel. to hormones after whole- and partial-body irrad. 78−48840
dynamic states, role of geometry and elastic strains 78−48745
dynein biochemistry, role in enkaryotic cell motility, book contrib. 79−16178
E. coli cells, iron-storage protein, Mossbauer spectra obs. 80−8022
edestin, protein-peroxide radicals, ^{17}O-labelled, EPR obs. 80−85345
elastase, globule, atomic density distrib. 79−79458
elasticity of polymer globule 77−70404
elastin, hydrated, dielectric relax. 79−5247
elastin ultrastruct., freeze-fracture electron microscopy 80−8036
electrical conductivity, self-consistent continued-fraction theory of cond. 79−69482
electrolyte solutions, interionic radial distrib. function approx. scheme 77−32796
electron diffraction, low dose, of wet protein cryst. 80−85550
electron microscopy, real-space filtering of images from optical autocorrel. patterns 78−8479
electron microscopy of nucleic acids, basic protein film method 80−104844
electron radiation damage on primary and secondary struct. evel 80−89808
electron transfer kinetics models 79−39339
electron transfer mechanism 79−96510
electron transport at large distances, role of proteins 79−34480
electron-transport type, H-bonding, ab initio MO 80−51039
electronic transport mechanisms, asymmetry role 78−6370
electrophoresis of proteins in intercellular bridges 80−89734
electrophoretic waveform analysis for blood serum protein composition determ. 78−64928
electrostatic effects on behaviour 79−53027
ellipsosomes in fish cones, ultrastruct. and staining props. 79−11924
endonuclease, rel. to DNA electron damage repair in E. coli mutants 78−31775
enzymatic active transport model 80−51049
enzymatic activity, quantum cooperative mechanism 77−40632
enzymatic activity in biomolecular nonequilibrium reactional scheme, limit cycle and dissipative structs. 77−1977
enzymatic catalysis, dynamic theory, conform. rearrangements 77−36858
enzymatic catalysis, orbital perturbation anal. 78−31623
enzymatic charge transfer across oil-water interface, effect of dielec. const. 77−70419
enzymatic digestion of γ-irrad. DNA, separation by ion exchange chromatography 78−85290
enzymatic fluoresceindiacetate hydrolysis in mammalian cells after UV and gamma irrad. 77−56333
enzyme, complexation, Mossbauer spectroscopy 77−12876
enzyme, diffusion-controlled reaction rate to buried active site 78−35796
enzyme, nucl. quadrupole interaction parameter related to structure-function 77−8472
enzyme activities, effects of whole-body X-irrad. on creatine biosynthesis, rat 78−3559
enzyme activity, kinetic assay, progress curve algorithm for spectrophotometric meas. 78−20083
enzyme activity rate reduction by EM fields *(Russian)* 78−61142
enzyme dynamics, statistical phys. 80−21439
enzyme microwave inactivation system, electronic control to reduce dose variability 78−40285
enzyme reaction kinetics modelling 77−4979
enzyme reaction rate determ. by capacitance meas. 78−31997
enzyme reaction systems, nonequilib. transitions, probability distrib. 79−12720
enzyme reactions in tissue sections, quantitative microscopy using microdensitometry 77−86728
enzyme supports, method for determ. amino and isothiocyanate groups on surface 79−61920
enzyme synthesis, simulation of cellular response to methotrexate 77−40647
enzyme-linked immunosorbent assay, apparatus for meas. light absorbance of small vols. of liquids 80−72387
enzyme-mediated multidimensional inflection points in nonequilib. linear behaviour 80−72122
enzyme-substrate interaction forces influence on reaction rates 78−31765
enzyme-substrate interactions rel. to limit cycle model for brain waves 77−73520
enzyme-substrate reactions in differential scanning calorimeter, digital simulation 79−74794
enzymes, membrane bound, influence of membrane fluidity on activity, book contrib. 80−30688
enzymes, membrane-bound, activity on exposure to 2450-MHz microwave radiation 80−56126

proteins continued
enzymes, molecular struct. reconstruction from electron microscopy images 80−89715
enzymology in subzero temp. range, air-bath cryostat 78−48949
EPR absorption of tissue constituents, colour correlation, using mouse liver 77−90727
erythrocyte integral membrane protein lateral mobility, human cells 77−66805
erythrocyte membrane protein alterations in Huntington's disease, EPR 77−56347
erythrocyte membranes, human, elec. cond. characts. 77−9180
erythrocytes, bound water in frozen solns., proton mag. relax. 77−28472
erythrocytes, human, effect of hydration on water content 77−16921
erythrocytes, membrane protein vertical displacement, rel. to microviscosity changes 77−44608
evolution, molecular clock test using Panamanian sea urchins 79−92134
eye, intact bovine lens protein, Raman spectroscopy with intensified Vidicon detectors 79−29525
eye lens low molecular weight protein obs. and prep. 80−16921
eye lenses, crystalline, of humans, fish and birds, state of water, NMR meas. 79−48212
eye striated muscle, bovine, physico-chemical anal. of contractile proteins 77−90819
factor VIII, native and modified, surface adsorption and mol. interactions, ellipsometric obs. 80−104555
fatty acid synthetase, from yeast, three-dimens. electron microscopy, struct. and image reconstruction 77−12883
Fc-fragment crystals, low-temp. study, effect on flexibility, temp. factor, mosaic spread, extinction and diffuse scattering 80−54214
ferredoxin, Fe atoms at active centre, exchange integral of antiferromag. interaction 80−76697
ferredoxin, from Clostridium pasteurianum, Mossbauer effect, ESR, and mag. susceptibility meas. 80−40961
ferredoxin, from Halobacterium, Mossbauer and EPR spectrum 78−76998
ferredoxin, pulse-radiolysis study of conformationally nonequilibrium states 79−70506
ferredoxin, S. platensis [2Fe-2S], struct. and evolution of chloroplast-type ferredoxins 80−94165
ferredoxin, soluble, investigation of 2 forms from pea leaves, EPR obs. 80−45851
ferredoxin of adrenal cortex, destruction of chromophore centre on exposure to X-irrad. 78−76993
ferredoxin synthetic analogues, $[Fe_4S_4(SR)_4]^{3-}$ clusters, Mossbauer effect, EPR, and mag. props. 80−41057
ferredoxin-like centres, membrane bound, in photosystem I of blue-green algae, Mossbauer and EPR study 80−40974
ferric cytochrome c, reson. Raman spectra, Fe^{3+} low-lying electronic levels 78−53335
ferric haeme complex of low spin, Mossbauer spectra, crystal field parameters 80−26203
ferric haeme protein, anal. of low-spin ESR spectra 77−60185
ferric haemoglobin, EPR studies before and after irradiation 79−29503
ferric haemoglobin chains, crystalline state disorder and hyperfine component line widths 79−34482
ferric haemoglobin single crystals, contribs. to EPR line width 79−34484
ferric leghaemoglobin a, proton-depend. anion binding, soybean, proton NMR study 79−74592
ferric myoglobin cpds., single cryst., Mossbauer studies 80−8016
ferricytochrome c, rate of interaction with negatively charged lecithin liposomes 77−16914
ferricytochrome c and c_3, ionis. pot. from VUV photoelectron spectra 79−43821
ferricytochrome c structure, effect of different phospholipids 78−68981
ferricytochrome-lipid interaction effect on struct. of artificial vesicular membranes 77−25385
ferrihaemoglobin hydroxide, nucl. hyperfine interaction, HF LCAO calc. 79−2002
ferrihaemoglobins, $(Fe^{3+})d^5$ config. 78−39071
ferritin particle, microanal. by energy loss spectrometry using field emission STEM 78−53286
ferritin particles, BeO supporting films in high resolution electron microscopy 78−12792
ferrocytochrome c_3, anhydrous, ionisation pot., UV photoelectron spectrosc. obs. 80−85328
ferrocytochrome c, ionis. pot. from VUV photoelectron spectra 79−43821
ferrocytochrome c, mol. dynamics simulation 80−87255
ferrohaemoglobin, R-T conformational change due to pseudo Jahn-Teller effect 79−70521
ferrohaemoglobin excited state wave functions *(Japanese)* 79−8475
ferrous nitrosylhaemoglobin, NO binding, spin distrib., orbital model and mag. props. 80−81534
ferrous porphyrin, intermediate spin, reson. Raman spectra 79−69820
ferrous rubredoxin, high spin, spin fluctuation rates from Mossbauer spectra 79−29506
fibres, natural, Brillouin scatt. shifts, comparison with synthetic polypeptide obs. 80−55991
fibrinogen, adsorbed layers on polystyrene, contact angle meas. 80−61508
fibrinogen, bovine, high energy-induced aggregation, time resolved spectra 80−61655
fibrinogen, liq. cryst., layer, shear orientation 77−27807
fibrinogen, native and modified, surface adsorption and mol. interactions, ellipsometric obs. 80−104555
^{123}I-fibrinogen scintigraphy for thrombosis detect. 78−7437
fibrinogen solution, effect of scavengers on radiation-susceptible sites 78−11701
^{125}I-fibrinogen uptake test for detect. of deep vein thrombosis, review of current practice 78−7436
film, at liq. interfaces, dilatational props. 80−94255
film, at liq. interfaces, shear rheological props. 80−94256
fluorescence, equilib. struct. mobility *(Russian)* 78−76986
fluorescence polarisation meas. at high press. 78−66576
fluorescence spectra, using 3-dimens. contour plotter 78−58046
fluorescent probe binding to proteins error in interpretation of double-reciprocal plot and Scatchard plot 78−24021
folded, models for H exchange 78−76981
folding, incorporation of 1-dimens. Ising model into 3-dimens. model 77−90723
formyl-triglycyl amide-H_2O, analytical pot., ab initio calc. 79−48206

proteins continued
Fourier refinement of structs. 80−51037
freeze-fracturing of capillary layers of cells, membranes, viruses, new hinged device 78−20327
β-galactosidase induction in X-irrad. E. coli B and B/r 78−28005
gamma globulin, effect on latex particles flocculation kinetics 80−11958
gel electrophoresis, 2-dimens., in study of somatic cell differentiation 80−46114
gel scanner for location of proteins separated by isoelec. focusing 80−30953
gelatin film, deuterated, IR absorpt. spectra, heat treatment and ageing *(Russian)* 78−39621
globin, human, isoelectric focusing method for chain separation 80−17219
globular, bend form., conformational space, statistical mech. anal. 77−68146
globular, compressibility in water at 25°C 80−40951
globular, crystalline, intermol. interactions, denaturation, DSC and X-ray diffr. obs. 80−16897
globular, diffusion in calcium alginate gels, heterodyne beat spectrum 79−1776
globular, in aqueous solutions, conformational mobility investigation 79−53033
globular, in water, proton NMR spin echo decay comparative investigation 80−81541
globular, intramol. relaxation 77−10798
globular, no. of turns and models of turn form. 77−77869
globular, prediction of β-turns by computer 79−83698
globular, rot. correlation times, photocounting pulse fluorimetric determ., statistical accuracy 77−61777
globular, surface and inside volume meas. 79−34477
globular and BPTI, folding, unfolding, expt. studies 79−2003
globular protein rotatory mobility meas. by spin probe method, soln. viscosity 77−16902
globular protein struct., large angle X-ray diffuse scatt. exam. 78−3444
globular proteins, micro- and macro-stabilities 79−92135
γ- globulin, single mol., fluoresc. tagging in optical microscope 77−21662
β-glucoronidase release by leucocytes exposure to shear stress 78−40125
glucose 6-phosphate dehydrogenase studies following partial body γ-irrad. glucose 6-phosphate dehydrogenase in testes after partial body γ-irrad. 78−80924
glutamate dehydrogenase:α-ketoglutarate, cross relax. effect on NMR spin-lattice relax. time 78−78723
glutamine synthetase, neg. stained, image reconstruction of low and high dose micrographs 80−85551
glutamine synthetase macromolecular struct., electron microscopy and image anal. 80−89716
glyceraldehyde-3-phosphate dehydrogenase radiolysis, active-site and SH loss 78−77000
glycogen phosphorylase b activity, struct. of cryst. and complexes 78−80830
glycophorin, of human erythrocytes, receptor function in lipid bilayers 78−48764
glycoprotein, Ca^{2+}-binding, inhibition of mitochrondrial Ca^{2+} transport by antibodies 77−4990
glycoproteins, fast axonal transport in guinea pig auditory neurons 80−104573
grain legumes, proton-induced X-ray emission and nuclear reactions for determ. of protein quality 78−20321
gramicidin A in biomembrane channel, IR spectroscopic obs. 80−16901
gramicidin ion pore, potential variation 79−34506
gramicidin-S, dissolved in deuterated ethylene glycol, interproton nuclear Overhauser effects 79−16123
GTPase, light-activated, in vertebrate photoreceptors 78−3481
guanyl ribonucleases of fungi, crystn. and X-ray diffr. 78−71718
haeme a, low-spin ferrous, MCD, LCAO MO SCR π-electron calcs., PPP approx. 78−9178
haeme disorder characterisation in haeme proteins, PMR method 79−92152
haeme protein, reson. Raman line intensity formulae applicability 77−83609
haeme protein, resonance Raman effect *(Hungarian)* 78−74666
haeme protein solns., resonance Raman spectra at low temp. 77−23588
haeme proteins, CO binding dynamics, flash photolysis 77−21472
haeme proteins, inversely polarized modes in reson. Raman scatt., depolarisation dispersion curves, vibronic interactions 78−78676
haeme proteins and metalloporphytins, redox chem. and oxygen binding 80−3573
haeme-liganded sickle cell haemoglobin, spin label detection of intermolecular interactions 79−16122
haemin-histidin, ^{57}Fe Mossbauer spectra, temp. depend. of quadrupole splittings, atom positrons *(Spanish)* 77−73098
haemoglobin, ^{15}N NMR determ. of residual struct. in backbone of unfolded mol. 77−90720
haemoglobin, ^{3}H distribution in glycogen, haemoglobin and chromatin of mice drinking tritiated water 78−31910
haemoglobin, absorpt. spectra, light scatt. method meas. *(Russian)* 78−21939
haemoglobin, allosteric effect, mathematical description 79−64125
haemoglobin, aq. soln., X-ray induced changes 78−11699
haemoglobin, bovine type A, γ-induced changes obs. 79−43811
haemoglobin, charge carriers origin and mobility, adsorbed water effects 79−92461
haemoglobin, charged effectors, indirect allosteric action mechanism 79−20503
haemoglobin, conformational change, relation with CO binding 79−8473
haemoglobin, deoxygenated, electronic term scheme using mag. susceptibility and Mossbauer data 77−44586
haemoglobin, deoxygenated, vibronic coupling effect on paramagnetisms 77−57899
haemoglobin, deoxygenated sickle cell, gels, liq. cryst. props. 78−3445
haemoglobin, dielec. transient response following UV irrad. 80−51166
haemoglobin, dielectric props. under UV excitation 80−6912
haemoglobin, dynamic characts. of conformational nonequilib. states, radiolysis investig. 78−58877
haemoglobin, effect of adsorpt. on struct. and props. 79−92121
haemoglobin, ferrous high-spin derivatives, MCD at room and liq. N_2 temps. 78−76997
haemoglobin, high resolution optical props. of blood 77−36869

proteins continued
haemoglobin, human, EPR spectrum, g-value during oxygenation-deoxygenation reaction 78−53333
haemoglobin, human, liganded, kinetics of alkaline tetramer-dimer dissoc., laser scatt. obs. 78−48749
haemoglobin, human, maleimide spin labeled, proton ENDOR spectra obs. 80−89719
haemoglobin, human and Lumbricus terrestris, conc. depend. of self-diffusion 78−68984
haemoglobin, hyperfine-shifted PMR, mag. field and temp. induced line broadening 77−60184
haemoglobin, in salt soln., diffusion rel. to intermol. interactions, light scatt. investig. 77−44585
haemoglobin, Jahn-Teller pseudo effect rel. to Fe release and conformational changes 80−76701
haemoglobin, low freq. modes and excitation profiles, reson. Raman spectra 80−94428
haemoglobin, metal substitution effect on mol. struct. and functional props. 79−53037
haemoglobin, modulated excitation meas. of quaternary conformation struct. change rate 77−44589
haemoglobin, mol. interactions, Fourier transform IR absorpt. spectra 78−96007
haemoglobin, mol. system, with N associating particles, free energy virial expansion 77−55336
haemoglobin, mutual and tracer diffusion coeffs., photon correl. obs. 80−72123
haemoglobin, nanosec. probe of dynamics using time resolved reson. Raman scatt. 80−94162
haemoglobin, O_2 linked Cl^- binding sites, pH dependence 79−62174
haemoglobin, picosecond transfer times meas., book contrib. 77−64166
haemoglobin, quaternary struct., hydration and self-association, ^1H NMR obs. 80−67040
haemoglobin, sickle cells, 3-dimens. reconstruction of fibres 78−44452
haemoglobin, sickling deer type III, macromol. struct. refinement by restrained least-squares and interactive graphics 80−28870
haemoglobin, structure and respiratory transport 79−57576
haemoglobin, subunit cooperative interaction, stereochemical trigger, Mossbauer study 78−53321
haemoglobin, suspending medium, dielec. props., human erythrocyte obs. 80−76716
haemoglobin, thermal and athermal effects on erythrocytes by microwave irradiation 79−70581
haemoglobin, US attenuation and dispersion, Kramers-Kronig relative 78−83135
haemoglobin+CO reaction kinetics, using various regimes of photolytic illum. 78−48753
haemoglobin aqueous solutions, γ-irrad. in air and Ar 80−41135
haemoglobin as a transducer for O_2 transport in fish 79−96505
haemoglobin concentration meas., in whole blood, using IR reflectance 77−52860
haemoglobin cooperativity, simple tension-displacement model 79−34472
haemoglobin equilibria in soln., surface free energy model 80−81535
haemoglobin Fe-N distance determ. by EXAFS 78−68989
haemoglobin g-value change obs., EPR *(Japanese)* 77−90724
haemoglobin haem structure after photo-deligation, Raman spectra 80−61510
haemoglobin in red cell suspensions, NMR relax., T_1 and T_2 meas. 78−80832
haemoglobin in solution, conc. depend. of diffusion coeff. 79−29546
haemoglobin macroporous particle study, photoacoustic spectrometry 80−85543
haemoglobin measurements using solid-state noninvasive tissue refl. oximeter 78−35919
haemoglobin oxygenation, cooperative phenomena 77−44577
haemoglobin reactions as interfacial phenomena, hydrophilic colloid model 77−9167
haemoglobin S, fibres, discs having six-fold symmetry, electron microscopy 78−76989
haemoglobin S solution, effect of deoxygenation on US absorpt., rel. to sickle cell blood 78−44477
haemoglobin solns., O_2 uptake during channel flow 77−81516
haemoglobin solution, facilitated diffusion of O_2 77−48747
haemoglobin solution, proton mag. relax. meas. 77−1975
haemoglobin-CO complex, absorpt. spectrum, electronic transitions, PPP calcs. 77−71811
haemoglobin-CO reaction kinetics, relax. meas. on photolytic illum. 77−70405
haemoglobin-erythrocyte membrane interaction, γ-ray effects, EPR 78−7402
haemoglobin-haptoglobin deoxygenated complexes, Mossbauer spectroscopy 78−24020
haemoglobin-methaemoglobin system, oxidative potential in preserved blood 77−81771
haemoglobin-O_2 equilibrium curve, instrument for determ. based on membrane diffusion 80−81761
haemoglobin-O_2 equilibrium curve determ., semipermeable membrane transport model 79−92418
haemoglobins and chlorocruorins, extracellular respiratory, physicochemical and functional props. 80−3581
haemoprotein, fine structure of Fe ions 80−30661
haemoproteins, allosteric effect, mathematical description 79−64125
haemoproteins, Fe-ligand binding and electronic struct., Mossbauer studies 80−8021
haemoproteins, highly oxidised Fe, electronic struct., Mossbauer spectroscopic obs. 77−88478
HeLa cell nuclei protein content, effect of hyperthermia 80−40972
α-helical protein molecules, solitons *(Russian)* 78−68990
helical structure reconstruction from projections, phage tail appl. 80−8237
helix-coil transitions in specific sequence biopolymers 78−35794
heme-proteins, general spin Hamiltonian for determ. of ligand nucl. Zeeman and hyperfine interactions 77−85617
high density lipoprotein-3 macromolecule observation using CTEM and STEM with negative staining 80−85561
high performance liquid chromatography 80−61174
high-potential Fe protein of Chromatium vinosum, low-lying excited state, EPR 78−3448
histidine-decarboxylase, molecular weight and form determ. by low angle X-ray scatter 78−76987
proteins continued
histidinedecarboxylase molecule, distance between heavy atom markers small angle X-ray scatt. determ. 79−55613
histone F2a solutions, effect of ionic composition of medium on struct. and effectiveness of intermol. interactions 78−48744
histone lysine-rich, molecular wt. determination via diffusion coeff. from laser scattering spectra 77−29095
histones, conform. state in water, circular dichroism 77−56335
histones, H2a and H4, aggregation ionic strength effect *(Russian)* 80−55697
hopping conduction, theory 79−24935
horseradish peroxidase cpd. II, high-field Mossbauer spectra, 4.2 to 120K 80−8026
horseradish peroxidase retrograde axonal transport in lateral geniculate nucleus rel. to monocular deprivation 77−52781
horseradish peroxidase transport revealing source of centrifugal fibres to eye in nonavian vertebrate 77−36921
human erythrocyte carbonic anhydrase, limiting viscosity number determ. *(French)* 77−12874
human serum and erythrocyte microwave complex permittivity meas. 80−3889
hydration dynamics, quasi-elastic neutron scattering 79−16127
hydrophilic side groups, linear H-bonded systems, proton conduction 80−40973
hydrophobic effect, organisation of living matter 79−11887
hydrophobic interactions, lipid-protein binding, thermodynamics, book contrib. 79−16129
15-hydroxy prostaglandin dehydrogenase activity in tissues of mice, X-irrad. effects 80−51169
hyperthermia effect on nonhistone proteins isolated with DNA 78−80843
immobilised enzyme membrane oscillations and pH fronts 77−25387
immobilised enzyme systems, hysteresis, oscillations and pattern formation 79−62173
immobilised enzyme systems, optimisation of porous glasses 77−12891
immobilised enzymes, glasses as bioactive materials, review 78−3698
immunochemical analysis, standardisation of light scatt. meas. 78−36081
immunoglobulin, human, high energy-induced aggregation, time resolved spectra 80−61655
immunoglobulin (Ig) κ chain m RNAs, identical 3′ non-coding sequences favour unique C_κ gene in mouse 80−8010
immunology slide, darkening, Mie scatt., Maxwell Garnett theory 77−9315
immunoresponsive membrane, pot. associated with immunochem. reaction between membrane-bound antigen and free antibody 77−86453
inducible enzyme synthesis in irrad. yeast, UV effects on regulation and activity 78−69157
inductive resonance energy transfer, struct. and conform. changes 79−27120
inelastic electron tunnelling spectroscopy appls. 78−92770
insulin, appl. of cryst. struct. refinement technique based or fast Fourier transform algorithm 78−91197
insulin, cryst. growth kinetics 80−35823
insulin, radioimmunoassay, improvement in precision and accuracy of commercial kit 78−48884
insulin, radioiodine labelling using dimethylsulphoxide as labelling agent *(Korean)* 78−88746
insulin and analogue, side-chain mobility and tyrosyl circular dichroism 78−15770
interaction with nucleic acids and sugars, studied by luminesc. 79−34476
intermediate states responsible for specific props. 79−96511
internal charge transfer, ascorbic acid adduct model systems, SCF calc. 80−69072
internal liberational motion, effect on ^{13}C NMR relaxation times 78−85293
invertase, S-containing glycoprotein, gamma-irrad., secondary radical reactions, EPR 77−9175
o-iodotyrosine, intramol. effects of ^{125}I decay 80−108973
isocitrate dehydrogenase in testes after partial-body γ-irrad. 78−80923
isomerisation, gel permeation chromatography of interacting multicomponent systems 78−68950
isomerisation kinetic consts. determ. by gel permeation chromatography of interacting multicomponent systems 78−68951
isorhodopsin, photochem. on picosecond time scale, bathorhodopsin form. 79−83706
isorhodopsin, physiological activity in rat rods 77−60204
isorhodpsin, resonance Raman spectra 79−92148
keratin, mammalian, organisation of polypeptide chains 77−4981
keratin-NaCl, Na Auger electron spectra 78−53339
kinase, membrane protein, acetylcholine receptor phosphorylation-in receptor-enriched T.californica membrane 77−56370
kinases, cAMP-depend., membrane-localised, and regulation, of slow inward current, frog heart 80−81567
kinases, in vitro phosphorylation of acetylcholine receptor 77−56371
kinetic constants of association and dissociation, theoretical determ. 80−51033
laccase, mag. susceptibility 79−92125
lactate dehydrogenase, H-forms, radioimmunoassay 80−67219
lactate dehydrogenase, O_2 effect in radiolysis obs. 80−72223
lactate dehydrogenase+free radicals, reactions, pulse radiolysis 78−7214
β-lactoglobin, adsorpt. meas. at interfaces by drop volume technique 78−60009
β-lactoglobulin, absorpt. spectra for complexes formed with vitamin-A 80−30664
large external transformation-sensitive proteins on cell surface, rel. to centripetal particle transport 77−32881
laser photo-CIDNP as surface probe for proteins in soln. 78−73138
lecithin vesicle shapes, rot. symmetric, opt. microscopy 77−64011
leghaemoglobin, thermal denaturing in cryst. and soln. 80−108849
leghaemoglobin of Lupinus luteus, cryst. struct. of first component 78−27893
leghemoglobin minimisation of functions of many variables appl. to X-ray struct. anal. 80−3589
leguminous plants, protein quality determ. by proton-induced radiation anal. 77−48978
lens protein composition obs. during senile nuclear cataract development 79−62236
leucine aminopeptidase crystalline aggregates, interpretation of electron microscope images 78−68988
leucine-binding protein, rat nerve, aggregation 79−62181

proteins continued
ligand binding parameters estimation from continuous ultrafiltration results 77−12878
ligase repair of single-strand breaks after irrad., role rel. to radiation chem. 77−12965
limiting viscosity number determ. *(French)* 77−12874
lipid extract from lung surfactant, IR spectra, H-bond lengths 79−24941
lipid interaction, surface tension meas. 79−24940
lipid-protein complex, effect of UV on free radical oxidation of lipids 77−36874
lipid-protein interaction in membrane bound Na^+, K^+-ATPase, spin label anal. 79−11902
lipid-protein interactions, review 77−90719
lipoprotein, high density, of human plasma, solubilisation of phospholipid membrane 77−16916
lipoprotein, low density, from human serum, STEM and FE-TEM obs. 78−100566
lipoprotein, very low density, particle distrib. by intensity correl. spectroscopy 78−21228
lipoprotein molecule transport to artery walls, in arteries with longit. ridges 77−44702
lipoproteins in water, density contrast, cross verification of X-ray scatt. and pycnometry expts. 79−10757
liver alcohol dehydrogenase, proton relay system, SCRF PCE theory, CNDO/2 calcs. 80−85325
liver growth protein metabolism and turnover, radiotracer obs. 79−88062
long-range interactions, approx. method 78−7317
luciferase, rel. to yellow light emission of luminous bacterium 77−66802
luminescent label Eu^{3+}, spectra and binding centres 78−15754
lumirhodopsin, photoconversion at 77K, quantum efficiency estimation 80−67081
lysosomal enzyme activation in gamma-irrad. mammary tumours 77−5050
lysosomal enzymes, pigeon tissue, effects of sub-lethal γ-ray dose 80−98022
lysosomal enzymes in lung, late biochem. changes after hemithoracic irrad. of rat 77−5053
lysosomal hydrolase redistrib. in rat spleen homogenates under γ irradiation 79−88132
lysosomal hydrolases of rat serum and spleen, gamma-induced changes 77−52848
lysozyme, 0.01% soln., mag. and radiofreq. effects on activity 78−61136
lysozyme, absorption mode spin-echo spectra appl. 80−78634
lysozyme, adsorpt. isotherm, at air-water and air-oil interfaces 79−79461
lysozyme, adsorpt. meas. at interfaces by drop volume technique 78−60009
lysozyme, adsorption kinetics, surface denaturation 79−79460
lysozyme, anomalous diamag. susceptibility and elec. cond. 79−29498
lysozyme, aq., Raman intensities, interac. 78−58704
lysozyme, aq. solns., H_2O ordering, NMR relax. investig. 79−62171
lysozyme, binding to bacterial cell wall trisaccharide NAM-NAG-NAM, X-ray cryst. struct. anal. 80−35834
lysozyme, computer simulation of solvent struct. 78−40113
lysozyme, cryst., dynamic sp. ht. capacity meas. 80−21447
lysozyme, cryst. growth kinetics 80−35823
lysozyme, dye-sensitized photoinactivation rate constant studies 79−79476
lysozyme, electric and mag. props. 77−44584
lysozyme, electron acceptor props. in photosensitized electron transfer, EPR study 79−79469
lysozyme, hydrated, dielectric props. at 9.9 GHz 78−15758
lysozyme, light-induced riboflavin binding 78−27899
lysozyme, molecular structure of adsorbed film 79−79462
lysozyme, nuclear Overhauser effect in ^1H spectra 79−43823
lysozyme, of hen egg-white, ^{13}C n.m.r., carboxyl group resonances, ionisation consts. 77−1978
lysozyme, search for superconducting regions 80−101149
lysozyme, sorption and desorption of water, thermal-stimulated press. and thermogravimetric anal. 80−8008
lysozyme, spin echo and spin lock ^{13}C Fourier transform NMR 79−43824
lysozyme, stepped character of thermal denaturing, optical density at 290 nm 78−15763
lysozyme, tryptophan residues, H exchange for D, relax., proton NMR spectra 80−35846
lysozyme and complex with trisaccharide inhibitor, struct. in soln. and in cryst. 77−81465
lysozyme aqueous solutions, viscosity and density 79−48208
lysozyme bound water, thermally-stimulated press. and current 78−15757
lysozyme complex with substrate-inhibitors, photosensitised electron transfer, role of Cu^{2+} 80−30638
lysozyme effect of pH on dimorphic crystal growth 79−14728
lysozyme hydration, correl. of diverse types of meas. 80−61507
lysozyme interaction with water, intermol. pot. calcs. 77−75250
lysozyme macroradicals, ultraslow diffusion in an aq. matrix, EPR obs. 79−92119
lysozyme solution as dye laser, threshold power for laser operation 79−68391
lysozyme spin-labelled preps., water-protein layer microstruct. study by mag. relax. 78−76980
lysozyme-lipid interaction effect on struct. of artificial vesicular membranes 77−25385
lysozyme-salt water soln., critical mixing point, turbidity and viscosity meas. 77−86437
lysozyme-water mixture, phase separation, rel. to cold cataract form. in young rat lens 78−11640
α-lytic protease, predicted model rel. to X-ray struct. 79−62178
α_2-macroglobulin values in serum of X-ray workers 78−28020
malic dehydrogenase isoenzymes in wheat shoots and chloroplasts, effect of light 78−11696
membrane, double layer mediated energy conversion using imposed freq. and wavelength 78−88695
membrane, interaction with lipids, ^2H NMR investig. 78−80826
membrane damage caused by light irradiation of fluorescent concanavalin A 80−56123
membrane integral proteins, mobility increase in spherocytic erythrocytes obs. 80−81569
membrane multilayers, thickness depend. of props. 80−89726
membrane protein, structure determination, electron microscopy, optical and digital anal. *(French)* 79−66594

proteins continued
membrane protein props. rel. to membrane functions, review 77−44601
membrane protein-lipid interactions 79−5254
membrane structural rearrangements due to anaesthetics 77−36873
membrane thin sectioning development for electron microscopy 79−74819
membranes, immobilised, H^+ ion transport, assoc.-dissoc. time-scale factor 79−34529
membranes, structural order of lipids and proteins, fluoresc. anisotropy data eval. 80−97873
met-myoglobin, struct. determ., neutron crystallography 79−43814
metal containing, chem. characts. of conformational nonequilib. states 78−95998
metallo-proteins and model systems, susceptibility and struct., SQUID magnetometer uses 79−53036
metalloenzyme, metal ion geometry and mechanism from PAC expts. 78−44449
metalloenzymes, ^{113}Cd as NMR active site probe 78−68999
metalloenzymes, model for biological active sites, ab initio calcs. 80−104551
metalloenzymes and carriers, hydration effect on mobility of Mossbauer atoms 80−35819
metalloprotein, modelling by low mol. wt. metal-peptide complexes, EPR 78−64937
metalloproteins, EXAFS, review, book contrib. 79−5436
metalloproteins, metal nuclei, biophysical appls. of NMR, review, book contrib. 80−109081
metalloproteins, recent EPR studies 78−64936
metalloproteins, site symmetry, X-ray absorpt. spectra using synchrotron radn. 78−64938
Cd-metallothionein, test object for dark field electron microscopy of protein struct. 78−11610
metaquohemerythrin, difference Fourier refinement 79−8472
metarhodopsin I-II transition obs. by absorpt. changes of eriochromblack T 77−44593
metarhodopsin transition, triggering of light-induced change in Ca binding, rod disk membranes 80−94211
metarhodopsin transitions rel. to visual response in barnacle photoreceptor 78−69050
methaemoglobin, solid lyophilised bovine, rot. frame proton $T_{1\rho}$ spin-lattice relax. 78−95995
methaemoglobin, struct. change on addition of inositol hexaphosphate 80−72130
methanol dehydrogenase, enzyme, electron spin echo, 35 GHz 80−13113
methanol dehydrogenase, enzyme powder, ESR and ENDOR, 9 and 35 GHz 79−70524
methine aromatic C sites, natural abundance ^{13}C NMR at high mag. field strength 77−86443
methionine sulfoxide in protein, ^{13}C NMR anal., method and expt. obs. 80−56305
metmyoglobin, dynamics study using Rayleigh scatt. of Mossbauer radiation 80−40963
microtubule polymerisation in vitro, effects of ^{60}Co gamma irrad. 78−20222
microwave effect observation prerequisite conditions 80−3592
mitochondrial cytochrome b, evidence for two or more components 79−24944
mitochondrial Fe-S proteins, EPR spectra of animal tissues in vitro, 13 to 43 K 77−16919
mitochondrial protein synthesis in rat liver after whole-body X-irrad. 78−80925
mitochondrion, elec. props. and struct. transitions 79−24943
mixed protein phospholipid films, viscoelastic behaviour and Marangoni effect 80−3602
mobility from spin-echo determ. of about T_2 values in proton-decoupled ^{13}C NmR 78−2769
model building procedure 80−51036
model chain, aperiodic, electronic spectra, hopping cond. 80−5641
molecular models, semiautomatic coordinate meas. device using laser beams 79−37573
molecular weight and ultrastruct. determ. in STEM 80−85562
molecular weight determ. by monolayer surface press. meas. technique 80−89526
molecular weight determination by STEM 79−92451
molecule, simulation of single mol. images combining computer and electron micrograph analysis 78−37781
molecule chain-folding mapping, new type of representation 77−44588
monolayer desorption 77−85053
motion, nonsteady hydrodynamics, damping effects 77−36861
multi-enzyme complex carrying out electron transfer, asymptotic anal. of functioning 80−81523
multivalent binding to substrate, linear differential equations in chemical equilibrium calculations 80−30279
murein, electron microscopic exam., reduction of radiation damage 79−34718
muscarinic acetylcholine receptor increase on exposure of dark-reared rats to light 78−24069
muscle contraction, protofibril reciprocal sliding and thick filament shortening 77−56331
muscle proteins, rot. motions, saturation transfer EPR obs. 80−94151
myelin sheath, thickness irregularities distrib., paracryst. struct. 77−12892
met-myoglobin:Cu^{2+}, single cryst., EPR, conform. changes 77−73505
myoglobin, appl. of cryst. struct. refinement technique based on fast Fourier transform algorithm 78−91197
myoglobin, Fe-O_2 bonding and oxyhaeme struct. 78−96006
myoglobin, ferrous high-spin derivatives, MCD at room and liq. N_2 temps. 78−76997
myoglobin, from Aplysia limacina, X-ray cryst. struct. determ. at 5 Å resolution 79−16131
myoglobin, hyperfine-shifted PMR, mag. field and temp. induced line broadening 77−60184
myoglobin, O_2 and CO bonds, flash light photolysis *(Hungarian)* 79−29501
myoglobin, rate of entry of O_2, CO 79−8471
myoglobin, refolding kinetics by diffusion-collision-adhesion model 80−94187
myoglobin, static and dynamic structure of biomolecules, Mossbauer effect 80−40952
myoglobin , oxyhaeme complex, single cryst., visible spectrum, electronic struct., coord. geometry 78−44456

proteins continued
myoglobin conformationally-nonequilibrium state reactivity obs. by pulse radiolysis 79−39353
myoglobin in solution, small angle scattering anal. using synchrotron radiation and energy dispersive techniques 79−12051
myoglobin solution, facilitated diffusion of O_2 77−48747
myoglobin solution, new method using X-ray diffuse scattering for investigation of conformation changes 79−12054
myoglobin-Fe^{3+} compounds, Mossbauer and suscept. expts. 78−24019
myoglobin-H_2O_2, high-field Mossbauer spectra, 4.2 to 120K 80−8026
myoglobin-O_2(CO), elec. field gradient tensor, Mossbauer meas. 80−8017
myoglobins, Fe-, Co-substituted, O_2 binding, comparisons, thermodynamic investig. 80−67030
myoglobins, kinetics studied by picosecond spectroscopy 79−43804
myosin, column-purified, struct. studies of synthetic filaments 79−92131
myosin, conformational changes induced by inorganic salts, Raman spectra obs. 78−96002
myosin, fast and slow, in developing muscle fibres 78−64961
myosin, interaction with adenosine 5′-diphosphate, intermolecular spin diffusion study 80−18951
myosin, interactions with HDO, intermolecular spin diffusion study 80−18951
myosin, muscle contraction process, 10 ms time resolution X-ray diffr. 80−61741
myosin, muscle cross bridge rotation during contraction, fluctuations in polarised fluoresc. 80−97856
myosin, removal of regulatory light chains rel. to Ca control of tension in scallop striated muscle 78−53360
myosin, struct. and functional changes in chronic cardiac insufficiency 77−36887
myosin, struct. changes in living muscle fibres, polarised UV fluoresc. microscopy 80−67037
myosin, synthetic, effects of C-protein on filament struct. 79−92132
myosin conformational conversions, using acetate and acetamide spin labels 77−52733
myosin head return to thick filaments after muscle contraction 78−7319
myosin heads, evidence for cooperative interaction from O_2 exchange meas. 77−32870
myosin heads movement during a heart beat 79−48207
myosin helical fragments, stepwise pattern of thermal denaturing 80−40966
myosin interaction with a spin-labelled ATP analogue 79−57563
myosin kinetic anal., review 80−21441
myosin molecule binding to two actin filaments 78−27884
myosin muscle filaments, crustacean, struct. of backbone 79−20512
myosin projection behaviour during staircase phenomenon in heart muscle 78−53362
myosin regulated muscle, changes in crossbridge attachment 78−53361
myosin rod, and subfragments, flexibility, birefringence relax. in soln. 78−53320
myosin S-1, mol. basis for chemomechanical energy transduction in muscle 80−72143
myosin subfragment-1 attachment to actin, effect on equatorial X-ray refls. 78−27880
myosin synthesis increased by elec. stimulation of skeletal muscle cell cultures 77−1988
NADH coenzyme, two photon absorpt. cross section meas., reaction rate modification 80−51043
negative resistance of biopolymers, rel. to living cell props. 78−64923
nerve excitability, interactions between intrinsic membrane protein and elec. field 78−53377
nerve membrane protein conform. and energy changes, rel. to action pot. 78−44497
nerve membranes, protein channels for Na and K ions, mol. mechanisms 77−4994
neuraminidase, effect on specific resist. and electrophoretic mobility of regenerating liver cells 77−25402
neurotoxin, snake venom, appl. mol. graphics to struct. determ. 78−27892
nicotinamide adenine dinucleotide, and reduced form, pH induced modification, Raman spectra 80−85343
nitrogenase, cofactor centres, Mossbauer spectra obs. 80−8023
nitrogenase active site, Mossbauer spectra of Mo-Fe-S clusters 80−45852
nitrosylhaemoglobin, electron spin distrib. 80−83528
NMR, ^{13}C, review 77−86449
NMR, resolution enhancement by digital filtering with sinusoidal window function 77−18060
NMR Fourier transform spectroscopy, high-field, of biological systems 79−39457
NMR spectroscopy study 78−88694
non-histone proteins, role in chromatin solubility 79−53021
nuclear non-histone protein interaction with DNA, γ-ray effect 78−7401
nuclear Overhauser effect, truncated driven, in presence of spin diffusion 80−1095
nuclear Overhauser effect in ^1H spectra 79−43823
S_1 nuclease detect. of DNA damage and repair in γ-irrad. rat brain tumour 78−48838
nucleic acid recognition, role of unspecific complexing 79−79449
nucleic-protein interactions in tobacco mosaic virus, spin label and fluoresc. obs. 80−40949
optical rotatory dispersion and circular dichroism, review 77−3497
origin of life, synthesis of proteins and nucleic acids 78−69461
ovalbumin aqueous soln., macromol. gel layer formed on ultrafiltration tubular membrane, charact. 80−14260
oxirane-acrylic bead, radical conc. gradient determ. by microinterferometry and microfluorometry *(German)* 79−100799
oxy- and deoxyhaemoglobin, optical spectra, dichroism 79−20514
oxyhaemoglobin, deoxygenation, Jahn-Teller effect 77−21474
oxyhaemoglobin, dilute soln., reson. Raman spectra, pulsed laser excitation; optical multichannel detection 78−76999
oxyhaemoglobin, evaluation of elec. field gradient tensor components 77−64004
oxyhaemoglobin, mag. props. and structure 78−48751
oxyhaemoglobin, mag. susceptibility of frozen aq. soln., 25 to 250K 78−6507
oxyhaemoglobin, normal and sickle cell, Raman spectra, polarisability difference 79−62191
oxyhaemoglobin-hydrazine (dimethylhydrazine) interaction, γ-reson. spectroscopy 80−81525
proteins continued
oxyhemocyanin, mag. susceptibility 79−92125
oxyhemoglobin, spectroscopic meas. after pulsed optical excitation 79−92150
oxymetalloproteins, electronic spectroscopic data review 80−52977
oxymyoglobin, evidence for conformational and diffusional mean square displacements 80−89713
oxymyoglobin, forzen soln., recoilless fraction, Mossbauer spectra meas. 80−8025
oxymyoglobin structure determ. by X-ray diffr. 78−56950
pancreatic trypsin inhibitor, bovine, 3D protein folding model 77−90723
pancreatic trypsin inhibitor, bovine, macromol. dynamics, high resolution NMR investig. 80−91708
pancreatic trypsin inhibitor, bovine, struct. fluctuations in 100 ps 79−34478
pancreatic trypsin inhibitor, PMR, nuclear Overhauser enhancement difference spectroscopy 78−81091
pancreatic trypsin inhibitor bovine, dynamics of folded globular protein 77−64003
pancreatic trypsin inhibitor tyrosine residues in soln., laser photo-CIDNP as surface probe 78−73138
papain inactivated by OH radicals and H_2O_2, optical density, amino acid composition and fluoresc. 78−53344
papain models, active site α-helix and ion pair stability 80−74265
parvalbumins, Ca-binding, lanthamide-substituted, of muscle, ^{13}C NMR obs. 79−96516
pepsin and rennin, relative orient. of mols. in unit cells, mol. replacement method 77−36866
pepsin crystal fusion, microcalorimetry 77−70413
peptide folding, model based on incipient 3_{10} helix in Piv-Pro-Pro-Ala-NHMe 79−100568
peptides, in soln., nuclear Overhanzer effect methods for total conformational anal. 79−16136
peptides, soln. conformation by intramolecular nuclear Overhauser effect 79−16135
periodic models, forbidden band gap calc. indicating insulating behaviour 77−25367
peroxidase, ferrous high-spin derivatives, MCD at room and liq. N_2 temps. 78−76997
peroxidase, immobilised, spectral charact. obs. 79−57579
peroxidase, low-temperature radioreduction, MCD and absorpt. spectra 78−31763
phage T7 RNA polymerase, base pair for recognition and initiation 79−74597
phenylalanine+chloranil, charge transfer interaction, equilib. const., enthalpy and entropy determ., mol. polarisability 80−89708
phonon density of states in linear disordered system, self-consistent continued-fraction method 77−69062
phospholipase A and mechanism of action of aldosterone 78−24053
phospholipid membrane thermotropic transitions, effects of bivalent cations and proteins 77−48765
phospholipid membranes, orientational order and integral protein struct. 80−45862
phosphoprotein in visual cell, rel. to proposed role of cyclic GMP 78−64997
phosphoryl transfer enzymes, biophysical appls. of NMR, review, book contrib. 80−109081
phosphorylase A crystals, automated struct. determ., from micrographs 80−92425
phosphorylase b, structure factor moduli, estimates from negative intensity obs. 78−75486
photoinduced electron transport across protein-containing membranes 80−30768
photoreceptor mutant of Drosophila, protein role in intermediate steps of phototransduction 77−48799
phycobilin pigment role in photosynthesis 78−48752
β-phycoerythrin crysts., twinned by merohedry, diffr. data treatment 80−108845
Physarum actin, amino acid sequence 79−16141
phytochrome, autoradiographic tryptic digest maps 79−16144
phytochrome, role of light in regulating plant growth and development, review 78−11695
phytochrome control of cell permeab., red light irrad. of moss 78−77025
phytochrome subunit, evidence for symmetry 78−27890
phytohaemagglutinin stimulated equine peripheral blood lymphocytes, X-irrad. 77−5032
pigment-protein complexes, oriented, of photosynthetic bacterium Chromatium minutissimum, linear dichroism 80−35841
plasma, filtration through capillary wall 77−32936
plasma fractionation, development of automatic continuous process 77−52955
plasma lipoprotein lipase in rabbit irrad. by 25 MeV photons, action of corticoids *(French)* 77−90859
plasma low density lipoproteins, human, size and surface effects rel. to phase transitions 78−3446
plasma low-density lipoprotein, human, molecules organisation of central core 77−90722
plasma membrane of mouse egg, effect of fertilisation on lateral diffusion of lipids and proteins 78−44480
plasma protein, human, labelling with ^{99m}Tc-pertechnetate, chemical method 79−29618
plasma protein interaction with polyion complex studied by circular dichroism and UV spectroscopy *(Japanese)* 80−12316
plasma proteins, ligand distrib. among multiple binding sites, computer program 77−12877
plasma proteins adsorbed on polymer surface, Fourier transform IR spectrometry 80−16899
plasminogen, ^{123}I or ^{131}I labelled, evaluation as imaging agent for pre-existing thrombi 77−21610
platelet adhesion to solid surfaces, effects of plasma proteins and substrate wettability 78−35814
poly O-carbobenzoxyl-L-tyrosine, in soln., conformation, helix-coil transition, circular dichroism, NMR spectra 77−31037
poly-γ-benzyl-L-glutamate solutions, calorimetric study of fusion of liquid cryst. struct. 79−53022
poly-γ-benzyl-L-glutamate-dichloroethane in conc. soln., mol. assoc., electro-opt. investig. 78−1973
poly-γ-methyl-L-glutamate, interfacial conformational modifications 78−2339
polyacrylamide gel, automated scanning of ^{14}C 80−17221

proteins continued
polyglycine chain with hydrated side group, electronic struct., transport props. 79−16146
polymerase-DNA complex, thiopyronine-sensitised photodynamic inactivation of RNA synthesis 77−29177
polypeptide chains, struct. of conduction and valence band 80−76700
polypeptide in conc. soln., mol. assoc., electro-opt. investig. 78−1973
polypeptides, α-helix asymmetry, circular dichroic spectra 79−16145
polypeptides, amide proton spin-lattice relax. 79−20502
polypeptides, electronic struct., side-chain disorder effect 80−76706
porphyropsin, visual pigment changes in rainbow trout, in response to temp. 77−48788
porphyropsin, visual pigment composition of rainbow trout 79−43899
prealbumin, human, struct., X-ray diffr., amino acid sequence, circular dichroism meas., comparison 77−42450
prealbumin, protein-DNA and protein-hormone interactions rel. to model of thyroid hormone nucl. receptor 77−66793
prealbumin-DNA-hormone interactions, X-ray studies, review 78−53322
precipitants and flocculants, dimensions of disperse forms of cross-linked polyelectrolytes 80−11957
prelumirhodopsin, psec. kinetics, primary photochem. event in vision, proton translocation 78−44508
pressure jump method for fast kinetics using optical rotation and circular dichroism 78−77175
primary structure, distrib. of identical amino acid residues 77−56334
protamine, electron microscopic recognition rel. to radiation exposure 79−62175
protamine cDNA plasmids, coding and non-coding nucleotide sequences, sequence divergence of rainbow trout protamine mRNA 79−74596
protein, X-ray struct. study using synchrotron radiation and multichannel detector 78−47210
protein-ligand equilibrium binding, mathematical models 78−48688
protein-lipid model systems, chemiluminesc. on exposure to formalin 77−56329
protein-membrane interactions probing using laser flash spectroscopy of indoles in presence of nitroxide radicals 79−87855
protein-methylglyoxal complex, electronic props., energy band cond. 79−24936
protein-water system dynamic model 77−21470
proteolytic enzymes and substrates, effect on elec. cond. of lipid membranes 78−15779
protohaeme, low-spin-ferrous, MCD, LCAO MO SCR π-electron calcs., PPP approx. 78−9178
purple membrane, polarized IR spectroscopic struct. study 79−43809
purple membrane fragment suspensions, elec. dichroism obs., trimer model interpret. 80−89728
purple membrane of Halobacterium halobium, energy transfer 78−44467
purple membrane particles, freeze-fractured, protein content 77−90735
purple membrane protein chromophore, fluoresc. 78−44454
purple membrane protein retinal chromophore, role of protein in photochem. 78−15772
purple membrane protein synthetic pigment analogues 77−73504
purple membrane structure, effects of bleaching and regeneration, H-halobium 77−86532
purple membrane topography of Halobacterium halobium 79−48211
pyrophosphatase, inorganic, of yeast, cryst. growth, derivatives formation, heavy atoms positions 80−108842
quartz fibres, possible role as templates for biopolymers 79−39345
quaternary structure modification, microwave irradiation requirements and role of temperature *(Russian)* 79−83851
radical limiting conc. on UV irrad. at 77K, effect of luminesc. quenchers 80−30662
radioactive tracers, improved labelling with 99mTc by stannous tartrate reduction of pertechnetate 80−72324
recognition model, stereochem. enhancement of specificity 77−81461
red blood cells of thalassemia, sickle-cell anaemia, and haemoglobin Hammersmith, ferritin-like Fe, Mossbauer study 80−8018
red cell membrane protein monolayers, viscoelastic props. 79−48224
redox enzyme, Fe-, Cu-, or Mo-containing, electron transfer peculiarities 80−16896
relaxation times in solid-state theory and one-dimensional molecular systems *(Russian)* 80−100640
relaxational experiments for proteins with memory 77−70406
rennin and pepsin, relative orient. of mols. in unit cells, mol. replacement method 77−36866
replica form., for wetting angles of invertible surfaces investig. 79−37900
representation, unique method 80−67036
retinal, proton donor-acceptor isomerisation coupling, bacteriorhodopsin as light driven proton pump 79−79473
retinal pigment epithelium, identification of membrane protein binding retinol 77−21515
retinol-binding proteins in retinal pigment epithelium 79−20525
review, plastic deformation during freeze-cleavage 78−14400
Rhacopholus embryo yolk platelets, freeze fracture study of crystalline struct. 80−104552
rhodopsin, α-helix orientation, spectroscopic study 80−89711
rhodopsin, bacterial compared with animal, H exchange 77−29096
rhodopsin, bathochromic shift origin 78−31767
rhodopsin, bathorhodopsin and isorhodopsin, mech. of photoconversion 78−53336
rhodopsin, bovine, conform. in situ and solubilised with detergent 77−44587
rhodopsin, bovine, interaction with Ca^{2+} 79−100564
rhodopsin, bovine, kinetics of intermediate photolysis processes 79−43608
rhodopsin, bovine, kinetics of $NaBH_3CN$ reduction 78−64926
rhodopsin, bovine, mol. wt. determ. by monolayer method 77−81492
rhodopsin, bovine, photochem. cis-trans isomerisation at liq. He temps. 78−64939
rhodopsin, bullfrog, thermosensitive prop. 77−25431
rhodopsin, cattle, phosphorylated, isoelec. focusing 78−15766
rhodopsin, charge stabilization mechanism in the visual and purple membrane pigments 79−34500
rhodopsin, cis-trans isomerisation on psec time scale 77−86498
rhodopsin, coherent states of flexible macromol., mol. basis of vision 79−79472
rhodopsin, conformeric states, spectrophotometry 77−90725
rhodopsin, excited state energy surface to explain photochemistry 79−48218
proteins continued
rhodopsin, isorhodopsin and bacteriorhodopsin, and photoproducts, temp. and wavelength effects on photochem. 78−11612
rhodopsin, photo- and thermo-bleaching rel. to heterogeneity problem 80−41114
rhodopsin, photochem. on picosecond time scale, bathorhodopsin form. 79−83706
rhodopsin, picosecond spectroscopy obs. of primary events 80−56312
rhodopsin, presence of two closely arranged SH groups in mol. 78−53323
rhodopsin, primary photophys. and photochem. processes in visual excitation 78−15773
rhodopsin, red-absorbing visual pigment of butterflies 80−3646
rhodopsin, resonance Raman effect *(Hungarian)* 78−74666
rhodopsin, resonance Raman spectra 79−92148
rhodopsin, solubilised, photoinduced conform. changes, spin-label method 77−81496
rhodopsin, thermal isomerisation rel. to visual transduction mechanism in retinal obs. 79−74651
rhodopsin, transient light-induced conform. changes 78−15774
rhodopsin, vertebrate, chromophore orientation obs. 80−40959
rhodopsin, visual pigment, mag. anisotropy estimation 80−51137
rhodopsin, visual pigment composition of rainbow trout 79−43899
rhodopsin and bacteriorhodopsin chromophores, modelling by retinal Schiff bases, Raman spectra 79−62190
rhodopsin and bathorhodopsin, theoretical analysis of optical activity 77−52783
rhodopsin and intermediates, absorpt. spectra and orientational change of chromophore 78−7321
rhodopsin and its photoproducts, directional absorpt. props. obs. 80−51090
rhodopsin and other proteins in artificial lipid membranes 77−90730
rhodopsin and thermal intermediates, fast struct. fluctuations in protein component 80−72137
rhodopsin bleaching, cooperative conform. change in rod photoreceptor disc membrane 77−81499
rhodopsin bovine, interaction with Ca^{2+} 79−100563
rhodopsin chromophore, and desmethyl analogues, theory 80−94169
rhodopsin conformation, spectral studies 78−15765
rhodopsin content and behaviour threshold rel. to vitamin A deprivation in rat 77−70463
rhodopsin content and electroretinographic sensitivity in light-damaged retina 77−64033
rhodopsin flash photolysis, rabbit retina 78−76996
rhodopsin formation, opsin recognition of longit. length of retinal isomer 78−61137
rhodopsin in digitonin, isolation of 3 isochromic forms 77−52951
rhodopsin in model membranes, charge displacements in interfacial layers 77−52785
rhodopsin kinetics at room temp. meas. by picosec. spectroscopy 77−64036
rhodopsin lateral diffusion in surface membrane of rat retina rod external segment 78−15828
rhodopsin orientation in photoreceptor membrane, model 77−90775
rhodopsin $P499_1$ and porphyropsin $P522_2$, paired visual pigments in goldfish 79−53111
rhodopsin phosphorylation as possible mechanism of visual adaptation 78−15836
rhodopsin photochemistry, relevance of Halobacterium photosensory mechanism 77−90738
rhodopsin photolysis, retinal rod external segment mag. anisotropy decrease 77−52838
rhodopsin photoproduct kinetics in frog retinas, rapid scanning microspectrophotometer meas. 78−92763
rhodopsin photosensitivity, thermal stability and metarhodopsin prod., extractant effects 78−7355
rhodopsin stability in rods and dark noise in retinal bipolar cells 78−11644
rhodopsin thermal stability in photoreceptor membrane, role of lipids, PMR spectroscopy 80−35874
rhodopsin thermal stability in photoreceptor membrane and Triton extracts, squid rhodopsin 77−32893
rhodopsin visual pigment, photochemical transformations 79−66472
rhodopsin-containing bilayer membranes, light-induced transmembrane channel form. 77−52784
rhodopsin-lipid interactions in photoreceptor membranes 80−12094
rhodopsin-lipid interactions on peroxide oxidation of lipids in photoreceptor membrane 77−21522
rhodopsins of oceanic decapods, absorpt. spectra 78−61182
rhodospin carbohydrate component on intradiscal surface of retinal rod discs 77−4998
ribonucleare, PMR spectra, line narrowing, convolution and pulse methods 78−78729
ribonuclease, positron annihilation, temp. depend. meas. 79−66448
ribonuclease, STEM struct. anal. studies 79−16147
ribonuclease A, bovine, cryst. struct. determ. by X-ray and neutron diffr. 80−108841
ribonuclease A, lyophilized, heat of soln. depend. on H_2O content of solid 79−24938
ribonuclease A, microviscosity, mobility profile 80−91710
ribonuclease A, thermodynamics of interaction and unfolding in transfer to aq. consolute solns. 79−24939
ribonuclease inactivation cross-sections for slow heavy ions 80−26286
ribonuclease model, β-cyclodextrinylbisimidazole, catalysis of cyclic phosphate substrate 78−85287
ribonuclease T_1 in soln., phosphoresc. at 293K *(Japanese)* 77−44595
ribonuclease-A, solid, PMR spin-lattice relax., mol. dynamics 80−51041
ribonucleotide reductase of E.coli, in vivo photoinactivation by near-UV 77−52841
ribosomal protein S4 from Escherichia coli, circular dichroism obs. of conformation 78−96003
ribosomal subunit 30 S, of E coli, meas. of location and radii of gyration of proteins by neutron scattering 79−11892
ribosomal subunit proteins from E. coli, 16S ribosomal RNA conformational changes induction 79−79466
ribosome solution, periodic conversions, optical mixing method obs. 78−96029
ribosomes, E. coli, complexes of individual components, small angle X-ray scatt. study 79−11895
ribosomes, E. coli, contrast variation neutron scattering studies, reassembled subunits 79−20510

proteins continued
ribosomes, E. coli, form. of covalent linkages between RNA and proteins due to gamma irrad. *(French)* 77−56340
ribosomes, E. coli, neutron small-angle scatt., contrast variation study 79−16138
ribosomes of Escherichia coli, partially deuterated subunit, protein and RNA distrib., neutron scatt. 78−77021
ribulose bisphosphate carboxylase, two-layered square-shaped mol. 77−56336
rigid assemblies of spheres, creeping flow translational resistance 80−54086
RNA, molecular motions investigated by ^{31}P and ^{13}C NMR relaxation 80−63657
t-RNA, simplified molecular model for use as teaching aid 77−78936
RNA polymerase system, effect of UV irrad. on λ DNA transcription 77−66827
RNase, damage and energy deposition by low-energy ions 77−9172
RNase, effect on specific resist. and electrophoretic mobility of regenerating liver cells 77−25402
RNase inactivation due to elastic nucl. collisions 78−28008
rotational motions, large-scale, detection by EPR and fluorescence 79−16120
rubredoxin, forzen soln., recoilless fraction, Mossbauer spectra meas. 80−8025
rubredoxin, reduced analogue, EHT calc., Mossbauer parameters, zero field splittings 77−79544
rubredoxin, X-ray diffr. expts., synchrotron radiation appl. 77−52936
sarcoplasmic Ca pump, efficient ion translocating system 77−90746
SCF-LCAO-ASMO and CI calcs. of low-lying multiplets and excited states 80−94155
secondary struct., IR, Raman spectral data, review 78−90330
secondary structure determ. by circular dichroism spectra 80−30653
secondary structure determ. by laser Raman spectroscopy 77−23587
secretion by pancreas, accounted for by diffusion-like process 80−21457
sequencing, solid-phase techniques 77−56557
serine proteases, enzymatic reaction mech. mol. orbital studies 77−60183
serine proteases, enzymatic reaction mechanism, CNDO/2 mol. orbital calcs. 78−27751
serium albumin, bovine, high energy-induced aggregation, time resolved spectra 80−61655
serum albumen, bovine, adsorption kinetics, surface denaturation 79−79460
serum albumin, bovine, 2 types of soluble complexes with polyelectrolytes 79−92120
serum albumin, bovine, adsorpt. isotherm, at air-water and air-oil interfaces 79−79461
serum albumin, bovine, binding of spin-labelled stearic acid 79−96506
serum albumin, bovine, hydrated, dielec. and elec. props. 80−97854
serum albumin, bovine, labelling with ^{57}Co, expts. 80−85495
serum albumin, bovine, molecular structure of adsorbed film 79−79462
serum albumin, bovine, mutual and tracer diffusion coeffs., photon correl. obs. 80−72123
serum albumin, diffusion and sedimentation in conc. solns. 77−48749
serum albumin, human, ^{125}I labelled, geometrical dilution *(French)* 80−104742
serum albumin, human, ^{99m}Tc labelled kits, evaluation for cardiac blood pool imaging 80−17130
serum albumin, human, mechanism of eosin-sensitised photochemiluminescence 79−53044
serum albumin, human, prep. of ^{68}Ga-labelled microspheres 80−17131
serum albumin, human hydration, pH depend., water self-diffusion obs. *(French)* 79−34475
serum albumin, permeability of vascular walls, physical theory 80−16908
serum albumin solns., X-ray induced chemiluminesc. intensification by dye addition 79−79470
serum interaction with poly(N^{α},N^{ϵ}terephthaloyl-l-lysine) membrane for artificial red blood cells *(Japanese)* 80−12061
serum low density lipoprotein, human, anomalous permittivity behaviour 80−81540
serum of human, density meas., improved mech. oscillator technique *(German)* 78−28098
SHG study of non-centrosymmetric character 79−74599
sickle haemoglobin gelation, reaction order and crit. nucleus size 78−76983
silk fibroin films, conformational changes induced by water immersion 80−10498
single ligand binding constant computation, règulatory enzyme exponential model 79−79454
small molecules in protein solns., spin-lattice relax. times, inversion recovery spin-echo sequence 80−21446
small peptide antibiotic and protein solns., US absorption 79−48286
small protein struct. anal. by electron microscopy, valinomycin, bacitracin, LMW-CSA N and B 79−92453
solid, PMR spin-lattice relax., mol. dynamics 80−51041
solution, gel conc. and diffusivity at gelling determ. by ultrafiltration 80−21325
solution, propagation of surface shear waves 79−77146
solutions, nuclear mag. relax. dipole-quadrupole nuclei interaction, quasi-rigid and tumbling lattice 77−66434
solutions, quasielastic light scatt. in small wave vector limit 80−45088
solutions, small-angle neutron scatt. using time of flight method, spectrometer 79−1371
solvated, spectroscopic meas. of energy barrier to electron transfer 77−38766
solvent accessibility properties of complex proteins 79−83696
solvent systems, dynamics investigation by nucl. gamma-resonance 79−62166
soya protein gels and sols, PMR relax. times rel. to temp., pH and conc. 78−56952
spectrin-actin monolayer, adsorbed at Hg-H_2O interface, ionic permeability 80−12064
spin diffusion and proton magnetic resonance 77−28470
spin-lattice relax. time, role of cross-relax. 78−35800
stratum corneum basic protein, epidermal keratin filaments, aggregation expts. 79−16142
stress-induced struct. and activity changes 79−43812
structural differences evaluation from electron micrographs 79−53040
structural dynamics, temp.-depend. X-ray diffraction 79−92133
structure, areas, vols. and packing, review 77−86441
structure and bonding, quantum theory, ab initio calcs. 80−61509
proteins continued
structure determination, crystal bending, electron-diffraction data 78−53325
structure factors from electron density, test on model crystal 78−47204
structure factors from electron density distrib., theoretical foundations 78−47203
structure of proteins involved in active membrane transport, review, book contrib. 80−108844
structure prediction from amino acid sequence 78−24026
subtilysin, globule, atomic density distrib. 79−79458
succinic dehydrogenase Fe-S centre of submitochondrial particles, ubisemiquinone interaction, EPR 78−69016
superoxide dismutase, increased level in erythrocytes rel. to radiosensitivity 77−44726
superoxide dismutase, O_2^- as cause of O_2 effect in X-ray induced cell lethality 77−25513
superoxide dismutase, role in lipid photoperoxidation in isolated chloroplasts 78−77016
supramolecular structure, ordered, electron micrographs, image processing 80−89923
supramolecular structures, calorimetric and van't Hoff enthalpies of assembly comparison 77−90717
synaptic proteins after electroconvulsive stimulation 80−56011
synthesis, stochastic eqns., ribosome translation along mRNA and tRNA selection processes 79−66440
synthesis 77−32965
synthesis control studies, exptl. probe using psoralen and near UV light 77−66881
synthesis in human fibroblasts in vitro, US stimulation, role of cavitation 80−8100
synthesis in root meristem cells, 2 MHz US effects, Pisum sativum 77−9218
synthesis mechanisms, genetic codes 77−56353
Tanford-Kirkwood theory of protein titration, proposed extensions 80−101147
testes, γ-irrad., glycogen a metabolising enzymes following radiation-induced atrophy 78−15869
testes, inorganic pyrophosphatase and pyrophosphate following γ-irrad. of rat 78−15868
thaumatin antibodies as model of sweet taste receptor 78−27975
thermal denaturation, use of high heating rates to separate denaturation and aggregation 77−81470
thymidine kinase kinetics, gamma-ray response of leucoagglutinin stimulated lymphocytes 78−57041
thymopoietin active fragment in H_2O, soln. conformation by DNMR spectroscopy 80−89710
titrations by NMR, pH depend. of internal reference 77−86727
tobacco mosaic virus, data quality collected using modified mirror monochromator for rotation photography 79−9269
tomato bushy stunt virus, 3-D coordinates from stereodiagrams 80−64824
transfer across microsomal membranes reassembled from separated membrane components 78−69029
transferrin, ^{111}In labeled, perturbed angular correls. study 79−39342
transferrin, human, ^{57}Fe Mossbauer obs., λ and D values 77−21481
transferrin, human anal. density gradient equilib. centrifugation for determ. of mol. wt., sp. vol., preferential hydration 77−64160
transferrin, use in meas. of plasma total Fe-binding capacity by EPR 77−17003
transferrin bound Fe^{3+} during rat lymphosarcoma development, EPR 77−77878
transport across endothelial membrane 80−3601
transport in agargel electrophoresis, stochastic model 77−77769
tripeptides, synethetic, hormone models, field desorption mass spectrometry using needleless emitters 79−34398
triplet state energy transfer 78−20143
tropocollagen macromolecule form., effect of soln. pH 78−95999
tropomyosin, cryst. struct. and molecular interactions 79−48210
tropomyosin, isotopic H exchange as function of state of ionisation of side groups 78−68979
α-tropomyosin, specific splitting at cysteine-190, physicochem. study of fragments 80−30647
tropomyosin, thermal denaturing, causes of heterogeneity in fusion curves 79−53023
trypsin, bovine, accuracy of two independent refined models 79−92128
trypsin, bovine, activation, activity and inhibition *(German)* 79−79465
trypsin, inactivation role of tryptophanyls singlet and triplet states 79−57564
trypsin, photoluminescence after UV irradiation *(German)* 79−92137
trypsin crystal fusion, microcalorimetry 77−70413
trypsin inhibitor, mol. dynamics, computer simulation 78−9932
trypsin inhibitor, soybean, folded, models for H exchange 78−76981
tryptophanase induction in X-irrad. E. coli B and B/r 78−28005
tryptophon+chloranil, charge transfer interaction, equilib. const., enthalpy and entropy determ., mol. polarisability 80−89708
tubulin antigens, agarose gel electrophoretic determ. of mol. weights 80−67313
tyrosin+chloranil, charge transfer interaction, equilib. const., enthalpy and entropy determ., mol. polarisability 80−89708
tyrosinase in buffer soln., UV effect on biological activity 80−30791
tyrosine aminotransferase activity circadian rhythm, mouse liver, X-ray effects 80−41121
tyrosine fluorescence at 345 nm in proteins lacking tryptophan 79−39360
UDPG-dehydrogenage, rat liver, struct. alterations and functional vars. due to γ radiation 78−15873
urease shear inactivation, metal ion effect, rel. to shear deform. effects in enzyme catalysis 78−76982
US absorpt. and vel. in mammalian tissue, dependence on constituent proteins 80−61621
UV fluorescence detect. of conformational rearrangements in plants 79−53031
UV fluorescence spectra, resolution of components of complex spectra by Alentsev-Fok method 80−1097
UV fluorescence spectra, resolving of components, Alentsev-Fok method 80−1096
UV irradiated, luminesc. quenching, EPR and absorpt. spectra 78−15768
UV irradiated, paramag. centre accumulation, kinetic eqn. 77−21476
vasopressin, dark field electron micrographs, image array filtering in reciprocal space 77−74557

proteins continued
visual pigment retinal chromophore, role of protein in photochem. 78−15772
visual pigment unprotonated chromophore-protein bond, ^{13}C NMR spectra 78−11607
visual pigments, resonance Raman studies of the primary photochemical event 80−41020
visual pigments of Gekko, ionochromic behaviour 77−36928
water adsorbed on proteins, new programme for NMR study of diffusion 79−92139
water interactions in aq. solns., Raman spectroscopy 77−6792
wheat germ agglutinin, struct. of binding sites, ligands with heavy atoms, phosphoresc. changes 79−24947
X-ray crystallographic data measured on oscillation camera, collection and reduction method 79−29672
X-ray crystallography, book contrib., review 77−40958
X-ray crystallography, synchrotron radiation appl., anomalous scatt., absolute intensity, and polarisation 77−52936
X-ray diffraction data collection on macromolecules, FORTRAN program 77−51279
X-ray diffuse scattering curves, nature of 4.5 Å max. 78−31769
X-ray precession photography, thermal gradient problems 77−27781
X-ray scattering, large-angle diffuse, rel. to globular protein struct. anal. in soln. 77−86723
X-ray scattering data, Soule-Porod plots 77−51273
zein, protein-peroxide radicals, ^{17}O-labelled, EPR obs. 80−85345
Na^+,K^+-ATPase, brain, soluble, interaction with plane phospholipid membranes 80−35851
^{211}At protein labelling technique using an acylation reaction 80−36130
CO myoglobin struct. determ., neutron crystallography 79−43814
CO-haemoprotein photolysis, transient Raman study, quantum yield origin 80−67155
CO-myoglobin, mol. tunnelling, isotope effect, time resolved IR Fourier transform obs. 80−72126
^{13}C, NMR of peptides and proteins, review 78−24023
$(Fe_4S_4(SH)_4)^{0/2-/3-}$, HFS-LCAO calcs., 4-Fe active site model in high pot. Fe protein and ferredoxin 80−42929
H^+-ATPase, soluble mitochondrial, thermal stability obs. 80−55992
H_2 exchange kinetics and internal motions 80−21440
^3H-labelled, fluorography in immunoelectrophoresis 80−17220
^3H-methyl acetimidate preparation for protein labelling 79−53246
HeLa cell chromatin, effects of hyperthermia on protein-to-DNA ratio 79−11905
Mo-containing (2Fe, 2S) protein, isolation from Desulphovibrio gigas, sulphate reducer 77−86375
Mo-containing enzymes, investigation using EPR 77−86373
NO-Fe(II)haemoproteins, orbit-orbit interaction, low temp. mag. circular dichroism obs. 80−30645
O_2 biomolecular transport proteins and metabolism 79−24946
$^{239}PuO_2$ inhalation, rat pulmonary connective tissue modification by internal α-irrad. 79−92302

proton absorption
Al(p,$\bar{p}\pi^-$), 10 GeV, $\bar{p}$ weak absorpt., $\bar{p}$ and π^- yields *(Russian)* 79−75987
Au(p,$\bar{p}\pi^-$), 10 GeV, $\bar{p}$ weak absorpt., $\bar{p}$ and π^- yields *(Russian)* 79−75987
Be(p,$\bar{p}\pi^-$), 10 GeV, $\bar{p}$ weak absorpt., $\bar{p}$ and π^- yields *(Russian)* 79−75987
Cu(p,$\bar{p}\pi^-$), 10 GeV, $\bar{p}$ weak absorpt., $\bar{p}$ and π^- yields *(Russian)* 79−75987

proton accelerators
see also cosmotrons
14UD Pelletron accelerator at ANU, energy calib. using $^{12}C(p,\alpha)$ 78−17449
28 GeV proton synchrotron and intersectig storage rings, interconnected vacuum system 78−86706
800 MeV proton synchrotron for pulsed spallation neutron source 77−67930
applications for intense 10-20 GeV proton beams 79−85838
AVF cyclotron, electromagnet 77−3198
beam cooling effect of electrons 77−23334
beam energy distribution control technique for proton synchrotron 79−72128
beam lifetime in KEK PS main ring 77−83278
beam-beam interactions in e-p storage rings 78−78889
beam-beam interactions in p-p storage rings 78−78900
beam-beam simulation for modest Fermilab proton colliding beam expt. 77−83337
BNL linear accelerator development 77−38484
Brookhaven 200 MeV proton linear accelerator 79−31245
Brookhaven accelerator-reactor breeder concept 77−54294
CERN, 25 years history and equipment *(French)* 80−98778
CERN, 50 MeV proton linac injector, performance 79−67972
CERN, Intel 8080 microprocessor development system 77−83314
CERN, international scientific cooperation *(Dutch)* 77−45669
CERN 400 GeV proton accelerator 78−70651
CERN 400 GeV Super Proton Synchrotron, multipurpose He refrigerator/liquefier 79−58737
CERN 400 GeV super proton synchrotron, review *(Dutch)* 77−46432
CERN 400 GeV superproton synchrotron, facility description 78−37471
CERN 50 MeV linac, beam emittance meas. in matching 77−38479
CERN 50 MeV linac, beam optics 77−38477
CERN 50 MeV linac for proton synchrotron, operation and modification 77−38442
CERN accelerators, radiation protection *(Dutch)* 77−46434
CERN linac, computer control system 77−38480
CERN proton synchrotron, improvement project for computer assisted controls 79−72209
CERN proton synchrotron, stand alone control system for continuous transfer ejection to SPS 78−82552
CERN proton synchrotron booster, improved recombination of 20 PSB bunches and merging to 5 dense bunches 79−76192
CERN proton-antiproton colliding beam facilities 79−67996
CERN PS, collective phenomena at very high intensity 79−76193
CERN PS booster, reliability and maintenance anal. 77−83281
CERN PS booster, simultaneous dynamic stopband compensation and correction lens location 79−76191
CERN SPS, 200 MHz accelerating systems and 800 MHz Landau damping cavity 79−72063

proton accelerators continued
CERN SPS, collective transverse beam instabilities damper description 79−72143
CERN SPS, control systems operating experience, suggested principles for future accelerators 79−72211
CERN SPS, external proton beams and splitter system 77−83386
CERN SPS, fast resonant extraction 79−72137
CERN SPS, high energy polarisation parameters, feasibility of future expt. 77−30738
CERN SPS, target stations and beam dumps 77−83385
CERN SPS, zer flux DC current transformer 77−88306
CERN SPS system, travelling wave drift tube structure 77−38517
CERN super proton synchrotron, experimental programme *(Dutch)* 77−46431
CERN super proton synchrotron, experiments with light particles *(Dutch)* 77−46433
CERN super proton synchrotron, review 78−78529
chemical anal. appls. 78−85239
Cockcroft Walton 860 keV preaccelerator for SIN high current injector cyclotron 79−67975
Cockroft-Walton, use in X-ray high intensity sub.-kV calib. facility 77−71714
collective accelerator, superconducting resonators and solenoids, Q-values and field profiles 78−46188
collective accelerator, superconducting solenoids, resonators and cryogenic system 78−46187
collective ion acceleration from rotating relativistic electron beam injection into neutral H 79−76167
collective ion accelerators and power balance in intense electron beams in neutral gas 77−83171
collective proton acceleration in system with insulated anode 79−31246
collectively accelerated protons, nucl. activation, time-of-flight, and foil activation meas. 79−4195
colliding beam facility, 1000 GeV on 1000 GeV, proposal at Fermilab 77−83201
cooling channel for injection into linear accelerator 80−68973
CPS at CERN, pulse to pulse modulation, extraction modes, beam intensity 77−83277
cyclic, Monte Carlo determ. of intensity of positronium beams *(Russian)* 77−388
cyclotron, TRIUMF, beam props. improvements 77−83397
cyclotron beam emittance measurements with a dispersion-matched magnetic spectrograph 79−54732
depolarisation during acceleration and storage of polarised protons and deuterons 78−58519
Doubler-Tevatron, charact., points of interest 79−72038
electron cooling method, proton-antiproton colliding beam appl. 79−18067
electron cooling of proton beam in storage ring 77−14281
electron-proton facility in CERN SPS 77−83203
electron-proton project TRISTAN, design features 77−83204
Fermilab, acceleration development 77−38478
Fermilab, appl. of NMR cct. to superconducting mag. field meas. using signal ave. 77−83231
Fermilab, microprocessor based timed reading and time plot CAMAC modules 77−54484
Fermilab, multi-user control and data acquisition systems 77−54480
Fermilab 500 GeV accelerator, operating experience 77−83280
Fermilab 500 GeV main accelerator RF cavity 128 MHz mode damper 77−83299
Fermilab booster, transverse instabilities suppression, fast feedback system 77−83298
Fermilab booster beam, longitudinal dipole oscills., effects, damping 77−83259
Fermilab booster bunches, linac bunch struct. during adiabatic capture and accel. 77−83261
Fermilab capacitor tree 77−83242
Fermilab electron cooling expt., design and construction of electron beam 79−72138
Fermilab facilities, future projects, perspective 79−85841
Fermilab linac, microprocessor-based preaccelerator control system 77−38481
Fermilab main accelerator quadrupole transistorised regulators 77−83243
Fermilab main ring power supply, minicomputers control system 77−83303
Fermilab POPAE, 6 T superconducting dipole mag. design 77−26898
Fermilab synchrotron, attainment of 500 GeV proton beam 77−83275
fissile material spallation breeding by high power accelerators 77−83162
future technologies in high-energy physics, collective accelerators, laser accelerators, single-pass collecters 80−78466
Hall accelerator, four-lens, pure ion beam struct. 78−66441
Harvard Univ. 160 MeV proton beam, clinical experience and implication for designers 79−54693
HEPI accelerator, active filter of annular electromagnet 78−33338
high gradient proton linac, high energy accel. structs. 77−83144
high-current pulsed linear ion accelerators, insulated drift tube 78−50417
IFVE accelerator, coherent beam instability 78−837
Intense Pulsed Neutron Source (IPNS-1) accelerator 500 MeV fast kickers 79−72131
Intense Pulsed Neutron Source (IPNS-1) accelerator RF system 79−67998
intersecting storage accelerator ISABELLE, review 80−32545
ionising radiation produced during operation, dosage and shielding *(Czech)* 79−89505
ISABELLE, charact., points of interest 79−72038
ISABELLE, pp intersecting storage accelerator facility at BNL 77−83344
ISABELLE full cell, ultrahigh vacuum system 80−77798
ISABELLE ISR, computer based control and monitoring system 78−46191
ISABELLE ultrahigh vacuum system, self-modulating ion gauge 80−82786
ISR, longitudinal bunch dilution due to RF noise 77−83260
ISR at CERN, beam stability, coupling impedance, meas. by RF excitation 77−83269
IUCF control system 79−54702
Karlsruhe supercond. proton linear testaccelerator, performance characteristics 79−72006
KEK, 750 keV beam line construction 77−38438

proton accelerators continued
KEK, 750 keV beam monitoring 77−38439
KEK, beam position monitor system, design, operation 77−83306
KEK, harmonic current AC filters 78−33333
KEK 12 GeV proton synchrotron, voltage flicker suppression 77−83230
KEK 12 GeV synchrotron, and current status of accelerator facilities in Japan 79−72041
KEK 20 MeV injection linac, operational behaviour 77−38441
KEK 500 MeV fast cycling booster synchrotron 77−83282
KEK booster, beam loss in initial acceleration 79−76182
KEK booster, longitudinal beam behaviour 79−76184
KEK booster, transverse coherent instability anal. 79−76183
KEK booster to main ring beam transfer system, construction operation 77−83264
KEK main ring, dipole magnets field meas., B-clock system 77−83308
KEK main ring, prototype multipole magnets, design, field uniformity 77−83220
KEK main ring, RF acceleration 79−68048
KEK projector operation 77−38437
KEK proton synchrotron, initial operation, 12 GeV energy, peak intensity 77−83272
KEK proton synchrotron, power supply 77−83245
KEK proton synchrotron, synchronous beam transfer from booster to main ring 77−83263
KEK proton synchrotron vacuum system design and construct. 77−83225
KEK proton synchrotrons, coupling resonance $2\nu_H$-$2\nu_V$ 79−76185
KEK synchrotron, proton attenuation lengths in paraffin, concrete and iron around targets 80−102412
KEK synchrotron, simple Q-measurement 77−83316
Kiev isochronous cyclotron, beam extraction and transportation 79−54717
LAMPF, effect of perturbation in low-β proton accelerating structures 77−34485
LAMPF, neutron physics programme 77−26951
LAMPF, status 77−18715
LAMPF, status 77−38447
LAMPF, status of injector complex 77−38440
LAMPF Alvarez sections, high-power low-freq. klystron as drive 77−83174
LAMPF high power pion prod. target mechanism 77−83387
LAMPF line-D fast deflector system 77−83157
LAMPF radiation effects facility, total neutron flux, energy spectrum, meas. and calc. 77−23331
linac, accelerating structure of meson factory 77−38482
linac, generators for Medical Applications 77−38474
linac, ion sources and injector development 77−38470
linac, KEK preinjection accelerating column 77−38436
linac, low cost RF struct. 77−88293
linac, pion generator for medical applications, beam dynamics 77−38475
linac, source of neutrons for radiotherapy 77−81569
linac bunch shape meas. and double drift harmonic buncher 77−38471
linac cavity, calc. methods for field distrib. 77−38505
linacs for protons and heavy ions, loss reduction 77−83120
linear, appl. to reactor fuel breeding 78−29630
linear, high current, appl. in nuclear power 77−38450
linear, high-energy section modelling by graded-β Electron Test Accelerator 77−38467
linear, increase of beam radius and image ellipsoid 77−65360
linear, non-destructive bunch length monitor 77−376
linear, optimum particle bunching 78−5068
linear, USSR Radiotechnical Institute developments 77−38448
linear, with quadrupole RF focusing, URAL-15 78−82543
linear, with variable phase focusing, calc. parameters 77−46426
linear, with variable phase focusing, space charge effect 79−13561
linear, [conference, Ontario, Canada (Sept. 1976)] 77−38445
linear accelerator simulation, code PARMILA, longitudinal tuning of LAMPF 77−83159
linear accelerators, struct. reson. 77−83158
linear high energy, possible use of quadrupoles with permanent magnets 77−23320
low energy proton accelerator, voltage or energy calibration using (p,γ) reaction 77−50316
meson factories, status and survey in 1977 77−83161
muon beam channel, 40 GeV/c, Serpukhov, lens guide reflector, filter 77−18729
neutrino experiments, facility, particle loss and radiation environment 79−9930
neutrino experiments facility, focusing, pulsed power supply 79−9974
neutrino target complex at Fermilab, operating experience 80−23230
Nevis proton synchrocyclotron extraction system, design, operation 77−83265
non-neutral proton ring, const. radius mag. accel. 78−46192
Orsay 200 MeV proton synchrocyclotron, beam optics and beam monitoring in beam lines 79−54636
Orsay 200 MeV synchrocyclotron, machine parameters, beam handling and extraction, current status 79−54635
personnel neutron dosimetry using cellulose nitrate film and LiF as radiator and TLD 77−64132
photon dose rate from induced activity in the beam stop of a 400 GeV proton accelerator 78−94144
PIGMI, 250 kV proton injector system 79−45467
PIGMI, accelerator control system 79−45475
PIGMI, linear pion generator, mechanical technologies 79−72008
PIGMI, linear proton accelerator, mechanical description 79−45474
PIGMI program at LASL, proton linac development for medical appl. 79−45471
PIGMI prototype, linear pion generator, initial performance 79−72007
polarised proton acceleration in CERN synchrotron 77−38509
polarised protons, acceleration by 12 GeV synchrotron at KEK, possibilities 79−63846
POPAE, lattice insertions 77−83328
proton beam in storage ring or synchrotron, monitoring by narrow band synchrotron radiation 77−83293
proton double extraction for irradiation of Mirabel and Lyudmila bubble chambers 78−839
proton injection into a large amplitude space charge wave 79−71990
proton storage ring, NAP-M, accelerating system and beam parameters monitoring 77−65364
proton synchrotron, radioactivity of subsurface water in ground shield 77−67907
proton accelerators continued
proton-proton colliding beam facility at Brookhaven, ISABELLE, design status 77−83322
PS booster at CERN, longit. active damping system electronics, tracking band pass filters 77−83297
pulse generation, 0.2TW 77−22618
pulsed H injection, vacuum system with magnetic discharge pumps 77−23318
pulsed proton gun, microsec. operation 79−89510
pulsed source, Penning type, beam parameters 80−87001
pulsed spallation source for neutron scattering research 77−83351
radiation loading and heating of struct. 80−42883
relativistic proton beam, energy monochromation using laser 78−90010
RF accel. in KEK booster synchrotrons 77−83279
RF field induced by a charged beam in a multigap resonator 80−52804
Saturn 2, 100 MeV-3 GeV proton accelerator *(French)* 80−32547
SATURNE II proton synchrotron, magnet design and meas. 77−83241
scanning microprobe, digitally controlled for p and heavy ions 79−13571
secondary electron amplification in high energy accelerators 78−46193
separated-sector cyclotron multidisciplinary facility 77−83196
SIN 590 MeV ring cyclotron, recent and future developments 79−54642
SIN accelerator facility 79−85836
SIN accelerators, operational experience and improvement programs 77−83284
SPS, FODO separated function lattice, design 77−83262
SPS, real-time control system, operating system principles 80−875
SPS, second order effects in sextupole-corrected SPS lattice 79−76196
SPS beam instrumentation, closed orbit correction 77−83305
SPS computer control system, operational experience 77−83292
SPS magnet system, nonlinear fields and their compensation 77−83268
storage ring, operation of Fermilab accelerator 77−83330
storage ring 400 GeV facility, CERN design 77−83202
storage ring lattice design 77−83190
storage rings, low energy current accumulator 77−83329
storage rings, proton beam interaction with ion wake 77−83345
super-proton-synchrotron at CERN, microtechniques *(Swedish)* 77−65370
superconducting accelerator structs. for medium energy protons 77−83151
superconducting dipole magnet, quench levels induced by proton beam spray meas. 77−26906
superconducting magnet, 400 GeV proton damage to stabilising material 77−37948
superconducting magnets in synchrotron, quench thresholds after proton beam exposure 79−31254
superconducting proton-linac, Karlsruhe, 1.8K cooling circuit 79−58707
superconducting quadrupole magnets for Karlsruhe proton linac 77−26889
synchrontron at CERN, low-momentum high-intensity separated antiproton beam 77−14292
synchrotron, beam, 70 GeV channel, shaping system, for Protvino Inst. neutrino expts. 78−37476
synchrotron, beam parameter diagnostics via IR undulator emission *(Russian)* 78−836
synchrotron, intense beam, bunched, optimum critical energy transition 77−83346
synchrotron, KEK 12 GeV, beam profile meas. 77−83404
synchrotron, proton beam 70 GeV, for Protvino Inst. neutrino expts., characts 78−37475
synchrotron, proton recapture and moderation on magnetic field decay 79−68062
synchrotron, pulsed neutron facility at Rutherford 78−29208
synchrotron accelerator theory 77−67925
synchrotron for intense pulsed neutron source facility 77−83191
synchrotron radiation prod. in visible narrow band 77−58241
synchrotron slow extraction beam parameter monitoring and control system in CAMAC standard online with ES 1010 computer 78−29674
synchrotrons, bunches with local elliptic energy distribs. 79−76565
synchrotrons, feedback-stabilised proton synchrotron, beam interaction 78−78527
synchrotrons with short accel. time, accelerating resonators 77−46429
target and collimator precision position control and monitoring via CAMAC 77−67927
tevatron, Fermilab proton accelerator with supercond. mag. ring 78−835
Texas A&M polarised proton beam meas. 80−102360
trace element analysis appl., characteristic X-ray emission excitation *(German)* 77−25348
TRIUMF, 500 MeV, 100 μA isotope production facility 80−68985
TRIUMF 100 μA beam, achievement and control 79−54699
TRIUMF data interface 77−88304
TRIUMF facilities and kaon factory designs 79−85837
TRIUMF isochronous cyclotron, recent developments and thermal neutron facility 79−54643
TRIUMF meson factory, preliminary research results on few body problems 77−18721
UNK project, 3 TeV accelerator, constructional problems *(Czech)* 80−869
vacuum diodes, accelerating mechanisms, induced radioactivity 79−97470
Van de Graaff, focusing electrode improved ion source extraction system 79−76179
Van de Graaff, proton beam resolution improvements 77−75008
ZGS, external proton beams 80−91307
ZGS at Argonne, depolarising resonances effects on circulating polarised proton beam 77−83274
ZGS booster, intensity and position meas. systems 77−83307
ZGS polarized beam facility, supercond. solenoids, magnet and cryostat design 79−31252
ep colliding beams 78−78531
pp colliding beams at Fermilab, phase space cooling 77−83324
π factories, multidisciplinary role 78−21791
Al vacuum chamber and bellows, proton synchrotron appl. 79−68056
Fermilab, H^- ion program 77−38506

proton affinity
amino acid protonation ab initio Hartree-Fock-Roothaan SCF calcs. 80−9503
dichlorocarbene, new value for proton affinity 79−18312
electronegativity equalisation in atom-atom reactions 79−66272
B(I) hydrides, ab initio calcs., proton and hydride affinities 79−10029

proton affinity continued
$C_2H_3O^+$ and $C_2H_5S^+$, stability, proton affinity, ab initio SCF, CEPA PNO, MINDO/3 and MNDO calcs. 79−59357
HBr, proton affinity, mol. beam photoionisation method determ. 79−89622
HCl, proton affinity, mol. beam photoionisation method determ. 79−89622
HF, proton affinity, mol. beam photoionisation method determ. 79−89622
H_2S, proton affinity, ab initio HF calcs. 79−31371
NH_2 radical, heat of form., a diabatic electron affinity, from proton affinity meas. 79−91987
NH_3, gas phase proton solvation energetics, mol. beam-photoionis. obs. 79−29345
O_3H^+, isomeric structs. ab initio MO calcs. 80−83270

proton angular distribution
see also proton spectra
elastic scattering of protons, ang. distrib., cross section, anomaly rel. to shell struct. of target 78−54752
nuclear photoemulsion obs. at E_π=115 MeV, ang. distribs. and cross sections *(Russian)* 79−13352
^{2}H(p,p), theoretical anal. of nucleon-nucleon forces 79−9554
pp elastic scatt., ISR energies, spin behaviour of ang. distribs. at large momentum transfer *(Russian)* 79−80849
pp elastic scattering, up to 27.4 GeV, simple Regge model for ang. distribs. 79−75799
pp scatt., polarisation paramater and ang. distribs. meas. at 100 and 300 GeV 78−89738
π^--nucleus, 3.9 GeV/c, backward proton emission *(Russian)* 77−38302
Al(Ne,X), proton inclusive spectra, direct plus thermal model 80−57799
^{10}B(d,p)^{11}B, 1 to 2 MeV, ang. distribs., reduction factor, spectroscopic factors 77−41977
^{10}B(d,p)^{11}B, E_d=0.8 to 2.4 MeV, reaction mechanism 79−17910
^{10}B(t,p)^{12}B, 0.5 to 1.25 MeV, excitation functions and ang. distribs. 78−13109
^{11}B(γ,p)^{10}Be, 18 to 31 MeV, photoproton spectra and ang. distrib., excited state transitions 78−13056
^{9}Be(p, p) and ^{9}Be(n, t), 18.3 MeV, ang. distribs. 77−18539
^{12}C(^{7}Be,p) at 11.4 MeV c.m. energy 80−9302
^{12}C(α,p_0), 17.5-18.7 MeV, p ang. distribs. and integrated cross section 79−30846
^{12}C(α,p)^{15}N (3/2$^-$, 6.328 MeV) transition, giant resonance effects 79−9601
^{13}C(^{3}He,p), 20 MeV, p ang. distrib., ^{15}N energy levels 78−21581
^{A}Ca(α,p)$^{A+3}$Sc, 25 MeV, population of $f_{7/2}{}^4$ states 79−59077
^{40}Ca(p,p), imaginary spin-orbit term in proton optical potential, ang. distribs. 78−58273
cc ^{42}K levels and ang. distribs., spectroscopic factors, DWBA anal. from ^{41}K(d,p) 79−17806
^{140}Ce(d,p)^{141}Ce, 17 MeV, spectra and ang. distrib. obs., DWBA anal. 77−38283
Cl(Ar,X), proton inclusive spectra, direct plus thermal model 80−57799
^{50}Cr(p,p′γ), 2.00-3.03 MeV, proton and γ-ray ang. distrib. meas., p-wave reson. obs. 77−41961
^{19}F(t,p)^{21}F, 0.9 and 1.1 MeV, proton ang. distribs., possible compound nucl. form. 78−17218
^{54}Fe(τ,d), (τ,dp), spectroscopic study of ^{55}Co 77−88029
^{2}H(d,N), 50-85 MeV, ang. distribs., PWBA anal. 79−76005
^{2}H(p,2p)n, 8.5 MeV, n-p final state interaction, cross section, ang. distrib. 78−21560
^{2}H(p,p), 6,8 MeV, ang. distrib. meas. *(Russian)* 78−21566
^{3}He(e,e′p)^{2}H, 1.2 GeV, p angular distrib., recoil nucleus momentum distrib. *(Russian)* 79−9550
^{3}He(p,p), 18-48 MeV, elastic differential cross section ang. distribs., four body problem 79−75998
K(Ar,X), proton inclusive spectra, direct plus thermal model 80−57799
^{6}Li(d,α), (d,p), simultaneous determ. of p and α particle ang. distribs., cellulose nitrate detector 79−737
^{6}Li(n, p)^{6}He, 6.77-4.71 MeV, ang. distrib. excitation function, DWBA, optical model, anal. 77−18539
^{6}Li(π^+, 2p), 85 MeV, ang. depend. of cross section *(Russian)* 77−34349
^{7}Li(π^+, 2p), 85 MeV, ang. depend. of cross section *(Russian)* 77−34349
^{24}Mg(α,p)^{27}Al, 25-26 MeV, high spin selectivity 77−23097
^{26}Mg(γ,p), 16-23 MeV, proton ang. distrib. meas. 77−41946
^{26}Mg(p,p′), 6 MeV, spin-flip probability, ang. distrib., energy depend. 78−13078
^{14}N(d,p)^{15}N, 0.309-0.638 MeV, differential cross-section, ang. distrib. meas. 77−6396
^{15}N level excitation functions, resonance, p ang. distribs. from ^{13}C(^{3}He,p), 3.6-6.6 MeV 78−93942
^{142}Nd(e,e′p), spectra and ang. distribs. meas., $T_>$ giant reson. anal. 78−13069
^{20}Ne, levels, J^π and ang. distribs. from ^{18}O(t,p) 80−18204
^{16}O(d,p)^{17}O, anal. using deuteron deform. effects *(Japanese)* 78−37355
^{16}O(γ,p), 40-105 MeV bremsstrahlung, ang. distribs. meas. 77−41945
^{16}O(p,p), imaginary spin-orbit term in proton optical potential, ang. distribs. 78−58273
^{16}O(π^+,p)^{15}O, 66 MeV, ang. distrib. meas. 77−10438
^{18}O deduced levels and ang. distribs., cross sections from ^{12}C(^{7}Li,p), 16, 18 MeV 79−6686
Pb(α, p), 3.6 GeV, max. in p ang. distrib. *(Russian)* 79−36253
^{96}Ru(d,p), 16 MeV, spectra and ang. distribs. meas., ^{97}Ru levels anal. 77−38284
^{31}S, excited states, ang. correl. meas. 77−38239
Si, ang. distribs. of 6.6 MeV protons, 12.5 MeV deuterons, and 24 MeV α-particles 78−29720
^{28}Si(d,p)^{29}Si, 1.0 to 2.5 MeV, excitation functions and angular distribs., DWBA anal. 78−62543
Ti(p,p), 6 MeV, A=46,48,50, cross sections, excited states, ang. distribs. 77−61410
U(Ne,X), proton inclusive spectra, direct plus thermal model 80−57799
Xe+π^+ → p+..., 2.34 GeV/c, proton angular distrib., shock-wave effect *(Russian)* 77−38304
Xe(π,p), E_π=2.34 and 3.5 GeV/c, energy and angular distrib. obs. *(Russian)* 79−9633

proton angular distribution continued
Xe(π^+,pπ^0), E_π=2.34 GeV/c, momentum distrib. function estimate for internuclear nucleons *(Russian)* 79−9634
^{66}Zn(d,p)^{67}Zn, 12 MeV, levels, ang. distribs., spectroscopic factors meas. 77−22891

proton beam effects *see proton effects*

proton belt *see radiation belts*

proton detection and measurement
acoustic signature of proton beams in fluid media 79−59317
beam burst width and phase drift at the Indiana University cyclotron facility 79−76216
beam detector assembly for the Fermilab Energy Doubler 79−72156
cellulose acetate solid state track detectors, catalytic oxidation sensitization *(Chinese)* 80−102399
cellulose nitrate, proton, H_2^+ mol. ion, and heavy ion irrad., track prod., etching obs. 78−86757
cellulose nitrate track detector, simultaneous determ. of p and α particle ang. distribs., (d,α) and (d,p) reactions 79−737
cellulose nitrate track detectors, detect. of efficiency and range meas. of alphas and protons 78−17524
cellulose proton track visualisation detectors *(French)* 80−74080
cerenkov counter for spacecraft application 78−86734
CERN 2m HBC, automatic meas. of 12 GeV/c p̄p interactions 79−36471
collectively accelerated protons, nucl. activation, time-of-flight, and foil activation meas. 79−4195
counter telescope, efficiency for 89-466 MeV protons 77−57843
dose buildup from secondary protons and recoil electrons, 185 MeV protons 78−15898
energy-range relations for heavy protons and heavy quarks, use in detection 78−58566
fluorescent intensification screen+photographic film combination, response to proton exposures, radiography 78−20268
Havar foil, stopping power and multiple scatt. for low energy protons 79−31339
helical channel electron multiplier, characts. *(Russian)* 79−3324
intense proton beam current measurement via prompt γ rays from nuclear reactions 78−93784
Kapton foil, stopping power and multiple scatt. for low energy protons 79−31339
KEK, beam position monitor system, design, operation 77−83306
liquid Ar calorimeters, props. of EM and hadronic showers 79−45599
low energy α and proton spectra, simultaneous detect. *(Russian)* 77−50332
Melbourne proton microprobe 80−42302
multilayer gas proportional counter system, CM CERN external particle identifier 79−45530
photometric calorimeter for proton flux measurements 80−4718
photonuclear reactions, Saclay linac, photon beam prod., 10-100 MeV, giant dipole resonance *(French)* 79−523
polarimeter for nucleons between 100 and 500 MeV 78−82599
polarisation meas. for ^{12}C(p,p) at 40-75 MeV 80−52840
position sensitive proportional counter, resistive wire, multi-anode, focal plane detector 80−63464
proportional counter tests at TREAT 80−58072
rem-dose measurement of mixed p-n radiation using solid state detectors of fission fragments 80−36137
resistance strip electron multiplier, protons and H atoms detect. efficiency 77−10552
scintillation counter response, 2.43-19.55 MeV, NE-228A, NE-228, NE-224, and NE-102 scintillators 78−58542
secondary electron emission method, test of KCl layers with 400 to 750 MeV protons 77−54475
secondary emission chamber at Brookhaven AGS 79−72187
slow proton detectors, 10-30 keV range 79−68137
spectrometer for proton directional distrib. meas. in space 79−58252
SPS beam instrumentation, closed orbit correction 77−83305
surface barrier detector, peak changes under particle irrad. 80−58077
XTR-detector, Monte-Carlo simulation, 0.5-5 TeV cosmic ray hadron interactions *(Russian)* 79−49564
ZGS booster, intensity and position meas. systems 77−83307
(e,e′p) coincidence expts. at Saclay 600 MeV electron linac ALS 79−72035
γp→π°p, recoil polarisation meas. using C plate and liq. H_2 polarimeters 79−93898
Λ hyperon polarisation, meas. by hybrid Monte Carlo tech. 80−99431
p-γ coincidence expt., use of Ge(Li) detector near 400 MeV intense proton beam 80−5452
Ar, liquid, calorimeter, electron and proton response 80−47832
C polarimeter, proton analysing power, 300-560 MeV 80−23279
CsI(Tl) crystal light output when exposed to protons at 3-15 MeV 78−78570
Cu foils, activation by p, d, ^{3}He, ^{4}He from cyclotron beam, monitoring props. 77−38578
D depth profiling with D(^{3}He,p), proton detection at backward angles 80−30309
$FeSO_4$ Fricke dosemeter solns., G-value determ. for 20 MeV protons 77−52884
^{1}H(n,n)^{1}H, 10 keV-20 MeV, use for neutron flux meas., proton-recoil detectors 79−9960
He polarimeter, low temp., 20 to 50 MeV proton polarisation analysing apparatus *(Russian)* 79−76318
^{7}LiF TLD, efficiency for H^+ and Ar^{18+} detect. 78−53504
NaI detectors, proton react. losses determ. 78−74540
Ni foils, activation by p, d, ^{3}He, ^{4}He from cyclotron beam, monitoring props. 77−38578
^{58}Ni+p, 5.65 and 6.50 MeV, compound nucleus time evolution meas. 78−50160
Si, axially channelled protons, transmission meas. using two-dimensional position-sensitive detector 79−1471
Si detection system for fusion products in migmacell II 77−83089
Si detector, energy response differences for p and α particles 79−6805
Si detector, proton spectra, noniterative method for fitting Gaussian to peaks 77−57840
Si dosimeter, proton beam dosimetry in C, Al, Fe, mylar and H_2O 80−47733
Si semiconductor counters, response to relativistic pions, electrons and protons 79−13597
Si surface barrier detector, Fano factor for protons 79−36480

proton detection and measurement continued
U liquid Ar calorimeter, response to high energy protons, calc. 78−46224
U plastic calorimeter, response to low GeV protons 79−93882

proton-deuteron interactions
see also proton-deuteron scattering
break-up reaction anal. at 1.825 GeV/c 77−71525
charged particle multiplicity distribs. and rescatt. effects at 19 GeV/c 79−36107
charged-particle multiplicity distribs. at 400 GeV/c 80−13337
charged-particle multiplicity distribs. in 100 GeV interactions 78−33101
coherent elastic and inelastic pd scatt. at 2800 GeV^2, cross sections, momentum transfer squared depend. 78−37233
diffractive excitation at high energies and small momentum transfer *(Russian)* 78−17036
double scattering in pd collisions, hadron struct. probs. 77−74732
multiplicity distribs. and rescatt. effects at 200 GeV/c 78−82255
neutron fragmentation and inclusive charge exchange, 195 GeV/c 77−22814
pd→Xd, diffraction dissociation, high energy 78−25087
polarized proton-neutron total cross sections from proton-deuteron data 80−22633
rescattering effects in 19 GeV/c interactions, ΔΔ component of D 80−42500
secondary proton momentum spectra, 4.3 to 8.9 GeV collisions *(Russian)* 79−3039
single particle distribs. with large momentum transfer at 3.3 GeV/c *(Russian)* 78−41596
spin dependent total cross sections, rescattering corrections, Glauber theory 79−49536
dp→dp$\pi^+\pi^-$, 11.9 GeV/c, d* effect and resonance prod. 77−22805
dp→pX, relativistic d inclusive p spectrum, cross section 77−82783
dp→ppn, 8.5 MeV, n-p final state interaction, cross section, ang. distrib. 78−21560
p+d→p+d+γ, 6.3 to 6.9 MeV, bremsstrahlung, cross-sections 78−62429
p+d→π+t, 470 MeV, importance of NN→NNπ in backward scatt. peak at 470 MeV 79−30744
pd, 28 GeV, multiplicity distrib., double scatt. in deuterium 79−36114
pd, 350-1000 MeV, neutron prod. double differential cross section in meson generation reactions *(Russian)* 80−42490
p̄d, 355-1066 MeV/c, total and annihilation cross sections, S meson search 80−68473
pd, 70 GeV, $\pi^\pm$, $K^\pm$, p, p̄ prod. with 0.5-2.2 GeV/c transverse momenta, yield ratio, QCD *(Russian)* 80−83012
p̄D, S-resonance anal. 79−63509
p̄d, total cross section determ., 200 to 370 GeV/c 79−26352
pd→(Nπ)$^+$d, Deck model anal. 77−22757
pd→(p$\pi^+\pi^-$)d, diffr. dissoc. and interactions of diffractive produced systems 79−45107
p̄d annihilation, double-scatt. effects 77−61313
p̄D annihilation, pion rescatt. effect at intermediate energies 80−5010
p̄d annihilation, p̄n mass spectrum enhancement, double scatt. effect 80−78090
p̄d atom formed in liquid deuterium, mechanism, quasinuclear meson *(Russian)* 77−50569
pd bremsstrahlung near breakup threshold, initial and final state amplitude interference 79−67588
pd→d'N*, backward N* prod., 1.0 to 5.0 GeV, exam. of N* exchanges 78−21448
pd→d+X, high energy, screening effect in diffr. dissoc. anal. 77−71541
p̄d double inelastic interactions, 1.6 to 4.3 GeV/c, multiplicity distribs. 79−58969
pd→dπ^+n, 585 MeV, Glauber theory, NN and NΔ amplitudes 78−62525
p̄d dynamics, rescatt. effect, annihilation product, resonances 78−62431
p̄d exclusive reactions, 5.7 GeV/c, impact parameter anal. exclusive reactions, 4.72 to 14.6 GeV/c, impact parameter anal. 77−46073
pd→$K^\pm$+anything, large p_T, 200 to 400 GeV 77−22816
p̄d→Λ+X, cross section calc. for quasinuclear ΛN meson generation *(Russian)* 79−9398
pd→n$_3\pi$d, 800 MeB, cross-section meas. 77−6358
p̄d→NX, <500 MeV/c, narrow NN state search 80−57627
pd→ndπ^+, 585 MeV, reaction mechanisms 79−548
pd→npp, 1 GeV, final-state interactions 77−82900
pd→npp, 1.65 (GeV/c)^2, evidence for Δ-nucleon virtual state 77−10274
pd→npp, exotic final state interaction, intermediate Δ, ΔN threshold parameters 78−50043
pd→p$_1$p$_2$n, 156 MeV, test on p_1-n-p_2 collinearity reson. 79−75996
p̄d→p$_s\pi^-\pi^-\pi^-\pi^0$, 0.4 to 0.9 GeV/c, meson resonance production 79−93447
pd→p(p̄)+anything, large p_T, 200 to 400 GeV 77−22816
pd→pd$\pi^+\pi^-$, 19 GeV/c, two and three pion coherent prod. 79−36095
pd→pd$\pi^+\pi^-\pi^-$, 19 GeV/c, two and three pion coherent prod. 79−36095
pd→pnp, 12.5 MeV, angular distrib. of p-n final state interaction in ^{2}H(p,pn)^{1}H 80−52672
pd→ppn, 1 GeV, OPE contrib. to elastic backward scatt. cross section *(Russian)* 79−9395
pd→ppn, 1.67 GeV/c, secondary particle ang. distribs. and correlations *(Russian)* 80−27646
pd→ppn, 28.5 MeV, collinearity effect 79−75995
pd→ppn, 50 MeV, expt. and theoretical cross sections 79−75994
pd→ppn, 650 MeV, differential cross sections, expt. study *(Russian)* 77−10277
pd→p$\pi^+\pi^-$d, interference phenomena in coherent production, nucleon diffractive amps., helicity-flip 80−47329
pd→π^0X, large transverse momentum, π^0 prod. cross section, ISR energies 79−3055
p̄d→$\pi^+\pi^-$(n), stopped antiprotons, p̄p annihilations from p state 77−18314
pd→$\pi^\pm$+anything, large p_T, 200 to 400 GeV 77−22815
pd→$\pi^\pm$($K^\pm$)pX, 11.75 GeV/c, meas. of left-right asymmetry far inclusive $\pi^\pm$, $K^\pm$, p prod., polarised p-beam 79−22155
pd→tπ^+, 410-809 MeV, ang. distrib. meas. 78−29466
pd→tπ^+, microscopic model using realistic nuclear wavefunctions 79−85465
pd→V^0X, 18 GeV/c, K^0s, γ, Λ, Λ̄ prod. 77−87993
pd→Xd, diffractive interaction, test of finite mass sum rule 77−22819
pol→ppn, inelastic scatt. mechanism at moderate energy *(Russian)* 78−41723

proton-deuteron interactions continued
π, super-fast prod. in relativistic deuteron-proton and nucleus collisions 77−18362
π production in pd collisions, 19 GeV/c, cross sections, mass distrib. 77−71537

proton-deuteron scattering
see also proton-deuteron interactions
analysing power 0.68 to 1.53 GeV 78−93901
back-angle, effect of anti-symmetrisation 77−10273
backward elastic scatt., one nucleon exchange mechanism in light front dynamics *(Russian)* 79−40799
backward elastic scatt. in Δ-reson. region, and OPE formfactor *(Russian)* 79−54353
coherent elastic and inelastic pd scatt. at 2800 GeV^2, cross sections, momentum transfer squared depend. 78−37233
Coulomb interaction in nonrelativistic quantum mech. 79−25906
diffraction cone region, elastic scatt. at 30 GeV *(Russian)* 77−13985
double scattering on H target, d alignment, spin struct. of NN amplitude 78−45937
elastic backward scattering, detection of d relativistic wave function dependence on additional variable *(Russian)* 79−58973
elastic pd scattering at 51.6 GeV/c, scatt. amplitude, slope parameter 78−33093
elastic scatt., 53, 63 GeV, inelastic intermediate state effects, Glauber multiple scatt. theory 79−36104
elastic scatt. anal. at 1.825 GeV/c 77−71525
EM effects, separation, Coulomb problem 77−23014
forward scattering amplitudes, 50 to 400 GeV, ratio of real to imaginary parts 78−70410
Glauber versus final state interaction theory, inelastic/elastic scatt. cross sections 77−57554
inelastic propagators, evidence in elastic scatt. at $\sqrt{s}$=63 GeV, Glauber theory comparison 78−89739
intermediate inelastic states and triple-Regge couplings, Pomeron 80−4972
large angles, resonance one-pion-exchange model *(Russian)* 77−34306
non flip amplitude, real part determ. using derivative analyticity relns. 77−71535
one-pion-exchange model description 79−80834
parity conservation at 15 MeV 77−30445
parity non-conserving effects, predictions 79−93448
phase shifts near deuteron break-up threshold *(French)* 80−73728
potential pd scattering, total cross section calcs., 200-1000 MeV, Glauber model 77−61309
relativistic corrections to two-body pot. 78−74301
rescattering in p-d and π^+-d 100 GeV/c collisions 77−50011
theoretical anal. of nucleon-nucleon forces 79−9554
total cross sections in pure spin states, Coulomb interference and rescatt. corrections 80−432
p(p̄)+d, high energy cross section calc., complex ang. momentum theory *(Russian)* 78−46067
pd→dX, associative multiplicity at high momentum transfer *(Russian)* 77−61333
^{2}H(p,p), energy spectrum, detector, telescope design and performance 78−13384

proton effects
accelerator, radiation loading and heating of struct. 80−42883
accelerometer, high sensitivity, CACTUS, in-orbit electrification of proof mass *(French)* 77−64589
acoustic signature of proton beams traversing fluid media 78−38162
alumina, intense pulsed neutron source, vacuum system bonding methods 79−63261
Artemia eggs, effects of 645 MeV and 9.2 GeV protons 80−45969
benzene, fluoresc. quenching by pulsed proton irrad. of cyclohexane soln. 78−5270
benzene, soln., fluoresc., quenching in pulsed proton and alpha particle irrad., radiation quality effects 80−66259
benzene in dilute cyclohexane solution, fluoresc. quenching on pulsed proton irrad., temp. depend. 80−21307
biological acute and late reactions, mice, comparison of heavy particles for therapy 78−85338
cell survival, OER and RBE, comparison of heavy particles for therapy 78−85337
cell survival vs. depth, comparison of heavy particles for radiotherapy 78−85336
cells, human, multinucleate and micronucleus formation obs. 80−72219
cellulose nitrate, proton, H_2^+ mol. ion, and heavy ion irrad., track prod., etching obs. 78−86757
channelling of relativistic protons in bent crysts., theory 80−96581
charge exchange in solids, studies with Van de Graaff tandem *(French)* 79−4339
charge states of fast protons, capture into and loss from bound states 77−43257
dental enamel, human, damage and exposure during activation anal. 79−70608
durability of cryst. materials for low-energy proton beams, instrumentation aggregate 77−76266
energy doubler dipole, sensitivity to beam induced quenches 79−68084
fast proton track energy deposition and ionisation calc. and obs. 80−12196
fluoride film, contamination by 1 MeV proton bombardment, backscatt. obs. 77−11811
fluorite, use of proton irrad. to reveal growth and deform. features 80−84216
glass, multicomponent Schott, proton-induced colouring 80−9974
graphite assembly exposed to 52 MeV protons, penetration of secondary neutrons and photons 79−76152
ice, monocrystalline, radiation damage, 100 keV proton channelling 80−34102
III-V semiconductors, radiation-induced defects, review 77−80544
ionosphere, channel lower hybrid resonance excitation by superthermal particle streams *(Russian)* 78−4025
local exposure to 200 MeV protons, contrib. of secondary particles to absorbed dose 79−100752
lunar regolite, Fe reduction on heating in vacuum, XPES spectra 80−41740
magnetotail, Alfven wave generation via proton accelerator 78−73582
metal, irradiation-induced creep strain measurement, design and construction of apparatus 78−15634

proton effects continued
metal, polycryst., irrad., coherent acoustic emission *(Russian)* 77—81355
metal, proton energy losses, Bohr equipartition rule 77—15467
metal and metal oxide spacecraft thermal control materials, low-energy proton effects 80—70288
metallic bar, 30 MeV proton excitation of reson. oscills. 80—64431
metallurgy, use of combined ion-, electron-beam techniques 79—43700
metals, 30 to 200 MeV, US wave generation *(Russian)* 77—7761
methanol, excitation of acoustic radiation by pulsed proton beam *(Russian)* 77—80580
MgO, temp. depend. of int. angles for proton axial channelling 80—10586
mica, proton induced giant halos round α-emitting inclusions containing water 77—51420
mirror, interference filters for improved solar radiation resistance 77—39015
monkey, mortality and latent effects, 9 year study 77—2026
neutral radical proton interactions, applic. of anisotropic HFS tensors for double zeta functions 77—35903
ovarian tumour types and incidence in mice after whole-body exposure 79—57724
Permalloy, proton radiation effects, Mossbauer obs. 80—40008
point defects of rad. damage to construction materials, math. modelling 79—90703
polarised nuclear target materials 78—29723
polymer spacecraft materials, electron and proton irrad. effects 80—70262
quartz, comparison of different radiation effects 78—26596
quartz, crystalline, thermolum. sensitivity 77—90205
quartz, ion bombardment, extrusion, evidence for radiation-induced stress relax. of silica network 77—24335
radionuclides prod. cross sections in Al, Si, Ti, Cr and stainless steel by 12-45 MeV protons 77—17310
rare-earth metals and oxides, very-short-lived radiation effects following Coulomb excitation 79—60411
RBE of protons rel. to γ-rays for human cells 80—30798
refractories, swelling on proton, deuteron and He ion bombardment 78—67750
refractory matrices, fast release of reaction products from 600 MeV irradiation 78—29652
relative biological effectiveness, microdosimetric interpretation of biological data 79—62306
relative biological effectiveness, microdosimetric parameters 79—62305
RNase, damage and energy deposition by low-energy ions 77—9172
scanning proton microprobe in atmospheric environment 77—70394
scanning transmission microscopy, proton vs. electron, ratio of elastic to inelastic cross-sections 77—22625
semiconductor, proton energy losses, Bohr equipartition rule 77—15467
silicate glasses, swelling on proton, deuteron and He ion bombardment 78—67750
solar cell proton damage ratio obs., 2 to 10 MeV 79—96476
solar system, early proton irradiation rel. to H and O isotope study in chondritic meteorites 80—36518
spacecraft thermal control coatings, electron and proton irrad. effects 80—70262
stainless steel, type 316, deuteron and proton bombarded, irrad. creep under stress 80—39209
steel, stainless, irradiation creep during 4 MeV proton bombardment 77—43256
steel, stainless, irradiation-induced creep anal., proton simulation of first wall environment 79—24707
steel, stainless 310, proton induced radiation damage investigation by Mossbauer effect 79—1735
storage rings, neutraL molecule desorption from SS(304) and Al(6061) due to particle bombardments 79—76213
superconducting dipole magnet, quench levels induced by proton beam spray meas. 77—26906
superconducting dipole quenching by proton beam induced heating 79—30504
surface barrier detector, peak changes under particle irrad. 80—58077
synchrotron, beam parameter diagnostics via IR undulator emission *(Russian)* 78—836
tissue reactions and fractionated dose schedules, RBE 78—31858
tissue-equivalent gas, energy loss of H, C, N and O ions for elastic nuclear collisions 78—86759
tomography, proton beams computed reconstruction 78—48870
V, polycrystalline, 20 keV protons penetration depth, ultrasonic meas. technique 78—30677
vaporisation, partial wave propag., influence of rapid particle fluxes *(Russian)* 79—38696
Zircaloy-2, irradiation creep under H^+ bombardment at 5.5 MeV 78—14392
Ag film, energy depend. of defect production in displacement cascades 77—31700
Ag, proton irrad., radiation-annealing effects in energetic displacement cascades, film resist. meas. 78—26603
(Al,Ga)As DH injection lasers, sustained oscills. depend. on DC current bias 79—68392
Al, dislocation loops and pores due to 23 MeV proton irrad. *(Russian)* 80—54235
Al, proton flux depth-dose distribs., space-shielding appls. 80—39186
Al, proton irradiated, muon spin rotation study at low temps. 78—92011
Al, proton irradiation, Al atomic displacement position study 80—103401
Al, radiation damage due to protons, μSR 79—56702
Al, single cryst., primary knocked-out atom, energy of spatial distrib., modelling of 0.2 MeV proton trajectories 79—14864
Al target inside magnet, hadron cascades prod. by 300 GeV protons 77—10566
Al, vacancy distribution, interbonding atoms, heat peaks in scattered cascades *(Russian)* 80—39169
(AlGa)As DH, proton-striped, proton-induced defects, photoluminesc. study 80—48251
(AlGa)As DH lasers, comparison of 'normal' lasers and lasers exhibiting light jumps 80—106519
(AlGa)As heterostruct., proton irrad., photoluminesc. 80—29808
(AlGa)As stripe geometry, proton-bombardment delineated DH laser, lifetime 80—106520
AlGaAs-GaAs proton irradiated solar cells, deep-level defects, recombination mechanisms, performance characts. 80—81459
proton effects continued
AlGaAs-GaAs proton irradiated solar cells, deep level defects and recombination parameters 80—94032
$Al_xGa_{1-x}As$ DH stripe-geometry lasers, degraded, capacitance spectroscopy 77—14715
$Al_xGa_{1-x}As$ stripe geometry DH lasers, proton bombarded, intensity pulsations 79—94235
$Al_xGa_{1-x}As$ triggerable semiconductor lasers made by deep proton bombardment 80—69408
α-Al_2O_3, polarised luminescence in neutron- and proton-irradiated single crystals 80—66271
Al_2O_3-BaO-SiO_2 glass coatings in fission and fusion reactors, permeation, elec. cond. and dielectric breakdown 80—18439
Ar isotopes prod. cross sections in natural Ca by 12-45 MeV protons 77—17310
Au foil, optical transition radiation, bombardment by 29 MeV protons 78—2938
Au, proton impact, blocking profile calcs. 78—18694
Au, proton irrad., radiation-annealing effects in energetic displacement cascades, film resist. meas. 78—26603
Au, proton irrad. at 0.3K, resistivity annealing 77—76475
Au, scattering and radiation damage for 14 MeV neutrons and 10 to 20 MeV protons 77—15458
$BaTiO_3$:Co, voltaic current appearance on proton irrad. 80—104032
$Be_3Al_2Si_6O_{18}$, beryl, 350 keV proton irrad., superchannelling effects 79—4344
BeO, radiation induced detrapping of implanted D by ^3He and proton irradiation 80—32482
C accumulation on accel. target surfaces irradiated by protons 77—83380
C, foil, energy loss straggling meas. for low energy protons 78—47459
Cd, lattice defects studied by gamma ray angular correlation 79—51895
CdTe, thin film, stopping power for protons and alpha particles, proton energy straggle values 77—89489
Cr MIS solar cells on Si, proton radn. effects 79—92074
Cr-SiO_x-Si MIS solar cells, photovoltaic performance and interface states, nucl. radiation effects 80—94004
Cu, 400 GeV proton irrad., resist. meas., supercond. magnet stabilising material 77—37948
Cu, defect annealing around stage III, $\gamma\gamma$ ang. correlation expt. 79—14846
Cu, energy straggling of 6.74 MeV protons 78—79641
Cu, irradiated, small edge dislocation loops, electron microscope image contrast, Burger's vector determ. 77—76410
Cu, irradiated with protons, α-particles and C ions, increase of elec. resist. meas. 77—84808
Cu, positron-lifetime study of 4.5-25 MeV proton irrad. effects 79—33021
Cu, proton irrad., radiation-annealing effects in energetic displacement cascades, film resist. meas. 78—26603
Cu, proton irradiated, muon spin rotation study at low temps. 78—92011
Cu, proton irradiation, 10 to 16 MeV, isochronal annealing meas. 80—2083
Cu, proton irradiation, 10-16 MeV, neutron damage simulation 80—34089
Cu, proton irradition, 10 to 16 MeV, resistivity changes 80—2082
Cu, proton-irradiated, H_2 gas-bubble struct., study at 300K 80—92569
Cu, radiation damage due to protons, μSR 79—56702
Cu, radiation damage effect of 800 MeV protons on thin target 77—69016
Cu, scattering and radiation damage for 14 MeV neutrons and 10 to 20 MeV protons 77—15458
CuCl, H^+ irrad., luminesc., high density excitons in particle tracks 79—47020
D re-emission from C target, proton induced 80—70270
Fe, proton irrad., 10-16 MeV, neutron damage simulation 80—34089
Fe, proton irradiation, 10 to 16 MeV, isochronal annealing meas. 80—2083
Fe, proton irradition, 10 to 16 MeV, resistivity changes 80—2082
Fe, scattering and radiation damage for 14 MeV neutrons and 10 to 20 MeV protons 77—15458
$FeCl_2.4H_2O$, proton radiation effects, Mossbauer spectra meas. 77—11603
(GaAl)As DH laser, low-current, proton-bombarded, design and characts. 78—87059
GaAlAs DH lasers, proton-bombard., nonradiative recomb., luminesc. time-response meas. 79—98371
(GaAl)As, Zn diffused proton bombarded stripe laser 79—98392
GaAs, H ion bombard., carrier removal effects 80—92542
GaAs, H^+ irradiation, effect on electrical props. 80—65567
GaAs, irrad., lattice strain, precision X-ray meas. 77—27922
GaAs, modification of Zn diffusion profiles by proton irrad. 78—43043
n^+-GaAs, multiple energy proton bombard. effects on elec. characts. 77—39853
GaAs, optical modulation spectra, proton damage effect 78—76487
n-GaAs, proton irrad., E_p=30 MeV, defect form., orientation depend. 78—55898
GaAs, proton irradiated, low energy, deep level defects and hole diffusion length meas. 80—60000
GaAs, radiation damage caused by proton bombardment, observation using TEM 80—75276
GaAs, range calcs. 77—76479
GaAs Schottky barrier structure, defects from proton irradiation, thermal transients and optical capacity *(French)* 80—59534
GaAs solar cells, electron and proton radiation damage 80—94034
n-GaAs, undoped, proton radiation defect detect. by transient capacitance spectroscopy 79—11089
GaAs:Cr, optical modulation study of proton bombardment 78—6720
GaAs:Cr, optical modulation spectra affected by 150 keV proton beam 78—10871
GaAs:Sn, proton implantation and annealing behaviour *(Chinese)* 80—44224
GaP, 1 MeV proton bombardment, lattice deformation investigation by Kossel effect 78—22775
GaP surface barrier structure, breakdown voltage exam., effect of proton irradiation 79—11225
Ge coaxial detectors with reverse electrode, radiation damage resistance 79—41076
Ge, high parity detectors, 6 GeV/c proton irradiation 78—37508
n-Ge, proton and γ irrad., minority carrier recombination 80—65591

proton effects continued
Ge, proton bombardment damage, irrad. energy depend., channelling meas. 80−24511
Ge, single cryst., proton irradiated, defect study using X-ray diffuse scattering 79−95048
Ge single cryst., radiation piezoelec. effect 78−19419
p-Ge:Ga(Sb), proton irradiated, kinetics of accumulation of radiation defects, minority carrier lifetime 79−10885
He isotopes prod. cross sections in natural Mg, Al, Si, CaF_2 by 12-45 MeV protons 77−17310
Hg, thick target, proton and deuteron irradiation, Tl yield determ. 78−2174
InP, proton bombard. effects on resist. 77−80552
InSb, ion bombard. and defect annealing, n- and p-type cond. layer prod. 78−26606
n-InSb, proton irrad. defects energy level scheme, transport props. meas. 80−96576
p-InSb:Ge, proton irrad. defects energy level scheme, transport props. meas. 80−96576
K salts, spectral refl. changes and luminesc. during 2-10 keV proton bombardment, implications for Io 79−96950
KBr, proton irrad., divacancies, positron capture, ionic cond. and TSC study 80−54289
KCl, ion bombard., damage profiles, track effect anal. 77−15465
KCl:Tl and KCl, F-centre production by positive ions and X-rays 78−38760
KCl-KH, F- and U-centre redistrib. at end of proton tracks, microspectrophotometric anal. 80−10583
LiF, high-energy particle bombard., F-centre creation, optical meas. and model 77−47497
Mg silicates, effects of irradiation with MeV protons 77−45534
Mo cathode, H_2 glow discharge, FCC surface layer form., electron diffr. obs. 77−55311
Mo, irradiated, small edge dislocation loops, electron microscope image contrast, Burger's vector determ. 77−76410
Mo, proton irradiated, annealed and rolled, void form. 78−22774
NH_3, solid, proton irradiated, dynamic nucl. polarisation below 0.5K 79−78569
^{13}N species formed by proton irradiation of water 80−45532
Na salts, spectral refl. changes and luminesc. during 2-10 keV proton bombardment, implications for Io 79−96950
NaCl, F-centres near monoenergetic proton stopping region, space charge effect 78−18640
NaCl preirradiation effect on proton channelling, thermoluminescence study 80−19860
Nb, flux pinning by proton irradiation damage 77−47947
Nb foils, polycryst., proton irrad., diffusion of nuclear react. products *(German)* 77−35756
Nb, fusion neutron damage effects on mech. props., simulation by 16 MeV protons 78−71768
Nb, proton irrad., dislocation loops and mag. flux pinning 79−56463
Nb, radiation damage from 16 MeV protons, effect on microstruct. and mech. props. 79−46721
Nb, radiation hardening and yield strength correlations for 16 MeV H^+ and (D,T) neutron effects 78−14389
Nb, scattering and radiation damage for 14 MeV neutrons and 10 to 20 MeV protons 77−15458
Nb simulation of 14 MeV neutrons by higher energy protons 79−1469
Nb_3Sn, 2-MeV proton-irradiated, Mossbauer effect studies 79−69757
Nb_3Sn, filamentary conductors, type-II, low temp. 30 GeV proton effects on critical props. 78−52178
Nb_3Sn, proton and γ-irradiated, lattice dynamics from ^{119}Sn Mossbauer studies 78−39458
Nb_3Sn, proton irradiated, Mossbauer effect at 78K 78−19394
Nb_3Sn, radiation damage effect on superconducting props. 78−52127
NbTi, filamentary conductors, type-II, low temp. 30 GeV proton effects on critical props. 78−52178
Ne isotopes prod. cross sections in natural Mg, Al, Si by 12-45 MeV protons 77−17310
Ni, anodically oxidised, 100 keV proton channelling investig. of oxide layer struct. 77−84820
Ni, fusion neutron damage effects on mech. props., simulation by 16 MeV protons 78−71768
Ni, magnetisation effect on channelling and blocking of proton beam 77−69022
Ni, pure, irradiation creep during 4 MeV proton bombardment 77−43256
Ni, radiation damage due to protons, μSR 79−56702
Ni, radiation damage from 16 MeV protons, effect on microstruct. and mech. props. 79−46721
Ni, radiation hardening and yield strength correlations for 16 MeV H^+ and (D,T) neutron effects 78−14389
Ni, scattering and radiation damage for 14 MeV neutrons and 10 to 20 MeV protons 77−15458
Ni-Si, proton irrad., γ' precipitation, early stages 80−34096
PLZT ceramics photosensitivity enhancement by H- and He-ion implantation 80−96934
Pb, radiation damage and recovery processes 77−69002
Pb-Cu, damage and recovery processes 77−69002
PbS-base photodetectors, struct. invest. by proton irrad. 80−104388
$Pb(Zr,Ti)O_3$, excitation of mechanical vibr. by ionising radiation beams 77−24799
n-Si, 300 keV proton irrad., temp. depend. of defect prod. 78−6113
Si, diffusion of self-interstitials and As, B and P, radn.-enhanced 80−29216
Si, divacancies due to proton irrad., IR absorpt., annealing effects 80−20673
Si, EPR of radiation damage due to complete stopping of 30 MeV protons 77−65994
Si, feeding-in and blocking of 2 MeV protons, simple diffusion model 78−22782
n-Si, interaction of disordered regions with point defects 79−19296
Si, irradiation damage 78−34556
Si, monocrystal, channelling of 5 MeV protons *(Rumanian)* 79−14863
Si, proton damage, depth profile anal. by channelling 78−43054
Si, proton irrad., efficiency of form. and nature of defects, Hall meas. 80−6444
p-Si, proton irrad. magnetiodiode effect, heat treatment, photocond. spectra 79−69591
Si, proton irradiated, IR absorption 79−33742
proton effects continued
Si, proton irradiated and annealed, hydrogen containing radiative recomb. centres 77−24896
Si, proton irradiation, energy depend. of rate of degradation of cond. 77−62944
Si, proton random and aligned stopping powers, 80 to 300 keV, backscatt. meas. 77−27931
p-Si radiation defects due to 30 MeV proton irrad., rel. to solar energy convertors 78−71776
Si, Schottky barrier structs., proton bombarded, defect states 80−29356
Si solar cells, proton irradiated, processing influence on elec. performance 80−94001
Si solar cells, ultrathin, electron and proton effects 80−94002
Si:Al(Ga), O_2 diffusion, conc. profile meas. 80−79990
Si:As, 1.5 MeV H^+ and He^+ irradiations of As diffused layers 78−47447
Si:B, influence of proton beam irrad. on concentration profiles *(French)* 77−51402
Si:B, proton-irrad.-enhanced diffusion 80−29227
Si:B ion implantation, proton channelling effects, anal. using Promiss protonograph 80−19823
Si:B(P), impurity-peak form. during proton-enhanced diffusion 79−55772
Si:B(P), proton enhanced diffusion, vacancies diffusion length 80−29226
Si:B(P), proton-irrad., impurity uphill diffusion, vacancy mechanism 80−92719
Si:C, disorder profiles by proton backscattering, proton bombardment annealing 78−47449
Si:C, H^+ and He^+ beam impact phemomena, damage annealing rates 78−47450
Si:P(B)(As), proton enhanced diffusion and vacancy migration 78−67747
SrO, irradiated, low temp. photocond. 77−39891
SrO, neutron- or proton-irrad., F^+ centre fluoresc. yield and lifetime, 5 to 140K 80−55181
Ti ferrite, magnetisation effect on channelling and blocking of proton beam 77−69022
Ti, K-shell ionisation probability, for 150 keV protons, impact-parameter depend. 79−10189
U, irradiation growth during fission fragment and proton bombard. 80−92568
V, proton bombard. induced blistering 77−7770
V_3Ga, filamentary conductors, type-II, low temp. 30 GeV proton effects on critical props. 78−52178
W, axial to planar channelling transition, proton induced X-ray yield meas. 77−31704
W, channelled proton energy losses 77−1161
W, proton bombard., radiation damage, proton backscatt. obs. *(Russian)* 79−46720
W, single cryst., proton integral dechannelling functions *(Russian)* 78−10111
ZnO, spacecraft thermal control material, low-energy proton effects 80−70288
$ZnSiP_2$, 1 MeV proton bombardment, lattice deformation investigation by Kossel effect 78−22775
$ZnSiP_2$, proton induced Kossel effect *(German)* 77−84601
ZnTe, thin film, stopping power for protons and alpha particles, proton energy straggle values 77−89489
Zr, proton irradiation, 10 to 16 MeV, isochronal annealing meas. 80−2083
Zr, proton irradition, 10 to 16 MeV, resistivity changes 80−2082
Zr, scattering and radiation damage for 14 MeV neutrons and 10 to 20 MeV protons 77−15458

proton excited X-ray emission *see ion microprobe analysis*

proton interactions *see electron-proton interactions; kaon-proton interactions; lepton-nucleon interactions; photon-proton interactions; pion-proton interactions; proton-deuteron interactions; proton-nucleus reactions; proton-proton interactions*

proton magnetic moment
gyromagnetic ratio, review of last 15 years and latest meas. 78−57887
gyromagnetic ratio and derived value of fine struct. const., QED test 79−71674
hadron mag. moments, colour mag. moments and transition M1-moments, quark mass parameter 79−97596
magnetic monopole struct., observational limits, from 42 cm neutral galactic H absorpt. 79−53717
ME-EM field model of free electron state 78−49988
MIT bag model, M1 transition calcs. low lying hadrons 79−13080
polarizabilities of proton and pion, sum rule relation *(Russian)* 79−93420
quark bag model in 3+1 dimensions 77−10214
straton model, wave functions without SU(6) symmetry, P anomalous mag. moment *(Chinese)* 79−49489
SU(3) subalgebras of SU(4), generalised U-spin charmed baryon magnetic moment 79−36078
SU(6) broken summetry model, baryon mag. moment values 79−49417
virtual charge displacement model 78−54633
$\gamma p \rightarrow \pi^0(p^+)p$, energy independ. multipole anal. through second resonance region 78−62410
μ_p:μ_p, discrepancy between direct and indirect determinations of μ:p mag. moment ratio 77−18287
$\bar{p}$ mag. moment and mass determ. 78−45990
π^0 emission by protons with anomalous mag. moment in const. EM field, Furry formalism *(Russian)* 78−410
H_2O, Bohr magneton electron and proton g-factor ratio determ. 78−33526

proton magnetic resonance
acenaphthenequinone, solid phase NMR spectra, 77-430K 79−15360
acetic acid-H_2O, assoc. liq., struct. props., static and dynamic phys. props. meas. 79−70316
acetone, solid, effects of tunnelling on spin-lattice relax. of methyl protons 77−12216
acetone, soln. in EBBA, nematic liq. cryst., NMR, orientation 77−1605
acetonitrile-d_2, liq., intermol. ^1H spin-lattice relax. and pair-diffusion 79−99781
N-acetyl-D-alloisoleucine, soln. struct., dynamics, proton relaxation mechanisms 80−76708
acetylacetonatobutyl halides, equilib. reacts. redistribution of −F, −Cl monofunctional groups *(French)* 78−64816

proton magnetic resonance continued
adamantane, mol. reorientation activation parameters, determ. by NMR method under press. 77−89393
adamantane, orientation and deform. in nematic liq. cryst., PMR obs. 77−71815
L-alanine, solid, H bonding, wide line NMR obs. 78−52362
l-alanine powder, short dipolar relaxation time meas. by saturation method 80−60441
albumin denaturation, investigation by PMR 80−3582
aliphatic alcohols-2,2,6,6-tetramethylpiperidine nitroxide radical complexes, EPR, PMR, hyperfine coupling consts. 79−65736
alkali metal difluoride, MHF_2, free induction decay 78−2753
alkanes and cycloalkanes, saturated hydrocarbon chains characterisation *(Portuguese)* 80−5562
p-alkanoyl-benzylidene-p'-aminoazobenzenes, liq. cryst., proton mag. relax., self-diffusion 77−84632
p-alkoxybenzoic acids, nematic liq. cryst., proton spin lattice relax., mol. dynamics 78−34425
alkylamines coordinated to Ni(II) acetylacetonate, ^1H and ^{13}C NMR, hyperfine coupling const. 79−41187
alkylammonium cadmium tetrachloride, struct. phase transition, PMR, spin-lattice relax. time 77−35688
alkylene diammonium cadmium tetrachloride, struct. phase transition, PMR, spin-lattice relax. time 77−35688
amino acids, polycryst., proton mag. relax. and mol. motion 78−20139
ammonium salts, reorientation of NH_4^+, PMR relax. and inelastic neutron scatt. 79−82167
amniotic fluid, human proton relax. times in low field range, appl. to nucl. magnetography *(French)* 78−3574
anilinium chloride, NH_3^+ intraionic C_3 reorientation, NMR and rot. frame expt. 79−28630
anilinium halides, and anilinium sulphate, proton mag. relax. obs. 80−34800
p-anisidine, polycryst., intramol. reorientations, PMR 78−64279
anthracene-TCNB, 1:1 charge transfer complex, phase transition at 206K, NMR meas. 79−7690
anthranilic acid, solid, amino group reorientation, PMR second moment obs. 78−35046
aromatic hydrocarbons, proton chem. shifts with ring currents, π-bond model 79−81215
aromatic polyesters, broad-line NMR, dynamical mechanical behaviour 77−55718
asbestos, dehydroxylation, PMR investigation 80−21269
bacteriochlorophyll cation in soln., N atom ENDOR and proton triple resonance 78−96018
basic pancreatic trypsin inhibitor, methyl group PMR, 360 MHz 78−27887
benzene, ^1H chem. shift tensor, proton mag. shielding anisotropy 78−19348
benzene, unlabelled and ^{13}C labelled PMR, oriented in liq. crysts., r_α struct., solvent effects 79−94017
benzene submonolayer on silica gel, PMR and DMR dynamics and surface heterogeneity 79−69735
benzene-2,5-dibromothiophene, self-association, proton mag. relax. 77−28471
benzene-d_1, -(d_2)(-d_3), oriented, order, D nucl. quadrupole coupling, mag. reson. spectra 78−74683
benzenes, di- and mono-substituted, NMR spectral data, aromatic proton chemical shifts 77−79632
benzenesenol, CCl_4 soln., PMR, barrier to internal rot. 78−1006
biological cells, classical diffusion to explain ^1H spin relax. 79−83721
biological macromolecules, PMR, nuclear Overhauser enhancement difference spectroscopy 78−81091
biological systems, hydrated, PMR spin-lattice relax. of water, cross-relax. effects 79−34496
biomedical target relaxation time measured by magnetic focusing method 79−34621
biomembrane, water transport determ. methods *(Rumanian)* 80−94435
biomolecular components, proton relaxation; solid state, activation energies, relax. consts., 50-500K 78−68998
biomolecules, conformation and struct., ESR, NMR and optical meas. 80−26201
2,2'-bipyrimidine, in nematic solvent, conformation, ab initio and PMR determ. 80−47869
α-bis (N-methylsalicylaldiminato) copper II, one-dimens. spin-$^1/_2$ Heisenberg antiferromag., high-field spin dynamics 80−71224
bis-methyldigermyl chalcogenide, ^1H and ^{13}C NMR study, chemical shifts 80−71201
bis-methyldisilyl chalcogenide, ^1H and ^{13}C NMR study, chemical shifts 80−71201
bispenol-A epoxy resin, glass transition temp., effect of absorbed water, PMR line width 79−90766
block copolymer in soln., molecular motion study by high resolution PMR 78−55803
blood, normal and pathologic, NMR T_2 relax. time studies 80−81682
blood, peripheral, in cancer patients, spin-lattice relax. time 77−86579
blood flow measurement using NMR flat crossed-coil detector 79−83880
blood flow measurements by NMR of the intact body 80−81680
blood flowmeter, cylindrical crossed-coil, for noninvasive measurement 79−62328
blood plasma ^1H NMR relax. rates, cancer-induced decrease obs. 80−56075
bone powder and ash, PMR and IR spectra, chem. anal., bond lengths 78−3414
boroxines, trioxadiborolanes, evidence for aromaticity from mass spectral and NMR meas. 78−9172
breast carcinoma imaging with line scanning technique 79−48314
9-bromo-meta-carborane, mol. reorientation, ^1H and ^{11}B NMR 77−16185
bromobenzene, in EBBA, ^1H NMR and NQR of D, geometric struct. 78−17689
n-butane, solid, mol. reorientation, PMR 77−8431
n-butanol, microemulsion, dynamical and structural props., by chem. physics method 79−79308
2-butanol adsorption on Al_2O_3, PMR spectra 79−19457
butyl boron halides, equilib. reacts., redistribution of −F, −Cl monofunctional groups *(French)* 78−64816
calcium copper acetate hexahydrate, PMR at low temp., atomic position determ. 77−20728
calcium formate, intermolecular shielding contributions, proton mag. shielding 80−34783

proton magnetic resonance continued
calcium formate, selective high resolution ^1H NMR 79−61245
cancer detection, behaviour of different nuclear probes 79−62326
cancer diagnosis, FONAR scan of live human abdomen 80−8122
carborane, ortho- and para-, phase transition and mol. reorientation, isomer effects, PMR obs. 80−80628
carboranes, small cage, antipodal H-H coupling 80−1003
cellulose, mobility of adsorbed water, NMR pulse obs. 80−108835
cement pastes, binding props. 78−23355
cement pastes, setting at positive, subzero temps., PMR exam. 80−55625
chlorobenzene in EBBA, ^1H, D NMR and NQR, geometric struct. 78−17689
o-chlorobenzoic acid, solid, H bonding, wide line NMR obs. 78−52362
chloroform, liq., crit. fluctuations, proton spin relax. obs. 78−19358
chloroform diluted in CS_2, proton transverse relax. time and reorientation of chloroform *(French)* 77−32280
chloroform-hexamethylphosphoramide complex, mol. motion and assoc., PMR obs. *(French)* 78−72429
chloromethane, low density gas, proton spin-lattice relax., mol. reorientation 79−3462
chlorophyll radical cations, NMR, hyperfine coupling 79−8482
2-chloropyrimidine, CS_2 soln., mol. reorientation, ^1H, ^{13}C nucl. mag. relax. 78−27105
chloroquine-biopolymer binding interactions, PMR effects 80−55982
cholesteric liquid crystal, proton NMR spectra, angular depend. of second moment *(Russian)* 77−62478
choline salts, mol. motion, proton spin-lattice relax. 77−59474
chromophore orientation in micellar, liposome solns., liq. cryst. phases, dichroism, NMR 79−53059
clathrate deuterohydrates, ^1H NMR lineshape of tunnelling methyl group, <5K 78−46370
collagen, hydrated, PMR spin-lattice relax. of water, cross-relax. effects 79−34496
collagen, native, phasic transition 77−25363
collagen-water system, phasic transition invesitgation by calorimetry and NMR 79−62167
computerised tomography, human whole-body line scan imaging system 79−66502
copolymer, ^{13}C and ^1H NMR, monomer unit distrib. *(Russian)* 77−46664
copper benzoate, spin 1/2 system, one-dimensional nucl. relax. 78−39427
copper formate tetradeuterate, paramag., induced staggered magnetisation, NMR 77−12212
copper oxalate, two dimens. antiferromag., proton reson. exam. 77−28453
CpApUpG, self complementary oligoriboncleotide, double helix form., PMR obs. 79−22873
cyanoacetylene, liquid, ^1H relax. rate using pulsed NMR *(French)* 79−38394
n-pcyanobenzylidene-p-n-octyloxyaniline, liq. cryst., proton FFT of aromatic and alkyl motions 77−15302
cyanopentyl-d_{11}-biphenyl-d_4, ordering matrix, proton dipolar coupling obs. 78−63671
cyclobutanone, ^1H NMR anal., deconvolution technique 80−58289
cyclododecane, force field, PMR of deuterated isotopomers 79−45695
cyclohexane, mol. motion, press. and temp. depend., PMR relax. obs. 78−64289
cyclohexane-d_0, -d_{11} ^{13}C-^1H coupling constant 78−13519
cyclooctane, solid, NMR lineshape and spin-lattice relax. 77−24757
cyclooctane-d_{14}, in oriented solvent, conformation, NMR determ. 77−61770
cytidine, pulse Fourier transform proton mag. resonance, equivalent to CW INDOR 77−32293
cytochrome c, PMR, eight-ring current model heme ring, conformation depend. shifts 80−74185
n-decylammonium cadmium chloride, perovskite-type layer cmpd. n-decylammonium chain dynamics 79−99313
decylammoniumchloride and bromide, lyotropic nematic struct. 78−51410
delayed Fourier transformation technique for resolution enhancement 80−74181
deoxyhaemoglobin, proton NMR, modified DEFT technique for obs. hyperfine shifted line, T_1 values meas. 80−76871
deoxymyoglobin, low temp. PMR, low-lying Fe^{2+} states model 78−68997
dextran, aq. soln., conc., PMR *(Russian)* 80−71225
dextrane, aq. solns., H_2O diffusion, PMR investig. *(Russian)* 79−51290
di-t-butyl nitroxide radical, in soln., proton relax., meas. of H-bonding 78−27103
di-t-butylnitroxide radical, solid, nucl. and electron spin relax. times meas. 78−60350
di-tert-butyl radical, ^1H NMR in organic solvents, press. depend. 79−31546
diamantane, NMR meas. of mol. motion 79−42858
diamine oxidase solutions, proton mag. relax. dispersion obs. 80−51136
diastereomeric compounds, nonrigid mols., in soln., conform. determ., NMR, lanthanide shift reagents 77−30887
o-dibromobenzene, r_α-struct. determ. from PMR with ^{13}C satellites, bond lengths and angles 78−25560
2,3-dichloro-1,4-napthoquinone in EBBA, PMR obs., mol. struct., orientation and solute-solvent interactions 77−27806
p-dichlorobenzene, orientation and deform. in nematic liq. cryst., PMR obs. 77−71815
o-dichlorobenzene, r_α-struct. determ. from PMR with ^{13}C satellites, bond lengths and angles 78−25560
3,5-dichlorobenzyl mercaptan, PMR, barrier to rot. about C-C bond 78−17696
1,2-dichloroethane, enclathrated, conform., reorientation, PMR line shape anal. 79−91300
3,6-dichloropyrazine, orientation and deform. in nematic liq. cryst. 77−71815
diheptyloxyazoxybenzene, smectic-C phase, proton NMR 77−11474
2,4-dihydroxy benzoic acid, PMR obs., proton second moment, 77 to 383K effect of OH group rot. 78−10784
o-diiodobenzene, r_α-struct. determ. from PMR with ^{13}C satellites, bond lengths and angles 78−25560
dimethyl cadmium, partially oriented in nematic EBBA, mol. geom., PMR obs. 77−71819

proton magnetic resonance continued
dimethyl mercury, coupling consts., solvent depend., ^{1}H, ^{13}C and ^{199}NMR 78−76334
dimethylammonium copper chloride bromide, mag. props., pulsed NMR expts. 80−11292
2,6-dimethylbenzoic acid, ^{1}H chem. shift recovery from combined multiple pulse NMR and sample spinning 80−32738
4-4′ dimethylbenzophenone, ^{1}H spectrum using multiple pulse decoupling-magic angle spinning NMR probe 78−12735
N,N-dimethylformamide, in nematic solvent, PMR spectrum 77−90049
N,N-dimethylmethanesulphonamide+phenol (chlorophenol), assoc., PMR 78−23941
dipalmitoyl lecithin-water system, lyotropic liq. cryst., pretransitional effects, PMR second moment meas. 78−91234
DNA, gamma-ray effects on hydration, PMR of frozen and liq. solns. 78−27900
DNA, proton mag. relax., methyl group reorientation 77−64009
DNA hydration characts. in H_2O/D_2O frozen solns., γ irrad. effects, PMR 78−31772
DNA internal motions, ^{31}P NMR and PMR 80−97855
E. coli cells, anaerobic metabolism, ^{1}H correlation NMR spectra 79−43978
EBBA, binary systems with non-nematic solutes, phase transition behaviour and ^{1}H NMR anal. 80−34174
EBBA, isotropic phase, order fluctuations, self-diffusion, and rot. motion, proton spin relax. meas. 79−87328
EBBA, liq. cryst., rapid cooling and mag. field effects on NMR relax. and thermal behaviour 79−82321
elastomer, segmented block, morphology, pulsed proton NMR study 80−33907
electrolyte solutions, NMR relaxation of ^{1}H, ^{2}D, ^{23}Na *(Russian)* 78−15053
electrolyte solutions, preferential solvation, NMR obs. 78−95919
electrolyte solutions, preferential solvation and mol. motion, NMR obs. 78−95920
epoxy resin, mobility of sorbed water, low resolution PMR method 80−11276
erbium triethyl sulphate, single cryst., H^{+} coords., NMR 80−97152
erythrocyte membrane, pulse meas. of water exchange 79−43826
erythrocytes, bound water in frozen solns., proton mag. relax. 77−28472
ethane, solid, PMR line shape, band width and second moment, phase transition 77−85584
1,2-ethanediol, aq. soln., proton NMR study of H-bonding 79−78545
ethanol$_{(l)}$, hydroxyl proton chem. shift, density and temp. effects 77−1607
ethyl-trimethyl phosphines, $(C_2H_5)_{3-n}P\{E^{IVB}(CH_3)_3\}_n$, ($E^{IVB}$=C;Si;Sn; n=0,1,2,3), ($^{1}H$, ^{13}C, ^{29}Si, ^{31}P, ^{119}Sn) NMR 80−32744
ethylene copolymers with acrylic monomers, NMR investig. *(Russian)* 80−54959
ethyliodide-d_2, NMR, spin-torsional spectra 79−15363
eye lens, normal and senile cataractous, PMR study of state of water 78−64987
fatty carboxylic acids, C_{15} to C_{19}, solid phase, ^{1}H and ^{13}C NMR spectra 79−95653
ferric leghaemoglobin a, proton-depend. anion binding, soybean 79−74592
ferrous porphyrin, intermediate (S=1) spin state, PMR characterisation 80−48014
ferrous porphyrins, 4-coordinated, PMR 77−58044
Fischer-Tropsch wax, NMR investigation 80−7186
fluoranil-macrocyclic polyether mol. complexes, configs., IR and NMR obs. 78−33529
2-fluoropyridine, natural abundance ^{1}H coupled ^{15}N NMR spectra, selective population transfer method 79−95682
FONAR scans of cancer patients 79−62327
formic acid, liq., microdynamic behaviour, struct., nucl. spin-lattice relax. 77−76270
furfuryl alcohol resins, PMR study of mol. motion 79−8062
furil + pentachlorophenol, photochem. reduction, cross-relax. and CIDNP, PMR relax. obs. 79−52694
gas chromatography-IR-PMR optimised method anal. 77−86392
gas chromatography/PMR spectroscopy anal. system 77−52690
L-glutamic acid, solid, amino group reorientation, PMR second moment obs. 78−35046
glycerol, aq. soln., proton NMR study of H-bonding 79−78545
GpApGpC:GpCpUpC duplex set, helix form., PMR obs. 79−22872
gramicidin-S, dissolved in deuterated ethylene glycol, interproton nuclear Overhauser effects 79−16123
graphite, adsorbed methanol, proton mag. relax. times obs. 77−51590
graphite lamellar derivatives, KC_{24}(tetrahydrofuran)$_m$, (m=1 and 2) ^{1}H NMR study 80−44932
guadinium aluminium sulphate hexahydrate, high resolution multipulse NMR appls. 78−60345
haeme disorder characterisation in haeme proteins, PMR method 79−92152
haemoglobin, hyperfine-shifted PMR, mag. field and temp. induced line broadening 77−60184
haemoglobin, quaternary struct., hydration and self-association obs. 80−67040
haemoglobin solution, proton mag. relax. meas. 77−1975
halobenzenes in potassium laurate mesophase, proton distance ratios and order tensor elements calcs. 80−63672
hexafluorobenzene-n-paraffins, binary liquid solns., self diffusion, spin echo meas. 80−65263
hexamethyldialuminium, methyl group rotation and bonding, CW proton second moment and line shape studies 79−47346
hexamethyldisilane, mol. motion, press. and temp. depend., PMR relax. obs. 78−64289
hexamethylenetetramine, orientation and deform. in nematic liq. cryst., PMR obs. 77−71815
hexamethylenetetramine in oriented mesophases, mol. distortion, PMR 77−6802
hexamethylethane, mol. motion, press. and temp. depend., PMR relax. obs. 78−64289
high resolution PMR in solids, improvement in resolution 77−48060
high-resolution multipulse NMR spectrometer 78−58000
homonuclear coupled spin system, inversion-recovery data anal. 79−33554
hornblendes, refinement of struct. characts. by reference to PMR data 78−22704
proton magnetic resonance continued
hydrate, struct. I clathrate hydrate, H_2O mol. reorientation and diffusion, PMR and dielectric relax. 77−36142
hydrate layered chalcogenide, anisotropic mobility of water, NMR, for $A_x^{+}(H_2O)_y[TaS_2]^{2-}$, (A=Na, K, Cs) 79−65744
hydrocarbons, proton NMR chem. shifts, mag. shielding effect of neighbouring C atoms 77−27094
hydrogen-bonded systems, investigation by NMR high resolution of solids method 78−76323
p-hydroxybenzoic acid, lattice rigidity, mol. motions, wide-line NMR at room temp. 77−51967
N-(2-hydroxythiobenzoyl)morphiline, ^{1}H NMR, spin decoupling by torsional transitions 78−62832
ice, polycryst., natural abundance PMR, chem. shift meas. 79−67365
inert gas liquids, H_2 diffusion and NMR 79−61249
intramolecular H-bonds, H, D and T NMR, isotope effects and pot. energy surfaces 79−76447
ionic solvation, in methanol, spectroscopic study *(French)* 79−70363
kidney, tissue water freezing study, ^{1}H NMR obs. 80−8027
lanthanum ethyl sulphate=Gd^{3+}, proton position determ. by ENDOR 77−51992
lanthanum nicotinate dihydrate:Nd^{3+} cryst., H coords., EPR and ENDOR determ. 77−59005
lechithin-cholesterol interaction, effect of lecithin struct. 78−64922
lecithin bimolecular leaflets, incorporated fluoresc. probes, PMR 77−90734
lecithin liposomes, binding sites for $Fe(CN)_6^{3-}$ ions, PMR obs. 79−79481
lecithin-deoxycholate mixed micelles, surface curvature and mobility, PMR study 80−21452
linear polyethylene melt, PMR spectrum 77−51979
liquid binary mixtures, proton mag. relax. and mol. motion 77−28471
liquid crystal, spiral-like, struct., PMR of dissolved mols. 78−1981
liquid crystal, thermotropic, diffusion and nucl. mag. relax. 80−24362
liquid crystals, protonated multiple quantum transitions, excitation detection, Fourier transform multiple quantum NMR 80−31819
liver tissue and tumour proton mag. relaxation rel. to Fe content 79−39355
low-temperature thermometer for ^{1}H, ^{19}F, and ^{13}C spectroscopy 78−65949
2,6-lutidine, H bonding to iso- and tert-butyl alcohols, PMR obs. 79−27008
lysine vasopressin, amide H exchange rates in aq. soln. 79−83692
lysozyme, tryptophan residues, H exchange for D, relax., proton NMR spectra 80−35846
magnetic shielding constants calc. by GIAO method using Gaussian functions 80−1001
magnetometer, precision field averaging, for low and high fields, using PMR in flowing water 79−67359
malignant cells, evidence for a condensed phonon state 79−62214
manganese zinc formate dihydrate, two-dimens. antiferromag., anomalous crit. phenomena, neutron scatt. and PMR obs. 80−50104
MBBA, isotropic phase, order fluctuations, self-diffusion, and rot. motion, proton spin relax. meas. 79−87328
MBBA, nematic, freq. depend. of proton T_1, rot. diffusional mechanism interpret. 77−12219
MBBA, nematic phase, elec. field induced biaxiality, PMR study 79−90532
MBBA, order fluctuations, self-diffusion, rot. motion, proton spin T_1 relax. 77−32285
MBBA, proton spin-lattice relax. in crit. regime 80−80631
MBBA, ring deuterated, dipolar spin system exam. 77−39533
MBBA-d_{13}, ^{1}H spin-lattice relaxation, intermol. and intramol. contribs. 80−75873
MBBA-d_8, H and D spin-lattice relax. 77−59475
medical, fast scan proton imaging 77−21591
medical imaging, H tomography and pot. for imaging other body constituents 80−98062
medical imaging, in vivo study of human fore-arm and hand 79−20605
medical imaging, mice and phantom expts. 77−86584
medical imaging, multiple sensitive point method 80−81679
medical imaging, multiple sensitive point technique 79−11993
medical imaging by NMR, book 80−31426
medical imaging by NMR, book contrib. 80−36064
medical imaging techniques, developments, review 80−26324
mesogen compounds, melting behaviour, proton NMR spectra 78−15044
methane, ^{13}C and proton medium shifts in gas phase and in soln. 77−88467
methane, solid, high press. PMR, second moment 79−8059
methane, solid, rot. ordering and proton spin-lattice relax. 78−91967
methane, solid-state phase transitions, 5-80K, PMR spin-lattice relax. up to 3 kbar 77−40137
^{13}C-methane-d_1:O, annealed, spin conversion and proton 2nd moment time-depends. 80−11283
methane-d_1, solid, ^{13}C and ^{1}H NMR, spin conversion obs. 77−20731
methanol solns., IR spectroscopic detection of free lone-pair groups or terminal methanol mols., PMR 79−19869
methanol-β-quinol clathrate, orientation and reorientation dynamics, dielec. and NMR obs. 79−99783
methanols, labelled, proton T_1 in presence of intramol. rots., intermol. relax. rate 80−2656
methyl ammonium aluminium sulphate, ferroelec., proton spin-lattice relax. time anomaly 80−60440
methyl group, ^{2}H quadrupole coupling const., from ^{1}H and ^{2}H NMR data 78−25563
methyl group, internally rot., attached to symm. top mol., NMR relax. 78−13515
methyl group, proton spin relax. due to intermol. proton coupling, reorientation 78−25564
methyl group, proton tunneling reson. at low temp. 80−108087
methyl groups, detection of proton NMR at arbitrary temps. of tunnelling system 78−39432
methyl piperidines, PMR spin-lattice relax. times and lineshapes, 100-300K 77−81027
methyl protons, in solids, spin-lattice relax., torsional vibr. effects calcs. 77−16196
4-methyl-2,6-ditertiarybutyl phenol, proton spin relax., 80-340K methyl rot. 79−78553
4-methyl-2,6-ditertiarybutylphenol, proton spin-lattice relax. and activation energies of tunnelling CH_3 groups 77−48071

proton magnetic resonance continued
methyl-containing mol. solids, proton NMR line shape, methyl group tunnelling 78−6588
methylammonium bromide, solid, phase transitions, PMR, DTA study 80−107421
methylene bromide-d_0-d_2, liq., nucl. spin-lattice relax., rot. correl. times 77−59476
methylene chloride, in EBBA-d_{23}, intermol. dipolar random field cross-relax. term obs. 80−60438
methylene chloride, partially deuterated, NMR, T_1 meas. and anal., −96 to 40°C 78−80237
methylfluoride, anomalous behaviour of proton chemical shift in gas-liquid crit. region 78−39419
1-methylimidazole complexes, with ferriporphyrins, PMR obs. 77−12214
methylmercury nitrate, in nematic and lyotropic liq. crysts., r_α-struct. and anisotropy of Hg-C coupling const. 80−43071
methylpyridines, rot. tunnelling, NMR relax. and inelastic neutron scatt. 79−4733
α-bis(N-methylsalicylaldiminato)-copper (II), ^{1}H NMR spin-lattice relax. time, spin dynamics 79−99786
mica, Fe^{2+} distrib. on octahedral sites, PMR investig. 78−15041
microemulsions, PMR spin-lattice relax. time meas., inversion recovery method *(French)* 78−48066
mitochondria and submitochondrial fragments by high resolution NMR 77−16918
molecular spectroscopic laboratory strategies, queueing theory and digital simulation use 80−30299
molecule, large, ^{1}H spin-spin coupling consts., accurate meas. method 79−31555
monochlorobenzene, partially oriented, r_α-struct., ^{13}C satellite PMR obs. 79−50048
multiple proton spin echo at two pulse excitation *(Russian)* 77−4577
muscle, frog, spin-spin relax. times rel. to temp. and water content 78−56952
muscle, hydrated, PMR spin-lattice relax. of water, cross-relax. effects 79−34496
muscle, mouse, ^{13}C NMR and PMR 77−86463
muscle, mouse, NMR multiwindow anal. and proton local fields and magnetisation distrib. 80−21444
muscle, of barnacle, transverse nucl. mag. reson. relax., bounds on bound water 77−4989
muscle, skeletal, water protons NMR relax. times anisotropy obs. 80−85341
muscle water, anal. in mouse above and below freezing 80−56073
muscle water, frog, varied mag. field, multiple-pulse and magic-angle spinning ^{1}H NMR obs. 80−51135
muscle water transverse and longit. NMR relax. rates 78−35810
myoglobin, hyperfine-shifted PMR, mag. field and temp. induced line broadening 77−60184
naphthalene in EBBA, PMR obs., mol. struct., orientation and solute-solvent interactions 77−27806
1,4-naphthoquinone in EBBA, PMR obs., mol. struct., orientation and solute-solvent interactions 77−27806
β-naphthylamine, cryst., amino group reorientation, PMR obs., 77-373K 79−82881
nematic liq. cryst., PMR line breadth temp. depend. 77−8419
nematic liquid crystals, continuum theory of disorder, nuclear magnetic relaxation 77−31592
neuroradiography by NMR imaging 80−51197
NH_4Cl, PMR free induction decay shape and moments 78−68394
nitrobenzoic acid, lattice rigidity, mol. motions, wide-line NMR at room temp. 77−51967
t-nitrobutane, plastic cryst., proton spin-lattice relax. time meas. 77−90058
nitromethane, liq., NMR relax. obs. of internal mol. rot. 79−95668
nonadecane, mol. motion in solid, ^{1}H spin relax. 78−15048
nucleic acid bases, proton mag. relax., methyl group reorientation 77−64009
Nylon 66, stress-oriented NMR expt. using multiple impulses to achieve line narrowing *(German)* 77−28457
OBPA, liq. cryst., proton spin-lattice relax., freq. cut-off effect 77−20738
4-octyloxy-4′-heptyl-α-cyanstilbene liquid cryst., mag. props. 78−87615
one-dimensional charge transfer conductors, press. effects on mag. props., review 78−6505
order parameter fluctuation spectrum, central peaks near ferroelectric phase transitions, review 79−19851
organic compounds, electron donating, PMR spectra, paramag. shifts induced by N_2O_4 *(Russian)* 78−21946
organic free radicals, solid, selective pulse NMR expts. 80−60452
organic liquids, NMR spin energy transfer using zero mag. field, spin echoes 79−95675
organic ortho compounds, solid, H bonding, wide line NMR obs. 78−52362
organic solid, exciton motion effect on proton relax. 78−14671
organonitrogen derivatives of Si, Ge and Sn, prep. and props. 78−60456
organotin compounds, mol. and cryst. struct., X-ray diffr., NMR and Mossbauer spectra meas. 77−47441
oxalic acid diamide, mol., PMR and IR spectra, easy polarisable H-bonds 79−31516
α-oxalic acid dihydrate, H_2O proton shielding tensor, multiple pulse proton NMR obs. 80−63655
oxalic acid dihydrate, PMR, water mols., reorientation 79−42856
oxalic and dihydrate, monocrystals, high resolution PMR 78−64283
oxytocin, amide H exchange rates in aq. soln. 79−83692
PAA, methyl deuterated, dipolar spin system exam. 77−39533
PAA, methyl deuterated, nematic liq. cryst., soft-mode dynamics 78−79749
PAA, nematic, freq. depend. of proton T_1, rot. diffusional mechanism interpret. 77−12219
PAA, selectively deuterated, proton spin-lattice relax. temp. freq. depend., diffusion 77−43132
PAA, smectic-C and nematic long chain homologues, H-spin-lattice relax. *(German)* 78−87610
PAA-d_6, -d_8, H and D spin-lattice relax. 77−59475
PEBAP, nematic liq. cryst., PMR line breadth temp. depend. 77−8419
pentacoordinated ferrous porphyrins, ^{1}H and ^{19}F NMR, hyperfine shift, π electron binding 78−78719
pentofuranosyl nucleosides, isomeric, ^{1}H NMR coupling consts., SCF FPT INDO approx. calc. 80−14156
peptides, α-aminoisobutyric acid containing, ^{1}H NMR conform. obs. 79−81311
phase-sensitive displays for proton 2D J spectra 80−77830
phenol, PMR in absence of intermol. proton exchange, long-range coupling and conformations 77−34660
phenols, orthosubstituted, proton acceptor soln., PMR of H-bonding 78−13517
phenols, substituted, proton NMR chem. shift in aprotic solvents 79−47342
phenylphosphines, and derivatives, ^{1}H, ^{13}C and ^{31}P NMR studies 80−87152
phlogopites, mica, Fe^{2+}, F^-, and OH^- distrib. in octahedral sheet, NMR study 79−82183
phosphatidylcholine hydration, adsorpt.-desorpt. isotherm and PMR 78−15781
phosphatidylcholine-cholesterol vesicles interacting with lucensomycin 80−40954
phospholipid bilayer membrane, spin $^1/_2$-nuclei, in chain methylene groups 77−48767
phospholipid bilayers, struct. dynamics from deuterium spin-lattice relax. time meas. 79−79485
phospholipid vesicles, NMR determs. of maleic acid permeation coeffs. 79−83711
phosphoric acids, proton n.m.r. rel. to glass transition temps. 77−4050
phthalic acid diamide, mol., PMR and IR spectra, easy polarisable H-bonds 79−31516
phthalozine, oriented in lyotropic mesophase, proton NMR spectra 79−82886
γ-picoline, proton Zeeman relax., CH_2D groups effect 79−8067
piperazines, PMR spin-lattice relax. times and lineshapes, 100-300K 77−81027
pleural liquids in weak fields, relaxation times, appl. to medical diagnosis *(French)* 78−73187
PMMA, stereoregular, assoc. in dilute soln., PMR obs. 78−76321
PMMA, syndiotactic, solns. in toluene, NMR obs. of struct. and dynamics of associates 80−75867
PMR relaxation times vs. water content for tumour and normal tissue 77−12884
poly(α-methylvinyl alkyl ether)s, ^{1}H-, ^{13}C-NMR spectra, stereoregularity 80−48112
poly(methacrylic acid)-D_2O soln., proton and deuteron relax. rates, temp. and freq. depends 77−88472
poly-β-benzyl-L-aspartate, soln., ^{13}C and ^{1}H NMR dynamic study 79−69737
poly-γ-benzyl-L-glutamate, soln., ^{13}C and ^{1}H NMR dynamic study 79−69737
polyalkyleneoxide polymer, proton nuclear mag. relaxation *(Rumanian)* 78−91977
polybutyl acetate-polyvinyl acetate crosslinked compositions, proton mag. relax., forced compatibility *(Russian)* 80−44950
polycrystalline solids, selective high resolution ^{1}H NMR 79−61245
polydimethylsiloxane fluid, irradiated, NMR anal. of cross-linked and entangled networks 77−51980
polydimethylsiloxane proton spin-lattice relax., chain motions 78−70987
polydimethylsiloxane-bisphenol-A polycarbonate block copolymer, PMR spin diffusion effects 77−66431
polydimethylsiloxanes, liq., proton spin relax., mol. motion, network form. 79−15369
polyethylene, amorphous, struct. from NMR line shape analysis and MAR-NMR 80−28931
polyethylene, amorphous fraction determ., multiple pulse NMR 77−77107
polyethylene, bulk-crystallised, linear, PMR, phase struct. 77−84665
polyethylene, chlorinated, ^{1}H and ^{13}C NMR microstructural investigation *(German)* 77−55246
polyethylene, liq., very high mol. wt., pulsed NMR obs., entanglement, crosslinking, irrad. effects 78−66702
polyethylene, molecular motions, exam. by PMR line shape anal. 79−41982
polyethylene, pulsed NMR obs., crystallinity effects 78−76342
polyethylene cocrystals, partially and fully deuterated, chain folding, ^{1}H NMR solid echo technique 80−20507
polyethylene glycols, ^{1}H NMR in presence of shift reagent 79−99779
polyethylene melt, dynamics anal. by three components, proton relax. 79−65754
polyethylene melts, entanglement effects in NMR spin-spin relaxation 79−19795
polyethylene oxide, dilute solns., mol. motion, EPR and NMR investigations 79−94863
polyethylene oxide in benzene solns., ^{1}H relaxation times, intermol. interactions 77−32281
polyethylene oxide-Co^{2+} solution, complex struct. *(Russian)* 77−40140
polyisobutylene, relax. modes of short range fluctuation, n.m.r. meas. 77−3502
polyisobutylene, soln., ^{1}H NMR relax. 77−24759
polyisocyanates, rigid backbone, ternary phase relationships obs. 80−59371
polyisocyanides, solns., struct. and acidification 80−19915
cis-polyisoprene, ^{1}H NMR, T_1 and T_2 meas., −50-170°C 79−69738
cis-polyisoprene, ^{1}H NMR of γ-induced cross-linked polymer 79−69739
polyisoprenes, partly deuterated, ^{1}H-NMR spectra, struct. 80−50202
polymer, cryst., broadline PMR spectra, math. separation procedure 80−2647
polymer gel, magic angle rot. H NMR spectra meas. by variable temp. probe 80−31830
polymers, magic angle rotation ^{1}H NMR, appls. 78−43649
polymers, semicrystalline, partially and fully deuterated, chain folding, ^{1}H NMR solid echo technique 80−20507
polymethacrylic acid aq. solns., PMR line breadths 78−27099
polymethinecyanines, symm. solvent effects on electronic struct., ^{1}H, ^{13}C NMR 78−13516
polymethyl acrylate, head-to-head, high-resolution PMR spectra 79−73834
polymethyl cinnamate, head-to-head, high-resolution PMR spectra 79−73834
polymethyl crotonate, head-to-head, high-resolution PMR spectra 79−73834
polymethylacrylate, tacticity from peak-eliminated Fourier transform NMR 77−563

proton magnetic resonance continued
polynucleotide hydration characts. in H_2O/D_2O frozen solns., γ irrad. effects, PMR 78−31772
polynucleotides, gamma-ray effects on hydration, PMR of frozen and liq. solns. 78−27900
polypeptides, amide proton spin-lattice relax. 79−20502
polypropylene terephthalate prepolymer, PMR 79−38392
polysaccharide gel, anomalous behaviour of PMR line width of water *(Russian)* 80−11962
polysaccharide gels and sols, PMR relax. times rel. to temp., pH and conc. 78−56952
polystyrene, head-to-head, high-resolution PMR spectra 79−73833
polystyrene, head-to-head high-resolution PMR spectra 79−73833
polystyrene in dil. sol., solvent depend. of molecular motion, proton mag. relax. meas. 79−41932
polystyrene soln., macromolecular chain dynamics, C^{13} and NMR 78−55267
polystyrene solution, conc., diffusion and NMR relax. times 77−55725
polyvinyl acetate-vinyl acetate, partially polymerised, ^1H-, ^{13}C-spin lattice relax. time meas. *(German)* 79−28633
polyvinyl cyclohexane, head-to-head, high-resolution PMR spectra 79−73833
polyvinyl cyclohexane, head-to-head high-resolution PMR spectra 79−73833
porphyrins, reduction reactions intermediate products 79−53019
Portland cement, absorbed H_2O, pulsed NMR study 80−84665
potassium hydrogen malonate, carboxylic proton chem. shift tensor 80−58280
powders with spin 1/2 nuclei arranged in isosceles triangular mag. config., shape function 80−2648
probe for high-resolution NMR 78−89517
1,2-propanediol, aq. soln., proton NMR study of H-bonding 79−78545
propylene-butadiene, alternating copolymer, struct., fractional composition obs. *(Russian)* 79−65011
protein, globular, in aqueous solutions, conformational mobility investigation 79−53033
protein, proton magnetic reson. and spin diffusion 77−28470
proteins, globular, in water, proton NMR spin echo decay comparative investigation 80−81541
proteins, line-narrowing, convolution and pulse methods 78−78729
proteins, solid, PMR spin-lattice relax., mol. dynamics 80−51041
proteins, spin-lattice relax. time, role of cross-relax. 78−35800
protocatechualdehyde, PMR, 77-427K, OH group rot., struct. 77−30886
proton chemical shifts, combined pulse NMR and magic-angle spinning 80−44934
pyromellitic and dianhydride, intermolecular shielding contributions, proton mag. shielding intermolecular shielding contributions, proton mag. shielding 80−34783
PVC, proton spin-lattice relax. dispersion, quadrupolar dip 77−16197
pyrazine, cryst., mol. reorientation, NMR meas., pot. energy calc. 78−76335
pyridinium molten salts, ^{1}HNMR rel. to transport props. 77−73087
pyrogallol, PMR, OH group rot., H-bonds 79−47339
pyrrole, liq. and nonaq. solns., ^{14}N NQR, ^1H line shape anal. 78−6598
pyrrole, natural abundance ^1H coupled ^{15}N NMR spectra, selective population transfer method 79−95682
quinoxaline, oriented in lyotropic mesophase, proton NMR spectra 79−82886
quinuclidine, plastic phase, mol. reorientations, ^1H and ^{14}N NMR relax. 79−69039
rare gas liquids, nucl. spin relax. of H_2 79−56623
resolution enhancement in FT NMR by digital filtering with sinusoidal window function 77−18060
retinal rod outer segment membranes and liposomes of extracted phospholipids, proton spin-lattice relax. rates 77−90782
rhodopsin thermal stability in photoreceptor membrane, role of lipids, PMR spectroscopy 80−35874
ribonuclease-A, solid, PMR spin-lattice relax., mol. dynamics 80−51041
ring current theories, chem. shifts in conjugated systems 80−53020
$tRNA_{yeast}^{phe}$, Fourier transform PMR in aq. soln., ^1H exchange and relax. rates meas. method 78−15049
$tRNA^{Phe}$, yeast, in soln., H-bonded protons in tertiary struct., PMR, assignments 77−90728
1,2,5-selenadiazole, partially oriented in mesophase, r_z struct. PMR obs. 78−58719
silicate glass, hydrated, proton and ^{23}Na wide-line NMR study 80−84659
skin, rat, ^1H and ^{13}C NMR obs. 80−40965
sodium biphthalate, water of crystn. detection 77−35546
sodium dodecyl sulphate, microemulsion, dynamical and structural props., by chem. physics method 79−79308
solid-state NMR, deuteron spin decoupling from protons 79−61266
soya protein gels and sols, PMR relax. times rel. to temp., pH and conc. 78−56952
spectrometer for quantitative analysis, microprocessor-controlled digital integrator 80−11971
sphingomyelin bilayer systems, monolayer coupling, choline methyl proton line width 78−35807
spin imaging, review 77−5877
spin warp NMR imaging and appls. to human whole-body imaging 80−101250
spin-lattice relax. effects of hindered rotation of NH_4^+ 77−8433
spin-lattice relax. in ^{13}C nuclear Overhauser enhancement reduced value interpret. 77−46581
spin-lattice relaxation and activation energies of tunnelling CH_3 groups 77−48071
spin-lattice relaxation meas., variable nutation WEFT, biochemical appl. 80−20482
spin-lattice relaxation times from CW spectroscopy, phys. chem. lab. expt. 80−17775
spin-lattice relaxation times prolongation, regionally ischemic dog heart tissue 80−101216
squaric acid, dielec. const. and PMR near struct. phase transition 79−10946
starch, H_2O mol. transverse PMR, temp. effects *(German)* 77−60186
steam, supercritical, compressed, proton spin-lattice relax. time meas. 80−22403
styrene, thermal polymerization, PMR obs. 80−3342
substituted benzoic acids, comparative study 80−39881
succinic acid, partially deuterated, ^1H and ^2H distant ENDOR obs. of mol. struct. parameters 80−23445

proton magnetic resonance continued
succinic acid diamide, mol., PMR and IR spectra, easy polarisable H-bonds 79−31516
TANOL, linear chain antiferromagnet, long-range order, magnetisation, PMR 78−23266
TBBA, smectic, spin-lattice relax., self-diffusion, mol. rot. 78−35055
TCNQ, salt, $Me\phi_3As(TCNQ)_2$, nonOhmic elec. cond., tunnelling model and expt. 79−99558
TCNQ salt, $(N(CH_3)_3H)(I)(TCNQ)$, proton spin-lattice and spin-spin relax. times 79−8065
TCNQ salt, pyridinium $(TCNQ)_2$, low temp. mag. phase transition, ESR study 80−25139
TCNQ salt, $Qn(TCNQ)_2$, phase transition, paramag. shifts and PMR line width *(Russian)* 77−43892
TCNQ salts, PMR, electron-proton couplings, local susceptibilities 79−82883
TCNQ salts, proton nucl. relax. meas. 80−20484
TCNQ-DIP Φ_4, electronic diffusion coeffs. in chains, proton spin-lattice relax. and dynamic nucl. polarisation 80−25241
TCNQ-HMTSeF, nucl. spin relax. obs., diffusive character of response function and interchain coupling 78−10797
TCNQ-NMP, incomplete charge transfer, NMR relax. and line-shift meas. 80−20485
TCNQ-NMP, nucl. relax. and spin dynamics 78−52370
tetramethyl gruop VIa cation silicon hexafluorides, ^1H and ^{19}F nucl. spin lattice relax. 78−80234
tetramethylammonium octahydrotriborate, NMR study of proton and B dynamics 80−93200
tetramethylammonium zinc tetrachloride, ^{13}C NMR and PMR study of incommensurate phase transition 80−34863
tetramethylgermanium, Zeeman spin-lattice relaxation rate maxima 80−84666
TGS, proton spin-lattice relax. time, temp. depend., near transition pt. 78−43668
TGS, spin-lattice relax., ferroelec. transition 77−1646
TGS, temp. depend. of spontaneous polarisation, microscopic mechanism, NMR expts. 77−81070
TGS deuterised, radiospectroscopic studies, NMR of $^2D_1$ and $^1H_1$ nuclei 79−15341
thiopen-2,5- dicarboxaldehyde, in lyotropic mesophase, mol. struct. and orientation 78−1004
thiophen-2-carboxaldehyde, in lyotropic mesophase, mol. struct. and orientation 78−1004
thiourea-cyclohexane inclusion compound, thiourea-d_4 derivative, temp. depend. of cyclohexane spectra, cyclohexane molecular motion 78−31116
thylakoid membranes of wheat chloroplasts, proton spin-lattice relax. time, −8°C phase transition 80−108853
thymopoietin active fragment in H_2O, soln. conformation by DNMR spectroscopy 80−89710
tissue, living and ischaemically damaged, longit. relax. decay 77−12895
tissue, rabbit, comparison of NMR water proton T_1 relax. times 80−101221
tissue molecular dynamics and freezing phase transition studied by proton spin relax. 78−68983
tissue of newt, proton spin-lattice relax. time study, blood, liver and tail samples 79−20515
tissues, normal and malignant, pulsed NMR obs. 80−94171
TMMC, 3d ordering, effect of mag. field, PMR meas. 77−4569
TMMC, field-suppression of spin fluctuations, NMR obs. 78−91971
TMMC, impurity doped, antiferromag. three-dimensional ordering, proton NMR meas. 79−78414
TMMC, linear antiferromag., 3D ordering and spin correlations, mag. field effect 78−19262
TMMC, symmetry crossover in spin dynamics, proton spin lattice relax. calc. 77−40147
toluene, microemulsion, dynamical and structural props., by chem. physics method 79−79308
transition metal complexes, proton NMR chem. shift, covalency parameters calcs. 78−42098
transition metal hexaaquo ions, proton mag. relax., spin delocalisation effects 78−62827
2,3,4,- tri-O-acetyl-1,6,-anhydro-β-D-mannopyranose, pulse Fourier transform proton mag. resonance equivalent to CW INDOR 77−32293
s-triazine, in nematic soln., ^1H NMR, struct. ^1H, ^{13}C, ^{15}N direct coupling meas. 77−50452
sym-triazine, molecular reorientation in cryst. 79−73114
1,3,5-tribromobenzene mesophase, spiral-like, struct., PMR of dissolved mols. 78−1981
trichloroacetic acid, proton chem. shift tensor 79−24224
1,2,3-trichlorobenzene, oriented mols., ^{13}C satellites use in proton spectra, r_0-structure 80−18872
1,3,5-trichlorobenzene mesophase, spiral-like, struct., PMR of dissolved mols. 78−1981
triethylacetic acid, high resolution ^1H and ^{13}C NMR spectra at liquid-solid phase transition 80−11281
1,2,3-trifluorobenzene, ^{13}C, ^{19}F, and ^1H NMR spectral anal. 78−37659
trifluorobenzene, symmetrical ^1H and ^{19}F NMR, cross relax. 79−38406
trimethyl ammonium cobalt chloride, magnetisation temp. depend. 80−7128
trimethylacetic acid, high resolution ^1H and ^{13}C NMR spectra at liquid-solid phase transition 80−11281
trimethylammonium cadmium chloride, $(CH_3)_3NHCdCl_3$, struct. phase transitions 79−1502
trimethylammonium cobalt chloride, low-dimensional Ising-like system, nucl. spin-lattice relax. of protons meas. 77−85609
trimethylphosphate, plastic and hard crysts., liq., nucl. spin-lattice relax. mol. motion 78−48065
trioxane, NMR proton relax., mol. rot., rel. to polymerisation 79−73843
trithiane, NMR proton relax., mol. rot., rel. to polymerisation 79−73843
tryptophan, Fourier transform PMR in aq. soln., ^1H exchange and relax. rates meas. method 78−15049
DL-tryptophan, polycryst., amino group rot., reorientation, mol. struct., 77-555K, PMR obs. 78−35047
TTF salts, PMR, electron-proton couplings, local susceptibilities 79−82883
TTF-^{13}C, mol. struct. determ. from PMR in nematic solvents 77−88468
TTF-CuBDT, inter- and intra-chain exchange couplings, proton spin-lattice relax. time meas. 80−71220
TTF-TCNQ, nucl. spin relax. obs., diffusive character of response function and interchain coupling 78−10797

proton magnetic resonance continued
TTF-TCNQ electronic props. 78−2763
tumour development kinetics obs., relaxation method 79−70578
tumour-bearing animals, spin-lattice relaxation study 79−70577
tunable notch filter for solvent elimination 80−22405
two-dimensional, representation using cross sections, projections 79−3464
uridine, pulse Fourier transform proton mag. resonance, equivalent to CW INDOR 77−32293
valinomycin conformation in a phospholipid bilayer 80−40958
vesicle membrane, large unilamellar, ^{1}H NMR study of acetic acid permeation 80−8031
vesicular bilayer membranes, gangliosides orientation, ^{1}H NMR, viscometric and ultracentrifugation obs. 79−92162
vinyl acetate, pulse Fourier transform proton mag. resonance, equivalent to CW INDOR 77−32293
vinyl polymer solutions, proton spin-lattice relax. and Overhauser enhancements 77−55721
water, adsorb3d on Mg vermiculite, elec. pot. calc., rel. to spectra interpretation 78−26763
water, adsorbed on cellulose, NMR relaxation times 79−78552
water, compressed, supercritical, NMR ^{1}H relax. 78−60349
water, direct observation in rotating frame *(Russian)* 78−39422
water, in presence of nonreson. field, interpretation *(French)* 78−72421
water, liq., NMR proton spin-lattice relax. and shear viscosity press. depend., −15 to 10°C 77−40144
water, liq., proton spin-lattice relax. by slow proton exchange 80−60437
water, self-diffusion coeff., pressure and temp. depend. meas. by proton spin echo 80−39328
water, studies in biological systems 80−3886
water adsorbed in kaolinite dispersions, PMR exam. *(Russian)* 78−35058
water diffusion in wheat grain endosperm tissue, ^{1}H NMR obs. 80−8001
water diffusion through narrow pores of biomembranes, ^{1}H NMR obs. 79−92194
water in biological systems, pulsed NMR obs. 80−35930
water mobility in blood plasma, NMR determ., viscosity correl. to $1/T_2$ 80−67176
water molecules in biological systems, relax. rel. to vol., pulse NMR obs. 80−40960
water PMR obs. in obligately halophilic blue-green alga 79−96526
water-formic acid (acetic acid)(propionic acid)(n-butyric acid), PMR relax. obs., mol. assoc. 79−33553
wideband detectors, R-LC and autodyne types, performance comparison 77−74473
wrist, human, radiographic thin-section image by NMR 78−24112
yeast cell membrane, water transport study, pulse NMR obs. 80−40981
yttrium ethylsulphate, rare earth doped, NMR of protons adjacent to impurity 77−85589
zirconocene dichlorides, alkyl-substituted, ^{13}C and ^{1}H NMR, chemical shifts prediction 80−63671
AgI, sol, water PMR meas., 3 to 60°C 78−76930
$(Ag(NH_3)_2)Ag(NO_2)_2$, and deuterate, proton and deuteron mag. reson., reorientation 79−11351
$Ag(NH_3)_2Ag(NO_3)_2$, phase transition, mol. motion, PMR obs. 78−88203
$Ag_2SO_4.4NH_3$, mol. motion, proton mag. reson. 79−47349
β-Al_2O_3-H_3O^+, pulsed ^{1}H NMR study, 77 to 440K 79−87329
β-Al_2O_3-NH_4^+, NH_4^+ jump diffusion and rotational tunnelling, proton NMR, spin isomerism theory 79−99778
β-Al_2O_3-NH_4^+, PMR relax. time obs. of ionic motion 80−71213
β-Al_2O_3-NH_4^+ and β''-Al_2O_3-NH_4^+-H_3O, single cryst. PMR and proton motion 80−108101
γ-AlOOH, boehmite, proton pair obs. from NMR absorpt. spectra 80−75866
Ar:H_2, nuclear spin relax. of H_2, crystal field meas. 79−51875
$BaFHF_2$, free induction decay 78−2753
BaH_2, proton chemical shift tensor, heavy ion effects 79−19791
$BeSO_4.4H_2O$, p-p vector orient., PMR obs. 78−52361
^{13}C-enriched mols., proton relax. and nuclear Overhauser effect from NMR meas. 77−68058
$CaF_{2-x}H_x$, ionic conductivity study by NMR experiments *(French)* 80−29210
CaH_2, proton chemical shift tensor, heavy ion effects 79−19791
$Ca_x^+(H_2O)_y[NbS_2]^{x-}$, hydrate layered chalcogenide, anisotropic mobility of water, NMR 79−65744
$Ca(NO_3)_2$ hydrous melts, proton spin relax. and mobility 77−77118
$Ca(NO_3)_2$, hydrous melts, correl. times, conc. depend., proton NMR relax. obs. 77−90059
$CaSO_2.2H_2O$, few thermodynamic invariants, proof from PMR 78−43657
$CaSO_4.2H_2O$, mol. reorientations and mol. diffusion, PMR 78−43671
$Ca_2[B_5O_9]Cl.H_2O$, hilgardite, PMR of water mol. 80−84655
Cd complex, aminoacetate, proton spin-lattice relaxation, temp. depend. 78−31119
Co complex, $Co(NH_3)_5FCl_2$, mol. motions, NMR 77−36145
$CoCl_2.2H_2O$, magnetisation temp. depend. 80−7128
$CoCl_2.2NC_5H_5$, magnetisation temp. depend. 80−7128
$CoCl_2.6H_2O$, paramag., PMR 78−91962
Co(II)-containing aq. electrolyte soln., nucl. mag. relax., hydration shell *(Russian)* 80−54966
$Co(NH_3)_6Cl_3$, proton second moment meas., 96 to 404K 79−95652
$Cs_x^+(H_2O)_y[TaS_2]^{x-}$, hydrate layered chalcogenide, anisotropic mobility of water, NMR 79−65744
$(Cu,Zn)Cs_2(SO_4)_26(H,D)_2O$, thermal contact between nucl. Zeeman and electron dipole-dipole interaction system 77−90065
$(Cu,Zn)Cs_2(SO_4)_2.6(H,D)_2O$, proton spin-lattice relax. exam., rel. to EPR 77−90064
$(Cu,Zn)Cs_2(SO_4)_2.6(H,D)_2O$ Tutton salt, proton spin-lattice relax. time, proton conc. depend. and spin diffusion role 80−71221
Cu complex, α-CuNSal, one-dimensional $S=^1/_2$ Heisenberg system, nucl. relax. at high temp. 77−85610
Cu complex, $CuCl_2.2NC_5H_5$, spin 1/2 system, one-dimensional nucl. relax. 78−39427
Cu complex, Cu(II) dimers. temp. depend. PMR relax., singlet-triplet separation determ. 80−43073
Cu complex, L-alanyl-L-serine, PMR, EPR and absorpt. spectra 78−46367
$CuK_2Cl_4.2H_2O$, proton spin-lattice relax. and exchange interactions, temp. depend. 79−95663
$CuM_2X_4.2D_2O$, MX=alkali or ammonium halide, quadrupolar interaction, 4-300K, reorientation 79−73848
$Cu(NO_3)_2.2^1/_2H_2O$, ^{1}H spin-lattice relax. time, 4.2K, 5-60 kOe 79−15371
$Cu(NO_3)_2.2^1/_2H_2O$, long-range ordered state, mag. props. 78−39417
$Cu(NO_3)_2.2.5H_2O$, linear Heisenberg antiferromag., proton spin-lattice relax. times 79−61257
$Cu(NO_3)_2.2.5H_2O$, single cryst., $S=^1/_2$ alternating linear antiferromag. spin dynamics 79−51793
$Cu(NO_3)_2$(pyrazine), single cryst. PMR 78−2761
$CuSO_4.5H_2O$, low freq. spin dynamics, proton relax. study 80−71218
$CuSeO_4.5H_2O$, antiferromag. chain system, proton spin-lattice relax. near saturation field 79−61256
dimethylammonium cadmium chloride, proton-^{14}N double reson. exam. of struct. phase transitions 77−4583
$ErCl_3.6H_2O$, single cryst., H^+ coords., NMR 80−97152
$Fe_2(CO)_6(HC_2R)_2$, R=H, Bu^t, Ph, binuclear complexes, isomer identification and stability *(Italian)* 77−54620
$Fe(ClO_4)_3$-DMSO, solvation spheres, exchange kinetics, PMR *(French)* 77−58045
$FeSO_4.n\ H_2O$ (n=1,4,5,7), Fe^{2+} ion mag. interaction with crystallisation water protons, proton NMR obs. 80−60447
H halides, spin-orbit coupling effect on proton mag. shielding 80−23440
H_2 in organic solvents, proton chem. shift, Van der Waals solvent effect contrib. 77−68062
H_2, proton spin relax., gas at 77.5K 79−72335
p-H_2, solid, NMR lineshape due to unpaired o-H_2 mols. 79−47341
H_2, solid, nuclear magnetism at reduced ortho conc. 78−10787
H_2-N_2 mixtures, 300K, proton spin relax., single relax. time approx. 77−61766
HCl and $(HCl)_2$, matrix isolated, pulsed NMR 79−22730
$HClO_4.H_2O$, wide line PMR spectra, oxonium ion motion *(French)* 79−56616
HIO_3, cryst., ^{1}H NMR, −165 to 25°C 79−73828
HIO_3, PMR spectra, homonuclear and heteronuclear broadening separation 80−77828
$H_{0.36}MoO_3$ and $H_{1.71}MoO_3$ bronzes, NMR relax. obs. at 77<T<450K, H diffusion 80−108089
$H_{1.6}MoO_3$ bronze, proton shift tensors PMR meas. 80−71202
$H_{1.8}MoO_3$ bronzes, proton mobility 78−39426
HN_4^+, in crystalline cpds., tunnelling, PMR, generalised line shape, theory 79−73827
HNO_3-graphite intercalation cpd., proton relax. meas., two-dimens. system model 77−51968
$HNO_3.H_2O$, wide line PMR spectra, oxonium ion motion *(French)* 79−56616
$HN(SO_2Cl)_2$, physical props. meas. 79−51293
H_2O in biological samples, PMR, fast-exchange model interpretation via differential kinetics clarified 80−67033
H_2O, liq., proton NMR chem. shift, press. depend. 77−8428
H_2O, nuclear magnetic relax. of protons at identically oriented planar interfaces 77−36148
H_2O powder, PMR chem. shift anisotropy, nucl. mag. screening tensor 78−17687
H_2O, supercooled, longit. proton relax. times, press. and temp. depend. 77−85598
H_2O:HF ice, pulsed NMR 77−28467
$H_2Os_3(CO)_{10}$, and $H_4Os_4(CO)_{12}$, polycryst., PMR chem. shift 79−95655
$H_2PtCl_6.2H_2O$, wide line PMR spectra, oxonium ion motion *(French)* 79−56616
$H_4Ru_4(CO)_{12}$, polycryst., PMR chem. shift 79−95655
H_2S, powder, PMR chem. shift anisotropy, nucl. mag. screening tensor 78−17687
$H_2SO_4.H_2O$, wide line PMR spectra, oxonium ion motion *(French)* 79−56616
$H_2SeO_4.H_2O$, wide line PMR spectra, oxonium ion motion *(French)* 79−56616
$HTaWO_6$, and $HTaWO_6.H_2O$ defect pyrochlores, NMR study of proton motion 79−82889
$H(UO_2P(As)O_4)4H_2O$, H motion, PMR obs. 78−80239
^{1}H spin systems, NMR, two-dimensional Fourier transform. of spin echoes 79−3463
^{2}H spin lattice relaxation, mols. with multiple internal rots., limiting behaviour 79−39356
$HfV_2H_{2.1}$, proton NMR relax. time and Knight shifts, diffusional activation energies meas., sorption props. 80−75871
hydrate layered chalcogenide, anisotropic mobility of water, NMR, for $A_x^+(H_2O)_y[NbS_2]^{x-}$, (A=Na, K, Cs) hydrate layered chalcogenide, anisotropic mobility of water, NMR 79−65744
K^+ salts, diamag. ion solvation in methanol soln., NMR relax. obs. 78−56389
KB_3H_8, NMR study of proton and boron dynamics 80−71210
KCl:NH_4Cl, PMR, NH_4^+ ion proton spin-lattice relax. time temp. depend. 78−27104
$K_2CuCl_4.2H_2O$, and isomorphous cpds., mag. interactions of H and D nuclei, NMR obs. 79−87251
$K_2CuCl_4.2H_2O$, nucl. dipole interaction and transferred hyperfine tensors determ. *(Korean)* 78−19342
$K_2CuCl_4.2H_2O$, paramag. single cryst., PMR temp. depend., hyperfine const. and exchange interaction *(Korean)* 80−29630
KH_2AsO_4:Cr^{3+}, lateral proton config., ENDOR spectra 77−59483
$KHCO_3$, PMR, proton shielding tensor proton ionis. in H-bond 77−1606
KH_2PO_4, paraelectric, dynamic central peak depend. on deuterium content 79−65752
$KH_3(SeO_3)_2$, ferroelastic, central peak in local proton fluctuation spectrum 78−23363
$KH_3(SeO_3)_2$, high-resolution PMR 78−35053
$K_xRb_{1-x}HF_2$, nuclear spin-lattice relax. and internal motion mechanism 79−99787
$K_2[MoO_{1-x}(OH)_{2x}(H_2O)_{1-x}O(MoO_4)_2].2H_2O$, proton NMR for chem. comp. at −195°C 78−38651
La hydrides, proton mag. relax. temp. depend. meas. by pulse NMR 78−88217
$LaH_{2.69}$ two-phase behaviour 80−93189
$LaNi_5$, Pauli paramagnet, adsorption of H, proton and ^{139}La NMR 79−78535
Li^+ salts, diamag. ion solvation in methanol soln., NMR relax. obs. 78−56389
LiCl, aqueous, proton, deuteron and ^{7}Li relax. times, mol. motion obs. 79−28632

proton magnetic resonance continued
LiH, solid, anion and neutron diffusion, NMR relax. and linewidth obs., Schottky disorder 80−15815
$LiNH_4SO_4$, phase transitions, temp. depend. of NMR, spontaneous polarisation, birefringence and SHG 78−10191
$LiNbO_3$, OH^- ion conc., PMR calibration method, IR determ. *(German)* 77−55712
$Li_2O.3MoO_3.5.7H_2O$, fibrillar cryst., IR and NMR investig. of water bonding 77−12370
$Li_2SO_4.H_2O$, linear pyroelectric, temp. depend. of polarisation 79−99821
$Mg(NH_3)_6(ClO_4)_2$, solid, mol. rot., Raman contour, quasielastic neutron scatt., and PMR obs. 79−87444
Mg_2NiH_x, PMR exam. of motion of H 78−56383
Mn complex, $Mn(SCN)_2(C_2H_5OH)_2$, two-dimens. Heisenberg magnet, cryst. struct. and mag. props. 79−60337
Mn II complex with amino acids and peptides in D_2O, NMR line widening 77−56328
$MnSO_4.4H_2O$, p-p vector orient., PMR obs. 78−52361
NH_4 Br single cryst., low temp. PMR lineshapes of tunnelling NH_4^+ ions 80−25223
NH_4 salts, relaxation time of dipolar energy of proton spins 78−76333
NH_4^+ ions undergoing slow tunnelling rotations, proton NMR line shapes 79−90576
NH_4^+, NMR absorpt. lineshape rel. to ion reorientation 77−48074
NH_4^+, NMR line shapes at low temp., composite tunnelling, reorientation 78−48054
NH_4^+, tetrahedrally coordinated four-spin-$^1/_2$ system, PMR absorpt., semiclassical anal. 77−8425
NH_4AlCl_4, crystal struct., X-ray, Raman, IR and NMR 78−63720
$(NH_4)_2Al(SO_4)_2$, ^1H spin-lattice relax., 100-500K 79−38398
NH_4Br, proton spin-lattice relax., temp. depend. 79−42859
N_2H_5Br, mol. ion motion and barriers to rot., PMR and neutron scatt. meas. 79−24226
$(NH_4)_2Ce(NO_3)_6$, proton spin-lattice relax., temp. depend. 79−42859
NH_4Cl, proton spin resonance relaxation time near ordering transition 79−61251
N_2H_5Cl, mol. ion motion and barriers to rot., PMR and neutron scatt. meas. 79−24226
$NH_4Cl(Br)(I)$, NMR under high press. 78−84485
NH_4ClO_4, with 0.015% and 0.1% D, proton Zeeman relaxation 78−6592
$(NH_4)_2Cr_2O_7$, proton spin-lattice relax., temp. depend. 79−42859
$NH_3(D_3)$, liq., longitudinal proton and deuteron relaxation rates, press. and temp. depend. 80−44941
$(NH_4)_2HAsO_4$, $(NH_4)_2HPO_4$, molecular motion, PMR meas. 77−85591
NH_4HF_2, powder, proton and fluorine 2nd moments meas., 77-395K 80−34803
$(NH_4)_x{}^+(H_2O)_y[NbS_2]^{x-}$, hydrate layered chalcogenide, anisotropic mobility of water, NMR 79−65744
$(NH_4)_x{}^+(H_2O)_y[TaS_2]^{x-}$, hydrate layered chalcogenide, anisotropic mobility of water, NMR 79−65744
$(NH_4)_2HPO_4$, NH_4^+ motions, PMR relax. times obs., 77-430K, struct. transition 77−85599
$(NH_4)_2HPO_4$, nonexponential proton relaxation 77−69716
$NH_4H_2PO_4$, ^1H spin-lattice relax. in paraelec. and antiferroelec. phases 79−33555
NH_4HSO_4, NH_4^+ movement 77-388K 77−28524
$(NH_4)_3H(SO_4)_2$, movement of NH_4^+ in all phases over 77 to 388K, NMR study 77−28524
NH_4I, NMR, spin-torsional spectra 79−15363
NH_4LiSO_4, ferroelec., PMR line shape and spin-lattice relax. 78−88205
$(NH_4)_2MoO_4$, ^1H spin-lattice relax., 100-500K 79−38398
$NH_4NH_2SO_3$, ^1H spin-lattice relax., 100-500K 79−38398
NH_4NO_3, proton spin-lattice relax., temp. depend. 79−42859
NH_4ReO_4, PMR, NH_4^+ tunnelling, ground torsional level struct. 78−27097
NH_4ReO_4, polycryst., ^1H spin-lattice relax. by mech. sample rot. 77−16200
NH_4ReO_4, proton absorpt. lineshape and spin-lattice relax., ^{187}Re anomalous temp. depend. 78−48067
NH_4SCN, proton spin-lattice relax., temp. depend. 79−42859
$(NH_4)_2SO_4$, ferroelec., ion group reorientation temp. and press. depend., PMR obs. 78−72470
$(NH_4)_2S_2O_8$, proton spin-lattice relax., temp. depend. 79−42859
$(NH_4)_2SnCl_6$, ^1H spin-lattice relax., 100-500K 79−38398
NH_4TaWO_6, rapid ionic motion, spin-lattice and spin-spin relax. times meas. 79−38396
$(NH_4)_2TiF_6$, ^1H-^{19}F coupled NMR, line shapes, spin-lattice relax. 79−73839
NOH polycryst. radicals, low temp. PMR 80−25220
^{15}N-$^1H^+$ NMR, coupling consts., double reson., difference proton Fourier transform spectroscopy 79−3467
Na^+ salts, diamag. ion solvation in methanol soln., NMR relax. obs. 78−56389
$Na_8Al_6Ge_6O_{24}(CO_3).3H_2O$, water molecule dynamics and hydrogen bonds 79−90577
$Na_8Al_6Ge_6O_{24}(CO_3).3H_2O$, H_2O molecule orientation determ. 79−90631
$Na_{7.5}Ca_{0.5}(AlSiO_4)CO_3.2H_2O$, cancrinite, proton-containing groups, PMR meas. 78−2094
$NaClO_4.H_2O$, ^1H NMR second moment, H_2O dynamic disorder 80−25221
$Na_8(Ge_6Al_6O_{24}).CO_3.nH_2O$, linear pyroelectric, temp. depend. of polarisation 79−99821
NaPtY zeolite, proton spin relax., adsorbed H_2O effect on Pt distrib. 78−88216
$Na_2Si_3O_7.xH_2O$, amorphous, pulsed NMR study 79−78555
NaY zeolite, proton spin relax., adsorbed H_2O effect on Pt distrib. 78−88216
$Na_2[MoO_{1-x}(OH)_{2x}(H_2O)_{1-x}O(MoO_4)_2].2H_2O$, proton NMR for chem. comp. at −195°C 78−38651
Nb, proton diffusion, NMR obs., 120-480K 80−34812
NbH_x, proton Knight shift and mag-suscept., high resolution meas. 77−55716
NbN_xHy, diffusion of H, PMR obs. 79−69287
Ni^{2+} aqueous complex, EPR, PMR and spin-spin relax. 79−69713
$Ni(CN)_2$-dodecylamine, lamellar paraffinic system, phase transitions, wide-line NMR obs. *(French)* 80−44929
$NiS_2O_3.6H_2O$, p-p vector orient., PMR obs. 78−52361
Np(IV)-tetracyclopentadienide complex, H^1-NMR studies, paramagnetic moments, temp. depend. 80−93186
OH, correlation between chem. shift and charge in organic cpds. 77−18946
proton magnetic resonance continued
Pb complex formation with oxyacids, IR and PMR study *(Russian)* 77−28582
Pd complex, L-alanyl-L-serine, PMR, EPR and absorpt. spectra 78−46367
PdH, electronic struct. and proton spin-lattice relax. calc. 78−67937
PdH, stoichiometric, rel. to supercond. T_c 78−72430
$PdH_{0.76}$, ^1H spin-lattice relax. meas. 78−43672
PdH(D), superconducting, electronic spin density, isotope effects 78−39262
Pd(II)-Gly-Tyr complexes, aq. soln., PMR obs., conform. 77−50450
Pt, adsorption of cyclopropane, NMR and PMR obs. 77−51591
RbCl:NH_4Cl, PMR, NH_4^+ ion proton spin-lattice relax. time temp. depend. 78−27104
$Rb_2CuBr_4.2H_2O$, dynamic props. in paramag. state, spin-lattice relax. time meas. 80−71214
$RbNH_4SO_4$, ferroelec., ion group reorientation temp. and press. depend., PMR obs. 78−72470
$Sb_2O_{5.n}H_2O$, crystalline, ^1H NMR study of proton transport 80−60446
Si:H, plasma-deposited amorphous film, proton mag. reson. 80−44931
Si:H film, amorphous, H-associated disorder modes, PMR spin-lattice relax. time meas. 80−93202
SiH_4, NMR linewidths and relax. times at 6.7 to 124K 77−85602
SiH_4, proton spin relax. rate, centrifugal distortion 77−75184
SiH_4, solid, NMR direct detection of tunnel splittings 78−56396
SiO_2:Co(II), adsorption of H_2O, coord. lifetime, surface effect, NMR obs. 80−34299
$SrFHF_2$, free induction decay 78−2753
SrH_2, proton chemical shift tensor, heavy ion effects 79−19791
$Sr(NH_3)_6$, PMR linewidth, proton tunnelling and NH_3 rot., rapid NH_3 diffusion 78−35045
$Sr(NO_3)_2.4H_2O$, p-p vector orient., PMR obs. 78−52361
TaH_x, H diffusion and electronic struct., pulsed NMR obs. 80−54967
TaH_z, proton Knight shift and mag. suscept., high resolution meas. 77−55716
TaS_2-NH_3 intercalation complex, press. induced diffusion effects, NMR study 79−19797
Ta_6SH_x, H locations and motions, PMR linewidth meas. 77−77115
$TaS_2(NH_3)$ intercalation complex, wideline NMR obs., translational and reorientational effects 77−1602
$TaS_2(NH_3)_x$, NMR spectral densities and two-dimens. diffusion 80−50215
Te compounds, dihalides, organometallics, ^{125}Te, ^{13}C, ^1H NMR spectra, nucl. coupling, exchange processes 79−95658
Th complexes, O-donor complexes of cyclopentadienyl Th (IV) halides, prep. and characterisation 79−15974
Th complexes, Th(IV) poly(pyrazol-1-yl)borate complexes, prep. and characterisation 79−15978
Th_4H_{15}, and ThH_2, NMR relax. expts., diffusion processes and hyperfine fields 79−8066
Ti-H, H diffusion and phase consistution, V influence, proton spin-lattice relax. meas. 78−27484
Ti-H, proton spin-lattice relaxation time, band struct. 78−56395
Ti-Nb-H, proton spin-lattice relax. time, conc. depend., diffusion effects 77−4576
TiCuH, PMR obs. of H diffusion 78−91978
$TiH_{1.45}$, PMR study of spin correl. and saturation effects 77−59477
TiH_x, H diffusion, NMR obs. 80−34813
$TiS_2(NH_3)$, intercalation complex, wideline NMR obs., translational and reorientational effects 77−1602
$TiS_2(NH_3)_{1.0}$, NMR spectral densities and two-dimens. diffusion 80−50215
TlH_2AsO_4, proton spin-lattice relax. study of structural phase transition 79−19796
$TlHF_2$, free induction decay 78−2753
U complex, tetrakis(dipivaloylmethanato)uranium IV, in CS_2 soln., ^1H NMR, intromol. rearrangement 79−19784
VH_x, Knight shift and spin-lattice relax. of proton NMR, local electronic environment of protons 77−16194
VH_z, proton Knight shift and mag-suscept., high resolution meas. 77−55716
W, with H adatoms, PMR meas. of adsorption state, surface migration 78−10275
Xe hydrate, reorientation and diffusion of H_2O, PMR and dielectric relax. 77−36142
Y-H system, solid soln. phase, wide-line PMR 80−25226
YH_2, location of H, PMR rigid-lattice second moment meas. 80−71198
Zn complex, aminoacetate, proton spin-lattice relaxation, temp. depend. 78−31119
$ZrBrH_n$, (n=0.5, 1), ^1H NMR, shielding tensors 79−69731
$ZrBrH_x$, PMR exam. of H-location and diffusion 78−56382
ZrClH, ^1H NMR shielding anisotropy 80−20466
$ZrClH_n$, (n=0.5, 1), ^1H NMR, shielding tensors 79−69731
$ZrClH_x$, PMR exam. of H-location and diffusion 78−56382
$ZrMn_2H_x$, proton NMR relax. time and Knight shifts, diffusional activation energies meas., sorption props. 80−75871

proton-nucleus reactions
for inelastic proton-nucleus scattering, see "proton-nucleus scattering" see also neutron-proton interactions; proton-proton interactions; proton radiative capture
0.7-8 GeV, scaling and nonscaling of inclusive π prod. 79−22296
1 GeV, neutron production *(Russian)* 79−85477
20 to 200 GeV, secondary particle multiplicity distribs. characts. *(Russian)* 77−74740
100 GeV/c, multiplicities and pseudorapidity distrib. 78−82241
A=21 to 44, spectroscopic factors for single-nucleon transfer, review 77−71563
A=54-82, ground state transition strengths from (p,t) reactions 80−95305
A(p,d)X, A(p,t)X, inclusive reaction clustering phenomena, scaling behaviour, knockout mechanism, review 79−6441
A(p,p)X, quasi-two-body scaling appl., single scatt. model validity 79−3151
accelerator proton collisions, 200 to 400 GeV, review of charm particle prod. in nuclear emulsions 79−63534
actinide fission product X-rays in micas, comparison with superheavy elements K- and L-shell ionisation estimates 77−50581
activation analysis, 11 MeV protons 78−88686
backward inclusive prod. of high energy p,d,t 78−66275
backward inclusive scattering of polarised protons from nuclei 78−17206

proton-nucleus reactions continued
backward p,d,t production, p-p correlations 80−529
beam dump experiments, prompt neutrinos and charm particle lifetime 79−63535
beam dump neutrino experiments, promp neutrino meas. 79−63537
CD ^{90}Zr(p,π^+)^{91}Zr, 160 MeV, ang. distributions 78−37345
channelling, modulation of high energy interactions 80−37373
charged particle cross sections, exotic fusion fuels 77−23293
charm particle search at 300 GeV/c 77−18348
cluster cascade model, single particle distributions and two-particle correlations 80−18300
clusterisation and secondary particle correl. *(Russian)* 78−33133
coherent recoil dominance, basis for quasi two-body scaling 78−50140
collective tube model, credibility of criticism by Azimov et al., effects of target fragmentation 78−93982
collective tube model of high energy proton scatt. on polarised nuclei 80−32273
collision number, rel. to angular distrib. of black and grey prongs *(Rumanian)* 79−63677
conference on high energy physics and nuclear struct. Vancouver, Canada (Aug. 1979) 80−41936
correlation strength at 400 GeV, dependence on target size, multiplicity and cluster size 80−78287
cosmic ray, around 20 TeV, momentum and energy spectra 77−22029
cosmic-ray-nucleus reactions, hadron multiple prod., muon time-correl. meas. *(Russian)* 77−14133
cross sections characts. appl. to calc. of muon sea level momentum spectrum and charge ratio 77−41275
cumulative effects, phenomenological model for pion prod. and elastic scattering involving deuterons 78−58267
cumulative pion production models, comparison 78−13092
DC (p,2p) reaction, three body model anal. of two step process 79−40911
differential cross sections meas. by SPES I 79−75983
dimuon prod. at 400 GeV, ψ and ψ' signals 77−10399
dimuon resonance obs. at 9.5 GeV in 400 GeV interactions 77−74847
early solar system, local proton irradiation model for isotopic anomalies 78−93128
EAS, violation of scale invariance in hadron interactions, 10^{15} to 10^{17} eV 78−7849
effective target mass distribution in relativistic proton-nucleon inelastic interactions 78−66162
emulsion, 400 GeV ang. distribs. of secondaries 79−36232
emulsion, nuclear, p-N interaction at 70 GeV 79−13288
emulsion, particle production by clusters at 200 GeV/c 79−89302
emulsion nuclei, 200 GeV proton interaction, charged particle prod., multiplicity, ang. distrib. 77−50123
emulsion nuclei, 200 GeV/c, transverse momenta of secondary particles 79−13301
emulsion nuclei, 23 GeV, probability of proton emission *(Spanish)* 77−30564
emulsion nuclei, 400 GeV/c proton interactions, charged particle multiplicity 78−21558
emulsion nuclei, inelastic interactions of 400 GeV protons 79−6596
emulsion nuclei, shower ang. distribs., anisotropy coeffs., multiple prod. mechanism 10^{10} to 10^{13} eV/nucleon *(Russian)* 77−79385
emulsion nuclei+p, 400 GeV, shower particle multiplicity 79−3145
emulsion nuclei+p, 400 GeV/c, diffractive coherent prod., inclusive and exclusive channels 78−62530
emulsion nuclei+p, correlations between secondaries 77−57654
emulsion nuclei+proton, 300, 400 GeV 78−54756
emulsion nucleus, 400 GeV, two particle correlations between produced particles *(Russian)* 79−3157
emulsion reaction, 300 GeV/c, new stars containing only black tracks 80−78285
emulsion stars of 200, 300, 400 GeV protons, multiplicities, ang. distribs. 78−596
energy dependence of two-particle rapidity correls. 77−34292
exact finite range calculations of light-ion induced two-neutron transfer reactions 79−63639
fast particle production on nuclei in quark model *(Russian)* 79−6612
fireball coplanar decay, 24 GeV/c 78−50157
fission of medium mass nuclei induced by 1 GeV protons 77−71627
fissionability, target mass depend. for π, γ, α, p, cascade-evaporation and liquid drop calcs. *(Russian)* 80−106089
fragmentation, clustering and absorption mechanisms in p and π induced reactions 79−6546
fragmentation velocity, source vel. mass independ. correlation 78−93979
fragmentations at high-energy, search for stable neutronium isotopes 77−22904
fragmented analogue states produced in proton-nucleus reactions, fine struct. anal. 77−6391
Frankel events observation in streamer chamber 79−85505
Glauber screening eqns. in fast backward particle prod. in high energy processes, role of short range nucleus struct. 79−63670
hadron mean charged multiplicities, universality in particle and nuclear collisions 77−54086
hadron production on nuclei, incoherent-multiple-collision effects 77−50037
high energy, evidence against multiple collision models 77−50128
high energy knock-out reaction, rel. to cluster structure *(Hungarian)* 77−50124
high energy p-nucleus collisions, impact parameter anal. of multiplicity distrib. 77−79369
high energy reaction temp., kinematic props. of nuclear fragments 78−54761
high energy reactions, secondary particle multiplicity 79−93597
high-energy, at Saturne I, five years of expts. *(French)* 79−3262
high-energy, correlation between fast target protons and hadron+nucleon collisions 78−41681
high-energy, two-particle rapidity correlations in produced particles 77−18545
high-energy reactions in astrophysics, comparison of methods for cross-sections calc. 78−28505
high-energy similarity of pion and proton induced reactions 77−67747
hole states, continuum shell model approach for (p,2p) and (e,e'p) reactions 79−22162
hydrodynamic model 80−68671
hydrodynamic model predictions for arbitrary vel. of sound in nuclear matter 77−50070
proton-nucleus reactions continued
hydrodynamical model, secondary energy distrib. at very high energies 77−88136
hydrodynamical model calcs. at E>200 GeV 79−550
inclusive, very large momentum transfer, cluster representation 79−93615
inclusive π prod., 0.78 to 5 GeV, relation to NN π prod. 78−78384
inclusive correlation functions, 300 GeV proton interactions on emulsion nuclei 78−58279
inclusive hadron production in high energy particle+nucleus collisions, sum rules, scaling law 77−57673
inclusive production of large-transverse-momentum hadrons and hadron pairs 79−89310
inclusive production of neutral strange and charged particles, collective tube model 80−52538
inclusive proton prod. at 180°, correlated cluster model 77−71600
inclusive proton spectra A depend. at large transverse momenta, multiple collisions theory *(Russian)* 77−38215
inclusive single particle prod. of $\pi^\pm$, $K^\pm$, and $p^\pm$ at 28.5 GeV 77−18346
intermediate energy reactions as struct. probes with p,πK,γ,e projectiles 77−88107
large momentum pion prod., nuclear density fluctuation 77−38267
large transverse momentum hadron prod. by 200-400 GeV protons, atomic no. depend. 77−41967
leading proton spectrum at high energies in (p,X) reactions, intranuclear cascade model anal. 80−5139
light and intermediate nuclei, polarisation phenomena interpret. 78−13051
light nuclei, three and four nucleon low energy scatt. expts., review 79−80945
light nuclei (p,π^+) reactions, π distortion effect on asymmetry 78−50176
light relativistic ion-target interactions, particle emission 80−102193
linear acceleration reactors, anal. of neutron yield produced by high-energy protons 80−22895
Maxwell distrib. and mass motion to account for ang. distrib. anisotropy, ~600 MeV 77−61425
medium mass nuclei systematics of 80-160 MeV proton bombardment 77−74846
meson exchange current effects in hadron-nucleus scatt. 79−26380
momentum wave function determ. in atomic, molecular and nuclear systems 77−88556
multi-nucleon removal by 400 MeV p, p-γ coincidence spectra 79−6549
multiparticle production data anal. using charged particles created as variable 79−3155
multiphoton events distribs., 300 GeV/c 77−10283
multiplicity distribs. of compound shower and grey track, proton-emulsion interaction 78−591
multiplicity of secondary particles, 7 GeV/c *(Russian)* 77−88146
multiplicity ratios, Landau's relativistic hydrodynamical model 77−46169
neutrino-like particle prod., limits from calorimetry meas. 79−85473
nuclear emulsion, 70 GeV, primary energy estimation 79−30826
nuclear emulsion, pp and pn inelastic interactions, 69 GeV/c 78−66161
nuclear emulsion expts. on particle prod., 200 to 400 GeV 77−30433
nuclear fissility at intermediate energy cascade-evaporation and liquid drop model anal. 78−70579
nuclear size dependence of π^- prod., unified pattern 78−82349
nuclear size dependence of particle prod., hydrodynamical model 80−22593
nucleon knockout, off-shell effects, momentum-space wavefunctions 77−88122
nucleonic mass distrib. using mag. spectrometer *(French)* 79−449
one-nucleon transfer reactions, high energy, reaction kinetics and struct. determ. *(French)* 79−535
(p,2p) reactions, intermediate energies, distorted wave impulse approx. anal. review, ^{40}Ca(p,2p)^{39}K illustration 78−62541
(p,^{3}He) with A=21-39 T_Z=1/2 targets, S=1 two-nucleon quenching 77−14128
(p,α), α-cluster preformation coeffs. and level densities 77−71579
(p,α) direct reactions on light nuclei, alpha cluster breakup effects 79−6550
(p,t), rare earths, 18-20 MeV, Q effects on cross section, DWBA anal., A dependence 79−63675
(p,t) reactions, ang. momentum selection rules in DWBA theory 77−46154
(p,t) reactions, exact finite-range DWBA calcs. 77−71597
(p,t) with A=21-39 T_Z=1/2 targets, S=1 two-nucleon quenching 77−14128
p+emulsion, 200 GeV, star event containing single electron, charmed particle generation, anal. 77−61414
particle momenta spectra fits from streamer chamber expt. with two temp. Boltzmann model 79−85507
particle-stable neutral nuclei prod. search, multi-GeV energies 78−25189
photoemulsion+p, 400 GeV/c, decay of short lived charmed particles produced *(Russian)* 79−3022
photoemulsion nuclei, 70 and 250 GeV, hypernuclei formation *(Russian)* 80−9297
photon, electron and positron prod. from primary proton beams, Monte Carlo calcs. 80−32555
pion production, Fermi motion effects, multiplicity distribs. and inclusive cross sections 79−93622
polarisation meas. with low energy proton and deuteron beams 77−2970
pre-equilibrium decay of nuclei of mass ≃90 in 10-100 MeV reactions 78−17171
primary cosmic ray interactions with photoemulsion nuclei using satellite Intercosmos-6 *(Russian)* 78−93063
production of particles with lifetimes 10^{-12}-10^{-14} sec., by 400 GeV protons 77−46163
prompt μ production in p-nucleus collisions, multiple prod. model based on lepton-hadron relation 78−29362
proton-emulsion collisions, 67 to 400 GeV/c, energy independence, pseudorapidity distribs. for shower particles 79−75808
proton-induced fission, 70 to 200 MeV compound nucleus formation, fragment ang. anisotropy *(Russian)* 79−13359
pseudorapidity distribution, energy and target depends., 24 and 70 GeV/c 80−5138
pseudorapidity distribution for 50, 100, 200 GeV/c beams, energy proton, target depend. targets ranging from C to U 78−17202
QCD, μ pair transverse momentum distrib. in Drell-Yan processes 78−62374

proton-nucleus reactions continued
QCD, transverse momentum distribs. of μ pairs from pN interactions, p-nucleus study 78−62375
radiochemical solar neutrino detectors using (ν,e$^-$) reaction, (p,n) background from cosmic ray muons 77−61650
rapidity intervals of secondary charged particles from nuclear emulsion, 70 GeV/c 78−54750
relativistic nuclear collisions, p, d, and t inclusive energy spectra 80−63199
relativistic particle angular distribs., inelastic proton-nucleus interactions, 20 to 200 GeV/c *(Russian)* 78−46065
secondary particles angular distribution, 400 GeV/c *(Russian)* 77−46173
shower particle multiplicity distribs. at 6.2-300 GeV, scaling hypothesis 77−50019
shower particles average number in 300 GeV p-nucleus emulsion interactions 77−50018
single particle nuclear density struct., Hartree-Fock and model independent anal. *(Russian)* 79−80941
slow body emission, 200 and 300 GeV, mass estimates 77−41959
slow particle charact., relation to high energy interaction models 78−58269
spallation cross sections for medical radioisotope preparation 77−23052
spherical nuclei, excitation of collective states in high-energy proton interactions 78−17073
spin effects in inelastic p-nucleus scatt., diffractive minima 78−89875
thermonuclear reaction rate data for intermediate mass nuclei 80−31427
trimuon events, probability of production by short lived source of neutrinos 78−37343
two step (p,d) (d,t) process, Strum-Liouville state asymptotic convergence 79−54414
Be+p, 200 GeV, d, $\bar{d}$, t, $\bar{t}$, ^{3}He, $^3\bar{H}e$ prod. 79−9563
C+p, 24 GeV, J/ψ prod. cross section 78−46055
d and t quasifree knockout at 62 mrad, differential cross sections *(Russian)* 79−30819
D^0(1.865) production in proton-nucleus collisions at 400 GeV/c 78−13099
emulsion nucleus, 250 GeV, $_\Lambda{}^{12}$C hypernucleus detection, Λ hyperon binding energy *(Russian)* 78−89816
γ spectra, high energy, anal. of 303 GeV/c p+nucleus reactions in emulsion chambers 78−70521
H+p, 24 GeV, J/ψ prod. cross section 78−46055
K subthreshold prod., struct. function 78−21564
L^0 prod. in pN collisions, 400 GeV/c upper limit on cross section 78−37243
μ pair prod. in 200-400 GeV interactions, scaling 78−82344
μ^+ longitudinal polarisation in direct prod. from 70 GeV protons 77−2995
n pickup reaction, intermediate and high energies, review 78−94010
N̄-nucleus optical pot. strong interaction effects, implications for N̄N interaction 77−18402
(p,2p), 1p shell nuclei, high lying one hole states *(Russian)* 79−59004
(p,2p), backward inclusive prod. mech. probing, differential cross section 80−68668
(p,2p), distorted momentum distrib., and pp collisions, geometry choice for independent study 79−6597
(p,2p), distorted wave t-matrix anal. 78−50169
(p,2p), off shell effects using optimum geometrical conditions 79−6598
(p,2p), off-shell effects in distorted wave off shell impulse approx. 77−6376
(p, 2p), pol. p, quasi-free scatt. on closed shell nuclei, effective polarisation 80−91173
(p,2p) 800 MeV high resolution reactions, proposed studies 77−88123
(p,2p) coplanar symmetric reaction, impulse approx. for peak cross section 79−45257
(p,2p) DWIA calcs., N-N off shell t-matrix, optical model from N-N 77−88124
(p,2p) high-energy knockout reactions, factorisation corrections 79−17885
(p,2p) knockout, DWIA and PWA mechanisms 77−88120
(p,2p) knockout experiments at Maryland, DWIA anal. 77−88118
(p,2p) knockout expts. at E>100 MeV 77−88119
(p,2p) knockout reactions, single particle momentum states 77−88117
(p,2p) quasi-free reactions, analysis of distortion in momentum distribs. 78−54762
(p,2p) reaction for slightly deformed nuclei 77−57657
(p,α), 72 MeV, ^{27}Al, ^{59}Co, ^{90}Zr, ^{197}Au, ^{208}Pb, ^{232}Th targets, spectra and angular distribs. 80−68660
(p,α), continuous α-spectra, meas. and anal. 79−6585
(p,α), polarised p, anal. power, direct 3-nucleon transfer reactions, microscopic approach review 79−6545
(p, α) microscopic form factors, DWBA cluster form factor replacement 80−47478
(p,α) preformation coeffs. for mass range 27-123 77−54209
(p, α) reaction, statistical direct reaction model 79−80913
(p,χ), inclusive backward collision, intermediate energies, correlated nucleon clusters 79−40914
(p,d), 51.9 MeV, forbidden transition ang. distribs., CCBA and DWBA anals. 80−86848
(p,d), 52 MeV, deeply bound hole state transition strength giant resonance, DWBA anal. 80−47426
(p,d), (p,t), deep hole states observed in particle transfer reactions 80−68511
(p,d), intermediate energy study review 80−42653
(p,d), pol. p, 65 MeV, A=12-94, differential cross sections and anal. powers, pickup 80−91172
(p,d), Q values, $1f_{7/2}$ shell isobaric analogue states, displacement energies 79−13207
(p,d) backward pick-up react. for inclusive deuteron spectra at 180° 78−17203
(p,d) cross-section, effect of nuclear vertex form factor in peripheral model *(Russian)* 77−82889
(p,d) reaction, nuclear cluster effects 79−6576
(p,d) reactions on light nuclei, differential cross sections, peripheral and distorted wave model calcs. 79−9560
(p,d) reactions on spherical nuclei, form factors, Pauli principle *(Russian)* 77−6393
(p,f) on pre-Actinide nuclei targets, 24-30 MeV range, fission barriers *(Russian)* 77−82978
(p,γ) proton energy straggling determ. in thin Au and Ag films 79−4354
proton-nucleus reactions continued
(p,^{3}He), Q-values, $1f_{7/2}$ shell isobaric analogue states, displacement energies 79−13207
(p,Λ^0), inclusive cross section, constituent-constituent multiple scatt. model for dependence on atomic number 80−83101
(p,n), 1 GeV, A=7-212, charge exchange scatt., Glauber diffractional theory anal. *(Russian)* 80−83103
(p,n), 1 GeV, quadrupole moment, isovector component, nuclear spin reorientation effect 80−52573
(p,n), 120 MeV, 0° cross sections, Gamow-Teller matrix elements for A=7-90 80−86860
(p, n), 22.2 MeV, A=27-197, neutron spectra, direct and equilib. processes *(Russian)* 80−52648
(p,n), 2.5-5.8 MeV, A=89-130, cross sections, sub-Coulomb proton anomalous optical pot. 80−32278
(p,n), A=12, 24, 28, isovector M1 excitations, current and spin contribs. 80−68582
(p,n), A=88 to 124, reaction rates of reaction important to nucleosynthesis 79−45253
(p,n), A=89-130, anomalous optical pot. for sub-Coulomb protons 80−102190
(p,n), A=89-130, sub-Coulomb protons, anomalous optical pot. 80−102191
(p,n), A=90 region, reaction cross section, statistical model calcs. 80−68674
(p,n), anomalous optical potential for sub-Coulomb barrier protons, 2 particle 1 hole states 80−105948
(p,n), atomic excitation effects on nuclear resonances and Q values 79−45226
(p,n), charge exchange reaction, mean energy regions, diffraction model *(Russian)* 78−82352
(p,n), high resolution neutron spectroscopy in near threshold region 79−45251
(p,n), on ^{7}Be and ^{7}Li, lifetimes of first excited levels meas. 77−22943
(p,n), pion exchange at intermediate energy 80−63179
(p,n), Q-value atomic excitation corrections 79−40918
(p,n) cross section needs for solar physics studies 77−25997
(p,n) cross sections on nuclei with A=89 to 130, anomalous optical model pot. 78−25188
(p,n) elastic and inelastic scatt., deformation of neutron excess, coupled channel anal. 79−93480
(p,n) excitation functions for A=45 to 80, proton optical pot. at sub-Coulomb energies 80−9292
(p,n) quasielastic reaction, cross section and polarisation, Lane model extension to light nuclei 79−85449
(p,n) quasielastic reactions with polarised 22.8 MeV protons, targets A=49-208 77−6382
(p,n) reactions, alignment and decay of IAS, depend. on higher multipole contrib. 77−3003
(p,n) reactions, associated activity method, calibration of flat response neutron detectors 79−9979
(p,n) reactions, black and grey neutron detectors 79−9971
(p,n) scattering, charge exchange, isobaric analogue state, giant resonance effect, semimicroscopic model 78−89868
(p,N*), high energy reactions, Glauber scatt. theory study *(Chinese)* 79−93626
(p,p) 800 MeV, polarised p, n density uncertainties from optical model anal. 79−22185
(p,p'), on ^{40}Ca, ^{48}Ca, ^{90}Zr, and ^{208}Pb, (in)elastic scatt., self-consistent calcs. of nuclear density *(Russian)* 79−80928
(p,p'), on ^{7}Be and ^{7}Li, lifetimes of first excited levels meas. 77−22943
(p,p'), study of pion condensation in finite nuclei, precritical phenomena 79−85377
(p,p'd), quasifree scatt., break-up cross section at high energies 80−99174
(p,pα) comparison with (α,2α) reactions, antisymmetrisation effects 79−6575
(p,p$\pi^+\pi^-$), isobar prod. in proton diffractive dissociation *(Russian)* 79−80836
(p,pπx) reaction, pion production, flucton mechanism anal. 79−6590
(p,π), 4.2, 4.5 GeV/N, pion multiplicities and theoretical models, review 80−42657
(p,π), exclusive single nucleon transfer, theoretical status 80−42652
(p,π), hopes and realities, review, book contrib. 80−73849
(p,π), pion prod. in proton-nucleus collisions, expt. and theoretical results, book contrib. 79−75991
(p,π), polarised p, light nuclei, cross sections, ang. distribs. and anal. power 79−85460
(p,π), production models 77−10393
(p,π) reactions, nucleon-nucleus distorted wave, small component role, relativistic effects 79−40919
(p,π) reactions near threshold, relativistic effects in one-nucleon model 77−34302
(p,π^+), 1p-shell nuclei, inclusive cross sections near threshold 79−85462
(p,π^+), 8-16 MeV, inclusive cross sections near threshold, A depend. 80−27644
(p,π^+), differential cross-section, current theories 77−6445
(p,π^+), light nuclei, 0.5-10 MeV, total cross sections near pion Coulomb barrier 80−32280
(p,π^+), polarised p, 200 MeV, p distortion and asymmetries 79−22285
(p,π^+), π threshold prod. and absorption, pseudoscalar-pseudovector equivalence 79−80877
(p,π^+) cross-section calcs., model relating to (π^+,π^+) cross-section 77−61422
(p,π^+) reaction anal. at momentum transfer below 600 MeV/c 77−79376
(p,$\pi^\pm$), 320-800 MeV protons on ^{2}H to ^{10}B targets, coherent pion production *(French)* 79−533
(p,$\pi^\pm$), 585 MeV, A=1-208, differential cross section and pol. parameter 80−106056
(p,$\pi^\pm$), 585 MeV, cross sections, polarisation parameter for H, D, Be, C, O, Al, Ni, Cu, Mo, Pb targets 80−73848
(p,π^-), 154 MeV, production on ^{10}B, ^{13}C, ^{14}N, ^{25}Mg, ^{28}Si, ^{32}S and ^{40}Ca 77−10391
(p,πx) in emulsion, 70 GeV/c, Lorentz invariant kinematical anal. 80−47474
(p,π^+X), 4.3 GeV/c, inclusive pion prod., nuclear mass number depend. 79−76029
(p, spallation), 480 MeV, medium to heavy mass targets, deep spallation products 80−83085

proton-nucleus reactions continued
(p,t), deformed nuclei, quadrupole vibr. excitation in two nucleon transfer reactions *(Russian)* 79−30780
(p,t), even actinides, lowest 0^+ state excitation, collective phonon state, spectroscopic factors 80−13410
(p,t), medium mass vibr. nuclei, 22 MeV, polarised p, anal. power systematic nuclear struct. depend. 79−22265
(p,t), pol. p, strong ground state transitions, anomalous anal. power, direct and sequential processes 80−5115
(p,t), Q-values, $1f_{7/2}$ shell isobaric analogue states, displacement energies 79−13207
(p,t), radioactive targets, for study of nuclei far from stability 77−22990
(p, t) ang. distrib., zero-range DWBA calc., volume absorptive optical pot. singular prop. 80−523
(p, t) ang. distrib. with deep minima, DWBA calcs. geometrical aspects 80−522
(p,t) reaction for investigating shape transition and core-excitation 77−54212
(p,t) reactions, two stage processes in direct reactions, (p,d)(d,t) *(Dutch)* 78−29439
(p,t) reactions on Ge isotopes, 26 MeV spectroscopy of transitional nuclei using transfer reactions 78−86480
(p,τ), 72 MeV, ^{27}Al, ^{59}Co, ^{90}Zr, ^{197}Au, ^{208}Pb, ^{232}Th targets, spectra and angular distribs. 80−68660
(p,X), 0.6-21 GeV, ^{A}Rb, A=83,84,86 prod. cross sections and recoil props. 80−9295
(p̄,X), 20, 37 GeV/c, ang. distribs., multiplicity distribs. and particle correlations 79−93664
(p,X), 200 GeV/c in emulsion, fireball parameters and π emission 80−95317
(P,X), 22.6 GeV/c, pion p_T distrib. in emulsion 80−95319
(p,X), 400 GeV, A=6-180, p̄,$\pi^{\pm}$ and $K^{\pm}$ backward prod., invariant cross sections 80−102188
(p,X), 400 GeV, in emulsion, two-particle rapidity correlation 80−63054
(p,X), 400 GeV/c, deuteron prod. mechanism, pick up reactions 80−83096
(p,X), 5-9 GeV/c, total inelasic and knock-out cross sections, nuclear RMS radius *(Russian)* 80−32175
(p,X), 50-200 GeV/c, ang. distrib. of charged shower particles *(Korean)* 80−27641
(p,X), 640 MeV, fast proton emission, two particle differential cross sections *(Russian)* 80−106058
(p,X), 70 GeV/c *(Russian)* 80−52681
(p,X), 70 GeV/c in emulsion, forward-backward rapidity correl. and asymmetry 80−95320
(p,X), A=10-152, thermonuclear reaction rates, thick target meas. 80−73108
(p, X), A=12-209, pol.p, 65 MeV, continuum spectra anal. powers 80−102178
(p̄,X), antiproton as nuclear probe 80−42704
(p,X), complete fusion barrier and evaporation from ^{194}Hg 80−68715
(p,X), experimental information review, polarisation phenomena 80−42655
(p,x), few nucleon correlations in nuclei, cumulative particle production *(Russian)* 80−5145
(p,X), high energy, Glauber anal., produced particle-A relation *(Chinese)* 80−102192
(p,X), inclusive one- and two proton spectra by statistical model 79−93624
(p,X), inclusive pion prod., forward and backward π spectra 79−85484
(p̄,X), multi-chain model, charged particle distrib. 80−83098
(p,X), neutron excess isotope prod. in fragmentation reactions ^{6,8}He, ^{7,8,9,11}Li *(Russian)* 80−86888
(p,X), relativistic collisions, slow and fast fragment correlations, multiplicity association 80−86886
(p,X) 400 GeV, p, d, t, π, ^{3}He, α backward prod., inclusive cross sections 79−85475
(p,X) 90 MeV, inclusive spectra, 'quasi-two-body scaling' and 'hot spots' 80−5142
(p,X) emulsion, 400 GeV/c slow deuteron and proton prod. 80−52666
(p,X) in emulsion 24 GeV, clusters in rapidity interval method, multiperipheral model 80−5135
(p,X) on light nuclei, 1.55, 2.89 GeV/c, total and inelastic cross sections 79−6610
(p̄,X), p̄ annihilation on heavy nuclei, nuclear matter props. 80−63185
(p,xn) on heavy elements, K X-ray and nucl. satellites 80−27599
(p,xn) reactions, cross-sections and astrophysical appls. 78−28504
(p,xnγ), rare earth nuclei, complete fusion process n and γ multiplicity 80−18363
(p,Z), 250 GeV, heavy emulsion nuclei, ^{8}Li fragment formation, yield and energy spectra *(Russian)* 79−59072
p̄ absorption cross section on nuclei, 60-280 GeV/c 79−22293
p̄ annihilations in heavy liquid bubble chamber, effects of complex nuclei reactions 77−79373
p̄ subthreshold prod., struct. function 78−21564
p+A→p+X, 800 MeV, inclusive cross sections, analysing power 78−70524
p+A→p+anything, A=C, Al, Ti, Cu, Cd, Pb, inclusive backward emission of protons, 1.5 to 9.0 GeV *(Russian)* 77−10278
p+A→p$\pi^+\pi^-$+A, 2.25 and 15.3 GeV, coherent diffr. reaction, Glauber model fits 77−22809
p+Be(Cu), 70 GeV, π^+, K^+, p large p_T yields *(Russian)* 77−82778
p+Be→Δ^0+X, 300 GeV/c, Δ^0 polarisation meas. 77−30458
p+Be→φ+X, 400 GeV/c, φ decay modes, OZI rule 78−599
p+Cu 400 GeV large $p_\perp$, quark search 77−79290
p+emulsion, 200 GeV, data anal. hydrodynamical model 79−551
p+emulsion collisions, charged particle multiplicity distrib., high energy, KNO scaling 78−70568
p+emulsion nuclei, 300, 400 GeV, search for short lived charmed particles 77−50023
p+emulsion nucleus, 60 and 200 GeV, shower particle multiplicity distrib. parametrisations 78−62524
p+nuclear emulsion, 400 GeV nonwhite stars 78−13097
p+nucleus→$\mu^+\mu^-$+anything, 400 GeV, high-mass dimuon continuum 78−37344
pA high-energy collision yields, evidence for composite quark model *(Russian)* 79−9636
pA→π^-+X, scaling invariance of interactions of relativistic nuclei, the cumulative effect *(Russian)* 79−93611
pC→p(pol.)X, 100 to 400 GeV, proton polarisation in inclusive processes 79−58983

proton-nucleus reactions continued
pD, phenomenological relations between large-p_T meson spectra 79−26349
pN, 70 GeV, forward prompt muon yield, μ/π yield ratio *(Russian)* 79−97641
pN interaction in nuclear emulsion with single electron emission, possible charm particle prod. *(Russian)* 77−252
pN reaction, subthreshold p̄ production, interpretation by cumulative process 'gathering' model 78−58268
pp total cross section from cosmic ray p-nucleus and pp data anal. *(Russian)* 78−17064
p$\pi^+\pi^-$ systems in coherent and incoherent collisions, 18.6 GeV/c 77−41866
$\pi^{\pm}$ prod. in 0.8-4.89 GeV collisions, energy depend. of 180° prod. 80−22834
W boson search in p+nucleus 70 GeV muon yields 77−18367
W+p, 24 GeV, J/ψ prod. cross section 78−46055
^{208}Pb+p, 100-1050 MeV, optical pot. real part, nuclear matter approach 77−82890
^{6}Li(p,n), 144 MeV, one pion exchange and PCAC expt. test 80−528
^{42}(p,n), ^{42}Sc weak neutral current props., search for 0^- isomer 79−45126
^{127}(p,xn) and ^{127}I(p,pxn), excitation functions, yields for ^{123}Xe prod. 78−594
Ag (p,X), 400 GeV/c, multiplicity and ang. distribs. of relativistic and slow particles *(Russian)* 79−40931
Ag break-up in relativistic proton collisions, ^{4}He emission 77−10410
Ag, emulsion nuclei, 28 GeV proton interactions *(Korean)* 80−18299
Ag, proton-induced fission at 400 GeV, ternary to binary event ratio 78−13170
Ag+p, 1 to 28.5 GeV, production of 43≤A≤51 nuclides, reaction mechanisms 77−34301
Ag+p, 200 GeV, data anal. hydrodynamical model 79−551
Ag+p, 300 MeV, 450 MeV, 24 GeV, cross-section meas. 77−67740
Ag+p, 300 MeV, heavy fragment evaporation yields 79−6584
Ag+p, inelastic interactions, 6.0 GeV/c, in emulsions 78−86530
Ag+p, role of pick-up processes in prod. of fast t and ^{3}He 80−27632
^{A}Ag(p,n), A=107,109, 2.0-6.7 MeV, cross sections, Hauser-Feshbach optical calcs. for p absorption systematics 80−47483
^{107}Ag+p, 24 GeV/c, in nucl. emulsion, particle emission freq. variation 78−37335
^{107}Ag(p,αX), 20-45 MeV, α spectra, exciton model anal. 80−18306
^{107}Ag(p,α), 20 to 44 MeV, energy spectra and α-particle angular distrib. 79−49630
^{107}Ag(p,n)^{107}Cd, preequilib. emission of neutrons, ang. distrib. 78−62542
^{108}Ag+p, 70 GeV/c central collisions, s-particles ave. multiplicity 78−21567
^{109}Ag(p,n)^{109}Cd, ^{110}Cd, n spectra of isobaric analogue resonance decay *(Russian)* 78−89841
^{109}Ag(p,n)^{109}Cd, 6 and 7 MeV, neutron spectra meas. *(Russian)* 78−54764
Ag(p,^{3}He), 210-480 MeV, implications of statistical theories of fragmentation 78−82347
Ag(p,^{4}He), 210-480 MeV, implications of statistical theories of fragmentation 78−82347
Ag(p,X), X=N to Ar, 2.1 and 4.9 GeV, fragment energy spectra, Maxwellian functional form 78−70529
Ag(p,α)X, direct knockout model for fragmentation, (p,pα) predictions 80−18275
Ag(p,f), 1 GeV, binary fission, possible mass instability of correlated fragments 80−83133
Ag(p,f), 600 MeV, binary fission process 77−3060
Ag(p,f), 600 MeV, fragment energies, cross sections level density and barrier heights 80−42723
Ag(p,f), 600 MeV, mass yields in binary fission 78−8819
Ag(p,f), product event cross-sections at 14, 18, 23 GeV 77−10411
Ag(p, spallation), 300 GeV, radionuclide prod. cross sections, charge dispersions and mass yield curves 79−67735
Al+p, 200 GeV, data anal. hydrodynamical model 79−551
Al+p, 200 GeV, jet production 79−54438
Al+p, 200 GeV/c, relative yields of $\pi^{\pm}$, $K^{\pm}$, p, p̄ 78−93995
Al+p, 600 MeV, pion production, energy spectra, A depend. *(Russian)* 78−17213
Al+p, 7 GeV/c hadron multiple prod. *(Russian)* 79−22298
Al+p, 82-800 MeV, production of ^{7}Be, ^{22}Na, and ^{28}Mg 77−6388
Al+p, relative yields of K-mesons, p̄ and d̄ with 25 GeV/c momenta *(Russian)* 77−38277
Al+p, search for massive, long-lived, fractionally charged particles produced by 300-GeV protons 79−89311
Al+p→p, 640 MeV, proton inclusive spectra and ang. distrib. meas. 77−67751
^{27}Al, gas phase proton irradiation, condensation, isotopic anomalies generation 79−13289
^{27}Al+hp, 400 MeV, multinucleon removal in quasifree process, p-γ coincidence expt. 78−37342
^{27}Al+p, 1 GeV, neutron production *(Russian)* 79−85477
^{27}Al+p, 35-100 MeV, excitation function for ^{24}Na prod. 78−74356
^{27}Al+p, 62 MeV, complex particle emission, pre-equilibrium exciton model anal. 78−66280
^{27}Al+p, 660 MeV, H and He isotope prod. 77−18544
^{27}Al(p, 2p)^{26}Mg, average cross section for 6 to 15 MeV *(Japanese)* 77−57656
^{27}Al(p, α), 6.44 MeV, ^{28}Si resonance wave functions and differential cross sections 80−18261
^{27}Al(p, α)^{24}Mg, average cross section for 6 to 15 MeV *(Japanese)* 77−57656
^{27}Al(p, n), 6.44 MeV, ^{28}Si resonance wave functions and differential cross sections 80−18261
^{27}Al(p,X), 400 GeV, absorption cross sections and multiplicity distribs., A-depend. study 79−67748
^{27}Al(p,X), 90 MeV, charged light particle energy spectra exciton and evaporation model anal. 79−40923
^{27}Al(p,X), X=p,n,α, 6.44 MeV, ^{28}Si resonance wave functions from differential cross sections 80−78239
^{27}Al(p,α$_0$), automatic spark counting of α-tracks in plastic foils 77−79524
^{27}Al(p,α$_0$), E_p=887.8 keV, blocking lifetime meas. comparison 79−59041
^{27}Al(p,α$_0$)^{24}Mg, 1.12-3.08 MeV, ^{28}Si resonances 78−13091
^{27}Al(p,α$_0$)^{24}Mg, Al conc. as a function of depth in epitaxially grown Si layers on sapphire substrates 79−4328

proton-nucleus reactions continued

^{27}Al(p,α), ^{28}Si 4$^+$ state lifetime by blocking effect method *(Russian)* 80−91152
^{27}Al(p,α), 0.731 MeV, ^{28}Si 12.291 MeV level width, axial blocking meas. 80−63086
^{27}Al(p,α), 937 and 885 keV resonance lifetime meas. using crystal blocking technique 79−63671
^{27}Al(p,α)^{24}Mg, 1.35 to 1.46 MeV, test of detailed balance at isolated resonances and time reversibility 79−45260
^{27}Al(p,α)^{24}Mg, finite-range cluster-model description, DWBA approach 80−52667
^{27}Al(p,α)^{24}Mg, Q-value determ. 78−66205
^{27}Al(p,α)^{24}Mg resonance, nuclear lifetime meas. problems in single cryst. blocking expt. 77−47500
^{27}Al(p,α)X, direct knockout model for fragmentation, (p,pα) predictions 80−18275
^{27}Al(p,αx), 50 MeV, pre-equilib. alpha emission 78−70518
^{27}Al(p,γ)^{28}Si, 2.4-2.74 MeV, γ-spectra, isobaric analogue states 77−57646
^{27}Al(p,γ)^{28}Si, expt. γ-ray yield curves from H_2^+ and H_1^0 beams, material anal. 79−3530
^{27}Al(p,n), realistic complex nuclear matter t-matrix anal. Hamada-Johnston pot. 79−9564
^{27}Al(p,n)^{27}Si, cross sections and thermonuclear reaction rates 80−73852
^{27}Al(p,n)^{27}Si, threshold energy meas. 77−79375
^{27}Al(p,n)^{27}Si, threshold energy for accelerator calibration 79−36241
^{27}Al(p,n)^{27}Si, yield and (p,n) threshold meas., detector geometry effects 77−54221
^{27}Al(p,n)^{27}Si neutron yield meas. with sphere counter 77−23381
^{27}Al(p,pα), 600 MeV, α-cluster quasielastic knockout, expt. methods, separation energy spectra 79−13275
Al(p,X), 400 GeV, p backward prod. invariant cross section 79−93623
Al(p,X), 400 GeV/c, light ion backward prod., invariant cross section 80−32279
Al(p,X), 70 GeV/c, $\pi^\pm$, K$^\pm$, p and $\bar{p}$ relative yields *(Russian)* 79−40930
Al(p,X), X=He to Na, 2.1 and 4.9 GeV, fragment energy spectra, Maxwellian functional form 78−70529
Al(p,$\bar{p}\pi^-$), 10 GeV, $\bar{p}$ weak absorpt., $\bar{p}$ and π^- yields *(Russian)* 79−75987
Al(p,x), spallation by 300 GeV protons, activation cross section meas. rel. to ^{12}C(p,pn)^{11}C 79−40898
Al(p,xpX), x=1, 2, 640 MeV, energetic backward p emission, inclusive differential cross section 80−9290
A(p,Nd)B quasifree scatt. at backward angles, one-pion-exchange model description 79−80834
^{38}Ar(p,n), threshold meas., ^{38m}K β-end point energy determ. 78−46030
^{40}Ar, fission by 1 GeV protons, ang. distrib. of products *(Russian)* 77−46200
^{40}Ar(p,X), 1 GeV, deep inelastic interaction, reaction product angle and energy spectra *(Russian)* 79−75988
^{40}Ar(p,d), 35 MeV, DWBA anal., spectroscopic factors 78−17204
^{40}Ar(p,n), 8.3 meV, ^{40}K excitation energy, γ decay, of lowest T=2 state 78−8769
^{40}Ar(p,t), 52 MeV, ^{38}Ar levels, J$^\pi$ and transition strengths, DWBA anal. 80−47378
^{42}Ar(p,n)^{38}K^m threshold meas. using gaseous target 79−93619
^{75}As(p,2nγ), 17-28 MeV, ^{74}Se quasi-γ bands and negative parity levels 80−456
^{75}As(p,3n)^{73}Se, production yields, excitation curves 80−36131
^{73,74}As, yields in α, d and p interactions on Ge, Ga and As 77−54223
Au fragmentation, 200-800 MeV, excitation function for ^{24}Na prod. 77−38301
Au, proton-induced fission at 400 GeV, ternary to binary event ratio 78−13170
Au+p, 300 MeV, 450 MeV, 24 GeV, cross section meas. 77−67740
^{196}Au, fission, 1 GeV, cross section meas. *(Russian)* 78−94041
^{197}Au, 62 MeV, complex particle emission, pre-equilibrium exciton model anal. 78−66280
^{197}Au+p, 10-90 MeV, exciton model, pre-equilibrium decay calcs., excitation functions 77−82922
^{197}Au+p, 11.5, 300 GeV, formation cross sections for nuclides ^{22}Na to ^{196}Au 77−2999
^{197}Au(p,^{3}He x), 72 MeV, pre-equilibrium emission *(German)* 80−68657
^{197}Au(p,X), 0.2-6.0 GeV, product cross sections, mass yields, spallation products 80−83088
^{197}Au(p,X), 11.5 GeV, ^{24}Na fragment ang. and energy distribs., two-step model anal. 80−52678
^{197}Au(p,X), 20-48 MeV, proton total reaction cross section 79−80934
^{197}Au(p,X)^{149}Tb, target fragmentation momentum transfer, collective tube model, collectivity effects 80−37359
^{197}Au(p,αx), 72 MeV, pre-equilibrium α-emission 79−26440
^{197}Au(p,αx), 72 MeV, pre-equilibrium emission *(German)* 80−68657
^{197}Au(p,f), 1 GeV, fission fragment ang. correlation, kinematically different events search *(Russian)* 79−59103
^{197}Au(p,n), 11.2 MeV, spin cut-off parameters from neutron ang. distribs. *(Russian)* 79−80940
^{197}Au(p,n)^{197}Hg, preequilib. emission of neutrons, ang. distrib. 78−62542
^{197}Au(p,x), 197-800 MeV, ^{24}Na fragment emission excitation functions cascade-evaporation anal. 79−6553
^{197}Au(p,x) ^{22}Na-^{196}Au, 1-100 GeV radionuclide recoil props., fission, fragmentation and spallation 79−3149
^{197}Au(p,xn)$^{197-x}$Hg, excitation function meas., for ^{194}Hg half-life determ. 79−45214
Au(p,$\bar{p}\pi^-$), 10 GeV, $\bar{p}$ weak absorpt., $\bar{p}$ and π^- yields *(Russian)* 79−75987
B, 20 to 50 MeV, total reaction cross sections compared to opaque-nucleus model 78−33174
$\bar{p}$+P, A=10, 11, 660 MeV, H and He isotope prod. 77−18544
^{5}B(p,2α)α, possibility of thermonuclear fuel in relativistic plasma *(Russian)* 80−37573
^{A}B(p,X), A=10, 11, 740 MeV, ^{7}Be prod. cross section for cosmic ray anal. 79−93625
^{A}B(p,π^+), A=10,11, 200 MeV, pion energy spectra for discrete final states, cross sections 80−106057
^{10}B(p, π^+)^{11}B, 140 to 200 MeV, π^+ ang. distrib., energy depend. 79−63667
^{10}B(p,$\alpha_1\gamma$), 2.0-4.1 MeV, ^{11}C levels and resonance, γ-ray excitation curves 80−9280
^{10}B(p,p$_1\gamma$), 2.0-4.1 MeV, ^{11}C levels and resonance, γ-ray excitation curves 80−9280

proton-nucleus reactions continued

^{10}B(p,π^+), 320-605 MeV, cross sections, pion exchange model anal. 80−27676
^{10}B(p,π^+), differential cross sections, DWBA calc. 79−85415
^{10}B(p,π^+), near threshold, reaction energy dependence 79−85461
^{10}B(p,π^+)^{11}B, 163 to 186 MeV, expt. and theoretical study of π^+ prod. 79−59061
^{10}B(p,π), microscopic model anal., stripping model test for (d,p) 79−85436
^{11}B+p→^{4}He+^{8}Be→3(^{4}He) fusion power feasibility 77−38310
^{11}B+p→3 ^{4}He+6.8 MeV, calcs. of use in fusion reactor 77−83092
^{11}B(p, n)^{11}C, steel B depth distrib. meas. using time of flight method 80−71986
^{11}B(p,^{6}Li)^{6}Li, 51.9 MeV, five nucleon transfer mechanisms, DWBA calcs. 80−73845
^{11}B(p,2α)α, reaction characts., potentiality for controlled thermonuclear fusion 77−30667
^{11}B(p,3α), 35.4-1500 keV, resonance cross sections, astrophysical S-factor, fusion fuel 79−36213
^{11}B(p,3α), E$_p$=2 to 4 MeV, energy depend. of interference phenomena 78−13084
^{11}B(p,α)^{8}Be, continuous energy spectra of α-particles 77−30567
^{11}B(p,α)^{8}Be 6.0-18.0 MeV, isoscalar giant reson. 77−46152
^{11}B(p,$\alpha\alpha$)^{4}He, E$_p$>2.5 Mev, reaction mechanism 77−6362
^{11}B(p,$\alpha\alpha$)^{4}He, Q=8.68 MeV, quasi-free effect search 78−4947
^{11}B(p,n)^{11}C, 3-49 MeV, cross section, ang. distrib., ^{12}C level spin assignment 78−93996
^{11}B(p,n)^{11}C, analogue reaction at 16.3 to 26.5 MeV, polarisation transfer meas. 77−26735
^{11}B(p,n)^{11}C, B concentration profiling in solids by neutron TOF 79−51131
Ba(p,X)^{A}Xe (M=124-136), excitation functions, 38-600 MeV, lunar samples appl. 77−57661
Ba(p, t), 52 MeV, ^{A}Ba, A=132, 134, 136, negative parity states, J$^\pi$, transitions, DWBA anal. 80−86810
Be (p, X), 2.2, 6, 8.5 GeV, p and d inclusive spectra at 162° *(Russian)* 79−97710
Be, absolute neutron yield meas. for protons from threshold to 3 MeV 77−79498
Be+p, 12 GeV/c, direct e$^+$e$^-$ prod. 78−78221
Be+p, 150 GeV, inclusive muon pair prod. parameters, statistical interpretation 79−30820
Be+p, 200 GeV/c, relative yields of $\pi^\pm$, K$^\pm$, p, $\bar{p}$ 78−93995
Be+p, 400 GeV/c, dihadron prod., A depend. of prod. cross sections for massive dihadron states 78−33180
Be+p, 400 GeV/c, search for long-lived heavy particles, 4 to 10 GeV/c^2 78−78380
Be+p, 400 GeV/c, two hadron correlations at large transverse momenta 78−46060
Be+p, 7 GeV/c hadron multiple prod. *(Russian)* 79−22298
Be+p, direct muon prod. in 70, 50 and 35 GeV collisions 77−2872
Be+p, high mass symmetric hadron and pion pair prod., scaling props. 79−22291
Be+p, high transverse momentum scatt., two particle correlations and ϕ prod., jet trigger 78−78225
Be+p, relative yields of K-mesons, $\bar{p}$ and $\bar{d}$ with 25 GeV/c momenta *(Russian)* 77−38277
Be+p collisions 400 GeV, meas. of dihadron mass continuum and search for narrow resonances 78−33178
Be+p($\bar{p}$), 200 GeV/c, forward inclusive prod. spectra of K$_s$, Λ^0, $\bar{\Lambda}^0$, n, 200 GeV/c 78−82393
Be+p→Λ^0(K_S^0)($\bar{\Lambda}^0$)+X, neutral strange-particle prod. by 300 GeV protons 79−17905
Be+P→μ^++μ^-+anything, 400 GeV, high-mass dimuon continuum 78−37344
Be+p→p, 640 MeV, proton inclusive spectra and ang. distrib. meas. 77−67751
^{9}Be (p,π^+), 200 MeV polarised protons, differential cross sections, analysing power 78−78382
^{9}Be+p, 1 GeV, neutron production *(Russian)* 79−85477
^{9}Be+p, 660 MeV, H and He isotope prod. 77−18544
^{9}Be(p,^{3}H)^{7}Be, 75 MeV, continuous spectra phase space model anal. 79−76000
^{9}Be(p,^{3}He)^{7}Li, 75 MeV, continuous spectra phase space model anal. 79−76000
^{9}Be(p,α)^{6}Li, 30 MeV, continuous spectra phase space model anal. 79−76000
^{9}Be(p,α)^{6}Li, 30-75 MeV, obs. of ^{6}Li highly excited states 77−6244
^{9}Be(p,α)^{6}Li, 75 MeV, continuous spectra phase space model anal. 79−76000
^{9}Be(p,α)^{6}Li, appl. to Be concentration profiles determ. in Be implanted GaAs 79−4335
^{9}Be(p,α)^{6}Li, α ang. distrib. determ. by Doppler γ-line broadening method 77−61407
^{9}Be(p,α)^{6}Li, depth profiling Be in alloys in low energy reactions 79−5203
^{9}Be(p,α)X, direct knockout model for fragmentation, (p,pα) predictions 80−18275
^{9}Be(p,$\alpha\gamma$)^{6}Li, 2.56 MeV, ^{10}Be 8.89 MeV reson. J$^\pi$ 77−50098
^{9}Be(p,d^{3}He), DWIA anal., α-spectroscopic factors, quasifree process 77−79378
^{9}Be(p,d)^{8}Be, depth profiling Be in alloys in low energy reactions 79−5203
^{9}Be(p,n), 14-23 MeV, thick target neutron yields 77−57791
^{9}Be(p,n), 14.8-23 MeV, thick target neutron yields 77−26752
^{9}Be(p,n), cross sections and polarisation from Lane model anal., multichannel constraints 79−80914
^{9}Be(p,n) comparison of neutron spectra expt. obs. 79−59056
^{9}Be(p,pα), 100 MeV, absolute spectroscopic factors 77−30574
^{9}Be(p,pn), 47 MeV, excit. energy spectra, energy sharing spectra 77−50132
^{9}Be(p,pn)^{8}Be, 10-24 MeV, cross section, reaction mechanism, ^{9}Be level excitation 79−22284
^{9}Be(p,pn)^{8}Be$_{gs}$, ^{9}Be-^{9}B isobaric doublet asymmetric excitation 77−26678
^{9}Be(p,π^-)^{10}C, 613 MeV, residual nucleus excitation levels, cross section 78−78383
^{9}Be(p,π^+), 320-605 MeV, cross sections, pion exchange model anal. 80−27676
^{9}Be(p,π^+), 800 MeV, ^{10}Be, ^{10}C ang. distribs. to isobaric analogue states cross section ratio 79−89274
^{9}Be(p,π^-), 800 MeV, ang. distribs. 79−85463

proton-nucleus reactions continued
^{9}Be(p,π), 200 MeV, proton distortion and asymmetries 79−85464
Be(p,X), 200, 300, 400 GeV, hadron prod. at large p_T invariant cross section 79−40926
Be(p,X), 200, 300 GeV/c direct photon prod., η/π^0 and γ/π^0 prod. ratios 80−27618
Be(p,X), 400 GeV, p backward prod. invariant cross section 79−93623
Be(p,X) 400 GeV, search for new massive particles 78−89877
Be(p,X), 400 GeV/c, light ion backward prod., invariant cross section 80−32279
Be(p,X), 400 GeV/c, nucleon number depend. of inclusive dihadron prod. 79−49626
Be(p,X), 400 GeV/c, two particle quantum number corrections, p$\bar{p}$ and K^+K^- correlations 79−49625
Be(p,X) 70 GeV/c, $\pi^{\pm}$, $K^{\pm}$, p and $\bar{p}$ relative yields *(Russian)* 79−40930
Be(p,2π^-X), 28.5 GeV, fireball model comparison 79−59059
Be(p,h^+), 200 to 400 GeV, inclusive production of large-transverse-momentum hadrons and hadron pairs 79−89310
Be(p,n), 35 and 46 MeV, neutron spectra 80−524
Be(p,pπ^-), 10 GeV, $\bar{p}$ weak absorpt., $\bar{p}$ and π^- yields *(Russian)* 79−75987
Be(p,xpX), x=1, 2, 640 MeV, energetic backward p emission, inclusive differential cross section 80−9290
^{209}Bi, 62 MeV, complex particle emission, pre-equilibrium exciton model anal. 78−66280
^{209}Bi, fission, 1 GeV, cross section meas. *(Russian)* 78−94041
^{209}Bi+p, 39 MeV, intranuclear cascade model 78−33185
^{209}Bi+p, nucleon losses on high-energy fission *(Russian)* 78−46120
^{209}Bi(p,X), 90 MeV, charged light particle energy spectra exciton and evaporation model anal. 79−40923
^{209}Bi(p,X) *(Russian)* 79−80964
^{209}Bi(p,4n), simple formula for excitation functions 78−93978
^{209}Bi(p,n) pre-compound process, 18 to 64 MeV, cross sections, hybrid models anal. 79−3140
^{209}Bi(p,n)^{209}Po, preequilib. emission of neutrons, ang. distrib. 78−62542
^{209}Bi(p,p'(d)X), pol. p, 65 MeV, anal. powers of continuum energy spectra 80−68637
^{210}Bi^m(p,t), 18.4 MeV, ^{208}Bi two-particle, two-hole configuration, levels, J^{π} and excitation energies 80−32190
Br, break-up in relativistic proton collisions, ^{4}He emission 77−10410
Br, emulsion nuclei, 28 GeV proton interactions *(Korean)* 80−18299
Br+p, inelastic interactions, 6.0 GeV/c, in emulsions 78−86530
Br+p, role of pick-up processes in prod. of fast t and ^{3}He 80−27632
^{A}Br(p,pxn) A=79,80, 10 to 85 MeV, excitation function meas. 79−63673
^{A}Br(p,xn) A=79,80, 10 to 85 MeV, excitation function meas. 79−63673
^{79}Br+p, 24 GeV/c, in nucl. emulsion, particle emission freq. variation 78−37335
^{79}Br(p,3n)^{77}Kr excitation function meas. 79−88191
^{79}Br(p,3n)^{77}Kr→^{77}Br production excitation curves 79−85468
^{79}Br(p,3n)^{77}Kr→^{77}Br production, separation and radiopharmaceutical labelling 79−79649
^{79}Br(p,4n)^{75}Kr excitation function meas. 79−88191
^{79}Br(p,5n)^{75}Kr→^{75}Br excitation function meas. 79−88191
^{79}Br(p,nγ)^{79}Kr, low lying levels 80−105972
^{79}Br(p,p4n)^{75}Br excitation function meas. 79−88191
^{80}Br+p, 70 GeV/c, s-particles ave. multiplicity 78−21567
^{81}Br(p,d), 22.8 MeV, ^{80}Br level struct. and transitions, DWBA anal. spectroscopic factors 79−3084
^{81}Br(p,nγ), ^{81}Kr low lying levels from γ spectra, γ-γ coincidences 78−25195
^{81}Br(p,nγ), 1.8-5.5 MeV, ^{81}Kr levels, transitions and J^{π} assignments, first excited state lifetime 79−75849
Br(p,X), 400 GeV/c, multiplicity and ang. distribs. of relativistic and slow particles *(Russian)* 79−40931
Br(p,2nγ), 17-28 MeV, ^{78,80}Kr quasi-γ bands and negative parity levels 80−456
Br(p,xn)^{77}Kr, prep. of carrier free ^{77}Kr using natural Br 78−29678
^{11}Bu(p, α)$\alpha\alpha$, sputtering yield meas. *(Japanese)* 80−25513
C, 180° prod. of protons in high-energy reacts. 78−8816
C (p, X), 2.2, 6, 8.5 GeV, p and d inclusive spectra at 162° *(Russian)* 79−97710
C+p, 225 GeV/c, J/ψ and ψ'(3.7) prod. study using muon pair meas. 77−57694
C+p, 28.5 GeV, prompt dimuon prod., cross section, atomic number depend., mass distrib. 78−89858
C+p, 300 GeV, nuclear fragment prod., p:d:t ratio, ^{3,4}He abundances 78−70513
C+p, 50 to 275 GeV/c, inclusive particle prod., nuclear size depend. 77−46168
C+p, 52 MeV, spectral meas. of secondary neutrons and photons from thick targets 78−58282
C+p, 600 MeV, pion production, energy spectra, A depend. *(Russian)* 78−17213
C+p, 7 GeV/c hadron multiple prod. *(Russian)* 79−22298
C+p, inelastic interactions, 6.0 GeV/c, in emulsions 78−86530
C+p, massive muon pair prod., test of Drell Yan model 77−57695
C+p, props. of prompt muons prod. by 28 GeV protons 79−17906
^{A}C(p,π^+), A=12,13, 200 MeV, pion energy spectra for discrete final states, cross sections 80−106057
^{A}C(p,$\pi^{\pm}$), A=12,13, 200 MeV, analogue and nonanalogue state cross sections 80−99130
^{12}C, proton total cross section, 0.15 to 1 GeV, α-particle model and Glauber multiple scatt. theory 77−18538
^{12}C+p, 1 GeV, neutron production *(Russian)* 79−85477
^{12}C+p, 1 GeV, prod. of Li isotopes, meas. with online mass spectrometer *(Russian)* 77−10409
^{12}C+p, 40, 50, 150, 600 MeV, 25 GeV, ^{10,11}B prod., cosmic-ray propag. appl. 77−79380
^{12}C+p, 4.3 GeV/c, search for d knockout 79−6580
^{12}C+p, 50 MeV, three particle final state *(Russian)* 78−29471
^{12}C+p, 62 MeV, complex particle emission, pre-equilibrium exciton model anal. 78−66280
^{12}C+p, 660 MeV, H and He isotope prod. 77−18544
^{12}C+p, secondary proton momentum spectra, 4.3 to 8.9 GeV collisions *(Russian)* 79−3039
^{12}C+p(d)(α), transparency in composite particle-nucleus reactions 80−9273
^{12}C(p, 2p), 400 MeV, quasifree knockout cross sections 79−93614
^{12}C(p, pn), 400 MeV, quasifree knockout cross sections 79−93614
proton-nucleus reactions continued
^{12}C(p, spallation), Li, Be, B prod., 45-100 MeV, nucleosynthesis and space radiation effects implications 77−23053
^{12}C(p, X), 50 MeV, effective cross sections for charged particles in outgoing channel 80−18294
^{12}C(p,^{3}He)^{10}B, angular distrib. exam. at 51.9 MeV 77−30566
^{12}C(p,^{6}Li)^{7}Be, 36 to 56.8 MeV, differential cross section meas., reaction anal. 79−85467
^{12}C(p,^{6}Li)^{7}Be, 51.9 MeV, DWBA anal. of angular distribs. 78−46058
^{12}C(p,X), 4.2 GeV/c, multitudes of secondary negative particles, momentum distrib. ratios *(Russian)* 80−63178
^{12}C(p,X), 50 MeV, effective cross sections 80−78284
^{12}C(p,X), reaction and scatt. dynamics, optical and coupled channel anal. 80−78297
^{12}C(p,2p), 100 MeV, ^{11}B states, spectroscopic factors from DWBA anal. 80−5057
^{12}C(p,2p), 400 MeV, DWIA check using quasifree (p,pn) comparison 79−93621
^{12}C(p,2p), 45-50 MeV, distorted wave t-matrix anal. 78−50169
^{12}C(p,2p), asymmetric energy-sharing mode, half distorted-wave formalism, intermediate giant resonance 80−68656
^{12}C(p,2p)^{11}B, single nucleon form factor between deformed nuclear states 78−93999
^{12}C(p,3p), quasielastic ejection of proton pairs at 640 MeV *(Russian)* 79−59067
^{12}C(p,α), 45.2 MeV, cross sections, finite range DWBA anal., cluster form factors 80−68666
^{12}C(p,α) for energy calib. of 14UD Pelletron accelerator at ANU 78−17449
^{12}C(p,α)^{9}B, knockout mechanism 78−29474
^{12}C(p,α)^{9}B$_{gs}$, 45.2 MeV comparison to ^{12}C(p,α^*)^{9}B$_{gs}$ 79−6586
^{12}C(p,d^{3}He), DWIA anal., α-spectroscopic factors, quasifree process 77−79378
^{12}C(p,d), 4.3 GeV, deuteron knockout search *(Russian)* 79−3158
^{12}C(p,d) at 65 MeV, deuteron break-up effects 77−18535
^{12}C(p,d)^{11}C, 185 MeV, one- and two-step processes 77−38282
^{12}C(p,d)^{11}C, 700 MeV, transitions confirm multistep processes 78−46110
^{12}C(p,n), 144 MeV, charge exchange, one pion exchange and PCAC tests 80−78299
^{12}C(p,n), 144 MeV, one pion exchange and PCAC expt. test 80−528
^{12}C(p,n), 62, 120 MeV, isobaric analogue states, differential cross sections 80−18202
^{12}C(p,n)^{12}N, test of Monte Carlo efficiency calcs. for scintillation counters 80−37713
^{12}C(p,p') proton polarisation and natural parity level excitations *(Russian)* 80−5144
^{12}C(p,p')X, 316, 516 MeV, analysing powers at backward angles 78−46062
^{12}C(p,pα), 100 MeV, absolute spectroscopic factors 77−30574
^{12}C(p,pα), 600 MeV, α-cluster quasielastic knockout, expt. methods, separation energy spectra 79−13275
^{12}C(p,pα)^{8}Be, DWIA calc. 77−34273
^{12}C(p,pd), ^{12}C(p,pt), ^{12}C(p,p^{3}He), 75 MeV, expt. setup, DWIA anal. 77−322
^{12}C(p,pd), (p,pt), (p,pα), spectroscopic data on quasielastic ejection on nucleon clusters from 1p shell nuclei 79−80931
^{12}C(p,pd)^{10}B, energy level determ. of ^{10}B at 58 MeV 79−6578
^{12}C(p,pd)^{10}B, quasi-elastic cluster knock out, cross section calc. 78−46042
^{12}C(p,pn), pol. nucleon quasi-elastic scatt., nuclear wave function and model tests 80−42656
^{12}C(p,pt)^{9}B, quasi-elastic cluster knock out, cross section calc. 78−46042
^{12}C(p,px), x=d,t, ^{3}He, 75 MeV, spectroscopic factors, cluster model, DWIA 77−54214
^{12}C(p,π^-)^{13}O, 613 MeV, residual nucleus excitation levels, cross section 78−78383
^{12}C(p,π^+), 185 MeV, relativistic PWIA 77−10394
^{12}C(p,π^+), 200 MeV polarised protons, differential cross sections, analysing power 78−78382
^{12}C(p,π^+), optical model orthogonality constraints for bound and continuum waves 79−89306
^{12}C(p,π^+)^{13}C, 185 MeV, DWBA with Kisslinger type optical pot. 78−4938
^{12}C(p,π^+)^{13}C, π distortion effect on asymmetry, polarised protons 78−50176
^{12}C(p,π^+)^{13}C, relativistic stripping model in plane wave impulse approx. 77−325
^{12}C(p,π^+)^{13}C, relativistic pion stripping formalism 78−41717
^{12}C(p,t) 80 MeV, ^{10}C low lying level ang. distribs., zero range DWBA anal. 79−67656
^{12}C(p,t)^{10}C, angular distrib. exam. at 51.9 MeV 77−30566
^{13}C(p,α)^{10}B$_{g.s.}$, 65 MeV, pol. p, DWBA form factor 80−52559
^{13}C(p,d), 200, 500 MeV, differential cross section scaling, reaction mechanism 80−42625
^{13}C(p,d), 800 MeV, cross sections, DWBA anal. 80−42667
^{13}C(p,d) modified DWBA anal., optical model parameter influence on vertex consts. *(Russian)* 78−78340
^{13}C(p,π^-), 185 MeV, differential cross section, two-nucleon model *(Chinese)* 79−59069
^{14}C(p,n), 35 MeV, ^{14}N 1$^+$ state cross sections, effective two nucleon interaction, isovector tensor component 80−18208
^{14}C(p,n)^{14}N, n polarisation ang. distrib., R-matrix anal., ^{15}N excited states 78−4937
^{14}C(p,t), 27.6 MeV, ^{12}C lowest T=2 state, excitation energy 78−66211
^{A}Ca+p, A=40, 44, 48, 700 MeV, total reaction cross section meas., matter radii 79−40924
^{A}Ca+p, A=40,44, 1 GeV, neutron production *(Russian)* 79−85477
^{A}Ca(p,α)k, A=40, 42, 35 MeV, ^{37}L (sd)$^{-3}$ g.s band investigation 79−6587
^{A}Ca(p,p), 800 MeV, polarised p, A=40, 42, 44, 48, differential cross sections and anal. powers 79−36244
^{40}Ca (p,2p), polarised p, 200 MeV, quasi-elastic scatt., asymmetry meas. 79−67755
^{40}Ca (p,pα), 157 MeV, quasifree scatt., α spectroscopic factors, SU(3) predictions 77−6370
^{40}Ca+P, 100-1050 MeV, optical pot. real part, nuclear matter approach 77−82890
^{40}Ca+p, energy dependent radial functions formalism of continuum shell model 78−25185
^{40}Ca+p(d)(α) transparency in composite particle-nucleus reactions 80−9273

proton-nucleus reactions continued

^{40}Ca(p, 2p)^{39}K, 148.2 MeV, factorisation approx., energy states of ^{39}K, DWIA calcs. 78−62535
^{40}Ca(p, π^+)^{41}Ca, 140 to 200 MeV, π^+ ang. distrib., energy depend. 79−63667
^{40}Ca(p, ^{17}Ne^{22}Na^{28}Al), 40-85 MeV, ^{24}Na yields in 'fission-like' reactions 78−598
^{40}Ca(p,^{3}He), 42.5 MeV, ^{38}K low lying 1^+, T=0 states, DWBA anal. 80−470
^{40}Ca(p,X), multiple scattering theory, validity of closure approx. 79−45269
^{40}Ca(p,2p+n)^{39}K, partial-body Ca determ. in body by proton activation anal. 77−86605
^{40}Ca(p,2p), 200 MeV, cross section and asymmetry meas. 79−6583
^{40}Ca(p,2p) 200 MeV polarised p, spin-orbit effects 79−89222
^{40}Ca(p,2pn)^{38}K, prod. of uniform ^{38}K yield using range modulator 77−40735
^{40}Ca(p,2pn)^{38}K, total cross section, 20-160 MeV 78−86536
^{40}Ca(p,α), polarised p, 22.0 MeV, analysing power J dependence 79−67740
^{40}Ca(p,nπ^+), ≃500 MeV, NNπ vertex function 79−59066
^{40}Ca(p,pα), 600 MeV, α-cluster quasielastic knockout, expt. methods, separation energy spectra 79−13275
^{40}Ca(p,pα)^{36}Ar, 157 MeV, energy spectra, SU(3) model comparison 77−88121
^{40}Ca(p,π^+), 163 to 186 MeV, expt. and theoretical study of π^+ prod. 79−59061
^{40}Ca(p,π^+), differential cross sections, DWBA calc. 79−85415
^{40}Ca(p,π^+), near threshold, reaction energy dependence 79−85461
^{40}Ca(p,π^+)^{41}Ca, relativistic pion stripping formalism 78−41717
^{40}Ca(p,t)^{38}Ca 51.9 MeV and configuration mixing 77−26684
^{42}Ca(p,d), form factors, Pauli principle *(Russian)* 77−6393
^{42}Ca(p,t) form factor, hole and continuum contribs. for pick-up reactions 80−78256
^{44}Ca(p,α)^{41}K l-forbidden M1 decay from 1st excited state 78−13024
^{44}Ca(p,n)^{44}Sc, 4.49-7.57 MeV, cross sections 79−85470
^{44}Ca(p,n)^{44}Sc, reaction rates in stars 80−82183
^{44}Ca(p,p'γ), inelastic proton amplitudes for fragmented analogue state in ^{45}Sc 79−17882
^{45}Ca(p, n)^{45}Sc, 0.95-2.7 MeV, cross sections and thermonuclear reaction rates, Hauser-Feshbach calcs. 79−36239
^{48}Ca(p,αn), 18-45 MeV, ^{44}K excited levels, J^π, transitions and lifetimes 80−68544
^{48}Ca(p,n), 160 MeV, ^{48}Sc spin-flip isovector giant resonance, $T_>$ Gamow-Teller strength 80−106019
^{48}Ca(p,n), nucleon optical potential from Lane model 80−83097
^{48}Ca(p,n)^{48}Sc, 0.76-2.20 MeV, absolute cross sections and yields, statistical model anal. 79−26432
^{48}Ca(p,nx), 45 MeV, preequilib. ang. distrib., generalised exciton model 77−10407
^{48}Ca(p,t), 40, 20 MeV, two step (p,d)(d,t) process, second order DWBA 78−66276
^{48}Ca(p,t), (p,^{3}He)(^{3}He,t) two step process calcs., two step cross section 79−36245
^{48}Ca(p,t)^{46}Ca, 20, 40 MeV, finite-range effect in (p,d)(d,t) process 78−74365
^{48}Ca(p,t)^{46}Ca two-step (p-d-t) process anal. 78−62534
^{48}Ca(p,t)^{46}Ca(0$^+$,g.s.), 20 and 40 MeV, two step process, deuteron break-up effect 80−73844
Ca(p,α), 40 MeV, ^{A}K, A=37,39, levels, excitation and microscopic form factors, DWBA calcs. 80−32185
Cd+p, 7 GeV/c hadron multiple prod. *(Russian)* 79−22298
^{A}Cd(p,t), A=106, 104, at high excitation, observation of hole states 78−25187
^{106}Cd(p,t)^{104}Cd, 42 MeV, hole states at high excitation 78−50158
^{110}Cd(p,n)^{110m,g}In, anal. of isomer ratios in preequilibrium statistical model 77−6361
^{111}Cd(p,nγ)^{111}In, E_p=6 MeV, γ-ray spectra and ^{111}In level scheme 78−13083
^{111}Cd(p,nγ)^{111}In, internal conversion electron spectra, rotational band detect. in ^{111}In 79−6362
^{112}Cd(p,α)^{109}Ag, 22 MeV, analysing power, J-depend., DWBA 78−70523
^{112}Cd(p,n)^{112m,g}In, anal. of isomer ratios in preequilibrium statistical model 77−6361
^{112}Cd(p,n)^{112}In, $0_1^+ \rightarrow 0^+$ elec. monopole transition in low-lying ^{112}Cd levels prod. in ^{112}I decay 79−54406
^{112}Cd(p,nγ), ^{112}In low lying levels, transitions, $T_{1/2}$, multipolarities and mixing ratios 80−68545
^{113}Cd(p,n), 11.2 MeV, spin cut-off parameters from neutron ang. distribs. *(Russian)* 79−80940
Cd(p,nγ), ^{111,113}In energy levels, spins, lifetimes, Hauser-Feshbach anal. 77−320
Cd(p,t), 11-15 MeV, ^{A}Cd, A=104-116, low lying level scheme, mass excess 80−73807
^{140}Ce(p,X), 17.5-48 MeV, proton total cross section 78−8809
^{140}Ce(p,2n), ^{139}Pr medium spin states, J^π, transitions and shape 80−86779
^{140}Ce(p,2nγ), 20 MeV, ^{139}Pr isomeric $11/2^-$ state, half-life, g-factor, and nuclear orientation relaxation 79−75837
^{140}Ce(p,n), ^{140}Pr isobaric analogue resonances, de-excitation cascade, K-shell ionisation, spin depend. 80−78202
Ce(p,t), 30 MeV, DWBA, ^{138,140}Ce levels, spin, parity, enhancement factors 77−54217
^{A}Cl+p, A=35, 37 below 52 MeV, cross sections, excitation functions 78−89864
^{35}Cl(p,n)^{35}Ar, threshold energy, reln. to vanishing Cabibbo angle 78−50167
^{35}Cl(p,n)^{35}Ar threshold energy, ^{35}Ar→^{35}Cl β-decay endpoint energy 77−74807
^{36}Cl prod. in proton induced high-energy spallation, cosmic ray effects 77−61421
Co, absolute neutron yield meas. for protons from threshold to 3 MeV 77−79498
^{59}Co(p,X), 12-45 MeV, reaction cross section and hybrid model analysis 79−67749
^{59}Co(p,d), 50 MeV, fine struct. of ground hole-state analogues 78−50065
^{59}Co(p,d), fragmentation of hole-state analogues in ^{58}Co 78−54731
Co(p,^{3}He x), 72 MeV, pre-equilibrium emission *(German)* 80−68657

proton-nucleus reactions continued

Co(p,X), 10-60 MeV, long lived radioisotope prod. cross sections and excitation functions 79−89305
Co(p,αx), 72 MeV, pre-equilibrium emission *(German)* 80−68657
C(p,X) *(Russian)* 80−52649
C(p,X), 400 GeV, p backward prod. invariant cross section 79−93623
C(p,X), 400 GeV/c, light ion backward prod., invariant cross section 80−32279
C(p,X), 400 GeV/c, multiplicity and ang. distribs. of relativistic and slow particles *(Russian)* 79−40931
C(p,X), 4.2 GeV/N, multiple π^- proc., mean multiplicity *(Russian)* 80−27647
C(p,X), 740 MeV, ^{7}Be prod. cross section for cosmic ray anal. 79−93625
C(p,X) X=He to C, 2.1 and 4.9 GeV, fragment energy spectra, Maxwellian functional form 78−70529
C(p,3p), 640 MeV, proton pair quasifree knock-out 80−22795
C(p,π), 600 MeV, backward π^+ prod., momentum depend., scaling, Monte Carlo calcs. 79−13305
C(p,π^+) 240 MeV inclusive pion production *(Russian)* 80−86908
C(p,π^+), 400-500 MeV, cross-sections meas. 77−10392
C(p,xpX), x=1, 2, 640 MeV, energetic backward p emission, inclusive differential cross section 80−9290
^{A}Cr(p,n), 11.2 MeV, A=52, 53, 54, spin cut-off parameters from neutron ang. distribs. *(Russian)* 79−80940
^{50}Cr(p,d), 55 MeV, ^{49}Cr ground analogue state fine struct., l=3 states differential cross section 80−63152
^{53}Cr(p,α), 35 MeV, ^{49}V proton hole, analogue and high spin states, distorted wave anal. 79−9482
^{53}Cr(p,nγ), 6.3-7.3 MeV, populating ^{52}Mn low-lying levels 77−14028
^{54}Cr(p,γ), 1.0-3.8 MeV, γ-yields, cross sections, predicted (p,n) cross section, Stat. anal. 80−5136
^{133}Cs(p,pxn), 550 MeV cross-sections meas. and Monte Carlo calcs. 77−41969
^{133}Cs(p,xn) 550 MeV, cross-sections meas. and Monte Carlo calcs. 77−41969
^{137}Cs, 10 GeV proton spallation for transmutation of radioactive waste, calc. of transmutation number 80−13470
Cu (p, X), 2.2, 6, 8.5 GeV, p and d inclusive spectra at 162° *(Russian)* 79−97710
Cu (p,π^-) 240 MeV inclusive pion production *(Russian)* 80−86908
Cu, absolute neutron yield meas. for protons from threshold to 3 MeV 77−79498
Cu spallation by 28 GeV protons, mass yields 77−6435
Cu+p, 1 GeV, neutron production *(Russian)* 79−85477
Cu+p, 1.2-4.6 MeV, (p,n) thresholds and radiative capture, A=63, 65 78−89856
Cu+p, 300, 400 GeV, prod. of massive μ pairs 77−6379
Cu+p, 400 GeV, charm prod. cross section and particle lifetimes, Monte Carlo anal. 78−89679
Cu+p, 400 GeV, dimuon and trimuon prod., prompt ν source, D$\bar{D}$ prod., axions 78−89860
Cu+p, 400 GeV, prompt ν prod., axion prod. upper limit 78−89859
Cu+p, 52 MeV, spectral meas. of secondary neutrons and photons from thick targets 78−58282
Cu+p, 600 MeV, pion production, energy spectra, A depend. *(Russian)* 78−17213
Cu+p, 7 GeV/c hadron multiple prod. *(Russian)* 79−22298
Cu+p, dimuon prod., struct. in Υ region near 9.5 GeV 78−17201
Cu+p, direct muon prod. in 70, 50 and 35 GeV collisions 77−2872
Cu+p, relative yields of K-mesons, $\bar{p}$ and d with 25 GeV/c momenta *(Russian)* 77−38277
Cu+p collisions, 400 GeV, prompt ν prod. 78−46061
Cu+p→Δ^0(K_S^0)($\bar{\Lambda}^0$)+X, neutral strange-particle prod. by 300 GeV protons 79−17905
Cu+p→$\mu^+\mu^-$+anything, 400 GeV, high-mass dimuon continuum 78−37344
Cu+p→p, 640 MeV, proton inclusive spectra and ang. distrib. meas. 77−67751
^{63}Cu(p, 2nγ), 22-31 MeV, in beam gamma spectroscopy of ^{62}Zn 77−6297
^{63}Cu(p,nγ), 6 MeV, ^{63}Zn level scheme, spin and parity assignments 79−465
^{63}Cu(p,p3n)^{60}Cu, 30-47 MeV, cross-section meas. 78−13090
^{63}Cu(p,pnγ), 22-28 MeV, ^{62}Cu high spin states, level scheme *(French)* 78−21496
^{64}Cu(p,X), 400 GeV, absorption cross sections and multiplicity distribs., A-depend. study 79−67748
^{65}Cu(p,α_0)^{62}Ni, 1.1-3.6 MeV, Wigner cusps 78−41719
^{65}Cu(p,n), cross sections and spectra, exciton model *(Russian)* 78−21536
^{65}Cu(p,nγ), 3.4-4.0 MeV, ^{65}Zn lifetimes 77−74804
Cu(p,X), 400 GeV, p backward prod. invariant cross section 79−93623
Cu(p,X), 400 GeV/c, light ion backward prod., invariant cross section 80−32279
Cu(p,X), 70 GeV/c, $\pi^\pm$, $K^\pm$, p and $\bar{p}$ relative yields *(Russian)* 79−40930
Cu(p,$\bar{p}\pi^-$), 10 GeV, $\bar{p}$ weak absorpt., $\bar{p}$ and π^- yields *(Russian)* 79−75987
Cu(p,π), 0.7-8 GeV, scaling and nonscaling of inclusive π prod. 79−22296
Cu(p,π^+), 400-500 MeV, cross-sections meas. 77−10392
Cu(p, spallation), 200, 350 MeV, radioactive residual nuclei prod. cross sections at (3,3) resonance 79−3130
Cu(p, spallation), 28 GeV, mean kinetic props., momentum transfer, target recoil props. 79−3129
Cu(p,xpX), x=1, 2, 640 MeV, energetic backward p emission, inclusive differential cross section 80−9290
D(p,π^-)T, 410, 605, 809 MeV, pion angular distrib. 78−29466
^{158}Dy (p,t), 29.9 MeV, possible two-phonon $\beta\gamma$ vibr. 77−14018
^{158}Dy(p,t)^{156}Dy, 29.9 MeV, populating levels below 2.3 MeV, collective struct. 77−74747
^{160}Dy(p,3n)^{158}Ho, isomeric state and rotational band in ^{158}Ho 77−2890
^{162}Dy(p, α), statistical direct reaction model calc. 79−80913
^{A}Er(p, α), A=166.168, statistical direct reaction model calc. 79−80913
^{151}Eu(p,pxn), x=2-5 up to Ep=52 MeV, excitation functions 77−38261
^{151}Eu(p,xn), x=1,3-6, up to Ep=52 MeV, excitation functions 77−38261
^{153}Eu(p,xn), x=1,3,5 up to Ep=52 MeV, excitation functions 77−38261
^{19}F+p, 1 GeV, neutron production *(Russian)* 79−85477
^{19}F(p, α)^{16}O, 12.4 to 18.0 MeV, exit channel effects 77−14124

proton-nucleus reactions continued
^{19}F(p,α) pol. p, ^{20}Ne 13482 keV level, parity violating effects in two resonance interference 80−83033
^{19}F(p,α)^{16}O, ^{20}Ne quartet states 80−105973
^{19}F(p,α)^{16}O, 1.5 to 2 MeV, [211] quartet state in ^{20}Ne 78−46006
^{19}F(p,αγ), analytic appl. of protons from 3 MV Dynamitron accelerator 77−81453
^{19}F(p,αγ), determ. of F conc. profiles in Mg alloy scales 78−88678
^{19}F(p,αγ), determ. of F density distrib. in human enamel 77−56292
^{19}F(p,αγ)^{16}O, 872 keV resonance, appl. of H molecular ion beams 79−36452
^{19}F(p,αγ)^{16}O, F conc. profiles determ. in corroded MAGNOX fuel canning materials 79−92035
^{19}F(p,αγ)^{16}O, intense proton beam current meas. 78−93784
^{19}F(p,αγ)^{16}O, reson. reaction, teaching expt. using Van de Graaff generator 77−74178
^{19}F(p,d), 19.3 MeV, ^{18}F levels, J$^{\pi}$ and ang. distribs. DWBA anal. 80−42545
^{19}F(p,p′γ)^{19}F, determination of fluorine in food samples 79−5218
Fe, proton bombardment, stable nuclide form. and separation 78−20045
Fe+p, 28.5 GeV, prompt dimuon prod., cross section, atomic number depend., mass distrib. 78−89858
Fe+p, 400 GeV, missing energy associated with $\mu^+\mu^-$ prod. 80−22833
Fe+p, 52 MeV, spectral meas. of secondary neutrons and photons from thick targets 78−58282
Fe+p, high energy spallation, prod. cross sections of stable, long-lived nuclides 77−2998
Fe+p, props. of prompt muons prod. by 28 GeV protons 79−17906
Fe+p inclusive react., structure function of conserved hadrons, 100-1600 GeV *(Russian)* 78−41611
Fe+p→$\mu^+\mu^-$+anything, enhancement in μ pair mass spectrum at 9.5 GeV, Υ prod. 79−432
^{A}Fe(p,X), A=54, 56, 57, 58, 12-45 MeV, reaction cross section and hybrid model analysis 79−67749
^{A}Fe(p,n), 11.2 MeV, A=56, 57, spin cut-off parameters from neutron ang. distribs. *(Russian)* 79−80940
^{19}Fe(p,α$_0$)^{16}O, 1.5 to 3.8 MeV, Hauser-Feshbach anal., level density of ^{20}Ne *(Spanish)* 77−30562
^{54}Fe+p, 62 MeV, complex particle emission, pre-equilibrium exciton model anal. 78−66280
^{54}Fe(P, α)^{51}Mn, 21 MeV analogue state, excitation 80−13471
^{54}Fe(p,α)^{51}Mn, 9 to 13 MeV, γ-ray spectroscopy study of ^{51}Mn structure 77−18471
^{54}Fe(p,α)^{51}Mn, multi-step-direct-reaction anal. 78−8818
^{54}Fe(p,d)^{53}Fe, 40 MeV spectroscopic factors, ang. distrib., DWBA anal. 79−22287
^{54}Fe(p,p′), cross sections and spectra, exciton model *(Russian)* 78−21536
^{54}Fe(p,t), 45 MeV, ^{52}Fe levels, ang. distrib., spin, parity, $f_{7/2}$ shell model 78−74362
^{54}Fe(p,t), 80 MeV, ^{52}Fe, low lying level ang. distribs., zero range DWBA anal. 79−67656
^{54}Fe(p,t)^{52}Fe, 52 MeV, ^{52}Fe levels, J$^{\pi}$ 77−50058
^{54}Fe(ρ,α)^{51}Mn, 35 MeV, nuclear struct. study 79−75980
^{56}Fe+p, 39 MeV, intranuclear cascade model 78−33185
^{56}Fe(p,2n)^{55}Co carrier-free positron-emitting label for bleomycin 79−79648
^{56}Fe(p,α), 34 MeV, ^{53}Mn low lying states, DWBA anal., shell model wave functions 80−32211
^{56}Fe(p,n)^{56}Co in steel surface, wear loss from activity loss meas. 77−4881
^{56}Fe(ρ,α)^{53}Mn, 35 MeV, nuclear struct. study 79−75980
^{57}Fe(p,p′)^{57}Fe*, excited 5/2$^-$ state mag. moment 79−93512
^{58}Fe(p,n) 20.2 MeV, ^{58}Co 1$^+$ level population, shell model calcs., (t,^{3}He) and (e,e′) comparison 79−9481
Fe(p,X), 10-60 MeV, long lived radioisotope prod. cross sections and excitation functions 79−89305
F(p, α), (p, α γ), microanal. of F depth profile 80−45607
^{69}Ga(p,nγ) 3-5.6 MeV, ^{69}Ge excited states, spin and γ-decay, parity state struct. 79−464
^{159}Gd(p,n)^{158}Tb, 7.4 MeV, equilib. and nonequilib. contribs. 78−21565
Gd(p,α), 17 MeV, ^{153,155}Eu single proton hole states in pickup reactions 80−78128
Gd(p,α)^{153,155}Eu, 17 MeV, direct and sequential reaction mechs., (t,α) comparison 79−540
Ge, 15 GeV/*c* pions, nucl. interactions under random and channelling conditions in single crystals 79−13348
^{70}Ge(p,t), 26 MeV, t spectra, ang. distribs., ^{68}Ge energy levels, spin, parity 77−54216
^{72}Ge(p,γ)^{73}As, 2213 keV energy levels of ^{73}As meas. 78−93939
^{72}Ge(p,nγ), 5.0-6.3 MeV, ^{72}As level scheme determ. 77−14032
^{76}Ge(p,nγ), ^{76}As level structure 80−47379
^{76}Ge(p,nγ), 1.8-2.7 MeV, ^{76}As excited states, excitation functions and decays ang. distribs., cross sections *(Russian)* 80−63089
Ge(p,nγ), 6.5-14 MeV, ^{A}As, A=70, 72, level scheme, transitions, J$^{\pi}$ and lifetimes 80−22695
Ge(p,t), ^{A}Ge A=68,70,72,74, deformations and collective spectra, reaction mechanisms 79−22168
Ge(p,t), 26 MeV, ^{70,72,74}Ge excited states, spins, parities 78−25194
Ge(p,t), shape transition obs. 78−25190
Ge(p,xnγ), 25 MeV, ^{A}As, A=71, 73, levels, J$^{\pi}$, transitions, T1/2 80−57684
H+p, 200 GeV, data anal. hydrodynamical model 79−551
H+p, 200 GeV, jet production 79−54438
H+stopped p̄ meas. on bound NN̄ systems 79−68336
^{1}H(^{15}N,αγ), for H detection in metals 80−55767
^{1}H(p,e$^+$)^{1}H, bounds on rate, impulse approx. 77−3000
^{1}H(p,pπ$^+$)n, 800 MeV, Δ^{++} prod. and cross sections 79−22294
^{1}H(p,π$^+$)^{2}H, Low eqn. approx. soln., field theory propagator modification 79−85546
^{1}H(p,π$^+$)^{2}H, NN pot., isobar configurations and π prod., inelastic cross sections 79−63666
^{1}H(p,π$^+$)^{2}H, pol. p, total cross section, ang. distribs. and asymmetry parameters 80−63182
^{1}H(p,π$^+$)^{2}H, SIS, 578 MeV, pol. beam and target, spin depend. parameters 80−42651
^{1}H(p,π$^+$)pn, polarised p, 305, 330 MeV, pion production differential cross section 79−67754
^{2}H breakup, 156 MeV protons NN multiple scatt. anal. 77−18546
^{2}H breakup, 45 MeV proton induced, np final state interaction ang. distrib. 77−18552
proton-nucleus reactions continued
^{2}H breakup induced by 12.5 MeV protons, Ebenhoh code anal. 77−18547
^{2}H breakup induced by 8.5 MeV protons, Faddeev calcs. 77−18548
^{2}H breakup using 156 MeV protons, test for special kinematic conditions 77−18551
^{2}H disintegration, energies up to 50 MeV *(Russian)* 78−89848
^{2}H+p, 200, 300, 400 GeV, hadron prod. at large p_T invariant cross section 79−40926
^{2}H(d,n)^{3}He, 12.3 MeV, neutron spectra normalisation, differential cross-section meas. 77−88106
^{2}H(p, 2p), 400 MeV, quasifree knockout cross sections 79−93614
^{2}H(p, dπ$^+$)n, 585 MeV, d momentum spectra 78−41718
^{2}H(p, n), 50 MeV, neutron polarisation meas. 78−70726
^{2}H(p, pn), 400 MeV, quasifree knockout cross sections 79−93614
^{2}H(p, pn)n, 8.5 MeV, ang. distrib. of final state interaction 78−54751
^{2}H(p,Nπ)^{2}H, Deck model anal. 77−22757
^{2}H(p,2n)n, 50 MeV, expt. and theoretical cross sections 79−75994
^{2}H(p,2p), 156 MeV, kinematic collinearity condition 77−30547
^{2}H(p,2p), 156 MeV d$^3\sigma$ and d$^4\sigma$ spectra for collinear nucleon system 78−17175
^{2}H(p,2p)n, 13.25 MeV, meas. of total breakup cross-section 77−18555
^{2}H(p,2p)n, 15 MeV, polarised p, cross section in non-coplanar geometry 78−93997
^{2}H(p,2p)n, 20 MeV, cf. Faddeev eqn. calcs. 77−18549
^{2}H(p,2p)n, 22.7 MeV, proton analysing power 80−78302
^{2}H(p,2p)n, 23, 39.5 MeV, noncoplanar reaction, breakup cross section 80−530
^{2}H(p,2p)n, 28.5 MeV, collinearity effect 79−75995
^{2}H(p,2p)n, 28.6 MeV, breakup cross sections in collinear geometry 80−9296
^{2}H(p,2p)n, 45 MeV, sensitivity to various separable S-wave NN potentials 77−313
^{2}H(p,2p)n, 585, 800 Mev, n-p final state interactions 77−41965
^{2}H(p,2p)n, 8.5 MeV, n-p final state interaction, cross section, ang. distrib. 78−21560
^{2}H(p,2p)n, high energy, final state np interaction 77−18533
^{2}H(p,2p)n, interference effects for const. NN relative energies 77−26774
^{2}H(p,dπ$^+$), 800 MeV, pion prod. with spectator neutron, cross section 80−9294
^{2}H(p,γ) and ^{3}He(γ,pd) anal. using Reid soft-core pot. 77−26664
^{2}H(p,n)2p, pol. n and p, 10.6-15.1 MeV, transverse polarisation transfer at 0° 80−42630
^{2}H(p,np)^{1}H, 1.825 GeV/c anal., Glauber theory comparison 77−71525
^{2}H(p,nπ$^+$), 585 MeV, differential cross sections, reaction mechanisms 79−548
^{2}H(p,nπ)^{2}H, 800 MEV, cross-section meas. 77−6358
^{2}H(p,pX), 19 GeV/c, Thomas Reiche Kuhn sum rule appl., mean energy losses 80−91192
^{2}H(p,p) cross section, d wave function with spin at light front *(Russian)* 79−85478
^{2}H(p,p)^{3}He, four-body problem calc. 78−516
^{2}H(p,p)pn, polarised p, vector anal. power in final state interaction region 79−71836
^{2}H(p,pn), 156 MeV, kinematic collinearity condition 77−30547
^{2}H(p,pn), 156 MeV d$^3\sigma$ and d$^4\sigma$ spectra for collinear nucleon system 78−17175
^{2}H(p,pn), 47 MeV, excit. energy spectra, energy sharing spectra 77−50132
^{2}H(p,pn)^{1}H, 1 GeV, final-state interactions 77−82900
^{2}H(p,pn)^{1}H, 12.5 MeV, angular distrib. of p-n final state interaction 80−52672
^{2}H(p,pn)^{1}H in relativistic description of moving composite particles 77−46156
^{2}H(p,pn)p, 15 to 156 MeV, attenuation of quasifree scatt., empirical rules 77−61415
^{2}H(p,pn)p, 1.67 GeV/c, secondary particle ang. distribs. and correlations *(Russian)* 80−27646
^{2}H(p,pp)n, 50 MeV, pp coincidence meas. 77−18556
^{2}H(p,pp)n, polarised p, polarisation effects in 3-body system 79−80946
^{2}H(p,π$^+$)^{3}He, 377, 462, 576 MeV, possible forward peak in cross section 78−89874
^{2}H(p,π^0)^{3}He, (p,π$^+$)^{3}H, 250-800 MeV, distorted-wave impulse-approx. calc. 77−82932
^{2}H(p,π$^+$), 400, 470, 600 MeV, microscopic model calcs., reaction cross section 79−40916
^{2}H(p,π$^+$), 400-470 MeV, backward π differential cross sections and anal. power 80−86905
^{2}H(p,π$^+$), polarised p, 305, 330 MeV, pion production differential cross section 79−67754
^{2}H(p,π$^+$)^{3}H, 400, 470, 600 MeV, differential cross section using isobar model 80−9291
^{2}H(p,π$^+$)^{3}H, microscopic model using realistic nuclear wavefunctions 79−85465
^{2}H(p,π$^+$)^{3}H, NN pot., isobar configurations and π prod., inelastic cross sections 79−63666
^{2}H(p,π$^+$)^{3}H, studied via pp→π$^+$d amplitude and triangle graph 77−38265
^{2}H(p,π)^{3}H, pion prod. models for medium energies 77−18563
^{2}H(p$_0$,p$_1$p$_2$)n, 156 MeV, test on p$_1$-n-p$_2$ colliniarity reson. 79−75996
^{3}H (p,n)^{3}He, determ. of π^{3}He^{3}He coupling constant from differential cross section 78−89801
^{3}H(p,n), ^{4}He continuum microscopic calcs. cross sections and levels 80−57702
^{3}H(p,n), 1.24, 1.8 GeV, differential cross section, spin independ. Glauber model interpretation 80−63183
^{3}H(p,n), signal to background ratio for 10 to 14 MeV neutron prod. 77−30683
^{3}H(p,n)^{3}He, 13.6 MeV, neutron spectra normalisation, differential cross-section meas. 77−88106
^{3}H(p,n)^{3}He, 6 to 17 MeV, n prod. absolute differential cross sections 78−74373
^{3}H(p,n)^{3}He, associated particle methods for neutron flux monitoring 79−9977
^{3}H(p,n)^{3}He, coupled channels anal. of neutron polarisation 77−18560
^{3}H(p,n)^{3}He, R-matrix anal. of polarisation and analysing power 77−88142
^{3}H(p,n)^{3}He charge exchange reaction, multifold diffr. scatt. theory *(Russian)* 80−78303
^{3}H(p,n)^{3}He in associated particle apparatus for neutron detector calibration 77−26939

proton-nucleus reactions continued
^{A}H(p,π), A=1,2, 0.7-8 GeV, scaling and nonscaling of inclusive π prod. 79−22296
He, Ne, Ar isotopes and ^{238}U prod. by solar cosmic ray protons in lunar materials 77−17311
He+p, 1.5 to 2.5 GeV interactions in streamer chamber 79−6709
He+p, particle multiplicity correlations in streamer chamber 79−85506
^{3}He breakup, 156 MeV protons, NN multiple scatt. anal. 77−18546
^{3}He breakup induced by 156 MeV protons, pd final state interactions 77−23013
^{3}He target, expt. to observe excited states of nucleons in nuclei *(French)* 79−3179
^{3}He(p,2p)^{2}H, 155 MeV, multiple scatt. diffraction theory anal. *(Russian)* 77−10408
^{3}He(p,2p)d, 590 MeV, in noncoplanar geometry, two particle spallation, diffr. description *(Russian)* 78−33160
^{3}He(p,2p)d(d*), 136 MeV, d/d* ratio, PWIA anal. 79−75999
^{3}He(p,dp), (p,2p), and (p,pn), 156 MeV $d^{3}\sigma$ and $d^{4}\sigma$ spectra for collinear nucleon system 78−17175
^{3}He(p,dp)p, 156 MeV, p-d scatt. at small rel. energy in FSI region 79−85441
^{3}He(p,p)^{3}He, cross-section anal. using four-body integral eqns. 77−18577
^{3}He(p,pd)p, 35 and 45 MeV, four-body break-up calcs. 77−57667
^{3}He(p,pp)d, 35 and 45 MeV, four-body, break-up calcs. 77−57667
^{3}He(p,π^{-})^{4}He, 300-400 MeV, virtual pion exchange 77−74848
^{3}He(p,π^{+})^{4}He, 415, 716 MeV, DWIA calcs. of differential cross-section 77−6359
^{3}He(p,π^{+})^{4}He, 415, 716 MeV, differential cross-section meas. 77−6360
^{3}He(p,π^{+})^{4}He, 415 MeV, angular distrib., microscopic description, generalisation of (π,π) *(Chinese)* 80−63188
^{3}He(p,t)Δ^{++}, 850 MeV, search for (Δ^{++},2n) in the ^{3}He wave function 78−82345
^{4}He+p, 18.6 GeV/c, coherent prod. of low mass p$\pi^{+}\pi^{-}$ states 78−33175
^{4}He+p, 50 MeV, deuteron production possibilities, astrophysics importance 79−40928
^{4}He+p, 8.56 GeV/c, two pronged events, cross sections and prod. features 79−3152
^{4}He(p,^{3}He), ^{2}H, large momentum transfers, π exchange effects 80−5143
^{4}He(p,X), multiple scattering theory, validity of closure approx. 79−45269
^{4}He(p,X)^{3}He, 6.85 GeV/c, inclusive angular distributions 77−74845
^{4}He(p,X)^{3}He, 6.85 GeV/c, Glauber multiple model 79−63664
^{4}He(p,2p), 250, 350, 500 MeV, cross section energy depend., DWIA calcs. 80−37375
^{4}He(p,2p), pol. nucleon quasi-elastic scatt., nuclear wave function and model tests 80−42656
^{4}He(p,2p)^{3}H, 350 and 500 MeV, energy sharing spectrum, symmetric angular distrib. 79−6582
^{4}He(p,d), intermediate energies, pion exchange currents in DWBA anal. 80−32199
^{4}He(p,d), reaction mechanism, effect of Pauli principle and channel coupling 77−65219
^{4}He(p,d) pickup reaction, isobar configurations and short range correlations 80−22798
^{4}He(p,d)^{3}He, 275-500 MeV, large angle meas. 78−41713
^{4}He(p,d)^{3}He, 3.98 GeV/c, ang. distrib. meas., comparison with DWBA 77−61416
^{4}He(p,d)^{3}He, 770 MeV, calcs. 77−6357
^{4}He(p,d)^{3}He, 770 MeV, differential cross section meas., DWBA anal. 77−46166
^{4}He(p,d)^{3}He, 770 MeV, exact finite range DWBA, cross sections 78−70531
^{4}He(p,d)^{3}He, 770 MeV, multiple-scattering approach 80−27636
^{4}He(p,d)^{3}He, direct-reaction mechanisms 78−581
^{4}He(p,d)^{3}He, energy depend. and cross sections 200-500 MeV 79−13296
^{4}He(p,d)^{3}He, large momentum transfers, π exchange effects 80−5143
^{4}He(p,nπ^{+}), 18.6 GeV, invariant mass distrib., double Regge pole model comp. 79−3144
^{4}He(p,nπ^{+}), $\simeq$500 MeV, NNπ vertex function 79−59066
^{4}He(p,nπ^{+}), pion prod. operator non-relativistic approx. 79−85500
^{4}He(p,nπ^{+}), pion prod. operator non-relativistic approx. 80−27640
^{4}He(p,p'), high energy, nonlocal imaginary pot. in one channel approx. 78−592
^{4}He(p,pn)^{3}He, ^{3}He momentum spectra determ. by cluster model interpretation 79−6577
^{4}He(p,pπ^{0}), 18.6 GeV, invariant mass distrib., double Regge pole model comp. 79−3144
^{A}Hf(p, α), A=176,178,180, statistical direct reaction model calc. 79−80913
^{176}Hf(p, n), 6.7, 10 MeV, ^{176}Ta level properties, rot. bands, transitions and level lifetimes 79−36158
^{202}Hg+p, 10-90 MeV, exciton model, pre-equilibrium decay calcs., excitation functions 77−82922
^{204}Hg(p,t)^{202}Hg, 17.5 MeV, transfer strengths 78−94005
$^{1-5}$Ho(p,4nγ), 30-51 MeV, energy levels of ^{162}Er 77−61348
^{165}Ho(p, xnypγ), 60 MeV, preequilibrium and equilibrium de-excitation processes 78−50185
^{165}Ho(p,αX), 20-45 MeV, α spectra, exciton model anal. 80−18306
^{165}Ho(p,α), 20 to 44 MeV, energy spectra and α-particle angular distrib. 79−49630
^{165}Ho(p,xn), 30-51 MeV, energy levels of ^{162}Er 77−61348
^{165}Ho(p,xnypγ), 60 MeV, n and γ energies and ang. distribs. 78−89872
^{123}I production from ^{123}Xe formed in spallation reactions by 660 MeV protons, medical appls. 80−85494
^{127}I(p,5n)^{123}Xe, ^{123}I prod., excitation function 77−2981
^{127}I(p,5n)^{123}Xe, ^{123}I prod. from ^{123}Xe—^{123}I, at 58 MeV 80−94369
^{127}I(p,5n)^{123}Xe, for large scale ^{123}I prod. from flowing liq. target 77−29203
^{127}I(p,5n)^{123}Xe→^{123}I statistical model based computation 79−26416
^{127}I(p,5n)^{123}Xe→^{123}I 79−79649
^{127}I(p,5n)^{123}Xe→^{123}I production of di-iodomethane target 79−79651
^{127}I(p,n)^{127}Xe statistical model based computation 79−26416
^{127}I(p,xn)Xe→(β)→I reactions, yield curves for cyclotron prod. of ^{123}I, ^{125}I and ^{121}I 78−44611
In+p, 1 to 28.5 GeV, production of 43≤A≤51 nuclides, reaction mechanisms 77−34301
^{115}In(p,n), 11.2 MeV, spin cut-off parameters from neutron ang. distribs. *(Russian)* 79−80940
proton-nucleus reactions continued
^{115}In(p,n), 2.0-6.7 MeV, cross sections, Hauser-Feshbach optical calcs. for p absorption systematics 80−47483
^{115}In(p,n), 5 to 9 MeV, neutron spectra of ^{115}Sn, TOF meas. *(Russian)* 79−9579
^{115}In(p,n)^{115}Sn, ^{110}Cd, n spectra of isobaric analogue resonance decay *(Russian)* 78−89841
^{191}Ir(p,4nγ), 38 MeV, low lying and high spin states in ^{188}Pt side band 78−4936
^{191}Ir(p,n), 10 MeV, ^{191}Pt level scheme, γ, conversion electron spectra, spins, parities 78−25149
^{191}Ir(p,t), 34.7 MeV, ^{189}Ir low lying positive parity bands, state anomalous angular distribs. 78−66212
^{193}Ir(p,t), 34.7 MeV, ^{191}Ir low lying positive parity bands, state anomalous angular distrib. 78−66212
Ir(p,t)^{189,191}I, 18 MeV, ground state rot. band, 7/2 gamma vibr. levels 78−74360
^{39}K(p,^{3}He), 40 MeV, DWBA anal. 78−66278
^{39}K(p,n) 7480-7530 keV, threshold energy, ^{39}Ca β-decay Gamow-Teller interaction renormalisation constant 79−6601
^{39}K(p,t), 40 MeV, DWBA anal. 78−66278
^{84}Kr(p,n), ^{84}Rb prod. at Manitoba Univ. 79−54695
Kr(p,X), 2-400 GeV A=3-14 fragment energy distrib. 79−17901
Kr(p,X), fragment prod. by two body breakup 79−85440
Kr(p,xn)^{81,82m}Rb, ^{87,82m}Rb prod. for positron emission tomography 80−98068
^{139}La(p,αn)^{135m}Ba, ^{135m}Ba yield depend. on energy of bombarding particle 80−5151
^{139}La(p,f), 600 MeV, fragment energies, cross sections level density and barrier heights 80−42723
La(p,f), 600 MeV, mass yields in binary fission 78−8819
Li, absolute neutron yield meas. for protons from threshold to 3 MeV 77−79498
^{6}Li, 180° prod. of protons in high-energy reacts. 78−8816
^{6}Li+p propagating fusion fuel cycle 80−37629
^{6}Li(p, ^{3}He)^{4}He, 100 to 700 keV, cross sections and angular distrib. meas. 79−93618
^{6}Li(p,^{3}He), 0.1-3.0 MeV, absolute differential and total cross sections, astrophysical S-factor 80−27642
^{6}Li(p,^{3}He), 3-12 MeV, absolute cross sections 77−23297
^{6}Li(p,X), 400 GeV, p backward prod. invariant cross section 79−93623
^{6}Li(p,X), 400 GeV/c, light ion backward prod., invariant cross section 80−32279
^{6}Li(p,2p)^{5}He, appl. of break-up reaction theory to resonant final states 77−10381
^{6}Li(p,3p), quasielastic ejection of proton pairs at 640 MeV *(Russian)* 79−59067
^{6}Li(p,α)^{3}He, 1.0-2.6 MeV, cross-section meas. 77−34295
^{6}Li(p,α)^{3}He, Li isotopic comp. determ. using coincident meas. of complementary particles 79−5201
^{6}Li(p,d^{3}He), DWIA anal., α-spectroscopic factors, quasifree process 77−79378
^{6}Li(p,dπ^{+})^{5}He, 800 MeV, momentum spectra enhancement 77−10395
^{6}Li(p,n), 144 MeV, charge exchange, one pion exchange and PCAC tests 80−78299
^{6}Li(p,p')X, 800 MeV, cluster recoil mechanism for inclusive nuclear reactions 78−93998
^{6}Li(p,pα)np, ^{6}Li ground state, cluster struct. 77−88129
^{6}Li(p,pd), 590 MeV, α-d motion, impulse distrib., cluster momentum distrib. 80−52679
^{6}Li(p,pd), 670 MeV, large angle quasifree scatt., spectroscopic factor, momentum distrib., cluster model 80−63184
^{6}Li(p,pd)^{4}He, results in relation to (p,2p) 800 MeV high resolution proposed studies 77−88123
^{6}Li(p,pd)α, 156 MeV, relative wave function of d and α clusters, PWIA, DWIA anal. *(Chinese)* 79−59068
^{6}Li(p,pt)^{3}He, 1 GeV, knock-out of clusters, distorting factors, microscopic approach *(Russian)* 78−58285
^{6}Li(p,π^{+})^{7}Li, 600 MeV, comparison with π,p exchange calcs. 77−79377
^{7}Li (p, n), 50 MeV 78−70726
^{7}Li, dσ(p,p'd)/dσ(p, nd), 670 MeV, cross section ratio, cluster model estimate 80−22829
^{7}Li+p, 1 GeV, neutron production *(Russian)* 79−85477
^{7}Li+p→$\alpha\alpha^{*}$→αtp, 4.5-12 MeV, ^{8}Be, highly excited $\alpha\alpha^{*}$ states 78−78262
^{7}Li(p, α), 45 MeV, nuclear vertex constant in peripheral model for virtual decay ^{7}Li→α+t 80−18295
^{7}Li(p, n)^{7}Be, absolute yield and neutron spectra 79−40929
^{7}Li(p,α), 21-28 MeV, ^{8}Be resonant state, $\alpha\alpha^{*}$ cluster and sympletic model anal. 79−9537
^{7}Li(p,α), 45 MeV, ^{7}Li→αt virtual decay vertex constant 80−78231
^{7}Li(p,α)^{3}He, Li isotopic comp. determ. using coincident meas. of complementary particles 79−5201
^{7}Li(p,αt), 4.5-12 MeV, ^{8}Be high spatial symmetry excited states, resonances, rot. band 80−86780
^{7}Li(p,d^{3}He), DWIA anal., α-spectroscopic factors, quasifree process 77−79378
^{7}Li(p,d), 800 MeV, cross sections, DWBA anal. 80−42667
^{7}Li(p,γ)^{8}Be, polarised p, 380-960 keV, ^{8}Be level, J$^{\pi}$ 77−88131
^{7}Li(p,n,γ)^{7}Be, associated gamma-ray technique for neutron fluence meas. 79−9978
^{7}Li(p,n$_{1}\gamma$), are as standard in neutron flux determ. by associated gamma-ray technique 77−10562
^{7}Li(p,n), 14-23 MeV, thick target neutron yields 77−57791
^{7}Li(p,n), 14.8-23 MeV, thick target neutron yields 77−26752
^{7}Li(p,n), 24.8-45 MeV, ^{7}Be effective for charge exchange analogues of Gamow-Teller transitions 80−57726
^{7}Li(p,n), cross-section contrib. from ^{8}Be 3^{+} states, isospin mixing model 78−89789
^{7}Li(p,n) 77−30602
^{7}Li(p,n)^{7}Be, activation and ang. distrib. meas., absolute neutron yield determ. 78−17199
^{7}Li(p,n)^{7}Be, microscopic multi-channel calcs. to 2.5 MeV c.m. 78−4934
^{7}Li(p,n)^{7}Be as therapy neutron source especially for small cyclotrons 80−26335
^{7}Li(p,n)^{7}Be neutron yield using sphere counter 77−23381
^{7}Li(p,n)^{7}Be source of fast neutrons for small cyclotrons, neutron therapy appl. 79−57755
^{7}Li(p,n)^{8}Be reaction for determ. Li conc. in glass 77−35582
^{7}Li(p,nα), 7-10 MeV, neutron spectra meas. 77−26741
^{7}Li(p,np), 7-10 MeV, neutron spectra meas. 77−26741

proton-nucleus reactions continued
^{A}Li (p, nd), A=6,7, 670 MeV, quasifree scatt., PWIA anal., cross sections 79−75985
^{A}Li(p,pα), A=6,7, 600 MeV, α-cluster quasielastic knockout, expt. methods, separation energy spectra 79−13275
^{6,7}Li(p,n)^{6,7}Be, 800 MeV, high-resolution n-spectra meas. 77−61423
Li(p,n), neutron spectra from thick target bombardment, for therapy 78−28049
Li(p,pα), A=6,7, at 100 MeV, absolute spectroscopic factors 77−30574
Li(p,pn), 47 MeV, excit. energy spectra, energy sharing spectra 77−50132
^{176}Lu(p,t)^{174}Lu, energy levels and rotational bands in ^{174}Lu 78−37346
Mg+p, 82-800 MeV, production of ^{7}Be, ^{22}Na, and ^{28}Mg 77−6388
^{A}Mg+p, A=24,25,26, 1 GeV, neutron production *(Russian)* 79−85477
^{A}Mg+p, A=24-26, gas phase proton irradiation, condensation, isotopic anomalies generation 79−13289
^{24}Mg+p, 400 MeV, multinucleon removal in quasifree process, p-γ coincidence expt. 78−37342
^{24}Mg(p,X), 17.5-48 MeV, proton total cross section 78−8809
^{24}Mg(p,α), near threshold, total cross section, reaction rate, astrophys. significance 77−82929
^{24}Mg(p,d), 49.5 MeV, ^{23}Mg j-forbidden $^{7}/_{2}^{+}$ state excitation, CCBA calculations, two step processes 79−26369
^{24}Mg(p,d), 94.8 MeV, ^{23}Mg hole states, transitions and spectroscopic factors, DWBA anal. 80−32161
^{24}Mg(p,f), 22 to 42 MeV 79−6717
^{24}Mg(p,pα), 157 MeV, quasifree scatt., α spectroscopic factors, SU(3) predictions 77−6370
^{24}Mg(p,pα), 600 MeV, α-cluster quasielastic knockout, expt. methods, separation energy spectra 79−13275
^{24}Mg(p,pα), 600 MeV, quasi-electric knockout reaction, PWIA calcs. 79−6581
^{24}Mg(p,pα)^{20}Ne, 157 MeV, energy spectra, SU(3) model comparison 77−88121
^{24}Mg(p,pα)^{20}Ne, DWIA calc. 77−34273
^{24}Mg(p,t), CCBA anal. using shell model wave functions 77−321
^{25}Mg(p,n)^{25}Al, cross sections and thermonuclear reaction rates 80−73852
^{26}Mg(p,n), 24.6-45 MeV, ^{26}Al 1^{+}T=0 states, isobaric analogue state, spin-isospin effective interaction 80−68553
^{26}Mg(p,n)^{26g}Al(7.3×10^{5} yr), ground state cross section, statistical compound model 79−30827
^{26}Mg(p,n)^{26m}Al(6.35s), ground state cross section, statistical compound model 79−30827
^{26}Mg(p,n)^{26}Al^{g}, 5.2-6.9 MeV, cross section via accelerator mass spectrometry 80−99175
^{26}Mg(p,π^{+}), isobar configuration effects, p→$\Delta^{0}\pi$ model, ang. distribs. *(Chinese)* 80−47484
^{26}Mg(p,π^{+}), 180 MeV, effect of Δ^{++} components in nuclei 78−33181
^{26}Mg(p,t), ^{24}Mg ground and γ-bands, direct and multistep processes 80−102094
^{28}Mg carrier-free production by 50-180 MeV protons on Si, P, S, Cl, Ar and K 79−83934
Mg(p,n), 35 MeV, ^{A}Al, A=24,25,26, giant M1 strength, comparison with cross sections 80−86878
^{55}Mn(p,α)^{52}Cr, 35 MeV, nuclear struct. study 79−75980
^{55}Mn(p,n)^{55}Fe, 1.35-5.42 MeV, total cross section and isobaric analogue resonances, shape anal. 79−6604
^{55}Mn(p,n)^{55}Fe, neutron polarisation at isobaric analogue resonances 78−54759
Mo, activation in cyclotron by p, d, α, ^{3}He 79−30839
Mo bombardment, yields of Tc isotopes, energy depend. 77−23098
^{A}Mo(p,n), 5.82 to 6.14 MeV, A=94 to 98, γ-ray multipolarities, internal conversion coeffs., energy levels 79−63625
^{A}Mo(p,n), A=94-96, 98, 1.7-6.7 MeV, total cross sections, p strength functions, optical model anal. 80−18301
^{A}Mo(p,p'), (A=92,94), 20 MeV, polarisation effects on nuclear excited states *(Russian)* 80−27645
^{92}Mo(p,d), 50 MeV, fine struct. of ground hole-state analogues 78−50065
^{92}Mo(p,p'3n), 60 MeV, ^{89}Mo^{m} levels, transitions and half life 80−86858
^{95}Mo(p, nγ)^{95}Tc, energy levels of ^{95}Tc 80−37372
^{96}Mo(p,nγ), 3.7-5.8 MeV, ^{96}Tc energy level diagram, γ transitions and parities 79−9479
^{97}Mo(p,nγ), 1.5-8.0 MeV, ^{97}Tc levels, decay props., mixing ratios and J$^{\pi}$, from directional correlations 79−89240
^{95}Mo(p,α)^{92}Nb, nuclear structure determ. 77−46118
^{98}Mo(p,n), 3-6.3 MeV, ^{98}Tc 14 μs isomer, low lying levels and transitions 80−73802
^{98}Mo(p,n), 4-5 MeV, ^{98}Tc, lifetimes of isomeric states 78−82314
^{98}Mo(p,n), obs. of ^{98}Tc low-lying levels 77−88076
^{100}Mo+p, cyclotron production of ^{99}Mo, ^{99m}Tc, excitation functions, target yields 77−46170
^{100}Mo(p,α)^{97}Nb, transfer reactions, nucl. struct. obs. 77−46118
^{100}Mo(p,n), 3-5.2 MeV, ^{100}Tc μs isomers, isomeric transitions and mean lives 80−73803
^{100}Mo(p,n), 3.7 MeV, ^{100}Tc internal conversion, isomeric level half life 78−78313
^{100}Mo(p,nγ), 4-6.8 MeV, ^{100}Tc low lying and isomeric levels, transitions and mean lines 80−42548
N+p, inelastic interactions, 6.0 GeV/c, in emulsions 78−86530
^{14}N+p, 50 MeV, three particle final state *(Russian)* 78−29471
^{14}N(d,p$_{0}$)^{15}N, N depth distrib., in barley grains and chromium steel samples 79−5221
^{14}N(p, X), 50 MeV, effective cross sections for charged particles in outgoing channel 80−18294
^{14}N(p,X), 50 MeV, effective cross sections 80−78284
^{14}N(p,X), 7.3 GeV, differential fragmentation cross sections 79−54442
^{14}N(p,α)^{11}C, light element profiling of tapered corrosion sections 79−92036
^{14}N(p,d) at 65 MeV, deuteron break-up 77−18535
^{14}N(p,d) modified DWBA anal., optical model parameter influence on vertex consts. *(Russian)* 78−78340
^{14}N(p,γ), 1.742 MeV, 8.92 MeV doublet and 8.98 MeV level in ^{15}O anal. 77−38243
^{14}N(p,γ)^{15}O, 3.15-3.5 MeV, ^{15}O reson. widths and branching ratios meas. 77−38244
^{14}N(p,n), 144 MeV, charge exchange, one pion exchange and PCAC tests 80−78299
^{14}N(p,n), 144 MeV, one pion exchange and PCAC expt. test 80−528
^{14}N(p,n)^{14}O, threshold energy 77−26625
proton-nucleus reactions continued
^{14}N(p,pd), (p,pt), (p,pα), spectroscopic data on quasielastic ejection on nucleon clusters from 1p shell nuclei 79−80931
^{14}N(p,pd)^{12}C, quasi-elastic cluster knock out, cross section calc. 78−46042
^{14}N(p,pt)^{11}C, quasi-elastic cluster knock out, cross section calc. 78−46042
^{14}N(p,t)^{12}N, 52 MeV, ^{12}N 2.43 MeV level study 77−6235
^{15}N+p reactions, ^{16}O energy levels near 15 MeV excitation, R-matrix anal. 78−29460
^{15}N(p,α$_{0}$)^{12}C, 93 to 418 keV, remeas. of low energy cross section, astrophys. S-factor determ. 79−63665
^{15}N(p,α) (p,αγ), 0.9-1.25 MeV, ^{16}O levels, J$^{\pi}$ 78−509
^{15}N(p,α)^{12}C, <1.25 MeV polarised protons, ang. distribs. 77−3009
^{15}N(p,α)^{15}N, 2.50-5.14 MeV, 3^{+} ^{16}O reson. state excit. 78−580
^{15}N(p,αγ)^{12}C, anal. of protein quality of leguminous plants 77−48978
^{15}N(p,αγ)^{12}C, isotopic anal., estimation of ^{15}N/^{12}C conc. ratio 79−48014
^{15}N(p,n$_{0}$)^{15}O, 8.5-19.0 MeV, resonance struct., excitation functions, cross sections 78−50164
^{15}N(p,n), 3.75-7.5 MeV, continuum shell-model coupled-channel calcs. 77−34269
^{15}N(p,n)^{15}O, continuum random phase approx. 80−27635
^{17}N yields from Mg, S, Ca, Ni, Sn isotope targets, isotope depend. *(Russian)* 77−61429
^{20}Na(p,α), 1-2.5 MeV, ^{20}Ne non-isolated resonances, excitation functions and ang. distribs. *(Chinese)* 80−22788
^{23}Na(p,α), lowest T=2 level of ^{24}Mg narrow resonance, isospin forbidden particle decays 78−89871
^{23}Na(p,α)^{20}Ne, 4-8 MeV, ^{24}Mg coherence width, intermediate structure effects 79−45133
^{23}Na(p,n), threshold to 6.3 MeV, total n prod. cross sections, statistical model parameters, nucleosynthesis 79−9602
^{23}Na(p,n)^{23}Mg neutron yield meas. with sphere counter 77−23381
^{24}Na, carrier-free production by 50-180 MeV protons on Si, P, S, Cl, Ar and K 79−83934
Nb simulation of 14 MeV neutrons by higher energy protons 79−1469
^{93}Nb(p,αX), 20-45 MeV, α spectra, exciton model anal. 80−18306
^{93}Nb(p,α), 20 to 44 MeV, energy spectra and α-particle angular distrib. 79−49630
^{93}Nb(p,n), direct neutron decay of analogue resonances in ^{94}Mo *(Russian)* 79−3128
^{93}Nb(p,n)^{93}Mo, direct neutron decay of analogue resonances of ^{94}Mo 80−22824
^{142}Nd(p,2n), ^{141}Pm medium spin states, J$^{\pi}$, transitions and shape 80−86779
^{145}Nd(p,p), (p,p'), 8.7-10.3 MeV, isobaric analogue reson. and seniority model 77−57642
^{146}Nd(p,2n), 14.9-20.2 MeV, ^{145}Pm level struct., J$^{\pi}$ and lifetimes, cluster-vibr. model anal. 80−91125
^{146}Nd(p,t), 30 MeV, obs. of ^{144}Nd levels 77−6241
^{148}Nd(p,2nγ), 12.1-20.2 MeV, γ-spectra, deduced ^{147}Pm level struct. 78−510
^{148}Nd(p,n), 9-45 MeV, ^{148}Pm^{m,g} isomeric pair prod. 77−88144
^{150}Nd(p,2nγ), ^{149}Pm levels, bands, transitions, in-beam spectroscopy, particle-rotor anal. 80−78125
^{150}Nd(p,2nγ), 12.1-15.8 MeV, ^{149}Pm high spin states and bands, rot. description and in-beam study 80−32153
Ne+p, 1.5 to 2.5 FeV interactions in stream chamber 79−6710
Ne+p, particle multiplicity correlations in streamer chamber 79−85506
^{20}Ne(p,α), near threshold, total cross section, reaction rate, astrophys. significance 77−82929
^{20}Ne(p,γ)^{21}Na, 1.7 MeV, DSA lifetime of 2425 keV state in ^{21}Na 77−82860
^{21}Ne(p,t), 40 MeV, ^{19}Ne $3/2^{+}$ state config. from ang. distribs. and cross section 79−9473
^{21}Ne(p,t), 40 MeV, ^{19}Ne 5.09 MeV level parity 79−45155
^{22}Ne(p,t), CCBA anal. using shell model wave functions 77−321
Ne(p,γ)Na, Ne(p,pγ)Ne, 0.5-2.0 MeV, absolute reson. strengths in ^{21,22,23}Na meas. 77−38272
Ni+p reactions, 12 to 45 MeV, excitation functions for Cu, Ni, Co, Mn isotopes prod. 78−66283
^{A}Ni, (p, X), A=58, 64, E$_{p}$=7.5 GeV, yields of hydrogen and helium isotopes *(Russian)* 79−93627
^{A}Ni(p,X), A=58, 64, 7.6 10 GeV/C, isotopic cross section ratios, He, Li fragments isotopic effects *(Russian)* 80−63154
^{A}Ni(p,α), A=58, 60, 30 MeV, α-particle angular distrib. 79−6588
^{A}Ni(p,α), A=58,60,62,64, 15-17 MeV, ^{A}Co A=55,57,59,61, level direct and compound cross sections 79−9474
^{A}Ni(p,α) A=60,62, polarised p, 22.0 MeV, analysing power J dependence 79−67740
^{A}Ni(p,α)$^{A-3}$Co, A=60,62,22 MeV, analysing power meas. in L=0 transfer reactions 79−45268
^{A}Ni(p,n), 11.2 MeV, A=60, 62, spin cut-off parameters from neutron ang. distribs. *(Russian)* 79−80940
^{A}Ni(p,π^{+}), A=58, 64, 660 MeV, pion energy spectra, isotopic effects *(Russian)* 80−42669
^{A}Ni(p,xγ), 80-164 MeV, A=58, 60, 62, 64, prod. cross sections, pre-equilibrium phase 80−78301
^{A}Ni(p$_{pol}$, α), A=58, 60, 62, 22 MeV, analysing power and cross sections, Co proton-hole states 80−68663
^{58}Ni spallation by 1 GeV protons, reaction channels *(Russian)* 78−74370
^{58}Ni+p, 1 GeV, alpha-particle decay channels 80−22826
^{58}Ni(p,X), 90 MeV, charged light particle energy spectra exciton and evaporation model anal. 79−40923
^{58}Ni(p,d), 121 MeV, DWBA applicability test, d D-state contribs. 79−13261
^{58}Ni(p,d), 50 MeV, fine struct. of ground hole-state analogues 78−50065
^{58}Ni(p,d) form factors, Pauli principle *(Russian)* 77−6393
^{58}Ni(p,d)^{57}Ni at 52 MeV, deuteron D-state effect, calcs. 79−54434
^{58}Ni(p,γ)^{59}Cu, 3547 and 1833 keV resonances, lifetime meas. 77−26621
^{58}Ni(p,p'(d)X), pol. p, 65 MeV, anal. powers of continuum energy spectra 80−68637
^{58}Ni(p,p'), 5.65 to 6.13 MeV, resonance and statistical mechanisms *(Russian)* 79−80911
^{58}Ni(p,pα), 157 MeV, quasifree scatt., α spectroscopic factors, SU(3) predictions 77−6370
^{58}Ni(p,pα)^{54}Fe, 157 MeV, energy spectra, SU(3) model comparison 77−88121

proton-nucleus reactions continued
^{59}Ni(p,t), 40 MeV, ^{57}Ni energy levels, spin and parity assignments 79−9475
^{59}Ni(p,t)^{57}Ni, 40 MeV, mass excess of ^{57}Ni determ. 77−18376
^{60}Ni+p, 400 MeV, multinucleon removal in quasifree process, p-γ coincidence expt. 78−37342
^{60}Ni(p,α)^{57}Co(3/2$^+$), anomalous analyzing power, DWBA calc. 80−86894
^{60}Ni(p,d), fragmentation of hole-state analogues in ^{59}Ni 78−54731
^{60}Ni(p,p′), near 6 MeV, spin-flip probabilities distorted wave and statistical anal. *(Russian)* 79−80939
^{62}Ni(p,γ), study of $g_{9/2}$ isobaric analogue state in ^{63}Cu 79−22258
^{62}Ni(p,n)^{62}Cu, 5.5-7.2 MeV, gamma transitions from ^{62}Cu excited levels obs. *(French)* 77−26615
^{64}Ni(p,nγ), ^{65}Cu analogue resonance direct n decay, ^{64}Cu levels and transitions *(Russian)* 80−5104
^{64}Ni(p,p), (p,p′), 5.0-6.2 MeV, isobaric analogue reson. in ^{65}Cu anal. 78−78351
Ni(p,α), 30 MeV, ^{A}Co, A=55,57,59,61, deduced levels, proton-hole states, semimicroscopic model 79−45171
Ni(p,d) 50 MeV, ^{57,61,63}Ni, ground hole-state analogues fine struct., isospin mixing 80−13401
Ni(p,d), A=60, 62 and 64, 50 MeV, fine struct. of ground hole-state analogues 78−50065
Ni(p,t), A=60, 62, at 27 MeV, two step processes, finite range effects 78−58281
N(p,X), 340, 660 MeV, ang. distribs., proton quasi-elastic knockout *(Russian)* 80−52649
N(p,X), 400 GeV/c, multiplicity and ang. distribs. of relativistic and slow particles *(Russian)* 79−40931
N(p,X), 740 MeV, ^{7}Be prod. cross section for cosmic ray anal. 79−93625
^{237}Np(p,f), 11-26 MeV, product yield 80−91197
O+p, inelastic interactions, 6.0 GeV/c, in emulsions 78−86530
^{16}O+p, 1 GeV, neutron production *(Russian)* 79−85477
^{16}O+p, 50 MeV, three particle final state *(Russian)* 78−29471
^{16}O+p, 62 MeV, complex particle emission, pre-equilibrium exciton model anal. 78−66280
^{16}O+p, energy dependent radial functions formalism of continuum shell model 78−25185
^{16}O+p fragmentation reaction, 2 GeV, three-stage model anal. 79−6551
^{16}O+p(d)(α) transparency in composite particle reactions 80−9273
^{16}O+p($\bar{p}$), total cross section calc., complex momentum theory anal. with $\alpha_P{}^0>1$ *(Russian)* 79−9638
^{16}O(p, X), 50 MeV, effective cross sections for charged particles in outgoing channel 80−18294
^{16}O(p,^{3}He)^{14}N(2.31 MeV), 27-30 MeV, isospin conservation 78−50170
^{16}O(p,^{6}Li)^{11}C, 51.9 Mev, five nucleon transfer mechanisms, DWBA calcs. 80−73845
^{16}O(p,X), 50 MeV, effective cross sections 80−78284
^{16}O(p,X), 50-90 MeV, contribution to Li, Be, B nucleosynthesis, cross sections 79−40978
^{16}O(p,2p), 200 MeV polarised beam reaction, possible knockout polarisation 77−88099
^{16}O(p,2p), 320 MeV polarised protons, quasifree scatt., spin orbit coupling 78−66272
^{16}O(p,2p), 45-50 MeV, distorted wave t-matrix anal. 78−50169
^{16}O(p,2p)^{15}N, 200 and 380 MeV, momentum distribs. calc. 78−54762
^{16}O(p,2p)^{15}N, single nucleon form factor between deformed nuclear states 78−93999
^{16}O(p,α), near threshold, total cross section, reaction rate, astrophys. significance 77−82929
^{16}O(p,α)^{13}N, in-cyclotron ^{13}N prod., water loop target 80−23201
^{16}O(p,p′), proton polarisation and natural parity level excitations *(Russian)* 80−5144
^{16}O(p,pd), ^{16}O(p,pt), ^{16}O(p,p^{3}He), 75 MeV expt. setup, DWIA anal. 77−322
^{16}O(p,pd), (p,pt), (p,pα), spectroscopic data on quasielastic ejection on nucleon clusters from 1p shell nuclei 79−80931
^{16}O(p,pd)^{14}N, quasi-elastic cluster knock out, cross section calc. 78−46042
^{16}O(p,pt)^{13}N, quasi-elastic cluster knock out, cross section calc. 78−46042
^{16}O(p,px), x=d,t, ^{3}He, 75 MeV, spectroscopic factors, cluster model, DWIA 77−54214
^{16}O(p,π$^+$)^{17}O, polarised protons, π distortion effect on asymmetry 78−50176
^{16}O(p,t)^{14}O(g.s.), 27-30 MeV, isospin conservation 78−50170
^{16}O($\vec{p}_{pol}$,2p), cross section, analysing power, energy sharing spectra, distorted wave impulse approx. 80−78291
^{17}O(p,α), ^{18}F J^π=3$^-$ doublet at 6241 keV, isospin mixing 80−511
^{17}O(p,α), 0.4-1.4 MeV, ^{18}F levels and resonances, cross sections in R-matrix formalism 80−18267
^{17}O(p,α), 1.4-2.8 MeV, ^{18}F levels and resonances, J^π assignments 79−9480
^{17}O(p,γ), 0.56 MeV, populating ^{18}F 5603 keV level, isospin mixing 78−543
^{17}O(p,t), ^{15}O T=3/2 levels 78−78264
^{18}O(p,α$_0$)^{15}N, 6.6 to 10.4 MeV, partial wave anal. of differential cross sections 79−93609
^{18}O(p,α), 661 to 223 keV cm, cross section meas. and S-function extrapolation using R-matrix theory 78−82341
^{18}O(p,α) 72 to 935 keV, astrophysical reaction rate, ^{19}F resonances 79−26439
^{18}O(p,α)^{15}N, applic. to high temp. oxidation studies of alloys 79−87912
^{18}O(p,d) reaction at 52 MeV, ang. distrib., DWBA anal. 77−26679
^{18}O(p,γ)^{15}N prompt reactions, lattice location meas. of O in Nb 79−86813
^{18}O(p,n), 3.75 MeV, ^{18}F 1.04 MeV state lifetime and γ-transition polarisation 80−106016
^{18}O(p,t), 20 MeV, ^{16}O form factor effects, zero range DWBA calcs. 80−491
^{18}O(p,t), exact finite range DWBA calcs., realistic triton and nuclear wave functions 80−63191
^{18}O(p,t), finite range DWBA anal. with realistic triton wave function 80−78300
^{18}O(p,t), polarised p, 24.4 MeV, two-step reaction to unnatural parity state, anal. power 79−67739
^{18}O(p,t)^{16}O, 20 to 45 MeV, energy depend. of two-step DWBA for unnatural parity state excitations 78−70528

proton-nucleus reactions continued
O(p,X), 340, 660 MeV, ang. distribs., proton quasi-elastic knockout *(Russian)* 80−52649
O(p,X), 400 GeV/c, multiplicity and ang. distribs. of relativistic and slow particles *(Russian)* 79−40931
^{182}Os(p,xnγ), K-isomer population levels 78−93927
^{192}Os(p,2nγ) 12 to 24 MeV, ^{191}Ir levels, Coriolis coupling model and asymmetric rigid rotor model 79−22164
(p,n) for A between 27 and 238, 800 MeV, n prod. systematics, π associated cross section 79−3153
p+pN, 640 MeV, obs. of correl. between backward emitted protons and forward outgoing protons 79−17902
^{31}P(p,n)^{31}S, 6.38 to 13 MeV, polarised protons, β-decay asymmetry meas. 77−18482
^{31}P(p,pn)^{30}P short-lived positron emitter production obs. 79−76236
Pb (p, X), 2.2, 6, 8.5 GeV, p and d inclusive spectra at 162° *(Russian)* 79−97710
Pb+p, 1 GeV, neutron production *(Russian)* 79−85477
Pb+p, 1 to 28.5 GeV, production of 43≤A≤51 nuclides, reaction mechanisms 77−34301
Pb+p, 3.6 GeV, emitted proton vel. spectra max. *(Russian)* 79−9571
Pb+p, 52 MeV, spectral meas. of secondary neutrons and photons from thick targets 78−58282
Pb+p, 600 MeV, pion production, energy spectra, A depend. *(Russian)* 78−17213
Pb+p, 7 GeV/c hadron multiple prod. *(Russian)* 79−22298
Pb+p superdense nuclei search, cross-section limit in 60-70 GeV range 77−26638
Pb+p→Λ^0($K_S{}^0$)($\bar{\Lambda}^0$)+X, neutral strange-particle prod. by 300 GeV protons 79−17905
Pb+p→p, 640 MeV, proton inclusive spectra and ang. distrib. meas. 77−67751
^{4}Pb(p,t)Pb, A=204, 205, 206, 17.5 MeV, transfer strengths 78−94005
^{A}Pb, A=206-208, fission at 1 GeV, cross section meas. *(Russian)* 78−94041
^{205}Pb(p,t), 35 MeV, ^{203}Pb multiplet struct., DWBA anal. 79−17784
^{207}Pb+p, 70 GeV/c, s-particles ave. multiplicity 78−21567
^{208}Pb(p,α), 20 MeV, ^{5}H pick-up, ^{208}π transition strengths and ang. distribs. 79−13271
^{208}Pb(p,α), 35 MeV, ^{205}Tl, level excitation energies and ang. distribs. cluster model DWBA calcs. 79−17814
^{208}Pb(p,d), 121 MeV, DWBA applicability test, d D-state contribs. 79−13261
^{208}Pb(p,d), two stage processes in direct reactions *(Dutch)* 78−29439
^{208}Pb(p,γ) fast capture, direct-semidirect model excitation function calcs. 78−94004
^{208}Pb(p,n), 120,160 MeV, ^{208}Bi M1 isobaric analogue resonances and giant spinflip resonances 80−106030
^{208}Pb(p,n), nucleon optical potential from Lane model 80−83097
^{208}Pb(p,nx), 45 MeV, preequilib. ang. distrib., generalised exciton model 77−10407
^{208}Pb(p,π$^+$), 180 MeV, ang. distribs., discrete states, differential cross section 79−13298
^{208}Pb(p,π$^+$), differential cross sections, DWBA calc. 79−85415
^{208}Pb(p,π$^+$)^{209}Pb, 160 MeV, ang. distributions 78−37345
^{208}Pb(p,π$^±$), semiclassical models, multiple scatt., nucleon recoil effects 77−2996
^{208}Pb(p,π), microscopic model anal., stripping model test for (d,p) 79−85436
^{208}Pb(p,t), 80 MeV, ^{206}Pb low lying level ang. distribs., zero range DWBA anal. 79−67656
^{208}Pb(p,t), finite range DWBA anal. with realistic triton wave function 80−78300
^{208}Pb(p,t), simple unitary estimate for multistep processes, cross section bounds 79−40922
^{208}Pb(p,t)^{206}Pb, successive and simultaneous transfer processes, on-shell, DWBA methods 78−8812
^{208}Pb(p,t)^{206}Pb, unnatural parity transitions, finite range DWBA anal. 77−67750
^{208}Pb(p,t)^{206}Pb(3$^+$), pol. p, 22 MeV, anal. power and (p,d)(d,t) sequential transfer processes 80−5119
Pb(p,X), 400 GeV/c, nucleon number depend. of inclusive dihadron prod. 79−49626
Pb(p,d), 9 GeV, nuclear emulsion expt. 80−78292
Pb(p,n), A=207,8, proton decay of isobaric analogues of ground states 77−26692
Pb(p,t), A=204,6,8, E=35 MeV, spectra and ang. distribs. meas. DWBA anal., sum rules 78−13101
Pb(p,t), pairing vibr. band, microscopic struct. and wave functions 80−91126
Pb(p,xpX), x=1, 2, 640 MeV, energetic backward p emission, inclusive differential cross section 80−9290
^{A}Pd(p,X), 6 MeV, A=102,104,106,108,110, quadrupole deformation, cross sections, direct processes, optical parameters *(Russian)* 79−67753
^{A}Pd(p,t), A=104, 102, at high excitation, observation of hole states 78−25187
^{104}Pd(p,t)^{102}Pd, 42 MeV, hole states at high excitation 78−50158
^{105}Pd(p,nγ)^{105}Ag, γ-spectra, level scheme *(Russian)* 77−74801
^{106}Pd (p,t), 30 MeV core-coupling model 77−57672
^{108}Pd(p,nγ)^{108}Ag, E_p=2.6-3.95 MeV, level struct. of ^{108}Ag 77−18392
^{108}Pd(p,t), 30 MeV, core-coupling model 77−57672
^{110}Pd(p,nγ)^{110}Ag, E_p=2.6-3.95 MeV, level struct. of ^{110}Ag 77−18392
^{110}Pd(p,t)^{108}Pd(2$_1{}^+$), analysing power difference from ^{110}Pd(p,t)^{108}Pd(2$_1{}^+$) 78−37341
Pd(p,2nγ), 19, 25 MeV, ^{A}Ag A=99, 101, 103, levels, transitions and J^π 80−47383
Pd(p,n), ^{A}Ag, A=104, 106, levels, J^π, and isobaric analogue resonances 80−32180
Pd(p,t)Pd, A=104, 108, 110, at 52 MeV, direct and indirect interf. 77−54220
^{210}Po(p,d), 17.8 MeV, ^{209}Po deduced levels, J^π assignments, spectroscopic factors 79−22197
Pt+p, 4-18 GeV, Υ″ prod., search for new narrow resons. 79−30833
Pt+p, dimuon prod., struct. in Υ region near 9.5 GeV 78−17201
Pt+p→μ^++μ^-+anything, 400 GeV, high-mass dimuon continuum 78−37344
Pt+p→$\mu^+\mu^-$+anything, massive lepton pair prod., Υ family 78−78368
^{A}Pt(p,d), A192-198, even, 26 MeV, levels obs. 78−50089
^{190}Pt(p,t)^{188}Pt reaction, 25 MeV ^{188}Pt states population 78−86532
^{194}Pt(p,n), conversion electron and γ-ray spectra, isomeric states in ^{194}Au anal. 77−71582

proton-nucleus reactions continued
^{195}Pt(p,2n), conversion electron and γ-ray spectra, isomeric states in ^{194}Au anal. 77−71582
^{195}Pt(p,t), 25 MeV, ^{193}Pt low lying negative parity states and shape 80−68540
Pt(p,d) ^{193,195,197}Pt, l-assignments, spectroscopic factors 78−8810
Pt(p,t), 35 MeV, ^{192,194,196}Pt states, J^{π}, ang. distribs. and transitions, DWBA anal. 80−468
^{226}Ra(p,f), 12 MeV, prompt neutron energy distrib. meas. 78−13182
^{226}Ra(p,f), 12 MeV, prompt γ-ray spectra meas. 78−13183
^{81}Rb-^{81}Kr generators, aspects of production, elution and automation, medical appls. 80−61696
^{85}Rb, excitation functions, medical appls. 80−78286
^{85}Rb(p,2nγ), 17-28 MeV, ^{84}Sr quasi-γ bands and negative parity levels 80−456
^{85}Rb(p,d), level location, spin and parity determ. in ^{84}Rb 78−82338
^{85}Rb(p,nγ) ^{85}Sr reaction, meanlifetimes of ^{85}Sr levels 79−36196
^{87}Rb(p,nγ), 3.8 MeV ^{87}Sr excited levels, spin, parity, branching ratios, lifetimes 77−50076
Re, p bombardment 15-160 MeV, long lived isotope prod., high temp. graphite thickness gauge calibration 77−23054
^{100}Ru (p,n), ^{100}Rh short lived isomer, decay scheme 79−75920
^{102}Ru (p,3n), ^{100}Rh short lived isomer, decay scheme 79−75920
^{33}S(p,^{3}He), 40 MeV, ^{31}P transition cross sections 79−67660
^{33}S(p,γ), 1.0, 2.0 MeV, reson. excit., Q-value *(French)* 77−26612
^{33}S(p,t), 40 MeV, ^{31}S level J^{π} assignments, transition cross section 79−67660
^{34}S(p,α)^{31}P, 35.5 MeV, DWBA, coherence effects 77−38271
^{34}S(p,n)^{34}Cl, threshold energy, ^{34}Cl superallowed beta-decay Q-value 77−34298
^{121}Sb(p,n)^{121m,g}Te, 4-24 MeV, yield meas. 78−37349
^{123}Sb(p,n)^{123m}Te, 4-24 MeV, yield meas. 78−37349
Sc+p, ^{45}Ti prod. in cyclotron 78−80966
^{45}Sc(p,^{17}Ne^{22}Na^{28}Al), 40-85 MeV, ^{24}Na yields in 'fission-like' reactions 78−598
^{45}Sc(p,α), 2.5-3.8 MeV, reaction rates and stellar nucleosynthesis 77−88134
^{45}Sc(p,γ)^{56}Ti, stellar reaction rates 78−93090
^{45}Sc(p,n), source of monoenergetic 10-50 keV neutrons 77−54387
Se+p→ ^{77}Br production excitation curves 79−85468
^{76}Se(p,nγ)^{76}Br, 5.8 to 6.8 MeV, level scheme deduced for ^{76}Br 78−50091
^{77}Se(p,nγ), levels of ^{77}Br 79−6407
^{80}Se(p,d)^{79}Se, 22.8 MeV, level structure study of ^{79}Se 78−93993
^{80}Se(p,n), 2.7-5.4 MeV, ^{80}Br isobaric analogue resonances and spectroscopic factors 79−36212
^{78,76}Se(p,t)^{76,74}Se, 33 MeV, J^{π}, level assignments to 4.64 MeV 77−67700
Se(p, d), 33 MeV, ^{A}Se, A=75, 77, 79, 81, levels and ang. distribs., spectroscopic factors 80−22696
Se(p,nγ)Br, A=80,2, energy levels of Br anal. 77−71609
SiO_2+p, 82-800 MeV, production of ^{7}Be, ^{22}Na, and ^{28}Mg 77−6388
^{A}Si+p, A=28, 29, gas phase proton irradiation, condensation, isotopic anomalies generation 79−13289
^{28}Si+p, 400 MeV, multinucleon removal in quasifree process, p-γ coincidence expt. 78−37342
^{28}Si(p,d) reaction at 52 MeV, ang. distrib., DWBA anal. 77−26679
^{28}Si(p,p'(d)X), pol. p, 65 MeV, anal. powers of continuum energy spectra 80−68637
^{28}Si(p,p), 6.9 GeV/c, elastic and inelastic differential cross sections, spin flip probability *(Russian)* 79−59071
^{28}Si(p,pα), 157 MeV, quasifree scatt., α specroscopic factors, SU(3) predictions 77−6370
^{28}Si(p,pα)^{24}Mg, 157 MeV, energy spectra, SU(3) model comparison 77−88121
^{28}Si(p,π^{+}), ^{29}Si $3/2^{+}$ and $5/2^{+}$ states population, (d,p) comparison 80−95307
^{29}Si(p,α), 13.5-15.5 MeV, ^{30}P level width isospin depend., excitation functions, statistical anal. 80−78152
^{30}Si(p,α), polarised proton, reaction struct. depend. 80−18296
^{30}Si(p,α)^{27}Al, 17 MeV, polarised p, cross-section and analyzing power ang. distrib. 79−54427
^{30}Si(p,α)^{27}Al, 40.75 MeV, differential and relative cross sections, distorted wave direct pickup calcs. 78−94009
Sm, fission, 1 GeV, cross section meas. *(Russian)* 78−94041
^{A}Sm(p,t), A=148, 150, 152, 154, 40 MeV, two neutron transfer strengths, IBA model predictions 79−85474
^{147}Sm(p,2n) 19 MeV, ^{146}Eu 9^{+} isomer, γ-decay, high spin particle-hole multiplet population 80−63066
^{147}Sm(p,p), (p,p'), 7.5-10.8 MeV, isobaric analogue reson. and seniority model 77−57642
^{150}Sm(p,2nγ), 18-26 MeV, level struct. of ^{149}Eu, spin, parity 78−21561
^{152}Sm(p,2nγ), 18-28 MeV, ^{151}Eu level scheme from excitation functions, rotor and interacting boson anals. 79−45163
^{154}Sm(p,t), ^{152}Sm ground and γ-bands, direct and multistep processes 80−102094
Sm(p,α), 17 MeV ^{147,149,151}Pm single proton hole states in pickup reactions 80−78128
Sm(p,α) ^{147,149,151}Pm, 17 MeV, direct and sequential reaction mechs., (t,α) comparison 79−540
Sm(p,n), 20-26 MeV, ^{A}Eu, A=144,148,150,152, ground and excited state analogues, two-phonon coupling effects 79−89277
Sm(p,t), even isotopes, high energy neutron pairing strength, two neutron holes, resonances 80−78116
Sn+p, 225 GeV/c, J/ψ and ψ'(3.7) prod. study using muon pair meas. 77−57694
Sn+p, massive muon pair prod., test of Drell Yan model 77−57695
^{A}Sn+p, A=116,124, 1 GeV, neutron production *(Russian)* 79−85477
^{A}Sn(p,X), A=112, 124, 7.6, 10 GeV/C, isotopic cross section ratios, He, Li fragments isotopic effects *(Russian)* 80−63154
^{A}Sn(p,n), A=112, 116, 124, 35.3 MeV cross-sections, test of forward scatt. amplitude approx. 79−6599
^{A}Sn(p,π^{-}), A=112, 124, 660 MeV, pion energy spectra, isotopic effects *(Russian)* 80−42669
^{A}Sn(p,t), 52 MeV, A=117,119, angle integrated cross sections, blocking effect ^{115,117}Sn transition strengths 79−89307
^{A}Sn(p,t), A=122, 120, 124, 116, 118, at high excitation, observation of hole states 78−25187
^{116}Sn(p,α)^{113}In, 22 MeV, analysing power, J-depend., DWBA 78−70523
^{116}Sn(p,t), 20 MeV, two step (p,d)(d,t) process, second order DWBA 78−66276
proton-nucleus reactions continued
^{116}Sn(p,t)^{114}Sn, 20 MeV, finite-range effect in (p,d)(d,t) process 78−74365
^{117}Sn(p,d), polarised p, 12.9 MeV, anal. power 80−5114
^{118}Sn(p,αX), 20-45 MeV, α spectra, exciton model anal. 80−18306
^{118}Sn(p,α), 20 to 44 MeV, energy spectra and α-particle angular distrib. 79−49630
^{118}Sn(p,α)^{115}In, 20 MeV polarised protons, DWBA calcs. 78−41714
^{118}Sn(p,t). ang. distribs. and cross sections full finite range CCBA anal. 80−5141
^{119}Sn(p,X), 400 GeV, absorption cross sections and multiplicity distribs., A-depend. study 79−67748
^{119}Sn(p,n')^{119}Sb, 17-19 MeV, analogue state excitation and decay 79−6542
^{119}Sn(p,n)^{119}Sb, 16-20 MeV, isobaric analogue state, ang. distrib. meas. 78−29468
^{120}Sn, 62 MeV, complex particle emission, pre-equilibrium exciton model anal. 78−66280
^{120}Sn+p, exciton model of pre-equilib. decay 77−18487
^{120}Sn(p,n), statistical multistep direct emission, p-h and DWBA calcs. 80−106035
^{120}Sn(p,n)^{120}Sb, nuclear alignment of ^{120}Sb temp. depend. 78−41720
^{120}Sn(p,nγ), 3.4-4.1 MeV, ^{120}Sb low lying level scheme, J^{π} assignments 79−22196
^{120}Sn(p,nx), 45 MeV, prequilib. ang. distrib., generalised exciton model 77−10407
^{120}Sn(p,p3n), 52 MeV, ^{117}Sn^{m} E5 transition, branching ratio 79−45200
^{122}Sn(p,n), 11.2 MeV, spin cut-off parameters from neutron ang. distribs. *(Russian)* 79−80940
^{124}Sn(p,t), 54.9 MeV, ^{122}Sn excitation of 6^{+}, 8^{+}, 10^{+} and 9^{-} states, DWBA anal. 79−89264
Sn(p,2nγ)Sb, A=111, 3, 5, excited states of Sb anal. 77−2911
Sn(p,d), 52 MeV, deeply bound hole states, isobaric analogue states in ^{115,117,119,123}Sn 77−30570
Sn(p,n), 3-7 MeV, competition of gamma ray and neutron emission 77−23022
Sn(p,n), 6-9 MeV, ^{119,122}Sb level density, neutron spectra and ang. distribs. nonequilib. processes *(Russian)* 80−37376
Sn(p,n) (A=112,116,124), 22.8 MeV, ang. distribs. to isobaric analogue states, nuclear matter distrib. 77−10405
Sn(p,n), even isotopes, 4-10 MeV, cross sections, optical parameters and nuclear radius A-depend. 80−57773
Sn(p,n) for A=117-124 at 2.6-7 MeV, p-wave size reson. optical model fit 77−30575
Sn(p,n), microscopic description 77−57670
Sn(p,n)Sb, Sb, A=120, 122, 3^{+} isomeric states quadrupole moments (p,n) excited, TDPAD method 78−41635
Sn(p,n)Sb, A=115-120, between analogue states via (p,p) and (p,np̄) anal. 77−88132
Sn(p,n)Sb reson. reaction, direct neutron decay of isobaric anal. reson. *(Russian)* 77−88145
Sn(p,n)^{116,118}Sb, threshold region, thick-target cross sections, statistical theory, Q values 77−54218
Sn(p,np̄)Sn, A=115-120, 14-18 MeV, IAS, p branching ratios 77−88132
Sn(p,t), 89 MeV, ^{118,120,122}Sn deep hole states, excitation energies and ang. distribs. 80−86792
Sn(p,t), A=116, 118, 120, 122 and 124, 42 MeV, hole states at high excitation 78−50158
Sn(p,t), bump at 8-9 MeV excitation 78−74366
^{88}Sr(p,2nγ), 22.8 MeV, ^{87}Y level struct., γ-spectroscopy and J^{π} 80−83040
^{88}Sr(p,d), two step processes, excitation of core coupled states, in ^{87}Sr 77−88150
Ta, 180° prod. of protons in high-energy reacts. 78−8816
Ta+p, 28.5 GeV/c, backward particle emission, energy depend. 78−25236
Ta+p, 300 MeV, 450 MeV, 24 GeV, cross-section meas. 77−67740
^{180}Ta, ground state spin, (p,d) cross-sections 79−26368
^{181}Ta (p, n), 6-10 MeV, ^{181}W, level absolute density from n spectra, statistical anal. *(Russian)* 79−97657
^{181}Ta (p,X), 4.2 GeV/c, multitudes of secondary negative particles, momentum distrib. ratios *(Russian)* 80−63178
^{181}Ta, fission, 1 GeV, cross section meas. *(Russian)* 78−94041
^{181}Ta+p, 1 GeV, neutron production *(Russian)* 79−85477
^{181}Ta(p,X), 20-48 MeV, proton total reaction cross section 79−80934
^{181}Ta(p,2nγ), 16 MeV, ^{180}W, rot. and vibr. bands, γ-vibr. band, metastable state half life 79−54378
^{181}Ta(p,2nγ), 17 MeV, ^{180}W ground and $K=2^{-}$ octupole band ang. momenta coupling, lifetimes 80−9214
^{181}Ta(p,2nγ), CC ^{180}W, $K=2^{-}$ octupole alignment, ground-band angular momenta 78−78237
^{181}Ta(p,4n)^{178}W radionuclide production and purification 80−12252
^{181}Ta(p,d), evidence for Gallagher-Moszkowski doublets in ^{180}Ta 78−58233
^{181}Ta(p,n), 11.2 MeV, spin cut-off parameters from neutron ang. distribs. *(Russian)* 79−80940
^{181}Ta(p,n), 5.76-9.83 MeV, ^{181}W level density, n spectra and ang. correls., direct and nonequilib. processes *(Russian)* 80−68631
^{181}Ta(p,n)^{181}W, 10.2 MeV, CC neutron spectra and angular distrib. meas. *(Russian)* 78−25198
^{181}Ta(p,n)^{181}W, multi-step compound and direct reactions, statistical theory 80−57761
^{181}Ta(p,p')X, 800 MeV, cluster recoil mechanism for inclusive nuclear reactions 78−93998
Ta(p,X), 400 GeV, p backward prod. invariant cross section 79−93623
Ta(p,X), 400 GeV/c, light ion backward prod., invariant cross section 80−32279
Ta(p,X), 4.2 GeV/N, multiple π^{-} prod., mean multiplicity *(Russian)* 80−27647
Ta(p,X), 4.2 GeV.c^{-1}, inelastic cross section meas. and multiplicities obs. *(Russian)* 79−9580
Ta(p,X), 8 GeV, β-active superdense nuclei search *(Russian)* 80−42535
Ta(p, spallation), 1 GeV, ^{A}Lu, neutron deficient isotopes, A=157, 158, 160, 161, 163 79−75957
Ta(p, xn), 23 MeV, n energy distribs. *(Russian)* 78−86537
^{159}Tb(p,X), 20-48 MeV, proton total reaction cross section 79−80934
^{159}Tb(p,4nγ), 27-51 MeV, ^{156}Dy rotational levels 77−6199
^{159}Tb(p,f), 600 MeV, binary fission process 77−3060
^{159}Tb(p,f), 600 MeV, fragment energies, cross sections level density and barrier heights 80−42723

proton-nucleus reactions continued
Tb(p,f), 600 MeV, mass yields in binary fission 78−8819
^{99}Tc(p,d), 15,19 MeV, ^{98}Tc excit. in 0.43-1.32 MeV range 77−18370
^{99}Tc(p,d), 22.9 MeV, ^{98}Tc energy levels, l-values, spectroscopic factors, parities 78−25183
^{30}Te(p,α), 35.2 MeV, ^{127}Sb states, collective neutron excitation role, spectroscopic factors and form factors 79−67622
^{124}Te (p,n)^{124}I, excitation functions and target enrichment vs. nuclidic purity 77−60252
^{124}Te(p,2n), ^{123}I prod. at Manitoba Univ. 79−54695
^{124}Te(p,2n), ^{123}I product radionuclidic purity, reply 79−29622
^{124}Te(p,2n), ^{123}I product radionuclidic purity and quality, comments 79−29621
^{124}Te(p,2n), 26 MeV, routine prod. of ^{123}I at Karlsruhe isochronous cyclotron 79−54694
^{124}Te(p,2n)^{123}I, excitation functions and target enrichment vs. radionuclidic purity 77−60252
^{124}Te(p,2n)^{123}I, improved targetry and radiochem. for ^{123}I prod. 78−28064
^{124}Te(p,2n)^{123}I, new approach to target chem. for ^{123}I prod. 77−60250
^{124}Te(p,2n)^{123}I statistical model based computation 79−26416
^{124}Te(p,n)^{124}I, improved targetry and radiochem. for ^{124}I prod. 78−28064
^{126}Te(p,n), $2_2^+ \rightarrow 2_1^+$ transition multipole mixing ratio 80−78198
^{128}Te(p,t)^{126}Te(2_1^+), analysing power difference from ^{110}Pd(p,t)^{108}Pd(2_1^+) 78−37341
^{232}Th, fission, 1 GeV, cross section meas. *(Russian)* 78−94041
^{232}Th(p, f), 35-85 MeV, light mass nuclide charge dispersion curves for A=76-79 80−18349
^{232}Th(p, spallation), spallation cross section and recoils, range calcs. computer code MARLOWE 79−93736
^{232}Th(p,X), 10-100 MeV, spallation residue excitation functions, fissionability 80−18353
^{232}Th(p,f), 28 GeV, charge dispersion, mass yields 77−3062
^{232}Th(p,f), 29-97 MeV, Rb, In and Cs relative independ. yields, charge division 80−102218
^{232}Th(p,f), 4-7 MeV, cross sections *(Russian)* 78−41794
^{232}Th(p,f), 9.5-17 MeV, symmetric to asymmetric mass ratios for fragments 80−5178
^{232}Th(p,p'f), 52.5 MeV, fission probability 80−99195
Ti, 20 to 50 MeV, total reaction cross sections, compared to optical model prediction 78−33174
^{46}Ti(P,n)^{46}V, threshold and ^{46}V(β^+)^{46}Ti ft value 77−10371
^{46}Ti(p,n), ^{46}V weak neutral current props., search for 0$^-$ isomer 79−45126
^{46}Ti(p,p'γ), 2.25-3.10 MeV, ^{47}V 3/2$^-$ analogue state decay amplitudes, common doorway state phase relation 79−89276
^{46}Ti(p,t) 42 MeV, ^{44}Ti, lowest T=2 state decay, branching ratios 78−78304
^{48}Ti(p,^{17}Ne^{22}Na^{28}Al), 40-85 MeV, ^{24}Na yields in 'fission-like' reactions 78−598
^{48}Ti(p,n), 4.7-5.4 MeV, cusp behaviour of cross-section obs. 78−29470
^{49}Ti(p,n), 0.74-3.25 MeV, cross section and thermonuclear reaction rates, nucleosynthesis 80−102187
Ti(p,X) 200, 300, 400 GeV, hadron prod. at large p_T invariant cross section 79−40926
Ti(p,2π$^-$X), 28.5 GeV, fireball model comparison 79−59059
Ti(p,d), A=46,48,50, DWBA calcs., rms radius pick-up reaction cross sections 79−541
Ti(p,x), 13 to 45 MeV ^{48}V $^{43-48}$Sc, ^{43}K, production excitation functions, statistical equilib. calcs. 79−36220
Tl+p, ^{201}Tl and ^{203}Pb radioisotope preparation 79−88184
^{203}Tl(p,3N)^{201}Pb→^{201}Tl, E_p=15 to 60 MeV, yields and excitation functions 79−5369
^{205}Tl(p,5n)^{201}Pb→^{201}Tl, E_p=15 to 60 MeV, yields and excitation functions 79−5369
^{205}Tl(p,5n)^{201}Pb→^{201}Tl, yields and excitation functions for Pb radioactivities, medical appls. 80−67249
^{203}Tl(p,d), 26.1 MeV, ^{204}Tl neutron hole states, J$^\pi$ and spectroscopic factors 80−86783
^{169}Tm(p,αX), 20-45 MeV, α spectra, exciton model anal. 80−18306
^{169}Tm(p,α), 20 to 44 MeV, energy spectra and α-particle angular distrib. 79−49630
^{169}Tm(p,n), cross sections and spectra, exciton model *(Russian)* 78−21536
U, proton-induced fission at 400 GeV, ternary to binary event ratio 78−13170
U+p, 1 to 28.5 GeV production of 43≤A≤51 nuclides, reaction mechanisms 77−34301
U+p, 7 GeV/c hadron multiple prod. *(Russian)* 79−22298
U+p, 700 MeV, search for polyneutron systems 77−50064
U+p, fragmentation, 800 MeV beam, obs. of new nuclides ^{27}Ne, ^{31}Mg, ^{32}Mg, ^{34}Al, ^{39}P 77−61419
U+p, particle-stable neutral nuclei prod. search, multi-GeV energies 78−25189
^{A}U, A=235, 238, fission at 1 GeV, cross section meas. *(Russian)* 78−94041
^{235}U(p,f), 13.7-14.2 MeV, isobaric analogue resonances, fission width 78−21616
^{236}U(p,t), cranking model anal., validity 77−18517
^{238}U, (p,f), 1 GeV, fission fragment ang. correlation, kinematically different events search *(Russian)* 79−59103
^{238}U, deuteron and proton bombardment, excitation function determ. 78−41709
^{238}U, proton-induced fission, asymm. region, nucl. charge distrib. 78−4967
^{238}U+p, 0.8-11.5 GeV, energy depend. of Sc fragment ang. distribs. 78−70527
^{238}U+p, 1-300 GeV, production props. of Sc nuclei 77−6389
^{238}U+p, nucleon losses on high-energy fission *(Russian)* 78−46120
^{238}U(P,X), 11.5 GeV, heavy fragment energies and masses, reaction mechanism 80−5140
^{238}U(p,X), 0.8-11.5 GeV, formation of A=131 isobaric nuclides 80−9293
^{238}U(p,X), 0.8-400 GeV, Sc fragment differential ranges and energy spectra 80−42666
^{238}U(p,X), 0.8-400 GeV 80−83099
^{238}U(p,X), 11.5 GeV, Ba fragments, differential ranges and ang. distribs. 79−67790
^{238}U(p,X), 400 GeV, ^{A}Sc, A=44m,46,47,48, fragment emission, two-step model applicability 80−99177

proton-nucleus reactions continued
^{238}U(p,X), 400 GeV/c, unusual backward enhancement in product ang. distrib. 80−514
^{238}U(p,X) *(Russian)* 79−80964
^{238}U(p,2n), production of ^{237m}Np fission isomer, statistical model anal. 78−25256
^{238}U(p,f), 11-29 GeV, three dimens. charge dispersion curves, isobaric yields 80−102111
^{238}U(p,f), 11.5 GeV, He and heavy fragment energy and ang. correlation 79−45310
^{238}U(p,f), 35-85 MeV, nuclear charge dispersion in light mass region 78−8864
^{238}U(p,f), 4-7 MeV, cross sections *(Russian)* 78−41794
^{238}U(p,f), 9.5-17 MeV, symmetric to asymmetric mass ratios for fragments 80−5178
^{238}U(p,f) 12 MeV, estimation of neutron yield from individual fragment in medium-excitation fission 80−542
^{238}U(p,nf), multiple scatt. effect due to filling in of blocking patterns 78−21617
^{238}U(p,t), 1 GeV, meas. of total fission cross-section *(Russian)* 77−341
^{238}U(p,t), 400 GeV, ang. distrib. of Sc fragments in thick targets 77−6472
^{238}U(p,xnf), lifetime of second chance fission at threshold, in UO_2 single cryst. 78−17259
U(p,X), X=F to Ar, 2.1 and 4.9 GeV, fragment energy spectra, Maxwellian functional form 78−70529
U(p,f) 300 to 660 MeV protons, neutron multiplication 79−59099
U(p,f), 600 MeV, fragment energies, cross sections level density and barrier heights 80−42723
V+p, 1 to 28.5 GeV, production of 43≤A≤51 nuclides, reaction mechanisms 77−34301
^{A}V(p,X), A=50, 51, 12-45 MeV, reaction cross section and hybrid model analysis 79−67749
^{50}V(p,α), 13.85 MeV, level density parameters, statistical model anal. 78−13130
^{51}V(p,X), X=γ or n, 0.93-4.47 MeV, cross sections, competition effects, Hauser-Feshbach calcs. 80−91184
^{51}V(p,d)^{50}V, 51.9 MeV, symm. pot. anal. 78−33182
^{51}V(p,n), 1.56-5.53 MeV, total cross section, excitation functions, isobaric analogue resonance 78−4943
^{51}V(p,n)^{51}Cr, 2.34 MeV, shell model anal. of analogue resonance 77−14122
^{51}V(p,n)^{51}Cr, neutron polarisation at isobaric analogue resonances 78−54759
^{51}V(p,nγ), 3.95-4.65 MeV, ^{51}Cr bands, levels, EM transitions, J$^\pi$, branching and mixing ratios 80−52606
V(p,^{17}Ne^{22}Na^{28}Al), 40-85 MeV, ^{24}Na yields in 'fission-like' reactions 78−598
W, 24 GeV proton irradiation, obs. of ^{72}Zn in nearby Zn sample, existence of bound neutral nuclei 77−30502
W, activation in cyclotron by p, d, α, ^{3}He 79−30839
W+p, 25 GeV, antiproton prod., flux optimisation using hadron cascade calcs. 77−83411
W+p, 25 GeV, search for neutral nuclei *(Czech)* 78−29454
W+p, 28.5 GeV, prompt dimuon prod., cross section, atomic number depend., mass distrib. 78−89858
W+p, 400 GeV/c, dihadron prod., A depend. of prod. cross sections for massive dihadron states 78−33180
W+p, 400 GeV/c, dimuon mass spectrum, ϒ signals 78−89857
W+p, 50 to 275 GeV/c, inclusive particle prod., nuclear size depend. 77−46168
W+p, props. of prompt muons prod. by 28 GeV protons 79−17906
W+p, relative yields of K-mesons, p̄ and d̄ with 25 GeV/c momenta *(Russian)* 77−38277
W+p→muons, 28.5 GeV, large transverse momenta, μ polarisation meas. 77−71542
^{183}W(p,t), 21 MeV, ^{181}W levels (neutron and collective) and J$^\pi$, ang. distribs. 80−78160
^{184}W(p,X), 400 GeV, absorption cross sections and multiplicity distribs., A-depend. study 79−67748
^{187}W+p, 2 to 5 GeV/nucleon, multiplicities of secondary particles *(Russian)* 78−46066
W(p,X), 10-60 MeV, long lived radioisotope prod. cross sections and excitation functions 79−89305
W(p,X) 200, 300, 400 GeV, hadron prod. at large p_T invariant cross section 79−40926
W(p,X), 400 GeV, particle mean multiplicities 80−13473
W(p,X), 8 GeV, β-active superdense nuclei search *(Russian)* 80−42535
W(p,2π$^-$X), 28.5 GeV, fireball model comparison 79−59059
W(p,p'e$^+$e$^-$), 1.0-2.5 MeV, e$^+$e$^-$ pair prod. search 80−27637
W(p, spallation), 1 GeV, ^{A}Lu, neutron deficient isotopes, A=157, 158, 160, 161, 163 79−75957
W(p,t), 21 MeV, ^{A}W, A=178, 180, 182, 184, levels and J$^\pi$, ang. distribs. 80−78159
W(p,t), pairing excitations in even nuclei, anal. 79−93532
W(p,t)W, A=182, 180, 178, at 21 MeV, pair excitations 77−88032
Xe prod. cross sections with protons of 320-590 MeV, nuclear medicine appl. 80−36133
^{125}Xe production by 1 GeV proton spallation on Cs, Ba, La 79−63676
^{125}Xe production by 1 GeV proton spallation on Cs, Ba, La 79−63676
Xe(p,X) 10-400 GeV A=3-14 fragment energy distrib. 79−17901
Xe(p,X), fragment prod. by two body breakup 79−85440
^{89}Y+p, 62 MeV, complex particle emission, pre-equilibrium exciton model anal. 78−66280
^{89}Y(p,α), microscopic anal. of low lying ^{86}Sr levels 78−70449
^{89}Y(p,γ$_0$)^{90}Zr, 14-27 MeV, E_2 and E_3 radiation anal. in direct-semidirect model 77−38266
Yb, fission, 1 GeV, cross section meas. *(Russian)* 78−94041
^{89}Yb(p,2nγ), 22.7 MeV, high spin states of ^{88}Zr 78−74383
^{170}Yb(p,α)^{167}Tm, α spectra and ang. distribs. calc., statistical knock-on model 77−79371
^{171}Yb(p,4n), 40 MeV, interpretation with level scheme of ^{167}Lu 77−88026
^{176}Yb(d,xnγ), 14 MeV, γ-ray spectra angular distribs. and γγ coincidences 79−75838
^{176}Yb(p,3n), 22.7 MeV, ^{174}Lu isomeric levels, γ-spectra, T 1/2 and decay modes 80−99151
^{176}Yb(p,α), 16 MeV, ^{173}Tm level and band struct., spin assignments, ang. distribs. 79−474
^{176}Yb(p,xnγ), 66 MeV, γ-ray spectra angular distribs. and γγ coincidences 79−75838

proton-nucleus reactions continued
^{176}Yb(p,xnγ), 6.6 MeV gamma-ray spectra *(Russian)* 78−54720
Yb(p,n), 13 MeV, ^{A}Lu A=171, 173, Nilsson state transitions from 1/2 life, Coriolis coupling matrix 79−6485
^{A}Zn(p,α), 12.5 MeV, A=64,66,68,70, compound and precompound α emission spectra 78−82367
^{64}Zn(p,d), 18 MeV, ^{63}Zn level scheme, spin and parity assignments 79−465
Zn(p,X), A=64, 66, 68, 17.5-48 MeV, proton total cross section 78−8809
^{A}Zr(p,4pxn)Rb, A=90, 91, 94, spallation reactions, nuclear structure influence on yields of product nuclei 80−22794
^{A}Zr(p,6pxn)Br, A=90, 91, 94, spallation reactions, nuclear structure influence on yields of product nuclei 80−22794
^{A}Zr(p,n), 11.2 MeV, A=90, 91, 94, spin cut-off parameters from neutron ang. distribs. *(Russian)* 79−80940
^{A}Zr(p,n), 5.055, 5.27 MeV, A=92, 94, γ-ray multipolarities, internal conversion coeffs., energy levels 79−63625
^{A}Zr(p,n), A=92, 94, 1.7-6.7 MeV, total cross sections, p strength functions, optical model anal. 80−18301
^{A}Zr(p,p′), (A=90,92), 20 MeV, polarisation effects on nuclear excited states *(Russian)* 80−27645
^{90}Zr (p,n)$_{g}$ nucleon optical potential from Lane model 80−83097
^{90}Zr (p,π^{+}), 180 MeV, ang. distribs., discrete states, differential cross section 79−13298
^{90}Zr(p,X), 90 MeV, charged light particle energy spectra exciton and evaporation model anal. 79−40923
^{90}Zr(p,d), 121 MeV, DWBA applicability test, d D-state contribs. 79−13261
^{90}Zr(p,d), 50 MeV, fine struct. of ground hole-state analogues 78−50065
^{90}Zr(p,n), 120 MeV, ^{90}Nb giant particle hole resonances, Gamow-Teller strength 80−86877
^{90}Zr(p,n), IAS transition, 18.5 to 45 MeV, microscopic model anal. 77−82927
^{90}Zr(p,nx), 45 MeV, preequilib. ang. distrib., generalised exciton model 77−10407
^{90}Zr(p,π^{+}), differential cross sections, DWBA calc. 79−85415
^{91}Zr(p,nγ), 3.5-4.8 MeV, ^{91}Nb lifetimes, branching ratios, multipole mixing ratios 78−13011
^{92}Zr(p, n), 4.25-5.30 MeV, ^{92}Nb energy levels, spins, parities 77−14125
^{92}Zr(p,α), ^{89}Y gamma transitions, microscopic finite-range anal. 80−63181
^{92}Zr(p,α), 35 MeV, polarised p, DWBA anal., anal. power, optical pot., J-depend. 79−3143
^{92}Zr(p,α)^{89}Y, 35 MeV, analysing power study *(French)* 79−75981
^{92}Zr(p,α)^{89}Y, 35 MeV, microscopic DWBA anal. of three particle transfer 79−9567
^{92}Zr(p$_{pol}$, A)^{89}Y, finite-range cluster-model description, DWBA approach 80−52667
^{94}Zr(p,n), 6-9 MeV, ^{94}Nb level density, neutron spectra and ang. distribs. nonequilib. processes *(Russian)* 80−37376
^{94}Zr(p,n)^{94}Nb, differential cross section, 1.7-3.0 MeV 79−9551
^{94}Zr(p,nγ), 1.7-30 MeV, ^{94} Nb excited states, spin, parity, γ-spectra 77−88125
Zr(p,4pxn)Rb spallation reactions, 1 GeV, meas. with online mass spectrometer *(Russian)* 77−10409
Zr(p,n), 11.2 MeV, ^{A}Nb, A=90,91,94 neutron spectra, level density, direct processes *(Russian)* 79−67666

proton-nucleus scattering
see also neutron-proton scattering; proton-proton scattering
^{16}O(p,p), spin orbital interaction and nucl. matter density distrib. *(Russian)* 79−22176
^{18}O(p,p), polarised p, elastic and inelastic, 6.1-16.6 MeV, ^{19}F resonance parameters and J^{π} values 79−45232
A=9 to 70, 14 to 45 MeV, differential cross sections 79−45273
A>4, elastic and inelastic scatt., intermediate and high energies, research review 78−94010
A(p,p′)X, inclusive reaction cluster emission models 79−6441
angular distribs. and energy spectra of elastic and inelastic scatt. 78−62674
angular momentum depend. optical pots., physical interpretation for p elastic scatt. 79−26431
central p-wave parameter meas., p+polystyrene 5.9-9.9 MeV, nucleon-nucleon force 77−67748
compound nucleus (p,p′) cross-sections in Ni region, 12 MeV 77−74864
deep inelastic processes as multi-step direct reactions, (p,p′) appl. 77−26652
differential cross sections meas. by SPES I 79−75983
diffraction scatt., polarization of nucleons *(Russian)* 79−89285
double magic nuclei, self consistent description of low lying collective states *(Russian)* 78−89783
effective inelastic cross-section for high-energy protons 77−61412
eikonal anal. of high energy scatt. *(Russian)* 77−22908
elastic, spin-rotation effects 79−26441
elastic and inelastic proton-nuclear scatt. at high energy *(Chinese)* 78−13074
elastic proton and neutron, cross sections, microscopic optical model pot. calcs. 78−593
elastic scattering amplitudes at 1 GeV, target matter and neutron radii 78−70515
elastic scattering of protons, ang. distrib., cross section, anomaly rel. to shell struct. of target 78−54752
elastic scattering theory, multiple scatt. test review 80−42654
emulsion, 400 GeV, inelastic scatt., secondary charged particle multiplicities *(Russian)* 78−89880
emulsion, 400 GeV, shower particle ang. distribs. from inelastic collisions, Glauber-Gribov model *(Russian)* 78−89881
emulsion, 67-400 GeV, leading baryon pseudorapidity distribution, leading particle props. 79−6611
emulsion nuclei, proton inelastic interactions, 22.6, 24 and 70 GeV/c 78−74351
Ericson fluctuations in polarised (p,p) reactions *(Rumanian)* 80−5113
even-even spherical nuclei, 2_1^+ state deformation parameter from (p,p) and EM excitation 80−27549
gamma-ray line emission from nucleus de-excitation following energetic particle reactions 80−18219
giant quadrupole resonances in light nuclei excited by α or p inelastic scatt. 78−624
Glauber model calculations at 1 GeV 79−13260
Glauber theory of high-energy proton elastic scattering 77−41966

proton-nucleus scattering continued
Glauber theory of spin-orbit interactions 1 GeV (p,p) scatt. 78−37336
high energy elastic scatt., prediction from nucleon density distrib. 78−54738
high energy hadron-nucleus scatt., correl. and isospin effects, multiple diffr. theory 78−94000
high resolution proton scattering 79−45252
high-energy elastic and inelastic scatt. by light nuclei, mechanism and struct. determ. *(French)* 79−534
high-resolution elastic scatt., techniques and results 77−75008
inelastic p scattering, two step process, three body model, (core+n)+p system 78−62537
intermediate atomic weight nuclei, 6 MeV proton scatt. anal., quadrupole deform. 78−13076
intermediate energy nuclear physics, review of recent expts. 78−50061
isoscalar giant monopole resonance systematics from 60 MeV (p,p′) 79−17879
L-depend. optical pots., local density models 79−93583
light and intermediate nuclei, polarisation phenomena interpret. 78−13051
light ion scatt., optical pot. and proximity pot. comparison 79−3121
microscopic optical model anal. of (n,n) and (p,p) cross sections 78−29434
multiple Coulomb scattering angle meas. 50 to 200 GeV/c 80−9315
multiple scattering with rearrangement 79−504
N=82 nuclei, elastic and inelastic polarised proton scatt., isobaric analogue states 77−74825
neutron disrib. anal. from 0.8 to 1.5 GeV data 79−26429
neutron distribution in nuclei, elastic and inelastic proton scattering, review 80−22649
optical model pot. with l-depend., elastic and polarisation anal. 77−61394
optical model proton scatt. parameters at subcoulomb energies 79−93584
optical potentials, vol. integrals calc. 77−10403
polarised proton elastic scatt., 30 MeV, optical model anal. 78−597
quasi-elastic multiple scatt. 78−62515
quasielastic scatt. at 800 MeV, detection of α- and D-clusters 79−6579
radiography, medical application *(French)* 79−2128
relativistic particle production on nuclei at large angles, multiple interaction mech. *(Russian)* 77−74822
review, hadron-nucleus interactions at high energies, phenomenological models 78−8859
review, high resolution scatt., 1 GeV protons 78−70536
review of proton scattering at 1 GeV 79−26428
scattering of amplitude, physical constraints 79−71824
solar flare energy spectrum simulation from monoenergetic incident proton beam 78−12786
spin flip effects at high energy *(Chinese)* 77−74840
spin zero nuclei+polarised proton, Coulomb multiple scatt. anal. 79−22277
spline interpolation method appl. to optical potential 80−32272
stable isotope tracer analysis by proton scattering 80−104487
summed scattering (elastic and inelastic with no meson production), 2.1 GeV/c, asymmetry meas. *(Russian)* 79−89313
(α,n,p) elastic scatt., ^{6}Li structure three body model 79−75875
^{2}H(p,p), theoretical anal. of nucleon-nucleon forces 79−9554
(p,n), centre-of-mass spuriosity in continuum shell-model calculations 80−32210
(p,n) transitions to anti-analogue states, fluctuations in Lane pot. 78−8815
(p,p), 0.1-1 GeV, optical pot., vol. integrals and root mean square radii 80−106054
(p, p), 1 GeV, polarisation data, Glauber anal. spin-orbit parameters, matter distribs. 80−52655
(p,p), 1 GeV, polarisation features, Glauber model calcs. 79−40915
(p,p), 1 GeV elastic and inelastic scatt., diffr. minima filling mechanism *(Russian)* 80−86907
(p,p), 10 to 50 MeV, scatt. data on nuclei of A≤70 79−93633
(p,p), 100-2200 MeV, total and reaction cross sections from optical pot. 80−18303
(p,p), 600, 750 MeV, polarisation and cross section, Glauber model calc., NN matrix test 80−47485
(p,p), <100 MeV, Coulomb corrections to NN coupled states, nonrelativistic scatt. theory 80−78114
(p,p), A=9 to 70, differential cross sections, struct. effects, optical and coupled channel anal. 80−47482
(p,p), centre-of-mass spuriosity in continuum shell-model calculations 80−32210
(p,p), cross section and polarisation, Lane model extension to light nuclei 79−85449
(p,p), elastic, inelastic polarised and unpolarised, intermediate energy study review 80−42653
(p,p), isobaric analogue resonances, microscopic and phenomenological parameters, S-matrix eval. methods 78−13045
(p,p), knock-on exchange, local equivalent methods 78−33184
(p,p), microscopic optical model pot 78−54729
(p,p), new type of parameter systematics 79−93630
(p,p), on ^{40}Ca, ^{48}Ca, ^{90}Zr, and ^{208}Pb, (in)elastic scatt., self-consistent calcs. of nuclear density *(Russian)* 79−80928
(p,p), pol. p, sd, fp shell nuclei, 65 MeV, effective two-body interaction range 80−32201
(p,p), polarisation in elastic scatt., multiple diffraction approx. 79−97696
(p,p), polarised p, 0.8 GeV, neutron isotopic density differences and RMS radii 79−67643
(p,p), reduced normalisations 78−86522
(p,p), semi-phenomenological anal. 79−93632
(p,p), single particle bound state, energy independ. optical model, asymmetry term 80−37316
(p,p), small distances, new electrodynamics approach 80−63180
(p,p), statistical significance of spreading widths for doorway states, reply to comments 80−63147
(p,p̄) and (p,p), from Be, C, Al, Cu, Sn, Pb, 70, 125, 175 GeV/c 80−83128
(p,p) elastic and inelastic on s-d shell nuclei, polarised p, nuclear matter distrib. 78−78297
(p,p) isotopic effects, cross sections and polarisation ang. distrib. *(Russian)* 79−36246
(p,p) on Li, Be, C, Al, Cu, Sn, Pb, 30 to 50 GeV/c, nuclear radii, real/imaginary forward scatt. amplitude ratio *(Russian)* 77−34351
(p,p) quasifree scatt., polarised p, nuclear state information 79−75846

proton-nucleus scattering continued
(p,p) scatt., with polarised protons, ang. distribs. anal. 77−2973
(p,p) scatt. on light nuclei, 6 MeV, optical model anal. *(Russian)* 78−25200
(p,p) total cross sections, 180 to 560 MeV, Galuber model calcs. 79−40917
(p,p′), 800 MeV, cross sections, quasifree knockout mechanisms, PWIA calcs. 80−78294
(p,p′), A=6 to 208, 800 MeV, proton spectra, quasifree scatt., DWIA anal. 80−52677
(p,p′), compound nucleus lifetimes from X-ray method, statistical properties 80−78295
(p,p′), deformed nuclei, ground state rot. band, shape meas. and exchange contrib. 79−451
(p,p′), deformed nuclei, local approx. results for exchange effects 79−452
(p,p′), direct, and multistage processes, DWBA anal. *(German)* 78−25202
(p,p′), ground state correlation, continuum spectra 78−94007
(p,p′), hadronic transition operator for collective state transition rates 79−45262
(p,p′), light and intermediate nuclei, analysing capacity, 2^+ state excitation 79−6558
(p,p′), polarised p, cluster struct. of 2s-1d shell nuclei 79−6557
(p,p′), scatt. of 32 MeV polarised protons, spin-flip 77−71601
(p,p′), single neutron states, two step process and effective interaction 80−78290
(p,p′), transition strengths, unnatural parity state excitation of stretched configs., NN forces 79−63626
(p,p′), unnatural parity states excitation, π-condensate instability effects, DWBA anal. 80−78168
(p,p′) and (e,e′) scattering, core polarisation, microscopic models, transitions, cross sections, form factors 78−604
(p,p′) inelastic spectra in high energy continuum, single and multiple scatt. mechanisms 80−57777
(p,p′) on light nuclei, analysing power, primary factors 79−6559
(p,p′) on light nuclei, polarised protons, analyzing power ang. depend. 77−61411
(p,p′) to collective states, medium energies, spin-orbit deformation from DWBA calcs. 79−9565
(p,p′γ), low energy scatt. by medium weight nuclei, statistical theory *(Russian)* 77−319
(p,X), experimental information review, polarisation phenomena 80−42655
p($\vec{p}$)+light nuclei, high energy cross section calc., complex ang. momentum theory *(Russian)* 78−46067
p-H_2O 6 GeV/c scatt. with polarised protons, helicity-depend. and P-violation 77−30403
p+complex nuclei, 10 GeV, inelastic emulsion scatt., optical model anal. *(Korean)* 78−50165
p+Z→Z+W^++n, high energy total cross sections calcs. *(Russian)* 77−46086
pd, elastic scatt. analysing power meas. 78−93901
pp, low energy scatt., spin depend. EM force effects, Coulomb DWBA anal. 79−9568
^{12}C(p,p), 11.5-18 MeV polarised protons, ang. distribs. 77−3010
^{116}Sn(p,p), 0.8 GeV polarised p, differential cross section and analysing power data anal. 78−70526
Ag+p, inelastic interactions, 6.0 GeV/c, in emulsions 78−86530
^{A}Ag(p,p), A=107,109, 2.0-6.7 MeV, cross sections, Hauser-Feshbach optical calcs. for p absorption systematics 80−47483
^{109}Ag(p,p′), pol.p, 6.06 MeV, anal. powers, large absorption pot., optical model 80−83092
^{27}Al (p,p_0), elastic resonance scatt., 0.85-3.0 MeV, excitation functions 77−14121
^{27}Al(p, p′), 6.44 MeV, ^{28}Si resonance wave functions and differential cross sections 80−18261
^{27}Al(p,X), X=p,n,α, 6.44 MeV, ^{28}Si resonance wave functions from differential cross sections 80−78239
^{27}Al(p,p), (p,n) threshold anomaly 78−94003
Al(p,p), 36.2 MeV, differential cross section, asymmetries, 0 to 7° scatt. 78−94002
^{40}Ar(p,p), 18-44 MeV, differential cross sections, phase shift anal., energy depend. 80−47481
^{40}Ar(p,p)^{40}Ar, E_p=1 MeV, cross section meas. 78−13089
^{197}Au, 16 MeV, coherent optical model analysis 77−26750
^{11}B(p, p), 1 GeV, quadrupolar effect, cross sections *(Russian)* 79−30834
^{11}B(p,n)^{11}C, shell model anal. of polarisation-analysing power differences 80−22804
^{11}B(p,p), 1.9 to 3.0 MeV, polarisation map, R-matrix study, ^{12}C 17.77 and 18.36 MeV state struct. anal. 79−9435
^{11}B(p,p), polarisation behaviour near (p,n) threshold, virtual scatt. mechanism feasibility 79−6592
^{11}B(p,p), polarisation effects for elastic scatt. near (p,n) reaction threshold 78−13075
^{11}B(p,p)^{11}B, resonant scatt., determ. of ^{12}C analogue states 77−38260
^{138}Ba(p,p′), 10-11.7 Mev polarised protons scatt. at IAR 77−2991
^{9}Be(p, p), 1 GeV, quadrupolar effect, cross sections *(Russian)* 79−30834
^{9}Be(p,α), meas. of second excited state excitation energy in Li 77−57619
^{9}Be(p,p′), 6.4 MeV, two stage mechanism described by square Feynman diagrams *(Russian)* 79−22299
^{9}Be(p,p), 22-8 MeV, polarised protons, R-matrix theory 77−82921
^{9}Be(p,p), cross sections and polarisation from Lane model anal., multichannel constraints 79−80914
^{9}Be(p,p), polarisation effects for elastic scatt. near (p,n) reaction threshold 78−13075
^{9}Be(p,p)^{9}Be, 2.56 MeV, ^{10}Be, 8.89 MeV reson. J^π 77−50098
^{9}Be(p,p)X, 0.8 GeV, inclusive cross sections, quasi-two-body scaling 79−3150
^{9}Be(p,pn)^{8}Be, kinematically complete exam. of ^{9}B and ^{9}Be levels 78−21550
Br+p, inelastic interactions, 6.0 GeV/c, in emulsions 78−86530
C+p, inelastic interactions, 6.0 GeV/c, in emulsions 78−86530
^{A}C(p,p), A=12, 13, 0.8 GeV, elastic and inelastic, ang. distribs., states, optical and DWBA anal. 79−3154
^{12}C, excitation cross sections induced by 1 GeV protons and electrons, Glauber theory *(Russian)* 78−41684
^{12}C, high energy scatt., deformed translationally invariant model 79−58996
proton-nucleus scattering continued
^{12}C, penetration range, 200 MeV to 2 GeV *(French)* 78−4964
^{12}C, quasielastic scatt. of polarised 635 MeV protons, depend. of left-right asymm. on nucl. momentum *(Russian)* 77−79384
^{12}C+p, 9.5 MeV, optical pot., inverse scatt. method *(Russian)* 79−552
^{12}C(p, p), 1 GeV, quadrupolar effect, cross sections *(Russian)* 79−30834
^{12}C(p, p), 1.7-1.89 MeV, bremsstrahlung spectra, soft photon and Feshback-Yennie approx. 79−80937
^{12}C(p, p), excitation function at 14.232 MeV, proton beam energy spread determ. 78−70669
^{12}C(p,X), reaction and scatt. dynamics, optical and coupled channel anal. 80−78297
^{12}C(p,2p)^{11}B, 1 GeV, quasi-elastic multiple scatt. 78−62515
^{12}C(p,p′), 0.8 GeV, DWBA and coupled-channels anal. 78−74367
^{12}C(p,p′), 0.8 GeV, polarised p, spin orbit deformation effects, DWBA anal. 79−30832
^{12}C(p,p′), 1 GeV, multiple scatt. expansion 78−50156
^{12}C(p,p′), 1 GeV, proton polarisation in natural parity level excitation *(Russian)* 80−42634
^{12}C(p,p′), 1^+(T=1, 15.1 MeV) state excitational pionic modes, M1 form factor 80−78195
^{12}C(p,p′), 122 MeV, level excitation, cross sections, effective NN interaction, DWIA anal. 80−78197
^{12}C(p,p′), 122 MeV, precritical phenomena 80−83089
^{12}C(p,p′), 16-40 MeV, ^{13}N giant dipole reson. as doorway-states 77−6336
^{12}C(p,p′), 185 MeV, elastic and inelastic scatt., proton polarisation and ang. distribs. 79−59060
^{12}C(p,p′), 22-27 MeV, 1^+ state de-excitation γ-ray ang. distrib., tensor force effects, DWBA anal. 80−68580
^{12}C(p,p′), 45, 155 MeV, high lying continuum states, multipolarities, strengths 77−82925
^{12}C(p,p′), 50, 65 MeV, isospin depend. on analysing powers 78−82343
^{12}C(p,p′), 62, 120 MeV, isobaric analogue states, differential cross sections 80−18202
^{12}C(p,p′), 64 MeV, direct reaction, model t-matrix test, cross section and anal. power 79−93594
^{12}C(p,p′), 800 MeV, 15.11 MeV state diff. cross section, nuclear critical opalescence search 80−105984
^{12}C(p,p′), 800 MeV, multistep processes, ang. distribs., Glauber model anal. 80−47475
^{12}C(p,p′), Glauber model, shell model wave functions, EM form factor, spin effects 77−46164
^{12}C(p,p′), non-eikonal effects in high energy inelastic scatt. 80−42608
^{12}C(p,p′), pair decay of 7.65 MeV level meas. 78−29469
^{12}C(p,p′), pol. p, 800 MeV, unnatural parity states excitation, anal. powers and isospin 80−68538
^{12}C(p,p′), single proton distrib. anal. 78−603
^{12}C(p,p′), spin flip excitation of 1^+ T=0 state 78−8817
^{12}C(p,p′)^{12}C, PWIA anal. and bound-state momentum distribs. 78−601
^{12}C(p,p′)^{12}C*, pol. p., 19-23 MeV, giant resonances as doorway states, virtual excitation 80−5102
^{12}C(p,p′)^{12}C*, test of Monte Carlo efficiency calcs. for scintillation counters 80−37713
^{12}C(p,p′γ), 23.5-27 MeV, 1^+ state spin flip meas. DWBA anal., cross sections 80−68529
^{12}C(p,p′), 20-40 MeV, pol. p, anal. powers, imaginary spin-orbit pot., coupled channels anal. 80−102179
^{12}C(p,p′), 65 MeV, 2^+ (4.43 MeV) state, transition DWA anal. 79−67704
^{12}C(p,p′), polarised p, 20, 30, 40 MeV, anal. power and cross sections, spin-orbit deformation 79−75963
^{12}C(p,p), 0.3-2.0 MeV, level parameters ^{13}N anal. 77−3007
^{12}C(p,p), 0.8 GeV, analysing powers 78−54760
^{12}C(p,p), 0.8 GeV, ang. distrib. meas. 78−25186
^{12}C(p,p), 0.8 GeV, polarised p, differential cross section, anal. power, nuclear matter densities 79−13299
^{12}C(p,p), 1 GeV elast. and inelast. scatt. and nuclear deform., Glauber theroy 77−6377
^{12}C(p,p), 11.5 to 18 MeV polarised beam, ^{13}N level structure 77−315
^{12}C(p,p), 14-45 MeV, differential cross section and spin-flip probabilities, giant resonances 80−73850
^{12}C(p,p), 144 MeV, elastic scatt. cross sections, optical pot. 80−42660
^{12}C(p,p), 3-61.4 MeV, α-cluster contribs., semi-classical model 79−36233
^{12}C(p,p), 3.0 MeV, elastic scattering, discrepancies from optical model, possible α-cluster struct. 78−62528
^{12}C(p,p), 40-75 MeV, polarisation meas., differential cross sections 80−52840
^{12}C(p,p), 50-160 MeV, energy depend. optical pot. 80−22830
^{12}C(p,p), 6-8 MeV polarised proton calib. standard 77−10573
^{12}C(p,p), 60 to 183 MeV, folded potentials for d intermediate channels 79−17868
^{12}C(p,p), 635 MeV, left-right asymmetry depend. on residual nucleus momentum *(Russian)* 78−54765
^{12}C(p,p), 6.9 GeV/c, elastic and inelastic differential cross sections *(Russian)* 79−59071
^{12}C(p,p), analogue resonances to ^{13}C parent states 78−13046
^{12}C(p,p), below 8 MeV, iterative R-matrix in collective rot. model, phase shifts, inelasticity 79−3141
^{12}C(p,p), bremsstrahlung near 1.7 MeV resonance 80−68670
^{12}C(p,p), elastic and inelastic scatt., 185 MeV, polarisation, diffraction model anal. 79−75943
^{12}C(p,p), hadron induced semicoherent scatt., excitation of ^{12}C(2^+, 4.4 MeV) level 78−70569
^{12}C(p,p), multichannel quasi-separable pot. approach 78−37320
^{12}C(p,p), optical potential, spin-orbit term 80−52668
^{12}C(p,p), pol. p, 14.23 MeV resonance broadening, nuclear recoil, atomic excitation effects 80−102165
^{12}C(p,p), pol. p, 450-600 keV, Mott-Schwinger interaction existence, anal. power 80−22805
^{12}C(p,p), radial sensitivity of optical pot. 80−86869
^{12}C(p,p), spin rotation angle meas. appl. to phase shifts 77−3011
^{12}C(p,p), spin-flip probability to first 2^+ level 80−78288
^{12}C(p,p) dispersive effects in ground state rot. band excitation, coupled channel calcs. 79−40828
^{12}C(p,p) forward scatt., dispersion anal., ^{12}C and ^{13}N ground states 77−34297
^{12}C(p,p) quasielastic scatt., 635 MeV polarised protons, asymm. meas. *(Russian)* 77−74852

proton-nucleus scattering continued
^{12}C(p,p) spin 0-spin 1/2 phase shift anal. discrete ambiguities 80−18307
^{12}C(p,p)^{12}C, 1 GeV, polarisation meas. 77−88103
^{12}C(p,p)^{12}C, elastic and inelastic, 1 GeV, α-particle model in Glaüber multiple scatt. theory 77−30577
^{12}C(p,p)^{12}Cm bremsstrahlung near 1.7 MeV resonance 79−45249
^{12}C(p,pγ), bremsstrahlung cross section near 1.7 MeV resonance, Feshbach-Yennie approx. 80−42662
^{12}C(p,pγ), meas. of bremsstrahlung spectra to determ. reaction time delays of 10^{-20} sec. 77−6378
^{13}C(p, p), 1 GeV, quadrupolar effect, cross sections *(Russian)* 79−30834
^{13}C(p,p), 9.1-18.4 MeV, polarised p, cross section phase-shift anal., ^{14}N possible resonances 79−6602
Ca (p,p), 1 GeV, neutron and proton RMS radii differences in matter 79−54403
^Ca(p,p′), pol. p, A=40,48, 800 MeV, diff. cross sections, anal. powers, DWIA anals., high spin levels 80−83067
^Ca(p,p), 0.6, 1 GeV, A=40,42,44,48, matter density, Glauber model anal. 79−93500
^Ca(p,p), 30.3 MeV, A=40,44,48, cross section ratio, optical model anal. 79−54441
^Ca(p,p), A=40,42,44,48, elastic and inelastic scatt. cross-sections from Hartree-Fock densities *(Russian)* 79−13287
^Ca(p,p) A=40,48, static and transition densities, self consistent RPA theory test in fast scatt. *(Russian)* 79−49604
^{14}Ca(p,p), A=40, 42, 44, 48, 1 GeV, cross sections using nuclear densities from self-consistent methods *(Russian)* 78−41724
^{14}Ca(p,p), A=40-48, elastic scatt. cross section ratio meas. 79−93634
^{40}Ca (p,p), elastic scatt., polarisation and spin-orbital amplitude parameters, 1 GeV *(Russian)* 78−17208
^{40}Ca, penetration range, 200 MeV to 2 GeV *(French)* 78−4964
^{40}Ca+p, fine struct. levels sign meas., off-diagonal strength function, analogue state broadening theory test 78−78381
^{40}Ca+p, optical model potential, spin-orbit component from internucleon pot. 78−46039
^{40}Ca(p, p′), isovector dipole strength excitation in giant resonance region 80−83066
^{40}Ca(p,p′), 25-46 MeV, effects of two-step process determ. 78−21569
^{40}Ca(p,p′), 800 MeV, high energy octupole giant resonance, ang. distribs. 80−86879
^{40}Ca(p,p′), giant resonances from antisymmetrised DWBA anal. 79−85432
^{40}Ca(p,p′), realistic complex nuclear matter t-matrix anal. Hamada-Johnston pot. 79−9564
^{40}Ca(p,p′)^{40}Ca, 185 MeV, scatt. from 3$^-$ and 5$^-$ states, DWIA anal. 77−18537
^{40}Ca(p,p′γ), 6.02-6.48 MeV, ^{41}Sc 2p-1h intermediate struct. resonances, anal. powers, J^π 80−86883
^{40}Ca(p,p′γ), 6.25 MeV, triple ang. correlation, 3$^-$ exit channel, resonances, single particle states 80−68626
^{40}Ca(p,p), 1 GeV, Glauber approx. corrections, differential cross sections 78−50166
^{40}Ca(p,p), 1.04 GeV elastic scatt., polarisation 78−21549
^{40}Ca(p,p), 30 MeV, optical pot. imaginary part calcs. 80−86868
^{40}Ca(p,p), 30.3 MeV, microscopic anal. 79−93631
^{40}Ca(p,p), absorbing optical pot., Coulomb correction term 80−73831
^{40}Ca(p,p), E_p=1 GeV, elastic differential cross sections 78−13082
^{40}Ca(p,p), elastic and inelastic scatt., 185 MeV, polarisation, diffraction model anal. 79−75943
^{40}Ca(p,p), elastic scatt. at medium energies, microscopic optical pots. 79−97703
^{40}Ca(p,p), evidence for ang. mom. depend. optical model pots. 79−13290
^{40}Ca(p,p), high energy differential cross sections, nucleon density distrib. 78−54738
^{40}Ca(p,p), imaginary spin-orbit term in proton optical potential, ang. distribs. 78−58273
^{40}Ca(p,p), optical potential from realistic Hamada-Johnston internucleon pot., binding energy 78−54730
^{40}Ca(p,p), spline interpolation method appl. to optical potential 80−32272
^{40}Ca(p,p)^{40}Ca, 1.04 GeV, nuclear matter density calc. 77−34303
^{40}Ca(p,p′), DWIA test in Glauber theory, transition density 80−99173
^{42}Ca(p,p), 1.2 to 3.0 MeV, cross-section meas., ^{43}Sc struct. 77−6374
^{42}Ca(p,p), E_p=1 GeV, elastic differential cross sections 78−13082
^{44}Ca(p,p), E_p=1 GeV, elastic differential cross sections 78−13082
^{48}Ca(p,p′γ), 28 MeV, lifetime of 5147 keV, 4504 keV, levels determ. 77−79381
^{48}Ca(p,p), 1 GeV, elastic scatt. differential cross section calc. 80−47480
^{48}Ca(p,p), 5.55 to 8.4 MeV, ^{49}Sc isobaric analogue states and resonances, J^π 80−13426
^{48}Ca(p,p), E_p=1 GeV, elastic differential cross sections 78−13082
Ca(p,p), 1 GeV, neutron densities 78−17087
Ca(p,p), 30 MeV, A=40, 48, pick-up and inelastic scatt. contributions to p optical pot. 78−25182
Ca(p,p), A=40,48, 1 GeV, spin-effects, Coulomb interactions, Glauber theory 77−82931
Ca(p,p) for A=40,42,44,48 isotopes, 1.044 GeV, elastic and inelastic, Glauber theory anal. 77−18536
Ca(p,p′), 19 MeV, nuclear struct. anal. 78−17197
^{106}Cd(p,p′), 10, 12 MeV, compound nucleus lifetime by X-ray spectroscopy 80−22831
^{106}Cd(p,p′)^{106}Cd, simultaneous nucl. and K-shell excitation, ^{107}In lifetime meas. 80−63130
^{112}Cd(p,p′), 30 MeV polarised proton inelastic scatt., phonon states 77−2982
^{114}Cd(p,p′), 11 MeV, polarised p, differential cross sections, anal. powers, spin flip prob. 79−89284
^{114}Cd(p,p′), optical pot. deform. effect on analysing power and p-γ ang. correlations 79−17903
^{116}Cd(p,p′γ), 5-20 MeV, lowest 3$^-$ collective level identification from decay excitation function 79−9444
Cd(p,p)Cd, A=110, 112, 5-9 MeV, isobaric analogue reson., QRPA calc. 78−576
^{140}Ce(p,p′), 30 MeV, DWBA, Ce levels, spin, parity, deform. parameters, enhancement factors 77−54217
^{35}Cl(p,p), (p,n) threshold anomaly 78−94003
^{59}Co(p,2p)^{58}Fe, 17 MeV, search for double-direct reaction 77−30576
^{59}Co(p,p′), 6 MeV, level energies, branching ratios lifetimes and spins 80−63093

proton-nucleus scattering continued
C(p,p), 36.2 MeV, differential cross section, asymmetries, 0 to 7° scatt. 78−94002
C(p,p′), 0.6-25 GeV, backward emitted proton inclusive spectra, short range correlation 80−32281
^Cr(p,p′), 6 MeV, A=50, 52, p spin flip probability 79−9561
^Cr(p,p), A=50, 52, 6 MeV, elastic and inelastic differential cross sections, spin flip probability *(Russian)* 80−91187
^{50}Cr(p,p′γ), 2.00-3.03 MeV, proton and γ-ray ang. distrib. meas., p-wave reson. obs. 77−41961
^{50}Cr(p,p), (p,p′), 3.2 to 4.4 MeV, high resolution, study of ^{51}Mn levels 77−54151
^{50}Cr(p,p) and (p,p′), E_p=6 MeV, cross sections, opt. pot. parameters 78−13086
^{52}Cr(p,p′), 4.7-5.4 MeV, cusp behaviour of cross-section obs. 78−29470
^{52}Cr(p,p) and (p,p′), E_p=6 MeV, cross sections, opt. pot. parameters 78−13086
^{63}Cu(p,p′), 40 MeV, octupole states, weak coupling model 79−93495
^{63}Cu(p,p′) negative parity level excitation, gamma ray obs., test for core excitation model 80−68534
^{63}Cu(p,p′γ), 4.2-6.0 MeV, ^{63}Cu levels 78−78378
^{63}Cu(p,p′γ) 5.0 MeV, ^{63}Cu EM props. 77−74800
^{65}Cu(p,2p)^{64}Ni, 17 MeV, search for double-direct reaction 77−30576
^{65}Cu(p,p′γ), 5.25, 6.0 MeV, levels, transition energies, lifetimes, branching ratios determ. 77−41960
Cu(p,p′), 0.6-25 GeV, backward emitted proton inclusive spectra, short range correlation 80−32281
D(p,p), 630 MeV, asymmetry in scatt. polarised protons *(Russian)* 78−46064
^Eu(p,p′), A=151-3, 12 MeV, rot. states, deformation parameters, DWBA and coupled channel anal. 79−9459
^{154}Eu(p,p′), 12 MeV, ground band rot. states, deformation parameters, coupled channels anal. 80−9195
^{19}F(p,p′), 5.5 MeV; time differential obs. of perturbed γ linear polarisation distrib., Hanle effect 78−78360
^{19}F(p,p′γ), 1459→110 keV transition, E2/M1 mixing ratio 80−106013
^{19}F(p,p′γ)^{19}F, 5 to 9 MeV, levels, J^π, lifetimes, branching 77−297
^{19}F(p,p), 17.5 and 30 MeV, low lying level cross-sections, coupled-channel method 80−42649
^Fe(p,p′), A=54, 56, 6 MeV, resonances, spin flip and cross section depends., Hauser Feshbach anal. *(Russian)* 80−83084
^{54}Fe(p,p′), 39, 62 MeV, DWBA anal., collective spectra, direct process contrib. *(Russian)* 80−13408
^{54}Fe(p,p′), 3.25-4 MeV, ^{55}Co isobaric analogue resonances, J^π, partial widths and spectroscopic factors 79−85431
^{54}Fe(p,p′), 62 MeV, effect of nucleon mean free paths on intranuclear cascade calc., 77−67749
^{54}Fe(p,p′), pol. p, 800 MeV, diff. cross sections, anal. powers, DWIA anals. 80−83067
^{54}Fe(p,p′), testing self consistent models of collective and single particle struct. 78−82300
^{54}Fe(p,p′γ), ^{55}Co f-wave resonances, inelastic p amplitudes, analogue state spectroscopic factors 80−47451
^{54}Fe(p,p), 3.28-4.53 MeV, ^{55}Co IAR, J^π assignments 78−574
^{54}Fe(p,p), 5.5-6.2 MeV, resonance effects, deformation, spectroscopic factors, statistical, optical and DWBA anal. 79−6593
^{54}Fe(p,p), 800 MeV, polarised differential cross sections and anal. powers, n density 79−13297
^{56}Fe(p,p′), 4.7-5.4 MeV, cusp behaviour of cross-section obs. 78−29470
^{56}Fe(p,p), 6 MeV, elastic and inelastic, quadrupole deformation, IAR excitation, optical pots. *(Russian)* 80−63149
^{56}Fe(p,p), elastic scatt. in giant reson. region of ^{57}Co 77−18542
^{56}Fe(p,p), elastic scatt. in giant reson. region of ^{57}Co 77−18543
^{56}Fe(p,p), evidence for ang. mom. depend. optical model pots. 79−13290
Fe(p,p), 36.2 MeV, differential cross section, asymmetries, 0 to 7° scatt. 78−94002
Fe(p,p′), A=54,6, E=17.2, 20.4, 24.6 MeV polarised protons, optical model, DWBA anal. 78−13094
^{69}Ga(p,p′γ), 3.0-5.1 MeV, low lying state struct., lifetimes, spin and parity 79−467
^Ge(p,p′), A=70, 72, 74, appl. of crystal blocking technique to study highly excited nuclear continuum 79−45261
^{70}Ge(p,p′γ), 4.95-5.19 MeV, ^{71}As intermediate struct., resonance spin from ang. correlations 79−67729
^{70}Ge(p,p), 3.5 to 5.3 MeV, ^{71}As, isobaric analogue reson. 79−75951
^{74}Ge(p,p) elastic and inelastic scatt. at 3.3-5.4 MeV, IAR excit. 77−34278
^{1}H(p,X), elastic, inelastic and charge exchange cross sections in optical model 80−68665
^{1}H(p,p), 0.35-1.0 MeV, differential cross section meas. 78−78379
^{1}H(p,p), 1-3 GeV/c, pol. p, spin parameters A and A_{nn} 80−95304
^{1}H(p,p), 225, 327, 520 MeV, analysing powers 79−75961
^{1}H(p,p), 398-572 MeV, analysing power meas., EM-nuclear interf. 77−23008
^{1}H(p,p), 6.14 MeV, cross sections and anal. power for noncentral reaction 79−85444
^{1}H(p,p), 6.141 MeV, anal. power, Paris pot. predictions 80−63156
^{1}H(p,p), EM effects, separation 77−23014
^{1}H(p,p), pol.p, 9.57 MeV, spin correlation parameter, phase shift anal. 80−102112
^{1}H(p,p) 647 and 800 MeV, absolute differential cross-section meas. 77−6390
^{1}H(p,p)^{1}H, E_p=1 MeV, cross section meas. 78−13089
^{2}H, elastic scatt. of protons and α-particles *(Russian)* 78−21566
^{2}H+p, 50 MeV polarised p scatt., analysing power meas. 77−71608
^{2}H+p, polarised projectile, parity nonconservation in low energy scatt. 78−66271
^{2}H+p, polarised projectile, parity nonconservation in low energy scatt. 78−70522
^{2}H(p, p′) d bag, nuclear bag states containing quarks, detection 78−70465
^{2}H(p,2p)n, inelastic scatt. mechanism at moderate energy *(Russian)* 78−41723
^{2}H(p,p′), 0.6-25 GeV, backward emitted proton inclusive spectra, short range correlation 80−32281
^{2}H(p,p), 10 MeV, differential cross section, p and d analysing powers 78−46063
^{2}H(p,p), 10 MeV, differential cross section, (n,n) comparison for Coulomb force 79−71793
^{2}H(p,p), 40-1000 MeV backward scatt., N-exchange model 77−18562
^{2}H(p,p), 600 MeV and 1 GeV, noneikonal theory 79−80930

proton-nucleus scattering continued
^{2}H(p,p), 800 MeV, differential cross sections and anal. powers 80−83091
^{2}H(p,p), back angle elastic cross sections in Kerman-Kisslinger model, inelasticity corrections 80−106060
^{2}H(p,p), backscattering, large momentum transfers, π exchange effects 80−5143
^{2}H(p,p), Coulomb corrections near elastic threshold 77−34282
^{2}H(p,p), EM effects, separation, Coulomb problem 77−23014
^{2}H(p,p), large angle scatt., cross section and anal. power 79−80917
^{2}H(p,p), near threshold, on-shell two-body model 77−34283
^{2}H(p,p), pol.p, spin rot. and depolarisation, NN amplitude double spin flip part 80−78271
^{2}H(p,p), polarisation effects in 3-body system 79−80946
^{2}H(p,p), polarised p, 14.1 MeV, analysing power 79−71831
^{2}H(p,p), polarised p, 2.5-6.5 MeV, vector and tensor anal. powers 79−63653
^{2}H(p,p), polarised p, 316, 516 MeV, anal. powers in resonance region, backward angle scatt. 79−71834
^{2}H(p,p), polarised p, medium and high energies, polarisation phenomena 79−85448
^{2}H(p,p), precise low energy cross section meas. with polyethylene targets 78−82342
^{2}H(p,p), rank-1 pots. using shielded Coulomb pot., separable nuclear forces 79−71854
^{2}H(p,p), resonance amplitudes in light nuclei 77−18561
^{2}H(p,p), tensor asymmetries, deuteron D-wave and non-eikonal effects, Glauber model 80−78296
^{2}H(p,p) 17, 20, 24 MeV, polarised p and d, analysing power data 79−71830
^{2}H(p,p) elastic backward scattering, detection of d relativistic wave function dependence on additional variable *(Russian)* 79−58973
^{2}H(p,p) Glauber versus final state interaction theory, inelastic/elastic scatt. cross sections 77−57554
^{2}H(p,p) large angle elastic scatt., d form factor at large q^2 80−102189
^{2}H(p,p)^{2}H, 1.5-3 MeV, extraction of dnp coupling constant, Cutkosky method 77−10404
^{2}H(p,p)^{2}H, 1.825 GeV/c anal., Glauber theory comparison 77−71525
^{2}H(p,p)^{2}H, 316, 516 MeV, backscatt. anal. power meas. 78−74368
^{2}H(p,p)^{2}H, determination of Coulomb corrections 77−10400
^{2}H(p,p)^{2}H, large angles, resonance one-pion-exchange model *(Russian)* 77−34306
^{2}H(p,p)^{2}H backward elastic scatt., resonance region, double-scatt. mechanism *(Russian)* 77−74854
^{2}H(p,p)np, 13-19 MeV, p energy spectrum shape 79−6594
^{2}H(p,pγ), elastic cross sections, bremasstrahlung, threshold and Coulomb effects 80−91186
^{2}H(p,pp)n, 6.4 to 25.8 MeV, pn final state interaction, cross sections 78−54757
^{3}H(p, p), 600 MeV, Glauber formalism study *(French)* 79−93616
^{3}H(p,p), ^{4}He continuum microscopic calcs. cross sections and levels 80−57702
^{3}H(p,p), 0.6 to 1.04 GeV, differential cross sections calcs. *(Russian)* 78−54763
^{3}H(p,p), 1-10 MeV, isospin splitting of 1p-1h excitation in ^{4}He 78−41622
^{3}H(p,p), 156 MeV, differential cross section, diffr. theory of multiple scatt. 77−61404
^{3}H(p,p), 1.24 GeV, differential cross section, spin independ. Glauber model interpretation 80−63183
^{3}H(p,p), 1.26-3.71 MeV polarised p, spin depend. N-N forces 79−6634
^{3}H(p,p), 4-12 MeV, Amado model quasi-three body calc. 78−25191
^{3}H(p,p), 5.8 and 6.8 MeV, phase shift anal. *(Russian)* 77−65225
^{3}H(p,p), 8 to 17.1 MeV, cf. neutron polarisation in ^{3}He(n,n) 78−25171
^{3}H(p,p) four-nucleon integral eqn. solns. using effective UPA 79−71794
^{3}H(p,p), microscopic optical pot. calc. 79−85423
He+p, A=3,4, polarised projectile, parity nonconservation in low energy scatt. 78−66271
He+p, A=3,4, polarised projectile, parity nonconservation in low energy scatt. 78−70522
^{3}He(p, p), 1 GeV, differential cross section minimum, Glauber model description 79−80938
^{3}He(p, p), 600 MeV, Glauber formalism study *(French)* 79−93616
^{3}He(p,p), 0.6 to 1.04 GeV, differential cross sections calcs. *(Russian)* 78−54763
^{3}He(p,p), 156 MeV, differential cross section, diffr. theory of multiple scatt. 77−61404
^{3}He(p,p), 18-48 MeV, elastic differential cross section ang. distribs., four body problem 79−75998
^{3}He(p,p), 19-30 MeV, spin anal. power and phase shift anal. 79−13295
^{3}He(p,p), 1.75 to 4.13 GeV/N, small angle scatt., Glauber model *(Russian)* 78−41726
^{3}He(p,p), 1.75 to 4.50 MeV polarised protons, analysing power meas. for ^{4}He T=1 level ordering 79−26438
^{3}He(p,p), 415-800 MeV, large angle differential cross-sections 77−30573
^{3}He(p,p), 6.8 to 16.2 MeV, optical model pot. calcs. of cross section and polarisation data 79−63672
^{3}He(p,p), charge independ. R-matrix anal. of four nucleon system 79−85479
^{3}He(p,p), forward dispersion relations and wave function models 79−75956
^{3}He(p,p), generator coord. method study of ^{4}Li 80−27581
^{3}He(p,p), pol. p, 0.3-1.0 MeV, differential cross section, anal. power, and phase shifts 80−42629
^{3}He(p,p), polarised p, 6.8-10.7 MeV, polarisation transfer coeffs. 79−17889
^{3}He(p,p), polarised p, below 6 MeV, anal. power meas. for four nucleon system levels 79−71837
^{3}He(p,p) virtual scatt. from ^{4}He+p two pronged events 79−3152
^{3}He(p,p)^{3}He, 2.3 to 13.6 MeV data, phase shift anal. 78−78376
^{3}He(p,p)^{3}He, 2.3 to 8.8 MeV, ang. distribs. of analysing power 78−78375
^{3}He(p,p)^{3}He, four-body calc. solns. 79−71855
^{3}He(p,p)^{3}He, four-body model of the four-nucleon system 79−63643
^{3}He(p,p)^{3}He, four-body problem calc. 78−516
^{3}He(p(polarised),p)^{3}He, nuclear force and T-violation effects 78−4797
^{4}He (p,p), 200, 350, 500 MeV, differential cross-section and analyzing power meas. 78−17195
^{4}He (p,p), effective channel approach, N* resonance effects 79−9570
^{4}He (p,p), high and intermediate energies, polarisation, research review 78−94010
proton-nucleus scattering continued
^{4}He+p, 8.56 GeV/c, two pronged events, cross sections and prod. features 79−3152
^{4}He+p, elastic scatt. of intermediate energies, polarisation, momentum transfer effects 77−30408
^{4}He+p, interaction potential from inverse scatt. problem method *(Russian)* 78−46068
^{4}He+p(p), high energy cross section calc., complex ang. momentum theory *(Russian)* 78−46067
^{4}He(p, p), 1.05 GeV, cross sections and polarisations, correlation effects calcs. 80−57774
^{4}He(p, p), 225, 327, 520 MeV, analysing powers 79−75961
^{4}He(p,p), 0.35-23.1 GeV, differential cross section and polarisation, Glauber theory *(Chinese)* 79−49628
^{4}He(p,p), 0.4 GeV, nucleon-nucleon data inputs 78−74369
^{4}He(p,p), 0.5-1.7 GeV, differential cross section and polarisation meas. 79−22295
^{4}He(p,p), 0.56-1.73 GeV, differential cross-section meas. 77−88138
^{4}He(p,p), 0.58, 1, 2.1 GeV, corrections to Glauber model calc. 77−79379
^{4}He(p,p), 1 GeV, Glauber theory 77−41966
^{4}He(p,p), 185 to 500 MeV, large angle cross section, analysing power 78−74363
^{4}He(p,p), 1.05 GeV, backward peak, differential cross section meas. 78−70525
^{4}He(p,p), 20-55 MeV, anal. power, cross sections, phase shift anal. 79−9569
^{4}He(p,p), 200-500 MeV, differential cross section and anal. power 80−68640
^{4}He(p,p), 2.68 GeV, elastic differential cross section 79−17900
^{4}He(p,p), 45, 52, 60, 65 Mev, cross sections and polarisation meas. 79−97706
^{4}He(p,p), 45-65 MeV, phase shift anal. 80−22832
^{4}He(p,p), 560-1730 MeV, Dirac eqn. optical model anal. 78−29467
^{4}He(p,p), 5.75 GeV, meas. of $d\sigma/dt$, t=0.18 to 2.2 $(GeV/c)^2$ 78−70532
^{4}He(p,p), 600, 1050 MeV, optical model partial-wave anal. 77−10406
^{4}He(p,p), 68-125 MeV, resonating group anal. 77−88139
^{4}He(p,p), 788 MeV, back angle diffraction struct., Dirac, eqn. optical model 80−68667
^{4}He(p,p), 788 MeV, cross section, backward diffr.-like struct. evidence 78−94008
^{4}He(p,p), (p,p), 24, 50 GeV quasieikonal model, complex momenta theory *(Russian)* 78−29473
^{4}He(p,p), differential cross-section, multifold diffr. scatt. theory *(Russian)* 80−78303
^{4}He(p,p), differential elastic scatt. cross-section, 1 GeV protons *(Russian)* 77−79382
^{4}He(p,p), elastic scatt., medium energies, effective channel anal. 77−2997
^{4}He(p,p), elastic scatt. at medium energies, microscopic optical pots. 79−97703
^{4}He(p,p), intermediate energies, energy depend. of optical model 77−23006
^{4}He(p,p), intermediate energy, microscopic momentum space optical pot. calc. 79−71853
^{4}He(p,p), medium energy, anal. power, relativistic optical model anal. 79−40925
^{4}He(p,p), resonance amplitudes in light nuclei 77−18561
^{4}He(p,p) 18.6 GeV 79−3144
^{4}He(p,p) elastic scatt., 11.1-14.2 MeV, differential cross-section meas. 77−38270
^{4}He(p,p) elastic scatt., 1.05 GeV, shape around first interference minimum 77−57662
^{4}He(p,p) elastic scatt., polarisation meas. 0.56 to 1.73 GeV, $0.006 \leq -t \leq 1.2$ $(GeV/c)^2$ 77−57664
^{4}He(p,p) elastic scatt. near 1 GeV, Glauber theory calcs. 77−57663
^{4}He(p,p)^{4}He, 0-18 MeV, statistical anal., data fluctuations, error estimation 78−25196
^{4}He(p,p)^{4}He, calc. with Glauber model optical potential in Schrodinger eqn. 77−50093
^{4}He(p,p)^{4}He, elastic data for 350-1150 MeV 77−61424
^{4}He(p,p)^{4}He, optical model anal. 78−78369
^{4}He(p,p)^{4}He elastic scatt., 11.93, 17.00 MeV, analysing power meas. 77−38269
^{4}He(p,p)^{4}He forward amplitude real part, 1.5-10 GeV, from dispersion relns. 77−314
^{A}He(p,p), A=3,4, backscattering, large momentum transfers, π exchange effects 80−5143
^{A}He(p,p)^{A}He, A=3,4, depth profile meas. of He in Ni and Nb 79−14839
He(p,p), A=3,4, backward p elastic scatt. anal. using D and T exchange models 78−58270
H(p,x), direct and charge transfer scattering processes, second quantisation 80−78289
^{115}In(p,p), 2.0-6.7 MeV, cross sections, Hauser-Feshbach optical calcs. for p absorption systematics 80−47483
^{41}K(p,p'), ^{41}K l-forbidden M1 decay from 1st excited state 78−13024
^{41}K(p,p'), impurity in Co, hyperfine field calc. by gamma ray ang. corr. method 78−6340
^{41}K(p,pγ), 1.58 MeV, parity doublet gamma lifetimes, 3/2 levels, parity mixing 80−78209
^{A}Kr(p,p'), 51.9 MeV, A=78, 80, 82, 84, 86, 2_2^+ and 4_1^+ state excitation 79−54389
^{86}Kr ions accelerated in UNILAC, energy meas. by recoil proton technique 78−58527
Kr(p,p'), 51.9 MeV, low-lying octupole states anal. 78−21497
^{139}La, level props., Coulomb excitation obs. 80−13378
^{6}Li(p,p'), 185 MeV, optical model anal. of inelastic scatt. to 1st excited state, deformation parameters 79−22300
^{6}Li(p,p'X, 800 MeV, cluster recoil mechanism for inclusive nuclear reactions 78−93998
^{6}Li(p,p'), meas. of second excited state excitation energy in Li 77−57619
^{6}Li(p,p), 144 MeV, elastic scatt. cross sections, optical pot. 80−42660
^{6}Li(p,p), 635 MeV, left-right asymmetry depend. on residual nucleus momentum *(Russian)* 78−54765
^{6}Li(p,p) 0.6, 1.04 GeV, α-d cluster model and Glauber multiple scatt. theory 79−85476
^{6}Li(p,p) quasielastic scatt., 635 MeV polarised protons, asymm. meas. *(Russian)* 77−74852
^{6}Li(p,p)^{6}Li, 3-12 MeV, absolute cross section 77−23297

proton-nucleus scattering continued
^{6}Li(p,p)^{6}Li, four body approach 79−75933
^{6}Li(p,p)X, 0.8 GeV, inclusive cross sections, quasi-two-body scaling 79−3150
^{7}Li(p, p′), microscopic calc. for 1/2$^-$ level excitation, isoscalar quadrupole renormalisation 77−14046
^{7}Li(p,p), ^{8}Be lowest negative parity state, shell and cluster model calcs. 80−18205
^{7}Li(p,p), polarisation effects for elastic scatt. near (p,n) reaction threshold 78−13075
^{7}Li(p,p′)^{7}Li, microscopic multi-channel calcs. to 2.5 MeV c.m. 78−4934
^{A}Mg(p, p′), A=24, 26, isovector dipole strength excitation in giant resonance region 80−83066
^{A}Mg(p,p), A=24, 26, 6.9 GeV/c, elastic and inelastic differential cross sections, ^{26}Mg spin flip probability *(Russian)* 79−59071
^{24}Mg, microscopic model of 2_1^+ and 3_1^+ states, inelastic p scatt. test 79−26358
^{24}Mg(p,p′), 0.8 GeV, rot., γ and β bands, ground state deformation, DWBA, coupled channels anal. 80−9198
^{24}Mg(p,p′), 135 MeV, cross section, population of unnatural parity high spin states 78−54753
^{24}Mg(p,p′), 135 MeV, high spin unnatural parity states, anal. 78−37334
^{24}Mg(p,p′), 135 MeV, large momentum transfer, excitation of high-spin particle-hole states in ^{24}Mg 77−61420
^{24}Mg(p,p′), 20, 40, 800 MeV, γ-vibr. band, coupled channels anal. 80−9194
^{24}Mg(p,p′), 22.5 to 28.5 MeV, giant reson. effects 78−4923
^{24}Mg(p,p′), 40 MeV, two step pickup-stripping process, negative parity states 80−32256
^{24}Mg(p,p′), polarised p, 20.3 MeV, cross section and analysing power, DWBA and coupled channel anal. 78−82287
^{24}Mg(p,p′) 15-35 MeV, low lying state differential cross sections, two step effects 79−89304
^{24}Mg(p,p′)^{24}Mg, 20 MeV, excitation energies up to E_x=13.2 MeV 77−317
^{24}Mg(p,p′)^{24}Mg*, 9.1 MeV, DWBA and Hauser-Feshbach anal. 77−316
^{24}Mg(p,p′γ), 6.9 MeV, spin flip probability 77−88127
^{24}Mg(p,p'), 40 MeV, DWBA anal., positive parity states, transitions and giant resonance 79−6419
^{24}Mg(p,p'), 49.5 MeV, consistent folding model, HF calc. for E2, E4 transitions 79−22288
^{24}Mg(p,p') 17.5 MeV 79−22288
^{24}Mg(p,p), 14-45 MeV, differential cross section and spin-flip probabilities, giant resonances 80−73850
^{24}Mg(p,p), 15 Mev, excitation functions 80−22825
^{24}Mg(p,p), 18-44 MeV, differential cross sections, phase shift anal., energy depend. 80−47481
^{24}Mg(p,p), 22.5 to 28.0 MeV, differential cross sections, optical, coupled channel, core excitation anal. 79−6613
^{24}Mg(p,p), 40 MeV, natural parity transitions 78−66277
^{24}Mg(p,p), 5.65-6.25 MeV, isospin-forbidden T=3/2 reson., isospin mixing 77−18507
^{24}Mg(p,p)^{24}Mg, 9.1 MeV, optical model and Hauser-Feshbach anal. 77−316
^{25}Mg(p,p′)^{25}Mg*, 8.8 MeV, J^π=1/2$^+$, line shape 77−54211
^{25}Mg(p,p′)^{25}Mg*, 9.1 MeV, DWBA and Hauser-Feshbach anal. 77−316
^{25}Mg(p,p′)^{25}Mg*, E_x=8.838 MeV, lineshape model calc. *(German)* 77−22989
^{25}Mg(p,p)^{25}Mg, 9.1 MeV, optical and Hauser-Feshbach anal. 77−316
^{26}Mg(p, p′), pol.p, 5.5-17.5 MeV, cross sections and anal. powers, autocorrelations 80−106042
^{26}Mg(p,p'), 24 MeV, rot. description of low lying states, coupled channels anal. 79−54376
^{26}Mg(p,p′), 6 MeV, spin-flip probability, ang. distrib., energy depend. 78−13078
^{26}Mg(p,p′)^{26}Mg, 20 MeV, excitation energies up to E_x=11.2 MeV 77−317
^{26}Mg(p,p′)^{26}Mg*, 9.1 MeV, DWBA and Hauser-Feshbach anal. 77−316
^{26}Mg(p,p), 1.54-3.06 MeV, high resolution study, excited analogue states of ^{27}Mg 78−78377
^{26}Mg(p,p), 1.9-4.0 MeV, ^{27}Al isobaric analogue resonances, spectroscopic factors and γ-rays 80−86873
^{26}Mg(p,p), polarised protons, direct reaction contrib. in fluctuating cross sections 77−50102
^{26}Mg(p,p)^{26}Mg, 9.1 MeV, optical and Hauser-Feshbach anal. 77−316
Mg(p,p), A=24, 26, 5-6 MeV, polarisation in elastic scatt., thick target method 78−13079
Mg(p,p′), giant quadrupole resonance strength, p- and α-inelastic scatt. and α capture 78−37323
^{55}Mn(p,p), (p,p′), cross section fluctuations anal. 78−21551
^{92}Mo, elastic and inelastic scatt. of 30 MeV polarised protons 77−23004
^{92}Mo(p,p′), time development function at isobaric analogue resonances, compound nuclear level decays 79−3124
^{100}Mo(p,p′), 6.975 MeV, E0 transition probability for 0_1^+-0^+ transition 77−41963
Mo(p,p), unified optical model anal., Lane model breakdowns 79−17873
Mo(p,p′γ), odd isotopes, excited d-states from analogue resonances and p-γ correlations 80−68546
N+p, inelastic interactions, 6.0 GeV/c, in emulsions 78−86530
^{14}N(p,p′), 122 MeV, level excitation, cross sections, effective NN interaction, DWIA anal. 80−78197
^{14}N(p,p′), 25-40 MeV, level cross sections, optical parameters, DWBA anal., tensor effective interaction 80−68555
^{14}N(p,p')^{14}N at E_p=21 MeV, two-step process, spin depend. interaction 79−89301
^{14}N(p,p), 144 MeV, elastic scatt. cross sections, optical pot. 80−42660
^{14}N(p,p), average geometry optical model potential, doorway state effects 77−79367
^{14}N(p,pd), excitation spectrum of ^{12}C, exchange processes effect, impulse approx. 77−61405
^{15}N, anal. by proton scatt. 79−61926
^{15}N+p reactions, ^{16}O energy levels near 15 MeV excitation, R-matrix anal. 78−29460
^{15}N(p,p), 18-44 MeV, differential cross sections, phase shift anal., energy depend. 80−47481
^{15}N(p,p)^{15}N, 2.50-5.14 MeV, 3$^+$ ^{16}O reson. state excit. 78−580
^{16}N(p,p′)^{16}N*, 5.7 MeV, J^π=1$^+$, line shape 77−54211
^{16}N(p,p′)^{16}N* (E_x=3.226 MeV), lineshape model calc. *(German)* 77−22989
^{23}Na(p,p′)^{23}Na, 20 MeV, excitation energies up to 11.2 MeV 77−317
^{23}Na(p,p), (p,n) threshold anomaly 78−94003
proton-nucleus scattering continued
^{23}Na(p,p), lowest T=2 level of ^{24}Mg narrow resonance, isospin forbidden particle decays 78−89871
^{143}Nd(p,p), (p,p′), 8.7-10.3 MeV, isobaric analogue reson. and seniority model 77−57642
^{20}Ne(p,p′), differential cross-sections, analysing powers in direct reaction theory 77−65223
^{20}Ne(p,p') 24.5 MeV, consistent folding model, HF calc. for E2, E4 transitions 79−22288
^{20}Ne(p,p), polarised protons, obs. of ^{21}Na levels near 5 MeV 77−2913
^{21}Ne (p,p′γ), 0.4 to 1.6 MeV, study of resonances 77−18540
^{21}Ne(p,p), 0.4 to 1.6 MeV, study of resonances 77−18540
^{A}Ni(p,p), 1 GeV, A=58,60,62,64, elastic and inelastic, Glauber anal., matter distribs. 79−75883
^{58}Ni (p,p), 1.04 GeV, elastic scatt. 78−21549
^{58}Ni (p,p) 100 MeV, systematic optical model anal. 78−66274
^{58}Ni, comparison with electron scatt., large momentum transfer 77−38262
^{58}Ni+p, 5.65 and 6.50 MeV, compound nucleus time evolution meas. 78−50160
^{58}Ni+p, K-shell X-ray photon proton coincidences, nucl. time delay 79−18281
^{58}Ni(p,p′), 0.8 GeV, coupled channels effects 79−63669
^{58}Ni(p,p′), 15 MeV polarised protons, surface delta description of analysing power 77−61397
^{58}Ni(p,p′), 60 MeV, analysing power for excitation of giant resonance region of continuum 77−6387
^{58}Ni(p,p′)^{58}Ni, medium energy, DWBA calc. 77−6380
^{58}Ni(p,p), 0.8 GeV, analysing powers 78−54760
^{58}Ni(p,p), 0.8 GeV, ang. distrib. meas. 78−25186
^{58}Ni(p,p), 0.8 GeV, polarised p, differential cross section, anal. power, nuclear matter densities 79−13299
^{58}Ni(p,p), 1 GeV, Fresnel and two-body correl. effects 78−82353
^{58}Ni(p,p), 1 GeV, Glauber theory 77−41966
^{58}Ni(p,p), 1 GeV, neutron densities 78−17087
^{58}Ni(p,p), 178 MeV, ang. distribs., cross sections and polarisation, coupled channels calcs. 79−75984
^{58}Ni(p,p), 20.4 and 30.3 MeV, elastic and inelastic scatt. multishell model description 78−86533
^{58}Ni(p,p), 800 MeV, elastic and inelastic, cross section, deformation lengths, optical and DWBA anals. 80−68664
^{58}Ni(p,p), 800 MeV, non-eikonal corrections to Glauber diffraction approx. 79−71851
^{58}Ni(p,p), 800 MeV, polarised differential cross sections and anal. powers, n density 79−13297
^{58}Ni(p,p), evidence for ang. mom. depend. optical model pots. 79−13290
^{58}Ni(p,p), inelastic and elastic scatt., 17.1-20.6 MeV, cross section fluctuations 78−58286
^{58}Ni(p,p), pol. p, 40 MeV, elastic and inelastic, asymmetries and differential cross sections *(Russian)* 80−27623
^{58}Ni(p,p)^{58}Ni, high-resolution meas. of scattering cross section, 3.0 to 4.0 MeV 77−10397
^{60}Ni(p,p′), 15 MeV polarised protons, surface delta description of analysing power 77−61397
^{60}Ni(p,p)^{60}Ni, high-resolution meas. of scattering cross section, 3.0 to 4.0 MeV 77−10397
^{61}Ni(p,pγ)^{61}Ni, 3.0-4.5 MeV, low-lying levels study 77−26610
^{62}Ni(p,p), 20 MeV, elastic and inelastic scatt., analysing powers *(Dutch)* 78−29464
^{62}Ni(p,p), elastic and inelastic scatt., 5.2 to 6.05 MeV, scatt. cross section energy depend. 79−9559
^{62}Ni(p,p)^{62}Ni, high-resolution meas. of scattering cross section, 3.0 to 4.0 MeV 77−10397
^{64}Ni(p,p), (p,p′), 5.0-6.2 MeV, isobaric analogue reson. in ^{65}Cu anal. 78−78351
^{64}Ni(p,p) 800 MeV, polarised differential cross sections and anal. powers, n density 79−13297
Ni(p,p), 36.2 MeV, differential cross section, asymmetries, 0 to 7° scatt. 78−94002
Ni(p,p), A=58, 60, 5.65, 6.5 MeV, time evolution of compound elastic scatt., cryst. blocking technique 78−62531
Ni(p,p)Ni, A=58,60,62,64, at 1.047 GeV, neutron matter densities 77−54171
Ni(p,p′), A=58,60,62, E=17.2, 20.4, 24.6 MeV polarised protons, optical model, DWBA anal. 78−13094
O+p, inelastic interactions, 6.0 GeV/c, in emulsions 78−86530
^{16}O (p,2p) 200 MeV polarised protons, j-dependence obs. in quasifree scatt. 77−10401
^{16}O, quasielastic scatt. of polarised 635 MeV protons, depend. of left-right asymm. on nucl. momentum *(Russian)* 77−79384
^{16}O(p,p′^{16}O) at 27.2 MeV, 6.05 MeV 0$^+$ level excit., meas. and microscopic calc. 77−26687
^{16}O(p,p′), 1 GeV, proton polarisation in natural parity level excitation *(Russian)* 80−42634
^{16}O(p,p′), 135 MeV, high spin particle-hole states, 4$^-$ states 80−9217
^{16}O(p,p′), 150 MeV, spin-orbit interaction within collective model and DWBA 79−45128
^{16}O(p,p′), 25-46 MeV, effects of two-step process determ. 78−21569
^{16}O(p,p′), 40 MeV, retarded isoscalar M2 strength obs. 78−93962
^{16}O(p,p′), 45 MeV, giant dipole and quadrupole 77−2965
^{16}O(p,p′), giant resonances from antisymmetrised DWBA anal. 79−85432
^{16}O(p,p′), microscopic anal. of doorway states in giant resonance region 77−2966
^{16}O(p,p′), polarised p, ^{17}F 14.174 MeV T=3/2 level, spin assignment 79−67648
^{16}O(p,p'), 135 MeV, 4$^-$ particle-hole states, J^π ambiguity removal 80−5036
^{16}O(p,p'), 20-40 MeV, pol. p, anal. powers, imaginary spin-orbit pot., coupled channels anal. 80−102179
^{16}O(p,p'), polarised p, 20, 30, 40 MeV, anal. power and cross sections, spin-orbit deformation 79−75963
^{16}O(p,p')^{16}O*, 42.5-49.3 MeV, octupole GR strength, polarised proton 77−57644
^{16}O(p,p), 1 GeV, cross sections using nuclear densities from self-consistent methods *(Russian)* 78−41724
^{16}O(p,p), 1 GeV, Glauber approx. corrections, differential cross sections 78−50166
^{16}O(p,p), 1 GeV, Glauber theory 77−41966
^{16}O(p,p), 1 GeV, spin-effects, Coulomb interactions, Glauber theory 77−82931

proton-nucleus scattering continued
^{16}O(p,p), 20-50 MeV differential cross section, polarisation ang. distrib., optical model exchange terms 80−27638
^{16}O(p,p), 49.48 MeV, elastic scattering, discrepancies from optical model, possible α-cluster struct. 78−62528
^{16}O(p,p), 50-160 MeV, energy depend. optical pot. 80−22830
^{16}O(p,p), 635 MeV, left-right asymmetry depend. on residual nucleus momentum *(Russian)* 78−54765
^{16}O(p,p), 6.9 GeV/c, differential cross section *(Russian)* 79−59071
^{16}O(p,p), average geometry optical model potential, doorway state effects 77−79367
^{16}O(p,p), evidence for ang. mom. depend. optical model pots. 79−13290
^{16}O(p,p), high energy differential cross sections, nucleon density distrib. 78−54738
^{16}O(p,p), imaginary spin-orbit term in proton optical potential, ang. distribs. 78−58273
^{16}O(p,p), nucleon distrib. in nuclei, self-consistent anal. 79−9556
^{16}O(p,p), spline interpolation method appl. to optical potential 80−32272
^{16}O(p,p) 25 MeV, macroscopic description of exchange effects 77−57635
^{16}O(p,p) polarised p, 800 MeV, differential cross section and anal. power, microscopic anal. 79−80915
^{17}O(p,p$_1\gamma$), 1.4-2.8 MeV, ^{18}F levels and resonances, J$^\pi$ assignments 79−9480
^{17}O(p,p), finite-range coupled-channel calcs. 77−10377
^{17}O(p,p)^{17}O, 1.4-3.0 MeV, spin-parity assignment in ^{18}F 78−29391
^{18}O(p,p'γ), 3-3.5 MeV, γ-ray ang. distrib., for ^{19}F reson. and bound levels 78−89790
^{18}O(p,p), 18-44 MeV, differential cross sections, phase shift anal., energy depend. 80−47481
^{190}Os(p,p'), 16 MeV, γ-ray spectra, energy level scheme 77−34243
(p,p), small-angle scatt. of polarised protons at 36.2 MeV 77−30603
^{31}P(p,p), 5 to 8 MeV, anomaly at (p,n) reaction threshold energy *(Russian)* 78−94011
^{31}P(p,p), 65 MeV polarised protons, asymm. in elastic and inelastic scatt. 78−54754
^{31}P(p,p), (p,n) threshold anomaly 78−94003
^{206}Pb(p,p$_0$), polarised p, 13.6 MeV, analysing power near ^{207}Bi 3p$_{1/2}$ isobaric analogue resonance 78−78346
^{207}Pb(p,p$_0$), polarised p, 13.6 MeV, analysing power near ^{208}Bi 3p$_{1/2}$ isobaric analogue resonance 78−78346
^{207}Pb(p,p'), 135 MeV, DWIA test 78−33186
^{207}Pb(p,p'), excitation of neutron-hole states, 61.2 MeV protons 78−8724
^{207}Pb(p,p), polarised p, 13.5-18 MeV, ^{208}Bi isobaric analogue resonances, spin assignments, decay amplitudes 79−75946
^{208}Pb (p,p'), 635 Mell protons, meas. of energy spectra of secondary protons 79−97708
^{208}Pb (p,p), 1 GeV, spin-effects, Coulomb interactions, Glauber theory 77−82931
^{208}Pb (p,p), 1.04 GeV elastic scatt., polarisation 78−21549
^{208}Pb (p,p) elastic scatt., polarisation and spin-orbital amplitude parameters, 1 GeV *(Russian)* 78−17208
^{208}Pb, eikonal anal. of high energy proton and electron scatt. *(Russian)* 77−22908
^{208}Pb(p,P'), pol. p, 9, 10 MeV, vol. integrals for optical pots., real symmetry pot. 80−42659
^{208}Pb(p,p'), 135 MeV, normal parity level excitation, J$^\pi$, differential cross sections 80−57690
^{208}Pb(p,p'), 24 MeV, mag. dipole states, spin, parity, transition strengths 77−14129
^{208}Pb(p,p'), 39, 62 MeV, DWBA anal., collective spectra, direct process contrib. *(Russian)* 80−13408
^{208}Pb(p,p'), 40, 45 MeV, fine struct. in giant resonance region, collective dipole spin flip excitation 78−46056
^{208}Pb(p,p'), 5 to 8 MeV, hyperfine reson. struct., Feynman diagrams 79−6589
^{208}Pb(p,p'), 61.2 MeV, low lying normal parity excitations 77−74843
^{208}Pb(p,p'), 800 MeV, high energy octupole giant resonance, ang. distribs. 80−86879
^{208}Pb(p,p'), giant resonances from antisymmetrised DWBA anal. 79−85432
^{208}Pb(p,p'), precritical behaviour in pionlike excited states in nuclear matter 79−49593
^{208}Pb(p,p')^{208}Pb, medium energy, DWBA calc. 77−6380
^{208}Pb(p,p), 0.8 GeV, analysing powers 78−54760
^{208}Pb(p,p), 0.8 GeV, ang. distrib. meas. 78−25186
^{208}Pb(p,p), 0.8 GeV, cross sections, optical anal. np RMS radius difference, Δr_{np} 80−63187
^{208}Pb(p,p), 0.8 GeV, elastic and inelastic, ang. distribs., states, optical and DWBA anal. 79−3154
^{208}Pb(p,p), 0.8 GeV, polarised p, differential cross section, anal. power, nuclear matter densities 79−13299
^{208}Pb(p,p), 1 GeV, cross sections using nuclear densities from self-consistent methods *(Russian)* 78−41724
^{208}Pb(p,p), 1 GeV, Fresnel and two-body correl. effects 78−82353
^{208}Pb(p,p), 20-50 MeV differential cross section, polarisation ang. distrib., optical model exchange terms 80−27638
^{208}Pb(p,p), 30 MeV, optical pot. imaginary part calcs. 80−86868
^{208}Pb(p,p), 30 MeV, pick-up and inelasti scatt. contribution to p optical pot. 78−25182
^{208}Pb(p,p), elastic and inelastic, static and transition densities, self consistent RPA theory test *(Russian)* 79−49604
^{208}Pb(p,p), elastic and inelastic scatt., 185 MeV, polarisation, diffraction model anal. 79−75943
^{208}Pb(p,p) 100 MeV, systematic optical model anal. 78−66274
^{208}Pb(p,p)^{208}Pb, 1 GeV, neutron and nuclear matter space distribs. *(Russian)* 78−502
^{A}Pd(p,X), 6 MeV, A=102,104,106,108,110, quadrupole deformation, cross sections, direct processes, optical parameters *(Russian)* 79−67753
^{102}Pd(p,p'γ,γ), population of low spin levels, level scheme 79−36153
^{102}Pd(p,p'γ), 8 MeV, ang. correl. meas. to determ. level scheme 78−21559
^{102}Pd(p,p'γ), long lived O$^+$ state, E0 transitions 80−73804
^{195}Pt(p,p'), single proton distrib. anal. 78−603
^{A}Ru(p,p'γ), A=96, 98, 5-8 MeV, level schemes, transitions, vibr. state, mixing ratios 80−18199
^{32}S (p,p), 5-6 MeV, polarisation in elastic scatt., thick target method 78−13079
^{32}S(p,p), 14-45 MeV, differential cross section and spin-flip probabilities, giant resonances 80−73850
^{33}S(p,p), 3-3.8 MeV, isospin-forbidden T=3/2 reson., isospin mixing 77−18507
proton-nucleus scattering continued
^{32}S(p,p), spin-flip probability to first 2$^+$ level 80−78288
^{34}S(p,p), 1.45-2.85 MeV, high resolution differential cross-sections 77−65222
^{34}S(p,p), (p,n) threshold anomaly 78−94003
^{45}Sc+p, low-lying negative parity levels, Coulomb excitation 79−93552
^{45}Sc(p,p'), 2.5-3.8 MeV, reaction rates and stellar nucleosynthesis 77−88134
^{45}Sc(p,p'), levels, J$^\pi$, transitions and lifetimes 80−63091
^{A}Se(p,p), A=76-82, doubly even nuclei, deformation parameters 79−97705
^{82}Se(p,p) elastic, inelastic 4.5-77 MeV scatt., IAS, ^{83}Se low-lying states 78−573
^{A}Si(p,p'), A=28,29,30, 51.9 MeV, blocking effect and core-excitation DWBA and optical model 78−82336
^{25}Si(p,p), 14-45 MeV, differential cross section and spin-flip probabilities, giant resonances 80−73850
^{28}Si (p,p'), 14-40 MeV, low lying states, optical and statistical model anals., giant resonances 79−40894
^{29}Si, microscopic model of 2$_1^+$ and 3$_1^+$ states, inelastic p scatt. test 79−26358
^{28}Si(p, p'), isovector dipole strength excitation in giant resonance region 80−83066
^{28}Si(p,p'), 135 MeV, cross section, population of unnatural parity high spin states 78−54753
^{28}Si(p,p'), 135 MeV, high spin unnatural parity states, anal. 78−37334
^{28}Si(p,p'), 135 MeV, large momentum transfer, excitation of high-spin particle-hole states in ^{28}Si 77−61420
^{28}Si(p,p'γ)^{28}Si, 3.5-3.8 MeV, spin-flip probability in resonance region *(Russian)* 78−41725
^{28}Si(p,p') 3.1-3.8 MeV, interference effects, β_2 and optical parameters 77−26685
^{28}Si(p,p), 2.0-3.8 MeV polarised protons, analysing powers meas. 77−3012
^{28}Si(p,p), pol. p, 12-18 MeV, cross section, anal. power and states, ^{29}P resonance coherence widths 80−32258
^{28}Si(p,p), spin-flip probability to first 2$^+$ level 80−78288
^{28}Si(p,p) 5.6-5.9 MeV, isospin-forbidden T=3/2 reson., isospin mixing 77−18507
^{30}Si(p,p), 1.1-3.0 MeV, analogue reson. obs., Coulomb energies, spectroscopic factors determ. 77−2988
^{30}Si(p,p), polarised proton fluctuation expt., compound elastic enhancement factor determ. 79−519
Si(p,p), A=28, 29, 30, 65 MeV polarised protons, asymm. in elastic and inelastic scatt. 78−54754
Si(p$_{pol}$,p$_{pol}$), giant multipole resonance region, optical model anal. 80−57779
Sm isotopes, A=148,152,154, 16 MeV, coherent optical model analysis 77−26750
^{A}Sm(N,N') A=152,154, deformed nuclei struct., rot. model with optical pot., coupled channel formalism 79−3146
^{A}Sm(p,p'), A=144,154, 67 MeV, giant isoscalar monopole resonance excitation 79−22259
^{A}Sm(p,p), 1 GeV, A=152, 154, dispersive effects in ground state rot. band excitation, coupled channel calcs. 79−40828
^{147}Sm(p,p), (p,p'), 7.5-10.8 MeV, isobaric analogue reson. and seniority model 77−57642
^{154}Sm (p,p')^{154}Sm, 1 GeV, giant reson. excit., Glauber calc. 77−82891
^{154}Sm(p,p'), 0.8 GeV, ang. distribs. and multipole moments, DWBA and coupled channel anals. 80−105969
^{154}Sm(p,p'), 35 MeV, extraction of deform. parameters 78−54755
^{154}Sm(p,p'), 35 MeV, ground state rot. band and multipole moment 80−32178
^{154}Sm(p,p'), 1 GeV, possibility of observing giant resonances with high multipolarities *(Russian)* 78−78350
^{A}Sn(p,p'), A=115, 117, 119, 18 MeV, state spin assignment, particle-vibr. coupling 80−32160
^{A}Sn(p,p'), A=116, 124, 0.8 GeV, polarised p, spin orbit deformation effects, DWBA anal. 79−30832
^{A}Sn(p,p), A=116, 120, 4-9 MeV, proton optical pot. low energy behaviour 79−85469
^{112}Sn(p,p'), 20.51, 25.0 MeV, energy levels, excitation functions and ang. distribs. 80−32184
^{112}Sn(p,p') 10, 12 MeV, ^{113}Sb mean nuclear lifetime from X-ray spectrum 80−9267
^{116}Sn(p,p'), 800 MeV, high energy octupole giant resonance, ang. distribs. 80−86879
^{117}Sn(p,p), polarised p, 12.9 MeV, anal. power 80−5114
^{120}Sn(p,p) 100 MeV, systematic optical model anal. 78−66274
^{122}Sn(p,p') 54.9 MeV, ^{122}Sn excitation of 6$^+$, 8$^+$, 10$^+$ and 9$^-$ states, DWBA anal. 79−89264
^{122}Sn(p,p), 20 MeV, elastic and inelastic scatt., analysing powers *(Dutch)* 78−29464
^{124}Sn(p,p), 0.8 GeV polarised p, differential cross section and analysing power data anal. 78−70526
Sn(p,n), 4 to 10 MeV polarised protons, optical model parameters 77−2972
Sn(p,p), 8.8 MeV polarised protons, optical model parameters 77−2972
Sn(p,p$_0$), pol.p, 6.77-8.8 MeV, cross sections, optical parameters and nuclear radius A-depend. 80−57773
Sn(p,p)Sn, A=115-120, 14-18 MeV, optical model parameters, (p,n) analogue state reaction relevance 77−88132
^{87}Sr(p,p'), 20.5 MeV, level scheme, ang. distribs., transitions and deformation parameter 79−22195
^{88}Sr(p,p')^{88}Sr(2$_1^+$), 7-7.5 MeV polarised protons, scatt. at IAR 77−318
^{88}Sr(p,p), polarised protons, direct reaction contrib. in fluctuating cross sections 77−50102
^{48}T(p,p'), 4.7-5.4 MeV, cusp behaviour of cross-section obs. 78−29470
^{181}Ta(p,p')X, 800 MeV, cluster recoil mechanism for inclusive nuclear reactions 78−93998
^{181}Ta(p,p)X, 0.8 GeV, inclusive cross sections, quasi-two-body scaling 79−3150
^{181}Ta($\pi^\pm$,p), ($\pi^\pm$,d), E=100, 220 MeV, p and d spectra meas. 78−648
Ta(p,p'), 0.6-25 GeV, backward emitted proton inclusive spectra, short range correlation 80−32281
^{232}Th(p,p'), 35 MeV, extraction of deform. parameters 78−54755
^{232}Th(p,p'), 35 MeV, ground state rot. band and multipole moment 80−32178
^{233}Th(N,N'), deformed nuclei struct., rot. model with optical pot., coupled channel formalism 79−3146

proton-nucleus scattering continued
^{48}Ti(p,p), 1 GeV, cross sections using nuclear densities from self-consistent methods *(Russian)* 78−41724
^{48}Ti(p,p), 1 GeV, elastic scatt. differential cross section calc. 80−47480
^{48}Ti(p,p), 1.044 GeV, elastic and inelastic, Glauber theory anal. 77−18536
^{48}Ti(p,p), E_p=1 GeV, elastic differential cross sections 78−13082
^{48}Ti(p,p), elastic and inelastic scatt. cross-sections from Hartree-Fock densities *(Russian)* 79−13287
Ti(p,p), 5.2-6.0 MeV, A=46,48,50, energy depend. of cross sections 77−61409
Ti(p,p), 6 MeV, A=46,48,50, cross sections, excited states, ang. distribs. 77−61410
^{235}U(N,N'), deformed nuclei struct., rot. model with optical pot., coupled channel formalism 79−3146
^{238}U(p,p'), 22 MeV, rot. band, multipole deformation parameters from coupled channel anal. 80−13369
^{238}U(p,p'), 35 MeV, extraction of deform. parameters 78−54755
^{238}U(p,p'), 35 MeV, ground state rot. band and multipole moment 80−32178
^{238}U(p,p'), isobaric analogue reson., modified KASTOR code calc. 77−14132
^{49}V(p,p'), 3/2$^-$ resonances, inelastic proton channel 79−93586
^{51}V(p,2p)^{50}Ti, 17 MeV, search for double-direct reaction 77−30576
^{51}V(p,p'), 6 MeV, levels, spins and EM props., shell model anal. 80−63092
^{137}Xe(p,p_i), 10.26 to 11.82 MeV, anal. by ^{137}Cs analogue resonance and parentage coeffs. in ^{137}Xe states 78−66282
^{88}Y(p,p), (p,p'γ), 4.5-8.0 MeV polarised protons, IAS spectroscopy of ^{87}Y 77−61396
^{89}Y (p,p'), 62 MeV, effect of nucleon mean free paths on intranuclear cascade calc. 77−67749
^{89}Y(p,p'), two stage processes in direct reactions *(Dutch)* 78−29439
^{89}Y(p,p), 0.8 GeV, elastic and inelastic, differential cross sections, relativistic optical model anal. 79−45270
^{89}Y(p,p), 185 MeV, ang. distribs., polarisation, cross section, optical pot. 78−89873
^{89}Y(p,p), 65 MeV polarised protons, asymm. in elastic and inelastic scatt. 78−54754
^{89}Yb(p,p), 20 MeV, elastic and inelastic scatt., analysing powers *(Dutch)* 78−29464
^{176}Yb(p,p'), 0.8 GeV, ang. distribs. and multipole moments, DWBA and coupled channel anals. 80−105969
^{176}Yb(p,p'), 35 MeV, extraction of deform. parameters 78−54755
^{176}Yb(p,p'), 35 MeV, ground state rot. band and multipole moment 80−32178
^Zn(p,p), A=66,68, 20-50 MeV differential cross section, polarisation ang. distrib., optical model exchange terms 80−27638
^{64}Zn(p,p'), 15 MeV polarised protons, surface delta description of analysing power 77−61397
^{70}Zn(p,p'), 3.825 MeV, E0 transition probability for 0_1^+-0^+ transition 77−41963
Zn(p,p'), A=64-70 even, 12.5 MeV, compound and pre-compound processes 77−34296
^Zr (p,p), A=92, 94, 2-6.5 MeV, optical and Lane model anal. comparison 80−18302
^Zr, A=90, 92, elastic and inelastic scatt. of 30 MeV polarised protons 77−23004
^Zr(p,p'), A=94,96, 11.2-13.4 MeV, anal. power and excitation function T$^-$ fluctuations 80−42626
^Zr(p,p) A=90, 92, elastic and inelastic, 40 MeV polarised protons, cross sections and anal. power 79−54428
^{90}Zr, 1 GeV, Glauber approx. corrections, differential cross sections 78−50166
^{90}Zr (p, p'), 57.5 MeV, polarised p, low lying level and giant resonance excitation 79−36157
^{90}Zr (p,p'), 0.8 GeV, low energy giant octupole resonance excitation, deformation length 79−93593
^{90}Zr (p,p) 100 MeV, systematic optical model anal. 78−66274
^{90}Zr, giant resonance levels, study by proton and electron scatt. *(Russian)* 79−3127
^{90}Zr(p,p'), polarised protons, compound nuclear contribs. to IAR inelastic decay 78−8813
^{90}Zr(p,p), 0.8 GeV, analysing powers 78−54760
^{90}Zr(p,p), 0.8 GeV, elastic and inelastic, differential cross sections, relativistic optical model anal. 79−45270
^{90}Zr(p,p), 0.8 GeV, polarised p, differential cross section, anal. power, nuclear matter densities 79−13299
^{90}Zr(p,p), 1 GeV, spin-effects, Coulomb interactions, Glauber theory 77−82931
^{90}Zr(p,p), 4.5-9 MeV polarised protons, reaction cross-section near (p,n) threshold 77−3015
^{90}Zr(p,p), 65 MeV polarised protons, asymm. in elastic and inelastic scatt. 78−54754
^{90}Zr(p,p), elastic and inelastic, static and transition densities, self consistent RPA theory test *(Russian)* 79−49604
^{90}Zr(p,p), elastic and inelastic scatt., 185 MeV, polarisation, diffraction model anal. 79−75943
^{90}Zr(p,p), polarised protons, direct reaction contrib. in fluctuating cross sections 77−50102
^{90}Zr(p,p), spin orbital interaction and nucl. matter density distrib. *(Russian)* 79−22176
^{90}Zr(p,p)^{90}Zr, 1 GeV, neutron and nuclear matter-space distribs. *(Russian)* 78−502
^{92}Zr(p,p'), 40 MeV polarised protons, 2$^+$ states excitation 79−6600
Zr(p,p'γ), odd isotopes, excited d-states from analogue resonances and p-γ correlations 80−68546

proton polarisation
2s-1d shell nuclei, cluster struct. and inelastic scatt. of polarised protons 79−6557
acceleration of polarised protons in CERN synchrotron 77−38509
axially polarised proton target, for A and R parameter meas. in π^-p→K$^0\Lambda^0$ 79−63834
beam profile monitor, determ. of intensity and polarisation profiles 79−76251
2,3-butanediol doped with Cr(V)-complex, materials with adjacent hydroxyl groups, dynamic proton polarisation 77−79492
calibration standard using ^{12}C+p polarised scatt. 77−10573
conference on high energy phys. with polarised beam and target, Argonne, USA (Oct. 1978) 79−63526
depolarisation during acceleration and storage of polarised protons and deuterons 78−58519
display and calibration using automatically tuned NMR spectrometer 80−37669
eikonal description of nucleon-nucleon elastic polarisation data 77−13948
elastic scattering at high energy, polarisation meas. apparatus, target, spectrometer, polarimeter 77−30439
EM polarisabilities and $\gamma\gamma\to\pi\pi$ amplitude, dispersive approach 77−82743
EM polarisabilities from γN scatt., $\pi^0\to 2\gamma$, $\eta^0\to 2\gamma$ decay rates 77−18289
final state polarisation in pp elastic scatt. 209-515 MeV 78−461
frozen polarised proton target 79−26795
high energy beam from lambda decays, possibilities 79−63845
high energy polarisation parameters, feasibility of future CERN SPS expt. 77−30738
high intensity beam by radiation quenching and photoionisation by H atoms *(Russian)* 78−46202
hyperon decay, high energy, polarised proton beam production 78−58517
lepton-nucleon isobar prod. by neutral current, polarisation effects 77−18220
light and intermediate nuclei, proton-induced reactions, polarisation phenomena interpret. 78−13051
longitudinally polarized ep elastic scatt., 6.5 GeV, cross section asymm., p form factors 77−6131
low-energy protons, polarisation meas. using orientation effect in inner-shell atomic ionisation 80−9482
Massachusetts Univ. polarised proton target for strange particle phys. 79−63833
matter current density and R parameter meas. 77−30544
measurement methods, symmetry errors *(Rumanian)* 79−59322
nuclear diffraction scatt. of nucleons *(Russian)* 79−89285
PANSI, polarisation anal. neutron scattering instrument, description and appls. 80−23280
parton distribution functions for polarised protons, SLAC polarised ep data anal. 77−82747
polarimeter designs for high energy p and d beams, polarised beam spin anal. 78−58516
polarised proton beams, higher energy, conf., Ann Arbor, MI, USA, Oct. 1977 78−58514
pp elastic scatt., 7.9 GeV/c, polarisation parameter meas. 77−82759
pp elastic scatt. at 6 GeV/c, cross section, spin meas. 77−38189
proton electric polarisability 79−49524
QCD, asymmetries in inclusive hadron prod., polarised beam and target 78−50057
quadrupole lens, spin precession of polarised proton beam, analytic soln. 77−30692
recoil polarimeter for zero gradient synchrotron 77−38511
slow proton beam spin polarisation meas. by Lamb shift 78−78031
spin refrigeration of $(Yb,Y)(C_2H_5SO_4)_3.9H_2O$ cryst. in nonuniform mag. field 77−83435
spin-flip amplitude in 300GeV elastic scatt. 79−93461
sum-rule relating polarizabilities of proton and pion *(Russian)* 79−93420
superconducting magnet polarised proton target 77−14291
superconducting magnet system, polarised proton target, for pion photoproduction 79−22508
synchrotron, spin flip by adiabatic passage of depolarisation resonances 80−5415
ZGS, acceleration of polarised protons 77−34488
ZGS at Argonne, depolarising resonances effects on circulating polarised proton beam 77−83274
ZGS polarized beam facility, supercond. solenoids, magnet and cryostat design 79−31252
$e^-e^-\to p\bar{p}$, asymm. and polarisation of p,$\bar{p}$, neutral weak currents *(Russian)* 78−58195
ep deep inelastic asymmetry meas., Bjorken sum rule, p spin struct. models 78−70376
ep→epρ^0 or eX, polarised beam and target, cross section asymm., vector-meson dominance model 77−6135
ep longitudinally polarised deep inelastic scatt., asymm., depolarisation, p struct. functions 77−6133
γd→pn, 350-700 MeV, p polarisation meas. 78−82215
γd→pn, 400 to 650 MeV, ang. depend. of proton polarisation and partial wave anal. of possible dibaryon resonances 79−58967
γd→pn, proton polarisation energy depend., 400-700 MeV *(Russian)* 80−63000
γp→nπ^+ reaction, with polarised protons and photons at 340 MeV *(Russian)* 79−89170
γp→π^0p, 360-500 MeV, secondary proton polarisation meas. *(Russian)* 78−54637
γp→π^0p, 480-800 MeV, proton polarisation at second πN resonance *(Russian)* 78−78192
γp→π^0p, below 1 GeV, polarised target asymmetry meas., comparison with phenomenological anal. 78−62409
γp→π^0p, proton polarisation vector components *(Russian)* 79−85305
γp→π^0p, recoil polarisation, review *(Russian)* 78−54636
γp→π^+n below 1.02 GeV, polarized target asymm. meas. 78−17029
γp→π^0p, recoil polarisation meas. using C plate and liq. H_2 polarimeters 79−93898
γp scattering, proton polarisability determ. 78−17025
$K^-p\to K^-p$, elastic scatt. at low energies, polarisation parameter 78−12932
K^+p, elastic scatt., 6 and 12 GeV/c, polarisation meas. using CERN polarised d target 79−49542
K^+p at 45 GeV/c, polarisation parameter *(Russian)* 77−34179
n-p spin-correlation parameter at 50 MeV 77−49993
NN spin-polarisation meas. 78−74272
np charge exchange amplitudes, Regge behaviour of imaginary parts, polarisation 77−38145
np elastic scatt., phase shift anal. and mixing parameters at 325 MeV 77−79277
np→np, 6 GeV, spin-spin forces 80−433
np→pn, charge exchange models, polarisation 77−30444
np scatt., analysing power meas. at 14 MeV, multiple scattering effects 77−10572
np scatt. at 1.03 GeV 78−82245
$\nu_\mu(\bar{\nu}_\mu)$p→$\nu_\mu(\bar{\nu}_\mu)$p hadronic neutral current, final-proton polarisation 78−82200

proton polarisation continued
p-H_2O 6 GeV/c scatt. with polarised protons, helicity-depend. and P-violation 77−30403
p+A→p+X, 800 MeV polarised protons, inclusive cross sections, analysing power 78−70524
p+α, elastic scatt. of intermediate energies, polarisation, momentum transfer effects 77−30408
pC→p(pol.)X, 100 to 400 GeV, proton polarisation in inclusive processes 79−58983
pd, elastic scatt. analysing power meas. 78−93901
pn elastic scatt., 11.8 GeV/c, polarisation parameter meas. 78−66158
pN→pX, 28.3 GeV/c, Pt target, polarisation of inclusively produced protons at p_T=1.5 GeV/c 78−93917
pp, low energy scatt., spin depend. EM force effects, Coulomb DWBA anal. 79−9568
pp, polarisation analyzing power, 643-796 MeV scatt. 78−78207
pp, polarisation data interpretation for high energy elastic scatt., eikonal model, spin parameters 79−3048
pp→($\pi^{\pm}$,$K^{\pm}$,p,d)X, 6 and 11.8 GeV/c, polarised proton, L-R asymmetry meas. 77−30455
pp and pn, elastic, inelastic, inclusive reactions, polarisation studies with effective mass spectrometer 77−30412
pp→dπ, 1.03 GeV, analysing power 78−93901
pp→dπ$^+$, polarised beam and target, NΔ intermediate states, coupled channel method 79−9392
pp→Δ^{++}n, polarised proton, spin effects in SU(3) and quark model 77−30399
pp→$\Delta^{++}\pi^-$p, polarised proton, spin effects in SU(3) and quark model 77−30399
pp elastic, inelastic, and inclusive interactions, spin effects, polarisation 77−30434
pp elastic and inclusive interactions, 7.9 GeV/c, polarisation, scatt. asymm., spin depend. effects 77−30413
pp elastic collisions, polarised, 6 GeV/c, absorpt. model 77−2858
pp elastic scatt., 11.8 GeV/c, polarisation parameter meas. 78−66158
pp elastic scatt., 20 to 200 GeV/c polarisation parameter meas. 78−50054
pp elastic scatt., 6 GeV/c, spin-spin correlation parameters 78−62433
pp elastic scatt., energy depend. and scaling of spin-correl. and polarisation 77−34173
pp elastic scatt., polarisation normalisation between 200 and 520 MeV 78−70397
pp elastic scatt., spin effects at 150 GeV/c 78−66157
pp elastic scatt. and inclusive reactions, polarisation phenomena 78−78224
pp elastic scatt. at 45 GeV/c, polarisation parameter *(Russian)* 77−34179
pp elastic scattering, 100 GeV/c, polarisation meas. 77−30440
pp elastic scattering, 24 GeV/c, polarisation parameter meas. 77−30437
pp elastic scattering, 24 GeV/c, small momentum transfer, polarisation parameter meas. 77−46081
pp elastic scattering, 2.1 GeV.c^{-1}, polarisation meas. of scatt. protons in small momentum transfer region *(Russian)* 79−9397
pp elastic scattering 3-spin cross sections, 6 GeV/c, polarised target and beam expt. 77−30411
pp elastic scattering at 6 GeV/c, polarised beam and target, spin correl. 77−30410
pp elastic scattering at 6 GeV/c, polarisation parameters 77−38188
pp elastic scattering at 610 MeV, spin correl. parameter 77−30406
pp elastic scattering in pure initial spin states, 11.75 GeV/c, spin correl. 77−30436
pp̄→γγ annihilation, influence on sum rule proton polarisability 80−18143
pp→K^-K^+, 1.0 to 2.2 GeV/c, polarisation parameter 77−87995
pp→$K^0(\Lambda)(\Delta^{++})$X, 6 GeV/c, polarised proton 77−30400
pp→n̄n, charge exchange models, polarisation 77−30444
pp→pX, high p_T, spin-spin asymmetries, polarisation, hard scatt model with QCD 80−13339
pp→pX, polarised 6 GeV/c projectile, L-R asymmetry 77−49995
pp→p(pol.)X, 100, 200, 300, 400 GeV, outgoing p polarisation 79−63543
pp→p(pol.)X, 100 to 400 GeV, proton polarisation in inclusive processes 79−58983
pp→p($p\pi^-\pi^-$)($n\pi^+$)($p\pi^0$), polarised protons at 6 GeV/c, low mass enhancements 77−30400
pp phase shifts at 2 GeV/c using polarisation spin correl. cross section data 77−41852
pp polarisation asymmetry in high p_T inclusive prod., QCD and gluon$^-$ models 79−40819
pp→pp, high P_T^2 elastic scatt., 11.75 GeV/c, spin depend. from polarised p 79−3049
pp→pp, triple-spin correl. parameters and spin transfer parameters at 6 GeV/c using polarised beam and target 79−89179
pp→pp spin-spin interactions in high-$p_\perp^2$ elastic scatt. at 11.75 GeV/c 77−88009
pp→$\pi^-\pi^+$, 1.0 to 2.2 GeV/c, polarisation parameter 77−87995
pp̄→$\pi^-\pi^-$, polarised targets, p̄ parity meas. 77−2860
pp̄→$\pi^+\pi^-$, polarised target, charge parity determ. 77−57567
pp scatt., high energy, impact picture for polarisation and rotation parameter 78−70341
pp scatt., low energy, test of quantum mechanics limits of validity *(French)* 79−406
pp scatt., polarisation meas. in scatt. at 52.34 and 68.19 MeV 78−54641
pp scatt., polarisation paramater and ang. distribs. meas. at 100 and 300 GeV 78−89738
pp scatt., polarised beams, Wolfenstein parameter meas. near 1 GeV *(Russian)* 77−49997
pp scatt., spin correlation meas., local hidden variable theory, quantum theory 78−54649
pp scatt., spin correlation parameter at high energies 79−97636
pp scatt., spin-spin correlation param. meas. at 6 GeV/c 77−18327
pp scatt., total cross section difference in longitudinal spin states, 1.2 to 6.0 GeV 78−62432
pp scatt. at 1.03 GeV 78−82245
pp scatt. spin-dependent eikonal model for 5.5 GeV/c-2000 GeV/c calcs. 77−26545
pp scattering, 0.97 GeV, polarisation and depolarisation parameters *(Russian)* 79−30745
pp small angle scattering, 398-572 MeV, polarisation, amplitude anal. 77−30407

proton polarisation continued
pp total cross section, spin dependence, relativistic model of Δ(1232) prod. 78−62436
πp→π^{0}p, 650 and 700 MeV, angular depend. of secondary p polarisation *(Russian)* 78−78191
πp radiative scattering, calc. of polarisation asymmetries using Lagrangian isobar model 79−89184
π$^+$p backward elastic scatt., 3.5 GeV/c, polarisation parameter, isospin anal. 77−13974
π$^-$p→π$^-$p, 291.5 and 308 MeV, polarisation parameters meas. 79−6347
π$^-$p→π^{0}n, charge exchange polarisation parameter meas., 617 to 2267 MeV/c 78−82231
π$^+$p, elastic scatt., 6 and 12 GeV/c, polarisation meas. using CERN polarised d target 79−49542
π$^+$p at 45 GeV/c, polarisation parameter *(Russian)* 77−34179
π$^+$p elastic scattering, 100 GeV/c, polarisation meas. 77−30440
π$^-$p→ρ$^0\Delta^{++}$(ωΔ), ΔJ=1 rule, model tests from polarisation expts. 77−30471
π$^+$p scatt., 291.4 and 310.0 MeV, polarisation parameter 78−41571
π$^+$p, 100 GeV/c scatt., polarisation param. meas. 77−71534
QCD, q̄ polarisation in quark sea of proton 78−12867
^{12}C(p,p′), 185 MeV, elastic and inelastic scatt., proton polarisation and ang. distribs. 79−59060
Cr complex, Cr^V, doping agent for polarised targets 78−46198
Cr(V) complex, paramagnetic, dynamic polarisation of protons and deuterons 79−36453
^{63}Cu(α,p)^{66}Zn, proton polarisation calc., distorted wave method 77−6404
D(p,p), 630 MeV, asymmetry in scatt. polarised protons *(Russian)* 78−46064
Fe complex Fe(NO)[$S_2CN(C_2H_5)_2$]$_2$ in frozen toluene, for dynamically proton polarised target 78−52378
H$^-$ polarised beam production by 800 MeV spin precessor 79−68096
H$^-$ polarised ion source, pulse operated, Lamb shift type, for acceleration of polarised protons *(Japanese)* 77−67929
^{1}H(γ,n)p, 50 MeV, polarisation parameter meas. 78−50148
^{2}H(γ,np), 325-725 MeV, proton polarisation anomalous struct. 77−30551
^{2}H(γ,np), <800 MeV, proton polarisation in γn→π$^-$p *(Russian)* 78−41700
^{3}H(p,p), 8 to 17.1 MeV, of neutron polarisation in ^{3}He(n,n) 78−25171
He polarimeter, low temp., 20 to 50 MeV proton polarisation analysing apparatus *(Russian)* 79−76318
^{6}Li(^{3}He,p)^{8}Be, 14 MeV, p-^{8}Be optical model parameters 78−25208
^{16}O(p,2p), 200 MeV polarised beam reaction, possible knockout polarisation 77−88099
Si polarimetry facility, proton polarization meas. 79−31346
^{28}Si(α,p)^{31}P, proton polarisation calcs., distorted wave method 77−6404

proton production
causality, Regge behaviour, proton electroprod. struct. function, Bjorken limit of sum rule 77−67662
central high energy heavy ion collisions, possible finite particle number effects, p spectra 80−99181
cumulative proton production in neutrino and antineutrino interactions with freon, 2 to 30 GeV *(Russian)* 80−4980
depolarisation during acceleration and storage of polarised protons and deuterons 78−58519
electroproduction, inclusive particle ratios on H and D targets 77−18291
electroproduction struct. function and constituent-particle scatt. 78−45931
fast stable particles from light emulsions nuclei following 1.5 GeV/c K$^-$ interactions 78−17245
hadron-nuclear interactions, fast proton backward emission mechanism *(Russian)* 79−63706
hadron-nucleus collisions, backward particle emission, energy depend. 78−25236
hard scattering process, parton model, p to π ratio at large transverse momentum 80−62934
heavy-ion proton-proton correlations in relativistic collisions 77−88170
(HI,X), inclusive one- and two proton spectra by statistical model 79−93624
hyperon decay, high energy, polarised proton beam production 78−58517
inclusive electroproduction of forward protons in fireball model 78−41554
inclusive particle production in C+p and W+p reactions, nuclear size depend. 77−46168
large p_T proton production, parton models 79−40743
nuclear inclusive photoprod., A-dependence, momentum spectra, max. bremsstrahlung energy 2.0 to 4.5 GeV *(Russian)* 77−34287
nuclear multi-particle rescatt. effects, cumulative π, p, K prod. *(Russian)* 80−52638
particle and antiparticle prod. by 200 GeV/c p is CERN SPS charged hyperon beam 79−71768
polarised proton beams, higher energy, conf., Ann Arbor, MI, USA, Oct. 1977 78−58514
pulsed source, Penning type, beam parameters 80−87001
QCD predictions for large momentum transfer baryon prod. 79−89125
relativistic heavy ion collisions, central and peripheral, p emission patterns 80−73860
relativistic light ion collisions, two-fireball model improvements, p and π spectra 80−5158
relativistic nuclear collisions, p, d, and t inclusive energy spectra 80−63199
residual proton production in deep inelastic electron scatt. 78−70381
sub-Coulomb barrier protons from Al+n, Ti+n reactions at 14 MeV 77−30597
total pion absorption cross section, A depend., proton yields 80−106081
(e, e′p), eN interaction in quasifree scatt., nonrelativistic Hamiltonian through 2nd order 80−52663
(e,e′p) quasi-free scatt., spectral function, sum rule discrepancy, shell model deviation 80−42641
ed, 2.3 GeV, inclusive electroprod. cross sections for final state nucleons 77−34159
e$^\pm$d→e$^\pm$np, polarised, parity violating asymmetry 80−78080
e$^+$e$^-$ annihilation, inclusive Λ and p yield 79−9369
e$^+$e$^-$→hadrons, 12, 30 GeV, π,k,p,p̄ production 80−105916
e$^+$e$^-$→p̄X, 13 and 25 GeV^2, cross sections, scaling 77−49989
e$^+$e$^-$→pX, at CERN ISR with x=0 77−18303
e$^+$e$^-$→pp̄, 1925-2180 MeV total energy, form factors and cross sections 80−427

proton production continued
e^+e^-→pp̄, asymm. and polarisation of p,p̄, neutral weak currents *(Russian)* 78−58195
e^+e^-→pp̄, neutral current effects in Weinberg model 77−18310
eN→pX, ^{1}H, ^{2}H targets, forward protons to Q^2=9.5 GeV^2 77−74690
e⁻p→e⁻p+anything, virtual photon photoprod. invariant cross section 77−46058
(γ,p), >100 MeV, using monochromatic photons, leading to final nuclear states 80−22814
γd→np, 300 MeV, dibaryon resonance manifestation, pseudoindependent amplitude elimination *(Russian)* 80−57612
γd→pn, 250 to 800 MeV, differential cross-section and proton polarisation, theoretical models 80−78081
γd→pn, 400 to 650 MeV, ang. depend. of proton polarisation and partial wave anal. of possible dibaryon resonances 79−58967
γd→pn, proton polarisation energy depend., 400-700 MeV *(Russian)* 80−63000
γN→p+anything, 9-18 GeV, forward hemisphere 77−6134
γn→π⁻p, 700 to 1200 MeV, recoil proton polarisation 80−78075
γn→π⁻p reaction cross-section asymmetry in photon energy range 0.9 to 1.65 GeV *(Russian)* 80−32108
γp→p̄pp, threshold −4.8 GeV, elastic photoprod. cross section 80−52521
γp→π⁰p, 450 to 800 MeV, proton polarisation, Walker-type anal., P_{11}(1470), D_{13}(1470), S_{11}(1535) resonances 80−73721
K⁻d→Ξ⁻K⁰p, 1.45, 1.65 GeV/c, Ξ⁻p invariant mass enhancement 80−57639
Kp→π(K)(p)X, 4-250 GeV/c, Pomeron factorisation 77−14005
K⁺p→pK⁰X, 32 GeV/c, total cross section and structure functions 79−40809
K⁺p→pX, 32 GeV/c, total cross section and structure functions 79−40809
K⁺p→p+anything, 16 GeV/c, study of slow inclusive protons 77−65184
(μ,pxn), reaction probabilities on targets from ^{23}Na to ^{209}Bi 78−29451
(N,N′X), shower proton and meson transverse momenta, intranuclear cascade model 80−102185
(n,pπ⁻) reactions on nuclei, 8 to 24 GeV/c, coherent diffractive prod., cross sections 78−41711
n→pπ⁻π⁰, diffractive dissociation induced by 12 GeV K⁻ 79−40805
np→px, baryonium exchange, triple-Regge couplings 80−86763
$\nu_\mu(\bar\nu_\mu)$p→$\nu_\mu(\bar\nu_\mu)$p hadronic neutral current, final-proton polarisation 78−82200
νn→=νpπ⁻, neutral current process, excitation function, cross section ratio 80−78053
νn→μ⁻p, bounds on outgoing baryon transverse polarisation, T-odd effects 77−87966
(p,2p), backward inclusive prod. mech. probing, differential cross section 80−68668
(p,X), 400 GeV, A=6-180, p̄,π± and K± backward prod., invariant cross sections 80−102188
(p,X), 640 MeV, fast proton emission, two particle differential cross sections *(Russian)* 80−106058
(p,X), 70 GeV/c *(Russian)* 80−52681
(p,X), inclusive one- and two proton spectra by statistical model 79−93624
(p,X) emulsion, 400 GeV/c slow deuteron and proton prod. 80−52666
p̄ prod. in W+p, 25 GeV, flux optimisation using hadron cascade calcs. 77−83411
p+A→p+anything, A=C, Al, Ti, Cu, Cd, Pb, inclusive backward emission of protons, 1.5 to 9.0 GeV *(Russian)* 77−10278
p+Be(Cu), 70 GeV, π⁺, K⁺, p large p_T yields *(Russian)* 77−82778
p+Z→π⁻(K,p,p̄)X, 28.5 Gev/c, invariant cross-sections, for P_T 0.75-2.25 GeV/c 77−30456
pC→p(pol.)X, 100 to 400 GeV, proton polarisation in inclusive processes 79−58983
pd, 70 GeV, π±, K±, p, p̄ prod. with 0.5-2.2 GeV/c transverse momenta, yield ratio, QCD *(Russian)* 80−83012
pd→p(p̄)+anything, large p_T, 200 to 400 GeV 77−22816
pd→π±(K±)pX, 11.75 GeV/c, meas. of left-right asymmetry far inclusive π±, K±, p prod., polarised p-beam 79−22155
pN, 67 GeV/c, in Be, Al, Cu, inclusive π±, K±, p, p̄ prod. cross sections *(Russian)* 80−86769
pN, 67 GeV/c, nuclear targets, π±, K±, p,p̄ yields *(Russian)* 80−68501
pn→pX, 100 to 400 GeV/c, slow-proton prod., Regge trajectory 80−22646
pN→π⁻pX , 9 GeV/c, inclusive π⁻p prod. below 188 mrad *(Russian)* 79−49538
pN reaction, subthreshold p̄ production, interpretation by cumulative process 'gathering' model 78−58268
pp, 70 GeV, π±, K±, p, p̄ prod. cross sections, QCD-parton model anal. *(Russian)* 80−63044
pp̄ annihilation, 100 GeV/c, general features of charged particle prod. 79−75803
pp inclusive and semiinclusive interactions, 69 GeV/c, π⁺, π⁻ and p prod. 77−79289
p̄p→pX, 6.94 GeV/c, momentum distribs., triple Regge model predictions 78−66170
pp→pX, polarised 6 GeV/c projectile, L-R asymmetry 77−49995
pp→p̄X, search for new long lived particles with masses 1.4 to 3.0 GeV at CERN ISR 79−40810
pp→pX or π±X, 7.9 GeV/c, polarised target, spin depend. 79−3056
pp→p̄+anything, parameter free exchange model 77−10293
pp→p(p̄)+anything, 100-400 GeV, expt. techniques and data analysis 78−58216
pp→p(p̄)+anything, large p_T, 200 to 400 GeV 77−22816
pp→p(pol.)X, 100 to 400 GeV, proton polarisation in inclusive processes 79−58983
pp→pp, pp̄, πp, double differential cross-section meas. 77−82776
pp→π±(K±)pX, 11.75 GeV/c, meas. of left-right asymmetry far inclusive π±, K±, p prod., polarised p-beam 79−22155
pp→π(K)(p)X, 4-250 GeV/c, Pomeron factorisation 77−14005
(π,p), A=12-181, proton yields, number of nucleons involved in pion absorption 80−63209
(π, πp), emulsion light nuclei, 112 MeV, cross sections and mechanisms *(Russian)* 79−97733
π⁻+A→p+anything, A=C, Al, Ti, Cu, Cd, Pb, inclusive backward emission of protons, 1.5 to 9.0 GeV *(Russian)* 77−10278
π⁻d→π⁻pn final state interactions and d breakup for 438 MeV/c π⁻ impulse *(Russian)* 80−18145

proton production continued
π⁻n→pX⁻⁻, 21, 205 and 360 GeV/c, reggeised one-pion-exchange 80−57649
π⁺n→pX, 100 to 400 GeV/c, slow-proton prod., Regge trajectory 80−22646
πp→π(K)(p)X, 4-25 GeV/c, Pomeron factorisation 77−14005
π⁻p, 200, 300 GeV, relative π⁺, K⁺, p, p̄ prod., charge ratios, high p_T 80−47335
π⁻p inclusive reactions, 147 GeV/c, average charged particle multiplicities 79−40818
π⁻p→p_{slow}+X⁻, 147 GeV/c, differential cross sections, triple Regge anal. 79−40811
π⁻p→pX, 12 GeV/c, absorbed Mueller-Regge model for backward inclusive p prod. 80−73752
π⁻p, 32 GeV/c, slow proton and Δ⁺⁺(1236) inclusive prod. *(Russian)* 80−63046
π⁺p→p+anything, 6 GeV/c, unitary bounds on ang. distribs. 77−30466
Π⁻ ρ→p̄d, p̄ prod. obs. near 3.75 GeV/c threshold momentum 80−52533
^{107}Ag+p, 24 GeV/c, in nucl. emulsion, particle emission freq. variation 78−37335
Al+p, 200 GeV/c, relative yields of π⁺, K±, p, p̄ 78−93995
^{27}Al(γ,p)^{26}Mg, energy and angular distribution *(Korean)* 80−18289
^{27}Al(π,π′p), 255 MeV, quasielastic knockout, proton yield, σ(π⁺)/σ(π⁻) cross section ratio 80−32305
Al(p,X), 400 GeV, p backward prod. invariant cross section 79−93623
^{197}Au(^{16}O,p)X, 315 MeV, high energy p emission, fireball and preequilibrium anals. 80−91194
Be+p, 200 GeV/c, relative yields of π±, K±, p, p̄ 78−93995
Be(γ,p), intermediate energy bremsstrahlung, cross sections 78−13061
Be(p,X), 400 GeV, p backward prod. invariant cross section 79−93623
^{79}Br+p, 24 GeV/c, in nucl. emulsion, particle emission freq. variation 78−37335
^{12}C+π, 5 GeV/c, momentum spectra and mechanism of proton emission *(Russian)* 79−89334
^{12}C+π⁻→p+X, 40 GeV/c π⁻ momentum *(Russian)* 79−89335
^{12}C(e, e′p), eN interaction in quasifree scatt., nonrelativistic Hamiltonian through 4th order 80−47469
^{12}C(e, e′p), quasifree scatt., spin-orbit distortion of emerging nucleon 80−52664
^{12}C(e,e′p), cross sections from DWIA, optical, and shell model calcs. *(Russian)* 80−32270
^{12}C(γ, π⁻p), final state interaction, plane and distorted wave momentum distrib. 80−18286
^{12}C(γ,π⁻), (γ,π⁻p), knockout p interaction, optical model and quasifree π photoprod. mechanism *(Russian)* 80−42638
^{12}C(γ,π⁻p), 340-380 MeV, quasi-free photoprod., impulse and shell model anal. *(Russian)* 80−5124
^{12}C(γ,π⁻p), final state interaction, distorted and plane wave momentum distribs. 80−78275
^{12}C(π⁻p) in Δ(1232) region, differential yield, impulse and shell model anal. *(Russian)* 79−67744
^{A}Ca(α,p)$^{A+3}$Sc, 25 MeV, population of $f_{7/2}{}^4$ states 79−59077
C(p,X) *(Russian)* 80−52649
C(p,X), 400 GeV, p backward prod. invariant cross section 79−93623
Cu(p,X), 400 GeV, p backward prod. invariant cross section 79−93623
^{3}He(e, e′p) electrodisintegration by 1200 MeV electrons *(Russian)* 80−37370
^{4}He (π⁻, π⁻p), 5GeV/c, quasielastic scatt., cross section, form factor, final state interactions 80−99190
^{6}Li(p,X), 400 GeV, p backward prod. invariant cross section 79−93623
^{A}Li(πp), A=6, 7, 75, 175 MeV, diffential cross sections, reaction mechanisms 80−78332
(n,pπ⁻), neutron coherent dissociation using nuclear targets, comparison of expt. data with Deck model 79−89309
NaF+^{20}Ne, 800 MeV nucleon^{-1}, inclusive proton production, classical many-body calc. 79−17918
^{20}Ne+emulsion nuclei, Monte Carlo simulation pion and proton multiplicities 78−37363
^{A}Ni(^{3}He, p), 8, 10 MeV, A=58, 60, 62, p spectra compound nucleus contrib., odd-even effect 80−106061
^{58}Ni(^{40}Ar,X), 280 MeV, deep inelastic, light fragments, thermal equilib., ang. momentum transfer 80−63203
^{60}Ni+π, 70 MeV, γ+charged particle coincidence spectroscopy, cross section, p multiplicity 78−46111
N(p,X), 340, 660 MeV, ang. distribs., proton quasi-elastic knockout *(Russian)* 80−52649
^{16}O+emulsion nuclei, 75-200 MeV/nucleon, pion and proton multiplicities 78−37363
O(p,X), 340, 660 MeV, ang. distribs., proton quasi-elastic knockout *(Russian)* 80−52649
^{208}Pb(π,π′p), 255 MeV, quasielastic knockout, proton yield, σ(π⁺)/σ(π⁻) cross section ratio 80−32305
^{28}Si(γ,p), 18.1-29 MeV, photoproton energy spectra, contribs. to giant dipole resonance 80−78242
Ta(p,X), 400 GeV, p backward prod. invariant cross section 79−93623
U+^{20}Ne, 250 and 400 MeV nucleon^{-1}, inclusive proton production, classical many-body calc. 79−17918
U+^{4}He, 400 MeV nucleon^{-1}, inclusive proton production, classical many-body calc. 79−17918

proton-proton inclusive interactions
$\Delta\sigma_L$(pp), 400-600 MeV 79−97632
absorption role in πp and pp multiplicity differences 78−66172
accelerator proton collisions, 200 to 400 GeV, review of charm particle prod. in nuclear emulsions 79−63534
antibaryon and baryon inclusive spectra, quark model anal. 77−88018
azimuthal correl. of high $\rho_T\pi^0$ and η with second π⁰ 79−85347
baryonium exchange, evidence from pp and pp̄ reactions, total cross section differences 78−66171
beam dump experiments, prompt neutrinos and charm particle lifetime 79−63535
beam dump neutrino experiments, promp neutrino meas. 79−63537
Bose-Einstein statistics, wave packet formulation of multiparticle production at high energies 80−13338
channel coupling effects and resonance phenomena in pp interactions, N/D eqn. study 79−71765
charged hadron production 100-400 GeV, expt. techniques and data analysis 78−58216
charged hadron trigger at large transverse momentum at CERN ISR 79−45117

proton-proton inclusive interactions continued
charged multiplicity distributions, comparison of $\bar{p}p$, pp, and e^+e^- interactions 77−57577
charged particle associated multiplicities at ISR energies 78−21473
charged particle average multiplicities comparison in $\pi\pm$p and pp collisions, quark model *(Russian)* 78−17065
charged particle correlations between forward/backward hemispheres in pp collisions at ISR energies 78−29366
charged secondary particles average multiplicities, total cross sections, lepton-hadron relation 78−33100
charged-particle multiplicities associated with large p_T photons 77−18358
charmed baryon diffractive prod. at ISR energies 77−41818
charmed particle production from two-gluon annihilation in proton-proton collisions 79−347
cluster mass spectrum 80−37307
clusterisation, role of rapidity interval distrib. *(Russian)* 77−10220
colliding beam experiments, double pomeron cross sections 77−14007
constituent transverse-momentum fluctuations and hard scatt. expansion 79−17749
correlations between two identified charged hadrons at CERN ISR 77−14006
credibility of criticism by Azimov et al., misuse of CTM 78−93980
cross section meas. for 100-3000 GeV using hadron-Fe collisions 79−49549
deep inelstic pp, πN, eN scatt., lepton-hadron relation, multiparticle prod. phenomena, average multiplicities 78−37247
depolarisation parameter, dominance of natural parity exchange 80−78088
dihadron high mass continuum, phenomenological anal. of Fermilab data 80−42511
dimuon continuum production in hadron collisions, nonscaling behaviour 79−22156
direct electron prod. 10-25 GeV, anomalous behaviour in e/π ratio 77−14004
Drell-Yan processes, perturbative versus asymptotic-freedom convections 79−63446
dynamical model for multiplicity distribs. in πp and pp-collisions, pion prod. 78−21469
eikonal mechanisms at high energy 78−82256
elastic differential scattering cross section, 30-250 GeV/c 79−13166
fast hadrons at low $p_\perp$, parton model, quark recombination, pp scatt. appl. 78−54618
final state struct. prod. in association with large transverse momentum π^0 79−45115
final states containing high p_T π^0 at CERN ISR 79−45119
final states structure, charged hadron of high transverse momentum at 90°, forward particles 78−58214
fireball model three component, appl. to $\bar{p}p$ interactions above 9 GeV 80−62946
hadron prod. 23.4 to 63.4 GeV, charged multiplicity density for various p_T 78−70414
hadron production, phase transition in Feynman-Wilson analogue fluid, multiplicities, plateaux, cross-sections 80−73744
hadronic jets, possible intermediate bosons 80−18149
hadronic multiple prod. and average charged multiplicity, strato-gluon mechanism in pp, Kp, πp *(Chinese)* 80−22586
hadronic production of charmed particles, review 79−67610
hadronic two-jet events, momentum unbalance, parton transverse momentum 80−57652
heavy black and grey prongs in nuclear emulsions, scaling in multiplicity distribs. 79−49555
Higgs bosons from two-gluon annihilation in pp collisions 78−41501
high momentum $\pi^\pm$ and $K^\pm$ prod., 45 GeV, cross sections 78−93910
high p_T direct single photon prod., 30-62 GeV 80−9189
high p_T spectra and ang. multiplicity correls., phenomenological anal. 77−10292
hydrodynamical approach, large p_T distrib. in pp interactions 79−49490
intermediate boson and heavy lepton prod. and detection possibility in pp and $p\bar{p}$ 77−54072
jet and background multiplicity distribution associated with high $p_\perp$ particle in pp-collisions 79−26350
jet fragmentation in large p_T events at ISR 79−45118
jet structure in high p_T events, importance of parton transverse momentum 78−432
jet thrust spectrum, 3-jet structure, QCD calc. 80−47333
large p_t hadron production, lowest subprocess model, two body reactions 78−4887
large p_T two-particle correlation, hadron composite struct. 77−54085
large transverse momentum hadron+hadron collisions, particle-jet correls., quark scatt. model 78−4883
large transverse momentum pions prod., correls., fireball model 78−66174
lepton-hadron relation and a new KNO-type of scaling 79−9414
longitudinally-polarised beam and target, total cross-section meas., 3, 6, GeV/c 78−4870
many particle correlations, multiperipheral cluster model interpretation *(Russian)* 78−74285
massive lepton pair prod. by polarised p, constituent spin prop. test, QCD 79−89201
massive lepton pair production, review of parton model 77−57498
mean charged hadron multiplicities in high energy collisions 79−93467
meson large p_T distrib. formula, from pre-equilib. fireball state and fireball spin 79−13170
meson prod. with large transverse momentum, effective gluon model 78−8717
meson production, multimeson inclusive spectra and recombination model, multiquark structure functions 80−73751
meson production at large p_T, comparison with πp results 77−50030
meson resonance prod. 77−34198
Monte Carlo approach to multiparticle prod. in a quark-parton model 79−13171
multihadron production, gluon matter hadronisation 79−45047
multiperipheral cluster model comparison with data for 28.5 GeV/c interactions *(Russian)* 79−9424
multiplicities, charged and neutral, associated with large transverse momentum π^0s in pp collisions, expt. obs. 79−3058
multiplicity distrib. formula in 10-405 GeV range 77−13998
multiplicity distribs. of charged particles at ISR energies 78−8709
multiplicity distribs. of negative particles, energy depend. of KNO scaling parameter *(Russian)* 79−80860
proton-proton inclusive interactions continued
multiplicity distributions, 50-400 GeV/c, multi-Regge model with threshold factor for cluster prod. 77−18256
multiplicity distributions associated with charged hadron prod., ISR energies 79−3053
multiplicity of particles, production, correl, with increasing primary energy 79−58979
multiplicity ratios, Landau's relativistic hydrodynamical model 77−46169
narrow resonances, search in 53 GeV interactions 77−2881
narrow vector meson hadroprod., ϕ, J, ψ, charmoniumlike states 77−57573
neutral particle production in 4 to 2100 GeV interactions, review *(Russian)* 80−68489
nondiffractive collisions, 52.5 GeV, density, charge and transverse momentum correls. 79−80853
nonleading particle distrib., contributions to direct lepton spectra 77−2880
nucleon charge exchange, reggeized one pion exchange model *(Russian)* 77−2888
one-dimensional cascade model of interacting nuclei using Glauber theory 78−17233
particle and antiparticle prod. by 200 GeV/c p is CERN SPS charged hyperon beam 79−71768
parton-parton interaction in high transverse momentum collisions, phenomenological description 77−57574
perturbative QCD and exptl. signatures of weak bosons 78−93916
perturbative reggeon calculus, topological cross sections 78−8632
phenomenological model of pion prod. *(Russian)* 79−30763
phenomenological two-component model for hadron constituents, large p_T spectra, pp inclusive reactions 78−25086
phenomenology of pp semiinclusive collisions, hypergeometric distrib., KNO scaling 77−2883
pion multiplicity distribs. in impact parameter space, multi-Regge model 77−14001
pN collision, 200 GeV/c, production of long-lived hadrons and leptons, antinuclei production 80−13342
polarisation, recent results from Fermilab 78−78224
polarised beam, P violating asymmetries and estimates of W prod. 79−63538
pp→ΛX, Λ longit. polarisation determ. QCD anal. 79−63559
pp→Xp, diffraction dissociation, high energy 78−25087
pp collisions, high energy, fireball mass, rapidity, spin distribs. 80−57645
probabilistic quark-model approach to p fragmentation 80−63049
prompt μ and $\mu\mu$ prod. 400 GeV, possible charm prod. 78−89750
prompt lepton emission, 53 GeV, e/π ratio, charm particle total inclusive cross section 78−93914
prompt neutrino production in beam dump expt., cluster anal. 79−49556
Pure spin total cross sections 79−63539
QCD perturbation theory, asymmetries in inclusive hadron prod. 78−50057
quantum chromodynamics, hadroprod. of lepton pairs and real photons 78−50056
quark cascade model, inclusive meson and baryon spectra in pp, πp, e^+e^- 77−50025
quark model and π^+p-pp multiplicity difference 79−40813
quark parton model, total cross sections 78−45859
quark-antiquark recomb. in fragmentation region 77−67690
quarks, search for fractionally charged particles in pp collisions at 62.2 GeV 77−65183
radial scaling analysis in single particle inclusive reactions 77−18351
rapidity correlations in pp collisions at 102 and 400 GeV/c 77−46088
rapidity distribs., three and higher order at 200 GeV/c 77−18337
scaling-in-the-mean hypothesis 80−68497
sea-quark distrib. in proton, from pp inclusive interactions 78−66090
six prong pp interactions, 25 and 200 GeV/c, particle clustering using parameter invariant quantities *(Russian)* 79−80857
sphericity distribution, in 70 GeV/c inelastic collisions, multiplicity depend. 79−80852
thermodynamic model calcs. of single particle distribs. 77−30453
total cross section, CERN ISR precision meas. 79−17769
total cross section and small angle elastic scatt. 23.5-62.5 GeV, diffraction peak 79−424
total cross section at cosmic ray energies up to 100 TeV 79−96868
total cross section difference for scatt. in longitudinal spin states 77−41870
total cross section from cosmic ray p-nucleus and pp data anal. *(Russian)* 78−17064
total cross section in pure spin states, Coulomb nuclear interference corrections 79−40822
total cross section rise, critical character of pomeron 77−50029
total cross sections in pp interactions, 1 to 3 GeV/c, transverse spin depend. 77−30409
total cross-section asymptotics, stable approach, timelike and spacelike behaviour, vacuum polarisation 80−47332
total inclusive cross sections for δ^0, g^0, K^{*0} and $\bar{K}^{*0}$ at 53 GeV 79−17771
transverse momentum distrib. anal., at 24, 70 GeV/c 77−82781
transverse spin depend. of total cross-section at 1-3 GeV/c 78−33078
triple scattering in exclusive and inclusive processes at wide angle 79−45104
two-component model and geometric picture for high energy P-P collisions 79−58948
two-jet calorimeter experiment at Fermilab 79−45116
two-stage model, parton distribs. and Q^2 depend. 78−66078
vector meson dominant prod., 53 GeV 77−67685
vector meson production, OZI rule violation 79−58929
vector meson production in pp interactions, constituent-interchange model 80−22579
X-particles and their backgrounds in 400 GeV/c proton interactions 79−63548
ap→cX, a, c=$\pi^\pm$, $K^\pm$, p, $\bar{p}$, low P_t hadron fragmentation at 100, 175 GeV/c 79−85346
d and $\bar{d}$ production in pp collisions at CERN ISR 78−33099
D^0 meson prod., search in 53 GeV interactions 77−30462
Δ prod. and spin depend. of pp total cross sections 77−82794
e production in pp collisions at 53 GeV, small transverse momenta electrons 78−29367
η production, 30 to 50 GeV 80−5023
η/π^0 prod. ratio at high transverse momenta 78−41602

proton-proton inclusive interactions continued
$f^0(1270)$ prod. cross section in 53 GeV interactions 77−30462
γ production in pp collisions, quark parton model 79−429
K^0 production, inclusive and exclusive, 6 GeV/c, polarised beam 77−65171
$K^{\pm}$, single particle spectra in 100-400 GeV pp interactions 78−17059
$K^*(890)$ and $K^*(1420)$ prod. in 405 GeV/c pp interactions 79−30757
$K^{*\pm}(890)$ production in 205 GeV/c pp interactions 78−54659
$K^{*\pm}(892)$ production at 12 and 24 GeV/c 80−86765
Λ, $\bar{\Lambda}$, $\Sigma^{\pm}(1385)$ prod. in 405 GeV/c interactions 78−21477
Λ production, inclusive and exclusive, 6 GeV/c, polarised beam 77−65171
Λ production, polarisation effects, effective mass spectrometer studies 77−30412
Λ^0 polarisation in inclusive prod. by 24 GeV protons on Pt 77−67691
NN cluster prod., pion inclusive cross section 77−71545
p, single particle spectra in 100-400 GeV pp interactions 78−17059
$\bar{p}$ annihilations in heavy liquid bubble chamber, effects of complex nuclei reactions 77−79373
$p(\bar{p})p \rightarrow W^+Z^0(\gamma)X$, high energy behaviour and hard photon prod. 80−5028
$p(\bar{p})p \rightarrow \gamma X$, large angle real photon prod. at large p_T, QCD anal. 80−22644
$p(\bar{p}p) \rightarrow W^{\pm}X$, QCD perturbative predictions 79−40812
p-nucleus interactions, 20 to 200 GeV/c relativistic particle angular distribs. *(Russian)* 78−46065
p-nucleus interactions, energy dependence of two particle rapidity correls. 77−34292
p+Be, inclusive proton spectra anal. 78−21480
$p+Be \rightarrow \phi+X$, 400 GeV/c, φ decay modes, OZI rule 78−599
p+emulsion nuclei, 300, 400 GeV, search for short lived charmed particles 77−50023
p+H target, high transverse momentum π^0 and jets prod. 78−70417
$p+^{187}W$, 2 to 5 GeV/nucleon, multiplicities of secondary particles *(Russian)* 78−46066
$pC \rightarrow p(pol.)X$, 100 to 400 GeV, proton polarisation in inclusive processes 79−58983
pN, charm-pair production 80−22643
$pN \rightarrow R\bar{R}+X$, R-hadron prod. bounds from calorimetry expts. 79−13167
$\bar{p}p$, 100 GeV, inclusive cross section ratio is a function of effective mass hypothesis 78−78227
pp, 100 GeV, topological cross-sections and multiplicity distribs. meas. 77−30464
$\bar{p}p$, 100 GeV/c, $\Delta^{++}(1236)$, $\bar{\Delta}^{++}$ inclusive prod., interaction mech. 79−3054
$\bar{p}p$, 100 GeV/c, inclusive meson and strange particle prod., energy partition 80−95289
pp, 147 GeV/c, inclusive Δ^{++} prod., cross section energy depend. 80−57651
$\bar{p}p$, 14.75 GeV/c, inclusive and semi-inclusive $K^{*\pm}(890)$ and $\Sigma^{\pm}(1385)$ prod. 80−5027
pp, 200, 300, 400 GeV, hadron prod. at large p_T invariant cross section 79−40926
pp, 200 GeV/c, high p_T charged particle prod. and correlations 79−89199
pp, 200 GeV/c in Be, inclusive ω prod. at large p_T, η′ prod. upper limit 80−52547
$\bar{p}p$, 22.4 GeV/c, azimuthal correlations and secondary transverse momentum alignment *(Russian)* 80−42509
$\bar{p}p$, 22.4 GeV/c, charged particle average energy, mass independ. calc., multiplicity depend. *(Russian)* 80−63045
$\bar{p}p$, 22.4 GeV/c, γ, K_S^0 and Λ inclusive prod., structure functions *(Russian)* 79−58985
$\bar{p}p$, 22.4 GeV/c, inclusive γ, K_S^0, Λ $\bar{\Lambda}$ production, KNO scaling test *(Russian)* 79−30759
$\bar{p}p$, 22.4 GeV/c, multiparticle prod., Monte Carlo quark-parton model 79−97639
$\bar{p}p$, 22.4 GeV/c, multiplicities and forward-backward correls. 78−17061
$\bar{p}p$, 22.4 GeV/c, single-particle inclusive spectra of charged particles 77−50024
pp, 27 GeV/c, resonant prod. of high $p_\perp$ back-to-back gluon jets 79−93470
pp, 28 GeV, in H, D, Be, inclusive Λ polarisation 80−47337
pp, 300 GeV/c, inclusive prod. of K^0, Λ^0 $K^{*\pm}(890)$ and $\Sigma^{*}\pm(1385)$ 80−95290
pp, 31-63 GeV, direct photon prod. at large p_T, π^0/γ prod. ratio 80−63038
$\bar{p}p$, 32 GeV/c, π and neutral strange particles inclusive prod. 78−4881
pp, 400 GeV/c, inclusive and semiinclusive prod. of π^0, K_s^0, Λ^0, $\bar{\Lambda}^0$, Σ^0, $\bar{\Sigma}^0$, η^0, ω^0 79−93472
pp, 405 GeV/c, pion local number distrib. fluctuations, higher order correlations 80−18152
pp, 405 GeV/c, ρ^0, f, g^0, h meson prod., cross sections 80−105930
pp, 52.6 GeV, large transverse momentum charged hadron at 90°, jet like structs. 80−18150
pp, 53, 62 GeV, forward prod. of Λ^0, $\bar{\Lambda}^0$, Ξ^-, $\Sigma(1385)^{\pm}$, $\Lambda^0\bar{\Lambda}^0$ simultaneous prod. 79−89206
pp, 53, 63 GeV, massive electron pair prod., Υ ang. decay, scaling function 80−68495
pp, 53, 63 GeV, Υ and ψ prod., dielectron decay angles 80−68496
$\bar{p}p$, 5.7 GeV/c, single particle inclusive spectra, Mueller-Regge approach 80−73727
pp, 60 GeV/c cross-sections and charged-particle multiplicity meas. 77−30463
pp, 62 GeV/c, multiparticle prod. mech., e^+e^- comparison in parton model 80−78103
pp, 62.4 GeV, e^+e^- massive pair prod., continuum and Υ resonance cross sections 80−18153
pp, 63 GeV, Λ_c^+ diffractive prod. at CERN ISR, $\Lambda_c^+ \rightarrow K^-p\pi^+$ decay mode 79−89204
pp, 69 GeV/c, charged backward π prod., inclusive baryon resonance prod. cross section *(Russian)* 79−30760
pp, 69 GeV/c, two particle correlation functions, multiperipheral cluster model *(Russian)* 79−30762
pp, 70 GeV, $\pi^{\pm}$, $K^{\pm}$, p, $\bar{p}$ prod. cross sections, QCD-parton model anal. *(Russian)* 80−63044
pp, 93 GeV, $\bar{p}p$ narrow enhancement at 1940 MeV, S(1936) mass 80−52542
$\bar{p}p$, 9.1 GeV/c, annihilation and inelastic final states cross-sections 77−30415
$\bar{p}p$, 9.1 GeV/c, inclusive prod. of vector and tensor mesons 79−6355
proton-proton inclusive interactions continued
pp, $\sqrt{s}$=30.6, 53.2 GeV, direct photon prod., γ/π^0 ratio 79−71771
$\bar{p}p$, azimuthal correlations at 22.4 GeV, ρ^0, Δ^{++} reson. prod. 79−67611
$\bar{p}p$, charge transfer reactions, 22.4 GeV/c 78−89762
$\bar{p}\bar{p}$, equal sign lepton pairs, cleaner W-signal 79−13012
pp, high energies, $\Sigma^{\pm}(1385)$ inclusive prod., minimised wave function model calcs. *(Russian)* 80−63047
pp, ISR energies, high p_T π^0 and single photon events, associated charged particle multiplicity 80−63039
pp, ISR energies, inclusive high p_T ω^0 and η′ prod. 80−42504
pp, ISR energies, Λ_c^+ production total cross section, decay modes 79−89150
pp, ISR energies, p fragmentation, D^+ prod. from Λ_c^* and Λ_b decay 80−102080
pp, large P_T $pion^0$ prod., meson structure functions, quark distrib. functions 80−86714
$\bar{p}p$, mean charged multiplicity, energy depend., modified Heisenberg calcs. 79−40806
pp, polarised p, W prod. estimates for hadron jet decay detection, parity violating asymmetries 79−40821
$\bar{p}p$, pp, 12-405 GeV, low p_T meson prod., quark-antiquark formation model 80−63056
$\bar{p}p$, pp, 130, 200 GeV, jet prod. cross sections, QCD anal. and scale breaking 80−99111
pp, $\bar{p}p$, 200 GeV/c, high p_T jet prod., QCD expt. test 79−89200
$\bar{p}p$, pp, 540 GeV, Υ and ψ transverse momenta from QCD 2→3 processes, gluon subprocesses 80−52546
$\bar{p}p$, pp, multiple production processes regularities, Monte Carlo model 80−102082
$\bar{p}p$, pp, pol. and unpol. beams, hadronic jets, vector bosons, QCD and weak interference 80−57648
pp, $\bar{p}\bar{p}$ inclusive interactions, lepton pair prod. and Drell-Yan mechanism 78−8718
pp, π^+ structure from two jet events, parton scatt. anal. 79−49491
$\bar{p}p$, $\pi^{\pm}$ inclusive prod., annihilation component estimation 77−82790
$\bar{p}\bar{p}$, $\pi^{\pm}$ inclusive spectra, comparison with Monte Carlo quark-parton model 79−30755
pp, secondary hadron absolute yield, L=1 meson prod., quark model *(Chinese)* 80−99113
$\bar{p}p$ 12 GeV/c search for D, D* and λ_c charmed particles, charmed pair prod. 79−426
$\bar{p}p$ 14.75 GeV/c, search for $K_s^0\pi^{\pm}\pi^+\pi^-$ resonance near 2.6 GeV/c 78−74289
pp 4-prong interactions, 25 and 200 GeV, anal. using parameter invariant quantity *(Russian)* 79−49559
$pp \rightarrow (K_s^0, \Lambda, \text{or } \bar{\Lambda})\pi^{\pm}+X$, 405 GeV/c cross section determ., vector meson dominance 79−89207
$pp \rightarrow (K^-\pi^+p)X$, scalar field with isospin, IR asymptotic behaviour of one-fermion Green's function 79−89205
$pp \rightarrow (\Lambda^0\pi^+\pi^+\pi^-)X$, scalar field with isospin, IR asymptotic behaviour of one-fermion Green's function 79−89205
$pp \rightarrow (\pi^{\pm}, K^{\pm}, p, d)X$, 6 and 11.8 GeV/c, polarised proton, L-R asymmetry meas. 77−30455
$pp \rightarrow (\pi^{\pm} \text{ or } K^{\pm})+X$, fast-meson production and the recombination model, proton multiquark structure functions 79−89208
$pp \rightarrow (\pi\pi)+X$, cross sections for large longitudinal momentum interactions 78−82254
$pp \rightarrow (\pi\pi\pi)+X$, cross sections for large longitudinal momentum interactions 78−82254
$pp \rightarrow aX$, a=p, $\pi^{\pm}$, Λ, K_s^0, $\Sigma^{\pm}$, 24 GeV/c, transverse momentum depend. 77−61327
pp and $\bar{p}\bar{p}$, Higgs-boson production at large transverse momentum in quantum chromodynamics 79−40745
pp and $\bar{p}p$ evidence for inclusive cross section ratio effective mass relationship 78−82185
$\bar{p}p$ and pp reactions, μ prod., Drell Yan prod. of intermediate vector bosons 78−29364
$\bar{p}p$ annihilation, 0 to 100 GeV/c, statistical and multiperipheral models, π^0 prod. 79−63507
$\bar{p}\bar{p}$ annihilation, 100 GeV/c, general features of charged particle prod. 79−75803
$\bar{p}p$ annihilation, low energy, prompt e^+e^-, ω^0 and η^0 prod., inclusive prod. rates 80−42506
$\bar{p}p$ annihilation, π^+, π^- and π^0 probability distrib. 78−41604
$\bar{p}\bar{p}$ annihilation at rest, γ-ray spectrum 78−21450
$\bar{p}\bar{p}$ annihilation channel as a prototype for the central fireball in pp production processes 79−75802
$\bar{p}p$ annihilation relative multiplicity moments, dual unitarisation scheme verification 79−89203
$\bar{p}p$ annihilation with polarised beams 79−36111
$\bar{p}p$ annihilations, 0.76 GeV/c, inclusive $K^{*\pm}(892)$ and K_S^0 prod. 78−62465
$\bar{p}p$ annihilations, 0.76 GeV/c, $K\bar{K}$ correls., effect of resonance prod. 78−78205
$\bar{p}\bar{p}$ annihilations, multipion distrib., statistical bootstrap model 80−68472
$pp \rightarrow cX$, scaling parameters at ISR energies, cosmic ray muon charge ratio 78−58212
$pp \rightarrow$charm particles, 400 GeV, evidence for prompt single muon prod. 79−63536
pp collision inclusive spectra, fast pionisation at high energies, z-scaling *(Russian)* 80−47339
pp collisions, 300 GeV, correlations between neutral and charged pions 79−36115
pp collisions, charged particle multiplicity, Bose distrib. 77−50022
$pp \rightarrow D\bar{D}X$, 53, 63 GeV, inclusive prod. cross section anal. 79−54368
$pp \rightarrow D\bar{D}+X$, upper limit for $D\bar{D}$ prod. at 55 GeV 78−89758
$pp \rightarrow dX$, search for new long lived particles with masses 1.4 to 3.0 GeV at CERN ISR 79−40810
$pp \rightarrow D+$anything, parameter free exchange model 77−10293
$pp \rightarrow \Delta^{++}X$, triple Regge anal., role of absorptive corrections 77−18340
$\bar{p}p \rightarrow \Delta^{++}(1232)X$, 32 GeV, cross sections 80−105937
$pp \rightarrow \delta^{++}(1236)$, Λ^0, 100 GeV/c, one-meson-exchange mechanism anal. 78−8712
$\bar{p}p \rightarrow \Delta^{++}(1236)X$, 22.4 GeV/c, inclusive and semiinclusive cross sections, one pion exchange contrib. 79−49548
$pp \rightarrow e^-+$anything, 23-62 GeV, cross section meas. 77−2877
$pp \rightarrow e^-h^{\pm}+$anything, 23-62 GeV, cross section meas. 77−2877
$pp \rightarrow e^+X$, direct prod. at 256 and 800 MeV 77−251
$pp \rightarrow e^+e^-X$, 52, 63 GeV, cross section, ψ′ prod. cross section, continuum cross section 79−425

proton-proton inclusive interactions continued
pp→e^+e^-X, 53 and 63 GeV, prod. of high transverse momentum low mass e^-e^+ pairs 79−54365
pp→e^+e^-X, J/ψ prod. at $\sqrt{s}$=52 GeV 77−65181
pp→e^+e^-X, J/ψ prod. in $\sqrt{s}$=23.5 to 62.5 GeV range 77−79293
pp→e^+e^-X, large p_T, reference to Υ(9.5), ξ(3.5) and direct γ-prod. 78−89749
pp→e^+e^-X, limits on prod. of large transverse momentum direct photons 79−9418
pp→e^+e^-X, review of CERN-Columbia-Rockefeller-Saclay expt. 77−263
pp→e^+e^-+anything, 23-62 GeV, meas. 77−2877
pp→$e^\pm\mu^\mp$X, CERN ISR energies, production limits, D(1.87) leptonic decay 77−65186
pp→$e^\pm\mu^\mp$+X, charmed meson pair semileptonic decay, inclusive charm prod. cross section 78−89759
pp→eX, origin of small p, direct electrons 78−21474
pp→eX, review of CERN-Columbia-Rockefeller-Saclay expt. 77−263
pp→ηX, inclusive η prod. at high p_T at the ISR, η/π^0 cross section ratio 79−71770
$\bar{p}p$ gluon jet prod. 79−63554
$\bar{p}p$→γ, Z^0+X, charge asymmetry, QCD-parton model study 79−93349
pp→γX, 24 GeV/c, inclusive π prod. 77−14003
pp→γX, large p_T direct photon prod., QCD scale violation effects 79−71772
pp→γX, perturbative QCD anal. 80−63042
$\bar{p}p$→γ+X, 4.6, 9.1 GeV/c, inclusive total, topological and invariant differential cross sections 79−408
pp→hX large p_T multiplicities 77−10289
pp→hadrons, quark processes, interaction with hadronic sea, Lorentz transformation 80−37236
pp→hadrons, scaling violation in fragmentation region in quark model, 10^6 GeV *(Russian)* 79−3051
$\bar{p}p$ high energy annihilation in nuclei, multiple scattering models 80−102079
pp in emulsion, 70 GeV/c, four-momentum transfer between groups of secondary particles 78−58211
pp in W, 400 GeV, particle mean multiplicities 80−13473
$\bar{p}p$ inclusive prod. of π^-,η,ρ^0,ω,f, mesons at 0.7 GeV/c 77−65170
pp inclusive π^0 large p_T prod., quark subprocesses 77−2885
$\bar{p}p$ interaction at 22.4 GeV/c, identical pion pair interference obs. *(Russian)* 79−9420
$\bar{p}p$ interactions, 100 GeV/c, inclusive distribs. for γ, K_s, Λ^0, $\bar{\Lambda}^0$ prod. 77−38213
pp interactions, 52.5 GeV, search for fractionally charged quarks 78−70416
pp jet prod., π^0 fragments, jet fragmentation function and momentum 80−443
pp→jet+X, P-violating weak effects in high transverse momentum collisions, QCD anal. 79−63559
pp→jets, 400 GeV, p_T plots, Monte Carlo and parton model predictions 78−89747
pp→K_S^0X, 147 GeV/c, cross-section, scaling 80−52539
pp→K_S^0X, 69 GeV/c, cross-section 77−22812
$\bar{p}p$→K_S^0X(ΛX) ($\bar{\Lambda}$X), 3.6 GeV/c, cross section anal. and Λ polarisation 79−45095
$\bar{p}p$→K_S^0+X, 4.6, 9.1 GeV/c, inclusive total, topological and invariant differential cross sections 79−408
pp→$K_1^0K_3^0X^{++}$ 19 GeV, strong dynamic correlations 79−93468
pp→$K_s^0\pi^-$+anything, 28.4 GeV/c, cross-sections and mass distribs. meas. 77−38212
pp→K^-X, pK^- exotic, triple-Regge formalism, Pomeron exchanges 80−63041
$\bar{p}p$→K^0X or ΛX or $\bar{\Lambda}$X at 12 GeV/c 78−4885
pp→$K^0(\Lambda)(\Delta^{++})$X, 6 GeV/c, polarised proton 77−30400
pp→K^+K^+X, search for narrow six quark resonance 78−89757
pp→K^-+anything, large p_T, 200 to 400 GeV 77−22816
$\bar{p}p$→K*(890)X, $\Sigma^\pm$(1385)X, $\bar{\Sigma}^\pm$(1385)X, or S*(993)X, 12 GeV/c, prod. cross sections 78−93911
$\bar{p}p$→K*(892)X, 3.6 GeV, factorisation hypothesis test 80−102055
pp→l^+e^-X, asymptotic free gauge theory calc. 77−74734
pp→l^+l^-X, massive lepton pair prod., quark-gluon-parton model, scaling 79−428
pp→l^+l^-X, parton density scale violations and quark-gluon correction to Drell Yan formalism 79−63560
pp→l^+l^-X, QCD quark-quark correction for Drell-Yan formalism 79−75731
pp→l^+l^-x, QCD corrections to Drell-Yan formula 80−22578
pp→l+anything, single lepton cross sections from decays of intermediate bosons 77−41868
pp large p_T reactions, jets, dual-string approach 80−32136
pp→llX, hadronic mass scales 77−71543
pp→llX, p_T behaviour and scaling violations with conventional ideas 77−74691
pp→Λ^0X, 53 and 62 GeV, Λ^0 polarisation at CERN ISR 79−49550
pp→Λ^0X, high energies, semiclassical model for polarisation 79−89202
pp→Λ^0X, small-angle production from nuclear and nucleon targets, collective tube model and triple-Regge picture 80−52538
pp→Λ^0X^{++}, 69 GeV/c, triple Regge anal. 77−74730
pp→$\Lambda K_s^0X^{++}$, 19 GeV, strong dynamic correlations 79−93468
pp→ΛK_s^0X, 19 GeV/c, single particle props. 80−32139
pp→ΛX, 147 GeV/c, cross-section, scaling 80−52539
pp→ΛX, 19 GeV/c, polarisation at high transverse momenta 78−37246
pp→ΛX, Λ polarisation and Regge cuts 77−2876
pp→ΛX, natural and unnatural parity exchange in triple-Regge region 77−65182
pp→ΛX and Λ polarisation, Mueller Regge model 77−30454
$\bar{p}p$→Λ+X, 4.6, 9.1 GeV/c, inclusive total, topological and invariant differential cross sections 79−408
pp→$\Lambda(K^0)$X, 12 GeV/c, beam polarisation induced asymmetries 80−42507
pp→$\bar{\Lambda}(\bar{\Sigma}^0)$X, 69 GeV/c, cross-section 77−22812
pp multiple hadron prod. up to 1500 GeV, hadronic matter eqn. of state *(Russian)* 80−32085
pp multiplicities, viscosity effect in Landaus hydrodynamical model 80−63055
pp→$\mu^+\mu^-$X, 62 GeV, ψ and γ cross sections, scaling function 80−105932
pp→$\mu^+\mu^-$X, dimuon prod. using polarised beam, Drell-Yan parton model anal. 79−58981
pp→$\mu^+\mu^-$X, gluon corrections to Drell-Yan model 79−36037
proton-proton inclusive interactions continued
pp→$\mu^+\mu^-$X, muon pair ang. distrib., QCD model study 79−36035
$\bar{p}p$→$\mu^+\mu^-$X, neutral current effects, $SU_L(2)\times SU_R(2)\times U_{L+R}(1)$ theory 78−17060
pp→$\mu^+\mu^-$X, parity violating effects in dilepton production using polarized targets 79−67613
pp→$\mu^+\mu^-$X, polarised p, polarisation direction, structure functions and Drell-Yan parton model test 79−63544
pp→$\mu^+\mu^-$X, QCD, parton and dimuon intrinsic transverse momenta 79−13038
pp→$\mu^+\mu^-$X, spontaneously broken colour gauge theory effects in Drell-Yan process 79−26344
pp→$\mu^+\mu^-$+anything, Drell-Yan formalism 78−78229
pp→$\mu^+\mu^-$+anything, muon pair production, M quiescent mass determ. *(Hungarian)* 79−13163
pp→$\mu^-e^\pm$+X, possible charmed meson pair prod., D$\bar{\text{D}}$ cross section 78−89751
pp→$\mu^+\mu^-$X, large mass, QED calc. with massive photon *(Russian)* 77−30468
pp→NN+nπ, kinematical constraints on particle correls., independent emission model 77−18344
pp→nX, baryonium exchange, triple-Regge couplings 80−86763
pp→NX, ISR energies, low p_T secondary prod. and lepton-hadron relation 79−45112
pp→nX or ΛX, 12, 24 GeV/c, n/Λ ratio, cross sections 78−58213
pp→n+X, triple-Regge region, absorpt. corrections to inclusive spectrum 78−78230
pp→n+anything, inclusive charge exchange, parameter-free model 77−18336
$\bar{p}p$ off shell annihilations from K^-p→λ+pions at 4.2 GeV/c 79−45101
pp or $\bar{p}p$ colliding beams, inclusive W^+W^- and Z^0Z^0 pair production 79−40820
pp→pX, 205 GeV/c, leading p spectrum, random walk hypothesis, geometric bremsstrahlung model 80−68493
pp→pX, 28.5 GeV/c, π charge multiplicity, scaling and Hagedorn temp. 77−26553
pp→pX, 50-400 GeV, differential cross sections, P diffractive dissociation *(Russian)* 80−5030
pp→pX, 500 GeV, cross section, mass spectrum of diffractive peaks 77−10291
pp→pX, 55-400 GeV/c, small momentum transfer, mass spectrum and cross section 78−58215
$\bar{p}p$→pX, 6.94 GeV/c, momentum distribs., triple Regge model predictions 78−66170
pp→pX, associated multiplicity, and pomeron-pomeron cross section 79−17770
pp→pX, bremsstrahlung model and recoil mass distrib. 78−70418
pp→pX, Deck effect contribution 78−21471
pp→pX, deep inelastic scatt. in nuclei, bare particles, multiple scatt. theory *(Russian)* 80−52549
pp→pX, diquark fragments, large transverse momentum baryon production 80−47330
pp→pX, high p_T, spin-spin asymmetries, polarisation, hard scatt model with QCD 80−13339
pp→pX, intermediate and high energy, black/almost black constituent quark anal.. *(Russian)* 79−54325
pp→pX, large $p_\perp$ QED calc. *(Russian)* 77−30468
pp→pX, leading proton spectrum, associated multiplicity distrib. in geometric bremsstrahlung model 80−37309
pp→pX, polarised 6 GeV/c projectile, L-R asymmetry 77−49995
pp→$\bar{p}$X, pp exotic, triple-Regge formalism, Pomeron exchanges 80−63041
pp→$\bar{p}$X, search for new long lived particles with masses 1.4 to 3.0 GeV at CERN ISR 79−40810
pp→pX, triple-Regge fits, duality struct. of inclusive diffr. dissoc. 78−8715
pp→$\bar{p}$X, upper atmosphere, p/$\bar{p}$ flux ratio calc. 78−40783
pp→pX or $\pi^\pm$X, 7.9 GeV/c, polarised target, spin depend. 79−3056
pp→p+X, multiplicity dependence on transverse momentum and missing mass, multiperipheral diagram anal. 79−365
pp→p+X, or $\pi^\pm$+X, 7.9 GeV/c polarised target, scatt. asymm., spin depend. effects 77−30413
$\bar{p}p$→$\bar{p}$+anything, 50 to 175 GeV/c, cross sections, factorisation 77−50027
pp→p+anything, beam fragmentation region, spin correls. *(Russian)* 77−79292
pp→$\bar{p}$+anything, parameter free exchange model 77−10293
pp→p+μ+X, 200 and 240 GeV, charmed particle forward prod. search 77−22818
pp→p($\bar{p}$)+anything, large p_T, 200 to 400 GeV 77−22816
pp→p(pol.)X, 100, 200, 300, 400 GeV, outgoing p polarisation 79−63543
pp→p(pol.)X, 100 to 400 GeV, proton polarisation in inclusive processes 79−58983
$\bar{p}p$→p(slow)+X, 22.4 GeV/c, associative multiplicity *(Russian)* 80−5031
pp($\bar{p}$)→$W^\pm(Z^0)$X, QCD perturbation theory struct. function predictions 80−42505
pp($\bar{p}$)→$\mu^+\mu^-$X hadronic fragmentation initiated by pointlike probes 79−49551
pp phase shifts and dibaryon resonances 79−63540
$\bar{p}p$→pions, 1.6 GeV/c, branching ratio meas. 78−17038
pp polarisation asymmetry in high p_T inclusive prod., QCD and gluon models 79−40819
pp→ppX, cross sections at ISR energies, ρ, ω, A_2 and f meson prod. 79−40815
pp→ppX, double pomeron exchange in high energy collisions 79−3057
pp→ppX, two particle distrib. and Pomeron-Pomeron total cross section 77−22811
pp→pp(ϕ,ω), estimate of ω, ϕ and baryonium mixing at t≈0 79−40814
pp→pp$\bar{p}_{forward}$+anything, observation of qq with qq$\bar{q}$ bound states, pseudobaryons and baryonium 78−58219
$\bar{p}p$→p$\pi^\pm$X, 8.9 GeV/c, comparison with leptoprod., quark-parton model anal. 79−63512
$\bar{p}p$→pπX, 22.4 GeV.c^{-1}, inclusive production of pπ^+, pπ^- systems, OPE model anal. *(Russian)* 79−9422
pp→π^-X, Dao scaling model appl. to sea level muon spectrum 78−61694
pp→π^-X, polarised p, inclusive π^- scatt. asymmetries near X=0 79−63541

proton-proton inclusive interactions continued
pp→π⁻X, search for new long lived particles with masses 1.4 to 3.0 GeV at CERN ISR 79−40810
pp→π⁻X⁺⁺⁺ inclusive double-charge-exchange π⁻ prod., 100 GeV/c 78−37250
p̄p→π⁻X(ΔX), 22.4 GeV/c, test of factorisation hypothesis for leading Regge trajectories *(Russian)* 79−49561
pp→μ⁻+X, ISR energies, scaling variable, derived sea level muon spectrum 77−13995
pp→π⁰, large transverse momentum jets investig. at 52.4, 62.7 GeV 80−18151
pp→π⁰X, 100, 200 GeV/c high transverse momentum π⁰ prod., quark scatt. 78−45976
pp→π⁰X, 100 and 200 GeV, ang. depend. of π⁰ prod. 78−41603
pp→π⁰X, 50-400 GeV, cross sections, 0.3 to 4 GeV/c π⁰ transverse momenta 77−18350
pp→π⁰X, 52.7, 62.4 GeV, inclusive prod. at very large p_T at the ISR 79−71769
pp→π⁰X, 53, 63 GeV, inclusive π⁰ prod. at very large transverse momenta 78−45980
pp→π⁰X, intermediate $p_\perp$ distribution through a QCD resummation mechanism 80−83010
pp→π⁰X, large p_T phenomena, Bjorken scaling violation models of quarks with substructure 79−26305
pp→π⁰X, large p_T processes, pion exchange model anal. *(Russian)* 80−27527
pp→π⁰X, large transverse momentum, π⁰ prod. cross section, ISR energies 79−3055
pp→π⁰X, one-gluon-exchange quark scatt. 78−8714
pp→π⁰X, parton model, polarised proton, large p_T π⁰ prod. asymm. 78−12936
pp→π⁰X, pol.p, 24 GeV/c, high p_Tπ⁰ prod., spin. depend. 80−105935
pp→π⁰X, scaling in the mean hypothesis and Feynman variable energy depend. 80−42501
pp→π⁰X/π⁻p→π⁰X ratio at high-p_T, quark model explanation 77−10290
p̄p→π⁰+X, 4.6, 9.1 GeV/c, inclusive total, topological and invariant differential cross sections 79−408
pp→π⁰+X, large p_T-π⁰ spectra, quark model anal. 78−89756
pp→π⁰+X, secondary neutral pion-nucleon flux ratio at atm. top 80−8500
pp→π⁰+anything, √s=52.7 and 62.4 GeV, prod. of high transverse momentum π⁰'s 78−78226
pp→π⁰+anything, large p_T, clustered parton model 77−67688
pp→π⁰π⁰X, high transverse momentum, correlations 80−105933
pp→π⁰π⁰X, ISR π⁰-π⁰ azimuthal correlation data, comments 80−52543
pp→π⁰π⁰X, large p_T, azimuthal correlations 78−89749
p̄p→π⁺X, 22.4 GeV/c, invariant cross section, average multiplicity and annihilation spectra 79−6354
pp→π⁺X, non-plateau behaviour in central region 77−6182
pp→π⁺X, P-violating weak effects in high transverse momentum collisions, QCD anal. 79−63559
pp→π⁺+X, inclusive reactions, ISR energies, scaling variable 77−50021
pp→π⁺(K⁺)X, particle exchanges, coupling consts. *(Russian)* 77−50035
p̄p→π⁺π⁻X, 100 GeV/c, tests of factorisation in Pomeron and Reggeon exchange 77−74731
pp→π⁺π⁻X, 405 GeV/c, indictive ρ⁰ and f meson prod. 79−45111
pp→π⁺π⁺X, constituent hard scatt. processes, spin correl. 79−63558
p̄p→π±K_s⁰X⁺, low energy, thermodynamical anal. of charged pion momentum spectra 77−65169
pp→π±X, charge ratio for cosmic pion spectrum in atmosphere 78−28463
pp→π±X, primary proton energy rel. to pion energy, Landau parameter 79−54364
pp→π±+anything, large p_T, 200 to 400 GeV 77−22815
pp→π⁺(K⁺)pX, 11.75 GeV/c, meas. of left-right asymmetry far inclusive π±, K±, p prod., polarised p-beam 79−22155
pp→π±π±+anything, 69 GeV/c, study of rapidity gaps *(Russian)* 77−54125
pp→π±π±X, 24 GeV, high transverse momentum inclusive interaction 79−13169
pp→π°X reaction, quark-quark inelastic collision model *(Russian)* 80−32141
p̄p→πX, 22.4 GeV/c, charged particle spectra 77−13997
pp→πX, 23 GeV, Monte Carlo anal., parton Fermi motion 78−45977
pp→πX, 24 GeV/c, direct γ-yield 77−14003
pp→πX, crucial spin tests of QCD approaches to large transverse momentum processes 79−63558
pp→πX, large P_T, transversely polarised beam and target, QCD predictions 79−49553
pp→πX, large-P_T reactions in broken color gauge theory 80−95292
pp→πX, Pomeron struct., effects on one particle inclusive cross sections 79−89210
pp→πX, π± average transverse momentum energy depend., scaling relation 80−91116
p̄p→πX or ρ⁰X, central region, Regge Mueller approach, inclusive cross sections *(Russian)* 78−58218
pp→π+X, high p_T jet prod., QCD perturbation theory 79−89209
pp→π+anything, pion spectrum at top of atmosphere 78−53780
pp→π(K)X, 50-175 GeV, Regge parametrisation 77−14002
pp→π(K)(p)X, 4-250 GeV/c, Pomeron factorisation 77−14005
pp→ππX, √s=63 GeV, high momentum meson correlations 80−32138
pp→ψDDX, suppression and OZI rule 77−65185
pp→ψX, cross-section and quark energy distrib. 77−22813
pp→ψX, pψ exotic, triple-Regge formalism, Pomeron exchanges 80−63041
pp→ψX 70 GeV to ISR energies, pion exchange model anal. *(Russian)* 79−40823
pp→ψX or p̄p→ψX, J/ψ prod. mech., p gluon distrib. determ. 79−430
pp→ψX→μ⁺μ⁻X, Drell-Yan mechanism in colour quark model 77−6181
pp→ψ+anything, parameter free exchange model 77−10293
pp→ρ⁰X, study of ρ⁰ prod. using Heisenberg uncertainty relation *(Russian)* 79−49560
p̄p→ρ⁰+X, 22.4 GeV/c, cross section, average transverse momentum 78−62468
pp→ρ⁰+X, $S^{1/2}$=23.6 to 63.0 GeV, inclusive cross section meas. 79−75805
pp→ρ⁰(φ)(J/ψ)X, OZI rule violation 79−58929

proton-proton inclusive interactions continued
pp single-lepton spectra at high p_T, parton p_T and gauge invariance 77−18352
p̄p soft annihilation, parton description in three chain model 80−83009
p̄p→Σ(1385)X, 3.6 GeV, factorisation hypothesis test 80−102055
pp total cross-section difference of pure helicity states, 2100 to 2500 MeV, obs. of structs. 78−78206
p̄p→W±X, front back asymmetry in QCD and Weinberg-Salam model 79−97579
pp→W±γX, mag. moment parameter meas. 79−97640
pp→XΔ⁺⁺, absorption corrections to three Reggeon formulas *(Russian)* 79−9423
pp→Xp diffractive interaction, test of finite mass sum rule 77−22819
p̄p→xπ, model of excited hadronic matter 78−74288
pp→xπX, QCD radiation and mean scaling, longitudinal and transverse momentum 80−42405
p̄p→Z⁰→ll+anything, cross section for Z⁰ production, Weinberg model *(Russian)* 77−10296
p̄p→Z+anything, front-back asymmetry differential cross section, W± prod. 79−6352
pp-pX, Regge cut contribs. in triple-Regge region 77−38146
p⁻p, high-energy, reaction differences and annihilations 78−74279
pp.p̄p, polarised and unpolarised, jet cross sections vector boson signals, QCD-weak interference 80−5026
π distribs. in 205 GeV/c reacts. 78−8716
π prod. in pp collisions at 102, 400 GeV, transverse momentum props. 78−8713
π⁻ multiplicity distribs. *(Russian)* 78−41742
π⁻ prod., 13 to 300 GeV/c, inclusive distribs. *(Russian)* 78−45946
π⁻ semi-inclusive cross sections to 300 GeV/c in pp 77−13999
π⁰ and π± produced in pp collisions, correl., multiparticle prod. mech. 78−8708
π⁰ inclusive resolved high p_T meas. at CERN ISR 79−63555
π⁰ pair prod., high transverse momentum, azimuthal correlations 78−62469
π⁰ prod. at large p_T, parton model 77−46090
π⁰ prod. at large p_T, pp and π±p collision 77−79287
π⁰ prod. at large p_T at CERN ISR 79−13168
π⁺, π⁻, and p prod. in pp interactions at 69 GeV/c 77−79289
π± single particle spectra in 100-400 GeV pp interactions 78−17059
π± prod. in 100 GeV/C interactions, R-distrib. 77−50028
π± single particle distribs. in pp, πp collisions, transverse momentum, rapidity depend. hard scatt. models 78−29361
ρ⁺, ρ⁻, ρ⁰ inclusive prod., cross sections, quark model, pp interactions, 24 GeV 78−93912
Σ±(1385) inclusive prod. at 12 and 24 GeV/c 79−6356
W-boson production, Weinberg-Salam model 80−9186
X° pair production and decay in 400 GeV/c proton interactions 79−17768
Z⁰-boson production, Weinberg-Salam model 80−9186
Be+hadrons, 200 GeV/c, high transverse momentum jets and single particles 77−61329
Be+p, 400 GeV/c, two hadron correlation at large transverse momenta 78−46060
Be+p, high transverse momentum scatt., two particle correlations and φ prod., jet trigger 78−78225
p̄p annihilations, studied using topological cross-section differences between p̄p and pp at 48.9 GeV/c 80−83011
pp→D⁺X, 53 GeV, D⁺→K⁻π⁺π⁺ *(Polish)* 80−9187
p̄p→Λ, 10 to 300 GeV, triple Regge framework 78−21472
pp→μ pairs, 200, 300, 400 GeV, test of scaling hypothesis 78−4888
p̄p→μ⁺μ⁻X, scale violating effects in large q_T interactions 79−22125
pp, p̄p, 100 and 175 GeV/c, inclusive scatt. results from Fermilab single arm spectrometer 78−89746
pp→π⁺π⁻X, QCD testing by high energy hadroprod. of lepton pairs 79−26343
pp→π°X, quark-quark cross-section, dynamic amplitude factorisation model *(Russian)* 79−22067
pp→πX, large p_T π prod., QCD theory 78−45861

proton-proton interactions
see also proton-proton inclusive interactions; proton-proton scattering
$\Delta\sigma_L$ (pp) between 400 and 600 MeV 79−45097
bremsstrahlung, 1.38 GeV/c, differential cross section meas. 79−40796
bremsstrahlung from pp interactions, ω-radiative decay contrib. 78−70386
charged secondary production, 69 GeV/c^{-1}, transverse and rapidity distribs. 79−9409
charged secondary transverse momentum depend. on multiplicity, eikonal model 77−6177
charged-particle multiplicity distribs. at 400 GeV/c 80−13337
cluster cascade model, single particle distributions and two-particle correlations 80−18300
cluster production, field theoretic model 77−6091
conference on high energy phys. with polarised beam and target, Argonne, USA (Oct. 1978) 79−63526
correlations between potentials and observables in the NN interaction 79−67577
cross sections characts. appl. to calc. of muon sea level momentum spectrum and charge ratio 77−41275
current-carrying target, Monte Carlo anal. 77−82775
dibaryon resonance behaviour, nonadiabatic rotational bands in light nuclei 80−13353
dibaryon resonant states, narrow peaks in cross-section 80−63016
diffraction dissociation, 25 and 200 GeV/c, parameter invariant quantities *(Russian)* 78−54655
diffractive cross-section determ. for six-prong interaction at 205 GeV/c 78−33097
diffractive dissociation of 200 GeV/c protons, 4 and 5 particle final states *(Russian)* 77−34188
diffractive excitation at high energies and small momentum transfer *(Russian)* 78−17036
Dirac monopole search in 70 GeV proton synchrotron 77−14011
double differential cross sections for ππ and pπ prod. 77−82776
Drell-Yan lepton pair prod. processes, π structure function and scaling phenomena 80−405
dual model, vacuum exchanges, double pomeron poles with exotic Regge poles 78−89686
effective target mass distribution in relativistic proton-nucleon inelastic interactions 78−66162
electron pair production cross section, and Υ(9.5 GeV) prod. 78−25085

proton-proton interactions continued
EM phase shift calc. within relativistic model, isospin non-conservation 78−62438
energy depend. of cross sections, quark model anal. 78−62458
exotic mesons and p-p̄(e⁺-e⁻) annihilation 78−21393
explosive quark matter, hypothesis for Centauro event 80−22648
Fermilab energies, proton struct. anal. 78−62457
fireball model, cosmic γ-ray spectrum 77−18364
flavour state production in pp and p̄p interactions, QCD estimates 79−54301
four quark states and open charm production 79−63443
fragmentation at high energies, quark constituents 77−34185
fragmentation model and minimal rule 78−25019
hadron prod. at large p_T, multiplicities, quark model *(Russian)* 77−262
heavy long lived particles, 4 to 10 GeV/c, search 78−78380
Higgs meson prod., possible signals in high energy collisions, gauge groups 78−89649
high energy, particle prod., energy distrib., fragmentation, diffractive dissociation 77−71533
hydrodynamic model, nonlinear pion+pion chiral Lagrangian, e⁺+e⁻ and p+p collisions 78−32966
hydrodynamic theory of high energy interactions *(German)* 80−406
inelastic, and inclusive interactions, spin effects, polarisation 77−30434
inelastic Δ and N* production, polarisation studies with effective mass spectrometer 77−30412
inelastic charge exchange, quark interchange 80−86759
inelastic cross section in proton-proton interactions 78−4939
inelastic diffraction, unitarity bounds, evaluation including real parts 77−82724
inelastic diffraction dissociation cross section, const. fraction of unitary bound 77−10286
ion-cyclotron instability driven by oppositely directed proton streams in magnetosphere 79−62690
ISABELLE, pp intersecting storage accelerator facility at BNL 77−83344
KNO scaling, automodel behaviour of multiplicity distrib. as function of inelasticity factor *(Russian)* 79−89213
large inelastic diffraction in the quark-glue model 79−89138
large transverse momenta interactions, quark cascade model anal. 79−36101
lepton direct prod. in pN via hypothetical hadron and heavy lepton prod. *(Russian)* 77−46074
lepton direct production in hadron-hadron collisions, interaction models review 77−236
local compensation for transverse momentum, Pomeranchuk trajectory 77−18326
local potentials for pp scatt. in $^3P_0$ and $^3P_1$ states 77−38186
Lorentz-invariant method, 24 and 70 GeV/c interactions, including pionisation 79−80848
mag. monopole search, CERN ISR 78−66176
massive lepton pair prod., constituent interchange model 78−8611
massive muon pair data, cf asymptotically free parton model 78−8605
meson exchange currents role, and the solar ν *(Russian)* 77−74710
Monte Carlo calcs. on cascades prod. at 10^{13} eV 77−61322
multiparticle production in photoemulsion plates, rapidity space distrib. for 70 GeV incident protons 78−58205
multiperipheral process, interference terms in transition, amplitudes, correlation expansions 80−62953
multipion production, charge correl. cluster effect *(Chinese)* 77−57500
multiple particle generation, Monte Carlo model of proton high energy collisions *(Hungarian)* 80−13336
multiplicities of pion, kaon or proton prod. at ISR 77−259
multiplicity distribution, Markov and log-normal models 78−89753
multiplicity distributions, two channel multiperipheral model 77−6100
muon pair prod. and new parton radiative processes 79−17766
nuclear emulsion, pp and pn inelastic interactions, 69 GeV/c 78−66161
p̄p annihilation, 3.0 GeV/c, differential cross sections and polarisation of Λ^0 and K_s^0 78−58197
phase shifts at 2 GeV/c using polarisation, spin correl. cross section data 77−41852
pion-quark scattering model for lepton pair production from qq̄ annihilation 79−13056
polarised p, resonant like structs. in mass region 2100 to 2800 MeV 78−89745
pp→2γ+anything, $\sqrt{s}$=52 GeV, 2 photon mass spectra 78−21470
pp and p̄p, associated prod. cross section for Higgs and Z particles 79−410
prompt neutrino search in 70 GeV collisions 79−13160
protonium annihilation widths from coupling channel boundary condition model 79−36803
protonium formation in flight, p̄p, antiproton+neutral and negatively ionised hydrogen atoms 79−85319
QCD, μ pair transverse momentum distrib. in Drell-Yan processes 78−62374
quark-fusion model, direct prod. of large transverse momentum photons 77−30465
quark-lepton interactions and ēe (p̄p) annihilation 77−22746
rapidity distributions, rising plateau from longit phase-space 77−88017
scalon production and detection *(Chinese)* 80−47324
secondary proton momentum spectra, 4.3 to 8.9 GeV collisions *(Russian)* 79−3039
single direct photon prod. at 53.2 GeV in p_T interval 2.3 to 5.7 GeV/c 79−45110
single photon direct prod. in collisions at $\sqrt{s}$=53.2 GeV 78−78222
slow body emission, 200 and 300 GeV, mass estimates 77−41959
spin dependence of products 80−434
statistical bootstrap model anal. of NN annihilations 78−37224
$SU_L(2)\times U(1)$ and $SU_L(2)\times SU_R(2)\times U(1)$ predictions at high Q^2, neutral currents, Z-bosons 80−63029
t-flavoured meson production in photonuclear and pp collision 80−22623
thermodynamical approach to few body hadronic interactions, pion prod. 77−74704
third correlation moment and increasing cluster size, 50-400 GeV/c 78−66166
topological cross section and charged secondary ang. distrib. at 69.0 GeV/c 78−78219
transverse momentum fluctuations and high p_T processes in QCD 79−36014
two-body correlations at high-energy 77−54124
unitary impact-parameter model for multicluster prod. 78−33091

proton-proton interactions continued
charged hadron prod. with large transverse momentum at 90°, 52.6 GeV interactions 79−17763
D meson semileptonic decays, contrib. to single lepton spectra and dilepton invariant mass distribs. 77−2820
D^0(1.865) production in proton-nucleus collisions at 400 GeV/c 78−13099
$^1D_2$ diproton, resonance criteria 77−18312
Δ(1232) prod. region, parity violation 78−62435
e production in small-p_T pp interactions at 2800 GeV², multiparticle prod. mech., lepton-hadron relation 77−2868
e⁺e⁻ direct production in pp and Be+p 12 GeV/c collisions 78−78221
K^0 production, inclusive and exclusive, 6 GeV/c, polarised beam 77−65171
K⁻p→ΔX, 8.25 GeV/c, off shell KK̄ and p̄p interactions, KNO scaling 80−52534
Λ production, inclusive and exclusive, 6 GeV/c, polarised beam 77−65171
μ-pair, W and Z prod., asymptotic freedom and scaling violations 77−26554
N-Δ reson. with T=1, $J^P=2^-$ obs. in pp scatt. 78−17041
np observables, ^{3}P-waves effects, phase shift anal. of pp expts. 78−33077
(p,2p), distorted momentum distrib., and pp collisions, geometry choice for independent study 79−6597
p̄ annihilation in nucl. emulsion, statistical theory of multiple prod. *(Spanish)* 77−67669
p+Cu 400 GeV large $p_\perp$, quark search 77−79290
p̄d→π⁺π⁻(n), stopped antiprotons, p̄p annihilations from p state 77−18314
phenomenological relations between large-p_T meson spectra 79−26349
pN→N*N coherent dissociation via p+A→pπ⁺π⁻+A 22.5 and 15.3 Gev, Glauber anal. 77−22809
p̄n:p̄p annihilation ratio, low energy and stopped p̄ in C, p̄N system resonance 77−18313
p̄p, 0.76 GeV/c, lower limit on p̄ lifetime 78−45968
p̄p, 100 GeV/c, inclusive ρ^0 and f^0 prod. 78−41605
pp, 12 and 24 GeV/c, strangeness transfer distribs. 79−22142
pp̄, 12 GeV/c, automatic meas. in CERN 2m HBC 79−36471
pp̄, 12 GeV/c, evidence for narrow peak in $K_s^0\pi^\pm\pi^+\pi^-$ at 2.6 GeV 77−30452
p̄p, 12 GeV/c, search for K3π at 2.6 GeV/c² 78−25090
p̄p, 1.6 GeV, comparison with empirical model 78−25060
p̄p, 1.6 GeV/c, search for direct single electron production 77−49994
pp, 24 GeV/c, final states with large transverse momentum particle, π and N emission 79−13159
p̄p, 2.32 GeV/c, cross-sections, C-invariance, π and ρ^0 multiplicities anal. 78−41569
p̄p, 2.99-3.14 GeV, cross-section upper limits for new particles 77−30416
pp, 350-1000 MeV, neutron prod. double differential cross section in meson generation reactions *(Russian)* 80−42490
p̄p, 355-1066 MeV/c, total and annihilation cross sections, S meson search 80−68473
p̄p, 373-734 MeV/c, total cross section enhancement, 1936 MeV narrow resonance 80−13324
p̄p, 400-850 MeV/c, annihilation and elastic cross-sections meas. reson. obs. at 1939 MeV 77−46082
pp, 62.4 GeV/c, direct single photon prod. at large p_T 80−91113
p̄p, 8.8 GeV/c, exclusive annihilation processes, cross sections, quark model anal. 80−105920
p̄p, 9.1 GeV/c, single pion prod. anal. 78−54645
p̄p, charmed meson prod. at 12.4-15.0 GeV/c 77−6176
p̄p, χ_J P-wave charmonium states, hadronic prod. cross section 80−37292
pp, D, B, K prod., QCD model for heavy flavour prod., two gluon annihilation 80−86744
pp, diffraction dissociation, dip and kink structs., differential cross sections 80−95284
pp, effects of hard gluon bremsstrahlung in dimuon and Υ prod., QCD anal. 79−13058
p̄p, heavy lepton prod. and decay, supersymmetrical model of weak and EM interactions *(Russian)* 80−86748
pp̄, high energy process, with strong absorption, elementary quantum mech. 78−86053
p̄p, internal target expts., 1 TeV antiquark-heavy nucleus collisions 80−52536
p̄p, low, energy scatt., one-boson exchange pot. model 77−74705
pp, massive lepton pair prod., pion exchange model anal., quark parton interpretation *(Russian)* 80−82993
p̄p, pp, beauty prod. total cross section from perturbative QCD 80−32080
p̄p, pp, Drell-Yan processes, scaling violation effects 80−382
pp, p̄p, fireball mass and pion multiplicity 78−45974
pp, p̄p, integrated cross section compilation 80−32121
p̄p, pp, lepton pair prod., transverse momentum distrib., QCD calcs. to leading logarithms 80−42486
pp, p̄p high energy, impact parameter props. from σ_{tot}, σ_{el} data 77−6183
pp̄, Q production, Breit-Wigner parameters, decay modes 77−57560
p̄p, resonance in cross section, rescatt. effect in d, annihilation product 78−62431
p̄p, soft-pion amplitude for π^0 emission 78−41570
p̄p, three-body annihilations, rel. to quark rearrangement model 78−21444
p̄p, total cross section determ., 200 to 370 GeV/c 79−26352
pp, two component fireball model 78−45965
pp,p̄p, Z^0 high p_T bremsstrahlung, Higgs versus quark or gluon jets 80−32063
pp→^{2}He⁺ν_e, pionic exchange current contribs. 77−10329
p̄p→2π⁺2π⁻, 5.7 GeV/c, pion ang. distribs., ρ^0, f^0, prod. rates 77−2857
p̄p→2π⁺2π⁻π⁰, 0 to 700 MeV/c, interference correls. between like pions 77−61311
pp→(nπ⁺)p diffraction dissociation, Deck model with absorption 77−26548
pp→(pπ⁺)(pπ⁻), 23-63 GeV, charge exchange double dissociation reaction anal., $\Delta^{++}\Delta^0$ prod. 79−6350
pp→(pπ⁺)(pπ⁻), observation of charge exchange double dissociation 78−25079
pp→(pπ⁺π⁻)(pπ⁺π⁻), 24 GeV/c, double diffraction dissociation reaction, cross sections, mass spectra 78−93908
pp→(pπ⁺π⁻)(pπ⁺π⁻), s-depend. of double diffraction dissociation 78−25084

proton-proton interactions continued
pp→(π⁺n)p, π energy and transverse momentum distrib., DHD model with nucleon exchange *(Russian)* 80−13327
p̄p and pp, annihilation and non-annihilation processes 77−88008
p̄p and pp, effective radius and total cross sections Pomeranchuk theorem confirmation *(Russian)* 78−89737
p̄p annihilation, 2 GeV/c, search for prompt electron prod. 79−54351
p̄p annihilation, asymptotic props., parton model, kaon prod. *(Russian)* 78−466
p̄p annihilation, γ spectra, evidence for quasinuclear bound states 78−54642
p̄p annihilation at rest, branching ratio Γ(p̄p→e⁺e⁻)Γ/(p̄p→total) determ. 77−2861
p̄p annihilation at rest, maximum final particle momentum projection direction reference frame 77−57553
p̄p annihilation cross sections, corrected differences, fireball model, diffraction cross sections 80−91108
p̄p annihilation mechanisms, 2.5 to 9.1 GeV/c, pion prod., quasi two body process 78−17039
p̄p annihilations, 1 GeV/c, multiplicity independ. of single π mean scaled distribs. 77−30414
p̄p at 7.3 GeV/c, ionisation meas. with HPD, track density and particle separation 77−10543
p̄p atom formed in liquid hydrogen, mechanism, quasinuclear meson *(Russian)* 77−50569
pp→baryons by diquark-quark fusion model 80−102065
pp bremsstrahlung, 730 MeV, γ-energies of <300 MeV, differential cross section 80−99108
pp bremsstrahlung, criteria for expt. choice 79−67587
pp bremsstrahlung, Δ isobar excitation and radiative decay 79−67586
pp bremsstrahlung, field theory calcs. 79−67584
pp bremsstrahlung with polarised p, soft photon approx. 79−67585
p̄p̄ channel narrow resonances, baryonium degeneracy, qqq̄q̄ or NN̄ existence 79−58971
pp collisions, real photon prod. at large p_T, cross section calc. 79−13149
pp→DD̄ cross sections, Monte Carlo anal., particle lifetime for detection in emulsion 78−82229
pp→de⁺ν, effect of vac. polarisation on solar reaction rate 77−57555
pp→Dev, in Sun, exchange current contrib. *(Russian)* 78−93195
pp→dπ, 1.03 GeV, analysing power 78−93901
pp→dπ, 400 to 600 MeV, production cross sections 80−78091
pp→dπ⁺, 0.8 GeV, differential cross section and polarisation asymmetries 80−27519
pp→dπ⁺, 0.8 GeV polarised proton energy, analysing power 79−85315
pp→dπ⁺, 305 to 425 MeV, differential cross section meas., d-wave π production contrib. 78−62440
pp→dπ⁺, 305 to 425 MeV, differential cross section and analysing power, using polarised protons 79−36094
pp→dπ⁺, 750 MeV, T=1 NN phase shifts and total cross section 80−22630
pp→dπ⁺, 800 MeV, comparison between expt. momentum spectra and theoretical models 78−62441
pp→dπ⁺, 800 MeV 77−6141
pp→dπ⁺, ang. distribs., sensitivity to nuclear wavefunctions 79−85314
pp→dπ⁺, deuteron polarisation, isobar model anal. 79−49535
pp→dπ⁺, differential cross section, polarisation asymm., threshold to 750 MeV 78−54648
pp→dπ⁺, differential cross-section and polarisation 78−8683
pp→dπ⁺, field theory treatment 78−93898
pp→dπ⁺, P-wave meson prod., calc. of total and differential cross section 77−6143
pp→dπ⁺, polarised beam and target, NΔ intermediate states, coupled channel method 79−9392
pp→dπ⁺ or pπ⁺n, 800 MeV, cross sections, n-p final state interactions 78−70387
pp→dρ⁺, N and N* exchanges 77−22804
pp→Δ⁺⁺Δ⁰ up to 1500 GeV/c, Reggeised absorption model 77−6170
p̄p→Δ̄⁻⁻Δ⁺⁺, 3.6-12 GeV/c, cross sections and decay, parity exchange contribs. from quark model 79−13146
p̄p→Δ̄⁻⁻Δ⁺⁺, quasi eikonal model anal., πP cut contribution, enhancement coefficients *(Russian)* 79−40798
pp̄→Δ⁺⁺+anything, 9.1 GeV/c, Mueller-Regge theory test, fragmentation process expt. 77−61312
pp→Δ⁺⁺n, polarised proton, spin effects in SU(3) and quark model 77−30399
pp→Δ⁺⁺pπ⁻, 4 GeV/c, mass spectra, ang. distribs. and momentum transfer *(Russian)* 80−42489
pp→Δ⁺⁺π⁻p, polarised proton, spin effects in SU(3) and quark model 77−30399
pp→Δ⁺p, radiative corrections and vacuum pole exchange *(Russian)* 79−58964
pp̄→e⁺e⁻, magnetic nucleon form factor, p-meson type contribs. 80−57596
p̄p→e⁺e⁻ annihilation, weak neutral current effects *(Russian)* 80−105837
p̄p exclusive reactions, 5.7 GeV/c, impact parameter anal. 77−46073
p̄p→F₁ω, F₁ spin-parity anal., boson spin tests from sequential decays 78−29345
pp̄→γγ annihilation, influence on sum rule proton polarisability 80−18143
p̄p hyperon-antihyperon prod. at 3.6 GeV/c with ≥3 final state particles 77−38187
pp inelastic interaction, ISR energies, impact parameters *(Russian)* 79−93463
p̄p inelastic reactions, 22.4 GeV/c, charge asymm. at large p_t 78−476
p̄p interactions, 48.9 GeV, elastic and topological cross-sections 80−83007
pp interactions, charmed D⁺ prod., total cross section, D⁺→K*⁰π⁺ observation 79−36102
pp̄ interactions, test of charge-conjugation invariance 78−66145
p̄p→$K_S^{0\pm}\pi^{\mp}$, K*(890), EM mass difference determ. 79−390
p̄p→K⁻K⁺, 1.0 to 2.2 GeV/c, polarisation parameter meas. 77−74711
p̄p→K⁻K⁺, 1.0 to 2.2 GeV/c, polarisation parameter 77−87995
p̄p→K⁻K⁺, differential cross sections, evidence for meson reson. existence 2.1 and 2.5 GeV/c² 78−93897
p̄p→$K^0_SK^0_S$+pions, 700-760 MeV/c, $K^0_SK^0_S$ threshold enhancement in final states 78−82228
p̄p→K⁺K⁻, evidence for $J^P=3^-$ and 4^- meson resonances from differential cross section 78−70399
pp̄→K⁺K⁻, geometrical Schrempp model 77−74659
p̄p→K⁺K⁻ 6.2 GeV/c, ang. distrib. 77−18330
p̄p→K⁺K⁻π⁺π⁻, 2.32 GeV/c, cross section, C conservation, errors 78−21446
pp→K⁺K⁺+missing mass, stable six quark state search, mass range 2.1-2.4 GeV 78−89742
pp→KK, 12 and 24 GeV/c, strangeness transfer distribs. 79−22142
p̄p→KKππ, 700-760 MeV/c, D(1285) an E(1420) resonance prod. 78−54646
pp→l⁺l⁻+hadrons, lepton pair prod. in hadronic collisions, review 80−5022
p̄p→ΛΛ, 1.50-2.06 GeV/c, polarisations, cross sections, spin correl. coeffs. 78−74271
p̄p→ΛΛ, 6 GeV, cross sections and polarisations 79−407
p̄p→ΛΣ⁰, 6 GeV, cross sections and polarisations 79−407
p̄p→Λ+missing mass, trigger accepted polarisations 79−407
pp→meson+lepton pair, transverse momentum distrib. and branching ratios, proton gluon distribution 80−52537
pp→NΔ, parity violation in Weinberg model 78−8701
pp→NΔ or pp, 1.25, 1.66 GeV/c, spin depend. total cross sections, elastic and inelastic effects 78−62453
pp→nΔ⁺⁺, 6 GeV/c, polarised p, spin density matrix elements, beam polarisation induced effects 79−93451
pp→nΔ⁺⁺, 6-1500 GeV/c, differential cross-section 78−8700
pp→nΔ⁺⁺, quasi eikonal model anal., πP cut contribution, enhancement coefficients *(Russian)* 79−40798
pp→nΔ⁺⁺, unconventional behaviour of isospin-one exchanges 78−21445
pp→nΔ⁺⁺(1232), 23-53 GeV, charge exchange anal. 77−74724
pp→NNπ⁰, consideration of p→nπ⁺ forbidden reaction threshold case 78−62442
p̄p→neutral meson+π⁺π⁻, or neutral meson+p̄p, 7.2 GeV/c, quark model anal. 78−41561
p̄p→n̄n, 0.119-1.046 GeV/c, charge exchange cross section 80−63015
p̄p→n̄n, 1-3 GeV/c, scintillation-counter study 78−41567
p̄p→n̄n, 5-25 GeV/c, charge exchange scatt., πNN vertex function, one pion exchange 80−37291
p̄p→n̄n, 8 GeV/c, Regge anal. of charge exchange scatt. 77−22756
p̄p→n̄n, 8 to 23.5 GeV/c, test of Veneziano-type πNN form factor in fitting dσ/dt data 79−17725
p̄p→n̄n, charge exchange models, polarisation 77−30444
p̄p→n̄n, charge exchange processes, baryonium trajectories, Regge pole description 80−9180
pp→npπ⁺, 647-805 MeV, neutron momentum spectra obs. 77−30417
p̄p→nπ's, multiplicity distrib. and charmed meson hadronic decays 77−10288
pp→pΔK⁺, 12, 24 GeV/c, diffr. dissoc. 77−82779
pp→pN*(1400), duality prediction for cross-section 77−13940
pp→p(nπ⁺), 28.5 GeV/c, t-depend. and struct. 77−22802
pp→p(pπ⁰), 28.5 GeV/c, t-depend. and struct. 77−22802
pp→p(pπ⁺π⁻)(nπ⁺)(pπ⁰), polarised protons at 6 GeV/c, low mass enhancements 77−30400
pp(p̄)→μ⁺μ⁻, 60 and 200 GeV, implications of light neutral gauge boson 78−58154
pp→pnπ⁺, 19 GeV/c, nucleon dissociation and spectator concept 77−30447
pp→pnπ⁺, 800 MeV 77−6141
pp→pnπ⁺, mass spectra at 28.5 GeV/c 77−22801
pp→pnπ⁺, two nucleon mechanism for pion production 79−85286
p̄p→p̄ωp or p̄pπ⁺π⁻π⁰, 9.1 GeV/c, cross sections, momentum depend. 78−29344
pp→pp, high energy collisions, EM-hadronic interference, spin depend. phenomena 79−422
pp→pp, medium energies, inelasticity and struct., pure spin total cross section data 78−62439
pp→ppĜG, mag. monopole search with plastic detectors 79−6351
p̄p→p̄p2π⁺2π⁻, 100 GeV/c, diffraction and ρ⁰ prod. in exclusive interactions 78−93909
pp(pp̄), heavy flavoured states, assoc. prod. QCD calcs. 79−85274
pp→ppγ, applicability limit of Low theorem for pp bremsstrahlung 79−85323
pp→ppp̄p, 11.75 GeV/c, baryonium states, cross section and branching ratio 80−95288
pp→ppπ⁰, 800 MeV, Δ⁺ prod., π and ρ exchange 79−85316
pp→ppπ⁰, 800 MeV 77−6141
pp→ppπ⁰, mass spectra at 28.5 GeV/c 77−22801
p̄p→p̄pπ⁰(p̄nπ⁺)(n̄pπ⁻), 8.8 GeV/c, one pion prod. cross sections, Deck model anal. 80−105919
pp→ppπ⁺π⁻, $s^{1/2}$=31 GeV, double pomeron exchange, dipion mass 77−13993
p̄p→p̄pπ⁺π⁻, 100 GeV/c diffraction and Δ⁺⁺ prod. in exclusive interactions 78−93909
pp→ppπ⁺π⁻, 23, 45 GeV, double-Pomeron exchange anal. 77−65180
p̄p→p̄pπ⁺π⁻, 32 GeV/c 78−4881
pp→ppπ⁺π⁻, 4 GeV/c, Reggeised one pion exchange model anal. *(Russian)* 79−30746
p̄p→p̄pπ⁺π⁻, 7.2 GeV/c, diffraction dissociation and double resonance prod. 79−89177
pp→ppπ⁺π⁻, double Pomeron exchange, 23.4 to 63.4 GeV 79−3050
pp→ppπ⁺π⁻ or ppX, cross section, double pomeron exchange 77−18333
p̄p→p̄pππ, 12 GeV/c, final state diffraction dissociation, cross section 80−99109
pp→pπ⁺n, 800 MeV, Δ⁺⁺ prod. study 78−70385
pp→pπ⁺n, 800 MeV, Δ⁺⁺ prod. and cross sections 79−22294
p̄p→φ(ω)π⁺π⁻, 0.70 to 0.76 GeV, effect on OZI rule 79−22124
p̄p→φ(ω)ρ⁰, 0.70 to 0.76 GeV, effect on OZI rule 79−22124
p̄p→π⁻X⁻, 6 GeV/c search for narrow states in X⁻ decay 78−89708
p̄p→π⁻π and π⁺p→pπ⁺ line reversed channels, 6 GeV/c, differential cross section comparison 77−74708
p̄p→π⁻π⁺, 10.1 GeV 78−66160
p̄p→π⁻π⁺, 1.0 to 2.2 GeV/c, polarisation parameter meas. 77−74711
p̄p→π⁻π⁺, 1.0 to 2.2 GeV/c, polarisation parameter 77−87995
p̄p→π⁻π⁺, 2020-2580 MeV/c, differential cross section zeros 77−41854
p̄p→π⁻π⁺, 6 GeV/c, differential cross sections, line reversal symmetry test for baryon exchange 78−78202
p̄p→π⁻π⁺, amplitude anal., 2020 to 2580 MeV/c², spin 3, 4 and 5 mesons 77−41853
p̄p→π⁻π⁺, amplitude anal., meson prod. in 2020-2580 MeV/c² region 77−46075
p̄p→π⁻π⁺, differential cross-section zeros 77−38191
p̄p→π⁻π⁺, polarised targets, p̄ parity meas. 77−2860
p̄p→π⁻π⁺(π⁰π⁰), 1-2 GeV/c, partial wave determ. and resonance struct. 79−93449

proton-proton interactions continued
pp→$\pi^-\pi^+$pp, 800 MeV, integrated cross section meas. near threshold 78−62441
$\bar{p}p\to\pi^0\pi^0$, 1.1-2.0 GeV/c, differential cross sections in T and U meson region 79−9393
$\bar{p}p\to\pi^0\pi^0$, 2.12 to 2.43 GeV, 2.15 GeV resonance from partial wave amplitude anal. 79−9394
$pp\to\pi^0\pi^0$, up to 10 GeV/c, correlation of momentum of π^0 pairs 80−5011
$pp\to\pi^+d$, 400-800 MeV, anal. by neutron exchange, ΔN intermediate states, diproton resonances 80−27518
$pp\to\pi^+d$, 515 and 575 MeV, spin depend. parameter meas. 80−73734
$pp\to\pi^+d$, di-proton resonances 80−22631
$pp\to\pi^+d$, interaction anal. by neutron exchange Born terms, ΔN states, diproton resonances 79−93391
$pp\to\pi^+d$, NΔ(1232) state contrib., K matrix theory anal. 80−5013
$pp\to\pi^+d$, SIS, 578 MeV, pol. beam and target, spin depend. parameters 80−42651
$pp\to\pi^+d$, up to 1 GeV, differential cross section using polarised beam and target 79−17748
$pp\to\pi^+pn$, 1 GeV/c, momentum spectra ang. depend., one-particle-exchange model comparison *(Russian)* 77−10276
$pp\to\pi^+pn$, 800 MeV, comparison between expt. momentum spectra and theoretical models 78−62441
$\bar{p}p\to\pi^+\pi^-$, 6 GeV/c, differential cross sections, line reversal symmetry 78−41564
$\bar{p}p\to\pi^+\pi^-$, 6 GeV/c, differential cross sections, line reversal symmetry test for baryon exchange 78−78202
$\bar{p}p\to\pi^+\pi^-$, polarised target, charge parity determ. 77−57567
$\bar{p}p\to\pi^+\pi^-$ 6.2 GeV/c, ang. distrib. 77−18330
$\bar{p}p\to\pi^+\pi^-$ or K^+K^- annihilation cross-section at 300 MeV/c 77−82757
$pp\to\pi^+\pi^-(K^+K^-)$, 1.0-2.2 GeV/c, polarisation parameter 77−30401
$p\bar{p}\to\pi^+\pi^-\eta$, quark-line rule for η-η' complex 77−30330
$\bar{p}p\to\pi^+\pi^-\pi^+\pi^-\pi^0$ 1950 MeV/c^2, experimental evidence 80−27516
$\bar{p}p\to\pi^+\pi^-\pi^+\pi^-\pi^0$ 1950 MeV/c^2, properties evidence for $\bar{p}p\to\omega^0\rho^0$ 80−27517
$\bar{p}p\to\pi^+\rho$, 6 GeV/c, differential cross sections, line reversal symmetry test for baryon exchange 78−78202
$\bar{p}p\to\pi^+\rho^-$, 6 GeV/c, line reversed reaction, Δ exchange, ρ^- decay 78−12926
$pp\to\pi d$, π^+ negative parity assignment 80−32117
$\bar{p}p\to\pi\pi$, 1-2 GeV/c, Barrelet zero anal., resonant struct. 80−73735
$\bar{p}p\to\pi\pi$, 1-2 GeV/c, resonance region, partial waves, positivity constraints 80−99107
$pp\to\psi\gamma$, inclusive prod. anal. 78−25091
pp reaction, exchange current corrections to π and ρ exchange 80−26733
$\bar{p}p$ resonant annihilation, η_c charmonium state prod. cross section 80−82991
$pp\to\rho^0_0$+n charged, 300 GeV/c, high multiplicity search 77−22807
$\bar{p}p\to\rho^0\rho^0,\omega\rho^0,\rho^0 f$, or ωf, T(2200) region, partial wave anal. 77−34171
$\bar{p}p\to S\to\bar{p}p$, S meson as baryonium state 80−62938
$p\bar{p}$ scatt. at low momenta, simple approach emphasising absorption, pot. model 79−13145
$p\bar{p}$ system, possible evidence for narrow bound states below threshold, mesonic struct. 78−62443
pp total cross section, spin dependence, relativistic model of Δ(1232) prod. 78−62436
$\bar{p}p\to V^0\pi^0\to e^+e^-\pi^0$, annihilation at rest, heavy vector meason prod., ρ' (1250), ρ'' (1600) existence 77−13971
$p\bar{p}$ very high energy collisions, cooling and storage of $\bar{p}$ beams 78−54654
pp→virtual gamma+hadrons soft bremsstrahlung, external emission dominance model 78−62430
p^+p, high-energy, reaction differences and annihilations 78−74279
$p^+p\to p^++X$, 140-175 GeV, differential cross-section meas. 77−18345
$P_1p_2\to p_3N_4$+mesons, 28.5 GeV/c, space-time extension of centrally produced matter, intensity interferometer technique 77−50017
$\bar{p}p+\bar{n}n$, energy depend. of np charge exchange, phenomenological anal. 78−25082
$pp_{\pi^-}d\pi^+$, 3.2 GeV, forward scatt. relativistic study, reaction cross section 79−97633
$ppe\to D\nu$, in Sun, exchange current contrib. *(Russian)* 78−93195
π cluster central prod., 28.5 GeV/c, props. 77−10287
π distribs. in 205 GeV/c reacts. 78−8716
π pairs, dynamical and Bose-Einstein inclusive correlations, explanation of bubble chamber data 78−62463
π prod., invariant-mass depend. of correl. functions 77−34181
π prod. in pp, np, πp interactions, mass quantisation *(French)* 78−25059
ψ prod. cross-sections in pp collisions at E_{cm}=23-63 GeV 77−57572
ρ-dominance in model for inelastic pp collisions 78−37238
ρ-meson production and charged-neutral correlations in high energy pp interactions 79−17760
S(1936), evidence against existance from $\bar{p}p$ interaction 80−78089
Υ(9.4) family, gauge theory mass anal., harmonic oscillator pot. 78−82186
Υ production cross sections, colour excited states in Han-Nambu model *(Chinese)* 79−49480
W-boson prod. cross sections and hadronic jets in pp and $\bar{p}p$ collisions 78−8707
W-boson prod. in ep and pp collisions 77−61247
$\bar{p}p$, 5.7 GeV/c, nonannihilation channels Δ^{++}, $\bar{\Delta}^{++}$, Δ^0, $\bar{\Delta}^0$ prod. cross sections 80−27515
pp bremsstrahlung, intermediate nucleon isobars contrib., relativistic model, nuclear force significance 78−93899
$pp\to pn\pi$, exclusive pion prod. OPE and VME amplitudes 79−85336
$pp\to pp\pi^+\pi^-$, 12, 24 GeV/c, p dissociation into $(p\pi^+\pi^-)$, partial wave anal. 79−22148
$\bar{p}p\to\pi^+\pi^-$, 5.7 GeV/c, two-pion correls., interference effects 80−32116
$p\bar{p}\to\pi^+\pi^-(K^+K^-)$, T, U and V resonances 80−68485

proton-proton scattering
see also proton-proton interactions
3-spin pp elastic scattering cross sections of 6 GeV/c, polarised target and beam expt. 77−30411
400 GeV, energy and angle dependence at high momentum transfer 78−93905
$^1D_2$ state, multichannel N/D formalism 79−63506
$\Delta\sigma_L$(pp), 400-600 MeV 79−97632
absolute differential cross section meas., at large momentum transfer, 23 to 63 GeV 79−45103
asymmetry meas. with polarised beams and targets 78−62459

proton-proton scattering continued
bell's inequalities from the field concept in general relativity 80−105771
Bounds on slope of diffraction peak and zeros of absorptive differential cross sections 78−74282
bremsstrahlung, ω radiative decay contrib. at 158-400 MeV 77−74706
bremsstrahlung, bounds on external emission amplitude, cross section values 78−62450
bremsstrahlung, field theoretic calc., treatment of OBE external emission processes 78−62451
bremsstrahlung, forbidden asymmetries and choices of geometry 79−58972
bremsstrahlung, review of Low theorem soft photon approach 78−62452
bremsstrahlung cross sections, 11 and 13 MeV *(German)* 77−10275
central p-wave parameter meas., p+polystyrene 5.9-9.9 MeV, nucleon-nucleon force 77−67748
Chou-Yang model anal., structure of second dip 77−54120
Coulomb corrections in pp scatt., phase shift contrib. 78−70391
Coulomb interaction effects on calc. of scatt. characts. 79−9529
Coulomb-nuclear interference, influence of proton charge form factor 79−49534
cross section structureless behaviour, 53 GeV, disagreement with diffraction models 77−22798
depolarisation parameter, dominance of natural parity exchange 80−78088
dibaryon resonance existence 78−45939
differential cross section, pp at 200, 1500 GeV, second min. 78−66159
differential cross section dip, ISR energies, dual absorptive model with peripheral pomeron 77−79281
differential cross section energy dependence, large angles, 2-9.7 GeV/c 78−37227
differential cross sections, diffraction model account of absence of dip struct. 78−82246
differential cross-section meas. at 53 GeV 77−65178
diffraction elastic scatt., Lorentz-contracted geometrical model 77−74722
diffraction elastic scatt. 200-2000 GeV/c total cross section, energy depend. 79−30753
diffraction pattern of pp elastic scatt., quark-glue model description 77−61323
diffraction scattering, convergent polynomial expansion and scaling 79−40797
diffractive inelastic scatt. at 42.5 and 52.2 GeV/c *(Russian)* 77−82777
diffractive many-channel problem, absorptive s-channel unitarisation for inelastic scatt. 79−17700
diproton resonance in pp system 78−4871
dispersion theoretic analysis of pp helicity amplitudes at t=0 78−62340
Drell-Yan process, quark-quark contrib. 80−73731
dual unitary scheme calc. of pp and $p\bar{p}$ scatt. 77−6168
eikonal model, energy depend. anal. 20 to 60 GeV 79−89190
eikonal model, spin depend. at high energies 77−22710
elastic cross section from dressed quark model, Glauber multiple scatt. expansion 79−2977
elastic differential and total cross-sections, 50 to 175 GeV/c 77−74721
elastic differential cross section break, 90° scatt., duality satisfying lepton-hadron relation 79−3035
elastic multichannel eikonal model, diffractive dissociation 77−10229
elastic scatt., 10 MeV, A_{yy} component of spin correlation tensor 79−67592
elastic scatt. in Coulomb-nuclear interf. region at 42.5 and 52.2 GeV/c 77−18332
elastic scatt. slope at small momentum transfer between 5-2000 GeV/c 77−18328
elastic scattering, high P_t, spin interactions meas. 79−67608
elastic scattering in pure initial spin states, 11.75 GeV/c, spin correl. 77−30436
EM corrections at low energy *(Japanese)* 78−17023
EM effects, separation, Coulomb problem 77−23014
exchange degeneracy violating A_1-Z Regge amplitude and dibaryon resonances 80−4971
Faddeev approach, 0-1200 MeV pp scatt., πNN dynamics 80−57625
final state polarisation in pp elastic scatt. 209-515 MeV 78−461
fixed pole pomeron, high energy phenomenology of pp elastic scatt. 78−25080
forward elast. scatt., 4-10 GeV/c 78−8682
forward scatt. amplitude, real part, CERN ISR meas. 77−30443
forward scattering amplitudes, 50 to 400 GeV, ratio of real to imaginary parts 78−70410
Froissart bound saturation, logarithmic rise of total cross-section 80−47328
geometrical model for scatt. at ultrahigh energies, existence of dips 79−89191
geometrical scaling real part effects in pp elastic amplitude 78−37232
glass correlation parameter at high energies 79−97636
gluon distribution in proton from result anal. 80−82939
hadron-nucleon total cross-section, regularities and systematics 77−38205
high energy, 50 to 2050 GeV, additive eikonal quark model 79−67606
high energy, 53 GeV, differential cross-section meas. 78−66155
high energy, impact picture for polarisation and rotation parameter 78−70341
high energy diffraction scatt., model with shielded pomeron, pp, πp, Kp investigation 78−17004
high energy elastic pp scatt. at large momentum transfer, diffraction model with nucleon core 78−74281
high energy elastic scatt., unitarity bounds, slope parameter t-depend. 78−93907
high energy elastic scattering and constituent multiple scatt. model 79−67607
high energy pp elastic scatt., ang. depend., generalised droplet model 78−82243
high P_T^2 elastic scatt., 11.75 GeV/c, spin depend. from polarised p 79−3049
high-energy, amplitude energy independent component, TeV region cross-section prediction 78−66156
high-energy 100 to 2048 GeV/c, based on Van der Walls type eqns. 78−29358
impact param. anal. of pp and $p\bar{p}$ scatt. from 50-175 GeV/c 77−22799
impact parameter analysis of pp elastic scatt., 23, 62 GeV, opaqueness function 78−78217
impact parameter distribution of pp inelastic overlap integral from pp elastic scatt. and total cross-sections 80−83001

proton-proton scattering continued
impact parameter representation *(Russian)* 80−5019
impact parameter space, study of pomeron models 77−10226
large |t| scatt., and quark-quark scatt. 79−13161
large angle elastic factorisation in quark model *(Russian)* 77−57497
large angle elastic scatt., quark elastic scatt. model 79−17751
large angle elastic scatt., unitarity condition and partial cross sections 80−82990
large momentum transfer, multiple-scattering model, three-quark proton 80−63031
large momentum transfer struct. in pp elastic scatt. at 201 GeV/c 78−8697
large scale scatt. of particles with spin, nonautomodel corrections, Logunov-Tavkhelidze quasipot. approach *(Russian)* 79−54360
large transverse momentum, spin-spin forces 78−78216
large-angle pp elastic scatt., 7.9 GeV/c, polarisation parameter meas. 77−82759
longitudinally-polarised beam and target, spin-spin correl. parameter meas., 6 GeV/c 78−4870
low energy, up to 30 MeV, precision analyses 77−34172
low energy (0.35-1 MeV) cross-sections determ., ang. distrib. data determ. 78−62423
low energy discrepancies, relativistic, radiative and finite proton size effects explanation 79−17747
low energy scatt., spin depend. EM force effects, Coulomb DWBA anal. 79−9568
low-energy, simultaneous polarisation meas., test of quantum mechanics limits of validity *(French)* 79−406
multiple Regge model, up to 5.10^3 GeV *(Russian)* 77−61324
multiple scatt. of quarks, elastic pp cross-section 78−4868
multiple scattering model anal. including inelastic intermediate states 79−89189
natural and unnatural parity exchanges, exact separation, A, exchange 79−13144
off-shell p-p T matrix for Graz separable interactions 79−40795
opaqueness at high energy, factorisable eikonal model and scaling hypothesis comparison 78−74280
parity conservation at 15 MeV 77−30445
parity violating observables in low energy pp scatt. 78−50045
parity violation at 50 MeV *(German)* 80−68471
parity violation meas. at 45 MeV 80−78092
phase shift anal. 78−62425
phase shift analyses, 1 to 500 MeV 77−54115
phase shifts, 25 to 70 MeV *(Japanese)* 78−17037
phase shifts and diproton resonances, 2.1 to 2.8 GeV mass range, $^3F_3$ (2.22 GeV) diproton 79−36093
phase shifts at 3 GeV/c 77−54114
phase shifts at 4 GeV/c 80−22632
polarisation, high energy, feasibility of future CERN SPS expt. 77−30738
polarisation analyzing power, 643-796 MeV scatt. 78−78207
polarisation and depolarisation parameter, 0.97 GeV *(Russian)* 79−30745
polarisation and energy dependence 80−63030
polarisation asymmetry in pp elastic scatt., effective mass spectrometer study 77−30412
polarisation correlation coeff. meas., 610 MeV *(Russian)* 77−30419
polarisation data interpretation for high energy elastic scatt., eikonal model, spin parameters 79−3048
polarisation expts., 6 GeV/c, pure spin cross sections, Wolfenstein parameters 78−41568
polarisation expts., Regge and diffraction descriptions 77−57564
polarisation in 1.03 GeV scatt. 78−82245
polarisation in elastic scatt., correlation coeff. at 550 and 630 MeV *(Russian)* 78−12929
polarisation in elastic scatt., meas. from Fermilab and CERN 78−78224
polarisation in high energy elastic scatt., meas. apparatus, target, spectrometer, polarimeter 77−30439
polarisation in pp elastic scatt. at 100 GeV/c 77−30440
polarisation in pp elastic scatt. at 20 to 200 GeV/c 78−50054
polarisation in pp elastic scatt. at 6 GeV/c 77−38188
polarisation in pp elastic scatt. at 7.9 GeV/c, spin depend. effects 77−30413
polarisation in small angle pp scatt., 398-572 MeV, amplitude anal. 77−30407
polarisation meas., 100 and 300 Gev 79−63527
polarisation meas. in scatt. at 52.34 and 68.19 MeV 78−54641
polarisation measurement at 6.14 MeV 79−67591
polarisation normalisation between 200 and 520 MeV 78−70397
polarisation paramater and ang. distribs. meas. at 100 and 300 GeV 78−89738
polarisation parameter for pn and pp elastic scatt. at 11.8 GeV/c 78−66158
polarisation parameter in pp elastic scatt. at 24 GeV/c 77−30437
polarisation parameter meas. in 24 GeV/c pp elastic scatt. at small momentum transfers 77−46081
polarisation phenomena in close-to-forward scatt., intermediate energy region 80−78086
polarisation structure and Pomeron flip, Regge pole model 80−102073
polarised beam, P-violation, longit. asymmetry meas., at 15 MeV 79−63499
polarised beams, Wolfenstein parameter meas. near 1 GeV *(Russian)* 77−49997
polarised cross-sections for high-P_T^2 pp scatt. at 11.75 GeV/C 78−8698
polarised protons elastic collisions, 6 GeV/c, absorpt. model 77−2858
pomeron pole+cuts, power series formula 78−8631
preasymptotic effects in large angle elastic scatt. amplitudes, quasipot. scatt. *(Russian)* 80−57631
proton-proton potential models obtained from the Virginia phase-shift analysis 80−47401
Pure spin total cross sections 79−63539
quark structure of proton by multiple scatt. model 79−13072
Regge cuts and large |t| pp scattering 78−41587
Regge model for ang. distribs. in elastic scatt. up to 27.4 GeV 79−75799
relativistic quantum field theory, improved impact picture for 14 to 2000 GeV/c 79−89178
residual phase shifts, Coulomb contrib., for potential model calc. comparison 79−67589
resonance, possible existence in the $^3F_3$ state 78−4869
resonance in $^1D_2$ (2.17 GeV) state, phase shifts 79−58970

proton-proton scattering continued
S-wave scatt., Coulomb distortion effects on phase shifts and effective range parameter 79−85322
scattering amplitudes, 6 GeV, phase shift anal. 80−37290
scattering matrix determ. from scatt. meas., exptl. technique 78−25063
second dip development in elastic pp scatt., Chou-Yang model current-current interaction 79−89192
SIN expts., 400 to 600 MeV 80−73733
small angle elastic scatt., 312, 392, 493 MeV, Wolfenstein and polarisation parameters 79−67593
smooth interpolation between Orear- and fixed angle scaling behaviour of the scattering amplitude 80−105873
spin behaviour of ang. distribs. at large momentum transfer *(Russian)* 79−80849
spin correlation A_{nn}, polarisation, 400 to 600 MeV 79−63503
spin correlation meas., local hidden variable theory, quantum theory 78−54649
spin correlation parameter in polarised pp elastic scatt. at 610 MeV 77−30406
spin correlation parameter in pp elastic scatt. at 6 GeV/c, polarised beam, polarised target 77−30410
spin correlation parameters for 6 GeV elastic scatt., eikonal model anal. 80−5012
spin correlations, $\Delta\sigma_T$ energy depend., 1 to 3 GeV region 79−63504
spin correlations in low energy meas., test of Bell's inequality 77−13633
spin correlative parameters $A_{nn}(\theta)$ at 643 and 796 MeV 79−63502
spin dependence at large P_T^2 80−42493
spin dependence in strong interactions at very high energy 78−58203
spin dependent eikonal amplitude, extension to pseudoscalar exchanges 79−17698
spin dependent forces in 6 GeV polarised scatt. in eikonal model 80−37246
spin effects and polarisation in pp elastic scatt. 77−30434
spin effects in polarised pp elastic scatt. at 150 GeV/c 78−66157
spin measurement in pp elastic scatt. at 6 GeV/c,cross section 77−38189
spin parameters meas. in pp scatt. at 2, 3, 4, 6 GeV/c 78−25078
spin rotation parameter meas. in 45 GeV/c scatt. *(Russian)* 77−6169
spin-correlation and polarisation, energy depend. and scaling 77−34173
spin-dependent eikonal model for 5.5 GeV/c-2000 GeV/c calcs. 77−26545
spin-flip amplitude in 300GeV elastic scatt. 79−93461
spin-spin corel. parameter, energy depend. 79−13147
spin-spin correlation param. meas. at 6 GeV/c 77−18327
spin-spin correlation parameters at 6 GeV/c 78−62433
spin-spin forces, energy depend. in 90° elastic scatt. 78−45941
spin-spin interactions in high $p_\perp^2$ elastic scatt. at 11.75 GeV/c 77−88009
string model, string geometrical shape and overlapping functions 79−13073
strong van der Waals interaction in low energy pp scatt. 78−41563
thermodynamical approach to few body hadronic interactions, pion prod. 77−74704
three gluon exchange contribution to forward high energy scattering 79−26310
three-gluon exchange contribution to forward high-energy scattering 79−54324
total cross section difference in longitudinal spin states, 1.2 to 6.0 GeV 78−62432
total cross sections in pure spin states, Coulomb interference and rescatt. corrections 80−432
transversity amplitude formalism for pp elastic scatt., complete expts. planning 78−54647
triple scatt. parameters meas. 78−62420
triple scattering in exclusive and inclusive processes at wide angle 79−45104
triple-spin correl. parameters and spin transfer parameters at 6 GeV/c using polarised beam and target 79−89179
two-component model and geometric picture for high energy P-P collisions 79−58948
unitarity, large-angle elastic scatt. *(Russian)* 77−61221
urn model, modified, dimens. counting rule, pp elastic scatt. appl. 80−27485
Van der Waals type model for high energy large momentum transfer pp scattering 80−73740
van der Waals type model for pp elastic scattering at high energies 79−58977
Veneziano-like model with 2q2q̄ meson trajectory and pp scattering at 90°c.m 79−13087
Wolfenstein parameters meas. for small angle scatt. at 310, 390, 490 MeV 78−62422
Wolfenstein parameters meas. in range 150 to 515 MeV, phase shift anal. 78−70396
$^1D_2$ diproton, resonance criteria 77−18312
polarisation parameter in elastic 45 GeV/c reactions *(Russian)* 77−34179
pp, 1 GeV, elastic scatt. amplitude, phase shift anal. *(Russian)* 80−86746
pp, 1-3 GeV/c, total cross section differences, singlet and triplet contribs. anal. 80−68474
pp, 100, 200 GeV, elastic scatt., polarisation effects at large momentum transfer, quark model *(Russian)* 80−83005
pp, 100, 300 GeV/c, polarisation parameters and ang. distribs. for elastic scatt. 80−95287
pp, 1.5 GeV/c, phenomenological anal., dibaryon resonances 79−17750
pp, 2-9.5 GeV/c, wide angle elastic scatt., differential cross section 80−73730
pp, 23.4-62 GeV, scatt. amp., differential cross section from eikonal model *(Russian)* 80−57642
p̄p, 400-850 MeV/c, annihilation and elastic cross-sections meas. reson. obs. at 1939 MeV 77−46082
p̄p, 406-922 MeV/c, backward elastic scatt. cross section, resonance search 80−32119
pp, 45 MeV, longitudinally pol. p, parity nonconservation in anal. powers 80−57626
p̄p, 5.7 GeV/c, parton-cluster model, hadron struct. and non-diffractive collision impact parameters struct. 80−27454
pp, 970 MeV, Wolfenstein polarisation rotation, coeff., phase shift anal. *(Russian)* 80−86747
p̄p, elastic differential and total cross-sections, 50 to 175 GeV/c 77−74721
p̄p, elastic differential cross-sections at 8 and 16 GeV/c 77−71536

proton-proton scattering continued
$p\bar{p}$, elastic events separation in bubble chamber at 5.7 GeV/c 78−13379
pp, elastic scatt., 12 to 24 GeV, leading effective trajectories, residues, anal. 79−421
pp, elastic scatt., 150 GeV/c, $-t=0.2$-3.0 GeV^2, polarisation meas. 79−85343
pp, elastic scatt., teaching expt. using Van de Graaff generator 77−74178
pp, elastic scatt. amplitude in quark diquark model 80−102075
$\bar{p}p$, forward elast. scatt., 4-10 GeV/c 78−8682
pp, high energy elastic scatt. cross sections, pomeron-nucleon coupling vertex, pomeron residue *(Russian)* 80−42492
pp, $\bar{p}p$, 39, 44.5 GeV/c, differential cross section meas. 77−74720
pp, $p\bar{p}$, 50, 100, 200 GeV/c, differential cross sections meas. 77−18329
$\bar{p}p$, pp, elastic scatt. and diffractive dissociation, Regge model with $\alpha_P(0)>1$ *(Russian)* 80−57630
$\bar{p}p$, pp high energy elastic scatt., cross section rise and polarisation, Regge model *(Russian)* 80−37301
pp, simple Coulomb correction for phase shifts, on-shell approx. 80−82989
pp $^3F_3$ resonance as resonance in πNN system 78−45940
pp and $\bar{p}p$ elastic scatt., dominant exchanges using Reggeon-photon coupling analogy 78−78204
$\bar{p}p$ and pp elastic scattering, relativistically invariant scaling law 77−13986
$p\bar{p}$ and pp elastic scattering, 39, 44.5 GeV/c, polarisation, spin rot. meas. 77−30438
pp elastic, 2.1 $GeV.c^{-1}$, polarisation meas. of scatt. protons in small momentum transfer region *(Russian)* 79−9397
pp elastic, differential and total cross sections, proton model, gluon-gluon annihilation 80−91114
pp elastic, evidence for a proton core of valence quarks 79−17682
pp elastic C_{LL} scatt., interpretation of dibaryon resonances at 2140, 2260, and 2430 MeV 79−75781
pp elastic scatt., 1-3 GeV/c, pol. p, spin parameters A and A_{nn} 80−95304
$p\bar{p}$ elastic scatt., 1.9 to 2.6 GeV, differential cross-section zeros 78−29346
$\bar{p}p$ elastic scatt., constituent interchange model 77−2856
pp elastic scatt., current-current interaction, spin depend. differential cross section 80−18147
$\bar{p}p$ elastic scatt., FESR constraint on baryonium resonances, S, T, U, contrib. 80−27520
pp elastic scatt., improved unitarity bound on slope parameter 79−49537
PP elastic scatt. at 20-750 MeV, EM effects 77−74707
pp elastic scatt. at $\sqrt{s}=53$ GeV, three-quark struct. 77−88010
pp elastic scatt. at high energy and large momentum transfer, cross-sections 78−62460
pp elastic scatt. at high energies and large momentum transfer, review *(Russian)* 80−105926
$\bar{p}p$ elastic scatt. complex zeros, 2.0 to 2.6 GeV, evidence for 3^{--}, 4^{++}, 5^{--} resonances 77−74712
$\bar{p}p$ elastic scattering, repulsive long range force, dispersion relation calcs. 78−25061
pp high p_T polarised elastic scatt., QCD explanation of asymmetries 80−13323
$\bar{p}p$ interactions, 48.9 GeV, elastic and topological cross-sections 80−83007
pp large angle elastic scatt., cross section beyond 2nd maximum, unitarity condition *(Russian)* 80−83004
$\bar{p}p$ large-angle elastic scatt., 1.5-2.06 GeV/c, optical model anal. 78−74270
$\bar{p}p \rightarrow \bar{n}n$, Regge parametrization of NN differential cross sections and polarizations 79−17746
$\bar{p}p \rightarrow \bar{p}p$, 8 and 16 GeV/c, cross-section anal. in O(3,1) scheme 77−61310
$pp \rightarrow pp$, high energy, polarisation, spin correls., s-channel helicity amplitudes 77−30435
$pp \rightarrow pp$, universal function for large angle cross sections of exclusive hadronic reactions 77−50010
$pp \rightarrow pp$ or $N\Delta$, 1.25, 1.66 GeV/c, spin depend. total cross sections, elastic and inelastic effects 78−62453
$pp \rightarrow pp\gamma$, 200 MeV, cross section meas., bremsstrahlung at small angles 78−62446
$pp \rightarrow pp\gamma$, 730 MeV, total and elastic cross sections for bremsstrahlung, Low theorem discussion 78−62448
$pp \rightarrow pp\gamma$ bremsstrahlung, 730 MeV, differential cross section 77−46072
pp scatt., <300 MeV P-odd asymmetry for pol. ρ *(Russian)* 80−102063
pp scatt., intermediate energy, polarised p, three body model 79−67590
pp scatt. amplitude, phase anal. ambiguities, cross sections and polarisation parameter *(Russian)* 80−86749
pp scatt. at higher energies, differential cross section ratio scaling 80−73741
pp scatt. cross section at high momentum transfer, geometrical scaling, energy depend. *(Russian)* 80−102064
pp small angle scatt., 312-575 MeV, pol. p, Wolfenstein and polarisation parameters 80−57629
$\bar{p}p$ total elastic cross sections, 0.69-2.43 GeV/c 78−12928
$p\bar{p}$ total elastic cross sections, 0.69 to 2.43 GeV 78−25067
p^-p, peripheral reaction model, large angle behaviour 78−442
$^3F_3$ resonance, composed of $\pi^+ + p + n$ system 78−66142
$^1H(p,p)$, 0.35-1.0 MeV, differential cross section meas. 78−78379
$^{208}Pb(p,p')$, 135 MeV, normal parity excitations, microscopic description, NN interaction shape 80−57691
pp, 40-45 GeV, Regge anal. differential cross sections *(Russian)* 78−25081

proton radiative capture
γ-ray angular distrib., radiative capture of fast nucleons 77−41964
capture by A=50 to 100 nuclei, stat. anal. of differential cross sections 79−9555
collective excitations, role in fast capture 77−23024
direct and resonance capture, giant dipole and quadrupole resonances 80−37385
E1-E2 direct-semidirect model for fast nucleon radiative capture, γ ang.-distribs. 78−62536
giant dipole resonance region radiative nucleon capture, expt. ang. distrib. coeffs., direct-semidirect theory 78−74354
implantation type accelerator, 400 kV, energy resolution, stability and calib. using (p,γ) react. 79−30604

proton radiative capture continued
low energy proton accelerator, voltage or energy calibration using (p,γ) reaction 77−50316
proton induced γ-ray yields, chemical anal. appl. 80−45608
quadrupole isoscalar and isovector capture of 5-50 MeV nucleons 77−2994
radiative nucleon capture, pure resonance model, direct-semidirect model, pure semidirect model 80−78257
sd shell nuclei, (p,γ) resonance strengths 80−22786
spherical even nuclei, role of doorway states in gamma decay of highly excited states 77−30581
target composition determ. from α-scatt. and (p,γ) meas. 77−75019
γ-emission spectrum for 50 MeV nuclear excitations 79−59065
(N,γ), ang. distribs. from direct-semidirect model 79−71852
(N,γ) reactions in giant dipole resonance region, role of exchange forces 77−88126
np doubly radiative capture, M1-M1 transitions and cross section calcs. 79−13292
(p,γ), $(p,\gamma\gamma)$, recent experiment review, future experiment suggestions 80−37382
(p,γ), exclusive single nucleon transfer, theoretical status 80−42652
(p,γ), isobaric analogue doorway states, excitation functions 80−47388
(p,γ), resonance broadening anal. of N in Ta 78−38918
(p,γ) resonance broadening meas. of light ion ranges 77−69023
(p,γ) resonances, use in Dynamitron fault diagnosis 78−29671
(p,γ_0), polarised p in giant dipole resonance region on ^{14}C, ^{30}Si, $^{54,56,58}Fe$, ^{59}Co, ^{88}Sr 78−82346
$\pi^-p \rightarrow n\gamma$, test of pion range monitor, medical appls. 80−72317
$^{208}(N,\gamma)$, pol. N, anal. power and giant multipole resonances, direct-semidirect model 80−18265
$^{26}Al(p,\gamma)^{27}Si$, reaction rate in explosive H burning 80−85929
$^{27}Al(p,\gamma)$, 0.5-2.1 MeV, determ. of ^{28}Si levels and resonances 78−66205
$^{27}Al(p,\gamma)^{28}Si$, 0.5 to 0.9 MeV, resonance strengths of selected resonances in s-d shell 78−66281
$^{27}Al(p,\gamma)^{28}Si$, 12917 and 12924 keV ^{28}Si level gamma-gamma directional correl. 79−536
$^{27}Al(p,\gamma)^{28}Si$, 2046 keV, gamma-ray intensity calibration standard 77−30698
$^{27}Al(p,\gamma)^{28}Si$, $E_p=992$ keV resonance, γ-ray intensity standard 78−17472
$^{27}Al(p,\gamma)^{28}Si$, radiative capture of intermediate-energy protons to high-lying states 79−36243
$^{27}Al(p,\gamma)^{28}Si$, standard resonance strength 77−30565
$^{10}B(p,\gamma)$, 1.11 MeV, ^{11}C negative parity states lifetime limits and transition strengths 80−5092
$^{11}B(P,\gamma)^{12}C$, radiative capture of intermediate-energy protons to high-lying states 79−36243
$^{11}B(p,\gamma)$, 163 keV, ^{12}C radiative transition and isospin mixing 77−38242
$^{11}B(p,\gamma)$, 30-100 MeV, meson exchange and nucleon correlation process calcs. 79−549
$^{11}B(p,\gamma)$, 6-23 MeV, capture to ground state and first three exited states of ^{12}C 77−74842
$^{11}B(p,\gamma)$, pol.p, ^{12}C p_0 channel E2 strength 80−22790
$^{11}B(p,\gamma)$ 40,60,80 MeV, photon spectra direct reaction calc. 79−89281
$^{7}Be(p,\gamma)$, low energy cross section from direct, capture potential model 80−102184
$^{7}Be(p,\gamma)^{8}B$, cross section, 360 keV 77−61432
^{9}Be (p,γ), 1.29 MeV, ^{10}B 3590 keV excited state lifetime 79−9510
$^{A}C(p,\gamma)$, A=12, 13, isotopic anal., estimation of $^{13}C/^{14}C$ conc. ratio 79−48014
$^{12}C(p,\gamma_0)$, pol. p, ^{13}N giant dipole resonance population amplitude and phase, E1 reaction amps. 80−63145
$^{12}C(p,\gamma)$, 16-40 MeV, ^{13}N giant dipole reson. as doorway-states 77−6336
$^{12}C(p,\gamma)$, direct capture to unbound states 77−61418
$^{12}C(p,\gamma)$, precise determ. of Q-value 78−17200
$^{12}C(p,\gamma)^{13}N$, intense proton beam current meas. 78−93784
$^{12}C(p,\gamma)^{13}N$, pol. p, 10-17 MeV, ^{13}N electric quadrupole strength semi-direct capture model calcs. 80−47370
$^{13}C(p,\gamma)$, ^{14}N DSA lifetimes determ. from exptl. stopping powers 78−17142
$^{13}C(p,\gamma)$, 1701 keV resonance, ^{14}N 9.13 MeV state 78−41641
$^{13}C(p,\gamma)$, Doppler shift attenuation anal., ^{14}N unbound states 78−25184
$^{13}C(p,\gamma)$, pol. p, 6.25-17.0 MeV, anal. power and cross section ang. distribs., E1, E2 amplitudes 80−47461
$^{13}C(p,\gamma)^{14}N$ energy levels up to 11.05 MeV, transitions and resonance decay 80−47376
$^{42}Ca(p,\gamma)$, 0.7-5.5 MeV, cross section and stellar nucleosynthesis reaction rates 79−13294
$^{42}Ca(p,\gamma)^{43}Sc$, 0.66-5.39 MeV, cross sections 79−85470
$^{42}Ca(p,\gamma)^{43}Sc$, below 2.75 MeV, resons., γ-decay schemes and level energies 78−13072
$^{42}Ca(p,\gamma)^{43}Sc$, reaction rates in stars 80−82183
^{44}Ca (p,γ), 1.644, 1.650 MeV, ^{45}Sc resonance decays, energy levels and J_π values 79−80908
$^{44}Ca(p,\gamma)^{45}Sc$, 1.62-2.18 MeV, e.m. decay of fragmented analogue states of Sc 77−2987
$^{48}Ca(p,\gamma)^{49}Sc$, 0.6-2.7 MeV, cross sections and thermonuclear reaction rates, Hauser-Feshbach calcs. 79−36239
$^{48}Ca(p,\gamma)$, 0.76-2.20 MeV, absolute cross sections and yields, statistical model anal. 79−26432
$^{110}Cd(p,\gamma)$ γ-22 MeV differential cross-section meas. 79−93617
$^{140}Ce(N,\gamma_0)$, 2-10 MeV, giant M1 resonance in direct-semidirect model 79−17898
$^{35}Cl(p,\gamma)$, decay of first T=2 state in ^{36}Ar 77−6294
$^{35}Cl(p,\gamma)^{36}Ar$, 0.5 to 0.9 MeV, resonance strengths of selected resonances in s-d shell 78−66281
$^{52}Co(p,\gamma)$, shell model anal. of GDR 78−78345
$^{59}Co(p,\gamma_0)$, polarised p, 5.8 to 16.5 MeV, cross section and analysing power ang. distrib., model comparison 78−70533
$^{50}Cr(p,\gamma)$, 0.6 to 3 MeV, captive cross section, statistical theory anal. 79−9557
$^{52}Cr(p,\gamma)$, ^{53}Mn fragmented $g_{9/2}$ isobaric analogue resonance, γ-spectra and excitation functions 80−68627
$^{52}Cr(p,\gamma)$, 4.08-4.32 MeV, ^{53}Mn fragmented $g_{9/2}$ isobaric analogue resonances, γ-transitions 79−85430
$^{52}Cr(p,\gamma)^{53}Mn$, resonant react. appl. to Cr depth distribs. 79−33011
$^{53}Cr(p,\gamma)$ 4.11-4.19 MeV; ^{53}Mn fragmented $g_{9/2}$ isobaric analogue resonance, transitions, J^π assignments 79−45240
$^{54}Cr(p,\gamma)$, 1040-2560 KeV, ^{55}Mn energy level excitation curve, bound state and resonance γ-decay 79−476

proton radiative capture continued
^{54}Cr(p,γ), 1.0-3.8 MeV, γ-yields, cross sections, predicted (p,n) cross section, Stat. anal. 80−5136
^{54}Cr(p,γ)^{55}Mn, 0.83-3.606 MeV, cusp in excitation function 78−66273
^{54}Cr(p,γ)^{55}Mn energy levels, bound state mean lifetimes and spins 80−42586
Cu+p, 1.2-4.6 MeV, (p,n) thresholds and radiative capture, A=63, 65 78−89856
^{65}Cu(p,γ)^{66}Zn, 1.1-3.6 MeV, Wigner cusps 78−41719
Cu(p,γ), 1.7-7.2 MeV, ^{A}Zn, A=64, 66 levels and primary E1 transition strength functions 80−91149
^{19}F(p,γ), ^{20}Ne, deformed nuclei, giant multipole resonances, and transitions, microscopic theory 79−513
^{19}F(p,γ), 0.2-1.2 MeV, ^{20}Ne resonances, J$^{\pi}$, excitation functions and branching ratio 80−22787
^{19}F(p,γ), pd. p, ^{20}Ne E1 resonance 80−22790
^{19}F(p,γ), pol. and unpol., 3.5-10 MeV ^{20}Ne giant E1 resonance intermediate struct. 80−78251
^{19}F(p,γ)^{20}Ne, 668 keV, γ-ray transitions to ground state, rel. to stellar nucleosynthesis 78−17191
^{19}F(p,γ)^{20}Ne, calculated cross sections to ground and first excited state 77−54139
^{19}F(p,γ)^{20}Ne, giant multipole reson., microscopic theory 77−22987
^{A}Fe(p,γ$_0$)Co, A=54,56, giant dipole resonance splitting, direct-semidirect capture model anal. 80−106055
^{54}Fe (p,γ), 3450 keV, ^{55}Co, 1 g$_{9/2}$ analogue state fragmentation using analogue resonances 78−70506
^{54}Fe(p,γ), 1.1-1.75 MeV, ^{55}Co resonance decay schemes branching ratios, analogue states 80−52643
^{54}Fe(p,γ), 1.5-2.9 MeV, excited levels and isobaric analogue states in ^{55}Co 77−18509
^{54}Fe(p,γ), 3.40-3.48 MeV, ^{55}Co isobaric analogue resonances, J$^{\pi}$, partial widths and spectroscopic factors 79−85431
^{56}Fe(p,γ), ^{57}Co g$_{9/2}$ isobaric analogue resonances 78−82332
^{56}Fe(p,γ), 2-4 MeV, ^{57}Co, state alignment, γ-transitions and ang. distribs. 80−73797
^{56}Fe(p,γ), g$_{9/2}$ IAR in ^{57}Co 78−70504
^{56}Fe(p,γ) ^{57}Co, 3.7 to 3.8 MeV, γ-decay of g$_{9/2}$ isobaric analogue reson. 79−63674
Fe(p,γ), absolute resonance strengths meas. using separated targets 77−79374
Ge(p,γ), 2-3 MeV, ^{71,73,75}As E1 γ-ray strength function 79−75902
^{2}H(p,γ), 7-15 MeV, polarised and unpolarised p, cross section and anal. power 79−40921
^{2}H(p,γ)^{3}He, existence of excited states of A=3 nuclei 79−9553
^{2}H(p,γ)^{3}He, 450, 550 MeV, differential cross sections, inverse reaction comparison 80−86904
^{3}H(p,γ), 17-31 MeV, ^{4}He 2^{+} resonance evidence at 40 MeV 80−86880
^{3}H(p,γ), 30-100 MeV, meson exchange and nucleon correlation process calcs. 79−549
^{3}H(p,γ), 6 to 16 MeV polarised protons, ^{4}He excited states 77−18559
^{3}H(p,γ)^{3}He, intermediate energy, ang. distribs., reaction amplitude and ^{3}He vertices 80−22835
^{115}In(p,γ) γ-22 MeV differential cross-section meas. 79−93617
^{40}K(p,γ), ^{41}Ca giant dipole resonance, isospin struct., direct-semidirect anal. 80−47449
^{6}Li(p,γ), 200-1200 keV, cross section 80−13478
^{6}Li(p,γ), cross section and spectroscopic factors from direct capture pot. model 80−99171
^{7}Li(p,γ$_0$), ^{8}Be 1^{+} and 1^{-} levels, expt. and shell model calcs. 80−63095
^{7}Li(p,γ), cross-section contrib. from ^{8}Be 3^{+}states, isospin mixing model 78−89789
^{7}Li(p,γ)^{8}Be, intense proton beam current meas. 78−93784
^{24}Mg(p,γ)^{25}Al, ^{25}Al T=3/2 states γ-decay 77−26608
^{25}Mg(p,γ), 0.3-0.4 MeV, ^{26}Al T=1 states, resonances, J$^{\pi}$ and transitions 80−99131
^{25}Mg(p,γ), 80-350 keV, ^{26}Al low energy resonances, decay and J$^{\pi}$ assignments, branching ratios 80−42624
^{25}Mg(p,γ) reaction, relative yields of ^{26}Al^{g} and ^{26}Al^{m} 79−101058
^{25}Mg(p,γ)^{26}Al, reaction rate in explosive H burning 80−85929
^{25}Mg(p,λ)^{26}Al, stellar reaction rate, rel. to ^{26}Al prod. during C burning 79−70948
^{26}Mg(p,γ), 1.6-3.95 MeV, ^{27}Al isobaric analogue resonances, spectroscopic factors and γ-rays 80−86873
^{26}Mg(p,γ), 80-355 keV, ^{27}Al levels, resonances, J$^{\pi}$, branching and mixing ratios 80−99132
^{27}Mg(p,γ) resonances, ^{27}Al bound state parity and spin assignments, level struct. 78−66206
Mg(p,γ), 0.3-2.1 MeV, ^{A}Al, A=25,26,27 levels, resonances, γ-ray branching ratios 80−86875
Mg(p,γ), 0.3-2.1 MeV, stellar H burning in explosive C burning 80−86875
^{55}Mn(p,γ), ^{56}Fe isobaric analogue resonance levels, branching ratios 80−68617
^{55}Mn(p,γ), 1660-1710 keV, ^{56}Fe isobaric analogue resonances corresponding to ^{56}Mn 335.5 and 340.9 keV states 78−78342
^{94}Mo(p,γ), 4.4 MeV, γ-ray multipolarities, internal conversion coeffs., energy levels 79−63625
^{96}Mo(p,γ), 3.9 MeV, γ-ray multipolarities, internal conversion coeffs., energy levels 79−63625
^{14}N(p,γ), 1.74, 2.35 MeV, lifetimes of ^{15}O bound states 77−82928
^{14}N(p,γ)^{15}O, isotopic anal., estimation of ^{15}N/^{14}N conc. ratio 79−48014
^{15}N(p,γ$_{0,1,2}$), 6-22 MeV, ang. distrib. and correl. meas., ^{16}O excited state giant resonance 77−82926
^{15}N(p,γ$_0$), 8.6-18 MeV, giant E1 resonance in ^{16}O 78−66256
^{15}N(p,γ), ^{16}O excited state GDR, coupled channels version of continuum shell model 79−542
^{15}N(p,γ), 30-100 MeV, meson exchange and nucleon correlation process calcs. 79−549
^{15}N(p,γ), pol p, ^{16}O E1 and p$_0$ channel E2 strength 80−22790
^{15}N(p,γ), polarised p, ^{16}O mag. dipole strength, M1 resonances 79−80898
^{15}N(p,γ)^{16}O, anal. of ^{16}O giant dipole reson. struct. 78−4942
^{22}Na(p,γ), 1.1-2.0 MeV, ^{23}Na levels, resonance strengths, γ-decays and level lifetimes 79−45229
^{23}Na(p,γ) resonance reaction, 3906 keV, ^{24}Mg lowest T=2 state, total width 78−89870
^{23}Na(p,γ)^{24}Mg, ^{24}Mg T=2 state props. 78−8767
^{23}Na(p,γ)^{24}Mg, 0.5 to 0.9 MeV, resonance strengths of selected resonances in s-d shell 78−66281
^{20}Ne(p,γ), depth profiling of implanted Ne 79−7621
proton radiative capture continued
^{21}Ne(p,γ), 0.4 to 1.6 MeV, study of resonances 77−18540
^{21}Ne(p,γ) 0.5-6.0 MeV, ^{22}Na bound and analogue state lifetimes, branching ratios, DSA method 78−93967
^{21}Ne(p,γ)^{22}Na, γ-ray ang. distrib. and mixing ratios, analogue resons. 78−62504
Ne(p,γ), absolute resonance strengths meas. using separted targets 77−79374
^{58}Ni(p,γ)^{59}Cu, time struct. of the 2d$_{5/2}$ analogue state 79−6591
^{58}Ni(p,γ)^{59}Cu, γ-decay of ^{59}Cu analogue resons. 78−13005
^{60}Ni(p,γ)^{61}Cu, 1800 to 290 KeV, γ-ray spectra and j$^{\pi}$ assignments 79−59063
^{62}Ni(p,γ), 2-4 MeV, ^{63}Cu state alignment, γ-transitions and ang. distribs. 80−73797
^{62}Ni(p,γ), 3766-3865 keV, ^{63}Cu g$_{9/2}$ analogue state fragmentation from γ-transitions 79−22202
^{64}Ni (p, γ), 3.2 MeV, ^{65}Cu analogue P$_{1/2}$ resonance, γ-decay and energy levels 79−80907
^{64}Ni(p,γ), 2.05-2.55 MeV, ^{65}Cu levels and transitions, γ-strength function using average resonance capture 80−13411
Ni(p,γ), ^{A}Cu A=29,63, Doppler shift attenuation factors, level lifetimes, resonances 80−57741
Ni(p,γ)^{59,61}Cu, analogue to antianalogue M1 transitions 77−67718
^{16}O(p,γ), 12-15 MeV, ^{17}F T=$^{3}/_{2}$ states resonance energy, γ-decay and J$^{\pi}$, capture strength 79−67728
^{17}O(p,γ), 0.67 MeV, ^{18}F J$^{\pi}$=3^{-} doublet at 6241 keV, isospin mixing 80−511
^{17}O(p,γ), 1.4-2.8 MeV, ^{18}F levels and resonances, J$^{\pi}$ assignments 79−9480
^{18}O(p,γ), 630-2260 keV, γ-ray decay scheme, for ^{19}F reson. and bound levels 78−89790
^{31}P(p,γ)^{32}S, 0.5 to 0.9 MeV, resonance strengths of selected resonances in s-d shell 78−66281
^{31}P(p,γ)^{32}S, ang. distribs. of γ-rays from decay of ^{32}S reson. states 78−13085
^{208}Pb(N, γ$_0$), γ-ray ang. distribs., giant E3 resonances, direct-semidirect model 79−67727
^{208}Pb(N,γ$_0$), 2-10 MeV, giant M1 resonance in direct-semidirect model 79−17898
^{208}Pb(p, γ), γ ang. distrib., isovector giant quadrupole resonance, direct-semidirect model 79−63647
^{208}Pb(p,γ), 6 to 40 MeV, dipole/quadrupole interference, direct-semidirect model, γ ang. distrib. 78−93994
^{208}Pb(p,γ), γ-ray ang. distribs. asymmetry effects through IAR, direct-semidirect model 80−42581
^{34}S(p,γ)^{35}Cl, determ. of ^{35}Cl resonance level spin and multipolarity mixing coeff. 79−9552
^{34}S(p,γ)^{35}Cl, E$_p$=700 to 2100 keV, γ-ray angular distrib. 79−9466
^{45}Sc(p,γ), 0.7-4.2 MeV, cross section, statistical model anal., stellar interaction rate 79−17897
^{A}Si(p,γ)$^{A+1}$, A=28,29,30, resonance strength determ. for H burning of ^{29,30}Si in explosive C burning 79−22289
^{28}Si(p,γ), 1.3-2.3 MeV, resonant and direct capture, ^{29}P excitation functions and spectroscopic factors 79−80912
^{29}Si(p,γ), 0.73, 1.75 MeV, ^{30}P T=1 state decay, lifetimes and branching ratios, analogue E2 transitions 80−68598
^{30}Si(p,γ), pol.p, 6.4-15.0 MeV, cross section and anal. power ang. distribs. 80−99168
Sn(p,γ), 3.4 MeV, ^{A}Sb, A=121,123, levels below 2 MeV, spins, transitions and mixing ratio 80−32191
Sr(p,γ), 2-3 MeV, ^{85,87,89}Y E1 γ-ray strength function 79−75902
^{49}Ti(p,γ), 0.74-3.25 MeV, cross section and thermonuclear reaction rates, nucleosynthesis, IAR effects 80−102187
^{50}Ti(p,γ)^{51}V, 2.1 to 3.1 MeV, ^{51}V, γ-strength function, γ-ray spectra, average resonance method 80−9257
^{51}V(p,X), X=γ or n, 0.93-4.47 MeV, cross sections, competition effects, Hauser-Feshbach calcs. 80−91184
^{51}V(p,γ), 0.7-2.0 MeV, ^{52}Cr isobaric analogue states 78−70503
^{89}Y(p,γ$_0$)^{90}Zr, 14-27 MeV, E$_2$ and E$_3$ radiation anal. in direct-semidirect model 77−38266
^{89}Y(p,γ), 2-3 MeV, ^{90}Zr E1 γ-ray strength function 79−75902
^{A}Zn(p,γ), A=64, 66, g$_{9/2}$ isobaric analogue resonances 79−63663
^{68}Zn(p,γ), 2-4 MeV ^{69}Ga state alignment, γ-transitions and ang. distribs. 80−73797
^{68}Zn(p,γ), 3.8 MeV, ^{69}Ga, IAR corresponding to 1/2^{-} and 9/2^{+} ^{69}Zn states 78−66257
Zn(p,γ)^{67,69}Ga, 3 MeV, γ-ray ang. distrib. 78−74353

proton scattering *see electron-proton scattering; kaon-proton scattering; lepton-nucleon scattering; photon-proton scattering; pion-proton scattering; proton-deuteron scattering; proton-nucleus scattering; proton-proton scattering*

proton spectra
alpha-particle breakup on various nuclei at 140 MeV 78−46080
atmosphere, secondary nucleon spectra, 2-component model *(Russian)* 78−41612
atmospheric cosmic rays, 50 MeV≤E≤100 GeV, Monte Carlo simulation *(German)* 77−13197
collectively accelerated protons, nucl. activation, time-of-flight, and foil activation meas. 79−4195
cosmic radiation, theoretical proton spectra at atm. depths 40 g cm^{-2}≤h≤350 g cm^{-2} *(German)* 79−12367
fireball model for proton inclusive spectra, heavy-ion collisions 77−6339
heavy ion central collisions, 800 MeV/A, wide angle inclusive proton spectra 79−40951
high energy, emerging from 680 MeV synchrocyclotron shielding 78−17530
inclusive spectra in nuclear high energy collisions 78−70557
magnetosphere inner radiation belt proton spectra from Kosmos 721 satellite 80−72699
nuclear π^{-} capture, p, d and α inclusive prod. spectra 79−22338
nuclear isotopes far off stability line, production, props., review *(Hungarian)* 79−9927
odd-odd neutron deficient nuclei, spectra of delayed protons and α-particles in β^{+} decay *(Russian)* 78−46034
proton-nucleus elastic and inelastic scatt. 78−62674
inner radiation belt protons, energy and pitch angle distrib. analytic study 80−67471
solar flare energy spectrum simulation from monoenergetic incident proton beam 78−12786
d stripping, inclusive p spectrum, d wave function behaviour 79−17884

proton spectra continued
d+A, 6.3 GeV/c, A=H, D, C, Al and Bi, inclusive spectra of fast p and d *(Russian)* 78−46075
(e,e'p) reactions on ^{6,7}Li, ^{9}Be, ^{10}B, 700 MeV, proton spectral functions, momentum distribs., DWIA anal. 78−41701
nd→pnn, 800 MeV, quasielastic charge exchange, p spectra meas. 78−70389
np→pX, 800 MeV, proton spectra, πN(1232) resonance 78−62437
(p,p'), A=6 to 208, 800 MeV, proton spectra, quasifree scatt., DWIA anal. 80−52677
(p,p'), ground state correlation, continuum spectra 78−94007
p+nucleus reactions, 400 MeV, multi-nucleon removal, p-γ coincidence spectra 79−6549
pp scatt., spin correlation meas., local hidden variable theory, quantum theory 78−54649
π⁻-nucleus, 3.9 GeV/c, backward proton emission *(Russian)* 77−38302
Ag+α, 720 MeV, correlated energy spectra of light fragments, fireball and coalescence models 78−62555
Al+α, 720 MeV, correlated energy spectra of light fragments, fireball and coalescence models 78−62555
Al+p→p, 640 MeV, proton inclusive spectra and ang. distrib. meas. 77−67751
Al(Ne,X), proton inclusive spectra, direct plus thermal model 80−57799
^{22}Al(π,πpγ), 190 MeV, quasi-free single nucleon removal, p and π spectra 79−85519
^{27}Al+n, 15 MeV , sub-Coulomb-barrier spectra 77−23007
^{27}Al(^{3}He,p) 9-14 MeV, stat. multistep compound emission, residual two-body interaction 80−47493
^{27}Al(d,pX), 25.5 MeV, inclusive p spectra and cross sections from d breakup 79−13303
^{27}Al(d,pX) 80 MeV, inclusive proton spectra, d break-up, DWBA anal. 80−91190
^{27}Al(π⁻, pxγ), 300 MeV, proton-gamma ray coincidence spectra 79−6704
^{27}Al(π⁺,p), (π⁺,d), E=100, 220 MeV p and d spectra meas. 78−648
Al(d,p), 6.3 GeV/c, p momentum spectra from d breakup 78−89887
^{32}Ar, isobaric analogue states via β-delayed protons 78−558
^{40}Ar+^{58}Ni, deep inelastic collision at 280 MeV, fragment energy and spin 78−21599
^{197}Au(d,pX), 80 MeV, inclusive proton spectra, d break-up, DWBA anal. 80−91190
^{10}B(d,p)^{11}B, E_d=0.8 to 2.4 MeV, reaction mechanism 79−17910
^{11}B(γ,p)^{10}Be, 18 to 31 MeV, photoproton spectra and ang. distrib., excited state transitions 78−13056
Ba, A=117, 119, 121, delayed proton emitters, positron-proton coincidence meas. 78−78326
Be+p→p, 640 MeV, proton inclusive spectra and ang. distrib. meas. 77−67751
^{9}Be(p,pn)^{8}Be$_{gs}$, ^{9}Be-^{9}B isobaric doublet asymmetric excitation 77−26678
Bi (d,p), 6.3 GeV/c, p momentum spectra from d breakup 78−89887
Bi(d,p), 6.3 GeV, proton momentum spectra 79−6621
^{12}C, quasielastic π scatt., recoil proton spectra obs. 77−14198
^{12}C+^{12}C, 800 MeV/nucleon, two-fireball model for p and π inclusive spectra 79−13323
^{12}C+π±, proton spectra, cross section, π. absorpt. mechs. 78−25239
^{12}C(α,p)^{15}N, 50 MeV, proton spectra, excitation of high-spin states *(Russian)* 77−6209
^{12}C(e,e'p), 700 MeV, proton spectral function, independ.-particle shell model, DWIA anal. 77−6353
^{40}Ca, α-and p-spectra from giant reson. region via ^{40}Ca(α,2α) and ^{40}Ca(α,αp) 77−30523
^{40}Ca(p, 2p)^{39}K, 148.2 MeV, factorisation approx., energy states of ^{39}K, DWIA calcs. 78−62535
C(d,p), 6.3 GeV/c, p momentum spectra from d breakup 78−89887
Cd, A=97, 99, β delayed proton emission, spectra, branching ratio, half life 78−86517
^{140}Ce(d,p)^{141}Ce, 17 MeV, spectra and ang. distrib. obs., DWBA anal. 77−38283
^{252}Cf spontaneous fission, proton origin 77−38309
Cl(Ar,X), proton inclusive spectra, direct plus thermal model 80−57799
^{59}Co(p,2p)^{58}Fe, 17 MeV, search for double-direct reaction 77−30576
Co(n,n'), 9.1 MeV, equilib., pre-equilib., direct process anal. *(Russian)* 77−46172
Cs, A=114-118, neutron deficient isotopes, half lives, β⁺,γ, delayed p and α meas. 78−70489
CsI crystal, neutron bombardment, p and α emission spectra, yields, pree-quilib. mech. 77−50139
Cu+p→p, 640 MeV, proton inclusive spectra and ang. distrib. meas. 77−67751
^{63}Cu, quasielastic π scatt., recoil proton spectra obs. 77−14198
^{65}Cu(p,2p)^{64}Ni, 17 MeV, search for double-direct reaction 77−30576
^{54}Fe(p,p'), cross sections and spectra, exciton model *(Russian)* 78−21536
^{56}Fe+^{12}C, 192 MeV, energy spectra and yields of p,d and t 78−66306
H+H⁺, differential energy loss cross-sections 77−46630
^{2}H+π⁺, proton spectra, cross section, π. absorpt. mechs. 78−25239
^{2}H(n,p)nn, 13.95 MeV, proton spectrum, neutron-neutron scatt. length 77−26704
^{2}H(p,p)np, 13-19 MeV, p energy spectrum shape 79−6594
H(d,p), A=1,2, 6.3 GeV/c, p momentum spectra from d breakup 78−89887
^{4}He+π±, proton spectra, cross section, π. absorpt. mechs. 78−25239
^{4}He(d,p), 6.8 , 7.8 MeV, continuous proton spectra obs. 78−37352
K(Ar,X), proton inclusive spectra, direct plus thermal model 80−57799
^{78}Kr, charged particle evaporation following form. from ^{58}Ni+^{16}O 80−47453
^{24}Mg(p,p'), 135 MeV, large momentum transfer, excitation of high-spin particle-hole states in ^{24}Mg 77−61420
^{25}Mg(p,p')^{25}Mg*, 8.8 MeV, $J^{\pi}=1/2^{+}$, line shape 77−54211
^{16}N(p,p')^{16}N*, 5.7 MeV, $J^{\pi}=1^{+}$, line shape 77−54211
^{93}Nb(d,pX), 25.5 MeV, inclusive p spectra and cross sections from d breakup 79−13303
^{93}Nb(d,pX), 80 MeV, inclusive proton spectra, d break-up, DWBA anal. 80−91190
Nb(n,n'), 9.1 MeV, equilib., pre-equilib., direct process anal. *(Russian)* 77−46172
^{142}Nd(e,e'p), spectra and ang. distribs. meas., $T_>$ giant reson. anal. 78−13069
^{62}Ni+π±, proton spectra, cross section, π. absorpt. mechs. 78−25239
^{52}Ni(d,pX), 25.5 MeV, inclusive p spectra and cross sections from d breakup 79−13303
proton spectra continued
^{62}Ni(π±,p),(π±,d), E=100, 220 MeV, p and d spectra meas. 78−648
Ni(γ,p), 17.5-32.0 MeV, isospin effects in decay of highly excited ^{58,60}Ni states 77−61398
Pb+p, 3.6 GeV, emitted proton vel. spectra max. *(Russian)* 79−9571
Pb+p→p, 640 MeV, proton inclusive spectra and ang. distrib. meas. 77−67751
^{208}Pb, quasielastic π scatt., recoil proton spectra obs. 77−14198
^{96}Ru(d,p), 16 MeV, spectra and ang. distribs. meas., ^{97}Ru levels anal. 77−38284
^{32}S(γ,p$_0$), giant dipole resonance decay model, cross section and p spectrum 79−6563
^{36}S(d,p), 3.2 MeV, proton spectra meas., ^{37}S energy level scheme *(Russian)* 78−41733
^{69}Se, decay, T=1/2 β-delayed proton precursor 77−88082
Si detector, proton spectra, noniterative method for fitting Gaussian to peaks 77−57840
^{28}Si(n,p), 21.6 MeV, cross-sections, proton spectra, ^{28}Al analogue dipole state 77−30571
^{28}Si(p,p'), 135 MeV, large momentum transfer, excitation of high-spin particle-hole states in ^{28}Si 77−61420
^{119}Sn(d,pX), 25.5 MeV, inclusive p spectra and cross sections from d breakup 79−13303
Ta+α, 720 MeV, correlated energy spectra of light fragments, fireball and coalescence models 78−62555
^{181}Ta+π±, proton spectra, cross section, π. absorpt. mechs. 78−25239
^{181}Ta(d,pX) 25.5 MeV, inclusive p spectra and cross sections from d breakup 79−13303
^{46}Ti, ^{48}Ti+n, 15 MeV, sub-Coulomb-barrier spectra 77−23007
^{47}Ti(α,p), 15.35 MeV, level density parameters, statistical model anal. 78−13130
Ti(p,p), 6 MeV, A=46,48,50, cross sections, excited states, ang. distribs. 77−61410
U(Ne,X), proton inclusive spectra, direct plus thermal model 80−57799
^{238}U(d,p), 12 MeV, ^{239}U level assignments 78−66209
^{238}U(e,p), 40 MeV, p spectra, deduced ternary fission cross section 79−9549
^{51}V(p,2p)^{50}Ti, 17 MeV, search for double-direct reaction 77−30576
Xe(π,p), E_π=2.34 and 3.5 GeV/c, energy and angular distrib. obs. *(Russian)* 79−9633
Xe(π⁺,pX), 2.34 GeV/c, gauge props. of proton emission *(Russian)* 77−38303
Xe(π⁺,pπ⁰), E_π=2.34 GeV/c, momentum distrib. function estimate for internuclear nucleons *(Russian)* 79−9634
^{172}Yb(d,p)^{173}Yb, 14 MeV, proton spectra and ang. distrib. meas. level struct. determ. 78−29482
Y(n,n'), 9.1 MeV, equilib., pre-equilib., direct process anal. *(Russian)* 77−46172
^{90}Zr, breakup of alpha particles in nuclear field 78−46080

proton-surface impact *see ion-surface impact*

protonium *see protons*

protonosphere *see upper atmosphere*

protons
see also cosmic ray protons; delayed protons
antiprotonic atoms, X-ray transition energies, strong interaction and p̄ mass meas. 78−25759
asymptotically free SU(5) grand unification, proton stability, renormalisation group 80−82929
beam production, ~1 MeV, pinched electron-beam diode 77−10521
beams in NAP-M storage ring, accelerating system and parameters monitoring 77−65364
charge form factors, K_{min} approx. in ^{16}O, and ^{40}Ca 79−9456
charge radius from H Lamb shift meas. 77−50047
decay, baryon number nonconservation, expt. status 80−57594
decay, confirmation of unification of forces, book contrib. 80−42383
decay, search techniques for lifetimes of order 10^{34} years 80−47287
decay, unified theory of elementary-particle forces 80−105827
decay lifetime in SU(5) grand unified theory 79−71749
decay modes in SU(5) and SO(1) theories 80−13301
deep inelastic structure function, large-x depend. in GVMD 77−30350
deep structure, renormalisation group approach, review 79−85302
dielectric medium, impurity dispersion self energy calcs. 78−52536
Dirac form factor and QCD 78−45864
disintegration, concepts of leptons and quarks, unified field theory *(French)* 80−91038
Earth bow shock energetic protons meas. in upstream solar wind 80−90308
electric mean square radius, from ep scatt. at 4.5 GeV *(Russian)* 79−49525
electric polarisability, from photoabsorption cross-section 80−57597
electric polarisability 79−49524
electron cooling of protons at CERN 80−9443
electroproduction struct. function, elastic form factor, scaling function, causal representation 79−13138
EM form factors from MIT bag model 79−93419
EM polarisabilities difference contribs. from N$\bar{N}$→ππ and ππ→γγ 79−3023
EM structure functions from electron scatt. data 80−13306
finite energy sum rule for nucleon polarizabilities difference *(Russian)* 79−58905
flavour symmetry breaking in antiquark distribs. 79−36006
flux anisotropies, Pioneer 10 obs. near Jupiter 79−53762
form factor, harmonic anal. with Lorentz group *(Russian)* 77−46051
form factor extraction from high energy scatt., Chou-Yang model 77−6127
form factor extrapolation using Pade type approximants 79−6341
form factors, hadron distributions in quark jets 79−54317
gluon distribution from elastic pp scatt. 80−82939
half life, Dirac approach to large number coincidences 80−27501
inner structure, observation in collisions producing jet of debris 80−57569
interplanetary medium, proton number density and flux energy rel. to shock waves thickness 80−90314
intrinsic charm from non-negligible uudcc̄ Fock component 80−86691
Jupiter, proton flux along magnetic field lines in middle magnetosphere 79−53763
Jupiter mid-magnetosphere, equatorial protons instability 80−67642
lifetime predictions in grand unified SU(5) model 79−49441
magnetosheath and magnetotail, energetic protons and electrons simultaneous meas. 79−16760

protons continued
magnetosphere, dynamics of protons trapped in geomag. field 79−16756
in magnetosphere, IPDP source regions and resonant proton energies 79−53673
magnetosphere, low energy electrons and protons obs. 78−36407
magnetosphere, pitch angle dispersion of drifting energetic protons at synchronous orbit 78−77428
mass and ρ-meson lifetime relationship, quantum of time 77−22716
matter-antimatter asymmetry of Universe, review of speculations and data *(French)* 79−35439
neutron-proton mass difference, classical electrodynamic model 77−6123
O(10), SU(4) colour subgroup, fractional charged gauge boson, proton half-life 80−73644
parton gas model, degenerate, quark-lepton identification 80−68416
parton structure and charge distrib. in multiparticle production 77−6088
proton-neutron mass difference, Cottingham formula simplification with causality conditions 77−61286
proton-neutron mass difference, higher intermediate hadronic states 78−45920
proton/electron mass ratio, limits to past variability from quasar absorpt. line redshifts 77−61338
QCD, ratio of mag. to elec. form factors 78−70340
QCD perturbation theory for confined quarks and gluons, p glue content 80−52460
radiation belt, equatorial α/p ratio near 1 MeV 80−4205
inner radiation belt protons, energy and pitch angle distrib. analytic study 80−67471
radiation belts, proton fluxes, critical levels in outer boundary 78−16246
radiation therapy, high-energy proton beam, physical meas. using tissue substitutes 80−81720
rest frame proton, colour gluon content, bag model and QCD calcs. 79−335
Saturn radiation belt protons, rings ice particles sputtering 78−89116
scaling behaviour of struct. functions in parton model 78−16988
semileptonic decay in nuclei, pion attenuation 80−47286
size, lower limits in general relativity 80−22245
solar wind, obs. of backstreaming protons near Earth bow shock 80−90309
solar wind, proton-driven EM instabilities in high-speed streams 79−53701
solar wind protons, non-bi-Maxwellian distrib. function rel. to ion cyclotron instability 78−96375
solar wind protons cooling, evidence from Mariner 2 data 78−40789
spin, outcome of violent collisions 80−434
stopping power in H_2, He, N_2, O_2, CO_2, Ne, Ar, Kr, Xe 80−14057
strong gravity explanation of proton mass 78−12852
structure function, higher order asymptotic freedom corrections, from deep inelastic scatt. 80−105905
structure function nonsinglet moments from deep inelastic lepton scatt., QCD 80−62980
structure function parametrisation 77−22734
SU_N gauge group uniqueness in grand unified model, U_1 color, proton stability 79−316
SU(5), SU(6) vectorlike unified theories with unitary groups, Fermi oscillators, proton stability 77−67608
SU(5) and SO(10) grand unification, flavour mixing and proton instability *(Russian)* 80−68413
SU(5) grand unification, p lifetime and branching ratio, bag model wavefunctions 80−78004
SU(5) grand unification, superheavy fermions and proton lifetime *(Russian)* 80−91036
SU(5) grand unified theories, proton decay, flavour mixing effects 80−377
SU(5) grand unified theory, proton lifetime estimate accuracy 80−101967
subcomponent models of quarks and leptons in SU(3) subcolour, proton decay 80−78035
teaching, from Compton effect to quarks, at., proton, and nucl. struct. 78−24596
three photon structure function, quark-parton model, inelastic electron scatt. data 77−46022
transport across charged membrane and pH oscills. 80−61516
unified theory with right handed currents, SU(6) based vector-like gauge theory, proton stability 77−49890
universe ultimate fate, effect of finite proton lifetime 80−82560
Uranus radiation belt protons, rings ice particles sputtering 78−89116
e⁻p mass ratio, direct determ. using cyclotron resonance technique 78−70093
μp, 219 GeV, proton struct. function determ. 78−82216
$\bar{p}$, parity determ. from ang. momentum anal. 78−4889
$\bar{p}$ decay, baryon number of universe 77−91422
$\bar{p}$ decay and baryon number of universe 77−49964
p EM form factors calc. 77−67654
$\bar{p}\rightarrow e\pi^0$, lifetime meas. using counter technique at ICE 79−93413
$\bar{p}$ instability, implications for symm. big-bang cosmologies 78−41104
$\bar{p}$ lifetime, lower limit determ. 78−45968
$\bar{p}$ lifetime using ICE storage ring 78−89768
$\bar{p}$ mag. moment and mass determ. 78−45990
$\bar{p}$ properties and interaction 78−54654
p-n mass difference, quark-parton model anal. 78−93859
p-$\bar{p}$ symmetry, mass difference, Dirac and CPT theory test 78−82125
pn mass difference, effects of EM mixing, Λ−Σ^0, η−π^0, ω−ρ^0 *(Russian)* 78−74255
pp, ISR energies, p fragmentation, D^+ prod. from Λ_c* and Λ_b decay 80−102080
$p\bar{p}$ atom, nucl. level shift and radiative transitions *(Russian)* 80−28121

proving, theorem *see theorem proving*

proximity effect
barrier effect at supercond.-normal metal interface 77−59357
bidimensional junction lattices, proximity effects *(French)* 80−49998
bifurcation theory and order of phase transition for proximity effect sandwiches 78−84353
bridge, thermal effects 77−63030
coupled superconducting weak links, voltage locking and other interactions 80−39719
DC Josephson current temp. depend. in proximity junction 79−78271
DC Josephson effect, proximity systems with magnetic impurities 80−100554
DC Josephson effect for supercond. proximity systems 79−56425
proximity effect continued
DC Josephson effect for superconducting proximity Kondo alloys 80−88690
dirty proximity-effect sandwich system, theoretical investigation of transition temp. 79−73638
dirty superconductor, microscopic theory of current-voltage relationship across normal-superconducting interface 79−73637
elastic scattering, appl. of Anderson theorem 80−84568
electron-phonon interaction function of normal metal determ. by proximity effect *(Russian)* 77−89902
electron-tunnelling junction fabrication technique 79−38261
energy gap anisotropy, normal layer proximity effect 80−84558
energy gap in tunnelling density of states for supercond.-normal metal sandwich 77−40006
exciton insulator, proximity effect at low temp. 79−73643
film, with spatially varying order parameter, far IR absorption 77−28284
finite geometry, microscopic investigation of proximity effect 79−33402
finite geometry, supercond.-normal metal interface study 79−33404
first-order phase transition in supercond. sandwiches 77−40004
hysteresis in nonequilibrium superconducting proximity-effect bridges 79−15258
inhomogeneous superconductivity, Ginzburg-Landau theory 80−88672
intermediate state, reflectivity of S-N interface, application for Rowell-Tomasch oscills. amps. and thermal cond. 78−91822
Kondo alloys and supercond. proximity effect 78−19190
Kondo alloys in supercond. proximity, localised bands 78−10613
localised states, nonmag. at interface, effect on supercond. proximity effect 78−64170
McMillan tunnelling model 79−73639
McMillar tunnelling model of proximity effect, sp. ht. jump 79−87201
metal-insulator-metal-superconductor junction, phonon struct., proximity effect tunnelling 79−82721
microjunction, supercond.-normal metal-supercond., microwave enhanced crit. current 79−82720
multifilamentary superconducting wires, in situ, anal. of continuity proximity effect conductivity 79−60997
N-S boundary resistivity, tunnelling contact resistance *(Russian)* 80−93048
N-S sandwich, theory 79−1646
normal metal-superconductor boundary excess resist. temp. depend., quasiparticle Andreev reflection *(Russian)* 79−73640
normal metal-superconductor double-layer, photon struct. induced into normal side by proximity effects 79−99659
normal-superconductor interface, boundary conditions, theory 80−39708
p-state supercond., anal. using proximity effect 79−56407
parametrically coupled Josephson bridges, resistive state, proximity effect *(Russian)* 80−100550
phonon structure in tunnelling characts. of thin proximity effect sandwiches 77−28304
review *(French)* 78−2625
S-wave and P-wave superconductors, absence of proximity effect 80−93033
sandwich system, near transition temp., proximity effect and Josephson current 80−7039
semimetal and semiconductor to exciton phase transition 79−28296
series array of proximity coupled bridges, mode locking 77−51852
spin density of states of proximity effect supercond. sandwiches in high fields 77−85394
superconducting bridges, Josephson effect and collective modes 79−56435
superconducting junction proximity sandwich, mag.-supercond.-mag., phase diagram 78−95399
superconducting microbbridges and point contacts, nonstationary Josephson effect 79−38256
superconductor, with mag. impurities, proximity effect at low temp. 79−73643
superconductor tunnelling, sum rules *(Russian)* 79−87195
superconductor with mag. impurities, longit. elec. field penetration, kinetic proximity effect *(Russian)* 79−19694
superconductor-metal-insulator-metal-superconductor system, Josephson current, weak supercond. *(Russian)* 80−54842
superconductor-normal metal contacts, nonlinear electric phenomena *(Russian)* 79−78268
superconductors, magnetic impurity low temp. behaviour, transition temp., specific heat, free energy 80−88691
superconductors containing transition metal impurities, tunnelling conductance calc. 78−52160
thermodynamics of second order phase transitions in proximity sandwiches 79−56408
transition metal impurities in normal metal of supercond.-normal metal structure 77−59356
tunnel junctions with amorphous Nb-Si(Al) barriers 79−65614
weak links, control of characts. 79−65615
weak links, steady-state and RF props. 80−84563
weak links, thermal switching times 78−76191
Ag, Fermi velocity from proximity effect tunnelling 78−51875
Ag-In (Sn) multilayers, vapour quenched, supercond. transition temp. 80−20346
Ag-Mn film, supercond. proximity effect and pair breaking, normal state mag. interactions 77−63035
Ag-Pb sandwich, mag. field depend. of tunnelling characts. 77−20501
Ag-Sn, supercond. proximity-effect bridge, thermal effects 79−78265
Ag-Sn proximity effect bridge, crit. current anomaly 78−76194
Ag-Sn proximity effect bridges, long, voltage anomaly 79−51725
Ag-Sn proximity effect bridges, nonequilibrium state, hysteresis of crit. current 79−56411
Ag-Sn proximity-effect bridges, crit. current hysteresis under phonon injection 79−87206
Ag-Sn proximity-effect bridges, T* anomaly under phonon injection 80−34566
Ag-Sn proximity-effect bridges, phonon-injection-induced first-order transition obs. 80−39718
Al, thick film, supercond., tunnelling characts., geometrical reson. in Al-Pb struct. 79−38260
Al-Al_2O_3-Nb, quantitative proximity tunnelling spectroscopy 79−91193
Al-oxide-Mg-Al, thin proximity effect sandwiches, spin-polarised tunnelling obs. 80−50007
Al-Pb proximity sandwiches, Josephson and quasi-particle tunnelling expts. 79−65616
Au/In proximity effect bridges, finite size array 79−78270

proximity effect continued
Au/In proximity effect bridges, square arrays, transition temps. 80−84557
Bi-Sb film, tunnel conductivity, proximity effect *(Russian)* 79−51726
Cu alloy-Nb composite wires, resist.-temp. meas., percolation theory 79−28490
Cu-Nb filamentary composites, powder metallurgy prod., supercond. props. 79−56477
Cu-Pb proximity sandwiches, tunnelling expt., barrier transmission effects 80−50002
Cu-V-Ga dil. alloys with V_3Ga particles, supercond. props. and microstruct. 78−39278
In film, Josephson arrays, proximity effect junctions 80−84553
In superconducting microbridge, voltage locking and other interactions 80−39720
In-CdS-In, tunnel junction light-induced DC Josephson current 79−47204
Nb and Nb_3Sn, inhomogeneity detection by penetration depth meas., proximity theory 77−28288
Nb Josephson junctions, excess current anal. 79−28465
Nb, proximity electron tunnelling spectroscopy 80−107964
Nb, superconducting phonon struct. obs. in proximity tunnelling 77−77008
Nb tunnel junction, temp. dependent props., 2-9L 77−24642
Nb wire, Cu clad, proximity effect, Meissner screening length meas. 79−60996
Nb wire, Cu-clad, temp. sensor below 1K using proximity effect 79−85139
Nb/Ta thin film proximity effect bridge 79−82712
Nb-Al, tunnelling expts. on normal metal backed by Al 80−65751
Nb-Al proximity sandwiches, supercond. transition temp. and tunnelling meas. 80−7045
Nb-I-Pb junction, double-peak structure *(Russian)* 79−82716
Nb-Nb_xO_y-Pb, tunnelling junction, current-voltage charact., knee struct. 79−38261
Nb-Nb_xOy-Cu/Pb supercond. proximity junction, max. DC Josephson current, thickness depend. 79−82719
Nb-NbO_x-Al/Pb supercond. proximity function, production by RF sputtering and photolytographic techniques 77−43787
Nb-NbO_x-Pb tunnel junction, temp. depend. of effective Nb energy gap 80−80454
Nb-NbO_x-PbIn tunnel junctions with ultra-thin Nb electrodes 79−56398
Nb-Pb supercond. tunnel junction proximity effect, theory 80−65752
Nb-Pb tunnel junction, crit. Josephson current, proximity effect model 80−93047
Nb-Si amorphosamorphous thin film tunnel junctions 79−28473
Nb_3Ga Josephson junctions, excess current anal. 79−28465
Nb_3Ge film, in supercond. proximity sandwich, energy gap struct., appl. to electron-phonon spectra 79−56401
Nb_3Ge, high T_c films, electron tunnelling and AES anal. 79−28471
$NbSe_2$ microbridges, current-voltage curves, hysteresis of crit. current *(Russian)* 77−69452
Nb_2Sn, filamentary segments, flux pinning, proximity effects, percolation thresholds 78−56269
NbTi superconducting wire, Cu clad, proximity effect, Meissner screening length meas. 79−60996
$Nb_{0.75}Zr_{0.25}$, supercond. energy gap, proximity tunnelling method determ. 79−56404
Pb film, conducting coating effect on supercond. transition temp. and normal-state cond. 77−16007
Pb on Cu and Ag substrates, tunnel conductivity, proximity effect *(Russian)* 79−51726
Pb, supercond. phonon struct. in ultra-thin proximity effect tunnel junctions 78−80101
Pb/Bi-I-Al tunnel injected nonequilibrium supercond. struct., diffusive quasiparticle instability, multiple gap states 80−50005
Pb/Cu(Ag) proximity effect semiconductor, US surface wave attenuation 79−60994
Pb-Cd, electron tunnelling study 78−10616
Pb-Cd eutectic composite, mag. flux entry in proximity effect regime 79−33418
Pb-Cd thin films, electron tunnelling study of supercond. proximity effect 80−2525
Pb-Cu contacts, proximity effect *(Russian)* 80−34558
Pb-Cu(Ag) double layers, intermetallic boundary effects, tunnelling 80−88692
Pb-In/Sn-In proximity sandwiches, crit. currents 79−60992
Pb-Sn, lamellar eutectic alloy, entropies, free energies and transition temps. 77−51849
Pb-Sn eutectic alloy, diamag. Sn lamellae up to 7K *(French)* 77−51858
Pd-CdS-In, tunnel junction, light induced DC Josephson current 79−47204
Sn-Pb sandwich, mag. field depend. of tunnelling charact. 77−20501
Ta-Ta_xO_y-Pb, tunnelling junction, current-voltage charact., knee struct. 79−38261
Ti-V (19 at.%), aged ω-phase precipitation, incomplete proximity effect 78−60252
Zn-Pb proximity sandwiches, tunnelling charact. 79−56396

pseudobinary semiconductors *see II-VI semiconductors; III-V semiconductors; III-VI semiconductors; IV-VI semiconductors; semiconductor materials*

pseudopotential methods
A15 compounds, plasma energies, tight-binding energy-band model 78−84159
ab initio effective core pot. method appl. to F_2, Cl_2 and LiCl 80−32625
ab initio effective core potential studies, relativistic effects, appl. to $HgCl_2$, AuCl, and PtH 79−93933
ab initio molecular fragment calculations with pseudopotentials 79−93905
ab initio pseudopotential for FSGO calcs., appl. to Li compounds 77−75043
adparticle on substrate, pseudopot. near second-order phase transition 80−80065
AKNS system 79−97243
alkali atom, in inert-gas solid, at level struct. calc. pseudopot. method 80−9532
alkali halides, elastic constants, temp. depend.; pseudopot. calc. 80−65120
alkali halides, F-centre absorption energy calc. 79−78715
alkali hydrides, ionic-covalent config. mixing, pot. curves 77−34576
alkali metal, Ashcroft pseudopotential, unified study of props. 80−39239

pseudopotential methods continued
alkali metal, atomic props., accuracy of description depenxence on pseudopotentials *(Russian)* 78−38997
alkali metal, ideal electrical resistivity, temp. depend. 78−64022
alkali metal, law of corresponding states, pseudopotential theory 77−59095
alkali metal, liq. struct., from 1st-principles pseudopot. calc. 79−41941
alkali metal, local Heine-Abarenkov-type model pot. 79−87031
alkali metal, thermal expansion, elastic constants, phonon freq. anisotropy *(Russian)* 79−1516
alkali metal+inert gas, adiabatic pots. 79−81254
alkali metal anions, photodetachment cross-sections and multipole polarisabilities, extended asymptotic model 78−42028
alkali metal atom, perturbed by rare gases, dipole moments of S-P transitions 80−27979
alkali metal atom, polarisability calc. using Laplace method *(Russian)* 79−89803
alkali metal atom+alkali metal atom, interatomic potential 79−68294
alkali metal atoms, in solid matrix, bistable state, optical trapping between levels 79−81187
alkali metal atoms, positive ion Rydberg states, pseudopotentials, local exchange approx. calcs. 77−14337
alkali metal hydride, variational time-dependent H-F calcs. in pseudopot. framework 77−10588
alkali metals, atomic properties, pseudopot. calcs. 77−89512
alkali metals, bulk modulus and eqns. of state under press. 80−88293
alkali metals, density of states effective masses, liq. and solid phases, model pseudopot. calc. 77−76738
alkali metals, effective ion-ion potential, compressibility and force consts. 80−70158
alkali metals, elastic and thermal props. by pseudopotential method 80−19899
alkali metals, elastic constants, temp. depend. 78−51603
alkali metals, equation of state and vol. depend. of thermodynamic props., pseudopot. theory 78−18738
alkali metals, Fermi surface topological changes due to uniaxial stresses 80−92810
alkali metals, Gruneisen parameter and temp. depend. of elastic consts. 80−39317
alkali metals, Gruneisen parameters, influence of press. on lattice anharmonicity and temp. depend. 80−79905
alkali metals, heavy, crystal structure, effect of Van der Waals forces 79−99111
alkali metals, ideal thermal resist. and Lorenz number due to conduction electron-phonon scatt. 80−29377
alkali metals, lattice dynamics, a priori pseudopot. calc., cond.-core exchange approxs. 77−72662
alkali metals, lattice sp. ht. and thermal vibrs. 78−30768
alkali metals, liq., Fermi energy, density of states, electronic props., exchange and correl. effects 80−96774
alkali metals, mode Gruneisen parameters, ab initio calc. 77−20091
alkali metals, paramag. and electronic susceptibility calc. 78−52205
alkali metals, partial pressure contributions to equation of state 80−107401
alkali metals, phonon dispersion binding energy, compressibility, elastic consts. electron screening and Ashcroft pot. calcs. 80−65174
alkali metals, pressure influence on absolute zero isotherms, polymorphic transform., phonon spectra *(Russian)* 80−49363
alkali metals, pseudopotential calcs. of binding energy, compressibility and resistivity 79−65025
alkali metals, relation between ion-ion pot. and phonon spectra 77−80591
alkali metals, third order elasticity moduli, temp. depend. *(Russian)* 78−63798
alkali metals and alloys, liq., internal energy, chem. pot., critical consts. 78−34422
alkali-alkali dilute alloys, lattice relax., energy of mixing 77−84936
alloy, theory of ordering, crystal lattice parameters rel. to composition and order *(Russian)* 79−77543
alloys, crystalline, liq., amorphous, stability and structure, pseudopotential calcs. *(German)* 80−38913
alloys, nearly free electron like, indeterminacy of a priori pseudopots., effects on form factors 80−103608
alloys, short-range order, electronic theory using pseudopot. approx., review 79−47004
angular momentum projector pseudopots., 1st principle HF and local density functional schemes comparison 78−62702
anisotropic normal metal, thermopower calc. 80−24879
atomic core radius and pseudopotentials 78−95248
atomic correlations energy calcs. 77−30788
atomic dynamic polarisability, variational calcs. with mode pot. *(Russian)* 78−902
atomic model potentials soluble in closed form 80−23287
atomic nonlocal pseudopotentials, density functional formalism calcs. 79−41096
atomic properties of solid state *(Russian)* 79−60674
atomic three parameter pseudopots., Li to Kr, and hydrides, PSIBMOL algorithm 77−26963
B-32 superstructure, instability in absence of many-particle interactions 77−58972
barriers to internal rotation, pseudopot. calcs. 77−14352
binary alloy, determ. of distortion field 80−44536
binary alloy, electron theory of short range order 78−10390
binary alloy, of simple metals, with non-homovalent impurities 80−44464
binary alloy, solid-liquid transition theory 78−6144
binary alloys, and intermetallic cpds., struct. and stability, ab initio pseudopot. calcs. 78−34460
binary alloys, form factors of pseudopot., OPW calc. *(Russian)* 79−19498
binary compounds, structural stability, nonlocal density-functional atomic pseudopot. method 80−49174
binary semiconductors, general model pseudopot. 77−62800
bond orbital model, model pot. approach, appl. to Li_2 and LiH 79−49923
brass, α and β phases, Hume-Rothery rules for phase stability 79−99292
β-brass, phonon spectra pseudo potential calcs. rel. to long range order and composition *(Russian)* 79−99279
β-brass (40 to 50 at.% Zn), elastic shear consts., comp. depend., pseudopot. calc. *(Russian)* 80−24525
chemical bonding in crystals, modern theories 78−2064

pseudopotential methods continued
coherent pseudopotential approximation 77−15735
cohesive energy calcs., frozen core approx. and pseudopotential theory validity 80−64949
completely orthoganalised plane waves in pseudopotential theory, formalism *(Russian)* 77−1345
completely orthogonalised plane wave method, model pseudopotentials *(Russian)* 78−34740
completely orthogonalised plane waves, class of pseudopotentials constructed *(Russian)* 77−1346
coreless pseudopots. for atoms K through Zn 78−55121
covalent bonding, covalent charge distrib. concept 77−51345
covalent crystals, lattice dynamics 77−43295
covalent crystals, local Heine-Abarenkov model potential 78−42949
covalent semiconductors, electronic interface states in intrinsic stacking-faults 80−75522
cubic metals, press.-vol. relations calc., pseudopotential method 77−11662
Density-functional pseudopotential approach to crystal phase stability and electronic structure 78−72058
development and appl. of pseudopotential theories in solid state and condensed matter physics 79−90933
diamond:N, effect of displacement upon impurity levels, pseudopotential calc. 77−39803
diamond, surface electronic struct., self consistent pseudopotential calc. 78−47842
diamond Schottky barrier, electronic struct., pseudopot. calc. 78−95364
diamond Schottky barrier, electronic struct., pseudopotential method, jellium model 79−38162
diamond type crystals, semicond.-metal transition 78−72072
diatomic mol., Hellman pseudopot. calcs., dissoc. energy, ionis. pot., bond length 77−10577
diatomic molecule, with 2nd row atom, core pseudopot. valence electron method 79−72233
dilute alloy, electron scatt. by impurity cluster, lattice distortion and back-scatt. effects 77−20306
dilute binary alloy, residual resistivity 77−1406
dilute binary alloys, formation energy, lattice relax. and zero-point vibrations 78−83771
dilute binary alloys, formation energy, lattice relax. and zero-point vibrations 78−87646
dimethyl zinc, valence band and Zn 3d levels, electric field gradients 77−88495
disordered simple metal, electronic and cohesive properties, review 80−44475
disordered solid, l-depend. pseudopot. in theory of band struct. 78−84124
disordered system, orbital mag. susceptibility of conduction electrons 78−76217
effective hamiltonians, pseudopotentials and applics. 77−30754
elastic properties, of Al and Pb *(Russian)* 78−56678
electric current, determ. by time correlation functions force-force and force-momentum, pseudopot. method 78−95275
electrical conductivity of high temp. imperfect gas *(Russian)* 80−100072
electron effective mass calc., self-consistency 79−77990
electron energy spectrum in crystals, use of atomic scatt. form factors 80−6688
electron gas, dense high-temperature, classical modelization of symmetry effects 78−65869
electron scatt. at low energies, phaseshift evaluation by pseudopotential method 79−22830
electronic structure and solid props., rel. to chemical bonding, book 80−86044
electronic structure of solids, self-consistent mixed-basis approach 79−69394
electrons in disordered metals and at metallic surfaces, conf., Ghent, Belgium (Sept. 1978) 80−41946
elemental semiconductors, model pseudopotential, band struct. calcs., liquid semicond. resistivity calcs. 80−20075
energy-dependent pseudopot. method for Fermi surface distortion and phonon dispersion calc. 77−15737
exchange interaction and correlation effects on ion pseudopot. form factor 80−49639
extended Hartree-Fock Hamiltonian, nearly free electron approx. and pseudopotential method 78−60047
first-principles pseudopotential in the local-density-functional formalism, appl. to C and W 79−59328
first-row atoms, local density formalism calcs. using pseudopots. 77−75047
fluoromethane, core energy levels, pseudopot. calcs. *(French)* 79−49935
form factor, analytic expression 78−10330
form factors of free ion pseudopot., calc. 80−59849
formaldehyde, MC SCF method in full and pseudopot. versions 77−83487
formic acid, H bonding, electronic struct., geometries, moments, dimerisation energies, charge distrib., pseudopotential calcs. 80−27942
FSGO calcs. on methane using pseudopotentials 77−26971
GaAs-$Ga_{1-x}Al_xAs$, ultrathin layer heterostruct., pseudopot. calcs. 78−95343
graphite intercalation compounds, C_nK, electronic struct. and elec. props. 80−44471
ground state atoms, Van der Waals coeffs., polarisabilities and oscill. strengths calcs. 79−93913
group IV hydrides, pseudopot. FSGO calc. 79−22591
group IV semiconductors, acoustic deform. pot. determ. 77−1363
halogen molecule, orbitals calc., correlation effects, force const., dissoc. energy, bond length 77−26964
halogen molecule negative ion, Cl_2^-, Br_2^-, I_2^-, $ClBr^-$, ClI^-, pot. curve calc. 77−10596
Hartree-Fock approximation with pseudowavefunctions 79−3357
HCP metals, phonon dispersion relations, effect of different dielec. functions on model pseudopot. calc. 79−33055
heavy elements, relativistic model pot. 78−75978
hydrides, first-row, pseudopot. calcs. using FSGO 78−9062
hydrocarbons, double-zeta quality ab initio mol. fragment calcs. with pseudopots. 79−85879
5-hydroxyindole, near ab initio and pseudopotential calcs. 77−71749
hydroxytryptamines, near ab initio and pseudopotential calcs. 77−71749
II_3V_2 semiconductors, spin-orbit and cryst. field splittings of valence band 78−63980
pseudopotential methods continued
II-IV-V_2 semiconductors, electronic band struct., general model pseudopot. 78−39020
II-VI semiconductors, acoustic deform. pot. determ. 77−1363
II-VI semiconductors, electronic theory, cryst. energy and bulk modulus 78−72104
III-V semiconductor, electronic theory, cryst. energy and bulk modulus 78−72104
III-V semiconductor, localised defects, one-electron pseudopot. 77−24533
III-V semiconductors, acoustic deform. pot. determ. 77−1363
imidazolium cation, near ab initio and pseudopotential calcs. 77−71749
inert gas atom photoelectron ang. distribs., theoretical calcs. comparison 79−59412
inert gas solids, luminesc., self-trapped exciton 79−38605
interface state models, appl. of Green's function matching procedure 77−59320
intermetallic alloys and compounds, solid solubility 79−60514
intermolecular interactions, short range, non-additivity, pseudopot. anal. appl. to Ar_2, Ar_3, and Ar_4 79−50179
ionic crystal, surface parameter calc. by pseudopotential method *(Russian)* 78−76130
ionicity and struct., interrelation, appl. to zincblende, rocksalt and wurtzite structs. and amorphous semiconductors 77−1093
IV-VI compounds, orthorhombic, atomic pseudopots. 79−42453
IV-VI semiconductors, transverse effective charge from one dimens. band struct. calc. 80−15038
IV-VI semiconductors, transverse effective charge from three dimens. band struct. calc. 80−15039
lattice dynamics, microscopic theories, developments 78−59870
Lie algebras, solitons and pseudopotentials 77−26131
liquid alloy, binary, interatomic forces, thermodynamic props. and alloying 77−47324
liquid alloy, thermodynamic ab initio calcs. 77−47602
liquid alloys, binary, entropies, ab initio calcs. 77−47599
liquid alloys, electromigration, driving force, pseudopot. calc. 77−55373
liquid alloys, vapour pressure, pseudopot. and Gibbs-Bogoliubov calcs. 78−83935
liquid metal, conductivity calculation with regard for nonlinearity of electron-ion interaction screening *(Russian)* 78−43351
liquid metal, effective interionic interaction, many particle effects *(Russian)* 77−39530
liquid metal, electron momentum density, perturbed Green's function method 78−60052
liquid metal, electronic density of states, pseudopotential calcs. 80−70578
liquid metals, elec. cond., effect of multiparticles interionic correls. *(Russian)* 79−28333
liquid metals, elec. resist. calcs. 77−85190
liquid metals, mixing volumes, pseudopotential method 79−37846
liquid metals, nonlocal pseudopot. calc. of Knight shifts 78−91965
liquid metals, nucl. quadrupole relaxation, Sternheimer antishielding and fluctuating elec. field gradients 77−55726
liquid metals, spin-orbit interactions effect on mag. susceptibility, effective pseudohamiltonian 80−29299
liquid metals, vapour pressure, pseudopot. and Gibbs-Bogoliubov calcs. 78−83935
liquid metals of groups IIB, IIIB, and IV, thermoelectric power, pseudopotential calc. 80−59959
liquid polyvalent metals, struct. factors with shoulder 80−19686
localised fixed orbitals, construction, pseudopot. method using multi-config. SCF theory 77−14334
localising pseudopotentials for local moments and certain virtual bound states 78−34959
many-valence-electron pseudo-wavefunction, ats. and mols., exact theory 77−79534
many-valley semiconductor, Mott transition, critical carrier conc. 77−47747
metal, BCC, stacking fault and twin boundary energies 77−76420
metal, classical cleavage energy, layer summation method 77−85287
metal, d-band, generalized pseudopotential theory, density functional formulation 78−10389
metal, elec. resist., correction from non-Hermiticity of pseudopotential 79−7815
metal, electron gas kinetic energy and cryst. pseudopot. orthogonalisation *(Russian)* 77−85160
metal, electron-impurity scattering, lattice distortion effects, phase shifts, calc. 80−96860
metal, electron-ion interaction model, appl. to K and Na props. 78−26486
metal, electronic structure, optical absorption 79−38566
metal, free-electron-like, XPS lineshape asymmetries 78−14681
metal, liquid, resistivity, thermoelectric power, Harrison nonlocal pseudopot. calcs. 78−23069
metal, liquid, resistivity at MP, general model pseudopot. method 77−55508
metal, Mossbauer isomer shift, pseudopot.-Born-Oppenheimer theory development 78−2775
metal, normal and magnetic, temp. depend. of plasma freq. 78−56100
metal, plasmon dispersion, effect of band struct., dielec. function calc. 78−26825
metal, positron density distribution, temp. effects 78−47739
metal, pseudopotential theory, completely OPW method and orthogonalised hole conception *(Russian)* 77−62792
metal, simple, cohesive energy, many-electron correl. 77−51393
metal, simple, long-wavelength plasmon width, pseudopot. theory 77−11864
metal, simple, vacancy and divacancy form. energies and divacancy binding energy 77−35554
metal, surface energy calc. in model of discrete positive charge *(Russian)* 78−38911
metal, valency electron density and total energy, weak pseudopotential calc. *(German)* 77−59241
metal, work function, pseudopot. calc. 80−96970
metal surface electronic struct., linear response theory, appl. to Na 78−56197
metal-diamond interface, Schottky barrier theory, ionicity depend. 78−52086
metallic glasses, stability, microscopic calcs. 79−32914
metallic glasses, structure and formation, thermodynamic props., cluster relaxation approx. 80−54143

pseudopotential methods continued
metallic radii, of group I, II, III and IV elements, rel. to ionic radii, based on pseudopotential method 79−86738
metals, binding energy using pseudopot. method 79−60749
metals, cohesive properties, energy density functional-pseudopotential method 79−73462
metals, compressibility local pseudopot. approach 80−65129
metals, compressiblities, general pseudopotential approach 80−54631
metals, cubic, monovacancy resist. using pseudopot. models 80−29378
metals, cubic, vol. depend. contrib. to elastic consts., pseudo-pot. theory 77−72646
metals, effect of alloying on Fermi surface and Dingle temp. 77−47719
metals, energy-independ. model for elec. cond., second order elastic consts. and phonon spectra 77−62890
metals, free electron approx. and symm. Hermitian pseudopot. *(Russian)* 79−28263
metals, Gruneisen parameters, interatomic forces, pseudopot. calc. 80−44165
metals, HCP, vacancy and interstitial config. 79−65071
metals, lattice dynamics and three body interaction 78−10139
metals, liquid, electron transport nonlocal pseudopot. calc., appl. to Cd 77−1404
metals, monovalent, mechanical ideal strength, pseudopot. model calcs. 79−77670
metals, pseudopotential study of electronic props. 80−20149
metals, simple, binding energy, compressibility, interionic pot. and transition temp. 79−46598
metals, simple, elastic moduli, chem. trends, pseudopot. method 80−107355
metals, simple, interion interaction and interion force constants, effective pots. in nonlocal pseudopot. method *(Russian)* 78−22684
metals, simple, static props., Thomas-Fermi-pseudopotential approach 80−75514
metals, small-core approx. and structural phase stability 79−99498
metals and alloys, pseudopotential investigation of phys. props. 77−43526
methanol, H bonding, electronic struct., geometries, moments, dimerisation energies, charge distrib., pseudopotential calcs. 80−27942
methyl halides, mol. force fields, IR intensities, and vibr. props. 80−47879
migration energies of point defects, in pure metals and dilute alloys, calc. 78−47572
mixed crystal, disorder scatt. theory using model pseudopot. 77−15811
molecular calculations, use of pseudopots. 79−31384
molecular calculations applications, reliability 79−31367
molecular consts., di and triatomic mols., mol. model pot. calcs., SCF approx. 77−65420
molecular core energy levels, pseudopot. calcs. *(French)* 79−49935
molecular ions, negative, polar, thermally stable 79−7033
molecular models of condensed systems and interfaces *(German)* 80−20062
molecular spinors from the quasi-relativistic pseudopotential approach 79−97963
molecules, pseudopot. theory calcs. of electronic struct. 77−42230
molecules of rows 1-3, equilib. geometries, orbital energies, ab initio rel. to pseudopot. calcs. 78−82613
multivalley semiconductor, donor binding energies calc. 78−23041
nearly free electron metal surface, at. chemisorption 78−14588
noble metal, electron-ion interaction, model pseudopot. 78−34785
noble metal, proton diffusion, config. and activation energies 79−37878
noble metal based, disordered alloys, dil., virtual bound states, reson. model pot. theory 79−23934
noble metal dilute alloy, residual resist. calc. 77−28156
noble metal lattice dynamics, pseudopotential method, Cu, Ag phonon spectra 77−89508
noble metals, electronic properties, form. factors, phonon freq. and elastic consts. 77−4168
noble metals, Krasko-Gurskii model potential, test of validity for Cu 80−39485
noble metals, pseudopot. exam. of electronic props. 78−51960
nonideal plasma theory, using Hellmann pseudopotential 78−75260
nonparametrised, for Hartree-Fock-Slater calcs. 77−57859
nontransition metals, binary alloying tendencies 78−2261
nontransition metals, calculated contribs. to elec. field gradients 78−39079
nontransition metals, electron density, bulk and surface props. relation 80−103609
norm-conserving pseudopots. 80−14066 .
nucleic acid bases, Zn^{2+} binding, ab initio SCF (pseudopot.) calcs. 80−12052
one-dimensional conductors, Peierls instability, dynamics, structural energy, pseudopot. calc. 80−54676
one-dimensional periodic system, energy spectrum of defects, pseudopot. approach *(Russian)* 80−59909
Phillips-Kleinmann pot. derivation, many-valence-electron mols., appl. I_2 77−65418
phonon dispersion calc., dielectric screening theory, closure approx. 79−77700
phonon spectra calcs., exact normalization of single OPW conduction electron states 77−7803
photoemission, angle-resolved, from bulk bands of solids 79−4895
polar molecules, electron affinities, ab initio calcs., dipole moments 79−89623
polar semiconductor, conduction states, pseudopot. and tight-binding calcs. 80−24785
polar semiconductor, impurity pseudopotential screening 79−15121
positronium, formation in positron+alkali metal atom collisions, first Born approx. 80−83525
positronium formation in positron+alkali metal atom collisions, pseudopot. calcs. 80−83524
quantum chemistry course problems using model pseudopots. 79−30165
α-quartz, valence electron states and X-ray emission spectra, pseudopot. and OPW calcs. 77−35866
α-quartz, valence electron states calc. by pseudopotential method 77−20239
α-quartz electron states, self-consistent pseudopot. calc. 77−62823
rare earth metal, lattice dynamics and scatt. reson. 78−59872
relativistic model pseudopot. yielding mag. model pseudopot. and effective Hamiltonian 80−29299
relativistic norm-conserving pseudopotential 80−70584
pseudopotential methods continued
relativistic pseudopotential theories and corrections to Hartree-Fock method 80−63523
reliability criteria, for pseudopot. approaches to molecule, solid and surface electronic struct. 80−49563
resistivity of grain-boundary joint by pseudopot. method *(French)* 79−51539
Schottky barrier theory at jellium-semicond. interface, role of ionicity, pseudopot. method 77−47888
self consistent pseudopot. method with Gaussian orbitals, appl. to Si band struct. 79−90928
self-consistent atomic pseudopotential, appl. to band struct. determ. 80−59846
semiconductor, dynamical effective charges, pseudopotential calc. 78−30881
semiconductor, multiband calcs. of effective masses 77−51644
semiconductor band structure under high stress, nonperturbative calc. 78−10344
semiconductor heterojunctions, discontinuities predicted from bulk band structs. 77−20409
semiconductor solid soln., bending parameters calc. by pseudopot. method 78−26813
semiconductor surface electron states, calc. based on chemical pseudopotential 77−69393
semiconductor-metal interface, electronic struct. self-consistent pseudopot. method 77−20428
semiconductor-vacuum interface, electronic struct. self-consistent pseudopot. method 77−20428
semiconductors, amorphous, chem. bonding, struct., pseudopot. theory *(German)* 78−30581
semiconductors, amorphous, liquid, glassy, random field parameters and pseudopotential calc. 80−29316
semiconductors, optical props. above band edge, book contrib. 80−84425
semilocal technique, testing of arbitrariness and limits 80−91446
short range atomic order, size effect in electron theory, static conc. waves approximation *(Russian)* 78−39049
short range order, many electron effects 78−79954
short-range order, electronic theory 77−80717
short-range order, size effect in electronic theory *(Russian)* 77−15339
Simons-type model potentials, mol. calcs. appls. 78−5120
simple liquid metals, elec. resist. and thermoelec. power calc. 77−76788
simple metals, electronic charge density, OPW-based pseudopot. calc. 78−87896
simple metals, model pseudopot. appl. to various props. 80−59845
simple metals, pseudopot. theory of k-depend. plasmon line width 77−85169
simple metals, solid and liq., electronic struct., mag. susceptibilities calc. 78−52204
simple metals, volume forces 80−15178
single metals, monovacancy formation parameters, temp. depend., pseudopot. theory 78−75658
smooth analytical model potential for positive ions 77−35844
solid solution, deform. interaction of interstitial atoms, pseudopot. calc. *(Russian)* 78−18636
solid solution, dilute, residual resistance, pseudopotential calc. *(Russian)* 79−33276
solid with thermal or static disorder, one electron props. 79−37957
solids, total energy calcs., momentum space formalism 80−15468
solitons, geometrical interpretation from generation of eqns. solvable by pseudopotentials 78−24684
spherical system, relativistic pseudopotential 78−82653
spin-dependent correlated atomic pseudopotentials 80−107686
steel, austenitic stainless, Mn-N interaction, internal friction obs. 78−84883
structural pseudoion form factors 77−62617
superconducting transition temp., electron-phonon mass enhancement, pseudopot. calcs. 78−2604
superconducting transition temperature, of simple metals 79−99650
superconductivity, pseudopotential, Bragg planes, effect on superconducting pairing and crit. temp. 80−15648
superconductivity theory, HF cut offs of Coulomb interaction, real freq. Coulomb pseudopotential derivation 80−49980
superconductor, Gaspari-Gyorffy theory, non-local extension 78−80093
surface and interface calcs. 80−49853
ternary semiconductors, defect tetrahedral crystals band structure 77−11850
Tomonaga model, correlation function 77−1342
transition metal, adsorption of CO, electronic struct., localised orbital pseudopot. method 80−39653
transition metal, lattice dynamics and scatt. reson. 78−59872
transition metal, model potential, generalised APW formulation 78−91579
transition metal impurities in transition and noble metal hosts, electronic struct. 78−75990
transition metal-carbonyl cluster molecules, electronic struct., localised orbital pseudopot. method 80−39653
transition metals, local pseudopotential theory 78−30863
transition metals, partial resonance, Hubbard's theory of phase shifts 79−28264
trihalide anions, VB pseudopot. calcs. on electronic states 77−26984
tryptamine, near ab initio and pseudopotential calcs. 77−71749
twin and stacking fault energies 79−38018
vacancy, self-consistent electronic states 80−29354
vacancy model theory, melting temperature-av. energy of interaction correl. 79−28080
valence-shell MO calc. with pseudopot. 78−907
Veljkovic Slavic model, modified, appl. to Si, Ge, Sn 79−56121
void formation energy, pseudopot. calc. 77−68961
Xα method with pseudopotentials 80−83282
zinc blende-type semiconductors, interstitial PDs, electronegativity diff. and effective ionic charges 77−76766
zincblende compounds, (111) face, dangling bond surface state 78−84278
α-$ZnIn_2S_4$, and related polytypes, electron band struct. 79−51485
NN interaction, coupling const. singular points for approx. Bethe-Salpeter eqns. with a nonlocal pseudopotential 78−25062
Ag (110), electroreflectance, surface state contrib. 80−80755
Ag, electronic contribution to thermal cond. at low temps. 79−95384
Ag, mag. susceptibility, Animalu model pot. calc. 80−75711
Ag, model pseudopotential method for phonon dispersion 79−23685
Ag, nonlocal model pseudopotential 78−14659

pseudopotential methods continued
Ag, phonon dispersion, binding energy, compressibility, pseudopot. calc. 77−4164
Ag, phonon limited elec. resist., temp. depend. 80−24876
Ag, pseudopot. optimised form for phonon dispersion study 80−10611
Ag-Au(Cu), residual elec. resist., pseudopot. calc. 80−6813
α-Ag-Zn, atomic short-range order determ., X-ray scatt. and pseudopot. calc. 78−2067
α-Ag-Zn, short-range order calc. *(Russian)* 77−43175
Al alloys, dil., depend. of electron scatt. rate on lattice relax. 77−69311
Al, dielectric function pseudopot. theory, vol. plasmon dispersion 79−23917
Al, dynamic susceptibility, model pot. theory 80−75710
Al, elastic consts., third order, pseudopotential calc. by method of homogeneous deformation 80−29106
Al, electronic Gruneisen parameter in shock Hugoniot eqn. of state 80−10635
Al, empirical pot. methods, use of Wedepohl pot., vacancy form energy 80−39230
Al, energy and elastic constants 80−59435
Al, Fermi surface under homogeneous strain, local pseudopot. model 80−29308
Al, Gruneisen coeff. depend. on specific volume, phonon spectra calcs. 79−65165
Al, impurities heat of solution, pseudopot. calc. 77−51393
Al, impurity low-field galvanomag. coeffs., 4 OPW calcs. 77−69304
Al, K X-ray absorption, K-emission spectrum, band struct. using APW method 80−97380
Al, lattice thermal cond. at low temps., Ashcroft pseudopotential method 80−19897
Al, liq., radial distrib. function calc., pseudopot. method *(Russian)* 79−19138
Al, liq., thermodynamic props., pseudopot. calc. *(Russian)* 79−46549
Al, liquid, dynamical struct. factor calc. 80−64880
Al, liquid, electron momentum density, correlations and ionic potentials 78−60052
Al liquid, molecular dynamic simulation of static and dynamic structural factors *(Russian)* 79−69005
Al, model pseudopotential 78−91582
Al, monovacancy thermodynamic parameter calcs., temp. dependence 78−2114
Al, plasmon dispersion, effect of band struct., dielec. function calc. 78−26825
Al, polycryst., anisotropy of plasmon dispersion, pseudopotential method 78−23039
Al, pseudopot. band struct. calc. 79−56119
Al, singular struct. in density of levels 79−77997
Al, solid, binding energy and compressibility 79−99650
Al, symmetrical high-angle tilt boundary energy calcs. 77−27892
Al:H, impurity energies and geometrics, self-consistent jellium calc. 79−99507
Al:He, pseudopotential calc. of screening of He atom 78−51917
Al-Ge(Mg)(Zn)(Ga), dil., electronic transport coeffs. for point defect scatt., 4-OPW calc. 79−42531
Al-Mg, determ. of distortion field, induced by substitutional defect 80−44536
Al-Mg, dil., form of distortion field produced by Mg substitution, pseudopot. calc. *(German)* 79−42092
Al-Mg, dil. alloy, residual resistivity, model pseudopot. form factors 77−8062
Al-Mg, liquid alloy energy of soln. pseudopotential calcs. *(Russian)* 79−66330
Al-Zn (10 at.%), short-range order parameter calc. in pseudopot. approx. *(Russian)* 80−49183
AlAs-GaAs (110) interface, self-consistent calc. of interface states and electronic struct. 78−52066
AlAs-GaAs abrupt (110) interface, electronic struct. 78−95339
AlCl, pseudopot. calcs. 80−91446
AlF, pseudopot. calcs. 80−91446
$Al_xGa_{1-x}As$, energy band struct. calc. 78−23019
AlH, pseudopot. calcs. 80−91446
AlH, valence excited states, pot. curves 78−41973
Al_cMg_{1-c} liquid alloys, vols. and entropies of mixing, calc. 80−75363
AlN, (^4P)Al-(^4S)N, (^2P)Al-(^2D)N, nonempirical pseudopotential, configuration interaction calcs. 79−93930
Ar, photoemission angular distribution, atomic pseudopotentials for soft X-ray excitations 77−23478
Ar, solid, self-trapped exciton, pseudopotential method 79−82529
Ar, valence electron distrib., pseudopotential calcs. 80−2335
As, amorphous, electronic struct. of defects using cluster-Bethe-lattice method 79−73471
As, band structure and cryst. energy, pseudopot. calc. 79−90954
As, band structure on Jones zone boundary, pseudopot. calc. 80−54603
As, cryst. struct. calc., pseudopot. expansion method 77−27848
As, pseudopotential, self-consistent, band struct. 78−84141
As, rhombohedral, electronic struct. and optical props. var. with internal displacement parameter 79−60702
As, struct., pseudopotential method calcs., using untruncated pot. 78−18582
Au (110), electroreflectance, surface state contrib. 80−80755
Au, local pseudopotential, phonon frequencies, binding energy and liq. metal resist. calc. 77−20216
Au, mag. susceptibility, Animalu model pot. calc. 80−75711
Au, model pseudopotential method for phonon dispersion 79−23685
Au, nonlocal model pseudopotential 78−14659
Au, phonon dispersion, binding energy, compressibility, pseudopot. calc. 77−4164
Au, phonon limited elec. resist., temp. depend. 80−24876
Au, pseudopotential, fitted to elastic data 78−75705
Au-Cu, residual elec. resist., pseudopot. calc. 80−6813
BN, electronic energy band struct., X-ray spectra, pseudopotential calcs. 79−78008
Ba-Cd system, short-range order calc. *(Russian)* 79−23566
Be, magnetic suscept. anomalous temp. depend. *(Russian)* 79−4650
Be metal, electron distribution and momentum density, Compton scatt. 80−11502
Be, twin and stacking fault energies 79−38018
Be, twin boundaries, computer simulation 80−39109
Be:Li, ion-implanted, interstitial props. 79−37876
BeO, F-centre exam., pseudopotential calc. 78−43328
Bi, band struct., temp. and press. depend. 78−18955
pseudopotential methods continued
BiI_3, band struct., empirical pseudopotential calc. 77−15766
CO, core pseudopot. valence electron calc., orbital energy and bond length 79−72233
CO, Hartree-Fock-Slater calcs., using pseudopot. method 77−57859
CS, core pseudopot. valence electron calc., orbital energy and bond length 79−72233
CaF_2, electronic energy bands calc. 78−34762
$CaMg_2$, phonon spectra 77−20031
CaO, electronic band struct., combined tight-binding and pseudopot. approach 77−47728
Cd, de Haas-van Alphen effect under press., Fermi surface and pseudopot. form factors 77−43475
Cd, magnetic susceptibility, temp. depend., electron-phonon interaction effects 79−61046
Cd, nuclear quadrupole interaction theory using first-principles pseudopotential 79−73482
Cd, phonon spectra and eqn. of state, pseudopot. method *(Russian)* 77−24367
Cd, spin-orbit interac. contrib. to mag. susceptibility of interacting electrons 77−63084
Cd, temp. depend. Knight shift 80−2655
Cd, twin boundaries, computer simulation 80−39109
Cd_3As_2, energy band structure calc. 80−75504
Cd_3As_2, inverted band struct. 79−90958
$Cd_3(As_xP_{1-x})_2$, $0 \leq x \leq 1.0$, band struct. calc. near Brillouin zone centre 80−107703
CdF_2, electronic band struct., combined tight-binding and pseudopotential calc. 77−43495
CdF_2, electronic energy bands calc. 78−34762
$CdGa_2(S_{1-x}Se_x)_4$ solid solns., band struct. behaviour w.r.t. comp. *(French)* 80−107699
$CdGa_2S_4(Se_4)$, band struct., pseudopot. method 80−92816
$Cd_{1-x}Hg_xGa_2S_4$ solid solns., band struct. behaviour w.r.t. comp. *(French)* 80−107699
$CdIn_2S_4$ cubic spinel, electronic band struct. and chem. bonds 78−34768
α-$CdIn_2Se_4$, defect zincblende struct., electronic props. 77−15767
$Cd_{1-x}Mg_x$, energy spectrum pseudopotential calcs., mag. props., impurity scatt. *(Russian)* 80−65430
Cd_3P_2, energy band structure for real $D_{4h}{}^{15}$ symmetry 79−56124
$CdSiP_2$, pseudodirect chalcopyrite semicond., electronic band struct. 80−20079
$CdSnP_2$, optical props., band struct. calcs., real space atomic potential parameters 79−95325
Cl_2, Hartree-Fock-Slater calcs., using pseudopot. method 77−57859
Cl_2, pseudopot. calcs. 80−91446
Cl_2, pseudopot. theory calcs. of electronic struct. 77−42230
^{35}Cl, nucl. mag. screening in ClH, pseudopot. calcs. 79−6879
Co-Os, short-range order parameters, ordering energy on first coordination sphere *(Russian)* 79−69058
Cr-Ge liquid and amorphous alloys, struct. props., cond., viscosity, surface tension *(Russian)* 80−54119
Cs, absolute zero isotherms and polymorphic transition 79−73310
Cs halides, F-centre energy levels, ion-size effects, calc. 80−96519
Cs phonon freqs. and Gruneisen parameter, model pseudopotential calc. 77−35643
Cs, phonon spectral density, pseudopotential calcs. 80−39234
Cs, relativistic model pseudopot., appl. to elec. resist. calc. in liq. phase 78−51866
Cs, structural energies, pseudopotential formalism 80−39519
$Cs_{2,2}^+$ pot. energy curve, pseudopot. calc. 77−6703
Cs_2^{2+}, interaction potential determ., comparison between all-electron frozen core and psuedo-potential results 80−69054
CsH^+, Σ state pot. energy, Hellman pseudopot. calcs. 78−70764
CsI:Na, electronic struct. and luminesc. 80−16080
Cu (110), electroreflectance, surface state contrib. 80−80755
Cu, dynamic susceptibility, model pot. theory 80−75710
Cu, electronic contribution to thermal cond. at low temps. 79−95384
Cu, energy band calc. by model-pseudopotential method 79−7779
Cu isoelectronic series, hard-core pseudopotentials and struct. maps 80−44168
Cu, Krasko-Gurskii model potential, test of validity 80−39485
Cu, liq., effective interionic interaction *(Russian)* 77−84622
Cu, mag. susceptibility, Animalu model pot. calc. 80−75711
Cu, model pseudopotential method for phonon dispersion 79−23685
Cu, nonlocal model pseudopotential 78−14659
Cu, phonon limited elec. resist., temp. depend. 80−24876
Cu-Al, short range order and static distortion contribution to residual elec. resistivity *(Russian)* 80−70672
Cu-Al (15 wt.%), residual resistivity, influence of short range order and size effect *(Ukrainian)* 79−99528
Cu-Au, elec. resist., pseudopot. calc. *(Russian)* 78−2460
Cu_2, bonding, ab initio pseudopot. calcs. 79−6857
Cu_2NiZn, atomistic approach to ordering 79−94944
Cu_2NiZn, boundary energies by effective interatomic potential methods 79−65082
Cu(111) surface 77−62979
F_2, pseudopot. calcs. 80−91446
$F(^2P_{1/2})+H^+(Xe)$, nonadiabatic collision processes, electronic degrees of freedom, classical model 79−64062
Fe, valence electronic struct., pseudopot. method 79−68184
Fe^{n+}, valence electronic struct., pseudopot. method 79−68184
Fe-Al, residual elec. resist., contrib. from static lattice distortions and short-range parameters *(Russian)* 79−51548
Fe-Ni(Cu)(Al)(Si) liquid alloys, thermodynamic characts. calc. *(Russian)* 80−15264
FeH^+, valence electronic struct., pseudopot. method 79−68184
GE, microscopic inverse dielec. matrix, local field correction and acoustic sum rule 77−84863
(Ga, Al, As) heterostructures and compounds, electronic props., empirical pseudopot. calc. 80−80366
Ga, de Haas-van Alphen effect, expt. and interpretation 78−84132
Ga, vacancy equilib. config., pseudopot. estimation 77−39582
Ga-GaAs heterojunctions, electronic struct., tight-binding and pseudopot. models 79−42633
$Ga_{0.5}Al_{0.5}As$, heterostructure, band struct. calc. 79−1570
$Ga_{1-x}Al_xP$, bending parameters calc. by pseudopot. method 78−26813
GaAs (110), self-consistent pseudopotential calcs., electronic struct. and atomic co-ords. 80−49848
GaAs (110) relaxed surface, electronic states 79−51649

pseudopotential methods continued
GaAs (110) surface, electronic struct., pseudopot. calc., surface relax. model 80−29456
GaAs, energy bands and wavefunctions, localised orbital description 78−18942
GaAs:O, effect of displacement upon impurity levels, psuedopotential calc. 77−39803
GaAs-AlAs and related monolayer heterostructures, pseudopot. calc. 78−60198
GaAs-AlAs mixed crystals, valence charge distrib. and elec. field gradients 80−80239
GaAs-$Ga_{1-x}Al_xAs$ repeated monolayer heterostructure, electronic struct. 77−66197
GaAs-GaSb, threshold energies for impact ionisation by electrons and holes 78−6390
GaAs-ZnSe (110) interface, electronic struct., self-consistent calc. 79−95486
$(GaAs)_n$-$(AlAs)_n$, multilayer heterostructure, band struct. calc. 79−1570
$GaAs_{1-x}P_x$, bending parameters calc. by pseudopot. method 78−26813
GaP, electronic structure of neutral phosphorus vacancy, empirical pseudopotential 79−78042
GaP, localised states in presence of P vacancy, pseudopot. calc. 78−18992
GaP:O effect of displacement upon impurity levels, pseudopotential calc. 77−39803
GaP:N, electron binding by N pairs 79−90990
GaP_xAs_{1-x}:N, impurity electron states, binding energies and wavefunctions 79−42488
GaSe polytypes, electronic band struct. calcs. 77−51650
Ge, Compton profile anisotropy, pseudopot. calc. 79−28854
Ge, electronic and struct. props., nonlocal pseudopot. calc. 80−34349
Ge, energy bands and wavefunctions, localised orbital description 78−18942
Ge, lattice stability, pseudopot. theory and problem of covalent bonding 77−55490
Ge, nonlocal pseudopotentials 77−11848
Ge, Schottky barrier, electronic struct., pseudopot. calc. 78−95364
Ge Schottky barrier, electronic struct., pseudopotential method, jellium model 79−38162
Ge, surface electron states, relaxed (111), self consistent pseudopot. calc. 77−47880
Ge, surface electronic struct., self consistent pseudopotential calc. 78−47842
Ge:H, interstitial impurity levels, pseudopot. calc. 80−44533
Ge-GaAs (110) interface, relax., self-consistent pseudopotentials 78−30981
Ge-GaAs (110) interface, self-consistent calc. of interface states and electronic struct. 78−52066
Ge-GaAs (110) junction, interface states and electronic struct. 77−69408
Ge-GaAs abrupt (110) interface, electronic struct. 78−95339
Ge-Si, phase diagrams near melting point, Helmholtz free energy, heat of solution 80−70379
Ge-ZnSe abrupt (110) interface, electronic struct. 78−95339
GeS, angular resolved UV photoemission and band structs. 77−85144
H, excited states, pseudopotential calcs., teaching approach 79−84893
H_2, ionic-covalent config. mixing, pot. curves 77−34576
H_2, metallic, solubility of He, Gibbs energy, fluid state model, He conc. in giant planets 79−60602
HCl, pseudopot. calcs. 80−91446
HF, potential curve calc. using angular momentum depend. of pseudopot. 77−30804
HF, pseudopot. calcs. 80−91446
H_2O, H bonding, electronic struct., geometries, moments, dimerisation energies, charge distrib., pseudopotential calcs. 80−27942
H_2O, pseudopotential calculations, parameter fitting scheme appls. 78−41928
H_2S, pseudopotential calculations, parameter fitting scheme appls. 78−41928
^{4}He film, Bose-Einstein condensation, thermodynamic functions 79−82399
^{4}He, superfluid, excitation spectrum, RPA calc. involving simple pseudopot. 80−92738
Hg+Cs(K)(Na)(Rb), scatt. cross-sections, pseudopot. calcs. 78−9225
Hg_2, pseudopot. theory calcs. of electronic struct. 77−42230
$HgGa_2Se_4$, energy band struct. calc., empirical pseudopot. method 80−24793
HgH, pseudopot. theory calcs. of electronic struct. 77−42230
I_2, band system, MC SCF pseudopot. calcs. 78−78632
I_2, vertical valence excited states, CI nonempirical pseudopotential calc. 77−71757
In, lattice dynamics, pseudopot. computation *(Russian)* 80−92617
InAs-GaSb (100) superlattice, electronic struct., self-consistent pseudopot. method 80−49884
InAs-GaSb superlattice, electronic struct., self-consistent pseudopot. calc. 80−29470
InP, electronic structure of neutral phosphorus vacancy, empirical pseudopotential 79−78042
InSb, at Γ-point, spin depend. wave functions and band parameters 77−72818
InSb, semiconductor, Brillouin zone spin dependent wave functions calcs. 79−56126
InSe, layer semicond., electronic props. 79−28275
InSe, three-dimensional band structure 80−24799
β-In_3Sn, band struct. and Fermi surface calc. using model pseudopot. 77−28103
$In_{0.69}Tl_{0.31}$, supercond. transition temp., specific heat, pseudopotential form factor 80−97026
K, absolute zero isotherms and polymorphic transition 79−73310
K, atomic, smooth pseudowavefunctions calc. 77−43542
K, binding energy and equilib. struct., pseudopot. calc. *(Russian)* 79−47037
K, elec. resist., effect of energy depend. of electron relax. time 77−69296
K, electrical and thermal resistivity determ. from first principles 79−69493
K, Fermi surface distortion 80−2325
K, interatomic function from phonon-dispersion curves and Heine-Abarenkov-Shaw optimised model pot. 79−19185
K isoelectronic series, hard-core pseudopotentials and struct. maps 80−44168
pseudopotential methods continued
K, liquid, interionic interaction theory, pseudopotential calcs. *(Russian)* 80−79675
K, mechanical ideal strength, pseudopot. model calcs. 79−77670
K, mode Gruneisen parameters, calc. 77−4180
K, phonon frequencies, normal mode Gruneisen parameters, pseudopot. calcs. 79−42184
K, phonon spectral density, pseudopotential calcs. 80−39234
K, solid, dynamical structure factor S(Q, ω), molecular dynamics simulation 77−7806
K, structural energies, pseudopotential formalism 80−39519
K, thermopower, high temp., first principles calc. 79−65447
K-Rb, liq., form factors and transport coeffs., pseudopot. perturb. theory 80−44561
K-Rb(Cs), liquid, resistivity calc. using general model pseudopot. 77−55506
K+He, 4^2P state $j_1m_1 \rightarrow j_2m_2$ Zeeman transition, total cross section energy depend. 80−83475
K_2^+, pot. energy curve, pseudopot. calc. 77−6703
KCl, F-centre, wave functions and spin densities, pseudopot. calc. 79−4533
KCl, F-centre hyperfine interaction parameters, press. shifts 77−8043
KCl, press. shifts of F-centre hyperfine interaction parameters 78−79957
KCl:Na, F_B centre energy levels 80−107738
KCl(Br)(I), electronic struct. of self-trapped excitons calc. 77−39784
K_7Cs, Laves phase, chemical bonding, electronic charge density distrib. pseudopotential calcs. 79−77549
K_7Cs_6, μ-phase variant, chemical bonding, electronic charge density distrib. pseudopotential calcs. 79−77549
KH^+, Σ state pot. energy, Hellman pseudopot. calcs. 78−70764
K_3Sb, and Na_2KSb, photocathode materials, band struct., empirical pseudopotential calc. 78−10346
K_3Sb, optical and dielectric props., energy spectra, density of states calcs. 80−20083
Kr, 4p asymmetry parameter and cross section photoelectron energy depend. pseudopot. method 78−9130
Kr, solid, self-trapped exciton, pseudopotential method 79−82529
Li, atomic, smooth pseudowavefunctions calc. 77−43542
Li, binding energy and atomic radius calc., effect of nonlocalised charact. of pseudopot. *(Russian)* 78−18575
Li, binding energy and equilib. struct., pseudopot. calc. *(Russian)* 79−47037
Li, energy and elastic constants 80−59435
Li, impurity and conduction electron scatt. at 4.2K *(Russian)* 77−35931
Li, interatomic function from phonon-dispersion curves and Heine-Abarenkov-Shaw optimised model pot. 79−19185
Li isoelectronic series, hard-core pseudopotentials and struct. maps 80−44168
Li, isoelectronic series, model potential field, pseudopotential calcs. 79−59339
Li isoelectronic series, relativistic pseudopot. appl. in HF calcs. 80−27960
Li, liq., elec. resistivity and thermoelec. power, orthogonalisation hole pseudopotential calc. 80−29376
Li, liq., temp. and density depend. of struct., improved pseudopot. theory 79−14669
Li, martensitic phase transitions, and phase diagrams at moderate press. 78−72775
Li, mechanical ideal strength, pseudopot. model calcs. 79−77670
Li, phonon limited resistivity struct. depend., Umklapp scatt., elastic consts. 80−88532
Li, phonon spectral density, pseudopotential calcs. 80−39234
Li, photoionis., one-electron pseudopotential calc. 79−18166
Li, plasmon linewidth, k-dependent, anomalous behaviour explanation, interband transitions 78−47721
FCC-Li, symmetrical high-angle tilt boundary energy calcs. 77−27892
Li to Ne, coreless Hartree-Fock pseudopotential method 79−68188
Li, twin boundaries, computer simulation 80−39109
Li+He(Ne), inelastic collisions, Baylis-Gombas pseudopot. appl. 77−58151
Li_2, floating spherical Gaussian orbital, Hartree-Fock-Roothaan and pseudopot. calcs., comparison 78−46262
LiAl, pseudopotential method and ordering problem 77−35500
LiCl, press. shifts of F-centre hyperfine interaction parameters 78−79957
LiH_2F hypothetical crystal, existence, total energy calc., pseudopot. calc. 78−2442
LiNa, ground and excited states, model pseudopot. calcs. 77−75069
LiTl, pseudopotential method and ordering problem 77−35500
Mg, phonon spectra and eqn. of state, pseudopot. method *(Russian)* 77−24367
Mg, twin and stacking fault energies 79−38018
Mg, twin boundaries, computer simulation 80−39109
Mg:H, impurity energies and geometrics, self-consistent jellium calc. 79−99507
Mg-Al, dil. alloy, residual resistivity, model pseudopot. form factors 77−8062
Mg-Cd, thermodynamic props., order-disorder transitions based on Helmholtz free energy 79−37853
Mg-In dil. alloys, effect of alloying on Fermi surface, pseudopot. model 77−76733
Mg-Li dil. alloys, effect of alloying on Fermi surface, pseudopot. model 77−76733
MgO, electronic band struct., combined tight-binding and pseudopot. approach 77−47728
MgO, valence electron distrib., pseudopotential calcs. 80−2335
Mg_2Si, valence band density of states, pseudopot. calc. 78−72067
$MgZn_2$, struct. exam. using Shaw's model potential calc. 77−19906
$Mg_{70}Zn_{30}$ metallic glass, struct. and dynamics 79−37632
Mo (001), self consistent electronic struct., pseudopotential calcs. 79−42606
Mo (001) surface with saturated H adsorption, band structure self-consistent calc. 80−15585
Mo, binding energy, lattice parameters bulk modulus, self-consistent pseudopot. calc. 79−60748
Mo, electronic and struct. props., nonlocal pseudopot. calc. 80−34349
Mo, electronic props., first-principles nonlocal pseudopot. approach 79−95319
Mo-W system, short-range order calc. *(Russian)* 79−23566
Mo(001), H chemisorbed, self-consistent electron struct. 80−44693

pseudopotential methods continued
Mo(001) surface, electronic struct., self-consistent pseudopot. calcs. 78−76128
Na (001) surface electronic struct., linear response theory 78−56197
Na, atomic, smooth pseudowavefunctions calc. 77−43542
Na, binding energy and equilib. struct., pseudopot. calc. *(Russian)* 79−47037
Na, electrical and thermal resistivity determ. from first principles 79−69493
Na, equilibrium struct. and phys. props., pseudopot. method 80−96778
Na, Fermi surface distortion 80−2325
Na, interatomic function from phonon-dispersion curves and Heine-Abarenkov-Shaw optimised model pot. 79−19185
Na isoelectronic series, hard-core pseudopotentials and struct. maps 80−44168
Na, linear potential and phonons 79−82293
Na liquid, interionic interaction theory, pseudopotential calcs. *(Russian)* 80−79675
Na, martensitic phase transitions, and phase diagrams at moderate press. 78−72775
Na, mechanical ideal strength, pseudopot. model calcs. 79−77670
Na, monovacancy thermodynamic parameter calcs., temp. dependence 78−2114
Na, phonon limited resistivity struct. depend., Umklapp scatt., elastic consts. 80−88532
Na, phonon spectral density, pseudopotential calcs. 80−39234
Na, photoionis., one-electron pseudopotential calc. 79−18166
Na, thermopower, high temp., first principles calc. 79−65447
Na-K, liquid alloy energy of soln. pseudopotential calcs. *(Russian)* 79−66330
Na-K(Cs), liq., form factors and transport coeffs., pseudopot. perturb. theory 80−44561
Na-K(Rb)(Cs), liquid, resistivity calc. using general model pseudopot. 77−55506
Na_2^+, pot. energy curve, pseudopot. calc. 77−6703
Na_n ($n \leq 8$), equilibrium geometries and ionization energies calcs. 80−1099
NaCl, F-centre, wave functions and spin densities, pseudopot. calc. 79−4533
NaCl, press. shifts of F-centre hyperfine interaction parameters 78−79957
NaCl, valence electron distrib., pseudopotential calcs. 80−2335
NaCl-type crystals, ionic polarisabilities, pseudopot. calc. 80−88913
NaF, F-centre, wave functions and spin densities, pseudopot. calc. 79−4533
NaH^+, Σ state pot. energy, Hellman pseudopot. calcs. 78−70764
NaK, ab initio and pseudopot. energy curves 78−90068
Na_3Sb, and Na_2KSb, photocathode materials, band struct., empirical pseudopotential calc. 78−10346
NaTl, pseudopotential method and ordering problem 77−35500
Nb (001) ideal surface, self-consistent pseudopot. calcs. 77−76894
Nb, (001) surface electron states 77−8167
Nb, band structure, self-consistent pseudopot. calc. 77−43487
Nb, optical properties and electronic props. 79−42439
Nb-H system, screening of H impurity and lattice distortion *(Russian)* 79−1577
Nb_3Al, band struct. and density of states from self-consistent pseudopotentials 79−69401
$Nb_3Al(Ge)$, bonding, electronic charge distribs. and struct. transform. from self-consistent pseudopotentials 79−69054
Nb_3Ge, band struct. and density of states from self-consistent pseudopotentials 79−69401
Ni, chemisorption of O(S)(Se)(Te), orbital energy spectrum of chemisorbed electrons 78−2542
Ni complex, nickel-bis-dithiolene, pseudopot. MCSCF and limited CI calcs. 80−83292
Ni compound, $[Ni_3(CO)_6]_n^{2-}$, n=1,2, one-electron states in polynuclear carbonyls 79−95358
Ni, phonon dispersion, model pseudopotential approach 77−11646
Ni, pseudopotential calculations, parameter fitting scheme appls. 78−41928
Ni-Os, short-range order parameters, ordering energy on first coordination sphere *(Russian)* 79−69058
Ni-Pt, short-range order parameter calc. in pseudopot. approx. *(Russian)* 80−49183
Ni-Ta(7 at.%), short-range order, pseudopot. calc. and diffuse X-ray scatt. *(Russian)* 77−28008
Ni_2, Hartree-Fock-Slater calcs., using pseudopot. method 77−57859
β'-NiAl, self consistent embedded cluster model for Fe, Co, Ni mag. impurities 80−2549
$Ni(CO)_4$, valence orbital energies, pseudopot. calcs. 78−37546
Ni_3Fe, short-range order parameter calc. in pseudopot. approx. *(Russian)* 80−49183
O, pseudopotential calculations, parameter fitting scheme appls. 78−41928
O_2, electronic struct., self-consistent pseudopot. calc. 80−9508
P, black, pseudopotential crystal-struct. stability calcs. as function of press. 79−60503
$POCl_3^+$, ion states assignments, from He I(II) XPS spectra comparison, pseudopot. calcs. 77−61794
Pb, electronic thermal Gruneisen parameters 80−39242
Pb, Fermi surface, uniaxial stress depend. 79−65362
Pb, liq., elec. resist., temp. depend., calc. 78−14701
Pb, liq., elec. resist. calcs., pseudopot. depend. 80−96840
Pb, pseudopot. band struct. calc. 79−56119
Pb, relativistic model pseudopot., appl. to elec. resist. and phonon spectra calc. 78−51866
PbO, appl. of effective pots. to relativistic HF calcs. of mol. props. 78−74559
Pd (111), electronic states calc. and adsorbate-induced photoemission struct. interpretation 78−60179
$Pd(CO)_4$, ab initio LCAO MO SCF results invalidate pseudopot. calc. 77−6675
$Pd(CO)_4$, valence orbital energies, pseudopot. calcs. 78−37546
Pd(111) chemisorption of H, photoemission spectra, SCF electronic struct. 79−33320
Pt compound, $[Pt_3(CO)_6]_n^{2-}$, n=1,2, one-electron states in polynuclear carbonyls 79−95358
Pt, phonon spectrum, Kohn anomaly 79−46766
$Pt(CO)_4$, valence orbital energies, pseudopot. calcs. 78−37546
Rb, absolute zero isotherms and polymorphic transition 79−73310
pseudopotential methods continued
Rb, interatomic function from phonon-dispersion curves and Heine-Abarenkov-Shaw optimised model pot. 79−19185
Rb, lattice dynamical props., conduction-core exchange, Lindgren approx. 79−1481
Rb, liq., static struct. and electronic transport props., pseudopotential calc. 79−7543
Rb, phonon freqs. and Gruneisen parameter, model pseudopotential calc. 77−35643
Rb, phonon spectral density, pseudopotential calcs. 80−39234
Rb, structural energies, pseudopotential formalism 80−39519
Rb_2^+, pot. energy curve, pseudopot. calc. 77−6703
RbH^+, Σ state pot. energy, Hellman pseudopot. calcs. 78−70764
$Rh_2Cl_2(CO)_4$, non-empirical pseudopot., PSIBMOL algorithm 79−76335
S, pseudopotential calculations, parameter fitting scheme appls. 78−41928
$(SN)_x$, electronic struct., X-ray and UV photoemission obs., OPW and pseudopot. calcs. 78−6832
$(SN)_x$, electronic struct. and opt. props. 78−6256
$(SN)_x$, polymeric, electronic structure, semi-empirical pseudopotential calc. 77−72812
SO, pot. energy curves, pseudopot. multi-struct. valence bond calcs. 78−9094
Sb, electronic band struct. changes due to plane straining effects *(Russian)* 80−54602
Sb, electronic struct., depend. on hydrostatic pressure 80−80158
Sb, electronic structure change with press., pseudopot. calcs. *(Russian)* 79−47006
Se, amorphous, defect states, SCF pseudopot. and tight-binding calc. 79−65415
Se, amorphous, electronic struct. and optical props., pseudopot. calc. 80−65428
Se, bonding coordination defects 80−59927
Se, charge density, self-constent OPW and pseudopot. calcs. 80−92813
Se, electronic struct. of cryst. phases and hydrostatic press. effects 80−59865
Se, glassy, structural excitation energies of defects, pseudopot. approach 80−107061
Se, trigonal, electronic props. under press. 77−31939
Se, trigonal, electronic struct., near metal transition, press. depend. 78−34758
Si, (001) (2×1) reconstructed surface, dimer model self consistent calcs. 80−88613
Si (111), with chemisorbed Al, electronic struct., self-consistent pseudopotential calc. 78−34880
Si (111) 1×1, chemisorption of Cl in surface vacancies 79−77910
Si (111) surface, Al overlayers, theoretical study 78−95366
Si (111) surface states, step depend., self-consistent pseudopot. calcs. 77−20384
Si (111) surface with Al overlayers, electronic struct., self-consistent pseudopotential method 79−4595
Si (111)-Cl(7×7), angle resolved secondary emission and electron energy loss study of electronic struct. 79−61477
Si (111)-1×1, electronic struct. of surface, model pseudopot. calc. 80−65651
Si, ab initio effective pots. 77−69222
Si, atoms, density functional theory, energy calcs., core effects 78−72106
Si, band structure, self-consistent pseudopotential *(Japanese)* 77−43491
Si, bulk and surface equlib. props., self-consistent pseudopotential calcs. 79−60750
Si, chemisorption of H on (111) 77−62743
Si, Compton profile anisotropy, pseudopot. calc. 79−28854
Si, covalent semiconductor, electronic response to high symmetry lattice vibr. 80−10619
Si, dielectric screening, microscopic theory, phonon dispersion, moment expansion calcs. 79−55839
Si, electronic and struct. props., nonlocal pseudopot. calc. 80−34349
Si, electronic energy levels strain depend., pseudopot. method 77−39775
Si, electronic struct., non-spherical local pseudopotential calcs. 80−39496
Si, electronic structure at high press. near semicond.-metal transition 80−49586
Si, electronic vacancy states by chemical pseudopot. method 79−23929
Si, energy bands and wavefunctions, localised orbital description 78−18942
Si, ground state props. in density-functional pseudopot. approach 80−92803
Si, lattice energy, pseudopotential calc. 78−23002
Si, lattice stability, pseudopot. theory and problem of covalent bonding 77−55490
Si, local pseudopotential, Gaussian band charge model 80−88477
Si, microscopic inverse dielec. matrix, local field correction and acoustic sum rule 77−84863
Si, neutral undistorted vacancy 78−91638
Si, nonlocal pseudopotentials 77−11848
Si, pseudopotential calculation of phonon dispersion curves 80−10620
Si, pseudopotentials for band struct. and cryst. energy calcs. 79−82514
Si, Raman cross section and its press. depend., theoretical study 79−91448
p-Si, Raman spectra, pseudopot. calc. of discrete-continuum interference 80−2747
Si, screening of ions, band struct. calcs. with screening variants 78−67938
Si, self-consistent pseudopotential cal. of electronic states associated with reconstructed vacancy 79−73465
Si, semiconductor charge densities with hard-core and soft-core pseudopotentials 79−33266
Si, structural props., self-consistent calc. 80−28947
Si, structural props. using electron-ion Hamiltonian using density-fundamental methods 79−82177
Si, structurally related bulk and surface props., self-consistent pseudopot. method 80−54632
Si surface, ideal and 2xl chain-reconstructed, electronic struct. determ. 78−52050
Si, total energy calcs. by r-space method, Wannier functions 80−88503
Si, valence band model, nonlocal exchange and correl. pot. 77−43492
Si, with non-spherical pots. for two basis atoms, electronic struct. 78−72069
Si:Ga(Zn), impurity ground states 79−28313
Si:H, interstitial electronic struct., self-consistent pseudopotential calcs. 79−73469

pseudopotential methods continued
Si_2, charge density and pseudo charge density, pseudopot. and SCF calcs. 78−70740
Si_2, density functional theory, energy calcs., core effects 78−72106
Si_2, pseudopotential charge densities calcs. 79−31367
Si_2, SCF Xα calcs. using pseudopots. and PW basis set 77−34558
$Si_{1-x}Ge_x$ system, lattice energy and consts., virtual cryst. approx., pseudopot. calc. 80−44166
SiO, core pseudopot. valence electron calc., orbital energy and bond length 79−72233
SiO_2, pseudopotential study of bonding and structure 78−75622
SiO_x, electronic struct., mixed-crystal and random-bonding models 79−65029
SiS, core pseudopot. valence electron calc., orbital energy and bond length 79−72233
Si(111) ideal and relaxed surface, electronic struct. 79−60901
Si;O, effect of displacement upon impurity levels, pseudopotential calc. 77−39803
α-Sn, lattice stability, pseudopot. theory and problem of covalent bonding 77−55490
Sn, white, band masses and deformation pots., OPW pseudopotential model 80−100430
SnS_2 (2H), band struct. press. depend. 78−43292
SnS_2, band struct., effect of polytypism 78−43293
SnS_2, conduction and valence band density of states 77−62817
SnSe, electron states anal. by pseudopotential method 77−66115
SnSe, electronic band struct. determ. 78−51890
^{119}Sn temp. depend. isomer shift, pseudopot. approach 80−84675
SrF_2, band struct. determ. 77−89700
Ta, electronic props. and reflectivity, iterative empirical pseudopot. calc. 77−76745
Ta, optical properties and electronic props. 79−42439
Te, amorphous, electronic struct. and optical props., pseudopot. calc. 80−65428
Te, electronic struct. of cryst. phases and hydrostatic press. effects 80−59865
Te, monoclinic, electronic states above high-press. phase transition 79−99476
Te, trigonal, electronic and optical props., press. depend., self consistent pseudopotential formalism 79−65838
Te, trigonal, electronic struct., near metal transition, press. depend. 78−34758
Te_4^{2+}, pseudopot. SCF-MO calcs., spectrum assignments 80−83269
Th, lattice dynamics in reson. model pseudopot. theory 79−19334
Th, local model pseudopotential applic. to lattice dynamics 77−39646
TiO_2, cond. and valence band struct., gap anisotropy 77−47729
α-U, lattice dynamics 79−95101
V, dynamic susceptibility, model pot. theory 80−75710
V, electronic density of states, effective mass, electron-phonon interaction, Coulomb pseudopot. *(Russian)* 78−26804
V, optical properties and electronic props. 79−42439
V-Rh alloys, short range atomic order exam. *(Russian)* 78−63696
W, binding energy, lattice parameters bulk modulus, self-consistent pseudopot. calc. 79−60748
W, electronic and struct. props., nonlocal pseudopot. calc. 80−34349
Xe, solid, self-trapped exciton, pseudopotential method 79−82529
Zn, cyclotron mass and superconducting energy gap calc. as a function of Fermi surface position 79−69625
Zn, de Haas-van Alphen effect under press., Fermi surface and pseudopot. form factors 77−43475
Zn, electrical and thermal resist. calc. 79−69489
Zn, electronic band struct., pseudopotential calcs. 79−19510
Zn, spin-orbit contrib. to mag. susceptibility of interacting electrons 77−63084
Zn, twin boundaries, computer simulation 80−39109
Zn-Al, dil., impurity quasi-particle lifetimes and pseudopotential form factor 78−47734
$ZnCl_2$, pseudopot. calcs. of mol. electronic props. 77−30779
$ZnGa_2S_4$, band struct., pseudopot. method 80−92816
$ZnIn_2S_4$, electronic props. of polytypic forms, pseudopot. calc. 80−38997
ZnO, electronic struct. calc., appl. of O nonlocal ionic pseudopot. 77−51659
ZnO, F-centre exam., pseudopotential calc. 78−43328
ZnS, F-centre exam., pseudopotential calc. 78−43328
ZnSb, band struct. calc. 78−39015
ZnSe-Ge (100) interface, electronic struct., self-consistent pseudopot. calc. 78−91747
$ZnSiP_2$, band struct. calc., empirical pseudopotential method 77−1362
$ZnSiP_2$, pseudodirect chalcopyrite semicond., electronic band struct. 80−20079
Zr, BCC, phonon vibrs., pseudopot. method 80−15204

pseudoternary semiconductors. *see ternary semiconductors*

psi mesons
$^1P_1$ charmonium state, decay modes, prod. mechs. 77−10247
$\Gamma(\psi\to\phi\pi^+\pi^-)/\Gamma(\psi\to\omega\pi^+\pi^-)$ and Okubo-Zweig-Iizuka rule 77−6119
ϕ^4 (rubber bag) model, hadron mass spectra and J/ψ family *(Chinese)* 79−80812
ψ(J) particle, discovery, props., experimental apparatus develop. *(Czech)* 78−78232
ψ/J(3100)$\to\eta'$(958)γ, e^+e^- storage rings expt., upper limit on partial decay width 77−49956
A dependence of inclusive distrib. in Be(π^-, Ψ), Cu(π^-, Ψ), W(π^-, Ψ) *(Russian)* 78−45983
asymptotic SU_3 and a new mass constraint for the ω, ϕ, ψ and Υ mesons 79−36001
charm, fourth quark, ψ-meson family 77−57492
charm hypothesis, early experiments 77−65167
charmed triplet and leptonic decays 77−67622
charmonium, $^1D_2$ level at 3.5 GeV 77−2826
charmonium, ψ and χ states, hyperfine struct. 78−12878
charmonium, generation of spin depend. forces through scalar-vector admixture 78−33038
charmonium, masses of 2P and higher levels, sum rules 78−4805
charmonium, non-singular confining pot., order of levels anal. 77−65189
charmonium, rel. to gluons, quantum chromodynamics theory 78−62362
charmonium, Todorov's quasipotential eqn., quark confinement 78−8593
charmonium atomic physics, ψ, ψ', η_c, η_c' masses and $\psi\to\eta_c\gamma$ decay 79−40740
charmonium level struct., superheavy quarks, bound state spectroscopy 78−8614
psi mesons continued
charmonium model, tensor force affects on ψ' and χ 77−87943
charmonium model anal. 77−71490
charmonium model and the ψ and Υ families 80−47253
charmonium model of ψ family 78−78143
charmonium photoprod., gluon-exchange model 78−74214
charmonium psion states, confining pots. and inverse scatt. problem, Υ mass 80−4946
charmonium quark-antiquark pots., flavour independ., γ, γ', ψ and ψ' appls. 80−47254
charmonium spectroscopy, spin forces, obs. in ψ'(3.68)-ψ''(3.77) struct. in e^+e^- annihilation 79−36047
charmonium spectrum, relativistic and nonrelativistic theory 78−50010
charmonium spin struct. and quark gluon effective interaction 77−13922
charmonium states, multimesonic decays, statistical quark model 78−82171
charmonium-like models, order of first energy levels 78−29311
classification scheme with colour-antisextet quarks 77−10225
colour diquark excitation model 77−18234
colour symmetry and ψ particles 77−57493
colour symmetry breaking, ψ(3.1) and ψ(3.7) 77−18233
conference on particle physics, Honolulu, Hawaii (Aug. 1977) 79−49485
confining potentials, order of levels theorem, two body nonrelativistic interacting system 77−49634
conserved vector current hypothesis, extension to gluons 77−71480
cryptoexotic states of the four-quark system 79−40762
data summary and interpretation 77−82798
decay, stiff quark line hypothesis, strong interaction suppression, Zweig Iizuka rule origin 77−2792
decay modes in Han-Nambu colour model 77−18307
decay modes of ψ resonances, neutral and radiative 77−57530
decay properties, intermediate states, Iizuka model 77−2825
decay rate in charmonium models 79−22061
decays, data anal. using quark model and VMD 77−54101
decays, hadronic, asymptotic freedom, one-photon or three-gluon exchange 80−62971
decays, QCD, inclusive hadronic annihilation of heavy quark-antiquark bound states 78−45866
decays and intermediate states from SPEAR, LBL-SLAC expts. 77−242
decays of ψ/J (3100) and ψ' (3700), results from DASP collaboration/DORIS 77−61282
decays violating Zweig Iizuka rule, asymptotic freedom phenomenology 78−451
dimuon prod. in proton-nucleus 400 GeV collisions, ψ' and ψ signals 77−10399
discoveries during 1974-7, and associated theory *(Czech)* 78−86103
discovery, experimental details, personal recollection 77−54112
discovery, expt. details, charm particles, review 77−54113
discovery, personal recollection by Ting *(Polish)* 78−73820
e^+e^- annihilation, phenomenological interpretation, ψ prod. and props. 77−67668
EM decay, contact terms 79−63481
EM decays, relativistic corrections in potential model 79−49522
EM transition rates, geometrodynamical quark model 80−47295
energy spectra using quark model, leptonic decay widths, spin depend. forces 79−13109
equality of radii characterising ρ and ψ Regge trajectories 79−63457
excitation models from $e^+e^-\to\mu^+\mu^-$ reactions with polarised e^+,e^- 79−13095
experiments, 1975 and 1976 *(Czech)* 79−26288
five-quark model, masses of charmed hadrons *(Russian)* 77−61263
flavour independence of forces between quarks, ψ and Υ spectra 80−22569
flavour symmetry breaking and production processes in dual unitarisation, ϕ and ψ prod. 79−45080
gluon contrib. to hadronic ψ prod. 78−66084
hadron suppressed decays and non-charmed meson spectroscopy 77−26519
hadron-hadron inclusive interactions, charmed particle production, η_c, ψ and other $c\bar{c}$ bound states 80−63036
hadronic and photonic decays, pseudoscalar mixing effects, cylinder dominated model 77−6120
hadronic collisions, ψ/J and ψ' prod., quark-antiquark annihilation, cascade process 78−25013
hadronic collisions, production of D- and ψ-mesons, QCD calc. *(Russian)* 79−9348
hadronic decay, energy crisis interpretation, anomalous neutral component 78−41540
hadronic decay, generalised Veneziano model 78−58182
hadronic decay, one photon intermediate state 79−54337
hadronic decays and soft pion theorems in charmonium model 77−6117
hadronic decays from DORIS, DASP expts. 77−243
hadronic decays of J/ψ, dynamics, SU(3) violation, dispersion relations, mass splitting 79−382
hadronic prod., lepton pair ang. distribs., cross section χ contribution 80−42487
hadronic prod., role of ^{3}P charmonium states 77−22744
hadronic prod. *(Chinese)* 78−8696
hadronic production of heavy quark bound states, quark fusion, fluon processes, for J/ψ, Υ prod. 79−349
hadronic production of heavy quark bound states 79−63435
heavy quark potentials, effect on triplet $c\bar{c}$ charmonium and triplet $b\bar{b}$ upsilonium systems 79−49456
heavy quark system prod. in QCD, duality predictions 79−13074
heavy quark-antiquark bound states, short distance anal., appl. to ψ and Υ 79−93345
heavy quarkonium states, hadronic transitions, QCD anomalies for Υ'' and ψ' 80−105888
history and significance 79−80409
inclusive J/ψ production in 43 GeV/c π^- on Be, Cu, W, A-depend. 78−62581
inclusive prod. in pp and πp, quark energy distrib. 77−22813
inclusive production cross sections, correlating quark rearrangement model 79−54320
J particle discovery, personal recollection 77−65166
J particle discovery, review *(Hungarian)* 79−17778
J/Ψ production in NN interactions, failure of Drell-Yan parton model 79−89106
Klein paradox and the mass spectra of the neutral vector mesons 79−26299
lectures given at CERN School of Physics (6-19 June 1976) 77−61173

psi mesons continued
lepton pair width regularity of vector mesons, ρ, ω, φ, ψ and γ 79−63472
leptonic decays, spectral-function sum rules 78−4857
$M_\psi - M_{\eta(c)}$ and $M_\Upsilon - M_{\eta(b)}$ lower bounds, concave and convex pots. 80−91057
magnetic dipole transitions in atomic and particle physics: ions and psions 79−9322
mass formula, SU(4) algebraic realisation *(Russian)* 78−45895
mass spectra, quasipotential calcs. *(Russian)* 80−47268
mass spectra and radiative decay in light-quark model 77−18258
masses and leptonic-decay widths, one-parameter potential 80−13279
masses of new mesons and effects of the fifth flavour 78−66098
mesonic decay branching ratios, two-, quasi-two- and three-body decays 77−49959
multimesonic decays of charmonium states in a constant matrix element quark model 79−26298
multimuon prod. in conjunction with ψ particles in π(p)+nucleus reactions 77−30460
multiple charmed quark model, mixing effects, leptonic widths of ψ meson 77−22687
narrow hadronic widths, extended flavour symmetry, new conserved quantum no. 79−22064
narrow resonances by strong coupling 77−30370
neutral decays, identification of $\psi \to \gamma\eta \to 3\gamma$ and $\psi \to \gamma\eta' \to 3\gamma$ modes 77−49968
neutral radiative decay, possible intermediate states 77−241
new elementary particles, theoretical predictions, recent expt. results 77−57475
'new particle' searches and discoveries, 'Review of Particle Properties' 1976 supplement 77−57515
nonrelativistic pot. models for heavy quark systems, Υ and ψ hadronic decay 78−89688
off-mass-shell coupling consts. and radiative decays in VDM 78−70371
overlapping resonances with variable channel struct., ψ prod. 79−22118
OZI rule, pseudo-dimension rule and ψ(3770) decay 79−40724
OZI rule breaking in decays 79−97597
P-state dominance in hadronic production 77−46024
PCAC and dual resonance amplitudes, old and new mesons, charm 78−45885
phenomenology and quark confinement 78−29308
photoprod. and helicity conservation from $\psi \to l^+l^-$ ang. distrib. 77−18297
photoprod. from Be and Ta targets, mass no. depend. of cross-section meas. 77−26668
photoproduction, direct peripheral mechanism *(Russian)* 77−46056
photoproduction, two-gluon exchange model 78−21437
photoproduction on nucleon, peripheral model of diffraction mechanism *(Russian)* 77−38180
prod. and decay, book contrib. 78−82208
production, gluon-gluon fusion model, gluon distrib. *x*-depend. 80−62922
production and decays, probability calcs. *(Chinese)* 77−65153
production by coalescence of strange particles, ferromagnetism analogy 77−13951
production cross-sections by $\pi^\pm$, $K^\pm$, p, and p̄ beams at 39.5 GeV/c 77−57571
pseudoscalar and vector meson decays, triangular quark diagram anomalies, ψ, η and η′ appl. *(Russian)* 80−42455
QCD, asymptotic freedom, energy levels J/ψ and Υ mass difference *(Chinese)* 80−52480
QCD, heavy-vector meson-nucleon scatt., cross section suppression, Υ and ψ 80−22564
QCD and ψ parameters, charmed quark current in quark-gluon coupling *(Russian)* 80−13277
QCD low energy tests, gluon non-zero effective mass, ψ decays 80−91054
QCD quark-gluon plasma, hadronic prod. of leptons, photons and ψ *(Russian)* 78−89672
QCD quark-gluon plasma, hadronic prod. of leptons, photons charm and ψ 78−89669
quantum chromodynamics psi-spectroscopy model *(Hungarian)* 79−13068
quark bag model with finite potential barrier, S-wave mass spectra of QQ̄ and leptonic widths 80−47242
quark model anal. of two-body hadronic decay 78−25040
quark model of ψ, ψ′, relative magnitudes of wave functions at origin calc. 77−87947
quark-confining string model, ψ spectrum determ. 77−6094
quark-parton model relns. for dilepton and ψ meson prod. 77−82711
quarkonium, quantum mechanical applications, masses and leptonic widths of ψ and Υ 80−27484
quarkonium decay into heavy quark flavours, ψ (J) energy distrib., QCD perturbation theory 78−82146
quarkonium pot., ψ data and Υ′-Υ mass splitting fit, Υ leptonic widths 78−89666
quarkonium spectroscopy in a potential model with vacuum-polarization corrections 80−78038
radiative decay, gluonic bound state O^- width 80−37272
radiative decay, radial excitations and q^2 depend. in VDM 78−452
radiative decay and heavy quarks 77−2798
radiative decay in spectrum-generating SU(4) 77−34152
radiative decay to η′(958)+γ, upper limit to width 77−38173
radiative decay width from glueball model 80−62941
radiative decays, charmonium model 77−38174
radiative decays, possible intermediate states from inclusive photon spectra 77−10246
radiative decays, unified mechanism, form factors *(Chinese)* 77−57540
radiative transitions anal. in nonrelativistic quark model 78−8607
reciprocal effects and other quark theories, charm quarks, J/ψ discovery, gauge theories *(Danish)* 79−30698
Regge trajectories for narrow meson resons. 78−82178
review of discovery, charm 77−22680
review of expt. results and interpretation *(Russian)* 77−269
review of three years e^+e^- research at SPEAR 79−63490
seven quark model, leptonic widths 77−22685
soliton model of ψN interactions and ψ photoprod. *(Russian)* 77−46071
spectroscopy in quark confining two-step pot. 77−26492
strong and radiative decays, SU(3)′×SU(3)″ scheme of three triplet model 77−30371
SU(3)′×SU(3)″ scheme of three triplet model, colour symm. ψ-mesons descript. 78−78151

psi mesons continued
SU(3) model for strong interactions quark excitation and ψ mesons 77−18198
SU(8) symm. mag. moments of charmed vector bosons 78−4794
subnuclear physics, review 77−67623
suppression factor in the decays of the ψ family 79−13112
tensor force effects on ψ family in charmonium model 78−89675
two neutral vector gluon model explanation of data 77−226
two-body photonic decays, 16-plet mixings in SU(4) quark symm. 78−33062
unitarity effect of ψ′(3684) on shape of ψ″(3772) 79−434
vector Ψ_b hadronic prod., b-quarks 78−8613
vector meson radiative decay evaluation in spectrum generating SU_4 scheme 79−54342
Veneziano model anal., KK̄π Dalitz-plot density calc. 79−26331
wave functions mol. partial decays in SU_4 model *(Chinese)* 77−65152
Zweig rule in two-dimensional QCD, ψ and Υ decays 80−52479
Zweig suppression and statistical factors 77−46025
B→J/ψ+hadrons, branching ratio, b quark decay calcs. 80−32095
b quark→ψ(η_c)+X, B branching ratios assuring colour suppression 80−37259
C+p, 24 GeV, J/ψ prod. cross section 78−46055
cc̄ bound states, e^+e^- decay processes, relativistic harmonic oscillator model 78−62393
χ(3.45)→π⁺π⁻X(2.83), test of cc̄ dynamics 77−74685
χ production properties from inclusive electron pair and J/ψ prod. at CERN ISR 79−36113
χ→ψγ, charmonium E1 radiative transitions and quark mag. moments 80−86721
χ/ec→ψγ, scalar and tensor meson dominance 79−3019
$\chi_J \to \gamma\psi$, charmonium states radiative and hadronic widths, gluon spin 80−4998
$(e^+e^- \to \text{hadrons})/(e^+e^- \to \mu^+\mu^-)$ cross sections ratio, differential dispersive anal., narrow resonances 78−37223
e^-e^+ annihilation, >2 GeV, production of charmed particles and charged τ lepton, review 78−17006
$e^-e^+ \to \psi(z)$, spin correlations, spin 0, $^1/_2$, or $^3/_2$ pair prod. *(Russian)* 79−22117
e^+e annihilation, 3.1-5.2 GeV, DASP results 80−42483
e^+e^-, annihilation, production of new particles, J/ψ, ψ′ and τ props. 80−5008
$e^+e^- \to 3\gamma$, 3.6 GeV and ψ′ reson., comparison with QED 77−46066
$e^+e^- \to 3\gamma$, ψ radiation decay and new heavy reson. obs. 77−46065
e^+e^- annihilation, anomalous lepton prod., charmed mesons and heavy leptons 78−66134
e^+e^- annihilation, gluon jets and heavy quarkonium prod., QCD test, ψ prod. 80−42479
e^+e^- annihilation at SPEAR, total hadron cross section, ψ prod., μe events 77−57548
e^+e^- annihilation experiment review, ψ spectroscopy and charmed particles D and F 79−49533
e^+e^- colliding beam technique, from psi to charm 1975 and 1976 *(Polish)* 78−74297
$e^-e^+ \to e^+e^-(\mu^+\mu^-)$ EM processes, vector resons. cross sections *(Russian)* 77−57517
$e^+e^- \to$hadrons, scaling and quark binding anal., generalised vector dominance 77−249
e^+e^- interactions, review 79−80833
$e^+e^- \to J/\psi X$, 4.0-5.0 GeV, Zweig rule violation 77−61305
$e^+e^- \to \psi$, review of expts. (1975 and 1976) 77−87991
$e^+e^- \to \psi X$, EM corrections, low energy theorem, unitarity, dispersion relations *(Russian)* 77−49982
$e^+e^- \to \psi X$, estimate of inclusive ψ and $\psi\eta_c$ prod., QCD anal. of cross section 79−85308
$e^+e^- \to \psi(3,1) \to e^+e^-$, leptonic creation and decay processes, radiational effects *(Russian)* 77−46060
$e^+e^- \to \psi(3770)$, cross section, ψ mass, total width and e^+e^- partial width 80−73696
$e^+e^- \to \psi \to 2\gamma(3\gamma)$, charmonium model calcs. 77−30387
$e^+e^- \to \psi \to l^+l^-$, leptonic creation and decay processes, radiational effects *(Russian)* 77−46060
$e^+e^- \to \psi\pi\pi$, radiative corrections, model estimates 77−10271
$e^+e^- \to \tau^+\tau^-$, neutral-current effects on ψ-like resonance 78−74239
$e^+e^- \to X$, theory from renormalisable field theory differential dispersion relations 77−26535
η decays of ψ's, VMD and colour model coupling const. calcs. 77−26516
η-η′ mixing angle and relative radiative decay rates $\Gamma(\psi \to \eta\gamma)/\Gamma(\psi \to \eta'\gamma)$ 80−9173
γN→ψN, spin and mass depend. of constituent and phenomenological models 77−61304
γN→ψ(3.1)+anything, cross section and N charmed quark composition 80−423
H+p, 24 GeV, J/ψ prod. cross section 78−46055
hadronic production, gluon contrib. in QCD framework, quark fusion, gluon fusion 78−78139
J particle, tensor meson decays in SU_4 model *(Chinese)* 79−75767
J/ψ decay, gluon source, search for scalar gluonium, QCD 80−47296
J/ψ decay, via ω, φ, ρ^0 poles and cascade decays, vector meson pole dominance 79−85295
J/Ψ prod., valence- and sea-quark distribs., deep inelastic scatt. and Drell-Yan processes 79−13069
J/ψ→η_cγ, radiational decays in charmonium *(Russian)* 80−13308
J/ψ→η(η′)γ decay rate, QCD sum rules 80−52497
μ⁻μ⁻ pair system, meson reson., leptonic decay *(Russian)* 77−67646
μN, 209 GeV, ψ diffractive prod. cross section, ψ→μ⁺μ⁻ decays 80−102054
μN→(xμ)X, dimuon and trimuon prod., heavy quark and 4 diffractive prod. 79−93429
μN→μψX, diffractive and non-diffractive ψ leptoprod. in QCD 80−424
μ⁻N, 280 GeV/c in Fe, Ψ virtual photoprod. 80−37279
νN→νψX, neutral current ψ prod., Z^0-gluon fusion model 80−78015
p+Be→e⁺e⁻X, 30 GeV, J/ψ prod. and decay into e⁺e⁻ 77−57570
pN in Fe, 400 GeV/c, ψ(3100) prod. 80−57650
p̄p, 2.99-3.14 GeV, cross-section upper limits for new particles 77−30416
pp, 53, 63 GeV, Υ and ψ prod., dielectron decay angles 80−68496
p̄p, pp, 540 GeV, Υ and ψ transverse momenta from QCD 2→3 processes, gluon subprocesses 80−52546
pp→e⁺e⁻X, 52, 63 GeV, cross section, ψ′ prod. cross section, continuum cross section 79−425
pp→e⁺e⁻X, J/ψ prod. at √s=52 GeV 77−65181
pp→e⁺e⁻X, J/ψ prod. in √s=23.5 to 62.5 GeV range 77−79293

psi mesons continued
pp inclusive interactions, narrow vector meson hadroprod., ϕ, J, ψ charmoniumlike states 77−57573
pp→J/ψX, OZI rule violation 79−58929
pp→$K_s^0\pi^-$+anything, 28.4 GeV/c, cross-sections and mass distribs. meas. 77−38212
pp→$\mu^+\mu^-$X, 62 GeV, ψ and γ cross sections, scaling function 80−105932
pp→ψX 70 GeV to ISR energies, pion exchange model anal. *(Russian)* 79−40823
pp→ψX or $\bar{p}p$→ψX, J/ψ prod. mech., p gluon distrib. determ. 79−430
pp→ψX→$\mu^+\mu^-$X, Drell-Yan mechanism in colour quark model 77−6181
pp→ψ+anything, parameter free exchange model 77−10293
φ(3100) two-body decays and SU(3) breaking 77−18277
πN→J/ψ+X, 27 and 40 GeV, total (J/ψ) production cross sections on Cu target *(Russian)* 78−25249
π^-N, 150 GeV/c, prod. of J/ψ and ψ′ mesons 79−40804
π^-N, 217 GeV, dimuon prod., prod. of γ associated with χ→ψγ 79−36081
π^-N→J(ψ)+X, 27 and 40 GeV/c total cross-section for Cu nucleus 78−25088
π^-N→$\mu^+\mu^-$+hadrons, 225 GeV, ψ and charm prod. 78−25092
πp→ψX, 70 GeV to ISR energies, pion exchange model anal. *(Russian)* 79−40823
π^-p→J/ψ+n or χ+n, 27-40 GeV/c, nuclear proton, upper limit on cross section *(Russian)* 78−78218
$\pi\bar{p}^-$→ψ+X, ψ(3.1) inclusive prod. in fragmentation region 79−13150
π^-p→ψn, generalised Veneziano models, ψ/d production mechanism 80−22638
ψ, ψ′→$\pi^+\pi^-$, K^+K^-, decay suppression, dimensionality based selection rule 78−33061
ψ,ψ′→$\eta_c\gamma$ rates, suppression in SU(4) multiplet mixing 77−18195
ψ(3095)→pp̄ or ΛΛ̄, branching ratios, quantum numbers, final state resonances 78−74252
ψ(3100) decay into muon pairs, e^+e^-→$\mu^+\mu^-$ study at J/ψ energy, ang. distrib. 77−2846
ψ(3100) N total cross section from modulus dispersion relation anal. of photoprod. 77−18300
ψ(3100) prod. cross section from μN in Fe 79−75779
ψ(3684), radiative decay into high-mass states 78−66113
ψ(3684) radiative decays, energy correlation 80−13307
ψ(3684)→DD̄ decay width from e^+e^-→hadrons multistate approach anal. 77−71521
ψ(3772)→DD̄, $D^{0,?}$ masses, branching fractions 78−17009
ψ(3.095), ψ′(3.684), appl. of quarkonium system inverse scatt. formalism, interquark pot. 78−82154
ψ(3.1), nucleon EM struct., ψ(3.1) in VDM of nucleon form factors 78−50034
ψ(3.1) photoproduction, vector dominance model 77−18302
ψ(3.1)-quark-antiquark coupling calc., dimens. regularisation technique 77−41812
ψ(3.1)→fω, ψ(3.1)→Bπ, branching ratios meas. 78−17011
ψ(3.1)→νν̄, neutral current decays, possibility of expt. obs. 77−18276
ψ→3γ, dispersion sum rule charmonium theory, decay probability lower bound *(Russian)* 78−89716
ψ→3γ, dispersion theory of charmonium, self consistency test, decay probability *(Russian)* 78−89717
ψ→3γ, heavy narrow state search, η′ and η_c branching ratios 80−57600
ψ→3π, generalised Veneziano model, 3π Dalitz plot 79−381
ψ→3π, ρ recurrences, quantitative study 77−79266
ψ(4.0 to 4.5 GeV) decay to D, F charmed mesons 79−17719
ψ(4.03)→DD̄, suppression problems, model-independent approach 80−52494
ψ(4.03)→DD̄(D*D̄, DD̄*, D*D̄*), vector state strong decay 80−78057
ψ(4.1)→ψ(3.1)+π+π, coloron model, quark composite struct. 78−29332
ψ(4.414), width anal. in quark model 78−17010
ψ(4.42)→DD̄, suppression problems, model-independent approach 80−52494
ψ(4.42)→FF̄, suppression problems, model-independent approach 80−52494
ψ (3100) decay, inclusive γ and π^0 momentum spectra, direct γ prod. at large x 80−42466
ψ (4.03), isospin and G-parity, model indeperdent prediction 80−86689
ψ and ψ′ (3684) hadronic production, charmed straton content of straton sea *(Chinese)* 79−63434
ψ and ψ′ charmonium spectroscopy anal. using square root pot., decay widths 78−82182
ψ associated with gluon, hadronic prod. 80−105846
ψ→χγ_2 radiative width calc. 77−71508
ψ→DD̄ radial excitations of charmonium 80−102046
ψ decay, high energy direct photons, γ, π^0 momentum distribs., QCD calcs. 80−32098
ψ decay into baryon-antibaryon pairs 77−71510
ψ→$\eta_c\gamma$, charmonium, hyperfine interaction, nonperturbative treatment 80−62944
ψ→$\eta_c\gamma$, η_c hadronic decay, charmonium model 78−41502
ψ→$\eta_c\gamma$, quark-string model anal. 78−33065
ψ→η′γ, QCD, width, exclusive OZI violating radiative decay 80−68458
ψ→η′(ηγ), Okubo mass formula, η(cc̄) component 77−6116
ψ→η(η′)γ, SU_3 violation, symmetry breaking and decay amplitudes 80−52499
ψ→η(η′)γ, Ward identity anal., η,η′ quark-glue struct. 80−42449
ψ→ηγ, conflict with single parameter scheme for radiative decays of vector mesons 80−86720
ψ→πγ, pseudoscalar meson mixing and M1 radiative decays 77−30329
ψ→$f^0\gamma$, meas. of f^0(1270) polarisation 78−74251
ψ→$f^0\gamma$, ψ→ρπ, branching ratios meas. 78−25043
ψ→$f^0\gamma$, prod. and decay distribs. 78−89765
ψ family, VDM anal. of contrib. to total photon cross sections 79−22083
ψ→fγ, f′γ, ππγ, KKγ, meas. using DASP detector at DORIS 78−45922
ψ→fγ, form factor depend. in relativistic harmonic oscill. model 79−89156
ψ→fγ, intermediate one photon state description 78−62397
ψ→gravitino+antiphotino, gravitino mass lower limit, light gravitino weak interactions 79−75698
ψ→γf, tensor dominance for γ decays of new particles 78−66112
ψ meson prod. by π⁻-mesons with momentum 43 GeV/sec in Be, Cu and W nuclei *(Russian)* 78−8863
ψ→$\mu^+\mu^-$, search for extra μ in (π^-, ψ CC̄), 225 GeV/c 80−82967

psi mesons continued
ψ→nn̄, pp̄, simultaneous meas. of decay channels at J/ψ resonance 78−93893
ψ→pp̄, nucleon form factors at t=9.58 GeV^2 77−6118
ψ prod. cross-sections in pp collisions at E_{cm}=23-63 GeV 77−57572
ψ propagator, relativistic dispersion anal. of R in 4 GeV region 77−45989
ψ→$\pi^0\gamma$, two body photonic decays, SU(4) scheme, ideal mixing angles, amplitudes, quark sectors 78−54630
ψ(ψ′)→$B_8\bar{B}_8$ and $B_{10}\bar{B}_{10}$ modes, decay widths 77−6118
ψ(ψ′)→vector meson+pion+pion, disconnected quark diagram, decay widths 77−2824
ψ radiative decays, generalised quark line rule, SU_4 symm. scheme 78−54614
ψ→ρπ, ψ→γη′, branching ratios meas. 77−2827
ψ→X(2830)+γ, E1 amd M1 radiative decays using the geometrodynamical approach 78−86452
ψ→X(3410)+γ, means of J^r determ. of X(3410) *(Chinese)* 77−57581
ψ/J, charmed particles, particle multiplicity distribs. in hadronic decays 77−46044
ψ′, ψ decay branching ratios, isospin and flavour symmetry breaking 80−95264
ψ′, radiative M1 transitions with charmonium model 79−13132
ψ′, suppressed hadronic decay and particle degeneracies 77−76684
ψ′(3684)→χγ, χ→ψ(3095)γ, inclusive γ spectra in e^+e^- colliding beam expts. 77−57549
ψ′(3684)→γγJ/ψ(3093), cascade decays, evidence for new C=+ intermediate state 79−13115
ψ′(3685)→γP_c/χ→γγJ/ψ(γπ⁺π⁻)(γK^+K^-), investig. of γγ$\mu^+\mu^-$ final state 80−18132
ψ′(3.7)→ψπ^0, isospin violating decays 78−37205
ψ′ and ψ decay ratios, composite particle matrix elements 80−95266
ψ′→χ$_1\gamma$, radiative decay widths of charmonium states, superconvergent sum rules 78−21422
ψ′→χ/$e_c\gamma$, scalar and tensor meson dominance 79−3019
ψ′→χ(3455)+γ, E1 amd M1 radiative decays using the geometrodynamical approach 78−86452
ψ′→χγ, charmonium E1 radiative transitions and quark mag. moments 80−86721
ψ′→χγ, decays of 0^{++} scalar mesons 77−13963
ψ′ decay, Higgs bosons, five-quark model, P and T nonconservation 77−74686
ψ′→ηJ/ψ(π^0J/ψ), investig. of γγ$\mu^+\mu^-$ final state 80−18132
ψ′→ηγ, ψ→η′γ and η-cc̄, η′-cc̄ coupling consts. *(Russian)* 77−49962
ψ′→ηψ, ψ′→π′ψ, forbidden decays anal. 78−66114
ψ′→γ$\chi_{1,2}$, radiative decays of 2^{++}, 1^{++} mesons 78−21420
ψ′→γγ→γγψ, radiative decay width in charmonium model 77−18283
ψ′→π^0ψ, isospin isolating decay, branching ratio 80−57601
ψ′→ψ+2π, decay width dynamical calc. 77−18278
ψ′→ψ+η, two gluon mechanism, T dynamics test 78−89665
ψ′→ψη, Ward identity anal., η,η′ quark-glue struct. 80−42449
ψ′→ψη(π^0), decay branching ratios 80−105889
ψ′→ψπ^0(η), SU_2 violation, symmetry breaking and decay amplitudes 80−52499
ψ′→ψππ, charm model 78−74250
ψ′→ψππ, current algebra techniques, pole plus remainder model, chiral symmetry breaking and QCD 80−62972
ψ′→ψππ mass spectrum, hadronic cascades between QQ̄ bound states, QCD anal. 79−85261
ψ″(4.414) GeV, third radial excitation of cc̄ $^3S_1$, unorthodox branching ratios 79−17720
ψ″(4.42)→DD̄, FF̄, decay suppression, pseudo-dimension selection rule 80−9163
ψ″, Schwinger phenomenological and dyon description 78−82109
ψ″(3770), mass width from quark model 80−73723
ψ″(3770) in cross section for e^+e^-→hadrons 78−45934
ψ″(3770) isospin and G-parity 79−63569
ψ″(3772), radiative decay nonoccurrence 80−4997
ψ″(4.028)→DD̄, or DD̄*+D̄D* or D*D̄D*, strong decay theory, radial excitation of charmonium 78−12909
ψ″(4.4)→Ω⁻Ω̄⁺, Ω′→$\Xi^0e^-\nu_e$ or $\bar{\Xi}^0\mu^-\nu_\mu$, explanation of anomalous lepton prod. in e^+e^- annihilation 77−41834
ψ″ (3.772), ground state admixture in potential model 80−102033
ψ′→ψη, OZI rule violating transition, unitary corrections using dual model 79−26330
ψψ prod., correl. effects in large p_T pion events 77−26549
qq̄ prod., quark-mass effects, ψ and T mesons 78−66130
T (3.1), instantons and spin forces between massive quarks 78−37173
W+p, 24 GeV, J/ψ prod. cross section 78−46055
C+p, C+$\pi^\pm$, 225 GeV/c, J/ψ and ψ′(3.7) prod. study using muon pair meas. 77−57694
Cu+π^-→ψX, 16, 22 GeV, cross section, quark fusion model 79−36278
Cu(π^-, ψ′(3700)), 50 GeV, formation cross-sections *(Russian)* 80−106082
π^-N→J/ψ+X, 43 GeV/c, cross-sections for W, Cu, Be targets 78−25089
ψ→$\rho^0\pi$, meas. of ρ^0(770) polarisation 78−74251
ψ′→$\chi_0\gamma$, radiational decays in charmonium *(Russian)* 80−13308
Sn+p, Sn+$\pi^\pm$, 225 GeV/c, J/ψ and ψ′(3.7) prod. study using muon pair meas. 77−57694

PSK *see phase shift keying*

psychological optics *see vision*

psychology
acoustical research into life sciences, review 80−97925
aircraft noise index, psychological assessment 78−55507
American contemporary fiction, world view, influence of physics 79−58517
artificial sensory feedback system, stimulation freq. discriminability 78−44714
astigmatism and orientation preference in human infants 80−61542
attentional processes study, contrib. of EEG spectral band anal. *(French)* 80−61721
auditory sensations evoked by pulsed microwave fields, some pecularities 80−61636
behaviour patterns in cod released by elec. stimulation of olfactory tract bundlets 80−97951
behavioural sensitivity of a domestic bird to 60-Hz AC and to DC mag. fields 80−61622
biofeedback, student demonstration 79−44677

psychology continued
biofeedback diagnosis system, physiological parameter meas. considering psychic effects 79−100774
biofeedback process principle and appl. *(Japanese)* 77−44830
classical conditioning of microwave-induced hyperthermia, rat obs. 80−61629
coloured surrounds, effects on colour naming and luminosity 80−56054
conditioning auditory stimuli and the cutaneous eyeblink reflex, human obs. 80−67090
decision making, split-second, electrophysiological signs, auditory stimuli 80−89771
duration subjective impression rel. to ambient noise 78−44554
education, Piaget's cognitive psychology rel. to science teaching 79−58460
education, psychoacoustical expts. with all pass networks 79−25787
EEG patterns during cognitive tasks, controlled tasks anal. 80−67059
EEG patterns during cognitive tasks, methodology and complex behaviours anal. 80−61531
eye and hand motor systems, optimal response in pointing at a visual target 80−61567
eye fixations and cognitive processes 77−25438
eye movement recorders, problems, use in laboratory 80−41331
eye movements, cognitive psychology, on-line computer applications 80−41329
form recognition, scale invariant, in man and machines 78−40176
frequency perception, colour as a pervading principle over pitch, rhythm, and form 80−56059
hearing, combination tones and relation with suppression, psychophysical meas. 80−108910
hearing, contralateral cueing effects in backward masking 80−61587
hearing, difference tone perception at low freqs. 80−67087
hearing, forward masking, mechanism and freq. distrib. of two-tone suppression 80−108909
hearing, frequency discrimination for masked tones 80−76754
hearing, precedence effect, possible role in avoidance of interaural ambiguities 80−61588
hearing, psychophysical 2-tone suppression, stimulus component level effects 80−61584
hearing aids, perceived sound quality obs. 80−41050
higher cortical functions, EEG correlates 79−100591
human brain functions rel. to foundations of physics, science and technology 78−73823
hypnotic suggestion, meas. of effects in elec. induced muscle contract *(Slovenian)* 80−81571
immersion in various liquids, anal. of dynamic cold sensation *(Japanese)* 80−21448
industrial noise onset effects on physiological and psychological functions 80−91959
intellectual activity, classification of normal and anomalous forms, quantised-wave theory of coherent brain appl. *(Russian)* 80−76722
intellectual activity, psychoheuristic relationship of psychotism structs. and giftedness structs. introduction, quantised wave theory of coherent brain appl. *(Russian)* 80−76723
ionising radiation induced behavioural and physiological changes in rats, hormonal radioprotection 80−98026
Laser ballistic missile destructor and weapons technology 77−50710
magnetophosphenes, quantitative determ. of thresholds 80−61620
manic depression, abnormal red cell membrane Li transport 80−61525
melody perception, computer program for music transcription 77−5009
mental activity evoking pupil dilation, link with intelligence 80−61532
microwave chronic exposure, physiological and behavioural effects, rat obs. 80−67152
microwave exposed rats and mice, behavioural obs. 80−61631
microwave irradiation and ambient temp. interaction, rat behavioural alterations 80−67153
microwave radiation and dextroamphetamine, combined effects on rat behaviour, expt. obs. 80−61635
moment of inertia, human sensitivity, psychophysical study 80−72180
neocognitron, self-organising neural network model, pattern recognition mechanism unaffected by shift in position 80−76745
neural signal space entropy, neurodynamic basis of Weber's and Steven's laws 77−73516
noisy office work interruption and psychological effects 78−42492
object perception criteria, information theory appl. 78−44444
occupational physiology and psychology laboratory 77−48885
olfaction, bilateral interaction 77−66819
olfactory perception, neurophysiological correlates rel. to amygdalotomy 79−100637
operant behaviour and rectal temp. during 2.45-GHz microwave irrad., squirrel monkey obs. 80−61630
operant behaviour induced by microwave radiation, effect of psychoactive drugs 80−61632
perception, rel. to complementarity of living and lifeless matter 79−66436
perception mechanisms, rel. to brain evoked pots. 78−11627
physics teaching and personality development assessment *(German)* 80−67966
Piaget, J., research and theory 79−49000
picture processing, eye tracking, computer raster graphics device 80−41330
psychoacoustic experiments using freq. and amplitude modulated stimuli 80−94236
psychophysical 2-tone suppression as function of input level for $f_2/f_1>1.0$ 80−76756
psychophysical and VEP increment obs. of light adaption in a normal and a rod monochromat 80−16939
psychophysical evidence for sustained and transient channels in the monkey visual system 80−35896
psychophysical stress from long term ECG recording, hardware evaluation of parameters *(German)* 80−26388
psychophysical tuning curves for combination tones $2f_1$-f_2 and f_2-f_1 80−76755
psychophysics as method of meas. of biosystems *(Japanese)* 78−53591
psychophysiological techniques applied to aircraft design and other operational problems 80−26384
psychosomatic clinic audio-visual communication system 79−83997
punctuate pressure sensitivity rel. to skin surface temp., cutaneous cross-model interactions 78−3527
quantum interference effects in psychology, Schrodinger's cat, review 80−73158
radiation exposure, perception of harm 80−85450
psychology continued
reaction time, N1-P2 correls. at the single-trial level 80−85389
reading without a fovea 80−76748
reasoning development, influence of studying physics 77−29971
RF radiation exposed chicks, behavioural obs. 80−61633
scientific creativity 79−49010
sensorineural hearing loss, freq. selectivity and speech discrimination 80−61593
sleeping rhythm of mouse, classification using compact accelerator 80−56309
spatial contrast sensitivity in albino and pigmented rats, behavioural obs. 80−41013
spatial frequency tuning studies, psychometric curves description by probability summation 80−61576
spatial localisation during pursuit eye movements 80−51081
spatial vision, psychophysical investigation, normal and reeler mutant mouse obs. 80−41032
speech reception threshold, reliability in the determ., psychometric function 80−61657
subjective experiments (e.g. aircraft noise anal.), use of changeover designs 77−82380
subjective noise annoyance by low level sound 80−35902
subliminal communication for behaviour therapy and education, audiovisual technique 78−73293
tactile senses pattern discrimination power meas. 79−83971
trichromatic colour matching, high-level, rel. to pigment-bleaching hypothesis 80−35891
vibrotactile pattern perception extraordinary observers 77−64065
vision, apparent contrast matching, narrow-band spatial mechanism 80−61571
vision, associative learning model, voltage-dependent Ca^{2+} and K^+ conductances 80−72166
vision, Bezold-Brucke hue shifts, short-flash obs. 80−72170
vision, colour-contingent movement aftereffect, interocular transfer obs. 80−61578
vision, cone spectral mechanisms, ERG and psychophysical obs. 80−61565
vision, grating induction, a new type of aftereffect 80−72175
vision, gratings moving in opposite directions, summation and discrimination 80−72169
vision, human recognition system with thinking, model 80−76744
vision, McCollough effect, role of test pattern background hue; 80−41036
vision, saturation enhancement in coloured Hermann grids varying only in chroma 80−72168
vision, simultaneous and successive contrast obs. 80−76742
vision complex pattern discrimination, learning by young kittens, expt. obs. 80−56049
visual acuity, infant, underestimation as near threshold gratings are not preferentially fixated, expt. obs. 80−56053
visual illusion, geometrical, analysis in terms of perceptual field 77−2002
visual pattern matching, human performance, spatial freq. anal. model 78−40177
visual psychometric discrimination of spatial freqs. in different orientations 80−81590
visual stimuli generation, microprocessor based system 80−41328
visually guided locomotion, psychophysical evidence for neural mechanism sensitive to flow patterns 80−51107
voice tremor EMG correlation, psychological stress evaluators 77−9214
PTC thermistors *see thermistors*
p.t.m. *see pulse time modulation*
public utilities
see also water supply
involvement in solar energy Project SAGE 79−57452
publishing
American Journal of Physics, nature of journal 79−58456
astronomy, cost effectiveness in terms of publications and citations of Kitt Peak National Observatory telescopes 80−90334
geophysics and astrophysics research worldwide growth, 1967-75 period 77−66884
Indian scientific and technical Journals critical evaluation 80−94906
scientific citation study of Argentina, Brazil and Norway 79−97180
scientific journals significance, Science Citations Index anal. 77−9831
scientific papers, refereeing system 77−33719
pulp industry *see paper industry*
pulsars
see also neutron stars; radiofrequency cosmic radiation
A0535+26, transient slow X-ray pulsar, spectrophotometric survey 78−4263
acceleration by asymmetric radiation, observational evidence 77−60783
accretion possibility 79−75237
angular momentum and energy loss, physical processes 77−91557
apsidal motion in highly evolved stars 77−45483
atmosphere with arbitrary mag. and rot. axes, qualitative features 78−57569
atmospheres, numerical solns. of trans-relativistic shock relations 80−31202
atom motion in very strong mag. fields, mass anisotropy effect *(Russian)* 80−67557
atomic statistical model thermodynamics in strong mag. field, pulsar crust condensed matter 79−2741
Australian Astronomical Society, conf. Melbourne, Australia (May-June '77) 78−69655
axisymmetric magnetosphere, model 79−84813
axisymmetric magnetosphere models, Fourier transform method 79−92794
baryon star magnetospheres, inclined rotator case 80−26887
binary, relation between speed ups and variation of gravitational constant 78−73728
binary pulsar, secular relativistic change in pulsar period 77−5542
binary pulsar origin and asymmetric supernova explosions 78−69816
binary pulsar PSR 1913+6, dissipative effects connected with gravitational radiation, indirect evidence 79−75236
binary pulsars, neutrino emission 79−2550
binary star containing eruptive star assoc. with pulsar, gamma-ray source *(French)* 78−20913
binary X-ray pulsars, review 77−29869
birthrate, rel. to supernovae occurrence freq. and long-lived remnants, prod. 77−64784

pulsars continued
birthrate and z-distribution from 2nd Molonglo Survey 79−8940
book, review of six years of work 78−8035
CG 195+4 (Geminga) pulsating γ-ray source, neutron star models 78−4402
characteristics and evolution, from radio, X-ray, and γ-ray obs. 77−37611
charge-separated magnetospheres, props. 78−40981
charged particle accel. to extremely high energies in far field 77−29868
charged particle motion in an electromagnetic field on Kerr background geometry 79−9167
charged particle trajectories in mag. field in Schwarzschild geometry 77−41296
Cherenkov radiation from charge separated magnetic plasma 77−47163
Cherenkov radiation of charged particle moving in mag. cold plasma 79−62736
classification into groups with similar properties *(Russian)* 77−60787
classification method from period change and radio luminosity *(Chinese)* 80−85963
classification scheme 78−12262
close binary systems in quiet stage, detect. from γ-ray emission 79−67058
coherent curvature radiation 80−56704
coherent radiation, relativistic soliton model *(Russian)* 78−77568
coherent radiation mechanism 79−53848
coherent radio emission, source 80−82403
coherent radio emission from pulsars, review 80−46596
coherent radio emission in nature, theory, solar system and pulsars appl. 80−46393
coherent radio radiation by antenna mechanisms, theory 77−49414
compact supernova remnants, possible γ-ray emission from pulsars 78−45435
composition of outer crust, influence of mag. field 80−101610
conference, Sydney, Australia, (April 1978) 79−75230
constrained atmosphere, min. energy state 79−25622
cosmic betatron model, general relativistic induction accelerator 77−37793
cosmic ray sources, evidence from Galaxy cosmic rays and mag. field distrib. 80−4207
cosmic rays injection into dense supernova shells 78−65638
Crab, electron-positron flux at neutron star surface 77−64789
Crab, pulsed emission prod. by synchrotron mechanism 79−35283
Crab Nebula, disrupted the star in close binary containing neutron star, model 79−25696
Crab pulsar, Cherenkov radiation from charge separated magnetic plasma 77−47163
Crab pulsar, gravit. radiation revised estimate 78−32501
Crab pulsar, momentum distrib. of high energy particles 78−73727
Crab pulsar, proper motion 77−82269
Crab pulsar, relativistic particles injection into Crab Nebula 78−36678
Crab pulsar, upper limit for gravit. radiation energy flux 78−73730
crust, infinitely magnetised H atom theory 80−77282
crust superfluid, pinning and threading of quantized vortices 77−45475
Cygnus X-3, cocooned X-ray binary pulsar model 78−36723
Cygnus X-3, young pulsar in binary system model 77−29955
decametric radio emission, similarity with Jovian emission *(Russian)* 80−77333
detection at 22.7 GHz 77−33539
discovery, structure, and physical props., general introduction 78−16450
discovery story 78−65644
dispersion and Hα emission meas., limits on interstellar electron density and ionized gas filling factor 78−8078
dispersion data anal., scale height determ. 80−85965
distribution, birthrate and flux density distrib. 80−98681
dynamics of differential rotating sphere 77−37609
education, suggested expts. 78−61982
electron cap, electrons accel. in internal zone 80−46592
electron-positron pair annihilation in strong mag. field *(Russian)* 79−17705
electrostatic shear flow instability of relativistic nonneutral beams 79−53847
elliptical cross section and linear polarization of pulsar radio beams 80−56865
EM ion waves in cold relativistic plasmas, astrophys. appl. 80−21910
EM vars. in curved space-times 80−56866
emission geometry and pulse-width statistics 80−26893
emission mechanism, AC Josephson effect hypothesis 80−82404
emission regions location, obs. limits 78−65637
energy emission 80−82450
energy spectra and pulse shapes at metre wavelengths, obs. 79−75233
EUV thermal radiation, upper limits for nearby pulsars 77−22259
evolution, initial magnetic moments rel. to decay times 79−62861
evolution rel. to torques, magnetic moment and pair production 80−62169
exercises, period, distance and dispersion calc. 77−53725
Fermi quantum crystals, melting curves low temp. anomalies 78−24757
finite force face cold plasma atm. models, plasma differential rot. 80−77378
flux observations, long-term intensity and spectral vars. 78−4268
force-free aligned atmosphere, response to perturbations 78−53974
force-free magnetosphers, temp. stabilisation of instabilities 77−49413
force-free wind zone, stability 78−49468
formation, from evolution of mass-accreting white dwarfs 80−77281
formation frequency, results from search for galactic supernova remnants 79−29998
fundamental luminosity 79−5850
galactic distrib. 77−60785
galactic distribution, determ. from second Molonglo survey 79−75231
galactic distribution and evolution 78−4260
galactic magnetic field scale and strength from pulsar data 78−28752
galactic nucleus radio source, pulsar hypothesis 77−5572
gamma ray emission, theoretical model 78−65641
gamma-ray emission, contrib. to diffuse flux from galactic disc 77−67143
gamma-ray emission, contrib. to galactic gamma-ray flux 79−25763
gamma-ray emission, observational and physical review 79−80373
gamma-ray emission, production and beaming 78−4266
gamma-ray emission, theory 78−53975
gamma-ray light curves, geometrical anal. 80−36653
gamma-ray luminosity influence on pulsar models 78−4262
gamma-ray obs. of galactic small-scale structure 80−98743
gamma-ray observations *(German)* 77−60853
gamma-ray production mechanism 80−77433
gamma-ray pulsars, curvature radiation-pair prod. model 79−5852
gamma-ray pulsars, observability 78−81646
gamma-ray sources, supernova shells of young pulsars *(Russian)* 77−74077
gamma-ray spectra 79−30083
geometries, hollow-cone radiation model 77−9761
Goldreich-Keeley radiative instability, physical mechanism 79−12400
gravitational cyclotron instability, mechanism for cosmic radio emission 78−65724
gravitational radiation, collapsed objects and exact solns., Einstein Centenary Summer School, Perth, Australia, 1979 January 80−105434
gravitational red-shift according to the bi-metric theory of gravitation 79−35119
gravitational wave emission from rotating and precessing rigid bodies, simple model, appl. to pulsars 79−97271
gravitational wave noise, from spontaneous prod. of gravitons, energy density distrib. *(Russian)* 79−12551
gravitationally redshifted γ-rays, neutron star mass constraints 78−4274
Hercules X-1, hard X-ray pulsation obs. 78−12293
Hercules X-1, heliocentric pulse period, OSO 8 obs. 77−91573
high energy neutrinos of extraterrestrial origin, possible detection with DUMAND 79−80179
hollow-cone beam models *(Russian)* 78−16451
hydromagnetic eqns. for infinitely long plasma cylinder, unstable soln., pulsar mag. fields 80−96352
induced Compton scattering in pulsar winds 78−96497
information sources for neutron star, dense matter and gravitational collapse physics 80−36657
integrated pulse profiles and mean fluxes, obs. at 2.388 GHz 79−92791
interpulse emission, structure 80−36652
interpulses, single-pole emission model 78−16449
interpulses and other off-pulse emission 77−87467
interstellar electron density determ. from decorrel. bandwidth of pulsar scintillation 77−78850
interstellar scintillation, analytic soln. of second-order moment eqn. 80−26726
JP 1953, period var. rel. to Dirac cosmology 77−22334
JP 1953+29, timing data anal., spinup/spindown 78−24522
lepton processes in supercritical mag. fields *(Russian)* 78−78159
long-period pulsars, absence rel. to force-free mag. fields instabilities 78−49425
low freq. radiation in interstellar medium 77−26044
low-velocity pulsars, OB binaries and X-ray stars, tugboat model for evolution 77−56915
luminosities, upper bounds for narrowband and broadband emission processes 80−51797
luminosity function and spatial density *(Russian)* 78−93290
magnetic alignment, classification system 77−45476
magnetic dipole moments secular variation 77−9764
magnetic field calculation of cosmological bodies 79−12399
magnetic field generation, inertial mechanism *(Russian)* 77−82268
magnetic field lines, behaviour in rot. system 78−20848
magnetic fields evolution 77−78808
magnetic monopoles, creation 79−35287
magnetic monopoles creation, theory 79−44516
magnetic polar cap region, hadronic photoabsorpt. and pair production 78−12261
magnetic pole model for pulsar emission 79−48838
magnetogyro ratios, calcs. and rel. to evolution 79−8937
magnetosphere, EM wave dispersion relations for charge-separated plasma 77−7549
magnetosphere, generalised Ohm law 77−37610
magnetosphere, magnetoactive plasma equilib. in gravit. field *(Russian)* 80−26895
magnetosphere, natural wave modes, rel. to radio emission polarization 78−69822
magnetosphere, nonaxisymm., relativistic plasma streaming, particle inertia 79−21320
magnetosphere, plasma, dissipation phenomena formalism 79−4111
magnetosphere, plasma waves propag. along mag. field in strongly anisotropic relativistic plasma 80−67542
magnetosphere, relativistic particle curvature radiation 80−77434
magnetosphere, relativistically streaming plasma, flux conservation, MHD and force-free approxs. 79−19081
magnetosphere, vibrations generation by klystron mechanism 78−53971
magnetosphere boundary layer phenomena 80−36776
magnetosphere emission, mag. bremsstrahlung of ultrarelativistic particle beam in relativistic plasma 80−46390
magnetosphere interaction with plasma flow, review of studies 78−65496
magnetosphere model, cylindircal, with particle inertia but no dissipative forces 80−51796
magnetosphere models, interior and exterior struct., pair prod. 80−46594
magnetosphere numerical modelling 77−29871
magnetosphere pair prod. 79−44515
magnetosphere plasma, instability 78−53976
magnetosphere radio emission, plasma supply and elec. forces, review 80−46595
magnetospheres, axisymmetric, finite inertia and resistivity effects 78−24521
magnetospheres, axisymmetric, method of soln. of self-consistent description 80−94825
magnetospheres, axisymmetric, self-consistent description 80−31318
magnetospheres, basic props., models *(Polish)* 77−17608
magnetospheres, consequences of polar cap model *(Russian)* 79−101169
magnetospheres, cosmic ray acceleration mechanisms *(Russian)* 78−16448
magnetospheres, electron cap shape of rot. neutron stars with strong mag. field 78−12265
magnetospheres, photon absorpt. by electrons, quantum mechanical treatment 79−1296
magnetospheres, plasma co-rotation 78−12258
magnetospheres, power-law electron and ion distributions in a strong magnetic field 79−96908
magnetospheres, quasi-steady, Vlasov-Maxwell eqns. 77−13375
magnetospheres, relativistic MHD wind or plasma wave 80−31317
magnetospheres, stellar-wind model for plasma-EM fields 80−22031
magnetospheres and radio emissions, conf. Snowmass, Colorado, USA (Aug. 1978) 80−41939

pulsars continued
magnetospheres physics, limitations on force-free approximation 77−5541
magnetospheres with arbitrary geometry, force-free approx. 77−64788
magnetospheres with parallel electric fields 78−65643
micropulses, drifting subpulses and nonradial oscills. 80−67766
microstructure, radiowave propag. in turbulent shearing plasma 80−94822
model pulsar plasma, MHD, Lorentz covariant eikonal method 77−27663
multiple-ring structure in hollow-cone emission 78−12259
neutrino and cosmic ray source, energy spectra 80−31319
neutrino and photon pair prod. in strong mag. field 78−407
neutrino luminosity, photodecay contrib. *(Russian)* 77−17360
neutrinos, high energy, emission from point sources and detect. techniques 79−2484
neutron crystals, review rel. to pulsars *(Polish)* 77−61369
neutron star magnetospheres, charged particle distribs. 77−13379
neutron star magnetospheres, laboratory modelling 79−75240
neutron stars, postglitch behaviour of quantum plasma 79−35289
neutron stars and compact X-ray sources, properties, general description *(Danish)* 77−67106
new discoveries, 102.5 MHz obs. of three objects *(Russian)* 80−67764
newly born pulsars with expanding dense envelopes, high energy neutrino sources 78−8034
northern sky, 17 new discoveries at 400 MHz 79−5853
NP0532, contrib. of Crab Nebula to dispersion meas. 77−74122
NP 0531, distrib. model of press., density, ang. vel., matter rot., grav. field *(Ukrainian)* 80−12775
NP 0531+22, review of gamma ray obs. *(Russian)* 78−41097
NP 0532, COS-B satellite obs., appl. of X-γ synchronisation to nonparametric anal. 78−73729
NP 0532, Crab Nebula, pulsar, radiofrequency, pulse arrival times 77−71123
NP 0532, Crab Nebula pulsar, variability of dispersion and scatt. 77−49409
NP 0532, Crab pulsar, ang. size at 74 MHz 78−12260
NP 0532, Crab pulsar, Compton emission model using gamma-ray data 80−67902
NP 0532, Crab pulsar, gravit. redshifted γ-rays, neutron star mass constraints 78−4274
NP 0532, Crab pulsar, influence on Crab Nebula small-scale polarisation 79−25656
NP 0532, Crab pulsar, lunar occultation obs. at decametre wavelengths 80−62248
NP 0532, Crab pulsar, magnetized cracks in crust rel. to matter flow, radio, X-ray and optical emissions 80−72990
NP 0532, Crab pulsar, mass and radius from supernova remnant physical theory 80−51834
NP 0532, Crab pulsar, model, X-ray, optical and radio emission 78−4265
NP 0532, Crab pulsar, model for unpulsed light 79−44518
NP 0532, Crab pulsar, nature of radiating particles *(Russian)* 78−12351
NP 0532, Crab pulsar, nonlinear plasma waves parametric instabilities 79−66915
NP 0532, Crab pulsar, nonlinear space charge waves rel. to coherent radio emission 77−41386
NP 0532, Crab pulsar, optical and X-ray pulses, Compton effect 79−53849
NP 0532, Crab pulsar, peculiarities, He outflow from surface layer *(Russian)* 77−60786
NP 0532, Crab pulsar, pulsed and unpulsed light 79−17005
NP 0532, Crab pulsar, pulsed X-ray emission obs. during lunar occultation 78−8032
NP 0532, Crab pulsar, random walk timing noise anal. 80−77432
NP 0532, Crab pulsar, relativistic material ejection rel. to Crab Nebula model 80−62230
NP 0532, Crab pulsar, resolution of peak of optical pulse 78−93292
NP 0532, Crab pulsar, search for coherent ELF radiation at pulsar freq., upper limit 79−16728
NP 0532, Crab pulsar, search for pulsed gamma-rays of energy 10^{13} eV 77−13373
NP 0532, Crab pulsar, search for X-ray polarisation 79−5851
NP 0532, Crab pulsar, transient structure of high-energy X-ray emission 77−33541
NP 0532, Crab pulsar, ultrahigh energy γ-rays, detect. by obs. of Cherenkov flashes of EAS 79−80368
NP 0532, Crab pulsar, X-ray and gamma-ray radiation 80−41885
NP 0532, Crab pulser, gravitational radiation obs., energy flux upper limit 80−36655
NP 0532, NP Crab pulsar, 1-10 MeV obs. in 1971 August 77−45605
NP 0532, rotation parameters, temporal var. 80−62170
NP 0532 magnetosphere, cyclotron instability rel. to origin of radiation *(Russian)* 80−8645
nuclear neutrino pair photoprod. in strong mag. field, pulsar neutrino luminosity *(Russian)* 80−68648
nuclear physics of neutron stars, review 79−92797
number density, rel. to rate of stellar collapses in Galaxy 77−71122
observational data 80−77435
observational parameters and dispersion measures 77−9763
observational properties, rel. to use as cosmic laboratories for study of neutron stars and hadron matter 80−77442
observations at 14.8 and 22.7 GHz 78−81645
observations of intensity vars. and timing irregularities 79−12485
optical pulsations, obs. of southern pulsars 78−77569
origin and z-distribution *(Italian)* 79−53850
oscillation period, increase with time, gravit. mechanism 80−67765
P_3 period, correl. with mag. field and age 80−90461
pair formation above pulsar polar caps, struct. of low altitude accel. zone 79−92790
pair production discharges above polar caps 77−53618
particle acceleration by DC electric fields 80−31316
period derivatives, distrib. in sky rel. to existence of solar companion star 78−12198
period jumps, prod. by neutron star thermal-timing instability 79−35293
periodic gravitational waves, focusing effects *(Russian)* 79−6032
periodic source absolute timing, limiting standard deviation 77−45314
periods, positions and proper motions determ. from pulse arrival times, UHF, obs. 80−77431
pulsars continued
phenomenological model, for coherent and incoherent radiation 78−40979
planetary systems, post supernova survival 80−56860
plasma, relativistic, longit. waves and beam instability *(Russian)* 79−60158
plasma collective effects and pulsar emission models 79−25461
plasma coupling, boundary conditions 80−94823
plasma instabilities *(Russian)* 80−36656
plasma oscillations in polar caps 77−60784
polar cap, inhomogeneous struct. and radiation processes 79−25623
polar caps, particle acceleration and radio emission 80−51794
polar caps as foil-less diodes, nonneutral relativistic beam accel. 80−17604
polarisation, rot. induced by non-Minkowskian spacetime 79−35115
polarisation charact. at 400 MHz 77−64787
polarisation charact. at 640 MHz for 43 southern pulsars 78−65642
polarisation fluctuations at 430 MHz with microsec. time resolution 78−16446
polarised radiation at 430 MHz, statistical summary 80−67760
polarization, intrinsic posn. angles for 40 objects 79−44517
positron production, galactic 511 keV gamma-ray line from positron annihilation 80−46590
potential drops above pulsar polar caps, nonneutral beam accel. 78−4267
potential drops above pulsar polar caps, ultrarelativistic particle accel. along curved mag. field 78−53970
proper motions, velocities and lifetimes 79−35284
proper motions from timing obs. 77−33540
proper motions from timing obs. 79−17003
PSR 0031−07, drifting subpulses obs. and implications for pulsar models 80−67763
PSR 0239+54, four-freq. study of single-pulse structure 78−53972
PSR 0329+54, binary motion to explain freq. variations 80−26894
PSR 0329+54 and 1133+16, obs. of single pulses at 327 and 2695 MHz 79−8939
PSR 0355+54, pulse shape change, 11 cm obs. 80−67761
PSR 0525+21 occulted by solar corona, Faraday rot. at 1720 MHz 80−46526
PSR 0531+21, Crab pulsar, γ-ray obs. with COS-B *(Danish)* 80−82544
PSR 0531+21, Crab pulsar, light curve, 1973 to 1976 period *(Russian)* 78−12263
PSR 0531+21, Crab pulsar, optical light curve changes in 1970-7 period 80−36654
PSR 0531+21, in Crab Nebula, SAS-2 gamma-ray obs. 77−33688
PSR 0531+21, interplanetary scintillations at 74 MHz 78−36625
PSR 0531+21, radiation generation mechanisms *(Russian)* 79−58370
PSR 0531+21 (Crab pulsar), pulsed γ-ray emission, COS-B obs. 78−8033
PSR 0531+21 X-ray pulse ground-based obs. 77−91444
PSR 0611+22, short time scale integrated pulse shape vars. 80−105267
PSR 0809+74, phase stability in drifting subpulse pattern 78−40980
PSR 0820+02, long-period binary pulsar, discovery from timing obs. 80−56867
PSR 0826−34, 408 MHz obs. of unusual profile and sporadicity 79−40207
PSR 0833−45, Veal pulsar, optical pulses detect. 77−49417
PSR 0833−45, Vela pulsar, γ-ray obs. with COS-B *(Danish)* 80−82544
PSR 0833−45, Vela pulsar, age determ. 80−77436
PSR 0833−45, Vela pulsar, Compton emission model using gamma-ray data 80−67902
PSR 0833−45, Vela pulsar, HEAO-1 pointed obs. 78−7856
PSR 0833−45, Vela pulsar, nature of assoc. X-ray source 79−17138
PSR 0833−45, Vela pulsar, optical pulse profile 80−46593
PSR 0833−45, Vela pulsar, pulsed and unpulsed light 79−17005
PSR 0833−45, X- and gamma-ray emission from Vela SNR *(Russian)* 80−94861
PSR 0833−45 (Vela pulsar), period change (1978 June-July) 78−89215
PSR 0833-45, review of gamma-ray obs. *(Russian)* 78−41097
PSR 0833-45, Vela pulsar, position determ. 77−49416
PSR 0833-45, Vela pulsar, pulsed high energy gamma rays 80−41848
PSR 0833-45, Vela pulsar, pulsed soft X-ray flux, upper limits 80−105268
PSR 0833-45, Vela pulsar, radio and γ-ray pulses, relative phases 78−85966
PSR 0833-45, Vela pulsar, SAS-2 high-energy γ-ray obs. 77−49411
PSR 0833-45 (Vela pulsar), pulsed γ-ray emission, COS-B obs. 78−8033
PSR 0950+08, ghost SNR, 327 MHz obs. 79−12506
PSR 0950+08, micropulses freq. struct. 80−22030
PSR 0950+08, PSR 0531+21, high-energy pulsed gamma rays obs. 78−45346
PSR 0950+08, submicrosecond time resolution obs. 79−8941
PSR 1133+16, high time resolution obs. of high freq. radio emission microstruct. 78−45348
PSR 1133+16, pulse microstruct. direct. obs. at timescales down to 6 μs 78−28711
PSR 1641−45, large period discontinuity in long period pulsar 78−77570
PSR 1747−46, gamma-ray emission obs. by SAS-2 77−2450
PSR 1822−09, balloon-borne gamma-ray obs. 80−105269
PSR 1858+03, distance 77−64785
PSR 1913+16, astrometry and photometry of stars in vicinity of binary pulsar 78−93219
PSR 1913+16, binary pulsar, appl. of bimetric gravit. theory 78−45347
PSR 1913+16, binary pulsar, companion star possible optical obs. 79−84823
PSR 1913+16, binary pulsar, components min. projected distance calc. 80−26904
PSR 1913+16, binary pulsar, confirmation of existence of gravit. waves *(French)* 79−80495
PSR 1913+16, binary pulsar, digital area photometry 77−49410
PSR 1913+16, binary pulsar, dipole gravitational radiation, Rosen's theory 77−26021
PSR 1913+16, binary pulsar, general relativistic effects meas. 79−35286
PSR 1913+16, binary pulsar, gravit. radiation in alternative metric theories 77−60589
PSR 1913+16, binary pulsar, nature from observational data 80−77435
PSR 1913+16, binary pulsar, optical pulses upper limit 77−26020

pulsars continued
PSR 1913+16, binary pulsar, optical source and general relativistic effects 80−56868
PSR 1913+16, binary pulsar, origin rel. to supergiant/neutron star double core evolution 78−53980
PSR 1913+16, binary pulsar, origin through X-ray binary double core evolution 79−84816
PSR 1913+16, binary pulsar, Poincare gauge theory of gravitation 79−75434
PSR 1913+16, binary pulsar, post-Newtonian timing effects 78−4261
PSR 1913+16, binary pulsar, relativistic observable effects 80−77438
PSR 1913+16, binary pulsar, report 79−75234
PSR 1913+16, binary pulsar, test of new dispersion-removing radiometer 79−35142
PSR 1913+16, binary pulsar obs. at 327, 408, 610 and 1420 MHz 77−78810
PSR 1913+16, binary system, test of relativistic effects *(Dutch)* 80−62172
PSR 1913+16, evidence for gravitational waves emission 79−92664
PSR 1913+16, Hulse-Taylor binary pulsar and gravitational spin precession 78−12264
PSR 1913+16, optical candidate, astrometry and high-speed photometry 80−101609
PSR 1913+16, optical candidate discovery, position, magnitude 78−69819
PSR 1913+16, X-ray and timing meas. correlations, grav. radiation, gas cloud friction 80−62171
PSR 1913+16b, binary pulsar, rel. to 4 BC Aquila supernova and Christmas Star 78−81781
PSR 1913+6, binary pulsar, relativistic astrophysics *(German)* 79−80213
PSR 1919+21, interpulse radio emission at freqs. 16.7-38 MHz 78−16447
PSR 1919+21, P_3 period temporal variability 78−36626
PSR 1919+21, pulsed radiation at 16.7, 20 and 25 MHz 77−87466
PSR 1952+29 and 1929+10, evidence of binary system disrupted by supernova explosion 79−35285
PSR 2016+28, radiation patterns, data reduction and two frequency study 77−57004
PSR 2020+28, orthogonal polarisation modes obs. 78−93291
PSR 2045−16, multiple-ring struct. in hollow-cone emission 78−12259
PSR 2223+65, rel. to supernova-induced star form. in Cepheus OB3 assoc. 78−12306
pulse analysis and development of models 77−71124
pulse polarisation patterns, rel. to quasi-transverse propag. theory 80−46591
pulse shape scattered in interstellar medium *(Russian)* 77−78855
pulse structure obs. at 102.5 MHz with 10 μsec time resolution 79−62862
pulse timing measurements, appl. to search for gravit. waves 80−56743
pulse timing obs. from Arecibo Observatory 79−8938
pulse width and period relations for various models 78−28714
quasars, multiple pulsar model rel. to colour variability 79−9021
radiation, polarised shot noise model 77−13374
radiation, subpulse and micropulse emissions rel. to neutron star crusts torsional oscills. 80−90464
radiation 79−97015
radiation from pulsars accelerates supernova envelope 79−62859
radiation mechanism, coherent amplification 77−78809
radiation mechanism, relativistic beam-plasma system, electrostatic excitation level 77−9762
radiation patterns, objects without synchronised drift across window 77−67105
radiation patterns, obs. of objects with synchronised drift across window 77−57005
radiation patterns, observational results rel. to physical mechanism 78−53973
radiation source form. mechanism, mag. annihilation *(Chinese)* 80−77440
radiation transfer through moving astrophysical plasmas 78−65489
radio and X-ray, review 78−69820
radio emission, amplified linear accel. emission mechanism 79−8936
radio emission, curvature radiation absorpt. theory 79−75090
radio emission, effects of superfluidity in neutron star 80−77441
radio emission, generation in neutron star mantle *(Russian)* 79−101168
radio emission, mag. field, energisation, comparison with Jupiter 80−46466
radio emission, millisecond intensity var. 80−98682
radio emission, possible mechanism 78−20847
radio emission, possible mechanism 79−84812
radio emission, propagation effects on polarisation 79−75235
radio emission appl. to possibility of detecting mag. charges 79−75704
radio emission beaming, possible relation with rot. braking 79−92793
radio emission from relativistic electron beams 77−5540
radio emission mechanism, model 78−12257
radio emission mechanism model, by electron/positron-magnetosphere EM ineteraction 78−8036
radio emission microstruct., qualitative model 77−49415
radio emission microstructure, propag. effects in shearing field-free plasma 80−17483
radio emission models, relativistic clock error effects 77−64786
radio emission polarization at 3.5 m wavelength 78−28713
radio emission rapid variation, mechanism *(Russian)* 80−77437
radio emission scintillation, decorrelation bandwidth rel. to dispersion measure 80−85964
radio emission spectra, 17-1420 MHz 79−62863
radio flux density and pulse profile at 102.5 and 61 MHz, obs. 80−17601
radio halos, search at 11, 21 and 40 cm wavelength 77−5539
radio pulsar, model involving neutron star elec. field 80−109453
radio pulses production mechanism 77−13372
radio radiation, as result of modulation instability in relativistic plasma *(Russian)* 77−22258
radio signals spectra and microstruct., relativistic electron beam model 78−65639
rapidly rotating rapidly slowing pulsars, rel. to short-lived Crab-type supernova remnants (plerions) 79−12504
relativistic and nonrelativistic gas flows, general symm. soln., low press. limit 77−9655
relativistic astrophysics, pulsars, supernovae, and X-ray sources *(German)* 79−101060
pulsars continued
relativistic beaming process rel. to pulses 77−29870
relativistic centrifugal winds 78−96473
relativistic degenerate electron plasma, dielectric response in mag. field, plasma oscillations 80−54022
relativistic electrons in strong mag. field, Raman scatt., pulsar radiation *(Chinese)* 77−53418
relativistic Langmuir soliton appls. 79−17004
relativistic spin-spin interaction theory for two concentric shells 80−46148
relativistic streaming plasma, generalised Ohm's Law, pulsar magnetosphere relevance 78−9823
review, cosmic gamma radiation, sources and detection 78−12059
reviews, galactic and intergalactic astronomy *(Russian)* 77−57061
rotating magnetosphere, charge bunching mechanism for coherent curvature radiation 77−33538
rotating neutron stars, general relativity, exact solns. for slow rot. 79−75239
rotation measures, determ. of galactic mag. field components 80−85966
rotation periods, long-term changes rel. to neutron star interior plasma 80−22029
rotational behaviour rel. to superfluidity 80−98683
rotational energy loss, slowing down index and time derivs. 80−67762
rotational history of pulsars in massive X-ray binary systems 77−49412
rotational velocities, effects of neutrino ang. momentum losses in stellar collapse 77−56916
Ruderman-Sutherland model, emission zone limits 80−51795
scintillation, freq.-time struct., means for detecting interstellar electron density irregularities 80−101608
scintillation, modified Rickett diagram for charact. freq. scale versus dispersion meas. wavelength parameter 77−17609
scintillation theory, mathematical anal. of physically thin screen 78−28501
scintillations, cosmic ray streaming or mirror instability effects 80−51845
scintillations, freq. cross-correl. and finite bandwidth effects 80−4392
scintillations, interstellar density fluctuations effect 80−46649
scintillations, interstellar medium mirror instability growth effects 80−46648
second Molonglo survey, 155 discoveries 79−12486
signal microstructure, periodicities, polarisation and pulsar magnetospheres probing 79−75232
signal scattering by turbulent interstellar plasma 79−5854
size limit, for uniformly pulsating EM radiation sources 79−84656
slowly rotating stars, gravit. collapse, supernova explosion, neutron star or pulsar remnant 78−96472
Smith's model, inconsistent with obs. 78−28712
in southern hemisphere, polarisation obs. at 1612 MHz 80−90462
southern sky survey, progress report 78−69821
space velocities rel. to evolution 78−4264
space velocity vector orientation rel. to spin axis 77−53619
spatial distrib. and birth-rate 79−25624
spectra, charact. feature interpretation 80−109451
spectra, nature of low-freq. dropoff 80−17602
spectra and flux densities in 61-1420 MHz range for 9 objects 79−12487
spectrum, charact. freqs. rel. to pulsar models *(Russian)* 79−58369
spin-down rates, distrib. in sky rel. to reality of Sun companion star 78−57475
SS 433, massive black hole and pulsar models rel. to precessional motion origin of 164^d period 80−62138
SS 433 as veiled pulsar 80−41842
static plasma polarisation in Schwartzschild gravitation field *(Russian)* 79−16825
stimulated linear acceleration bremsstrahlung, unlikely mechanism 79−92658
stress-deformed state of rotating neutron star *(Russian)* 77−37612
subpulse drift rel. to particle acceleration at magnetic poles of neutron star 78−93295
subpulse polarization pattern theory 79−48837
subpulse widths derivation from integrated profiles equivalent widths 78−65640
subpulse widths lower bound 77−17607
Sun, pulsation with 2^h40^m period, possible magnetospheric origin 78−7961
superconducting vortex systems in pulsar nucleus *(Russian)* 79−8935
superdense stars in quantum limit of ultrastrong frozen-in mag. fields 77−53620
superfluid dynamics, rotating, lab. expts. 78−49469
superfluid liquid rotation, theory, relativistic effects in vortices *(Russian)* 78−61876
superfluid phase transition for neutron star matter 80−101607
superfluid system, rotating, dynamics of Onsager-Feynman vortices *(Russian)* 77−82270
supernova light curves, pulsar theory, dynamical effect and thermalisation of strong waves 78−8028
supernova light curves rel. to existence of central pulsar 78−4256
supernova off-centre explosions, rel. to high vel. pulsars form. 80−46587
supernova remnant/pulsar associations, possible origin in close binary systems 78−85965
supernova remnants, pulsar-driven isothermal blast-wave models 77−78847
supernovae, rel. to origin of pulsars 77−87455
surface structure, props. of condensed matter in huge mag. fields 80−82187
synchro-Compton radiation damping of linearly polarised plasma waves 78−61877
timing observations, rel. to neutron stars thermal/timing instability 79−92795
timing observations at NASA Deep Space Station, Tidbinbilla 77−33542
trigonometric parallax meas., electron density determ. in solar neighbourhood 79−88694
3U 0833−45, Vela pulsar X-ray flare obs. 77−22260
3U 1223−62, binary X-ray pulsar, Ariel V obs. 78−96566
4U 1538−52, binary X-ray pulsar, early B-type supergiant as counterpart 78−93472
3U 1626−67, X-ray pulsar, X-ray position and optical candidate 77−67139
3U 1626−67, X-ray pulsar as accreting neutron star in compact binary 78−49470

pulsars continued
ultrahigh-energy neutrinos production, fluxes and detect. techniques 78−49264
ultrarelativistic beam quasilinear relativistic plasma relax. in strong mag. field, magnetobremsstrahlung *(Russian)* 80−38669
ultrarelativistic electron-positron plasma, wave prod., rel. to pulsar radiation 78−20629
Universe, high density matter, many body treatment, pulsars 80−26738
vacuum gaps in magnetospheres 79−30082
Vela, detect. of change in rot. measure 77−29867
Vela, pulsed emission prod. by synchrotron mechanism 79−35283
Vela pulsar, assoc. extended X-ray source obs. 78−41095
Vela pulsar, gravit. radiation revised estimate 78−32501
Vela pulsar, ultrahigh energy γ-rays, detect. by obs. of Cherenkov flashes of EAS 79−80368
Vela pulsar (PSR 0833−45), radiation model 80−94824
velocities, critical review 77−78811
wave forms, anal. rel. to hollow-cone beam models 77−2449
X-ray pulsars, accretion torques 77−49505
X-ray pulsars, effect of vacuum birefringence on X-ray polarisation 78−4408
X-ray pulsars, radiating accretion column model 77−53710
X-ray pulsars, relativistic accretion 79−9032
Fe atoms and condensed matter in strong mag. fields, var. calc. ground-state energy 77−75046
H I absorpt., meas. in seven low-latit. pulsars 80−101606
H I absorption in spectra of four low latitude pulsars, interstellar electron density determ. 79−92792
H I radio recombination lines obs. in direction of pulsars 77−74155
H_2-He plasma interface in strong gravit. field, bremsstrahlung, neutron stars and pulsars appl. *(Russian)* 79−67048

pulsatile flow
see also peristaltic flow
air flow, time-averaged stagnation pressure probe design 78−14116
air flow in pipes, heat transfer coeff. 77−62252
air flow over rearward facing step, flow separation meas. 80−69885
air in heated channel, turbulent flow, velocity and temp. pulsation characteristics 80−14820
aneurysm, pulsatile pressure and flow distrib. using latex fusiform models 77−21547
aortic and mitral valve prostheses, in vitro flow visualisation 77−86703
aortic coarctation distal flow profiles 78−44528
aortic shear stress reduction by cardiac pacing 78−40239
aortic valve opening, haemodynamics 78−20208
aortic valve prosthesis, Hancock porcine xenograft, comparison of models 242 and 250 77−56532
aortic valve prosthesis, Reul-Ghista optimal tri-leaflet, in vitro performance tests 79−92432
arterial blood, incompressible flow, stability *(French)* 77−5023
arterial curvature sites anal. of unsteady component of pulsatile flow 77−56408
arterial dynamics, model of multilayered shell with fluid flow 77−29171
arterial flow lipid transport model 78−44552
arterial stenosis, math. model 80−72202
arterial stenosis and stenotic atherosclerosis, dynamic press.-flow diagrams 80−3658
arterial stenosis model, pulsatile flowfield downstream 80−17001
arterial stenosis models, initiation of turbulence, steady and pulsatile flow 79−79577
arterial system, elastic non-uniformity using hydraulic model 77−29164
arterial system, elec. simulation 77−25501
arteriosclerotic flow models, velocity fluctuation and shear stress obs. *(German)* 79−16226
binary boundary layer with press. pulsations, friction and heat and mass transfer 80−14653
blood pulsatile viscous flow, O_2 transport to diseased coronary arteries of man 78−40220
blood, arterial flow, linear theory *(Chinese)* 79−39427
blood, particle paths and stasis in unsteady flow through bifurcation 78−20206
blood, pulsatile viscous flow through diseased coronary arteries of man 77−90835
blood, studies in model of human aortic arch 80−104633
blood, thin walled collapsible vessels 79−25020
blood, through tube containing rigid and distensible sections, num. soln. technique 77−56419
blood, turbulent flow through natural human vitral valve 77−36975
blood, unsteady viscous flow in non-uniform channels, numerical anal. 77−52830
blood analogue in curve tube, flow visualisation 78−44546
blood electric impedance, effects of pulsatile flow *(Japanese)* 80−21513
blood flow, laminar-turbulent transition, in pulsatile flow *(French)* 77−5022
blood flow calc. by indicator dilution, pulsatile error analysis 77−60225
blood flow in artery, math. model 78−31831
blood flow in artery, pulsatile flow 80−106845
blood flow in channel of small exponential divergence, flow separation 77−86528
blood flow in frog web arteriole 80−16964
blood flows, oscill. freq. effects in plane wavy conduit flows 78−20209
blood pressure control model 77−21557
blood pump, pulsatile, stabilisation of unsteady ball valve motion 78−44708
blood pump, vortex diode used as outflow valve 78−44724
blood pump development and characteristics 77−81659
branching pipeline system pressure pulsation calc. and expt. *(Japanese)* 79−90337
bubble motion in viscous liquid half-space near boundary with inviscid liquid 80−19494
buoyancy effects, heat transfer and flow over semiinfinite plate 77−80152
capillary blood volume flow determ. by improved photoplethysmograph, Hemorheograph 78−31934
cardiovascular flow disturbance, US detection 77−60231
channel, with diverging walls, blood streaming viscous-convected inertia effect 77−52828
channels, constricted or dilated, pulsatile flow at high Reynolds number 80−74985
conjugated nonstationary heat exchange with pulsating fluid flow in circular tube *(Russian)* 79−68817

pulsatile flow continued
coronary flow model, of horse, method of characts. calc. 77−86524
couple stress fluid pulsatile flow through circular tubes 79−62275
curved tube, axial velocity profile meas. 80−41088
cylinder in pulsating air-water spray, forced convective heat transfer *(French)* 79−7274
cylindrical cavity in incompressible fluid, rel. to detonation *(Russian)* 77−24001
cylindrical pipe, pulsating flow type of entry effects 79−37400
drag plate flowmeter, for pulsating flow, design and evaluation 79−68863
duct flow in presence of orifice plate, discharge and press. drop coeffs. eval. 78−30306
ducts, eddy motions induced by water waves and periodic flows 80−33679
ducts, noncircular straight, steady and unsteady flow 77−65795
dusty fluid through constricted channel 79−14468
electrolytic method of mass transfer meas., appl. in oscill. and pulsating tube flows 79−68828
flow rate meas. error using US phase flowmeter 77−72388
flowmeter, for pulsating flow, design and evaluation 79−68863
fluid filled tubes, pressure pulse propag. 77−65797
free moving drop in pulsating liquid, mass transfer *(French)* 77−27588
furrowed channel, flow patterns calc. 79−23367
furrowed channels with pulsatile flow, Navier-Stokes soln. flow patterns, separation 80−33672
furrowed channels with pulsatile flow, observed flow patterns, separation and vortices 80−33673
gas phase catalytic reactions, periodic press. cycling, viscous flow effects 80−19521
gas transport in duct, variable periodic flow *(French)* 77−72315
gas-liquid cocurrent downflow in fixed bed in pulsed regime, mass transfer fluctuations 80−19485
gas-solid mixture, pulsating flow, hydraulic resistance, heat transfer 78−38392
harmonically oscillating visco-elastic boundary layer flow 79−55401
Hartmann-Sprenger tube, air jet from convergent nozzle, air column oscillations generative mech. 80−14828
heart valve prosthesis mean press. gradient meas. under in vitro pulsatile flow 77−56531
heat exchanger radial tube bank vibration in transverse liquid flow *(Russian)* 79−81973
heat transfer and skin friction, pulsating laminar-boundary layer 78−94711
heat transfer in porous channel 77−19604
Helmholtz resonators with grazing flow, dye streamlines 78−63511
Hiemenz flow, pulsatile, struct., and temporal variation of wall shear stress near stagnation point 77−62303
Hiemenz flow struct., wall shear stress temporal var. near stagnation point 77−75929
horizontal gas-liquid stream, flow vel. meas. 80−96301
hot-film probe, in reversing flow, forced convection, finite difference soln. 80−12177
hydraulic lines, wave phenomena, coupled vibrations in bending and branching lines 80−14778
hydraulic lines, wave phenomena, freq. characts. between press. and flow rate 79−32669
ideal fluid small oscillations, mass forces in elastic shell, simulation of blood vessels 79−77253
incompressible liquid oscills. in variable cross section viscoelastic tube due to pulsating press. 80−31519
jet, air, subsonic, fully pulsed, near field vel. meas. 80−19540
jet, turbulent, plane, impinging on solid wall, spectral characts. of pulsations 78−9668
laminar, velocity meas. for flow in 90° branch, appl. to atherogenesis 78−38277
laminar channel flow, heat transfer 77−31297
laminar compressible flow in cylindrical pipe with through flow 77−80216
laminar flow in tubes, heat tranfer 78−30289
laminar heat transfer between two parallel plates, pulsation effects *(German)* 80−33681
laser Doppler velocimeter signal analysis for pulsatile arterial flow meas. *(Japanese)* 79−2156
laser velocimetry technique, for phase inhomogeneous medium, appl. to pulsed flow *(Russian)* 78−30375
liquid, immiscible, pulsating, stability of interacting cylindrical liq. jet 78−83444
mass transfer to drops moving in pulsating flow, renewal-penetration model 77−31369
measurement, using automatically controlled static plate flowmeter 79−68870
MHD pulsating viscous flow superposed on steady laminar motion 80−92228
micropolar fluid, model for blood flow 77−7359
n-incompressible and immiscible rarefied gases, pulsating flow between two plates 80−10306
non-Newtonian pulsatile laminar flow in tube 78−79346
non-Newtonian pulsatile laminar pipe flows, multiviscous approx. 77−3871
nonisothermal streams, turbulent velocity pulsations meas., procedure 80−19514
orifice meter, pulsating incompressible flow, anal. and expt. 78−34230
oscillating flow past flat plate, heat transfer, viscous dissipation effect 77−80151
periodic helical flow in pipe, linear stability, Hermitian forms and eigenvalue bounds 79−37401
pipe, laminar pulsating flow, heat transfer 79−94621
placenta, human, detect. of pulsatile flow in situ by impedance meas. 80−104799
plane channel with parallel walls, turbulent flow stability *(Russian)* 79−37295
polymeric fluids, in circular pipes, Maxwell model 78−90937
polymeric liquid flow in circular tubes, flow enhancement, Goddard-Miller model 78−30324
post-stenotic turbulent wall pressure fluctuations, spectral and temporal characts. 80−16994
pressure pulsation in pipelines, resonant amplitudes 78−9646
pressure waves of finite amplitude in elastic tubes, water expt. 77−27596
propagation rate of pulse wave in arteries 80−41099

pulsatile flow continued
prosthetic aortic valves, press. drops under steady and pulsatile flow, in vitro meas. 78−44731
prosthetic mitral valve, pressure drop and flow pattern obs. 79−92430
pulmonary haemodynamics, quasi one-dimens. unsteady nonlinear fluid flow eqns. soln. 80−41104
pulmonary vascular response to hypoxia, online impedance analysis system 77−52943
pulsating turbulent pipe flow, velocity field and press. gradients 80−64641
quantitative representation of nonrepetitive temporal behavior 80−92101
renal branch unsteady blood flow simulation 78−27983
resonant gas oscillations in open pipes due to moving piston 79−68805
resonant hydraulic circuit pulsatile water flow meas. using laser Doppler velocimeter 80−103091
roller pump for pulsatile blood flow 78−44721
rotating pipe flow 77−62258
sinusoidally curved pipe, pulsating laminar flow, anal. 78−87390
spherical oscillating gas bubbles in fluids, fluid compressibility influence *(German)* 79−37383
stenoses model disorder distal, steady and pulsatile flow 79−57688
stenosis model, flow disorder distal to mild stenoses 78−44551
stenosis model, pulsatile flow downstream 79−92279
stenosis model, turbulence development in pulsatile flow through partially occluded tubes 78−44531
stratified gas-liq. film flow, eqns. of motion 79−37376
suction and wall injection effects on flow in a tube, Navier-Stokes eqns. 78−38403
suspension, oscillating parallel flow in channel 77−68677
suture line stress in end-to-side anastomosis, math. assess. in pulsatile flow 80−97986
thermal convection in step wake with pulsating jet *(French)* 80−10240
transitional turbulent pulsatile flow in channel 77−46993
tube, oscillating and pulsating flow, critical Reynolds numbers *(German)* 80−1687
turbulent flow onto elastic surface, boundary-value problem *(Russian)* 78−75153
turbulent gas flow in channel, wave attenuation factor 77−42852
turbulent pipe flow, press. and vel. distribs. 77−24023
turbulent pipe flow, vel. distrib. 79−32666
turbulent pulsatile flow, wall region periodicity 77−54978
turbulent pulsating tube flow, friction resistance and energy losses *(Russian)* 77−51039
unstaggered tube bank vibration induced by viscous liquid flow *(Russian)* 80−33677
unsteady flow in a porous, elastic rectangular tube *(Japanese)* 80−6143
unsteady pipe flow of viscoelastic fluids−possibilities of volume discharge increase *(German)* 79−50797
unsteady viscous flow curved elastic tube model 80−16998
unsteady viscous flow in curved elastic tube, Fourier analysis 79−92281
vapour bubbles, analysis of oscillation 80−19487
vapour bubbles, evaporation-condensation resonance frequency 80−19488
ventricular volume determ. from indicator dilution curves, dog expts. 79−57696
viscoelastic fluid, fluctuating flow in a porous channel 79−64774
viscoelastic liquid, pulsatile flow in elliptic cross-section channel 79−7392
viscoelastic tube, pulsatile flow, non-Newtonian effects *(French)* 80−59113
viscous fluid in rotating channel 80−10311
viscous sublayer and near wall turbulence struct., stroboscopic visualisation 80−19349
wake structure of two-, three-dimensional flame holders 80−53786
water, turbulent flow, effect of polymeric additives 79−1216
water flow vel. meas. in oscillating pipe 77−68691
water pulsating flow in heat exchanger effect of pulsations on heat transfer 79−94614
Ar, supersonic pulsed flow from conical nozzle 80−103056

pulse amplifiers
300 W wideband pulse amplifier 78−86302
automatic simple pulse echo tracking apparatus, US absorpt. meas. appl. 77−22571
charge sensitive high resolution amplifier 77−88352
DC couple linear pulse amplifier, fast, gain and phase response design 80−58088
delay line readout for drift chambers 79−3317
fast charge sensitive amplifier, input circuit response anal. 79−13609
fission ionisation chamber, high-speed, in pulsed current regime 77−6620
Gaussian filter for nuclear pulse amplifiers, direct synthesis, freq. domain anal. 77−3239
linear, for X-ray spectrometer, cct., features 78−78595
linear accelerator, pulse amplifier with digital gain control 80−68977
NMR pulsed spectrometer wideband preamplifier 79−71502
parametric convertor type pulse amplifiers, AC Josephson effect appls. 78−19184
photoconduction decays, fast, measurement, DC-10 MHz low noise amplifier system 80−57326
scintillation detector amplifier for widely varying input amplitudes 77−50335
transresistance amplifier for CdTe radiation detector 79−13594
US receiver response, optimised by fast-attack detector 77−80034
voltage sensitive, noise meas. 77−88353

pulse amplitude analysers *see pulse height analysers*

pulse amplitude modulation
linear convertor, for acoustic emission signals 78−9512
microwave field dosimetric device 80−3818
multistep laser excitation, pulse modulation, Schrodinger eqn. anal. 78−63046
optical fibre digital communications, PAM-PPM signalling format 79−27190
optical fibre transmission expts. at 34 Mb/s with HDB3 line code 80−64198
telemetry, low power PAM/FM system for ventricular press. and cardiac dimension meas. 78−44747
He-Ne laser pulsed internal modulation 77−61985

pulse analysers
see also pulse height analysers
alpha particle assay, liquid scintillation with energy and pulse shape discrimination 77−23350
amplitude and time analyzer for flaw detect. 79−70288

pulse analysers continued
digital differential pulse rate meter, nuclear plant radiation monitoring appl. 78−37451
digital lock-in detection technique and appls. 79−49303
discriminator, high-speed nonoverloading, for pulse counting 77−401
electron spectrometers, pulse shape anal. in fosfich detector 77−65387
flash counter and interval recorder 78−88928
high-speed broadband amplitude discriminator that does not change pulse duration 79−26842
implanted cardiostimulator pulse recording 77−78041
Munich pulse shape discrimination cct., low energy performance 78−46233
picosecond trigger system for mode-locked laser pulse meas. 77−26406
picosecond waveform meas. 78−57923
pulse counter, four-function pocket calculator adaption, for teachers 78−12497
radiation detectors pulses, review of time position meas. methods 77−65410
shape discrimination cct. for n and γ multidetector meas. 78−70709
single channel analyser, temp. stability, resolution 78−33399
α-γ separation using pulse shape discrimination, trans-stilbene scintillator 78−13386

pulse circuits
see also demodulators; digital circuits; modulators; pulse generators; pulse shaping circuits
Auger electron spectroscopy blanking resistive heating cct. 77−29078
counting circuit, in time-interval series meter 78−176
current and voltage measurement in pulsed X-ray device, voltage divider and Rogowski coil *(Japanese)* 78−93788
direct display of gas-gun projectile velocity 78−177
electric conductivity meters with automatic correction of charact., seawater appl. *(Russian)* 78−65426
gating, medium speed, of Intensified Silicon Intensified Target (ISIT) tubes 78−12766
gyrowave interaction experiment, synchronising, triggering 77−45191
high-resolution multipulse NMR spectrometer 78−58000
high-speed amplitude spectrometry, overlapping pulse elimination 78−78544
klystron self excited oscillator with short time delay microwave pulse 77−6578
laser isotope separation pulse power requirements 79−13972
LF meter used for measuring period between pulses 79−85128
linear pulse selector for US investigs. 78−5623
noise suppression circuit for automatic flaw indicator 79−5111
octave synthesizer, teaching appl. 79−44680
optical multichannel analyser for picosecond spectroscopy, synchronisation circuit 77−38022
oscilloscope low repetition trigger cct., for high speed pulse observation *(Spanish)* 80−62657
passive notch circuit for pulsed-off fusion power compression fields 77−23266
rate recorder providing printed record 78−3644
ratio analogue pulse height module for fluorescence activated cell sorter 79−20734
semiconductor spectral noise meas. between 30 and 400 MHz, pulse technique device *(German)* 79−47134
series coupled power crowbar system for Tokamak devices *(Japanese)* 78−55755
spectroscopic light curve *(Russian)* 78−46740
standard signal transmission over long cables, using ESL ICs 78−5102
statistically distributed flow conversion into pseudorandom flow, counting cct. appl. 77−18753
stroboscopic method for picosecond diagnostics of rapid processes 78−47159
synchroniser clock circuit, improves signal-to-noise quality of evoked response measurements 78−24155
temperature measurement, pulsed thermistor operation method 77−82510
ten-channel differential discriminator for radiation detection spectra 78−78593
time coder with variable channel width for time-of-flight expts. 78−33403
time to digital convertor, wide-range 79−18090
time-amplitude convertor for leading-edge spectrometer 77−6607
time-domain electromagnetics and its appl. 78−71010
time-to-amplitude convertors, spectral distortion *(Japanese)* 77−46469
US receiver response, optimised by fast-attack detector 77−80034
Xe pulsed light source, programmed command unit 77−79163

pulse-code modulation
see also delta modulation
adaptive differential, speech digitisation and bandwidth compression techniques *(Korean)* 79−59876
ADPCM, for speech waveform coding, developments in Japan 80−33353
ADPCM coded speech, segmental SNR measure as indicator of quality 80−33359
data transmission performance study in optical fibre communication system 78−38028
digital image coding techniques, performance analysis 77−58277
digital speech interpolation system called adaptive DPCM with time assignment speech interpolation 80−99903
encoding and decoding for optical memories 80−102658
holography, binary digital hologram synthesis, PCM method 78−17876
Information Measuring System error computation considering communication channel charact. 78−73957
LANDSAT multispectral sensor image adaptive coding techniques 78−45060
laser PCM, injection laser radiation, optimal conditions 79−59733
modulation schemes for optical transmission systems *(German)* 79−36994
monochrome picture signal, digitally coded, level reassignment technique 78−55307
optical computing for image bandwidth compression, analysis and simulation 78−94373
optical fibre systems, Australian development 77−65630
optical fibre transmission experiment, 800 Mb/s, using single-mode fibre 77−88917
optical fibre transmission experiments, 100 Mb/s and 400 Mb/s PCM signals 77−88918
optical fibres, 0.95 Gbit/s PRS signals regeneration after transmission over 0.91 km of fibre, regeneration cct. 79−59807

pulse-code modulation continued
optical links development of basic units for PCM transmission *(Dutch)* 79−68365
PCM audio disc *(Japanese)* 79−27484
semiconductor laser direct PCM improvement by optical feedback 78−1287
speech, sub-band coding with adaptive bit allocation 80−28386
speech digitization and bandwidth compression, ADPCM and ADM *(Korean)* 79−55273
speech encoding, freq. domain techniques using APCM 80−33355
speech transmission, forward and backward prediction in adaptive differential PCM over nonideal channels 80−99902
speech waveform coders, objective quality meas. equipment and method 80−91981
tape recorder, wideband, Space Shuttle Orbiter appl. 77−64614
telemetry systems, air pollution detection/control appl. *(German)* 78−93003
Viking Lander camera design 77−41285
CO_2 TEA Laser pulse, PCM with CdTe crystal Pockels modulator 80−102742
GaAlAs DHS laser, direct modulated from 260 Mbit/s to 1.4 Gbit/s, monomode operation 78−46601
$Ga_{1-x}Al_xAs$:GaAs LED 640 mbit/s PCM optical fibre source, expt. 78−37998
GaAs-$Al_xGa_{1-x}As$ injection laser, direct modulation and spectral props. *(German)* 78−37921
He-Ne laser, internal pulse-code modulation, 0.6328 μm at 150 Mbits s^{-1} 79−76725
InGaAsP-InP 1.27 μm CW DH injection lasers, 1.1 Gb/s pseudorandom PCM 78−55390

pulse-code modulation links
9 km fibre-optic telephone transmission system 78−42435
400 Mb/s optical transmission expts. 77−88954
400Mb/s SELFOC fibre transmission system expt. 78−1419
coded and transmitted images, optimum restoration technique 77−58278
digital transmission system for Deutsche Bundespost using fibre-optic link, PCM 480 system 80−38120
fibre-optic system repeater error rate calc. approaches compared 77−54672
optical, with envelope modulation, pulse detection characteristics 77−11010
optical communication expt., graded index fibre, 1.12 Gbits/s 77−83967
optical fibre communication system numerical aperture optimisation *(German)* 78−38017
optical fibre digital transmission error probability, quantum noise effects *(Italian)* 77−23623
optical fibre transmissions of 100 Mb/s and 400 Mb/s PCM signals 78−1323
power station fibre-optic system installation 79−37028
random noise, optical PCM communication system, Poisson and Gaussian analysis *(Italian)* 77−50759
telephone carrier system, optical fibre cable development 78−9458
GaAs-$Ga_{1-x}Al_xAs$ DH strip CW laser for optical transmission *(German)* 77−68222

pulse control systems *see sampled data systems*

pulse frequency modulation
dielectric optical waveguide, chirp pulse transmission characts. 78−9438
Doppler blood flowmeter modulation *(Japanese)* 79−2115
fibre optical video transmission, noise performance, cable attenuation 77−65634
fibre-optic video transmission to and from undersea vehicles 80−46310
FM pulse sound holographic imaging 79−55270
heart natural pacemaker, modelling as pulse-freq. modulator 78−40135
neural communication system model, single signed integral PFM and PPM comparison 79−5268
optical repeater using PFM at 1 GHz, GaAs-GaAlAs laser system 79−98395
resonant e.m. pulse freq. modulation 77−734
wideband subcarrier PFM analogue optical communications channel 77−27378

pulse generators
see also multivibrators; square-wave generators; time bases
1 kV SCR pulse generator for US pulse echo excitation 79−70290
40 ns 55 A pulses for heterojunction laser, cct. *(Polish)* 79−3701
100 ps risetime, for GaAs laser drive 77−7149
600 kV repetitive stacked line transformer pulse generator 78−77935
1200 pF fast-response pulse voltage generator for spark chamber 77−54444
accelerator modulator charging system upgrade for 5 MeV electron accelerator 80−23182
acupuncture diagnostic system *(French)* 79−62397
additive pulses from internally stressed magnetostrictive wire bundle 79−99742
alternate polarity HT fields, appl. to Ne flash tubes 77−10539
atom probe FIM evaporation pulse generator 78−78041
automatic threshold following pacemaker concept and application 77−81671
avalanche transistor pulser for fast-gated operation of microchannel plate image intensifiers 78−37527
betatron electromagnet pulsed power supply 78−82546
bipolar square,for investigation of ferroelec. switching characts. 80−62687
calibrated electrical pulse production for meas. of electrical props. of conductors 78−8416
calibration, spectrum amplitude measurement 77−18017
cardiac arrhythmia simulator 79−100755
cardiotachometer calibrator appl., precision 77−86682
coaxial relay current pulse generator for laser pumping 78−59014
colour sensing optoelectronic device, neural mechanism modelling 80−12128
computer programmable digital pulse generator for Fourier NMR spectroscopy 80−98959
computer-controlled stimulator for ventricular myocardial function analysis 77−60267
constant current electrosurgical generator, load independent 78−44684
current pulse generator, to direct prolonged burst of betatron-accelerated electrons onto target 78−5072
delayed-pulse generator, ten-channel 78−4634
demand pacemaker, with adjustable-pulse-width, clinical experience 77−81697

pulse generators continued
demand pacemaker, with variable-pulse-width, clinical experience 77−81696
diadynamic current therapy, portable apparatus 79−57809
digital, programmable, for proton enhanced ^{13}C high-resolution NMR spectrometers 79−58762
digital pulse programmer cct. 77−74474
digital signal generator for rapid scan differential pulse voltammetry 80−61182
digitisers, nonlinear clock 79−18091
diode circuit for high bit rate pulse regeneration and injection laser modulation 77−79935
dual integrated gate generator 78−55112
electrocardiostimulator parameter tester 77−21658
electroconvulsive therapy pulse instrument 78−53562
electrostimulator, portable, for transcutaneous analgesia 78−36032
electrostimulator for leg muscles to correct defective walking 78−36051
electrostimulator for muscles, Stimul-1 78−36035
electrostimulator three-mode control unit 79−20693
exploding wire, MHD calc. 77−55196
fast digital two channel pulse generator, for controlling time resolved expts. 78−93670
fast-rising, time-domain reflectometry, development *(German)* 79−6148
functional generator of controlling voltage of energy modulator for synchrocyclotron injector 80−68975
fusion reactor, TEXT, motor-generator power supply system 80−99292
fusion reactor power supply using air powered fibre optic coupled pulser 78−13342
gas-discharge lamp, current pulse formation using thyristor keys *(Bulgarian)* 78−33795
gastrointestinal tract electrostimulator, Endoton-1 78−36033
HF oscillator with single coil transducer, for NMR spectrometer 79−2802
high average power pulser, for Cu halide laser systems 78−5497
High Density Z-pinch pulse power supply 79−14603
high speed image intensifier gating circuit 79−37044
high voltage pulsed system, designed for small labs. 78−86079
high-voltage pulse generator, controlled spark gaps 78−5965
HV, generation using chemically enhanced opening switch 77−49744
HV, Kirlian photography appl. *(Italian)* 78−49916
HV high-speed, centre aperture, disc capacitors, spark chamber appl. 77−34511
HV pulse generator for modulation spectroscopy 78−77995
HV pulser development for CS_2 laser cavity 80−23707
HV pulser for discharge into CS_2 laser cavity, with triggered spark gap 79−13973
HV staircase generator, modulated fast bump for CPS continuous transfer 77−83240
impulse generator, for exciting acoustic waves 79−10441
inductor for high power impulse production, features *(German)* 78−50293
infrared detector, pulsed LED source detects objects on a conveyor belt 78−45700
injection diode modulated laser pulse generator and digital control cct. *(Russian)* 80−14372
injection laser pumping by thyristor oscillator 79−13982
laser digital communication system, 100 Mb/s, optical receiver and pulse generator *(Russian)* 79−94170
LF pulsed NQR spectrometer transmitter 77−61101
line source of pulsed EM radiation in two-media configuration, incident, refl. and transmitted waves 79−64153
linear accelerator with S-band subharmonic prebuncher for picosecond single electron pulse *(Japanese)* 80−78460
linearly varying amplitude, Ge(Li) spectrometer calibration appl. 77−10526
low-impedance high-voltage pulsers, for travelling wave excitation of UV gas lasers 77−3608
Marx type fast rise impulse generator using laser triggered gap switches *(Japanese)* 78−94940
mass spectrometer, double step pulse-forming circuit for ion extraction 77−18124
metal electroplastic deformation meas. pulse generator *(Russian)* 80−25931
multichannel commutator, for HV spark gaps, investigation in Torus accelerators 77−71708
multichannel commutator for thermal analysis data transfer to single recording instrument 79−52821
multichannel nanosecond pulse generator for cyclotron stroboscopic system 79−68168
multifunctional programming unit for self-contained oceanographic instruments 79−2391
multiple pulse NMR in solids, pulse programmer for high resolution expts. *(German)* 77−41660
multiple-cct., for high repetition rate rare gas halide lasers 78−94399
MW impulse generator system, for ion cyclotron heating, fusion reactor 78−70635
nanosecond, high-power, wave processes 77−18730
nanosecond pulse electron and bremsstrahlung generator 78−21308
nanosecond pulses, two-channel type generator 78−4652
nanosecond pulses with sharp leading edge 78−4651
nanosecond source for semiconductor laser pumping 77−14746
neuromuscular system electrical stimulator using biopotential amplifier 79−48315
neurostimulator, with improved rectangular pulse cct. *(Rumanian)* 77−21637
neutral beam, pulsed, arc (arc filament) power supplies, for fusion reactor 78−70637
NMR, two channel analogue pulse generator design 78−45665
NMR appl. of pulse programmer 80−57347
NMR pulse programmer, microprocessor-based 80−52289
output pulse generator, for US seismoscopes 77−9537
pacemaker pulse generator design, manufacture and performance documentation for reliability 77−81715
pacemaker pulse generator replacement and other problems 77−81705
pacemaker pulse generator replacement indicator 77−81692
pain relief via implantation in human body 78−96112
physiological stimulator, rabbit heart stimulator, variable frequency/width and amplitude oscillator 78−31991
picosecond pulse generation scheme for injection lasers 80−87418
plasma probe, using discrete stepped pulse generator 77−39454
Pockels cell drive pulser in multiarm laser 79−14001

pulse generators continued
power systems for high energy gas laser 78−9390
precision integral linearity measurement instruments for nuclear spectroscopy 77−67951
programmable pulse sequence generator for pulse NMR 80−17979
programmed, for excitation of electrochemical luminescence 78−74026
programmer for high power nuclear resonance equipment 77−10079
pulse echo transducer, uses ultrasonic pulser that requires no step up transformer 78−79182
pulse source using transition radiation (for optical and UV receiver calibration) *(Russian)* 77−58409
pulsed acoustic sinusoids generated with phased-array speakers, transient free 77−54847
Q-switched Nd:YAG oscillator for stable time-tunable operation in nanosec. regime 80−99759
random, physiological uses 78−24189
random tail pulse generator for simulation of nuclear radiation detector signals 80−74093
ratio analogue pulse height module for fluorescence activated cell sorter 79−20734
recirculating, meas. of acoustic surface wave velocity changes 78−5619
rectangular bipolar voltage pulses generator, for electrochemical excitation of electron levels in organic compounds 77−28629
rectangular pulse generator using 555 IC 79−48998
rectangular pulses generator for pumping injection semiconductor laser oscillators 77−27299
reversing rectangular pulse generator for transient electric birefringence 78−45657
RF, high power, for US vibration excitation, contactless electromagnetic acoustic method 79−5110
RISK 5 m magnetic spectrometer streamer chamber, bipolar voltage pulse generator 79−68131
sawtooth, IC cct. for monitoring scintillation counters *(German)* 78−25395
self-diffusion NMR pulsed-gradient meas. noise pulse generator 77−53965
semiconductor laser pumping appl., cct. parameters 78−74919
semiconductor laser pumping thyristor current pulse generator 78−79024
semiconductor laser pumping thyristor nanosecond current pulse generator 78−79025
short-time measurement instruments calibration, checking appl. *(German)* 78−12728
sine squared waveform generator for cardiac pacemaker sensitivity testing 77−25612
smooth pulse oscillator for single mode operation in I laser 78−59057
SPEAR transport line toroids, intensity monitors calib. system 77−88295
square root of time mark generator using TTL digital ccts. for chronocoulometry 80−35588
steel surface HF inductive pulse hardening *(German)* 78−27687
stimulator for electrophysiological expts., constant-current device 77−21663
synchrotron, Sirius, shaping of highly stable flat top in excitation current pulse of electromagnet 78−5075
thyratron pulser, high-power, HF, for photo-impulse ionised lasers 79−18444
timing circuit subnanosecond walk adjustment using pulse generator 79−76306
Tonus 2M accelerator, high-voltage pulse generator of stored energy 135Kj 78−5067
transistor generator of square pulses for image convertor shutter control 78−4653
travelling wave excitation of H_2 laser discharge 78−9370
triggered light pulse generator for recording fast processes 80−105727
two-channel instrument for pulsed elec. discharge prod. *(Russian)* 78−1946
two-stage opening switch technique, for high inductive voltage generation 78−55034
ultrashort current pulse generation and meas. using Josephson devices 80−90827
US pulse excitation method for solids 78−5624
ventricular programmed pulse generator, testing by waveform generator and cardiac simulator 79−16351
versatile pulse generator and coupled fast signal averager for pulse-echo expts. 78−21188
voltage, Arkad'ev-Marx type, time characteristics stabilisation, spark chamber appl. 77−34512
voltage, for production of modulated beam of H atoms, 3 to 15 keV 79−18315
Wiegand effect voltage pulse generation 79−81322
X-ray, with thyristor based power supply, bell shape pulses generation 80−57446
X-ray source, 1-10 Å, for calibration and adjustment of X-ray pulse detectors 79−2902

pulse height analysers
aerosol classification pulse amplitude analyser 78−61587
AI-128-2 in multichannel counting mode, operational organisation of storage 79−26843
automatic channel-width switching in NTA-512B analyzer in multichannel counting mode 79−26840
automatic differential deadtime correction 79−22559
automatic simple pulse echo tracking apparatus, US absorpt. meas. appl. 77−22571
biomedical rectilinear scanner, multichannel analyser interface 80−101254
buffer store for multichannel analyser, 4096 channel sequential memory, control circuitry 77−57829
CAMAC based linear pulse height anal. 77−87749
CAMAC data acquisition interface 79−3336
composite amplifier-discriminator cct., RMS noise meas. 77−54473
computer compatible conversion for printing multichannel analysers 78−90036
computer system 79−9975
computerised, windowless stabilisation scheme 79−9976
constant fraction differential discriminator for use in fast timing coincidence systems 79−45580
constant fraction discriminator, time resolution meas. with conical scintillators 77−65408
count rate optimisation for maximum precision 77−54463
damping decrement determ. of multichannel analysers 79−68167
DC coupled single channel pulse height analyser, dynamic range 78−21825
dead time correction by the pulser method for single channel nuclear counting systems 79−13611
dead time correction system using standard modules 78−17532
dead time corrections in coincidence measurements by time-to-pulse-height converters or standard coincidence systems 80−9472
differential discriminator with full channel logic using two integrated ccts. 77−10555
digital events analyser of low-cost construction 80−57267
digital multidiscriminator for use in gamma-gamma coincidence experiments 78−70707
discriminator principle slow neutron counting 78−29717
drift chamber electronics for time and pulse height meas. 79−3326
eight-channel unit, automatic, for recording tracer activity 78−86751
electron microprobe anal. using energy dispersive spectrometry 80−55765
emission nebulae, first obs. with optical multichannel analysis of Sao Paulo University 80−26743
energy analyser for charged particle energy and angle meas. in ultrahigh vacuum 78−86750
four fold coincidence system, simultaneous counting of true and random events 79−81140
gamma ray spectroscopy, time dependent deadtime and pile up corrections 77−23385
gamma-ray high-rate spectroscopy system using low noise DC coupled prefilter 77−10527
high resolution fast neutron spectrometry without time-of-flight using a broad window pulse shape discriminator 79−45523
high speed photometer of Asiago Observatory, multichannel analyser data logger 79−25505
high-speed single-input system for pulse indentification 80−891
hodoscope containing scintillation counters, and small FEU-87 photomultipliers, charged particle meas. 78−78562
HTGR coated-particle fuel, irrad. performance determ. by irradiated microsphere gamma analyzer (IMGA) 79−54543
IR pulse power, nanosecond recorder for 10.6 μ radiation 77−37990
laser microphotometry with laminar hydrodynamic focusing 77−37965
linear accelerator pulse amplitude instability meas. apparatus 78−82537
linear gate with prescaled window 78−74548
loss-free counting, real time compensation of dead time and pile up losses 78−17465
magneto-optical stroboscope with pulse height analyser for rapid magnetisation variations 79−67356
MAS-1 multichannel amplitude selector, for dense pulse flow anal. 77−75029
megachannel gamma-gamma coincidence system using PDP-8/E computer and moving-head discs 77−57834
megachannel pulse height analyser for gamma-ray coincidence analysis 80−99430
meteorology, wind direction gauge based on pulse height analyser 79−25351
microcomputer-controlled multichannel analyser for spectral measurement of short light pulses 79−93890
microprocessor based digital controller 79−3335
microprocessor multichannel analyzer laboratory project 80−101685
microprocessor-controlled, transfer of blood pressures and neural activities for computer anal. 80−72356
microwave single pulses of ns duration, amplitude and shape meas. instrument 77−45863
miniature multichannel analyser with LED matrix display 78−25400
modules of 'Summa' system for information output to oscilloscope, digital display and digital printing 77−3244
Mossbauer effect work, function generator using IC 80−68334
multi-channel analyzer using a dedicated CAMAC memory 79−45592
multichannel, digital, time interval distrib. meas. 78−81950
multichannel, random signal flow intensity levelling using analogue memory device 77−18752
multichannel analyser, built from microcomputer 79−58490
multichannel analyser, live time clock testing 78−86749
multichannel analyser, versatile programmable power supply 77−42218
multichannel analyser adaptation for 4096×4096 two-parameter meas. 77−14316
multichannel analyser appl. to simultaneous meas. of synchronous processes 79−26839
multichannel analyser to computer interface 79−93904
multichannel analysers for X-ray spectroscopy *(Hungarian)* 80−95205
multichannel charge-exchange energy analyser with high time resolution, plasma energy spectrum 79−41882
multichannel spectra, discrimination of counting fluctuations 79−36494
multichannel time-digit conversion modules of 'Summa' system for spark chambers 77−3236
multidetector meas. of ang. correl. 79−41084
multitrack pulse height electronics 79−3325
MWPC, IC tapped delay line readout 80−5455
MWPC, position sensitive, pulse shape from cathode RC Lines, zero-cross time meas. 80−58038
MWPC appl. to energy loss meas. 79−3330
neural spike window discriminator confirmation by analogue delay cct. 77−21664
neutron activation anal., ion microprobe surface anal., control and data analysis software 79−11860
neutron irradiation short-lived products, rapid anal. using minicomputer based pulse height analyser 79−11866
nuclear data, multichannel analyzer data processing by minicomputer systems 79−36497
nuclear laboratory instruction with multichannel analyser/microcomputer system 80−31471
nucleonic dual charge sensitive preamplifier 78−55110
on-line method for peak area determ. 79−755
optical MCA, use in simultaneous multi-element atomic emission spectroscopy 77−40607
optical system, multichannel time analyzers for luminescence spectroscopy 79−85185
partial discharge spectra meas. by multichannel amplitude analyser system *(Italian)* 80−33847
particle size distrib. display system, Coulter counter input 79−70716
peak detector circuits, use with single-particle detectors and multichannel analysers 80−37707
phoswich detectors in space borne hard X-ray expts. 80−36501

pulse height analysers continued
photoelectronic spectrometer and coincidence instrum., use of AI-4096 analyzer 80−22473
portable neutron spectrometer/kerma-rate meter, design, performance 78−33361
precision gated current integrator and live time meter system 79−9973
programmable calculator as alternative to minicomputer-based analyser 79−9985
proportional counter, pulse shape discrimination technique *(Chinese)* 79−93867
proportional drift tube for large calorimeter ν detector 79−13592
proton detection, helical channel electron multiplier, charact. *(Russian)* 79−3324
pulse height store for A/D conversion 80−14054
pulse shape discrimination system, performance meas., figures of merit applicability 77−83468
pulse shape discriminator for n,γ separation, appl. to TOF spectroscopy 79−6786
radiation monitoring, multi-channel analyser, portable microprocessor controlled, accessories, data acquisition 80−63474
recoil electron signals, pulse height anal., indication of low energy γ and ν direction of incidence 80−52823
Royco aerosol particle counter 225, data processing system and modified system props. 80−37005
scintillation spectroscopy, organic, use of logarithmic pulse height and energy scales 80−37690
scintillator, NE 213, pulse shape discrimination, appl. to neutron spectrometry 80−27862
semiconductor detectors, pulse height and time analyser 78−78592
shape analysis of fast pulses out of a broad pulse height spectrum 78−70710
shaper for optoelectronic aerosol classifier 79−16049
single channel pulse height analyser, control and meas. system contruction appl. 79−93891
spectral distortion due to peak pile-up calc. of true spectra from observed spectra 77−14327
spectral distortion for double sum pulses of arbitrary shape 77−14326
spectrometer system for investigating light polaris. dynamics in nanosecond band 79−2834
successive approximation A/D convertor for pulse height analyser, rapid coding 77−23386
TGS vidicon tube, used with optical multichannel analyser as IR detector 78−86329
time to amplitude converters, precision 1 GHz time calibration 80−27903
time to pulse height convertors, theoretical and experimental spectra comparison 80−102406
two-dimensional buffer store based on a multichannel amplitude analyzer 79−26838
Voyager Cosmic Ray Experiment, telescopes, electron energy meas., pulse height analysers 79−48643
wind speed and direction meas., automatic distrib. meas. system 79−96839
wind speed intensity distrib. anal. appl. 78−88937
X-Y recorder for Auger spectrometer using pulse height analyser, computer interfaces 78−49942
Ge intrinsic detector and multichannel analyzer in 5.1 cm borehole probe 80−63451
Ge(Li) detectors, energy meas. source position effect 79−13579
Ge(Li) spectrometry, pulser method limitations in pile-up and dead-time corrections 77−23384
NaI detector system, front end electronic, pulse height anal. 79−45587
NaI(Tl) scintillation detectors, microprocessor-based multichannel analyser 80−91378

pulse modulation
see also demodulators; modulators; pulse amplitude modulation; pulse-code modulation; pulse frequency modulation; pulse time modulation
CPS at CERN, pulse to pulse modulation, extraction modes, beam intensity 77−83277
dynamic props. of pulse spectra *(Russian)* 79−97335
Faraday tarotion, effects of pulsewidth 78−71540
laser diode 1ns pseudo-random pulse modulation cct. 78−50836
laser pulse generation and modulation devices 78−25899
noise intensity measurement, using modulation radiometer 77−61048
NQR pulse spectrometer modulator 80−17971
optical fibre transmissions direct modulation of semicond. laser *(Japanese)* 79−41402
Pockels double shutter in ruby laser with active phasing of spectrum *(Russian)* 79−98419
radiometer limiting sensitivity formula correction *(Russian)* 78−58030
SAW EM transducer range resolution improved by pulse compression 77−19509
semiconductor laser, single mode criteria at high speed pulse modulation 79−10305
semiconductor laser, single-wavelength oscillation at high speed pulse modulation 79−7129
thyristor current modulator for cyclotron arc ion source 77−46438
GaAs diode laser in communication system using PPM methods *(Rumanian)* 77−68260
Hg low-pressure pulse-modulated discharge optical and electrical parameters 78−67491
PbS mosaic array pulse-bias modulation 80−86414

pulse motors *see stepping motors*

pulse oscillators *see pulse generators*

pulse position modulation
data transmission performance study in optical fibre communication system 78−38028
decimal/residue/decimal optical converters 79−22905
interval modulation semiconductor laser communication system 78−9331
multiple beam gratings produced by PWM and PPM, high efficiency, beam splitter appl. 79−81515
neural communication system model, single signed integral PFM and PPM comparison 79−5268
nonlinear image processing, binary pulse position encoding 78−29906
optical communication, TDM pulse analogue modulation, diode laser nonlinearity 78−55455
optical discrete PPM signal reception accuracy *(Russian)* 79−94171
optical fibre digital communications, PAM-PPM signalling format 79−27190
telemetry system, implantable, single-freq., physiological parameter monitoring appl. 77−86688

pulse repetition rate modulation *see pulse frequency modulation*

pulse shaping circuits
1200 pF fast-response pulse voltage generator for spark chamber 77−54444
discharge power source for CO_2 laser, pulse forming network 78−74928
ECG arrhythmia simulator for monitor testing 78−61270
fast coincidence, with Ge(Li) detectors 78−41864
frequency counter modification, for pulse duration below 1 μsec meas. 77−10060
gamma camera/computer pulse-stretching interface 78−40380
Gaussian filter for nuclear pulse amplifiers, direct synthesis, freq. domain anal. 77−3239
high voltage microsec. pulse-forming network for CO_2 laser 78−5494
high-power long-pulse thyratron modulator with small off-duty factor 78−86380
high-speed pulse shaper/discriminator for scintillation and Cherenkov counters 78−86748
high-speed shaping device, for address control of laser beam deviation 78−5554
HV pulser development for CS_2 laser cavity 80−23707
ionospheric recording pulse expander IC 79−70892
laser pumping lamp ignition pulse semiconductor shaper 79−72585
mass spectrometer, double step pulse-forming circuit for ion extraction 77−18124
microwave spectrometer control pulse shaper for two-pulse relaxation time meas. 79−67363
modular coincidence circuits and shapers, parameters 79−3320
nanosecond pulse stretcher, appl. to laser-excited time-resolved fluorescence spectrometer 79−67390
nuclear radiation measurement, pulse processing technique, pulse shaping *(Japanese)* 79−81138
optimum filter responses for liq. Ar total absorpt. detectors 78−46215
for optoelectronic aerosol classifier 79−16049
power supply inductive pulse shaping for periodically pulsed CO_2 laser 80−53311
pulse compression using SAW components *(German)* 79−81639
quadrupole mass spectrometer with elliptical electrodes, 3-dim. 80−31931
RISK 5 m magnetic spectrometer streamer chamber, bipolar nanosec. pulse shaper 79−68166
scintilation spectrometer signal shaper-discriminator 78−33387
scintillation beta spectrometer with compound detector 80−23243
scintillation spectrometric path, switch shaper 77−6641
shaper amplifier for proportional chambers, logical microcircuits and high time resolution 78−5103
synchrotron, Sirius, shaping of highly stable flat top in excitation current pulse of electromagnet 78−5075
transversal filter approach of trapezoidal pulse shaping for silicon live targets 79−36487
US pulse-echo system, chopping circuit 77−67162
Van de Graaff accelerator subnanosecond pulsing using passive coaxial pulse shaper 78−46186
Si semiconductor switch using laser-excited solid-state plasma for pulse shaping, expt. 77−19397
Xe pulsed arc lamp with adjustable plateau slope 79−68422

pulse time modulation
see also pulse position modulation; pulse width modulation
high-power long-pulse thyratron modulator with small off-duty factor 78−86380
laser, passive mode locking, two laser amplifiers with slow saturable absorber 80−33041
laser passive pulse shaping by delayed superposition using grating 77−75580
microprocessor based telemetry demodulation system 79−20738
optical fibre communication system field expt. 78−1424
pulse interval modulation for optical fibre communication system 78−50917
sonar, rel. resolution with linear-period-modulated pulse 77−54825

pulse transformers
5 MeV electron accelerator modulator charging system 79−13563
250 kV water Blumlein, off-resonance transformer charging 79−13564
600 MW pulsed energy convertors for toroidal field coil, design philosophy 78−58496
air core shielded spiral transformers, pulse forming transmission line charging appls. 80−63419
automatic resistance thermometer bridge 80−98913
electron gun voltage supply, for a linear induction accelerator 77−75007
Fermilab neutrino focusing horn, 10 msec. 150 kA pulsed power supply 79−68092
high voltage impulse transformer for pulser-sustained laser appls. 80−1263
HV power supply system of streamer chamber 78−5095
pulse forming transmission line charging, 3 MV transformer 79−76173
semiconductor laser pumping with combined pulse transformer 78−1255
signal coupling of semiconductor detector to cold resistance preamplifier through cable or delay-line transformer 78−33401
toroidal core pulse current transformers, pulse permeability and loss in Ni-Fe cores 78−43615

pulse width modulation
acoustooptical modulators, computer controlled laser interferometer 80−56294
blood circulation apparatus, improved electromechanical drive regulator 80−3871
CAMAC encoding system for MWPC remote readout 79−26847
DC motor drive system control, electric wheelchair appl. *(German)* 77−56491
Doppler blood flowmeter modulation *(Japanese)* 79−2115
EEG physiological data teletransmission system 77−86687
HPLC, two-pump gradient, accuracy and reproducibility 80−16742
liquid level-to-frequency converter 79−6080
magnetic tape recording, time reference signal, IRIG and NASA code formats 80−57262
multiple beam gratings produced by PWM and PPM, high efficiency, beam splitter appl. 79−81515

pulse width modulation continued
muscle contraction strength control during elec. stimulation, using PWM and FM 77−40929
optical fibre PWM multilevel pulse transmission, theory and expt. 79−55078
optical fibre transmission expts. at 34 Mb/s with HDB3 line code 80−64198
optical pulse, freq. chirped, compression by strongly dispersive grating pair 79−50373
optics, band-limited function approx. realisation by low-pass filtering sequence of width-modulated pulses 80−95836
telemetry system, implantable, multichannel, inductively powered, for animal cardiovascular data recording 77−86662
temperature telemetry system for small animals, miniature CMOS 4-channel PWM design 78−44751
thyristor modulator with periodically interrupted supply, microtron appl. 78−55061
Nd:YAG regenerative amplifier, variable-duration synchronized pulse generator 79−45967

pulverised coal *see pulverised fuels*

pulverised fuels
see also coal
coal, low sulphur, US assisted drying in vacuum filtration 77−32539
coal combustion, in combustion chambers of steam generators, digital simulation *(German)* 78−27758
coal conversion, by flash hydropyrolysis and hydrogasification 79−52868
coal conversion, solvent refined, pilot plant experiences 79−52867
coal dust mass flow meas. methods *(German)* 80−92242
coal liquefaction, 1978 status and development trends in US 79−48061
coal liquefaction processes, research status 79−48060
coal pyrolysis, in entrained bed flow reactor, theoretical exam. with aid of physical models 79−48062
coal reactors, cold flow mixing rates with recirculation 79−50762
fossil-fuelled power stations, air pollution detection and control, opacity monitoring 79−100557
gas flow distrib. in manifolds of uniformly variable section *(Russian)* 80−33666
CO concentration meas. in coal pulverising plant, IR gas analysers 80−89572

pumped-storage power stations
cascade static stability and critical velocity *(German)* 78−79306
compressed air and underground pumped hydro storage, comparison 80−40910
geologic conditions 80−30577
Pakistan, hydroelect. pot. for future electricity demand, review 79−34423
underground pumped hydroelectric storage plants, high-head turbomachinery, cost anal. 80−61432

pumping *see pumps*

pumping (optical) *see optical pumping*

pumping plants
horizontal-axis wind-turbine system for pumping duties in Third World agriculture, design 80−61259
irrigation pump Rankine cycle solar engine and wind turbine comparison 79−57448
solar, based on Rankine cycle, performance prediction model 79−70460
solar, based on Rankine cycle principle 79−70459
solar photovoltaic energy powered deep well irrigation system 79−92082
solar power appls., passive system using organic working fluid 79−70439
solar-powered, for water, air- or water-cooled, development and performance 79−70441
water level computations, method of characts. for slowly varying nonstationary flows *(German)* 79−5515

pumping stations *see pumping plants*

pumps
see also vacuum pumps
20 kbar pressure system using reciprocating hand pump, for magnetic resonance studies 79−67335
150 kW solar powered irrigation facility, design 79−96427
AC conduction pump with Na working fluid, performance characts., freq. depend. *(Japanese)* 80−13092
air sampling pump, personal, for hospital operating staff 79−12019
ambulatory blood pressure recording in man, transducer and perfusion system 79−53271
artificial blood circulation pump unit redesign for sterilisation 77−48932
artificial blood pump fabrication for durability 79−84026
artificial heart, pneumatically actuated, echographic anal., air chamber inlet design 77−48943
artificial pancreas programmed control technology *(German)* 79−16346
atrio-aortal left ventricular bypass, haemodynamics in calf *(German)* 78−88763
auger-centrifugal pump entry sections, cavitational cavities and cavitational resistance, return flow effects 79−18921
autotransfusion, variable speed pump head control 77−52918
autotransfusion, variable-speed pump head control 78−57121
auxiliary blood circulation pump, electronic control circuit 77−78050
axial piston pump, suction performance 78−8389
Batfish active towed body system development 77−5374
Baylor left ventricular bypass pump, calf expts. 78−73295
Baylor left ventricular bypass pump, recent experience 78−44718
bimorph vibrator micropumps, cylindrical and plane types 79−48182
biomedical pumps for pulsed insulin delivery, modification 80−101290
birth monitoring by cardiotocography, interference effect by infusion pumps *(German)* 78−85416
blade type, cavitational oscill., linear math. model 77−35187
blood, pressure servovalve control, moving coil system *(German)* 78−24182
blood, total artificial heart development 77−25599
blood damage by artificial part-hearts and pumps, dwell minimisation model *(German)* 79−16345
blood intermittent pump with linear motor drive *(German)* 79−5401
blood pump, biventricular, brushless DC motor powered, development and in vivo evaluation 79−53285
blood pump, controlled high pressure, for heart support systems *(German)* 79−8580
blood pump, experiences with miniaturised press.-controlled servo *(German)* 78−88762
blood pump, pulsatile, in vitro eval. of erythrocyte bulk lysis 77−44840
blood pump, pulsatile, stabilisation of unsteady ball valve motion 78−44708
blood pump artificial heart valve *(German)* 78−81065
blood pump for completely implantable circulatory assist systems 78−44723
blood pump implantations in animals, regulation mechanisms in circulation and fluid balance *(German)* 78−81064
blood pump manufacture for total heart replacement, using polyurethane with seamless interior *(German)* 79−8581
blood pump regulation electropneumatic servo operation *(German)* 79−8579
blood pumps, pneumatic, closed-loop control system 77−52930
cardiac assist system, intrathoracic, self-sufficient instantaneous haemodynamic control 77−44842
cavitating, dynamic characts., bubbly flow model 79−32646
cavitating screw pump nonsteady-state press. component 80−19455
centrifugal, impeller flow, quasi two-dimens. method of singularities 78−46986
centrifugal blood pump for cardiac support 78−44709
centrifugal liquid H_2 pumps, submerged 77−22560
centrifugal pumps in two-phase flow, characts. correlation 79−98790
chromatography, pump design reviews of HPLC apparatus 78−80800
closed system gas circulating pump 77−2641
closed system gas circulating pump without moving parts 78−180
closed-circuit water jet pump construction 79−67272
compound parabolic concentrator heat transport to storage 79−62102
conducting liquid, eddy current induced pumping, longit. current in corrugated tube *(Russian)* 78−75216
conduction centrifugal EM pump for nuclear reactor coolants, characts., operation 78−86246
conduction MHD pump with current leakage, equivalent circuit *(Russian)* 78−26346
constant pitch inducer pumps, solidity effect limits 80−6108
contactless MHD pump with EM asymmetry, max. press. calc. *(Russian)* 78−26340
corrosive liquids pumped circulation, vacuum-tight elec. drive with gear pump 77−74376
cylindrical inductive MHD pump, external mag. field, dipole calcs. *(Russian)* 77−3884
d.c. electromagnetic pump, flow of conducting liquid *(Rumanian)* 80−28574
DC electromagnetic pump using supercond. magnet, performance characts. 77−82994
double-acting Hg-piston gas circulation pump 79−67270
dredging, shaft breakage, US detection 77−77716
EHD, expt. investigation *(Russian)* 79−37405
EHD, in attraction mode, efficiency 80−52187
EHD pumping of cable oil 78−87414
electrofluidic, appl. of elec. field to dielectric fluid, evaluation *(German)* 79−94724
electronically controlled insulin pump and valves for diabetes patients 78−53565
electroosmotic pump for regulated release of medicaments *(German)* 78−7518
electropneumatic blood pump with electronic control, features *(German)* 78−53564
EM, DC, channel dimensions optimisation, minimum current consumption *(Russian)* 77−22581
EM induction pumps, fluids, laminar flow, characts. anal. 79−32699
EM pump and plant with liq.-metal working fluid, review *(Russian)* 77−19639
EM pumps for liquid metal fast breeder reactor, review 78−94074
fibre-optic glass manufacture using polypropylene sump pumps 80−14410
gas pumping arrangement, for relativistic electron-beam pumped lasers 77−701
gas-lift pump design, <8 mm riser dia. 80−10324
glass circulating pump for gaseous mixtures 78−41292
haemofiltration control system *(German)* 79−5403
helical induction machine, laminar flow in channel, boundary effects *(Russian)* 77−47105
hydraulic, airborne noise meas. methods 79−79433
hydraulic pump for laboratory high pressure installations 79−93159
hydraulic pumps, standard methods for airborne noise meas. 79−50548
hydraulic transport of fragile nonspherical solids, algae aqueous suspensions 77−73618
incompressible fluid flow, one dimensional, calc. 80−79402
induction MHD machine, integrated characts. *(Russian)* 78−26342
induction MHD pump, active zones, effective forces, EHDA integrator study 80−43797
induction MHD pump channel, EM field and longit. boundary effect, 2-dimens. theory *(Russian)* 78−47188
induction MHD pumps, with transverse mag. flux, active element optimisation *(Russian)* 78−94840
induction pump, linear, cylindrical EM field distrib. *(Russian)* 78−5820
infusion pump, biological appl. 78−31987
infusion pump control by labour and foetal heart rate *(German)* 78−85415
infusion pump interference on foetal heart rate recording *(German)* 78−85414
insulin infusion system, portable and precise 79−25148
intra-aortic balloon pump controller, within computerised evaluation system 77−56538
intra-aortic balloon pump simulator for dynamic demonstration and teaching 77−56537
intra-aortic balloon pumping apparatus trials 79−48368
intra-aortic balloon support, prognostic indices, rel. to left ventricular assist device use 77−56536
Isaacs wave-energy pump, field tests around Hawaii 79−57354
jet, circulation of the two-phase mixture 80−82771
jet, finite-difference performance anal. 77−31348
jet thermal, head discharge charact. 79−18924
left ventricular assist device, diaphragm-type, factors affecting pumping dynamics 78−44706
left ventricular assist device long-term expts., maintenance of efficient pump performance 78−44722
left ventricular assist device testing using calf model 78−73296
left ventricular assist mech. pump effectiveness in acute myocardial failure model 78−44719

pumps continued
linear induction MHD pump, cylindrical, electrodynamic forces *(Russian)* 78−94843
linear induction MHD pump, DC, mag. field obs. *(Russian)* 77−7469
linear induction MHD pump, liq. metal flow, energetic charcts. *(Russian)* 77−3882
linear induction MHD pump, liquid metal flow and energy charcts. *(Russian)* 77−47104
linear induction pumps, cylindrical, for liq. Na *(Russian)* 78−94839
linear induction pumps, cylindrical, research and development studies 79−77276
liquid He jet pump, for circulating refrigeration systems 79−205
liquid metal MHD induction pump, transversely closing mag. flux, optimisation of parts 79−77278
liquid metal MHD pump, performance indices channel geometry *(Russian)* 78−5821
LMFBR, equipment design, Na-NaK engineering handbook 79−97815
LMFBR, large EM induction pump for high-temp. appl. 78−17291
mechanism of the development of noise in hydro-systems as the result of fluctuations in delivery flow *(German)* 79−7256
MHD, compensated, two channel conduction MHD pump with leakage current, obs. *(Russian)* 78−75228
MHD, for Hg transfer in chlorine and caustic soda production 80−43787
MHD AC conduction pump for ferrous metal 80−33701
MHD channel uncompensated DC cond. pump, pumping and generating charcts. *(Russian)* 79−1352
MHD conduction pump for filling casting mold 80−43798
MHD induction pump channel press. loss, laminar liq. metal flow friction losses *(Russian)* 78−75224
MHD induction pump with side bars, thrust-flow charcts. at large Re_m *(Russian)* 78−75231
MHD linear induction pump, cylindrical with inclined coils, electrodynamic force calc. 79−77281
MHD linear induction pump, instabilities at low flow rates 79−77279
MHD liquid metal pump, conical MHD channel of single-phase inductor 79−77280
MHD pump, direct-current uncompensated conduction-type, exptl. charcts. 79−77283
microejector, charcts. calc. 80−77809
non-Newtonian fluids, Prandtl-Eyring law appl., jetstream pump parameters *(German)* 78−30331
nonequilibrium parametric pump, steady state predictions 77−49736
nuclear power reactor, austenitic stainless steel, appl. 77−3102
nuclear reactor coolant pump, seismic anal. by response spectrum method 77−3183
nuclear reactor pump coolant tests, computerised monitoring 78−70585
osmotic pump for drug delivery, design and operating principles 77−56544
parathoracic ventricular assist device for use with nucl. or elec. actuation systems 77−48941
perfusion, EM drive, features 78−7532
perfusion pump, low-compliance, for oesophageal manometry 79−53272
peristaltic, lab. appls. 80−98905
piston and diaphragm type dosing pumps for high press. use *(German)* 79−21762
piston pumps, double-acting, for cryogenic He and N_2 79−58716
pneumatic amplifier pump, for supercritical fluid chromatography, control and programming 78−88665
pulsatile blood pump development and characteristics 77−81659
PWR, reactor coolant pump failure investig. at Arkansas Nuclear One 80−9336
PWR cooling and heat recovery, circulating pump development 77−82993
reciprocating, flow measurement, control system, high performance liquid chromatographic detectors appl. 78−92559
reciprocating circulation pump for withdrawal of liquid He from liquefier 79−58745
reversible pump-turbine, axial, for tidal power plants 79−43735
rigid-vane artificial heart development 79−84025
roller pump for pulsatile blood flow 78−44721
roller pumps, clinical, automatic safety shutdown 78−44720
solar, below actuated, based on Rankine cycle principle, analysis and expt. data 79−74504
solar, economic comparison with wind power, petrol engine and electric water pump 79−74507
solar, for lift irrigation, modified design analysis, with working fluid and water separation and internal insulation 79−70440
solar, irrigation, 1978 status review 79−74506
solar, irrigation, India's 1978 development trends 79−74509
solar and wind powered, desalination plants appl., based on reverse osmosis *(French)* 80−55807
solar energy drive, turbo-pack based on Rankine cycle, low-cost design 79−62021
solar photovoltaic system appl., optimisation *(Spanish)* 79−96428
solar powered, using biomass as auxiliary heat source, Indian development 79−70461
solar thermal engine, irrigation, 7.5 W, with liquid piston, design and analysis 79−74537
solar-powered, 1 kW, reciprocating engine development, for rural appl. 79−74536
solar-powered, for water, air- or water-cooled, development and performance 79−70441
spirally-wound, EM processes in secondary medium, model *(Russian)* 77−3881
thermal oscillating pump for nuclear powered artificial heart 78−20317
Toepler pump, all-metal automated, for laboratory use 80−52180
two channel DC EM pump, expt. study 80−43791
valveless shock tube pumping mechanism 79−14337
vapour/gas joint flow, kinetic model of cavitational oscill. 77−35186
ventricle type blood pump, blood damage 78−44707
vertical pumps, solving the vibration problem 78−87186
water pumping, by means of flat solar energy collectors *(French)* 80−55902
water pumping windmill, low-cost, using sail-type Savonius rotor 80−21367
wave power generation, Mauritius 'passive' project, electro-mechanical aspects 79−43724
wind pumps, development programme 80−55792
wind-operated, reciprocating water pump, stroke adjusting mechanism for rotor speed control 80−50930
pumps continued
windmill for use in irrigation, with horizontal axis sail 80−21368
windpump ITDG development program, for small-scale manufacture and use in under-developed arid regions 80−26106
wing, wear anal. when using flash-resistant hydraulic fluids *(German)* 79−83331
zero mechanical work thermal compressor or pump, in high speed rotating frame 78−57962
He, liq., design and construction, applic. in supercond. mag. system 77−45849
^{4}He pumping lines, low press. safety value 78−32822
punched paper tape equipment *see punched tape equipment*
punched tape equipment
chronometric system using punched tape for star transit obs. *(Russian)* 78−4110
data logging digital system 77−22538
data recorder for F5080 freq. meter, oceanological appl. 77−49175
ECG digital voltmeter with output to punched tape 77−21646
holographic document retrieval and conversion to photographic microforms 79−76643
X-ray diffractometer data, automatic attachment for punching to tape 78−34385
purification, crystal *see crystal purification*
Purkinje effect *see vision*
push pull amplifiers *see differential amplifiers*
push pull microphones *see microphones*
p.w.m. *see pulse width modulation*
pylons *see poles and towers*
pyroelectric devices
camera tube, material limitations and improvements 77−8519
ceramic, high power continuous laser emission meas. appls. *(Russian)* 78−16845
chemically sensitive devices for trace level anal. 77−52720
conference, ferroelectric materials and their applications, Kyoto, Japan, Nov. 17-19, 1977 79−19846
conference, Minneapolis, MN, USA (June 1979) 80−77535
connectivity and piezoelectric-pyroelectric composites 78−80290
detector, background noise limited 80−82820
detector, direct meas. of IR laser radiation multiphoton mol. absorpt. 80−102545
detector, performance evaluation method 80−82819
detector, thin film, temp. fluctuation noise 80−77861
detector, use in horizon sensors 80−37086
detector, use of $PbHPO_4$ cryst. 77−82600
detector array for IR and far-IR studies, improvement of sensitivity using digital averaging technique 79−49290
detector for subnanosecond CO_2 laser pulse meas. 80−78884
detector of transmitted power, coordinate-sensitive, for laser beam displacement determ. 79−75599
detectors, sub-100 ps, 10.6 μm damage threshold meas. 80−77859
detectors, user's guide 79−35823
dicalcium lead propionate, improper ferroelectric, dielectric props., IR radiation pyroelectric detection 80−80711
differential calorimeter, for meas. of absorbed energy in laser-produced plasmas 78−5942
electret applications, book contrib. 80−80709
far IR thin crystal pyroelectric detector development 77−37994
ferroelectric materials for dielectric power conversion, dielectric prop. anal. 80−80712
ferroelectric thin film, pyroelectric radn. detector development *(Russian)* 79−47394
gamma-ray pulse calorimeter 78−860
homodyne detection at 100 GHz with a pyroelectric detector 80−105650
imaging tube, sensitivity and geometrical resolution improvement *(German)* 80−105715
ionisation upconvertor for IR detection 80−77860
IR detector, temp. noise 78−89542
i.r. detector, temperature noise and dielec. loss 77−17975
IR detector arrays, self-scanning 79−58785
IR detectors, effect of substrate on current responsivity 80−73454
IR detectors, survey of different detector charcts. 77−10106
IR detectors, technology review 79−2827
IR imaging appl., development trends *(Czech)* 79−97383
IR pulse temporal contours obtained with pyroelec. detector 78−37056
IR signature classification system 80−86430
IR visualisation gauges 79−68432
laser beam profile monitor system using photodiode or pyroelec. array 77−58364
laser spatial profile meas. by pyroelectric vidicon camera 80−87425
leaf temp. meas., infrared thermometer method in connection with plant physiology *(Japanese)* 78−31993
matrix pyroelectric detector for laser oscills. investigation 77−74502
millimetre wave detector using the pyroelectric effect of PVF_2 *(Japanese)* 78−8444
photodetector spectral response measurement 79−21812
polymer film transducer, piezoelec. and pyroelec. response rel. to dipole polarisation 80−7267
polymer IR detector *(Japanese)* 80−105713
polyvinylidene fluoride, optimised target for IR vidicon camera tube 79−32050
polyvinylidene fluoride, piezoelec. and pyroelec., rigid dipolar model *(French)* 79−8090
polyvinylidene fluoride film, pyroelec. camera tube for IR imaging, thermal diffusivity of Bi-Bi_2O_3 black layer 80−57369
PVDF IR detector *(Japanese)* 80−105714
PVF_2, plastic film sensors 79−99826
PVF_2 detector, MM waves at 100 GHz, high-sensitivity *(Japanese)* 79−97432
PVF_2 film pyroelectric radiation detector sensitivity *(Japanese)* 79−93222
pyroelectric detectors and materials 78−49901
pyroelectric high power density heat engine, dielectric losses, polarisation 80−80689
pyroelectric target performance improvements 77−39103
pyroelectric vidicons, figures of merit, material parameters 80−77855
pyroferroelectric energy convertor under thermocycling 78−15102
pyrothermometer in scanning calorimeter, heat cond. eqn., model 77−10026
radiation detector, 40-1100 nm range 77−87834

pyroelectric devices continued
radiation detector, lag correction network ccts. 78−288
radiation detector for dosimetry of pulsed γ-radiation 77−71725
radiation detectors, principle, materials and charact. *(Czech)* 79−40611
radiation detectors, review 77−45889
radiation pyrometer, near-infrared, using standard temp.-calibrated lamp with filter 77−53915
radiometer, electrically calibrated, description 78−29140
radiometer/photometer appl., commercial devices survey and classification 78−16830
radiometry, optical calibration system 77−61106
solid state pyroelectric IR detector array 80−9036
spectral response and sensitivity, comparison with other detectors 79−35832
submillimetric-wave detectors 79−30545
surface resistivity measurement, at 890 GHz, using modified pyroelectric detector 77−34004
TGS, proper and improper ferroelec., direct meas. of figure of merit 79−95711
TGS, pyroelectric figures of merit 77−59519
TGS IR detectors, permanent polarisation due to X-rays, optimum non-ferroelec. behaviour 77−41684
TGS pyroelectric detector, compared with W-C point contact, appl. to temporal coherence meas. of HCN laser 80−31871
TGS thin film pyroelectric detectors, far IR absorption 77−38010
TGS vidicon tube, used with optical multichannel analyser as IR detector 78−86329
for thermal imaging system, review 77−14794
thermal imaging with pyroelectric vidicon camera 80−86288
thermal radiation detectors, thin-film technique *(German)* 78−62226
three-dimensional thin pyroelectric IR detector simulation 80−57375
triglycine sulphate, deuterated, reticulated target for pyroelectric vidicon, IR imaging 80−77858
TV camera for instrum. with IR lasers 78−59150
vidicon, appls. 77−65635
vidicon, CO_2 laser beam meas. 78−49907
vidicon, thermal props. of reticulated sensing layers, design parameters 78−49897
vidicon, thermography appl. 77−54798
vidicon, ultrafast photography, with 10.6 μm radiation 78−38035
vidicon camera, use as medical thermograph 79−25060
vidicon for thermal imaging *(Japanese)* 77−27359
vidicon target, TGS-Ge contact, thermal resist. 77−4226
vidicon thermal imager principles and performance 77−39093
vidicons for thermal imaging 77−19449
$Ba(NO_2)_2.H_2O$, pyroelectric IR radn. detector 79−80685
$Ba_{0.25}Sr_{0.75}Nb_2O_6$, fast-response pyroelec. cryst. detector 78−49904
$Fe_3B_7O_{13}I$, improper ferroelectric, dielectric props., IR radiation pyroelectric detection 80−80711
$LiKSO_4$, thermal and dielec. props., use as pyroelectric detector 80−34860
$LiTaO_3$ monolithic pyroelectric array, IR detectors 80−77857
$LiTaO_3$ pyroelectric detectors, temp. noise effects on performance 77−79156
$LiTaO_3$/CCD hybrid focal plane, IR imaging and detection, crosstalk 80−77856
PLZT pyroelectric detectors, fast response to MW CO_2 laser pulses 79−54187
$PbZrO_3$ pyroelectric detector, low temp. behaviour, expt. 80−31869
$SrTiO_3$ ceramic, electrocaloric effects for refrigeration at cryogenic temp. 80−77789
$Tb_2(MoO_4)_3$, improper ferroelectric, dielectric props., IR radiation pyroelectric detection 80−80711
$Tb_2(MoO_4)_3$, proper and improper ferroelec., direct meas. of figure of merit 79−95711

pyroelectricity
adiabatic depolarization under cryogenic conditions 80−55045
atomic displacements, in pyroelec. and piezoelec. crysts., temp. and stress depend. conds. 79−24265
automated simultaneous meas. of electrical properties 80−57335
1,6-bis(2,4-dinitrophenoxy)-2,4-hexadiyne, obs. of apparent ferroelec. transition 80−66121
charge storage, charge transport and electrostatics conference, Kyoto, Japan (Oct. 78) 80−7252
Costa Ribeiro effect, role of pyroelectricity 78−56431
crystal nonlinear electroacoustics, dynamical eqns. and constitutive relations 79−56734
l-p-decyloxybenzylidene-p'-amino-2-methylbutylcinnamate, (l-DBC); liq. cryst., pyroelec. const. stationary value over ferroelec. temp. range 79−65801
l-p-decyloxybenzylidene-p'-amino-2-methylbutylcinnamate, ferroelec. liq. cryst., pulsed pyroelec. effect 79−15405
detector, background noise limited 80−82820
detector materials, thermal noise and dielec. response 80−75952
dicalcium strontium propionate, cryst. symmetry in low temp. phase 79−37693
dielectrics, thermoelect. conversion using solid state heat engine 80−35707
disilicate, piezoelectric glass ceramic, recrystallisation, pyroelectric response, permittivity 80−80703
DOBAMBC, chiral smectic phases, pyroelectric and dielec. props. 79−91380
electrets, piezo- and pyroelectric props. 80−80685
electrets and dielectrics, conf., Sao Carlos, Brazil, Sept. (1975) 80−7251
electrocaloric effect meas. apparatus 78−213
electrocaloric refrigeration, for 4 to 15K 79−80624
electrocaloric refrigeration for 4-20K range 78−93703
ferroelectric, tetragonal, irradiated by laser pulses, spatial temp. and bound-charge distrib. 80−103927
ferroelectric crystal, non-linear pyroelec. effect in phase transition region 79−47393
ferroelectric films, pyroelectric response to step radiation signals 80−7302
ferroelectric liquid crystals, kinetics of spontaneous polarisation *(Russian)* 79−8101
ferroelectric materials for dielectric power conversion, dielectric prop. anal. 80−80712
ferroelectric semiconductor, solid solution, phys. charcts. nonlinearity near phase transition 78−43812

pyroelectricity continued
ferroelectric thin film, dynamic pyroelectric effect, radn. detector development *(Russian)* 79−47394
ferroelectrics, quantum transition suppression, pyroelectric, electrocaloric effects, specific heat 80−75984
film, origin of pyroelectricity 78−88258
glass, pyroelectric, low-temp. behaviour 78−56432
guanidinium aluminium sulphate hexahydrate, pyroelectric coeff., 1.8-300K, dynamic method *(French)* 79−19844
HOAB, smectic C-phase pyroelectric effect 78−79522
holographic grating recording, pyroelectric mechanism 78−42300
homogeneous ferroelectrics; bulk photovoltaic effect 79−42578
insect, Periplaneta americana, pyroelectric coeff. and permittivity obs. 80−51315
insulator, pyroelec., role of surface ions in contact electrification 80−54762
internal energy relationship to moment 77−16028
langbeinite-type crystals, phase transitions, dielec. props. obs. 78−6643
leaf epidermis of palm-like plant Encephalartos Villosus, anomalous behaviour 78−44755
leaves of palmlike plant Encephalartos villosus, pyroelec. and induced pyroelec. polarisation 77−77876
leaves of rhododendron and encephalarts, pyroelectric coeff. and permittivity obs. 80−51315
liquid crystal, ferroelectric, review of props. 77−85667
literature fuide, 1976 to 1977, references, bibliography, authors list, key word index 78−43797
literature guide, 1974-1975 77−12323
literature guide, 1975-6 77−59515
literature guide, 1977-78 79−19843
literature guide, 1979 80−57019
literature guide, (1978-9) 80−62404
literature guide (1977) 78−95552
lithium formate monohydrate, elec. props. 79−87371
Maxwell's eqns. in matter, covariant formulation 78−57798
NOBAMBC, chiral smectic phases, pyroelectric and dielec. props. 79−91380
noncentrosymmetric crystals, subjected to strong elec. field, theory of transport phenomena 79−11136
nonlinear electroacoustics, fundamentals and appl. 80−34489
nonlinear electroacoustics of dielec., piezoelec., and pyroelec. crysts. 78−79155
nylon 11, pyroelectricity and piezoelectricity 77−69780
PET, pyroelectric effects and depolarisation currents, illumination effects 80−34859
photovoltaic bulk effect due to electron-phonon coupling 77−20358
photovoltaic effect due to electron-phonon coupling 78−14757
phthalocyanine metal free films, TSC, ferroelectric-semiconductor transition 80−66105
polar polymer, piezoelectricity and pyroelectricity 80−7267
polar polymer, pyroelectric response rel. to dipole polarisation 80−7267
polarized dielectric appl. *(French)* 79−51902
poly(vinylidene fluoride) film, pyroelectric coefficient determ. using dielectric heating 78−35096
poly vinylidene fluoride, injection process nature during poling, rel. to pyroelectricity 78−19422
polyacrylonitrile, elec. polarisation 80−7275
polyacrylonitrile, polaris., pyroelec., electret film, solar energy conversion *(Russian)* 78−39507
polycrystalline materials; pyroelec. temp. anal. as method for studying ferroelec. transitions 79−38502
polymer, piezoelectricity and pyroelectricity, review 77−8514
polymer film, pyroelectric coefficient determ. using dielectric heating 78−35096
polymer film, space charge, thermal expansion and pyroelectricity 77−4603
polymer film transducer, piezoelec. and pyroelec. response rel. to dipole polarisation 80−7267
polymer films, electronic cond., electro-, photoresponsive effects, review 79−56261
polymer materials, piezoelectricity and pyroelectricity and anal. *(Japanese)* 78−88257
polymers, electrical phenomena, nature and appl., book contrib. 80−50254
polypropylene, electron bombarded, radical formation, piezoelectric and pyroelectric effects, ESR study 80−7169
polypropylene film electret, space charge injection 77−12324
polyvinylidene fluoride, γ-phase containing films, thermocurrent spectra 79−42555
polyvinylidene fluoride, ageing effects on thermally stimulated currents 77−1634
polyvinylidene fluoride, elec. field induced phase changes 79−11387
polyvinylidene fluoride, electrocalorific effect *(French)* 79−47392
polyvinylidene fluoride, film, piezoelec., pyroelec., thermal expansion, elastic consts. 78−84529
polyvinylidene fluoride, piezoelec., pyroelec., and improper ferroelec. 80−7301
polyvinylidene fluoride, piezoelec. and pyroelec. props., struct. model 79−11386
polyvinylidene fluoride, plasma poling, piezoelec. and pyroelec. responses 80−71296
polyvinylidene fluoride, poling by corona charging, pyroelec. effect 78−19423
polyvinylidene fluoride, poling process, kink propag. model 80−80679
polyvinylidene fluoride, poling process, solitary wave propagation model 79−87398
polyvinylidene fluoride, polycryst. ferroelec., microstruct., piezoelec. and pyroelec. props. 80−7303
polyvinylidene fluoride, pyroelectric transient response 80−75956
polyvinylidene fluoride, pyroelectricity, low temp. behaviour, due to origin 80−88932
polyvinylidene fluoride, struct. study, piezoelec. and pyroelec. props. 80−7300
polyvinylidene fluoride, thermodynamic model and appl. 80−75955
polyvinylidene fluoride, thermodynamical model, applications *(French)* 80−39315
polyvinylidene fluoride, uniaxially stretched, piezoelec. and pyroelec. 77−40181
polyvinylidene fluoride film poling rates, 20 to 100°C 77−77138
polyvinylidene fluoride films, 200 ps laser pulse heating, pyroelectricity meas. 79−4768

pyroelectricity continued
polyvinylidene fluoride films, corona-charged, struct. changes, piezo- and pyroelec. props. 79−11389
polyvinylidene fluoride films, pyroelectric current freq. depend., thermal diffusivity 79−78630
polyvinylidine fluoride, corona charging at 12.5 kV, obs. 78−92027
potassium acetylacetonate, polycryst., elec. cond., pyroelectricity, phase transition, UV spectrum 78−76392
primary and secondary, review 80−93243
primary coefficient, low temp. behaviour 78−39506
PTS, pyroelectric effect, 76 and 300K 78−95554
PVDF dielectric, piezoelec. and pyroelectric props. rel. to crystalline forms 80−15982
PVF_2 pyroelectric coeff., depolarisation current meas. 79−56737
pyroelectric high power density heat engine, dielectric losses, polarisation 80−80689
pyroelectric materials, photovoltaic effect, photoelectron transport 79−4582
rare earth molybdates, cryst. growth, cryst. chem., and phys. props., book contrib. 80−44194
saccharose, far IR absorpt. spectra, pyroelec. coeff. temp. depend. *(French)* 78−72503
saccharose, far IR absorption, low temp. pyroelectricity 78−80348
saccharose, single cryst. low-temp. pyroelectricity 79−42906
saccharose crystal, low temp. pyroelectricity 79−42909
sodium benzoylacetonate, pyroelectric effect, peak near Curie temp. 79−8096
TGFB, deuterated, single cryst. growth from soln., dielec. and pyroelec. props. 79−24422
TGS:α-alanine, single crysts., pyro- and dielectric props. *(Russian)* 77−59520
TGS: nitroaniline, dielec. and pyroelec. props. 80−75916
TGS, deuterated, undoped and alanine-doped, growth by rotating disc method and elec. props. 79−47611
TGS, deuterated and undeuterated, pyroelectric, dielectric and thermal props., temp. depend. 78−43809
TGS, effect of aniline in aqueous crystal growing soln. on physical props. 78−43810
TGS, emission of free charge carriers in vacuum as symptom of pyroelec. props. 79−42908
TGS, ferroelectric, domain pattern using pyroelectric effect 77−40196
TGS, ferroelectric crystal, non-linear pyroelec. effect in phase transition region 79−47393
TGS, ferroelectric hysteresis, dielectric and pyroelectric props. *(Chinese)* 80−88938
TGS, growth from solution containing aniline, dielec. and pyroelec. props. 78−6639
TGS, pyroelec. effect in phase transition region *(Russian)* 79−87401
TGS, pyroelec. signal, domain struct. determ. 77−43951
TGS, pyroelec. single cryst., elec. field meas., thermally stimulated charges 80−45012
TGS, pyroelectric coeff., 1:8-300K, dynamic method *(French)* 79−19844
TGS, pyroelectric coeff., polarising field effect 79−47391
TGS, pyroelectric figures of merit 77−59519
TGS, pyroelectric props. with internal bias field 78−72466
TGS crystals, influence of domain struct. on pyroelec. props. 78−31159
TGSe, pyroelectric coeff., 1.8-300K, dynamic method *(French)* 79−19844
thiourea, pyroelectric coeff., 1.8-300K, dynamic method *(French)* 79−19844
thiourea formaldehyde polymer, pyroelectricity and dielec. props. 79−91379
tourmaline, struct. mechanisms 78−10850
triglycine fluoberyllate, pyroelectric, dielectric and thermal props., temp. depend. 78−43809
triglycine sulphate-Ge contact, thermal resist. 77−4226
uniaxial pyroelectric, nonlinear optical susceptibility 77−23705
uniaxial pyroelectric, spontaneous polarisation calc. from results of optical meas. 78−27162
vinylidene fluoride copolymer electret, charge and polarisation distribs. meas. 78−35081
vinylidene fluoride-tetrafluoroethylene copolymer, two types of pyroelectricity 80−11346
vinylidenechloride-acrylonitrile copolymer, amorphous, pyroelectricity due to space charge mechanism 79−87400
vinylidenefluoride/tetrafluoroethylene copolymer, piezoelect. and pyroelect. response rel. to dipole polarisation 80−7267
wheat, pyroelectric props. 77−12322
Ag_3AsS_3, proustite, cryst., pyroelec. coeff. vs. constant elec. field at 26K 79−61317
Ag_3AsS_3, proustite, light effects on dielec. props., elec. resist. 80−49816
Ag_3AsS_3, proustite crystals, stoichiometric composition derivation influence on phase transition 79−95715
β-$AgSbS_2$, phase transitions, electrophysical props. 80−44316
Al-SiO_2-Si, pyroelectricity 80−100524
$BaCoF_4$, low temp. magnon effects on polarisation 79−42905
$BaMgF_4$, low temp. phonon effects on polarisation 79−42905
$BaMnF_4$, dielectric props. near 250K phase transition 77−12335
$BaMnF_4$, low temp. phonon, and exciton effects on polarisation 79−42905
$BaMnF_4$, phase transitions review 79−78378
$BaMnF_4$, spectroscopy, ferroelectric/ferromagnetic coupling, high temp. pyroelectric props. 79−19845
$Ba(NO_2)_2.H_2O$, pyroelec., room temp. cryst. struct. 80−96491
$Ba_2NaNb_5O_{15}$, ferroelec. phase, thermally stimulated light flashes, surface elec. props. effects 79−73885
$BaNiF_4$, low temp. magnon effects on polarisation 79−42905
$BaNiF_4$, obs. of anomalous pyroelec. behaviour due to cooperative mag. singularity 77−59517
$(Ba_xSb_{1-x})TiO_3$ 80−60514
$Ba_{0.725}Sr_{1.775}Li_xNb_{5-x}Ti_xO_{15}$, solid soln., prep., struct., dielec. props. *(French)* 77−69782
$Ba_{1.35}Sr_{0.65}NaNb_5O_{15}$ crystals, struct., dielec. and pyroelectric charact. 79−51913
$Ba_{0.60}Sr_{0.40}TiO_3$, sputtered film on Pt, pyro-effect for laser registration *(Russian)* 77−20804
$Ba_{1-x}Sr_xTiO_3$ ceramic pyroelec. responsivity, −140° to +160°C obs. 78−23405
$Ba_2TiGe_2O_8$-$Ba_2TiSi_2O_8$, pseudobinary system, pyroelectricity and related props. 78−95553
pyroelectricity continued
$BaTiO_3$ and $BaTi_{0.08}Sn_{0.02}O_3$ films, pyroelectric response to step radiation signals 80−7302
$BaTiO_3$, controlled surface layers 78−48120
$BaTiO_3$, exam. of anomalous pyroelectric effect above Curie point 79−33613
$BaTiO_3$ film, struct. and dielec. props. 80−60514
$BaTiO_3$ films, ferroelec., effect of elec. field on dielec. props. 79−33642
$BaTiO_3$:Cu, photoferroelec. props., Jahn-Teller effect, laser irrad. effect on pyroelec. props. 78−60400
$BaTiO_3$:Mn^{2+}, electrooptical effect, charge transfer mechanism, defect. pair form. 79−38519
$Ba_2TiSi_2O_8$, fresnoite, Czochralski growth and phys. props. 78−3026
$Ba(Ti_xSn_{1-x})O_3$ film, struct. and dielec. props. 80−60514
$BaZnF_4$, low temp. phonon effects on polarisation 79−42905
BeO ceramic TLD, operational charact. and problems 77−42216
BeO, emission of free charge carriers in vacuum as symptom of pyroelec. props. 79−42908
$BiFeO_3$, pyroelectric-antiferromag., magnetoelectric effect *(Russian)* 78−43625
Bi_2WO_6 film, RF sputtering, possible piezoelec., pyroelec. and photolithography appl. 77−15705
CdS-Au structure, work function of {0001} faces of CdS, pyroelec. charcts. 78−23164
Cr_2BeO_4, magnetoferroelectricity, weak pyroelectric effect 79−42914
$CsCuCl_3$, phase transition, refr. index, electrooptic coeff., pyroelec. signal, and NQR meas. 80−70386
CsH_2AsO_4, pyroelectric investig. in ferroelec. phase 77−12321
CsH_2PO_4, single cryst. growth, struct. and elec. props. 78−71693
Cu-Cl boracite, pyroelec. coeff. meas. 80−75951
Cu-Sb-S-I amorphous film formation and stimulated crystallisation, electrophysial props. *(Russian)* 78−30838
Fe-I boracite, pyroelec. coeff. meas. 80−75951
$Fe_3B_2O_{13}I$, boracite single cryst., nucleation control density growth 80−80955
FeI boracite single crystals, dielectric, pyroelectric props., vapour phase transport growth 80−80673
Fe_3O_4, lattice parameters, NMR freqs., and magnetoelec. pots. near 12K 80−71146
$FeSb_2S_4$, berthierite cryst., anomalies in elec. and dielec. props. 77−47821
$K_2Cd_2(SO_4)_3$, langbeinite type cryst., search for ferroelec. phase transition 77−59535
$K(H_{1-x}D_x)_1P_4$, polarised impurity cluster effects in light scatt. expts. 80−71431
KH_2PO_4, ferroelec., change of sign in pyroelec. coeff. 79−82929
KH_2PO_4, polycrystalline materials; pyroelec. temp. anal. as method for studying ferroelec. transitions 79−38502
KH_2PO_4, powder sample, pyrocharge temp. depend. near phase transition 79−87399
KH_2PO_4, pyroelectric investig. in ferroelec. phase 77−12321
KH_2PO_4, pyroelectric coeff., 1.8-300K, dynamic method *(French)* 79−19844
$KH_3(SeO_3)_2$, phase transition, acoustic phonon softening 77−27997
$K_2Mg_2(SO_4)_3$, langbeinite type cryst., search for ferroelec. phase transition 77−59535
$K_2Mn_2(SO_4)_3$, langbeinite type cryst., ferroelec., phase transitions, dielec., elastic and pyroelec. meas. 77−59535
$KNbO_3$, spontaneous polarisation and pyroelec. effect meas. 77−90107
$K_2SbNb_5O_{15}$, dielec. and pyroelec. props. 79−99841
$KTaO_3$, sp. ht. and electrocaloric props. at low temps. 77−84945
$K_2Zn_2(SO_4)_3$, langbeinite type cryst., ferroelec., phase transitions, dielec., elastic and pyroelec. meas. 77−59535
$3La(IO_3)_3.HIO_3.7H_2O$, pyroelec., cryst. struct. 79−1410
$3La(IO_3)_3.HIO_3.7H_2O$, pyroelec. p_3 and piezoelec. d_{33} coeffs. 79−19840
$LiClO_4.3H_2O$, absolute sign of piezoelec. d_{33} and pyroelectric p_3 coeffs. 78−43793
$LiClO_4.3H_2O$, pyroelec. and piezoelec. coeffs., struct. refinement 78−18602
$LiCsSO_4$, thermal and dielec. props. 80−34860
$Li_2Gd_4(MoO_4)_7$, ferroelec. and paramag. props. 78−39517
Li_2GeO_3 piezoelectric glass ceramic, recrystallisation, pyroelectric response, permittivity 80−80703
$LiKSO_4$, thermal and dielec. props. 80−34860
$LiKSO_4$, uniaxial crystal, pyroelectric, thermal expansion, phase transition 80−19966
$LiNH_4SO_4$ and $LiND_4SO_4$, dielec. pyroelec., and thermal props. 80−60509
$LiNbO_3$ crystal, elec. cond., optical quality, impurity depend., space charge pyroelectric field compensation 79−64295
$LiNbO_3$, laser induced optical damage, pyroelec. contrib., electrostatic obs. 78−37935
$LiNbO_3$, $LiTaO_3$ transition metal doped, photovoltaic and photorefractive effects, origin 77−20364
$LiNbO_3$, optical damage induced by X-irradiation 77−20814
$LiNbO_3$, partially clamped single cryst., secondary pyroelectricity, electrostatic meas. 79−82927
$LiNbO_3$, partially clamped single cryst., tertiary pyroelectricity, electrostatic meas. 79−82928
$LiNbO_3$, pyroelectric induced optical damage 78−52446
$LiNbO_3$, vitreous, anomalous dielectric behaviour and reversible pyroelectricity 77−85658
$LiNbO_3$:Fe, exoelectron emission in pyroeffect regime 80−76158
$LiNbO_3$:Fe, unipolar Malter emission under pyroelectric effect conditions 80−29862
$LiNbO_3$:Fe^{3+}, electrooptical effect, charge transfer mechanism, defect. pair form. 79−38519
$LiNbO_3$:Fe(Cu), pyroelectric, photorefractive props., optical absorption, EPR and Mossbauer spectra meas. 77−32403
$LiNbO_3$:Ti optical waveguides, pyroelectric loss meas. 79−46046
LiNb0$_3$:Fe, anomalous photovoltaic effect and diffraction efficiency *(Russian)* 79−15190
$Li_2SO_4.H_2O$, electrocaloric cooling effect, low temp. behaviour of primary pyroelectric coeff. 78−39506
$Li_2SO_4.H_2O$, linear pyroelectric, temp. depend. of polarisation 79−99821
Li_2SiO_4, piezoelectric glass ceramic, recrystallisation, pyroelectric response, permittivity 80−80703
$Li_2Si_2O_5$, pyroelectric glass-ceramics 80−75950
$LiTaO_3$, primary pyroelec. effect, lowest order mode contrib. 78−15103
$LiTaO_3$, vitreous, anomalous dielectric behaviour and reversible pyroelectricity 77−85658

pyroelectricity continued
$Li_{1+y}Ta_{1.5y}Ti_{6y}O_3$ ($0 \leq y \leq 0.028$), non-stoichiometric phase, crystallographic and dielec. props. 80−75212
$Mg_3B_7O_{13}Cl$, pyroelec. effect, spontaneous polarisation, domain struct. 77−8520
$NH_4H_2PO_4$, polycrystalline materials; pyroelec. temp. anal. as method for studying ferroelec. transitions 79−38502
$NH_4H_2PO_4$, powder sample, pyrocharge temp. depend. near phase transition 79−87399
NH_4HSeO_4, ferroelec. phase transition, pyroelec. props. 80−60513
NH_4HSeO_4, ferroelec., phase transitions, permittivity and pyroelectricity meas. 80−71350
NH_4NBeF_4, successive phase transitions, dielec. and optical props. obs. 80−50275
$(NH_4)_2SO_4$, polycrystalline materials; pyroelec. temp. anal. as method for studying ferroelec. transitions 79−38502
$(NH_4)_2SO_4$, powder sample, pyrocharge temp. depend. near phase transition 79−87399
$Na_9(Al_6Si_6O_{24})(OH)_2.6H_2O$, hydrosodalite, ferroelec. transition, pyro- and piezoelec. activity 79−15421
$Na_2CO.2CaCO_3$, shortite, cryst. struct. and space group, pyroelec. effect 79−23573
$Na_8(Ge_6Al_6O_{24}).CO_3.nH_2O$, linear pyroelectric, temp. depend. of polarisation 79−99821
$Na(H_3O)(I(OH)_3O_3)$, pyroelec., cryst. struct. at room temp. 79−10835
$Na(H_3O)[I(OH)_3O_3]$, piezoelec. and pyroelec. ionic displacements 79−38456
$NaH_3(SeO_3)_2$, phase transition, pyroelec. current meas. 79−82934
Na_2SO_4, high temp. phase, DTA and dielec. meas. 79−82333
$Nd(BrO_3)_3.9H_20$, single cryst. low-temp. pyroelectricity 79−42906
$Ni_3B_7O_{13}Br$, boracite single cryst., nucleation control density growth 80−80955
NiBr boracite single crystals, dielectric, pyroelectric props., vapour phase transport growth 80−80673
PLZT pyroelectric detectors, piezoelectric oscillations, in response to CO_2 laser pulses 79−61305
PLZT pyroelectric detectors, delayed onset of piezoelec. oscills. 80−75953
PLZT, RF sputtered thin film, ferroelectric props. 79−69780
PLZT, thin, elec. cond. and pyroelectric behaviour 80−75954
PVF_2, film, origin of pyroelectricity 79−99828
PVF_2, film, static and dynamic pyroelectric coeffs. from 90-370K 79−99827
$Pb_{5-x}(Cs, Bi)_2Ge_3O_{11}$ 80−75960
$Pb_3Ge_2O_7$, dielectric thin film, obtained by sedimentation, exam. of dielectric props. and structure 80−2282
$Pb_5Ge_3O_{11}$ single crystals, switching behaviour and hysteresis 80−40077
$Pb_3(Ge_{1-x}Si_x)_2O_7$, optical SHG and pyroelectric effect 77−10982
$Pb_{5-x}Nd_xGe_3O_{11}$, ferroelec. props. 80−75960
PbO, disordered photoconductor, dielec. props., temp. depend. anomalies 78−43765
PbO-GeO system, pyroelec. and TSC props. 78−43798
PbO_x, photoconducting, phase transitions, occurrence of ferroelectricity, pyrocurrent obs. 79−11395
3PbO.2GeO, TSC in thermoelectret state during ceramic synthesis, pyroelec. currents and energy struct. of capture centres 80−55014
$Pb_{0.95}Sr_{0.05}(Zr_{0.53}.Ti_{0.47})O_3$, low temp. internal friction in ferroelectric ceramic 77−21200
$Pb(Ti,Zr,[Fe_{1/2}Ta_{1/2}])O_3$, pyroelec. props. at transition between ferroelec. phases 78−52447
$Pb(Ti,Zr)O_3$, pyroelectric props., addition effects 79−33608
$PbTiO_3$, anomalies in elec., photoelectric and mechanical props. 80−55051
$Pb(Zn_{1/3}Nb_{2/3})O_3$ single cryst., pyroelec. props., meas. under laser beam illum. 80−66117
Pb(Zr,Ri)O_3:Ni-silicon rubber flexible composite pyroelectric, dielectric props. 80−80704
$Pb(Zr, Ti)O_3$ ceramics for IR detectors, pyroelectric charact. 79−56736
$Pb(Zr,Ti)O_3$, PCD ceramic, pyroelectric props. 80−100635
$Pb(Zr,Ti)O_3$ pyroelectric ceramics 79−47649
$PbZrO_3$-Pb_2FeNbO_6-$PbTiO_3$, pyroelectric props. of ferroelec. rhombohedral transition 77−12336
$Rb_2Cd_2(SO_4)_3$, pyroelectric and dielectric props., ferroelectric transitions 79−38458
RbH_2AsO_4, phase transition, dielec. pyroelec. and internal friction meas. 77−16261
$RbH_2PO_4(AsO_4)$, pyroelectric investig. in ferroelec. phase 77−12321
$RbHSeO_4$, ferroelec. props. and domain struct. 79−78637
$Rb_2Mg_2(SO_4)_3$, langbeinite type cryst., search for ferroelec. phase transition 77−59535
$Rb_3MoO_3F_3$, ferroelec., phase transitions, crystallographic, DTA, dielec. and pyroelec. meas. *(French)* 77−85671
$SbNbO_4$ single crystals, pure and doped, growth and pyroelec. and ferroelec. props 80−40248
$SbNbO_4$:CoO(Fe_2O_3)(TiO_2), growth, pyroelectric and ferroelectric props. 79−73886
SbSI, ferroelectric, dark current and spontaneous polarisation, ferro-paraelectric transitions obs. 80−60521
$Sn_2P_2S_6$, ferroelec. and pyroelec. props. meas. 78−35107
$Sr_{0.5}Ba_{0.5}Nb_2O_6$ crystals, ferroelec., dislocation free, pyroelec. props. 79−42907
$Sr_{0.5}Ba_{0.5}Nb_2O_6$, ferroelec., primary pyroelectricity 77−63371
$Sr_{0.5}Ba_{0.5}Nb_2O_6$:Fe(Mn)(Cr)(La), ceramic, additive effects on ferroelec. and pyroelec. props. 77−16256
$Sr_{1-x}Ba_xNb_2O_6$, and Nd doped growth of low dislocation density cryst., dislocation struct. 77−40348
$Sr_4NaLiNb_{10}O_{30}$, electro-optic, pyroelec., dielec. and piezoelec. props. *(Chinese)* 79−69810
$SrTiO_3$ ceramic, electrocaloric effects for refrigeration at cryogenic temp. 80−77789
$SrTiO_3$ ceramic, sp. ht and electrocaloric effects at low temps. 77−59518
TGFB, emission of free charge carriers in vacuum as symptom of pyroelec. props. 79−42908
TGSe, emission of free charge carriers in vacuum as symptom of pyroelec. props. 79−42908

pyrolysis
acenaphthylene pyrolysis, carbonaceous mesophase and disc-like liquid crystals 80−79687
acetylene pyrolysis, nucleation of C black particles *(French)* 79−52648
$AgBi(CrO_4)_2$, synthesis, thermolysis, crystallography *(French)* 80−33946
aluminium acetylacetonate, pyrolysis rel. to Al_2O_3 film prod. 77−85943
ammoniates, appl. to solar energy storage 80−76656
asbestos, dehydroxylation, PMR investigation 80−21269
atactic polypropylene waste, pyrolytic conversion to fuel oil 80−35627
azoethane, pyrolysis, master eqn. for rate coeff. 78−48612
barium titanyl oxalate exam. of chemical production and thermal dissocation *(German)* 79−4935
bauxite reduction at 800-1800°C, corundum recrystallization 77−86296
benzene, liq., laser pulsation kinetics, optical damage effects 80−58614
bioenergy conversion systems, efficiency improvements 80−30511
n-butyl nitrite, pyrolysis at low-press., 590-750K, n-butoxy radical isomerisation 79−20355
cellulose char, O_2 chemisorpt. kinetics 80−96730
coal, C isotope effects in gaseous products 79−84263
coal, laser pyrolysis in He or H_2, products exam. 79−20356
coal, liquefaction by hydrogenation, developments 79−92051
coal gasification using COGAS pyrolysis process 80−30342
coal tar and petroleum pitches, press. effects on coke yield and microstruct. form. 77−70289
complex formate, spray-dried, thermal treatment to produce $Li_{0.5}Fe_{2.5}O_4$ spinel ferrite 79−24482
complex systems, pyrolysis and combustion charact., Fourier transform IR spectroscopy 80−86462
concrete, thermal decomposition in interaction with molten nuclear core materials 80−22946
copper molybdates, oxidation, reduction and thermal decomp. mechanisms 80−50847
Curie point pyrolysis of polymers, determ. of kinetic parameters *(German)* 78−85155
Curie point pyrolysis system for hydrocarbon anal. 77−77854
diacetate-nitrocellulose, long period struct., 180-265°C, X-ray diffr. obs. *(Russian)* 79−24556
diamond powder, consolidation by thermal decomposition of methane and benzene 80−66448
o-diazonaphthoquinones, thermal decomposition of light sensitive materials *(Russian)* 80−73504
dispiro compound I, pyrolysis, CIDNP, S-T mixing, nuclear Overhauser effect 77−6803
dolomite, powders sintering, decarbonisation cycle effect 80−104102
Earth mantle elements compounds and modifications, high press. and temp. thermodynamics 80−81874
elastomers, vacuum compatible, chem. character correl. with physical charact., review 78−24804
epoxy resin, pyrolysis products, anal. by MS-GC *(Japanese)* 78−35767
epoxy resins analysis, cured, combination of pyrolysis, gas chromatography and conventional analytical techniques *(Japanese)* 79−87914
ethane, pyrolysis, thermodynamics and kinetics 79−43577
ethyl cyanide, kinetics and mechanism 79−24728
ethylidenimine, pyrolysis product, microwave spectra, rot. distortion and electric quadrupole const. and rot. barriers determ. 80−78608
ferrites, Li-containing, conditions for obtaining high-density one-phase mag. ceramic 79−52141
gas chromatography, for analysis of tyre rubber blends, computer-controlled 79−96396
gaseous hydrocarbons in fluidised beds, quantitative model conceptions *(German)* 77−73448
graphite, laser pyrolysis in He or H_2, products exam. 79−20356
graphite tubes, for at. absorpt. spectroscopy, pyrolytic coating method optimisation 78−76940
H_2O decomposition using S-I cycle, process eng. and bench-scale studies, for H prod. 80−35770
hexamethylcyclotrisilazane film, plasma-polymerised, TEM study 80−44456
HTR fuel particle coating with pyrocarbon by pyrolysis in fluidised beds *(German)* 79−59247
hydro carbon pyrolysis, C particle growth, model 79−91919
hydrocarbons, coating nuclear fuel particles for HTR *(German)* 80−18585
hydrocarbons, gas phase oxidations and pyrolysis, wall-less reactor technique 80−45500
hydrocarbons, gaseous, pyrocarbon deposition, kinetic model *(German)* 78−23851
hydrocarbons, Ni-catalysed decomp., morphologies and growth mechanisms of carbons 78−35679
1-iodopropane, pyrolysis, intermol. energy transfer in two-channel unimol. reaction 79−11769
isotope compounds, conversion to metals by reduction-distallation methods 80−23223
Kapton, pyrolysed, cond. polymer, transport and mag. props. 80−96887
laser beam pyrolysis of organic liqs. *(Russian)* 77−56226
laser specific and thermal reactions classifications 80−11919
laser-probe, microanalysis trace contaminants in substrates appl. 78−92553
layer compound, expansivities and thermal degradation 77−89554
lead-containing stabilisers in PVC, degradation obs. using X-ray diffr. *(German)* 79−34297
light pyrolysis of polymers, determ. of kinetic parameters *(German)* 78−85155
magnesite, powders sintering, decarbonisation cycle effect 80−104102
mean first-passage time, steady-state and equilib. rate consts. 78−35673
metal azides, modeling of elementary step of chemical transform. of crysts., appl. to decomp. 79−15985
metal sulphates, thermochem. approach to gas-phase reduction by H_2 79−5147
methane, pyrolysis, spiral growth of pyrolytic C *(German)* 78−42931
methane pyrolysis, AC arc discharge plasma temp., electron density meas. 79−87843
methanetrithiol, pyrolysis, dithioformic acid prod. and microwave spectra 78−58671
methanol, adsorption and decomp. on Al, UPS, XPS and thermal desorption obs. 79−82441
methanol, adsorption and decomp. on Ni (100) 80−66876
mica, natural, high γ- and electron-irrad. doses effect on annealing behaviour, thermal decomp. resist. 80−60897
monomethylamine, dilute mixtures, decomposition, shock tube studies, IR emission obs. 79−96301
neopentane, steady state in flow pyrolysis, determ. individual rate consts. 78−35650

pyrolysis continued
perfluoroalkyliodide, pyrolysis of vapour due UV irrad. 78−73070
perylenetetracarboxylic dianhydride pyrolysis for synthesis of C films with high conductivity 80−80983
petroleum feedstocks and cokes, graphitisability 80−93580
plastic materials, waste, pyrolysis to produce organic raw materials *(German)* 80−3307
PMMA sheets, flame spread in laminar forced oxidising gas flow 80−35535
poly-α-deuteroacrylonitrile, thermal degradation under reduced press., Fourier transform IR studies 79−87437
poly-α-methylstyrene-polybutadiene, light beam and Curie point pyrolysis investigation *(German)* 79−57223
polyacetylene:AsF_5, thermal decomp. kinetics, elec. cond., ESCA and mass spectra 80−50830
polyacrylonitrile, pyrolyzed, elec. cond. and dielec. const. in AC regime 78−60173
polyacrylonitrile, thermal degradation, Fourier transform IR obs. 78−92474
polyamide-Cu(Ni) oxalate, oxalate decomposition kinetics, in polymeric medium, thermogravimetry and DTA 78−52749
polyatomic molecules decomposition, pseudocanonical description of non-Boltzmann excited ensemble of oscillators 79−29331
polyborodiphenylsiloxane, synthesis and thermal decomposition 77−40541
polybutadienes, radiation chemically cross-linked, charact. by pyrolysis gas chromatography *(German)* 80−81348
polychlorinated biphenyls waste disposal by pyrolysis, plasma torch appl. 80−76487
polydiacylthiosemicarbazides, synthesis and thermal cyclodehydration *(Japanese)* 80−108388
polyethylene sulphide, thermal stability and stability against solvents *(Russian)* 78−51449
polymer, transparent, high-temp. zone form. in laser induced mech. breakdown 77−56086
polymers, high-temp. pyrolysis, heat transfer processes at gas/solid surface *(Russian)* 80−61152
polymers, light and Curie point pyrolysis, determ. of kinetic parameters *(German)* 78−85155
polymers, pyrolysis-IR anal. 78−3404
polymers, pyrolysis-mol. wt. chromatography−vapour phase IR spectrophotometry, on-line system, reviews 80−55768
polymethylene sulphide, thermal stability and stability against solvents *(Russian)* 78−51449
polyorganosiloxane-asbestos composites, high-temp. transitions 79−38802
polyquinazolones containing pendant imide groups, prep. and props. *(Japanese)* 80−104111
polystyrene, thermal degradation, kinetic study *(Japanese)* 79−39139
propane pyrolysis, model, kinetics *(French)* 79−52649
propellant solid, pyrolysis craters due to laser pulse heating 78−23921
PTFE, pyrolysis surface layer ablation, analytical model 77−52637
PVC, pyrolysis, HCl anal. in off-gases using ion-selective electrode 77−60146
pyrocarbon coating deposition by gaseous hydrocarbon pyrolysis, theoretical anal. 77−40459
pyrochemical process chemistry, appl. to nuclear fuel reprocessing 80−18578
pyrochemical processing for purification and recovery of spent reactor fuels 80−18577
pyrochemical reprocessing of nuclear fuels, process technology for Zn distillation, melt refining and salt transport 80−18579
pyrochemical reprocessing of spent nuclear fuels, evaluation of proliferation-resistant process 80−18580
radioactive liquid waste, thermal decomp. of Harvest feed slurries 80−52757
radioactive slagging pyrolysis incinerator, off gas treatment system 80−37514
radioactive waste heat treatment, effluent gas purification techniques *(French)* 77−23230
radioactive waste processing, volume reduction of organic alpha waste by pyrohydrolysis 80−95366
rare earth oxyphosphates, x Ln_2O_3.y P_2O_5, synthesis, characterisation and thermal stability 80−16256
reinforced organic composite, graphite, or C-C, ablation, mathematical modelling 79−41564
rotational effects, analytical model 79−24741
silane compounds prep. of pure and doped β-SiC 78−44018
silylene, decomp. kinetics under shock tube conditions 79−34292
solar cell materials, ternary and quaternary, spray pyrolysis 79−70004
solid particle, cyclic dynamics 79−47897
solid waste utilization in integrated community energy systems 79−100359
SOS early growth, transmission electron microscope obs. 77−76703
sphalerite materials, complex, spray pyrolysis 79−43574
spray pyrolysis, aerodynamics of nozzles 79−68782
stainless steel, ferritic SUS 410 type, coated with organometallic complexes and Ti alkoxides 80−34078
styrene-α-methylstyrene copolymers, prep., charact. by pyrolysis gas chromatography *(German)* 79−29355
2,2,3,3-tetramethylbutane, pyrolysis, 699 to 735K and 3 to 19 torr 78−92478
Th-based nuclear fuels, pyrometallurgical reprocessing using Al alloys for proliferation resistance 80−18582
thermal decomposition reactions, H_2O vapour evolution detection device 80−3440
thermochemical instability in optically heated condensed medium 79−66282
triacetate-nitrocellulose, long period struct., 180-265°C, X-ray diffr. obs. *(Russian)* 79−24556
trifluoroiodomethane, pyrolysis in Ar:O_2 matrix, forming trifluoromethylperoxy radical 80−50845
trifluoroiodomethane, vap. phase photolysis, UV irrad. 78−73070
1,3,5-trinitrohexahydro-1,3,5-triazine, thermal decomposition, mass spectra obs. 79−79340
tyres, used, pyrolysis to produce organic raw materials *(German)* 80−3307
unsteady heat conduction accompanied by an endothermic solid reaction *(Japanese)* 79−76939
urea phenolic resins, long term thermal stability *(German)* 79−91943
very low pressure pyrolysis, gas-gas and gas-wall average energy transfer 80−93739

pyrolysis continued
viscose, long period struct., 180-265°C, X-ray diffr. obs. *(Russian)* 79−24556
volume reaction model, of single solid particle accompanied by consecutive reactions 79−47896
waste reduction in controlled atmosphere 78−35658
water, for H prod., development of two new thermochem. cycles at ORNL 80−35780
water, thermochem. H prod. using the Mark-13 process, status report 80−30606
wood, hybrid poplar, direct hydrogenation to liq. and gaseous fuels 79−87945
wood energy in W.Virginia 80−72006
wood sawdust, flash pyrolysis, cyclone, solar gas-solid chemical reactor *(French)* 80−61296
wood wastes, gasification, using flash pyrolysis and concentrated solar energy *(French)* 80−61226
$3NO \rightarrow N_2O + NO_2$, irreversible thermal decomposition, rate consts., 440 to 650°C *(Russian)* 79−70322
AgN_3 pyrolysis, 513 to 558K 80−7787
Al, coating prod. by thermal decomp. of Al alkyls 80−104076
Al-organic compounds for Al_2O_3 technical ceramics, extraction and prep. *(German)* 78−53200
AlH_3, photo-and thermochem. reactions, 200-350K, UV Induced local states 78−31667
$Al_2In_{12}S_{21}$, thermal decomposition 78−20016
Al_2O_3, high temp. gas phase equilib. formation enthalpy, dissoc., mass spectra 78−23925
Al_2O_3, thermodynamics 77−90595
Al_2O_3:$CrCl_3$, calcination, mag. and optical studies of CrO_n 79−24736
β-Al_2O_3-H_3O^+, high press. thermal stability 79−23678
β-Al_2O_3-NH_4^+, high press. thermal stability 79−23678
β-Al_2O_3-NH_4^+, single cryst. characts. and AC cond. obs. 80−107514
$Al(OH)_3$:Fe^{3+}, thermal decomposition, EPR obs. 78−40047
γ- AlOOH, boehmite, dehydration to γ-Al_2O_3 80−21277
$3.5Al_2O_3.2SiO_2$, mullite, decomposition by SiO_2 volatisation 80−61082
Al_2SiO_5, kyanite, sillimanite, mullitisation, effect of gaseous atm. 79−11604
B compounds, prep. of amorphous B, review, book contrib. 78−48358
B thermistor preparation and properties 77−12536
BBr_3-$SiBr_4$ mixture, prep. of B-Si thermoelec. materials 80−20862
$BaB_{12}H_{12}.10H_2O$, struct. dehydration, intermediate phases and thermooxidative degradation 80−33951
$Ba(N_3)_2$, thermal decomp., role of defects 78−73033
BaO-$BaCO_3$, thermal dissociation 77−86297
$BaPt(OH)_6 \rightarrow BaPtO_{3(5)}$. 77−80486
(BaTi) citrates, thermal decomp., thermal anal., IR and X-ray diffr. obs. 79−24735
$BiH(PO_3)_4$, condensed, thermal behaviour and IR spectra 80−19912
$Bi_2Mo_2O_9$, thermal decomp. rel. to catalytic oxidation 80−35520
BiOI, synthesis, thermal decomposition in dry O_2 *(French)* 78−53205
C fibre reinforced C, fibre-matrix interactions 78−84725
C, glassy reticulated struct., low temp. thermal cond. meas. 79−86938
C, pyrolysis mechanism, electron microscopy, DTA, IR, ESR obs. 78−56593
C/C composite with S-modified pitch binder precursor, carbonisation and mech. props. *(German)* 77−44183
^{11}C-acetylene, production by methane pyrolysis and irrad. 80−36129
Ca-Mn-O system, isobaric phase diagram and subsolidus phase relations 79−24508
$CaB_{12}H_{12}.10H_2O$, struct. dehydration, intermediate phases and thermooxidative degradation 80−33951
$CaCO_3$, thermal decomp. in vacuo, ultrastruct. and crystallography 78−71864
β-CaO.Al_2O_3, onset temp. of decomp. 77−81244
CaO.$6Al_2O_3$, thermodynamic stability, reaction with Ti, Cr and Zr oxides 80−92687
$CaSO_4$, thermal decomposition, torsion-effusion cell obs. 77−77741
Cd_3As_2, thermal dissoc., 550-850°C 80−35512
CdS film, spray pyrolysis prep., elec. transport props. 78−2590
CdS spray pyrolysis film prep. and characterisation 78−64492
$CoFeF_5.7H_2O$, thermal decomp. 77−81394
CoO on Co_3O_4, oriented growth following Co_3O_4 pyrolysis 78−80739
Cr complex, bis(ethylbenzene) chromium, thermal degradation, high purity Cr production *(Russian)* 80−35128
Cr pyrolytic coating, effect of support metal mech. props. on formation *(Russian)* 80−7713
$Cr_{1-x}Fe_xOOH$, thermogravimetric anal., thermal decomp. to obtain rutile type oxides 79−24740
CrO, reduction by powdered graphite, mechanism 77−4748
$CsCd(NO_2)_3$, pure and metal ion doped, cryst. struct., reflectance spectra and thermal decomp. 79−51081
$Cs_2Ni_3(P_2O_7)_2.nH_2O$, thermal dehydration 80−35513
Cu-H, evolution of gas during heating, mass spectroscopic exam. 80−30221
$CuCr_2O_4$, thermal decomp. mechanism *(French)* 80−50834
$CuGaSe_2$, film, spray pyrolysis prod. 79−95953
$CuInS_2(Se_2)$, film, spray pyrolysis prod. 79−95953
Cu_2S layer spray preparation and CuCl-thiourea complex formation 78−64471
$CuSO_4.5H_2O$, dehydration into trihydrate obs. using monocryst. platelets, product domains shape 80−71905
D_2-Ar, thermal dissoc. of dilute mols., vibr. bias mechanism 79−61854
$Dy_2(SeO_4)_3.8H_2O$, thermal decomp. and IR spectra 80−3319
$Er_2(SeO_4)_3.8H_2O$, thermal decomp. and IR spectra 80−3319
EuF_3, thermal stability in vacuum 78−7183
$FeCl_3$ pyrolysis, effect of CO presence 79−43623
$Fe_2F_5.7H_2O$, thermal decomp. 77−81394
$Fe_3(HCOO)_6(OH)_2HCOO.4H_2O$, thermal decomp. 78−80741
α-Fe_2O_3, prep. by evaporative decomposition of $Fe(NO_3)_3.6H_2O$ soln. 79−20011
Fe_3O_4, partial thermal dissociation in air, using solar concentrator *(French)* 79−20015
δ-FeO(OH), study of thermal decomp. by X-ray diffr., electron diffr. and TEM 80−66790
GaAlAs-GaAs lasers, channelled substrate, prepared by combination of organometallic pyrolysis and LPE 80−99745
$GaCl_3$ and GaI_2 ammoniates, for GaN film deposition 77−36402
$Ga_{1-x}In_xAs$ epitaxial layer growth by organometallic pyrolysis, homojunction LED prep. 80−76194

pyrolysis continued
GaN film, preparation by pyrolysis of $Ga(CH_3)_3$ in NH_3, cathodoluminesc. 77−4691
$GaNbO_4$ decomp. due to electron beam heating in electron microscope 78−35711
$GaPO_4.2H_2O$, orthorhombic, thermal dehydration 79−79234
$GdCl_3.6H_2O$, X-ray emission luminesc. *(Japanese)* 80−55763
Ge, epitaxial layer deposition by vacuum pyrolysis 78−52676
Ge-pyrolytic SiO_2 system, carrier trapping, GeO_2 sublayer effect 78−91775
H thermochemical prod. by H_2O decomposition, review 80−45800
H, thermochemical prod. using General Atomic S-I cycle for H_2O decomposition 80−55941
H_2-Ar, thermal dissoc. of dilute mols., vibr. bias mechanism 79−61854
HBr decomposition using $FeBr_2$ and Fe_3O_4 for H prod. 80−35778
HBr, pyrolysis for H prod. 80−35772
HI decomposition and H separation in S-I thermochem. prod. of H 80−35771
H_2O, Br-Ca-Fe cycles for H production 80−35784
H_2O, computer thermodynamic anal. and optimisation of thermochem. cycles for H prod. 80−45766
H_2O decomposition by Ce-Cl cycle for H prod. 80−35783
H_2O decomposition for H prod., equilibrium effects in high press. prod. 80−35775
H_2O decomposition using S compounds, feasibility anal. for H prod. 80−35768
H_2O decomposition using S-I cycle for H prod. 80−35769
H_2O decomposition using S cycles, thermochem. anal. of energy balance for H prod. 80−35779
H_2O decomposition using Mg-I cycle for thermochem. H prod. 80−35786
H_2O direct thermal decomposition utilising solar energy for H_2 prod., thermodynamics, review 80−61450
H_2O dissociation using solar thermal energy for H prod. 80−45770
H_2O, for H prod. optimum temp. conditions utilizing HTGR nuclear heat 80−35781
H_2O, for thermochem. H_2 prod. 80−55928
H_2O, high temp. H prod. using solar energy 80−45822
H_2O pyrolysis, solar-H_2 energy systems, theory 80−61448
H_2O pyrolysis using Fe-Cl thermochem. cycle for H_2 prod., chem. engineering anal. 80−97811
H_2O, thermochemical cycles of high temp. decomposition, thermodynamic method of research *(French)* 79−96295
H_2O, thermochemical water-splitting cycles based on Ce and alkaline earth phosphates for H_2 prod. 80−55945
HO_2NO_2, thermal decay kinetics 79−5135
H_2Se decomposition 673 to 748K, appl. to thermochem. H prod. using ZnSe cycle 80−35782
HfS_2, layer compound, expansivities and thermal degradation 77−89554
$HgH+M \rightarrow Hg+H+M$, reaction rate temp. depend., chemiluminescence 78−68885
$Ho_2(SeO_4)_3.SH_2O$, thermal decomp. and IR spectra 80−3319
InAs-InP, phase equilib. and dissoc. 80−35170
InP, thermal degradation and its control in LPE growth 79−100343
$K_2Ca(SO_4)_2.H_2O$, syngenite, thermal dehydration under nonisothermal conditions 80−3324
$KEuHP_3O_{10}$ acid, exam. of thermal decomposition 80−55638
$K_2Mg(S_2O_3)_2.6H_2O$, isolation, struct., decomposition *(French)* 78−52506
$K_2Ni_3(P_2O_7)_2.nH_2O$, thermal dehydration 80−35513
KO_2, non-isothermal decomp. kinetics 80−16649
$KYbHP_3O_{10}$, thermal decomp., thermogravimetric and X-ray obs. 80−101013
KrF_2 in duralumin reaction vessel, for F atom source 79−24724
LaIr(g), thermodynamic stability, high-temp. mass spectra obs. 80−7781
$La_7(OH)_{18}Br_3(I_3)$, hydrothermal phase equilib., cryst. struct. 78−35372
La_2S, unsaturated and saturated vapour press., 673-1173K, thermal dissoc. pattern 80−104457
Li_2O_2, thermal decomposition and heat capacity 301 to 566K, enthalpy 80−3322
LiOH(D)(T), thermal decomposition rates 530-690K, activation energy and enthalpy meas. 80−3321
$Lu_2(SeO_4)_3.8H_2O$, thermal decomp. and IR spectra 80−3319
$Mg(AlH_4)_2$, prep., thermal decomposition, molar heat capacity, heat of form. 80−3325
$MgB_{12}H_{12}.10H_2O$, struct. dehydration, intermediate phases and thermooxidative degradation 80−33951
$MgCa(CO_3)_2$, dolomite, partial thermal decomp. into MgO and $CaCO_3$, product cryst. growth 80−108706
$Mg(OH)_2$, thermal decomposition, oxidising properties 79−100339
$MgSO_4$, thermal decomposition, torsion-effusion cell obs. 77−77741
$MgSO_4.7H_2O$, thermo-electrochemical H_2 prod. using solar energy *(French)* 79−24918
$MnO-P_2O_6$ system, formation of manganese phosphates 77−90331
MnOOH, α- and γ-phase, thermal decomp., 20 to 670°C 80−35521
$Mo(CO)_6$, pyrolysis for CVD of Mo_2C, laser fusion target appls. 78−60861
MoS_2, prep. and mag. props. *(French)* 80−93072
Mo_3Sb_7, Sb decomp. press. and enthalpy of form., Knudsen effusion meas. 79−87840
NH_3, decomposition by Re filament at low press. above 500K 79−61906
NH_4ClO_4, elec. field effect on decomp. 79−15987
$(NH_4)_2Mg(S_2O_3)_2.6H_2O$, isolation, struct., decomposition *(French)* 78−52506
$(NH_4)_2Ni_3(P_2O_7)_2.nH_2O$, thermal dehydration 80−35513
NO_2, thermal decomposition, kinetics in medium pressure region *(Russian)* 79−70321
NO_2, thermal decomposition kinetics *(Russian)* 80−3329
β-Na, O-Al_2O_3, onset temp. of decomp. 77−81244
NaCl:Sr, high temp. phenomena Cottrell effect and thermal decomposition 79−20351
NaN_3, thermal decomp., N_3 generation 79−100351
$Na_2Ni_3(P_2O_7)_2.nH_2O$, thermal dehydration 80−35513
NaO_2, non-isothermal decomp. kinetics 80−16649
NaO_2, thermal decomp. macrokinetics, differential thermal anal. 80−16650
NbO_x, phase comp. on heating 2000-4000K 80−21267
$Nd_7(OH)_{18}Br_3(I_3)$, hydrothermal phase equilib., cryst. struct. 78−35372
Ni-Zn-Co ferrites, synthesis from solid solns. of schoenite-type salts 80−93511

pyrolysis continued
Ni_3C films, on graphite, thermal decomp., AES lineshape study 79−79293
$NiFeF_5.7H_2O$, thermal decomp. 77−81394
O electrode, reaction in alkaline soln. on transition metal oxides prepared by thermal decompositions 79−61864
O_2, thermal decomposition, vibr.-rot. state depletion, Monte Carlo calc. 80−35506
O_2-Ar, thermal dissoc. of dilute mols., vibr. bias mechanism 79−61854
PZT ceramics, PbO content estimation using analytical procedure *(German)* 78−53279
$Pb(SCN)_2$, thermal decomposition, kinetic parameters from thermogravimetric data 79−61859
$PdH_{1.18}$, $PdH_{1.20}$, prep., cryst. struct., chem. comp. determ. by thermal decomp. 80−34334
$Pr(OH)_3$, thermal decomposition, exam. 80−55640
$Pr_7(OH)_{18}Br_3(I_3)$, hydrothermal phase equilib., cryst. struct. 78−35372
$Rb_2Ni_3(P_2O_7)_2.nH_2O$, thermal dehydration 80−35513
S_4N_4, pyrolysis products, mass spectrometric obs. 78−60994
SO_2, thermal decomposition in shock waves, infrared measurements 79−47903
$SO_3+Ar \rightarrow SO_2+O+Ar$, rate const. of spin forbidden dissoc. in shock wave 79−57214
$S_2O_6F_2$, heating and laser excitation fluorosulphate radical prod. and spectrum 78−35647
Sb, new autoionised series, flash pyrolysis IR absorption obs. 79−85937
Sc_2O_3, reduction in Li vapour, 1800-2500K, thermodynamics 77−90595
Si, polycryst. film from low. temp. pyrolysis of SiH_4 78−31342
Si powders, laser synthesis using SiH_4 79−74119
Si production from rice husk ash for solar cells 79−62008
Si:H, amorphous hydrogenated film, decomp. kinetics 79−100342
Si-Al-O-N compounds, decomposition in N_2 atm. at high temp. 79−57226
SiC fibres obtained from polycarbosilane fibre 80−50582
β-SiC, powder, synthesis by chemical vapour phase reaction from methylsilane, exam. of props. *(German)* 79−4938
SiC powders, form. by vapour phase method 80−25623
SiH_4, at low temps. and atm. press., Si deposition kinetics 79−91595
SiH_4, silane, decomp. kinetics under shock tube conditions 79−34292
SiH_4-NH_3 mixture, deposition of Si_3N_4 film *(French)* 77−40382
Si_3N_4 powders, laser synthesis using NH_3-SiH_4 gas mixtures 79−74119
Si_2N_2O, thermal decomp. 80−81311
SiO_2, appl. to solar energy storage 80−76656
SiO_2 film deposition on high-resistance Ge substrate by pyrolysis of tetraethoxysilane 77−1818
SiO_2, gel, pyrolysis, for low-temp. silica glass synthesis 79−43194
SiO_2, low-pressure deposition from tetraethylorthosilicate, modelling 79−87582
SiO_3:B, P films doped by pyrolisis and ion implantation, IR absorpt. obs. of impurity conc. 77−72802
$SnS_2(Se_2)(SSe)$, layer compound, expansivities and thermal degradation 77−89554
$SrB_{12}H_{12}.10H_2O$, struct. dehydration, intermediate phases and thermooxidative degradation 80−33951
SrO-$SrCO_3$, thermal dissociation 77−86297
$Tb_2(SeO_4)_3.8H_2O$, thermal decomp. and IR spectra 80−3319
$TeO_{11}Cl_2$ thermal decomposition, matrix isolation IR and mass spectra 80−81306
TiD_2, film, AES detection of decomp. 79−91937
$Ti(OC_4H_9)_4$, pyrolysis, autocatalysis, TiO_2 film form. 80−55311
TiS_2, layer compound, expansivities and thermal degradation 77−89554
$Tm_2(SeO_4)_3.8H_2O$, thermal decomp. and IR spectra 80−3319
UF_6, gas phase thermal decomp., dissoc. energy of U-F bond *(German)* 79−29353
UO_2, sintered, production by gel calcination and drying, thermal anal. *(Czech)* 80−45260
WC_x formation during pyrolysis of WCl_6 and toluene, coating props. 77−36682
Y_2O_3, reduction in Li vapour, 1800-2500K, thermodynamics 77−90595
$Y_2(SeO_4)_3.8H_2O$, thermal decomp. and IR spectra 80−3319
$Yb_2(SeO_4)_3.8H_2O$, thermal decomp. and IR spectra 80−3319
$ZnCl_2(NCR)_2$, R=CH_3 or C_2H_5, thermal decomp., thermogravimetric and differential thermal anal. *(Chinese)* 80−81291
$Zn_{0.2}Co(Ni)_{0.8}O$. $1.1Al_2O_3$ powders, ZnO vaporisation from 80−16675
$ZrCl_3$ disproportionation reaction sequence, and Zr lower halide formation enthalpies 79−15973
ZrS_2, layer compound, expansivities and thermal degradation 77−89554

pyromagnetic effects *see magnetocaloric effects*

pyrometers
see also temperature measurement
band radiation pyrometry for error reduction in transmission coeff. calc. of IR radiation energy depend. on atmospheric props. *(German)* 80−105649
bench for metrological certification and testing of radiant-flux sensors (RFS) 80−98977
blackbody for energy calibration of infrared equipment 80−86377
calibration and standards 79−85141
calibration device for radiation-pyrometer systems 79−80623
calorimeter, scanning, with pyroelec. heat sensor, heat cond. eqn., model 77−10026
chemical vapour deposition conditions, quick survey method 78−44019
chopping pyrometer for remote meas. below 200°C *(German)* 80−86313
colour temperature, wide range, operational principles *(Russian)* 78−74004
contactless temp. meas. thermometers and appls. *(Dutch)* 77−53916
contactless temperature meas., IR techniques and detectors *(German)* 80−86314
contactless temperature meas. methods *(Dutch)* 77−67433
corrections to new method of temp. meas. 79−203
digital pyrometry in solar furnace *(Japanese)* 78−32821
effective wavelength formula evaluation for total radiation pyrometer 78−41311
electrical temp. meas. methods and trends *(German)* 78−93681
electro-optical pyrometer single-pulse calibration flash tube 78−12702
emission factor and luminance temp. considerations *(French)* 79−17424
fast, wide ratio pyrometer, construction and appl. *(Chinese)* 79−30483
fast optical pyrometer at many colours, detonation product temp. *(French)* 77−71330
fast-response pyrometer, calibration 80−90852

pyrometers continued
figure of merit for comparison of types of thermal detectors *(German)* 78−57954
flame temperature meas. by 3 wavelength pyrometer 79−93141
Funk net pyrradiometers for shipboard net radiation meas. 79−21055
furnace temperature meas. with suction pyrometer, accuracy 77−5845
GATE aircraft radiation instrumentation, anal., IR irradiance meas. 78−32134
high speed and resolution pyrometer design 79−21755
high-temperature meas. and calibration, above 1000°C, based on Au melting point *(Rumanian)* 80−47061
hot-wire pyrometer, highly sensitive system 78−65936
image quality in temp. meas. of nonisothermal objects 78−41312
industrial IR detector markets and device limitations 80−86432
industrial IR instrumentation sources and optical components 80−87453
injection moulding, melt temp. meas., appl. of thermocouples or pyrometers 79−58694
International Practical Temperature Scale 1968, fixed point determination 78−41270
IR, performance parameters and applications *(German)* 80−86315
IR, portable, for temp. rise meas. of live connections *(Swedish)* 77−17981
IR, portable instrument for noncontact temp. meas. *(German)* 80−42229
IR pyrometers for translucent materials *(Russian)* 79−88959
IR pyrometry, calc. method for true temp. from expt. readings 80−13081
IR pyrometry for measuring target temps. in solar furnace 77−41603
IR spectro-pyrometer, for condensed system combustion obs. *(Russian)* 77−36756
IR thermometer and pyrometer calibration methods and standards 79−88958
laser heated surface colour temp. meas. pyrometer 78−57956
logarithmic photoelectric receiver for spectral ratio pyrometers *(Russian)* 80−57302
low-temperature, total-radiation, UNT-74 apparatus for checking, 20° to 300°C 79−67387
melting pool surfaces, temp. meas. by ratio pyrometers 78−82471
methodological error elimination 77−126
modular form, for white- and band-limited radiation *(Russian)* 80−90853
monochromatic, industrial type, principal parameters evaluation *(French)* 77−5846
monochromatic pyrometer with silicon photocell as a detector *(Japanese)* 79−93145
multiwavelength optical pyrometer for shock compression experiments 80−52229
multiwavelength radiation pyrometry where reflectance is measured to estimate emissivity 80−31757
operating principles survey and error sources *(German)* 78−49841
optical, accuracy improvement using photography 80−62673
optical, cylindrical cavity blackbody radiators, effect of surface roughness on quality of radiator 80−52228
optical, extension of use of UP0-6M2 equipment 80−8991
optical and photoelectric pyrometry, measurement correction, reference wavelength 77−45847
optical IR pyrometer, combustion gas flow instantaneous temp. meas. *(French)* 79−30482
optical pyrometer for meas. of specimen temp. in controlled-atmosphere electron microscopy 78−93690
particles in flight, temp. meas. by monochromatic photographic pyrometry *(French)* 80−27312
photoelectric, for domestic oven temp. meas. *(Russian)* 78−70128
photoelectric, for temp. gradient meas. in Si cryst. growth 77−40359
photoelectric, using non-cooled $Hg_{1-x}Cd_xTe$ detector, 0-700°C range *(Polish)* 78−41313
photoelectric micropyrometer for rapid temp. var. meas. 77−41618
photoelectric pyrometer, for Oxford spectroscopic furnace temp. meas. 79−36584
photoelectric pyrometer 80−22364
photoelectric pyrometry, radiance temp. direct calc. 80−73367
photoelectric radiation, near-infrared range, calibration using standard temp.-calibrated lamps with filter 77−53915
photoelectric transducers with astatic characts., statistical errors determ. 78−93760
photoelectronic, using radiation invariant method, true temp. meas. of metals 80−52223
photographic, in aeroballistic range, track facilities of von Karman gas dynamics facility 78−37094
photographic pyrometry technique and external calibration 79−93144
photon counting, 1400K to above 2200K within 0.5K and 1.0K 80−52232
photovoltaic cell, Si, for ultrahigh vac. system 77−5908
PPT and PChD pyrometers *(Russian)* 80−68203
precision, with filament and optoelectronic transducers, 400-900°C range 77−87766
precision pyrometer, residual aberration effect calc. 79−71456
pulsed plasma source temperature calibration spectropyrometer 77−7590
radiant heat flux portable direct reading measuring device, CERL flux-probe features 78−45633
radiation, for metrological standard, 50°C to 150°C range 79−30471
radiation pyrometer, for molten cast Fe, design and field test *(Japanese)* 80−98917
radiation pyrometer, use in automatic control of molten glass temp. in feeders 77−49729
radiation pyrometry, high speed, review of problems and technology 77−26299
radiation thermometry, applied precision, current status 80−52224
ratio pyrometer, hot surface radiation flux measurements *(German)* 78−41310
remote temp. meas. of high-power radiation-generating equipment 78−24799
shock wave radiation, low inertia pyroprobe meas. *(Russian)* 77−31333
sighting device for reduction of measurement errors and industrial furnace appls. 79−71455
solar furnace temp. meas., computer aided 77−37896
spectral global and diffuse radiation and atm. aerosols, pyranometer meas. errors 79−21050
spectral radiances multiplicative comparator performance and realisation *(Japanese)* 78−8407
spectral ratio, scale correction by electric method *(Russian)* 80−37040
pyrometers continued
spectral ratio pyrometers, rated conversion characteristics *(Russian)* 80−42258
spectral ratio pyrometers of Spektropir 7 and 8 types *(Russian)* 80−90854
spectropyrometer effective wavelength value, narrowband interference filter background transmission effect 79−72687
spectropyrometers, threshold sensitivity 80−8990
spectropyrometric unit, for vibr. relax. meas. in supersonic flow 78−9275
standard temperature lamps, with W ribbon filaments 80−95102
state of art, radiation laws and detectors *(German)* 77−5844
suction pyrometer, corrections to local values of the flame temp. 77−22551
surface temperature meas., poor thermal conductors *(German)* 77−5832
surface temperature meas. errors due to emission and ambient temperature limitation *(German)* 77−82522
surface temperature meas. through radiance temp. and emissivity, algorithm for calc. 80−52209
temp. meas. of bodies heated in solar furnaces 80−86312
temp. meas. of rotating object, non-contact method with thermistor and pyrometric voltmeter 79−35742
temperature meas., contactless, potential and limitations, characts. *(German)* 78−62203
temperature meas., contactless, problems *(German)* 77−82507
temperature meas., effect of aberrations on metrological characts. 78−77920
temperature meas. principles and appl. *(German)* 78−32819
turbine blade surface temperature meas. IR pyrometer 77−17983
two-colour, modification of emissivity response 79−93142
two-colour, operation and appls. 78−65937
two-colour, principle, appls. 79−6129
vapour pressure meas. up to 5000K, pyrometric-laser heating technique 77−1239
visual pyrometric systems, optoelectronic convertor characteristics *(Russian)* 78−77919
wide range, temp. scale calc. 78−217
Bi-Sb film thermopiles for radiation pyrometry 78−214

Q *see Q-factor*

Q-factor
accelerating structure with plane symmetry, reson. freq. and quality factor meas. *(French)* 77−30676
acoustic resonance, definition and errors arising 80−69572
capacitive 1 MHz Q standards, calculable accuracy 78−21176
charged particle recoils rel. to neutron energy 80−63397
composite bulk acoustic resonator properties and applications 77−27434
cylindrical TM_{010}-mode cavity, meas. of dielectric parameters at microwave freq. 80−9002
driven magnetic fusion reactors, conf., Erice-Trapani, Italy (Sept. 1978) 80−41948
Earth, pore fluids and Q rel. to earthquakes brittle fracture model 79−39671
Earth, results from seismic studies 79−39682
Earth crust and upper mantle, inversions of high freq. $Q_\gamma^{-1}(f)$ 77−33000
Earth crust beneath SW.Honshu, Japan, Q-factor derived from explosion seismic waves 80−17242
Earth interior, Q-factor freq. depend. rel. to seismic pulse propag. 80−72438
Earth lower mantle, Q-factor from seismic P-waves amplitudes 77−86797
Earth mantle, Q-factor for Rayleigh waves from great circle attenuation and group vel. 77−49030
earth mantle, Rayleigh waves, regional differences in phase velocity and Q-factor 79−16413
Earth Q-factor, determ. from Moon tidal accel. 79−16849
Earth upper mantle, high-Q zone in Pamir and Hindu Kush from earthquakes spectral content 77−86795
Earth-ionosphere cavity, Q-factor and elec. cond. profiles from expt. Schumann reson. data 80−36360
flextensional transducer design trends 80−43588
fusion reactor, driven Tokamak, plasma parametric studies and appl. 80−42865
fusion reactor, using toroidally-linked mirrors 80−42858
grooved reflective array SAW compressor and resonator performance 77−23820
high-power US transducer performance rel. to ceramic location 79−50561
Jupiter convective interior, turbulent viscosity and tidal Q 77−29713
Kamchatka active zone, Q-factor of upper mantle 77−44929
magnetostrictive materials, compression effects on acoustic Q-factors 77−40109
mirror hybrid reactors 80−42860
mirror reactors, economic significance of Q 80−47722
neutron spectra, Q-factor calcs. for spectra below 4 MeV, dosimetry appls. 79−79654
opening switch, chemically enhanced, for generating high-voltage pulses, quality factor meas. 77−49744
optical ring resonator, high-Q, asymmetric three-layered dielectrics, design 78−83118
peridotite, high-temp. anelasticity and elasticity 80−17256
phosphate glass laser, statistical props. and stabilisation 80−48266
piezoceramic aperiodic transducer, mech. load study 80−87700
piezoceramic elastic compliance and mechanical Q-factor at high drive levels 78−60395
planetary satellites, Q-factor rel. to tidal friction effects on rot. 79−8860
plasma dielectric, in cylindrical condenser, carrier density enhancement meas. 77−58891
polyvinylidene fluoride piezoelectric film, acoustic Q meas. 77−81058
polyvinylidene fluoride piezoelectric thin films, US atten. at high freqs. 79−65798
quartz, IR radiation extinction coeff. rel. to mechanical Q 80−100653
quartz crystal gravitation radiation antenna 78−16715
quartz crystals with TTC-cut *(Danish)* 80−60504
SAW resonator Q rel. to fabrication tolerances 77−27452
seismic shear waves, Q estimation from S-SS spectral ratios 77−64218
tandem mirror reactors, fusion power reactor and fusion-fission hybrid reactor 80−42856
TCNQ salts, $Li^+(TCNQ)^-$, $Cu^+(TCNQ)^-$ and $Cu^+(TCNQ)_2^-$, low temp. EPR of impurity reson. 77−85548

Q-factor continued
two-junction Josephson interferometer, reson. phenomena, anal. 78−47910
Al alloy disc, quality factor of vibr. rel. to gravit. radiation detector 78−75093
Fe-Co (5 to 25 wt.%), exam. of damping capacity of Gentalloy 78−72800
$Fe_5Co_{70}Si_{15}B_{10}$, amorphous ribbon, žero magnetostriction, low residual mag. loss 77−12157

Q-factor measurement
acoustic resonator in finite-amplitude sound wave field 78−1469
AT-cut quartz plate vibration anal. using light modulated oscillator 78−71255
capacitor loss measurement, using Q-bridges or resonant coaxial lines 77−34002
coils by damped oscillation method *(Japanese)* 78−89492
digital Q-meter, automatic, design procedure 78−70155
Earth, surface waves phase vel. and attenuation simultaneous inversion, Love waves appl. 78−85491
feedthrough waveguide resonator 77−10053
microwave cavity, analytic method using reflection coeff. vs. freq. 80−98937
microwave cavity, EPR spectrometer appl. *(Polish)* 78−93728
microwave meas. system 78−54396
neutron measurements of Oak Ridge National Labs. Dosimetry Appls. Research Facility 80−83237
oscillating quartz crystal stress distribution meas. by laser probe 77−20803
piezoelectrics, Q-factor determ. method 77−87788
quartz, synthetic, characterisation by IR adsorption 79−56824
quartz intrinsic Q estimation 80−43578
sediment classification by ocean subbottom acoustic Q meas. 80−46168
single-ended cavity resonator loaded Q-factor meas. using reflection bridge 78−54405
solid dielectric props. meas. with superconducting resonators 78−21180

Q-meters
digital, automatic, design procedure 78−70155
high nuclear polarisation of targets using automatic phase control and tuning 79−228
measurement range expansion method 78−74023
NMR spectrometer modification, servomechanism for automatic tuning *(French)* 77−18061

Q power factor *see Q-factor*

Q-switching
see also lasers
axial mode selector for laser with active Q-switching 79−13996
controlled flashlamp illuminated phototropic switch 77−88735
double pulse laser oscillator with continuously variable time interval between pulses 79−10321
dye DFB laser, N_2 laser pumped, self Q-switched, tunable picosecond pulse generation 80−69432
dye laser, flashlamp pumped, freq. tunable ns duration pulses by pulsed Q-modulation 79−41403
dye laser, ultrashort pulse generation, self Q-switching mechanism 80−58612
dynamic electro-biased laser Q-switch with SCRs *(Chinese)* 79−45977
electrooptic polarization modulated injection laser 80−58591
FET Q-switch circuit for pulsed NMR 77−49760
fluoromethane TEM_{00} far IR laser with integrated pump laser 80−43348
fluoromethane TEM_{00} far IR laser with integrated pump laser 80−58578
four level laser, Q-switched, dynamics and lifetime of terminal energy level *(Chinese)* 78−66832
frustrated total internal reflection switches and modulators 77−39066
gamma-ray laser, conditions for laser threshold, use of polarized nuclei 78−37868
holography of moving object, using Q-switched ruby laser freq. chirp 79−7093
inertial feedback laser, T-modulated giant pulses 77−19353
intraresonator, mirrors optimal reflection coeff. selection 80−48302
introductory concepts and results, Q-switching and mode-locking, book contrib. 80−106504
Kerr shutters, for Q-switching and radiation pulse shaping in Nd-glass lasers 79−3729
large-aperture laser, resonant vibrating mirror system 78−87082
laser acousto-optical Q-switching, for interferometer light source 77−7489
laser beam divergence in short interferometers 77−27310
laser microspectral analysis, forensic appl. 80−81385
laser passive Q-switching, criterion 78−94406
laser pulse generation and modulation devices 78−25899
laser pumping lamp trigger circuit 79−68403
laser resonator fourth harmonic generation cascade process *(Russian)* 80−99797
laser with nonlinear active medium, transient intracavity SHG, giant pulse generation 80−9948
microprocessor-controlled 64-cell pulsed optical receiver for crosswind sensing 77−18096
Nd:glass multichannel laser with plasma shutter 80−64088
operation of two individually Q-switched lasers *(Japanese)* 77−691
optical Kerr effect modulator, for laser passive mode-locking and Q-switching 78−9403
oscillator-based powerful laser, GOS-1001 with film resonator Q-switch 79−3705
output energy stabilisation of Q-switched laser, appl. to Nd:YAG oscillator 78−83003
passive mode locking with fixed moment of stimulated emission 77−61973
passive switch of KS-19 glass for controlling time of appearance of laser giant pulses 77−38959
physical model and techniques *(Slovenian)* 78−63138
plasma Q-switch in laser cavity 80−28259
PLZT ceramic modulator for 1064nm laser Q-switching 77−38964
POPOP solution dye lasers, multiplate reflectors 80−83606
pulse synchronization in Q-switched and mode-locking regime 78−5510
rate equations for Q-switched operation, theory 77−38948
ruby, unstable Q-switched resonator in negative branch confocal config. 79−13980
ruby laser, μs pulse laser with negative feedback 77−714

Q-switching continued
ruby laser, continuously pumped, repetitive self-Q-switching 78−50781
ruby laser, passive Q-switching by I_2 vapour bleaching 77−79872
ruby laser, Q-factor passive modulator unloading, in resonator with prism *(Russian)* 77−68234
ruby laser, Q-switched, parameter depend. on ruby quality 78−46608
ruby laser, Q-switched, power dependent freq. sweep 77−19256
ruby laser, radiation automodulation with passive switching of electro-optical shutter *(Russian)* 78−74936
ruby laser, radiation self-modulation with passive closing of electro-optic shutter 79−64258
ruby laser, spectroscopic props., operation modes, pulse amplification *(Rumanian)* 80−48265
ruby laser, using colour centres in SrF_2 78−71157
ruby laser, weak passive Q-switching in spherical resonator 78−50834
ruby laser ns pulse generation by electrooptic gating *(Russian)* 77−79871
ruby laser with electrooptical shutter, emission spectrum narrowing and single freq. giant pulse lasing 80−78877
ruby laser with high-frequency control of lasing conditions 80−74363
ruby laser with special resonator Q-switching 77−38958
ruby lasers, freq. synchronisation and locking by passive modulator 80−1249
ruby lasers with stable operation in pure transverse natural oscillators *(German)* 77−14761
ruby passive Q-switched oscillator, damage limited pulsewidth 78−83004
ruby pulsed laser real-time holographic interferometry 80−74319
ruby Q-switched laser, photographic film calibration for energy meas. 78−5517
semiconductor acoustic DFB laser, high speed repetitive Q-switching 78−83007
semiconductor laser, transient effects 77−75513
semiconductor laser, using electro-optical props. of Bragg reflectors 77−19345
single heterostructure laser, spatial distrib. of radiative recomb. rate, time delays and Q-switching 79−22953
solid laser, nanosecond and microsecond pulse generation, review 78−71130
solid laser, pulse train stability with periodic Q-switching 80−28239
solid laser, subnanosecond and picosecond operation 80−28262
solid laser characts. control, using optical delay lines, free-generation, Q-switching and mode-locking regimes 80−99758
solid laser Q-switching by optomechanical shutter 79−72609
solid-state ring laser, generation of microsecond pulses 80−9913
spherical cavities, Q-switching by rotating mirror in ruby and Nd:glass lasers 80−28261
stimulated Brillouin scatt. mechanism of laser resonator Q-switching 80−106552
TOPOT vapour dye lasers with multiplate reflectors 80−83606
transition-metal dithiene complex dyes for 0.9 to 1.4 μ lasers 80−1200
tricarbocyanine dye passive Q-switch for Nd^{3+} lasers 79−10333
unstable resonator Q-switched laser, transient processes 77−75576
(Al,Ga)As DH laser, pulsations produced by saturable absorber Q-switching, possible model 79−81426
CO laser, electron-beam-controlled, short high-power pulse generation 78−25863
CO laser, liq. N_2 cooled, extended spectral distrib. of lasing transitions 79−89894
CO laser passive Q-switching, intracavity Zeeman modulation detect. of NO 80−9597
CO_2 high-pressure Q-switched electron-beam-controlled laser characts. 79−59669
CO_2 IR laser, transients obs. by modulation of intracavity absorber 78−74933
CO_2 laser, 10 ns pulse generation, rotating mirror technique 80−33042
CO_2 laser, mode locking obs. by intracavity plasma injection 80−83624
CO_2, laser, passive Q-switching by CH_3F 78−9402
CO_2 laser, passive Q-switching using heated CO_2 saturable absorber 78−25900
CO_2 laser, passive Q-switching by FIR laser gas CH_3I 80−1246
CO_2 laser, Q-switched, single rot. line-selection *(German)* 78−46562
CO_2 laser, single mode locked pulse selection, semicond. refl. switching 77−3609
CO_2 laser, with intracavity Stark cell, for pulsed and Doppler laser radar 77−19320
CO_2 laser modulation, plasma injection into cavity 80−83626
CO_2 lasers, IR saturable absorpt. in benzene, chlorobenzene and bromobenzene 80−69465
CO_2 Q-switched laser pump source for CH_3OH/D, CHOOH and CH_3F lasers 80−69383
CO_2 rotating-mirror Q-switched TEA laser, mode sweeping effects 80−99769
CO_2, short-pulse oscillator, variable pulse repetition freq., pulsewidth and wavelength control 77−88801
CO_2, submillimetre wave laser operating in passive Q-switched intracavity pump mode 77−83885
CO_2 waveguide laser, electrooptically Q-switched 79−98416
$CoCl_2.6H_2O$ solution in ethanol, thin absorbing film, nonlinear optical props., Q-switch appl. 80−91836
Cr^{3+}:$BeAl_2O_4$, tunable laser performance, 701 to 794 nm, long-pulse and Q-switch operation 79−72573
Cr^{3+}:$BeAl_2O_4$ alexandrite laser, high gain performance 80−53299
Er^{3+}:YAG pulse periodic laser with high activator conc. 79−10320
(GaAl)As injection lasers, self-pulsations, Q-switching and mode-locking effects 78−66827
GaAs junction laser, theory 77−3587
GaAs junction laser long time delays, internal Q-switching 77−79822
HF laser with flow-through chem. active medium, pulsed-periodic regime realisation 80−106513
HF multiline laser pulses, ns switching, amplification 77−38910
Ho:$LiYF_4$ laser, TEM_{00} mode and Q-switched operation 80−74395
I laser, emission at two frequencies 79−18413
I photodissociation laser, characts. of new dye comps. for passive switches 80−91826
I photodissociation Q-switched laser, optically thick active medium, chemical kinetics and gasdynamics 79−64218
$LiNbO_3$, nonstationary intracavity stimulated Raman scatt. by polaritons 79−18473
$NH_4H_2PO_4$ total internal reflection intercavity laser switch 77−38955
$NH_4H_2PO_4$, total internal refl. diffr.-type modulator as laser cavity switch 78−5511

Q-switching continued
N_2O IR laser, transients obs. by modulation of intracavity absorber 78−74933
Nd laser, bleaching-spectrum widths for dyes used in Q-switching 77−42573
Nd laser, giant nanosecond pulse chain stabilisation 79−13998
Nd laser, with mirror plasma-optical Q-switch *(Russian)* 80−33028
Nd:glass, oscillator, short laser pulses *(Rumanian)* 79−7165
Nd:glass, Q-switched laser, radiation polarisation 77−27293
Nd:glass, subnanosecond pulse oscillator, investigation by high-speed oscillography 80−74411
Nd:glass laser, mode locked, picosec. pulse form., expt. technique 77−38957
Nd:glass laser, resonant reflectors in laser cavity, freq. selection 78−55369
Nd:Glass laser, sub ns periodically Q-switched 78−17995
Nd:glass laser, with nonlinear absorber, pulsed Q switching 78−9400
Nd:glass laser with periodic Q-switching, mathematical model 80−33043
Nd:glass laser with US Q-switch 80−64034
Nd:glass lasers with stable operation in pure transverse natural oscillations *(German)* 77−14761
Nd:glass Q-switched laser, feasibility of tuning range widening 79−59724
Nd:glass Q-switched laser controlled by external signal, stimulated emission characts. 79−10312
Nd:glass Q-switched laser emitting polarised radiation 79−45974
Nd:glass ring laser, actively mode-locked and Q-controlled, props. 79−18445
Nd:glass ultrashort pulse length, passive switch relax. time effect 77−38960
Nd:$La_2Be_2O_5$, laser crystal properties 77−19260
Nd:YAG, actively AM mode-locked Q-switched laser, pulse compression by liq. Kerr cell 79−22990
Nd:YAG, CW laser gain switching for intracavity pulse amplification 77−88771
Nd:YAG, laser fusion system, short pulse generation, active mode-locking and Q-switching 77−79868
Nd:YAG, operational characts. of $LiNbO_3$ Q-switch for generating single laser pulse *(Korean)* 77−704
Nd:YAG, unstable resonator, Q-switched laser, operating characts. 79−36928
Nd:YAG high performance laser system efficiency and beam uniformity 77−19327
Nd:YAG laser, acousto-optic Q-switches 79−7166
Nd:YAG laser, actively modelocked and Q-switched, fusion reactor appl. 79−45980
Nd:YAG laser, mode self locking with combined Q-switching 78−1284
Nd:YAG laser, passive Q switching at 1.3 μm 79−72610
Nd:YAG laser, Q-switched, pulse stretching using Pockels cell 80−95927
Nd:YAG laser, reduction of passive Q-switch output jitter 78−46648
Nd:YAG laser pulse tailoring/synchronization system for laser-plasma interaction expt. 79−98404
Nd:YAG master oscillator, spectral comp. form. of high-power laser radiation 78−71115
Nd:YAG mode-locked laser picosecond pulse profile and power meas. 77−7112
Nd:YAG oscillator, flashlamp pumped, const. gain Q-switching to improve stability 78−50837
Nd:YAG oscillator, generation of high-power ns pulses 80−23730
Nd:YAG Q-switched laser beam and waist, knife-edge profiling 79−45982
Nd:YAG repetitively Q-switched laser, fifth harmonic generation for mW 213 nm source 79−55178
Nd:YAG unstable-resonator oscillator, stable single-axial-mode operation by injection locking 80−53331
Nd^{3+}:glass laser, Q-switching by exploding PbS film 78−42361
Nd^{3+}:glass laser, stabilised, single-mode, Q-switched, continuous frequency scanning 79−31922
Nd^{3+}:YAG, Q-switching mechanism by intracavity stimulated Brillouin scatt. 80−106552
Nd^{3+}:YAG continuously pumped pulse-periodic laser, stability 80−28241
Nd^{3+}:YAG electro-optically Q-switched pulse-periodic laser 79−45975
Nd^{3+}:YAG electrooptically Q-switched laser pulse duration increase by intracavity SHG 79−94255
Nd^{3+}:YAG laser, contrast and configs. of $LiNbO_3$ electrooptic switches 80−33012
Nd^{3+}:YAG laser, high repetition rate electrooptic Q-switching, birefringence 80−69430
Nd^{3+}:YAG multimode laser radiation noise 80−74366
Nd^{3+}:YAG Q-switched picosecond laser radiation, pulse duration and energy fluctuations 79−89949
Nd-YAG laser, Q-switched, freq. doubled, 200 kW output 80−33026
Ni complex, BDN, saturable absorber, degenerate four-wave mixing, amplification and phase conjugation 80−43394
Ni complex, BDN II in tetrahydrothiophene-1,1-dioxide, saturation behaviour, Q-switching appl. 80−48354
Ni:MgF_2, tunable transition-metal-doped solid state lasers 80−58549

QC *see quality control*

quadratic programming
constrained finite element solns., convergence proof 78−54168
elastic-plastic plane stress finite element analysis 77−42740
frictionless elastic contact problems, approximate soln. 78−16646
linear elastic half-space, frictional unloading problem, variational soln. for stress analysis 78−59350
nuclear reactor core 78−54860
optimisation in subspaces, appl. to kinetic rate const. determ. 78−53185
PWR, core control optimisation for scheduled load changes 79−71911
space vehicle orbit determ. with incomplete inform. on error covariance matrix and expectation 79−8808
unbounded contact problems analysis 77−2533

quadrupole crystal field interactions *see crystal hyperfine field interactions*

quadrupole lenses *see electron lenses; electrostatic lenses; magnetic lenses*

quadrupole mass analysers and filters *see mass spectrometer components and accessories*

quadrupole moments
see also atomic electric moment; molecular moments; nuclear electric moment; nuclear quadrupole resonance
charmonium hyperfine quadrupole moment, orbital mixtures, quarkonium system phenomenology in potential models 79−49496
crystals, NMR quadrupolar effects, RF energy absorpt., relaxation times *(Russian)* 80−71235
deuteron, EM quadrupole form factor peak value, determination of percentage D-state 78−93950
finite ligand size and the Sternheimer antishielding factor γ_∞ 80−103653
linear gyrotropic media, E2, M1 moment contribs. to linear polarisation *(Russian)* 77−8540
molecular torsional oscills., NQR freq. temp depend. electric field gradient asymmetry 80−18868
muonium, hyperfine quadrupole moment, orbital mixtures, quarkonium system phenomenology in potential models 79−49496
nuclear quadrupole moments and rms charge radii, shell model calcs. 80−47369
organic molecules, quadrupole moments, dipole quadrupole A and C polarisabilities, perturbation theory anal. 80−27934
phenazine, first excited state ^{14}N quadrupole tensor by ODNQR 78−50561
polar liquid, electric double layer at surface 78−53212
rare earth metal, anisotropy of carrier scatt. by disorder in quadrupole moments 79−69494
(rare-earth)Al_2Ga_2, synthesis, NMR and X-ray absorpt. studies 80−108083
sigma phase alloys, NMR and electric-field gradients 80−108109
spin-1 particle, quantum gravity corrections to anomalous mag. and quadrupole moments 77−65130
tellurium-thiourea compounds, Mossbauer investig. of ^{129}I, quadrupole interactions and bonding 77−48111
transferrin, ^{111}In labeled, perturbed angular correls. study 79−39342
trinuclear exchange clusters, Dzyaloshinsky coupling effects in Mossbauer spectra *(Russian)* 80−108142
d, $^3S_1$-$^3D_1$, $^3D_2$ phase parameters and deuteron quadrupole moment, pot. reconciliation 79−67575
W boson, Weinberg model 77−30383
Al($^2P_{3/2}$), at. quadrupole shielding factor 79−10222
As, $np^2(n+1)s$ excited-state config. quadrupole moments, Sternheimer shielding factor 80−37755
^{A}Ba,(A=134-138), quadrupole moments and change in mean square radii of charge distrib. 79−50154
CO_2 IR Zeeman spectra utilizing copropag. wave reson., diamag. shift obs. 80−53055
^{43}Ca, nucl. quadrupole moment, HFS in at. beam mag. reson. 79−63940
Cd, nuclear quadrupole interaction theory using first-principles pseudopotential 79−73482
$CuFe_2O_4$, Jahn-Teller type crystal distortions 80−103904
D, calc. from elec. field gradient of D_2 79−93511
Dy, visible spectra obs., hyperfine struct., mag. dipole and electric quadrupole interaction const. anal. 80−91698
^{166}Er, Skyrme-HF calcs., deformation, electric moments, spin-orbit potentials 78−62480
Ge, A=70, 72 and 74, dynamic deformation theory, energy levels 78−58235
H-like atoms, quadrupole moments 78−90072
H_2, $S_0(3)$ pure rot. quadrupole transition, obs. using tunable diode laser 78−82723
^2H, quadrupole moment and percentage D state lower bounds 78−37286
^{165}Ho in $HoVO_4$, NMR predictions of properties, dipolar interactions and antiferromagnetic exchange 80−50203
LiF, H_2 scatt. from surface, qudrupole interaction and rot. transitions 79−74041
^7Li electric quadrupole moment, from Coulomb scatt. of aligned ^7Li ions 80−78141
^{24}Mg+e, 21 to 32 MeV, E0 and E2 excitations, fission into two $^{12}Cg.s.$ nuclei 78−54744
^{A}Mo, A=94, 96, 98, multiparticle states, method of generalised seniority 80−22759
N, $np^2(n+1)s$ excited-state config. quadrupole moments, Sternheimer shielding factor 80−37755
$(NH_4)_2BeF_4$ crystal, macroscopic quadrupole moment anomalies in incommensurable phase *(Russian)* 79−65808
Na I $3^2P_{3/2}$ meas. beyond natural linewidth by beam laser quantum beats 77−50399
Nb complexes, ^{93}Nb quadrupole coupling tensors form EPR meas. 80−88866
P, $np^2(n+1)s$ excited-state config. quadrupole moments, Sternheimer shielding factor 80−37755
$Pd_{0.7}$, D spin-lattice relaxation time, D quadrupole coupling, D atom diffusion 79−73844
^{108}Pd, vibr. states study, elastic and inelastic electron scatt., anharmonic vibrator model 78−62520
$RbH_3(SeO_3)_2$ crystal, incommensurable phase, quadrupole moment study 80−97213
^{A}Ru, A=96, 98, 100, multiparticle states, method of generalised seniority 80−22759
Sb, $np^2(n+1)s$ excited-state config. quadrupole moments, Sternheimer shielding factor 80−37755
^{A}Sb, A=121, 123, elec. and mag. hfs. 79−10224
^{154}Sm, Skyrme-HF calcs., deformation, electric moments, spin-orbit potentials 78−62480
^{181}Ta, elec. quadrupole interactions in 482-keV level, meas. using Ge detector 79−40842
TbP (As)(Sb)(Bi), mag. transitions, quadrupolar interaction effects 80−80512
V complexes, ^{51}V quadrupole coupling tensors form EPR meas. 80−88866
V-Ni sigma phase alloys, NMR and electric-field gradients 80−108109
Zn, nuclear quadrupole interaction theory of ground state of ^{67}Zn nucleus 79−73481
$ZnMn_{1-x}Cr_xFeO_4$, Mossbauer effect, quadrupole splitting 80−29664
^{A}Zr, A=92, 94, 96, multiparticle states, method of generalised seniority 80−22759

quality control
see also reliability
acoustic cleaning, electrolytic method for quality control 79−34233
acoustic emission detection technique, industrial NDT appl. *(Japanese)* 78−27721
acoustic emission transducer for inspecting weld quality 79−94444
advanced fibre composite, ultrasonic scanning, C-scan technique for fibre misorientations, delaminations, bond failures 78−95882

quality control continued
airframe material defectometry, quantitative test specifications *(German)* 80−89427
anemograph data 80−56642
anodic oxide coatings in Al, testing *(German)* 77−28943
anti-HBs quantitative determination computer analysis by AUSAB procedure 77−13036
application in industrial analysis 79−52609
automatic test equipment for material props. determ. and quality control 77−86236
automation of measuring equipment state-inspection results, USSR Krasnodar territory 80−52152
biomedical engineering component quality control system 77−48884
biomedical measurement systems, metrological support, state-of-the-art and development 79−16318
BWR containment vessels of prestressed concrete, pressure tests 80−81254
camera objectives, quality testing by semiautomatic modulation transfer coeff. meas. 79−14124
capacitor dielectric fluid test and anal., quality assurance 78−80272
cast stoneware, quality control, use of US methods 78−11490
casting defects, NDT 78−27690
casting-pit refractories, quality control, specific non-standardized test development *(French)* 77−90297
coal, continuous nuclear analyzer development 79−52851
colorimetry, quality control appl., theory and practice *(German)* 79−80665
colour control of ultramarine pigments 80−62711
complete computer program in FORTRAN, for analysis of variance and means 80−98792
component checking after heat treatment, steady magnetising field 78−60958
computed tomography scanner, fourth-generation, performance evaluation 80−46035
concrete, acceptance tests comparability for separation charact., quality control *(German)* 78−68848
concrete, quality control, construction of operating charact. curves *(German)* 77−28960
conductance meter classification and quality assurance 77−12857
conference, nuclear power quality assurance, Knoxville, USA (Oct. 1978) 79−97773
consumer product quality assurance, colorimetric theory and equipment *(German)* 80−86372
destructive examination of materials with data processing, microprocessor application *(German)* 80−93714
diamond turned surface production, interferometric test repeatability 80−74538
dielectric loss of polymers meas., automatic, at 100 MHz to 300 MHz and 2°C to 40°C 80−68219
diesel nozzle sprayer castings, heat treatment quality inspection 80−35471
distribution law for normal production processes of known standard deviation *(German)* 79−52554
electro-medical servicing, quality maintenance 78−77126
electromagnetic inspection review 80−35468
electron beam processing, dosimetry and quality control 79−49871
environmental radioassay, Italy 79−25117
ferrous metallurgy, nondestructive inspection and quality control review 80−21201
FFTF, quality assurance appl. to design procurement and construction 79−97786
fission reactor, criticality safety anal., quality assurance for computer programs 79−63766
fission reactor, criticality safety calcs. quality assurance plan 79−63767
fission reactor criticality safety program, role of computers in quality assurance 79−63765
fission reactor criticality safety quality assurance, need for exptl. studies 79−63770
fission reactor Sphere-Pac fuel rods, techniques for quality assurance 79−93805
flaw detection in welded joints, X-ray television systems appl. and characteristics 77−81380
fluoropolymer components, pulsed US quality control of heat treatment 78−60953
fuel elements, quality inspection by eddy currents, unit 79−100315
gamma flaw detector, appl., multichannel 77−90565
glass fibre reinforced polyacetal mouldings, injection, shape testing, projection of optical gratings *(German)* 79−29322
glazed ceramic insulators, surface quality monitoring 79−61813
glossiness of curved surface, physical and psychological, meas. method 80−37074
heat treatment, electromagnetic quality inspection with specified intensity of internal field 80−108677
heterogeneous materials, conc. inhomogeneities control, electron and ion probe testing 79−43505
hierarchical systems, calibration errors influence on end item performance 80−98788
holographic interferometry appl. *(French)* 78−42305
holography, industrial, principles, applications *(German)* 80−95841
HTGR fuel rod fabrication, estimation and control 80−83215
HTGR fuel rod length meas. and control microcomputer system 79−71942
IC PSG film, P determ. by X-ray fluorescence technique 77−40612
industrial ear protectors, standardisation of testing, current developments 78−22225
instrument quality not maintained by frequent calibration, statistical evidence 79−93090
large monocrystal X-ray reflection/scanning and transmission topographic methods 80−96415
large-spot laser damage meas., multibeam apparatus 77−19286
LWR, quality assurance of fuel and fuel elements *(German)* 79−49810
manufacturing processes, industrial visual testing, photographic methods as technical aid *(German)* 80−31923
mass-produced camera objectives, effects of cosmetic defects 80−47135
materials testing, planning and evaluation by statistical methods *(German)* 80−93725
materials testing machines, historical development of Instron Ltd. 80−35452
measuring equipment, state control in USSR 80−52150
measuring equipment, state control in USSR 80−52151
medical engineering, appl. of automatic meas. and automata 79−62381
quality control continued
medical instruments, mass production appl. *(Hungarian)* 79−48354
metal, US quality control standardisation 78−53142
metal corrosion meas. specifications and quality assurance 77−12764
metal sheet parity, pressed, X-ray TV system for automatic analysis *(German)* 77−90536
metal surface cleanness control by photoemission recording *(Russian)* 80−49839
metalworking rectilinearity and planarity deviations meas. 79−97348
meteorology, surface synoptic obs., automatic real-time quality control 78−92920
metrological support to quality-control management 80−184
micro-optics quality testing 79−27368
monitored parameters choice for unification of measurements 80−186
multilayer components, thermal quality control 78−85107
multilayer parts, thermal quality inspection two dimensional problem soln. 79−70283
natural and industrial objects, chem. anal., future programme, computer appls. 80−104484
NDT, book 78−44340
NDT, data processing and acquisition for product quality control 80−11862
NDT appl. to castings 79−29321
NDT inspection reliability 79−66229
nondestructive, magnetic inductive method appl. *(German)* 78−48581
nuclear component manufacture, quality control problems 79−22453
nuclear fuel characterisation and quality control, conf. Karlsruhe Germany (June 1978) 79−49794
nuclear fuel pins, computer controlled meas. 80−5300
nuclear fuel reprocessing and refabrication, quality control 79−13506
nuclear medicine, computer applications 79−16295
nuclear plant operation, quality assurance, cost effective programs 79−97863
nuclear plant operations, quality assurance program 80−783
nuclear plant outage management and quality assurance 79−97862
nuclear plant quality assurance criteria, international standardisation 80−780
nuclear plant quality assurance standards in USA, present status and appl. 80−781
[nuclear plant] construction sequence scale model an aid to productivity and quality assurance 79−97777
nuclear power industry in Japan 77−61628
nuclear power plant, contrib. of quality assurance to safety and reliability 79−22438
nuclear power plant, quality assurance as method of technology transfer 77−61631
nuclear power plant, quality assurance requirements for reliability in developing countries 79−22452
nuclear power plant, quality systems standards comparison 79−22439
nuclear power plant in developing countries 77−61633
nuclear power plant in Iran, initiation 77−61629
nuclear power station, inservice examinations, effective quality assurance 79−97861
nuclear power station pressure vessels, exam. for compliance with safety regulations 78−89954
nuclear power stations, by French Elec. Board *(French)* 77−3155
nuclear power stations, safety, management *(French)* 77−3154
nuclear power system, as management commitment and personnel indoctrination 77−61632
nuclear reactor components, weld seam inspection, steam supply system, quality assurance *(German, English)* 77−83052
nuclear reactor pressure vessels, strain measurements 80−79865
nuclear reactor pump coolant tests, computerised monitoring 78−70585
nuclear technology, West German practice *(German)* 77−75004
nuclear technology transfer in Iran 77−61630
nuclear [Nuclear] fuel components QC reports 79−97883
optical element production start up, operational control optimisation 78−18078
optical fibres, measurement of refractive-index profiles in optical-fibre preforms by spatial-filtering technique 80−48403
optical instrument control life test design 80−87572
optical microscopes for quality control and industrial production 80−82816
optical shop interferometric instrumentation as a cost-effective production tool 80−74535
optical surface quality standards based on total integrated scatt. 80−48391
particle size distrib., on-line measurement techniques, instruments *(German)* 78−60895
particle size measurement techniques, rapid response, online methods, continuous industrial processes appl. 78−89429
pharmaceutical, automated 79−52798
pharmaceutical 79−97449
photographic paper, using laser-operated device *(German)* 80−57412
photographic pulp quality control using He-Ne laser scanning system *(German)* 80−3272
physical methods 79−79202
pipes, hot-rolled, automatic mag. quality control on prod. line 80−108661
pipes, soldered, device for automatic scrapping 79−29308
planar diode characterisation using SEM with movable Faraday cup, illuminator and backscatt. diode detectors 78−21292
polyethylene ageing prediction, by isothermal differential scanning calorimetry 78−11485
polymers, quality control method based on solid surface wetting 79−52534
portal film duplication using instant photography 79−30591
precision manufactured components using X-ray gauging system 77−10156
precision measurement, image analysis of precison components *(German)* 80−42193
pressure vessels weld quality assessment, NDT methods and equipment 78−56871
printing, appl. of microdensitometry *(Czech)* 79−30524
product appearance, CIE Standard Observer colour specification 80−61539
production testing, multiple shaker considerations 80−79047
purification system for Ne circulating in spark chambers 77−14309
PWR, quality assurance by Framatome 80−782
PWR, quality assurance during operation, France 77−61526

quality control continued
PWR components, pressure vessels and boilers for Framatome plant 77−38323
PWR fuel production *(French)* 77−3110
pyrocarbon, quality control techniques 77−79461
radiation processes 77−67905
radiation therapy, weekly localization films and field placement error detect. 79−43985
radiochemical and chemical trace analysis, in environmental materials, reliability aspects 78−40106
radiochemical purity quality control by rapid feedback system 77−90900
radiograph quality control programme, economic analysis 78−73236
radiographic control of MTR fuel production, use of X-ray paper 78−5001
radiographic equipment, computer-assisted quality assurance 80−89838
radiography, processor control using preexposed control strips and visual comparative densitometry 78−69210
radioimmunoassays in clinical chemistry laboratory, computerised approach 77−90878
radiology diagnostic facilities, quality assurance programme, proposed recommendation 78−73235
radome and backstructure design improvements 78−57449
raw material acceptance testing for dielectric applications 80−97646
reactor components, quality control systems by acoustic emission 79−93758
refractory materials, thermal analysis appl. *(German)* 78−35337
refractory metal refining, at. absorpt. spectroscopy for continuous process control *(Russian)* 77−56302
refractory products, apparent density determination, using surface γ densimeter 80−35464
refractory slabs, radio wave phase method for quality control 80−40667
reliability aspects in metrology, appl. to Weibull distrib. *(Rumanian)* 79−40524
retail equity, NBS Standard Reference Materials 80−86249
rolled stock, stat. quality control w.r.t. mech. props. 79−43510
roughness of periodically shred surfaces, on-line meas. technique using He-Ne laser *(German)* 80−33014
ruby rods, quality control, EPR method 79−14047
Safe Drinking Water Act, microbiology, QC for the Water Supply Lab., USA 79−74558
sapphire and Si surfaces, using IR and UV specular reflectance meas. 80−108684
scanning electron microscope appl., ISI Model (7) 79−89044
semiconductor device characterisation using electron beam induced current technique, review 78−21302
sintered metal parts and powders standardisation of quality control methods 79−96266
spectacle lens inspection apparatus *(French)* 79−7235
spectrochemical anal. appl. *(French)* 77−90703
sphalerite, hydrothermal single crysts., feasibility of optical methods for quality control 80−89065
stators, using thermovision flaw detector 'Stator-1', meas. channel 80−76449
steel, 20A, melt, tube blanks, mech. props., statistical determ. 79−29316
steel, 38KhS, heat treatment quality inspection by magnetic method 79−52574
steel, 45, case hardening quality control by ferromagnetic coercive force transducer probes 78−53151
steel, coercive force measurement method of quality inspection of heat and thermomechanically treated parts 79−5113
steel, crack detection using image quality indicators, comparison 77−25232
steel, flocculation detectability factor in US inspection in quality control 78−3268
steel, heat treated, electromagnetic device for quality inspection 78−53104
steel, high speed, anode potential determ. of tempering quality 78−53139
steel, tubes, helical welded, computerised US quality control 78−35601
steel 40 G, coercimeters with attached electromagnets used for quality control 80−108672
steel products, production line X-ray fluoresc. anal., coating thickness meas. 77−54029
steels, heat treatment of 30KhN2MFA and 40Kh, nondestructive mag. quality control method 80−108662
structural material analysis by computerized tomography 80−101001
surface configuration control by conc. loads applic., mirrors case 79−94317
surface configuration control of nonuniformly heated shells, actuators effectiveness 79−94318
surface metrology using peak counting, quality control 80−95065
testing of measuring instruments, determ. of valid interval between tests values 80−57284
thermal analysis applications in electrical and electronics industries 79−75531
thermal analysis precise temperature programming using microprocessor 79−54127
thermal NDT of large shells under prod. conditions CCTV system with combined scanning 79−11751
thermometers, resistance, transformer bridge cct. 77−53906
thermoplastic moulding quality assurance using holography and speckle photography 78−27720
thin walled bearing races eddy current inspection of hardening and tempering quality 78−95892
thremosetting resin quality control by dynamic mechanical analysis 79−74319
thyroid function radioimmunoassay, computer program *(French)* 80−94348
TV microscopy system for teaching and quality control 80−82817
tyre rubber blends, analysis using computer-controlled pyrolysis gas chromatography 79−96396
u.s. automatic inspection system, computer aided *(German)* 77−4877
US exam. *(German)* 79−91903
US imaging equipment, quality control problems 78−69171
US nondestructive inspection system, microprocessor utilization 80−71845
US rail monitoring, by mirror-shadow method using EM acoustic convertors 77−90551
US spection, with given reliability, optimal conditions 78−95895
US testing appl., acoustic emission technique 77−12767
US testing of contact welds 78−56854

quality control continued
US transducers, appl. of ultrasound visualisation technique 77−14863
water quality trends, statistical tests for dependent obs. 77−29513
water-moderated-water-cooled reactor VVER-1000, power plant technology 78−82501
weld joint of high-pressure vessel, radiography inspection 79−100313
weld quality testing, US, in spiral-welded gas pipes 77−90550
welded joints, German specifications *(German)* 79−83415
welding seams, automatic US inspection system 79−29310
welds, ultrasonic testing techniques review 77−74899
wind power plant development, low cost approach 80−61268
workpiece quality control by optical correlation 77−50644
X-ray fluorescence spectrometer for industrial quality assurance 79−70398
X-ray quality control, automatic exposure relay 78−95893
X-ray spectrometry improvement 79−54240
X-ray testing of pneumatic type inspection, in automated production line *(French)* 77−5969
Be bronze, BrB2 grade, heat treatment quality evaluation, using eddy current device 77−90562
Cr-Mn-Si steel, heat-treatment quality, higher harmonics of EMF obs. 78−60941
Fe, coercive force measurement method of quality inspection of heat and thermomechanically treated parts 79−5113
Fe nodular parts, comparison of sonic-resonance and US velocity techniques for quality control 80−97654
$Ga_xAl_{1-x}As$-GaAs heteroepitaxial layer distortion characterisation by X-ray multiple diffr. 80−96754
Li-I cell solid state, cardiac pacemaker power source, testing 79−66584
Li-I_2 battery, construction, performance and reliability 80−97771
MnO_2 batteries, type LR9, cathode composition, quality effects *(Polish)* 79−52920
Nb-Ti, multifilamentary, Mirror Fusion Test Facility, superconductor core manufacturing and quality 80−93521
PbTe layers, quality control of carrier conc. using Hall effect graphical representation 77−1500
Pt-Au, thick film, adherence meas. and evaluation 80−50813
Si devices, oxidation induced stacking fault detection by refl. X-ray topography 77−84767
Si, optical reflectance rel. to surface damage 79−14985
Si, surface potential spread rel. to chemical treatment *(Russian)* 78−11363
Si wafers layers, multilayer ellipsometry, layer thickness and refr. index determination of layers 80−95121
Sm-Co alloy magnets, operational control of residual induction, maximum mag. energy 79−15324
^{99m}Tc radiopharmaceuticals, rapid miniaturised chromatographic quality control procedures 78−28070

quality factor *see Q-factor*

quanticule theory of chemical binding *see bonds (chemical)*

quantisation
't Hooft-Polyakov monopole, zero energy eigenvalues for quantum fluctuations, quantisation 79−9318
*-quantisation as deformation for a system of identical particles 79−30274
Abelian gauge field, $A_0=0$ gauge, canonical and path-integral quantisation 78−70277
action-angle variables in quantum mechanics, appl. to harmonic oscill., linear (triaxial) rotors 80−31543
anharmonic oscillator, 3-term recursion relations and quasienergies, WKB method, quantisation rules 79−97257
antisymmetric tensor gauge field, action principle quantisation 79−71623
antisymmetric tensor gauge fields, covariant quantisation, Faddeev Popov ghosts 80−27406
approximate spectral decompositions associated with a family of harmonic oscillators *(French)* 79−44761
area preserving maps, quantisation 80−12924
atom+molecule, collision dynamics, classical trajectory problem Fourier transform method 79−98189
bilocal theory, constraints, centre of mass and quantisation 78−89619
Bohr-Sommerfeld quantisation condition, appl. to steep walled single-well pots. 78−86180
Bohr-Sommerfeld quantisation rule, relativistic corrections using Dirac eqn. semiclassical approx. *(Russian)* 78−89645
Bohr-Sommerfeld quantization of n-dimensional neutral and charged pulsons *(Russian)* 79−49092
Bohr-Sommerfeld quantization of pseudospin Hamiltonians 80−105537
Bose description of fermions 78−89402
boson field in neighbourhood of classical solution, quantisation by appl. of Bogolyubov's method 78−8566
canonical formalism on lightlike hyperplane, neutral scalar field, Dirac's theory 77−79214
canonical Hamiltonian system, different quantisations and classical limits 78−8271
canonical quantisation and independent coordinates, for teachers 79−16
canonical quantisation of gauge fields, gravitational field *(Chinese)* 80−22266
canonical quantisation of non-Abelian gauge theories, axial gauge 78−70279
canonical scalar field quantisation, higher derivative couplings, Lorentz invariance of scatt. operator 78−4526
canonical transformations and quantization rules 79−44789
charge quantisation condition with N strings, charge monopole systems 77−65121
charge quantisation in curved spacetime, Kaluza-Klein background, Mandelstram field 79−2695
charged particle in mag. field, phase operator 80−8827
classical moving extended object, quantisation in one space dimension 77−79217
classical systems with non-integrable constraints, quantisation 80−36901
classical V-A theory and non-conservation of the dynamical parity 79−54014
closed systems with nonconservative internal forces, Lie admissible quantisation, hadron struct. 80−37174
CM(3) collective model, geometric quantisation 80−5078
compact group gauge fields, breaking of symmetry and dual charges *(Chinese)* 79−35918
computerised hologram generation, quantisation error minimisation method 77−83836
conformal group, quantisation and Kepler problem 77−17872

quantisation continued
conformal symm. breaking, quantisation in curved space-time 78−41434
constrained dynamical systems, quantisation by Weyl correspondence 80−77650
constrained Hamiltonian systems, generators of symmetry transformations 80−57138
constrained systems, quantisation, path-integral nonlinear effects 79−21574
constrained systems, quantization in paths integral formalism 80−94966
constraint formalism of classical mechanics, covariant relativistic quantisation, two-body problem 79−2622
continuous Heisenberg spin chain, semi-classical quantisation and spectrum 79−85084
coordinate covariant second quantisation, quantum processes in black hole evaporation 77−82670
correspondence and opposition between quantum theory and classical physics, temporal logic 80−27176
cosmology, particle pair creation, canonical quantisation for Chitre-Hartle model 80−62342
Coulomb-like quantization of the electromagnetic field on spacelike hyperboloids 79−306
covariant quantisation of quark binding string 78−4829
covariant scheme of quantisation for one-soliton sector 78−8265
curved space-time of rotating star, instability of quantum field, particle creation 78−69790
damped harmonic oscillator, non-equilibrium quantum statistical mechanics, system quantisation 80−52070
deformation theory 77−17867
deformation theory and quantisation, sympletic struct. 78−45493
deformation theory and quantisation 78−45494
dielectric solids, quasiequivalence of annihilative e^+e^- and ionisative e^-e^- interactions 78−72633
Dirac bra-ket notation for second quantisation 78−41910
Dirac charge quantisation and ang. momentum in curved spacetime 78−70045
Dirac monopole, relativistic theory, canonical quantisation 78−45517
Dirac propagator from path integral quantization of the pseudoclassical spinning particle 80−86577
Dirac quanta detection in Rindler and black hole space times, ξ quantisation scheme 80−31651
Dirac quantisation of a massive spin-3/2 particle coupled with a magnetic field 79−75703
Dirac quantisation of spin-2 field 79−12652
Dirac string Lagrangian in A^0-0 gauge, path integral quantisation 80−32007
dissipative dynamical system, stochastic quantisation 77−56
dissipative systems, calc. of propagators in the Caldirola-Karai-Schrodinger equation 79−6009
dissipative systems, canonical quantisation, von Neumann equation 80−52132
dissipative systems, exclusion of time dependence 79−92981
dissipative systems 77−22445
double soliton solutions for multidimensonal eqn., quasiclassical quantisation 78−54569
droplet model and neutral currents, operator form 80−91043
dual charged solution in curved space time, Dirac quantisation, SU(2)×U(1) gauge theory 78−12827
dual string with internal spin, second quantisation 78−440
dynamic system, classical quantisation conditions with stochastic behaviour anal. 80−8922
dynamical group quantisation 78−4520
dynamical prequantisation, spectrum-generating algebra, Kepler and harmonic oscill. problems 77−17870
education, magnetic charge quasiclassical quantisation 77−87595
education, waveguides, quantisation of radiant energy 78−36757
Einstein-Cartan theory, with anticommuting variables, quantisation in Diracs Hamiltonian formalism 79−93017
Einstein-Maxwell instantons charge quantization 79−80489
elastic wave analytic quantisation 79−88815
electric charge quantisation in elementary matter, generalized quaternion struct. of general relativity 78−29013
electrodynamics, gauge invariance and mass without spontaneous symmetry breaking 79−89088
electron-dipole system, semiclassical quantisation, for teaching 79−25799
elementary particle theory, mathematical method, conf., Liblice, Czechoslovakia (June 1978) 79−21891
EM field algebraic quantisation 79−63391
EM field in dispersive medium, phenomenological quantisation 80−13240
EM field in half space bounded by perfect mirror *(French)* 77−78994
EM field quantisation, Lorentz gauge, QED treatment of scalar and longitudinal photons 77−34111
EM field without indefinite metric, relativistic invariance 78−8565
EM wave, evanescent, quantisation, near dielectric surface, field momentum 80−43231
embedding classical fields in QFT, electrodynamics, Yang-Mills theories, gravit. appls. 78−54223
Epstein-Nesbet partitioning of full Hamiltonian, second-quantisation representation 77−3254
equation of motion, commutation relations for quantum mechanics and QFT, quantisation 80−105541
equivalence theorem, validity in nonperturbative context 79−26214
ergodicity, classical, quantum mech. implications 80−8898
Fermi quantisation of EM field, model for quantum field theory 77−79208
Fermi quantisation of Landau gauge 78−54591
fermion field with broken SU_2 symm., two-dimensional isotopic model *(Russian)* 80−73616
fermion fields with $(\sin\phi)_2$ interaction, quantum solitons 77−41780
ferromagnet, one-dimens., quasiclassical approach to many-magnon bound states *(Russian)* 78−23222
Feynman path integral formulation using geometric quantisation techniques 80−31588
Feynman quantisation in curved space, molecular vibr.-rot. spectra *(Russian)* 77−75121
fluid semiclassical statistical mech., quantum effects nonperturbative incorporation 79−64819
Fock quantisation for indefinite metric gauge fields 80−77942
Fokker-Planck equation, stochastic quantisation, path integral formulation 78−86228
free fields in stationary space times 77−67335
free massive anticommuting spin 3/2 field, quantisation using Dirac's Hamiltonian method 78−58113
free relativistic field in curved space, quantisation *(French)* 79−30639
friction, stochastic quantisation, nonlinear Schrodinger equation 80−27164
friction, stochastic quantisation, nonlinear wave eqn. 80−98825
functorial geometric quantization and Van Hove's theorem 80−86108
Galilean and Lorentz particles, quantisation, a new approach 80−12951
gauge field, for spin 3/2 fields 77−2735
gauge fields, canonical quantisation in axial gauge with indefinite metric, perturbation calc. 80−101928
gauge fields, procedure avoiding path-integral formalism 77−13863
gauge fields, quantisation, renormalisation, and fluctuations 79−30670
gauge fixing ambiguities, flux strings, and the unconstrained Yang-Mills theory 79−35927
gauge invariance in second quantisation, Hartree-Fock and random phase approximations 79−75395
gauge quantisation of Yang-Mills theory around classical solns. 78−29245
gauge theories, quantisation, without fixing gauge, functional technique 80−57471
gauge theories, using path integral procedure, physical state Hilbert space construction 78−82106
gauge theories with open gauge algebra, covariant quantisation 79−12947
general system quantisation, rigid sphere appl., wave eqn. using correspondence principle 78−57801
geometric, representation spaces 78−36869
geometric quantisation, book 77−41510
geometric quantisation, corrected Sommerfeld-Wilson rule 77−67318
geometric quantisation, correl. between classical and quantum mech. in geometric language 79−25905
geometric quantisation, pairing of polarisations 78−28974
geometric quantisation, review 77−17866
geometric quantisation and twistor theory 77−17898
geometric quantisation and wave functions 77−17869
geometric quantisation for multidimensional harmonic oseillators and Kepler problem, Maslov theory 80−17833
geometric quantization and gravitational collapse 80−90752
geometric quantization and quantum mechanics, book 80−94908
geometric strings, quark binding, quantisation in GL(2,C)/SL(2,C) struct. group 79−40727
geometry and quantisation of space-time 77−33924
geometry of the quantization of angular momenta (l,s,j) in fields of central symmetry 80−105530
global properties of systems quantized via bundles 79−75385
Godel universe, scalar perturbations 78−57709
Grassmann variant of classical mechanics, particle spin dynamics 77−41495
gravitational field, quantisation, Hilbert space of quantised system 80−52113
gravitational field 77−26220
gravitational field quantisation method *(French)* 79−30341
gravitational instantons 79−21639
gravity, sum over paths quantisation, 2-submanifold boundary value problem 80−105566
Gribov degeneracies, Coulomb gauge, conditions and initial value constraints 79−58864
Gross-Neveu type models, quantisation of a nonlinear phase space classical mechanics 79−6255
group actions on quantum bundles, geometric quantisation theory 80−17837
group-induced, in central mechanics problems 78−36866
halftone image coding rel. to visual performance characteristics 77−58280
Hamilton G-spaces, quantisation of A-bundles 77−26139
Hamiltonian dynamics in symplectic phase space, Nambu's formulation 77−26168
Hamiltonian with ergodic behaviour, classical quantisation 80−86148
harmonic oscillator, damped, quantization of inequivalent classical Hamiltonians, for teaching 79−35466
harmonic oscillator model, non-equilib. quantum statistical mechanics 77−5750
Hilbert space, operator of second quantization, classification of domains, Fock space 78−12606
holomorphic, appl. of hyperdifferential operators 79−30287
hyperbolic-type dynamics, second quantisation 77−6035
hyperquantisation of multi-mass vector spinor field in EM interaction, S-matrix unitarity 77−61232
imprimitivity systems, quantisation and superselection rules 80−4592
information test for uniform quantisation, meas. error determ. 77−79048
integral transform related to quantization 80−94978
interacting relativistic particles in phase space, manifestly covariant theory, central force system 79−6031
Kemmer-β formalism for spin-1/2 particles, removal of nonphysical components 77−74571
Kepler problem, 1-D, invariant *-product quantisation 80−17831
Klein Gordon field, covariant, in external fields, quantisation, stationary case 1-particle struct. 78−89389
Lagrangian, with higher derivatives, arbitrary spin fields 79−17596
Lagrangian-Hamiltonian systems, partial quantisation *(Portuguese)* 80−77653
Lagrangians with quadratic depend. fields and derivative couplings, covariant quantisation 77−65089
lattice quantisation of Sine-Gordon system, single-site approx. 79−17603
layered crystal, mag. quantisation investig. *(Russian)* 78−23054
Lie admissible quantisation in a self-interacting scalar field theory, deformation distribs. 78−74169
Lie algebra, quantisation of momenta and Hamiltonian 79−44775
Lie superalgebraic approach to second quantisation 79−21654
light-cone quantisation, massless propagators 78−8538
light-cone quantisation of scalar field, current nonconservation 80−47220
linear gauge theory algebraic struct., spontaneously broken symmetry, quantisation, massive gauge field 79−2906
linearised non-linear evolution eqns., integral solns. 78−93512
linearised supergravity, supersymmetric quantisation, ghost fields and superpropagation 79−93022
linearly damped harmonic oscillator, quantisation 78−21068
Liouville eqn. quantisation using correspondence principle and gauge invariance 78−4509

quantisation continued
Liouville generalised eqn. solns., density matrices 78−27739
Liouville mechanics for systems with singular Lagrangian, quantisation 78−62096
Lippmann-Schwinger type integral eqn. of motion, quantum corrections 78−62318
magnetic monopoles in compact simple Lie groups, quantisation condition 77−13869
magnetic monopoles with no strings, action principle and canonical quantisation 80−31990
manifold with affine connection, quantisation using Weyl correspondence 78−86186
many-body problem, dissipative system wave eqn. 80−86104
mapping and deformation of polynomial observable classical algebra 80−27155
massive Gross-Neveu model, semi-classical quantisation by inverse scatt. method 79−2924
massive spin-1 particles in external symmetrical tensor field, quantisation and noncausality 80−105790
massless antisymmetric tensor gauge fields, second rank, free field theory quantisation 79−257
massless fields in asymptotically flat space-time, null surface quantisation and quantum theory 80−4625
massless fields with fixed arbitrary spin, quantisation 80−31992
massless QED, dimensional regularisation in spherical spacetime 79−40698
massless Rarita-Schwinger field, covariant canonical quantisation 79−97280
massless scalar field, conformal symmetry breaking and quantisation in curved spacetime 79−97523
massless spin 3/2 field, covariant canonical quantisation in general covariant gauges 79−40440
massless spin 3/2 theory, noncanonical coordinate-covariant Lagrangian procedure 77−18163
massless spin two field, covariant quantisation in general covariant gauge 78−66027
matter quantisation without quantising related fields 80−105525
Maxwell field, quantisation and Poincare group extensions of zero mass representations 79−30685
Maxwell field, stochastic mechanics in Euclidean formulation 80−42081
Maxwell field quantisation in linear conformal invariant gauges 79−71666
mechanical system with second order constraints, quantisation procedure, nonrelativistic H atom appl. 79−75
meson field theory, second quantisation, in linear and angular momentum bases 77−22633
metastable vacuum states in SU(2) Yang-Mills theory, quantisation in $A_0=0$ gauge 79−250
method of action-angle variables and the classical dynamics of a nonlinear Lagrangian 78−77702
molecular crystal, second-quantisation representation of exciton states 78−23030
momentum observables, quantisation and measurement 80−98815
monopole theory without strings 77−49625
Moyal quantum mechanics formulation and Weyl. quantisation generalisation, Lie algebras 80−17835
Moyal-Vey bracket, quantisation, quantum mech. as nontrivial deform. of classical mech. *(French)* 77−5685
multispecies Tani transorm., kinematical props. 79−17333
Nambu's mechanics, rel. to quantisation of Dirac's singular theory *(Czech)* 77−30030
Nelson's stochastic field, tensor field quantisation 80−105574
Nelson's stochastic mechanics on Riemannian manifolds, classical dynamical system 78−57860
Noether's theorem and exact invariants for time-dependent systems 80−86114
non local theory, canonical quantization, with form factor in interaction Lagrangian 79−75691
non-Abelian gauge fields, gauge fixing and canonical quantisation 79−35947
non-affine path algorithm in the functional integral calculus of Schrodinger kernels 80−31593
nonAbelian gauge field theories, flux quantisation and angular momentum 77−74594
nonAbelian gauge theories, quantisation 78−78066
nonAbelian gauge theory quantisation, nonclassical field configs., broken symmetries, gauge copies 79−49373
nonadiabatic collision processes, electronic degrees of freedom, classical analogue, appl. to mol. system 79−64063
nonlinear Hamiltonian systems of Vlasov and Hartree type, uniformisation method 79−21588
nonlinear O(3) invariant theory, quantisation in neighbourhood of classical soln. 79−97522
nonlinear problems, consistent quantisation procedure 80−4586
nonlinear Schrodinger eqn., Moller operator construction, Lax pair operator quantisation 79−97250
nonlinear super-Poincare fermion, quantisation in bag like formulation 80−4923
nonlinearly realised supersymmetric theory, canonical quantisation 79−97283
nonlinearly realised supersymmetric theory 77−65088
nonlocal field theory and space-time quantisation 77−34078
nonrelativistic free particle, half integral or integral helicity particles by canonical quantisation 79−6020
nonrelativistic Markoff field, stochastic quantisation 79−67181
nonrelativistic quantum mechanics, fibre bundles *(German)* 80−90699
nonrelativistic singular quasilinear system, canonical quantisation 77−37770
nonseparable bound system, quantisation rules, classical trajectories, degenerate case 77−9904
nonseparable system semiclassical quantisation, invariant tori and energy levels calc. scheme 79−97225
null plane quantisation and Hag's theorem 77−64959
null surface quantization and quantum field theory in asymptotically flat space-time *(German)* 79−25959
null-plane quantisation in nonlinear Lagrangian theories 77−61194
O(3) nonlinear σ-model, quantisation ambiguity and nontrivial vacuum struct. 79−40662
'On the theory of the Schrodinger equation', Leontovich and Mandel'shtam, 50th anniversary 79−49090
one-dimensional field theories with odd-power self-interactions 79−254
quantisation continued
open system, new classical Hamiltonian-Lagrange mechanics 80−36900
optical spatial filters from binary computer generated holograms 77−50774
para-Bose coherent states 79−96
para-Fermi quantization in the representation of SO(n) 80−86554
parafermi statistics, Lie algebraic aspects of quantum statistics 79−54045
path integral quantisation and cosmological particle prod. 78−12440
path integral quantisation in curved space, independent of form of Hamiltonian 80−68071
path integral quantisation in nonrelativistic quantum mechanics *(Japanese)* 79−9138
periods on manifolds, quantisation, gauge, comments on Kiehn's work 78−8508
periods on manifolds, quantisation, gauge, topological props. of phys. theories 77−49826
perturbative expansion of quantum states of extended objects 78−54536
phase integral quantisation conditions for bound states in 1-dimens. single-well pots. 78−86181
phase space quantisation of interacting vortices in two demensions 80−4634
phase space quantization of the linearly damped harmonic oscillator 79−35627
phased-array US scanners, coarse phase quantisation effects 79−57739
photon field quantisation and dipole ghosts *(Chinese)* 80−101929
photons, antibunching effect, and direct-action quantum absorber theory 80−57535
point canonical transformations and path integral 77−38090
point transformations and non-linear system quantisation, S-matrix from perturbation theory 79−109
Poisson Lie algebra deformation and quantisation 80−8854
polarons, Frohlich, mean field theory, phase transitions 80−34371
postulate, operator functions 78−72
potential scatt., amplitude, quasiclassical asymptotic behaviour, quantum correction 78−62325
projective geometry for polarisations 80−52053
QED, charge quantisation, vac. degeneracy in two dimens. 78−405
quadratic friction quantisation, point object in viscous field 80−68076
quantisation around superparametrised finite-energy classical solutions 79−242
quantum crystals, approx. second quantisation method 79−23804
quantum field theoretical study of tachyons, book contrib. 79−58887
quantum spin systems, Fermi systems and group extensions in Weyl quantisation procedure 80−8905
quantum transport effects in DC elec. resistance of solids, review 79−40500
quasi-classical quantisation of multidimens. systems, adiabatic invariants *(Russian)* 79−3343
relativistic Brownian motion, space-time approach to quantum mechanics 80−31567
relativistic constrained system, compensating functional and quantisation, S-matrix 79−97527
relativistic free field quantisation geometrical approach 78−81885
relativistic particles, with isotopic spin, kinematics, geometric quantisation 80−62871
relativistic scattering theory, a covariant approach for the one-soliton sector 79−17640
relativistic second quantisation, extension of Hamiltonian formalism 79−244
relativistic string, longitudinal vibr. 79−13061
relativistic wave equations derivation, elementary domains theory, stochastic quantisation procedures 77−41502
Riemannian manifolds, quantisation in spaces of constant curvature 78−12602
rigid sphere quantisation, appl. to charged sphere in EM field, Pauli eqn. 79−82
Robertson-Walker cosmologies, Kostant-Souriau quantisation 80−12838
rotation quantisation in spherical coords. *(Russian)* 78−21012
S-matrix for interaction of gravitational and Yang-Mills fields 80−42315
scalar field propagators in isotropic universe 78−74137
scalar field quantisation, alternative approach, augmented quantum field theory 77−6018
scalar field quantisation in anti-de Sitter space-time 79−21641
scalar field theory in lattice space, analogy to random walk 78−21325
scalar mesonic fields on a curved space, quantisation *(French)* 79−30640
scalar-spinor instanton, systematic quantisation 78−21331
scale-covariant operator field eqn. 78−32984
Schrodinger's variational quantisation method in stochastic framework 80−105532
Schrodinger eqn., nonlinear, comparison of exact quantum and quasiclassical results 77−64965
Schrodinger kernel as functional integral, non-uniqueness 80−31594
Schrodinger-Infeld-Hull factorisation, quantisation condition, matrix elements and selection rules 78−41909
Schwinger boson representation, quantised rotator 80−18164
second quantisation and symplectic geometry, field theory 77−45977
second quantisation scheme for strongly coupled fields 79−97502
second quantization for composite particles, reactive collisions, and unstable particles 80−57116
Segal quantization of dynamical systems 79−88826
Segal-Weinless approach to linear Bose fields, uniqueness result 80−98
self-coupled vector fields, calcs. using Dirac quantisation procedure 78−89610
semiclassical, periodic orbit role for the quantal bound state 80−8831
semiclassical quantisation of nonrelativistic logarithmic theory 78−49708
semiclassical quantization of nonseparable systems 79−58567
semiconductors, semimetals, electron heating by phonons, acoustic absorpt. and acoustoelectric current quantum oscills. *(Russian)* 79−19639
Serre duality for polarised symplectic manifolds 78−29004
sesquiholomorphic functions, symbolic calculus and second quantisation *(French)* 77−53804
sine-Gordon supersymmetric model, quantisation of conservation laws and superrenormalisation 79−89058
singular Lagrangian systems, canonical transforms. and quantisation 79−9140
Slavnov-'t Hooft identities in Mandelstam's formalism 78−45776
soliton, extended particle, quantisation, degeneracy of eigenstates 80−73594

quantisation continued
soliton, non-topological, non-Abelian internal symmetry in 3+1 dimensional space-time, quantisation, collective coord. and Lorentz covariant methods 80−47199
soliton mass, surface tension, in $(\lambda|\phi|^4)_2$ quantum field theory 77−30240
soliton quantisation, cancellation of zero-mode singularities 77−49838
soliton quantisation in gauge models, Feynman rules 77−2734
soliton quantisation using Bogolyubov transformation 78−16695
soliton soln. of generalised discrete nonlinear eqn. 79−17261
solitons, radiative corrections in infinite volume 77−13865
space quantisation, classical explanation 80−42082
space-time quantisation, based on quantum mechanics and general covariance 79−71343
spacetime quantisation, generalised relativistic mechanics and Mach's principle 78−73867
spin 3/2 fields in presence of external gravitation, quantisation, soln. 77−22446
spin angular momentum of field interacting with plane interface 79−81399
spin projection operators for fields of any spin *(Japanese)* 78−32733
spin systems and Fermi systems quantisation 79−58627
spin-3/2 field, Hamiltonian formulation and quantisation 78−8325
spinning string, quantisation by Grassmann variables conversion to Clifford algebra elements 78−66095
spinor field quantisation, fermion-boson correspondence in quantum field theory 78−8496
spinor field quantisation 78−45777
still-picture real-time Hadamard transform coding quantiser design 77−27263
stochastic, connection with Euclidean-Markov field theory 77−17877
stochastic quantisation of wave fields, appl. to dissipatively interacting fields 78−86184
stochastic quantisation processes, review, Markov processes, Martingales, quantum dynamics 80−94969
stochastic quantization and detailed balance in Fokker-Planck dynamics 80−4645
SU(2) harmonic analysis as basis for quantisation 80−9116
SU(2) spontaneously broken gauge theory, canonical quantisation *(Chinese)* 79−49406
SU(2) Yang-Mills theory in Coulomb gauge, quantisation 78−54546
SU(2) Yang-Mills-Higgs system, classical finite energy solns. embedding in supersymmetric extension 79−2950
super Riemannian space quantisation, perturbation theory rule derivation 78−77790
supercritical reggeon field theory, classical kink state quantisation 78−16952
supergauge theory, geometric aspects, broken gauge invariance 78−8506
supergravity, covariant quantisation 78−41470
supergravity, Hamiltonian formalism, quantisation and S-matrix 78−16972
supergravity, unitarity, Ward identities, and new quantisation rules 78−54279
synchrotron radiation quantum corrections, radiated power of spin $^1/_2$ particle 79−21995
systems with curved phase space, quantisation and global props. 79−74
tensor fields, valency ≤5, extension of Segal's rules 78−29003
tensor properties of second-quantization operators and analysis of composite physical systems 79−25903
time depend. Hartree eqn. quantisation, boson expansion, particle hole excitations 79−13230
time depend. Hartree-Fock and functional approaches, anal. using Lipkin model 79−36178
time depend. self consistent fields and finite boson representations for many fermion systems 79−6048
time dependent Hartree eqn. quantisation, finite and infinite boson expansions 79−13231
time quantisation, discrete space-time model 78−20999
time quantisation, relation between proton mass and ρ-meson lifetime 78−76
torsion and matter fields, quantisation procedure 79−35615
transition from classical mechanics, nontrivial deformation *(Czech)* 78−86171
trilocal theory, constituent mass, free limit condition and quantisation 79−2984
twistor flag spaces as phase spaces of conformal particles 79−97239
twistor theory, particle models 80−13278
twistors and geometric quantisation theory 79−104
two-body relativistic systems 78−69977
universal metaplectic structures and geometric quantization 79−25881
unstable particle decay, second quantisation representation 80−4568
weak exchange interaction between atoms or ions orbitally degenerate ground states, atomic second quantisation method 80−32604
weak quantization in a nonperturbative model 79−88825
Weyl, classical limit 80−93
Weyl's quantisation rule, generalisation 77−17871
Weyl quantisation, bounded operators 80−90697
Weyl quantisation, classical limit 78−54219
Weyl quantisation and metaplectic representation 78−49712
Weyl quantization of classical spin systems quantum spins and Fermi systems 80−31585
Yang-Mills and gravitation, Ward identities and Green's function eqns. 77−67552
Yang-Mills field, canonical quantisation, interaction Lagrangian *(Chinese)* 79−21950
Yang-Mills field and Mandelstam's theory in gauge-independent path-dependent formalism 77−30249
Yang-Mills fields, quantisation by separation of gauge variables 79−67474
Yang-Mills fields, quantisation without fixing gauge 80−13207
Yang-Mills theory, conversion of isospin degree of freedom into spin degree of freedom 78−89617
Yang-Mills theory, unconstrained temporal gauge 78−45790
Yang-Mills theory in temporal guage, quantisation and asymptotic freedom 79−80754
zero frequency mode contributions in soliton quantisation general scatt. amplitude 78−29234
e^+e^- processes, photon quantisation 79−12995
$K^-p \rightarrow \Lambda^0\pi^0$, strong reaction asymmetry and mass quantisation, particle struct. *(French)* 79−3043
$K^+p \rightarrow \Sigma^+\pi^+$, strong reaction asymmetry and mass quantisation, particle struct. *(French)* 79−3043

quantisation continued
Ω^- spin, centrifugal barriers, quantisation of l=0 baryon levels 77−18221
$p\pi^-$ interaction, K+hyperon prod., mass quantisation anal. *(French)* 78−70401
π prod. in pp, np, πp interactions, mass quantisation *(French)* 78−25059
ZnO accumulation layers, electrolytic contact quantisation effects, self consistent quantum calcs. 79−60920

quantisation (communications) *see analogue-digital conversion*

quantitative analysis *see chemical analysis*

quantum beat spectra
^{14}N II ground state hyperfine structure quantum beats via ion-beam surface interaction at grazing incidence 79−10233
aromatic molecules, phosphoresc. triplet spins phase coherence, ESR 79−31559
atom, quantum beats in two-photon resonance fluorescence 80−91488
atomic coherent populations, RF elec. field reson. interactions, quantum beats 77−46542
atomic hyperfine struct. quantum beats, intensity profile, ang. momentum theory graphical method 78−25497
atomic light absorption, modulations derived semiclassically 78−25499
atomic sublevels, magnetically tuned, quantum beat phenomena 79−13682
aza-aromatic molecules, intersystem crossing, quantum interference effects 80−53037
biacetyl, single rovibronic state fluoresc., quantum beats 79−31570
bromochlorofluoromethane, narrow saturated reson. absorpt., weak current detection 77−14433
cascade effects on Zeeman quantum beats 79−89631
cascade quantum beats, intensity profile calculation 79−89630
connection between atomic and nuclear physics 78−70772
lifetime meas. in atoms, mols., ions 77−30832
microemulsion, H_2O-toluol-sodium dodecylsulphate-alcohol, diffusion coeff., light scatt. data 78−15722
molecular system, coherent three-level beats, theory 77−23526
multi-level atom, quantum beats in correl. functions of spontaneous emission and transition rates 77−75080
multilevel atom, quantum beat effect on emission rate 77−18840
n-level system, cooperative behaviour, quantum beats 77−34861
nitrobenzene, steady state electroconvection, self beating laser spectroscopy 78−87408
photon echoes, mixing collisions and quantum beats 77−34914
polyatomic mols., quantum beats 80−37826
polymer solns. and gels, dynamics, photon heat expts. 80−55727
polystyrene coils, benzene soln., internal modes by photon beat 78−10905
quantum beats, in phosphorescence 80−63704
recoil-free γ-radiation, quantum beats 80−37142
resonance fluoresc., probe of intramolecular relax., density matrix formalism, lifetimes and quantum beats 80−32757
source field detection and quantum beats, QED 79−26917
superfluorescence, quantum beats 77−42275
superfluorescence quantum beats, chirping role, Lamb shift sign change 79−31474
tetramethyl pyrazine in durene, phosphorescent mols., quantum beats in triplet states 80−58312
tetramethylpyrazine-d_{12}, photoexcited triplet state, in durene, phosphoresc., spin coherence and quantum beats 78−76517
tetramethylpyrazine-d_{12}, photoexcited triplet state, phosphoresc., quantum beats 77−71827
three level atom at high photon densities, reson. fluoresc. interference effects 80−87073
Ar, cascade effects on Zeeman quantum beats 79−89631
Ar^++C, beam-foil spectra, Ar^+ ion orientation, ang. variation 78−86944
$^{40}Ar^+$, excited state polarisation transfer due to optical cascades 78−9238
Ba I, Stark quantum beats under pulsed dye laser excitation 77−42277
^{13}C V, high energy hyperfine struct. meas. 77−57915
Cs, $7P_{3/2}$-$6S_{1/2}$ transition, photon-echo quantum beats obs. 80−23373
Cs, superfluorescence quantum beats 77−42275
^{133}Cs, high-field quantum beats for $7^2P_{3/2}$ state 79−13682
^{133}Cs, Rydberg S and D states, hyperfine struct., lifetimes, depopulation cross sections 77−42270
Ge, electron-hole drop velocities, excitation wavelength depend. 78−88358
H, beam-foil excitation of 2P-state, alignment meas. 80−14215
H, beam-foil excited, zero-field quantum beats in H_β emission, polarisation energy depend. 80−14218
H, electric field-induced quantum beats, fringing fields effect 77−42307
H, excited state, J=3/2-J=5/2 transition, fine struct. interval meas. 77−46542
H, s-p coherence quantum beats, following H^+ electron capture in gas 79−89773
H, Stark-induced quantum beats in H_β 80−9757
H^++He(Ar), H(n=4) s-d coherence, zero-field quantum beats obs. 80−32676
H^++He(Ar)(O_2), charge transfer to H(n=2), mixed parity elec.-dipole oscillations 79−31678
^2H nuclei, spin-1 particle, eight-dimensional spin space determ. by NMR 80−60428
He, depolarising collision cross sections, quantum beat obs. 80−87203
He, double excited states, lifetime meas. by beam-foil technique 78−74590
He I, $3p^3P$ level decay, zero field quantum beats 78−961
He I, interf. beat period determ. of nondegenerate states 78−70807
He, Lande g-factor determ. from free radn. beats 77−18880
He^+ impact on C foil, quantum beat pattern depend. on foil thickness 80−58343
He^++C, beam-foil spectra, He atom orientation, ang. variation 78−86944
HeH^+ impact on C foil, quantum beat pattern depend. on foil thickness 80−58343
^4He, $3p\ ^3P$ state alignment and orientation as function of foil tilt angle, quantum beat spectra 79−94071
^4He, beam foil and quantum beat spectra *(Chinese)* 80−32638
$^4He^+$, quantum beats in C foil interaction *(French)* 79−59544
Hg+Cd, quantum beats under transfer of orientation 79−98206

quantum beat spectra continued
$^{191}Hg^{m}$, and $^{190m-185m}Hg$, nucl. spins, on-line quantum beat spectrosc. determ. 80−9562
^{215}In, $8P^2P_{3/2,1/2}$, HFS and lifetimes, fluoresc. decay and quantum beats, beam 80−32657
$LaF_3:Pr^{3+}$, photon-echo quantum beats in $^3P_0$-$^3H_4$ transition 79−86219
^{14}N II, $2p3p\ ^1P_1$, hyperfine struct. after ion beam surface impact at grazing incidence 80−58403
$^{15}NH_3$, modulated coherent Raman beats 80−23464
^{14}N III, hyperfine struct. of quadruplet levels *(French)* 77−19103
^{15}N, beam foil and quantum beat spectra *(Chinese)* 80−32638
Na, ^2D highly excited states, fine struct. splitting, field ionisation quantum interference 80−18835
Na, coherent ground state transients, beat meas. 80−948
Na, hyperfine splitting, fluoresc. after two-photon excitation 79−18307
Na I $3^2P_{3/2}$ meas. beyond natural linewidth by beam laser quantum beats 77−50399
Na, mag. field quantum beats in two-photon free-induction decay 79−13692
Na, optical heterodyne spectra, hyperfine struct. 77−30841
Na, oriented vapour, RF transitions and laser beat reson., expt. technique 77−27005
Na, quantum beats of hyperfine levels observed in photoionisation 80−32690
Na, Rydberg states, high resolution spectroscopy 80−52901
Na, two-photon optical free-induction decay 78−90138
Na, vap., two-photon echo, quantum beats, superposition relax. 78−83041
Na vapour, superradiance, quantum beat spectra 80−106311
Ne, g-factors meas. by quantum beat spectroscopy 79−93955
OH, $A^2\Sigma^+_{1/2}$ state, g-factor meas. by quantum beat obs. 79−18176
Se_2, Lande factor meas. by Zeeman quantum beats *(French)* 79−45761
$^{80}Se_2$, B $^3\Sigma_u^-$ state, Lande factor meas., mol. perturbations 79−45756
SiH_4, second-order stark effects, RF-IR double reson. 78−58739
Sm, coherent ground state transients, beat meas. 80−948
Yb, Zeeman quantum beats in $6s6p\ ^3P_1$-$6s^2\ ^1S_0$ transition 79−13682
Yb(6^1P_1), Zeeman splitting, high-resolution time-resolved quantum beat spectra 78−58640

quantum beat spectroscopy
atomic systems, beam-foil interaction process, quantum beats, alignment and orientation obs. 80−14252
atomic transitions, 0 and 2π rotations distinguished by quantum interference 80−91485
collisionless sources, Forrester effect, light-beating spectroscopy 77−34034
delayed quantum beat subnatural linewidth spectroscopy 80−77879
Doppler-free laser spectroscopy seminar 78−302
gamma radiation, recoil-free, quantum beats 78−43748
laser spectroscopy uses and applics. 77−57397
light beating spectroscopic instrument for continuous meas. of tissue blood flow 80−41160
nuclear spin polarised ion beam use, hyperfine structure of ^{14}N 77−42396
optical heterodyne simulation expts., first order correlation meas., fluctuating laser beam 78−83008
photoionisation, quantum beats, origin 80−52954
recoil-free γ-radiation, quantum beats 80−22498
review 80−22444
Rydberg states, fine struct. splitting, quantum beat and double reson. spectroscopy 78−86979
scanning technique and exptl. arrangement for quantum beat obs. 80−9757
Stark quantum beats under pulsed dye laser excitation 77−42277
superfluorescence beats, theory incl. quantum fluctuations and finite sample size 80−102686
superhigh-resolution spectroscopy based on interference of states 80−102687
synchrotron pulse nuclear excitation 78−88239
time-resolved high-resolution polarisation spectroscopy in transmission, technique 78−58640
Cs, superfluorescence, comparison with theory, quantum beat spectroscopy appls. 78−86837
Na vapour, Zeeman coherence, transient and stationary, polarisation spectroscopy 80−58212
^{23}Na, P sequence, hyperfine structure 79−89632
SmI, Zeeman coherence, transient and stationary, polarisation spectroscopy 80−58212

quantum chemistry
see also chemical reactions; orbital calculation methods; perturbation theory; potential energy surfaces for collision processes; pseudopotential methods; quantum statistical mechanics; quantum theory; reaction kinetics; wave functions
Clebsch-Gordan coefficients, chain $SU(2)\supset D_{\infty}'\supset D_4'\supset D_2'$ 78−17552
electron density mapping in mols., cyrsts., conf., Rehovot, Israel, (Apr. 1977) 78−71622
molecular tunnelling in chemical reactions *(Russian)* 77−52615
photographic reactions *(German)* 78−53229
symposium, Florida, USA (March 1979) 80−51946

quantum counters *see photon counting*

quantum electrodynamics
see also electromagnetism
(1+1) dimens. Todd chain and $e^{\phi}+e^{-2\phi}$ model, exact factorised S-matrices 80−18094
(1+1) dimensional model field, fermion-boson correspondence, Klein transformation 80−42379
(2+1) dimensional compact QED, combined WKB-variational method, vacuum tunnelling 80−101960
(2+1) dimensional Georgi-Glashow model, critical Higgs mass, clustering, monopoles 80−52441
ϵ separation method in formulation of QED on lattice 78−41453
$\eta\rightarrow\pi^+\pi^-\gamma$, one-loop approx. in quantum chiral theory 78−25041
θ-vacua and confinement in two-dimensional models 80−77990
$g\phi^4$ field theory, strong coupling expansion, appl. to $g\phi^{2N}$, $g(\bar{\psi}\psi)^2$ and QED 79−58880
ψ collapse and locality 80−372
't Hooft transformation, explicit solns. 80−345
't Hooft-Polyakov monopole, zero energy eigenvalues for quantum fluctuations, quantisation 79−9318
$\hbar\rightarrow 0$ limit of QED 78−74191

quantum electrodynamics continued
n-bubble diagram contrib. to electron $g-2$, zeta function coeffs. 80−62897
$A_0=0$ gauge, propagation of fermions 79−71669
Abelian and non-Abelian gauge theories, mass generation, renormalisation, chiral and unified theories 80−4871
Abelian gauge theories, QED_2 generalisation, quark confinement 79−71605
Abelian gauge theory description *(Russian)* 77−6038
Abelian gauge theory supersymmetric aspects, Becchi-Rouet-Stora supertransformation, QED reformulation 77−34103
Abelian lattice gauge theories, θ-vacua construction in compact gauge theories 79−58874
Abraham's and Minkowski's electrodynamics, equivalence 79−80773
Abraham and Minkowski expressions 79−97550
Abraham force, comment and observation 80−73626
achiral molecule, laser induced circular differential scatt., QED anal. 78−46409
Aharanov-Bohm effect, possible nonexistence 80−27434
Aharonov-Bohm effect, first-order perturbation theory, for teachers 79−21497
Aharonov-Bohm effect, nonexistence condition, inaccessible fields 80−37194
Aharonov-Bohm effect revisited 80−32040
angular momentum of scalar isodoublet in magnetic monopole field 78−41428
anisotropic universe, particle generation and vacuum polarisation 77−74626
anomalous dimension and infrared behavior for high energy QED 80−101958
anomalous electron mag. moment near conducting plane, non-relativistic calc. 77−61229
anomalous magnetic moment calcs., spin induced mass 77−61228
arbitrary plane wave EM field, electron motion, radiational corrections, mass operator *(Russian)* 80−57534
arbitrary spin particles 78−89637
arbitrary spin particles in EM field, mag. dipole g-factor 78−93829
Aspect experiment, local and quantum theories 80−32051
Aspect experiment, objective reality, causality in QED 80−99076
asymptotic estimates in QED, fermion determinant 78−54593
asymptotic estimates QED 78−8564
asymptotic freedom, zero charge, point charges in quantum electrodynamics *(Polish)* 78−45822
asymptotic photon propagator in nonperturbative iteration scheme for finite theory 79−40702
atom, heavy and superheavy, K-electron binding, self-energy correction 77−18802
atom, relativistic, level shifts, transition probabilities, perturbation theory 79−10067
atom system, path depend. electrodynamics 79−21985
atomic electron binding energies, determ. from relaxed-orbital relativistic Hartree-Fock-Slater calcs. 77−42255
atomic energy levels, calcs. one-electron atoms 77−79529
atomic ionisation pots. in EM field, Kramers-Henneberger transformation, QED and semiclassical 77−23481
atomic pair polarisability, retardation effects 77−30744
atomic physics applications of strong field QED, Dirac eqn., autoionisation model, QFT 77−54495
atomic reson. fluoresc., QED calcs. 78−41995
atoms, photon exchange between neutral neighbours and cooperative radiation 77−27141
atoms, resonance properties, intense photon beam interaction, QED calcs. 77−27033
augmented quantum field theory, systems containing derivative coupling and/or vector fields 79−63367
axial currents, supercurrents and anomalies in supersymmetric QED 80−46933
axially gauge-covariant electrodynamics 79−17644
axion−e^+e^- after emission from ^{12}C excited state 80−32235
bagged complex scalar field, EM interaction, fine struct. const., possible dynamic origin 80−86635
Bernard Gregory 1979 lectures 80−77992
Bertotti-Robinson metric, pair production, semi-classical treatment 79−2702
Bethe-Salpeter equation, reduction to equiv. Schrodinger eqn., appl. to muonium and positronium 79−2933
Bianchi type I anisotropic universe, quantum gravitational effects *(Russian)* 78−24588
Bloch electrons in external electric field, evolution operator 79−49426
Bogoliubov transformations for systems of relativistic charged particles 77−45998
Borel singularities, effective one-loop Lagrangian in constant elec. field 78−16917
boson field in neighbourhood of classical solution, quantisation by appl. of Bogolyubov's method 78−8566
bound state formalism, modified functional formalism, self-energy and renormalisation effects 77−26463
bound states, variational approach 79−21992
bound states in quantum nonrelativistic Coulomb systems 78−41452
bound states near limit of lower continuum 77−49638
bound states near limit of lower continuum 77−49885
bounded motion in central field of force, O_4 covariant Hamiltonian formalism 79−6012
bremsstrahlung, quasiclassical limit 77−67606
bremsstrahlung and pair prod. in Coulomb field 78−4811
bremsstrahlung of vector particle in nucl. field 80−37198
broken supersymmetry mass formula, quantum corrections 80−27424
C* algebra, gauge transformation formulation for EM field 79−6307
canonical formalism for Dirac field, Lagrangian formalism basis 78−49989
canonical Yang-Mills theory with invariant gauge families 78−74140
cascade showers, three-dimens., Landau-Pomeranchuk-Migdal effect 78−49993
Casimir effect in dielectrics using source theory, surface tension and latent heat 79−8109
causal independence in local relativistic free quantum fields 79−21894
causality and renormalisation group 77−18165
centre of mass motion, atomic field eqns. for particle ensembles, multipolar Hamiltonian 77−17876
channelled electrons and positrons, quantum theory of spontaneous and stimulated emission *(Russian)* 78−49999

quantum electrodynamics continued
charge confinement, Schwinger model compared with $(QED)_4$ 80−62902
charge current commutator in framework of analytic regularisation 78−54592
charge quantisation, theorem *(Russian)* 79−63390
charge quantisation, vac. degeneracy in two dimens. 78−405
charge quantisation condition with N strings, charge monopole systems 77−65121
charge sectors, local observables framework 79−58908
charge-electric dipole interaction in 1 dimens. 80−42005
charge-field formulation of quantum electrodynamics (QEMED) 80−95232
charge-monopole system, mech. model 78−62343
charged black hole, QED effects, Cauchy horizon *(Russian)* 80−51803
charged bosons in Lorentz gauge, QED 77−49884
charged linear harmonic oscillators, interaction between two one-dimensional oscillators 78−16963
charged particle, stimulated radiation emission mechanism 80−42374
charged particle in mag. field, phase operator 80−8827
charged particle interaction, mag. field energy, spatial distrib. of interaction contrib. 80−73625
charged particle motion in fixed mag. monopole field, quantum mech. treatment 78−66062
charged particle scatt. in laser radiation field, S-matrix theory 79−12996
charged particle scattering by mag. monopoles, SO(3), gauge theory 77−13907
charged particle self-interaction 80−373
charged photons of magnitude αe (α=fine structure constant) 79−97551
charged scalar meson pair prod. by two virtual photons *(Russian)* 77−6069
charged sectors and scatt. states 79−80775
charged spin-zero particles in time-independent pots. 77−13899
charged tachyon in dispersive medium, EM radiation *(Russian)* 78−74187
charged tachyon in dispersive medium, radiation energy *(Russian)* 78−74186
charged vector meson electrodynamics *(Russian)* 78−66057
charges, magnetic, self-dual Lorentz covariant Lagrangian 80−57525
charmonium and charmed mesons on QCD, sum rules 77−30327
Cherenekov and Doppler effects, quantum theory paradoxes 78−45824
Cherenkov radiation, momentum-energy Minkowski and Abraham tensors 78−45825
Cherenkov radiation of Dirac particle in crystalline medium 77−32463
Cherenkov radiation polarisation 77−79241
circuits at ultralow temp., QED verification 80−13247
coherent bremsstrahlung, energy and momentum spectral function 80−22546
coherent hadron radiation at TeV energies *(Russian)* 79−92641
coherent hadron radiation interpretation of cosmic ray anomalous events *(Russian)* 79−92642
coherent states of a nonrelativistic charged particle in a constant electric field 80−18103
coherent states of an electron in a quantized electromagnetic wave 79−22000
compact QED in 3-dimens., Josephson effect comparison 77−79238
completely integrable class of mech. systems, Korteweg-de Vries eqns., multicomponent Schrodinger eqns. particle motion 78−54218
complex ϕ^4 theory, Euclidean path integrals and Feynman-Dyson-Wick perturbation expansion 78−49957
Compton amplitude, parity violating part 77−2840
Compton bound electron state scatt., binding and off-mass shell effects, relativistic anal. 78−17637
Compton effect, analogy to reflection from moving mirror 78−82218
Compton effect, multiple scatt., operator formalism, nonstationary electrons 78−12846
Compton effect, multiple scatt. corrections, error bounds 78−16959
Compton effective wavelength, high energy QED approach 78−37213
Compton electron wavelength, determ. by cryogenic metrological technique 78−37165
Compton scattering by unmagnetised electrons in ambient mag. field, vacuum polarisation effects 80−86631
condensed monopoles and Abelian confinement 78−78140
conducting medium, Cherenkov and ohmic losses of relativistic charge, unified treatment 79−12998
conference, nonlinear problems in theoretical physics, Jaca, Gain 1978 80−4478
conference, quarks and leptons as fundamental particles, Schlamding, Austria, (Feb.-Mar. 1978) 80−17709
confinement of compact QED for low couplings 80−18095
confining gauge theories, quark correlation functions in massive QED_2 80−105845
conformal field equations 80−46881
conformal invariance in quantum field theory 79−63377
conformal invariant QED, electron propagator, gauge parameter 77−45999
conformal-invariant finite QED, electron and photon self-energies 77−41797
conformally covariant spinor field equations 79−22004
conformed invariance 80−99074
conserved opposite parity currents, coupling to single vector field 79−21990
constant SU(2) non-Abelian gauge pot., vacuum polarisation by fermions, integral representation 80−22543
construction of two-dimensioanl quantum electrodynamics 80−86627
constructive quantum field theory models of QED_2 77−18210
continuum Dirac electron, Coulomb field, simple asymptotic wave function 78−41455
continuum QED, implementation of Gauss's law in A_0=0 gauge 78−41458
coordinate asymptotic behavior of (3→3) wave functions for a system of three charged particles 79−21980
cosmological redshifts, QED rel. to photon interaction field hypothesis 77−9828
cosmological relic radiation, as possible product of quantum era in universe expansion *(Russian)* 78−81717
cosmology, quantum effects, black and white holes 78−12441
cosmology pair creation in presence of EM fields 80−41924
Coulomb amplitude, integral representations 78−78118
Coulomb and Landau gauges interpolation in Hilbert space of free QED 78−24987
Coulomb energies of particles, lower bound 79−58912

quantum electrodynamics continued
Coulomb gauge description of large Yang-Mills fields 78−54555
Coulomb gauge QED, dimensional regularization and renormalization 79−89087
Coulomb gauge vac. degeneracies in (2+1) dimensions 79−2928
Coulomb off shell two body amplitudes, numerical computation 80−46858
Coulomb off-shell Jost functions, simple analytic expressions 78−62121
Coulomb pot. exact bound w.r.t. Dirac operator 79−21988
Coulomb scattering, Lee-Nauenberg theorem analysis 78−54595
Coulomb spheroidal functions, integral eqns. and relations 78−409
Coulomb T-matrix, modified integral eqn. using Green's functions 79−35976
Coulomb-like quantization of the electromagnetic field on spacelike hyperboloids 79−306
coupling constant singularities in QED 79−21991
covariance group in presence of external EM field 77−18211
covariant EM projection operators, covariant description of charged particle guiding centre motion 78−58145
covariant field equations for an electromagnetic string with mass points at the ends 79−309
covariant formalism for a relativistic string in a constant homogeneous electromagnetic field 79−21546
covariant inverse problem of calculus of variations, corrigendum 78−77773
covariant method, for calc. of intense radiation resulting from charged particle motion *(Russian)* 78−33007
CP^{N-1} σ-model, N-component scalar QED model, renormalisation group functions 79−97500
CPT invariance, permutation symmetry and crossing symmetry 79−55176
critical screening length for static screened Coulomb pot. 78−49706
current commutator anomaly, regularised dimensionally using hyperfunctions 78−12845
current density and electric and magnetic multipole-moment operators in quantum mechanics 80−27433
current status in elementary particle physics 79−40651
cyclotron lines in Hercules X-1 spectrum, quantum theory of struct. and higher harmonics 78−20912
Delbruck scattering, elastic scatt. of photons by Coulomb field 78−21541
density matrix in QED and the Hawking effect *(Russian)* 78−89644
density matrix in quantum electrodynamics, equivalence principle and Hawking effect 78−66060
DESY e^+e^- experiments, QED checks, τ and Υ studies 80−18111
deuteron relativistic wave equation in EM fields *(Russian)* 79−89248
dichroism, circular, laser-induced, quantum electrodynamical anal. 77−75193
Dicke model, two-level atoms, phase transition 78−5442
dielectrics, relativistic effects, ponderomotive laws 77−41519
differential scattering theory, Raman scatt. of circularly polarised light, two chromophores model 78−9158
differential scattering theory, Rayleigh scatt. of circularly polarised light, two chromophores model 78−9157
dimensional regularisation and current commutators 78−12843
dimensional renormalisation, trace and axial anomalies, Zimmermann like identities, massive QED 80−101959
dipole Cherenkov effect in doubly anisotropic 77−38790
Dirac's extended electron model 79−26269
Dirac's time dependent perturbation theory, appearance of singularities 79−21984
Dirac charge Ze particle scatt. by mag. monopole, helicity amplitudes 77−65123
Dirac distinguished self adjoint extensions 79−25880
Dirac electrons, moving in periodic mag. fields, one-photon emission 78−12844
Dirac eqn., exact solutions of eqns. of motion of charge *(Russian)* 78−49954
Dirac eqn., spinor field eqn. conformal covariance 80−52442
Dirac eqn. for EM vector and scalar pot., soln. 79−63398
Dirac eqn. for particle bound by short-range forces in electric field 79−2963
Dirac eqn. for particle in const. elec. field with plane EM wave 77−30297
Dirac equation, accurate solns., for charge moving in crossed homogeneous fields *(Russian)* 77−30289
Dirac equation, normalisable solutions in the presence of magnetic monopole 79−67488
Dirac equation, two-component first-order equations for the quantum-relativistic electron 79−17649
Dirac equation, WKB approximation at Z>137 79−17650
Dirac equation derivation, inhomogeneous media electrodynamics refraction *(German)* 79−13005
Dirac field in curved spacetime, geometrodynamical superHamiltonian and supermomentum 78−45518
Dirac fields in a curved space-time 80−18070
Dirac monopole, with and without strings 77−41794
Dirac monopoles and the Hopf map $S^3 \to S^2$ 80−32042
Dirac particle, charged scalar field, strong coupling theory 78−16976
Dirac particle in mag. field, symmetry breaking by monopole singularities 78−16977
Dirac particles, creation in general relativity with torsion and electromagnetism, general formalism 79−88856
Dirac particles, massless bound state, Coulomb potential 80−37189
Dirac particles in Minkowski space with torsion 78−57824
Dirac quantisation of a massive spin-3/2 particle coupled with a magnetic field 79−75703
Dirac quantum field, scatt. automorphisms, external field perturbations 78−58112
Dirac singletons, equivalence with massless particle 79−21903
Dirac type essentially self adjoint operators 78−16957
Dirac-Coulomb functions, asymptotic expansions of radial integrals 79−308
dispersive medium, QED and multiphoton processes at impurity centre *(Russian)* 78−71141
Doppler and Cherenkov effects, quantum theory paradoxes 78−45824
Doppler effect in refracting medium, classical and quantum interpretations *(Russian)* 79−13002
Dreel-Yan processes, gluon corrections 78−8597
dressed electron propagator solution without renormalisation 79−312
dynamical rearrangement of symmetry 77−65122

quantum electrodynamics continued
dynamical spontaneous symmetry breaking, in scalar electrodynamics and Yang-Mills fields, scalar particles 79−97536
Dyon spin and statistics, fibre bundle theory for interacting charges 80−32049
Dyson's perturbation theory analogue for processes with pair creating external field 78−4813
Dyson-Salam scheme subtractions, counterterm equivalence 80−13241
e^+e^- spontaneous creation in inhomogeneous magnetic fields 80−22540
effective Lagrangians at finite temp. for scalar and spinor QED 79−71668
effective potential derivation 79−12994
effective potentials in gauge field theories containing scalar bosons 78−21330
eikonal formula, spin corrections using functional methods 77−13900
Einstein's field theory with teleparallelism and Dirac's electrodynamics *(German)* 79−40418
einstein dynamics compatible with Galilean kinematics 80−27437
Einstein-Dirac equation, soln., neutrino representation 79−58596
electric dipole radiation interactions, implications of gauge invariance 79−30268
electrodynamics, quantisation, gauge invariance and mass without spontaneous symmetry breaking 79−89088
electrodynamics with strings and monopoles, book contrib. 79−58916
electron, anomalous magnetic moments, eighth order contrib. calcs., QED tests 78−45821
electron, free, motion in uniform mag. and elec. fields, Schrodinger eqn. soln. 78−24985
electron, in mag. field, intrinsic mag. moment, measurement possibilities *(Russian)* 78−86430
electron, photon and mag. monopole interactions, quantized theory 79−13004
electron, relativistic model 79−35975
electron 78−37160
electron anomalous mag. moment, dispersive approach, 6th order contrib. 79−9316
electron anomalous magnetic moment, Pauli eqn. in crossed mag. electrostatic fields *(Russian)* 78−16962
electron anomaly, radiative corrections, vac. polarisation insertions, ladder graphs 79−2959
electron beam, quantum modulation in field of opposite EM waves 78−74188
electron bremsstrahlung spectrum in point Coulomb field, classical and nonrelativistic quantum theory 78−65792
electron charge and velocity, independence limit, atomic neutrality 79−97549
electron g-factor, sixth order contributions, anal. evaluation of graphs 77−6066
electron gas interacting with radiation in mag. field, relaxation 80−17489
electron gravitational interaction corrections 77−30305
electron in coherent EM field, null-plane formulation, Volkov soln. expansion 77−13898
electron in external EM field, radiative corrections 78−41449
electron in magnetic field, induced angular momentum, classical and quantum calcs. 78−86060
electron in quantised plane EM wave, integrals of motion *(Russian)* 77−38108
electron in strong randomly rotating mag. field 78−37163
electron induced radiation in plane wave in mag. field 80−37196
electron inertial mass, asymptotic soln. of Dirac eqn. 79−2961
electron internal dynamics, rel. to Lamb-Rutherford shift and microwave generation 80−13239
electron magnetic moment anomaly determ. using two level dual vac. polarisation model 78−54632
electron mass, calc. in left-right-symmetric model 79−26282
electron mass, possibility of determ. from finite QED 78−12841
electron mass, truncated, gauge dependence 80−22542
electron mass operator in 2-D QED approx., radiative convections 80−4900
electron mass operator in plane wave field, near cyclotron reson. region *(Russian)* 78−86432
electron model, semiclassical, Casimir self-stress in dielectric and conducting balls 80−86625
electron modelling by phase-locked cavity 79−63089
electron motion in standing wave fields 80−22539
electron moving in quantised field of plane wave, exact soln. *(Russian)* 77−45995
electron moving in strong EM field, radiational corrections to mass and mag. moment *(Russian)* 77−61226
electron nonrelativistic scatt. in quantised EM field 80−77993
electron optics, quantum phenomena in dense electron beams, soln. of Schrodinger eqn. 79−76568
electron pair photoproduction, at nucleus, in field of plane EM wave *(Russian)* 77−61225
electron pair photoproduction, in field of bichromatic plane EM wave *(Russian)* 77−30291
electron pair prod., point-Coulomb calc., analytic continuation to tip of positron spectrum 77−26475
electron pair prod. in field of bichromatic plane EM wave *(Russian)* 79−6299
electron plasma in mag. field, photon absorpt. quantum mechanical treatment 79−1296
electron propagator, Dyson-Schwinger eqn. solns. 78−24984
electron propagator, truncated electron self-energy calc. 79−89086
electron propagator singularities, using Runge-Kutta method 79−49427
electron radiation in quantised field of nonmonochromatic EM wave *(Russian)* 78−82132
electron self mass in semiclassical limit 78−33008
electron self-energy, vacuum polarization, and vertex correction 80−47222
electron self-energy in non-local QED and correspondence principle 77−22671
electron self-energy problem, correspondence principle 79−93321
electron spin equations of motion in external field 80−18102
electron wave packet in uniform electric field for teachers 78−61983
electron with anomalous moments, motion in parallel elec. and mag. fields *(Russian)* 78−37161
electron with anomalous moments in EM field 80−37197
electron-dipole system, semiclassical quantisation, for teaching 79−25799

quantum electrodynamics continued
electron-mag. monopole interactions, without Dirac strings, quantum-mech. formulation 79−21994
electron-muon symmetry of Callan-Symanzik function: two-lepton case 80−73627
electron-photon scattering, symmetrical formulation in relativistic quantum mech. 77−67599
electron-positron field, interaction with classical static EM field 78−41445
electron-positron gas in external mag. field, polaris. tensor *(Russian)* 79−35982
electron-positron internal pair formation following heavy ion collisions, conversion coeff. calcs. 78−50135
electron-positron pair production in field of longitudinal electric wave *(Russian)* 79−6300
electron-positron pair stimulated annihilation, coherent γ-emission 79−55104
electrons and positrons as quantum rotators 79−35981
electrons in logarithmic pots., Dirac eqn. soln. 78−41448
electrons in logarithmic pots., Schrodinger eqn. soln. 78−41447
elimination of the electric charge and current as primitive notions 79−97552
EM field algebraic quantisation 79−63391
EM field in dispersive medium, phenomenological quantisation 80−13240
EM field in space with torsion, semi-minimal coupling principle 80−77675
EM field quantisation, canonical variables 80−32045
EM field quantisation, Lorentz gauge, QED treatment of scalar and longitudinal photons 77−34111
EM field without indefinite metric, relativistic invariance 78−8565
EM fields, generalised, second quantisation 80−99072
EM fuzzy ball, motion in free space 77−74622
EM potential, two degrees of freedom quantisation for any gauge 77−22670
EM radiation-charged particle stimulated interaction, classical and quantum theory study *(Russian)* 78−86431
EM response of electron gas and vacuum in strong mag. field 77−13641
EM soliton in weak and EM unified field theory 79−9323
EM vacuum fluctuations, interaction with an atom between two perfectly conducting plates 78−78122
EM wave absorpt. in degenerate semiconductors 79−33307
EM wave propagation, nonlinear, in strong mag. fields, second harmonic generation 80−77988
energy levels in gauge theories, modified functional measure, scalar QED 78−49973
energy-momentum tensor, trace coupling to two photons 77−41796
energy-momentum tensor anomalies in spherical space-time for massless QED 80−73628
energy-momentum tensor vac. expectation values, depend. on manifold geom. and topology 80−355
energy-momentum-tensor trace anomaly calc. 77−46002
equal-time commutators in continuous dimensions 79−71730
Euclidean formulation, H-like energy levels for scalar and spinor fields 77−88378
Euclidean massless spin 0, spin 1/2 electrodynamics, Fredholm determinant zeros 78−24988
Euclidean QED_2 on lattice, continuum limit, Schwinger functions, vacuum expectation values 80−73624
Euclidean QED_2 on periodic lattice, continuum limit 80−18092
evolution operator, quark struct. of states, two dimensional massless electrodynamics *(Russian)* 80−73630
exotic atoms: a new method in nuclear and elementary particle physics, review *(German)* 79−76536
expanding universe, high freq. EM field propag., with Dirac coupling 79−58913
expanding universe effect on quantum mechanics of electromag. bounded spin 1/2 particles 78−54271
experimental status of quantum electrodynamics, review 79−63399
experimental tests *(Chinese)* 80−77997
exponential interaction in R^n 79−63361
external EM fields, time-dependent, particle interpretation, Fock representations of Fermi field operators. 80−52439
external field, quantum processes in strong EM field *(Russian)* 77−13902
external fields, interpretation as temp. 78−8562
external fields creating pairs, problems 80−42375
external interaction of two charged particles with quantised field, relativistic invariance 78−74189
Fermi quantisation of Landau gauge 78−54591
fermion, massless, quantum electrodynamics of Schwinger model, perturbation anal. 77−65109
fermion charged fields in nonlinear approach to QED 79−97545
Fermion determinant in two-dimens. QED 79−97548
fermion fields, spin 1/2, 3/2, accelerated states, stress-energy tensor vac. expectation value 78−70313
fermion thermal radiation from an accelerated wall 79−54265
fermion-antifermion eqn., appl. to positronium, Breit eqn. 78−62963
fermions, charged relativistic, semi-classical; two-body problem, new approach 78−29284
fermions, massless, isospin 3/2, coupled to N-pseudoparticle field 79−6298
Feynman graphs, generation by computer 77−6065
field theory of electric and magnetic charge 79−6306
fine structure constant, virtual EM processes and Aharonov-Bohm fields *(French)* 79−2958
fine structure constant, Ward-Takahashi relation and eigenvalue eqn. 79−17648
fine-struct. const., Wyler's calc. anal. 78−37162
fine-structure const. value from EM field as 42 state superposition 77−30293
fine-structure constant, coupled Maxwell and Dirac eqns., lepton and quark-like solutions 80−62894
finite formulation based on improved operator products 78−58147
finite photon rest mass, theorem of effect on observable EM fields, comment 79−12999
flat rotator in field of circularly polarised wave, quasienergy states 78−54596
Fock spaces for man-zero helicity-one particles described by antisymmetrical two-tensor 77−13903

quantum electrodynamics continued
Foldy Wouthuysen transformations and Volkov states, unitary in 2-component forms 79−30688
formulation without vacuum state stability principle *(Russian)* 79−49435
formulations, with magnetic monopoles, book contrib. 79−58915
four dimensional symmetry framework, additional concepts and universal time 78−74184
free charge-EM field interaction, Thomson scatt. and energy shifts 77−74625
free charged particle interacting with intense laser pulse, energy momentum gain 80−101963
free electromagnetic potentials in Minkowsku and Euclidean regions 79−93323
free electron as localised stationary state of vacuum EM polarisation *(Polish)* 77−38107
free EM field quantisation, gauge invariant fields 80−105817
free tensor potential equivalence in QED 80−73579
frequency-dependent electric and magnetic multipole moments and Siegert's theorem 80−27432
fundamental length hypothesis, concept in gauge vector field theory 78−93836
fundamental length hypothesis for QED finite theory 79−71665
fundamental length hypothesis in a gauge theory context 80−9101
Furry procedure for quantum processes in strong EM field *(Russian)* 77−13901
Furry representation on null plane *(Russian)* 78−33012
gamma quanta spontaneous emission by channelled charged particles *(Russian)* 77−52198
gauge, field intensity and relativistic effects 79−54287
gauge and basis sets for EM interaction representation 80−42371
gauge covariant approx., Dyson-Schwinger eqns. i.r. behaviour 78−16918
gauge covariant approx., Dyson-Schwinger eqns. soln. 77−57477
gauge dependence of spectral functions 80−37191
gauge field theory formulation in quantum field theory framework 79−21908
gauge invariance, diagrammatic proof 78−74183
gauge invariance and pseudoperturbations 80−22545
gauge invariant formulation of QED using local currents 77−45997
gauge invariant QED construction in stochastic space 79−21998
gauge invariant wave mechanics and the Power-Zienau-Woolley transformation 80−99073
gauge models of weak and EM interactions, quantisation and renormalisation of gauge theories, book contrib. 79−30669
gauge technique appl. 79−35925
gauge theories, large transverse momentum behaviour 77−71429
gauge theories of weak, EM, and strong interactions, book contrib. 79−30694
gauge theory field strength and dual variable formulations 79−35946
Gaussian fluctuations: 't Hooft's method and an approximate method 79−85236
Gell-Mann-Low function and Borel summations in renormalizable theories 79−40670
generalised Dicke model for matter interacting with EM field 78−5441
generalized two-dimensional QED and functional determinants 80−42373
generating scattering amplitude, coherent representation 78−50527
geometrical gauge theory of gravit., strong interactions, EM interactions 78−70041
ghost-field formalism, spin 3/2 and 2 fields, EM interaction 78−70315
global characterisation on space time lattice *(Hungarian)* 80−37192
gluon bremsstrahlung and multiperipheral cluster models 79−22082
Goppert-Mayer gauges for intense-field electrodynamics 80−99075
Gordon decomposition and tidal interaction 78−8324
graphical evaluation of relativistic matrix elements 79−58586
gravitational creation of odd numbers of fermions 80−32048
gravitational trace anomaly renormalisation in QED 80−57532
Green's function in external elec. field and combination with mag. field and plane-wave field 80−101964
Green's functions for spinor and scalar particles in mag. field *(Russian)* 78−49997
Gupta-Bleuler and infrared-coherence subsidiary conditions 79−13001
Gupta-Bleuler condition and infrared-coherent states 79−13000
gyromagnetic ratio, light-cone formulation for arbitrary spin particles 77−13961
gyromagnetic ratio and Galilean symmetries, light cone formulation 77−13962
gyromagnetic ratios for muon and electron 80−22548
hadron polarization operator insuperrenormalizable model, rainbow approx. of $(\lambda/2)\Phi^2\phi$ model 80−105821
hadronic atoms in momentum space, including vacuum polarisation 79−872
Hamiltonian form of non-relativistic motion eqns. 79−313
Hamiltonian formalism, construction of 2-D QED 79−21987
hamiltonian formulation in generalized linear electrodynamics 79−97543
Hamiltonian formulation of mag. and electric charges, string and non-string model 77−22429
Hamiltonian QFT, renormalisation group anal. 77−82662
Hamiltonian variational approach to physics of weak-coupling region 79−35979
hard-soft renormalization of massless fields 80−13214
harmonic oscillator, EM field interaction, initial value problem 80−47223
harmonic oscillator in random EM field radiative corrections stochastic electrodynamic treatment 77−45736
harmonic oscillators, relativistic two-body interaction, exactly soluble system 78−16955
harmonically bound radiating electron, nonrelativistic wave equation 79−40701
heavy ion collisions, positron prod. 78−50198
heavy ion molecular collisions, QED test in strong elec. fields, pair creation 78−45829
heavy ion quasimol. collisions, electron pair prod., vacuum polaris. shakeoff 77−30945
heavy ion reactions, dynamical properties, field overview 80−18327
heavy lepton production in e^+e^- annihilation, QED background 79−75706
heavy leptons, existence in quantum theory 78−21363
heavy particle effects, factorised local operators, renormalisation group 80−62898
quantum electrodynamics continued
heavy particle effects, factorised local operators, renormalisation group 80−62899
heavy particle effects through factorisation and renormalisation group, QED appl. 80−13243
heavy quark-antiquark potential, effect of vacuum polarisation at long distances 79−6304
Higgs boson decay, QED and QCD radiative corrections 80−95275
Higgs effect, supergravity and supersymm. massless QED 78−29268
high order estimates 77−67603
high-energy scatt., new formalism 78−66063
history of quantum field theory, search for unity 78−28904
how and why it works 80−18093
Hubbard model with half filled band, fermion mass spectrum 79−21955
hydrogenic atoms, metastable 2S state in weak elec. field, radiative decay, bound state QED 80−42959
hyper-Raman effect, vibr. mode classification and spectral line assignment, QED method 78−58703
hypergeometric partial solutions in the problem of two Coulomb centers 80−4582
inclusive Coulomb scatt. cross section in 4th order of QED 78−78117
indefinite metric axioms, Markov property failure 78−41444
index theorem, axial-vector anomalies, in Schwarzschild and Taub-NUT spaces 78−93832
induced $2s_{1/2} \rightarrow 2p_{1/2}$ + one photon transition, rate calcs. 77−50384
induced radiation in time-periodic EM field 77−38109
induced vacuum decay in scalar field theory 80−42372
infrared attractive fixed points, gauge symmetries, QED and anti-grandunification 80−95213
infrared behaviour of electron Green's function, renormalisation group use 79−35977
infrared catastrophe averted by Hertz potential 79−85250
infrared divergences, dimensional regularisation 77−10179
infrared singularities, Feynman diagram investigation for e^+e^- annihilation 79−71671
infrared structure, derivation from first principles 80−101962
intense field, perturbation theory expansion parameter 80−62900
intense field, rel. to QED at small distances *(Russian)* 77−87926
intense field QED in continuous medium, appl. to Thomson scatt. and Cherenkov radiation 80−27435
intermediate vector boson decay, QED and QCD radiative corrections, hadronic jets 80−73759
internal $GL_{2c} \times GL_{2c}^*$ symmetry of Dirac equation with external electromagnetic field 79−93324
inverse bremsstrahlung, high energy, nucl. mag. contribs. 78−74350
IR behaviour in QED and QCD, IR equiv. and non-perturbative solns. 77−74579
IR behaviour with Weinberg and 't Hooft renormalisation group eqns. 79−89085
IR divergence, rearranged perturbation theory appl. to spinor QED 77−67602
IR regularisation of massless scalar free field in two dimens. space time, Lorentz expansion 78−12818
IR singularities for arbitrary Euclidean external momenta 79−58861
isolated 1 MeV electron, meas. of axial, magnetron, cyclotron and spin cyclotron beat frequencies 77−30300
isotropic cosmological models, vacuum stress energy tensor and particle creation *(German)* 80−94901
isotropic universe, particle creation and vacuum polarisation, cosmological models 80−90582
jet and lepton-pair production in high-energy lepton-hadron and hadron-hadron scattering 79−17729
Josephson-junction capacitor, QED theory 80−93049
Klein Gordon eqn. for particle in mag. field *(French)* 79−53994
Klein paradox and vacuum polarization 78−8329
Klein paradox as many-particle problem 77−2717
Klein-Gordon eqn. for particle in const. elec. field with plane EM wave 77−30297
Klein-Gordon eqn. soln., appl. to Green function construction for scalar QED *(Russian)* 79−54288
Klein-Gordon equation, identical motion in relativistic quantum and classical mechanics 77−61177
Klein-Gordon particles, massless bound state, Coulomb potential 80−37188
Klein-Gordon particles in deep square wells 80−31982
Kramers-Heisenberg dispersion formula, Dirac transformation generalisation 78−16960
Lamb shift in ^{35}Cl XVI, precise meas. 80−9549
Lamb shift in Cl^{16+} meas. 80−9551
Lamb shift in hydrogenlike Ar meas. 80−9550
Landau gauge realisation 77−22672
large-complex-charge behaviour of the Dirac determinant 79−93328
laser field, generalised LF scatt. approx. 79−58590
laser radiation pressure for e^+e^- pair prod. 79−40700
laser-induced optical activity, QED theory of multiphoton processes 79−31794
lattice Dirac eqn., spectral degeneracy as function of lattice shape 78−376
lattice field theory Dirac eqn. 78−24924
lattice gauge theory with fermions, renormalised phases, vacuum polarization 80−13198
lattice Higgs models, (non)Abelian, diamag. and crit. props. 79−67465
lattice Schwinger model, massive QED for fermions in 1+1 dimens. 78−78121
lattice theory for fermions, Adler anomaly nonexistence 79−71667
Lauricella function, analytic continuations 79−17645
lepton bound in Coulomb field of nucleus 79−94115
lepton mass determ., self-energy formula with grav. self-energy 79−9314
lepton pair production, leading logarithms technique, correl. with hard scatt. approaches 79−45072
lepton wave packets produced by strong short-range potentials 78−45828
leptonic mass generation model 80−375
light cone formulation of two-dimens. QED 77−57476
light rays in QED 79−63395
light-magnetic field interactions *(Russian)* 80−73632
linear response theory, macroscopic vs. microscopic, appl. to electron in periodic pot. 78−65813
Lippmann Schwinger eqns. for three charged particles 80−4580
local field theory of solitons 79−12953
local operators and charged states 77−54063

quantum electrodynamics continued
local structure of functional spaces and dynamical variables of gauge-invariant fields 80−9099
locally supersymmetric extension of QED 77−18212
long range potentials, EM polarisabilities, interacting systems, neutral, spinless, with mag. moment 77−6058
Lorentz condition in Hilbert space, zero dressed photon rest mass 79−6302
Lorentz covariance in gauge independ. formulation 78−54594
Lorentz group, IR problem and spontaneous breaking in QED 80−32047
Lorentz invariance, nonphysical variation in QED 78−93828
lorentz invariance from classical particle paths in quantum field theory of electric and magnetic charge 79−49431
Lorentz invariance of quantum field theory of electric and mag. charge 78−33010
lorentz transformations of observable and ghost particle states in quantum electrodynamics and in a massive gauge theory 78−66061
low energy e^6 Compton scatt. 78−45925
lowest-order EM correction in point particle scatt. 77−87978
magnetic charges, quantum strings and gauge invariance 78−33009
magnetic circularly polarised emission from luminesc. mol. system, QED formalism, orientation relax. 77−46589
magnetic dipole transitions in atomic and particle physics: ions and psions 79−9322
magnetic fields, flux string and monopole, geometric configuration, compared to O(3) nonlinear σ-model 80−57527
magnetic fields $>10^{20}$ gauss, existence in astrophysical systems 78−4094
magnetic monopole, relativistic classical eqns. of motion, electric dipole moment case 80−37195
magnetic monopoles and charges, nucleon struct. *(Norwegian)* 77−34109
magnetic monopoles with no strings, action principle and canonical quantisation 80−31990
Mandelstam-'t Hooft duality in Abelian lattice models 78−78057
many photon collective phenomena, finite QED formalism 78−9352
many-body electrostatic potential vanishing in QED 78−54270
many-electron atoms, foundations of relativistic theory, Hamiltonian H_+ and h_+ and related relativistic HF eqn. derivation 80−99458
mass divergences in annihilation processes, cut vac. polarisation diagrams 78−70285
mass divergences in annihilation processes, cut vac. polarisation processes, diagrams 78−74157
mass formula of charged leptons 80−13244
mass singularities and coherent states in gauge theories, QED and QCD results 79−12948
massive electrodynamics limit, and two component photon field theory 79−63393
massive photon magnetic bremsstrahlung *(Russian)* 78−41461
massive photons, rel. to hot gas stability in clusters of galaxies *(Russian)* 79−44614
massive QED, gauge invariant subtraction scheme 79−21993
massive QED, renormalisation in Veltman gauge, supersymmetric transformation 77−46000
massive Schwinger model, decay of metastable vacs. 78−24989
massive Schwinger model 77−6063
massive Schwinger model in infinite momentum frame, phys. particles spectrum 77−49886
massive vector boson field theory with spontaneous symmetry breaking 80−52443
massless, calc. of Feynman integrals arising in $F_1(\alpha)$ 77−46001
massless Abelian gauge theory, infrared problem and boson suppression 77−2742
massless boson, unified nonlinear theory 80−376
massless BPHZ renormalised QED, IR finiteness 77−74623
massless electrodynamics, two-dimens., disappearance of charged states *(Russian)* 79−17651
massless electrodynamics, vacuum instability, bare coupling constant Gell-Mann-Low eigenvalue condition 78−89643
massless fermion coupled to single axial vector field in U(1) model, AAA triangle diagram 79−35965
massless limit in the ladder approximation 79−21953
massless QED, appl. of conformal symmetry for calc. gauge invariant Green's functions 79−63394
massless QED, dimensional regularisation in spherical spacetime 79−40698
massless QED, dimensional regularisation of gauge fields in spherical spacetime, free field trace anomalies 79−40699
massless QED, IR divergences 78−29285
massless scalar classical solns. for large external charge with total screening 77−79237
massless scalar QED, colour confinement model 78−33027
Maxwell field quantisation in linear conformal invariant gauges 79−71666
Maxwell theory, quantised, rosette of rosettes of Hilbert spaces 80−32043
ME-EM field model of free electron, determ. of electron parameters 78−29281
ME-EM field model of free electron state 78−29280
ME-EM field model of free electron state 78−49988
metals and semimetals in strong mag. fields, EM excitations, review 77−8130
minimal coupling, symplectic mechanics of classical particle in Yang-Mills field 78−74136
minimal EM coupling in elementary quantum mechs., group theoretical derivation 78−54590
minimally nonlocal quantum electrodynamics without potentials for bound electrons 80−86626
molecule, electric circ. dichroism, QED 78−37666
Moller cross section in strong laser field, resonances and intensity depend. shifts 79−45918
Moller scatt., high intensity, scatt. energies 80−22541
monopoles, elec. and mag., without strings, heuristic pot. theory, teaching approach 79−5931
motion and radiation of a charge in a plane wave and a magnetic field *(Russian)* 79−21986
moving scale dimension pole in quantum electrodynamics 79−26270
multi-mass vector-spinor field in EM interaction, hyperquantisation, S-matrix unitarity 77−61232
multiparticle production in chromoelectric flux tube model in 1+1 dimens. field theory 80−73666
multiphoton absorption by electrons 80−6224
quantum electrodynamics continued
multiphoton ionisation by lasers, localised and dispersive states 77−27041
multiphoton stimulated Compton scattering of relativistic electrons 80−48198
muon g-factor anomaly, review of theoretical contribs. 77−30384
muon mass 78−33011
muonic atom, heavy, $1s_{1/2}$ levels, self-energy corrections 78−55262
muonic atom energy levels, $\alpha^2(Z\alpha)^2$-vacuum polarisation contrib. 79−22867
muonic atom transition energy meas., tests of high-order vac. polarisation corrections 77−71895
muonic atoms, vac. polarisation pots. calc. 77−26476
muonic He, hyperfine struct., relativistic, radiative and recoil corrections, QED test 80−14256
mutually interacting charge fields, photon quantisation in e^+e^- processes 79−12995
N-level atomic system interaction with quantised EM field, algorithm for numerical calcs. 79−64187
n-vertex loop diagrams in superstrong calc. field, calc. method 77−71472
near mass shell IR singularities in QED 78−37164
Nelsons stochastic mechanics, spinning particles and relativistic particles 80−31587
neutrino and photon pair prod. in strong mag. field 78−407
neutrino bremsstrahlung in an intense magnetic field 79−30055
neutrino form factors in 2-D approx. of QED 80−9132
neutrino wave equations in conformal space, Dirac theory 78−21364
nine-quark, nine-lepton model of weak and EM interaction 77−74631
non Abelian gauge theories in external electromagnetic fields *(Russian)* 80−57533
non conventional monopoles in field theory, book contrib. 79−58919
non-analytic mass behaviour, renormalisation group 77−67558
non-relativistic fermions, Ward identity 80−86633
nonAbelian gauge theory, unification of weak and EM interactions 77−18188
nonlinear approach, conformal invariance and fine-structure constant 80−91023
nonlinear approach, magnetic dipole moment, corrections to g-2 80−42370
nonlinear Dirac equation, spinor solitons or bags 78−12817
nonlinear effects in theory of erratic electron 78−93825
nonlinear electrodynamics, photon-gravitation coupling 79−97276
nonlinear electrodynamics, testability using present day instrumentation 79−71675
nonlinear EM effects induced by vacuum polarisation and gravitational interaction, a comparison 79−97544
nonlinear gauge, for processes involving soft photons 77−79236
nonlinear photoionisation, testable Noyes-like interpretation of Panarella's effective-phonons theory 77−61929
nonlinear problems due to self-field of electron 80−4901
nonlocal, relativistically invariant, bubble electron model, fundamental length and causality 79−30687
nonlocal stochastic equation of motion with damping in electrodynamics 80−17872
nonmonochromatic EM wave field, quantum effect probability *(Russian)* 77−41799
nonperturbative gauge technique soln. for Schwinger model of 2-dimens. electrodynamics 78−78120
nonrelativistic, infrared problem 80−52440
nonrelativistic, Kramers-Heisenberg dispersion formula 78−42015
nonrelativistic particle scatt. in presence of strong EM wave, Schwinger variational principles 79−93329
null change and asymptotic freedom *(Czech)* 79−45002
null-plane quantum field theory, consistent formulation, absence of vac. polarisation 77−54050
numbers and weights of Feynman diagrams, ϕ^N, QED and non-Abelian theories 79−2937
O(3)⊗U(1)⊗U(1) internal symmetry in massless vector field theory *(Russian)* 80−22531
observable phase factors and symmetry of electric and magnetic charges 78−86428
octonions and exceptional groups in field theory, unified interaction model *(Russian)* 79−67491
one degree of freedom for photon field 78−54589
one loop effective potential for scalar and spinor QED, finite temp. effects 79−54286
one loop effective potential in QED, in presence of magnetic (electric) field 79−67487
one loop effective potential with anomalous moment, electron Lagrangian 78−58146
one scalar charged particle QED 80−99071
one-loop effective pot., radiative corrections to electron propagator 77−45996
operator Schwinger term in zero-mass photon QED 78−41450
orbit-orbit interaction, new tensor expansion, matrix and graphical forms 80−14064
orthopositronium, vac. polarisation corrections in muonic molecules 78−78841
orthopositronium decay rate, O(α) corrections, graph theory 77−31029
orthopositronium three photon decay rate, vertex angle and electron self-energy radiation corrections *(Chinese)* 77−75342
oscillator strengths, velocity and length forms and unitary transforms. 78−74615
pair creation in strong EM field, quantum processes *(Russian)* 77−30288
pair production in slowly varying and constant fields, diagrammatic approach 80−374
pair production on photon scattering by intense EM wave in homogeneous mag. field *(Russian)* 80−47227
paramagnetic conjecture counter-example based on Bohm-Aharonov effect 80−32046
paramagnetism for nonrelativistic electrons and Euclidean massless Dirac particles 79−63396
particle creation and scattering by nonstationary EM field in canonical formalism 77−30298
particle creation by black hole due to Casimir effect 79−35607
particle creation by singularities in asymptotically flat spacetime 78−54260
particle creation or Hawking effect in nonstationary black holes 78−4278
particle self-interactions 79−67486

quantum electrodynamics continued
particles, creation in general relativity with torsion and constant electric field 79−88857
particles with anomalous moments, motion in external EM field *(Russian)* 79−9321
path group appl. to gauge theory and quarks 80−31985
path-dependent quantum formulation of electromagnetism with magnetic charges 80−86628
perturbation expansion of quantised composite field theory, gauge invariance *(Chinese)* 78−82156
perturbation series, asymptotic estimates and guage invariance 77−87925
perturbation series in QED, Dyson instability, asymptotics 78−62342
PETRA QED tests, implications for weak neutral current struct. 80−86657
phenomenological ideas toward a field theory of matter, unification of EM and gravity fields 80−378
phonon splitting in the magnetised vacuum 80−4897
photon, Dirac-like eqn., transform. props. 79−58914
photon, invariant struct., wave function 77−71475
photon antibunching, at. resonance fluorescence, quantisation of light 78−66791
photon antibunching in reson. fluoresc. from two-level atom, quantum nature of light 79−85251
photon coalescence at an electron in plane wave approx. model 80−18100
photon coalescence in process of interaction between quantized plane EM wave and electron *(Russian)* 77−30287
photon coalescence in quantised plane EM wave interaction with electron *(Russian)* 77−30292
photon dispersion in asymptotically strong magnetic fields 77−82697
photon fission, in intense laser fields and nuclear Coulomb field, QED test 80−4895
photon form factor, asymptotic behaviour in QED 80−18096
photon gravitational interaction, QED corrections 77−65131
photon interference, quantum field theoretic description using QED methods 78−12464
photon nonlocal form factors, extended extremal approach 77−61227
photon polarisation in superstrong mag. field calc. *(Russian)* 77−30299
photon propagation in mag. field, radiative correction to polarisation operator *(Russian)* 78−8567
photon propagator and pair production in steady electric field *(Russian)* 79−9320
photon propagator in general EM cavities *(German)* 79−93320
photon scattering, elastic large-angle, Delbruck and Rayleigh scattering below 5 MeV 80−13456
photon splitting cross sections in nucleus Coulomb field 80−32041
photon splitting into three components by electron in quantised plane EM field 80−18101
photon-intensive EM wave interaction in uniform mag. field *(Russian)* 80−86636
photon-photon, dimensional scatt. amplitude and gauge invariance in lowest order 77−71471
photon-photon scatt., pair and photon prod. *(Russian)* 77−22673
photon-photon scatt. in strong mag. field, pair creation 78−4816
photons, antibunching effect, and direct-action quantum absorber theory 80−57535
photons as para-fermion composites, limitations 79−40704
photons interaction with nonstationary EM field *(Russian)* 79−98327
photoproduction of relativistic parapositronium, and muonium perturbation expansion *(Chinese)* 79−49432
photoproduction polarisability sum rules in QED 79−2960
physical states in indefinite-metric space 77−13906
planar model electrodynamics, phase diagram, continuum limit, and mass spectrum 79−63426
Planck's constant, and finite struct. const. calc. 78−82135
Planck's constant, origin of quantum theory 80−27179
plane wave, moving along mag. field, radiative effects 78−29283
plasma, thermalisation of energetic charged particles in fusion plasma, QED effects 77−65834
plasma, Thomson cross sections, vacuum polaris. effects 79−10646
plasma-wave dispersion rels., modification due to magnetic monopoles, pulsar emission 79−75704
Poincare invariance without Poincare group 79−12992
Poincare invariant differential equations for particles of arbitrary spin 79−30689
Poincare self-stresses, model and field Lagrangian densities 80−52438
Poincare stresses, dynamical basis 79−6303
Poincare-invariant motion equations for arbitrary spin particles *(Russian)* 79−2964
Poisson equation for relativistic streams of charged particles, analytical soln. *(Russian)* 79−9319
polarisation of relativistic particles in plane wave fields *(Russian)* 78−74192
polarisation operator in ladder approx., renormalisation group 80−73629
polarisation tensor for magnetised vacuum 77−61230
polarised electron bremsstrahlung γ-quanta from ultrarelativistic electrons in mag. field *(Russian)* 78−46502
polarised photon splitting on unpolarised electron *(Russian)* 79−371
ponderomotive meter of EM energy, quantum features *(Russian)* 78−8273
positive ion behaviour in strong mag. field 79−35978
positron emission in Pb+Pb(U) collisions, evidence for strong field QED processes 78−93833
positronium, Bethe-Salpeter equation, Coulomb like kernel 78−93831
positronium, ground state splitting, more $\alpha^6 \ln\alpha$ terms 77−14621
positronium, hyperfine interval, α^2 corrections, three-photon virtual annihilation contrib. 78−41451
positronium, hyperfine splitting, contrib. of ground state quasipot. approach 79−59606
positronium, QED predictions rel. to expts. 77−58213
positronium, triplet, asymmetrical decay, two- and threefold polarisation correlation of photons 80−57536
positronium annihilation in field of plane EM wave *(Russian)* 80−14259
positronium annihilation in strong magnetic fields 79−17007
positronium hyperfine splitting, anomalous contribs., radiation gauge 77−83771
positronium hyperfine struct., $m\alpha^6$ contribs. from two photon virtual annihilation 78−89642
positronium hyperfine struct., three-photon virtual annihilation 77−68143
quantum electrodynamics continued
Poynting's theorem, nonrelativistic and 2-component spin, transition probability 78−24986
proton gyromagnetic ratio and derived value of fine struct. const., QED test 79−71674
proton in mag. field and quantised EM field *(Russian)* 79−49433
proton magnetic moment and EM struct. 78−54633
pseudoclassical and quantum Foldy-Wouthuysen transform. for electron in non-homogeneous mag. field 77−2781
pseudoclassical relativistic electron and supersymmetries 77−13845
pseudoparticle fields, role of fermionic zero modes 78−74159
pulsars, hadronic photoabsorpt. and pair production 78−12261
QCD, energy levels of 1+1 dimensional lattice gauge theory 78−4828
QCD contributions to vacuum polarization 80−91059
QCD contributions to vacuum polarization 80−105834
$(QED)_2$, functional determinant absolute bound 80−68402
qualitative methods in problem solving, graduate text book 77−71239
quantised electric charge as purely EM phenomena 80−37190
quantised lattice gauge field construction, mass generation and Abelian Higgs models 80−4831
quantum action method in quantum field theory 79−40659
quantum effects in systems with accelerated mirrors 80−22508
quantum effects in the Bertotti-Robinson space-time 79−35930
quantum electronics within limit cavities, Fain Chanin vs. infinite R_3 formalism 77−38839
quantum field theory methods and models review using Schwinger source theory *(German)* 78−86406
Quantum particle production in the formation of naked Kasner-type singularities 79−97546
quantum scalar electrodynamics, nonlinear approach 79−80776
quantum theory, stochastic electrodynamics formulation *(Spanish)* 80−82925
quantum theory evolution law approach appl. *(Russian)* 79−80866
quark confinement and instanton-like Euclidean field configurations 77−49910
quark confinement criteria, QED_2 model with SU(n) flavour 78−45840
quarkonia, spectra, decays, levels, jets, sum rules 80−18112
quasipotential eqn., nonlocals in terms of retarded functions 78−29282
quasipotential eqn. for wavefunction, drived by Fock-Podolsky method 77−65127
radiating electron, covariant semiclassical theory 77−26478
radiation corrections to quantum processes in an intense electromagnetic field 80−4899
radiation damping classical limit, photon, meson scatt. 77−67605
radiation effects in field of plane EM wave 77−82696
radiation entropy estimation by weight functions 78−408
radiation reaction in nonrelativistic QED 77−65125
radiation theory, multipolar Hamiltonian QED and quantum optics 80−86634
radiation-matter interaction Hamiltonians 78−54114
radiative corrections, exponential factor of soft photons 80−47225
radiative corrections to classical Lagrangian and dynamical symmetry breaking 77−18196
radiative corrections to electron form factors, book contrib. 78−82213
radiative corrections to motion of e^- in non-monochromatic EM field *(Russian)* 79−22002
radiative decays of fermions and photon mass 78−41456
radiative effects in field of EM wave with allowance for action of stationary mag. field *(Russian)* 77−2782
radiative effects of intense constant field, mass operator eigenfunctions *(Russian)* 79−17652
radiative polarisation in particle accelerators, review 78−33335
radiative transfer equation for partially polarised light, QED derivation 77−79235
Rayleigh scattering spin depend., circ. polarised γ-rays on magnetised Fe-Co 77−59637
real-photon spectra weight functions, imaginary part of vacuum polarization, and electromagnetic vertices 79−21997
regular external fields in QED 78−89640
relative scattering and time delay in presence of a uniform electric field 79−13003
relativistic barriers for two spin-1/2 particles, from Breit eqn. 78−62339
relativistic beams, quantum spectroscopy *(Russian)* 78−33013
relativistic causality in QED 79−71670
relativistic charged particle, effect of multiple scattering on synchrotron radiation *(Russian)* 80−13245
relativistic classical and quantum dynamics 80−22192
relativistic electron field theory 77−2779
relativistic electron model from the introduction of the chronon 78−93827
relativistic electron scattering from a two-centre potential 78−66058
relativistic electron wave diffraction by cylindrical capacitor 80−5671
relativistic electron-positron gas, polarisation in strong mag. field, EM wave propag. 80−4896
relativistic electrons, radiation in periodic mag. array, wavelength and polarisation 78−58149
relativistic eqns. for massless particles, new invariance algebras 79−58909
relativistic free-electron in uniform mag. field, Green's function of Dirac eqn. 80−18098
relativistic magneton, convective and radiation fields *(Russian)* 78−66056
relativistic particle EM interaction using universal laboratory time 79−71672
relativistic particle in field of waves with non-zero proper mass *(Russian)* 78−21365
relativistic particle motion in standing wave fields 79−58910
relativistic particle physics, book 80−41966
relativistic quantum electrodynamical plasmas, covariant Wigner function calcs. 79−4175
relativistic scalar boson in Redmonds field, coherent states *(Russian)* 78−41460
relativistic string in a constant homogeneous electromagnetic field 79−22073
relativistic two particle bound state energy levels, gauge invariance 80−77989
relativistic two-electron atom, level shifts, transition probabilities, perturbation theory 79−22001
relativistic wave eqn. of electron *(Hungarian)* 79−12928
relativistic wave functions and diffr. 77−10207
relic 't Hooft Polyakov mag. monopoles in the Universe 79−9317

quantum electrodynamics continued
renormalisation, dimensional, coupling constants and masses 80−57523
renormalisation and R-operation 79−26273
renormalisation constants, small mass behaviour 77−2780
renormalisation group equations, invariant charge function 80−57529
renormalisation group formulation 78−93830
renormalisation group invariant charge and confinement 78−45791
renormalisation group techniques and study of near mass shell behaviour 77−45965
renormalised theories of particles with spin J=1 described by antisymmetric tensor *(Russian)* 77−13876
renormalised transition amplitudes, gauge independence, Green functions 80−57530
renormalizable field theories with multiple fermionic excitations 79−49428
renorminvariant charges in QED 77−10208
resonance Compton scattering in intense EM wave field 77−34803
resonance radiation redistribution, elastic and inelastic collisions effect 79−62734
review, classical limit of QED 78−8563
review, QED and general relativity, physics of strong fields 78−8561
Robertson-Walker universes, particle creation, self-interacting quantised fields 80−17699
S-matrix anal. as three-body interaction Klauder phenomenon interpretation 79−80777
S-matrix construction for QED in external gravitational field 78−78116
S-matrix electrodynamics, low-frequency photons in processes involving particles with spin 80−9131
S-matrix evaluation for QED in an external gravitational field, pair prod. 78−82131
S-matrix theory, n-body potentials in QED and quantum gravity 78−24969
saturation of gauge invariant Schwinger model correlation functions by instantons 77−30296
scalar, asymptotic estimates 77−30295
scalar conformal invariant QED, conformal group spontaneous breaking in Abelian Higgs model 78−49960
scalar electrodynamics, gauge invariant approx. 77−71469
scalar electrodynamics, Green's function perturbative expansion higher orders 77−87923
scalar electrodynamics, IR divergences, rearranged perturbation expansion 77−67601
scalar electrodynamics in nonsimply connected space-time, topological mass generation 80−82924
scalar field, carrying quaternion charge, props. 78−4757
scalar field Reggeisation in scalar QED 79−26272
scalar gravitational field interactions, nonelimination of divergences 78−93834
scalar one-loop integrals, soft bremsstrahlung and radiative corrections 79−75682
scalar particle in Coulomb and uniform mag. field *(Russian)* 79−3385
scalar particle inverse bremsstrahlung in triple collision processes 80−47226
scalar QED, bound states, lump solns. of classical eqns. 77−53
scalar QED, Green's functions in external elec. field *(Russian)* 79−49434
scalar QED on lattice, correl. inequalities, infinite vol. limit 77−61233
scalar quantum electrodynamics on lattice as classical statistical mechanics 78−16956
scale and conformal covariance in QED 77−6067
scale invariant regularisation for QED 79−93326
scale-covariant gravity theory, electrodynamics involvement 80−109350
scale-invariant gauge theories, instanton role in QCD, QED and $CP^{(N-1)}$ 80−27400
Schrodinger electron-photon interaction, gauge and hybrid transforms. 80−22544
Schwartz's method and Goldstein's eigenvalue problem 78−4814
Schwarzschild space-time, vacuum polarisation induced by gravitation 80−82410
Schwinger model, canonical surface formalism, axial anomaly, chiral symm. breaking 78−12816
Schwinger model, equivalent boson theory, anomaly-free Ward-Takahashi identities 80−82873
Schwinger model, Ward identity, fermion axial vector current divergence, chiral invariant regulator field 80−57524
Schwinger source theory, hypercomplex number approach 77−71416
Schwinger-Dyson equation for massless vector theory, absence of fermion pole and cut 77−13855
screened Coulomb T-matrices, absolute values 78−66059
screening corrections in electron pair production by intermediate- and low-energy photons 79−30686
second-quantised Dirac and Klein-Gordon eqns., external fields 77−26472
self-consistent classical field theory of electrodynamics, QED in limit 78−49683
self-duality, helicity, and supersymmetry: the scattering of light by light 79−93327
semi-inclusive scattering in QED 79−63388
semiclassical radiation theory within quantum mechanical framework, book contrib. 79−75705
semiclassical representation of EM field density matrix 77−61234
semiinfinite plasma interaction with charged nonrelativistic particle 77−38110
sine-Gordon massless quantum eqn. in 2 space time dimens. 78−32754
small angle scatt. 79−21999
small distances and QED, review *(Russian)* 77−217
soft photon emission, and electron form factors in two-dimens. QED *(Russian)* 77−46003
soft-photon emission transverse momentum distrib. from Bloch-Nordsieck method 77−71473
solids, EM field quantum field theoretical treatment *(German)* 80−91022
soluble model, four-dimens. field theory of electrons, photons 78−41457
solution of the Dirac equation with anomalous magnetic moment 78−82133
source field detection and quantum beats 79−26917
source theory, Casimir effect 77−22639
sourceless quantum EM field in multiply connected asymptotically flat background metric 79−25946
space time *(Italian)* 78−12840
quantum electrodynamics continued
space translation, gauge invariant, spinor field-electromag. pot. (quantised or unquantised) interaction 78−62296
space-time structure of jet hadronization 80−91024
spacelike features and asymptotic behaviour of e^+e^- annihilation 80−86630
spatially dispersive media, generalised Kramers-Kronig formula, vac. polarisation tensor 77−17798
spin 1/2 particle, motion in field on mag. monopole 80−18097
spin $^1/_2$ charged particle, in two-dimens. mag. field, quantum ground state 79−80778
spin motion eqn. in external field, Dirac particle quasiclassical theory 80−18099
spin-1 theories, consistency in external EM fields 79−45043
spin-1/2 system, mag. resonance in arbitrarily oriented fields 77−42263
spin-mass trajectories and QED in null plane, free field theories 78−29259
spinless particle interaction with electromag. field, path integrals, Klein-Gordon eqn. 78−58144
spinning charge, torsion contrib. to magnetic field 80−77676
spinor, role of eikonal approx. in IR domain 77−26477
spinor bound states, nonradiation gauges, using Bethe-Salpeter type equation 78−78058
spinor electrodynamics, anomaly free and axially coupled, bilinear gauge renormalisation 79−307
spinor electrodynamics, infrared and fixed angle domains, eikonal approx. rule 79−49424
spinor electrodynamics, quasiclassical approx. *(Russian)* 78−49996
spinor electrodynamics in Riemann-Cartan space, dynamical theory of axial vector torsion propag. in vac. 78−73889
spinor eqn. of pure EM field 78−86429
spinor fields in four dimensional space-time 79−6271
spinor functional determinate in Yang-Mills potential, upper bound of 1 79−311
spontaneous breaking of elec.-mag. charge symmetry in local theories 77−18209
spontaneous symmetry breakdown induced by quantum effects 79−63379
static EM angular momentum, in vacuo obs. 80−73631
statistical mechanics of relativistic dense matter, QED plasma appl. 78−89814
Stern-Gerlach quantum-like behaviour of a classical charged particle 79−85913
stimulated Compton scattering and collisionless Landau damping 77−34802
stochastic, approach to quantum harmonic oscillator 79−49077
stochastic, derivation of quantum mechanics 77−74252
stochastic foundations of quantum mechanics, harmonic oscill. in stochastic electrodynamics 77−9910
stochastic nonlinear electrodynamics, partial in central field of force 80−86629
stress tensor, reln. to Poincare identities 77−13904
stress-energy tensor of vacuum created particles from homogeneous electric field *(Russian)* 79−80779
string-like topological excitations of the electromagnetic field 78−93835
strong and supercritical fields, heavy-ion collisions, review 78−74193
strong external fields, fermion and boson interactions 78−49987
strong field QED, nonrelativistic treatment *(Russian)* 77−6064
strong gravity and Dirac numbers 78−21372
strong localised EM potential interactions with charged leptons or vac. state, critical pots., weak currents 78−54597
strong quantised EM field, statistical description 78−16961
SU_2 monopole harmonics 79−17646
$SU(2)_L \times SU(2)_R \times U(1)$ Higgs scalars, vacuum expectation values, quark mass ratios 79−49404
$SU(2) \times U(1)$ gauge theories, successes and current issues 80−18064
$SU(2) \times U(1)$ gauge theory of weak and EM interactions, quark model 77−26458
$SU(3) \times U(1)$ gauge theory, charged intermediate boson mixing 77−87910
subsidiary condition and local gauge transformations 78−4815
superconducting ring with weak links, critical voltage for flux tunnelling 80−75685
supercritical fields and dynamic confinement of heavy fermions 79−12997
supercritical nuclear composites, spontaneous vacuum decay 78−25235
superdense magnetised astrophysical objects, electron-positron pair prod. 80−17603
superheavy atom, critical nucl. charge, electron shells, positron creation in collisions 79−9603
superheavy ion+atom collision, positron form. 78−62873
superselection rules, for free quantum EM field 78−78119
supersymmetric, absence of radiative corrections to axial current anomaly 80−13242
supersymmetric, renormalised supercurrents and scale anomaly 80−105818
supersymmetric, supercurrent gauge invariance, α-independ. 80−95233
synchrotron radiation, quantum corrections 80−37193
synchrotron radiation, quantum corrections to power spectrum 78−21362
synchrotron radiation directed beam, possibility of obtaining from relativistic charge *(Russian)* 78−1139
synchrotron radiation field, statistical states 78−66736
synchrotron radiation quantum corrections, radiated power of spin $^1/_2$ particle 79−21995
synchrotron radiation transition rates in intense-field regime 80−77991
synchrotron spectral tip calc. refinement, transition rates for mag. bremsstrahlung, computing techniques 79−49430
temporal gauge quantisation of QED 79−49425
tests of electron propagator, vacuum polarisation 80−77994
Theiss' regularisation procedure appl. 80−9129
thermal plasma cyclotron radiation depend. on vacuum polarisation by strong mag. fields *(Russian)* 79−89089
thermodynamic pot. at finite temp. and density, QED and QCD 78−8535
thermodynamic potential in QED, path integral methods 78−41459
Thirring-model effective pot., EM contribs. 77−30294
Thomson scattering in strong mag. field, vacuum polarisation effects 80−86632
three photon vertex in QED, renormalisation group anal., Callan-Symanzik eqn. 80−105822
three-level atom, optical double reson., QED eqns. 77−10652
three-photon coalescence at electron 80−91026

quantum electrodynamics continued
three-photon couplings 77−71474
topological fluctuations and chiral breaking in gauge theories involving massless fermions 77−38088
total pair prod. cross-sections for hydrogen in range 330-910 MeV 77−2783
trace identity and self-stress in QED 79−97547
transition and Cherenkov radiation interference at dielectric media interface 79−49429
transition-radiation energy distribution, comparison with expt. data 79−63397
tripositronium ion splitting into electron and two photons, polarisation effect *(Russian)* 79−72448
two fermion eqn. with form factors and EM high mass resonances 79−93322
two jet processes, asymptotic cross sections *(Russian)* 77−6068
two lepton (eμ) case for Gell-Mann-Low and Callan-Symanzik functions 79−310
two-dimensional Dirac eqn. on spatial lattice 79−93325
two-dimensional massive QED in unitary gauge as renormalisable theory 77−57478
two-electron system, QED, Foldy-Wouthuysen transform. and transition operator relativistic corrections 77−74624
two-particle system in QED, Dyson-Schwinger eqn. 79−2962
two-photon annihilation stimulation of relativistic electrons and positrons 79−64195
two-photon single-mode laser, radiated EM field statistics 79−98334
two-potential description of the electromagnetic field 79−71673
two-potential formulation of electrodynamics with magnetic monopoles *(Russian)* 80−62893
two-quantum radiation of a particle travelling uniformly in a refracting medium *(Russian)* 80−62901
$U_L(1)\times U_R(1)\times R_R$ group, mass ratio and symmetries of electron and muon, model 79−58917
U(1) lattice gauge model, phase transition in four-dimensional compact QED 80−105820
ultrarelativistic particle channelling in crystal lattice *(Russian)* 79−30690
ultrarelativistic particle in homogeneous mag. field, trajectory, radiation damping 80−18104
ultrarelativistic particles, Lorentz factor determ. by ionisation loss 79−35551
unambiguous field-strength formulation and dual potentials for gauge theories 79−35938
undulators, spin effects during electron movement *(Russian)* 78−13652
unified field theory with homotopic charge 79−13006
unified formulae for EM decays, electroprod., e^+e^- hadron pair prod. for arbitrary spin 77−57535
unified parity-conserving interactions based on SU4 77−74629
unified theory of elementary-particle forces 80−105827
unitarising high energy scatt. amplitudes in field theories 78−62341
unitarity violation in finite theory 77−65124
Universe, isotropy, vacuum polarisation contrib. to energy content of Universe 80−73083
unrenormalised vacuum polarisation tensor calc. in lowest order 77−45938
UV-stable fixed point behaviour in QED, expt. aspects 78−21367
vacuum, empty, fields and quanta, strong gravity, particle-antiparticle annihilations 80−68400
vacuum behavior in two-dimensional scalar electrodynamics 80−105819
vacuum birefringence, magnetic field induced, expt. detection method 79−85252
vacuum copies and perturbation theory in the 't Hooft-Veltman gauge of QED 79−21989
vacuum decay, near superheavy atomic nucleus 80−32050
vacuum field press. on electron 79−35973
vacuum instability in massless electrodynamics, Bethe-Saltpeter eqn. tachyon solns. *(Russian)* 79−12993
vacuum polarisation, accurate fourth order computation by VAC4 subroutine 78−89639
vacuum polarisation, breakdown of normal threshold dispersion relation, naive quark model 77−2849
vacuum polarisation, influence on confinement 79−71715
vacuum polarisation, influence on radiation propagation in plasma *(Russian)* 78−47100
vacuum polarisation, long distance behaviour, linear approx. 77−13905
vacuum polarisation, test using heavy muonic atom X-ray meas. 78−29287
vacuum polarisation in background grav. field, effect on photon vel. 80−91025
vacuum polarisation in Fock space 78−41446
vacuum polarisation in intense EM fields, perturbation theory, renormalisation group calcs. *(Russian)* 80−52444
vacuum polarisation in one-loop approx., SLAC fermion lattice action 79−85249
vacuum polarisation in parallel homogeneous elec. and mag. fields 78−70314
vacuum polarisation in strong fields, π condensation 79−314
vacuum polarisation induced by intense gauge field, renormalisation group method 78−49994
vacuum polarisation potential, calc. method to order $\alpha(Z\alpha)$ *(German)* 79−85248
vacuum polarisation potential calculations 77−10209
vacuum polarisation tensor, fourth rank, gauge invariance 77−41795
vacuum polarisation under external field, renormalised scalar Euclidean functional determinant 78−78061
vacuum polarization and non-Newtonian gravitation 80−62896
vacuum polarization and particle creation in a non-stationary homogeneous electromagnetic field *(Russian)* 80−13246
vacuum polarization connection to atomic spectrum in a strong magnetic field 80−42369
vacuum polarization effects on radiative opacities in a strong magnetic field 79−85032
vacuum polarization in a nonsimply connected spacetime 80−57531
vacuum polarization in Delbruck scatt. 80−18288
vacuum polarization in uniform non-Abelian gauge fields 80−4898
vacuum polarization potential for two heavy ions, calc. in first order, numerical method 78−21594
vacuum quantum effects analogy in gravitational and EM fields 80−32044
vacuum radiation in presence of Coulombic interaction 78−406

quantum electrodynamics continued
vacuum stability and quantum electrodynamics at short distances 79−35974
vacuum stability problem 78−41454
vacuum structure of indefinite-metric quantum field theory 78−45782
vacuum tunelling, field theoretic alternative derivation 79−35980
vacuum tunneling in spontaneously broken gauge theory 79−40703
vacuum with spin in the ECSK-theory of gravitation 79−44830
vacuum-polarization-corrected long-distance static quark-antiquark potential 79−49475
vacuum-to-vacuum transition probability, with pair-producing external field *(Russian)* 78−12842
valdity test precision meas. of muonic 5-4 transitions in Pb and 4-3 transitions in Ba 78−33642
vector meson, in quantised monochromatic EM plane wave field, exact solns. 78−89638
vector meson in a quantized electromagnetic field 79−40705
vector mesons, effective electric charge and asymptotic freedom *(Russian)* 78−45827
vertex form factor radiative corrections in 2 dimensional QED approx. *(Russian)* 80−418
vertex function, spectral representation, ghostless electron propagator, infra-red and ultraviolet behaviour considerations 79−58911
vertex function expansion parameter, two-dimens. approx. QED *(Russian)* 79−6301
virtual annihilation processes, appl. of Gegenbauer integration techniques 79−21996
Ward identities, anomalous axial vector, renormalisation group in QED 77−61231
Ward identity, axial vector current divergence, chiral invariant regulator field 80−57526
Ward identity of dilation current 80−68401
wave function of charged particles near mag. monopole *(Chinese)* 77−67600
Weinberg power counting theorem, inapplicability in finite QED 77−87924
Weisskopf-Wigner theories, causality 77−67598
Weisskopf-Wigner type theory, graphical representation 77−71470
Weyl neutrino, translation props. 79−63392
X-ray pulsars, vacuum polarisation effect rel. to radiative transfer and X-ray spectra 80−27015
X-ray scattering by free and bound electrons in strong laser field 78−58148
X-Y model, gauge theory analogue, 4-D self-dual gauge model, phases and transitions 80−27399
Yang-Mills temporal gauge struct. by Feynman propagation kernel 80−37162
Yang-Mills theory, covariant canonical formalism, quark confinement, absence of localised coloured/charged physical states 80−57573
Yang-Mills theory, Regeisation of scalars and dual model struct. 78−16927
Z>137, WKB approximation for Dirac's equations, spontaneous positron production *(Russian)* 78−78123
zero charge and asymptotic freedom *(Hungarian)* 78−37159
zero mass renormalisation and triangular anomalies 78−16915
zero mass system, generalised EM field, reduction and second quantisation 80−27436
zero-charge and asymptotic freedom 77−65126
zero-energy eigenstates for the Dirac boundary problem 80−101961
e, anomalous magnetic moment, QED test 80−77996
e, finite self-mass in nonperturbative iterative scheme of QED 78−89641
e in superstrong mag. field, $\nu\bar{\nu}$ pair emission *(Russian)* 78−49991
e moving in polarized EM wave, anomalous mag. moment determ. *(Russian)* 78−49998
e scatt., in presence of intense EM field 78−33014
e:μ mass ratio, EM coupling const., flux quantization model 77−79240
e^+ production by Coulomb centre in homogeneous mag. field *(Russian)* 77−41798
ee scattering, energy depend. scale dimens. in QED 77−79239
e^-e^+ colliding beam physics, review 77−74700
e^+e^-, asymmetry of prod. by circularly polarised protons *(Russian)* 78−29286
$e^+e^-\rightarrow\mu^+\mu^-\gamma$, neutral current effects and hard photon correction 79−13096
e^+e^- calorimetric experiments, γγ processes, tests of QCD 80−22628
e^+e^- creation from vacuum induced by variable elec. field *(German)* 77−82695
$e^+e^-\rightarrow e^+e^-$, 13 and 17 GeV, test of QED 79−54289
$e^+e^-\rightarrow e^+e^-$, 9.4 to 31.6 GeV, QED test 80−101965
$e^+e^-\rightarrow e^+e^-$, γγ, $\mu^+\mu^-$, 5.2 GeV, tests of QED 78−66064
$e^+e^-\rightarrow e^+e^-X$, virtual 2 photon processes, luminosity functions, rapidity distrib., QED factors 80−86734
$e^+e^-\rightarrow e^+e^-X$, $X=e^+e^-$, $\mu^+\mu^-$, $\pi^+\pi^-$, η', photon-photon interactions, QED test 79−93425
$e^+e^-\rightarrow e^+e^-$+gluons, gluon jet production, quark models 80−22576
$e^+e^-\rightarrow e^+e^-(\gamma\gamma)$, 27.7-31.6 GeV, QED test, Weinberg angle 80−77995
$e^+e^-\rightarrow e^+e^-(\mu^+\mu^-)(\gamma\gamma)$, 12-31.6 GeV, QED test and Weinberg angle 80−91027
e^+e^- experimental tests 77−57551
e^+e^- final states, qq̄ decay, semiclassical model, vacuum polarisation by colour field 80−63011
$e^+e^-\rightarrow\gamma\gamma$, Einstein-Podolsky-Rosen nonseparability, Feynman nonlocality 77−34110
$e^+e^-\rightarrow\gamma\gamma$, weak interaction effects, QED tests, SU(2)×U(1) gauge theory 79−40767
$e^+e^-\rightarrow\gamma\gamma$ at 6.2-7.4 GeV CM, comparison with QED predictions 77−49942
$e^+e^-\rightarrow$hadrons, R problem, QED and QCD corrections, quarks and leptons 80−95281
e^+e^- interactions, anomalous eμ and μ events, anal. *(Chinese)* 77−67641
$e^+e^-\rightarrow\mu^+\mu^-$, 30 GeV, charge asymmetry, QED and weak corrections 77−61266
$e^+e^-\rightarrow\mu^+\mu^-$, 9.4 GeV, QED test 80−101965
$e^+e^-\rightarrow\mu^+\mu^-$, early weak gauge boson restrictions from PETRA QED cut-off 80−52487
$e^+e^-\rightarrow\mu^+\mu^-$ 6.2-7.4 GeV CM, comparison with QED predictions 78−74194
$e^+e^-\rightarrow\mu^+\mu^-$ or e^+e^-, EM corrections for μ pair prod. and Bhabha scatt., QED processes 77−18259
$e^+e^-\rightarrow\mu^+\mu^-\gamma$, QED distribs. for hard photon emission 77−61265

quantum electrodynamics continued
e^+e^- pair creation by free EM field in vac. *(Russian)* 77−71467
e^+e^- pair creation in strong EM fields, gravitational effects 80−42376
e^+e^- pair formation, identical photons in nuclear field *(Russian)* 77−30290
e^+e^- pairs and equilib. radiation in quantising mag. fields *(Russian)* 78−49990
e^+e^- photoprod., radiative corrections calc. 78−45823
e^+e^- prod., quantized magnetic field influence, equilib. *(Russian)* 78−4812
e^+e^- prod. by p+Ne at 300 GeV/c, comparison with QED theory 78−8569
e^+e^- prod. by photons in constant electromagnetic field in general relativity 78−8568
e^+e^- production, intermediate energy, Coulomb correction to total cross section 78−21540
e^+e^- transversely polarised annihilation, heavy lepton prod. and decay 77−18261
$e^+e^-\rightarrow\tau^+\tau^-$ near Z^0 pole, heavy lepton polarisation and radiative effects 79−22085
$e\gamma$ scatt., coherent states and quantum nonperturbing measurements 79−315
$e\mu$ system in QED with internal fermion excitations 80−9130
$\gamma\rightarrow e^-e^+$ generalised conservation laws of physics, electron energy spectra theory 79−85246
$\gamma\rightarrow e^-e^+$ generalised conservation laws of physics, electron energy spectra theory 79−85247
$\gamma\gamma$ pair, polarisation correl. 78−49995
$\gamma\gamma e\rightarrow e\gamma$, fusion of two antiparallel photons into one *(Russian)* 77−26473
μ, anomalous mag. moment, sixth order, photon-photon contrib. 78−16958
μ, anomalous magnetic moment, QED test 80−77996
μ, sixth-order anomalous mag. moment 78−74190
μ atoms, vacuum polarisation, $\alpha(Z\alpha)^3$ correction to energy level shifts 78−21366
μ g-factor, (g−2) expts., review, book contrib. 80−68403
μ:p magnetic moment ratio, discrepancy between direct and indirect determinations 77−18287
μ^- to e^+ conversion in nuclei, mediation by Majorana lepton 80−22547
$(\mu^-{}^4He)^+$ ion, meas. of $2S_{1/2}$-$2P_{3/2}$ splitting, QED vacuum polarisation 77−34785
$\mu^-N\rightarrow\mu^+\mu^-N$ in Pb, 10.5 GeV/c, short lived particle search, QED tridents 80−37275
(n,γ), γ-rays, QED test review 80−37199
n dipole polarisation, possible detection in U(n,n) small angle scatt. 77−22674
pp elastic scatt., total cross-section asymptotics, stable approach, timelike and spacelike behaviour, vacuum polarisation 80−47332
$\bar{p}$p nP bound states, black sphere model for linewidths 78−42252
pp scatt., EM corrections, vacuum polarisation effect *(Japanese)* 78−17023
π condensation, vacuum instability in external fields 78−50114
π^0 decay, Compton electron scatt., 0.1 to 5.0 GeV 79−397
π^0 emission by protons with anomalous mag. moment in const. EM field, Furry formalism *(Russian)* 78−410
$\pi\mu$ atom, energy levels, fine struct. and Lamb shift calc. *(Russian)* 79−31744
π^-p, 360 GeV/c, direct e^+e^- pair prod. in liquid H, comparison with QED calcs. 77−10285
$q\bar{q}$, fine-hyperfine splittings and Lorentz structure of confining potential with vacuum polarisation corrections 80−78041
$q\bar{q}$ pair energy modification in Wilson loop formalism 80−18122
^{35}Cl XVI, n=2, Lamb shift, fine struct. 79−13675
H, excited state interaction with photon field, simultaneous eqns. 78−66481
H, induced $2s_{1/2}\rightarrow 2p_{1/2}$+one photon transition, rate calcs. 77−50384
H, self-interaction of excited at. with radiation field 78−86794
H+e^- interactions in intense EM field, one photon absorpt., 1s-2s transition 79−36765
He liquid, Hamiltonian of interaction with quantised EM field 79−46853
He muonic atoms, $2S_{1/2}$-$2P_{3/2}$ level splitting, test of QED predictions on electronic vacuum polarisation 77−3494
Pb, muonic high-lying states transitions, electron screening effects 77−34786
Ta (γ,γ), 2.754 MeV, elastic scatt. diffr. cross section, Rayleigh, Thomson, Delbruck scatt. interference 79−528

quantum electronics *see quantum optics*

quantum field theory
see also axiomatic field theory; Bethe-Salpeter equation; dispersion relations; gauge field theory; meson field theory; nonlinear field theory; quantisation; quantum field theory of elastic scattering; quantum field theory of interactions; Reggeon field theory; relativistic quantum field theory; renormalisation; scaling phenomena; Schwinger source theory; unified field theories
1+1 dimensional field theories, bound state problem, S-matrices 79−71609
θ model in quantum corrections to classical confinement 78−29297
$\lambda\phi^4$ theory, high temp. expansion, crit. exponent γ calc. 77−2743
σ model, explicit renormalisation in Goldstone mode 77−79218
σ model, linear, collective phenomena in supercond. models, renormalisability 77−18179
σ model, symmetry restoration through finite temp. phase transformation 77−67587
σ model, vacuum stability, strong dynamical symm. breaking 77−13856
ϕ^3 and ϕ^4 scalar nonrenormalisable field theories, scale-invariant solns. *(Russian)* 77−34097
abnormal nuclear matter, many body forces, σ-model Lagrangian field theory 77−6277
abstract equipartition of energy theorems 79−71273
accelerated detectors, thermal like behaviour, quantum noise 79−139
aesthetic field equations, sinusoidal solns. 80−77937
aesthetic field theory, new solns., bounded particle systems 77−61179
affine fields and operator formalism of augmented scalar fields 78−8272
anharmonic oscillator, multipseudoparticles, perturbation theory in ground state energy calcs. 79−17622
associative algebra of tensor fields, duality and Dirac identities 79−71618
quantum field theory continued
asymptotic behaviour in quantum field theory, renormalisation group analysis 80−68378
asymptotic behaviour in renormalisable QFT, Green's functions 78−70254
asymptotic estimates in quantum field theory, Lipatov method 79−21895
asymptotic estimates of perturbation theory at large orders 79−21901
asymptotic expansion in coupling const. 79−71595
asymptotic field, fundamental props., Robinson-Greenberg theorem 78−45787
asymptotic series summing *(Russian)* 77−82683
augmented quantum field theory, systems containing derivative coupling and/or vector fields 79−63367
baryons with arbitrary spin, generalisation of Dirac eqn., group scheme 80−73615
base space topology, implications for construction of classical and quantum fields 79−63353
Baxter model and scale invariant field theory 78−32764
Bianchi IX model, spectral asymmetry and QFT in curved spacetime 80−56982
bibliography, probabilistic ideas in field theory and statistical mechanics 78−8230
bilinear QFT, uniqueness connection between charge conjugation and statistics 78−37130
bilocal quantum field theories, conservation laws 79−12931
black hole, rotating, in mag. field, particle creation 77−2452
Bogolyubov's operator S(g) for some two-dimens. models 77−60981
bootstrap eqns. in conformal invariant field theory *(Russian)* 78−58142
Borel summation of perturbation series 78−16683
boson condensation, solvable quantum field theoretic model 77−57447
boson system coherent states 77−17911
bosonization in positive definite Hilbert space 78−49974
bound states in field theoretical model without elementary particles 77−22636
bound states in quantum mechs. and AFT, eqns. of motion, variational principles, WKB approx. 78−54540
bound states of two dimens. O_N model at finite temps. 78−41409
boundary-value problems, numerical solns. 77−2526
canonical formalism for field theory with singular Lagrangian *(Russian)* 78−54563
canonical quantisation of finite two dimens. model field theory with Schwinger term 77−45946
Casimir forces, appl. of analytic regularisation 78−81887
causal theory, removal of Einstein's objections to quantum theory, unification 80−31572
causality and renormalisation group 77−18165
causality condition in field theory with momentum space of const. curvature 78−395
chiral models in three space dimens., finite energy static solns. 77−203
chiral symmetric two-dimensional σ-model, semiclassical and of multiparticle bound states 77−6028
classical soln. quantisation, zero-mode problem of kink translations 79−75404
classical sources, conditions for quantum scalar field with higher order derivatives 79−63365
cohomology groups with coefficients in sheaves of holomorphic functions, vanishing theorems 79−49405
collective co-ordinate of a quantized field 79−67192
collective coordinate method in the canonical formalism: Bogolubov's transformation 80−105776
collective quantum fields for many body systems, appl. to BCS, ^{3}He and type II superconductors *(German)* 79−35917
coloured null flags and para-Fermi fields 77−5993
completely integrable theories as theories of spontaneous breakdown 79−49416
completely positive mapping families in *-algebra 80−94971
complex mass and field operator for unstable particle 80−9105
complex one dimens. field, solitary-wave soln. 77−5707
complex space-times, real geom. 78−77684
composite field theory, proof of two identities, order of integrations interchange *(Chinese)* 80−47196
composite quantised field theory and bound states *(Chinese)* 80−86543
conference, fundamentals in quantum theory and field theory, Flagler Beach, FL, USA (Feb.-Mar. 79) 80−57114
conformal anomalies using dimens. regularisation in general metric 77−57454
conformal invariance, constants of motion 77−2730
conformal invariance in quantum gravity 77−17896
conformal invariant 2- and 3-point functions for tensor fields with arbitrary spin 78−49977
conformal invariant quantum field theory, composite field operators 78−81886
conformal invariant quantum field theory, review 78−86420
conformal superfields, two- and three-point functions 79−40674
conformal symmetry and the vector four-point function 79−49394
conformally covariant quantum field theories, transformation behaviour *(German)* 77−71240
conformally invariant free fields, functional representations 77−5708
conserved chiral charge on Schwinger model 78−49961
convergent expansion about mean field theory, mean field cluster expansion 77−5706
convergent expansion about mean field theory, nearly Gaussian quantum field theory 77−5705
cosmological singularity avoidance and quantum conformal anomalies 77−67148
counterterms in normal product formalism, Zimmermann identities 77−30268
covariant 'in-out' formalism for creation by external fields 79−107
covariant inverse problem of calculus of variations, corrigendum 78−77773
critical exponents by quantum field theory methods *(Russian)* 80−4869
crystal, SCF theory, boson transform. 77−80430
crystals and dislocations, spontaneous breakdown of spatial translation invariance *(German)* 79−7653
crystals and extended objects, quantum field theory, review 79−42164
curved static space-times, quantisation of conformally coupled scalar fields, particle emission *(French)* 78−77771
d'Alambert's equation, canonical formulation of field solns., Dirac's field 80−68343
Deser-Gilbert-Sudarshan representation, existence 80−37167

quantum field theory continued
diatom+atom (electron) scatt., vibr.-rot. excitation, generalised field theory method 77−23537
dilations and interactions 77−57445
dimensional reduction and axial anomalies 80−86561
dimensional regularisation, positivity vs. gauge invariance 77−45938
dimensional regularization of composite operators in scalar field theory 80−73573
Dirac matrices, compact evaluation of traces 77−17750
Dirac particle creation by gravit. fields 78−33021
Dirac quantisation of spin-2 field 79−12652
Dirichlet forms, construction of stochastic processes 80−8921
disconnectedness problem in field theory model of NNπ system, three-body problem 78−29276
discontinuous perturbations in singular dynamical systems 77−10169
disordered systems as quantum field theories 79−65354
dispersion relation in terms of localisable field theories *(Russian)* 77−74618
dual symmetry of general type vector field, quaternion formulation *(Russian)* 78−58107
duality and quantum field theory 77−30236
Dyal symmetry of vector and spinor fields *(Russian)* 79−30673
dynamical equation for scattering operator 79−12936
dynamical symmetry breaking, extended structs., generation in field theory 77−6026
dyon-dyon nonrelativistic scatt., classical and quantum anal. 77−5985
effective action, quantum mechanical definition using time depend. variational principle 80−57457
effective potential anomalous behaviour 80−32023
effective potential calculation to order $\hbar$ using functional Schrodinger Rayleigh-Ritz approach 77−74257
elementary particle and math. physics, conf., Austria (Feb. 1976) 77−5974
elementary particle theory, unified description *(German)* 77−41803
elementary particles, physical fields, symmetry, causality props. 79−6270
EM field quantisation, C*-algebra formalism 77−49827
EM moments of spin J-1 particles, and equivalency of wave eqns. *(Russian)* 77−65113
energy eigenvalue problem, adiabatic perturbation theory using QFT techniques 78−93551
energy eigenvalues lower bounds for quantum Hamiltonians in lattice field theories 78−45575
equation of motion, commutation relations for quantum mechanics and QFT, quantisation 80−105541
equivalence of field theories with/without boson kinetic energy terms 79−9148
essential quantum field theory for expt. particle physicists 78−82118
Euclidean fermion-boson systems on lattice, appl. to field theory 78−45559
Euclidean loop expansion 79−5989
Euclidean massless free lattice field as approx. of plane rotator model 77−28351
Euclidean QFT, appl. of virial expansion derivation 78−37131
Euclidean scalar field theory, asymptotic behaviour of Feynmann integrals 78−388
exponential momentum-space growth, generalization of local commutativity 78−21013
extended supersymmetry, derivation of unextended superfields 79−89076
Fermi quantum fields, derived from Bose quantum fields, applications 78−36928
fermion field with broken SU_2 symm., two-dimensional isotopic model *(Russian)* 80−73616
fermion Green's functions, functional integral representation construction 79−21941
fermion-boson correspondence in field theory, spinor field quantisation 78−8496
fermions, micro- and macrocoherence relation *(German)* 80−31660
fermions constructed from bosons, remarks on Kalnay theorem 77−65074
Feynman measurements, continuous displacements *(Russian)* 79−35954
Feynman path integrals, conference, Marseille, France, 1978 80−31422
Feynman path integrals, generalised meas. 78−384
Feynman path integrals, mathematical theory, book 77−41511
feynman path integrals and the corresponding method of stationary phase 80−31583
fibre bundle struct. of thermodynamic states 78−8370
field embedding problem *(Russian)* 78−12828
field operator for unstable particle and complex mass description in local QFT *(German)* 80−90981
field theory, massless equations, first-order, conformally covariant 78−29265
Fierz-Pauli field theories, smooth massless limit 80−73590
finite integration range for zero modes 80−86150
Finzi unified field eqns., wave solutions 78−70036
fluctuations in gravitational collapse and cosmology 78−49571
Foldy-Wouthuysen and Cini Touscheck transformations, free spin 1/2 particle 78−62291
four-point theories in UV asymptotics, conformal-invariant behaviour *(Russian)* 77−45978
Fourier analysis on space-like surfaces, mass $\neq 0$ 77−29995
free electron laser, classical, semiclassical and quantum field theories 77−14684
free scalar charge field, local nets of algebra of observables 80−99039
free vector field, canonical formulation, zero mass field connection 80−52388
frequency solutions of massive vector field eqns. in curved static space-time 78−36909
Frohlich model, method of functional derivatives 78−51909
froissarton coupling constant, s-channel unitarity *(Russian)* 78−45799
functional methods, introduction to use 77−57458
functional methods *(French)* 79−54016
Galilean supersymmetry 79−17625
general, two-particle structural eqns. for four, five and six-point functions 78−54524
generalised Fenyes-Nelson model for free scalar field theory 80−105769
global conformal transformations and dynamics 77−26460
global operator product expansions for free fields of arbitrary mass 77−49641
Goldstone bosons in two dimens., ground state, IR divergences 78−12815
quantum field theory continued
Grassman functional Schrodinger equation appl. to perturbation theory 79−21915
Green functions and diffusion kernels, quantum field theory on cone 77−18161
Gross-Neveu model on lattice, bound state spectrum 78−29236
group theory approach to dynamical quantisation 77−18183
Hamiltonian formalism for harmonic oscillators and free fields 78−29005
Harish-Chandra eqns. for composite particles with spins 1/2 and 3/2 77−71418
Heisenberg eqns. of motion for spin-3/2 field with interactions 78−370
Higgs field and mag. monopoles *(Chinese)* 77−10174
Higgs model, impenetrability of vortices 77−34091
high energy physics, conf., Schladming, Austria (Feb.-Mar., 1977) 78−8494
high-spin field with indefinite metric 78−74156
higher Euler operators and some of their applications 79−49101
higher order field equations, Green's functions limit props. 77−34085
higher-order Hamiltonian formalism in field theory 80−105766
history of quantum field theory, search for unity 78−28904
holonomic quantum fields, deformation model 79−25907
holonomic quantum fields, model 79−25909
holonomic quantum fields, model 79−25908
holonomic quantum fields, Riemann-Hilbert problem on complex sphere 79−25910
holonomic quantum fields, symplectic version of 2-dimens. operator theory 79−49102
holonomic quantum fields 79−25911
homogeneous covariant equations, mass and uniqueness conditions 77−18160
hyperbolic-type dynamics, second quantisation 77−6035
indefinite-metric quantum field theory, vacuum struct. 78−45782
infinite and T products of exponentials 77−74602
infinite nuclear matter, response function, quantum field theory of fermion systems 78−70480
infinite-component conformal fields, spectral representation of two-point function 77−13836
instantons and antiinstanton forces in sigma model and Yang-Mills theory 77−26462
intersoliton forces in weak-coupled quantum field theories 77−71430
intrinsic coupling between gravitational wave and quantised EM radiation 78−54268
invariant field equations solns. in (4,1) de Sitter space-time 78−93563
invariant props. of n-point functions and functionals due to translationally invariant formal measure 78−45500
invariant regularization 79−45020
invariant renormalisation method for non-linear realisations of dynamical symmetries 79−108
inverse scattering transform as an operator method in quantum field theory 79−85229
Ising model, D=2, direct construction of quantum field operators 78−32773
Ising model, two-dimens., quantum field theory calc. of correl. function 77−32205
Ising n-spin correlation function for 2-dimens. model in quantum field theory 77−37821
Ising two-dimens. model and quantum field theory 77−69471
Kemmer-β formalism for spin-1/2 particles, removal of nonphysical components 77−74571
Kemmer-Duffin equation with proper time, diagonalisation *(Russian)* 77−61200
kernels and symbols of operators 79−236
kernels and symbols of operators for fermion fields 79−30644
Klein-Gordon field in naked-singularitiy background 78−70274
Kondo problem, low-temp., Nozieres-Wilson relation, renormalisable quantum field theory 79−95572
Lagrange formulation of symm. theory of massive spin-3 fields 78−41423
lagrange multiplier formalism for spin-2 fields 80−90982
Lagrangian, conditions for existence, analytic representations of tensorial field eqns. 77−22632
Lagrangian, conditions for existence, tensorial field eqns. 77−22631
Lagrangian, generalised analytic representations of tensorial field eqns. 77−61175
Lagrangian, with higher derivatives, arbitrary spin fields 79−17596
Lagrangian formulation for noninteracting high spin fields, Lorentz group representations 77−49825
lattice Hamiltonian results for (1+1) dimens. asymptotically free field theory 77−6021
lattice Schwinger model, new states 77−2759
Lie admissible quantisation in a self-interacting scalar field theory, deformation distribs. 78−74169
Lie groups, octonion/quaternion hypercomplex numbers, nine-vectors and real world 78−37151
Liouville equation, Goursat problem regular solns. 80−105795
local algebra type in QFT 77−45932
local class field theory, generalisation by K-groups 79−25875
local class field theory generalisation using K-groups, Abelian extensions 79−44799
local cohomology and superselection struct. 77−10192
local field theory based on improved operator products, finite and covariant formulation 77−41755
local QFT, higher symm. interpretation, spontaneous symm. breaking, quarks and flavours 78−16942
local quantized superfield, local commutativity from spin and statistics 77−57435
local supersymmetry in (2+1) dimens., spinning membrane 78−58138
magnetic charges, one pot. formulation 80−22512
magnetic monopoles, review 79−26234
magnon fields, finite temp. effective pot. methods, loop expansions 78−2640
Markov systems of imprimitivity 78−8347
Markovian homogeneous multicomponent Gaussian fields 80−77933
mass divergences in annihilation processes, cut vac. polarisation processes, diagrams 78−74157
mass scales, confinement, nonperturbative approach, self-consistent method 78−33033
massive Gross-Neveu model, semi-classical quantisation by inverse scatt. method 79−2924

quantum field theory continued
massive particle decoupling in field theory, scaled mass, Feynman amplitudes 79−71585
massive particles with any spin. consistent eqns., Klein-Gordon divisor, review 80−73577
massive scalar field coupled to gravit. field, stress-tensor trace anomaly 77−41768
massive scalar field in curved background, vacuum expectation value of stress tensor 77−13658
massive scalar field in Einstein universe, vacuum stress tensor, finite-temp. effects 77−41769
massive spin-2 theory, nonuniqueness 77−65075
massive spin-3 fields, first order formalism 77−22638
massive spin-3 particles, construction of Euclidean field which is Markovian 78−86414
massive spin-3/2 field, Lagrange multiplier formalism 77−61182
massless field quantum fluctuations, IR props. of quantum determinants 79−85237
massless fields with continuous spin, quantisation 78−4525
massless fields with fixed arbitrary spin, quantisation 80−31992
massless free field in two space-time dimens., bound states 77−13846
massless modes interacting with quantum harmonic oscillator, correlation function, long time limit 78−65814
massless scalar free field, local von Neumann algebras 78−45778
massless spin two field, covariant quantisation in general covariant gauge 78−66027
massless spinor field/massive pseudoscalar field interaction, mass perturbation around exact soln. 79−63368
matrix superpropagators, second order theory for nonlinear chiral Lagrangians 77−57442
mesonic topological amplitude products, an algebraic soln. 78−81884
metastable vacuum states, lifetime, semiclassical approx. 78−54542
microcausality, lack of consistency with exponential growth in momentum representation 78−16931
microcausality principle in QFT *(Chinese)* 78−86195
minimal EM coupling for massive spin-two fields 78−70270
modified renormalisation conditions, two-point Green functions 80−9089
modular operator, local observables, in von Neumann algebras, duality in QFT, CPT invariance 78−81793
molecular scattering, distorted wave formalism 79−3513
multi-mass vector-spinor field in EM interaction, hyperquantisation, S-matrix unitarity 77−61232
multilocal quantum field theory, Fock-space technique, particle creation effects 80−77945
multiparticle system interacting with boson field, calc. of quasimeans 77−13695
multiplication of distribs. by non-standard anal. 79−30292
multiplicative struct. of giant fields 77−65070
multispinor Lagrangian, symm. group 78−58115
n→0 models, reformulation using anticommuting scalar fields 80−52071
N-quantum approx. method, bound state problem appl. 79−21943
N-quantum approximation in Bronzan-Lee extended-source static model 78−8507
Nambu Jano-Lasinio model, symm. restoration above critical temp. 77−54054
neutral scalar massive field theory, two-dimensional soluble models 78−58129
non local theory, canonical quantization, with form factor in interaction Lagrangian 79−75691
non-basic fields with arbitrary spin, conformal invariant two point functions 77−45930
non-Lagrangian field equations, variational principles 79−21565
non-linear point transformation, regularisation 77−49839
noncritical polynomial theories, block-field distribs. 77−2733
nonequilibrium statistical field theory, renormalisation of closed time path Green's functions *(Chinese)* 79−80758
nonlocal field theory, structurological generalisations 77−34080
nonlocal field theory and space-time quantisation 77−34078
nonlocal fields characterized by internal variables, geometrical theory 78−29014
nonlocal or gradient type theories, a matter of convenience 79−67457
nonlocalisation, field theory in Finsler spaces, internal variable 78−49963
nonperturbative Green's function approach to quantum field theory 77−34079
nonperturbative techniques for QFT, topological props. of classical fields 77−82400
nonrelativistic field theories, functional methods, finite temp. behaviour 79−12952
nonrenormalisable QFT models, summing of perturbation theory 78−74129
nonrenormalisable quantum field theory, generic interactions 79−40655
nonrenormalizable quantum field models in four-dimensional space-time 79−110
normal liquids, quantum field theory 78−91213
normal-product methods, functional formalism 78−29252
nuclear field theory, appl. to ^{209}Bi struct. 77−67692
nuclear field theory, functional approach, schematic model, monopole pairing, particle-hole forces 78−50095
nuclear field theory perturbation expansion for strongly anharmonic systems, convergence, phonons 78−62490
null planes, field struct., restricted field operators, commutation props. 77−37784
null-plane quantisation in nonlinear Lagrangian theories 77−61194
null-plane quantum field theory, consistent formulation, absence of vac. polarisation 77−54050
O(10) spontaneous symmetry breaking for Higgs fields 80−105812
O(3)⊗U(1)⊗U(1) internal symmetry in massless vector field theory *(Russian)* 80−22531
O(N) model, 1/N expansion summability 80−73582
open systems theory, appl. to unstable particles 79−17281
optical cavity with output coupling, one-dimens., quasimodes as field eigenvalue 80−9911
orbital symmetry conservation, chem. appl. of field theory *(Chinese)* 79−63884
Pade approx. and low-energy Lagrangian field theory 77−61220
Pade-Borel summation of perturbation series, Gell-Mann-Low function 78−86416
para-Bose algebra representations using single Bose field 79−49157
para-Fermi algebra representation 78−65867
quantum field theory continued
paraboson field, uniqueness for infinitely many degrees of freedom 77−57443
parafield current algebra, Lagrangian quantum field theory *(Russian)* 77−13891
parafield theory and supergroup transformations 80−9124
particle creation in generic external fields, particle definition 78−8498
particle limit to field theory, strong-coupling expansion 78−24940
particle solution in aesthetic field theory, intense singularity-free field 77−61178
particle-hole propagator, order analysis 77−38602
path dependent field operator based on characts. of displacement operators 77−30227
path integral formalism, barrier penetration effects on wave functions and energy spectrum 78−62117
Pauli spin matrices, generalised, commutation rules 79−17597
periods on manifolds, quantisation, gauge, topological props. of phys. theories 77−49826
perturbation expansion of quantised composite field theory, gauge invariance *(Chinese)* 78−82156
perturbation theory, convergent integral representation for summing 79−9146
perturbation theory, higher order, appls. to quantum mech. and field theory *(Russian)* 78−36886
perturbation theory, large order estimates 79−26237
perturbation theory at large order, choice of integration contour 79−6263
perturbation theory at large orders, role of vacuum instability 77−41504
perturbation theory at large orders 80−32022
perturbation theory series divergence, quasiclassical theory *(Russian)* 77−30272
perturbative expansion, contrib. of very high orders, functional methods 77−30241
perturbative expansion of quantum states of extended objects 78−54536
perturbative oscill., ground state energy calc. infinite coupling limit 77−74582
perturbative unorthodox expansions in quantum field theory 78−49759
phase transitions, Goldstone bosons, topological superselection rules 77−5977
photon field quantisation and dipole ghosts *(Chinese)* 80−101929
Planck's constant, numerical value, dynamic mechanism, classical/quantum physics borderline 79−21573
Poincare group representations in the free quantum field framework *(German)* 78−77772
point splitting technique, canonical formalism extension 79−6262
polynomial conservation laws in (1+1) dimens. classical and quantum field theory, nonlinear Schrodinger eqn. 78−54224
position operators constructed from free spin-1/2 fields 77−2566
probabilistic concepts in field theory, stochastic processes 77−5975
proceedings of the 1977 CERN-JINR School of Physics, Nafplion, Greece (May-June 1977) 78−81726
propagators in multiply connected spaces 77−17868
pseudoparticles, conformal symm. Lagrangian models in four dimens. space 78−374
qualitative methods in problem solving, graduate text book 77−71239
quantisation around superparametrised finite-energy classical solutions 79−242
quantised rotator, classical correspondence of Schwinger boson representation 79−9492
quantum coherence effects and the second law of thermodynamics 79−6025
quantum many-particle systems in curved spacetime 80−98751
quantum mechanics, experiments on reinterpretation, new ideas 77−26204
quark confinement, quantum corrections to classical confinement 77−2796
quasiclassical expansion and solitons 78−94
random phase approximation for the four fermion interactions 79−12653
regular QFT, minimal wave-packet representations 78−81883
regularisation schemes in perturbation calcs., comparisons 77−82663
renormalisable field theory differential dispersion relations, theory of ψ particles 77−26535
renormalisation group appls. to critical phenomena 77−57296
renormalised Feynman amplitudes for fields with fixed masses 77−49860
Robertson-Walker spacetime, trace anomaly of energy-momentum tensor of quantised scalar fields 79−63360
rotating black hole, Kerr metric, spontaneous creation of massive spin 1/2 particles 78−89217
rotational symmetry in Hamiltonian dynamics 78−74134
scalar field in Bianchi I anisotropic space-time, particle prod. anal. 77−30238
scalar field interactions, in Green's function formalism 77−57436
scalar field propagators in homogeneous expanding universe, particle creation 77−17733
scalar field propagators in isotropic universe 78−74137
scalar field quantisation, alternative approach, augmented quantum field theory 77−6018
scalar field theories, path integral derivation of the self-consistency condition 80−27408
scalar field theory with Gaussian propagator, perturbation series 78−70268
scalar field with isospin, IR asymptotic behaviour of one fermion Green's function 79−89067
scalar fields on lattice, lower bound for ground state energy density, to Φ^4 theory 77−6012
scalar quantum field theories, noncanonical self-coupled, Green's functional eqns. 77−65104
scalar theories, perturbation theory divergence, pseudoparticles *(Russian)* 77−30273
scalar-gluon field theory, variational approach to bound states 77−6025
scale-covariant operator field eqn. 78−32984
scaling variable in simple field theory 78−70269
scaling violation, field-theoretic pattern 78−66037
scattering medium, with quasistatic fluctuations, average field weakening calc. 79−71367
Schwinger model, reconstruction of Lowenstein-Swieca soln. from asymptotic field soln. 78−41411
second Noether theorem, extension for locally invariant Lagrangians 79−93290
Segal-Weinless approach to linear Bose fields, uniqueness result 80−98

quantum field theory continued
self-consistent field theory, diagrammatic review and implications 77−74313
self-coupled vector fields, calcs. using Dirac quantisation procedure 78−89610
self-interacting boson field, interaction with classical current, S-matrix elements 79−21963
semiclassical bound-state methods, four dimens. field theory, trace identities, mode sums, renormalization 77−6020
semiclassical quantisation of nonrelativistic logarithmic theory 78−49708
semiclassical theory of scalar field in globally hyperbolic universe 78−54250
sesquiholomorphic functions, symbolic calculus and second quantisation *(French)* 77−53804
sine-Gordon equation, exact mass spectrum, WKB approx. 77−33896
sine-Gordon field, spectral sum rules 77−6000
sine-Gordon theory, soliton mass 77−13848
single-loop divergences in six dimens., Ricci-flat Riemannian spaces 77−38081
singular potentials, divergence problem in quantum field theory, pot. theory analogy 77−67556
singularities in Feynman integrals of quantum field theories 79−40661
solid state physics, book 77−31922
soliton mass two-loop quantum correction in scalar field theories 77−10175
space derivatives, scalar and vector fields 77−37785
spin 3/2 field, canonical variables and Heisenberg eqns. of motion 79−26225
spin 3/2 field theories, constraints, positivity and obscure representations 79−2909
spin 3/2 fields quantisation in presence of external gravitation 77−22446
spin $^3/_2$ massive/massless particles, field theory, wave eqns. and actions 79−75687
spin projection operators for fields of any spin *(Japanese)* 78−32733
spin wave, propagation in ferromagnetic metal, quantum field theory method 79−7982
spin-1 fields, supersymmetric non-polynomial vector multiplets and causal propagation 80−91012
spin-2 field, free, canonical formulation 80−42316
spinor and scalar fields in 4-D non-Euclidean momentum space, eqns. of motion, vacuum momentum 80−68379
spinor field quantisation 78−45777
spontaneous breakdown of fermion number conservation and supersymm. 77−30248
spontaneous breaking of conformal invariance and the Higgs mechanism 79−40687
spontaneous breaking of elec.-mag. charge symmetry in local theories 77−18209
spontaneous particle creation in strong gravitational field, semiclassical theory 78−54281
spontaneous symmetry breakdown and group contractions 77−13883
spontaneous symmetry breakdown induced by quantum effects 79−63379
spontaneous symmetry breaking in chiral quantum field theory, covariant formulation 78−21347
state vector distinguished component eqn., decay in one dimens. model 77−45929
statistical and classical fields, quantum aspects 79−58585
stringlike object in quantum field theory 77−2738
strong EM field, quantum theory, c-number semiclassical description 80−105540
summer school, methods in field theory, Les Houches, France (July-Sep. 1975) 77−57457
superalgebra in (0,1) integration of supersymmetrical Liouville eqn. *(Russian)* 80−101947
superconducting systems, electrodynamics and quantum theory 80−60134
superfields with arbitrary spin, spectral representation of two-point function 77−6050
superrenormalizable theories with higher derivatives 79−63344
superspace, effective potential calc. 78−16944
supersymmetry and classical particle spin dynamics 77−82690
supersymmetry and pseudoclassical dynamics for particle with arbitrary spin 77−57464
supersymmetry charges in theory of scalar and spinor free fields 77−6049
supersymmetry in QFT, spontaneously broken 78−54582
symmetry groups in QFT, supersymm., space-time symm., internal symm. groups *(Russian)* 77−49871
symmetry restoration in the early Universe 78−73782
symplectic framework for field theories, book 80−22130
tensor field quantisation, valency ≤5, extension of Segal's rules 78−29003
tensor fields invariant under subgroups of the conformal group of space-time 79−2603
thermal states, KMS states, of vector meson model in two dimens. space time 77−5987
time and space structures conference on quantum theory, Starnberg, W.Germany (July 1978) 80−27044
time-asymptotic particle interpretation in the Friedman-de Sitter space 78−81720
time-dependent variational principle and effective action 79−63359
topological solitons and instantons 79−12924
tunnelling decay, classically stable state, local potential minimum 78−16693
two-dimens. quantum kinks, spin and statistics 77−49841
two-dimensional pre-Schwinger model, operator soln. in asymptotic fields 78−29237
ultralocal quantum fields, symmetries 77−65076
ultralocal static field theory with imaginary bare mass 78−8499
unitarity and causality eqns., remarks on solns. 77−9917
unitarity and causality eqns. soln. 79−40413
unstable particles, vacuum structure 77−54041
unstable particles description in quantum field theory, S-matrix poles 77−6024
vacuum energy in two-dimens. curved space-times 77−30239
vacuum instability, appl. to Goldstone and Weinberg models 77−65107
vacuum instability 78−41419
vacuum states in static space-times with horizons 77−57243
vector spherical harmonics of unit hyperboloid in Minkowski space 78−32732

quantum field theory continued
vertex functions of chronological exponential, renormalised system of equations 79−30661
von Neumann's theorem, generalisation to irreproducible meas. in field theory *(Russian)* 78−62115
von Neumann's theorem on irreproducible measurements, generalisation *(Russian)* 78−73888
von Neumann algebra, unbounded derivations and invariant states 78−45456
von Neumann theorem, generalisation to irreproducible meas. 80−62862
von Neumanns theorem for irreducible measurement 80−91007
Ward-like identities in canonical field theory 77−67562
Wess-Zumino model as linear σ-model of spontaneously broken conformal and OSp(1,4) supersymmetries *(Russian)* 79−93315
Weyl's m-coefficient in a B*-algebra 79−63374
Weyl neutrino, translation props. 79−63392
Weyl theory, position operator written in terms of Dirac matrices 78−58123
Wick-Cutkosky model, eigenvalue refl. symmetry 77−61193
Wigner representation, gauge invariant, electrodynamics of scalar particles 78−29251
Wilson expansions using counterterm technique 77−71241
Yukawa$_2$ field theory construction with large external field 77−57440
zero eigenvalues for quantum fluctuations, instanton, spontaneous breakdown of conformal symm. 78−12821
zero-point energy of fields in finite volume 77−13867
Zwanzigers local Lagrangian quantum field theory, electric and mag. charge, Lorentz invariance 79−6286
$B\bar{B}$ narrow states in QCD 77−57494
$\eta \to \pi^0\gamma\gamma$ decay width and processes in chiral QFT *(Russian)* 80−32099
ψ and ψ' decays violating Zweig lizuka rule, asymptotic freedom phenomenology 78−451
^{209}Bi, effect of pairing modes in multiplet struct. 78−12973
^{3}He-^{4}He mixtures, tri-critical phenomena, Callan Symanzik study of $\lambda\phi_3{}^4+g\phi_3{}^6$ theory 77−35788

quantum field theory of elastic scattering
see also elementary particle scattering; relativistic scattering theory
3→3 forward amplitude, analytic struct. determ. 79−30296
σ models, nonlinear, soft mass renormalisation of 1/N expansion 80−47164
't Hooft electromagnetic tensor for Higgs fields of arbitrary isospin 80−68364
Abelian Higgs model in 2-dimens., confinement and massless fermions 79−22047
Abelian Higgs models, disorder parameter approach 80−27411
amplitudes for fermion exchange processes in nonAbelian gauge theories *(Russian)* 77−61204
analytic struct., of distribs. and essential support theory 77−10191
asymptotic bounds on derivatives of elast. scatt. amplitudes 78−12892
asymptotic conditions, field and Hamiltonian props. 80−13222
asymptotic expansions in motion of two electrons in nuclear field 78−66459
Ball-Zachariasen model of diffractive scattering, numerical soln. near singularity of Frechet derivative 80−9158
Bethe-Salpeter, eqn. exact three dimens. reduction, off mass shell amplitudes 78−70247
bilinear Bose Hamiltonian diagonalisation, Heisenberg field asymptotic behaviour 80−47201
binary $q\bar{q}$ system and local field 80−47244
bounds on scatt. amplitudes and form factors 77−13878
causality, generalized integral condition for S-matrix, reln. to algebraic approach 78−37150
charged particle scattering by mag. monopoles, SO(3), gauge theory 77−13907
chiral invariance for asymptotic momenta, elastic scatt. of hadrons, helicity amplitudes 78−4800
Chou-Yang model and s-channel helicity conservation 79−63449
classical and prequantised field theories, analyticity of scattering operator 80−73611
Coulomb scattering, Lee-Nauenberg theorem analysis 78−54595
cut-off potential, asymptotic energy behaviour of Green function 80−27165
differential scatt. cross section, influence of amplitude singularities 78−49984
diffraction peak width, upper bound derivation 78−12831
Dirac quantum field, scatt. automorphisms, external field perturbations 78−58112
dispersion relations with two substractions in frames of field localisable theories *(Russian)* 78−41433
divergent perturbation and partial wave expansions in scatt. theory, summation methods 79−67485
dynamical impact parameter in quantum theory 79−21982
Dyson-Jost-Lehmann representation, scaling for large-angle scatt. 77−67580
elastic scattering, Sommerfeld poles and backward peaks 78−21357
electron+monopole, scatt. through small angles, Dirac-Schwinger monopole 80−68398
electron-molecule scatt., adiabatic nuclei theory 79−45846
EM and gravitational two-particle potentials, fourth order, from scattering operator 80−73598
Federbush model, absence of induced counterterms e^+e^- scatt. amplitudes 78−50023
Federbush model, perturbation theory, induced interaction terms 77−13853
finite nonpolynomial field theories, renormalisation group, scatt. amplitudes 78−16901
functional S-matrix, unitarity and causality in renormalised QFT 78−4793
geometrical unification of gauge and Higgs fields 80−99077
Ginzburg-Landau equations, N-vortex solutions, Higgs field 80−82863
Haag-Ruelle scattering theory as scattering theory in different state spaces 80−4593
hadrons on Regge trajectory, ϕ^3 interaction, bootstrap and quark interpretation 77−54046
Higgs and gauge fields, group actions on principle bundles and dimensional reduction 80−105770
Higgs coupling constraints from axionatics, Weinberg-Salam model Higgs extension 79−40706
Huyghen's principle, quantum field theory version, appl. to massless particle scatt. *(German)* 78−70017

quantum field theory of elastic scattering continued
impact parameter expansion of scalar and Dirac fields 77−26471
impact-parameter group, realisation on cone functions *(Russian)* 78−45817
instantons and vacuum tunnelling, canonical formalism in $(1+1)_\varepsilon$dimens. Higgs model 79−63348
interactions with strong cutoff, asymptotic fields algebra, scatt. operator 77−61198
inverse scattering problem 78−363
left-right symmetric model from general horizontal symmetry, Cabibbo angle, CP violation 80−101972
local relativistic quantum field theory, additive conservation laws 80−22507
Low eqn. multiple scatt. effects of π-nucleus 77−41998
many boson non-relativistic systems, classical field limit of scatt. theory 79−80501
mass divergences of wide angle scatt. amplitudes 79−49402
mass shell applications of renormalisation group with arbitrary interpolating fields 77−13879
massive Thirring model, quantized renormalized, dynamical charges, soliton, antisoliton, breather states 77−18171
massless limit in the ladder approximation 79−21953
multichannel potential scattering theory with permanently confined channels, quark model appls. 77−13634
neutron matter-quark matter phase transition, QCD and extended Higgs model, instantons 80−91062
non-Abelian gauge theories, Born helicity amplitudes and cross-sections 77−2777
non-Abelian gauge theory of strong interactions, EM current renormalisation 79−63350
nuclear elastic scatt. with optical potential, complex angular momentum methods, poles and zeros of S-matrix, REGGE 80−47445
overlapping function and scatt. amplitude phase connection *(Russian)* 78−41431
path integral representation of QFT for S-matrix, meson field-nucleon field interaction 79−2947
Pomeranchuk-type theorems for total and elastic cross sections 79−21972
reggeization of vector mesons for non-Abelian theories with arbitrary symmetry 77−2740
Reggeon field theory, ordered phase, Hamiltonian formulation, scatt. amplitude calc. 78−4807
renormalisation group method, upper bound on total cross section 77−18177
S-matrix and Yang-Feldman relations 77−30276
S-matrix asymptotic perturbation expansion, time ordered functions in relativistic theory 77−6039
S-matrix for interacting extended boson fields, scatt. amplitude, self energy 78−66047
scalar quantum field in an external gauge field 79−97489
scaling property of shrinking diffraction peaks, elastic unpolarised differential cross section 77−18206
scattering amplitude at high energies on power type singular potl. 77−30053
scattering amplitude zeros 79−21983
sine-Gordon N-soliton quantum scatt. 77−34084
soliton-soliton scattering amplitudes, three dimens., semi-classical approx. 79−49091
solitonlike fields, gauge phase factor operators, extended Higgs models and 't Hooft algebra 80−42324
space-dispersion approach to the explanation of the Higgs-mechanism 80−90975
spinless particle scatt. by medium, elimination of divergencies, Lippmann-Schwinger eqn. 78−62320
strong coupling theory, scatt. on nonrelativistic particle 79−40675
SU_2 Yang Mills theory, high energy scatt. amps. 79−63346
supergravity, super Higgs effect, gravitino masses and couplings 80−62562
symmetry scalar theory in strong coupling limit, Bogolyubov transformation method 77−49862
tachyons and virtual fields elementary particle strong interactions 79−12970
total cross sections, upper bound 78−12839
two particle system, interaction through action-at-a-distance force, relativistic mechs. 78−66055
unitary bounds on elastic absorptive parts in terms of diffraction peak width 77−54092
vector boson elast. scatt., Lorentz covariant scatt. amplitude and Compton scatt. 77−2776
Yang-Mills fields, finite-diagram theory, sixth-order scatt. amplitudes 80−73585
Z_2 lattice gauge Higgs theories, Monte-Carlo calcs. 80−86593
ed elastic scatt. at high momentum transfer 80−82977
$\gamma NN \rightarrow \gamma NN$ forward scatt. amplitude and generalised optical theorem, dispersion relations 79−93446
hh scattering, geometrical model for scatt. at ultrahigh energies, existence of dips 79−89191
$\bar{\nu}_\mu e^- \rightarrow \nu_e \mu^-$, exotic lepton number violation and neutrino Majorana masses, Higgs sector 80−86615
pp elastic scattering, 14 to 2000 GeV/c, improved impact picture 79−89178
pp elastic scattering, eikonal model, energy depend. anal. 20 to 60 GeV 79−89190
pp scatt., high energy, impact picture for polarisation and rotation parameter 78−70341
πN scattering amplitude at high energy in localisable quantum field theory *(Russian)* 77−74603
πNN vertex operator for πN elastic scatt. phase shift calcs. 77−54118
$\pi\pi$ phase shifts, nonlinear σ model Pade calcs. 78−8695
$q\bar{q}$ binary confined systems, elastic scatt. amplitudes 79−97576

quantum field theory of gravitation
see also elementary particle gravitational interactions; gravitons; supergravity
$2+\varepsilon$ dimens. quantum gravity, one loop counterterms and asymptotic freedom, β function 79−9173
$\lambda\phi^4$, momentum space renormalisation in curved space time 80−37158
$\lambda\phi^4$ field theory, renormalisation in curved space-time 80−42320
$\lambda\phi^4$ field theory renormalisation in curved space-time 80−42319
σ-model, nonlinear, supersymmetric, Ricci-flat Kahler manifolds and supersymmetry 80−90994

quantum field theory of gravitation continued
Abelian Higgs and Goldstone models, no-hair theorems for black holes 79−17016
action integrals and partition functions, Kerr-Newman and de Sitter examples 77−64984
advances and significance of quantum theory of gravity 79−93028
anisotropic cosmological solutions in the theory with quadratic invariants *(Russian)* 77−91673
antenna sensitivity, quantum mech. anal. *(Russian)* 79−75436
antisymmetric tensor fields coupled to gravity, renormalisability 80−90765
Arnowitt-Deser-Misner quantisation of metrics with two parameter isometry groups 77−45779
arnowitt-deser-misner quantization of metrics with at-least-two-parameter isometry groups 77−45779
asymptotic field theory and non-abelian gauge theories 77−22653
asymptotic field theory approach to gravit. quantisation 77−22653
asymptotically flat quantum grav. field, spin $^1/_2$ 80−68121
axial and conformal anomalies for arbitrary spin in gravity and supergravity 78−70040
axial anomaly and boundary terms for general spinor fields 79−63122
axial anomaly for Majorana spin 3/2 loop with external gravitons in supergravity 78−8580
axial superfield and the supergravity group *(Russian)* 79−17319
axial vector anomaly and index theorem 78−29293
axisymmetric gravitational problem, chiral connection with ferromagnetism and SU(2) vacuum gauge field 78−70258
back reaction of quantised field in gauge treatment of gravity 78−16711
background curved space-time in indefinite metric QFT 79−85049
baryon number generation mechanism in expanding universe 80−51931
Becchi-Rouet-Stora transform. for gravitational field 78−93590
Belavin Yang-Mills pseudoparticle soln., metric representation, isotropic Universe relation 80−27404
Bertotti-Robinson metric, pair production, semi-classical treatment 79−2702
Bianchi IX metrics, self-dual asymptotically Euclidean, quantum gravity 78−65857
Bianchi type I anisotropic universe, quantum gravitational effects *(Russian)* 78−24588
Bianchi type I universe, quantized scalar field 78−4549
Birkhoff's theorem andDunn theory of gravitation 80−42132
Birkhoff theorems for $R+R^2$ gravity theories with torsion 80−82705
black hole, generation of pairs by collapsing body *(Russian)* 77−13234
black hole, quantum gravitational fluctuations, energy dissipation mechanism 78−57572
black hole+heat bath, thermal equilib. possibility, thermal Green functions 78−12275
black hole formation by collapsing cloud of quantal particles 79−2552
black holes, gravitation, charges, cosmology and coherence, elementary particles and Dirac large numbers 79−2477
black holes, quantum processes, especially Hawking thermodynamic emission process 78−12284
black holes, quantum vacuum effects rel. to fall into another universe 78−32748
black holes, small, quantum mechanical approach 78−16453
black holes, unpredictability 78−54277
black holes of strong gravity, identification with elementary particles 78−16973
black-hole, Kerr-Newman, quantised massless field, instability 80−82409
Bogoliubov transformations, propagators, and the Hawking effect 79−2698
Bondi-Metzner-Sachs group, lifting of projective representations 78−21028
boson field, equal-time commutator, general relativity, indefinite-metric 80−68119
broken symmetric theory, unified gauge field breaking 79−30343
canonical commutation relations anal., BRS transform. 79−12700
canonical many-time quantisation of gravitation 78−8328
canonical quantisation of gauge fields, gravitational field *(Chinese)* 80−22266
canonical quantisation of gravity, QFT in curved spacetime, Bianchi I cosmology 80−27202
causal unification of relativity, gravitation and quantum mechs. 77−33923
causality in homogeneous spaces 79−2699
charge quantisation in curved spacetime, Kaluza-Klein background, Mandelstram field 79−2695
charge renormalisation constant in quantum gravity near two dimens. 78−41222
chirally extended supergravity, Maxwell-Einstein supergravity, auxiliary field struct. 78−78126
chronos principle and interactions of fields of spin 0 and 1 78−8286
classical and quantum gravitational collapse, torsion, wave field, cosmology *(Russian)* 78−53815
classical and quantum gravitational collapse *(Russian)* 78−49311
classical and quantum gravitational collapse *(Russian)* 79−9039
classical pseudoparticle solutions in general relativity 78−89390
Clifford-Klein space times, effective Lagrangian and vac. stress-energy tensor 79−2674
coherent beam interference, phase shift in gauge and grav. fields 80−4627
collapse, quantum uncertainty in final state 77−82433
collapsing shell, Schwarzschild-de Sitter space-time, thermodynamics and radiation 80−17607
collective phenomena of fermion-antifermion pairs 79−12687
commutation relations in vierbein formalism 80−27205
complex line bundles 78−49732
complex pp waves and the nonlinear graviton construction 79−130
composite model of the graviton 79−35621
conformal and gauge spontaneous symm. breaking, cosmology quantum effects 80−37185
conformal and superconformal gravity and non-linear representations 79−17308
conformal anomalies, observations 77−74298
conformal anomalies, off-mass-shell corrections 78−32749
conformal anomalies and Hawking effect, gravit. instantons, asymptotic freedom 77−74298
conformal gravity in SO(4,2) gauge *(Chinese)* 79−93027
conformal invariance and asymptotic freedom in quantum gravity, renormalisation group anal. 78−86213
conformal invariance in quantum gravity 77−17896

quantum field theory of gravitation continued
conformal supergravity, superconformal group, nonlinear representation 79−12695
conformally, related space times, field theories, global considerations 79−67473
conformally flat space, strong gravity field coupled to SO(3) gauge field 80−62563
constraints, Hermiticity, and correspondence 79−71344
contact interactions in the Einstein and Einstein-Cartan-Sciama-Kibble (ECSK) theories 77−5719
cosmic gravitational radiation having the characteristics of noise *(Russian)* 79−12551
cosmical coherent avalanche catastrophes 78−85844
cosmological constant, time dependent 79−88865
cosmological evolution, homogeneous anisotropic models 77−17735
cosmological models and quantum effects *(Russian)* 80−27206
cosmology, anisotropic solns. in theory with quadratic invariants *(Russian)* 77−91673
cosmology, effective Lagrangian and pair prod. 80−22123
cosmology, quantum effects, black and white holes 78−12441
cosmology pair creation in presence of EM fields 80−41924
coupling of O(2) supergravity with vector multiplets, Yang Mills field appl. 78−33020
covariant CP^2 non-linear σ-model, classical solns. 79−54020
covariant quantisation of gravitation 78−8327
CP^2 properties compared with SU(2) Yang-Mills instanton, gravit. instanton 78−81909
CP^2 vierbien singularities in half integral spin fields with EM background 80−73572
current trends in the theory of fields, conf., Tallahassee, Florida, 6-7 April 1978 79−12923
de Sitter gauge theory for gravitation *(Chinese)* 79−80487
de Sitter gauge theory of gravitation 79−97285
de Sitter space, renormalisation by point-splitting 78−29035
decoupling of fields from escaping sources in a de Sitter universe 79−12698
development, book contrib. 80−22267
differential geometry methods in gauge and gravitational theories 80−90768
dimensionally reduced quantum gravity, one-loop counterterms 80−86193
Dirac's constraints, geometric approach *(Italian)* 78−21044
Dirac fields in Riemannian space time, geom. props. 79−75430
Dirac fields in Riemannian space-time, geom. props. 79−75431
Dirac particle creation in Einstein-Cartan-Sciama-Kibble theory 80−4622
Dirac quanta detection in Rindler and black hole space times, ξ quantisation scheme 80−31651
discrete space structure dynamics 80−52392
dual spinor model, low energy region, supersymm. Yang-Mills theory, supergravity theory 77−49923
dualism of field and matter in the general theory of relativity *(German)* 80−90748
duality of gravitation in the quantization problem 79−30344
dust ball, nonsingular collapse in quantum conformal geometry 79−97284
dynamical affine symmetries and covariant perturbation theory 77−49661
dynamical affine symmetry and covariant perturbation theory *(Russian)* 77−49661
dynamical affine symmetry and renormalisation in gravity 79−85048
early Universe, gauge theories, grav. constant time depend. and antigravity 80−90591
ECSK theory, fibre bundle struct. 77−37799
Eguchi Hanson metric equivalence to Gibbons Hawking metric 79−58612
Eguchi-Hanson instanton, TP inversion in quantum gravity, appl. to scatt. theory 79−58613
Einstein's gravitation field quantisation procedure avoiding path-integral formalism 77−13863
Einstein's impact on theoretical physics 80−77677
Einstein's theories extended, book 80−22164
Einstein's unified field theory, field equations soln. for H-atom space-time struct. 79−21634
Einstein action of Riemannian metrics, rel. to quantum gravity and thermodynamics 77−45778
Einstein action of riemannian metrics and its relation to quantum gravity and thermodynamics 77−45778
Einstein field equations, covariant splitting, spherical symmetry models *(German)* 79−21616
Einstein relativistic particles, construction of quantal theories, appl. to two particle system 78−62347
Einstein theory, unitarity, gauge invariance test 77−13673
Einstein theory of gravity, quantized, test of gauge invariance and unitarity 77−13673
Einstein vacuum and Einstein-Maxwell space-times, infinitesimal holonomy group structure and geometrization 80−73252
Einstein-Cartan theory, with anticommuting variables, quantisation in Diracs Hamiltonian formalism 79−93017
Einstein-Cartan theory in the spin coefficient formalism 80−101742
Einstein-Klein-Gordon equations, Killing field vectors, theorem *(French)* 79−30340
Einstein-Klein-Gordon equations in stationary axially symmetric space-time *(French)* 79−25921
Einstein-Maxwell equations: gauge formulation and solutions for radiating bodies *(German)* 80−27194
Einstein-Schrodinger eqn. of quantum gravity, soln. by linear approx. 77−60997
Einstein-Yang-Mills pseudoparticles and electric charge quantization of dyon black hole 79−12703
Einstein-Yang-Mills system, Feynman-quantised, null-gauge functional measures 79−12702
Einstein-Yang-Mills system in six dimensions, static solution 80−8883
Einsteinian manifold, quantisation of gravitation 78−54254
electrogravitational conversion cross sections in static EM background fields 78−24711
electrons and gravitational instantons 79−25961
electrostatic potential in gravitational field 78−54270
elementary particle theory, mathematical method, conf., Liblice, Czechoslovakia (June 1978) 79−21891
quantum field theory of gravitation continued
EM and gravitational two-particle potentials, fourth order, from scattering operator 80−73598
EM fields in space-times with local rotational symmetry 80−82694
EM phenomena induced by weak grav. fields, possible gravitational wave detector 80−82692
embedding classical fields in quantum field theory 78−54223
energy density commutator for massless spin 3/2 field in covariant gauge 79−71335
energy momentum tensor of massless scalar quantum field in Robertson-Walker universe 78−12635
energy-momentum tensor vac. expectation values, depend. on manifold geom. and topology 80−355
equivalence principle, stress tensor, and long-range 77−13676
equivalence principle, stress tensor, long-range behaviour of gravitational interactions 77−13676
equivalence principle, test using neutron elec. dipole moment 77−57265
equivalence theorem, validity in nonperturbative context 79−26214
Euclidean gravity, asymptotically flat self-dual solns. 78−45834
expanding universes, positive frequency and Hamiltonians 80−4624
experimental tests for quantum effects 77−87684
experimental tests of quantum effects in gravit. 77−87684
extended inertial frames, de Sitter space, projective relativity, quantisation on curved manifold 80−90764
extended supergravity, eqns. of motion in terms of geometrical quantities in superspace 78−65856
extended supergravity, higher order invariants in Riemann curvature tensor 79−35614
extended supergravity, three loop counterterms, nonrenormalisability 78−65854
f-g fields, class relevant to quark confinement 80−125
fermion pairs created near Friedman singularity, energy and pressure *(Russian)* 77−57114
fermionic Goldstone-Higgs effect in (2+1) dimens. supergravity 78−29291
Feynman diagrams, dimensionally regularised, symbolic evaluation, quantum gravity application 80−13259
fictitious-particle vertex in quantum gravity 78−24720
field equations of fourth order and supersymmetry 79−12674
field quantisation, the necessity 77−26220
field theory approach 77−60998
Fierz-Pauli program for spin-2 fields in de Sitter space 79−21637
Finsler spaces, physical aspects underlying the field theory 80−101745
flat space as a gravitational instanton 79−17661
flat superspace with supertorsion, supergravity, quantisation, renormalisable theory 79−2705
formalism, using vector field 78−89385
fractional winding numbers and surface effects 78−8579
free gravitational field quantisation 80−90767
free relativistic field in curved space, quantisation *(French)* 79−30639
Friedmann cosmological model, explicit canonical quantisation 79−21644
Friedmann model, quantum effects 77−79025
functional measure 77−45780
functional measure for quantum gravity 77−45780
functional measure for quantum gravity in light-cone gauge 78−73914
gauge conditions for quantum gravity 77−87682
gauge conditions in quantum gravity 77−87682
gauge field theories 79−80493
gauge field theory, renormalisable, cosmological implications 79−44839
gauge field theory formulation in quantum field theory framework 79−21908
gauge fields resulting from compact internal symmetry groups 80−95022
gauge formulations, relationship to Riemannian holonomy struct. 80−42131
gauge symmetry, max. 4-dimens., and general covariance, implications 79−63115
gauge theories, facts and prospects, conf., Schladming, Austria (Feb.-Mar. 1978) 79−26203
gauge theories of gravitation 79−26209
gauge theory of conformal and superconformal group 77−74300
gauge theory of gravity and supergravity on a group manifold 79−21635
gauge theory with alternative to black holes 80−57168
gauge theory with no black holes 80−82702
Gauss-Bonnet and Bianchi identities in Riemann-Cartan type gravitational theories 80−86190
general covariance group, unitary representations 79−21970
general relativity, indefinite metric quantum field theory, Poincare generators 79−35618
general relativity, path-integral formulation, DeWitt-Morette measures 78−123
general relativity, quantum mechanical one-particle state, interfering neutron beam expt. 80−95025
general relativity, quantum version, spin-spin contact interactions, comparison with Einstein-Cartan-Sciama-Kibble theory 77−5719
general relativity, SL(2,C)Yang-Mills field theory description, in curved twistor space 79−21602
general relativity, symmetry aspects 78−62139
general relativity, vierbein formalism 80−22263
general relativity and field theory approach to gravitation 78−81910
general relativity as a generalized Hamiltonian system 80−31650
general relativity conference, Trieste, Italy, 1975, July 78−8285
general Taub-NUT-De Sitter metric, self-dual Yang-Mills soln. of gravity 80−46946
general-relativistic and gauge field theories 78−86212
generalised gravitation theory, with electromagnetism, derivation of conservation laws 79−49146
generalised spin structure 78−29036
geometric gravity Lagrangian, SP(4) and general coord. transforms. 78−70039
geometric quantisation and general relativity 78−8288
geometric quantisation and internal symm. in gravit. 77−79022
geometric quantization and internal symmetry 77−79022
geometrical gauge theory of gravit., strong interactions, EM interactions 78−70041
geometrodynamics, knot wormholes 77−67612
geometry, gravity and dual strings 77−18242
geometry and quantisation 77−33924
geometry and quantization 77−33924
geometry of first-quantized theories 77−37799
ghost free axial gauge, infrared gravitons 79−67214
Gordon decomposition and tidal interaction 78−8324

quantum field theory of gravitation continued
Goto-Imamura difficulty, resolution without Schwinger term 80−86191
Gowdy universes, particle creation 80−56990
graded orthosymplectic group $OSp_{8;1}$ and fundamental fermionic twistor variables 79−35617
graded spin extension of the algebra of vol. preserving deformation 78−65855
gravitation as gauge theory of Poincare group 80−86189
gravitational bubbles, radiative corrections to covariant massless quartically self-interacting meson theory 80−62826
gravitational charge of uniton-quark 79−63400
gravitational collapse, classical and quantum problems *(Russian)* 77−56822
gravitational collapse, classical and quantum problems *(Russian)* 77−87258
gravitational collapse, final state, quantum uncertainty 77−82433
gravitational creation of odd numbers of fermions 80−32048
gravitational field, thermodynamic comments 79−2701
gravitational field gauge theories, review 80−98848
gravitational field stochastic fluctuations 79−44837
gravitational field with torsion, renormalisation *(Chinese)* 79−93026
gravitational index theorems and super theorems 79−75432
gravitational instanton contribution to spin 3/2 axial anomaly 79−17321
gravitational instanton symmetries, classification 79−63110
gravitational instantons and their interactions 80−90766
gravitational instantons and universal spin structs. 78−78128
gravitational interaction, spin, rotation and quantum effects, review 80−37203
gravitational monopoles, path depend. approach for Einstein's eqn. 80−77682
gravitational multi-instanton scalar fields, Greens functions 79−85050
gravitational multi-instantons 79−2693
gravitational radiative corrections as the origin of spontaneous symmetry breaking 80−86192
gravitational solitons 79−44838
gravitational trace anomaly renormalisation in QED 80−57532
gravitational waves detector, appl. of photon-graviton resonance, technical problems, expt. possibilities 78−73905
gravitational-field equation for quantum gravity 80−124
gravitationally induced CP effects, quantum gravidynamics, QCD quark sector 80−86616
gravitino, axial current anomaly, Faddeev-Popov ghosts 80−68120
graviton, impossibility of non-zero rest mass 80−95023
graviton creation in isotropically expanding Universes 78−16588
graviton loop calc. in general gauge 80−27204
graviton production in the early Universe, effective pot. approach 78−24587
graviton scatt. amplitude, gauge invariance 80−82700
graviton self-energy, general gauge calc. 79−133
graviton-graviton scatt., one loop scalar field contrib. and helicity nonconservation 80−52114
graviton-matter interaction, Zitterbewegung interpretation 80−122
gravitons, Einstein eqn. soln., on nonsingular positive definite metric 79−49150
gravitons, exact masslessness from quantum gravity canonical formalism 79−80492
gravitons, trace anomaly 79−2709
gravitons from a spinning rod 78−62137
gravitons in Minkoswki space-time, review 77−87683
gravitons in Minkowski space-time 77−87683
gravitons photoproduction in a static mag. dipole field due to currents 78−62138
gravity and spin 1 gauge fields 79−21923
gravity as a Goldstone field in the Lorentz gauge theory 80−31655
gravity as Hilbert space of quantised system 80−52113
gravity Lagrangian with ghost-free curvature-squared terms 79−21640
Green's exponential functions, chiral and gravitational 79−97490
H-spaces, gravitational instantons, spin coeff. method 80−31654
hadron strong interactions, theory from general relativity 79−49143
hadrons' band-spinor representations GL(N,R), gravitational interaction 78−50000
Hawking particles produced by black hole evaporation Higgs particles 79−2553
Hawking radiation and strong gravity black holes 79−67213
hidden ghosts in antisymmetric tensor gauge fields coupled to gravity 80−82889
Higgs effect, supergravity and supersymm. massless QED 78−29268
Higgs mechanism in (1+1) supergravity 78−74199
Higgs scalar effects on gravity, Nambu Jona Lasinio type model 78−41467
high energy stability and renormalisability of gravitation, Einstein Lagrangian supplement 79−25935
high-energy gravity and the very early universe 80−98847
higher spin fields in curved space-time 78−62140
indefinite metric quantum field theory of general relativity 78−65853
indefinite metric quantum gravitation theory, subsidiary conditions and physical S-matrix unitarity 79−9171
indefinite metric theory, supplementary remarks 80−42133
indefinite-metric QFT of general relativity 78−89391
indefiniteness of gravitational action, path integrals convergence, one-loop approx. 78−70318
index theorem boundary terms for gravitational instantons 80−123
infinite conservation laws for EM and asymptotic gravitational fields 79−21613
instantons, gravitational, flavour currents of QCD, Green's functions, foam-like structure of space-time 80−62825
instantons, gravitational, self-dual soln. to Euclidean gravity 80−68118
integral relations for invariants constructed from three riemann tensors 77−30074
internal rotations of spinning particles 79−22011
invariant states, quantised gravitational perturbations 79−136
isotropic closed universe, quantised scalar field formulae 79−12550
isotropic universe, particle creation and vacuum polarisation, cosmological models 80−90582
isotropic Universe, quantum gravitational effects, spontaneous particle production *(Russian)* 80−94711
K3 gravitational instanton, physical interpretation 79−17320
Kerr-Schild's gravitational fields, quantisation 80−31653
Killing vectors in gauge supersymmetry 79−131
Klein Gordon field, covariant, in external fields, quantisation, stationary case 1-particle struct. 78−89389

quantum field theory of gravitation continued
Klein paradox and vacuum polarization 78−8329
Klein-Gordon system, gravit. equilib. 78−24719
knot wormholes in quantum geometrodynamics 77−67612
Lagrangian field theories of gravitation without gauge invariance to first order 79−63121
lagrangian for general relativity in presence of a quantized scalar field 77−45762
Lagrangian for general relativity with quantised scalar field 77−45762
Lagrangian formalisms in scalar pregeometry, quantum mechanical equivalence 79−54024
Lagrangian formulation, conservation laws, relativistic gravitation *(Russian)* 80−68337
lattice massive dual fields for gravity 80−105779
Lie algebras, BRS transform. 78−93591
linear zero-spin fields in external gravit. and scalar fields, perturbation theory 80−31969
linearised gravitational pot., Euclidean and Minkowski space formulations 80−121
linearized Einstein theory, twistors, plane fronted impulse wave backgrounds 79−30329
local structure of functional spaces and dynamical variables of gauge-invariant fields 80−9099
locally flat space-time, quantised metric, spontaneous dilatation asymm. 78−16713
lorentz gauge invariant vacuum functionals for quantized spinor fields in non-simply connected space-times 79−89061
Lorentzian gravity, appl. to hadron struct. and galaxy clusters 79−97288
Lorentzian manifold, Kahler-metrics 80−73251
mach principle and the quantal response of the Universe 79−12549
Mansouri-Chang gauge theory of gravitation, comparison with general relativity 78−36919
mass-zero spin-two particles, covariant quantum field theories 79−17322
masses from extra dimensions 79−71332
massive quantum field theory in two-dimensional Robertson-Walker space-time 79−25962
massive scalar multiplet coupling to supergravity, generalisation 78−82137
massive supergravity, from spontaneous breaking orthosymplectic gauge symmetry 78−77787
massive supergravity nonlinear realisation of orthosymplectic gauge symm., coupling to spin 1/2 spin 1 multiplet 78−33019
massive vector multiplet coupled to supergravity 80−17855
massless and massive spin 3/2 field in general covariant gauges, canonical quantisation 79−71334
massless boson fields, group theory 77−34098
massless conformal quantum fields in hyperbolic universes, stress tensor vacuum expectation value 79−2708
massless fields in asymptotically flat space-time, null surface quantisation and quantum theory 80−4625
massless quantum fields in curved asymptotically flat space-time, particle creation near black hole *(Russian)* 78−57846
massless spin 3/2 field, covariant canonical quantisation in general covariant gauges 79−40440
massless spin 3/2 field, irreducibility 79−35620
massless Thirring model is curved space, black holes, thermal states, conformal anomaly 79−26221
matrix, superpropagators, asymptotic behaviour 78−54276
matter couplings in supergravity theory 77−17895
matter-antimatter accounting, thermodynamics, and black-hole radiation 79−49136
Maxwell equations, in Minkowski space-time and Poincare group 79−30301
methods in field theory 77−57457
Minkowski space, conformal geometry, hyperbolic world lines 80−57167
mixing of weak and gravit. interactions, massive gravitino 78−8578
momentum space techniques for curved space-time quantum field theory 79−71341
monopole solutions for strong gravity coupled to SO(3) gauge fields 80−4621
moving mirror effects, back-reaction 80−46944
mutually interacting Bose fields, external potential problems, geometrical approach 80−101744
N=1 supergravity, chiral invariance in four dimensions 79−40441
N=2 extended supersymmetry, Noether current multiplets, extended supergravity 79−40438
N=2 supergravity with gauged central charge 78−62349
n=4 supergravity theory with local SU(2)×SU(2) invariance 78−66067
N=8 supergravity theory, lagrangian 79−17311
neutrino, Maxwell, and scalar fields in the cylindrical magnetic or plasm universe 80−120
non-distinguishable field and space variables in QFT, supergravity appl. 80−98845
non-inertial framed space-time configurations, gauge theory appl. 80−22262
non-integral gauge theories 79−12675
nonlinear EM effects induced by vacuum polarisation and gravitational interaction, a comparison 79−97544
nonlinear gauge fields and the structure of gravity and supergravity theories 78−77791
nonlinear graviton unprimed spinor description 80−8892
nonlinear graviton-photon interaction in Einstein-Maxwell space-time 79−30338
nonlinear Heisenberg-Klein-Gordon equation, localised solns. in flat Schwarzschild space-time 80−4620
nonlinear realisation of general covariance group, massless tensor graviton and massive vector tordion 79−54030
nonlinear spinor theory, gravit. interaction *(Russian)* 77−79023
nonlinear spinor theory, gravitational interaction 77−79023
nonlinearity, Newton constant's role 80−90761
nonlocal field theory and space-time quantization 77−34078
nonlocal properties of fermionic matter in strong gravitational fields 79−26210
nonlocalisation, connection with geometrical theory of gauge fields 80−82696
nonrenormalisability, one-loop divergences 80−4626
normal flat space-time, embedding hadronic microuniverses 80−9135
null surface quantization and quantum field theory in asymptotically flat space-time *(German)* 79−25959
observability differences between classical EM and gravitational gauge fields 80−36925

quantum field theory of gravitation continued
one loop finiteness of quantum gravity off mass shell 78−62142
one-dimensional gravitational gas, ground state energy 77−5757
one-dimensional gravitational gas' estimate of ground state energy 77−5757
one-loop counter terms, system with derivative couplings to fermions 79−249
pair production by collapsing body *(Russian)* 77−13234
pair production by gravitational waves in the field of a black hole 77−22474
pairing model, dynamical method for generating gravit. 78−70042
particle creation and geometry 78−12442
particle creation by black hole due to Casimir effect 79−35607
particle creation by time depend. elec. and gravitational fields 80−4623
particle creation by time-depend. gravitational field, quantum equivalence principle 80−41925
particle creation in curved space-time, covariant treatment 78−12443
particle creation in curved spaces 77−13857
particle creations in the pseudoparticle gravitational fields 79−2704
particle emission rates from nonrotating black hole 78−24718
particle propagation in spacetime foam 79−93029
partition function for two-dimensional solitons 79−6039
path integral quantisation and cosmological particle prod. 78−12440
Pauli-Villars regularisation trace anomalies 78−45548
PCAC, dimensional derivation of gravitational correction 78−21371
perihelion anomaly 77−22473
perturbation theory anal. of gravit. collapse *(Russian)* 77−87258
Petrov's type III, N and O solutions, renormalisable theory, trapping of physical gravitons 80−31652
phenomenological ideas toward a field theory of matter, photons which satisfy Maxwell's eqns. for EM waves 80−378
phenomenological ideas toward a field theory of matter, unification of EM and gravity fields 80−378
photon gravitational interaction, QED corrections 77−65131
Planck energy nonconserving fluctuations and strong forces 80−57551
plane wave Einstein-Maxwell space-times, soln. of zero rest mass field eqns. 78−62140
Poincare gauge theory of gravitation, translational part of Lagrangian 79−2710
Poincare gauge theory of gravitation 79−75434
Poincare group gauge theory, geometric meaning, equivalence to Einstein-Cartan gravitation 80−62845
Poincare supergravity as broken superconformal gravity 78−62348
point splitting in curved space-time background 79−80491
positive action conjecture and asymptotically Euclidean metrics 79−58611
positive-action conjecture, failure for spacetimes with horizons 79−12701
positive-action conjecture, proof 79−30322
post-Newtonian approximation of the Poincare gauge theory of gravitation 80−52115
post-Newtonian charged n-body problem, centre of inertia and coord. transforms. 79−93025
pregeometry, gravity with composite metric 79−35619
probabilities of quantum processes in external gravit. fields 80−36932
projective geometry, Langrangian subspaces, and twistor theory 80−52112
projective geometry for polarisations 80−52053
pseudoinvariant gauge Lagrangians for Einstein gravity and supergravity 79−12680
pseudoparticles in higher rank gauge theories 77−45960
quadratic lagrangians in a space with torsion and the theory of the spinor gauge field 80−91006
quantisation method for gravitational field *(French)* 79−30341
quantisation of gravit. field 77−26220
quantised singularities in gravitational field 77−2595
quantization of gauge fields without the path-integral formalism 77−13863
quantized singularities in the gravitational field 77−2595
quantizing gravitational instantons 79−21639
quantum effects and evolution of cosmological models 77−17735
quantum field theory approach to gravitation 77−60998
quantum fluctuations near the classical space-time singularity 80−8893
quantum gravity, choral of symmetries in general relativity 80−105565
quantum gravity and path integrals, supersymmetric theory, virtual Planck-mass black holes 79−2706
quantum gravity and quark confinement 77−22681
quantum gravity and world topology 77−5729
quantum gravity on Wilson lattice, gauge invariant cutoff 79−30342
quantum linearization instabilities 79−44835
quantum mechanics and gravitation 79−12699
quantum numbers for Dirac spinor fields on a curved space-time 79−97277
quantum process probability in external gravitational fields, Green's function calcs. 80−36931
quantum stress energy in nearly conformally flat spacetimes 80−57170
quantum theory of gravitation 77−60998
quark confinement, event horizons around a particle surrounded by a static confinement potential 78−66075
quark confinement, unified theory of gravity and strong interactions 77−22681
quaternionic multi $S^4 \approx HP(1)$ gravitational and chiral instantons 80−31656
recursive calculation of axially symmetric stationary Einstein fields 80−77661
regularisation 77−49834
Reissner naked singularity 78−24990
Reissner-Nordstrom space, EM field of point discharge *(Russian)* 77−82432
Reissner-Nordstrom space, point discharge, E M field *(Russian)* 77−82432
renormalisable model of quantum gravity, higher derivative terms 78−77789
renormalisation and 1/N expansion, graviton propagator calc. 78−8320
renormalisation of gravit. constant, and fermion pair creation in nonstationary gravit. field *(Russian)* 79−17323
renormalisation of higher-derivative quantum gravity 78−8326
renormalisation of quantum gravit. without matter 77−37798
renormalised, evolution of anisotropic and homogeneous cosmological models 79−2703
renormalised quantum stress tensor calc. by adiabatic regularisation in Robertson-Walker space times 78−32747
quantum field theory of gravitation continued
renormalization of quantum field theory in curved space-time 77−49834
renormalization of quantum gravitation without matter 77−37798
Riemann tensor products, integral relations 77−30074
riemannian spaces with local duality and gravitational instantons 79−25938
right translation invariant metrics and variational principles on principal bundle, gauge theories *(Chinese)* 80−101743
Robertson Walker metric, pair prod., propagator method appl. 80−105564
Robertson Walker universes, quantised gravit. wave perturbations 78−12636
Robertson-Walker cosmologies, Kostant-Souriau quantisation 80−12838
Robertson-Walker metric, covariant point-splitting regularisation for scalar quantum field 77−82434
Robertson-Walker space-times, nonconformal renormalised stress tensors 78−65852
Robertson-Walker spacetime, vacuum expectation values, perturbation technique in curved space 79−97286
Robertson-Walker Universe, covariant point-splitting regularisation 77−82434
Robertson-Walker universe, pair-creation of particles 80−22265
Robertson-Walker universes, field interaction effects on particle creation 80−42130
Robertson-Walker universes, IR divergences 78−8323
Robertson-Walker universes, particle creation, self-interacting quantised fields 80−17699
rotating fluid, spontaneous symmetry breaking and bifurcations from the Maclaurin and Jacobi ellipsoids 79−35616
S wave kinks of Dirac-Weyl eqn. 78−29292
S-matrix existence in curved space time 79−63120
S-matrix for interaction of gravitational and Yang-Mills fields 80−42315
S-matrix theory, n-body potentials in QED and quantum gravity 78−24969
scalar field quantisation in anti-de Sitter space-time 79−21641
scalar fields, improved gravit. coupling 79−49151
scalar matter production, global effects in quantum cosmology 79−92903
scalar quantum field in an external gravitational field 80−31974
scale invariance in superspace 79−17313
Schwarzschild-de Sitter space-time vacuum energy-momentum tensor 80−52091
second order field equations for grav. field theory 80−27203
self-dual gauge fields and space-times 80−9108
self-duality in supergravity *(Russian)* 79−44831
semiclassical relativity, weak field limit 80−57169
semiclassical theory, appl. book contrib. 80−22268
single-loop divergences in six dimensions 77−38081
singularities and rule of unanimity 78−4529
singularity and unanimity 78−4529
SL(2,C) exterior forms and quantum gravity 79−35622
SL(2,C) gauge theory, Palatini-type variational principle 78−78059
SL(2n,C)⊗SL(2,C), invariant gravitational model, spontaneous symmetry breakdown 77−46009
SO_2 extended supergravity, geometrical interpretation 77−49660
SO(1,3)-gauge theory of gravity 79−129
SO(8) extended supergravity 78−16970
soft graviton emission in scatt. processes, linearised gauge theory 78−49746
solitary-wave motion for gravitating particles 80−62565
soliton solutions of stationary axi-symmetric gravitational fields 80−73253
some thermodynamical remarks on the theory of gravitational field 78−81899
sourceless, impossibility of geon analogues 78−361
sourceless quantum EM field in multiply connected asymptotically flat background metric 79−25946
space-time, foam-like structure, Bjorken scaling violation due to gravitational field 80−77939
space-time, geometric quantization theory appl., covariant field theory 78−12637
space-time quantisation, based on quantum mechanics and general covariance 79−71343
spacetime foam, mathematical framework 79−9172
spacetime structure theory at very short distances, nonlinear sigma model 80−12979
spin, supersymmetry, and square roots of constraints 79−12676
spin 3/2 field, axial and trace anomalies 79−2690
spin 3/2 field and Cartan's geometry 78−16712
spin 3/2 particles with minimal EM interaction, inconsistencies of Glass's eqn. 79−67207
spin test for the equivalence principle 77−57265
spin-1 particle, quantum gravity corrections to anomalous mag. and quadrupole moments 77−65130
spin-2 gluon-graviton model with baryon-number nonconservation 80−57565
spin-2-gravity coupling, consistency problems 80−77681
spin-3/2 axial anomaly, Feynman graph, point splitting, topological and zeta function methods 78−93588
spin-3/2 field, Hamiltonian formulation and quantisation 78−8325
spin-3/2 theory of gravitation 79−49148
spinning particle in grav. field with torsion, eqns. of motion *(Chinese)* 80−62546
spinor electrodynamics in Riemann-Cartan space, dynamical theory of axial vector torsion propag. in vac. 78−73889
spinor field theory, generalized spin structures on 4-D space-times 80−62564
spinor formalism 80−90762
spinor gravity, tree ghost 77−71260
spinor space, quantum phenomena 79−17192
spinor theories in curved space-time, nonlinear invariances 79−54029
spinor theory of general relativity, without elementary gravitons 78−8321
spinor-spinor scatt., graviton ghost pole 77−71260
spontaneous breaking of gauge symmetry in a nonstationary isotropic metric 79−21643
spontaneous origin of Newtons const., modified Einstein eqns., matter interactions in weak gravit. fields 78−12853
spontaneous particle creation leading to black hole evaporation 78−40986
spontaneous symm. breaking due to gravitational interaction 78−36918

quantum field theory of gravitation continued
spontaneous symmetry breakdown in an SL(2N,C) SL(2,C)-invariant gravitational model 77−46009
stimulated emission processes in gravitational fields, regions of constant shift 80−82703
stress tensor of conformally invariant field in conformally flat spacetime, axiomatic renormalisation 78−29034
stress-energy tensor of scalar field in curved spacetime 79−12697
strong gravity, field equations, strong interactions, de Sitter microsphere idea of hadrons 80−68111
strong gravity, short range pots., type II solns. 80−77683
strong gravity, spherically symmetric solns., multipole expansion appl. 79−75433
strong gravity, supersymmetric theory for f- and g-gravitons and massive gravitinos 78−62141
strong gravity and Dirac numbers 78−21372
strong gravity equations, spin and torsion effects, rel. to spin of Universe 79−97116
strong gravity explanation of proton mass 78−12852
strong spin-two interaction and general relativity, review 79−45046
strong-gravity model, stability under perturbation, Hamiltonian formalism 80−52453
strong-gravity solns. for Einstein's eqns. 78−24705
SU(2) gauge fields coupled to strong gravity, Coulomb like solutions 80−82701
SU(4) and SO(4) supergravity relations, anomalies and field transformations 79−9170
SU(N) conformal supergravity, gauge theories for extension 78−8577
sum over paths quantisation, 2-submanifold boundary value problem 80−105566
summer school, methods in field theory, Les Houches, France (July-Sep. 1975) 77−57457
super Riemannian space quantisation, perturbation theory rule derivation 78−77790
super Weyl transformations in two dimensions 79−25953
super-gauge symmetry in general relativity, Einstein's A transformation *(German)* 78−86199
superconformal gravity, local geometry 79−44836
superconformal invariance of superspace with nonminimal auxiliary fields 79−17317
superconformal supergravity and internal symm., proliferation of gauge fields 77−54056
superfield formulation of supergravity 79−17312
superfield supergravity formalism of Wess Zumino, constraints 79−2970
superfields in higher-dimensional spacetime 79−17316
superfluid as a source of all interactions 79−21620
supergauge theory, geometric aspects, broken gauge invariance 78−8506
supergravity, and superconformal gravity linearisation 79−12679
supergravity, auxiliary fields, matter coupling, BRS transformations 78−93837
supergravity, auxiliary fields and UV divergences, supersymmetric Yang-Mills-Einstein system 78−78127
supergravity, auxiliary fields for closed algebra using S-matrix 78−81911
supergravity, canonical formulation 78−29016
supergravity, Cartan's geom. struct. 78−49745
supergravity, constraint-free superfield formalism 79−17309
supergravity, covariant quantisation 78−41470
supergravity, critique of superfield theories 79−54028
supergravity, elimination of redundancy in superspace eqns. 79−12678
supergravity, exact plane wave soln. to coupled field equations 79−30337
supergravity, failure of minimal coupling, superfield covariant derivative 79−6035
supergravity, fundamental supergeometrodynamic theory of hadron 79−40725
supergravity, ghost counting on one-loop level of Rarita-Schwinger field, gauge fixing 78−93589
supergravity, Hamiltonian formalism, quantisation and S-matrix 78−16972
supergravity, Hamiltonian formulation 78−24722
supergravity, introduction 79−49149
supergravity, locally invariant supersymmetric gauge field theory 78−49742
supergravity, modified Feynman rules and Ward-Slavnov-Taylor identities 79−132
extended supergravity, N=2, auxiliary fields in 5, 6 space-time dimens. 79−30339
supergravity, one-loop divergences 77−13674
supergravity, one-loop renormalisability 77−5730
supergravity, Poincare and conformal, multiplication rule and supersymmetric densities for multiplets 78−70037
supergravity, Poincare and conformal models with closed algebra 78−74198
supergravity, prepotentials in superspace formulation, superconnections 79−12683
supergravity, relation between vector and scalar multiplets and gauge invariance 79−12684
supergravity, renormalisability props., superinvariant local counterterms 77−34087
supergravity, rigid simple and extended 79−30336
supergravity, S-matrix difficulties, graviton elastic scatt. amplitude 79−135
supergravity, SO(3)-invariant extended 77−22475
supergravity, SU(4) invariant theory 78−41471
supergravity, supercurrent anomaly 78−29267
supergravity, superfield Lagrangian 78−41468
supergravity, superspace formulation, component formalism transform props. 79−12688
supergravity, superspace formulation, consistency checks 78−37170
supergravity, superspace-time local symmetry, Ferru torsion preservation, renormalisability 79−12689
supergravity, supersymmetric generalisation of differential geometry tensors 78−45546
supergravity, symmetry breaking by instantons 79−21625
supergravity, total energy positivity at second quantised level 77−74299
supergravity, two-loop renormalisability 77−17897
supergravity, unified theory of basic forces 78−50001
supergravity, unitarity, Ward identities, and new quantisation rules 78−54279
supergravity, Weyl and Einstein, unified approach to matter coupling 78−54275

quantum field theory of gravitation continued
supergravity and gravity, BRS gauge and ghost field supersymmetry 77−38116
supergravity and gravity as gauge theories on group manifold 78−41469
supergravity and S-matrix 77−46010
supergravity and spinor dual model 77−13675
supergravity and Yang-Mills theory unification 77−46011
supergravity as gauge theory of supersymmetry 78−8576
supergravity coupled to scalar multiplet 77−46012
supergravity coupling to nonlinear realisations of supersymmetry in two-dimens. 77−79024
supergravity field eqns., exact plane wave solns., vacuum Einstein eqn. soln. generalisation 79−2707
supergravity group structure 79−21619
supergravity groups, struct., complex conjugated superspace general covariance groups 79−6036
supergravity in 11 dimens., action and transform. laws 78−70038
supergravity in superspace, algebraic approach 79−17314
supergravity review, phenomenological appls., and lower spin fields unification 78−77788
supergravity spin 5/2 with SO_9 inernal symmetry 79−21624
supergravity structure, gauge actions, multiplets 79−2971
supergravity theories, background metric, conformal anomalies calc. 78−70043
supergravity with complex spin-3/2 gauge fields, invariant under local complex supersymm. 77−5731
supergravity with general scalar interactions, super Higgs effect, gravitinos, spontaneously broken supersymmetry 79−6037
supergravity without cosmological constant, spontaneous symmetry breaking and Higgs effect 79−17310
superspace formulation of supergravity using vierbeins 79−2972
supersymmetric black holes in supergravity, spin 3/2 perturbation of Schwarzschild black hole 78−93300
supersymmetric Yang-Mills theory in superspace 79−12979
supersymmetry concept, physico-geometrical considerations, superfield theory 78−74172
superunified theories, geometry of gauge invariance 78−24723
superunified theories in superspace 80−8886
tadpole diagrams, Ward identities, induced cosmological term in quantum gravity 78−125
taming of the dipole ghost in relativistic quantum field theory 78−66035
Taub-NUT instanton with an horizon 78−89392
tensor calculus for vector multiplet coupled to supergravity 78−86214
tetrad Palatini formalism and quadratic Lagrangians in gauge theory of gravitation 79−2697
thermal and nonthermal particle production without event horizons 80−4628
thermal effects for accelerating observer in empty Minkowski space 78−8322
thermal particle production in a radiation dominated Robertson-Walker universe 78−81721
thermal propagators and accelerated frames of reference 79−67211
Thirring model coupled to gravity, classical solns. in generally covariant model with fermions 80−9091
time reversability 80−82704
torsion and gravitational Meissner effect 80−8894
trace and axial vector anomalies, for spin 3/2 Majorana field, derivation using zeta function regularisation procedure 79−2700
trace anomaly for neutrinos in Ricci-flat space-time of six dimens. 78−57847
trace anomaly of a conformally invariant quantum field in curved space-time 78−54278
translational gauge theory of gravity: post-Newtonian approximation and spin precession 80−46945
twisted quantum fields in a curved space-time 78−73913
twister space, complex fibration, fibration structure deformation, Einstein vacuum eqns., Maxwell's eqns. 78−12854
twistor theory, particle models 80−13278
twistor theory and geometric quantisation 77−17898
twistor theory and geometric quantization 77−17898
U_4 theory of gravity, unique spherically symmetric soln. in teteparallelism limit 80−90763
unification of fermions and bosons, math. structures and phys. questions 79−21630
unified affine gauge theory of gravity and strong interactions, GL(4,R) spinor fields 79−93331
unified gauge theory of gravitational and strong interactions 80−95016
unified Lagrangian formulation for massive and massless tensor fields 79−12686
unified scalar-free theory, order-R vacuum functional, with spontaneous scale breaking 80−78003
unified theory of gravitation, particle masses, instantons 78−37168
unitary field theory, preliminaries and recent developments, review 79−35613
unitary inequivalence of various theories 80−52111
unitary spin, colour and unified theory, consideration of many-dimensional space-time 78−8570
universal metaplectic structures and geometric quantization 79−25881
use of FORMAC73 in general relativity 77−41522
vacuum, conformally flat space-time, quantum cosmology 77−5728
vacuum, empty, fields and quanta, strong gravity, particle-antiparticle annihilations 80−68400
vacuum cosmology 77−5728
vacuum decay, quantum and semiclassical gravitational effects 80−86194
vacuum definition in external grav. field 79−21642
vacuum polarization and non-Newtonian gravitation 80−62896
vacuum quantum effects analogy in gravitational and EM fields 80−32044
vacuum structure for a quantum field theory in curved space-time 79−21638
vacuum symmetries of gauge supersymmetry, quantum effects 79−17634
vacuum with spin in the ECSK-theory of gravitation 79−44830
vector boson model from SL(2,C) gauge theory of gravitation and Yang-Mills theory 79−322
vector graviton and metric fields *(Chinese)* 79−71324
vector superfield generated by supercurrent, supergravity formulation 77−71453
weak gravitational field, connection between Dirac and Dixon eqns. 78−124

quantum field theory of gravitation continued
Weinberg-type fields in curved spacetime, stress tensor conformal anomaly 79−25960
Weyl tensor diagonalisation, Lorentz transformation of gravitational superenergy flux 79−134
Wheeler's 'rule of unanimity' in quantum cosmology 80−98846
world topology, quantum gravity, instanton number 77−5729
Yang's gravitational gauge field, plane wavelike solns. *(Chinese)* 79−80486
Yang-Mills and gravitational fields, quantisation 77−67552
Yang-Mills equations, Cauchy problem 80−13206
Yang-Mills formulation, gravit. dynamics 78−24721
Yang-Mills gauge theory of gravity, gravit. field of spherically symm. matter distribs. 78−4773
Yang-Mills gauge theory of gravity, SO(1,3), self-gravitating cosmons 77−82431
Yang-Mills higher-derivative theory, ghost problem 80−31970
Yang-Mills instanton in Taub-NUT space 79−2691
Yang-Mills instantons, space-time topology 78−8522
Yang-Mills theory, broken symmetry soln., Higgs fields and Einstein gravity action 80−101746
Yang-Mills theory, fibre bundle struct. 77−37799
Yang-Mills theory of gravity 80−42134
Zitterbewegung of Dirac particle in time-asymmetrical gravit. field 77−54067
e^+e^- pair creation in strong EM fields, gravitational effects 80−42376

quantum field theory of interactions
see also elementary particle coupling constants; elementary particle interactions; Feynman diagrams; quantum electrodynamics; quantum field theory of gravitation; quantum field theory of strong interactions; quantum field theory of weak interactions; vertex functions
1/N expansion for N-component scalar field interactions, nonleading order, bounded interaction appl. 79−6275
γ^5-invariant eqns. for massive particle 78−29262
$\lambda\phi^4/N$ theory, vac. stability, quark confinement 77−82677
$\lambda\phi^4$, spontaneous symmetry breakdown, approx. ground state, variational approach 77−79229
$\lambda\phi^4$ theory, bound states, RPA anal. 77−6008
σ model, gauge invariant extension with EM interactions, SU(2) symm. breaking 77−30258
σ-model, bilinear symmetry-breaking, meson mass and decay const. 77−49877
$\phi^{3,4}$ theory, conformal anomalies for interacting scalar fields in curved spacetime 79−49396
ϕ^4 scalar theory, mean field perturbation theory, path integral formulation 78−12803
$(\bar{\psi}\psi)\psi\psi$ model field theory anomalous dimens., 1/N expansion 78−379
Abelian Higgs model, classical vortex soln. 77−2752
Adler zeros, as group theoretical consequence of mass zero asymptotic free fields 77−22655
arbitrary-spin particles, field theory 77−34075
asymmetric creation of matter and antimatter in the expanding Universe 79−75302
asymptotic evaluation of high energy cross sections, appl. to 0^4 theory 78−54551
asymptotically free massless field theory, self-consistent β functions 78−16911
atom+diatom scattering, field theoretic calcs. 77−50484
atomic radiation model 79−238
axial vector meson model, quasi-renormalisation using BPHZl approach 80−13208
Bianchi-type I universe, causally connected DeWitt's two vacuum states 78−12608
Bjorken asymptotic behavior of deep inelastic scattering form factors and the general principles of field theory 79−21958
Bogolyubov transformation in the theory of strong coupling of a heavy particle to a scalar field 79−21592
boson-fermion interacting system, coherent states on Lie groups and evolution operator 78−36932
bound state formalism, modified functional formalism, self-energy and renormalisation effects 77−26463
C*-algebras of two body interactions, existence of scatt. theory of time automorphism groups 80−31972
chaotic isospin zero state of one mode isovector field 78−12883
charged Bose condensates in supercritical external fields, relativistic field theory 78−8766
charged particle scattering by mag. monopoles, SO(3), gauge theory 77−13907
charged particle self-interactions 79−67486
chiral Lagrangian model, linear and nonlinear σ models, pion polarisabilities, Compton scatt. 78−21323
chromatic principle, interaction quantum fields 77−34086
collective excitations, fermion Lagrangian 77−71426
composite operator anomalous dimens. in $2+\epsilon$ dimens. Gross-Neveu model 77−67660
composite particles, second-quantised representation 77−49830
conformal invariance, two-point function of arbitrary spin 78−21316
conformal invariant field theories, new approach 77−2728
conformal pot. in N dimens. (N>1) 77−74271
conformal spin-1/2 systems, vertex functions and form factors 77−38085
conformal superalgebra, new representations 77−61199
conformally invariant theory, calc. of coupling consts. 77−41776
continuous one-dimensional many-component Gibbs system with regular two-body interaction pot., transfer matrix 78−8342
coordinate covariant second quantisation, quantum processes in black hole evaporation 77−82670
correspondence and opposition between quantum theory and classical physics, temporal logic 80−27176
coupling parameter trajectories 78−8519
covariant loops and strings in positive definite Hilbert space 77−30233
critical exponents, three dimensional system with short-range interaction, calc. 80−42348
crossing properties of scattering operators 80−32028
curved space-time, renormalisation 77−49834
deep inelastic lepton-hadron scatt. in massive vector gauge models 78−74262
deep inelastic scatt., field theoretical description, QCD, quark-parton, and light cone algebra *(Russian)* 80−42388
derivative-coupling model, 2 dimens., zero mass limit and induced interactions 79−49397

quantum field theory of interactions continued
dimensional symmetry rearrangement in renormalised quantum field theory 77−5982
Dirac quantum field, scatt. automorphisms, external field perturbations 78−58112
Dirac self-interacting field, soliton solns. in three-dimens., quark confinement 77−26461
double Wilson expansions of products of three-spinor operators 77−30232
dual string with internal spin, second quantisation 78−440
dual theory space-time geometry, graviton coupling to fermion string 77−18242
Dyson eqn., exact soln. for mean value of Green's function 78−4559
effective potential at finite temperature 77−30269
Einstein's impact on theoretical physics 80−77677
electroproduction structure functions studied using light cone expansion via O_4 symm. 77−41845
factorised completely X symmetric S-matrix characterisation, multicomponent field theories 80−105800
Federbush model, absence of induced counterterms e^+e^- scatt. amplitudes 78−50023
fermion fields with $(\sin\phi)_2$ interaction, quantum solitons 77−41780
fermion-fermion scattering in supersymm. field theory, high energy behaviour 77−13887
fermionic interaction models, classical solns. 79−67463
fermions, quantum field theory, large order perturb. theory, more than one coupling constant 80−77940
fermions as solitons in extended particle field theory 77−26454
fixed point structure, renormalisation group appls. 77−57461
Friedmann universe, photon gas 78−4543
$g\phi^4$ theory, strong coupling limit 77−87911
gauge group theory of combined gravitational and e.m. interaction 77−80
gauge invariance in operator-product expansion in non-Abelian gauge theory 77−2751
gauge theories, facts and prospects, conf., Schladming, Austria (Feb.-Mar. 1978) 79−26203
gauge theories, quantised, large time behaviour, asymptotic anal. 80−27395
generalized Weizsacker-Williams method, single variables description 77−49937
geometrical description of fields 79−67462
Goldstone fermions and supersymmetry breaking 77−22659
Goldstone particle spin values and spontaneous symmetry breaking *(Russian)* 77−212
Gross-Neveu model, exact S-matrix theory 78−24937
hadron inclusive electroprod. in current fragmentation region 79−30741
Hagedorn model, topological cross sections in multiplicity asymptotics *(Russian)* 80−9154
Higgs models with fermions, vortex-like solns. 77−13850
homogeneous interactions, perturbation theory 77−49836
identical particle indistinguishability, field quantisation Lie algebraic approach 80−77984
inclusive processes, bremsstrahlung approx. 77−50033
inclusive processes with large momenta, quark-parton model *(Russian)* 77−71538
infrared divergences in non-Abelian gauge theory 77−6001
instanton solutions for scalar isotensor fields and interacting isovector+-gauge fields *(Russian)* 78−393
interacting Rarita-Schwinger field on light front 78−4786
inverse scattering problem 78−363
isovector scalar meson interaction, static source, variational method, coherent states 78−16921
$J^\mu J_\mu$, mean field perturbation theory, path integral formulation 78−12803
Klauders augmented quantum field theory, Green's function formalism, Yukawa model, σ-model 79−6277
Klein-Gordon equation and scattering theory 77−5986
knot wormholes in quantum geometrodynamics 77−67612
ladder models, dynamical symmetry and asymptotic scale invariance 79−21959
Lagrangian, effective, in path integral quantisation formalism 80−42325
Lagrangian field theory, divergence identity and dynamical symm. rearrangement 77−45963
Lagrangians with quadratic depend. fields and derivative couplings, covariant quantisation 77−65089
lattice Hamiltonian for arbitrary couplings, variational methods calcs. 78−16746
Lee model, V-V sector 78−24967
light-cone quantisation, massless propagators 78−8538
limit $\hbar\to 0$ in quantum field theory, rel. to scatt. amplitudes, differential cross section *(Russian)* 77−61202
linear stochastic dynamic systems, appl. of Green's function method *(Russian)* 78−16722
linearisations of theories with spontaneous symmetry breaking 77−54043
local supersymmetry of spinning particle 77−2768
localised classical solution for fermions+scalar bosons in field theory, Yukawa coupling const. 78−24928
log-concave functions and convex interaction terms 77−57232
long range forces in quantum theory, book contrib. 78−82811
low-energy meson physics in theory with chiral Lagrangian 77−65110
Majorana-Weyl fields, development of unified models 78−33015
massive Schwinger model, θ-parameter 78−49967
massive Thirring model, conserved charges 77−199
massive Thirring model, conserved currents 77−198
massive Thirring model, effective potential, reality symm. 77−2731
massive Thirring model, particle scatt. in perturbation theory 77−82674
massive Thirring model, scattering solns. using pot. derived from bound state solns. 77−22641
massive Thirring-Schwinger model, convergence of perturbation theory and particle structure 77−10173
massive U(1) Thirring model, S-matrix and dynamical supersymm. 77−67586
massless boson collision theory in local field theory 77−18155
massless scalar and spinor field theory in curved space-time 78−21321
mean field perturbation theory, path integral formulation 78−12803
meson and baryon trajectory slopes based on multilocal model 77−87944
multimass field hyperquantisation, S-matrix unitarity 77−22645
multiparticle scatt. operators representation satisfying unitarity and crossing props. 80−32029

quantum field theory of interactions continued
Nambu Jona Lasinio model renormalisation in mean field expansion 79−26219
noncausal wave propagation in spin-0 theories with external field interactions 77−41770
nonleading mass singularities, two dimens. Federbush model 77−5988
nonlinear quantum field, self-interacting theory 78−70251
nonlinear scalar interactions, 1/N expansion 78−16903
nonlocal, field theory, form factor props. 77−87903
nonlocal nonpolynomial interactions, strong coupling 78−21319
nonlocal quantum field theory, quark confinement and scaling 77−13915
nucleon σ-model and spontaneously broken conformal symm. 77−2729
null plane field and algebra struct. 77−18154
null plane theory of n-particles, two-time Green's function props. 78−93
numbers and weights of Feynman diagrams, ϕ^N, QED and non-Abelian theories 79−2937
one-dimensional model with four-fermion interaction particle mass *(Russian)* 77−41781
Pade approximants in Wick Cutkosky model 77−18162
particle-boson interactions and the weak coupling limit 79−49100
particle-field Hamiltonians, sequences of transformations 78−24691
parton model in renormalisable field theory, anomalous dimension 77−22682
parton model interpretation of cut vertex formalism 80−86566
path integral quantisation of field theories with second-class constraints 77−202
path integrals and semiclassical propagator approx. 77−87664
Penrose theory in particle physics 78−29321
perturbation theory at large orders, ϕ^{2N} interaction, anharmonic oscillators 77−45735
plasma, two-component, third sum rule and local mean-field theory 78−5982
pole search problem of scatt. amplitudes in L^2 norm 77−41756
Pomeranchuk-type theorems for total and elastic cross sections 79−21972
Potts model 79−6055
precocious scaling in field theories 78−8525
pseudoclassical Lagrangian for 2 interacting spinning particles 78−86426
QED_2 models in constructive quantum field theory 77−18210
quark confinement, dynamical and topological considerations, review 79−26296
quark trapping in quantized bag model based on SLAC Lagrangian 77−13920
Reggeon field theory, quantum spin model 77−45974
Reissner naked singularity, spontaneous pair creation 78−24990
relativistic Hamiltonian theory, covariant formulation, on light cone, fields with spin *(Russian)* 80−9087
relativistic Hamiltonian theory on light cone, covariant formulation 79−2942
relativistic many-body bound systems, electromagnetic props. 77−74765
relativistic quantum mechanics, elimination of phase angle uncertainty, charged Dirac particle+mag. monopole scatt. *(Chinese)* 78−78100
relativistic two body Schrodinger equation, generalisations of quasipot. eqn. for scalar interactions 77−13871
renormalisable theories from nonrenormalisable interactions 78−383
renormalisation group appls. in high energy physics 77−57461
Sakata-Taketani spin 0 theory with external field interactions 77−41748
scalar one-loop integrals, soft bremsstrahlung and radiative corrections 79−75682
scalar particle interaction with quantised field, nonrelativistic model 79−25912
scalar particle light scattering 77−49822
scaling of inclusive form factors with respect to a generalized scaled variable 80−417
Schroer model, operator solution in asymptotic field formalism 77−54053
Schwinger variational principle for bound states and scatt. problems 78−16932
second-class currents, general treatment 77−67590
second-class currents and matrix elements in renormalisable field theory 77−10197
series expansions, low and high temp., for quantum fields on lattice 78−29061
SO(3) gauge group, monopoles, spontaneously broken gauge theory 77−2753
soliton, static, mass formulae in two-dimens. scalar field theory 77−204
soliton quantisation in gauge models, Feynman rules 77−2734
space-like fields, asymptotic props. and appl. to hadron physics 77−18158
spin-1 field theory, lack of relativistic covariance 77−2720
spin-3 field theory, free massive Lagrangian, zero-mass limit of higher spin theories 80−52402
spinning strings, addition of scalar and spinor fields 77−49833
spontaneous symmetry breaking in interaction of scalar field with external vector field 78−8545
statistical mechanics, operator formulation 78−24734
statistical mechanics appl., analytic props. of causal Green's function *(German)* 77−45787
strong-coupling theory of point particle with neutral scalar field 77−67575
SU(2)×SU(2), dynamical rearrangement of symmetry 78−49979
SU(2)-flavour Schwinger model on the lattice, Hamiltonian lattice perturbation exam. 78−16747
superconductivity unified model of weak, EM and strong interactions 77−49888
superrenormalisable interactions, struct. of infrared divergences 79−40663
supersymmetric relativistic harmonic oscillator, model 77−38086
supersymmetric Sine-Gordon model, infinite set of local quantum conservation laws 80−47207
supersymmetry, field theory, fermion (meson)-meson scatt., high energy behaviour 79−295
symmetry dynamics and invariant coupling const. behaviour *(Russian)* 77−34096
symplectic geometry and second quantisation 77−45977
Thirring model, massive, higher conserved current determ. 77−38087
Thirring model, symm., anomalous dimens. and Schwinger term 77−87900
Thirring model Lagrangian, generalised, interacting fermions, interacting solitons 77−45937
quantum field theory of interactions continued
two-body interacting Lagrangians invariant under world line independ. reparametrization, nonexistence 79−97491
two-body relativistic systems 78−69977
two-dimens. field theories, static solns. 77−2755
two-dimens. light-cone coords., noncovariance of fermion fields 77−71448
two-dimens. Thirring and Schwinger models, solitons and confinement *(German)* 77−82665
two-dimensional massless Fermi field, symm. couplings 78−29228
two-dimensional model, pseudoparticles and massless fermions 78−24974
two-particle Green's functions, bound states and poles 78−16694
two-particle irreducibility in single channel 77−49821
unified parity-conserving interactions based on SU_4 77−74629
vector coupling, bound states, Dirac fermions in three dimens., interacting via gluons 77−34090
vortices topology of unified intrinsic field quantities for elementary particle systems 79−40653
ep deep inelastic scatt., density matrix appl. to scaling props. 78−8673
ep deep inelastic scatt., EM form factors asymptotic behaviour, Fourier transform singularities 79−40789
ep scatt., deep inelastic, Lorentz invariant generalized functions, rel. to EM form factors 78−8544
γp interactions, Thomson limit calc. using rising total cross sections 79−22103
μp deep inelastic scatt., charm effects, field theory anal. 78−21435
$\nu(\bar{\nu})N \rightarrow \mu^-(\mu^+)$+hadrons, renormalisable field theory, high energy behaviour 77−61279
ϕ^3 theory, multiparticle Regge poles *(Russian)* 77−6057
πN-interaction, linear wave eqn. with energy-depend. pot. 77−18317
$\pi^+n \rightarrow p(\pi^+\pi^-)$s, direct channel diagram of $(\pi^+\pi^-)$s atom prod. *(Chinese)* 79−81308

quantum field theory of strong interactions
see also elementary particle strong interactions; Lee model
0(N) nonlinear σ model, constrained systems, absence of classical lumps 79−2904
(3,3*)⊕(3,3*) bilinear symmetry breaking in linear σ-model, symmetry breaking Lagrangian 79−300
$\eta \rightarrow \pi^+\pi^-\gamma$, one-loop approx. in quantum chiral theory 78−25041
$\lambda\Phi^4$ model of meson-meson interactions, dynamical symmetry restoration 77−5989
σ model, $SU_2 \times SU_2$, modified Goldberger-Treiman relation, pseudoscalar form factor 80−27421
σ models, nonlinear, perturbative approach to symmetry restoration 80−37163
σ-model, finite energy solution 79−17618
σ-models, two-dimens. nonlinear, on Riemannian and Hermitian symmetric spaces 80−52404
ϕ^4 model, strong-coupling expansion in the large-N limit 80−346
ACD off light-cone, transverse momentum cut-off 78−381
asymptotic behaviour in strong coupling for solvable model field theory 77−54048
asymptotic fields, colour confinement in QFT 78−70331
asymptotic freedom, quark-parton model 77−82675
asymptotic freedom, zero charge, point charges in quantum electrodynamics *(Polish)* 78−45822
asymptotic freedom and charmonium 78−54534
asymptotic freedom and local duality 77−71518
asymptotically free gauge theories, massive lepton-pair prod. 77−74734
axial gauge, QCD, differential identities and soft-gluon singularities 77−74585
bag model and QCD, quark-antiquark sea 77−71481
baryon system, strong interacting, finite temp. many body theory, phase transition 77−65210
bi-local field interaction with external field 78−66030
bi-local field on space-like surface 80−27403
bilocal models of hadrons, relative time depend. as gauge freedom 77−74584
Borel singularities, effective one-loop Lagrangian in constant elec. field 78−16917
Bose description of fermions 78−89402
boson field in neighbourhood of classical solution, quantisation by appl. of Bogolyubov's method 78−8566
boson scattering, variational method 79−255
canonical $SU_4 \times SU_4$ pseudoscalar meson matrix, nonlinear chiral Lagrangian 78−397
Caratheodory's canonical theory for fields, quark confinement 77−87941
charged relativistic boson field, coherent state representation 79−71708
charged soliton long range interactions 79−63373
charmonium, rel. to gluons, quantum chromodynamics theory 78−62362
charmonium and asymptotic freedom in QCD 79−6327
charmonium and QCD, review 78−82157
charmonium spectroscopy, explicit soln. of wave eqn. for arbitrary power pots. 80−403
chiral gauge invariant Lagrangian, relationship to strong interactions *(Chinese)* 79−21968
chiral properties of fermionic determinant in two-colour QCD, symm. breaking 78−25015
chiral symmetry and pion-nucleus interactions 79−80961
chromomagnetic and electromagnetic hyperfine interaction, charm meson spectrum 78−12879
composite hadrons, field theoretical model, quark field operators in motion, interaction vertices 79−342
composite hadrons, field theoretical model, quark field operators, Dirac Hamiltonian at rest 79−341
Compton effect in QCD 77−74656
condensation of extended structures 78−78141
conformal-invariant field theory, anomalous dimensions, coupling consts. 80−4870
Coulomb gauge vac. degeneracies in (2+1) dimensions 79−2928
covariant σ models, first order system of differential eqns. 80−31978
CP invariance and pseudoparticles 77−61213
cross sections, inclusive and semi-inclusive, auxiliary field theory classical solns. 79−49388
current trends in the theory of fields, conf., Tallahassee, Florida, 6-7 April 1978 79−12923
cylindrical gauge field configurations, confinement in QCD 78−12870
Dashen-Frishman model free-field-like behaviour and singularity of Callan-Symanzik function 78−16928
deep inelastic lepton-hadron interactions, scaling deviations 78−32991

quantum field theory of strong interactions continued
deep processes in non-relativistic confining potentials 79−9329
dimensional regulation, SU_2 gauge theory, instantons 80−18066
dipole ghost, taming, four dimens. field theory 79−22019
discriminative deep inelastic tests of strong interaction field theories, QCD scaling violations 79−89105
Drell-Yan formula in QCD, lepton pair prod. 78−33025
Drell-Yan processes, perturbative versus asymptotic freedom convections 79−63446
dressing the nucleon propagator, nested bubbles approx. in Bethe Salpeter eqn. 77−6032
echo hadrons, colour confinement and fractionally charged states 79−67506
eikonal pionisation graph summing in Lagrangian field theory 80−4973
eikonal theory, interacting Pomeron production by retaining Feynman graphs 78−8633
elastic scattering between binary quark-antiquark system and local field 80−47244
energy momentum tensor of quantised fields, vacuum averages, bag model of hadrons 80−91005
extended baryon fields and meson-baryon interaction 77−41751
extended meson model, Euler-Lagrange eqn. bilocal field theory conservation laws 79−21938
factorisation in the 2 dimens. linear σ model in 1/N expansion 79−35936
Faddeev-Popov procedure and Gribov copies in gauge theories, QCD appl. 78−32979
fermion confinement and bosonisation, quantum sine-Gordon field theory, quark confinement 78−86442
fermion-pseudoparticle interactions, non-generation of quark masses 78−37175
Feynman-Wilson gas, statistical model for multiparticle physics 79−22071
fibre bundle geom., hadronic currents 77−79204
fibre bundle with Cartan connection, group contraction 77−74573
flavour nonsinglet structure function, $F_3^{\nu N}$, strong-interaction field theory discrimination, QCD 79−75774
flexible Jordan admissible algebra, dimens. seven, hadron physics appl. 78−93792
four-dimensional σ-model on quaternionic projective space 80−9092
G-parity and exchange degeneracy breaking 77−71449
gauge field theory formulation in quantum field theory framework 79−21908
gauge theories and strong gravity 79−58869
gauge theories of weak, EM, and strong interactions, book contrib. 79−30694
general principles of QFT at high energies 79−239
generalised Low eqn. approach to reaction matrix 79−85491
geometrical gauge theory of gravit., strong interactions, EM interactions 78−70041
glueball singularity, flavour loops and the Harari-Freund picture 80−42433
gluon distrib. function, tests of QCD 78−45796
gluonic decay of heavy quarkonium states, QCD test, three jet struct. 78−62365
gluons, nonlinear field theory *(Chinese)* 79−58923
Grassmann spaces, model for supersymmetric quark-twistor string 79−22018
Gross-Neveu model and self-consistent β-function method, fermion mass generation 79−49466
hadron+hadron$\rightarrow\mu^+\mu^-$X, QCD anal. jet recoil on large p_T muon pair 79−9416
hadron+hadron elastic scatt., >100 GeV, asymptotic theorems review *(Czech)* 78−29357
hadron jets from quantum chromodynamics 78−25056
hadron plasma theory *(Russian)* 78−37148
hadron strong interactions, theory from general relativity 79−49143
hadronic potentials, field theoretical interpretation, Poincare invariance, causal solns. 79−26266
hadronic structure using parton anal. of deep inelastic scattering and rel. processes 79−80803
hadrons, extended, second-quantisation of strongly interacting fields 80−13270
hard processes, parton model and QCD, review 80−47258
heavy quark potential, non-perturbative contrib., appl. to QCD 79−13025
heavy quarks, widths of neutral vector mesons 78−8602
high energy physics as infrared phenomenon, strong interactions in 6-ϵ dimens. 77−10182
history of quantum field theory, search for unity 78−28904
impulse approximation in QCD, partons p_t distrib., appl. to deep inelastic electron scatt. 78−62368
inclusive cross section density matrix and scaling props., many-body problem 77−41872
inclusive cross sections in scatt. angle, anal. props., ladder models with dynamical symmetry 79−93390
instanton effects on static $\bar{Q}Q$ potential 79−9333
instantons and infrared divergences 78−70284
isotopic spin and coherent states 80−4843
isotopic symmetry group in strong interactions, possible geom. origin 79−17628
jet processes in QCD 78−82104
jet production by a gluon source in QCD 79−22056
large NO(N) σ-model of meson-meson interactions, dynamical symmetry restoration 77−5989
large Q_T transverse momentum lepton pairs and hadron jets prod., reaction mech., perturbative QCD 79−2999
lattice gauge theory with fermions, renormalised phases, vacuum polarization 80−13198
liquid neutron matter, pion condensation and the linear σ-model 79−59027
local operator products, gauge invariance and renormalisation 78−358
secret long range force in QFT with instantons 79−9283
low energy light particle processes in spontaneously broken gauge theories, heavy particle effects 80−22521
low equation, solns. in no-crossing approx. 80−32012
Mandelstam-'t Hooft duality in Abelian lattice models 78−78057
mass singularities factorisation for polarised parton legs in low order QCD perturbation theory 79−40737
massive CP^n sigma models, topological struct., finite action configurations 80−57476
quantum field theory of strong interactions continued
massive Schwinger model, decay of metastable vacs. 78−24989
mean spherical model in 1+1 dimens., strong and weak coupling connection 80−82888
meron configurations in two dimens. O(3) σ model 78−32983
meson-baryon scatt. lengths in chiral Lagrangian model, πN coupling const. 77−88001
MIT Bag model, field theory Lagrangian 78−89670
MIT bag model, quantum corrections to classical confinement 77−74643
MIT bag model, two-dimens., confined massive field vacuum fluctuations 80−4921
MIT bag theory, microscopic derivation with spontaneously broken symmetry 79−264
modified renormalisation conditions, two-point Green functions 80−9089
multicolour QCD as dual resonance theory, mesons on rising Regge trajectories 78−16987
multilegged propagators in strong-coupling expansions 80−4861
multilocal fields in relativisitic quantum field theory 78−37125
Nambu-Goldstone realisations of dynamical groups and nonlinear eqns. *(Russian)* 78−89632
Nielsen-Olesen vortices in coherent state approx., creation and annihilation operators 79−9284
non-Abelian gauge theories and quark confinement 79−13022
non-Abelian gauge theory, colour-singlet quark form factor anal. 77−65084
non-Abelian gauge theory of strong interactions, EM current renormalisation 79−63350
non-Abelian vortex-bond model of hadrons 78−4827
non-asymptotically free theories, scaling in deep inelastic processes 77−67568
nonlinear σ model, 2-D, topology and higher symmetries 79−26241
nonlinear σ models with instantons, 1/n expandable series 79−21909
nonlinear σ-model, finite action solns. 79−80739
nonlinear σ-model with quadratically broken symmetry, cross-over behaviour 79−17601
nonrelativistic persistent model, Schrodinger and Klein Gordon interacting fields with Chew-Low coupling, renormalisation props. 79−54250
nontopological solitons, hadron appl. 80−47191
nuclear field theory of Fermi systems in an external field, path integrals 78−93954
null change and asymptotic freedom *(Czech)* 79−45002
O(3) σ-model, confinement in two dimens. models with factorisation 79−36011
O(5) nonlinear σ-model as a SU(2) gauge theory 79−35937
O(N)ψ^4 interaction, strong coupling limit, rel. to renormalizability of chiral field 78−386
O(N) nonlinear σ-model, two-dimens., fifth Painleve transcendent 80−32002
operator products near light cone, expansion in terms of regular bilocal operators 77−87899
P and T invariance in colour gauge theory of strong interactions 78−37153
parton model, asymptotically-free, $W^{\pm}$, Z^0, μ-pair prod. 78−12865
path group appl. to gauge theory and quarks 80−31985
path integral representation for U- and S-matrix, scalar meson model renormalised S-matrix elements 78−78103
perturbative field theory effects and Regge pole representation, QCD, dual topological unitarisation 80−42434
phenomenological Lagrangian construction 79−63356
physical vacuum and physical one-particle state based method 77−41775
pion condensates, supercond. props., σ model anal. with nucleons 79−59029
Planck energy nonconserving fluctuations and strong forces 80−57551
pre-Schwinger model, Lorentz transforms. if operator solns. 80−47171
propagator of binary quark and antiquark system 79−45053
proton fragmentation functions, Q^2 depend., lowest order QCD calcs. 78−62359
pure gauge fields on coset space 79−40673
$Q^2\bar{Q}^2$ states, mass levels in (3+1) dimens. lattice gauge theory 79−58942
QCD, μ pair transverse momentum distrib. in Drell-Yan processes 78−62374
QCD, axial gauge, mass shell behaviour 78−49966
QCD, charm contrib. to electroprod. struct. functions 78−58170
QCD, charm photoprod., ψ, D, F etc. prod., sum rules, cross sections 78−58169
QCD, decays of heavy leptons and intermediate weak bosons 78−8524
QCD, dynamical props. 78−70332
QCD, E_7 model, quark and lepton assignments 78−8590
QCD, e^+e^- annihilation energy, asymptotically free perturbation theory 78−66045
QCD, effective quark pot. in baryon reson. 78−16910
QCD, energy of classical sources, finite confinement from Pade approximants 78−41478
QCD, expt. test 78−8601
QCD, field strength and action copies in any axial-like gauge 78−82143
QCD, gauge invariance and perturbative calcs. 79−63417
QCD, gluon colour screening by Higgs mechanism 78−93861
QCD, hadron prod. at large transverse momentum 77−87949
QCD, hadronic and supersymm. string states 79−75724
QCD, hard processes, universality of mass singularities 78−82101
QCD, inclusive hadronic annihilation of heavy quark-antiquark bound states, Υ, ψ decays 78−45866
QCD, inclusive production at large transverse momentum, cross section 78−62369
QCD, infinite-mass limit determ. 78−66039
QCD, infrared, near-mass-shell, behaviour of non-Abelian gauge theories 78−24947
QCD, infrared behaviour, colour-singlet quark form factor 78−24948
QCD, IR behaviour of higher order derivative field theories 79−30699
QCD, IR struct. of quark-antiquark scatt. kernel, quark binding pot. 78−8588
QCD, lattice-gauge theory calc. of π and ρ-meson decay consts. 78−74154
QCD, long-range correl. in forward quark-quark scatt. 78−4779
QCD, massless, two dimens., bound states 78−62371
QCD, massless two-dimens. model, operator soln., local colour SU(n) symm. 78−41480
QCD, Migdal's regularisation scheme, hadron struct. 78−4782
QCD, modified, exact global colour SU(3) symm., asymptotic freedom 78−41493

quantum field theory of strong interactions continued
QCD, multicolour, series expansion for meson masses 78−21315
QCD, new quarks and hadrons 78−8591
QCD, parton and gluon distribs. 78−16981
QCD, parton transverse momentum distribution 78−29301
QCD, photoprod. of heavy quark flavours 78−21384
QCD, positivity constraints on quark and gluon momentum distribs. 78−74205
QCD, quantised electric flux tubes 78−45844
QCD, renormalisation group invariant charge and confinement 78−45791
QCD, review 78−37146
QCD, soft gluon radiation 77−13921
QCD, static potential QQ̄ model in weak coupling expansion 77−74647
QCD, strong interaction gauge theory, SU(3) colour gauge vector mesons, confinement 78−78136
QCD, struct. functions, perturbation theory *(Russian)* 78−8595
QCD, three gluon jets as test 78−25001
QCD, transverse momentum distribs. of μ pairs from pN interactions, p-nucleus study 78−62375
QCD, transverse momentum of jets in electroprod. of hadrons 78−62367
QCD, two dimens., bound state eqns. on null planes, Hamiltonian approach 78−37137
QCD, two dimens., renormalisation group functions 78−29242
QCD, two dimens., with SU(N) gauge symm., N→∞ limit 78−41489
QCD, two dimens. light-like gauge formulation, hadronic reactions 78−21388
QCD, two-dimens., bare pomeron graph 78−4824
QCD, two-dimens. extrapolation to four-dimens. 78−78081
QCD, unconfined quarks and gluons 78−45850
QCD and heavy quarks *(German)* 80−37214
QCD and particle-string variables 78−24939
QCD and polarised quarks *(Russian)* 78−74217
QCD and the string model 79−26292
QCD calc. of three-jet processes in leptoprod. and hadronic μ-pair prod. 78−21338
QCD diagrammatic structure, deep inelastic scatt. in asymptotically free theories 79−2996
QCD estimates for heavy-particle prod. 78−82108
QCD gluon contribs. to large p_T reactions 78−41504
QCD in two colours, virtual quark-quark scatt. in pseudoparticle background 78−12823
QCD IR divergences exponentiation 78−41492
QCD observables in higher order calcs. 79−9334
QCD of hadron struct. 78−93849
QCD on mass shell, Ward identities 78−16913
QCD perturbation theory, high energy behaviour of jet and lepton-pair prod. 79−2932
QCD perturbation theory, quark decay functions, heavy hadron prod. 78−62364
QCD perturbation theory predictions, applications and expt. verification, review 79−13026
QCD phase transitions, chiral symmetry breaking, confinement, as tunnelling through singular barriers 78−82145
QCD predictions for large p_T hadron prod. by polarised hadrons 78−82148
QCD test, prod. of heavy quark flavours in hadronic interactions 77−45957
QCD theory prediction of jet structure in e^+e^-→ hadrons 78−12920
QCD vacuum props., strong interaction theory 79−26233
quantum chromodynamics, field strength formulation 78−16924
quantum chromodynamics, review 79−67498
quantum chromodynamics, scale violation in presence of instantons 77−61196
quantum chromodynamics psi-spectroscopy model *(Hungarian)* 79−13068
quantum fluctuations and particle struct. in field theory model 79−30659
quark bound states in field theory 78−25006
quark confinement, analyticity of parton model, QCD_2 calc. 78−41484
quark confinement, bag models, field theoretic, renormalisation and translation invariance 80−62932
quark confinement for gluon generation 78−25008
quark confinement in (1+1) dimensions and fermions 79−63422
quark confinement in condensate of non-Abelian vortices 78−70328
quark confinement potential, infinite order metric multipole fields,theory 78−29295
quark decay patterns, liberated QCD and confined QCD theory 79−9328
quark field quantum fluctuation computation in arbitrary Yang-Mills instanton background 80−13268
quark hyperfine interactions in negative parity baryons, QCD 78−16984
quark model, wave eqns. for mesons and baryons *(Chinese)* 78−86444
quarkonium decay into heavy quark flavours, ψ (J) energy distrib., QCD perturbation theory 78−82146
quarks, observation, calcs. using relativistic quantum field theory 78−24933
quarks and leptons, fermion physics in terms of SU(2)×SU(1) gauge theory 78−74197
radiation gauge static pot. between fermion and antifermion, non Abelian gauge fields 78−89621
Reggeon field theory, Pomeron intercept anal. 77−6003
relativistic bound state of fermion and antifermion, fermion fields, quark model 78−82151
relativistic dense matter, statistical mechanics using phenomenological quantum field model 78−89814
relativistic equations for bound states of quarks 78−70333
relativistic generalisation of linearly rising pot. 78−4768
relativistic local renormalizable field theories, basis for quark confinement and QED 79−21893
relativistic many body theory, finite temp. and density., elementary particle symmetries 79−49403
relativistic many-body theory, quantum chromodynamics and neutron stars/supernova 79−40752
relativistic quantum field theory of finite nuclei 79−6466
relativistic quantum theory of composite systems, nonlocal field theory of quark model 78−70253
relativistic string theory in external field 79−97574
scalar field theory, solvable models of vac. polarisation 78−385
scalar U(N) QCD in the large-N limit, hamiltonian method 80−37212
scaling, model-independ. anal. of electroprod. data 77−5999

quantum field theory of strong interactions continued
Schwinger model, canonical surface formalism, axial anomaly, chiral symm. breaking 78−12816
Schwinger theory, vacuum struct. generators in Lowenstein-Swieca gauge 79−6259
second quantisation scheme for strongly coupled fields 79−97502
semiempirical mass formula for hadrons in quark model and QCD 78−74236
separable nucleon-nucleon potentials and minimal relativity 80−27495
sine-Gordon equation and nonlinear σ model on a lattice 79−21932
soft CP violation, renormalisable gauge model for strong, weak and EM interactions 78−74196
soft gluons in Drell Yan and deep inelastic processes, large const. terms, asymptotic behaviour 79−6326
space-like fields and non-unitary representations of the Poincare group 79−85238
spacetime structure theory at very short distances, nonlinear sigma model 80−12979
spontaneous symmetry breakdown and finite struct. const. calc. 77−22707
spontaneously broken Yang Mills theories, high-energy gauge meson exchange reactions, factorisation, Reggeisation 77−18172
spurion boson model in solvable regularised quantum field theory 77−54047
static potential energy of a heavy quark and anti-quark 79−13028
string, with confined 3/2 spin field 77−41822
string model, critical dimension 77−49925
string theory, relation to field theory, strong coupling expansion 77−87953
strings in the embedding space 78−89654
strong coupling theories, fermions and gauge fields on lattice 77−6009
strong coupling theory, scatt. on nonrelativistic particle 79−40675
strong-coupling calcs. of hadron spectrum in QCD, lattice Hamiltonian 77−41819
strong-coupling limit of renormalisable interacting quantum fields 78−49968
SU_3 symmetry breaking, dynamical 78−21346
SU(2)×U(1), P and T invariance violation suppression, quark mixing angles 79−54278
SU(2)×U(1) gauge theories, successes and current issues 80−18064
SU(2) gauge fields, interaction Hamiltonian for quark source interactions 79−67466
SU(6) quark model of hadron struct., field theory treatment 79−49483
SU(N) σ model, 2 dimens., Gross Neveu model as a Z_3=0 limit 79−35949
SU(N) invariant non-linear σ models 79−17613
superdense nuclei, search for and synthesis, review of expts. and π-condensation theory 79−6463
tachyons, role in strong interaction field theory 79−9353
tachyons and virtual fields elementary particle strong interactions 79−12970
testing strong interaction theories 79−97569
thermodynamic pot. at finite temp. and density, QED and QCD 78−8535
Thirring field confined to MIT bag 77−65099
three-body nuclear forcesin σ-model, nuclear matter and triton BE 77−71568
topological problems in gauge theories, appl. to quark confinement 79−63351
triple spinor model of hadrons 79−13044
two particle inelastic scatt., mass divergences, QCD and parton model 79−22049
twobody crossing elastic and inelastic scatt., asymptotic theorems and polarization phenomena 79−63334
U(N,r) σ models, generalisations of σ and CP^N models, and instantons 79−49377
unified affine gauge theory of gravity and strong interactions, GL(4,R) spinor fields 79−93331
unified theory of gravity and strong interactions, quark confinement 77−22681
vacuum spontaneously broken symmetry of Higgs field and Bose condensation 80−82912
Yang-Lee edge singularity in the hierarchical model 79−35933
Yang-Mills SU(2) high-energy scatt. amplitudes to arbitrary perturbative orders 77−67571
Yang-Mills theory, nonleading IR divergences in QCD, renormalisation group function 77−71422
Yukawa field renormalisation group eqns., asymptotic freedom 77−30314
Yukawa-type interactions of strongly coupled fields 78−49969
e^+e^- annihilation, hadronic jet structs., QCD tests, max. directed momentum parameter 78−25057
e^+e^- annihilation, jet struct., test of QCD and quark-confining string 78−33040
e^+e^-→hadrons, asymptotically free QCD perturbation theory for multijet final states 78−74267
e^+e^-→hadrons, finite energy sum rules, cross section, QCD calcs. 78−62413
e^+e^-→hadrons, inclusive distribs., jets, 1+1 dimens. QCD 78−66137
e^+e^- pair creation in strong EM fields, gravitational effects 80−42376
ep→e+hadron+x, parton picture from QFT, structure function scaling behaviour 79−402
η' mass and quark mass ratio 78−8584
μ pair prod., QCD ang. correl. 78−49976
μ pair production in hadron-hadron collisions, gluon effects, QCD predictions 78−78148
(NΔ) quasi bound state, T=J=2 79−45007
NN interaction, field theoretical approach with stress on OBE pot. *(German)* 78−78203
NN→NNπ, lowest order Feynman diagram calc. 79−63508
NN scatt., high-energy, effect of anomalous mag. moments in quantum field theory 78−465
Nπ scatt., high-energy, effect of anomalous mag. moments in quantum field theory 78−465
ν deep inelastic scatt., four flavour quark model, asymptotic freedom 78−45905
ν-nucleus reactions, multimuon events, QCD predictions for associated prod. of charm 78−25034
νN reactions, field theory phenomenology 79−54304
pp, high energy interactions, field theoretic model of cluster production 77−6091

quantum field theory of strong interactions continued
pp bremsstrahlung, field theory calcs. 79−67584
pp collisions, constituent transverse-momentum fluctuations and hard scatt. expansion 79−17749
pp→dπ$^+$, field theory treatment 78−93898
pp interactions, cluster mass spectrum 80−37307
pp→$\mu^+\mu^-$X, spontaneously broken colour gauge theory effects in Drell-Yan process 79−26344
pp→$\mu^+\mu^-$+anything, Drell-Yan formalism 78−78229
pp scatt., high energy, impact picture for polarisation and rotation parameter 78−70341
π decays and π electromag. form factor, σ-model with quarks 79−22100
π form factor, expt. behaviour, influence of left-hand cut on second Riemann sheet 80−13304
π N forward scattering amplitudes high energy, integral axiomatic upper bounds for coupling const., logarithmic sensitivity *(Russian)* 77−13984
π-nucleus scatt., nonrelativistic QFT formulation, Low eqn., optical pot. definition 79−6700
πd field theoretical model, effective semi-relativistic three-body problem 78−86454
πd semi relativistic field theroretical model, extended Fadde'ev and Amado-Lovelace eqns. 78−89729
πN field theoretic aspects, disconnectedness problem 79−85335
πN→γπN, recoil corrections to static model, interaction current 78−25072
πN low energy interaction, field theoretic approach 79−67602
$(\bar{\psi}\psi)^2$ model, kinks, S-matrix elements 78−93809
QCD, q̄ polarisation in quark sea of proton 78−12867
σ model, pion condensation, use of chiral symmetries, reply to comments 79−297
τ particle properties, QCD type gauge theories, absence of $\tau^+\tau^-$ resonance in e^+e^- annihilation 78−37144
ϒ(9.5) hadronic prod., parton distrib. and QCD 78−78142
ϒ→photons+gluons, QCD perturbation theory 78−33028

quantum field theory of weak interactions
see also elementary particle weak interactions; Weinberg model
asymptotic particle states, local definition in flat space-time 79−21906
asymptotically free theories of deep inelastic muon, and electron scatt. 78−21430
Cabbibo angle and quark mixing 78−74207
charged current Fermi four field point interaction, weak interaction theory, rescatt. graphs consequences 77−67555
conformal invariant Fermi weak interactions and weak bosons as collective modes 79−89094
CP violation and instantons 80−354
CP violation in weak interaction, vector-like theories 78−62333
Dirac particle, charged scalar field, strong coupling theory 78−16976
Dirac particle in mag. field, symmetry breaking by monopole singularities 78−16977
Euclidean QFT, n-particle irreducible functions 80−13199
Fermi universal coupling and gravit. in general relativity 77−79
fermion-fermion scatt., very high energy weak interaction effects 79−9327
gauge models of weak and EM interactions, quantisation and renormalisation of gauge theories, book contrib. 79−30669
gauge scheme of weak and electromagnetic interactions, review *(Russian)* 79−26278
gauge theories, facts and prospects, conf., Schladming, Austria (Feb.-Mar. 1978) 79−26203
gauge theories local operator products 78−12804
gauge theories of weak, EM, and strong interactions, book contrib. 79−30694
Higgs-Boson mass, weak interactions at very high energies 78−8540
history of quantum field theory, search for unity 78−28904
lattice gauge theory with fermions, renormalised phases, vacuum polarization 80−13198
left-right-symmetric theory of weak interactions in unified gauge theory, constraints on phenomenology 78−21369
lepton models, dynamical symm. breaking 77−5980
mixing of weak and gravit. interactions, massive gravitino 78−8578
neutral currents and gauge theories, review 79−13011
neutral-current processes, test of single-Z-boson hypothesis 77−74639
nine-quark, nine-lepton model of weak and EM interaction 77−74631
nonAbelian gauge theory, unification of weak and EM interactions 77−18188
pure leptonic weak interaction with induced shadow states, renormalisable theory 78−37136
quarks and leptons, fermion physics in terms of SU(2)×SU(1) gauge theory 78−74197
renormalisable model on gauge group $SU(2)_L\times SU(2)_R\times U(1)$ 78−12855
review of weak interaction theory 78−4822
second threshold related to Higgs mechanism 77−57483
semileptonic neutral currents as higher order effects in Fermi-type charged current theory 78−41474
short distance analysis of weak interactions, asymptotically free theory 77−54068
six-quark theory, calc. of t-quark mass and flavour mixing angles based on $SU(2)\times SU(2)_R\times U(1)$ 79−80811
six-quark theory, weak interaction mixing 78−41475
soft CP violation, renormalisable gauge model for strong, weak and EM interactions 78−74196
Sp(4)×U(1) gauge symm. for weak interaction, $\Delta I=1/2$ rule 77−34093
SU(2|1) electroweak interactions, implications for 6 extra time dimensions 80−77998
SU(2)×U(1), gauge theory of weak interactions 78−21328
SU(2)×U(1) gauge theories, successes and current issues 80−18064
SU(2)×U(1) gauge theory of weak and EM interactions, quark model 77−26458
SU(2)⊗U(1)⊗U(1)′ gauge model of weak interactions, $\Delta I=1/2$ enhancement 77−6073
SU(3)×U(1) gauge model of weak interactions, quark triplets, charmed hadron decay 77−2789
SU(3)×U(1) gauge theory, charged intermediate boson mixing 77−87910
SU(3)×U(1) gauge theory of weak and EM interactions 78−70317
universal CP noninvariant superweak interaction and baryon asymmetry of the universe 78−66072
vector boson model from SL(2,C) gauge theory of gravitation and Yang-Mills theory 79−322

quantum field theory of weak interactions continued
vectorlike theory of weak interactions 77−67613
weak coupled gauge field formulation using quaternions and p, n, λ quark fields 79−63349
weak interactions of quark fields, quark masses, spontaneous parity violation 77−34115
e-μ permutation symm., lepton number conservation in gauge theories 78−4777
$\mu^-\mu^-\mu^+$ events in ν_μ reactions, SU(3) gauge models 77−74674
ν mass, second-order effect in Higgs coupling 79−75716
ν-induced multilepton events, weak interaction model 78−41533
ν_μ mass limit in absence of muon-lepton-number conservation, unified gauge theories 78−21368
ϒ(9.5), implications of ϒ for ν interactions in weak gauge theories 78−70271
H parity violations, fundamental struct. of weak current, unified gauge theories 78−12849

quantum fluids
see also boson systems; fermion systems; liquid helium
boundary-value problems, quantum statistical mechanics *(Rumanian)* 78−86219
critical behaviour and generalised phase diagrams 77−31815
degenerate quantum gases in the binary collision approximation, two-particle density matrix 79−71358
density fluctuations in classical and quantum liquids, general theory 79−35628
dynamic structure function, deep inelastic behaviour 77−69129
gas-liquid transition, quantum crossover effect 77−7839
Gibbs mixing entropy paradox, quantum gases 78−49588
Gross Pitaevskii eqn., generalised solns. 80−49437
hot nuclear matter, eqn. of state determ. 79−93538
hydrodynamics, canonical eqns. 78−91497
hydrodynamics equations in presence of vortices *(Russian)* 79−33141
hyper-netted chain eqn., Kohn-Sham theory derivation 78−47225
ideal gases, paradoxes associated with mixing 77−13728
impurities, surface bound states, quantum and classical liquids 78−18859
ion structure in fluids, Atkins model revision 77−7921
liquid, computer modelling 80−54472
liquid physics, book 79−60245
many body theory, appls. review of development 80−46968
Monte Carlo methods and results, book contrib., review 79−82405
neutron scattering 78−59990
nonlocal exchange-correlation pot. for inhomogeneous electron gas and quantum fields 78−65870
phase space quantisation of interacting vortices in two demensions 80−4634
polymer expansion for quantum many-body problem 80−57181
quasiparticle kinetic eqn. construction 80−53905
relaxation, renormalized perturbation expansion in kinetic theory 78−21061
superfluid mechanics for high density of vortex lines 78−54290
surface, atomic processes, book contrib. 79−60605
vortex formation and dynamics, Magnus force *(Russian)* 80−10719

quantum generators (optical) *see lasers*

quantum mechanics *see quantum theory*

quantum numbers *see quantum theory*

quantum optics
see also photon counting
absorption spectrum windows, of oscillator ensemble with embedded impurity oscill. 79−6045
absorptive optical bistability, transmitted light spectrum and dynamic response function 80−99789
absorptive optical bistability transient, analytical treatment 80−19077
absorptive optical bistability transient, local relax., quantum statistical treatment 80−91838
active and passive particles, extinction 80−102684
active particles, Lorenz-Mie scatt. theory paradox 80−74324
active particles, Lorenz-Mie scatt. theory paradox 80−102683
adiabatic following solutions of Bloch equations, rel. to Pauli type master eqns. 79−13940
amplified spontaneous emission in spherical and disk-shaped laser media 80−1177
anharmonic oscillator model for dispersive optical bistability 80−58623
anti-Stokes luminescence, quantum statistics 79−915
antibunching in two-photon absorption 78−78980
anticorrelation effect in optical parametric processes, quantum statistical props. 79−7177
atom, canonical dressing by intense radn. fields 80−1173
atom, multiphoton ionis., r-photon reson., theory 79−49998
atom, resonance light scattering, intensity effects 80−91511
atom, spontaneous radiation, near field calcs. 80−99493
atom, two- and three-level, transition in stochastic field, saturation and Stark splitting 80−9546
atom in strong EM field, characts. calc. using quantum theory of Markovian processes 80−32943
atom-evanescent wave interaction, exchanged momentum meas. *(French)* 78−37603
atom-photon interaction quantum fluctuations, at. beam focusing by radiation press. 80−58217
atom-strong field interactions, generalised dressed atom approach, laser theory and Bloch-Siegert shift 77−71964
atomic and molecular collisions in intense light beams, quantum aspects *(Russian)* 79−6903
atomic coherent state representation, operator eqn. mapping to C-no. differential form 77−58304
atomic cooperative system, intensity correlation functions 79−59663
atomic cooperative system, light scatt. spectrum, coherent-state representation, numerical results 80−23650
atomic engines, efficiency of coherent amplification 78−33717
atomic fluorescence sideband prediction 78−55139
atomic hyperfine struct. transitions, nonstationary RF coherence signals *(Russian)* 79−98011
atomic level shifts in laser fields and space-translation Hamiltonian 77−34858
atomic momentum distrib. in resonance fluoresc. 79−72271
atomic momentum distrib. modification by travelling wave reson. light field 79−72280
atomic motion in resont fluctuating laser radiation 80−43310
atomic movement, reson. light press. due to strong standing wave 78−50529

quantum optics continued
atomic number fluctuations, intensity correlations in resonance fluorescence, photon antibunching 78−50499
atomic state, superradiant, excitation by pulse of quantum field 80−87359
atomic systems, coherent transients theorem 80−99808
atomic three-level system, collisionally aided radiative excitation 79−98022
atomic translational motion, coherent radiation effect *(Russian)* 77−27035
atoms, motion in optical freq. radiation trap 80−78818
bistability, absorptive and dispersive, in Fabry-Perot and ring-cavity geometries 80−95942
bistability, cooperative effects and fluctuations 78−17885
bistability, exact semiclassical treatment of ring cavity 80−58627
bistability, in lasers containing saturable absorbers, semiclassical and quantum theory 79−3674
bistability equations for standing wave cavity, analytic solns. 80−48328
bistability in bad cavity limit, Fokker Planck eqn. approach 80−64116
bistability in resonant two photon absorber 78−90448
bistability through nonlinear dispersion and absorpt. 79−76653
bistable absorber system, in ring cavity, photon statistics 79−31847
bistable optical system, phase transitions induced by white noise 79−18388
bistable optical system, stochastic master eqn. description 79−76652
bistable steady states in optical subharmonic generation, Wigner distrib. 80−53370
bistable system, noise transform. 79−59746
bistable systems, fluctuations when driven by coherent external light field 79−18387
black-body radiation field interaction with photoconductor, noise, Langevin method 78−30950
Bloch coherent states derivation from SU(2) van der Waerden invariant 79−3671
Born-Oppenheimer and true eigenstate prep. by coherent light, large mol. nonradiative relax. 77−88490
broad band reson. light press., basic eqns. 80−28182
cavity, optical bistability, long-time behaviour 80−78892
cavity with outout coupling, one-dimens., quasimodes as field eigenvalue 80−9911
charged dust grain, light scatt., quantum approach 80−48196
charged particle, pot. scatt. in low-freq. laser field 79−41311
charged particle self-interaction 80−373
coherence, classical and quantum theory 77−58306
coherent and nonlinear optics, Conf., Leningrad, USSR (June 1978) 80−27027
coherent emission, caused by pulsed laser in low-density gas 79−18389
coherent multiphoton intense interactions, convergent perturbation anal. 80−1037
coherent multiphoton processes, effective two level hamiltonian 78−29921
coherent optical spectroscopy 78−1112
coherent propagation, two-photon quasi-reson. pulses, multi-level atom medium 77−68196
coherent properties of two oscillators, elec. and mag. transitions of arbitrary multiplicity *(Russian)* 77−46712
coherent spontaneous and stimulated emission, quantum theory 77−3557
coherent state, necessary condition to remain coherent 78−73879
coherent states, time evolution 77−61930
coherent states and quantum nonperturbing measurements 79−315
collective atomic system population inversion driven by classical field 80−63964
collective atomic systems, transient and steady-state behaviour in classical external fields 79−13939
collective radiation and the near-zone field 80−37977
collective radiative phenomena in two level systems *(Russian)* 80−1174
communication channels, statistical model, asymptotic relations 78−33687
communication theory, appl. of generalised quantum meas. theory 78−13668
conference, New York, USA (Jun. 1980) 80−90614
cooperative cascade emission, linear stochastic theory 80−74326
cooperative cascade emission theory, nonlinear evolution 80−74327
cooperative combination scattering, light pulse propag. effects 79−81485
cooperative emission by polyatomic system, homogeneous and inhomogeneous broadening *(Russian)* 77−46713
cooperative multiphoton ionisation, bistability effects, Bonifacio-Lugiato model 80−19010
cooperative resonance fluorescence, multiple sidebands, semiclassical calcs. 80−99685
cooperative resonance fluorescence, photon statistics and absorption spectrum 78−42311
cooperative spontaneous emission theory 79−27223
coupled system, time depend. projection operator anal., classical gas and quantum systems 78−16720
degenerate parametric amplification 77−58380
degenerate parametric generation from quantum noise, photon statistics 79−81398
degenerate states, magnetoelec. susceptibilities, ang. momentum theory 78−55142
degenerate states, magnetoelec. susceptibilities, numerical calcs. 78−55143
degenerate two level system, reson. light scatt., transient polarisation characts. 78−94382
degenerate two-level system interacting with pulse of radiation, time depend. 79−59662
detective quantum efficiency and granularity rel. to quantum noise 79−21829
diatom+molecule, laser-induced vibr. excitation 79−98205
diatomic system, spontaneous emission, photon correls. *(German)* 80−5711
Dicke maser model, dynamical struct. 80−37985
Dicke maser model, equilibrium states for mean field models 80−46961
Dicke maser model, radiation damping, phase transition, presence of phonons 77−19224
Dicke maser model-van der Waals spin system thermodynamic equivalence 80−83572
Dicke model, compressible, exact soln. 77−34857
Dicke model, equilib. and nonequilib. crit. props. 78−63049
Dicke model, generalised, canonical transform theory 77−19216
Dicke model, lack of transition with external fields 77−10878
quantum optics continued
Dicke model, modification for long wave photons 80−1169
Dicke model, nonlinear extensions, second order phase transitions 77−34855
Dicke model, reson. freq., temp. doubling 77−14681
Dicke model, soft mode 77−42515
Dicke model, spontaneous polarisability of two-level atoms 80−1167
Dicke model, two-level atoms, phase transition 78−5442
Dicke model for a multicomponent system 80−74329
Dicke model Hamiltonian, coherence props. of radiation field 78−58959
Dicke model of maser, phase transition, counter rot. and $(A)^2$ terms in Hamiltonian 77−23641
Dicke model of phase transitions, rel. to optical bistability 79−81402
Dicke model phase transition, thermodynamic Green's function method 80−5715
Dicke model with external fields, simple Green function approach, lack of phase transition 78−9353
Dicke state N two level atom assembly, radiation emission theory 80−69350
Dicke-maser model dynamics, phase transition to the spontaneous coherent state 78−66792
Dicke-type Hamiltonians with hidden variables 78−74874
discrimination, of quantum optical fields 77−10879
dispersion effect on optical bistability, master eqn. generalisation 79−31845
dispersive optical bistability with inhomogeneous broadening, exact soln. 80−53360
distinguishing close quantum signals 77−7044
distributed feedback due to meeting of oppositely propag. noise waves, beats *(Russian)* 77−71965
double radiooptical resonance, signal propag. and shape 80−87360
dressed atom system, energy levels and reson. phenomena, universal algorithm 80−69111
dynamic behaviour of optical bistability, time depend. Fokker-Planck eqn. soln. 80−37980
dynamic self-diffraction of coherent light beams; review 80−102777
effective photon hypothesis, expt. test 77−46709
effective photon scattering cross section, high intensity laser radiation+-matter interactions 78−74872
electric dipole interaction 80−19011
electron-laser photon elastic scatt., Coulomb background 77−74666
EM field, eigensolutions of field strength operator *(German)* 78−83028
EM field momentum very close to plane interface 79−13936
EM field quantification near plane mirror *(French)* 77−34854
EM fluctuations in dielec. slab resonator 79−3672
energy trapping in atomic systems metastable states, continuous rad. source 78−78669
F-centres, struct., quantum optics, laser spectra 77−52147
Fabry-Perot cavity, dispersive optical bistability 80−78889
Fabry-Perot cavity, instabilities for coherently driven absorber 80−53387
Fabry-Perot cavity, optical bistability, standing wave effects 80−91837
Fabry-Perot interferometer, optical bistability, inhomogeneous broadening, mean field approx. 80−90885
ferroelectric transition, photon condensation effect 77−68201
field fluctuations of two-photon coherent states 79−13937
Fokker-Planck equation, for parametric process 79−3663
Fokker-Planck equation, for parametric processes, photocounting statistics 79−3664
Fokker-Planck equation for optical bistability 79−75456
four-photon processes stimulated by fluctuating pump in dispersive medium 79−23017
free electron laser, coherent quasi-classical states 80−53251
free electron laser, multiphoton analysis 80−78826
free electron laser, quantum theory 80−23656
free electron laser, quantum theory for strong fields 80−83583
free electron lasers, quantum mechanical and classical theories 80−83579
free-free transitions in quantum electronics 80−28183
gamma-Lorentzian intensity fluctuations, integrated, statistics 80−102685
gas, spontaneous emission and absorpt. of weak wave, radn. capture effect 80−939
gaseous dipolar media, semiclassical theory, appl. to gas laser 80−83586
gaseous medium, two-photon-absorbing, polarised light propag., quantum effects 80−103107
gaseous system, third harmonic generation, quantum theory 80−99795
gaussian beam resonator, optical nutation 80−99807
Gaussian light, partially polarised, photon statistics 80−19012
generalised Dicke model for matter interacting with EM field 78−5441
generalised P-representations in quantum optics 80−87356
generating functions calc. 80−1168
generating functions calc. from characteristic functions 79−914
Glauber mode statistical props. 79−98326
Goldstone mode in stationary state of non-equilibrium dissipative system *(Chinese)* 80−87365
harmonic generation, quantum statistics 77−58379
harmonic oscillators, charged, interaction with transverse EM field mode 80−5712
hidden variables, quantum mechanics, and stochastic electrodynamics *(French)* 78−62107
higher order nonlinear optical processes, quantum statistical props. 77−46753
homogeneously broadened three level atoms, intense standing wave saturated, spatial inhomogeneity, mode competition 80−23646
hyper-Raman scattering, degenerate, quantum statistical props. of photon and phonon fields 79−89873
hyper-Raman scattering, non-degenerate, quantum statistical props. of photon and phonon fields 79−89872
impurity atoms in solids, photon antibunching in reson. fluorescence 79−43025
indeterminancy, of phase and number of photons *(Russian)* 79−18390
inelastic light scattering conference, Santa Monica, CA, USA (Jan. 1979) 79−95762
injection laser quantum noise in optical fibre communication systems 80−48259
intensity fluctuation linewidth, Jakeman-Pike approx., black-body and laser models 78−58960
intensity fluctuation spectrum, theory of registration *(Russian)* 78−1199
interaction processes between atoms and EM fields in presence of static mag. field 78−55143

quantum optics continued
interatomic correlation effect on spontaneous Raman light scatt. *(Russian)* 77−46711
intersection of quasistationary levels *(Russian)* 77−3561
Josephson junction, coherently driven, bistability model 80−15661
laser, multimode, containing saturable absorbers, bistable operation 80−91862
laser cavity resonator, photon lifetime and reflectance meas., phase-shift method 80−38039
laser excitation, stepwise, coherent Schrodinger vs. incoherent rate eqn. approaches 78−74871
laser field interaction, Floquet theory 80−63716
laser fields, stochastically fluctuating, saturation and Stark splitting of resonant transitions 80−53245
laser pump fluctuations, influence on resonance fluoresc. radiation intensity correlation 80−37981
laser saturation spectroscopy, time-resolved, free induction decay of two-level resonances 80−102775
laser system qualitative change in threshold range, analogy with phase transition *(Czech)* 80−32949
laser-induced line shifts and double-quantum Lamb dips 78−86825
laser-photocond. layer system, optical amplification coeff. *(Russian)* 77−24585
laserlike systems, stochastic master equation description 80−53243
lecture on introduction to quantum optics 78−25843
lectures on interaction of radiation with condensed matter, Trieste, Italy (Jan.-March 1976) 78−27172
Lie algebra representations and coherent states, Trotter limits 80−22238
light beam interaction with atomic system, description by irreducible tensorial sets 77−68195
light beam quantum fluctuations meas. using nonlinear interferometer 79−80672
light evolution of quantum statistics 78−58964
light generation at impurity atoms in ferroelectrics and LC, fluctuation effects *(Russian)* 80−91767
light scattering, intensity correlations, general theory 79−50267
linear interaction processes between atoms and EM fields of laser wave 78−55142
local heating, quantum transitions in coupled electron-vibr. system 79−15514
many photon collective phenomena, finite QED formalism. 78−9352
many-atom system, coherent radiation processes, renormalisation calcs. 77−3560
many-level molecules, unitary dynamical symmetry for superadiance, classical limit 78−9355
many-mode optical fields, photon statistics 78−42310
many-particle systems, reson. weak light field scatt., intensity correl. function 80−95855
many-photon ionization, resonance scattering on a nonstationary potential, and complex poles of the S-matrix 79−22677
master equation derivation for optical bistability 78−74873
matter system irradiated by coherent light quasi-stationary states *(Japanese)* 77−42514
matter-photon interaction renormalisation, coherent states in matter-photon systems 77−68199
mean field models, equilib. states 80−46961
meson fields, classical coherent component 78−78082
microscopic radiation field measurements, phase-difference operator analysis 77−42517
modulation concept rel. to degrees of coherence, for quantum optical field 77−83840
molecular collision processes in multimode laser field, intensity time variation effect 79−31620
molecular gas, rot. temp. decrease due to stimulated transitions *(Russian)* 79−86152
molecular near-resonant fluoresc. and Raman scatt. theory 79−3446
molecular rotational coherence, reson. collisional exchange, time-resolved microwave obs. 80−23525
molecular system interacting with radiation field, equilib. mean values 79−27224
molecule, quantum nonlinear resonance, theory 77−65587
molecules, large optical free induction decay, photon echoes 78−37945
Moller cross section in strong laser field, resonances and intensity depend. shifts 79−45918
Moller scatt., high intensity, scatt. energies 80−22541
monochromatic EM wave, passing through reson. medium, characteristic modulation 79−27220
moving atoms interacting with laser fields, self consistent approach to transport eqn. 78−42016
multi-level atom with Raman reson., time-delayed laser scatt. 80−48343
multi-level excitation theory, analytic approximations 78−29922
multilevel atomic system, thermally relaxing, coherent radiation reson. scatt. and absorpt. 79−81401
multilevel equidistant system, excitation by elec. field 80−37983
multilevel molecular system, excitation by laser IR field 78−55212
multilevel relaxing systems, multitime correl. in scatt. and fluoresc. 80−1166
multilevel system, band type, excitation dynamics in laser field *(Russian)* 78−21980
multilevel system, equidistant, coherent excitation in reson. monochromatic field *(Russian)* 77−61933
multilevel system, group theoretical method for coherent effects calc. 80−106502
multilevel system, nontransient phase coherent light absorpt. effects 77−498
multilevel system, quasienergy states 77−75462
multimode attenuation due to two photon absorption 79−13933
multimolecular system, two-level mols., coherent trapping of single excitation 79−89875
multiparticle system, effects of powerful coherent radiation on spontaneous emission *(Russian)* 78−46554
multiphoton absorption and emission processes, photon statistics calcs. 80−78819
multiphoton absorption influence on photon statistics 79−13931
multiphoton stimulated Compton scattering of relativistic electrons 80−48198
multiple coherent interaction in optical separated fields, superhigh resolution spectroscopy 80−52338
multiplication of spontaneously emitted photons by means of quantum mech. amplifier *(Russian)* 77−75463

quantum optics continued
N two-level atom system, single-mode reson. radiation field interaction 80−78817
N two-level atoms, interaction with radiation field in restricted rotating wave approx. 80−5713
N two-level atoms, quantum theory of nonlinear optical phenomena 80−5790
N-atom system, superradiance and energy transfer 77−3558
N-level atom, mol., coherent dynamics, periodic anal. 79−94200
N-level atom (molecule), coherent dynamics, two- and three-level behaviour 80−23649
N-level atomic system, reson. excitation by strong coherent radiation 79−68374
N-level atomic system interaction with quantised EM field, algorithm for numerical calcs. 79−64187
N-level atoms, coherent dynamics, anal. solns. 78−22105
N-level atoms, coherent dynamics, numerical expts., 78−22104
N-level molecules, coherent dynamics, anal. solns. 78−22105
N-level molecules, coherent dynamics, numerical expts. 78−22104
n-level quantum system, coupled to photon reservoir, polychromatic field interaction 77−75460
n-level system, cooperative behaviour, energy states, coherent states, classical limit theories 77−34860
n-level system, cooperative behaviour, quantum beats 77−34861
N-level system in strong monochromatic field 78−29923
n-photon resonance phenomena, finite laser bandwidth effect 80−58230
N-two level atoms, interaction with radiation field in restricted rotating wave approx., numerical anal. 80−5714
negative light absorption by medium with selective freq. modulation of quantum oscillators 80−106501
NMR system, multi-level, coherent phenomena, review *(Japanese)* 79−73831
non-centresymmetric media, phase transitions into spontaneous coherent state *(Russian)* 80−69353
nonequilibrium quantum statistics of lasers and nonlinear optics 79−31848
nonlinear, Fokker-Planck eqn., rel. to path sums, Feynman proof 77−2629
nonlinear oscillator excitation by harmonic force, numerical computation 78−50743
nonlinear photoionisation, testable Noyes-like interpretation of Panarella's effective-phonons theory 77−61929
nonlinear quantum oscillator, stochastic instability 79−85007
nonlinear quantum systems, wave packet behaviour in pseudo-coherent state method *(Russian)* 80−1175
nonlinear wave rectification, quantum limit 80−83634
nonradiating partially coherent sources, scalar theory 79−64189
nonradiative transitions of excited atoms located near absorptive medium surface 77−61692
nonresonant excitation, ensemble of two-level systems, rel. to multiphoton spectra, polyatomic mols. 80−5585
one-dimensional cavity with output coupling, field quantisation 77−7144
one-dimensional optical cavity with output coupling, fluctuation-dissipation theorem 79−89876
one-mode fields, greatest lower bounds for degree of coherence of higher order 78−71068
optical bistability, Fokker-Planck eqn. from master eqn. 79−13935
optical bistability, nonlinear polarisability model 80−37976
optical bistability, photon statistics and spectrum of transmitted light 78−46298
optical bistability, scatt. light spectrum atomic fluctuations 78−94383
optical bistability and spectrum of fluctuations, quantum anal. 78−71067
optical bistability with dispersion 80−78893
optical Bloch equation, stochastic incoherences 79−68373
optical cavity, one-dimens., with output coupling, thermal radiation, fluctuation-dissipation theorem 79−978
optical communication using two-photon laser, optimum control of quantum noise 78−71049
optical equivalence theorem, new type of discrete diagonal coherent state representation 78−55328
optical field quantisation from absorber theory 80−43309
optical nutation in gases *(Russian)* 79−27225
optical triple resonance, semiclassical anal. 79−93963
oscillatory superradiance, quantum fluctuations effect 77−14682
parametric interaction with reson. medium, EM field statistics 80−1171
partially coherent light interpretation, optical theorems 80−53210
phase measurement anal., for microscopic radiation fields 78−17887
phase relations, bremsstrahlung struct. *(Russian)* 78−74870
photoelectron statistics, book 78−25842
photoelectron time-interval distrib., effect of higher-order intensity correl. 77−61932
photon antibunching, polaris. depend. 80−1170
photon antibunching enhancement by interf., Young's interf. expt. 79−27313
photon antibunching simulation 79−72543
photon behaviour in high intensity coherent laser beams 80−28185
photon emission from mol. and electronic transitions, quantum dynamics, semiclassical description 80−105466
photon existence testing by photoelectric counting and nonexistence of photons 80−9842
photon field equation, effect of A^2 term omission in conventional Hamiltonian 77−7043
photon impulse in medium with negative group velocity *(Russian)* 79−3670
photon nonexistence, expt. test 77−31082
photon position observable, Ludwig axiomatic quantum mechanical formulation, quantum optics 80−73206
photon reflection at the boundary of an inverted medium 79−36869
photon stationary distribution in optical bistability 80−48197
photon statistics, unsaturated k-photon absorption, exact soln. of master eqn. 80−37984
photon statistics after destructive interf. of two-photon absorbed light 80−48199
photon statistics and quantum optics 77−34864
photon statistics change by one-photon and two-photon absorpt. 78−22103
photon synchronisation effect on intensity interference *(Russian)* 80−48200
photon-anticorrelation effect calc. in degenerate optical parametric amplifier 80−33079

quantum optics continued
photon-electron scattering, opacity due to electron and quantum correls. 77−64634
photon-matter system, polariton instability and thermodynamic phase transition 79−86150
photon-photon scattering, effective-photon theory for cross-section 78−58962
photons interaction with nonstationary EM field *(Russian)* 79−98327
polyatomic mol. gas, laser-induced rate processes, collision-free dynamics 77−30934
population inversion, with freq. chirping, pulse shape depend. 78−17886
probe frequency gain in optically bistable system, quantum theory 79−98435
pulse excited multilevel system, diffr. grating effect in luminesc. 79−50272
quantum electronics and Einstein's theory of radiation 80−98782
quantum electronics within limit cavities, Fain Chanin vs. infinite R_3 formalism 77−38839
quantum meas. realisable with photoemissive detectors 80−53220
quantum oscillator interacting with quantised radn. field, Brownian motion effects 77−34856
quasi-energetic spectra of quantum systems in classical monochromatic fields 78−78981
Rabi oscillations, double-pole decay 79−86151
Rabi oscillations, mag. sublevel degeneracy effects 78−63048
radiation fluctuations from light source 80−95857
radiation theory, multipolar Hamiltonian QED and quantum optics 80−86634
Raman effect, spontaneous, three-level system in intense laser fields 78−86802
Ramsey resonance, of two-level mols., in three separated fields produced by corner reflector, theory 80−74166
reflection of light, from spatially nonuniform amplifying medium 80−106444
resonance atom, spontaneous diffr. of light 80−91512
resonance fluorescence, detailed balance, Lyapunov stability and entropy 79−13941
resonance fluorescence, multiat. and transit-time effects on photon-correlation meas. 78−86812
resonance fluorescence, optical bistability and cooperative effects 79−3668
resonance fluorescence, photon correlation laser linewidth effects 80−83316
resonance fluorescence in Markovian stochastic fields 80−83573
resonance light scattering, two level density matrix description 78−25840
resonance phase transition in two-level lattice system, thermodynamics 80−69351
resonance radiation, diffuse and selective reflection 77−50611
resonance scattering and fluorescence, time and spectral resolution 77−58305
resonant media, pulse counterpropagation and nonlinear interaction, transverse effect computation 80−106563
resonant medium, interferograms form. by nonoverlapping pulses of coherent light 79−64191
resonant optical phenomena in fluctuating laser fields, quantum statistical theory 79−14042
resonant Raman scattering in laser fields of arbitrary strength, antibunching effects 80−23653
resonant scattering line, unshifted, of strong quasimonochromatic field, shape var. *(Russian)* 77−61934
resonant scattering of intense beam of radiation by assembly of atoms in small vol. 77−34853
resonant transitions in strong chaotic fields, saturation and Stark splitting 79−72542
review of work at Ukrainian SSR Acad. of Sci. *(Russian)* 79−45950
ring cavity, dispersive bistability in homogeneously broadened systems 80−14306
ring cavity, dispersive optical bistability 79−18386
ring cavity, dressed mode dynamics of optical bistability 80−19013
rotator, plane, in intense EM field, scatt., emission, and absorpt. 78−78982
rotator, rigid, power of induced radiation in quantum transitions *(Russian)* 78−74875
saturable optical amplifier, quantum theory 80−78916
scattering in laser field, generalised LF approx. 79−58590
second order optical processes, stochastic theory 79−94201
self pulsing in absorptive optical bistability, analytical description 80−78891
self pulsing in dispersive optical bistability in ring cavity 80−78890
self-induced transparency *(Russian)* 79−98448
simple quantum model, periodic spontaneous collapse and revival 80−73208
single mode laser, photon statistics, intracavity two-photon absorption effect *(German)* 77−10933
single-beam two-photon absorbed light, off diagonal density matrix 78−30009
solid, quantum EM processes, population var. and natural radiative decay *(Russian)* 77−32343
spatio-temporal correlation measurements, exciting light effects 79−50268
spectral density of resonance fluorescence, two level atom in intense radiation fields 78−58961
spherically symmetric molecules, many-photon excitation in IR laser field 80−95596
spin angular momentum of field interacting with plane interface 79−81399
spin-1 system, periodic perturbation, analogue of Shirley's eqn. 77−3248
spontaneous and stimulated emission intensities, depend. on radiation field 79−3662
spontaneous emission, 2 particle system in strong reson. field *(Russian)* 77−50646
spontaneous emission, line widths and energy shifts *(Chinese)* 79−89874
spontaneous emission by large system of identical atoms, math. treatment 77−50396
spontaneous emission near plane mirror, quantum formalism *(French)* 77−27267
stable coherent states, evolution operator 77−42516
Stark effect in high-frequency fields for resonant modulation 79−10274
statistical, struct. and representation of correlation functions and density matrix 79−98325
quantum optics continued
statistical theory of one-photon and two-photon processes, density matrix formulation 78−42313
stimulated versus spontaneous emission as cause of photon correlation 77−34862
sub-Poissonian radiation field construction 79−13932
sub-poissonian statistics of an anharmonic oscillator in thermal equilibrium 80−82669
subharmonic lasers, quantum theory, first order non-equilib. phase transition 80−83584
superfluorescence, phase-wave fluctuations 80−23652
superfluorescence, two-level atoms system, quantum theory, incl. propag. effects 80−58491
superluminescence polarisation obs. of high-current pulsed discharge in gas with anisotropic gain 79−14515
superradiance, octupole and hexadecapole dynamics, algebraic struct. 77−88682
superradiance, subharmonic, two-level atom system 79−18385
superradiance from extended systems, propag. in ab initio theory 77−642
swept-grain amplification, semiclassical theory 79−31846
thermally excited quantum oscillators and second law of thermodynamics 77−34863
three boson field modes with trilinear interaction, statistical behaviour 78−87093
three level atom, reson. fluoresc. fluctuation-regression theorem 77−10629
three level atoms, coherent nonlinear mechanism for optical bistability 80−102756
three level medium, ultrashort pulse propag., transient processes 78−18024
three level molecular system interaction with two laser fields 77−54685
three level system, coherently pumped, cooperative relax. 80−78816
three level system, interference between one and two photon processes, occupation probabilities 80−63965
three level system, two-photon reson. scatt. in strong field *(Russian)* 78−58967
three two-level atoms system, continuously incoherently-pumped, radiation rate, spectrum 80−5716
three-level atom, Doppler free two-photon absorption, near reson. intermediate state 77−71788
three-level atom, multiphoton absorpt., finite bandwidth laser influence 78−25841
three-level atom, nonmonochromatic chaotic field, double optical reson. and reson. fluoresc., AC Stark splitting 80−9547
three-level atom, reson. fluoresc. spectrum 79−54804
three-level atom in radn. field, resonance processes *(Russian)* 79−45687
three-level atom reson., vector model, comparison, with exact two-photon soln. 77−57957
three-level atom reson. fluorescence, statistical props. 78−78661
three-level atom system, distortionless optical pulse propag. 78−22179
three-level molecular system, populations, rate equations 80−37975
three-level system, adiabatic following in two-photon transitions refr. index, line asymmetry 77−57956
three-level system, coherently driven, collisional contrib. to dynamic Stark effect 79−13765
three-level system, free induction decay, in time-delayed laser saturation spectroscopy 78−86976
three-level system, interacting with two strong EM fields, steady-state population distrib. and complex susceptibility 80−37978
three-level system, interaction with pump fields 78−33718
three-level system, rel. tuned two- and three-photon processes 77−68198
three-level system, stimulated Raman scatt. and stimulated collision induced fluoresc. 78−87103
three-level system, strongly-excited, statistical broadening and population loss 79−41359
three-level system, two-photon mag. circ. dichroism 79−76457
three-level system, two-photon transition in two pulsed fields 79−68215
three-photon vector model, resonant coherent interaction *(Chinese)* 80−43306
three-wave reson., self-induced transparency effect 78−33716
time evolution of coherent states 79−50271
transient response in optical bistability 79−3666
transition phenomena, review 80−32944
transition probability in two level systems, damping of states, crossing terms *(Russian)* 80−78820
triple optical resonance, N-level system, N-1 photon reson., steady state level population calcs. 78−17888
two level atom, two-photon reson. fluoresc. 79−780
two level atom system, coherently driven, cooperative fluoresc. 80−87357
two level atoms, method of separated optical fields 78−30008
two level atoms, reson. fluoresc., cooperative effects, bistability 77−10628
two level system, microwave SHG, at. correlations and line shape 77−19219
two level system, microwave SHG, at. correlations and line shape 77−19220
two level system, relax. consts. meas., two travelling waves reson. interaction 77−38644
two level system, temp. in strong radiation field 77−79791
two level system interacting with two optical fields, generalised theory 79−36866
two level three dimensional system, phase transitions analogy with lasers 78−58965
two photon coherent states in degenerate four wave mixing 80−5717
two-(three-)level systems, steady and transient behaviour 78−1200
two-atom resonance fluorescence, in strong EM field, excitation spectrum 78−82778
two-atom system, continuously pumped, radiation props., master eqn. 78−86828
two-atom system, cooperative, reson. fluoresc. spectrum. sidebands 80−43000
two-atom two-photon resonance fluorescence 79−22645
two-level atom, driven by reson. multimode laser, light scatt., statistical props. 80−91489
two-level atom, EM radiation interaction, elec.- and mag.-dipole contribs., reaction field 78−94215
two-level atom, excited state, decay, radiative emission-autoionisation interference 79−26945
two-level atom, intensity effects in reson. fluoresc. 79−59661
two-level atom, interaction with laser pulse 78−86827

quantum optics continued
two-level atom, interatomic force depend. on intense radiation fields 80−53100
two-level atom, multiphoton reson. fluoresc. in strong low-freq. field 78−55154
two-level atom, phase transition induced by laser field *(Russian)* 78−29924
two-level atom, radiative decay, external static perturbation effect 79−93949
two-level atom, rel. redistrib. by standing waves 78−55327
two-level atom, reson. fluoresc., atomic operators 80−63579
two-level atom, sub-Poissonian photon statistics in resonance fluorescence 79−76650
two-level atom in resonant bichromatic field *(Russian)* 79−36588
two-level atom interaction with EM field, quasi-classical approx. *(Russian)* 77−27031
two-level atom plane, one-dimens. $\delta l=1$, $\Delta m=0$ decay, soluble semiclassical model *(Portuguese)* 80−18809
two-level atom saturated by resonant laser beam, at. fluoresc. 77−18835
two-level atom system, absorptive optical bistability, photon antibunching 80−58486
two-level atom system, reson. fuoresc., photon antibunching, propag. effect 80−9843
two-level atomic system, superfluoresc. fluctuations 80−23651
two-level atomic system, weak probe field absorption spectra in coherent laser field 80−23758
two-level atomic system two-photon transverse reson. in RF spectra 77−79594
two-level atoms, Dicke model, nonradiative relax. *(Russian)* 79−50273
two-level atoms, multiphoton cooperative radiation, SCF approx. calcs. 80−95856
two-level atoms, saturation in chaotic field 80−37982
two-level atoms, spontaneous emission, semiclassical model 77−19221
two-level atoms in solids, resonant interaction model for long-wavelength photons 80−91765
two-level atoms interacting with single-mode radiation field 77−65586
two-level Doppler-broadened medium in Fabry-Perot, optical bistability 80−102759
two-level electron system with electron-phonon interactions in field of strong EM wave 77−24524
two-level ensemble interacting through EM field, phase transition, collective polarisation 77−19218
two-level gas, reson. radiation press. in travelling EM wave field 79−13681
two-level molecular ensemble, cooperative decay 77−88681
two-level molecules, cooperative energy transfer 77−83838
two-level spin system, mag. moment dynamics in mutually perpendicular mag. fields, of arbitrary freq. 79−3415
two-level system, adiabatic rapid passage, narrow IR saturation resons., book contrib. 78−9419
two-level system, atomic coherence decay due to interaction with strong coherent radiation 77−71963
two-level system, Doppler broadened, vel. tuned reson. as multi-Doppleron process 77−79789
two-level system, in monochromatic field, quasienergy calcs. 79−10276
two-level system, in noise pumping field, absorpt. of probing rad. 77−68197
two-level system, in nonstationary field, fluctuation and relax. props. 78−33715
two-level system, in strong reson. field, saturation, temp. and spectrum characts. 80−99690
two-level system, multi-doppleron processes, probe spectroscopy 79−81400
two-level system, nonmonochromatic radiation excitation, nonlinear optical phenomena *(Russian)* 78−87101
two-level system, optical coherent transients 77−19222
two-level system, optimal control of resonance radiation processes 80−106498
two-level system, quantum transitions in nonmonochromatic external fields *(Russian)* 79−36865
two-level system, Rabi oscillations in partially coherent field 80−102688
two-level system, spontaneous emission, non-Markovian effects 80−58487
two-level system in coherent field, reson. scatt., quantum description 79−64053
two-level system in high power pulse field, dynamics 77−7045
two-level system in radiation field, dynamics, temp. depend. props. 78−66793
two-level system in resonant multifrequency field with structureless noise *(Russian)* 80−91766
two-level system in sinusoidal elec. field *(Russian)* 78−58966
two-level system in strong field, kinetics of states, analogue modelling *(Russian)* 78−74876
two-level system in two periodic fields, kinetics 79−64188
two-level system in two RF fields, saturation effects 79−59660
two-level system interaction with strong monochromatic wave and thermostat *(Russian)* 78−78983
two-level system resonant processes in presence of nonresonant fields *(Russian)* 80−14308
two-photon absorption, from polychromatic stationary radiation field, light coherence 78−74626
two-photon absorption with coherent and partially coherent driving fields 78−5191
two-photon ionisation, by finite bandwith laser 79−81193
two-state atom, in low-freq. laser field, charged particle scatt. 79−41241
ultracooled atoms in reson. laser field, quantum motions 77−61931
ultrashort light pulse propagation in resonant medium 80−43308
VUV radiation, narrowband tunable, at Lyman-α wavelength 80−78907
wavefront reversal in four-photon process, two-quantum reson. conditions *(Russian)* 80−106574
weak quantization in a nonperturbative model 79−88825
Wigner-Weisskopf approximation, derivation using principle of averaging 77−19217
Wigner-Weisskopf system, irreversible behaviour in thermodynamic limit 77−65584
X-ray quantum statistics limited electrostatic imaging 78−7451
Ba I, light shift induced zero-field level crossing 80−58220
Cs, multiphoton ionisation, rel. to light statistics 79−72287
Cs quantum current-frequency convertor, operation principles *(Russian)* 79−10275
H, self-interaction of excited at. with radiation field 78−86794

quantum optics continued
H-like atom, photon coalescence and splitting at 1s electron, low-energy limit 79−10082
NH_3, two-photon population inversion, adiabatic rapid passage 78−78763
$^{15}NH_3$, modulated coherent Raman beats 80−23464
Na atom, resonance fluorescence, photon antibunching, quantisation of light 78−66791
Na beam, optical amplification without population inversion 77−50645
Na beam deflection by reson. standing wave radiation 79−98056
SF_6, coherent resonance in pulsed fields 79−68375
$Sr(^1S)+Ar$, $Sr(^1P)$ collisional excitation in nonreson. laser field, four-state model 79−10191

quantum solids
see also solid helium
Boson system, hard spheres, condensed phase, Jastrow wave function 78−84018
critical behaviour and generalised phase diagrams 77−31815
crystal, computer modelling 80−54472
crystals, appl. of method of quasiaverages 80−10737
defectons in quantum crystals, theory *(Russian)* 78−60004
diffusion, of impurities and defects, review 77−7945
discontinuous orientational phase transitions, thermodynamics, isotope effects 80−6590
Einstein-Kanzaki model of static and dynamic lattice relax. 78−34676
fermi crystal, mag. props. of vacancies *(Russian)* 79−46881
Fermi quantum crystals, melting curves low temp. anomalies rel. to neutron stars 78−24757
Fermi solid, collective modes, vacancy motion-lattice vibr. coupling 79−86960
Kirkwood-Monroe approx., quantum solid energy 79−33155
lifetime-under-load, temp. depend. 77−15487
magnetically ordered, phenomenological theory 77−7944
molecular crystal, quantum quadrupolar phase theory *(Russian)* 78−22929
Monte Carlo methods and results, book contrib., review 79−82405
nonlinear null vibrations *(Russian)* 78−6194
one-dimensional, solitary defectons 78−2332
phonon spectrum of quantum crysts. 77−11766
superfluidity, microscopic and hydrodynamic theory, for perfect one-component periodic solids 77−43405
superfluidity on Bose-condensed quantum crystal 78−75905
superharmonic approximation for quantum crystal 80−92615
thermal conductivity, role of defectons 77−35796
translational symmetry spontaneous breakdown, quasi-averages and averages, phase transitions 78−30811
vacancy delocalisation, local phase stratification and impurity free region creation *(Russian)* 78−47637
H, metallic, Hartree-Fock and correlation energies 78−34674
H_2, and isotopes, review of properties *(Dutch)* 77−62704
H_2, short-range corre. and motional renormalisation of anisotropic interactions as function of density 80−34272
H_2, solid, neutron scattering expts. 78−79693
O_2 solid, α-β transition, mag. susceptibility *(Russian)* 80−6592

quantum statistical mechanics
see also jellium; many-body problems; quantum fluids; quantum solids; quantum theories of fluid structure
$\lambda_0\Phi^4$ field theory, 3 space-time dimensions, renormalisation, analytical continuation to imaginary time 80−86563
$\lambda\pi^4$ field theory with internal symm., string representation 78−70266
$(\lambda\phi^4\text{-}\sigma\phi^2\text{-}\mu\phi)_3$ quantum field models, Euclidean approach 77−5978
$(\lambda|\phi|^4)_2$ quantum field model, soliton mass and surface tension 78−58109
ϕ^4 system, metastable state, decay rate calc. 80−22301
A^4-phonon theory, free energy and phase transition 78−41257
adatom interaction with solid substrate, effect of mechanical stress on chem. pot. 80−10784
adiabatic perturbation theory for quasilevels 79−40457
adsorption process 79−40460
Alfven wave system, eqn. of state, thermodynamic props., Bose-Einstein statistics 78−87397
algebraic approach, equilib. states and hierarchy of stability 77−22491
anharmonic crystals, Debye-Waller factor, specific heat thermal behaviour 80−54335
anharmonic oscillator, perturbative approach 79−80464
anharmonic oscillator, trial Hamiltonians for quantum statistical treatment 80−77652
anharmonic oscillators, partition function, statistical variation perturbation method 80−77648
anharmonic quartic oscillators, statistical mechanics 80−98817
asymptotic commutation problem, correlation weakening principle formulation 79−85070
atom+diatom, stochastic one-dimens. model 78−42159
atomic radiation model 79−238
atomic statistical model thermodynamics in strong mag. field, pulsar crust condensed matter 79−2741
Baierlein's entropy theorem, limitation on quantum-mechanical extension 77−83
baryon interactions through scalar meson field viar Yukawa-like interaction 79−67225
bath-system correlation functions, Lugiato theory 77−74316
binary correlations in random matrix spectra 79−44851
Birkhoff's pointwise ergodic theorem on operator algebras, extension to quantum mech. 78−86218
black body radiation, photon occupation numbers 79−88869
black-body radiation, infinite slab resonator, low temp. behaviour 77−82458
black-body radiation field interaction with photoconductor, noise, Langevin method 78−30950
blackbody radiation between parallel plates, coherence props. 79−85107
Bogolyubov's method in quantum theory of crystal with many-particle interaction 77−31928
Boltzmann's theorem 79−40459
Boltzmann equation, quantum form, one-particle Γ_+-distrib. function 78−45579
Boltzmann gas, moderately dense, momentum distrib., quantum corrections for smooth pots. 77−13692
Boltzmann gas, moderately dense, momentum distrib., quantum corrections for hard-sphere pots. 77−17903
book, axiomatic QFT, PCT, spin and statistics 78−78102

quantum statistical mechanics continued
Born-Green-Yvon equations, for strongly interacting Fermi systems 79−49161
Bose's second paper, conflict with Einstein, history of science 77−33813
Bose 1-D gas with point interaction 78−49762
Bose condensate, bounds in dimensions $\nu \geq 3$ 78−54294
Bose condensate in dimensions $\nu \geq 3$, bounds 79−54051
Bose description of fermions, model 77−53833
Bose description of fermions 78−89402
Bose expansion for general spin, exact 80−31662
Bose fluid, degenerate, Lee and Yang formulation extension 78−45563
Bose fluid, degenerate, very low temp., equilib. props. 78−45564
Bose fluid, structure factor determ. 78−34667
Bose gas, ideal, virial series 80−42139
Bose gas, impenetrable, one particle reduced density matrix, Painleve-type eqn. 80−62576
Bose gas, spatially inhomogeneous, kinetics in presence of condensate 78−16730
Bose gas, weakly interacting in restricted geometries, low-temp. thermodynamics 80−34261
Bose imperfect gas, condensed state, limit Gibbs state 80−52124
Bose modes, spin-1/2 approx. in quantum theory 79−6047
Bose partition functions, functional integral representations and inequalities 80−31667
Bose statistics, para-, Lie superalgebra, osp(1,2n), creation and annihilation operators 80−62572
Bose superfluid, pot. depend. of pairing soln. 79−55977
Bose system, nonideal, condensation, momentum, correlation function 80−46966
Bose-Einstein condensate dynamics, two-fluid hydrodynamics, Mori theory 77−28061
Bose-Einstein condensation, in 3-dimens. system, at const. press. 79−6049
Bose-Einstein condensation, role of cosmology in elementary particle physics 80−27430
Bose-Einstein condensation, suppression in restricted geometries, coherent states 79−46854
Bose-Einstein condensation in an Einstein universe 78−77797
Bose-Einstein condensation in confined ideal systems, onset criteria 77−37812
Bose-Einstein condensation in Einstein universe 80−46959
Bose-Einstein condensation of a relativistic gas in d dimensions 80−8902
Bose-Einstein condensation of ideal gas 80−22272
Bose-Einstein ideal gas, review 77−87692
Bose-Einstein statistics, wave packet formulation of multiparticle production at high energies 80−13338
boson, integrals of motion for δ-function interaction pot. *(Russian)* 78−21069
boson expansions, convergence of various methods 79−93037
boson fluid, distribution functions within hypernetted-chain approx., appl. to liq. ^{4}He 80−24696
boson gas, interacting, approx. equilib. states 80−46962
boson gas, rigorous second-order cumulant expansion 79−44853
boson magnetised ideal gas, effect of confinement, anal. 80−12987
boson operators, exponential ordering of quadratic forms 78−77800
boson operators, transform. between normal and antinormal expansions 79−97295
boson system, λ-transition, renormalisation-group theory 80−143
boson system, condensed, canonical ensemble approach 78−89400
boson system, scaling equation of state, renormalisation group transformation 78−12643
boson system coherent states 77−17911
Boson theory, quantum soliton and classical soliton 80−12986
boson trimer, bound state, pair-pot. in two-dimens. 79−58632
boson-fermion interacting system, coherent states on Lie groups and evolution operator 78−36932
bosons, analytical treatment of hypernetted-chain and Percus-Yevick eqns. 79−30359
bosons with attractive interaction 79−12717
bound state spectra in ϕ^4 theory and Gross-Neveu model, temp. depend. 78−4770
bound states, in multi-dimens. nearly 1:1 degenerate systems, semiclassical calcs. 77−82454
bound states near limit of lower continuum 77−49885
boundary-value problems *(Rumanian)* 78−86219
bures distance and relative entropy 80−84
C*-algebra, KMS condition and asymptotic Abelianness 77−17910
C*-algebra applications, conference, Varenna, Italy (July-August 1973) 77−17753
canonical commutation relns. and stochastic regularity 77−33939
canonical ensemble, appl. to equilib. between black hole and radiation field 80−52121
canonical ensemble partition function, hidden connections and functional integral representation 79−30361
canonical ensemble partition function, incorporation of long range electrostatic effects 78−21065
canonical ensemble theory, for equilib. states of quantum system 77−86
Casimir forces, appl. of analytic regularisation 80−36939
causal Green's function, analytic props., Feynman diagram technique in thermo-field dynamics *(German)* 77−45787
cell model, generalised for strong spatial correls. 77−57276
channel coupling equations of Bencze and Tandy, spurious soln. discussion 78−57857
channelling, quantum theory, generated transport eqns. 78−10110
chaotic phenomena and statistical physics, review of the contributions made by J. Schwinger 79−63135
charge-monopole composites, system of identical particles, statistics 78−93796
chemical potential, algebraic theory for usual gauge group 80−31661
chemical reaction diffusion systems, quantum statistical theory, multichannel reactive scatt. 80−81284
chemical reactions, quantum statistical theory, formulation, lowest order results 77−60045
chemical reactions in dense systems 78−73016
chemically reacting quantum gases, kinetic eqns. 78−19997
chemostress effect in ionic crysts. and metals 79−28193
class of sum rules for system of identical particles 80−91019
classical and quantum statistical mech., common Liouville space 78−32758
classical limit of quantum nonspin systems 79−63134
cluster expansion for pots. with exponential fall-off 77−41527

quantum statistical mechanics continued
cluster expansion formalism, independ. pair correlations 78−73922
cluster expansion in statistical mechanics, S-matrix formulation *(German)* 78−41256
clustering prop. for arbitrary primary state 77−30097
coherence and randomness in quantum theory, uncertainty relations 80−22231
coherent states, time evolution 79−50271
coherent states of Fermi operators and the path integral 79−2717
collective radiative phenomena in two level systems *(Russian)* 80−1174
collective subspace of many-body Hilbert space, generator coord. approach, kinematics 78−70055
collective variable approach to many-boson high-density systems 77−49676
collective variables and path integrals *(Russian)* 77−85
collective vibrs., generator coord. description, double perturbative theory 77−79031
commuting macro-observables, entropy conserving eqns. 79−44855
composite particle ensemble, fixed ion plasma model, projection technique 77−27649
condensates and Bose-Einstein correlations, quantum optics formalism 79−59028
condensation model 79−42232
conference, Haifa, Israel, 1977 79−30353
constraints, flexible vs. rigid 80−31658
continuous dipole system in grand canonical ensemble, lack of screening 80−22273
continuous one-dimensional many-component Gibbs system with regular two-body interaction pot., transfer matrix 78−8342
continuous quantum systems, variational principle for pressure, entropy, free energy, convexity consequences 79−40453
continuous systems, correl. inequalities and thermodynamic limit 78−57848
continuum calculus, Skorohods weak distribs. in Feynman path integral determ. 79−93
correlation inequalities hierarchy, relation to equilib. states 78−21064
correspondence and opposition between quantum theory and classical physics, temporal logic 80−27176
Coulomb energies of particles, lower bound 79−58912
counting processes valid for quantum point processes 78−21066
coupled harmonic oscillators, diagonalisation of general quadratic Hamiltonian 79−49158
coupled linear chains, dynamics 78−89403
coupled quantum systems, statistical inference 79−54042
coupled system, time depend. projection operator anal., classical gas and quantum systems 78−16720
coupled systems, dynamic correls., master eqn. 77−13698
coupled systems, dynamic correls. master eqn. 77−13697
Cramer-Rao inequality in quantum meas. theory, noncommutative analogues 77−26209
created boson multiplicity distribs., method of combinants 78−81917
critical scattering theory, book 79−25913
crystal, ground-state lattice vacancies and Bose-Einstein condensation 77−7943
damped harmonic oscillator, eqns. of motion in quantum statistical theory *(French)* 78−89399
damped harmonic oscillator, non-equilibrium quantum statistical mechanics, system quantisation 80−52070
Davies model of heat cond., entropy prod. in open quantum systems 79−88899
decay of unstable quantum system, survival probability 80−46965
degenerate (non)quadratic functional, partition function 79−67458
degenerate Fermi gas, distrib. functions with allowance for pairing correlations 79−40458
degenerate quantum gases in the binary collision approximation, two-particle density matrix 79−71358
delocalisation, statistical and stochastic aspects 77−30759
delocalisation, statistical and stochastic aspects 77−30760
dense, quadrupolar, hard sphere fluid, integral eqn. approx. 78−63652
density matrices, generalised integrals, Green's functions 77−79029
density matrix, coherent-state basis 78−21060
density matrix, semiclassical phase space representation 79−9135
density matrix calc. of entropy 78−62148
density matrix for arbitrary spin, equations of motion for new SU(n) parameters 80−52592
density of states in disordered one-dimensional systems 79−58640
density of states of particle in Gaussian random pot. 78−81915
density operators, equations of motion in external fields 80−36944
density operators in external fields, dynamic eqns. 79−85069
density spatial distrib. of free particles in triangular pot. well 77−17905
desorption, multiphonon processes, quantum-statistical theory 80−107641
diagonalisation of the quadratic fermion Hamiltonian with a linear part 79−40445
diatomic mol. gases, quantum partition functs., virial coeffs., by path integration 77−15146
Dicke-like model structural stability of 2nd order phase transitions 77−26259
diffusion equation for semiclassical bosons and fermions 79−40446
diffusion equations, generalised, derivation 77−87705
diluted black body radiation, conversion thermodynamics 79−40507
dipole plasma oscillations, Bose-Einstein condensation of excitons *(Russian)* 78−84155
Dirac operator, virial theorem and spectral shift function 79−17339
Dirac particles, interaction, and generalised phase factors 80−27168
Dirichlet's integral formula and the evaluation of the phase volume 80−17744
Dirichlet forms, construction of stochastic processes 80−8921
discontinuous perturbations in singular dynamical systems 77−10169
discrete ϕ^4 chain 79−75463
discrete Gaussian model, position-space renormalisation transformation 78−93617
disorder variables and para-fermions in two-dimensional statistical mechanics 80−98853
disordered assembly, partition function 77−9957
disordered system, divergence of partition function of attractive Frisch-Lloyd model 80−136
disordered systems, simple inequality for free energy 77−47593
dissipative heavy ion collisions, transport equation for microscopic Wigner functions 79−13329
dissipative system, description, soln. of Liouville eqn. 78−16725
dissipative system, nonlinear von Neumann equations 79−25976

quantum statistical mechanics continued
dissipative systems, noise operator approach 77−30099
dissipative systems with a Liapounov function, quantum rules 78−89611
distinguishable quantum particles in one-dimens. box, continuous system, dynamics, phase transitions 78−32755
distribution functions and Green functions *(Russian)* 78−65890
distributive processes in discrete systems 79−80504
dominant partition method 80−47455
donor-acceptor energy transfer, quantum statistical calcs. 77−1713
donor-acceptor transition kinetics, with allowance for vibr. struct. 80−144
double well oscillator, nonlinear contribs. to the partition function 79−12963
dynamical cluster properties in the quantum statistical mechanics of phase transitions 80−77693
dynamical semigroups, approach to equilibrium 78−49710
dynamical transformation of density matrices, general form 77−49678
dynamics of molecules in contact with an external medium at equilibrium 79−9179
education, domain and range of operator 79−97149
education, one-dimens. many body model with two- and three-body forces, exact Hartree soln. 79−9065
Einstein, quantum mechanics, conceptual problems 80−46783
Einstein and the quantum theory, review 80−22237
electron gas, degenerate, distrib. function in periodic field 79−23914
electron gas, degenerate, static density response function calc. by QHNC 80−49633
electron gas, grand partition function, first order term temp. depend. anomaly 79−21656
electron gas, magnetised, confinement effects 79−28494
electron gas, relativistic degenerate in strong mag. field, transport props., covariant relaxation-time model 77−41531
electron gas, self-diffusion (spin diffusion) coeff., proper connected diagram expansion 78−21067
electron gas, Tomonaga model, response function calc. method 80−22279
electron-phonon system, complete nonstationary density matrix in functional integration representation 79−55846
elementary particle and math. physics, conf., Austria (Feb. 1976) 77−5974
EM field density matrix, semiclassical representation 77−61234
energy exchange between subsystems, nonequilib. statistical operator method 77−61013
energy levels, statistical mechanics method, perturbative variational approach 80−62513
energy loss by test ions to plasma electrons 79−94804
energy moments, analytic continuation of generalised zeta function 80−36938
ensemble density matrix form., with off-diagonal (coherent) constraints 77−74314
ensemble of two-body random Hamiltonians, nonzero mean matrix elements, eigenvalue density, Monte Carlo calcs. 78−81920
ensemble of two-body random Hamiltonians, spectrum shape, Monte Carlo calcs. 78−81919
ensembles for random matrices of Hamiltonians with small time reversal noninvariant part 80−77694
equilibrium between solid and vapour state, for Cd *(Croatian)* 79−95154
equilibrium states description, m-particle density matrices of canonical ensemble 77−61016
equilibrium states in lattice systems 77−17909
equilibrium statistical mech., inequalities for mean values 77−64999
equivalence of canonical and grand canonical ensembles 79−30360
ergodic theory in von Neumann algebras 80−9104
ergodicity, classical, quantum mech. implications 80−8898
Euclidean Yukawa$_2$ quantum field theory, FKG correlation inequality 80−68357
excitons, condensation effects, review 78−2427
exclusion principle extended, particle classification anal. 78−49690
exponential quadratic phonon operators, ensemble averages 78−54293
extended objects, correl. functions in one-dimens. kink-bearing systems 80−86204
Fermi fluids, nonlinear response of equilibrium strongly coupled fluids 77−7930
Fermi fluids, nonlinear response of strongly coupled fluids, appl. to polarisation diags. 77−7931
Fermi fluids, propagation techniques for equilibrium strongly coupled fluids 77−7932
Fermi gas, one-dimensional theory, correlation functions 80−22278
Fermi golden rule and Markov master eqns. 78−36935
Fermi liquid, T-approximation, viscosity coeff. of ^{3}He *(Russian)* 79−21655
Fermi quantum crystals, melting curves low temp. anomalies rel. to neutron stars 78−24757
Fermi quantum fields, derived from Bose quantum fields, applications 78−36928
Fermi system of charged particles, collective variables method 79−88873
Fermi-Dirac integral, approx. by 12th order polynomial *(French)* 79−11109
Fermi-Dirac integrals of arbitrary order, expansions and approx. 79−85065
fermion clusters, many particle correlations, method of transition density operators 78−49763
fermion N-representability density operators, necessary conditions 77−5759
fermion nonrelativistic, self-energy and inter-fermion Coulomb-Yukawa forces, quantum theory 78−29047
fermion systems level densities, appl. of cluster expansion theory *(Spanish)* 79−88868
fermion thermodynamic system, high-order perturbation expansion 80−4635
fermion-boson isotopic mixture, ground state configuration, theory 80−107601
fermions, constrained variation in Jastrow method at high density, neutron system, liquid ^{3}He appls. 77−5753
fermions, independent, 1-dimens. density-pot. rel., local density approx. 78−29045
fermions, quantum mechanics of ground state 80−82713
fermions with gravitational interaction, press. 79−63138
Feynman path integrals, mathematical theory, book 77−41511
quantum statistical mechanics continued
Feynman path integrals, white noise approx., inertialess Brownian system 78−57859
Feynman postulates, modifed set, superposition principle 80−82657
Feynman-Wilson gas, KNO scaling, phase transitions 77−30094
Feynman-Wilson gas, statistical model for multiparticle physics 79−22071
field quantisation, number operators for distinguishing Bose, Fermi and parastatistics 78−93562
finite closed systems, relaxation, algebraic approach 77−29985
finite system, order parameter and sp. ht. for epitaxial ordering renormalisation-group calc. 80−17862
finite volume statistical mechanics for highly singular two body pots., many particle interactions 77−5752
fireball dimension determ. in hadron collisions, Bose-Einstein correlations 79−22069
fireballs, quantum-statistical chain decay, pion clusters 78−430
fluid model of quantum statistics with irregular stochastic fluctuations, derivation of Nelson equations 79−40450
Fock-Tani representation for the quantum theory of reactive collisions 79−80505
Foldy Wouthuysen transform. group content, nonrelativistic limit for arbitrary spin 79−75387
free energy, order-parameter expansion appl. to some phase transition model 78−43099
Friedmann universe, photon gas 78−4543
Friedmann universe, statistical model, geometrical props. determined by neutrino gas 77−53717
fuzzy spin spaces, probability theory, spectral densities 77−37811
Gaussian quantum stochastic processes on the CCR algebra 80−12985
Ge, heavily doped, dislocation vel., electronic effects 77−11547
general algebraic treatment of identical particles in scattering processes 78−81891
generalisation of exactly soluble models 77−82446
generalised density matrices and Wigners distribs. 77−82455
generalised hydrodynamics construction by nonequilibrium statistical operator method 77−30116
generalised master eqn. and generalised Langevin eqn. equivalence 77−13699
generalised statistics and quark model 77−13690
generalised two-level quantum dynamics, nonHamiltonian state evolution 78−36854
generating functionals in nonequilibrium statistical mechanics *(German)* 80−12981
geometric methods and appl. to bound state spectrum 77−82452
Gibbs condition, positive cone, Radon-Nikodym theorem, relative Hamiltonian, appl. of Tomita Takesaki theory 77−17758
Gibbs ensemble, approach to equilibrium 77−41553
Gibbs formula for elementary quantum systems, thermodynamical proof 79−58628
global thermodynanic stability and correlation inequalities 78−45560
grand partition function, multi-species cluster expansion 77−82459
Grassman number systems, Hamiltonian formalism, canonical quantisation by Feynman path-integral 80−77697
Green's function coupling, rel. to ladder vertex function and screened pot. 77−5754
Green's function defined in phase space, using Wigner operator eigenfunctions and eigenvalues 78−24728
Green's function for surface physics, partial differential eigenvalue eqn. 80−6929
Green's functions, finite temp., dynamical picture and causality 79−63144
Green's functions determ. using ab initio calcs. 79−80506
Green function low frequency asymptotics, reduced description of nonequilibrium states *(Russian)* 77−5760
ground states of quantum spin systems charact. by minimum local energy principle 79−12714
hadronic matter, thermodynamic props. of class of solvable statistical models 79−63452
hard sphere Fermi gas Jastrow correlations 79−40451
hard sphere gas interacting with hard wall, density profile, virial expansion 78−63928
hard sphere problem on lattice, moment method, uniform chain 79−97311
hard wall potentials, semiclassical statistical mechanics, transformed pot. approach 79−32870
harmonic oscillator, classical phase-space distribs. for approximating quantum states 79−63145
harmonic oscillator, driven and stochastically modulated, reduced eq. of motion 78−77764
harmonic oscillator, kinetic formulation for random pots. 78−32756
harmonic oscillator system spontaneous emission, master eqn. 79−17277
harmonic oscillators, charged, interaction with transverse EM field mode 80−5712
Hawking effect, temp. relativity, axiomatic field theory 80−109456
heat conduction, stochastic theory of atomic chain coupled to two reservoirs 78−54319
heat engine, quantum open system model 79−44894
heavy particle, quantum Brownian motion, adiabatic expansion 78−49768
Heisenberg eqns. on C* algebra of quasilocal observables, boson and fermion systems 78−57854
Heisenberg model, long-range interaction, asymptotic behaviour 78−56282
Heisenberg nonautomorphic dynamics, covariant representations 77−67375
helicity modulus at low temperatures 78−70052
heteroaromatic mol. radiationless transition decay rate freq. shift depend., quantum statistical mechanics anal. 78−74691
HF approximations, thermodynamic Fermi systems 80−4642
hidden variables and proper mixtures for multivalued observables, correlation function results 78−57853
hidden variables controversy 79−62975
hierarchical model, renormalisation group anal., book 78−81921
higher virial coeffs. in case of Boltzmann states 77−5751
hydrodynamics, vel. operator 77−82449
hydrogenic partition function, compensation of bound and scatt. state contribs. 77−61012
hyper Raman effect, quantum statistics 80−23754
hyper-netted chain eqn., Kohn-Sham theory derivation 78−47225

quantum statistical mechanics continued
hyper-Raman effect, master eqn. approach, quantum statistical treatment 78−82736
hypernetted chain approx. anal. 77−64998
ideal gas, external pot. effects, time evolution of response 77−71268
ideal gas, time evolution, microscopic hydrodynamics in nonlocal pot. 78−73920
ideal relativistic gas, cluster decomposition appl., statistical bootstrap eqn. 77−30095
infinite, irreversible dynamics 77−82451
infinite chain, quantum mech. irreversible motion 80−4633
infinite macrosystems in standard representation, dynamical symmetries 80−4590
information theory density matrix for a simple quantum system 79−58470
information-theoretic, system in contact with heat reservoir, for teachers 78−36770
inhomogeneous fluids, quantum statistical mechanical eqns. 78−34414
inhomogeneous systems, multiple density correlation functions 78−49757
intensity of average field relaxation, in medium with quasi-static fluctuations *(Russian)* 79−2715
interacting boson problem, appl. to diffusion constant of Brownian particles 79−164
interacting bosons, statistical mechanics, temp. depend. energy levels 77−59163
interacting quantum gas, nonequilibrium entropy, low-density approx. 79−21684
inversibility, decay, and asymptotic dynamics 80−57172
ionized gas, thermodynamic props., classical one-component Coulomb gas calcs. 77−5777
irreversible behaviour in quantum statistical mechs., singular coupling and weak coupling limits 77−45790
irreversible conservative motion in generalised, two-level quantum dynamics 78−36927
irreversible kinetic eqn. for strongly interacting system, increasing entropy 78−54300
irreversible processes, study via spectral deformation techniques 79−30357
irreversible processes, time asymmetry 80−22215
irreversible processes, time evolution for large quantum systems in superspace 78−62172
irreversible processes and dissipative systems in quantum theory 80−8906
Ising magnet, kinetic processes, 1-D chain, magnetic relaxation, quantum stat. mechs. 80−80471
Ising magnet, kinetic processes, reduction of statistical description of system during evolution 80−80470
Ising model eigenvalue analytic continuation and free energy 77−26236
Ising transverse 1-D model, dynamics 80−29515
isotopic molecules, reduced partition function ratio, generalised finite polynomial approx. 78−66529
Jastrow theory, momentum distrib. of boson and fermion systems 78−45561
jet model, uncorrelated, implications of Bose-Einstein statistics 79−22070
K-systems, kinetic description, stochasticity condition 79−85080
Keldysh's perturbation formalism 80−13217
kinetic eqns., quantum virial expansions 77−49677
kinetic equations, derivation, nonlocal Uehling Uhlenbeck eqn. 78−70054
kinetic equations, derivation by collision expansions, three particle term 78−70053
kinetic equations for system with weak interaction *(Russian)* 77−64992
KMS states, stability properties, KMS condition 78−81916
Kolmogorov entropy, quantum generalisation 78−86232
Kubo-Freed relaxation theory generalisation, appl. to mol. absorption peaks 79−49156
Landau's hydrodynamic model, further aspects 78−82173
Landau-Zener problem, random nature of motion role in intersecting terms problem 80−8937
Langevin eqn. extension 77−61011
large mol. reaction with intermediate complex, vibr. distrib., R-matrix, hybrid quantum statistical mechanics 77−52611
laser, single mode, nonequilibrium statistical operator method 79−89881
laser, two-photon, inhomogeneously-broadened, quantum statistical anal. 79−59666
laser theory, open systems *(Japanese)* 79−76658
laser theory, open systems *(Japanese)* 79−76659
laser with saturable absorber, stationary state, nondiffusive approx. 80−19076
laser- or black-body radiation, strong electron coupling, limitation of Fermi-Dirac statistics 80−29843
lattice Coulomb-gas representation of two-dimensional problems 79−58650
lattice gases, quantum corrections 77−17920
lattice models with a solvable symmetry group 79−17616
lattice spin theory, Jastrow wave functions 79−25999
lattice system equilib. states, semi-quantum, AF algebra 78−45576
lattice systems, metric space of interactions, grand canonical pressure, thermodynamic limit 78−12652
lattice systems with short-range and Coulomb interactions 80−82715
Lennard-Jones gas, second virial coeff. calc. using equilib. Wigner distrib. function variational principle 80−4685
Lie superalgebraic approach to second quantisation 79−21654
linear hard core fluid as limit of lattice fluid 80−38882
linear quantum channel with thermal noise, quasiprobability distribs. 80−12984
linear relaxation equations in the nonequilibrium statistical operator method 79−30362
linear response dynamics in quantum statistical mechs. 78−49758
linear response theory, many-body van Hove limit 78−62156
linear response theory, master eqn. approach 80−31663
linear stochastic dynamic systems, appl. of Green's function method *(Russian)* 78−16722
linearly damped harmonic oscillator, quantisation 78−21068
Liouville dynamics for optimal stochastic phase-space representations of quantum mechanics 78−21062
Liouville equation, renormalised, simplified derivation 77−57275
Liouville operator spectra 77−9952
Liouville problem, quasi-particle dynamics from a given kinetic eqn., inverse 80−101749
liquids, nonrelativistic scattering, quantum statistical theory 77−4030
local harmonic approx. 77−53832
local limit theorem for Gibbs random fields of particles and unbounded spins 79−97296
local thermodynamic stability and KMS conditions of quantum lattice systems 77−71275
local thermodynamic stability of quantum lattice, KMS conditions 77−17902
locally equilibrium correlation function calc. method 80−36943
Luttinger model, preservation of sum rules for 1p-Green function 77−9956
macroobservables, reconstruction in embedding method 80−77691
macroscopic observables, treatment procedure 80−17864
macrovariables, microdynamics and eqns. of motion 77−45795
magnetised Bose gas, confinement effects 79−54050
magnetism in superdense stars, quantum theory 79−92753
many body theory, appls. review of development 80−46968
many boson non-relativistic systems, classical field limit of scatt. theory 79−80501
many boson systems, representation of coherent states 79−30363
many fermion systems, energy lower bound 80−17860
many-boson absorption, nonreson. maximum 78−8343
many-boson model, spontaneous symmetry breakdown and restoration 80−52123
many-fermion systems, partial level density for widely varying values of the range of interaction 80−58120
many-fermion theory, expS or coupled cluster form 78−29048
many-particle Hamiltonians in symmetry spaces, finiteness of discrete spectrum 79−2719
many-particle systems, distrib. functions and thermodynamic functions 77−57273
many-spin system, group approach in dynamics *(Russian)* 80−44900
Markov fields in noncommutative probability theory on W* algebras 79−97260
Markov processes in quantum lattice systems 79−40476
Markov subdynamics in quantum dynamic systems 77−2604
Markovian eqns., transportation theory, using group theory 78−21063
Markovian master eqns. 79−144
Markovian master eqns. for unstable particles, weak coupling limit 77−45794
Markovian processes 78−29049
mass degeneracy at fixed particle number, differential eqn. for bootstrap degeneracy 78−24732
master eqn. for quantum systems with strong interactions *(Chinese)* 78−86229
master equation treatment of single reservoir limit 78−29050
master kinetic equation for a particle in the field of randomly varying scatterers 79−58634
mathematical model for a set of microsystems 79−25971
matrix order and W*-algebras in operational approach 80−77690
matter formation, photon condensation, treatment using Bose-Einstein statistics 78−12435
Mayer cluster function and quantum two-body t matrix 80−17859
mean field models, equilib. states 80−46961
measurement sequences, Everett interpretation 78−32707
metal, positron thermalisation by non-equilibrium statistical operator method 79−15551
metallic particles, spectrum fluctuations in two-dimens. model, specific heat calc. 77−82447
metastable states of quantum lattice systems 77−71276
microcanonical ensemble, the quantum lattice and conditional entropy 79−80555
microcanonical system, pressure anal. 79−40454
Mielnik's generalised quantum mechanics, nonlinear model, simplex for mixed states set 78−57852
mixtures, general formulation and appl. to binary hard-sphere system 77−87691
model system classes with a lowering of power in thermodynamic limit 79−88874
model systems, generalised theorems 79−21658
model systems in which particles interact with definite conservation laws 79−21659
modified cluster expansion method, appl. to multicomponent system 77−2609
molecular relax. phenomena, quantum statistical mechanical approach, irreversible thermodynamic theory for radiationless decay 80−48028
molecular relaxation phenomena, non-exp. decay and external disturbance 79−44850
molecular wavefunctions, Schrodinger eqn. random walk soln., electron spin effects 77−18780
molecule-molecule reaction, ergodic energy transfer, vibr. quantisation effects 78−85137
momentum distrib., binary cluster term evaluation, 3D Lennard Jones gas, 1D hard rod gas 77−37808
Monte Carlo method, Green's function path integrals with hard boundaries 79−67223
Monte Carlo methods, quantum mechanical corrections to classical equilibrium statistical-mechanical results 80−135
motion of quantum particle in medium with dynamical disorder 80−68125
multicomponent large system time evolution, numerical anal. 77−22490
multielectron configuration, evaluation of matrix elements of energy operator 79−63895
multiparticle scattering operators, cluster decomp. 80−22592
multiphonon relaxation, statistical anal. 79−79223
multispecies Tani transorm., kinematical props. 79−17333
multispinor basis of Fermi-Bose transformations 79−75676
N-body scatt., filter operators in linked-cluster formalism 79−45040
n-component spin system, energy-energy correl. function calc. 80−31697
N-fermion problem, improved lower bounds 78−54292
N-level systems in contact with singular Bose or Fermi reservoir 77−22487
N-mode laser, emitted light correlations 78−63051
N-particle distrib. functions, space- and time-depend., possible appl. to black holes 77−26237
N-particle problem, reduced density operators, theory, historical review 79−5945
neutral radiant gas, kinetic eqns. with allowance for radiation polarisation 79−23399
neutrino+antineutrino system, relativistic kinetic theory, Wigner functions 77−26239

quantum statistical mechanics continued
neutrino component of $e\bar{e}\nu_e\bar{\nu}_e$ mixture, transport eqn. 77−33941
neutrino system, relativistic transport eqn. 77−33940
neutrino systems, relativistic kinetic theory of transport processes 80−73283
neutron matter, test of Wu-Feenberg and F_2 approximations 79−40873
neutron star model, appl. of Schrodinger eqn. 77−49418
neutrons, relativistic, ultra-degenerate, non-interacting gas, Fermi energy and eqn. of state in intense mag. field 78−89401
non-equilibrium, harmonic oscillator model 77−5750
non-equilibrium, stochastic transport processes, K-flow, K-entropy 77−5749
non-equilibrium quantum statistics validity of Fourier expansion method 77−53829
non-Hamiltonian systems, detailed balance condition 77−30096
non-interacting electron system, of finite number of particles, pressure at zero temp. 79−97301
nonequilibrium, classical Markov stochastic process 77−33938
nonequilibrium, exactly solvable models 79−30365
nonequilibrium, stochastic processes 77−82456
nonequilibrium density matrices, calc. using quantum integrals of motion 77−61009
nonequilibrium quantum statistics of lasers and nonlinear optics 79−31848
nonequilibrium state, Langevin type eqns. applic. to linear response theory, scatt. cross section 78−16726
nonequilibrium statistical operator method, existence of ε-limit *(Russian)* 78−49781
nonequilibrium statistical operators, theory 77−13696
nonequilibrium system, strongly driven, linear response theory 77−2606
nonequilibrium systems, cluster expansions with contraction for homogeneous systems 80−46964
nonequilibrium systems, existence of thermodynamic limit 79−54084
nonequilibrium systems, statistical mechanical theory from generalised phase space and damping theory 79−75481
nonequilibrium systems, theory of irreversible processes 80−46963
nonlinear, stochastic differential eqn., perturbation theory, projection operator method, statistical linearisation 78−41229
nonlinear Bose systems, Dyson-Wick expansions 78−73921
nonlinear hydrodynamical eqns., external fields, Einstein relations for kinetic coeffs. *(Russian)* 78−50
nonlinear Langevin eqns., and time-convolutionless master eqn. 79−40502
nonlinear lattice, quantum corrections for a system of interacting phonons and the modified Korteweg-de Vries equation 79−60454
nonlinear oscillators, 1-D, intramolecular vibr. energy transfer, quantal, classical and statistical behaviour 80−91641
nonlinear quantum oscillator ensemble excited by external periodic force, statistics *(Russian)* 80−27213
nonlinear response of a system in connection with entropy maximum 80−95047
nonlinear systems, canonical perturbation theory 79−17338
nonlinear systems, stochasticity condition 78−49760
nonlinear waves in cold plasma, classical Vlasov plasma description through quantum numerical methods 80−92288
nonMarkovian stochastic model of non-relativistic wave mechanics *(French)* 77−82450
nonrelativistic electron in const. parallel elec. and mag. fields, thermodynamic characteristics 80−90777
nonrelativistic para-Fermi gas, thermodynamic and mag. props. 79−25974
nonstationary systems, invariants and radiation 78−36929
nuclear and molecular collisions 79−30821
nuclear dynamics of heavy-ion reactions 77−41996
nuclear matter, thermodynamic model, shear viscosity temp. dependence 78−62499
nuclear-spin subsystems, cross-relax., nonequilib. thermodynamics 79−58662
one component classical charged particle gas, thermodynamic grand function using collective coordinates 80−73289
one dimensional conductors, Fermi gas model, reviews 79−78083
one dimensional continuous quantum systems, limit Gibbs state 78−93599
one particle reduced density matrix of impenetrable bosons in one dimension at zero temperature 80−17863
one-dimensional ϕ^4 and double quadratic systems, kinks 80−47197
one-dimensional ϕ^4 system in external field 79−63136
one-dimensional Fermi gas with backscattering, coupling between charge and spin degrees of freedom 80−17861
one-dimensional sine-Gordon system, kinks 80−46969
one-dimensional solitary-wave-bearing scalar fields, statistical mechanics, ideal-gas phenomenology 80−105792
one-dimensional system, Bose-Einstein condensation at const. press. 80−22276
one-dimensional system, correl. functions, limiting relationships 77−62790
one-particle quantum mechanics, duality between confining pots. and $(R+L_c^{\infty})$ pots. 80−31574
open BSC model, dynamics in weak coupling limit 79−2738
open N-level system, algebras, condition for approach to equilibrium 78−16678
open quasi-free systems, time evolution 80−95030
open system, current-carrying states in quantum statistics 80−90802
open system, exact master equation 77−71270
open systems, generalised master eqn. struct. 77−9972
open systems, generalised regression theorem for multitime correl. functions 77−9973
open systems, S-matrix and density matrix formalism 79−88872
open systems, stochastic quantisation, Schrodinger-Langevin eqn. derivation 77−30090
operator algebra and quantum statistical mechanics, book 80−41965
operator formalism of statistical mechanics of gauge theory in covariant gauges 80−86591
operator formulation of statistical mechanics 78−24734
optic mode second sound in distortive phase transitions 79−73366
optics, generating functions calc. 80−1168
optics, struct. and representation of correlation functions and density matrix 79−98325
orthonormalisation method, appl. to j-j coupling of fermions in single j-shell 78−81922

quantum statistical mechanics continued
oscillator ensemble with embedded impurity oscillator, absorption spectrum windows 79−6045
$P(\phi)_2$ Euclidean field theory, boundary conditions rel. to ferromagnetic spin systems 77−54036
parafermi statistics, Lie algebraic aspects of quantum statistics 79−54045
paragas thermodynamics *(Russian)* 78−49754
paragas thermodynamics at intermediate temps. 80−46970
parametric amplification and generation, quantum statistical properties 78−46717
parastatistics description of magnons and excitons at high concentrations 77−51674
particle collision inclusion in extended time dependent HF approx. 78−49780
particle displacement momenta, quantum equilib. distrib. in molecules and solids 78−32751
particle in Gaussian random pot., density of states, quantum mechanical correction 79−63132
particle lattice models, physical signals speed of propagation, bounds 78−93613
particle mobility in Gaussian pot. at high temp. *(Russian)* 79−30364
particle motion in a viscous medium 78−24731
n-particle quantum system, energy operator discrete spectrum 79−85006
particle scattering from target, spin-spin interaction calcs. 78−81730
partition functions, classical limit 80−52120
partition functions, coherent states and upper bounds in Hilbert space 80−57173
path integrals, distrib. definition 80−31595
path integrals and lower bounds for density matrices 80−138
path-integral approach to time-dependent self-consistent field theories 79−59023
Pauli master equation, derivation 78−89397
periodic vacuums, functional integrals, classical sine-Gordon solns., Coulomb gas props. 79−26226
perturbation expansion for Fokker-Planck dynamics 79−88879
perturbation theory, large-order behaviour, critical exponents, Callan-Symanzik eqns. 79−30397
perturbative unorthodox expansions in quantum statistical mechanics 78−49759
phase space distributions and quantum state determinations, simultaneous meas. 80−90774
phase space quantisation of interacting vortices in two demensions 80−4634
phase space quantization of the linearly damped harmonic oscillator 79−35627
phase space quantum mechanics, Liouville operator eigenfunctions 77−45792
phase space quasi-distribs. in quantum mechanics 78−54291
phase space sampling approach, semiclassical statistical mech. 78−32753
phase transitions and reflection positivity, Peierl contour probabilities, long range lattice models 78−89398
photodetection, open system theory, dynamics of field and atomic moments 78−70185
photon statistics, unsaturated k-photon absorption, exact soln. of master eqn. 80−37984
pion gas, relativistic, kinetic props., non-equilib. statistical operator method 79−30718
pion relativistic quantum gas, crit. temps., Bose-Einstein clustering 77−54084
planar spin system with annealed bond disorder 80−57212
Planck's law and the light quantum hypothesis 77−13564
plasma, hot, dense, change from Fermi-Dirac statistics to strong coupling at $kT=mc^2$ 78−55716
plasma, hydrogenic, statistical mechs. of composite particles, projection technique 78−47090
plasmas, nonideal, quantum-statistical conductance theory, force-force correlation function method 80−79440
polarised radiation field, statistical equil. eqns., density matrix technique 77−5425
polyatomic molecules, isotopic reduced partition function ratio approx., by polynomial perturbation method 78−66530
polymer expansion for quantum many-body problem 80−57181
position operators for relativistic non-interacting n-particle system 78−41182
probability calculus, statistical theory, wave mechanics 78−54301
process characterisation by method of local specifications *(French)* 80−31597
pseudoclassical dynamics in terms of min. uncertainity states 79−63143
pseudopotential in statistical thermodynamics 79−85109
pulsars, superfluid liquid rotation, theory, relativistic effects in vortices *(Russian)* 78−61876
pure quantum states, single system and ensemble interpretations 78−8340
pycnonuclear reactions, and pair correl. function in dense plasma 78−32445
quadratic boson Hamiltonian, diagonalisation 78−93600
quadrupole phonon states, fifth label values, exact derivation 80−31664
quantum amount of information and maximum work 79−63142
quantum crystals, appl. of method of quasiaverages 80−10737
quantum fluid relaxation, renormalised perturbation expansion in kinetic theory 78−21061
quantum friction and statistical mechanics 80−77649
quantum harmonic oscill. chain, relaxation dynamics *(Russian)* 80−94992
quantum mechanical addition, statistical distribs. 80−22274
quantum oscillator interacting with quantised radn. field, Brownian motion effects 77−34856
quantum partition functions, explicit classical bounds 80−90775
quantum statistical thermodynamics, rigorous information theoretic derivation 77−74338
quark confinement and vacuum struct. of nonlinear σ-models, statistical fluctuation effects 79−89101
quasi-one-dimensional systems, statistical mech., thermodynamic props., mag. transition 77−26246
quasiaverages, hybrid systems, phase transition description 77−41532
quasibound state contributions to the second virial coefficient 79−71364
radial distribution function of fluid, quantum corrections 77−3906
radiation field in flat parallelepiped, ideal photon gas eigenvalue spectrum 78−8344
radiation law, phenomenological extension *(German)* 77−41533

quantum statistical mechanics continued
radiationless transitions, proximity effect, vibrational tuning, vibronic interaction probe, QSM approach 78−94274
Raman scattering by phonons, anticorrel. effects, Heisenberg eqns. of motion 79−95747
random potential, behaviour of Wiener integrals as t→∞ and density of states 79−2720
random system, dispersion theory approach to scaling function 78−70071
reacting fluid mixture, kinetics, BBGKY hierarchy in arrangement channel quantum mechanics 79−70299
regular invariants class, asymptotic limits or ergodic means *(French)* 78−70051
relative entropy, information-theoretic discussion 79−71360
relativistic dense matter, statistical mechanics using phenomenological quantum field model 78−89814
relativistic harmonic oscillator imbedded in random stochastic thermostat, stable states 79−49033
relativistic kinetic eqns. 77−67376
relativistic kinetic gas theory, electron-neutrino system 77−5756
relativistic kinetic theory, $e\nu_e$ $e\bar{\nu}_e\nu_e$ mixture 79−63140
relativistic kinetic theory of $e\nu_e$ and $e\nu_\mu$ systems, transport coeffs. 79−21680
relativistic paramagnetism, statistical mechanics in strong mag. field 80−17865
relativistic quantum Hamiltonian for directly interacting particles 78−16729
relativistic quantum ideal gas of massive particles, eqns. of state 79−2721
relativistic quantum mechanics formulation of space and time 78−65796
relativistically invariant generalised quantum kinetic eqn., Liouville eqn. basis 78−54299
relaxation processes, initial slips and transient effects, theory 78−24729
representability conditions for rotationally invariant density matrices, group theory appl. to generation 79−88870
resonance radiation redistribution, elastic and inelastic collisions effect 79−62734
resonance transfer rate of electron excitation, model of convergent terms, effect of diffusional motion of particles 80−8936
response function and effective potential, self consistent theory 79−35628
Robertson-Walker Universe, quantum statistics 79−88769
RPA and pairing vibration approximations, multiple basis set calcs. 77−5755
scattering and dynamics, classical and quantum statistical mechs., unified treatment 78−45522
Schrodinger fluid velocity field, fermion system moments of inertia 78−65868
Schwinger variational principle for dynamic susceptibilities 80−4639
second virial coeff., in weak coupling limit, temp. depend. upper bound on partial wave contrib. 79−30356
second virial coefficient, trace formulas for time delay 77−82476
second virial coefficient from the scattering operator 78−24730
self-consistent field theory, diagrammatic review and implications 77−74313
self-interacting boson field, interaction with classical current, S-matrix elements 79−21963
semiclassical canonical density matrix, approx. semigroup props. 78−16723
semiclassical densities in phase space, Wigner's distrib. function for thermodynamic equilibs. 79−58565
semiclassical wave functions, regular and irregular 78−20998
semiconductor junctions, quantum statistical theory in thermal equilibrium 78−39197
separable many-particle interactions, free energy calcs. 77−9954
short-range asymptotic wave function method, appls. 78−24727
SHRIMP energy lower bound model, derivation for translation-invariant many-fermion systems 78−29046
silicate glasses, model of struct. element, calc. of physicochem. props. 79−69016
sine Gordon theory, equivalence to z-dimens. ferromag. classical X-Y model low temp. behaviour 77−13873
sine-Gordon chains, role of breather solns. in statistical mechanics 79−85212
sine-Gordon massless quantum eqn. in 2 space time dimens. 78−32754
sine-Gordon system, breathers, extended object QSM 80−42347
single eigenvalue distrib. for non-zero mean matrix ensembles, correct form 80−73198
singularity structure, of partition function, in complex coupling constant plane 79−12716
Slater determinants, energy functional, extremum problem, Hartree-Fock equations, gradient method 80−62573
small system in thermostat, reduced description 77−5783
SO(2N+1) algebra, time-dependent Hartree-Bogoliubov theory, quantisation 80−62575
solid, high-density, quantum statistical model 79−55824
solid in equilibrium with radiation field, reconciliation of photon noise statistics with electron statistics 79−23014
solids, classical and quantum scaling 79−35626
space density functions, positive phase, position and momentum joint distribs. 80−62509
space time inhomogeneous Gibbs ensembles, dynamics of macro-observables 79−9182
spatial Bose-Einstein condensation, teaching examples 79−71176
spectral distributions and subsystem density matrix *(Russian)* 78−65891
spectral properties of products of projections in quantum probability theory 80−98807
spin and pseudospin lattice systems, Green's functions diagrammatic technique 78−8355
spin and pseudospin lattice systems, Green's functions diagrammatic technique, Pauli operators 78−8356
spin dynamics differential eqns., asymptotic expansion of quantum averages near classical limit *(Russian)* 77−53831
spin model with unstable stationary states 77−67382
spin system propagation properties study 78−12642
spin traces, nature of S-depend. 79−17331
spin-1 system, lattice of verifiable propositions 77−45789
spinless particle scatt. by medium, elimination of divergencies, statistical mechanical averaging 78−62320
spinning particles, canonical approach, path integral expression 79−97298
quantum statistical mechanics continued
spinor fields in an Einstein universe, finite temp. effects 79−21614
square-well fluid, nonclassical crit. behaviour 80−44291
static space-times, finite temp. and boundary effects 78−54526
stationary nonlinear Hartree eqn., asymptotic soln. 78−49723
statistical sum calc. by coherent states method *(Russian)* 77−13691
steady states of weakly dissipative systems, Fokker-Planck eqn. soln. 78−81918
stochastic electrodynamics, derivation of Schrodinger eqn. 77−82411
stochastic fields, functional integral methods 79−25973
stochastic interpretation of quantum mechanics, review 78−70056
stochastic Liouville equation for quantum-mechanical scatt. for particle in field of variable scatterers 78−140
stochastic phase space, generalised functions 78−77796
stochastic phase spaces and master Liouville spaces in quantum statistical mechanics 79−85076
stochastic processes, thermodynamic limit, master equation 77−37814
Stratonovich-Hubbard scheme for grand canonical partition function determ., linearization by functional integral 79−63141
strong quantised EM field, statistical description 78−16961
structure and order evolution of many-body systems 77−41528
subdynamics theory, dissipative processes in dynamical systems 77−9951
subdynamics theory of non-equilibrium statistical physics 77−53828
superfluid viscous liq., hydrodynamics and transport coeffs. 77−69134
superfluidity, macroscopic systems, linear response theory, Thomas-Kuhn sum rule 77−28060
superfluorescence, oscill., quantum statistics 79−917
supernovae, thermodynamic of nucleon, lepton, photon mixture, quantum mechanical calcs. 80−77273
symmetries and statistics in many-particle systems, group theory aspects 77−18452
symmetrised density operator treatment of quantised dissipative systems 77−9959
synchrotron radiation field, statistical states 78−66736
teaching, statistical thermodynamics, partitions 79−58496
thermal mechanics: a quantum mechanical analogue of nonequilibrium statistical thermodynamics, stochastic processes 80−52125
thermal radiation, parity violating currents 79−17633
thermal states, KMS states, of vector meson model in two dimens. space time 77−5987
thermodynamic density fluctuations effect on low of mass action and kinetics *(Russian)* 78−60990
thermodynamic Green's functions, eikonal approxs. 77−9958
thermodynamic processes induced by coherent radiation 78−32752
thermodynamics, relativistic, and temperature 79−63182
thermodynamics of N particle system, quantum corrections 78−70082
thermodynamics of quasi relativistic electron gas, pathway integral application *(Russian)* 80−22277
thermodynamics rigorous information theoretic derivation 77−37837
thermostat-subsystem contact, density matrix, exact kinetic eqn. 79−85068
third cluster coefficient for square well discs 79−85072
Thomas-Fermi model, review 77−84
Thomas-Fermi thermodynamic functions, quantum and exchange corrections *(Russian)* 77−9953
time correlation function calc. and generalization of Wick's theorem 79−25975
time-reversal noninvariance of the quantum-mechanical kinetic equation of Kadanoff and Baym 79−17332
Toda, quantum mechanical lattice 80−46983
Tomonaga fermions and three-dimens. Dirac eqn. 79−58633
transfer coefficients of ultrarelativistic gas of elementary particles *(Russian)* 78−8635
transport equation for electrons in nonmonochromatic EM field 80−10937
triangular lattice, self-avoiding walks 79−40478
two-body scatt. T matrix in real-time formalism 78−41230
two-component system, catalytic reactions, time evolution 77−45791
two-component systems, density evolution, nonlocal potential 78−81914
two-dimens. Coulomb gas, low-temp. behaviour 77−45788
two-dimensional square Ising model in transverse magnetic field, renormalisation-group method 80−20428
two-level molecule interacting with light, Dicke model asymptotic behaviour 79−3508
two-level system, damped and stochastically modulated, reduced eq. of motion 78−77764
two-level system, kinetics at diffusion modulated local interactions *(Russian)* 79−2716
unbounded operators in statistical mechanics, *-algebras for quantum mechanics formulation 79−6046
uncorrelated jet model, quantum statistical correls., Bose-Einstein statistics, pion prod. 78−16992
uncorrelated jet model with Bose-Einstein statistics, statistical bootstrap model 78−86445
uncorrelated jet model with Bose-Einstein statistics for π prod. anal. 78−82172
unimolecular reaction rate theory, nonequilib. quantum statistical mechanics 77−44463
uniqueness theorem for anticommutation relations and commutation relations of quantum spin systems 79−12713
unstable quantum systems, decay theory review 78−65871
unstable systems, decay *(German)* 77−71265
van der Waals eqn. of state theory generalised 78−38602
van Hove master equation, derivation 78−89397
variational principles 79−75452
velocity of light Markov process, Klein-Gordan quantum statistic, quantum mechanics 80−98808
virial eqn., generalised quantum 77−37810
virial theorem and Born-Oppenheimer approx. at different order of perturbation *(French)* 77−49617
virial theorem and scale transformations, for teaching 80−17763
virial theorem derivation, for teachers 79−71193
viscosity, quantum phenomenology 78−54298
von Laue's theorem of partially coherent radiation entropy, quantum statistical proof 79−17373
wavefunctions of identical particles 78−49756
weakly coupled non equilibrium systems, time asymptotics and reversibility 79−54049
weakly interacting systems, S-matrix, density matrix, Pauli and Boltzmann eqns. 79−88871
Weyl's commutation relation, implied generalized statistics 77−82408

quantum statistical mechanics continued
Widom-Rowlinson lattice gas, grand partition function zeros 80−31681
Wiener processes, analogue, existence and uniqueness theories for canonical processes 78−57856
Wigner's distribution function in spherical coords. 77−61017
Wigner distribution and quantum ergodicity 80−82711
Wigner distribution function, temporal positivity conservation 79−9183
Wigner distribution function and its factorisation 77−9955
wigner function and normal ordering 80−57176
Wigner-Weisskopf atom in one-dimens. radiation field, relax. to equilib. 78−62769
Wigners 3j symbols, quasiclassical asymptotic behaviour 79−21660
WKB wave function, systems with many degrees of freedom, solitons and pseudoparticles 78−29255
e^+e^- pairs and equilib. radiation in quantising mag. fields *(Russian)* 78−49990
$e\bar{e}\nu_e\bar{\nu}_e$-mixture, reactive collisions influence on bulk viscosity 77−74637
$K^+p\rightarrow K^+p2\pi^+2\pi^-$, 16 GeV/c, azimuthal correls., Bose Einstein symmetrization effects 78−37239
ϕ^3 field theory in $6+\epsilon$ dimensions, anomalous dimens. calc. 78−134
H, condensed, spin-aligned, props. from variational calcs. 80−4637
H, optically thin plasma, UV spectral emission coeff., quantum statistics of recomb. continuum *(Russian)* 79−77348
H, spin-aligned, and its isotopes, ground-state energy and finite temp. props. 77−61014
H, spin-polarised, density, magnetisation, compression and thermal leakage 80−44391
H_2, liquid, perturbation theory and quantum effects, thermodynamic props. and quantum stat. corrections *(Russian)* 78−22867
He, liq., ground state in Kirkwood superposition approx. 77−15650
He, superfluid, statistical thermodynamics of cubic system below 0.5K 79−86939
$^4He_3$, gas, Efimov effect 77−30042
^{3}He, liquid, test of Wu-Feenberg and F_2 approximations 79−40873
^{3}He, superfluid A-phase, Cooper pairs vs. Bose condensed mols., ground-state current 80−49451
^{3}He-^{4}He mixtures, hard sphere model 77−89614
^{3}He-^{4}He mixtures, tri-critical phenomena, Callan Symanzik study of $\lambda\phi_3{}^4+g\phi_3{}^6$ theory 77−35788
^{4}He atomic Bose system, equilibrium superradiance 78−55994
^{4}He, liq., exchange effects on excitation spectrum 78−10236
^{4}He, liquid, condensed phase, long-range order of one- and two-body density matrices 80−10726
^{4}He, superfluid, quantum lattice gas as microscopic model 78−59986
^{238}U, nuclear excitation rate in high-temp. environment 78−66244

quantum statistics *see quantum statistical mechanics*

quantum statistics of many-particle systems *see quantum statistical mechanics*

quantum theories of fluid structure
see also liquid theory; quantum fluids
Bose fluids, normal, conserving evaluation of dynamic struct. factor 79−14975
cavity-biased (T,V,μ) Monte Carlo method, computer simulation 80−92434
dilute aqueous solutions, Monte Carlo studies of struct., review 80−54101
fluid with nearly spherically symmetric molecules, thermodynamic perturbation theory 80−14985
Green's function Monte Carlo method for quantum hard spheres radial distrib. function 79−54005
hard sphere, semiclassical fluid, equilib. props., quantum corrections 78−18522
hard sphere fluid, thermodynamic props., quantum corrections 79−4219
hard spheres, quantum mechanical virial coeff., two point Pade approx. 80−79657
hard wall potentials, semiclassical statistical mechanics, transformed pot. approach 79−32870
hard-sphere fluid, eqn. of state, quantum corrections 78−34592
hyper-netted chain eqn., Kohn-Sham theory derivation 78−47225
inhomogeneous fluids, quantum statistical mechanical eqns. 78−34414
inhomogeneous systems, multiple density correlation functions 78−49757
macromolecular fluid, 77−7496
molecular theory, Kihara pot. *(Spanish)* 77−68902
Percus-Yevick pair correlation function for hard sphere fluid, series representation 80−103232
periodic boundary conditions, error in computer simulation determ. 77−15296
superfluid Fermi systems, appl. to low density hard sphere systems 79−51339
superfluid Fermi systems, binary expansion in microscopic theory 79−51338
tunnel theory, appl. to specific heats of liquid metals, Ar, and water 79−33095
van der Waals eqn. of state theory generalised 78−38602
virial theorem derivation, for teachers 79−71193
water, liq., Monte Carlo studies of struct., review 80−54101
Yukawa-tail fluid, semiclassical fluid struct. and thermodynamics props. 79−27895
HF+HF, interaction energy, multipole anal., charge overlap, orientation and bulk props. 77−34715
LiH+LiH, interaction energy, multipole anal., charge overlap, orientation and bulk props. 77−34715
N_2+N_2, interaction energy, multipole anal., change overlap, orientation and bulk props. 77−34715

quantum theory
see also Clebsch-Gordan coefficients; complementarity; correspondence principle; indeterminancy; perturbation theory; quantisation; quantum field theory; spin hamiltonians; wave mechanics
0(3) dynamic symmetry of neutron in linear current mag. field, hidden symm. *(Russian)* 77−210
2n-degree forms, semipositive definiteness 77−30050
3 wave bound state in spherically symmetric potential, inequality with correct coupling constant depend. 77−82405
3-j symbols, general set of relns. 78−41183
3j and 6j coeffs., recursive computation 77−5687
3j coefficients, computation 79−49076
3j symbols, T coeffs. and D function *(Russian)* 77−30055
3j-coeff., symmetries 78−41181
4-atomism, theory 80−94967
6j symbol calculation for compact groups 80−8856

quantum theory continued
α^{-1}=137.0324, physical interpretation 79−25891
absorbing boundary method, Golden Rule generalisation 79−97226
acoustic superradiance, quantum theory 78−10128
action-angle variables in quantum mechanics, appl. to harmonic oscill., linear (triaxial) rotors 80−31543
adiabatic hypothesis, old quantum theory, rel. to classical electrodynamics, zero-point EM radiation 79−2661
adiabatic theorem 80−31546
adsorption of isolated adatoms 78−22957
affine algebraic groups, automorphisms 79−17269
affine symplectic group, generating functions 78−41149
Aharanov-Bohm effect, possible nonexistence 80−27434
Aharonev Bohm effect 80−36893
Aharonov Bohm effect 79−63076
Aharonov-Bohm effect, commutation relations, irreducible representations 80−57132
Aharonov-Bohm effect, Feynman path integral approach 80−31578
Aharonov-Bohm effect, nonexistence, quantum mechanics consequences 79−12641
Aharonov-Bohm effect, physically observable consequences 79−92978
Aharonov-Bohm effect in toroidal solenoid *(Russian)* 78−77770
Aharonov-Bohm effects nonexistence, discussion of significant experiments 79−63081
Aharonov-Bohm scatt. by thin impenetrable solenoid 79−9058
Aharonov-Carmi thought expt., inertial and EM vector potentials 80−52051
Airy functions, asymptotic behaviour of derivatives 80−17830
algebra (CCR), quasi-free states and automorphisms 77−5686
algebra of physical magnitudes 80−82658
algebra of pseudodifferential operators and the asymptotics of quantum mechanics 78−93547
algebraic, dilations of irreversible evolutions 78−65794
algebraic generalisation, based on the comparison of classical mech. with quantum mech. 78−81881
alkali metal atom, valence electron ground states, model potentials 78−50476
alkaline earth positive ions, valence electron ground states, model potentials 78−50476
ambiguity group for classical canonical transforms, role in quantum mechanics 80−8839
analytic continuation of a group of eigenvalues 79−6010
angle and phase quantum description, nonhermitian operators 77−5682
angle-angular momentum variables in quantum mechanics, commutation relations 80−86112
angular momentum, average for two-body system, lower bound 77−57514
angular momentum, Wigner operators in phase space 78−4511
angular momentum Helmholtz theorem, decomposition of solenoidal vectors 77−2556
angular momentum projection in nuclear physics 77−50066
angular momentum projection operator, finite sum representation 79−92993
angular momentum theory, generalised equivalent operator products 79−49071
angular structure of unique spherical shells, appl. to ang. momentum quantisation 78−73873
anharmonic damped oscillator and coherent state representation 79−97236
anharmonic oscill., classical versus quantum case *(Spanish)* 80−73210
anharmonic oscill., residue-squaring diagonalisation meth. 77−49635
anharmonic oscillator, analytic theory of continued fractions, Green's function 79−6019
anharmonic oscillator, Feynman-Dyson series asymptotic expansion 80−62503
anharmonic oscillators, nonseparable problem with exchange, classical limit 80−57120
anharmonic oscillators, quantum theory, independent to spherically coupled, level crossing 78−77747
anharmonic oscillators, single and coupled, with quartic coupling energy levels 79−35587
anharmonic oscillators, transition moments 78−12601
anharmonic-oscillator energies using operator recursion mech. 77−22443
anisotropic dispersive media, generalisation of Planck's law 78−18153
anisotropic harmonic oscillator, accidental degeneracy of energy levels 78−8263
anisotropic harmonic oscillator, n-dimens., accidental degeneracy, semi-direct product representation 78−4506
anisotropic harmonic oscillator group, quantum mech. representation 78−8262
anisotropic potentials, rainbow scatt. 77−82407
anisotropy damping through quantum effects in early universe 78−57708
antimatter, defn. in quantum theory of perception 78−24674
area preserving maps, quantisation 80−12924
associative Hamiltonian algebras 78−69975
asymmetric systems described by a pair of local covariant wave equations 79−75391
asymptotic $\hbar$-expansions of stationary quantum states 77−67313
asymptotic eigensolutions of fourth and sixth rank octahedral tensor operators 79−93975
asymptotic expansion in coupling const. 79−71595
asymptotic expansions in motion of two electrons in nuclear field 78−66459
asymptotic forms of radial wavefunctions and Jost functions for cutoff potentials 79−71278
asymptotic series by H^0 strictly singular perturbations 80−62498
asymptotical level density of a physical system, Lanczos method 79−5977
atom, unitary group generators representation matrices calcs. 78−78610
atom scattering by corrugated potential wall, appl. to diffr. by cryst. surface 80−42104
atom-surface scatt., inelastic, eikonal approx. 80−50499
atom-surface scatt., inelastic, energy transfer and sticking coeff., classical and quantum treatments 80−40209
atomic electron scatt., analyticity and dispersion relations 77−23561
atomic four-body problems, Faddeev eqns. in momentum representation 79−59524
atomic inner shells, physics, quantum mech. appls., history 77−18773
atomic interactions, retarded energy shift and pair polarisability, field theoretical perturbation theory 80−102560

quantum theory continued
atomic momentum distrib. modification by travelling wave reson. light field 79−72280
atomic pair polarisabilities, continuum electrostatic theory 78−86769
atomic RF spectroscopy, nonlinear and parametric effects, review 80−18816
atoms and atomic spectra theory, conference, Leningrad, USSR (Feb. 1977) 79−10059
automorphisms of quantum logics 77−30049
axiomatic operational quantum mechanics 80−57139
axiomatic quantum mechanics 78−12594
axiomatic quantum theory and resonances 79−2907
axiomatic theory 80−76
axioms for nonrelativistic quantum mechanics 78−12595
Backlund transformations, canonical struct. 80−86141
Backlund transformations for AKNS inverse method 77−71243
barrier, two-dimens., quantal and semiclassical anal. 77−74243
Bell's conditions sufficiency in four-dimens. 79−54010
Bell's inequalities, generalised 78−12598
Bell's inequality, a limitation 79−58558
Bell's inequality, hidden parameters and probabilities, meas. theory 78−54244
Bell's inequality, joint measurability, real and imagined nonlocalities 80−46861
Bell's inequality, test of meas. of spin correl. in low-energy pp scatt. 77−13633
Bell's inequality violations, possible sources 79−54009
Bell's theorem, generalisation 78−36860
Bell's theorem. Experimental tests and implications, review 79−17280
Bell's theorem without hidden variables 77−37777
Bells inequality, quantum generalisations for different space-time regions 80−101728
Bessel functions, asymptotic approx. 80−31562
bibliography, probabilistic ideas in field theory and statistical mechanics 78−8230
biharmonic oscillator, coincident energy levels, for teachers 79−40324
biological membranes, mol. transport, quantum mech. theory 79−8489
biological replication by quantum mechanical interactions 77−40626
biorthonormal systems, Parserval's identity 78−16669
black body monochomatic emissive power, fast calc. by nomograph 78−22257
black hole, particle prod. 78−81647
black hole quantum processes, review 77−17614
black holes, particle escape by tunnelling 77−82272
blackbody radiation from incipient black hole 77−9767
blackbody spectrum, interpretation of quantum theory, for teaching 78−54130
blackhole-particle scatt., Reissner-Nordstrom metric 77−57267
Bloch electron continuous spectrum instability, N-band Stark ladder 77−57220
Bloch electrons in mag. field, energy spectrum, struct. of Landau levels 80−54623
Bloch electrons in magnetic field, quantum numbers 80−96768
Bloch Hamiltonian one-dimens. bands by fibres 77−31934
Bloch reduced Hamiltonians, spectral props. and bands 77−24509
Blume-Emery-Griffiths model, renormalisation group centred, tricriticality 80−42165
Bogolyubov-boson transform., coherent states 78−32715
Bohr-Sommerfeld quantization of n-dimensional neutral and charged pulsons *(Russian)* 79−49092
bonding of particles of quantum systems 80−101724
book, elements of quantum theory 77−60979
book, first course standard 79−97259
book, undergraduate text 79−97258
Borel summation appl. to quantum mechanical models 80−90718
Borel summation of perturbation series 78−16683
Born's discovery of the quantum-mechanical matrix calculus 80−82615
Born series generalisation, sparse-matrix version 78−77751
Born series in scatt. theory, rearrangement, convergence improvement, orthogonal projections basis 77−60974
Born series rearrangement in model space, resolvent operator expansion 80−13422
Born-Oppenheimer approx., perturbation theory 77−26988
Bose-like oscillator, uncertainty relation for canonical variables 80−62539
boson expansion method, appls. 78−36884
boson trimer, bound state, pair-pot. in two-dimens. 79−58632
bosons, bilinear Hamiltonian, diagonalisation methods 78−32716
bound spectrum by action-angle variables path summation 77−30038
bound state decay in external field in semiclassical approx. 80−12941
bound state energy levels, quantum mechanical formalism, convergent perturbation theory *(Russian)* 80−4573
bound state wave function explicit normalisation, decay widths calc. 80−18116
bound states, bound on number, spherically symm. pot. 77−2564
bound states, orthogonalised plane wave set construction method 79−25894
bound states, semiclassical, in one-dimension, perturbation formalism 80−12937
bound states, WKB approx. from Heisenberg matrix mechanics 78−32717
bound states and resons. from separable pots., T matrix 77−30036
bound states for r^{-2}-like potentials in one and three dimensions 79−2645
bound states for the symmetric shifted Coulomb potential 79−6007
bound states in continuum, local pot. and normalisable wavefunction construction 77−49632
bound states in quantum mechs. and AFT, eqns. of motion, variational principles, WKB approx. 78−54540
bound states in weak pot. fields depend. on free particle density of states *(Russian)* 78−62091
bound states of bispherical and toroidal potentials *(French)* 80−75
bound states of weakly coupled long-range one-dimens. quantum Hamiltonian 77−87656
bound three and four particle systems, two particle resonance poles and energy spectra 78−41204
boundary-value problems, numerical solns. 77−2526
bounded motion in central field of force, O_4 covariant Hamiltonian formalism 79−6012
bounded operators with discrete spectrum 77−26193
branching diagram for particles with arbitrary spin 77−30027
quantum theory continued
Brownian motion, connection with quantum theory 80−90786
Brownian motion, Fokker-Planck and Kramers-Chandrasekhar eqn. 79−9186
Brownian motion in external field, effect of fluctuations 77−49687
bures distance and relative entropy 80−84
C* algebra, completely positive maps 78−49716
C*-algebras and Jordan algebras, spectral theory 77−9893
C*-dynamical systems, small perturbations 79−80458
CAI via graphics 77−67164
canonical anti-commutation relations, probability and harmonic anal. on representations 79−9145
canonical approach to particle motion with dissipative forces 77−57227
canonical description of solitary quantum decay 78−36881
canonical form of bilinear Hamiltonians *(Russian)* 78−57804
canonical Fourier transform of quantum-mechanical pair 79−44781
canonical Hamiltonian system, different quantisations and classical limits 78−8271
canonical mechanics, admissible forms 78−16691
canonical Schwartz spaces and generalized operators 79−30284
canonical transformation framework, non-perturbative approach to effective interactions 78−12603
canonical transformation of the Hamiltonians quadratic in coordinate and momentum operators 79−84991
canonical transformation to action and angle variables and their representations 79−58563
canonical transformations, development from Hamilton's principle 79−71185
canonical transformations, nonlinear and nonbijective to action and angle variables 80−105517
canonical transformations to action, angle variables, their representations in quantum mechs. 79−77
canonical transformations to action and angle variables, quantum mechanical representation, Coulomb problem 79−92965
Carter separable spacetimes, characteristaion 78−36867
cascade decay processes, probability theory calc. 79−44670
Casimir operator eigenvalues and Lie algebra canonical realisations 77−5697
catastrophe and stochasticity in semiclassical quantum mechanics 80−8861
causal explanation for quantum phenomena in macroscopic physics 77−57229
causal interpretation of quantum mech., superluminal propag. of quantum pot. 79−40400
causal nature of the motion of wavelets 79−67176
causal unification of relativity, gravitation and quantum mechs. 77−33923
causality, localisation and spreading of wave packets 80−90715
causality, macroscopic, Einstein correlation, CPT symmetry, decreasing probabilities, advanced waves, antiparticles 80−68073
causality and transformations of physical systems, decay, molecular rearrangement 77−2551
cavity of entropy 80−27158
Cayley quantum theory, new aspects in eight-dimens. Clifford algebra 80−8846
charge and action polarity and their order props. 77−37771
charge current density of Pauli eqn. using vel. operator method, nonrelativistic derivation 78−73872
charge-monopole system, mech. model 78−62343
charged linear harmonic oscillators, interaction between two one-dimensional oscillators 78−16963
charged particle motion in fixed mag. monopole field, quantum mech. treatment 78−66062
chemical bonding in inorganic complexes, quantum mech. ideas development and use 80−12878
chemical bonding in inorganic complexes, quantum mech. ideas development and use 80−12879
chemical bonds, quantum theory 78−54243
chemical exchanges, quantum reactive scatt. theory, nonorthogonal bases and coordinates 79−91909
chemical reactivity, reliability of quantum mechanical predictions, config. of reaction prod., H-bonded species 80−108691
chiral invariant theory, quantum mech. 78−81880
chronometric redshift theory, erroneous presentation correction 78−85839
chronon, fundamental time interval, in quantum theory 77−41500
chronon in quantum theory of electron, existence of heavy leptons, neutrino spectrum 78−70008
classical and relativistic limits 77−33901
classical content of many-body quantum mechanics 79−53998
classical dynamics, quantum analogs, book 80−41969
classical gauge transforms and quantum theory 77−5681
classical groups, invariant operators 79−21585
classical limit for arbitrary commutation relations in quantum theories 79−25877
classical limit for quantum theories defined by real Lie algebras 78−65807
classical limit of quantum dissipative generators 79−58572
classical realisation of quantum mechanics, experimental predictions 78−73868
classical two fluid process, relationship with Schrodinger quantum theory 79−40385
closed linear operators, matrix representation, extension of Von Neumann's theory 79−40396
closure approximation, appl. to perturbation theory, muon capture and pion electroproduction 78−16680
coherent hyper-Raman scattering from isotropic material, quantum theory 80−106327
coherent state, necessary condition to remain coherent 78−73879
coherent state representation of linear operators 78−16677
coherent states, $\hbar \to 0$ limit 80−31538
coherent states, time-dependent invariants 79−44791
coherent states and conserved charges 79−17275
coherent states and induced representation 78−49713
coherent states and lattice sums 79−2650
coherent states and projective representation of the linear canonical transformations 80−82662
coherent states and stochastic formulation of quantum mechanics 78−57810
coherent states for general potentials; three dimensional systems 80−90716

quantum theory continued
coherent states for general potentials, time evolution 80−90717
coherent states for general pots. with harmonic oscillator props. 78−73883
coherent states of nonaxial quantum mech. top *(Russian)* 77−45739
collapse postulate for observables with continuous spectra 80−36885
collective inertiae, in variational frameworks, canonical approach for auxiliary Hamiltonian *(French)* 77−87657
collision theory integral, analytic determ. 78−28987
collisional ionisation in intense laser field, quasimol. state reson., quantum mechanical anal. 78−33589
combined algebra for classical and quantum mechanics 78−85
communication channels, quantum 78−28998
commutation and uncertainty relations, deterministic interpretation, Planck's const. as coupling condition 78−73875
commutation relation [A, B]=−icI for one parameter unitary groups 78−65811
commutation superoperator of state, appl. to noncommutative statistics 78−28997
commutator acting on finite space with discrete spectrum 77−64
commutators and eqns. of motion, noncommuting operators on Heisenberg ring 77−79002
commuting tensor operators, and state labelling problem for SO(4)⊃P 78−28980
complete sets of observables on the sphere in four-dimensional Euclidean space 78−70015
completely integrable field theory models, quantum-mech. approach 80−4574
completely integrable systems connected with semi-simple Lie algebras 78−12599
completely positive mapping families in *-algebra 80−94971
completely positive mappings on algebras of unbounded observables 77−45674
completeness value for eigenfunctions of second order differential eqns. 80−31564
complex Airy functions, evaluation algorithm 79−58562
complex Bell's inequality, quantum meas. expts. 78−54217
complex coord. method, error bounds 78−49705
complex diffusion processes, transforms., and nonrelativistic quantum mechanics 80−82670
complex diffusion processes and nonrelativistic quantum mechanics 80−90707
complex pot. barrier scatt. in semiclassical theory 77−9915
complex versus quaterionic quantum theory, note on Peres' proposed test 80−31576
composite particles, exchange Hamiltonian spin component diagonalisation, second quantisation method 77−71236
composite systems, relativistic centre of mass variable and Lie algebra of Poincare group 79−71245
composite systems states, prep. *(Russian)* 79−44770
conceptual anal. in microchannels theory, Hilbert space representation 80−22217
conceptual analysis method in microchannel theory, quantum theory appl., fundamental concepts 79−84981
conditional probability of a generalised probability theory, quantum mech. foundations 80−12949
conditioning of states 79−6008
conference, fundamentals in quantum theory and field theory, Flagler Beach, FL, USA (Feb.-Mar. 79) 80−57114
conference, group theoretical methods in physics, Austin, Texas, USA (Sep. 1978) 80−4474
conference, group theoretical methods in physics, Netherlands, (June, 1975) 77−17862
conference, Starnberg, W.Germany (July 1978) 80−27044
conference on Lie admissible formulations, Cambridge, USA, (Aug. '79) 80−36765
confining potentials, peculiar prop. of wavefunctions 80−46863
conformal invariance in quantum mechanics 77−2730
conformal spinors, $O_{2,4}$ transformations in $E_{2,4}$, components obeying Dirac eqn. 78−45504
conjugate momentum of ang. momentum modulus 78−16673
connected partially ordered set of events in time measurement 80−77640
constrained systems, quantum treatment using path integrals based on distrib. theory 78−65815
continuous measurement 78−78
continuous observations and decay process regeneration 77−17834
continuum calculus, Skorohods weak distribs. in Feynman path integral determ. 79−93
contractions of expansions of fermion operators 80−17834
controllability, optimisation of quantum systems, pure states and mean values 80−22210
controversial problems of measurements within quantum mechanics 79−53999
convergence properties of generalized inner projections to dynamic polarizabilities 79−5999
convex sets of states for spin 1/2 and spin 1 systems, geometrical description 77−26196
cooling of quantum oscillator 78−32728
Copenhagenism, a defence 79−25820
correlation functions of nondynamic interacting systems 78−57814
correspondence rules and path integrals 80−31590
cosmological particle pair creation as above barrier reflection, WKB approx. 79−80377
cosmological quantum theory, a general framework 79−9043
cosmology, quantum turbulence near singularity rel. to universe expansion law 78−77629
Coulomb+rational separable pots., T-matrix, effective range functions 77−57221
Coulomb and Coulomb-like off-shell Jost functions 79−75388
Coulomb and Yamaguchi pot. scatt., bound states 77−57222
Coulomb coupling, strong, group SO(2,1), Klein Gordon eqn. 77−17837
Coulomb Green function for extended, uniformly charged nucleus 79−13199
Coulomb integral and quantum mechanical exchange redefinition from atomic and molecular orbitals 79−44787
Coulomb interaction in nonrelativistic quantum mech. 79−25906
Coulomb phase shift, for teachers 79−97135
Coulomb problem, symm. technique appls. 77−45731
Coulomb problem, zero-energy 78−62097
Coulomb scatt. in N dimensions, algebraic approach 79−75386
quantum theory continued
Coulomb systems, stability of atoms and bulk matter, thermodynamic limit 77−45716
Coulomb two-centre problem, review *(Russian)* 77−30056
Coulomb wave function, in u representation 79−58584
Coulomb wave functions, completeness in quantum mechanics 78−89278
coupled anharmonic oscillator energy levels, large quantum number behaviour, path integral method 80−91
coupled anharmonic oscillators, level density 77−30044
coupled nonlinear oscillators, large amplitude vibr. motion, coherent state representation 77−87698
coupling of logics 78−62104
covariance for quasi-probability distribs. 77−9901
covariance operators, reflection positivity using Dirichlet or Neumann boundary data 80−131
covariance principle in quantum physics 78−4496
covariant coherent states for quantized systems with nilpotent symmetry group *(German)* 78−73865
covariant formalism for a relativistic string in a constant homogeneous electromagnetic field 79−21546
covariant formulations of eqns. of motion 77−45723
covariant interactions of spinless particles, covariant Hamiltonian quantum mechs., local solns. 78−41186
covariant observables and instruments 80−8842
covariant quantum equations in curved spacetime, Lorentz covariance and tachyons, book contrib. 79−44725
covariant representation of the causal logic 79−97235
CPT invariance, quantum mechanical interpretation 80−105805
cranked harmonic oscillator pot., self-consistent condition 78−17122
creation and annihilation operators in Gauss plane and quantum friction 79−67183
crystallisation, activation energies of mass transfer at phase boundaries, quantum theoret. calcs. *(German)* 78−67671
crystallisation, activation energies of mass transfer at phase boundaries, quantum theoret. calcs. *(German)* 78−67673
cubic harmonic functions, actual forms to 16th order, quantisation axis in [111] direction 77−60971
currents and local currents in Galilean quantum mechanics 80−77641
curved space path integral, quantal Lagrangian and Hamiltonian for harmonic oscillators system 78−41193
curvilinear coordinate and momentum operators in configuration representation 80−105521
damped harmonic oscillator, quantum friction in c-number picture 80−94980
damped particle motion, dissipation 79−63071
damped quantum system, pseudostationary states, existence and props. 78−41177
damping, anal. of Kanai Hamiltonian and nonlinear pots. 79−63070
damping, quantum mechanical 80−46862
Davidson's generalization of the Fenyes-Nelson stochastic model of quantum mechanics 80−62531
de Broglie's thesis, critical retrospective 77−13520
de Broglie wave packet, nondispersive 78−36858
de Broglie waves, dispersion relation 80−67949
de Broglie waves of the second kind 79−6004
decay of quantum states and systems 78−62112
decay processes and dynamical subgroups 80−8848
decaying states, using Kapur-Peierls and Siegert resonant states and extended Hellmann-Feynman theorem 78−4503
decaying states as complex energy eigenvectors in generalized quantum mechanics 79−12645
decaying states in rigged Hilbert space formulation 80−62521
deformation of symplectic structure and quantization 80−8853
degenerate discrete levels, periodical perturbation *(Russian)* 80−86152
degenerate energy levels, adiabatic and time-independ. perturbation theory diagrammatic anal. 79−2642
degenerate perturbation theory, continued fraction solns. 77−17840
degenerate perturbation theory, electron in strong mag. field, example for teaching 77−33801
degenerate perturbation theory 78−65799
delocalisation, organic chemistry courses 78−4426
density functional theory, quantum mech. system, accurate pot. and energy functionals 80−52849
density matrices convergence and entropy 77−30046
density matrices with continuous entropy for quantum mechanical system 80−13024
density matrix, asymptotic high temperature expansion 78−54115
density matrix approach to problems in time-dependent perturbation theory 79−92973
density matrix characterisation, geometric and other methods comparison 79−6001
density matrix formulation, physical interpretation 80−57115
density matrix geometry, definitions, N matrices and 1 matrices 78−65816
density matrix geometry, reduced density matrix and N-representability 78−65817
density matrix of scattered particles, comments on 80−22219
density matrix of scattered particles 80−22218
derivation from stochastic electrodynamics 77−74252
description of quantum mechanics, first kind states, local hidden variables 78−28990
Deser-Gilbert-Sudarshan representation, existence 80−37167
desorption, laser stimulated, quantum theory 78−79876
determinism, temporal and formal *(Hungarian)* 79−44766
deterministic and probabilistic local theory equivalence 79−17272
diamagnetic band structure, first principles calc. 80−88470
diatomic molecule, quantum mech. model 78−86050
Dicke laser model, semi-classical theory in presence of focal points 77−37774
differential equations, first-order, symm. and first integrals, Hamiltonian system *(Russian)* 77−30034
differential equations, second order, without first derivatives, fourth-order numerical method 80−86107
differential inequalities, comparison theorem 80−31549
diffraction in quantum physics, formulation, representations, relativistic and high energy, mixed systems 78−36885
diffraction problem, non-homogeneous media, non-stationary problem 80−22211
diffusion, particle in fluctuating medium, memory effects 79−49180
diffusion coefficient of elementary particles, intrinsic 80−22222

quantum theory continued
dimensionality of physical space, assumption of three-dimensionality 78−93515
dipole interaction of an oscillator with scalar field 80−94
Dirac brackets for dynamical systems with redundant constraints 79−63078
Dirac distributions, perturb. of self-adjoint Hamiltonians, Green's functions and wavefunctions, scattering theories 80−62514
Dirac eqn., Bunge-Kalnay position operator 78−36864
Dirac matrices, compact evaluation of traces 77−17750
Dirac operator non-self-adjoint, connected with completely integrable Hamiltonian systems *(Russian)* 79−12630
Dirac-Faddeev method, existence theorem of constraints 77−17843
direct reactions, semiclassical theory, complex paths and uniform approximations 77−71244
Dirichlet's integral formula and the evaluation of the phase volume 80−17744
Dirichlet forms, construction of stochastic processes 80−8921
discontinuous perturbations in singular dynamical systems 77−10169
discrete spacetime, quantum numbers, uncertainty and min. entropy 77−87659
discrete spectrum of the n-body quantum mechanical Hamiltonian. I 79−86
discretization problems of functional integrals in phase space 79−97254
disjointness of β-KMS states with different chemical potential 80−62530
dissipation and quantum theory 79−63077
dissipative oscillator, time relaxation approx. anal. *(Russian)* 79−5997
dissipative system, nonlinear von Neumann equations 79−25976
dissipative systems, dynamical description 80−17867
dissipative systems, geometrical mechanics for particles in dissipative systems 79−49087
dissipative systems, time evolution of state vector 80−12935
distorted wave Glauber approximation, Pauli eqn. soln. 78−57809
donor-acceptor energy transfer, temp. dependence *(Russian)* 77−73161
Doppler-shifted photons, origin of increased energy explained by mechanics of source 78−28897
double group theory, half-shell and two-level system, optical polarisation 78−49594
double group theory, half-shell and two-level systems, rot. and half integral spin states 78−45447
double groups and projective representations, Clebsch-Gordan coeffs. calcs. 79−92977
double groups and projective representations 79−88833
double well anharmonic oscillator, 1-d system, effect of fermions upon tunnelling 78−16689
double well anharmonic oscillator, no horn of singularities 78−73884
driven damped oscillator, path integral treatment 79−80457
dynamic Stark effect, absorber theory approach 79−54807
dynamic system, classical quantisation conditions with stochastic behaviour anal. 80−8922
dynamic systems, deformation and quantification *(French)* 80−31598
dynamical impact parameter in quantum theory 79−21982
dynamical instability of nonrelativistic many-body systems 77−49619
dynamical maps asymptotic behaviour for finite systems 78−73
dynamical semigroup for time evolution of finite system 77−30045
dynamical semigroups, approach to equilibrium 78−49710
dynamical semigroups, dilations, open quantum mech. system embedded in closed system 77−2508
dynamical semigroups and spin multipole relaxation in isotropic surroundings 78−86813
dynamical spin spreading of unstable particles in four models 79−54003
dynamical symmetries in spherical geom. 79−40394
dynamics in state space, Heisenberg equations 77−37782
dyon-dyon nonrelativistic scatt., classical and quantum anal. 77−5985
E_7 exceptional group, calc. of 6_j symbols 78−57800
E-indepent model Hamiltonian, diagrammatic construction 77−53796
Eastern mystical philosophy, quantum mechanics and the bootstrap-quark controversy 79−84883
education, angular momentum operators, derivation in spherical polar coords. 77−78932
education, canonical transformation to the free particles 77−49521
education, classical and quantum uncertainties, particle in box, harmonic oscill. and atom 79−25789
education, composite potential well, energy level determ. using Green's function factorisation theorem 79−97148
education, Dirac γ matrices 77−45637
education, electron spin, nonrelativistic quantum mechanics derivation from Schrodinger eqn. 78−69942
education, EM wave interaction with matter, gauge invariant formulation 78−62006
education, extended Galilean transformation 79−25788
education, Kac ring model, illustrative calcs. using projection tech. 77−78918
education, Maxwell fish-eye pot. and Coulomb pot. from mechanics 78−49585
education, non-Hermitean Hamiltonians, dissipative forces 77−33763
education, nonspreading wave packets, physical interpretation of Berry Balazs wave function 80−57040
education, orthogonal curvilinear coord. representation of quantum mechanical operators, exterior differential form 79−9049
education, Pauli's σ matrices, intuitive understanding 79−97153
education, plane rotator, degenerate perturbation theory, Zeeman and Stark effects 79−9059
education, quantum mechanics, mechanical model 78−49591
education, quantum mechanics, spherically symmetric pots., ladder operators, energy levels and degeneracy 78−62013
education, quantum mechanics and perturbation theory, perturbed harmonic oscillator *(Spanish)* 78−36786
education, relativistic quantum mechanics, free localised Dirac particle, Zitterbewegung 80−17739
education, renormalisation rule for WKB-type wave functions 78−69944
education, rigid rotator, account suitable for basic quantum mechanics course 77−33773
education, rotations, Lorentz transformations, and arbitrary axes 79−97155
education, Schrodinger eqn. for free particle, wave packet spreading in coord. representation 80−17736
education, self-adjointness and spontaneously broken symmetry 77−87593
education, semiclassical quantization, Bohr-Sommerfeld quantization rule 77−78930
quantum theory continued
education quantum mechanics, computer graphic presentation for non-physical science students 77−49526
educational course, PSI, with optional lectures on videocassettes 77−64951
efimov effect in an analytically solvable model 79−63083
eigenstate decay into continuum in presence of elec. field 77−13631
eigenvalue perturbation theory, remarkable examples 78−93558
eigenvalue perturbation theory divergence, quantum mechanical counterexample 79−92982
eigenvalues and eigenvectors, computational method 77−26206
eigenvalues lower bounds for quantum Hamiltonians, classical limit of quantum theories 78−41200
eigenvalues of matrix operator $S.\pi$ for spins 1/2, 1, 3/2, const. mag. field 78−32712
eikonal, Rytov high-energy approx. 77−53802
eikonal approximation, analytic props. 80−32038
eikonal description of scatt., appl. to heavy-ion scatt. 77−41938
eikonal eqn., underlying geom. struct. 77−60957
Einstein, Podolsky and Rosen paradox, resolution using density matrix calcs. 79−35588
Einstein's contribution to development of science *(Russian)* 79−84926
Einstein's part in the development of quantum concepts 80−98781
Einstein's work and effect on atomic physics at the turn of the century *(German)* 80−90648
Einstein and the quantum problem *(German)* 80−90725
Einstein and the quantum theory, review 80−22237
Einstein correlation, S-matrix and Feynman zigzag 78−77761
Einstein correlations, S-matrix, ψ collapse *(French)* 78−77742
Einstein equation dynamics modified by fourth derivative terms, radiation from charged test particles 78−41216
Einstein locality, generalised inequalities, deterministic approach 79−21577
Einstein locality, inequalities 78−36855
Einstein locality, with correl. function $P(0) \neq -1$ 79−67173
Einstein paradox, time symm., photon polarisation in cascade transitions 78−21008
Einstein paradox and intrinsic time symmetry 79−71287
Einstein Podolsky Rosen experiment, Bell inequality for spin s 80−90713
Einstein Podolsky Rosen nonseparability, nonlocality in Feynman's antiparticle theory, e^+e^- annihilation *(French)* 77−41498
Einstein Podolsky Rosen paradox, propagator theorem calc. 78−77
Einstein-Bohr debate, who was right 80−90724
Einstein-Podolsky-Rosen gedankenexperiment *(German)* 77−41508
Einstein-Podolsky-Rosen paradox, causal superluminal interpretation 80−45
Einstein-Podolsky-Rosen paradox, contradiction between classical quantum theory of meas. and total ang. momentum conservation *(French)* 80−52042
Einstein-Podolsky-Rosen paradox, experimental evidence, quantum theory predictions 77−57225
Einstein-Podolsky-Rosen paradox, formal statement 79−44769
Einstein-Podolsky-Rosen paradox 77−74241
elastic scatt., variationally optimised T matrices 78−74
elastic unitarity eqn., new uniqueness condition for soln. 79−58950
elasticity, linearised eqns., acoustic tunnel effect 77−26188
elasticity, resolving functions and potentials for linearised eqns. 77−22425
elasticity equations, natural vibrations of rectangular parallelepiped and plate 77−27483
electrical conductivity, quantum theory, appls. 78−84181
electron conductivity in random pot., diffusive mode existence 79−65421
p-electron density matrix, spin-tensorial components, geometric consequences 79−84986
electron diffusion by positive ion, waveguide theory *(French)* 77−74240
electron gas, inhomogeneous, virial and Hellmann-Feynman theorems 80−88494
electron interference effects, Lande approach experimental contradictions 79−49081
electron penetration, single-barrier transmission, phase-integral. approx. 80−86140
electron plasma with nonparabolic energy dispersion relation, EM fluctuations 80−2413
electron-phonon antiresonant system, closed form canonical transformation calcs. 77−31741
electronic wavefunctions in a space of constant curvature 80−5466
electrons in helical mag. fields 79−80470
elementary length and elementary time interval, existence *(French)* 80−8815
elementary length and time interval *(French)* 78−77743
elementary particle classification, selection maps for quantum logics 78−29320
elliptic operator, partition function as functional integral over eigenspace 79−75394
EM potentials, arguments against Aharonov-Bohm effect, Marton expt. 80−73205
EM potentials, effect on an internal degree of freedom 80−42101
EM wave interference, new quantum interpretation, solns. to Maxwell eqns. 77−33882
EM wave propagation, propagator derivation by quantum mechanical technique 78−73886
energetically stable systems 79−2647
energy calculation, converging approximations, in terms of Planck's constant 79−25889
energy dispersion relation in valence band of quantum pendulum, semiclassical calc. 78−41199
energy eigenvalue problem, adiabatic perturbation theory using QFT techniques 78−93551
energy eigenvalues of Coulomb and oscillator potentials, connections 79−12637
energy forms, Hamiltonians and distorted Brownian paths 77−57279
energy levels, lower bounds determ. 78−16672
energy states of finite square well pot. 78−32723
entropy in operational statistics and quantum logic 80−17903
entropy of observable, continuity props. 77−60970
entropy of systems undergoing time evolution 77−30051
entropy prod. for quantum dynamical semigroups 78−57883
entropy which does not increase, quantum logic 77−17850
enveloping subspaces and superposition of states 77−2549
epistemological and mathematical foundations 77−37769

quantum theory continued
EPR, symmetry adaptation and operator equivalents *(French)* 78−91924
EPR paradox, breaking of restricted relativistic Einsteinian causality by quantum mechanics 79−63079
EPR paradox, quantum correlations and separability 80−31571
EPR paradox, reduced density matrix method, review 78−77766
equation of motion, commutation relations for quantum mechanics and QFT, quantisation 80−105541
equations of change 78−70003
equations of motion, deterministic model 78−24689
equations of motion, quantization method 79−85008
equations of motion 77−64958
equivalence of projective representations 77−17863
equivalence principle, evolution to general relativity 80−98779
equivalence principle test for spin-1/2 particles 79−12707
equivalent electrons, J allowed values in jj coupling, teaching 80−90624
Ermakov systems, nonlinear superposition, and solutions of nonlinear equations of motion 80−86125
Escoufier's operator, construction and appl. to principal components anal. 77−26146
Euclidean semiclassical methods, use limitations 80−42102
event phase space structure, alternative to quantum logic 80−42093
Everett interpretation 78−86175
evolution law approach, appl. to nuclear physics, QED and QFT *(Russian)* 79−80866
evolution of semiclassical quantum states in phase space 79−44774
exceptional gauge groups and quantum theory 79−35983
exclusion principle, undergraduate teaching approach 78−81746
expectation values as averages on fuzzy phase space 77−33888
expectation values variational calc., second order error 77−33894
experimental test for distinguishing real, complex quaternion quantum theory 79−35580
experimental tests of quantum mechanics versus local hidden variable theories 78−77750
experimental verification of quantum theory, hidden variables 78−54245
exponential operator approximants, many-body appl. 77−9896
extended relativity, T-violation and new particle 80−37182
extension theorems for operator-valued measures 79−49075
extremum sufficient condition in classical action integral, eigenvalue problem, education 80−105462
factored irreducible symmetry operators 77−26197
Fenyes-Nelson stochastic model of quantum mechanics 80−86
Fermi's 'golden rules' and exact long-term transition probability 77−30037
Fermi gas, 1-D planar theory 78−45519
fermion in pseudoscalar field, nonrelativistic model 77−67329
fermion systems, operator ordering, functional integrals 80−62574
fermion-field nontopological solitons 77−45970
fermions, precession in mag. field, test of equivalence principle *(Norwegian)* 77−64986
few body dynamics analytical continuation, nuclear shell model, resonances and bound states *(Russian)* 79−40860
few-body scatt. in quantum mechanics, soln. methods 79−85010
Feynman's path integrals, continuum calculus 77−5691
Feynman diagrams, appls. in advanced quantum theory, book 80−22157
Feynman Lagrangian for short diffusion processes 80−31551
Feynman maps and the Wiener integral 78−77758
Feynman measurements, continuous displacements *(Russian)* 79−35954
Feynman path integral, polygonal path formulation 80−31584
Feynman path integral and gauge invariance 80−82601
Feynman path integral and quantum mech. as $\hbar \to 0$ 77−2557
Feynman path integral and theory of forms 80−31586
Feynman path integral formulation using geometric quantisation techniques 80−31588
Feynman path integrals, classical limit 78−12476
Feynman path integrals, conference, Marseille, France, 1978 80−31422
Feynman path integrals, generalised meas. 78−384
Feynman path integrals, mathematical theory, book 77−41511
feynman path integrals and the corresponding method of stationary phase 80−31583
Feynman path integrals on/near caustics, semiclassical approx. using catastrophes 79−53992
Feynman path integrals with Gaussian measure, Laplace transform method 80−62522
Feynman-type integrals defined in terms of general cylindrical approximations 80−31591
fine structure constant, theory 79−12647
finite closed systems, relaxation, algebraic approach 77−29985
finite group representations, method of commuting operators *(Chinese)* 78−8257
finite integration range for zero modes 80−86150
finite propositional lattice, impossibility in quantum mechanics 79−84982
finite-dimensional Hilbert space theory 78−89356
five-body equation, wave function treatment for binary partitions 78−16686
fluctuations in quantum systems, spectral props. of physical processes of Markov-correlated events 79−21665
fluid, with square well+hard core pot., quantum corrections to eqn. of state 79−7535
Fock, V., development of ideas in atomic phys. and quantum theory 80−22183
Fock-Tani representation for the quantum theory of reactive collisions 79−80505
Foldy Wouthuysen transform. group content, nonrelativistic limit for arbitrary spin 79−75387
force on nucleus in non-stationary state, definition and anal. 80−105526
forced quantum oscillator equation, time-depend., soln. in coordinate representation 80−52044
formulae derivation for $y_{lm}(r_1 \times r_2)$ 80−98811
formulae for $y_{lm}(r_1 \times r_2)$ 80−98810
formulation in geometric picture 80−36895
foundations of quantum mechanics and uncertainty principle, book 78−29000
four-velocities in quantum theory, K-space 78−49720
Fourier transform, fractional order, appl. to quantum mechanics and electron motion in magnetic field 80−82665
free Dirac field, algebraic struct. of set of local observables 79−58883
free electron laser, quantum description 79−98330
free electron pair, possible ferromagnetism of triplet state 79−30272
quantum theory continued
free relativistic spin-1/2 particle energy-momentum invariants and kinetic moment *(French)* 78−62287
Freidrichs model, Lyapunov function evaluation 78−73876
frequencies, differences from classical freqs. *(Russian)* 78−4498
friction in quantised Langevin systems, Schrodinger eqn., damped harmonic oscill. solns. 79−21570
frictional quantum mechanical system, one-dimens. scatt. model for coherence in stopping power problem 80−101736
Frohlich Hamiltonian without cut-off, self-adjointness and other properties 78−38995
function integrals over anticommuting variables and 1-D scatt. problem 78−62103
functional differentiation, heterogeneous, continuous, appl. to Feynman path integral 78−4504
functional integration through inverse scattering variables 80−52065
fundamental constants, self-consistent values *(German)* 79−12758
fundamentals in quantum theory and relativity, conf. 78−54233
fuzzy observables, quantum meas. with residual expt. errors 78−77746
fuzzy spin spaces, probability theory, spectral densities 77−37811
Galilean system quantisation 78−70
Galilei covariant theory, minimal EM coupling 80−77634
gamma photon detection processes, statistics of radiation 77−65010
Gamow state vectors as functionals over subspaces of the nuclear space 80−32227
gas in closed container, relativistic thermodynamics 77−45812
gauge equivalence of representations of symmetry groups in quantum mechanics 78−77752
gauge invariant interpretation 77−5680
Gauss and Mainardi-Codazzi eqns. generalisations, appls. to quantum and classical mechanics 78−62092
Gaussian fluctuations: 't Hooft's method and an approximate method 79−85236
Gaussian path integrals and semiclassical propagator 77−22432
Gaussian wave packet propag. in uniform gravit. field, accelerating transformation operator calcs. 77−74239
gedanken expt., observation without interaction, effects 78−89362
Gel'fand lattice polynomials and irreducible representations of U(n) 78−49700
Gel'fand-Levitan equations with comparison measures and comparison potentials 80−12931
Gelfand-Levitan eqn. and Korteweg-de Vries eqn. 78−32708
Gelfand-Levitan method for operator fields 80−57136
geminal expansions, symmetrised, N-completeness 79−63068
generalised 3j symbols 78−36876
generalised 6-j symbols 80−31557
generalised coherent states, geometrical props. 77−17873
generalised coherent states, irreducible representations of Lie groups, anal. and applications 78−62114
generalised coherent states closest to classical states *(Russian)* 79−67189
generalised effective Hamiltonian, time scale separation with semiclassical formalism 78−65800
generalised Fenyes-Nelson model for free scalar field theory 80−105769
generalised Poisson bracket and associated natural one-form 77−37719
generalised polarisabilities, new variational bounds 78−45502
generalised quantum defect, energy and radius depend. 80−14067
generalised quantum logics, geometry 80−42085
generalised transition probability derived from physically motivated axioms 79−12631
generalised two-level quantum dynamics, nonHamiltonian state evolution 78−36854
generalized absorber theory and the Einstein-Podolsky-Rosen paradox 80−90714
generalized deformations of nonassociative algebras. Definition and some simple examples 80−36887
generalized Hamiltonian theory: central coordinates 80−105538
generalized quantum spins, coherent states, and Lieb inequalities 79−67172
generating functions for characters of group representations and their applications 80−8840
generating functions for integrals involving harmonic oscillator functions 79−35577
generating scattering amplitude, coherent representation 78−50527
generator coordinate method in natural state formalism, appl. to harmonic oscill. 77−17831
generators of infinite direct products of unitary groups 78−24677
geometric quantisation, correl. between classical and quantum mech. in geometric language 79−25905
geometric quantization and internal symmetry 80−42089
geometric quantization and quantum mechanics, book 80−94908
geometric struct. of charged fields, Aharanov-Bohm effect 78−28994
geometrisation into classical Hamiltonian form on symplectic struct. 79−40390
geometrodynamic approach via Hilbert space affine connection 77−60962
geometry, physical, group manifold 80−105522
Gleason's theorem generalisation 80−36889
graded algebras, finite dimensional irreducible representations, appl. to (Sp(2n); 2n) 79−49074
gradient method in quantum mech., one-dimens. harmonic oscillator appl. 77−82831
graphical spin algebra, differential operators 77−60964
Grassmann variables, possible interpretation of theories 77−79001
gravitation, neutron interference fringes due to gravitational potential, role of gravity in quantum mechanics 80−62495
gravitational collapse, predictability breakdown, principle of ignorance 77−17356
gravitational interactions in Brownian motion theory 79−12699
gravity role, neutron interferometer expt. 80−86176
gravity wave detection, quantum nondemolition meas. schemes 79−67218
Green's function defined in phase space, using Wigner operator eigenfunctions and eigenvalues 78−24728
Green function equations, normal phase-space coords. 77−45738
ground state properties, energy level lower bounds, particle in mag. field and external pot. 78−8260
group extensions, appl. to quantisation 77−37765
group representation theory, intuitive approach for teaching 79−25804
group representations and appls., book 78−32652
group theoretical foundations, elementary systems 79−30282

quantum theory continued
group theoretical foundations of classical and quantum physics, kinematical symmetry groups and state spaces 80−52008
group theory, postgraduate textbook for physicists 77−41455
group theory applications to physical and chemical systems in relation to struct. and substructs. 80−42921
group theory approach to dynamical quantisation 77−18183
group theory solution to problem of particle motion, field of two Coulomb centres *(Russian)* 79−92992
hadron microstructure, de Sitter microuniverse, relativistic Hooke group and nonrelativistic quark model 80−27480
hadronic matter, string junction model and spectrum energy density of string 80−57556
hadronic quantum numbers beyond charm as possible source of neutrino induced trimuons 78−12903
Hamilton-Jacobi equation solns. in Coulomb pot. and quasiclassical approx. 80−46765
Hamilton-Jacobi generalised theory, phase space approach 80−36891
Hamiltonian, information content of exact eigenfunction of physical system 79−30280
Hamiltonian, quantification of geodesic flow of sphere S^n *(French)* 78−54151
Hamiltonian determ. in presence of constraints 79−30289
Hamiltonian eigenvalues in Weyl correspondence limit, Turschner's formula 79−84988
Hamiltonian evolution, sufficiency condition, semigroup formalism 77−30047
Hamiltonian model for N, π and Δ in many body problems 79−85417
Hamiltonian model of computers 80−101727
Hamiltonian of single variable systems, asymptotic behaviour of bound eigenfunctions 78−77754
Hamiltonian operator, discrete spectrum calc. method *(Czech)* 80−17823
Hamiltonian operators, class of lower bounds 79−40393
Hamiltonian $P^2+A|X|^\nu$, exact eigenvalues 79−40392
Hamiltonian path integral in polar coords. 79−49079
Hamiltonian repres., absolutely and singularly continuous subspaces 77−64952
Hamiltonian system dynamics, Lie group symm. *(Russian)* 77−30033
Hamiltonian systems, additional integrals of motion 78−49711
Hamiltonian systems, props. of charact. exponents *(French)* 79−25888
Hamiltonians, approximate relativistic, for interacting particles, canonical formalism 77−13897
Hamiltonians, quadratic, classes of quadratic invariants, interrelations and symmetries 80−31565
Hamiltonians, time depend. linear canonical transformations 77−74213
Hamiltonians perturbed by pulses, quantum dynamics 80−17829
Hamiltonians with x^{-2} singularity 77−26201
Hanle effect, level-crossings effect on He I D_3-line polarization in solar prominences 80−94772
harmonic anal. on Lorentz group as dynamical relativistic Fourier anal. 77−82406
harmonic oscill. chains, vel. correl. functions 77−82403
harmonic oscillator, driven and stochastically modulated, reduced eq. of motion 78−77764
harmonic oscillator, extended Feynman path integral formula 80−36890
harmonic oscillator, quantum action angle variables 80−46842
harmonic oscillator, time-dependent 80−8826
harmonic oscillator, two dimens., q equivalent particle Hamiltonian 78−93525
harmonic oscillator brackets, derivation of new expression 78−20997
harmonic oscillator Brownian motion, quantum dynamical semigroup formalism 77−30100
harmonic oscillator in box, quantum-mechanical soln. 77−13632
harmonic oscillator relaxation, Gaussian identities 78−4524
harmonic oscillators, continuous observation, quantum restrictions 79−97252
harmonic oscillators, position and momentum eigenstates, superposed coherent states 80−57135
harmonic oscillators, time-dependent, exact invariant determ., direct method 78−12597
harmonics on 3-sphere, Lie group SU(2) 78−57813
Hartree equations, time-dependent, global solutions, and nonlinear Schrodinger eqn. 80−73193
Hartree-Fock accuracy, nuclear charge dependent perturbation theory, Hellmann-Feynman theorem, virial theorem 79−44776
heavy charged particle elastic scatt., Debye expansion and JWKB approx. 77−53803
Heisenberg, development of quantum mechanics 77−9844
Heisenberg's principle, distinguishing test from de Broglie's relation 80−42092
Heisenberg algebra commutation relation, general representation, Schrodinger eqn. soln. 79−2653
Heisenberg commutation relations, Hermitian phase operator *(Russian)* 78−73870
Heisenberg infinite classical and quantum models, intertwining, Trotter approx., coherent state formalism 79−44713
Heisenberg matrix mechanics and variational principles in quantum theory 79−63085
Heisenberg operators, Laplace transformations in finite dimens. spaces *(Russian)* 77−49640
Heisenberg/Lie/symplectic formulations, problematic aspects 80−62497
Hellmann-Feynman theorem, appl. in surface physics 79−95262
Hellmann-Feynman theorem for limited CI wave function, 1st-order props. 79−59329
Helmholtz equation, 1-D three-body problem, Sommerfeld Maluzhinetz transformation 80−62524
Helmholtz flat space eqn., non orthogonal separable coordinate systems 79−75416
Hermitian, antiHermitian and unitary operators, basic props. 78−54113
Hermitian matrix, disorder effect on spectrum 80−31547
hermitian matrix, large, eigenvectors determ., new approach 77−37717
Hermitian metrics and the Weyl-London approach to the 'quantum theory' 79−67179
Hermitian operator low lying eigenvalue calcs., iterative method 77−60965
hermitian operators, upper and lower bounds to eigenvalues, variational calcs. 78−36882
heterodyning of elementary particles, radiation meas. method 80−42898
hidden parameters problem, exptl. classification 78−57821
hidden parameters problem, exptl. test *(Chinese)* 78−16676

quantum theory continued
hidden symmetries in dynamical systems 80−37168
hidden variables, algebraic constraints 78−65797
hidden variables, quantum mechanics, and stochastic electrodynamics *(French)* 78−62107
hidden variables and locality 77−58
hidden variables and proper mixtures for multivalued observables, correlation function results 78−57853
hidden variables controversy 79−62975
hidden variables model, proposed test 80−86109
hidden variables theory, probability measure in Hilbert space 80−62508
high energy process, with strong absorption, elementary quantum mech. 78−86053
higher-order Levinson's theorems and the high-temperature expansion of the partition function 80−4558
Hilbert space, commutativity of two projections 80−68083
Hilbert space, embedded orthomodular partially ordered set, probabilities from standard trace formula 78−86183
Hilbert space, quantum mechanics and integration, functional integrals 79−97246
Hilbert space, unbounded measures on the closed subspaces 79−12639
Hilbert space and probability meas. 77−57223
Hilbert space field 77−74247
Hilbert space formalism for probability theory 77−60955
Hilbert spaces, Gleason measures on infinite tensor product 77−26200
Hill-Wheeler integral for rotational energies, polynomial expansion 79−95
history, 1901 to 1911, Einstein and Planck *(Russian)* 79−84933
hot cavity, thermal ionisation 78−70677
Hunziker's theorem, proof 77−26190
hydrodynamical formulation, Aharonov-Bohm effect 79−71288
hydrogenic atom, nonrelativistic, linear response to external linear polarised EM wave 78−8258
hypergeometric partial solutions in the problem of two Coulomb centers 80−4582
hypervirial relations, giving recurrence relations for radial matrix elements 78−4502
hypervirial theorem, form of intermediate operators 79−44784
hypervirial theorems and co-ordinate transformation in quantum mechanics 80−86137
hypervirial theorems and symmetry, optimal variational wave function 80−17841
identical particles, theory, quantisation of two particle system, spin 77−26203
implicate order, algebras, and the spinor 80−52047
impulse approx., neglect of binding 79−112
individual properties of individual particles, theory, teaching approach 78−57721
induced projective unitary-antiunitary representations, selection rules, Clebsch-Gordan series 78−54214
infinite component wave equations, composite system internal struct. 77−65102
infinite macrosystems in standard representation, dynamical symmetries 80−4590
infinite systems, symmetry, isotropic representations, Galilei-group 78−93553
infinite systems, symmetry, state space and group action 78−93552
infinitesimal symplectic relations and generalized Hamiltonian dynamics 79−25878
information theory, comment on recent studies 77−17851
information theory and open systems 77−17848
information theory of quantum measurement 78−36863
inner-shell vacancy system, saddle point calcs. 80−23292
integral Schrodinger eqn. for atomic evolution operator, transitions to continuum, Fredholm method 79−72223
integral transforms, alternative forms using hyperdifferential operators 77−49570
integrals of motion, dimensionality of commutative subalgebra of observables *(Russian)* 77−17835
integrating factors for single systems, general nonconservative systems 80−90706
intelligent spin states, compact representation, time evolution and radiative props. 77−5690
intelligent states, group-theoretic study and computation of matrix elements 78−62100
interacting particles system, nonrelativistic classical and quantum mechanics conservation laws 78−89328
interference, gravitational and rotational effects 77−45734
interference and phase shift due to Earth's rotation 80−82679
intermediate states spectrum, Sturm expansions of Green's functions 79−9132
intermediate system lifetime in quantum mech. collisions 78−45521
internal Galilei group for a two-particle system 79−75406
interpretation, spin and uncertainty, teaching approach 79−58481
interpretation and conceptual basis 78−12588
intramolecular dynamics, criteria for stochastic nonstochastic flow 80−53082
intrinsic geometry of quantum mech. phase space Hamiltonian systems, correspondence principle 79−83
intrinsic temperature of confined systems 79−85271
invariance principle in scatt. theory, proof 79−75378
invariant phase space integral evaluation via Laplace transforms 80−31573
invariant props. of n-point functions and functionals due to translationally invariant formal measure 78−45500
inverse Noether theorem, general formalism for symmetry and conservation 80−46850
inverse power singular pot. with complex coupling const., phase shift 78−41176
inverse problem at high energies, ambiguities by JWKB method 79−85419
inverse scatt., Newton's method modification at fixed energy 80−73207
inverse scatt. problem, two discrete forms 77−78995
inverse scattering problem, N-soliton of eqn. $\sigma_{xt}=e^{\sigma}$ 78−8269
inverse scattering problem, nonuniqueness 78−65820
inverse scattering technique of soliton theory, Lie algebra, Poisson-Moyal bracket, rotating rigid body 77−9908
inverse scattering transform, Wronskian technique, isospectral flow eqn. 78−8275
inverse scattering transforms, Zakharov-Shabat and Schrodinger-type, connection 78−21006

quantum theory continued
involution and differentiation generalised functions, 3-D, associative algebra 80−68080
IO(n), lowering and varing operators and normalisation consts. 79−58569
ion, singly-charged, sufficient conditions for finite no. of bound states 79−10047
ion cyclotron resonance, collision-dominated, quantum mech. description 79−2666
ion cyclotron resonance power absorption, quantum theoretical treatment 78−317
IR radiation, interaction with molecular system, classical/semiclassical theory challenged 80−43117
irreducible tensor operator methods in strong-field coupling 79−7811
irreversibility, time and anisotropies, cosmological origin 77−13510
irreversible processes, time asymmetry 80−22215
irreversible processes and dissipative systems in quantum theory 80−8906
ISO(n), explicit determ. of representation functions 80−31561
isolated quantum system, consequences of more general theory of symmetries 78−49718
isotonic oscillator, coherent states for nonharmonic potentials 80−52061
isotopic spin and coherent states 80−4843
isotropic harmonic oscillator, n-dimensional, noninvariance group 78−8264
IU(n), lowering and varing operators and normalisation consts. 79−58569
J^2 eigenvalues 80−17742
jarring of quantum system, theory of sudden perturbations 80−17839
JBD theory, exact cosmological soln. with particle creation 78−96576
joint distributions of observables on quantum logics 79−71270
joint probabilities, study of Wigner's theorem 79−67175
joint probability distributions for quantum observables 79−12650
Jordan algebra state space characterisation in quantum mechanics 80−86105
Jordan-Wigner representation of CAR algebra, boson expansions 78−36850
Jost function, off-shell, for Coulomb, Hulthen and Eckart pots., limiting relations 78−81875
Jost function treated by the F-matrix phase integral method 79−25884
jump processes, Cauchy problem for Schrodinger eqn. *(French)* 80−31596
K-harmonics in one dimension 79−2584
K-matrix, off-shell 2-body scatt. with Woods-Saxon pot. 78−21002
Kampe de Feriet function expansion in terms of generalised prolate spheroidal wave function 79−17259
Kepler stationary orbits of electron with velocity-depend. oscillatory perturbations 80−52062
Killing trajectories, intrinsic geometry, appl. to real quantum mechanics 77−22393
kinetic equations, linear and nonlinear, quantum mech. theory 77−9969
kinetic theory, three-particle collision term 77−64994
Klein-Gordon eqn., essential spectrum selfadjointness and invariance 77−18157
Klein-Gordon equation, identical motion in relativistic quantum and classical mechanics 77−61177
Klein-Gordon equation, nonlinear, oscillating particle-like solutions *(Russian)* 77−9916
Klein-Gordon equation applic. to quasi-classical wave function, conservation laws for ensemble of noninteracting particles 77−64962
Klein-Gordon particles, charged, quantum kinetic theory, linear kinetic eqn. 80−57178
Klein-Gordon particles in deep square wells 80−31982
KMS condition for Schrodinger dynamics 80−36896
Korteweg-de Vries generalised systems, rels. 79−58551
kq representations in quantum mechanics 79−84990
Kramers rate theory, quantisation using Wigner representation 80−52054
Krolikowski-Rzewuski eqn., unstable system state vector 77−53794
ladder operators of group matrix elements 80−31555
Lagrangian, objective interpretation 78−24686
Lagrangian and dissipation, teaching approach 79−84892
Lagrangian and Hamiltonian eqns., prob. distribs. anal. 77−26191
Lagrangian formalisms in scalar pregeometry, quantum mechanical equivalence 79−54024
Lanczos tridiagonalisation in bounding eigenvalues 77−53798
Langevin eqn., canonical quantisation 79−12640
large-angle potential scattering in variable phase approach 78−91
lattice, orthocomplemented quasi modular, quantum logic interpretation 80−12950
lattice structure of quantum logics 79−73
lattice structure of sublevels for pseudo-internal product *(Italian)* 78−12586
Lee-like models decay parameter calcs. 77−30026
Legendre moments calc. from partial waves 79−17273
Legendre Pade approximants, and appl. to pot. scatt. 78−28982
Legendre Pade approximants, convergence, to Coulomb and other scatt. amplitudes 78−28983
Legendre Pade approximants to scatt. amplitudes, convergent sequences 79−85014
lepton-quark system, quantum number laws, classification of weakly interacting particles, decays 78−82138
level clustering in regular spectrum 77−71237
level spacings, lower bound for single particle in neg. potential 77−22430
Levinson theorem and its generalization in relativistic quantum mechanics *(Chinese)* 79−92988
Levinsons theorem, generalisation to abstract scatt. systems, appl. to pot. scatt. systems 78−62090
Lewis Riesenfeld harmonic oscillator, unitary declension of dynamical symmetries 79−89074
Lie algebra, canonical realisations 77−41453
Lie algebra, equivalence of deformations and associated *-products 79−97237
Lie algebra representations, contraction 79−80767
Lie algebras in Schrodinger picture and radial matrix elements 77−2560
Lie group, path integral and quasiclassical asymptotic behaviour 78−54230
Lie group Sp(8,R), Lorentz subgroup anal. and null plane boson realisation 78−62116
Lie groups, associated observables 77−74249
quantum theory continued
Lie groups and algebras, geometrical theory of contractions of groups and representations 79−58566
Lie-admissible symmetry, representation theory 80−62870
Lie-Backlund operators, exam. of isomorphic correspondence between classical and quantum-mech. invariants 80−90700
light wave resonant interaction with atoms and molecules *(Ukrainian)* 78−66515
limits of validity, test in low energy pp scatt. *(French)* 79−406
linear potential, energy eigenvalue eqn. 79−2646
linear potential eigenenergy equation, $K_n(3l')$ coeffs. 79−44762
linear response theory, macroscopic vs. microscopic, appl. to electron in periodic pot. 78−65813
linearly perturbed parameter dependent systems, energies calcs. 79−25893
Liouville dynamics for optimal stochastic phase-space representations of quantum mechanics 78−21062
Lippman-Schwinger eqn. for non-central pots., appl. of Fredholm theory 77−71232
Lippman-Schwinger equation, soln. for n delta-shell pots. 78−41112
Lippmann Schwinger eqns. for three charged particles 80−4580
liquid-gas critical point, quantum mechanical effects, theory 80−103452
local bound states *(Russian)* 77−71227
local causality and quantum mech. state vector 77−22438
local commutativity, possible expt. test 77−74266
local hidden variable theory test completeness, Bohm-Aharonov system 79−71276
local kinetic energy, phase space formulation 79−44771
local theories, probabilistic and deterministic, inequalities of Einstein locality 80−82656
local two-body interaction, off-shell phase shift 78−45516
localisation concept of relativistic particles, consistency with causality 77−33883
localised crystal, quantum theory, causal Green's functions 79−42338
locality concepts, Bell's theorem, quantum theory predictions and interpretations 78−93550
localizability of relativistic particles in fuzzy phase space 77−63
logarithmic Schrodinger equation, soliton dynamics 80−57130
logic, quantum, Schrodinger cat paradox 79−97170
logical and mathematical structures of quantum mechanics, review 77−33904
logical interpretation of quantum mechanics, and significance of hidden variable proof 79−71271
logical problems of quantum mechanics 80−12883
logical structures and hidden models in quantum theory 78−41190
long range interactions, range definition 79−54001
long-range potentials, vac. fluctuations and retardation effects 79−3522
Lorentz group, linear representations and matrix element computation formulas 79−58571
Lorentz group in oscillator realisation 78−77755
Lorentz space relativistic path integrals, Dirac electron perturbation expansion 79−85000
Lorentz-covariant formulation on projective planes 79−58577
loss energy states of nonstationary quantum systems 78−49719
low intensity interference effects, hidden variable theories 78−70009
low-energy scatt. by velocity depend. potls. 77−49631
Lyapunov variable, entropy and meas. in quantum mechs. 80−77739
macroobservables, reconstruction in embedding method 80−77691
macroscopic observables, treatment procedure 80−17864
magnetic Aharonov-Bohm effect 79−71281
magnetic monopole-electric charge scatt., rotationally invariant approx. 78−54225
magnetic monopole-electric charge scatt. amplitude, analyticity 78−54226
magnetic resonance, symmetry adaptation and operator equivalents *(French)* 78−91924
magnetic resonance problems, semi-classical approach 79−35586
magnetism, ferro- and para-, review of use of quantum mechanics 78−76215
magnetism, key to understanding by quantum mechanics 79−24125
magnetism, quantitative understanding *(Polish)* 79−51733
magnetism theory, sole of quantum mechanics in development *(Czech)* 79−44765
many particle systems, time inversion and mobility 80−101722
many-body equilibrium configuration for one-dimens. problem, pair pots. 78−4513
many-body fermion energy lower bound models 77−37809
many-body problem, vertex function and crossing symmetry 80−62515
many-body problems, orthogonal polynomials, asymptotic density of zeros 79−30286
many-fermion quantum mechanics, coherent-state representation 80−94988
Markov classical processes, nonequivalence to quantum mechanics 80−62583
maser with beam of inflying atoms, spectral line broadening mechanism 80−106503
Maslov index, explicit construction, applications *(French)* 77−17875
mass and Pontecorvo oscillations of neutrinos using chronon concept in electron theory 78−36879
mass centre separation in homogeneous mag. fields 79−80
mass formula of charged leptons 80−13244
mass spectrum in relativistic extended models of elementary particles 77−34116
mathematical basis, observed vel. statistical definition 79−88831
mathematical basis 77−49630
mathematical foundations of dimensional analysis and the question of fundamental units 80−42086
matrix diagonalisations via involutional transforms. 80−17827
matrix diagonalisations via reduced characteristic eqns., appl. to ang. mom. coupling 80−17828
matrix elements between unbound states, for radial Schrodinger eqn. 79−97240
matrix order and W*-algebras in operational approach 80−77690
matrix Pade approximants, applics. in pot. theory 79−78
matrix representation of unbounded operators 79−97231
Matrix variational Pade approximants and multi-step square-well potentials 79−71283
matter stability despite catastrophic Coulomb forces 80−22212
maximum overlap and shape instabilities 79−40401
maximum square variance of finite dimensional Hamiltonian 79−71269
Maxwell's equations, derivation from local gauge invariance 78−54109

quantum theory continued
measure theoretic ergodic theory in quantum mechanics 80−52069
measurement, consciousness and environment 77−61
measurement, Newman's theorem, Bell's hypothesis *(Hungarian)* 77−71226
measurement, quantum logics 78−54237
measurement in perception quantum theory 78−49689
measurement perturbations, repeated, quantum system decay and reduction laws 80−62496
measurement problem, collapse of wave function 77−62
measurement problem of quantum mechanics 80−12948
measurement process, interpretation problems 80−57117
measurement sequences, Everett interpretation 78−32707
measurement techniques, interaction between classical and quantum systems 80−42099
measurement theory, argument against superluminal transmission 80−52055
measurement theory, ideal expts. appl. 80−42087
measurement theory, initial correl. and observables with continuous spectra 77−33885
measurement theory, interaction between classical and quantum system 80−92
measurement theory, interrelation of quantum theory and gravitation 78−54235
measurement theory, mechanism of reduction of wave packet 80−86146
measurement theory, peculiarities and postulational excesses 80−27174
measurement theory, proposed Einstein-correlation experiment with a timelike separation of detections 79−58574
measurement theory, wave packet reduction 80−105536
measurement theory 80−17824
measurement theory noncommutative analogues of Cramer-Rao inequality 77−26209
measurements, interactive computer program, for teaching 78−41113
measurements, quantum and classical correlations 78−73866
measurements, simulation using programmable pocket calculator 80−41982
measuring units system, electromagnetic phenomena, relativistic aspects *(Rumanian)* 79−17382
Melosh transformation, Eriksen like form, group theoretic interpretation 80−8859
metal particles, small, dielectric function and IR absorption 80−60607
metastable lifetimes, level crossings and vertical cuts 79−90
microphysics, stochastic basis for quantum mechanics 79−53997
microphysics foundations, use of Bell inequalities in expt. test 79−102
microrealistic explanation of quantum phenomena 80−82659
microsystems, nondistributivity, empirical correctness 78−28989
minimal EM coupling in elementary quantum mechs., group theoretical derivation 78−54590
minimal time-energy uncertainty relation 79−67174
minimally coupled N-particle scatt. integral eqns. 77−88090
minimum uncertainty states and pseudoclassical dynamics 79−103
minimum uncertainty states and pseudoclassical mechanics 77−45733
mixed crystal or alloy, graded, effective Hamiltonian theory 80−34344
model systems, generalised theorems 79−21658
molecular beam in Stern-Gerlach apparatus, state reduction hypothesis 78−77765
molecular charge distrib., quantum topology, bonding theory and molecular structure 80−5463
molecular internal stresses, stress tensor, one electron system 78−62686
molecular physics, quantum mechanical description of high resoln. expts. 77−6862
molecular physics, quantum tunnelling process 79−63894
molecular quantum mechanics, $F_m(y)$ function, improved computation 79−63892
molecular quantum systems, time dependent Born-Oppenheimer approximation 80−105518
molecular spectra, full quantum mechanical theory, mol. eigenstates generator coordinate method 78−21895
molecular struct. defn. in quantum mechanics 80−52843
molecular structure, quantum theory, interpretation problems 80−106248
molecular structure and shapes, quantum mechanical view 80−102422
molecular structure as postulate of quantum theory 78−62684
molecular structure hypothesis, quantum mechanical aspects 80−102421
molecular structure quantum theory 78−58568
molecular structure theory, quantum topology 80−106247
molecule, diatomic, hyperfine struct. transitions, quantum theory, for undergraduate demonstration 80−17762
Moller operator, rel. to superoperator, algebraic proof 78−28977
moment of inertia in quantum mechanics, Harris cranking model, for teachers 79−35475
momentum operator, in nonCartesian coords., for teaching 78−24620
momentum operator in curvilinear coordinates *(Russian)* 78−36862
momentum operators for curvilinear coordinate systems 80−17743
monatomic gases, quantum corrections to transport coeffs. 77−15148
Morse oscillator, matrix elements calcs. with Sturm-Liouville eqn. eigenfunctions 79−2660
motion group, completeness theorem 78−4519
Moufang plane and octonionic quantum mechanics 78−69999
Moyal quantum mechanics formulation and Weyl. quantisation generalisation, Lie algebras 80−17835
multi-level system in strong mag. field *(Russian)* 78−49696
multichannel, time-depend., nonrelativistic quantum scatt. theory for identical particles 79−44798
multichannel quantum scatt., two-Hilbert space formulation 78−28986
multichannel scatt. theory in two spaces 79−88839
multichannel scattering, time independent theory 77−17859
multidimensional problems, WKB approx. 77−82412
multidimensional WKB wavefunctions, local and global semiclassical approximations 78−73880
multimode quadratic expression in boson operators, ordering or exponential 77−45728
multiparticle scatt., time depend., arrangement-channel quantum mech. 77−41503
multiple pot. scatt., soln. by finite iteration 78−28993
multiple scatt. of waves from lattice, theory 78−16697
multiple scattering approximations in 3-body problems, comparison 79−84
multiple scattering with three-body forces 78−63
multiplicity free 6-j symbols and Weyl coeff. of U(n) 78−65809
multiply connected spaces, quantisation in terms of Feynman path integrals 80−52060

quantum theory continued
multipole states, tensor struct., transition operator 80−36907
multisoliton formula for completely integrable two-dimensional systems 79−67166
multivalued observables, new tests 77−57226
multivalued observables, reinterpretation and extension of Bell's inequality 77−60959
Muskhelishvili-Omnes equation and final state interactions 80−17821
mutual observation, impossibility 79−44793
N-body integral eqns. and orthogonality scatt. 77−17861
n-body quantum system, time depend. scatt. theory for infinite delta function pots. 78−49704
N-body scatt. in two-cluster region 78−28975
N-body scatt. theory, form factor approach 79−79
N-body scatt. theory in two Hilbert spaces, asymptotic limits 78−65808
N-level systems, approach to equil. for completely positive dynamical semigroups 77−30048
N-particle system in arbitrary EM field, eqn. of change in config. space 79−36705
N-representability, rels. between necessary conditions 79−6000
N-representability problem, operator endomorphisms 77−33892
N-representability problem, operator endomorphisms 77−33893
narrow resonances, high energy mag. resonances, exactly soluble model 80−86134
natural modes, completeness for quantum mech. pot. scatt. 79−30283
Nelsons stochastic mechanics, spinning particles and relativistic particles 80−31587
Neother's theorem, time-dependent invariants and nonlinear equations of motion 80−12932
Neumann algebra, completely positive maps, semigroup generators 78−93545
neutron in magnetic field of linear current, system with latent symm. 0(3) *(Russian)* 77−67588
neutron interference, gravity and inertial effects, principle of equivalence at quantum level 80−77669
neutron interferometry, Earth rot. affecting wave function phase 79−54012
neutron star, relativistic quantum mechanical model for solid core 77−33546
neutrons in helical mag. fields, quantum theory Schrodinger eqn. solns. 79−35581
new gauge transformation for a generalized quantum representation 80−86136
Newton's first law, appl. to particle detect. probability *(German)* 77−67309
Newton and Heisenberg eqns. of motion relation, harmonic and anharmonic oscill. 79−6018
Newton-Wigner position operator, non existence for quanta with zero mass and nonzero helicity 78−62099
Newton-Wigner position operator derivation 80−98821
nilpotent Lie groups, coherent state representation 77−49618
nodeless wave function quantum theory 80−57119
non relativistic quantum mechanics, quantum microsystem evolution, nonconservation effects 80−22515
non-Abelian dyons, Nambu mechs. descript. 78−41490
non-completeness argument, EPR anal. 80−105533
non-conservative description of evolution in physics *(French)* 79−97328
non-Gaussian wave packet time evolution 80−57133
non-Hamiltonian systems, detailed balance condition 77−30096
non-hermitian potls., completeness relns. in scatt. theory 77−17854
non-locality as implied by quantum theory 78−54241
nonadiabatic transition amplitudes, semiclassical calcs., adiabatic theorem in complex plane 78−20993
nonassociative algebra, bibliography 80−36793
nonbijective canonical transformations, representation in quantum mechanics 78−45501
noncanonical operators, determ. of eqns. of motion from action principle 78−4515
noncausal world model; can an effect precede its cause? 78−73824
noncompact groups, equiv. problem to 2-centre integrals in quantum mechanics *(Russian)* 78−89367
nonconservative systems, irreversible behaviour 79−81
nondecay probability, small-time behaviour and Zeno's paradox 79−97241
nonequilibrium effects, Fokker-Planck eqn., rel. to path sums, Feynman proof 77−2629
nonergodic classical statistical theory 80−77646
nonexistence of signal going backwards in time 80−42105
noninertial reference frame, laws of motion in invariant form *(German)* 80−36886
nonintegrable quantum system, irregular part of discrete energy spectrum, statistical theory 80−82667
nonlinear approach to electrodynamics spin and stability props. anal. 78−49682
nonlinear differential difference eqns. with N-depend. coeff. 79−71274
nonlinear functional theory of particles, general conservation formulae 80−46860
nonlinear lattice quantum corrections for a system of interacting phonons and the modified Korteweg-de Vries equation 79−60454
nonlinear oscillator, quasiclassical theory of excitation time 79−40411
nonlinear oscillator in harmonic force field, averaged quantum eqn. of motion 78−54232
nonlinear quantum mechanics, appl. of Gauss tranformation to $^1/_2$ fields 79−63082
nonlinear quantum mechanics, Gauss transform. appl., Schrodinger eqn., nonlinear integro-differential eqn. 79−6013
nonlinear quantum oscillator, stochastic instability 79−85007
nonlinear resonance in quantum system, perturbation and quasiclassical theory 77−13640
nonlinear response of some simple quantum systems 77−49620
nonlinear reversible dynamical evolution, entropy and superposition 77−60961
nonlinear spin relaxation theory 80−90701
nonlinear systems, semiclassical quantisation methods, review 77−71238
nonlinear systems mobility 80−31566
nonlinear wave equation for quantized frictional forces 79−85
nonlocal continuous potentials, theory of integral operators and eigenvalue anal. 78−8274
nonlocal interactions, generalised Levinson theorem and spectrum struct. 77−74250
nonlocal interactions and Bell's inequality 77−22442

quantum theory continued
nonlocal models and QM comparison 78−4510
nonlocal pot. scatt., off energy shell results 79−49104
nonlocal pot. scatt., off energy shell results 79−49105
nonlocal potential scatt., phase shift and extra nodes 77−74265
nonlocal theories satisfying Bell's inequality 79−12642
nonlocality detection, rel. to game of quandice 80−86143
nonradiative transitions, solvent effects, dynamic coupling model, quantum mechanical theory 80−29787
nonrelativistic multichannel quantum scattering theory in two Hilbert space formulation 78−57822
nonrelativistic perturbation theory, new approach 79−71289
nonrelativistic quantum mechanics, fibre bundles *(German)* 80−90699
nonrelativistic quantum mechanics and anomalous part of g-factor 77−74238
nonseparability for systems composed of identical constituents 77−57230
nonseparability of quantum mechs., workable expt. scheme 77−5695
nonseparable system, energy levels, semiclassical method using Birkhoff-Gustavson normal form 79−97224
nonseparable system semiclassical quantisation, invariant tori and energy levels calc. scheme 79−97225
nonsingular integral eqn. for three body scatt. problem 78−62106
nonspreading wave packets 79−44672
nonstandard model of two dimens. quantum system, axioms 78−28972
nonstationary effects, obs. in ultracold neutron interaction with time-depend. pot. *(Russian)* 77−9913
nonstationery quantum systems, loss-energy states 79−75399
nontunnelling particle penetration through potential barriers, Lee model calcs. 80−73213
normal and anomalous intellectual activity classification, coherent quantum-wave brain model *(Russian)* 78−27922
normal ordering, identities 78−86059
normal states and unitary equivalence of von Neumann algebras 77−17754
nuclear decay, γ-decay of coherent rotational states, random quantum meas. 80−73855
nuclei, classification of states, unitary scheme 80−42550
nucleon-nucleon hard-core system, bound states and scatt., for teaching 78−41115
O(2) Heisenberg gauge invariant model, eigenfunctions and energy spectrum 79−58875
O(3) irreducible representation bases, for systems with finite symm. group 77−9902
O(3) shift operators, general anal. 79−94
objective, Copenhagen interpretation and Popperism 77−37772
observable differences between proper and improper mixtures 77−82410
observables, relation between quantum and classical 80−31537
observables, relative compatibility and joint distributions 80−105524
observables on infinite-dimens. Hilbert spaces 77−33884
observables with continuous spectra, hidden variables problem 78−16690
octonionic quark confinement 79−17669
octonions in quantum mechanics 80−27479
off-shell scattering by Coulomb-like potentials 80−31560
on-shell three-body multiple scatering eqns. 78−28988
one dimens. symmetrical quantum systems, exact local states 80−46870
one dimensional particle, quantum, for teachers 79−35473
one-dimensional equation in method of phase functions *(Russian)* 78−45499
one-dimensional many-body problems, exact results, review *(Russian)* 79−80460
one-dimensional molecular chain, collective model for conformons 80−15456
one-dimensional particle-in-the-box problem, perturbation theory illustration using champagne bottle situation 80−36816
one-dimensional scatt. theory, stability of direct and inverse problems 78−4523
one-dimensional singular potentials 77−13522
one-dimensional three body system, δ-interaction, exact bound-state soln. 77−5694
one-electron density matrix, optimisation 77−79532
one-system formalism of quantum mechanics, locality and joint probabilities 78−54238
Onsager-Casimir symmetry, geom. of roots of matrices 79−100
open N-level system, algebras, condition for approach to equilibrium 78−16678
open system, new classical Hamiltonian-Lagrange mechanics 80−36900
operational logics, state-generated effects measures 79−75401
operator construction, in Fock space 78−24688
operator equivalents, diagonal and off-diagonal, formula for derivation 80−22233
operator equivalents, polynomial formula, derivation in terms of ang. momentum operators 79−6014
operator functionals and path integrals 77−33736
operator manifolds, expansion and completeness theorems 79−59331
operator ordering and perturbation expansion, path integral formalism 78−16682
operator orderings rel. to functional formulations, quantum and stochastic dynamics 77−45740
operator symbols in the description of observable-state systems 80−57140
optical anal. of resonances in velocity depend. square well pot. 78−62098
optical group Opt(3,1) and its subgroups 78−77759
2 orthogonal time dimensions for concept reconciliation, speculation 80−31582
orthonormalization, polar decomposition, and transformation to an effective Hamiltonian. 79−6811
oscillating pots., no. of bound states, inequalities 77−45717
oscillator, quartic, zeta function 80−62532
oscillator in coherent state, quantum nondemolition meas. 78−54228
overlapping avoided crossings, rel. to quantum stochasticity 80−90694
Pade and Pade-Borel perturbation theory series summation methods *(Russian)* 79−2663
paradoxes, interpretation and time symmetry 77−59
parameter-dependent system, energy soln. method 80−8828
parametric amplification, quantum-mechanical 80−42097
parity operator, explicit derivation 78−86191
parity violating potentials, fermion scattering 77−79245
partial inner product spaces, compatibility relns. 80−46855
partial inner product spaces, topological considerations 80−94977
partial wave expansion summations in scatt. by long range pots. 78−49707
quantum theory continued
partial wave expansions summation in scatt. by short range pots. 80−31570
particle beam, potential scatt. into cone 79−97234
particle bound to a Coulomb potential, mag. field effect on polarisability 79−5933
particle dechannelling with phonon scatt. 78−18695
particle detection in de Sitter curved spacetime 77−30040
particle diffusion and scatt. length, Green's function methods 77−13629
particle in 1-D deformed lattice, energy depend. on quasimomentum 77−30052
particle in rot. frames, current circulations lattice struct., rot. fluid 78−45498
particle motion in axially symm. pot. with arbitrary deformation, Lippmann-Schwinger eqn. soln. *(Russian)* 77−9912
particle motion in potential channel, waveguide-optical analogy 80−12942
particle penetration through multiple pot. barriers 78−36871
n-particle quantum system, energy operator discrete spectrum 79−85006
particle stationary states, in uniform gravit. field, accelerating transformation operator calcs. 77−74239
particle statistics from induced representations of a local current group 80−57129
particle system in rot. frames, rigid flow impossibility 78−45497
particle trapped in rectangular potential, simple computing system, undergraduate expt. 78−28891
particle wave behaviour, experimental observation system 80−62535
particle with spin n/2, classical and quantum dynamics *(Russian)* 79−44796
partition functions asymptotic expsn., local dynamic charges 79−58582
passive states and KMS states for general quantum systems 78−41178
path integral, canonical to covariant change 78−73877
path integral for Reggeon quantum mechanics 79−26259
path integral method, operator formalism 77−17844
path integrals, distrib. definition 80−31595
path integrals, examples from quantum mechanics 77−60980
path integrals and ordering rules 77−2559
path integrals and semiclassical propagator approx. 77−87664
path integrals and stationary-phase approximations 79−71290
path integrals covariant interpretation, nonlinear pt. transformations 79−84945
path integrals for waves in random media 79−63049
path integrals in quantum theory, basic concepts, review 80−52066
path integrals in Riemannian spaces, smooth path spectral anal. 80−52059
path integrals on curved spaces, method of determination 80−31589
path integrals with a periodic constraint: entangled strings 79−2651
path integration in non-relativistic quantum mechanics 79−40405
path sums for Brownian motion and quantum mechanics 80−36882
path-integral evaluation of the space-time propagator for quadratic Hamiltonian systems 79−88824
Pauli algebra, first order power-associative deformations 79−75400
Pauli eqn. for particle in metric and EM fields *(German)* 77−78997
Pauli equation with differential operators for the spin *(German)* 79−2664
Pauli spin matrices, higher dimensional extensions 79−92969
Pauli spinor theory, axiomatic deduction 78−12593
Pauli-Lenz vector, extension of SO(3) to SO(4) 80−31550
pendulum, representation of canonical relns. 80−42084
penetration through and reflection on two thin potential barriers 78−65793
percolation problems, quantal 80−31554
perfect measurements in microchannel theory by conceptual anal. 80−17825
periodic exponential lattice, soliton quantum theory 77−30110
periodic vacuums, functional integrals, classical sine-Gordon solns., Coulomb gas props. 79−26226
permutation operator, explicit representation, for teaching 79−35469
permutation symmetry, geometrical approach 78−21001
perturbation anal. of variation method 77−82404
perturbation formulas for energy, derivation 78−86051
perturbation theory, almost degenerate, partitioning type treatment 78−32701
perturbation theory, convergence props., energy series 78−80
perturbation theory, higher order, appls. to quantum mech. and field theory *(Russian)* 78−36886
perturbation theory, many-body, arbitrary point group symmetry, wave operator matrix elements 80−23311
perturbation theory, projected, simple non-hermitian choices for standardisation operator 77−33903
perturbation theory anharmonic oscillator, strong coupling regime, appl. to Φ_4^4 model 78−89622
perturbation theory at large orders, ϕ^{2N} interaction, anharmonic oscillators 77−45735
perturbation theory at large orders, role of vacuum instability 77−41504
perturbation theory for Green's functions, effective mass formalism 78−28915
perturbation theory within variation method 78−41180
perturbations, continuous and discontinuous 78−62113
perturbed eigenvalues, perturbation expansions and variational constraints 78−16670
perturbed ladder operator method, analytical determ. of generalised central field energies and wavefunctions 78−32704
phase eqns., new class 77−37783
phase equiv. potls., invariant physical props. 77−17855
phase integral formulae for level densities, normalisation factors and quantal expectation values 78−54222
phase scattering, quasiclassical approximation *(Russian)* 79−89
phase shifts, stability in spherically symmetric pot., Coulomb-strong interference 77−74237
phase space formulation of quantum mechs., linear transformations 78−45508
phase space functional integrals of quantum mechs., Hamiltonian quantization 78−41194
phase space path integrals, without limiting procedure 78−32718
phase space quantum mechanics, Wigner distrib. function unicity 77−9906
phase space quasi-distribs. in quantum mechanics 78−54291
phase space quasidistrib. serving infinite set of polynomials, construction 78−77741

quantum theory continued
phase space representation of quantum and classical mechanics *(Russian)* 79−25882
phase-amplitude method for complex pot., generalised approach 77−53800
phase-integral calc. of quantal matrix elements, numerical method 77−49622
phase-integral calcs. of matrix elements without wavefunctions 77−57219
phase-shift anal. ambiguities 77−18208
phase-space approach to relativistic theory, coherent-state representation 77−57441
phase-space formulation, variational principle, harmonic oscill. ground state 77−2558
phase-space projection identities for diffraction catastrophes 80−27162
phase-space quasi-distrib. in quantum mech. 78−81868
philosophical aspect, its cognitive repression in contemporary physics 79−97169
philosophical review 79−44698
philosophically different interpretations and their consequences *(Spanish)* 78−41202
photoelectron counting statistics, theory, fully quantum, review 80−52312
photon, stochastic phase space kinematics 79−2649
photon counting as basic research tool 79−7105
photon counting distribution, quantum mech. derivation 77−58302
photon interference, quantum field theoretic description using QED methods 78−12464
photon linear polarisation following positron annihilation, quantum mech. test 77−69932
photon position observable, Ludwig axiomatic quantum mechanical formulation, quantum optics 80−73206
photon position operator, Galilean components 77−33906
photon-scalar boson scatt., impact on Planck's radiation law and Hubble effect 78−54212
photons, quantum mech. theory 77−13519
phsyical and intrinsic states in quantum mechanics 79−84978
physical foundations, stochastic formulation, proposed expt. test 80−52049
physical justification of using tensor product to describe two quantum systems as joint system 79−84984
physical nonexistence of signals going backwards in time 80−42094
physical operations, diagram operations 80−46846
physical symmetry groups, subgroups and invariant EM fields and potentials 80−8841
planar channelling, yield oscills. of inelastic processes at angles greater than crit. angle 79−77657
Planck, Max Karl Ernst Ludwig (1858-1947), quantum and relativity theories 80−68008
Planck's constant, numerical value, dynamic mechanism, classical/quantum physics borderline 79−21573
Planck's constant, origin of quantum theory 80−27179
Planck's constant, time invariance 78−93556
Planck integral, non evaluation in terms of finite series of elementary functions 80−31563
Planck thermal radiation spectrum in quantum theory, relativistic free particle Boltzmann distrib. inconsistency 79−85001
plethysms of finite and continuous groups, generating functions 80−31548
Poincare and Galilei groups, quantum mechanics 78−49701
Poincare group, irreducible unitary representation, velocity operator 78−32713
Poincare group representations, momentum and position variables, complete decomposition theory 80−62511
Poincare group representations on phase space 79−88827
Poincare sphere sample space 77−60958
point defects as model of quantum object 77−22433
Poisson brackets, on extension 79−63080
Poisson Lie algebra deformations, quantum mechan. 77−74261
Poisson summation formula, generalisations 80−4565
Polish groups, splitting and representation groups 78−36874
polyatomic molecules, electron density, generalised Berlin diagram appl. to H_2O internal modes 79−98001
polymer molecules, irreducible representations of symmetry groups 79−3603
polynomial class $R_n^{\mu}(x)$, integral formulae, series relations, recurrence relations 79−25899
position as only observational quantity, review 80−52048
position operator, relation between momentum and rel. for elementary systems 77−60967
position operators, systems exhibiting special relativistic relation between momentum and vel. 78−89335
position operators for relativistic non-interacting n-particle system 78−41182
positive-definite-matrix-conjugate vector, construction and constrained variation 78−8267
positron annihilation quanta, nonlocality and polarisation correlations 77−2563
positron atomic shells, quantum mech. anal. 79−10235
potential barrier, axially symmetric, tunnelling calc., appl. to energy level splitting and well broadening *(Russian)* 79−58588
potential barrier shape from tunnelling transmission coeff. 79−6017
potential scatt., asymptotic completeness, geometrical and spectral transformation approaches 79−80459
potential scatt., gauge transform. for variational method 77−65
potential scatt., inverse problem at fixed energy 78−41203
potential scattering, inverse problem formal solns. 77−2555
potential scattering, K-matrix in distorted wave theory 77−22439
potential well particle escape, time-depend. Schrodinger eqn. soln. 80−86118
power series soln. of coupled eqns. and three-body problem 80−86145
prequantum bundles and projective Hilbert geometries 78−36799
presymmetry in relativistic quantum mechanics, absence of kinematics 80−8843
presymplectic Lagrangian system, constraint algorithm and equivalence theorem 79−75377
presymplectic manifolds and the Dirac-Bergmann theory of constraints 79−2652
principle of identity of indiscernibles, photon violation, discussion 79−25817
principles of advanced mathematical phys., book 79−63090
quantum theory continued
probabilistic anal. of unification of quantum theory and relativity 78−86176
probabilities in quantum theory and probability theory 79−97223
probability amplitudes of transitions between not necessarily stationary states, coupling const. 80−36902
probability calculus of quantum theory 78−54236
probability concept in theory of elementary particles 77−49882
probability foundations, modal frequency interpretation 80−12885
probability in logical space 80−31579
probalistic descriptions in classical and quantum theories 80−36899
Proca's eqn. stochastic derivation, Weyssenhoff top fluid considerations, velocity of light random fluctuations 79−97247
process characterisation by method of local specifications *(French)* 80−31597
product operators, closed basic diagram generation program 80−8817
projection of wave functions on states with definite ang. momentum 78−12590
projection operators and properties *(German)* 77−67334
projection-operator method, mathematical foundations 80−85
projective limit of projective system of state operators 80−80
propagator with friction 80−8821
propagators in multiply connected spaces 77−17868
propensity microrealistic interpretation 77−9899
proper and improper mixtures, observable differences 77−67325
proportional system, structure preserving maps 79−84983
propositional system sublattice representation of physical subsystem with physical interpretation 79−49083
propositional systems and meas., quasi-tensor-products of certain orthomodular lattices 78−81871
protein, structure and bonding, quantum theory, ab initio calcs. 80−61509
proton transfer reactions, kinetic isotope effects, quantum theory 80−3301
pseudo Nilsson quantum numbers, goodness in asymptotic limit 80−99138
pseudo-Hamiltonians, theory of minimal unitary dilations 80−27153
pseudoparticle contrib. to energy spectrum of 1-D system, comparison with WKB result 78−4517
psi function recovery, nonrelativistic quantum mech. 77−64966
psychology, quantum interference effects, Schrodinger's cat, review 80−73158
QED, Aspect experiment, local and quantum theories 80−32051
quadratic Hamiltonians, exact propagators 78−49709
quadratic Hamiltonians, quadratic invariants and SU(n) symmetry group 78−36873
quadrupole perturbation of harmonic oscill. pot. 77−60978
qualitative methods in problem solving, graduate text book 77−71239
quanta from a diachronical aspect 80−90723
quantal Coulomb excitation calcs., error anal. of code AROSA 77−2550
quantal nonrelativistic N particle systems, appl. of variational techniques to bound states 79−35579
quantal tunneling through a rectangular barrier using $|\psi|^2$ and flux, education 80−105457
quantisation, semiclassical, periodic orbit role for the quantal bound state 80−8831
quantised space-time, rel. to radiation physics and chemistry 77−67327
quantization rules and Dirac's correspondence 79−21579
quantum correlation calculation programs 79−30275
quantum friction equations from Schrodingers equation 79−49069
quantum friction in a uniform magnetic field 79−67180
quantum interference and the quantum potential 79−80466
quantum logic and Jauch-Piron states 77−33887
quantum logics, extended characterisation theorem 77−87658
quantum logics and orthomodular lattice embedding in Hilbert space 80−89
quantum measurement as a communication with nature 79−17253
quantum measurement process, classical and quantum interaction using superselection principle 79−21581
quantum mechanical Brownian particle, tunnelling and transport problems 80−4644
quantum mechanical description of scatt. by dissipative and diffusive scatt. centre 79−75410
quantum mechanical particle in random potential, inverse participation ratio in $2+\epsilon$ dimens. 80−36908
quantum mechanical perturbation problems, resolution using integral eqn. 80−58112
quantum mechanical quasidistributions 79−44764
quantum mechanical system dynamic polarisability, van der Waals constants 80−46867
quantum mechanical tunnelling, historical survey 78−54141
quantum mechanical two centre problem, noncomplete integral algebra *(Russian)* 80−86154
quantum mechanics, description of operators 80−8820
quantum mechanics, experiments on reinterpretation, new ideas 77−26204
quantum mechanics, logical foundation 80−94975
quantum mechanics, rel. to reality 80−27172
quantum mechanics in non-inertial reference frames *(German)* 77−45720
quantum mechanics representation based on Radon and Euler transforms 79−63087
quantum numbers as hidden parameters, in causal interpretation of wave mechanics *(French)* 80−68062
quantum oscillators, matrix element diagrams 80−105455
quantum pendulum as spin 1/2 79−58578
quantum radiation inelastic scatt., correlation functions and higher order coherence 78−32721
quantum radiation inelastic scatt., reduced field density operator 78−32722
quantum recurrence theorem, step in proof using Pioncare recurrence theorem 79−21580
quantum state decay rates, absorbing boundary method calcs. 79−54004
quantum state entropy using covariant and contravariant symbols 80−52068
quantum system coupled to thermal reservoir, generator in weak coupling limit 79−88883
quantum systems with elevated stability of stationary state, struct. and props. 80−4576
quantum theory, conditional probabilities and statistical independence 78−77757

quantum theory continued
quantum transition concept in undergrad. courses, explanation of photon creation and absorpt. 80−36807
quantum-mechanical kinetic energy as measure of information in distribution 80−101725
quarkonium, quantum mechanical applications, masses and leptonic widths of ψ and T 80−27484
quasi-degenerate Rayleigh-Schrodinger perturbation theory, calc. of effective Hamiltonians 79−71284
quasi-energetic spectra of quantum systems in classical monochromatic fields 78−78981
quasi-light-cone frame and approx. Galilean symmetries 77−13844
quasi-probability coordinate and momentum operator *(Russian)* 78−49695
quasiclassical approx. in scatt. problem, wave function representation by functional integral 78−87
quasiclassical estimates on moments of the energy levels 80−98806
quasimodes associated with stable periodic orbits 77−17833
quasiperiodic boundary conditions, vac. struct., in gauge theories, quantum mech. analogue 78−70255
quasipotential governing time evolution of projection of state-vector onto one-dimens. subspace 78−20988
quasiprobability distrib. in quantity operators correspondences 80−78
quasiprobability distribs. in quantum mechanics, dynamic eqns. 80−27157
quaternion quantum mechanics as the description of tachyons and quarks 79−30273
R-separable solutions of wave eqn. $\psi_{tt}-\Delta_3\psi=0$ 78−62293
radiation of relativistic channelled particles 78−22779
radiative transfer, quantum mechanical description, radiation processes 79−53713
radiative transfer equation, quantum mechanical derivation 79−80546
radioactivity and quantum mechanics unification, probabilistic conceptions 80−12946
radius perturbation theory, appl. to NN system and pionic atoms 78−21007
random pulses in quantum systems, Schrodinger eqn. soln. 78−86189
ray representation of scattering amplitude in the presence of resonances 79−21587
realist interpretation, indeterminancy and measuring process 77−9898
recasting of quantum theory 78−54240
recoupling coeff. and isoscalar factors, for chain of compact topological groups 78−20939
reduced mass for relativistic quantum-mechanical problems 78−4809
reformulation, modification and EPR paradox 77−22441
Regge pole theory, reasons for survival, review 78−24977
relative compatibility in conventional mechanics 77−60956
relativistic, conserved four-vector currents for free particle 77−37778
relativistic, curved space-time, generalised quaternion formulation 78−366
relativistic, Levinson theorem generalisation *(Chinese)* 79−80461
relativistic, localisation and causality 78−4514
relativistic, phase space formulation 78−36878
relativistic, successive observations 79−88830
relativistic π-mesic atom, eigenfunctions and eigenenergies, N-space dimensions calcs. 80−41988
relativistic Brownian motion and the foundations of quantum mechanics 79−63084
relativistic classical and quantum dynamics 80−22192
relativistic electron wave equation 80−101702
relativistic Hamiltonians, diagonalisation of Dirac and Sakata eqns. with const. mag. field 77−34081
relativistic harmonic oscillators and hadronic struct., 1st year graduate quantum mechs. 78−61971
relativistic invariance in classical limit 79−21586
relativistic isolated unstable system, extended variables 80−62525
relativistic localisation and operator density current 78−32709
relativistic Markov processes in quantum mechanics, Feynman path integrals 79−21576
relativistic models of nonlinear quantum mechanics 79−12927
relativistic particle physics, book 80−41966
relativistic path integral formulation, for particles with spin 79−53995
relativistic quantum kinematics on stochastic phase spaces for massive particles 79−2648
relativistic quantum mechanics, algebraic approach, nonrelativistic limit 78−41188
relativistic quantum mechanics, elimination of phase angle uncertainty, charged Dirac particle+mag. monopole scatt. *(Chinese)* 78−78100
relativistic quantum mechanics, Galilean limit, group contraction, probabilistic interpretation 78−77760
relativistic quantum mechanics, localisation problem 77−49616
relativistic quantum mechanics, role of wave fronts and torsion *(French)* 77−53795
relativistic quantum mechanics, semigroup 80−27180
relativistic quantum mechanics, space-time formalism for spin-zero particles 79−21974
relativistic quantum mechanics formulation of space and time 78−65796
relativistic quantum theory, role of position 78−36852
relativistic quantum theory with correct conservation laws 80−82677
relativistic spin 1/2 particle dynamics 78−70001
relativistic spinless particles, one particle quantum theory 79−17255
relativistic string with massive ends, classical and quantum theory 78−62073
relativistic wave functions and diffr. 77−10207
relativistic wave mechanics, hypothesis on origin of quantum potential *(French)* 78−86405
relativistic Wigner superoperator and its distribution 77−33897
relativity and quantum mechanics 78−54242
relativity principle in quantum mechanics 79−6003
relativity theory comparison 80−27175
renormalized plane wave-projected and Coulomb-projected T-matrices 79−17267
representation groups for semiunitary projective representations of finite groups 80−12933
representation of linear operators in L^2 spaces, generalised matrices 78−62095
representation theorem and communicability of observations 77−74246
resolvent operator on dense set of quantum states, spatial localisation, second-sheet singularities 80−77645
resolvent operator theory of sequential quantum processes 80−46849

quantum theory continued
resonance states theory based on analytical continuation in coupling const. 79−17279
resonances, scattering theory and rigged Hilbert spaces 80−94987
resonances and complex scaling: a rigorous overview 79−17258
resonances in quantum mechanics over phase space, group theory aspects 80−8852
resonant states, completeness props. 80−46857
resonant states in pot. scatt. theory, wave packet description 79−40391
retardation effects in motion of quantum systems, atomic energy level broadening in turbulent plasma 77−60975
retroactive influence, EPR paradox, quantum theory of spin meas. 78−70000
Riemannian struct. on states of quantum-like system 78−67
rigged Hilbert space and decaying states 80−4591
rigorous lower bounds to energy levels, Brillouin Wigner perturbation theory, finite summations 78−54216
role of mathematics in a physical theory *(German)* 80−90726
rotation group irreducible representations, spin-1/2 representation, teaching approach 79−58488
rotation group realisations, orbital ang. momentum and massless particles 77−37776
rotation operators, time-depend. aspects, teaching 80−90634
rotational symmetry in Hamiltonian dynamics 77−75791
rotations, nonlinear vector products calc. methods. 77−71201
rotator, plane, in intense EM field, scatt., emission, and absorpt. 78−78982
S-matrix, Debye expansion convergence 79−40679
S-matrix near bound states in the continuum 77−87663
S-matrix theory, determinant and its relation to number of eigenvalues due to perturbation 78−58132
s-wave resonances with square well pots. 77−9914
Saito pot., zero energy continuum bound state 79−9151
scalar particles creation in isotropic universe, Feynman propagator behaviour 78−45445
scattering, inelastic, of ats. and mols., coupled eqns. soln. method in adiabatic approx. 79−3524
scattering, one-dimens., variable amplitude nonlinear eqns. 77−22431
scattering, struct. of many-body wavefunctions 78−62119
scattering amplitude at high energies on power type singular potl. 77−30053
scattering amplitudes and complex scaling 79−17257
scattering by central field, quantum-mechanical virial theorem 79−80469
scattering cylinder of finite conductivity, symmetry group and natural resonances 79−45888
scattering operator of few-body quantum mechanical system, sum of two-body potential operators 80−62516
scattering phase shifts, first order error estimates in approx. calcs. 79−58573
scattering problem as eigenvalue problems 78−28971
scattering resonances, tunnelling decay, absorbing boundary layer 80−57121
scattering subspace defn. in nonrelativistic quantum theory 77−33889
scattering theory, nonsingular potential, scatt. length by iterative-perturbation method 80−27160
scattering theory, some fundamental problems 78−86174
scattering theory, variable interval variable step method for soln. of linear second order coupled differential eqn. 80−105527
scattering theory, variational principles and virial theorem 78−54231
scattering theory for Stark Hamiltonians involving long range pots. 78−41184
scattering theory of ≥ 4 particles, on the unique soln. 78−21005
scattering theory with different state spaces of perturbed and free system 79−40406
scattering with δ-function pot. 77−17849
Schlesinger systems, isomonodromy deformation, integrable Hamiltonian systems 80−22229
Schmidt orthogonalisation in the continuum 78−8266
Schnurs, combinatorial hierarchy, spin dichotomy and conservation of quantum numbers 80−68383
Schrodinger's cat paradox, separation of macroscopic and microscopic domains 77−33742
Schrodinger's factorization method for Sturm-Liouville operators 79−21582
Schrodinger equation, Brownian motion interpretation challenged 80−94974
Schrodinger equation, energy approximants and perturbation theory 80−22232
Schrodinger equation, new type, evolution of wave function with respect to position 80−27178
Schrodinger equation, perturbation problem, two-level atom interacting with EM field 80−52056
Schrodinger equation, polynomial factor eigenfunctions, corresponding pots. *(Chinese)* 80−22236
Schrodinger equation, random walk calcs., method of successive corrections 79−68180
Schrodinger equation and the accel.-gravity equivalence principle, for teaching 78−24614
Schrodinger equation eigenvalues, perturbation theory calc. without complete set of eigenfunctions 80−105519
Schrodinger fluid, single-particle formulation 77−54165
Schrodinger wave functions at pot. discontinuities, continuity conditions, for teaching 80−27077
Schrodinger-type eqn. for dissipative system 79−49085
Schwinger equations, compact description 80−13204
Schwinger variational principle *(Russian)* 78−89361
screened Coulomb pot., perturbation theory and hypervirial theorem, sixth order atom energy levels 80−14071
second order matrix element eval., trial function linear transformation 80−62529
secondary school education, review of Dutch program *(Hungarian)* 79−44657
Segal entropy and principle of least interference 77−79043
self turbulence in free particle motion 78−86177
self-mass of electron, eqn. of motion calc. 78−28995
semi-classical approach to elastic scatt. and direct reactions 78−32706
semi-classical correspondence relns. 79−75384
semiclassical approximation in the Weyl picture by path summation 79−2644
semiclassical approximation to quantum dynamics 80−12927

quantum theory continued
semiclassical densities in phase space, Wigner's distrib. function for thermodynamic equilibs. 79−58565
semiclassical eigenvalues from classical trajectories for non-separable bound systems 77−50342
semiclassical energy levels, degeneracies 78−4500
semiclassical expansion of the anharmonic-oscillator propagator 79−63072
semiclassical functional methods for arbitrary Hamiltonians, path-integral method 77−30043
semiclassical Green's function, energy-representation 80−90692
semiclassical path integral methods, at finite temp., double well pot. problems 79−97256
semiclassical path integrals in terms of catastrophes 80−8860
semiclassical propagator, focal points, phase 79−76
semiclassical radiation theory within quantum mechanical framework, book contrib. 79−75705
semiclassical scattering theory, spurious excitation 80−73142
semiclassical theory, phase space interpretation 78−20991
semiclassical wave functions, regular and irregular 78−20998
semiclassical WKB approx. for arbitrary Hamiltonian 77−49628
semiconductor doped surfaces, inversion layers, quantum model 78−30961
semigroups, irreducible and ergodic props. 77−64956
semigroups and the density matrix formulation of quantum mechanics 80−57118
sensitivity analysis in quantum dynamics, Green's function method 79−67178
separable quasipotential formulation of the relativistic dynamics for three point particles 79−12989
sequential decay processes, quantum and classical calcs. of level occupation numbers 79−97242
sequential decay processes, quantum theory 79−25896
sequential events and objectivistic probabilities, quantum logic 80−94973
sets of propositions, compatibility or otherwise with quantum theory 78−54239
shift parameter estimation on quantum state 79−6024
short-range long-range action dilemma *(Russian)* 78−16692
simple quantum model, periodic spontaneous collapse and revival 80−73208
simplified anharmonic oscillators, energy levels 77−64961
simultaneous measurement and joint probability distributions in quantum mechanics 79−30278
simultaneous verifiability of yes-no measurements 79−44768
sine-Gordon eqn., soliton creation-annihilation operators as canonical transformation 77−30041
single system and ensemble interpretation of pure quantum states 77−33878
single system movement and description 77−22440
single-well pot. quantisation condition, Wentzel's proof 77−26199
singular continuous measures in scattering theory, examples of potentials and physical interpretation 78−57802
singular oscillating potentials, number of bound states 77−33899
singular pot., variable phase eqn., formal series method 77−67330
singular potentials, bound states, WKB approx. 77−82402
singular potentials, divergence problem in quantum field theory, pot. theory analogy 77−67556
singular potentials, inhomogeneous boundary value problem, eigenvalue equation 79−58530
singular potentials in the non-relativistic quantum theory *(Russian)* 79−63063
singular quasipotential eqn. for bound states, soln. 77−60973
singular state problems, monopole pair energy levels, charged monopole-electron system *(Chinese)* 80−101733
SL(2,*C*), new nonlinear realisations 79−88828
SL(3,R) symmetry, coupling of self-conjugate systems 79−97228
SO(n), Weyl coeff. 78−45503
SO(n) symmetric tensor representations, analytic functions on complex cone 77−60895
solid state physics, historical aspects, symposium, London, England (Apr.-May 1979) 80−56999
solid state physics based on quantum theory, shaping ideas *(Hungarian)* 77−87608
solids, classical and quantum scaling 79−35626
solids, total energy calcs., momentum space formalism 80−15468
soliton quantum mechanical mass in supersymmetric theories 80−22536
soliton solutions, quantum expansion generalisation *(Chinese)* 78−24915
solitons, Backlund transformation for higher order Korteweg-de Vries equation 77−78999
solitons, pulsating, energy of n-particle bound state *(Russian)* 77−74267
solitons geometrical interpretation, rigid body motion along helical space curves 78−24684
soluble quantal problems, for pedagogic appls. 77−67307
sound, quantum mechanical treatment of structural information 77−14822
SP(4) and SP(3,1) groups, unified treatment using spinor calculus 77−53797
Sp(n,R) discrete series, harmonic oscill. eigenstates, nuclear collective model 78−71
space density functions, positive phase, position and momentum joint distribs. 80−62509
space group representations, complex conjugation 79−90583
space-time approach, relativistic Brownian motion 80−31567
space-time operators, quantum mechanics incompatibility in special relativity 79−12592
space-time structure operational anal. in quantum-relativistic theory 77−67322
spacetime code, quantum topology 78−36859
special relativity and quantum theory 77−26192
special symmetries of jm factors and j symbols 79−84989
spectral properties of products of projections in quantum probability theory 80−98807
spectral theory of $(p^2+m^2)^{1/2}-Ze^2/r$ operator 77−45719
spin measurement on spin 1/2 particle, model of hidden variable 80−27167
spin permutation group, representation matrices 78−28976
spin permutation group representations, transformation matrices, graphical approach 77−71224
spin systems, functional method *(Chinese)* 79−63064
spin traces, nature of S-depend. 79−17331
quantum theory continued
spin-1 matrices, props., for teaching 79−67128
spin-1 problems, algebraic solns. 77−64957
spin-1 problems, soln. using spin-1/2 methods 78−73793
spin-1 system, lattice of verifiable propositions, Hilbert space formulation of quantum mechs. 77−45789
spin-1 system, periodic perturbation, analogue of Shirley's eqn. 77−3248
spin-free quantum chemistry, alternacy quantum no. assignment 79−9988
spin-free quantum chemistry, particle-hole and pairing symmetries 79−6812
spin-orbit potentials, quantum scattering theory inverse problem, fixed energy Jost functions *(Russian)* 80−68082
spin-rotation model, for adiabatic anal. of collisions 79−40402
spinless elastic scatt., phase-shift ambiguities 77−9905
spinless particle, point form of quantum dynamics and 4-vector coord. operator 79−17213
spinless particle many-body problem, multiconfigurational approx. 78−4518
spinors in Hilbert space 77−13569
spins, arbitrary no., quantum mech. vector addition 80−57134
spontaneous state reduction criterion, meas. problem in quantum mechanics 77−26205
spontaneous symmetry breaking and metastable state blocking, various appls. 78−45510
stability of atoms and bulk matter, review 77−5696
stability of matter anal., Thomas-Fermi theory 77−5678
star-product representation of path integrals 79−97253
state props. in quantum logic, Hilbert-space formulation 80−12947
state reduction in passage of mol. beam through Stern-Gerlach apparatus, calculational example 79−36696
state space transition probability of *-algebra 77−5699
state vectors, second-type, observable consequences 78−69
states and preparation procedures 77−67321
static screened Coulomb potential, high-accuracy eigenvalues 79−40403
stationary path integrals appl., bound state energies and wave functions 78−12587
stationary perturbation theory, commutator possible appl., nth order expectation values 80−86116
stationary state, standing de Broglie wave, Aharonov-Bohm effect 80−22228
stationary state scatt. theory for density operators 77−26207
stationary states of quantum dynamical semigroups 79−12632
statistical inference and quantum mech. meas., information theory 78−20990
statistical inference and quantum mech. meas. 78−36856
Stern-Gerlach expts., observability of arbitrary spin operators 80−31568
Stieltjes moment problem, Borel summability and indeterminacy, anharmonic oscills. 78−62094
stimulated effects upon electron jarring in external EM field 77−79737
stimulated Raman scatt. quantum theory 80−106565
stochastic behaviour of quantum pendulum under periodic perturbations 80−8834
stochastic dynamics, dissipative forces with vel. depend. pot. 77−33891
stochastic electrodynamics, derivation of quantum mechanics 78−36801
stochastic electrodynamics and quantum mechanics *(French)* 77−50
stochastic electrodynamics formulation *(Spanish)* 80−82925
stochastic formulation, quantum operator algebra origin 80−88
stochastic foundations of quantum mechanics, harmonic oscill. in stochastic electrodynamics 77−9910
stochastic Hamiltonian classical and quantum, systems, Volta Memorial Conf. 80−8738
stochastic interpretation of quantum mechanics 79−40399
stochastic mechanics of Bopp-Haag spin model, higher spin states 77−30039
stochastic methods and techniques for quantum mechanics, book 80−4584
stochastic model of quantum mechs., equivalence to Markov processes 78−86188
stochastic parallel displacement of tensors, geodesic correction 80−8920
stochastic physics, quark bag model 79−54000
as stochastic process in phase space 77−64964
stochastic processes in quantum mechanics, equivalence of two theories 79−80468
stochastic quantisation of wave fields, appl. to dissipatively interacting fields 78−86184
stochastic quantum mechanics, dissipative forces, operator algebra 80−98826
Stokesian and non-Stokesian vector potentials, Aharonov-Bohm effect 79−88832
strong EM field, quantum theory, c-number semiclassical description 80−105540
structural stability in physics (conference, Tubingen, Germany, May and Dec. 1978) 80−8739
structure and order evolution of many-body systems 77−41528
Sturmian operator, four Euclidean conformal group struct. 80−87
SU(1,1) non-compact group, existence of intelligent states 78−77753
SU(2), eigenstates of complex linear combinations of J_1, J_2, J_3 78−58139
SU(2) coherent state representation, path integrals 80−62502
SU(2) Yang Mills multi-instanton paths, tunnelling pots. and WKB wave functionals 79−248
SU(3) broken symmetry group in central force problems 77−60960
SU(4)⊃SU(2)×SU(2), commuting missing labels operators, equivalent sets 77−60896
SU(N)⊃O(3), angular momenta multiplicities in system of N-dimensional harmonic oscillators 78−32702
SU(N) symmetric quantum dynamical systems, N→∞, energy spectrum for singlet and adjoint states 80−62880
subdynamics theory, dissipative processes in dynamical systems 77−9951
subspace quantum dynamics and the quantum action principle 78−65798
subspace quantum mechanics and the variational principle 78−70002
subsystem characterisation in physics 79−49082
subsystems, bilinear maps between generalised Hilbert spaces 80−62507
super Clifford algebra 79−98
superfluorescent decay, large time behaviour 78−46296
superluminal communication through wave function collapse in quantum theory 80−27166
superluminal connections of events, a theorem 77−67324
superoperator method for weak interaction of oscillator with non-particular medium 79−30290

quantum theory continued
superposition principle and entropy 77−60969
superposition principle and sectors in quantum logics 80−94970
superselection rule nonexistence, 'frame of reference' definition 79−54002
superselection rules, quantum measurement, and the Schrodinger's cat 80−86103
superselection rules, state restriction violation proposal 79−84980
superselection rules, subensemble selection 80−17826
superselection rules for quantum theories *(Russian)* 79−17252
supersymmetric mag. monopoles and dyons, quantum corrections 78−62334
supersymmetric theories with solitons, algebra including topological quantum numbers as central charges 78−89630
symmetric groups, generation algorithms 80−98813
symmetries in indefinite metric spaces 77−33907
symmetries in quantum logics 78−77745
symmetrised density operator treatment of quantised dissipative systems 77−9959
symmetry breaking and Euclidean group subgroup 77−26198
synchrotron radiation quantum corrections, second order effects 78−1136
system influenced by time dependent electric field, fourth order variation perturbation theory 80−22230
T-ordered exponentials, appl. to mag. dipole in field 77−17832
tachyonic scalar waves in Schwarzschild space-time 78−45558
tachyons, complex physical quantities and space-like states, book contrib. 79−44723
tachyons, quantum mech. aspects, book contrib. 79−44721
TDHF eqns. for quantum mechanical many body systems 78−78296
teaching, from Compton effect to quarks, at., proton, and nucl. struct. 78−24596
teaching *(Hungarian)* 78−36753
temperature of a gravitational field 79−85055
tensor harmonics in the helicity basis 79−49080
tensor operators, reduced matrix elements for L-S coupled, N-electron configurations 79−13625
tensor product of the octonionic Hilbert spaces and colour confinement 79−2982
tensor spherical harmonics and multipoles in Euclidean space 77−2515
tensor virial theorem, quantum mechanical generalisation for Born-Oppenheimer approx., atoms, mols. 78−86182
tensorial theory for higher order constants of motion 80−46852
term entry into continuum in presence of Coulomb field 79−21583
test using Bell-type inequality for nondicotomic observables 78−36865
theoretical frameworks, dichotomic observables and quantum mechanical single state 78−62105
thermal mechanics: a quantum mechanical analogue of nonequilibrium statistical thermodynamics, stochastic processes 80−52125
thermodynamic partition function, semiclassical expansion 79−84993
thermodynamics and mech. unified theory, irreducible dispersions 77−60
thermonuclear reactions, quantum theory of screening effect in relativistic electron plasma *(Russian)* 77−17350
thin film heterostructures, optical transition selection rules 80−66319
third-order constants of motion in quantum mechanics 79−6002
third-order JWKB approximation method applic. to absolute continuity criteria derivation, approx. operators construction 78−12591
third-order JWKB approximation method applic. to absolute continuity criteria derivation, approx. operators and estimates 78−12592
Thomas Fermi model, free boundary 79−93906
three body problem in quantum mechs., singularities, Lavine's method appl. *(French)* 77−67310
three particle nuclear molecular states, Schrodinger eqn., wave functions and energy spectrum *(Russian)* 78−86497
three particle scatt. rates, double scatt., T-matrix singularities 78−32727
three resonantly interacting particles, level spectrum 77−17860
three-body one-dimens. three-force problem, path integration 77−49624
three-body problem, bound state and scatt. problems 78−16684
three-body quantum system, negative point spectrum 77−5683
three-body system, conditions for absence of bound states 77−45725
three-body system S energy levels, functional integration 77−67323
three-particle scatt. rates, disconnected T matrix singularity 78−32726
three-particle scattering without divergence difficulty 78−93555
three-particle system, orthogonal projection 78−90
time asymmetries and classical and quantum physics 80−22216
time delay in N-body scattering 79−75389
time dependent Hamiltonian, scale gauge transforms., adiabatic approx. principle, suitability for teaching 78−45506
time dependent quantum systems, approx. method *(French)* 78−57816
time evolution of dynamical system under continuous obs. 77−49626
time evolution operator, derivation and appl., for teaching 79−58476
time evolution operator in quantum mechanics 80−82610
time operators, need for accurate derivation 80−27170
time periodic perturbations, calc. of mean energy 80−46869
time reversal in classical and quantum mechanics 80−42090
time-dependent Hamiltonian systems with one degree-of-freedom, exact invariants 78−54215
time-dependent invariants with applications in physics 80−57131
time-dependent multi-level system with new calc. method 77−67314
time-dependent polynomial Hamiltonians, nonlinear transform. 79−40395
time-dependent three-dimensional harmonic oscillator, generalised invariants 77−49623
Tomita-Takesaki theory, classification of type III factors 77−17756
Tomita-Takesaki theory for von Neumann algebras with separating and cyclic vector 77−17755
topological shifts in the Aharonov-Bohm effect 80−82674
total scatt. cross section, time depend. approach 79−84992
total scattering cross sections for optical pots., quasiclassical calcs. 78−8270
traces of products of ang. mom. operators in spherical basis 78−32705
transfinite ordinals as axiom no. symbols for unification of quantum and EM wave functions 77−5688
transition probability, second order, time-independent perturbation asymptotic formalism 80−27159
transition probability between not necessarily stationary states 80−73212
transition probability between states of two different Hamiltonians *(French)* 78−86170
transition to classical theory 80−105523
transitions, without quantum jumps, theory 77−67306
translation-invariant atomlike identical particles systems, lower energy bounds, nonrelativistic quantum mechs. 78−86187

quantum theory continued
translation-invariant quantisations phase space algebraic structs. 77−17846
translationally invariant nonrelativistic Hamiltonian, for atom 77−5700
transmission past rectangular barriers or wells, $|\Psi|^2$ and flux anal. 79−71183
transparent pots. in classical approx. 77−50872
triviality of continuous multipliers for the real line 79−44767
tunnelling, reaction coord. method 80−62500
tunnelling, stochastic quantisation, escape over barrier 78−57819
tunnelling, time dependent stochastic quantisation theory 78−41197
tunnelling theory in more than one dimension *(Russian)* 77−33879
turbulent medium, photon interactions *(Russian)* 79−88
twistor theory and particles, book 79−97485
two and three-body problem, boundary condition model *(Russian)* 77−34237
two centre problem, elementary solns. and O(4)⊗O(2,2) group representations *(Russian)* 79−21590
two centre problem, linear algebra of integrals *(Russian)* 78−89368
two loop calculation about quantum mech. instanton, test of tunnelling 78−58126
two or three electrons, interacting with localised mag. moment, wave function determ. *(French)* 79−12636
two photon reson. third harmonic generation, quantised field theory 80−43397
two spinless particles, scatt. amplitude and cross-section, relativistic correction *(Russian)* 78−36889
two-body bound state and half off-shell t-matrix parametrisation 77−18424
two-body quantum systems asymptotic completeness, decoupling of finite singularities 77−9919
two-centre problem, discrete and continuous spectra, nonadiabatic matrix elements 77−45726
two-centre problem for Dirac eqn. 77−67328
two-centre scattering amplitudes, var. determ. 77−78998
two-level quantum dynamics, representations of Kossakowski conditions 78−20989
two-level system, damped and stochastically modulated, reduced eq. of motion 78−77764
two-level system, kinetic of induced relax. *(Russian)* 77−30054
two-potential formulae for rearrangement scattering 78−4512
two-state quantum system, time-dependent perturbation by sinusoidal field 77−5703
U(n), multiplicity free Wigner and Racah coeff. 80−31556
U(p,q), matrix elements and Casimir operators of discrete series representations 79−97238
unbounded Hermitian operators, low-lying eigenstates, method 80−98812
unbounded operators in statistical mechanics, *-algebras for quantum mechanics formulation 79−6046
uncertainty measure for compact Lie group, minimised for max. weight vectors 78−20996
uncertainty relation for successive measurements 79−75396
uniaxial spin systems, quasiclassical method appls. 80−8931
unified atom limit, adiabatic approx. for transitions between l=2 states 79−22781
unified formalism for quantum and classical scattering theories 80−100
unified theory of reality 77−45722
uniqueness of number operators for certain symmetries 78−20987
unitarily equivalent multiparticle Hamiltonian systems yielding equal scattering for corresponding states 78−77756
unitary group formulation of many-electron theory and quantum organic chemistry 80−106270
unitary group representations, appl., book 79−30198
unitary groups, functional integral representation *(Russian)* 79−9309
unitary interpretation of quantum physics and relativity 77−87641
unitary quantum mechanics, nonlinear and relativistic invariant fields 80−4567
unitary-antiunitary group representation, type and standardform 79−54008
unitary-antiunitary group representations 80−98809
Universe creation as quantum phenomenon, fireball model 79−9038
unstable particles in electric field, Zel'dovich dipole moment 77−74627
unstable quantum states, time evolution, resolution of Zeno's paradox 78−8560
unstable quantum states and rigged Hilbert spaces in nonrelativistic scatt. theory 80−8849
unstable quantum systems, decay theory review 78−65871
vacuum bubble evaporation and thermodynamics, surface oscill. consideration 80−62608
vacuum polarisation function 79−21578
variable phase method for scatt. on non-local spheroidal pot. 80−95
variational bounds to excited states from generalised Brillouin-Wigner eqn. 78−45507
vector operators and spherical harmonics 79−44674
velocity of light Markov process, Klein-Gordan quantum statistic, quantum mechanics 80−98808
vertex function multipolar development in arbitrary reference frame *(French)* 77−49614
virial inequalities, quantum and relativistic 80−62609
vitalism, nonlinear transforms in Hilbert space 78−73133
von Neumann's measurement theory, phase relationship observation 80−105539
von Neumann's theorem on composite systems, group theoretical interpretation 79−71189
von Neumann algebra for quantum model of single spin system 78−45459
von Neumann algebras, complete normal dissipations 78−89358
von Neumann algebras, conditional expectation and commutativity 78−36789
vortices, quantised, ang. momentum, creation and significance 78−24675
wave calculus based upon wave logic 79−71268
wave diffraction, stationary problem in non-homogeneous media 80−68
wave fields and wave propag. description by quantum mech. techniques 79−80471
wave function, inclusion of observer, geometrodynamics 78−54234
wave mechanics, origin, pedagogical approach *(Portuguese)* 80−22166
wave operator asymptotic completeness for singular and long-range potentials 79−71264
wave operators for momentum depend. long range potential 77−64953
wave packet, charact. features determ. 79−71267

quantum theory continued
wave packet reduction and measurement uncertainty principle, proposed expt. test 79−84979
wave packet reduction as medium of communication 77−74242
wave packet reduction in quantum mechanics: a model of a measuring apparatus 79−84977
wave packets, propag. and spreading theory 77−13521
wave packets, simultaneous localisation in energy and configuration space, impossibility 77−45737
wave packets in unidimensional pot. fields, computed graphical representation *(German)* 77−49534
wave particle duality problems, photon propag. *(Hungarian)* 77−67317
wave-corpuscle duality, Planck's, Einstein's, de Broglie's, Schrodinger's contributions to development *(German)* 80−68016
wave-packet, position probability, classical and quantum spreading, for teaching 78−24606
wave-particle duality and quantum theory, attitudes, 1900-1920 80−57061
weak coupled system, decay, general theory 80−36884
weakly interacting particle system, quantum field divergence disappearance in modified quantum dynamics 80−62537
Weierstrass-Mandelbrot fractal function 80−52063
Weisskopf Wigner formula derivation from Krolikowski Rzewuski eqn. for state vector 78−41175
Weyl, normal, and antinormal ordered forms of exponential of quadratic in boson operators 77−45727
Weyl's association, Wigner's function and affine geometry 80−98823
Weyl's commutation relation, implied generalized statistics 77−82408
Weyl relation, generalisation, props. 78−21003
Weyl theory, position operator written in terms of Dirac matrices 78−58123
Weyl transform between quantum-mech. and phase-space operators 77−60977
Weyl transform inversion 79−99
Whiteheadian approach to quantum theory and the generalized Bell's theorem 79−30276
Wiener diffusion process generalisation, functional Stieltjes measure 77−74317
Wigner's function, semiclassical mechanics in phase space 78−12600
Wigner's theorem generalisation, struct. of projection-valued states 78−36868
Wigner 9-j symbol 79−97229
Wigner distribution for ang. coords., for teaching 79−35472
Wigner distribution function, temporal positivity conservation 79−9183
Wigner distribution functions, canonical transformation representation in quantum mechanics 80−90702
Wigner distribution in quantum mechs., algebraic struct. 78−77767
wigner function and normal ordering 80−57176
Wigner representation, semi-classical ergodicity of quantum eigenstates 80−8833
Wigner-Weyl isomorphism, group theoretical aspects and basic props., $E^{(2)}$ symmetry group 78−62089
WKB approx. and scaling behaviour for Hellmann-Feynman and virial theorems 78−86193
WKB energy levels determ. via path integral 78−77763
WKB expansions in curved spaces, functional integrals, higher order corrections 79−71280
WKB method, generalised, soln. for three-dimens. case *(Russian)* 77−13626
WKB method, generalised, three-dimens. case, separation of variables *(Russian)* 77−26194
WKB method improvement 79−75383
work and energy in electrostatic and magnetic systems 80−52050
Young operators invariance groups, Pauling numbers 77−18774
Yukawa pot., s-wave off shell T and K matrices by Ecker-Weizel approx. 79−63074
Yukawa potential function, determ. of phase shifts 78−58237
Zeeman effect, linear, relativistic correction, Coulomb field 80−102484
zero probability problems, teaching approach 77−41499
α-particle emission as violation of usual interpretation of quantum mechanics 78−62108
p+H atom, low energy, quantum theory, integrated cross sections, phase shifts 77−30957
$pp \rightarrow \rho^0 X$, study of ρ^0 prod. using Heisenberg uncertainty relation *(Russian)* 79−49560
pp scatt., spin correlation meas., local hidden variable theory, quantum theory 78−54649
Θ_2^4 quantum field theory, numerical methods, anharmonic oscillator approx. 80−52390
^{12}B polarisation, quantum mechanical explanation for $^{100}Mo(^{14}N,^{12}B)$ 79−17890
CO, energy levels for perturbed Morse oscillators 80−78676
$F_2+X \rightarrow XF+F$ (X=Mu,H,D,T), isotope effects, quantum mech. and information theoretic calcs. 78−44360
H atom, Green's function path integral soln. 79−67187
H atom, relativistic model of spin 1/2 particles interacting with external EM field 78−70756
H atom, relativistic quantum mech. as weak-field limit of nonlinear theory 79−6878
H atom, variations, quantum theory calcs., generator coord. calcs. 80−41987
H atom energy spectrum in expanding Robertson-Walker universe 78−73869
H atom in box, 2-D Schroedinger equation, influence of constant elec. field, finite-element method 80−31544
H, eigenfunctions and eigenenergies, N-space dimensions calcs. 80−41988
H, Kepler problem regularisation on quotient of conformally flat manifold 80−82663
H, perturbation theory and Pade approx. in electric field 80−91493
H, spin flipping, quantum mech. eqns. of change 78−70003
H_2, Bender-Wu formula, SO(4,2) dynamical group and Zeeman effect, perturbation coeffs. determ. 80−95674
H_2, ortho-para conversion, magneto-catalytic reaction, quantum formulation 80−108750
o-H_2, solid FCC, orientational ordering, SCF approx. 78−2029
H_2^+, ground state energy inverse power expansion of two proton distances 79−97976
He atom, one-dimensional, bound states, for teachers 79−40317
He atoms, S-state eigenfunctions, Konishita's expansion 78−16674
He like systems, ground state one electron density decay 79−76337

quantum theory continued
He+Ne pot., differential cross section, quantum mechanical inversion 78−70896
^{3}He, liq., interface with nonmag. solid, Kapitza resist., quantum perturbation treatment 80−88385
^{4}He truncation influence, using recurrence relations for reaction matrices 79−489
ICN, rotational distribs. in photodissociation 77−9097
^{6}Li, appl. of four-body atomic Faddeev eqns. 79−59569
molecular pair polarisabilities, continuum electrostatic theory 78−86769
NO molecular predissociation, quantum mechanics expt. test 79−17274
$^{208}Pb+^{16}O$, classical, semiclassical and quantum mechanical scatt. and reaction calcs. 79−566

quantum theory of light *see quantum electrodynamics*

quantum theory of many-body problems *see many-body problems*

quark confinement
(2+1) dimensional Georgi-Glashow model, critical Higgs mass, clustering, monopoles 80−52441
ΔI=1/2 rule in QCD, higher order gluon corrections, diagrammatic anal. 80−4945
η' meson as pseudoscalar gluon, current sum rule saturation in QCD *(Russian)* 79−71718
θ model in quantum corrections to classical confinement 78−29297
θ-vacua and confinement in two-dimensional models 80−77990
$\lambda\rho^4/N$ theory, vac. stability, quark confinement 77−82677
$\lambda\phi^4$ theory, bound states, RPA anal. 77−6008
ν-dimensional Yang-Mills and (ν-1)-dimens. nonlinear σ-model connection, quark confinement, dual strings 80−90978
σ models, nonlinear, perturbative approach to symmetry restoration 80−37163
σ-model supersymmetric dynamics on pre-QCD level with elementary quarks and composite gluons 80−82886
$(\phi^3)_6$ theory, IR behaviour, gluon confinement mech., nonperturbative approach 78−24954
ϕ^4 (rubber bag) model, hadron mass spectra and J/ψ family *(Chinese)* 79−80812
ϕ^4 theory exact soln., model of confinement 77−41811
ϕ^4 type bag model of hadrons, rubber bag model theory *(Chinese)* 79−49479
't Hooft's disorder parameter, meson like configurations contribution, confinement phase 80−86574
$A_0=0$ gauge canonical formalism, gauge degrees of freedom, external charges, quark confinement 79−2936
Abelian gauge theories, (1+1) dimens., instanton effects 79−261
Abelian gauge theories, QED_2 generalisation, quark confinement 79−71605
Abelian Higgs model, lattice version, phase transitions and confinement 79−49398
Abelian Higgs model, two dimens. quark confinement 79−263
Abelian Higgs model in 2-dimens., confinement and massless fermions 79−22047
Abelian lattice gauge theories, θ-vacua construction in compact gauge theories 79−58874
Abelian lattice gauge theory, quark confinement 78−66040
action at a distance and relativistic wave equations for spinless quarks 79−36030
Airy functions, asymptotic behaviour of derivatives 80−17830
algebraic approach to hadrons without seeing quarks 80−9143
anomalous muon capture and lepton number conservation 80−68654
appl. of quark model to hadron spectroscopy and high-energy phenomena 78−82162
asymptotic catastrophe, temporary freedom in lepton and quark interactions 79−85253
asymptotic fields, colour confinement in QFT 78−70331
asymptotic freedom, for teaching 80−17761
asymptotic freedom in the infinite-momentum frame, SU(N) Yang-Mills theory renormalisation 80−22519
asymptotic freedom infrared instability 80−73678
asymptotically free nonAbelian gauge theory 77−2794
asymptotically free SU(2)×SU(2)×SU(4) model of unified interactions 78−16968
asymptotically non-free Yang-Mills theory, IR divergences 80−37166
bag and multimeron solutions of the classical Yang-Mills equation 80−4853
bag model, analogy to bubbles in liquid 80−22587
bag model, boundary motion, P-wave baryonic excitation spectrum 77−13925
bag model, deformation energy, quark-antiquark separation 78−45851
bag model, description of nucleons and isobars 79−49452
bag model, hadronic deformation energy, two-nucleon interaction 78−45852
bag model, isobaric ensemble and multiplicity distrib. *(Russian)* 80−82952
bag model, large transverse momentum processes of hadrons, EM form factors *(Russian)* 79−26308
bag model, multibaryon states, SU(6) mass formulae 78−45848
bag model, primordial transverse momentum, σ_L/σ_T ratio 80−82938
bag model, quark 78−45921
bag model, quark-quark interaction anal. 78−33029
bag model, quark-sea percentage under constraint of quark-line rule 78−24998
bag model, radial and breathing excitations 78−70330
bag model, spectroscopic appls., baryonium, gluonium, quark phase of matter, review 78−50008
bag model, spin-depend. struct. functions in deep inelastic scatt. 78−8589
bag model, variational principle description *(Russian)* 79−40757
bag model and QCD, quark-antiquark sea 77−71481
bag model for hadrons, classical interpretation, solns. of Maxwell eqns. 78−37183
bag model of hadrons, review 79−75736
bag model of quark confinement 77−79248
bag model of quarks *(Hungarian)* 79−13032
bag model $Q^4\bar{Q}$ states, meson-nucleon low-energy S-wave scatt., P-matrix formalism 80−13271
bag model with finite potential barrier, S-wave mass spectra of $Q\bar{Q}$ and leptonic widths 80−47242
bag model with toroidal glueballs 80−102009
bag models, field theoretic, renormalisation and translation invariance 80−62932

quark confinement continued
bag theory, excited states of confined quarks 77−6080
bag-bag scatt., interquark interaction effects 77−30315
bagged hadronic matter 80−73664
baglike potential, one dimens. extended hadron model, modified sine Gordon equation 77−30323
baglike struct., ϕ and ψ interacting scalar fields 79−22046
bare Pomeron in four-dimensional quantum chromodynamics 79−336
baryon magnetic moments calc. using quark confinement ideas 77−57539
baryon pionic transitions, MIT bag model anal. 78−82155
baryon pionic transitions in MIT bag model using PCAC hypothesis 80−37228
baryon spectrum, s-wave, phenomenological quark-quark interaction 80−101984
baryon spectrum, second excited level in harmonic oscillator model, experimental situation 80−37233
baryon spectrum and the forces between quarks 80−102004
baryon synthesis from unconfined primordial quarks 80−57566
baryonium, narrow states, mass formula, selection rule, quark model 78−66089
baryonium, nuclear and quark confinement forces 80−68431
baryonium four body problem, Schrodinger eqn. soln. by stochastic variational method 79−36008
baryonium model from $qq\bar{q}\bar{q}$ hadron spectrum, T- and M-diquonium 78−58172
baryonium spectroscopy based on duality and unitarity 79−58947
baryons, binding energy and rest mass of constituents, total symmetry effects *(French)* 80−63068
baryons, gluon exchange corrections in model with confining potentials 78−21379
baryons, relativistic quark model, confining force saturation 79−93336
baryons, with scalar raising pot., relativistic model 80−37231
bi-scale theory of gravitational and strong interactions 79−12696
bilocal fields, quark confinement and conservation laws 78−74120
bilocal gauge field theory 80−31986
binding, explained by strong gravity with cosmological const. 78−4820
binding energy in model classical field theories 80−4927
bootstrap model harmonic oscill. pot. 77−49912
bottomium, potential models, non-relativistic description 80−68426
bound state form factors, rel. to binding pot. using nonrelativistic Schrodinger eqn. 78−58187
bound states in field theory 78−25006
bound triquark nucleon model, mag. moment and weak interaction coupling constant ratios 79−67517
Breit equation, Klein paradox 80−57506
bremsstrahlung contrib. to $q\bar{q}$ sea polarisation 79−67507
broken symmetry restoration, topology of gauge theories 77−41808
bubble dynamics, motion of relativistic membrane, relevance to quark confinement 79−2989
Cabibbo angle in the $SU(2)_L \times U(1)$ gauge theories 79−35991
canonical field theory, quark binding 78−32994
canonical field theory, quark-binding 78−29264
canonical scaling in hadronic high-p_T processes, parton Fermi motion 78−45977
Caratheodory's canonical theory for fields, quark confinement 77−87941
central potentials, wave function at origin for large-n S-wave levels 79−35585
charge confinement, Schwinger model compared with $(QED)_4$ 80−62902
charge invariance, QCD, renormalisation group, confining and asymptotically free soln. 80−62881
charge screening, extended model of hadrons 78−37179
charge-monopole duality and nonAbelian gauge theory phases 79−71625
charged and neutral current coupling 78−89651
charged relativistic boson field, coherent state representation 79−71708
charged soliton long range interactions 79−63373
charges, vortices and quark confinement, confinement phase transition 79−36004
charm, elementary particle theories, properties *(Spanish)* 80−73681
charm particles, inclusive production cross sections, correlating quark rearrangement model 79−54320
charm photoprod. with linearly pol. photons, QCD calcs., gluons 80−68464
charmed particle production from two-gluon annihilation in proton-proton collisions 79−347
charmed quark semileptonic decay, gluon corrections to charged lepton spectrum 79−75765
charmonium, ψ and χ states, hyperfine struct. 78−12878
charmonium, generation of spin depend. forces through scalar-vector admixture 78−33038
charmonium, mass in QCD 80−105867
charmonium, masses of 2P and higher levels, sum rules 78−4805
charmonium, potential models, non-relativistic description 80−68426
charmonium, Todorov's quasipotential eqn., quark confinement 78−8593
charmonium and asymptotic freedom in QCD 79−6327
charmonium fine struct., confining pot. anal. 78−50007
charmonium photoprod., gluon-exchange model 78−74214
charmonium psion states, confining pots. and inverse scatt. problem, Υ mass 80−4946
charmonium spectroscopy, explicit soln. of wave eqn. for arbitrary power pots. 80−403
charmonium spin structure, and possible origin of quark spin depend. forces 79−30707
charmonium wave function, coloured glue effects using MIT bag model 79−75735
charmonium-like models, order of first energy levels 78−29311
chiral symmetry breaking in gauge theories 80−95244
chiral symmetry breaking in quark confining theories 79−63423
chromelectric-flux-tube model, finite time corrections 80−32083
classical massless scalar electrodynamics, charge confinement by classical instabilities 79−58933
classical quark confinement from general relativity 78−45842
classical quark confinement from general relativity 78−58162
classical quark matter, one dimens., Abelian approx. 78−41491
classical quark statics, $q\bar{q}$ pot. in Prasad-Sommerfield background, colour flux line focusing 79−49467
classical solutions of quark confinement model 79−13084
classical Yang-Mills field of a quark source 78−78077
classical Yang-Mills point charges, interaction, rel. to quark confinement *(Russian)* 78−32995
classically massless string, quark confinement 79−22041
quark confinement continued
cluster model of ordinary and exotic hadrons 79−40759
coherent quark-gluon jets in coherent state formalism 79−97580
color field model with nonzero-mass quanta, lattice calc. by Monte Carlo methods 79−13023
colour, confinement, ferroelectric mechanism analogue *(Russian)* 80−13274
colour, jet prod., exponentiation of leading logarithmic cross sections 79−63445
colour confinement, possible mechanism gauge invariance 79−54311
colour confining forces and effects saturation 80−73672
colour confining pot., upper bound, Yang-Mills theory and lattice QCD 79−2992
colour geometrodynamics, eightfold way, review 80−95243
colour SU(N) gauge theory 78−8592
colour zitterbewegung, non-Abelian Wilson loop integral evaluation 79−36007
coloured SU(3) scheme of three quark binding in baryons, mass formulae 78−12876
composite particle EM form factors, asymptotic behaviour 80−62927
compound quarks, gluons and parton confinement 79−22017
condensate of non-Abelian vortices 78−70328
condensation of extended structures 78−78141
condensed monopoles and Abelian confinement 78−78140
conference, quarks and leptons as fundamental particles, Schlamding, Austria, (Feb.-Mar. 1978) 80−17709
conference on hadron struct. and lepton-hadron interactions, Cargese, France (July 1977) 80−4473
configuration space renormalisation to phase space, gauge coupling 80−18074
confinement criteria for gauge invariant, lattice, and Abelian models 79−22023
confinement in (1+1) dimensions and fermions 79−63422
confinement in Z_n lattice gauge theories implies confinement in SU(n) lattice Higgs theories 79−58930
confinement model from eqn. with higher order derivatives 79−85265
confinement pots. in Schrodinger theory, analytic continued fraction theory 79−44786
confining gauge theories, quark correlation functions in massive QED_2 80−105845
constituent particle scattering in the Regge region 80−37244
constituent rearrangement model and hadron reactions review 79−26294
cosmological f-g fields relevant to quark confinement 80−86659
coupling constant inverse, energy perturbation expansion and eigenvalue 80−86658
coupling strengths and renormalization scale parameter in QCD by dimensional transmutation 79−6316
covariant parton model, jets, quark confinement large p_T and leptonic inclusive processes 77−30317
covariant quantisation of quark binding string 78−4829
covariant wave equations of two spinning particles harmonically bound 79−71692
CP^{N-1} model, QCD toy model, instantons θ vacua and confinement 80−9138
CP^{n-1} model with quarks, confinement and chiral symmetry breaking 79−54302
CP^{n-2} models in more than 2-dimens., confinement props. 80−86570
CP invariance, QCD confinement of colour, modification of axion scheme 80−73663
current definition and nonconservation, geometrodynamics for quarks and hadrons 78−45809
current trends in the theory of fields, conf., Tallahassee, Florida, 6-7 April 1978 79−12923
cylindrical mixing phenomena in dual topological unitarisation, pomerons, reggeons and gluonic states 80−86696
D and F charmed meson decay and evidence for $(\bar{c}s)_R$ current 78−58167
deep inelastic scatt., incusive observables and hard gluon emission 80−99094
deep inelastic struct. functions, direct method for QCD predictions of scaling violations 79−80800
deep processes in non-relativistic confining potentials 79−9329
dense neutron matter, quark percolation theory of phase transitions 80−77277
DESY e^+e^- experiments, QED checks, τ and Υ studies 80−18111
deuteron, six-quark state and EM struct., two nucleon bound state model *(Russian)* 79−13031
diffractive bumps, gluonic excitation Regge trajectories from bag and dual models 79−2978
dilute gas approximation, higher order corrections, appl. to gluon propagator and static quark pot. 79−49400
dipole ghost gauge theory as gluon model, confinement 78−66079
diquark constituents of baryons and baryonium 79−93383
diquark spectrum in two-dimens. chromodynamics 79−71719
Dirac's magnetic monopole string theory 77−13927
Dirac equation in a linear potential 80−27392
Dirac equation with quadratic scalar potential 80−27459
Dirac equation with relativistic linear potential, baryon properties, SU_6 representations 80−47261
Dirac particle, charged scalar field, strong coupling theory 78−16976
Dirac self-interacting field, soliton solns. in three-dimens. 77−26461
Dirac strings, monopoles, duality, triality 78−12864
discriminative deep inelastic tests of strong interaction field theories, QCD scaling violations 79−89105
disorder×order operator combination, quark confinement and gauge theories 79−85270
division of matter, confinement of quarks and gluons *(Polish)* 80−68417
double-logarithmic quark and form factors and the evolution of parton jets 80−68421
Dreel-Yan processes, gluon corrections 78−8597
Drell-Yan formula in perturbation theory, Abelian gluons 79−30702
dressed fermions in Abelian gauge theories 78−82093
droplet model for quark confinement phase transition, reduction to string statistical mechanics 79−2991
dual string theory, local currents *(Russian)* 78−25024
dual topological unitarization, correspondence with quark-parton model and QCD 79−93361
dual topological unitarization, glueball exchange effects, pomerons and reggeons 80−52482
dynamic confinement from vel. depend. interactions, appl. to quark-quark interactions 80−46800

quark confinement continued
dynamic models and subnuclear phenomena 77−67614
dynamic models with confinement and linear trajectories without parity doubling 77−2797
dynamical and topological considerations, review 79−26296
dynamical preon model from primordial QCD 80−105840
dynamical theory of quark confinement and hadron spectrum 77−82701
dynamics in low energy hadron-hadron scatt. 79−93366
dynamics on basis of stochastic Γ geom. 78−50009
Dyson equations, Ward identities, and the infrared behavior of Yang Mills theories 80−42353
echo hadrons, colour confinement and fractionally charged states 79−67506
effective Lagrangian with two color-singlet gluon fields 80−86680
electric and magnetic confinement schemes for mesons and baryons 80−4960
electric confinement and magnetic superconductors, appl. of QCD 78−58157
electrodynamics, Coulomb law, extension to 4-dimens., confining potentials 79−36012
EM model for charge confinement 78−78078
energy momentum tensor of quantised fields, vacuum averages, bag model of hadrons 80−91005
Euclidean gauge theory, four dimens. QCD, quark confinement mechanism 77−30321
exchange degeneracy breaking, hadronic selection rules 80−37248
exotic atoms, conf., Erice, Sicily, (1979) 80−67939
exotic quark states 80−73679
expanding bag model, effective quark mass 79−97604
extended hadrons, creation and annihilation thermodynamics 80−62925
extended hadrons and quark confinement, description using nonlinear De Sitter symmetry 78−58140
extended meson fields, alternative approach 77−22642
extended objects from Goldstone bosons in relativistic quantum field theory 79−285
extended systems, classical action, generalised London eqns. 77−49911
f-g fields, class relevant to quark confinement 80−125
fermion collective motions, quark currents, Green's functions 79−93348
fermion confinement and bosonisation, quantum sine-Gordon field theory, quark confinement 78−86442
fermion field, nonlinear, origin of four quark flavours, quantum numbers, isosymmetry breaking 80−62920
Feynman rules for lattice gauge theory of quark confinement, Green's functions, review 78−93850
Feynman rules of QCD inside hadron 79−63425
field theory and quark confinement, conf., Rochester, USA, (June, 1976) 77−71440
finite confinement potential and relativistic field theories 77−79249
finite quark mass effects on superdense quarkion configurations 80−105852
fixed sphere MIT bag model, b-quark mass, zero-point energy, gs b-flavoured hadron masses 79−63429
fluxon solutions in non-abelian gauge models 79−9287
forces between leptons and quarks, a gauge field phenomena 80−91008
forces holding quarks inside other particles *(Polish)* 78−45843
forces preventing free quark production 77−26488
form factors of composite states, relation to Regge trajectories 77−82742
four quark mesons, recoupled wave functions, phase inconsistency 80−68425
four quark states and open charm production 79−63443
fragmentation, trigger side momentum distrib. in large P_T processes 80−42422
free quarks 80−13289
free-spinor field on Regge trajectory as representation of strongly interacting quark field 80−32067
gauge field theories, Hamiltonian formalism, quark confinement eqn. 78−41488
gauge field theory formulation in quantum field theory framework 79−21908
gauge fields, chiral fields on loop space, colour-electric flux rings 80−42327
gauge independ. two body amplitudes, VDM of EM form factors 77−74645
gauge invariant gluons, Hamiltonian operator 80−105843
gauge lattice systems, transition, duality 79−262
gauge theories, an introduction for experimental particle physicists 78−82119
gauge theories, confinement model 79−89109
gauge theories and strong gravity 79−58869
gauge theories of weak, EM and strong interactions 77−13835
gauge theory for 2-D statistical mechanics 79−30713
geometric strings, quark binding, quantisation in GL(2,C)/SL(2,C) struct. group 79−40727
geometrical approach to elementary particles 80−105865
geometrodynamical model of extended baryons 77−79251
giant MIT bag, hot quark matter, from relativistic ideal Fermi gas 80−99083
glue bag model, unification of bag models *(Chinese)* 79−35998
glueball pomeron singularity cancellation 80−73687
glueball singularity, flavour loops and the Harari-Freund picture 80−42433
glueball spectra, prod. and decay for QCD and SU(n) gauge theories 80−62941
glueballs, production and properties of gluonium 80−73674
gluon and quark jets in a recursive model motivated by quantum chromodynamics, Υ decay 80−62936
gluon and quark observation, QCD interactions and confinement 79−2981
gluon and quark population evolution in QCD jets, numerical estimates 80−101987
gluon bremsstrahlung, nucleon structure functions in QCD 79−49469
gluon bremsstrahlung and multiperipheral cluster models 79−22082
gluon chain model in QCD 77−26487
gluon chains and multiquark hadrons 79−93337
gluon collective excitations, nonabelian gauge theories, effective chiral Lagrangian 79−22034
gluon colour charge measurement 79−22028
gluon condensation and QCD 80−102007
gluon distribution in hadrons, colour cancellations and coherence effects 79−40746
quark confinement continued
gluon distributions in QCD, definitions 80−37227
gluon exchange in meson spectroscopy 80−102013
gluon exchange in short distance hadron-antihadron pot., quark motion, Schrodinger eqn. 79−328
gluon fragmentation functions from quark jets 79−49453
gluon generation 78−25008
gluon jets, G→GG and G→qq̄ 80−37209
gluon jets from QCD, jet ang. radius and energy depend. 78−89662
gluon mass shell Ward identities verification in axial gauge 79−13037
gluon matter hadronisation, pp-collision multihadron production 79−45047
gluon momentum fraction, colour élec. tube and linear potential model anal. 79−17679
gluon observation in P-wave quarkonium decay 80−32068
gluon operator coefficients in electroproduction 79−58926
gluon propagation in non-Abelian gauge theories, IR props. 79−2983
gluon-gluon interactions, hadron prod. and σ(total) growth at high energies 80−91049
gluonic bound states, masses and decay widths, X(2.8) as possible candidate, γγ decay 79−93364
gluonic boundary conditions, quark mass depend. and quark condensation 80−86671
gluonic jets, heavy meson associated prod. in e^+e^- annihilation 78−93892
gluonic long-range forces between hadrons 79−9339
gluonic stream origin processes. azimuthal asymmetry *(Russian)* 79−45065
gluons, nonlinear field theory *(Chinese)* 79−58923
gluons in e^+e^- annihilation, QCD anal. of strong interaction dynamics 79−9386
gluoproduction of heavy quark flavors in hadronic scattering 79−9330
Grassmann spaces, model for supersymmetric quark-twistor string 79−22018
gribov ambiguity, perturbation theory, and confinement 79−21934
hadron bags, interactions under strict quark-line rule 78−41495
hadron beam jets structure at small P_T 80−102014
hadron collective model based on quantum chromodynamics 77−13926
hadron collisions, theory and phenomenology of lepton pair production, review 78−82159
hadron constituent dynamics, nonconservative quantum character, quark dynamics, nonrelativistic limit 79−17671
hadron dissociation, diffractive dissociation model, quark states 79−75752
hadron EM mass differences, quark behaviour 79−58941
hadron high energy struct. models *(Hungarian)* 80−4924
hadron masses in bag model with surface tension 78−70337
hadron matrix elements in relativistic quark model 80−37238
hadron properties from quark models and confinement schemes 80−105864
hadron spectroscopy, quark models and SU(5) grand unification scheme 80−4958
hadron spectroscopy with covariant Coulomb and confining interactions 80−32090
hadron states, quark sea and non-Abelian gauge field contrib. 79−327
hadron stream generation by quarks and gluons, transverse impulse *(Russian)* 79−85280
hadron total cross sections in quark parton model 78−45859
hadron-hadron 3-jet collisions, charge conjugation asymmetries and trilinear gluon coupling 80−105934
hadron-hadron low energy scatt., anal. of internal quark-gluon eigenstates, Wigner-Eisenbud formalism 79−63525
hadronic bag quark confinement through tensor gauge fields, de Sitter microuniverses 79−22045
hadronic cascades between QQ̄ bound states, QCD anal. 79−85261
hadronic multiple prod. and average charged multiplicity, strato-gluon mechanism in pp, Kp, πp *(Chinese)* 80−22586
hadronic structure 77−34118
hadronic structure theory, derivation of static bag and bag constant estimation 79−58932
hadronic structure using parton anal. of deep inelastic scattering and rel. processes 79−80803
hadronic wave eqns. from lattice gauge theory, breathing modes 79−97586
hadrons and their constituents, wave-particle quality 80−9136
hadroproduction of quark flavours, extension of conserved vector current hypothesis to gluons 78−58159
Hamilton-Jacobi formalism for strings, string-gauge theory link 80−78048
harmonic confinement, hard gluon exchange corrections, meson mass spectrum 78−86440
harmonic confinement, relativistic approx. to meson spectrum 78−29303
harmonic oscill. covariant model, baryon reson. decay matrix elements 77−61284
harmonic oscill. covariant wavefunctions, chiral config. mixing 77−49913
harmonically confined q q̄ system, relativistic wave eqn. 80−95247
heavy 1^{--} quark-antiquark bound state decays, fast gluons 79−85297
heavy baryon spectroscopy in the QCD bag model 80−105866
heavy meson weak decays, heavy quark decay, QCD corrections, real gluon role 80−57586
heavy qq̄ systems, fine struct. and axial vector gluons 79−63431
heavy quark bound states, production and decay 80−102008
heavy quark bound states of top quark and antiquark pairs, QCD test 80−68430
heavy quark bound system, vibr. states 78−29300
heavy quark dynamics in non perturbative QCD vacuum 79−80795
heavy quark effective potential, non-perturbative semi-classical calc. 79−13053
heavy quark infrared safe weak decay, dimensional regularisation techniques, gluonic corrections 80−102087
heavy quark potential, non-perturbative contrib., appl. to QCD 79−13025
heavy quark potentials, effect on triplet-cc̄ charmonium and triplet bb̄ upsilonium systems 79−49456
heavy quark prod., nonperturbative gluoprod. versus perturbative QCD fusion models, B and ψ 80−91058
heavy quark semileptonic decays, gluon corrections 79−17688
heavy quark-antiquark potential, effect of vacuum polarisation at long distances 79−6304
heavy quarkonium states, decay rate to lepton pairs, gluonic corrections 80−102043

quark confinement continued
heavy quarks, EM shift of energy levels due to confinement, bag model 80−13287
heavy quarks and new particles 80−73661
heavy quarks in QCD *(French)* 80−78017
heavy vector meson annihilation rate to lepton pairs, hadronic corrections 80−4943
heavy vector meson annihilation to lepton pairs, hadronic corrections 80−68424
hidden colour and the isobar content of the deuteron 80−102024
Higgs boson decay, gluon final states, differential spherocity and thrust distrib. 80−86655
Higgs bosons from two-gluon annihilation in pp collisions 78−41501
Higgs lattice abelian model, finite temp. behaviour 80−13260
Higgs self coupling effects on asymptotic freedom 79−266
high p_T hadronic jet photoprod., QCD anal., quark and gluon jets 80−42474
hydrodynamical model based on baglike Lagrangian 77−57496
hydrodynamics and the bag model, multiparticle production, finite geometry effects 79−22044
hypercomplex quark fields and quantum chromodynamics 79−93344
inclusive vector meson production in fragmentation regions of meson at small P_T 80−105931
inelastic Compton scatt., hadronic contrib., two-dimens. QCD calcs. 79−45062
infinite momentum frame formulation 79−36026
infinite relativistic string with a point-like mass 79−13036
infrared divergences in non-Abelian gauge theory 77−6001
infrared struct. of QCD, quark confinement, perturbation theory 77−71443
instanton, group theoretical aspects 79−97494
instanton correction to vac. energy densities and bag const. 80−37211
instanton effective size estimate from gluon field strength tensor vacuum expectation value 78−70326
instanton effects in bound state dynamics, quark-antiquark binding, gluon-instanton interactions 79−6280
instanton effects in pure Yang-Mills theory, perturbation theory rules 78−58125
instanton effects on quark-antiquark potential 78−93847
instanton effects on static $\bar{Q}Q$ potential 79−9333
instanton suppression as origin of quark confinement 79−9338
instanton system weakly interacting with anti-instanton system, external electric fields, structure and stability 80−77956
instantons, dynamical role in quarkless chromodynamics, bag model test 80−47246
instantons, numerical significance at short distances 78−70339
instantons, relationship to confinement, one-dimens. quantum mech. model anal. 79−12962
intrinsic temperature of confined systems 79−85271
inverse problem for confining potentials, zero ang. momentum 79−30704
inverted charmed meson multiplets as a test for scalar quark confinement 78−70325
IR singularities, spin $^1/_2$ quark confinement in three dimens. 79−337
IR singularity quark confinement model, coloured bound state absence 79−338
Jaffe model, lowest states, appl. to $q^4\bar{q}$ in SU(6) 79−13060
jet asymmetry in polarized proton collisions *(Russian)* 79−17685
jet quantum number, identification model 80−42423
jet quantum number identification event by event, original parton and gluon jets 80−52466
Klein-Gordan equations with logarithmic nonlinearities, classical theory 79−5996
Kuti-Weisskopf model, quark distrib. in mesons *(Russian)* 80−13291
ladder model of QCD, hadron struct. 80−37213
large $p_\perp$ photoproduction, gluon fragmentation function extraction, scaling 80−105853
large p_T hadron prod. off nuclei, QCD parton model, nucleus as gluon filter 79−89110
large p_T hadronic collisions, QCD sensitive test, quark and gluon jets 80−57647
large p_T interactions, quark existance studies 80−37235
large p_T production and hard rearrangement of quarks 79−63454
lattice algebra for light and heavy hadron constituents 78−16978
lattice approx. of gauge field theories 78−29225
lattice confinement, gauge fixing and transfer matrix 77−41766
lattice gauge field theories in 2-dimens., continuum limit 77−41765
lattice gauge models in strong coupling regime, quark confinement 77−49835
lattice gauge theories, two dimens., static quark confinement 79−35916
lattice gauge theories with fermions, cluster expansion 78−58119
lattice gauge theory, 4-D Z_2 gauge, verification of first order phase transition 79−58876
lattice gauge theory, extreme environments and duality transform., review 79−13024
lattice gauge theory, strongly coupled, confinement of fermions 79−2905
lattice gauge theory, Z_N Abelian group, phases, duality 80−42323
lattice Higgs models, (non)Abelian, diamag. and crit. props. 79−67465
lattice Higgs-Villain model 79−26289
lattice models of quark confinement at high temperature 80−32082
lattice QCD, mass levels of boxiton (glueball) states 79−54259
lattice QED with low coupling confinement studies 80−18095
lattice Schwinger model, form factors of dipole states 78−66029
lattice SU(N) gauge theory, vacuum structure, large-scale 80−57470
lattice U(1) gauge fields, quark trapping 77−18175
lattice Yang-Mills theory, convergence of strong coupling expansion and linear pot. 78−45847
Lee model, SLAC bag method, skin- and δ-confinement *(Chinese)* 79−80757
lepton-nucleon deep inelastic scatt., quark-parton model 77−57545
leptoquark bosons, confinement in SU_4 theory 79−45052
liberation from chromodynamical confinement, possibilities 79−30708
light hadron mass in bag model, quark-gluon coupling constant *(Russian)* 79−67514
light meson radiative decay, Zweig law *(Russian)* 80−102051
light quark spectroscopy, review 80−42424
limiting spectra from confining potentials 79−84895
linear confining pot., soln. with combinatorics functions 78−32719
link operator formulation and string breaking for confinement without van der Waals forces 80−101994
local covariant gauge quantum field theories, cluster property 78−70265
local spin-$^1/_2$ wave equations and harmonic confinement 80−4926
quark confinement continued
long lived hyperstrange multiquark droplets in MIT bag model 80−9137
secret long range force in QFT with instantons 79−9283
long range forces between hadrons 79−67503
Lorentz structure of confining quark-quark interaction, asymptotic freedom, new particle spectroscopy 78−66077
low transverse momentum fragmentation processes, quark-gluon struct. of hadrons 80−22561
M_2 baryonium state decays, baryonium assignment scheme 79−71691
$M_\psi - M_{\eta(c)}$ and $M_T - M_{\eta(b)}$ lower bounds, concave and convex pots. 80−91057
magnetic monopoles, non-Abelian, stability analysis, Yang-Mills equations 80−31987
magnetic quark confinement, flux tube in gauge field model 77−6084
Mandelstam-'t Hooft duality in Abelian lattice models 78−78057
manifestly gauge invariant gluon eqns. from Yang-Mills fields 80−86681
mass scales, confinement, nonperturbative approach, self-consistent method 78−33033
mass spectrum for integral isospin monopoles, bag model as high isospin limit 78−24935
massive gauge-invariant QCD, quark confinement and vortices 80−384
massive gluinos 79−2987
massive lepton pair production at large q_T, large p_T jet props. 79−54326
massive Schwinger model, saturation, fermion confinement and instantons 80−47175
massive Schwinger model, vacuum degeneracy and confinement 78−78090
massless 't Hooft model, tachyonic modes, vanishing of scalar density 80−77949
massless non-abelian gluon confinement and rising total cross sections 80−13264
massless scalar QED, colour confinement model 78−33027
meron pairs, quark confinement phase transition in SU(2) Yang-Mills quantum field theory 78−37174
meson hyperfine splittings and asymptotic freedom 77−79252
meson mass spectrum, planar bootstrap, and Regge approach 80−22581
meson masses of radial excitation for ρ, ω, ϕ-mesons, potential model calcs. 78−93860
meson model, quark-antiquark-gluon bound state 78−45877
meson photocoupling in quark model 80−82954
meson resonance leptonic decay, quark confinement potential 78−41536
meson scattering, quark model asymptotic completeness 80−73738
meson spectroscopy, review of SU_3 quark model, quark confinement and bound states 78−74228
meson spectroscopy, spin struct., effective scale quark confinement in QCD 79−17684
meson spectrum, quark-antiquark relativistic two-body wave eqn. bound states 77−30328
meson three-dimens. wave eqn. from Bethe-Salpeter eqn., comment 77−65136
meson weak and EM decays, relativistic confined quarks, MIT bag model 80−47277
mesons, deformations and spectral props. 80−13203
mesons, heavy, one-parameter potential 80−13279
mesons, $SU_{1,4}$ as dynamical group, discrete representations anal., masses 77−74642
mesons with heavy quark constituents, lifetime and branching fraction determ. 79−93404
MIT bag, 1-dimens., structure function L_0 approx. correction 80−101985
MIT bag, 2-dimens., force between two point colour charges 79−334
MIT bag, one-dimens., Bjorken scaling, mass corrections 78−62356
MIT bag, structure functions in a translationally invariant approx. 79−36023
MIT bag model, approx. QCD lower bound for bag constant B 79−17681
MIT bag model, charmed and b-flavoured hadron mag. moments 80−95271
MIT bag model, chiral symmetry breaking 79−63408
MIT bag model, coloured quark and gluon constituents of mesons 80−4929
MIT Bag model, field theory Lagrangian 78−89670
MIT bag model, first order formalism for scalar fields 78−16986
MIT bag model, G_2 struct. function 80−4947
MIT bag model, instanton effects on light quark spectroscopy, hadron mass 78−62372
MIT bag model, M1 transition calcs. low lying hadrons 79−13080
MIT bag model, parton dynamics 78−74204
MIT bag model, PCAC effects, pion field exchange energy, η mass 79−93378
MIT bag model, quantum corrections to classical confinement 77−74643
MIT bag model, quark and parton phys., introduction, book 79−85276
MIT bag model, radiative transitions of baryons, resonance photoprod. 79−40722
MIT bag model, tensor component of two-nucleon interaction 79−49471
MIT bag model, two-dimens., confined massive field vacuum fluctuations 80−4921
MIT bag model, zero-point energy of fields 77−13867
MIT bag model and Roper resonance 77−82705
MIT bag model cavity approx., parton distribs., Bjorken scaling 78−89664
MIT bag model cavity approx., prediction of radially excited baryon states 79−89127
MIT bag theory, microscopic derivation with spontaneously broken symmetry 79−264
MIT bag with de Sitter geometry 79−2988
MIT confinement scheme, geometrodynamical approach 78−89657
mixing matrix and CP violation for n quark generations 80−101986
mixing of gluon bound states and quark-antiquark states, η and η' appl. 80−47255
Moufang plane and octonionic quantum mechanics 78−69999
moving mirror effects in hadronic reactions 79−54303
multibaryonic systems, 3n-quark systems, MIT bag model 78−70321
multichannel potential scattering theory with permanently confined channels, quark model appls. 77−13634
multilocal theory and relativistic string 78−93845
multipole fields of infinite order, indefinite metric 78−29295
multiquark meson states, struct. 80−9146
multiquark states: Q^3 baryon resonances, mass spectrum from MIT bag model 79−67510
multiquark states, obs. in $p\bar{p}$ formation and prod. expts. 80−9153

quark confinement continued
naive model, pre-flavour states, quark searches 80−18110
Nambu Goldstone realisation for vector gluon-quark theories, gluon vertices 80−68415
Nambu string model, scatt. amplitude *(Russian)* 80−86695
neutral-current quark coupling determination using neutrino-neutron and neutrino-proton deep-inelastic cross sections 79−89122
neutron charge radius and deep inelastic struct. functions 78−70334
Nielsen-Olesen vortices in coherent state approx., creation and annihilation operators 79−9284
non-Abelian Block-Nordsiech conjecture, counter-example 80−78021
non-Abelian gauge theories, coupling constant IR props., glue propagator 80−31999
non-Abelian gauge theories, local covariant operator formation, quark confinement 80−47190
non-Abelian gauge theories and mag. monopoles, strong interaction models and quark confinement 79−49367
non-Abelian gauge theories and quark confinement 79−13022
non-Abelian gauge theory, mag. charges, quark confinement 77−49849
non-Abelian two-dimens. theories, novel inconsistency, quantum chromodynamics 77−65097
non-Abelian vortex-bond model of hadrons 78−4827
non-Abelian Yang Mills field, infrared behaviour, gluon decoupling 79−85215
nonAbelian gauge theories, Faddeev-Popov ghost decoupling, QCD gauges and gluons 80−52406
nonAbelian gauge theory, topological symmetry breakdown and quark confinement 79−71611
nonet mixing and gluon effects in current quark framework 79−80799
nonlinear Klein-Gordon eqns., non-dissipative character, confinement principle 78−62361
nonlinear super-Poincare fermion, quantisation in bag like formulation 80−4923
nonlinear superfields and quark confinement *(Chinese)* 80−42346
nonlocal quantum field theory, quark confinement and scaling 77−13915
nonlocal quark model in $SU(3)\times SU^{c}(3)\times U(1)$, meson decay and mass correction *(German)* 80−27456
nonperturbative gluon jet model, gluon fragments, meson prod. 80−68420
nonperturbative QCD, large N_c, QCD bag model, instantons and η' mass 80−57559
nonrelativistic bound s-states in linear central potential 80−82936
nonrelativistic quark model with one gluon exchange pot., baryon spectroscopy in $SU(6)\otimes O(3)$ 78−78147
nuclear bag states containing quarks, detection 78−70465
nuclear matter, phase transitions from nucleon to quark matter 79−63617
nucleon form factors, asymptotic relations from quark-gluon model, scaling violation 80−42463
nucleon structure function, quark and gluon moments, gauge theory 78−50036
nucleons, quark-diquark model 77−87937
O(2) Heisenberg gauge invariant model, eigenfunctions and energy spectrum 79−58875
O(3) σ-model, confinement in two dimens. models with factorisation 79−36011
octonionic quark confinement 79−17669
one dimensional gauge field theories, at finite temp. and densities, props. and quark confinement 79−49468
opposite-side angular correlation of high-p_T particles as a probe of gluons 79−71703
orthoquarkonium decay, Dalitz plot population and thrust ang. distrib., scalar gluon nonexistence 80−27470
OZI rule, justification in QCD 80−62924
pairing theory of Yang-Mills field and string phase 79−13047
particle struct. studies, book 80−41952
parton confinement: A different perspective 78−86437
parton transverse momentum dependence on longitudinal momentum 78−25016
pathological lattice field theory for interacting strings 80−47186
Pati-Salam neutral vector gluons, possible expt. search in e^+e^- collisions 80−37202
permanent quark confinement without van der Waals forces 79−97582
perturbation theory and QCD, quark binding 77−71444
perturbative aspects of QCD, an introduction 79−30714
perturbative QCD, gluon bremsstrahlung by confined sources 79−45067
perturbative QCD, hard hadronic processes, e^+e^- annihilation, lepton-hadron deep inelastic scatt. 80−52477
PETRA results for fluons, nuclear forces, t-quarks and quark-lepton symmetry 80−86731
phase transition in nonAbelian quantised gauge field theories, permanent quark confinement 78−70322
phase transitions in two dimens. and quantum field theory, analogies, review 80−52149
planar bootstrap model calcs., $Q\bar{Q}$ and QQQ mass spectra 78−89685
planar model electrodynamics, phase diagram, continuum limit, and mass spectrum 79−63426
pole-dipole relativistic string model 80−386
positive parity excited baryons in quark model with hyperfine interactions 78−82161
potential model, Dirac eqn. with linear confining pot., symmetric model 79−364
potential model based on Dirac eqn. with linear confining pot., asymmetric model 79−363
potential models, tunnelling and quark leakage through the confining pot. 79−6317
power law confinement potentials, bound states 80−18123
pre-quarks and fractional charges 80−91048
preconfinement as a property of perturbative QCD 79−54310
proceedings of the 1977 CERN-JINR School of Physics, Nafplion, Greece (May-June 1977) 78−81726
propagator in a theory with confinement 79−71689
propagator of binary quark and antiquark system 79−45053
proton core evidence, from muon pair p_T distrib. and elastic pp data 79−17682
pseudomesoniums, spectroscopy, prod. and decay props. 79−45058
pseudoparticle physical mechanism for quark confinement, Yang-Mills theory confinement 79−49463
pseudoscalar gluon, role in hadron struct. *(Chinese)* 79−75745
Q^2 dependence for quark and gluon fragmentation functions, QCD predictions, Altarelli-Parisi eqns. 80−78018
quark confinement continued
Q^2 dependence of quark and gluon fragmentation functions in a parton picture based on QCD 79−9336
$Q^2\bar{Q}^2$ states, mass levels in (3+1) dimens. lattice gauge theory 79−58942
QCD, 2-D, evidence against colour confinement 79−26293
QCD, 2-dimens., Bose form, SU(N) confining phase 80−52463
QCD, 2-dimens., confinement effects on analyticity meson inelastic form factor, scatt. amplitude 79−333
QCD, 2-dimens. multiflavour, local colour symmetry breakdown, massive gluons and quarks 80−82942
QCD, baryons in 1/N expansion, mesons and glue states 80−13267
QCD, bound on MIT bag constant and Nielsen-Olesen unstable mode 79−89100
QCD, colour ferromag. vacuum states, two loop energy densities, MIT bag constant 80−99085
QCD, confinement and long range gauge fields 80−73668
QCD, confinement and quark theory, introductory review 79−67502
QCD, effective quark pot. in baryon reson. 78−16910
QCD, energy of classical sources, finite confinement from Pade approximants 78−41478
QCD, field theoretical aspects, perturbative effects 79−26286
QCD, gauge independ. approach to hard processes, structure functions, gluons 80−86665
QCD, gauge invariance and the quark-antiquark static potential 79−97587
QCD, ghost gluon bound state and pseudoscalar mixing 80−86685
QCD, gluon colour screening by Higgs mechanism 78−93861
QCD, hadron interaction effective string lagrangian, Regge slope, charmonium pot. model 80−4939
QCD, hadron masses, behaviour of constituent quarks 80−57557
QCD, hadron struct. theory, expt. tests 79−93367
QCD, heavy quark-antiquark bound systems, effective potential 79−49477
QCD, higher order, charge conjugation asymmetries from two gluon exchange 80−4935
QCD, IR behaviour of higher order derivative field theories 79−30699
QCD, modified, exact global colour SU(3) symm., asymptotic freedom 78−41493
QCD, nonperturbative, fundamental scale of strong interactions 79−36002
QCD, perturbative, colour singlet distribs. and mass damping 79−63418
QCD, quark and gluon fragmentation functions, quarkonium decay inclusive hadron spectrum 79−97584
QCD, quark and gluon propagators 80−52469
QCD, quark confinement, background theory 80−18113
QCD, renormalisation group and infrared behaviour 79−58931
QCD, spin depend. quark-antiquark forces 79−49476
QCD, stagnant gauge for gluon propagator 80−57554
QCD, static potential $Q\bar{Q}$ model in weak coupling expansion 77−74647
QCD, strong interaction gauge theory, SU(3) colour gauge vector mesons, confinement 78−78136
QCD, testing of gluons by energy-energy correlations in heavy quarkonium decay 79−71690
QCD, three gluon jets as test 78−25001
QCD, three gluon vertex 79−49454
QCD, universal multiplicity hypothesis, bounds on quark gluon coupling, quark mass, and confinement region 78−74213
QCD, universal multiplicity hypothesis, quark-gluon coupling constant 79−6319
QCD, vector gluon propagator using gauge technique 79−45049
QCD, weak coupling approx. Schwinger-Dyson eqn. *(Chinese)* 80−52476
QCD and dual resonance model vertices, string prod. operators, singlet colour states *(Russian)* 80−42410
QCD and hadronic structure 80−42416
QCD and superdense matter, quark and gluon plasma, hadronic structure, neutron stars, hadron collisions, review 80−73683
QCD at high temp., MIT bag model and thermodynamic pot. 79−30706
QCD hadronic μ pair prod., gluon gauge depend., struct. func. calc. 79−80810
QCD higher-order asymptotic freedom, corrections, γ struct. function calc. 79−89130
QCD in 2-D quark confinement and parton model 79−17670
QCD low energy tests, gluon non-zero effective mass, ψ decays 80−91054
QCD model for gluon jet fragmentation, oblate transverse momentum struct. 79−9340
QCD of hadron struct. 78−93849
QCD of quark matrer to nuclear matter transition at neutron star density 78−54608
QCD opposite two hadron correl., scale violations in quark/gluon fragmentation functions 79−54299
QCD perturbation theory, asymmetries in inclusive hadron prod. 78−50057
QCD perturbation theory for confined quarks and gluons, p glue content 80−52460
QCD perturbation theory for confined quarks and gluons 80−401
QCD phase transitions, chiral symmetry breaking, confinement, as tunnelling through singular barriers 78−82145
QCD phenomenological model of high- and low-energy behaviour 79−63439
QCD phenomenology, quarks and gluons in medium energy nuclear physics 80−42563
QCD polarisation operator at finite temps. and densities, one loop approx., gluons *(Russian)* 80−68427
QCD predictions, parton and gluon transverse momenta for large p_T particle prod. 79−40723
QCD processes, large IR corrections, soft gluon emission 80−78028
qCD scattering processes with hard gluon emission, jet prod. 80−62939
QCD screening discussion from QED massless scalar problem 77−79237
QCD spectrum, infinite number of colours at fixed coupling, interacting string model 79−2993
QCD theory for the strong interaction 80−4962
QCD transverse lattice theory, confinement and hadron bound states 80−4961
QCD two-dimens. 't Hooft Hamiltonian spectrum 77−65106
QCD vacuum, asymptotic freedom, quark confinement, Yang-Mills theory for strong interactions 80−73638
QCD vacuum in strong external gauge fields, spontaneously, broken chiral symmetries 80−57555

quark confinement continued
QCD vacuum nonperturbative fluctuations, bag effect in low P_T hadronic spectra 80−37218
QCD vacuum of background SU(2) gauge field, colour mag. permeability 80−78023
QED_2 confinement and instanton-like Euclidean field configurations 77−49910
QED_2 model with SU(n) flavour, quark confinement criteria 78−45840
QQ states, P wave decays, jet ang. distrib. and kinematics 79−75737
quantised dual string theory, string functional and propagators 80−32088
quantised strings and chromodynamic IR behaviour, Yang-Mills electric flux lines 77−30316
quantized scalar SLAC bag model, quark trapping 77−13920
quantum chromodynamics, hadroprod. of lepton pairs and real photons 78−50056
quantum chromodynamics, IR struct. perturbation theory calcs. 77−74577
quantum chromodynamics, nonperturbative approach 77−67617
quantum chromodynamics, two dimens., confinement form factors, deep inelastic scatt. 77−30322
quantum chromodynamics, unified approach to gauge, dual, Gribov theories 77−18223
quantum chromodynamics in two dimens. 77−74590
quantum corrections to classical confinement 77−2796
quantum mechanical applications to quarkonium 80−27484
quantum relativistic strings and the multiplicative dual model *(Russian)* 80−82958
quantum-chromodynamic phenomenology of gluon jets 80−4941
quark and gluon jet longitudinal momenta, QCD anal. 80−22571
quark antiquark pot. in QCD 78−4825
quark charges in QCD 79−97575
quark confinement, event horizons around a particle surrounded by a static confinement potential 78−66075
quark decay patterns, liberated QCD and confined QCD theory 79−9328
quark electric dipole moment in Kobayashi-Maskawa theory with gluonic corrections *(Russian)* 80−86688
quark jet fragmentation, semiclassical model 79−45071
quark jets in e^+e^- annihilation, forward-backward asymmetries 79−97605
quark liberation in (1+1)-dimensions 79−324
quark matter, phenomenological equation of state, neutron star appl. 79−63424
quark pair condensation and confinement 79−17677
quark recombination mechanism in multi-hadron production 80−18114
quark-gluon field coupling const., meson mass differences *(Russian)* 80−105898
quark-gluon phase transition 80−27475
quark-nucleon phase diagram and quantum chromodynamics 80−105855
quark-nucleon phase transitions, rel. to density fluctuations in early Universe 79−75301
quarklei, free quarks saturated with nucleons, existence and detection 79−6315
quarkonia, S- and P-wave, gluon jets, perturbative QCD anal. 80−32070
quarkonia, spectra, decays, levels, jets, sum rules 80−18112
quarkonium, almost degenerate P-wave charmed-bottom meson multiplet, scalar confinement test 79−13052
quarkonium, observed dynamical groups 80−9149
quarkonium, scaling and prescaling 79−40726
quarkonium and extended constituent quarks, confining pots. 79−13021
quarkonium mass spectra, one gluon exchange corrections, gauge invariance and choice 80−52483
quarkonium systems, binding energy effect on mass spectra 80−37229
quarkonium systems, inverse scatt. formalism for confining pots., 1-dimens. formalism 78−82153
quarkonium systems, sum rules 80−68423
quasi-confinement of quarks 77−13923
quasi-relativistic quark model with confining pot., hadron form factors 77−46020
quasiconfinement in colour gauge symmetry, unconfined quarks and gluons 80−86686
quaternionic Hilbert space and colour confinement, admissible symmetry groups 80−27458
quaternionic Hilbert space and colour confinement 80−27457
radiative transitions and gluon-exchange contributions in QCD 79−45074
Regge trajectories families, S-matrix theory, nonrelativistic linear pot. quark binding model, comparison 78−33048
Regge-pole approach to charmonium and bottonium 80−86697
relativistic confining potential model, current spectral functions, meson dominance calc. 79−71734
relativistic equations for bound states of quarks 78−70333
relativistic local renormalizable field theories, basis for quark confinement and QED 79−21893
relativistic membrane, quantum dynamics 80−57552
relativistic quark model, Lagrangian form of relativistic mechanics for bilocal and trilocal structs. 77−41809
relativistic quark model, with linear scaling pot. 77−38125
relativistic radial equations for two spin-1/2 particles consistent with the hole theory 79−93272
relativistic string, longitudinal vibr. 79−13061
relativistic string dynamics, Lorentz invariant quantum theory, review *(Russian)* 79−22020
relativistic string in a constant homogeneous electromagnetic field 79−22073
relativistic string model generalisation in geometrical approach, Yang-Mills approx. 80−383
relativistic string with massive ends, dynamical eqns. 78−4826
relativistic strings and electromagnetic flux tubes 79−49494
relativistic vortices interacting through scalar field, solns. for nonlinear coupled equations 79−22039
relativistic wave equation and mass spectrum of gluonium 80−73596
resonance-saturation picture, scaling violation patterns 80−82940
rest frame proton, colour gluon content, bag model and QCD calcs. 79−335
review 77−34121
review of quark model with SU(n) symmetry, 3 colours and 5 flavours 79−9343
review of quarks, appl. to hadron spectroscopy quark parton model 79−22052
quark confinement continued
Roper resonance photocoupling in relativistic quark model with scalar confining pot. 80−4936
saturation property of quark potential *(Chinese)* 79−17672
scalar field theory in lattice space, analogy to random walk 78−21325
scaling, nonrelativistic Schrodinger eqn. charmonium 78−54613
Schrodinger wave equation soln. for logarithmic pot. 80−32065
Schwinger theory, vacuum struct. generators in Lowenstein-Swieca gauge 79−6259
screened confinement force and e^+e^- annihilation 77−22692
semi-classical models for gluon jets and leptoproduction based on the massless relativistic string 80−105861
semiclassical model for rotational states of mesons containing massive quarks 79−36038
sine-Gordon type field eqn., two-dimens., solitons, quark confinement 78−74160
singular gauge transformations, monopole vortex line systems, Nielsen Olsen SU(2) Higgs model, Nambu model 78−66034
singularities in parton-hadron wave function needed for confinement 78−41484
six quark s-wave states, props., depend. on number of quark flavours 79−45060
six- and eight-quark models, weak interactions 80−99086
soft gluon resummation formulae for hard parton processes in QCD 80−105842
soft gluons in Drell Yan and deep inelastic processes, large const. terms, asymptotic behaviour 79−6326
solitons in some geometrical field theories 80−27390
space-like fields and non-unitary representations of the Poincare group 79−85238
space-like fields for quark confinement 80−42426
space-time structure of jet hadronization 80−91024
spin depend forces in semiclassical model of confinement 79−67500
spin structure of the quark-confining potential 79−22042
spin-2 gluon-graviton model with baryon-number nonconservation 80−57565
static bags, parton distrib. divergence 79−54313
static confinement conditions, two-dimens. anal., SO_2 mesons 80−13262
static Euclidean SU(2) solns., global struct. 80−4862
static potential energy of a heavy quark and anti-quark 79−13028
static quark forces in classical chromodyanamics, bag models, SU(2) Yang-Mills field 79−2990
statistical fluctuation effects on confinement and vacuum struct. of non-linear σ-models 79−89101
stochastic physics, quark bag model 79−54000
strange particle nonleptonic decay, asymptotic freedom, light quarks and $\Delta T=1/2$ rule 77−38164
string, quark confinement 78−25004
string dynamics in external field 78−8585
string in static field, conservation laws 79−21969
string junction in hadron reactions 77−49907
string operator eqns. of motion in QCD 80−4953
string reconnections and quark matter 80−37226
string representation of gauge fields, chiral field topological props. 80−52410
string representations and hidden symmetries for gauge fields 79−49378
string-junction model and width of baryonium 79−58928
strings in non-Abelian gauge theories 80−52403
strong and gravitational interaction unified theory, hierarchy of universes, large numbers explanation 79−17654
strong-coupling limit of gauge theories, Fermion-Boson decoupling, quark confinement 79−35924
structure functions, bounds for the ratio of anomalous dimensions, scalar gluon theories 80−57595
structure functions for quarks, gluons, hadrons in QCD 79−54318
SU_n colour gauge group, confinement with regular cutoff 77−6083
$SU(2)_L \times SU(2)_R \times U(1)$ Higgs scalars, vacuum expectation values, quark mass ratios 79−49404
$SU(2)_L \times U(1)$ with four flavours, relation between Cabibbo angle and quark masses 80−105872
$SU(2) \times U(1)$, P and T invariance violation suppression, quark mixing angles 79−54278
SU(2) and SO(2) gauge fields in 4-, 5- space-time dimens., confinement, critical dimensionality 79−89064
SU(2) colour Yang-Mills theory, quark source charge screening, confinement 80−22565
SU(2) gauge fields in interaction with static extended quark sources 79−30709
SU(2) symmetry, classical quark confining solns. incorporating colour 79−339
SU(3)-symmetric gauge theory, static gluon pots., appl. to fermions 79−12967
SU(5) electroweak-strong interaction model, broken colour symmetry and gluon mass 80−73650
SU(5) grand unification, nucleon lifetime, bag model calc. 80−52450
SU(5) grand unification, p lifetime and branching ratio, bag model wave-functions 80−78004
SU(6) configuration mixing symmetry breaking, one gluon exchange potentials 79−40739
SU(n), SU(2n) three quark coupling coeffs., diagrammatic group theory 79−331
SU(N) Georgi-Glashow model, electric quark confinement in 2+1 dimens. 79−85263
SU(N) Georgi-Glashow model, electric quark confinement in 3+1 dimens. 79−97583
SU(N) lattice gauge model, weak coupling, monopole condensation and quark confinement 79−75683
SU(N) lattice gauge theories, Wilson and 't Hooft loop behaviour 80−57493
SU(N) scalar QCD in two dimens., and the parton model 78−93856
sufficient condition, model-independent 80−91050
sum rules and moments of dimuon prod., valence quark transverse moments 78−54660
superconformal confinement 77−65134
superfluid quark matter 79−93340
supergravity, fundamental supergeometrodynamic theory of hadron 79−40725
superrenormalisable abelian gauge model with confinement in four dimens. 80−31998
symmetry breaking mechanism in baryons, universal confining forces between quarks 78−50013

quark confinement continued
tensor and vector meson decay, relativistic confined quark model anal. 79−13116
tensor gauge theory with steeply-rising pot., rising Regge trajectories 77−49858
tensor product of the octonionic Hilbert spaces and colour confinement 79−2982
thermal props. of gauge fields and quark liberation 78−24936
thermodynamics of confined quarks 80−95249
thermodynamics of gas of MIT bags 77−79247
Thirring field confined to MIT bag 77−65099
three gluon coupling hadronic signature, η' in gluon jets, QCD vertex 79−75727
time space structure and quark confinement 80−4964
topological approach to high-energy large transverse momentum interactions 79−22057
topological problems in gauge theories, appl. to quark confinement 79−63351
transverse momentum variation with x in MIT bag model 77−74648
trilocal theory, constituent mass, free limit condition and quantisation 79−2984
triple gluon vertex meas. 79−71695
triple gluon vertex meas. from gluon jet spread 80−82946
truthful hadrons, mag. moments, transition moment, using state vectors and quark additivity principles 79−71723
two gluon jets in e^+e^- annihilation, scaling limit ang. distrib. 79−54314
two photon processes, manifestation strength of colour below and above colour threshold 80−381
two-body equal-time wave eqn., quark-antiquark system 78−32992
two-dimens. Thirring and Schwinger models, solitons and confinement *(German)* 77−82665
two-gluon annihilation of quark-antiquark pair *(Russian)* 78−45856
U(N) lattice gauge theories with quarks, string eqns., Dyson-Schwinger eqns. 80−4857
U(N) lattice gauge theory, string representation, Wilson loop amplitudes 80−4856
U(N) lattice Yang-Mills theory, Schwinger-Dyson eqns., string model equivalence 80−4855
unconfined quarks and gluons, quasiconfinement model, confining and nonconfining phase transition 80−86687
unconfined unstable quark, decay characts. 77−30311
unconfined unstable quarks in unified gauge theory 77−13916
unified gauge theory with Abelian massless gluons, binding of fractionally charged quarks 78−29296
unified theory of gravity and strong interactions, quark confinement 77−22681
unified theory of strong and gravitational interactions 79−17662
unified Yang-Mills-Einstein-Higgs gauge theory, hadron struct., quark confinement 79−9275
universal confining pot. and symmetry breaking in baryons. SU(8)⊗0(3) symmetry 79−13051
universal Regge slope α' from the QCD gluon propagator 80−78026
vacuum polarisation, influence on confinement 79−71715
vacuum-polarization-corrected long-distance static quark-antiquark potential 79−49475
valence gluon admixture effect on hadron ground state spectrum *(Russian)* 78−45879
valence gluons, possible evidence from SLAC e-p deep inelastic scaling 77−30310
valence quark-parton transverse momentum distrib. 78−12862
van der Waals forces associated with quark confinement pot. 78−82152
Van der Waals-like forces between hadrons induced by color confining potentials 79−49460
vector and tensor meson decays in relativistic confined quark model 77−79256
vector gluon-quark theories, Nambu-Goldstone realisation proof 80−22563
vector meson leptonic decay and gluon condensate *(Russian)* 78−33060
vector meson spectroscopy in quark confining two-step pot. 77−26492
vortex condensation mechanism for static quark confinement, Abelian gauge theories 80−52457
vortex string picture and large p_T reactions 79−63415
weak neutral current couplings calc. of u and d quarks, ν interaction input data 78−54603
Werle type confining models, soliton-soliton interactions 79−85272
Wilson loop expectation value, area low and loop wave eqn., quark confinement 80−47185
Yang-Mills fields, quark confinement and Gribov ambiguities in Coulomb gauge 78−62297
Yang-Mills gauge theory, classical soln. in colour meson model 78−45780
Yang-Mills instability, colour-screening 77−45951
Yang-Mills instanton gas, bag-to-vacuum phase transition, mean field approx. 80−9097
Yang-Mills lattice gauge theories, comparison with gauge groups SU(2) and Z_2 80−31966
Yang-Mills quark prod. processes, mass singularities 77−26459
Yang-Mills static Euclidean anti-self-dual SU(2) eqns., small deformation of Prasad-Sommerfield soln. 79−71633
Yang-Mills theories, quantum dual string wave functional 79−21921
Yang-Mills theory, covariant canonical formalism, quark confinement, absence of localised coloured/charged physical states 80−57573
Yang-Mills theory, equations of motion finite range classical solns., confinement 80−57474
Yang-Mills theory, infrared struct., perturbative study 77−38089
Yang-Mills theory, quark confinement and observables in covariant canonical formalism 79−6322
Yang-Mills theory, saturated Euclidean vacuum functional, instanton distrib. 79−22029
Yang-Mills theory, vortex condensation 79−6272
Z(N) topological excitations in Yang-Mills theories: duality and confinement 79−12938
Zweig suppressed decay of heavy 1^{--} vector mesons, two gluon exchange 78−54616
$\chi(3.45)$, radiative M1 transitions with charmonium model 79−13132
$\chi_J \rightarrow \gamma\psi$, charmonium states radiative and hadronic widths, gluon spin 80−4998
d, gluon distrib. from elastic dd scatt. 80−82939
D_s mesons, charmed, hadronic decay, MIT bag model calcs. 78−82207
D^0, D^+ decays, gluon enhancements in charmed-meson decays 80−95265
$D^0 \rightarrow K^- p^+$ signals, evidence for$(\bar{c}s)_R$ current 79−71745
quark confinement continued
$D^0 \rightarrow K^0\pi^0$, branching ratio from final state soft gluon exchange 80−52498
$D^0 \rightarrow K^*\pi^-$ signals, evidence for$(\bar{c}s)_R$ current 79−71745
$D^\pm$, weak decay constant from bag model extension 80−62967
$\Delta(1232)$ decay width using little bag dynamics and axial vector current 79−75771
$\Delta_{D35}(1925)$ baryonic degrees of freedom, nonrelativistic, harmonic oscillator quark model mass formula 80−91066
e+e annihilation, sum rules for Υ-family formation, QCD anal. *(Russian)* 79−54347
ed elastic scatt., EM form factors, relativistic harmonic oscillator model 79−54327
e^+e^-, annihilation, polarised gluon bremsstrahlung as QCD test 80−32077
e^+e^-, vector and axial vector gluon prod., as signatures for axial chromodynamics 79−40729
e^+e^-, weak corrections to three-jet angular distributions 80−22629
$e^+e^- \rightarrow$ jets, transversely polarised annihilation, charged gluon jets, Pati-Salam model 80−86739
■ $e^+e^- \rightarrow$3 jets, integer charge quark model, gluon jets 80−91101
$e^+e^- \rightarrow$3 jets, three gluon coupling in perturbative QCD 80−105913
e^+e^- annihilation, charge current asymmetry as QCD test, neutral gluons 80−57616
e^+e^- annihilation, gg and qg coupling equality on resonance, QCD calcs., expt. tests 80−389
e^+e^- annihilation, gluon jets and heavy quarkonium prod., QCD test, ψ prod. 80−42479
e^+e^- annihilation, gluon jets, multiplicity and ang. distribs. asymmetries 80−91105
e^+e^- annihilation, hadronic final state charge current asymmetry, QCD test, neutral gluons 80−37289
e^+e^- annihilation, hard gluon bremsstrahlung from heavy quarks, jet cross section 80−32078
e^+e^- annihilation, jet struct., test of QCD and quark-confining string 78−33040
e^+e^- annihilation, meas. of gluon spin 79−30701
e^+e^- annihilation, meson pair prod., multichannel formalism 77−22747
e^+e^- annihilation, QCD and jet acollinearity, quark-gluon coupling 80−105914
e^+e^- annihilation, two and three gluonic jet prod., perturbation theory *(Russian)* 80−52525
e^+e^- annihilation, vector or scalar gluon jets 80−27474
e^+e^- annihilation at high energies and search for the t-quark continuum contribution 80−102012
$e^+e^- \rightarrow$charmed hadrons, quark mass effect on fragmentation functions 80−91098
$e^+e^- \rightarrow e^+e^-$+2 gluon jets from $\gamma\gamma$ interactions cross section, gluon role in QCD 80−4976
■ $e^+e^- \rightarrow e^+e^-$gg, gluon jet polarisation in photon-photon scatt., QCD test 80−52550
$e^+e^- \rightarrow$gluon and quark jets 80−91100
$e^+e^- \rightarrow \gamma^* \rightarrow$hadrons, hadron calorimetric meas., QCD predictions, gluon emission 80−91102
$e^+e^- \rightarrow \gamma \rightarrow q\bar{q}g$, charge distrib., Sterman-Weinberg criterion, QCD test 79−71694
$e^+e^- \rightarrow$hX, high energy predictions from perturbative QCD 80−42417
$e^+e^- \rightarrow$hadrons, 12, 30 GeV, jets, quark fragmentation and coupling constant, QCD comparison 80−105915
$e^+e^- \rightarrow$hadrons, 13-31.6 GeV, gluon bremsstrahlung evidence, seagull effect, one sided jet broadening 80−430
$e^+e^- \rightarrow$hadrons, energy correls. in QCD, asymptotically free perturbation theory 79−63497
$e^+e^- \rightarrow$hadrons, planar events, gluon jet identification 80−47317
$e^+e^- \rightarrow$multihadrons, planar three jet events, gluon bremsstrahlung, strong coupling constant 80−57617
$e^+e^- \rightarrow Q\bar{Q}$, heavy quark study approach 80−105859
$e^+e^- \rightarrow q\bar{q}$ chromoelectric-flux-tube model of particle production 79−89176
$e^+e^- \rightarrow q\bar{q}g$, cross sections and ang. distrib. 80−102061
$e^+e^- \rightarrow q\bar{q}g$, energy-momentum distrib. 79−71696
$e^+e^- \rightarrow q\bar{q}g$, gluon bremsstrahlung, neutral current and beam polarisation effects 80−99106
$e^+e^- \rightarrow q\bar{q}q \rightarrow$jets, ang. energy flow in perturbative QCD 79−49455
$e^+e^- \rightarrow$three jets, acoplanar angle relative to beam polarisation, vector/scalar gluons 80−63005
$e^+e^- \rightarrow \Upsilon$, suggested search for gluon hadronic states in collinear gluon jets 78−89663
eN, deep inelastic scatt., quark model, field-theoretic, quark indistinguishability, nucleon structure function 80−62993
ep, deep inelastic scatt., σ_L/σ_T ratio from quark model 80−82979
ep, sea quark and gluon momentum distribs., perturbative vs. asymptotic freedom corrections 79−17736
η Dalitz decays, excitable colour gluons 78−58181
η_c associated with gluon, hadronic prod. 80−105846
η', QCD sum rules for mass, possible pseudoscalar gluonium, instanton effects 80−388
$F^+ \rightarrow \tau^+\nu$, gluon enhancements in charmed-meson decays 80−95265
$F^\pm$, weak decay constant from bag model extension 80−62967
$\gamma^*N \rightarrow \psi N$, gluon momentum, spin, parity and coupling 80−42395
γp, heavy quark particle photoprod., QCD model, vector dominance implications 80−86730
J/ψ, inclusive production cross sections, correlating quark rearrangement model 79−54320
J/ψ, radiative M1 transitions with charmonium model 79−13132
J/ψ decay, gluon source, search for scalar gluonium, QCD 80−47296
$K \rightarrow 3\pi$, relativistic quark model anal. 80−99096
K charge radius, coloured quark field theory 80−62945
$K \rightarrow \pi e(\mu)\gamma$, quark mass ratios 80−105884
$K_S^0 \rightarrow \pi^0\pi^0$, MIT bag model 78−33066
$K^0 \leftrightarrows \bar{K}^0$ transition amplitude, and $K_L K_S$ mass difference, in MIT bag model 79−63450
Λ^0 octet baryon mag. moment, MIT bag model 80−47290
Λ_c^+ lifetime, semileptonic branching fractions, nonspectator quark interactions 80−37260
μN deep inelastic scattering, gluon jets 80−105862
$\mu N \rightarrow \mu X$, broken colour gauge theory of integer charge quarks 80−13313
n, EM form factors from MIT bag model 79−93419
N,N* resonances, radiative decays, static quark bag model *(Russian)* 80−47299

quark confinement continued
nd→pπd, interference phenomena in coherent production, nucleon diffractive amps., helicity-flip 80−47329
NN, 12 GeV, spin depend., quark exchange evidence 80−102074
NN interaction, quark MIT bag model anal. 79−80806
NN large angle elastic scatt., spin depend., quark confinement short distance behaviour 79−97598
NN short range interaction, six quark symmetry props., nucleon colour mag. attraction *(Russian)* 80−42411
NNπ amplitudes, parity violating, QCD calc. in Weinberg-Salam model and SU(4) flavour symmetry breaking 79−67520
NNρ couplings, parity-violating, QCD and MIT bag model, $1/2^-$ resonance contribs., $SU(6)_w$ symmetry 80−57540
ν deep inelastic scatt., four flavour quark model, asymptotic freedom 78−45905
νN, charm and strangeness production, role of gluons 79−13104
νN, quark properties and existance studies, book contrib. 80−42441
νN, two gluon mechanisms, quarkonia, glueballs and Higgs scalars 80−78077
$\nu N \rightarrow \nu\psi X$, neutral current ψ prod., Z^0-gluon fusion model 80−78015
$\bar{\nu}p \rightarrow$charm quarks 80−102040
Ω^- nonleptonic decay branching ratios from Weinberg-Salam and MIT bag models 80−37261
p, degenerate parton gas model, quark-lepton identification 80−68416
P, EM form factors from MIT bag model 79−93419
p, gluon distrib. from elastic pp scatt. 80−82939
p charge form factors, linear pot. model with gluon exchange 78−45873
p electroprod. struct. function and constituent-particle scatt. 78−45931
$p+N \rightarrow \mu^+\mu^-X$, 400 GeV, charged gluon effects, broken colour gauge model study 79−49473
$pd \rightarrow p\pi^+\pi^-d$, interference phenomena in coherent production, nucleon diffractive amps., helicity-flip 80−47329
pp, 27 GeV/c, resonant prod. of high $p_\perp$ back-to-back gluon jets 79−93470
pp, D, B, K prod., QCD model for heavy flavour prod., two gluon annihilation 80−86744
$\bar{p}p$, pp, 540 GeV, Υ and ψ transverse momenta from QCD 2→3 processes, gluon subprocesses 80−52546
pp elastic, differential and total cross sections, proton model, gluon-gluon annihilation 80−91114
$\bar{p}p$ gluon jet prod. 79−63554
$pp \rightarrow l^+l^-X$, parton density scale violations and quark-gluon correction to Drell Yan formalism 79−63560
pp large p_T reactions, jets, dual-string approach 80−32136
$pp \rightarrow \mu^+\mu^-X$, gluon corrections to Drell-Yan model 79−36037
$pp \rightarrow pp\bar{p}_{forward}$+anything, observation of qq with qqq̄ bound states, pseudobaryons and baryonium 78−58219
$pp \rightarrow \rho^0(\phi)(J/\psi)X$, OZI rule violation 79−58929
π charge radius, coloured quark field theory 80−62945
π struct., gauge model, confinement scheme 78−45841
πN coupling const. determ. in MIT bag model 78−78149
$\pi^-N \rightarrow \psi X$, 225 GeV, bottom meson pair production limit 80−73750
$\pi^-p \rightarrow \pi^+\pi^-n$, 1.33-1.38 GeV, isobar prod. near threshold, isobar model partial wave anal., bag model 79−93456
ψ, OZI rule breaking in decays 79−97597
ψ, radiative decay, gluonic bound state O^- width 80−37272
ψ associated with gluon, hadronic prod. 80−105846
$\psi \rightarrow \eta(\eta')\gamma$, Ward identity anal., η,η' quark-glue struct. 80−42449
ψ hadronic production of heavy quark bound states 79−63435
ψ meson, phenomenology and quark confinement 78−29308
ψ meson spectroscopy, charmonium model, quark-confining string 78−8625
ψ production, gluon-gluon fusion model, gluon distrib. *x*-depend. 80−62922
ψ′, radiative M1 transitions with charmonium model 79−13132
$\psi' \rightarrow \psi+\eta$, two gluon mechanism, Υ dynamics test 78−89665
$\psi' \rightarrow \psi\eta$, Ward identity anal., η,η' quark-glue struct. 80−42449
$qg \rightarrow 1^{++}$, high P_T photon polarisation as QCD test 80−4934
QQ̄, bound system, dynamics 80−73676
qq̄, eikonal speculations on infrared confinement 79−36027
qq̄, fine-hyperfine splittings and Lorentz structure of confining potential with vacuum polarisation corrections 80−78041
QQ̄, potential energy, gluon distrib. 80−62929
qq̄ binary confined systems, elastic scatt. amplitudes 79−97576
QQ̄ mass, approx. scheme is QCD 80−42398
qq non Abelian gluon interactions, long distance behaviour of chromostatic potential 79−17676
qq̄ pair energy modification in Wilson loop formalism 80−18122
$q\bar{q}(q^2\bar{q}^2)$ mesons, mass formula 80−62958
qq̄ spectra, heavy systems, equaltime relativistic wave eqn. with confining potential 80−77977
QQ̄ systems, two gluon decay widths, short range quark gluon effective vertex 80−86669
$Q^2\bar{Q}^2$ resonances in baryon-antibaryon systems, NN̄ scattering and $N\bar{N} \rightarrow \pi^+\pi^-$ 78−58171
qqq confinement, by infrared singularities 79−36028
qqq̄q̄, suppressed decays, strings, bags, baryonium 78−21385
Σ^+ octet baryon mag. moment, MIT bag model 80−47290
$\Sigma^+ \rightarrow p\gamma$, $1/2^-$ resonance poles to parity-violating amplitude, two-quark weak transitions 80−78062
t-quark, properties and signatures 80−37223
t-quarkonium decay props. *(Russian)* 80−105856
θ vector particles, calibration interaction macroscopic confinement radius *(Russian)* 80−47257
Υ, hadron production of heavy quark bound states 79−63435
Υ, heavy quark bound states in potential model with relativistic corrections 80−37247
Υ, production and decay in quark fusion model 80−102018
Υ(9.46) orthoquarkonium decay, jet profiles, three gluon structure 80−73698
Υ(9.46)→hadrons, gluon spin and colour, QCD nontrivial test 80−82971
Υ(9.4)→charmonium, quarkonium prod. via one gluon mechanism 80−95263
$\Upsilon \rightarrow e^+e^-$, harmonic oscillator model, QCD gluon-bottom quark coupling 79−3016
Υ production, photon-gluon fusion model, gluon distrib. *x*-depend. 80−62922
Υ spectroscopy, asymptotic freedom 78−45865
$\Upsilon' \rightarrow \Upsilon+\eta$, two gluon mechanism, Υ dynamics test 78−89665
$V \rightarrow p\mu^+\mu^-$, vector meson decay EM form factors in bag model *(Russian)* 80−62982

quark confinement continued
X(2.83), radiative M1 transitions with charmonium model 79−13132
Ξ^0 octet baryon mag. moment, MIT bag model 80−47290
Z^0, prod. in e^+e^- collisions, important landmark 79−97567
η_c(2830), OZI rule breaking in decays 79−97597
^2H nuclei, spin-1 particle, eight-dimensional spin space determ. by NMR 80−60428

quark models
see also colour model
0^{++} scalar mesons radiative decays 77−13963
$0^-1/2^+ \rightarrow J^P 3/2^+$, universal impact parameter hypothesis and quark model 77−49914
0^- meson, EM form factor in straton model *(Chinese)* 80−22616
1/N dual unitarisation convergence due to SU(4) breaking, charm and strangeness implications 79−6321
$3/2^+$ charmed baryons, mass splitting by weight diagrams, parallelogram law sum rules 77−49915
27-plet mesons, mass sum rules using SU_4 dynamical-group scheme 77−26505
$^3P_0$ generalised model, reln. to Melosh transform. 78−12885
ΔS=0 weak hadron neutral current, quark parton model, νN and e^+e^- interactions 78−12859
ΔS=1 nonleptonic weak decays, ΔI=1/2 rule, quark models and current algebra 80−47282
η_q prod. cross section ratio in quark parton model *(Korean)* 80−27466
Λ magnetic moments, rel. to quark mass and hadron mass 79−13050
ν_μN, charged heavy muonic lepton production, explanation of Kolar events 79−9364
$(\phi^4)_4$ theory, semiclassical infrared emission processes 78−29257
ϕ^4 (rubber bag) model, hadron mass spectra and J/ψ family *(Chinese)* 79−80812
φ-ω mixing and violation of Okubo-Zweig-Iizuka rule 77−87948
ψ production and decay, book contrib. review 78−82208
additive diquark spectator model for meson-baryon quasi-two-body reactions, addendum 79−89114
additive diquark spectator model test in meson-baryon quasi-two-body reactions 79−40742
additive eikonal quark model anal. of various hadron-hadron cross-sections 77−26493
additive quark model and multiparticle production off emulsion nuclei at 50 GeV 80−68491
additive quark model in quasi-two-body hadronic reactions, Δ and vector meson prods. relation 78−41494
additive quark model with six flavours 80−27455
additive quark parton model, hadronic fragmentation distribs. 78−8711
Adler-Weisberger relation and quark model 78−45849
algebraic approach to hadrons without seeing quarks 80−9143
antiquark sea role in determ. of $\sin^2\theta_W$ from total neutron cross sections *(Russian)* 80−4910
appl. of quark model to hadron spectroscopy and high-energy phenomena 78−82162
asymptotic freedom, quark-parton model 77−82675
asymptotic freedom and charmonium 78−54534
asymptotic freedom without non-Abelian gauge theories, renormalisation group eqns. 77−30314
asymptotic SU_3 and a new mass constraint for the ω, φ, ψ and Υ mesons 79−36001
asymptotically free gauge theories, higher twist effects, four quark operator anomalous dimensions 80−105848
asymptotically free gauge theories, scaling violations in leptoproduction 78−4769
asymptotically free theories of deep inelastic muon, and electron scatt. 78−21430
axes and scalar measures of two-jet and three-jet events 79−45069
axial vector mesons decoupling from local currents 77−87938
axial vector multiplets, mass spectrum, mixing angles, pseudoscalar mesons, decay consts. 77−13892
axion, implied by U(1) symm. 78−33037
axions, evidence against from ν reactor expts. 78−45904
b-quarks, possible obs. in $\bar{\nu}$ interactions, nonleptonic decays and vector Ψ_h hadronic prod. 78−8613
B-S equation, approx. soln. in quark-gluon model 77−87940
bag model, connection with optical theorem violation 77−26504
bag model, D meson EM mass differences calcs. 77−6124
bag model, description of nucleons and isobars 79−49452
bag model, lightest state mass determ. 80−42414
bag model, meson and massive photon production 80−105850
bag model, primordial transverse momentum, σ_L/σ_T ratio 80−82938
bag model, spectroscopic applications, baryon excitations 77−22699
bag model, spin-depend. struct. functions in deep inelastic scatt. 78−8589
bag model and QCD, quark-antiquark sea 77−71481
bag model of confinement, analogy to bubbles in liquid 80−22587
bag model of hadrons, review 79−75736
bag model of hyperon nonleptonic decays, octet enhancement 77−10249
bag model $Q^4\bar{Q}$ states, meson-nucleon low-energy S-wave scatt., P-matrix formalism 80−13271
bag model solns. in 3+1 dimensions, proton mag. moment, bag mass 77−10214
bag model with finite potential barrier, S-wave mass spectra of QQ̄ and leptonic widths 80−47242
bagged hadronic matter 80−73664
baryon bound state in two-dimens. SU(N) gauge theory 77−13918
baryon classification in straton model *(Chinese)* 79−22075
baryon electric dipole moments in CP noninvariant Kobayashi-Maskawa theory *(Russian)* 80−105897
baryon EM mass differences in charmed quark model 77−82741
baryon magnetic moment, incorrect value from static compound quark models 80−9169
baryon magnetic moments, ground-state, SU(6) symmetry 80−78064
baryon magnetic moments, implications for quark model 80−13290
baryon mass relations in internal SU(6) symmetry 80−82962
baryon mass spectrum anal. using quark shell model 78−4833
baryon mass splitting by the 'strong hyperfine interaction and SU(3) breaking 78−82184
baryon model based on Dirac eqn. with confining pots., independent quark model 78−425
baryon nonleptonic decay pseudo-connected line diagrams 78−45918
baryon nonleptonic weak decay, SU(4)-20″-dominance 78−45917
baryon pionic transitions, MIT bag model anal. 78−82155

quark models continued
baryon pionic transitions in MIT bag model using PCAC hypothesis 80−37228
baryon reson. photocouplings, single quark transition anal. 77−82751
baryon resonance decay, π emission, quark model, widths, amplitudes, sum rules 77−57534
baryon resonance decay, l-broken $SU(6)_W$ model equivalence to relativistic harmonic oscillator quark model 78−41546
baryon resonance decay, unified interactions in relativistic quark model 78−41547
baryon resonance photocoupling anal. in relativistic quark model 78−66086
baryon resonance photoexcitation amplitudes, relativistic corrections, harmonic oscillator quark model 77−13935
baryon resonances, EM transitions, multipole moments in single quark transition model 80−62985
baryon resonances, even-parity, harmonic oscill. quark model 77−10224
baryon resonances in gluon perturbed linear potential 77−46023
baryon spectroscopy and photoproduction couplings using new baryon wavefunctions 80−102016
baryon spectrum, second excited level in harmonic oscillator model, experimental situation 80−37233
baryon struct. in quark geometrodynamics, current and meson couplings 79−6320
baryon structure functions, dynamic relationship to baryonium trajectories 79−40763
baryon structure involving the u, d, s quarks 79−63414
baryon SU_3 dynamical model, gravit. bound linear rotator 77−49904
baryon-lepton symmetry, quark mass spectrum 79−54306
baryon-lepton symmetry model, μ-number and flavour nonconserving neutral currents 78−66069
baryon-lepton symmetry model, neutral current test 77−61248
baryonia, decay properties and L=1 state width approx. 79−75773
baryonia mass spectra calc. incl. spin-dependent forces 79−26309
baryonic $(56,1_3^-)$ supermultiplet and new ΔD35(1925) reson. 77−82718
baryonic and electric charge distribs. in multiparticle prod., quark-parton model 77−79285
baryonium, broad resonance states, S(1963), T(2190), U(2350), expt. evidence review 78−89764
baryonium, empirical evidence and theoretical interpretation review 80−42394
baryonium, exotic nuclear state or four quark boson resonance? 79−325
baryonium, geometrical approach 80−91065
baryonium, ground state hyperfine splitting, harmonic oscillator potential anal. 80−68422
baryonium, importance of isospin *(French)* 79−85260
baryonium, mass and selection rule, string model 78−29319
baryonium, molecular model, quark-diquark picture of baryon 80−27462
baryonium, narrow states, mass formula, selection rule, quark model 78−66089
baryonium, nuclear and quark confinement forces 80−68431
baryonium, S-matrix representation 80−399
baryonium, Schwinger partial symmetry, quark flavour EM interaction 79−93335
baryonium interaction, dual amplitudes 78−25022
baryonium interactions, string model, dual amplitudes *(Russian)* 78−54620
baryonium masses in a quark model 80−37241
baryonium model, spectrum of $q\bar{q}q\bar{q}$ hadrons 78−62363
baryonium Regge trajectories exchange in medium and high energy scatt., expt. evidence 78−50022
baryonium spectrum, SU(4) mass formulae, degenerate clustering 79−93393
baryonium spectrum classification based on duality and unitarity 78−45869
baryons, b-quark, magnetic moments, broken SU(5) symmetry 80−95257
baryons, charmed, mag. dipole moments and mag. quarks 79−97573
baryons, five quark models and mag. moments 79−26297
baryons, leptonic decays and mag. moments in nonlocal quark model *(Russian)* 80−86711
baryons, linear string model, flavour symmetry, exchange degeneracy and spin structure 79−89118
baryons, mag. moment calcs. in quark models 80−27505
baryons, quark diagrams 77−87939
baryons, spin $1/2^+$, mag. moment sum rule, in SU_3 for u-, d- and c-quark sector 78−21428
baryons, with scalar raising pot., relativistic model 80−37231
baryons and mesons, parton distribs. consistent with naive quark model and QCD 80−62937
beautyonium bound states, Υ, Υ′, Υ″, dispersion sum rules *(Russian)* 80−13235
Bethe Salpeter model for strong, EM, and weak meson decays effective quark mass 78−70336
Bethe-Salpeter eqn. approx. soln. 77−54080
Bethe-Salpeter formulation for baryon matrix elements in hadronic weak decays 79−386
bi-local field interaction with external field 78−66030
bi-local model, Poincare group and position operator 78−93844
bilocal fields for study of quantum corrections to dynamically broken symmetries 78−16985
bilocal models of hadrons, relative time depend. as gauge freedom 77−74584
bilocal theory, constraints, centre of mass and quantisation 78−89619
Bjorken scaling law violation, mass dependent, quark-quark interactions 80−9160
Bjorken scaling violation, model of quarks with size and excited states 78−74208
Bjorken scaling violation, QCD and models of quarks with substructure 80−105851
Bjorken scaling violation models of quarks with substructure 79−26305
Bjorken scaling violation study of quark substructure 79−17674
bootstrap theory of quarks 79−49451
bootstrap topological approach to quarks and leptons 80−95253
Bose description of fermions 78−89402
Bose quark model, mass spectrum of exotic particles 78−62358
Bose quarks, exciton model, exotic states anal. 78−16983
bottom hadrons, masses and allowed decays, SU(5) quark model 80−62954
bottom mesons, weak decays, strong correction meas. 80−82970
bottomium, potential models, non-relativistic description 80−68426

quark models continued
bound and rebound states, relativistic eikonal approximations 80−27491
bound state wave function explicit normalisation, decay widths calc. 80−18116
bound triquark nucleon model, mag. moment and weak interaction coupling constant ratios 79−67517
bound-state model of charmed meson threshold prod. by virtual photons 77−10269
broken SU(6) parton model, spin depend struct. functions, deep inelastic lepton+nucleon appl. 78−428
broken SU(8) symm., charmed meson pair prod. in e^+e^- annihilation 77−38182
Cabbibo angle and quark mixing 78−74207
Cabibbo angle, CP violation quark masses 78−33016
Cabibbo angle, gauge invariant rearrangement and theory, SU(2) symmetry breakdown 79−22027
Cabibbo angle and quark masses in the Weinberg-Salam model 79−93332
Cabibbo angle calc., $SU(2)\times SU(2)\times U(1)$ gauge theory 78−4776
Cabibbo angle calcs., mass matrices in Weinberg-Salam model 80−86674
Cabibbo angle in six quark $SU(2)_L\times SU(2)_R\times U(1)$ gauge model 79−17683
Cabibbo angle physical interpretation, weak interactions nonleptonic ΔI=1/2 rule, four-quark scheme 77−22679
Cabibbo current and CP violation in a six quark gauge model 78−70329
Cabibbo-suppressed nonleptonic D decays, ΔI=1/2 rule 80−52501
Callan-Gross relation, instanton violation, nonperturbation correction asymptotic behaviour 80−27409
Cartan conformal semi-spinor quark representation 79−97572
cascade model, comparison with hadron prod. in quark fragmentation region 79−22065
cascade model, decay distrib. functions 79−36033
cascade model, inclusive meson and baryon spectra in pp, πp, e^+e^- 77−50025
cascade model, meson-nucleon collisions, meson spectra in meson fragmentation region 77−67689
cascade models, bootstrap eqn. and diffusion eqn. 78−29317
cascade models, transverse momentum depend. of quark fragmentation functions 79−45068
causal model of quark fragmentation, charge retention in hadronic jet 78−29313
centauro, Geminion and multipion events, quark matter hadronisation, prod. cross sections 80−47331
Centauro event, high density nuclear matter, and quark model interpretation 79−63565
CERN bag model, effects of SU(3) breaking 77−38121
Chao-Yang statistics, particle ratios and quarks 80−27486
charge, fractional and integral models, effect of colour oscillations 79−75725
charge conjugation, signature, twists, of quark diagrams 78−29310
charge screening, extended model of hadrons 78−37179
charge transfer in multiparticle production processes and the quark cluster model 78−93858
charge transfer in the uncorrelated cluster production model *(Russian)* 79−40755
charm classification in SU(4), quark-lepton analogy *(Norwegian)* 77−34137
charm particle prod. by photon-gluon fusion 78−45923
charm particle spectroscopy 80−73680
charm particles, inclusive production cross sections, correlating quark rearrangement model 79−54320
charm particles, review 78−17035
charm particles photoproduction, asymptotically free field theories 77−13934
charm quark mass in asymptotically free gradient theory *(Russian)* 77−30333
charm quark prod., scaling violation as threshold effect 78−66088
charm scheme of subhadronic constituents, weak decay processes 78−25012
charm-strange spin in SU_3 symm. for c-, s-, d-quark sector 78−37172
charmed, baryon spectrum due to chromomagnetic and electromagnetic hyperfine interaction 79−13123
charmed axial vector meson prod. in e^+e^- annihilation, nonrelativistic quark model 78−25055
charmed baryon, EM mass differences in charmed-quark model 77−71515
charmed baryon and antibaryon bound states 78−8608
charmed baryon decays, nonleptonic, parity-violating, single-quark and two-quark transitions 80−68453
charmed baryon diffractive prod. at ISR energies 77−41818
charmed baryon prod. by neutrinos, quark-model calc. 78−45909
charmed baryon reson. prod. cross-sections in νN reactions 77−26513
charmed baryons, dipole mag. moments, new U_3 scheme using u, d, c quarks 78−58165
charmed baryons, dynamical group selection, SU(1.4) 78−37178
charmed baryons, elec. and mag. quarks rel. to Dirac mag. monopoles 80−402
charmed baryons, mag. moments in quark model 77−30332
charmed baryons, magnetic moments, broken SU_3 subsymmetries of SU_4 79−63382
charmed baryons, magnetic moments by SU_3 and SU_4 symmetry 78−82209
charmed baryons, static and transition magnetic moments in quark model 77−46050
charmed baryons, SU(4) symmetric 20-plet representation, mass, EM splitting 78−54615
charmed baryons, weak decays, quark model framework 80−62976
charmed hadron masses, from effective quark masses, sum rules 80−4965
charmed hadrons, mag. moments, additive-quark-model 77−82707
charmed meson, non-leptonic decay in SU(3) Bose quark model 79−85278
charmed meson decays and right handed currents 78−8662
charmed meson mass, effect of u and d quark differences calc. 77−46019
charmed meson mass spectrum, quark model calc. 77−26491
charmed meson mass splitting in universal confining potential model 80−4967
charmed meson masses, effects of fifth flavour 78−66098
charmed meson prod. in e^+e^- annihilation 78−8680

quark models continued
charmed meson prod. in quark exchange model 78−8600
charmed meson spectra from effective quark-quark interaction, D^0 mass 79−36018
charmed mesons, dynamic SU(4,1) symmetry, mass spectra, anal. *(Russian)* 78−70350
charmed mesons, review of three years e^+e^- research at SPEAR 79−63490
charmed particle-antiparticle system, bound states near charm threshold 78−45857
charmed particles lifetime, semileptonic decay rate calc. 79−9366
charmed particles weak decays, generalised charge symm. 78−37184
charmed quark d-wave $c\bar{c}$ in e^+e^- charm prod. 77−22749
charmed quark fragmentation functions in a Monte Carlo quark recombination model 79−97570
charmed-meson decay, massive quark model 78−33067
charmed-strange exotic mesons, quark model 77−87946
charmonium, $^1P_1$ state, mass, branching ratios, decay rates 78−62370
charmonium, potential models, non-relativistic description 80−68426
charmonium, Schwinger partial symmetry, quark flavour EM interaction 79−93335
charmonium decay, effective strong coupling constant for timelike Q^2 80−99091
charmonium electromagnetic decay, relativistic eval. 80−68459
charmonium hyperfine quadrupole moment, orbital mixtures, quarkonium system phenomenology in potential models 79−49496
charmonium level struct., superheavy quarks, bound state spectroscopy 78−8614
charmonium mass spectrum using oscillator pot., Υ and Υ' masses 79−97595
charmonium model, tensor force affects on ψ' and χ 77−87943
charmonium model anal. 77−71490
charmonium model and the ψ and Υ families 80−47253
charmonium model calc. of $e^+e^-\rightarrow\psi\rightarrow 2\gamma(3\gamma)$ 77−30387
charmonium model of ψ hadronic decays, soft pion theorems 77−6117
charmonium models, energy perturbation series from Schrodinger eqn. 79−6005
charmonium narrow states, hadronic and EM decays 78−70343
charmonium photoprod., ψ_c, η_c ang. distribs., non-Abelian gauge gluon exchange 77−57546
charmonium psion states, confining pots. and inverse scatt. problem, Υ mass 80−4946
charmonium quark-antiquark pots., flavour independ., γ, γ', ψ and ψ' appls. 80−47254
charmonium resonances above open charm threshold, nonrelativistic quark model 80−78039
charmonium singlet state, possible resolution 78−74225
charmonium spectroscopy, explicit soln. of wave eqn. for arbitrary power pots. 80−403
charmonium spin struct. and quark gluon effective interaction 77−13922
charmonium state decay, nonrelativistic and relativistic theory 78−58221
charmonium states, multimesonic decays, statistical quark model 78−82171
charmonium states with small hyperfine splitting, coupling constants 79−97599
chiral invariance for asymptotic momenta, elastic scatt. of hadrons, helicity amplitudes 78−4800
chiral SU(4)⊗SU(4) symmetry breaking parameter, meson mass 78−12838
chiral symmetry breaking, connection with quark model, unification of baryon and meson constraints 77−65116
chiral symmetry breaking, current and constituent quarks 79−13033
chiral symmetry breaking, effect of distinction between current and constituent quarks 77−61210
chiral symmetry spontaneous breaking, using vacuum stability condition 79−35986
Chou-Yang model and s-channel helicity conservation 79−63449
classical solutions of quark confinement model 79−13084
classification of new particles, scheme with colour-antisextet quarks 77−10225
closed string as source of Yang-Mills field, gluon gauge field vortex 78−41413
cluster concept in multiple hadron prod. 78−66177
cluster formation in multiparticle prod. processes 77−13931
clustering aspects of nuclear struct. and nuclear forces, review 79−80887
coherent state model for electron-positron annihilation 80−13321
collective reson. in hadronic matter, hydrodynamic model 77−71491
coloured, quantum chromodynamics, asymptotic freedom, zero charge, point charges in quantum electrodynamics *(Polish)* 78−45822
composite hadrons, field theoretical model, quark field operators in motion, interaction vertices 79−342
composite hadrons, field theoretical model, quark field operators, Dirac Hamiltonian at rest 79−341
composite heavy quarks, Υ and Υ' structure 79−36020
composite heuristic model of leptons and quarks 79−93354
composite leptons and quarks, anomalous mag. moment, flavour as dynamical quantum number 80−105854
composite leptons and quarks, mag. moment 80−105896
composite models, mag. moments of quarks, leptons and hadrons 80−32081
composite quark and lepton model 80−27473
compound quarks as an explanation for a possible quark mass spectrum 79−17673
conference, lepton-hadron physics, Karlsruhe, Germany (Sep. 1978) 80−73098
conference, quarks and leptons as fundamental particles, Schlamding, Austria, (Feb.-Mar. 1978) 80−17709
conference, trends in physics, York, England (Sep. 1978) 80−31416
conference on few body systems and nuclear forces, Graz, Austria (Aug. 1978) 79−67567
conference on hadron struct. and lepton-hadron interactions, Cargese, France (July 1977) 80−4473
conference on nuclear structure and reactions, clustering aspects, Winnipeg, Canada (June 1978) 79−3099
conference on particle physics, Honolulu, Hawaii (Aug. 1977) 79−49485
conformal group as broken symm. for quarks with charm 77−10193
conserved vector current hypothesis, extension to gluons 77−71480
conserved vector current hypothesis for gluons, hadroprod. of quark flavours 77−74617
constituent interchange model, appl. to meson-baryon scatt. and baryon-baryon scatt. 77−255

quark models continued
constituent interchange model of pp high p_T spectra and ang. multiplicity correls. 77−10292
constituent quark model and production of particles from nuclear targets 80−380
constituent quarks in SU(3) and SU(6), current algebra., hadron decays, review, book contrib. 80−47259
constituent rearrangement model and hadron reactions review 79−26294
core valence quark model, vector meson dominance total photoproduction cross section 79−49497
correlating quark rearrangement model, large p_T hadron jets 79−2997
cosmic ray high energy interactions, Centauro event(s), quark hotspot scenario 79−67618
Coulombic $q\bar{q}$ bound states, short range behaviour, quark mass 80−78033
counting rules and determination of quark masses in chiral $SU_4\otimes SU_4$ 79−63437
coupling S^* and ϵ to $\pi\pi$ and $K\bar{K}$ 80−22580
coupling strength of meson-baryon interactions in u-, d- and c-quark sector 78−25011
covariant harmonic oscills., parton model 77−34117
covariant inclusion of quark spin into the dual resonance model *(Russian)* 79−22074
CP noninvariance test in nonleptonic decay of mesons containing one 6-quark 79−71654
CP violation, radiative symm.-breaking, fermion and Higgs boson masses 78−41435
cryptoexotic states of the four-quark system 79−40762
current conservation and quark light-cone model 78−21386
current induced reactions, conf. 77−34106
current quark masses and symmetry-breaking effects 80−4952
current-induced reactions, dual unitarisation 78−74233
DC K^+p, 32 GeV/c, resonance inclusive prod. cross sections, quark model comparison 78−93913
DCI vector meson resonances, $q\bar{q}$ excitation explanation using quark pair creation model 78−70342
decays of charmed pseudoscalar mesons and heavy leptons 77−61281
deep inelastic $F_2^n(x)/F_2^p(x)$ near $x=1$, chirality 77−10258
deep inelastic hadron electroproduction, charge retention, quark-parton and jet models 79−45090
deep inelastic hadronic final states, sum rules, quark parton model 77−87981
deep inelastic lepton-nucleon scattering, quark cascade model, struct. functions 78−25051
deep inelastic leptroproduction, meson bound state contrib. to σ_L/σ_T 80−78029
deep inelastic scatt., hadron secondary average transverse momentum, comparison with e^+e^- annihilation 80−37281
deep inelastic scatt., naive quark model 77−61251
deep inelastic scatt., quark-parton model 77−79270
deep inelastic scatt. test of model, $e^+p\rightarrow e^+\gamma X/e^-p\rightarrow e^-\gamma X$ 77−41846
deep inelastic struct. functions 80−42461
deep-inelastic leptoproduction off nucleons, struct. function model in asymptotically free gauge models 79−40786
deformed shell model for quarks 80−62919
dense quark matter, thermodynamic functions, instanton contrib. 80−52464
dense stellar matter in asymptotically free gauge theories, high density limit 77−53421
density oscillations within hadrons 77−22689
DESY e^+e^- experiments, QED checks, τ and Υ studies 80−18111
deuteron, eight quark model, ang. momentum group anal. 79−89098
deuteron, six-quark state and EM struct., two nucleon bound state model *(Russian)* 79−13031
di-nucleon exotics and quark statistics 79−13071
dibaryon resonances, quark cluster model 79−13081
dibaryonic six-quark states as possible model for deuteron 78−21378
diffractive bumps, gluonic excitation Regge trajectories from bag and dual models 79−2978
diffractive dissociation processes and quark-antiquark jets 80−95246
diffractive dissociation processes enhancements, quark-gluon interpretation 78−45839
diffractive scatt., field theoretic model with quark field operators 79−26318
dihadron production spectra prediction using quark model and Chao-Yang statistics 79−89124
dilepton production in $\nu(\bar{\nu})$ reactions, bottom quark excitation contrib. 80−42439
dilepton production in hadronic collisions, review 79−49547
dimensional-counting model of elastic form factors at large momentum transfer 77−18235
dimuon continuum origin and space-time evolution of hadron collisions 77−88015
dimuon enhancement at 9.5 GeV, vector meson family with hidden 'beauty' *(Russian)* 78−33030
dimuon events with identical sign, signal of creation of heavy leptons in neutrino expts. *(Russian)* 77−82729
dipole ghost gauge theory as gluon model, confinement 78−66079
diquark and quark jet fragmentation model, meson and baryon production 79−2979
diquark clustering in baryon spectrum, $(56,1^-)$ and $(70,0^+)$ multiplets 78−41503
diquark constituents of baryons and baryonium 79−93383
diquark contribs. to scaling violation and deep inelastic σ_L/σ_T, structure functions, QCD 80−22573
diquark jets in leptoprod. and large p_T reactions, fragmentation functions 78−82149
diquark model and baryonium, location of mesons with exotic quantum numbers 79−63436
diquark-antidiquark model, explanation of narrow mesonic states 1.4 to 2.0 GeV region 79−17692
diquark-antidiquark states, mass difference in lattice gauge theory 79−2985
diquarks of 0^+ or 1^+, group theoretical props. 77−22683
disconnected quark diags., forbidden coupling and inhibited decay 77−22686
discrete mass eigenstates and hadron-hadron low energy scatt. 80−42415
discrete symmetries, Cabibbo universality, flavour mixing angles, in gauge model with six quarks 78−62346
distribution function modification to describe scale breaking and anomalies in deep inelastic scatt. 77−57543

quark models continued
distribution of masses of leptons and hadrons 80−99093
division of matter, confinement of quarks and gluons *(Polish)* 80−68417
double-beta decay, electron-neutrino pair emission via Δ(1232) resonance 78−54722
Drell ratio and the existence of a second heavy lepton 79−13048
Drell-Yan annihilation, threshold effects and quark masses 77−54076
Drell-Yan annihilation processes, transverse momentum distribs., gauge theory predictions 79−97585
Drell-Yan contrib. to lepton pair prod., incident hadron qq̄ correlation function 78−89668
Drell-Yan model, hadroprod. of muon pairs 78−45872
Drell-Yan processes, A-depend. of valence and sea quark contribs. 80−86684
Drell-Yan processes, nonleading qq̄ and qg contribs. 79−85269
Drell-Yan scaling, absorptive corrections, for initial and final hadronic state interaction 80−4950
dual models of weak interactions of leptons and quarks 78−66070
dual quark pattern for multiplicities, inclusive distribs., in hadron or lepton induced reactions, quark jet universality 78−41476
dual unitary approach of associated strange and charm prod. 77−41824
duality, diagram topological expansions incorporating baryons and mesons 77−57505
duality between resonances and free quark-antiquark pairs 79−63448
duality diagram struct. of particle prod. 77−22696
dynamic models of confined quarks and subnuclear phenomena 77−67614
dynamical generation of effective degrees of freedom, flavours 79−22026
dynamical Higgs mechanism, weak $\Delta I = 1/2$ rule, sum rules, heavy quarks and leptons 80−27442
dynamical model, spectra and decays of radial excitations 78−93840
dynamical theory of quark confinement and hadron spectrum 77−82701
E_6 model of unified interactions, asymptotically free, mass relations and interactions 80−73642
E based vector-like unified theory, group theoretical anal. of symm. breaking 77−87929
Eastern mystical philosophy, quantum mechanics and the bootstrap-quark controversy 79−84883
education, group theory of covariant harmonic oscillators, interacting quarks 78−61970
education, S-matrix theory, quark as redundant concept, order concept, review 79−25786
effective gluon model description of inclusive meson prod. in $\pi^{\pm}$p and pp collisions 78−8717
effective strong interaction Lagrangian 77−46018
eight quark model, CP violation, heavy quark degeneracy, explanation of $K_L \to 2\pi$ 77−26490
eight quark model, modified left-handed currents, ν reactions and e^+e^- annihilations 78−16982
eight quark model by adding horizontal SU(2) gauge to Weinberg-Salam model 79−71682
eight-flavour model of hadrons based on two quartets, heaviness quantum number 78−82142
eight-lepton and eight-quark unification based on Grassmann algebra 80−105824
Einstein's special relativity and Pauli's exclusion principle, verification within a hadron 78−89655
elastic scattering between binary quark-antiquark system and local field 80−47244
electric dipole moment from CP noninvariant gauge theory, left handed currents *(Russian)* 78−74218
electroproduction, spin-dependent, sum rules, test of relativistic constituent quarks 78−25050
electroproduction and symmetric quark model 77−79272
electrostatic interpretation of light quark empirical parameters in elementary particle geometrical model 78−74203
electroweak and strong interactions without the t quark 80−73640
elementary particle classification and quark model, symmetry breaking gauge theories, unified theories 79−346
elementary particle mass, mag. quark models 79−26312
EM form factor and Zweig rule, anal. props. *(Russian)* 79−9374
EM form factors and integral representation of wave function in straton model *(Chinese)* 77−34124
EM mass differences, one gluon exchange contrib. 79−3024
EM mass differences in MIT bag model calcs., charm particles 77−49965
EM mass splittings in quark model 77−18285
EM mixing of narrow baryon-antibaryon states 77−87979
EM probes of nucleons, photo- and electro-excitation, quark model anal. of nucleon struct. 79−49520
entropy prod. in very early universe 78−32624
even-wave harmonic oscill. theory of baryon decay 78−45853
evolution operator, quark struct. of states, two dimensional massless electrodynamics *(Russian)* 80−73630
exclusion principle for quarks, momentum distrib. in nuclei anal. 77−38236
exotic baryon interpretation of narrow mass enhancement at 1360 MeV, diffr. dissociation 78−12888
exotic meson mass formulae in $SU_{1,3}$ 77−65147
exotic mesons and p-p̄(e^+-e^-) annihilation 78−21393
exotic NN resonances, joined spring model, Bose quark model anal. 79−89120
explosive quark matter, hypothesis for Centauro event 80−22648
extended quark model, large p_T hadron prod. 78−29342
f-quark, five quark models and baryon magnetic moments 79−13020
factorising quark model, elastic scatt. of hadrons at large angles *(Russian)* 77−57497
fast hadrons at low $p_\perp$, parton model, quark recombination, pp scatt. appl. 78−54618
fast mesons as dressed quark fragmentation products, Kuti-Weisskopf model 80−91061
fast particle production on nuclei in quark model *(Russian)* 79−6612
fermion inelastic form factor, gauge theory, quark scatt. *(Russian)* 78−45883
fermions, charge density phase transitions in gauge theories with spontaneous symmetry breaking *(Russian)* 79−2969
fifth quark and $\nu(\bar{\nu})$N dimuon prod. 77−61276
finite spectrum relativistic wave eqn. models of quark and lepton masses 78−74130

quark models continued
five quark model, b-flavour prod. by flavour changing neutral currents 79−75720
five quark model, b-quark prod. by flavour changing neutral currents 79−45073
five quark SU(2)×U(1) gauge theory weak current model with $\Delta C \neq 0$ neutral current 77−54069
five-quark model, spin-spin coupling 78−45876
fixed sphere MIT bag model, b-quark mass, zero-point energy, gs b-flavoured hadron masses 79−63429
flavor unification, τ decay, and b decay within the six-quark-six-lepton Weinberg-Salam model 79−35990
flavor-changing effective neutral-current couplings in the Weinberg-Salam model 80−86649
flavour, crude numerical estimate in SU(2)×U(1), SU(3)×U(1), SU(2)×SU(2)×U(1) models 79−13059
flavour, unified theory with SU(5) subgroup 79−89102
flavour and colour quark groups, unitary symmetry links 80−9151
flavour and spin effects in the quark sea 79−80794
flavour changing neutral currents with b quarks and/or τ leptons 80−73656
flavour changing self energies, contrib. to $\Delta S = 1$ hadronic weak decays 79−71713
flavour conservation, natural, in neutral weak currents, symm. $SU_2 \times U_1 \times U_{1'}$ model 78−12858
flavour content of quark sea 77−61252
flavour independence of forces between quarks, ψ and Υ spectra 80−22569
flavour number determination using Higgs scalar particle 80−13288
flavour quantum numbers, dynamical origin 79−17678
flavour symmetry breaking and isovector parity-violating potentials 79−80780
flavour transfer in quark and gluon exchange, Pomeron models 77−49917
flux quantization model, e:μ mass ratio, EM coupling const. 77−79240
forbidden ghost states in non-Abelian gauge theories 79−2929
form factor, asymptotic behaviour 78−89660
form factors, conformal invariance breaking and quark counting rule 77−30381
form factors of hadrons 78−21429
forward hard scattering in hadron-hadron collisions in the energy region $\sim 10^{14}$ eV 80−86773
four-flavour model and deep inelastic ν and $\bar{\nu}$ data 77−71505
four-quark model, $SU_{2L} \times SU_{2R} \times U_1$ gauge group, Cabibbo angle and quark masses 78−25002
four-quark scheme, $\delta I = 1/2$ rule, existence of K_L^0, K_S^0 77−22688
four-quark static bag model in two dimensions 80−78037
fragmentation distribs., meson, baryon and photon reactions 77−74655
fragmentation function, low transverse momentum hadron fragmentation 80−13261
fragmentation function for charmed quarks from $\mu^+\mu^-$ and μ^-e^+ event data 78−62355
fragmentation functions for pion electroproduction, parton-quark model consistency 77−79254
fragmentation functions in high-p_T deep inelastic processes 77−61295
fragmentation functions in Monte Carlo quark parton model of e^+e^- annihilation 79−80791
fragmentation functions of heavy quarks into hadrons, ν reactions, e^+e^- annihilation appls. 79−3013
fragmentation functions ratios in inclusive electroprod. 77−54079
fragmentation in quark combinatorics, hadron prod. processes *(Russian)* 78−89671
fragmentation products parity-odd correls., longit. polarisation 78−433
free quark search, possible method 79−40749
free quarks 80−13289
free-particle Dirac eqn. generalisation theory with internal coords. 77−65135
gauge Bosons struct., quark-antiquark pair 77−30308
gauge model with heavy lepton, muon number nonconservation 77−61239
gauge models with V+A currents, higher order effects in strangeness changing processes 77−22677
gauge theories, box diagrams with nonvanishing external four-momenta, massive-external-quark 80−22525
gauge theory, dressed quark-gluon vertices, instantaneous approx. 78−78091
gauge theory anal. of integral versus fractional charges 77−18226
gauge weak interaction model with left-handed 8 quarks and 8 leptons 77−18218
gauge-group singlet quark form factor, infrared structure 77−45964
Gelfand pattern, charmed hadrons and magnetic moment 80−398
generalised quark line rule, SU_4 symm. scheme, reaction of hadrons containing charm quarks 78−54614
generalised quark parton model, deep inelastic scatt., Drell Yan process 78−62373
generalised statistics and quark model 77−13690
generalized quark-parton model study of σ_L/σ_T and large k_T 78−29306
geometrodynamics, baryon states 77−61254
Glashow-Iliopoulos-Maiani mechanism, horizontal and vertical quark flavour mixing 79−67512
Glashow-Iliopoulos-Maiani model, charge symmetry violation 77−18194
Glashow-Weinberg theorem, neutral currents 78−8582
glue bag model, unification of bag models *(Chinese)* 79−35998
gluon contrib. to hadronic ψ prod. 78−66084
gluon fragmentation, polarised, in e^+e^-, e−q and hadron scattering 80−82988
gluon fusion model, hadronic charm prod. 78−66081
gluon mass, lower bound in integer-quark-charge model 80−78042
gluon model, approx. soln. of Bethe-Salpeter eqn. 77−41816
gluon model, large $P_\perp$ data anal. 78−8615
gluon properties in high energy hadron reactions 78−66076
gluon-quark dynamics 78−25018
gluonic resonances in hadronic spectrum, scalar mesons, pomerons 78−21394
gluoproduction of heavy quark flavors in hadronic scattering 79−9330
goldstino couplings and neutral currents, mass relation for lepton and quark superpartners 79−75717
grand unified O(10) model, quark mass formulae and number of flavours 79−75730
Gross-Neveu model, mass generation, renormalisation 80−27393

quark models continued
Gross-Neveu model and self-consistent β-function method, fermion mass generation 79−49466
ground-state baryons in a quark model with hyperfine interactions, masses 80−4944
hadron, fragmentation from heavy quark partons 78−8603
hadron+hadron, jet production, large transverse momentum 80−42503
hadron+hadron→meson+X, quark elastic scatt. as high transverse momentum meson source 77−57575
hadron+hadron interactions, Drell-Yan dynamics, lepton pair from $q\bar{q}$ collision, energy scaling breakdown 78−54610
hadron+nucleus interactions, yields of projectile fragments, quark model calcs., A-depend. 78−41499
hadron classification, quark model, SU(4) symmetry 78−12861
hadron collisions, D-meson emission, two-gluon charm form. *(Russian)* 77−71489
hadron collisions, lepton pair production, $q\bar{q}$ annihilation within same hadron, structure function anal. validity 80−57622
hadron decay, ν sources, right hand weak currents and direct neutrinos *(Russian)* 77−82699
hadron decay, relativistic quark model and SU(4) 78−62366
hadron diffractive dissociation in the quark model *(Russian)* 79−2994
hadron distribs. in reactions with very heavy quarks 78−41486
hadron dynamics, consequences of quark theory 77−54078
hadron elastic scatt., high energy, review 77−257
hadron EM interactions, review 80−412
hadron EM mass differences, quark behaviour 79−58941
hadron EM mass differences and struct. 80−27502
hadron geometry and quark coordinates 77−34122
hadron high energy struct. models *(Hungarian)* 80−4924
hadron inclusive prod. cross sections at large P_T A-depend., quark-parton model *(Russian)* 80−86771
hadron interactions, effective radius quantum number depend., quark sum rules *(Russian)* 80−102062
hadron interactions, inclusive processes, multiplicity and scaling, resonance production, additive quark model, SU(6) theory, review 80−63043
hadron interactions, local thermodynamic equilibrium *(Russian)* 80−9155
hadron interactions, neutral heavy lepton detection probability 78−8612
hadron isospin classification, same finite group for mesons and baryons *(Chinese)* 80−62887
hadron lepton model interpretation of particle resonance states 80−4957
hadron low $|t|$ elastic scatt., polarisation effects and forward amp. in quark model *(Russian)* 77−258
hadron mag. moments, colour mag. moments and transition M1-moments, quark mass parameter 79−97596
hadron magnetic dipole transition, quark anomalous mag. moments *(Russian)* 80−82975
hadron matrix elements in relativistic quark model 80−37238
hadron microstructure, de Sitter microuniverse, relativistic Hooke group and nonrelativistic quark model 80−27480
hadron nonlinear string model 77−87901
hadron photoproduction total cross-section, VDM and Lipkin's 'third component' 77−82745
hadron production, hadron- and nucleus-nucleus collisions in quark model 77−67681
hadron production, inclusive, quark fragmentation and triple Regge models, quark decay functions 80−62921
hadron properties from quark models and confinement schemes 80−105864
hadron spectroscopy, quark model explanation 79−30710
hadron spectroscopy, quark models and SU(5) grand unification scheme 80−4958
hadron total cross section, role of string junction 78−89676
hadron total cross sections, semiempirical formulae, three component model with SU(3) components 78−41600
hadron wave functions, one-gluon corrections, hadron EM characteristics, bag model *(Russian)* 79−93380
hadron-hadron collisions, dilepton ang. distribs., QCD and quark model anal. 79−80801
hadron-hadron collisions, fragmentation processes, treatment in quark models 79−58940
hadron-hadron collisions, hard and soft processes in small p_T inclusive reactions 78−41599
hadron-hadron interactions at high energy, generalised hydrodynamical models 79−89131
hadron-hadron large p_T collision, weak interaction effects 78−21462
hadron-hadron low energy scatt., anal. of internal quark-gluon eigenstates, Wigner-Eisenbud formalism 79−63525
hadron-hadron two-body SU(3) quark model for all angles 77−49916
hadron-induced and e^+e^- annihilation, multiplicity ratio 80−105877
hadron-lepton deep inelastic scatt., review, book contrib. 80−47260
hadron-nucleon total cross-section, regularities and systematics 77−38205
hadron-nucleus (nucleon), relativistic secondary multiplicities, constituent quark rescatt. 80−63034
hadron-nucleus collisions, massive muon pair prod., test of Drell Yan model 77−57695
hadron-nucleus collisions, relation between low mass dimuon and meson prods., quark-antiquark interactions 78−41477
hadron-nucleus interaction, quark-parton model *(Russian)* 79−22066
hadron-proton amplitudes, real parts from 3-universality 77−49926
hadronic and electromagnetic widths of mesons in the style schemes, Sp(8) and SO(8) schemes 79−45051
hadronic collisions, jet structure, two-jet events, glueball-Pomeron identity, dual field theory 80−63051
hadronic coupling constants and the nonrelativistic quark model with charmonium potential 80−37207
hadronic cross section strength, nonlinear unitarity eqn., internal symm. restriction 78−33042
hadronic form factors, asymptotic behaviour *(Russian)* 77−61289
hadronic fragmentation processes, valence quarks 80−101982
hadronic interiors, meas. and charge distrib., hadronic diffraction scatt. 80−73817
hadronic large p_T reactions, K^+ and K^- prod. as model test, hard quark scatt. 79−40735
hadronic matter, phase transition of second band, anal. in one-loop theory in renormalisable field theory 80−4930
hadronic matter exponential mass spectrum, incompatibility with weakly interacting quark phase 80−37219

quark models continued
hadronic processes, intermediate and high energy, black/almost black constituent quark anal. *(Russian)* 79−54325
hadronic prod. of large-P_T leptons and large-Q^2 lepton pairs 77−22810
hadronic production of heavy quark bound states, quark fusion, fluon processes, for J/ψ, Υ prod. 79−349
hadronic quantum numbers beyond charm as possible source of neutrino induced trimuons 78−12903
hadronic structure 77−34118
hadronic structure functions at $x\to1$, quark-gluon model *(Russian)* 78−54617
hadronic structure using parton anal. of deep inelastic scattering and rel. processes 79−80803
hadronic total cross sections, model, using covariant harmonic oscillator pot. wave functions 79−26306
hadronic wave eqns. from lattice gauge theory, breathing modes 79−97586
hadrons, parton distribs. calc. 78−421
hadrons and baryonium, geometrical approach 80−91065
hadrons and quarks in high energy collisions, review 79−49482
hadrons of absolute stability, quark mixing and discrete symm. considerations 78−33036
hadrons with charm, beauty and taste, mass sum rules and SU_3 subalgebras of SU_6 80−9152
hamiltonian for the nonrelativistic two-fermion bound state 80−13273
hard scattering models, large transverse particle prod., cross section constraints from opposite side rapidity distribs. 78−29360
hard scattering models comparison for large transverse momentum meson prod. 78−41498
harmonic oscill. covariant model, baryon reson. decay matrix elements 77−61284
harmonic oscillator model, pseudoscalar and vector meson structure wave functions *(Chinese)* 77−34123
heavy b and t quarks, weak decay, lifetimes and branching ratios 79−97588
heavy charged quark system decays, CP noninvariance, six-quark model/QCD anal. 79−80826
heavy lepton model for rare μ and K decay modes 78−45898
heavy meson inclusive semileptonic decays, lifetime estimates, quark-parton model difficulties 80−86704
heavy meson spectroscopy, centrifugal and harmonic oscill. pot. 79−17699
heavy mesonic resonance prod. quark model *(Russian)* 78−45881
heavy neutral strange lepton predicted by mag. quark model 79−75738
heavy $q\bar{q}$ systems, fine struct. and axial vector gluons 79−63431
heavy quark, next, semileptonic decay distribs. 79−45066
heavy quark (b,t) bound states, phenomenological estimates 80−47262
heavy quark and gluon two jet prod. in e^+e^- annihilation *(Russian)* 78−89696
heavy quark and heavy lepton mass spectra similarity 79−67508
heavy quark infrared safe weak decay, dimensional regularisation techniques, gluonic corrections 80−102087
heavy quark mesons, inclusive hadronic prod. *(Russian)* 80−86770
heavy quark pot., instanton effects, effective Hamiltonians 79−22048
heavy quark potentials, effect on triplet $c\bar{c}$ charmonium and triplet $b\bar{b}$ upsilonium systems 79−49456
heavy quark states, weak decays and prod., jet like distrib. in $SU(2)\times U(1)$ model 79−75746
heavy quark-antiquark bound states, short distance anal., appl. to ψ and Υ 79−93345
heavy quark-antiquark bound states, short distance anal., diagrammatics 79−89103
heavy quark-antiquark pair, pot. energy, static model 79−85273
heavy quark-antiquark spectra in e^+e^- annihilation 77−26494
heavy quarkonium decay in the presence of instantons 79−85296
heavy quarkonium decays, renormalisation group approach, exclusive two meson and inclusive decays 80−82972
heavy quarkonium states, EM decays, relativistic corrections in potential model 79−49522
heavy quarks, elementary particle physics developments, review 79−22053
heavy quarks, mass power law 80−62955
heavy quarks, possible exotic charge or baryon number 80−47245
heavy quarks ($M>200$ GeV/c^2) in $SU(2)\times U(1)$ theory, maximal CP violation, kaon decays 77−38123
heavy quarks and new particles 80−73661
heavy quarks and radiative decay of new particles 77−2798
heavy quarks to explain behaviour of $\sigma(e^+e^-\to\text{hadrons})/\sigma(e^+e^-\to\mu^+\mu^-)$ *(Russian)* 77−57550
heavy triply charmed spin $3/2^+$ baryon, radial excitation spectrum 80−27482
heavy vector meson annihilation rate to lepton pairs, hadronic corrections 80−4943
heavy vector meson weak decays 79−13110
heavy vector mesons associated with $\Upsilon(9.4)$ and the nature of $\Upsilon'(10)$ 78−82187
heavy-quark channels and threshold prediction, pomeron hypothesis, sum rules relating NN, πN, KN cross sections 78−89755
heavy-quark content of light hadrons, implications for Υ-family 78−93853
hierarchical fermion masses from grand unification 80−105832
hierarchy of quark masses, Cabibbo angles and CP violation 79−22030
Higgs boson interactions with nucleons 79−2973
Higgs bosons from two-gluon annihilation in pp collisions 78−41501
Higgs charged bosons and decays of heavy flavoured mesons 79−22014
Higgs induced neutral currents, natural flavour conservation and quark mixing angles 80−42392
Higgs induced neutral currents, symmetries leading to flavour conservation, Cabibbo angle 79−63407
high energy collisions, cumulative particle prod., parton recombination and quark-parton models 80−82956
high energy hadron-nucleus interactions, inclusive prod., quark-quark elastic scatt. model 78−45858
high energy interactions, quark role, appl. of quark parton model 79−30715
high energy lepton pair prod. with pol. hadrons, P and C violations 80−99068
high energy neutrino interactions, quark parton model anal. 79−30730
high energy neutrino physics, recent expt. results 80−4982
high energy neutrino physics, recent results, influence of quark concept on understanding 79−93402

quark models continued
high mass dilepton prod., comparison with Drell-Yan formula in asymptotically free theories 80−4942
high transverse momentum π^0 and jets from p+H and π+H events. 78−70417
high transverse momentum processes, quark-parton model anal. 78−82163
high-energy inclusive spectra near phase-space boundary using quark fragmentation model 78−89658
high-energy physics, particles and interactions, accelerators 80−77944
horizontal-quantum-flavor-dynamics approach to the fermion mass spectrum in $[SU(2)\times U(1)]_{WS}\times U'(1)$ gauge 80−52474
hydrodynamical model based on baglike Lagrangian 77−57496
hydrodynamical quark model of extended hadrons, Dirac type quark fluid 79−49465
hypercharge-exchange reactions, K^-p and π^+p at 10 and 16 GeV/c, comparison with additive quark model prediction 80−13335
hyperfine struct. in relativistic fermion-antifermion system 77−71432
hypermomentum in hadron dynamics and gravit. 78−41487
hyperon hadronic decay, absolute magnitude and EM hyperfine splittings 78−17016
hyperon hadronic decay, quark-diquark model 79−13120
hyperon-nucleon elastic scatt., quark model with factorizability assumption, differential cross section 78−471
hyperon-nucleon elastic scatt., slope parameter 79−9399
inclusive γ production in pp collisions, quark parton model 79−429
inclusive ν deep inelastic scatt. in SKAT bubble chamber, 2-30 GeV 78−62390
inclusive electroproduction of hadrons, virtual photon prod., quark fragmentation region 78−54634
inclusive processes with large momenta, quark-parton model *(Russian)* 77−71538
induced strangeness changing processes, quark mass restrictions 77−57491
inelastic diffraction cross section, quark model and three reggeon limit 80−102035
inelastic processes, cluster model with repulsion and correlation anal. *(Russian)* 80−102026
infrared behaviour of pure Yang-Mills fields, fermionic representation 77−71445
instanton effective size in dilute gas model, $q\bar{q}$ spin exchange force 79−6258
instanton effects in bound state dynamics, quark-antiquark binding, gluon-instanton interactions 79−6280
instantons and spin forces between massive quarks 78−37173
instantons in a quark plasma, superheavy hadrons and neutron stars *(Russian)* 79−36039
instantons in quark plasma, multibaryon hadrons and neutron stars 79−40733
integer-charged quarks in the SU(5) grand unified theory 80−68410
integral and fractional charged quark model test using η and η' props. 80−32074
interference terms, phases, 1/N expansion, Lee-Veneziano model 77−18247
internal coordinates in quark theory, Dirac eqn., Bethe-Salpeter eqn. 77−18224
internal quantum numbers for quarks and leptons in bootstrap approach 80−95254
internal quark motion and SU(6) breaking effects on baryon ground state props. 77−38128
interquark potential, instanton contrib. in dilute gas approx. 80−37220
invariance groups in quark models, internal symms. and ghost symms. 78−25007
isoscalar axial-vector current matrix elements 78−66051
isospin-violating mixing in meson nonets, $d\bar{d}$-$u\bar{u}$-$s\bar{s}$) mass differences 80−32096
$J^P=0^-$, 1^- and 2^+ multiplets, level shifts and chain mass, test of asymptotic planarity 77−38130
Jaffe model, lowest states, appl. to $q^{4-}q$ in SU(6) 79−13060
jet cross sections and quark current-photon pointlike coupling, sum rules 80−32104
jet fragmentation universality in lepton processes 78−434
jet model, uncorrelated, implications of Bose-Einstein statistics 79−22070
jet model with quantum statistics, Touschek invariant meas. 79−22068
jet studies and large transverse momentum collisions, review 79−22143
jets in hadron collisions 78−54612
$K^0\rightarrow K^0$ transition in the standard SU(3)⊗SU(2)⊗U(1) scheme *(Russian)* 80−82951
Klein paradox and the mass spectra of the neutral vector mesons 79−26299
Kobayashi-Maskawa model, Cabibbo-like parameter and quark mass relation *(Chinese)* 80−42408
Kobayashi-Maskawa six quark model, mixing angles, mass matrix and CP violation 80−13284
Kuti-Weisskopf model, quark distrib. in mesons *(Russian)* 80−13291
Lagrange formalism, direct and inverse variational characterisation of linear non conservative systems 78−93527
large |t| proton-proton scattering and quark-quark scattering 79−13161
large momentum transfer behaviour in two-body scatt., hadron quark struct. 77−22690
large momentum transfer reactions, quark jet fragmentation, implication of large vector meson prod. 79−345
large p_T inclusive photoprod. and hard scatt. model 79−9417
large p_T proton inclusive prod., quark-quark elastic scatt. 79−17773
large p_t hadron production, lowest subprocess model, two body reactions 78−4887
large transverse momentum hadron+hadron collisions, particle-jet correls., quark scatt. model 78−4883
large transverse momentum inclusive cross sections magnitude, hadron struct., constituent interchange model 79−431
large transverse momentum physics review, diagnosis and prognosis 78−78215
large transverse momentum trigger, multiplicities and rapidity distribs. 78−62376
lattice algebra for light and heavy hadron constituents 78−16978
lattice gauge theory, hadron mass spectrum 78−74139
lattice gauge theory, string model, hadron spectrum, Regge trajectories 77−57452
leading fragment momentum distrib. functions in light and heavy-quark fragmentation 78−74221
quark models continued
leading logarithms technique, correl. with hard scatt. approaches 79−45072
lectures given at CERN School of Physics (6-19 June 1976) 77−61173
left handed weak doublets with mixed quark states, appl to $\nu N\rightarrow\mu^+X$ 77−26514
left-handed quarks, phenomenology 78−21383
left-right symmetric model from general horizontal symmetry, Cabibbo angle, CP violation 80−101972
left-right symmetry breaking and fermion masses 80−105810
left-right-symm. unified theory of quarks and leptons 78−41466
lepton+hadron collisions, hadronic contributions to trimuon prod., quark-+antiquark annihilation 78−41551
lepton+hadron deep inelastic scatt., evidence for quarks 79−93430
lepton and quark model constraints in SU(2)×U(1) theory 77−61238
lepton and quark spectra difference eqns., τ and toponium mass 80−22589
lepton induced multimuon prod. phenom. anal. in (V-A) scheme 79−17707
lepton pair prod., hard-scatt. expansion 78−66091
lepton pair production, where the Drell-Yan picture breaks down 79−93372
Lepton pair production cross section using Drell Yan formula, sum rules, moments 78−54611
lepton-hadron hard reactions, scaling features, correlating quark rearrangement model 79−58939
lepton-hadron scattering, ang. correls. of outgoing particles, quark-gluon dynamics 79−395
lepton-nucleon deep inelastic scatt., quark-parton model 77−57545
lepton-nucleon deep inelastic scatt., SU(4) duality and quark parton models 77−61293
lepton-pion deep inelastic scatt. from composite particle in scale-invariant quark model *(Russian)* 77−22740
lepton-quark and space-time symmetry 78−16967
lepton-quark correspondence scheme 79−35999
lepton-quark interactions and $\bar{e}$-e ($\bar{p}$-p) annihilation 77−22746
lepton-quark model, supermultiplet of weak bosons and Higgs scalar 78−62345
lepton-quark symmetry, theoretical ideas about charm and flavour mixing 79−49486
leptonic and stratonic spectra conjectures *(Chinese)* 79−49481
light hadronic spectroscopy, expt. and quark model interpretations, review, book contrib. 80−68438
light quark mass spectrum in QCD 79−63427
light quark meson spectroscopy, recent results 78−78134
light quarks, generation of second-class currents, suppression via confinement 77−10213
light vector mesons, mass spectra and Regge trajectories in relativistic quark model *(Russian)* 78−93864
lightlike wave function and wave eqn. on null-plane using Bethe Salpeter eqn. 78−41412
linear baryonic string model, dynamical SU(3) symmetry breaking 79−22036
local symmetry groups and fermion families 79−13030
localised classical solution for fermions+scalar bosons in field theory, Yukawa coupling const. 78−24928
long lived hyperstrange multiquark droplets in MIT bag model 80−9137
Lorentz groups, homogeneous and inhomogeneous, teaching method to illustrate difference 80−17766
Lorentz transformation for quark processes, interaction with hadronic sea 80−37236
Lorentz type internal symmetry 78−50005
low energy hadron dynamics with medium mass quarks 78−21390
low quark scheme and narrow resonances 77−34130
low transverse momentum fragmentation processes, quark-gluon struct. of hadrons 80−22561
$m_{\pi^0}^2=m_{\theta}^2-(m_{\theta}^2-m_{\pi}^2)=(3000\pm20\ MeV)^2$ after all 79−85288
magnetic dipole transitions in atomic and particle physics: ions and psions 79−9322
magnetic field topology in particle physics, implications on quark model 78−8583
magnetic monopoles, elementary particle energy level calcs., Coulombian field approx. 79−26311
many-quark models, weak interactions *(Russian)* 78−33023
mass corrections to scaling in deep inelastic processes 77−13929
massive μ pair prod. in hadronic collisions, ang. distrib, quark-partons+gluons model 77−82706
massive gauge theories, with instantons, wave functions, energies, vacuum and heavy quarks, WKB Schrodinger eqn. 79−35951
massive lepton pair prod., constituent interchange model 78−8611
massive quark model, charmed meson decay 79−93376
massive quarks from discovery of upsilon particle 79−40753
massless 't Hooft model, tachyonic modes, vanishing of scalar density 80−77949
massless up quark, SU(2)×SU(2) symmetry improvement 78−70323
matter at supernuclear densities, neutron star test of quark bag models 77−78812
Melosh transform. in interacting quark theories, U(6)×U(6)×O(3) group on null plane 79−49464
Melosh transformation, Dirac eqn., group theoretical anal. 77−2749
Melosh transformation, re-examination of Miura-Minamikawa-Pati-Woo theorem 79−93377
Melosh transformation, SU_2 symm. 77−87914
Melosh transformation determ. 77−13919
meron pairs, quark confinement phase transition in SU(2) Yang-Mills quantum field theory 78−37174
meson and baryon prod. sum rules in quark recombination model 80−4922
meson electroproduction in correlating quark rearrangement model 80−86666
meson isosinglets, mixing angles, non-relativistic quark model, Schwinger-type mass relations for SU_4 and SU_5 80−18125
meson isosinglets, mixing angles, non-relativistic quark model, SU_5 and SU_n 80−22591
meson jet generated by fast outgoing quark, parametrisation of props. 78−58168
meson jets from quark fragmentation, flavour, power counting rules at $x\rightarrow1$ 78−37185
meson leptonic decay, quark spinors in bound quark system, small component effects 80−73694

quark models continued
meson mass formula, quark line rule in u-, d-, and c-quark sector 78−8596
meson mass formulae in broken $SU(8)_w$ symmetry 78−37191
meson mass hierarchy, quark flavours 78−429
meson mass spectra based on bilocal model 79−67521
meson mass spectrum, planar bootstrap, and Regge approach 80−22581
meson mass spectrum and unitarity in quark model 80−18115
meson multiplicity prod. at large p_T, quark rearrangement model 77−61259
meson P-wave radial mixing, effect on E1 radiative decays, charmonium mass 80−37271
meson radiative decay, consistency with vector dominance, quark models 77−79265
meson radiative decay, decay widths, relativistic quark models anal. 79−13118
meson radiative decays 78−21419
meson Regge trajectories in the quark-gluon model 79−13042
meson relativistic model with instantaneous interaction, spectra, mag. moment 77−61255
meson resonances, radially excited total widths calc. 77−38126
meson scattering, quark model asymptotic completeness 80−73738
meson spectra interrelations, heavy quarks 77−18231
meson spectroscopy, a review using quark models 78−25010
meson spectroscopy, case against pseudoscalar nonet and SU(4) symmetry 77−41817
meson spectroscopy, review of SU_3 quark model, quark confinement and bound states 78−74228
meson spectrum calc. from quark model 77−71485
meson states, four-quark model 79−54307
meson strong decay, 2 quark-antiquark pair model 80−52496
meson structure constants in quark diagram model *(Russian)* 79−30717
meson theory with internal coords., Dirac eqn., Bethe Salpeter eqn., quark model 77−13937
meson three-dimens. wave eqn. from Bethe-Salpeter eqn., comment 77−65136
meson wave functions, spinor struct., inter-straton potentials 79−12969
meson-baryon large angle elastic scatt. calcs. 80−83002
meson-meson inelastic collisions, Glauber multiple-quark scatt. model, quark-quark scatt. amplitudes 78−21459
meson-meson scattering, resonating group calcs., low energy limit 78−424
mesonic Bethe-Salpeter eqn. for different mass straton and antistraton, SU(4) mass relations *(Chinese)* 79−58934
mesonic topological amplitude products, an algebraic soln. 78−81884
mesons, composite model in relativistic space, masses, leptonic widths *(Russian)* 77−74658
mesons, heavy, one-parameter potential, linear confinement 80−13279
mesons, low-lying positive-parity, radiative transitions, VMD and single-quark selection rules 77−18279
mesons, $SU_{1,4}$ as dynamical group, discrete representations anal., masses 77−74642
mesons in O^{++} nonet, quark struct. 77−49906
mesons with heavy quark constituents, lifetime and branching fraction determ. 79−93404
mesons with non-zero charm, inclusive prod. in meson-nucleon and nucleon-nucleon interactions *(Russian)* 77−14008
MIT bag model, gluon exchange corrections to nucleon magnetic moment 77−26528
MIT bag model, M1 transition calcs. low lying hadrons 79−13080
MIT bag model, $q\bar{q}g$ states, exotic mesons energy, spin, parity, mass spectrum *(French)* 79−80807
MIT bag model, radiative transitions of baryons, resonance photoprod. 79−40722
MIT bag model, static electroweak props., PCAC 80−73645
MIT bag model, widths of strong decays $\rho^+ \rightarrow \pi^+\pi^0$, $\Delta^{++} \rightarrow p\pi^+$, calc. 77−74681
MIT bag model cavity approx., prediction of radially excited baryon states 79−89127
MIT fixed-sphere bag model, various predictions 77−18232
mixing angles in sequential Weinberg-Salam model, new generalised Cabibbo fit 79−17655
mixing matrix and CP violation for n quark generations 80−101986
mixing models, mass formulas and OZI rule isolation 77−71498
mixing of gluon bound states and quark-antiquark states, η and η' appl. 80−47255
mixing of neutral leptons 78−4847
mixing of states containing heavy quarks 78−422
model parameters from pion electroprod. data 77−57488
modern atomic and nuclear physics (book) 80−11
modified Han-Nambu and SUB models 80−22562
molecular charmonium prod. in e^+e^- annihilation into hadrons 77−30394
momentum distrib. of quarks inside hadrons 78−74209
multi-channel baryonium and some peculiarities of its decays *(Russian)* 80−105857
multi-particle and inclusive reaction at high energies, review 79−17777
multibaryonic systems, 3n-quark systems, MIT bag model 78−70321
multichannel potential scattering theory with permanently confined channels, quark model appls. 77−13634
multigeneration $SU(2)_L \times U(1)$-based model, quark-lepton correspondence 80−22584
multihadron production in matter connection with hadron quark-glue model 79−356
multilepton configurations in b and t decays from $t\bar{t}$ and $b\bar{b}$ 80−18130
multilepton events, nucleon dissociation and quark and gluon decays 77−46014
multilocal field theory description of hadron struct. 80−9148
multilocal models and string theory 79−2986
multilocal theory, relativistic mechanics of interacting particles 78−16638
multimesonic decays of charmonium states in a constant matrix element quark model 79−26298
multiparticle prod. in quark-parton model, Monte Carlo method 78−41607
multiparticle production meson ratios, statistical quark model *(Chinese)* 79−49558
multiparticle reactions, quark model predictions of η and η' prod. 78−423
multiple charmed quark model, mixing effects, leptonic widths of ψ meson 77−22687

quark models continued
multiple hadron production and struct. from 10 GeV to 10 TeV interactions 80−57653
multiquark baryons and the MIT bag model in SU(6), coupling const. and decay modes 79−97600
multiquark hadrons, Regge slope factorisation 79−22021
multiquark meson states, struct. 80−9146
multiquark models and imbedding of groups 77−49903
multiquark states, metastable, mass and decay prediction using chemistry concepts 78−82158
multiquark states, octonionic interpretation in dual string picture 79−49449
multiquark states and the breaking of exchange degeneracy, dual approach 79−45061
multiquark systems, logarithmic extension, depth and range dependence of energy 79−54309
multiquark systems in Feynman's bremsstrahlung analogy, Regge intercepts 79−97590
multparticle decay theoretical models for heavy hadrons containing charmed quarks 78−70344
muon scattering at Fermilab, inclusive scatt., quark models, scaling violation 80−5001
muonium, hyperfine quadrupole moment, orbital mixtures, quarkonium system phenomenology in potential models 79−49496
N resonance electroproduction, helicity structure and quark motion effect 78−398
naive model, pre-flavour states, quark searches 80−18110
naive quark model predictions for meson mass and baryon mass and mag. moment 80−78036
naive three-point-quarks model, deep inelastic data and n charge radius contradiction 79−355
Nambu Goldstone realisation for vector gluon-quark theories, gluon vertices 80−68415
Nambu mechanics, relation to generalised Hamiltonian mechanics 78−93526
Nambu-Goldstone realisations of dynamical groups and nonlinear eqns. *(Russian)* 78−89632
narrow states in $\bar{p}p$, $qq\bar{q}\bar{q}$ mesons, $\bar{B}B$ bound states, duality, expt. 78−62378
natural flavor conservation and the absence of radiatively induced Cabibbo angles 79−97581
natural flavour conservation in neutral weak interactions, SU(5) and SO(10) unified models 78−4817
neutral current, P-violation in nuclear transitions 79−13243
neutral current P-violation, gauge flavours, Weinberg model testing 77−61240
neutral current quark flavour natural conservation in $SU(2) \times U(1)$ theories 77−49899
neutral current reactions, (V-A) model, mixing between ordinary and heavy leptons 78−41472
neutral currents, effect of quark-antiquark sea *(Russian)* 77−6078
neutral currents, flavour- and muon-number changing in $SU(2) \times U(1)$ model with CP isolation 77−26484
neutral currents, flavour-changing, Wienberg-Salam model 80−22553
neutral currents, P-violating flavour changing and natural $\Delta S=0$ in vector like theories 77−18217
neutral currents and quark charge origin 78−21373
neutral currents natural flavour conservation, determ. of Cabibbo angle 79−22015
neutral diagonal currents, possible strangeness changing effects 77−49900
neutral mesons, quark flavour mixing 78−426
neutral pseudoscalar meson radiative decays, K_{l4} decay in chiral quark model *(Russian)* 80−105900
neutral transitions, vector-like weak currents, parity violation *(Russian)* 78−24995
neutrino, inclusive charged current scatt., new quark flavours and scaling 77−82731
neutrino anomalies, renormalisation effects on $\sigma\bar{\nu}/\sigma\nu$ and $\langle y \rangle \bar{\nu}$ in four quark model 77−18230
neutrino deep-inelastic scatt., asymptotic freedom effects 77−79262
neutrino expts., quark charged current tests 77−22726
neutrino flux from quark matter at core of collapsed stars 80−22028
neutrino interactions and six-quark model, right hadronic currents *(Russian)* 77−82736
neutrino neutral current couplings in $SU(2) \times U(1)$ gauge theories, natural relations, flavour dynamics 79−89095
new elementary particles, quark and composite models *(German)* 80−57570
new elementary particles, theoretical predictions, recent expt. results 77−57475
new flavours beyond charm, evidence in ν-$\bar{\nu}$ cross-sections 77−18268
nine-quark, nine-lepton model of weak and EM interaction 77−74631
non conventional monopoles in field theory, book contrib. 79−58919
non-Abelian dyons, Nambu mechs. descript. 78−41490
non-Abelian gauge fields and nonrelativistic bound states 77−71425
non-Abelian lattice gauge theories, composite hadrons anal. 77−13852
non-Abelian quark-gluon theory, energy-momentum tensor 77−38122
non-Abelian theories, struct. of leading IR divergences 78−4785
non-Abelian vortex-bond model of hadrons 78−4827
non-asymptotically free theories, scaling in deep inelastic processes 77−67568
non-leptonic hyperon decays and the baryon spectrum, S- and P-waves, quark model description 79−36073
nonAbelian gauge theory, light quarks and instantons, chiral symmetry breaking 79−63332
nonet mixing and gluon effects in current quark framework 79−80799
nonleptonic charm decay and u-s symmetry 79−13078
nonleptonic decay, lightlike chiral struct. of hadrons 78−17014
nonleptonic decays, Weinberg-Salam and harmonic oscillator quark model 80−102048
nonleptonic decays of ordinary and charmed hadrons, gauge model with right handed current 78−41545
nonleptonic hyperon decay, octet dominance in nonrelativistic quark model 79−388
nonlinear relativistic strings, exceptional waves and characteristic shocks 78−89618
nonlocal quark model in $SU(3) \times SU^c(3) \times U(1)$, meson decay and mass correction *(German)* 80−27456
nonrelativistic bound s-states in linear central potential 80−82936

quark models continued
nonrelativistic multichannel potential scattering model, confined channels, Hamiltonians 77−5684
nonrelativistic potential models of hadrons 79−22038
nonrelativistic quark model, $\eta\eta'$ and $\omega\phi$ mixing in meson decay 78−21423
nonstrange exotic meson production via baryon exchange, cross section upper limit meas. 77−50015
nontopological solitons, hadron appl. 80−47191
nuclear collisions, hadron prod. in quark-parton model 78−12868
nuclear decays as test of elementary particle theory, review 78−21361
nuclear force, parity violating, unified treatment 80−47400
nuclear force from quark exchange 78−41648
nuclear forces, N struct., deep inelastic scatt. effects *(Russian)* 77−61299
nuclear forces, nonrelativistic quark model study, resonating group method 80−47403
nuclear form factors, dispersion relation approach, pole and quark-counting model 77−26568
nuclear leptoproduction, phenomenological model 79−63660
nuclear structure, quark exchange model for binding energy calcs. 79−93533
nucleon, constituent quarks and deviations from Bjorken scaling 77−6089
nucleon form factors and light front dynamics *(Russian)* 77−38172
nucleon ground state wave functions, O(3)×SU(6) symmetry, hyperspherical method 78−62352
nucleon internal structure, expt. evidence from lN collisions, book contrib. 80−42413
nucleon production in quark parton model, e^+e^-, ep and large $p_\perp$ reactions 78−21391
nucleon structure functions from quark distrib. functions anal. of μp and μd interactions 78−50035
nucleon weak interaction pots. in the Weinberg-Salam model *(Russian)* 80−13258
nucleons, quark-diquark model 77−87937
null change and asymptotic freedom *(Czech)* 79−45002
O(10) theory of strong, weak and EM interactions, masses and mixing 80−13248
observable quarks, gluons and leptons 77−34120
Ochs-Stodolsky jet profile in iterative quark cascade models and low $p_\perp$ meson fragmentation 79−75733
off-shell amplitude singularities in position-space and momentum-space 77−13941
Okubo Zweig Iizuk, quark line rule, consequences 78−25014
Okubo Zweig Iizuka rule phenomenology, rule-violating transitions 77−224
Okubo-Zweig-Iizuka rule, unitary constraints on resonance mixing 79−22024
Okun-Zakharov-Pontecorvo model of CP nonconservation 77−67621
one boson exchange model, OZI rule, nucleon-nucleon-boson coupling 80−32066
operator mixing in asymptotically free theories, deep inelastic scattering 78−37145
ordered hadron S-matrix, quark interpretation, selection rules 78−62322
ordered S-matrix theory, quark struct. and charge conjugation connections, hadron zero triality 79−12973
origin of lepton and quark flavours 79−13043
orto-charmonium spectrum, relativistic potential model, linear potential 79−58922
OZI relations for SU(4) coupling constants with applications to tensor mesons 79−80793
OZI rule, pseudo-dimension rule and ψ(3770) decay 79−40724
OZI rule violation, analyticity and duality 78−24978
para-charmonium spectrum, relativistic potential model, linear potential 79−58922
paracharmonium states, corrections to two-gluon annihilation rates 78−33039
parity-violating nucleon-pion amplitude in unified gauge-invariant models 77−6070
particle correlations in multiperipheral resonance prod. model, broken SU_3 theory 78−45891
particle struct. studies, book 80−41952
parton model and Bethe-Salpeter wave function 77−41820
parton transverse momentum dependence on longitudinal momentum 78−25016
parton-quark model for nucleon deep inelastic struct. function in rest frame 77−87942
Pati-Salam $SU(2)_L\times SU(2)_R\times SU(4)$, gauge-c 78−12851
penguins in $\Delta S=1$ nonleptonic weak decays 80−91086
Penrose theory in particle physics 78−29321
photoprod. of charged intermediate vector bosons 78−45855
photoprod. of heavy hadrons, peripheral and VMD models 78−33074
pion EM props., dressed quark model *(Russian)* 80−52508
pionisation influence on beam hardness, beam evolution eqns. for hadronic processes *(Russian)* 80−42407
Poincare group representations for relativistic extended hadrons 79−89099
point like spin-3/2 quarks, contrib. to deep inelastic struct. functions 80−47250
polarisabilities of hadrons, quark models 77−82703
Pomeron and critical temp. 80−22566
pomeron current model for diffraction dissociation 78−4843
pomeron flavouring and rising total cross sections 77−38102
pomeron-quark relative coupling strengths 77−65145
potential-model mass formulae for hadrons 78−70349
pre-quarks and fractional charges 80−91048
proceedings of the 1977 CERN-JINR School of Physics, Nafplion, Greece (May-June 1977) 78−81726
propagator in a theory with confinement 79−71689
properties in relativistic quark model with strong binding 80−102023
proton, inner structure, observation in collisions producing jet of debris 80−57569
proton struct. function determ. from Lorentz deformed wave function 79−13070
proton structure, high energy p-p scatt. and multiple scatt. model 79−13072
proton-hadron high energy collisions, hadron struct. 79−67614
proton-lepton deep inelastic scattering in four-quark model *(Russian)* 77−26530
protons, flavour symmetry breaking in antiquark distribs. 79−36006

quark models continued
pseudo-Goldstone bosons in Pati-Salam model 77−87933
pseudobaryons, narrow bound states of qq with qqq 78−45870
pseudoscalar and vector meson decays, triangular quark diagram anomalies, ψ, η and η' appl. *(Russian)* 80−42455
pseudoscalar heavy meson decay by t and b quarks 79−380
pseudoscalar meson masses, quark model with 4 quarks 77−46021
pseudoscalar meson masses and sum rules, 4 quark model 77−10233
pseudoscalar mesons, EM mass shifts, quark-parton model, SU_3 quark triplet 80−42459
pseudoscalar mesons in the c-$\bar{c}$ and b-$\bar{b}$ systems 79−93359
$Q^2\bar{Q}^2$ states, mass levels in (3+1) dimens. lattice gauge theory 79−58942
Q^6 dibaryon resonances, orbitally excited mass spectrum, decays 80−73670
QCD, confinement and quark theory, introductory review 79−67502
QCD, E_7 model, quark and lepton assignments 78−8590
QCD, energy levels of 1+1 dimensional lattice gauge theory 78−4828
QCD, scale breaking for quark and gluon distribs., diagrammatic anal. 79−71706
$Q\bar{Q}$ systems, new flavours, internal parity and the quark line rule 79−13034
quantised space, quark kinematics, colour, geometric interpretation 79−89116
quantized scalar SLAC bag model, quark trapping 77−13920
quantum chromodynamics, review *(Dutch)* 77−46016
quantum field scatt. theory of hadrons on Regge trajectory, bootstrap and quark interpretation 77−54046
quantum field theory of extended hadrons 80−13270
quantum flavour dynamics, quark masses and flavour mixing angles in six quark model 78−74211
quantum flavour dynamics, renormalisability conditions 80−42404
quantum fluctuations of quark fields, in arbitrary Yang-Mills instanton background 80−13268
quantum mechanical applications to quarkonium 80−27484
quantum number distribs. and fluctuations in multiparticle prod., quark-parton model 78−82249
quantum-number-exchange reactions, phenomenological quark model, appl. to K^+N scatt. 77−87950
quark and hadron jets, charge and energy flow in cascade models 80−102017
quark and lepton couplings in the weak interactions 79−17665
quark anomalous magnetic moments and meson radiative decays in naive quark model 79−17693
quark attenuation and recombination in nuclear matter, hadron-nucleus reactions 80−52601
quark density model, SU(3) symmetry breaking and nonleptonic decays 79−13079
quark diagrams as spectral representations of quark masses *(Russian)* 80−82953
quark fragmentation functions in inclusive hadron muoproduction 79−67565
quark fusion model, strange and charmed quark numbers, vector meson description 78−58158
quark jet fragmentation 79−45063
quark lattice and QCD in nuclei 80−5101
quark liberation in (1+1)-dimensions 79−324
quark line rules, quark rearrangement model, energy dependence 78−70320
quark mass differences in high energy collisions 78−45868
quark mass ratio, chiral perturbation in new key 80−37208
quark masses and Cabibbo angles 79−9332
quark matter, phenomenological equation of state, neutron star appl. 79−63424
quark pair creation, $\delta^0 e$ transition mass and $\eta\to 3\pi$ decay 77−41841
quark parton distribs. for deep inelastic scatt., calc. from 1-D Dirac box 78−45845
quark parton model, review 79−93368
quark parton model with large parton k_T 80−42412
quark physics, theoretical speculations, empirical data 77−18227
quark recombination mechanism in multi-hadron production 80−18114
quark recombination model, vector meson prod., effect on $\pi^\pm$ and $K^\pm$ fragments from proton 78−82160
quark string model, hadron spectrum, semiclassical approach, baryons and exotic hadrons 79−40747
quark strong interactions as weak interaction symmetry breaking mechanism 80−18117
quark-antiquark pot., charmonium model modifications, spin forces and instantons 78−93842
quark-antiquark systems combined by Coulomb type attractive force 78−89677
quark-cascade model, particle ratios at large p_T 77−10218
quark-gluon coupling constant, perturbation theory appl. to $e^+e^-\to$hadrons 77−38127
quark-gluon coupling constant renormalisation, unified gauge theories containing Pati-Salam model 77−6072
quark-gluon interaction in pN collisions, dimuon prod. at large transverse momenta 78−29355
quark-gluon phase transition 80−27475
quark-gluon-parton model, constituent quarks as clusters 77−30318
quark-lepton correspondence in neutral current interactions 80−27450
quark-lepton unification in SU(N>5) 80−73646
quark-nucleon phase transitions, rel. to density fluctuations in early Universe 79−75301
quark-parton, charge transfer in multiparticle prod. 77−57490
quark-parton distrib. functions and sign of neutron charge radius 77−22694
quark-parton distributions model, large transverse momentum hadrons, logarithmic scale breaking 78−16989
quark-parton fragmentation, support from data on μ^+p inclusive hadron distribs. 77−61296
quark-parton model, Large-p_T correlations in scale-breaking model 77−82704
quark-parton model, leading proton-large p_T particle and proton-lepton pair correlations 79−353
quark-parton model, strong interactions of quarks, weak interaction *(Russian)* 77−82710
quark-parton model, three photon struct. function of proton, inelastic electron scatt. data 77−46022
quark-parton model, with scaling violations, large p_T processes anal. 78−45927

quark models continued
quark-parton model description of neutrino data, particle prod. in $\bar{\nu}$N and νN interactions 77−18270
quark-parton model of charged π electroprod., fragmentation functions 79−13136
quark-parton model predictions of $e^+e^-\rightarrow\gamma+$hadrons, sum rules, charge asymm. 77−10219
quark-parton model relns. for dilepton and ψ meson prod. 77−82711
quark-parton model results for $\sigma(e^+e^-\rightarrow\text{hadrons})/\sigma(e^+e^-\rightarrow\mu^+\mu^-)$, asymptotic freedom predictions leading to paradox 77−49988
quark-parton model with charm for dimuon prod. in high energy νN and $\bar{\nu}$N interactions 77−57520
quark-quark scatt. models for Be+p at 400 GeV/c 78−46060
quark-string model, meson mass spectra 78−33065
quark-vector-gluon, chiral SU(3) breaking for pseudoscalar meson nonet 77−6046
quarklei, free quarks saturated with nucleons, existence and detection 79−6315
quarkonia, spectra, decays, levels, jets, sum rules 80−18112
quarkonium leptonic decay rates for 1S and 2S states, constraints 80−37252
quarkonium level spacings 78−8604
quarkonium level splittings, scaling behaviour, semiclassical methods 79−75742
quarkonium mass spectra, one gluon exchange corrections, gauge invariance and choice 80−52483
quarkonium origin, prediction of new quark masses 79−36003
quarkonium pot., ψ data and Υ'-Υ mass splitting fit, Υ leptonic widths 78−89666
quarkonium spectroscopy in a potential model with vacuum-polarization corrections for ψ, Υ 80−78038
quarkonium system inverse scatt. formalism, appl. to ψ, ψ' and Υ 78−82154
quarks and leptons, fermion physics in terms of SU(2)×SU(1) gauge theory 78−74197
quarks and leptons, high energy and nuclear physics interface 80−41974
quasi-relativistic quark model with confining pot., hadron form factors 77−46020
quaternion model, gauge theory *(Russian)* 78−62315
quaternion model, quark mass matrix, CP violation and Cabbibo angle *(Russian)* 79−40751
quaternionic chromodynamics as a theory of composite quarks and leptons 80−82948
radially excited states, photon and hadron interactions 78−82170
radially excited states in baryon resonance pionic decays, relativistic quark model 80−95268
rearrangement model, unified description of nonleptonic hyperon decays 77−54104
rearrangement model for large p_T hadron inclusive prod. 77−50026
reciprocal effects and other quark theories, charm quarks, J/ψ discovery, gauge theories *(Danish)* 79−30698
recombination model, π^+/π^- ratio in meson-proton inclusive interactions 80−102022
Regge cuts, not applicable to multigraph and baryon models 80−27464
Regge formalism, quark fragmentation functions for inclusive hadron production 80−68462
Regge pole exchange amplitudes 80−404
Regge slopes factorisation, ordinary and new hadron, spectroscopy, four flavour model 77−82722
Regge trajectories, dual unitarisation scheme, SU(3)-breaking and baryon exchange effects 79−26316
Reggeisation of meson trajectories quark-gluon gauge theories 78−25005
Reggeised valence-core exchange model 77−26485
reggeon and photon coupling relns. 79−13063
Reggeon exchange degeneracy and quark model 77−13944
relativistic, hadron matrix elements of two- and four-quark operators 79−97578
relativistic, K_{e4} decay form factors 77−38160
relativistic, light cone dynamics, nuclear wave function *(Russian)* 77−6085
relativistic, meson mass differences 77−26489
relativistic, parity violating vector meson-pseudoscalar meson interaction 77−54102
relativistic bound state of fermion and antifermion, fermion fields, quark model 78−82151
relativistic constituent quark model in four dimens., construction remarks 78−62360
relativistic covariant formulation, meson form factors *(Russian)* 80−9140
relativistic generalisation of quark model minimal boosting of SU(6) scheme, meson, baryon props. 77−41814
relativistic hadron couplings, unified framework, symms., quark models *(German)* 78−50012
relativistic harmonic oscillator model, baryon reson. radiative decays 79−85277
relativistic harmonic oscillator model, hadron EM interactions and props. 80−37225
relativistic harmonic oscillator quark model, N and $\Delta(1236)$ form factors 78−93852
relativistic heavy-ion collisions, nuclear matter to hot quark matter phase transition 79−3170
relativistic mechanics of two or three point particle systems 78−4481
relativistic motion of massive quarks joined by massive string 78−74206
relativistic nuclear collisions, pulsating blobs of quark matter in hydrodynamical model 80−83122
relativistic oscillator formalism for hadron struct. and props. 80−9144
relativistic quantum theory of composite systems, nonlocal field theory of quark model 78−70253
relativistic quark model, Lagrangian form of relativistic mechanics for bilocal and trilocal structs. 77−41809
relativistic quark model, origin of spin-orbit and spin-spin coupling forces 79−13046
relativistic quark model for mesons, symm. breaking via quark mass differences 77−79253
relativistic quark models, $c\bar{c}$ and $b\bar{b}$ singlet triplet splitting, mass formulae *(Russian)* 80−37232
relativistic quark pair creation model for $V\rightarrow P\gamma$, $P\rightarrow\gamma\gamma$ reduced decays and enhanced EM tadpoles 79−67555
relativistic string with massive ends, classical and quantum theory 78−62073
quark models continued
relativistic strings with massive end quarks, boundary condition solns. 79−49493
renormalisation group methods in statistical mech. treatment of quark and string systems 77−54075
renormalisation group techniques, quarks and strings on lattice 77−22654
resonances, quark model, $SU_6\times O_3$, form factors review 77−67624
review of quarks, appl. to hadron spectroscopy, quark parton model, book contrib. 79−22161
review of quarks, appl. to hadron spectroscopy quark parton model 79−22052
right handed currents, $\Delta I=1/2$ rules, nonleptonic decays, heavy-quark expansion, Zweig's rule 77−61217
rishon model of quarks and leptons with double SU(2) symmetry and Dirac magnetic moments 80−82943
Roper resonance photocoupling in relativistic quark model with scalar confining pot. 80−4936
S_3-symmetrical model, use of permutation symmetry 79−26280
scalar mesons, $J^{PC}=0^{++}$ partial waves self-consistent anal. 79−71711
scaling violations and $\nu,\bar{\nu}$ cross-sections 77−87970
scaling violations in deep inelastic lepton scatt., charm quark prod. 78−21436
schematic composite model of quarks and leptons 79−93353
Schrodinger equation for central potentials, energy levels and level ordering 79−80463
sea, evaluation of bubble contribution to quark sea 78−93851
sea quarks, null plane current anticommutators, sum rules and appls. 80−52436
sea-quark distrib. in proton, from pp inclusive interactions 78−66090
second class currents and anomalies in neutrino reactions 77−57522
semi-classical models for gluon jets and leptoproduction based on the massless relativistic string 80−105861
semiclassical model for rotational states of mesons containing massive quarks 79−36038
semileptonic decay of charmed particles, formalism using helicity amplitudes 78−4852
semileptonuc decay spectra of charmed mesons pairs produced in γN collisions 77−49952
sequential flavour dynamics, flavour mixing and quark masses 79−80802
sequential particle order, fundamental concept for hadron physics 79−80762
sequential particle order, fundamental concept for hadron physics, S-matrix theory 79−80763
sequential Weinberg-Salam model, neutral current flavour conservation, fourth generation 79−97561
seven quark model for hadron spectrum 77−22685
sextet model phenomenology, interpretation of ψ and χ states 77−22684
shell model, meson spectroscopy 79−6328
short distance analysis of weak interactions, asymptotically free theory 77−54068
single quark transition model, parity violating charmed hadron decays, current-current interaction 78−12907
singlet quark form factor exponentiation in leading logarithm approx. 80−91091
six flavour model, mixing at small angles 80−27453
six quark model, b-flavour prod. by neutrinos 79−75720
six quark model, b-quark prod. by ν and $\bar{\nu}$ 79−45073
six quark model, CP nonconservation upper bounds in neutral theory meson systems 80−42397
six quark model, quark mixing angle bounds 79−71686
six quark model, t-quark prod. in νN collisions, calcs. 79−93371
six quark model without right handed currents 77−6081
six quark models, group theoretic anal. 80−9150
six quark models with broken SU(12) symmetry, hadron mass relns. 77−22693
six- and eight-quark models, weak interactions 80−99086
six-quark model, for weak and EM interactions *(Russian)* 77−67658
six-quark model, mixing angles, mass depend. on q^2 80−37224
six-quark model, SO(4)×U(1) gauge group 77−49905
six-quark model, spontaneous CP violation *(Russian)* 79−93379
six-quark model of quantum flavourdynamics, Cabibbo angle and quark masses 78−33017
six-quark symmetric model and associated neutral currents 77−18216
six-quark theory, calc. of t-quark mass and flavour mixing angles based on $SU(2)\times SU(2)_R\times U(1)$ 79−80811
six-quark theory, weak interaction mixing 78−41475
sixth quark mass in $SU(2)_L\times SU(2)_R\times U(1)$ gauge group 79−26291
SL(3,R) symmetry, coupling of self-conjugate systems 79−97228
small p_T hadronic collisions, jets, quark, fragmentation universality and rising rapidity plateaus 79−40734
SO(4)×U(1) model of weak and electromagnetic interactions 79−13009
soft gluons in Drell Yan and deep inelastic processes, large const. terms, asymptotic behaviour 79−6326
soft hadronic collisions and fragmentation on nucl. targets, quark dynamics 79−22063
soliton models of hadrons, semiclassical approach to quantum field theory 77−5981
Sp(4)×U(1) gauge symm. for weak interaction, $\Delta I={}^1/_2$ rule 77−34093
space-like fields, asymptotic props. and appl. to hadron physics 77−18158
space-like fields for quark confinement 80−42426
spectral function sum rules in relativistic quark model 79−63428
spectroscopy from bag and nonrelativistic pot. models 78−8594
spectrum law for leptons and quarks 79−93338
spin dependence, composite hadrons, S-matrix theory, TeV energy range 78−58164
spin dependence in strong interactions at very high energy 78−58203
spin structure of effective quark Hamiltonian, hyperfine splittings of charmonium 78−12871
spin system for b-universality and additive quark model 77−13914
spin-orbit terms of the heavy-quark potential in the presence of instantons 79−71710
spontaneous CP nonconservation in theories with more than four quarks 80−47212
stable hadrons containing massive stable quarks, cosmological constraints 79−54308
standard 4-quark model and beyond, review 79−80805
standard weak-EM gauge model, six-quark phenomenology and Grand Unification 80−37204
static quark potentials from Yang-Mills equations 79−45056

quark models continued
Sterman-Weinberg formula for quark jets and gluon jets, leading log version, master equation 80−22552
stiff quark line hypothesis, strong interaction suppression, Zweig Izuke rule origin 77−2792
strange baryonium, spectrum, decay, production 78−93854
strange particle production by $\nu(\bar{\nu})$ in quark model 79−13103
strange quarks, Regge exchange building, K^-p data anal. 79−2995
straton model, wave functions without SU(6) symmetry, P anomalous mag. moment *(Chinese)* 79−49489
straton model anal. *(Chinese)* 78−86438
string junction model and spectrum energy density of string 80−57556
string model, string geometrical shape and overlapping functions 79−13073
string model and hadron spectrum, semiclassical approach 79−13082
string model for fermions 77−2803
string model of mesons with two massive quarks 77−10212
string reconnections and quark matter 80−37226
string-junction model, hair pin line rule and baryonium decay 80−27487
string-junction model and width of baryonium 79−58928
strings, bags, baryoniums 78−29307
strings and membranes in external field 79−93341
strong interaction formalism with internal coords., partial unification of quantum theory and SU(3) classification 77−65137
strong interaction theory, development from the Fermi-Yang model to the quark model *(Chinese)* 79−30711
structure functions for hadrons, Drell-Yan model anal. of $pN\rightarrow l\bar{l}X$, $\pi N\rightarrow l\bar{l}X$, $eN\rightarrow eX$ 78−21476
structure functions of mesons in quark-parton model, appl. to hadron prod. in e^+e^- annihilation 78−41482
structure of hadrons containing heavy quark, MIT bag model 80−86672
structure of quarks and quark systems in hadrons, form factors 77−41810
$(SU_2\times U_1)\times S_n$ flavour dynamics, flavour number bound, n quark and n lepton generations unification 80−4907
SU_7 grand unification model, two (V−A) and one (V+A) generations of quarks and leptons 80−57538
$SU_L(3)\otimes U(1)$ gauge model, exact Cabibbo universality, τ^- and X^- 80−4852
$SU_L(4)\times SU_R(4)\times U(1)$ model, generation of u- and d-quark masses 79−63419
$SU_L(4)\times U(1)$ four-quark model, lepton quartets and W bosons 77−87934
SU_n flavour symmetry of quark sea 78−54606
$SU(10)_{flavour}\times SU(10)_{colour}$ unified hadron lepton theory 79−67509
$SU(2)_L\times SU(2)_R\times U(1)$ gauge with permutation symmetry, quark mass and Cabibbo angles 80−47232
$SU(2)_L\times SU(2)_R\times U(1)$ six quark gauge models, flavour violation 80−4951
$SU(2)_L\times SU(2)_R\times U(1)$ six quark model, mixing angle derivation, comments 79−75729
$SU(2)_L\times U(1)$, mass hierarchies and Cabibbo angle formula 79−63420
$SU(2)_L\times U(1)$, natural flavour conservation of Higgs couplings and Cabibbo mixing conflict 80−37200
$SU(2)_L\times U(1)$ gauge model, mixing angles and CP violation 80−73648
$SU(2)_L\times U(1)$ gauge theory, four flavours, Cabibbo angle natural relations and bounds 80−57550
$SU(2)_L\times U(1)$ primitive particle model 79−40708
$SU(2)_L\otimes SU(2)_R\otimes U(1)$ model, implications of absence of parity nonconservation in atomic physics 77−41758
$SU(2)_L\otimes U(1)$ models, implications of absence of parity nonconservation in atomic physics 77−41758
$SU(2)_L\otimes U(1)$ theory, CP violation and Cabibbo angle 80−52447
$SU(2)\times U(1)\times U(1)$ model, Cabibbo angle and Higgs coupling strangeness conservation 80−47233
$SU(2)\times U(1)\times U(1)$ model, neutral current, quark mass reactors, spontaneous broken Lagrangian 79−97563
$SU(2)\times U(1)$ gauge model, chiral $SU(2)\times SU(2)$ symmetry and electron mass 80−57542
$SU(2)\times U(1)$ gauge model predictions for neutral current reactions 77−71424
$SU(2)\times U(1)$ gauge models, ν and $\bar{\nu}$ neutral current events 77−74632
$SU(2)\times U(1)$ gauge models, with diagonal neutral currents 77−71433
$SU(2)\times U(1)$ gauge theory, μ-e mass ratio and CP violation as quantum effect 79−30691
$SU(2)\times U(1)$ gauge theory of weak and EM interactions, quark model 77−26458
$SU(2)\times U(1)$ model, fermion and Higgs multiplet structure, universality 80−62909
$SU(2)\times U(1)$ model, quark mass matrix and discrete symmetries 78−54607
$SU(2)\times U(1)$ models, hadronic neutral currents, low energy neutrino reactions, constraints 77−13912
$SU(2)\times U(1)$ scheme, CP violation parametrization, quark n-doublet weak interaction *(Russian)* 80−13231
$SU(2)\times U(1)$ vectorlike model: new leptons, quarks, and the axion question 79−40711
$SU(2)\otimes U(1)_y\otimes U(1)_c$ gauge model, neutral current and $\Delta I=1/2$ rule 79−6257
$SU(2)\otimes U(1)$ gauge group theory tests from neutral current phenomena 78−24992
$SU(2)\otimes U(1)$ gauge model, strange baryon weak radiative decays and CP violation 79−6260
SU(2) quark diagram struct. of prod. amplitudes 77−22662
$SU(3)\times U(1)\times U(1)$ model, suppression of flavour changing neutral currents 78−21350
$SU(3)\times U(1)$ gauge model of weak interactions, quark triplets, charmed hadron decay 77−2789
$SU(3)\times U(1)$ gauge models, generalised mixing and CP violation in hadron decays 78−41473
$SU(3)\times U(1)$ models, massless and supermassive quarks 79−9331
$SU(3)\times U(1)$ modified model, quark and lepton mass hierarchy 78−89653
SU(3) 27-plet mesons masses, existence of low-mass long lived exotics in quark model 78−33032
SU(3) gauge model of weak and EM interactions, Weinberg angle, Han-Nambu quarks 80−52452
SU(3) model for strong interactions quark excitation and ψ mesons 77−18198
SU(3) quark sectors, weak hadronic and radiative decays of nonstrange charmed baryons 79−22092
quark models continued
SU(3) subalgebras of SU(4), generalised U-spin charmed baryon magnetic moment 79−36078
SU(3) symmetry breaking and partial conservation of axial vector current 77−2773
SU(3) symmetry in more than 3 quarks world, nonet struct., quark line rule 79−36022
SU(3) wave eqns. for quarks 80−57571
$SU(4)_L SU(4)_R\times U^Y(1)$ gauge group for lepton and quark weak interactions *(Russian)* 79−97566
SU(4), broken Zweig rule and null plane 77−18225
$SU(4)\times SU(4)$ broken symm. in quartet model, D- and F-meson masses and decay consts. 78−66087
$SU(4)\times SU(4)$ current two point functions, meson decay consts. and bare quark masses from duality 78−8598
$SU(4)\times SU(4)$ symmetry breaking, Cabibbo angle, nonlinear hadronic Lagrangian, PCAC *(Russian)* 80−42360
$SU(4)\otimes SU(4)$ broken chiral model, based on $SU(4)\supset SU(2)\otimes SU(2)$, Glashow-Weinberg model extension 78−12836
$SU(4)\otimes U(1)$ broken gauge theory, muon number nonconservation 77−74638
SU(4) 16-plet boson mass formulas, flavour symmetry breaking 80−37250
SU(4) Clebsch-Gordan coefficients for the formation of baryonium and exotic baryons 79−75739
SU(4) mass splitting, group theory and quark model comparison 79−6290
SU(4) mixing angles and quark-loop anomalies 77−34104
SU(4) six-quark models, meson masses and EM decays 77−38129
SU(4) symm. model, mag. moments of 20-plet baryons, charm quantum numbers 77−61257
SU(4) symmetry predicted $^1/_2{}^+$ charmed baryons, $C_1{}^{++}$, $C_1{}^+$, $C_1{}^0$, $X_u{}^{++}$, $X_d{}^+$, possible observation 79−40758
SU(5), Clebsch-Gordan series, quark model appl. 80−47256
$SU(5)\times SU(2)$ unification, horizontal symmetry due to quantised motion along internal axes 80−62905
SU(5) and SO(10) grand unification, flavour mixing and proton instability *(Russian)* 80−68413
SU(5) asymptotic symmetry, b quark flavour from Weinberg spectral function sum rules 79−67495
SU(5) grand unification, flavour number estimate 79−85264
SU(5) grand unification embedding in SU(N), SU(9) theory, flavour unification 80−32059
SU(5) grand unified theory, flavour number limit from fermion mass higher order corrections 80−4904
SU(5) mass formulae, bb states masses, mass differences and splitting 79−17691
SU(5) symmetry with beauty quark, baryon and meson mass spectra 79−45079
$SU(6)_w$ analysis of sums of baryonic partial widths 77−30378
$SU(6)_W$ decay anal. of $[70, 1^-]$ and $[56, 2^+]$ multiplets 77−22733
$SU(6)_W$ models and baryon resonance decays 77−22700
$SU(6)_W$ symmetry, ang. constraints and collinearity breaking, free quark model 79−30679
$SU(6)\times O(3)_L$ multiplets, semilocal duality, quark-orbital Regge trajectories 80−27490
$SU(6)\times O(3)$ baryon multiplet, linear string model 78−8624
$SU(6)\times O(3)$ harmonic oscillator model, comparison with $\bar{K}N$ data 77−22782
$SU(6)\times O(3)$ multiplet masses, relativistic quark model 78−8552
$SU(6)\times O(3)$ quark shell model, L=1 meson mass spectrum 78−89678
$SU(6)\times SU(3)$ as classification group for baryons, Poincare group and quarks 77−18246
$SU(6)\supset SU(3)\otimes SU(2)$ Wigner coefficients 79−97607
SU(6) classification of states, quark model with interaction 77−74651
SU(6) exotic gauge model, lepton-quark symm., CP-violation and k^0 decay and $\mu\rightarrow e\gamma$ decay 78−12875
SU(6) model of weak interactions, neutral weak currents at high energy *(Russian)* 78−45836
SU(6) multiplet, connection with semi-local duality in quark model 79−93386
SU(6) quark model of hadron struct., field theory treatment 79−49483
SU(6) scheme of relativistic quark model, hadron electromag. and weak form factors 78−41500
SU(6) unified gauge field theory of weak, EM and strong interactions 79−17658
SU(8) non-leptonic decay of hyperons and charmed baryons 77−49963
SU(8) symm., mag. moments of charmed vector bosons 78−4794
SU(8) symmetry and the baryon mass spectrum 79−80814
SU(9) grand unification of flavor with three generations 80−13251
SU(n), SU(2n) three quark coupling coeffs., diagrammatic group theory 79−331
SU(N) gauge theory consistency in two Euclidean spacetime dimens., quark-gluon theory 77−74598
SU(N) model, unitary invariant generalisations *(Russian)* 78−66024
subnuclear structure concept via dilepton prod. in hadronic collisions, historical review 79−93365
subquark model of leptons and quarks, unification, currents and exotic states 80−86683
superconducting quark model quantum corrections 77−6082
superconductivity phase transition in meson states, quark quasiparticle model *(Chinese)* 80−102021
superconformal group and quark-like fermionic coordinates 80−9145
superheavy quarks and possible quasistable hadrons 77−49893
supersymmetric sine-Gordon model and two-dimens. bag 78−21382
T′ (10040) as an I=1 vector meson resonance 80−47241
T-baryonium system, four-body potential in multiquark states 80−101996
t-flavoured meson production in photonuclear and pp collision 80−22623
t-quark mass in O(10) unified field theory 79−75708
taming of the dipole ghost in relativistic quantum field theory 78−66035
tensor force effects on ψ family in charmonium model 78−89675
tensor meson radiative decay in $SU(6)\times O(3)$ broken symmetry quark model 80−73710
thermodynamical quark bootstrap, hadron prod. 77−30336
thermodynamical quark model, hadron prod. cross sections, boiling quark soup 78−420
Thomas-Fermi type picture of EM structure of π and N 80−9170
three quark operators, anomalous dimensions, baryon form factors and quantum numbers 80−22568
three quark oscillator model for baryon spectrum 77−22698

quark models continued
three-body mechanism for narrow resonances 77−74654
three-component model extended, total cross sections 78−24999
three-quark systems, dynamics, linear mass spectra baryon models 80−42390
top mesons, weak decays, strong correction meas. 80−82970
topological approach to high-energy large transverse momentum interactions 79−22057
topological expansion for baryons and mesons, Veneziano scheme 78−70335
topped and bottomed hadrons, mag. moments in additive quark model 80−52478
trajectory slopes based on multilocal model 77−87944
trilocal theory, constituent mass, free limit condition and quantisation 79−2984
trimuon prod. mechanism, $\nu(\bar{\nu})$ interactions 78−82199
triple jet production in hadronic collisions at large transverse momentum 78−93919
twister flat-space theory, possible bearing on quark models 77−22719
two body reactions, spin system constraints, quark additivity, geometrical hypothesis 78−29309
two-gluon jets from Υ(10.00) 78−29302
two-hadrons inclusive reactions and correl., large p_T, scale-violating quark model 78−74292
U_3(W)-gauge unified EM-weak theory, neutral current neutrino interactions 77−26481
U_A(1) symmetry and flavor mixing, Cabibbo angle and quark mass ratio relation 79−93355
$U(1)\times SU_L(2)\times SU(3)$ theory, integer charge quarks, lepton hadronic processes *(Russian)* 80−86653
unconfined unstable quarks in unified gauge theory 77−13916
unified gauge theories, restrictions on possible supergroups and flavour groups 77−65129
unified lepton-quark model of Nambu-Jona-Lasinio type for weak, EM and strong forces 77−30304
unified quartet quark model extensions, weak interactions and right-handed currents 77−22678
unified U_3 gauge theory of weak and EM interactions, six quark flavours and lepton types 77−18215
unified vectorlike gauge theory based on group SU(6) for quarks+leptons 78−4818
unified Yang-Mills-Einstein-Higgs gauge theory, hadron struct., quark confinement 79−9275
unitarity and hadron self-energy, mass shifts, and SU_6 symmetry breaking in meson spectrum 79−17687
unitarity corrections to the vector-meson masses and mixing angles 79−49487
unitary symmetry in baryon-antibaryon systems *(Chinese)* 80−102000
universal multihadron jets, quark interactions 77−38132
universal neutral current interactions and urbaryon-lepton correspondence 78−66068
up-quark zero mass, critical anal. in current algebra framework 78−82144
urbaryon rearrangement, SU(4) symmetry breaking in hadronic reactions 77−13932
V+A current of charmed quarks for nonleptonic processes 77−30307
V+A currents coupling old quarks to new quarks 77−26486
vac. struct. of two-dimens. Higgs model, quark pair prod. 78−29254
vacuum polarisation, breakdown of normal threshold dispersion relation, naive quark model 77−2849
vacuum polarization effects in lattice gauge theories 80−13211
valance quark distribs. in π, K, D, Regge trajectories, SU(3), SU(4) breaking 79−30703
valence gluons, existence in nucleons 79−13029
valence gluons and quarks *(Russian)* 77−74657
valence quark clusters in nucleon structure functions from neutrino scatt. 80−95252
vector coupling, bound states, Dirac fermions in three dimens., interacting via gluons 77−34090
vector gluon exchange model of pomeron, diffraction scatt. 77−30345
vector gluon models, implications of pair prod. in intense mag. fields 77−13505
vector gluon-quark theories, Nambu-Goldstone realisation proof 80−22563
vector meson decays to $e\bar{e}$, constituent quark spinors, small component effects 79−85279
vector meson mass predictions, SU(3) formalism of S quark model 78−37177
vector meson photoprod., Carlitz-Green-Zee mechanism and vector meson dominance model 79−13137
vector meson photoproduction from nucleons, quark rescatt. effects *(Russian)* 77−65160
vector meson production in pp interactions, constituent-interchange model 80−22579
vector meson strong decay widths in relativistic quark model 77−57529
vector mesons, leptonic decays, six-quark sequental model 80−52490
vector mesons, two body photonic decays, SU(4) scheme, ideal mixing angles, amplitudes, quark sectors 78−54630
vector mesons, two-body photonic decays, 16-plet mixings in SU(4) quark symm. 78−33062
vector-like models and nuclear parity violating effects 77−61249
vectorlike SU(3)×U(1) gauge model of weak interact. $\bar{\nu}$ reactions, neutral currents 77−41805
vectorlike theory of weak interactions 77−67613
VV+AA type gauge models, effective ν interactions 78−66038
W-boson propagator effects in the neutrino-nucleon scattering 79−13098
wave eqns. for mesons and baryons *(Chinese)* 78−86444
weak and EM interaction unification with strong interactions following τ and Υ, book contrib. 80−47235
weak and EM interactions at high energy [conf. Les Houches, France (July 1976)] 79−80785
weak and EM radiative corrections to low-energy processes 80−95274
weak charmed-baryon resonance prod., neutrino inclusive interactions, scaling behaviour 78−8645
weak coupled gauge field formulation using quaternions and p, n, λ quark fields 79−63349
weak hadronic current in models with 4 and 6 quarks *(Russian)* 77−74616
weak interaction model with 8 quarks and 8 leptons, neutrino experiment heavy leptons *(Russian)* 79−67494
quark models continued
weak interaction orientation to strong interaction, quark mass spectrum, dynamical symm. breaking 77−74640
weak interaction scheme, charmed hadrons expt. data, four flavour model explanation 78−45860
weak interaction theory, review 78−4822
weak interactions, five-quark model with right handed current 77−57485
weak interactions, renormalisable model on gauge group $SU(2)\times SU(2)_R\times U(1)$ 78−12855
weak interactions, spontaneous symm. violation, strong quark interaction mechanism *(Russian)* 79−71659
weak interactions, vectorlike model with right handed mixing 78−416
weak interactions of quark fields, quark masses, spontaneous parity violation 77−34115
weak interactions of ultra heavy fermions 78−93838
weak interactions vectorlike model with six quarks, gauge theory, $SU(2)\times U(1)$, νN appl. 77−57480
weak neutral couplings to hadrons in neutrino inclusive, semi-inclusive and elastic reactions 79−36064
weak nonleptonic decays, $\Delta I=1/2$ rule and strong interactions 77−46046
weak production of charmed baryons by neutrinos, relativistic quark model 78−41496
weak-current angles of six quark model, constraints, from K^0-$\bar{K}^0$ system 79−71685
weak-interaction mixing in the six-quark ambidextrous model of quantum flavourdynamics 79−36000
Weinberg's model of CP violation in gauge theories, valence quark hypothesis 79−12940
Weinberg-Salam model, D_5 group, 2 values of Cabibbo angle, 4 quark flavours 80−68405
Weinberg-Salam model, extended, Higgs-induced neutral processes, natural-flavour conservation, K-symmetries 80−57539
Wigner coefficients for $SU(6)\supset SU(3)\otimes SU(2)$ 79−45025
Wilson loop critical point behaviour in gauge and lattice guage theories 80−90993
y anomaly in $SU(2)\times U(1)$ vector like model, with parity violating neutral current 79−13013
Yang-Mills theory, mass singularities, cancellation mechanism 77−82676
Yang-Mills theory, real and virtual IR divergences 77−45943
Zweig forbidden processes, intermediate vector particle model, neutral vector mesons *(Chinese)* 80−62918
Zweig rule model for couplings, quark conservation at meson vertices, multiRegge phenomenology 77−82709
A_1 meson in quark model and chiral symm. 78−12834
$\alpha\alpha$ and NN scatt. analogies, quark struct. and clustering connections 79−6442
$B\rightarrow J/\psi$+hadrons, branching ratio, b quark decay calcs. 80−32095
$B\rightarrow\psi pK^-$, search for b flavoured baryons 80−42450
b quark$\rightarrow\psi(\eta_c)$+X, B branching ratios assuring colour suppression 80−37259
b-quark interaction with τ^--lepton, gauge model 79−40738
b-quark mesons, mass, quark model predictions 80−95256
$B\bar{B}$ annihilation process, simple geometrical picture 80−95291
$B\bar{B}$ channel narrow widths, use of 'mock' diquoniums, quark-pair-creation model 79−75734
$b\bar{b}$ meson state lifetimes, R predictions above bottom threshold, quark model 80−99097
$B^0\bar{B}^0$ mixing in six quark model, decay, mass mixing and CP nonconservation 80−42406
$c\bar{c}$ and $b\bar{b}$ states, spectra and strong decays 80−52502
$c\bar{c}$ bound states, e^+e^- decay processes, relativistic harmonic oscillator model 78−62393
$c\bar{c}$ meson radiative decays, generalised VMD mechanism 78−8606
$c\bar{c}$ $q\bar{q}$ states, decay, hadronic and photo-prod., e^+e^- annihilation prod. 80−99092
χ(3.45), γ-transitions in charmonium system 78−78138
χ(3.45) resonance, time-like $c\bar{c}$ excitation 78−8599
χ particles, radiative decay widths calc., broken SU(4) model 78−62395
χ_c radiative decay, ψ and ψ' prod., straton coupling constants *(Chinese)* 80−42467
χ_J P-wave charmonium states, hadronic prod. cross section in K^-p, $\bar{p}p$, and π^-p 80−37292
d, 6 quark system, wave function, elastic form factor, NN forces, spectroscopy *(Russian)* 78−50015
d, six-quark model, form factors and struct. functions 78−45871
D, two-body hadronic decays, six-quark model mixing angle constraints 79−97618
D and D* prod. from e^+e^- annihilation, form factors and free quark model 78−37222
d EM form factors at large transferred momentum, six-quark state *(Russian)* 78−89715
d in six-quark model, isobaric component determ. 78−21377
$D\rightarrow K\pi(K\pi\pi)$, nonleptonic decay rates, quark diagrams and pole approx. 80−86707
$D\rightarrow K\pi l\nu$, charm-changing weak hadronic current, models 80−57585
D mesons, anomalous Cabibbo suppressed decay ratios, simple model 80−42452
D mesons, colour triplet diquark states 77−30325
D mesons, decay const. using current algebra with Lagrangian model 78−58176
D two body nonleptonic decays, quark model predictions 80−9164
D-meson decay, hadronic, role of free-quark pairs 80−78059
D-meson EM mass difference in quark model, quark mass difference 77−71516
D^0 Cabibbo suppressed hadronic decays, Cabibbo universality fake violation, RH currents 80−73699
D^0 decay enhancement mechanism, quark diagram with gluon prod. 80−105891
$D^0\rightarrow K^-\pi^+$, Cabibbo suppressed decay compatibility with weak interaction mixing angles, branching ratios 79−97620
$D^0\rightarrow K^-\pi^+$, quark total number conservation, D^+ lifetime longer than D^0 80−57590
$D^0\rightarrow K^0\pi^0$, $\Delta T=1$ constraints and final state interactions 80−95267
$D^0\rightarrow K^0\pi^0$, quark total number conservation, D^+ lifetime longer than D^0 80−57590
$D^0\rightarrow K^+K^-$, Cabibbo suppressed decays, Penguin diagram contribution, mixing angles 80−22604
D^0 nonleptonic decay, quark annihilation hypothesis test 80−102044
$D^0\rightarrow\pi^+\pi^-$, Cabibbo suppressed decays, Penguin diagram contribution, mixing angles 80−22604

quark models continued
$D^0 \rightarrow \pi^+\pi^-$ 79−97620
D^0-$\bar{D}^0$ mixing, flavour-changing Higgs bosons 80−62915
D^+, D^0, weak nonleptonic decays, SU(3) symmetry and quark diagrams *(Russian)* 79−93411
D^+ decay, Cabibbo suppression, strong 20-plet dominance and W exchange 80−42453
$D^+ \rightarrow K^0\pi^+$, $D^0 \rightarrow K^-\pi^+$, two body decays of charmed mesons, quark recombination scheme 78−37207
$D^+ \rightarrow K^0\pi^+$, quark total number conservation, D^+ lifetime longer than D^0 80−57590
D^+-D^0 charmed mesons EM mass difference estimate, quark pair creation model 77−10250
$D^0-D^\pm$ lifetime difference, possible mechanism $D^0 \rightarrow s+\bar{d}+$gluon 80−37255
$^3D_1$-charmonium decay into $e\bar{e}$ and relativistic effects of constituent quarks 79−3017
DD molecular charmonium from dual diagram and Schrodinger eqn. 80−86660
Δ(1236) isomer production, by charged and neutral currents 79−17711
Δ(1236) νN neutral current prod., quark model anal., isovector vector and axial-vector neutral-current couplings 77−61278
Δ(1236) production in νp reactions, multipole struct. of weak prod. by charged currents 78−29328
δ(980)→γγ decay rate implying δ is four-quark state 79−93422
Δ assignments, π^+p elastic scatt. partial wave anal. up to 10 GeV/c with impact parameter approach 77−22769
Δ mass, three quarks bound state, variational method calcs. 78−21396
Δ-Δ resonance in nonrelativistic quark model 80−86692
δ-meson four quark nature *(Russian)* 80−101999
Δ_{D35}(1925) baryonic degrees of freedom, nonrelativistic, harmonic oscillator quark model mass formula 80−91066
e/π ratio at low p_T in high energy hadronic collisions, possible $Q\bar{Q} \rightarrow e^+e^-X$ mechanism 79−71687
eD, 19.4 to 22.2 GeV, unpolarised target, parity violation in inelastic scatt. of polarised electrons 79−63482
ed, elastic and deep inelastic scatt. at large momentum transfer, quark model *(Russian)* 78−86529
ed, elastic and inelastic scatt., quarks and dimensional scaling 77−6132
ed deep inelastic scatt., p-violating asymmetries, neutral current couplings, sea quark contrib. 79−97630
ed scatt., P-violation calc. in weak interaction theory 80−42469
$(e^+d^- \rightarrow$ hadrons$)/(e^+e^- \rightarrow \mu^+\mu^-)$ cross sections ratio, differential dispersive anal., narrow resonances 78−37223
e^-e^- annihilation, parton model, finite energy results 78−419
e^+e^-, annihilation, weak neutral currents of quarks hadron prod. cross section P-odd depend. *(Russian)* 79−93445
e^+e^-, jet cross sections and quark current-photon pointlike coupling, sum rules 80−32104
$e^+e^- \rightarrow$ hadron jets, 13-31.6 GeV, planar events evidence, transverse momentum and broadening 79−93441
$e^+e^- \rightarrow$ hadrons, dual unitarisation and quartz model 77−10272
$e^+e^- \rightarrow$ hadrons, quark existence and theory 80−37234
$e^+e^- \rightarrow$ hadrons, scaling and quark struct. 80−425
$e^+e^- \rightarrow$3 jets, integer charge quark model, gluon jets 80−91101
e^+e^- annihilation, 6 GeV, η_c existence, possible $c\bar{c}c\bar{c}$ state 77−82755
e^+e^- annihilation, axial vector meson prod. rate, non-relativistic quark model 77−38184
e^+e^- annihilation, charge polarisation of quark jets 77−38183
e^+e^- annihilation, charmed baryon pair prod., symm. quark model, $c\bar{c}$ pair creation model 77−54111
e^+e^- annihilation, hadron secondary average transverse momentum, comparison with deep inelastic scatt. 80−37281
e^+e^- annihilation, hadron/muon pair prod. ratio, nonasymptotic contribution to quark-parton model 77−34169
e^+e^- annihilation, heavy quark fragmentation functions from inclusive hadron spectra *(Russian)* 79−40756
e^+e^- annihilation, heavy vector meson prod., quark model estimations 77−18306
e^+e^- annihilation, prod. of orbitally charmed hadrons, free quark model anal. 79−22120
e^+e^- annihilation, Q^2 duality test with nonrelativistic potentials 80−102011
e^+e^- annihilation, quark jet fragmentation into mesons and baryons, chain decay model 80−63001
e^+e^- annihilation, ratio of secondary baryon and meson yields and quark combinatorics *(Russian)* 79−49532
e^+e^- annihilation, superheavy flavour prod., weak current effects, Z^0 effects 80−57614
e^+e^- annihilation and hadron-induced events, multiplicity ratio 80−105877
e^+e^- annihilation and quark fragmentation functions, Monte Carlo quark-parton model 79−22119
e^+e^- annihilation in upsilon region, quark model predictions 78−54640
$e^+e^- \rightarrow b\bar{b}$, single lepton spectra, coupling strengths 79−49461
$e^+e^- \rightarrow e^+e^-K\bar{K}$, δ and S^* meson interf., S^*-ε mixing angles, and K^+K^-, $K^0\bar{K}^0$ cross sections *(Russian)* 79−80832
e^+e^- EM annihilation into quarkonium states with even charge conjugation, vector dominance 79−93438
$e^+e^- \rightarrow$hadron jets, quark helicities, neutral current vector and axial couplings 80−32114
$e^+e^- \rightarrow$hadrons, asymptotically free quark model predictions in complex plane 77−71522
$e^+e^- \rightarrow$hadrons, cross-section constraints in asymptotically free theories with anomalous dimens. 77−30393
$e^+e^- \rightarrow$hadrons, multiplicity, scaling, inclusive spectrum, simple hadron cascade model 78−66135
$e^+e^- \rightarrow$hadrons, new flavour search at PETRA 80−37282
e^+e^- inclusive two-particle final states ang. distrib., simple quark model 77−49984
e^+e^- interactions, review 79−80833
$e^+e^- \rightarrow$jets, high energy, $q\bar{q}$ pair conversion model, seagull effect 80−5007
$e^+e^- \rightarrow$jets, particle ratios from quark statistical model 80−73724
$e^+e^- \rightarrow$jets, t-quark pair prod. effects in annihilation, Kobayashi-Maskawa model 80−86733
$e^+e^- \rightarrow M+X$, M = pseudoscalar meson, forward-backward asymmetry from neutral currents 79−71759
$e^+e^- \rightarrow$multiple lepton+hadron final states, flavour changing neutral currents 77−30363
$e^+e^- \rightarrow n\pi$, jet struct., lightlike (zero mass) quarks anal. 79−63496
quark models continued
$e^+e^- \rightarrow$O particle, decay, mass, prod. from Zweig rule intermediate vector particle model *(Chinese)* 80−73697
$e^+e^- \rightarrow pX$, weak neutral current, polarisation effects, asymm. parameters *(Russian)* 78−459
$e^+e^- \rightarrow \pi^0\gamma$ or $\eta\gamma$, reaction rate, weak neutral current corrections, 3γ background 77−46069
$e^+e^- \rightarrow$quarkonium state, D,F, ϒ mesons, importance as experimental tool in new particle searches 80−42425
e^+e^- total hadronic cross-section in 4 GeV region, quark model with broken colour symmetry 77−22748
$e^+e^- \rightarrow t\bar{t}$, single lepton spectra, coupling strengths 79−49461
eN, deep inelastic scatt., quark model, field-theoretic, quark indistinguishability, nucleon structure function 80−62993
eN deep inelastic scatt., parton model anal. 78−62405
eN→e meson boson, nature of gluons, spin, helicity struct. of amplitudes 77−18293
ep, deep inelastic scatt., σ_L/σ_T ratio from quark model 80−82979
ep deep inelastic inclusive K_s^0 and Λ electroproduction, quark fragmentation 78−66123
ep deep inelastic scatt., p-violating asymmetries, neutral current couplings, sea quark contrib. 79−97630
ep deep inelastic scatt., pol. p and e, straton model, sum rule *(Chinese)* 80−42475
ep inclusive reactions, eμ event, associated charm quark pair creation 77−2841
$ep \rightarrow W^+(Z^0)+X$, inclusive cross sections, quark-parton model calcs. 79−71755
$\epsilon(700)_{\bar{d}}$ four quark bag model, high statistics data anal. 78−82147
$\eta \rightarrow 3\pi$, decay rate, up quark masslessness 79−40761
η(549), η′(958) with inert component, gluon bound state 78−74226
η(η′)→γγ, quark model tests 80−78067
η meson large mass, quark-gluon model, virtual annihilation mech. 79−351
$\eta \rightarrow \pi\pi\gamma$, quark loop model, SU(3) splitting of quark masses 80−62990
η-η′, pseudoscalar meson mixing, phenomenological model with radial excitations in mass matrix 79−54316
η-η′ complex, quark-line rule in $\pi^+p \rightarrow \eta\Delta^{++}$, $\pi^-p \rightarrow \eta n$, $p\bar{p} \rightarrow \pi^+\pi^-\eta$ 77−30330
η_c, predictions of existence by extrapolation methods 78−93863
η_c prod. and hadronic decay, charmonium model 78−41502
η′(957) meson, quark model description for prod. and decay 80−62970
η′(958), three triplets of fractionally charged quarks 80−9172
$\eta'(958) \rightarrow 4\pi$, decay mode in broken $SU_6 \times O(3)$ quark model 79−36071
η′ EM decay, η-η′ mixing and gluons 80−62981
$\eta' \rightarrow \eta\pi\pi$, amplitude satisfying Adler conditions, relativistic quark pair creation model 80−95262
$\eta' \rightarrow \eta\pi\pi$, current algebra calcs. with symmetry breaking, inconsistency with expt. 79−13114
$\eta' \rightarrow \pi\pi\eta$, $\delta\eta'\pi$ and $\delta\eta\pi$ coupling constant ratio, δ(980) quark content 80−82955
F mesons, mass and decay const. using current algebra with Lagrangian model 78−58176
F-meson decay, hadronic, role of free-quark pairs 80−78059
F^+, weak nonleptonic decays, SU(3) symmetry and quark diagrams *(Russian)* 79−93411
F^+ decay widths and branching ratios, quark recombination widths, free quark model 80−27500
F^+ nonleptonic decay, quark annihilation hypothesis test 80−102044
$F^\pm \rightarrow 3\pi$ or $K^\pm K_S^0$, charmed pseudoscalar meson nonleptonic decays, right handed c+λ quark doublet 77−49958
f′-f mass mixing sign from gluonic annihilation model, OZI rule violation 79−71722
γ(10.0), two-body hadronic and radiative decays, pseudo-dimension rule, ππ and KK̄ suppression, SV_1 singlet 80−52495
γγ, jet cross sections and quark current-photon pointlike coupling, sum rules 80−32104
γγ collision, deep inelastic, helicity method 80−22606
γN, cross sections, contrib. of $q\bar{q}$ and $c\bar{c}$ vector mesons 78−58192
γN, exclusive photoprod. reactions, Okubo-Zweig-Iizuka rule 80−95277
γN, inelastic virtual Compton scatt., quark struct. 79−89164
γN→ψN, spin and mass depend. of constituent and phenomenological models 77−61304
γN→ψ(3.1)+anything, cross section and N charmed quark composition 80−423
$\gamma_v N \rightarrow \pi^\pm X$, current fragmentation region, quark cascade model of deep inelastic lepton-nucleon scatt. 78−25052
γp→hX, quark jet model and total cross section 79−13133
$\gamma p \rightarrow W^+(Z^0)+X$, inclusive cross sections, quark-parton model calcs. 79−71755
$\gamma q \rightarrow \pi q'$ inclusive pion production in γN and e^-N collisions, quark-parton model *(Russian)* 80−78073
J/Ψ, EM transition rates, geometrodynamical quark model 80−47295
J/ψ, inclusive production cross sections, correlating quark rearrangement model 79−54320
J/ψ meson hadronic prod., role of ^3P charmonium states 77−22744
J/Ψ prod., valence- and sea-quark distribs., deep inelastic scatt. and Drell-Yan processes 79−13069
$J/\psi \rightarrow \eta_c\gamma$, radiational decays in charmonium *(Russian)* 80−13308
K, deep inelastic structure functions in massive quark model 80−86717
$K \rightarrow 2\pi$, comment of appl. of current algebra and bag model 79−97622
$K \rightarrow 3\pi$, CP violation, current algebra anal., six quark Weinberg-Salam model 80−47281
$K \rightarrow 3\pi$, relativistic quark model anal. 80−99096
K charge radii, quark model relation 78−4835
K decay, mixing of p-wave axial vector resonances 77−30374
K electric charge radius determ. in nonrelativistic quark model 78−16990
k form factor, quark-antiquark systems combined by Coulomb type attractive force 78−89677
$K \rightarrow \pi\pi\pi$ in relativistic quark model 77−10248
K structure functions from inclusive prod. data, nonstrange quark distribs. 80−86715
K^0, charge radius, quark models 78−45854
$K^0 \rightarrow \pi\pi$, six-quark model, $\Delta I = 1/2$ rule and CP violation 79−54323
$K^+ \rightarrow \pi^+e^+e^-$, pole contribs., test of theory by comparison with expt. 78−70360
$K_L \rightarrow 2\mu$, K_L-K_S mass difference, strong interaction effects from short-dist. gluons 77−82737
$K_L \rightarrow \mu\bar{\mu}$, quark mixing angle upper bounds in standard 6 quark model 80−18131

quark models continued
$K_L \rightarrow \pi^+\pi^-(\pi^0\pi^0)$, CP violation parameters in six quark model *(Russian)* 80−62974
K_{l4} decay in relativistic quark model, axial vector form factors and decay rate 78−66109
$K^* \rightarrow K\gamma$, quark loop model, SU(3) splitting of quark masses 80−62990
$K^0 \leftrightarrows \bar{K}^0$ transition amplitude, and K_LK_S mass difference, in MIT bag model 79−63450
$K^0 \rightleftharpoons \bar{K}^0$, weak neutral current diagonality, mixing amplitude, multi-quark gauge model *(Russian)* 80−68414
K_SK_S pair rapidity correlations, quark level strangeness compensation in multiparticle production 79−36024
KN, below 1 GeV/c, Y* states, SU(6)⊗O(3) quark model classification 80−27523
KN scatt., Blankenbecler-Sugar multichannel eqn., $J=1/2$ partial wave soln. 78−37230
kp, large P_T pion^0 prod., meson structure functions, quark distrib. functions 80−86714
K^-p, 32 GeV/c, vector and tensor meson prod., with quark model anal. 79−80854
$K^-p \rightarrow (\pi^+\pi^-)_{s\text{-wave}}\Sigma^0(1385)$ amplitude anal., additive quark model and duality diagram predictions 77−30430
$K^-p \rightarrow K^*(890)\,\Delta(1236)$, 10 GeV/c, multidimens. anal., reaction subchannel separation 80−32127
$K^-p \rightarrow \Lambda X$, 4.2 GeV/c, Λ polarisation, quark diagrams 78−45948
$K^-p \rightarrow M^0+\Lambda(2^0)(2^0\text{-}1385)$, 4.2 GeV/c, quark model relations 78−82233
$K^-p \rightarrow \rho^0$+anything, or f+anything, 10, 16 GeV/c, central and fragmentation contribs., quark model predictions 78−62467
$K^\pm$p, 32 GeV/c, ρ, K*, φ inclusive prod., quark fusion model 80−32135
$K_L{}^0p \rightarrow K_S{}^0\pi+\pi^-$ p, up to 17 GeV/c, $Q^0\bar{Q}^0$ prod., cross sections 80−32129
$l^\pm$N, deep inelastic scatt., EM corrections to hadronic and neutral currents, systematic effects *(Russian)* 79−49526
Λ(1405) and kaonic H atom, $\bar{K}N$ interaction model 80−68479
$\Lambda \rightarrow pe^-\bar{\nu}_e$, $|g_A/g_V|$ calc. in quark model, 56-70 octet mixing 79−389
$\mu N \rightarrow (x\mu)X$, dimuon and trimuon prod., heavy quark and 4 diffractive prod. 79−93429
μN deep inelastic scatt., asymm., quark proton model evaluation, gauge theories test 78−62408
μN scatt., deep-inelastic, EM production of trimuons 80−22619
μ^-N→hadron shower, charm-pair production effects 80−73748
$\mu^-N \rightarrow \nu tX$, six-quarks model, upper bounds for t-quark production 80−13297
μp charged current interactions, hadron production, quark-parton model comparison 79−40769
N, N*, evidence for core of valence quarks 79−36025
n charge distrib., NΔ mass difference, quark model anal. 77−67653
n charge radius and quark-parton model, deep inelastic e-N struct. functions 77−71488
n charge struct., form factor in quark-parton model 77−54106
n electric dipole moment, CP violation in gauge theories 80−91041
n electric dipole moment, quark and gluon corrections 80−4994
N form factor, isovector, meson field theory, pseudoscalar πN interaction 80−62986
N form factors, parton separation determ. 78−33026
N struct. functions, scaling violation dynamical anal. 77−49976
N structure function model from hard consistent quark interactions, scaling violations 80−86719
N*(1470), Roper resonance, quark pair creation model soln. 80−47252
NN̄, baryonium, internal struct. *(Norwegian)* 79−36032
NN interaction, field theoretical approach with stress on OBE pot. *(German)* 78−78203
NN̄ interaction, low energy, meson exchange forces, one boson exchange potential, dual quark models 78−62444
NN interaction, quark MIT bag model anal. 79−80806
NN large angle elastic scatt. spin depend., pure vector for q-q interactions 79−13049
NN large angle elastic scatt., spin-spin asymmetries and flavour depend., quark interchange 80−86743
NN̄ narrow meson resonances near threshold, theoretical approaches 80−9157
NN negative-parity reson., six-quark bag 78−74210
NN parity-violating π-exchange pot. 77−65133
NN potential short range behaviour with the quark model 80−47409
NN scattering in the nonrelativistic quark model, total elastic cross section *(Russian)* 80−68475
NN̄ system, single γ and π emission rates, meson quantum number assignments 78−78208
NNπ coupling, parity violating, quark, model calc. in Weinberg Salam model 79−35987
np→dγ, γ-polarisation, NN weak pot. in simple gauge model 78−54644
np elastic scattering data, comparison with theory, large transverse momentum processes 77−57566
ν, charmonium and strangeonium, linear+Coulomb pot. study, high α_S regime 80−62935
ν, massless, left-right symmetric gauge models, $SU_{2,L}\times SU_{2,R}\times U_1$ 80−27461
ν and $\bar{\nu}$ inclusive processes for neutral currents, sea quark effects, meson prod. 79−22088
$\bar{\nu}$ anomalies and right-handed currents 78−8654
ν data, exotic quarks and high gauge groups 77−74583
ν deep inelastic scatt., four flavour quark model, asymptotic freedom 78−45905
ν elastic and inelastic scatt., quark-lepton models of weak neutral currents 77−18272
$\nu(\bar{\nu})$ high-energy interactions, dimuon distrib. anal., quark-parton model 78−33056
$\nu(\bar{\nu})$N, pol.N, deep inelastic processes from valence straton distrib. functions *(Chinese)* 80−99095
$\nu(\bar{\nu})$N neutral current interaction, charm prod. in quark parton model 77−61246
$\nu(\bar{\nu})N \rightarrow l^-(l^+)X$, differential cross section in scaling limit, sea quark contribution 78−37196
$\nu(\bar{\nu})N \rightarrow \mu^+\mu^-X$, dimuon rate and strange quark sea 80−62961
$\nu(\bar{\nu})N \rightarrow \mu(\mu^+)+c\bar{c}+X$, like sign dimuon prod., and b-quark prod./decay limits 79−85290
$\nu(\bar{\nu})N \rightarrow \nu(\bar{\nu})\pi+X$, determ. of neutral current coupling consts. 78−8649
ν reactions, dilepton events, neutral heavy lepton, rising $\sigma(\bar{\nu})/\sigma(\nu)$ 77−57523
ν-induced multilepton events, weak interaction model 78−41533
quark models continued
ν-induced new particle prod., heavy quark fragmentation function 77−87968
ν-N scatt., relativistic quark oscill. model, N* weak prod. *(Russian)* 77−220
$\nu_\mu(\bar{\nu}_\mu)$N, prod. of hadrons with new quantum numbers, quark parton model *(Russian)* 77−82735
$\nu_\mu(\bar{\nu}_\mu)N \rightarrow \mu^-(\mu^+)X$, struct. functions meas., quark-parton model anal. 79−58951
$\nu_\mu(\bar{\nu}_\mu)h \rightarrow \mu^\pm l^\pm+X$, charm contrib. to prod. of opposite sign dimuons 79−377
νN, $\bar{\nu}$N interactions muon prod., quark model anal. 78−4850
νN, scaling violation, quarks with size and excited states 78−74242
$\bar{\nu}$N deep inelastic scatt., net charge in current fragmentation region, quark fragmentation 80−62964
νN→hadron shower, charm-pair production effects 80−73748
νN inclusive interactions, nondiagonal neutral currents, six quark model with slow rescaling 77−49949
νN inelastic scattering, possible soln. with weak neutral currents to ρ-π puzzle 79−17714
νN interactions, dimuon prod., quark-parton model, threshold effects of charm prod. 77−46041
$\bar{\nu}$N interactions at high energy, deviations from quark-parton models 77−30361
$\bar{\nu}$N(νN) CERN data, inconsistency with e-N in quark-parton model *(Russian)* 77−49951
νN tetramuon prod. sources, heavy quark and lepton cascades, charm prod. 78−70356
ν_μN→multiple lepton+hadron final states, flavour changing neutral currents 77−30363
$\nu_\mu N \rightarrow \mu^-X$, 2 to 30 GeV, characts. of deep inelastic processes *(Russian)* 79−80821
$\nu_\mu N \rightarrow \mu^-$+hadrons, restraint on weak four-fermion interaction constants, quark-parton model *(Russian)* 77−6110
$\bar{\nu}\bar{\nu}$, y-distrib. energy and x-depend., quark right handed coupling 79−26325
$\bar{\nu}$p charged current interactions, quark fragmentation, quark-parton model test 80−68444
νp elastic scatt., neutral current struct. anal. 77−61273
$\bar{\nu}p \rightarrow \mu^+X$, deep inelastic scatt., MQM description 80−47305
$\bar{\nu}p \rightarrow \mu^+$+X, 4.5 GeV^2, p struct. functions x depend., quark distrib. 80−32097
ω-φ-baryonium mixing model 80−32072
Ω^- decays and right-handed currents 78−17015
Ω^- spin, centrifugal barriers, quantisation of l=0 baryon levels 77−18221
$\Omega^- \rightarrow \Theta e(\mu)\bar{\nu}$ or $\Theta^* e(\mu)\bar{\nu}$, branching ratios and lepton energy spectra 80−73701
ω′(1.78) vector meson props., quark model, VDM 77−54103
ω*-φ* interference in multi π prod., origin of Iizuka-Zweig-Okubo rule violation 78−70324
ωN elastic scatt., and meson size, in quark multiple scatt. model 79−54349
$P \rightarrow \gamma l^+l^-$, EM characts. for pseudoscalar meson decay in nonlocal quark model *(Russian)* 80−102050
p-n mass difference, quark-parton model anal. 78−93859
p+nucleus→μ^-+μ$^-$+anything, 400 GeV, high-mass dimuon continuum 78−37344
pγ, one-gluon exchange, quark loop contrib. to photon total cross sections 80−4999
pn, 195 GeV/c, inclusive π^+/π^- ratio and quark distributions 79−54367
pN, 300 GeV, quark fragmentation functions in additive model 80−37222
pN, charm-pair production 80−22643
pn, inelastic charge exchange, quark interchange 80−86759
pN, p̄N, 200 GeV/c, dimuon prod. cross section, Drell-Yan predictions, struct. functions 80−37300
pN→hadron shower, charm-pair production effects 80−73748
$pN \rightarrow \Lambda^0X$, Λ^0 polarisation and quark prod. mechanisms 79−63542
$pN \rightarrow \mu^+\mu^-X$, 225 GeV/c, muon pair prod., qq̄ annihilation model 79−63552
pn→$\mu^+\mu^-$+anything, review of data, explanation using quark models, new quarks 78−74202
$\bar{p}n \rightarrow \bar{p}p\pi^-$, 2.98 GeV/c, $\bar{\Delta}^-$ prod. in additive quark model framework 80−52529
pp, 100, 200 GeV, elastic scatt., polarisation effects at large momentum transfer, quark model *(Russian)* 80−83005
p̄p, 22.4 GeV/c, multiparticle prod., Monte Carlo quark-parton model 79−97639
pp, 53 GeV, elastic scatt. differential cross-section meas. 78−66155
p̄p, 8.8 GeV/c, exclusive annihilation processes, cross sections, q̄uark model anal. 80−105920
pp, direct prod. of large transverse momentum photons, quark-fusion model 77−30465
pp, elastic scatt. amplitude in quark diquark model 80−102075
p̄p, equal sign lepton pairs, cleaner W-signal 79−13012
pp, ISR energies, p fragmentation, D^+ prod. from $\Lambda_c{}^*$ and Λ_b decay 80−102080
pp, inelastic charge exchange, quark interchange 80−86759
pp, large P_T pion^0 prod., meson structure functions, quark distrib. functions 80−86714
pp, large p_T two-particle correlation, hadron composite struct. 77−54085
p̄p, pp, 12-405 GeV, low p_T meson prod., quark-antiquark formation model 80−63056
p̄p, pp, Drell-Yan processes, scaling violation effects 80−382
pp, probabilistic quark-model approach to p fragmentation 80−63049
p̄p, $\pi^\pm$ inclusive spectra, comparison with Monte Carlo quark-parton model 79−30755
pp, secondary hadron absolute yield, L=1 meson prod., quark model *(Chinese)* 80−99113
p̄p, three-body annihilations, rel. to quark rearrangement model 78−21444
pp, three-gluon exchange contribution to forward high-energy scattering 79−54324
pp,p̄p, Z^0 high p_T bremsstrahlung, Higgs versus quark or gluon jets 80−32063
pp→($\pi^\pm$ or $K^\pm$)+X, fast-meson production and the recombination model, proton multiquark structure functions 79−89208
pp and p̄p reactions, total cross section differences evidence for baryonium exchange 78−66171
pp→baryons by diquark-quark fusion model 80−102065

quark models continued
pp collisions, Monte Carlo approach to multiparticle prod. in a quark-parton model 79−13171
pp cross-sections, energy depend. determ. 78−62458
pp→DD̄ cross sections, Monte Carlo anal., particle lifetime for detection in emulsion 78−82229
p̄p→Δ⁻⁺⁺Δ⁺⁺, 3.6-12 GeV/c, cross sections and decay, parity exchange contribs. from quark model 79−13146
pp elastic cross section from dressed quark model, Glauber multiple scatt. expansion 79−2977
pp elastic cross-section, multiple scatt. of quarks 78−4868
p̄p elastic scatt., FESR constraint on baryonium resonances, S, T, U, contrib. 80−27520
pp elastic scatt., multiple scatt. model anal. including inelastic intermediate states 79−89189
pp elastic scatt., quark-glue model description 77−61323
pp elastic scatt. at $\sqrt{s}$=53 GeV, three-quark struct. 77−88010
pp hadron prod. at large p_T, multiplicities, quark model *(Russian)* 77−262
pp→hadrons, scaling violation in fragmentation region in quark model, 10^6 GeV *(Russian)* 79−3051
pp high energy elastic scattering and constituent multiple scatt. model 79−67607
pp inclusive π^0 large p_T prod., quark subprocesses 77−2885
pp interaction, quark-antiquark recomb. in fragmentation region 77−67690
pp interactions, antibaryon and baryon inclusive spectra, quark model anal. 77−88018
pp→K^+K^+X, search for narrow six quark resonance 78−89757
pp→K^+K^++missing mass, stable six quark state search, mass range 2.1-2.4 GeV 78−89742
pp→l^+l^-X, massive lepton pair prod., quark-gluon-parton model, scaling 79−428
pp large angle elastic scatt., quark elastic scatt. model 79−17751
pp large inelastic diffraction in the quark-glue model, gluon distrib. in parton model 79−89138
pp large transverse momentum interactions, quark cascade model anal. 79−36101
pp→mesons, multimeson inclusive spectra and recombination model, multiquark structure functions 80−73751
pp multiple hadron prod. up to 1500 GeV, hadronic matter eqn. of state *(Russian)* 80−32085
p̄p→neutral meson+$\pi^+\pi^-$, or neutral meson+p̄p, 7.2 GeV/c, quark model anal. 78−41561
pp→ppp̄p, 11.75 GeV/c, baryonium states, cross section and branching ratio 80−95288
p̄p→pπ^-X, 8.9 GeV/c, comparison with leptoprod., quark-parton model anal. 79−63512
pp→π^0X, one-gluon-exchange quark scatt. 78−8714
pp→$\pi^0X/\pi^-p\to\pi^0X$ ratio at high-p_T, quark model explanation 77−10290
pp→π^0+X, large p_T-π^0 spectra, quark model anal. 78−89756
pp→π°X reaction, quark-quark inelastic collision model *(Russian)* 80−32141
pp→ψX or p̄p→ψX, J/ψ prod. mech., p gluon distrib. determ. 79−430
p̄p→S→p̄p, S meson as baryonium state 80−62938
pp scatt., Drell-Yan process, quark-quark contrib. 80−73731
pp scatt. high energy, 50 to 2050 GeV, additive eikonal quark model 79−67606
pp single-lepton spectra at high p_T, parton p_T and gauge invariance 77−18352
pπ→baryons by diquark-quark fusion model 80−102065
φ decays, hadronic, asymptotic freedom, one-photon or three-gluon exchange 80−62971
φ→ηγ, quark loop model, SU(3) splitting of quark masses 80−62990
φ meson, two-body hadronic decay, quark model 78−25040
φ-ω mass mixing sign from gluonic annihilation model, OZI rule violation 79−71722
φN, cross sections and quark multiple scatt. model 79−54350
φπ prod. in e^+e^- annihilation and diffractive photoprod., 4 quark state signature 79−6324
π, deep inelastic structure functions in massive quark model 80−86717
π, effective-bare quark mass distinction 78−12866
π, modified quark loop model, form factors, struct. functions, radiative decay 80−91088
π, structure functions from inclusive prod. data, nonstrange quark distribs. 80−86715
π Bethe Salpeter wave function in ladder model, light cone behaviour 77−18176
π decays and π electromag. form factor, σ-model with quarks 79−22100
π EM form factor, asymptotic behaviour in scale-invariant quark model 78−37211
π EM form factor, large-Q^2 behaviour 77−6002
π electroprod., quark light cone current algebra 78−41556
π electroproduction inclusive processes, quark fragmentation function ratio determ. 77−61294
π→$e\nu_e\gamma$, isospin-breaking, chiral limit, conserved-vector-current violation, σ model 80−62988
π→$e\nu\gamma$, PCAC and quark model 77−30366
π→$e\nu\gamma$ and SU(3)×SU(3) σ-model 80−78054
π inclusive electroproduction, quark-parton model comparison with expt. data 78−37218
π mass in improved static bag model 80−73667
π structure function expt. determ., quark distrib. 79−89154
π structure functions, determ. sea-valence quark contribs. from $\nu\pi^\pm$ deep inelastic scatt. 79−26323
π^0 electroproduction, test of quark parton model 78−8672
$\pi^0\to\gamma\gamma$, u-d quark mass difference effects, form factors 79−89159
π^0 inclusive photoprod. and quark-parton model 78−78189
$\pi^+\to e^+\nu\gamma$, u-d quark mass difference effects, form factors 79−89159
πA high-energy collision yields, evidence for composite quark model *(Russian)* 79−9636
πN in Al, quark jet multiple production 80−9188
πN σ term in hybrid chiral bag model, PCAC and SU(3)×SU(3) symmetry violation 80−78096
πN total cross section sum rule, reln. of sea quark distrib. and pomeron 79−63441
π^-N in Ne, 25, 50 GeV/c, secondary particle multiplicity and multiple scatt. model anal. *(Russian)* 80−83014
π^+n, 195 GeV/c, inclusive π^+/π^- ratio and quark distributions 79−54367

quark models continued
$\pi^\pm$N, 16 GeV, dimuon prod., qq̄ annihilation contrib., exact scaling deviations 79−89196
$\pi^\pm$N, 200 GeV/c, dimuon prod. cross section, Drell-Yan predictions, struct. functions 80−37300
$\pi^\pm N\to\mu^+\mu^-X$, 225 GeV/c, muon pair prod., qq̄ annihilation model 79−63552
πω→ππ *(Russian)* 79−9408
πp, direct photon prod., Compton and annihilation process contrib. 80−105925
πp, large P_T pion^0 prod., meson structure functions, quark distrib. functions 80−86714
πp→$\mu^+\mu^-X$, quark transverse momentum effect in bag model 80−86668
π^-p, 200 GeV/c, valence and sea quark distribs. in the pion, quark recombination model 79−63556
π^-p, 40 GeV/c, charge particle asymmetry and quark model *(Russian)* 77−266
π^-p, large p_T inclusive π^0 prod., quark subprocesses 77−2885
π^-p→$D^0\bar{D}^0$n, 40 GeV, D^0 hadronic decay search for associated prod. of charmed particles 77−13990
π^-p→$\mu^+\mu^-$+hadrons, π^-p→hadrons, quark-parton model 78−74222
π^-p→φn, quark line rule, violations 80−52530
π^-p→φn, violation of Iizuka-Okuba-Zweig rule 77−65173
π^-p→φφn, 22.6 GeV/c, cross section meas. 78−37242
π^-p→π^0X, large P_T collisions, quark cascade model anal. 79−36110
π^+p, inclusive yields, transverse spectra, of nonstrange mesons, direct π prod. 78−4886
π^+p→(π^+pp̄)p 50 GeV/c, narrow baryonium states, diffractive prod. cross sections 80−442
π^+p→K^+X, pion struct. function from low p_T hadron prod. 79−13129
π^+p→ΛX, 32 GeV/c, cross section, quark recombination model 80−52541
π^+p-pp multiplicity difference 79−40813
$\pi^\pm$p, 150 GeV/c, multiparticle prod., quark parton model anal. 79−30756
$\pi^\pm$p, 2-9 GeV/c, large angle elastic scatt. cross sections, parton and bootstrap model test 78−78209
$\pi^\pm$p and pp collisions, charged particle average multiplicities comparison, quark model *(Russian)* 78−17065
$\pi^\pm$p→p$\pi^+\pi^\pm\pi^-$, 16 GeV/c, clustering, multidimens. study using Yang variables 80−5020
$\pi^\pm$single particle distribs. in pp, πp collisions, transverse momentum, rapidity depend. hard scatt. models 78−29361
ψ, ψ′, relative magnitudes of wave functions at origin calc. 77−87947
ψ(3.1)-quark-antiquark coupling calc., dimens. regularisation technique 77−41812
ψ(4.414), width anal. in quark model 78−17010
ψ (4.03), isospin and G-parity, model independent prediction 80−86689
ψ and χ mesons, radiative transitions anal. in nonrelativistic quark model 78−8607
ψ and ψ′ (3684) hadronic production, charmed straton content of straton sea *(Chinese)* 79−63434
ψ decays, hadronic, asymptotic freedom, one-photon or three-gluon exchange 80−62971
ψ→ηγ, pseudoscalar meson mixing and M1 radiative decays 77−30329
ψ family, VDM anal. of contrib. to total photon cross sections 79−22083
ψ hadronic production of heavy quark bound states 79−63435
ψ mass spectra and radiative decay in light-quark model 77−18258
ψ meson, radiative decays, charmonium model 77−38174
ψ meson, two-body hadronic decay, quark model 78−25040
Ψ meson decay rate in charmonium models 79−22061
ψ narrow hadronic widths, extended flavour symmetry, new conserved quantum no. 79−22064
ψ particles and charm, 1975 and 1976 expts. *(Czech)* 79−26288
ψ photoproduction, two-gluon exchange model 78−21437
ψ prod. in pp and πp inclusive interactions, quark energy distrib. 77−22813
ψ(ψ′)→vector meson+pion+pion, disconnected quark diagram, decay widths 77−2824
ψ/J, expt. results and interpretation, review *(Russian)* 77−269
ψ/J and ψ′ decay properties, intermediate states, Iizuka model 77−2825
ψ/J and ψ′ production in hadronic collisions, quark-antiquark annihilation, cascade process 78−25013
ψ/J discovery, expt. details, charm particles, review 77−54113
ψ-family in $e^+e^-\to X$, theory from renormalisation field theory differential dispersion relations 77−26535
ψ-meson family, fourth quark, charm 77−57492
ψ-particles, five-quark model, masses of charmed hadrons *(Russian)* 77−61263
ψ′, ψ decay branching ratios, isospin and flavour symmetry breaking 80−95264
ψ′ and ψ decay ratios, composite particle matrix elements 80−95266
ψ′ decay, Higgs bosons, five-quark model, P and T nonconservation 77−74686
ψ′→ψππ, charm model 78−74250
ψ″(3770), mass width from quark model 80−73723
Q_1(1290), Q_2(1400) vector-pseudoscalar decay rates and SU(3) implications 77−61283
Q_1-Q_2 mass difference and mixing, A_1-B mass difference, predictions 79−13122
qq̄, fine-hyperfine splittings and Lorentz structure of confining potential with vacuum polarisation corrections 80−78041
QQ̄ bound states mixing with Z^0 intermediate boson 79−75719
qq interactions and nonrelativistic quark model 80−73682
qq̄ p-wave systems, fast decay anal. 78−50030
qq̄ prod., quark-mass effects, ψ and Υ mesons 78−66130
qq̄($q^2\bar{q}^2$) mesons, mass formula 80−62958
qq̄ recombination model with resonance prod. 79−75740
QQ̄ relativistic bound states, mass formula, unification of linear Regge trajectories 79−89141
qq̄ static interaction, instanton contribs. 79−12961
qq̄ system, $^3S_1$ levels anal. 78−25003
QQ̄ systems, inequalities 80−78022
$Q^2\bar{Q}^2$ states with relatively narrow widths 79−54300
$q^m\bar{q}^n$, multiquark hadrons, bag model anal. 77−34127
qqq̄, baryonium states, spectrum calc. in quark-gluon model 78−16991
qqq confinement, by infrared singularities 79−36028
qqqq̄, suppressed decays, strings, bags, baryonium 78−21385
qqqq̄ diquonium states, production in e^+e^- processes 80−57615
qqqq̄ mesons, spectra and decay couplings anal. in bag model 77−30331
R-hadron prod. bounds from calorimetry expts. 79−13167

quark models continued
ρ/ω amplitude ratio for radiative decay, sea quark γ emission 79−63440
ρ^+, ρ^-, ρ^0 inclusive prod., cross sections, quark model, π^+p, pp interactions 78−93912
ρN elastic scatt., and meson size, in quark multiple scatt. model 79−54349
S* scalar meson, four-quark nature *(Russian)* 80−68432
s$\bar{s}$ vector mesons, hadronic decays and props., nonrelativistic quark model 80−105892
$\Sigma^- \rightarrow ne^-\bar{\nu}_e$ $|g_A/g_V|$ calc. in quark model, 56-70 octet mixing 79−389
$\Sigma^0 \rightarrow \Lambda\gamma$, transition moment, SU(6) breaking and strange quark mass 77−18284
$\Sigma^+ \rightarrow p\gamma$, radiative weak decays of baryons as single-quark transitions 79−40776
t-quark mass predictions from Glashow determinant condition 80−86677
t-quark mesons, mass, quark model predictions 80−95256
t$\bar{t}$ states, t threshold, potential model predictions 80−86682
t$\bar{t}$ vector meson, proposed 40 GeV mass 80−62942
τ and b-quark spin value, implications for quark and lepton theories 80−32076
τ heavy lepton, possible interactions, quark description 79−45054
τ prod. and decay anal. 78−54605
$\tau \rightarrow \rho\pi\nu_\tau$, quark model, current algebra model, divergence of axial vector current 80−57655
u-quark masslessness, consequences for SU(2) and SU(3) 79−22022
T, EM mass splitting in nonrelativistic quark model 79−89152
T, hadron production of heavy quark bound states 79−63435
T, narrow high mass resonance formation in e^+e^- annihilation at 9.46 GeV, heavy q$\bar{q}$ bound state 78−62414
T, production and decay in quark fusion model 80−102018
υ, Schwinger partial symmetry, quark flavour EM interaction 79−93335
T(9.46), prod. in e^+e^- interaction at DORIS, quark parton model agreement 79−93443
T(9.46) orthoquarkonium decay, jet profiles, three gluon structure 80−73698
T(9.54) and broken SU_3 in nonstrange quark sector, vector mesons 78−58166
T(9.5), cascade-gluon model, bound state of heavy quarks 78−4834
T(9.5), nature of heavy particle anal. *(Chinese)* 78−86443
υ(9.5), prod. in e^+e^- annihilation, photoprod., decay modes, quark model 78−12877
T (9.5), heavy quark charge 78−37180
T (9.5), implications of T for ν interactions in weak gauge theories 78−70271
T (9.6) constituents, heavy quarks as colour sextets, possible weak decay 79−2998
T and charmonium spectra, common pot. fit, T″-T mass difference 80−86712
T decay, photon spectrum, branching ratios, leptonic-, hadronic widths, quarkonium model 79−3020
υ decays, hadronic, asymptotic freedom, one-photon or three-gluon exchange 80−62971
T→e^+e^-, widths and b-quark interpretation of peaks 79−63435
T energy spectra using quark model, leptonic decay widths, spin depend. forces 79−13109
T family, EM transition rates, geometrodynamical quark model 80−47295
T flavoured vector mesons, production in e^+e^- annihilation at DORIS energies 78−93890
T leptonic decay widths, determ. of new quark 78−50029
T meson, bottom quark mass inequality 79−9345
T mesons, level struct., masses, new quarkonium state 78−33031
T observation, charmonium, c-quark and new elementary particles *(Danish)* 79−45048
υ p-wave ground state, mass scaling inequalities for quarkonium levels 80−32071
T→photons+gluons, QCD perturbation theory 78−33028
υ prod. from duality and new quark charge 78−74224
T resonances, mass splitting, bound states of exotic quarks 78−70338
T states with small hyperfine splitting, coupling constants 79−97599
T structure, new heavy quark-antiquark system 78−78138
T′(10.02), prod. in e^+e^- interaction at DORIS, quark parton model agreement 79−93443
T″ leptonic and total width 79−40760
T9.5 GeV dimuon resonance, evidence for fifth quark of 4.7 GeV 78−29312
W-boson prod. cross sections and hadronic jets in pp and $\bar{p}$p collisions 78−8707
X(2.82), γ-transitions in charmonium system 78−78138
$X^0(958) \rightarrow \eta\pi\pi$, ηX^0 mixing angle, broken SU(6)×O(3) quark model 79−17721
ξ(2800) as a four-quark 0^+ scalar meson, SU(5) dynamical group anal. 79−67497
$Z^- \rightarrow \Sigma^-\gamma$, radiative weak decays of baryons as single-quark transitions 79−40776
ζ energy spectra using quark model, leptonic decay widths, spin depend. forces 79−13109
Be+hadron, 200 GeV, quark-quark scatt. model 78−45975
$^{12}C(\pi^-, \pi^\pm)X$, 40 GeV, multiparticle prod. mechanism, additive quark model 79−573
Cu+p, dimuon prod., struct. in T region near 9.5 GeV 78−17201
$Cu+\pi^- \rightarrow \mu^+\mu^-X$, 16, 22 GeV, quark annihilation model interpretation, scaling 79−36277
$Cu+\pi^- \rightarrow \psi X$, 16, 22 GeV, cross section, quark fusion model 79−36278
D^0, D^+ decay widths and branching ratios, quark recombination widths, free quark model 80−27500
$D^0 \rightleftharpoons \bar{D}^0$, weak neutral current diagonality, mixing amplitude, multi-quark gauge model *(Russian)* 80−68414
Δ(1236)-N(939) mass difference from deep inelastic scatt. quark wave functions, hyperon masses 80−47289
^{3}He(e,e), form factors and dimensional scaling quark model 78−93991
^{4}He(e,e), form factors and dimensional scaling quark model 78−93991
K→πe^+e^-, six-quark model, CP violation 80−78055
N struct.functions, $(1-x_s)^4$ behaviour 78−74227
^{16}O, α-cluster model, clustering and nuclear forces in terms of quark struct. 79−6443
pp, polarised p, resonant like structs. in mass region 2100 to 2800 MeV 78−89745
pp→π^0X, quark-quark cross-section, dynamic amplitude factorisation model *(Russian)* 79−22067
Pt+p, dimuon prod., struct. in T region near 9.5 GeV 78−17201

quark models continued
$\psi' \rightarrow \chi_0\gamma$, radiational decays in charmonium *(Russian)* 80−13308
S^*-δ^0 scalar meson mixing as threshold phenomenon from coupling constants 80−27477

quarks
see also quark confinement; quark models
affinity to water molcule, centre expansion SCF calcs. 80−43213
anapole moments, source of odd-parity electron-nucleon interactions *(Russian)* 79−45093
angular momentum group of four quarks 78−16980
anomalous magnetic moments and meson radiative decays in naive quark model 79−17693
atomic spectral line shifts for heavy quark atoms 78−62965
axial-vector-current divergences in constituent-quark basis 78−8557
b quark, a possible member of a colour sextet 79−71712
b quark, weak interactions and multilepton final states 79−49516
b-quark, SU(5), broken, meson mass formulae 80−47267
bare quark masses from transverse cut-offs in e^+e^- interactions 77−18309
baryon mesonic decays, two quarks transition amplitude, baryons taken as symmetric three quark states 78−17013
baryon-quark phase transition, asymptotic freedom studied using renormalised coupling constant 78−4830
bottom mesons, weak decay struct., multilepton production 79−54319
bottom quark mass inequality 79−9345
broken chiral $SU_4 \times SU_4$ symmetry at infinite momentum, have quark mass ratios 79−80768
c-quark mass determ. from nλZ vertex in Weinberg-Salam model *(Russian)* 77−2821
Cabibbo angle and quark spectroscopy *(Russian)* 78−62351
character, possibility of simple constituents 80−42437
characteristic features *(Hungarian)* 79−13180
charge meas. from deep inelastic bremsstrahlung *(Russian)* 78−41555
charges in QCD 79−97575
charges of quarks, η-problem of meson masses, $\eta \rightarrow 2\gamma$, colour model 77−57542
charm particles, implication for unified theory of elementary particles *(French)* 79−67522
charmed quark mass 78−45991
charmed quark semileptonic decay, gluon corrections to charged lepton spectrum 79−75765
classical quark matter, one dimens., Abelian approx. 78−41491
Clifford algebra based unified theory for quarks and leptons 80−47228
collapsed stars of low mass quarks, eqns. of state 78−73725
colour and flavour properties, review *(Czech)* 77−41807
colour magnetic moment 80−42400
composite leptons and quarks, mag. moment 80−105896
composite model of quarks, large P_T hadron prod. 78−62472
composite models, mag. moments of quarks, leptons and hadrons 80−32081
composite quark and lepton model 80−27473
composite quarks and leptons, mag. moments 80−91056
cosmic ray quarks, search by Sydney Univ. particle telescope 78−25388
cosmology, quark era in primaeval Universe 80−36746
current quark masses and symmetry-breaking effects 80−4952
current status in elementary particle physics 79−40651
deep inelastic lepton scatt. in nuclei, energetic quark beam prod. 80−47304
detection using Nb balls *(Czech)* 79−26850
division of matter, confinement of quarks and gluons *(Polish)* 80−68417
dynamical quark mass generation and the mean instanton density 79−54305
dyonic models of hadrons, quark mag. charge allowed values *(Russian)* 80−13275
E6 unified gauge model, breaking patterns, quark-lepton symmetry and mass scales 78−86434
E_6 model of unified interactions, asymptotically free, mass relations and interactions 80−73642
education, elementary particles, quarks and the concept of particle, Richtmyer memorial lecture 78−62286
effective mass from charmed baryon semi-leptonic decay SU_4 symmetry 78−58185
effective mass in expanding bag model 79−97604
eikonal model of hadronic matter distribution of particles and nuclei 79−26317
electric dipole moment in Kobayashi-Maskawa theory with gluonic corrections *(Russian)* 80−86688
electric fractional charge, $^1/_3$e, expt. determ. on Nb sphere 79−21694
electric neutrality of matter at milligram level, quark search 80−105939
electron-hadron interactions, P-invariance, lepton, quark anapolar moments with pol. e *(Russian)* 80−52518
electrostatic forces, Lagrangian model with colour brightening 77−6079
electrostatic interpretation of light quark empirical parameters in elementary particle geometrical model 78−74203
electroweak symmetry group, B-L U(1) generator and quark-lepton symmetry 80−57549
elementary particle physics, information from astronomical observations 80−51935
elementary particle physics, review 78−8493
EM fine struct., Fermi weak coupling, Newtonian grav. constants, unified relation 80−101974
EM form factors 80−99102
energy-range relations for heavy protons and heavy quarks, use in detection 78−58566
evolution operator, quark struct. of states, two dimensional massless electrodynamics *(Russian)* 80−73630
existence of quarks, monopoles, tachyons, etc., review of expts. 78−12872
exothermal nuclear reactions, quark catalysis 79−30873
exotic atoms, conf., Erice, Sicily, (1979) 80−67939
experimental searches, crit. anal. 77−46015
Fermi-Bose couple of coloured preons, primordial QCD, leptons and quarks 80−52461
fermion masses and hierarchy of symmetry breaking, u and d quarks 80−86618
fifth quark, elementary particle physics *(Polish)* 79−54372
fine-structure constant, coupled Maxwell and Dirac eqns., QED 80−62894

quarks continued
finite spectrum relativistic wave eqn. models of quark and lepton masses 78−74130
fixed sphere MIT bag model, b-quark mass, zero-point energy, gs b- - flavoured hadron masses 79−63429
flavour detection using e^+e^- collision jet angular distrib. eccentricity 78−70383
flavour-changing neutral-current process in gauge models and strong interactions 78−8541
fourth generation of quarks and leptons, mass formula 80−105876
fractional charge on matter, obs. by mag. levitation of Nb spheres 77−49709
fractional charge on W particles, Millikan method search 77−74349
fractionally charged, test of existence via meas. of electric neutrality of matter 77−57579
fractionally charged in matter, existence searches 80−42513
fractionally charged ions, search in He gas 80−8954
fragmentation function universality, inclusive hadron interactions 78−66082
fragmentation in field-theoretic model of composite hadrons and e^+e^- annihilation 80−82986
free quark existence, theoretical possibilities 79−17744
free quark search, possible method 79−40749
free quarks, production in early universe 80−393
fundamental constituents of matter and unification of weak and electromagnetic interactions 80−62940
G_1, spin depend. struct. function, scaling violations 78−93880
gauge theories, large transverse momentum behaviour 77−71429
gauge theories, quark fragmentation 78−21340
grand unification with exceptional group E_6, symmetry breaking, SU(5) relations, quark masses 80−68407
grand unified model, Yukawa coupling radiative corrections, lepton and quark masses 79−97555
grand unified wave function for quarks and leptons 80−91034
hadron leptoproduction, nuclear targets, quark-nucleon inclusive cross section, heavy lepton pairs 80−57607
hadron magnetic dipole transition, quark anomalous mag. moments *(Russian)* 80−82975
hadronic charmed particle decays, quark and particle helicities, charm changing current chirality 80−37256
hadronic decays of quark-antiquark resonances, suppression 80−9163
hadronic transitions between $q\bar{q}$ bound states, colour gauge field theory 78−37181
hadronic two-jet events, momentum unbalance, parton transverse momentum in pp, πp 80−57652
hadrons consisting of quarks, form factors in terms of inelastic Jost functions 77−2831
Hagedorn's big-bang model, strongly degenerate heavy neutrino decay, free quark-baryon ratio 78−16589
Han-Nambu, integrally charged quarks expt. search 78−25094
heavy b and t quarks, weak decay, lifetimes and branching ratios 79−97588
heavy quark leptoproduction in QCD, characts. 79−17733
heavy quark physics, practical appls. in energy sources and storage 79−9426
heavy quarks, EM shift of energy levels due to confinement, bag model 80−13287
heavy quarks, possible exotic charge or baryon number 80−47245
history of search for fundamental constituents of matter *(Polish)* 78−54588
horizontal cosmic ray penetrating particles identification, fractional charge search *(Chinese)* 80−101514
infrared properties of quark gas 80−395
interacting, Melosh transform applicability *(Russian)* 78−66116
isospin violating mass differences and mixing angles, quark mass and QCD 80−52505
Kobayashi-Maskawa model, Cabibbo-like parameter and quark mass relation *(Chinese)* 80−42408
LEP, design, tests of unified field theories and quark properties, search for new quarks and leptons 80−74048
lepton and quark spectra difference eqns., τ and toponium mass 80−22589
lepton bound states of sub-hadronic dimens., quark lepton relation 78−54609
lepton model, heavy lepton+quark pair 77−49895
lepton-hadron inelastic scatt., bremsstrahlung of gluons *(Russian)* 77−2839
lepton-quark mass relation in unified theory 79−97560
lepton-quark system, quantum number laws, classification of weakly interacting particles, decays 78−82138
leptons and quarks, EM and weak interactions, flavour $SU_3 \times U_1$ gauge model 79−97554
leptons and quarks, unification within conformal relativity 79−93343
leptoproduction, $\mu N \rightarrow \mu X$, broken colour gauge theory of integer charge quarks 80−13313
local QFT, higher symm. interpretation, spontaneous symm. breaking, quarks and flavours 78−16942
long lived heavy particles with fractional charge, evidence in cosmic ray events 79−2447
long-lived heavy particles, 4 to 10 GeV/c^2 78−78380
low lying baryons, anomalous mag. moment contrib. from quarks 80−42462
magnetic form factor and heavy quark-antiquark pot. form quark-instanton interaction 78−70339
magnetisation of quark gas in intense magnetic field 79−85061
magnetism in neutron star superdense core 80−8646
mass, chiral charge space, statistical analysis 80−42428
mass, electroweak contrib. 80−101990
mass, symmetry-breaking in hadron spectra 80−42436
mass dependence ambiguities in gauge theory renormalisation 79−21913
mass dependence on QCD parameters 79−17675
mass determination in unified weak and EM theory without scalar fields 79−75709
mass differences of up and down quarks, grand unification 80−62978
mass from SU(6) based renormalisable unified gauge model 78−89647
mass generation by pseudoparticles, spontaneous breaking of chiral symm. 77−74646
mass of charmed current quark from D-meson semi-leptonic decay, current algebra treatment 79−97577
mass of third and fourth generation quarks, prediction 80−18133
mass of u and d quarks from weak and EM interaction model 80−13254
quarks continued
mass ratio, charm-to-strange 79−93312
mass spectra, $Q\bar{Q}$ and QQQ, planar bootstrap model calcs. 78−89685
mass spectrum from broken SU(6) symmetry 79−45057
masses, quantitative meas. 79−93311
masses, restrictions imposed by induced strangeness changing processes 77−57491
masses from Weinberg-Salam model renormalisation group eqns. 80−42377
masses in scalar dynamics, gluon theories compared with QCD 80−57553
mesonic processes and quarks in nuclei 80−42564
mesons with heavy quark constituents, lifetime and branching fraction determ. 79−93404
molecular ionisation potential, quark influence, ab initio SCF calcs., appl. to H_2O and SO_2 79−10058
momentum subtraction scheme, quark mass depend. cancellation in anomalous dimens. 80−77965
muonic charge and quark-lepton analogy *(Russian)* 77−219
neutrino induced dilepton events, extraction of heavy quark and heavy lepton signals 78−74243
neutron matter-quark matter phase transition, QCD and extended Higgs model, instantons 80−91062
neutron stars, baryon to quark matter transition 77−5424
neutron stars, quark beta decay and cooling 80−82406
'new particle' searches and discoveries, 'Review of Particle Properties' 1976 supplement 77−57515
nucleon Fermi motion in deuteron, smearing effects, (West β correction), on expt. results. 80−32107
O(10) theory of strong, weak and EM interactions, masses and mixing 80−13248
observable quarks, gluons and leptons 77−34120
observation, calcs. using relativistic quantum field theory 78−24933
observation of fractional charges on Nb ball, exptl. reliability 78−12666
PCAC, chiral anomalies and quark masses 78−8556
PETRA results for fluons, nuclear forces, t-quarks and quark-lepton symmetry 80−86731
physical pion low energy photo- and electroprod., photoprod. phenomenology, quark mass 80−5004
polarised lepton-hadron scattering, lepton and quark anapole moments *(Russian)* 79−17730
preon model for hadron and lepton struct. 78−78124
QCD, confinement and quark theory, introductory review 79−67502
QCD, hadroprod. of heavy quark flavours 79−22062
QCD, heavy quark semileptonic decay, gluon radiative corrections 79−75743
QCD, long-range correl. in forward quark-quark scatt. 78−4779
QCD, new quarks and hadrons 78−8591
QCD, perturbative contributions to quark masses 80−47249
QCD of highly condensed matter 78−70267
QCD theory of three-jet prod. in large momentum transfer reactions 79−93373
QDD, quantum dath dynamics, SU(3) model for composite quarks and leptons 80−91055
$Q\bar{Q}$ bound states, hadronic decay, azimuthal correlations 79−93442
quantum electrodynamics review *(Hungarian)* 78−37159
quark distributions and quark jets from the CERN bubble chamber neutrino experiments 79−45085
quark masses and Cabibbo angles 79−9332
quark masses in QCD, one loop approx. calc. in axial gauge 79−58925
quark-antiquark pairs, role within hadron, analogy with superconductivity theory 78−37176
quarkonia from charmonium and renormalization group equations 79−22055
quarks and leptons, fermion physics in terms of SU(2)×SU(1) gauge theory 78−74197
quaternion quantum mechanics as the description of tachyons and quarks 79−30273
relativistic cosmology, interactions with leptons 80−90590
relativistic quark gas, ground-state energy 78−8537
relativistic quark model for mesons, symm. breaking via quark mass differences 77−79253
restored symmetries, quark system, Pomeron as Josephson current 77−61211
rishon model for quarks and leptons, topological bootstrap approach 80−78047
rishon model of quarks and leptons with double SU(2) symmetry and Dirac magnetic moments 80−82943
scale dependent quark mass in colour gauge theory, $e^\tau e^- \rightarrow$hadrons anal. 77−30320
search for +1/3e fractional charges in Nb, W, and Fe metal 78−66186
search for occurrence in seawater, ocean sediment deposits and volcano lava *(Russian)* 77−64288
search for quarks in matter, mag. levitation electrometer results 80−102088
search for quarks in matter 78−488
search in p+Cu 400 GeV large $p_\perp$ collision 77−79290
singlet quark form factor exponentiation in leading logarithm approx. 80−91091
six-quark theory, calc. of t-quark mass and flavour mixing angles based on $SU(2) \times SU(2)_R \times U(1)$ 79−80811
SO(10) unification, composite structs., quark and lepton composite models 80−57547
spectral function sum rules for quark and baryon fields, using lightlike charges 78−93822
spin, relation to isospin, strangeness and charm 80−37183
spontaneously broken chiral SU(3)⊗SU(3) symmetry, quark mass ratios, Goldstone pseudoscalar meson pairs 79−80770
stable quark detection using cyclotron mass spectrometer *(Czech)* 78−86375
stable quark stars, possibility of existence 77−45471
stars, beta decay 80−82398
stars containing quark matter, nonexistence 79−62855
structure, weak interactions model 77−30313
structure and radius, consequences of second class nucleonic currents 77−18200
structure functions for quarks, gluons, hadrons in QCD 79−54318
$SU_L(4) \times U(1)$ as gauge symm. for quark, lepton quartets, weak and EM interactions, weak currents 78−74174
$SU(2)_L \times SU(2)_R \times U(1)$ gauge model for weak/EM interactions, u-d quarks mass difference 78−12850

quarks continued
$SU(2)_L \times SU(2)_R \times U(1)$ gauge with permutation symmetry, quark mass and Cabibbo angles 80−47232
$SU(2) \times U(1)$ gauge model, eigenvalue condition for Weinberg mixing angle, new leptons and quarks 78−41463
SU(3) colour gauge theory, effective scale depend. quark masses in chiral limit 77−18222
SU(3) quark-meson σ-model, quark masses 80−47178
SU(3) wave eqns. for quarks 80−57571
SU(4) symmetry, meson-quark interactions, mag. moments *(Russian)* 78−45804
SU(5), unification of weak, EM and strong interactions, review 80−105814
SU(5) combined quark-lepton decuplets, particle families *(Russian)* 80−47217
SU(5) gauge model, masses, mixing angles, CP violation and b-quark decay 80−78006
SU(5) grand unification, heavy coloured Higgs scalars, b-quark mass 80−57543
SU(5) grand unification, strong CP violation, quark-lepton mass ratio 80−32057
SU(5) grand unified theory, t-quark mass 79−97559
SU(5) without symmetry constraints, unified model of quarks and leptons, conservation laws 80−101968
SU(n) decomposition theorem, appl. to CP violation through quark mass diagonalisation 80−47216
SU(N) grand unification with several quark-lepton generations 80−27443
subcomponent models of quarks and leptons in SU(3) subcolour, proton decay 80−78035
subquark model of leptons and quarks, unification, currents and exotic states 80−86683
superconducting quark matter, asymptotically high density 78−12863
supergrand exceptional unification and quark-lepton constituents 80−91030
supergrand unification in E_8, quark-lepton assignments, symmetry breaking scheme 80−68408
t quark, prod. in νN collisions, six quark model calcs. 79−93371
t-quark production by ν and $\bar{\nu}$ seimileptonic decay 80−13297
teaching, from Compton effect to quarks, at., proton, and nucl. struct. 78−24596
top quark production, deep inelastic νN scatt., Bjorken scaling law violation 80−9160
tumbling gauge theories with chiral fermion fields, symmetry breaking 80−99042
U(1) problem and zero-mass quarks 78−82124
unbound, attempts to reconcile recent evidence for existence in stable matter 78−58160
unconfined unstable quark, decay characts. 77−30311
unconfined unstable quark, unified gauge theory predictions, selection rules 77−61253
unification of EM, weak and strong interactions, quark and lepton mass, quark fractional charge, baryon asymmetry 80−73637
unified description of quarks and leptons using colour and flavour degrees of freedom 80−27445
unified field theories, proton and neutron disintegration, concepts of leptons and quarks *(French)* 80−91038
unified field theory bounds on number and masses of quarks and leptons 78−58151
unified model, mesons and numbers of quarks and leptons 78−21370
unified models of quarks and leptons, B-L conservation and B nonconservation 80−95229
unified theory of weak interactions of leptons and quarks, gauge model 80−22556
unit charge, search for anomalous isotopes of H 77−61879
up quark mass 79−63461
up quark mass and chiral symmetry at infinite momentum 79−40685
up quark masslessness and $\eta \rightarrow 3\pi^0$ decay 79−40761
up-quark zero mass, critical anal. in current algebra framework 78−82144
weak hadronic $\Delta S = 0$ baryon-π amplitudes, Melosh transformation 78−12857
weak interactions, quark masses, spontaneous violation of parity 77−6054
weak interactions of quark fields, quark masses, spontaneous parity violation 77−34115
weak quark and lepton chiral symmetries, dynamical breaking gauge interaction 80−47215
Yang-Mills theory, magnetic monopoles in the presence of quark sources 80−13213
b quark prod., left-handed currents and lepton number nonconservation 77−67616
b quark weak isospin and possible non-existence of t-quark 79−36010
b-quark, evidence in Υ, SU(5) mass formula, spectroscopic and FM props. 79−17691
b-quark production from νN, $SU(2) \times SU(2) \times U(1)$ gauge group mixing angles 80−68445
$b\bar{b}$ prod. and decay in e^+e^- data at PETRA 79−63492
C-quark, mass difference to be quark 80−78022
c-u mass difference, baryon mag. moments 80−37240
$\chi \rightarrow \psi\gamma$, charmonium E1 radiative transitions and quark mag. moments 80−86721
d-quark mass generation from $SU_L(4) \times SU_R(4) \times U(1)$ gauge models 79−63419
$e^+e^- \rightarrow$charmed particles, contrib. of d-wave charmed quark pair 77−26534
$e^+e^- \rightarrow$ jets, on-shell QCD quark form factor from two particle correlations 80−86740
e^+e^- annihilation, hadron and lepton prod., τ-lepton decay, $K^{\pm}$, p, $\bar{p}$ yields, quark flavours 80−73725
e^+e^- annihilation, heavy quark jet ang. distribs., quark mass, QCD anal. 80−42481
$e^+e^- \rightarrow b\bar{b}$, heavy quark masses and C- and P-odd asymmetries, Weinberg-Salam model *(Russian)* 80−102060
$e^+e^- \rightarrow$hadrons, 33-35.8 GeV, new quark flavour search, cross sections and thrust 80−86736
$e^+e^- \rightarrow$hadrons, R problem, QED and QCD corrections, quarks and leptons 80−95281
$e^+e^- \rightarrow$hadrons, scaling and quark binding anal., generalised vector dominance 77−249
$e^+e^- \rightarrow q\bar{q}$ chromoelectric-flux-tube model of particle production 79−89176
$e^+e^- \rightarrow V(b\bar{q}$ or $\bar{b}q)$, $b\bar{q}$ resonance prod. below $b\bar{b}$ threshold via flavour-changing neutral currents 79−89123
η' mass and quark mass ratio 78−8584
$K \rightarrow \pi e(\mu)\gamma$, quark mass ratios 80−105884
K_{l3} decay, scalar form factor, quark mass ratio determ. 79−93409
neutral current couplings of u and d quarks 78−86435
$\nu(\bar{\nu})$+p interactions, ratio of down to up quarks in proton determ. 77−71504
$\nu_\mu(\bar{\nu}_\mu)$N, charm meson prod. and decay, lepton inclusive distrib., c-quark fragmentation function *(Russian)* 80−52493
$\bar{\nu}_e e$ annihilation in Weinberg-Salam model, number of quarks and leptons *(Russian)* 80−102041
νN, heavy-quark production, t and b-quarks, $SU(2) \times SU(2) \times U(1)$ gauge group mixing angles 80−68445
$\bar{\nu}$N, K^0 and π^- prod. rates, SU(3) symmetry violation in quark jet 80−82966
νN interactions at CERN SPS, search for quarks 78−74240
$\nu N \rightarrow \mu^-\mu^-\mu^+ N$, 350, 400 GeV, event origin, heavy lepton or quark cascade upper limit 78−89698
$\bar{\nu}p \rightarrow$charm quarks 80−102040
pp collisions at 62.2 GeV, search for fractionally charged particles 77−65183
pp interactions, 52.5 GeV, search for fractionally charged quarks 78−70416
ψ and ψ' decays violating Zweig Iizuka rule, asymptotic freedom phenomenology 78−451
ψ spectroscopy, quark-confining string model 77−6094
ψ-meson family, fourth quark, charm 77−57492
$\psi' \rightarrow \chi\gamma$, charmonium E1 radiative transitions and quark mag. moments 80−86721
$\bar{q}$ polarisation in quark sea of proton, QCD anal. 78−12867
$q\bar{q} \rightarrow$3 gluons$\rightarrow$3 jets, jet kinematics and observability 79−45070
$Q\bar{Q}$ annihilations in QCD, strong radiative corrections 79−80809
$q\bar{q}$ states, decay with large mass in 2-D QCD, appl. to meson decay anal. 79−89126
t-quark, grand unified field theories, mass relations and renormalisation effects 79−49436
t-quark, mass in SU(3) horizontal symmetry 80−37230
t-quark, properties and signatures 80−37223
t-quark detection from associated equal sign dileptons 79−67528
t-quark mass, generalised Cabibbo angle, predictions 79−49447
t-quark mass in $SU(2) \times U(1)$ 79−40710
t-quark mass in super unified O(10) model 79−49439
t-quark mass predictions from Glashow determinant condition 80−86677
t-quark production from νN, $SU(2) \times SU(2) \times U(1)$ gauge group mixing angles 80−68445
u-quark mass generation from $SU_L(4) \times SU_R(4) \times U(1)$ gauge models 79−63419
H-quark interaction, var. method calcs. 78−37771
^{2}H, EM struct. in terms of meson currents, quarks and Heitler-London-Cutkosky picture 77−10326
$U + {}^{20}Ne$, quark matter, signature in nuclear fireball model 80−37395
W, fractional charge search using a Millikan type apparatus 78−54334
W ions, fractionally charged, search 78−29083

quartz
α-crystal quartz as IR dichroic laser mirror 79−36908
α-phase, constitutive eqns. by group theoretic methods 80−1954
acoustic activity, Bragg light scatt. at elastic waves *(Russian)* 77−62587
acoustic activity, elastic wave polarisation plane rotation, Bragg scatt. of light investigation 79−65142
acoustic activity, inelastic neutron scatt. obs. *(French)* 80−103431
acoustic interferometer for determ. of acoustic parameters of fused quartz 79−41532
acoustic mode converter in three-dimens. Fabry-Perot interferometer 79−23152
acoustic phonon geometric propag., anisotropic continuum acoustics 77−4169
acoustic resonance vibrations, Berg-Barrett X-ray diffr. method 80−40063
acoustic surface wave diffraction, temp. depend. 77−15674
acoustic surface waves, power densities approximation 77−79987
acoustic wave attenuation by vacancy mechanism at high temp. 79−86846
adsorbed multilayers of water, surface forces 80−6597
adsorption of water, appl. of Hill-de Boer eqn. 79−15008
alpha particle induced radiation defects, EPR and thermoluminescence study 80−20461
alpine metamorphism study using fluid inclusions in quartz crystals *(German)* 77−25677
amethyst, α-β phase transition interaction of Dauphine and Brazil twins 77−62641
amethyst, Fe^{3+} diffusion, associated phenomena 77−36269
amethyst, natural form. conditions and optimum artificial growth conditions *(French)* 79−33911
amethyst crystals, dislocations, selective etch method 78−75674
amethyst large cryst. growth from hydrothermal fluoride soln. 78−11098
amorphous and crystalline, surface polaritons and splitting of optical frequencies 78−72090
amorphous layer on mech. treated single crysts. electron microscope and RHEED obs. 80−24721
anisotropic circular plate initial stress effect calc. 79−55300
anisotropic diffraction by acoustic waves, induced anisotropy 77−50614
anisotropic material elements in optical systems, point and line image intensity distribs. *(German)* 79−55058
annealing effect on optical props. of neutron-irradiated quartz *(Russian)* 77−32381
anthracene-quartz interface exciton luminescence, Frenkel exciton metallic quenching *(Russian)* 80−50421
antireflection film, vacuum-etched high-transmittance 80−74449
AT quartz plate resonators and filters, discrete element model 79−55297
AT-cut plate, bevelled, thickness-shear vibrations 79−90166
AT-cut quartz plate vibration anal. using light modulated oscillator 78−71255
atmospheric dust, imaginary refr. index rel. to particle size 78−7763
atomic reference frequency stability transfer to quartz crystal oscillator 79−54108

quartz continued
ball mill grinding, rate constant determination *(Japanese)* 78−95828
ball mill grinding, wet, dry, rate constant determination *(Japanese)* 78−95827
beach sand, spectral reflectance/grain size relationship 78−16005
bent perfect crystal, diffractional focusing, X-ray spectroscopy *(Russian)* 80−54076
birefr. and opt. rot. near structural phase transition points 78−75823
birefringence, normalised dispersion 79−28713
birefringence measurement using photoelastic modulator 80−31838
Bragg reflection enhancement due to X-ray irradiation under high elec. fields 79−14643
Brazil twins, twinning prod. by successive shears 79−19263
Brillouin spectroscopy of induced phonons 77−28588
c-axis fabrics in metamorphic rocks, anal. via photometric method 80−101456
c-axis orientation in Saxony Granulites, petrofabric anal. by optical and X-ray diffr. studies 80−21740
capillary, viscosity of thin interlayer of aq. soln., between ice and quartz capillaries 79−55913
cathodoluminescence microscopy and spectrometry appl. 77−69919
cell parameter variations between 94 and 298K 80−96497
ceramic, elastic property changes on sintering 77−90301
ceramic, physicomech. props., influence of surfactant incorporated during synthesis 80−20856
ceramic, quartz glass based, organosilicon binder, spalling-resistant, prod. 80−40313
ceramics, thermal and temp. cond. in range 500-1900K 80−39370
chalcedonies, structural disorder by IR spectroscopy 79−87450
chalcogenide glass IKS-25-quartz boundary, mech. of contact interaction, mech. and optical props. 78−88375
circular quartz resonators, parameter calc. with energy trapping *(Russian)* 78−30141
CNDO/2 MO calc. of SiO_2 polymorphs 80−6386
coexistence of α and β phases, elastic light scatt., birefringence 79−47412
colour centre form. by UV irrad., afterglow, thermolum. and EPR obs. 78−10047
complex dielec. const. at audio freqs., 5.5 to 380K 80−25272
crack propag. and bifurcation 78−72888
crazing resistance, particle size effect *(Japanese)* 79−39014
creep and mechanism by which water accommodates dislocation glide 77−90414
cristobalite transform. kinetics 78−11223
crossed fibres, mol. attraction forces meas., depend. on air gap width 77−27216
crystal, AT-cut, ion plating of Ag film, crystallographic structure obs. 80−2280
crystal, charact., operation mode and struct. *(German)* 79−61306
crystal, influence of tabs thickness on resonating props. 78−18140
crystal, oscill. props., mag. field effects 77−59516
crystal, particle track formation and minimal energy loss *(German)* 77−18757
crystal, rotated Y-cut, with two different electrodes as one dimens. acoustic composite resonator 77−84098
crystal flexure bars and tuning forks, frequency-temp. charact. 80−5971
crystal gravitational radiation antenna, Q factor 78−16715
crystal growth, defects induced by seed orientation 80−96454
crystal growth, hydrothermal, appl. of O isotope doping technique 77−28706
crystal growth in fluoride environment, growth features and props. 80−6373
crystal impedance and admittance bridge development 77−37944
crystal intergrowth condensation-crystallisation contact bridge, between dissimilar crystals 79−65332
crystal irrad., optical absorpt. spectra, computer calcs. *(Russian)* 78−92091
crystal lattices of SiO_2 system, spatial symmetry laws 80−19784
crystal microbalance with coatings of finite viscosity, transmission line analogy 80−17933
crystal orientation determ. by Laue method, computer calc. *(Chinese)* 79−32853
crystal resonator nonlinear analysis 79−55299
crystal structure, α-phase, determ. up to 68×10^8 Pa by X-ray diffractometry 79−37668
crystal structure, pattern-fitting struct. refinement method for X-ray powder diffractometer patterns 77−76251
crystal structure rearrangement due to neutron irrad. 80−64981
crystal units, vacuum system for cleaning and cold welding *(Polish)* 80−31776
crystal US vibrations, SEM obs. 79−56733
crystal with electrode-tab config., simultaneous mass and temp. determ. 78−54353
crystalline, birefringence, temp. depend., intracavity method meas. 80−78931
crystalline, far IR complex refr. index spectra determ., new method, for transparent solids 77−28566
crystallinity index 77−17080
crystals orientation in shear zone from Castell Odair, Scotland, re-investigation 78−77216
crystals quartzite breccia, Onaping Formation, Sudbury Basin, preferred orientations 77−9402
crystals with TTC-cut *(Danish)* 80−60504
cultured, hydrothermal growth, prism face develop. rel. to microcryst. form. 77−72572
cultured, prism faces growth and development, attached microcrystals role 77−31612
cultured crystalline, vacuum UV transmittance before and after electron irrad. 78−83044
culturing process for optical grade quartz 79−81494
Dauphine twinning, reversible elastic, in α-quartz 78−87684
Dauphine twinning, stress-induced, acoustic emissions 80−6414
decrepitation recording for gas-liquid inclusions in quartz powder temp. meas. method 77−71325
defects growth, study by X-ray diffr. topography *(French)* 80−39095
deformed rocks, quartz preferred orientation and quartz content inter-dependence 78−88818
delay line second harmonic generation in SAW *(French)* 80−34285
density of states, bulk electronic struct., tight binding calcs. 80−44502
dental composites, acrylic acid grafted on particles by gamma-radiation 80−66840
quartz continued
deposited thin film-resonating quartz crystal substrate interaction, energy transfer model 79−88914
determination by X-ray diffr. on PVC membrane filters 77−70392
diffusion of Ag, radiation stimulated diffusion *(Russian)* 77−39694
digital quartz crystal thermometer principle and technical parameters *(Polish)* 78−24791
digital quartz thermometer *(Russian)* 79−49229
digital thermometer using crystal oscillator, high accuracy achieved 78−65932
dislocation fine structure under electron irrad. 80−70213
dislocation free and low dislocation quartz, preparation by hydrothermal crystallisation 78−72712
dislocation structures in deformed grains, etching technique 77−39590
dislocations, elastic energy *(French)* 79−14807
dislocations, electron irrad. induced vitrification 80−107252
dislocations, inclined, in synthetic quartz 79−99200
dissociated 'a' dislocations, TEM exam. 78−47379
dissociated a-dislocations, effect on plastic deformation 79−7610
dissociated dislocations, appl. of weak beam technique *(French)* 79−42070
dissolution in liq. Si, effect of C, rel. to melt growth of Si 80−70414
dissolution of grown synthetic quartz inside the autoclaves 78−63911
distribution in Atlantic sediments relation to climate, last glaciation 80−8308
doubly rotated α-quartz plate vibration, polarising effect 79−14186
doubly rotated α-quartz plates vibrating in thickness, zero polarizing effect 80−55038
doubly rotated crystal frequency and temp. coeff. angular dependence 77−39142
doubly rotated plates, angle-of-cut goniometry 79−54098
doubly-rotated-cut, numerical anal. of props. of SAWs 80−74616
dust, in situ absorption meas. using reson. CW laser spectrophone 77−73860
dynamic wetting angle of dry lyophilic surface 80−88405
E_1' centre formation and regeneration, α and γ radiation efficiency 79−32992
elastic coefficients, independent fourth-order, determ. 77−20003
elastic constants, fundamental, first temp. derivatives 79−77667
elastic constants and piezoelec. props. 80−92590
elastic plates, rotated-Y-cuts, high frequency vibrations 80−96216
elastically bent crystal plate, diffr. of pulsed thermal neutron beam 77−43116
elasto-optical birefringence modulator construction method *(Japanese)* 77−54809
electrical charact., neutron effects *(Russian)* 77−48119
electrical conductivity var. during heating of quartz veins of various textures 77−53040
electro-optical props. near phase transition 80−80756
electroded doubly-rotated thickness-mode resonators, temp.-induced frequency 79−55298
electrodeposition mech., onto metal electrodeposit, cermet prop. 79−33992
electrogyration effect, electric field depend. of optical activity 77−32352
electrokinetic behaviour in solns. of inorganic electrolytes *(Spanish)* 77−70306
electron beam evaporation, SiO_2 stoichiometric condensate form., optical, dielec. props., struct. 77−16496
electron beam irrad., defect form., annealing and migration effects, ESR obs. 80−50180
electron capture by impurity ions, cross sections eval. using thermolum. data 79−95855
electron irrad., defect struct. and radiolysis 80−107321
electron irrad. fused and cryst., transient absorpt. on pulse radiolysis 79−1779
electron irradiated, optical and anelastic absorptions and resonator freq. 78−64385
electron irradiation effects on optical, dielec., elastic props. 80−59521
electron pulse irradiation effect on defect formation 80−15155
electron states, self-consistent pseudopot. calc., for α-quartz 77−62823
electron-hole centres, energy charact. assoc. with point radiation defects 79−32991
electronic energy band struct. calc. 79−23894
electronic structure of α-quartz, local disorder influence 80−59870
energy level schemes, Fermi level-electrochemical potential level coincidence, quantum yield spectrum 79−69400
EPR of Al-Ag centres in α-phase 78−88186
EPR of E'_4-centre 79−73810
equation of state, derivation from shock wave meas. with allowance for phase transitions 79−88347
erosion of windblown quartz sand on Mars 80−17525
etch features for determ. of quartz grain source 77−70650
etching characteristics of a natural quartz track detector 80−91401
etching in HF, theory 78−27666
fading rel. to lattice deformation *(German)* 78−63760
far IR diagnostic quartz beam splitters 77−39470
far IR ordinary-ray optical constants 80−45025
Faraday effect in transducer material, comparison with glass 78−48149
fast neutron irradiated, saturation of 9.4 GHz hypersonic attenuation 79−23682
fast neutron irradiated, spin-lattice relax., 0.1 to 4.2K 79−78519
ferrobielastic twinning, electrical and acoustic emissions 79−56731
ferrobielastic twinning coercive stress obs. 78−59854
ferroelastoelectricity, expt. 80−40078
ferruginous quartzites of Ukrainian shield, magnetic props. at high press. and temp. *(Russian)* 78−15999
fibre, ESR and IR obs. of microinhomogeneities 77−8401
fibre, torsion balance, sat up by welding fused quartz rods and fibres *(Japanese)* 80−31738
fibres, polar orientation, stereospecific twisting 78−42930
fibres, possible role as templates for biopolymers 79−39345
fibres crossed in air, mol. attraction meas. as function of dist. 78−13566
film, microcrack growth, electron microscope obs. 77−69037
film acoustic surface waveguides, electrically controllable polarisation conversion and its appl. 79−76924
film thickness monitors, effect of accumulated film layers on accuracy 78−72734
filter resonators with energy trapping, optimum design 78−32663
finite strain theory appl. to evaluation of compression curves *(French)* 77−69028
first order transition, coexistence states, optical obs. 80−75350

quartz continued
fission fragment track registration development efficiencies, etchant (etching conditions) depend. 78−66454
fission track dating, grains from Oklo uranium ore deposit 78−20555
flash lamp shell transparency changes and dynamic colour *(Russian)* 79−10370
Fourier transform spectroscopy of obs. states at high temps. 80−97256
frequency control 32nd Annual Symposium, Atlantic City (1978) 79−54100
frequency spectrum determ. for cryst., new method 78−23402
fundamental elastic constants, temp. derivatives 79−55810
fused, γ-irrad., paramag relax. of E′ centres 79−99770
fused, absorption edge, temp. depend. 77−20867
fused, continuous laser emission effects on surface, spectroscopic obs. 79−94271
fused, cylindrical fibres in regular struct., multiple frustrated total internal refl. calc. 78−83094
fused, damage by UV laser radiation, avalanche ionization mechanism 80−76110
fused, dielec. const. meas. at 40-1500 MHz *(Japanese)* 77−87780
fused, elastic wave excitation by charged particle beam 77−89474
fused, electronic struct. determ. by X-ray spectroscopy 79−8210
fused, fracture toughness testing, plane strain, simple meas. method 77−73381
fused, laser torch effects, spectroscopic investig. *(Russian)* 78−76560
fused, light scatt. by SAW on refl. and transmission 79−24288
fused, longit. phonon lifetimes, thermal Brillouin scatt. obs. 77−36255
fused, phonon lifetimes at 2.4K 77−62605
fused, photoelastic light scatt. from surface Rayleigh waves 80−97235
fused, picosecond-pulse optical breakdown, direct obs. of dynamics 78−6629
fused, piezooptic data, precision interferometry 77−26384
fused, positronium form. and decay, elec. field effect 80−97369
fused, second press. derivatives of elastic moduli, US vel. meas. 79−23670
fused, substrate for ZnS, Na_3AlF_6 films, H_2O absorpt., IR anal. 80−75446
fused, thermal cond., temp. depend. at low temps. 80−65322
fused, waveguide struct. form. by H_2^+ ion irrad. 78−18072
fused and cryst. laser pulse breakdown freq. depend., self-focusing elimination 77−55855
fused quartz tube, thermal expansion in a dimensional stability test facility 79−58779
fusion reactor toroidal and helical tubes, forming machine 78−54886
g-tensor and ^{29}Si hyperfine tensors of E_1'-centre for model of O^- vacancy 79−19777
gamma irradiated α-quartz:Al, thermal cond. below 10K 79−51320
gas-solid interface, EPR centres induced by microwave gas plasma 78−80215
glass, boron-containing, struct. investig. using ESR spectra 77−7673
glass, crystn., effect of fusion temp. and time 77−36441
glass, effect of boundary refl. and selectivity of optical characts. on radiative-conductive heat transfer 78−1554
glass, effect of O vacancies and hydroxyl-group concs. on crystn. 77−16533
glass, hydroxyl-free, for low-loss fibre waveguides, γ-irrad. effects 78−13773
glass, IR emissivity, 673-1673K 80−24623
glass, laser breakdown and absorption, 1800-2400K 79−64296
glass, optical breakdown by sharply focused laser beam 79−69776
glass, Si^+O^- defect bands, Raman intensities, thermal treatment effects 79−15444
glass, spectral absorpt., 3000-4000K 80−25401
glass, spectral absorpt. coeff., 0.25 to 1.25 μ and 1300 to 1700K 80−20622
glass, spectral absorption coeff. in 2.0 to 4.8 micron region, up to 800°C 77−43985
glass, surface energy evaluation, by a microindentation method 80−16473
glass, thin layer, interaction with gas-discharge plasma *(Russian)* 78−14178
glass, Ti-doped, acoustic props., thermal stability 77−24356
glass, water vapour influence on crystn. stability 77−36440
glass fibre waveguides, low-loss, radiation-optical stability 79−64345
glass inclusions in quartz and anorthoclase from Pantelleria peralkaline lavas *(French)* 77−9389
glass struct. study using small-angle X-ray scatt. 80−84071
glass-ceramic, atm. influence on sintering rate 79−38784
glass-ceramic second-order microstresses 78−27468
glass-water suspensions, electrolytes effect on viscosity, pH and zeta pot. props. 79−34365
glasses, crystallisation in different gaseous media 77−24269
glasses, spectral absorptance in 0.25-1.25 μ wavelength, 293-1273K temp. ranges 77−36212
glasses, viscosity rel. to crystallisation 77−24386
glasses of various grades, natural luminescence and lattice vacancies *(Russian)* 77−28625
glassy, surface, in vacuum, mechanism of appearance of elec. charges 79−69743
glassy quartz, thermal expansion coeffs., represented by Gaussian spline polynomials 80−44341
grains, from coastal plain of Rio Grande do Sul, Brazil, coaxial crescentic marks *(Spanish)* 78−92816
grains, thermolum. dating, β-dose attenuation correction factors 79−75669
graphite-quartz junction, thermal cond., 6 to 95K, junction rectification 78−63890
gravitational wave antenna, Q-factor 79−35623
ground single crystal, stressed surface layer depth *(Russian)* 79−79133
ground surface, structure features of dull layer 77−54763
growth from soln., mechanism 78−83763
growth layers on natural quartz microcryst. faces, electron microscope obs. 78−14634
growth rate from soln., depend. of mech. Q 78−9978
Gruneisen constants for optical modes, neutron irrad. and press. effects, α-phase obs. *(Russian)* 78−22815
Gruneisen parameter, meas. at high press. 80−8299
handedness determination for electron diffr. convergent beam patterns 78−34498
heat transfer at low temps., lattice thermal cond. 80−92729
quartz continued
heat treatment of dense moving layer, heat exchange development 79−20075
hemicylinder-air-quartz system, semi-infinite crystal, dispersion of surface phonon polaritons 78−71939
HF acoustic losses, measurement using Fabry-Perot acoustic interferometer 80−5887
HF quartz crystal unit frequency/temp. and activity/temp. anomalies 77−39139
high grade quartz, low-temp. impurity band IR absorption spectra 79−56825
high purity, impurity distrib., neutron activation anal. 80−24485
high-frequency phonon lifetimes 80−70338
high-performance quartz crystal oscillators, systems approach 79−54109
HV measurement using quartz electrogyration effect 77−41656
hydrogenic trapped hole species in α-phase, EPR studies 80−44915
hydrolytic weakening of natural and synthetic crystals, emch. and IR study 78−61410
hydrophone quartz transducer stability analysis 77−11102
hydrothermal crystallisation, new natural nutrient sources 77−8738
hydrothermal crystallisation, role of soln. density 80−10516
hydrothermal crystallization at 250°C and 15 kbar, mechanisms 78−49014
hydrothermally grown single crystals, real struct. investig. of rhombohedral faces *(German)* 78−2348
impurity C determ. by isotopic spectral method 80−26093
impurity content and lattice consts. of crysts., electrolysis influence 77−35580
impurity microdefects. electron capture cross-sections *(Russian)* 78−76025
inclusion morphology for thermolum. dating, effect of HF etching 78−70240
inclusion obs., solid-liquid-gas, Raman microprobe-microscope appl. 80−62737
incommensurable phase near α⇄β transition *(Russian)* 78−79768
incommensurate phase near α⇄β transition pt. 79−90748
induced elliptic double refraction, separation into linear and circular components *(German)* 77−24817
infinite piezoelec. plate, on elastic Al, transient response to pot. pulse 78−52442
interatomic forces and lattice dynamics in α-phase 77−7802
interdigital transducer on piezoelectric half space, spectrum of emanating acoustic waves 80−79044
interface with liq. ^4He, saturation effects in phonon reflection 80−92736
internal friction, depend. on strain amplitude, role of dislocations 77−27939
interstellar, radiation effects rel. to diffuse interstellar bands origin 77−13432
intrinsic luminescence 80−16098
intrinsic Q estimation 80−43578
ion beam etching, for SAW refl. struct. fabrication, role of redeposition 77−56123
ion bombardment, extrusion, evidence for radiation-induced stress relax. of silica network 77−24335
ion implanted, radiation defects and optical props. 80−107293
ion-etching of grooves for SAW devices 78−95822
ion-implanted, SAW velocity 0.9 to 6K 78−84040
ion-implanted layers, total X-ray reflection investig. of clustering 78−6081
IR absorption in α-phase 79−42959
IR radiation extinction coeff. rel. to mechanical Q 80−100653
IR reflection spectra of rough surfaces *(Russian)* 77−48175
IR total internal refl. spectrum, surface polaritons *(Russian)* 77−20861
irradiated, fused, crystalline, absorpt. spectra, colour centres 80−7384
large optical component antireflection and protective coatings 79−72660
laser plasma X-ray spectroscopic diagnostics using high-quality quartz and Si crystals 79−68953
laser Raman line polarisation meas. for α-phase 77−4641
laser wave propag. in crystal slab between two linear media 77−14769
laser-induced spherical defects 77−44093
lattice attenuation of longitudinal sound 79−86847
lattice constants, impurity effects 80−39034
lattice thermal conductivity at mantle press. and temp. 78−69338
light scattering by α-β coexistence state 77−69086
light scattering by crushed quartz particles in water 78−40565
light scattering polarisation props. at α-β phase transition 80−108220
lightguide resonator for Nd^{3+}:YAG laser, Raman generation 80−99735
loess-formed quartz silt thermoluminescence and dating *(Chinese)* 78−57226
low, CC Si-O bond characteristics 80−84132
low, ionicity of Si-O bond 80−84133
luminescence centres at 396 and 280 nm 80−103996
lunar impact structures, peak shock press., X-ray diffr. investig. 78−7002
magnetic field effect on fundamental and overtone modes 77−12182
magnetic separation for thermolum. dating of ancient kiln 77−34070
magnetoelectric resonances *(Russian)* 79−42904
mechanically activated, reactivity *(German)* 79−29395
melt, irrad., optical absorpt. spectra, computer calcs. *(Russian)* 78−92091
metallic overlay films for temp. compensation SAW device appls. 80−79043
microstructure and fabric development in quartz-feldspar mylonite 78−96201
microtopographical obs. of 2nd order prism faces, hydrothermally-grown crysts. 80−54481
microwave phonon attenuation in quartz at low temperatures 79−19324
molten, stimulated Mandel'shtam-Brillouin scattering in a magnetic field 79−76762
monidisperse quartz fractions from soils in completely dry state, local stability criterion 77−49060
morphology, detailed discussion on forms *(French)* 79−4266
multiple reflection, correction for single cryst. intensities for average values 79−23488
muonic atoms, hyperfine splitting frequency *(Russian)* 79−91332
muonium EPR transitions by muon-spin rot. 80−29668
muonium hyperfine splitting meas., muon spin rot. technique 80−50246
muonium precession, in α-quartz, quadrupole splitting 79−42879
muonium precession, quadrupole splitting 79−56678
muonium spin precession quadrupole effects 80−75910

quartz continued
natural, dosimetric props., possibility of thermolum. dating of geological objects 79−12288
natural, gamma-irradiated, stress effect on thermolum. sensitivity 80−11482
natural, virgin (γ-irradiated), polarisation effect on thermolum. sensitivity 80−11483
natural and synthetic, 3400 cm^{-1} IR spectra fine struct., H impurities 78−43910
natural crystals, fission fragment track development anisotropy 77−1149
naturally deformed, dynamic recrystn. during creep, dislocation substruct., Mg alloy comparison 80−109142
neutron diffraction experiments with macroscopic objects 79−23503
neutron irradiated, thermal spikes 78−38757
neutron irradiated, X-ray cryst. struct. anal. 79−14853
neutron irradiated α-phase and quartz glass, struct., neutron diffr. meas. 78−22769
neutron track retaining props. for high temp. in-core neutron fluence meas. 77−75032
nonlinear crystals, interference of optical harmonics 80−64102
nylon-quartz fibre support for low temp. mag. suscept. meas. 78−65947
opalescence near α-β transition, static model rel. to domain wall form. 80−11420
optical absorption power after irrad. and annealing *(Russian)* 77−36273
optical constants of pure fused quartz in far IR, 20 to 120 cm^{-1} 78−79080
optical fibre, hollow, with liquid core, stimulated Raman scatt. 78−30087
optical fibre, stimulated Raman scatt., Stokes components recording opposite to pump wave 80−106569
optical fibre waveguide, quartz glass, material dispersion meas. 79−18545
optical fibres, acoustic modulation of light propagation 80−33209
optical fibres, liquid core tetrachloroethylene filled, transmission loss meas. at 3.39 μm 79−81532
optical quartz glass fibres, B and P radial doping profiles 77−50771
optical SHG with surface plasmons 78−18008
optical waveguide, anisotropic, for IR expts. 77−34938
orientation of industrially cut alpha quartz AT plates 80−92008
oscillating crystals, electron contrast effects in SEM 78−88255
oscillating quartz crystal stress distribution meas. by laser probe 77−20803
oscillator microbalance, high resolution, appl. to Al oxidation 77−70219
oscillator plate, surface treatment by 100 keV B ion implantation *(Japanese)* 78−59826
oscillator quartz cuts for improved temp. stability 79−55292
overgrowths, on quartz, cathodoluminescence and microstruct., SEM exam. 79−25239
particle, EM wave irradiated, evaporation, diffusion approx. 80−44308
particles, embedded in NaCl, IR spectra, rel. to state of O impurity in Si 79−19914
periodic laminar structure, optical SHG *(Japanese)* 77−72029
permittivity, X-band 77−2664
phase equilibrium in shock compressed quartz 77−62584
phase transform. in brittle materials, plane stress anal. 77−86024
phase transition, α→β, obs. from nonlinear optics and bond polarisability model 77−15336
phase transition, α-β, in natural and synthetic quartz crystals, effect of impurities 80−20928
phase transition, α-β, lattice dynamical study 79−65168
phase transition, α-β, struct. aspects, light scatt. *(Russian)* 78−47521
phase transition, high-low, effect on compressional and shear wave velocities in rocks under high press. 80−12380
phonon dispersion curves, rel. to $AlPO_4$ lattice dynamics 78−75750
phonon heat conduction of single crysts. by quantum acoustic method 77−11748
phonon polariton dispersion in reststrahlen bands 77−35647
phonon polaritons, bulk, dispersion meas. by IR refl. in α-phase 78−59902
phonon transmission from incoherent radiator into cryst., anisotropic continuum acoustics 77−47521
phonon-polariton modes for freq. chirped optical pulse compression 78−46689
photochromic fused quartz, LITMO, optical props. 80−1287
photoconductivity, 78−76103
photoelectric and photoluminescent props. in fundamental absorpt. region 78−39596
piezo quasi-mosaic struct. effect obs. on X-ray diffr. *(Russian)* 77−89349
piezoelectric, twinning and tailored domain patterns 77−40197
piezoelectric, var. of elastic consts. under gamma irradiation 77−36180
piezoelectric 79−78626
piezoelectric β-quartz roots of frequency eqn. 78−56428
piezoelectric constant measurement, at frequencies up to 50 kHz, by interferometric method 79−63270
piezoelectric constants determ. from dynamical X-ray diffr. curves, α-phase 77−77153
piezoelectric crystal, electron-acoustic signal processing *(Russian)* 77−62111
piezoelectric crystal microbalance for sorption studies under dynamic conditions 80−73323
piezoelectric layer, non-crystalline characteristics after ion implantation *(French)* 77−73117
piezoelectric material for electrostatic voltage sensor *(Japanese)* 80−105632
piezoelectric surface excitation by far IR laser beam 79−46906
piezoelectric surface wave velocity, flexural biasing state influence 79−56730
piezoelectric transducer, acoustic field distrib., Bragg diffr. method 80−97231
piezoelectric transducer, multimodality influence on US vel. and attenuation meas. 77−11100
piezoelectric transducers with tunable working freq. 78−51035
piezoelectricity and gamma-ray diffr. props. 77−20801
Pioneer Venus Programme stable quartz oscillator 77−41288
planoconvex AT-cut quartz resonator vibration displacement meas. by laser interferometry 77−37976
plant deform. and recrystallisation textures 78−68708
plate, z-cut, light transmission, linear polarisation conversion 77−8542
plate frequency changes rel. to electroelastic tensor, polarising effect 78−60398
quartz continued
pleochroic amethyst, optical absorpt. of d^1 ion Fe^{4+} 78−15201
PMMA, quartz- and glass-particle reinforced, abrasive wear 80−97594
podzols, quartz grains surface texture, SEM study 78−36151
porcelain, fast fired, development of microstruct. *(German)* 78−60625
porous, Hugoniot synthesis at high pressures 79−95080
position annihilation radiation, two-dimensional ang. correlation, momentum density meas. 78−10331
positron annihilation, phase composition determ. *(Russian)* 79−91527
positron annihilation in α-form., positronium effective mass and annihilation probability 79−28858
positron annihilation in α-form., positronium quasiparticle damping effect on momentum distrib. 79−28859
powder, dry ball milling, breakage parameters variation with ball and powder loading 80−80999
powder, RF dynamic polarisation echo obs. 77−16254
powder on piezoelec. substrate, dynamic SAW reflecting struct. 80−74565
powdered, hydrothermal reactivity *(Japanese)* 78−23938
powdered, thermal effects of Fe contamination, adsorbed H_2O, annealing on DTA 79−100161
powders, CaO soln. chemisorpt. rel. to lattice parameters, work function 79−37918
preferred orientation, review and outlook 79−83220
preferred orientations of ⟨a⟩ axes in tectonites, flow kinematics 78−96200
pressure sensor, qualification as deep sea gauge *(German)* 79−74980
pulsed RF radiation produced by scratching *(Russian)* 78−19607
quantitative X-ray anal., standardisation, milling effect on degree of disorder *(German)* 78−11176
α-quartz:^{57}Fe, anomalous hyperfine splitting 80−103650
α-quartz:$Ag^{2+}(Cu^{2+})$, γ-irradiated, stabilisation of impurity atoms 79−8047
α-quartz:Ag, Ag atom paramagnetic centre, $A_{Ag\text{-}Si}$ 78−76308
quartz:Ag glasses, EPR of atomic Ag centres 79−15349
quartz:Co^{2+}, far IR absorption spectra, effect of phonons *(French)* 78−31186
quartz:Cu, glassy and cryst., luminesc. centres 77−4679
quartz:Cu(Ag), paramagnetic centre formation after α-irradiation *(French)* 77−69690
quartz:Fe^{3+}, EPR for phase transform., reduced signal above 670K 77−90016
quartz:Fe absorption spectra and structural state of Fe^{3+} ion 80−16071
quartz:Ge, optical and piezoelectric props., ang. distrib. *(Russian)* 78−23404
quartz:Mn, X-ray and thermally stimulated luminesc. *(Russian)* 78−84626
quartz:Nd^{3+} fibre, stimulated radiation generation and amplification 77−88729
α-quartz:P, dynamic interchange among 3 states of P^{4+}, EPR obs. 80−66010
quartz:Ti^{3+}(Li), ENDOR 77−90067
quartz:Ti tube for I photodissoc. laser, C deposit elimination 77−10945
α-quartz, CNDO/2 calcs., electronic props. of perfect cluster, EPR parameters of O^- vacancy 80−107701
α-quartz, compression to 120 kbar 77−15493
α- quartz, ferrobielastic hysteresis 80−19869
quartz, fused, rel. to hyper-Raman scatt. and longit.-transverse splitting of vibrs. 79−73953
quartz, grinding and surface treatment by ball mill in cetyl alcohol *(Japanese)* 80−25890
quartz, isentropic compression by ultrastrong mag. field *(Russian)* 78−47468
quartz, nonlinear polarisation plane rotation due to ruby laser irrad. *(Russian)* 80−53390
γ-quartz, reaction, with NaCl-kCl melt, exam. of struct., IR absorption spectra 80−55706
α-quartz, Renninger effect, forbidden X-ray reflections 80−64980
quartz, single crysts., Ar and O_2 interaction at high temp., surface struct. changes *(German)* 80−96725
α-quartz, temp. in high-press. shock state 80−72490
quartz grains, from sub-glacial and assoc. environments, characterisation using SEM 79−25238
α-quartz surface skimming bulk wave theory 79−56064
quartzite, naturally deformed, textural and microstructural development, metallurgical approach 79−83228
quartzite, shock compressed, vel. of sound meas. 78−10123
quartzite, vitrified, and quartzite based refractory concretes, prep. and props. 80−89188
radiation damage in birefringent samples, meas. using photoelastic modulator 78−87724
radiation defects, effect of annealing on absorpt. spectrum *(Russian)* 77−47495
radiation effects, comparison of different radiations 78−26596
Raman FTIR spectra, surface layer and vol. spectra comparison 78−52491
Raman spectra, anharmonic effects, α-phase *(Russian)* 77−32382
Raman spectral lines of α-phase, radiation and temp.-induced changes in width and intensity 78−2859
Raman spectrum, piezospectroscopic behaviour, for α-phase 78−35138
Raman spectrum of optical phonon mode, stress splitting and wave-vector depend. 77−77214
reaction and bonding with Pd, below MP of starting materials, obs. in TEM 77−21419
rectangular AT-cut plates with patch electrodes, vibration modes 79−55295
rectangular AT-cut quartz resonator frequency rel. to mass loading and electrode geometry 77−39140
rectangular electrode and array dimensioning on AT-cut quartz crystals 77−39169
reflection and surface polariton spectra, ion implantation effect *(Russian)* 79−47451
reflective dot array for high-performance signal processing, development 80−74623
reflector-array-compressor devices, use of Y-cut quartz 80−74625
refractive index distrib. normal to polished surface, ellipsometric meas. 79−86965
resonant powder, stimulated phonon echo, ang. and powder depend. 79−8093
resonator, AT-cut, operating at 270 MHz 77−42671
resonator, electron irrad., optical absorpt. 77−8609

quartz continued
resonator, for thin film thickness monitor 78−11116
resonator, growth sector boundaries 77−39595
resonator, nonlinear thermoelastic couplings *(French)* 80−34118
resonator, second-order phenomena and polarising effect with plates of orientation 78−72463
resonator, X-ray double crystal topographic assessment of defects 79−50943
resonators, AT-cut, temp. depend. of oscillation freq. between resonance and antiresonance freqs. 79−46749
resonators, thickness-mode, thermal stress effects on reson. freq., theory 80−50272
ring gap sizer, characterisation of particle shape in sieve range 78−84732
rocks, quartz-bearing, search for piezoelec. effect 77−73728
rose, charge transfer mechanism for origin of colour, EPR and optical expts. 78−52537
rose quartz, uncompensated Ti^{3+} centre, annealing, X-irrad., EPR meas. 79−65731
rotated elastic consts., coupling factors and conversion efficiencies for AC and BC crysts. 79−19838
rotated Y-cut quartz surface skimming bulk wave analysis 79−56065
rotated Y-cuts, higher-order effects of initial deform. on cryst. vibrs. 77−46862
sand, high-conc. suspension, prod. principles 80−66463
sand, pilot tests of acoustic device for dressing 78−7271
sand, press. soln. expt. 77−60370
sand from Lasko Polje, determ. of Th, U, and K from spectrometry of natural γ-activity 78−20408
SAW, temp. depend. for α-quartz 78−51813
SAW and SBAW on doubly-rotated cuts 80−74584
SAW cut with orthogonal temp. compensated propag. directions 80−10770
SAW delay, zero temp. coeff. 79−86972
SAW diffraction 80−38160
SAW dispersive delay lines, new cut of quartz for temperature stability 80−19185
SAW generation, use of analytical calc. for semi-infinite piezoelec. 78−51809
SAW generation by nonlinear mixing of bulk waves in isotropic fused samples 79−50490
SAW GHz quartz transversal filters, fabrication limits and characteristics 80−43562
SAW oscillator higher-order temp. coefficients 79−55291
SAW propag., effects of He ion implantation 80−75421
SAW propag. characts. on quartz with zero temp. coeff. of delay 80−75420
SAW propagation, acoustoelectric methods 80−84359
SAW propagation, temp. coeffs., piezoelectric coupling *(French)* 78−35093
SAW resonator deep etching 78−59248
SAW resonator design with Al metallisation 77−39147
SAW resonator transverse modes, SEM obs., phase effects 79−68452
SAW resonator tuning by shorted reflector opening 78−59246
SAW velocity, influence of annealing for He^+ ion implanted quartz 79−14996
SAW velocity in Al or Au film on α-quartz, temp. depend. 77−31861
SAW velocity/temperature dependence calc. 79−56062
secondary Dauphine twinning in α-phase, visualisation method 79−51121
secondary electron spin echo obs. *(Russian)* 78−80191
shallow bulk acoustic wave excitation by interdigital transducers 78−59251
shear elastic waves, conical refr. and collinear interaction 77−62588
SHG of ruby laser in quartz slab 77−7159
shock adiabatics at ultrahigh press. *(Russian)* 77−27941
shock-loaded, IR spectroscopic studies, solid-state glass prod. 79−19157
shock-loaded, y-cut shear-wave particle vel., interferometer technique 79−99268
Si-quartz boundary, mech. of contact interaction, mech. and optical props. 78−88375
silt, resistance to isotopic exchange when buried and weathered 79−39709
slit, wetting angle by water, aq. solns. of electrolytes 79−37899
smoky, γ-irrad., electric dipolar echoes 80−20604
smoky, gamma-irradiated, short-time-scale sp.ht. meas. 80−59672
smoky, HF US relax. 78−71796
smoky, sp. ht. 78−71867
smoky quartz, thermal props. at very low temp. 80−24610
space group $C3_12$-$C3_22$, habit variation 80−107090
specific directions of plane elastic waves in thin quartz crystal plates 80−92601
spectral excitation in inert gas medium, detection limits of contaminants 80−55746
spherical ground samples, extinction effects, inhomogeneous mosaicity 78−75494
square wave grating with μm dimensions, reactive sputter etching 78−33921
ST plate, efficient bulk wave excitation 77−15502
ST-quartz SAW resonators and coupled resonator filters 77−39174
stimulated Brillouin scatt. correlation with laser induced damage 77−38984
stishovite, synthetic polycrystalline, thermal diffusivity meas. 79−39706
stress buildup due to UV irrad. *(Japanese)* 79−19278
stress compensated quartz resonator calculations 77−39137
stress gauge, shorted guard-ring, measurement of current and stress profiles 79−58680
stressed, Dauphine twinning growth, thermodynamic theory 79−23619
structural transitions, optical SHG and γ-ray diffr. results 78−14459
subgrain boundaries, theoret. predictions and microscopic obs. methods 80−84187
substrate, adherence of Ti and Cr films 80−7496
substrate, anthracene ultrathin film deposition 80−59812
substrate, chemical vapour deposition of TaB_2 80−29880
substrate, polycrystalline Si film deposition, using double cathode sputtering system *(Japanese)* 77−55889
substrate, SAW attenuation due to platelet defects 79−95253
substrate, slightly rough, ellipsometric meas. of water film thickness, error estimation 78−32856
surface, action of glow discharge *(Russian)* 80−25886
surface, adsorption of chlorosilanes and n-alkanes 79−4466
surface, chemical polishing by etching 78−60858
quartz continued
surface, nonlinearly-absorbing, laser-induced evap. 78−80438
surface, oscillation ground, amorphous zone distribution *(German)* 79−64995
surface, polymolecular adsorbed layers of water, IR absorption spectra 80−9595
surface, seasoned, cyclobutene decomp., variable encounter method calcs. 80−50885
surface, viscosity of nonfreezing thin interlayer between ice column and quartz capillary 80−54475
surface, XPS study 80−93451
surface and bulk acoustic waves excited by interdigital transducers, optical diffr. study *(Chinese)* 78−50965
surface conductivity, adsorbed gas effects 77−85297
surface damage by X-rays, γ-rays, neutrons, SEM study 80−79837
surface defect studies, AES, theoretical model, and expt. 79−7738
surface fluctuation, obs. by laser-induced damage of Au evaporated film 77−1279
surface heating by laser, optical temp. meas. 79−55911
surface irregularities in quartz plates due to mechanical, chemical treatment, piezoelectric resonators appl. *(Polish)* 80−89380
surface irregularity statistics for laser component materials 79−14057
surface polariton dispersion of Au film coated α-quartz 78−48249
surface quality, determ. using Ag diffusion and neutron-activation method 79−51401
surface skimming bulk wave propag. in Y-rotated cuts 80−74583
surface skimming bulk waves, excitation and detection on rotated Y-cut quartz 80−43492
surface space-charge layer form. on γ-irrad. 80−10575
surface structural modification by high temp. gases, computer simulation of RHEED patterns *(German)* 79−95251
surface waves, perturbation anal. of attenuation and dispersion 78−47653
surface-skimming bulk wave controlled quartz crystal oscillator 78−59250
surfaces joined by optical contact, spectral absorpt. of water layer 78−46852
synthetic, Al centres conc. and anomalous pleochroism depend. on crystn. parameters 80−107311
synthetic, annealed, light scatt. centres 77−11586
synthetic, as-grown and etched cobbled Z-surfaces, SEM obs. *(French)* 80−24719
synthetic, connection between lattice deform. and coloration pattern 78−10930
synthetic, cryst. growth, review *(German)* 79−33926
synthetic, crystallisation and defects *(Chinese)* 79−69041
synthetic, deuterisation, EPR and IR absorpt. characterisation 80−92721
synthetic, discoloration rel. to lattice deform. 77−24872
synthetic, dislocations obs. by light scatt. tomography 80−49229
synthetic, electron beam irrad.-induced interstitial ion mobility, ESR centres and IR spectra meas. 80−39153
synthetic, Fe-doped prisms, refr. index study of α-β transition 77−1225
synthetic, Ge doped, refr. index and α-β phase transition 78−83945
synthetic, growth forms and interface molecular group waviness correlation *(Chinese)* 79−51027
synthetic, growth sector boundary between −X and Z sectors 78−59774
synthetic, growth sector boundary between −X and Z sectors 78−59775
synthetic, growth spirals on prism faces, electron and optical microscope obs. 77−7723
synthetic, lattice distortions, optical inhomogeneities by X-ray topography and optical birefringence meas. 78−55887
synthetic, line defects, etch tunnels and X-ray topography 77−76406
synthetic, local variations meas. in spacing and orientation of lattice plane, X-ray anal. 79−52099
synthetic, metallic impurity incorporation 79−19167
synthetic, structure bound water in microinclusions, influence of hydrostatic press. on precip. 78−75838
synthetic α-phase seed plate fracture strength, etching and annealing effects 77−36661
synthetic crystal manufacture, Z-plate, Japanese technology 79−91575
synthetic crystals, observation of growth defects by light scatt. tomography 78−71743
synthetic crystals production, using large autoclaves with 400 kg/batch capacities 79−91576
synthetic hydrolytically-weakened crystals, α-β phase transform. effects on creep props. 77−43274
synthetic piezoelectric quartz, precision meas. of elastic characts. 78−6638
synthetic quartz, characterisation by IR adsorption 79−56824
synthetic single crystal, impurity content 77−11583
temperature-stable shallow bulk acoustic wave devices 79−55293
TFTR diagnostic windows, radiation damage 80−34063
thermal conductivity and diffusivity measurement using non-steady-state method 79−50572
thermal expansion near α-β transition under uniaxial stresses 80−70429
thermal phonon radiation from Au and Cu films into α-quartz substrates 79−42363
thermally excited state relax., acoustic and EM pulse obs. *(Russian)* 77−40293
thermoluminescence, γ-irrad. sample, heat treatment 78−64418
thermoluminescence, glow curves and spectral characts., γ-ray effects 78−2927
thermoluminescence, sensitivity, heat treatment effects 77−59622
thermoluminescence, superlinear accumulation of light sum *(Russian)* 79−52030
thermoluminescence dating, effect of radioactivity within quartz 78−70241
thermoluminescence output intensity depend. on γ-and X-irrad. temp. 77−59623
thermoluminescence sensitivity, proton and gamma induced 77−90205
thermoluminescence sensitivity change due to stress 77−59627
thickness monitor, low temp. film thickness meas. 77−79052
thickness monitor, low temp. film thickness meas. 78−41275
thickness monitor nonlinearity for vac. deposited film meas. 78−29091
thin film deposition, by low pressure, high freq. induction plasma *(Russian)* 79−69992
time dependent phonon irrad. of detector area from pulsed incoherent phonon radiator 78−38790
torsional vibration frequency temp. depend. 80−70294
transducer for shear US meas. of aqueous liquids 80−53599

quartz continued
transducer measurement time extension using fused quartz housing 78−54354
trapping levels 78−91703
tube orifice leaks for local, fast-response gas sampling to mass spectrometers 80−35609
tuning forks, quartz crystal, finite element analysis of displacement at base portion 79−68470
twin boundaries, phase transformations and domain structures *(French)* 78−27509
twinned crystals, after Japan Law, investigation of regrowth 80−54162
two-layer disc, quartz/Permalloy, bending reson. vibrs. *(Russian)* 77−24797
two-port quartz SAW resonator construction and performance 77−39145
Twyman effect in plane-parallel plates, effective surface tension *(Russian)* 77−31867
Twyman effect in quartz and optical glasses, temp. effect 79−4784
ultrafine capillaries with diameters between 0.5 and 60 μm, fabrication and calibration 77−30135
US absorption, influence of plastic deform. and electrostatic field *(Russian)* 80−39226
US shear wave attenuation, 9.4 GHz, AC-,BC-cut, 15-35K 78−26627
US shear wave propagation in γ-irradiated quartz cryst., beat obs. 77−43283
US velocity in X-cut plate, meas. via phase shift freq. depend. 77−14866
UV optical constants, cryst. and fused 77−81078
UV/O_3 cleaning of surfaces, procedure and results 77−25168
valence electron states and X-ray emission spectra, pseudopot. and OPW calcs. 77−35866
valence electron states calc. by pseudopotential method 77−20239
van der Waals forces for interacting mica and quartz plates, calcs. from complete dielectric data 77−32340
Van der Waals interaction, between two crystalline samples, influence of optical absorpt. 79−95273
veins in Stavelot massif, pyrophyllite, dickite and kaolinite 79−34813
wafer, use in simultaneous mass and temp. determ., optimised cryst. cut improvement 79−49205
wafers, surface contaminant estimation methods, cleaning process appl. *(Polish)* 80−89381
water content from mass spectroscopy 77−86401
water saturated, plasticity, rel. to dislocation theory 79−34104
waveguide layer form. on bombardment by B^+ ions 79−27454
weak anharmonic modes detection, multicryst. reson. freqs. 77−81061
wedge, refl., transmission and conversion of normally incident SAW 80−2257
wetting by Au-Si eutectic melt 77−31840
X-irradiated α-quartz, paramag. Ag_2^+/AlO_4 centre, EPR obs. 79−28612
X-ray diffr. obs. of α to β transform. *(French)* 79−96234
X-ray interferometers in quartz crystal *(Russian)* 79−44995
X-ray optical props. determ. using novel X-ray polarimeter 79−6251
X-ray spectra, correlation between cryst. perfection and refl. intensity for analyser cryst. 78−48259
X-ray topographical chamber for work by the Lang extinction method, appl. to quartz *(Russian)* 78−83649
y-cut, impact, appl. of transverse-displacement interferometer 78−12747
Z-cut crystal with Ge additive, radiation attenuator appl., 0.25 to 1 μm, with attenuation coeff. up to 10^3 80−48415
α-quartz:Ge, Ge^{3+} centres, dynamic interchange, EPR obs. 79−19776
Al_2O_3-B_2O_3-SiO_2 system, liq. phase calc. for commercial quartzite powders 80−25671
$CaF_2+SiO_2+Mg(OH)_2$ matrix, quantitative anal. of multocomponent powders, full-profile refinement of Guinier-Hagg X-ray film data 79−39249
Fe^{2+} absorpt. spectra in polarised light and struct. position 79−43007
H concentration profiles by nuclear reaction method 79−60396
MgF, polycryst., quartz particle impacts no. effect on erosion in elastic-plastic response regime 80−81209
OH^- impurity IR absorpt., electron irrad. effects 79−99913
Pt coatings on glass, quartz, ceramic or sitall, method 77−44376
α-quartz:Ge,Ag^+, Ag-compensated Ge centre, EPR meas. 77−77098
α-quartz:P, X- and γ-irradiated, EPR studies of phosphoric ion 77−63263
Rb-Sr ages of weathered and stream transported quartz grains from Harney Peak Granite, S.Dakota 79−74865
SiO_2 bricks, quartz estimation using IR spectra 78−48718
SiO_2:Ag, fused, crystalline, luminescence and colour centre props. 78−10954
SiO_2:Ag, X-ray induced EPR and luminesc. centre 80−65043
SiO_2:Fe, vitreous and cryst., with or without Al_2O_3, Na_2O additions, exam. of Fe^{2+} coordination, IR spectroscopy 78−88344
SiO_2-Cr_2O_3-TiO_2, ceramics, creep and porosity, for ceramics with different structures 80−21011
β-SiO_2-MgO reaction, diffusion controlled 78−6882
Sn film-quartz substrate interface, anomalous transmittance for thermally radiated phonons of thin metal films *(Russian)* 80−103664
WC-Co cemented composites, abrasion by quartz 80−16495
ZnO/quartz for SAW device materials, expt. study of props. 80−80050

quartz resonators *see crystal resonators*

quasars
see also BL Lacertae-type objects; cosmology; galaxies; radiofrequency cosmic radiation; stars
1 mm continuum emission, obs. 78−36720
3C 345, apparent superrelativistic vel. redeterm. in chronometric cosmology 79−25768
0043+389, strong emission line quasar with redshift z=0.189, spectrum and photometry 80−8710
0241+622, possibly associated with CG 135+1, low-energy γ-ray obs. 80−31392
0241+622, very high resolution radio obs. 79−88758
0241+62, nearby quasar, radio props. 79−25752
0254−334/2, high-redshift QSO without Lyman α emission or absorpt., spectroscopic obs. 79−92886
0420−01, correlated time-delayed radio-optical outburst 79−25750
0933+733, redshift determ. from low dispersion objective prism plates 79−2485
0957+561, radioastron. obs. of assumed double quasars 80−105381
0957+561 A, B, twin QSOs, spectroscopic obs. with multiple-mirror telescope 80−12827
quasars continued
0957+561 A, B, twin quasistellar objects or gravit. lens theories 79−67114
0957+561A, B, double quasar, IR obs. of quasar and intervening galaxy 80−73065
0957+561A, B, double quasar radio study rel. to gravit. lens hypothesis 79−88762
0957+561A and B, twin QSOs, direct imaging rel. to gravit. lens interpretation 80−17686
1229−021, H I 21 cm absorpt. at redshift z=0.395 79−62928
1331+170, 21 cm absorpt. detect. at Z≈1.8 79−75292
1400 Å emission feature, rest wavelength and identification 80−12825
1610−771, radio QSO with steep optical spectrum, obs. 80−94887
1633+38, very high resolution radio obs. 77−33663
1978 Halley Lecture 79−40292
2005+403, spectroscopic obs. of associated optical object 77−2484
2A 2251−179, X-ray quasar, UBV photometry 80−82349
absolute magnitude correlation with ejected gas velocities 78−28839
absolute magnitude-volume diagrams, appl. to cosmology *(French)* 80−8705
absolute magnitudes, and Hubble plot 77−91662
absorbing regions in QSOs, extended Lyman α emission obs. 79−44631
absorption line clouds, radiative accel. 78−57683
absorption line features of Fe II and Mg II 78−16559
absorption line redshifts, distrib. 80−90563
absorption line redshifts, limits to past variability of proton/electron mass ratio 77−61338
absorption line redshifts, selection effect 79−92885
absorption line regions, physics 78−57680
absorption line spectra, accidental redshift system estimation 78−16562
absorption line spectra, implications of disc galaxies sizes in Virgo and Hercules clusters 79−75269
absorption line spectra, origin in galactic coronae 77−13448
absorption line spectra and redshift systems, obs. 77−13488
absorption line spectra origin 77−33679
absorption line systems, lack of dust 77−49493
absorption line systems, wind driven shell model 79−21461
absorption lines, line-locking hypothesis, intervening galaxies absorpt. and z=1.95 peak in redshifts 78−57685
absorption lines, origin 78−57684
absorption lines, redshifts statistics and line-locking effects 78−57681
absorption lines, rel. to galactic coronae and intracluster medium origin 80−31355
absorption lines and galaxy Faraday rotation *(Russian)* 79−40273
absorption lines and intergalactic clouds 80−62311
absorption lines due to intervening interacting galaxies 77−17714
absorption lines in QSOs of small and intermediate emission redshift, homogeneous survey results 80−31218
absorption lines in spectra of quasi-stellar objects, review 78−57679
absorption lines shortward of Lα emission, redshifts, origin in moving H I clouds 79−9025
absorption redshifts, evidence for large-scale uniformity of physical laws 80−73079
absorption spectra, effects of intervening galaxies 78−16561
absorption spectra and Wu states, plasma-laser star model 79−48950
absorption spectra in QSOs, line shape analysis 78−36718
absorption systems in high redshift QSOs 78−28843
accreting black holes model, theory 78−57678
accretion disc model, rel. to optical props. 77−64872
accretion discs, thermal continuum as optical emission source 78−54075
accretion disks in quasars and active galactic nuclei, theoretical review *(Polish)* 80−26739
accretion from gas-rich dwarf galaxies, rel. to quasars cosmological evolution 80−31349
accretion on massive black holes in galactic nuclei 79−80335
accretion wake model of galactic and quasar jets in clusters 79−71135
accurate positions of quasars and quasar candidates from $\delta<-45°$ zone 77−87566
active centre, relativistic astrophys. *(Russian)* 77−13233
active galactic nuclei, conference, Cambridge, (England 1977) 79−75281
active nuclei, line transfer calcs. 79−48902
active nuclei, role of UV obs. *(Italian)* 78−32577
active nuclei contrib. to diffuse X-ray background 78−36733
activity, scheme for quasars, radio galaxies, N galaxies and Seyferts 77−45541
alignment of quasars across galaxy NGC 3384 79−53927
angular diameter-redhsift test for large redshift objects 78−28841
angular diameter-redshift relation for matter and radiation filled universes 78−20917
angular positions correl. with Lick galaxy counts, from extragalactic objects catalogues statistical anal. 79−25700
anisotropic radio emission model 80−62304
annihilation model of quasi-stellar objects 80−22109
antimatter model for galactic nuclei and quasars *(Chinese)* 78−73771
AO0827+25, absorpt. lines in optical spectrum 78−4390
AO 0235+16.4, another source exceeding the speed limit 77−2482
Arp QSO-galaxy associations, nature 80−90564
associations with galaxies, statistical analysis 79−9024
astrometric reference frame, ALSEP-quasar differential very long baseline interferometry technique 78−45245
astrometry using Palomar Sky Survey prints 77−87274
atmosphere instability rel. to cool regions in relativistic plasma 80−17486
B2 1225+317, IR and optical spectrophotometry, Hα/Lα ratio 79−25749
B2 1225+31, abundances in z=1.7941 absorpt. line system 80−12826
B2 1225+31, high-luminosity quasar, H emission line intensity ratios 79−25748
B2 1225+31, spectrum of bright quasar 78−93447
B2 catalogue quasars, radio structs. at 1415 MHz 79−35422
B2 quasars, radio spectral props. 79−44632
black hole in galactic nucleus, sustenance 78−57632
black hole model, supercritical accretion on disc theory 80−105272
black hole model *(Japanese)* 80−22114
black hole model of quasar-like objects, appl. to IR and optical emission 78−20905
black hole supercritical disc accretion model 80−41850
black holes, possible existence in quasars 79−48842
black tide model, destruction of stars in isothermal sphere 77−78884
bright optical PG quasars, radio emission at 2.7 and 8.1 GHz 78−45424
bright QSOs, linear polarization survey 78−41077

quasars continued
bright quasars discovery program, preliminary results 77−17715
brightness, cyclic depend. on parameter ln (1+z) 80−105382
brightness fluctuations, source size limits 77−45585
brightness rapid variability, search in eight quasars and BL Lacertae objects 80−90567
broad line emission from black hole accretion disc 77−60819
broad line regions, luminosity and radio emission in active nuclei and quasars 80−105340
3C273, COS B high-energy gamma-ray obs. 78−93454
3C273, gamma-radiation, X-ray source size limitations 79−30143
3C273, HEAO 1 (A4) obs. of 13-120 keV X-rays 79−44633
3C273, spectroscopic obs. and redshift of associated galaxy 78−77606
5C3 sources, optical idents., spectroscopic results 80−46689
5C4 radiosources, search for optical identifications 78−73767
3C 119, 286, 345, 454.3, 5 milliarcsecond resolution maps at 1.67 GHz 80−82531
3C 120, 273 and 345, structure from hybrid maps 79−92883
3C 120, 273 and 345, superluminal vars. 79−92882
3C 147, 3C 286, VLBI obs. at 329 MHz 80−67898
3C 147, 3C 380, milli-arcsecond struct. determined by hybrid mapping with five-station array 80−46694
3C 147, hybrid mapping on Very Large Array, SHF obs. 80−82534
3C 147, radio struct. determ. by multi-element very long baseline interferometry 78−4391
4C 19.31, absorpt. line spectrum obs., evidence for spectrum var. 77−13488
3C 232 spectrum, Ca II absorpt. lines due to galaxy (NGC 3067) 78−36719
3C 249.1, quasar, spectroscopic obs. of assoc. nebulosity 77−33677
4C 25.05, H_2 lines identification in spectrum *(Russian)* 78−69905
3C 270.1 and 3C 275.1, radio maps at 15 GHz 78−93452
3C 273, 3C 454.3, very high resolution radio obs. 77−33663
3C 273, detailed UV obs. with IUE 80−94886
3C 273, far UV spectrophotometry of quasar using Faint Object Telescope 79−25481
3C 273, gamma-ray emission from Penrose powered black hole 80−56925
3 C 273, H I spectral line intensities *(Russian)* 79−88763
3C 273, interplanetary scintillation spectra obs. 80−72741
3C 273, IR polarisation obs. 78−4360
3C 273, IUE obs. of spectrum 79−71149
3C 273, light curve interpretation 78−8143
3C 273, non-thermal radiation *(Russian)* 79−35426
3 C 273, optical vars., shot noise model 77−2480
3C 273, quasar, second-order Compton interpretation of X-rays and γ-radiation 80−22106
3C 273, quasar, UV emission line spectrum 77−87567
3C 273, quasar containing dust, IR spectra obs. 80−56970
3 C 273, radio and X-ray spectra, model, Maxwellian synchrotron source 79−35107
3C 273, rapid fluctuations of radio flux and circular polarisation and optical linear polarisation 77−91663
3C 273, scintillation at 25 MHz rel. to ang. struct. 78−65711
3C 273, search for 1-20 MeV gamma rays, balloon-borne obs. 80−67912
3C 273, spectrophotometry at optical and IR wavelengths 79−17123
3C 273, UBV obs., (1975 to 1979) 80−62309
3C 273, UV spectrophotometry 78−12401
3C 273, UV spectrum, 1200-1700 Å, cosmological implications 78−45425
3C 273, UV spectrum from International Explorer Ultraviolet Explorer (IUE) obs. 78−96540
3C 273, X-ray spectrum, 2-60 keV 80−12824
3C 273, X-ray variability, spectrum and position 79−62929
3C 273, X-ray variability of quasar 79−67112
3C 273 (3U 1224+02), weak X-ray source, ANS meas. 80−46701
3C 273 B, small-scale structure and variability, 2.8 cm obs. 77−33672
3C 273 jet, imaging polarimetry 78−41076
3C 279, variable quasi-stellar source, IR and visible polarimetry and photometry 78−16528
3C 286, radio absorpt. line obs. and appl. to cosmological deceleration meas. 78−20902
3C 286 spectrum, optical absorpt. lines obs. 80−4454
3C 303, double radiosource, radio struct. and optical field 78−16519
3C 303, QSO group in cluster, gravit. lens effect 77−78878
4C 32.69, quasar with radio jet, high resolution radio obs. 80−105375
3C 345, colour variability during flare-ups 79−9021
3C 345, compact radiosource obs. 78−12399
3C 345, large 2.2 μm polarisation obs. 79−80367
3C 345, optical spectrum variability 80−8709
3C 345, optical variability 77−74157
3C 345, optical variability meas. 77−78886
3C 345, quasar, time dependent radio fine structure 77−17711
3C 345, relation between optical and radio VLBI 77−64876
3C 345, VLBI obs. at 1.67 GHz 80−94885
3C 345, VLBI obs. of circular polarizations at 8 GHz 78−41075
3C 345 and 3C 454.3, D2-type QSOs 77−64875
3C 345 and 454.3, 102 MHz obs. of interplanetary scintillations *(Russian)* 80−94889
3C 351, search for periodic components in light variations *(Russian)* 79−53931
3C 351, VLA maps and outer lobe optical emission search 80−105376
4C 38.41, optical variability meas. 77−78886
4 C 39.25, compact radio source, search for time-depend. radio fine struct. 80−90552
4C 39.25, compact radiosource obs. 78−12399
4C 39.46, optical variability meas. 77−78886
3C 395, compact radio source, high resolution obs. at 1671 MHz 80−56960
3C 446, 1980 June outburst, UBV photometry 80−86010
3C 48, emission-line spectrum 79−71147
3C 48, nature of assoc. nebulosity 77−13487
3C 48, search for variability at 408 MHz *(Russian)* 77−17710
4C 55.27, redshift and spectrum 77−45596
4 C 61.20, optically active extragalactic radiosource 77−17712
3C 84, 3C 273, vars. in circular polarisation at 8 GHz 77−33673
3 C and 4C catalogues quasars, obs. with Cambridge 5 km telescope at 5 GHz 78−12391
3C catalogue faint red QSO candidates, spectrophotometry and red shifts 80−67897
4C catalogue quasars, radio structs. of complete sample 79−75293

quasars continued
4C radiosources, brightness and polarisation distrib. 77−26076
4C radiosources, optical identifications 77−26077
4C radiosources, search for variable quasars by image tube photography 77−22326
3C radiosources, systematic optical identification 78−36709
3C sources, depolarization parameter and H II mass 79−35420
catalogue of 403 QSOs 77−26080
CG 135+1, search for 1-20 MeV gamma rays, balloon-borne obs. 80−67912
characteristics and evolution, from radio, X-ray, and γ-ray obs. 77−37611
charge exchange model for broad emission line prod. 77−53681
Cherenkov line radiation, emission line spectra *(Chinese)* 79−80366
Cherenkov line radiation, QSO emission-like spectra *(Chinese)* 80−105378
Cherenkov radiation amplification 77−41294
chronometric cosmology, tests using galaxy and quasar samples 80−86022
classification of extragalactic star-like objects 79−97071
classification using method of principal components 79−97096
clustering and pairing, theory 78−16564
coherent curvature radiation 80−56704
coherent curvature radiation driven by plasma waves 77−60848
collapsed objects models with large central gravit. redshifts, physical props. 77−5588
colliding-cloud system, struct. and spectrum and relationship to QSOs 78−28836
collision strengths of UV emission lines 77−82318
colours in near IR, interpretation 78−69904
GQ Comae, low redshift, optically variable quasar discovery 77−33676
GQ Comae Berenicis, QSO or N galaxy, spectrophotometry obs. 80−77488
compact double radio sources, relativistic blast-wave model for superlight motion 78−28807
compact extragalactic source model, stellar collisions near Kerr black hole 79−12490
compact group of QSOs in Leo 80−27006
compact quasars from Parkes survey, high resolution obs., spectra 79−75295
compact radio sources, relativistic jets model 80−4448
compact radio sources, struct. and time vars. 78−57669
compact radiosources, flux density and linear polarisation at 3.7 and 11.1 cm wavelength 77−49490
compact sources, vars. in intensities and sizes at 13 cm wavelength 77−78876
compact star, radiation, anisotropic fluid in spherical spacetime 77−56821
compact synchrotron sources variability, model of knots spontaneous form. in relativistic flows 80−105369
complete samples, volumes analysis 80−51899
compositions, C/Si, Al/Si and Fe/Mg abundance ratios 78−20903
Compton scattering in sources with synchrotron reabsorption 80−72761
Comptonised spectrum, Monte Carlo simulation 80−90566
condensations in expanding envelopes 77−29946
condensed nucleus rel. to successive supernovae in Seyfert galaxy 77−91652
conference on high redshift objects, IAU Symposium 92, Los Angeles (August 1979) 80−101669
conformally invariant gravit. theory, astrophysical appl. 77−82428
continuous optical spectra, of QSOs and galaxies active nuclei 78−57644
cosmological distance determination, new method, appl. to weighing of Universe 79−9003
cosmological evolution 78−57688
cosmological evolution of extragalactic radiosources 78−28799
cosmological evolution of flat-spectrum quasars 77−64873
cosmological objects in nonradial motion, redshifts, special and general relativistic anal. 79−80212
3CR and 4C quasars, comparative study of props. 77−67136
3CR identifications 78−28825
3 Cr radio sources, spectral index breaks 79−67108
3CR radio sources counterparts, optical field investigations to faint limiting magnitudes 78−54067
CTA 102, 5 milliarcsecond resolution maps at 1.67 GHz 80−82531
CTIO 4 m survey, visible and UV spectrophotometry 80−86009
CTIO Curtis Schmidt survey −40° zone, discoveries and spectrophotometry 80−73064
CTIO surveys of large redshift objects 78−57692
Curtis-Schmidt thin prism survey for extragalactic emission line objects, Univ. of Michigan list I 77−71012
D2 radio structure sources, 11 cm obs. 80−67895
D2-type, alignment of radio structure and magnetic field 79−12540
decimetre flux density vars. time scale 79−53930
dense clouds form. and confinement in QSOs 79−30117
diffuse gamma-ray emission from active galaxies 80−12806
digital speckle interferometry 77−53641
discovery and spectroscopic obs. of high redshift quasars 77−45594
discovery and theories, review 77−60847
distance determ. from quasars to absorbing clouds 79−35421
distance determination, from correl. anal. of radio luminosity features and optical light curve *(Russian)* 80−51880
distribution in depth 80−105383
double extragalactic radio sources, central radio component 78−77617
double radio components, separation vel. *(Chinese)* 78−69903
double radio source structures, form. and superluminal expansion 78−8141
double radio sources, collimation 80−22098
dust opacity and photoionization in far UV 80−46696
emission line clouds, radiation pressure-driven Rayleigh-Taylor instability 79−35419
emission line objects, classification system and list of 116 objects 77−22308
emission line objects from Curtis Schmidt thin prism survey, second list 78−28537
emission line redshift, and true redshift differences 77−64853
emission line redshift distrib. 77−53698
emission line redshift distrib. gaps, trend analysis 78−45423
emission line redshifts distribution periodicities 77−60842
emission line spectra, of newly discovered quasars (with $2.5<z<3.1$) 77−9806
emission lines, photoionisation models, dust in or near quasars 80−27009

quasars continued
emission spectra, photoionisation anal. 78−16560
emission spectra and radio struct. relations 79−40290
emission-line clouds, Rayleigh-Taylor stability of radiation-supported surfaces and slabs 77−53697
emission-line filaments interaction with highly energetic explosions 79−17120
emission-line objects, Univ. of Michigan List IV 78−77494
emission-line objects in Curtis Schmidt thin prism survey, third list 78−28538
emission-line regions clouds, absorpt. spectrum synthesis 80−62308
emission-line spectra, luminosity indicators 77−57103
emission-line spectra and redshift distrib., review 78−57677
emissive regions, self-consistent models 78−57686
energy generation, theoretical explanation *(French)* 77−57104
energy loss by resonance line photons in an absorbing medium 80−56699
energy mechanism, Penrose photoproduction processes 80−31365
energy source, rel. to supernovae relativistic particles total energy upper limit in early explosion stages 79−71059
energy source, supermassive black holes 79−40213
energy source and time variation, accreting massive black holes 79−40214
energy source models and cosmological evolution 80−27002
energy sources, choice between, magnetoid, black hole and compact star cluster *(Russian)* 77−78885
energy sources, review 77−87539
energy sources in quasars and nuclei of galaxies 77−60849
energy supply and press. balance 77−41417
ESO 113-IG45, galaxy and/or quasar, spectrum, photometry and struct. 78−28782
ESO 113-IG 45, interacting galaxy, Type 1 Seyfert spiral with bright central quasar 78−8126
evolution rel. to galactic evolution 78−57693
evolution with resolved components, deceleration parameter determ. 80−31386
evolutionary constraints from galaxy star counts 80−82507
explosions, off-centre, in spheroid 78−63450
extended and compact radio sources, interpretation and theory 78−57670
extended radio sources, VLBI obs. of compact components 80−17680
extended radio sources (>1 arcsecond), large-scale struct. 78−57668
extended sources, radiatively driven winds 80−51901
extragalactic astronomy meeting (Paris, 11-13 December 1978) 79−97121
extragalactic radio sources, problems and advantages *(German)* 77−67134
extragalactic radiosources, bent beams and overall size 79−21452
faint blue objects, nature and distrib. 80−82476
faint blue objects in field of open cluster M67, spectroscopic obs. 77−22329
faint blue objects in high galactic latits., candidate QSOs catalogue near South Galactic Pole 80−46415
faint components, VHF and SHF obs. 80−90547
faint emission line quasar candidates 78−8146
faint quasars, spectroscopy and props. of CTIO 4 metre survey 78−32592
faint quasars number, limits 79−92884
Fairall-9 (ESO 113-IG 45) nucleus, IR and visible photometry 79−25720
Faraday rotation of radio emission, evidence on origin 77−5584
fast spectral line variability interpretation *(Russian)* 80−77286
flat spectrum quasars, evidence for cosmological evolution 78−54074
flat spectrum quasars, rel. to faint radio source counts at 5 GHz 78−32588
flat-spectrum quasars, variability at 962 MHz 77−82317
flux densities and variability at 1.35 cm of quasars with short wavelength radio emission excess *(Russian)* 78−57666
forbidden lines in quasars and active galaxies, theory 78−93408
G-varying cosmology, galaxy and QSO magnitude/red shift relations 80−56980
galactic nuclei, rotating supermassive magnetized disc model 79−84849
galaxy-quasar associations, ang. separations 77−60846
galaxy-quasar associations, search using Jodrell Bank 966 MHz survey 78−24566
galaxy-quasar pairs and surface density of quasars 78−12404
gas and high energy particle interactions, B line search 78−4388
gas clouds, containment by particle flux 79−8820
gas clouds, radiatively driven, dynamics and stability of plane parallel slabs 80−22107
general problems 79−97068
giant black holes, mass-density diagram *(French)* 80−94828
gravitational and Doppler redshifts, interpreted as massive black holes ejected from galaxies 80−46695
gravitational lens effect, focusing by slowly rotating relativistic spherical mass 80−105155
gravitational masers model 78−54071
gravitational mirage *(French)* 80−94710
gravitational radiation 77−9825
gravitational red-shift according to the bi-metric theory of gravitation 79−35119
gravitational screens and superluminal separation 80−51896
gravitational-inertial field of Universe, crit. systems struct. 80−8720
gravity power model, black hole accretion disc rel. to quasar struct. 78−57667
hard X-ray spectra, models of unsaturated Compton accretion discs around supermassive black holes 80−22033
HEAO-2 data, open Universe supported 79−62946
V396 Herculis, low redshift, optically variable quasar discovery 77−33676
HIA 2344+094, new possible quasar near quasar (PKS 2344+09) 77−37659
high energy neutrinos of extraterrestrial origin, possible detection with DUMAND 79−80179
high redshift quasars, existence rel. to gravit. const. var. 78−69892
high redshift quasars, search for 21 cm absorpt. 80−4453
high redshift quasars selected optically and by radio characts., emission line spectra 77−53696
high-redshift QSOs, emission-line regions props. 79−21458
high-redshift QSOs, optically-selected, Image Dissector Scanner (IDS) spectrometry 80−22111
quasars continued
high-redshift quasars from CTIO survey 78−4389
historical light curves, shot-noise interpretation 77−37666
Hoyle-Fowler model, photon emission critical angle 80−31383
Hubble's law, galaxies recession and quasar redshifts *(Swedish)* 77−71144
Hubble diagram for QSOs 78−77616
Hubble diagram statistics, form of luminosity function and density vars. 79−97093
Hubble diagram statistics, q_0 determ. and luminosity evolution rel. to quasars 79−71102
Hubble diagrams, nonparametric statistics 79−40289
Hubble diagrams 78−57691
Hubble diagrams and optical luminosity functions 78−61930
Hubble diagrams for brightest quasars 78−28845
Hubble law isotropy test 79−97111
IC 4329A, spectrophotometry of extreme Seyfert, possible quasar 79−101190
identification and spectroscopy of distant radiosources 77−17705
image doubling, assoc. with absorpt. systems 80−22112
information sources for neutron star, dense matter and gravitational collapse physics 80−36657
interferometer observations of quasars from Jodrell Bank 966 MHz survey 79−5915
intergalactic absorption, rel. to Dirac cosmology and microwave background 78−8176
intrinsic spectra rel. to reddening 79−67113
IR energy distribs., obs. 78−57645
IR sources, optical identification problems 80−105392
IR spectra, H I line ratios 80−105391
jets, models and current-carrying beams 78−49313
large redshift quasi-stellar radio sources, angular dia.-redshift test 78−24565
Lemaitre Universes, Jeans instability 78−12445
line identifications, red shifted UV lines or violet shifted IR lines 80−8707
line profiles in expanding envelopes 79−44464
linear polarisation meas. at 99 GHz 78−93439
local space density, of quasars galaxies active nuclei 78−57676
low absorption line redshift quasars, search for nearby faint objects 79−17121
low-red shift quasars fields, photoelectric UBV stellar sequences *(French)* 80−51904
low-redshift, morphology, electronographic obs. *(French)* 79−88759
low-redshift quasars, optical struct. 78−32596
low-redshift quasi-stellar objects spectra, absorpt. lines obs. 79−21459
luminosity, X-ray to optical ratio, determ. ratio 80−94719
luminosity function, const. density model with luminosity evolution 77−5586
luminosity function evolution ion Friedman model with zero pressure solns. *(Chinese)* 80−51905
luminosity functions for complete samples, observational magnitude cutoff bias elimination 80−56940
luminosity model, galactic nucleus evolution with stellar coalescence and supernovae 77−87568
Lyman α/Hβ intensity ratio in QSOs spectra 77−45600
M82 nucleus, obs. of compact radio source 77−78869
M87 jet, imaging polarimetry 78−41076
magnetic flare model, magnetised accretion disc around massive black hole 80−22113
magnetised accretion disc model, for quasars and active galactic nuclei 79−35425
magnitude estimation from Palomar Sky Survey prints 80−36510
magnitude-redshift relation for matter and radiation filled universes 78−20917
Markarian 231, Seyfert galaxy, obs. and similarity to quasars 77−45558
Markarian 813, photoelectric UBVR photometry *(Russian)* 80−36721
Markarian 992, galaxy with UV continuum, identification as quasar *(Russian)* 77−91445
massive black holes, existence in quasars and galaxy nuclei 79−25713
massive black holes binary systems, model for quasars and active galactic nuclei 80−109546
massive extreme Kerr black holes, Penrose pair production 79−21322
master list of non-stellar objects 77−78668
MCS 141, 232, 275, spectra interpretation, visible obs. 80−90562
MCS QSOs, radio obs. of 70 optically selected objects 80−105377
Michigan-Tololo quasars, spectrophometry 80−22105
millimetre temps. of planets, galactic and extragalactic sources 78−28556
millimetre wave emission, rapid variability obs. *(Russian)* 80−90559
millimetre-wave emission, 90 GHz obs. 78−16548
mm emission from extragalactic objects, luminosities, spectra, microwave background contrib. 77−17677
MO758+120, extended radiosource identification with quasar 77−87563
model, accretion disc around supermassive black hole 79−25466
models, rel. to solar flare physical mechanisms 77−17499
models of radiogalaxies and quasars 78−16557
Molonglo Deep Survey QSOs, optical spectra and redshifts 80−94884
Molonglo Deep Survey sources, radio and optical spectra and red shifts 78−69900
Molonglo radiosource catalogues MC2 and MC3, optical identifications, 11^h28^m to 17^h00^m right ascensions 78−20900
Molonglo radiosources optical counterparts, spectrophotometric obs. 78−4375
MR2251−178, X-ray QSO discovery, 2 Ariel 2251−179 optical counterpart 78−24567
MR 2251−178, nearby QSO in cluster of galaxies 80−67900
MR 2251−178, X-ray QSO, spectrophotometric obs. 79−17122
MR 2251−178, X-ray quasar, companion galaxies redshift data 79−84861
MR 2251−178, X-ray quasar, IR obs. 79−44642
NAB 0137−01, spectrophotometry of possible X-ray quasar 77−13490
NAB 0137−01, UBV photometry and brightness vars. 80−56967
narrow line absorption systems, form. model 80−82535
narrow line region physical conditions 80−31364
neutrinos, high energy, emission from point sources and detect. techniques 79−2484
NGC 1073 field, obs. of three QSOs lying in galaxy spiral arms 80−22110
near NGC 7714−7715, peculiar pair of galaxies, discovery of two quasars 78−28835

quasars continued
nonuniform radial distrib. regardless of redshift 78−32593
NRAO 512, optical variability meas. 77−78886
NRAO 512, VLBI obs. of circular polarizations at 8 GHz 78−41075
NRAO 5 GHz and 4C catalogues, optical spectra and redshifts 78−8145
nuclei, gamma-ray source model 79−25747
nuclei, VLBI hybrid mapping 80−105356
null radiation gravitation deflection by relativistic spherical masses 79−58600
number counts and X-ray background 79−75294
number-magnitude relation rel. to luminosity function and cosmological evolution 80−77507
OA 33, photometric obs., optical candidate 77−9744
OE323 (4C 34.13), extended radiosource identification with quasar 77−87563
OF-024 optically active extragalactic radiosource 77−17712
OH 471, gravit. and cosmological redshifts 77−13229
Ohio radio sources, optical identification using radio and optical positions meas. by Texas interferometers 78−28808
optical and near UV spectrum synthesis for average quasar 77−60843
optical and radio luminosity function evolution 78−86035
optical and radio props. rel. to identifications of 3CR sources 78−28830
optical and UV spectra 79−97094
optical catalogue 77−49492
optical counterparts of 5C radiosources and blue objects, spectrographic obs. 79−101212
optical counterparts of extended radiosources, improved optical positions 78−93444
optical counterparts of radiosources, galaxies and quasars, astrometry 80−90551
optical identifications of extragalactic radio sources 80−105373
optical monitoring, three-colour photographic photometry of BL Lacertae 78−16525
optical polarisation, alignment with radio struct. 79−25751
optical polarisation model, synchrotron radiation 77−2479
optical positions of extragalactic radio sources 77−78881
optical quasars, radio and optical obs., redshifts, luminosity function 78−49552
optical surveys, electronographically recorded low-dispersion slitless spectra 78−57467
optical variability, survey of objects from 17-22^h RA 78−41079
optical variability and absorption line correl. 77−5589
optical variability of quasistellar objects in 13^h+36° field, blue magnitudes obs. 79−40291
optical variability on long time scale 77−22328
optically discovered, search for radio emission 80−90561
optically selected QSOs, accurate positions 79−9022
optically selected QSOs, radio study 80−82536
optically variable quasars, distrib. of ang. distances from bright galaxies 79−58438
optically-selected objects at large redshift, observed props. 78−96562
OQ 172, H_2 lines identification in spectrum *(Russian)* 78−69905
OQ 172, H_2 lines in absorpt. spectrum 80−36734
OS210 (4C 28.40), extended radiosource identification with quasar 77−87563
OTL source positions and struct. form 327 MHz obs. of lunar occultations 80−73061
OV-236 (1921−29), radio outburst obs. 80−51906
paradoxical redshifts compatibility with gravitation theory 78−73757
parallaxes, meas. via radiointerferometric techniques 78−53796
Parkes 2700 MHz survey, optical identifications 77−49489
Parkes 2.7 GHz selected area survey sources optical identifications 77−17701
Penrose pair production as power source 79−44352
PG 0026+129, Lα/Hβ/Pα ratio following IUE UV obs. 79−12537
PG 0026+129, spectrophotometry at optical and IR wavelengths 79−17123
PG 1115+08, triple QSO, probable gravitational lens 80−86012
PHL 1070, spectrum of quasar and surrounding halo 78−28771
PHL 1092, narrow line quasar, discovery of extreme Fe II emission 80−77508
PHL 5200, absorption-line spectrum and relevance of 4C −05.93 source 79−88760
PHL 938, continuum spectrum reddening due to dust 78−96561
PHL 957, H_2 and CO absorpt. lines obs. in quasar spectrum *(Russian)* 79−101216
PHL 957, limits on H I emission in quasar direction 77−91659
PHL 957, Lyman α emission halo upper limit 77−33678
PHL 957, upper limits on Lyman α halo 80−51907
photon splitting into 3, cosomological limits, spectral broadening, frequency-dependent and multiple red-shifts 80−77284
physical conditions and spectra, role of inelastic collisions 77−45599
physical problems assoc. with QSOs 78−57649
PKS 0237−23, absorpt. spectrum obs., absorpt. lines origin 78−41074
PKS 0237−23, absorption redshift analysis 79−35417
PKS 0237−23, Lymanα/Hα intensity ratio from IR obs. 78−41078
PKS 0438−43, high radio luminosity quasar, identification 79−17124
PKS 0528−250, abundances in absorbing material towards QSO 79−40288
PKS 0537−286, high-z QSO with extreme Lyman continuum cutoff 79−12538
PKS 0736+01, optical spectrum variability 80−8709
PKS 0837−12, resolved optical structure 78−81704
PKS 1157+014, spectral obs., of QSO with no Lα emission 80−31384
PKS 1158+007, redshift from QSO spectrum 79−58440
PKS 1402+044, dissector scanner obs. of red object with 3.20 redshift 78−65710
PKS 1510−08, large radio outburst at 2.8 cm 79−30144
PKS 1954−388, brightening 78−77615
PKS 2126−158, absorption spectrum, high resolution study 79−53928
PKS 2126−15, bright quasi-stellar object with neutral colour and redshift of (3.27) 78−93450
PKS 2126−15 (z=3.27), JHK photometric obs. 80−94888
PKS 2134+004, highly luminous QSO, historical light curve 78−54072
PKS 2135−14, photographic obs., assoc. faint optical features 79−9026
PKS 2344+09, obs. of nearby radio sources 77−37659
plasma laser star model, analysis 79−58437
plasma laser star model of QSOs 78−96558
plasma-laser star model, O VI and He II emission lines 77−45597
polarisation properties, of extragalactic radio sources 79−53920
quasars continued
polarised compact radio sources, physical conditions 78−4384
pregalactic black holes as power source 80−56978
primaeval giant elliptical galaxies, observable props. and resemblance to quasars 78−89260
primeval galaxy model, appl. to galaxy form. 77−33645
Q0000−398, angular size of high-redshift quasar 79−44634
Q0000−398, high redshift, large angular size, 2695 MHz obs. 77−45601
Q0002−422 and 0453−423, QSO absorption spectra, high resolution study 79−62925
Q0353−383, QSO abundance anomalies, UV and visible spectral obs. 80−82532
Q0453−423, absorption line spectrum 78−8144
Q0957+561, double quasar, components brightness ratio var. 80−77509
Q2227.6−3928, highest redshift quasar from Tololo deep survey 78−12403
Q2228.1−4033, high redshift quasar from Tololo deep survey 78−12403
Q 0002−422, QSO with $z_{abs} \ll z_{em}$ 78−16565
Q 0420−338 (z=3.13), JHK photometric obs. 80−94888
Q 0420−388, IR obs. of most luminous quasar 78−89272
Q 0932+501, bright quasar with broad absorption features 80−46697
Q 0957+561, double quasar, intervening galaxy obs. rel. to gravit. lens hypothesis 80−27005
Q 0957+561 A,B, UV spectra and gravit. lens interpretation 80−82537
Q 1011+25, C III spectral lines, IUE obs. 79−71089
Q 1246−057, absorpt. line spectrum, presence of outflowing material 78−93453
Q 2204−408, IUE UV spectrum of high redshift radio-quiet quasar 79−35424
Q 2240.9-3702, Q 2238.9-4115, optically selected QSOs with broad-lined absorpt. systems spectra 80−4456
QSO 0241+622, nearby X-ray quasar, extended radio emission search 80−31382
QSO 0242+622, spectrum and luminosity of low redshift object 78−93451
QSO 0752+258 and 1049+616, new redshifts 80−46661
QSO 0957+561, double quasar, 6 cm wavelength obs. 80−62312
QSO 0957+561, double quasar, visible spectrophotometry, gravitational lens interpretation 80−82533
QSO 0957+561, double quasar as gravitational lens, 6 cm VLA obs. 80−101647
QSO 0957+561, H I 21 cm radio absorpt. line redshifted to 594 MHz 80−36735
QSO 0957+561 A, B, 1.666 GHz VLBI meas. and gravitational lens hypothesis 80−27007
QSO 0957+561 AB, double quasar, IR spectrum confirms gravitational lens 80−77510
QSO 0957+561 AB, flux var. and image splitting by stars 80−27008
QSO 1038+528 A,D, close pair of radio-emitting quasi-stellar objects, radio and optical obs. 80−51902
QSO 1756+237, absorbing regions, physical conditions from visible obs. 79−71146
QSO absolute spectral energy distrib. in 0.3−10 μ range 79−62926
QSO absorption line spectra for six high-redshift objects 78−93449
QSO absorption line systems, radiation-driven outflow models 78−57687
QSO absorption redshift systems, central gravitational redshift model 79−25753
QSO absorption spectra 78−86036
QSO absorption spectra origin, intervening galaxy hypothesis 79−5894
QSO absorption spectra origin 80−105387
QSO candidates, spectroscopic obs., indentifications 80−31385
QSO candidates and radio galaxies, optical spectroscopy 80−56966
QSO clustering, pairing and anisotropy 78−57689
QSO emission line asymmetry 79−101214
QSO emission lines, hard X-ray effects 80−26974
QSO emission-line, radiatively accelerated clouds, structure, shape and evolution 80−17685
QSO energy source, tidal disruption by a massive black hole and collisions in galactic nuclei 78−77597
QSO identifications from Molonglo radio survey 78−28842
QSO line spectra, review 77−26081
QSO near NGC 5296/7 galaxy pair, radio obs. 78−93419
QSO pairs, spectroscopic obs. 77−5587
QSO radio emission, Faraday rotation and cosmological magnetic fields 80−22087
QSO redshift $(1+z_i)/(1+z_j)$ distrib. 78−65715
QSO redshift data, statistical 78−32598
QSO redshifted 21 cm absorption line clouds 80−62310
QSO redshifts and field galaxies 78−89271
QSO resonance lines as luminosity calibrators 80−105388
QSO revised optical catalogue 80−105177
QSO spectra, catalogue of absorpt. line lists for 108 objects 78−53840
QSO spectral indices and cut off energy determ. from photoionisation of cold dense universes 80−77526
QSO-galaxy and QSO-QSO pairs, discrepant red shift assocs. statistical anal. 79−8999
QSO-galaxy group assoc., 3C 273 field obs. 80−105385
QSO/galaxy associations, redshifts and distances 80−31369
QSOs, black flash model 78−57673
QSOs, JHKL obs. of four objects 79−40270
QSOs, linear polarisation meas., SHF obs. 80−73058
QSOs, luminosity and emission line intensity ratios 80−86011
QSOs, new type, identified through IR meas. 80−8708
QSOs, optical and radio props. 78−28829
QSOs, permitted Fe II emission, obs. 79−35361
QSOs, redshifts for 24 optically selected objects 78−54073
QSOs, relativistic jets and continuum emission 80−51898
QSOs, survey of optical variability of compact extragalactic objects 79−101215
QSOs 79−2577
QSOs 1548+056, 1721+343, 1722+33, historical light curves 78−32594
QSOs and evolution of galaxies 79−97095
QSOs and Seyfert galaxies, He I lines in spectra 78−36717
QSOs assoc. with clusters of galaxies, radio source morphology appl. 78−93434
QSOs from 4C and Parkes catalogues, complete samples, radio structs. 79−62927
QSOs model, stellar tidal disruption by black hole 77−33674
QSOs near bright galaxies, non-cosmological redshifts 80−105386

quasars continued
QSOs near S.Galactic Pole, photometry and 5000 MHz emission 79−88761
QSOs number density excess and initially inhomogeneous cosmologies 79−2576
QSOs possible assoc. with radio galaxies and rich clusters of galaxies 78−8142
QSOs with assoc. galaxies, spectroscopic search 80−105355
QSOs with flat radio spectra, apparent absence of evolution 77−2481
quasar near companion galaxy NGC 5296, photometry and redshift 77−13489
quasar-galaxy association, massive black hole ejection from galaxies 77−22263
quasar-galaxy cluster associations, rel. to compact galaxies redshifts 77−71143
quasar-like objects in early universe, rel. to D prod. by high energy particles 77−33709
quasars and galaxies active nuclei, conference, Copenhagen, Denmark, (1977 June 27 to July 2) 78−57675
radial distribution, uniformity in chronometric cosmology rel. to X-ray background 80−105409
radiation field, spectral shape effect on ionisation equilib., thermal equilib. and radiative accel. 80−41909
radiation from relativistic blast waves 77−74156
radiation pressure in spectral lines in gaseous systems with axisymm. motions, kinematics 79−88579
radiative acceleration of gas above luminous disc 77−49373
radiative transfer, reson. line form. in decelerating spherical flow 77−78624
radiatively driven winds for different power law spectra 80−90565
radio emission, comparison with emission of active and normal galactic nuclei 78−57646
radio emission, flux densities at 1.35 cm wavelength *(Russian)* 77−64868
radio emission, from intense EM beam-plasma system 79−84663
radio emission, from quasar group selected for optical brightness 80−41910
radio emission, variable, temporal charact. *(Russian)* 80−62307
radio emission from optically selected quasars, search at 1415 MHz 78−20904
radio emission linear polarisation obs. at 7.2 cm wavelength 77−64870
radio emission search from high-redshift optical QSOs 77−64874
radio intensity and polarisation distribs., meas. at three freqs. 78−96560
radio polarization of quasars with optical absorption spectra 78−12405
radio quasars, compact, apparent magnitude-redshift relations for resolved and unresolved sources *(Chinese)* 80−105380
radio quiet quasistellar objects, obs. at 3.3 mm wavelength 78−81703
radio recombination line obs. 79−101193
radio recombination lines, stimulated emission 78−86030
radio sources, ang. size-redshift diagram interpretation 80−22101
radio sources, compact, ripple radiation rel. to low-freq. variability 79−21450
radio sources, compact, strong mag. dipole model 79−17115
radio sources, double, separation depend. on redshift 80−22096
radio sources, extended, MHD instabilities and electron accel. 80−27000
radio sources, extended, relation between radio luminosity and spectrum 80−51894
radio sources, extended, statistical evidence on dynamical evolution 79−88757
radio sources, jets configuration and propag. 80−31374
radio sources, optical identifications using accurate radio and optical positions 77−37660
radio sources, position coincidence optical identifications using Texas Interferometer radio positions 79−88753
radio sources, quasi-stellar, from 4C and Parkes catalogues, studies of complete samples 78−65714
radio sources from B2 catalogue, optical identifications and 5 GHz flux meas. 79−40283
radio sources from NRAO-Bonn 5 GHz survey, optical identifications 77−78880
radio sources from NRAO-MPIfR 6 cm surveys, 21 cm flux density meas. 79−88754
radio sources in south polar cap, optical identifications 79−75284
radio sources of Parkes 2700 MHz survey, new optical identifications 79−75289
radio sources south of declination −75°, QSO candidates optical identification 77−64863
radio sources superlight velocities, model 77−29944
radio structures at 6 cm wavelength 77−60845
radio var. timescale, redshift effect 77−29947
radio-quiet QSOs and superluminally expanding radiosources 79−30142
radio-quiet quasars, Hubble diagram, luminosity function and density evolution 80−51903
radioastrometry, Z *(French)* 80−46411
radiosources, optical identifications, spectrophotometric obs. 79−92879
radiosources from 13th part of Parkes 2700 MHz survey, optical identifications 78−20901
radiosources optical identifications, statistical anal., data selection 78−61928
rapidly varying radio sources, relativistic plasmoids dynamics theory 78−93438
recession vels. greater than light 77−87585
red shift controversy rel. to Seyferts and quasars 77−2476
red shift parameter ln (1+z), periodicity 80−17687
red shift-magnitude link for strong interplanetary scintillation *(Chinese)* 80−12828
red shifts, anal. for randomness 78−12400
red shifts, composite Hubble diagram rel. to cosmological origin 77−22333
red-shift hypothesis implies Earth-centred universe 78−16563
redshift, rejection of photon-photon interaction explanation 79−35423
redshift and 3 GHz radio magnitude correl. 78−45422
redshift data, cosmological interpretation using V/V_{max} test 78−28844
redshift determ. from low dispersion objective prism plates 79−2485
redshift distrib. periodicity, selection effects 78−57690
redshift distribution, implications for evolution of galaxies 80−90527
redshift distribution, selection effects 78−57674
redshift distribution periodicity 77−22327
redshift doublets in absorpt. spectra, model 77−22325
redshift-apparent diameter relation for extragalactic radiosources 77−87559
quasars continued
redshift-magnitude relation, statistical study and chronometric cosmology 78−93455
redshift-magnitude relation for quasars with radio structure *(Chinese)* 77−67135
redshifted clouds, 21 in line studies 80−105389
redshifts, anomalous, and quasar-galaxy associations, examples 79−25722
redshifts, Doppler shifts distrib. for relativistic gas 78−65492
redshifts, evidence for random distrib. 78−54070
redshifts, ln(1+z) periodicity 78−12406
redshifts, teaching consideration 80−90621
redshifts and Hubble diagrams of QSOs 78−96559
redshifts clumping and geocentric universe 77−87565
redshifts cosmological nature, new test 77−17713
redshifts distributions, periodicity 80−62313
redshifts for 19 QSOs 79−97060
redshifts of 24 southern quasars 77−13491
redshifts rel. to parent galaxies masses 77−49480
regular optical variability 77−45598
relationship to BL Lacertae objects, review 78−89259
relative luminosities determ. from emission line strengths 78−61931
relativistic and nonrelativistic gas flows, general symm. soln., low press. limit 77−9655
relativistic blast waves in two dimensions, adiabatic case solns. 80−22108
relativistic plasmon ejection as activity indicator *(Russian)* 80−67870
retarded core model, cosmological role of weak currents 77−5605
rotation measure, intergalactic contrib. 78−20906
rotation measures and data processing 80−86006
Seyfert 1 galaxy nuclei, luminosity function and implications for X-ray background 80−8682
shock waves generated in intergalactic medium at large redshifts 79−21442
size limit, for uniformly pulsating EM radiation sources 79−84656
southern, optical monitoring, data reduction 79−58439
southern Molonglo radio sources, optical spectra 78−96555
southern Parkes radiosources, redshift obs. 78−20899
southern QSOs, redshift meas. 77−26075
southern quasars, optical monitoring 80−56969
southern quasars, spectra and redshifts 77−67137
southern quasars and quasar candidates, UBV photometry 78−32595
southern radiosource identifications 77−45591
space density evolution 79−9027
space distrib. of high-luminosity quasars 78−8147
spatial distribution anisotropy from MC2 and MC3 catalogues 79−53929
spectra, absorpt. effects due to intergalactic pyrolitic graphite whiskers 80−94866
spectra, continuous and emission-line, and relationship to Seyfert galaxies 79−2571
spectra, H absorpt. lines rel. to intergalactic medium struct. 77−67129
spectra, Mg II and Fe II lines excitation 80−67896
spectra, permitted Fe II lines 79−44602
spectra, profiles and redshifts of broad lines 78−16566
spectra, statistical tests for line-locking evidence 77−33675
spectra of large red shift quasars, implications of neutrino rest mass for H I obs. problem *(Russian)* 80−105414
spectral charact. of three high redshift objects 80−4455
spectral line profiles, interpretation from envelope model *(Russian)* 79−101203
spectral props. of 85 quasars from spectrophotometry 80−51897
spectrophotometric survey of radiogalaxies and quasars 78−28828
spectrophotometry of optically selected quasars with $3.0<z<3.5$, appl. to absorpt. line problem 79−25746
spectroscopic study of quasars with absorption redshifts greater than emission redshifts 77−45595
in spiral arms of galaxy NGC 1073 79−53904
star clusters, isotropic relativistic, multi-term trial function stability anal. 78−73742
steep LF radio spectra search among quasars and clusters of galaxies 77−45583
steep spectrum radiosources, spectral index dependent props. 80−36730
stellar debris clouds, in quasars and related objects 78−32597
structure of quasars from 5C2 survey 78−28837
submillimetre photometry 78−4353
super-luminal velocities and chronometric redshift theory 79−9023
supercritical accretion discs winds struct. and appearance, numerical models 80−21984
superfine radiostructure determ. using interstellar scintillations *(Russian)* 80−77297
superluminal expansion, appl. of ang. appearance of white hole 78−45352
superluminal radiosources, structure monitoring 79−44626
superluminal velocities in quasars, review 77−78882
surface density of QSOs 80−8706
surface distribution, intergalactic dust effects in visible, extinction 80−17651
synchrotron radiation model for IR emission 80−31387
systematic surveys with slitless spectrum technique 80−105384
Tautenburg catalogues blue objects, real number of suspected quasistellar objects (QSO) 79−80365
Tautenburg objective prism survey quasars, high-resolution spectra and redshifts 80−4436
theory of H line emission from dense plasmas 80−51900
Tololo deep survey, apparent red shift cut-off unreal 79−12539
Tololo objects, follow up visible spectroscopy 79−17125
Tololo quasar candidates, comparison with positions of bright galaxies 80−77506
Ton 1542, electronographic photometry *(French)* 77−45547
Ton 1542, optical polarisation *(French)* 77−26053
transverse motions, determ. from relativistic Doppler formula for redshift *(Chinese)* 80−105379
two-point angular correlation function between quasars and rich clusters of galaxies 79−80364
4U 0241+61, optical and radio identification, luminous low-redshift QSO 78−61940
4U 0241+62, identification with QSO or Seyfert nuclei-like object 78−16572
UBV photoelectric photometry, of low-red shift quasars *(French)* 80−51904

quasars continued
ultralow dispersion spectroscopy 79−53733
unidentified high latitude radiosources 78−57672
UV continuum source in list of galaxies with UV continua, identification as probable QSO 80−67585
UV emission lines, photoionization model analysis 79−71148
UV excess objects, ubvi photometry 80−46698
UV excess objects in region of NGC 2639 companion galaxy, discovery and redshifts 80−56965
UV obs., implications 80−105390
variable, strong gravity effect on light curve 79−16812
variable compact object discovery in Perseus, bright blue N-galaxy, photometry and spectrum 79−12524
variable quasars as pulsating accretion discs 80−46693
variable quasi-stellar objects, photometry and completeness of faint blue objects in Sandage-Luyten field 78−54069
variable quasi-stellar objects, photometry and completeness of faint blue objects 78−93446
variable radio emission, nature of cm radiation quasisteady component 79−21456
variable radio sources, obs. at 0.95 and 1.65 cm wavelength 78−16552
variable radio sources, ten-year study at centimetre wavelengths 78−89267
variable radio sources search at 18 cm wavelength, complete sample obs. 78−89268
visual magnitudes rel. to radio luminosity of components *(Chinese)* 78−28840
weak radio nuclei in galaxies and quasars 77−17680
white holes, appearance rel. to quasars and BL Lacertae objects 78−81650
WSRT deep surveys, identifications 78−28826
X-ray background contrib. 80−105405
X-ray background source possibility 80−94898
X-ray detection of cosmological objects 80−62323
X-ray emission detectability, deep surveys predictions and strategies 78−96567
X-ray emission from radio quasars, deep search by Ariel V 78−12402
X-ray observations of objects at cosmological distances from the 'Einstein' observatory 80−105171
X-ray properties from Einstein Observatory obs. 80−27004
X-ray quasar 0241+622, IR obs. 79−44642
X-ray quasars, evolution rel. to contrib. to X-ray background 80−82551
X-ray quasars, new obs. 79−62930
X-ray sources, low redshift, visible spectra and UBVRI photometry 80−105397
X-ray spectral lines profile evolution due to Comptonisation, Monte Carlo computations 79−66916
young galaxies and quasars, review 78−32582
young objects in hot big bang model 77−29968
$Z_{abs} > Z_{em}$ systems, props. rel. to origins of QSO absorpt. line systems 78−57682
III Zw 2, spectrophotometry of assoc. galaxies and nebulosity, redshifts 79−21460
C lines, charge exchange reaction effect 79−58243
Fe II emission obs., spectrophotometry 78−4347
Fe II emission profiles interpretation 77−9791
Fe II lines, permitted, form. and relative intensities rel. to low excitation region parameters 80−62278
Fe II permitted emission, excitation mechanism 79−21412
Fe II UV lines, spectrophotometry obs. of 11 QSOs 80−73063
H emission line ratios, implications 80−56968
H emission-line spectra, theory 78−96557
H I absorption in QSO spectra, search for absorption by clusters of galaxies 78−93448
H I and Mg II absorpt. lines obs. in QSOs 78−28838
H I Lα/Hα ratio for flares, quasars and prominences 78−61826
H I Lyman α absorpt. line distrib., intergalactic origin 80−67899
H I Lyman α/Balmer β intensity ratio interpretation 79−35418
H, line and continuum emission calcs. 80−27003
He I 584 Å in quasars and gaseous nebulae, line transfer problem and line strength 80−67550
Mg II 2798 Å and Hβ emission, line profiles 80−12807
Mg II 2934 Å emission in QSOs, possible identification 78−41073
O VI 1035 A emission and Lyman β 77−2483
Si II spectrum calc. 77−60844

quasi-particles
see also excitons; helicons; magnons; phonons; plasmons; polaritons; polarons; ripplons; rotons; solitons
3d system, configuration based quasi-particles 78−91648
alkali metal, electron-electron scatt. in terms of dielec. and vertex functions 79−95351
amorphous solids, low-energy excitations of phonons, magnons, electrons rel. to struct. factor 80−44488
Anderson model, quasiparticle lifetimes 80−44532
atomic and mol. systems, breakdown of quasiparticle picture, inner valence electrons 78−5112
binary boson system, variational calc. of ground state props., appl. to dil. ^{3}He-superfluid ^{4}He mixtures 79−73372
Bose fluid, interacting excitations 77−43401
Bose gas, temp. depend. of quasiparticle sound velocity 77−69128
Bose gas, two-dimens., charged, in zero mag. field, quasiparticle energy spectrum and damping 80−142
boson system, strongly interacting, excitation spectrum 78−71897
boson-soliton scatt., sine-Gordon model 80−9109
Brownian quasiparticle model 80−46976
classical system, backflow effect 79−27614
clean superconductor, effect of impurity scatt. on thermally induced charge imbalance 80−60135
correlation functions, time and temperature, calc. method with quasiparticle appls. *(Russian)* 78−12641
Coulomb superconductor with inverse quasiparticle distrib., behaviour in mag. field 77−20490
covalent crystal, dynamical correlation effects on quasiparticle Bloch states 80−88499
DC resistivity as functional of generalised dynamical susceptibilities, solid state model 79−28330
de Haas-van Alphen effect, quasiparticle approach 80−10897
de Haas-van Alphen effect, quasiparticle picture 78−91592
dense gas, quasiparticle kinetic eqn. construction 80−53905
quasi-particles continued
density of states, in anisotropic flat slab, in effective mass tensor approx. 79−28266
disordered systems, phonon-like excitations, dispersion and damping 80−49331
doped semiconductor plasma, inelastic light scatt., spin diffusion 77−36241
dynamics, inverse Liouville problem, quasi-particle dynamics from a given kinetic eqn. 80−101749
electron gas, ground state, functional spin-density method *(Russian)* 78−51914
electron liquid, plasmon dispersion 78−56099
Enskog quasiparticle, non-Hamiltonian dynamics 80−101750
even nuclei with A=228 to 240, anharmonicity of vibr. states, quasiparticle+phonon interaction influence 77−61340
exciton insulator, coherence factors and transport props. 79−28291
Fermi and Bose quasi-particles in lattice system *(Russian)* 79−75462
Fermi glass, theory for localised electrons 77−39807
Fermi liquid, transverse sound, soln. to dispersion eqn., with nonzero Landau F_2 77−20150
fermion systems, quasipartic renormalisation of memory function approach for response functions 78−8345
ferromagnetic metals, dislocation drag by conduction electrons 80−24451
ferromagnetic metals, Fermi liquid effects 77−51897
ferromagnetic semiconductor, doped, electron spin polarisation and conduction band struct. 80−65449
gas-metal interactions, scatt. dynamics 80−92787
granular metal, supercond. transition, increased resistance rel. to quasiparticle tunnelling 80−88689
hadron microstructure, de Sitter microuniverse, relativistic Hooke group and nonrelativistic quark model 80−27480
Hubbard model, magnetic instabilities, influence of short-range correlation effects 79−7963
Hubbard model, narrow-band region, quasiparticles, electron relax. and transport props. 80−80151
Hubbard model, quasi-particle energy in weak correlation regime 79−28305
Hubbard model, split-band solution and energy gap, narrow-band region 80−75484
instanton interactions, inequivalent embedding of SU(2), gauge fields 77−10180
interface of two media, quasiparticle interaction 79−65532
Josephson junctions, collective excitations in superconductors below T_c, tunnel current fluctuations 79−33403
Josephson tunnel current, Bogolyubov quasi-particle calc. 79−1647
Josephson tunnel junction, interference current component, Riedel peak width *(Russian)* 80−11137
Josephson tunnel junction, quasi-particle heterodyne mixing 79−56395
long superconducting bridges with variable thickness, Josephson effects 78−14897
magnet symmetry, and quasiparticle spectra at low momenta 79−42726
magnetic semiconductors, excitation spectrum, temp. and band occupation depend. 80−49588
magnetic soliton, in one-dimensional mag. systems, obs. *(Japanese)* 80−2555
many-body medium, quasiparticle pairing at arbitrary densities, soluble model 77−6252
metal, quasiparticle bands, cond. electron mixing with impurity d(f) ions *(Russian)* 78−10409
metals, electron resonances and energy spectrum, quasi-particle approach 79−61225
metals, simple, quasiparticle props., density functional approx., electron gas calc. 80−96808
metals, superconductivity studied by electron-phonon and Coulombian e-e coupling strength and quasi particle mass 80−88666
metals and alloys, electrons at Fermi surface, book 80−105445
molecular crystals with several sublattices, exciton-phonon interaction and Bose-Einstein condensation of Frenkel excitons 80−107713
multiband system, electron pairing, radiation effect 80−88679
n-type semiconductor, inelastic light scatt. from magnetoplasma oscills., Landau quasi-particle model 77−12385
nonequilibrium double tunnel junction, anal. 79−19698
nonequilibrium superconductivity, oscill. of order parameter caused by quasiparticle injection 79−42697
nonequilibrium superconductor, effect of pair breaking on branch relax. 79−78257
nonequilibrium superconductor, optical pumping, transition point *(Russian)* 77−12064
nonequilibrium superconductor with optical and tunnel quasiparticle pumping, threshold instability and inhomogeneous states *(Russian)* 79−87209
nonequilibrium superconductors, ferromag. ordering of quasi-particles and rise of domains 80−107958
nonequilibrium superconductors, mag. field depend. of relax. times 79−28477
nuclear collective model, two-phonon states, effect of Pauli principle 80−68565
nuclei in 2p-1f shell, quasi-particle-phonon interaction 80−22770
one-dimensional system, electron-phonon interaction, soliton solns. 79−23691
oxide-barrier tunnel junctions, single-sideband mixer noise temp. for quasiparticle mixing model 79−51722
pairing rotations and quadrupole modes, many-quasiparticle excitations 80−18165
para-Bose states, generalised Bogoliubov transform. coeff. 80−27211
paramagnet, electron state density for narrow-band model with Coulomb interaction 80−10852
photon-photon bond state via magnons in ferromagnet 79−61458
quantum crystal, soln. of Fermi-Bose quasiparticle 79−28173
quantum crystal, thermal cond., role of defectons 77−35796
quarks as quasiparticles of bound states *(Russian)* 78−25009
scattering, kinetic eqns. in statistical T-matrix approx. 77−65011
Schrodinger equation for quasi-particles with variable effective mass *(Russian)* 78−4497
semiconductor, electron excitation spectra in field of two travelling waves 80−65514
semiconductor, multiphoton absorption of intense EM waves 77−1648
semiconductor submillimetric-wave spectroscopy 79−33221
sine-Gordon equation, two soliton solutions, breather solution 80−12945
solid containing spin-1/2 triads undergoing hindered reorientation, quasi-quadrupolar echoes 79−4744

quasi-particles continued
solid solution theory, quasi-particles method 80−24560
spin wave damping, magnetic materials with canted mag. struct., thermodynamic and high freq. props. 80−11184
superconducting film, acoustic coupling and effective quasiparticle lifetime 77−20499
superconducting film, gap enhancement due to microwave irradiation 78−14892
superconducting film, gap enhancement due to quasiparticle tunnel injection 78−56262
superconducting film, illuminated, heating model and spectral characts. of phonon emission 79−28442
superconducting film, optically excited, spatial instability driven by quasiparticle diffusion 77−80870
superconducting film, photoexcited, phonon spectrum 80−11132
superconducting film, surface impedence, effects of quasiparticle redistrib. 80−44764
superconducting film, thermal induced potential, quasiparticle thermal transport coeffs. 77−85385
superconducting film containing single flux vortices, tunnelling 77−59360
superconducting films, optically irrad., quasiparticle energy distrib. function 80−2527
superconducting phase slip centre, charge imbalance waves and nonequilib. dynamics 80−54830
superconducting phase slip centres, interactions obs. using coupled microbridges 77−47940
superconducting states out of thermal equilib. stability 80−2526
superconducting tunnelling function, quasi-particle injection and disappearance of supercond. 77−20497
superconducting tunnelling junction, quasi-particle recomb. and 2Δ-phonon-trapping 77−8236
superconducting weak link, short, with distinct chem. potentials at boundary 80−2528
superconducting weak links, gapless, coupled dynamics of order parameter and quasiparticle distrib. 79−56422
superconducting weak links, quasiparticle-injected, simple-heating-induced Josephson effects 80−70904
superconducting-normal interface, boundary resist. 80−50006
superconducting-normal-superconducting film struct., quantised resistances 79−56426
superconductive tunnelling with spin polarised electrons 79−4627
superconductivity, electron-hole, influence of struct. defects 77−20489
superconductivity, enhancement by quasiparticle tunnelling 78−76197
superconductivity, nonequilibrium, quasiparticles and phonons 78−52146
superconductivity, two-band model, tunnelling density of states 77−51854
superconductor, 2-dimens. fluctuation-induced cond. above crit. temp. 78−10608
superconductor, bulk, absorption of SAW in presence of supercurrent 79−28443
superconductor, formation of nonequilibrium distribution, electron-electron collisions effect *(Russian)* 80−7033
superconductor, kinetic eqns. for electron excitations and phonons 80−7032
superconductor, nonequilib., with wideband source of quasiparticles, kinetic theory 80−80442
superconductor, nonequilib. distrib. function 78−91810
superconductor, nonequilibrium distribution functions of quasiparticles and phonons calc. 77−89904
superconductor, nonequilibrium excitation of quasiparticles and phonons 77−43783
superconductor, quasiparticle and phonon lifetimes, theory 77−20488
superconductor, quasiparticle charge imbalance induced by supercurrent with thermal gradient 80−34546
superconductor, strong coupling, finite-freq. US attenuation 77−51846
superconductor, tunnelling potentials, thermoelectric quasiparticle transport 79−47200
superconductor, weakly illuminated, nonequilib. props., theory 77−66224
superconductor film, nonequilib. states induced by quasiparticle tunnelling injection 77−47925
superconductor nonequilibrium state, large quasiparticle injection from external current source 78−10614
superconductor-insulator junction, quasiparticle nonlinear relax. to nonequilib. state *(Russian)* 80−7040
superconductor-insulator-superconductor quasiparticle mixers, conversion gain prediction 80−70901
superconductor-insulator-superconductor quasiparticle tunnel junctions, as microwave detectors 80−65744
superconductor-normal-superconductor film struct., quasiparticle scatt. and current-volt. characts. 78−10615
superconductors, kinetic eqns., nature and decay rate of new mode 80−49978
superconductors, nonequilib. distribs., review *(Russian)* 79−19688
superconductors, nonequilibrium, T^* model of quasiparticle and phonon distribs. 80−25039
superconductors, nonequilibrium, BCS-Boltzmann and Ginzburg-Landau descriptions 79−65589
superconductors, nonequilibrium, phase transitions induced by quasiparticle injection 78−91808
superconductors, nonequilibrium states, narrow nonequilibrium sources *(Russian)* 80−88687
superconductors, quasiparticle charge imbalance relax. 79−60960
superconductors, relaxation and collective motion two-fluid theory 79−73625
tensor quasiparticle interaction and spin-isospin sound in nuclear matter 79−63618
thin optical irradiated superconductors, phonon spectrum and phonon temp. definition 80−93037
vacancion, Bose-Einstein condensation *(Russian)* 77−85014
weak-coupling supercond., quasiparticle, charge and energy conservation 79−19685
weak-coupling superconductor, effect of electron-phonon renormalisation on thermodynamics 79−99655
yrast-band of odd nuclei, quasi-particle-phonon interaction 80−22651
^{164}Er, populated via ^{150}Nd(^{18}O,4n)^{164}Er, quasineutron $i_{13/2}$ bands 78−37257
Al alloys, dil., depend. of electron scatt. rate on lattice relax. 77−69311
Al film, supercond., meas. of effective quasiparticle recombination times, density of electronic states at Fermi level 79−38264
Al film strips, radiation stimulated supercond. 77−28298
quasi-particles continued
Al particles, small supercond. nuclear spin-lattice relax. meas. 80−88681
Al, quasi-particle properties, anisotropic, electron-phonon interaction study 77−43480
Al, supercond. film, intrinsic and expt. quasiparticle recomb. times 77−15999
Al, supercond. film, quasiparticle branch mixing rates 79−78269
Al, supercond. order-parameter relax. time calc., quasiparticle lifetime 79−4618
Al, superconducting, energy gap enhancement by tunnelling extraction 80−34564
Al, superconducting, quasiparticle charge distrib. due to tunnel injection 80−44771
Al, thick film, supercond., tunnelling characts., geometrical reson. in Al-Pb struct. 79−38260
Al-AlO_x-PbBi tunnel junction, quasiparticle energy distrib. in nonequilib. supercond. 77−80881
Al-Mn(Cr)(V), dil., supercond., nucl. spin relax. and quasiparticle excitations 80−88680
Al-PbBi superconducting tunnel junctions, optically illuminated, quasiparticle energy distribution 80−75688
Al_2O_3, doped, phonon spectroscopy in supercond. tunnel junctions 79−90738
Ba odd neutron isotopes, microscopic struct. of low lying collective excited states *(Japanese)* 79−3065
Cd, surface impedance, Gantmakher-Kaner oscills. *(French)* 77−66195
Cs, Fermi surface and quasiparticle props., density functional approx. 80−96771
$CsNiF_3$, nonlinear excitations, 1D-ferromag., neutron scatt. 80−70949
EuO magnetic semiconductor, quasiparticle lifetimes, CPA study 80−65443
EuS, absorpt. spectrum, change near mag. saturation using quasi-particle multi-band theory 79−61342
EuS, conduction band density of states, redistrib. near ferromag. saturation 78−67939
He, dense gas, transport eqns., shear viscosity and acoustic vel., quasiparticle kinetic eqn. calcs. 80−53906
^{2}He, liq., 0.015K, elementary excitations, neutron scatt. study 79−46874
^{3}He, liq., dynamic form factor, particle density, spin density correlation, RPA calcs. 79−46873
^{3}He, liq., interface with nonmag. solid, Kapitza resist., quantum perturbation treatment 80−88385
^{3}He, liq., longitudinal zero-sound dispersion, thermal cond., and Landau F_2 78−2327
^{3}He, liq., normal phase, Landau Fermi liquid theory and low temp. props., book contrib. 79−99386
^{3}He, liq., polarisation potentials and elementary excitations 78−91502
^{3}He, liq., quasiparticle interactions and superfluid transition temps. 79−51356
^{3}He liq. and ^{3}He-^{4}He dil. soln., quasiparticle theory of surface tension for normal systems 79−56012
^{3}He, liquid, polarisation potentials, viscosity, thermal cond., spin diffusion 80−88389
^{3}He, normal, diffusive heat flow and sum rules in the hydrodynamic limit 78−56012
^{3}He, normal, overdamped modes and transport 78−56011
^{3}He, normal, paramagnon exchange and quasiparticle interaction 79−95231
^{3}He, normal liquid, elementary excitations, density and spin density, zero sound mode, press. depend. RPA model calcs. 80−59749
^{3}He quasiparticle excitation spectrum and second sound vel. meas., dil. soln. of ^{3}He in superfluid ^{4}He 80−24708
^{3}He, quasiparticle interactions, superfluid transition temps. 79−95233
^{3}He, quasiparticle interactions, transport coeffs. and superfluid free energy 79−95234
^{3}He single quasiparticle near surface of liq. ^{4}He, binding energy 79−77853
^{3}He, superfluid, A phase, theory of sound propag. 78−38896
^{3}He, superfluid, bound states of one-particle excitations near vessel walls 77−31826
^{3}He, superfluid, orbital dynamics, homogeneous systems 79−33144
^{3}He, superfluid, pair breaking by electron bubbles 79−51352
^{3}He, superfluid, second viscosity and attenuation of fourth and second sound near transition temp. 77−31830
^{3}He, superfluid, sound propag. and kinetic coeffs., book contrib. 80−2237
^{3}He, superfluid, transport and relaxation properties, kinetic eqn. and Bogoliubov quasiparticle relax. rate 78−79838
^{3}He, superfluid, transport and relaxation properties, viscosity, thermal, cond. and normal fluid density relax. 78−79839
^{3}He, superfluid A-phase, ion mobility tensor, ion-quasiparticle scatt. 80−59753
^{3}He, superfluid A-phase, orbital dynamics 80−2232
^{3}He, superfluid B-phase, low-temp. spin relax. 79−55989
^{3}He superfluid β-phase, negative ions mobility 79−86956
^{3}He-^{4}He, liq., excitation spectrum and quasiparticle interactions, perturbation theory 78−10250
^{3}He-^{4}He, solid soln., struct. of vacancies 80−2242
^{3}He-^{4}He, superfluid, osmotic and mag. props., review *(French)* 80−10733
^{3}He-^{4}He dilute solns., number density calc. 78−43205
^{3}He-^{4}He mixtures, excitation spectrum, neutron inelastic scatt. study 79−46877
^{3}He-^{4}He quantum solns., spatial separation of opposite charges and dipole complex form. *(Russian)* 80−6588
^{3}He-He II mixture, dil., weak bound state for ^{3}He quasiparticles 78−22925
^{3}He-superfluid ^{4}He mixture, dispersion law of ^{3}He quasi-particles under press. *(Russian)* 79−42336
^{4}He, liq., quasiparticle model, finite temp. 77−39715
^{4}He, superfluid, bubblons, speed camera obs. 79−65272
^{4}He, superfluid, density fluctuation spectrum at finite temps. 79−82403
^{4}He superfluidity, macroscopic quantum waves, bound quasi-particles 80−39378
^{4}He-^{3}He, dil. soln., ^{3}He quasiparticle interaction, conc. depend. 77−15655
In whiskers from Sn-In alloys, current carrying, superconductivity breakdown 80−60133
K-Na, dil., dynamical props. of quasiparticle excitations, de Haas-van Alphen effect meas. 78−84128
$La_{1-x}Ce_xAl_2$, supercond., nucl. relax. and impurity magnetism 77−20495

quasi-particles continued
$La_{1-x}Gd_xAl_2$, supercond., nucl. relax. and impurity magnetism 77−20495
Li_x Fermi surface and quasiparticle props., density functional approx. 80−96771
Nb, quasiparticle velocity, anisotropic many-body effects 79−33223
Nb_3Ge, superconducting thin films, energy gaps from tunnelling meas. 80−25050
Nb_3Sn, cavities, quasiparticles in energy gap corresponding to weak spots 79−56386
Nb_3Sn, superconducting, inelastic scattering of light, one- and two-electron excitations 79−33390
Nb_3Sn, superconducting thin films, energy gaps from tunnelling meas. 80−25050
^{93}Nb, 1 quasiparticle 2 phonon multiplet, microscopic quasiparticle cluster phonon coupling model 77−2908
Ni, quasi-particle energies, two-hole XPS satellite 80−66399
Pb, film, first order transition due to quasiparticle injection 78−23208
Pb film, supercond., meas. of effective quasiparticle recombination times, density of electronic states at Fermi level 79−38264
Pb, laser irradiated tunnel junction, nonequilibrium quasi-particle distrib. function, thermal regime *(Russian)* 79−42700
Pb, supercond., quasi-particle recomb. time, Kapitza resistance 78−68123
Pb, supercond., quasiparticle and phonon propagation 79−42689
Pb, supercond., surface bound state, microwave surface impedance 77−12059
Pb, supercond. film, intrinsic and expt. quasiparticle recomb. times 77−15999
Pb, supercond. single cryst., quasiparticle propag. and recomb. 77−32126
Pb superconducting film, anomalous temp. depend. of quasiparticle injection-induced voltage onset 78−56256
Pb superconducting film, quasiparticle and phonon lifetimes, tunnel junction and meas. 77−20498
Pb-PbO_x-Pb small supercond. tunnel junctions, effect of capacitance in I-V characts., high-freq. obs. 80−80448
$Pb_{0.98}Bi_{0.02}$-Cd, superconductor-normal-metal boundary resist., mag. field depend. 80−44772
Rb, Fermi surface and quasiparticle props., density functional approx. 80−96771
Rb, quasiparticle dynamics, density-functional approx. 79−60682
Rb-K, dil., dynamical props. of quasiparticle excitations, de Haas-van Alphen effect meas. 78−84128
Si, inversion layer, temp. depend. of subband energies, exchange and correlation effects 80−20281
Si MOSFET, surface quantum states, two-dimensionality of many-body effects 80−103740
Sn film, supercond., energy gap reduction by quasiparticle injection 77−47941
Sn, odd isotopes, number-projected three-quasiparticle description 78−93953
Sn, supercond., quasiparticle recomb. time and normal electronic density of states at Fermi surface from tunnel junction expts. 79−24108
Sn, supercond. film, charge imbalance generation by supercurrent 79−95548
Sn, supercond. film, intrinsic and expt. quasiparticle recomb. times 77−15999
Sn, supercond. tunnel junction, quasiparticle excitation by α-particles 80−103791
Sn, superconducting current carrying film, resistive region boundary movement, ambient media depend. 80−44763
Sn, superconducting film, energy gap suppression and instability under strong quasiparticle injection 80−7042
Sn superconducting thin-film bridge, IV curves oscill. instability and quasi-particle recomb. *(Russian)* 80−44769
Sn, superconductor, bulk non-equilib. quasiparticles probed by ballistic phonons 79−56391
Sn, thin film, supercond., acoustic wave absorpt., quasiparticle distrib. 78−10603
Sn-In, dil., supercond., current-induced resistive state 79−51712
Sn-SnO-Pb, excess quasiparticles, equilib. distrib., influence of illumination 79−15262
^{95}Tc, 1 quasiparticle 2 phonon multiplet, microscopic quasiparticle cluster phonon coupling model 77−2908
Te odd neutron isotopes, microscopic struct. of low lying collective excited states *(Japanese)* 79−3065
V_3Si, superconducting thin films, energy gaps from tunnelling meas. 80−25050
W-Re amorphous alloys, phase-slip and localisation diffusion lengths 80−107747
Xe, odd neutron isotopes, microscopic struct. of low lying collective excited states *(Japanese)* 79−3065
Zn-Al, dil., impurity quasi-particle lifetimes and pseudopotential form factor 78−47734

quasi-stellar objects *see quasars*

quasi-stellar sources *see quasars*

quasimolecules
alkali + inert gas molecule, far wing line broadening, quasistatic theory 79−22762
alkali atom (ion)+inert gas, collision studies of quasi-one-electron systems 80−63750
alkali atom collisions, photon absorpt. cross-section and quasimol. transitions *(Russian)* 77−75285
alkali metal-inert gas mol., gaseous transient, D-line emission obs. 77−38688
alkali-inert gas system, mol. band profiles of induced dipole transitions 78−42135
alkaline earth dimens., heteronuclear, matrix-isolated, laser photoluminesc., van der Waals ground state 79−41192
alkane dimer, PCILO calc. of geom. struct. and energy 79−63930
9,10-anthraquinone, phosphorescence, external heavy atom in mol., 4.2 to 77K, quasiline spectra 78−82773
atmosphere Van der Waals mol. comp., 5-90 km altitude 80−85699
atom+atom (ion) collisions, low energy, ionisation cross sections, diffusion eqn. calcs. 77−54605
atom+atom collisions, adiabatic satellites of at. lines 77−50513
atom+ion collision, low energy, ionisation, total cross-section meas. 77−54606
atom+ion collisions, continuum photon emission, radiative electron capture, mol. orbital emission 77−42401
quasimolecules continued
atom+ion collisions, electron capture, quasi-molecular binding corrections 78−90287
atom+ion collisions, MO, radiative electron capture X-ray emission 77−19043
atom-atom collisions, X-ray continua from coalescing atoms 77−530
atom-atom slow collisions, electron translational effect, diagonalisation calcs. 77−3441
atomic collision intermediate, superheavy, X-ray emission empirical scaling rule 79−76502
atomic collisions, absorption spectrum oscill. struct. due to quasimol. states 79−64093
atomic collisions, close, slow, Σ-Π transitions, united-atom approx. 79−22794
atomic inelastic scatt., quasimol. states phase interference 78−62902
atomic inner shell ionisation phenomena, conf., Freiburg, West Germany (Mar.-Apr. '76) 77−27040
autoionisation, electron spectra *(Russian)* 77−79690
autoionisation states decay 79−64058
colliding atoms, optical excitation to state of quasibound motion *(Russian)* 78−58784
collision systems $\alpha(Z_1+Z_2)\gtrsim 1$, quasimolecular 1 sσ orbital, excitation and spectroscopy 80−87199
collisional excitation cross section oscillations, unequal spacing 79−27079
collisional ionisation in intense laser field, quasimol. state reson., quantum mechanical anal. 78−33589
double molecules, with weak reson. bond, quasilinear *(Russian)* 78−74640
electronic struct. calc., CNDO approx., computer program 78−86789
ethylene dimer, PCILO calc. of geom. struct. and energy 79−63930
exchange interactions of atoms with valence s electrons 77−83677
formation in heavy ion collisions, X-ray radiation *(Russian)* 78−33568
heavy collision systems, vacancy prod. in strongly bound quasimol. states, impact parameter depend. 78−22003
heavy ion+atom, 1sσ MO excitation probability and binding energy, X-ray coincidence 78−94316
heavy ion+atom, 3dπ-2pπ radial coupling, symm. and near symm. collisions 77−71857
heavy ion+atom collisions, mol. M-X-rays, self-consistent relativistic HF-Slater many electron correl. diagrams 77−14567
heavy ion+atom collisions, quasimol. X-ray line tails 77−14564
heavy ion collisions, 3dσ mol. orbital ionisation 78−94311
heavy ion collisions, Doppler shift of continuum X-rays from quasimols. 79−22808
heavy ion collisions, electron EM field interaction, quantised field formalism 80−83478
heavy ion collisions, electronic states in rot. two-centre Coulomb systems 77−14561
heavy ion collisions, molecular-orbital X-rays yield 78−13587
heavy ion collisions, quasimol. KX-ray spectra, Doppler shift 77−19044
heavy ion collisions, rotational transitions, effect of spin-orbit coupling 78−13573
heavy ion quasimol. collisions, electron pair prod., vacuum polaris. shakeoff 77−30945
heavy-ion collision, quasimolecular L X-rays, relativistic self-consistent correlation diagram 78−5247
heavy-ion collisions, intermediate L-K mol. orbital radn. spectral distrib. 77−50511
heavy-ion collisions, K-vacancy production, 1sσ excitation of transient mol. orbital 77−83718
heavy-ion collisions, K-vacancy production, 2 pσ mol. orbital, single and multiple collisions 77−83717
heavy-ion collisions, nuclear charge movement induced, X-ray transitions in quasimolecule spectrum 77−50510
inert gas binary mixture, unlike mol. force consts. from viscosity data, thermal cond. 78−33565
inert gas complexes spectroscopic data, geometry, pot. energy curve, dissoc. energy, equilib. internuclear distance, determ. 80−53018
inert gas dimer+atom, IOSA calc. for total integral cross sections for excitation, exchange and dissoc. 80−1044
inert gas dimer formation, free-jet expansions, rate coeffs. 77−66745
inert gas dimers., photoionis. cross sections of excited states 78−66523
ion+atom collision, diatom. quasimolecule form., shielded-orbital model 79−10165
ion+atom collision, electron spin coupling in rot. frame, X-ray emission 79−36724
ion+atom collisions, diabatic correl. diagrams for quasi-mol. description 79−3525
ion+atom collisions, mol. X-ray anisotropy 77−19046
ion+atom slow collision, atomic excitation by quasimolecular orbital rot. coupling, uniform Airy approx. 78−25644
ion-atom collision, electron capture, at. expansion method 79−45833
ion-atom collisions, relativistic effects in variable-screening model 77−14516
K X-ray anisotropy peaks, Z-depend. 77−58043
kinematic dipole model for the anisotropy of quasimolecular X-rays 79−13814
molecular orbital X-ray emission, from primary exciting collision 77−50449
molecular orbital X-rays, scaling law derivation 79−18284
molecular orbital X-rays from atomic and molecular impact on solid targets 79−36750
molecular X-rays from heavy-ion collisions, superheavy quasi-molecule spectroscopy 80−23509
molecule excited state lifetimes time-resolved spectra 78−17704
quasistationary states decay, electron and photon spectra *(Russian)* 79−49969
relaxation times in intermediate quasimolecules 78−42170
single-electron atom+single-electron ion.(atom), exchange splitting at large separation 78−46480
superheavy, electronic states, spectroscopy 78−37706
superheavy and intermediate atomic collision systems, UNILAC expts. 80−63751
superheavy collision system, radiative processes, search for positron emission 80−63752
superheavy ion-atom collisions, quasiats., K-vacancy form., positron emission 80−63753
superheavy quasi-molecules, positron creation from K-shell vacancy 77−58220
superheavy quasimolecules, Bang Hansteen scaling rule, $K\alpha_1$ line anal. 79−10126

quasimolecules continued
superheavy quasimolecules, binding energy of inner-shell electrons, monopole approx. 78−62949
superheavy quasimolecules, inner shell electronic states calc. 79−89817
superheavy quasimolecules, inner-shell ionisation, scaling behaviour 78−25691
superheavy quasimolecules, inner-shell vacancy formation, coupled channel anal. 80−48116
superheavy quasimolecules, M-like X-ray transitions 79−6951
s-tetrazine, cooled supersonic jet, Van der Waals complex, isotope effects, fluoresc. obs. 78−55194
three atom dipole moment, large separation, perturbation theory 78−62946
triatomic van der Waals complex, vibr. predissoc. and photodissoc. lifetimes 80−9661
triatomic van der Waals mols., rot. predissoc. 80−63721
triatomic van der Waals mols., vib. predissoc. 78−55215
van der Waals complex, formation, role of entropy 80−7840
Van der Waals complex, PCILO calc. of dispersion energy and geom. conf. 79−63930
van der Waals complex, prod. and rot. spectra assignments 80−5532
van der Waals complexes, IR continuum spectrum at low temps. 80−980
Van der Waals dimers, intermol. V-V energy transfer in vibr. predissoc. 79−94060
van der Waals dimers, intramolecular vibr. dynamics, vibr. predissociation 80−28083
van der Waals dimers, struct. rel. to dielectric second virial coeffs. 77−46611
van der Waals mol. rot. predissociation study, complex coord. method 80−74205
van der Waals molecules, mol. fluoresc., vibr. predissoc. model 78−42120
van der Waals molecules, vibr. level spacings calc. from Lennard-Jones pot. 77−42369
van der Waals molecules, vibrationally excited, lifetimes, momentum gap 80−5601
van der Waals T-shaped mol., perpendicular vibr. predissoc., vibr. relax., Morse pots. 78−82659
variational calcs., 1 s σ orbitals 78−37707
X-ray emission in heavy-ion collisions, electron slip effects 77−19040
X-ray spectra, collision dynamic effects 77−19045
X-ray spectra from ion+atom collisions 77−19041
Ag+Ag symmetric collisions, MO-2pσ radiation anisotropy, quasimolecular nature 78−70924
Ar-HCl, Van der Waals mol., far IR spectrum, anisotropic intermol. force effects 78−62869
Ar-O_3 Van der Waals complex, struct. and props., RF and microwave obs. 80−32704
Ar-Xe gaseous mixtures, collision-induced microwave absorpt. 78−78680
Ar+K^+, inelastic collisions, emission cross sections, quasimol. state interference 77−61848
Ar^++Ar, 1-500 keV, inelastic energy loss, ionis. phenomena, theoretical model 77−34747
Ar^++Ar, quasimol., Auger transition probability, internucl. distance effect *(Russian)* 77−75116
Ar^++He, $X^2\Sigma$ and $A^2\Pi$ states, CI pots. 78−74727
Ar^{x+}+Sn(Sb)(Xe), vacancy sharing between K and L shells in 3dσ mol. orbital 79−22807
Ar_2 $^1\Sigma_u^+$ excimer state, photoionis. cross section 78−70882
Ar_2, collision-induced Raman spectrum, absolute cross sections 78−46349
Ar_2, collision-induced Raman scatt., polarisability anisotropy 78−46350
Ar_2, emission continua in VUV, new oscill. struct. 79−54905
Ar_2, emission spectra, VUV region 79−31543
Ar_2, in electron-beam excited supersonic Ar jet, continuous VUV spectrum origins 79−6964
Ar_2, near IR absorpt. spectra 78−66547
Ar_2, photoionisation 77−54578
Ar_2, Raman spectra, press. broadened transitions, calc. 79−64009
Ar_2, short range interactions between two rare gas atoms 79−26888
Ar_2 van der Waals dimer, intermol. pot., SCF CI ab initio calcs. 80−106274
Ar_2^+, electronic states, pot. curves, with/without spin-orbit interaction 78−33443
Ar_2^+, electronic struct., pot. energy curves, spectroscopic consts. 79−18114
ArCl, neutral and negative ion states SCF pot. energy curves 78−62745
ArH, neutral and negative ion states SCF pot. energy curves 78−62745
ArHCl, ab initio FGO calc. 78−50467
ArHF, van der Waals complex, ab initio RHF calc., struct. 79−76339
ArHO, van der Waals complex, ab initio RHF calc., struct. 79−76339
ArI_2, van der Waals mol., fluoresc. spectrum, predissoc. 78−66584
Ar.HCl bond energy from IR spectra 77−27061
Ar.HCl, Van der Waals mols., SCF energies and dispersion forces 80−74279
Ar.HF, Van der Waals mols., SCF energies and dispersion forces 80−74279
Ar.H_2O, Van der Waals mols., SCF energies and dispersion forces 80−74279
Au+I, noncharacteristic X-ray emission, self-consistent relativistic many-electron correl. diagram 77−19023
Ba+Ba, atomic pair absorpt. obs. with white-light source 79−63944
Ba+Tl, atomic pair absorpt. obs. with white-light source 79−63944
Ba^++inert gas atom collision, polarisation of emitted radiation, quasimol. interf. effect *(Russian)* 77−46633
Ba^++Kr, quasimolecular states interference, degree of polaris. oscill. *(Russian)* 77−6917
$BeAr^+$, long range pot., pot. inversion method 78−21992
(Br,Zr) system, 1 s σ orbital, variational calc. 78−37707
Br, ion collisions, 12-60 MeV, K-vacancy production, multiple and single collisions in mol. orbital excitation 77−83717
Br ion+target collisions, K-X-ray yields, 1sσ excitation 77−19051
Br, ion+target collisions, X-ray yields, K-L level matching 77−19052
Br ions+target collisions, K-X-ray yields, K-vacancy sharing 77−23548
Br K-X-ray yields, 2pσ excitation 77−23549
Br+Br, symmetric collisions, MO-2pσ radiation anisotropy, quasimolecular nature 78−70924
Br^{25+}+Br^{25+}, correlation diagrams, inner-shell vacancy prod., characteristic X-rays 77−83503
BrF_2^--, $BrFCl^-$-, $BrCl_2^-$, inert gas cpds., localised MOs and bonding nature 78−9061
quasimolecules continued
CO_2, negative Van der Waals polymer mols., formed by nozzle expansion 78−90307
CO_2^-, hydrated anion stable gas phase heteronuclear clusters, mass spectra, autodetachment rates 80−14266
$^{12}C+^{16}O$, 12.8 to 18.2 MeV, reactions and inelastic scatt., resonance anomalies due to quasimol. states 78−4955
Ca-Ca symmetric collisions, molecular-K-X-ray anisotropy spectra, discrete struct. 77−14560
Ca^++inert gas atom collision, polarisation of emitted radiation, quasimol. interf. effect *(Russian)* 77−46633
Ca_2, laser-excited fluorescence in inert gas matrices 78−94273
CdHg(Mg), Ar matrix absorpt. spectra, vibronic spacing and bonding 79−3453
Cl+Cl collisions, impact parameter dependence of emitted noncharacteristic rad. 77−14563
Cl^{x+}+Sn(Sb)(Xe), vacancy sharing between K and L shells in 3dσ mol. orbital 79−22807
ClF_2^--, ClF_4^--, ClF_6^--, inert gas cpds., localised MOs and bonding nature 78−9061
ClF_n-, ClF_n^+-, ClF_n^--, inert gas cpds., n=1-6, localised MOs and bonding nature 78−9061
Cs-inert gas molecule, excimer transitions, absorpt. spectra 77−475
Cs-Xe molecular bands, time-resolved fluoresc., lifetimes 77−58068
Fe+Fe, symmetric collisions, MO-2pσ radiation anisotropy, quasimolecular nature 78−70924
Fe+Fe symmetric collisions, molecular-K-X-ray anisotropy spectra, discrete struct. 77−14560
Ge+Ge, quasimolecular K X-ray anisotropy and ang. distrib. 78−1073
Ge+Ge, symmetric collisions, MO-2pσ radiation anisotropy, quasimolecular nature 78−70924
(H,H) system, 1 s σ orbital, variational calc. 78−37707
H_2-H_2, overlap parameters from IR spectrum in binary collision-induced H_2 band 77−54561
H_2-inert gas, bound complex form., anisotropic intermol. pot., IR spectra anal. 78−37634
$(H_2)_2$, ab initio calcs., perturbation dispersion energy versus CI treatment 77−26976
H_2Ar, van der Waals complexes, lifetimes calcs. 78−13564
H_2O, Van der Waals polymer mols., negative ions formed in nozzle expansion 78−90296
H_2^*+H_2, van der Waals mols., mol. fluoresc., vibr. predissoc. model 78−42120
He pair, dispersion interaction, independent particle model, polarisabilities 80−37732
He-Ar, van der Waals pot. determ. 79−10167
He-Ar mixture, translational IR spectrum at 165K, binary and ternary absorptances 77−68042
He-Ar(Kr)(Xe), 208 and 707K, intermol. forces, virial, diffusion, and viscosity coeffs. 77−75256
He+Ar mixture, collision induced absorpt. calcs. 77−6777
He^++Ar, charge exchange, quasimolecule model, four-state calcs. 77−14571
He^++He, interference struct., optical emission interpretation 79−45816
He^{2+}+He, two-electron excitation of quasimol. states 79−18274
He_2, 600 Å emission continuum 80−1012
He_2, electronic and rot. energy relax., reactive collisions by isotope selective excitation 78−33541
He_2 formation of He_2 in afterglow of pulsed discharge 77−15259
He_2, He_2^+, MO correlation diagrams 77−61689
He_2, in electron-beam-produced supercooled plasma, emission spectrum 77−84501
He_2, molecular spectrum and structure, singlet Π states 4pπ-9pπ 78−42080
He_2, photoionis. cross sections of excited states 78−66523
He_2, pot. curve using CEPA-PNO correl. wavefunction 79−63932
He_2, Raman spectra, collision-induced, diatom polarisability 79−64011
He_2, short range interactions between two rare gas atoms 79−26888
He_2, vibr.-rot. interaction factor 78−42036
He_2^+, $^2\Sigma_g$ states effect in charge exchange collisions, close-coupled calcs. 77−50524
He_2^+, rate coeffs. for bimol. and termol. ion-mol. reactions 78−53188
He_2^{2+} quasimolecular states, radial and rot. coupling terms 79−26896
He_2^{2+}, static polarisability determ. by optimised rot. method 79−54990
$^4He_2$, bound state at small and large separations, variational calcs. 78−50609
He_3, dipole moment, large separation, perturbation theory 78−62946
$HeCrCl_2O_2$, vibr. predissoc., spectroscopic origin identification appl. 78−5239
HeH, neutral and negative ion states SCF pot. energy curves 78−62745
HeH^+, collisional formation, SCF calcs. 77−6893
HeH^+, spectroscopic characts. in ground and first excited triplet states, Dunham pot. approach 77−42234
HeH^{2+}, lowest 20 states, eigenvalues, electronic wavefunctions, w.r.t. internuclear separation 77−18811
$^4HeH^+$, ro-vibr. quasi-bound levels of $X^1\Sigma^+$ state, eigenenergies, dissoc. 77−26997
HeH_2 collision induced dipole IR spectra, ab initio SCF LCAO calc. 79−89737
He(He_2)+Ar, metastable destruction rates 78−37728
$He_2(He_2^+)$, variational electronic struct. calcs. using Hylleraas type wavefunctions 77−88375
HeI_2, rot. fluoresc. spectra, nonlinear equilib. struct. 78−37672
HeI_2, Van der Waals mol. vibr. predissoc. anharmonicity effects 80−52971
HeI_2, vibr. excited mol., dissoc., predissoc., quasiclassical trajectory obs. 79−87839
$HeNO_2$ van der Waals complex, fluoresc. spectrum 77−46591
HeNe, detection in nozzle beam, total collision cross section determ. 77−61826
$HeNe^+$, collisional form., excitation, pot. energy curves calcs. 77−6697
$HeNe^+$, visible spectrum obs. in discharge 79−13729
$HeSr^+$ states population probability in $He(2s^3S_1)$+Sr Penning collision 80−23533
$He_2(^3\Sigma_u)$+Ne(Ar)(N_2)(CO)(C_2)(CH_4), excitation transfer reaction rates 78−5332
$He_2^+X^2\Sigma_u^+$ state, ab initio CI calc., pot. energy curve, vibr. and rot. levels 77−3263
$(^3He)_3$, quantum exchange effects in Lennard-Jones 12-6 pot. 78−1117
$^4He_2$+^4He, zero-energy, Faddeev-unitary pole expansion theory 78−37572

quasimolecules continued
$^4He_3$, bound states, Faddeev-unitary pole expansion theory 78−37572
$(^4He)_3$, Faddeev theory, binding energy 77−26995
$He^*(1s2s,^3S)$+Ar, Penning ionis., discrete-continuum states coupling 79−10193
$He_2(2^3\Sigma_u^+)$+He_2(Ne), reaction rate consts. meas. in afterglow 78−7173
Hg+Xe^{n+}, single and multiple collisions, charact. and quasimolecular X-rays 77−83713
HgXe, excited molecule formation 77−23519
HgZn(Cd), Ar matrix absorpt. spectra, vibronic spacing and bonding 79−3453
I, ion collisions, 15-80 MeV, K-vacancy production, multiple and single collisions in mol. orbital excitation 77−83717
I ion+target collisions, K-X-ray yields, 1sσ excitation 77−19051
I ion+target collisions, K-X-ray yields, K-vacancy sharing 77−23548
I ion+target collisions, K-X-ray yields, 2pσ excitation 77−23549
I ion+target collisions, X-ray yields, K-L level matching 77−19052
I^{25+}+Te^{24+}, I^{43+}+Au^{69+}, I^{25+}+Au^{51+}, correlation diagrams, inner-shell vacancy prod., characteristic X-rays 77−83503
I_2Ar^*, product state distrib. and binding energy 80−63857
I_2He, van der Waals mol., photodissoc. 80−63765
I_2He^*, product state distrib. and binding energy 80−63857
I_2Ne^*, product state distrib. and binding energy 80−63857
Kr, ion collisions, 200-330 MeV, K-vacancy production, multiple and single collisions in mol. orbital excitation 77−83717
Kr, ion+target collisions, K-X-ray yields, 1sσ excitation 77−19051
Kr ion+target collisions, X-ray yields, K-L level matching 77−19052
Kr ion+target collisions, K-X-ray yields, 2pσ excitation 77−23549
Kr+Ar^+(Kr^+) collisions, quasimol. Auger transitions 77−19070
Kr+Kr(Xe), X-ray prod. cross sections for Kr L-shell vacancies 79−10190
Kr+Ti, 200 MeV, collision, quasimol. bremsstrahlung, semiclassical calcs. 77−88530
Kr_2, collision-induced Raman spectra, absolute cross sections 78−46351
Kr_2, near IR absorpt. spectra 78−66547
Kr_2, photoionisation 77−54578
Kr_2^+, electronic states, pot. curves, with/without spin-orbit interaction 78−33443
Kr_2^+, electronic struct., pot. energy curves, spectroscopic consts. 79−18114
Kr_2^{+*}, formed in 50 keV Kr^++Kr collisions, Auger transitions obs. by electron-scattered-ion coincidence method 80−74243
KrAr*, quasimolecule Auger spectra 79−68269
KrF*, oscillatory bound-free emission spectra, semiclassical anal. method 80−7799
KrHCl, van der Waals complex, prod. and rot. spectra assignments 80−5532
KrX, (X=He, Ne, Ar, Xe), VUV absorpt., van der Waals mols. props. 78−13513
^{84}Kr ions+target collisions, K-X-ray yields, K-vacancy sharing 77−23548
Kr_2^*, form. and UV fluoresc. under monochromatic excitation and collision processes 78−9237
Li^++He, quasimol. study of collisions in 0.3-50 keV range 77−88529
Li^++He collisions, K-shell vacancy sharing, ab initio LCAO-SCF, CI calcs. 77−19054
Li^++K, rot. coupling, Fraunhofer diffraction effects 77−65526
Li^++Ne, low energy, ionisation, total cross-section meas. 77−54606
Mg_2, Ar matrix isolated laser photoluminescence spectra, electronic absorpt., emission, vibronic and vibr. relax. 78−82744
Mg_2, pot. energy curve for $X^1\Sigma_g^+$ state, many-body perturbation calcs. 78−55216
MgZn(Cd), Ar matrix absorpt. spectra, vibronic spacing and bonding 79−3453
$(NO)_2$, heat of form., UV spectrum temp. depend. 78−64872
N_2O, negative Van der Waals polymer mols., formed by nozzle expansion 78−90307
NO*+NO, van der Waals mols. in mol. fluoresc., vibr. predissoc. model 78−42120
$N^{2+}(^2P^0)$+H, charge transfer, ab initio CI pot. curves and coupling-matrix elements 80−37878
Na-He model pot. calcs., fluoresc. line profile 79−36723
Na+Ne, Na(3p) excitation 80−1056
Na^++Ne, quasimolecular states, coherent population *(Russian)* 77−10718
Na^++Ti(Ni)(Zn)(Fe), 0.2-3.0 MeV, united-at. limits, mol.-orbital continua 77−19030
NaAr, $X^2\Sigma$, $A^2\Pi$ and $B^2\Sigma$ state, ab initio CI calcs. 78−9085
NaK, $C^1\Pi$ state, spectroscopic consts., vibr.-rot. struct., K fluoresc. obs. 77−18901
NaNe, laser spectroscopy, interat. pot. curves 78−86871
NaNe, van der Waals mol., form., laser spectroscopy 78−29797
NaNe, $X^2\Sigma$, $A^2\Pi$ and $B^2\Sigma$ states, model pot. calcs. 78−78776
$NaNe^+$, pot. energy surface for inelastic Na^++Ne collision 79−68314
Nb+Kr, excitation of 1sσ and 2pσ quasimolecular radiation 78−78801
Nb+Nb, selected MO X-ray coincidence with separated at. K X-rays 80−43148
Nb+Nb symmetric collisions, MO-2pσ radiation anisotropy, quasimolecular nature 78−70924
Ne-Xe gaseous mixtures, collision-induced microwave absorpt. 78−78680
Ne^++Kr, low vel. collision, enhanced K-L vacancy sharing ratios, X-ray prod. cross section 78−78790
Ne_2, emission continua in VUV, new oscill. struct. 79−54905
Ne_2, near IR absorpt. spectra 78−66547
Ne_2, pair polarisability tensor, extended Gaussian basis set, perturbation coupled HF calc. 77−75058
Ne_2, short range interactions between two rare gas atoms 79−26888
Ne_2, vibr. spectra, calc. from pot. curve 80−1040
Ne_2^+, electronic struct., pot. energy curves, spectroscopic consts. 79−18114
Ne_2+Ar, total integral cross sections for excitation, exchange and dissoc. 80−1044
Ne_2+Kr total integral cross sections for excitation, exchange and dissoc. 80−1044
Ne_2^++e, in recombination afterglow, line intensity decay complex struct. 79−7503
NeAr, detection in nozzle beam, total collision cross section determ. 77−61826
Ne*+Ne, differential elastic scatt., rainbow max., mol. states 77−38710
Ni+Ni, 12-90 MeV, molecular orbital K X-rays ang. distrib. 79−10125
quasimolecules continued
Ni+Ni symmetric collisions, molecular-K-X-ray anisotropy spectra, discrete struct. 77−14560
Ni+Ni(Nb), Doppler shift of continuum X-rays from quasimols. 79−22808
O^-+Ne(Ar)(Kr), 0.2-1 keV, elastic and inelastic reduced differential cross-sections 80−32829
$(O_2)_2$, van der Waals mol., WKB vibr. eigenvalues 78−33498
O(Se)(S)+inert gas, ^1S-^1D collision-induced transitions 78−33588
O_4^* van der Waals complex, radiative lifetime, dimole intensity press. depend. 78−58741
Pb, ion collisions 90-110 MeV, K-vacancy production, multiple and single collisions in mol. orbital excitation 77−83717
Pb-Pb quasimolecular states, inner shell ionis. spectra during form. 78−33592
Pb+Pb quasimolecules ab initio calc. of K X-ray spectra 78−21941
Pb^++Z (42≤Z≤92), 1sσ MO excitation probability and binding energy, X-ray coincidence 78−94316
Rb-Ar, oscill. strength, for induced dipole transitions, pot. energy curve 77−75100
Rb-inert gas molecule, excimer transitions, absorpt. spectra 77−475
Rb+Ne(Ar), spin relax., van der Waals mols. form. 77−19027
Rb+Xe system, reson. fluoresc., quasimol. states *(Russian)* 79−85935
RbHe(Ne), spin relax., Rb hyperfine interaction in Van der Waals mol. 78−94201
S+inert gas (N_2)(H_2), rare gas sulphide S(^{1}S) emissions 78−82828
S^{n+}+Ar, molecular K-X-ray production, projectile charge depend. 78−90188
Sr^++inert gas atom collision, polarisation of emitted radiation, quasimol. interf. effect *(Russian)* 77−46633
U+Pb, K-vacancy form., rot. coupling effect in quasimol. L-shell 78−25692
U+U, superheavy quasimolecule, direct Coulomb formation of 1sσ vacancies 77−3450
U^{+}+U^{+}, critical two-centre distance, HFS relativistic calc. 79−22801
^{238}U+^{238}U (^{136}Xe), nuclear Coulomb excitation, inner shell ionisation and internal conversion, quasimol. formation 78−94026
Xe, 326-470 MeV, ion collisions, K-vacancy production, multiple and single collisions in mol. orbital excitation 77−83717
Xe ion+Hg vapour (Au foil) collisions, quasimol. M-radiation 77−14566
Xe^++Ag, quasimolecular L and Ag L X-ray excitation thresholds, electron correl., calc. and expt. 78−78793
Xe_2, collision-induced Raman spectra, absolute cross sections 78−46351
Xe_2, effective core pot., Hartree-Fock calc., relativistic and nonrelativistic effects 78−46281
Xe_2, near IR absorpt. spectra 78−66547
Xe_2, obs. in Xe-inert gas far UV spectra, press. (temp.) depend., interaction const. 77−61698
Xe_2, time-resolved excitation using synchrotron radiation *(French)* 77−88483
Xe_2, VUV radn. emission, radiative lifetimes 79−27089
Xe_2, van der Waals mol., photoelectron spectra 78−66599
Xe_2^+, bound ground state, pot.energy curves 78−66599
Xe_2^+, effective core pot., Hartree-Fock calc., relativistic and nonrelativistic effects 78−46281
Xe_2^+, electronic states, pot. curves, with/without spin-orbit interaction 78−33443
Xe_2^{+*}, electronic struct., pot. energy curves, spectroscopic consts. 79−18114
XeAr, obs. in Xe-inert gas far UV spectra, press. (temp.) depends., interaction const. 77−61698
XeCl, B-X and D-X band systems, vibr. anal. 79−59482
XeF,(Cl)(Br) matrix isolated, absorpt. and emission spectra 77−14446
XeF, effective core pot., Hartree-Fock calc., relativistic and nonrelativistic effects 78−46281
XeF, ground state dissoc. vibr. equilibrium 80−9652
XeF^+ form. by Xe^++NF_3 reaction 78−27737
XeH^+, pot. energy curves, VB calcs. 77−61688
XeI*, emission spectrum, from Xe-I_2 77−6843
XeNe, obs. in Xe-inert gas far UV spectra, press. (temp.) depends., interaction const. 77−61698
XeO, emission kinetics 77−34684
XeX, (X=He, Ne, Ar, Kr), VUV absorpt., van der Waals mols. props. 78−13513
Xe_2(−Kr,He), time-resolved excitation spectra, 1500 Å region, fluoresc. lifetime 77−75195
^{136}Xe ion+target collisions, K-X-ray yields, 1sσ excitation 77−19051
^{136}Xe ion+target collisions, X-ray yields, K-L level matching 77−19052
^{136}Xe ion+target collisions, K-X-ray yields, K-vacancy sharing 77−23548
^{136}Xe ion+target collisions, K-X-ray yields, 2pσ excitation 77−23549
Xe_2^*, form. and UV fluoresc. under monochromatic excitation and collision processes 78−9237
ZnHg(Mg), Ar matrix absorpt. spectra, vibronic spacing and bonding 79−3453

quench hardening
austenite, quenched and tempered, effect of bainitic decomp. products on mech. props. 77−56007
β-brass, quenched single crystal, deform. and slip 79−79026
diamond-metal strip, strength props. 79−61678
Elinvar, γ to γ′ transformation and γ′ phase form. kinetics, lattice consts. 80−35191
HF heated cylindrical component temperature field computation for quench control 78−90632
high-C steel, strength characts. with controlled hardenability after bulk-surface hardening 77−56156
measurement and control problems *(German)* 77−44267
metals, FCC, hardened, plasticity, review 79−11683
steel, austenitic, AISI 4340, effect of step quenching on microstruct. and fracture toughness 78−84834
steel, austenitic N31, mechanical instability in premartensitic state *(Russian)* 77−73273
steel, austenitic stainless, Cr-Ni, Mn and Mo effect on mech. props. rel. to treatment 79−96039
steel, austenitic-ferritic Ni-Cr, 12Kh21N5T, phase and struct. transform. *(Russian)* 78−95748
steel, C type 45 hardened layer structure and props. with intensive spray cooling and hardening 79−38859

quench hardening continued
steel, cold rolling, effect of transformations during quench hardening and tempering 77−55989
steel, cutting, high-speed, nondestructive testing 77−90559
steel, die type, vacuum quenching parameters 79−38861
steel, hardening, mathematical model including phase changes 79−4950
steel, low C, quench-hardened, plastic deform. effect on mech. props. and struct. *(Russian)* 77−70102
steel, low-alloy, case carburised, retained austenite effect on contact fatigue strength 80−30096
steel, low-C, with Nb-B addition, transform. characts. and mech. props. *(French)* 79−43253
steel, maraging, hardening mechanism of quenched samples, tempering *(Czech)* 79−78989
steel, martensitic transformation kinetics 79−87630
steel, medium C, static and dynamic stress effect on hardenability and grain growth *(Korean)* 78−35404
steel, plain C, quench ageing avoidance, critical cooling rate *(German)* 79−52244
steel, quench-hardened, exam. of anomalous plasticity when deformed *(Russian)* 79−11663
steel, ultrahigh C, heat treated, mechanical properties and microstructure 79−57012
steel, ultrahigh strength, near-threshold fatigue crack propagation, load cycle and cyclic strength effects 78−11331
steel, water soluble polymer quenchants 79−100190
steel case depth after quench hardening, inspection using coercimeters 80−104377
steel dies, durability improvement using isothermal hardening in salt bath 80−35198
steel hardfaced, effects of quenching on structure and wear resist. 77−21175
steel parts, martensite form., hardening cracks, acoustic emission investig. possibility 79−29177
steel R6M5, tempering after quenching with rapid heating 77−56002
steels, thermal hardening stress determ. by thermoplasticity theory 79−29076
water soluble polymer quenchants 79−100190
Al, quenched, irradiated, and quenched plus irradiated, grain boundary hardening 80−3162
Al-Cr, quench hardened, Cr effects on resoftening 77−66657
Al-Cu-Mg-Mn(-Zn-Cr), low temp. deformed, ageing and mech. props. 79−1881
Al_2O_3, effect of quenching hardening on mech. strength, for various quenching mediums *(German)* 78−35403
Cr-Ni-Mo 40KhN2MA, magnetostriction used in inspection after heat treatment 80−108673
Cu-Al (11.47 wt.%), high temp. phase transforms., effect of pre-exposure to neutrons 79−20045
β-Cu-Zn(-Ni)(-Mn), order-disorder transformation temperature effect on quench hardening 78−95745
Cu_2S, molten, oxidation, exam. of product phase composition by X-ray anal. *(Russian)* 79−34166
KBr, quench hardening of single crystals 79−43261
KBr, quench hardening related to dislocation density and slip 78−52855
KCl, hardness increase mode, effect on dislocation mobility 79−51114
KCl, quench hardening behaviour and quenching temp. 78−64550
KI, quench hardening behaviour and quenching temp. 78−64550
LiF, hardness increase mode, effect on dislocation mobility 79−51114
MgO, hardness increase mode, effect on dislocation mobility 79−51114
NaCl, hardness increase mode, effect on dislocation mobility 79−51114
NaCl, quench hardening of single crystals 79−43261
NaCl, quench hardening related to dislocation density and slip 78−52855
NaCl:Ca(K), impurity state from heat treatment on microhardness 77−80532
NaCl:X (X=Ca, Sr, Ba, Mg, K, Li, Tl, Ag), impurity conc. effect on mech. and elec. props. 78−47469
steels, Cr-C-Mn(Ni), struct. prop. rel., design of struct. steels for high strength and toughness 80−97491
Ti alloy, hardening heat treatment, alloying element effects development trends 78−95759
$\alpha+\beta$Ti alloy VT3-1, drop forgings, grain orientation and props., combined mech. working, hardening and high-temp. heat treatment influence *(Russian)* 80−20973
Ti-Al-Cr-Mo-V, alloy VT22M, exam. of ageing and phase transitions *(Russian)* 79−11641
Ti-Mo-Zr-Sn (11.5, 6, 4.5 wt.%), β III, mech. props. rel. to heat treatment 80−84961
Ti-Nb, cold strained, exam. of ω and α phases, precipitated during ageing *(Russian)* 79−11620
Ti-Nb alloys, Fe, Mo, V, Ta alloying additions on microstruct. after combined treatment *(Russian)* 77−59826
Ti-Ni (48 to 53 at.%), heat treatment and deviation from stoichiometry 80−104192

quenching (optical) *see radiation quenching*

quenching (thermal)
see also quench hardening
actinide alloys, metastable phases production by splat cooling 77−21134
α-$AgSbS_2$, X-ray diffr. study of phase transitions in quenched samples 77−15577
alkali glasses, rapidly quenched, alkali ion cond. 80−107559
alloy, austenitic, mechanical changes after electrolytic quenching *(Russian)* 80−50653
alloy, binary, quenched, computer simulation of cluster dynamics of two dimensional model systems 78−31434
alloy, binary, quenching, cluster growth, first order phase transition, computer simulation anal. 79−34039
alloy, binary, theory for initial stage of grain growth and unmixing kinetics 78−19714
alloy, quenched, binary, time evolution, computer simulation of three-dimensional model system 78−31433
alloy, quenched to sufficiently low temp., struct. function, long time behaviour 77−84886
alloy, splat-quenched, grain size, isothermal transform. 77−77463
alloy solidification, kinetic model, appl. to liquisol quenching 78−44116
alloy steel, complex, X-ray diffr. determ. of fine struct. changes during quenching and tempering 77−56004
alloys, magnetic, amorphous, magnetic strip appl. *(German)* 77−16700

quenching continued
alloys, rapidly quenched crystalline, struct., and heat treatment effects 80−76292
amorphism, techniques for determ. very short room temp. lifetimes 80−84981
amorphous alloy ribbons manufacturing, chill-block metal spinning process 80−29898
amorphous ferromagnetic alloys, form. and stability 77−16515
amorphous metal ribbon form. by cylindrical jet on flat moving substrate, uniformity 78−52718
amorphous structure, computer simulation 78−30541
austenitic solid solution, chem. evaluation of B and its correlations with hardenability and hardness *(German)* 79−39230
austenitic steel, ageing after deform. in pre-martensitic state, internal friction meas. *(Russian)* 77−77477
binary alloy, model quenched computer simulation of time evolution in nucleation region 79−82344
binary alloy, quenched, time evolution, computer-simulation of three-dimensional model system 77−48422
binary alloy, quenched, time evolution of struct. function free energy 78−55937
binary alloys, quenched, vacancy concs. 80−107212
binary mixture, early stage evolution, kinetic Ising model 77−69468
boiling, solid quenching in subcooled water, propag. of wetting front *(French)* 79−77108
boiling, transition type, in forced convective flow, boundaries meas. 79−27499
borosilicate glass, phase separated, depolarised light scatt. in terms of Rayleigh-Gans theory 79−87452
brass, α and $\alpha+\beta$ type, positron annihilation, short-range order, clustering and lattice defects influence 79−29107
brass, crystal structure and morphology of thin needle-like martensite 78−31425
brass, LANKMts, solid soln. range of existence 77−12653
brass, martensitic transform., short range order effect 79−61586
α-brass, quenched, chemical composition in stacking fault tetrahedron 77−21183
α-brass, quenched, secondary defect form. during ageing, TEM obs. 78−88482
β-brass, quenched single crystal, deform. and slip 79−79026
α-brass, single crystal, obstacle strength variation during stress relaxation 78−68723
brass LMtsSKA 58-2-2-1-1, heat treatment, struct. and props. 79−83239
brittle ceramics, effect of data scatter on apparent thermal stress failure mode 80−60949
butadiene nitrile, soot filled, thermal treatment influence on mech. props. *(German)* 80−30000
ceramic, structural integrity in severe thermal environments 77−36544
ceramics, brittle, heat-transfer variables effect as thermal stress resist., meas. by quenching expts. 80−79871
coal dissolution at short reaction times, fast-dump reactor apparatus 77−44575
composite superconductors, triple-phase phenomena, during quenching by pressurised superfluid ^4He 80−20364
cryolite, molten, struct. charact. by IR spectroscopy and splat cooling *(French)* 79−69835
cylindrical specimens in underheated media, calc. of heat transfer during quenching *(Russian)* 78−39821
dilatometric method for study of dimensional anomalies in metallic materials rel. to crystal struct. *(French)* 79−52563
disordered metal ribbon production by ultrarapid quenching 80−71612
electric vacuum furnaces for quenching developed in USSR 78−84872
Elinvar, Cr addition effect on modulus of elasticity and thermoelastic coeff. 77−90387
Elinvar, Curie point, magnetisation and susceptibility, heat treatment effects *(Russian)* 78−47973
energy spike development and quenching depend. on thermal diffusion 80−88367
EPR of thermally induced defect 77−81005
filament reinforced hypoeutectoid C steel, strength characts. after deform. and quenching 80−35271
film boiling instability, during quenching in subcooled water *(French)* 79−46167
first-order phase transitions, influence of quenched impurities 79−73289
fluoroplastics, mech. props., accumulation of submicrocracks, thermal treatment effects 77−4850
foil, preparation apparatus, for X-ray diffr. study of lattice defects 79−37585
freeze-fracture specimen temp. changes during rapid quenching in liq. coolants 78−57140
n-GaAs, neutron irrad. and thermally induced defects, annealing stages 77−51409
gases, thermal shock prod. with conc. solar energy *(French)* 78−91056
glass, coloured, toughening process, spectral characts. 80−43416
glass, flat, dependence of creep, viscosity on cooling intensity, during quenching 80−20964
glass, horizontal quenching, technological parameters rel. to optical properties 80−45264
glass, liquid quenching equipment 78−84854
glass formation, Taylor wire prod. by rapid quenching 78−44045
glass interferometer rod, inhomogeneity rel. to tempering 77−34919
glass thermopolishing, by use of low temp. plasma radiation *(Russian)* 80−45406
glassware, stress distrib. calc. using finite element anal. 79−66087
glassy alloys, splat cooling prep., new, transition-metal free *(German)* 79−28989
glassy material, phase transform. in steep thermal gradients, apparatus 78−84767
graphite nucleation, role of pre-heat treatments *(Japanese)* 80−35220
HBT, liq. cryst., phase transitions, quenching effects obs. 78−22833
heat transfer between high temp. solid and boiling water *(French)* 77−62136
heat treated, stresses and cracks form. *(Czech)* 80−20977
heat treatment apparatus 79−79005
high strength steels HT80, HY130, quenching and tempering effect on H_2 diffusion *(Japanese)* 78−64565
high-Si corrosion-resistant steel, 02Kh8N20S6, mech. props. and heat treatment 77−56003
hot surface quenching rates, wetting of outer tube walls by water 77−82996
Incoloy 903, microstruct. and effect of H_2 charging 77−86143

quenching continued
ingots, quenching technique, for studying formation of macrosegregations 78−52793
interface segregation, influence of cooling rate 78−72010
ion bombardment induced amorphisation, energy spike generation and quenching processes 78−47448
Ising model, quenched-bond disorder, cluster extension of effective-interaction approximation 80−93130
isoprene rubber elastomers, thermal treatment influence on mech. props. *(German)* 80−30000
KBr, thermally processed cryst., optical absorption bands *(Russian)* 78−76513
Kh20N40 alloys, phase composition after quenching, tempering 78−60650
Leidenfrost effect, demonstrations 78−81744
Lennard-Jones fluid, phase separation by spinodal decomposition, mol. dynamics computer simulation 79−10766
levitation splat-quenching device 77−52261
liquid alloys, rapid quenching prep. of metastable solids, apparatus *(German)* 79−28990
low temperature techniques and devices 80−76291
low-alloy cast steel, high-strength, fracture toughness 77−56109
low-alloy steel, abrasive wear resistance, effect of C content, annealing quenching 77−56115
luminescent screens, resolution determ. with thermal quenching 78−21131
LWR fuel rod quenching, two-dimensional heat conduction model 79−93815
magnetic amorphous alloys, props. improvement and appl. 80−7693
magnetic field, cooling capacity of quenching liquids 79−38867
α-martensite, quenching in const. magnetic field, struct. peculiarities *(Russian)* 79−52204
melt extraction technology, advances 80−76207
metal, nucleation of vacancy precipitation during quenching 77−72612
metal, vacancy defect mobilities and binding energies obtained from annealing studies 78−47325
metal ribbon, amorphous, fluid-flow-temp. model for casting by melt extraction 79−56942
metal ribbons, amorphous Newtonian-quenched, formed by melt spinning and melt extraction, dimens. variations 79−56943
metallic alloy, prediction of glass-forming ability after melt-quenching 79−23524
metallic coatings, electric field atomisation from melt 80−76174
metallic glass, current exptl. data on struct., review 80−88058
metallic glass, prep. and phys. props. development 80−81003
metallic glass, splat cooled, mag. props. 80−80491
metallic glass ribbons, quenching stabiliser to improve geometrical uniformity and cross-section 80−55343
metallic glass Taylor wire prod. by rapid quenching 78−44045
metallic glasses, formation and rapid quenching techniques 80−76214
metallic glasses, mats. props. review 77−4043
metallic glasses, polymer model 80−6361
metallic glasses, prep., characterization, review struct., formation, electronic, mag. and mechanical props., review 78−3074
metallic glasses, stability 80−75184
metallic glasses, structure, stability and prod., elec., mag. and mech. props., review 80−44134
metallic thin films, optical props., effect of quench condensation 79−78773
metals, quenched, vacancy cluster form. process 80−92706
metals, rapidly quenched, conf., Brighton, England (July 1978) 80−67934
metals, residual stress and deformation, due to quenching, elastic-plastic anal. *(Japanese)* 78−83268
metals and alloys, FCC quenched, form. of prismatic loops 77−65979
$Mg_{70}Zn_{30}$, amorphous alloy 77−27835
microcrystalline alloys, metastable, produced by rapid particulate quenching, props. and appls. 80−84887
mixture, binary, off-critical, quenched, struct. functions and mobilities renormalisation 79−82343
Ni, high purity 78−48432
Ni-Cr-Mo and Ni-Cr, impact strength, effect of modified ausforming *(Japanese)* 79−11692
Ni-Cr-Mo-Ti-Al, quenching and ageing effects on props. of type 36NkhTYuM8 79−52275
nonisothermal devitrification kinetics 80−92465
nylon 6, relationship between morphology and dynamic mech. props. 79−4992
oxide phase equilibria, high temp. appl. 79−8416
phosphate glasses: Ti^{3+}, $MO(M_2O)$-TiO_2-P_2O_5 M=K, Ca, Be, elec. resistivity *(Japanese)* 77−12719
phthalic anhydride spherulites, cryst. growth from melt 79−32930
piezoelectric semiconductor, influence of thermal quenching of photocond. on US amplification 77−4410
piston and anvil liquisol apparatus, electronic device design 78−23905
plasma industrial utilisation, synthesis, powder, metallurgical and surface treatments, review *(French)* 80−96398
polycarbonate, glassy state, rel. between thermal pre-treatment and viscoelastic behaviour 79−79038
polycarbonate, TSC anal. by activation energy spectra 80−20579
polyester-organic solvent mixtures, phase diagrams, eutectic props., devitrification, crystn. *(French)* 80−3015
polyethylene, annealed, crystallinity effect on mech. props. *(German)* 80−35230
polyethylene, high density, crystallisation struct. revealed by solvent extraction 78−42922
polyethylene, high density extruded fibres, morphology effect on physical and mech. props. 79−83235
polyethylene, irradiation, crystallinity and crosslinking efficiency 80−66843
polyethylene, linear, bulk-crystallised, morphology study 79−32918
polyethylene, linear, crystallised from melt, effect of crystallisation time on density, mech. props., X-ray scattering 80−25680
polyethylene, linear, glass transition temp. 80−15225
polyethylene, linear, quenching of thin films to amorphous state 80−28929
polyethylene, rapid crystn. from melt rel. to struct. 80−44152
polyethylene, shrinkability, orient. 79−11660
polyethylene, ultraquenched, electron diffr., morphology and thermal anal. 79−15640
polyethylene film, elec. props. 77−73114
polyethylene-paraffin wax, blends, rapid cooling processing techniques 80−84905
polymer solution, ZSP-1 78−23739
polyoxymethylene, rapid crystn. from melt rel. to struct. 80−44153
polypentene-1, isotactic, polymorphism of form I 79−19159
polypropylene, quenched form, struct., X-ray obs. 78−67661
polystyrene, glassy, light scattering, quenching effect 80−20649
polystyrene, isotactic, normal vibrational anal. 78−43869
polyvinylidene chloride, vibr. spectra, amorphous and cryst. state conforms. 79−27930
porcelain wave, crazing resistance, glaze fitness *(Japanese)* 79−74278
PVC, enthalpy determ. of order 79−7556
PVC, rigid, viscoelastic props. rel. to thermal, mech. history 79−5016
quartz, thermoluminesc., sensitivity, heat treatment effects 77−59622
quenching-tempering apparatus with recirculation tempering furnace, thermal charact. 77−67438
random sink models, vacancy loss during quenching 78−60698
rare earth oxide (R_2O_3)-M_xO_y glassy systems (M=Ti,Nb,Ta), rapid quenching by laser beam, exam. of composition and crystallization 78−52856
rare earth oxide containing systems, highly refractive, phase equilib. and metastable phases 80−97467
real liquids, quenched to glassy state, struct., one dimens. Ising model appl. 80−54134
Recalloy, Fe-Nb, semihard magnetic alloy, magnetic props., hardness, microstruct. 78−56660
rewetting model using generalised boiling curve 79−9675
ribbon-form material, rapid quenching from melt *(Japanese)* 78−92210
rocks, fracture propagation by transient cooling 79−84236
roller-plate technique, for thin film prep. from melt 80−71607
rotating mill fast quenching device 77−32600
sapphire, neutron bombard., F-centre fluorescence, photoluminescence 80−100676
p-Si, interstitial Fe and thermal defects, Hall effect and resist. meas. 79−82200
solid surfaces, effects of pressure and materials, rel. to LWR emergency core cooling system 79−31061
spinodal decomposition, light scattering, depend. on method of quench 78−18782
splat cooling process, using piston and anvil technique, mathematical model 80−11679
splat quenching, electron transparent area prod., comment 77−4755
splat quenching, electron transparent area prod. 77−4754
splat-cooling devices, quenching efficiency 79−29106
splat-quenching device, refractory metals, alloys, in magnetic levitation furnace *(Croatian)* 79−11639
spray cooling technique 78−23738
steel, 0.54% C, fatigue crack accel. and closure in rotating bending tests, in annealed or quenched/tempered state 79−43383
steel, 0Kh12G14N4Yu2, struct. after deformation under conditions of superplasticity 80−21031
steel, 10Kh11N20T3R, brittle fracture susceptibility rel. to grain size *(Russian)* 77−59901
steel, 18 Kh2N4MA, grain size effect on mech. props. 78−44207
steel, 30CH2GMT and 35CHG2SV, thermomechanical hardening *(Czechoslovakian)* 77−32602
steel, 30KhGSA, fracture toughness, tempering effects 77−90463
steel, 30N9K4, effects of Mo, V, and N on grain growth, tempering, hardenability, strength and toughness 78−44202
steel, 3.5% Ni neutron irrad. effects on tensile props., microstructure effects 77−69005
steel, 36NKhTYu, ageing to produce ultrafine grains, discontinuous precipitation *(Russian)* 77−81277
steel, 37Kh12N8G8MFT, precipitation hardening, hardness meas. and electron microscope exam. *(Russian)* 79−38843
steel, 38KhMYuA, brittleness of nitrided case 77−21418
steel, 40Kh, heat-treated, wear during friction under extreme conditions 78−85007
steel, 4140, fatigue crack initiation and microcrack growth 79−24617
steel, 4340, quenched, tempered, and austempered, effect of plastic strain followed by ageing on elastic limit 78−31446
steel, 45 and U7, deform. microheterogeneity and ductility 77−73309
steel, AISI 4340 toughness evaluation austenitized at high and low temps. 77−86155
steel, Al, quenched, tempered, orientation of precipitated Fe_xC particles, X-ray obs. *(Russian)* 79−29063
steel, alloy, 300M, fracture toughness and strength, effect of heat treatment on microstruct. 78−15436
steel, alloy, 37KhGSTF and 44KhGSTF, quenched X-ray diffr. testing of heat treatment 78−56834
steel, alloy, austenitic, grain size, tempering effect on brittle fracture susceptibility 80−55534
steel, alloy, carburized case parameters, effect on props. of 20Kh3MVFA and 12Kh2N4A 78−52989
steel, alloy, cluster formation susceptibility in 40 KhN, influence of isothermal working in H_2 *(Russian)* 78−56643
steel, alloy, cyclic strength after strain hardening and tempering, precip. hardened 40FT and 40 78−52988
steel, alloy, fracture and fracture energy, subject to static, impact and repeated impact bending 77−63799
steel, alloy, high C, amorphous, produced by rapid quenching from melt, hardness and strength 78−59764
steel, alloy, high speed, rapid stepless cyclic method 80−16352
steel, alloy, high-speed, struct. changes investigation by hot hardness and quench dilatometry *(French)* 80−76249
steel, alloy, low C, effects of pre-treatment on graphitisation behaviour *(Japanese)* 78−84860
steel, alloy, medium and low C, quenched and tempered, fracture resist., nonmartensitic transformation products effect 79−96054
steel, alloy, Ni-Cr-Mo-V, exam. of temper embrittlement susceptibility 78−76737
steel, alloy, nonmartensitic decomposition of austenite, fracture strength of high tempered products *(Russian)* 78−11304
steel, alloy, nonsteady temp. fields during cooling, calc. 80−16346
steel, alloy, quenched, high strength, shot blast hardening effect on repeated impact bending 79−1914
steel, alloy, quenched carbonitrided, multicycle fatigue failure 80−104283
steel, alloy, toughness evaluation inconsistency of AISI 4340 austenitised at increasing temp. 78−52982

quenching continued
steel, alloy, type 36NKhTYu, plastic deformation, effect of surface condition on initial stage 78−84929
steel, alloy, type 60 ND 11, martensitic transform. effect on stress development during quenching *(French)* 79−91712
steel, alloy, U20Kh6T2D, structural transformations during heat treatment, and wear resistance 78−88484
steel, alloy, ultrahigh-strength, near threshold fatigue crack propag., microstructure effects 77−86168
steel, alloy maraging, type Kh13N8D2TM, conditions for formation of stable austenite 78−84868
steel, and alloy, fatigue strength improvement 78−44153
steel, austenitic, 30KhGSA, grain size before quenching rel. to mech. props. 79−24553
steel, austenitic, 30KhGSA, heat treatment, preliminary, cold deform., elec. heating rel. to mech. props. 79−24554
steel, austenitic, 33N25Yu3F, hardening, effect of quenching and ageing temps. *(Russian)* 77−81267
steel, austenitic, alloyed with N, decomposition of solid solution 78−23712
steel, austenitic, Cr-Ni (18,12 wt.%), containing coarse grain boundary precipitates, thermomechanical treatment 78−27545
steel, austenitic, Cr-Ni (20, 25 wt.%), containing B and Ti additions, splat quenching, X-ray and TEM study 79−74186
steel, austenitic, Cr-Ni-Mo, Mo effect on lattice parameters and chem. comp. of σ-phase and $M_{23}C_6$ carbides 77−70072
steel, austenitic, martensitic transform., alternating elastic stressing effects 77−86029
steel, austenitic, martensitic transform., mechanism and kinetics, TEM, X-ray and optical obs. *(Rumanian)* 78−19746
steel, austenitic, phase composition of Kh14N16 with Zr, Ti, Nb and N additions after quenching and tempering 77−90378
steel, austenitic, phase transform to pearlite and martensite, kinetics, stresses due to quenching, anal. *(Japanese)* 78−27508
steel, austenitic, press. effect, distrib. of temp. fields analysis 79−38860
steel, austenitic, quenched state, influence of austenite stability on impact strength *(Russian)* 80−81146
steel, austenitic, strength, ductility and fracture toughness, N and Cr effects 80−100878
steel, austenitic, supercooled, decomposition by heat treatment, carbide particle morphology *(Russian)* 77−70076
steel, austenitic, supercooled ShKh15, stability, effect of spheroidising carbides *(Russian)* 77−25074
steel, austenitic Mn, existence of carbide M_5C_2 phase, electron microdiffr. analysis *(Russian)* 78−23727
steel, austenitic Mn-Ni ageing , alloying element influence on struct. and mechanical props. *(Russian)* 80−35256
steel, austenitic stainless, cavitation erosion resistance, martensitic transform. effect *(Russian)* 78−35524
steel, austenitic stainless, cold worked, 20%, heat treatment effects on mech. state, load-relaxation expts. 77−52350
steel, austenitic stainless, dynamic recrystallization kinetics 79−47731
steel, austenitic stainless, irradiation induced creep by alpha particles, in type 316 steels *(French)* 78−72791
steel, austenitic stainless, matrix precipitation of Cr_2N, due to P addition, TEM exam. 79−4973
steel, austenitic stainless, stabilized, creep improvement, effect of B precipitation and hyperquenching *(French)* 78−23784
steel, austenitic stainless, type 00Kh18N20S3M3D3B, anticorrosion props., heat treatment effects 80−30168
steel, austenitic stainless, type 316, hydrogen embrittlement, tensile testing 80−7671
steel, austenitic stainless B-containing, decomp. of solid solns., effect of cooling conditions 77−44256
steel, austenitic type 110G13L, preliminary strengthening inheritance, exam. 78−44137
steel, bainitic, low C and alloy, quenched microstruct. effect on mech. props. *(French)* 79−79003
steel, borided, 45, 20Kh, 30KhGSNA and Kh12F1, relative wear resistance 77−73351
steel, C1020, dual phase, mech. behaviours and structs. *(Korean)* 80−25779
steel, C, bainitic hardenability, overheating effect 79−38866
steel, C, contact fatigue strength, effect of austenite grain size 79−100254
steel, C, corrosion fatigue resistance in cavitations, bainitic and martensitic structs. *(Russian)* 78−56815
steel, C, diffusion of H_2, effect of quenching and tempering 77−7908
steel, C, diffusion of H_2, SCC via martensite form. cooling rate changes on Mn and Ni addition *(Russian)* 78−56813
steel, C, martensitic by quenching 80−3038
steel, C, massive martensitic transformation kinetics 80−81060
steel, C, pressure vessel and piping, factors affecting notch toughness 79−61730
steel, C, quenched, restoration of austenite grains during rapid heating *(Russian)* 80−76272
steel, C, quenched and tempered, ductility, effect of hydrostatic press. 78−44190
steel, C, rubbed surface, continuous hard layer *(Japanese)* 77−52501
steel, C, tempered martensite embrittlement, and retained austenite, exam. 78−56754
steel, C, transform. kinetics, heat cond. and elastic-plastic stresses during quenching *(Japanese)* 80−25688
steel, C and alloy, wear resistance, change through hardened layer 79−96153
steel, C and Co, carbide transitions during post-strain ageing and tempering *(Russian)* 78−95741
steel, C type U10A, X-ray diffr. investig. of carbide residues after deform. and tempering *(Russian)* 77−81275
steel, C-Cr (1.0, 1.5 wt.%), 52100 bearing steel, control of surface residual stress by heat treatment 80−97501
steel, C-Mn and C-Mn-Nb, weldable, high temp. thermomechanical treatment 79−15709
steel, C-Mn-(Cr), structural changes during stress cycling after heat treatment and cold rolling *(Russian)* 78−19787
steel, C-Ni-Cr (0.6, 1, 1 wt.%), grain boundary segregation of S, N, P, As, Sb and Bi *(Japanese)* 78−15405
steel, carburised, alloying effect on props., mathematical-statistical determ. 78−19794
steel, carburized and quenched, residual stresses *(Japanese)* 80−89262
quenching continued
steel, casecarburized and hardened, relationship between fatigue strength and case hardness distrib. *(Japanese)* 79−61782
steel, cast, high tensile strength, heat treatment 80−16358
steel, CC Cr-Mo-V, creep fatigue interaction 78−60841
steel, cementite migration in temp. gradient 78−44151
steel, Co-Cr-Ni-Mo-Mn (39.65, 20.25, 15.33, 7.08, 1.9 wt.%) carbide formation during tempering after plastic deformation 80−16330
steel, commercial C, stress corrosion cracking susceptibility in liquid NH_3 *(Japanese)* 78−11411
steel, complex alloy, exam. of temper brittleness 78−44209
steel, Cr, corrosion resist., tempering after air-hardening in rolling heat *(German)* 80−45324
steel, Cr, high C, in situ transform. of cementite to M_7C_3 and internal defects of M_7C_3 by tempering 78−31412
steel, Cr (12 wt.%), thermomechanical treatment, high temperature, effect on props. and struct. *(Czechoslovakian)* 77−32603
steel, Cr (13 wt.%), tempered, quenched, fatigue resistance in corrosive medium *(French)* 78−23870
steel, Cr maraging, internal friction, 120 to 700K *(Polish)* 79−96075
steel, Cr modified, heat resist. rel. to thermomech. treatment 79−20084
steel, Cr-Al (12, 6 wt.%), ferritic stainless, high temp. treated, strengthening mechanisms 80−3106
steel, Cr-C, segregation of P, C, and Cr to γ-boundary and carbide/γ-interface *(Japanese)* 79−61593
steel, Cr-C (18, 0.9 wt.%), cavitation, abrasion resistance, effect of unstable austenitic struct. *(Russian)* 77−16695
steel, Cr-Mn, unstable austenite, martensitic transform., effect of alloying, heat treatment, and deform. 78−19751
steel, Cr-Mn type, martensite struct. after quenching and HTMT, X-ray diffr. obs. 80−84975
steel, Cr-Mo, Mn-V, V, fracture toughness, pressure vessel appl. *(Czech)* 79−79094
steel, Cr-Mo (2.25, 1 wt.%), quenched and tempered, diffusion and solubility of H_2 *(Japanese)* 79−65255
steel, Cr-Mo (2.25, 1 wt.%), temper embrittlement trace elements, Mo, intercritical heat treatment effects 77−36634
steel, Cr-Mo (2.25, 1 wt.%), thermal fatigue cracking caused by repeated quenching from high temps. 77−52469
steel, Cr-Mo (9,1 wt.%), austenitized in $\gamma+\delta$ phase field, secondary hardening and tempering 78−11247
steel, Cr-Mo-V, heat treated, mech. props. *(German)* 80−25724
steel, Cr-Mo-V, medium strength, correlation between crack initiation, propag. and microstruct. 78−60787
steel, Cr-Mo-V, press. vessel, fracture, effect of tempering 78−60799
steel, Cr-Mo-V pressure vessel, microstruct. parameters and yielding rel. to plastic deform. 80−89318
steel, Cr-Ni, effect of tempering under load on mech. props. 80−16354
steel, Cr-Ni, microstruct. effect on temper brittleness *(Korean)* 79−70092
steel, Cr-Ni, pendant drop melt extracted, struct. and props. 80−76242
steel, Cr-Ni (32.8 wt.%), tensile props. and fracture of two phase Fe alloy austenite and ferrite *(Japanese)* 79−8344
steel, Cr-Ni (32,8), two phase austenite-ferrite alloy, fatigue behaviour *(Japanese)* 79−79091
steel, Cr-Ni-Mo-Cu, ε phase particle precipitation from martensite, local internal stress relaxation *(Russian)* 79−78969
steel, Cr-Ni-Mo-V, austenite form. during heating, influence of recrystn. during tempering *(Russian)* 80−104188
steel, Cr-Si-Mn-Ni-Mo-C, resist. to deform. and fracture, C effect 80−71757
steel, Cr-W(Mo), quenched, carbide reactions during tempering 80−89229
steel, cracking resistance of high-strength 40Kh and 35KhGSA, tempering temp. influence *(Russian)* 79−52252
steel, cylinder, quenched without transform., residual stresses *(German)* 80−25725
steel, die, with high heat resist. and toughness 78−84989
steel, duplex ferritic/ martensitic, design for improved mech. props., heat treatment, TEM obs. 77−63697
steel, embrittled N18K8M3TYu, toughness enhancement by double quenching 77−59922
steel, eutectoid notch toughness, tempering at moderate temps., effect of quenching temp. 77−21193
steel, fatigue strength of 30 KhGSNA, 12 KhN3A, effect of friction in abrasive medium after hardening 78−35507
steel, Fe-C martensite, quenched, and heated to 293K, struct., Mossbauer obs. *(Russian)* 77−59784
steel, ferritic, with interstitial N, continuous precipitation and clustering 80−7585
steel, ferritic martensitic, effect of ductility of second phase on ductile fracture 78−19847
steel, ferritic stainless, embrittlement 80−85041
steel, ferromagnetic, U8, magnetic method of martensite transform. study *(Russian)* 79−87631
steel, free plate elastoplastic stress condition during phase transformation 78−95781
steel, H_2 effect on yield 78−15474
steel, hardened and casecarburized, fatigue crack initiation, propag. and termination, notch depth effects *(Japanese)* 78−7022
steel, heat treated, deform. due to thermal gradient *(French)* 79−61631
steel, high alloy Cr-Mo-W, splat quenched, formation of metastable austenite 80−84974
steel, high C, high alloy, $M_{23}C_6$ type carbides, effect of alloying elements on defect struct. and hardness 80−16481
steel, high C, quenched and tempered, hydrostatic press. effect on brittle fracture stress 79−61727
steel, high Mn alloy G22, phase transform. during plastic deform. 77−16576
steel, high Mn mandrels, wear resist., surface layer chem. comp. influence *(Russian)* 79−52444
steel, high Ni (19 wt.%), thermal stabilisation of austenite 78−15397
steel, high purity, low S content, for tough semi-finished products in nuclear power plant *(German)* 80−45393
steel, high speed, anode potential determ. of tempering quality 78−53139
steel, high speed, atomised powder, defects in parts produced by hot isotactic pressing 78−60612
steel, high speed, microstruct. effect of splat cooling 79−61624
steel, high speed, type R6M5K5, secondary and red hardness of marquenching 80−16350

quenching continued
steel, high speed, wear resistance of white layer formed by vacuum oil quenching *(Japanese)* 78−11336
steel, high speed M2, charact. of solidification struct. within dendritic core 78−27504
steel, high speed R8F8K7M6, cast, forged, sintered, struct. and props. 77−77516
steel, high speed tool rapidly quenched, exam. of solidification struct. 78−39758
steel, high strength, 300-M, slow fatigue crack growth, threshold behaviour, temper embrittlement, impurity segregation effects 77−86152
steel, high strength, fine grained, quenched and tempered, residual welding stresses, stress relieving temp. *(German)* 78−72793
steel, high strength, increasing resistance to cracking, use of overheating before quenching *(Russian)* 77−25135
steel, high strength, surface work hardening effect on life 77−70234
steel, high strength, thermally strengthened by rolling heat, H_2 embrittlement *(Russian)* 77−77562
steel, high strength, treatment effect on ductility and strength 80−60880
steel, high strength HP 9-4-20, retained austenite influence on fatigue crack propag. 80−21106
steel, high-speed, quenched and tempered notch toughness, ultimate and yield strength in tension and compression 78−95782
steel, high-speed cutting, struct. and props. Co addition effects *(Russian)* 77−21177
steel, high-speed tool, splat quenching, props. and struct. 80−76294
steel, high-strength low alloy, Nb(CN) precipitation and coarsening during hot compression 80−97514
steel, homogenisation of sulphide inclusions 77−32605
steel, induction hardened, static bending strength and correlation between static strength and endurance limit *(Japanese)* 77−70108
steel, Kh17N2, endurance limit, effect of residual stresses caused by Cr plating and cyaniding 77−86184
steel, Kh18N9T, strengthening by vibrational stirring effect 80−40405
steel, KhVG, quenched change in structure under influence of cyclic loads 78−56676
steel, lath martensite, elastic interaction of H_2 with precipitates 78−3129
steel, low alloy, 18KhMVTCh, corrosion cracking resistance in sulphide environments *(Russian)* 78−31571
steel, low alloy, acoustic emission during ductile fracture, isothermal tempering effect 79−83241
steel, low alloy, B, quenchability and microstructure *(French)* 79−47727
steel, low alloy, bainitic and martensitic transform., isothermal studies 77−36497
steel, low alloy, brittle fracture, quenched and tempered 80−11677
steel, low alloy, formation of stony fracture during forging 79−79059
steel, low alloy, pressure vessel and piping, factors affecting notch toughness 79−61730
steel, low alloy, quenched, tempered martensite embrittlement, role of retained austenite and cementite 79−74251
steel, low alloy, radiation embrittlement, heat treatment effects 78−19893
steel, low alloy, SNCM 8, quenched, tempered, prior austenite grain size effect on stress corrosion cracks *(Japanese)* 79−66215
steel, low alloy, tempered martensite embrittlement mechanisms 79−8351
steel, low alloy, thermally fatigued, fracture toughness 78−72872
steel, low alloy, toughness, effect of packet size and lath width 77−16677
steel, low alloy, type 4340, quenched and tempered, effect of plastic strain followed by ageing, on torsion fatigue resistance 78−92360
steel, low alloy structural, pre-treatments to enhance graphitisation, dilatometric and optical microscopy study *(Japanese)* 79−78992
steel, low and medium C, tempering 79−61629
steel, low C, bainitic, optimal struct., heat treatment effects 77−16624
steel, low C, effect of heat treatment on resistance to fatigue crack propag. 80−11675
steel, low C, grain size effect on fatigue strength, high temps. 78−68759
steel, low C, high C, bainite transform. heat treatment effects *(Czech)* 77−63661
steel, low C, high strength, thermomech. treatment, strengthening mech. 79−57014
steel, low C, low alloy, Mossbauer study of retain austenite 78−48434
steel, low C, martensitic, fracture toughness variations during tempering 78−60812
steel, low C, Mb-Nb, reheated, quenched, tempered, microstruct. 77−36550
steel, low C, microalloyed, heat treatment, mech. props. 79−24551
steel, low C, Mn effect on recrystallisation and texture *(French)* 80−3110
steel, low C, Mn-Nb, quenched and tempered, microstruct. and props. 77−36549
steel, low C, packet martensite struct. and localisation of residual austenite, electron microscope obs. *(Russian)* 80−25695
steel, low C, quenched, interphase precipitates obs. *(Russian)* 80−29957
steel, low C, quenched, struct. and props. after plastic deform. and tempering 78−23734
steel, low C, tempered, lath martensite, Ni (5 wt.%), microstruct./yield strength relationship 77−21234
steel, low or medium alloy, work hardening effect on martensitic transform. cond. *(French)* 80−16329
steel, low-alloy structural 16G2 and 16GFR, struct. and props. after quenching and tempering 80−76280
steel, low-C, Cr, ferritic, optimal heat treatment development 79−38869
steel, low-C, gas nitrocarburised, aged, fatigue behaviour 80−40514
steel, magnetic field effect on retained austenite transformation 77−16580
steel, maraging, effect of deformation on props. 80−21032
steel, maraging, thermally embrittled, TiC precipitation 77−25055
steel, maraging N18K9M5T, crack propag. resistance under stress corrosion 77−70224
steel, maraging stainless, phase transformation and mech. props. rel. to heat treatment *(Chinese)* 80−66501
steel, martensite, brittle fracture resistance, struct. after quenching effects, tempering effects 79−57104
steel, martensitic, ageing, thermal recovery 77−56011
steel, martensitic, ageing of 05kh3N2MD2, hardness depend. on tempering temp. *(Russian)* 79−24544
steel, martensitic, Cr-Co-Ni-Mo, notch toughness, rel. to sensitivity to stress conc. 78−31532
quenching continued
steel, martensitic, Cr-Ni deform., effect of phase composition and struct. *(Russian)* 77−25102
steel, martensitic, high C, Co addition effect on strength *(Korean)* 78−68736
steel, martensitic, low C wire, strain tempering by rapid heating *(Japanese)* 78−31428
steel, martensitic, medium alloy, quenched state, deform. hardened, ageing effects *(Russian)* 77−21179
steel, martensitic, quenched, strength variation rel. to H behaviour 77−59924
steel, martensitic, sp. ht. and magnetisation meas. 1.2 to 10K 80−71059
steel, martensitic, tempered, C and low alloy, hardness, effect of alloying additions 78−27629
steel, martensitic transform., orientation relationships *(German)* 77−25050
steel, martensitic-aged, plastic deformation influence in type N17K12M5T steel on mech. props. *(Russian)* 80−76305
steel, medium C, isothermally quenched, high-temp. deform. effects on struct. and props. *(Russian)* 80−25760
steel, medium C, structural changes and elastic-plastic stresses during quenching *(Japanese)* 79−38858
steel, medium C, tempered, normalised or quenched, statistical property of fatigue limit, press-fitted axles *(Japanese)* 77−12693
steel, medium C 80−11752
steel, medium C quenched, tempered, relation between wear and work surface layers *(Japanese)* 77−52499
steel, medium Cr, B effects on struct. and toughness 77−21265
steel, medium strength plate, quenched and tempered, fracture toughness in ductile-brittle range 78−7036
steel, microalloyed, alloy carbide precipitation during isothermal ageing 80−3077
steel, middle and low C, clad plate, inhomogeneity and residual stresses, heat treatment effects *(Japanese)* 78−6955
steel, mild, semi-killed, tempering, effect of microstruct. and hardness 77−21184
steel, mild, tempered and quenched, dynamic fracture toughess 77−36665
steel, mild, yield strength and fracture toughness, microstruct. effect, heat treatment 78−27615
steel, Mn-B-V, low alloy, transform. singularities *(Russian)* 80−104116
steel, Mn-C (1, 0.1 wt.%) strip, hot rolled, P effect on mech. props. 78−27532
steel, Mn-C-Si-Cu (0.95, 0.85, 0.25, 0.16 wt.%), fibrous-banded fracture mechanism 80−104280
steel, Mn-Cr-V, tool, quenched and tempered, fracture toughness *(German)* 80−25726
steel, Mn-Mo-Ni-Cr, bainitic, microstruct. and mech. props. *(French)* 80−16362
steel, Mn-Ni-Cr-C, supercooled austenite, influence of constant mag. field on diffusional decomp. *(Russian)* 79−4964
steel, Mn-Ti-B-rare earth, distrib. of B *(Chinese)* 78−84811
steel, Mo-W high speed, best quenching heat treatment 78−84852
steel, Ni, 11.6%, quenched cylinder residual stresses, boring/turning and X-ray diffr. obs. *(German)* 80−93586
steel, Ni, high-strength, impact fatigue strength, heat treatment conditions effect 80−76285
steel, Ni, sintered, physical and mech. props. rel. to homogeneity 79−38762
steel, Ni(9 wt.%), isothermal bainitic transform., thermomechanical effects on mech. props. *(German)* 80−40383
steel, Ni (9 wt.%), mech. props., effect of alloying 77−48462
steel, Ni and W, recrystallisation mech. during laser treatment 80−50658
steel, Ni-(Cr)-Ti, thermomechanical and heat treatment effects on retained austenite *(Russian)* 77−66661
steel, Ni-Co-Cr, high-strength medium C, Cr effect on props. 80−76339
steel, Ni-Cr, temper embrittled, electron microscope and X-ray microstruct. obs. 79−38870
steel, Ni-Cr-Mo, quenched and tempered, nothced bar tensile tests *(German)* 80−35247
steel, Ni-Mn-Al-V, nonmagnetic, ageing, dispersion hardening, microstruct., phase comp., mech. props. *(Russian)* 79−34046
steel, Ni-Mo-C (2.0, 0.2, 0.4 wt.%) sintered, struct. transforms. and mech. props. after quenching 80−66557
steel, Ni-Mo-C (5, 0.5, 0.5 wt.%), sintered, effects of powder and sintering variables on props. 80−104093
steel, pearlitic, heat treatment effect on fracture resistance, microstruct. and mech. props. 80−104191
steel, platelike parts, quenching, temp. field calc. 80−60889
steel, quench ageing effect of Mn content on C and N precipitation and mech. props. *(German)* 78−31409
steel, quenched, adsorption of P on austenite grain boundaries rel. to tendency to delayed fracture of type 18Kh2N4VA *(Russian)* 80−45378
steel, quenched, corrosion cracking in NaCl soln. *(Russian)* 78−56801
steel, quenched, exam. of phenomena taking place during tempering by positron annihilation *(Russian)* 79−24543
steel, quenched, local H distrib. and internal microstresses *(Russian)* 80−50654
steel, quenched, martensite, tensile and compressive deform. resist. *(Russian)* 78−19819
steel, quenched, notch sensitivity, effect of tempering temp. 77−1846
steel, quenched, reheating, to improve plasticity and notch toughness 77−63701
steel, quenched, tempered, intergranular failure during fatigue crack growth 79−8357
steel, quenched, tempering treatment, ultimate tensile strength and yield point *(Russian)* 77−32599
steel, quenched 40Kh2N5SM and 18KhNVA, nature of delayed fracture 77−90456
steel, quenched and tempered, microstructure effect on cleavage fracture toughness 79−74252
steel, quenched and tempered 52100 bearing, plastic deform. in compression 77−40437
steel, quenched and tempered sheet, first operation cupping *(German)* 78−72788
steel, quenched surface layer hardness rel. to adsorption contact fatigue *(Ukrainian)* 80−40478
steel, quenched-tempered, relationship between half value breadth and hardness *(Japanese)* 77−52366

quenching continued
steel, quenching, computer anal. of thermal processes 77−70085
steel, quenching to form martensite, morphology and struct., electron microscope and electron diffr. study *(French)* 77−73291
steel, residual quenching stress determ. in cylinder, consideration of transform. *(German)* 80−35213
steel, Rheocast high performance alloy, solid-liquid phase charact. 77−28803
steel, Si-Cr-Mo-W-V (2,4,1,3,2 wt.%), heat treatment and props. 80−16349
steel, Si-Mn, 27SG, heat treated sheets, underwater explosive forming *(Polish)* 79−34052
steel, Si-Mn-Cr-C (1.1, 0.9, 1.0, 0.29 wt.%) 30KhGSA, heat treatment effect on strength and toughness 78−15437
steel, silver, elastic limit, bending strength, and ductility rel. to tempering temp. after quenching 78−95764
steel, spring alloy, microstruct. and props. at low temps. 77−44286
steel, stainless, 304, deformed in torsion, annealed, static recrystallization and restoration after hot deform. 79−47735
steel, stainless, 95Kh18, vacuum quenching 78−85047
steel, stainless, C-Cr-Ni-Mn-V , non mag., aged, struct. and mech. props. *(Russian)* 78−56666
steel, stainless, dislocation struct. adjacent to fatigue crack tips 77−36643
steel, stainless, ferritic Ti stabilised, changes in structure and mech. props., after alkali bath etching *(Russian)* 79−29271
steel, stainless, filament produced by glass coated melt spinning, new metastable tetragonal struct. 79−20072
steel, stainless, fusion reactor He embrittlement simulation, splat cooling in development of B doping 80−30072
steel, stainless, martensitic 403, heat treated struct. effect on H_2 diffusion 77−63703
steel, stainless, prestrained, heat treatment effect on fatigue strength *(Czech)* 78−60747
steel, stainless, two phase, variation of tensile and impact strength with heat treatment 79−34085
steel, stainless, type 07Kh16N6, heat treatment 79−66158
steel, stainless, type 304, exam. of H_2 induced cracking 78−76738
steel, stainless, type Kh17N13M2T, strengthening by plastic deformation and cold working *(Russian)* 78−52839
steel, stainless, XM19, stress corrosion resistance 80−16558
steel, stainless 18KhNMA, microplastic deform. *(Russian)* 77−66681
steel, stainless Cr (17 wt.%), hot rolled sheets, martensite distrib. effect on ridging phenomena 79−1887
steel, stainless fracture character under tension, in S-H_2 atmosphere *(Russian)* 79−34198
steel, structural, 34KhN3M, heat treatment effect on magnetostriction 80−104306
steel, structural, brittleness susceptibility rel. to heat treatment 79−24620
steel, structural, CrN-modified, tempering and quenching effects on struct. and props. 77−59835
steel, temp. field exact calc. in large pieces, computer use 77−70086
steel, tempered or quenched, exam. of fracture toughness tests, for C shaped specimens 79−29215
steel, tempered StE70, water quenched, residual stress field in centrally welded plates *(German)* 78−72794
steel, thermal processes 77−63699
steel, thermomechanical treatment effect on mech. props. and microstruct. *(French, German)* 79−66090
steel, Ti (0.1 to 0.55 wt.%), strengthening by carbide precipitation 77−25062
steel, tool, high-strength, mech. props. in compression, tempering temp. effect 79−83240
steel, tool, quenching procedure effect on distortion, tool life 80−50657
steel, tool, type KhBG, carburising and quenching, effect on fracture toughness 80−29997
steel, tool, W-Mo, heat treatment effect on props. 80−50656
steel, tufftrided, S15CK smooth specimens, fatigue strength, strengthening mechanisms *(Japanese)* 78−27609
steel, type 20Kh deformed, austenite grain size, inheritance effect with quenching and tempering 80−60881
steel, type 27KhGSNL, castings, exam. of cracks due to treatment 78−44205
steel, type 28Kh3SNMVFA, strain hardened martensite, resist. to tempering, exam. 80−16348
steel, type 52100, heat treatment effect on microstruct. and mech. props. 80−29993
steel, types 15Kh2NMFA and 45, fatigue tests, low cycle, material variance distrib. law 79−91799
steel, ultra high strength, P induced 350°C embrittlement 79−57099
steel, ultrahigh C, superplastic struct. development by heat treatment 80−11703
steel, ultrahigh strength, Si addition and retain austenite effect on SCC, quenched and tempered 78−48567
steel, W, high C, amorphous, rapidly quenched from melt, mech. and thermal props. 79−38874
steel, W alloy, microstruct. and hardness, splat quenching effect 80−76293
steel, W-Co-Mo-Cr-V-C (8.5, 8.1, 4.5, 3.5, 2.2, 1.02 wt.%), phase composition, struct. and props. 80−104163
steel, W-Mo, sintered high-speed, naphthalenelike grain form., quenching effect on fracture toughness 80−30103
steel, water soluble polymer quenchants 79−100190
steel, wear resistance of 30KhGSA and 40 kHNMA after thermal and thermomech. treatment 77−70087
steel, with 4% Al, κ'-martensite struct. and $\kappa' \rightarrow \alpha_m$ transform., X-ray diffr. *(Russian)* 77−59786
steel *(French)* 80−66670
steel 1095, quenched, Mossbauer study of surface martensite 77−32578
steel 12Kh1MF, fine struct., effect of isothermal transform. temp. 77−21137
steel 14Kh2N3MA, brittle fracture susceptibility, heat treatment effects 77−21190
steel 18Kh2N4MA, phase transformations and props. 77−12614
steel 30khGSNA, low alloy, quenched, grain refinement influence on impact strength *(Russian)* 80−20974
steel 40 KhSN2MVF, chemical micro-inhomogeneity recovery during thermal working *(Russian)* 78−15442
steel 40Kh, notch sensitivity under cyclic impact loads 78−3220
quenching continued
steel 45, effect of low temps. and heat treatment on growth rate of fatigue cracks 79−57027
steel 52100, compressive strain induced austenite transform. 77−86027
steel AF1410, wear against stainless steel, repetitive impact, microstruct. effect 79−74263
steel Cr-Mo, Ni-Cr, Ni-Cr-Mo, Cr, quenched and tempered struct. effect on H diffusion coeff. and solubility *(Japanese)* 78−52857
steel fine structure after heat treatment, X-ray diffr. exam. 80−60890
steel forgings, expt.-calc. model of quenching, temp. meas. across cross section 80−16345
steel hardfaced, effects of quenching on structure and wear resist. 77−21175
steel high strength, Cr, Cr-Mo, Ni-Cr, and Ni-Cr-Mo, diffusion of H_2, effect of quenching and tempering 77−90384
steel JIS SNCM8, enhancement of delayed failure resistance by partial unloading method, environment effects 79−79146
steel Kh18N9T, fractographic features of rupture, rel. to struct. changes 77−63801
steel low C, fatigue strength of notched specimen, low-temp. quenching and quench ageing effects 79−100173
steel M16C, low C, natural discrete microlamellar composite *(Russian)* 78−39810
steel N22, crack movement rate during cyclic deform., internal microstress effects 78−3225
steel nitride phase hardening, precipitation and solution kinetics after heat treatment 78−95756
steel ShKh15, austenite, grain growth, melting procedure effects 77−12650
steel tubes, square section, collapse in bending 80−25792
steel VNS-2, damping capacity, magnetomechanical, phase transform. effects 78−31445
steel-cast Fe cam-roller pair, wear resistance after strengthening treatment *(Russian)* 78−31542
steels, austenitic, microdefect accumulation during creep, effects of heat treatment, hardening 79−24550
steels, C, quenched and tempered, struct.-prop. relationships 80−7599
steels, Cr and Cr-Ni-Mo refining effect on low cycle fatigue strength, resistance to hydrogen embrittlement 78−44208
steels, induction hardened bearing, rolling contact strength *(Japanese)* 80−93568
steels, low C S25C, medium C S45C, Cr-Mo SMC3, statistical fatigue props. eval., heat-to-heat variations 78−7048
steels, low-C, aged after quenching, rel. between micro-cracks and coaxing effect *(Japanese)* 80−81159
steels, tempered with different Ni contents, scaling behaviour obs. 80−71817
structural steel, microstruct. and brittleness, rel. to austenizing and heat treatments 77−56091
superconducting magnet, effect of adhesion between turns 78−89507
superconducting metastable alloys, review of current work 80−81002
superconductors, composite, by various states of ^4He 79−61633
temperature field, exact calc. in large pieces, computer use 77−70086
Ticonal, two- and one-dimens. modulated struct. after thermomag. treatment and water quenching *(Russian)* 80−29983
Ticonal-type alloys, struct. after quenching from 800-850°C *(Russian)* 77−59822
transition boiling curves from quenching expts., two-dimens. model with axial conduction 79−19360
transition metal alloys, domain struct. of diffuse ω-phase formed in quenching, 1D model 78−27523
transition metal amorphous alloys, mag. props. 80−29576
transition metals and alloys, high-melting-point, fast cooling from melt, cooling rate influence on struct. *(German)* 79−43287
Udimet 700 superalloy, laser melt quenching and alloying 79−69919
vacanacy trapping by foreign atoms in FCC crystals 79−90696
vacancies, quenched-in, stochastic theory for clustering, general mathematical props. 79−65073
vacancies, quenched-in, stochastic theory for clustering, solvable model 79−65074
vacancies, quenched-in, stochastic-theory for clustering, continuum model 79−77593
vacancy defects, quenched-in, behaviour, electron microscopy study 77−1120
vacancy loss during quenching of low dislocation density cryst. 78−75656
water soluble polymer quenchants 79−100190
water-isobutyric acid (2,6-lutidine) mixtures, critically quenched, phase separation and coalescence 80−24581
Zircaloy-2, neutron irrad., low temp. deform. studies 79−47757
Zircaloy-4, β-transformed, flow stress and dynamic strain ageing 80−3101
Zircaloy-4, strain ageing 77−25071
Zircaloy-4-O alloys, rapidly heated and quenched, transform. charact. 79−20041
Ag chalcogenides, single-phase, preparation 78−35293
Ag-Cu (50 at.%), splat-cooled, struct. of η' extended solid solution 78−3147
Ag-Cu (6.6% at.wt.), laser melt quenching and alloying 79−69919
Ag-Cu alloy filaments, prod. by glass coated melt spinning, microstruct. and tensile strength 79−91667
Ag-Cu surface alloyed films, laser melt quenched, microstruct. 80−76423
Ag-Ga (27 at.%), cooling rate depend. of thermal arrest, transform. temp. 79−29053
Ag-Ge alloy, liq.-quenched, metastable phase formation and evolution 77−90338
Ag-In alloys, rapidly quenched from melt, stacking faults, TEM and X-ray diffr. meas. 77−59768
Ag-Mg, low temp. internal friction, 150 to 300K *(Polish)* 79−96077
Ag-Sn, splat-quenched, X-ray diffr. study 80−81094
Ag-Sn (6,11 at.%) alloy, splat-quenched, X-ray diffr. study of microstruct. 77−8860
Ag-Sn (6(8.2)(11) wt.%), splat-quenched, X-ray line broadening 80−40397
Ag-Sn alloys containing Au, splat cooled ribbons, electron microscope exam. 78−39987
AgAu, quenched, short range order effects on specific heat 80−29181
$AgGaSe_2$, growth by Bridgman method, optical charcts. 77−69980
AgI/Ag oxysalt system, vitreous solid electrolytes, conductance mechanism 80−107560

quenching continued
AgZn, β' to ζ_0 and β to ζ_0 phase transform. 79−34026
Al alloy, cast struct. form. in continuous casting *(German)* 78−92256
Al alloy, heat treatment of semifinished products of alloy 01420 before cold deformation 78−84873
Al alloy, high-strength, using water-soluble polymers 79−38862
Al alloy, precipitation hardening, creep deform. effect 77−16601
Al alloy 01205, mech. props. at cryogenic temps. 79−29206
Al alloy 2024, relief of residual quenching stresses *(Korean)* 79−70091
Al alloy 2024-T3, work hardening in surface layers and bulk during fatigue 78−48428
Al alloy 6061, thermomechanically treated elev. temp. mech. props. 79−8310
Al alloy 7001, ageing effect on hardness and tensile props. rel. to delay time till quenching 78−92286
Al alloy AZ5G, age hardening heat treatment effect on mech. props. microstruct. *(French)* 77−52370
Al alloy RR58, low cycle fatigue at 423K, prior treatment effect 80−104254
Al alloys, dil., quenched, foreign element effects on dislocation loop form. 80−54239
Al alloys, metastable microcrystn., appl. 80−84887
Al alloys, quenching rate rel. to mech. props., residual stresses, optimum quench coolings *(French)* 78−64562
Al and Al alloys, quenched, multiple-faulted dislocation loop config., TEM 77−27887
Al binary alloys, rapid quenching, struct. and decomp. 80−76244
Al foil, electron-irrad., interstitial trapping on impurities 79−99242
Al foil, quenched, anomalous annealing phenomena, quantitative study 78−80565
Al, interaction between ^{57}Co atoms and quenched-in vacancies, Mossbauer meas. 80−7234
Al, positron annihilation, effects of quenching, annealing and neutron irrad. 80−20732
Al, positron annihilation rel. to thermocyclic treatment 79−52040
Al, quenched, diffusion solution for point defects in stress field, steady state and transient 78−30780
Al, quenched, irradiated, anisotropic electron scatt. on defects 79−95397
Al, quenched, muon$^+$ trapping at vacancies, compared with positron annihilation 80−15937
Al, quenched, positron annihilation study, vacancy clustering 78−27348
Al, quenched, vacancy agglomeration, elec. resist., splat-cooling effects 77−51365
Al, quenched, vacancy annihilation at surface and dislocation loops 79−60351
Al, quenched, vacancy-Fe interactions 78−47412
Al, quenched-in lattice defects, Mossbauer anal. of associated ^{57}Co 78−39820
Al, rigidity modulus, neutron irrad. and quenched, point defects 78−27546
Al, splat cooled, vacancy transformations, resist. meas. 77−59770
Al, splat-cooled, grain-size distrib. function, TEM study 80−40396
Al steel, austenite, martensite cryst. struct. changes on γ irrad. 79−90699
Al, superpure, anomalous primary creep behaviour, precipitate form. 80−7646
Al, vacancy annihilation to non-uniformly distributed dislocations 78−6096
Al, vacancy loop formation, quenched-in vacancy clustering, continuum model 79−77594
Al wire, hot and cold deformation drawing strengthened, thermal EMF study *(Russian)* 80−54674
Al, zone refined, vacancy annihilation to dislocations, annealing profiles 77−80536
Al-Ag, type-II superconductor, torque oscillations in mag. field *(Russian)* 80−103800
γ'-Al-Ag (15 wt.%), dislocation splitting mechanism, cessation above critical temp. 78−26572
Al-Ag (15 wt.%), precipitate growth kinetics 77−28817
Al-Ag (16 wt.%) alloy, quenched, early stages of decomposition, small-angle X-ray scatt. meas. 77−59740
Al-Ag (7.27 wt.%), peculiarities exhibited during fatigue loading *(Chinese)* 80−71723
Al-Ag (up to 40 at.%), exam. of anelastic phenomena and structural state 78−76693
Al-Al_2Cu, aligned eutectic, precipitation, TEM and microhardness meas. 78−27529
Al-alloy plates, type VAD23, thermomech. parameters effect on struct. and props. 80−20988
Al-Ce (0.06 at.%) alloy, rapidly quenched from melt, vacancy loops and precipitates, TEM 77−59769
Al-Cr, rapidly solidified, crystalline and amorphous structures 77−44274
Al-Cr (0.1 wt.%), exam. of pre precip. behaviour, by elec. resistivity meas. and TEM exam. 78−48406
Al-Cu, partially solidified, viscosity and struct. *(Japanese)* 79−14950
Al-Cu, splat quenched, amorphous regions 77−4047
Al-Cu, splat quenched, amorphous regions, comment 77−4048
Al-Cu, splat-quenched, microstruct. thickness and comp. depend., TEM 77−8863
Al-Cu (0.5 to 40 wt.%), morphology of quenched solid-liquid interface *(Czech)* 77−86021
Al-Cu (3 wt.%) single cryst., stress aging, oriented precipitation *(Japanese)* 80−71652
Al-Cu alloy, microsegregation *(Japanese)* 77−16589
Al-Cu alloys, quenched rapidly, microstruct. 78−56668
Al-Cu liquid alloys, rapid quenching prep. of metastable solids, apparatus *(German)* 79−28990
Al-Cu samples (0.5, 2.0 and 4.0 wt.%) polycryst., precipitation, positron annihilation and TEM 80−50639
Al-Cu-Mg, dil. alloys, ageing response *(Korean)* 77−28832
Al-Cu-Mg, string ghost form. during solidification *(Japanese)* 79−100130
Al-Cu-Mg (1.3, 1.3 at.%) alloy, natural ageing, meas. of quenching vacancy dislocation loops 79−15704
Al-Cu-Mg type 2036, thermomech. treatment, flow stress anal., effect in mech. props. 80−93584
Al-Cu-Mg-Mn-Fe-Si, alloy D16, effect of mechanisothermal treatment on mech. props. 78−56674
Al-Cu-Mg-Si-Mn (2.5, 0.7, 0.7, 0.5 wt.%), alloy AK6, US inspection of heat treatment quality 78−76681

quenching continued
Al-Cu-Mg(:Fe,Si) alloys, double-ageing, resist., hardness meas. 77−28822
Al-Cu-Mn-Mg-Fe-Si (4.48, 0.66, 1.55, 0.43, o.23 wt.%), alloy D16, relationship between intercrystallite corrosion depth, and elec. cond. 79−20220
Al-Cu-Sn (3.4, 0.28 wt.%), Mossbauer anal. of Sn behaviour during ageing 78−31431
Al-$CuAl_2$, directionally solidified eutectic alloy, effect of heat treatment 77−55977
Al-Cu(Si)(Mg) binary and ternary alloys, dimensional changes in heat treatment. 80−89271
Al-Cu(Zn, Ag, Mg_2Si), intermediate precipitates, stability, X-ray, elec. resist. and hardness study 80−3063
Al-Cu(0-10 wt.%) sintered compacts, mech. props. rel. to sintering 80−76210
Al-Fe (0.02 at.%), rapidly quenched, ^{57}Fe Mossbauer spectrum associated with vacancy 78−23378
Al-Fe (0.02 wt.%), Mossbauer spectrum of ^{57}Fe associated with vacancies 77−85636
Al-Fe alloy, dil., quenched secondary defects, Mossbauer spectroscopy 77−28491
Al-Ge (2 wt.%), quenched and aged, deform. slip line obs. 78−51544
Al-Ge (6.8 at.%), quenching from mushy state for production of metastable phases 80−35223
Al-Li, alloy, ageing, δ'-phase precip., effect of quenching conditions *(Russian)* 78−19761
Al-Li alloy, annealing of vacancies and ageing, resist. and TEM obs. 77−21172
Al-Li alloy, dil., quenched and irrad., recovery, resist. and internal friction obs. 78−52848
Al-Li alloy, thermal anal. of precipitation 78−15417
Al-Li solid soln., decomposition exam. by secondary ion ion emission *(Russian)* 78−68696
Al-Mg (33 at.%), liquisol quenched, decomposition 79−61622
Al-Mg (4 wt.%), struct. and strengthening in hot working 80−84968
Al-Mg (5.7 wt.%) alloy, pre-precipitation, elec. resist. investig. 77−32601
Al-Mg_2Si (1 wt.%), precipitation reactions 80−11652
Al-Mg_2Si (1 wt.%) secondary recrystallisation by grain boundary unsewing 79−1886
Al-Mg_2Si(1.42 wt.%), aged, dislocation structs. caused by plastic deformation 80−25786
Al-Mg-Be, solid soln. decomposition, metallographic study 77−16577
Al-Mg-Si, effect of quenching on recrystn. after hot working 79−43289
Al-Mg-Si, type 6010, microstruct. characts. influence on formability, heat treatment 80−81090
Al-Mg-Si (0.52, 0.58 wt.%), ductile fracture intergranular mechanism 79−15784
Al-Mg-Si alloys, DTA exam. of zone form. and other solid phase conversions 77−86057
Al-Mg-Si alloys, DTA meas. of struct. changes in zones after quenching and isothermal heat treatment 79−52248
Al-Mg-Zn alloys, liq./solid phase equilibria determ. *(German)* 80−50601
Al-Mn (0.35 wt.%), quenched exam. of Mn-vacancy interaction 78−76676
Al-Mn(Cr), quenched, thermal stability *(Russian)* 80−20976
Al-Ni (2 at.%) alloy, rapidly quenched from melt, vacancy loops and precipitates, TEM 77−59769
Al-Ni (3-18wt.%), gun-quenched from melt, struct. 80−76225
Al-Pd, rapidly solidified, new ordered phase, electron microscope obs. 79−11645
Al-Si, dilute, anomalous primary creep behaviour, precipitate form. 80−7646
Al-Si, hypereutectic Ostwald ripening of Si crystals during solidification *(Japanese)* 79−4962
Al-Si, internal friction and Si precipitate nucleation 78−60690
Al-Si (0.57 at.%), Si precipitate dissolution kinetics 80−84935
Al-Si (35 wt.%), Cr, Co, Si addition effects on strength of powder 77−24983
Al-Si hypereutectic alloy, dissolution and primary crystallization of Si *(French)* 77−59832
Al-Si melt, microheterogeneity *(Russian)* 80−103238
Al-Sn, dil. alloy, vacancy-impurity interaction, exam. by electrical resistivity meas. at 77K *(German)* 78−83846
Al-Zn, formation of Guinier-Preston zones, and their limit temp. *(Japanese)* 78−84861
Al-Zn, G.P. zone form., temp. limit 80−16317
Al-Zn (0.041 to 4.4 at.%), clusters, electrical resistivity meas. *(Japanese)* 77−21168
Al-Zn (10 wt.%), ageing at low temp., solute conc. fluctuation effects *(Japanese)* 79−4969
Al-Zn (10 wt.%), solute conc. fluctuation effects on ageing at low temp. 79−57023
Al-Zn (12.5 wt.%) alloy, retardation of precip. reaction by DC stress 77−55969
Al-Zn (2 and 4 wt.%), ageing and elec. cond. reversion *(Japanese)* 79−4983
Al-Zn (30 wt.%), metastable phases, transformation kinetics, quenching rate effects meas. 77−55960
Al-Zn (40 wt.%), mechanical properties after thermal cycling 78−3150
Al-Zn (7 at.%), liquid quenched, early stage phase separation, exam. 78−68698
Al-Zn alloys, interfacial stability of planar solid-liq. interface during solidification 80−104145
Al-Zn eutectoid, superplastic, fracture, electron microscope obs. 78−31533
Al-Zn-Mg, duplex ageing effect on tensile props. 79−91721
Al-Zn-Mg, plastic deform. influence on structural transform. and mechanical props. *(Russian)* 80−7623
Al-Zn-Mg, polygonized struct. in extrusions, thermal stability and mech. props. 80−50659
Al-Zn-Mg, precipitation of η' phase, heat treatment, electron microscope obs. 78−68699
Al-Zn-Mg, TEM and calorimetric study 80−76290
Al-Zn-Mg, zone composition change during ageing 79−29110
Al-Zn-Mg (4.8, 1.1 wt.%), second phase dissolution, calorimetry study 79−100193
Al-Zn-Mg (5,1 wt.%), decomp. process, TEM study 80−71660

quenching continued
Al-Zn-Mg alloy, Ag addition and pre-precipitation treatment, influence on GP zone growth 80−71658
Al-Zn-Mg alloys, role of dispersed transition metal intermetallic compounds 79−96088
Al-Zn-Mg granules and bands rolled from them, heat treatment 80−100862
Al-Zn-Mg-Cu alloys, heat treatment optimisation 80−60888
Al-Zn-Mg-Cu-Cr-Zr, high strength Cr and Zr addition effects 77−59820
Al-Zn-Mg-Li alloys, effect of Li on thermal props. 79−24515
Al-Zn-Mg(3.2, 2.2 wt.%), deform. strengthened by Guinier Preston zones 77−52343
Al-Zn(10 at.%), supersaturated solid soln., structural charact. of decomposition 77−70027
Al-Zr (1-13 wt.%), rapidly quenched, extended solid solubility, grain refinement and age-hardening 80−76266
Al_2O_3 rods, quenched, exam. of contact induced strength degradation 78−76731
α-Al_2O_3:V^{3+}(V^{4+})(Co^{3+})(Co^{2+}), optically and thermally stimulated reactions, absorpt. spectra 80−80825
Al_2O_3-Dy_2O_3, phase diagram at high temps. *(Japanese)* 80−50619
Al_2O_3-ZrO_2, microstructure effect on friability 78−64515
AlZn alloys, ageing zone stage duration depend. on quenching temp. *(Russian)* 77−55993
As_2S_3 glass, melt-quenched, reversible photostruct. change 77−68925
As_2S_3, secondary electron emission, fluctuation state effect 80−40193
As_2Se_3 bulk glass, physical parameters anisotropy, cooling effects 77−36545
AsTeCu, ($0 \leq x \leq 0.4$) glass, effect of Cu on elec. cond. and thermoelectricity, 100 to 370K 78−87978
Au, electron and neutron irrad., quenched, Doppler broadened positron annihilation meas. *(German)* 77−62563
Au, hardening mechanisms, grain size effect 80−35302
Au, magnetoresist of quenched and annealed metal, defect scatt. 79−4981
Au, pure metal and Au-Sn dil. alloy, vacancy clusters, quenching and ageing 78−76671
Au, quenched and annealed, cond. electron scatt., de Haas-van Alphen Dingle temp. meas. 77−89688
Au, quenched and annealed, conduction electron scattering 78−47774
Au, quenched polycryst., vacancy loss at grain boundaries 80−59477
Au quenched single crysts., vacancies, diffuse scatt. and resist. obs. 80−33994
Au, stacking fault tetrahedra, critical nucleation temp. 78−26581
Au, stacking fault tetrahedra formation, quenched-in vacancy clustering, continuum model 79−77594
Au, thin foil, growth of stacking fault tetrahedra 80−19815
Au-Cd (47.5 at.%), effect of cooling rates on stress-strain behaviour 78−76721
Au-Co, electron scatt., spin-orbit effects 80−65533
Au-Co electrodeposits, heating effect on microstruct. and surface topography 77−43456
β-Au-Cu-Zn, martensitic transformation temps. ageing and quenching effect 79−47687
Au-Fe alloys, magnetism and atomic clustering 80−103810
Au-Fe ion implanted alloy, Mossbauer conversion electron scatt. 80−88898
Au-Ge, liquid quenched, exam. of phase decomposition 78−48371
Au-Ni, fast liq. quenched, anomalous sp. ht. near ferromag. crit. comp. 77−80947
Au-Ni-Cu-Zn, white gold, metallographic struct., heat treatment and plastic working effect 80−40403
Au-Pd (1(50) wt.%), quenched, vacancy annihilation and short-range order formation, elec. resist. 80−108487
Au(-Cu)(Sn) vacancy cluster form. in quenched pure Au and dil. alloys 77−62546
$Au_{11}Mn_4$ ordered phase formation, electron diffr. and microscopy study 80−107418
Au_4Mn, high resolution dark field electron microscopy exam. of ordering 79−7615
Au_5Mn_2, monoclinic, ordering, high resolution electron microscopy 79−43290
$Au_{35}Ni_{65}$, vapour quenched amorphous alloy, atomic arrangements 80−100173
Au_3Si, room temp. dissociation 78−35672
$Au_{35}Si_{65}$, amorphous vacuum-deposited and liquid-quenched films, diffusion and crystn. 80−84094
$Au_4Si.m$, metastable phase, substruct. unit cell *(German)* 80−88091
B-Mg-N system, precipitation mech. of BN 79−70068
B_2O_3-BaO, liquid immiscibility region, equilibration and quenching expts. 80−45288
B_2O_3-Li_2O-Fe_2O_3, prep. by quenching methods, exam. of microcrystalline precipitates of Li_2O-Fe_2O_3 *(French)* 79−20019
BaF_2:La^{3+}, relaxation processes, studies by ionic-thermocurrent techniques 79−69769
BaO-Fe_2O_3, splat quenching struct. and crystn. mechanism *(French)* 78−51426
BaO-Fe_2O_3-B_2O_3 glass, splat cooled, low temp. micromagnetism 80−34660
BaO-Fe_2O_3-(Na_2O) glass, rapidly quenched, mag. and ferrimag. props. 80−75744
Ba_2RF_7, (R=Dy, Ho, Er, Tm, Yb, Lu, Y), superstructure phases, prep., thermal characterisation and X-ray powder diffr. 80−96494
$BaTiO_3$, acceptor doped, exam. of electrical conductivity 130 to 300°C 79−33286
$BaTiO_3$-CeO_2 liquid immiscibility region, X-ray diffr. anal. 80−50611
Be bronze BrB2, quenched deformed, substruct. and props., effect of prerecrystallisation annealing *(Russian)* 78−60677
Be-bronze BrB2, struct. and phase transform. during mechano-thermal treatment *(Russian)* 80−11667
Bi foil, splat quenched, preferred orientation 80−40381
Bi, quenching and annealing of defects, elec. resist. meas. 78−87973
Bi:Sb(Te), quenching and annealing of defects, elec. resist. meas. 78−87973
Bi_2O_3, polymorphic transformation and elec. resistivity *(Japanese)* 80−93555
Bi_2Te_3-$SbTe_3$, ordered structure formation, heat treatment effect on thermal cond. 80−54448
C, noncrystalline conversion to diamond, diffusion conversion enhanced rate due to shock compression 80−39221

quenching continued
C steel, abrasive wear resistance, effect of C content, annealing, quenching 77−56115
C steel, fatigue crack propagation, effect of mean stress on crack closure 77−73315
Ca containing alloy systems, prep., glass form., thermal props. 79−24461
$CaAl_2Si_2O_8$, anorthite, quenched from 1530°C, struct. refinement 77−15355
CaF_2:Er, defect structure, quenching effect, dielec. relax. and optical absorption 80−65031
$CaF_{2-x}H_x$, ionic cond. determ. from admittance and dielec. loss meas. *(French)* 80−107479
CaO:Li, thermally quenched, generation of Li^0 centres 80−50382
CaO:OH^-, room temp. IR spectra, heat treatment and electron irrad. effects 79−51992
CaO-Al_2O_3-SiO_2 melt, at 1723 to 1823K, determ. of inter diffusivities matrix 78−43161
Cd foil, splat quenched, preferred orientation 80−40381
Cd, lattice defects studied by gamma ray angular correlation 79−51895
Cd-Ag, polycryst. quenched foil, the influence of Ag on the recovery spectrum 78−76661
Cd-Ge-As system, quenched samples, phase diagram, DTA after annealing 79−69226
Cd-Zn alloys, splat-quenched, X-ray diffr., SEM and TEM study of struct. 79−66077
$CdGeAs_2$, amorphous, thermal gradient expts., recrystn. 80−55438
$Cd_xHg_{1-x}Te$, high-speed quenching of melt *(German)* 79−65997
$Cd_{1-x}M_x$ (M=Mg, Ca, Sr), solid soln., phase equilib. diagrams 80−108412
CdS:Li, thermochemical changes in microstructure of anisotropic centres, polarisation modulation method meas. 79−38027
Co, levitation quenching 77−59711
Co-B-Si amorphous alloy, liq. quenched, elec. resist. and cyclic deform. 80−59949
Co-Fe amorphous alloys, high permeability props. *(Japanese)* 77−51927
Co-Ga β' quenched single crystals, annealing-out of point defects 80−55426
Co-Nb-C, obtained by liq. quenching, superconductivity 80−75699
Co-Sn system, phase Co_3Sn obtained by splat cooling *(German)* 80−104147
Co-Ti alloys, martensitic transformation depend. on ageing, cryst. struct. 79−91649
Co-Ti-C, secondary precipitation and allotropic transform., TEM obs. 80−108453
Co-WC, levitation quenching 77−59711
Co-WC hard alloys, rapidly quenched struct. 80−76233
Co-X-Co (X=Cr,Mo,W) systems, crystn. temp. and hardness 79−77529
β-CoGa, Cu addition effects on defect struct. *(German)* 77−11546
$Co_{0.54}Ga_{0.46}$, frequency depend. magnetisation, superparamagnetic behaviour 80−84624
CoGe, vacancy conc. in B2 phase exhibiting triple defects 79−42058
Co_5Ge_3, phase and struct. charcts. 77−36450
$Co_{74}Si_{10}B_{16}$, amorphous ferromagnetic alloy, isothermal annealing effect on static magnetic props. *(Japanese)* 79−52398
countercurrent single- and two-phase flow effects on hot surface quenching rate 78−59451
Cr-Al alloy KH40NYu3, microplastic deform. *(Russian)* 77−66681
Cr-C, binary alloy formation of nonequilib. Cr_3C in alloys quenched rapidly from melt 80−7581
Cr-Co-Fe permanent magnet anisotropic alloys, plastic deform., ageing, particle alignment temp. 80−35254
Cr-Ni steel, carburised, effect of atm. during heating to quenching temp. on austenite decomp. 77−56157
Cu block, by liq. N_2 for N_2 boiling curve 79−14232
Cu chalcogenides, single-phase, preparation 78−35293
Cu, defect annealing around stage III, $\gamma\gamma$ ang. correlation expt. 79−14846
Cu, dislocation damping strain amplitude depend. on 1 MeV electron irrad. and quenching 79−95023
Cu foil, electron-irrad., interstitial trapping on impurities 79−99242
Cu, quenched, Hall coefficient, relaxation times, Fermi surface 80−84460
Cu, types MOb and M1, primary recrystallisation kinetics depend. on state of impurities *(Russian)* 79−66069
Cu, wires, effect of heat treatment during drawing 78−56659
Cu-Ag, ion implantation as an ultrafast quenching technique for alloy production 77−55902
Cu-Al, α_2 phase form. process 77−48464
α-Cu-Al, binary substitutional, short-range ordering kinetics, vacancy behaviour 78−55867
α-Cu-Al, short range order effect, atomic potential appl. 77−27850
Cu-Al (10 wt.%) alloy, water-quenched, tensile fatigue strength at high temp. in vacuo *(Japanese)* 78−72837
Cu-Al (15 at.%), vacancy migration, and short range ordering, comparison of exp. results with theory 78−47356
Cu-Al (21 at.%) transition state *(French)* 80−55392
α- Cu-Al (6 to 17 at.%), short-range order investigated by diffuse X-ray scatt. *(Russian)* 80−104187
Cu-Al alloy, vacancy formation energy, determ., using new method, elect. cond. meas. 78−47345
Cu-Al alloy UA10, heat treatment *(French)* 80−35225
Cu-Al-Fe, mech. props. rel. to heat treatment 80−50682
Cu-Al-Ni, phase diagram associated with stress induced martensitic transform. 79−8272
Cu-Al-Ni (14, 4.5 wt.%), premartensitic alterations 77−12655
Cu-Al-Ni (14.3, 4 wt.%), ω-phase form. during quenching and ageing *(Russian)* 80−25686
Cu-Al-Ni Marmen alloys, rapid solidification and ageing 80−76245
Cu-Al-Zn, structural phenomena preceding martensitic transform. 77−12624
Cu-Au, vacancies and divacancies, quenching effects and elec. resist. meas. 80−39072
Cu-Au alloys, vacancy and divacancy migration activation energies, elec. cond. meas. 80−88140
Cu-Be, SCC in NH_3 80−104326
Cu-Be (2 wt.%), alloying addition effects on grain boundary reaction *(Japanese)* 80−49236
Cu-Be-Ni-Zr, anodic behaviour of intermetallic phase 78−72895
Cu-Co, solid soln., mag. susceptibility near solubility boundary *(Russian)* 79−15281

quenching continued
Cu-Cr (0.75 wt.%), deformation characts., fully reversed cyclic strain with fatigue cracks and dislocation struct. 80−81148
Cu-Fe, precipitation processes during aging, TEM, resistivity, hardness study *(Japanese)* 80−35221
Cu-Fe, thermal treatment effect on thermoelec. power *(French)* 77−32000
Cu-Fe (0.2 at.%), quenched, Fe dimers and defects 80−40007
Cu-Fe (2.46 wt.%), reversion phenomena and cold-working effect *(Japanese)* 80−35204
Cu-Fe alloy, cluster form., Fe solubility determ., 450 to 1000°C, Mossbauer spectra obs. *(German)* 79−29021
Cu-Fe system, ageing and reversion phenomena study 80−89274
Cu-Mn (10 at.%), meas. of mag. viscosity below freezing temp. 79−24171
Cu-Mn alloy, effect of ageing on mag. props. 77−28366
Cu-Mn ferrites, heat treatment effect on props. 77−28838
Cu-Nb (0,4 at.%), splat quenched, aged, superconductivity *(Japanese)* 77−63018
Cu-Nb composite superconductor produced by rapid quenching 78−48351
Cu-Nb-Sn dil. alloys containing Nb_3Sn precipitates, superconductivity 78−43507
Cu-Ni-Al, ageing charact., optical TEM, X-ray, hardness obs. 79−29079
Cu-Ni-Al, grain boundary reaction under isothermal ageing at 623 to 973K *(Japanese)* 79−70090
Cu-Ni-Be (30, 0.5 wt.%), grain boundary reaction after ageing and quenching, obs. *(Japanese)* 79−70089
Cu-Ni-Cr (28, 2.8 wt.%), spinodal alloy, microstruct. and tensile props. 78−39858
Cu-Ni-Fe, magnetic properties, heat treatment and compressive stress effects 80−60367
Cu-Ni-Fe alloy, quenched and aged, deformed, low-temp. elec. resist. meas. *(Russian)* 77−52514
Cu-Ni-Nb-Al, formation of γ' and γ'' precipitates 78−76655
Cu-Ni-P, precipitation hardening 77−12633
Cu-Ni-Sn, thermal decomposition after prior cold work 78−15427
Cu-Pt, quenched, microdomain model anal. of diffuse X-ray scatt. 79−52276
Cu-Sb alloy, splat-quenched, energy dispersive X-ray diffr. 78−23728
Cu-Sc alloy, dil., impurity effects on annealing and resist., vacancy-Sc interaction 79−51142
Cu-Sn (25 wt.%), struct. after ultrahigh-speed quenching *(Russian)* 78−80563
Cu-Sn(-Al), quenched and aged, struct. of phases *(Russian)* 80−49184
Cu-Ti, lattice parameter change during ageing *(Japanese)* 78−35411
Cu-Ti (1.07 wt.%), containing coherent precipitation, observations of flow and fracture 78−80643
Cu-Zn (30 wt.%), slip band growth, thermally activated 80−40457
β-Cu-Zn-Al, electron microscope exam. of premartensitic state 78−72801
Cu-Zn-Al, martensitic transform., short range order effect 79−61586
Cu-Zn-Al (26, 4 wt.%), martensitic transform. temp. variation after low temp. ageing 79−15666
β-Cu-Zn-Si, premartensitic instability 77−12625
Cu-Zr, vapour quenching prod. (thermal evaporation and r.f. sputtering), amorphous film for electron microscopy 78−6851
Cu-Zr amorphous alloy, splat cooled, local order and amorphous struct. 80−88061
Cu-Zr amorphous alloys, mech. props. *(Japanese)* 77−86179
Cu_3Al-Al_2O_3 dispersion hardenend, short range order, quenching effect on yield stresS 78−35399
CuAu(Pt), quenched, short-range order X-ray diffuse scatt., microdomain model anal. 79−96043
$CuCrS_2$ single cryst., spectral study and phys. props. *(French)* 80−29002
$Cu_{0.5}Fe_{2.5}O_4$, ferrite, determination of specific heat at 298-800K 80−2579
$Cu_{1-x}Fe_{2+x}O_4$, cation distrib. and valence state 78−63732
Cu_3Ga, transition state between long range order and short range order, model, computer simulation *(French)* 80−49371
$CuInS_2$, region of existence, determ. by quenching and X-ray anal., phase transition 79−66054
$Cu_2MnIn_{1-x}Sn_x$ alloy, compositional SRO, hyperfine interactions 80−71065
$Cu_{40}Nb_{30}X_{30}$ (X=Ti, Zr, Hf), superconductors with metastable ordered structs. 80−108484
Cu_2O, Cu inclusions and annealing, optical and IR absorpt. obs. 80−60630
CuPt equiatomic alloy, effects of quenching temp. on ordering, study by elec. resistivity meas. *(Japanese)* 79−43285
CuPt, quenched, state of local order 79−47722
$Cu_{0.57}Zr_{0.43}$ amorphous alloy, neutron diffr. obs. of struct. 80−88060
(Fe,Co,Ni)-Si(B), amorphous mag. alloy, magnetostriction rel. to soft mag. props. 80−84633
Fe based alloy, amorphous, liq. quenched, struct., thermal stability and mech. props. 80−88059
Fe based amorphous alloys, Invar effects, mag. and elastic props. *(Japanese)* 79−20100
Fe, cast, dispersed with interdendritic graphite, eutectoid transformation of austenite during cooling 78−84800
Fe, cast, ferritic grey, exam. of ordering kinetics by elastic modulus meas. 79−100136
Fe, cast, steel cam-roller pair, wear resistance strengthening treatment *(Russian)* 78−31542
Fe, cast, white, high Cr, phase composition, B effect 80−104172
Fe, cast alloyed, struct., props., heat treatment 77−16623
Fe, cast grey, effect of quenching conditions, on elastic modulus 78−56675
Fe, H_2 effect on yield 78−15474
α-Fe, influence of C and ZrH_2 on static and cyclic creep behaviour 78−39856
Fe, pure, splat-quenched, martensite morphology, SEM study 80−7547
α-Fe, quench ageing of N_2, effect of soln. heating and quenching temps. *(German)* 77−55991
Fe, quenched-in hydrogen, yield stress decrease of prestrained specimens 80−16454
α-Fe, quenching from high temps., form. of C atom pairs 77−36540
Fe, splat-quenched, microhardness and martensite 80−76359
α-Fe-(Ni,Mn,Cr,Mo,W)-P (1 wt.%). grain boundary segregation, temper brittleness, AES study *(Japanese)* 79−78981

quenching continued
Fe-(Ni)(Si)-C, cast, spheroidal graphite, metallography of solidification 78−19737
α-Fe-Al, migration of C, mag. permeability disaccommodation meas. 77−36100
Fe-Al (15 at.%), short range order form. kinetics *(Russian)* 78−3146
Fe-Al (25 at.%), anomalous magnetic behaviour *(Japanese)* 77−48011
Fe-Al (51 at.%), crystal vacancies, dilatometric and field ion microscopy exam. 78−47346
Fe-Al alloys, rapidly quenched, mag. props. 80−29579
Fe-Al-C, low C, precip. of carbides and cementite after quenching and ageing 78−52814
Fe-Al-C steel, singularities of struct., electron microscope and electron diffr. analysis *(Russian)* 77−77476
Fe-B, amorphous alloy, mag. props. 80−84618
Fe-B, eutectic, crystallisation *(Russian)* 79−70087
Fe-B, rapidly quenched, metastable phases 80−76234
Fe-B alloys, rapidly quenched metastable solid solns., prop. and mag. props. 78−92218
Fe-B amorphous ribbons formation, high-speed photography investigation 80−76216
Fe-B metallic glasses, density, mech. and thermal props. 78−31432
Fe-B metallic ribbons, correl. between quenching temp. and mech. and mag. props. 80−89373
Fe-B ribbon, microhardness, and static coercive force, melt overheating effect 80−84978
Fe-B-Si amorphous alloy, liq. quenched, elec. resist. and cyclic deform. 80−59949
Fe-B(C), amorphous phase form. by rapid quenching from melt *(Russian)* 77−66664
Fe-C, martensite, struct., Mossbauer meas. 80−40000
Fe-C (4.3 wt.%), splat cooled, amorphous phase form. and crystn. 77−15323
Fe-C single crystals, effect of heat treatment prior to cold rolling on recrystn. texture 79−83232
Fe-C-Al steels, law of variation of cryst. lattice parameters, X-ray diffr. analysis *(Russian)* 77−52322
Fe-C-Ni-Cr(Cu), dynamically hot pressed, mech. props., additives effect 78−60620
Fe-C-Si, struct. and constitution on quenching from liquid state *(Russian)* 77−52309
Fe-C-Si alloy, lattice parameters of cementite after quenching 78−11198
Fe-C-X, glasses and metastable cryst. phases, third element effect 80−75171
Fe-C-(Si), splat quenched, electron diffr. and Mossbauer study of retained ε-phase 77−52354
Fe-C(0.001 to 0.44 wt.%), C effect on low temp. brittleness *(Japanese)* 80−50711
Fe-Co, equiatomic, atomic order, Mossbauer study *(French)* 78−27135
Fe-Co-Cr, Cr effect on struct. of ordering 78−35407
Fe-Co-Ni-W alloy, 45KKhVN, plastic deform., electron microscope obs. *(Russian)* 78−80584
Fe-Co-Si-B alloy, amorphous, mag. heads appl. *(Japanese)* 80−54922
Fe-Co-V alloys, effect of V on struct., electron diffr. and Mossbauer meas. *(Russian)* 77−77507
Fe-Co-W-C steel, M_6C carbide behaviour during ht. treatment *(Russian)* 77−66658
Fe-Co(Al), B_2 superlattices, point defect investigations 78−47357
Fe-Cr (25wt.%), continuously cooled, embrittlement 77−36636
Fe-Cr-C alloys, equilibrium partition coeffs. for ferrite/liquid, austenite/liquid 78−39744
Fe-Cr-Co (28, 10.5 wt.%) ductile magnet alloy, humidity-induced H_2 embrittlement 80−89406
Fe-Cr-Co-Mo, melted in open induction furnace, microstruct. and magnetic props. 79−61626
Fe-Cr-Co-Mo, microstruct., hardness, mag. props., influence of isothermal tempering and heat treatment 79−79129
Fe-Cr-N (5.9, 0.5 wt.%), martensitic, tempered, fine struct. 77−25079
Fe-Cr-Ni-Nb-C, austenitic, splat quenching 78−72798
α-Fe-Cr(V)(Ti)(Mo)(W), morphology and growth kinetics of δ-eutectoid produced by carburisation 77−16618
Fe-Cu, ageing, hardness depend. on tempering temp. *(Russian)* 79−24544
Fe-Cu alloys, transform. substruct., lath microstructure after quenching 80−16298
Fe-Cu(2, 4 and 6 wt.%), sintered, precipitation hardening 77−66653
Fe-Ge (10 to 50 at.%), phase diagram rel. to heat treatment, supercooling diagram *(German)* 78−92240
Fe-H, recovery of hydrogenated and quenched alloy, solute diffusion 77−77510
Fe-Mn, γ to ε phase transform. induced by high press. and plastic deform. 78−68686
Fe-Mn (2 to 8 wt.%) alloys, phase transformations, tempering influence *(Russian)* 80−25735
Fe-Mn (8 wt.%), quenched, exam. of intergranular embrittlement 78−76745
Fe-Mn alloy, splat-quenched, martensite formation obs. 77−44247
Fe-Mn alloys, high-purity, martensitic transform., heat treatment effect 79−56979
Fe-Mn-C (11.5, 0.2 to 1.6 wt.%), water quenched, effect of C on phase composition, abrasion, plasticity *(Russian)* 78−35445
Fe-Mn-Cr-C (20, 4, 0.5 wt.%), hyperquenched and predeformed, mech. props. *(French)* 78−23786
Fe-Mn-Cu-C, Cu effect on ε'-martensite, X-ray obs. of heating effects *(Russian)* 79−87667
Fe-Mn-Nb-V, high Mn, dispersion strengthening 77−16602
Fe-Mn-Ni, fracture toughness, thermomechanical treatment effects 78−60794
Fe-Mo (15.5 and 19.5 at.%), modulated struct., heat treatment effects, TEM obs. 79−100192
Fe-Mo-C alloy, splat cooling, microstruct. changes 78−84855
Fe-Mo-CaF_2 sintered composite, struct. and mech. props., heat treatment effect 80−66526
Fe-Mo(W), semihard magnetic alloys, magnetic, elec. mech. props. *(Japanese)* 79−70078
Fe-N, hexagonal, ferromag. Mossbauer spectroscopy 77−63331
Fe-N (0.022 wt.%), quenched, N precipitation during isothermal ageing 77−28820
α-Fe-N solid soln., N precipitation kinetics, defects effect 77−59789
Fe-Nb(Ta)-Co, Recalloys, semihard mag. alloys, mag. and elec. props., hardness, thermal expansion *(Japanese)* 79−5066

quenching continued
Fe-Ni, $\alpha \rightarrow \gamma$ conversion, electron microscope and X-ray spectral microanal. 79−78966
Fe-Ni, influence of hydrogen press. on temp. of martensitic transform. *(Russian)* 78−27514
Fe-Ni, quenched irreversible alloy, zero or negative thermal dilatation 79−4419
Fe-Ni (32.86, 30.65 wt.%), characts. of quenched struct. formed in textured sheets, TEM and optical microscopy study 79−34084
Fe-Ni Invar alloys, splat quenched, mag. props. 80−75799
Fe-Ni martensitic alloys, age hardening 79−47736
Fe-Ni system, ferro-antiferromag. transition, γ phase mag. struct. 79−91231
Fe-Ni-Al-Co-Cr-Ti, YuNDK35T5BA, exam. of hypodissociation process *(Russian)* 79−11547
Fe-Ni-Al(2.5, 7.5 at.%), fracture surface morphology, ageing temp. effects 77−16600
Fe-Ni-B glassy ribbons melt spinning, gas boundary layer effects 80−76217
Fe-Ni-C, martensitic, internal friction 77−16633
Fe-Ni-C alloy, splat-quenched, martensite formation obs. 77−44247
Fe-Ni-C austenitic alloy, banded struct. formed by deform. 80−71713
Fe-Ni-C-Mn (3.56, 3.25, 0.6 wt.%), solid soln., quenched, changes during annealing to crystal structure, mech. props. *(Russian)* 79−34076
Fe-Ni-Co-B-P soft magnetic metallic glasses, status report 78−64226
Fe-Ni-Co-Ti, martensite cryst. lattice tetragonality, $\gamma \rightleftharpoons \alpha$ transform. *(Russian)* 79−61587
Fe-Ni-Mn alloy, martensitic transform. kinetics *(Russian)* 77−81262
Fe-Ni-Mo, ferrite plus martensite structures, exam. of mech. props. 78−56709
Fe-Ni-P-B amorphous ribbons, form. by melt spin technique 80−76215
Fe-Ni-Ti, martensite, tetragonality, X-ray obs. 77−63665
Fe-Ni(Mn)-Al-C, form. of ductile Ni_3Al by split quenching, mech. props. 79−100197
Fe-P, P equilib. grain boundary segregation 79−38835
Fe-Pd Invar alloy, Young's modulus, magnetostriction, Curie temp. 80−65988
Fe-Si (3 wt.%), grain oriented, MnS-AlN-inhibited, precipitate morphology 77−12648
Fe-Si (3 wt.%) high-permeability grain-oriented steel, quenching effect on primary recrystn. texture development 80−84956
Fe-Si (6.5 wt.%), effect of ordering on mag. props. 79−51833
Fe-Si (6.5%) alloy, struct. and rolling texture 79−79006
Fe-Si ribbon, prep. by rapid quenching 79−33957
Fe-Si-Al, Sendust, ribbon-form, prep. by rapid quenching, mech. and mag. props. 80−71611
Fe-Si-Al ribbon-form Sendust alloy made by rapid roll quenching, mag. props., recording head appls. 80−81001
Fe-Si-Al Sendust alloy ribbon form, rapid quench prepared, elec. cond., coercive field, permeability 79−83151
Fe-Si-Mn, effect of Mn addition on mag. props. and elec. resist. 78−91890
Fe-Si(6.5 wt.%) ribbon, prep. by rapid quenching and mag. props. 80−45251
Fe-Ta alloy, mech. drawn and aged, exam. of electrical resistivity, hardness, microstruct., and mag. props. *(Japanese)* 78−48545
Fe-Ti-C, rapidly quenched by splat-cooling 80−84923
Fe-X-C (X=Cr, Mo, W), quenched rapidly from melts, nonequilib. phases *(Japanese)* 80−71630
Fe-Zn, crystallographic relations by X-ray diffr. 80−24408
Fe-Zn, quenched, martensite struct. and hardness, electron microscope exam. *(Russian)* 80−66619
Fe_3Al, phase separation 77−63664
Fe_3Al, vacancy conc. and ordering conc. 78−18639
$Fe_{80}B_{20}$, amorphous, crystn. temp. under press. 79−23523
$Fe_{80}B_{20}$, amorphous, crystn. 80−75187
$Fe_{80}B_{20}$ amorphous alloy, low field magnetic props. 77−55690
$Fe_{80}B_{20}$ metallic glass, crystn. kinetics 80−84083
$Fe_{83.4}B_{16.6}$, amorphous, mag. props. and microstruct., cooling rate and melt overheating effects 80−65965
$Fe_{83.4}B_{16.6}$ amorphous, mag. props., melt overheating and cooling rate effects 80−89371
FeC_x ($x \leq 0.05$), splat-quenched, struct., elec. and mag. props. 77−21187
$Fe_{80}(C_{1-x}B_x)_{20}$ amorphous alloy, α-Fe crystn., morphology 80−70129
FeCo, isothermal annealing effect on lattice const. *(Japanese)* 79−20076
$Fe_{50}Co_{50}$, disordering by laser irradiation, Mossbauer transmission spectroscopy and electron microscopy study *(French)* 79−23639
$Fe_5Co_{70}Si_{15}B_{10}$, amorphous ferromagnetic alloy, isothermal annealing effect on static magnetic props. *(Japanese)* 79−52398
$(Fe_xCo_{1-x})_{100-y}(Si_{0.4}B_{0.6})_y$ amorphous alloy zero magnetostrictive, mag. props. 79−99743
$(Fe_{0.6}Ni_{0.4})_{100-x}B_x$ and $(Fe_{100-x}Ni_x)_{80}B_{20}$ amorphous alloys, X-ray diffr. struct. determ. 80−64906
$Fe_{40}Ni_{20}B_{20}$, metallic glassy ribbon, casting conditions *(Japanese)* 80−55386
$Fe_{40}Ni_{40}B_{20}$, amorphous, processing conditions effect on mag. props. 79−73775
$Fe_{40}Ni_{40}B_{20}$, amorphous, casting conditions effect on mag. props. *(Japanese)* 80−34698
$Fe_{40}Ni_{40}B_{20}$, amorphous ribbon prod., apparatus parameters effect on dimens. 77−12570
$Fe_{40}Ni_{40}B_{20}$, amorphous ribbon, anal. of casting conditions 79−95965
$Fe_{40}Ni_{40}B_{20}$, metallic glass, embrittlement kinetics and crystn., quenching influence 78−68766
$Fe_{80-x}Ni_xB_{20}$ and $Fe_{80-x}Ni_xP_{14}B_6$ amorphous alloys, microhardness correl. with mag. props. 80−88826
$Fe_{40}Ni_{40}B_{20-x}P_x$ metallic glasses, local struct. and dynamic disorder of Fe and Ni, EXAFS obs. 80−89088
$Fe_{40}Ni_{40}P_{14}B_6$, amorphous, resistometric study of short-range ordering rel. to heat treatment 80−70140
$(Fe_{1-x}Ni_x)_{78}Si_{10}B_{12}$ amorphous alloys, cold rolled and as-quenched, mag. anisotropy 80−97089
$Fe_{1-x}O$, quenched, decomposition and ordering, electron diffr. and microscopy 77−31635
$Fe_{1-x}O$, surface struct., XPS study 80−20759
Fe_3O_4, partial thermal dissociation in air, using solar concentrator *(French)* 79−20015
$Fe_{80}P_{13}C_7$, amorphous and crystalline, electrochemical and semicond. behaviour *(Russian)* 80−101021
quenching continued
$Fe_{80}P_{13}C_7$, amorphous ferromagnetic alloy, isothermal annealing effect on static magnetic props. *(Japanese)* 79−52398
Fe_3Pd, quenched, or annealed exam. of magnetostriction, galvano- and thermomagnetic props. *(Russian)* 79−19757
$Fe_xPd_{82-x}Si_{18}$ metallic glass, mag. transitions, weak ferromagnetism 80−100583
$Fe_{0.545}Sb$, temperature effect on lattice consts., Mossbauer spectra and density 80−88124
$Fe_{75}Si_{15}B_{10}$, amorphous ferromagnetic alloy, isothermal annealing effect on static magnetic props. *(Japanese)* 79−52398
Ga-As-Sb system, two- and three-phase fields obs. 80−55373
Ga-Cu, fast quenching of A15-phases *(German)* 77−36014
GaAs, complex luminesc. centres at 1.20 and 1.30 eV 77−16386
GaAs, luminesc. emitted by deep centres, illumination-induced change in internal quantum efficiency 79−91495
GaAs:Cd, lattice defects caused by quenching, elec. cond. 79−56160
Ga_2O_3:Mg(Zr) single crystals, quenched, ionic and elec. props. 78−30922
Ga_2O_3-R_2O_3:Nd^{3+} glass, prep., characts., X-ray diffr., absorpt. and thermal anal. obs. *(French)* 78−19704
n-GaS, Bridgman crysts., hole traps, photocond. and thermal quenching study 80−75580
Ga_2S_3-PbS system, phase diagram and crystallographic study *(French)* 80−29937
Gd-Co-B system, phase composition, struct., phase equilibria 78−35355
$Gd_3Al_5O_{12}$ phase obtained by crystallisation of amorphous $Gd_2O_3.5/3Al_2O_3$ by quenching 78−92224
Ge, acceptor complex spectra, tunnelling H systems 80−89036
Ge, entropy and enthalpy of vacancy form., comparison of theory with quenching expts. 77−11872
Ge, fast and slow quenching defects 78−39052
p-Ge, neutron irrad. quenched sample, lattice defects 79−19284
Ge, quenched n- and p-type, intrinsic defects migrating near 100°C 77−62670
Ge, quenching temp. effect on annealing rate of quenched-in acceptors 79−82590
Ge, shallow acceptors produced by quenching 79−51523
Ge:As, thermally induced defects properties obs. 77−63692
Ge:Cu, quenched, interaction between shallow-level defects and Cu atoms, Hall effect meas. 78−64002
Ge:Sb, annealing stages of thermal defects, elec. meas. 77−55282
Ge-S glass, melt-quenched photoinduced ESR, annealing behaviour and glass comp. depend. 80−71156
Ge-S-Se, glass formation 80−103251
Ge-Se-Te amorphous alloys, prep. and calorimetric obs. 77−11675
Ge-Te, exam. of new compound, using light microscopy and X-ray diffr. exam. 78−48383
GeO_2 glass, nonisothermal devitrification kinetics 80−92465
$GeSe_2$ amorphous semicond., DC conductivity, calorimetric, and X-ray diffr. meas. 79−78107
$GeSe_2$-As_2Se_3-Sb_2Se_3, quenched glass system, elec. cond., low temp. heat treatment effect 80−39586
GeTe, effect of phase transition on mech. and elec. props. 77−51746
GeTe, quenched, phase transitions and electrophysical props. 79−51250
H_2, quenching method *(Japanese)* 80−7604
He quenching method *(Japanese)* 80−7604
Hf-V foil, rapidly quenched and heat treated, supercond. props. 80−54852
HfO_2-TiO_2, phase relations and thermal expansion 77−21121
Hg-Ar quench condensed system, annealing effects on elec. cond. 79−60880
Hg-Tl, metastable system, prep. by quenching, phase struct. 78−52762
In-Sb, cryst. struct. after appl. of high press., supercond. transition temp. 80−70169
In-Sb-Bi system, solid solns., solubility limits, microhardness, microstruct. investig. 78−35368
InAs, exam. of decomposition of donors 79−1605
Ir_3Cr, yield stress and saturisation magnetisation 80−16389
KBr, quenched, absorpt. spectra, role of Schottky defects 77−59599
KBr, quenched single cryst., hardness var. with load 80−76337
KCl, doped, elec. conductivity and optical absorpt., quenching from 750°C 78−2289
KCl, pure and Pb^{2+}-doped, X-irrad., quenching effects on thermal glow curves 78−27333
KCl:Ba(Ca)(Sr), microstruct. and hardness, impurity distrib. effects 79−24529
KCl:Ca^{2+}, Z,-centre thermolum. 80−80879
KCl:Pb, lead aggregation effect on yield stress, incoherent precipitates, solubility determ. method 80−50645
KCl:Sn^{2+}, thermally stimulated space-charge decay 78−48111
KCl:Sr, thermally pre-treated, glow curves 80−25470
KCl(Br)(I), single cryst., quenched, microstruct. around indentations 80−7628
KI, quenched, absorpt. and emission spectra, α-centres 80−11442
$KMg_2(AlSi_3O_{10})F_2$-$KMg_{2.5}Si_4O_{10}F_2$, solid soln., melting and crystn., quenching and DTA study 80−39263
$KNbO_3$ glass, quenched, ionic cond., appl. as solid electrolyte 79−1522
$KTaO_3$ glass, quenched, ionic cond., appl. as solid electrolyte 79−1522
La-Al amorphous alloys, internal friction, relaxation process 80−92607
La-Au, splat-quenched, Mossbauer effect and elec. resist., amorphous struct. 80−84676
La-Fe, liquid quenched, X-ray diffr. and Mossbaeur effect exam. of structure 78−76678
La-Re-B, annealed and quenched, X-ray structural and phase anal. 78−11207
LaF_3-$La(OH)_3$, high pressure phases, X-ray diffr. and IR spectroscopic anal. 79−47679
La_2O_3-WO_3, melt, glass formation on rapid quenching 77−20055
(Li,Na,K) (Nb,Ta)O_3, pseudo-binary and ternary systems quenched metastable glassy and cryst. phases 80−29935
Li-Sn, phase relationships between Li_7Sn_2 and LiSn, microcracking obs. in quenched alloys 79−78933
$Li_2B_2O_4$-$LiFe_5O_8$, borate glass, mag. props. of Fe^{3+} cations 80−100599
$Li_2B_2O_4$-$LiFe_5O_8$ glass, rapidly quenched, mag. and ferrimag. props. 80−75744
LiF:Co, flow stress changes during precipitation 80−92594
LiF:Mg, origin of dislocations *(Russian)* 77−15425
LiF-AlF_3-Na_3AlF_6-Al_2O_3 system, phase equilibrium, X-ray diffr., DTA, quenching, optical microscopy study 80−50610
Li_2MgSiO_4-Li_2ZnSiO_4, form. of solid soln. *(Japanese)* 77−25037

quenching continued
$LiNbO_3$, amorphous ribbons, prep., electron and X-ray diffr. obs., dielec. const. temp. depend. 79−50993
$LiNbO_3$ glass, quenched, ionic cond., appl. as solid electrolyte 79−1522
$LiNbO_3:Cr^{3+}$ glass, roller quenched, crystn. kinetics 80−44143
Li_2O-Al_2O_3, rapidly quenched glasses, Li ion cond., elec. cond. 80−100346
Li_2O-Al_2O_3(Ga_2O_3)(Bi_2O_3), quenched glasses, crystn. and ionic cond. 80−33899
Li_2O-Bi_2O_3, rapidly quenched glasses, Li ion cond., elec. cond. 80−100346
Li_2O-Ga_2O_3, rapidly quenched glasses, Li ion cond., elec. cond. 80−100346
$LiTaO_3$ glass, quenched, ionic cond., appl. as solid electrolyte 79−1522
$Li_2Ti_3O_7$ growth by Bridgman-Stockbarger technique 80−25548
Mg alloy, quenched-in defect behaviour, effect on flow stress 79−61625
Mg cast iron, effect of heat treatment on phase comp., microstruct., wear resistance 77−56006
Mg, quenched to 4.2K, presence and mobility of H_2 77−28042
Mg-Fe alloy film, quench-condensed, resistance meas. 79−15235
Mg-Li-Al (31, 1 at.%), heat treated, precipitation 80−40364
Mg-Y-Nd-Zn-Zr (2,2,0.3, 0.7 wt.%), heat treatment effect on casting dimensional stability, alloy mech. props. 78−44146
MgCd wire, elongation during disorder-order transform. *(Russian)* 80−104148
MgF_2-Na_3AlF_6 thin film deposits, quenched ageing by chopping 80−97364
MgO, electron irradiation induced mobility of substitution H 77−55390
MgO, pure and doped, luminesc. of free and relaxed excitons 79−74008
MgO:Li, $[Li]^0$ defect, high temp. and ionisation induced effects 78−34509
MgO:Li^+, quenched, elec. polarisation, thermal depolarisation and dielectric loss meas. 79−1738
MgO:OH^-, room temp. IR spectra, heat treatment and electron irrad. effects 79−51992
MgO:S, cathodoluminesc. spectrum *(Russian)* 80−55197
MgV_2O_4-Mg_2VO_4 spinel solid soln., quenching and lattice const. 77−90307
$Mg_{74}Zn_{26}$, glass, exam. of crystallisation 78−71681
Mn-Al-C, ferromag., transform. kinetics 80−34627
Mn-Al-C, ferromag. alloy, transform. kinetics 80−76229
Mn-Cu, alloying behaviour and high damping capacity 80−35160
Mn-Cu structural alloys, physicomechanical props. 77−12652
Mn-Cu-Zn system, optimum heat-treatment routine for max. damping 79−87670
Mn_3Ga, formation of DO_{22} superstruct. and para-antiferromag. transition 79−19737
MnZn ferrite, microstructure and initial permeability, presintering process effect 80−89367
MnZn ferrites, post sinter-cooling rates effects 80−89369
Mo, high purity single crystal doped with C, low temp. mech. props. 77−77544
Mo, quenched sample, UV photoelectron spectra, exoelectron-like emission 79−15587
Mo-based metallic glass development 80−89172
Mo-Re, solid soln., dislocation internal friction *(Russian)* 78−23748
Mo-Re, σ phase alloy, critical mag. field, elec. resistance 80−54850
Mo-Ru(-Si), amorphous superconductors, prep. by electron beam evaporation and liq. quenching, crit. temp. 80−103776
Mo-Tc system, supercond. behaviour, quick-quench production technique 78−56251
Mo-Zr-Ti-C(0.1, 0.15, 0.004 wt.%), alloy TsM2A, cavitation failure mechanism 77−70169
$(Mo_{1-x}Ru_x)_{80}P_{20}$, amorphous alloys, superconductivity, mag. susceptibility and electronic props., liq. quenching 78−88057
$Mo_{70}Si_{20}B_{10}$, amorphous alloys obtained by liq. quenching, superconductivity 80−75670
Na-NH_3 film, quench-condensed, anomalous elec. cond. obs. 77−32057
NaBr, thermally processed cryst., optical absorption bands *(Russian)* 78−76513
NaCl, dislocation rosettes around Vickers diamond pyramid indents, quenching effect 80−11740
NaCl, rock salt, quenched, residual stresses, optical study 80−55061
NaCl, X-ray irrad., vacancy conc., thermal expansion meas. 80−6431
NaCl:Ca, precipitate form., transform. after annealing, critical flow stress 78−38848
NaCl:Mg^{2+}, radiation-induced colouring, room temp. kinetics 79−55736
NaCl:Sn^{2+}, thermally stimulated space charge decay 78−48111
NaCl+Pb, Pb aggregation effect on yield stress, incoherent precipitates, solubility determ. method 80−50645
6NaCl.$CdCl_2$, 60 wt.% powders, Suzuki phases prep. and stability 80−35123
Na_2O-Al_2O_3-P_2O_5, exam. of subsolidus structure 79−4954
Na_2O-SiO_2 glass drops, quenched from liq. state, thermally treated, density profile 80−81085
$(Nb,Ti)N_x$, metastable supercond. phase, effects of rapid quenching on transition temp. 78−2611
Nb alloys, non-metallic inclusion form. during quenching from liquid state 78−95766
Nb, H_2 diffusion, low temp. recovery 79−73342
Nb-Al(Ga,Si,Ge,Sn)-Cu, equilib. and rapidly quenched, struct. and props. 80−76235
Nb-Al(Ga)(Ge), fast quenching of A15-phases *(German)* 77−36014
Nb-Ga-Cu, fast quenching of A15-phases *(German)* 77−36014
Nb-Ge-Sn(Pt)(Ir), A15 cpds. prod. by liq. quenching, phase stability and supercond. props. 79−95538
Nb-Ir(Rh) system glasses, form., crystn. and microhardness, resist. obs. 80−89178
Nb-Nb_3Al superconductor, fabrication by quench-age method 77−40403
Nb-Ni, amorphous thin film, vapour quenched, elec. resistivity and thermoelectric power 79−33275
Nb-Si film, superconductivity close to A15 stoichiometric phase 79−95540
Nb-Si-Sn(Pt)(Ir), A15 cpds. prod. by liq. quenching, phase stability and supercond. props. 79−95538
Nb-W-X-C, X=Ti, Zr, Hf, quenched from liquid state, formation of non-metallic inclusions *(Russian)* 79−57007
Nb_3(Al,Ge) and Nb_3(Al,Si), liq. quenched, supercond. props. 80−84580
Nb_3Al, BCC struct., cold working and converting to A-15 struct. 78−64553
Nb_3Al, liq.-quenched, crit. current density and T_c 77−72957
quenching continued
Nb_2O_5-TiO_2, splat cooled, crystallization and ordering 77−68953
Nb_3Si A15 phase from amorphous Nb-Si alloys, high-press. synthesis 80−93516
Nb_3Si, substituted, splat cooling influence on supercond. T_c and stoichiometry 80−80439
NbTi superconducting state, stability under localised heat pulses 79−73611
$Nb_{20}Zr_{80}$, supercond., US attenuation 80−44766
Ni alloy EI617, creep, effect of preliminary heat treatment on struct. and props. 77−21195
Ni base Rheocast high performance superalloy, solid-liquid phase charact. 77−28803
Ni base superalloys, rapid solidification, use in gas turbine engines 80−84888
Ni based alloy, amorphous, liq. quenched, struct., thermal stability and mech. props. 80−88059
Ni, C precipitation 80−29958
Ni, cathodically H charged, isothermal ageing 79−15703
Ni ferrite, quenched, Neel temp. and initial susceptibility 80−75762
Ni, H diffusion in H_2 quenched sample, elec. resist. recovery 78−2299
Ni, quenched vacancies, effect of oxidation *(French)* 78−27686
Ni, splat quenched, gaseous impurities effect on struct. 77−4042
Ni:H thin plate, recovery of quenched-in solute H 77−62673
β_2-Ni-Al, elastic consts., supersaturated thermal vacancy effects 80−54298
Ni-Al (6.05 wt.%), prediction and meas. of precipitate number density 78−19756
Ni-Al solid solutions, Ni-rich, phase transforms. during quenching 77−32577
Ni-Al-Mo (12.7, 21.6 wt.%), directionally solidified eutectic composite, precipitation 80−108454
Ni-C, quenched, struct. of graphite precipitates, TEM obs. *(Russian)* 78−68695
Ni-C-W-Cr(-Mo), Vickers hardness and crystallisation temp. 80−16361
Ni-Co (25 at.%), polycrystalline, mech. damping 77−28850
Ni-Cr, ordering in the vicinity of Ni_2Cr 79−38819
Ni-Cr, solubility limit determ., X-ray method 79−43199
Ni-Cr alloy, structural changes, during thermal stress cracking, X-ray and microhardness meas. *(Russian)* 78−35496
Ni-Cr complex alloy with good creep resistance, friction stress/flow stress relation 79−8337
Ni-Cr-Al-Ti alloy type ZhS6U, effects of heat treatment in high vel. gas streams on props. 79−57025
Ni-Cr-Ti (19.51, 4.2 wt.%), quench-ageing and fracture *(German)* 77−70088
Ni-Cr-Ti rapidly solidified superalloys, surface segregation 80−76263
Ni-Cr-Ti-Al-Fe-Co (19.65, 2.40, 1.37, 0.78, 0.52 wt.%), strength of γ' hardened alloy, ageing exam. 78−88501
Ni-Fe, influence of atomic ordering on spin waves 79−7987
Ni-Fe-H, Curie points, mag. props. of H solutions FCC metal sublattice parameter behaviour 79−69671
Ni-Fe-Nb-Al(-Mo), wear resisting mag. head material, mag. props. and struct. 80−35350
Ni-Mo (20.8 wt.%), order, heat treatment effects 80−40406
Ni-Mo-C(-Cr)(W), Vickers hardness and crystallisation temp. 80−16361
Ni-Mo-W, type N55M20V25, quenched at various cooling rates, phase transformations *(Russian)* 79−66052
Ni-Nb-C, obtained by liq. quenching, superconductivity 80−75699
Ni-NiAl solid soln., high temp. transforms *(Russian)* 79−56973
Ni-P amorphous alloys, electrodeposited and melt-quenched atomic and electronic structures 80−88062
Ni-Ti alloy, shape memory effect mechanism 77−28865
Ni-Ti-Al superalloy, pendant drop melt extracted, struct. and props. 80−76242
NiAl, quenched and annealed, void formation 79−46652
β'-NiAl, single cryst., quenched and annealed, ω-like diffr. effects, TEM and X-ray diffr. study 79−60216
$Ni_{100-x}B_x$, rapidly quenched, mag. moment, temp. and comp. depend. 78−47957
$Ni_{0.75}Fe_{0.25}$, influence of atomic ordering on spin waves, inelastic neutron scatt. 77−69516
Ni_3Fe, short range order determ. after heat treatments 79−96044
Ni_3Fe, single cryst. ordered and quenched, stress relax. *(Russian)* 77−44282
$Ni_{40}Fe_{40}B_{20}$ glass alloy, rapidly quenched, explosive welding to A516-70 steel and to itself 78−39954
NiGa, vacancy conc. in B2 phase exhibiting triple defects 79−42058
Ni_3Mn, order-disorder transform. *(Russian)* 77−59776
Ni_3Mn, ordered at below Kurnakov temp. then deform., a/2⟨110⟩ dislocations and deform. antiphase boundaries *(French)* 77−51384
Ni_3(Mo,Ta), quenched alloys, DO_{22} type ordered phase form. 78−95768
Ni_4Mo, quenched, short-range order, electron diffraction study 77−39560
Ni_4Mo, stoichiometric and quenched, short range order and order-disorder transform. 79−78955
$(Ni_{0.5}Pd_{0.5})_{82}P_{18}$ amorphous alloy, liquid-quenched, crystn. kinetics, effect of thermal history 80−100175
$(Ni_{0.5}Pd_{0.5})_{82}P_{18}$ amorphous alloy, liquid-quenched, crystn. kinetics, nucleation 80−100176
$(Ni_5Pd_5)_{82}P_{18}$, amorphous alloy, crystallisation 77−89382
$(Ni_5Pd_5)_{82}P_{18}$ amorphous alloy, glass transition temp. 77−84909
NiPt, quenched, ordering kinetics and domain struct. form. during isothermal tempering *(Russian)* 80−66502
$Ni_{1.1}Sb$, temperature effect on lattice consts., Mossbauer spectra and density 80−88124
Pb, splat quench in vacuum 79−52268
Pb, splat-cooled and vapour-deposited, metastable structs. 79−87018
Pb, vacancy and divacancy props., exam. via quenching and annealing 78−47343
Pb-Ag, solid soln. hardening due to metal interstials 77−52337
Pb-Ag (0.068 wt.%), Ag precipitation kinetics and activation energy 80−66517
Pb-Au (0-0.0918 at.%), lattice parameter changes due to Au dissolution 79−77558
Pb-Bi, splat quenched, solubility limit, vacancy conc. and supercond. transition temp. 77−12046
Pb-Bi, supercond. tunnelling, effect of phase composition and press. 79−15261
Pb-Sb, influence of quench deform. on precipitation *(German)* 77−86064

quenching continued
Pb-Sb (1 wt.%), highly averaged, fracture behaviour 79−8366
$Pb_{1-x}Al_xF_{2+x}$, ionic cond. of quenched and annealed specimens, interstitial cond. mechanism 80−2199
PbF_2-AlF_3 glass, optical props., crystn. and thermal expansion 80−48367
PbF_2-AlF_3 glass, prep. and props. 80−49120
$Pb_{1-x}Mn_xTe$ (x=0.005, 0.001, 0.05), solid solns., exam. of electrical and thermal props. 79−1599
$PbNb_2O_6$, O defects and elec. props. anomalies 79−42898
$PbO-B_2O_3-SiO_2$, glass enamel, heat treated, exam. of microstructure and chemical durability 79−29254
$PbTiO_3$, $(PbTiO_3)_{0.9}(B_2O_3)_{0.1}$ amorphous ribbons, prep., electron and X-ray diffr. obs., dielec. const. temp. depend. 79−50993
Pd-Cu-Si, glass form., crit. cooling rate 80−75169
Pd-Cu-Si, laser melting and splat quenching to form foils for TEM obs. 80−29986
Pd-Si, amorphous thin films, laser irrad., metastable phases 80−96622
Pd-Si-Sb, mostly crystalline, rapidly quenched, mech. props. 79−61610
$Pd_{82-x}Ag_xSi_{18}$, amorphous, roller-quenching conditions determ. 77−21051
$Pd_{77.5}Cu_6Si_{16.5}$ metallic glass, diffusion of Au 78−55983
$Pd_{77.5}Cu_{6.0}Si_{16.5}$ metallic glass, glass transition temp., cooling rate depend. 80−75181
$Pd_{781}Cu_{55}Si_{164}$, liquid quenched metallic glass, wear resistance 79−66079
$Pd_{80}Si_{20}$, vapour quenched amorphous alloy, atomic arrangements 80−100173
Pt foil, quenched, 1.2 MeV electron irrad., subthreshold irrad. effects 78−51585
Pt, interstitial thermal conversion study by elec. cond. meas. 80−15096
Pt, quenched, coprecipitation of vacancies and C atoms 79−78978
Pt, quenched, deviations from Matthiessen's rule 77−69289
Pt-Co, magnetically hard, struct. and morphology, electron microscope study 79−82171
Pt-Cu (49.37 at.%), coexistent phases in homogeneous ordering 79−29052
Pt-Si, amorphous thin films, laser irrad., metastable phases 80−96622
Sb, film, liquid and vapour quenched, metastable struct. 79−56974
Sb, liquid-quenched, stabilisation and transformation kinetics of metastable phases 80−3022
Sb, splat-cooled and vapour-deposited, metastable structs. 79−87018
Sb_2Te_3-Sb_2Se_3, ordered structure formation, heat treatment effect on thermal cond. 80−54448
Se, vitreous, temp. depend. of sound vel. 77−84855
Se-Te-$Ge_{0.5}Sb_{0.5}$, DTA, critical cooling rates determ. *(French)* 77−72682
Si, carrier lifetime degradation at room temp. 78−95301
Si, deep centres associated with plastic deform. and quenching *(French)* 77−28145
Si, divacancy charge states, photoconductivity spectra 77−15899
Si, EPR of quenched-in defects 80−29620
p-Si, elec. props. and thermal defects, influence of high temp. treatment 79−69531
Si, entropy and enthalpy of vacancy form., comparison of theory with quenching expts. 77−11872
n-Si, fast electron irradiated, annealing of defects 80−89259
Si ribbon, prep. by rapid quenching 79−33957
Si ribbons, roller quenching method of prep., grain sizes and carrier conc. 80−40275
Si ribbons for solar cells, ultra high speed growth, elec. props. 80−89162
Si, thermally induced donors due to heat treatment and Fe contamination 79−78035
Si with defects produced in quenching, photocond. and elec. props. 80−6837
p-Si:B, Fe, 0.45 eV majority carrier trapping level after quenching 78−18990
n-Si:B,P, radiative recombination at thermal defects, luminescence centre electron struct. 79−91496
Si:Co, substitutional Co and Co precipitates, identification by Mossbauer spectroscopy 79−11631
Si:Fe_0 solubility study by EPR and neutron activation anal. 80−75361
Si:Fe_0, solid soln. decomp., Fe deposition on dislocations 77−51943
Si:Fe^0 interstitial localisation, EPR spectrum 79−1582
p-Si:Li, dislocation free, minority carrier lifetime, effects of heat treatment *(Japanese)* 79−65492
Si-Au films, quenched condensed, elec. resist. and supercond. 80−54669
Si-C-O-Ar, high temp. plasma, prod. quenching mol. dynamics simulation 78−39711
n-SiC, thermal defects, ESR study 80−88876
Si_xFe_{100-x} polycryst. ribbon, prep. by rapid quenching, and props. 80−75803
Si_3N_4, reaction bonded and hot pressed. exam. of thermal shock behaviour *(German)* 78−64561
SiO_2 glass, strengthened by ion exchange and quenching brittle destruction theory 80−45398
SiO_2, vitreous, Raman active defects, thermal equilibration 80−55092
SiO_2-Al_2O_3 refractories, thermal shock props., fracture mech. appl. *(French)* 79−96109
SiO_2-Al_2O_3-CaO-MgO-NaO-K_2O-B_2O_3-ZrO_2, glaze, exam. of zircon crystallisation 79−19155
SiO_2-Al_2O_3-CaO-MgO-Na_2O-K_2O effect of partial substitution of Na_2O by K_2O, on crystallisation 80−10499
Sm, metastable phase modification formation during quenching from molten state *(Russian)* 79−91636
$Sm(Co_{0.84}Cu_{0.16})_{6.9}$, microstruct. and domain struct., mag. reversal *(Russian)* 80−20429
$Sm(Co_{0.81}Cu_{0.15}Fe_{0.04})_{6.9}$ and $Sm(Co_{0.84}Cu_{0.16})_{6.9}$ powders, mag. props. *(Russian)* 80−20434
Sn droplets, on Bi, Zn and Al, heterogeneous nucleation 80−44294
Sn melt fragmentation on quenching in n-pentadecane and water 79−15706
Sn molten drops, gas evolution on quenching 78−39818
Sn-Bi, crystal struct. and superconductivity after appl. of high press. and quenching 80−10531
Sn-Bi alloy, splat-quenched, energy dispersive X-ray diffr. 78−23728
Sn-Ni electrodeposited equatonic alloy, cryst. struct., X-ray, electron diffr. anal. 80−79748
Sn-Pb (5 wt.%) ingots, quenching technique, for studying formation of macrosegregations 78−52793
Sn-Sb (10 wt.%), decomposition of supersaturated solid soln. 80−29960
Sn-Sb-Ag, splat cooled foils, TEM study 80−40344

quenching continued
SnS(Se)(Te)(S_2)(Se_2), oxidation, thermal decomp., Mossbauer spectra 79−11713
Sr containing alloy systems, prep., glass form., thermal props. 79−24461
SrO-Fe_2O_3, splat quenching struct. and crystn. mechanism *(French)* 78−51426
Ta, low temp., diffusion of H and D from quenching and annealing study 80−6555
Ta, low temp. diffusion of H and D from quenching and annealing study 80−6555
Ta-Ir(Rh) system glasses, form., crystn. and microhardness, resist. obs. 80−89178
Ta-N, domain configurations of new phase *(French)* 78−56648
Te, amorphous, obtained by splat cooling crystallisation 77−65949
Te thin film, thermoelec. EMF, Seebeck coeff., elec. cond. structural depend. 79−78230
Te-Ge-Sn(Pb), Te rich, structural phase transformation concurrent with glass crystallisation, thermal evidence 79−4965
Te-Pb, amorphous, obtained by splat cooling, crystallisation, TEM obs. 77−66638
$Te_{80}Ge_{20-x}A_x$ glasses, rapid melt cooled, glass transition and stability range 80−75170
Ti alloy, VT22, thermomechanical treatment, effects on struct. and props. *(Russian)* 78−19785
Ti alloy, VT23, ht. treatment effects on fracture *(Russian)* 78−80623
Ti alloy AT-3, crack development in air, H_2, aq. H_2SO_4, electrochem. charact. *(Russian)* 77−70209
Ti alloy VT20, phase composition and structure effect on mech. props. 79−38958
Ti alloy VT23, quenched decomposition of metastable phases during heating *(Russian)* 78−15432
Ti alloy VT3-1, fracture toughness, rel. to struct. 79−79105
Ti alloys, β-annealing and controlled rate quenching effects 78−80568
Ti alloys, domain struct. of diffuse ω-phase formed in quenching, 1D model 78−27523
$\alpha+\beta$ Ti alloys, fracture, influence of phase comp. in VT16 and VT9, quenching effects *(Russian)* 78−56665
Ti alloys, types VTZ-1 and VT8, two phase, mechanism and kinetics of metastable β and α'' phases dissociation *(Russian)* 79−74152
Ti base alloys, melt-extracted polycryst., mech. props. 80−76360
Ti-Al alloy system, quenched from β-region, struct. obs. *(Russian)* 77−21146
Ti-Al-Cr-Mo-Fe(V)(Zr), effect of structure and heat treatment on tensile strength, ductility, fatigue limit and notch sensitivity 78−56711
Ti-Al-Cr-Mo-U, alloy VT22, phase composition and fatigue strength 78−3219
Ti-Al-Cr-Mo-V, VT22 alloy, metastable β-phase decay under continuous heating, plastic strain effect *(Russian)* 80−71656
Ti-Al-Mo-Cr-Fe (6.4, 2.7, 1.6, 0.4 wt.%), quenched VT3-1, decomposition kinetics of α'' and β in annealing *(Russian)* 77−66662
Ti-Al-Mo-Sn-Si (2.25, 4, 11, 0.25 wt.%), type IMI 680, internal friction study of martensitic transformations 80−7573
Ti-Al-Mo-Sn-Si (2.25, 4, 11, 0.25 wt.%), type IMI 680, stability of martensitic phases 80−7574
Ti-Al-Mo-Sn-Si (4, 4, 4, 1/2 wt.%), type IMI 551, internal friction study of martensitic transformations 80−7573
Ti-Al-Mo-Sn-Si (4, 4, 4, 1/2 wt.%), type IMI 551, stability of martensitic phases 80−7574
Ti-Al-Mo-V (8, 1, 1 wt. %), stress corrosion cracking and slow strain rate H_2 embrittlement 78−48569
Ti-Al-V (6, 4 wt.%), type IMI 318, internal friction study of martensitic transformations 80−7573
Ti-Al-V (6, 4 wt.%), type IMI 318, stability of martensitic phases 80−7574
Ti-Al-V (6, 4 wt.%) cylinders, residual stresses introduced by quenching elastoplastic anal. *(French)* 80−45355
Ti-Al-V (6,4 wt.%), quenched, struct. and age hardening rel. to treatment temp. 80−11657
Ti-Al-V-Fe-Si, alloy VT6; phase transform. kinetics and Young's modulus *(Russian)* 77−81258
αTi-Al-(Zr), embrittlement due to ageing 78−56673
Ti-Al(Fe) microprobe anal. of alloying addition distrib. 80−55358
Ti-alloy, VTZ-1 and VT8, decomposition of metastable phases, effect of plastic deform. *(Russian)* 78−39770
Ti-Be, metallic glass form. and props. 80−16219
Ti-Be-Si glass ribbons, physical and mech. props. 78−95767
Ti-coated C steel, effect of heat treatment on struct. and props. 77−56159
Ti-Cr(Mo), alpha precipitation kinetics 78−68697
Ti-Cu-Al(Zr)(Sn)(Nb)(Mo), heat treatable alloys, effect of alloying on strength, tensile props. 78−56671
β-Ti-Fe, (7.1 wt.%) exam. of ω phase formation, by X-ray diffr. and Mossbauer spectroscopy 78−52800
α-Ti-Fe, solubility, resistivity variation rel. to quenching temp. 79−99324
Ti-Mn base beta alloys, H effect on stability solid soln., hardness *(Japanese)* 77−81261
Ti-Mo, martensitic transform., water quenched from β-region 79−38826
Ti-Mo-Fe-Cr-Al, alloy VT3-1, influence of constitution on fracture toughness *(Russian)* 77−77559
Ti-Mo-V-Al-Cr-Fe (4.8, 4.7, 5.2, 1.1, 1.0 wt.%), structural changes during heating up to 1000°C, DTA study *(Russian)* 80−93552
β-Ti-Mo-Zr-Sn (10.2, 5.8, 4.7 wt.%) heat treated, tensile yield, fracture behaviour, primary deform. mode, exam. 78−60724
Ti-Mo-Zr-Sn (11.5, 6, 4.5 wt.%), β III, mech. props. rel. to heat treatment 80−84961
Ti-Mo-Zr(-Al) (15, 5 (3) wt.%), quenched and aged metastable β-phase, crystallography, morphology and decomposition 80−76262
Ti-Mo(V), metastable diffusionless equilibria, high press. conditions 80−71627
Ti-Nb-Zr (35, 3 wt.%), martensitic τ phase, X-ray diffr. obs. 80−16300
Ti-Nb-Zr-Fe-Mo-V, cold worked, struct. and phase transform. during ageing 78−3153
Ti-Ni, laser melting and splat quenching to form foils for TEM obs. 80−29986
Ti-Ni (48 to 53 at.%), heat treatment and deviation from stoichiometry 80−104192
Ti-Ni-Si metallic glass, prep., thermal and mech. props. 78−64497
Ti-Ru (0.05 to 90 wt.%) hardness, thermal EMF, electrical conductivity, in annealed or quenched state *(Russian)* 77−55998
Ti-Si amorphous alloy, melt-quenched, transform. studies and mech. props. 80−100838

quenching continued
Ti-V (27 and 30 wt.%), fatigue crack propag., in single and poly. crystals 79−5048
Ti-V-Si (30, 1 at%), quenched and aged, hardness, tensile behaviour and phase transform. 79−11646
βTi-V-Si (40, 1 at.%), Si effect of precipitation and age hardening 77−63676
Ti_3Al-(Mo) (0.5 at.%), ordering, Mo effects 77−28841
Ti_3Al-(Nb), ordering transform. and mech. props. 78−31402
$Ti_{50}Be_{40}Zr_{10}$ glass, mech. props., X-ray diffr. exam. 78−11292
TiC, tool carbide, thermal shock resistance and fracture strength 77−21257
TiC-steel alloy, struct. form. during sintering, strength, rel. to heat treatments 77−59717
TiC-steel composite, effect of method of Cr additions on props. 78−15341
TiO_{2-x}, reduced, cond. between elec. props. in equil. at 1100°C and after quenching, defects role *(French)* 80−44582
TiO_{2-x} reduced, crystallographic shear planes, dislocation struct. 80−107175
$TiO_{1.95}$iFe, quenched near melting point, transverse composition waves 79−99220
Tl_2S-SnS, phase equilibria exam. 80−55369
$Tl_2SeAs_2Te_3$, secondary electron emission, fluctuation state effect 80−40193
Tl_5Te_3-Tl_4SnTe_3-Tl_4PbTe_3, phase equilib., DTA, SPA and microhardness meas. 80−96628
U-Mo (2 wt.%), depleted, effect of microstruct. on mech. props. 80−108497
U-Mo-Nb-Zr-Ti (0.75, 0.75, 0.75, 0.5 wt.%), heat treatment effect on microstruct. and mech. props. 78−23729
U-Mo(Nb) and U-Mo(Nb)-Zr alloys, shear martensitic transform. during quenching, plastic deform. and annealing 77−28815
U-Nb (14 at.%), exam. of shape memory effects 78−76694
U-Nb (14 at.%), martensitic and polymorphic transformations 80−60861
U-Ti (0.75 wt.%), quench rate sensitivity, effect on microstruct., mech. props., ageing 77−70077
UC, quenched-in defects, formation, migration and resistivity 80−64990
UCN, quenched-in defects, formation, migration and resistivity 80−64990
UO_2, isothermal crack healing and strength recovery, thermal shock effects 77−36625
V and V-Mo, mechanical properties, O, N_2 and C addition effects 79−52356
V-Al(Ga,Si,Ge,Sn)-Cu, equilib. and rapidly quenched, struct. and props. 80−76235
V-C-O, phase relations 79−96012
V-Ga(Ge)(Si), fast quenching of A15-phases *(German)* 77−36014
V-N, BCC solid soln., superperiodicity of lattice in quenched ordered struct. *(Russian)* 78−56662
V-N α-solid solution, struct. transform. during annealing and quenching *(Russian)* 77−81257
V-O alloys, quenched, local ordering of O, electron microscopy and diffr. 80−59453
V-S system, quenched, order-disorder transition of metal vacancies, DTA and X-ray analysis 78−30576
V-Se system, quenched, order-disorder transition of metal vacancies, DTA and X-ray analysis 78−30576
VC, metastable supercond. phase, effects of rapid quenching on transition temp. 78−2611
V_3Ga, supercond. A15 phase, prep. by controlled precip. 80−81000
V_2O_5, amorphous semicond., solubility and fibrous texture 80−75162
V_2O_5, water in noncryst. solid, quenching of molten V_2O_5 *(French)* 78−42912
V_3Sn, ultrafast quenched and subsequently tempered, supercond. T_c 78−64162
V_3Ti, metastable supercond. phase, effects of rapid quenching on transition temp. 78−2611
W, electron irradiated, or quenched, point-defect mechanism for Stage III recovery, field ion microscope study 79−60403
W, vacancies, quenching and recovery invest., resist. and TEM study 80−39074
W, vacancy-defect clustering, due to annealing and quenching, TEM and elec. cond. exam. 78−47344
W-Ni-Fe(Cu), liquid phase sintered, interfacial embrittlement 79−57101
WC, tool carbide, thermal shock resistance, fracture strength 77−21257
WC-Co hard alloys, hot-pressed, wear resist. under abrasive friction, heat treatment effect 80−66555
$W_{70}Si_{20}B_{10}$, amorphous alloys obtained by liq. quenching, superconductivity 80−75670
Y-Re-B, annealed, and quenched X-ray structural and phase anal. 78−11207
Y_2O_3:Eu, fluoresc., cathodoluminesc. and thermal quenching 79−47488
Y_2O_3-Fe_2O_3 systems, solid-phase reacts., $Y_3Fe_5O_{12}$ form. 78−44062
$Y_{2.6}Sm_{0.4}Fe_{5-x}Ga_xO_{12}$, epitaxial, domain wall crit. vel., effect of material parameters 79−99740
YVO_4:Eu, fluoresc., cathodoluminesc. and thermal quenching 79−47488
Zn based alloys, preferred crystal orientations, rot. mill device investig. 79−57006
Zn foil, splat quenched, preferred orientation 80−40381
Zn, preferred crystal orientations, rot. mill device investig. 79−57006
Zn-Al (22 at.%), heat treatment and straining effect on fracture and corrosion 79−87672
Zn-Al eutectoid alloy, straining at elev. temp., whisker crystal 79−29087
Zn-Al-Cu-Mg (22, 0.5, 0.01 wt.%), superplastic alloy, strengthening mechanism *(Japanese)* 77−55975
Zn-As system, homogeneity range of $ZnAs_2$ and electrophys. props. 80−60833
ZnS:Cu crystal, powder, epitaxial film, luminescence anomalous thermal 80−76077
ZnSe MIS diode, blue electrolum., heat treatment effects 78−19569
ZnSe, near band edge photoluminescence, electron-hole recombination 80−80835
ZnSe:Al, vapour phase doped, thermodynamics 79−90686
ZnTe, dominant acceptors, annealing and quenching 80−24463
ZnTe, effect of quenching on electrical props. 79−1920
ZnTe, reson. secondary radiation 79−99886
ZnTe, TEM obs. of precipitates, shape of Te solidus line 80−25703
ZnTe:Li, impurity segregation during short annealing and quenching, SEM, TEM and elec. meas. 80−10676
ZnTe-Ga_2Te_3, phase diagram 78−35360

quenching continued
Zr alloys, domain struct. of diffuse ω-phase formed in quenching, 1D model 78−27523
Zr, crept single crystal, nature of γ-hydride 77−21147
Zr, martensite, furnace cooled and water quenched, strength and deform. 79−20101
Zr TA6V6E2, tensile and toughness props. after isothermal quenching and continuous cooling *(French)* 77−59833
Zr-Al (14 at.%), martensitic, discontinuous precipitation, TEM obs. 79−34040
Zr-Al (4.6 wt.%), microstruct. effect on mech. props. 79−20080
Zr-Be, metallic glass form. and props. 80−16219
Zr-CR (1.9 wt.%), β-quenched and tempered, tensile props. rel. to tempered conditions, SEM study 79−66109
Zr-Cr (1.9 wt.%), β-quenched and tempered, optical and TEM study 79−66061
Zr-Cr (1.9 wt.%), β-quenched and tempered, $ZrCr_2$ precipitation, TEM study 79−66062
Zr-Cu, amorphous alloy, sheet production by plasma spray quenching 77−44193
Zr-Cu, dil. martensites, struct. and strength 79−29077
Zr-Cu (1.6 wt.%), near eutectoid, active eutectoid decomposition ageing and quenching effects 80−2993
Zr-Fe, amorphous alloy quenched by levitation method, crystallisation 79−55669
Zr-Mo(-Al) (3, 1 wt.%), β-phase stability 78−39742
Zr-Nb (2.5 wt.%), quenched-and-aged, neutron irradiated, 573 to 923K, damage struct. 79−99247
Zr-Nb (2.5 wt.%), strain ageing 77−77511
Zr-Ru, alloy Zr rich, Ru solubility, eutectic decay, $\alpha \rightleftarrows \beta$ transform., struct. *(Russian)* 80−65227
Zr-Ru(Pd), heat treated, mech. props. and struct. 78−80571
Zr-Sn-Mo (6, 1 wt.%), creep and creep rupture 78−23778
Zr-Ta (5 wt.%), martensitic transform. by rapid cooling, non-equilib. precipitation 79−34075
Zr-Ti martensites, furnace cooled and water quenched, strengh and deform. 79−20101
Zr-V foil, rapidly quenched and heat treated, supercond. props. 80−54852
ZrO_2-Cr_2O_3 system, react., phase diagram 1600-2400°C 79−11580
ZrO_2-SiO_2 (11 to 13 wt.%), X-ray phase anal. 80−35195
$ZrSiO_4$, plasma dissociated, quenching rate effect on microstruct. 79−38854

queueing theory
cell classification multistage systems, stochastic models 78−77143
coronary care unit equipment failure finding and prediction 78−44648
cyclic queue models of semiconductor noise and vehicle fleet operations 80−80336
EEG alpha and non-alpha intervals alternation model 78−96040
M/G/1 queue with finite capacity, inter-arrival times of accepted customers 77−2518
M/M/S queueing system, finite discrete transform 79−67144
Markovian queueing system central limit theorem 78−32658
molecular spectroscopic laboratory strategies, queueing theory and digital simulation use 80−30299
waiting time in stationary state for queue with server of walking type (autonomous service) 80−90657

queuing theory *see queueing theory*

R and D management *see research and development management*

R-centres
alkali halide crystals, binding energy of F_{c+}', M_{c+}' and R_{c+}' centres, positron trapping 79−69460
alkali halide crystals, capture and annihilation of positrons at M- and R-centres *(Russian)* 77−85829
alkali metal halides, analysis of spin-Hamiltonian parameters of heteronuclear XY^- defects 80−88509
radiation damage tetragonal R2 centre, optical and EPR spectra 78−2888
CaF_2, additively coloured, new type of F_3-centre, absorption bands obs. 78−35172
CaS phosphor, deep capture centres obs. 78−10951
CdS laser irrad. native defect formation, influence on photoelectric props., IR luminescence *(Russian)* 80−11039
CdS, low temp. IR-induced flash of green edge luminescence 77−63457
CdS, optical quenching of noise photooscillations, connection with photoconduction *(Russian)* 77−20363
CdS:Cu, fast electron irradiated, isochronous annealing of IR photocond. quenching spectra 77−1450
CdS:Cu, photosensitivity degradation mechanism 80−107851
CdS:In(Cl) concentration quenching mechanism of luminescence 80−97336
CdS:Li, nature of recombination centres responsible for 0.95 μm luminesc. band 77−69908
n-GaAs, intrinsic luminescence intensity, effect of 0.94, 1.0, 1.2 and 1.3 eV radiative centres 78−23517
KCl, absorption spectra of F-aggregate centres, 2K 77−48207
KCl, F_3-centre quartet state, IR emission spectra 78−43930
KCl, luminesc. excitation spectra of F-aggregate centres, 400-900 nm. *(Russian)* 78−10980
KCl, MCD, magneto-optical parameters of R-centre in H_3-mol. model 77−77253
KCl, MCD of R_1 band 77−8551
KCl, mag. circular dichroism of R-center, point-ion lattice model 79−69814
LiF, 3 MeV electron induced F, F_2, F_2^+, R_1, R_2 and F_2 colour centre obs., IR spectra obs. *(Russian)* 77−48210
LiF, irrad. at pile temp., higher F aggregate centres produced during thermal annealing 77−43212
LiF-Li_2O, F-aggregate centres *(Russian)* 78−64394
NaCl, F_3-centre quartet state, IR emission spectra 78−43930
NaCl, gamma irradiated, optical bleaching of colour centres, F-aggregate centre form. 79−95813
NaCl plates, γ-irrad., optical absorption spectra, hologram recording samples 78−17878
NaCl:Ca, hologram recording on R-centres 80−1157
NaF, F_3^+ centre zero-phonon line, photochem. and population hole burning 79−42997
NaF, F_3^+-centre decay by optical free induction 78−68555

R-centres continued
$RbNgF_3$, radiation defect F,M,R-centre absorpt., emission, excitation spectra 79−43000
ZnS phosphor, deep capture centres obs. 78−10951
R waves *see Rayleigh waves*
Racah coefficients *see angular momentum theory*
radar
see also Doppler effect; optical radar
35 GHz short-range pulse radar, effects of precipitation *(German)* 77−49147
acoustic, meteorological appl. *(Spanish)* 78−88944
aerospace systems and electronics, IEEE conference, Washington D.C., USA, 26-29 Sept (1976) 77−5420
biological effects of radiation impact on human systems 77−40710
coherent optical processing techniques 78−75018
delay parameter estimation following robust detection 79−55267
digital sensor simulation 77−33213
Doppler processing of HF backscatter radar and mode structures of ionospheric propagation 79−16753
Doppler radar data analysis in meteorological obs. 80−41564
Doppler weather radar, development of weather echo props. 80−26645
dual-polarisation radar for rain targets, rel. of diff. reflectivity to correl. 79−62556
historical development, effects on advance of astronomy 78−36471
interstellar communication via radio leakage, Earth model 78−57474
MF/HF backscatter radar for sea surface meas. *(Japanese)* 78−16210
mm wave radar, measurements of effective sea reflectivity and attenuation due to rain at 81 GHz 79−80001
non-spherical hydrometeors scattering properties *(French)* 78−53676
ocean surface, radar echoes of second order from waves, first inversion 78−49032
ocean wave synthetic aperture radar imagery rel. to surface structure 80−46197
optical folded spectrum processor, signal demodulation and radar processing appls. 78−5429
optical signal and image processing, conference, San Diego (1977) 78−74853
propagation anomalies, Bass Strait, Australia 77−49131
random media causing pulse spreading and wandering 80−37942
reflected waves, reln. to lightning and hail storm *(Chinese)* 77−66968
reflectivity gradients in the atmosphere 77−91229
reflectivity profile, Z-factor, classification by rain types 80−101420
remote sensing imagery, spatial filtering 78−90385
sideways-looking radar using synthetic aerial, remote sensing appl. 78−69537
signal processing, fibre and integrated optics techniques 77−27379
SLAR imagery correction for flight path curvature distortion 79−53553
symposium, London (Oct. 1977) 78−24395
synthetic aperture radar, satellite-borne, optical decoding 78−90384
synthetic aperture radars, speckle reduction 77−19191
synthetic aperture system, coherent optical simulation 77−27260
tropospheric studies, microbarographs, sodar, FM-CW radar, review 77−91332
VHF radar signals, partial refl. and scatt. from clear atmosphere 78−81278
wave and particle descriptions of light, equivalence, rel. to radar freq. shift 80−101692
weather radar matched filter criteria and range weighting 79−25341
^{222}Rn conc. monitoring by proportional counter, study of thermal diffusion in Rn-CO_2 mixture 79−50839
radar altimeters *see radioaltimeters*
radar antennas
acoustic, based on existing microwave dish-antenna, for acoustic remote sensing 79−72770
echosonde antennas, echo carrier freqs. and antenna dimensions rel. to performance 78−1474
Fresnel zone and diffraction fields anal. near boresight of acoustic radar antennas 80−64318
geological stratum sounding by UHF radar *(German)* 79−8702
HF radar system for ocean surface currents mapping, new antenna concept 80−94626
large reflector antenna structural design for gravity and wind loading 78−57448
Mills' cross array antenna, digital baseband processing 80−36500
multibeam synthetic aperture radar, global oceanography appl. 79−84506
Ondrejov meteor radar, antenna radiation pattern 77−78634
radiation effects on maintenance and repair personnel investigation 77−81529
side-looking airborne radar, Earth surface remote sensing appl. 78−20561
radar applications
active microwave sensing *(Japanese)* 78−16213
active microwave sensing of Earth surface *(Japanese)* 78−16214
aerosol measurements with calibrated two- and three-freq. lidars 78−36334
air flows in clouds, radar study 77−91243
air pollution detection, using optical methods *(Czech)* 78−81359
airborne lidar, continuous long-distance system, flight tests *(German)* 78−36338
airborne lidar, multidisciplinary, planned operation 78−36335
Antarctic bedrock mapping *(German)* 77−56770
Arctic lakes, L-band imaging radar obs. 77−21816
Arctic Ocean ice characteristics meas. by microwave scatterometry 79−84298
Arecibo radar meas. of tropical winds 79−100975
asteroids, radar detectability, opportunities for 1977-87 period 77−82149
astronomy, obs. of meteorites, Moon and planets *(Spanish)* 79−5759
astronomy, radar meas. in solar system 77−25947
atmosphere, precipitating clouds observed by RONSARD radars 80−51568
atmosphere frontal systems passage, obs. via VHF radar 79−53482
atmosphere observations at Kingston, Jamaica, using lidar system 78−36284
atmosphere radar technique, for dynamic struct. of middle atmos. 80−105078
atmosphere study, MST radar at Poker Flat, Alaska 80−90254
atmospheric meas., humidity and clouds drop phase charact. 79−74991
atmospheric measurement by VHF pulsed Doppler method, lower atmos. 80−46277
radar applications continued
atmospheric precipitation, depth-area relations from digitised radar returns 77−91249
atmospheric research, high power VHF radar appl. *(German)* 80−46294
atomosphere winds and turbulence continuous meas. using VHF Doppler radar, preliminary results 80−8444
aurora, radar signatures of substorm expansive and recovery phases 77−25812
auroral Doppler data, interpretation rel. to auroral electrojet curvature 77−41266
auroral electric fields, meas. from E-region irregularity drifts via backscatter radars 77−33262
auroral substorms, radar signatures of auroral east-west motions 77−29535
backscattering coefficient and wind speed meas., determ. of winds at sea 80−26644
borehole radar exploration in coal seams 78−28235
cartography radar image interpretation, line detection technique 78−61630
cloud and clutter targets observed by radar, broad-band noise technique 80−51454
cloud and precipitation particle observation, vertical X- and K_a-band system 80−46273
cloud seeding, radar reflectivity/rainfall rate relation 77−45099
clouds and precipitation study form correl. and spectral anal. of radar signals 80−12529
clouds meas., comparison of simultaneous studies by satellite 79−58077
coastal radar system appl. to tsunami prediction and magnitude 80−82101
coherent polarization-diversity radar techniques in meteorology 79−58111
containerisation of heavy lidar system for environmental protection control 78−36336
correlation function and averaged power of radar signals reflected from sea waviness 80−46190
crop and vegetation remote sensing, X-band scatterometer 79−25370
crop types monitored by side-looking radar 80−46280
digital data compositon for satellite and radar imagery 80−67413
directional sea spectrum determ. using HF Doppler radar techniques 77−17229
Doppler radar, wind profiles meas. compared with rawinsonde balloons meas. 78−44916
Doppler radar obs. of gust front evolution and tornado genesis 77−91219
duroral zone ionospheric modification, incoherent scatter radar obs. 77−82083
Earth-sounding radar obs. of EM lateral waves 77−44909
Eiscat radar, appl. to stimulated Brillouin scatt. prod. in ionosphere 77−37478
electrojet, equatorial, plasma instability and electron density irregularities, HF radar obs. 80−105112
equatorial anomaly, counter electrojet assoc. changes, upward drift reversal obs. 80−109297
equatorial counter-electrojet, electron drift vel., radar obs. 80−82126
equatorial electrojet, three metre irregularities depend. on Zenith angle, radar obs. 80−105109
exploration, ionosphere and planets 78−73663
frontal precipitation forecasting, contrib. of weather radar network, case study 77−56692
geodesy, SEASAT radar altimeter resolution capability 80−72645
geological interpretation, from composited radar and Landsat imagery 80−56647
geological stratum sounding by UHF radar *(German)* 79−8702
geology, discrimination using dual freq. and polarization imaging radar 79−12293
geophysical exploration by Electromagnetic Transient Underground Radar 77−17262
geophysical prospecting by pseudobaseband pulse radar 78−24398
geophysical reflection factor data, cartesian interpolation and display 80−31136
glaciers, vertical probing, signal depolarisation 77−9557
global oceanography, multibeam synthetic aperture radar 79−84506
ground imaging from satellite by synthetic-aperture, digital processing techniques 80−61914
Gulf Stream surface waves, radar obs. program 80−85679
hail detection technique, quasilinear discriminant function 80−21861
hail identification by radar, ice samples backscatter matrix 79−58046
hurricane dection by Doppler radar for coast of U.S.A. 80−67414
ice sounding, studies by Arctic and Antarctic Research Institute, Leningrad 80−4504
iceberg detection and characterisation, using synthetic aperture radar 80−26622
iceberg sounding by impulse radar 78−24388
incoherent scatter technique appl. to lower thermospheric dynamics 79−8734
ionosphere, incoherent scatt. radar for correl. meas. of electron and ion temps. 77−25820
ionosphere, incoherent scatter radar studies 77−22001
ionosphere measurement 78−49225
ionospheric chirp radar, transmit receive switching, effect on ambiguity function 79−84504
ionospheric pulsed sounding, historical review 77−5395
land use mapping using radar imagery 77−73886
lava flow terrain, radar imaged by satellite 80−98285
lidar temperature profiling of planetary atmsopheres 77−33352
lightning, cloud-to-ground discharges, radar cross section meas. 77−2279
mapping of rainfall by radar 78−24397
marine research from outer space, take-off of first ocean observation satellite *(German)* 79−74979
maritime surveillance, airborne, LASR-2 77−29507
Mars, Viking 1 landing sites, radar obs. rel. to site choice 77−13272
mesosphere remote sensing, VHF signal detection 80−46274
meteor bursts, forward scatt. technique, obs. over India 78−89132
meteor ionisation trails, charact. from radar obs. 77−71069
meteor radar research, growth and decline 77−78722
meteor radar system, Illinois University, description and results 77−41205
meteor tracks, initial radius measurement, simultaneous radar observations, three wavelengths *(Russian)* 77−22108
meteoradiolocator echo signals, optical spectral processing *(Russian)* 79−100968

radar applications continued
meteorites, velocity meas. by radar technique *(Spanish)* 79—5759
meteorological radar network optimal positions, multiple-Doppler system 80—31140
meteorological service in Poland 78—92992
meteorology, airborne pulse Doppler radar 80—85757
meteorology, differential reflectivity and differential phase shift rel. to hydrometeor size and shape determ. 78—57270
meteorology, line convection, radar obs., high resolution colour display 78—88894
meteorology, radar echo systems for upper midwestern U.S., analysis 78—16183
meteorology, review of radar appls. in atmospheric behaviour research 78—77371
meteorology, Ronsard Doppler pulse radars, G-band 77—87086
meteorology, Ronsard radar for investigation of vertical rising winds *(Dutch)* 78—81447
meteorology, wind field in frontal system, determ. from single-Doppler radar 79—21057
meteorology radar, echoes from distributed targets, averaging of time, angle and range 80—109264
meterological radar data acquisition system at Spino d'Adda ground station 78—69468
microwave attenuation through rain, correl. with predicted values using radar 77—5279
microwave radars, appls. to ocean wave detect. and direction meas. 79—5685
middle atmosphere struct. and dynamics from VHF radar obs. 80—105032
mine workings, roof and walls condition study *(Russian)* 79—62602
modelling of influx of meteoric matter with radar observations *(Russian)* 80—67664
Moon, radar contact in 1946 80—85866
mosaicing of radar images, side-looking 77—13135
nightglow, 6300 Å emission profiles from incoherent scatt. radar and photometry *(Portuguese)* 80—41591
ocean, microwave scattering signature, aircraft measurements 77—17112
ocean internal wave obs. with airborne synthetic aperture imaging radar 77—17110
ocean surface currents and gravity waves, directional spectra, remote sensing by microwave radar 78—57364
ocean surface currents mapped by coastal HF radar system 78—28351
ocean surface currents mapping, HF radar system appl. 80—94626
ocean surface imaging, spaceborne SAR, phase and Doppler errors 77—2323
ocean surface imaging, synthetic aperture radar, effects of random phase changes 77—17242
ocean surface imaging, synthetic aperture technique 78—77334
ocean surface wave imaging, synthetic aperture radar mechanism 79—5651
ocean surface waves, radar imaging method using SAR 80—77173
ocean surface waves imaging, models 77—17237
ocean surface waves imaging, models 77—25689
ocean surface wind field mapping, high-resolution, skywave radar 77—17159
ocean surface wind speed meas. from HF sea scatter by skywave radar 77—17160
ocean wave detection by microwave radar, gravity-capillary wave modulation 78—77333
ocean wave height determ. by synthetic aperture radar imagery 77—70845
ocean wave height statistics, dual frequency correlation radar measurements 77—17236
ocean wave height statistics, meas., dual freq. correl. radar 77—29478
ocean wave radar monitoring, ground wave and sky wave sensing techniques 80—109256
ocean waves, growth decay of 80 m waves, radar obs. 80—98344
ocean waves, pollution and ice, microwave meas. using SLAR 78—77245
ocean waves, remote obs. using HF skywave radar technique 80—90241
ocean waves, synthetic aperture radar imaging, focusing effects 78—40555
ocean waves and wind meas., HF and microwave techniques 78—81418
oceanographic remote sensing, using computer-controlled surface contour radar 79—80063
oceanography, appl. of radio obs. of polar regions 78—81419
oceanography, beam-limited target-referenced radar limitations 77—41194
oceanography, colloquium (Hamburg 1976 Sept. 29-Oct. 6) 78—77239
oceanography, directional sea wave spectrum determ. using HF Doppler sea wave spectrum determ. 77—29476
oceanography, large scale, radar altimetry contribs. 78—77337
oceanography, SEASAT synthetic aperture microwave-imaging radar expt., overview 80—46267
oceanography, SEASAT-A satellite scatterometer data regional integration, validation and appl. 79—5680
oil contaminations on sea surface, radar detect. *(Russian)* 77—49089
precipitation forecasting 0-6 hours ahead, radar and satellite imagery, FRONTIERS plan 80—12509
precipitation mapping with airborne synthetic aperture imaging radar 77—87106
precipitation parameter meas. method using radar reflectivity and optical extinction *(French)* 78—53729
radioaltimeters on automatic lunar stations, expts. 77—53438
rain attenuation measurements in conjunction with drop size measurements 79—62542
rain attenuation study on terrestrial microwave link 77—41130
rain cell monitoring, algorithms for automatic detection and tracking 80—51544
rain measurement and forecasting in UK using radar as part of integrated system, progress and plans 80—98490
rain measurement by dual-polarisation radar, drop size and fall rate 80—72650
rain precipitation strength obs. by radar rel. to ETS-II satellite wave propag. *(Japanese)* 78—85669
rain-rates, estimates for attenuating radar 78—73540
rainfall, convective, meas. over small areas using high-density raingauges and radar 80—77157
rainfall estimate using S-band radar during cyclonic storm, Calcutta 78—32157
rainfall measurement, combined usage of radar and radiometry techniques *(Chinese)* 80—109272
radar applications continued
rainfall measurement by radar, methods and interpretation of data 80—81959
rainfall monitoring, dual-freq. radar *(Japanese)* 78—57358
rainfall on convective days, analysed with respect to radar obs. atmos. parameters 80—109205
rainfall rate determ., effect of vertical air motions 77—45098
raingauge system, weather radar and real-time data processor combination 77—91326
remote sensing, 5-4 GHz region, microwave active spectrometer capability 79—25368
remote sensing, tetrahedral scan for tri-Doppler radar 78—16184
remote sensing and telecommunication, book 80—36431
remote sensing by stereo side-looking radar, accuracy anal. 80—56646
remote sensing in Irish and Celtic Seas using MF radar 79—16725
remote sensing of atmosphere by VHF radar expts. 78—88938
remote sensing of Earth's surface, techniques, review 79—12294
river management operational system development using weather radar 78—40718
RONSARD atmospheric radar, calibration techniques 80—46278
rough surface average impulse response, appl. to satellite radar altimetry 77—17235
salt domes, N.Louisiana, imaging radar mission 79—66833
salt mines, radar propag. in rock salt 78—96215
salt mining, radar detection of boreholes 78—96305
SAR imaging systems, holographic display 79—31843
satellite radiosounding, appl. to Venus atmosphere and surface investigation by (Venera 9 and 10) 80—101543
scatterometer, pulse compression system, experimental study 77—17240
sea ice and open water in Bering Strait, radar monitoring 77—87100
sea ice types, radar scatterometer discrimination 77—41198
sea return backscattering CW dual-freq. X-band radar studies 77—25687
sea state and wind sensing by HF skywave radar 78—24396
sea state estimation, ocean wave models and microwave scatter 78—77244
sea state radar, long-range sensing using HF sky wave, minimisation of ionospheric disturbance 80—21857
sea state remote sensing, HF sea echo Doppler spectra statistical props. 77—29312
sea surface waves, remote sensing using one and two freq. microwave techniques 80—94622
sea surface wind speed and significant wave height meas. using short pulse radar 77—17234
sea wave meas. using HF radio scatter 77—25789
sea wave profile meas. by radar altimeter, computer simulation 77—5367
sea waves, height, length and velocity, radar and Doppler effect, OREME project *(French)* 80—94625
sea-state parameter extraction from sample-averaged data, accuracy 80—51561
severe storm warning using Doppler radar 78—49148
severe-storm identification, multimoment Doppler display 77—56756
SHF signal attenuation by rain, monitored by radar 80—51567
short pulse radar ocean wave sensing, preliminary results 80—46315
side-looking airborne radar, Earth surface remote sensing appl. 78—20561
smoke plume concentration meas. by optical radar *(Chinese)* 78—58006
snow, radar backscatter in 1-8 GHz range, MAS expt. 77—86946
snow drift meas. *(Japanese)* 77—82032
space station, scheme for automatic rendezvous with unmanned (or manned vehicle) 80—77249
Spacelab incoherent scatter radar for atm. field-aligned currents meas. 77—21946
squall lines, radar obs. during GATE 78—20474
storm motion in three dimensions, detection by conventional weather radar 78—57360
stratosphere and mesosphere, UHF radar echoes, for wind and turbulence obs. 77—33135
stratosphere and mesosphere radar studies, UHF and VHF, review 80—90180
stratosphere turbulence near tropopause, review of radar obs. 80—90179
subsoil exploration, role of electronics *(Spanish)* 78—20552
subsurface radar for Earth's surface remote probing 79—8724
subsurface radar using video pulse for deep probing in Earth, pulse propag. in lossy media using LF window 80—74282
subsurface sounding of ground water in deserts and glaciers 80—67437
surface current mapping by Coastal Ocean Dynamics Radar 80—46316
surveillance, large sea areas, using side looking airborne radar system *(Dutch)* 80—12560
synthetic aperture radar, sea ice/lake L-band imagery computer processing 78—36311
synthetic aperture radar for remote sensing, technology trends 79—5655
synthetic aperture radar imaging in geosynchronous orbit 78—65442
synthetic-aperture radar, tutorial review, ocean surface imaging appls. 78—81445
thunderstorm classification, automated data acquisition and analysis 78—7772
thunderstorm observed by two-channel polarisation diversity radar 80—51453
thunderstorms, evolution studies using m and cm radars *(Russian)* 79—88405
tidal currents, meas. by two-site HF Doppler radar system by using two-site HF 80—72533
tornado-parent storm relationship from dual-Doppler radar anal. 77—21830
tornadoes probing with pulse Doppler radar 78—20558
tropopause detection, by partial specular refl. with VHF radar 80—8411
troposphere, radar obs. during clear air conditions, review 80—90178
troposphere and stratosphere sounding by pulsed VHF radar 80—51566
tropospheric studies, microbarographs, sodar, FM-CW radar, review 77—91332
upper atmosphere, meteor wind study at Kyoto University 79—48595
upper atmosphere studies 80—72661
urban effects on precipitation initiation in convective clouds, radar first echoes appl. 79—16601
Venus, distance from Earth determ. using radar, appl. to space craft navigation 80—109386
Venus, radar mapping by Pioneer Venus orbiter 79—48723
Venus atmospheric precipitation detect., remote sensing radar and radio techniques 80—56741
Venus radar mapping, Pioneer Venus Orbiter mapper design and operation 80—67495

radar applications continued
VHF backscatt. from blanketing E_s-layers in equatorial electrojet, gradient instabilities 77−29577
VHF coherent radar sounding of lower atmosphere 78−28281
weather forecasting processing of radar and satellite imagery data 80−109252
weather radar, airborne, return anal. 77−53108
weather radar, Doppler, estimation of echo spectral moment 80−51563
weather radar, signal anal. *(French)* 80−36418
weather radar, storm precipitation estimated with dual-wavelength radar 80−46220
weather radar calibration, correl. with rain gauge data *(Japanese)* 78−85670
weather radar data transmission using VHF satellite links, expt. 78−20569
weather radar detection of area precipitation *(German)* 80−46227
weather surveillance near airports using Doppler radar 80−46272
wind, off-shore meas. by HF Doppler ground-wave radar 78−77295
wind, strong shear obs. using pulse compression radar 78−32193
wind meas., new microwave radar 77−33195
wind measurement (absynoptic scale) using dual Doppler radar and vel. azimuth display 80−109263
wind measurements in clear air by microwave radar 77−13136
wind obs. in clear air using FM-CW Doppler radar 78−57271
wind profile determ. X-band solid-state radar system 78−12028
wind shear detection radar, for airport use 80−51565
wind vertical component in lower atmos., clear air Doppler methods 80−72642

radar clutter
cloud noise reduction, broad-band noise technique for fast-scanning radar 80−51454
MM wave radar, environmental effects on performance 79−80065
random path detection, Gaussian noise hypotheses testing 78−58551
sea return backscattering CW dual-freq. X-band radar studies 77−25687
weather clutter, Weibull-distributed, observations using L-band long range ARSR 80−36353
weather radar, airborne, return anal. 77−53108

radar cross-sections
active remote sensing with radar, radiative transfer theory, half-space random media appl. 79−8721
Arctic Ocean ice characteristics meas. by microwave scatterometry 79−84298
backscatter from metallic sphere in radially inhomogeneous plasma sheath, anal. *(Russian)* 77−7558
backscatter from water waves, induced current effects on microwave backscatter, expt. 77−25688
echo intensity and target cross-section relations, drifting snow meas. appl. *(Japanese)* 77−82032
effective scattering area of objects, average-value estimation in real-time *(Russian)* 77−83790
EM wave scattering by finite wedge with linearly varying surface impedance, anal. 77−61901
ground meas., for land and vegetation, influence of soil roughness *(French)* 77−49065
Gulf Stream roughness var. from radar cross section obs. 78−36194
HF radio wave backscatter by artificial ionised clouds 77−56788
infinitely long circular cylinder, backscatter of arbitrarily polarised EM wave 80−9778
nonconvex body, mode-matching method calc. 78−58887
North Sea, surface film, 13.9 GHz radar backscatter cross section meas. 79−39764
ocean surface, radar backscatter, friction vel. depend. 78−77246
ocean surface waves radar imaging, models 77−25689
precision measurement, as function of freq. 77−18014
rain, drop-size and temp. effects on forward and backward scattering on microwaves 80−17317
scattering properties of arbitrarily shaped lossy dielectric bodies of revolution 78−22072
scatterometer on satellites and aircraft for investigating underlying surface, optimization of characts. 80−67436
sonar coated hollow cylinder in water 77−46844
spot size of radar return from radar-acoustic sounding system, refractive turbulence effect 79−39821

radar displays
see also cathode ray tube displays; fluorescent screens
ambiguity function display and one-dimensional correlation/convolution by coherent optical processors 78−78950
geophysical reflection factor data, cartesian interpolation and display 80−31136
mapping of rainfall by radar 78−24397
polar coordinate display CRO 78−86253
SAR imaging systems, holographic display 79−31843
side-looking radar mosaicing, mapping errors and their reduction 77−13135
speckle noise, min, detectable contrast 77−19411
three-dimensional density function reconstruction, inverse problem 79−27197
weather detection and groundmapping using colour 79−92608

radar echo areas *see radar cross-sections*

radar equipment
airborne radar for oceanographic remote sensing, computer controlled 79−80063
Altair incoherent scatter radar for equatorial spread-F meas. 80−61927
Chatanika incoherent scatter radar, use of high-speed correlator and filter bank for plasma line meas. 80−98507
fibre-optic delay line signal processing devices 80−48443
French meteor radar facility 79−2386
HF radar system, for ocean surface currents mapping 80−94626
high resolution pulse-limited radar altimeter, appl. to ocean wave heights meas. 78−81172
linear array acousto-optical modulator devices 77−39072
meteorological radar equipment, pulse-wise interpretation of echo-signals *(Russian)* 80−67432
meteorology radar signal recording on video machine, coherent Doppler radar 80−46275
microwave, satellite borne, remote sensing of Earth physical parameters 79−80060
microwave radar for wind meas. 77−33195
oceanographic radar instruments, on experimental satellite Seasat-A 78−77455

radar equipment continued
Pioneer Venus Orbiter, radar mapper design and operation 80−67495
polarimeter, for study of air flows in clouds 77−91243
pulse compression using SAW components *(German)* 79−81639
radar meteor A/D filter charcts. *(Italian)* 79−80032
radar reflectivity variations with height due to wind shear on rain cells *(French)* 78−53682
radio meteor wind facility at Christchurch, New Zealand 79−2387
RONSARD atmospheric radar, for precipitation obs. 80−51568
SAW filter design for TV, CATV and radar appls. 80−53579
SAW slanted device technology for radar system appl. 80−19181
scatterometer on satellites and aircraft for investigating underlying surface, optimization of characts. 80−67436
SEASAT radar altimeter 80−56613
Seasat synthetic aperture radar system 80−94686
SEASAT-A satellite radar altimeter design 77−5415
SEASAT-A satellite scatterometer (SASS), data regional integration, validation and appl. 79−5680
SEASAT-A satellite synthetic aperture radar 77−5418
spectrum analyser for radar signal processing 78−78942
synthetic-aperture-radar processor, England (Oakhanger) sited, for US Seasat-A satellite 79−21128
X-band scatterometer, for crop and vegetation studies 79−25370
Ni-Fe polycrystalline film cross-tie memory for shipborne radar/sonar 80−42204

radar interference
see also radar clutter
HF sky wave radar remote sensing of sea state, minimisation of ionospheric disturbance 80−21857
parallel-polarised and cross-polarised radar returns from rough sea surface 80−51408
turbulnce effects, scintillation detection using monopulse techniques 78−85717
VHF echoes from equatorial E-region irregularities, sudden disappearance 78−40738

radar measurement
acoustic-microwave Doppler radar system, wind and wind shear meas. at Dulles Airport 78−32233
altimeter height and timing bias report 80−46326
Arctic sea ice, layered struct. study by radar sounding *(Russian)* 78−16023
Arctic sea ice, surface-based radar scatterometer results 79−92544
arterial wall movement monitoring by microwave Doppler radar 79−96647
Askja Caldera, Iceland, imaging radar meas. of surface roughness 79−16426
atmosphere frontal passage, VHF radar obs. 79−53482
atmosphere study, MST radar at Poker Flat, Alaska 80−90254
atmospheric precipitation properties using radar polarisation techniques 80−61925
atomosphere winds and turbulence continuous meas. using VHF Doppler radar, preliminary results 80−8444
attenuation in rain, iterative correction 78−92923
aurora, Doppler vel. meas., radio aural spectral charcts. and incident incoherent scatter meas. 80−56663
auroral currents, magnetometer array and radar backscatt. joint obs., N.Scandinavia 78−85768
auroral echoes, maximum entropy spectral anal. 78−93006
auroral electrojet, Chatanika radar meas. compared with Anchorage VHF backscatt. obs. 78−12048
auroral electrons energy distrib., incoherent scatter radar and photometric meas. comparison 78−77390
auroral radar echoes drift meas. using radar auroragraph 78−65436
Chatanika incoherent scatter radar obs. of field-aligned ionospheric currents 78−57387
clouds, radar reflectivity rel. to cloud dynamics and microphysics 80−61877
convective storm, triple-Doppler radar obs. 79−39886
cross-section measurements from satellites and aircraft for underlying surfaces, scatterometer 80−67436
differential-absorption lidar technique for remote meas. of atm. gases 78−61603
Doppler radar meas. of wind in extratropical cyclones, colour display system 78−61594
Dynasonde virtual height meas. methods, comparisons, accuracy and interpretation 80−94643
echo intensity and target cross-section relations, drifting snow meas. appl. *(Japanese)* 77−82032
EM wave attenuation and rainfall rates dual-polarisation radar meas. technique, precision 79−25371
equatorial counter-electrojet, two-stream instability, HF radar meas. 80−26671
equatorial electrojet, radar obs. rel. to auroral and equatorial dynamos global scale coupling 79−44297
floating ice layer thickness meas. using nanosecond impulse X-band radar 78−62178
Galilean satellites, radar obs. during 1976, results 78−61788
Geminid meteor shower, radar obs. statistical modelling 78−61816
Geos 3, radar altimeter data rel. to large-scale Gulf Stream frontal study 79−5488
glacier thickness and water content, radar measurement technique 80−98369
Greenland ice sheet topography from satellite radar altimetry 78−81233
Gulf of Alaska SeaSat Experiment synthetic aperture radar wave imagery 80−46199
hail, dual wavelength Doppler radar obs. at vertical incidence 79−79952
hailfalls kinetic energy, 10 cm radar and hailpad meas. 79−79951
hailstone trajectories determ. from crystallography, D content and radar backscatt. 78−61614
hailstorms, Switzerland, time-resolved hailstone size distrib. and radar struct. 78−49109
Harang discontinuity electric field, auroral radar and rocket double-probe obs. 78−88971
HF oblique radar obs. of plasma instabilities in equatorial electrojet over Africa 78−49205
HF peculiar lunar echoes, guided wave propag. in ionosphere and magnetosphere 78−93032
HF radio acoustic sounder, atm. wind and temp. remote meas. 78−32235

radar measurement continued
HF sea-echo Doppler spectra, extraction of wave height and period 77−78474
hurricane Ava, Skylab scatterometer meas., anomalous data correction 79−29881
hydrometeor size and shape determ., differential reflectivity and differential phase shift 78−57270
ice-cover thickness on rivers and lakes, pulsed radar meas. method 78−92862
iceberg sounding by impulse radar 78−24388
iceberg underwater shape determ., impulse radar appl. 80−26621
immature cyclonic storm struct. in Bay of Bengal revealed by radar 78−85628
ionosphere, auroral, field-normal plasma-line scatt. detect. expt. 78−73580
ionosphere, auroral zone, irregularities, simultaneous rocket probe, scintillation and incoherent scatter radar obs. 80−94640
ionosphere, equatorial radar backscatter plumes spatial relationship with plasma bubbles 80−67457
ionosphere, lower, wind obs. by Kyoto meteor radar 80−67444
ionosphere, props. meas. at Arecibo Observatory 78−81488
ionosphere, stimulated Brillouin scatt. detect. by Jicamarca radar 78−77412
ionosphere equatorial bubbles, topside sounder obs. 79−16737
ionosphere photoelectrons flux, low-altitude plasma line anisotropy theory 78−77414
ionosphere plasma line, meas. at Chatanika with high-speed correlator and filter bank 80−98507
ionosphere travelling disturbances, detect. by auroral zone incoherent scatter radar 79−48610
Kelvin-Helmholtz instability, jet stream generated, radar obs. and model 80−90165
lake ice, microwave radar and radiometric remote sensing meas. 80−85691
lakes, ice-covered (North Slope, Alaska), radar return differences 79−2298
lidar, simultaneous nighttime meas. of Na and K abundances 78−36239
lunar subsurface layering in Maria Serenitatis and Crisium, orbital radar evidence 78−85868
lunar surface using bistatic radar surveillance with FM signal 79−5758
mapping of rainfall by radar 78−24397
marine research from outer space, take-off of first ocean observation satellite *(German)* 79−74979
Mars, radar altimetry of S.Tharsis 80−98591
Mars, radar characts. of rough planar surfaces 80−98589
Mars, surface props. obs. by Earth-based radar at 70, 12.5, and 3.8 cm wavelengths 77−91457
Mars, surface slopes, roughness and reflectivity, radar obs. during 1975 opposition 78−45254
mesopause, ion-neutral collision freqs. and mean temps., Arecibo radar meas. 78−88957
mesosphere neutral winds, incoherent scatter spectrum meas. in 60 to 90 km region 79−16569
mesosphere turbulence structures, high-resolution VHF radar obs. 79−100895
mesosphere vertical velocities, first VHF radar meas. at temperate latits. 79−16572
meteor echo rates, correl. with zonal winds at 95 km altitude 80−56775
meteor tracks, initial radius measurement, simultaneous radar observations, three wavelengths *(Russian)* 77−22108
meteor trail, maximum ionization height detect. method 80−8487
meteor wind automatic meas. set, drift obs. accuracy *(Russian)* 77−41248
meteor wind automatic meas. set, programming and systems interaction *(Russian)* 77−41247
meteor winds, anal. using finite element approximation 78−81475
meteorological radar of Spino d'Adda 78−69467
meteors, echo drift deceleration 78−36538
meteors, head echo heights 78−36537
meteors, simultaneous visible and radar obs. technique 80−77354
meteors ionisation columns, initial radii meas. 80−94762
microwave scattering signature of ocean surface, aircraft meas. 77−25790
Moon, 3 cm radar obs. from Luna 16 to 24 spacecraft 80−77302
Moon, Earth-based radar mapping, review 80−12694
ocean surface currents and gravity waves, directional spectra, remote sensing by microwave radar 78−57364
ocean surface wind obs., SeaSat scatterometer/scanning radiometer/altimeter comparison 80−46249
ocean surface wind speed meas. from HF sea scatter by skywave radar 77−17160
ocean wave height meas. with satellite radar altimeter 79−44253
ocean wave height measurement by radar, airborne method 80−85771
ocean wave height statistics, dual freq. correl. radar meas. 77−29478
ocean wave heights, meas. by high resolution pulse-limited radar altimeter 78−81172
ocean wave parameters using pulse compression radar scatterometer system, expt. 77−29483
ocean wave spectra derivation by integral inversion of second order radar echoes 77−78475
ocean waveheight nondirectional spectrum from inversion of HF sea-echo Doppler spectrum 78−16203
ocean waves, comparison between synthetic aperture radar imageries and surface truth 79−5497
ocean waves, detect. and direction meas. via microwave radars 79−5685
ocean waves, remote obs. using HF skywave radar technique 80−90241
ocean waves and wind meas., HF and microwave techniques 78−81418
oceanic wind fields, high resolution mapping using skywave radar 77−29480
oceanic wind speed meas. using HF skywave radar sea scatter 77−29481
oceanography, directional sea wave spectrum determ. using HF Doppler sea wave spectrum determ. 77−29476
pack ice, drift observed using radar buoys *(Japanese)* 78−96224
Pc 5 geomagnetic pulsations, Stare auroral radar obs. 79−96862
peat bog and sapropel bed thickness meas. by radar 80−21860
phase tracking meteor radar ambiguity elimination algorithm *(Russian)* 77−41311
precipitation patterns structure, radar derived statistics 78−57260
pulse Doppler radar obs. of severe thunderstorms 78−85651
radar precipitation maps as lightning indicators 78−85652
radio oceanography using aircraft, inherent problems 77−25792
radar measurement continued
radiometeors, forward scatter, amplitude distrib. index, D-region absorpt. effect 78−65552
rain, radar reflectivity rel. to path diversity for Earth-space communication links 78−69424
rain slant path attenuation statistics prediction at various locations 78−24344
rainfall, convective, meas. over small areas using high-density raingauges and radar 80−77157
rainfall results of simultaneous surface precip. meas. at 3.2 cm and 5.4 cm *(German)* 77−82038
rangefinder with fluctuating phase shift, systematic averaging error elimination 77−67469
remote sensing and profiling of lower atmosphere using radiowaves, ground-based 80−56628
satellite remote sensing, CCD data handling system 77−91328
sea echo radar spectra resolution limitation inferred from ionospheric Doppler broadening 78−81489
sea ice, anisotropic props. in 50-150 MHz range 80−17274
sea ice, microwave remote sensing in AIDJEX main expt. 78−81173
sea ice, ocean waves SAR imaging 79−5496
sea ice, radar anisotropy due to horizontal c axes preferred aximuthal orientation 79−34836
sea ice field of Okhotsk Sea coast of Hokkaido, divergence and rot. meas. *(Japanese)* 78−96223
sea return backscattering CW dual-freq. X-band radar studies 77−25687
sea roughness radio measurement at Ukrainian Academy of Sciences 77−29313
sea state remote sensing, HF sea echo Doppler spectra statistical props. 77−29312
sea surface characts. rel. to radar returns at near-vertical sighting angles 79−57969
sea surface signal interpretation and energy transfer calc. 78−28241
sea surface using MF/HF backscatter radar *(Japanese)* 78−16210
sea surface wind speed and significant wave height using pulsed radar 77−29477
sea wave meas. using HF radio scatter 77−25789
sea wave space and time structure measurement from Doppler frequency shift 77−29482
sea-surface wind, from Skylab at 13.9 GHz 77−91304
SEASAT altimeter wave height comparisons 80−46201
SEASAT-A satellite project 77−5414
severe thunderstorms internal struct., dual-Doppler radar meas., tornado generation 78−61504
snow penetration and backscatter of millimetric waves 77−21877
snowfall meas., accuracy assessment 79−12316
soil moisture sensitivity of cross-polarized radar backscatt. 79−25282
sporadic meteors, ionisation height meas., VHF obs. 80−82312
subglacial lake, Antarctica, radar sounding 79−29798
summer rainshowers statistical models from fine-scale radar obs. 78−85650
surface soil moisture remote meas. 79−70896
Sydney thunderstorms of 10 November 1976, radar data 79−79995
thermosphere, middle, incoherent scatter radar studies 80−72654
thermosphere, winter motions radar in S.hemisphere meteor region 80−109287
thermosphere neutral winds, radar meas. at Millstone Hill and mathematical model 79−39995
thermosphere neutral winds deduced above Millstone Hill, seasonal vars., (1970 to 1971) 79−39996
thermosphere temperatures over Malvern, incoherent scatter data comparison with two global thermospheric models 80−8467
tidal currents, meas. by two-site HF Doppler radar system by using two-site HF 80−72533
tropopause, detect. by partial specular refl. with VHF radar 80−8411
troposphere, refractivity turbulence struct. const., Sunset Radar obs. comparison with theoretical model 79−8673
troposphere velocities and irregularities, VHF radar studies using spaced antenna techniques 79−16701
tropospheric temperature meas. by radio-acoustic sounding methods 78−53728
Venus, astrometric radar meas. in 1977, results 80−17522
Venus, equatorial zone surface topography, radar obs. from USSR 77−87303
Venus, radar mapping by Pioneer Venus orbiter 79−48723
Venus, surface bistatic radar survey, using Venera 9 and 10 satellites 77−87304
Venus atmosphere, radio waves attenuation investigation by bistatic radar method 80−62061
Venus surface, bistatic radar meas. by Venera 9 and 10 satellites 80−101543
Venus surface, geologic interpretation of new radar obs. 78−20666
VHF radar aurora and strong HF backscatt. comparison 80−61960
VHF radar signals partial refl. from troposphere 78−85656
warm frontal region, wind and precipitation struct., Doppler radar study 80−81995
waves in lower stratosphere, radar meas. 78−44917
waves in lower stratosphere, radar meas. 78−81292
weather radar systems, receiver bandwidth effect on refl. and Doppler vel. estimates 79−53549
wind measurements in Arctic troposphere and stratosphere 78−49172
wind obs. in clear air using FM-CW Doppler radar 78−57271
wind profiles, comparison of Doppler radar and rawinsonde balloons meas. 78−44916
wind vertical profile, high-altitude meas. with IR radar 79−70865
winds in lower stratosphere over Jicamarca, full-day radar meas. 79−25308

radar receivers
acousto-optic real-time radar and sonar signal processing 79−72515
logarithmic, for meteor radar, operating at 37.5 MHz *(Czech)* 79−21188
pulse Doppler processing with low-loss SAW delay line 77−31184
RONSARD atmospheric radar, calibration techniques 80−46278
weather radar systems, receiver bandwidth effect on refl. and Doppler vel. estimates 79−53549

radar stations
meteorological acoustic (MARS) and EM wave scattering studies 78−32210

radar stations continued
meteorological radar, vertical precipitation structure recording appl. *(German)* 80−17358
STARE: a new radar auroral backscatter experiment in northern Scandinavia 79−39977

radar systems
acoustic FM-CW radar for atmospheric sounding 79−74972
acoustic radar systems, microcomputer appl. 80−106685
active microwave systems for remote sensing 77−56776
air pollution meas. using laser radar data processing system 79−57559
attenuation and cross polarisation meas. at 20 GHz on satellite radio path caused by hydrometeors 79−20912
BASORA secondary radar, sounding ballon tracking appl. 80−17357
beam-limited target-referenced radar limitations on oceanographic use 77−41194
combined synthetic aperture radar/LANDSAT imagery 79−5650
CW dual-frequency X-band radar, backscattered sea-return studies 77−17232
Doppler, digital phasemeter optimal threshold determ. meteorological meas. appl. *(Russian)* 78−20560
dual frequency, directional gravity wave spectra and surface currents, remote sensing 78−96323
fast-scanning radar, cloud and clutter targets noise, reduced by broadband method 80−51454
Geos 3 tracking systems, intercomparison 80−4227
HF phased array radar for ionospheric and diagnostic appls. 79−5639
HF radar system, for ocean surface currents mapping 80−94626
interferometry, linear phase detect. *(Italian)* 78−85855
L-band air-route surveillance radar for observations of Weibull-distributed weather clutter 80−36353
LASR-2, 100 kW airborne maritime surveillance radar 77−29507
meteor radar system, Illinois University, description and results 77−41205
meteor wind radar, semiautomatic display and photographic recording system 79−8712
meteorological, performance as device for propagation studies, at Spino d'Adda 79−84342
meteorological and ATC radar system development 80−26651
meteorological radar of Spino d'Adda 78−69467
meteorology, radar echo systems for upper midwestern U.S., analysis 78−16183
MM wave, conf., London (Apr. 1980) 80−67441
MM wave, for remotely sensing atmospheric pressure from satellite 80−67443
MM wave radar, environmental effects on performance 79−80065
nanosecond impulse X-band radar, used for measuring floating ice thickness 78−62178
nonlinear coded waveforms, optical signal processing 79−72517
ocean wave height statistics, meas., dual freq. correl. radar 77−29478
optics utilisation in radar systems, conference, Huntsville (1977) 78−78939
passive detection system for wide class of illuminator signals 79−64408
passive mm wave detection of metallic objects in snow 79−84467
pulse compression radar, appl. to strong wind shear obs. 78−32193
Radar-Acoustic Sounding Systems, range limitation due to atmospheric refractive turbulence 77−41195
raingauge, weather radar and real-time data processor combination 77−91326
remote sensing techniques for ocean surveillance used by US coastguard 79−34991
Ronsard meteorological radar for investigation of vertical rising winds *(Dutch)* 78−81447
SAR imaging systems, holographic display 79−31843
satellite remote sensing, CCD data handling system 77−91328
sea surface contour airborne radar as remote sensing instrument 80−51562
SEASAT synthetic aperture microwave-imaging radar expt., overview 80−46267
space based radar systems, development, appl. 78−81525
spaceborne SAR, ocean surface imaging, phase and Doppler errors 77−2323
SPACETRACK, USAF, satellite-referenced ionospheric propagation correction 79−58131
subsurface radar for Earth's surface remote probing 79−8724
surveillance, large sea areas, using side looking airborne radar system *(Dutch)* 80−12560
synthetic aperture radar, satellite borne, terrestrial surface mapping appl. 80−12572
synthetic aperture radar image coherent-optical simulation 77−50632
synthetic aperture radar imagery for oceanography, random phase changes effects 77−25793
synthetic-aperture, Spacelab expts., for active remote sensing from space 80−36409
synthetic-aperture radar, tutorial review, ocean surface imaging appls. 78−81445
Venus Orbital Imaging Radar, aerobraking appl. 80−109338
VHF Doppler radar, appl. to atmospheric winds and turbulence continuous meas. 80−8444
Viking lander radar system mechanical design 78−57427
weather radar network, contrib. to local precip. forecasting, case study 77−56692
weather radar systems, receiver bandwidth effect on refl. and Doppler vel. estimates 79−53549
Zephyr, meteorological meas. appls. 80−90228

radar telescopes *see radiotelescopes*

radar theory
ambiguity function, optical processing techniques 78−78938
backscatter, from scatt. cells located in random medium 77−39428
backscattered pulse shape, small-angle multiple scatt. in random media 80−77079
chirp radar, transmit receive switching, effect on ambiguity function 79−84504
correlation function and averaged power of radar signals reflected from sea waviness 80−46190
cylinders in translational motion, Fourier spectrum evaluation 78−9300
Doppler shift formula derivation without transformation eqns. 77−82344
dual-Doppler radar, meteorological, coverage area as function of meas. accuracy and spatial resolution 80−82093
echoes scattered by random fluctuating surface, statistical model *(French)* 77−11066

radar theory continued
frequency scanning electronic imaging system 77−42589
general relativity, gauge field theory 78−36897
ground cover remotely sensed by radar, backscatter cross-section 80−46279
image simulation, point scatt. model, remote sensing appl. 79−12296
interferometry, linear phase detect. *(Italian)* 78−85855
microwave sea backscatter intermittency at extreme grazing angles, model 78−24307
modulated backscatter from reed switch loaded dipole 77−75386
ocean wave height statistics, meas., dual freq. correl. radar 77−29478
optical radar signal processing, multichannel optical correlator 78−74847
pulsed optical radar system using photodetector with lag, characts. 79−13918
quantum-information theory, expressions for Shannon quantity of information 79−55075
resistive strips scattering E- and H-polarised waves 80−37941
rough surface, average impulse response, satellite radioaltimeter appl. 77−25791
scattering from turbulent cylindrical plasma, model 78−22512
sea ice, radar wave reflected power intensity reduction with range *(Japanese)* 80−36329
sea surface scattering theory for large incident angles 77−86911
signal reflection from sea surface, spatial intensity fluctuations 80−109170
solar corona reflection of radar signal, efficiency of four-plasmon interactions 80−101582
speckle reduction in synthetic aperture radar processors by moving diffuser 77−34838
synthetic aperture imaging of ocean wave, focusing effects 78−40555
synthetic aperture radar imagery for oceanography, random phase changes effects 77−25793
time-domain computation of mean and variance of Doppler spectra 79−100972
weather radar, Doppler, estimation of echo spectral moment 80−51563

radar transmitters
Ondrejov meteor radar, antenna radiation pattern 77−78634

radarscopes *see radar displays*

radiance *see brightness*

radiation
see also atmospheric radiation; beta-rays; cathode rays; electromagnetic waves; heat radiation; radiation effects; radiative transfer; stellar radiation
acoustic radiation by instability waves in turbulent shear layer 80−79341
atomic collision processes, mixing and quenching cross-sections 77−61821
contaminated live steam release into turbine hall at Brunsbuttel *(German)* 79−89388
energy standards *(Japanese)* 80−62620
flux through successive spaced apertures 78−93542
gas flows, selfgravitating, thermodynamic processes and radiation, numerical method 80−14848
interstellar polarisation rel. to grain size, polarimetric obs. of four deviating stars 80−12792
ionising radiation, SI units introduction in Hungary aspects *(Hungarian)* 78−8379
PWR containment building, design and anal. of cavity shield system 80−18713
radiating particles of finite size, Dirac's subtraction formalism *(German)* 80−91740
radiogauging, use of ionising radiation 79−41086
risk to health assessment 80−41124
simultaneously radiating elec. and mag. sources, generalised EM field props. *(Russian)* 79−27131
Therac 6 linear accelerator, computer controlled evaluation for X-ray therapy 79−5363

radiation belts
see also atmospheric electron precipitation; atmospheric proton precipitation
Alfven waves and trapped particles nonlinear bounce resonant interaction 79−48624
alpha particles, energy spectrum between 18-70 MeV 77−64537
charged particle fluxes, obs. by JIKIKEN scientific satellite *(Japanese)* 80−94654
cosmic rays, element ions, interval $6 \leq Z \leq 28$, energies composition, Skylab study 80−8501
dynamics of outer belt during 1971, December 17 storm, Kosmos 426 obs. 77−33281
electron beams, counterstreaming, at altitudes of 1 R_E over auroral zone 80−67474
electron dynamics, influence of power-line harmonic radiation 79−80098
electron echoes, from conjugate regions of magnetosphere, distrib., Araks expt. *(Russian)* 79−40019
electron flux, high energy, obs. and comparison with VLF emissions by EXOS-B satellite *(Japanese)* 80−94652
electron flux variations, in inner radiation belt 80−67470
electron fluxes >0.7 MeV near belt boundary during substorm 78−96349
electron fluxes at outer trapping boundary, Kosmos 426 satellite obs. 77−64530
electron intensity fluctuations meas. from Cosmos 484 satellite 80−72698
electron leakage, artificially stimulated, optical and VLF emission obs. 77−64549
electron lifetime and VLF emission 79−62682
electron pitch angle distrib. determ. using Molniya 1 omnidirectional detectors 80−8437
electron pitch-angle diffusion rel. to morphological scheme of post-storm event 79−88523
electron precipitation, energetic, natural depletion mechanism for stratospheric O_3 77−41134
electron spectra in Earth's radiation belts during mag. storms 77−53314
electron-coherent whistler wave interaction, rel. to precipitation 80−46349
electrons, bounce-averaged collisional transport coeffs. 77−9624
electrons, evidence for trapped flux limit from pulsating aurorae 80−72666
electrons, loss cone distributions 77−29593
electrons, struct. of atmospheric loss cone 77−33294

radiation belts continued
electrons and protons equatorial pitch angle distrib., transient localised sources effects 77−64538
electrons pitch angle diffusion, instabilities rel. to pulsating aurora 3 Hz modulation 79−25391
electrons precipitation, struct. of loss cone 78−40774
electrons with energy 0.3 to 3 MeV, Prognoz 4 obs. 79−62693
energetic electrons, chorus generation during substorms 78−96356
energetic electrons, dynamics of high latit. trapping boundary during substorm 77−91374
energetic electrons in plasmasphere, distrib. function parameters 78−4035
energetic electrons precipitation rel. to maintenance of mid-latit. nocturnal D-region 77−25856
energetic electrons undisturbed trapping boundary at low altitudes 79−2441
energetic He ions obs. at geomag. equator during quiet conditions 78−88999
energetic ions expected charge states 79−80105
energetic particles, instabilities rel. to EM wave propag. in magnetosphere 77−87186
energetic proton and electrons in outer radiation belt, open drift envelopes, satellite meas. *(Russian)* 79−12358
energy selective precipitation of inner zone electrons 79−2428
equatorial pitch angle anisotropy in outer radiation belt, adiabatic modulation 78−89003
equatorially mirroring radiation belt protons, equilib. struct. 77−87192
equatorially trapped MeV ions, quiet time obs. 79−2445
equilibrium magnetic flux distrib. in moving force tube 78−69618
general study of upper atm. *(Chinese)* 79−75039
high-energy electrons, behaviour during reson. interaction with geomag. pulsations 78−28422
injection location affecting energetic particle spectra 80−72711
inner, energetic electron spectra before and after STARFISH nuclear explosion 77−2305
inner, proton spectra from Kosmos 721 satellite 80−72699
inner belt, max. radiation dose following 1962 STARFISH explosion 78−69612
inner zone electron precipitation, meas. 80−67452
inner zone electrons induced precip., obs. 78−88996
inner-zone protons, energy and pitch angle distrib. analytic study 80−67471
interfering background influence on orbiting IR sensor systems 77−22011
inverse loss cone electrons, temp. anisotropy quasi-linear relaxation due to interaction with electrostatic waves *(Russian)* 80−109314
ionosphere-protonosphere interaction, dynamic model 77−45220
leakage protons, meas. of spacecraft-produced neutron fluxes on Skylab 78−28486
low-energy charged particle ring around equator in 400-1100 km altitude range 77−49213
magnetic mirror vars., classical surface of section determ. 77−13231
magnetosphere, global fine structural forms. development during substorms 79−58190
magnetosphere dayside cusp, particle fluxes rel. to thermal electron densities and temps. 77−78574
magnetosphere morning sector, auroral electron discontinuity location meas. by Molniya-1 satellite 79−8778
magnetospheric physics, review of selected topics 78−65466
Molniya 1 satellite, radiation doses meas. 79−8774
nuclear and ionic charge distrib. particle expts. on International Sun-Earth Explorer spacecraft 78−85790
outer, dynamics during strong mag. storm 79−62678
outer, electron intensity increase, link with magnetosphere disturbance 80−77225
outer, electron vars. during substorm 78−40767
outer, energetic electrons dynamics during 1972 Dec. 12 Mag. storm 77−9619
outer, energetic heavy ions, origin in solar wind 79−40020
outer, fast electrons long-term vars. 78−49226
outer, influence of Jovian electrons 79−88548
outer belt behaviour after 1971 December 17 magnetic storm 78−16248
outer boundary variations, Kosmos 426 data 78−69614
outer electron boundary location, strong pitch angle scatt. effects, satellite obs. 77−70944
outer radiation belt, maximum fluxes of electrons with E>1 MeV (1958-1971) 80−61968
outer radiation zone struct. in simple model of convecting magnetosphere 77−25877
outer trapped electron belt, self-modulated VLF wave-electron interactions 80−41658
outer zone electrons, evidence for very weak pitch angle diffusion 78−28399
particle trapping by vertices of lines of force and lateral trapping 77−91377
particles radial diffusion, coeffs. from geomagnetic field fluctuations at synchronous orbit 78−96359
penetrating radiation composition, Cosmos 721 obs. 77−53279
permanent trapping in phase space 80−72709
pitch angle diffusion eqn. of trapped particles in presence of loss. cone, finite difference integration 79−70931
planar magnetic binaries problem, areas of motion 78−96386
proton auroral precip. and electrostatic ion-cyclotron instability during quiet times 77−33256
proton fluxes, critical levels in outer boundary of radiation belts 78−16246
proton ring current during storms, magnetic effect 78−96348
proton spectrum and spatial distrib. in Earth's radiation belts 77−53313
protonosphere, coupling fluxes from phase and group path meas. of VLF whistlers 78−49234
protonosphere, electron conc. inhomogeneities meas. by whistler method 77−67011
protonosphere-F-region nighttime proton fluxes 78−93034
protonosphere-ionosphere, plasma fluxes, ATS-6 obs. 78−28409
protonospheric replenishment after geomagnetic storm 78−28452
protons, cross-sections for (p,xn) reactions 78−28504
protons and α-particles with energy >1 MeV/nucleon, satellite meas. 79−8773
protons and He ions, equatorial α/p ratio near 1 MeV 80−4205
protons angular distribution and energy spectra at inner boundary, equatorial latits. 77−33293
radiation belts continued
protons trapped in geomagnetic field, dynamics 79−16756
pulsations of electrons trapped in inner geomag. field 77−53315
radial diffusion coeff. near L=6, electric field fluctuations 79−101022
radiation belts trapped electrons structure, effects of man-made VLF waves 78−45150
relativistic electron precip. spikes at midlatits. 77−29599
ring current, protons precip. rel. to auroral E-layer seasonal vars. 79−8746
ring current electrons, 1-30 Hz waves generation near plasmapause by reson. instability 78−49235
ring current field, determ. from D_{st} index 79−53658
ring current of magnetic storm, origin by inward displacement of trapped particles 80−72708
ring current particles, drift instabilities rel. to auroral precip. 79−12351
ring current plasma injection, correl. with solar wind parameters 78−96363
South Atlantic Anomaly spatial shift 78−28449
stability of invariant tori 80−31177
substorm associated particle fluxes, vars. at L=6 to 8 obs. by (GEOS-1) 79−35067
substorm protons, energisation and movements rel. to IPDP pulsations 79−25404
trapped electrons, energies above 100 MeV, produced by primary cosmic rays 78−36409
trapped electrons, energy >40 keV, pitch angle diffusion rate 79−21104
trapped particles, accel. by magnetosphere macroscopic elec. fields 78−49238
trapped photoelectrons and secondary electrons in mid-latitude plasmasphere 78−16244
trapping boundary at midnight, sharply defined L depend. energy threshold for anisotropy 80−41649
trapping region, quasiperiodic electron density pulsations, satellite detection 80−4198
Van Allen, mapping technique, student computing exercise 80−27076
VLF power line radiation effects on trapped electrons 79−12357
X-ray aurorae prod. by energetic electrons precip., imaging from Spacelab 78−61608
α-particles in inner belt, Prognoz 5 meas. 79−84587
C, N and O populations rel. to atm. blow-off mechanism 77−29524
H^++H charge exchange reactions, as source of energetic interplanetary H 77−9645
He^+, He^{2+}, nonadiabatic behaviour during quiet time conditions, theory and obs. 78−45158
O ions, energetic, in radiation belts, charge states theory 78−77427

radiation biology *see biological effects of radiation*

radiation chemistry
see also chemical effects of nuclear reactions and scattering; photolysis; radiochemistry; radiolysis
β source laboratory apparatus for radiation chemistry research 79−34340
acenaphthene single crystals, radicals produced by γ irrad., room temp. EPR study 78−84483
acetone, γ-irrad., isothermal luminesc. decay, temp. depend. 79−66322
N-acetyl-DL-valine, monocrystal, γ-induced free radicals at 77K 79−24774
acridine, single cryst., X-irrad., ENDOR obs. 79−87330
acrylourethane coatings, radiation curable, tensile, elongation and modulus props. appl. techniques 80−66847
adamantane, γ-irrad., free radicals EPR and ENDOR 80−69170
air, dissoc. by field-accelerated electrons, macroscopic props., rel. to pure O_2 80−61118
air, irrad., N_2^+ 1st negative band reson. absorpt. calcs. 77−30850
L-alanine:Cr^{3+}, X-irrad., thermoluminesc., ESR, UV photobleaching 77−9104
alcohol dehydrogenases, yeast and horse-liver, radiation chem. evidence for differences in amino acid composition 78−40116
alcohol glasses, X-irradiated, electron scavenging mechanism 77−56235
alcohols, trapped electron spectral relax., random-walk model 78−60493
alkali borate and silicate glasses, γ-irrad., paramag. SO_3^- radicals 79−42838
alkaline frozen solutions, polycryst. and glassy, photocond. and radiometric obs. 80−45531
alkaline glass: tryptophan (tyrosine), γ-irrad., electron traps, stimulated luminesc. 78−11536
alkaline glassy state, aq., density determ., radiation chem. 80−42197
alkaline ice, trapped electrons, photostimulated decay, time-depend. rate const. 79−52692
alkanes, glassy, radiation chem., D isotope effects 77−36767
alkanes, polycryst., radiation chem., D isotope effects 77−36767
alkoxy free radicals, produced by X-irrad. of hydroxy containing cpds., characterisation by ESR and ENDOR 78−95938
allyl free radical decay, in irrad. polyethylene, const. diffusion controlled rate const. 78−15651
amino acid, in polycryst., γ-irrad. induced radical pair form., 77K, EPR obs. 78−85292
amino acid formation by reactor irrad. of ethanol and aqueous ammonia 79−66305
amino acid radioracemisation, geochem. and cosmochem. implications 80−45975
α-aminoisobutyric acid, cryst., γ-irrad., cation radicals, ESR obs., SCF-MO-INDO calcs. 78−11537
anthracene, α-induced radical production beyond Bragg peak 79−24773
anthracene, γ-irrad., radical pairs EPR detection 78−31664
anthracene, radiation-induced radicals, EPR and optical absorpt. obs. 77−12816
anthracene, radiation-induced topotactic conversion from di-para-anthracene, low temp. TEM obs. 78−35710
and applications, review *(Japanese)* 77−73456
L(+)arabinose, irradiated single crystals, electron trapping, ESR obs. 78−88646
arabinose, X-irradiated single crystal, intermol. electron trapping, hyperfine ESR pattern 79−39166
aromatic polycrystals, γ-irrad., radical pair form., EPR meas. 78−80757
aspartate transcarbamylase, solid, enzyme activity and allosteric charact. after gamma irrad. 78−53341
aspartate transcarbamylase, solid, sedimentation and subunit interactions, after gamma irrad. 78−53342
bacterial single-strand breaks at short times after irrad., repair 77−12965

radiation chemistry continued
barium formate, γ-irrad., ESR of free radicals 79−65737
benzene, γ-irrad., radical pairs EPR detection 78−31664
benzene, fluoresc. quenching by pulsed proton irrad. of cyclohexane soln. 78−5270
benzene cryst., electron irrad., phenylcyclohexadienyl radical form., absorpt. and fluoresc. spectra study 80−89035
benzene in dilute cyclohexane solution, fluoresc. quenching on pulsed proton irrad., temp. depend. 80−21307
beta-decay, chem. and biological consequences 78−28018
biological photochemical and photophys. processes, conf., New Delhi, India, (Jan.' 72) 78−11694
biologically active compounds, MM-wave interactions 80−16707
biphenyl single crysts., γ-ray induced radicals, EPR and optical absorpt. studies 80−44921
1,2-bis(p-tolysulphonyloxymethylen)-l-buten-3-inylen, ESR of X-irrad. cryst., 77K 79−11806
Bowman-Birk soybean proteinase inhibitor, gamma irrad. 78−53343
5-bromodeoxyuridine, single cryst., X-irrad. at 77K, C_5-centred deoxyribose radical 78−20032
N-bromosuccinimide, X-irrad., ESR study of Br and σ* radical 80−66037
n-butanol, gamma-irradiated, trapped electrons, conc. of mol. vacancies determ. 77−65948
cadmium formate, γ-irrad., ESR of free radicals 79−65737
calcium tartrate tetrahydrate, X-ray irrad. single cryst., free radical EPR 77−63936
carbohydrate solutions, irradiated, lyoluminesc. and carbohydrate peroxy radical reactions 77−48665
carboxylic acids+urea, γ-irradiated reactions under high pressure *(Japanese)* 79−52707
carboxylic esters, γ-irrad. glass, trapped radical photolysis, ESR 78−85178
carcinogenesis, redox model 80−26298
cellulose acetate-g-polyacrylamide membranes, radiation grafted, appl. in water desalination by reverse osmosis 80−45548
cephalosporins, radiation-sterilisation by γ-irrad. 80−66822
ceric/thallous dosimetry at less than 1000 rad 80−63400
α-chloroacetamide, alkoxy radical form., effect, of α-hydroxyacetamide, ESR study 80−80610
chloroacetamide, X-irrad., ESR of $CH_2ClCO^{\cdot}$ radical 78−76882
5-chlorodeoxyuridine, single cryst., X-irrad. at 77K, C_5-centred deoxyribose radical 78−20032
5-chlorodeoxyuridine, X-irrad., α-chloro radical ESR and ENDOR 77−4916
choline bromide, radiation sensitivity, cryst. struct. depend., calorimetric investig. 78−88647
choline chloride, radiation sensitivity, cryst. struct. depend., calorimetric investig. 78−88647
choline iodide, radiation sensitivity, cryst. struct. depend., calorimetric investig. 78−88647
chondromucoprotein, effects of ^{60}Co γ-irrad. 78−7400
combustion gases, radiation treatment to remove SO_2 and NO_x 77−70322
coumarin, aqueous solution, fast neutron irrad., dosimetry appl. 78−44613
creatine monohydrate, single cryst., radiation damage, ENDOR obs. 78−96016
cyclodextrin, trapped electrons in cryst. matrices, ESR, optical absorption spectra 78−80768
cyclohexane, cation-electron pair distrib. irrad. and elec. field effects 77−81419
cyclohexane, neutron irradiation, radical distribution, ESR study *(Japanese)* 80−44920
cytosine, cryst., electron damage, electron microscope study 78−22762
cytosine monohydrate, single cryst., γ-irrad., ion radical recomb., EPR 78−15776
cytosine monohydrate single cryst., X-irrad., OH addition radical and decay product 77−86447
cytosine.H_2O crystals, radical form. by X-irrad. at 77 and 300K 77−12886
Czechoslovakia, past history and present status *(Czech)* 79−21516
n-decane-n-decane-d_{22}, γ-irrad., H_2/D_2 product ratio mass spectra, mechanism 77−40558
deoxycytidene 5'-phosphate-H_2O, cryst., X-irrad., ESR and ENDOR obs. 79−34330
deoxycytidine 5'-phosphate, H_2O, X-irrad., 3αH radial. form., ENDOR, ESR 77−73453
deoxyribonucleoprotein, gamma-ray protein damage 78−53338
diacetylenes, urethane substituted, polymer conversions in γ-ray polymerisation 80−26014
dicarboxylic acids, low-energy electron irrad., ESR obs. 79−95646
5,5'-diethylbarbituric acid, EPR and INDO-MO study of radical formation after irrad. 80−93774
5,6-dihydro-6-methyluracil, X-ray irrad., free radical form; ESR spectra obs. 80−50189
dimethyl sulfone, X-irrad. cryst., ESR spectrum 78−3351
2,4-dimethylpentane, glasses, γ-irrad., trapped electron yields, mol. struct. and temp. effects 77−40561
dimethylsulphide, liq., solvated electrons, optical absorpt. spectrum obs. 80−97250
1,3-dimethyluracil, non-hydrogen bonding crystal, radical formation 80−35552
dipotassium glucose-1-phosphate, X-irrad., ESR-ENDOR obs 80−60419
DNA, γ-irrad., 2-deoxy-D-erythro-pentonic acid isolation from alkali-labile site 78−20144
DNA, gamma-ray effects on hydration, PMR of frozen and liq. solns. 78−27900
DNA, single-stranded, alkali-labile sites and post-irrad. effects induced by H radicals 78−68994
DNA, transforming, X-ray sensitivity rel. to presence of free radicals 78−68995
DNA hydration characts. in H_2O/D_2O frozen solns., γ irrad. effects, PMR 78−31772
dodecane-tributyl phosphate solns., radiolysis, liquid products 80−40723
dulcitol, X-irradiated single crystal, intermol. electron trapping, hyperfine ESR pattern 79−39166
n-eicosane, single cryst., electron irrad., free radical pair form., ESR 77−4913
elastomers, continuous radiation vulcanisation, exam. *(German)* 78−92231

radiation chemistry continued
electron linac chemistry facility, 140 MeV 80−37640
electron reaction with scavengers in nonpolar liquids, rate const. 77−52654
electron track end effects in water 80−11932
enantiomeric compounds, optical purity, prod. by β-decay 78−40459
energetic ions in gas phase 77−25290
ESR studies of transient free radicals in irradiated food components 79−52699
ethanol, semiquantitative model for electron conc.-dose depend. in glassy matrix 78−20034
ethanol glasses containing anion radicals of fluorene and isologs, γ-irrad., optical absorpt. and EPR obs. after photobleaching 77−44491
ethanol-d_0, -d_1, -d_5, γ-irrad., trapped electron spin-lattice relax. 77−60089
ethylene glycol-water glass, γ-irrad., temp. depend. photobleaching of trapped electrons 79−66320
ethylene propylene/polyolefin blends, radiation cross linking 80−66801
ethylene-Co copolymers and -SO_2 copolymers prep. by catalysis and ^{60}Co γ-radiation, mech. props. 80−66841
ethylene-vinyl acetate copolymers, extrusion and heavy duty films, radiation crosslinking, struct. effect 80−66844
fibre reinforced polymer, soaking, wetting and compounding of materials during production *(German)* 80−93535
flammability resistance by radiation processing 78−95942
fluorene ketone polycryst., radical pair formation, 77K, EPR study 79−56610
formaldehyde, polymer formation in interstellar space 77−78858
Fricke dosimeter, influence of methanol and t-butanol on ferric yield 78−11736
frozen acid solutions, aq., irrad., at. H trap struct., spin echo obs. 79−42824
frozen salt solutions, aq., irrad., at. H trap struct., spin echo obs. 79−42824
G-value, dependence on scavenger conc., theory 78−20038
glasses, electron scavenging, hopping controlled time-depend. reaction rates 80−108723
glasses, electron scavenging kinetics, random walk hopping model 79−74401
glasses, gamma-irradiated, trapped electron form., dose effect on conc., empirical eqn. 79−34325
glassy matrices, electron tunnelling in radiation chem. 79−91980
glassy matrix, trapped electron decay time as function of preirrad. annealing time 79−66323
glassy organic matrices, electron spin-lattice relax. of radiation-produced Ag atoms, temp. depend., tunnelling relax. 79−34331
glutaric acid, γ-irrad. single crysts., free radical EPR obs. at 77K 80−81340
glycine-$AgNO_3$, single cryst., X-irrad., oxidation product form. 77−48660
glycyl anion radical, in α-glycine cryst., struct., ESR obs. 78−33530
dGMP γ-irrad. in frozen soln., free radical form., computer EPR spectra anal. 78−31774
halogermane radical anions, ESR spectra and struct. 80−87153
5-halouracils, solid, radiation damage, free radicals in 5-fluorouracil single crysts. 80−71926
s-halouracils, solid, radiation damage obs., deoxyribose ring opening in single crysts. 80−71929
heavy ion and He inactivation of mammalian cells, radiobiological characterisation 79−20585
heavy-particle track structure rel. to radical physical distrib. and chemical effects 80−11933
p-n-hexadecyloxycinnamic acid, liq. cryst., radiation stability 78−85184
hexafluoropropylene, radiation chem. alkylation with adamantane in liq. phase 77−48663
n-hexane, geminate ion scavenging yield, external elec. field effect 79−47909
high-energy electrons, theory of chemical effects 79−52700
hippuric acid, X-irrad. single cryst., ^{14}N and ^{1}H ENDOR study; 80−71240
hydrocarbon liq., effect of mol. struct., temp. and elec. field on electron mobility 78−2535
hydrocarbons, glasses, γ-irrad., trapped electron yields, mol. struct. and temp. effects 77−40561
hydrocarbons, in residual gas, polymerisation by electron bombard. *(German)* 77−40315
hydrocarbons, pulsed irrad. electron mobilities and reaction rate consts. for electron-solute reactions 79−91112
1-hydronaphthyl radical, in naphthalene single cryst., anisotropic oscill. strength 78−50591
4-hydroxy-2,2,6,6-tetramethylpiperidine, radiation-induced oxidation to paramag. nitroxide free radicals 80−81341
hydroxyproline HCl, X-irrad., free radical products, ENDOR meas. 78−76883
ice matrices, polycryst., electron spin-lattice relax. of radiation-produced Ag atoms, temp. depend., tunnelling relax. 79−34331
imidazole, Z-irrad., EPR study of H exchange 80−40718
inositol, X-irrad., deuteration effects, ENDROR and ESR meas. 78−73067
inositol, X-irrad., radical form. detection by ESR and ENDOR, oxidation process 78−27797
instrumentation, in Inst. Nuclear Res., Warsaw 78−76888
insulating and sheath materials for wire and cable, crosslinking by irradiation 80−66845
invertase, S-containing glycoprotein, gamma-irrad., secondary radical reactions, EPR 77−9175
β-iodophenylacetylene radical, PhC_2I^-, from γ-irrad. morpholine β-iodophenylacetylene complex, EPR obs. 77−52652
ion exchange membranes, production by electron irrad., cross linking, graft polymerisation *(Japanese)* 77−81403
ion implantation for chem. synthesis, review 77−43236
isocitrate dehydrogenase from Azotobacter vinelandii, essential amino-acid residues identification 80−76538
isopropyl vinyl ether, chem. initiated soln. polymerisation and radiation-initiated bulk polymerisation 79−91952
kinetic model for electron tunnelling in frozen irradiation systems 77−52655
D-leucine, preferential removal by polarised beta-rays rel. to origin of biological chirality 77−86445
linoleic acid, lipid membrane model, dose-rate and O_2 effects 77−48841

radiation chemistry continued
lipid peroxide formation in irrad. synthetic diets, storage effects 80−101025
liquids, electron scavenging and ion recomb. processes, 3-dimens. continuous time random walk model 78−7216
magnesium formate, γ-irrad., ESR of free radicals 79−65737
malic acid+formamide, γ-irradiated reactions under high pressure *(Japanese)* 79−52707
meat, biochemical procedure for detect. of radiation treatment 78−65075
6-mercaptopurine, electron beam irrad., free radical formation at 77K 79−5165
methanol, β-irrad., radical truck struct., electron spin-echo obs. 80−93776
methanol, solvated electron lifetime and reaction with hydroxymethyl radical, dose and base effects 78−20043
methanol, solvated electron yield and spur decay following electron irrad. 78−20042
methanol-2-methyltetrahydrofuran mixed glasses, annealed, γ-ray produced electrons transfer from IR to bisible traps 80−11440
methyl cyanide-water (methanol), Ag^+ ion solvation, γ-irrad., ESR obs. 80−97726
1-methyl cytosine: 5-fluorouracil X-irrad. at 300K, EPR 78−64941
4-methyl-2,6-di-tert-butylphenol, γ-irrad. cryst., ENDOR transitions, ELDOR detect. 78−95531
α-methyl-D-glucopyranoside, X-irrad., ESR and ENDOR study of free radicals 80−45526
methylamine liquid, 293K, solvated electron decay kinetics obs., IR spectra 80−71928
methylcyclohexane, γ-irrad., isothermal luminesc. decay, temp. depend. 79−66322
6-methylmercaptopurine riboside, 4 MeV electron irrad., 77K radicals form., EPR obs. 78−39405
methylmethacrylate soln., aqueous, polymerisation under pulse electronic accelerator irradiation 80−66802
12-methylpentane, γ-irrad. glass, trapped electron yield, elec. field effects 77−16848
3-methylpentane, glassy insulator, γ-irrad., IR enhancement of carrier radiation yield 77−76870
3-methylpentane glassy matrix, localised electrons, cavity model 80−107743
13-methylpentane-d_{14}, glass, γ-irrad., solvated electron struct. obs. 77−9101
3-methylpentane-d_{14}, glass, trapped electron optical spectra, wavelength selective bleaching 79−83480
2-methyltetrahydrofuran, glass, trapped electron optical spectra, wavelength selective bleaching 79−83480
molecules in degenerate electronic state, IR laser radiation effects 80−81351
monochlorobenzene, in KOH-2-propanol soln., chain dechlorination by γ-rays 78−56904
muonium atoms reactivity in aq. soln. 78−80774
muonium formation and charged particle tracks 79−57259
muonium-substituted transient radicals observed by muon spin rotation 78−74678
N-acetyl-L-leucine, single crysts., X-ray induced free radicals 80−45525
naphthalene, γ-irrad., radical pairs EPR detection 78−31664
negative muons, transport properties in matter, energy spectra 77−56239
negative muons, transport properties in matter 77−56238
neutron-gamma absorption, in blanket region of fusion reactor, chem. appls. 78−5021
nitrosourea compounds, 2, anal. of interaction with X-radiation in rat brain tumour cells 80−72230
non-radical processes, exptl. method for elucidation 78−27802
nonpolar solvent, o-Ps yield in chlorinated ethanes, ethenes and cyclohexanes 79−70357
nonsolvated electron reactions, positron annihilation method 77−81417
nucleosides, X-irrad., alkoxy radical form., ESR, INDO calcs. 77−90623
nucleotides, X-irrad., alkoxy radical form., ESR, INDO calcs. 77−90623
o-phosphorylethanolamine, ESR of phosphite radicals in X-irradiated single crystals 79−51857
octadecylacrylamide films, oriented ultrathin, radiation-induced solid state polymerisation 80−80128
p-n-octyloxybenzoic acid, liq. cryst., radiation stability 78−85184
olefines, radiation chem. alkylation with adamantane in gas phase 77−48663
organic compounds, irradiated single crystals, electron trapping, ESR obs. 78−88646
organic crysts., γ-irrad., positron lifetime rel. to free radical conc. 78−72635
organic reactions in solid state 80−21309
organosilicon ladder polymers, effect of γ-rays on props. *(Russian)* 78−76891
papain inactivated by OH radicals and H_2O_2, optical density, amino acid composition and fluoresc. 78−53344
particle stopping power dependence on physical and chemical states 80−9480
pentachlorobenzene, in KOH-2-propanol soln., chain dechlorination by γ-rays 78−56904
pentane:octane, γ-irrad., octane radical cations ESR 77−36765
peptide aqueous solution, EPR of spin-trapped radicals, OH radical reactions 78−68993
4-phenyl-3-thiosemicarbazide, single cryst., X-irrad., EPR, ENDOR, radical identification 79−31560
1-phenyl-3-thiosemicarbazide, X-irrad., radical prod., ESR, ENDOR 77−36770
L-phenylalanine.HCl, X-ray induced radical form. 78−48755
p-phenylene-di-p-n-heptyloxybenzoate, liq. cryst., radiation stability 78−85184
phosphoranyl radicals, Ph_3PBr, trapped in X-irradiated triphenyliminophosphonium bromide, ESR study 79−56611
photoabsorption data appls. 80−93778
photochromic polymer, thermal effect in photomech. conversion 80−16706
phthalocyanine, cryst., electron damage, electron microscope study 78−22762
2,5-piperazinedione, X-ray damaged, ENDOR, δ proton hyperfine interaction 77−9103
PMMA, neutron and gamma irradiation effects 80−66839
PMMA, neutron irradiation, radical distribution, ESR study *(Japanese)* 80−44920
radiation chemistry continued
PMMA crosslinked by dimethacryloxymethylanthracene, radiothermoluminesc. *(Russian)* 78−73068
PMMA electron resists, molecular weight depend. of developed contours 79−87859
polar liquids, MM-wave interactions 80−16707
polyacrylamide, high mol. wt., prep. by electron beam irrad. 80−76222
1,2-polybutadiene crosslinked in strain states; entanglement networks, stress-birefr. relations 80−66590
polybutadienes, radiation chemically cross-linked, charact. by pyrolysis gas chromatography *(German)* 80−81348
polycarbonate, irrad., electron spin-lattice relax. at low temp. 78−68382
polydiacetylene, crystalline and amorphous, γ-ray effects, gel form. and crosslinking 80−93777
polyester resin, unsaturated, glass fibre reinforced, polymerisation by UV irrad. *(German)* 79−100367
polyethlene crosslinking by electron beam radiation *(Japanese)* 79−70353
polyethylene, γ-irrad., alkyl radicals ESR and hindered oscill. 78−85182
polyethylene, γ-irrad. induced allyl chain free radical, decay kinetics, state depend. 78−76855
polyethylene, cross linking by energy rich radiation, mech. and elec. props. *(German)* 78−20035
polyethylene, deform. mechanism, γ-irrad. induced cross-linking effects 78−15469
polyethylene, electron beam crosslinking process for high voltage power cable 80−66846
polyethylene, ionising radiation effects crosslinking with accelerated electrons, ageing, SCC *(Polish)* 79−52701
polyethylene, irrad., trapping regions, allyl radical distrib. 78−91957
polyethylene, irradiated, far IR spectrum rel. to crystallinity 78−27216
polyethylene, irradiation, crystallinity and crosslinking efficiency 80−66843
polyethylene, liq., very high mol. wt., pulsed NMR obs., entanglement, crosslinking, irrad. effects 78−66702
polyethylene, low-density, γ-irrad., spin trapping reaction 80−39873
polyethylene, low-temp. relax., effects of chem.- and electron irrad.-crosslinking 79−4990
polyethylene, neutron irradiation, radical distribution, ESR study *(Japanese)* 80−44920
polyethylene, vinyl group reactions during γ-irrad., crystallinity effect, absorbance obs. 80−81346
polyethylene matrix, trapped free radicals, decay in single crystal and diffusion 77−52657
polyethylene terephthalate, irradiated with radiations with linear energy losses, peculiarities in chemical etching 78−39934
polyethylene-glass fibre composites, gamma-irradiated filler 80−66840
polyethylenes, extrusion and heavy duty films struct. parameters influence on cross-linking by radiation 80−66844
polymer, charged particle detect., graft-and-dye method 78−17520
polymer materials, appls. *(Japanese)* 80−55413
polymer network, crystn. and form. through crystn., crystallinity influence on radiation induced form. 80−38964
polymer radiation chemistry, computer modelling 79−74382
polymer systems for adhesive applications, radiation curing, lap shear strength props. 80−66842
polymer track detector, form. of heavy ion latent tracks 78−17522
polymeric cable insulation, radiation modification using electron beams 80−66848
polymerisation, γ-ray induced, control by dose rate regulation 77−32787
polymerisation, radiation-induced, solid state, computer modelling 79−66294
polymethacrylates degradation obs., due to UV, gamma-ray, and electron beam irrad. 78−27795
polymethacrylic acid, stereoregular, synthesis, ^{13}C NMR obs. 80−58422
polynucleotide hydration characts. in H_2O/D_2O frozen solns., γ irrad. effects, PMR 78−31772
polynucleotides, gamma-ray effects on hydration, PMR of frozen and liq. solns. 78−27900
polyolefin, cross-linked, irradiation appl. to provide improved insulation props. to wires and cables 80−66850
polypropylene, electron bombarded, radical formation, piezoelectric and pyroelectric effects, ESR study 80−7169
polypropylene, electron bombarded electret, trapped charges ESR study 80−7170
polypropylene fibres, EPR during glass transition, γ-irrad. 79−8445
polysiloxene, irrad., linear, IR and solubility obs. 80−93775
polysytene, neutron and gamma-irradiation effects 80−66839
polytetraoxane, polymerisation temp. effects on texture, and NMR obs. of mol. motion in tetraoxane cryst. 77−84663
polyvinyl alcohol, γ-irrad., ESR of trapped free radicals 78−85183
positronium formation in polar liquids, unsolvated electron effects 78−17826
propane, radiative thermal cracking on porous glass *(Russian)* 79−39205
1-propanol, electron traps, prestabilised electron relax. model 78−27803
n-propanol, gamma-irradiated, trapped electrons, conc. of mol. vacancies determ. 77−65948
protein, radical limiting conc. on UV irrad. at 77K, effect of luminesc. quenchers 80−30662
PTFE latex, emulsion polymerisation, radiation-induced *(Japanese)* 78−80747
pulsed NMR technique for meas. radiation effects in polymer 80−66051
purine, powder, γ-irrad., dose-response curves 78−7215
PVC, cross-linked, irradiation appl. to provide improved insulation props. to wires and cables 80−66850
PVC, Cu evaporated film, electron-induced metallochromic reaction for metal image formation 80−86476
PVC, plasticisers effect on behaviour under γ-irrad. *(Russian)* 79−87864
PVC materials, cross-linkable, for wires and cable insulation 80−66849
pyrene single crystals, γ-irradiated, free radical form. ESR spectra 78−72410
pyrene-naphthalene complex radical cation, in γ-irrad. glass, visible spectrum obs. 78−44385
pyrimidine powder, γ-irrad., dose-response curves 78−7215
pyrolytic C, energy depend. of methane prod. during deuteron bombardment 78−95939
pyrrole, free radicals produced by X-irrad. and decay of tritium atom, EPR study 78−48676

radiation chemistry continued
quartz dental composites, acrylic acid grafted on particles by gamma-radiation 80−66840
radiation processing, conf., Miami, FL, USA (Oct. 1978) 80−36772
radiation stability of 'nuclear class' ion-exchange resins 79−43609
radiation techniques and technology development in the Soviet Union 79−685
radical pair recombination kinetics, low conc. in solid matrix, 1, 2 and 3 dimens. 78−27793
radical radiation formation in solid organic compounds 80−85201
recoil T atoms+H_2O, neutron effects, apparent phase effect 77−63935
review of present status, future trends and applic. *(Japanese)* 78−31659
silica gel, effect of gamma-rays, electron scavenging by N_2O 79−24762
silicone rubber biomaterial, filler free, radiation chemical and physical evaluation 79−39608
silicone rubber with radiation-grafted methacrylate, for burn wound dressing 79−29657
sodium 10-undecanoate, γ-ray induced polymerisation in aq. micelle solns. 80−61093
styrene solutions, polymerisation initiation by intense pulsed electron beam 79−15997
succinamic acid, X-irrad., primitive radn. damage, ESR, ENDOR 78−3352
dl-tartaric acid, radiation products, ESR-ENDOR OBS. 80−55682
tartaric acid salts, and deuterated forms, irrad.-crysts., primary reactions, EPR obs. 80−3370
2,2,3,3-tetramethylbutane, γ-irrad., EPR spectrum assignment 80−15800
thiamine (vitamin B_{12}), aq. soln., radiation induced reactions 80−93779
l-thioproline single cryst., X-irrad., ESR and ENDOR study of radicals 80−45528
thymidine monophosphate, gamma irradiated, inorganic phosphate release, in presence and absence of O_2 80−67168
thymidine monophosphate aqeous solution, gamma irrad. effect on base damage, phosphate release 80−89806
thymine+muonium, radical form. in aq. soln., spin reson. obs. 78−74679
thymine fragment damage retained in DNA polynucleotide chain after γ irrad. in aerated soln. 78−31773
toluene in ethanol-d_0-d_1, dry electron scavenging efficiency, isotope effect on electron localisation 78−27784
transition metal sulphides, ion bombardment damage, XPS obs. 80−97404
trapped electron yields, close effects, tunnelling processes 79−39161
trapped electrons in glassy hydrocarbons, gamma ray irrad., relax., spectral obs. 80−23416
trifluoroacetamide, single cryst., X-irrad., transient radical form., INDO and ESR calcs. 77−12814
trifluoroacetamide, X-irrad., CF_3...F radical ESR 78−73066
2,2,5-trimethyl-1,3-dioxane-4,6-dione, cryst., X-irradiated, methyl group hindered rot. tunnelling, EPR, ENDOR, and ELDOR 79−68328
triphenylseleniumchloride, X-irrad. cryst., forming Ph_2SeCl, ESR study 79−39167
trypsin, in suspension, radical form. and inactivation after Γ-irrad. 78−3564
L-tryptophan-HCl radical form. after X-irrad. 78−64940
uracil, aq. soln., fast electron induced radical identification 79−24870
urea+acrylic acid (acrylamide), γ-irradiated reactions under high pressure *(Japanese)* 79−52707
uridine 5'-phosphate (Na salt), NO_2 species in an irrad. single crystal, EPR obs. 80−40719
uridine-5'-monophosphate gamma-irrad. solutions, short-lived radical detect. by spin-trapping method 77−21479
l-valine, cryst., electron damage, electron microscope study 78−22762
n-vinyl carbazole, radiation induced polymerization ESH study 80−7817
n-vinyl carbazole-acrylamide, post radiation induced polymerisation 80−7818
n-vinyl carbazole-acrylamide, radiation induced polymerization, monomer crystallinity effects 80−7819
vinylidene chloride, radn. induced emulsion polymerisation 79−74383
waste waters of paper manufacture, radiative purification, polymer prod. *(Russian)* 78−61035
zeolites, Y-type, EPR triplet assignment, NO_3^{2-} vs. H_2O^- 78−11534
$AgClO_3$, γ-irrad., ESR of O_3^-, ClO_2 and $(ClO_2\text{-}Cl)^-$ paramag. centres 77−9102
Ag(I) ions, in methyl cyanide, electron loss and capture, ESR spectra 79−33531
$AgNO_3$-KF in ice matrix, γ-irrad., Ag at., form., solution, ESR 77−59454
Al, electron irrad. induced aqueous corrosion 77−81343
Al, superpure, anodic oxide film growth kinetics, UV radiation effect 79−34190
AlH_3, effect of 1 MeV Co^{60} γ-irrad. on isothermal decomp. 78−92472
Ar, energetic electron degradation spectra and initial yields 80−95724
Ar, gas, electron thermalization time and position distribution meas. 80−93771
$BeHHe^+$, from BeHT β-decay potential energy curves 78−56910
$BeO\text{-}P_2O_5\text{-}RO(R_2O)$ (R=Li,Na,K,Mg,Ca,Sr,Ba) glasses, gamma irrad., cation modifier effect on radiation centre formation 80−40720
C-bearing gases, K-shell X-ray yields, proton-induced, chem. effects 80−37820
$CdO\text{-}Al_2O_3\text{-}P_2O_5$ glass, γ-irrad., EPR study 80−84639
2-chlorothiophene, σ^* anion radical, prod., ESR spectrum assignment 78−11539
Cl_2^-+HO_2, reaction in pulse irrad. aq. soln. containing Fe^{2+} and Cl^- 78−20036
$CoFeCN.xH_2O$, electron irrad., Mossbauer spectra 80−29652
$CsAsF_6$, γ-irrad., EPR spectra, hyperfine interactions and g-value determ. 77−81416
$CsAsF_6$:BiF_6^-, gamma irrad., BiF_6^{2-} prod., EPR meas. 78−19329
$CsSbF_6$, γ-irrad., EPR spectra, hyperfine interactions and g-value determ. 77−81416
$CuClO_4$, neutron activated, radiation annealing 80−93569
D, stabilised in low temp. frozen aqueous acidic solns., two-proton forbidden transitions, EPR meas. 78−27804
1,6-di-(N-carbazolyl)-2,4 hexadiin, cryst. struct., luminesc., γ-ray polymerisation 78−18629
$GaNbO_4$ decomp. due to electron beam heating in electron microscope 78−35711
$GaNbO_4$, electron beam induced decomp., high resolution lattice imaging obs. 78−6161
H_2, liberation from aqueous solns. irradiated in nuclear reactors 79−100416

radiation chemistry continued
H_2O, crystalline ice, localised excess electrons yield studied as function of dose rate 80−97712
H_2SO_4 glass, γ-irrad., trapped H ESR, vol. relax. effects 79−52703
H_2SO_4, glass, trapped H spin-lattice relax., modulation, saturation ESR 77−9095
^{125}I+methane, γ irrad. effects on organic iodide form. and decomp. *(Japanese)* 77−81418
KBr, NO_3^- centre form. by γ-bombardment in air *(Russian)* 78−31668
KCl, NO_3^- centre form. by γ-bombardment in air *(Russian)* 78−31668
$KClO_4$, ClO_3^- detection by EPR of ClO_3 radicals created by X-irrad. 78−76311
$KClO_4$, X-irrad., ESR spectra of O_3^- and ClO_3 exchange-coupled to O_2 78−64856
K_2CrO_4, ice, γ-irrad., electron trap depth, ESR 79−66317
$K_2Fe(CN)_6$ ice, γ-irrad., electron trap depth, ESR 79−66317
$K(H_{1-x}D_x)_2PO_4$, single cryst., 77K, γ-radiation damage centres, and EPR obs. 78−68379
KPF_6, γ-irrad., trapped free radicals EPR obs. 80−63683
Kr, gas, electron thermalization time and position distribution meas. 80−93771
^{85}Kr source, use for liq. phase radiation chem. 77−60091
$LiHe^+$, from LiT β-decay, pot. energy curves 78−56910
$Li_2O\text{-}Al_2O_3\text{-}SiO_2(P_2O_5)$:$Cd^+$ glasses, γ-irrad., EPR study 80−84639
$Li_2O\text{-}P_2O_5$:Cd^+ glass, γ-irrad., EPR study 80−84639
Mg, electron irrad. induced aqueous corrosion 77−81343
MgO, dissoc. under heat and electron bombardment 80−7834
MgO, irrad. effects, O_3^- ion form. 79−100431
MnO_2, oxidation under UV irradiation rel. to Viking gas exchange reaction on Mars 80−72831
Mo surface, H^- production by low energy H atom bombardment 79−100006
Mu+F_2→MuF+F, 300 to 400K in N_2 moderator, reaction rate determ., tunnelling 78−48682
N_2, radiation chem., primary neutral dissoc. excitation, isotopic exchange mechanism 78−48670
NH_3, liq., irradiated, solvated electron yield, partially diffusion-controlled ion recomb. 79−100409
NH_4ClO_4, γ-irrad., trapping and motion of NH_3^+ radical in cryst. lattice 79−33538
NO decomp. in industrial exhaust gases by electron beam irradiation 79−29490
NO, oxidation by electron beam irrad., appl. to exhaust gas treatment 78−80765
NO_2 decomposition by electron beam irradiation treatment of exhaust gases 79−79423
NO_2, reduction by electron beam irrad., appl. to exhaust gas treatment 78−80765
^{13}N species formed by proton irradiation of water 80−45532
Na (111) surface, epitaxial film, electron induced dissociation 80−6646
$Na_4Fe(CN)_6.10H_2O$, single cryst., X-irradiated product ESR, 4.2K 77−48659
$NaClO_3$, γ-irradiated, ESR of trapped O_3^- 79−29381
$NaClO_3$, X-irrad., thermal stability of radiation damage products 79−34324
$NaClO_3$:O_3^-, form. by γ-irrad., reson. Raman scatt., temp. depend. 78−92062
$NaClO_4$, aq. glass, formation of trapped H-atoms and electrons on X-irrad. 80−35559
$NaH_2PO_4\text{-}NH_4Cl\text{-}NiCl_2$, soln., Ni yield, factors affecting, pot. use as radiographic media 79−52702
$NaNO_3$, γ-irrad., electron trap depth, ESR 79−66317
$NaNO_3$, pure and Ca^{2+} doped, γ-irrad., damage species annealing 79−66324
$Na_2O\text{-}P_2O_5$, metaphosphate glass, active solute doped, absorpt. spectra of radiation products 78−64865
NaOH, electron tunnelling to NO_3^- scavenger sites 77−52655
NaOH ice, γ-irrad, ESR and absorpt. spectra of trapped electrons 79−66318
NaOH ice, γ-irrad., electron trap depth, ESR 79−66317
Nb film, ion bombardment with N_2^+, Ar^+, struct. changes, chemical compound formation *(Russian)* 78−95084
Ne, gas, electron thermalization time and position distribution meas. 80−93771
$NiClO_4$, neutron activated, radiation annealing 80−93569
O_2, dissoc. by field-accelerated electrons, macroscopic props., rel. to dry air 80−61118
O_2 radiobiological effect, molecular and cellular basis 80−26211
O_2^-, in nonpolar liqs., laser photodetachment, elec. cond. obs. 79−64057
O_2+hydrated electron, rate const., Arrhenius parameters 78−20041
O_2+muonium, aq. soln., reaction rate const., spin-conversion 79−100422
l-proline monohydrate single cryst., X-irrad., ESR and ENDOR study of radicals 80−45528
SF_6, breakdown at high pressure, possible cosmic ray effects 78−87577
SF_6, γ-irrad., SF_5 anisotropic ESR spectrum 77−21400
SF_3BF_4:SF_3, cryst., γ-irrad., radical form., EPR 78−91955
SO_2, oxidation in moist O_2-N_2 mixture by electron irrad., appl. to exhaust gas treatment 78−80766
Si+$XeF_2(F_2)(Cl_2)$ plasma etching, electron or ion bombardment, Ar^+ enhancement 79−82073
$SiCl_4^-$, γ-irrad. of $SiCl_4$ in adamantane matrix, ESR spectra 79−27011
SiF_4Cl_{4-n}, in γ-irradiated solid solution of tetramethysiline, EPR spectra obs. 80−80611
$SiF_3Cl^-(Br^-)(I^-)$ in γ-irradiated solid solution of tetramethysiline, EPR spectra obs. 80−80611
SiH_3X^-, X=Cl, Br, I, and isotopic forms, EPR spectra, mol. struct. 79−94023
Si_3N_4+$XeF_2(Cl_2)(F_2)$, plasma etching, electron or ion bombardment, Ar^+ enhancement 79−82073
SiO_2, fused, irrad., O_2^- radical defect centres, ESR obs. 79−61222
SiO_2, vitreous, H impregnated, γ radiation effects, hydride, hydroxyl formation 79−87874
SiO_2:H(D), γ-irrad., hydroxyls and hydrides form., detect. by Raman scatt. 77−32817
Ta film, ion bombardment with N_2^+, Ar^+, struct. changes, chemical compound formation *(Russian)* 78−95084
Ti film, ion bombardment with N_2^+, Ar^+, struct. changes, chemical compound formation *(Russian)* 78−95084
TiD_2, nucleation and growth in D_3^+ implanted Ti, TEM study 80−97717

radiation chemistry continued
V_2O_5, electron beam induced decomposition, appearance pot. spectroscopy 80−85203
W ribbon, with adsorbed CO, CO_2, or methane electron beam induced C deposition, AES obs. 77−89651
Xe, atom-diatom paradox, phenomenological description of spectroscopic props. 78−78766
Xe, gas, electron thermalization time and position distribution meas. 80−93771
ZnO_2 electron beam induced decomposition and desorption, AES and contact pot. difference meas. 78−79893

radiation counters *see counters*

radiation damage *see radiation effects*

radiation detection and measurement
see also alpha-particle detection and measurement; beta-ray detection and measurement; electron detection and measurement; gamma-ray detection and measurement; hyperon detection and measurement; meson detection and measurement; muon detection and measurement; neutrino detection and measurement; neutron detection and measurement; particle detectors; proton detection and measurement; radioactivity measurement
ΔE-E sample particle ddentification with wide dynamic range 80−14058
A/D converters, cyclic scale compensated 80−14039
acoustic detection of high energy particle showers in water 79−85862
acoustic noise production in polar medium, possible radiation detection method 80−63493
activated samples, simultaneous two-sample meas. immune to detector intercalibration 77−57835
air sampling system at HFEF/N 79−45441
angular correlation experiments, design and construction of stabilised variable temp. system 79−13614
angular distrib. meas. with positron sensitive detector 80−27899
apparatus spectrum decomposition, universal method 77−57800
avalanche parallel plate detector, appl. to photofission expts. 79−76263
average solid angle subtended by right circular cylinder from distrib. sources, Monte Carlo calc. 77−67950
beam time saving technique for measuring excitation functions in heavy ion reactions 78−70721
bi-dimensional drift chambers with flexible PC balanced delay lines 79−3300
bibliography (1972-76) *(German)* 80−95510
bubble chambers, elastic events separation, appl. to pp̄ interactions at 5.7 GeV/c 78−13379
calibration, appl. of monoenergetic standard X-ray sources 77−38078
calibration, mobile laboratory design 77−38582
calibration program using NPL secondary standard ionisation chamber dosimetry system 77−38584
calorimeter, double compensated, for absolute beam intensity meas., design, accuracy 77−6631
calorimeter, segmented, hadron shower struct. meas. 79−63870
calorimeter resolution effect on high P_T particle distribs. 79−59323
calorimetric measurements, method to distinguish between electromagnetic and hadronic showers 79−748
cellulose nitrate, proton, H_2^+ mol. ion, and heavy ion irrad., track prod., etching obs. 78−86757
channel electron multipliers, microchannel plates, props., development, appls. 78−46221
charge plunger technique, nuclear lifetime meas. 78−29698
charged hadrons, modular drift-chamber vertex detector at the CERN ISR 79−3302
charged particle counters in the pre-modern period, historical perspective 79−72190
charged particles, identification from nuclear reactions *(Rumanian)* 78−58564
charged particles prod. by neutrons, detection system 78−29712
charmed particles and short lived new particle obs. in bubble chamber 79−22543
Cherenkov, liquid differential counter, for proton and kaon, 2 to 9.5 GeV.c^{-1}, or kaon and pion, to 5 GeV.c^{-1}, separation 79−731
Cicoil personal RF radiation hazard detector, evaluation 80−5337
cloud chambers, factors affecting registration efficiency in low level activity counting *(Russian)* 80−27875
coincidence counting, improved correction formulae 78−70717
coincidence spectra from three particle reactions, projection on kinematical curve 77−10564
coincidence two-dimens. spectral data, offline treatment 79−97960
composite exponential decay curve anal. 78−46241
computer-based data acquisition system for multi-station teaching laboratory 78−4446
conference, meas. for safe use of radiation, Gaithersburg, USA (Mar. 1976) 77−40794
conference, radiation physics, Calcutta, India (30 Nov. to 4 Dec. 1974) 77−54128
contamination detectors assessment, w.r.t. German 1977 protective measures *(German)* 78−86693
cosmic ray anisotropy, COS approx. appl. to expt. data, computer simulation 77−5457
cosmic ray Fe group nuclei, detection in CR-39 plastic track detector 79−80154
cosmic ray high energy interactions in emulsion stack combined with ionisation calorimeter 78−49263
cosmic rays, electron-photon cascades in inhomogeneous absorbers 77−61669
cosmic rays, studies using gas Cherenkov counter with ionisation spectrometer 80−94662
counting statistics, with extended variable dead time *(French)* 77−57842
counting statistics with non-extended variable dead time *(French)* 77−30735
counting statistics with uniform dead time distrib. *(French)* 78−58560
dead time, corrections on long interval meas. of short lived activities 77−57836
dead time correction by the pulser method for single channel nuclear counting systems 79−13611
dead time correction for a counting rate measured with a system of buffer memories 78−86756
dead time correction of measurements using scaledown units 79−93892
dead time corrections in coincidence measurements by time-to-pulse-height converters or standard coincidence systems 80−9472
dead time effect on power spectral density estimates of discrete time series 79−18096

radiation detection and measurement continued
dead time effects, bibliography 77−37679
dead time meas., error risks in two oscillator method *(French)* 79−22567
dead time meas. in counting equipment, two-oscillator method *(French)* 78−50445
dead time meas. of individual detecting system 80−9470
dead time of detection systems, determination method *(Slovenian)* 80−47815
dead-time estimation method 79−6807
deadtime perturbed doubly stochastic Poisson counting system, information, error and imaging 79−22901
deconvolution of exptl. curves. Fourier series 77−54493
degree meter for radiation meas. 80−87024
delay line, cable, controllable microsecond, particle lifetime measurement appl. 77−18756
delayed coincidence expts., precision of half life estimation 80−27908
delayed coincidence method, spectra distortion of accidental coincidences in time meas. 78−86755
delayed coincidence spectra anal. without knowledge of resolution curve 79−22566
detection systems for intermediate energies 77−18750
detector, unconventional, data for X-rays, pions and protons 77−88341
detector systems for LEP 79−97952
detectors, effects of averaging within field of view on recording equipment 78−53098
deuteron beam polarimeter, ^{3}He(d,p) 80−47834
deuterons, secondary electron emission method, test of KCl layers 77−54475
digital data logger, microprocessor-based, for radiation detectors 79−26848
digital data processing using integer arithmetic 80−27917
digital radiation monitoring, plant-wide systems, design alternatives 79−41082
direct reading pen dosimeters, radiation exposure meas. aspects *(German)* 78−5050
dosimeter, aq. coumarin soln. response to high LET radiation from ^{10}B(,nα)^{7}Li reaction 78−24149
dosimetry, fluence of secondary photons generated by attenuation in thin walls 80−18699
dosimetry, primary standards for industrial radiation processing 80−5356
dosimetry, the computer as an active element 79−67961
dosimetry standardisation in Japan, review 80−5359
dosimetry standardisation in UK, review 80−5358
double filter system for Rn/Th measurements in environment and exhaled breath 80−57988
drift chamber, particle jet detection from e^+e^- reactions 79−3312
drift chamber, transition radiation detection 79−22546
drift chamber for multitrack particle identification 79−3276
drift chamber vertex detector for intersecting storage rings 79−3310
drift chambers, B-depend. of space-drift time relation and space resolution 79−3309
drift chambers, cylindrical, with two-dimensional read-out 79−3308
drift chambers with PC cathodes, design and props. 79−3303
drift tubes, quadratic and triangular, drift time and amplitude meas. 79−3314
Earth Radiation Budget Expt. solar constant obs. 79−58066
EAS Cherenkov radiation meas. by photomultiplier, cosmic ray induced noise 77−18735
effects meas., units selection 80−98870
efficiency calc. for extended flat sources 80−9469
electron, superheated superconducting suspension as transition radiation detector 77−6628
electron and energy fluxes meas., 5 to 50 MeV, Soviet primary standard 77−75031
electron beam, parameters meas. in adherer during compression via two-coil pickup 77−65393
electron beams, in-line energy monitoring by C and graphite monofilaments 77−61159
electron beams, meas. by beam-position pickup 77−65392
electron detection efficiency of compact high press. gas Cherenkov counter 77−6630
electron dose measurement, Zener diode dosimeter 77−50331
electronic measurement apparatus development at ATOMKI *(Hungarian)* 80−18768
electronics in nuclear science and technology 80−9347
electrons, secondary electron emission method, test of KCl layers 77−54475
electrons, thermally stimulated, elec. instrumentation for detection *(Spanish)* 77−32958
electrostatic sparks detection and characts., by radio methods 80−68217
EM non-ionising radiation standardisation 77−38013
emulsion plastic sandwich stack event, cosmic ray nucleus interpretation 78−69635
energy deposition measurement by thin film resistors 78−29719
energy irradiance from pulsed source, curve fitting problems 77−71377
energy-range relations for heavy protons and heavy quarks, use in detection 78−58566
environmental radioactivity, determ. for dose assess. 80−85321
fast electron collection ionisation chamber, principles of operation and appl. 79−68151
federal regulatory agency and radiation meas. system, US 77−37713
fission cross section meas. on short lived α-emitters using ionisation chamber 77−23380
fission fragment atomic number identification using gas ionisation chamber 80−27863
fission fragment position and nucl. charge identification in ionisation chamber telescopes 79−36478
fission fragments, kinetic energies and fly-off angles, ionisation method of meas., online numerical processing *(Russian)* 80−52838
fission fragments with high KE, mass separation based on TOF spectra 78−46209
fission track annealing characts. in crystals 79−26863
fission track visualisation, multi-detector electrochemical etching and automatic scanning system 79−26837
fission tracks, anisotropic track etching in olivine crystals using WN solution 79−26836
fission tracks, quantitative assessment of geometry factors 79−26860
fluctuating analogue quantities averaging device 79−68170
fringing field effects in a cylindrical condenser 80−52821
fuel reprocessing plant instrumentation for internat. safeguards 78−721

radiation detection and measurement continued
galactic neutrino sources, expt. neutrino astronomy, test of stellar evolution theories 77−70964
gamma spectrometry, secondary standard prep. 80−18701
gamma-flash suppressed solid state detector for fission fragments 79−26857
geometrical factors optimisation, symm. considerations, appl. to neutron and γ-ray polarimeters 77−54478
glass detectors, appl. to α-particle and fission fragment ranges in air 79−45597
glass dosemeter reader, design improvements *(French)* 80−57970
gravitation radiation detection, active resonant antennas, sensitivity and noise 79−30346
gravitational wave EM two level parametric detector 79−6041
hadronic cascades induced by high-energy muons in iron/plastic calorimeters, calibration calcs. 77−54477
hadronic transmission through Fe absorbers, 0.8 to 100 GeV calcs. 78−90041
heavy ion deep inelastic processes fragments, element identification in ΔE-E telescope, computerised method 77−57839
heavy ion identification, using modified Zaidins empirical range-energy relationship, power law type algorithm anal. 77−57838
heavy ion physics, expt. methods for radiation detection and meas., review *(Russian)* 79−49900
heavy ion track lengths in solid dielectric track detectors 79−59319
heavy leptons in cosmic radiation underground, search using scintillation+Cherenkov detectors 78−65470
heavy particle high-energy beam calib. with plastic track detectors 77−79525
heavy-ion timing with channel plates 77−14305
heliometric station operating data 79−58069
heterodyning of elementary particles, radiation meas. method 80−42898
high energy physics, appl. of solid state nuclear track detector, emulsion technique 78−17501
high power lamp, meter features *(Polish)* 79−26130
historical development of need for radiation protection and meas. in USA 77−37708
historical perspective of early detectors and counters 79−72189
human internal radiation counting, Los Alamos multiple simultaneous system 80−61709
hybrid focal plane detectors for heavy ions 79−68163
Incoloy 800, contamination and decontamination of samples from KFA experimental duct of DRAGON reactor 79−45600
infralow frequency signals, apparatus for running dose and mean value meas. 79−83936
instrumental variations during continuous detection of nucleons and ionising components 77−14323
internal contamination monitoring in GDR 80−67259
international radiation standards, role of ICRU 80−9414
international standard reference radiations and their application to the type testing of dosimetric apparatus 80−9416
ion, multiple scatt. effects on coincidence yield, inner shell ionisation probability meas. 79−31670
ion beam scanning device for rapid meas. of emittance and brightness 78−58522
ion beams, position location and profile measuring system for ion accelerators *(Croatian)* 77−75025
ion identification with detector telescopes 79−72180
ionisation chamber dose meter unit for emergency operations *(French)* 80−57977
ionising gases, meas. of m-values 80−18694
ionising particle beam interactions with liquids, acoustic effect, laser beam simulations 80−23262
ionising radiation, detection device, electret based *(French)* 80−57971
ionising radiation, metrology and calibration, French system *(French)* 80−5351
ionising radiation, primary standards and transfer methods in France, review *(French)* 80−5352
ionising radiation, traceability in meas. systems 80−5355
ionising radiation, USA national standards 77−38588
ionising radiation meas. system and standards lab., US 77−38581
ionising radiation metrological work automation 77−75033
ionographic detectors, identification of nuclear reactions, computation 77−3243
isotope conveyor weigher, errors caused by profile variations and shift of material 77−67933
jet bias effect due to small detector size 79−22562
jet structure events at LEP energy, detector system 79−97953
laboratory course at Purdue University 78−4443
large-area gas-scintillation proportional counters for in-vivo measurement of plutonium and americium 80−58086
legislation in West Germany, standards aspects *(German)* 78−5049
Lexan spectrometry, relativistic projectile fragments, imaging and identification 80−63442
light distribs. within light diffusion boxes, algorithm 79−49908
limiting accuracies in multiwire proportional and drift chambers 79−3298
linear radiation-flux functionals, estimation of local perturbations using Monte Carlo method 80−5457
liquid ionisation detectors, design, perf. and appl. 79−68152
liquid scintillation techniques, appl. in low level activity assessment 80−58082
long lived heavy particles with fractional charge, evidence in cosmic ray events 79−2447
loss-free counting, real time compensation of dead time and pile-up losses 78−17465
low-count radiation spectra, LSF processing 78−50448
low-energy recoil meas. in high-energy physics, review 77−38593
magnetic quadrupole and solenoidal spectrometers, optical props. and experimental techniques 79−68127
magnetic spectrographs for nuclear reaction studies, resolving power, kinematic broadening 79−68126
medical detectors, Ge rel. to Na(Tl), imaging efficiency and scatter rejection 79−83915
medical dosimetry standards programme of the National Bureau of Standards, USA, review 80−8187
medical facilities, US state and federal regulatory meas. responsibilities 77−40765
microphotometer, MF-2 type, scatt. light effects on optical densities of electron-photon cascade tracks 77−61655
minimum detectable activity concept 77−38586
radiation detection and measurement continued
mixed radiations, device for dose-equivalent index determ. *(Russian)* 80−57976
modern atomic and nuclear physics (book) 80−11
monitoring system, counting strategy 78−50444
Monte Carlo method for the analysis of low statistics experiments 79−18095
Monte Carlo study of the scanning problem with a visibility distribution 79−49915
Muller statistics for counting systems for non-extending dead time, exptl. test 78−94173
multichannel plate, detectors, operation, struct., performance charact. 78−12758
multichannel scattering chamber for polarisation anal., adapter for securing detectors 77−6654
multichannel spectra, discrimination of counting fluctuations 79−36494
multidetector technique readings, interpetation for dose equivalent determ. 79−49875
multigap proportional wire chamber system for multiparticle spectrometer 79−3271
multiplicity measurements, statistical algorithm 78−29721
multiwire drift chambers, left/right ambiguity and double track resolution 79−3307
multiwire proportional quantameters, performance predictions by Monte Carlo methods 79−3294
MWPC, heavy ion timing at very low pressure 79−93884
MWPC, localisation of minimum ionising particles using cathode induced charge centre of gravity readout 80−32576
MWPC appl. as focal plane detection system for mag. spectrograph 79−3295
MWPC for beam definition in precision total cross section meas. 79−3268
MWPC in synchrotron beam spectrometer, performance under very high fluxes 79−3272
MWPC rotated, drift time relations and their advantages 79−3306
MWPC with cathode read-out for separation of EM and hadronic showers 79−3273
neutrino detection, high-energy, using acoustic pulse from hadron shower *(Russian)* 77−38580
neutron collimated fast beam, radiation quality local distrib. 80−12247
neutron induced charged particle reactions, experimental techniques, applications 77−23031
non-polar liquids, elec. charges, appl. to high energy radiation detectors 80−20217
nuclear counting, method to reduce cosmic background 80−897
nuclear emulsion tracks, detection and meas. by inexpensive microscope television 79−3290
nuclear emulsion type BA-2, pulsed electric field effect on cosmic ray detection 79−26829
nuclear gauge, with digital response, statistical method for stability testing *(Rumanian)* 80−9459
nuclear lifetime meas., plunger device piezoelec. fine adjustment and PLL distance regulation 79−6806
nuclear medicine and metrology of ionising radiations *(French)* 80−17057
nuclear NDT methods, sensitivities and detection limits 77−32756
nuclear power plant containment buildings, integrated leak rate testing *(Spanish)* 79−54518
nuclear radiation characteristics, mathematical programming methods to obtain internal estimates 78−5105
nuclear radiation detection lab., desk top calculators 80−36821
nuclear reaction thresholds and half-life meas., computer controlled system 78−55114
nuclear resonances prod. in (γ,π^-p) reacts. 78−877
nuclear spectrometry, detector signal and noise parallel meas. 77−61667
optimum design of expts. on exponential absorpt. statistical errors anal. 78−885
optimum resolution by matching beam handling and detection systems 79−45494
paralyzable event counters, method for partial recovery of lost events 79−18094
particle identification statistics using ionisation 79−36491
particle identification systems including magnetic analysis, review 79−72181
particle motion through matter, fluctuations in cascade processes 80−5456
particle passage through medium, cascade process fluctuation 80−18769
particle tracks, search statistics, Monte Carlo study of random scatt. problem 78−58561
peak-detection probability for line spectra, stochastic model 78−78597
personal monitor for uranium and thorium in uranium mine dust 80−52792
phase sensitive amplifiers, appl. to interference suppression and light detection *(Czech)* 78−86331
photocounting distributions statistical props. for intensity modulated sources 79−72541
photographic film detectors, γ-exposure efficiency, focal distance depend. *(Czech)* 79−89518
photomultiplier tube instability, consequences for radioactivity meas. accuracy 79−76272
photons, 6-7 MeV, exposure rate and absorbed dose meas. 79−26766
photonuclear reaction N-fold coincidences, on-line acquisition 77−79527
photonuclear yield function anal. by modified least struct. method 77−79521
pictorial drift chambers, recent developments and particle identification 79−3307
plastic detectors, appl. to α-particle and fission fragment ranges in air 79−45597
plastic detectors, calib., heavy cosmic ray charge distrib. 78−17500
plastic detectors, meas. of high-linear-energy transfer particles on Apollo, Skylab and ASTP space missions 77−41272
plastic film detectors for light and heavy element fission studies 79−72193
plastic flash chambers, particle identification 79−59301
plastic scintillation counter response to relativistic heavy ions 79−36473
pocket radiation chirper, CdTe crystal and electronics 79−68165
polarisation meas., set of efficient estimators 80−27909
polished metal sphere and microaccelerometer, for absolute meas. of Earth's radiation balance *(French)* 79−29900
polycarbonate foils, detection of low energy ^{4}He, ^{12}C, ^{14}N, ^{16}O ions, etching props. 78−13391

radiation detection and measurement continued
position sensitive detectors, pseudostructures in spectra caused by digital data acquisition 79−76320
position sensitive proportional tube with helical delay line 79−3313
positron annihilation detectors ring, wobbling mathematics 79−63867
power spectral density and coherence functions, leakage and reduction, resolution increase 79−18097
precision integral linearity measurement instruments for nuclear spectroscopy 77−67951
projected proton method for heavy ion energy meas., device for 3-6 MeV beams *(French)* 78−82567
proportional counter, pulse shape discrimination technique *(Chinese)* 79−93867
proton beams in NAP-M storage ring, accelerating system and parameters monitoring 77−65364
proton spectrometer/polarimeter for photoreactions below 1 GeV 80−18751
pulse height analysis programs for high event rates, organisation 77−407
pulse height on-line gain stabilisation 78−74551
pulse height spectral distortion due to peak pile-up, calc. of true spectra from observed spectra 77−14327
pulse height spectral distortion for double sum pulses of arbitrary shape 77−14326
pulse meas. systems, relative variance of distrib. function of events 79−63880
pulse meas. systems, self checking of count losses 79−63879
pulse meas. systems, self checking technique based on waiting file theory 79−36492
pulse pile-up, role of waveform 77−88358
pulse pile-up in detection systems with rapidly varying counting rates 77−88359
pulse sequence fast A/D conversion 78−55119
pulse shaper, fast coincidence, with Ge(Li) detectors 78−41864
pulse spectroscopy, loss free counting performance 79−76312
pulsed laser radiation beams, energy flux density meas. based on thin-film thermometry 79−81472
pulses time positions, meas. methods review 77−65410
pyroelectric detector, 40-1100 nm range 77−87834
radiation absorption measuring instrument characts. evaluation with reference to information theory *(German)* 78−86753
radiation calorimetry of single electron pulses from a LINAC 80−42872
radiative decay curve anal., computer applications *(Hungarian)* 79−45617
radioactive element conc. from γ-ray intensity meas., numerical method 79−18059
radioisotope direct detection using accelerators 80−63468
radioisotope identification by coincidence methods *(German)* 78−90038
radioisotope transport in terrestrial food chains, dynamic modelling using RAGTIME code 80−104776
radionuclide concentration determ. in ground level air 79−24927
radionuclide distribution, selective determ., mathematical modelling *(Rumanian)* 79−81098
radionuclides in reactor circuits, continuous meas. techniques *(French)* 79−97857
radiophotoluminescence detector reading device, glasses for fluoresc. standards 77−67944
radiotherapy quality control recommendations 77−40778
random search algorithm for 2-D data fitting 80−27915
random summing in multi-detector counting system meas. radionuclide mixtures 80−36097
ratemeters, with variable time const., error determ. 80−95507
reactor core radiation transport code, comparison of electron transport models 80−23030
recoil distance lifetimes, comprehensive anal. formalism, computer code 77−6653
recoil products of high-energy nuclear reactions ang. distrib. meas., geometry calcs. 77−6596
resistive unidimensional detectors employing rise time readout method, position resolution and linearity 80−14048
review of 30 years work by Nuclear Reactions Lab. Dubna, USSR 79−36204
review of the evolution and use ot nuclear detectors and systems 79−72188
RF radiation, pulsed, recording during heating of periclase and glass *(Russian)* 77−55837
ring point detector, Monte Carlo flux-at-a-point estimates for axisymmetric problems 79−59282
rocket engine plume radiation, measurements in space simulation chamber 79−97437
scattering expts., estimation of asymmetries from incomplete azimuthal angular distributions 79−81142
secondary particle beams from accelerators, average momentum and comp. meas. 77−65382
secondary particles from high energy reactions, detection losses correction by generator functional technique 77−6650
secondary radiation excited in air, using ionisation chamber *(Czech)* 79−67967
semiconductor detectors, spectroscopy and applied phys. appls. 78−46218
semiconductor detectors, use in high energy physics *(Russian)* 77−50325
semiconductor detectors for charged particles and γ-rays, principles of operation and appl. 79−68154
semiconductor detectors of nuclear radiation, effect of trapping on response 80−5447
semiconductor radiation detector, development 79−68153
shape analysis of fast pulses out of a broad pulse height spectrum 78−70710
shielding experiments, cross section adjustment procedures 79−31345
short lived particle decay detection in nuclear track emulsion 79−97947
SI units in radiochem. and radiology 78−81939
simultaneously-produced scintillation and Cherenkov radiation separation method 79−93893
small angle scattering, axially symmetric geometry, main features 80−52836
solar irradiance meas. using optical fibres and Si detectors 79−100960
solar neutrino radiochemical detectors, cosmic ray muon induced proton background effects 77−61650
solar neutrinos, proposed Earth flux determ. by mass spectrometry of ^{205}Pb in Tl minerals 77−5447
solar radiation and wind power measuring instrument design 79−57404
solid angle integrals for rad. detectors, Monte Carlo solns. 80−9468
radiation detection and measurement continued
spatial noise reduction in detector arrays, controlled lateral shifts 80−53436
spectra unfolding code COOLC 78−5090
spontaneous fission fragment detection in on-line system of ionisation chambers 78−46226
spontaneous fission low background detection system 79−36475
standardisation in nuclear radiation meas. technology with SINUPERM system 78−50410
state responsibilities and radiation meas. system, US 77−37714
statistical evaluation and measuring strategy for extremely small line shifts 78−86234
statistical theory of asymmetry detection 79−26853
statistics of counting equipment, choosing goodness-of-fit test 78−46238
submillimetre wavelengths, techniques and devices for the detect. and sensing of radiation 78−93759
superconducting double multivibrator used as near- and medium-infrared radiation detector *(German)* 80−90892
superheavy primary cosmic ray nuclei, obs. with solid-state track detectors and X-ray films *(Japanese)* 78−61688
surface barrier detector, pulse height response to mass and energy separated fission fragments 77−57812
surface barrier detectors, pulse height defect and window energy loss of low energy ions 78−74541
tandem accelerators and nuclear phys. conf. 78−13349
tensor polarimeter using ^{3}He(d,p)^{4}He at 430 keV 77−3242
thermal defect in materials determ., using total-absorption calorimeters 80−99427
thermally stimulated luminescence application, radiation dosimetry, book contribution 80−80882
thermoluminescent dosemeter service in United Kingdom 79−59268
thick target meas. technique for reaction rate determ. 77−23392
thick-target thick catcher nucl. recoil expts., anal. 78−55115
thickness measurement by backscattered radiation 80−47829
threshold detection equivalence with and without dead time 80−32580
time of flight detectors for heavy ions, review 79−72178
TLD-04B reader, meas. of TL materials for health phys. appls. *(Russian)* 77−86648
track shape of normally incident particles, use of microtome cuts in SSNT detectors 79−26862
track structure theory in radiobiology and radiation detection 78−50446
transceiver, inexpensive, use in cosmic ray time coincidence expts. with long baselines 80−52837
transition-radiation energy distribution comparison with expt. data 79−63397
triple scanning search statistics 78−94172
two-phase fluid velocity meas. by radiation intensity correlation 77−75996
undisturbed meas., Monte Carlo study of rejection of outliers on estimated mean value and standard deviation 79−26856
US power meas. with radiation balance 79−83863
use of gridded ionisation chamber for measuring fission fragment angle 79−85865
UV radiation meas. in agricultural production, instrument *(Russian)* 78−65969
variable sampling-time technique for improving count rate performance of scintillation detectors 79−22565
velocity filter SHIP, a separator of unslowed heavy ion fusion products 79−49893
Voyager Cosmic Ray Experiment, telescopes, electron energy meas., pulse height analysers 79−48643
whole body counters, international intercomparison 80−78504
width of Lorentzian convoluted with Gaussian 77−79528
wire chamber conf., Vienna, Austria, 1978 79−3291
wrist watch dosemeter for ionising radiations, practicality tests 80−57972
X-ray recording focusing spectrograph for laser plasma 78−1891
α-γ angular correlation in ^{18}O(t,αγ) using Plurimat 20 data acquisition system *(French)* 77−41579
Al, electron spatial absorbed-dose distrib. for 25 MeV beam 77−88289
Ar, liquid, scintillation decay due to α-particles and electrons 78−55099
Ar liquid calorimeter with very thin sampling 77−34518
C, electron spatial absorbed-dose distrib. for 25 MeV beam 77−88289
^{60}Co radiation therapy, eval. of dosimetric accuracy and uniformity 80−12269
Fe calorimeter, hadronic cascade curves between 20 and 8000 GeV 80−36464
Ge detector, charge collection characteristics, influence on timing performance 80−47820
Ge detector system for inhaled radionuclide detection and meas. 80−57990
H isotopes, transition radiation from neutral beams, beam foil ionization 79−18299
H_2O, electron spatial absorbed-dose distrib. for 25 MeV beam 77−88289
^{3}H, absolute efficiency of phosphate glass channel electron multiplier 77−67945
^{3}H contamination monitoring using centralized control *(French)* 80−63407
He backscattered ions, electrostatic anal., electronic reduction of charge state energy doublets 80−27870
He beam, magnetic spectrom. meas. using automatic tracking NMR system 80−27869
He jet system for radioactivity studies 79−93855
^{131}I thyroid activity meas., improvement in precision 79−29635
LiF dosimeter, radiothermoluminescence dosimetry of 10 MeV electrons *(Italian)* 77−81582
LiF, TLD for low dose meas. 79−13538
^{7}Li(γ,t)^{4}He, N-fold coincidences, on-line acquisition 77−79527
Nb, supercond. point contacts, freq. and voltage depend. in noise background 79−58796
^{32}P-Cherenkov radiation, counting efficiency improvement, wavelength-shifting compounds investigation 80−90893
Pu accountability, nondestructive assay using neutron counting, calorimetry and gamma spectrometry 80−63266
Pu, accountability and control, field nondestructive assay measurements as applied to process inventories 80−63265
Pu detectors in activation anal., reading method 79−93896
Pu nondestructive assay meas. using NaI(Tl) detectors during fabrication plant decommissioning 80−63495
^{226}Ra, determ. of tap water pollution *(Czech)* 79−34675

radiation detection and measurement continued
Rn and daughters meas. methods in underground and free atmosphere air 80−57987
Rn, long term average level meas. instrument 80−58085
^{222}Rn, atmospheric, two-filter continuous monitor 80−58097
^{222}Rn, conc. in air, absolute determ. using cellulose nitrate track detector 80−63492
Si microcalorimeter dosimetry system for transient radiation effects, radiation induced temp. rise meas. 77−26885
Si surface barrier detectors, direct meas. of plasma delays due to fission fragments and α-particles 78−58546
Si surface barrier detectors, meas. of plasma delay differences due to ^{252}Cf fission fragments and α-particles 78−58547
Si surface barrier detector, fission fragment pulse height defect 79−76292
Si surface-barrier detector in lava or teflon housing, production 78−17481
T monitoring using scintillation chamber 79−89519
^{235}U decay heat meas. and calcs., review 80−13732
^{238}U, 1.4 MeV/amu, position and pulse height resolution, and pulse height study for gas-scintillation drift chamber 78−86730
W scintillator ionisation spectrometer, meas. of cascades initiated by 5 to 300 GeV hadrons 77−34526
^{186}W(^{12}C,^{16}C) ^{184}W, reaction mechanisms, use of accelerators and detection methods *(Norwegian)* 79−13316
Xe probe for contamination monitoring 80−27826
^{136}Xe, 1.4 MeV/amu, position and pulse height resolution, and pulse height study for gas-scintillation drift chamber 78−86730

radiation detectors *see particle detectors*

radiation dosimetry *see dosimetry*

radiation effects
see also acoustic wave effects; alpha-particle effects; beta-ray effects; biological effects of radiation; deuteron effects; electron beam effects; gamma-ray effects; hyperon effects; ion beam effects; laser beam effects; meson effects; neutron effects; proton effects; radiation chemistry; radiation hardening; voids (solid); X-ray effects
A15 compounds, disordered, reordering kinetics 80−96678
A-15 compounds, radiation damaged, supercond. crit. temp. 78−76185
acrylic scintillator and wavelength shifter material, radiation induced degradation 80−5442
actinide carbides, lattice defects and rel. to phys. props., review 77−27874
alkali halide, crystal, irradiation-induced defects 80−107316
alkali halide, Frenkel defect pairs formation mechanism *(Russian)* 80−10542
alkali halide, irrad., colloidal centre growth, model 77−19946
alkali halide, irradiated crystal, recombination of radiation defects *(Russian)* 80−39151
alkali halide crystal, irrad., chemiluminesc. process during dissolution *(Russian)* 78−92133
alkali halide crystals, radiation damage review, impurities and colour centers *(German)* 78−10086
alkali halides, defect form., model of excitonic mechanism 78−38696
alkali halides, defect formation, kinetics 78−67713
alkali halides, divalent cation doped, irradiated, first-stage F-centre prod. 80−107231
alkali halides, F-centre accumulation, radiation induced, temp. depend. 80−59460
alkali halides, interstitial motion during radiation damage and sputtering processes 80−54230
alkaline earth phosphate (MO-Al_2O_3-P_2O_5) irradiated electret glasses, relax. of external field intensity on heating 80−25282
alloys, clustering and ordering, radiation induced atomic rearrangements, conf. Atlanta, GA, USA (March 1977) 79−42099
alloys, conc., theory of radiation-induced segregation 79−77633
alloys, irradiated, effect of defect trapping and solute segregation, on defect recombination rates and void swelling 78−47369
alloys, radiation effects on ageing and precipitation, review 80−29956
aluminophosphate glass:Mn:Mg(Sr), optical props. H_2O effects 77−28600
amorphous metals, computer simulations of tensile deformation and radiation damage *(Japanese)* 79−42137
anthracene, cryst., radiation induced radicals, optical absorpt. bands, SCF-CI MO calc. 79−91463
atom-atom collision cascades localisation, impurity and thermal vibr. influence, computer simulation method 80−88227
ATS-6 solar cell flight expt., radiation damage, summary results 80−94005
beryl, channel constituents, electronic absorption spectra of Fe^{2+} 79−69863
biomaterials, radiation processing appls. to biomedical engineering 77−70542
birefringent samples, use of photoelastic modulator in radiation damage meas. 78−87724
blistering, interpreatation based on radiation stimulated vacancy migration 80−49265
Boltzmann transport eqn., role in radiation damage calcs. 79−77653
BWR radioactive corrosion products behaviour 78−21661
cables, mineral insulated, radiation induced currents 80−65037
cascades, validity of energy partitioning 78−43056
cellulose, fibres, membranes and composites, polystyrene used for modification of props. 78−95727
ceramics, TEM study of radiation damage, review 79−86816
chalcogenide amorphous semiconductors, ESR studies of doped Mn, review *(Japanese)* 77−90019
channelling backscattering use for radiation damage studies, review *(Japanese)* 77−72640
channeltrons and channel plates, influence of radiations, review 77−26933
characterisation by DPA function 78−87708
coatings for nuclear fuel particles, irradiation performance, additives effects *(German)* 80−27748
collector diffusion isolation bipolar technology, assessment of radiation tolerance 79−45430
collision cascades, fast charged particle bombard., of solid. defect prod. *(Russian)* 77−89492
collision cascades initiated by fast charged particles *(Russian)* 77−80561
coloration and bleaching of Schott optical glasses temp., time depend. 77−19981

radiation effects continued
computer experiments and their applications *(Polish)* 78−89420
conf., nucl. and space radiation effects, Williamsburg, USA (July, 1977) 78−26594
conference, atomic collisions in solids, Hamilton, Canada (Aug. 1979) 80−62375
conference, nuclear and space radiation effects, San Diego, Calif., USA (July 1976) 77−20376
conference on fusion reactor materials [Miami Beach, Florida, Jan. 1979] 80−31407
cosmic dust, radiation effects rel. to diffuse interstellar bands origin 77−13432
creep testing, extensometric method, for inside nuclear reactor channels 80−100998
crystal, subjected to high-energy, particle flux, point defects, change in mobility 79−7708
crystal lattice, beam instability and collective disturbance *(Russian)* 77−8676
crystalline solids, defect cluster nucleation 79−42051
crystals, computer modelling methods of radiation damage 77−7760
CTR first wall materials, irradiation effects 77−6561
CTR first-wall materials, ionisation-assisted damage processes 77−34432
current physics status in USSR 79−95049
1,1-cyclobutanedicarboxylic acid, X- and γ-irrad. cryst., EI-EPR overlapping spectra resolution 77−16179
damage cascades, stochastic theory of particle transport 80−54291
damage energy functions for compounds and alloys 78−86692
defect clusters, in particle-irradiated crysts., TEM identification 79−69108
defect clusters, nucleation and growth due to energetic particle radiation, chemical rate reaction theory, computer program 80−49263
defect processes, theory, rate eqns., chemical rules 80−33990
defect prod. and annealing, radiation-induced, computer expts. 78−87710
defect production, exact solns. of models for continuous and pulsed irrad., implications for stability and fluctuations 80−65041
defect superlattices, hardening influence, computer simulation *(Russian)* 79−83206
defect theory and processes, review 80−2009
defects, X-ray diffraction study, review *(Japanese)* 80−15152
defects and surfaces in bulk metallic, covalent and ionic systems, review 80−34049
deformation due to stress induced perferred adsorption induced dislocation anisotropy 80−75265
desorption fission fragment induced, method for correlated events in TOF mass spectrometry 78−58089
diamond, defects and impurities 80−29017
diamond, dynamic Jahn-Teller distortions at trigonal optical centres 79−87069
diamond, irradiated, optical spectrum 78−6719
diatomic materials, displacement function calc. 80−34047
dielectric, radiation induced currents and cond. 78−30927
diffusion processes, distrib. functions of point defects and moving gas filled holes 77−55302
diffusional mass transport, irrad. enhanced 79−14844
dislocation climb, in modulated structs. under irradiation conditions 80−70195
dislocation loops, elastic fields near stress-free surface, loop-point defect interaction 79−4301
displacement damage, analytical calc. 80−70250
dissociative diffusion, radiation-stimulated, model 79−23785
doped semiconductor, radiation defect, form. mechanism associated with electron transitions 79−69155
dose rate dependent effects of total ionising dose irradiation, annealing 80−70249
Earth mantle materials, radioactivity rel. to vacancies creation and creep rate 79−92520
education, undergraduate course evaluation on radiation and the environment 78−1
elastometer materials, selection for vacuum seals 80−77797
electrets, radiation-induced charge storage and polarisation effects 80−80684
electrometer operation in ionizing photon radiation fields by compensation method 77−79110
electron beam radiation processing on commercial scale 77−73281
electronic components, space radiation environment effects, laboratory simulation 80−94689
elemental semiconductors, group IV, Mossbauer spectroscopy of defects, radiation damage and deep levels 80−59533
energetic heavy particles, radiation damage, cascade formation *(Japanese)* 80−29094
enhanced diffusion mechanisms, review 78−67847
evaporation of drop, in EM field, theory 79−72787
fast negatively charged particles, resonance scatt. phenomena in single cryst. 80−65047
FBR carbide fuels, comparative irradiation tests of pellet and sphere-pac fuels 80−643
FBR fuel element structural materials, consequences of improved behaviour under irradiation 80−640
FCC crystal, interstitial and solute concentration gradients, flux expression derivation *(French)* 80−54219
FCC lattice, computer simulation of low energy displacement cascade 78−47367
Fermilab energy doubler/saver mag., radiation damage limitations 77−83238
fibre optics data link, radiation testing, degradation, transient outage time performance 77−19405
first wall of thermonuclear reactor, diffusive action of radiation *(Russian)* 78−29639
fission reactor materials, ion penetration distance calculations with multigroup transport computer codes 80−102246
fission reactor oxide fuel, irradiated, physical processes *(Japanese)* 80−27742
forward and backward Boltzmann eqns., use in radiation damage calcs. 79−17360
Frenkel pairs, unstable, mechanism for radiation stimulated processes in solids 80−34050
fusion and fast breeder reactors, a comparison, book 78−78430
fusion materials development, appl. of simulation expts. 78−46167
fusion reactor design, nuclear data requirements 77−23291
fusion reactor first wall, radiation damage simulation using fission reactor test facilities 80−57950

radiation effects continued
fusion reactor first walls, temp. and displacement transients 78−58427
fusion reactor first-wall performance under ion bombardment and cyclic stresses, in-reactor materials testing 80−104407
fusion reactor materials, appl. of dynamical computer models to high energy cascades 80−34046
fusion reactor materials, ion implantation for radiation damage studies 77−80530
fusion reactor materials, microstructure evolution under irradiation 80−34041
fusion reactor materials, radiation damage simulation using triple ion beams 79−45410
fusion reactor materials, range calculations using multigroup transport methods 80−34070
fusion reactor materials, surface erosion, review 77−57741
fusion reactor structural materials, accident-related dose rate calc. 80−95411
fusion reactor wall problem, reactor modular set up *(German)* 78−54879
fusion reactor wall radiation blistering, material distortion *(Russian)* 77−76160
fusion reactors, inertial confinement, first walls, void growth, analytical model 80−63377
fusion reactors, inertial confinement, interstitial loop formation, point defect clustering 80−63378
gas bubbles in solids, simultaneous hetero- and homogeneous nucleation model 80−2066
gas implantation and deposition rate, simultaneous irradiation, injection expts. 78−83855
gas-filled microballoons, radiation effects MEDUSA code calcs. 80−83220
GCFR pressure-equalised fuel irradiation program 80−648
glass, inorganic, radiation stability origin *(Russian)* 77−55300
glass, light effects, history of development of photosensitive and polychromatic glasses 80−40080
glass track detectors, NaO_2-SiO_2, phosphate, quartz glasses, nuclear phys. spectrometric appls., track diameter 78−17466
glass-clad optical waveguides, ionizing radiation effects, temp. depend. 79−18519
graphite, fusion reactor applications, mechanical constitutive laws for irradiation behaviour 80−32448
graphite, irrad., lattice expansion, vacancies and interstitials contrib., bond order role 80−65042
graphite, irradiated, thermal conductivity at elevated temps. by calc. 79−28163
graphite, radiation damage and its relevance to reactor design 79−33016
graphite, radiational size stability, effect of technological factors 79−26527
growth of point defect aggregates during irradiation, model 77−89468
H′ colour centre, radiation-tunnel decay 80−103327
high-level liquid waste, damage to organic extractant in positioning process 80−9345
high-silica fibre-optic waveguide, sensitivity to low-dose radiation *(German)* 78−33869
IC, junction isolated, ionising radiation performance, black box modelling 77−83467
ICF reactor, first wall protection schemes 80−32437
ICTR walls, thermal response and stress problems 78−813
II-VI semiconductors, radiation effects, optoelectric props. control 80−25458
impure solids, pulsed irrad., point defect generation 77−1150
Incoloy 800, from KFA experimental duct at 700°C and 480 d in DRAGON reactor, mech. props. before and after contamination 79−47777
infrared multiphoton processes, apparent step cross-sections, pulse spatial structure, irradiation techniques 80−32792
inorganic solids, high energy irradiation, energy storage meas. 78−51581
insulator, radiation induced cond., analytic solns. 77−80781
insulators, transient ionisation effects 77−80788
interaction with matter, review and bibliography *(Japanese)* 80−39149
interstitial and vacancy dislocation loops, diffusion growth in supersaturated soln. of point defects 77−68974
interstitial cluster nucleation at the onset of irradiation 78−79635
interstitial loop finite, modelling of growth under irrad. 79−23607
ionic crystalline materials, radiational stability *(Russian)* 77−80539
ionic crystals, defects, computer modelling, review 80−107205
ionic crystals, electronic excitation decay into radiation defects, review 78−47420
ionic crystals, influence of defect interaction upon their recomb. 80−84206
ionic crystals, lattice defects, conference, Canterbury, England (Sept. 1979) 80−105420
ionic crystals, radiation defect accumulation temp. depend. 80−19803
ionic crystals, spatial separation of components of primary radiation defect pairs 78−14376
ionisation damage monitoring, by means of 80 keV electron scatt. 77−4127
ionizing radiation and cavitation threshold 78−94774
irradiated metal, elec. cond. tensor calcs. 79−87079
irradiation growth, contrib. of grain shape to anisotropy 80−92556
irradiation induced crystalline to amorphous transition, Gibbs energy 80−70371
irradiation induced precipitation, thermodynamic approach 79−78975
irradiation-induced swelling, and creep, effects of pt. defect trapping and solute segregation 79−79040
Kapron fibres, elongation and tensile strength rel. to UV irradiation 80−25796
Kevlar 49, fibre, mech. props., environmental effects incl. sunlight, ionising rad. 77−36560
laser mirrors cooled by open pore structures, radiation damage 79−72603
latent photographic images, effect of longwave radiation *(Russian)* 77−49801
latex films, surface struct., vulcanisation, radiothermoluminesc. obs., 100-230K 78−75575
lattice atom displacements near end of implanted μ^+ tracks 78−55890
Lexan polycarbonate, thermolum. radiation-induced EPR of free radicals and track etchability 79−76295
light influence on thermoluminescent BeO and other TL-phosphors 79−76293
radiation effects continued
LMFBR claddings with axial fins, stress anal. including creep effects 77−88224
LMFBR materials, interstitial loop nucleation and growth during irradiation, Fokker-Planck equation, numerical soln. 80−57857
LMFBR materials, interstitial loop nucleation and growth during irradiation, Fokker-Planck equation, numerical soln. 80−68796
LMFBR MX-type highly rated advanced fuels, fission gas release and correl. with fuel restructuring 80−642
LMFBR performance, effects of irradiation creep and swelling 78−78482
LMFBR reactor materials, simulation of void swelling and radiation-induced creep 78−8907
low dose, void incubation, rate theory approach 79−77635
macromolecules, nonlinear laser photomodification, radiation damage 80−61120
magnon-photon interaction in ferromagnets, construct. and radiation effects 80−71188
many-bodied displacement cascade simulation up to 1 keV 78−87711
mass flux, irradiation enhanced, dislocation interactions 80−88206
materials science, phys. and mech. props. 80−25538
measurement units selection 80−98870
metal, cavity growth in irrad. sample under stress 79−73211
metal, diffusion, radiation effects 78−47555
metal, FCC, irrad., annealing, Frenkel pair annihilation in discrete mattice model 77−59009
metal, HCP, long-range interstitial migration rel. to c/a ratio 79−28125
metal, He migration and defect interactions, role in radiation damage processes 77−28041
metal, irrad., containing pre-existing dislocations, interstitial loop form. kinetics 80−65040
metal, irrad., containing self-interstitials and vacancies, electronic transport props. 78−60105
metal, irrad., self-interstitial type defects, combined single-double alignment channelling backscatt. 78−34561
metal, irradiated, determ. of time threshold energy for Frenkel pair creation 77−47444
metal, irradiated, surface plasmon modes of voids 79−60617
metal, radiation damage effects, neutrons and heavy ions, rel. to reactor technology, review 77−43255
metal, radiation defects, localized deformation of electronic state *(Russian)* 79−87061
metal, radiation induced damage, review 78−51580
metal, threshold energy displacement, depend. on bombarding particle energy *(Russian)* 79−90697
metal, threshold energy displacement, depend. on energy of bombarding particles *(Russian)* 79−90698
metal, void growth in irrad. sample, fully dynamic rate theory 79−73212
metal colloids in ionic cryst., preparation, optical, mag. resonance, elec. props. 80−59459
metal damage by intense EM radiation, kinetic mechanism 77−20167
metal surface, slow-positron emission 78−95079
metal swelling, max. point on temp. scale rel. to point defect generation *(Russian)* 78−38751
metal-insulator multilayer structures, model for calc. of electrical response 77−24607
metals, acoustic effect of fast particles, dynamic, thermoelastic, Cherenkov contribs. *(Russian)* 77−7761
metals, irrad., multiple atom displacements 79−46701
metals, irradiated, solute segregation and annealing kinetics at sinks 79−23640
metals, irradiated, validity of rate theory, point defect diffusion eqns. 79−55777
metals, irradiated, void growth, appl. of Langevin method 79−77632
metals, irradiation induced swelling, bias factor 80−2062
metals, point defect and microstruct. behaviour during irrad., appl. to fusion reactors 79−23638
metals, point defect simultaneous clustering during irrad. 79−95000
metals, radiation damage, FIM and atom probe FIM expts., review 78−35623
metals, radiation damage production in stage II, temp. and impurity effects 77−68997
metals, radiation defect treatment at annealing stages V and VI *(Russian)* 80−71676
metals, radiation induced vaporisation, press. behaviour 80−84288
metals, radiation-induced creep and swelling, radiation dose depend. *(Russian)* 80−29050
metals, thermal instabilities due to recomb. of radiation-induced Frenkel pairs 79−23597
metals, void growth and time-lag, statistical theory 80−88208
metals, void lattice form, spinodal decomp. of vacancies 78−92234
metals and alloys, radiation damage prediction and measurement 78−75693
metals radiation damaged long term strength curve forecasting *(Russian)* 80−34040
metaphosphate glasses with Ag activator, radiophotoluminesc. 79−38596
microcontroller, radiation tolerant, design, elec. and radiation tests, performance 77−18709
microprocessor, SBP9900, radiation test 77−75002
microwave, power transmission from solar power satellite, environmental aspects 79−52896
minerals, irradiated, differential thermal anal. rel. to radiation damage 79−62484
mirror, interference filters for improved solar radiation resistance 77−39015
MIS dielectrics, charge centres, removal by RF annealing 78−88035
MIS structure, RF annealing method for removing radiation damage 78−39224
MIS structure, surface states, dielec. deposition temp. effect 77−89872
MNOS structure, non-biased, charge storage by irradiation with UV light 77−43735
Moliere potential, ion transport theory, differential cross sections 80−88209
MOS, charge build-up due to radiation, mathematical model 79−19667
MOS capacitors, electron injection studies of radiation induced positive charge 77−20441
MOS capacitors, irrad., interface state buildup depend. on hole generation and transport 77−20446
MOS capacitors, irradiated and avalanche injected, trapping effects 79−19669
MOS devices, degradation due to induced conductivity 77−80788

radiation effects continued
MOS oxides, ionising radiation effects on mobile-ion density 79−28411
MOS radiation sensitivity, influence of Si surface defects 77−20445
MOS structure, Si-SiO_2, specific memory effect, radiation effects 79−51680
MOS structures, radiation-induced positive charge, thermal annealing 80−75648
MOS structures, thickness dependence of radiation charging, hole trapping model 77−20442
MOS structures, total dose effects on surface state density, carrier conc. and mobility 77−20443
Mossbauer effect appl., conference, Kyoto, Japan (Aug.-Sept. 78) 80−7199
Mossbauer resonance, obs. through Coulomb excitation, effect of thermal spike 78−27132
multipurpose radiation service centre, AEG, Germany 77−59796
muon single and multiple scatt. in continuous media with focusing mag. field 77−24328
naphthalene, cryst., radiation induced radicals, optical absorpt. bands, SCF-CI MO calc. 79−91463
narrow-band semiconductor, growth of epitaxial layers, activation by UV and IR radiation 80−71598
Nimonic, irradiated, void nucleation, numerical evaluation 80−70252
Nimonic alloy PE-16, irradiated, numerical simulation of void nucleation, dislocation densities, pt. defect conc. 79−73208
Nomex, fibre, mech. props., environmental effects, incl. sunlight and ionising rad. effs. 77−36560
non-metallic crystals, electric field influence on defect creation mechanism 80−70251
non-metals, low-temperature strong enhancement of diffusion and defect generation 79−28149
normal metal-constriction-superconductor microbridge, I-V characts. and excess current 79−73641
nuclear and space radiation effects, conf., Albuquerque, USA (Jul. 78) 79−19276
nuclear microprobe as analytical tool, review 79−87913
nuclear power plants, radiation exposure and protection 78−25301
nuclear reactor, corrosion product reduction program 78−21665
nuclear reactor driver fuel, irradiation behaviour 80−32346
nuclear reactor materials, depend. of evolving cavity distrib. functions on cavity growth kinetics 79−3206
nuclear reactor pellet-cladding interaction induced by radiation-induced dilation, mech. anal. 78−13302
nuclear reactor stainless steel and Na shield radiation heating expt. 79−9903
nuclear technology aspects of radiation physics 77−54373
nuclear track etching, review of appl. in other scientific fields 79−97934
O-ring compounds, resistance to heat and ionizing radiation 78−29584
Oklo fossil nuclear reactors, radiation damage of minerals 80−21751
Oklo fossil reactor, review 77−60377
Oklo natural fission reactor materials, thermoluminesc. props., effect of radiation damage 80−21750
op amp, type 108, radiation hardening by modified processing, failure anal. 77−18751
optical components in radiation environment, review 78−83054
optical fibre waveguide, low loss, ionizing radiation effect on attenuation 80−38112
optical fibre waveguide, low loss, radiation induced transmission loss behaviour 80−38111
optical fibre waveguides in 0.4 to 1.7 μ region, radiation response 79−18518
optical fibres, nuclear pulsed thermal radiation effects, hardening techniques 80−33170
optical fibres, nuclear radiation effects 79−27413
optical fibres, reversible photobleaching of radiation-induced losses 79−94356
optical fibres, UV radiation-induced losses rel. to colour centre form. 80−87517
optical glass, radiation protection by cage effect *(Russian)* 77−83938
optical glass fibre development, large-core, for military appls. 80−48451
optical materials and components, space charged particle environment effect 80−69472
optical waveguides, low loss, transient radiation effects, Cherenkov radiation, absorpt., in fibres 78−30055
oxide fuels, in-pile densification by vacancy boil-off and vacancy knockout, model 79−8259
oxide fuels and cladding in LWR, FBR, irrad. behaviour, chemical process, densification, corrosion *(Japanese)* 77−83033
PAC method appl. *(German)* 80−2679
particle beam, high current, producing Cherenkov radiation in amplifying medium 79−22926
particle transport, stochastic theory, appl. to radiation damage cascades 78−153
PBI fibre, mech. props., environmental effects, incl. sunlight and ionising rad. effs. 77−36560
phase stability, radiation disorder model 80−16297
phase stability under irradiation, review 79−77722
phase stability under irradiation, theory 79−77634
phosphate glasses, P_2O_5-Al_2O_3-Mg(Ba)(Sr)(Ca)O, struct. energetics and charging under irrad. *(Russian)* 77−84791
phosphors, halophosphate, recombination processes effect *(Russian)* 80−7424
photodetector optimisation for radiation environments 78−29158
planetary spacecraft, Jovian environment simulation, materials hardening and mass shielding 80−36472
plasma-wall interactions in controlled fusion devices conf., Abingdon, England (April 1978) 78−94917
plastic surface modification using 200 keV electron accelerator with specimen transport system 77−57776
PMMA, space radiation effects evaluation 80−70263
point defect diffusion, radiation enhanced, solns. of chem. rate eqns., appl. to expts. 79−73344
point defect diffusion in stress field of edge dislocation of irrad. solid 78−51720
point defect production in irradiation, swelling, cascade diffusion theory 80−34044
point defect trapping and void growth for irradiated materials 79−7626
point-defect clustering during irradiation 80−92521
polarised target materials, radiation damage, clean materials and dynamic polarisation 79−63832
radiation effects continued
poly(ethylene terephthalate), surface props. rel. to UV irrad. *(Japanese)* 78−79859
poly Si gate MOS capacitor post-irradiation flat-band shift expts. 77−76939
polyatomic materials, damage energy functions 80−49264
polycaprolactam, pure and TiO_3 filled, radiation effects *(Bulgarian)* 79−33015
polyethelene tubes and sheets, light resistance investigation under natural climatic conditions 80−21127
polyethylene, EPR and differential thermal anal. *(Bulgarian)* 79−46698
polyethylene, irrad., thermophys. characts. of amorphous phase, effects on crystallinity 77−7870
polyethylene, low density, UV and heat treatment effects, DSC obs. 79−14915
polyethylene, molecular chain mobility, UV irradiation effect 77−84792
polyethylene, photodegradation mechanism, from yield strength, elongation and mol. wt. studies *(Japanese)* 80−76311
polyethylene, pretreated surface, nitrobenzene contact angle, H_2O environment *(Japanese)* 78−79858
polyethylene, resist. to stress corrosion cracking, ionising radiation effect *(German)* 80−81224
polyethylene, space radiation effects evaluation 80−70263
polyethylene single crystals, STEM advantages over TEM, microarea diffraction patterns specimen radiation damage 79−55620
polymer, UV curing, lamps. 78−88443
polymer cable insulating materials for nuclear power stations, expt. 78−59835
polymer composite matrix materials, spacecraft, space radiation effects evaluation 80−70263
polymethacrylates degradation obs., for PMMA, PBMA, PMA and PMA AN under UV irrad. 78−27795
polystyrene films, UV irrad., struct. changes, gel permeation chromatogram computer manipulation, substraction 79−96387
polyvinylidene fluoride, relax., influence of monomeric unit conform. and supermol. struct. *(Russian)* 79−23537
pore nucleation in radiation damaged solid solns. 79−99237
porous glass, irradiated, accumulation and decay of paramagnetic centres *(Russian)* 77−85570
positron implantation from radioactive sources, profiles and absorpt. coeffs. 79−55781
power reactors, coolant circuit contamination 78−21666
precipitate re-solution in low dose irradiations 80−93559
pressure vessel components reliability, conf. Vienna, Austria, 1977 79−17986
primary knocked-on atoms effect, computing method 80−107318
pulsed irradiation, annealing and accumulation of defects 78−47419
pulsed radiation effect on void growth and swelling 80−34043
PWR pressure components reliability and residual life evaluation and precipitation 79−20191
quantum diffusion in crystals, radiation enhancement conditions 78−47607
quartz, cryst. and melt, irrad., optical absorpt. spectra, computer calcs. *(Russian)* 78−92091
quartz, electron-hole centres, energy characts. assoc. with point radiation defects 79−32991
quartz, irradiated, fused, crystalline, absorpt. spectra, colour centres 80−7384
quartz, photocond., X-ray and other irrad. effects 78−76103
quartz, stress buildup due to UV irrad. *(Japanese)* 79−19278
radiation damage, meas. of loss of gaseous elements from thin samples 80−96568
radiation induced exchange reaction kinetics of H_2, D_2 and T_2, review 78−61005
radiation-induced segregation in binary and ternary alloys 79−78970
radioactive waste, high-level, thermal and radiation effects on borosilicate glasses 77−61557
radiotherapy machine ionising radiation and EM interf. effects on cardiac pacemakers 79−62406
rate equations, transport theory formulation for fusion reactor materials 79−95050
reactor pressure vessel material, radiation embrittlement, current regulation assessment 78−52966
refractory multiphase systems, infusible, some novel effects, rel. to practical appls. 80−55460
research on radiation damage, (1950-60) 80−62446
ring laser gyroscope, nuclear radiation vulnerability 80−9935
risk evaluation model, on-site meteorological data, environmental consequences 80−36155
satellite orbits, perturbation by solar radiation press. general expansion of disturbing function 77−78605
satellite solar cell power plant, operating experience 80−94055
satellite solar cells radiation damage obs., GaAs and Si 79−48134
segregation of impurities to voids, kinetic model 77−43245
semiconductor, defect interactions, radiation physics *(Russian)* 79−46702
semiconductor, influence of electronic excitation on atom displacement 78−2158
semiconductor, ionisation effects in damage production 77−7772
semiconductor, irradiated, Hall mobility, dark and photo-conductivity calc. 78−47835
semiconductor, kinetics of defect cluster annealing 80−84209
semiconductor, radiation damaged, residual defects rel. to back reaction annealing kinetics 78−3161
semiconductor, radiation defects, formation kinetics, successive capture of vacancies by impurities 79−10873
semiconductor, radiation dose for amorphisation, max. point defect conc. 77−55301
semiconductor, recoil enhanced diffusion 77−89567
semiconductor crystals, role of nonequilibrium state in radiation treatments 80−39152
semiconductor displacement energy threshold 77−89430
semiconductor with inhomogeneous impurity distrib., irrad. effects 79−10875
semiconductors, annihilation processes of radiation-produced vacancies and interstitials 77−89432
semiconductors, conference, Dubrovnik, Yugoslavia (Sept. 1976) 77−80540
semiconductors, cryst. defects induced by radiation, review 79−55776
semiconductors, defect processes, electronic stimulation 80−24665

radiation effects continued
semiconductors, defects and radiation effects, conf., Nice, France (Sept. 1978) 80−22140
semiconductors, doped and amorphous, ionised centre diffusion accel. by electrostatic fields 80−70473
semiconductors, fast particle irrad., Frenkel defect formation threshold energy 80−6404
semiconductors, glassy, diamag., photostructural changes, mechanism 80−92557
semiconductors, point defect studies, new developments 77−19980
semiconductors, Watkins-type radiation defects, low temp. form. mechanism 80−15153
semiconductors and insulators, radiation damage, mechanisms, review 80−107315
semicorductors, elemental and binary, under subthreshold irrad. conditions, defect formation ionisation mechanism possibility 80−6430
shielded cables, nonlinearities and multiple exposure anomalies at CASINO, MCCABE code verification 78−58502
shock wave effects, possibility of imitation of radiation damage *(Russian)* 78−95107
silica, fused, ion implantation for radiation damage studies 77−80530
silicate glass darkening due to UV radiation from laser produced plasma jet 78−52598
silicate glasses:Cu^{+}, effect of UV irrad., absorption bands 78−31222
silk, natural, elongation and tensile strength rel. to UV irradiation 80−25796
sink strengths for thin film surfaces and grain boundaries 80−88207
sink-absorpt. terms in reaction-rate-theory analysis 78−79633
solid, radiation defects, vacancies and interstitial atoms recombination *(Russian)* 79−1429
solid solution, binary, radiation-induced instability, contrib. of dissipative processes 80−65039
solid solutions, ordering and disordering under irradiation 79−87626
solids, defect production, book 77−39615
solute redistribution and precip., radiation-induced, model 79−19277
sound generation, by suddenly heated matter 77−34977
space environment, multiple radiation effects facility 79−48644
spacecraft materials, appl. to Jupiter mission 79−92648
spatial pore lattice, parameter of vacancy pores, temp. depend. 79−27976
stainless steel, 316, long term radioactivity minimisation 78−772
steel, austenitic stainless, fusion reactor, first wall material, radiation damage by simultaneous accelerator microscope irrad. 79−45402
steel, austenitic stainless, irradiation induced creep by alpha particles, in type 316 steels *(French)* 78−72791
steel, austenitic stainless, postirradiation mechanical props. of honeycomb spacer grids 79−36324
steel, austenitic stainless oxide film morphology, irradiation effects in N_2O_4 *(Russian)* 79−33209
steel, corrosion, Na loop system, analysis of radioactive corrosion product transfer 78−78464
steel, heat resistant, tensile strain and endurance, normal and radiation conditions, linear load variation 80−81189
steel, I_2 adsorption on steel in HTGR He environment 80−44233
steel, non-irradiated and irradiated specimens, autoclaves for fatigue crack growth tests *(German)* 80−45467
steel, stainless, constitution changes due to radiation effects 80−34048
steel, stainless, dilation and bowing in EBR II ducts and cladding 80−625
steel, stainless, GCFR ribbed cladding, post-irradiation creep rupture tests 80−18430
steel, stainless, irradiated, void nucleation, numerical evaluation 80−70252
steel, stainless, laser fusion reactor first wall, void growth charact. 80−34042
steel, stainless, nucl. reactor driver fuel, irradiation behaviour 80−32346
steel, stainless, radiation-thermal treatment, N_2O_4 coolant action, intergranular corrosion *(Russian)* 78−58357
steel, stainless, sigma phase stability and irradiation effect 78−11200
steel, stainless, type 304, previously irrad. in fast neutron flux 78−80600
steel, stainless, type 316, point defect simultaneous clustering during irrad. 79−95000
steel, stainless type 316, temp. effects on swelling 80−32347
steel, type X16H15M3B, radiation swelling, predictions for conditions in fast reactors *(Russian)* 79−67870
strain measurement, extensometric method, for inside nuclear reactor channels 80−100998
strain-gauge transducer sensitivity to directional thermal gradient error 77−74382
structural materials, review 80−49267
superconducting phase transition variation with irradiation *(Russian)* 78−76181
superconductor, crit. temp., micropower-induced enhancement *(Russian)* 80−93023
superconductor critical temp. depend. on radiation defects, electron density of states calcs. 80−44758
superconductor film, nonequilib. states induced by optical and microwave irrad. 77−47925
superconductor-normal metal-superconductor microjunctions, microwave enhanced crit. current 79−82720
superconductors conf., Argonne, Il., USA (June 77) 78−52120
surface effects in controlled thermonuclear fusion 77−26866
surface erosion phenomena in CTR appl. 77−71695
technical superconductor radiation damage obs. 79−33422
temperature fields in radiation absorb. bodies Julich reactor expts., finite element calcs. *(German, English)* 77−82998
temperature spikes stochastic analysis, contribution towards component damage exposed to nuclear radiation environment 79−7627
thermal defect in materials determ., using total-absorption calorimeters 80−99427
thermoregulative coatings, radiation effects on reflectivity, space vehicle appl. *(Russian)* 78−76542
thermostatic air chamber, influence of radiation *(Japanese)* 78−37007
THTR fuel element, irradiation testing in DRAGON reactor *(German)* 78−25295
Tokamak fusion reactor, effects of blanket-shield penetration on performance 78−21765
Tokamaks, lifetime of reactor components 80−32445
TTF-TCNQ, Matthiessen's rule, effective defect resistivity 80−6821
tunnelling spectroscopy, appls., review 78−92588

radiation effects continued
type II superconductors, radiation-induced changes in crit. props., radiation defects *(Russian)* 80−25027
undersaturated alloys, irradiated, solute segregation kinetics, via drift and defect-solute complexes 80−60872
unsaturable trap model for defect accumulation in recovery stage II 77−47481
UV curing using electrodeless lamps 77−70199
UV exposure in environmental gases, effect on track etching rate of polycarbonate film 79−76296
vacancies and interstitials, irrad. induced, recombination rate 80−96516
vacuum system, outgassing rate during particle bombard. of walls 79−44911
vibrational spectra crystals with split configuration interstitial *(Russian)* 78−76450
void arrays in crystals, TEM contrast 80−14975
void coalescence kinetics in cryst. with dislocations and volumetric generation of point defects 77−68996
void generation, radiation cascades 79−73210
void growth and incubation, stress effect 79−51147
void growth kinetics, effect of surface energy barriers 79−51146
void sink strength depend. on mutual recombination, point defect loss to fixed sinks 80−33995
void swelling, nucleation theory 80−65038
void swelling, role of divacancies 79−99236
void swelling in metals and alloys under irradiation, theory 78−75692
void swelling simulation in reactor materials 78−8906
voids, sink strength of random array, steady-state diffusion problem, variational technique 80−49266
Voyager Sun sensor, CdS detector, evaluation of radiation interference, simulation 79−23644
water-acid ices, UV irrad., EPR of H and D, nucl. electron effects 79−83488
X-ray, and neutron small-angle scattering, structural defect studies, review 79−10752
X-ray standing wave field excitation, meas. apparatus, appls. 77−15285
Zircaloy, irradiated spent fuel cladding, annealing effects 79−89382
Zircaloy, irradiation growth in annealed and cold worked samples 77−88225
Zircaloy, LWR cladding, I_2 stress corrosion cracking 79−89380
Zircaloy clad UO_2 fuel elements, irrad. effects 80−666
Zircaloy-2, effect of simulated fission products on elongation fractography and metallography 80−649
Ag, production and annealing of radiation defects 78−47362
Ag-^{112}In, dil., ^{112}In nucl. alignment, radiation damage, γ-ray spectra 78−19398
Ag-Zn(Cd), production and annealing of radiation defects 78−47362
AgI aerosol, ice forming activity, UV irrad. effect 80−71950
Al foil, solar wind ion bombardment, lunar surface modification 80−109325
Al, narrow superconducting bridges, microwave radiation stimulated T_c enhancement 80−84537
Al, supercond., stimulation and enhancement by external micropower irradiation *(Russian)* 78−95394
Al-Ge, effect of irrad. on the nucleation of incoherent precipitates 79−8303
Al-gelatin-GaAs, C-V charact., irrad. effects *(Russian)* 77−51823
Al-Si_3N_4-SiO_2Si, MNOS structures degradation under UV irradiation effect 80−107923
Al_2O_3, corundum, doped, induced absorption spectra, low temp. irrad. effects *(Russian)* 78−72570
Al_2O_3, displacement function calc. 80−34047
Al_2O_3 gate insulator, low temp. radiation response 78−26960
Al_2O_3, ion implantation for radiation damage studies 77−80530
Al_2O_3, thermoluminescence, optical bleaching/stimulation effects following irrad. 78−43940
^{241}Am metal, self damage, total energy stored 77−28019
As-Ge-S(Se), glass films, photostruct. changes 77−85822
As_2S_3:Ag film, Ag photodoping rate, localised struct. transform. effect, absorpt. meas. 77−31914
As_2S_3-Ag interface, photodissolution kinetics of Ag in amorphous films 77−15955
$As_{15}S_{40}Ag_{45}$ glass, photosurface deposition of metallic Ag discs 77−76650
As_2Se_3:Mn^{2+} film, reversible photostructural change, ESR obs. 77−32411
Au foil, radiation damage from sputtering by fission fragments 78−2968
Au-Ag, radiation damage and diffusion 80−24645
Au-Fe (17 at.%) alloy, fission fragment irrad., simulation of neutron effects 77−80549
$BaTiO_3$, rare earth doped ceramics, thermolum. and microwave induced thermolum. fading 79−1792
C stripper foil irradiation lifetime preparation by hydrocarbon cracking 79−76249
C stripper foils, lifetime enhancement, heavy ion bombardment 78−94156
C stripper foils, tests with 4.8 MeV Ar ions 79−76240
C, structure change, during thermal ordering, radiation disordering 80−54283
CO_2 laser range finder, performance in radiation environments 80−38054
CaF_2:Mn^{3+}, fluorite, radiation and thermal redox processes 80−55678
CaO, displacement function calc. 80−34047
$CaSO_4$:Dy, TLD during irrad. by γ-rays, X-rays, electrons, ambient atm. effect 78−19578
$CaSO_4$:Dy TLD, temp. effect during UV and gamma irradiation 79−38684
CdF_2, colour centres, IR absorpt. and photocond. after UV irrad. 80−79784
CdF_2:NaF(AgF), colour centres, IR absorpt. and photocond. after UV irrad. 80−79784
CsI:Na, UV irrad., thermoluminesc. 79−28846
Cu, He-vacancy clusters, computer simulation 77−39583
Cu irradiated, exam. of dislocation bias for interstitials to edge dislocations 78−79612
Cu, radiation damage and diffusion 80−24645
Cu, thermal vibr. and zero-point motion effects on low-energy collision cascades 78−87705
Cu, vacancy migration induced by subthreshold focused collisions 77−19982

radiation effects continued
Cu_3Au, under irradiation, microstructural-based estimate of disordering 80−2067
Fe, ^{235}U fission product irrad., elec. resist. *(French)* 79−51159
Fe, amorphous, radiation damage simulation 80−34045
α-Fe, point defects, short term annealing, computer simulation 80−54282
Fe, radiation induced defects, annealing exam. using channelling tech. 78−47316
Fe-Cr-Ni austenitic alloys, environment sensitive cracking, metallurgical variables effect 80−35391
Fe-Cr-Ni system, austenitic, energetic particle bombardment, thermodynamic and dimensional stability 77−27904
Fe_3Al, computer simulation of energy dissipation from near threshold knock-ons 78−30666
Fe_3Al, ordered binary alloy, computer simulation of radiation effects 78−87709
$Ga_{1-x}Al_xAs$-GaAs solar cell, radiation resist., theoretical evaluation and optimisation 80−35681
GaAs:Cr, effect of light on EPR centres 78−10767
Ge, cyclotron resonance 78−72416
Ge, electron-hole drop deform., accel. and luminesc. under influence of radiation press. 77−47739
Ge γ-ray detectors, material props., appls., radiation damage 78−13392
Ge, lattice disorder influence on optical spectra in interband transition region 79−43006
Ge, review of point defect charact. *(Japanese)* 77−89428
Ge-GeO_2 MIS structure, growth of GeO_2 from liq. phase, appl. of UV irradiation *(Russian)* 80−40273
H maser failure mode identification 77−37862
H_2O, acoustic rad. from ionising particles 78−71793
Hg-polymer interface, UV exposed, contact potential and charge exchange meas. 80−75642
HgCdTe, radiation effects on low-temp. carrier recombination lifetimes, photocond. meas. 78−6400
HgCdTe short-wavelength IR photovoltaic detectors, radiation testing 80−37084
HgTe, VPE growth control by EM irrad. *(Russian)* 80−34338
In, muon quadrupolar interaction expansion of crystal lattice *(Russian)* 79−15388
In, supercond., stimulation and enhancement by external micropower irradiation *(Russian)* 78−95394
InSb, irrad. real and clean surfaces, work function 78−95336
interstitial cluster nucleation, effect of trapping at onset of irradiation 79−78974
K ternary halides, A_2MX_6 type, radiation induced lattice defects and solid state reactions *(German)* 79−42101
KBr, V- and X-centres accumulation *(Russian)* 80−54228
KBr(Cl):OH^-, cc U_2 to H_2O^- defects conversion after UV photodecomp. 80−107230
KBr(I): $O^{2-}(S^{2-})(Se^{2-})(Te^{2-})$, low temperature photochemistry on chalcogen vacancy centres 78−18641
KCl, F- and H-centre production by nonradiative decay of self-trapped exciton 78−23042
KCl, γ-irrad., F-centre absorpt., flash-stimulated changes 80−92524
KCl, irrad., V_3-band in absorpt. spectra, model *(Russian)* 79−56821
KCl, irradiated crystal, determ. of oscillator strength of V_3-centre *(Russian)* 78−92095
KCl surface, vacuum UV radiation damage, spectroscopic study 78−71758
KCl, temp. depend. of F-colouring efficiency 80−44204
KCl, V- and X-centres accumulation *(Russian)* 80−54228
KCl:Ba, negative photoplastic effect, photodestruction of Z-centres 77−43272
KCl:H, dichroic H- and U-centres by polarised bleaching of interstitial H 80−29766
KCl:Na(Ag), UV irrad. anionic H and D atoms, ESR and optical absorpt. expts. 79−99187
KCl(Br), coloured, irrad. damage during positron bombardment 78−63791
K_2O-B_2O_3 glass, γ- and UV- irrad., thermodecolorisation and thermolum. 80−20721
LiB_4O_7, thermoluminescent dosimeters, high dose characteristic 78−35966
LiF TLD, re-estimation of absorbed doses below 1 rad using UV bleaching 77−16992
LiF, thermoluminescent dosimeters, high dose characteristic 78−35966
LiF:Mg, Ti TLD long-term annealing at 400°C, radiation and thermally induced damage, recovery 77−5085
α-$LiIO_3$:$Cr^{3+}(Mn^{2+})(Fe^{3+})$ and radn. induced defects, EPR spectra *(German)* 78−84480
Mg, SiO_4:Th TLD phosphor, γ-ray induced sensitisation and phototransfer 79−33851
MgF_2 coated Al mirrors, AES, UV irrad. effect 77−72047
MgO, displacement function calc. 80−34047
MgO, Fe^{3+} and Cr^{3+} impurity ions valence conversion in single cryst. by UV irradiation *(German)* 78−84620
MnF_2, photochemical introduced radiation damage 78−2161
Mo alloy, TZM, long term radioactivity minimisation 78−772
Mo, defect configurations, PAC study 79−86817
Mo, diffusion, volatile fission product, diffusion in Mo, 1400-2000K *(Russian)* 78−91485
Mo, fission fragment bombardment, channelling effects *(Russian)* 78−38762
Mo, irrad.-induced voids and dislocations, annealing, theory *(Russian)* 78−47418
NH_4ClO_4, photothermochemical process 79−24769
NO_2 in nonane, supersaturated gas, photoinduced nucleation 78−80760
NaCl, transient infrared absorption of bound polarons 78−91642
NaCl, V- and X-centres accumulation *(Russian)* 80−54228
NaCl:NaOH, $NaNO_3$, oxygen colour centres, spectral absorpt. and Xe lamp irradiation 77−69862
$NaMgF_3$, defects induced by X- and vacuum UV irrad., optical and elec. study 80−107319
NaN_3, UV irradiated, F-centre ESR 77−28444
NaN_3, UV irradiated, polarised optical absorpt. of F_2^+-, F-centres 77−28605
Na_2O-CaO-SiO_2, glass, formation of colour centres, linear absorption of UV radiation 80−103328
Na_2S-B_2O_3-GeO_2, darkening and fading in UV irradiation *(Japanese)* 77−36270
radiation effects continued
Na_2S-GeO, darkening and fading in UV irradiation *(Japanese)* 77−36270
Nb_3Ge(Sn) film, superconducting transition temp. var. under ^4He irrad. 77−8220
Nb_3Sn, irradiated, critical current density 79−38293
Nb_3Sn, supercond., fast particle irradiation effects, using anti-site defect model, electronic state influences 79−56346
Nd:YAG laser range finder, performance in radiation environments 80−38054
Ni alloy, GAB 286, austenitic energetic particle bombardment, thermodynamic and dimensional stability 77−27904
Ni alloys, constitution changes due to radiation effects 80−34048
Ni, effect of 2 MeV Xe^+ ion irradiation on pore distribution and size 79−71898
Ni, irradiated, numerical simulation of void nucleation 79−73208
Ni model material, defect buildup and solute segregation, in alloys under pulsed irradiation 78−71757
Ni, radiation damage and diffusion 80−24645
Ni-Al(Ti)(Mo)(Si), effect of solute misfit and temp. on irradiation induced segregation 78−72779
Ni-Si solid soln., radiation-induced solute redistribution and precipitation, model 79−19277
P_2O_5-SiO_2-GeO_2 graded-index optical fibre, UV induced losses 80−87518
PbSnTe long-wavelength IR photovoltaic detectors, radiation testing 80−37084
PbTe, and $Pb_{1-x}Sn_xTe$, VPE growth control by EM irrad. *(Russian)* 80−34338
δ-Pu alloys, at. vol. increase due to prolonged room temp. self-irrad. 77−19910
Pu and Pu-Np alloys, additional resist. due to self-radiation damage, Matthiessen's rule deviations 77−28170
Pu radioactive waste, oxidation by radiation, effect on migration rate 80−13714
$RbMnF_3$, photochemical introduced radiation damage 78−2161
Se, amorphous film, crystn., thermal and photo-effects 77−47692
Se-based chalcogenide glasses, band gap variation 78−90461
Si, A-centre formation by vacancy-O_2 recomb., acceptor impurity conc. effect 77−43243
Si, Au diffusion enhancement by photo- and electron irrad. 77−27901
Si, defect prod. by GeV muons, thermally stimulated current technique 78−5099
Si, doping, low temp. radiation induced impurity diffusion 77−15439
Si, models for irradiation effects on impurity diffusion 77−80654
n-Si plate, internal friction, illumination effects, 50-250°C *(Russian)* 77−20010
Si, radiation defect clusters, form. kinetics and parameters 77−11545
Si, radiation induced defects, IR absorpt. bands 80−25424
Si, radiation-stimulated dissociative diffusion of Au, model 79−23785
Si, review of point defect charact. *(Japanese)* 77−89428
Si solar cells, capacitance transient spectra of processing- and radiation-induced defects 80−61340
Si:H, amorphous, Schottky diodes, elec. props., light-induced effects 80−103741
Si-Al_2O_3, MIS structure, with dielectric film, from UV irradiation converted metalorganic compounds *(Russian)* 80−45245
Si-Ge junction, Si monocryst. and Ge film, elec. props. 79−51660
Si-sapphire, interface radiation induced charge trapping, rapid anneal phenomena 79−19666
Si-sapphire interface charge trapping, effects of sapphire type and epi growth conditions 77−20447
Si-SiO_2 boundary, origin of interface states and oxide charges generated by ionising radiation 77−20380
SiC (6H), IR absorpt., UV illumination effects, defect levels 80−66251
Si(Li) detector, improvement of time depend. instabilities by IR and γ-irradiation 79−36477
Si_3N_4, amorphous, ion implantation for radiation damage studies 77−80530
SiO_2 film on Si, irradiation behaviour anal. 78−26957
SiO_2 films, prep. from tetraalkoxysilanes, by activation pyrolysis 79−87583
SiO_2 glass, low press. plasma treatment, paramag. defect form. *(German)* 78−23341
SiO_2 in MOS struct., location of positive charged generated by UV and X-irrad. 77−51820
SiO_2, numerical anal. of kinetics of space charge formation, rel. to irradiation *(Russian)* 79−78243
SiO_2 thin films, radiation-induced trapping centres, rel. to MOS transistor technology 80−107804
SiO_2, vitreous, colour centres, dangling bond defects, radiation effects 78−71732
SiO_2, vitreous, intrinsic radiation defects, nonbridging O 80−19837
SiO_2, vitreous, semi-empirical mol. orbital model, appl. to radiation compaction 79−73433
SiO_2-Si interface of hardened MOS capacitors, radiation effects 78−26958
SiO_2-Si inversion layer solar cells, radiation effects 77−43244
SiO_x protected Al mirror, far UV refl., UV irrad. effect 79−7191
SiO_2-Ge, B, P, optical fibre, radiation induced optical absorpt. spectra, 0.4 to 1.7 μm region 80−58761
Sn, cross-like film structures, microwave irrad. stimulated superconductivity and Josephson effect 79−60988
Sn, supercond., stimulation and enhancement by external micropower irradiation *(Russian)* 78−95394
Sn, supercond. whiskers, HF radiation effects on current-voltage charcts. 79−65619
SrF_2:Tb, and pure, UV induced processes 77−32452
Ta, muon quadrupolar interaction expansion of crystal lattice *(Russian)* 79−15388
TaO, displacement function calc. 80−34047
ThO_2, lattice defects and irrad. effects, review 77−27873
Ti-70A superalloy, fusion reactor blanket structures, radiation resistance 80−63379
Ti-Al-V, fusion reactor blanket structures, radiation resistance 80−63379
$TiH_{1.8}$, tritiated, NMR of ^3He formed by β-decay, radiation damage, ageing 77−24751
$(U,Pu)O_2$, lattice defects and irrad. effects, review 77−27873
γ-U alloys, at vol. increase due to prolonged room temp. self-irrad. 77−19910

radiation effects continued
UO_2, commercial fuel pin, irradiation induced volume changes, comparison with model 78−78465
UO_2, lattice defects and irrad. effects, review 77−27873
UO_2, swelling and gas release at low and intermediate temps. 77−50241
$UO_{2\pm x}$, model of response of fission gas bubbles to dynamic behaviour of point defects 79−37735
$V_3Ge(Si)$ film, superconducting transition temp. var. under ^4He irrad. 77−8220
VO_2, film, IR induced metal-semicond. phase transition *(Russian)* 77−15769
W, threshold atomic displacement energy, temp. depend., computer simulation 77−1148
W-Re, sigma phase stability and irradiation effects 78−11200
Xe, gas, diffusion enhanced by radioactivity 79−60094
ZnO, photodesorption of CO_2, rel. to surface cond. and AES, band-bending model 77−47671
ZnO powder, adsorption of O_2, H_2, light effects *(Japanese)* 78−95230
ZnS evaporated film, refl. loss on UV irrad., ZnO form. 80−99813
Zr-H system, δ and ε phases, neutron irrad., radiation swelling investigation 78−18685
$ZrSiO_4$, natural, radiation defect centre, EPR obs. 80−75853
$ZrSiO_4$, natural zircon, nucl. radiation effect on elastic moduli 77−11616

radiation hardening
alkali halide, low temp. radiation hardening mechanism, dislocation-interstitial elastic interaction 79−23636
development trends and appl. 78−55041
EMP radiation, electronic systems, protection, book 77−54366
fast reactor materials, fast neutron damage 78−10093
graphite, irradiated ultimate tensile bending and compressive strength charact. 78−15479
hardened irradiated metal, flow stress temp. depend., effect of interstitial atom clustering and embrittlement *(Russian)* 78−34538
LWR materials, pressure boundary problems, corrosion, cracking and radiation embrittlement props. 78−46142
metals, effect of neutron irrad. on plasticity charcts. 78−64607
metals, FCC, hardened, plasticity, review 79−11683
metals and alloys, radiation damage prediction and measurement 78−75693
mica, natural, high γ- and electron-irrad. doses effect on annealing behaviour, thermal decomp. resist. 80−60897
radiation processing, conf., Miami, FL, USA (Oct. 1978) 80−36772
steel, AISI 1045, laser transform. hardening, fatigue and wear rates 79−70198
steel, alloy, Cr, austenitic boundary layers, form. by short laser pulse reaction 78−88555
steel, by focused laser beam *(Russian)* 78−27670
steel, ferritic, impurity defect interaction influence on radiation hardening and embrittlement 80−35199
steel, hardness, effect of laser irrad. in inert gas atm. *(Russian)* 79−38935
steel, ionic nitriding, procedure and equipment, nitrided layer hardness obs. 80−45414
steel, irradiation by neutrons, damage function for mech. props. 78−13228
steel, low-alloy structural, radiation hardening, rel. to embrittlement *(Russian)* 77−21243
steel, medium C, type 35 laser treatment effect on struct. and mech. props. 79−39041
steel, reactor pressure vessel failure and radiation damage *(Czech)* 80−619
steel, stainless, Type 316, neutron irrad. effects on tensile props. and microstruct. 80−65059
steel, type 1Kh18N9T, neutron irradiated, microstruct. and mech. props. *(Russian)* 80−24503
steel, US strengthening treatment effect on fatigue resistance 80−81193
steel 45 microstruct. and hardness after electron bombardment 79−38956
steel pearlitic, statistical anal. of joint effect of Ni, Cu, P on irradiation embrittlement 78−71770
steels for nuclear reactor pressure vessels, neutron irrad. embrittlement, temp. effects, annealing *(German)* 77−34384
thermo-plasticity of irradiated metals 77−4146
Al, quenched, irradiated, and quenched plus irradiated, grain boundary hardening 80−3162
Al, US hardening kinetics rel. to dislocations 80−50644
Al-Mg-Cu-Si-Cr (1,2.7,0.6,0.2wt.%), laser shock hardening of weld zones 78−39800
Al-Mg-Mn-Cr (4, 0.45, 0.15 wt.%), laser shock hardening of weld zones, exam. 78−39800
CdS, photoplasticity and photocond., excitation energy conc. near dislocations, hardening 77−24346
Cu, electron irrad. at 100K, dislocation vel. meas. etch pit technique 80−49271
Cu, electron irrad. at 100K, comparison of irrad. hardening with dislocation vel. 80−54284
Cu, US hardening kinetics rel. to dislocations 80−50644
Cu-Al (11.47 wt.%), high temp. phase transforms., effect of pre-exposure to neutrons 79−20045
Fe, Armco, microstruct. and hardness after electron bombardment 79−38956
Fe, nitrogen, impurity defect interaction influence on radiation hardening and embrittlement 80−35199
Fe, US hardening kinetics rel. to dislocations 80−50644
Fe-N, neutron irrad. effects on mech. props. 79−4338
Fe-Ni, dilute, irradiation softening effect on yield stress 80−76319
Fe-Si, dilute, irradiation softening effect on yield stress 80−76319
Fe-V, dilute, irradiation softening effect on yield stress 80−76319
KBr:Li, low temp. radiation hardening mechanism, dislocation-halogen interstitial interaction 79−23635
KBr:Li(Na), low temp. radiation hardening mechanism, single halogen interstitials as hardening agent, Ha annealing 79−23634
KCl, hardness increase mode, effect on dislocation mobility 79−51114
KCl, photoplastic effect *(Japanese)* 79−82279
KCl-KBr, mixed cryst., radiation hardening 79−99238
LiF, hardness increase mode, effect on dislocation mobility 79−51114
Mg, US hardening kinetics rel. to dislocations 80−50644
MgO crysts., radiation damage influence on deform. in HVEM 80−103391

radiation hardening continued
MgO, hardness increase mode, effect on dislocation mobility 79−51114
Mo, neutron irrad., radiation anneal hardening mechanism 80−71678
Mo, neutron irradiated, radiation softening and hardening 80−34083
Mo-Zr-B alloy, neutron irrad. at 780-1080°C, porosity, hardening and embrittlement *(Russian)* 80−29062
NaCl, hardness increase mode, effect on dislocation mobility 79−51114
NaCl, neutron irradiated, induced flow stress and optical absorpt. 77−62569
NaCl, photoplastic effect *(Japanese)* 79−82279
NaCl, X-ray irrad., F-centre accumulation and rad. hardening *(Russian)* 78−51538
Nb, neutron irrad., yield stress and activation vol. 77−90418
Nb, neutron irradiated, radiation anneal hardening *(Japanese)* 80−89243
Nb, radiation hardening and yield strength correlations for 16 MeV H^+ and (D,T) neutron effects 78−14389
Nb wires, neutron irrad., radiation anneal hardening 200 to 700°C 79−70077
Ni, acoustic hardening, influence of US treatment temps. and material purity *(Russian)* 80−11656
Ni, radiation hardening and yield strength correlations for 16 MeV H^+ and (D,T) neutron effects 78−14389
Ni-Cr-Fe alloys, radiation enhanced precip. and dissolution of precipitates, point defect kinetics and dislocation obs. 80−108467
Ni-Ti(Fe), neutron irradiated, thermally activated deform. 80−6438
Pb, reactor radiation-induced hardening, computer modelling *(Russian)* 79−37738
Si substrate, implantation effects on hardening and Si_3N_4 film stress reduction 78−71748
Si-SiO_2 interface, rad. hardness, carrier localisation in inversion layer 77−85332
V, neutron irrad., yield stress and activation vol. 77−90418
V, oxygen impurity defect interaction influence on radiation hardening and embrittlement 80−35199
V, radiation hardening and plastic instability *(Russian)* 78−39842
V-Zr-C, radiation hardening and plastic instability *(Russian)* 78−39842
Zn, US hardening kinetics rel. to dislocations 80−50644
ZnSe, photoplasticity and photocond., excitation energy conc. near dislocations, hardening 77−24346
Zr alloys, neutron irrad., yield strength changes and radiation hardening, damage annealing *(Italian)* 77−65269
Zr, and its alloys, TEM obs. of irradiation damage, critical review 79−10879

radiation hardening (electronics)
analogue fibre optic data link, hardened, construction and analysis 78−30057
coherent laser detection system, radiation effects analysis 78−30056
fibre optics data link, radiation testing, degradation, transient outage time performance 77−19405
microcircuits, radiation hardness design, SEM as diagnostic tool 79−21869
microcontroller, radiation tolerant, design, elec. and radiation tests, performance 77−18709
MNOS capacitors, effect of 2 MeV electrons at 80K 79−19668
MOS, charge build-up due to radiation, mathematical model 79−19667
MOS capacitor, neutron damage mechanisms in CCDs 79−19672
MOS capacitor structs. radiation hardness eval. using elec. meas. technique 80−34516
MOS devices, irradiated, low-temp. appl. 78−26961
MOS hardness characterisation, depend. on process and meas. variables 77−20444
MOS oxides, ionising radiation effects on mobile-ion density 79−28411
MOS structures, irradiated SiO_2 film, electron and hole trapping 80−11098
MOS thin capacitors, electron-beam irrad., enhanced flatband voltage recovery 79−19670
nuclear and space radiation effects, conf., Albuquerque, USA (Jul. 78) 79−19276
op amp, type 108, radiation hardening by modified processing, failure anal. 77−18751
optical fibre transmission system, 400 MHz bandwidth, linear response 77−23750
PMOS process with ion implanted threshold adjust, radiation hardening 79−46689
Sandia Laboratories nuclear weapon neutron environment simulation, hardening tests 79−22448
satellite shielded cables, hardening techniques for reducing X-ray response 79−23642
SOS capacitors, ion-implanted with negative charge gamma radiation effects 79−23645
VLSI processing, radiation, and hardening 79−24088
X-ray source, industrial, use for electronic component radiation effects work, calibration 80−63402
$Ga_{1-x}Al_xAs/GaAs$ heterostructure solar cell design for space usage 79−96450
In_2Te_3-type semicond. radiation-resistant fast-electron detectors 78−78559
Si, MOSFETs, Shubnikov-de Haas oscills. from electron irrad. induced two-dimens. leakage channel 79−19671
Si, radiation damage effects on charcts. *(Korean)* 79−60402
Si-sapphire, interface radiation induced charge trapping, rapid anneal phenomena 79−19666
Si-SiO_2 interface, inversion layer transport, radiation hardness effects, review 79−19673

radiation injuries *see biological effects of radiation*

radiation monitoring
see also dosimetry
800 MHz portable transmitters, meas. of energy deposition in simulated human operators, comments and reply 79−57777
^{222}Rn flux through multilayered covers cover U mill tailings 80−95487
α-particle, high altitude radiation obs., design and performance evaluation of Cherenkov telescope 78−86734
accelerated electron beam current monitor using secondary emission detection 78−78033
acoustic emission monitoring difficulties overcome by optical detectors 78−60968
adjustable single-fibre connector and output monitor *(German)* 78−38011

radiation monitoring continued
AECL commercial products, contrib. to nuclear medicine and radiation processing 80−81736
aerosol, radioactive charging, transient mean particle charge 78−23973
aerosol surveillance system evaluation 80−57984
AGR fuel plug maintenance facility, corrosion product contamination control 80−5388
air ionisation probe for α, β, γ hand and shoe monitor 80−58084
air monitoring system for α-activity and nuclide specific noble gas meas. 80−63408
air monitoring systems for radioiodine and inert gases, evaluation 80−95480
air sampling system at HFEF/N 79−45441
air traffic radiation safety, high-altitude 78−44620
airborne γ-ray spectrometer calibration, altitude effects 80−18754
airborne and liquid releases from nuclear facilities, systems 78−37450
airborne gamma-ray mapping and tracking system 77−38427
airborne radioactivity meas. in HFEF/N 80−18687
albedo neutron dosimetry 77−90914
alpha beams, high energy, using excitation functions for $^{27}Al(\alpha,4p+3n)^{24}Na$ and $^{27}Al(\alpha,4p+5n)^{22}Na$ 77−3021
alpha-emitting contaminants in environment, field monitoring using ZnS scintillator and phoswich detector 78−70646
alpha-in-air monitoring system, real-time 80−23155
alpha-particle spectrometer, portable, single-channel, for meas. of Rn daughter product concs. 77−30702
area monitoring, problems associated with the placement of fixed area monitors around irradiated fuel storage pools 80−18711
artificial radioactivity migration in environment, survey of models 79−96487
automatic monitor of effluents from nuclear facilities 77−61615
beta-emitter contamination, low-energy RNB-76 monitor 79−36486
biochemical indicators of radiation injury 79−34607
biological and ecological samples *(French)* 78−5052
breached element location from mixture of Xe tags, MIXTAG code 78−33274
BWR, control blade worth depletion meas. 80−719
BWR decontamination, research and development program 79−54539
BWR power plant stack effluent inert gas nuclide monitor 79−3255
BWR Vermont Yankee power station, external radiation field meas. 77−54368
calorimetric dosimeters, automation of calorimetric measurements evaluation 79−67965
CANDU irradiated fuel, monitoring for sheath defects in shipments 78−54864
Caorso nuclear power station airborne and liquid radioactive release monitoring systems 79−13553
N Carolina, survey of external environmental radiation levels 78−80968
CEGB nuclear power station emergency monitoring procedures 78−55053
centralized TLD service and record keeping in Canada 80−58003
cholesteric liquid crystal thermo-optical monitor, for nonionising radiation 78−11742
chromatography radioactive source leak testing under dynamic flow conditions 80−3432
Cicoil personal RF radiation hazard detector, evaluation 80−5337
class 1E reactor components radiation test facilities for LOCA anal. 79−59277
coal, bituminous, subbituminous and lignite, gamma-ray activity 77−25684
coal fired power stations, EPA regulations and radiological dose commitment 79−52980
coastal nuclear power stations, gaseous release dilution meas. 79−52981
computerised digital count-rate estimation using adaptive exponentially weighted moving averages [for radiation monitoring] 80−18689
computerised monitoring, distributed processor-based system for large scale power plant monitoring 79−59280
concepts of radiation dosimetry, photon and charged particle dose meas., book 79−81101
conference, radiation protection monitoring advances, Vienna, Austria (June 1978) 80−57007
contamination detectors assessment, w.r.t. German 1977 protective measures *(German)* 78−86693
continuous radiogauges with digital meas. system, dynamic charact. 79−59311
criticality accidents at facilities processing fissile material, charact., detect. and action procedures *(French)* 78−55054
Czechoslovak nuclear power station fluid radioactive release monitoring *(Russian)* 79−13555
Czechoslovak Rez Nuclear Research Institute airborne radioactive release monitoring 78−89991
data acquisition shelf monitor system for special nuclear material real-time inventory 79−45426
decommissioned nuclear facilities, radiation exposure pathways 80−13957
dental X-ray photographs, comparative study of patient exposure to radiation 78−92702
DePangher precision long counter and neutron dose-rate meters, calibration 80−47822
digital pathway options for radiation monitoring 79−59278
digital radiation monitoring, plant-wide systems, design alternatives 79−41082
digital radiation monitoring system, signal processing by distributed microcomputer data modules 79−59279
disposition assessments for decontamination and decommissioning of inactive nuclear sites, data requirements 80−95474
dose equivalent measuring instrument for rapid use in mixed radiation fields 78−15901
dose field monitoring by independent detectors in cassette 77−81578
dose from CT scan, meas. using pencil shaped ionisation chamber 79−20683
dose limitation system, application problems 80−47767
dose measurement, beta and photon, for radiation protection purposes 78−15908
dose rate, risk factors, natural and man-made radiation, Germany, (1974) *(German)* 79−9897
dose rate meter, use as X- and γ-ray secondary protection-level standard 77−81579
dose-rate conversion factors for external exposure to photons and electrons, modifications to DOSFACTER code 80−104775
dosimeter, pocket-sized electronic system 78−5100
radiation monitoring continued
dosimetry film evaluation by neutron activation and X-ray fluoresc. anal. 79−63820
double filter system for Rn/Th measurements in environment and exhaled breath 80−57988
Dungeness A, radiation and contamination control 80−5386
ecosystem analysis methods for the assessment of inactive nuclear sites 80−95476
edge effect in beam monitor 77−88317
effluent monitoring, purpose and value 78−89986
effluent monitoring programme design and organisation principles 79−13548
effluent sampling programme data statistical evaluation 79−13547
electret ionisation chamber dosimeter for long-term personnel monitoring 78−21810
electron beam processing, dosimetry and quality control 79−49871
electron linear accelerator, dose monitoring system 78−92710
EM radiation hazard instrums. 79−92378
EM radiation probes, implantable, design factors 78−73258
emergency conditions, monitoring and handling 78−57082
environment monitoring ground radioactive burial site *(Japanese)* 80−67015
environmental γ flux meas. method using NaI(Tl) scintillation counter and photomultiplier 78−21786
environmental and personnel monitoring, long-term, with solid-state dosimeters 77−50308
environmental gamma and beta meas. 77−38429
environmental gamma radiation in Norway, population doses 78−11745
environmental impact from radioactivity releases, dose commitments, how long 79−52960
environmental low level meas. with plastic scintillation detector system 77−38567
environmental measurements and US regulatory responsibilities 77−38430
environmental measurements made with integrating detectors, error anal. 77−38428
environmental monitoring at Lawrence Livermore Laboratory 79−85823
environmental radiation measurement *(Japanese)* 79−6772
environmental radioactive pollution by U industry, monitoring using analytical chemistry 80−95488
environmental radioactivity, meas. of water, soil, and foodstuffs 79−5378
environmental radioactivity, methods for determ. of radionuclides in environmental samples 79−48202
environmental radioactivity, radiation dosimetry control, exposure rate monitoring of natural radiation reference field 80−67017
environmental radioactivity meas. in the EEC, 1977, for air, deposition, water and milk 79−62162
environmental radioactivity prior to the Kori nuclear power plant operation 79−6773
environmental radioactivity standards, USA 77−38431
environmental radioassay, Italy, appl. of quality control procedures 79−25117
ERDA nuclear plants, radiation levels in environmental vicinity 78−9002
experimental radiation transport to large distances from a bare reactor 79−59275
fallout at Chilton, Oxon. (1951-1977) 79−6775
fast neutron criticality monitor, response to prompt critical bursts 80−63398
fast reactor burnup, correlation of $^{134}Cs/^{137}Cs$ 80−677
fast reactors, track detector determ. of fuel contamination of primary Na coolant 80−32394
fast-neutron detector for use as criticality monitor 77−65391
FBR fuel reprocessing, radiological protection problems 80−5376
fibre-optic dosimeter, for large areas 77−46423
field measurements, relationship to calibration values 80−58002
film dosimeter exposure anal. method *(Bulgarian)* 79−85831
film dosimetry, endurance of film in personnel monitoring 80−23171
fine γ spectrometry and release meas. *(French)* 79−3258
FIR laser, optically pumped, nearly transparent power monitors 80−5773
fission reactor, breached fuel element diagnosis, use of fractional release ratio ^{137}Cs to ^{131}I 78−21713
fission reactor, containment leak rate test duration time, acceptability of eight hour test 78−21700
fission reactor fuel, gamma-ray spectrometric determ. of fission product activity and activity ratios 78−37430
fluid radioactive waste monitoring equipment, USSR standards *(Russian)* 78−89998
free air chamber for X-ray exposure standardisation at high quantum energies 80−14053
French nuclear power plant gaseous and liquid effluent release monitoring *(French)* 79−13551
French nuclear power plant occupational radiation exposure meas. and prediction 79−9900
fusion reactor materials, nuclear response functions library, MACKLIB-IV 79−67950
gamma alarm device, portable, with audible/visual warnings 78−8390
gamma and X-ray, phys. quantities used 80−99344
gamma radiation monitor testing, compact set-up with ^{60}Co reference gamma source 77−10494
gamma-ray environmental measurements using standard Ge(Li) detectors 77−38568
gamma-ray flux measurement, NaI(Tl) scintillation counter *(Japanese)* 77−71732
gamma-ray natural flux spectral distribution, analytical approx. 78−815
gamma-ray spectrometer, remote computer-controlled, for nuclear power plant monitoring 79−9916
gamma-ray spectrometer systems, portable, in situ field meas. applications 79−9958
gamma-rays from extended sources, energy distrib. calc., rel. to remote spectroscopy of Earth surface 78−61586
gaseous reactor wastes, dispersal forecasting *(French)* 78−8995
gaseous release monitoring and γ spectrometric analysis *(French)* 79−3259
geothermal steam, ^{222}Rn emanations, rel. to seismic activity 78−11832
geotoxicity hazard index for radioactive waste storage 80−97822
graduate educational program to prepare science majors for career in radiation health physics 78−4427
graphite health physics monitor for high energy neutrons 77−83116
gross monitors, estimation of inhalation doses from airborne releases 79−13532

radiation monitoring continued
health physics aspects of 20- to 40-MeV LINAC operations 79−45482
heavy ion and He dosimetry and instrumentation 79−20675
HTGR block fuel elements, fuel zone location meas. using gamma scanning *(German)* 79−67847
HTR, fission chamber development 79−76112
human body monitoring, radioisotopes direct determination 79−54602
human internal radiation counting, Los Alamos multiple simultaneous system 80−61709
ICRP new concept of person dose, related to film badge exposure 79−29631
imaging alpha detector, radioactive contamination monitoring appl. 80−102384
in-plant radiation monitoring standards 79−59276
Indian nuclear power station effluent monitoring system requirements and experience 79−13552
inert gas release by nuclear reactors in West Europe 77−50305
inert gas treatment at nuclear power station 77−50306
infralow frequency signals, apparatus for running dose and mean value meas. 79−83936
inhaled heavy elements deposited in vivo, external counting, review 80−36152
integrated radiochemical laboratory for radiological environmental anal., design 80−57994
integrating radiation dosimeter, using polyethylene and Pirani vacuum gauge for range 10^4 to 10^8 rad. 79−747
internal contamination monitoring in GDR 80−67259
ionisation chamber, design, maximum permissible fluence instrument 79−22556
ionisation chamber for X, gamma rays, performance monitoring of radiation shielding 79−6797
ionising radiation, personnel exposures, dose limits 80−99350
IRT-2000 fission research reactor, personnel radiation monitoring and reactor radiation charact. 79−71927
isotope record monitoring system, computerised 79−70652
JOYO experimental fast reactor, radiation protection monitoring programme 80−57992
Kodak Type II film badges, gamma dose meas. in presence of thermal neutrons 79−39517
labelling of materials with short-lived radioisotopes produced at the place of application *(German)* 79−89503
laboratory computer system for routine, plant and environmental radiation monitoring appl. 79−9912
laser, far IR optically pumped, monitoring by piezoelec. transducers 80−102729
laser beam diameter fluctuations meas. 78−87086
laser light, dosimeter for health physics evaluation of operating conditions at laser installations 80−76835
leakage radiation charact., 18 MeV, clinical linear acceleration 79−5379
linear accelerator calibration monitor with a memory 80−3821
liquid activity meas. instrumentation in Czechoslovakia 79−49873
liquid effluent beta monitor 77−61656
liquid effluents, aquatic radiological impact anal., radiocaesium transport in sediment 80−95486
liquid waste, control of hospital waste using NaI(Tl) detectors *(Italian)* 80−56224
LMFBR, computer model for ^3H transport and release 79−36371
low level radiation monitors, calibration accuracy and precision 80−9428
low level radioactive waste disposal site, trench water study 79−52963
low-level transuranic storage, radwaste Sr, Cs, Co sorption meas. on soil sediment 80−95482
Lucens reactor accident, alarm and surveillance 78−50283
lung monitor for assessment of low energy photon emitters 79−25067
LWPR, radiological emergency monitoring and instrumentation, Federal guidance 80−57961
LWR, chemical factors controlling γ radiation fields around coolant circuits 80−5371
LWR, fuel reprocessing plant, NDT control methods 80−5314
LWR gamma-scanning meas. of spent fuel elements, appl. to reactor simulation *(German)* 79−67874
LWR plant, occupational radiation exposure, recommended limitations 79−59266
LWR plant, plume exposure monitoring system 80−42875
LWR power plant, radioisotope activity meas. in secondary loop coolant 80−5345
LWR power station radioactive unplanned dischage meas. 78−89995
metabolism and dosimetry of low energy β-emitters, ^{14}C labelled compounds 79−8551
microprocessor based digital system, communication techniques 79−49866
microprocessor based systems 77−67897
microprocessor controlled long lived alpha emitter monitor 80−58069
microwave instruments, evaluation and comparison 79−96667
microwave radiation hazard monitors, measurement standards for calibration 80−26374
microwave radiation monitor 77−26401
milk radioactive fallout monitoring in Britain 80−12283
monitor evaluation, techniques for producing standard EM fields 79−97341
moving electrode instrum. for radiation dosimetry and control 79−3244
multi-channel analyser, portable microprocessor controlled, accessories, data acquisition 80−63474
multi-site nuclear utilities, centralized in-house environmental laboratory services 79−85821
multielement α-spectrometry for individuals and environment monitoring 80−58024
natural radiation exposure, New Zealand, soil survey and air doses for ^{226}Ra and ^{232}Th daughters and ^{40}K 78−88747
natural soil radioactivity monitoring with portable gamma ray specstum. 80−31148
naturally occurring radioactive sources, external environmental radiation levels 78−9001
naturally occurring radionuclides in building materials, estimation and control of population dose 78−9000
neutrino channel monitoring system, acquisition of digital information 77−3199
neutron dosimeter and monitoring instrumentation calibration using ^{252}Cf and $^{238}PuBe$ sources 80−13946
neutron dosimeter based on ^{237}Np fission, for personnel 79−13539
radiation monitoring continued
neutron monitor calibration, standard fields at Physikalisch-Technische Bundesanstalt 80−57999
neutron personnel monitoring film, Kodak NTA, energy depend. 79−100753
neutron radiation damage simulation, effect of He preinjection on swelling of stainless steel 80−44236
neutron spherical survey meter response 80−18679
non-ionising radiation, cholesteric liquid crystal appl. 79−2818
nonionising RF and microwave radiation hazards *(French)* 80−3824
NRPB TLD and dose record keeping service 80−5344
nuclear accident dosimetry system for criticality accidents 77−88288
nuclear energy production, research review *(Hungarian)* 78−74414
nuclear facilities, off-site radiological impact assessment real-time computer program CEPADAS 80−95475
nuclear facility, optimisation of radiation detector position and number 78−55043
nuclear failed fuel element detection by delayed neutrons using solid state track-etch technique 80−5249
nuclear fuel motion measurement, HCDA simulation, time resolved coded aperture imaging system 78−45764
nuclear fuel nondestructive assay instruments, in-line evaluation 79−85589
nuclear fuel reprocessing plant, neutron monitors for process and safety control 80−5458
nuclear installations, radioactivity release, air monitoring, emergency procedures 78−70610
nuclear materials accounting, perimeter monitors 79−89509
nuclear plant, off-site emergency monitoring systems 78−46178
nuclear plant airborne effluent variable-trajectory puff advection model modifications 78−94149
nuclear plants, digital differential pulse rate meter 78−37451
nuclear power plant, digital systems 78−816
nuclear power plant, radiation monitoring systems, review 78−33292
nuclear power plant decommissioning, IAEA defined options 79−81071
nuclear power plant environmental monitoring programs design 78−70647
nuclear power plant monitoring meter 79−54604
nuclear power plant radioactive liquid direct meas. instrument design *(Russian)* 79−3250
nuclear power plant vent-air monitoring by nuclide-specific detection system 79−3249
nuclear power plants, personnel monitoring concepts 79−85822
nuclear power plants and the fuel cycle, conf., Bristol, England (Nov. 1978) 80−4471
nuclear power plants secondary system radioactivity monitoring 80−18445
nuclear power station, decentralised system using microprocessors *(Spanish)* 80−47727
nuclear power station, personnel dosimetry and access monitoring by process computers *(German, English)* 78−17440
nuclear power station, radiation monitoring system *(Russian)* 79−31230
nuclear power station, US metalwork flaw detection system *(Russian)* 78−25302
nuclear power station, Vermont Yankee, radiation field measurements 79−9893
nuclear power station, Zarnowiec, contamination monitoring station *(Polish)* 80−74033
nuclear power station radioactive emissions meas. and control, survey 79−85818
nuclear power station radioactivity meas. *(German)* 79−67876
nuclear power station stack effluents, radiation monitoring 78−46179
nuclear power stations, ambiental radiology, equipment and methods, review *(Spanish)* 79−45425
nuclear power stations, radiation dosage determination, monitoring and control for personnel safety *(German)* 80−842
nuclear power stations, radiation safety, doses to personnel, local population 77−71701
nuclear reactor accident risk calcs., models and data 80−47613
nuclear reactors, remote monitoring system 77−50307
nuclear site decontamination, radiochemical anal. of environmental samples 80−95477
occupational exposure at Millstone 2 PWR, long-term man-rem meas. program 80−5383
occupational exposure Taiwan (1973 to 1975) 77−16985
occupational radiation exposure, evaluation and control, US research program 80−5370
occupational radiation exposure at nuclear power plants, meas. and prediction 79−59182
ocean sedimentation rates determ. by nondestructive gamma-gamma coincidence spectrometry 78−85709
offshore environmental monitoring program for proposed nuclear power plant in Islote, Puerto Rico 78−11917
on-line computer application to radiological protection programme of Tokai-II nuclear power station 80−5391
on-line radiation monitoring at a nuclear fuel reprocessing plant 80−95469
on-line radiation monitoring at fuel reprocessing plant 79−85731
Ontario Hydro nuclear power plant stack effluent monitoring 79−3254
Oregon, meas. of natural radioactivity 80−37638
Parker, H.M., biographical note on medical physics contribs. 80−12
particle accelerators, radiation exposure, design of cooling and ventilation systems 80−5350
particle accelerators, radiological safety in design and operation, American National Standard 79−89511
particle beams, monitoring at high frequencies 77−88316
particulate contamination monitoring, recent developments 80−57985
PBF, temp. sensitivity of Co self-powered neutron detectors under PWR conditions 78−33275
person dose, ICRP concept, related to exposure in industrial radiography 79−5370
personal, effect of environmental radiation, thermoluminescent dosimeter *(Japanese)* 80−61707
personal dosimetry instrument for airborne radon daughter meas. *(French)* 80−57989
personal radiation monitor checker 79−16312
personal sampling devices for atmospheric contamination monitoring *(French)* 80−57986
personnel dosimeters based on film badges and TLDs, appl. *(Russian)* 78−20293
personnel dosimetric control in Hungary *(Russian)* 78−20292

radiation monitoring continued
personnel dosimetry, automatic film-badge reading system 78−40335
personnel dosimetry in USA, survey results 78−53500
personnel dosimetry methods introduced in the Czechoslovak national laboratories 80−57969
personnel monitoring for radiological protection, current status and developments, review 79−22490
personnel monitoring measurements 77−40782
personnel monitoring performance standards 77−40783
personnel thermoluminescence dosimetry reader, microprocessor controlled 79−45428
phoswich battery operated portable detector for field monitoring of transuranic contaminants 79−683
photon radiation meas. in nuclear power stations 80−63403
pion$^-$, sensitivity of personnel monitoring film 78−28079
pion range monitor, test using the radiative capture $\pi^- p \rightarrow n\gamma$ 80−72317
pocket radiation chirper, CdTe crystal and electronics 79−68165
pollutant release assessment, JEREMIAH computational system environmental transport and dose calcs. 78−94150
portable body monitoring system, NRPB experience 80−104773
portable radiation meters, accuracy checking facility at Berkeley Laboratories, UK 78−74507
power station, personnel dosimetry monitoring, use of evaluation device for rod and process computer *(German, English)* 78−17441
pressure vessel surveillance capsules, remote disassembly and examination 79−45463
programmes at Point Lepreau nuclear power station 78−29552
protection monitoring in tropical developing countries 80−57997
protective coatings, decontamination test procedures 77−34475
proton, high altitude radiation obs., design and performance evaluation of Cherenkov telescope 78−86734
proton beam 70 GeV, for Protvino Inst. neutrino expts., characts. 78−37475
proton spectra, high energy, emerging from 680 MeV synchrocyclotron shielding 78−17530
proton synchrotron, radioactivity of subsurface water in ground shield 77−67907
pulse processing technique, pulse shaping *(Japanese)* 79−81138
pulse shape discrimination for alpha-gamma separation with trans-stilbene 78−13386
purpose and aims 80−57968
PWR, normal operating radiation levels 77−88290
PWR, Oconee, occupational exposures, radiation levels and waste levels during operation 78−21726
PWR, power stations containing VVER-440 reactors, radiation safety of personnel and local population 77−71700
PWR, radionuclide surface activities meas. 80−13941
PWR, system for internal neutron meas. *(French)* 79−76113
PWR, T sources, releases, monitoring, management and environmental impact 80−18690
PWR containment air monitoring system 80−57965
PWR decommissioning, safety, cost and occupational radiation exposure estimates 79−67903
PWR radioactive gaseous effluents, relase trends in US 1977 80−95481
PWR steam generator, γ-dose rate distrib. meas. 80−5382
RA reactor fuel, gamma-spectrometric determ. of fission product activity ratio 78−33269
radiation exposure meas. in aircraft from transported radioactive goods 79−22488
radiation exposure near nuclear power plants, remote monitoring system 79−18055
radiation exposures from film dosimeters, analogue computer anal. *(Bulgarian)* 79−85877
radiation monitor, Pu wound, sensitive simple instrument 79−8547
radiation protection instruments for personnel dosimetry, area and environmental monitoring 78−66427
radiation protection progress report, EEC, 1978, book 80−22148
radiation safety monitoring instrumentation complex at the USSR nuclear power plants *(Russian)* 79−76108
radiation units in SI system, conversion problems 80−57244
radiative waste, low- and medium-level surface and concrete-lined trench storage, seven years' experience report *(French)* 77−61579
radioactive aerosol dispersiveness at nuclear power station 78−70650
radioactive aerosols, atmos. conc. monitoring, radionuclide anal. 80−21427
radioactive contaminant unplanned release meas. and countermeasures 78−89994
radioactive effluent, Pu and Am inventory of ecosystem near a nuclear facility 80−97820
radioactive effluent monitoring, sampling and measurement principles *(French)* 78−89996
radioactive effluent monitoring, symposium, Portoroz (1977) 78−89985
radioactive effluent monitoring problems, loss and error reduction procedures 78−89987
radioactive fallout on Milan 1976-7, influence of Chinese nuclear expts. *(Italian)* 78−58501
radioactive ores, specific sensitivity of NaI(Tl) scintillator in γ-ray meas. 78−81449
radioactive release monitoring equipment test gas standard production *(French)* 79−3252
radioactive waste, commercial burial site, radionuclide dynamics and health implications 77−61618
radioactive waste, control and accountability by gamma scan assay 79−9913
radioactive waste, high-level, leaching of radioactivity from glass blocks buried below water table 77−65312
radioactive waste, solidified, assessment of loss of isotopes 79−54541
radioactive waste in deepsea disposal sites, environmental surveys using submersibles 77−61617
radioactive waste processing, health physics implications 79−57727
radioactive waste storage, in situ instrumentation for meas. of radionuclide migration 80−95485
radioactive waste storage, integrated biological dose evaluation 80−5379
radioactive waste storage, long term subsurface migration of radionuclides 80−95483
radioactive waste storage, radionuclide migration determ., adsorption of Cs(I), Sr(II), Eu(III), Co(II), and Cd(II) by Al_2O_3 80−99240
radioassay services in developing countries, recommendations 79−31220
radiochromic-based monitoring system 77−70264
radiographic phototimers, acceptance testing and performance monitoring 77−5071

radiation monitoring continued
radioisotope transport in terrestrial food chains, dynamic modelling using RAGTIME code 80−104776
radioisotopes, identification, possible problems *(Chinese)* 79−89506
radiological assessment of inactive nuclear sites, statistical design and anal. 80−95473
radiological assessment of inactive nuclear sites 80−95478
radiological survey of inactive nuclear sites, quality assurance 80−95472
radiolyoluminescence, appl. to dosimetry of ionising radiation 79−62374
radionuclide migration from buried radioactive waste 80−95484
radionuclide migration in seawater and marine sediments *(French)* 78−11916
radionuclide transfer to crops and agricultural products *(French)* 78−8996
radiopharmaceuticals, γ-emitting, in rat blood, continuous monitoring technique 79−2129
radiowaste storage, soil homogeneity evaluation by radionuclide tracer breakthrough curve interpretation 80−97821
random summing in multi-detector counting system meas. radionuclide mixtures 80−36097
reactor containment air contamination, sampling and measurement techniques *(French)* 78−89997
reactor coolant activity monitoring, automatic on-line system 80−684
reactor integrated safeguards system, fuel labelling and perimeter monitors 80−37536
reactor neutron flux meas., high temp. neutron rad. detectors and cables 79−76111
reactor neutron flux meas., integrated cable detectors for use under flux and/or at high temperature *(French)* 79−76114
reactor neutron flux meas., self-powered neutron detector with enriched-U emitter 79−76115
reactor out-core components, field prediction 77−6571
reactor portal monitors, evaluation and vulnerability anal. 79−49722
reactor safety, quantifying plant availability, ALARA, and occupational radiation exposure relationships 79−59183
real-time environmental α-β-γ radiation monitoring system 78−94152
reference radiations for radiation protection dose meter calibration *(French)* 80−57998
refueling and fuel handling, ALARA occupational radiation exposure 79−67914
remote radiation monitoring apparatus for processes of extractive separation of transuranium elements 79−71983
remote working level monitor, microprocessor assisted calibration 77−61616
research animals, monitoring of airborne tritium evolution 79−39526
research reactor, self-protection criteria for reactor fuel elements 80−9361
review of nuclear fuel cycles and waste management 78−54863
RF environmental field intensity automated meas. system 77−37947
RF fields below 300 MC/s, legislation proposals for workers' protection 80−56223
rod dosimeters, automatic evaluation of staff dosimeters during reactor shut down *(German)* 79−67960
routine environmental radiation monitoring at WNRE 78−82533
sampling sites, criteria for minimum number 79−53013
self-powered detector responses, detailed analysis by Monte Carlo methods 77−46360
semiconductor radiometer-spectrometer for meas. of surface contamination by α-radioactive materials 77−38423
Serpukhov proton synchrotron shield, mixed radiation dose equivalent outside 80−32530
shadow-shield background reduction method 80−108999
single channel counting rate monitor 77−30729
Sizewell power station 80−5387
sky-shine computational procedure *(German)* 80−74036
soil residual contamination levels and decommissioning nuclear facilities, radiological criteria 78−11747
solar, precision meas. instrum., biological response study applic. 77−52839
solid-state nuclear track detectors, development and use for reactor phys. expts. 78−41886
source level flux monitor expts. 77−54337
spent nuclear fuel inventory confirmation technique using Cherenkov light intensity meas. 80−78419
stack effleunt monitor in-place testing 79−3257
stack gas monitor, β scintillation detector+Ge(Li) detector system, environmental γ dose *(Japanese)* 79−3246
stack release radioactivity monitoring with digital processing 79−3253
standardisation in nuclear radiation meas. technology with SINUPERM system 78−50410
statistical errors in continuous collecting and counting 79−54603
statistical methodology for radiological surveying 80−57993
submillimetric wave noise interaction with rainy atmospheres 77−41138
superheated drop detector 79−72201
surface contamination meter 79−22494
surface contamination monitoring, test surface method 78−50409
surface contamination monitors for hospital use, calibration 80−36153
Switzerland, radioactivity surveillance and descent of Kosmos 954 *(German)* 78−77119
synchrotron, alternating gradient, efficient slow extraction, nonlinear growth of betatron oscillations, magnetic septum 80−47793
Tarapur Atomic Power Station radioactive waste discharge monitoring 78−89989
Tennessee Valley Authority occupational radiation exposure data management system 79−9899
TFTR, isodose contour map construction using DOT 3.5 computer code 79−67949
Thailand's first nuclear power plant, radiation monitoring programme 80−57996
thermoluminescence dosimeter, personal monitoring, judgement of uncleanness in elements by residual value method *(Japanese)* 80−21546
thermoluminescent TDP-2 instrument, improved sensitivity 79−89504
thermoluminescnece environmental monitoring methods and techniques at nuclear facilities 79−85819
Three Mile Island, environmental radiation monitoring using pressurised ionisation chambers 80−37637
Three Mile Island malfunction, monitoring, radiation exposure 80−57960
tissue equiv. medium, simultaneous meas. of neutron and gamma ray spectra 78−5058
TLD, automatic readers for personnel monitoring 78−50408

radiation monitoring continued
TLD, neutron dose monitoring using multiple LiF TLD badge 77−90907
TLD cards based on $CaSO_4$:Dy Teflon discs, annealing and repeated readout 80−3812
TLD element, precise calibrator *(Japanese)* 80−23159
TLD personnel monitoring, occupational radiation exposure in Austria *(German)* 80−26352
TLD system, automated, for gamma radiation monitoring 80−57964
TLDs, use in personal monitoring, judgement of abnormal value by glow curve *(Japanese)* 80−106208
total α and β counting of thick samples, review 79−36488
total radiation monitoring using liquid crystals and thermoluminescence 80−3819
track-etch monitor for reactor power anal., evaluation 80−78418
transport of radioactive material, statistical anal. of low-radiation packages 77−88286
transuranic aerosol measurement system and its field results 80−58068
transuranic aerosols, online high sensitivity measurement system 77−65334
transuranic analysis requirements, suitability of current and methods 79−96400
transuranic elements in air at nuclear reprocessing plant, monitoring system 80−63409
transuranium and other radionuclides, conc. and distribs. in nuclear power plant environs 79−93841
tritium, permeation test facility at Julich, safety measures and monitoring 79−36428
tritium distribution in technological systems of Novovoronezh nuclear power station 80−32533
Trombay nuclear facilities, effluent release monitoring procedures 78−89993
troposphere, ^3H in water vapour, rel. to reactor release detect. 78−11988
UK nuclear power station radioactive effluent monitoring and public information 78−89992
university hot laboratory, radiation monitoring programme 80−57991
USA diplomatic courier radiation exposures 78−28078
USA Energy R&D Administration effluent date collection and reporting system 79−13545
UVB spectral irradiance monitoring at 9°, 39° and 71°N 79−58070
Victoreen 555 integral and rate exposuremeter, digital display plug-in module 77−405
virtual impactor aerosol separators, analytical study 80−42874
waste, packaged, Ci content determ. from meas. exposure rate 77−6566
waste water, radiation treatment, process control techniques appl. 79−96489
water cooled, water moderated reactor, coolant tritium content in first loop 80−32334
water pollution by reactor organic coolant, environmental effects 79−66425
water pool spent fuel storage units, neutron anal., criticality state *(Spanish)* 80−32517
West German LWR power plant stack monitoring, legal and technical aspects 78−89988
West German nuclear plant airborne radioactive effluent monitoring 78−89990
West German nuclear power plant liquid radioactive effluent monitoring 79−13554
Westinghouse PWR, radiation levels 80−5296
whole body counter, portable chair type for in vivo internal contamination monitoring 78−61260
whole body counters, international intercomparison 80−78504
wideband nuclear radiation monitor using photodiode and op-amps, cct. 78−78591
working level survey meter 3R-WL, meas. of α-particles from ^{218}Po and ^{214}Po 78−25330
wrist watch dosemeter for ionising radiations, practicality tests 80−57972
X-ray area exposure product monitor, DQ-20 *(Japanese)* 77−73578
X-ray solid-state beam monitor 79−36431
X-ray survey instruments, automated calibration and recordkeeping system 77−37876
Zircaloy solid wastes from fuel reprocessing plant, management 77−61591
α-emitting effluents from nuclear processing plant, detection and meas. 80−95468
γ ray natural background, exposure rate variations in open air *(Czech)* 77−67900
^{241}Am and $Pu/^{241}Am$ ratios, environment meas. using X-ray spectrometry 77−60265
^{241}Am soil concs., in situ gamma anal. and sampling data comparison, Nevada 77−64143
^{37}Ar form. from Ca in fission reactors 77−83048
^{41}Ar dose distributions due to atm. release from HWR 77−14271
^{41}Ar release from TRIGA reactor, comparison of γ-ray detectors 78−57309
B neutron capture therapy of brain tumours, simultaneous flux monitoring system 79−92352
B_4C-Al(silicone)(graphite), neutron shielding materials, long term radiation effects 80−9413
CO_2 laser Helios fusion system beam diagnostics 80−78882
^{14}C and ^3H, sensitive method *(German)* 77−372
CaF_2:Mn TLD, internal background build-up 77−54399
$CaSO_4$:Dy TLD, monitoring of environmental radiation levels 79−93839
$CaSO_4$:Dy TLD, thermal neutron and γ-ray meas. in mixed radiation field, activation and capture gamma technique 79−738
$CaSO_4$:Dy Teflon TL dosimeters, thin, development for β-dosimetry in personnel monitoring 80−63399
$CaSO_4$:Dy Teflon TLD discs, metal filters for compnesation of photon energy depend. 80−30901
CdTe detector for personal radiation chirper 79−45557
CdTe γ spectrometer, use in monitoring activity deposited in nuclear power stations 77−42193
^{252}Cf neutron source, dosimetry meas. technique tests 79−68113
^{60}Co gamma ray sources, exposure efficiency dependence on distance, theoretical interpretation *(Czech)* 80−850
^{60}Co long-lived γ-emitting aerosols, max. allowable emission rate from nuclear power station 80−32532
^{137}Cs contamination of external-radiation doses in USSR territory 78−86698
Ge detector system for inhaled radionuclide detection and meas. 80−57990
Ge detectors used for high resolution gas ray spectroscopy 79−6804
Ge on-line, hyperpure detector, radiation monitoring system 78−37493
Ge(Li) anticoincidence shielded spectrom. for environmental radionuclide meas. 79−6791
Ge(Li) in situ environmental spectrometer, spectrum-to-exposure rate conversion function 77−65379
Ge(Li) in situ spectrometry, exposure rates due to rainfall 80−42873
Ge(Li) system for low level radioactive gas monitoring 78−9038
Ge(Li) upward looking dip-stick type spectrom., in-situ environmental γ-ray meas. 78−37480
HT-HTO in air meas. system 80−21433
^3H, environmental surveillance, sensitivity to natural fluctuation of tritiated water vapour in troposphere 77−88287
^3H, in liquid media and working area air at nuclear power sations 77−71699
^3H intake during various processes in industrial, academic and medical institutions 77−73600
^3H levels in urine of occupational exposed persons, working environment effects 79−83947
^3H monitors, calibration technique *(Czech)* 80−74075
^3H urine analysis, liq. scintillation solns. 77−9273
^3He-filled proportional counter, for sensitive dose or dose equivalent meter 79−45427
I, radioactive, air sampling system, separation into gaseous and particulate fractions 80−57962
I radioisotopes, high efficiency mixed species air sampling, readout and dose assessment system 78−57074
I trapping in ventilation system, user guide to codes ITRAP-A(B)(S)(L) 79−93843
^{125}I airborne vapour detection 80−51027
^{125}I contamination monitoring using portable scintillation camera 78−85388
^{125}I iodination for immunoassay, thyroid uptake and film badge monitoring of workers 77−13013
^{125}I surface contamination meas., due to medical use of ^{125}I sources, detectors sensitivity comparison *(Czech)* 79−34673
^{125}I thyroid dose calc., air and water conc. limits 79−88195
^{125}I uptake minimisation and thyroid monitoring 77−40796
^{125}I worker thyroid meas. 80−36151
$^{129}I_2$ radioisotope detection in nuclear fuel cycle, intracavity selective absorpt. analysis 78−46182
^{131}I air concentrations, comparison of calculated and meas. values 77−34477
^{131}I, airborne conc. in nuclear medicine lab. 79−34674
^{131}I, environmental, in vivo thyroid monitoring 77−9264
^{131}I in human thyroid gland, rapid monitoring using Ge(Li) detector 79−2134
^{131}I transport from pasture to milk, modelling Dresden-Monticello data 79−88203
^{85}Kr concentration in atmosphere over USSR (1971-1975) 78−37453
^{85}Kr monitoring system with permselective membranes 79−3260
^7LiF-Teflon disc TLD, determ. of neutron fluence and γ-dose distribs. 79−45434
NaI(Tl) scintillation survey meter, for ^{131}I meas. in human thyroid gland 78−80970
^{237}Np dosimeter and spark counting system, for routine personnel monitoring 78−89984
^{210}Pb from nucl. explosions in environment 78−21774
^{212}Pb inhaled body burden calibration, general phantom procedure 77−64138
Pu air monitor with background compensation system 80−27824
Pu contaminated solid waste streams, passive neutron assay 79−36373
Pu fallout detection using fission tracks prod. with neutron irrad. spectra 80−95479
Pu handling, radiation protection and monitoring of personnel 80−5389
Pu holdup in glove-box exhaust filter, in-line monitoring by gamma ray detection 80−78458
Pu laboratory stack monitoring, computerised system 79−3256
Pu, nuclear fuel workers management 79−74763
Pu, safe working, safety measures 79−41040
$Pu/^{241}Am$ ratios, environmental meas. using X-ray spectrometry 77−60265
Pu-Am survey instrument, β-α-γ-X-ray scintillation detect. probe 78−33376
Pu-island element, B304, gamma scanning of power and burnup distrib. 80−721
^{239}Pu, evaluation of portal monitors for the detection of nuclear materials 80−63406
^{239}Pu soil concs., in situ gamma anal. and sampling data comparison, Nevada 77−64143
^{239}Pu-^{241}Am monitor for in situ soil surface and pond bottom assay 77−9546
Ra and daughter products, personal dosimetry and area monitoring *(Japanese)* 78−55044
^{226}Ra determination in water, sampling and meas. methods 77−9278
^{226}Ra in Taiwan buffalo bone and environmental samples of N. Taiwan power reactor site 77−64142
^{86}Rh releases, continuous air monitor appl. 77−46411
Rn and daughters meas. methods in underground and free atmosphere air 80−57987
Rn and Tn, air concentration in dwelling places *(Hungarian)* 77−78409
Rn, at active U mines and mills, emission and control 80−41264
Rn continuous monitor response to transient Rn concs. 80−32519
Rn, continuous monitoring system 79−76150
Rn daughter airborne conc. meas. in atmosphere 80−37636
Rn daughter time-integrating environmental TLD dosimeter 79−67962
Rn detection, effect of humidity 77−6647
Rn emanation from ground, statistical anal. 80−41259
Rn, long term average level meas. instrument 80−58085
Rn monitoring, TLD, passive detector, U mill field 80−57963
Rn monitoring instrumentation 80−106204
Rn release from geothermal resources 80−41263
Rn releases from nucl. power phosphate mining and coal burning 80−46072
^{222}Rn, conc. in air, absolute determ. using cellulose nitrate track detector 80−63492
^{222}Rn conc. in energy efficient buildings 80−41261
^{222}Rn conc. monitoring by proportional counter, study of thermal diffusion in Rn-CO_2 mixture 79−50839
^{222}Rn concentration in water, meas. by gamma counting 78−53733

radiation monitoring continued
^{222}Rn concentration meas. by plastic detectors to determ. environmental α-emitters from natural sources 80−91292
^{222}Rn daughters, meas. of low conc. in air 78−28308
^{222}Rn determination in air and water, sampling and meas. methods 77−9278
^{222}Rn diffusion through U mill tailings covers, coeff. meas., lab. techniques 80−95387
^{222}Rn, environmental sources in contiguous United States 80−41258
^{222}Rn flux measurement using charcoal canister 77−6646
^{222}Rn gas detection using Track Etch system for U exploration 80−98488
^{222}Rn, human exposure due to Ra bearing residues 80−41260
^{222}Rn, passive environmental monitor based on exoelectron dosimeter 78−82523
^{222}Rn, sources, distrib., exposure in residential buildings 80−41262
Ru, hazards and control in nuclear fuel cycle, review 79−36392
Si diffused junction detector for alpha air monitoring instrumentation 80−58083
^{89}Sr and ^{90}Sr, radiochem. determ., error anal. comparison of methods 77−16873
^{90}Sr bremsstrahlung radiation meas. for well logging using Ge spectrometer 80−94619
^{90}Sr contamination of external-radiation doses in USSR territory 78−86698
T in air, scintillation detection using liquid adsorbent 79−76291
T in water, flow cell type detector for continuous monitoring in high γ-background 78−82524
T monitoring at nuclear power stations 80−18691
T monitoring methodology using SiO_2 desiccant, appl. to research reactor facility 80−21434
T, sampling and meas. in environmental samples using gas-filled proportional counters 78−86699
T species, sources and reactions 80−21432
T storage and monitoring, CANDU heavy water reactors 80−5291
U, in porcelain dentures, rapid anal. by delayed fission neutron method 78−15907
U mill radiological effluent and environmental monitoring guidelines 78−94153
U mill tailings, meas. of surface Rn flux, effect of moisture content 78−5056
U mill tailings, radiation pathways and potential health impacts 79−85826
U milling operations, radiological assessment methodology 79−85827
U mines, radiological evaluation 80−42806
U personnel monitoring, 16 yrs. experience 79−76149
U, specific α radioactivity meas. rel. to size using aerosol centrifuge 79−76255
U surface mining, radiation exposures, meas. 77−64140
^{235}U, determ. of amount in urine by delayed-neutron counting 79−25118
^{133}Xe, simple method of air monitoring 79−83949

radiation monitors *see radiation monitoring*

radiation patterns, antenna *see antenna radiation patterns*

radiation pressure
see also acoustic streaming
acoustic, historical review 78−59178
acoustic, standing wave effects in He I, stable microscopic bubbles 78−91381
acoustic longitudinal wave propag., theory, radiation press. problems appl. 78−25998
acoustic radiation force on sphere in quasistationary wave field, expt. 79−41482
acoustic radiation force on sphere in quasistationary wave field, theory 79−41481
acoustic radiation load, coupling between two finite-sized spherical sources 77−79982
acoustic radiation press. on an absorbing sphere 78−79154
acoustic radiation pressure on a sphere 77−84035
acoustic radiation pressure on sphere in standing wave field, meas. 77−79989
aerosol, photophoretic motion, particles ≪ light wavelength, gas collisional effect 77−90646
aether drag and radiation press. in dispersive medium 79−35124
Ap and Bp stars, radiation forces and B abundance diffusion theory 79−88664
artificial satellite with ecliptic plane orbit, solar radiation orbit perturbation 78−4088
artificial satellites orbital perturbs. due to Earth radiation, new albedo model 79−21020
atmospheres, wave propag. with high radiation pressure 80−26729
atmospheric thermal balance meas. by radiation pressure on satellite microaccelerometer 79−2380
atom cooling and trapping by resonance radiation pressure 79−72291
atom in laser field, reson. light press. forces, cooling and trapping appls. 79−98045
atom-photon interaction quantum fluctuations, at. beam focusing by radiation press. 80−58217
atomic beam, focused with laser beam, Na beam and dipole forces 79−7066
atomic beam deceleration and monochromatisation laser radiation press. 80−102491
atomic beam separation by light press. in isotope-separation setup 80−52943
atomic gases, cooling by reson. EM radiation, kinetic theory 79−77327
atomic motion in resonant EM wave, two-level atom 79−18155
atomic motion in resont fluctuating laser radiation 80−43310
atomic movement, reson. light press. due to strong standing wave 78−50529
atomic transition, inverted, anomalous resonance-radiation press. 80−52946
atomic velocities, phasing in field of moving EM wave *(Russian)* 80−14253
atomic velocity distrib. hole-burning by EM radiation 80−64674
atoms, motion in optical freq. radiation trap 80−78818
atoms, reson. radiation force, quantum mech. fluctuations, influence on at. motion 80−58233
atoms in resonant laser fields, cooling, trapping and storage 79−59421
balloon satellites orbital vars. 77−78612
binary stars, critical surface, influence of radiation pressure, X-rays and asynchronisation 77−29880
radiation pressure continued
binary stars, equipotential surfaces, modification due to pressure of radiation of component *(French)* 80−56880
binary systems, radiation pressure force influence on critical surfaces 78−96505
blast waves, magneto-gasdynamic radiative, cylindrical, similarity soln. 79−37338
blood cell banding in US standing wave field 79−62291
body repulsion form water surface under laser irrad., optically generated vapour cushion 79−10339
broad band reson. light press., basic eqns. 80−28182
β Cephei stars, radiation pressure and pulsational instability 79−84806
cold magnetised plasma, radiation pressure forces 78−79437
Comet Ikeya-Seki (1965 VIII), polarization reversal, grain segregation due to radiation press. 79−8881
comets, radiation pressure accel. effect on neutral species brightness profiles, average random walk model 80−77351
cooling of ions in Penning EM trap 78−66527
Crookes radiometer, physics anal., for teaching 79−35504
dielectric cylinder, infinite, randomly oriented, radiation press. 80−58454
dielectric spheres, resonances in radiation press., dielec. surface wave obs., and size meas. 77−58256
drag and levitation forces on moving resistive sheet 80−18989
Earth, IR radiation press. on Castor satellite meas. from Cactus accelerometer results 80−77251
Earth's radiative balance, meas. by Cactus accelerometer on Castor satellite *(French)* 78−81530
Earth IR emission, Lambertian, of spherical surface, radiation press. on satellite *(French)* 78−81529
Earth radiation budget, accelerometer direct meas. *(French)* 80−46287
Einstein, light quanta, radiation, relativity in 1905 77−31
EM energy-momentum tensor and the properties of material media 79−55020
EM wave, plane, obliquely incident on moving media, radiation press. 78−71007
EM wave absorption/scatt. in moving layer, energy and momentum conservation 78−25775
EM wave packets, 2 dimensional in fluids, radiation pressure effects 77−17828
force exerted by a propagated wave on an obstacle 78−78869
gas, magneto-radiative, shocks 79−37423
gas acceleration above luminous disc, QSOs matter ejection mechanism 77−49373
gas cooling to broad band reson. light press. 80−48835
gas translational nonequilibrium in reson. EM field 80−96340
glass spheres levitated by two horizontal laser beams, stable equilib. positions 77−46743
gravitational wave interferometer, quantum mechanical radiation press. fluctuations 80−90770
HZ Herculis, light curve, radiation pressure effects in X-ray binary 80−105280
holographic interferometric demonstration of effects 79−5943
interplanetary dust, solar radiation effects on orbits 77−5493
interplanetary dust particles rot. bursting caused by solar radiation press. 77−9644
interplanetary H I, solar radiation press. from H Lyman-alpha profile meas. 79−2452
interplanetary small particles in solar system, radiation forces 80−17461
interplanetary submicron grain orbits, gravit. attraction, radiation press. and electrodynamics 79−8879
interstellar dust, grain growth by radiation pressure induced coagulation 80−94851
interstellar matter, radiation-driven instabilities 79−53880
Io Na cloud, solar radiation press. as cause of east-west asymmetries 80−36560
irradiated sphere absorption centres, temperature distribution theory, source function 79−50221
laser, radiation in plasma, nonlinear press. forces 80−28682
laser atomic motion control, vel. selection, cooling, trapping, spectroscopy appl. 77−30833
laser beam levitation of solid transparent spheres 77−7104
laser prod. plasma, radiation press. effects, interferometric meas. 78−51325
laser pulse amplification through energy exchange with electron beam via nonlinear radiation press. effects 80−95776
laser radiation effects on particle properties, radiation pressure effect on particle motion *(German)* 80−102755
laser spectroscopy, mechanical effects of light 79−35846
laser-plasma interactions, effects of pressure 78−38540
laser-produced plasma, light press. effects, steady-state mdoel 77−47234
light beam on refractive spheres *(French)* 77−61911
liquid, absorbing intense IR radiation, behaviour of pressure 80−102749
materials motion around a source whose luminosity changes 79−12394
meteor stream dissintegration, solar radiation and planetary perturbation effects *(Russian)* 80−46495
microwave irradiated materials, rel. to acoustic signal generation 78−24095
microwave ponderomotive effect on transverse electron beam, expt. 79−13886
Na atomic beam focusing and defocusing using reson. radiation press. 80−47143
neutral atoms, stimulated Coulomb interaction in external resonance field 80−83449
nonspherical particle, optical levitation for light scattering obs. 80−58455
OB supergiants, radiation-driven density waves rel. to mass transfer to X-ray binaries 77−9809
object experiencing force perpendicular to EM wave direction 79−22881
optical levitation and partial-wave resonances 79−27170
optical levitation of dielec. or metallic spheres, by TEM_{01}^{*} mode laser beam 79−983
optical levitation of single particle to study quasi-elastic light scatt. theory 80−99620
optical levitation of spheres by laser beam *(French)* 79−98428
optical motion control applied to Atmospheric Cloud Physics Laboratory on Shuttle/Spacelab 80−12634
optical radiation pressure in dispersive medium, photon momentum, drag 78−33666
optical radiation pressure meas. in dispersive media refractive index depend. 78−33665

radiation pressure continued
orbital perturbations of space structures, effect of solar radiation, analysis 79−5723
Pageos 1 balloon satellite, orbital effects of direct solar and Earth albedo radiation pressure 79−88566
particle properties, particle heating by radiation absorption, effect of radiation press. *(German)* 80−106556
photon impulse in medium with negative group velocity *(Russian)* 79−3670
planetary exospheres, collisionless, satellite atoms depletion by radiation press. 79−96933
planetary nebulae, radiation press. effects on structural development 77−64746
plasma flow, radiation press. effects 80−1763
plasma interaction with laser radiation, light press. nonlinear force, polarisation influence 80−100078
plasma waveguide, ion acoustic wave, excited by EM rad. press. 78−26298
Pleiades, radiation press. rel. to filamentary struct. of refl. nebulosity 78−8082
polished metal sphere and microaccelerometer, for absolute meas. of Earth's radiation balance *(French)* 79−29900
ponderomotive forces of EM radn. in sphere 79−76556
porous media, nonisothermal mass transport, thermal energy flux and radiation pressure theory 78−76916
QSO clouds, Rayleigh-Taylor stability of radiation-supported surfaces and slabs 77−53697
QSOs, ionisation equilib., thermal equilib. and radiative accel. near radiation sources with different spectral shapes 80−41909
quasar winds, radiative acceleration for different power law spectra 80−90565
quasars, absorpt. line clouds radiative accel. 78−57683
quasars, radiatively driven gas clouds dynamics and stability, plane-parallel slabs theory 80−22107
radiation pressure, appl. to satellites inertially fixed pitch stabilisation 80−101523
Rayleigh and Langevin radiation press. magnitude calc., longit. wave propag. theory appl. 78−25999
Rayleigh-Taylor modes in fluid accelerated by radn. pressure 77−51133
resonance light pressure, anal. of forces and applications, reviews 79−18156
resonance ponderomotive effects in EM wave scatt. and emission 80−69301
resonant impurity gas, translational nonequilibrium in resonance optical field *(Russian)* 80−106865
rigidly rotating star, influence of nonsphericity and radiation press. on moment of inertia 78−28658
rotating absorbing cylinder in light field, transverse ponderomotive effect 79−64171
satellite orbits, perturbation by solar radiation press. general expansion of disturbing function 77−78605
solar, effect on anomalistic period of artificial satellites 80−77255
solar, effects on interplanetary dust grains 78−20730
solar, for maximization of spacecraft orbital momentum and energy 80−12640
solar corona radiative origins 78−96448
solar Lyman alpha radiation pressure effects on interstellar H and D 79−92686
solar pressure effect on artificial satellite nodal period 77−70987
solar radiation effects on artificial satellite resonances 79−25456
solar radiation pressure, orbital perturbations of spheroidal satellite 80−4219
solar radiation pressure and orientation control of rotating spacecraft 77−53397
solar radiation pressure induced coupled librations of gravity stabilized artificial satellite 80−21888
solar radiation pressure induced orbital perturbation analysis 78−89041
solar sail trajectories, long-term evaluation 79−48641
spacecraft with solar sail, eqns. of motion from geocentric orbit 77−53394
spectral lines in gaseous systems with axisymm. motions, kinematics 79−88579
spectroscopy using action of radiation press. on atoms 77−79164
sphere, force exerted by laser beam, stable optical levitation conditions 79−76733
spherical accretion onto neutron star or black hole, radiation press. effects 78−61725
SS 433, radiation press. rel. to mass accel. and collimation mechanisms 80−4368
standing wave and pellicle, proposed design for very large space telescopes 79−92672
star, variable luminosity, radiation press. rel. to particles 79−44338
stellar expanding envelopes, radiative forces 78−28659
stellar rapidly rotating models with radiation press., struct. parameters calc. 80−67697
subatmospheric nonthermal storage modes vs. radiation pressure for stellar wind origin 77−33468
suprathermal grain production by radiation pressure 79−58391
Thomas-Fermi equation of state, radiation press., high temp., coupling to high-density electron plasma 77−3925
three-body problem, restricted classical case, generalisation for radiation press. 80−85843
transparent hollow sphere, radiation pressure in cylindrical beam *(French)* 78−29896
two-level gas, reson. radiation press. in travelling EM wave field 79−13681
universe, Friedmann model, effect of decoupled radiation field press. on density perturbations growth 80−109567
US perturbation obs. at cellular level 78−61214
US radiation force function, rel. to intensity determ. using elastic sphere radiometer 77−68342
US radiation force variation with differing propagating media gas content 79−32128
US transducer power output meas. using modulated radiation pressure 78−59230
water droplets, small, weakly absorbing, motion in bounded laser beam 79−12269
wave propagation in medium with high radiation press., basic eqns. for homogeneous media 79−88581
A- and B-type stars, radiation forces and B abundance diffusion theory 79−88664

radiation pressure continued
Ge, far IR photon drag and radiation pressure in refractive media 80−60048
Ge, radiation pressure, photon drag effect in far-IR 80−50452
H plasma hemispheric layer total radiation calc. *(Russian)* 78−34278
Mg atoms, cooling to broad band reson. light press. 80−48835
Mg^+ laser cooled ions bound in Penning trap, high-resolution optical spectra 80−102487
Na beam deflection by reson. standing wave radiation 80−52945
Na neutral atom beam, focusing and defocusing forces, radiation press. from CW dye laser 80−52944
Na vapour, laser induced diffusion *(Russian)* 80−6195
Na_2, mol. spectroscopy by photodeflection in supersonic nozzle beam 79−54995
SF_6 molecule drift mobility due to IR laser radiation *(Russian)* 80−69192
Si, far IR photon drag and radiation pressure in refractive media 80−60048
Si, radiation pressure, photon drag effect in far-IR 80−50452

radiation protection
see also radiation monitoring
14 MeV neutron generator, concrete shielding dose transmission factors 77−71702
100 kHz to 300 MHz radiation hazard probe requirements 77−44760
γ-irradiation installation, GOU-1 *(Bulgarian)* 78−82530
absorbed dose distrib. in thin layers rel. to electron beam incidence 80−83226
accelerator shielding problems *(Japanese)* 80−99343
accident casualties, organisation and planning of medical aid *(French)* 78−53528
accident casualty, organisational forms of medical care in German Democratic Republic 78−53529
accident features affecting emergency measures 78−55055
accident handling, conf., Vienna, Austria (Feb.-Mar., 1977) 78−53518
accident handling in Federal Republic of Germany 78−53530
accident investigation, advance prep. 78−57083
accident management, participation of nucl. medicine technologists 77−56486
accident phenomena, human elements *(French)* 78−57084
accidents, effects on public, casualty management 78−53519
accidents, follow-up study programme for irrad. persons 78−53522
accidents, operational organisation *(French)* 78−53531
accidents, use of mobile remote-handling equipment *(French)* 78−53525
achievement, standards and value judgements 80−101273
acoustic radiation, performance of custom-moulded earplugs 80−104774
actinide radioactive waste, biological hazards, consequences for LMFBR fuel recycling 80−86960
actinides, inhaled, research at Nat. Radiological Protection Board 77−48879
activation detectors for neutron flux and spectrum determination 77−71727
adjoint photon transport, Monte Carlo biasing scheme, Compton scatt. and absorpt. 78−77819
advanced fuel reprocessing, remote operation anad maintenance demonstration facility 80−18568
AGR, internal radiation shields, design and performance evaluation 80−5373
AGR, radiation protection during operation and maintenance of irradiated fuel route 80−5375
AGR fuel plug maintenance facility, corrosion product contamination control 80−5388
AGR pressure vessel, safeguards for man-access 80−27790
AGR pressure vessels, radiation protection for shutdown man-access 80−5374
air sampling system at HFEF/N 79−45441
air traffic radiation safety, high-altitude 78−44620
airborne radiactivity in reactor containment building, ^{133}Xe and ^{131}I activity following shutdown 80−47749
ALARA, effectiveness of design modifications 80−18546
ALARA, reactor inplant design, a regulatory viewpoint 80−23016
ALARA inplant design for occupational radiation exposure, cost-benefit anal. 80−18547
ALARA objectives, reactor design for occupational exposure 80−23017
ALARA occupational radiation exposure, utility design viewpoint 80−18548
alpha recoil aerosol penetration of HEPA filters 77−66867
ANS annual meeting, 1977 78−663
artifical satellite with multihundred watt isotopic thermoelectric power source, health physics 77−46414
atmospheric emissions from nuclear plants, applications related concept for radiation exposure calc. *(German)* 78−82531
Atmospheric Release Advisory Capability, 1977 update 78−49127
B-group vitamins in aqueous systems, protection against γ-rays 79−2006
Babcock & Wilcox hot cell facility 80−68910
barrier thickness, simplified calc. method for ^{60}Co radiation 79−36421
barytes concrete, gamma ray buildup factors 80−27823
basic safety standards, status 80−47774
benchmark experiments and sensitivity studies, neutron plus gamma library 77−26947
benchmark experiments for shielding data validation 77−23203
benchmark gamma-ray skyshine expt. 79−59274
benchmark problems by CSEWG 80−47736
benchmark shielding problems, American Nuclear Society Standards Committee, documentation of computational methods 80−47737
benchmark shielding problems obtained from integral tests of neutron cross sections 80−47740
Berger coeffs. for Eisenhauer-Simmons γ-ray buildup factors in concrete 78−78510
beta-ray protection-level dosimeters, calibration quantities 77−52888
betatron, radiation protection meas. 79−29636
biological protection in water-moderated, water-cooled nucl. reactors 78−818
biological shield removal, associated radiological protection problems 80−9431
biological shield wall for Caorso nuclear plant, design, construction and erection 78−86694
BN-350 reactor, radiation safety assessment at design stage *(Russian)* 79−97869
bremsstrahlung in bulk media, shielding study, Monte Carlo anal. of thick target spectra 78−59839

radiation protection continued
bremsstrahlung influence on γ dose buildup factors rel. to penetration depth *(Russian)* 79−13542
bronchopulmonary lavage 78−15910
BWR, anal. of occupational radiation exposure, design implications 80−5380
BWR, control of Fe feed rate into feedwater system to reduce shutdown radiation level 80−5384
BWR, shield design against neutron streaming in pressure vessel vicinity 80−13678
BWR feedwater nozzle cladding removal ALARA approach 79−59224
BWR power plant, routine checks and radiation protection 78−74462
BWR power plant shielding concept 80−18712
BWR power plant turbine building, radiation protection, calc. and obs. 78−74461
BWR shield wall penetrations, radiation shielding 80−13679
BWR-6 computer anal. of fission product release to containment via press. suppression pool 79−59223
cables insulated with Al_2O_3 and MgO, resistance to high-temp. and intense gamma radiation 78−25332
calibration, mobile laboratory design 77−38582
CANDU 600 MW(e) station, man-rem expenditures 79−13493
CANDU design program for exposure minimisation 77−6570
CANDU irradiated fuel storage, concrete canister programme, heat transfer and shielding effectiveness 78−58388
CANDU reactors, Atomic Energy of Canada report to Royal Commission on Electric Power Planning 78−25312
CEGB nuclear power station emergency arrangements 78−55050
cell membrane radiobiology, impact on radiation protection 79−70585
CERN accelerators, radiation protection *(Dutch)* 77−46434
CERN supersynchrotron, radiation protection *(German)* 77−14270
Chalk River Nuclear Laboratories research in radiation biology, environment and radiation protection 78−61222
chelation therapy, DTPA treatment schedules for ^{239}Pu decorporation from simulated wounds 77−64137
chelation therapy for transuranic elements using Ca-DTPA and desferrioxamine B, rats 77−44758
chelation therapy with inhaled Ca-DTPA, effect on long-term $Pu(NO_3)_4$ effects 77−66861
chemical carcinogenesis, redox model 80−26298
chemical pollutants and radiation, comparative biological hazards 79−25035
chromosome aberration of human lymphocytes, microdosimetric expts. 80−26289
cinefluorographic units, protection survey results of four X-ray units 79−20618
Clinch River breeder reactor, ALARA nature of design effluents 79−22420
coal, bituminous, subbituminous and lignite, gamma-ray activity 77−25684
coal power station fly-ash and slag, natural radioactivity meas. 78−17442
collective dose commitment, evaluation problems *(French)* 80−47760
collective dose equivalent, cost anal. 80−47761
collective dose equivalent concept for population exposures 77−2059
collective dose exposures during radiotherapy, optimisation, man-rem monetary value 80−51274
collective dose rate commitment in nuclear power industry, appl. to future dose rate eval. *(Spanish)* 79−63816
commercial reactor, control rod material behaviour 78−8918
community shelters for protection from radioactive fallout 80−5338
computerised radiation safety system 77−25562
concrete, albedo for low energy γ-radiation 80−32534
concrete, high density, radiation shielding below 1 MeV 79−13535
concrete, neutron reflection characteristics 77−71633
concrete and containment uptake of fission product I, sorption and diffusion 79−67898
concrete buildup factors based on the American National Standard for flux-to-dose-rate conversion 80−47732
concrete canister spent fuel storage facility, conceptual design study 79−45378
concrete shields containing iron, two dimens. cross section sensitivity anal. of Fe 77−23311
concrete-equivalent materials, shielding calcs. below 100 kVp 79−29637
concrete-paraffin shielding, fast neutron leakage, use of Monte Carlo method 77−23309
concretes, normal and ilmenite, neutron attenuation 77−23308
conference, Bologna, Italy (Oct. 1977) 80−62367
conference, dose limitation systems, Vienna, Austria (Mar. 1979) 80−46736
conference, meas. for safe use of radiation, Gaithersburg, USA (Mar. 1976) 77−40794
conference, radiation protection monitoring advances, Vienna, Austria (June 1978) 80−57007
conference, San Diego, Calif., USA (June 1978) 79−17972
conference, San Diego, Calif., USA (June 1978) 79−49650
conference on nuclear power and fuel cycle, Salzburg, Austria, (May 77) 79−26503
contamination detectors assessment, w.r.t. German 1977 protective measures *(German)* 78−86693
cosmic-ray shielding for manned interstellar arks and mobile habitats 77−49264
cost-effectiveness analysis applied to radioactive effluents *(French)* 79−93840
criticality accidents at facilities processing fissile material, characts., detect. and action procedures *(French)* 78−55054
cyclotron, variable energy, shielding calcs., concrete and earth shield design 77−61622
cylindrical source shielding eqns. including buildup, lateral dose rate, compact function use 78−89982
decommissioning of nuclear facilities, deform. of acceptable residual radioactive contamination levels 80−13973
decommissioning of nuclear facilities, establishment of activity limits for items to be released for unrestricted use 80−13972
decontamination of radioactive isotopes 80−13950
deep penetration problems, rebalance methods, effectiveness 80−47533
deep penetration shielding problems, calc. of contribution flux and current spatial distrib. 79−59283
derived standards, Euratom directive and ICRP recommendations 78−35969
determ. of levels of ^{54}Mn, ^{59}Fe, ^{58}Co and ^{60}Co 78−85608

radiation protection continued
devices for protection at urological fluoroscopy working stations 80−41254
diagnostic X-ray rooms, simplified shielding 79−16313
dielectric trapping, bremsstrahlung shielding meas. 78−78507
digital radiation monitoring, plant-wide systems, design alternatives 79−41082
dimethyl sulphoxide radioprotection of mammalian cells, exposed to X-rays, heavy charged-particle beams 79−79609
dose equivalent index, practical implications 80−47778
dose equivalent index, practicality for regulations 80−47777
dose limitation system, application problems 80−47767
dose meter calibration for radiation protection in European Community 80−58000
dosimeter calibration using radiochromic dye film dosimeter, radiation sterilizing, processing industries appl. 78−40330
dosimetry calibration problems in connection with radiation protection around nuclear facilities 80−9422
double-scattered γ energy spectrum simulation and expt. 79−9905
Dungeness A, radiation and contamination control 80−5386
Dutch reactor safety studies, Rasmussen report eval. *(Dutch)* 79−81016
ear, airborne sound destructive interference applicability for personal sound protection *(German)* 77−66817
ear protection systems, attenuation produced at each normal freq., Noise Reduction Rating calc. *(Spanish)* 80−109041
ear protectors, use of sound levels for assessing adequacy 80−104771
EBR-II cover-gas cleanup system 79−97874
education, undergraduate course evaluation on radiation and the environment 78−1
electron accelerator, shielding for high energy neutron dose 79−54609
electron accelerator irradiation facility, shielding system *(German)* 77−70244
electron accelerator systems, shielding and safety 77−67904
electron beam, dose and shielding parameters of electron-photon stray radiation 77−57755
electron linear accelerators, regulations, standards, and guidelines for use in medical radiation therapy 79−53258
electron microscope, conventional and HV, X-ray leakage 77−38066
electron radiation processing applications, aspects radiation shielding 77−54370
electron transport by the method of condensed collisions 80−47000
electrons, diffusion of pencil beam, ang. distrib. model 80−23273
EM fields, range 3-30 MHz, exposure, maximum permissible intensity and duration, physiological effects *(German)* 80−12179
EM non-ionising radiation, influence of quality on bioeffects, exposure standards 78−44558
EM radiation protection, in transmission stations, Polish and international regulations *(Polish)* 78−61263
emergency conditions, monitoring and handling 78−57082
Emergency Response Planning and Preparedness Training Programmes, USA 78−57079
emergency response training programme 78−57080
EMP radiation, electronic systems, book 77−54366
ENDF/B-V cross section data for shielding appls., Monte Carlo MCNP integral calcs. 80−47744
ENDF/B-V nuclear data for shielding appls., energy balance anal. 80−47745
energy, environment and health, Failla Memorial Lecture, learning from nucl. experience 78−80982
Environmental aspects of nuclear power *(Japanese)* 77−83112
environmental dispersion models, evaluation of uncertainties 80−46074
environmental modelling, techniques and appls. 77−48878
environmental mutagenesis, recommendations of Committee 17 and effect on radiation standards 77−66863
environmental protection, radioactive waste from power plants in USSR 79−26601
environmental radioactivity control, relevance to control of other environmental contaminants 79−9889
equipment safety in diagnostic X-ray departments 79−48346
ethics in protection from radioactivity 79−59270
European neutron dosimetry intercomparison project results, recommendations for biological and medical appls. 78−82532
European regulation in EEC countries *(French)* 79−48347
exposure limits, establishment bases 79−26770
external exposure from radiation facilities, control, designer-health physicist collaboration 77−81586
Exxon nuclear fuel recovery and recycling center, safety analysis 79−36389
exxon nuclear fuel recovery and recycling center facility description 79−36388
eye, effectiveness of ophthalmic lenses against beta radiation 77−66862
eye, human, holographic diagnosis, fail-safe shutter system 80−12209
eye irradiation, limitations in international recommendations 80−51278
eye lens, protection for patients and users 79−92393
eye protection from scatt. radiation during mantle-field therapy 79−92396
eye protection shield for the fluoroscopist 79−92398
eye shield for use during carotid angiography 78−44615
eye shields, individualised, for electron beam therapy and low-energy photon irrad. 80−109040
eyeglasses, conventional, value for X-ray protection 79−88202
fallout gamma radiation, effectiveness of soil as shielding 78−5059
fast neutron albedo for Fe, concrete and Fe-covered concrete radiation shields 79−76151
fast neutron pulses, time distrib. of doserate behind polyethylene/Fe layers *(German)* 77−26886
fast neutron therapy system using cyclotron beam, beam optics and shielding 79−57756
fast neutron transport through laminated Fe-H_2O shield 80−13931
fast reactor shields, neutron transport 77−61481
FBR, commercial demonstration reactor, radiation damage shielding 80−23178
FBR, neutron shielding, integral expt. and data correlation 78−5057
FBR fuel handling, radiation safety 80−73985
FBR fuel reprocessing, radiological protection problems 80−5376
FBR fuel reprocessing plant, radiation protection, containment and shielding 80−23179
federal regulatory agency and radiation meas. system, US 77−37713
fibrosis in the rat gut, protective effect of hypoxia 80−30772
field measurements, relationship to calibration values 80−58002
field prediction around out-core reactor components 77−6571

radiation protection continued
fifth international conference on reactor shielding, review 78−29599
filter material selection for airborne radioactive ^{131}I and methyl iodide sampling 79−83673
filter testing, Winfrith, double automatic Pollak counter 78−33301
fission product release calcs. from reactor containment building 77−79449
fission reactor fuel, mixed oxide, suitability of spent fuel shipping casks 80−27757
fission reactor water coolant decontamination *(Spanish)* 79−45345
fluorography with image intensifier, apparatus for mass stomach survey *(Japanese)* 77−73575
fluoroscopic installations, diagnostic X-ray survey procedures, automatic brightness controlled units 77−25560
fluoroscopic installations with undertable X-ray tubes, survey form and techniques 77−73597
Forschungs- und Messreaktor Braunschweig, operating experience *(German)* 77−61527
fuel cycle, radioactive material release, cost/benefit anal. 79−26605
fuel cycle and radioactivity, regulatory control in Canada 79−26620
fuel cycle plants, radioactive discharges, limits 79−26779
fuel fabrication and reprocessing plant, radiation protection device based on neutron detection *(French)* 78−66362
fuel reprocessing plant, radiation protection design considerations 77−46416
fusion power, radiological protection review 80−9411
fusion reactor, MFTF, intense neutron environment, test cell side wall design, shielding materials 80−102318
fusion reactor design, nuclear data requirements 77−23291
fusion reactor ignition, D-D neutron and X-ray yields from high-power deuterium beam injectors 79−67942
fusion reactor irradiation test facility, higher energy neutrons, shielding calcs. 80−13786
fusion reactor radiation attenuation meas., sensitivity response of liquid scintillator detector 79−67951
fusion reactor safety, radiation exposure and maintainability 80−13828
fusion reactor shield integral expts. at ORNL 80−47709
fusion reactor shielding concretes, neutron activation props. 80−13787
fusion reactor shielding experiment, cross-section sensitivity calcs., one- and two-dimensional models 80−27799
fusion reactors, reliability requirements for admissible radiological hazards 78−58447
gamma alarm device, portable, with audible/visual warnings 78−8390
gamma buildup factors for photons in air, water, iron, moments method code 80−27828
gamma exposure rate, real time simulation by puff model 80−47618
gamma radiation field induced in air by fast neutrons, intensity and absorbed energy calc. method 77−50310
gamma ray spectral penetration through radiation shields, review 80−5343
gamma rays, 6 MeV, penetrating shielding materials, energy and ang. flux density spectra 80−63393
gamma sources in walls of dwelling rooms, exposure rate calc. 78−73260
gamma-ray backscattering from various barriers, characts. and spectral ang. distribs. 77−61621
gamma-ray buildup factors for mats. with very low atomic numbers 80−27822
gamma-ray buildup factors for Pb/H_2O stratified radiation shields 80−86994
gamma-ray radiation in dwelling rooms, Monte Carlo code REBEL-2 77−40793
gamma-ray shielding, concrete wall cavities, compensation by Fe plates *(German, English)* 77−83109
gamma-ray spectrometry appl. in radiological protection meas., small computer system 79−9917
gamma-ray streaming through annular cylindrical duct, dose computation at exit 77−65342
gamma-ray streaming through ducts, spectral meas. 80−32523
Gammacell self-contained irradiators, safety programme 77−29211
GCFR, design of deep penetration integral expt. for ThO_2 blanket and radial shield mockup 80−23167
GCFR, prototypic grid-plate shield confirmation experiment 79−54562
GCFR, Pu fuelled, fission products and secondary gamma-ray spectra 78−676
GCFR benchmark shielding expts. 79−9902
GCFR grid plate shield design, anal. of confirmation expt. 80−23166
GCFR grid-plate shield design experiment 79−59226
GCFR shield anal., neutron-coupled γ-ray cross section requirements 77−23310
GCFR shielding expts. at Tower Shielding Facility, ORNL 80−47739
geologic waste repositories, long term safety assessment methodology 80−37487
German Democratic Republic, conclusions from unusual events in field of ionising radiation 78−53520
glass dosemeter reader, design improvements *(French)* 80−57970
glass fibre materials for radiation filtration 80−5341
glass lenses, effectiveness in reducing eye exposure 79−92394
glove box accident, surgical treatment of wound contaminated by ^{239}Pu and Am *(French)* 78−53521
glove box for sealed manipulator maintenance 80−18684
glove boxes, Pu-contaminated, size reduction and waste packaging 80−18469
graduate educational program to prepare science majors for career in radiation health physics 78−4427
graphite, neutron penetration, Monte Carlo calculations for 30, 45 MeV *(Japanese)* 80−18677
graphite, proton bombardment at 52 MeV, neutrons and photons penetration 80−27821
graphite assembly exposed to 52 MeV protons, penetration of secondary neutrons and photons 79−76152
gypsum wallboard, use as protective barrier for diagnostic rays 79−70650
gypsum wallboard, X-ray attenuation characts. 79−70651
health aspects of low-level radiation, radiation protection standards 80−26375
health physics, Faculty Institute in Applied Health Phys. at Oak Ridge National Lab. 78−49581
health physics aspects of 20- to 40-MeV LINAC operations 79−45482
health physics conference, San Francisco, USA, June/July (1976) 77−16983
health physics quantities and units 80−8193
radiation protection continued
health physics technicians, uniform approach for on-site training and qualification 77−64900
HFEF/S air cell, decontamination and refurbishment 79−45445
high intensity radiation equipment, radiation safety during operation, personnel dose 77−73601
high-level waste management systems in Germany, risk analysis 78−17354
high-speed cassette film fogging and shielding 78−8460
Hinkley Point B, AGR radiation protection, design criteria and operating experience 80−27832
hip radiography, bull, skin and gonadal dose reduction, Pb sheeting and Cu filtration 79−100743
historical development of need for radiation protection and meas. in USA 77−37708
Holifield 25 MV heavy ion tandem accelerator, radiation safety 79−45483
hospital staff, Delhi, behavioural aspects 79−39527
hot cell, rigid hoist articulated grapple system development for enhanced remote maintenance 80−68968
hot cell, shielding slab thickness calcs. 79−6752
hot cell complex, Japan, users comments *(Japanese)* 80−91296
hot cell complex for post irradiation exam. in Japan, O-arai Engng. Centre *(Japanese)* 80−47536
hot cell complex in Japan, University use *(Japanese)* 80−91295
hot cell for synthesis of labeled organic compounds 80−68970
hot cell laboratory, refurbishing β-γ cell line, upgrading operational routines 80−23160
hot cell liners, removable, design 80−18685
hot cell oil filled Pb glass shielding windows, maintenance and refurbishment 80−68969
hot fuel examination facility, auxiliary equipment for remote handling systems 80−18686
hot fuel examination facility/north, equipment repair room modifications 79−9723
hot laboratory design and construction *(Japanese)* 78−29623
HTGR fuel reprocessing plant, cost and environmental impact of radioactive waste treatment 77−46380
HTGR hypothetical accidents, consequences following breach of primary circuit and safeguard failure *(German)* 78−58390
HTR, direct cycle, radiation exposure during maintenance and repair of He turbine 80−18563
HTR, expt. JAERI, safety anal. of fission product behaviour and hypothetical accident *(Japanese)* 78−66330
HWR, accident prevention, effect on environment 78−29613
HWR, safety research and development 78−29614
HYLIFE converter concept, remote systems requirements 80−18614
ICRP (1977) recommendations, implementation problems in Korea 80−47779
ICRP dose limitation system *(French)* 80−47753
ICRP recommendation implication in Israel 80−47773
ICRP recommendations, applications in practice 80−47771
ICRU phantom neutron fluence to dose index conversion factors 79−9909
improved radiation shielding using packed mixed size Pb particles, nuclear plant maint. appls. *(Japanese)* 80−106207
impulsive and continuous noise, combined dose meas. 80−102929
indoor shelter for reduced radionuclide inhalation after nuclear accident 77−34478
industrial radiation safety programme for accelerators 77−83115
industrial radiography, accidental over-exposure to ^{192}Ir source 77−56472
inert gas release by nuclear reactors in West Europe 77−50305
inert gas treatment in nuclear plant for safe environment 77−50306
information centre on radiation shielding, international technology resource 78−17543
inhaled hot particle toxicity, recommendations of German Commission on Radiation Protection 78−69150
instrumentation, reliability and availability 80−18709
instrumentation reliability, non-instrumental constraints upon the performance of systems for radiological protection 80−18710
instruments for personnel dosimetry, area and environmental monitoring 78−66427
integral measurements, shielding cross section test 77−23305
integrated approach for protection from ionising rad. and other mutagens 80−51276
intense neutron source facility, skyshine anal. methods comparison 80−5349
International Commission on Radiological Protection, dose limits (1934-77) 80−12266
International Commission on Radiological Protection, recommendations 80−47752
international network of laboratories to improve standards of absorbed radiation dose meas. 77−67898
interplanetary electron shield anal. 77−78604
intracochlear interference effect applicability for personal sound protection *(German)* 77−66816
ionisation smoke detectors, risks to humans 78−15909
ionising radiation, detection device, electret based *(French)* 80−57971
ionising radiation, mortality of radiation workers 80−8108
Iran, past, present, future trends 77−65337
irradiated fuel rods, in-cell welding techniques 80−22956
irradiated nuclear fuel, transport, packaging, UK experience 79−26782
irradiated nuclear fuel transport, European experience 79−31235
irradiated nuclear fuel transport and handling, French nuclear power plants *(French)* 79−31233
isotope induction at LAMPF, fabrication, cladding, handling of irrad. targets 80−23231
isotopic generators of multihundred watt design, integration with LES 8/9 spacecraft 77−46413
Israel, surveillance and accident prevention of radionuclide users 78−57077
KS-150 reactor, radial shielding model, neutron and γ-ray spectra meas. *(Slovak)* 78−21624
laboratory-scale shielded cell for ^{252}Cf 80−63405
laboratory-scale shielded cell for ^{252}Cf 80−74035
laser fusion blanket, neutronics and photonics 78−5025
laser fusion power plant, protection of optical system 79−76136
laser fusion research, safety aspects, control measures and protective eye-wear 77−40711

radiation protection continued
laser IR pulse irrad. of human eye, max. permissible exposure for safety 77−37009
laser radiation, calc. of max. permissible exposure levels 79−96666
laser radiation hazards and protection standards 80−46069
laser safe operation control measures 80−9928
laser safety, basic classification concepts 79−39524
laser safety considerations 77−77940
laser safety eyewear, filter glasses 79−39525
Lawrence Livermore Laboratory accelerator safety program 77−83118
leakage radiation meas., effective energy determ. 78−28089
leaktight remote handling equipment for operations in an irradiating and contaminating environment 80−13951
legislation in West Germany, standards aspects *(German)* 78−5049
leukaemia risk from neutrons, rel. to max. permissible dose for occupational exposure 78−53448
life shortening of mice exposed to fractionated X-irrad., repair and biochem. protection 78−69153
life-expired LWR, neutron activation product density and dose rate calc. 79−9908
linear accelerator, local absorber in accelerating section to reduce radiation level 80−83229
LMFBR, intermediate Na activation, Monte Carlo anal. 78−4997
LMFBR, physics problems of fast reactor shielding 79−67873
LMFBR component decontamination, glycolic-citric acids process 79−93769
LMFBR fuel elements, remote exam. of shroud tubes 80−18470
LMFBR spent-fuel shipment cask, radiation shields 77−46313
LMFBR unirradiated assemblies, shipping containers 78−723
low irradiation dose risk evaluation *(French)* 79−89508
low-level radiation during development studies, implications for ICRP-26 80−51281
lung lavage for removal of inhaled radioactive particles, review 78−3618
LWR, chemical factors controlling γ radiation fields around coolant circuits 80−5371
LWR, effect of small pipe weld types on personnel exposure 78−4996
LWR, rem reduction plan for standard 1100MW(e) plant designs 80−745
LWR, technical safety rules, catalogue and classification for reactors and fuel cycle plants 78−58384
LWR chemical decontamination and cleaning for radiation control 79−54554
LWR concrete shielding, ANS coupled cross-section standards 79−59281
LWR containment vessel, I removal by spray after LOCA, MIRA-PB code 80−47593
LWR fuel reprocessing plant, radioactive waste treatment costs and environmental impact 77−46379
LWR irradiated fuel transport flasks, shielding and engineering aspects 80−27831
LWR plant, occupational radiation exposure, recommended limitations 79−59266
LWR power plants, protection of maintenance personnel 80−5368
LWR power plants, radioactivity release in LOCA uncertainties 79−26639
LWR radiation control techniques 79−59184
LWR radiation dose minimization during operation, maintenance and inspection 80−5294
LWR shielding, neutron transport anal. comparison of several multigroup libraries 80−23168
LWR-type fuel element shipping casks and storage facilities, criticality assessment 79−63789
magnetostatic shield fabrication 78−5053
Magnox power station, decommissioned, rad. levels, neutron activation, waste disposal 80−13976
Magnox reactors, influence of design and operation on personnel radiation dose meas. 80−5385
man-made EM fields and georadiations, effects on man *(Polish)* 80−67258
manipulation unit equipment for radiotherapy depts. 80−30903
manned space crew radiation, dosimetry, design and zero-G problems 77−30674
marine radioecology, radiobiological protection aspects *(French)* 78−11744
materials, benchmark radiation transport data, air-over-ground neutron and gamma spectroscopy 80−23161
maximum permissible conc. calc. using absorbed dose data of MIRD pamphlet 11 78−53516
maximum tolerable radiation doses recommended by Israel Advisory Committee on Nucl. Safety 78−53517
medical accelerators, international standards 80−51272
medical diagnostic X-rays, effects, risks and protection, review 78−3591
medical establishments, pilot radiological study 79−8552
medical facilities, US state and federal regulatory meas. responsibilities 77−40765
medical findings for GDR works, documentation to meet ICRP-26 80−51280
medical radiation practice, ICRP recommendations in worker medical monitoring *(French)* 80−51275
medical regulations and standards in France *(French)* 78−48897
medical science campus, control of radioactive materials 77−44759
medical standards for radiation workers 77−13012
β-mercaptoethylamine, protective effect in rat small intestine, crypt survival after X-irradiation 79−11979
meteorological information system for response to nuclear power station accidental release of radioactivity 80−16888
methyl iodide desorption kinetics from impregnated charcoal 80−52791
methyl iodide removal by Ag impregnated Al and zeolite 78−53719
microdosimetry, conf., Brussels, Belgium (May 1978) 80−4472
microdosimetry, energy deposition distrib. patterns, biological effects of ionising radiations 79−20600
microwave, standards and need for field measurements 80−26377
microwave and RF radiation protection, American and European standards 78−80973
microwave radiation, emission and exposure standards 78−44619
microwave radiation hazard assessment methodology for USA Army Radiation Protection Program 78−85389
microwave radiation safety, meas. and instrumentation 78−44618
microwave survey instrument evaluation and calibration 77−37946
millimeter range of wavelengths, personnel safety 79−92391
Millstone Unit No.2 neutron spectra and fluence determ. 79−9907
radiation protection continued
minicomputer-based radiation protection networks for nuclear plants 80−855
mixed β-γ dosimetry, ionisation and scintillation counters 80−57975
mixed oxide fuel fabrication, radiation protection and shielding 77−46417
mixed oxide fuel fabrication plant decommissioning, public radiation exposure 80−42800
mixed radiations, device for dose-equivalent index determ. *(Russian)* 80−57976
monitoring beta and photon radiations to ICRP recommendations 78−15908
Monte Carlo shielding calcs., biased selection of particle flight directions as variance resolution technique 78−29653
MPD reduction suggestion fo meet requirements of higher safety 80−85499
multi-attribute approach to the rationalization of radiation protection options *(French)* 80−47765
multi-channel dosimetric meas. system *(Hungarian)* 78−57072
multidetector technique readings, interpetation for dose equivalent determ. 79−49875
multigroup electron transfer cross-section method 80−46999
multigroup transfer coeffs., efficient eval. for shielding appls. 80−47747
multiway sorption filters, development and use for radioactive iodine removal from air 78−61543
N-reactor, radiation source control, chemical decontamination 80−23058
National Arrangements for Incidents involving Radioactivity, NAIR 78−65136
National Radiological Protection Board low-background laboratory, research summary 77−48880
natural and man made radiation exposure in daily life, review 77−49535
natural background approach to setting radiation standards 80−47782
natural radiation dose, variability as comparison point for acceptable radiation risk 80−51282
natural radioactivity in underground cavities, gas conc. and exposure levels *(Spanish)* 79−39322
neutron activation anal. of biological samples, device for opening quartz ampoules 78−61121
neutron and gamma transport, direct coupled-ray method for design oriented 3-D anal. 77−83111
neutron and gamma transport, expt. and theoretic results comparison 80−47750
neutron bomb radiation protection, calc. of rad. penetration in air and shielded human tissue dose equiv. 80−47743
neutron data in fission reactor appl., review 77−23192
neutron dose determ. using calculated neutron spectra 77−60263
neutron dosimetry for radiation protection, European workshop 80−23177
neutron field in fast reactor, spectral charact. *(Japanese)* 78−46222
neutron leakage spectra from critical assemblies, depth dose, dose equiv. and quality factor 78−58504
neutron leakage spectra from Fe, Nb, Be, polythene spheres, integral test of cross sections 77−23033
neutron medium-energy radiotherapy, shield design 79−12016
neutron monitor calibration for radiation protection at 24.5 keV and 2 keV 78−89983
neutron shield material tests 80−37543
neutron shielding, 14 MeV, iron-water combination 77−61614
neutron shields, homogeneous slabs, computer calcs. of transmitted, reflected spectra 77−3067
neutron shutter for cyclotron facility 78−21794
neutron therapy beam, dosimetry and radiation protection 79−48342
neutron therapy source shielding for Be(d,n) reaction 79−20617
neutron yield calcs., electron beam incidence, radiation protection implications for accelerators 78−95622
neutron-nucleus reactions, double differential cross-section, analytic expression 78−8825
neutron-photon multigroup cross sections for neutron energies $\leq$60 MeV 79−30880
neutrons, research associated with National Radiological Protection Board's accelerator 77−2060
new waste calcining facility, radiation shield integrity testing 80−13940
noise dose criteria for setting hearing loss risk estimates for industrial noise 78−1504
noise protection of occupationally exposed workers 79−92392
non-ionising EM radiation standardisation 77−38013
non-ionising radiation exposure control in Canada 80−36150
non-ionizing radiations, hazards 79−92390
nonionising radiation hazard definition problems 80−3823
nonionising radiation protection, international programme 80−3822
nuclear accidents in power stations of Electricite de France, protection organisation *(French)* 78−55049
nuclear energy and the environment 77−50304
Nuclear Energy Research Centre, Mol, Belgium, emergency plan organisation in event of major accident *(French)* 78−53527
nuclear engineering, optimisation of radiation protection, cost, risk *(Czech)* 78−33295
nuclear facilities, cost-benefit anal. problems 80−47770
nuclear facilities, forecasting of environmental impact *(French)* 78−8994
nuclear fuel centre, fuel and waste facilities, safety, protection and socioeconomic aspects 78−58395
nuclear fuel disposal safety in Switzerland *(German)* 78−74455
nuclear fuel reprocessing plant, radiation exposure due to exhaust air *(German)* 80−57940
nuclear fuel reprocessing plant safety aspects 79−26708
nuclear fuel reprocessing plant ventilation control 80−5318
nuclear installations, environmental surveillance programme, Spanish experience 77−65336
nuclear material transport, West Germany, status future aspects 79−31234
nuclear medicine, diagnostic, hazards to personnel 77−81587
nuclear medicine laboratory, radiation safety 80−104772
nuclear medicine procedures, screen for radiation dose minimisation to nursing staff 79−53259
nuclear plant and lab. operations, radiation protection and waste handling 77−65338
nuclear power plant, fast alarm system to optimise protection of public 78−55048
nuclear power plant, occupational radiation exposure minimisation at Yankee Atomic, USA 77−18712

radiation protection continued
nuclear power plant emergencies, prevention of excessive irrad. of staff and population *(Russian)* 78−50286
nuclear power plant operation, radiation exposure ALARA concept 80−32388
nuclear power plant radiation exposure reduction robotic approach 77−14275
nuclear power plant safety, West German policy *(German)* 80−57865
nuclear power plants, radiation exposure and protection 78−25301
nuclear power plants and the fuel cycle, conf., Bristol, England (Nov. 1978) 80−4471
nuclear power programme radioactive waste management 78−13258
nuclear power reactor emergency medical assistance programmes 78−53532
nuclear power station, Biblis, radiation protection during first refuelling shutdown of unit A 77−65335
nuclear power station, environmental protection methods *(Hungarian)* 79−88008
nuclear power station safety, regulatory control in UK 80−18707
nuclear power stations, ambiental radiology, equipment and methods, review *(Spanish)* 79−45425
nuclear power stations, contamination prevention methods *(Hungarian)* 79−88007
nuclear power stations, radiation dosage determination, monitoring and control for personnel safety *(German)* 80−842
nuclear power stations, radiation safety prediction 79−45435
nuclear power stations, recommendations review *(Hungarian)* 78−74508
nuclear power stations in Italy, district emergency exercises 78−55052
nuclear reactor, corrosion product reduction program 78−21665
nuclear reactor containment vessels, cement selection criteria *(Polish)* 79−49876
nuclear reactor remote siting as risk-reduction method, cost effectiveness 77−67178
nuclear reactor shielding anal., spatial channel theory, appl. to FFTF 77−6569
nuclear reactor shutdown system reliability, effect of operator performance 78−29611
nuclear reactor stainless steel and Na shield radiation heating expt. 79−9903
nuclear reactors, underwater repair for workers protection 79−3226
nuclear risk estimation methods and wider applications *(French)* 79−89492
nuclear risks, energy source health effects 79−85696
nuclear safeguard systems effectiveness, SNAP network analysis technique 79−26658
nuclear safety, radiation protection estimation of individual and collective equivalent dose *(Spanish)* 80−5336
nuclear safety issues in Japan *(Japanese)* 79−9894
nuclear sites, workers' protection against radiation hazards 79−59267
nuclear vessels, probabilistic model for assessment of collision likelihood 78−5063
nuclear waste containment vessel response to impact using PISCES finite difference codes 77−3097
nuclear waste disposal, social criteria 77−30652
nuclear waste disposal problems and safety 78−86636
nuclear waste management, radiological protection criteria 80−47780
occupational exposure, averaging, weighting, ICRP-2G recommendations 80−47781
occupational exposure, problems raised by International Commission on Radiological Protection recommendations *(French)* 79−26771
occupational radiation exposure, evaluation and control, US research program 80−5370
occupational radiation exposure at nuclear power plants, meas. and prediction 79−59182
occupational radiation exposure reduction techniques 79−9898
occupational radiological exposure at nuclear fuel prep. plants, UK regulatory control 80−18708
OPO fabric decontamination *(Czech)* 79−31223
optical cables, LED- and laser-fed, safety aspects 78−74968
optical cables, LED- and laser-fed, safety aspects 78−74969
optical radiation measurement, practical considerations, rel. to enforcement of Federal standards 77−38012
optimisation at nuclear research centre using ICRP recommendations 80−47759
optimisation methodologies *(French)* 80−47758
optimisation recommendations, implementation methodology 80−47766
optimization of radiation protection 80−47757
Parker, H.M., biographical note on medical physics contribs. 80−12
parotid gland, rat, radioprotection by WR-2721 chemoprotector 79−92300
particle accelerator decommissioning, radioactive waste management 80−18720
particle accelerator decommissioning, re-utilisation potential of components 79−72029
particle accelerators, cost optimization of structural design of radiation shielding 78−17443
particle accelerators, radiation control for health and safety act 1968, manufacturers' responsibilities 77−83114
particle accelerators, radiation exposure, design of cooling and ventilation systems 80−5350
particle accelerators, radiological safety in design and operation, American National Standard 79−89511
particle accelerators, state registration and inspection programmes 77−83117
particle accelerators ionising radiation produced during operation, dosage and shielding *(Czech)* 79−89505
patients, accompanying parent, computerised tomography appl. 77−70524
PDX Tokamak, neutron skyshine Monte Carlo calcs. 80−47711
penetration in heterogeneous systems 79−18050
penicillamine-treated mice, survival following whole-body irrad. 80−98030
PEP IR hall scale model, neutron and photon dose equivalents meas. 79−31227
permissible dose estimation based on biological risk 78−40352
personnel dosimetric control in Hungary *(Russian)* 78−20292
personnel dosimetry methods introduced in the Czechoslovak national laboratories 80−57969
personnel exposure minimisation at waste calcining factory 77−50312
personnel monitoring for radiological protection, current status and developments, review 79−22490
radiation protection continued
personnel radiation minimisation in nuclear power plants 78−21663
perturbation theory, higher order generalised 80−47731
PFR Dounreay, radiation and contamination control 80−27834
PFR Dounreay, utilisation of neutrons meas. for shielding calcs. 80−32538
phosphate and related industries, need for radiation controls 77−56483
photon calibration of radiation protection instruments in an authorized metrology service 80−9423
photon dose rate from induced activity in the beam stop of a 400 GeV proton accelerator 78−94144
photon dosimetry, practical problems 77−60261
Pilgrim power station, radiation source control activities 80−23059
plutonium, biologically important physicochemical props. and methods of human contamination *(French)* 80−98004
polyethylene, neutron penetration, Monte Carlo calculations for 30, 45 MeV *(Japanese)* 80−18677
population doses from reactor operation, compliance with appendix I 77−46410
portable instrumentation test and calibration 80−9420
potential radiation exposure, West German nuclear installations 79−26603
power station ashes, Th, U, and K conc. meas., dose rates in Poland 79−100754
prescription lenses, attenuation of diagnostic X-rays 79−92395
present trends, impact of ICRP-26 80−47783
profile optimisation, use of penalty functions 79−97909
progress report, EEC, 1978, book 80−22148
proton beam of neutrino experiments facility, particle loss and radiation environment 79−9930
public radiation exposure, optimisation, problems 80−47768
purpose and aims 80−57968
PWR, anal. of occupational radiation exposure, design implications 80−5381
PWR, cavity streaming problem, shield config. optimisation 80−9352
PWR, comparison of containment leak rate data analysis methods 77−42143
PWR, control of fission products activity in primary coolant, computer code 80−32537
PWR, determ. of typical accidents and consequences, rel. to emergency planning *(French)* 78−50285
PWR, evaluation of environmental and in-plant effects of T recycle and build-up 78−33273
PWR, low-pressure drop reactor cavity shield system 80−13677
PWR, normal operating radiation levels 77−88290
PWR, occupational radiation exposure 78−21664
PWR, Oconee, occupational exposures, radiation levels and waste levels during operation 78−21726
PWR, power stations containing VVER-440 reactors, radiation safety of personnel and local population 77−71700
PWR, reactor cavity shield system, design and anal. 79−59225
PWR, release of radioactive material, ability to meet appendix I to 10CFR50 77−46306
PWR, releases of radioactivity reported in the LER file (1971-1977) 79−85647
PWR, St. Lucie 850 MWe, neutron streaming meas. and shielding recommendations 78−70608
PWR cavity shield design, radiation streaming, calc., appl. of Monte Carlo and discrete-coordinates technique 79−89364
PWR coolant pH effect on radiation field buildup 80−23060
PWR decommissioning, public radiation exposure 80−42800
PWR decommissioning, safety, cost and occupational radiation exposure estimates 79−67903
PWR LOCA, cavity pressurization relief with rotating neutron shield tanks 79−31049
PWR occupational radiation exposure reduction techniques 79−9901
PWR power plant *(French)* 78−82521
PWR primary cct., corrosion product transport and radiation field growth 77−88256
PWR radiation shielding design 80−5372
PWR reactor cavity shield system, design and anal. 79−89366
PWR refuelling shutdown, control of ^{58}Co dissolution in coolant using H_2O_2 80−23066
PWR shield configs., concrete attenuation effectiveness, numerical studies 77−38356
PWR spent fuel calcs., neutron multiplication and shielding problems 77−74951
PWR spent-fuel shipping, neutron multiplication and shielding 77−46418
quality factor, lineal energy correction for saturation effects 80−26376
quality factor, proposal for revision 78−28091
quality factor and RBE for low doses of X-rays and gamma-rays 78−73175
quality factor recommendations and dose limits 80−26369
quantities used in radiological protection—an explanation 80−46070
radar antenna radiation, power density zones 77−81529
radiation calorimetry of single electron pulses from a LINAC 80−42872
radiation exposure resulting from radioactive gases released near the NRI Rez *(Russian)* 79−36427
radiation field functional calc. method for shielding parameters 79−71928
radiation hazards from emissions of thermal and nuclear power stations, comparative study 79−34460
radiation risk assessment, importance 80−47754
radiation risks in nuclear industry, comparison to other jobs 80−18680
radiation shield integrity testing 80−5390
Radiation Shielding Information Centre, available computer codes and data 77−65343
Radiation Shielding Information Centre, data activities 77−23307
radiation source reduction, potential benefits of occupational radiation exposure reduction 80−23057
radiation stability of 'nuclear class' ion-exchange resins 79−43609
radioactivation of shielding materials Fe, Benelex by fast neutrons, γ-ray spectra, decay rates 79−682
radioactive element conc. from γ-ray intensity meas., numerical method 79−18059
radioactive emission meas. and control *(German)* 77−79484
radioactive liquid waste elimination in hospitals, math. model for decay pond design *(Italian)* 79−48345
radioactive material transport, USA experience 79−31236

radiation protection continued
radioactive materials, IAEA transport information collection system, influence on improved safety measures 80−63413
radioactive materials, IAEA transport regulations, underlying radiation protection principles 80−63414
radioactive materials, reactor fuel transport requirements, Poland 79−31232
radioactive materials, safe transportation, using type A, exempt and LSA packages 80−63401
radioactive rare gas, removal from fuel reprocessing plant *(Japanese)* 79−93747
radioactive release into environment management, dose limitation system 77−14272
radioactive solid wastes disposal, benefit-cost anal. 80−18556
radioactive solution sampling, vacuum-bottle system 80−18688
radioactive waste, land disposal, repository, packaging and cost estimate, internal radiation dose *(Japanese)* 78−66351
radioactive waste calcining facility, radiation protection features 80−5377
radioactive waste processing, health physics implications 79−57727
radioactive waste solidification facility, radiological aspects of design 80−5378
radioactive waste solidification using urea-formaldehyde resins, technical eval. 79−67875
radioactivity warning symbol, design history 79−67135
radioassay services in developing countries, recommendations 79−31220
radiobiological effects of low doses, implications for radiological protection 78−15867
radiographers, safety training 78−81961
radiography, foetal vs. parenteral radiosensitivity 80−51271
radiography, held radiograph technique and radiation protection 78−73199
radiography, mobile, mass-miniature unit, protection survey using TLD 79−62375
radiography of breast, recent techniques *(French)* 77−81564
radioiodine volatilisation problem, soln. using plexiglas iodination box 77−56484
radioisotope thermoelectric generator, safety programme for LES 8/9 mission 77−46412
radioisotopes used in Hungary, development of protection *(Hungarian)* 80−90644
radiological implications of Pu recycling in HTGR fuels 80−68777
radiological protection system installation, code of practice and design principles 79−85832
radiological safety rules at CEGB 80−5369
radionuclide intakes by workers, limits, recommendation from ICRP 80−47762
radionuclide migration from repository sites, stochastic anal. 80−37486
radionuclides incorporated into stem cell DNA, biological damage, radiation protection implications 80−12187
radiopharmaceutical investigations, appl. of ten-day rule 77−21633
radiotherapy, evaluation criteria for neutron contamination of 25 MV photon therapy beam from Varian Clinac-35 77−86628
radiotherapy, medical usage factors for 4 MeV rot. linear accelerator 77−64139
radiotherapy, organ shielding using Pb-Sn-Bi-Cd low melting point alloy block *(Korean)* 80−36154
radiotherapy, secondary radiation from supervoltage accelerators rel. to patient protection 77−56471
radiotherapy electron accelerator neutron production, conf., Gaithersburg, USA (Apr. 1979) 80−46730
radiotherapy linear accelerator use factors 77−9275
radiotherapy neutron leakage characts. rel. to room shielding 80−51273
radiotherapy shielding, comparison of photoneutron and ^{252}Cf neutron spectra 79−59273
reactor, radiation source control programs at EPRI 80−23056
reactor accidents, struct. shielding against gamma-ray sources, dose reduction factors 78−13251
reactor accidents and the environment 79−30940
reactor airborne plume deposition estimation model evaluation 78−94148
reactor burnup determ., accuracy requirements for fuel cycle design, reactor operation and safety 78−58342
reactor cavity neutron shield design at Millstone Unit No.2 80−47748
reactor cavity radiation streaming, albedo Monte Carlo methods 79−89363
reactor coolant, automated system for radioiodine anal. 78−35768
reactor decommissioning, radioactivity limits for release of liquid radwaste, math. model 80−13737
reactor fuel reprocessing plant, radiation protection and shielding 77−46415
reactor incident duct plugging by aerosol deposits, simple model 79−49782
reactor loop, experimental, hazard and protection from tritium 79−36420
reactor radiation field reduction, several techniques 77−6572
reactor radiation streaming anal. using spherical harmonics expansion of albedo data 79−89367
Reactor Safety Study (Wash-1400) and implications for radiological emergency response planning 78−50284
reactor shielding, 6 MeV gamma photons penetration through Al, concrete and graphite determ. 80−5256
reactor spent fuel storage vault, criticality safety determ. *(Korean)* 80−37478
reactor waste disposal in geological form., long term risk assessment 78−58387
recursive Monte Carlo technique for generating importance functions 79−59272
reference Japanese man *(Japanese)* 78−35968
refueling and fuel handling, ALARA occupational radiation exposure 79−67914
regulatory control, implications of ICRP publication 26 80−18706
regulatory requirements for radiation protection 79−26774
regulatory requirements for radioactivity management in India 79−26775
remote maintenance to comply with new legislation limiting occupational radiation exposure, in United States 80−106210
removal-diffusion shielding code SHREDI, bidimensional, fundamentals and results 78−70645
residual activity levels allowing radioactive waste to be considered inactive 80−13735

radiation protection continued
respirable fraction definitions, matching air sampler penetration curves 77−90827
retinal injury mechanics, laser exposure limits 79−66485
reusable frame greenhouse, waste generation reduction 77−46409
review of nuclear fuel cycles and waste management 78−54863
RF and microwave exposure, USA occupational safety and health standards 80−3727
RF EM fields (300 KHz-100 GHz), human exposure safety level 80−89869
RF fields below 300 MC/s, legislation proposals for workers' protection 80−56223
RF radiation from portable and mobile telecommunication transmitters 77−40795
RF radiation levels in urban areas 78−40351
ring point detector, Monte Carlo flux-at-a-point estimates for axisymmetric problems 79−59282
risk assessment 79−25116
risk justification, theory and appl. 80−47755
rod dosimeters, automatic evaluation of staff dosimeters during reactor shut down *(German)* 79−67960
safety device for gamma ray source containers 78−5051
safety exercises carried out in French industrial facilities *(French)* 78−55051
safety glasses, physical factors determining the utility 80−46067
safety regulation impact on nuclear medicine *(French)* 80−47764
safety standards for X-rays and ionising radiation 80−98146
scattering expansion truncation error correction program 80−47001
scintillation counter, for gamma radiation, design calibration and construction *(Spanish)* 80−5437
second-order perturb. theory of distrib. of materials throughout radiation protective shield 79−54608
secondary neutron polarization via penetration through a ferromagnetic shielding wall 80−47742
SEM view port 79−75655
SEM with X-ray spectrometer, studies of radioactive samples, shielding design 77−189
Serpukhov proton synchrotron shield, mixed radiation dose equivalent outside 80−32530
SGHWR, radiation protection and plant maintenance 80−27789
SGHWR safety design and evaluation 79−26636
SHIELD computational system, nucl. fuel cycle appl. 80−37517
shield design objectives selection, optimisation calcs. 77−6565
shielded cables, nonlinearities and multiple exposure anomalies at CASINO, MCCABE code verification 78−58502
shielding, calc. of half-value layers for multiple sources 77−9274
shielding, Monte Carlo calcs., event-value path-length biasing 77−38421
shielding, radiation transport theory, tracklength biasing in Monte Carlo methods 80−5335
shielding design, two-dimensional discrete ordinates calc. characts. *(Japanese)* 79−93744
shielding of structures against initial nuclear radiation: Monte Carlo methodology 80−47741
shipping cask criticality safety, SCALE system, correl. with expt. 79−63775
SI units and ICRP recommendations 78−5054
SI units in radiological protection 78−86235
Sizewell power station, radiation and contamination control 80−5387
skin contamination, difficulties in applying ICRP-26 80−51279
skin irradiation, limitations in international recommendations 80−51278
SLAC, beam containment electronics operational experience 77−83466
sodium reactor experiment decommissioning, radiation protection 80−9432
soil affixants, effect on germination, emergence, growth of cheatgrass, Russian thistle 79−2140
solar cells, for space appl., coverglass development 79−48133
SOLASE laser fusion reactor, Monte Carlo shielding calc. for mirror-laser beam duct system 80−23174
solid dielectric detectors with breakdown phenomena and their applications in radioprotection 80−91388
solid neutron shield development, materials eval. for spent fuel shipping cask 80−13939
source definition for head shielding requirements in linear accelerators, effect on room shielding design 80−46068
South African radiation control, historical growth and development 79−67134
Soviet radiation safety standards *(Russian)* 80−47756
space colonies, radiation protection 77−86651
space flights, prolonged, radiation danger to man 80−61711
space station, radiation protection design considerations for man in geosynchronous orbits 78−28096
spacecraft thermionic reactors, neutron leakage control using boronated reflector drums leading to lower shielding mass 80−47663
Spanish research is radiological protection *(Spanish)* 77−38419
spectral and intensity distribs. of accelerator prod. neutrons in concrete room 79−49868
spectral parameter measurement for γ-rays using overtake effect 79−45436
spent nuclear fuel shipping casks, R and D sea going vessel requirements 79−31083
spent nuclear fuel transport problems *(Russian)* 79−31084
spent reactor fuel, risk analysis of alternatives from reactor pool until final disposal 78−17355
spent-fuel shipping casks, Monte Carlo radiative heat transfer 79−59193
spontaneously fissioning radionuclides, max. permissible conc. 77−73598
stainless steel, type 316, neutron induced charged particle spectra 78−5024
standards, implicit built-in safety factors 77−73596
standards, quantitative risk 80−61708
standards for low dose, low dose-rate exposure 78−80972
standards for people involved in more than one source of hazard *(French)* 80−47772
state responsibilities and radiation meas. system, US 77−37714
steam generator, multiple tube rupture, radiological consequences 78−74452
storage ring, SRS, shielding design 80−37659
surface coating, adsorpt. of Cs ions on constituent materials 78−23843
surface coating materials in nuclear generating stations, ionising radiation protection *(German)* 80−18681
surface decontamination efficiency, influence of carrier *(Czech)* 79−31222

radiation protection continued
Swedish State Power Board nuclear power stations, training of emergency organisation 78−50412
Swiss emergency organisation for nucl. and chem. accidents 78−57078
Swiss Federal Institute for Reactor Research emergency organisation 78−55047
synergism of radiation and other DNA damaging agents 80−26299
tandem, nuclear safety facility at Daresbury, shielding methods for insulators, ICs, other components 78−33318
technology transfer to developing countries on radiation protection and nuclear safety 77−65297
temporary confinement structures, design criteria and guidelines 80−18683
TFTR neutral beam injectors, concrete shielding calcs. 80−47734
TFTR neutral-beam injectors, shielding calcs. 80−23172
TFTR vacuum pump system, radiation exposures during maintenance 80−13788
therapeutic ^{131}I solutions, precaution for minimising exposure due to vaporisation 80−101274
thermal flash protective goggles, PLZT ceramic bonded lens assembly manufacture 80−79018
thermal flash protective goggles, PLZT ceramic thin wafer electrode slotting process 80−79017
thermal-flash protective devices for eye. PLZT electrooptic shutters 77−46808
thermoluminescent dosemeter, NRPB's new record keeping service 77−81577
thermoluminescent dosimeter monitoring post, concrete shielding to reduce background 78−817
Thoramat automatic thoracic radiography unit experience 80−12212
thymic region shielding in radiobiology expts., dosimetry in irrad. mouse cadavers 78−61257
thyroid irradiation and 1977 ICRP dose limits for medical radioisotopes 78−65135
thyroid protection during radioiodine-labelled pharmaceutical administration, computer simulation 78−44616
Tokamak divertor slot design to enhance mag. shielding 78−5028
Tokamak fusion reactor, effects of blanket-shield penetration on performance 78−21765
Tokamak fusion test reactor, cross section sensitivity, uncertainty anal. personnel dose rate 77−6554
Tokamak fusion test reactor, in-vessel maintenance remote manipulator system 80−18611
Tokamak reactor blankets, effects of neutral beam injection tubes, shielding calcs. 80−23173
tokamak reactors, radiation shielding of major penetrations, theory 79−36412
transport of nuclear material, especially nuclear fuel *(German)* 78−25314
transport of radioactive material, statistical anal. of low-radiation packages 77−88286
transport package design, criticality evaluation, appl. of SCALE system 79−63774
transportation of irradiated fuels and Pu, regulations *(French)* 79−26777
transportation of irradiated nuclear fuel, in Canada, emergency planning 78−50411
transportation of radioactive materials, safety anal. 79−63814
transuranium elements in general environment, USA EPA Guidance on dose limits 78−69223
tritiated water intake, calc. of committed dose equiv. 79−16311
tritium, permeation test facility at Julich, safety measures and monitoring 79−36428
tritium distribution in technological systems of Novovoronezh nuclear power station 80−32533
Tsuruga power station anal. of corrosion products 80−23062
UK legislation embodying ICRP-26 and IAEA safety standards 80−47763
UK population, sources of radiation exposure, review 80−36156
ultra-thin dosemeter for skin dose assessment, development 80−57974
underground high level radioactive waste disposal 79−9760
unfolded neutron spectrum and foil reaction rate computation and meas. 79−9904
university hot laboratory, radiation monitoring programme 80−57991
US Nuclear Regulatory Commission practices for assuring worker protection 80−5367
USA Environmental Protection Agency activities in radioactive waste management 78−94115
USA NRC reactions to ICRP (1977) recommendations, practical implications 80−47776
USA planning guides for major radiological accidents 78−53526
UV effects on eye 78−80917
UV hazards and protection standards 77−81588
UV radiation standards for health and safety 78−74056
Varian Clinac 4 MeV linear accelerator, radiation from U collimators, and shielding 78−24135
variance reduction techniques using adjoint Monte Carlo method in shielding problem 79−63759
vitamin C radioprotective effects obs. in Chinese hamster ovary cells 77−73546
vitrified high-level radioactive waste, associated hazards 78−13259
VVER type nuclear reactors, in Soviet Union, biological shielding problems 80−106127
waste air at nuclear plants, dose conversion factors for radiation exposure estimation *(German)* 77−70558
waste disposal compactor for dry solid waste, effectiveness in university health centre setting 77−66860
waste management policies, OECD countries 79−26596
waste storage devices, personnel radiation exposure reduction 79−16314
water, fast neutron angular penetration spectra, comparison with Monte Carlo calcs. 77−23303
West German nuclear fuel element factory licensing legislation *(German)* 79−89469
West German nuclear plant airborne radioactive effluent monitoring 78−89990
West German nuclear power plant airborne radioactive release control 79−13549
West German nuclear power plant liquid radioactive effluent control 79−13550
Windscale nuclear fuel reprocessing, shielding and radiation protection 80−18714
radiation protection continued
workers and the ICRP recommendations *(French)* 80−47775
working level survey meter 3R-WL, meas. of α-particles from ^{218}Po and ^{214}Po 78−25330
X-ray attenuation, effect on dose distrib. and choice of quantities for protection standards 80−51277
X-ray attenuation measurements on Y tong shielding material *(German)* 80−98145
X-ray baggage anal. equipment, radiation safety standards, Canada 79−2139
X-ray diffraction and fluorescence anal. equipment, radiation safety 79−12017
X-ray fluoroscopy, acute radiation injury caused by faulty use during cardiac procedures 77−9272
X-ray machines, pulsating pot., filter method for peak volt. and inherent filtration meas. 78−73201
X-ray production equipment, USA safety standard 78−29223
X-ray screening glass antireflection surfaces 77−21601
X-ray shielding arrangement, for diffr. equipment 80−849
X-ray shielding device, Pb glass, for use with ceiling mounted tube 79−92397
X-ray signal backscattered from semi-infinite reflector, quantitative analysis of intensity controlling factors 77−54371
X-ray tube thermal monitoring system, LOADIX, features 78−3658
X-rays, high energy photon absorption cross section for matter, review *(Japanese)* 78−74506
β-ray point source dosimetry using variable cavity chamber, appl. to protection instrument response 80−13942
Al, blanket/shield designs, minimum-activity, for D-T and D-^{3}He fusion blankets 79−85796
Al gamma-ray dose buildup factor functions, polynomial parameters 79−54607
Al min. activity blanket design for TFTR upgrade 78−58460
Al target inside magnet, hadron cascades prod. by 300 GeV protons 77−10566
Al-graphite two-dimensional shield, neutron penetration meas. 79−3245
Al-steel radiation shields, build-up factors for 6.2 MeV photons 79−81093
^{241}Am removal, Ca-DTPA vs. Zn-DTPA in beagles 77−73599
^{241}Am source ingestion, case report 78−28088
B_4C reflector-shield concept for fusion reactor designs 80−102293
B_4C-304 stainless steel cermet for nuclear shielding appls. 80−102352
B_4C-Al(silicone)(graphite), neutron shielding materials, long term radiation effects 80−9413
B_4C-Cu cermet fabrication for neutron shielding appls. 80−102354
B_4C-phenolic fibre reinforced composite for nuclear shielding appls. 80−102353
Ba plaster, X-ray absorption coefficients, from 100 to 400 keV 78−31283
^{14}C, formation, distrib. in nuclear fuel cycle *(Russian)* 80−5316
^{252}Cb, polyethylene pellets in design, construction of storage safe, transport vessel, portable shield 79−5380
Cd jacket, for shielding of sample from thermal neutrons in reactor 77−63991
^{252}Cf fission neutron, transmission through various shields, dose equivelent meas. 77−61620
^{252}Cf, heavy metal shielding for neutron sources 79−9892
^{252}Cf source projector for plesiocurietherapy 77−29197
$^{252}CfCl_3$, metabolism in rat and effect of in vivo DTPA chelation therapy 78−85387
^{242}Cm removal, Ca-DTPA vs. ZnDTPA as chelate, in rat 77−64141
$^{59}Co+n$, calc. using pre-equil. statistical model code GNASH 78−4946
^{60}Co 20 Ci source, site radiography incident 78−53523
^{60}Co 3000 Ci source accidental fall and retrieval in teletherapy room 78−53524
^{60}Co gamma ray absorbed-dose standards, comparison 78−74512
^{60}Co ion removal in waste water by oxine impregnated activated charcoal 79−26558
^{60}Co long-lived γ-emitting aerosols, max. allowable emission rate from nuclear power station 80−32532
^{60}Co retention in mouse, rat, monkey and dog, at tracer levels 77−9271
^{60}Co teletherapy unit, mech. fault affecting source position 77−73562
^{60}Co-charging of γ-irradiation installation *(Bulgarian)* 78−82558
Cs, in seawater, rapid determ. using Cs selective resin 78−85609
Cs sputter source, T beam prod. 78−29684
D-D fusion reactor blanket, nucl. characts., summary 78−89973
Fe gamma-ray dose buildup factor functions, polynomial parameters 79−54607
Fe radiation shielding, computational benchmark for deep penetration 80−47738
Fe radiation shielding, TLD meas. of neutron and gamma-ray energy deposition 80−23163
Fe shield, meas. of neutron and gamma ray penetration 80−47730
Fe+H shield, neutron flux meas., comparison with Monte Carlo calcs. 77−23349
H_2O, gamma-ray dose buildup factor functions, polynomial parameters 79−54607
^3H distribution between gas and liquid in isotope equilibrium in H_2O-H_2S and D_2O-D_2S systems 79−45376
^3H intake during various processes in industrial, academic and medical institutions 77−73600
^3H levels in urine of occupational exposed persons, working environment effects 79−83947
^3H personnel exposure, rapid evaluation using surface monitor 77−56485
^3H urine analysis, liq. scintillation solns. 77−9273
I, A=123 to 135, derived air concs. annual limits 78−31909
I, radioactive, adsorption on charcoal filter, safety evaluation *(Japanese)* 78−33267
I, radioisotopes, environmental and biological effects from nuclear fuel cycle *(Russian)* 80−52768
I radioisotopes, meas. of crit. environmental exposure for reactor accidents 78−57081
^{125}I accidental inhalation, bioassay and thyroid monitoring results 78−24151
^{125}I labelling hazards, reommended code of practice 80−51270
^{125}I, procedures for safe working in labs. 79−35698
^{125}I, shielding of *(Japanese)* 80−63404
^{125}I surface contamination meas., due to medical use of ^{125}I sources, detectors sensitivity comparison *(Czech)* 79−34673
^{125}I uptake minimisation and thyroid monitoring 77−40796

radiation protection continued
^{129}I, long-lived, immobilization by fixation of $Bn(IO_3)_2$ in Portland cement 79−59208
^{131}I filters, design against weathering 80−32524
^{131}I radionuclide pollution, protection of thyroid gland 79−66560
^{131}I waste in urine, filter system 77−60319
^{85}Kr, pressurised cylinder storage tests 80−5269
LiF tile and sheet for thermal neutron shielding *(Japanese)* 78−74510
^{6}LiH shielding for NaI gamma spectrometer, neutron background reduction 78−90012
MgO, GCFR shielding material, anal. of shielding effectiveness 80−47746
N_2 sphere surrounding D-T source, neutron and gamma-ray spectra 77−38422
PLZT thermal, flash, ferroelectric protective goggles 80−81746
PLZT/TFPD thermal/flash protective lens assembly, polarised delamination investigation 80−78929
Pb shield, effects of thickness and geometry var. on neutron spectra 78−33300
Pb-Al radiation shields, build-up factors for 6.2 MeV photons 79−81093
^{212}Pb inhaled body burden calibration, general phantom procedure 77−64138
^{210}Po contamination of surfaces, removal coeff. determ. 79−26769
^{210}Po intake through damaged skin and efficiency of methods preventing absorpt. 77−25561
Pt self-powered detector, neutron sensitivity calc. 78−37449
Pu body burden estimation from urine data influenced by DTPA therapy 78−73259
Pu fuel research facility for advanced LMFBR fuel *(Japanese)* 78−29624
Pu handling, radiation protection and monitoring of personnel 80−5389
Pu, high burnup fuels, shielding and handling problems 80−27833
Pu, reactivity effects of reflecting and interspersed concrete, composition effects 79−63788
Pu, safe working, safety measures 79−41040
Pu translocation from simulated wound sites in rat 78−77117
Pu-containing fuel, safety training program 79−18053
PuO_2 powder, leak rate determ. 80−42808
^{238}Pu, sources for cardiac pacemakers, manufacture and safety tests *(French)* 77−44751
^{239}Pu removal after inhalation of aerosol, bronchopulmonary lavage and chelation therapy 77−9270
^{239}Pu, use in weapons and energy prod., radiological hazards, security 77−10492
^{226}Ra source leakage testing by mailed track detector method 77−60264
Rn barrier, interior of building structs. foundations built on U mill tailings material 79−2138
Rn barrier to reduce indoor airborne Rn progeny 78−73262
Rn, concentration of ^{222}Rn, ^{220}Rn and decay products in room air, exhalation, ventilation and deposition effects 78−73261
Rn daughter concentrations in air of dwellings in Great Britain 78−77118
Rn diffusion, effectiveness of U mill tailing covers 79−93838
^{A}Rn A=220, 222, decay products attachment to polystyrene aerosols 80−41256
^{220}Rn and ^{222}Rn, decay products, diffusion coeffs. in air and Ar 79−90366
^{222}Rn conc. in energy efficient buildings 80−41261
^{222}Rn decay products, conc. in basement lab., working levels 77−40797
^{222}Rn diffusion in soil, moisture effects 80−37491
^{222}Rn, sources, distrib., exposure in residential buildings 80−41262
^{90}Sr, leaching behaviour in cement composites 78−37416
T concentration reduction for aquifer 80−21423
T control by glove box containment at fusion reactor plant 78−46169
T health effects during normal and off normal release in CTR's 78−774
T removal from air streams of reactors by catalytic oxidation and water adsorption 77−50292
T, role in radiation safety in nucl. fuel cycle *(Russian)* 80−56227
T sputter cone ion source for Minnesota MP Tandem, installation 78−29683
^{99m}Tc generators, comparison of weekly and biweekly systems rel. to radiation safety 77−2049
Ti alloy, radioactive structures, recycle time 78−58457
U fuel fabrication facility, integrated US/IAEA safeguards exercise 79−85736
U in vivo chest survey confirmation by autopsy specimen anal. 77−66859
U milling, radioactive waste treatment costs and environmental impact 77−46377
U mine radon control research 78−82525
U mines, dose limitations, ICRP recommendations, implementation problems 80−47769
U(VI) removal from rat body by DTPA, DTPP, EDDIP, decontamination efficiency 78−44617
W, radiation shielding material, integral tests of ENDF/B-IV high-energy neutron cross-section data 80−23162
^{127}Xe maximum permissible conc. in air 78−61262
^{133}Xe storage and dispensing device for nuclear medicine *(Czech)* 79−43986
Zn radionuclide dosimetry and permissible body burden ^{65}Zn and ^{69m}Zn 77−56474
Zn radionuclide dosimetry standards and crit. organs 78−35961

radiation quenching
acetaldehyde+CO_2, vibr. relax., search for unquenchable species, room temp., 5-2200 torr 78−9229
acetylene, triplet state quenching by foreign gases 80−91596
acetylenic hydrocarbons, cyclohexane soln., structureless fluoresc. 80−5575
acridene yellow, glycerol soln., luminesc. intensity and polaris., temp. and viscosity effects 79−56833
acridene-toluene-phenol, luminescence of complexes with hydrogen bonding at 4.2-77K 79−87486
acridizinium ion, fluoresc. quenching by external heavy atom, via charge-transfer complex 78−42112
adsorbate phosphor-silica gel substrate, oxygen quenching anomaly of afterglow 77−77275
albumin, human serum, interaction with luminol. chemilum. and fluoresc. 77−21471
albumin, human serum, kinetics of eosin-sensitised photochemilum. of solns. 78−68991
radiation quenching continued
alcohol solutions, fluoresc. damping curves in reson. quenching by one-photon counting method 78−10978
alkali halides, luminescence quenching of F-centres 80−50417
alkanes, liq., energy transfer rate parameters, emission intensity, lifetime meas. 79−86031
amines, aromatic, photochem. reactions with carbon tetrachloride, initiation mechanism 79−61888
9-aminoacridine fluorescence quenching method of chloroplast membrane proton gradient and osmotic vol. determ. 78−28143
2-aminopurine, in viscous soln., fluoresc. quenching, emission, intensity and reson. transfer *(German)* 80−91599
anthracene:tetracene, nonlinear quenching of fluoresc. 79−65924
anthracene, fluoresc. quenching by inorganic anions 78−74694
anthracene, fluoresc. quenching by triethylamine 79−50057
anthracene, in cyclohexane soln., triplet state decay consts. by sampling flash apparatus 79−51998
anthracene, pure and doped, singlet exciton diffusion lengths, fluoresc. quenching by dye 78−43923
anthracene, rarefied vap., fluoresc. spectrum shape distortion in presence of intense radiation 79−3487
anthracene, vap., line fluoresc. response to IR laser 79−54893
anthracene, vapour, fluoresc. spectra, mol. vibr. freq. reson. laser IR irradiation, quenching 80−18883
anthracene film, effect of struct. on luminesc. quenching *(Russian)* 80−7411
anthrone, 533 nm excited state absorpt. kinetic, triplet quenching solvent, internal conversion, vibr. relax. 78−21935
aqueous soln., ion luminesc. quenching by electron transfer 78−76511
aromatic hydrocarbon, quenched with Ag^{+} in ethanol, triplet state form. 79−11801
aromatic hydrocarbon-dicyanobenzene, aq. micellar soln., fluoresc. quenching mechanism 79−50063
aromatic hydrocarbon-N,N-dimethylaniline, aq. micellar soln., fluoresc. quenching mechanism 79−50063
aromatic hydrocarbons, aqueous micellar soln., triplet state room temp. phosphoresc., hydrophillic quenchers 78−9181
aromatic hydrocarbons, fluorescence quenching rate constant, undergraduate expt. using Spectronic 20 77−57119
aromatic hydrocarbons, oxygen quenching of triplet states, charge-transfer interactions 77−23516
atebrin fluorescence photo-induced quenching and photosynthetic electron transport, pea chloroplast 77−56351
bacteriochlorophyll a, stimulated fluoresc. and fluoresc. quenching, pump photon density 78−27895
benzaldehyde-biacetyl system, self-quenching and electronic energy transfer obs. 80−5571
benzene, fluoresc. quenching by pulsed proton irrad. of cyclohexane soln. 78−5270
benzene, soln., fluoresc., quenching in pulsed proton and alpha particle irrad., radiation quality effects 80−66259
benzene (S_1)+OCS, V-V reson. energy transfer, microscopic reversibility, level degeneracies role 79−86045
benzene in dilute cyclohexane solution, fluoresc. quenching on pulsed proton irrad., temp. depend. 80−21307
benzene triplet state, self quenching, effect on naphthalene internal conversion rate estimate 78−25586
benzene-aniline gas mixture, fluoresc. spectra, lifetimes, yields, electronic energy transfer 77−14477
1,12-benzoperylene, phosphoresc. in solid matrix, electronic transition multiplets 77−3413
9,9′-bianthryl, excited, proton-induced radiationless processes 77−88486
bimolecular reaction, partly diffusion-controlled, physical and chem. kinetics competition 79−43567
biomembrane, distance meas. by radiationless energy transfer, transition probabilities 78−24187
biphenyl, fluoresc. quenching by inorganic anions 78−74694
N-carbazolyl-$(CH_2)_n$-tetrachlorophthalimide, (n=2,3,4,7) intramol. electron donor-acceptor system, photophys. 78−82763
2-carbethoxy-5-chloro-7-aminoindole, soln., liq. scintillator, UV excitation, energy transfer and quenching 78−64395
carbocyanine dyes, triplet state quenching by nitroxyl radical, charge transfer complexing 78−25585
Cd+molecules collisions 80−58338
chalcogenide glasses, Luminescence, temp. depend. rel. to nonradiative transitions 80−71485
Cherenkov counting of plants for β-emitter radioassay, sample prep. 78−81088
chlorofluorocarbene, ($^{1}A''$) state, radiative lifetime, quenching rate, press. depend., laser-induced fluoresc. obs. 78−5259
chlorophyll, fluoresc. in bilayer lipid vesicles and liposomes, conc. quenching 77−4985
chlorophyll, fluorescence quenching, exciton annihilation excited state absorption and stimulated emission 79−98137
chlorophyll, transfer of electronic excitation energy from monomer to dimer *(Russian)* 78−27289
chlorophyll a: Cu^{2+}, in pyridine fluoresc. quenching mechanism 79−56837
chlorophyll a, stimulated fluoresc. and fluoresc. quenching, pump photon density 78−27895
chlorophyll fluorescence quenching by β-carotene 77−52735
chlorophyll in vesicles, energy transfer and fluorescence quenching 79−39349
chlorophyll photo-oxidation, spectral detect. of exciplex in triplet state 77−25368
chlorophyll-a, conc. quenching rel. to functional charge transfer 80−30666
chlorophyll-a, interaction with β-carotene in phosphatidyl choline bilayers, fluoresc. quenching 79−20506
chloroplast photosystems, exciton annihilation at 100K 77−25371
complex molecule solutions, stimulated emission, light quenching *(Russian)* 78−33735
complex molecules, fluoresc. quenching by strong radiation due to linear Stark effect 77−58074
complex molecules, photoinstability and quenching effect on laser generation kinetics 80−3390
counter-ion quenching of organic compound fluoresc. in micellar aq. solns. of surface-active substs. *(Russian)* 77−54573
crystal, radiationless relax. of excitation energy *(Russian)* 77−32418
CW narrow band dye laser quenching 77−50561
cyanine dyes, solns., excited states, duration meas. 77−65503

radiation quenching continued
9-cyanoanthracene, quenching of solid state photodimerisation reaction by cryst. doping 78−68547
cyanonaphthalene, fluoresc. quenching by inorganic anions 78−74694
cylcohexane, liq., energy transfer rate parameters, emission intensity, lifetime meas. 79−86031
decalin, liq., energy transfer rate parameters, emission intensity, lifetime meas. 79−86031
3,6-diaminophthalimide vapour, mol. electronic excitation energy degradation path depend. on pentane 80−74195
dichlorocarbene, $^1B_1$ state, radiative lifetime, quenching rate, press. depend., laser-induced fluoresc. obs. 78−5259
Dicke maser model, radiation damping, phase transition, presence of phonons 77−19224
dicyanoanthryl-naphthyl, intramol. exciplex, fluoresc. quenching by pyridine (γ-picoline), triple exciplex form. 79−50061
p-difluorobenzene, $^1B_{2u}$, quenching by cyclobutanone, fluoresc. lifetime meas. 77−75205
p-difluorobenzene+ketone reson. energy transfer cross section, 1st Born approx. appraisal 77−65519
9,10-dimethyl anthracene, excited singlet state quenching by nitroxyl radical, triplet form. 77−88487
dimethyl sulphoxide, UO_2^{2+} γ-irrad. frozen solns., radiothermolum. and temp. deactivation *(Russian)* 79−33854
p-dimethylaminoacetophenone, ps reversible isomerisation kinetics, O_2 quenching obs. 79−5133
9,10-dimethylanthracene, conc. solns., fluoresc. quenching by anthracene and derivatives 78−17711
9,10-dimethylanthracene derivative, intramol. fluoresc. quenching, attached CBr_3 groups 78−42113
1,5-dimethylnaphthalene, fluoresc. quenching by cyclic azoalkanes, micelle system probe 80−35578
dioxane liquid scintillators, scintillation yield, chloroform and carbon tetrachloride quenching effects *(French)* 77−3217
dioxane solutions, radioluminescence quenching in mixtures of solvents *(Russian)* 80−55192
9,10-diphenyl anthracene, excited singlet state quenching by nitroxyl radical, triplet form. 77−88487
2,6-diphenyl-1,4-benzoquinone+aromatic amine, triplet exciplex quenching, H-transfer mechanism 79−79228
1,3-diphenyl-5-(p-chlorophenyl)-2-pyrazoline, singlet excitation energy migration in cryst. and glassy states 79−95831
1,6-diphenylhexatriene, lower excited states fluoresc. quenching 80−1016
1,6-diphenylhexatriene soln., light quenching effect on fluoresc. band shape 79−98148
1,3-diphenylisobenzofuran, oxidation, dissoc. oxciplex relax., solute reencounter probabilities 79−34285
DMSO:Cr^{3+}, Nd^{3+}, energy transfer and migration, donor-acceptor interaction, phosphoresc. quenching conc. depend. 78−64403
dye, two-photon fluoresc. quenching, phase fluctuations and phase modulation effect 78−50570
dye laser, tunable, flashlamp excited, triplet quenching effect 79−31892
dye laser, tunable O_2 quenching effect 79−72564
dye soln., quenched, laser action *(Russian)* 78−25873
dye solution, luminesc. quenching, pulsed photoacoustic detection technique 77−85780
dye solutions, light-induced quenching of spontaneous and stimulated emission *(Russian)* 78−27290
dye solutions, liq. scintillation counting, rel. to colour quenching ability 79−1790
dye solutions, mixed, fluoresc. conc. quenching, sensibilisation 79−24347
dye vapour, fluoresc. meas., buffer gases effect 77−75503
dyes in micellar aq. solns., counter-ion quenching *(Russian)* 77−54573
electrolyte, excitation quenching in Coulomb attraction pot. 79−72351
electron irrad. effect on electrolum., defects form. and quenching obs. 80−55194
electronic energy transfer, in excited atom collisions, review, book contrib. 77−40543
electronic-vibrational energy transfer and quenching, modified model 77−14534
eosine^{2-}, in dimethylsulphoxide, transition metal ionic associations, fluoresc. quenching 77−73163
N-ethylphthalimide+olefins, photochemical reaction, absorpt., fluoresc., phosphoresc. and triplet-triplet absorpt. spectra 80−85197
europium B-diketone chelate solns., fluoresc. quenching by appl. voltage, display devices appl. 79−87497
exciplex, FMO calcs. 77−48655
exciplex fluoresc. decay, elec. field depend., quantum theoretical model 79−98133
exciplexes and excited aromatic molecules, donor-acceptor props., comparison of fluorescence quenching 80−69174
excitation quenching in electrolytes, Coulomb repulsive pot. 79−63927
excited single state kinetics on a subnanosecond time-scale 79−36677
finite positive column moving striations, excitation and asynchronous quenching 78−67515
flavin aqueous solns., fluorescence quenching by iodide ions, temp. and viscosity effects 77−34673
fluorene:benz(f)indan(anthracene), single cryst., γ-irrad. rel. to luminesc. decay 77−12417
fluorescein, fluoresc. quenching by rose bengal 79−78726
fluorescence, quenching meas. of pesticide uptake into membranes 78−7323
fluorescence of trypsin, photoluminescence after UV irradiation *(German)* 79−92137
fluorine, fluoresc. quenching by inorganic anions 78−74694
formaldehyde(-d_2), S_1 state, collisionless decay, vibr. relax., quenching 79−27019
formaldehyde in air, photodecomposition, CO and H_2 quantum yields 79−66311
formaldehyde-d_2, fluoresc. quenching *(Russian)* 79−50074
geminate recombination of radical ions in polar solvent, mag. field modulation, fluoresc. quenching 77−4912
glycerine solutions, fluoresc. damping curves in reson. quenching by one-photon counting method 78−10978
glyoxal, ^1A_u state energy transfer, D effects 77−58066
glyoxal, gas phase emission spectra, mag. quenching 77−18968
glyoxal, intersystem crossing in weak mag. field 78−78743
glyoxal, mag. quenching of fluoresc. 79−31582
glyoxal, radiationless transitions in weak mag. field, fluoresc. quenching 77−58062
glyoxal, $S_0 \rightarrow S_1$ band, opto-acoustic phase angle meas. 80−68256

radiation quenching continued
Group VIA photolytic laser systems, for fusion research 78−59002
halofluoresccin dyes, fluoresc. internal conversion, intersystem crossing 77−3405
heavy atom+H_2(HD)(D_2), intramultiplet transitions 77−54597
high temperature metallic species, absorpt. and fluoresc., high temp. fast flow reactor technique 80−42231
hydrocarbons, fluoresc. quenching by TMPD cations, diffusion effects 77−6823
impure crystal, sensitiser radiation quenching by activators, influence of collective phenomena 77−44052
indole, fluorescence quenching by chloromethanes due to electron transfer 79−94027
indole, pH dependent fluoresc., quenching by histidine *(Russian)* 78−90209
indole soln. containing histidine, fluoresc. rel. to soln. pH 80−2826
indoles, laser flash spectroscopy in presence of nitroxide radicals, protein-membrane interaction probing 79−87855
inert gas atom+halogen mol., halide form., relax. and quenching 80−81314
inert gas fluoride exciplex laser pumping efficiency 78−74892
inert gases, doubly charged ions, de-excitation coefficients 79−91946
instrument for quenching studies on rare gas and metal halide excited complexes 79−17511
intracavity dye laser quenching, quantitative detect. of Na absorpt. 77−36817
ketones, triplet-triplet absorption carbonyl group role 77−83641
laser, two-mode, mutual quenching of axial modes 79−13991
light quenching of mol. fluoresc. spectrum, spectral distrib. of polarisation 79−85989
liq. scintillator, UV excitation, energy transfer and quenching 78−64395
liquid, migration mechanism of approaching particles, energy transfer, luminesc. quenching study 80−100343
liquid scintillation counters, external standard quench correct. capability, inexpensive method for acquisition 80−47810
liquid scintillation counting, liq. scintillation counting, use of Aquasol in plastic Mini-Vials 77−26934
liquid scintillation counting, quench monitoring, H Number concept 78−82576
liquid scintillation counting, simultaneous meas. of ^{59}Fe and ^{51}Cr in blood 77−29195
liquid scintillation counting, single and double labels, absolute activity analyser vs. on-line computer 77−83470
liquid scintillation counting, single and double labels, quench correction with on-line computer 77−79520
liquid scintillation system ^{32}P Cherenkov effect detect. efficiency meas. using ^{60}Co external source 78−25387
luminescence decay times and bimolecular quenching, ultrafast kinetics expt. for students 77−26116
luminescence quenching, hopping mechanism, kinetics 80−7406
luminescence thermal quenching for linear and derivative nucl. operators 77−8631
magnetic quenching, enhancement of radiationless decay, direct and indirect mechanisms 77−42345
metal atom oxidation reactions, kinetics of chemilum. emitter form. and quenching 78−63107
metal-dielectric contact, exciton quenching and excited state props. 77−4416
metalloporphyrin triplet state quenching by Fe II- and Fe III-porphyrins 78−76992
methacrylate polymer, carbazolyl substituted, excimer and charge transfer complex trapping of excitons 80−34367
methoxynaphthalene, fluoresc. quenching by inorganic anions 78−74694
methyl thiyl radical, emission spectrum, collisional quenching 78−13543
m-methyl-p-cyanodimethylaniline, ps reversible isomerisation kinetics, O_2 quenching obs. 79−5133
9-methylanthracene, in acetylcellulose foil, time-depend. fluoresc. anisotropy, crit. transfer distance *(German)* 78−21964
methylated benzene+tetracyanobenzene, fluorescent exciplex form., electronic relax. 80−5573
1-methylpyrene, fluoresc. quenching by Cu^{2+} in micellar system, general kinetic model 80−32753
micellar aq. solns. of fluoresc. org. dyes, counter-ion quenching *(Russian)* 77−54573
micelle forming detergent solutions, fluoresc. quenching by O_2, dynamic parameters and solubility characts. 79−83513
micelle-confined molecules reaction, diffusion-controlled, luminesc. quenching, excimer form. 80−50890
molecular energy transfer processes involving distorted excited states 79−45794
molecular excited state natural lifetime determ. by fluoresc. light quenching 78−82775
molecular fluorescence, transient effects, kinetics 78−40022
molecular vibrational energy transfer, potential well depths 80−43156
molecule, photodissociation recomb. afterglow, quenching var., activator penetration to region inaccessible to quencher 80−64813
molecules in magnetic field, spin-orbit interaction 79−3483
molybdates, alkaline earth, U activated, scheelite struct. luminesc. props. vibr. modes and quenching temp. 80−60651
monolayer assemblies, molecular cooperation in photo-induced electron transfer 79−73985
N_2*+NO(H_2O), vibr. excited quenching temp. depend., flowing afterglow 77−54595
naphthalene, crystalline, singlet exciton diffusion coeff. meas., fluorescence quenching anal. 78−67945
naphthalene, doped, fluoresc., impurity centre struct. depend. *(Russian)* 77−48231
naphthalene, fluoresc. quenching by inorganic anions 78−74694
naphthalene crystal, inclined dimers as model for quenching centres 77−42237
naphthalene fluorescence by biacetyl, effect of viscosity 78−29810
2-naphthalensulphonate, fluoresc. and phosphoresc., external heavy atom effect 78−29812
2-naphthol-toluene-phenol, luminescence of complexes with hydrogen bonding at 4.2-77K 79−87486
naphthyl group, excited singlet state, intramol. fluoresc. quenching by halogeno substituents 80−102537
naphthylalanine polypeptides, fluoresc. quenching and energy transfer 79−34332
β-naphthylamine, fluoresc. quenching and spectra, excited state reaction, red edge effect obs. 80−83400

radiation quenching continued
β-naphthylamine, soln., fluoresc., photochem. quenching, excitation wavelength depend. 77−50470
naphthylamines, abnormal fluorimetric titration behaviour, kinetic anal., fluoresc. quantum yields and lifetime meas. 80−89560
naphthylamines, excited state pK_a^* values, proton-induced fluorescence quenching 78−21958
β-naphthylmethyl amine, solvent-induced intramol. exciplex fluoresc. 78−25592
nonlinear luminescence quenching at high pumping levels, microscopic theory 80−89040
α-NPO, fluoresc. spectrum light quenching factor wavelength depend. 80−18882
NQR scanning spectrometer, improved super-regenerative oscillator and quench generator 78−8429
optical waveguide, stimulated Raman scatt. quenching *(Russian)* 77−10983
organic compounds, fluorescence quantum yield, light quenching meas. 79−98147
organic excited singlet state fluoresc. quenching by metal ions, rate meas., mechanism 77−38685
organic gases, kinetics of intermolecular triplet-triplet electron energy transfer 79−10141
organic liquid scintillator, γ-irrad., energy transfer and quenching 77−8622
organic molecules, triplet state quenching by ruthenocene 77−83630
organic photoconductor, electric field-induced fluoresc. quenching 80−34967
organic scintillators, vap. phase dye laser media, photophysical parameters 80−95884
orthopositronium quenching by O_3, meas. by two-photon coincidence rate difference technique 80−74262
oxalyl fluoride, radiative and nonradiative transitions, self-quenching, unimol. dissoc. 78−17708
oxide:U^{6+}, struct. sensitivity of luminesc. 77−90187
Penning ionis., radiative, photoionis. depend. of continuum radiation 77−19034
perylene, excited singlet state quenching by nitroxyl radical, triplet form. 77−88487
phase fluorometry as a probe of diffusion-controlled molecular encounters in dense fluids 80−32799
phenanthrene, fluoresc. quenching by inorganic anions 78−74694
phenanthrene, triplet state conc. quenching in propan-1,2-diol 77−75196
2-phenylindole, in viscous soln., fluoresc. quenching, emission, intensity and reson. transfer *(German)* 80−91599
phosphate glass:Nd^{3+}, highly conc., electron energy deactivation and transfer *(Russian)* 80−29802
phosphor adsorbates, luminesc. quenching, activator location effects 77−52172
phosphor model system, thermal quenching, QMSCC calcs. 79−78731
photogeneration and fluoresc. quenching theory, appl. to x-metal-free phthalocyanine 79−65513
photoluminescence concentration depolarisation, by excitation transfer, selfquenching considerations 77−32413
photoluminescence concentrational depolarisation by excitation energy transfer 80−2821
photosynthetic membrane, in vivo, light collection and exciton dynamics 79−48215
photosynthetic unit, bimol. quenching of excitons and fluoresc. 77−16908
phthalamide derivative with aromatic amine, exciplex formation and fluoresc. quenching 79−87848
phthalimide, soln., triplet state accumulation and deactivation depend. on solvent polarity 79−85982
phthalimide acetyl derivatives in polar solvents, luminesc. kinetics and phosphoresc. quenching 80−18885
phthalimide solutions, fluoresc. optical quenching by ruby laser rad. *(Russian)* 77−12437
phthalocyanine, metal-free, singlet-triplet fusion rel. to carrier photogeneration 77−36276
phthalocyanine, X-metal-free in polyvinylacetate, elec. field induced fluoresc. quenching, carrier photogeneration 78−48207
phthalocynanine, doped photovoltaic cell, photoconductivity, elec. field induced flouresc. quenching, charge carrier photogeneration 80−84485
plasma, heavy-impurity control by light-impurity radiation, wall layer cooling 77−65879
poly-N-vinylcarbazole-biacetyl, triplet exciton quenching, exciton trapping model 80−66267
polyatomic molecules, collisional mag. quenching, collision-complex model 79−50059
polycyclic aromatic hydrocarbons, alternant and nonalternant, fluoresc. quenching by nitro cpds. *(German)* 78−21967
polycyclic hydrocarbons, alternant and nonalternant, fluoresc. quenching by electron transfer 79−6959
polyethylene terephthalate, photoexcited, thermoluminescence field quenching 78−43942
polystyrene, electron trap depth distribs., thermolum. data 78−11002
polystyrene, thermoluminescence glow curves, quenching and isothermal decay plots 77−48258
polyvinylcarbazole, fluoresc., photooxide quenching, exciton migration effects 79−56830
POPOP, fluoresc. spectrum light quenching factor wavelength depend. 80−18882
POPOP laser, bleaching of vapour 80−19027
porous Vycor glass, quenching by O_2 and NH_3, photoluminescence obs. 80−93773
porphyrin solns., quenching of excited states by nitro-cpds., donor-acceptor interactions 78−2899
porphyrins, solid solns., phosphoresc. rel. to solvent heavy ats. *(Russian)* 77−40286
positronium formation and quenching in Ar-O_2 mixtures, orthopositronium quenching cross section determ. 80−74261
protein, radical limiting conc. on UV irrad. at 77K, effect of luminesc. quenchers 80−30662
proteins, adsorbed at interfaces, fluoresc. spectroscopy study 80−12315
proteins, fluoresc., equilib. structural mobility *(Russian)* 78−76986
proteins, UV irradiated, luminesc. quenching, EPR and absorpt. spectra 78−15768
protoporphyrin: Cu^{2+}, in pyridine fluoresc. quenching mechanism 79−56837

radiation quenching continued
pyrene, distinction of delayed fluorescences $S_1 \rightarrow S_0$ and $S_2 \rightarrow S_0$ by selective quenching of $S_1 \rightarrow S_0$ 80−69175
pyrene, fluoresc. quenching by 1,4-diazabicyclo[2-2-2]octane in cyclohexane soln. 79−31575
pyrene, fluoresc. quenching by inorganic anions 78−74694
pyrene, in aq. micelle system, fluoresc. quenching by inorganic ion 77−10697
pyrene, in cyclohexane soln., triplet state decay consts. by sampling flash apparatus 79−51998
pyrene, in micellar environments, fluoresc. quenching by nitroxyl radical 79−13754
pyrene, micellar solns., fluoresc. quenching 78−25588
pyrene-DMA-methanol solution, photoinduced radical ion pair geminate recombination, triplet yield 78−76879
pyrene-h_{10}, -d_{10}, dual fluoresc. quenching by O_2 and NO 78−5266
pyrene-N,N-dimethylaniline heteroexcimer systems, micellar solns., fluoresc., photoinduced electron transfer 78−25590
quenched fluorescein solution, lasing props. *(Russian)* 77−27286
quinones, triplet quenching by organometal cpds., time resolved CIDEP and ESR obs. 80−95654
rare earth laser materials, linear conc. quenching of luminesc. 79−31908
retinals, prod. and quenching of singlet oxidation 80−35840
rhodamine, soln., triplet state accumulation and deactivation depend. on solvent polarity 79−85982
rhodamine 101, quenching of emission in methanol and latex particle suspensions 80−3374
rhodamine 6 Zh solution, radiant transport effect on luminesc. duration 80−103995
rhodamine 6G, aqueous soln., absorpt. spectra, ground and triplet state photoprotonation pH depend. 80−42961
rhodamine 6G, in glycerine-water solns., anti-Stokes fluoresc., conc. quenching 79−24349
rhodamine 6G, in methanol, fluoresc. lifetime meas. 78−29811
rhodamine 6G+malachite green, in low viscosity solvent, ps time resolved energy transfer 78−70910
rhodamine dye, intercombination conversion rate consts. from triple quenching by 1,4-diphenylbutadiene 79−956
rhodamine dyes, phosphoresc. quantum yields determs. 79−8179
rhodamine solutions, quenching of two-photon fluoresc. and stimulated anti-Stokes emission 79−72619
rhodamines, 5G, 6G, B, 3B in ethanol soln., luminesc. quenching by photoirradiation 80−87168
rubrene, excited singlets, O quenching, singlet O formation 78−27792
ruthenium tris-bipyridyl, excited state electron transfer quenching, H_2O photoreduction mediators effects 80−102536
scintillation counters, use of miniature glass vials in multi-functional standards 77−70370
scintillation quenching curves, solns. by second-order polynomial regression 77−3220
semiconductor, quenching of luminesc. by charged defects 78−23531
semiconductor laser, transient processes, external optical feedback influence 79−50297
β-SiC, optical quenching of luminesc., acceptor ionisation energy 80−55178
Smoluchowski equation, with Coulomb pot., appl. to fluoresc. quenching 78−73051
solar cell, absolute efficiency meas., effect of IR quenching 79−83597
solid, luminesc. quenching parameters, donor-acceptor exchange mechanism 80−2840
solution, electronic excitation energy transfer between like mols. *(German)* 78−21965
solution, luminescence quenching due to approaching particles transferring energy *(Russian)* 78−43933
solution, nonlinear luminesc. quenching kinetics, high excitation power 79−56834
solutions, containing quenching agents, emission spectra, temp. effects *(Russian)* 78−15227
trans-stilbenes, triplet energy, substituents effect, singlet-triplet absorpt. and electrochemilum. obs. 79−81225
stimulated Raman emission, mutual quenching of modes 79−36960
terbium chelate solns., fluoresc. quenching by voltage appl. 79−87498
p-terphenyl, fluoresc. quenching by 4-aminobenzophenone in different dielec. const. solvents *(German)* 79−83030
tetrabutylammonium europium yttrium isothiocyanate, conc.-depend. electron-phonon coupling, and self-quenching 80−60657
tetracene, single cryst., exciton interactions, ps laser pulse intensity depend. 77−63448
N,N,N′,N′-tetramethylparaphenylenediamine, recomb. fluoresc., elec. field quenching 78−92107
thin-film laser logic element, operation *(Russian)* 79−10413
thiocarbonyl chlorofluoride, second excited singlet state emission spectroscopy, resonance fluorescence obs. 80−69158
thionine-monohaloaniline triplet exciplex, quenching position dependent heavy atom effect, intersystem crossing 78−53197
thiophosgene vapour, fluoresc. from S_2 single vibronic states, quantum yields and quenching 77−34675
TMPD, 2,2,4-trimethylpentane, fluoresc. quenching by elec. field, above photoionis. threshold 78−33539
TMPD, fluoresc. in nonpolar organic liqs. for excitation energies above and below photoionis. threshold 78−1018
TMPD, nonpolar photoionised soln., geminate pair quantum field, recombination fluoresc. elec. field quenching 79−20389
toluene+O_2, fluoresc. quenching kinetics 77−18964
TOPOT, 1,4-bi[2-(5-p-tolyloxazolyl)]benzene laser, bleaching of vapour 80−19027
TOPOT, fluoresc. spectrum light quenching factor wavelength depend. 80−18882
transition metal complexes, electron energy transfer process 79−10143
transition-metal fluorescence-quenching mechanisms for organic compounds 79−56837
triethylamine, gas (soln.), fluoresc. quenching by 'inert' perfluoromethylcyclohexane 78−46438
trypaflavine, on silica gel, luminesc. quenching, activator location effects 77−52172
tryptophan, laser flash spectroscopy in presence of nitroxide radicals, protein-membrane interaction probing 79−87855
tryptophan, pH dependent fluoresc., quenching by histidine *(Russian)* 78−90209
tryptophan soln. containing histidine, fluoresc. rel. to soln. pH 80−2826

radiation quenching continued
tungstates, alkaline earth, U activated, scheelite struct. luminesc. props. vibr. modes and quenching temp. 80−60651
tungstates, U-doped, perovskite struct., luminesc. quenching, QMSCC calcs. 80−71470
uniaxial crystal, macroscopic exciton luminesc. characts., high reabsorption conditions 78−19545
uranine, intercombination conversion rate consts. from triplet quenching by 1,4-diphenylbutadiene 79−956
vinyl polymers quenched with electron donor (acceptor) in soln., ionic photodissoc. 79−11800
X-ray transitions for F and O ions moving in Ne, Ar, Kr gases and C foils and slabs 77−69020
xanthione, solns., triplet state quenching by ground state xanthione 78−42180
0 I, 63 μm emission and quenching cross section in thermosphere and ionosphere 79−16732
$AR(^3P_1)+H_2$, energy transfer rate const. expts., reverse reaction effect 77−65520
AgBr film coatings, luminesc. props. for H_2 and other reduction sensitisation 79−61886
$AgGaSe_2$ single crysts., opt. quenching of photocond., temp. depend., slow centres activation energy *(Russian)* 77−69370
Ag_2S layers, quenching of photocond. by UV radiation 78−68047
Ar atomic excited states collision radiative destruction in glow discharge, quenching rates 79−3528
Ar, hydrogenlike, Lamb shift meas. by motional elec. field quenching time-of-flight expt. 80−9550
Ar I, II, fission fragment excitation of optical radiation, quenching by UF_6 77−23665
Ar, metastable $^3P_2$ deactivation in afterflow, plasma characts. 78−55769
Ar saturated solutions, NO_3^- effects on spectral distribution and intensity of sonoluminescence 80−76091
Ar^{17+}, Lamb shift, elec. field quenching time of flight method 79−13674
Ar-F_2 mixtures, low-press. excimer form. and quenching by e-beam excitation 79−50071
Ar+Ca, quenching cross section of Ar atom for Ce reson. line 77−19021
$Ar+H_2(HD)(D_2)$ reson. energy transfer cross section, 1st Born approx. appraisal 77−65519
$Ar+N_2$, bimol. and three body quenching, reson. state $^1P_1$, $^3P_1$ and excimer Ar atoms 79−3540
$Ar+N_2(SF_6)$, 1s states deactivation 77−50398
$Ar+N_2(SF_6)$, proton excited, time resolved VUV, UV and visible emission 77−14547
ArCl*, excimer formation rate consts., B state radiative lifetimes, quenching, VUV excitation 80−55631
ArF, electron quenching rate consts. meas. by fluoresc. anal., laser implications 80−32969
ArF*, Ar_2F^*, kinetics of proton-excited Ar-F_2 mixtures, time-resolved and time-integrated spectra 79−36883
ArF*, formation and quenching kinetics 77−88482
ArF* laser, electron beam pumped, dominant formation and quenching processes 79−938
Ar_2F^*, radiative lifetimes, quenching rate consts., emission spectra 78−46577
$Ar(^3P_{0,2})+N_2$, rate consts. and $N_2(C):N_2(B)$ branching ratio 78−5327
$Ar(^3P_2)+F$, donor reagent, quenching, excimer form. 79−63953
$Ar(^3P_2)+N_2(C^3\Pi_u)$ excitation transfer cross section, radiative lifetimes, in N_2 laser, transitions 79−27246
$Ar_2(^2\Sigma_u^+)+N_2$, quenching, fast absorption spectrophotometry 79−54940
Ar*, quenching by $O(2p^4\ ^3P)$, population and depopulation of $O(3p^5P)$ 80−42958
Ar^{*+}+Kr, flowing afterglow, energy transfer reaction and quenching rates 80−23529
$Ar^*(3p^54p)_i+Ar(^1S_0)$, collisional population transfer rate coeffs., 300K 79−10177
$Ar(3p^5, 4p)$ and $(3p^5, 4p')$ states, radiative lifetimes, two-body deactivation rate consts. 79−10068
As $4p^3(^4S_{3/2})$, collisional quenching 78−33464
As_2S_3:Fe glass, photolum. and ESR, Fe impurities as non-radiative recomb. centres 80−29788
B, quenching of reson. radn. by Xe and Kr 77−30820
Ba, $(5d^2D_J)$state, quenching obs. 80−52926
Ba+CO, radiation quenching of metastable Ba $(5d\ ^1D)$ in gas 79−85932
$Ba+D_2$, radiation quenching of metastable Ba $(5d\ ^1D)$ in gas 79−85932
$Ba+H_2$, radiation quenching of metastable Ba $(5d\ ^1D)$ in gas 79−85932
$Ba+N_2$, radiation quenching of metastable Ba $(5d\ ^1D)$ in gas 79−85932
$BaBr_2:Sm^{2+}$, spectra, ^5D states, Lauer-Fong formula and SCC model 79−15513
$BaCl_2:Sm^{2+}$, spectra, ^5D states, Lauer-Fong formula and SCC model 79−15513
$BaO-Nd_2O_3-P_2O_5$ ultraphosphate glasses, Nd^{3+} conc. quenching of luminesc. effect 79−19931
$BaO-P_2O_5(SiO_2)$ glasses, quenching of Nd^{3+} luminesc. by transition metal and rare earth ions 80−25449
BaO*, quenching of excited species formed by $Ba+NO_2$ chemiluminesc. reaction 77−58140
Bi, $6p^3(^4D_{3/2}^0)$ and $6p^3(^2D_{5/2}^0)$, collisional deactivation 77−61702
Bi, metastable states collisional quenching, temp. depend. 77−88526
Bi_2, radiative lifetime and self-quenching cross sections meas. from laser induced fluorescence expt. 80−69189
$Br+CO_2(HCl)$, quenching of $4^2P_{1/2}$ state, vib. excitation, temp. depend. 78−58792
$Br+O_2(NO)$, quencher paramagnetism, deactivation rate const., spin-orbit relax. study 80−21263
Br_2, $B^3\pi o_u^+$ state deactivation efficiency, temp. depend. 78−70869
Br_2, kinetics of excited states using laser excitation, radiative lifetimes and collisional deactivation 80−74237
Br_2, single rot. states, lifetimes and collisional quenching cross sections determ. by obs. fluoresc. decay 80−91595
BrCl, $^1\pi_0^+$ state, time-resolved fluoresc. 77−34679
BrCl, time-resolved fluoresc. of $a^3\Pi_0^+$ state 78−63093
BrF, fluoresc. decay lifetimes and quenching cross-sections for excited $B^3\Pi(0^+)$ states 78−1030
$Br(4^2P_{1/2})+CO_2(COS)(CS_2)$, electronic to vibrational energy transfer rates 78−29839
$Br(4^2P_{1/2})+N_2O$, electronic-vibr. energy transfer obs. 78−55220
C_2 $a^3\Pi_u$ state quenching, laser-induced fluoresc. obs. 79−31574
C_2, conc. meas. in oxyacetylene flame rel. to saturation spectroscopy 77−60148
C_2, low lying $a^3\Pi_u$ state produced in intense IR field, fluoresc. and quenching obs. 80−11931
C_3, $(^1\Pi_u)$ radical excited state radiative lifetimes and the collisional deactivation 79−27018
$CH(A^2\Delta)$ radicals, electronically excited, lifetimes and quenching rate constants meas. 80−69188
CN, fluoresc. spectra, time resolved, radiative decay and radiationless deactivation in Ar 79−98142
CN, radical, $A^2\pi$ state, collisional deactivation, fluoresc. quenching obs. 77−83642
$CN(B^2\Sigma)$ shock wave excitation, emission, excited state populations, in $CO-N_2$-Ar mixtures *(Russian)* 78−74638
CN*, $B^2\Sigma^+$ state, fluoresc. decay dynamics, collisional quenching and radiative lifetimes 80−58306
CO, $b^3\Sigma^+$ state excitation, low-energy electron impact, $\nu'=3$ level lifetime 80−1072
CO, $d^3\Delta$ state, low energy electron impact excitation and radiative decay 80−91691
$^{12}C^{18}O$ 78−82768
$^{13}C^{16}O$, fluoresc. and electronic quenching cross sections 78−82768
CO-He-O_2 gas discharge laser plasma, positive ion generation mechanism *(Russian)* 79−99005
CO+aromatic molecule, vibr. energy transfer, quenching efficiency 79−3539
CO+CO, $d^3\Delta$ state vibr. relax. in glow discharges 79−18271
$CO+CO_2$, vibr. level depend. quenching of $CO(\nu=1\text{-}16)$ 80−32808
CO+inert gas, collision-induced intersystem crossing mechanism 78−74689
CO+O, vibr. deactivation 78−94305
CO_2, atm. press. laser pulse duration reduction by stimulated emission quenching 79−18400
$CO_2+N_2(CO)$, CO_2 1st vibr. levels collisional deactivation, photoacoustic study 79−98187
$CO_2(01^10)+N_2(CO)(O_2)$, collisional deactivation rate const., 160-375K, photoacoustic obs. 79−10179
CS, $A^1\Pi(\nu=0)$, radiative lifetimes and quenching rates, laser-induced fluoresc. obs. 79−59496
CS_2, mag. quenching of fluoresc. 79−31582
$CS(A^1\Pi)$ vibr. relax. in He 80−53106
$Ca+Ca(Mg)$(inert gas), metastable ^3P-state, quenching reactions, fluoresc. meas. 80−102477
CaF_2:Dy(Ho)(Pr)(Tb), V_k-centre recomb. kinetics, phosphoresc. 77−55817
$CaO:Ce^{3+}$, Gd^{3+}, sensitization of Ce^{3+} luminesc. by Gd^{3+} 80−97326
$C_2(a^3\Pi_u)$+methane(acetylene)(ethylene)(ethane)(O_2), reaction rate consts. and quenching, multiphoton UV photolysis, fluoresc. obs. 79−74355
$C_2(a^3\Pi_u)+NO$(vinyl cyanide)(ethylene), laser-generated radical kinetics 79−100352
CaSe: Sn^{2+}, dimer centre, emission and excitation spectra, temperature quenching *(French)* 79−99937
$CaWO_4$, type selfactivated luminophors, nature of optically active centres 77−69880
Ca($4p\ ^3P_1$)+Ba, collisional deactivation and optical lifetime 80−48070
Cd, 6^3P_1 level, relax. of alignment and population 78−70795
Cd+K(+N_2), optical excitation, rate consts., collisional energy transfer kinetics 80−32801
Cd_2, quenching and predissociation, possible excimer laser 80−32770
$CdCr_2Se_4$, photoferromag. effect quenching, photocond. 78−68488
$CdIn_2S_4$, photoluminesc., thermal quenching and recomb. centres 79−24362
$Cd(^3P_{0,1})+CO(CO_2)(NO)$, absolute quenching cross section, phase-shift method 80−58340
$Cd(^1P_1)$ excited state quenching by mols., cross sections, chem., phys. exit channels 79−779
$Cd(^1P_1)+N_2$(alkanes), laser excitation, absolute quenching cross sections and branching ratios 79−49979
$Cd(^3P_1)(^1P_1)+H_2(HD)(D_2)$ reacts., CdH(CdD) yields, quenching cross sections 79−1948
$C_2(d^3\Pi_g)$ shock wave excitation, emission, excited state populations, in $CO-N_2$-Ar mixtures *(Russian)* 78−74638
CdS, optical quenching of noise photooscillations, connection with photoconduction *(Russian)* 77−20363
CdS:Ag, Ni thermographic phosphor luminesc. screen, for IR laser pulse recording 79−64342
CdS:Cu films IR quenching of photocapacitance, deep level detection 79−56258
CdS:In(Cl) concentration quenching mechanism of luminescence 80−97336
CdS:Li, TSC and optical photocurrent quenching spectra, Auger excitation of recomb. centres 79−33294
CdS:Mn(Co), intensity and spectral distrib. of luminescence *(Russian)* 77−16392
CdS(Se)(Te):Co^{2+}, IR luminesc. quenching, Co^{2+} level position, ionisation energy 80−16079
CdTe, elec. and photoelec. props. due to double injection, quenching spectra 80−70765
CdTe, undoped and donor-compensated, cathodoluminesc. of 1.4 eV bands 77−40291
CdTe:Xe, anomalous Xe^+ ion implantation defect introduction, cathodolum. quenching 77−62554
$Cd(5^3P_{0,1})$+methane.$(H_2)(D_2)(N_2)$, absolute quenching cross sections 80−5604
$Cd(5^3P_1)$+POPOP, vap., electronic energy transfer, laser appl. 77−30980
Cl_2, fluoresc. quenching by collision-induced predissoc. 77−14472
ClFCS, second excited singlet state photophysics, laser excitation obs. 80−32758
$Cl(3p^5(^2P_{1/2}))$+carbon tetrachloride (Cl_2)(He), VUV metastable state quenching, absolute rate const. 77−79641
$(Co,Cr,Fe)_3O_4$, $(Co,Rh,Fe)_3O_4$ film magnetooptical switches, for laser beam synchronisation 80−58615
Cr complex, organic mol. singlet excited state energy transfer to complex quartet levels 77−25291
Cs, photoplasma, optical excitation in radiation diffusion conditions 78−55227
Cs, resonant 6P state, quenching by CO_2 mols. in He-CO_2-Cs discharge 80−43860

radiation quenching continued
Cs+Cs, Rydberg states collisional disalignment determ. by fluoresc. quantum beat damping 79−13789
Cs+X, (X=N_2, H_2, He, Ar, Xe), collisional relax. and population - - quenching of Cs 78−25467
Cs_2, fluoresc. spectra, kinetics, laser candidate 79−64027
Cu^{2+}-1,5-dimethyl-2,4-hexadiene, fluoresc. quenching method for determ. binding const. 80−89530
D, Lamb shift, from elec. field quenching radiation anisotropy 78−66502
DF, IR chemiluminesc. quenching, (V-V) and (V-T, R) energy transfer rates 78−20018
DF, IR chemiluminesc. quenching, (V-V) energy transfer rates 78−20019
DF+CO_2, vibr. relax. rate, chemiluminescence depletion method meas. 79−72399
DF($1 \leq n \leq 7$)+HF(0), vibr. deactivation calc., 300-3000K 79−31655
Dy^{3+}+$O_3(SO_5^{2-})(SO_2)$, in H_2SO_4 soln., electrochemiluminesc. emitters quenching by electrolysis products 79−1794
Eu^{2+} activated phosphors, luminesc. efficiency, temp. and high pressure 78−23508
$EuCl_3.6H_2O$-$NdCl_3.6H_2O$($HoCl_3.6H_2O$), in DMSO soln., Eu^{3+}→Nd^{3+} (Ho^{3+}) radiationless energy transfer 80−5499
$Eu(NCS)_3$ solns., luminesc. quenching of Eu^{3+}, charge transfer states 77−90190
$EuNa_3Mg_2(VO_4)_3$, disordered, thermal quenching of luminesc. 80−71472
F atomic laser, He+NF_3 collisional quenching rates 79−81410
F VIII, 1s2p $^3P_0$ and $^3P_2$ levels, lifetimes, hyperfine quenching effects, UV beam foil spectra 80−47931
F^{7+}, $1s2p\,^3P_1$ collisional quenching, perturbation theoretic calc. 77−54602
F+H_2, collision in intense laser field, formalism for mag. dipole interaction 79−98190
F+Xe, enhanced quenching in intense KrF laser light, computer modelling 78−55232
F+Xe(H)$^+$(H_2), ($^2P_{3/2}$) state quenching, Franck-Condon approach 78−66640
$F(^2P_{1/2})$+H_2(j=0) quenching, quantum mech. study, ortho-para mixing role 79−76485
$F^*(^2P_{1/2})$+H_2, appl. of classical model for electronic degrees of freedom 79−98192
$FeCN_6^{4-}$, triplet state quenching agent, in ZnO electrode dye sensitisation obs. 78−76869
GaAs:Cr, photoluminescence in strong electric fields 80−108270
GaAs:Cr, single cryst., optical quenching spectrum, disappearance of stationary high-field domain 78−47830
GaAs:Ge, vap. grown, diatomic complex donor and acceptor model 78−80003
GaAs-Au, quenching of exciton luminesc. by surface elec. field 80−29801
GaP:N, bound excitons, low temp. photoluminesc. thermal quenching 77−48228
$(Gd_{1-x}Tb_x)_2O_2S$ phosphor, concentration quenching of Tb^{3+} luminesc. 80−29785
Ge $4p^2(^1S_0)$, collisional quenching 78−33463
n-Ge:Ni, quasi-surface conduction effects on photocond. spectrum and IR quenching 77−1452
Ge:Sb, electron-hole drop lifetime, quenching temp. influence 80−59889
GeF, $A^2\Sigma^+$ state, time-resolved fluoresc. 78−58732
GeO, produced in Ge+N_2O reaction, kinetics of chemilum. emitter form. and quenching 78−63107
H (2s) elec. field-quenched radiation polaris., Bethe-Lamb theory justification 78−17603
H halides, $I^*(5^2P_{1/2})$ quenching, electronic-vibr. energy transfer 78−63114
H, metastable quenching, subsequent photoionis., polarised proton prod. *(Russian)* 78−46202
H, muonic collision quenching of 2S-state, distorted wave calc. 77−58211
H, subnatural linewidth resolution $2^2S_{1/2}$, $2^2P_{1/2}$ level crossing, Lambshift, pulse technique 79−22669
H^+, isoelectronic sequence, quenching radiation anisotropy calcs. 77−27021
H-like ions, fluoresc. polarisation of Stark quenched spin-polarised beam 78−66501
H+He, H Balmer-α fine-struct. line shift and broadening 80−37783
H_2 3s, 3d: $^3\Sigma$, $^3\Pi$, $^3\Delta$ complex, fine struct., Doppler-free laser spectroscopy 80−1087
H_2, $E,F^1\Sigma_g^+$ state, collisional and radiative props. 80−58357
H_2, metastable $c^3\Pi_u$ state, population densities and quenching times meas. 78−94296
HCN (001)+HCN(Ar)(N_2)(CO_2)(CO), relax. rate consts., using Cs vap. IR source 80−9696
HCl, overtone vibr.-rot. bands, intracavity dye laser techniques meas. 80−91532
HCl+CO_2, vibr. relax. rate, chemiluminesc. depletion method meas. 79−72400
HCl(ν=1,2)+$O(^3P_g)$, reaction and deactivation, laser-induced fluoresc. obs. 78−35669
$HD(^1\Sigma_u^+)$+He, fluoresc. quenching and energy transfer processes 79−86032
$H_2(E,F^1\Sigma_g^+)$,+He(H_2), quenching rates, IR fluoresc. obs. 78−37698
HF, IR chemiluminesc. quenching, (V-V) and (V-T, R) energy transfer rates 78−20018
HF, IR chemiluminesc. quenching, (V-V) energy transfer rates 78−20019
HF+CO_2, vibr. relax. rate, chemiluminescence depletion method meas. 79−72399
HF+$I^*(5^2P_{1/2})$, electronic-vibr. energy transfer fluoresc. decay meas. 77−71846
HF+$O_2(a^1\Delta_g)$, E-V energy transfer 77−30960
HF*+ethylene (fluoroethylenes), vibr. deactivation rate constant 78−50615
HF($1 \leq \eta \leq 7$)+DF(0), vibr. deactivation calc., 300-3000K 79−31655
HNO(A^1A''), state-selected fluoresc. lifetimes, collisional quenching rates 79−36674
H_2O+H(n=3), $O(3p^3P)$, radiation quenching in pulse radiolytically excited water vap. 79−89738
H(2S)+$H_2(N_2)(NH_3)$(acetone)(methanol), collisional quenching, mass spectral obs. 78−25685
H(2S)+inert gas, collisional quenching, mass spectral obs. 78−25685
radiation quenching continued
HbBr($B^2\Sigma^+_{1/2}$), rate coeffs. for collisional quenching, time resolved emission obs. 79−89705
He, ^3P level, excitation and decay study up to high press. pumped by intense relativistic electron beam 80−74250
He (2^3P)+Ca(Sr), collisional quenching of metastable states, excitation transfer cross sections 78−66653
He and He^+, 3^3P and 4^2F levels excitation with electron beams, radiation decay obs. 80−43188
He glow discharge, low press., excitation transfer and quenching of n=3 excited states 80−38743
He glow discharge, n=3 sublevel quenching and energy transfer, laser perturbation method 80−44060
He I glow discharge, low-press., quenching of singlet states by N_2 80−49030
He I spectral lines, radiation trapping in electron beam, spatial distrib. of line intensity 77−79572
He, metastable states, props., energy transfer mechanisms, exptl. techniques 80−27921
He^+ Lamb-shift measurement by the quenching-radiation anisotropy method 80−18824
He+water (cyanomethane), afterglow, excitation and quenching reactions, optical pumping 78−35690
He^++inert gas, collisional quenching cross sections, two-state theory calcs. 80−69217
$He(^1S_0)$+Na(Li) radiative Penning ionis., photoionis. cross section depend. of continuum radiation 77−19034
He(2^3S), quenching rates meas., in pure afterglow 77−75206
$He(2^3S_1)$+Hg_0→He_0+Hg^++e, in afterglow, rate const. meas. 78−17785
$He(2^3S_1)$+Na(K)(Rb)(Cs), Penning ionis. in stationary afterglow 78−42184
He(3^3S) decay rates in high-press. afterglow 79−41898
$He(3^3S)(3^3P)(3^3D)$+$He(1^1S)$, deactivation rate, 300-600K, time-resolved spectra 77−19037
$He(5^3D)$+He, collisional quenching probability, 2-250 mtorr 78−25679
Hg, $^3P_0$ quenching rates, laser fluoresc. meas. 77−46522
Hg, 6^3P_0 and 6^3P_1 states, relax. effects. 78−5272
Hg (metastable), quenching const. in He afterglow, by slow electrons *(Russian)* 78−29848
Hg+H_2(CO)(NH_3)(ethylene), quenching rate constants determ. with nanosecond light pulser with Hg vapour 80−100111
Hg+H_2(HD)(D_2), intramultiplet transitions 77−54597
Hg+halomethane, $^3P_1$-state total quenching 80−52927
Hg_2 excimers, photoassoc., spectroscopy and kinetic processes of high-lying vibronic states, laser applics. 80−9649
Hg_2, photoassociated, collision-induced predissoc. with Hg 79−31626
Hg_2, quenching and predissociation, possible excimer laser 80−32770
HgBr, green luminesc. and stimulated emission, prolonged optical pumping of $HgBr_2$ 79−18414
HgBr, laser photolysis prep., laser induced fluoresc., collisional quenching processes 80−38014
HgBr*, collisional quenching by inert gas (molecule) 80−42986
HgBr*, collisional quenching by inert gas (molecules) 80−43091
HgCl, $B^2\Sigma^+$ state, produced in photochem. of $Hg/Cl_2/Ar$ 79−39154
HgCl*, collisional quenching by inert gas (N_2) 80−42986
HgCl*(B1/2), fluoresc., collisional quenching kinetics 78−94269
HgI*, collisional quenching by inert gas (N_2) 80−43091
HgX (X=Br, I), B-state quenching rate consts. from radiative decay of photodissociated mols. 79−54877
$Hg(6^3P_2)$+Hg, aligned metastable ats., longitudinal and transverse relax. times, simultaneous meas. 78−13585
I excited atom ($5^2P_{1/2}$) quenching by mols. with C-I bonds 79−64076
I metastable atoms prod. from He-I_2, quenching rate const. by I_2 mols. 78−13691
I+H_2(HD)(D_2), intramultiplet transitions 77−54597
I+HCl, quenching of $I(5^2P_{1/2})$, temp. depend., time resolved at. absorpt. spectrophotometry 80−32655
I+methane $-d_0(-d_3),(-d_4)$, excited atoms, quenching, isotope effects, time resolved reson. fluoresc. 80−32656
I_2, $B^3\pi o_u^+$ state deactivation efficiency, temp. depend. 78−70869
I_2, fluoresc. and quenching of 3400 Å 77−3398
I_2, fluoresc. in 340 nm band, buffer gas press. depend. 79−13762
I_2, use as test mol. in modern spectroscopy, review 78−90317
I_2+CO_2, collisional energy transfer, quenching effects 80−14193
ICl, IF, fluoresc. decay lifetimes and quenching cross-sections for excited $B^3\Pi(0^+)$ states 78−1030
ICl($A^3\Pi_1$), zero-press. lifetimes, fluoresc. quenching 79−68266
$I(^2P_{1/2})$+n-iodopropane (iodoethane), quenching rate coeff., in UV photolysis of n-iodopropane (iodoethane) 79−11799
I*+$H_2O(D_2O)$(HDO), $5^2P_{1/2}$ electronic to vibr. energy transfer, quenching and time resolved IR fluoresc. 79−3537
$I^*(5^2P_{1/2})$+HF(HCl)(HBr)(HI), collisional quenching rate consts. meas. 77−3299
$I(5^2P_{1/2})$, time-resolved reson. fluoresc., quenching rate coeffs. 78−25466
$I(5^2P_{1/2})$+benzene-d_0(-d_6), fluoresc. quenching, spin-orbit interaction, isotope effect obs. 78−62763
$I(5^2P_{1/2})$+$H_2O(D_2O)$(HX)(DX), collisional quenching, isotope effects 77−34583
$I(5^2P_{1/2})$+H_2(HD)(D_2), electronic to vibrational energy transfer 79−68259
$I(5^2P_{1/2})$+HBr(DBr)(methane)(propane), collisional deactivation, rate consts. meas. 77−86300
$I(5^2P_{1/2})$+iodomethane-d_0(−d_3), temperature dependence for quenching 79−45755
K+inert gas, quenching cross sections of alkali n^2P states, 5-100 eV 79−76505
K+NaK reactive collisions studied using circularly polarised laser fluorescence 80−69215
K_2, $B^1\pi_u$ state radiative lifetime, quenching cross section, fluoresc., single photon counting 77−75202
$KAlSi_3O_8$:rare earth ion, glass, nonradiative energy transfer and fluoresc. quenching 77−20905
$K_xBi_{1-x}Nd_x(MoO_4)_4$ solid soln., growth, spectroscopic and laser props. 78−2901
KBr, interaction between F- and α-centres, luminesc. meas. 79−73988
KBr(Cl)(I):Tl^+, recomb. luminesc. kinetics 77−16366
KBr(I), photostimulated recomb., electron spin polarisation 80−60673
KCl:Sm^{2+}, spectra, ^5D states, Lauer-Fong formula and SCC model 79−15513
KI, exciton diffusion, luminesc. quenching, meas. 4 to 77K 77−32433

radiation quenching continued
KI, intrinsic luminesc. quenching, by X-ray induced coloration 78−19539
$K_6Nb_6Si_4O_{26}$, luminesc. bands, Stokes shift, rel. to crystal struct., stacking faults 80−34974
$K_8Nb_{14}Si_4O_{47}$, luminesc. bands, Stokes shift, rel. to crystal struct., stacking faults 80−34974
$K_5Nd(MoO_4)_4$, spectral and struct. props. *(Russian)* 79−52020
Kr, 6p levels, two-photon excitation, time resolved fluoresc., quenching, lifetimes and photoionisation cross section 80−78587
Kr I, saturated absorpt. profile of 557 nm line, collision effects 78−9121
Kr+F_2, KrF form., relax. and quenching 80−81314
KrCl*, excimer formation rate consts., B state radiative lifetimes, quenching, VUV excitation 80−55631
KrF, electron quenching rate consts. meas. by fluoresc. anal., laser implications 80−32969
KrF, laser, e-beam pumped Kr-F_2 mixtures, form. and quenching processes 78−42322
KrF, radiative lifetime and quenching 78−63063
KrF+He(Ne)(Xe)(NF_3), quenching rate consts. meas. 79−24718
KrF(B), excimer, collisional quenching rates, photolysis meas. 78−63066
KrF*, bound-free emission spectra, simulation 78−29806
KrF*, dominant quenching mechanism, in gas laser 78−33730
KrF*, Kr_2F^*, kinetics of proton-excited KrF_2 mixtures, time-resolved and time-integrated spectra 79−36883
KrF* laser, electron beam pumped, dominant formation and quenching processes 79−938
KrF*, three-body quenching by Ar and broad-band emission at 415 nm 77−75486
KrF*+Ar(Kr)+Ar(Kr), recomb. rate consts., 300 to 800K, appl. to KrF* laser efficiency 79−45930
Kr_2F^*, radiative lifetime and quenching rate consts. 78−63056
$Kr(^3P_2)$+F donor reagent, quenching, excimer form. 79−63953
Kr_2^*, radiative lifetime and quenching rate consts. 78−63056
$La_{1-x}Nd_xP_5O_{14}$, Nd^{3+} luminesc. anomalously weak quenching 77−75533
LaOCl:Sm^{3+}, conc. quenching of X-ray and UV-excited luminescence *(Russian)* 77−55829
$La_{1-x}Tb_xOBr$ phosphor, concentration quenching of Tb^{3+} luminesc. 80−29785
Li+inert gas, quenching cross sections of alkali n^2P states, 5-100 eV 79−76505
Li_2, $A^1\Sigma_u^+$ state, radiative lifetime 77−27104
LiBr, aqueous soln., NO_2^- impurity anions, temp. quenching of luminesc. *(Russian)* 77−1714
LiCl, aqueous soln., NO_2^- impurity anions, temp. quenching of luminesc. *(Russian)* 77−1714
Li_2O-Al_2O_3-SiO_2 glasses, Tb^{3+} ($^5D_3$) luminesc., cross-relax. quenching *(Russian)* 79−33836
Li_2O-Nd_2O_3-P_2O_5 ultraphosphate glasses, Nd^{3+} conc. quenching of luminesc. effect 79−19931
Li(^2P_j), quenching cross-sections, energy depend. 79−63952
Li*(2^2P_j)+H_2(D_2), collision induced quenching and fine struct. transition rate coefficients meas. 80−74221
Mg ($^3P_1$) metastable atom afterglow quenching rate consts. with various mols. 77−6720
N, $3p\,^4S^0$-state quenching in low-press. glow discharge 80−23355
N, ($2p^3\,^2P^0$) state, form. and depletion in N afterglow 79−49951
N_2, ($C^3\Pi_u$) state, radiative lifetime, collisional quenching, pulse radiolysis meas. 78−29813
N_2 afterglow, catalysis and quenching by SF_6 78−51376
N_2, $B^3\pi_g$ state excitation and deactivation in positive column 77−3482
N_2, fission fragment excitation of optical radiation, quenching by UF_6 77−23665
N_2, fission fragment excitation, delayed coincidence spectroscopy 77−24189
N_2, solid and matrix isolated mol., triplet state spectra *(Russian)* 80−5574
N_2^+, fission fragment excitation of optical radiation quenching by UF_6 77−23665
N_2-CO-OCS, liq. mixture, vibr. energy relax. and exchange, laser induced fluoresc. obs. 78−70905
N_2+alkali metal atom, temp. depend. of vibr. relax. time 77−34725
N_2+Cs, collisional relax. and population quenching of Cs 78−25467
N_2+HgX_2 (X=halide), $A^3\Sigma_u^+$-state quenching obs. 80−108693
N_2+I_2, ($A^3\Sigma_u^+$) state quenching 78−13580
N_2+methylmercury halides, $A^3\Sigma_u^+$-state quenching obs. 80−108693
N_2+N_2(Ar)(H_2), ($A^3\Sigma_u^+$, ν=0,1) metastable state quenching rate coeffs. 78−90206
N_2+SF_6, pulsed H^+ excitation, fluoresc. decay and press. depend. 77−14483
N_2^++O_2(H_2)(He), ($A^2\Pi_u$) Meinel band deactivation cross sections above thermal energies 78−66635
N_2^+($A^2\Pi_u$-$X^2\Sigma_g^+$) system in aurora, vibr. development and quenching effects 78−88967
N_2($A^3\Sigma_u^+$), auroral, quenching by O and O_2 from rocket meas. of emission 78−57380
N_2($B^3\Pi_g$-$A^3\Sigma_u^+$) system in aurora, vibr. development and quenching effects 78−88967
ND($b^1\Sigma^+$), quenching rate consts. *(German)* 79−41189
NH_2 (A^2A_1), excited state dynamics and bimol. quenching processes 80−9681
NH(ND), $b^1\Sigma^+$ state, collisional quenching, isotope effects, rate coeffs. 77−19018
NH($b^1\Sigma^+$), quenching rate consts. *(German)* 79−41189
NO, $A^2\Sigma^+$ two-photon excitation, radiation lifetime, quenching 77−3426
NO, electronic quenching rates, two-photon spectrosc. meas. 79−50097
NO, quenching rate const. for NO, He, H_2, CO, CF_4, N_2 and CO_2 78−80773
NO, Rydberg states quenching rate consts., two photon excitation method 80−5581
NO, two-photon excitation to levels near and above the dissoc. limit 79−10161
NO+formaldehyde(-d_2), laser beam-induced free radical reactions, quenching 78−44387
NO+Ne(Ar)(N_2)(H_2)(CO), $E^2\Sigma^+$ and $B'^2\Delta$ states fluoresc. collisional deactivation 79−6965
NO_2, fluoresc. lifetime and quenching mechanism 79−89701
NO_2, fluoresc. quenching mechanism 78−25599
NO_2, fluoresc. quenching mechanism in mag. field 78−74696
NO_2, laser-induced fluoresc. quenching rate const. and lifetimes 80−11930
NO_2, mag. fluoresc. quenching mechanism, up to 18 kG, press. and λ depends. 77−65498
NO_2, mag. quenching of fluoresc. 79−31582
NO_2, perturbed $^2B_2$ state fluoresc. lifetime, excitation energy depend. 78−90202
NO_2+Ar(CO_2)(NH_3), continuum quenching in upper atmosphere 79−88520
NO($B^2\Pi_r$), form., quenching 79−64038
NO($X^2\Pi$)+Cd($^1P_1$)→NO($A^2\Sigma^+$, ν=0) electronic energy transfer react., collisional fluoresc. quenching 77−14548
NO($X^2\Pi$)+Zn($^1P_1$)→Zn($^1S_0$)+NO($A^2\Pi^+$, ν=0,1), near-resonant electronic energy transfer, fluoresc. quenching 77−14549
NO($b^4\Sigma^-$), electron impact excitation energy, radiative lifetime, quenching in NO 77−79642
NO^+(ν=1,2)+N_2, vibr. transfer, vibr. absorption coeff. 79−6994
N_2^*+H_2O(H_2S)(methane), deactivation, from laser-induced CO_2 fluoresc. obs. 80−63776
N_2^*+SO_2, quenching of vibr. excited N_2, photoionis. detect. technique 78−46388
Na free atom cooling in resonant laser field at scanning freq. *(Russian)* 79−72272
Na, high Rydberg states, quenching in strong 1.06 μm laser field 80−95559
Na-fluorescein, glycerol-alcohol soln., luminesc. decay time, conc. depend. 80−34960
Na+inert gas, quenching cross sections of alkali n^2P states, 5-100 eV 79−76505
Na+N_2, higher Na s and manifold states deactivation cross sections 79−10176
$Na_8Al_6Si_6O_{24}$.Cl(Br)(I), cathodochromic sodalites, coloured crysts., tunnel and recomb. luminesc., temp. depend. *(Russian)* 80−66261
NaCl, influence of coloration on intrinsic luminesc. 78−80399
Na_2O-P_2O_5-Y_2O_3-Tb_2O_3 glass, conc. quenching of luminesc. in disordered system with dipolar interaction 80−89059
Na_2O-TeO_2:Ho^{3+} (Er^{3+})(Yb^{3+}), luminesc. quenching by OH and OD *(Russian)* 79−28839
Na(^2P), quenching cross-sections, energy depend. 79−63952
Na*+N_2, differential quenching cross-section, polarisation effects 77−27019
Na*(3p)+Na_2, collisional and radiative processes, fluoresc. decay obs. 78−66638
Na(3^2P), in O_2-H_2-Ar flame, atm. press., lifetime obs. 79−39149
Na(3^2P)+CO(X^2S^+), electronic-vibr. energy transfer reaction 79−64084
Na($3p^2P_{3/2}$)+$N_2(O_2)$(CO)(NO), electronic energy quenching dynamics, crossed beam expt. 80−9683
Nd^{3+}:glass, laser props., uncorrelated inhomogeneous broadening of 1.06 μm band induced luminesc. quenching 79−31914
$Nd_xLa_{1-x}P_5O_{14}$, Nd^{3+} stoichiometric materials, luminesc., conc. quenching 78−27315
Nd_2O_3-Y_2O_3-As_2O_5 glass, spectroscopic props., rel. to possible appl. in lasers 78−84624
NdP_5O_{14}, fluoresc. lifetime meas., IR and photoacoustic spectroscopy 80−60652
NdP_5O_{14}, laser materials, linear conc. quenching of luminesc. 79−31908
$Nd_xY_{1-x}P_5O_{14}$, fluorescence quenching 77−69903
$Nd_xY_{1-x}P_5O_{14}$, fluoresc. conc. quenching, decay rate consts. 78−64404
Ne-He and Ne negative afterglows, microwave quenching, Ne spectral emission 77−80307
Ne*+X, (X=Ar, Kr, Xe, H_2, CO, HCl, F_2Cl_2, NF_3, N_2F_4, N_2O), quenching rate const. for metastable Ne($^3P_2$), flowing afterglow 78−46295
O, ($^1D_2$) state, quenching, rel. to O_2 $b^1\Sigma_g^+$ prod. and deactivation 80−76493
O (^1D), collisional quenching by inert gas atoms 78−66648
O I 5577 Å meteoric forbidden line collisional quenching 77−17448
O I 6300 Å line meas. of O(^1D) quenching coeff. by molecular collision, optical meas. 79−2419
O II 7319-7330 Å dayglow, quenching rates 77−37475
O+N_2, quenching of O(^1D) state, at 300K, semiclassical study 79−45823
O+O_2, quenching of O(^1S) state, rate coeff. 80−41581
O_2, ($b^1\Sigma_g^+$-$X^3\Sigma_g^-$) system in auroras, quenching rel. to vibr. development 77−2293
O_2, $b^1\Sigma_{g+}^+$ state excitation by 0.75-6 eV electrons 78−86958
O_2 $b^1\Sigma_g^+$ state prod. and deactivation following O($^1D_2$) quenching 80−76493
O_2 in chloroform and carbon tetrachloride solns., sensitized luminesc. 80−32762
O_2, laser excited, quenching by CO_2, H_2O and I_2 80−99515
O_2 quenching by porphyrin singlet and triplet states 79−92141
O_2, quenching of luminescence by porphyrins and metalloporphyrins 79−50058
O_2, single state, quenching by Ni complexes 79−94028
O_2, singlet, energy transfer in quenching, kinetics 77−68072
O_2, singlet, energy transfer in quenching, statistical theory of vibr. energy distrib. 77−68073
O_2 singlet energy transfer in quenching, vibr. excited mols. 77−71828
O_2, singlet states, quenching by $O_2(N_2)$, shock tube study 80−23511
OCS, high-intensity laser photolysis at 157 nm, S(^1S) prod., photoionisation, and loss, laser appl. 80−21306
OCS laser, two-quantum excitation, photolysis, energy transfer, for fusion expts. 78−59003
OCSe, quantum yields for Se, $^1S_0$, $^1D_2$, and $^3P_{0,1,2}$ atoms determ. in photolysis, lifetime and quenching rate meas. 80−97741
O^+(^2D) quenching, N_2^+ recomb. effects on O^+(^2D)+N_2 charge exchange rate coeff. determ. 78−88954
O(^1D) quenching in Earth atmosphere, translationally hot O(^3P) energy distrib. 80−21811
O(^1D)+Ar(Kr)(Xe), inelastic collisions, spin-orbit coupling 80−5605
O(^1D)+N_2, electronic quenching resons., collinear collision, quantum mech. calcs. 77−60050
O($^1D_2$)+CO($^1\Sigma^+$), collisional quenching, energy transfer processes 80−23501
O_2($^1\Delta_g$)+O_2, deactivation rate const. meas. 78−5262
OH Meinel bands, in airglow, rot. temp., radiative lifetime 78−61643
OH Meinel bands intensity distrib. in airglow, OH* quenching mechanisms 78−65447

radiation quenching continued
OH+CO(trichloroethane), reaction rate consts. and quenching kinetics, reson. fluoresc. obs. 79−72349
$OH(A^2\Sigma^+)+N_2(O_2)(H_2O)$(air), quenching rates and fluoresc. efficiency, rel. to atmosphere 80−14199
$OH(C^2\Sigma^+)$, prod. by water radiolysis, time-resolved emission, quenching rate consts. 79−10138
$O(^1S)+N_2O$, quenching rate const. determ. 77−10626
$O(^1S_0)\rightarrow O(^1D_2)$, nightglow 5577 Å intensity latit. var. calc. 77−37474
$O_2(^1\Sigma_g^+)+H_2$, collisional relax. temp. depend. 77−32783
$O(2^1D_2)+N_2(O_2)(N_2O)(CO_2)(H_2O)$(methane), collisional deactivation meas., 295K, rel. to atmospheric processes 80−16663
$O_2(b^1\Sigma_g^+)$ quenching by $O(^3P)$ and O_3, rate coeffs. 79−70309
$O_2(b^1\Sigma_g^+)$, temp. dependent quenching, photochemical study by H_2-VUV laser 80−63702
$O_2(b^1\Sigma^+g)+O_2(X^3\Sigma)$, quenching rate coeff. meas., density depend. 77−38721
PH+He, collisional deactivation of $PH(b^1\Sigma^+)$, time resolved quenching 79−54948
$PH+N_2(CO)(NO)(H_2)$, collisional deactivation of $PH(b^1\Sigma^+)$, time resolved quenching 79−54948
PH_2 radical, laser-induced fluoresc. 78−94277
PH*+PH_3, collisional deactivation of PH $(b^1\Sigma^+)$ state, time resolved spectra 78−78750
$POCl_3$-$SnCl_4$, Sm^{3+} fluoresc. quenching temp. depend., near reson. interaction 79−65915
$PO(SCN)_3$:Nd^{3+} solns., spectroluminesc. props. 77−16362
Pb, $^3P_1{}^0$ state reson. radiation, collisional quenching cross-sections 77−435
Pb I, interchannel interactions and series quenching in 5d and 6s spectra 77−88418
$Pb+H_2(HD)(D_2)$, intramultiplet transitions 77−54597
PbF, laser-induced fluoresc. of $A^2\Sigma$ state, chem. laser eval. 79−81222
Rb, quenching cross sections, highly excited states 79−89761
RbI, intrinsic luminesc. quenching, by X-ray induced coloration 78−19539
RbI, photostimulated recomb., electron spin polarisation 80−60673
Rb(nP)+Rb(inert gas), collisional depopulation Rydberg P state 77−75281
Rb(nS, $nD_{3/2}$)+Rb(ground state), collisional quenching cross sections 80−43146
Ru complex, (2,2′-bipyridyl)$_3$ruthenium^{2+}, excited-state redox processes, electron transfer theory 79−39126
S_2, $B^3\Sigma_u^-$ state lifetime, fluoresc. decay rate meas. 77−42346
S_2, fluoresc. quenching by He, Ar, Xe, N_2, S_2, CF_4, C_2F_6, fluoresc. lifetimes 78−46386
$S_2(B\ ^3\Sigma_u^-)$+inert gas $(H_2)(N_2)(S_2)$, collision-induced energy transfer 79−3544
$^{32}SF_6$, multiphoton dissoc. by laser pulse, Ar, N_2 and CF_4 environments 78−73061
SO_2 ($^3B_1$), phosphorescent lifetimes, press. saturation effect on quenching by CO_2, CO, N_2 78−1017
SO_2, collisional quenching of $^3B_1$ state, 8-1300 torr 78−86906
SO_2, fluoresc. and photosensitised phosphoresc. of biacetyl, quenching and triplet theory transfer 78−25608
SO_2+alkane, $^3B_1$-state lifetime saturation, chem. and phys. quenching channels 79−814
$SO_2+N_2(CO_2)(H_2O)$, collisional quenching of $^3B_1$ state, 8-1300 torr 78−86906
Se, amorphous film, influence of wavelength on optical quenching of photoconductivity 80−60046
Se_2, photolysis by UV lasers, appl. to kinetics of group VI laser systems 80−7807
Se_2, photolytic dissoc. obs. using inert gas halide lasers 80−11935
$SeO_2+Ar(N_2)(CO_2)$, radiative lifetime and quenching rates 80−95685
$Se(^3P_1)$+inert gas, gas phase flash photolytic deexcitation obs., 1000K *(Russian)* 78−50626
$Se(^1S)$, quenching of high concs. prod. by photolysis 79−6904
Se*+OCSe, radiation quenching rates 79−86050
$Se(4^1D_2)$ atoms, electronically excited, direct obs., quenching by inert gases 78−25461
Si, amorphous, spin depend. recomb., luminesc. and light induced ESR 80−50393
Si amorphous film, dangling bond ESR, light-induced quenching 80−50162
Si, pure and doped amorphous, photolum. meas. 77−36285
SiS*, collisional quenching from Si+OCS 80−45505
Si*+$He(H_2)(N_2)(O_2)(Cl_2)(CO)(NO)(C_2H_2)(C_2H_4)$, collisional quenching, reson. line absorpt. expt. 78−46297
$Si(3p^2(^1S_0))+He(SiCl_4)(O_2)(N_2O)$, attenuation of reson. radiation, time-resolved kinetic obs. 78−5329
$Sn+N_2O$, oxidation chemiluminesc., quenching kinetics 79−52672
$Sn+N_2O\rightarrow SnO(a^3\Sigma)+N_2$, chemiluminesc. high temp. fast flow reactor obs. 80−45493
SnF, $A^2\Sigma^+$ state, radiative lifetime, quenching rates 79−98156
SnO, produced in $Sn+N_2O(O_2)(O)$ reactions, kinetics of chemilum. emitter form. and quenching 78−63107
Sr, 5^1P state quenching cross sections in CO-N_2O flames 77−18836
SrF_2:Dy(Ho)(Pr)(Tb), V_k-centre recomb. kinetics, phosphoresc. 77−55817
SrF_2:Sm^{2+}, spectra, ^5D states, Lauer-Fong formula and SCC model 79−15513
SrO, luminesc. band edge, 4-6.5 eV, optical absorpt., photoluminesc., cathodoluminescence, photocond. obs. 80−50411
Sr_2TiO_4:Eu, synthesis, luminesc. of materials 79−11534
$Tb^{3+}+O_3(SO_5^{2-})(SO_2)$, in H_2SO_4 soln., electrochemiluminesc. emitters quenching by electrolysis products 79−1794
$TbCl_3.6H_2O$-$PrCl_3.6H_2O$($ErCl_3.6H_2O$), in DMSO soln., $Tb^{3+}\rightarrow Pr^{3+}(Er^{3+})$ energy transfer mechanism 80−5498
Te+$H_2(HD)(D_2)$, intramultiplet transitions 77−54597
$Te(^3P_1)$+inert gas, gas phase flash photolytic deexcitation obs., 1000K *(Russian)* 78−50626
Tl, metastable atoms quenching, diffusion and decay in buffer gases 79−54953
Tl+$H_2(HD)(D_2)$, intramultiplet transitions 77−54597
TlBr:I, isoelectronic donor, broad-band photoluminesc. meas. 77−8636
UF_6, electronically excited, laser-induced time-resolved emission, self-quenching 78−42114
UF_6, electronically excited, emission quenching by organic mols. 78−42115
radiation quenching continued
UF_6, electronically excited, emission quenching by inorganic mols. 78−42116
UF_6, fluoresc. lifetime, temp. depend. 77−58065
UF_6, gas, laser-induced fluoresc., A-X band 78−94275
UF_6, photophysical props., laser study 80−28040
UF_6, UV photophysics, energy balance through quantum efficiency meas. 80−9634
UO_2^{2+}, excited, in liq. and glassy media, luminesc. decay processes, temp. activation 79−91978
UO_2^{2+} in aq. solns., luminescence quenching by metal ions 78−39588
UO_2^{2+} in aq. solns., luminescence quenching by H_2O mols. 78−39589
UO_6^{6-} group, in perovskite type hosts, luminesc. var. with chem. environment 77−16374
Xe, afterglow, $6s_{12}$ metastable atom density decay rate 78−63612
Xe afterglow, radiative and collisional deexcitation of reson. states, absorpt. and emission obs. 80−38742
Xe-$Br_2(Cl_2)$(HCl) mixtures, low-press. excimer form. and quenching by e-beam excitation 79−50071
Xe-N_2, afterglow, $6s_{12}$ metastable atom density decay rate 78−63612
$Xe+Cl_2(F_2)$, XeCl(XeF) form., relax. and quenching 80−81314
Xe+Ne, quenching of excited $Xe^*(^3P_2, {}^3P_1, {}^1P_1)$ states 80−63578
XeCl laser, B→X, form. and quenching kinetics 80−74341
XeCl, relax. and quenching rate consts., emission spectra modelling 80−28211
XeF, electron quenching rate consts. meas. by fluoresc. anal., laser implications 80−32969
XeF, relax. and quenching rate consts., emission spectra modelling 80−28211
XeF, transfer and quenching rate constants for (III, 1/2) and (II, 3/2) states 79−16003
XeF+He(Ne)(Xe)$(F_2)(NF_3)$, radiative lifetime and collisional quenching kinetics 78−94289
XeF(B), fluoresc. and quenching rel. to XeF_2 vac. UV photolysis 77−58061
XeF_2(C) state lifetime, quenching rate consts., photolysis in inert gas atmospheres 80−66816
XeF*, $B^2\Sigma^+$ and $C^2\Pi_{3/2}$ states, fluoresc. decay dynamics, collisional quenching and radiative lifetimes 80−58306
XeF*, electron impact excitation, temp. depend. quenching rate consts. 80−63701
XeF*, fluoresc. intensity, two- and three-body quenching by Ar, Xe 77−58053
XeF*, lifetime and collisional quenching meas., XeF_2 photolysis 78−33545
XeF*+F_2+Xe, temp. dependent quenching rate constants 80−63701
XeF*+He(Xe)$(NF_3)(F_2)$, quenching rates for XeF in (B) state 78−58730
XeI*, production via laser absorpt. processes at 193 nm, quenching kinetics 80−91466
$Xe^+(^2P)+Ca(Sr)$, collisional quenching of metastable states, excitation transfer cross sections 78−66653
$Xe(^1P_2)$+F donor reagent, quenching, excimer form. 79−63953
$Xe(6s,{}^3P_2)$+RCl, reactive quenching, XCl* emission spectrum obs. 79−100344
YE+AG:Er^{3+}, laser material, radiative and nonradiative transitions, conc. quenching 77−16391
Y_2O_3:Tb^{3+} (Dy^{3+}), conc. quenching of X-ray and UV-excited luminesc. *(Russian)* 77−55829
YOF:Tb^{3+}, conc. quenching of X-ray and UV-excited luminesc. *(Russian)* 77−55829
Zn, excited states, collisional quenching cross sections and exit channels, fluoresc, quenching obs. 80−18919
Zn_2, quenching and predissociation, possible excimer laser 80−32770
$Zn_xCd_{1-x}S$, resonance Raman scatt. involving exciton complexes 80−16039
ZnHg excimer, optical pumping of Zn reson. line, optical and kinetic props. 78−58991
ZnS, excited phosphor, IR stimulation and quenching of luminesc., review *(Russian)* 80−11455
ZnS, photoluminesc. quenching by weak alternating field 77−85778
ZnS, self-activated, IR sensitivity 78−6742
ZnS, zinc blende-wurtzite-zinc blende, optical quenching of photocond. *(Russian)* 77−28240
ZnS:Ag, Ni thermographic phosphor luminesc. screen, for IR laser pulse recording 79−64342
ZnS:Ag,Sm, recomb. centre interaction, luminesc. quenching 78−10946
ZnS:Cu, Al phosphors, mechanism of IR stimulated and quenching 77−69881
ZnS:Cu 79−24350
ZnS:Cu phosphor, electric field quenching of photoluminesc. and flashlike rise in luminesc. 78−2911
ZnS:Tb, Cu(Ag) phosphors, luminesc. props. 80−100690
ZnS-CdS system, IR luminesc. and absorpt. centres, donor-acceptor pair model 77−44043
ZnS-CdS:Tm,Ni, recomb. centre interaction, luminesc. quenching 78−10946
ZnS(Se)(Te):Co^{2+}, IR luminesc. quenching, Co^{2+} level position, ionisation energy 80−16079

radiation therapy
25 MV X-ray beam, fast and thermal neutron profiles 78−73246
27.12 MHz selective heating of cutaneous tumours 78−24179
220 MeV/c superconducting π spectrometer for tissue irradiation 79−34667
^{222}Rn, disssolved in Boisson spring water, physiological props. 79−48292
absorbed-dose computations for inhomogeneous media in radiation-treatment planning using differential scatter-air ratios 79−25115
accelerator dose field monitoring by independent detectors in cassette 77−81578
accelerator leakage measurements 80−89839
accelerator neutron leakage survey 80−51269
accelerator primary beam neutron contamination 80−51268
accelerators, international standards 80−51272
accelerators used for high energy photon radiotherapy, dose levels due to neutrons 77−13008
accuracy, errors in patient set-up 78−11726
adenocarcinoma of colon and rectum, current place of radiation therapy *(French)* 80−17075
afterloading applicator, dose distrib. around 79−53249
analogue tomography for tissue organ anal. 79−43984

radiation therapy continued
anatomical cross-section determ. using radiotherapy simulator, for treatment planning 78−61244
anatomy, 3D display for radiotherapy treatment planning 80−3773
aneurysmal bone cyst response to low doses of ^{60}Co gamma radiation with prolonged treatment 78−73196
arc technique for total-body irrad. by 42 MV betatron 78−24134
arterial O_2 partial pressure, chronic reduction, effect on radiation response of tumour in mice 79−16252
Artronix PC-12 implant dosimetry program, stero rel. to orthogonal options 79−62371
autoimmune reactions, non-organ specific, absence of after treatment 80−12185
automatic checking system, for treatment parameters in radiation therapy, punch-card and recording unit *(Japanese)* 77−73614
backscatter factors for X- and γ-rays, polynomial and power law of central axis values 77−2056
beam characteristics of a 22 MeV microtron 80−51260
beam scanning 3-dimens. systems for radiation therapy 77−86589
beam-flattening filter calcs. for high-energy X-ray machines 78−65126
Beclere, Antoine, pioneer of radiation therapy techniques, biography 79−62982
benign thyroid disease treatment, ^{131}I appl., review 80−36107
beta particle emitters used in therapy, figure of merit 80−36083
beta ray eye applicators, dose function calc. 77−60260
betatherapy of haemangiomata, young children *(French)* 79−5356
betatron, 25 MeV, fast neutron component and patient dose 78−3592
betatron bremsstrahlung field shaping apparatus for teletherapy 78−57062
betatron electron beam, characterisation for dosimetry calcs. 79−39519
betatron redundant solid-state controller 79−88163
Bevalac, computed tomographic radiotherapy beam profile reconstruction with multiwire proportional chamber 79−79631
Bevalac radiotherapy facility, dosimetry and beam handling apparatus 79−79630
biologic effect ratios for parallel opposing fields 79−62299
biophysical dose planning expts. 78−15879
bladder cancer management, value of computerised tomography 79−88160
bladder carcinoma, treatment planning using computerised tomography 79−88159
blood extracorporeal irradiation with ^{137}Cs, expt. research and clinical appl. *(German)* 78−69149
blood vessel photocoagulation using laser radiation 79−39467
bone and joint disease, radioisotope therapy 80−36111
bone metastases of prostatic gland carcinoma, ^{89}Sr therapy 80−36076
brachytherapy, radiation exposure of nursing personnel to patients 78−85384
brachytherapy program used with the Philips Treatment Planning System 80−81738
brachytherapy source, dose rate meas., fundamental accuracy limitation 80−3815
brachytherapy source calibration using $Fe(NH_4)_2(SO_4)_2$-benzoic acid-xylenol orange dosimeter 77−5081
brain, appls. of nuclear reactors *(Japanese)* 79−83913
brain low dose elective, in small cell lung carcinoma 80−67253
brain tumour therapy by RF field controlled temp. gradients 77−25522
breast and chest wall, comparison of radiation techniques 80−30837
breast cancer, conservative treatment method *(French)* 80−17076
breast cancers, microwave irradiation, EM energy and temp. distrib., numerical calculations 79−100697
breast carcinoma, appearance of non-specific suppressor cells in the blood after local irradiation 79−20597
breast carcinoma, cosmetic results anal. after primary therapy 80−3782
breast carcinoma, efficiency of postoperative radiation 80−46008
breast carcinoma, functional changes in peripheral lymphoid cells after irradiation 79−88125
breast carcinoma, radiation therapy as primary treatment, review *(Dutch)* 80−17078
breast treatment, modified 3-field technique 80−104737
breast treatment with tangential fields using 4 MV X-rays, superficial doses 78−11740
bronchial tumour reaction to combined neutron-telecobalt therapy 79−20642
bronchogenic cancer, small cell, undifferentiated, role of radiation therapy in treatment 80−67226
build-up curves of scanned high energy electron beams, Sagittaire linear accelerator 80−89864
build-up effect with ^{60}Co radiation and fast electrons *(German)* 78−20271
calibration and meas. standards in USA 80−8188
calibration discrepancies, US institutions, data anal. 79−20686
calibration of instruments used in radiology and radiotherapy, metrological problems *(Spanish)* 79−92377
cancer, by controlled local heating, 915 MHz or 2450 MHz 80−76860
cancer, using microwaves, economical and safety aspects 80−3754
cancer management, potential impact of particle radiation therapy 79−20620
cancer management, status of low linear energy transfer radiation 79−20621
cancer therapy, invasive microwave system localised hyperthermia 79−100700
cancer therapy, microwave hyperthermia, design of implantable radiators 80−41164
cancer therapy, particle accelerator appl., current status 79−74783
cancer therapy, physical hyperthermic techniques, EM coupling modalities 80−41163
cancer therapy facility, microprocessor based control system 78−40398
cancer treatment, survival times and response rates 80−72315
cancer treatment appl. of microwave arrays for localised tumour heating 80−94308
cancer treatment by local microwave hyperthermia system 79−83893
cancer treatment by microwave hyperthermia *(French)* 80−3764
cancer treatment by ultrasound with radiotherapy or chemotherapy 79−48299
cancer treatment using neutron 77−40733
cancer treatment using proton and pion beams *(Czech)* 77−44738
cancer X-ray sensitivity increased by 434 MHz EM irradiation 78−24180
carcinogenetic risk estimation, comparison of radiation therapy and chemotherapy 79−20592
radiation therapy continued
carcinoma of anterior tonsillar pillar and soft palate-uvula, treatment methods comparison 80−98121
Cathetron, high intensity Co, gynaecological cancer therapy 80−72300
cathetron for cervical cancer treatment, description for teaching 78−49617
Cathetron linkages, safer coupling collar 77−73612
cell killing by π^- on glass and plastic surfaces 79−92305
cell kinetic quantitative models for tumour response, equivalence 80−30770
cell lethality computation, dose-time relationship, fractionated irradiation 79−20598
cervical cancer, self-adjusting applicator 80−51208
cervical cancer treatment using RALSTRON technique, semicond. rectal dosimetry *(Japanese)* 77−73594
cervical carcinoma, external small-field X-irradiation 79−16269
cervical carcinoma, para-aortic irrad. 80−72307
cervical carcinoma, radiotherapeutic approaches 80−67227
cervical intracavitary applicators, computer program for optimisation of source loading 77−13005
cervical spinal cord, radiation myelopathy, time, dose and volume factors 79−20658
cervical stage III carcinoma treatment, two regimes with same TDF but differing morbidity 78−53474
cervix, 1B carcinoma, role of radiation therapy 80−67228
cervix carcinoma, extended field technique complications, correl. of radiation and surgical parameters 80−67225
cervix carcinoma, external irradiation and 1 Ra appl. 79−88158
cervix carcinoma, transvaginal cone electron beam technique 80−21531
chamber factor reliability review in United States institutions 79−20685
charged heavy particle therapy, desirability of treatment with multiple fields 78−73220
charged particle beam, influence of thin inhomogeneities 78−69219
charged particle beam, influence of thin inhomogeneities 78−69220
chest wall irradiation, technique to improve electron dose distrib. homogeneity 80−72332
chromosome aberration of human lymphocytes, microdosimetric expts. 80−26289
Clinac 4 skin sparing improvement using leaded glass electron filters 78−31885
Clinac-18, electron-beam energy charact. using magnetic anal. method 79−39514
Clinac-18, satellite digital display 78−3599
Clinac-18 linear accelerator, dosimetry of 10 MV X-rays 77−21631
clinical trials for radiation therapy *(Japanese)* 80−51179
collective dose exposures during radiotherapy, optimisation, man-rem monetary value 80−51274
compensating filter cutter, semi-automatic 77−13001
compensation filter for chest portals 78−31887
computed tomography, spectral artefact correction and determ. of electron density and at. no. 80−51231
computed tomography for radiotherapy planning 80−94334
computer assistance in planning seed implants 79−100711
computer control 79−25099
computer interface for a linear accelerator 80−51226
computer program for negative pion beam calcs. 80−46061
computer system, comprehensive, design and development 79−25078
computer-aided radiation treatment planning 77−9268
computer-controlled radiation therapy 79−92367
computerised dosimetry calcs., linear accelerator electron beam parametrisation 79−83945
computerised electron beam treatment planning algorithms 79−100733
computerised internal mammary lymphoscintigraphy in radiation treatment planning 80−12223
computerised tomography, treatment planning system 79−29588
computerised tomography, use in treatment planning 79−88174
computerised tomography, use in treatment planning *(German)* 80−17090
computerised tomography ^{153}Gd sources, radiation therapy planning 79−20626
computerised tomography and radiation therapy planning 78−77113
computerised tomography in childhood craniofacial sarcoma management 80−12221
computerised tomography radiation therapy treatment planning in coronal and saggital sections, feasibility study 79−62344
computerised tomography relevance and accuracy for radiotherapy planning 79−20627
computerised tomography scanner principles and problems 79−20625
computerised tomography treatment planning, aids for use with EMI CT5005 scanner 79−100704
computerised tomography utility, estimate of outcome 80−67229
computerised verification and recording of treatments 77−81554
computerized tomography, compensation for inhomogeneities 79−25065
computerized tomography, use in therapy program development *(French)* 80−85472
computerized tomography, used to improve therapy 79−20660
computerized treatment planning system utilising interactive colour graphics 79−62336
computers in radiation oncology review 79−25098
conference, international congress of radiology, Rio de Janeiro, Brazil (Oct. 1977) 79−16284
conference, Las Vegas, USA, (Apr. 77) 78−3583
Conference, Los Angeles, USA (Mar. 1979) 79−83901
conference, New Orleans, USA (Oct. 1979) 80−41931
conference, Philadelphia, USA (Apr.-May 1980) 80−94913
conference on cyclotrons and their appl., Bloomington, USA (Sept. 1978) 79−54626
conformal applicators, therapeutic potential for hyperthermia induction 79−100696
continuous external irradiation 80−3781
contour plotter, computer-compatible, for use in radiotherapy treatment planning 77−70567
contrast enhancement of high-energy radiotherapy films 80−8126
cranial irradiation in children with lymphoblastic acute leukemia 79−100709
cross section imaging for treatment planning, using radiotherapy simulator 77−13030
current field heating, localised, as an adjunct to radiation therapy 80−98056
cutaneous and spinal cord response to accelerated charged particles 79−20586

radiation therapy continued
cutaneous human tumours, selective RF heating at 27.12 MHz 79−2123
cutaneous telanagiectasia after electron beam radiation, dose-time relationships 78−3552
cyclotrons, machine criteria for treatment of cancer patients 79−54691
deep tissue temp. monitoring by ultraminiature thermistors 80−3761
depth dose and off-axis characts. of TLD in therapeutic pion beams 80−101271
depth dose function concept, definition and values 80−3814
dermatological high-intensity laser therapy *(German)* 79−2117
dermatological photobiology, fibre optic light guides for phototesting 78−53472
dermatology, photobiologic phenomena 78−35909
dermatology investigation and therapy with dye lasers 78−35910
developments other than heavy particle beams 79−20649
diabetic retinopathy therapy, laser photocoagulation efficiency factors 79−79622
diathermy, shortwave and microwave, for deep-tissue heating 80−17050
diathermy, temp. distribs. obtained with a phantom 80−17051
diathermy 2.45 GHz microwave direct-contact applicator 79−2122
diathermy 915 MHz microwave applicator for deep tissues in humans 79−2121
diathermy 915 MHz microwave direct-contact applicator for tissues 79−2120
dosage calculation and compensation, basic data 80−104765
dosage calculations for inhomogeneous media, direct use of computerised tomography numbers 79−83943
dosage selectivity by planning 3-D radiation treatment using computer 80−41178
dose calculation, based on computed tomography images use of scatt. radiation meas. 80−51265
dose calculation system, ^{192}Ir interstitial wires 79−16268
dose calculations, megavoltage beam representation method 79−92374
dose calculations from computerised tomography data 79−25062
dose compensation filter design using megavoltage radiography 80−3785
dose control, precision of dose meas. devices, therapy machines and patient dose delivery 77−40789
dose distributions, three-dimensional, external beam therapy 79−25064
dose distributions, wedge-shaped, computer-controlled collimator motion 79−5358
dose perturbation from Au dental fillings 80−12265
dose planning, revision of tissue-max. ratio and scatter-max ratio concepts 80−76840
dose response curves, methods of extraction 80−94374
dose-depth measurements, film rel. to ion chamber systems 79−53255
dose-response relationships, appl. of logistic regression model 78−11724
dose/cure relationships of irrad. tumours, statistical anal. 80−46052
dose/cure relationships study 80−56218
dosimeter, for routine meas. with X-ray therapy equipment between 10 and 250 kV 78−28084
dosimeters, choice of meas. quantity 79−92379
dosimetric considerations of very large ^{60}Co fields 80−104766
dosimetry, ^{60}Co total body irrad. at 220 cm source axis distance 80−104768
dosimetry, absorbed dose calc. corrections for tissue inhomogeneity 78−3610
dosimetry, algorithm for calc. of central ray TAR and TMR values 80−76844
dosimetry, automated data acquisition and anal. system at LAMPF pion therapy facility 78−53506
dosimetry, calibration instrumentation used by AAPM, Keithley-Farmer system 77−2055
dosimetry, comparison of methods of obtaining % depth doses 79−53250
dosimetry, LiF radiothermolum. dosimetry of 10 MeV electrons *(Italian)* 77−81582
dosimetry, procedures with electron and photon beams 80−101266
dosimetry, quality control recommendations 77−40778
dosimetry, rel. to recurrence rate discrepancies between centres 78−7426
dosimetry for irregularly shaped fields 77−70550
dosimetry in accordance with section 13 of X-ray regulations using TLD *(German)* 78−20289
dosimetry intercomparison of prescription dose delivery in New England region 77−40791
dosimetry of electron beams, NBS service 77−40792
dosimetry procedures at Northwest Medical Physics Center, USA 77−40790
dosimetry study of split beam technique 80−12264
dosimetry using Si diode detectors, energy compensating shield development 78−24142
Dynagen IV, compact high intensity neutron generator 77−86603
electron accelerator neutron prod. 80−51240
electron accelerator neutron production, conf., Gaithersburg, USA (Apr. 1979) 80−46730
electron accelerator photoneutron prod., survey of European meas. 80−51241
electron accelerator target, depth-dose obs. 79−70618
electron beam applicator, variable field, dosimetry evaluation 80−76839
electron beam collimation, wall-scattering effects 79−53208
electron beam collimation in SL 75 linear accelerator, design, appl. and performance 80−41204
electron beam dose distrib. modification by transverse mag. fields 78−65132
electron beam dose distributions, magnetic field modification 79−5376
electron beam dose profiles in tissue and air 77−40786
electron beam dosimetry for treatment planning 80−3817
electron beam photon contamination obs. 79−59285
electron beam therapy of lateralised lesions of oral cavity and oropharynx 80−12215
electron beam therapy with medium energy electrons, review 80−36069
electron beam treatment planning, computer algorithm 79−62351
electron beam treatment planning, patient specific data acquisition 79−100731
electron beam treatment planning, symposium, Cincinnati, USA (July 1977) 79−100730
electron beam treatment planning and execution, for 10 to 35 MeV beams 79−100732
electron beam treatment planning for 1 to 10 MeV beams 79−100735
electron beam treatment planning system, absorption equivalent thickness factor 79−100734
electron beams, 50 MeV, in treating deeply situated tumors *(Chinese)* 80−56209
radiation therapy continued
electron beams, output factor variation by secondary blocking 79−62350
electron collimation system for use with electron cones of Varian Clinac 18 accelerator 78−11725
electron depth absorbed dose distribs. meas. by extrapolation chamber 77−81573
electron depth dose distrib., central axis, analytic expression 80−3813
electron dose distrib. in radiation therapy, magnetic enhancement 77−81570
electron dosimetry below 50 MeV, Monte Carlo calcs. 78−7453
electron dosimetry in tissue equiv. phantoms 78−7454
electron dosimetry of irregular fields on the Clinac 18 79−100747
electron flux in slab geom., high-energy radiotherapeutic field 77−81585
electron linear 40 MeV accelerator, therapeutic and research appl. 79−57752
electron linear accelerators, regulations, standards, and guidelines for use in medical radiation therapy 79−53258
electron therapy, review *(German)* 79−43968
electron therapy, up to 20 MeV, phys. aspects 80−85474
electron therapy using ALIN linear accelerator *(French)* 79−9925
electron treatment planning, air-gap correction 79−53254
electron whole body superficial therapy, dose distrib. anal. 77−86633
electron-dose distrib. in tissue, lung phantoms, magnetic modification 79−5377
electronic timer for use with Farmer dosimeter type 2502/3 79−25114
electrons, high energy, depth absorbed dose distribs. 78−73256
elementary particles from 1 GeV range accelerators, medicine appl. *(German)* 80−41210
Elkind recovery rel. to sublethal damage 77−64085
EM, 27.12 MHz diapulse acceleration of healing processes 77−77964
EMI scanner picture automatic outlining, for radio therapy treatment planning 80−41206
emitted radiation, clarification of concept, brachytherapy dosimetry appl. 80−76843
endoscope for holographic diagnosis and laser therapy *(German)* 79−96645
endoscopic laser coagulator with recirculating gas-jet assist 78−48867
endoscopic laser photocoagulation, use of gas jet appositional pressurisation 78−53468
energetic heavy ion beam model for radiobiology 80−26293
engineering in medicine and biology, conf. Atlanta, USA (Oct. 1978) 79−39332
epithermal neutron field for ^{10}B neutron capture therapy, prod. using FBR 80−61692
epithermal neutron radiation field development for cerebral tumour therapy *(Japanese)* 78−88742
erythropoietic bone marrow recovery of Fe uptake following large field therapy 79−20616
exposure timer for use with tele Co units 79−20684
external beam, optimisation using computer 77−86632
external beam, planning using the Edinburgh algorithm 80−94316
external beam radiation dose distribution calculation, radiation therapy planning 79−62364
external beam radiotherapy, isodose planning, new suite of programs 80−41243
external beam radiotherapy optimisation, relative radiation effect and isoeffect pattern computer study 79−62368
eye protection from scatt. radiation during mantle-field therapy 79−92396
eye tissue coagulation, OK-2 laser ophthalmocoagulator 79−11991
eye tumour treatment, computerised X-ray tomography for post therapy control *(German)* 79−100727
fast electrons, computerised treatment planning, dose distrib. calc. 80−81740
fast neutron, scatt. radiation from neutron collimater 77−40788
fast neutron and photon therapy, randomised clinical trials 79−20638
fast neutron beam, computer generation of dose distribs. 79−39510
fast neutron beam build-up and depth-dose characts. 78−28072
fast neutron beam for medical use, production and definition *(French)* 80−69003
fast neutron beams, linear regression anal. of γ-dose 80−89866
fast neutron beams, spectra low energy component 79−49899
fast neutron dosimetry, in vivo, use of Si diode 77−73587
fast neutron dosimetry techniques 79−20677
fast neutron generator tube, Haefely-GFK, for radiotherapy 79−20652
fast neutron radiotherapy unit, AEG/RDI 79−20653
fast neutron sealed-tube radiotherapeutic installations, characteristics 79−20650
fast neutron sublethal damage and cell division delay expts. 79−20588
fast neutron teletherapy, preliminary clinical results 79−20639
fast neutron therapeutic dosage schedule development 79−20678
fast neutron therapy, radiobiological bases 80−35995
fast neutron therapy, use of ^{10}B to enhance tumour dose 78−73249
fast neutron therapy beam intercomparison using mouse testes as biological test system 78−20225
fast neutron therapy beam prod. by 26 MeV protons on Be, dose meas. 78−28054
fast neutron therapy equipment trials 79−20657
fast neutron therapy facility at the cyclotron 'Cyclone', Louvain-la-Neuve 80−41192
fast neutron therapy history 79−20634
fast neutron therapy system using cyclotron beam, beam optics and shielding 79−57756
fast neutron therapy using ^{252}Cf *(Japanese)* 80−98112
fast neutron therapy with medical cyclotron, clinical results 79−20643
fast neutrons, trial for mouth and throat cancer 77−25554
fast neutrons in normal tissue, early and late damage obs. 79−20590
fast particle therapy status and prospects in Europe 79−20641
Fermilab cancer therapy facility, status report after $2^1/_2$ years operation 79−79628
feto-placental tissues, irrad. effects after treatment of material genital carcinoma 80−45964
fibre optics in medicine, diagnostic and therapeutic appls. 79−39466
fibrosarcoma, hamster, absence of metastases following US treatment 80−35960
field overlap, clinical complications phys. and technical considerations 78−11741
film dosimetry of multiple electron beam ports with wedges 80−98138
fundus oculi tissue, thermal effects on exposure to laser radiation 80−26261
gamma, teletherapy unit, radiation head, temp. distrib. 79−72790

radiation therapy continued
gamma dose meas. in d(80)+Be neutron beam 79−70648
Gammatron S80 telecobalt unit, reduction of electron contamination in beam 79−92330
gastric lesion bleeding control using lasers, comparison of Ar and Nd laser damage 78−48831
Gaussian-beam launcher for microwave exposure studies, dielectric hemisphere-loaded scalar horn 80−12206
gliomas, malignant, anal. of dose-effect relationship 80−72331
gliomas, malignant, high dose radiation therapy 80−67254
glottic cancer, early, review 80−12217
glottic cancer, early, review 80−12218
glottic cancer, T3, anal. of close time-vol. factors 80−104764
grey matter calcification secondary to radiation therapy, computerised tomography evidence 77−56424
gustatory function, radiation-induced changes, neutrons rel. to photons 80−12184
gynaecological cancer, treatment tolerance and early complications with extended field irrad. 77−21564
gynecologic cancer, advanced, whole pelvis megavoltage irradiation 79−100708
haemangiomas of infancy, results of ^{90}Y interstitial therapy 79−88156
haematologic disorders, radionuclide therapy 80−36109
hard X-ray machine, RT 305, phys. aspects and appl. 80−81709
Harvard Univ. 160 MeV proton beam, clinical experience and implication for designers 79−54693
head and neck, advanced cancers, low dose rate irradiation 79−34649
head and neck cancer, advanced and recurrent, short course high fractional dose irrad. 80−72297
head and neck squamous-cell carcinoma, advanced, fractionation schedules 80−98123
head and neck tumours, treatment in air rel. to treatment in hyperbaric O_2 80−72298
head and neck tumours, unorthodox fractionation 80−3780
head holder for treatment of head and neck cancers 80−94333
heavy ion and He effectiveness on tumour systems 79−20587
heavy ion beam linear energy transfer distribution calc. 79−20630
heavy ion facility for radiation therapy 77−86588
heavy ion therapy, treatment planning programme 80−72295
heavy particle comparison for therapy, acute and late reactions in mice 78−85338
heavy particle comparison for therapy, cell survival, OER and RBE 78−85337
heavy particle comparison for therapy, cell survival vs. depth 78−85336
heavy particle comparison for therapy, depth-dose distribs. for π^-, n, p, He, C, Ne and Ar ions 78−85379
heavy particle microdosimetric data with high intensity beams, pion appl. 78−40331
heavy particle radiations appl. *(French)* 78−48890
heavy-ion and He fractionated radiation therapy, clinical trial 79−20632
heavy-ion radiography and autoactivation techniques 79−20624
heliotherapy unit, integral concentrator, irradiation technique improvement, medical physics 79−83885
HF tumor therapy, slotted cylinder antenna for selective heating inside human body 79−34629
high energy electron therapy using betatron *(Japanese)* 77−70544
high energy particle therapy of cancer *(Japanese)* 78−31897
high energy photon absorption cross section for matter, review *(Japanese)* 78−74506
high energy photon beams, absorbed dose from secondary electrons 79−92380
high energy photon beams, advantages and props. 80−51238
high energy X-ray and electron beams, appl. in radiotherapy, dose distribs. 79−53227
high energy X-ray machines, effect on tumour cure rate 80−36067
high LET radiation therapy beams, expt. microdosimetry 80−12280
high-energy accelerators, mixed photon-neutron field meas. 80−51267
high-energy linear accelerator photon beam exit design for neutron prod. minimisation 80−51242
high-energy X-ray beams, scatt. radiation rel. to leakage radiation 80−51266
historical development of need for radiation protection and meas. in USA 77−37708
HV therapy, neutron dose levels of 8 MeV linear accelerator and 18 MeV betatron *(German)* 78−69221
hyperthermia, deep local, induction by US and EM fields, problems and choices 80−94283
hyperthermia, localised, comparison of EM and US diathermy 80−104725
hyperthermia, nonintrusive meas. by US temperature tomography 79−53282
hyperthermia by local EM heating and conductivity change, cancer treatment appl. 77−86578
hyperthermia by magnetically induced currents, freq.-depth-penetration, comments and reply 80−108991
hyperthermia combined with radiotherapy, normal and cancer cell effects obs. 80−45972
hyperthermia dosage definition form in vitro thermal cytotoxicity data 78−24178
hyperthermia induced by microwaves, dose definition 79−2135
hyperthermia induction in small animals using microwave system 79−2118
hyperthermia of expt. mouse cancers using 2450 MHz microwaves 79−2119
hyperthermia research with dual-beam microwave applicator 80−17052
hyperthyroidism, absorbed dose to ovaries and uterus 79−79656
hyperthyroidism, childhood, role of radioiodine treatment 80−41182
hyperthyroidism, use of ^{131}I in treating children and adolescents 80−46013
hyperthyroidism treatment with ^{131}I, carcinogenesis, comparison with surgery 78−85374
hypothyroidism therapy, sealed radioactive sources appls. *(French)* 78−53497
immune function, effect of irradiation, patients with mammary, pulmonary or head and neck carcinoma 79−16251
implantation device, preloaded custom-designed, for T1-T2 carcinoma of the floor of the mouth 80−94335
International Microwave Symposium, San Diego, Calif., USA (June 1977) 78−5478
interstitial, dosimetric localisation, use of computerised tomography scanner 80−21540
radiation therapy continued
interstitial, using Angiocath-^{192}Ir afterloading technique 77−13002
interstitial dosimetry, utilisation of the computerised tomography scanner 80−104770
interstitial radiotherapy of tongue, improved afterloading technique 78−35922
interstitial tonsillo-palatine implants using ^{192}Ir ribbons 77−70527
intracavitary therapy, dosimetry of Cathetron applicators 78−69217
intracavitary uses of colloids 80−36110
intracavity implant therapy, appl. of linear programming to dose optimisation 80−72329
intracavity radiotherapy, interactive treatment planning using CT 80−8145
intracavity Rn applicators, localisation with Diagnost C 79−48331
intracavity therapy using remote afterloading technique *(Japanese)* 80−81730
ion linear accelerator development for neutron radiotherapy 79−20654
ionising radiation, external beams, for teaching 78−49616
ionising radiations, effects and sources *(French)* 79−66494
ionization-chamber-dependent factors for calibration of megavoltage X-ray and electron beam therapy machines 80−18704
isocentric fast neutron therapy facility at Edinburgh 80−30842
isodoses in human radiotherapy, automatic determ. using whole body computer tomography *(German)* 77−9236
juxtasellar tumour radiotherapeutic management, value of computed tomography 77−56450
kidney stone contactless destruction by US shock waves 79−48300
kidney transplant patients, effect of local irrad. on acute rejection process 78−24117
LAMPF biomedical project, pion beam development 79−79629
laryngo-pharynx, British Institute of Radiology fractionation study 78−44584
larynx carcinoma, primary therapy, review 80−12216
laser, CO_2, appls. and results 80−56155
laser, endoscopic Ar ion laser photocoagulator for bleeding digestive lesions 78−40287
laser, endoscopic photocoagulation in human digestive tract using Ar ion laser *(German)* 78−35915
laser, tumour irradiation, immunological processes *(German)* 78−40242
laser applications in clinical medicine *(Japanese)* 80−12211
laser applications in medical research, biophysical aspects 80−51201
laser applications in otology, review 78−48860
laser back pointer for ^{60}Co radiotherapy unit 77−86583
laser beam applications in medicine and surgery, review *(French)* 79−34626
laser beam operation in surgery and treatment, safety 78−35903
laser endoscopic coagulation in gastrointestinal hemorrhages *(German)* 78−69178
laser endoscopic photocoagulation of bleeding lesions, using Ar laser *(French)* 79−34627
laser endoscopy, associated ophthalmic hazards 79−79598
laser iridectomy, energy required, hazards and techniques 78−11713
laser irradiation healing of wounds *(German)* 78−35918
laser radiation effects on wound healing, immunological aspects *(German)* 78−35917
laser radiation on immunocompetent cells, abscess removal example *(German)* 77−77960
laser therapy in lower female genital tract disease medical and engineering problems 78−48865
laser therapy of skin defects using Ar ion laser *(German)* 78−35916
lasers, therapeutic appl. *(French)* 80−108996
lasers in medicine, appls. and equipment development 78−48862
lateral therapy portal placement, reproducibility improvement, simulator accessory 79−100710
leakage radiation characts., 18 MeV, clinical linear acceleration 79−5379
light-ion flux mixed with collimated fast-neutron beams 80−81723
LIGHTCAST tape use, var. of surface dose with number of layers 77−86635
linacs for radiation therapy, physical characts., marketing parameters and ideal accelerator 79−53226
linear accelerator, 4 MV, use for whole-body irrad. 80−109001
linear accelerator, 5.5 MeV Neptune, phys. characts. of beam *(French)* 77−29196
linear accelerator, SL 75-20, clinical results with 79−48332
linear accelerator, SL 75-20, neutron and gamma doses in entrance mazes of treatment rooms 80−85500
linear accelerator, Varian Clinac 18/10, use of polystyrene filters for electron energy modification 80−56168
linear accelerator beam profile scanner 80−101267
linear accelerator calibration monitor with a memory 80−3821
linear accelerator calibration using Si diode detector, high-energy photon dosimetry 78−24143
linear accelerator dosimetry control system, solid state 80−94371
linear accelerator neutron sources and characts. 80−51239
linear accelerator use factors 77−9275
linear accelerator used in high-energy photon radiotherapy, 10 MV, neutron prod. 77−16995
linear accelerator X-ray beams, off-axis beam quality change 80−78461
linear attenuation coefficients of biological materials, extrapolation from diagnostic energies to megavolt range 78−24145
linear electron accelerator NEPTUN-10p 78−88744
Lipowitz metal shielding thickness for dose reduction of 6-20 MeV electrons 80−76842
liver, appl. of ^{90}Y for cancer therapy 80−17098
Luer lock afterloading device for ^{192}Ir brachytherapy 80−104735
lung cancer, interstitial brachytherapy, 20 year experience 80−72302
lung carcinoma, extended fractionation study 80−72305
lung carcinoma treatment by local irrad. and Corynebacterium parvum, mice 78−65091
lung dose in half body radiotherapy, determ. by computerised tomography 80−104763
lung irradiation for pulmonary metastases prevention, expt. with model system 77−37021
lymphatic metastasis from primary tumour growing in foot, localised preinoculation X-irrad. influence 80−45976
lymphocytes, peripheral, population changes following radiation therapy to limited and extended fields 80−72236
lymphocytes irrad. in vitro, effect of radiotherapy on mitogenic response to phytohaemagglutinin 78−24100
lymphocytic leukemia, chronic, total body irradiation 80−3778

radiation therapy continued
lymphoma, non-Hodgkin's, total body irradiation 80−3779
lymphomas, depth-dose factors using a 4 MV linear accelerator 79−25066
lymphosarcoma, advanced, total-body irradiation 79−74741
magnetic enhancement of electron dose distrib. in phantom 77−48872
magnetic modification of electron beam dose distributions 80−30893
malignant disease and its treatment, changing patterns, review 77−56446
malignant growths treatment, optimisation 79−5337
malignant melanoma, dosimetric consideration 80−94372
malignant melanoma, relationship between total dose, fraction number, fraction size 79−5341
malignant melanoma treatment near optic disc using small ^{60}Co beams 78−35929
malignant thyroid disease treatment, ^{131}I appl. 80−36108
mammacarcinoma conservative radiotherapy, computer assisted dosimetric soln. *(Dutch)* 80−36139
mammary adenocarcinoma, combined hyperthermia and X-ray effect, mouse expt. 77−90852
mammary adenocarcinomas, effects on tumor cell survival after irradiation, mice 79−25036
mammary carcinoma, primary radiotherapy, review *(German)* 80−61693
mammary carcinoma stage II, postoperative therapy programme 80−72285
mammary tumours, mouse, cytokinetic basis for efficacious radiotherapy protocols design 79−88124
mandible, radiation necrosis, dental factors, radiotherapy complication 80−98021
mandible, radiation necrosis, factors influencing onset, radiotherapy complication 80−98020
manipulation unit equipment 80−30903
mantle fields, dose compensator for lymph bearing areas 79−43991
mantle treatment, absorbed dose meas. in patients compared with dose planning 77−9258
maternal cancer, internal irradiation technique, dose calcs. *(Dutch)* 80−3816
maxillary antrum, squamous cell carcinoma, cervical lymph node metastases 80−72304
medical cyclotrons for fast neutron radiotherapy and radioisotope prod. 79−53244
medical physics conference, Ottawa, Canada (Jul. 1976) 77−16897
medulloblastoma treatment technique and radiation dosimetry 78−35926
megavoltage depth-dose value corrections due to reduced backscatt. thickness 77−48871
megavoltage dosimetry, accuracy of LiF TLD 77−81574
melanoma, implications of radiosensitivity of melanoma cells in culture 77−73548
melanoma therapy regime study using athymic nude mice 77−48839
melanomas, effect of clinical irrad. regimes on human malignant tumours grown in athymic mice 78−24101
meningioma irradiation, prototype circumscribed tumour for planning high-dose brain irrad. 78−35925
meson factory, therapeutic use *(Japanese)* 80−26351
metastases, subclinical deposits, cell sensitivity in Lewis lung carcinoma model 77−12978
metastatic thyroid cancer, use of ^{131}I 80−36084
Mevatron 20, compact high-output linear accelerator 78−28035
Mevatron 60, X-ray linear accelerator 80−21530
microdosimetry, conf., Brussels, Belgium (May 1978) 80−4472
microdosimetry of the pion beam at TRIUMF 80−109037
microstrip antenna for biomedical applications 80−89826
microstrip slot radiator for medical appls. 80−108994
microtron, 22 MeV, design, beam transport, gantry and depth doses 77−81552
microtron, shuttle design, electron and X-ray therapy unit 77−83188
microwave, for cancer treatment 80−26320
microwave, Gaussian-beam launcher for producing focused exposure field 77−40728
microwave, multimode square waveguide applicator 79−34630
microwave, treatment of cancer by hyperthermia 77−52859
microwave antenna, invasive, for locally-induced hyperthermia for cancer therapy 80−67193
microwave applicator, broad band, for heating tumours 80−30830
microwave applicators, comparison of stray radiation patterns 80−61660
microwave applicators for localised hyperthermia treatment of malignant tumours 80−89824
microwave diathermy, circularly polarised direct contact applicator design and performance 78−7531
microwave diathermy applicator with choke, 2450 MHz, slab-loaded, direct contact 80−89825
microwave diathermy direct-contact applicators, comparative heating patterns 78−40286
microwave diathermy direct-contact circular aperture applicator with corrugated flange, design 80−67190
microwave effects research, medical appls. and hazards, 1940-60 80−86066
microwave enzyme inactivation system with electronic dose control 77−81762
microwave Gaussian beam launcher, focal region field aberrations 78−44580
microwave Gaussian beam launcher, for selective partial body exposure of biological substances 79−29578
microwave heating combined with radiation therapy, skin and tumor thermal enhancement ratios 80−67192
microwave heating patterns in spherical tissue models 77−86537
microwave hyperthermia, chemotherapy, and ^{60}Co radiation for hamster melanoma treatment 77−77931
microwave hyperthermia, localised, biomedical devices 80−104724
microwave hyperthermia, microwave leakage during treatment 80−76820
microwave hyperthermia applicators, development of 79−25059
microwave hyperthermia simulation *(French)* 80−3770
microwave hyperthermia to cancer treatment *(Spanish)* 80−89795
microwave hyperthermia treatment and thermometry system 80−72280
microwave induced hyperthermal therapy of tumours in mice, bolusing technique 77−77934
microwave induced hyperthermia in cancer treatment, apparatus and preliminary results 79−62296
microwave irradiated breast tumour thermal pattern calc. *(French)* 80−3759
microwave linear accelerators, systematic patient-dose errors 79−92387
radiation therapy continued
microwave power appls., conf., London, England (Nov. 1979) 80−21520
microwave radiation, 2450 MHz, and γ-radiation effects on flour beetle 79−2103
microwave radiation appls. in surgery and cancer therapy 79−5336
microwave system for controlled production of local tumour hyperthermia in animals 79−34624
microwave thermography and local heating by same system, clinical applications 79−100695
microwave tissue heating system for hyperthermia research 80−30829
microwaves, direct-contact heating of dielec. encapsulated mouse tumour using dual-beam TEM applicator 78−40245
microwaves appl., bio-clutter interference effects 79−11992
microwaves in cancer therapy, review of 4 years 80−56162
missing tissue compensator 80−3784
mixed fields, X-rays, electrons, method for optimal field separation 79−8538
model mouse cancer response to 2.45 GHz free-field hyperthermia 79−70584
Moire topography applied to treatment planning and manufacture of compensating filters *(German)* 77−12983
Moire topography camera, simulator mounted, for constructing compensating filters 80−46024
monitoring using $C^{15}O$ and $^{15}O_2$ steady state imaging 78−40298
monocyte function rel. to irrad. in breast cancer patients 80−72238
monocytosis observation during ^{60}Co radiotherapy 77−70501
MOS transistor dosimeter appl., response functions obs. *(Czech)* 79−49874
mouse lung tumour growth delay by bleomycin with 2.45 GHz local hyperthermia 79−83894
moving-strip therapy, comparison of ^{60}Co unit and Varian 4 and 10 MV linear accelerators 77−70553
multibeam microwave therapy with computer control 80−3766
multicell spheroid low dose-rate irrad. 79−62304
multiple daily sessions with ^{60}Co and 250 kV X-rays, clinical experience 78−53475
multiple murine tumours, simultaneous microwave irradiation bolusing technique 78−7422
multiple neutron fractions, RBE for late spinal cord injury 79−25051
mycosis fungoides, electron beam therapy 80−72286
mycosis fungoides, whole body electron therapy 79−48322
mycosis fungoides lymphoma, advanced, evaluation and therapy recommendations 79−88157
neck node metastases, effectiveness of microwave hyperthermia combined with ionising radiation 80−94307
neutron, cryogenic ^{2}H gas target design 77−75020
neutron, stripping-theory anal. of thick-target prod. using Be(d,n) 77−6600
neutron 14 MeV generator therapy facility 77−81568
neutron beam characterisation by radioactivation image transfer technique 79−88196
neutron beam dosimetry, prod. by Be(p,n) and Li(p,n) reactions with 26, 35 and 45 MeV protons 78−28083
neutron beam for cancer radiotherapy 77−81567
neutron beams, dosimetric props. of d(80)+Be and d(80)+(Be+Ta) neutrons 79−12009
neutron beams from D+d reaction, 6.8 to 11.1 MeV, dosimetric props. 78−53509
neutron beams prod. by Be+p, 30 and 40 MeV, polyethylene filtration 78−53494
neutron beams prod. by protons and deuterons on Be and Li, dosimetry 78−24141
neutron capture therapy of cancer in mice, long range effects, dose effect 78−48877
neutron collimated beam RBE for cell survival rel. to lineal energy spectral differences 80−12200
neutron collimated fast beam, radiation quality local distrib. 80−12247
neutron contamination of 25 MV photon therapy beam from Varian Clinac-35 77−86628
neutron contamination of photon beam, scintillation counter meas. system 77−77992
neutron dose changes due to inhomogeneities, correction factor calc. technique 79−39511
neutron dose distributions in pion$^-$ irradiated tissue, Monte Carlo calc. 79−16310
neutron dosimetric props. using D(d,n) reaction 79−70646
neutron dosimetry, basic constants and meas. principles 79−20676
neutron dosimetry, international intercomparisons 79−20636
neutron dosimetry in high energy X-ray beams of medical accelerators 79−83942
neutron energy spectra and close distrib. spectra of cyclotron-prod. beams 77−70554
neutron energy spectra of d(49)-Be and p(41)-Be neutron radiotherapy sources 79−62347
neutron generator appls., activation analysis, material investigation, radiotherapy *(Czech)* 79−31279
neutron generator design using D-T reaction 79−20656
neutron generator for cancer therapy, output monitoring using $^{16}O(n,p)^{16}N$ 79−3287
neutron intense high-energy sources for fusion reactors and radiotherapy 77−83419
neutron irradiation facility, TRIGA Mk.II reactor, remodelling and dosimetry 80−56200
neutron irradiation facility, TRIGA-II reactor *(Japanese)* 77−56459
neutron leakage characts. rel. to room shielding 80−51273
neutron medium-energy radiotherapy, shield design 79−12016
neutron production by 25-55 MeV protons on Be, spectra and yield 77−70539
neutron radiation therapy, cyclotron biological intercomparisons 79−20589
neutron radiation therapy, treatment planning corrections 79−20637
neutron radiobiology, review 77−5076
neutron radiotherapeutic source developments at Cyclotron Corporation 79−20651
neutron radiotherapy, 14 MeV, skin-sparing, effect of metal sheets 78−35923
neutron radiotherapy, nature and significance of radiation outside beam 78−53477
neutron radiotherapy beam, photon dose fraction meas. 78−3605
neutron radiotherapy beams, effects on cultured human kidney cell reproductive capacity 79−62307

radiation therapy continued
neutron radiotherapy planning and radiation quality definition 80−12246
neutron RBE, rel. to leakage from HV electron accelerators 80−51177
neutron relative biological effectiveness in different exptl. tumours, 15 MeV neutrons 79−20591
neutron secondary spectra prod. by high energy bremsstrahlung in C, N, O and tissue 80−41239
neutron source engineering problems and dose distributions 79−20635
neutron source for radiotherapy, gas target, energy spectra, flux, dose rates 78−92698
neutron source shielding for Be (*d*,*n*) reaction 79−20617
neutron source using ^{7}Li(p,n)^{7}Be, especially for smaller cyclotrons 80−26335
neutron sources, high-intensity, with rotating and gaseous targets, charcts. and appl. *(Slovak)* 79−68114
neutron sources for medical appl., survey 77−25547
neutron spectra from d and p bombardment of thick Li targets 78−28049
neutron spectra from d bombardment of Be and D 78−40319
neutron spectral meas. in intense photon field of high-energy X-ray therapy machine 78−24133
neutron teletherapy, effects of filters and wedges on skin sparing and γ/neutron dose ratios 80−46029
neutron therapy, review *(German)* 79−43968
neutron therapy beam, dosimetry and radiation protection 79−48342
neutron therapy clinical trial programme in USA 79−20640
neutron therapy hospital staff, occupational exposure report 78−96098
neutron therapy vs. existing therapy techniques in Switzerland, cost-benefit anal. 78−11718
neutron-irradiated tissue and equivalent material recoil spectra 80−17022
neutrons, 14.1 MeV, estimated dose to bone and whole body via ^{40}Ca and ^{31}P 79−53256
neutrons, 14 MeV, thermal neutron distrib. in bone in paraffin phantom, Au wire activation meas. 78−3616
neutrons, fast, in vivo meas. of lung corrections for radiotherapy 77−13007
neutrons, fast, review of current usage 79−16270
neutrons, up to 50 MeV, freq. of occurrence of nucl. reactions in tissue-equiv. material 77−9243
neutrons from ^{7}Li(p,n) for small cyclotrons 79−57755
nomianl standard dose for radiation therapy, practical nomogram, correction factors *(Italian)* 77−81581
nSD and cell survival in fractionated irradiation 79−74720
nuclear data requirements 77−25553
nuclear medicine growth, contribution of research reactors 79−11998
nuclear therapy, survey *(French)* 78−48889
ocular lens dose estimation in cranial irradiation of acute lymphocytic leukemia 79−88198
OER at low dose-rates 77−9223
oesophagus tumours, afterloading system 79−74742
oncological clinical research, data storage and retrieval system 79−48321
oncology, historical developments 80−81708
ophthalmological treatment with photocoagulation systems *(Croatian)* 78−44581
optical monofibres for medical practice, appls. *(French)* 79−39462
optimal fractionation for tumour cells with wide-shouldered survival curves 79−53192
optimal treatment schedules for fractionated irrad. of tumours, math. derivation 80−98078
optimisation of treatment 77−86593
oral tongue, postoperative split course treatment of carcinoma 80−12220
organ shielding and localisation in a diverging treatment beam, simple method 80−94317
organ shielding using Pb-Sn-Bi-Cd low melting point alloy block *(Korean)* 80−36154
oropharyngeal epithelioma treatment, role of radiation therapy *(French)* 80−41190
oropharynx, advanced carcinomas, fast neutron teletherapy, efficacy obs. 80−72296
oropharynx, squamous cell carcinomas 80−67925
orthogonal megavoltage field matching technique 79−88197
orthovoltage X-ray therapy, TLD dose intercomparison 80−12272
osteogenic sarcoma treatment, role of radiation therapy *(French)* 80−17077
output factors, scatter ratios, for radiotherapy units, ^{60}Co γ-ray and MV X-ray calcs. 78−92708
ovarian cancer, comparison of ^{32}P and ^{60}Co in treatment of intraperitoneal implants in mice 77−56457
ovarian cancer, stage III, maximal treatment technique 79−25063
ovarian cancer, whole abdominal irrad. by moving-strip technique 80−72301
paediatric malignancies, set-up and treatment techniques 78−35927
parasternal lymphoscintigraphy, radiation treatment planning implications, breast cancer 80−72299
parotid gland, rat, radioprotection by WR-2721 chemoprotector 79−92300
particle radiation therapy, low linear energy transfer alternatives 79−20648
particle radiation therapy constraints and requirements 79−20622
particles and radiation therapy, conference, Berkeley, USA (1976) 79−20619
patient's surface contour measuring device 80−104717
patient position monitoring during radiation treatment using transmitted X-ray beam 77−40894
patient-contouring, electronic device, for radiotherapy treatment planning 77−13029
patient-positioning laser alignment instrument 78−53471
pelvic radiation portal reproduction, errors 78−35928
pelvis, optimisation of box technique to reduce femur dose 80−12263
permanent implant dosimetry, time-dose factor anal. of dose rate effects 77−70549
Philips treatment planning system implementation for teletherapy 78−73244
photochemotherapy, absolute radiation dosimetry 79−12008
photochemotherapy, anatomical distrib. of UV radiation 77−86643
photochemotherapy of psoriasis vulgaris and mycosis fungoides 78−35908
photocoagulation using ruby laser, colour discrimination time variability 78−53401
radiation therapy continued
photodermatological uses of dye lasers, erythema production, psoriasis treatment, tumour destruction *(German)* 80−56164
photogramm.etry use in absorbed dose determ. 80−12222
photoluminescent thermometer probes, temp. meas. in microwave fields 80−104721
photon activation anal. for high energy radiation therapy 80−21534
photon and electron transport simulation, deceleration photons prod. using linear accelerator *(French)* 80−12282
photon beam, 10 MV, dosimetry charcts. and computerised treatment planning 77−48875
photon beam 18 MV, from Philips SL/75-20 linear accelerator, fast and slow neutron contamination 78−65127
photon beam charcts. of 20 MV accelerator for radiation therapy appls. 80−26430
photon beam fast neutron contamination obs. 79−59284
photon beams, high energy, depth of max. dose var. with fluid size 77−70555
photon beams, high energy, electrons as cause of d_{max} shift 79−83938
photon beams, high energy, improving buildup and depth-dose charcts. 79−83939
photoneutron production in neutron detectors in high energy X-ray beams 78−94174
phototherapy, effect of prolonged illum. on luteinising hormone concs. in human infants 78−69138
PIGMI, linear proton accelerator, mechanical description 79−45474
pineal region tumours, treatment results 80−12219
pion$^-$, biological effect prdiction, star distrib. for high LET dose determ. 80−12248
pion$^-$, biomedical experiences, conf., Brugg-Windisch, Switzerland (Dec. 1978) 80−22138
pion$^-$, dynamic rangeshifter for modifying depth-dose distribs. 78−3595
pion$^-$, energy deposition spectra and radiation therapy appl. 80−26363
pion$^-$, in vivo dosimetry using Al activation 80−46060
pion$^-$, pre-clinical studies at TRIUMF 80−26264
pion$^-$, radiobiological evaluation of suitability for tumour therapy 80−67166
pion$^-$, suitability for use, radiobiological obs. 80−26338
pion$^-$ and pion$^+$, stopping density distribs. in 1 and 2 dimensions 80−26340
pion$^-$ beam dosimetry, LAMPF 78−3606
pion$^-$ beams, dose patterns in irrad. cylinders, effects of tissue inhomogeneities 77−9266
pion$^-$ biological effectiveness and O_2 enhancement ratio obs. 79−20595
pion$^-$ biomedical beam line, CAMAC control 77−90886
pion$^-$ broad therapeutic beams, microdosimetric characterisation 80−12277
pion$^-$ cancer radiotherapy, RBE in and near large beam 80−12245
pion$^-$ cancer radiotherapy evaluation at LAMPF 79−53216
pion$^-$ clinical facilities, linear accelerator selection 79−20645
pion$^-$ dose studies, influence of beam charcts. and detector size 79−53253
pion$^-$ irradiation, dose outside treatment volume 78−53508
pion$^-$ peak expansion to range of depths useful in radiotherapy, chromosome aberration meas. 78−20243
pion$^-$ radiation, uniform depth-dose distrib. technique and cell survival obs. 80−17139
pion$^-$ radiation therapy, dosimetry and treatment planning 79−20646
pion$^-$ radiation therapy, preliminary treatment plans 79−20644
pion$^-$ radiation therapy dosimetry 79−20679
pion$^-$ therapy, neutron energy spectrum in stopping pion field 78−85386
pion$^-$ therapy, review *(German)* 79−43968
pion$^-$ treatment planning, simultaneous multiport irrad. 79−20647
pion$^-$end, in vivo beam localisation by positron activation 80−72316
pion, energy dependent mean free path length for star formation 77−23393
pion, simulated treatment planning for Stanford Medical Pion Generator 77−86634
pion, two-dimens. visualisation of stopping pion distribs. 77−12999
pion applicator, meas. at πE^3 single beam correl. to dosimetry and therapy-planning 80−26361
pion beam, appl. of thermolum. dosimetry 80−26362
pion beam, hydraulic servomechanism for shifting range 77−83358
pion beam radiobiology at Rutherford Lab., 1971-76 77−13003
pion beam treatment planning, deep seated tumours, computerised tomographic scans 80−41180
pion beams, meas. of effect of inhomogeneities and compensating bolus 79−39512
pion dose contours, high-LET, in cellulose-nitrate plastic track detectors 79−39513
pion production using linear electron accelerators, and appls. *(Japanese)* 78−78533
pion radiotherapy, electron linac design 77−83138
pion radiotherapy, review *(Japanese)* 78−40321
pion radiotherapy facility at TRIUMF, dosimetry and radiobiology 77−70526
pion radiotherapy studies with nucl. emulsions 78−73219
pion range shifter for clinical therapy 77−32953
pion therapy controller designed for patient irradiation at the SIN π^--applicator 79−57754
pion therapy planning, stopping power ratios meas. 79−83847
planar implants, effect of crossing needle location on dose distribs. 79−100742
planning and dosimetry for pion applicator 80−26360
planning programs development for SIN pion applicator 80−26339
planning technique for inclined lesions 79−74743
porta hepatis, anatomic and physiological considerations 79−20661
portal film duplication using instant photography 79−30591
prescribed schedule non-compliance clinical significance 78−11723
primary dosimetric standards at the Memorial Sloan-Kettering Cancer Center, NY, USA 80−8190
prior immobilisation and positioning, pion therapy expt. 78−31886
prostate, dog, microwave localised heat treatment, new applicator 79−100698
prostatic cancer, preoperative extended field radiation using ^{125}I seed implants 80−72303
prostatic carcinoma treatment planning, US imaging rel. to computerized tomography 80−3786
proton and heavy ion source capabilities 79−20629
proton and heavy-ion fractionated radiation therapy experience 79−20631

radiation therapy continued
proton and heavy-ion therapeutic advantages 79−20628
proton beam, 200 MeV, visualisation and transport of positron emission 79−20668
proton beam, high-energy, physical meas. using tissue substitutes 80−81720
proton beam absorbed dose determ. 80−46062
proton beam localisation using ^{15}O activation 77−48862
proton Bragg peak therapy, beam penetration and control in nonhomogeneous phantoms 77−70531
proton dose distribution fattening for large-field radiotherapy 77−73564
proton linac, source of neutrons for radiotherapy 77−81569
proton local exposure, 200 MeV, contrib. of secondary particles to absorbed dose 79−100752
proton relative biological effectiveness, microdosimetric interpretation of biological data 79−62306
proton relative biological effectiveness, microdosimetric parameters 79−62305
pulmonary gas exchange following irrad. of cervical, mediastinal, hilar and axillary nodes 77−73542
purpose and technology, radiotherapy department planning 78−28034
quality control, weekly localization films and field placement error detect. 79−43985
radiation biology conf., Sapporo, Japan (Sept. 1978) 80−8105
Radiation Oncology Research Program, recommended research proposals 80−3787
radiation techniques and technology development in the Soviet Union 79−685
radioactive seed implants, computation of dose distrib. 80−101265
radiobiological data for clinical dosimetry in pion tumour therapy 80−26266
radionuclide cumulative dose calcs., graphical representation 77−66852
radionuclide therapy, pot. future appl. 80−36031
radioprotective and radiosensitising drugs combined use in exptl. radiotherapy 77−86559
radioresistant malignant tumours, HF hyperthermia and γ-rays therapy results 79−100699
radiotherapeutic agents, props., dosimetry and radiobiologic considerations 80−36106
radiotherapy machine ionising radiation and EM interf. effects on cardiac pacemakers 79−62406
rat metastatic growth effect of local tumour hyperthermia 78−24115
re-irradiation tolerance of heavily irrad. human skin 77−73544
renal blocking, use of diagnostic US to determine renal size and position 78−31874
RF diathermy tumour eradication 77−70516
RF heating for solid tumour destruction, animal expts. 80−61637
risk due to unwanted neutrons, estimation by dose calcs. 80−81714
rotation therapy, automatic var. of field size and dose rate 78−11720
rotational 4 MeV linear accelerator, medical usage factors for radiation protection 77−64139
rotational ^{60}Co therapy, transit dosimeter system, electronic modification 77−2053
safety regulation impact on nuclear medicine *(French)* 80−47764
scanning electron beam, semi-empirical model for dose distribs. generation 80−94373
scatter air ratio eqn. anal. 79−83917
scatter dose distribs. for 6 MV photon beams 79−62370
scatter-air ratio equation for megavoltage calcs. 77−2054
scattered radiation to fetus for partial treatment of Hodgkin's disease 80−21533
secondary radiation from supervoltage accelerators rel. to patient protection 77−56471
secondary sections for radiotherapy plane section *(German)* 80−89841
sensitometry, review 78−20260
sensitometry in medical imaging applied in diagnosis and therapy 78−69193
sidelight using laser cross-hair image 78−35939
simulator, use of therapy accelerator 78−3581
simulator and linear accelerator meas. and control by microprocessor 77−40902
skin, electron beam rotation therapy 79−88172
skin γ and neutron responses, dose fractionation effects 79−20593
skin absorbed dose, physical factors affecting, ^{60}Co γ-rays and 25-MV X-rays 79−83937
skin acute response, human, pion$^-$ relative biological effectiveness 79−20596
skin carcinomata, electron beam treatment obs. 79−62335
skin melanoma therapy by laser irradiation *(German)* 80−12208
skin nodules, comparative effects of pion and X-irradiation 79−20659
small-animal microwave induced hyperthermia development system 78−11715
source definition for head shielding requirements in linear accelerators, effect on room shielding design 80−46068
source motion, calc. in intracavity moving-beam and multipositional irrad. 80−104759
Space Radiation Effects Laboratory 710-MeV He ion beam, biophysical aspects 80−30871
spleen lymphoma, renal consequences of γ-irradiation 79−20615
spleen radiotherapy and computed tomography in treatment planning 80−56180
spot scanning system for proton radiotherapy 80−89836
squamous cell carcinoma of head and neck, time-dose factors anal. 80−72333
stomach tissue, canine, temp. increase comparison for Ar and Nd:YAG laser irrad. 79−92290
superconducting cyclotron neutron source 79−20655
supervoltage beam films, optimisation 78−3580
techniques and modes of action, review *(French)* 80−21523
technology manpower needs, problems and potential in United States 77−86701
telecobalt collimators, design principles 78−15888
teletherapy alignment, simplified method of quality control 77−70528
teletherapy machine electronic dual timer 78−85358
temperature distrib. in microwave-irradiated cylinders simulating living tissues 80−3760
tethered float radiometer for US therapy equipment output power meas. 80−104691
Therac 6 linear accelerator, field elongation effects on depth-dose curves, central-axis output of X-rays 79−5361
therapeutic radiologists, training in USA, 1978 survey 79−84878
radiation therapy continued
Theratron 780, empirical table of equivalent squares of rectangular fields 77−48856
thick inhomogeneity effects on charged particle beams 79−25041
thoracic inlet tumours, new irradiation technique 79−34651
thyroid, volume and dose estimation by ^{131}I scintigraphy 79−16302
thyroid cancer, radiotherapy technique 80−94337
thyroid carcinoma, treatment by ^{131}I after surgery 78−85373
thyroid geometry influence on response of LiF and $CaSO_4$ TLD discs to ^{131}I and ^{125}I 78−73250
thyroid treatment with ^{131}I, air concs. 79−25122
thyrotoxicosis therapy, dose determ. by thyroid uptake meas., effect of gland parameters 78−61245
timer, digital, to verify mech. timers 77−21623
tinea capitis, X-ray epilation, dose var. 77−9267
tissue compensators, use in improving dose uniformity in total body irrad. 80−104767
tissue equivalent bolus, 1 to 10 GHz electrical prop. characterisation 80−3763
tissue heterodensity meas. for charged particle radiotherapy 79−20623
tissue response to multiple small dose fractions 78−15865
tissue-air ratios for whole body irrad. with ^{60}Co gamma-rays 78−61258
tissue-equivalent compensators for 4-MV X-rays, basic data 80−98069
tissue-equivalent liquid bolus, physiologically compatable, for microwave tissue heating 79−39465
tissue-maximum ratio expression fitted to Varian Clinac-6 and Clinac-4 accelerators 78−24148
tissue-maximum ratios for high-energy X-rays 78−3609
tissue-maximum ratios/scatter-maximum ratios, indirectly ionising beams 79−39515
tissue-phantom ratio rel. to percentage depth dose 77−21629
tolerance dose, treatment field size relationship 79−5359
tongue carcinoma, dose and dose rate in ^{192}Ir interstitial irradiation 79−16267
topography of patient's body surface by photogrammetric technique 77−77972
Toshiba LMR-16 linear accelerator, X-ray depth-dose characts. 79−62369
total body irradiation, radiobiological bases 80−104667
total body techniques for bone marrow transplanation, review 80−104738
toxic diffuse goiter, simultaneous treatment with ^{131}I and antithyroid drugs 80−56193
track detector direct dosimetry in fast neutron beams 78−20277
transkull transmission of axisymm. focused US beams, 0.5 to 1 MHz 80−51184
transport calculations for poins, neutrons, protons, α-particles, ions 77−25555
transuranic production and appls. *(French)* 77−42204
transverse axial film tomography with a therapy simulator 80−81716
treatment plan selection, complication probability factor 78−53476
treatment planning, ^{60}Co, correction for inhomogeneities, appl. of ACTA scanner 77−60259
treatment planning, absorbed dose calcs. method 79−92386
treatment planning, accuracy of a 2-sensor sonic digitizer 80−30806
treatment planning, appl. of US imaging *(German)* 78−53463
treatment planning, computational anal. and dosimetric evaluation of commercial irregular-fields computer program 78−24147
treatment planning, computerised, accuracy 80−72328
treatment planning, depth dose scaling using computerised tomography scans 80−30899
treatment planning, external therapy, use of computerised tomography *(French)* 79−66553
treatment planning, FORTRAN program for optimisation using complication probability factor 80−81686
treatment planning, inhomogeneity correction methods compared with Monte Carlo data 80−61698
treatment planning, inter-hospital interactive computerised system 80−36068
treatment planning, phys. charact. of 45 MV photon beams 77−48873
treatment planning, three dimensional model for CT radiotherapy 80−8192
treatment planning, use of computed tomography 77−12996
treatment planning, value of computerised tomography scanning 80−72294
treatment planning and follow-up of superficial tumours, US B-scan appl. 78−11721
treatment planning and the distortion of computerised tomography images 80−76830
treatment planning appl. of computed tomographic imaging 80−51232
treatment planning for cancer therapy, use of US imaging 77−12982
treatment planning for irregular fields 80−81739
treatment planning in ^{60}Co radiotherapy using computerised tomography techniques 78−35964
treatment planning interactive computer/ultrasound system 77−9269
treatment planning system, clinical experience *(German)* 77−77991
treatment planning system implemented in FORTRAN on interactive computer 77−5080
treatment planning using ^{137}Cs computerised tomographic scanner 79−48323
treatment planning using ACTA scanner 78−65104
treatment planning using microcomputer 80−8191
treatment time and sub-lethal repair, CHO cell obs. 80−30773
TRIUMF biomedical negative pion beam line, tuning 78−96113
tumor irradiation using focused microwave array system, feasibility 79−100689
tumour, feasibility of focused microwave antenna array system 80−21521
tumour blood flow changes due to microwave hyperthermia 78−24116
tumour cell optimal radiotherapy for exponential-quadratic survival curves and exponential repopulation kinetics 77−81555
tumour growth inhibition in mice, microwave irradiation, 3000 MHz 79−2101
tumour location by computerised tomography, use of masking lattice *(German)* 80−41213
tumour microwave heating with automatic temperature control 77−77963
tumour model, potentiation of radiation lethality by hyperthermia 79−25037
tumour registration system 80−81710
tumour response to neutron radiation therapy, animal expts. 79−20594

radiation therapy continued
tumours, biological effect of 27.12 MHz SW diathermy 79−2102
underdosing due to lack of electronic equilib. in upper respiratory air cavities, 10 MV X-irrad. 78−11739
US, sonoluminescence generation by US therapy equipment, in water and blood plasma 77−77930
US chemotherapy enhancement, time/intensity studies using cell suspension and mechlorethamine 77−29175
US hyperthermia, localised, design of heating protocols 80−104693
US in medicine and biology, review 77−66830
US induced hyperthermia, spontaneous tumour treatment in dogs and cats 79−62290
US induced hyperthermia in previously X-irradiated sites 79−62315
US ophthalmological diagnostics and therapy *(Croatian)* 78−44570
US probes, power meas. by use of semiconductor strain gauges 80−87679
US therapy device surveys, performance standard drafting 79−79613
US tumour irradiation, closed-loop energy and temp. control 79−83874
uterine adenocarcinoma, Paul Cogniaux Centre results, 1960-1970 *(French)* 80−41191
uterine cancer, dosimetry effect of position change 79−62362
uterine cervix carcinoma, dose rel. to tumour recurrence 79−100745
uterine cervix carcinoma, high rel. to low dose irradiation 79−74759
uterus, mouse, US irradiation at therapeutic intensities in standing wave fields 80−41112
UV light therapy for skin diseases 80−36057
UV radiation from lamps, medical appls. 79−66504
UV radiation source output monitoring detector for psoriasis photochemotherapy 78−53473
Varian 6 MV CLINAC-6X accelerator, beam charact. 78−3582
Varian Clinac 4 MeV linear accelerator, radiation from U collimators, and shielding 78−24135
vascular occlusion, effect on thermal sensitization and X-irradiation of mouse tumour 79−16253
Vena cava, superior, optimum radiation schedule in obstruction treatment, importance of ^{99m}Tc scintiangiograms 80−72334
vertical couch extender 80−3783
wedged field characteristics for Clinac-18 10 MV X-rays 78−3608
whole-body computerised tomography appl. *(German)* 78−35945
X-ray, computer simulation of central axis dose distributions 79−8531
X-ray, electron, Soviet medical requirements, review 77−37032
X-ray beam, 4 MeV linear accelerator, dosimetric aspects 80−17140
X-ray beam characteristics, 25 MV, from a 35 MeV linear accelerator 79−25110
X-ray half-value-layer meas., 5-40 MV, rel. sensitivities of water, Al, Cu, Sn and Pb 77−45927
X-ray high energy therapy, patient neutron dose 77−86642
X-ray high-energy therapy, activity induced in patients 77−40744
X-ray spectral quality specification, photoactivation ratios, 15 to 40 MV 77−21619
X-ray spectral quality specification, photoactivation ratios 4 to 15 MV 77−21620
xeroradiography for direct field control 77−81551
π^- beams, direct track detector dosimetry 78−20281
^{198}Au, use in ovarian carcinoma treatment 80−36087
B neutron capture therapy of brain tumours, simultaneous flux monitoring system 79−92352
^{252}Cf for interstitial radiotherapy implantations, clinical study 78−11722
^{252}Cf in radiotherapy, RBE-dose rate relationships 77−5030
^{252}Cf, RBE vs. dose-rate relationships 77−9222
^{252}Cf radiotherapy source dosimetry, appl. of liq.-dielec. ionisation chamber 77−13009
^{252}Cf source projector for plesiocurietherapy 77−29197
^{252}Cf, use for brachytherapy 78−20272
^{252}Cf wire neutron source distrib. meas. by autoradiography 77−61643
Co teletherapy, T3-carcinoma in Bilharzial bladder, hyperfractionation and conventional fractionation comparison 80−41179
^{60}Co 3000 Ci source accidental fall and retrieval in teletherapy room 78−53524
^{60}Co applicator treatment of retinoblastoma 77−81550
^{60}Co axial depth dose empirical formula 78−35965
^{60}Co beam lateral profile model 78−28085
^{60}Co beam model for radiotherapy treatment planning 77−66857
^{60}Co beams, cylindrical ion chamber A_c and A_{eq} factors exam. 79−81121
^{60}Co gamma-rays, calibration in water vs. calibration in air for teletherapy units 77−21630
^{60}Co, installations calibrations, US national evaluation 79−5360
^{60}Co radiation therapy, eval. of dosimetric accuracy and uniformity 80−12269
^{60}Co sources for total body irrad., uniformity and standardisation 80−94338
^{60}Co teletherapy, IAEA-WHO dosimetry service using mailed LiF, 1970-75 survey 77−16991
^{60}Co teletherapy, surface dose reduction using Ag filter 79−79641
^{60}Co teletherapy, weekly fractionation of treatment 79−34650
^{60}Co teletherapy build-up dose meas. using $FeSO_4$-benzoic acid-xylenol orange dosimeter 78−28081
^{60}Co teletherapy dosimetry, USA nationwide survey 77−56478
^{60}Co teletherapy dosimetry survey of facilities 79−62367
^{60}Co teletherapy head shutter irrad. timer 77−66836
^{60}Co teletherapy split fields, symm. and asymm., dosimetry 78−3611
^{60}Co teletherapy unit, mech. fault affecting source position 77−73562
^{60}Co teletherapy unit dose calibration, comparison of methods 80−30900
^{60}Co teletherapy units, γ-ray beam source configuration, spectral composition obs. 79−62341
^{60}Co therapy for Hodgkin's disease, gonadal and eye doses 79−96665
^{60}Co total body irradiation, dose distrib. meas. using thermoluminescent dosimeters 80−41245
^{60}Co, use of electron filters to improve buildup charact. of large fields 78−3612
^{134}Cs, as potential radiotherapy radionuclide, prod. and decay scheme 77−90875
^{134}Cs, for treatment of cervical cancer, isodose curves 77−90876
^{137}Cs gynecologic insertions, expt. derived algorithm for computer calc. dose rates 80−101264
^{137}Cs needle implants, miniaturized 79−11995
D ion accelerator, intense neutron source, design and operation 79−49883
He ion beam therapy expts. and prospects 79−20633
He^{2+} 650 MeV ions study for possible radiation therapy applications *(French)* 77−66835
I, radioisotopes, history of use 80−42032
^{124}I interstitial implants, dose inhomogeneity 79−100746
^{125}I interstitial seed implants, new afterloading technique 79−34652
^{125}I therapy, RBE of soft X-rays 78−7405
^{125}I thyrotoxicosis management, dosimetry, radiobiology, clinical aspects 77−2048
^{125}I, use of screened low energy radiation sources for moulds in mouth carcinoma treatment 77−48855
5-^{125}I-iododeoxyuridine as prototype for radionuclide therapy with Auger emitters 77−29186
^{131}I therapy, absorbed doses to marrow and blood 77−48869
^{131}I therapy, review of contamination and exposure hazards 80−41257
^{131}I therapy for toxic diffuse goitre, incidence of hypothyroidism within 1 year 78−65116
^{131}I therapy of hyperthyroidism, gonadal dose and genetic significance 77−5082
^{131}I thyroid therapy, estimating doses recorded by personnel dosimeters 78−15891
^{131}I-therapy of cancer or hyperthyroidism, absorbed dose to ovaries or uterus 80−36138
^{192}Ir afterloaded implant in retreatment of head and neck cancers 78−96083
^{192}Ir afterloading method using nylon tube 77−48857
^{192}Ir, specific γ-ray constant and exposure rate constant 79−36187
^{177}Lu organ distribution in mouse 78−48879
^{32}P-diphosphonate dose determ. in patients with bone metastases from prostatic carcinoma 78−61251
Pb sheets, thin, as tissue compensators for larger field irrad. 80−104736
Pb-Bi, X- and γ-ray attenuation obs. 79−61457
^{239}Pu, endosteal cell dose and relative distrib. factors compared to ^{226}Ra 78−96091
Ra needle implants, computer program for reconstruction and dose-rate calc. 77−40770
Ra source leakage testing 77−16977
^{224}Ra biological effects, conf., Alta, USA (July 1974) 78−96068
^{224}Ra, endosteal cell dose and relative distrib. factors compared to ^{226}Ra 78−96091
^{224}Ra injections into humans, soft-tissue effects 78−96070
^{224}Ra injections into humans, skeletal effects 78−96071
^{224}Ra preparation, for ankylosing spondylitis therapy 78−96089
^{224}Ra usage in radiotherapy and radiobiology, brief history 78−96085
^{224}Ra use in treatment of ankylosing spondylitis and rheumatoid synovitis 78−96086
^{226}Ra source leakage testing by mailed track detector method 77−60264
^{186}Re labelled EHDP preparation and possible use in osseous neoplasms treatment 80−56215
^{222}Rn curved plesiotherapy applicators, dosimetry 80−51261
^{222}Rn external plesiotherapy, dosimetry obs. 80−36135
Si diode neutron detector for meas. near high-energy accelerator, photon and electron response 78−35963
^{90}Y 25 Ci generator, preparation and use 77−40768

radiationless transitions *see nonradiative transitions*

radiative corrections
"radiative corrections" is distinguished in use from "electromagnetic corrections" by application to atomic and molecular spectra
see also electromagnetic corrections; radiative shifts
atom, bound state quantum fluctuations and variational method, relativistic HF calc. with radiative effects 80−42918
atom, heavy and superheavy, K-electron binding, self-energy correction 77−18802
atom, many-electron, in external mag. field, Hamiltonian and classical electrodynamics 77−79576
atom, multiphoton transition amplitudes, exact summation of higher-order terms 77−18878
atomic ground state energy, relativistic and radiative corrections *(Russian)* 77−67991
atomic K-shell photoeffect, radiative corrections 77−57940
atomic photoeffect, K-shell, radiative corrections and HF end of bremsstrahlung spectrum 77−23477
atoms, electron-electron interactions, radiative effects, canonical transformation calcs. 77−3275
bremsstrahlung, HF spectral region, radiative corrections 77−58242
Dreel-Yan processes, gluon corrections 78−8597
electron form factors, book contrib. 78−82213
electron in external EM field, radiative corrections 78−41449
electron in laser field, modification of quasilevels due to radiative corrections 77−26474
electron mass operator in 2-D QED approx. 80−4900
fermion, massless, quantum electrodynamics of Schwinger model, perturbation anal. 77−65109
harmonic oscillator in random EM field radiative corrections stochastic electrodynamic treatment 77−45736
inner-shell vacancy creation, ionised fragments probability distrib. 80−83274
molecular crystal, surface exciton levels, radiation corrections 80−34962
muonic atom, heavy, $1s_{1/2}$ levels, self-energy corrections 78−55262
muonic He, hyperfine struct., relativistic, radiative and recoil corrections, QED test 80−14256
non-relativistic limit, physical interpretations of electron radiative corrections 78−37567
nucleon-nucleon scattering 79−26335
orthopositronium three photon decay rate, vertex angle and electron self-energy radiation corrections *(Chinese)* 77−75342
parity violation in atoms induced by radiative corrections 78−78108
pion-nucleon scattering 79−26335
positronium, hyperfine structure, order-α^4R_∞ contribs., radiative corrections calcs. 79−76538
QED, strong and supercritical fields, book contrib. 78−74193
Stern-Gerlach quantum-like behaviour of a classical charged particle 79−85913
two-electron system, QED, Foldy-Wouthuysen transform. and transition operator relativistic corrections 77−74624
two-level atom, EM radiation interaction, elec.- and mag.-dipole contribs., reaction field 78−94215
unstable atoms, in time-depend. EM field, radiative corrections 80−23321

radiative corrections continued
$K^+ \rightarrow \pi^+\mu^+\mu^-$, radiative corrections in Weinberg model *(Russian)* 77−38163
Be, atom, ground state, accurate CI wavefunction 77−42245
D_2^+,(DT^+), IR transition freqs. calcs. 77−88452
Fe XXIV, spectra, radiative corrections 79−98015
H, n=2 levels, Lamb shift and fine struct. reson. meas. 80−23321
H, self-interaction of excited at. with radiation field 78−86794
H-like atoms, radiational displacement of energy levels in fields of extended nucleus *(Russian)* 79−10045
H-like ions, one-photon decay rates, general theory of radiative corrections 78−46282
H_2, energy levels accurate determ. 77−46503
H_2, $X^2\Sigma_g^+$ state, vibr. energy levels, radiative corrections calcs. 78−90094
H_2^+(HD^+)(HT^+), IR transition freqs. calcs. 77−88452
Li, ^2S ground state calc. using Hylleraas-type wavefunctions 78−33418
Li-like multiply charged ions, spectra, radiative corrections 79−98015
Mg, and isoelectronic sequence, relativistic effects on transition probabilities 77−54532
S compounds, one-electron binding and Auger energies 80−52872
S, one-electron binding and Auger energies 80−52872

radiative lifetimes
$1s2p\,^4P$ levels, lifetimes and line fluoresc. yields 78−74612
acetaldehyde, single vibronic level fluoresc., radiative lifetimes 78−82769
acetaldehyde+CO_2, vibr. relax., search for unquenchable species, room temp., 5-2200 torr 78−9229
acetaldehyde ($A,^1A_2$), laser induced fluoresc. 79−50075
acetone, mol., radiative lifetime of phosphoresc. state, influence of high lying triplet states 79−86006
acetylene, VUV multiphoton dissoc., electronically excited fragment emission 78−90238
acridene-toluene-phenol, luminescence of complexes with hydrogen bonding at 4.2-77K 79−87486
acridine, solvent depend. of radiationless relax., singlet lifetime, picosecond spectroscopy 78−66582
acridine, temp. depend. of fluoresc. decay meas. using picosecond techniques 80−99518
alkali halide:Tl^+-like ions, triplet state lifetime, hyperfine interaction 80−2844
alkali isoelectronic series, transition probabilities, oscill. strengths, lifetimes, branching ratios 78−33470
alkali metal, radial matrix elements and radiative lifetimes 79−59375
alkaline earth halides:Eu^{2+}, fluorescence lifetime and quantum efficiency for 5d⟶4f transitions 80−100681
anthracene, excimer fluoresc. lifetime nd quntul yield in soln. 77−6834
anthracene, lifetimes of exciton-polariton luminesc. 79−33761
anthracene, matrix isolated, vibr. relax., hot luminesc. obs. 79−85986
anthracene, pure and d_n, PMMA soln., triplet lifetimes, 77-300K 78−25594
anthracene, singlet and triplet excitons as probes for photochem. reactivity 79−74406
anthracene, singlet exciton annihilation kinetics 79−19926
anthracene, spectral evidence for green incipient dimers after photooxidation and photodimerisation 78−15687
antiferromagnet, radiation problem of parallel pumping, magnon-photon interaction 79−51934
antimalarial drugs, lifetime meas. via reiterative convolution using fluorescence decay curves 80−57380
aromatic hydrocarbons, ethanol-KI solns., fluoresc. affected by I^- 79−13749
atmospheric thermal plasma, continuous emission, ionisation potential lowering and total excitation cross section 80−38705
atom, multielectron, correlated transitions in decay of two inner-shell vacancies 80−37799
atom, rel. oscillator strengths determ. by combined absorption/emission meas., Ti appl. 80−37784
atom+diatom, energy correction of infinite order sudden approx., improved phase shift approach 80−95710
atom and ion, radiative lifetime laws 80−74150
atomic collisions, rotationally induced transitions in two-state model 80−47945
atomic inner shell bound-bound radiative transitions, analytical description 78−82684
atomic lifetime technique, laser ablation and selective excitation spectroscopy 78−17824
atomic metastable states, props., energy transfer mechanisms, exptl. techniques 80−27921
atomic radiative and radiationless yields, K and L shell 79−76376
atoms, distortions of decay curves in delayed coincidence techniques 78−17620
atoms, molecules and ions, lifetimes meas. 77−30832
atoms, monovalent, transition probabilities calcs. *(Russian)* 80−63594
atoms and molecules, cascade-free determ., using modulated or deflected CW dye laser 78−25754
azoalkanes, fluoresc., solvent isotope effect 78−25591
trans-azobenzene, $S_2 \rightarrow S_0$ fluoresc. 80−28044
azulene($-d_8$), ultrafast $S_2 \rightarrow S_0$ internal conversion 79−3474
Ba I, lifetime meas. of Rydberg states in 6snd $^1D_2$ series 78−33472
beam-foil lifetime measurement, cascading problem, ANDC method use and error limits 80−14249
beam-foil spectroscopy uses in atomic lifetime meas., review 80−14248
benzaldehyde, and substitution products, spectral props. 79−27007
benzene, phosphoresc., radiative and nonradiative decay routs, spin sublevel origin 77−58064
benzene, SVL fluoresc. band intensities, Franck-Codon factors, Fermi reson. 77−10700
benzene($-d_6$), in Ar-Kr matrices, phosphorescence decay, external heavy atom effect 79−10132
benzene($-d_6$) vapour, SV L fluoresc. lifetimes and quantum yields 77−10701
benzene cryst., electron irrad., phenylcyclohexadienyl radical form., absorpt. and fluoresc. spectra study 80−89035
benzene-aniline gas mixture, fluoresc. spectra, lifetimes, yields, electronic energy transfer 77−14477
benzenoid hydrocarbons, triplet state decay, kinetic spectroscopy, 220-250 nm 78−62820
benzophenomes, substituted, solvent independence of radiative rate consts. 77−30904

radiative lifetimes continued
p-benzoquinone($-d_4$), n-π^* excited states, distant intramol. interaction between identical chromophores 78−90203
biphenyl, in propylene glycol, mol. fluoresc., effect of mol. conformation 78−78736
bound states, beam-foil excitation and decay near ionis. limit 80−9552
bromofluoromethylene radical, laser-induced fluoresc., $^1A''$-$^1A'$ transition 80−91589
t-butylbenzene, α-substitution effect and radiative lifetime, solvent effects, rel. to ethylbenzene 79−98154
chain with light emitting ends, radiative lifetime, recombination kinetics 80−108260
charged particle scatt. in quantising mag. field 80−46853
Cherenkov radiation, emission probability of radiation from charged particles passing through crystals 79−99969
chlorofluorobenzene cations in gaseous phase, emission spectra and lifetimes in B(0°) states 80−63711
chlorofluoromethylene radical, gas phase laser-induced floresc. spectroscopy 80−14173
chlorophyll, -a and -b, fluoresc. fading curve of lowest triplet state 79−36691
chlorophyll, fluoresc. decay time depend. on luminesc. and excitation wavelengths 79−66447
chlorophyll, fluoresc. detection of triplet state kinetics 77−30903
chlorophyll a, fluoresc. decay rate obs., inhomogeneous struct. and relax. time effects 79−86007
chlorophylls a and b and pheophytins, fluoresc. and phosphoresc. 80−12057
chloroquinolines, photophys. behaviour, substituent and solvent effects 80−106342
cholesta-4,6,8(14)-triene, fluoresc. and absorpt. spectra in UV, lifetimes 79−27017
cholesta-5,7,9(11)-triene-3β-01, fluoresc. and absorpt. spectra in UV, lifetimes 79−27017
cofacial diporphyrins, electron transfer reactions following picosecond excitation, CT state lifetimes, optical difference spectra 80−25995
complex molecules, fluoresc. decay in nonhomogeneous level broadening conditions *(Russian)* 79−50073
conference, luminescence, Paris (July 1978) 79−33755
core polarisation effects on transition probabilities, multi-electron atoms 79−89638
coumarin 6 ultrashort vibr. population lifetime of ground state in vapour phase 77−30929
coumarin laser dyes, fluoresc. quantum yields and lifetimes, polar solvent effects 80−87054
coumarin laser dyes, in methanol, ethanol, and water, fluoresc. lifetimes meas. 79−27252
coumarin laser dyes, solvent effects on photophysical parameters 80−91598
curve crossing systems, two-state, non-adiabatic transitions, semi classical Magnus approx. 80−37756
9-cyanoanthracene excimer emission, in glassy and cryst. matrices 79−11445
deca-2,4,6,8-tetraene, fluoresc. and absorpt. spectra, forbidden transition 78−82764
diamagnetic band structure, second order calc. using Landau functions, optical transition probability determ. 80−24784
diatomic isovalent sequence, free-mol. electronic transition intensity consts., systematics 78−42137
diatomic mols., electronic transition probabilities, isoelectronic, isovalent correls. for transition strength and vibr. consts. 80−87182
4,10-diazachrysene, absorpt. spectra and luminesc. in cryst. and glassy matrices, 77K 78−37650
1,3- and 1,4-dichlorobenzene radical cation, emission and photoelectron spectra, lifetimes meas. 78−86905
2,3-dichloroquinoxaline, in tetramethylbenzene cryst., sublevel phosphoresc. spectra 78−70863
difluorocarbene, $\tilde{A}^1B_1$-$\tilde{X}^1A_1$ system spectrosc. and photophysics 80−5577
p-diflyorobenzene $^1B_{2u}$, quenching by cyclobutnone, fluoresc. lifetime mes. 77−75205
dihalogenoacetylene radical cations, $C_2X_2^+$, emission spectra, $A^2\Pi \rightarrow X^2\Pi$ band systems 78−17679
dilute systems, donor fluorescence at high trap concentration 80−71479
2,6,dimethylpyrazine, PMMA soln., fluoresc. and phosphoresc. quantum yield and lifetime, 20-120 kbar 79−54902
1,6-diphenly-1,3,5-hextriene, mol. derivatives, absorpt. and fluoresc. spectral props. 79−72344
1,6-diphenylhexatriene, radiationless transitions and natural lifetimes, solvent effects 80−63622
diphenylketyl radical, fluoresc. lifetime and quantum yield, organic matrix, 77-130K 78−42110
4-diphenylphosphenylstilbenes, fluoresc., photodimerisation 80−1015
dipole radial integrals in Coulomb approx., tables for computation of dipole transition probabilities 79−89639
discharge, running striation excitation, metastable atoms lifetime influence 80−38760
DNA bases, polarised fluoresc. and estimated lifetimes, room temp. and in −125°C soln. 79−39352
DODCI, absorption relax. lifetime, isomeas, pulse excitations 77−9098
DODCI in ethanol, DQOCI added, electronic energy transfer, real-time ps meas. 80−58311
DODCI in ethanol, malachite green added, electronic energy transfer, real-time ps meas. 80−58311
dye, fluoresc. lifetime meas. using synchronised ultrashort laser pulses and streak photography 79−44951
dyes, fast mode-locking, IR fluoresc. and laser action obs. 80−102717
dyes, vapour phase, down conversion of 351 nm radiation for fusion lasers 79−3695
energy transfer dye lasers and laser induced intermol. and intramol. energy transfer processes 80−9647
ethylbenzene, α-substitution effect and radiative lifetime, solvent effects, rel. to t-butylbenzene 79−98154
excitation spectroscopy, time-resolved photoluminescence emission and lifetime meas., synchrotron radiation use 78−66687
fluorescence lifetime meas. by ps. single photon counting 77−5883
fluorescence lifetime meas. with picosecond resolution, using synchrotron radiation 79−13841
fluorescence quantum efficiencies and lifetimes, environmental effects, semiclassical approach 80−7393
fluorobenzenes in Ne matrices, molecular cation electronic absorption spectra, new photolytic technique 80−58415

radiative lifetimes continued
forbidden decay modes of one- and two-electron ions, book contrib. 78−82679
formadelhyde(-d_2), S_1 rot. levels, collisionless nonradiative decay rates 79−72346
formaldehyde, $^1A_2$-state, SVL fluoresc.-spectra, absolute radiative lifetime, ab initio CI calcs. 79−63919
formaldehyde, and -d_2, lifetime of ($^1A_2$) rovibronic levels 79−3495
C_{2v}-formaldehyde, Tamm-Dancoff approx., relativistic correction, vertical excitation energy, radiative lifetimes 78−9090
formaldehyde, two-step photoionisation, $^1A_2$ state lifetime 77−10711
formaldehyde S_1 levels, collisionless single rot. level lifetimes, elec. field depend. 80−63566
formaldehyde-d_0, -d_1, -d_2, single vibronic level photochem., radiative and nonradiative processes 78−66583
formaldehyde-d_0(−d_2), S_1 single rot. level lifetimes, isotope, elec. field and vibr. state depend. 80−78655
formaldehyde-d_1 (-d_2), single vibronic levels, fluoresc. emission, radiative lefetimes and vibr. relax 80−23521
formaldehyde-d_2, inert gas and N_2 matrix fluoresc. spectra, radiationless transitions and lifetimes 79−3469
germanate glass: Tb^{3+}, luminesc. props. 79−33798
glyoxal, radiationless transitions in weak mag. field, fluoresc. quenching 77−58062
haloacetylene cations, electron impact excitation A→X band system assignment 80−32766
halogenoacetylene radical cations, C_2HX^+, emission spectra, $A^2\Pi \rightarrow X^2\Pi$ band systems 78−17678
heavy ion, beam-foil spectra from 20 to 238 MeV energy, 5 to 60 nm, lifetime meas. problems 80−9722
heavy ions, beam-foil decay curves for reson. transitions, simulation 80−9721
helicenes, fluoresc., intersystem crossing, rate parameters 77−3392
hydrogen-like ions, beam-foil excitation, relative initial populations, lifetime curves 80−14210
7-hydroxycoumarine, one- and two-photon absorption, fluoresc. obs. 78−46407
indoles, temp. effects on electronic transition moments in n-heptane and water 78−58744
induced electronic transitions, radiative lifetimes, non-Condon effects 80−53051
inert gas, at. excited states in discharge, Hanle effect 79−76394
inert gas atom, first excited config., intermediate coupling coeff. 80−83450
inert gas crystal, lattice vibrs. and radiative transitions of implanted ions *(Russian)* 80−69098
inert gas mixtures, high-press., collisional radiative recomb. 80−63595
inert gases, from collision induced absorption spectra, IR line broadening 78−33554
9-iodoanthracene, picosecond fluoresc. lifetimes, thermally activated $S_1 \rightarrow T_n$ intersystem crossing 80−28045
ion excited state lifetimes meas. using orientation transfer in Penning collisions *(French)* 78−50621
ions, multiply charged, highly excited states, parity nonconservation effects 80−52898
ions, multiply charged, level lifetimes relativistic calc., S-matrix approach 80−47942
2-isopropoxyphenyl-N-methyl carbamate, fluoresc. and phospheresc. in solns. 79−61426
K-shell Auger rates, level widths and fluoresc. yields, relativistic Dirac Hartree Slater calc. 80−52957
ketones, triplet triplet absorption carbonyl group role 77−83641
lanthanides in molten $LiNO_3$-KNO_3, transition probabilities in absorpt. and fluoresc. spectra 79−50085
laser-based methods for transient chem. events meas. 80−40801
long optical lifetimes meas., distortion effects 78−9276
measurement by photon-photon delayed coincidence technique 79−89640
mesoatoms in static electromagnetic fields, excited state lifetimes and population, nuclear moments *(Russian)* 80−53170
metal surface, fast ion scatt. by plasmons, theory 80−45190
methine dyes, spectral props., solvent effects 80−69181
methoxy radical fluoresc. spectra induced by laser, UV region 79−59498
molecular, calc. methods 80−23462
molecular collision, quasi-classical and quantum moments of distrib. of states, semiclassical comparison 80−23480
molecular collision processes in presence of picosecond laser pulses, radiative transitions 80−23479
molecular excited state natural lifetime determ. by fluoresc. light quenching 78−82775
molecular interaction with EM fields, classical theory 80−95686
molecular ions, radiative lifetimes, threshold electron-phonon coincidence meas. 78−13550
molecular metastable states, props., energy transfer mechanisms, exptl. techniques 80−27921
molecule, electron impact, K-shell electrons excitation with high energy resolution, review 80−37899
molecule excited state lifetimes time-resolved spectra 78−17704
molecules, transition probability evaluation in double asymmetric pot. well 80−69120
molecules (molecular ions), lifetimes and branching ratios 78−17725
multicharged ions, transitions between energy levels in strong external field, relativistic calcs. *(Russian)* 80−63547
multimolecular system, two-level mols., coherent trapping of single excitation 79−89875
$n \rightarrow \pi^*$ singlet-singlet transition probabilities 80−95689
2-naphthol-toluene-phenol, luminescence of complexes with hydrogen bonding at 4.2-77K 79−87486
1,3,5,7-octatetraene, UV, visible, and fluoresc. spectra and assignments, evidence for ^1A_g state 78−33518
optical collisions, solvable model 80−91638
oxide glasses:Sm^{3+}, optical transitions 79−61430
pentacene films, luminesc., struct. 80−11461
perfluorobenzene, electron attachment, radiative and dissoc., negative ion lifetimes, ion cyclotron reson. spectra 80−74251
perfluorocyclobutane, electron attachment, radiative and dissoc., negative ion lifetimes, ion cyclotron reson. spectra 80−74251
perfluoromethylcyclohexane, electron attachment, radiative and dissoc., negative ion lifetimes, ion cyclotron reson. spectra 80−74251
perfluorotoluene, electron attachment, radiative and dissoc., negative ion lifetimes, ion cyclotron reson. spectra 80−74251

radiative lifetimes continued
phenanthrenes, and dideuteroisomers, vapour phase fluoresc. lifetimes, position dependent D effects 77−30901
pheophytin-a, fluoresc. fading curve of lowest triplet state 79−36691
phosphate glass: UO_2^+, Sm^{3+}, energy transfer from UO_2^+ to Sm^{3+} 79−78732
phosphate glass:Tb^{3+}, luminesc. props. 79−33798
phthalimide, soln., triplet state accumulation and deactivation depend. on solvent polarity 79−85982
phthalocyanine, metal-free, solid, fluoresc., lifetimes temp. depend., polymorphic modification 78−80388
picosecond phase shift measurements at 358 MHz using synchrotron radiation 79−44949
plasma, Jeffries' level population ratios and Seaton's cascade matrix 80−52934
polarisation propagator approach 77−18844
poly-2-vinylnaphthalene, soln., lowest triplet props., flash photolysis and radiolysis obs. 80−32861
poly-N-vinylcarbazole-biacetyl, triplet exciton quenching, exciton trapping model 80−66267
polyatomic molecule, ultrafast vibr. using laser light pulses 80−9699
polyatomic molecules, radiative lifetimes from absorpt. spectral data 77−6852
polyenes, linear, radiative rate consts., environmental effects 79−72348
polymethine saturable absorbing dyes, dual component fluoresc. lifetime meas. 80−106359
porphin (-d_2,d_4,d_6,d_8,d_{10},d_{12},d_{14}), nonradiative transition probabilities, deuteration effects 79−3485
positronium formation and quenching in Ar-O_2 mixtures, orthopositronium quenching cross section determ. 80−74261
protochlorophyll, fluoresc. fading curve of lowest triplet state 79−36691
pyrazine, mol., radiative lifetime of phosphoresc. state, influence of high lying triplet states 79−86006
pyrazine, PMMA soln., fluoresc. and phosphoresc. quantum yield and lifetime, 20-120 kbar 79−54902
pyrazine, single vibronic level fluoresc., nonexpamential decay 77−27108
pyrene excimer formation in micelle, time-resolved spectra 79−79298
quantum oscillators, matrix element diagrams 80−105455
quinazoline, in n-pentane (isooctane) Shpolskii matrices, luminesc. props., vibr. struct. 79−22739
quinoline in alcoholic glasses, induced fluoresc. 79−33775
r-centroid approximation accuracy 79−89661
radiative collisions, solvable model 80−91638
rare earth halide vapours, discharge spectra, fluoresc. lifetimes meas. 79−27025
resonance fluoresc., probe of intramolecular relax., density matrix formalism, lifetimes and quantum beats 80−32757
rhodamine, soln., triplet state accumulation and deactivation depend. on solvent polarity 79−85982
rhodamine 6G, blue and UV luminesc., obs. and mechanism 79−3486
rhodamine 6G, in methanol, fluoresc. lifetime meas. 78−29811
rhodamine 6G+BBOT donor-acceptor system, intermol. electronic energy transfer 78−17702
rhodamine dyes, phosphoresc. quantum yields determs. 79−8179
Rydberg atoms, Stark ang. momentum transfer, hydrogenic model 78−17606
sputtered excited states, secondary photon emission, role of transition probability 80−102483
stilbene, cis and trans, transient spectra, radiative lifetimes and quantum yields 80−78640
stilbene, ps photoisomerisation, time-resolved spectra obs. 79−57252
trans-stilbene, soln., lifetime and anisotropic fluoresc., viscosity effects *(German)* 80−106352
styrene (-d_3, d_5, d_8), fluoresc. quantum yields and lifetimes, 298 and 77K 79−59500
tetrabutylammonium tetrahalomanganate, phosphoresc. lifetimes in fused salts and solids 78−72573
tetracene, fluoresc. fading curve of lowest triplet state 79−36691
tetramethylpyrazine, PMMA soln., fluoresc. and phosphoresc. quantum yield and lifetime, 20-120 kbar 79−54902
thiophosgene, B^1A_1-state, photophys., fluoresc. lifetime meas. 80−53033
three two-level atoms system, continuously incoherently-pumped, radiation rate, spectrum 80−5716
three-electron systems, transition probabilities calcs. 80−99479
three-level system, two-photon transition in two pulsed fields 79−68215
time-correlated picosecond laser pulses generation, rapid sampling of optical relax. phenomena 80−9969
transition metals, 3d, MIII excited states, radiative lifetimes, beam-foil obs. 77−30979
1,3,5-trichloro,2,4,6-trifluorobenzene radical cation, $B^2A_2' \rightarrow X^2E''$ laser-induced fluoresc. spectra 80−14172
1,3,5-trichlorobenzene radical cation, emission and photoelectron spectra, lifetimes meas. 78−86905
trifluoroformamide, radiationless pathways, time-resolved fluoresc. obs. 78−66577
two electron systems, coupling schemes, transition energies and probabilities of autoionising states 80−18828
two-photon spectra, dipole-forbidden transitions, CNDO-CI cross sections 79−81244
two-state collision problems, distorted-wave formula for transition probabilities 80−69212
vibronic state short lifetime, determ. from reson. Raman excitation profiles 79−98103
xanthione, solns., triplet state quenching by ground state xanthione 78−42180
$(\mu p)_{1S}$ muonic atoms in gaseous H, triplet state lifetime 80−23579
$^4He(3^3P)$, fine struct., level crossing obs. 78−82686
Al II, lower laser levels, natural lifetime determ. 77−6724
Ag I, resonance level, radiative lifetime, dye laser excitation 78−46300
Al I, $4s^2S_{1/2}$ reson. level, mean life 79−59400
Al I, resonance level, radiative lifetime, dye laser excitation 78−46300
Al II to Al VI, beam-foil obs. from 1100 to 1900 Å, lifetimes and oscillator strengths 80−14108
Al II to Al VI, beam-foil obs. from 300 to 2000 Å, mean lives and oscillator strengths 80−14109
Al II-VII, radiative lifetimes, beam-foil spectra 79−49986
Al IV, lifetimes of n=3 and 4 levels meas. and calc. *(French)* 80−9554
Al IV, transition probabilities and radiative lifetimes 79−76372
Al IV, V, beam foil spectra, 1100-1900 Å, lifetime meas. 78−70919
Al IX to Al XI, beam-foil obs. of lifetimes and oscillator strengths, 300 to 1000 Å 80−14110

radiative lifetimes continued
Al, oscillator strengths and radiative lifetimes 79−54811
Al XIII, $1s2p^3P_2$ and $1s2p^3P_0$ levels, radiative lifetimes and hyperfine induced decay 80−74149
Al^{7+}, $2s2p^3$ terms, mean lives, from beam-foil spectra 78−37601
AlD, $A'\pi$, spectral lifetime and predissociation 79−59515
AlGaAs DH, temp. depend. of intensities and times of radiative transitions 79−38660
(AlGa)As stripe geometry, proton-bombardment delineated DH laser, lifetime 80−106520
AlGaAs-GaAs heterostructures, luminescent characts., efficiency and radiative lifetime conc. depend. 80−55151
$Al_xGa_{2(1-x)}O_3:Cr^{3+}$, luminesc., lifetime, 77 and 4K, struct., energy transfer 79−28798
$Al_{2x}Ga_{2(1-x)}O_3:Cr^{3+}$, luminesc., lifetimes 79−33784
AlH, $A'\pi$, spectral lifetime and predissociation 79−59515
AlO, $B^2\Sigma$-$X^2\Sigma$, Einstein A coeffs., band strength and band oscillator strength 80−43113
α-$Al_2O_3:V^{3+}$, near IR spectra, line lifetime, 2, 10, 77K 78−10972
Ar, $3p^55p$ config. aligned in discharge, interf. signals, lifetimes and collision cross sections 78−70796
Ar atoms in Ne matrix, radiative and nonradiative lifetimes in excited states 80−69106
Ar, condensed, luminescence decay under α- and β-particle excitation 79−38678
Ar, condensed electron beam excited, exciton radiative lifetimes 80−6727
Ar high density plasma, highly excited atomic levels, spectral-line-blending study 80−48969
Ar, hydrogenlike, Lamb shift meas. by motional elec. field quenching time-of-flight expt. 80−9550
Ar II, lifetime meas. using photon-photon delayed coincidence 77−14389
Ar II, transition probabilities, lifetimes, intermediate coupling semiempirical calcs. 79−789
Ar II, transition probabilities and level lifetimes calc. 79−26935
Ar II arcs, transition probabilities, statistical inference 80−106357
Ar IV to Ar XII, beam-foil obs. of lifetimes and oscillator strengths, spectral identifications, 400-2000 Å *(French)* 80−9555
Ar, lifetimes of L and LM vacancy states, X-ray emission linewidth 78−17621
Ar, liquid and solid, absorpt. and luminesc. spectra of self-trapped excitons 79−65893
Ar, photoionisation, Auger processes, decay lifetime, line shift, profile, X-ray photoelectron spectra 80−37798
Ar radiative level lifetimes, photoionisation and photoexcitation rates, in shock tube 77−34594
Ar, trapping of nonreson. radiation, lifetimes of 4p and 5p levels 78−62766
Ar VIII, beam-foil lifetime meas. using ANDC anal. for reson. doublet 79−93964
Ar^{15+} and Ar^{16+}, beam-foil obs. of lifetimes of metastable states 80−14116
Ar^{x+}, high resolution spectroscopy of prompt and metastable decaying levels 78−33462
Ar+Kr, ($4p^55p$) and ($4p^55p'$) states, radiative lifetimes and two-body collisional deactivation rate consts. 80−95572
ArCl*, excimer formation rate consts., B state radiative lifetimes, quenching, VUV excitation 80−55631
Ar_2F excimer laser, electronic structure, pot. energy curves, radiative transition probabilities, quantum mech. calcs. 79−10284
Ar_2F^*, radiative lifetimes, quenching rate consts., emission spectra 78−46577
ArH^+, $^1\Sigma^+$ ground state, molecular consts. calc. from pot. curves 80−9680
ArI, transition probabilities calc. 80−32666
ArS, photoluminesc. in rare gas matrices 80−5568
Ar*(4p),(5p) states, lifetimes and two-body rate consts. meas. 78−63058
Ar($3p^5$, 4p) and ($3p^5$, 4p') states, radiative lifetimes, two-body deactivation rate consts. 79−10068
As, $4p^3$→$4p^25s$, transition probabilities 80−47943
As III, radiative lifetimes, calcs and beam-foil spectra 77−75223
B IV, V, beam-foil meas. of mean lives below 450 Å 78−90120
B-like ions, autoionisation states calcs. 80−43006
BH, $A^1\Pi$ state, fluoresc. decay radiative lifetime meas. 79−13771
BO, radiative lifetime, first excited state 78−62848
BO_2, radiative lifetime, first excited state 78−62848
Ba ($5d6p)^3D_3$ state, lifetime meas. by dye laser spectrosc. 80−78577
Ba II resonance level lifetime meas. by pulsed laser excitation of ion beam 78−25480
Ba^+, excited state lifetimes, fluoresc. decay meas. 77−79574
Ba^{++} ions confined in cylindrical RF trap, lifetime meas., laser probing 80−95573
Ba^{++}+Ba, $6p^2P$ level lifetimes, depolaris. cross-sections, Hanle effect obs. 79−26943
Ba_2^{2+}, very long lived vibr. states, lifetimes, WKB calc. 80−78560
BaO, excited electronic states, lifetimes and transition moments 80−87177
$^{138}Ba^+$, lifetime of $6p^2P_{3/2}$ level using stperilposed ion and lser beams 77−57933
Be isoelectronic sequence, highly ionised, beam-foil obs. of oscillator strengths for E1 transitions 80−14112
Be like ion, radiative decay of $2\ ^3P_0{}^o$ level 80−27984
Be sequence, $2s3p\ ^3P_1$-$2s^2\ ^1S_0$ intercombination line transition probabilities 80−18823
$BeF_2:Eu^{3+}$ glass, luminesc. of Eu^{3+}, transition probabilities 80−80845
Bi, radiative lifetimes of excited states 79−3410
Bi^+, radiative lifetimes of excited states 79−3410
Bi_2, lifetime and self-quenching cross sections meas. from laser induced fluorescence expt. 80−69189
$Bi_4Ge_3O_{12}$ crystals, doped with Dy^{3+}, Ho^{3+}, Er^{3+}, Tm^{3+}, Yb^{3+}, growth, spectral and laser props. 80−45115
^{209}Bi I, tunable CW dye laser spectroscopy, energy levels, lifetimes and hyperfine struct. 79−6905
Br_2, kinetics of excited states using laser excitation, radiative lifetimes and collisional deactivation 80−74237
Br_2, single rot. states, lifetimes and collisional quenching cross sections determ. by obs. fluoresc. decay 80−91595
BrCl, excited $B^3\Pi(0^+)$ state, laser-induced fluoresc., steady-state kinetics 78−66594
BrCl, time-resolved fluoresc. of $a^3\Pi_{0^+}$ state 78−63093
radiative lifetimes continued
BrF, $B^3\Pi(0^+)$ states, collision-free lifetimes laser fluoresc. obs. 78−94278
BrF, laser induced fluorescence 78−66591
BrF, laser induced fluorescence 78−66592
C foil, ion irrad., graphitisation rel. to lifetime, relevance to beam-foil spectroscopy 80−15166
C II, III, IV, radiative mean life meas. by beam-foil technique 78−90121
C IV (C V), UV line identifications and lifetime meas. 80−106288
C, radiative lifetimes of visible and near IR transitions, solar abundance 78−50506
C^{3+}, fine struct. and lifetimes, doubly excited quartet system 78−78827
C_2 vapour, Swan bands, oscillator strength 80−63712
C_2+acetylene, C_2 Swan band transition probabilities, collisional energy transfer effects 80−87214
C_3, ($^1\Pi_u$) radical excited state radiative lifetimes and the collisional deactivation 79−27018
CBr_2 emission in solid Ar, laser excitation spectra and lifetimes 80−48034
CBrCl emission in solid Ar, laser excitation spectra and lifetimes 80−48034
CF_2, fluoresc. and radiative lifetime obs. in dibromodifluoromethane UV laser photolysis 80−16703
CH, radiative lifetimes, electron-photon delayed coincidence meas. 78−50594
CH_2 radical, fluoresc. induced by laser 588.9-595.6 nm, (a^1A_1−X^3B_1) energy separation 78−42121
CH($A^2\Delta$) radicals, electronically excited, lifetimes and quenching rate constants meas. 80−69188
CHF radical, $\tilde{A}^1A''$-$\tilde{X}^1A'$ transition, laser induced fluoresc. 80−95660
$CH_2(b^1B_1)$, radiative lifetime from b^1B_1→a^1A_1 emission in electron irrad. methane 77−3476
CN, A- and B-state lifetimes, collisional transfers and perturbations 78−78756
CN, $B^2\Sigma^+$←$A^2\Pi$ 0-0 and 1-0 bands, laser excitation spectra 80−91588
CN, fluoresc. spectra, time resolved, radiative decay and radiationless deactivation in Ar 79−98142
CNN, matrix isolated, 3Π-$^3\Sigma^-$ system, laser-induced temporal and wavelength resolved spectra 77−83637
CN*, $B^2\Sigma^+$ state, fluoresc. decay dynamics, collisional quenching and radiative lifetimes 80−58306
CO, $b^3\Sigma^+$ state excitation, low-energy electron impact, $\nu'=3$ level lifetime 80−1072
CO, $d^3\Delta$ state, low energy electron impact excitation and radiative decay 80−91691
CO, fluorescence, lifetime meas. for rot. levels of (0,0) band, $A^1\pi$ to $X^1\Sigma^+$ transition 78−29808
CO, reson. transitions, radiative lifetimes, astrophys. appls. 78−62767
CO^+, $B^2\Sigma^+$ state, radiative lifetimes of 0, 1, 2, 3 vibr. levels, intensity decay meas. 79−98157
CO^+, fluoresc. spectra of ion beam, laser and electron excitation 79−45743
CO^+, vibr.-excited $A^2\Pi$ state, radiative and radiationless vibronic deactivation rates with He 79−10134
CO_2, 4854 cm^{-1} 201_{III}←000 band, intensities and half-widths, 197, 233, 294K 79−89713
CO_2, from collision induced absorption spectra, IR line broadening 78−33554
CO_2^+, radiative lifetimes, threshold electron-phonon coincidence meas. 78−13550
$C^3\Pi_u$ effective lifetime in N and air 80−102704
CS, $A\ ^1\pi$ state, collisional transfer and radiative decay, time resolved obs. 79−89809
CS, $A^1\Pi(v=0)$, radiative lifetimes and quenching rates, laser-induced fluoresc. obs. 79−59496
CS, nonexponential decay of $a^3\Pi$-$X^1\Sigma^+$ luminesc., Π sublevel radiative lifetimes, matrix isolated spin-orbit 79−89699
Ca, $4p^2\ ^1S_0$−$4s4p\ ^1P_1$−$4s^2\ ^1S_0$ cascade rate, two photon coincidence meas. technique 80−95576
Ca, $4s4p\ ^1p_1$ level Hanle effect density depend., lifetime 80−91494
Ca, atoms and ions, radiative lifetimes of excited states *(Russian)* 78−13472
Ca, forbidden transitions, radiative lifetimes, MCSCF and CI calcs., time of flight spectra for metastable state 80−91498
Ca II, lifetime extraction from beam-foil decay curves 80−14107
Ca+He, $^1P_1$ level lifetime, Hanle measurement 80−23365
$CaF_2:Ho^{3+}$, fluoresc., relative intensities, lifetimes 78−27296
CaF_2:Na, γ-irrad. cryst., spontaneous and induced colour centre emission 79−7131
CaO, photoionisation of F-centre, luminesc. and photocond. meas. 80−66270
Ca($4p\ ^3P_1$)+Ba, collisional deactivation and optical lifetime 80−48070
Cd,(4s7r),(5r6d),(5r7d) configs., triplet states lifetimes 77−3326
Cd, $5,6,7^1D_2$→5^1P_1 transition probabilities meas. be US pulverisation/flame emission *(French)* 80−42995
Cd, 6^1P_1 level, relax. of alignment and population 78−70795
Cd I, excited states radiative lifetimes 80−942
Cd $K\beta_3$I$K\beta_1$ and $K\beta_2$I$K\beta_1$ relative intensities 77−75088
Cd, transition probabilities, 5^1P_2 level lifetime meas. 80−91500
Cd_2,(Cd_3), fluoresc. kinetics, optical excitation, energy spacings and equilib. consts. 80−43090
CdH, lifetime, Λ-doubling and hyperfine struct. of $A^2\Pi$ excited states 77−58083
CdHg, fluoresc. kinetics, optical excitation, energy spacings and equilib. consts. 80−43090
Cd($^3P_1$) radiation imprisonment lifetime, inert gas effect, phase-shift method 80−58213
Ce_3 F states, radiative lifetime and g-factor determ. 79−41138
Ce^{3+} impurities in cubic crystals, 5d→4f radiative transition probability calc. 80−71474
Cl (IX-XV) allowed intra L-shell transitions, oscill. strengths and radiative lifetimes meas. 79−13676
Cl, core polarisation effects on transition probabilities 79−89638
Cl ions, multiply-charged, beam-foil obs. of allowed L-shell transitions 80−14113
Cl XIII-XV, $\Delta n=0$ transitions, lifetime meas. beam-foil spectra 78−78798
Cl^+, laser levels, radiative lifetimes meas. 78−42330
Cl^{16+}, Lamb shift meas. using beam-foil excitation, QED test 80−9551

radiative lifetimes continued
Cl^{n+}+Cu, effect on projectile charact. X-rays and REC of target thickness 79−45662
Cl^{q+}+Cu, K X-ray production and radiative electron capture, fluoresc. yield determ. 80−99553
Cl_2, and isotopic forms, $B^3\Pi(0_u^+)$ state, laser-induced fluoresc., collisional energy transfer rates 80−53038
Cl_2, fluoresc. quenching by collision induced piedissoc. 77−14472
Cl_2, laser-induced fluoresc., excited $B^3\Pi(O_u^+)$ states, collision-free lifetimes of ro-vibr. levels 79−94029
ClCF radical in solid Ar, emission and excitation spectra, vibr. anal. 78−9164
ClFCS, second excited singlet state photophysics, laser excitation obs. 80−32758
ClO_2, predissoc. mechanism determ. from rot. level lifetimes 79−13732
Cn free radical, $B^2\Sigma^+$ state lifetime, photon-photon cascade meas. 78−5273
Co, fluoresc. of interstate intramol. perturbations 79−41194
Co I, multichannel anal. techniques, appl. to beam-foil spectroscopy, 3000-3950 Å, lifetimes 77−58206
Co I and Co II, beam-foil obs. of lifetimes 80−14111
Co, radiative lifetimes and election ilpact absolute emission cross-sections 77−88503
Co, rel. at. transition probabilities, by flame at absorption spectroscopy 79−89642
Cr $^7P_0^0$ state, radiative lifetime in matrices, meas. using laser ablation and selective excitation 80−71959
Cr, radiative lifetimes, laser ablation and selective excitation spectroscopy 78−17824
Cr, rel. at. transition probabilities, by flame at absorption spectroscopy 79−89642
Cs, 85 level lifetime meas., cooperative effects in EM cascade 77−30818
Cs atom, direct meas. of 7P doublet state lifetimes by pulsed dye laser 79−786
Cs, cascade-free radiative lifetime, modulated or deflected CW dye laser method determ. 78−25754
Cs I, radiative lifetime of 8S, 9S and 7D levels 77−34588
Cs II, radiation lifetimes of excited states 80−9558
Cs, natural and effective lifetimes meas. for 10 P states 79−26934
Cs, resonantly excited in cylindrical discharge plasma, effective lifetimes 78−79413
Cs^+ excited levels, hyperfine struct. and lifetimes 80−63590
Cs-Xe, molecular bands, time-resolved fluoresc., lifetimes 77−58068
CsI, self-trapped exciton electronic struct., semi-empirical mol. orbital method 80−49605
Cu I, radiative lifetime meas. 79−3409
Cu IV, wavelength region 700-1200 Å, extended analysis 80−99473
Cu, isoelectronic series, semi-empirical oscillator strengths, lifetime, transition probability 80−32672
Cu^{18+}, Na-like, low-lying levels, radiative lifetimes, f-values obs. 78−25482
Cu-like ions, E1 transitions, wavelengths, oscillator strengths and transition probabilities, data tables 80−37780
CuCl, time resolved exciton-biexciton transitions, UV excitation, luminescence spectra 79−69883
CuF, from gas phase reaction, photon yields, chemi- and photo-luminesc., excitation spectra 79−5157
D_2, Lyman bands, morse Franck Condon factors and centroids 77−58088
$DBr(A^2\Sigma^+)$ vibrational states, lifetimes, emission cross-sections, prod. by electron impact 77−3419
Dy I excited states, lifetime meas. using single photon counting method 78−70793
$ErCl_3(AlCl_3)_x$, vap. complexes, absorpt. spectra, 6000-44000 cm^{-1}, relax. props. 78−62799
Eu chelate, fluoresç. lifetime, depend. on optical environment 80−9630
Eu II, lifetimes of $^7P_{2-4}$, $^9P_{3-5}$ excited levels 79−3407
Eu^{2+} impurities in cubic crystals, 5d→4f radiative transition probability calc. 80−71474
Eu^{3+}, nonradiative $^5D_1$-$^5D_0$ transition in various solvents 79−3479
Eu(III) complexes, f-f transition probabilities, ligand polarisation model, anisotropic contribs. 80−53049
EuP_5O_{14}, luminesc. of Eu^{3+}, transition probabilities 80−80845
F I, reson. transitions, radiative lifetimes, astrophys. appls. 78−62767
F II to VIII, mean lives, beam-foil spectrum in far UV 79−59389
F III, IV, beam-foil spectra, mean lives, 2150-3200 angstrom 78−55224
F, spin-orbit splitting and $^2P_{1/2}$ radiative lifetime, absorpt. spectrosc. meas. 80−87063
Fe I levels, mean radiative lifetimes determ. 79−49987
Fe II, Fe III, lifetimes, VUV beam-foil spectroscopy 79−22657
Fe, rel. at. transition probabilities, by flame at absorption spectroscopy 79−89642
Fe XXII, allowed transition CI wave functions, oscill. strengths and transition probabilities 80−32664
Fe XXII, intercomb. transitions, oscill. strengths, transition probs., rel. to solar spectra 80−52935
Fe XXIII and XXIV, reson. and intersystem transitions, oscill. strength, lifetime, beam-foil spectra 78−82685
FeV and VI, beam-foil lifetime meas., 1100-1900 Å 80−23532
Ga I, radiative lifetimes, calcs. and beam-foil spectra 77−75223
Ga II, $4s4d\,^1D$ and $4p^2\,^1D$ energies and lifetimes 79−59391
Ga, oscillator strengths and radiative lifetimes 79−54811
$Ga_{0.5}Al_{0.5}As$-GaAs(:Ge) DH structure, minority carrier lifetime and internal quantum efficiency of surface-free GaAs 79−43013
GaAs, acceptor bound exciton Auger and radiative transition rates, radiative recomb. 80−6733
GaAs, doped, radiative lifetimes, quantum mechanical model 80−55151
Gd atom, long-lived autoionisation state *(Russian)* 78−94216
^{155}Gd $L_{2,3}$ subshell X-ray fluorescence and Coster-Kronig yields from ^{155}Eu decay 80−69102
Ge II, radiative lifetimes, calcs. and beam-foil spectra 77−75223
Ge IV spectra, nonrelativistic oscillator strengths calcr. 77−83538
GeF, $A^2\Sigma^+$ state, time-resolved fluoresc. 78−58732
H, beam foil excitation, n=2 density operator and prod. probability meas., transition probabilities 80−14219
H like, metastable 2S state in weak elec. field, radiative decay, bound state QED 80−42959
H-like, average spectral lifetime, asymptotic expression 79−45671
H_2, $c^3\Pi_u$ metastable state, fine struct. lifetimes 79−64050
H_2, $E,F^1\Sigma_g^+$ state, collisional and radiative props. 80−58357
radiative lifetimes continued
H_2, electron impact, H_α and H_β lines emission, intensity decay curves meas. 80−83505
H_2, electron impact excited singlet-g states, optical and time resolved spectra, radiative lifetimes, quenching rates for rovibronic levels 80−23564
H_2, excited levels, lifetimes, measurement by photon-photon delayed coincidence technique 79−89640
H_2, from collision induced absorption spectra, IR line broadening 78−33554
H_2, Fulcher bands, radiative decay consts. 79−22722
H_2, Lyman gands, Morse Franck Condon factors and R-centroids 77−58088
H_2 predissociation probabilities of $4p\pi\,^1\Pi_u^+ v' \geq 1$ levels, dissoc. channels interference 80−28074
HB rot. relaxation, diffusion theory 80−106313
HBr ($A^2\Sigma^+$) vibrational states, lifetimes, emission cross-sections, prod. by electron impact 77−3419
HCl, rot. relaxation, diffusion theory 80−106313
HCl, transition probabilities, IR chemilum. obs. of form. channels in H+ClF reaction 80−26017
$HCl\text{-}Bi^{3+}$ soln., luminesc., quantum yield and lifetime *(Russian)* 79−33834
$H_2(E,F^1\Sigma_g^+)$, two-photon excitation, cross section, radiative lifetime, quenching rate, IR fluoresc. obs. 78−37698
HF, electron impact excitation, dissoc., emission spectrum 78−90305
HF, transition probabilities, IR chemilum. obs. of form. channels in H+ClF reaction 80−26017
$HNO(A^1A'')$, state-selected fluorcsc. lifetimes, collisional quenching rates 79−36674
H_2O^+, vibronic A^2A_1 states, lifetimes, delayed coincidence meas. 78−70874
$HbBr(B^2\Sigma^+_{1/2})$, rate coeffs. for collisional quenching, time resolved emission obs. 79−89705
$H_2(c^3\pi_u)$, theoretical radiative lifetime, from mag. dipole, elec. quadrupole interaction 78−33553
He and He^+, 3^3P and 4^2F levels excitation with electron beams, radiation decay obs. 80−43188
He, excited S, D and F state radiative lifetimes, electron impact method 78−94325
He I, 4^1F and 5^1F lifetimes 78−37599
He, I excited states decay, lifetime meas., lab. mag. fields effects 77−10640
He, lifetimes of doubly excited states, autoionisation and radiative decay 79−18146
He^+, lifetime of metastable state, ion beam meas. 78−55141
He-like ions, 2^3P_0-1^1S_0 and 2^1P_1-1^1S_0 freqs. and transition rates, relativistic calc. 79−68210
He-N_2 plasma, N_2 $B^3\Pi_g$ state excitation, role of long lived states, luminesc. 80−37829
He+Ne^+, impact excitation, cascade-fluorescence spectroscopy, level-crossing techniques 80−23357
$He(2^1S, 2^3S)$+$Ne(e^-)$, transition probs., pots. 80−58371
Hg, 6D levels excited by dye laser, lifetimes 80−42996
Hg II, $6p^2P$ and $6p^2D$ levels, radiative lifetimes meas. 80−78576
Hg, lifetimes and cross sections of depolaris. collisions of laser working levels 79−76387
Hg, positive column of discharge, alignment of Hg levels meas. 78−83639
HgBr, ab initio CI calcs., spectroscopic parameters 79−72245
HgBr, B→X transition radiative lifetime, charge transfer model 78−17719
$HgBr_2$, UV absorpt. cross-sections of vapour 78−25554
$Hg_{1-x}Cd_xTe$, acceptor bound exciton Auger and radiative transition rates, radiative recomb. 80−6733
HgCl, ab initio CI calcs., spectroscopic parameters 79−72245
HgCl, $B^2\Sigma^+$ state, produced in photochem. of $Hg/Cl_2/Ar$ 79−39154
HgCl, B→X transition radiative lifetime, charge transfer model 78−17719
HgCl laser, HgCl(B) state radiative lifetime meas. 78−94390
HgD, $A^2\Pi$ state radiative lifetime, pulsed dye laser excitation meas. 78−94288
HgH, $A^2\Pi$ state radiative lifetime, pulsed dye laser excitation meas. 78−94288
HgI, B-state radiative lifetime, determ. by photolysis of HgI_2 79−10130
HgI, B→X transition radiative lifetime, charge transfer model 78−17719
HgI_2, UV absorpt. cross-sections of vapour 78−25554
Ho I, Ho II, excited level lifetimes and oscillator strengths, visible spectra 80−63573
^{155}Ho $L_{2,3}$ subshell X-ray fluorescence and Coster-Kronig yields from ^{165}Er decay 80−69102
Hz, 3d complex, radiative lifetimes, hyperfine constants 78−70873
I I,II, radiative lifetime meas., rel. to I and He-I^+ laser transitions 79−54810
I VI and I VII, beam-foil obs. of lifetimes, spectral assignments, 400 to 1300 Å 80−9556
I VII, beam-foil lifetime meas., cascading problem 80−14249
I_2, dynamic friction coeff. meas. by saturation spectroscopy, radiative lifetimes 78−18368
I_2, in CCl_4 and cyclohexane solns., higher vibr. levels, dephasing lifetimes, from reson. Raman spectrum 78−42068
$IBr(B^3\pi_0^+)$, lifetimes determ. from time resolved fluoresc. 78−46385
ICl, lifetimes of $A^3\Pi_1$ state vibr. levels, 6070-7300 Å 78−66605
$ICl(A^3\Pi_1)$, zero-press. lifetimes, fluoresc. quenching 79−68266
IF, $B^3\Pi(0^+)$, radiative and predissoc. lifetimes, laser-induced fluoresc. 79−31589
IF emission spectrum and form. kinetics in electron-beam-produced plasma 80−102533
$I(^2P_{1/2})$+n-iodopropane (iodoethane), quenching rate coeff., in UV photolysis of n-iodopropane (iodoethane) 79−11799
In I, radiative lifetimes, calcs and beam-foil spectra 77−75223
In $K\beta_3/K\beta_1$ and $K\beta_2/K\beta_1$ relative intensities 77−75088
In, oscillator strengths and radiative lifetimes 79−54811
InP, luminescence, hot electron effects 80−66277
^{215}In, $8P^2P_{3/2,1/2}$, HFS and lifetimes, fluoresc. decay and quantum heats, beam 80−32657
Ir I, radiative lifetimes, beam-sputtering technique meas. 79−18142
K I isolectronic sequence, transition probabilities, cancellations 80−91503
K, resonantly excited in cylindrical discharge plasma, effective lifetimes 78−79413

radiative lifetimes continued
K, s and d state radiative lifetimes, time and wavelength resolved fluoresc. spectra 80−14104
K^+, direct excitation of levels, transition probs. and cross sections 80−37890
K_2, $B^1\Pi_u$ state lifetimes, Hanle effect 78−90218
K_2, in discharge plasma, anomalous 5725 Å band, photorecomb. mechanism 79−50088
KBr, F-centre radiative lifetime meas. near 65K 80−25439
KBr:Br_2^-, triplet luminesc. kinetics, 0.4-4.2K 79−87482
KBr:Tl, luminesc., decay model for A_T and A_X emissions 80−93379
KCl, absence of energy transfer between F- and M-centres 79−99935
KCl:Pb, photoluminesc. induced by Suzuki-like occlusions, ionic thermocond. 79−33808
KI:I_2^-, triplet luminesc. kinetics, 0.4-4.2K 79−87482
KI:In^+, luminesc. decay, excited state symm. and g-value 79−99922
KI:Sn^{2+}, red emission, mag. field effect on radiative decay time 79−33818
KI:Sn^{2+} luminesc. decay, excited state symm. and g-value 79−99922
$KMgF_3$:Ni, Co, emission from Ni-Ni and Ni-Co pairs, exchange coupling const. 79−33788
$K_5NdLi_2F_{10}$ (KNLF), spectroscopy and lasing 80−5737
KXe, dye laser induced emission, excimer bands and uses 80−9650
KY_3F_{10}:Eu^{3+}, fluoresc. decay, radiative and nonradiative transition probabilities 78−72581
Kr, 6p levels, two-photon excitation, time resolved fluoresc., quenching, lifetimes and photoionisation cross section 80−78587
Kr atoms in Ne matrix, radiative and nonradiative lifetimes in excited states 80−69106
Kr, fluoresc. lifetimes, time resolved VUV spectra 78−17601
Kr I, transition probabilities in transition arrays 80−32667
Kr I atom, $4p^5$ nd (n=4,5,6,7) configurations, experimental lifetimes 80−27981
Kr I electric dipole lines, absolute transition probabilities 80−9560
Kr II, calcs. of radiative lifetimes, absolute transition probabilities and oscill. strengths 77−50405
Kr II, excited levels, lifetimes, measurement by photon-photon delayed coincidence technique 79−89640
Kr, liquid and solid, absorpt. and luminesc. spectra of self-trapped excitons 79−65893
Kr plasma, of positive column, at. alignment, radiative lifetimes, collision cross sections 79−4203
Kr, reson. levels relax. consts. determ. by alignment method in discharge 79−26936
Kr VII, beam-foil excitation, $4s4p\ ^1P_1{}^0$ level decay simulation 80−78578
Kr VIII, beam-foil decay curves for reson. transitions simulation 80−9721
Kr VIII, beam-foil lifetime meas. using ANDC anal. for reson. doublet 79−93964
Kr XXXIII and Kr XXXIV, beam-foil obs. of transition wavelengths and oscillator strengths 80−14115
Kr_2, prod. and decay of 0_u^+ and 1_u states, synchrotron excited 80−43109
KrCl*, excimer formation rate consts., B state radiative lifetimes, quenching, VUV excitation 80−55631
KrF, ab initio CI calcs. 77−38619
KrF_2 radiative lifetime and quenching 78−63063
KrF* radiative lifetime, pulsed photolysis obs. 78−29819
KrF(B), excimer, collisional quenching rates, photolysis meas. 78−63066
Kr_2F^*, radiative lifetime and quenching rate consts. 78−63056
KrI, $4p^55p$ and $4p^56p$ configs., level radiative lifetimes meas. 78−58625
KrS, photoluminesc. in rare gas matrices 80−5568
Kr_2^*, radiative lifetime and quenching rate consts. 78−63056
Kr_2^*, VUV time resolved spectra, formation and decay kinetics 79−31544
La II $y^3F_{4,3,2}{}^0$ levels, lifetime meas. using beam-laser method 77−30827
La^+, cascade free lifetime meas., beam-laser method 78−17618
$LaBr_3$:U^{3+}, luminesc., fluoresc. lifetimes 79−33768
LaF_3:Dy^{3+}, laser excited fluoresc., lifetimes meas. 79−24353
LaF_3:Nd^{3+}, radiative transition rates of Nd^{3+}, Judd-Ofelt theory 79−33753
LaF_3:R^{3+}, R=rare earths, crystal field anal., intensity calcs. 80−100670
La_2O_2S:Eu, high press. effect on luminesc. efficiency and lifetime, charge transfer absorpt. 80−66266
Li, differential meas. using atomic ionoluminesc. 79−13672
Li, excited-state lifetime meas. using disc-shaped heat-pipe oven 80−52941
Li I, $2s^2sp$ and $1s2s^2$ decay rates many-body perturbation theory calc. 79−59376
Li, lifetime of $1s2p^2\ ^2P$ state, radiative autoionisation 78−78665
Li^+, 2^3S_1 metastable state radiative lifetime, fluoresc. meas. 80−42999
Li_2, $A^1\Sigma_u^+$-$X^1\Sigma_g^+$ band system transition dipole moments and radiative lifetimes, model pot. calcs. 78−9160
Li_2, radiative lifetimes of $B^1\Pi_u$ states, model pot. calcs. 78−46397
LiCl, radiation effects on decay time of F-centre emission 80−93381
LiF:U^{3+}, absorption and laser-excited fluoresc. 79−99927
^{7}Li, 2^2P and 3^2P states, level crossing method 78−66678
^{7}LiH, radiative lifetimes for vibr. levels of $B^1\Pi$ state 78−78753
Mg (Mg^+), lifetime meas., beam foil spectra, comparison with numerical coulomb approx. calc. 80−58367
Mg, Hanle effect density depend., $3s4p\ ^1P_1{}^0$ level, and oscill. strengths 79−72282
Mg I, ^{3}p triplet system, lifetime meas. 80−47946
Mg I fluoresc. lines polarisation and mag. depolarisation *(German)* 77−6719
Mg III, radiative lifetimes calc. 79−98037
Mg porphyrins, additional ligands deuteration effect on luminesc. characts. 79−99932
Mg, reson. line, Hanle effect, density depend. 79−6917
Mg^{++}, $2p^2np$-$2p^2ms$ (n=3, 4; m=3,4,5) transition probabilities calc. 79−6915
Mg_{9+}^{6+}, $2s2p^3$ terms, mean lives, from beam-foil spectra 78−37601
Mg^{9+}, beam-foil excited, spin orbit-forbidden X-ray transition obs. 80−23537
MgD, $A^2\Pi$ state radiative lifetime, pulsed dye laser excitation meas. 78−94288
MgH, $A^2\Pi$ state radiative lifetime, pulsed dye laser excitation meas. 78−94288
MgH, and MgD, $B'^2\Sigma^+$-$X^2\Sigma^+$ band system, ab initio CI calcs. 79−93970
radiative lifetimes continued
MnI, transition probability and solar abundance, beam foil TOF meas. 79−40154
Mo I spectrum, lifetime meas. of excited states of $4d^55p$ and $4d^45s5p$ config. 79−13683
Mo^{13+}, energy levels for transition probabilities, oscillator strengths, rad. lifetimes 78−17589
Mo^{32+}, dielectronic recomb. rate coeffs. in plasma 80−43853
Mo^{38+}, dielectronic recomb. rate coeffs. in plasma 80−43852
N, high Rydberg states, radiative decay rates, TOF meas 78−46302
N I plasma jet, spectroscopic diagnostics, Stark broadening and shift, study 80−38727
N, radiative lifetimes of visible and near IR transitions, solar abundance 78−50506
N V, beam-foil decay curves, mean lives determ. 80−9553
N^{4+}, fine struct. and lifetimes, doubly excited quartet system 78−78827
N_2, $^5\Pi_g$-$^5\Sigma_g^+$ transition, MC-SCF calcs. 79−76412
N_2, ($C^3\Pi_u$) state, radiative lifetime, collisional quenching, pulse radiolysis meas. 78−29813
N_2, electron excitation of Birge-Hopfield bands ($b^1\pi_u$-$X^1\Sigma_g^+$) 80−95731
N_2 in Ar matrix, luminesc. lifetime 79−36690
N_2^+, radiative lifetime of $B^2\Sigma_u^+$ state 78−90220
N_2-CO-OCS, liq. mixture, vibr. energy relax. and exchange, laser induced fluoresc. obs. 78−70905
N_2-He ion nuclear pumped lasers feasibility study and quenching 80−64001
N_2^+($B^2\Sigma_u^+$, ν'=0), in N_2 laser transitions 79−27246
N_2($C^3\Pi_{u1}$ ν'=0,1), in N_2 laser transitions 79−27246
ND, $b^1\Sigma^+$ state, radiative lifetime, Einstein coeff. 78−90217
NH, $b^1\Sigma^+$ state, radiative lifetime, Einstein coeff. 78−90217
NH, radiative lifetimes, electron-photon delayed coincidence meas. 78−50594
NH_2 (A^2A_1), excited state dynamics and bimol. quenching processes 80−9681
NO, $3s\sigma(A^2\Sigma^+)$, in Al Kl Xe matrices, Rydberg state 'bubbles', reson. fluoresc. obs. 77−83636
NO, $A^2\Sigma^+$ two photon excitation, radiation lifetime, quenching 77−3426
NO $C^2\Pi(\nu'=0)$, lifetime meas., predissoc. and non-predissoc. rot. levels 78−62849
NO, measured lifetimes of $A\ ^2\Sigma^+$, $D\ ^2\Sigma^+$ and $C\ ^2\Pi$ states 78−90219
NO_2, coherence time rel. to radiative lifetime, theory 79−18240
NO_2, laser excited fluoresc. lifetime 79−50076
NO_2, laser-induced fluoresc. quenching rate const. and lifetimes 80−11930
NO_2, perturbed $^2B_2$ state fluoresc. lifetime, excitation energy depend. 78−90202
NO_2, rot. cooled, vibronic band lifetimes, time resolved fluoresc. excitation spectra obs. 79−94025
N_2O, electron impact ionisation and dissociation, radiation emission 78−90304
N_2O^+, fluoresc. and dissociation lifetimes of vibr. excited states 78−42108
NO($A^2\Sigma^+$, ν'=0,1,2) lifetimes, $A^2\Sigma^+$-$X^2\Pi$ transition moment, oscill. strengths, internucl. separation depend. 78−82787
Na, energy transfer with 3P-excited atoms, fluoresc. spectrum 78−66498
Na II, radiative lifetimes calc. 79−98037
Na II, spectrum, config. superposition and transition probabilities calcs. 80−87082
Na like ions, dielectronic recombination rate, scaling props. 80−32668
Na, np radiative lifetimes, effect of blackbody radiation 79−41127
Na, rel. at. transition probabilities, by flame at absorption spectroscopy 79−89642
Na, reson. light scatt., theory of correl. meas. 78−42014
Na, spectra, emission and absorpt., inert gas matrix 78−90106
Na V(VI)(VII), beam-foil spectra, extreme UV mean lifes and oscillator strengths 79−31456
Na+N_2, collisional deactivation of Na excited states, time resolved fluoresc. 78−42197
Na_2, laser excited, atomic and molecular fluorescence with long radiative decay times 80−27976
NaBr:Cu^+, luminesc. and lifetimes, press. depend. 79−33809
NaCl:Cu^+, luminesc. and lifetimes, press. depend. 79−33809
NaH, $A^1\Sigma^+$ states radiative lifetime in HF discharge 77−6841
NaI-SVI isoelectronic series, radiative lifetimes calc. 79−72276
NaK, mol. transition dipole moment, from laser-induced fluoresc. spectra 79−94034
$NaPO_3$:Eu^{3+} glass, luminesc. of Eu^{3+}, transition probabilities 80−80845
N_2($a'^1\Sigma_u^-$) state radiative lifetime, VUV emission 79−18226
Na(3^2P), in O_2-H_2-Ar flame, atm. press., lifetime obs. 79−39149
NdP_5O_{14}, fluoresc. lifetime meas., IR and photoacoustic spectroscopy 80−60652
Ne $^3P_1$ state, radiative decay time 79−72277
Ne ($2p^53p$) states, radiative lifetimes, collisional deactivation rate consts. 80−69107
Ne, beam-foil excited ^4P state, delayed coincidence Auger electron lifetime meas. 80−14117
Ne I, transition probabilities in const. elec. field 80−37785
Ne I isoelectronic series, radiative lifetimes calc. 79−98037
Ne II, 2p43p levels, perdiative lifetime by delayed coincidence method 77−83545
Ne II, radiative lifetime and transition probability calc. 79−3408
Ne II, transition probabilities, lifetimes, intermediate coupling semiempirical calcs. 79−789
Ne, liquid and solid, absorpt. and luminesc. spectra of self-trapped excitons 79−65893
Ne, Townsend discharge afterglow, decay rate of metastable ats. 80−44011
Ne^{4+}, $2s2p^3$ terms, mean lives, from beam-foil spectra 78−37601
Ne-like ions, E1 and M2 transitions, HF calcs. 79−59401
Ni I, UV lines, oscillator strengths from hook method and absorpt. meas. in furnace 80−83319
Ni, rel. at. transition probabilities, by flame at absorption spectroscopy 79−89642
Np I, first ionisation pot., radiative lifetimes, high-lying energy levels, laser spectroscopy 79−76370
O, beam-foil excited ^4P state, delayed coincidence Auger electron lifetime meas. 80−14117
O, beam-foil spectra, multiply ionised O 80−42977
O II, III, IV, beam-foil spectra, mean lives, 270-490 angstrom 78−55223

radiative lifetimes continued
O II, relative intensities and lifetimes in nebulae, conventional radiation theory 80−109513
O IV bound states, oscillator strengths and photoionisation cross sections 80−106293
O IV(VI), circular polarisation of light emitted in beam-foil collisions, cascade free lifetimes 78−55228
O, radiative lifetimes of visible and near IR transitions, solar abundance 78−50506
O V, E1 transition probabilities, lifetimes, CI calc. 80−83321
O^{5+}, fine struct. and lifetimes, doubly excited quartet system 78−78827
O_2 in chloroform and carbon tetrachloride solns., sensitized luminesc. 80−32762
O_2, lifetimes and reactivity in aq. micellar system 78−46398
O_2 molecule, effect of spin orbit interaction on magnetic dipole transition intensity *(Russian)* 79−6948
O_2, singlet state lifetime in D_2O soln., decay of micellar system 78−46301
O_2 singlet state radiative lifetime, perturbation-variation calc. 77−14496
O_2^+, absorpt. linewidth of predissociated levels, lifetimes 79−36711
O_2^+, radiative lifetimes and UV spectra, $b^4\Sigma_g$-$a^4\Pi_u$, $A^2\Pi_u$-$X^2\Pi_g$ transitions 78−17724
OCSe, quantum yields for Se, $^1S_0$, $^1D_2$, and $^3P_{0,1,2}$ atoms determ. in photolysis, lifetime and quenching rate meas. 80−97741
OH, A-X system, rot. transition probabilities 80−43027
OH Meinel bands, in airglow, rot. temp., radiative lifetime 78−61643
OH, radiative lifetimes of $A^2\Sigma$ state and A-X Einstein coeffs. 79−36703
OH^+, $^3\Pi_i$ state, lifetime, delayed coincidence meas. 78−70874
$OH(C^2\Sigma^+)$, prod. by water radiolysis, time-resolved emission, quenching rate consts. 79−10138
$O(^1S)$, prod. and props. in liq. Ar and N_2, by N_2O photodissociation 80−43063
$O(^5S)$ metastable state, via 1356 Å radiation, time-of-flight technqiue 78−74614
O_4* van der Waals complex, radiative lifetime, dimole intensity press. depend. 78−58741
$O_2(c^1\Sigma_u^-, C^3\Delta_u, A^3\Sigma_u^+)$ generation from at. recomb. in O_2-He afterglow, fluoresc. obs. 79−31576
P, highly ionised, beam foil radiative lifetimes and EUV spectrum 80−32671
P II, reson. transitions, radiative lifetimes, astrophys. appls. 78−62767
PH, $(b^1\Sigma^+)$ state, radiative lifetime, time resolved spectra 78−78750
$POCl_3$:Pr^{3+}, fluoresc. and lifetimes of excited states 80−71466
Pb I and II, transition probabilities, Stark broadening parameters 80−23367
PbF, laser-induced fluoresc. of $A^2\Sigma$ state, chem. laser eval. 79−81222
PbO, vapour, photoluminescent decay, a(1) state 78−58745
PbS, molecule, Ne matrix environment effects on vibronic emission systems 77−58070
$PbS_{1-x}Se_x$ thin film, stimulated emission, temp. depend. 80−66232
Pt I, radiative lifetimes, beam-sputtering technique meas. 79−18142
Rb F states, highly excited, natural radiative lifetime meas. 79−3404
Rb, highly excited P-states, national radiative lifetimes 77−6727
Rb II, lifetimes in $4p^55p$ config., precision meas. and calc. 80−102488
Rb, radiative lifetime, time resolved laser induced fluorescence 80−37781
Rb, radiative lifetimes up to n=12 excited states, pulsed dye laser and superradiance excitation 80−83322
Rb, radiatively excited states, ionis. rate coeffs. in two atom collisions 80−43160
Rb, resonantly excited in cylindrical discharge plasma, effective lifetimes 78−79413
Rb^+, levels direct excitation, cross sections and transition probabilities determ. 80−52899
^{85}Rb, $5^2P_{3/2}$ state, Hanle effect *(French)* 78−42018
$RbMnF_3$:Fr, pure and doped, unirradiated and electron irrad., energy transfer 80−108254
$Re_2Cl_8^{2-}$, in acetonitrile and dichloromethane solns., 300K, emission spectra and lifetimes 79−59447
Ru complex, Ru(II)-polypyridine, excited charge transfer states, multiple emissions 79−3468
Ru complexes, luminescent, non-radiative pathways in solvents 77−3393
Ru complexes, $Ru(bipy)_3Cl_2.6H_2O$ and $Ru(bipy\text{-}d_8)_3Cl_2.6H_2O$, soln. electronic excitation energy, deactivation determ. 80−55173
S, core polarisation effects on transition probabilities 79−89638
S I, (II), (III), reson. transitions, radiative lifetimes, astrophys. appls. 78−62767
S III-VI, spectra, 1050-5500 Å, beam-foil expt. with 100-700 keV ions 78−50495
S IV, $3s^23p^2P$-$3s3p^2\ ^4P$ multiplet, energy levels and transitions, appl. to solar atm. 80−87028
S V, VI, beam-foil spectra, radiative lifetimes, oscillator strengths 77−30973
S VII, vuv beam-foil spectrum, lifetimes 79−81174
S^{6+}, spectra, 500-1200 Å, lifetimes 78−62756
S^{n+}, beam-foil UV spectra, elec. dipole transition probabilities, radiative lifetimes 77−6730
S_2, fluoresc. quenching by He, Ar, Xe, N_2, S_2, CF_4, C_2F_6, fluoresc. lifetimes 78−46386
SF_6+$Li^+(H^+)$, mode selective vibr. excitation 80−58351
SO_2, UV absorpt. spectrum, triplet states, phosphoresc. lifetime 79−50042
SO_2+alkane, $^3B_1$-state lifetime saturation, chem. and phys. quenching channels 79−814
$S(^1S)$, prod. and props. by OCS photodissociation in liq. Ar and N_2 80−43064
Sb, excited state lifetimes, crossed at. electron beams obs. 79−790
Sb II, radiative lifetimes meas. 79−54813
Sb III, radiative lifetimes, calcs and beam-foil spectra 77−75223
Sb $K\beta_3$|$K\beta_1$ and $K\beta_2$|$K\beta_1$ relative intensities 77−75088
SbI, ^2D state radiative lifetimes 79−3381
SbI, decay branching ratios meas., transition probabilities derivation 80−95642
SbII, ^3P, ^3D state radiative lifetimes 79−3381
Sc, rel. at. transition probabilities, by flame at absorption spectroscopy 79−89642
Se, exciton luminesc. in trigonal form 79−33802
Se IV, radiative lifetimes, calcs. and beam-foil spectra 77−75223
Se_2, photolysis by UV lasers, appl. to kinetics of group VI laser systems 80−7807
Se_2, photolytic dissoc. obs. using inert gas halide lasers 80−11935
SeO_2+$Ar(N_2)(CO_2)$, radiative lifetime and quenching rates 80−95685
Si, amorphous, photoluminesc. and radiative lifetimes 79−61419
Si, excited states lifetimes, fluoresc. decay curves 80−58175
Si, highly ionised, beam-foil lifetime obs. 80−32670
Si II, reson. transitions, radiative lifetimes, astrophys. appls. 78−62767
Si, III, IV, beam foil spectra, radiative lifetimes, oscillator strengths 77−30973
Si ions, multiply-charged, beam-foil obs. of $1s2p^3P_1$ lifetime 80−14114
Si V, transition probabilities and radiative lifetimes 79−98041
Si V, VI, beam-foil meas. of lifetimes, 500 to 1300 Å 78−9118
Si XI, allowed transitions, radiative lifetimes and oscill. strengths meas. 78−78797
Si XII, allowed transitions, radiative lifetimes and oscill. strengths meas. 78−78797
SiC, (6H), radiation damaged, luminesc. 80−25462
SiF $A^2\Sigma(\mu'=0)$ state, radiative lifetime meas. 77−27110
SiH, A state new predissociations, improved dissoc. energy value from rot. level lifetimes 79−3496
$Si(Si^+)(Si^{2+})(Si^{3+})$, excited levels, radiative lifetimes, beam foil spectra 80−58368
Sm II, lifetimes of $^8G^0_{5/2\text{-}15/2}$ excited levels 79−3407
Sn II, radiative lifetimes, calcs. and beam-foil spectra 77−75223
Sn $K\beta_3$|$K\beta_1$ and $K\beta_2$|$K\beta_1$ relative intensities 77−75088
Sn, Sn^+, transition probabilities and Stark-broadening parameters, shock tube meas. 79−93956
SnF, $A^2\Sigma^+$ state, radiative lifetime, quenching rates 79−98156
SnX_2 (X=Cl, Br, I), UV absorpt. cross-sections of vapour 78−25554
$Sn^+(5s5p^2)^4P_{1/2}$ level, lifetime and Lande g-factor *(French)* 80−52938
Sr I and II, excited states radiative lifetimes 79−98042
Sr II, resonance level lifetime meas. by pulsed laser excitation of ion beam 78−25480
Sr+He, $^1P_1$ level lifetime, Hanle measurement 80−23365
$Sr^+(^2P_{3/2})$, Penning ion, polarised emission, Hanle effect obs., radiative decay rate meas. 80−5520
Tb complexes, intermol. energy transfer to Eu complexes in aq. soln. 80−25426
Tb complexes, intermol. energy transfer to Eu complexes in aq. soln. 80−25427
TbAG, reson. electronic Raman effect, interferences, lifetime meas. 80−93294
$TbCl_3$-$AlCl_3$, vap., high-energy laser medium props., for fusion ignition 78−63075
Te IV, radiative lifetimes, calcs. and beam-foil spectra 77−75223
Te $K\beta_3$|$K\beta_1$ and $K\beta_2$|$K\beta_1$ relative intensities 77−75088
Ti atoms sputtered from Ti, Ti oxides, photon emission, nonradiative transition effects 80−58208
Ti II, oscillator strengths from combined hook and emission expts. 80−87081
Ti III, IV, V, radiative lifetime meas. using beam-foil technique, 700 to 1900 Å 80−78574
Ti, rel. at. transition probabilities, by flame at absorption spectroscopy 79−89642
TiO, $(C^3\Delta$-$X^3\Delta)$ system, radiative lifetimes, oscillator strengths, flame spectroscopy 78−42136
TiO, β-system, radiative lifetime determ. 77−58086
TiO, $C^3\Delta_3$-X^3D_3 α system, radiative lifetime meas. 78−55202
Ti($y\ ^3D_2^0$) lifetime, in rel. oscill. strengths determ. by combined absorption/emission meas. 80−37784
Tl, oscillator strengths and radiative lifetimes 79−54811
Tm I, lifetimes of excited states, and oscill. strengths 79−3411
Tm II, lifetimes of excited states 79−3411
U I, laser spectroscopy, using stepwise excitation and fluoresc. detect. 79−54802
U, radiative lifetime, appl. to laser isotope separation 79−50152
UF_6, fluoresc. lifetime, temp. depend 77−58065
UF_6, gas, laser-induced fluoresc., A-X band 78−94275
UF_6, UV photophysics, energy balance through quantum efficiency meas. 80−9634
UO_2^{2+} in aqueous solution, time resolved luminesc. for lifetime, $U_2O_4H^{4+}$ exciplex 79−61417
^{235}U, lifetime meas. of electron excited states, rel. to laser isotope separation 77−34591
^{238}U I, lifetime, branching ratio and absolute transition probability of 6395.42 Å transition 79−3402
V, hyperfine struct., laser-RF double-reson. obs. 79−41141
Xe atoms in Ne matrix, radiative and nonradiative lifetimes in excited states 80−69106
Xe, condensed electron beam excited, exciton radiative lifetimes 80−6727
Xe, fluoresc. lifetimes, time resolved VUV spectra 78−17601
Xe, high Rydberg states, radiative lifetimes and transition probabilities 78−86817
Xe II, beam-foil spectroscopy 80−18825
Xe II, excited levels, lifetimes, measurement by photon-photon delayed coincidence technique 79−89640
Xe II, influence of relativistic effects, excited states 79−72274
Xe II $5s5p^6\ ^2S_{1/2}$ state, lifetime meas. 79−13670
Xe, in gas discharge, collisional excitation, radiation lifetimes, macroscopic alignment obs. 80−33734
Xe, reson. levels relax. consts. determ. by alignment method in discharge 79−26936
Xe VIII, beam-foil lifetime meas. using ANDC anal. for reson. doublet 79−93964
Xe VIII, beam-foil lifetime meas., cascading problem 80−14249
Xe^{2+}, energy level radiative lifetimes using 1-5 MeV ions 80−47947
Xe_2, fluoresc. decay of O_u^+ and 1_u states, rad. decay consts. 79−86009
Xe_2, time and energy resolved fluorescence, radiative lifetime, collisional mixing, pulsed synchrotron radiation obs. 79−98136
Xe_2, time resolved excitation using synchrotron radiation 77−88483
Xe_2, VUV radn. emission, radiative lifetimes 79−27089
XeCl* spectra, for $Xe(6s,^3P_2)$+RCl vibr. energy disposal assignment 79−100345
XeF, C-A blue-green band, gain meas. at 488 and 475.9 nm 79−45929
XeF, spontaneous emission lifetime meas. of C→A band 79−31874
XeF+He(Ne)(Xe)$(F_2)(NF_3)$, collisional quenching kinetics 78−94289
XeF_2(C) state lifetime, quenching rate consts., photolysis in inert gas atmospheres 80−66816
XeF(Cl)(Br)(I), covalent and ionic states, spectroscopic props., ab initio CI calc. 78−90092
XeF* $(C_{1/2})$, 351 nm fluoresc. time behaviour 78−63087

radiative lifetimes continued
XeF*, $B^2\Sigma^+$ and $C^2\Pi_{3/2}$ states, fluoresc. decay dynamics, collisional quenching and radiative lifetimes 80−58306
XeI, visible lines, absolute transition probabilities 80−69108
XeS, photoluminesc. in rare gas matrices 80−5568
Xe_3*, synchrotron radiation excited, time resolved spectroscopy 80−69092
Xe_2*, Xe_2^+, Xe_2, pot. energy curves, relativistic ab initio effective core pots. 78−86800
Y I, Y II, lifetimes of excited states, rel. to solar abundance determ. 78−86815
Y_2O_2S:Eu, high press. effect on luminesc. efficiency and lifetime, charge transfer absorpt. 80−66266
Yb I, Yb II, excited states radiative lifetimes 79−76386
Zn I isoelectronic series, $4s4p\,^1P$ lifetimes meas. 80−42998
Zn II, lifetime extraction from beam-foil decay curves 80−14107
Zn I(II), low lying level lifetimes, beam foil spectra 79−36751
Zn, triplet state lifetimes, (4s6s), (4s5d), (4s6d) configs. *(French)* 78−5175
Zn-porphin($-d_4,d_8,d_{12}$), nonradiative transition probabilities, deuteration effects 79−3485
ZnH, lifetime, Λ-doubling and hyperfine struct. of $a^2\Pi$ excited states 77−58083
ZnI, II, excited states, radiative lifetimes, multi-channel delayed-coincidence method 80−32669
Zr I, lifetimes of excited states, rel. to solar abundance determ. 78−86815
ZrF_4:Eu^{3+} glass, luminesc. of Eu^{3+}, transition probabilities 80−80845
ZrO, $B^3\Pi$ state radiative lifetimes, transition rates and oscillator strengths, reson. fluoresc. decay 80−28053

radiative shifts
collective radiative phenomena in two level systems *(Russian)* 80−1174
two-level atom, reson. fluoresc., photon recoil shift 77−18839
H*, radiative magnetic energy shift, H in 2p state 78−58601

radiative transfer
absorbing medium, analytic solns. of integral eqns. 77−14886
absorbing-emitting, natural convection boundary layer flow 77−58808
absorbing-emitting media, integro-differential energy eqn. soln., validity range of differential approx. 78−5644
absorbing-scattering infinite slab, combined conductive and radiative heat transfer 78−71269
absorbing-scattering semitransparent planar layer, flat temp. waves 78−90683
absorption line profile of isothermal atmos., under general freq. redistrib. function 77−37500
absorption of trapped line photons by dust 79−25460
acceleration waves, growth and decay, radiative heat transfer 78−87243
accretion disc around binary star, polarisation effects in emission 79−35128
active galactic nuclei, X-rays from inverse Compton refl. 79−48920
active remote sensing with radar, radiative transfer theory, half-space random media appl. 79−8721
aerocolloidal flow, radiant heating, Knudsen no. effect 77−68704
aerosol particles influence on warming of urban and rural atm. 79−16671
aerosol size distribution retrieval, simulated aureole data inversion in presence of multiple scatt. 79−74957
aid functions, approx. calc. *(Russian)* 79−8817
air, radiative cooling behind strong shock waves 78−91030
air exploded by focused laser, emission processes affecting development of explosion 79−7417
air pollution, smoke plumes visual effects, computer simulation 79−66429
air pollution effects on urban-rural complex, two-dimens. numerical simulation 78−81369
albedo problem in inhomogeneous isotropically scatt. atmospheres, appl. of max. variational principle 80−36398
angular radiation coeffs., 2D, flow algebra method 77−84129
anisotropic dispersive media, generalisation of Planck's law 78−18153
anisotropic light scatt. in inhomogeneous atmosphere, small true absorpt. case 79−62742
anisotropic Milne's problem, soln. using H-functions 77−53840
anisotropic scatt. in one-dimens. system, radiative transfer parametric anal. 80−5920
anisotropically scattering two layer atmosphere, brightness coeffs. *(Russian)* 77−17349
annulus with permeable insulator, radiative and free convective transfer 78−94575
Ap and Bp stars, radiation forces and B abundance diffusion theory 79−88664
aqueous media, radiation transfer prediction techniques, assessment 80−33428
Arctic summertime stratus clouds, solar radiation pyranometric meas. 78−32165
atmosphere, absorpt. and emission over mean long optical paths 77−49163
atmosphere, absorpt. coeff. for line with Voigt profile *(Russian)* 77−64429
atmosphere, aerosol optical scatt. thickness from daytime sky UV light polarisation 78−20517
atmosphere, aerosol particles effects on CO_2 15μm radiance rel. to error in satellite retrieved temp. profiles 80−98449
atmosphere, aerosol-induced heating effects on convective boundary layer 78−69409
atmosphere, cloud effects on satellite upwelling radiances 78−32227
atmosphere, CO_2 increase effects on stratospheric O_3, photochem. and radiative transfer model 78−65370
atmosphere, comparion of theoretical and experimental long-wave IR fluxes *(Russian)* 80−94598
atmosphere, computer simulation of irradiance meas. from aircraft 77−70830
atmosphere, doubling initialization, interaction of ang. and initial-layer error 77−70996
atmosphere, doubling initialization and ang. discretization errors 77−70997
atmosphere, downward solar radiant flux obs. and predictions for urban area 78−57317
atmosphere, global daily radiation estimation for any surface 79−39805
atmosphere, grey, diurnally insolated, radiative transfer 77−22060

radiative transfer continued
atmosphere, haze and fog vertical struct., effects on visible and IR extinction 79−58086
atmosphere, high resolution IR spectra, ground based obs. 77−41167
atmosphere, high resolution IR spectra, numerical simulation 77−41166
atmosphere, ice and water content from Nimbus 6 IR sounder data 78−92925
atmosphere, inhomogeneous 9.6 μm O_3 band heating, new approx. method 78−88918
atmosphere, intensity of direct and scattered UV radiation at large air masses *(Russian)* 77−49166
atmosphere, IR cooling rate in standard atmosphere 80−26609
atmosphere, IR cooling rates, effect of tropospheric aerosols 78−88886
atmosphere, IR radiative transfer model, comparison of obs. and calcs. 79−2369
atmosphere, IR radiative transfer rel. to zonal radiation balance perturbation by stratospheric aerosol layer 80−56602
atmosphere, IR transmissivities for H_2O vapour, CO_2 and O_3 78−11998
atmosphere, longwave radiative transfer model rel. to CO_2 effect on heating rates 80−17376
atmosphere, Lorentzian coeff. approx. for efficient transmittance profile calc. 78−61552
atmosphere, model transmission function rel. to remote sensing 77−9498
atmosphere, mol. scatt. and refl. in photon fluxes and photodissoc. rates calcs. 79−53512
atmosphere, multiple scatt. effect on radiometric determ. of rain attenuation at millimetre wavelengths 80−90260
atmosphere, new formula relating optical parameters *(Russian)* 78−11999
atmosphere, O_2 induced absorption band effects on transmission in 6 μm region *(Russian)* 78−69446
atmosphere, O_3 9.6 μm band radiance calc., excitation processes 78−36350
atmosphere, optically thick, radiative transfer eqn., direct soln. 77−41170
atmosphere, perturbed, photochemical radiative convective model for thermal struct. and relaxation rates 80−8408
atmosphere, plane-parallel, appl. to 4.3 μm auroral arc 78−88917
atmosphere, radiances in absorpt. bands, calc. methods including multiple scatt. 78−61554
atmosphere, radiation attenuation spectral struct., depend. on atmospheric surface layer turbidity *(Russian)* 78−44997
atmosphere, radiation model of polluted boundary layer 77−49168
atmosphere, radiation under cumulus cloud conditions, Monte Carlo method *(Russian)* 80−21793
atmosphere, radiative heat exchange in tropics *(Russian)* 79−84476
atmosphere, radiative transfer model rel. to anomalous gray shades in DMSP visible imagery 80−77111
atmosphere, radiative transfer rel. to Earth surface vertical heat fluxes N.hemisphere distribs. 79−96804
atmosphere, Rayleigh optical depth, appl. to solar radiation problems 77−91269
atmosphere, shortwave spectral characts. over desert, calc. from CAENEX-70 data 79−100956
atmosphere, solar radiation absorpt., cloud and aerosol effects on heating rate 78−57319
atmosphere, solar radiation absorpt. by H_2O vapour, including multiple scatt. 78−61553
atmosphere, solar radiation transmission, Monte Carlo simulation *(Russian)* 79−12265
atmosphere, spectra of variables deduced from ground-based radiometry 79−92567
atmosphere, static radiative flux model rel. to anthropogenic CO_2 influence on temp. 80−51486
atmosphere, surface radiative flux, clear and cloudy conditions, parametrisation accuracy 78−77325
atmosphere, thermal sensing from Earth orbit, spatial temp. and geopot. fields 80−36429
atmosphere, transfer in CO_2 4.3 μm band with non-LTE *(Russian)* 78−88914
atmosphere, transfer of auroral O I (989 Å) and O I (1027 Å) 78−28367
atmosphere, turbid, multiple scatt. effects on refl. light pulses 77−29442
atmosphere, urban, radiative effects of elevated pollutant layers on temp. struct. and pollutant dispersion 80−97841
atmosphere, water vapour absorption in 8 to 13 μm spectral region 79−39855
atmosphere and ocean, radiative transfer theory 78−69458
atmosphere boundary layer, form. and evolution of radiative fog and stratus cloud *(Russian)* 77−49104
atmosphere boundary layer, IR radiation effects on dynamics 79−39815
atmosphere boundary layer, temperature inversion, characts. of stable nighttime layer 80−41533
atmosphere effects on radiative transfer, conference, San Diego, California (1979 August 29 to 30) 80−62376
atmosphere emergent radiation, computation method for region ranging from UV to IR 77−87069
atmosphere heat and radiation budget during solar eclipse, above pine forest *(German)* 80−46226
atmosphere microwave radiation, Nimbus 6 scanning spectrometer data parameterisation for atmosphere liq. water content 79−58047
atmosphere radiative transfer eqn., soln. using Elsasser scheme 80−77112
atmosphere thermal radiation, effect of hailstones on spectral depend. in 0.86 to 17 cm range *(Russian)* 78−36222
atmosphere with cloud, IR radiation flux approximation 79−39854
atmosphere-ocean system, matrix operator approach 80−8330
atmosphere-ocean system, radiation interaction with turbulence 78−92953
atmosphere-ocean system, turbidity and hydrosols refr. index effects on solar radiation flux 77−64303
atmospheres, spherical symmetry, radiative transfer, non-conservative problem 80−36492
atmospheres, variational and discrete ordinate calc. methods 77−53188
atmospheric, fixed cloud-top temp. and fixed cloud-top altitude approximations for temp. profile 80−72616
atmospheric boundary layer, vertical temp. profile determ. by ground-based microwave radiometry 79−79915
atmospheric diffuse radiation, effects on remotely sensed Earth images 79−58091
atmospheric elevated pollutant layers, radiative effects 78−65382

radiative transfer continued
atmospheric optical props., appl. to satellite remote sensing of phytoplankton 80−77105
atmospheric radiation climate of Thailand, calcs. from routine meteorological data 79−29814
atmospheric radiative transfer in solar, IR and microwave spectral range 79−53520
attenuating medium, basic internal characts. of radiation field 78−1555
auxiliary functions calc. for homogeneous media 79−88580
average emissivity of various shaped volumes 77−46897
axially symmetric explosion, thermal radiation effects, astron. radiosources appl. 77−87249
axially symmetric hollow collectors for high temp. solar installations, computation 78−79093
axisymmetric system, radiative angular coeffs. 79−90120
axisymmetrical body, min. radiative heat transfer contour under heating rate limitations *(Russian)* 78−67020
azimuth dependent terms of radiation intensity in deep layers of semiinfinite medium *(Russian)* 77−73851
Be stars, electron scatt. effects on Balmer emission lines 80−17589
bibliography of heat transfer 78−63425
binary stars, reflection effects evaluation, generalised approach 79−25631
black hole, spherically accreting, radiation near Eddington limit 79−48843
black hole accretion discs, radiative transfer rel. to Lightman-Eardley instabilities and disc thickening 80−31324
black holes, radiation hydrodynamics of high-luminosity accretion 78−77571
black spheres by transparent refracting layer 79−1096
blackbody function efficient computation, two-series approach 80−79128
blast wave, with transport props., self-similar soln. 77−68621
blast waves, magneto-gasdynamic radiative, cylindrical, similarity soln. 79−37338
Boltzmann linear eqn., Pade approximants 80−551
boundary layer, radiation-flow field interactions with injection of absorbing gas 78−5826
butane, total emissivity, press. depend. 78−90673
η Carinae, spherical circumstellar dust shell model, radiative transfer 78−36577
α Carinae (Canopus), chromospheric scattering and generalised Compton effect in spectrum 78−53938
cavity, single-mode photon emission/radiation, Gibbs vs. information theoretic entropies 78−16765
celestial masers, radiation transfer through interstellar mol. cloud 79−21455
β Cephei stars, theoretical models with new radiative opacities 77−13347
Chahine relaxation method extension to radiative transfer eqn. inversion 78−7794
chamber filled with absorbing medium, generalised zone method 77−39206
Chandrasekhar's H-functions, new representation 77−87251
Chandrasekhar H-equation, Banach space anal. 77−13224
Chandrasekhar H-equation, soln. by Newtons method 80−87710
channel, annular, long, free-mol. and radiative transport, approx. analytical soln. 80−6165
channels, internal radiative transfer *(Russian)* 78−38330
chlorofluoromethane IR radiation, effect on zonal atmospheric temp. 79−80019
chromosphere Fraunhofer line cores formation, empirical statistical model 79−12450
chromospheric-type stellar atmospheres, non-isotropic redistrib. rel. to spectral line form. 77−5522
circuit-breaking arc radiative transfer, magnetic stability, and turbulent heat exchange 78−75482
circumsolar radiation, single and multiple scatt. contribs. 79−25325
circumstellar dust shells, models rel. to compact IR sources spectra 77−29948
circumstellar dust shells, Monte Carlo simulation of polarised light transfer 78−81608
circumstellar dust shells, radiative transfer 77−13318
cirrus clouds, IR radiative transfer rel. to radiative props. in NOAA 4 VTPR channels 79−39853
classical novae, photospheric props. of optically thick winds 78−24516
clear atmosphere, radiative transport and thermal turbulence *(French)* 80−82018
climate contemporary changes due to solar const. aerosols and radiative transfer *(Russian)* 77−41140
climate modelling using radiative-convective models 79−74954
close binary stars, model atms. of components 79−62869
close binary stars, nonradial radiative transfer 77−91567
closely packed media, difference eqn. 78−12654
cloud diffuse reflectance, semiempirical model 79−80014
cloud droplet growth effects 80−8404
cloud droplets, 8-12 μm radiant energy transfer effects on mass and heat budget 79−5571
cloud modelling, isothermality 79−58076
cloud shape and mutual shading effects 80−101430
clouds, finite cubic cumulus model, simulated radiance patterns 77−33187
clouds, horizontally inhomogeneous, albedo and refl. radiance 77−78417
clouds, internal radiation field, cloud blackness determ. technique 79−58089
clouds, mathematical model of radiative transfer 80−90215
clouds, radiative properties parameterisation 80−56601
cloudy atmosphere, model solar radiation and cloud struct. 79−21016
cloudy atmosphere, scatt. and line absorpt. of radiation, interaction, analytical calc. method 79−100940
cloudy atmosphere, thermal radiation fluxes calc. *(Russian)* 80−4103
cloudy layers, monochromatic radiation transfer *(Russian)* 77−41168
cloudy sky, theoretical scheme for IR radiative transfer 80−51540
coal-dust aerosol, radiation-absorbing coeff., effect of spectral comp. of radiation and particle size 77−23859
cocoon stars, radiative transfer in envelope and IR spectra 77−64824
coherence and radiation laws, review 77−23612
coherence theory rel. to theory of radiative transfer 77−65568
coherent light beam, atm. propag. fluctuations, quantum phenomena 77−608
collimated radiation, two-dimens. media, single and double scatt. approx. 79−30390
radiative transfer continued
colour temperature of hot bodies, exact eqns. 77−35024
combustion flow, passive optical diagnostics of temps. and species concs. 77−44527
combustion system, Milne-Eddington absorpt. coeff. 78−90680
comoving frame eqn. in spherically symmetric flows, scatt. source functions 77−22056
comoving-frame eqn. of transfer in spherically symmetric flows, soln. for relativistic flows 80−82181
comoving-frame transfer eqn. in spherically symmetric flows, soln. for multilevel atoms 78−28499
compact X-ray sources, Comptonisation of Fe X-ray spectral features 78−20908
complex heat exchange, radiant and convective components meas. method 78−32809
complex heat exchange in scatt. laminar flow in cylindrical channel 78−83490
conical radiators, radiation field calc. 77−58539
convection, free, and radiative transfer, at vertical plane surface 78−55645
convective-radiative equilibrium, numerical soln. 78−32164
coupled radiative and conductive transfer thermokinetics *(French)* 79−1095
Crab Nebula, ionising radiation transfer rel. to emission line spectrum 80−22068
Curtis-Godson approx. for nonisothermally gas 78−67019
curvature radiation, absorpt. theory rel. to pulsar radio emission 79−75090
P Cygni Balmer line spectrum, equivalent two-level-atom approach rel. to mass loss 78−93255
P Cygni type line profiles, theoretical, atlas 79−80297
Cygnus X-1, photospheric scatt. model for optical polarisation orbital vars. 78−54077
cylinder, heat transfer by free convection and radiation 79−14209
cylinder, infinite isothermal, fitted with scatt. medium, radiation problem soln. 80−4676
cylinder row systems, variation of heat transfer characteristics with number of rows 78−9552
cylindrical media, numerical method for soln. to transfer eqn. 78−5642
cylindrical surface, local ang. coeff. calc. 78−83227
cylindrical surfaces, parallel axes, apparent radiative props. *(French)* 78−94569
dark clouds, chemical and thermal equilib. 78−61899
delta-Eddington approx. for absorbing-scattering atmosphere 77−45151
delta-M method, radiative flux calcs. for asymm. phase functions 78−32338
delta-two-stream approximation in radiative flux calculations 79−96811
detonation wave propag. with allowance for radn. and mag. field 79−64796
detonation waves, radiative MHD flow *(Russian)* 77−89207
diathermic medium, effect of selectivity of radiation characts. 77−35022
diatomic gas, vibr. nonequil., probabilistic modelling 80−33434
diatomic gas, vibr. nonequilib. radiation, master eqn. approxs. 78−33496
diatomic gas, vibr. nonequilib. radiation 78−33495
diatomic gases, emissivities calc. 78−90675
diatomic gases, oscill., relaxing and radiating, propag. of small disturbances *(Russian)* 77−27625
differential approx. for linear-anisotropic scattering 80−33429
diffuse radiation emerging from semi-infinite medium, intensity accounting for inner refl. *(Russian)* 79−8637
diffuse radiation view factors from differential plane sources to spheres 80−5921
diffuse reflection, mutual shadowing effect classical calc. extensions 79−84666
diffuse reflection and transmission in accordance with phase function $^3/_4(1+\cos^2\Theta)$ 79−44353
diffuse reflection and transmission problem, exact soln. using Laplace transform and linear singular operators 79−35116
diffuse reflection and transmission problem, soln. by Laplace transform and linear singular operators 79−21175
diffuse reflection and transmission problem with scattering function, soln. by Laplace transform and linear singular integral eqn. 79−21174
diffuse reflection for arbitrary phase function *(Russian)* 79−8816
diffuse reflection problem for combination of Rayleigh and isotropic scatt., exact soln. 79−84661
diffuse solar radiation field in cloud layer *(Russian)* 79−29851
diffuse wall cavity, radiation pattern, nonuniform temp. and emissivity 77−80053
diffusion approximation for large absorpt. 79−63170
diffusion equation, soln. by mixed finite elements *(French)* 77−71283
diffusion in two gas clouds *(Russian)* 77−41297
disks, radiation configuration factors 79−55320
dispersive media, geometrical optics, rel. to relativistic astrophysics and cosmology 77−61917
Doppler broadening atmospheres, stratosphere, mesosphere and thermosphere 77−78418
drop, diffusional evap. in EM radiation field 78−43112
drops, evaporating in vert. hot air tunnel, heat radiation effect 79−46400
dust laden gas in channel, combined heat transfer 78−91031
dusty gas, attenuation of radiant energy 78−94579
dynamic stella atmospheres, non-LTE radiative transfer 77−60752
early B-type stars atmospheres, LTE line blanketing by UV lines using accurate damping consts. 78−16419
early universe, photon and neutrino diffusion rel. to nonlinear primordial fluctuations 79−25773
Earth's atmosphere, IR transfer and CO_2, statistical model 78−26024
Earth's radiation balance, sensitivity to cloud changes, zonal model 77−78419
Earth's radiation balance, zonally averaged model, improvements 78−61559
Earth atmosphere, plane-parallel model appls. to multiple scattered radiation problems *(Russian)* 78−36275
Earth atmosphere non-LTE radiative transfer in 15 μm CO_2 band *(Russian)* 78−36341
Earth radiation balance meas. as instrument design problem 77−41173
Earth radiation budget expt., Nimbus-6 obs. 77−41106
Earth stratosphere and mesosphere, radiative equilib. temps. rel. to O_3 densities data 78−81280
Earth-atmosphere radiative heating effects on climate, NOAA radiometer meas. 80−8425

radiative transfer continued
eclipsing binaries, linearised limb-darkening coeffs. for light curves anal. 78−49480
Eddington's number, cosmic variability 79−80375
Eddington approx., radiative transfer for spherically symmetric atmospheres 78−77484
Eddington approx. range of validity 78−12086
Eddington tensor, maximum entropy soln. 79−23190
electron plasma, partially degenerate, at high temp., Compton scatt. opacity 77−11322
electron scattering in strong mag. field, approx. formulae 79−92662
Elsasser formulation and downward IR fluxes, comments on discussion 77−56729
emergent and internal intensities, exact soln. for known surface incoming intensity 79−53711
emergent intensity from semi-infinite atmosphere, Laplace transform and Wiener-Hopf technique, exact soln. 79−75095
emission frequencies simulation from angle-dependent partial freq. redistribs. 78−32333
emittance, directional, of semi-infinite scattering medium with refr. index >1 79−94471
emitting-absorbing-scattering layer, radiative transfer anal. using effective absorptivity 78−5827
energy balance model, climate sensitivity to radiation flux calcs. 80−8421
energy loss by resonance line photons in an absorbing medium 80−56699
energy transfer in a heat-conducting medium with arbitrary scattering of thermal radiation 78−94507
entropy variation to attain radiative equilib. 79−98599
equivalence of some integrals of radiation theory 77−49285
evaporating droplets, radiative absorption 80−33426
evaporation cooling, radiation effect on heat transfer and Lewis no. *(German)* 79−41562
evolved stars expanding envelopes, coupled radiative transfer eqns. for CO thermal and maser emission 80−82334
exact solution for semiinfinite plane-parallel isotropic scatt. atm. 79−12396
exchange factors for specular passages, simple approx. 77−39207
excited atom concentration distrib. near absorbent boundary 78−67327
exothermic waves in gas flows 77−68709
expanding envelopes, Lyman α quanta scattering *(Russian)* 80−67556
expanding homogeneous sphere, integral eqn. *(Russian)* 78−73945
expanding media, opacity, effect of spectral lines 77−49283
explosions in radiating stars, similarity solns. 78−32443
exponential integrals, Λ-transform determ. 79−35114
exponential integrals, general integral transform 79−88577
exponential-sum fitting, of radiative transmission functions 77−70995
exponential-wide band, intensity, radiative flux and flux divergence 77−31204
F_N method for problems in plane geometry 79−16814
F_N-method for problems with reflective boundary conditions 80−79124
F, G, K-type stars, giants and dwarfs chromospheres, wave dissipation of mechanical energy 80−82340
F-type stars, atm. models including OH opacity, comparison with TD1 satellite flux obs. 78−73700
fibreglass insulating materials, radiative heat transfer rel. to optical props. 80−100367
fibrous media, radiative transfer 78−94571
field crops, aspects of micrometeorology *(Dutch)* 77−64389
finite atmosphere, exact soln. of basic eqn. via Laplace transform 80−94702
finite media, new technique for exact and unique soln. 78−77479
finite medium freezing (melting), variational anal., radiation and convection effects 80−38244
finite plane parallel atmos., polarisation studies, F_N method 79−40070
fire, radiation augmented, within enclosure 79−32206
fission reactor spent-fuel shipping casks, Monte Carlo radiative heat transfer 79−59193
flame radiation, in IR porous perforated gas radiators 78−3335
flames, IR radiation 77−19513
flames, radiation measurement techniques 78−94506
flat layer of selective medium with semitransparent boundaries, radiative-conductive heat transfer 80−19227
flat solar collectors, thermal exchanges in glass absorber cavity *(French)* 79−24909
flow of radiating gas over blunt body with intense vaporisation 77−35255
fluidised bed, radiative contribution to total heat transfer 80−19384
fluidised bed, radiative heat flux absorbed in radiative heating 77−39362
fog model, 2D numerical soln. algorithm 78−71032
Fourier analysis limitations for radiative transfer soln. in small angle scatt. approx. 80−37952
free boundary problems with radiation boundary conditions 79−71386
free convection suppression, inclined air honeycomb, radiative coupling 77−58684
free EM field, radiative energy and momentum transfer, exact eqns. 77−42462
freeze-drying of food models, heat and mass transfer 79−1098
frequency redistribution, general law for noncoherent radiation scatt. 78−24746
frequency redistribution in externally excited medium, Monte Carlo method 78−20628
functional equations in emitting atmospheres 79−25465
fundamentals of momentum, heat and mass transfer, book 77−39294
furnace, gas fired, radiative heat transfer 78−1557
furnace, internally fired, radiative transfer 78−5643
furnace combustion chamber and radiative transfer, fuel substitution effects, review 79−3903
furnace heat transfer, 3-dimens, computer model predictions test 78−59504
galactic centre, radiation model, dust grains heating by O-stars and K-giants 78−36697
galaxies active nuclei, H emission lines radiative transfer and spectra 78−96557
Galaxy, UV radiation transfer model and dust scatt. albedo 77−13504
gas, absorbing and radiating, soln. of one-dimensional transfer eqn. by discrete ang. subdivision method 77−35256
gas, boundary layer combustion, combined heat transfer 78−91029
gas, heated by isotropic source of monochromatic radn., self-consistent motion 77−89014

radiative transfer continued
gas, propag. of ultrashort light pulse in region of absorpt. line *(Russian)* 77−47141
gas blast circuit breaker arcs, investigation 79−27864
gas blast circuit breakers, three nozzle arc models, review 79−27862
gas dynamics equation soln. *(Russian)* 80−64553
gas flow patterns in furnaces, composite heat transfer 78−90677
gas impinging on heated surface, radiative transfer 78−90674
gas tube flow, radiative and convective transfer 78−94576
gas-particle mixtures, effect of thermal radiation on shock wave 78−91032
gas-to-surface radiative exchange area for rectangular parallelepiped enclosure containing a gray mediummedium 77−80055
generalised direct exchange factors for isothermal mol. gases 77−39208
geocorona, Lyman alpha emission meas. rel. to exobase H density and temp. 77−29526
giant planets atmospheres, radiative transfer eqn. inversion for thermal struct. determ. 79−84735
gray, planar, absorbing-emitting-scatt. medium bounded by nonisothermal walls, radiative heat transfer 80−1413
gray atmosphere, absorpt. lines form. *(Russian)* 79−21177
gray surfaces bounding closed vol. 79−81702
grey bodies system, closed combined radiation convection heat transfer, two-layer gas model 78−75052
grey cavity, apparent emission and absorpt. factors *(French)* 78−30168
grey medium between concentric cylinders, 2 dimens. radiative equilib. 78−42523
H-function for anisotropic scattering, approx. form 80−36491
H-functions in multiplying media, remodelled representations 78−53808
Hanle effect in compact non-LTE radiative transfer 78−61728
Hartmann MHD flow, radiative transfer 80−6161
HCDA, radiological consequences, attenuation due to radiative cooling 78−13296
heat and mass transfer bibliography−Soviet works 79−23318
heat conduction, unsteady, in quarter plane, appl. to bubble growth 78−75045
heat exchange, iterative soln. of difference eqn. system *(Russian)* 77−58540
heat flux measuring devices, for radiant heat exchange investig. 78−94505
heat radiation, two-dimens. isotropic scatt. in semiinfinite medium 78−42521
heat transfer, with isotropic scatt. and gaseous absorpt., optical path length calcs. 80−79125
heat transfer bibliography, Japanese works 79−23317
heat transfer in planar medium, anisotropic scatt. and directional boundaries 78−90679
heat transfer integral theory with anisotropic scatt. and general boundary conditions 78−32339
Hercules X-1, line photons transfer rel. to cyclotron features in X-ray spectrum 80−86015
Hercules X-1, reson. Compton cyclotron scatt. rel. to cyclotron line form. 80−8711
α^2 Herculis, circumstellar lines form. rel. to location along line of sight 78−73739
high temp. heat exchangers, heat transfer improvements, radiation between walls, effects *(Japanese)* 78−87244
high vacuum system, radiative and mol. heat transfer 78−94574
hollow functions of a source in radiation gasdynamics 78−9554
homogeneous atmosphere of finite optical thickness, standard problem 80−51646
homogeneous isotropic Universe models, radiation theory 77−37501
homogeneous plane-parallel atmosphere, unified treatment of reflected and transmitted intensities 78−85838
homogeneous semi-infinite atmosphere with isotropic scatt., radiation field calc. *(Russian)* 77−70991
homogeneous semiinfinite atmosphere, radiation field calc. 78−7876
homogeneous semiinfinite atmosphere with anisotropic scatt., radiation field calc. 77−78630
hot matter, conductive opacities and free-free Gaunt factors 80−3361
hot plasma, X-ray emission and radiative transfer effect 78−36451
hydrodynamics basic eqn. soln. with large and small Bouguer number 77−68708
hydrodynamics opacity enhancement by Doppler shift 77−75991
hypersonic flow around blunt body, similarity law for radiant heat transfer coeff. 80−33705
hypersonic gas flow, radiant heat and evaporative cooling 78−91028
ice, cloudy layers, back-melting by radiative heating 79−76961
ice, horizontal clear layer, radiative melting, rel. to atm. icing *(German)* 79−18679
ice, radiative heating 77−84130
imperfect Rayleigh scattering in semi-infinite atmosphere, transport eqn. soln. 79−75094
infinite atmosphere, interrelations between angular distribs. of intensity *(Russian)* 77−49281
infinite medium, radiation transfer *(Russian)* 79−8819
inhomogeneous cosmic masers, numerical calcs. of saturation behaviour 78−20898
inhomogeneous gas layer, transmission calc. for model with exponential distrib. of line intensities 80−17899
inhomogeneous molecular gas radiation calc. using spectral comp. modelling 80−32697
integral equation spectrum, calc. for semi-infinite medium 80−67540
integral transfer problems, splines under tension calcs. 77−53419
integration over frequency method for radiative transfer calc. in real spectrum 80−33430
intensity distribution inside absorbing-isotropically scatt. semiinfinite medium 78−32335
interlocked multiplets, transfer eqns. exact soln. for noncoherent scatt. 78−77478
internal energy source, in plane-parallel finite media, scatt. functions 79−37138
internal radiation field in plane layer illuminated by parallel rays *(Russian)* 77−49282
interstellar C II region, narrow radio recomb. lines prod. around X-ray source 79−8972
interstellar clouds, diffuse UV radiation penetration 80−56901
interstellar clouds, radiation transfer in H to H_2 transition region 79−25672
interstellar clouds, spectral lines, form. and widths rel. to vel. fields 79−12398

radiative transfer continued
interstellar CS, numerical solns. to radiative transfer and statistical equilib. eqns. 78−12319
interstellar cylindrical clouds, radiative transfer rel. to two-dimensional collapse 79−40247
interstellar dark clouds, anisotropic scatt. and formaldehyde lifetimes 78−8080
interstellar dark clouds, UV radiation transfer rel. to chemical and thermal equilib. 79−44593
interstellar dense clouds, CO self-absorpt. towards embedded stars 77−53670
interstellar dense clouds mol. cooling and thermal balance 78−65666
interstellar dust clouds, grain temps. and IR emission 77−74119
interstellar intercloud medium, diffuse recomb. radiation transfer and ionisation 77−9782
interstellar medium, polarisation reversal by small particles over strong resons. 79−2564
interstellar molecular clouds, line formation, radiative transfer effects 79−5884
interstellar molecular clouds, microturbulence, systematic motions and spectral line form. 77−33586
interstellar molecular clouds, radiation transport and kinematics 78−93347
interstellar polarisation in irregularly fluctuating medium, statistical anal. 80−26926
interstellar radiative shocks and UV precursors, theoretical models 79−25660
interstellar spherically symmetric radially moving clouds, spectral line shapes 78−20865
invariant imbedding method for multiple scatt. calc. Venus CO_2 lines appl. 78−4095
inverse albedo problem for finite medium 79−17366
inverse Compton reflection, time-depend. theory, X-ray sources appl. 80−12652
inverse problem, for 3-term phase function 80−13007
inverse problem, two-term. scatt. law 79−75479
inverse problems in transport and filter theory, soln. method 79−29920
inversion problems, Backus-Gilbert formalism 78−89054
inward solidification with black body radiation at boundary, asymptotic and perturbation solns. 77−55346
Io plasma torus, radiative cooling and spectra 80−72850
IR cloud opacities averaging for climate modelling 79−8692
Ir dryers, spectral composition of radn., optimisation 78−90676
IR radiation spectral absorptance and transmittance, accurate modelling technique 78−91062
IR radiation transfer, radiative effects in clouds 79−100912
IR radiation transfer in inhomogeneous atmos., transmission function 77−91270
IR sources, effect of multiple grain components on radiation transfer and 10 micron silicate feature 78−36659
IR sources, radiative transfer rel. to middle IR polarisation by dust 79−67078
irreversible processes *(French)* 80−13002
isothermal slab with Rayleigh scatt. 77−46896
isotropically scatt. finite medium, approx. soln. 78−1553
isotropically scattering medium on diffuse substrate, radiative props. 79−76951
isotropically scattering semiinfinite medium, two-dimens. radiative transfer expansions 78−42522
Jupiter, atmosphere, $^{12}CH_4(^{13}CH_4)$ ν_4 band, line parameters, 7.7 micron transmission 78−85894
Jupiter, H quadrupole absorption, spatial and temporal variations 77−37561
Jupiter, thermal structure from IR spectral meas., filtered iterative inversion method 78−7918
Lambertian cavity with dielectric window, effective absorptivity 80−38237
laminar compressible boundary layers, radiative interactions 79−50812
laminar convection in forced upflow, with radiative transfer 78−47064
laminar gas flow, heat exchange to selectively emitting liq. in radn. field 77−84343
lamp radiator for uniform heating of substrates rotating in circle, photometric calc. 77−54765
laser beam off-axis propag. in low visibility weather conditions, non-small-angle scatt. 80−102621
laser beam propagation in particulate media 79−50222
laser light with time-varying intensity in optical medium, temp. field kinetics 78−59098
layered media, radiative transfer theory for scatt. 79−76553
layered random media, remote sensing, radiative-transfer theory 80−36413
light, polarized, radiative transfer eqns., adjoint Monte Carlo treatment 78−37799
light diffusion problem in optically finite shell, soln. *(Russian)* 77−13236
light scattering by dielectric particles, statistical theory 80−32913
light sources total luminous energy transfer, scatt. medium effect 77−65577
line formation, in expanding spherical media with partial freq. redistrib. function R_I 79−88643
line formation in expanding stellar atmospheres 77−56919
line formation in stellar spectra 77−53422
line photons, equality of mean escape probability and mean net radiative bracket 78−40815
line radiation transfer in collapsing molecular clouds 78−73626
line radiation transfer in heated gas, arbitrary initial conditions in kinetic eqn. 78−51051
line transfer, Monte Carlo calcs., appls. to active nuclei and novae 79−48902
line transfer, non-LTE, with convective transport of excited atoms 79−88584
line transfer in spherical media with partial freq. redistrib., soln. 79−16932
line wings, polarized radiative transfer, excited state interference 80−105158
linear Boltzmann eqn., Pade approximants, appl. to spherical geometry, luminosity and albedo problem 80−52143
linear Fredholm integral eqns. for finite plane parallel media, imbedding in infinite medium 78−81532
linear Fredholm integral eqns. for finite plane parallel media, imbedding in semiinfinite medium 78−81533
radiative transfer continued
linear transport equation, degenerate case, full range theory, appl. to Milne problem 78−57874
linear transport equation, degenerate case, half-range theory, appl. to Milne problem 78−57875
low frequency EM or gravit. radiation spectrum 79−44350
low-temperature blackbody source 80−73355
magnetic accreting neutron stars, light scatt. in strongly mag. plasma 79−62739
magnetic DA white dwarfs, calc. and obs. spectra 79−71032
magneto-radiative gas, spherical shock, exact similarity soln. 79−16815
magnetogasdynamics, propagation of weak MHD discontinuities 78−63505
mantle radiative cond. from shock compressed Fe^{2+} bearing MgO absorpt. spectrum 80−90039
Markov chain formalism, adding algorithm 80−21902
Mars, lower atmosphere modelling, multilayer radiative transfer 80−46451
Mars atmosphere, effects of suspended dust particles on radiative convective model 79−84717
Mars atmosphere, optical props. during 1971 dust storm *(Russian)* 78−93138
Mars atmosphere, thermal radiative transfer, numerical modelling 80−8574
Mars atmosphere thermal IR properties, dust and ice clouds detect. from Viking IRTM spectral meas. 79−84712
Mars dusty atmosphere, solar radiation transfer and heating rates 78−85878
Marshak wave problem, non-equilib. 79−37137
maser soure, two energy level transitions, temporal var. 78−53817
masers, time vars. and radiative stability 79−35340
massive protostellar clouds, radiative transport rel. to dynamical evolution 77−17543
maximal variational principle for transport theory 78−62166
melting solid, radiative ablation 78−94564
melting solids, radiative ablation, Biot's variational method 77−31203
mesosphere, aerosol layer contrib. to polar albedo 77−60467
metal cone, vaporisation, solution by wave front method 78−5640
metals, radiation flux polarised components 78−94566
methane, shock-tube oxidation, equilibrium and nonequilibrium radiation emission 78−27760
MGD flow, radiation-conditioned Gaussian induced cone field 78−67283
MHD channel flow, thermally radiative, stability 78−55695
microwave passive remote sensing of snowpacks, theory and expt. 80−26632
microwave remote sensing, thermal emission from terrain, theory 80−77151
Milne's integral eqn., general variational method 79−8828
Milne integral equation with Pincherle-Goursat kernel, Cauchy problem 77−2513
Milne problem and spherical albedo, law of darkening, forward and backward scatt. effects 78−77483
Milne problem for inhomogeneous atm. 79−21179
Mira variable stars, radiative momentum transfer rel. to supersonic mass flow 79−35270
mirror, radiative transfer between its surface and focal point 79−32020
model atmopshere, radiative transfer eqn. soln. methods 77−66986
modelling techniques extension using Bayes' rule 77−78443
molecular gas, IR radiation flux, Lorentz profile 78−71268
molecular line haze opacity in sunspots 79−75188
molecular medium, IR transfer, complex absorpt. coeff., statistical model 78−26024
moment method anal. *(Russian)* 78−59284
Monte Carlo method, ang. biasing of collision process in multigroup calcs. 78−4975
Monte Carlo method modification, radiative flux local characteristics calculation *(Russian)* 79−35648
moving astrophysical plasmas, radiation transfer 78−65489
moving inhomogeneous media, radiation transfer 78−65490
moving layer, heat exchange, numerical-anal. soln. 77−7291
moving medium, radiative diffusion with plane symmetry *(Russian)* 78−53820
multi-region problems 79−75096
multiband molecular gases, radiative equil. problem, approx. soln. procedure 77−42712
multidimensional inverse problem in transport theory 80−174
multidimensional media, physical effects of radiative transfer 80−72758
multidimensional non-LTE radiative transfer, new approach to soln. 77−22057
multidimensional radiative transfer in stratified atmosphere, grey radiative equilib. 80−26845
multilayer insulation, heat transfer model 79−94465
multilayer scatt., absorb. materials, radiant energy transport 77−7297
multiple nonstationary scatt. with curved surfaces 77−29641
multiple scattering, two-dimens., in absorbing medium 80−10126
multizone system with isotropic scatt. 78−5643
nebulae, dusty, non on-the-spot (OTS) models 78−85995
neutral radiant gas, kinetic eqns. with allowance for radiation polarisation 79−23399
neutron star, magnetised, atmosphere, cyclotron line form. 79−48839
neutron star X-ray emission models 80−62175
neutron stars, Eddington luminosity limit and supercritical accretion, time-independ. calcs. 80−67768
neutron stars, magnetic, surface layers, radiative heat transfer theory 80−94826
NGC 1068, Seyfert galaxy, radiative transfer in dust rel. to spectral flux distrib. 77−29914
nodal network of large circular fins, thermal radiation 78−94570
non-gray gases, radiative transfer, simple differential approx. 80−38240
non-LTE problems, Monte Carlo method appl. 79−44357
non-LTE transfer, asymptotic expansion for small ε 78−16287
non-LTE transfer, asymptotics of partial redistrib. 80−62008
non-LTE transfer, rapidly convergent iterative method for Wiener-Hopf integral eqns. 78−12089
non-Minkowskian spacetime, polarisation plane rot. 79−35115
nonequilibrium ionised radiating gas flow over blunt bodies 78−9727
nonequilibrium radiation interaction with diatomic gas, kinetic model 77−3891
nongray extended dust shell models, Eddington approx. generalization 78−73627
nongray gas, bulk radiative exchange approx. 79−32205

radiative transfer continued
nongrey media with boundary, thermal radiation relax. 79−32204
nongrey radiation, IR band model correls. 77−57286
nongrey radiative transfer in two-dimensional medium 77−35020
nongrey two-dimens. medium, band or line shape effect on radiative transfer 77−62139
nonisothermal band model theory 77−62328
nonisothermal gases, radiative transfer, mixed grey gas model 79−97323
nonisothermal inhomogeneous layers, exiting monochromatic intensity 79−37139
nonisothermal volume, intrinsic radiation, effective temp. determ. 77−42709
nonLambert surface emission, shape factor determ. 78−94568
nonlinear radiation transport, soln. by renormalisation group method 80−67555
nonplane geometry media, approx. and num. methods of eqns. soln. 80−33431
nonstationary radiative transfer in variable scatt. medium, statistical theory *(Russian)* 77−75368
nuclear reactor, BWR rod bundles, combined radiation and convection under emergency cooling conditions 77−14249
nuclear reactor, GCFR and LMFBR, thermal radiation effects on subassembly wall failure 78−8938
numerical model based on standard meteorological observations 79−34929
O-type stars atmospheres, UV reson. lines transfer rel. to existence of coronae 79−21293
O-type stars winds and coronae, radiative transfer rel. to Hα line profile 78−40947
ocean, absorpt. and scatt. props. determ. 77−9430
ocean, clear, effective IR optical depths 79−8635
ocean, continuously stratified, remote sensing of optical props. 78−77331
ocean, optical properties, one parameter characterisation for remote sensing 78−7644
ocean atmosphere system, sea foam effect on albedo 77−81899
ocean diffuse reflectance, effects of chlorophyll a fluorescence at 685 nm 79−66700
ocean inertial oscills. radiation damping, wind mixed layer turbulence 79−39730
ocean-atmosphere boundary layer, heat transfer meas. using radio thermal microwave systems 79−84546
olivine, optical absorpt. spectra and radiative heat transport at high temp. 79−79818
one-dimensional non-planar systems, approx. solns. 78−59283
one-dimensional transport problem, variant of shell-adding method *(Russian)* 77−13235
opaque gas medium movement, deformation of temp. fields 77−51132
opaque region, asymptotic limit to optical pumping 79−70947
optical depth, integral of Voigt function 79−25468
optically finite layer, quasiasymptotic solns. for nonconservative scatt. *(Russian)* 77−17348
optically thin medium, weak MHD discontinuity propag. 79−46438
organic liquids, radiant heat exchange effect 80−19996
outer planetary atmosphere, ionisational nonequilib. shock layer effects on entry heating 77−25979
ozonosphere, radiative-photochemical model for temp. coupling effects on O_3 depletion 78−57246
parabolic reflectors, diffuse-specular axisymmetric surfaces, radiative anal. 80−33438
partially redistributed resonance radiation, ang. depend. 77−42285
particle transport phenomena, theory, book 79−63176
particles in dilute cloud, radiant heat transfer 77−58537
particulate material, six-beam model 77−17924
particulate multiple-scatt. medium, radiance prod. by laser beams 78−9325
perforated wall, injection cooled, temp. 78−90671
phase-integral method for radiative transfer problems with highly-peaked phase functions 79−7278
photoelectron transport analytic approach 77−70932
photon energy averaging, diffusion type eqn. *(Russian)* 77−31400
photosensitised reacts. in continuous chem. processes, scatt. effects 78−73057
photosphere, response functions and contrib. functions of spectral lines 77−17462
pipe wall with radiative heating and working medium at supercritical pressure, temp. fields 77−7479
plane atmosphere, invariance principles and integral eqns. for radiation fields 80−67559
plane atmospheres, nonlinear eqns. in linear transfer problems 79−62741
plane layer, effect of boundary refl. and selectivity of optical characts. on radiative-conductive heat transfer 78−1554
plane layer of molecular gas, IR radiation 77−35021
plane parallel atmosphere involving energy sources internal radiation field *(Russian)* 77−91417
plane parallel atmospheres, radiative transfer eqn. soln. 80−67409
plane stratified dielectric 78−51050
plane system with shadow, radiant and molecular transfer, algorithm 77−58538
plane-parallel atmosphere with polynomial emission source distrib. 80−94700
plane-parallel scattering absorbing media, approximate method for radiative transfer 78−37805
planetary and terrestrial atmospheres, book 79−62568
planetary atmosphere, a^m and b^m functions of anisotropic scatt. 77−56848
planetary atmosphere, diffuse refl. and transmission, soln. for three-term phase function *(Russian)* 77−13260
planetary atmosphere, F_N method for polarisation studies 80−98540
planetary atmosphere, light scatt. by optically thin atmosphere rel. to brightness at zenith near terminator 80−109382
planetary atmosphere, Markov chain formalism 78−36447
planetary atmosphere, radiation field near reflecting surface 77−25962
planetary atmosphere, single-scatt. albedo determ. for Rayleigh-scatt. atmosphere with true absorpt. 80−94704
planetary atmosphere studies by occultations, wavelength depend. of turbulence effects on refr. angles 79−48697
planetary atmosphere with isotropic scatt., radiation field 77−13232
planetary atmospheres, azimuth-independ. multiple scatt. with rough surface 78−12085
planetary atmospheres, polarised radiative transfer in flat geometry media, soln. symm. 79−21180
radiative transfer continued
planetary atmospheres, Rayleigh scattering in spherical shells 78−85872
planetary atmospheres, turbulence effects on atmospheric profiles derived from radio occultations 77−60696
planetary atmospheres, turbulent, effects of inhomogeneous background on radiation propag. 78−69679
planetary atmospheres, two stream approx. 80−109383
planetary boundary layer, nocturnal evolution *(French)* 79−84397
planetary coronae, multidimens. radiative transfer 77−64638
planetary finite atmospheres, key eqn. exact soln., Laplace transform and linear singular operators method 80−67536
planetary nebulae, geometry effects on H Lyman α form. 78−20871
planetary plane-parallel optically thick atmosphere, Rayleigh scattering 77−73947
planetary ring, radiative transfer and multiple scatt. shadowing effect, theory 79−29987
planetary spectra, anisotropic scatt. effects 77−2357
planetary spherical shell atmospheres, appl. to Venus, line form. level 80−17487
planetary surface layers, validity of radiative-conductivity, theory 77−17354
plasma, expanding, laser produced, radiative transfer line intensities and stimulated emission 77−3988
plasma, multicomponent multiply ionised, mean radiation paths calc. 80−33754
plasma, non-LTE line transfer, excited atom diffusion effects 77−31435
plasma, radiative, with anisotropic permittivity, developing wavefronts 80−43896
plasma, radiative cooling rates, high-temp. low-density plasma $2 \leq Z \leq 92$ 78−83534
plasma, vol. emission coeff. meas. by fully automatic optical system 77−58893
plate, flat, optically thin boundary layer, of grey medium near leading edge, radiative-convective heat transfer 78−91027
plate, radiant, heating by high temp. gas flow *(Russian)* 78−18154
point explosion in arbitrary atmosphere with radiative heat transfer 78−53708
point source in finite sphere, radiation field calcs. 80−13006
polarisation effects on surface due to radiative transfer *(French)* 80−79127
polarisation of scattered radiation, in medium with internal energy sources 80−67541
polarisation transfer, in thermal radiation sources *(Russian)* 77−91656
polarisation transfer in inhomogeneous magnetised plasma, comments and reply 79−96905
polarisation transfer in inhomogeneous magnetised plasma, inclusion of non-orthogonality props. 79−84662
polarised light, response functions for mag. lines 77−45304
polarised light transfer problem in presence of absorpt., soln. 80−67561
polarised radiation, multi-dimensional non-LTE transfer in mag. flux-tubes 78−69673
polarised radiation, transfer through rarefied magnetoactive plasma 79−92669
polarised radiation field, statistical equil. eqns., density matrix technique 77−5425
polarised radiation propag. in shearing field-free plasma, rel. to pulsar microstruct. 80−17483
polarised radiation transfer in inhomogeneous media 80−99607
polarised radiation transfer in inhomogeneous self-absorbed synchrotron sources 77−78623
polarization transfer eqn. in inhomogeneous magnetized plasma, solns. 78−28506
polarized light, eqn. soln. method in relativistic cosmology 78−73781
polarized radiation field, asymptotic characts. for low absorpt., appl. to nonconservative Rayleigh scatt. 80−5686
polarized radiation in isotropic media, linear singular integral eqns. 77−45306
polarized radiation transfer in X-ray pulsars, analytical solns. 80−94894
polluted urban planetary boundary layer 78−7708
polydisperse layer, isothermal, thermal radn. 77−68374
polydisperse media, optical characts., approx. representation 80−63922
power plant, high-temp. efficiency enhancement using coolant with particle suspension *(Russian)* 79−68549
propane, total emissivity, press. depend. 78−90673
protostellar envelope evolution, radiative transfer and spectrum 80−77384
protostellar envelopes of masses 3 M$\odot$ and 10 M$\odot$, coupled radiative transfer/hydrodynamics eqns. and IR appearance 80−36616
pulsar magnetosphere, curvature radiation-pair prod. model for gamma-ray emission 79−5852
pulsar magnetosphere, electron absorpt. rel. to spectra low-freq. dropoff 80−17602
pulsar magnetosphere, radio propag. effects on pulsar emission polarisation 79−75235
pulsars, gamma ray emission and transfer problem 78−65641
pulsed radiation, small-angle scatt., appl. to X-ray bursts and interstellar dust 78−57433
PWR rod bundles, radiative heat transfer calc. method 80−33602
QED derivation of radiative transfer equation for partially polarised light 77−79235
QSO clouds, Rayleigh-Taylor stability of radiation-supported surfaces and slabs 77−53697
quadratic integrals of transfer eqn., for monochromatic isotropic scatt. 77−33332
quantum mechanical derivation of transfer equation 79−80546
quantum mechanical description of radiative transfer, radiation processes 79−53713
quasars, H emission lines radiative transfer and spectra 78−96557
quasars, radiative transfer theory for H line emission from dense plasmas 80−51900
quasars, radiatively driven gas clouds dynamics and stability, plane-parallel slabs theory 80−22107
quasi-stellar objects, fully interlocked transfer calcs. for H emission line ratios, implications 80−56968
quasimonochromatic radiation propag. in static gravit. field *(Russian)* 77−70992
quasimonochromatic radiation propag. in stationary gravit. field *(Russian)* 77−70993
radiant-convective heat exchange problems, nonstationary, analytical soln. method 80−33432

radiative transfer continued
radiating gas, nonlinear attenuation of plane pulses, shock wave formation *(Russian)* 77−35259
radiation field in deep layers of semi-infinite medium with elongated phase function *(Russian)* 79−35129
radiation field in semi-infinite medium with internal radiation sources *(Russian)* 77−29437
radiation intensity in finite slab, integral Fourier transform technique 77−67389
radiation pressure in spectral lines in gaseous systems with axisymm. motions, kinematics 79−88579
radiation problems transport eqns., using Wigner distribution 80−168
radiation shape factor determ., integrator with oblique scale 77−42711
radiation-convection interaction 77−80231
radiative cooling by use of inverse greenhouse effect 79−25329
radiative transfer for confined isothermal medium, asymptotically exact approx. method soln. 79−76953
radiative transfer for isothermal medium confined by isothermal enclosure 79−76952
radiative-conductive heat transfer in plane-parallel layer 78−22256
radiative-conductive heat transfer in slab, steady-state problem 78−38181
radiative-convective heat transfer, numerical methods 78−94577
radiative-convective heat transfer from extended surface, Monte Carlo method 78−67005
radiator optimal shape for near field in limited vol. *(Russian)* 77−74335
radio galaxies, polarised radiation transfer in magnetoactive plasma 78−24564
radioline series decrement for atomic levels with high quantum numbers *(Russian)* 78−28497
radiosources, decay excitation of plasma turbulence and nonlinear radiative transfer 77−17707
radiosources, self-absorbed synchrotron, polarized radiation transfer 77−53413
random velocity fields, radiative transfer and line form., intensity moment transfer eqn. derivation 80−52967
rarefied gas, convective heat transfer coeff. and surface emissivity, effect of degree of vac. 78−1693
Rayleigh atmosphere single-scatt. albedo, determ. from polarisation meas. 79−35117
Rayleigh scattering transport eqn. exact soln. by Laplace transform and Wiener-Hopf technique 79−8827
real gas, slug flow, radiative and convective transfer interaction 77−58529
rectangular enclosure, six-flux model evaluation 80−1415
redistribution effect in expanding atmospheres, angle averaged in comoving frame 77−17545
redistribution of scattered radiation by collisions in nonimpact region of spectral line profile 79−35109
reflection nebulae, multiple scatt., Monte Carlo approach 78−12320
reflection nebulae, scatt. multiplicity 78−12323
reflection nebulae, with embedded illuminating stars, multiple scatt. 78−12322
reflection nebulae, with foreground stars, multiple scatt. 78−12321
relativistic electron beam relaxation in dense gas, radiative energy transfer 80−69968
relativistic Maxwellian electrons, moment generated radiative transfer functions 78−24747
relativistic self-inductive radiative fluid, wave propag. 79−41772
relict radiation in anisotropic universe, transfer eqn. soln. rel. to polarisation and anisotropy 80−67917
remote sensing of two-layer media, microwave radiative transfer models 77−21908
resonance line nonstationary radiation in homogeneous infinite space *(Russian)* 77−79040
resonance line scatt. from optically thin structs. located above solar limb 78−65591
resonance line scattering in absorbing medium, scaling laws 80−98538
resonance radiation redistribution, elastic and inelastic collisions effect 79−62734
resonance radiation transfer in infinite isotropically expanding medium *(Russian)* 78−61721
resonance radiation transfer in moving media with large-scale radiative coupling *(Russian)* 78−93088
resonance radiation transport with varying Doppler width, thermosphere appl. 80−26737
resonance scattering with absorpt. or differential expansion, Monte Carlo calcs. 80−21901
resonant absorber, Planck spectrum 79−7279
resonant medium with small degree of ionisation, radiation transfer mechanism *(Russian)* 79−37453
rhodamine (6G-DTDC and 6G-CV) in alchohol solns., energy transfer by means of photobleaching 79−23031
S140 IR, far IR spectrum and radiative transfer model 78−93372
Sahara dust mass in atm., satellite radiance meas. 77−9456
Saharan dust radiative characts. at solar wavelengths 77−81969
scattering, conservative anisotropic, in planar medium with collimated radiation 79−55319
scattering functions, adding and invariant imbedding eqns. in matrix notation 78−24745
scattering indicatrix, expansion coefficient through Mie coeff., anal. 80−18993
scattering medium, transfer eqn. for layer with extended scattering indicatrix *(Russian)* 78−40660
scattering medium description by number of particles scattered 78−93623
schlieren interferometer, 3-D vol., radiation transfer, probability model 77−87818
Schuster-Schwarzschild approx. for media with spherical and cylindrical symmetry 80−23875
scintillations in astrophysics, analytic soln. of second-order moment eqn. 80−26726
α^2 Scorpii, circumstellar lines form. rel. to location along line of sight 78−73739
seawater, diffuse irradiance refl., two flow model 77−29301
seawater, optical transfer function meas. in Sargasso Sea 80−8328
selectively grey medium in cylindrical channel, generalized angle factors for wall elements and gas volumes 77−35023
semi-infinite atmosphere containing energy sources, radiation field calc. 80−21907
radiative transfer continued
semi-infinite atmosphere with albedo $\omega>1$, transfer eqn. 80−82184
semi-infinite cylindrical rod, temp. gradient at conical end, radiation effects 77−11106
semi-infinite layer boundary, excited atom conc. distrib. radiating particle motion effects 77−49694
semi-infinite Rayleigh scattering atmosphere, exact soln. using Laplace transform. and Wiener Hopf technique 79−35112
semi-transparent medium, melting rate, radiative transfer effects 78−94590
semigrey nondiffuse cone and V-groove, local temp. distribs. 77−65664
semiinfinite atmosphere, isotropically scatt., radiation field calc. *(Russian)* 78−28496
semitransparent high temp. constructional materials, free radiation contrib. to thermal condition *(Russian)* 79−59914
semitransparent medium, effect of radiation heat transfer in thermal cond. meas. 77−23858
semitransparent solid, temp. distrib., thermal radiation influence 79−76948
semitransparent solids, approx. band model for radiative transfer 79−37136
semitransparent thin cylinder, radiation-conduction heat transfer, light-guide approx. 80−96179
shock layer in gas, spectral lines calc. 78−5641
shock wave incident on wall, thermal radiation effects 78−5823
shock wave propag. across radiative deflagration 77−3846
shock waves in radiating gases, vorticity 79−4089
sky brightness during 26 February 1979 eclipse, radiative transfer model 79−92588
sky radiance during total solar eclipse, model 78−40652
slab, anisotropic radiative transfer, iterative soln. 80−33439
slab, planar radiative transfer with isotropic scatt. 80−23876
slab, radiative source function, approx. soln. 77−65665
slab, with boundary refl., Fourier transform soln. 79−90119
snow, two-stream theory of reflectance 79−88376
snow pack, impact of CO_2 on surface cooling 79−92569
Sobolev method, generalisation for flows with nonlocal radiative coupling 78−28500
soil, surface roughness effect on microwave emission 80−17264
soil moisture meas. by remote microwave radiometry 79−48526
soil thawing under polar conditions using synthetic film covers, thermal balance meas. on polymeric film covered surfaces 77−78244
solar absorbing working fluid properties obs., molten salt heat transfer fluid with solar-absorbing oxide particles 78−87112
solar atmosphere, model including OH continuum opacity 79−40162
solar atmosphere, opacity rel. to acoustic waves and chromosphere temp. rise 79−16911
solar atmosphere, polarisation in reson. lines cores 77−29744
solar atmosphere, scatt. effects on quiet Sun emission at freqs. <200 MHz 78−4183
solar atmosphere, spectral line profiles, acoustic wave effects 80−46517
solar C I multiplets at 1560 and 1657 Å, overlapping emission peaks obs. and theory 78−93178
solar chromosphere, anal. of S I 1807 Å and 1900 Å lines profiles 78−57517
solar chromosphere, Lyman α transfer rel. to Hα seven components and 9873 MHz line 78−89151
solar chromosphere, quiet and active, Lα spectra and models based on partial redistrib. diagnostics 79−75169
solar chromosphere, radiative relaxation time 79−30040
solar chromosphere plages, Ca II and Mg II lines partial redistrib. calcs. 78−89153
solar corona, He^+ 304 Å line radiation theory 77−91510
solar corona, radiation heat flux rel. to expansion 80−90377
solar corona, transfer of X-rays, reson. scatt. 79−16904
solar corona radiative origins 78−96448
solar diffuse radiation through series of parallel regions, transmittance calc. 79−88005
solar energy thermal storage, numerical simulation of energy transfer by conduction and radiation *(French)* 79−24916
solar EUV limb brightening, influence of spicules 77−22170
solar Fe I magnetosensitive lines, Stokes parameters *(Chinese)* 79−80289
solar filaments, radio radiation transfer 77−25995
solar flare H radiative transfer soln. and upper chromosphere semiempirical model 79−40148
solar flare plasma non-stationary heating by non-thermal electrons 77−17455
solar flares, Fe Kα fluoresc. radiative transfer problem 80−17569
solar flares, temp. struct. rel. to radiative cooling and heat cond. 79−40168
solar flares H emission in gasdynamic models 77−17531
solar Fraunhofer lines, effective form. depths calculated by various methods 79−12447
solar granulation, dynamical model 77−60736
solar Hα output coeff. influence on source function *(Russian)* 78−73690
solar hot box systems, efficiency increase by radiation reduction, dielectric/metal/dielectric coatings appl. 78−79195
solar input determination and irradiance maps, analytical model and simulation code 79−34426
solar irradiance three-dimens. transfer in clouds, finite geometry effect 79−58085
solar magnetic fluxtubes, multidimens. non-LTE radiative transfer 77−60741
solar non-isothermal atmosphere, linear hydrodynamical eqns. coupling with radiative transfer 78−20794
solar photosphere, linear hydrodynamical eqns. coupled with radiative transfer, Mg I 5172 Å line interpretation 78−77529
solar photosphere, radiative transfer calcs. rel. to north-south brightness asymmetry 78−45303
solar photosphere Ba II spectrum, partial freq. redistrib. 79−101128
solar prominences, H line radiation diffusion 80−67694
solar prominences, radiation diffusion integral eqns. rel. to H early Balmer lines emission *(Russian)* 80−12718
solar prominences with filamentary struct., radiation transfer 78−89154
solar radiation absorption in ponds, aspects 79−16530
solar radiation intraregional vars. in E United States 79−39804
solar radiative heating, in presence of aerosols 79−16665
solar resonance radiation, multiple scatt. in nearby interstellar medium 80−41874

radiative transfer continued
solar spectral lines, Stokes profiles appl. to vector mag. fields determ. 78−28611
solar spectral lines propagating through interplanetary medium, profiles modification 79−66973
solar transition region, Bowen fluoresc. 78−93179
solar water heater analysis, flat-plate type, domestic 79−62141
solid sheet with selective optical props., combined radiative and conductive heat transfer 78−90672
sonic wave propagation, thermally conducting and radiating gases 78−42679
soot-CO_2-water vap. mixture, in luminous flames and smoke, IR mean absorption coeffs. calc. procedure 78−91061
source function, isotropically scatt. medium, refr. index effect 77−83805
source function surface value derivation in non-LTE radiative transfer 79−35122
spectral line broadening by electron scatt., calc. methods *(Russian)* 77−17347
spectral line formation depth in mag. field, theory *(Chinese)* 80−105159
spectral line formation depth in solar atmosphere *(Polish)* 79−88639
spectral line formation in axisymmetric moving envelopes, numerical method and appl. to YY Orionis stars 80−41813
spectral line formation in YY Orionis envelopes 77−64741
spectral lines, radiative transfer in reson. multiplet lines 78−24460
spectral lines formation in inhomogeneous medium, appl. to solar photosphere *(Russian)* 80−72901
spectral models, applicability, radiative gas dynamics 78−14100
spectrum line contours in incoherent scatt. 79−88590
spectrum-integral emission field characts. 78−90669
between specularly and diffusely reflecting surfaces 77−7296
spheres, radiation and shape factors 79−32207
spherical accretion onto neutron star or black hole, radiation press. effects 78−61725
spherical dust shell around central star, two-shell moment method for radiative transfer 80−62001
spherical dust shells, generalised two-stream Eddington approx. 79−35120
spherical extended atmosphere, radiation transport with discontinuous source function 77−53417
spherical geometry, numerical soln. of radiation transfer eqn. 80−90329
spherical harmonic approximations 80−173
spherical shell atmospheres, asymmetric phase functions 79−2500
spherically symmetric flows with nonmonotonic vel. fields, radiative transfer 80−94699
stainless steel, cylindrical surface protrusions, apparent radiative props. *(French)* 78−94569
starlight interstellar polarisation, fluctuation theory 80−82442
stars, line form. in moving envelopes, radiation field and statistical equilib. eq. 77−87374
stars, line profiles in expanding envelopes 79−44464
stars with IR excesses, optical emission intrinsic linear polarisation origin 78−96481
steam, Curtis-Godson approx. 78−67019
steam, total emissivity, press. depend. 78−90673
Stefan problem, new expansion procedure 77−92
Stefan problem, solns. for separation of variables case 77−11119
stellar, extended envelopes with differential rot. and expansion, reson. radiation transfer *(Russian)* 77−64747
stellar atmosphere, departure from LTE 79−48777
stellar atmosphere, exact soln. of line scatt. intensity transfer eqn. 79−84784
stellar atmosphere, expanding, Feautrier method 79−25593
stellar atmosphere, extended, anisotropy of radiation field *(French)* 79−48776
stellar atmosphere, Green's function method for noncoherent anisotropically scatt. plane-parallel slab *(Russian)* 78−61723
stellar atmosphere, non-LTE line formation in mag. field, two-level atom with freq. independent source function 78−61726
stellar atmosphere, reson. line form. in decelerating spherical flow 77−78624
stellar atmosphere, thermal-convective instability, radiative transfer effects 78−53929
stellar atmosphere in statistical equilib., effects of deviations from LTE 80−31290
stellar atmospheres, C I as continuous opacity source in late B-type main-sequence stars 77−87393
stellar atmospheres, characts. lengths for moving media *(Russian)* 77−82117
stellar atmospheres, coherent scatt. 78−28667
stellar atmospheres, geometries other than plane-parallel layers *(Italian)* 78−81616
stellar atmospheres, H_2^- and N_2^- free free absorpt. rel. to opacity 78−81610
stellar atmospheres, H continua from radiative shock 78−40918
stellar atmospheres, line formation in microturbulent magnetic fields 80−31201
stellar atmospheres, LTE problems, numerical techniques 77−71108
stellar atmospheres, non-LTE diagnostics *(Italian)* 78−81615
stellar atmospheres, non-LTE line form. in presence of mag. field 78−7871
stellar atmospheres, noncoherent renormalisation group approach 78−65495
stellar atmospheres, opacity, H^- bound-free photodetachment cross section calc. 79−49996
stellar atmospheres, radiation scatt., approx. soln. *(Russian)* 80−36621
stellar atmospheres, radiative equilibrium departures, grey absorpt. 78−81531
stellar atmospheres, radiative heat transfer in presence of mag. field *(Russian)* 77−87247
stellar atmospheres, rotational darkening or brightening 77−60750
stellar atmospheres, transfer eqn. perturbation soln. 77−45404
stellar atmospheres with spherical symmetry, conservative Milne problem 78−49312
stellar envelopes, generalised Eddington approximation 79−80214
stellar expanding envelopes, radiative forces 78−28659
stellar expanding envelopes, two-level atom model 78−61849
stellar finite atmosphere, key eqn. exact soln., Laplace transform and linear singular operators method 80−72762
stellar interiors, opacity due to electron correls. 77−64634
stellar magnetic atmospheres, analytical soln. 80−36494
radiative transfer continued
stellar model atmospheres, line blanketing rel. to limb darkening coeffs. 79−35243
stellar moving atmosphere, spectral lines differential Doppler shifts rel. to vel. gradients determ. 78−57538
stellar spectral lines, geometric solns., diagnostic anal. 77−5423
stellar spectral lines form. depths calc., rel. to curve of growth method *(Russian)* 78−65604
stellar stmospheres, spherical transonic flow, reson. line radiative transfer 80−94698
stellar weak interaction rates for sd-shell nuclei, appl. to supernovae 80−82336
stellar winds, steady state transonic wind model, radiative cooling effects 80−77391
Stokes parameters and mag. field vector profiles *(Chinese)* 80−77386
stratified turbid medium, small-angle approx. soln. *(Russian)* 80−82057
stratosphere, aerosol layer visible and IR optical props. influence on global climate 77−2240
stratosphere, CO_2-O_3 coupling in Cl free atm., photochemical-radiative column model 80−85723
stratosphere, radiative-dynamic coupling, 3-dimens. circulation model 77−86965
stratosphere, seasonal climate, numerical simulation, energetics 79−5567
stratosphere, seasonal climate, numerical simulation, zonal temp. and wind 79−5566
stratosphere, upper, radiative damping, obs. evidence 79−84368
stratosphere aerosol, radiation transport model rel. to climatic effects of aerosol layer modification 80−98408
stratosphere and mesosphere, review 78−49105
stratosphere O_3-CO_2 coupling, photochemical radiative column model with Cl chemistry 80−85724
stratosphere photochemical-radiative damping and instability, numerical results 78−81286
stratus cloud, in Arctic regions, radiation trapping rel. to layering 77−5290
stream containing gasdynamic disturbances, shock wave effects on inversion 77−15137
strong shock with radiation near stellar surface 78−32442
sunlight under fractional cloud cover, two-stream approx. 80−51534
sunspot model, radiation transfer theory 80−21964
sunspots, magneto-optical effects rel. to linearly polarised intensity distribs. obs. with vector magnetograph 80−21965
supercritical accretion onto unmagnetized neutron stars rel. to galactic bulge X-ray sources 79−80331
supernova remnant optical emission spectra, effect of shock wave intermediate zone radiative cooling 80−109517
supernovae, radiation dynamics, envelope ejection and light curves 77−64783
supernovae, type I, conservative scatt. theory for effects of line overlapping on spectra *(Russian)* 80−105266
supernovae, type II, nonequilib. processes in evolution 80−46586
supersaturation during heat and mass exchange in stationary gas medium 79−94480
supersonic flow past blunt body, radn. effect on flow field and heat flux 77−47113
supersonic flows, probabilistic approach to radiative transfer 79−53712
surface heat flux, nonisothermal grey gas, complex grey walls 80−10125
surfaces in diathermal medium, radiation anisotropy modelling 80−33435
surrounding variable source of heating radiation, IR flux development 80−105324
suspension, thermal EM radn. 2-dimens. multiple scatt. 77−39209
swirling turbulent radiative arc heater flowfield, model 79−41764
synthetic scattering phase function 80−74294
synthetic scattering phase function for radiation transfer 80−98541
T Tauri nebula, Lyman continuum transfer rel. to ionisation and emission line spectrum 80−67820
temperature jumps in a transient radiative transfer problem 80−33427
Thailand tropical atmospheric radiation and sky temp. calc. 79−58084
theory and analysis methods, review 79−81703
thermal emission, doubling and superposition methods 80−1414
thermal microwave emission from random inhomogeneous layer over homogeneous medium 77−42726
thermal microwave emission from two-layer medium, theory 77−49170
thermal-convective instability of partially ionized plasma, radiative transfer, medium porosity and collisional effects 80−67538
thermoacoustic stability of high-temp. heat generating gas 77−75992
thermokinetics of coupled radiative and conductive transfer, Kalman filtering identification *(French)* 79−41558
thermotechnical equipment, radiant heat exchange modelling in rectangular chamber with attenuating medium 80−33433
Thomson scatt. in thick layer 77−82216
three-term radiative transfer, inverse soln. by F_N and Monte Carlo methods 80−109352
time dependent, two-level atoms and one level atoms plus continuum 77−29638
time-dependent radiative transfer, exact soln. of integro-differential eqn. via Laplace transform 80−94703
total solar radiant property evaluation from spectral data 79−76954
TPD-plasma, optical escape factors and population densities 79−37460
transfer equation solution for Rayleigh's phase function by principle of invariance 79−84660
transient radiation-conduction heat transfer in selectively absorbing media 78−90670
transient radiation-conductive heat transfer in selectively-absorbing media 78−94572
transient radiative heat transfer between two emitting-absorbing media 78−94573
transient temp. of body, surface radiation and convection, quasilinearization approach 77−80054
transparent turbulent gas flow past radiating plate, heat transfer anal. 77−35257
transpiration-cooled system, thermal response in radiative and convective environment 78−32323
transport equation with scattering albedo $\omega_0<1$, exact soln. using Laplace transform and Wiener-Hopf technique 79−35111
transport or diffusion calculations, appln. of multiband method 80−95333
transport theory, characteristic eqn. 77−82473
transport-diffusion interfaces in radiative transfer 79−98598

radiative transfer continued
transport-equation, with anisotropic scatt. in finite slab geometry 79−17364
troposphere, IR radiative exchange from six-layer general circulation model 80−101432
troposphere, IR transfer in partial cloud cover, model 80−12544
troposphere, O_3 effects on Earth-atmosphere system radiative energy budget and climate 80−36365
troposphere, radiative cooling rate and flux, theory 80−85711
troposphere and lower stratosphere, cirrus clouds influence on IR cooling rate 78−73455
troposphere and stratosphere, simplified radiative-convective model 77−5320
turbid atmosphere, single-scatt. solution 79−16663
turbid atmospheres, path length distrib. of scattered photons 77−45147
turbid estuarine waters, optics, approxs. and appls. 79−66712
turbid water 80−8331
turbid water bodies, radiation absorpt. and scatt., radiative transfer eqn. solns. 79−81704
turbulent jet, radiative transfer 78−94578
turbulent media, theory 78−94578
turbulent plasma, wave scintillations, fourth-order moment eqn., astrophys. appl. 80−46381
turbulent scatt. in exponential atmosphere, wave-optical soln. 77−60590
turbulent suspension, combined radiative and convective heat transfer 78−9724
turbulent-jet-diffusion flame, effect of mol. gas radn. 77−80232
two-dimensional isotropic scattering, semi-infinite cylindrical media 78−90678
two-dimensional radiative transfer, planar geometry theory 78−40810
two-dimensional radiative transfer in a finite scattering planar medium 79−90118
two-dimensional steady state heat transfer with surface heat sources, program *(Italian)* 79−37132
two-phase inhomogeneous media of cylindrical geometry 79−23377
two-phase media of cylindrical geometry, refl. power 79−90121
Unno-Kondo generalized Eddington approx. in extended atmospheres 80−21997
upper atmosphere, O I 1304 Å nadir intensity/column prod. rate rel. to airglow 77−45213
upper atmosphere radiation transfer eqn. approx. soln. *(Russian)* 77−13122
urban planetary boundary layer, pollution effects on thermal struct. and dispersion 78−11986
W Ursae Majoris stars, effects of photospheric convection on source function 78−49478
US assisted radiant heat transfer into water and air 79−46169
UV and integrated solar radiation received, influence of cloud layers 79−70883
UV backscatter expt., airborne, for O_3 distrib. determ., error anal. 78−92985
vacuum-powder insulation, radiative heat transfer determ. by IR spectroscopy 77−13759
variable star, luminosity changes rel. to orbiting particle motion, accretion and ejection 79−44338
vegetation reflectivity, effect on atmospheric radiance and polarisation 78−40650
Venus, cloud model using radiative transfer theory 77−82138
Venus, radiative transfer, far IR opt. consts. of H_2SO_4 droplets 77−8574
Venus atmosphere, interpretation of weak absorpt. lines 78−24481
Venus atmosphere, IR polarization interpretation 79−53745
Venus atmosphere, model based on Venera 10 data *(Russian)* 80−12698
Venus atmosphere, radiative transfer rel. to thermal balance 77−73994
Venus atmosphere, scatt. solar radiation in cloud layer, multiple scatt. theory inversion 79−8865
Venus atmosphere, scattered solar radiation fluxes spectral and altitude distrib. 80−62059
Venus atmosphere, thermal radiation in 2.86-4.16 μm window 79−8863
Venus atmosphere, thermal radiative transfer, numerical modelling 80−8574
Venus atmosphere, Venera-8 optical meas. interpretation 79−8864
Venus clouds, absorpt. lines curve of growth rel. to spectropolarimetric equivalent widths information content 80−31215
vertically nonuniform stratocumulus water clouds, radiation transfer 77−45146
view factor, diffuse radiation between the spheres exact and approx. calcs. 77−26252
viscous radiating gas, hypersonic flow over blunted cones 77−51131
viscous-shock-layer analysis for equilib. flow about blunt axisymm. body, effect of coupled ablation injection 77−24033
visible light model 77−39205
Voigt function, partial differential equations, for stellar atm. line profile calcs. 78−28507
Voigt line width, empirical fits 77−22059
water, deep evaporation characterisation, from homogeneous porous medium *(French)* 78−59468
water, impact of CO_2 on surface cooling 79−92569
water mass, inherent optical props. of Lake Ontario coastal waters 80−36337
water suspensions, radiative property measurements 80−9811
water vapour, radiance spectra, nonisothermal band models 77−62329
water vapour emissivity, simple parameterisation 77−42958
wave propagation in medium with high radiation press., basic eqns. for homogeneous media 79−88581
wedge flow, anisotropic radiatively coupled, Milne-Eddington approx. 77−31398
white dwarf star, GD229, cyclotron absorpt. 79−53813
Wolf-Rayet stars, laser action in distended envelopes 77−13354
X- and Y-equations, new representation using Wiener-Hopf technique 79−53710
X-ray binary system, Fe fluoresc. line struct. 77−78889
X-ray binary systems, K-fluorescence lines in spectra 78−93456
X-ray binary systems, models, X-ray transfer, Monte Carlo study 78−93463
X-ray pulsars, vacuum polarisation effect rel. to radiative transfer and X-ray spectra 80−27015
X-ray radiation emitted near black holes, relativistic radiative transfer and polarisation features 80−46700
X-ray sources, compact, optically thick radiative transfer rel. to X-ray spectra form. 80−22115
radiative transfer continued
X-ray sources, high-freq. EM waves propag. through magnetised plasma in curved space time 80−48894
X-ray sources, time-dependent Comptonisation and X-ray reverberations rel. to rapid time variability 80−86013
X-rays Comptonization by low-temp. electrons, Monte Carlo calc. 80−12653
X-rays transfer through optically thick shell 78−65488
Zeeman line profile, mag. field determ., appl. of radiative transfer problem soln. 80−82221
zenith observation, contrast reduction due to atm. extinction, calc. 79−84479
A- and B-type stars, radiation forces and B abundance diffusion theory 79−88664
Al, plasma, transfer eqn. soln. using freq. and angle averaged photon escape probabilities 80−64688
Au plasma, high-density, high-temp., radiative opacity, particle beam fusion system 80−10365
Au, thermal radiative props. at cryogenic temps., comparison with model predictions 77−15604
C, paint type coating layer with spherical pigment, radiative transfer theory 80−61405
C stars atmospheres, transfer eqns. and Li line form. 78−65615
C^-, free-free transitions, continuous absorpt. estimation 78−9098
CO_2 15 μ band radiant energy inflow in disturbed LTE *(Russian)* 78−40657
CO_2, Curtis-Godson approx. 78−67019
CO_2 ice spheres, IR scatt. and absorpt. props. 80−97269
CO_2 plasma, atm. press. opt. props., 400-1200 nm spectral range and 10^3-2×10^4K temp. 80−33753
CO_2, rot.-vibr. bands, absorpt. coeff. calc. method, Fermi reson. effect on spectral lines 80−32696
CO_2-N, nonequilib. mixture convective and radiational heat exchange during flow past body 80−14850
Cs, photoplasma, optical excitation in radiation diffusion conditions 78−55227
Cu plates, gap magnitude effect on their thermal interaction at cryogenic temps. 79−86323
Fe_2O_3, paint type coating layer with spherical pigment, radiative transfer theory 80−61405
H I Lyman α line formation in expanding spherical planetary nebula 79−30110
H II regions, compact inhomogeneous, radio recomb. line and continuum emission theory 79−62885
H II regions, effects of dust on radiative transfer and struct. 77−33588
H plasma, departures of electron energy distrib. from Maxwellian rel. to radiative transfer 77−80274
H plasma plane and cylindrical layer emission field calc. *(Russian)* 80−33755
H, scatt. in reson. line wings and hyperfine struct. levels excitation *(Russian)* 77−57930
H^- free-free absorption, target polarisation effects 79−66917
H-like ions, departure coeffs. from thermodynamic equilib., rel. to radio-sources recomb. lines 79−76369
H_2, gas, radiative light scatt., approx. line shapes 78−90221
H_2 plasma, nonequilib., radiative props., computer program 79−90388
H_2O-CO_2, IR radiation transfer 79−80028
He I 584 Å in quasars and gaseous nebulae, line transfer problem and line strength 80−67550
He plasma, cooling, nonequilib.-ionised radiating ats. 77−76128
Hg discharge, high-pressure, NaI and TlI additives, line broadening and radiative transport 80−74199
N_2-propane mixture, total emissivity, press. depend. 78−90673
Ne, reson. level lifetimes, Zeeman coherence radiative and collisional transfer between excited states 77−23466
O I emission resonance triplet lines form. in solar spectrum 78−24504
OH maser sources, interstellar, radiative transport effects on inversion 80−17681
SiO film on Al, radiative cooling surface 80−50439
Ta surface, nonstationary heating and oxidation in low temp. plasma flow, heat and charge transfer obs. *(Russian)* 80−104341
TiO_2, paint type coating layer with spherical pigment, radiative transfer theory 80−61405

radicals, free *see free radicals*

radio applications
see also radio direction-finding; radioastronomy; radiocommunication; radionavigation
atomic clocks synchronisation, VLBI obs. 78−29092
aurora, Doppler vel. meas., radio aural spectral charact. and incident incoherent scatter meas. 80−56663
auroral ionosphere, radio investigations via VHF bistatic Doppler system 78−28387
deep sea mining ship, telemedical treatment system development 78−77147
dielectric medium, strongly absorbing, local defect detect. 80−35481
Earth surveying 79−100805
geological prospecting using VLF surface mode, wave tilt meas. 80−77139
ice sheet radio echo sounding, polarisation of signal 77−56755
magnetosphere, electron density meas. via International Sun-Earth Explorers 78−85803
oceanography, large scale, radio techniques contribs. 78−77337
oceanography, meas. using radio interferometer techniques 79−53559
oceanography, short bibliography of Russian literature 78−77338
perinatel radio telemetry 80−104722
picosecond fluorescence spectroscopy using CW laser and radio 77−27200
solar wind, electron density meas. via International Sun-Earth Explorers 78−85803
synoptic meteorology, shipboard sounding system for GWE 80−17394
synoptic windfinding technique, Loran and VLF navaids used with radiosondes 80−17392
synoptic windfinding using Oméga VLF navaid, atmos. radiowave propag. 80−17309
synoptic windfinding using radiotheodolite system, of USA National Weather Service 80−17379
time correlation of seismic events 80−90253

radio broadcasting
astronomy, education by radio programmes 77−67157
auditory picture properties, psychological factors *(Polish)* 77−77917

radio broadcasting continued
F_2-layer ionisation through a solar cycle, SW communications appl. 80−41626
ionospheric cross-modulation of radio signals between two nearby stations 78−93048
LF band, daytime sky-wave propag. effect 78−61648
LF band, noise field and skywave propag. 79−5708
medium wave, interference fading *(Russian)* 79−40018
MF band, polarisation coupling loss and sea gain effects 79−5709
MW field strength meas., sunset, night, ionospheric radiowave propagation appl. 77−67010
Nigerian local radio strategy, rural communities education 79−40313
reference frequency, Cs freq. standard for receiver control 79−6099
RF radiation levels in urban areas 78−40351
speech and musical signals statistical props. 79−76919
studio architectural acoustics, 'Deutsche Welle' building construction and meas. *(German)* 80−106668
SW transmission, proportional effect of ionospheric damping, solar activity *(Hungarian)* 80−56675
time and freq. meas., users' manual 80−94934
time dissemination for public requirements and communication systems, Canada 78−41284
USSR, educational TV and radio programme development *(French)* 78−89286
VHF and UHF, influence of polarisation on transmission quality *(German)* 78−61518
weather forecasting on radio and TV, development in America 77−49549

radio direction finders *see radio direction-finding*

radio direction-finding
E.Asia, atmospheric noise source contour maps 77−91245
atmospheric sources location, via triangulation direction finding network 79−100981
LF source localization and polarization determination using satellite radioastronomy *(French)* 79−70940
lightning source directions, 34 MHz interferometry 79−79939
Pc 1 geomagnetic pulsation sources, location using ULF goniometer techniques *(French)* 79−70890
radiosource localisation with short electric antennas on spacecraft 79−21184
SARSAT, search and rescue satellite, ionospheric effects on Doppler frequency 79−58183
tracking receiver direction finder for whistler mode signals, initial results 78−77429
VLF signals, time-varying, determination of wave normal directions *(French)* 79−70927
whistler two-frequency direction finder development 79−53674

radio equipment
see also antennas; loudspeakers; transceivers
construction kits, practical hints including soldering 79−80591
digital frequency-to-temp. convertor for use in radio telemetry systems 80−8119
Hungarian developments, BEAG activities 78−46860
UHF, SAW oscillator 79−7272

radio links
see also microwave links; radiocommunication
atmospheric pollution centralised supervision system, computer station/capturing stations links 78−81410
attenuation meas. for radio delay system design *(French)* 78−53685
Earth-ionosphere waveguide parameter determ. by VLF transitional route meas. 77−91234
ELF/VLF goniometer receiver, remote, unmanned, in Antarctica, UHF telemetry link 80−21854
heart rate radio telemetry for rats, nonobtrusive system 77−90964
HF sky-wave received signal level determination for communication link 78−85758
ionospheric radiowave propagation conditions at decimetre wavelength 78−45136
LF/VLF, for time-freq. secondary standard comparison 77−87737
line-of-sight, experimental investigation by direct meas. of impulse response *(Italian)* 79−70867
line-of-sight, propag. characts. eval. using impulse analysis *(Italian)* 79−70868
microwave propagation in standard atmosphere, ducting, subrefraction effects *(Norwegian)* 79−29835
precise time dissemination via OMA-50 kHz 80−47032
radiosonde meas. and spectral anal. of LOS fading 80−56568
rain attenuation above 11 GHz 80−98410
rain depolarization at 11.6 GHz *(French)* 78−53687
remote automatic station on radio link for wind and temp. monitoring 78−85726
satellite transmission, distribution of sound, graphical pictures 80−31463
satellite VHF/UHF communications, effect of ionospheric scintillation 77−41264
SHF signal attenuation by rain, monitored by radar 80−51567
solar photovoltaic system feeding unusual length radio link, characteristics and design data 80−61383
solar powered microwave telecommunication links, Papua New Guinea, research 79−29449
standard long-range operating stations in shelters with integrated thermal-syphon system 80−53616
telemetry, vibration measurements in steam turbine blades 77−68538
terrestrial and Earth-space propagation paths, rain attenuation joint statistics 78−73490
time signal coding and clocks for private and industrial use *(German)* 78−89445
troposcatter, Doppler crosswind relations 77−5303
tropospheric effects on radio communication, book 80−62400
UHF/SHF tropospheric scatter radio links, scanning beams 78−81276
VHF signals, ionospheric radio fluctuation obs. from geostationary satellite 79−21091
VLF, phase reception/processing convertor, for time-freq. secondary standard service 77−87739

radio networks
HF transmission networks, use of ionosphere models in administration problems *(French)* 79−58175

radio receivers
see also superheterodyne receivers
AM, constructed from pie plates, for teaching 78−81771

radio receivers continued
ceramic filters appl., using $Pb(Zn_{1/3}Nb_{2/3})O_3$-$PbTiO_3$-$PbZrO_3$ and $Pb(Mg_{1/3}Nb_{2/3})O_3$-$PbTiO_3$-$PbZrO_3$ *(Japanese)* 80−60507
clock for reception and display of time code information 79−175
data output device using narrow tape recorder for radio receivers 79−29993
DCF 77 standard time and frequency receiver, display ccts. *(German)* 77−13737
Doppler receiver, dual freq., for NAVSTAR Global Positioning System satellites, accuracy 79−100803
ELF/VLF goniometer receiver, remote, unmanned, in Antarctica, UHF telemetry link 80−21854
heterodyne freq. analyzer, detection of 200 to 400 GHz weak microwave signals 80−94716
International Sun-Earth Explorer A, Stanford University VLF wave injection expt. receiver 78−85806
marine radiofacsimile weather chart receiver and recorder 80−46297
miniature radio interferometer terminals, for Earth surveying 79−100805
mm-wave, travelling-wave maser for 85-90 GHz, using slot-fed guide slow wave cct., radio-telescope applic. 77−5429
mm-wave, travelling-wave maser using Fe doped rutile for radio telescopes 77−3562
MM-wave spectral line receiver, low noise 77−41300
planetary LF radio emission meas., used in Voyager spacecraft mission 78−4075
powered superconductor MM range receiver for radio astronomy 80−21919
radiotelescope, Croce del Nord, front-end with 30 to 408 MHz amplifier-convertor *(Italian)* 79−2478
radiotelescope VLPA FIAN, antenna phased array equipment, characts. *(Russian)* 77−22065
SAW resonator filter 79−7271
standard frequency receiver XKE 2, 10 to 200 kHz, for regulating crystal and atomic freq. references 79−67259
time-code clock, date display, BST switch and alarm add on circuits 77−53866
tracking correlation receiver with feedback for radio astronomical interferometry 78−57445
uncooled millimeter wave receiver for radioastronomical observations *(Swedish)* 78−24461
VHF/UHF, remote frequency measurement appl. *(German)* 78−4631
VLBI, Japanese domestic system, receiver and local oscillator *(Japanese)* 80−21923

radio reception
see also atmospherics; jamming
amplitude scintillations of radio beacon signals in equatorial electrojet region 77−29578
interstellar probes communications, transmission and reception philosophy 79−21133
ionospheric layers E, F, and D, effect on SW reception 80−67451
ionospheric scintillation, effects on received signal level 78−93047
SHF signal attenuation by rain, monitored by radar 80−51567
superposed plane waves, complex angles of arrival 77−71908
time signals, Tokyo reception accuracy 78−69606
VLF signals, numerical study of satellite reception using waveguide concepts 80−90282

radio reception quality *see radio reception*

radio relay systems *see radio links*

radio studios
acoustic design of talks studios and listening rooms 79−37091
acoustics planning for SDR's Stuttgart Broadcasting House *(German)* 78−71243
architectural acoustics, 'Deutsche Welle' building construction and meas. *(German)* 80−106668
Broadcasting House, SDR, Stuttgart, sound engineering planning *(German)* 78−1512

radio systems
see also mobile radio systems
electromagnetic waves, transmission and propag., book 79−50198
emergency warning system, earthquake prediction appl. *(Japanese)* 78−85497
large-aperture radio system for meteor studies 80−85870
VHF bistatic Doppler system, for radio investigations of auroral ionosphere 78−28387

radio transceivers *see transceivers*

radio transmitters
see also radiosondes
77.5 kHz transmitter signal, derivation of standard frequencies *(German)* 77−53928
energy deposition in simulated human operators of 800-MHz portable transmitters 79−8525
implantable biotelemetry transmitter for 6 differential signals 77−48968
patient temperature monitoring, μA radiotelemetry transmitter 79−16356
radio buoy for tracking oil slicks 78−45034
RF energy absorpt. of simulated body material using portable transmitters 78−44614
RF radiation hazards to personnel, mobile and portable transmitters, US Citizen Band Service 77−40795
telemetering of high temperature, inside metallurgical furnace *(Czech)* 77−2659
telemetry, transmitter for small animal temp. meas. 79−83888
VHF, 15 W, covering 6 metre band *(Spanish)* 77−53310

radioactive age determination *see radioactive dating*

radioactive chemical analysis
see also radiochemistry
^{14}C determination, chemical anal., in HTGR spent fuel elements 80−42745
^{252}Cf based nondestructive assay system for fissile material 78−73119
activity evaluation and statistical accuracy in activation determ. of low element conc. 79−87928
air and water pollution detection appl. *(Hungarian)* 77−36840
alpha counting and spectrometry by liq. scintillation, appl. to bone and tissue samples 77−25617
aluminosilicate glass, diffusion of Sn(IV) 80−49417
autoionography of beta-emitting radionuclides distrib. on thin-layer chromatograms 78−20126
automatic evaluation of isotope anal. of nuclear fuels, isotope dilution, mass and α spectrometry 78−55120

radioactive chemical analysis continued
automotive exhaust gas catalysts, radiometric determ. of Pt and Pd attrition 78−31740
autoradiography and soft laser scanning in radioisotope work, appl. to metabolic studies 78−3576
biological sample ^{32}P and ^{45}Ca determ. by Cherenkov and liq. scintillation counting 80−98183
biological samples, neutron-activated, determ. of short-lived radionuclides 80−109067
biomedical radioassays, historical development 80−42034
biomedical radioimmunoassay for biopterin 80−36101
book 78−95986
building materials, conc. of ^{232}Th, ^{226}Ra, and ^{40}K from gamma-ray spectra 77−38424
citrinin distribution in tissues and serum protein, radioactive chem. anal. 79−53292
coal power station fly-ash and slag, natural radioactivity meas. 78−17442
coastal marine sediments and seawater, ^{134}Cs, ^{137}Cs, ^{210}Pb, ^{226}Ra and ^{228}Ra concs. determ. 79−88370
coincidence spectrometry, minicomputer system 79−11864
complex composition in two-phase system, anal. method, by radioactive tracers 79−87896
compositional analysis with inner-shell ionisation by radioisotopic β-rays 79−57323
computer-based radionuclide analyzer system for nuclear power stations 79−81100
coral, alpha emitter analysis by solid-state track detect., Bikini lagoon 78−53661
counting meas. calibration determs., statistical uncertainties of anals. 78−92533
counting techniques for analytical appls. in biology and medicine 80−81794
cytochemical leucocyte differentiation and radioimmune assay *(German)* 79−5412
dekryptonation thermal anal. using flow type GM detector 77−66786
determ. in coastal sediments and seawater, activity ratios, disequilib. 78−27851
distribution in extended medium, qualitative and quantitative anal., mathematical modelling 80−71985
domestic coal, radiometric method for determ. of heating value, rel. to moisture content 78−20111
environmental low activities determining appl. of present ashing methods, critical anal. *(Bulgarian)* 79−88043
environmental monitoring, radioactivity standards prep. 78−80816
fast reactor fuel consumption determ., automated techniques *(German)* 77−14236
FBR mixed oxide fuels, determ. of total H_2 content *(German)* 79−49809
fissile material assay by neutron coincidence process 80−76578
fission products in reactor coolant water, continuous radiochem. anal. 77−71652
gamma ray analysis of K, U and Th for dose-rate estimation in thermoluminescent dating 79−79333
gamma-ray activity of large vol. samples, determ. using Ge(Li) detector 77−90656
gas chromatograph-mass spectrometer system, gas proportional counter detector 77−36815
gas radiochromatography discharge flow counter for high temps. 79−24859
geophysical samples, ^{10}Be distrib. meas. using tandem van de Graaff accelerator 80−61924
heavy element analysis through absorption jump in interfering element 78−85263
human tissue, Br determ. by thermal neutron activation analysis using radiochem. separation 79−88219
inert gas analysis, calibration of Ge(Li) gamma-ray spectrometer 77−83442
insulin, radioimmunoassay, improvement in precision and accuracy of commercial kit 78−48884
isotope detection in terrestrial and extraterrestrial samples, tandem accelerator appl. 80−61923
isotope substitution analysis, sub-superequivalence method, theory 78−95983
isotopes, mass spectrometric, detection using tandem electrostatic accelerators 79−52806
lactate dehydrogenase, H-forms, radioimmunoassay 80−67219
liquid scintillation counting of aqueous and non-aqueous samples, solgel-characts. 77−38546
liver, radioimmunoassay for carcinoembryonic antigen as adjunct to radioisotope scan 79−100720
LWR mixed oxide fuels, determ. of H_2O, Hz content by hot extraction methods *(German)* 79−49808
metallic materials, nucl. methods use, conc. gradients determ. *(French)* 79−43665
mica, fissionable element impurities, nature and distrib., fission track method 78−44436
natural waters, radiotracer methods for speciation study 79−88490
niacin, biologically active forms, radiometric microbiologic assay 80−17208
NRX and process effluents, gamma ray spectrometric anal. 78−29656
nuclear accelerator spectrometry, appl. to ^{10}Be meas. in 1000 and 5000 yr Antarctic ice 79−2305
nuclear explosion, time distrib. and anal. fallout particles from 1977 Sept. 18 Chinese detonation 79−25796
nuclear fuels, wet chemical analytical methods, impurity specifications *(German)* 79−49690
nuclear power station effluent analysis methods for environmental monitoring 79−13556
nuclear reactor irradiated fuel, anal. of α-emitting isotopes through laser micro-boring 80−37444
nuclear site decontamination, radiochemical anal. of environmental samples 80−95477
obsidian from northern New Zealand, U, Th determ., archaeological sourcing method appl. 79−2239
organic compounds, ^{14}C-labelled, gaseous, anal., radioactivity meas. using piston type counter tube, automated 77−56281
organic compounds, ^{35}S-labelled, liquid-scintillation counting, automatic sample prep. 78−70688
oxytocin radioimmunoassay, human plasma 79−5353

radioactive chemical analysis continued
progesterone in crude serum extracts, radioimmunoassay using ^{3}H and ^{125}I labelled tracers 80−56185
prostatic acid phosphatase, human, development of determ. by radioimmunoassay *(Japanese)* 80−98110
radioactive contaminant unplanned release meas. and countermeasures 78−89994
radioassays, automated data processing 79−16299
radiochemical purity quality control by rapid feedback system 77−90900
radiochromatogram localisation detector for static direct meas. *(French)* 77−77842
radiochromatography, beta-ray imaging using a multiwire proportional counter 80−102387
radiogas chromatography, software package for data collection and processing 78−20086
radioimmunoassay, automated on-line system, Gammaflow 77−9247
radioimmunoassay, automatic reservoir for serial pipetting 79−100723
radioimmunoassay, fitting of general form of fundamental physical model 80−94150
radioimmunoassay, instrumentation developments 77−86614
radioimmunoassay, plasma renin activity estimation, microprocessor controlled 80−46023
radioimmunoassay, probe for fine struct. of biological systems, review 78−73217
radioimmunoassay, statistical evaluation of normal range data 77−90885
radioimmunoassay 79−43982
radioimmunoassay appls. of Philips gamma counter PW 4800 and scintillation counter PW 4700 80−56173
radioimmunoassay as aid to diagnosis, review *(French)* 80−21522
radioimmunoassay computer-assisted analysis 79−25100
radioimmunoassay data processing, semiautomated polylinear system 79−70614
radioimmunoassay detection limit 79−79318
radioimmunoassay for thromboxane B_2 with thromboxane B_2-^{125}I-tyramide 79−88222
radioimmunoassay of acute myocardial infarction markers 80−3809
radioimmunoassay of insulin receptor, receptor structure and function 79−88164
radioimmunoassay techniques development 78−88743
Radioimmunoassay Total System *(Japanese)* 79−92356
radioimmunoassays in clinical chemistry laboratory, statistical quality control, computerised approach 77−90878
radioimmunological assay of gentamycine *(French)* 79−96652
radiommunoassay, review, book contrib. 80−109021
radiopharmaceutical purity determ., adaptation of multichannel scalar device for radiochromatogram scanning 78−48894
radioreagent methods, review 78−80814
Ranney wells waters, interconnection with River Sava determ. by environmental T meas. 78−20447
reactor coolant, automated system for radioiodine anal. 78−35768
River Danube, radioactive pollution meas. 1972 to 1975 by γ-spectrometric anal. *(Bulgarian)* 79−88019
scanning ultra-low-level, radiochromatograms, multicounter system 77−88335
scintillation counters, use of miniature glass vials in multi-functional standards 77−70370
scintillation counting analysis, review of technique 78−82586
sealed sources application to industrial and analytical problems 79−85847
serum thyroxine, radioimmunoassay by the antibody-coated test tube method *(Japanese)* 80−67237
short-lived radiopharmaceuticals, radiochem. quality control 77−52876
silicate glaze, diffusion of Sn(IV) 80−49417
soil, fissionable element impurities, nature and distrib., fission track method 78−44436
soils of New Zealand, ^{238}U, ^{226}Ra, ^{232}Th and ^{40}K radionuclide conc., rel. to Fe, K content 77−86867
solid state structures, radioactive inert gases appl. 79−11834
specific activity determination, procedure optimisation and error anal. 77−6645
steel, stainless surface preparation for adhesive bonding, surface characteris. techniques 77−56132
steel purity investigation, nonmetallic inclusions, quantity and origin 77−56201
thyroid function radioimmunoassay, quality control, computer program *(French)* 80−94348
thyroxine, free, radioimmunoassay for quantitative meas. of serum conc. 80−94344
thyroxine, free, radioimmunoassay with prebound anti-T_4 microcapsules 80−46014
transuranic analysis requirements, suitability of current and methods 79−96400
transuranium elements in thermonuclear test debris, collected near Bikini Atoll 78−96103
transuranium nuclides, production in reactor, yields, nuclide fractional concs. determ. 77−63986
tritium activity meas., in exhaust gases from nuclear power stations *(German)* 77−25322
tritium detection in gases and liquids, state of art *(Czech)* 77−86403
water samples, U conc. determ. by fission track registration technique 80−12565
West German nuclear power plant liquid radioactive effluent monitoring 79−13554
X-ray diffr. studies of radioactive materials 80−3450
X-ray fluorescence, comparison with neutron activation using low intensity ^{252}Cf source 77−16885
X-ray fluorescence, radioisotope-induced 77−16886
X-ray fluorescence analysis, radioisotope-induced, applic. to Zn and Pb determ. 77−17214
β-ray quantitative microautoradiograhy, by X-ray emission microanal. 78−20545
$^{239,240}Pu(V)$ in alkaline freshwater pond, determ. by coprecipitation technique 80−71988
AgI, iodyrite, ^{129}I concs. determ. by radiogenic ^{129}Xe meas. 77−63983
Al alloy, surface preparation for adhesive bonding, surface characteris. techniques 77−56132
β-Al_2O_3, ^{22}Na labelled monocrystals, radiochemical anal. by isotope dilution method 80−11976
$BaSO_4$, crystal growth, effect of nitrilotri (methylenephosphonic acid) adsorption 78−88417

radioactive chemical analysis continued
^{209}Bi spatial distrib. on microscopic scale, ^{4}He 30 MeV ion beam 77−12859
^{209}Bi+^{12}C reaction, fission product charge distrib., 40 to 66 MeV 77−79406
^{210}Bi, determ. in human urine by direct extraction by Ni foil 79−100707
$^{14}CO_2$, activity meas. in air 79−66388
$^{14}CO_2$, respiratory, determ. by Ba$^{14}CO_3$ decomposition in sample oxidiser 79−88153
^{14}C dating using electrostatic accelerators and negative ions 78−32917
^{14}C determination in whole-body sections by liq. scintillation counting *(German)* 77−5114
^{14}C direct detection at natural concs. by mass spectrometry, for dating 78−32916
^{14}C low level liq. scintillation counting using small vol. teflon-Cu vial 80−16887
^{14}C-labelled compounds, continuous radio-scanning method for chromatograms and electrophoretograms 77−70367
^{45}Ca, liquid scintillation counting in plant and soil material 77−44536
^{252}Cf wire neutron source distrib., meas. by autoradiography 77−61643
^{36}Cl, Cherenkov counting using Teflon vials 78−858
^{36}Cl in environmental water samples, anal. using electrostatic accelerator 79−20895
CuI, marshite, ^{129}I concs. determ. by radiogenic ^{129}Xe meas. 77−63983
Es compounds, X-ray powder diffr. 80−2002
Fe, determ. in radioactive soln., sub- and super-equivalence isotope dilution anal. 78−95984
^{59}Fe/^{55}Fe activity ratio of blood, meas. using semicond. detector 80−17062
GaP:Cr epitaxial layers, Cr conc. profile determ. 80−65029
^{154}Gd, 2^{+} rot. states, time integral perturbed angular correl., meas. method 77−9154
^{3}H determination in whole-body sections by liq. scintillation counting *(German)* 77−5114
^{3}H, distrib. in irrad. UO_2 pellets, radiochem. anal. *(German)* 77−16880
^{3}H in aqueous samples, single solvent cocktail for liq. scintillation counting 78−856
^{3}H in water, low-level meas., inter-laboratory comparison 78−44888
Hg ores, determ. of Hg content using ^{57}Co isotope and scintillation counter 78−20539
^{129}I and organic compound determ. in LWR irradiated fuel solns. *(French)* 79−3230
^{131}I determination in vegetation, ashing procedure 78−15930
^{131}I in milk, extreme low level determ. 78−92703
^{131}I, low level detection in milk rel. to population dose 78−31911
K content in natural samples, γ spectrometric determ. *(Russian)* 78−92562
Mn nodules, from sea-bed, isotopic and elemental composition, U, Pa, Th, radiochem. anal. 78−77215
MnO_2:Li(Mo)(V), of Zn^{2+} ions, kinetics, ^{65}Zn γ-ray scintillation investig. 80−70529
Ni sheet, surface, adsorbed ^{3}H, ethylene-^{14}C determ., autoradiography method 77−63989
^{32}P, Cherenkov counting using Teflon vials 78−858
^{32}P-labelled compound, radiochromatographic scanning procedure 77−9151
^{231}Pa, determ. in coastal sediments and seawater, activity ratios, disequilib. 78−27851
^{233}Pa removal from ^{237}Np by coprecipitation with MnO_2 or sorption on silica gel 79−52733
^{206}Pb spatial distrib. on microscopic scale, ^{4}He 30 MeV ion beam 77−12859
^{210}Pb determination in lake and marine sediments 79−48582
^{210}Pb determination in sediment core from ocean floor off Californian coast 80−72101
^{210}Pb, radiochem. determ. in U ores, air dusts 77−56266
Pd, solubility of S, 600-1000°C, H_2-H_2S gas phase composition depend. *(French)* 78−87791
^{210}Po determ. in air, radiochem. separation and α-counting method 78−73113
^{210}Po, determ. in human urine by direct extraction by Ni foil 79−100707
^{210}Po/^{210}Pb concs. in rain determ., ^{210}Pb tropospheric residence time meas. 78−85396
Pu, alpha-energy and mass analyses, using single sample mount 78−15744
Pu assay, in vivo methods for humans 79−20674
Pu, determination by volumetric and coulometric methods, effect of Am on accuracy 79−52826
Pu extraction-spectrophotometric determination in spent fuel of first Czechoslovakian nuclear power station *(Czech)* 77−3105
Pu isotopes, in soil, determination using alpha-spectrometry 80−45601
Pu low-background assay using modified commercial liq. scintillation detector and sample changer 77−54474
Pu, remote contamination and total inventory from Rocky Flats, mass spectroscopic anal. 77−73739
^{247}Pu concentrations in Swedish reindeer lichens, radiochem. anal. 78−15912
^{241}Pu in ^{241}Am, determ. by γ spectrometry 79−52808
Ra content in natural samples, γ spectrometric determ. *(Russian)* 78−92562
^{226}Ra, determ. in environmental samples by ^{222}Rn separation, integral counting methods 77−63988
Rh, A=108-111, prod. by fission of ^{235}U, ^{238}U, ^{239}Pu, ^{249}Cf, separation, identification 78−89924
Rn in groundwater, radiochem. method appl. to Christchurch artesian wells 77−82039
^{222}Rn concentration in water, meas. by gamma counting 78−53733
^{222}Rn tracer measurement in aqueous samples by decay product filtration 77−60476
Ru, fission product, isotope anal., U and Pu fission investig. *(German)* 77−63996
Ru isotopes, A=107-113, prod. by fission of ^{235}U, ^{238}U, ^{239}Pu, ^{249}Cf, separation, identification 78−89924
^{35}S content of coolant gas in Windscale AGR, gas chromatographic and radiochemical anal. 78−73125
$^{35}SO_2$ interaction with atmospheric particulates 77−41137
Sb, A=131, 133 prod. by ^{232}Th reactor induced fission, yield, radiochem. separation, anal. 78−89923
^{125}Sb, in HCl solns., valency states investig., radioanal. tracer preparation, stability 77−63943

radioactive chemical analysis continued
^{152}Sm, 2^{+} rot. states, time integral, perturbed angular correl., meas. method 77−9154
Sn, A=131, 132 prod. by ^{232}Th reactor induced fission, yield, radiochem. separation, anal. 78−89923
^{89}Sr and ^{90}Sr, radiochem. determ., error anal. comparison of methods 77−16873
^{89}Sr assay in aqueous solutions by Cerenkov radiation 79−87895
^{89}Sr/^{90}Sr concs. in rain determ., ^{90}Sr tropospheric residence time meas. 78−85396
$^{90}Sr^{2+}$, adsorption on Cu surface, immersion time, conc. and temp. depends. 78−87863
T_2O, injectable soln., radionuclidic purity using liquid scintillation counter *(French)* 78−73118
^{99m}Tc, cyclotron production, isotope impurities determ. 77−46170
^{99m}Tc radiopharmaceuticals, rapid miniaturised chromatographic quality control procedures 78−28070
Th content in natural samples, γ spectrometric determ. *(Russian)* 78−92562
Th, prospecting method, using Ra accumulation in animal thyroid glands, anal. 78−27853
^{232}Th, assay in phosphate containing materials by solvent extraction-liquid scintillation method 79−22447
U analysis in phosphate fertilisers and other materials using liq. scintillation spectrometry 78−53280
U, assay in phosphate-containing materials by solvent extraction-liquid scintillation method 79−22447
U autopsy specimen analysis confirmation of in vivo chest survey 77−66859
U content in natural samples, γ spectrometric determ. *(Russian)* 78−92562
U determ. in natural water by ion exchange separation, delayed neutron counting 77−36847
U, in environmental samples, determ. by gamma spectroscopy of 1.0015 MeV radiation in ^{234}U 77−1954
U, in porcelain dentures, rapid anal. by delayed fission neutron method 78−15907
U isotopes, in soil, determination using alpha-spectrometry 80−45601
U ore, U content determ., radioisotopic X-ray technique using Compton scatt. 77−70357
U ores, dusts and mill tailings, simultaneous determ. of ^{238}U, ^{234}U, ^{230}Th, ^{226}Ra, and ^{210}Pb 78−15736
U, prospecting method, using Ra accumulation in animal thyroid glands, anal. 78−27853
UO_2, powder and pellets, determ. of f and metal impurities *(German)* 79−49807
UO_2-P-uO_2 rods, isotopic anal., gamma-ray spectrometric meas. calibration appl. 77−81440
^{235}U content in enriched samples, fission track registration technique, solid state detectors 77−56291
Zn, determ. by dithizone complex extraction and isotope substitution anal. 78−95983

radioactive dating
see also geochronology
achondrite meteorites, Rb-Sr and Nd-Sm dating rel. to chemical history 77−60639
allanite, metamict, phase changes on heating, age determ., x-ray fluoresc. anal. 77−51493
Allende meteorite, ^{40}Ar-^{39}Ar ages 80−98621
Allende meteorite, ^{40}Ar-^{39}Ar dating of pre-4550 Myr inclusions 79−35212
Angra dos Reis meteorite, Sm-Nd-Pu timepieces 77−82180
Antarctic igneous rocks, palaeomag. and K-Ar age 80−12332
apatite, fission track retention as function of heating time during isothermal expts. 80−36420
apatite, mean etchable fission track length, high fission track densities determ. 77−82041
Apollo 15 green glass, Sm-Nd evolution and lunar initial ^{143}Nd/^{144}Nd 79−35156
Archaean basic and ultrabasic volcanics Sm-Nd dating 78−11848
archaeologic ceramic samples age determining, using thermoluminescent dosimetry *(Czech)* 77−5972
archaeological ceramic dating by alpha-recoil tracks in mica 78−70237
archaeological radicarbon dating, review 78−58104
archaeology, scientific techniques, book 77−61172
Archean gneiss dating using zircon data in Labrador 80−3959
Azores, K-Ar age of oldest volcanics, volcanic history 80−46158
batholith between Princeton and Okanagan Lake Sr isotope study 77−17096
Binda howardite, ^{87}Rb-^{87}Sr meteorite chronology 80−26819
blueschists, from Ile de Groix, France, isotopic ages, metamorphic episodes determ. 77−66896
bone, inclusions as source of error in radiocarbon dating 78−346
bristlecone pine and ancient Egypt, rel. to calibration of radiocarbon dates 78−70234
Bruderheim, L6 chondrite, U-Pb age and 500 Ma shock event in L-group meteorites parent body 80−98616
E.Carpathians, crystalline nucleus evolution, radiometric dating *(Rumanian)* 77−33029
ceramic art objects, thermoluminescent dating 78−58503
ceramic sculpture from Oaxaca, Mexico, authentication by thermolum. and style 78−70238
Chesapeake Bay, pollution history 79−34445
chlorite, fission track annealing and age determ. 78−36307
chondrite Kirin H, inert gas content interpretation *(German)* 80−46505
chondrite Yamato-74191, inert gas composition and neutron capture effects 80−46504
chondrites, ^{40}Ar/^{39}Ar dating of collisional events in parent bodies 77−17452
clam from Galapagos Rise hot spring field, growth rate using natural radionuclide ratios 79−84300
Coast Plutonic Complex, British Columbia, geochronology and thermal history 80−12351
Coast Plutonic Complex, British Columbia, Rb-Sr geochronometry 80−12350
corals and shells, ^{230}Th, ^{231}Pa and open system dating 80−12434
cordierite-bearing rock, ^{40}Ar/^{39}Ar age spectrum, effects of excess radiogenic ^{40}Ar 77−29456
cosmic ray induced neutron background sources rel. to ^{14}C dating 78−40781

radioactive dating continued
cosmic rays, containment time from radioactive isotopes abundance 78−53781
cosmochronology, implications of Allende meteorite isotopic anomalies 80−4462
Cretaceous-Tertiary boundary sediments, Red Deer Valley, magnetostratigraphy, biostratigraphy and geochronology 79−57888
cyclospectrometry, ^{10}Be conc. criterion for dating geochemical remains *(French)* 80−21859
cyclotron, as high-energy mass spectrometer, appl. to chem. anal., radioactive dating and quark detection *(Czech)* 78−86375
cyclotron application as mass spectrometer 77−64489
cyclotron applications, radiation damage, radioisotope dating, and large-scale radioisotope prod. 79−54692
decay constants in geochronology and cosmochronology, IUGS Subcommission convention 78−28189
Deccan Traps volcanic rocks, India, ^{40}Ar/^{39}Ar date and volcanic history 80−46178
deep sea carbonates, thickness and ^{14}C age of mixed layer 79−29742
deep-sea cores, ^{231}Pa dating via ^{227}Th counting 78−32238
Dhajala meteorite, unequilibrated H3 chondrite, K-Ar and cosmic ray exposure ages 78−32425
digital ESR dating method 80−86542
Donegal granite, Ireland, emplacement age by isotope chronology 80−67356
dosimeter, high-exposure, use of photostimulated thermolum. in $CaSO_4$:Dy 77−9262
education, radioactive dating and population growth by dice game 80−57030
EPR method of dating minerals 80−36415
ESR dating, appl. to archaeological materials from Greek Petralona cave 79−26094
excess ^{230}Th dating of Late Brunhes geomag. polarity episodes 78−11797
Farmington chondrite, U-Pb abundances and Pb isotopic studies 80−56778
ferromanganese nodules, oriented, U-Th series nuclides rel. to growth rates and turnover times 79−29740
fission track annealing characteristics of epidote, appls. to geochronology, geol. 78−94038
fission track data reports standardisation 80−31436
fission track dating, geom. factor for external detectors 77−82040
fission track dating and estimation of U in garnets 78−94039
fission track dating method, standard error estimation 80−36419
fission track dating of Himalayan muscovites, Nepal, and U conc. estimation 78−40524
fission track dating of zircon, improved etching techniques 77−29457
fission track dating parameters, calibration 77−41207
fission track dating technique 80−36417
fission track dating technique for minerals 77−45203
fission track dating using U glasses, error analysis 80−95503
fission track retention as function of heating time during isothermal expts. 80−36420
fission Xe isotope dating technique 79−21043
floating tree-ring chronology from NE.Scotland, radiocarbon meas. 78−70236
Francevillian series, K-Ar radiochronology *(French)* 80−21692
Frontenac Axis dikes, Ontario, ^{40}Ar/^{39}Ar dating and implications for Grenville palaeomagnetism 79−62466
galactic cosmic rays, age derived from ^{10}Be abundance 78−12060
gamma ray analysis of K, U and Th for dose-rate estimation in thermoluminescent dating 79−79333
Giant Mascot ultramafic body, near Hope, British Columbia, K-Ar ages 77−5147
Governador Valadares, Nakhlite achondrite, age determ., 1.3 aeons 77−33428
granites, Nanling region, southern China, K-Ar and U-Pb dating 77−2132
granitic plutons, E. Newfoundland, ages rel. to Appalachian evolution 77−66894
Grenville and adjacent Palaeozoic formations Pb isotope ratios 77−44941
groundwater ^{14}C dating, possible subsurface prod. of ^{14}C 80−85690
Hawaiian glaciation chronology, K/Ar and ^{14}C ages 77−33113
Hawaiian lavas, contamination evidence from ^{230}Th-^{238}U data 77−5166
Himalayan muscovites, fission track dating 78−3736
Himalayan rocks, Rb-Sr age and initial Sr isotopic ratio *(Japanese)* 77−17060
hornblende and biotite, ^{40}Ar/^{39}Ar ages across Georgia Inner Piedmont, rel. to tectonothermal history 78−48990
igneous rocks from Gulquac Lake area, New Brunswick, Rb-Sr ages 80−31006
S.Indian Craton, Archaean gneiss Rb-Sr date of 3360 Myr old 80−46155
Indian culture, ^{14}C dating of samples 79−40650
isotope detection in terrestrial and extraterrestrial samples, tandem accelerator appl. 80−61923
Jomon pattern pottery from Japanese Taishaku valley, thermoluminescent dating 79−26196
Kakangari meteorite, unique chondrite, ages and noble gas chemistry 78−65570
Kapoeta howardite, ^{40}Ar/^{39}Ar chronology of lithic clasts 80−46501
KBS Tuff, E.Turkana, Kenya, K-Ar age estimate 80−56433
Kirin chondrite, Rb-Sr age and Sr isotopes *(Chinese)* 78−89135
Lakes Ontario and Erie, comparative ^{210}Pb, ^{137}Cs and -pollen geochronologies of sediments 79−66728
laser techniques for sensitive radioisotope dating 79−59707
late Quaternary lakes, Arabian Desert, ^{14}C chronology 77−5161
lava succession in N.Iceland, K-Ar dating, geological and palaeomagnetic obs. 80−109096
lunar breccia, ^{40}Ar/^{39}Ar dating of plagioclase clasts, rel. to early lunar differentiation 78−65514
lunar highland rocks, radiometric dating rel. to stratigraphy 77−60645
lunar KREEP-basalt formation ages determ. 78−32372
lunar mare basalts, ages rel. to two-stage generation model 77−60648
lunar maria, absolute time scale of form. and filling 77−60646
lunar rocks, early chronology rel. to early collisional history of solar system 77−60640
lunar rocks, Rb-Sr and Nd-Sm dating rel. to chemical history 77−60639
lunar samples, radiometric ages rel. to lunar chronology 77−60644
lunar samples from Luna 16 and 20, ^{40}Ar-^{39}Ar dating 77−22125

radioactive dating continued
malachite from patinas of ancient bronze objects, stable ^{13}C/^{12}C and ^{18}O/^{16}O ratios 79−26194
Mamontova Gore silt, Siberia, radiocarbon dates and late Quaternary non-glacial stratigraphy 78−44819
marine sediment, α-scintillation counting of ^{230}Th 80−72636
Marydale Formation, Kheis Group, South Africa, Rb-Sr age 78−32088
Mesozoic tholeiites from Antarctica, interpretation of discordant ^{40}Ar/^{39}Ar age spectra 77−49047
meteorite, Unter-Massing iron, cosmic-ray exposure age and preatmospheric size, *(German)* 80−46507
meteorites, ^{87}Rb-^{87}Sr chronology of enstatite chondrites 80−8596
meteorites, ^{87}Rb-^{87}Sr dating, shock and brecciation effects in L chondrites 80−51705
meteorites, excess K-Ar ages prediction in presolar grains 78−28761
Midway volcano, Hawaiian volcanic chain, age determ. 78−32041
minerals, fission fragment range and closing temp. for track retention 80−41566
minerals from Fleur de Lys terrain, Newfoundland, ^{40}Ar/^{39}Ar age spectra, rel. to metamorphism 77−70657
minerals spatial isotope distributions, recovery from stepwise degassing data 79−34967
Murray (C-2) carbonaceous chondrite, I-Xe age and trapped Xe components 80−98618
nepheline syenite, dating, Rb-Sr internal isochron, ^{39}Ar-^{40}Ar plateau age methods *(French)* 78−32031
Nipissing Great Lakes, radiocarbon dating of organic material, alluvial sediments 79−84251
Nordlinger Ries giant meteorite impact crater, K-Ar and fission track dating 78−28236
Norton County enstatite achondrite, ^{87}Rb-^{87}Sr history 77−5508
ocean sediments, radiocarbon dating by benzene variant method aboard ship 80−85770
Oklo natural fission reactor, dating from U-Pb isotopic data 80−21763
Oklo natural fission reactor, radioactive dating from Pb and Th meas. *(French)* 80−21762
Oklo natural fission reactors, U and rare earth migration in core sample, appl. to dating of reactions *(French)* 80−21760
ore mineralisation in Erma River Area, Bulgaria, age, genesis, Pb isotope and K-Ar investigs. 78−81115
Central Pacific Basin, ^{40}Ar/^{39}Ar ages of diabase sill and basalt, rel. to ocean floor history 77−66897
Pacific island and seamount ages rel. to volcanic chains origin 77−64242
Pacific Ocean sediments, ^{10}Be dating compared with palaeomagnetic ages 78−32058
painting and artist identity, autoradiography and gamma-ray spectroscopy appl. 80−26073
particle tracks, fission/α anal. of U and Th families 77−29497
pelitic sediments, Rb-Sr and K-Ar dating rel. to Sr and Ar isotopic homogenisation during metamorphism 79−62511
polar ice cap, low-level beta counting with an automatic sample changer 80−31147
Precambrian terrain, multiply deformed, Rb-Sr dating of discrete structural-metamorphic events 79−57895
Precambrian zircons, metamictization and U-Pb systematics by IR absorpt. spectrometry 77−17099
pumice from KBS Tuff, East Rudolf, Kenya, ^{40}Ar/^{39}Ar dating 77−5160
quartz, grains, fission track dating, Oklo uranium ore deposit 78−20555
quartz grains, thermolum. dating, β-dose attenuation correction factors 79−75669
quartz inclusion morphology for thermolum. dating, effect of HF etching 78−70240
Quaternary loess deposits of Banks Peninsula, New Zealand, radiocarbon dating 78−24271
radiocarbon age determinations, procedures for comparing and combining 78−70235
radiocarbon chronology and calibration of Late Minoan IB 79−26200
radiocarbon dates from Akrotiri, Thera 79−26201
radiocarbon dating, ^{14}C detect. via small van de Graaff accelerator 79−11844
radiocarbon dating, ^{14}C enrichment method 79−10220
radiocarbon dating discrepancies illustrated using Egyptian and Aegean samples 79−26199
radioisotope dating with cyclotrons 79−34990
rare-gas dating, evaluation of double-spiking procedure for K-Ar dating 77−60473
Richardton chondrite, U-Pb abundances and Pb isotopic studies 80−56778
rinneite, Rb-Sr dating of potash salt deposits 80−67429
Roberts Arm Group, Newfoundland, age rel. to phases of volcanism 80−12354
Roccamonfina Volcano, geochronology and palaeomag. *(Italian)* 77−49036
Rostherne Mere, Cheshire, ^{137}Cs dating confirmation by algal stratigraphy 79−12156
Saglek area, Labrador, Uivak II gneiss, zircon age meas. 80−3958
Sahara plateau, petrographic and radiometric dating *(Italian)* 78−7595
Saint Mesmin chondrite, ^{87}Rb-^{87}Sr age, and dating of gas-rich polymict breccia 79−53778
San Juan Capistrano meteorite, cosmic ray exposure age from ^{81}Kr-Kr dating 78−57512
scintillation counting analysis, review of technique 78−82586
seashells in coastal Zagros Mountains, Iran, ^{14}C dates rel. to Holocene folding rates 79−48445
sediment age determination, ^{210}Pb, plastic nuclear track detector 78−20554
sedimentation rates determ. in rapidly accreting salt marsh by ^{137}Cs dating 78−96247
sediments, α-spectrometric dating method, using ^{210}Po 78−28350
sediments, from Lake Constance, rel. to eutrophication effects 79−79889
sediments of deep-sea, ^{14}C age and vertical mixing 80−81865
Shergotty achondrite, ^{40}Ar/^{39}Ar age and post-shock thermal history 80−46502
Shergotty achondrite, Rb-Sr age and isochron age resetting 80−41774
Sm-Nd dating of continental volcanics, effects of crustal contamination 79−66693
St. Mesmin brecciated chondrite, noble gases, K-Ar ages and irradiation history 78−28593
Stillwater complex, USA gabbro Sm/Nd age and mantle evolution curve of Nd 80−41410
submarine basalts, sea water weathering effect on K-Ar age 77−86830

radioactive dating continued
Sudbury Ni Irruptive and Superior Province granites, ages 78−36126
tektites, fission-track plateau dating evidence of australites older than indochinites 80−56780
thermoluminescence dating, effect of radioactivity within quartz 78−70241
thermoluminescence dating, radiation dose-rate data 80−31964
thermoluminescence dating of pottery, ^{87}Rb dose-rate contrib. 78−70242
thermoluminescence glow curve simulation method of dating archaeological specimens 77−5973
TLD evaluation of internal beta-dose rate for archaeological dating 80−98478
tourmaline, fission track etching and annealing, thermal retention 77−82042
travertine from archaeological sites, Nahal Zin, Israel, U series dating 79−34781
tree rings, $^{12}C/^{13}C$ in cellulose and lignin as palaeothermometers 77−17253
Umfraville Gabbro, Ontario, palaeomag. study and K-Ar age 80−12330
Upper Cenozoic volcanism, central Andes, ages and volumes 79−29730
Ventura, California, high rates of vertical crustal movements 77−56614
volcanic rocks in Lesser Antilles island arc, palaeomagnetic survey 80−8265
Whitehorse map area, Yukon, plutonic rock dates 80−31005
Wisconsin reef on Daito Ridge, Philippine Sea, isotopic evidences, Late Quaternary tectonic history 79−84227
zircons from Early Precambrian rocks of W.Greenland and Minnesota River Valley, U-Pb ages 78−11845
zircons from gneisses, igneous and metamorphic events, Fiskenaesset region, Greenland 79−84250
^{26}Al dating, separation of ^{26}Al and ^{26}Mg isobars, via negative ion mass spectroscopy 80−31146
^{26}Al, decay in marine sediments, meas. with cyclotron, dating technique 79−71819
Ar-K isotopic dilution method for absolute age determ. *(Rumanian)* 78−20562
$^{39}Ar/^{40}Ar$ and $^{87}Rb/^{87}Sr$ ages of North Pyrenean metamorphism 79−34819
$^{39}Ar/^{40}Ar$ dating of rock fragments from Mare Crisium 78−65513
^{39}Ar-^{40}Ar dating, K-feldspar importance in polyorogenic areas 79−44152
^{40}Ar excess identification by $^{40}Ar/^{39}Ar$ age spectrum technique, comments 78−32237
$^{40}Ar/^{39}Ar$ age and irradiation history of Luna 24 basalts 80−82245
$^{40}Ar/^{39}Ar$ age spectrum technique, excess ^{40}Ar identification 77−5152
$^{40}Ar/^{39}Ar$ dating, appl. to Laschamp geomagnetic polarity reversal 78−81105
$^{40}Ar/^{39}Ar$ dating, appl. to Grenvillian palaeopoles calibration 79−20778
$^{40}Ar/^{39}Ar$ dating, appl. of isochron diagrams 79−29873
$^{40}Ar/^{39}Ar$ dating, felsic and mafic mineral separates from an Abitibi dike 80−17237
$^{40}Ar/^{39}Ar$ dating by step-heating method, appl. to E.Iceland lava 80−36273
$^{40}Ar/^{39}Ar$ radioactive dating, appl. to K-bearing sulphide minerals age determ. 79−29720
$^{40}Ar/^{39}Ar$ radiometric age determ. of rocks, shock press. effects 77−60360
$^{40}Ar/^{39}Ar$ stepwise outgassing method, applicability to slates age studies 79−29721
$^{40}Ar/^{39}Ar$ studies of deep-sea igneous rocks 79−53325
^{40}Ar-^{39}Ar dating, inert gas extraction system incorporating ultra-high vac. furnace 78−77918
^{40}Ar-^{39}Ar dating of magnetizations in Archaean Shelley Lake granite 80−30982
^{40}Ar-^{39}Ar systematics, temp. and pressure effects 79−44178
^{10}Be, mass spectrometric meas. with cyclotron, geochronological appl. 79−57338
C^- ion source for radiocarbon dating using tandem accelerators 80−94620
^{13}C record in tree rings, industrial CO_2 affecting ^{13}C assimilation 80−51586
$^{13}C/^{12}C$ dating of New Zealand kauri cellulose for last millennium 80−21819
^{14}C absolute dating using low altitude European tree-ring calibration 78−16195
^{14}C age errors for recent deposits with fluvially transported charcoal 78−36172
^{14}C age of N.Atlantic deep water 79−84285
^{14}C analysis of soil, dating 78−36299
^{14}C and T meas. of groundwater in Eaton River Basin and Mirabel area, Quebec 78−28249
^{14}C, based on oak trees dendrochronology *(French)* 79−96840
^{14}C beam meas. using cyclotron 79−25352
^{14}C calibration curve for dendrochronology Suess wiggles, confirmation 79−74952
^{14}C counter system using proportional counters of plastic scintillator 77−60491
^{14}C dating, apparatus for β-counting 79−80048
^{14}C dating, beta rel. to ion counting 79−74992
^{14}C dating, determ. of $^{14}C/^{12}C$ ratio, review of methods *(Hungarian)* 79−48578
^{14}C dating, Great Barrier Reef 79−84225
^{14}C dating, high energy mass spectrometer appls. 80−101917
^{14}C dating, meas. of ^{14}C abundance vars. in wines with 11-year solar cycle, (1909 to 1952) 80−109249
^{14}C dating, principles and disagreements with geophysical data *(French)* 77−37434
^{14}C dating, thermal diffusion enrichment, N. American glacial history extended to 75000 yrs ago 78−77284
^{14}C dating, time scale extension by thermal diffusion enrichment, appl. to NW. Europe climatology 78−77314
^{14}C dating method using 20 keV Kr ion beam for objects <65000 yrs. *(Danish)* 80−8440
^{14}C dating of CO_2 sample with accelerator, blind meas. 79−25362
^{14}C dating of coastal marine sediments, fossil C effect 80−98308
^{14}C dating of geological and archaeological samples 78−92993
^{14}C dating of groundwaters, mass transfer and isotope evolution theory 79−20882
^{14}C dating of mg geological samples with electrostatic accelerators 79−25361
^{14}C dating of New Zealand stalagmite, rel. to temps. and climate change during laser millennium 79−62574
radioactive dating continued
^{14}C dating of small samples via proportional counting 80−82102
^{14}C dating rel. to magnetic and other dating methods 78−57359
^{14}C dating technique using cyclotrons, or Van de Graaff as mass spectrometer 80−5414
^{14}C dating using electrostatic accelerators and negative ions 78−32917
^{14}C direct detection at natural concs. by mass spectrometry, for dating 78−32916
^{14}C, dissolved in groundwater initial activity determ., new model and review 80−8458
^{14}C meas. on submerged forest floating chronologies, rel. to atm. ^{14}C vars. 79−48563
^{14}C measurement in known age specimens, cosmic ray intensity determ. 80−101516
^{14}C of lake bottom core rel. to ice-free corridor in Late Pleistocene Alberta 80−26552
^{14}C temporal atmospheric fluctuations 79−5591
^{14}C time scale changes and Late Pleistocene geomagnetic var. 79−62433
^{14}C, use in dating, review of technique 79−49922
$^{14}C/^{13}C/^{12}C$ vars., Bermuda coral 200 yr. record 79−16570
^{41}Ca dating, feasibility and appls. 79−21063
^{36}Cl dating of environmental water samples, anal. using electrostatic accelerator 79−20895
Fe meteorites, $^{41}K/^{40}K$-$^{4}He/^{21}Ne$ cosmic ray exposure ages and age distribs. 79−30015
$^{3}H/^{3}He$ dating as meas. of O_2 utilisation rates, appl. to Sargasso Sea 77−56654
I-Xe dating of silicate and troilite in Fe meteorites, group IAB 80−17554
K-AR dating, revised consts. rel. to geomag. polarity time scale for interval 0 to 5 m.y. BP 79−57851
K-Ar ages for basalts from Great Meteor and Josephine seamounts 77−9399
K-Ar dating, evolution of excess ^{40}Ar in Alpine biotites from ^{40}Ar-^{39}Ar anal. 80−94521
K-Ar dating, press. depend. of radiogenic Ar loss from phlogopite mica 77−86861
K-Ar dating method for argillaceous sediments 79−8716
K-Ar dating of intrusion gas and scheelite mineralisation, Cantung, Canada 79−5460
K-Ar dating of volcanic rocks from Morocco *(French)* 80−51322
K-Ar dating using three-dimens. plots 79−62601
K-Ar isochron method for age of North Mountain Basalt, Nova Scotia 80−3960
K-Ar isochron method use and misuse, atmospheric ^{36}Ar contamination removal 77−66988
^{40}K-^{40}Ar mineral ages for rocks in SW.Brooks Range, Alaska 80−26469
Mn nodules, from Pacific Ocean growth rates from U series and hydration-rind dating 77−29280
$^{204}Pb/^{207}Pb$ ratio rel. to Earth age and chemical evolution 79−88315
^{210}Pb dating, results from Lake Ipea and Lough Erne sediment cores 78−28202
^{210}Pb dating of annually laminated Finnish lake sediments 79−74916
^{210}Pb determ. by direct gamma-ray meas. in lake sediments and air samples 77−5156
^{210}Pb technique for marine heavy metal sedimentation rate determ. 78−32063
Po haloes in rocks and geochronology 80−56468
^{226}Ra leaching from fossil bones 78−58562
Rb-Sr, ratio determ., by X-ray fluoresc., for radiometric age meas. 77−70356
Rb-Sr ages of dolerites from Canada and Greenland, palaeomag. and Grenville orogeny 79−34772
Rb-Sr ages of early Archean supracrustal rocks and Amitsoq gneisses Isua, Greenland 78−16013
Rb-Sr ages of rocks, Hopei, China *(Chinese)* 79−20776
Rb-Sr ages of weathered and stream transported quartz grains from Harney Peak Granite, S.Dakota 79−74865
Rb-Sr chronology of continental crust formation 79−12100
Rb-Sr dating, deformation in Hellroaring Plateau area, Beartooth Mountains, Montana 80−17238
Rb-Sr dating, geologically meaningless total rock isochron determ. 80−31014
Rb-Sr dating, half-life determ. by absolute counting 77−26943
Rb-Sr dating of Brazilian rocks, appl. of solid-source mass spectrometer 77−70840
Rb-Sr dating of continental volcanics, effects of crustal contamination 79−66693
Rb-Sr dating of eclogites in Munchberg Gneiss Massif 79−34774
Rb-Sr dating of transect of Chilean Andes, latit. 45-46°S 79−29723
Rb-Sr method, Rb and Sr separation from potash salts by ion exchange *(German)* 78−23940
Rb-Sr whole rock dating of metamorphic events, Iglesian Complex, Venezuelan Andes 77−81894
Rb-Sr whole rock isochron, Newry Granodiorite, N.E.Ireland 77−5162
Rb-Sr whole rock isochron age from Kangamiut dykes rel. to Hudsonian orogeny in W.Greenland 79−5459
Rb-Sr whole-rock isochron age, 2390 Myr, for Scourie dykes, NW.Scotland 79−39690
^{87}Rb, decay constant determ., Rb-Sr dating appl. 78−29424
^{87}Rb-^{87}Sr chronology of H chondrites, parent body evolution 79−44421
^{187}Re-^{187}Os systematics in meteorites, rel. to solar system early chronology and Galaxy age 80−41778
^{222}Rn scintillation counting, standard deviation estimation 77−79519
Sm-Nd, isotopic investigations of Isua supracrustals and implications for mantle evolution 78−36129
Sm-Nd dating, appl. to Onverwacht Group Volcanics, southern Africa 79−62469
^{230}Th-^{234}U dating of calcite speleothems, interglacial chronology of Rocky and Mackenzie Mountains 78−36120
U minerals, radiogenic Pb migration in hydrothermal metamorphism 77−56627
U ore dating from meas. of ^{238}U and Ru conc. 80−21863
U series dating, appl. to insular phosphorite from Ebon atoll, Micronesia 78−81121
U series dating, open system model appl. 79−29874
U series disequilibrium, mechanisms involving recoiling alpha-emitting nuclei 79−16466
U-Pb age method, calc. of uncertainties of U-Pb isotope data 80−46269
U-Pb age of uraniferous opals, Spor Mountain, Utah, USA 80−46149

radioactive dating continued
U-Pb ages of crystalline rocks, Burlington Peninsula, Newfoundland, Fleur de Lys metamorphism age 78−28188
U-Pb ages of pegmatites in Enderby Land, Antarctic 80−76946
U-Pb geochronology in Lac Seul region, English River Gneiss Belt 77−5148
U-Pb zircon dating in Munchberg Gneiss Massif 79−34774

radioactive decay periods
^{294}110, naturally occurring superheavy element search, alpha emission half-life 80−63139
^{298}114, high spin pot. energy surfaces, fission barrier, α-, γ-decay half lives, yrast spectrum 80−73764
A=215, nuclear data sheets, decay characteristics and level struct. 78−58224
A=219, nuclear data sheets, decay characts. and level struct. 78−58225
A=223, nuclear data sheets, decay characts. and level struct. 78−58226
A=227, nuclear data sheets, decay characts. and level struct. 78−58227
A=354, Z=126, spontaneous fission, α-decay, β-decay half-lives calc. 77−6469
A=79-145, β-delayed neutron emission probabilities, half-life 80−52634
alpha decay as a fission-like process, Q-value and half-life calc. 79−93566
alpha-decay, liq. drop model *(Russian)* 80−32246
alpha-decay of neutron-deficient isotopes at ISOLDE, CERN 77−22967
beta strength function, half life and delays, nuclear- and astro-physics consequences 80−102149
beta strength function structures, nuclear- and astro-physics consequences 80−99152
beta-decay, shell effects in gross theory 77−38251
calibration materials for X and γ-ray spectrometers, decay data 80−106221
chemical environment effect on lifetime meas., review 79−75911
compound nucleus lifetime using shadow effect in ^{238}U(^{27}Al,f) *(Russian)* 78−86563
constant, effect of chem. surroundings, electron capture 80−42601
cyclic activation method of determining short half-lives 80−47421
double-beta decay, electron-neutrino pair emission via Δ(1232) resonance 78−54722
education, radioactivity, binomial distrib. and Poisson statistics 77−49525
electronic analogue, demonstration apparatus circuit 78−41122
fission product gamma-ray and half-life 29≤A≤69, data collection 78−50134
fission products, short lived, estimation of nuclear decay heat 77−71594
fission products, short-lived, rapid paper electrophoretic separation, γ-rays and half-lives determ. 77−44498
fission products nuclear data from on-line mass spectrometer 77−22616
fission products of ^{252}Cf, masses, β decay energies, halflives, He jet TOF mass spectrometer 77−23355
gamma-rays, half-life vs. energy map, photon activation anal. appl. 77−16883
highly excited nuclei, lifetime *(Russian)* 78−29430
light nuclei, delayed proton precursors 77−22971
LMFBR burnup calc., allowance for ^{239}Np 78−89936
magnetic lens spectrometer+Ge(Li) detector, for nuclear decay schemes and halflives meas. 79−710
mixed Fermi and Gamow-Teller β-transitions, data tables 79−54407
neutron rich nuclei, beta decay half lives, expt. techniques 80−78224
neutron-rich nuclei in A∼100 region, decay props. 77−22961
nuclear data files of UK Chemical Committee, summary of data, available in ENDF/B format 78−82425
nuclides for Interlaboratory LMFBR reaction rate program 77−22928
odd mass nuclei with 51 neutrons or 51 protons, radioactivity, expt. theory *(French)* 77−293
quantum radiation, data handbook 80−94933
radioactivation of shielding materials Fe, Benelex by fast neutrons, γ-ray spectra 79−682
radioactive nuclide decay data for reactor calcs., activation products and related isotopes 78−82426
radionuclide, half-life meas. by ion implantation 78−70713
radionuclides, short-lived, meas., counting statistics 80−58098
semiempirical mass formulae, shell corrections, α-decay period estimates for heavy nuclei *(Russian)* 79−22184
shape isomers, spontaneous fission, static and decay props. and excitations, review, book contrib. 78−82402
short lived nuclei, He-jet chopper for half-life meas. 77−38532
spontaneous fission half lives, odd A nuclei, Z≥96 78−86556
spontaneous fission half lives for actinide and transactinide nuclei, dynamic calc. 77−23124
spontaneous fission of transuranium nucl. isomers, exptl. work review 77−79405
superheavy elements, stability rel. to Moon primaeval melting 78−24478
superheavy nuclei, α-decay lifetimes 79−36203
superheavy nuclei, alpha half-lives, alpha particle struct. effects 78−17158
superheavy nuclei, lifetime, theoretical prediction of nonoccurrence in nature 78−662
superheavy nuclei in Z=126 region, α-particle stability 77−300
T=1/2 mirror nuclei, half-lives and branching ratios meas. 77−74805
U isotopes, sensitivities to cross sections, decay constants flux and time, analytical evaluation 78−82427
Z=114-126, nuclear stability reexamination using deformed Woods-Saxon pot. lifetimes level density 79−3094
Z=37-43, neutron rich fission products, mass energy surface, decay props. 80−78228
α-decay lifetime for A=110 to 120 and 174 to 188 *(Russian)* 78−78283
α-decay lifetimes and resonance widths, comparison of calc. methods 78−78325
(K^-,π^-), hypernuclei generation, γ-spectroscopy and lifetimes 79−75890
^{A}Ag, A=97, 98 and 99^{g,m} decay spectral meas. 78−93976
^{100}Ag^{g,m} decay, ^{100}Pd levels and γ-transitions 80−83077
^{101}Ag, $T_{1/2}$ meas., decay scheme, ^{101}Pd levels 78−37311
^{110}Ag, decay period, least square fitting, pocket calculator program with variable precision 80−67976
^{122}Ag decay, struct. of neutron rich even-even Cd nuclei 78−66249
^{26}Al, decay in marine sediments, meas. with cyclotron, dating technique 79−71819
^{26}Al^{m}, super-allowed Fermi β decay, lifetime meas. 77−79336
^{31}Al, radioactive half-life and branching ratios 79−22240

radioactive decay periods continued
Am isotopes, sensitivities to cross sections, decay constants flux and time, analytical evaluation 78−82427
^{241}Am-Be thermal neutron flux standard density variation obs. 77−83409
^{243}Am half life and α-activity 80−102159
^{45}Ar, β-decay scheme and half life, K deduced energy levels 78−78319
^{46}Ar, β-decay scheme and half life, K deduced energy levels 78−78319
^{46}Ar decay, gamma-ray spectra meas., half-life determ. 78−21513
^{A}As, A=85-7, mass chain, half lives and n-emission probabilities of delayed-n precursors 78−70497
^{66}As half life of Fermi superallowed β^+ activities from ^{58}Ni(^{10}B,2n) 79−9518
^{68}As β-decay, γ coincidence and singles spectra, spin, parity assignments, half-life meas. 77−79333
^{69}As β-decay, struct. determ. of ^{69}Ge 79−22245
^{74}As decay, branching ratios and $T_{1/2}$ meas., K-fluorescence yield of Ge 77−3300
^{206}At→^{206}Po, EC-β^+ decay, Po excited levels 77−79340
^{211}At half life, branching ratio of electron capture and α decay modes 78−58253
^{A}Au, A=181, 182, alpha decay, half lives, decay energies and branching ratios 79−45215
^{12}B, β-ray branching and $T_{1/2}$ 78−41674
Ba and rare-earth neutron deficient isotopes, β^+ strength $T_{1/2}$, X-ray, γ-ray spectra 77−34260
Ba heavy isotopes, $T_{1/2}$ determ. 77−26633
^{A}Ba, A=143 to 148, β-decay half life meas. 79−67718
^{A}Ba, A=144 to 147, β-decay half life determ. 78−78318
^{133}Ba decay data and standardisation 77−88081
^{139}Ba, γ-ray emission profitabilities and half-life obs. 80−57723
^{147}Ba, neutron rich nucleus identification, $T_{1/2}$ meas. 77−26633
^{148}Ba, neutron rich nucleus identification, $T_{1/2}$ meas. 77−26633
^{12}Be core excited T=2 levels, spin, half life from ^{10}Be(t,p), 12 MeV 78−66210
^{188}Bi alpha decay half lives 80−57749
^{207}Bi, half life determ. from ^{211}At and ^{207}Po decays 78−58253
^{242}Bk electron capture half life and α-branching ratio from ^{238}U+^{10}B, ^{235}U+^{11}B, ^{232}Th+N 79−67716
^{250}Bk, β^- decay, half life and ^{250}Cf energy levels, bands and transitions 79−22205
Br series fission product isotopes, sensitivities to various parameters, analytical evaluation 78−82424
^{A}Br, A=89-91, delayed neutron emission probabilities, β-decay half-lives 80−83078
^{92}Br mass chain, half lives and n-emission probabilities of delayed-n precursors 78−70497
^{15}C beta decay transition rates and half life, ^{15}N excited states and transitions 80−18248
Cd, A=97, 99, β delayed proton emission, spectra, branching ratio, half life 78−86517
^{126}Cd, mass separated, decay scheme and half life, ^{126}In levels 79−3117
Ce isotopes, half-life meas. 77−6311
^{A}Ce (A=149,150), fission product, γ-spectra half-life meas. 77−38240
^{A}Ce, A=124-127, half lives, low energy γ-data, β decay probabilities 79−499
^{139}Ce, determ. from gamma-ray meas. 77−34498
^{141}Ce, determ. from gamma-ray meas. 77−34498
^{145}Ce, β^- decay scheme and $T_{1/2}$ determ. using γ coincidence counting techniques 79−93558
^{149}Ce, β-decay half life meas. 79−67718
^{252}Cf effective half-life 77−22966
^{242}Cm, α-activity, half-life 77−54193
^{54}Co, super-allowed Fermi β decay lifetime meas. 77−79336
^{56}Co, half-life meas. by counting neutrons from D(γ,n) 77−26622
^{58}Co, determ. from gamma-ray meas. 77−34498
^{60}Co, determ. from gamma-ray meas. 77−34498
^{60}Co, $T_{1/2}$ meas. using double ionization chamber for the differential method 79−22552
^{47}Cr, β-decay GT matrix elements, $T_{1/2}$ 78−557
^{47}Cr, β-decay half-life and GT matrix element 77−22950
^{47}Cr, half-life and log ft to ^{47}V 77−22951
^{55}Cr, half-life determ. 78−4915
^{57}Cr mass excess, half life, ground state spin and parity, from ^{48}Ca(^{11}B, pn) 78−70436
Cs, A=114-118, neutron deficient isotopes, half lives, β^+,γ, delayed p and α meas. 78−70489
Cs, A=118,120,122, ground isomeric states, β-decay, $T_{1/2}$, γ- and CE-spectra 77−57601
Cs heavy isotopes, $T_{1/2}$ meas. 77−26633
Cs precursors, half lives and delayed neutron emission probabilities 79−49610
^{A}Cs, A=142-146, β-decay half life meas. 79−67718
^{A}Cs, A=144-147, β-decay half life determ. 78−78318
^{114}Cs β-decay, half life and branching ratio, ^{114}Xe excited states and γ-rays 80−47436
^{114}Cs, neutron deficient isotopes, α-decay meas. 79−93567
^{124}Cs, β-decay, ^{124}Xe level struct. 78−13033
^{134}Cs, half-life, gamma-spectrometric determ. 78−93972
^{137}Cs $T_{1/2}$ determ. using new specific activity meas. 78−70714
^{145}Cs, mass chain, half lives and n-emission probabilities of delayed-n precursors 78−70497
^{62}Cu half life from ^{63}Cu(n, 2n) 79−13291
^{A}E, A=110-113, neutron deficient isotopes, α-decay meas. 79−93567
^{169}Er, β-decay half-life, γ-ray spectra 77−79330
^{252}Es, half-life, γ-ray decay obs. 78−4914
^{148}Eu, ^{148m}Eu β-decay props., J^π, decay energy, $T_{1/2}$ 77−82876
^{17}F, populated in ^{16}O(d,n), half life meas. 77−88085
^{51}Fe, β-decay GT matrix elements, $T_{1/2}$ 78−557
^{51}Fe, β-decay half-life and GT matrix element 77−22950
^{53}Fe half life from ^{54}Fe(n,2n) 79−3142
^{259}Fm, fission mass distrib. and half life 77−26776
^{A}Fr, A=201-203, alpha decay, branching ratios, mass excess and half life 80−99154
^{62}Ga superallowed Fermi β^+ decay half life from ^{58}Li(^{6}Li,Zn) 79−54410
^{62}Ga, superallowed Fermi β-transition, half life and β-ray end point energy 78−78320
^{67}Ga γ- and X-ray emission probabilities and half-life obs. 80−32242
^{67}Ga, half life and γ ray absolute intensities 78−70496
^{72}Ga half-life determ. by ^{56}Mn activation and decay obs. 79−26398

radioactive decay periods continued
^{73}Ga, β-decay rate for estimation of ultra-high pressure 78−77927
^{143}Gd^{m+g}, β^+ and EC decay 78−50130
^{65}Ge, delayed proton spectra, $T_{1/2}$ meas. 77−38254
^{3}H biological half-life estimation in man, model 79−20689
Hf, alpha decay studies of the isotope 79−63636
^{181}Hf, decay, perturbed $\gamma\gamma$ directional correlations, complex chem. 77−36774
^Hg, A=177-183, 188, alpha decay, half lives, decay energies and branching ratios 79−45215
^{180}Hg, $T_{1/2}$=3s decay chain, on-line γ-ray spectroscopy 78−13034
^{194}Hg, half life determ. 79−45214
^{153}Ho→^{153}Dy, decay scheme, lifetimes 80−22765
^{170}Ho β^--decay, $T_{1/2}$ meas., ^{170}Er level struct. 78−41675
^I, A=139-141, delayed neutron emission probabilities, β-decay half-lives 80−83078
^{132m}I, ^{134m}I, isomer yield ratios in ^{235}U(n,f) 77−38306
^In, A=104, 106, β-decay half lives and decay schemes 78−74333
^{115}In, β^- decay spectrum, measured $T_{1/2}$, E_β 79−40888
^{120}In, β-decay, half life and decay schemes, ^{120}Sn level struct. 78−86510
^{181}Ir, γ-ray spectra, half-life, decay scheme 78−41672
^{35}K decay, ^{35}Ar levels, transitions and β-delayed protons 80−91156
^{38}K^m superallowed Fermi β-decay half lives 78−82318
^{40}K, decay consts. for use in geochronology and cosmochronology 78−28189
Kr series isotopes, sensitivities to various parameters, analytical evaluation 78−82424
^{73}Kr, delayed proton spectra, $T_{1/2}$ meas. 77−38254
La heavy isotopes, $T_{1/2}$ determ. 77−26633
^La, A=123-125,127, half lives and low energy γ-ray data, β-decay probabilities 79−499
^La, A=144-149, β-decay half life meas. 79−67718
^{129}La β-decay, struct. of ^{129}Ba 79−22244
^{134}La, half-life meas. 77−6311
^{138}La, radioactive decay meas., half life, γ energies 80−13418
^{140}La, beta decay half life 80−47435
^{140}La half-life determ. by ^{56}Mn activation and decay obs. 79−26398
^{143}La, gamma-ray spectra, half-life 77−82859
^{144}La, radioactive decay meas., half life, ^{144}Ce levels 80−13417
^{8}Li β-decay half life from ^{7}Li(d,p) 80−13483
^Lu, A=160-163, decay and $T_{1/2}$, $^{160\text{-}163}$Yb transitions 80−102146
^{157}Lu, short lived α emitter, α energy, $T_{1/2}$ and branching ratio 80−501
^{164}Lu, β-decay, half-life, populating ^{164}Yb levels 77−82805
^{176}Lu β-decay half life 80−52633
^Mg, A=29-32, radioactive half-life and branching ratios 79−22240
^{52}Mn half-life meas. 78−17152
^{57}Mn half life 78−82321
^{59}Mn, β-decay scheme, $T_{1/2}$ and mass meas., astrophysical significance 77−26635
^{60}Mn, mass and β-decay half life, ground state spin and parity 78−78317
Mo, A=103-5, half-lives and γ-ray energies of short-lived isotopes following ^{235}U fission 78−17137
^{85}Mo, delayed proton spectra, $T_{1/2}$ meas. 77−38254
^{102}Mo, β-decay, T1/2, ^{102}Tc deduced levels, tentative J^π and transitions 80−52630
^{91g}Mo, ^{91m}Mo, decay anal., half-life meas., γ-γ coincidences 77−2937
^{12}N, β-ray branching and $T_{1/2}$ 78−41674
^{17}N, β-decay delayed neutron emission, ^{17}O levels, T1/2 meas. 77−18481
^Na, A=27-32, radioactive half-life and branching ratios 79−22240
^{24}Na half-life determ., $T_{1/2}$=(14.964±0.015) h 80−95311
^{24}Na half-life determ. by ^{56}Mn activation and decay obs. 79−26398
Nb neutron deficient isotopes, studied via heavy ion induced compound reactions 77−57621
^{92}Nb, half life determ. by gamma spectroscopy, comparison of ^{92}Nb, ^{94}Nb activities and abundances 78−29423
^{92}Nb^g, cross-section and half-life from ^{93}Nb(n,2n), 14.8 MeV 78−70491
^{93m}Nb, radioactive decay period meas. *(French)* 77−79341
^{55}Ni, β-decay GT matrix elements, $T_{1/2}$ 78−557
^{55}Ni, β-decay half-life and GT matrix element 77−22950
^{55}Ni, half life meas. 77−22951
^{252}No spontaneous fission, fragment mass and kinetic energy distribs. 77−46194
Np isotopes, sensitivities to cross sections, decay constants flux and time, analytical evaluation 78−82427
^{242}Np β-decay, half life, ^{242}Pu level scheme 79−67664
^{14}O, half life determ., precision meas. 78−90043
^{14}O, superallowed Fermi β-decay half lives 78−82318
^{171}Os, alpha decay, half lives, decay energies and branching ratios 79−45215
^{196}Os, $T_{1/2}$ and partial decay scheme 78−21527
^{32}P, half-life, integrated internal bremsstrahlung intensity meas. 77−57629
^{32}P, half-life and mean beta distintegration energy determ by low-temp calorimetry 80−5094
^Pa, A=215-218, 222, α-decay half life and energies from ^{151}Ta+^{40}Ar and ^{184}W+^{40}Ar 79−45216
^Pb, A=183,184, alpha decay half lives 80−57749
^{204}Pb populated by ^{204}Bi decay, isomeric transitions, J^π assignments 78−50122
^{205}Pb decay, orbital electron capture ratios, half-life 78−74340
^{109}Pd, ^{238}U fission product, gamma-ray spectra, half-life determ. 77−50084
^{111}Pd^{g,m} γ-ray decay, ^{111g}Pd half-life, ^{111}Ag levels and decay 78−541
^{112}Pd, ^{238}U fission product, gamma-ray spectra, half-life determ. 77−50084
^{139}Pm decay, states in N=79 ^{139}Nd 77−41929
^{152}Pm decay, β and γ rays, spins, half lives, ^{152}Sm levels 78−542
Po, A=202-210, isomeric levels, g, $T_{1/2}$ 77−14068
^{207}Po half life, charact. γ meas. 78−58253
^{215}Po, excited states, half-life meas. *(French)* 79−97679
^Pr (A=149,150), fission product, γ-spectra, half-life meas. 77−38240
^{148}Pr, β^- decay scheme and $T_{1/2}$ determ. using γ coincidence counting techniques 79−93558
^Pt, A=173-179, 188, alpha decay, half lives, decay energies and branching ratios, rot. struct. 79−45215
^{183}Pt fast β-transition, ^{183}Ir levels, J^π assignments, Nilsson states for N=105 isotones 79−22206
Pu isotopes, sensitivities to cross sections, decay constants flux and time, analytical evaluation 78−82427
radioactive decay periods continued
^{232}Pu, fission barrier determ., from β-delayed fission 78−29518
^{237}Pu , half-life determ. by gamma counting in NaI(Tl) 78−8775
^{238}Pu, α-activity, half-life 77−54193
^{238}Pu half-life determ. 77−22965
^{239}Pu, α-decay half-life by two independent methods 77−82881
^{239}Pu, calorimetric determ. of half-life 79−26405
^{239}Pu fission isomers produced in ^{240}Pu(n,2n), half lives 77−30641
^{239}Pu, half life determ. by isotope dilution mass spectroscopy of ^{235}U 79−26409
^{239}Pu half life meas. by calorimetry, mass spectrometry and α-particle counting 79−26403
^{239}Pu, half-life determ. from α-emission rates 79−26407
^{239}Pu, half-life determ. specific activity meas., mass spectroscopy of ^{235}U daughter growth 79−26408
^{239}Pu, half-life determ. using isotope dilution mass spectroscopy and α-specific activity meas. 79−26410
^{239}Pu, prep. and chem. charact. for half-life meas. 79−26404
^{239}Pu, specific power and half-life, calorimetric determ. 79−26406
^{240}Pu, half life and specific activity by α-counting 79−502
^{240}Pu^m, shape isomer, half-life and excitation function meas. *(Chinese)* 78−78253
^{241}Pu compound nucleus lifetime by the shadow effect in ^{238}U(^{3}He,f) *(Russian)* 78−86562
^{241}Pu half life from α-spectrometry and ^{241}Am ingrowth 80−68609
^{241}Pu half-live determ. by mass spectrometry 80−78232
^{242}Pu half life relative to ^{238,239}Pu, α-activity and atom ratios 80−5100
^{242}Pu, half-life meas. 78−17154
^{242}Pu halflife from precise low-temp. heat capacity meas. on PuF_3, PuF_4, PuO_2 77−2952
^{223}Ra, excited states, half-life meas. *(French)* 79−97679
Rb heavy isotopes, $T_{1/2}$ meas. 77−26633
Rb precursors, half lives and delayed neutron emission probabilities 79−49610
^Rb, A=91 to 98, β-decay half life meas. 79−67718
^Rb, A=96 to 100, half-lives and neutron emission probabilities in neutron rich isotopes 79−17864
^Rb, A=96-98, β-decay half life determ. 78−78318
^{74}Rb, N=Z nucleus with T=1, I^π=0$^+$, half life 77−26627
^{74}Rb, Z=N nuclide, superallowed beta decay meas. 77−22952
^{81}Rb, β^+-EC decay, $T_{1/2}$, ^{81}Kr levels 77−79309
^{82}Rb, half life meas. 79−17861
^{83}Rb, half-life meas. 77−34257
^{84}Rb, half-life meas. 77−34257
^{87}Rb, decay constant determ., Rb-Sr dating appl. 78−29424
^{87}Rb, decay consts. for use in geochronology and cosmochronology 78−28189
^{87}Rb, half-life determ. by absolute counting 77−26943
Re, alpha decay studies of the isotope 79−63636
Re isotopes, $T_{1/2}$ determ. for β-decay using moving tape apparatus 77−65411
^{187}Re, decay const. determ. from ^{187}Re-^{187}Os systematics in meteorites 80−41778
^{94}Rh decay, $T_{1/2}$ ^{94}Ru levels and γ-transitions 80−18244
^{108}Rh, level structure and half life 77−82827
^{109}Rh, half-life and decay props. 78−25154
^{93g}Ru, ^{93m}Ru, decay anal., half-life meas., γ-γ coincidences 77−2937
^{29}S β^+-delayed proton decay, half life, ^{29}P deduced levels 79−22241
^{34}S, beta-decay, half-life 77−54188
^{39}S decay, half life, ^{39}Cl excited states and transitions 80−42595
Sb isotopes, fission product conc., sensitivity anal. of decay const. effects 78−82428
^Sb, A=135-6, mass chain, half lives and n-emission probabilities of delayed-n precursors 78−70497
^{46}Sc, beta decay half life 80−47435
Se series fission product isotopes, sensitivities to various parameters, analytical evaluation 78−82424
^Se (A=85-8), fission product, γ-spectra, half-life meas. 77−38240
^{68}Se half-life 77−38292
^{69}Se, delayed proton spectra, $T_{1/2}$ meas. 77−38254
^{69}Se, delayed proton decay 77−22971
^{32}Si, half life determined from varved Gulf of California sediment core 80−91153.
^{32}Si half life from tandem accelerator mass spectrometry 80−95313
^{32}Si half life via accelerator mass spectrometry 80−95314
Sn isotopes, fission product conc. sensitivity anal. of decay constant effects 78−82428
^{113}Sn, chem. effect on electron capture probability and decay const. 79−54412
^{132}Sn, doubly magic, RPA calc. of level scheme 78−50087
^{117m}Sn, half-life and γ-ray intensities 78−4916
Sr heavy isotopes, $T_{1/2}$ meas. 77−26633
^Sr, A=96-98, β-decay half life determ. 78−78318
^Sr, A=99, 100, $T_{1/2}$ determ. 79−9524
^{77}Sr, delayed proton spectra, $T_{1/2}$ meas. 77−38254
^{82}Sr, half life meas. 79−17861
^{85}Sr, electron capture decay, K X-ray emission probability, half-life, decay scheme 79−17862
Ta, alpha decay studies of the isotope 79−63636
^{166}Ta, isotope identification in ^{159}Tb(^{16}O,9n) reaction, half-life and decay scheme 77−79331
^{180}Ta, radioactive decay and half-life of naturally occurring isotope 77−61377
^{180}Ta^m, β^- and EC branching ratios, K-internal conversion coeff., γ-intensities, T 1/2 80−68601
^{146}Tb decay and T1/2, ^{146}Gd lowest 2^+ state, J^π and transitions 80−105979
^{162}Tb β-decay, γ-spectra, $T_{1/2}$, deduced ^{162}Dy levels 77−34246
^{99}Tc lifetime in generator-produced ^{99m}Tc, calc. 79−88188
^{99}Tc^m, β-decay rate for estimation of ultra-high pressure 78−77927
^{99}Tc^m, $T_{1/2}$ meas. using double ionization chamber for the differential method 79−22552
^{91g}Tc, ^{91m}Tc, decay anal. half-life meas., γ-γ coincidences 77−2937
^{99m}Tc, in hexahalogen complexes, decay const. determ. 80−106020
Te isotopes, fission product conc., sensitivity anal. of decay const. effects 78−82428
^Te (A=135-7), fission product, γ-spectra, half-life meas. 77−38240
^Te, A=107-110, neutron deficient isotopes, α-decay meas. 79−93567
^{128}Te $\beta\beta$ decay ratio of ^{128}Te/^{130}Te half lives 78−66250
^Th, A=212, 213, 214, decay energies and half lives from ^{176}Hf(^{40}Ar,X) 80−47440

radioactive decay periods continued
^{230}Th alpha-decay half life from specific activity method 80−102157
^{232}Th, α-decay half-life, liq. scintillator expt. for students 78−12496
^{232}Th, decay consts. for use in geochronology and cosmochronology 78−28189
^{51}Ti, β-decay scheme, $T_{1/2}$ and mass meas., astrophysical significance 77−26635
^{51}Ti β-decay scheme 77−46139
^{184}Tl, half-life 79−97652
^{186}Tl, isomer and ground state half-lifes 79−97652
^{188}Tl, half-life 79−97652
^{195}Tl (1.13 h) decay, ^{195}Hg level scheme and transitions, band population 79−17807
^{197}Tl decay, half life and decay scheme, ^{197}Hg level scheme and transitions 79−67719
^{201}Tl γ- and X-ray emission probabilities and half-life obs. 80−32242
^{206}Tl, isomeric yrast states obs. 77−281
^{153}Tm, short lived α emitter, α energy, $T_{1/2}$ and branching ratio 80−501
U analysis, in geological samples, delayed neutrons method *(Rumanian)* 79−88507
^{232}U half-life from specific and relative activity methods 80−9270
^{233}U, half-life determ. 80−57750
^{238}U, ^{235}U, decay consts. for use in geochronology and cosmochronology 78−28189
^{238}U, muonic fission and electron decay 77−38754
^{238}U, spontaneous emission of heavy ions, half-life of process 77−74815
^{238}U, spontaneous fission, half life and fragment kinetic energy meas. using cylindrical ionisation chamber 78−86555
^{238}U, spontaneous fission decay const., calibration of fission track dating parameters 77−41207
^{239}U second-chance fission decay times from crystal blocking in ^{238}U(n,f) 79−85568
^{242}U β-decay, half-life, ^{242}Np levels, J^{π} and transitions 79−67664
^{46}V(β^+)^{46}Ti, superallowed Fermi decay half-life 77−34259
^{46}V(β^-)^{46}Ti superallowed Fermi decay, ft value 77−10371
^{50}V, half lives of β-decay and e$^-$-capture in $\Delta J=4$ transitions 79−22246
^{50}V, half-life limits for β-decay and electron capture 77−79334
^{54}V, β-decay scheme and $T_{1/2}$ determ. 78−21528
^{55}V β-decay scheme and $T_{1/2}$ determ., mass excess meas. 78−21528
W, alpha decay studies of the isotope 79−63636
^{A}W(^{12}C,f), A=182, 183, 184, 186, 80 to 115 MeV, lifetime meas. by crystal-blocking tech. 80−91198
^{A}W(^{16}O,f), A=182, 183, 184, 186, 80 to 115 MeV, lifetime meas. by crystal-blocking tech. 80−91198
^{A}W(^{19}F,f), A=182, 183, 184, 186, 80 to 115 MeV, lifetime meas. by crystal-blocking tech. 80−91198
^{228}X, primordial and other nuclei, shell model calc. 78−8752
^{A}Xe, A=111-113, neutron deficient isotopes, α-decay meas. 79−93567
Y heavy isotopes, $T_{1/2}$ meas. 77−26633
^{A}Y, A=96 to 98, β-decay half life meas. 79−67718
^{99}Y→^{99}Zr, half life and beta decay investigation 79−17863
^{100}Y, fission product, γ-spectra, half-life meas. 77−38240
Yb, A=153-158, neutron deficient isotopes, daughter products, α-decay, halflives 78−21533
Yb isotopes, A=160-165, decay spectra meas. 77−22959
^{169}Yb, identification 77−50075
^{81}Zr, delayed proton spectra, $T_{1/2}$ meas. 77−38254
^{99}Zr→^{99}Nb, half life, level schemes and β-decay investigation 79−17863
^{100}Zr, fission product, γ-spectra, half-life meas. 77−38240
^{100}Zr, levels, J^{π} via ^{100}Y β-decay 77−82878
^{85g}Zr, half-life, decay scheme 77−34258

radioactive decay schemes
see also nuclear energy levels
A=198 nuclei, struct., level props., decay, review 78−17077
A=214 nuclei, struct. info., energy levels, spin, parity, decay 78−17078
A=215, nuclear data sheets, decay characteristics and level struct. 78−58224
A=218 nuclei, nuclear struct. info., energy levels, spin, parity, decay 78−17079
A=219, nuclear data sheets, decay characts. and level struct. 78−58225
A=222 nuclei, nuclear struct. info., energy levels, spin, parity, decay 78−17080
A=223, nuclear data sheets, decay characts. and level struct. 78−58226
A=227, nuclear data sheets, decay characts. and level struct. 78−58227
A=234 nuclei, nuclear struct. info., energy levels, spin, parity, decay 78−17081
A=238 nuclei, nuclear struct. info., energy levels, spin, parity, decay 78−17082
A=242 nuclei, nuclear struct. info., energy levels, spin, parity, decay 78−17083
A=53 nuclei, struct., level props., ENSDF data 78−17076
characteristic function eqn. of Markov process, Langevin process applications 80−57192
characts., natural occurrences, technological enhancement and health effects 80−46071
conference on nuclear spectroscopy and structure, Alma Ata, USSR, (Mar. 78) 79−75809
data sheets for A=184 nuclei 78−12948
data sheets for A=231, 235, 239 nuclei 78−12949
fission product decay props. meas. using many-capillary gas jet system 77−88364
gamma emission, math. modelling 80−32236
Gardner analysis of decay components with strong fluctuations 80−102161
heavy element decay data, reactor related calcs., current status 79−97772
impulse approx. with nuclear current conservation, off-shell form factors 80−52632
magnetic lens spectrometer+Ge(Li) detector, for nuclear decay schemes and halflives meas. 79−710
nuclear data files of UK Chemical Committee, summary of data, available in ENDF/B format 78−82425
nuclear structure references 1975-7 79−30772
nuclei far from line of beta stability, mass spectroscopic anal. techniques, book contrib. 80−69014
odd mass nuclei with 51 neutrons or 51 protons, radioactivity, expt. theory *(French)* 77−293
proton decay, β-delayed proton radioactivity, book contrib. 78−82322
quantum radiation, data handbook 80−94933

radioactive decay schemes continued
radioactive nuclide decay data for reactor calcs., activation products and related isotopes 78−82426
radionuclide decay, computer simulation, levels, transitions, internal conversion 80−63136
radionuclide distribution, selective determ., mathematical modelling *(Rumanian)* 79−81098
serial decay, transient equilib. and secular equilib. 79−80901
superheavy elements, search for high energy α-particles 79−59040
superheavy nuclei, unusual decays in bubble chambers *(Russian)* 79−93568
β-delayed neutron decay, statistical model, Monte Carlo techniques, fictional pandemonium nucleus calcs. 78−89830
^{230}Ac, identification and β-decay meas. 77−22963
^{101}Ag, $T_{1/2}$ meas., decay scheme, ^{101}Pd levels 78−37311
^{110}Ag^{m} disintegration, scheme of ^{110}Cd *(French)* 78−58248
^{111}Ag^{m}→^{111}Cd decay 78−541
^{113}Ag, 5.3 h decay scheme, ^{113}Cd level scheme 78−46028
^{115}Ag, 20 min decay scheme, ^{115}Cd level scheme 78−46029
^{45}Ar, β-decay scheme and half life, K deduced energy levels 78−78319
^{46}Ar, β-decay scheme and half life, K deduced energy levels 78−78319
^{198}Au, radioactive decay, γ-ray energy meas. *(German)* 77−57633
^{126}Ba→^{126}Cs→^{126}Xe, meas. of decay spectra 77−6316
^{131}Ba, decay, electric monopole transitions 80−22752
^{133}Ba decay data and standardisation 77−88081
^{143}Ba decay to ^{143}La, β-branching and log ft values 78−50129
^{7}Be, electron capture radioactive decay probabilities in atoms and ions 79−59556
^{199}Bi→^{199}Pb, spectra meas. 78−78316
^{201}Bi→^{201}Pb, spectra meas. 78−78316
^{204}Bi, decay scheme 78−50122
^{210}Bi→^{210}Po→^{206}Pb, L-shell auto -ionisation 77−6739
^{248}Bk, 23.7 h, spectroscopic studies 78−78314
^{126}Cd, mass separated, decay scheme and half life, ^{126}In levels 79−3117
Ce isotopes, neutron rich, decay properties 78−13032
^{144}Ce, 284.3 D, decay scheme, energy levels and transitions in ^{144}Pr 77−14070
^{145}Ce, β^- decay scheme and $T_{1/2}$ determ. using γ coincidence counting techniques 79−93558
^{57}Co, radioactive decay, γ-ray energy meas. *(German)* 77−57633
^{60}Co, radioactive decay, γ-ray energy meas. *(German)* 77−57633
^{63}Co from ^{64}Ni(n,d), 14.3 MeV 78−46053
^{64}Co from ^{64}Ni(n,p), 14.3 MeV 78−46053
^{124}Cs, β-decay, ^{124}Xe level struct. 78−13033
^{124}Cs, EC and β^+-decay, exam. of Xe nuclear level struct. 78−21498
^{126}Cs, EC and β^+-decay, exam. of Xe nuclear level struct. 78−21498
^{127}Cs→^{127}Xe, study of γ-rays, ^{127}Xe level scheme 77−299
^{129}Cs, β decay, ^{129}Xe population, energy level scheme, γ spectra meas. 77−2936
^{134}Cs, as potential radiotherapy radionuclide, prod. and decay scheme 77−90875
^{137}Cs decay determ. by β-ray spectrometry 79−26397
^{137}Cs, radioactive decay, γ-ray energy meas. *(German)* 77−57633
^{153}Dy β-decay to ^{153}Tb, decay scheme, weak deform. in ^{153}Tb 77−41884
^{165}Er decay parameters and whole-body dose, for radioisotope scanning 77−70529
^{250}Es^{m} EC decay, ^{250}Cf two-quasiparticle states 77−46140
^{152}Eu, decay, gamma transitions and probabilities of beta transitions 80−22768
^{24}F, shell model anal. of decay schemes 77−14044
^{52}Fe→^{52}Mn^{m}→^{52}Cr, γ-ray spectra, ^{52}Cr levels 78−21529
^{61}Fe from ^{64}Ni(n,α), 14.3 MeV 78−46053
^{147}Gd, γ-transitions, internal conversion electron spectra meas. 79−6475
^{75}Ge, beta decay of 83 min ground state, decay characts. and scheme 79−67713
^{158}He^{g,m} decay, obs. of ^{158}Dy collective excitations 78−82270
^{180}Hg, $T_{1/2}$=3s decay chain, on-line γ-ray spectroscopy 78−13034
^{153}Ho→^{153}Dy, decay scheme, lifetimes 80−22765
^{170}Ho β^--decay, $T_{1/2}$ meas., ^{170}Er level struct. 78−41675
^{133}I, β decay, ^{133}Xe population, energy level scheme, γ spectra meas. 77−2936
^{A}In, A=104, 106, β-decay half lives and decay schemes 78−74333
^{114}In isomer decay, spin, excitation function, T_{112} γ-X-ray and γ-γ coinc. 77−6312
^{120}In, β-decay, half life and decay schemes, ^{120}Sn level struct. 78−86510
^{A}Ir, A=168-170, new isotopes from ^{63}Cu induced reactions 78−70563
^{A}Ir, A=169, 170, decay characteristics 79−503
^{181}Ir, γ-ray spectra, half-life, decay scheme 78−41672
^{194}Ir decay, ^{194}Pt level scheme 77−2900
Kr isotopes, A=88 to 91, decay rate determ. for ground state beta-branching 77−26634
^{143}La, decay, gamma-ray spectra *(French)* 77−30517
^{167}Lu→^{167}Yb, spin-parity determ. for ^{167}Yb levels 79−6380
^{169}Lu, radioactive decay, gamma ray and conversion electron spectra 80−22766
^{169}Lu, radioactive decay scheme 80−22767
^{172}Lu, decay scheme, γ-ray, conversion electron spectra 79−75913
^{179}Lu, level struct. of ^{179}Hf 77−54185
^{24}Mg lowest $J^{\pi}=0^+$, T=Z level from ^{23}Na+p reactions, narrow resonance, isospin forbidden particle decays 78−89871
^{52}Mn^{g}→^{52}Cr, γ-ray spectra and ^{52}Cr levels 78−21529
^{91g}Mo, ^{91m}Mo, decay anal., half-life meas., γ-γ coincidences 77−2937
^{16}Ne mass excess and diproton decay width from ^{20}Ne(^{4}He,^{8}He) 117 MeV 78−78245
^{26}Ne shell model anal. of decay schemes 77−14044
^{12}O mass excess and diproton decay width from ^{16}O(^{4}He,^{8}He) 117 MeV 78−78245
^{A}Os, A=165-168, new isotopes from ^{63}Cu induced reactions 78−70563
^{177}Os→^{177}Re decay scheme, lower excited states of ^{177}Re obs. 78−17145
^{179}Os→^{179}Re decay scheme, lower excited states of ^{179}Re obs. 78−17145
^{194}Os beta decay, X-ray/gamma relative intensities, L_1 subshell yields 78−4919
^{190}Os, identification and β-decay meas. 77−22963
^{196}Os, $T_{1/2}$ and partial decay scheme 78−21527
^{233}Pa decay emission probability of 312 keV gamma-ray 79−59035
^{204}Pb populated by ^{204}Bi decay, isomeric transitions, J^{π} assignments 78−50122
^{139}Pm decay, states in N=79 ^{139}Nd 77−41929
^{147}Pm decay, K-orbital shake off electrons and X-ray spectra 77−46141
^{151}Pm→^{151}Sm, β-decay, level scheme of ^{151}Sm 77−74792
Po isotopes, alpha-decay theory 77−61389

radioactive decay schemes continued
^{210}Po, excited, deformed, fission or neutron emission, shell-correction approach to nuclear densities 77−30483
^{146}Pr→^{146}Nd, decay scheme and energy levels, log ft values 78−4912
^{148}Pr, β^- decay scheme and $T_{1/2}$ determ. using γ coincidence counting techniques 79−93558
^{185}Pt^{m+g} decay, population of ^{185}Ir levels 80−9269
^{239}Pu muonic atom, n emission, bound μ influence on fission barrier 78−89845
^{224}Ra and daughters, radioactive props. and biological behaviour 78−96090
^{230}Ra, identification and β-decay meas. 77−22963
Rb isotopes, A=88 to 91, decay rate determ. for ground state beta-branching 77−26634
^{A}Re, A=166, 167, 168, α-branching ratios, decay characterics 79−503
^{A}Re, A=168 and 169, new isotopes from ^{63}Cu induced reactions 78−70563
^{182}Re, cryonuclear physics for radioactive decay studies *(Dutch)* 78−29416
^{221}Rn, decay scheme, α-, β-, γ-spectra meas. 79−6507
^{222}Rn, props. and behaviour of short lived daughter nuclides in the atmos. *(Japanese)* 80−72339
^{93g}Ru, ^{93m}Ru, decay anal., half-life meas., γ-γ coincidences 77−2937
^{114}Sb, 8$^-$, 210 μs state, mag. moment, PAC of liq. Sn: ^{114}Sb 77−26609
^{125}Sb, radioactive decay, ^{125}Te levels form. *(French)* 77−65202
^{75}Se, decay, electric monopole transitions 80−22752
^{83m}Se, decay scheme refinement, ^{83}Br levels 78−17147
Sm decay chain expansion significance 79−9712
^{141}Sm^{g} decay scheme, ^{141}Pm level struct. 77−46142
^{145}Sm, electron capture decay to ^{145}Pm, γ-transition decay rate and intensities 78−13030
^{153}Sm, radioactive decay, γ-ray energy meas. *(German)* 77−57633
^{106}Sn decay, ^{106}In level scheme determ. 78−93971
^{113}Sn, decay to levels of ^{113}In 77−38247
^{130}Sn→^{130}Sb, decay scheme, log ft values, spin-parity assignments 77−34264
Sr isotopes with A=96, 98, 100, decay scheme, level scheme of Y 77−26632
^{85}Sr, electron capture decay, K X-ray emission probability, half-life, decay scheme 79−17862
^{91}Sr, decay scheme, gamma-ray spectra 77−71587
^{168}Ta, isotope identification in ^{159}Tb(^{16}O,9n) reaction, half-life and decay scheme 77−79331
^{180}Ta, radioactive decay and half-life of naturally occurring isotope 77−61377
^{94}Tc→^{94}Mo, level spins and multipole mixing ratios from γ-γ correlation meas. 78−21517
^{91g}Tc, ^{91m}Tc, decay anal. half-life meas., γ-γ coincidences 77−2937
^{129}Te^{m,g} decay, ^{129}I energy levels, γ spectra, coincidence spectra 77−2935
^{232}Th muonic atom, n emission, bound μ influence on fission barrier 78−89845
^{190}Tl→^{190}Hg→^{190}Au, decay spectra and periods 77−6317
^{197}Tl decay, half life and decay scheme, ^{197}Hg level scheme and transitions 79−67719
^{201}Tl dosimetry, nuclide parameters and S factors 77−13011
^{157}Tm, ^{155}Tm decay, nucl. energy levels determ. of ^{157}Er and ^{155}Er *(French)* 77−57630
^{163}Tm, β-decay, ^{163}Er excited state obs. 78−17146
U mining, U refining and decay processes, radioactive mining waste disposal *(Dutch)* 80−21418
U- and Th-series, secular equilib. investigation method 79−2381
^{232}U→^{212}Pb decay chain, obs. of collective states fed by weak α-transitions 78−8786
^{235}U α decay and ^{231}Th β decay, γ-radiation study, energy level scheme *(Russian)* 78−17160
^{235}U, decay product radioactive accumulation, FORTRAN program 80−68611
^{235}U, radioactive series decay, computer simulation 80−102160
^{235}U, thermal neutron irrad., fission product decay power calc. 80−22868
^{236}U, as extinct natural parent of Th, premature falsification of correct theory 79−30186
^{238}U, decay product radioactive accumulation, FORTRAN program 80−68611
^{238}U, muonic fission and electron decay 77−38754
^{238}U, radioactive series decay, computer simulation 80−102160
^{52}V→^{52}Cr, γ-ray spectra and ^{52}Cr levels 78−21529
^{54}V, β-decay scheme and $T_{1/2}$ determ. 78−21528
^{55}V β-decay scheme and $T_{1/2}$ determ., mass excess meas. 78−21528
^{190}W, identification and β-decay meas. 77−22963
^{127}Xe decay, absolute gamma-ray intensities 78−548
Y isotopes with A=96, 98, 100, decay scheme, level scheme of Zr 77−26632
^{88}Y solution, standardisation using efficiency extrapolation method, β-γ coincidence meas. 78−21832
^{96}Y from ^{235}U fission, spectroscopic meas. *(German)* 77−67726
^{98}Y from ^{235}U fission, spectroscopic meas. *(German)* 77−67726
^{159}Yb, identification 77−50075
^{165}Yb, beta-decay to ^{175}Tm, γ-ray and conversion electron spectra 78−74334
^{85g}Zr, half-life, decay scheme 77−34258

radioactive lifetimes *see radioactive decay periods*

radioactive sources
see also radioisotopes
^{222}Rn, disssolved in Boisson spring water, physiological props. 79−48292
^{241}Am, medical and industrial sources and applications 77−26915
absolute, standardisation of radioactive sources and solns., 4π β-γ coincidence, program 77−18760
activity calculation from counting rates in single and coincidence photopeak 78−13371
alpha-particle sources, thin, prep. from solns. at low temps. 80−27843
analytical and industrial applications of sealed sources 79−85847
automatic radioisotope production devices adapted to a medical cyclotron 80−12260
beta particle emitters used in therapy, figure of merit 80−36083
beta sources, depth dose distribs. in varous materials 78−17462
beta-ray source deposit uniformity, meas. techniques 79−26792
brachytherapy source calibration using $Fe(NH_4)_2(SO_4)_2$-benzoic acid-xylenol orange dosimeter 77−5081

radioactive sources continued
chromatography radioactive source leak testing under dynamic flow conditions 80−3432
concrete calibration sources for radiometric field instruments, experiences 79−5633
cyclotron irradiated gaseous targets, optimum flow rate *(French)* 80−14025
cyclotron production of radiodiagnostic isotopes 80−51255
cyclotron production of radionuclei for medical appl., UC-Davis program 80−51257
fission products of ^{252}Cf, preparation and meas. with He jet TOF mass spectrometer 77−23355
fissionable source, size and uniformity determ. 78−86711
gamma active spikants in nuclear fuel for proliferation deterrence, practical aspects 79−93716
gamma mixed-radionuclide NBS sources for calibration of Ge(Li) detectors for environmental assay 77−38541
gamma ray source, solid angle, self-absorption factors, evaluation by Monte Carlo method *(Rumanian)* 78−58526
gamma ray sources for exposure rate meas. instrument calibration 80−32562
gamma source with flat surface, activity determ. using Ge(Li) detector *(German)* 78−58528
gamma-ray source properties, electron momentum density studies 80−14028
gamma-ray sources, 4.43 MeV, Am-Be or Pu-Be surrounded by hydrocarbon, for undergraduate laboratory 78−77648
gamma-ray volume shaped source, self-absorpt., for NaI detectors, Monte Carlo calc. 77−26909
Gammacell self-contained irradiators, safety programme 77−29211
gaseous, prod. by cyclotron irradiated gaseous targets *(French)* 79−76252
heavy element quantitative sample preparation 79−9936
IAEA regulations for safe transportation 80−63410
IAEA transport information collection system, influence on improved safety measures 80−63413
IAEA transport regulations, underlying radiation protection principles 80−63414
international regulatory control for safe transportation 80−63411
isotope induction at LAMPF, fabrication, cladding, handling of irrad. targets 80−23231
isotope production at LAMPF, hot cell chemistry 80−18674
isotopic generator, medical and non-medical appl. *(Spanish)* 78−15922
labelling of materials with short-lived radioisotopes produced at the place of application *(German)* 79−89503
manipulation unit equipment for radiotherapy depts. 80−30903
N-16 source, exposure rate and absorbed dose meas. for 6-7 MeV photons 79−26766
neutron appl. in industry and technology 77−25244
neutron therapy source shielding for Be(*d*,*n*) reaction 79−20617
nuclear experiments performed with intense radioactive ion beams, review 79−97922
nuclear spent fuel use as radiation processing source 77−57729
optimum conditions in radioactive measurements with the statistic accuracy taken into account 79−41083
package design, construction and testing for safe transportation 80−63412
photon, low-energy, spectrum shapes, in vivo detection 77−65377
polarised β-active nuclei prod. by polarised neutron capture 77−30695
positron annihilation within source holder 78−70667
preparation, adsorption of ^{90}Sr+^{90}Y on anodised Al 79−36454
preparation, EM separation coupled to electron and positron spectroscopy 77−23329
preparation for 4$\pi\beta$-γ coincidence counting using $AlCl_3$ 78−838
production by chemical reactions in heterogeneous systems *(Spanish)* 79−45490
production using electron linear accelerator, review *(Japanese)* 78−78534
radiation field of extended rectangular source, numerical integration 78−66424
radioactive waste source terms, calc. using computer code 79−54569
radiometric system design, mathematical modelling of relevant physical processes *(Rumanian)* 79−59313
receptor binding radiotracer preparation 80−51258
release monitoring equipment test gas standard production *(French)* 79−3252
safe transportation, using type A, exempt and LSA packages 80−63401
sealed radioactive sources, US leak and surface contamination tests *(Czech)* 80−27846
short-lived, appl. in well logging 79−53563
spectrometric source conversion peak half-width determ. 77−79499
standardisation using 4$\pi\beta$-γ coincidence method *(Rumanian)* 77−46472
standards for environmental monitoring, prep. 78−80816
transuranics for industrial and medical appl. *(French)* 77−42206
uniform sources of extended area using radiotoned photographic film 78−78537
X-ray fluorescence analysis, radioisotope sources, development, charact. 78−15741
X-ray low energy calibration sources for proportional counters using radionuclides 79−705
γ-ray sources, narrowly collimated, from betatron, radiation fields in Al and H_2O *(Russian)* 77−30549
^{108}Ag^{m}, neutron cross-section for production from ^{107}Ag 79−29625
^{108m}Ag, γ-ray energies meas. for Ge(Li) detector calibration 80−27865
^{28}Al radioisotope source, activation expt. 79−31
Am-Be neutron probe, underestimation of radiation exposure by film badges 78−15900
^{241}Am, alpha, X-ray, gamma-ray and neutron sources for medical use *(French)* 77−42205
^{241}Am, for preionisation of pulsed gas lasers 78−29963
^{241}Am, radioactive decay, 59.5 keV photon yield 77−6588
^{241}Am sealed source for smoke detection *(French)* 77−42204
^{241}Am source ingestion, case report 78−28088
^{241}Am thin source preparation 80−18730
^{241}Am-Be, C content in coal determ., by neutron inelastic scattering *(Czech)* 80−101048
^{243}Am, absolute yields of 43.5, 74.7 and 117.8 keV photons 80−32568
Au coating for radioactive source backing, spontaneous resistance variations 77−54386
Au-Pd coating for radioactive source backing, spontaneous resistance variations 77−54386

radioactive sources continued
^{198}Au, redetermination of γ-ray standards between 0.1 and 1.0 MeV 78−37472
^{199}Au, carrier-free extraction from neutron-irradiated ^{198}Pt, medical appls. 79−2130
^{131}Ba, decay, electric monopole transitions 80−22752
^{133}Ba decay data and standardisation 77−88081
^{140}Ba/^{140}La radio-nuclide generator, separation methods *(German)* 77−25298
^{76}Br production, excitation functions for neutron deficient isotope form. via high-energy d-Br reactions 78−44609
^{77}Br production, excitation functions for neutron deficient isotope form. via high-energy d-Br reactions 78−44609
^{11}C isotopes, production and transport system 78−46200
^{13}C(α,n), n and 6.13 MeV γ-ray emission for Ge(Li) detector calibration 79−13572
^{109}Cd nuclear transformation rate meas. using 4π proportional counter 78−21826
^{109}Cd, production in nuclear reactors by neutron irrad. of ^{107}Ag 80−52798
^{139}Ce, half-life determ. from gamma-ray meas. 77−34498
^{139}Ce→^{139}La, internat. comparison of activity meas. March 1976 79−13613
^{141}Ce, half-life determ. from gamma-ray meas. 77−34498
^{144}Ce/^{144}Pr miniature radioisotope generator 79−49885
^{252}Cf for interstitial radiotherapy implantations, clinical study 78−11722
^{252}Cf, H content in coal determ., by neutron inelastic scattering *(Czech)* 80−101048
^{252}Cf, medical and industrial sources and applications 77−26915
^{252}Cf, neutron source for medical use *(French)* 77−42205
^{252}Cf sealed source for medical and industrial applications *(French)* 77−42204
^{252}Cf source with high emission, n and γ dosimetry, safety *(Czech)* 78−33296
^{252}Cf wire neutron source distrib. meas. by autoradiography 77−61643
Co isotopes, thick-target yields in Ni due to proton bombardment up to 100 MeV 77−88312
$CoAl_2O_4$, compatibility with containment metals 79−13534
$Co_{0.5}Mg_{0.5}O$, compatibility with containment metals 79−13534
CoO, compatibility with containment metals 79−13534
^{55}Co, cyclotron prod. by ^{3}He bombardment of natural Fe, bleomycin complex synthesis 77−86629
^{56}Co standard source, relative γ-ray intensities 78−55069
^{57}CoO, compact single-line Mossbauer source preparation 77−10518
^{58}Co, half-life determ. from gamma-ray meas. 77−34498
^{60}Co 20 Ci source, site radiography incident 78−53523
^{60}Co, 2505 keV gamma ray intensity in β-decay 79−13249
^{60}Co 3000 Ci source accidental fall and retrieval in teletherapy room 78−53524
^{60}Co applicator treatment of retinoblastoma 77−81550
^{60}Co, exposure-rate calibration of small radioactive sources 78−41881
^{60}Co external source on liq. scintillation system for ^{32}P Cherenkov effect detect. efficiency meas. 78−25387
^{60}Co gamma radiation, filtration anal. of collimated beams 79−63861
^{60}Co gamma ray sources, exposure efficiency dependence on distance, theoretical interpretation *(Czech)* 80−850
^{60}Co gamma-rays, calibration in water vs. calibration in air for teletherapy units 77−21630
^{60}Co, half-life determ. from gamma-ray meas. 77−34498
^{60}Co isotopic γ-ray source, quantum yield of electrons from cylindrical casing 79−31289
^{60}Co radiotherapy unit, comparison with 4 and 10 MV linear accelerators in moving-strip technique 77−70553
^{60}Co, secondary radiation characts., generated by gamma radiation-air interaction *(Czech)* 79−67967
^{60}Co sources for total body irrad., uniformity and standardisation 80−94338
^{60}Co teletherapy unit, mech. fault affecting source position 77−73562
^{60}Co teletherapy unit dose calibration, comparison of methods 80−30900
^{134}Cs, activity meas. 79−59292
^{136}Cs, as potential radiotherapy radionuclide, prod. and decay scheme 77−90875
^{134}Cs, for treatment of cervical cancer, isodose curves 77−90876
^{134}Cs, standardisation (1977) AECL 78−25371
^{137}Cs, exposure-rate calibration of small radioactive sources 78−41881
^{137}Cs gamma radiation, filtration anal. of collimated beams 79−63861
^{137}Cs, narrowly collimated γ-ray sources, radiation fields in Al and H_2O *(Russian)* 77−30549
^{137}Cs, parametric definition 80−91346
^{137}Cs, secondary radiation characts., generated by gamma radiation-air interaction *(Czech)* 79−67967
^{137}Cs standardisation by 4π(PC)-γ efficiency tracing method 79−13577
^{137}Cs-^{137m}Ba generator, for nucl. medicine, preparation by ion exchange chromatography 78−28071
^{62}Cu generator for medical and biological uses 80−30890
^{244}Cu, neutron source for medical use *(French)* 77−42205
^{244}Cu, simulated neutron irradiation damage, He ion implantation 78−79648
^{165}Er decay parameters and whole-body dose, for radioisotope scanning 77−70529
^{152}Eu gamma source, uncertainties in peak area determ. for Ge detector calibration 80−5436
^{152}Eu, intercomparison of gamma ray emission rate meas., using Ge spectrometers 78−82568
^{152}Eu, X-ray emission probabilities per decay 80−14027
^{18}F, for labelling anhydrous fluorinating reagents, prod. by cyclotron accelerated p, d, ^{3}He, or α 79−2131
^{18}F, production from ^{18}Ne, carrier free H^{18}F acid 79−29626
^{153}Gd sources for computerised tomography scanners, radiation therapy planning 79−20626
^{153}Gd, use in tissue lipid content analysis by photon absorpt. 78−28041
^{68}Ge/^{68}Ga radioisotope generator system 78−78536
^{177}Hf production, recovery and purification for nucl. medicine use as ^{172}Lu generator 78−48893
^{197}Hg source for Mossbauer studies 79−26796
^{166m}Ho, relative intensities of gamma-rays 78−46201
^{A}I, A=121, 123 and 125, cyclotron prod. by ^{127}I(p,xn)Xe→(β)→I reactions, yield curves 78−44611
^{123}I, carrier-free, prod. from ^{127}I(p,5n)^{123}Xe using in-beam collection of ^{123}Xe 78−44610
^{123}I source sumpeak calibration absolute activity 77−57785
radioactive sources continued
^{123}I two-crystal coincidence counting 78−13394
^{125}I, encapsulated, and other photon sources, microdosimetric props. 80−36146
^{125}I surface contamination meas., sensitivity comparison with other detectors *(Czech)* 79−34673
^{125}I, use of screened low energy radiation sources for moulds in mouth carcinoma treatment 77−48855
^{113m}In generator with modified silica gel column 77−90897
^{192}Ir high intensity gamma-ray radiographic source development 77−2715
^{192}Ir industrial radiography source, accidental over-exposure 77−56472
^{192}Ir, interstitial radiation therapy, Angiocath afterloading technique 77−13002
^{192}Ir radioactive sources, field determ. of output and effective size 80−30193
^{192}Ir radiographic source, radiation accident 78−53514
^{192}Ir, redetermination of γ-ray standards between 0.1 and 1.0 MeV 78−37472
^{192}Ir ribbon interstitial tonsillo-palatine implants for radiotherapy 77−70527
K_2CoO_3:^{57}Co Mossbauer source 77−6592
^{40}K, exposure rates from gamma sources in dwelling room walls, Monte Carlo calc. 78−73260
^{40}K, γ-ray energies meas. for Ge(Li) detector calibration 80−27865
^{77}K, cyclotron prod. for regional cerebral blood flow meas. 77−56468
^{79}Kr production, excitation functions for neutron deficient isotope form. via high-energy d-Br reactions 78−44609
^{81}Kr^{m}, new type generator using cellulose chromatography paper, for hospital use 79−8541
^{81}Kr^{m} generator for lung ventilation studies, test for free Br in carrier gas 79−79642
^{172}Lu generator, ^{172}Hf production, recovery and purification for nucl. medicine use 78−48893
^{28}Mg producting using compact cyclotron 77−90894
^{28}Mg production with 50 MeV neutrons 77−90895
^{56}Mn, neutron generator, prep. by ^{56}Fe(n,p)^{56}Mn 78−50178
^{99}Mo fission product, sequential cation-exchange separation from neutron irrad. U_3O_8 77−90898
^{99}Mo-^{99m}Tc generators with (n,γ)-prod. ^{99}Mo, eluate contamination from ^{131}I, ^{103}Ru and ^{239}Np 77−5079
^{99}Mo-^{99m}Tc multiload generator, Multigen, prep. and testing 77−16982
NaI:Tl scintillator response determ. undergraduate expt. 78−49600
^{22}Na positron lifetime source, preparation in glass matrices 77−30689
^{22}Na, thick-target yields in Mg due to proton bombardment up to 100 MeV 77−88312
^{57}Ni, cyclotron prod. by ^{3}He bombardment of natural Fe, bleomycin complex synthesis 77−86629
^{63}Ni, for thickness determ. of supported metallic films 78−22989
^{32}P high-energy beta-rays, hazards to eye lens and gonads 78−65131
^{147}Pm, sealed sources for phosphor light sources *(Hungarian)* 80−91348
^{147}Pm small-size nuclear battery, characts. of luminophores and photoelements *(Bulgarian)* 80−72084
Pu-Be, for in vivo N determ. using neutron capture gamma anal. 77−86606
^{237}Pu gamma-emitting isotope, prep. of tracer by ^{238}U(^{3}He,4n) 77−34497
^{238}Pu for cardiac pacemakers, radioactive controls *(French)* 77−44752
^{238}Pu, medical and industrial sources and applications 77−26915
^{238}Pu, neutron source for medical use *(French)* 77−42205
^{238}Pu production from target elements based on MgO and NpO_2 *(French)* 77−42199
^{238}Pu production from targets in Celestin reactors, medical use *(French)* 77−42200
^{238}Pu sealed source for medical and industrial applications *(French)* 77−42204
^{238}Pu, sources for cardiac pacemakers, manufacture and safety tests *(French)* 77−44751
^{238}Pu-Be, C content in coal determ., by neutron inelastic scattering *(Czech)* 80−101048
^{239}Pu-Be, C content in coal determ., by neutron inelastic scattering *(Czech)* 80−101048
^{242}Pu preparation by EM isotope separation, for use as α-spectrometry and mass spectrometry tracer 78−9011
Ra needle implants, computer program for reconstruction and dose-rate calc. 77−40770
Ra radiotherapy source leakage testing 77−16977
^{228}Ra, calibration standard for Ge(Li) gamma ray spectrum 77−38543
^{226}Ra decay chain, γ-ray energies meas. for Ge(Li) detector calibration 80−27865
^{226}Ra, exposure rates from gamma sources in dwelling room walls, Monte Carlo calc. 78−73260
^{226}Ra, exposure-rate calibration of small radioactive sources 78−41881
^{226}Ra source leakage testing by mailed track detector method 77−60264
^{228}Ra-Be (α,n) source, neutron spectrum calc. from angular distrib. and cross-section data 78−41882
Rb neutron deficient radioisotope selective production in (α,xn) reacts. *(Croatian)* 78−44608
^{82}Rb generators for imaging studies, ion exchange resin comparison 77−21626
^{A}Re, A=181, 182, 187, magnetic moments meas. by PAC 80−22688
^{222}Rn daughter dose estimates from area sources 78−94151
^{38}S producting using compact cyclotron 77−90894
^{47}Sc preparation in carrier-free state by ^{48}Ti(γ,p) reaction for radiopharmaceutical appls. 77−90892
^{75}Se, decay, electric monopole transitions 80−22752
^{153}Sm, reactor prod. of curie strength photon beam 78−86709
^{113}Sn-^{113m}In generator, monitoring Zr and ^{113}Sn breakthrough in ^{113m}In eluates 77−5078
^{119m}Sn half-life, by X- and γ-ray intensity meas. 77−26620
^{82}Sr-^{82}Rb generator improvement using inorganic exchangers 80−17135
^{90}Sr/^{90}Y radioisotope generator, educational aid 78−78535
^{90}Sr-^{90}Y beta source absorbed dose, thermolum. dosimetry, appl. to dating 77−90911
^{90}Sr-^{90}Y high-energy beta-rays, hazards to eye lens and gonads 78−65131
^{177}Ta, magnetic moments meas. by PAC 80−22688
^{178}Ta, chemical separation from parent ^{178}W, applications to nuclear medicine 79−16301
^{178}Ta, short lived nuclide for nuclear medicine, production of the parent ^{178}W 79−16300

radioactive sources continued
^{181}Ta, 133-482 keV cascade, effect of source preparation technique on differential ang. correl. 77−71711
^{181}Ta, 6.2 keV level, Mossbauer spectroscopy, source prep. 78−25373
^{181}Ta 6.2 keV Mossbauer resonance, prep. of narrow line sources 79−76253
Tc isotopes, yield from irrad. of Mo and Nb targets 77−23098
^{99}Tc^{m}, simulated standard by ^{141}Ce 78−61261
^{99}Tc^{m} generator of higher activity 80−17136
^{99m}Tc generators, comparison of weekly and biweekly systems rel. to radiation safety 77−2049
^{132}Te, fission product, sequential cation-exchange separation from neutron irrad. U_3O_8 77−90898
^{228}Th, exposure rates from gamma sources in dwelling room walls, Monte Carlo calc. 78−73260
^{228}Th, selective separation of ^{212}Bi 77−40566
^{45}Ti production by proton bombardment of Sc in cyclotron 78−80966
^{201}Tl from Tl(p,xn)^{201}Pb→^{201}Tl, E_p=15 to 60 MeV, yields and excitation functions 79−5369
^{170}Tm, precise γ-ray energies from radioactive decay 79−45525
U-Ni dilute alloy fission product source design and use at EBR-II 79−9932
^{232}U electrodeposited sources, ejection of α-recoil atoms 78−50426
^{122}Xe-^{122}I short-lived positron emitter generator 79−100740
^{123}Xe-^{123}I generator production for radiopharmaceutical appls., high energy alpha reactions 77−37053
^{133}Xe, laboratory calibration standards preparation *(Czech)* 79−6782
^{90}Y 25 Ci generator, preparation and use 77−40768
^{169}Yb, precise γ-ray energies from radioactive decay 79−45525

radioactive tracers
^{26}Al in seawater rel. to oceanic residence times of dissolved Al 79−34856
^{55}Co for nuclear medicine, production by ^{3}He bombardment of ^{55}Mn 80−36132
^{99m}Tc labelled heparin for imaging of acute myocardial infarcts, dog expts. 80−81733
adrenal imaging agents, rationale, synthesis, formulation, metabolism 78−85370
adsorption and electrocatalytic phenomena, radiotracer method investig. appls. radiotracer 80−70525
aerosol, human inhalation administration technique, deposition/clearance expts. 77−60312
aerosol, radioactive charging, transient mean particle charge 78−23973
aerosol lung clearance studies, adjustable response detector 77−56451
air pollution and ventilation appls., review 78−28306
albumin, human serum, adsorption studies, feasibility of radiolabelling 78−85359
albumin microspheres, rapid method for labelling with ^{111}In, ^{113m}In 79−34669
antipyrine, radioiodinated, prep. and stability for use in local blood flow determs. 80−94366
applications in industry and science *(Czech)* 80−32554
astatine labelled proteins, prep. using electrophilic reaction 79−29627
autoradiography, double radionuclide methods for tissue sections or cell smears, using light microscopy 77−5113
autoradiography and soft laser scanning in radioisotope work, appl. to metabolic studies 78−3576
beta-decay in labelled molecule, chem. and biological consequences 78−11541
biological system simulation for tracer distribution determ. 77−40956
biotelemetry, semicond. memory systems for data storage 77−90877
bleomycin, effect of dose loading and double labelling with ^{57}Co and ^{125}I on animal tissue distrib. 80−67220
blood flow measurement using radiotracer, automatic bolus injector 77−9238
blood plasma radio-Fe kinetics in man, effect of plasma Fe conc. 79−25019
bone imaging radiopharmaceutical local accumulation model 78−24127
α-cellulose iodination for dietary fibre analogue tracing 79−48339
cerebral blood flow determination, computer assisted method for multi-exponential curve fitting 78−20246
cerebral blood flow meas. by radioisotope clearance, radiation scattering effect 78−3600
cerebral blood flow meas. in animals using ^{14}C-ethanol 80−41205
Cherenkov counting of beta emitter isotope pairs using performance number criterion 77−83471
chlormerodrin-203, radiochem. purity determ., electrophoretic method 77−56283
cholesterol, T-labelled, prod. by catalysed exchange with T_2 *(German)* 77−90599
cholesterol transmembrane movement in human erythrocytes, radioactive tracer expt. 78−3459
compartmental system identification by optimum sampling 77−86615
complex composition in two-phase system, anal. method 79−87896
concrete, leachability determ., radioactive tracer method 78−61135
coronary perfusion pressure programmable control circuit 79−92278
corrosion monitoring in chem. equipment, distant-reading radiometric method 80−50795
cosmogenic and artificial radioisotopes distrib. in ocean, turbulent exchange intensity determ. *(Russian)* 79−39744
crossed-beam meas. of reactive scatt. using short lived radioactivity 77−4969
crystallisation, activation energies of mass transfer at phase boundaries, quantum theoret. calcs. *(German)* 78−67671
cyclosporin A labelled with ^{123}I or ^{125}I, prep. and biodistrib. 80−85496
detection techniques, flow problems appl. *(Japanese)* 78−96320
diffusion coefficients, open-eded continuous capillary method determ. 78−75861
diffusion meas. in liq., closed capillary method 78−14491
diffusion rates in ionic solid, influence of transmutation products 77−89568
dilution method for discharge meas. in pipes 78−30396
distribution coefficient of radionuclides in sample soil and water, environmental effects 77−13092
double labelling method for radiotracer study of zone electrophoresis 79−79278
drug radioreceptor analysis applications 80−94315
EBR II gas-tagging anal., isotopic weighting factors 79−59221
ecological system model sampling/identification, input signal anal. 78−69267

radioactive tracers continued
Egypt's technological experience in radioisotope production 77−65358
eight-channel unit, automatic, for recording tracer activity 78−86751
epoxy meas. of H_2O diffusion by radionuclides, corrosion effects *(Czech)* 77−48566
fallout water deactivation using sorption props. of clinoptilolite, vermiculite, bentonite 79−43995
flow device to measure γ radioactivity uptake and size of microparticles 77−5074
gamma ray emitters, principles, techniques, appl. to engineering systems 77−65065
gas-solid chromatography, using radiotracers, appl. to adsorption meas. of volatile chlorides 78−76902
glomerular filtration rate and renal plasma flow, simultaneous meas. by radioisotope clearance 77−56458
groundwater flow, investig., using In-EDTA tracer and neutron activation anal. 78−11921
haemoglobin, mutual and tracer diffusion coeffs., photon correl. obs. 80−72123
heavy isotope labelled mols., isotopic distrib. calcs. 77−56265
homogeneous solids, leachability determ., radioactive tracer method 78−61135
hydrological investigations, nuclear radn. appls. 79−39981
hydrological pollution control, tracers appl. *(French)* 80−7995
hydrospheric trace elements, water pollutants 78−85266
inaccessible pipes, optimised procedure for leak detection 79−34217
indicator dilution measurements of flow parameters in curved tubes and branching networks 77−66824
inert gases, emanation thermal analysis of solid state structures appl. 79−11834
inferior colliculus of immature mouse, plastic reinnervation, autoradiography with ^{14}C-deoxyglucose 79−92233
insulin, radioiodine labelling using dimethylsulphoxide as labelling agent *(Korean)* 78−88746
insulin receptors on human platelets, ^{125}I-insulin binding meas. 79−92245
intravascular radioactive tracers, calc. of residence time distribs. in fields of external registration 80−72291
ion exchange, Zn^{2+}-Cl^{-} system, complex form. studied using radiotracer, effect of macroelectrolyte cation 80−16659
isotopes for oceanographic investigations *(Russian)* 77−60486
kidney filtration fraction, noninvasive determ. by dual tracer technique 77−86596
kinetics, a method of study 79−70609
kinetics of tracers, displays in nucl. medicine 78−85443
labelled release expt. on Mars in search for heterotrophic life 77−37548
labelling of materials with short-lived radioisotopes produced at the place of application *(German)* 79−89503
lake studies, isotope techniques appl., advisory group meeting, Vienna (1977 August 29 to September 2) 80−41950
laminar flow in small channels, liq. tracer method 77−58816
laminar flow in small channels, response model 77−58814
laminar flow in small channels, tracer-sphere method 77−58815
leucocytes, radioactive-labelled, appl. for proof of inflammations 80−67218
leukocyte uptake of radiolabelled compounds in whole blood, liq. scintillation method 77−90882
life sciences appl. 78−15882
liquid flow rates through pipes, applicability of experimental meas. methods 80−100044
liquid nuclear waste, simulated, ion exchange equilibration, radiotracer obs. 78−74444
liquid scintillation counting, single and double labels, absolute activity analyser vs. on-line computer 77−83470
liquid scintillation counting, single and double labels, quench correction with on-line computer 77−79520
liver growth protein metabolism and turnover, radiotracer obs. 79−88062
lung function studies, including effects of ozone, using short-lived positron emitters 77−25552
lung ventilation regional and whole, math. model for radioactive tracer studies 78−20249
marine pollution, solid pollutant dispersion analysis 77−41069
medical computing, compartmental models short parameter-fitting routine 77−82378
medicine, nuclear, production of useful radioisotopes, Los Alamos Meson Physics Facility 80−67251
molten salts, tracer diffusion coeffs., determ. methods 78−71873
multiple fuel failure resolution with gas tagging, barycentric coordinate technique 79−13485
neurophysiology, transmitter-specific retrograde labelling in the striato- and raphe-nigral pathways 80−51309
noble gases for geothermal tracing 78−69502
nuclear medicine, diagnostic, hazards to personnel, protection problems 77−81587
nuclear medicine, trends *(French)* 80−26327
nuclear medicine conference, Karlovy Vary, Czechoslovakia (May, 1979) 80−12840
nuclear medicine imaging principles, concepts and equipment 80−17113
nuclear techniques in hydrology, survey 77−37419
ocean, large-scale water transport, determ. from radionuclide obs. *(Russian)* 79−39742
oncology, role of radionuclides, review 77−9248
organ blood flow determ. using radioactive microsphere technique, PDP-11 interactive program 78−20247
ovum movement measurement in rabbit oviduct using radioactive surrogate and CdTe detector 78−36087
paeonol and urinary metabolites labelled with ^{13}C and D, synthesis and physicochem. props. 80−67250
particulate matter dynamics in industrial manufacturing processes, appl. of radiotracer techniques 78−41398
pentane, combustion, isotopic tracer studies of the further reactions of pentenes 79−8438
perhalo-compounds, labelled, high yields from ^{18}F and ^{38}Cl reactions with CCl_xF_{4-x} and C_3F_6 80−109025
physiological compartment tracer flow modelling and digital imaging 80−101257
physiological uptake in radionuclide imaging 79−48324
plasminogen, ^{125}I or ^{131}I labelled, evaluation as imaging agent for pre-existing thrombi 77−21610
plastics, leachability determ., radioactive tracer method 78−61135

radioactive tracers continued
plume diffusion at Rancho Seco Generating Station, LIDAR obs. 78−11991
pollution monitoring in petroleum refinery 77−41163
polyester resin, water diff. meas. by radionuclides, corrosion effects *(Czech)* 77−48566
polymer powder coatings, water permeability eval. by radioactive tracers *(Czech)* 78−11362
polystyrene monodisperse ^{51}Cr tagged aerosol prod. using aerosol centrifuge 78−92519
positron active tracer for liquid-flow measurement system, microcomputer-controlled 80−24113
production for biomedical uses, review *(French)* 80−17056
production technology transfer to developing countries 77−65357
proteins, improved labelling with 99mTc by stannous tartrate reduction of pertechnetate 80−72324
Pseudemys scripta hemibladder $^{36}Cl^-$ transport meas. system 79−96529
pulsed neutron measurement of single and two phase flow 79−50771
radioactive gas diffusion, adsorpt. in porous media *(Russian)* 77−27591
radioiodination, microelectrolytic, of polypeptide hormone, using Pt microcell 79−48340
radioisotope applications in agriculture, hydrology, medicine industry etc., booklet 78−35947
radioligand assays, in vitro diagnostic use *(Korean)* 79−39482
radiopharmaceuticals, γ-emitting, in rat blood, continuous monitoring technique 79−2129
radiopharmaceuticals, cyclotron prod. for nuclear medicine appls. 77−44753
radiopharmaceuticals preparation by Szilard-Chalmers labelling and radioprotection in ice lattice 80−51259
reaction products in proton irrad. Nb foils, diffusion *(German)* 77−35756
receptor binding radiotracer preparation 80−51258
red blood cells, ^{99m}Tc labelling 80−41236
red blood cells, in vivo labelling with ^{99m}Tc with stannous pyridoxylideneaminates 80−46049
renal extraction fraction determ. by double-tracer method 77−37045
sea water, current vel. determ. via neutron-activation method *(Russian)* 78−77358
sedimenting suspension, conc. distrib. determ. by radioactive solids 79−32634
separation processes, appl. of radioisotope tracer method 78−76896
serum albumin, bovine, mutual and tracer diffusion coeffs., photon correl. obs. 80−72123
short-life radionuclides and regional lung function, review 79−53211
soil moisture movement and groundwater recharge by T tagging technique 78−61438
soil samples, meas. trace radionuclide L X-ray detection 78−49020
solid-liquid pipe flow, cross correlation method anal. 79−32638
solvent extraction device using radioactive tracers 77−32819
stearic acid monolayers on HCl subsoln., surface diffusion by ^{14}C-tracer 78−34679
steel purity investigation, nonmetallic inclusions, quantity and origin 77−56201
subsoil hydrology investigations by radiotracer methods 79−34869
suspension, particles self-diffusion in shear flow 77−24015
tagged assembly failure location analysis program 79−13486
testing and measurements on industrial plant, appls. *(German)* 77−70522
tetrachloromethane-cyclohexane system, interdiffusion, ternary diffusion eqn., radioactive tracer obs. 78−79792
thymocyte, calf, tritiation by catalytic hydrogenation 79−88152
thyroid, radionuclide in vivo studies, technical considerations, developments, review 78−85372
thyroid uptake meas., influence of gland depth, mass and lobe separation 78−61245
triiodothyronine/thyroxine assay in unextracted serum using double tracer radioimmunoassay 77−37051
turbulent atmospheric transport, Monte Carlo simulation, radioactive pollution appl. 78−61550
water pollution, silt double-labelling technique for radioactive tracing *(French)* 80−7994
water pollution, treatment process anal. and mixing patterns in streams 77−25711
water resource research using Pennsylvania State Univ. reactor 79−12159
$^{18,19}F$ ion diffusion in dental enamel at pH 7, obs. 79−29553
$^{125}(p,5n)^{123}Xe \rightarrow {}^{123}I^-$ 79−79649
α-AgI, I_2 diffusion obs. using ^{131}I radiotracers 78−18830
Al, diffusion of ^{85}Kr *(Russian)* 79−65258
Al-Si alloys, modification by Na-containing agents, ^{24}Na radioisotope investigation *(Russian)* 77−40567
^{A}Ar, A=36, 38, appl. for PWR gas tagging 79−59222
$^{40}Ar(\gamma,2p)^{38}S$ production on recirculatory, Ar gas target 79−88185
$^{40}Ar(\gamma,p)^{39}Cl$ production on recirculatory, Ar gas target 79−88185
^{211}At protein labelling technique using an acylation reaction 80−36130
Au, sensitisation mechanism using tracer techniques 79−39171
^{7}Be, atmospheric, distrib. within high-press. systems in E.United States 80−4072
^{10}Be in seawater rel. to oceanic residence times of dissolved Be 79−34856
Br ion neutron activable tracers 78−85267
^{77}Br-labelled 5α-dihydrotestosterone, synthesis and distrib. in rats rel. to ^{77}Br-bromide 80−51247
$^{79}Br(p,3n)^{77}Kr \rightarrow {}^{77}Br^-$ production, separation and radiopharmaceutical labelling 79−79649
^{80}Br-bromohippuric acid preparation 79−88187
^{80m}Br labelling of tyrosine, uracil and cytosine 80−51248
$C^{15}O$, continuous inhalation, model for regional cerebral O_2 distrib. 78−65108
$C^{15}O_2$ continuous inhalation, model for regional cerebral O_2 distrib. 78−65108
$C^{15}O_2$ inhalation for left heart imaging 77−64126
^{11}C labelled molecules, examples of use in medical research *(French)* 77−66833
^{11}C methionine positron emission computerised tomography, pancreatic scanning obs. 80−30861
^{11}C, production by cyclotron, biomedical appls. *(French)* 80−56216
^{11}C, production for studies on photosynthesis, transport and metabolism in plants 79−39502
radioactive tracers continued
^{11}C, racemic [1-^{11}C]-alanine and partially resolved [3-^{11}C]-alanine synthesis 79−88186
^{11}C-1-aminocyclopentane carboxylic acid, tumour location, clinical trials with single photon detect. 78−31895
^{11}C-acetylene, production by methane pyrolysis and irrad. 80−36129
^{11}C-chlorpromazine, clinical results using short-lived radioisotopes prod. by medical cyclotron 79−57775
^{11}C-iodomethane remotely controlled synthesis 79−88192
^{11}C-l-lactic acid, enzymatic synthesis 80−61695
^{11}C-labelled amino acids for rectilinear and positron tomographic imaging of human pancreas 80−12258
^{11}C-lactic acid synthesis and scintigraphic evaluation of in vivo distrib. in dog 78−80965
^{11}C-lactonitrile synthesis and scintigraphic evaluation of in vivo distrib. in dog 78−80965
^{11}C-methionine, clinical results using short-lived radioisotopes prod. by medical cyclotron 79−57775
^{11}C-pyruvic acid, enzymatic synthesis 80−61695
^{13}C, kinetics obs. for CO oxidation over Pt 79−29400
^{14}C, autoradiography of thin laminars *(French)* 80−35438
^{14}C detection, $NaH^{14}CO_3$ liquid and $Ba^{14}CO_3$ gel suspension, scintillation cocktails efficiencies 79−3283
^{14}C fallout from nucl. weapons testing, use as biological tracer 77−64162
^{14}C labelled organic compounds, gaseous, anal., radioactivity meas. using piston type counter tube, automated 77−56281
^{14}C trace elements in seawater estimation *(Dutch)* 77−29459
^{14}C-labelled bumetanide, whole body autoradiography in dogs by round saw method 80−72399
^{14}C-uracil metabolism in golden hamster after irrad. 77−40714
$^{14}CO_2$, radiometric estimation of the replication time of bacteria in culture 79−16170
$^{14}CO_2$ breath analysis tests, plastic scintillation filament detector system 78−65122
CaO-SiO_2-Fe_xO system, liq., steel making slag, Ca and Fe tracer diffusivities, O_2 press. depend. 78−38863
$^{45}Ca^{2+}$ efflux from cerebral tissue, l.f. elec. field effects 77−1984
^{47}Ca, simultaneous in vivo determ. of Ca and P effective absorpt. in rat 78−48882
CdTe detector, biotelemetry appl. 77−86587
^{38}Cl+ethane (methane)(vinyl bromide), rate consts., stratospheric temps., radiotracer meas. 77−48632
$^{36}Cl^-$, self-diffusion in NaCl soln., β-active tracer, plastic capillary meas. method 77−50333
^{55}Co, carrier-free positron-emitting label for bleomycin from $^{55}Fe(p,2n)^{55}Co$ 79−79648
^{55}Co, cyclotron prod. by ^{3}He bombardment of natural Fe, bleomycin complex synthesis 77−86629
^{57}Co in bleomycin radioimmunoassay 77−37050
^{57}Co labelled $Co(acac)_3$, diamag., $^{57}Fe(III)$ species prod. by electron decay, spin relax. 77−63329
^{57}Co labelling of bovine serum albumin, expts. 80−85495
$CrSi_2$ formation on Pd_2Si and PtSi on Si, ^{31}Si tracer obs. 78−60578
^{51}Cr, tracer, Ni-Cr alloy component transport numbers determ. 77−62667
$^{51}Cr_2O_7^{2-}$ tracer solution preparation *(French)* 79−29385
^{51}Cr-EDTA, limitations of single sample tracer method for determ. glomerular filtration rate 79−16271
^{51}Cr-labelled lymphocyte autoradiographic detection problems 79−29592
^{130}Cs, low energy ions systematic range meas. in Ar and N_2 gases 79−1472
^{137}Cs fallout in arid watersheds, phys. and chem. parameters affecting transport 78−61461
^{137}Cs, radiotracer studies in equatorial Indian Ocean *(Russian)* 79−39743
Cu, electrodeposition from cyanide solns., interaction with 2-butynediol-1,4, obs. *(Russian)* 79−47936
^{18}F labelled anhydrous fluorinating reagent preparation using cyclotron accelerated p, d, ^{3}He, or α 79−2131
^{18}F labelled compounds, rat prostrate imaging expts. 80−51215
^{18}F recoil labelling of chlorofluoromethanes and tetrafluoromethane 79−52732
^{18}F, skeletal tracer kinetics in rats, evaluation of model 80−56188
^{18}F-F_3COF-^{18}F radiopharmaceutical synthesis procedure 79−29619
^{18}F-5-fluorouracil distrib. in tumour-bearing mice and rats 78−48878
^{18}F-5-fluorouracil studies in humans and animals 80−109000
^{18}F-labelled acetic acid, carrier-free, production via a recoil labelling method 80−104756
^{52}Fe and contaminant ^{55}Fe, combined use in bone marrow studies 77−56447
^{52}Fe, production for use in a radionuclide generator system 80−51253
^{55}Fe as contaminant in ^{52}Fe, use in bone marrow studies 77−56447
^{59}Fe tracer data analysis program and kinetics model *(German)* 79−5342
^{212}Fr, low energy ions systematic range meas. in Ar and N_2 gases 79−1472
$GaAs_{1-x}P_x$:Zn, diffusion profile determ., $^{32}P/^{65}Zn$ double tracer technique 78−55888
GaP:Zn, diffusion profile determ., $^{32}P/^{65}Zn$ double tracer technique 78−55888
^{67}Ga citrate, role in inflammatory disease 79−57770
^{67}Ga citrate, use in detect. and follow-up of extrapulmonary tuberculosis 80−46012
^{67}Ga imaging in abdominal disease 79−57772
^{67}Ga, metallic, prep. and appl. to tracer diffusion studies in liq. Ga 80−24629
^{67}Ga, use in diagnosis of pulmonary disorders 79−57771
$^{67}Ga/^{99m}Tc$, computerised double-tracer subtraction scanning for inflammatory diseases 79−70612
^{67}Ga-citrate, comparative evaluation of pulmonary lesions 80−94327
^{68}Ga, ionic, pot. column chromatography generators 80−46050
^{68}Ga labeling of albumin and albumin microspheres 80−17137
^{68}Ga-labelled human serum albumin microspheres, prep. 80−17131
H^3HO, $H_2^{18}O$, simultaneous self-diffusion in porous membranes, ionic solns., H_2O struct. 79−52765
^{3}H labelled biologically active compounds obtained using at. ^{3}H bundles, appls. 80−30888
^{3}H labelled retinal, inadequacy for visual pigment regeneration studies 80−41357

radioactive tracers continued
^{3}H, tracer for aquifer interconnection investigs. in Turtz mine *(Rumanian)* 77−53251
^{3}H-2-deoxyglucose, appl. to retinal neurones differential labelling 79−92447
^{3}H-methyl acetimidate preparation for protein labelling 79−53246
^{3}H-thymidine incorporation, for herpes simplex virus radiometric detect. 78−65117
^{197}Hg, labelling of human albumin microspheres 80−51251
$^{197}HgCl_2$, renal uptake meas., single tracer method for background subtraction 80−67217
^{203}Hg, tracer for Hg conc. in seawater expts., ^{75}Se tracer 80−21420
^{123}I, absorbed dose to thyroid from radioiodine impurities 77−29207
^{123}I labelled Hippuran dosimetry, physiological parameters 79−53251
^{123}I, labelling of o-iodohippuric acid for diagnostic nuclear imaging 79−39503
^{125}I labelled compounds, rat prostrate imaging expts. 80−51215
^{125}I labelled DNA, pot. tumour imaging agent 80−30892
^{125}I labelled DNA, prep. method and in vivo studies of tumour localisation 80−51249
^{123}I labelled estradiol, a γ-emitting estradiol analogue that binds to the estrogen receptor 80−61697
^{125}I labelled estrogen derivatives 80−81734
^{125}I labelled human serum albumin, geometrical dilution *(French)* 80−104742
^{125}I labelled prostaglandins *(Hungarian)* 80−94368
^{125}I, labelling facilities for biomedical appls. 80−41235
^{125}I microelectrolytic labelling of polypeptide hormones 80−12255
^{125}I, rel. to ^{99m}Tc in thyroid imaging 80−36077
^{125}I-7-iodo-6-demethyl-6-deoxytetracycline HCl use for bone mineralisation obs. 80−12214
^{125}I-fibrinogen, multiwire proportional chamber, low energy radionuclide distrib. 80−61679
^{125}I-iododeoxyuridine incorporation, for herpes simplex virus radiometric detect. 78−65117
^{125}I-labelled iodobenzoic and iodohippuric acids, NQR of ^{127}I, Mossbauer spectra of ^{125}I 77−12241
^{125}I-serum albumin, convective and diffusive transport through rabbit aortic tissue 78−44482
^{127}I prod., life sciences appl. 78−15882
^{131}I, blood plasma, vol. meas. in man using labeled serum albumin 79−29602
^{131}I labelled chorionic gonadotropin, use in ovarian imaging, rat expts. 80−41186
^{131}I labelled Hippuran, evaluation of renal grafts 80−46017
^{131}I labelled Hippuran dosimetry, physiological parameters 79−53251
^{131}I labelled ioglycamic acid, evaluation in hepatobiliary disorder scintiscanning 80−36072
^{131}I labelled o-iodohippurate, in vitro stability 80−16668
^{131}I-Hippuran transit times in kidney, renogram deconvolution 78−40317
^{131}I-4-iodoantipyrine preparation from ^{131}I-iodide 80−12256
^{131}I-fibrinogen for clot detect. in canine model of cervical carotid thrombosis 78−85363
^{131}I-ortho-iodohippurate absorbed kidney dose calc., literature review 80−76841
In, A=111, 113m, adsorbed on silica-alumina catalyst, mixing in fluidised bed investig. 77−35269
In-EDTA tracer, for groundwater flow investig., neutron activation anal. 78−11921
^{111}In 8-hydroxyquinoline labelling of human platelets 80−12259
^{111}In at active site of bovine carbonic anhydrase, γ-ray perturbed directional correl. obs. of conform. change 79−83700
^{111}In, human lymphocyte labelling 79−5354
^{111}In labeled transferrin, perturbed angular correls. study 79−39342
^{111}In labelled human platelets, dose obs. 80−94370
^{111}In oxinate, comparative study as abscess scanning agent 80−94328
^{111}In oxinate labelled autologous granulocytes, comparative study as abscess scanning agent 80−94328
^{111}In oxine, radiolabelled liposomes as metabolic and scanning tracers in mice 80−17073
^{111}In oxine cell damage resulting from labelling rat lymphocytes and HeLa S3 cells 80−56145
^{111}In-bleomycin, comparative evaluation of pulmonary lesions 80−94327
$^{111}InCl_3$, comparative study as abscess scanning agent 80−94328
^{115}In aerosol generation technique for atm. tracer obs. 80−26190
^{113m}In-labelled transferrin, use in meas. of blood vols. in rat, rabbit 80−3878
^{113m}In-tripolyphosphate, new radiopharmaceutical for bone scanning 80−67247
^{114m}In-EDTA complex, method of determ., use as tracer in hydrology 77−73458
Kr, self-diffusion coefficient, radioactive tracer meas. 77−13534
^{A}Kr, A=78, 82, appl. for PWR gas tagging 79−59222
^{81m}Kr, continuous carotid infusion for assessment of regional cerebral blood flow 78−20254
Mg tracer techniques for Pu nuclear fuel input accountability in reprocessing plants 80−73919
^{54}Mn radioactive tracer diffusion in Pt *(French)* 79−51306
^{13}N cpds., for environmental and biological research, cyclotron prod. 78−82551
^{13}N, production by cyclotron, biomedical appls. *(French)* 80−56216
^{13}N-labelled NH_3 and NO_3^- ions, prod. for biol. expts. using 3 MV Van de Graaff accelerator 80−26349
$^{13}NH_3$ intravenous injection, absorbed radiation dose calcs. 80−94375
^{16}N tag for water transient flow meas. 79−14504
NaBr, n-propanol soln., cond. and transference no. meas., radioisotope method 77−35735
^{22}NaCl, tracer diffusion meas. in aq. NaCl soln., closed capillary method 78−14491
NaI, n-propanol soln. cond. and transference no. meas., radioisotope method 77−35735
$Na^{125}I$ telemetric detection for biological rhythms in renal function 77−86586
^{24}Na exchanges in granuloma pouch during initial and final stages of inflammatory process 77−77886
$^{92}Nb^{m}$, production and impregnation in polystyrene microspheres for X-ray detector calibration 80−74065
^{1}Ne, A=21, 22 appl. for PWR gas tagging 79−59222
^{57}Ni, cyclotron prod. by ^{3}He bombardment of natural Fe, bleomycin complex synthesis 77−86629
^{63}Ni applications in biological research 80−12321
^{63}Ni tracer, Ni-Cr alloy component transport numbers determ. 77−62667
^{15}O, production by cyclotron, biomedical appls. *(French)* 80−56216
$^{15}O_2$ continuous inhalation, model for regional cerebral O_2 distrib. 78−65108
^{18}O tracer used to study growth mechanism of oxide scale 77−8964
^{32}P, simultaneous in vivo determ. of Ca and P effective absorpt. in rat 78−48882
^{32}P-labelled compound, radiochromatographic scanning procedure 77−9151
Pb tracer techniques for Pu nuclear fuel input accountability in reprocessing plants 80−73919
^{210}Pb, atmospheric fluxes determ. from soil profiles 79−2346
^{210}Pb, use as heavy metal tracer in Susquehanna River system 78−49046
^{237}Pu gamma-emitting isotope, prep. of tracer by $^{238}U(^{3}He,4n)$ 77−34497
^{242}Pu preparation by EM isotope separation, for use as α-spectrometry and mass spectrometry tracer 78−9011
$RbAg_4I_5$, I_2 diffusion obs. using ^{131}I radiotracers 78−18830
^{79}Rb, low energy ions systematic range meas. in Ar and N_2 gases 79−1472
$^{81}Rb/^{81m}Kr$ ratio as radioactive tracer study of organic bleeding *(Dutch)* 80−3807
^{81}Rb-^{81}Kr generators, aspects of production, elution and automation, medical appls. 80−61696
^{82}Rb generators, alumina-based, medical evaluation and appl. 80−41237
^{101m}Rh, cyclotron prod. through natural precursor ^{101}Pd 77−52875
Rn daughters as atmospheric tracers *(Spanish)* 77−9553
Rn decay products, appl. to atmos. diffusion props. anal. 79−84347
Rn decay products, appl. to atmos. diffusion props. anal. 79−84348
Rn decay products, stability index measurement by natural radioactive tracers *(Spanish)* 80−51448
Rn tracer determination of vertical mass diffusion coeff. in atm. *(Spanish)* 77−70717
^{222}Rn, and decay products, vertical distrib. in atmosphere, time-dependent calc. 79−84383
^{222}Rn content in air, diffusion in lower atm., U deposits prospecting appl. *(Spanish)* 77−78303
^{222}Rn measurement in aqueous samples by decay product filtration 77−60476
^{222}Rn potential appl. as tracer in ocean hydrophys. studies *(Russian)* 79−39745
^{97}Ru, preparation, separation from TC isotopes 77−37054
^{97}Ru preparation investigation 80−30891
^{103}Ru in determination of rate of passage of food through gut of captive wild birds 80−26425
SO_2 air pollution deposition to pine forest, meas. method 78−20508
^{35}S, effect on solubility of $BaSO_4$ in water 78−43126
^{38}S, for meas. SO_2 atm. removal rate *(German)* 79−53411
Sb, liq., self-diffusion, long capillary method obs., using radioactive Sb 77−89564
^{125}Sb, in HCl solns., valency states investig., radioanal. tracer preparation, stability 77−63943
^{75}Se, yield for various reactions and chem. processing 80−36131
^{75}Se labelled adenosyl selenomethionine, distrib. in rat and prostate scanning appl. 80−17132
^{75}Se, tracer for Se conc. in seawater expts., ^{203}Hg tracer 80−21420
^{31}Si, for silicide formation, Si self-diffusion and Si epitaxy obs. 79−4431
^{31}Si, radioactive marker in thin film silicide form. 77−62681
$SrSO_4$, activation energies for mass transfer during crystallisation, surface active agent effects *(German)* 78−63689
^{82}Sr-^{82}Rb biomedical generator, performance obs. 79−53247
^{90}Sr, conc. meas. in Caribbean Sea, vertical transport of admixtures determ. 79−53362
$^{90}Sr^{2+}$, adsorption on Cu surface, immersion time, conc. and temp. depends. 78−87863
T balance in surface water reservoir, molecular exchange 80−72565
T distribution in Weddell Sea water masses 79−39728
T_s in Pacific Ocean, source function for transport models 78−32122
^{178}Ta radiopharmaceuticals for lung and liver imaging, rat expts. 80−51254
^{178}Ta, scintigraphic imaging with the Anger scintillation camera 80−12231
TcP_2O_7, $Tc_4(P_2O_7)_3$, prep. and comparative biological props. 79−12000
$^{95}Tc^{m}$ for determination of ^{99}Tc accumulation by tumbleweed and cheatgrass grown on arid soils 78−80974
$^{99}Tc^{m}$-dimercaptosuccinic acid evaluation as static renal imaging agent 78−77102
^{95m}Tc, ^{96}Tc, skeletal uptake of pyrophosphate evaluated by autoradiography 79−29608
^{99m}Tc, assay of radioactive impurity in pertechnetate eluted from ^{99}Mo−^{99m}Tc generator *(Japanese)* 80−81735
^{99m}Tc, blood plasma, vol. meas. in man using labeled serum albumin 79−29602
^{99M}Tc DTPA, radiolabelled liposomes as metabolic and scanning tracers in mice 80−17073
^{99m}Tc, gamma camera array of ^{99}Mo impurities 80−36100
^{99m}Tc glucoheptonate, prep. using formamidine sulfinic acid 80−51252
^{99m}Tc labeled red blood cells and serum albumin, cardiac blood pool visualisation 79−29601
^{99m}Tc labelled 2,3-dimercaptopropansulphonate, prep. and distrib. in the rat 80−51244
^{99M}Tc labelled (Sn)DTPA, comparison of 4 commercial preps. in glomerular filtration rate meas. 80−81704
^{99m}Tc labelled bovine thrombin and streptokinase-activated human plasmin, in vitro assessment 80−41238
^{99m}Tc labelled DTPA and MDP, compensative value on brain lesion *(Japanese)* 80−67235
^{99m}Tc labelled EHDP, uptake quantification in sacroiliac scintigraphy, comparative study 80−94326
^{99m}Tc labelled erythrocytes, rat, factors affecting splenic deposition of heat damaged cells 79−29596
^{99m}Tc labelled human serum albumin kits, evaluation for cardiac blood pool imaging 80−17130
^{99m}Tc labelled pertechnetate, evaluation of renal grafts 80−46017
^{99m}Tc labelled pyrrolidino-methyl tetracycline, prep. and control 79−29623
^{99m}Tc labelled radiopharmaceuticals, comparison of 2 types for lymphoscintigraphy 80−41185

radioactive tracers continued
^{99m}Tc labelled red blood cells, ultrafiltration labelling technique 80−51243
^{99m}Tc labelled stannous pyrophosphate, mouse myocardial uptake obs. 80−46019
^{99m}Tc methylene diphosphonate, immediate renal imaging and renography, clinical evaluation 80−98126
^{99m}Tc p-isopropylacetanilidoiminodiacetic acid (Sn), hepatobiliary dynamic flow study 79−53217
^{99m}Tc phosphate complexes, femoral head activity in Perthes' disease 79−29606
^{99M}Tc, pyrophosphate and hydroxymethylene diphosphonate carriers, comparison in acute myocardial infarction 80−94342
^{99M}Tc pyrophosphate rel. to ^{99M}Tc methylene diphosphonate in acute myocardial infarction 80−17070
^{99m}Tc radiolabelling of mouse spleen leucocytes 79−100739
^{99m}Tc radiopharmaceuticals, rapid miniaturised chromatographic quality control procedures 78−28070
^{99m}Tc radiopharmaceuticals, As for P substitution, bone-seeking agent analogues 80−51250
^{99m}Tc, rel. to ^{125}I in thyroid imaging 80−36077
^{99m}Tc-DTPA, limitations of single sample tracer method for determ. glomerular filtration rate 79−16271
^{99m}Tc-HIDA, synthesis of 5 new isomers and comparison with ^{99m}Tc-(2,6-dimethyl)HIDA 80−72323
^{99m}Tc-MDP, lymphography appl. *(Japanese)* 80−94352
^{99m}Tc-Sn-phytate and ^{99m}Tc-S colloids, comparative values in splenomegaly 79−62342
^{99m}Tc-Ti-DTPA, prep., control and biological distrib. 80−51246
^{99m}Tc-1-hydroxy-ethylidene-1,1-disodium phosphonate labelling using Sn(II) reductant 79−88190
^{99m}Tc-(p-butyl) iminodiacetic acid, clinical evaluation in hepatobiliary imaging *(Japanese)* 80−67236
^{99m}Tc-bleomycin selective labelling for tumour imaging 79−53228
^{99m}Tc-citrate, comparative evaluation of pulmonary lesions 80−94327
^{99m}Tc-diethylentriaminepentaacetic acid freeze-dried kit prep. 79−88189
^{99m}Tc-fibrinogen, usefulness of phlebography for pulmonary embolism patients 80−36093
^{99m}Tc-glucoheptonate, use in brain tumour detect. 78−20253
^{99m}Tc-hepatobiliary agents, absorbed dose estimation 80−72330
^{99m}Tc-labelled erythrocytes, spleen scanning in humans 80−67230
^{99m}Tc-microspheres, bladder wall dose after administration 80−109030
^{99m}Tc-pertechnetate labelling of human plasma proteins, rapid chemical method 79−29618
^{99m}Tc-pyridoxal leucine, liver pharmacokinetic and imaging studies 79−29597
^{99m}Tc-pyridoxal-phenylalanine evaluation as hepatobiliary imaging agent 78−31893
^{99m}Tc-pyridoxal-phenylalanine evaluation as hepatobiliary imaging agent 78−31894
^{99m}Tc-radiopharmaceuticals, ligand determ., electrophoretic method 80−40699
$^{99m}TcO_4$, radiation damage to mouse testis cells 78−24103
^{99M}TcS colloid, bone marrow scanning in pediatric oncology 80−17067
^{99m}TcS colloid, muco-ciliary transport monitoring method, bronchiectatic patient appl. 80−30840
^{99m}TcS colloid lymphoscintigraphy 80−36114
^{99m}Tc(Sn)methylenediphosphonate uptake in canine tibia rel. to blood flow 80−56192
Te, self-diffusion in HgTe, layer stripping technique 79−37873
^{123m}Te-labelled adrenal-imaging agents, radiation dosimetry 80−101268
Th, stability index measurement by natural radioactive tracers *(Spanish)* 80−51448
Th(B) conc., appl. to atmos. diffusion props. anal. 79−84347
Th(B) conc., appl. to atmos. diffusion props. anal. 79−84348
$TlCl_3.(TlCl)_3$, labelled, exchange of Tl ats. rel. to γ-irrad., heat treatment, grinding 78−92470
^{199}Tl, production by ^{197}Au(α, 2n) reaction 80−51245
^{201}Tl dynamic analysis for regional myocardial blood flow determ. 79−70627
^{201}Tl, use in thyroid 'cold' areas scintigraphic evaluation 80−36078
^{201}TlCl, tumour scintigraphy by intraarterial injection *(Japanese)* 80−98111
$^{204}Tl^+$, diffusion in KCl, transmutation effect 77−89589
^{230}U, production, tracer appls., α-spectra 77−61644
Xe, self-diffusion coefficient, radioactive tracer meas. 77−13534
^{A}Xe, A=124, 126, 128, 129, appl. for PWR gas tagging 79−59222
^{133}Xe, cerebral regional blood flow meas., functional landscapes in brain 78−85356
^{133}Xe diffusion through frog skin, toad bladder and water boundary layer 77−66803
^{133}Xe in cerebral blood flow noninvasive regional meas. and computer analysis 78−35948
^{133}Xe, systemically administered, calc. of coronary blood flow from myocardial clearance 77−16967
^{133}Xe washout curve discriminant analysis for lower extremity vascular impairment 78−35949
$^{62}Zn/^{62}Cu$ generator, source of ^{62}Cu for radiopharmaceuticals 80−67248
^{65}Zn, in zinc oxalate, isothermal crystallisation from soln. 80−108336
$ZrH_mCe_n(PO_4)_2.XH_2O$, cryst., self-diffusion of Ce^{3+} ions 78−34648
α-$ZrH_{0.74}La_{0.42}(PO_4)_2.4.6H_2O$ cryst., self-diffusion of La^{3+} ions 78−34648
^{95}Zr from Chinese atmospheric thermonuclear explosions, appl. to stratospheric transport parametrisation 79−2342

radioactive waste
see also fission reactor materials; fusion reactor materials; materials handling; radioactivity; waste disposal
^{222}Rn flux through multilayered covers cover U mill tailings 80−95487
accountability, analytical methods and laboratories, present and future 79−81047
actinide, ^{233}U-^{232}Th reactor as burner 77−23235
actinide aqueous ions, chemical thermodynamics, book 77−60108
actinide burner, fusion-driven, design of superconducting toroidal coil 77−27693
actinide burning in very hard spectrum reactors 79−89414
actinide elements, chemical thermodynamics, book 77−60107
actinide elimination by fissioning in generic actinide burner reactor 79−93756
actinide elimination by nuclear transmutation 77−61569
actinide incineration, UK and European investigations 79−85702
actinide incineration and transmutation in thermal and fast reactors 79−85707
actinide incineration strategies, UK 79−85704
actinide lanthanide separation from high-level wastes by oxalate precipitation 79−49720
actinide partitioning, arguments against 77−61570
actinide partitioning in LWR fuel reprocessing, conceptual methods 79−85810
actinide recycling, neutron multigroup cross sections 77−23237
actinide recycling, nuclear data uncertainties 79−85711
actinide recycling in power reactor fuel cycle *(French)* 79−85714
actinide recycling strategies, burn-up and transmutation studies 79−85700
actinide removal for reprocessing wastes by solubilisation and solvent extraction 79−36384
actinide removal from HNO_3 waste streams, bidentate organophosphorous extractants 77−26861
actinide sensitivity studies and nuclear data requirements 79−85710
actinide separation from high activity liquid waste, OXAL process *(French)* 79−85813
actinide separation in highly active nuclear waste solns. *(French)* 79−85812
actinide separation in nuclear fuel and wastes, hazard assessment 79−85806
actinide transmutation, nuclear fuel cycle impact studies 79−85752
actinide transmutation, research activity status, Japan 79−85807
actinide transmutation, Swedish studies 79−85703
actinide transmutation and chemical separation from radioactive waste 79−85808
actinide transmutation in fission reactors 79−26584
actinide transmutation in nuclear power reactors, neutron physical feasibility 79−85701
actinide waste burning in laser fusion driven hybrid reactor 79−22421
actinides, biological hazards, consequences for LMFBR fuel recycling 80−86960
actinides, burn-up characteristics, feasibility study for nuclear incineration 79−85706
actinides, chemical separation from PUREX raffinates using organic solvents 78−66676
actinides, decay heat estimation, summation calcs. and Standard eqns., review 80−63317
actinides, fast reactor recycle as waste management alternative, performance calcs. 78−13269
actinides, long lived, disposal, irrad. expts, production assessment nuclear data 79−85712
actinides, man-made, health effects compared to natural radionuclides 80−61647
actinides, nuclear incineration feasibility study 79−85705
actinides, recycling and recovery in fission reactor wastes 79−85699
actinides, separation from high level radioactive fuel reprocessing waste 79−85809
actinides in aqueous solutions, oxidation state and complex formation *(French)* 77−26858
actinides in English Channel, transfer into S.North Sea 79−48519
active spent fuel storage, replacement of underwater storage racks 80−23035
adsorption of Co and selected actinides by Mn and Fe oxides in soils and sediments 79−66422
aerosol dipsersiveness at nuclear power station 78−70650
air pollution, laser-Raman microprobe anal. of suspended particulates 80−76687
air pollution, X-ray absorption spectra for chem. characterisation of atmospheric aerosols 80−61501
air pollution, X-ray absorption spectra for chem. characterisation of atmospheric aerosols 80−72121
air pollution over N.Atlantic obs. of fission products and ^{222}Rn 80−77074
airborne and liquid releases from nuclear facilities, radiation monitoring systems 78−37450
airborne discharges, use of census data in assessing collective doses 79−59271
alkaline, decontamination by ion exchange 78−50263
alpha bearing and high level wastes management 79−26597
alpha waste production and proliferation hazard of different fuel cycles 80−83214
alpha-active waste production calcs. for various fuel cycles 79−59209
alpha-radioactive nuclides separation from waste solution *(Japanese)* 77−54318
alternative waste management techniques, Pu and actinide burnup 79−59210
American Nucl. Soc. winter meeting 1977 78−58315
American Nucl. Soc. Winter Meeting 1977 78−82408
American Nuclear Society proceedings (conf. Las Vegas, NV, June 1980) 80−94920
ANS leachability standard, figure of merit determ. 80−47623
Antarctica, radioactive waste disposal, glaciological aspects 77−61523
Antarctica, radioactive waste disposal site 77−61522
aqueous tritiated waste management from fuel reprocessing 80−5272
aqueous wastes from reprocessing plants, long term planning for management 77−61532
area skyshine from radioactive waste, gamma-ray backscatt. photon spectra 80−31119
asphalt products for final disposal, safety evaluation *(Japanese)* 77−50254
Asse salt mine, disposal of radioactive waste 77−65308
atmospheric dispersion models, comparison between critical sector and overall-site techniques 80−16873
atmospheric pollutant dispersion 80−47621
atmospheric pollutant propagation anal., appl. of indicator activation method 79−88039
atmospheric pollution, concentration time integral *(German)* 80−26378
atmospheric pollution by radionuclides, diffusion calcs. *(German)* 80−61484
atmospheric radioactivity inside buildings, absorbed dose estimation *(Spanish)* 78−8998
atmospheric transport from large area sources, finite element method 80−16874
Austrian research and development, collection, treatment and storage *(German)* 77−10473
automatic monitor of effluents from nuclear facilities 77−61615

radioactive waste continued
basic electrolyte for low-level decontamination 80−37528
beneficial utilisation, programmes in 1977 78−8950
bentonite clay, Na enriched, buried radioactive waste isolation material appl. 79−81029
Biblis nuclear power station, waste production, storage and disposal 80−68903
biochemical and chemical processes leading to radionuclide transport from low-level waste burial sites 80−101275
biological effects, cancers and mutations 80−76791
biosphere, radioactive contamination, influencing factors, 1962-76, Hungary *(Hungarian)* 78−92711
bitumen salt mixtures for rad. waste containment, thermogravimetric anal. *(German)* 79−89391
bitumen solidification for low/medium level wastes 80−23094
bitumen-salt mixtures, thermal stress behaviour *(German, English)* 77−65290
bitumenisation development *(German)* 77−10474
bituminization program for PWR waste in Korea 80−23096
BOPSSAR plant, radioactive waste management, influence on standardised plant design 77−46307
borated concrete use in Hanford N-reactor spent fuel basin 77−42128
boric acid solutions, extractive purification from radioactive corrosion and fission products 80−18458
borosilicate glass for storage of radioactive waste, thermal cond. meas. *(Japanese)* 77−69124
breeder reactor security and environmental impact *(French)* 80−47614
breeder reactor spent fuel shipping cask design, heat transfer tests 79−85640
breeder reactor spent-fuel shipping cask design 79−9834
build-up minimisation, design, construction and operation aspects 80−23074
buildings, indoor airborne radioactivity calcs. 80−63305
burial, study of natural convection in porous media with heat, generation 77−51114
burial grounds, generic hazard evaluation 79−22418
buried transuranic waste, equipment system for retrieval handling 79−89415
BWR, Brunswick Steam Electric Plant, radwaste system operating experience 78−17392
BWR, off-gas explosions, minimisation procedures 80−9369
BWR, radioactive waste management 78−17389
BWR, spent fuel γ-ray spectrometry and chemical analysis 78−54841
BWR, transactinide buildup in nuclear fields, sensitivity anal. rel. to neutron flux and spectra *(Italian)* 79−45356
BWR, vol. reduction and bitumen solidification of low level waste 80−9380
BWR high density fuel storage 78−726
BWR irradiated fuel channel disposal 78−21730
BWR power plant stack effluent inert gas nuclide monitor 79−3255
BWR spent fuel element storage, neutron physical aspects 80−68841
BWR spent fuel safeguarding, nondestructive assay using gamma spectrometry 80−68802
BWR spent fuel storage and refueling La Crosse 80−23034
BWR steam turbine, blast cleaning to remove radioactive deposits 80−18554
calcination and vitrification for high level waste 77−61546
calcined simulated high level waste, prep. and characterisation of sintered glass-ceramics 77−28770
calcined waste solid spillage, recovery of U, erosion in solids transport system 78−13264
calcined zeolites, leaching rates of Cs and Sr *(Japanese)* 77−61515
calcining facility, construction material anal. 78−86647
calcining facility, process filters, remote handling system 79−45382
calcining facility, remote maintenance development facility installation 77−54342
calcining facility, remote maintenance equipment 78−13263
calcining facility at Idaho Chemical Reprocessing plant, design criteria 77−61549
calcining facility development 77−54341
Canada, radioactive waste management 77−61521
Canadian program for nuclear fuel waste disposal 80−37483
Canadian program for storage and disposal of spent fuel and high-level waste 77−61535
Canadian radioactive waste management, bibliography of published literature 80−36796
CANDU, energy, water, tritium budgets for Perch Lake 1975 78−29563
CANDU, future development 77−38381
CANDU−Canadian experience and expectations with the heavy-water reactor 79−26593
CANDU fuel storage in pods and air-cooled concrete canisters 78−89963
CANDU irrad. fuel bundles, sheathed in Zircaloy-4, long term stability investig. 80−13774
CANDU irradiated fuel, disposal in dry storage 80−27788
CANDU irradiated fuel, monitoring for sheath defects in shipments 78−54864
CANDU irradiated fuel storage, concrete canister programme, heat transfer and shielding effectiveness 78−58388
CANDU nuclear stations, decommissioning 77−74973
CANDU reactor waste disposal, development programme 79−13494
CANDU reprocessed fuel and high level waste radioactive decay props. 77−71656
CANDU wastes, disposal options in Canada 78−41826
CANDU-PHW, decommissioning cost, environmental impact hazards and size 77−61598
CANDU-PHW decommissioning, costs, environmental impact, radioactive waste management 80−13964
CANDU-PHW reactors, preparation and storage and solid radwaste 80−5262
canister materials for radwaste containment 80−102279
Caorso nuclear power station airborne and liquid radioactive release monitoring systems 79−13553
cask concepts for spent-fuel storage 80−5284
cement solidification at Ringhals, Sweden 80−23086
cemented radioactive wastes, stability improvement method 80−57869
centrifugal clarifier, appl. in BWR crud removal 80−23082
ceramics for high level waste, solidification and storage 77−6542
cermet approach to nucl. waste management 80−37516
cermet high level waste forms for repository storage 79−89411
radioactive waste continued
charact., natural occurrences, technological enhancement and health effects 80−46071
chemical and isotopic anal. of U, Pu, and Th in nuclear fuel materials 79−81046
chemical migration of radionuclides in soil 80−17144
chemical toxicity issues in high-level waste disposal 80−42798
chop-leach fuel hulls, chemical decontamination and melt densification 77−65319
chronic radioactive release assessment, models and computer codes 80−13710
clean fusion concepts, survey 77−83082
Clinch River breeder reactor, ALARA nature of design effluents 79−22420
cloud, external gamma dose model 79−85828
coal power station fly-ash and slag, natural radioactivity meas. 78−17442
coastal breezes, dispersive, monostatic acoustic sounding system *(French)* 78−7683
collective dose commitment for estimate of radioactive pollution, concept and calcs. *(German)* 78−74504
combustion in Julich Incinerator *(German)* 80−73976
commercial burial site, radionuclide dynamics and health implications 77−61618
commercial LMFBR spent fuel shipping system 79−9821
Commonwealth Edison's Zion Generating station, decontamination of radwaste evaporation 80−9376
computer-aided fuel cycle management, w.r.t. economics 77−14241
concrete canister spent fuel storage facility, conceptual design study 79−45378
conditining and storage costs estimation *(Italian)* 78−25303
conference, actinide nuclear transmutation, Ispra, Italy (April 1977) 79−85698
conference, Chattanooga, Tennessee, USA, August 1977 78−17266
Conference, nuclear materials, safeguards and accountability meas., Williamsburg, USA (May 1978) 79−81045
conference, on-site management, Zurich, Switzerland (Mar. 1979) 80−22143
conference, Osaka, Japan (Nov. 1979) 80−98756
conference, radioactive waste management, Vienna, Austria (Mar 1976) 77−61530
conference on nuclear engineering remote systems technology, San Francisco, USA (Nov.-Dec. 1977) 79−45438
confinement device for determ. of whole-body radionuclide concs. in live ducks 80−67299
confinement in glass, stability charact. *(French)* 77−61556
contact-handled transuranic waste transportation 80−37538
containers, struct. dynamic response anal., appl. of endochronic plasticity 80−16407
containment, Ti-alloy canister materials, corrosion in saline radioactive waste isolation environments 80−104349
containment materials, EPR investig. 80−97138
contaminated groundwater zone control by underground impermeable wall, radioactive waste site *(Japanese)* 79−34446
continuous vitrification of fission product solns. 77−61544
control and accountability by gamma scan assay 79−9913
COPRECAL conversion of $(Pu,U)NO_3$ to mixed oxide 80−37570
corrosion and fission products, ion exchange separation 80−18460
corrosion and fission products, liquid-liquid extractions with metal diethyldithiocarbamates 80−18459
Cosmos 954 crash in Canada, air pollution, obs. of lichens 80−55960
cost-effectiveness analysis applied to radioactive effluents *(French)* 79−93840
creep analysis of canisters for radioactive waste vitrification 78−86648
Creys-Malville centre, siting, operation, safety, containment and waste *(French)* 79−30945
critical arrays, effects of packaging materials 79−26567
CTR central power station waste management 78−773
CTR Monsanto-Mound Laboratory eng. development of T handling systems 77−50295
W.Cumbria, Pu and ^{137}Cs concs. in environmental samples and possible maritime effect 80−108817
Czechoslovak nuclear power station fluid radioactive release monitoring *(Russian)* 79−13555
Czechoslovak Rez Nuclear Research Institute airborne radioactive release monitoring 78−89991
deactivation of waste waters using granulated bentonites *(Russian)* 77−38369
deactivation of weakly active discharge water by fibrous ionites 77−56251
decay heat estimation, summation calcs. and Standard eqns., review 80−63317
decommissioned structural materials, long-lived activity and implications for containment 80−13739
decommissioning of commercial power reactors, technical feasibility, cost, environmental effects 79−67902
decommissioning of nuclear facilities, quantitative anal. of radioactive waste development 80−13974
decommissioning of Pu fuel fabrication plant, nondestructive assay meas. using NaI(Tl) detectors 80−63495
decommissioning of the surface facilities associated with repositories for the deep geological disposal of high-level nuclear waste 80−13734
decommissioning of U ore processing facilities, engineering eval. 80−13977
decontamination and waste management at shutdown reprocessing plant, experience 78−66354
decontamination facility for large reactor components 80−13740
deep ocean sediment thermal conductivity meas. platform rel. to nuclear waste storage 80−46175
deepsea disposal sites, environmental surveys using submersibles 77−61617
defense waste processing facility, anal. of radionuclides 80−37518
denitration of aqueous waste solns. from fuel reprocessing 80−5313
denitration with organic reductants, effect of nitrate addition 79−97880
density measuring meter, digital, remotely operated 80−68927
depository in West Germany, advance payment from users, legal aspects *(German)* 79−71903
development of techniques for radwaste systems in CANDU power stations 80−37547
disposal, conf. Montreal, Canada, 1973, Oct. 77−61520
disposal, Czechoslovak Research Institute activities *(Slovak)* 80−83188

radioactive waste continued
disposal, decision anal. 80−18488
disposal, economic considerations, transportation, land burial and containers 78−17393
disposal, hard rock repositories, soln. 78−78477
disposal, interaction with hydrologic cycle 78−94103
disposal, national programmes, aspects 78−697
disposal, operation of a pilot solid waste incinerator 80−22990
disposal, pilot plant concept for New Mexico site, deep salt form. 77−61577
disposal, popular assumptions, critical examination 80−106141
disposal, public acceptance 78−41824
disposal, safety and regulations *(German)* 78−54836
disposal, solidification of ion exchange resins in polystyrol, transport and storage *(German)* 77−23217
disposal, Spanish programme *(Spanish)* 79−31074
disposal, Swedish project on safety *(Swedish)* 77−38341
disposal, thermomech. impact around rock salt borehole 80−5278
disposal, US Federal disposal programs, 1978 status 79−36374
disposal, waste management and its role in Canadian fuel cycle 79−89393
disposal and reprocessing, West German solution *(German)* 77−38338
disposal and storage management 77−10476
disposal area, dose to rodent inhabitants 78−85383
disposal by bituminisation, fire safety and explosion prevention 79−71920
disposal by imbedding in glass blocks 80−18462
disposal by incineration in shaft furnaces *(German)* 80−47584
disposal by Julich incineration process *(German)* 80−47583
disposal by nuclear incineration, CEGB Research Division report 78−46145
disposal by solidification, evaluation of various techniques 79−31080
disposal by solidification and burial, geological aspects 80−63316
disposal by underground storage, geological aspects *(German)* 79−13431
disposal criteria proposals by EPA and NRDC, review 80−18484
disposal following decommissioning of nuclear facilities *(French)* 80−13736
disposal from nuclear power plants *(Russian)* 79−30966
disposal in Asse salt mine, Germany, results and future developments 77−61575
disposal in bedded salt, conceptual design of Waste Isolation Pilot Plant 79−26570
disposal in bedded salt, thermally induced movement of canisters 79−26573
disposal in bedded salt, Waste Isolation Pilot Plant environmental studies 79−26572
disposal in bedded salt, Waste Isolation Pilot Plant high-level waste program 79−26574
disposal in bedded salt, Waste Isolation Pilot Plant site evaluation 79−26571
disposal in bedded salt, Waste Isolation Pilot Plant transuranic wastes program 79−26575
disposal in deep geological formations, interactions between waste and surrounding rock 78−54853
disposal in geologic formations, site selection criteria 80−106142
disposal in geologic formations *(French)* 77−88230
disposal in geological formation, general considerations *(German)* 79−9757
disposal in geological formations 79−31070
disposal in hard rock, slow crack growth anal. of granite 79−89452
disposal in mines, Dutch policy *(Dutch)* 80−671
disposal in ocean rel. to deep sea biology 79−29638
disposal in sea 80−37472
disposal into deep ocean, hazard assessment 77−88233
disposal into internationally important waters, limit evaluation *(Russian)* 79−29488
disposal method including encapsulation in thick gold layer 78−74441
disposal methods, risk assessment 79−41021
disposal methods in German Democratic Republic, use of abandoned salt mine 77−61574
disposal of high level and α-bearing waste, international co-operative research programmes 79−36363
disposal of high-level and long-lived waste 78−29610
disposal of low- and intermediate-level radwaste, Canadian R and D program 80−99255
disposal of nuclear waste, social criteria 77−30652
disposal operations Peach Bottom power station system backfit considerations 80−5261
disposal options, modelling studies 78−41830
disposal problem and soln. *(French)* 79−93740
disposal problems and safety 78−86636
disposal problems and soln., fast reactor role in limitation and control of Pu prod. 79−9758
disposal safety criteria, choosing risk assessment methods 80−99247
disposal safety criteria, ORIGEN2 point-depletion and decay computer code 80−99248
disposal safety criteria, radionuclide chain transport through heterogeneous media 80−99250
disposal under seabed 80−89588
disposal using linear accel. 79−67980
distribution coefficient of radionuclides in sample soil and water, environmental effects 77−13092
dodecane-tributyl phosphate solns., radiolysis, liquid products 80−40723
doses to public from nuclear industry, health risks from various power sources 80−57899
dosimetric data tables 80−105438
dosimetry calculations due to radionuclides in aquatic food chains, NEPTUN interactive code in FORTRAN 80−109039
Dresden-1 chemical cleaning, radioactive waste treatment 78−17394
dry solid waste, effectiveness of commercial compactor in university health centre setting 77−66860
dry spent fuel cask handling system and transport 78−17348
dry spent fuel storage installation, design and operation 80−23036
dry storage pit for radioactive sources 78−13248
EBR-II cover gas clean-up system, transient anal. 77−46357
ecological search for radiation effects in Hanford nuclear waste ponds and streams 80−89804
educational module on nuclear reactor safeguards and waste management 80−36802

radioactive waste continued
effluent discharge data intercomparability and EEC harmonisation 79−13546
effluent discharges, European Community, 1972-76, radiological aspects 79−41019
effluent gases from nuclear power industry, ambient contamination *(Spanish)* 78−61540
effluent monitoring, symposium, Portoroz (1977) 78−89985
effluent monitoring problems, loss and error reduction procedures 78−89987
effluent monitoring programme design and organisation principles 79−13548
effluent sampling programme data statistical evaluation 79−13547
electrical energy and hydrogen production from fission product decay heat 79−18005
electricity production using radioisotope-powered photovoltaic generator 79−57432
EM filtration of crud in PWR primary circuits 80−23081
environment monitoring ground radioactive burial site *(Japanese)* 80−67015
Environmental aspects of nuclear power *(Japanese)* 77−83112
environmental dispersion models, evaluation of uncertainties 80−46074
environmental effects, survey *(French, English)* 77−83064
environmental impact assessment, of oceanic and geological disposal, use of box model method *(Japanese)* 80−9346
environmental modelling principles 79−79414
environmental pollution by nuclear fission products 78−85607
environmental protection, radioactive waste from power plants in USSR 79−26601
environmental protection, reactor safety and waste handling *(Hungarian)* 80−91224
environmental radioactivity, determ. for dose assess. 80−85321
environmental radioactivity control, relevance to control of other environmental contaminants 79−9889
environmental radioactivity near a radioactive waste disposal site 80−98148
environmental radiological surveillance, relative importance of environmental media 79−66421
environmental research, bibliography of AECL publications 79−34444
environmental risks associated with radioactive waste management 79−26604
ERDA long term waste management goals and programs 77−61531
European Community Commission (ECC) programme *(French)* 77−26853
European Nuclear Conf., Hamburg, Germany, May 1979 79−97841
evaporator concentrates, pretreatment before solidification 80−23079
ex-vessel storage tank design and fabrication for CRBRP 78−17347
exxon nuclear fuel recovery and recycling center facility description 79−36388
fast reactor fuel element regeneration by gas-fluoride method, highly active waste product behaviour 78−37425
FBR, Clinch River, design and fabrication of ex-vessel storage tank 79−30973
FBR fuel handling, radiation safety 80−73985
FBR safety and economics, leak detection, cooling, waste disposal 80−63303
FFTF fuel storage facility design 78−715
final disposal possibilities, waste conditioning, storage and safety, review 79−26554
fission gas release from high burn-up oxide fuel, predictions in ELESIM code 80−57864
fission materials, European nuclear industry situation, review *(Dutch)* 77−3073
fission product cold trapping in stainless steel Na loop 77−61514
fission product release calcs. from reactor containment building 77−79449
fission product waste solidification, high-level, for final storage *(German)* 80−22958
fission products, concentrated solns., continuous vitrification *(French)* 77−361
fission products, continuous vitrification process, industrial scale *(French)* 77−23228
fission products, decay heat estimation, summation calcs. and Standard eqns., review 80−63317
fission products, solubility rules based on lattice parameter differences 78−59953
fission reactor, radioactive waste disposal 77−74954
fission reactor fuel, mixed oxide, suitability of spent fuel shipping casks 80−27757
fission reactor fuel reprocessing, adsorptive removal of rare gases 79−31094
fission waste storage in glass and salt *(Dutch)* 78−29587
fixation in glass, laboratory expt. 77−74957
fixation in high-SiO_2 glass matrix prod. by porous glass process 79−49708
fluid, processing plant for long-term storage rel. to ocean dumping 80−5279
fluid radioactive waste monitoring equipment, USSR standards *(Russian)* 78−89998
French nuclear power plant gaseous and liquid effluent release monitoring *(French)* 79−13551
fuel and waste management schemes for nuclear power implementation 77−57773
fuel cycle, radioactive material release, cost/benefit anal. 79−26605
fuel cycle, transportation status and problems 79−59236
fuel cycle wastes, solidification and burial techniques, USSR *(Russian)* 79−31081
fuel cycles principle and state of art, critical review *(German)* 77−34408
fuel disposal safety in Switzerland *(German)* 78−74455
fuel elements of HTR, continuation store *(German, English)* 77−65289
fuel elements recycling and thermal re-irradiation, technical, economic and safety problems *(German)* 80−99269
fuel fabrication and reprocessing plant, radiation protection device based on neutron detection *(French)* 78−66362
fuel reprocessing, anal. of fundamental problems 79−26665
fuel reprocessing, safety problems re environment and operating staff 80−816
fuel reprocessing and waste treatment at Karlsruhe nuclear research centre 79−31143
fuel reprocessing plant instrumentation for internat. safeguards 78−721

radioactive waste continued
fuel reprocessing technology, development up to current status 78−58393
fuel reprocessing waste ^{137}Cs, ^{90}Sr and rare earth radioisotope separation by cation exchange 78−78486
fuel storage, close spaced racks 78−728
fuel storage, in-plant facilities, design considerations 79−67916
fuel storage basin water, chloride ion removal 79−30975
fusin power plant radioactive waste disposal 77−67876
fusion power reactor waste management 78−21766
fusion reactor, radioactive waste generation by neutron activation of struct. components 78−74476
fusion reactor air detritiation operations, computer modelling and bench-scale testing 79−85784
fusion reactor blanket material impurity hazardous activity and dose rates, biological hazard pot. 80−102315
fusion reactor fuel streams, impurity removal and recovery processes 79−85783
fusion reactor transmutation waste management program effectiveness, ^{90}Sr disposal case 77−34460
fusion reactor transmutation waste management system 80−37482
gamma-emitting activation products, plant uptake of ^{59}Fe, ^{58}Co, ^{54}Mn and ^{65}Zn 80−30614
gas permselective membranes, irrad. effects on permeation and separation performances 78−29591
gas processing with low temp. rectification for quasi-null release 79−67877
gas separation performance of tapered cascade with membrane 79−22478
gas-chromatography, beta radio effluents, window flow counter 80−93824
gaseous, from power plant, cryogenic rectification system for ^{85}Kr and ^{133}Xe removal 78−50268
gaseous core reactor power production with minimal transuranic wastes 79−9806
gaseous effluents from LWR and reprocessing plants, treatment and control 77−61589
gaseous effluents from reprocessing plants, treatment *(French)* 77−61588
gaseous fission products formation and behaviour, Kr and Xe separation and processing *(Czech)* 79−49707
gaseous reactor wastes, dispersal forecasting *(French)* 78−8995
geochemical aspects of radionuclide migration from waste repositories 80−13711
geologic depositories, safety criteria for high-level waste storage 80−95379
geologic disposal, geotoxicity hazard index 80−97822
geologic disposal, in situ expts. 80−5276
geologic disposal, migratory props. of waste elements 79−67893
geologic disposal, modelling of radionuclide transport and decay products 80−78415
geologic disposal, safety anal., functional relations of risk to input data uncertainties 80−83189
geologic formations, radionuclide migration 78−4994
geologic isolation for fuel cycle wastes, management perspective 77−42172
geologic isolation repositories, long-term safety assessment 79−49714
geologic media, radionuclide migration model 80−37499
geologic nuclear waste disposal, pathway anal. review 79−22424
geologic repositories, characteristics for radioactive waste acceptance criteria 80−18486
geologic repositories, computer anal. of long-term radiation hazards 80−18483
geologic repositories, feasibility study of granite formations, Stripa, Sweden 80−18481
geologic repositories, NRC waste disposal safety criteria 80−99246
geologic repositories, operation of the Waste Isolation Pilot Plant 80−99264
geologic repositories, risk assessment 80−95359
geologic repositories, survey methods for assessment of radiological release 80−18489
geologic repositories, US DOE program for terminal storage 80−95381
geologic repositories, US Earth Science Technical Plan 80−18482
geologic repositories, US Geological Survey Program [for nuclear waste geologic repositories] 80−22989
geologic repositories, waste disposal safety criteria 80−99245
geologic repositories for commercial nuclear waste, feasibility study of basalt formations 80−18479
geologic repositories for nuclear waste isolation 80−18584
geologic repository, methodology for repository siting in different geologic media 80−102268
geologic repository, site search and qualification process 80−18474
geologic repository, status report on Waste Isolation Pilot Plant 80−18478
geologic repository, US DOE site identification criteria for waste isolation 80−102267
geologic repository for nuclear waste at Nevada Test Site 80−18480
geologic storage, effect of adsorption of Tc and I radioisotopes by minerals 80−83203
geologic waste repositories, high level defence waste and spent fuel characterisation 79−89410
geologic waste repositories, long term safety assessment methodology 80−37487
geological and ocean nuclear waste disposal programme in UK 78−41829
geological disposal, chemical factors controlling environmental actinide sorption 80−13713
geological disposal, Netherlands programme 79−26609
geological disposal, sorption of actinides in igneous rocks 80−95367
geological disposal of high-level waste, Canadian program 77−3140
geological disposal of spent fuel, criticality considerations 80−37533
geological long-term disposal of high-level waste, Sweden 80−13712
geological storage, experience gained at Oklo natural fission reactors 80−21773
geological storage, natural retention experience at Oklo natural reactor 80−18561
geological storage and disposal in partially serpentinized ultramafic rock 77−61524
geosphere transport model for WIPP site 80−16854
German Government responsibility w.r.t. storage facility, legal aspects *(German)* 78−86701
German reactor safety study, consequence model 80−18524
radioactive waste continued
German Waste Management Centre, technical project design phase status *(German)* 79−13432
getter development for radiocaesium, obs. of $Cs\text{-}SiO_2\text{-}Al_2O_3$ system interactions 80−83208
glass, corrosion and devitrification, trace element anal. by neutron activation, rel. to ancient samples 78−12801
glass containment, effect of α-emitters *(French)* 77−26849
glass for high level waste, field leach test 77−6541
glass for high level waste disposal 77−6540
glass leaching, ^{90}Sr diffusion modelling 80−37519
glove box for sealed manipulator maintenance 80−18684
glove boxes, Pu-contaminated, size reduction and waste packaging 80−18469
ground waste disposal, sorption and migration studies for ^{90}Sr, ^{137}Cs 79−54523
groundwater flow models, mass transport models, dose models 80−16853
groundwater modelling, hydrogeologic conditions at radioactive waste burial sites 80−21550
groundwater system, transport of chain decaying radionuclides 80−51019
handling at Swedish nuclear power plants 79−26612
Hanford site, transuranic distrib. beneath retired underground disposal facility 80−42802
Harwell inactive vitrification pilot plant 77−61543
hazard indices for nuclear high-level waste in underground repository, rel. to naturally occurring toxic minerals 78−15913
hazards anal. due to Th fuel cycle use in power reactor systems 79−30941
health hazards, for teachers 79−35506
health hazards of waste disposal, EEC-JRC research 80−42786
health physics conference, San Francisco, USA, June/July (1976) 77−16983
heat source for steam prod. in nucl. waste boiler 78−41838
heat treatment, effluent gas purification techniques *(French)* 77−23230
high activity waste immobilisation, potential solidification material properties 79−49790
high level, conversion to glass, exptl. joule-heated ceramic melter 80−18471
high level, disposal in deep-sea bed, New Zealand 78−705
high level, immobilization, continuous glass melter 79−59214
high level, long term integrity of deep geologic repositories 80−37498
high level, solidified in borosilicate glass, γ-scanning as integrity test *(German)* 80−78426
high level, vitrification, industrial scale plant, France 77−365
high level incorporation of $3CaO\text{-}Al_2O_3$ cement 78−78485
high level liquid radioactive waste, denitration with formic acid, Pt group effects 79−36339
high level liquid waste evaporation and storage, lab. simulation 79−89409
high level nuclear reactor waste immobilisation in SYNROC 79−43794
high level radioactive liquid waste, disposal options, fuel reprocessing 79−49703
high level radioactive waste, disposal options 79−26610
high level radioactive waste management, safety and protection aspects *(French)* 79−26656
high level radwaste management, storage, transportation, disposal, review 79−54522
high level solid, from HTGR fuel reprocessing, long term isolation from environment 79−26576
high level waste, retrieval system design, Hanford 79−45380
high level waste containing granules coated and embedded in metal as an alternative to HLW glasses *(German)* 80−83186
high level waste disposal risk assessment 77−6532
high level waste form props. 80−37520
high level waste repositories, siting criteria, implications of policy/regulation changes 80−102269
high level waste reprocessing, management in France *(French)* 79−26598
high level waste solidification 77−67836
high level wastes, oxalate precipitation for separation of Am, Cm, and trivalent lanthanides 80−83202
high-level, characts. of glasses for solidification 79−63779
high-level, evaluation of products for solidification 77−61555
high-level, fixation in glass ceramics 77−61558
high-level, leaching of radioactivity from glass blocks buried below water table 77−65312
high-level, long-term storage and disposal in geological formations 79−93764
high-level, new waste calcining facility 79−59211
high-level, repository site selection, concerns of Michigan State 79−49716
high-level, stability of phosphate and borosilicate glasses used for solidification *(Russian)* 77−61560
high-level, thermal and radiation effects on borosilicate glasses 77−61557
high-level, ultimate disposal in salt domes, waterproof geometry on safety aspect 77−61576
high-level, use of DHDECMP for actinide partitioning 79−26583
high-level, vitrified, thermal, chemical and radiation stability *(Russian)* 77−61559
high-level and actinide contaminated, from fuel reprocessing, long-term radiotoxicity problems 77−61571
high-level liquid 79−59213
high-level liquid radwaste partitioning, radiation damage of organic extractant 79−67879
high-level liquid solidification, UK facilities 77−61542
high-level liquid waste, damage to organic extractant in positioning process 80−9345
high-level nuclear waste management from nuclear fuel reprocessing 77−65309
high-level radioactive waste, ultimate disposal on seabed, rel. to oceanographic circulation 78−13273
high-level radioactive waste disposal on seabed following reprocessing, feasibility study 78−13271
high-level radioactive waste management 80−37470
high-level radioactive waste storage, distribution calc. *(German)* 79−81014
high-level radioactive waste storage, temp. distribution simulation expts. *(German)* 79−81015
high-level tritiated aqueous waste, immobilization in polymer-impregnated concrete 78−13265

radioactive waste continued
high-level vitrified waste, risk anal. of repository in geologic salt formation 78−17362
high-level waste, hot cell facility and equipment for tests of radionuclide removal process 80−18675
high-level waste disposal in deep geologic formation, environmental aspects 79−49712
high-level waste disposal in salt formation, far-field temp. calcs. 80−5277
high-level waste management 77−34412
high-level waste management systems in Germany, risk analysis 78−17354
high-level waste solidification plant, contribs. to risk evaluation 78−17356
high-level waste solidification products, composition, struct., props. *(Russian)* 79−31082
high-level-waste disposal on ocean floor, prospects of international cooperation 78−13272
HLLW, safety analysis of tank storage 80−740
HLW fixation in SYNROC-B sintered ceramics, comp. and phase charact. 80−106126
HLW repositary, water intrusion scenario studies 80−52765
hospital radioisotope release to environment, model and meas. 78−96105
hospitals, radioactive liquid waste elimination, math. model for decay pond design *(Italian)* 79−48345
hot cell, shielding slab thickness calcs. 79−6752
hot cell liners, removable, design 80−18685
hot cell manipulator remote decontamination facility and repair station 79−9911
hot fuel examination facility, air cell decontamination and refurbishment 79−9910
HTGR, at Peach Bottom, gamma scanning the primary circuit at end-of-life 77−46419
HTGR, Peach Bottom, decommissioning and component removal 78−21756
HTGR fuel reprocessing, radioactive waste streams 77−42173
HTGR fuel reprocessing off gases, simulated, efficiency of CO_2 removal 79−26577
HTGR fuel reprocessing plant, cost and environmental impact of radioactive waste treatment 77−46380
HTGR reprocessing plant off-gas streams, ^{85}Kr removal 79−30972
HTGR spent carbide fuel storage, water-cooled storage concepts 80−22996
HTR and LWR Th, U, and Pu-separation, time-dependent alpha-activity curves determ. *(German)* 77−6546
Hudson River estuary, man-made radionuclides and sedimentation 77−2183
hydrodynamic dispersion in transport models 80−17146
IAEA regulations for safe transportation 80−63410
IAEA transport information collection system, influence on improved safety measures 80−63413
IAEA transport regulations, underlying radiation protection principles 80−63414
immobilisation, review of waste forms, and waste processing 80−102280
immobilisation of highlevel nuclear wastes, US program 80−13708
immobilisation using glass 80−42812
immobilised nuclear waste, disposal centre conceptual design 80−52774
in PWR and BWR 79−54570
in-situ transuranium element measurement technique for wastes associated with power reactor fuels 79−85715
incineration at reactor site 80−23093
incineration studies at Los Alamos 80−73963
incinerator for alpha solid waste, prototype operation 80−73964
incinerator for transuranic contaminated waste 79−49718
Indian nuclear power station effluent monitoring system requirements and experience 79−13552
industrial radioactive liquid waste processing by ion exchange at Westinghouse Waltz Mill Site, USA 77−54345
inert gas analysis, calibration of Ge(Li) gamma-ray spectrometer 77−83442
inert gas fission products, separation of ^{85}Kr from Xe by distillation *(German, English)* 77−61516
inert gas release by nuclear reactors in West Europe 77−50305
inert gas treatment at nuclear power station 77−50306
inert-carrier radwaste volume reduction and solidification system 80−23046
inertial confinement fusion pellet centre burnup of fission reactor actinide waste 79−31181
inorganic ion exchanges, appl. in U, Pu separation from fission product solns., reviews 79−85625
integrated system for solid and liquid waste conditioning 77−65311
interim storage and final disposal, French experience 77−38344
international regulatory control for safe transportation 80−63411
inventory report for reactor and fuel fabrication facility wastes 80−37532
Iodox process for iodine removal from air with hyperazeotropic nitric acid 79−31107
ion exchange resin, embedding in bitumen 77−10475
IRAN-1,2, plants, calc. of radioactive releases 79−18056
irradiated CANDU fuel, long-term storage under water 79−41020
irradiated fuel elements recycling plant design modifications and safety of used nuclear fuel during storage and disposal *(German)* 80−99219
irradiated fuel rods, storage options, comparisons 79−45383
irradiated fuel sipping, inspection and repair 79−9844
irradiated nuclear fuel, long range storage, American proposals *(French)* 79−49709
irradiated nuclear fuel storage, waste management implications 79−31079
irradiated nuclear fuel transport and handling, French nuclear power plants *(French)* 79−31233
irradiated nuclear reactor fuel rod components, EM separation, feasibility 80−99224
isolation repository, material control and accountability 79−85682
isotope concentration and precipitation via ion exchange methods *(Hungarian)* 80−18450
Japanese nucl. fuel cycle for LWRs 78−86670
JEN, Spain, work on nuclear fuel cycle *(Spanish)* 77−38376
Lac du Bonnet batholith, Canada, geological reconnaissance for nuclear waste disposal 80−73977
lake sediments, radionuclide geochronology and pollution history 78−61451
radioactive waste continued
land disposal, repository, packaging and cost estimate, internal radiation dose evaluation *(Japanese)* 78−66351
lanthanides (III), extraction with di-isodecyl phosphoric acid from HNO_3 soln. 79−22398
large fuel reprocessing plant, anticipated chem. emissions 78−5004
large pools for spent fuel, LUSH code cf with design methods for struct. load calc. 78−17337
large-scale nuclear power station safety consideration 78−8961
laser fusion driven actinide waste burner, neutronics anal. 78−58459
laundry, liquid wastes at BWR plant treatment 77−61540
laundry waste treatment system 78−17338
leach behaviour of hydrofracture grout 77−10478
leach rates, effect of temp. and leaching media 80−22991
leach rates determ. by activation anal. 80−37523
leach rates of high activity waste from borosilicate glass 79−36358
leach test methods for solidified radwaste 80−102277
leach tests interpretation 80−42810
leach-migration experiments to determine the mobility of radionuclides in geologic media 80−18487
leached hull monitor for determ. of transuranic content of spent reactor fuel 79−85606
leaching of solidified radioactive waste, rel. to diffusivity const. 78−5055
light-water waste management systems, vol. reduction and economics 80−9367
liquid, bituminisation process, physical and chem. props. of products 77−57727
liquid, decontamination by ion exchange and electrodialysis 79−71926
liquid, low level, treatment by precipitation and centrifugation 80−23084
liquid, management experience of Spanish nuclear energy board *(Spanish)* 77−61533
liquid, solidification processes, problems 77−364
liquid, solidification techniques by mobile units 80−23087
liquid, vitrification, thermal decomp. of nitrates and additives in glass-making *(Korean)* 78−86638
liquid, zero release, and treatment using ACEREN evaporator *(French)* 80−23083
liquid and solid, processing using fixation method *(Czech)* 77−74947
liquid discharge, radionuclide isotopic anal. *(Spanish)* 78−13250
liquid effluent beta monitor 77−61656
liquid effluents, aquatic radiological impact anal., radiocaesium transport in sediment 80−95486
liquid high level waste, vitrification *(Japanese)* 80−22971
liquid high level waste solidification 78−21669
liquid high-level waste at reprocessing plants, very long term storage of fission products *(French)* 77−61534
liquid low-level waste at BWR plant, treatment 77−61540
liquid nuclear waste, simulated, ion exchange equilibration, radiotracer obs. 78−74444
liquid radioactive waste, disposal in deep aquifers, USSR approach 79−29489
liquid radwaste system at Santa Maria de Garona nuclear power plant 77−42140
liquid scintillation counting waste vol. reduction by distillation 78−78556
liquid scintillation wastings, combustion system *(Japanese)* 80−63503
liquid scintillation wastings, vaporisation apparatus *(Japanese)* 80−63502
liquid scintillator, 1,4 dioxane based decontamination and recovery 79−22536
liquid waste, control of hospital waste using NaI(Tl) detectors *(Italian)* 80−56224
liquid waste, ion exchange with chem. treated vermiculites 79−45370
liquid waste from decontamination processes, reduction of quantity *(German, English)* 77−38345
liquid waste from nuclear reprocessing, vitrification, durability 78−54852
liquid waste handling facilities for LWR fuel reprocessing plant 79−36390
liquid wastes, solidification 77−83046
liquid with T contamination, packaging 77−6538
liquid-metal-cooled reactors, radionuclide trap in primary circuit 79−93768
LMFBR, borosilicate glass and glass ceramics with highly radioactive waste 80−5271
LMFBR, elimination of transuranium elements by neutron absorpt. 78−29628
LMFBR, fuel handling and storage system 79−45394
LMFBR, spent fuel shipping system 79−45385
LMFBR 79−26677
LMFBR coolant, decontamination by low-pressure distillation 80−13694
LMFBR fuel storage facilities, criticality calcs. 79−26568
LMFBR spent fuel shipping cask designs, subcriticality guidelines, Monte Carlo calcs. 78−82470
LMFBR spent fuel transportation 78−711
LMFBR spent-fuel shipment cask, radiation shields 77−46313
LMFBR spent-fuel shipping, organics as coolants 77−46312
LMFBR waste management, USA 80−23073
LMRBR spent fuel shipping casks, subcriticality design 78−706
long term facility failure hazards, preliminary examination 79−54533
long-lived, disposal in Trisaia clay formation, Italy 77−61573
long-lived, final disposal in underground clay formation, Belgium *(French)* 77−61572
long-lived fission product waste transmutation by spallation and neutron reactions using linear accelerator 78−13268
long-term entrapment, asphalt props. relevant to safe immobilization 80−9355
long-term risk assessment of waste disposed in geologic formation 78−17361
loop disposal system of sodium loop safety facility 80−18467
low and intermediate levels, current Canadian development programs, review 80−13733
low and moderate activity, bituminisation, French experience *(French)* 77−26852
low and moderate activity, conditioning by thermosetting resins *(French)* 77−23229
low level, solid/liquid waste, volume reduction, solidification technique 80−23092
low level, solidification in Dow processes 80−23090
low level, transport regulations, proposed changes 80−68896
low level contaminated metal waste volume reduction by melting 79−89412
low level disposal site, trench water study 79−52963

radioactive waste continued
low level long lived radioactive liquid waste, chem. treatments, decontaminability 77−54351
low level radioactive liquid wastes, chem. treatment, clay numerals, cation exchange capacity 78−33270
low level radioactive waste volume reduction and cost savings 79−36360
low level radwaste, on-site management options 80−13692
low level solid waste, vol. reduction in Ontario Hydro 80−9379
low level waste disposal technology, US DOE R and D program 80−99254
low level waste leachability, ANS standard 80−47622
low level waste leaching, material parameter defined by ANS standard 80−47624
low- and intermediate-level waste, risk anal. of road transport in Netherlands 78−17359
low- and medium-level, surface and concrete-lined trench storage, seven years' experience report *(French)* 77−61579
low-level, developments and studies for marine disposal 77−61578
low-level, from nuclear power plants, solidification 79−54540
low-level, radionuclide migration in soil 79−54610
low-level, shallow land disposal, microbiological aspects 79−85630
low-level, solid, land burial experience report 77−61581
low-level burial site, radionuclide migration model 78−21671
low-level commercial disposal sites, trench water survey 79−85629
low-level radioactive solid wastes disposal, benefit-cost anal. 80−18556
low-level radioactive waste, impact of decay daughters 79−52964
low-level radioactive waste management complexity and cost-effectiveness 78−94117
low-level radioactive wastes: public fears and political strategies 80−102272
low-level radwaste treatment, volume reduction systems, progress report 80−99260
low-level solid radwaste, regulations and guides 80−5263
low-level solute and gas transport from burial site 79−85628
low-level transuranic storage, radwaste Sr, Cs, Co sorption meas. on soil sediment 80−95482
low-level volume reduction, fluidised bed dryer/incinerator 80−9378
low-level waste, industrial processes for treatment and storage 80−5280
low-level waste, inert-carrier process for vol. reduction and solidification 80−9370
low-level waste, vol. reduction policy 80−9366
low-level waste burial facility at West Valley, correl. of water accumulation to operating practices 78−13266
low-level waste burial facility at West Valley, remedial work for trench water accumulation 78−13267
low-level waste burial grounds, nonradiological hazards 80−42797
low-level waste disposal alternatives 80−37527
low-level waste disposal guidelines using the RWDCS methodology 80−99262
low-level waste disposal in Japan, research and planning 78−86657
low-level waste management, US DOE strategy, public acceptance 80−102270
low-level waste management and safety, public acceptance 80−102271
low-level waste siting needs−an overview 80−99261
low-level waste transport and disposal, logical 80−23044
LWR, accidents, effects and damages 80−22961
LWR, borosilicate glass and glass ceramics with highly radioactive waste 80−5271
LWR, commercial, props. of solidified radioactive waste 79−59207
LWR, commercial, volume reduction system design and operation 78−21699
LWR, high-level radioactive waste prod. 77−26851
LWR, liquid effluent treatment 80−18444
LWR, low-level liq. and solid waste, vol. reduction and solidification 80−9368
LWR, radwaste solidification processes, safety aspects 80−13673
LWR 79−26677
LWR alkaline waste, evaporation by wiped-film evaporators 79−36391
LWR and coal power stations, effects on ambient media from mining to waste disposal *(Spanish)* 77−75005
LWR fuel, population dose calc. 80−46073
LWR fuel containing Pn, waste treatment cost/benefit anal. 77−46378
LWR fuel cycle, back end, projecting 1985 fuel cycle impact of government action 79−59237
LWR fuel cycle, high level waste, management 77−359
LWR fuel cycle costs, future trends, waste disposal and reprocessing 79−26696
LWR fuel cycle effluent model for ENFORM system 78−94111
LWR fuel fabrication plant, cost of controlling inorganic chemical releases 78−5003
LWR fuel reprocessing, hot cell studies 77−42169
LWR fuel reprocessing plant, intermediate and high level waste management 77−42171
LWR fuel reprocessing plant, radioactive waste treatment costs and environmental impact 77−46379
LWR fuel waste disposal using linear accelerator fission product transmutor 80−63365
LWR fuels, actinide removal from high level wastes 77−26860
LWR irradiated fuel pellets, leaching in deionized water, sea brine and typical groundwater 79−26581
LWR irradiated fuel transport flasks, shielding and engineering aspects 80−27831
LWR liquid radwaste treatment 79−54571
LWR nongaseous radwaste, collection, treatment and storage 79−54572
LWR power station decommissioning, radioactive waste decay behaviour 80−13738
LWR radioactive solid waste management 77−42130
LWR reprocessed fuel, EPMA 80−5306
LWR reprocessing solns., instabilities and solids formation 77−42170
LWR spent fuel, alpha spectrometric meas. for SNM verification 80−78424
LWR spent fuel, economics of away-from-reactor water storage basin 79−59201
LWR spent fuel, non-destructive anal. using inherent and induced neutron radiation *(Russian)* 80−68805
LWR spent fuel, nondestructive meas. and verification for materials safeguards 80−78420
LWR spent fuel assemblies, interim and long range storage 80−5286
LWR spent fuel elements, disposal in geologic isolation, feasibility study report 80−106140
radioactive waste continued
LWR spent fuel elements, gamma spectrometric meas. of burnup U/Pu ratio and cooling time for materials safeguards 80−78423
LWR spent fuel storage benchmarking expts. 79−63776
LWR spent fuel transportation 78−724
LWR spent fuel water storage basins, away-from-reactor design comparisons 79−59200
LWR spent-fuel heatup following loss of water during storage 79−59202
LWR spent-fuel processing and packaging options, for disposal in geologic repository 80−18485
LWR stowaway fuel cycle effluent projections 78−94110
LWR waste, leach tests of cement containers under high hydrostatic press. *(Japanese)* 79−63761
LWR waste management, cf. fusion plant 78−773
Magnox, development and radiation stability of glasses for vitrification 77−61554
Magnox power station, decommissioned, rad. levels, neutron activation, waste disposal 80−13976
management, advantages of regional centres 77−362
management, and plutonium, Swedish approach 79−31075
management, closed nuclear fuel cycle, W.Germany 79−619
management, EEC policy 80−95376
management, goals and criteria 79−31072
management, India's programme 79−26606
management, industrial aspects, Western Europe 79−31071
management, industry experience in low-level waste siting−regulatory, political, and business considerations 80−99257
management, Japan Atomic Energy Research Institute 79−26608
management, mathematical modelling 80−701
management, regional cooperation in India 77−57730
management, report on 1977 IAEA conference *(Dutch)* 77−79446
management, review of new technical standards in Japan *(Japanese)* 79−67880
management, shallow burial ground disposal for low- and intermediate level waste, French experience 80−95380
management, storage and transportation in Sweden 80−95378
management, technological progress, EEC conclusions and recommendations 80−106133
management, technological progress, EEC R&D programme 80−106132
management, US DOE organization for waste materials characterization 80−102273
management, US DOE program, role of Materials Characterisation Centre 80−102275
management, US DOE program, role of the Materials Review Board 80−102274
management, US DOE waste management program 80−95375
management, US NBS proposals for measurement standards 80−102276
management alternatives 77−46367
management alternatives for low-level waste using decision tree analysis 80−99259
management and disposal methods and policies 79−93757
management and environmental impact 77−86897
management and storage, review 80−5315
management at Point Lepreau nuclear power station 78−29600
management in $(U,Pu)O_2$ FBR fuel cycle 80−47682
management in Belgium *(French)* 79−26607
management in Canada, bibliography 79−6755
management in West Germany 79−31073
management of high-level waste, French research program for solidification and disposal in borosilicate glass 80−95377
management of irradiated fuel pond at Trawsfynydd power station 80−23072
management of low-level radioactive wastes in Illinois 80−99256
management of low-level radwaste, book 79−54568
management of nuclear industry waste, solidification, storage, dispersal control 77−10469
management of nuclear waste, storage, disposal, safety 77−65291
management of U mining and milling waste, N.Australia 79−31076
management practices in Federal Republic of Germany 80−23068
management practices in selected European countries 80−37471
management scheme involving actinide transmutation 79−26611
management schemes, criteria for assessing societal, moral and political implications 78−13270
management systems, engineering and operational principles 79−54576
management systems for reactor waste, economic considerations 79−54575
management technology, present European situation 80−106131
marine cephalopods, radioactive trace elements obs. 80−94379
material security, near-real-time accounting of strategic nuclear materials 79−85755
materials accountability, U and P NDA of crated waste by gamma-ray and neutron coincidence counting 80−83166
medical electron linear accelerator, radioactive and toxic gas production 80−94378
medium active waste, chem. treatment prior to evaporation 77−54327
medium-level, expts. on treatment, bituminisation 77−61563
medium-level, from power plants, cementation and bituminisation methods of solidification 77−65313
medium-level, from PWR, direct bituminisation technique *(French)* 77−61562
medium-level, incorporation into heat-hardened resins *(French)* 77−61566
medium-level, ion exchange resins from power plants, bituminisation and cementation 77−61565
medium-level, sedimentation method of bituminisation, thermogravimetric characts. of products 77−61561
medium-level and low-level, incorporation in polymer impregnated cement 77−61564
membrane filter appl. for crud separation in LWR waste water 80−23080
metal surface chemical decontamination 80−37530
metallic surfaces, radioactive waste electrodecontamination using a basic electrolyte 80−37529
metallic waste, decontamination by smelting 80−13741
methyl iodide, removal using Ag-alumina 79−85638
methyl iodide removal by Ag impregnated Al and zeolite 78−53719
methylradioiodide, catalytic trapping by beds of impregnated charcoal 78−21681
microbial prod. of tritiated and ^{14}C methane from radioactive waste 80−45868
migration velocities determ. from partitions coeffs. 80−37525

radioactive waste continued
Minch waters and sediments, Windscale effluent 77−91158
mobile radwaste processing systems, logistical advantages 80−18555
monazites, nuclear waste, synthesis, ideal actinide hosts for geologic disposal 79−22406
monitoring nuclear plants discharges, state of art *(German)* 77−42174
multistage counter current extraction with HDEHP, rare earth distrib. ratios calc. 79−49705
national waste terminal storage program waste packaging criteria 78−708
natural fission reactors, at Oklo (Gabon), origin hypotheses *(Dutch)* 78−33261
natural salt repositories, thermomigration of brine inclusions in NaCl single crystals 80−99251
neutron dosimetry characterization of spent thermal reactor fuel assemblies, using nondestructive methods 80−23164
neutron shield material tests 80−37543
neutron source intensity in random absorption medium *(French)* 80−74057
Nevada Nuclear Waste Storage Investigations, site evaluation activity 80−37489
new waste calcining facility, radiation shield integrity testing 80−13940
New Waste Calcining Facility process filter remote handling 79−9820
nitrate solutions, highly active, precipitation of Mo compounds during evaporation 78−37426
noble gases removal from contaminated gas streams in Japan, cryogenic distillation process 77−61538
non-fuel bearing components, engineered transport and burial system 77−61580
nondestructive analysis applications in the nuclear industry 80−13706
nonstationary heat processes in spent nuclear fuel element containers *(Bulgarian)* 80−69637
NRC high-level waste management program 80−13709
NRX and process effluents, gamma ray spectrometric anal. 78−29656
nuclear and fossil power plants effluent environmental impact comparison 78−96290
nuclear energy, technical economic and safety aspects *(Hungarian)* 78−82465
nuclear energy and the environment 77−50304
nuclear energy synergetics, characts. of integrated systems 79−13382
nuclear facilities, effluent monitoring, sampling and measurement principles *(French)* 78−89996
nuclear fuel burnup determination using Aragonic γ detector 80−63262
nuclear fuel centre, fuel and waste facilities, safety, protection and socioeconomic aspects 78−58395
nuclear fuel cycle *(Japanese)* 79−9766
nuclear fuel cycle environmental assessment methodology 78−94112
nuclear fuel fabrication, low level radioactive waste solns. containing NH_4NO_3, spray tower treatment *(German)* 79−93798
nuclear fuel reprocessing, radioactive waste elimination by nuclear transmutation *(Spanish)* 80−5298
nuclear fuel reprocessing and waste disposal, public issues 77−46375
nuclear fuel reprocessing in West Germany, case against suspension *(German)* 80−32418
nuclear fuel reprocessing technology status, large plants 78−21735
nuclear fuel waste, deep underground disposal, Canadian programme 79−22423
nuclear fuelled electric power supplies, radioactive waste handling *(Spanish)* 77−67821
nuclear fusion reactor materials, social aspects *(Dutch)* 80−106153
nuclear generating station, waste disposal and licensing *(German)* 80−99222
nuclear installations, ambient radioactivity, standards rel. to dose and radioactive waste limits *(Spanish)* 80−52789
nuclear material accounting, decision anal. 79−81049
nuclear material disposal planning and difficulties *(German)* 78−86630
nuclear materials, actinide determ. review of procedures at Rockwell Hanford Operations 79−81050
nuclear materials, nondestructive neutron assay for accountability and criticality control 80−66759
nuclear materials safeguards and materials control, meas. tech. conf. Charleston, SC. USA (November 1979) 80−77544
nuclear plant airborne effluent variable-trajectory puff advection model modifications 78−94149
nuclear plant and lab. operations, radiation protection and waste handling 77−65338
nuclear power, effect on the environment, general radiation level and waste product disposal 79−18051
nuclear power, radioactive waste management 79−9763
nuclear power plant chronic aq. releases, calc. rel. to meas. doses 79−54605
nuclear power plant laundry drain treatment system development 79−9788
nuclear power plant licensing procedures in the UK 80−27708
nuclear power plant radioactive waste water treatment by flocculation precipitation process 79−93797
nuclear power programme radioactive waste management 78−13258
nuclear power station, environmental protection methods *(Hungarian)* 79−88008
nuclear power station, radioactive waste management 77−74974
nuclear power station accidental activity release, effect of meteorological parameters 80−17142
nuclear power station decontamination, chelating agent appl., aspects 78−50280
nuclear power station effluent analysis methods for environmental monitoring 79−13556
nuclear power station stack effluents, radiation monitoring 78−46179
nuclear power stations, contamination prevention methods *(Hungarian)* 79−88007
nuclear power stations, disposal problem 77−363
nuclear power stations, fuel circuit review, radioactive conditioned waste final storage *(German)* 80−799
nuclear power stations, licensing procedure, public participation under Atomic Energy Act *(German)* 80−102256
nuclear power stations, waste management principles modifications *(German)* 80−102255
nuclear power stations prospects, w.r.t. environmental problems *(Hungarian)* 80−13742
nuclear power waste management problem *(German)* 79−13499
nuclear reactor gaseous effluents reprocessing, radionuclide management 79−76078
radioactive waste continued
nuclear reactor waste disposal rel. to fuel reprocessing 77−67853
nuclear reactors, decommissioning, main problems 80−676
nuclear safety in France, reactors, waste, and fuel cycle installations 79−71908
nuclear spent fuel shipping cask licensing 80−37545
nuclear spent fuel storage for Pacific Basin nations 78−86659
nuclear spent fuel use as radiation processing source 77−57729
nuclear spent fuel valuation, procedure appls. and analysis 80−738
nuclear transmutation of actinides, potential method for radioactive waste disposal 78−66428
nuclear waste constituents, stabilisation in Portland cement 80−13630
nuclear waste disposal, geological aspects 79−9759
nuclear waste disposal problems, present and future trends 78−66350
nuclear waste disposal R & D programmes by OECD countries 78−41823
nuclear waste incineration for destroying actinides, costs and risks 78−41825
nuclear waste isolation plant design studies in USA 78−46151
nuclear waste management, R and D concept, in W.Germany 77−61509
nuclear waste management problem, R&D efforts 78−4991
nuclear waste management research, UKAEA programme for Iran 78−4992
nuclear waste management safety assessment, use of safety indices 79−89413
nuclear water solutions, radioactive ion removal by electrodialysis 79−36338
ocean dumping of high level waste 80−32376
off-shore discharge, safety aspects *(French)* 77−18678
Oklo phenomenon, isotopic abundances, long-term radioactive waste storage information 80−52769
on-site facilities for processing and disposal 80−23095
on-site management, Canada 80−23069
on-site management at power reactors, India 80−23070
Ontario Hydro nuclear power plant stack effluent monitoring 79−3254
organic alpha waste, vol. reduction by pyrohydrolysis 80−5273
origin in power plants, average yearly quantities for LWRs 80−23067
ORNL interface and logistics studies 80−37540
oxyanions, in nuclear waste materials, laser Raman spectrometric determ. 78−35743
packaged, Ci content determ. from meas. exposure rate 77−6566
packaging containers, a survey 80−23097
packaging techniques, evolution in France *(French)* 80−23098
particle accelerator decommissioning, radioactive waste management 80−18720
particulates in gaseous effluents at nuclear fuel reprocessing facility 79−9848
partitioning, separation of transplutonium and rare earth elements 79−97881
partitioning of high level waste from fuel reprocessing *(Japanese)* 79−81019
pathway anal., RAMM computer programs 77−13015
Peach Bottom power station radwaste system backfit considerations 80−9351
Perch Lake Basin, Ontario, hydrological and geochemical studies conference, Chalk River, 1978 April 25 to 26 80−51955
permanent home search discussion 77−42113
personnel exposure minimisation at waste calcining factory 77−50312
Phenix fast breeder reactor fuel dismantling hot cell 77−50274
Phenix LMFBR, radioactive effluent release, operating team irrad. results *(French)* 79−31163
phosphate vitrification of liquid waste, KS-KT-100 plant *(Russian)* 77−61552
poisoned fuel rods, treatment on-site, France *(French)* 80−47674
polymeric solidification of low level radioactive waste, Dow process 80−37502
pool systems for spent-fuel interim storage facilities 80−5283
population doses from reactor operation, compliance with appendix I 77−46410
population radiation exposure, radioactive effluent from nuclear facilities in West Germany 79−26781
Port Granby radioactive waste storage site leakage into Lake Ontario, water quality obs. 80−97829
portable vol. reduction and solidification system 80−37515
post-LWR wastes, management alternatives 77−61536
pot vitrification of fully radioactive fuel reprocessing wastes 77−61547
processing, health physics implications 79−57727
processing, management and storage, INFCE report summary *(Dutch)* 80−52750
processing, volume reduction of organic alpha waste by pyrohydrolysis 80−95366
processing and encapsulation techniques, France *(French)* 80−47675
processing of high-level waste, consequences of separation of long-lived α-emitters *(Czech)* 80−5251
processing radioactive waste solution with zeolites, thermal transform. of Na, Cs, Sr type zeolites 77−10477
processing with zeolites, acid resistance, leachability of Cs and Sr *(Japanese)* 77−67828
programme in W.Germany *(German)* 78−8954
protective clothing, dry cleaning versus water wash 80−13691
public acceptance of a low-level waste burial facility 80−95382
public issues concerned with disposal 77−33822
public radiation exposure, optimisation, problems 80−47768
pulsating solvent extraction columns, computation and simulation methods 79−97882
Purex reprocessing plant, chemical separation of actinides from aqueous high level waste 77−26862
Purex solvent extracting system, monitoring and control instrumentation 80−37566
Purex solvent extraction process for treatment of gaseous and liquid waste 79−36387
PWR, CANDU, operation, status and prospects of nuclear power in Canada 78−86664
PWR, Oconee, occupational exposures, radiation levels and waste levels during operation 78−21726
PWR, Point Beach Nuclear Plant, spent fuel storage modification 79−30974
PWR, startup, secondary-side corrosion product transport 80−9377
PWR, two-unit, modification feasibility for radwaste volume reduction equipment 78−17395
PWR and BWR systems and fuel cycle in USA 79−26687

radioactive waste continued
PWR coolant pH effect on radiation field buildup 80−23060
PWR decommissioning, public radiation exposure 80−42800
PWR dismantling, management of radioactive waste 80−27756
PWR fuel storage pool, safety calcs. and benchmarking 79−26565
PWR liquid waste management 80−52758
PWR radwaste systems design, factoring operating experience 78−17390
PWR spent fuel calcs., neutron multiplication and shielding problems 77−74951
PWR spent fuel storage pools, graphic method for neutron multiplication factor comparison 79−26566
PWR spent-fuel shipping, neutron multiplication and shielding 77−46418
PWR/BWR power stations, waste-water treatment plants, engineering experience 77−6543
radiation exposure of UK population, review 79−62373
radiation protection features of waste calcining facility 80−5377
radio-nuclide transport in soil, conc. profile in groundwater, waste storage problems *(German)* 79−74556
radioactive, programme in Switzerland *(German)* 78−8953
radioactive acid digestion test unit, nonradioactive startup operations 79−49717
radioactive emission meas. and control *(German)* 77−79484
radioactive fuel and waste, review of treatment handling, storage and disposal *(Italian)* 79−63753
radioactive reprocessing, comprehensive system of major hazard control 80−818
radioactive waste source terms, calc. using computer code 79−54569
radioactive waste storage, integrated biological dose evaluation 80−5379
radioactivity in stored coal ash and in nuclear power waste 79−89417
radiochromatographic gas purification equipment, adsorptive capacity of activated C for inert gases 77−52673
radioisotope-powered photovoltaic generator 79−22495
radiological aspects of the design of a facility to solidify radioactive sludge 80−5378
radiological implications of Pu recycling in HTGR fuels 80−68777
radiological protection criteria for disposal 80−47780
radionuclide adsorption by manganese oxides and implications for radioactive waste disposal 78−69349
radionuclide chain migration in groundwater 78−85616
radionuclide conc. rel. to residence time in marine sediments near Maine Nuclear Power Reactor 78−49021
radionuclide disposal, GARD computer program for geochemical assessment 79−31068
radionuclide geospheric transport eqn., boundary conditions 80−47611
radionuclide migration at US ERDA Nevada test site 77−57752
radionuclide migration from buried radioactive waste 80−95484
radionuclide migration from repository sites, stochastic anal. 80−37486
radionuclide migration in seawater and marine sediments *(French)* 78−11916
radionuclide migration resulting from site intrusion 80−13701
radionuclide transfer in terrestrial animals 78−24152
radionuclide transfer to crops and agricultural products *(French)* 78−8996
radionuclide transport through heterogeneous media 80−32382
radwaste concentrator at Millstone Unit 1, decontamination and repair experience 80−13693
radwaste evaporator improvement 80−91232
rare gas separation, using cell with two membranse of differing permeability 78−29590
rare gas separation by membrane permeation, improvement in separation factor 80−18559
rare gases, separation perform. of two-unit series-type separation cell 79−41008
reactor airborne plume deposition estimation model evaluation 78−94148
reactor cladding waste, spent fuel contamination, composition and amounts arising in EC 78−66360
reactor decommissioning, radioactivity limits for release of liquid radwaste, math. model 80−13737
reactor effluent, radionuclide accumulation by oysters, math. model 77−81589
reactor fuel cycles and proliferation, resource conservation and waste management *(German)* 79−13500
reactor fuel element storage and transportation 80−13707
reactor near-stack dose calc., diffusion model applicability 78−94147
reactor spent fuel storage vault, criticality safety determ. *(Korean)* 80−37478
reactor unplanned release meas. and countermeasures 78−89994
reactor waste, storage, reprocessing and disposal, book 79−63780
reactor waste air plumes, diffusion in atmosphere 77−53183
reactor waste disposal in geological form., long term risk assessment 78−58387
reactor waste glasses, reaction with water and soda lime, ^{15}N H profiling method 79−54519
recycle nitric acid, trace contaminants removal 79−85733
recycling, prospects 77−71657
release into environment management, dose limitation system 77−14272
remote handling, history at Los Alamos 80−78417
repository in geologic primation 79−49713
repository siting, socioeconomic impacts, environmental decision making 79−49715
reprocessing, solidification vitrification of liquid waste, review 79−9762
reprocessing and disposal, ecological problems solution *(German)* 77−54344
reprocessing nuclear fuels, waste storage, nuclear burning and types of reactor *(French)* 80−91235
reprocessing of irradiated fuels, French and European policies *(French)* 80−809
reprocessing philosophy, German waste management *(German)* 79−54565
reprocessing plant off-gas, abatement techniques, control of ^{128}I, ^{85}Kr, ^{14}C, T 79−3221
reprocessing plants, Purex-type, schematic flowsheet comparison *(German)* 80−57936
reprocessing solvents, decontamination and clean-up process 80−5254
research programmes for radioactive waste management 77−67824
residual activity levels allowing radioactive waste to be considered inactive 80−13735
resuspended radioisotopes, possible importance of short-term exposure 80−85501
radioactive waste continued
resuspension models, chronic releases of radionuclides to atmosphere 80−16871
resuspension models, factors determining amount of material resuspended 80−16872
reusable frame greenhouse, waste generation reduction 77−46409
review of energy resources, reactor accidents, radioactive waste disposal 78−50413
review of nuclear fuel cycles and waste management 78−54863
risk anal. of high-level waste management systems in Germany 78−50272
risk anal. of transport using Monte Carlo and probability methods *(Norwegian)* 79−13437
risk analysis for management system, safe design 78−17351
risk assessment for potential accidental releases from nuclear fuel cycle operations 78−17353
risk estimation, evaluation, and management 78−17350
risk evaluation model, on-site meteorological data, environmental consequences 80−36155
risk evaluation of high level waste solidification plant 78−50273
River Danube, radioactive pollution meas. 1972 to 1975 by γ-spectrometric anal. *(Bulgarian)* 79−88019
rock salt storage, γ-radiation effects *(Dutch)* 77−88232
Rocky Flats waste packaging 77−6536
safe nuclear waste disposal route, Swedish utilities design 78−41827
safe transportation, using type A, exempt and LSA packages 80−63401
safeguards planning in plant design process 78−82423
safety assessment of radioactive waste disposal into salt deposits, fault tree anal. appl. 78−55046
safety criteria for LWRs 80−18472
salt formation, high radioactive waste disposal *(German)* 79−54566
salt mine waste disposal, experience in West Germany 78−41828
Sandia solidification process for high level aqueous wastes 77−61551
sea disposal of low level radioactive waste, preparations *(Japanese)* 79−9768
sediment-bound, absorpt. through digestive tract of marine demersal fish 79−92400
seismic design considerations for deep geologic repositories 80−23019
shale fracturing for radioactive waste disposal at ORNL 77−88251
shale investigation as radioactive waste repository, vermiculite role 80−32354
shallow earth burial stabilisation, natural loose rock as biobarrier to prevent waste transportation 80−95385
shallow land disposal of low-level radioactive waste, radionuclide sorption 80−16851
SHIELD computational system, nucl. fuel cycle appl. 80−37517
shipping cask criticality safety, SCALE system, correl. with expt. 79−63775
simulated high level radioactive wastes in borosilicate glasses, characterisation *(Japanese)* 79−93745
simulation of high level liquid waste evaporation and storage 80−37476
site selection and equipment planning for radioactive waste disposal at Gorleben *(German)* 80−68855
site selection criteria development and appl. 80−37484
siting, geologic studies of Paradox Basin 80−37485
slagging pyrolysis incinerator, off gas treatment system 80−37514
sludge dehydration using Funda filter *(Japanese)* 77−88234
sludge removal demonstration from Savannah River storage tank 80−73958
sludge sample collection system at Savannah River 80−73959
SNR spent fuel element storage tank *(French)* 79−97884
social and technical problems of nuclear waste disposal 79−39528
society effects of nuclear power developments 80−47590
sodium reactor experiment decommissioning, radiation protection 80−9432
soil affixants, effect on germination, emergence, growth of cheatgrass, Russian thistle 79−2140
soil interactions, radionuclide migration 80−42801
sol-gel technology for waste fixation 80−83207
solid, impact resistance test program 80−37521
solid combustible waste, Pu recovery 80−5274
solid high-level waste, evaluation of radiation stability 80−102278
solid neutron shield development, materials eval. for spent fuel shipping cask 80−13939
solid radwaste, current concerns, treatment system design changes 80−5258
solid radwaste combustion, development of wire cloth filter for flue gas scrubbing 79−71919
solid radwaste system utilizing cement 80−5260
solidifed high level wastes, storage in stainless steel bins, corrosion meas. 77−6535
solidification, anal. of concentrating and drying processes in thin-film evaporator 79−59215
solidification, composition, structure and properties of final product obs. *(Czech)* 78−66353
solidification, spray calcination system 79−59212
solidification facility for high heat SRP waste 80−73960
solidification in concrete, polymer impregnation 77−6537
solidification of evaporator concentrates by hydraulic binding agents *(French)* 80−23088
solidification of fission product solns. using a drum drier, FIPS method 77−61548
solidification of high level wastes at Karlsruhe nuclear research centre 77−61545
solidification of high-level radwaste, production facility 80−83201
solidification of highly active liquid wastes *(Korean)* 80−52759
solidification of waste water concentrates using a roller drier 80−23089
solidification process using vinyl ester resin with improved free-water and leachability characts. 80−99265
solidification products, radiolysis gases generation, mass spectrometric anal. 79−85626
solidification system, Dow, state-of-the-art 80−5259
solidification to phosphate glass-metal matrix blocks 77−61550
solidification using urea-formaldehyde resins, technical eval. 79−67875
solidified, assessment of loss of isotopes 79−54541
solidified, leach testing, background 80−42809
solidified, radionuclide migration in aerated zones, ^{90}Sr leaching from cement *(Japanese)* 77−42109
solidified low-level forms, leachability 79−85631
solution concentrator equipment for criticality safety 80−18432
solvent wash process to minimise radioactive waste volume 77−18681

radioactive waste continued
sorption of ^{106}Ru and ^{59}Fe on natural sorbents *(Russian)* 77−38370
sorption of technetium and iodine radioisotopes by various minerals 79−49721
Soviet disaster 1957-8, explosion of stored nucl. waste, causes 80−22974
Soviet nuclear disaster, 1957-8, radioactive waste origin 80−45823
space disposal of nucl. waste, waste mixes and forms 80−37534
spectrum in stellar spectra, means of detecting extraterrestrial civilisations 80−82230
spent fuel, bremsstrahlung spectra and average energies, analytic calc. method 80−22985
spent fuel, neutron interrogation 80−5307
spent fuel bundle counters for CANDU reactors, appl. of safeguards design principles 80−63347
spent fuel disposal in Germany *(German, English)* 79−9771
spent fuel elements storage in large pools, seismic load anal. 78−17400
spent fuel heatup following loss of water during storage 80−83205
spent fuel integrity in water pool storage 79−30976
spent fuel overheating in pool drainage accident, protection 79−85639
spent fuel pool natural convection, multichannel analysis 79−9786
spent fuel pools, regulatory aspects of structural evaluation for high-density storage 78−21727
spent fuel shipping casks, R and D sea going vessel requirements 79−31083
spent fuel shipping systems, full scale tests in extremely severe accident environments 79−26582
spent fuel storage, away-from-reactor facilities, Tennessee Valley Authority studies 80−18496
spent fuel storage, away-from-reactor storage basin design 80−22994
spent fuel storage, high-density, economic evaluation of alternatives 78−21732
spent fuel storage, remote underwater rack removal and installation 78−21729
spent fuel storage, requirements for away-from-reactor facility 80−22993
spent fuel storage, structural design problems with backfitting fuel racks to existing pools 78−21728
spent fuel storage, supercriticality through optimum moderation 80−57896
spent fuel storage, thermal anal. of metal-encapsulated fuel 79−36359
spent fuel storage, US licensing and regulation 80−23039
spent fuel storage, use of poisoned racks at Point Beach 80−23038
spent fuel storage 78−714
spent fuel storage and disposal and plant building and operating legislature *(German)* 80−99223
spent fuel storage and transportation, operators experience 80−23037
spent fuel storage at independent installations, comparative risk assessment of external source damage 80−23041
spent fuel storage at independent installations, licensing considerations 80−23042
spent fuel storage basins 78−725
spent fuel storage expansion, planning, site preparation, installation considerations 79−45381
spent fuel storage expansion planning, site preparation, and installation 79−9819
spent fuel storage facilities, design and operational charact. 79−36355
spent fuel storage facilities, methods of criticality anal. 79−63777
spent fuel storage in USA 78−713
spent fuel storage in water pools, technology assessment 79−36357
spent fuel storage optimisation 77−42129
spent fuel storage pool reracking, licensing experience at Trojan 80−23040
spent fuel storage pools, behaviour of B_4C reactor materials 80−42771
spent fuel storage racks, decontamination and disposal 78−21731
spent fuel storage racks, design, safety calcs. and benchmarking 79−22416
spent fuel subassemblies, nondestructive assay, comparison of calcs. and meas. 80−78421
spent fuel transportation, commercial experience in US 80−63310
spent fuel transportation, effect of AFR storage location 80−18497
spent fuel transportation logistics 79−89416
spent fuel transportation R and D in ERDA 78−710
spent fuel verification by gamma-ray spectroscopy for materials safeguards 80−78422
spent fuel waste products, delayed neutron nondestructive assay instrumentation, Monte Carlo calculational design 80−81271
spent fuel zero leakage storage pool design 77−42139
spent LWR fuel storage in Pacific Basin at Palmyra Island, decision making methods 80−27763
spent multicomponent fuel mixtures, comp. anal. by delayed-neutron decay 79−71899
spent nuclear fuel, long term storage, United States' scheme 79−45355
spent nuclear fuel, storage alternatives 78−74456
spent nuclear fuel elements, intermediary storage, stationary temp. level determ. calc. method 80−91223
spent nuclear fuel inventory confirmation technique using Cherenkov light intensity meas. 80−78419
spent nuclear fuel shipment, appl. of ALARA principles 80−37541
spent nuclear fuel shipping cask containment and accident impact limiters 77−46314
spent nuclear fuel storage in HI-CAP high-capacity fuel rack, design considerations 78−17349
spent nuclear fuel stored in basalt, chances of reintroduction into biosphere, analysis 80−106144
spent nuclear fuel transport problems *(Russian)* 79−31084
spent nuclear fuel transportation by barge and rail, risk anal. 80−18498
spent reactor fuel, risk analysis of alternatives from reactor pool until final disposal 78−17355
spent reactor fuel pool sizing, maximisation methods, cost comparisons 79−67915
spent-fuel assembly inspection plant 80−5285
spent-fuel rail cask system, high-speed impact and fire test 79−59206
spent-fuel shipping casks, Monte Carlo radiative heat transfer 79−59193
spent-fuel storage, time-integrated toxicity index 79−59203
spent-fuel storage, utility perspective 79−63794
spent-fuel storage facilities, capabilities for processing shipping casks 79−59199
spent-fuel storage program, US Dept. of Energy 79−63778
spent-fuel transportation required to implement the DOE spent-fuel policy 80−22995
steel waste form containers, corrosion 80−18493
storage, Am sorption on major rock-forming minerals 80−13716
radioactive waste continued
storage, control of stress corrosion cracking in carbon steel storage tanks 79−70226
storage, in situ instrumentation for meas. of radionuclide migration 80−95485
storage, interaction of actinides and humic acid 80−13715
storage, long term subsurface migration of radionuclides 80−95483
storage, materials considerations 77−6533
storage, migration of ^{137}Cs in Magenta dolomite by aquifer 80−13718
storage, mineral-contributed anion effects on the retention of trivalent actinides in the environment 80−13717
storage, problems and cost in W.Germany *(German)* 77−79452
storage, Pu oxidation by radiation, effect on migration rate 80−13714
storage, radionuclide migration determ., adsorption of Cs(I), Sr(II), Eu(III), Co(II), and Cd(II) by Al_2O_3 80−99240
storage, rock salt structure design *(Dutch)* 79−30953
storage, soil homogeneity evaluation by radionuclide tracer breakthrough curve interpretation 80−97821
storage, thermodynamics of free-convection air-cooled storages 80−5282
storage and disposal, development in Hungary *(Hungarian)* 78−13249
storage and disposal prospects, US policy prediction 79−49792
storage and shipment of spent fuel elements INFCE Working Group 6 *(German)* 80−102257
storage facility, radiological safety assessment 79−17995
storage glass properties, improvements, R&D in United Kingdom 79−59181
storage in crystalline rock, temp. distrib. calc. *(German)* 78−86631
storage in geological formations, studies in Switzerland *(German)* 77−13014
storage in monitored containers in a controlled underground tunnel environment 79−97820
storage in salt domes, conceptual design 80−106143
storage of fissile materials, use of neutron absorber for enhanced criticality safety 80−13609
storage of spent fuel elements in steel canisters, air cooling *(German)* 80−57867
storage of spent nuclear fuel, design studies, cost estimates 78−29615
storage on open-air bed at CAMEN in concrete containers *(Italian)* 80−78401
storage study, groundwater vel. estimation 80−82111
storage time evaluation for active solid waste produced in hospitals 80−26333
subsurface migration studies at Radioactive Waste Management Complex, Idaho 80−42805
subsurface nuclear waste disposal, groundwater modelling 80−16852
subsurface storage of commercial spent nuclear fuel 79−36356
subterranean gamma-ray in situ spectroscopy 77−57806
surveillance instrumentation, spent-fuel safeguards 79−85679
SYNROC-B ceramic for radwaste disposal, feasibility of subsolidus sintering 80−83198
synthetic mineral nuclear waste ceramics 80−42813
T immobilisation, possible solid mats. 80−27755
Tarapur Atomic Power Station radioactive waste discharge monitoring 78−89989
technology assessment and nuclear waste management 79−89392
temporary confinement structures, design criteria and guidelines 80−18683
thermal analysis of irradiated nuclear fuel transport flasks 80−5281
thermal reactor fuel cycles, actinide wastes toxicity limitations *(German)* 80−99220
thermal reactor stations in USSR, fuel reprocessing and waste disposal *(Russian)* 79−26592
THTR fuel reprocessing Pu and Np separation from aqueous soln. *(German)* 77−83067
time-tested underground structures suitable for isolating low-level waste 80−95383
toxicity reduction in Augean fusion reactor 80−106175
trace element analysis of radiological effluents from coal-burning power plants 80−21426
trace radionuclides in soil, L X-ray meas. using Si(Li)-NaI spectrometer 80−58020
trans Cm isotope build-up in thermal reactors 79−85709
transceramic, from nuclear power plants, storage vessels and methods *(Dutch)* 80−68845
transmutation of by-product actinides to reduce high-level radwaste storage times 80−95384
transmutation of fission product waste using DT neutrons 80−32383
transmutation of waste actinides in thermal reactors 80−18491
transplutonium element buildup and possible nuclear incineration 77−26856
transplutonium element separation with phosphororganic extractants 77−26854
transplutonium element symposium, Baden-Baden, Germany (September 1975) 77−28974
transport model for radionuclides through geologic media 80−786
transport of nuclear material, especially nuclear fuel *(German)* 78−25314
transport package design, criticality evaluation, appl. of SCALE system 79−63774
transport to reprocessing plant and final storage *(German)* 77−34403
transportation, DOE transportation technology centre 80−37537
transportation, new SF, HLW and CW shipping systems 79−59205
transportation, ORNL Nuclear Legislative Data Base program 80−37539
transportation, safety requirements 77−74956
transportation and burial of radioactive wastes 79−54574
transportation containers, struct. technology programs 78−707
transportation in Japan 78−86658
transportation in urban areas, radiological, nonradiological and economic environmental impact 80−18473
transportation of commercial low-level radwaste 80−99258
transportation of irradiated fuels and Pu, regulations *(French)* 79−26777
transportation of nuclear waste material, risk analysis 78−17357
transportation of radioactive materials, safety anal. 79−63814
transportation regulations 78−709
transportation SABRE II combat simulation model 80−37542
transportation security by railroad cask 77−74948
transportation status at fuel cycle end 78−712
transuranic analysis requirements, suitability of current and methods 79−96400

radioactive waste continued
transuranic element separation from radioactive waste and fuel reprocessing *(French)* 79−85811
transuranic elements, long term hazards, removal requirements *(French)* 77−26848
transuranic mobility in agricultural ecosystem 79−96668
transuranic nuclear waste management, evaluation of alternatives 80−18490
transuranic nuclide migration in earthen burial trenches at Savannah River Plant 80−42804
transuranic transport from environment to man modelling 79−96669
transuranic waste, retrieval of buried wastes and long-term management 79−49719
transuranic waste assay, low-level, Monte Carl calcs. of ^{3}He detector design 79−54542
transuranic waste assay instrumentation, Los Alamos Scientific Laboratory developments 79−85692
transuranic waste degradation under WIPP conditions 80−37526
transuranic waste disposal classification system 79−93763
transuranic wastes, interaction with soils 79−96488
transuranics, plant uptake, techniques for long term field studies 79−57821
transuranium and other radionuclides, conc. and distribs. in nuclear power plant environs 79−93841
transuranium concentration in solid waste from commercial power reaction 79−71929
transuranium elements, resuspension from contaminated surfaces 79−62376
transuranium processing plant, chem. process engng. 77−54338
transuranium processing plant, remote processing practices, equipment changing and modification facilities 77−54339
transuranium radionuclides in the foodchains 79−74554
treatment, handling, characterisation at Winfrith SGHWR 80−23076
treatment and burial, co-operation between member states of CMEA 77−61537
treatment and disposal *(French)* 80−99221
treatment and disposal methods *(German)* 80−57868
treatment and storage, review *(German, English)* 77−61517
treatment and storage, use of ceramic encapsulation process, based on powder metallurgy *(German)* 78−33281
treatment and storage problems *(French)* 77−23227
treatment at Czechoslovak nuclear power station 80−23077
treatment experience at Atucha, Argentina 80−23075
treatment experiences, Tarapur, India 80−23078
treatment prospects for ENEL's reference power station 80−23071
treatment system for low- and intermediate-level liquid radioactive wastes at CAMEN *(Italian)* 79−30952
treatment techniques for CANDU power stations 80−23085
trench leachates, low-level radioactive waste disposal sites, organic carbon content 80−17145
tritiated, gas generation by autoradiolysis 80−32384
tritiated waste materials, gas generation by self-radiolysis, container suitability 79−26579
tritiated water, fixation in silica gel, zeolite, leaching in cement 79−97851
tritium activity meas., in exhaust gases from nuclear power stations *(German)* 77−25322
Trombay nuclear facilities, effluent release monitoring procedures 78−89993
Trombay operational experience and developments and waste management 77−61539
Tsuruga power station anal. of corrosion products 80−23062
Tsuruga power station radioactive waste treatment system *(Japanese)* 78−74442
turbulent atmospheric transport, Monte Carlo simulation, radioactive pollution appl. 78−61550
UK nuclear power station radioactive effluent monitoring and public information 78−89992
UK standards and procedures 79−81032
underground disposal, solutes movement through aqueous fissures in porous rocks 80−94553
underground high level radioactive waste disposal 79−9760
underground nuclear waste repositories, risk assessment using reliability models 80−57898
underground repository, geotechnical assessment, hydrogeology, rock mechanics 79−26590
underground repository, summary of study feasibility 79−26591
underground repositroy of high-level radwaste, water intrusion scenario studies, anal. and re-eval. 80−73950
underground solidified high-level radioactive waste retrieval system development 79−9818
underground waste repository, design and operation 79−26589
underwater solution to nuclear fuel storage problem 80−86963
Urazoko Bay, ^{239}Pu, ^{137}Cs and ^{60}Co distrib. and behaviour 80−97825
US Nucl. Regulatory Commission high level waste management repository assessment methods and anal. 80−37497
US nuclear fuel cycle, review 79−54585
USA, comparison of military and civilian inventories 78−4995
USA Energy R&D Administration effluent date collection and reporting system 79−13545
USA Energy R&D Administration role in low-level waste management 78−94114
USA Environmental Protection Agency activities in radioactive waste management 78−94115
USA Geological Survey low-level radioactive waste burial site selection 78−94116
USA Nuclear Regulatory Commission low-level waste management programme 78−94113
utilisation, fertility value of gamma-irradiated sewage sludge 80−99243
utilisation, recovery of noble metals 80−99242
utilisation, sewage sludge treatment with gamma irradiation 80−102284
utilisation, sewage solids as supplemental feed for ruminants grazing rangeland forage 80−99244
utilisation of defence nuclear wastes as conservable resources 80−99241
vault, preliminary assessment of temp. distrib., model simulation 79−636
Vermont Yankee management system zero-liquid-release 80−13695
Vermont Yankee radwaste system 78−17391
vitreous matrices for high level Purex waste containment 77−360
vitrification, industrial scale plant, under construction in France 78−78478
vitrification, slurry feeding to an electric glass melter 80−18492
radioactive waste continued
vitrification, using microwave power, industrial process appl. 79−18008
vitrification for high level waste from LWR fuel 80−73961
vitrification for waste immobilisation 80−83199
vitrification of fission product soln. from spent fuel reprocessing *(German)* 80−73975
vitrification of fission product solutions at Marcoule [description and hot operation results] 80−5270
vitrification of highly active liquid waste, thermal decomp. of Harvest feed slurries 80−52757
vitrification system design 77−54340
vitrification techniques in France *(French)* 77−67835
vitrification using in-can melting process 80−83204
vitrification without precalcination, radionuclide behaviour *(Russian)* 77−61553
vitrified high level liquid waste, container design and specification 77−61541
vitrified high-level radioactive waste, associated hazards 78−13259
vitrified high-level radioactive waste, rail transportation, fault tree anal. and accidental release 78−17358
vitrified high-level waste, calcs. of radioactivity release due to leaching in final disposal 78−17360
vitrified waste, effects of post-devitrification leaching rel. to microstruct. 79−22417
volatile fission product atmospheric release from nuclear reactors and fuel reprocessing plants 79−34461
volatile fission products from nuclear fuel cycle and power stations, pollution effects *(Russian)* 79−31152
volume reduction and solidification of low level radioactive wastes 80−42794
volume reduction and solidification systems, economics 78−17396
volume reduction options, total cost sensitivity to fixed charge rate and inflation 80−99263
volume reduction techniques for radwaste management 80−23091
volumetric reduction techniques for low level waste 80−23045
WAK reprocessing plant, a design basis for large-scale reprocessing plant 80−5310
WAK reprocessing plant, chemical decontamination of highly active process cell 80−5312
Wase Isolation Performance Assessment Program 80−37496
waste air at nuclear plants, dose conversion factors for radiation exposure estimation *(German)* 77−70558
waste isolation Pilot Plant, deep geological nuclear waste disposal 80−5275
Waste Isolation Pilot Plant, retrieval methods and equipment 80−73962
Waste Isolation Pilot Plant, siting status 80−37488
waste isolation safety assessment methods, overview 80−37495
waste management, legal aspects 77−88229
waste management from nuclear fuels and power plants in Canada 79−26600
waste management in the Federal Republic of Germany. A survey of policy and research and development 79−26599
waste management policies, OECD countries 79−26596
water, low-level, ^{60}Co removal by ferric hydroxide coagulation-flocculation, improvement using diethyldithiocarbamate 78−37415
water pollution, computer anal. of relative potential hazards 80−21422
water pool spent fuel storage units, neutron anal., criticality state *(Spanish)* 80−32517
West German nuclear power plant airborne radioactive release control 79−13549
West German nuclear power plant liquid radioactive effluent control 79−13550
West German nuclear power plant liquid radioactive effluent monitoring 79−13554
Westinghouse high-density spent fuel rack design 78−727
Wylfa air-cooled dry store, design, operation, safety 80−57900
X-ray fluorescence anal. for solns. and slurries, feasibility study 79−81051
Zion Generating Station steam generator operating experience 79−9851
Zircaloy hulls, conversion to zirconate ion exchange materials for waste stabilisation 78−702
Zircaloy-4 spent fuel cladding, tensile props. and annealing charact. 79−22392
γ radiation dose rate calc. in building materials 79−18057
^{239,240}Pu(V) in alkaline freshwater pond, determ. by coprecipitation technique 80−71988
^{108}Ag^{m}, prod. in nuclear reactors by thermal neutron capture in stainless-steel structure 80−42747
Al liquid waste calcination using microwave technique 77−81594
Am, low conc. meas. in earth samples, appl. of Si(Li) X-ray detector 78−58505
Am release into estuarine-coastal sea ecosystem, assessment methodology 79−70471
Am retention by rock 77−71679
AmO_2-UO_2, target possibilities for waste incineration, simulation study 80−32419
^{241}Am sorption on USA subsoils from differing weathering intensity areas, ^{241}Am, ^{237}Np and ^{99}Tc 78−16014
^{37}Ar form. from Ca in fission reactors 77−83048
^{41}Ar, atmospheric turbulent transport Monte Carlo simulation and comparison with exptl. data 79−53479
C steel containers for nuclear process liquid waste, stress corrosion 77−46311
CANDU spent fuel, containment in concrete canisters, UO_2 oxidation 77−6539
CO, radioactive and stable, determ. in marine biological materials 80−36157
^{14}C activity and distrib. in gaseous effluents from PWRs 79−85829
^{14}C production and discharge in BWRs 79−52979
Co radioactive release from reactor cooling water, fixation by sandy soil *(Japanese)* 78−74443
^{60}Co contamination of freshwater food chains, direct water borne contamination of organisms *(French)* 79−20688
^{60}Co distribution in N_2O_4 condensate cooling circuit *(Russian)* 79−13491
^{60}Co, fixation on natural sorbents from phenol-polluted water 79−57506
^{60}Co, inhaled, long-term clearance 79−79663
^{60}Co ion removal in waste water by oxine impregnated activated charcoal 79−26558
^{60}Co leaching in cement composites 77−61508

radioactive waste continued
^{60}Co, migration by complexing agent ethylenediaminetetraacetic acid 79−20687
^{60}Co, radionuclide leaching from hardened cement grout, container dimension depend. 79−13439
^{60}Co removal from waste water, adsorption on activated charcoal with oxine 78−58365
Cs, A=134, 137, distrib. in Peach Bottom HTGR primary coolant circuit 78−13275
Cs, contamination in water, removal agent efficiencies *(Slovak)* 78−24319
Cs fraction encapsulation at Hanford 77−6534
Cs in basalt, migration velocities determ. from partitions coeffs. 80−37525
Cs volatilization from zeolites in radioactive waste soln. processing at high temp. *(Japanese)* 79−13441
$CsAlSiO_4$, and $CsAlSi_5O_{12}$, cryst. evap., mass spectral investig. 80−49353
$CsAlSiO_4$, prep. and X-ray characterisation 78−39728
$^{134}Cs/^{137}Cs$ activity ratio, spent fuel assembly 78−82487
^{137}Cs, 10 GeV proton spallation for transmutation of radioactive waste, calc. of transmutation number 80−13470
^{137}Cs accumulation and elimination by naturally contaminated wood ducks 77−66865
^{137}Cs, contents in coastal sediments 79−57974
^{137}Cs, coyote scats, Hanford Reservation, waste distrib. 79−25120
^{137}Cs, diffusion in bitumen block coating, radioactive waste treatment *(Russian)* 80−52771
^{137}Cs, distrib. in fuel elements of Peach Bottom HTGR 78−13274
^{137}Cs, fixation on natural sorbents from phenol-polluted water 79−57506
^{137}Cs immobilisation in cement-waste composites 78−82466
^{137}Cs leaching from ion-exchange resin incorporated in polyethylene or cement composite 77−65275
^{137}Cs, radionuclide leaching from hardened cement grout, container dimension depend. 79−13439
^{137}Cs, removal from nuclear power station liquid waste by zeolite 79−6749
^{137}Cs, seasonal cycling in reservoir 79−100881
^{137}Cs, separation from nucl. waste using sodium zirconate 80−27760
^{137}Cs, study of absorpt. by Lemna minor 80−30677
^{137}Cs, tilt-pour melt caster for encapsulation 79−26580
^{137}Cs transmutation in fussion reactor imploding liner blanket 78−17420
^{137}Cs, transmutation in high flux fission reactor, feasibility 79−85708
^{137}Cs, uptake by cotton rats inhabiting banks of liquid waste pond 79−25121
^{137}CsCl, use of $Cs_2O.Al_2O_3.4SiO_2$ (pollucite) for long term-storage 80−37467
H isotope removal from flowing Ar, U and Ce as hydriding materials 78−17438
H production from radioactive waste heat and utilisation in gas turbines 80−30326
^{3}H distribution between gas and liquid in isotope equilibrium in H_2O-H_2S and D_2O-D_2S systems 79−45376
I absorpt. on ion exchange resins in aqueous solns. 80−47610
I partition equilibrium between air and NaOH aq, effect of CO_2 conc. 78−78474
I radioactive isotopes, nuclear fuel cycle radiation safety problem, *(Russian)* 80−18560
I radioactive waste, solidification in conrete, leach rates 78−703
I, radioisotopes, environmental and biological effects from nuclear fuel cycle *(Russian)* 80−52768
I removal from fuel solns. as insoluble PdI_2 77−42164
^{129}I, dose to world population from nucl. power industry 80−47619
^{129}I in bovine thyroid glands, activation anal. obs. 80−94380
^{129}I, long-lived, immobilization by fixation of $Bn(IO_3)_2$ in Portland cement 79−59208
^{129}I radioisotope, fixation with Portland cement, radiation stability tests 80−83200
^{129}I storage, IO_3^- adsorption by hematite 80−22992
^{131}I in milk, rapid method of detect. 80−46106
^{131}I in nuclear power plant gaseous discharge, cumulative meas. *(Russian)* 79−3224
^{131}I, separation from water by ion exchange *(Japanese)* 77−60099
^{131}I waste in urine, filter system 77−60319
$^{131}I_2$ transport via pasture-cow-milk pathway, stat. anal., thyroid dose uncertainty 79−83950
Kr removal from contaminated gas streams in Japan, cryogenic distillation process 77−61538
^{85}Kr absorption in liquid CO_2 (KALC process), mass transfer efficiencies of packed columns 79−36354
^{85}Kr conc. determ. at high pressures using β-ray count, CaF_2 scintillation counter activated with Eu 78−13385
^{85}Kr entrapment in continuous-biased sputter-deposited glassy metals 80−24603
^{85}Kr immobilization, evaluation of methods 79−26578
^{85}Kr, pressurised cylinder storage tests 80−5269
^{85}Kr recovery system using cryogenic distillation 77−54331
^{85}Kr waste encapsulation, in amorphous alloy 80−47589
^{85}Kr waste management, strategy anal. 80−37531
^{85}Kr/Xe separation from nucl. engineering off-gases, low temp. distillation *(German, English)* 77−18671
^{54}Mg, removal from waste water by oxine-impregnated activated charcoal 80−9344
^{54}Mn distribution in N_2O_4 condensate cooling circuit *(Russian)* 79−13491
^{54}Mn radionuclide adsorption characts. in waste water on oxine-impregnated activated charcoal 79−89394
Na, contaminated, packaging and storage 80−18468
Na_2O-B_2O_3-SiO_2-MoO_3 glass containing high level radioactive waste, phase separation 80−25683
Np, environmental behaviour, chemical approaches 79−93765
^{237}Np migration potential 80−3537
^{237}Np, neutron activation anal., determ. of small amounts in solns. containing U, Pu and fission prod. 78−21682
^{237}Np, sorption on USA subsoils from differing weathering intensity areas 78−16014
Pb encapsulation of radioactive waste, risk assessment 80−99249
^{238,239,240}Pu, concs. in arthropods at a nuclear facility 80−30905
Pu and Am inventory of ecosystem near a nuclear facility 80−97820
Pu and trans-Pu element isotopes, accumulation and disposal 79−59187
radioactive waste continued
Pu and U extraction by reprocessing, methods and risks *(German)* 77−42157
Pu compounds 18B packagings for transportation 80−37544
Pu contaminated incinerator facility, decontamination and decommissioning 80−13987
Pu contaminated incinerator ash incorporated in cement, leach studies 80−37522
Pu contaminated soil, nondestructive anal. 79−11879
Pu contaminated solid waste streams, passive neutron assay 79−36373
Pu contamination assay using thermal neutron counter 79−85716
Pu contamination of soil near Rocky Flats plant 80−42803
Pu, contents in coastal sediments 79−57974
Pu dose to lung and bone from contaminated soils, statistical uncertainties 80−109028
Pu ecological export from reprocessing waste pond 78−53533
Pu, environmental behaviour, chemical approaches 79−93765
Pu environmental contamination, review 80−101136
Pu in lungs of pronghorn antelope near a nuclear fuel reprocessing plant 80−30906
Pu in situ array for electropolishing bath, Monte Carlo calcs. 80−37524
Pu in soil, meas. in respirable dust using different size fractionation methods 79−66836
Pu in waste, anal. of enhanced variance and twin gate methods 80−5454
Pu isotopes, maximum permissible inhalation values 79−70640
Pu, low conc. meas. in earth samples, appl. of Si(Li) X-ray detector 78−58505
Pu, lung 80−109042
Pu migration through soil 80−37490
Pu, neutron analysis in solid waste 80−42840
Pu processing for fast reactor fuel cycle 80−27793
Pu proliferation, comparison thermal, FBR reactors, nuclear power stations appl. 78−86641
Pu reclamation, precipitation-ion exchange scheme for actinide removal from salt waste soln. 79−49820
Pu recovery from nitric acid waste, comparison of anion exchange resins 80−681
Pu, recycling in mixed oxide fuel for LWR 79−36385
Pu, release into estuarine-coastal sea ecosystem, assessment methodology 79−70471
Pu retention by rock 77−71679
Pu transport, environmental impact 80−779
Pu, unmoderated, criticality safety practices for handling in glove boxes 79−26669
Pu-bearing materials, environmental impact of transportation, linear regression anal. 80−85308
Pu-contaminated, at fuel facilities, management techniques 77−61568
Pu-contaminated solid waste, operational techniques for minimisation, segregation and accounting 77−61567
$Pu(NO_3)_4$-nitric acid soln., direct denitration in screw calciner 80−37567
PuO_2 powder, leak rate determ. 80−42808
^{238}Pu, ^{239}Pu, ^{240}Pu, content in deer from integrated nuclear fuel cycle facility 79−57778
$^{238}Pu^{4+}$, $^{238}Pu^{6+}$, $^{239}Pu^{4+}$, $^{239}Pu^{6+}$, alga uptake rel. to isotope and oxidation state 80−30692
^{239}Pu, ^{240}Pu, concs. in fish and seawater from Kwajalein Atoll 80−26380
^{239}Pu citrate, internally deposited, pot. genetic dose, influence of testicular microanatomy 80−36147
^{239}Pu contamination in snakes inhabiting Rocky Flats plant site 77−81591
^{239}Pu in organic media, survey of criticality parameters 79−26670
^{239}Pu, isolation and characterisation of particles in atm. effluent 79−63757
^{239}Pu, use in weapons and energy prod., radiological hazards, security 77−10492
$^{239}PuO_2$, inhaled by baboons and dogs, comparison of early mortality 80−108977
^{226}Ra, assessment of quantities in North Carolina drinking water supplies 80−45826
^{226}Ra, conc. in water near a phosphate facility 80−45827
^{226}Ra leaching from contaminated soils, investigation of Ra bearing soils from Port Hope, Ontario 79−20900
Rn diffusion consts. for soil covers of U mill tailings 80−42807
Rn emanation from α-emitting waste, expts. 80−98314
Rn flux from U mill tailings, attenuation by consolidation 79−66563
^{222}Rn, conc. in water near a phosphate facility 80−45827
^{222}Rn, diffusion and exhalation meas. from U mill tailings pile 79−92109
^{222}Rn diffusion in soil, moisture effects 80−37491
^{222}Rn diffusion through U mill tailings covers, coeff. meas., lab. techniques 80−95387
^{222}Rn released by uranium tailings piles, potential population dose 79−85824
^{222}Rn releases associated with cultivation of agricultural land 80−16850
Ru, hazards and control in nuclear fuel cycle, review 79−36392
Ru, processing from nuclear fuel by aluminosilicate gels *(Japanese)* 80−22973
RuO_4, catalytic reduction in radioactive liquid waste processing 79−76092
SiO_2 based glass, packaging of radio-active waste appl. *(French)* 79−71910
^{90}Si transmutation in fusion reactors 79−26559
Sr fraction encapsulation at Hanford 77−6534
Sr, process for solidification *(Japanese)* 77−54319
^{90}Sr concentrations in pronghorn antelope bones near a nuclear fuel reprocessing plant 80−89875
^{90}Sr, coyote scats, Hanford Reservation, waste distrib. 79−25120
^{90}Sr, diffusion in bitumen block coating, radioactive waste treatment *(Russian)* 80−52771
^{90}Sr fission reactor waste management, by fusion reactor transmutation 78−70642
^{90}Sr, leaching behaviour in cement composites 78−37416
^{90}Sr migration in aerated zones, theoretical estimation *(Japanese)* 79−9896
^{90}Sr, radionuclide leaching from hardened cement grout, container dimension depend. 79−13439
^{90}Sr, transmutation in fusion reactor imploding liner blanket 78−17420
^{90}Sr, transmutation in high flux fission reactor, feasibility 79−85708
T control by glove box containment at fusion reactor plant 78−46169
T, handling facilities in US and Europe *(Japanese)* 79−9895
T leaching behaviour from hardened cement paste 80−18443

radioactive waste continued
T meas. with electrolytic enrichment cell and reduction system 78−20128
T removal from air streams of reactors by catalytic oxidation and water adsorption 77−50292
T removal from inert gases, feasibility of chemical getter beds 78−41861
T storage and monitoring, CANDU heavy water reactors 80−5291
T transport, storage and disposal, charact. of metal tritides 77−54343
Tc, environmental behaviour, chemical approaches 79−93765
Tc, radiochemical charact. and role in nuclear fuel reprocessing, review *(Czech)* 78−82496
^{99}Tc migration potential 80−3537
^{99}Tc, reduction and sorption in granitic bedrock, biological hazard estimation 79−79415
^{99}Tc sorption on USA subsoils from differing weathering intensity areas 78−16014
Th alternative fuel cycles, waste management aspects 79−59204
Th-contaminated waste water, decontamination with soap *(German)* 77−26846
Th-U spent fuel, disposal of long lived α-emitters 77−26855
Ti alloy, radioactive structures, recycle time 78−58457
(U,Pu)C, controlled oxidation for head-end step reprocessing 80−5308
U and UF_6, mining, manufacture and purification processes, safety and waste disposal *(Spanish)* 79−63785
U content in solid waste mats. using α-particle detectors, two layer proportional counter *(Russian)* 80−27904
U mill tailings, radiation pathways and potential health impacts 79−85826
U mill tailings, radiological criteria 78−82480
U mill tailings generated between 1975 and 2030, environmental impact 79−85825
U milling, radioactive waste treatment costs and environmental impact 77−46377
U milling operations, radiological assessment methodology 79−85827
U, milling waste management in USA 79−31077
U mills, radioactivity release meas. 78−82479
U mines, radiological evaluation 80−42806
U mining, U refining and decay processes, radioactive mining waste disposal *(Dutch)* 80−21418
U mining and milling, effects on groundwater in Grants Mineral Belt, New Mexico 77−56657
U, recovery in slags containing calcium and magnesium *(Spanish)* 78−8955
U tailings management, economic impact on nuclear fuel cycle 80−18494
U, Vitro Mill Tailings at Salt Lake City, Utah, remedial action 77−46315
$UO_2(NO_3)_2$, establishing traceability to standard reference material 79−81052
$UO_2(NO_3)_2$, preparation of uranium nitrate standards for X-ray fluoresc. anal. 79−81053
UO_2, irradiated, T loss during oxidative processing in air 79−97831
UO_2 low enriched fuel rods, storage and transportation, critical separation in water with fixed neutron poisons 80−73918
UO_2, Zircaloy-clad, stability during long-term storage 79−26588
$^{234}U \rightarrow ^{230}Th \rightarrow ^{226}Ra$, superposition soln. of transport of decay chain through sorbing medium 80−37500
$^{234}U \rightarrow ^{230}Th \rightarrow ^{226}Ra$ decay chain, hydrogeological migration anal. 80−37501
^{235}U enrichment by laser isotope separation 77−19113
^{A}Xe, A=133,135, interference with low-energy meas. systems 80−89872
^{133}Xe waste storage and retrieval, clinical use 77−86649

radioactivity
see also alpha decay; atmospheric radioactivity; beta-decay; radioactive decay periods; radioactive decay schemes; radioactive sources; radioactive tracers; radioactivity measurement; radiochemistry; spontaneous fission
activated metal foil experiments, teaching expts. 79−17165
aerosol particles, hot β active emission electrification in varying force fields 80−7868
aggregate recoil theory 80−57062
AVR reactor steam generator leakage, meas. of activities and their origin in leakage water 80−693
beta decay Rumanian standard *(Rumanian)* 80−68603
biosphere contamination, explosion and power plant influence *(Hungarian)* 80−21548
bone and muscle radioactivity separation by dermestid ingestion 80−30949
Canada Maritime Provinces, rocks radioactive heat prod. rel. to heat flow meas. 79−100819
Canon City meteorite, ^{37}Ar and ^{39}Ar radioactivities 80−36582
charged particle emission following μ capture in complex nuclei, A≳20 78−70490
coastal sediments, English Channel, distribution of fission products (1976-78) *(French)* 79−84219
comets, primordial, interiors radiogenic melting 80−67659
continental crust, radioactivity rel. to heat flow-age relation 77−21696
cooling orogen, magnetic and isotopic blocking temps. 78−65226
cosmic ray nuclei, electron capture decay rel. to time delay between nucleosynthesis and accel. 78−28455
Cosmos 954 satellite debris, airborne gamma-ray spectrometer detection 78−85784
cryonuclear physics for radioactive decay and neutron+nucleus reaction studies *(Dutch)* 78−29416
decay analysis method, comparison to least squares 80−102162
decay data, ENDF/B file, applications 77−22978
deep sea cores from Project FAMOUS, radiocarbon and ^{210}Pb distrib. 77−37179
delayed neutron spectra from separated fission products with A=88-144 77−34268
depositions, shallow, on body surfaces, meas. using M X-rays 80−67223
determ. in coastal sediments and seawater, activity ratios, disequilib. 78−27851
Dhajala meteorite, ^{37}Ar and ^{39}Ar radioactivities 80−36582
drinking water, Finland, internal radiation doses due to radioactivity 80−109029
drinking water, Finland, natural radioactivity 80−108819
dynamical sorption eqns. of radioactive substances, numerical soln. *(Russian)* 79−61907
Earth, radioactive heat generation, variation with depth 79−84202
radioactivity continued
Earth crust radiogenic heat production, model 80−85619
Earth crustal rocks, exponential relationship between seismic vel. and radioactive heat prod. 79−70793
Earth interior, convective stability with radioactive heat sources 77−9381
Earth mantle, natural radioactivity influence on creep rate 79−92520
Earth mantle, radioactivity rel. to geosynclinal processes energy sources *(Russian)* 78−96182
Earth mantle, radiogenic heating in convecting mantle rel. to oceanic bathymetry flattening 80−85642
education, stochastic model, radioactive decay, difference-differential eqns. 80−51992
education, undergraduate course evaluation on radiation and the environment 78−1
energy release, half life, radioactivity's early puzzles 78−13001
enriched heavy minerals in sand grains, enhanced natural radiation exposure *(German)* 80−51018
environmental radioactivity in W.Cumbria, Pu and ^{137}Cs concs. and possible maritime effect 80−108817
extinct radioactivities in meteorites, as trapped residuals of presolar grains 77−49342
extinct radioactivities in meteorites, trapped residuals of presolar grains 77−45367
fission products in reactor, decay power, sensitivity to uncertainty in yields 77−6494
gamma-ray spectrometry, correction for dead-time losses, mixture of short-lived radionuclides 80−42312
granites of E.United States, radioactive elements concs. rel. to low-temp. geothermal resources 80−85264
history, Frederick Soddy and the practical significance of radioactive matter 80−86068
incidents, national arrangements, review 80−102355
equatorial Indian Ocean, ^{137}Cs distrib. in upper layer *(Russian)* 77−60426
interstellar, gamma-ray energy spectra in 0.02-12.27 MeV range 77−2501
interstellar grains, effects of radioactivity on elec. charge 77−87499
isotopes, probability determ. of number of atoms at end of production 79−63637
Lake sediment radioactivity, mixing by benthic organisms 78−16060
lunar soil samples from Luna-24, radioactivity and cosmic ray dose rate, thermolum. obs. 80−67596
Mare Crisium, regolithic radioactivity 80−62045
medicine, residual activity in syringes after radiopharmaceutical injection *(Japanese)* 80−98113
metal surfaces, radioactive contamination 80−68771
meteorites, appl. to galactic cosmic ray solar modulation *(Bulgarian)* 80−72728
mica, Po anomalous haloes origin 79−44186
Moon, orbital gamma-ray data rel. to large-scale lunar problems 78−12123
Moon, radioactive elements distrib. rel. to thermal history 78−65522
Moon, superheavy elements radioactivity rel. to primaeval melting 78−24478
New Zealand soils, survey of naturally occurring radionuclude conc. 77−53057
nuclear decay chains, abundances evaluation method 78−45216
nuclear reactor, fluctuations in number of radioactive atoms, anal. 77−3076
ores, effective γ-ray attenuation coeffs. 77−25680
NE.Pacific, Columbia River discharge effect on radioactivity field *(Russian)* 79−39761
Pacific Ocean surface layer, radioactive admixture spreading studies *(Russian)* 77−60488
probabilistic description based on good-as-new postulate, for teaching 79−35471
pulse processing technique, pulse shaping *(Japanese)* 79−81138
quantum mechanics and radio activity unification, probabilistic conceptions 80−12946
radiation dosimetry, standardised radioactive decay data sets 80−13945
reactor decay heat uncertainties estimate 78−25263
reactor fission products, radioactivity reduction 79−26490
rock U isotope disequilibrium due to α-recoil and soln. effects 80−98314
rocks, altered mid-oceanic basalts, radioactive disequilibrium 78−96186
rocks, Scandinavian, giant and dwarf haloes rel. to unknown radioactivity 78−81157
Sakurajima volcano, ^{226}Ra-^{222}Rn disequilib. and pumice radioactivity 77−33033
seawater, radioactivity, and salinity changes with advection of water masses *(Russian)* 78−77275
seawater, vertical diffusion of radioactive admixture *(Russian)* 77−60417
seawater of Narragansett Bay, USA coast, radionuclide content 80−12399
secondary education, learning of radioactivity *(Japanese)* 80−4484
Singhbhum thrust belt (India), radioactive elements content rel. to heat flow 77−49050
soil, U and Ac series nuclides radioactive disequilibrium 80−4014
spring waters in Bulgaria *(Russian)* 77−41098
standards for medical use 80−67232
statistical density functions for radioactive decay and counting 80−73828
stony meteorites, cosmogenic ^{26}Al and ^{22}Na *(Russian)* 77−9719
Straits of Malacca, radioactivity in marine environment 79−12135
superdense radioactive nuclei, search in p-nucleus collisions, cross-section limit 77−26638
supernovae, Type I, radioactive excitation source model for late time spectra 80−105264
supernovae, Type I, radioactive excitation source rel. to interpretation of spectra 78−49467
synchrocyclotron hall, 680 MeV, induced activity of building and structural mats. 77−50319
teaching, dice games to illustrate probability 78−12515
terrestrial beta radiation field in natural environment, numerical evaluation 78−81161
UK population, sources of radiation exposure, review 80−36156
uraniferous materials, disequilib. variability and ^{222}Rn emanation factor 79−62498
water baseline radioactivity in Arizona 78−81230
wear measurement by thin layer activation 78−60932
Wyoming, heat flow and radioactivity 80−72469

radioactivity continued
$^{113}Cd^{m}$, in marine organisms and sediment around Marshall Island nucl. test site 80−109174
D abundance, Indian radioactive thermal spring water D content, mass spectrometric anal. 79−39765
^{40}K, isotope relative abundance, radioactivity expt. for schools 79−21511
^{231}Pa, determ. in coastal sediments and seawater, activity ratios, disequilib. 78−27851
^{223}Ra,^{226}Ra, activity ratio and separation from Indian spring water 78−86962
Rn short lived daughters meas., modification of three interval method 79−26754
^{24}Si delayed-proton emitter, search in (^{3}He,3n) 60 MeV reaction 77−22970
^{228}Th-^{228}Ra radioactive disequilib. rel. to coastal pollution in New York Bight 79−29784
U prospecting, geochemistry of inclosure radioactivity 80−85766

radioactivity measurement
see also radioactivity measuring apparatus
absolute, standardisation of radioactive sources and solns., 4π β-γ coincidence, program 77−18760
air monitoring systems for radioiodine and inert gases, evaluation 80−95480
air pollution control at Nulcear Research Institute, using scintillation probe and GM-tube *(Czech)* 78−88906
airborne and liquid releases from nuclear facilities, monitoring systems 78−37450
airborne radiometric data inversion, radioactive elements conc. mapping 78−77347
alpha-radioactive isotopes, radiometry via ARS-1 attachment 77−75022
atmosphere, surface layer, natural radioactivity continuous meas. method *(Flemish)* 78−61612
atmospheric radioactive gas monitoring by silicone oil absorbent scintillation counter 80−12044
autoradiography and soft laser scanning in radioisotope work, appl. to metabolic studies 78−3576
biological and ecological samples *(French)* 78−5052
body radioactivity, SABRE computer system for assessment 77−77998
bone-seeking radionuclide skeletal burden determ. from in vivo scintillation meas. of head 78−15915
borehole γ-ray logging, exact inverse filters 80−94609
bulk sample gamma-ray assay, equipment specification 78−24158
CANDU, energy, water, tritium budgets for Perch Lake 1975 78−29563
cellulose nitrate α-particle detector for Rn short lived daughters, results and calibration *(Czech)* 78−62663
Cherenkov counter, liq.-filled, for gamma-ray counting of large samples 78−53491
Cherenkov counting of beta emitter isotope pairs using performance number criterion 77−83471
Cherenkov counting of plants for β-emitter radioassay, sample prep. 78−81088
chromatography radioactive source leak testing under dynamic flow conditions 80−3432
coal power station fly-ash and slag, natural radioactivity meas. 78−17442
counting small sample of radioactive atoms 78−17535
counting statistics with non-extended variable dead time *(French)* 77−30735
cumulative sum charts, for background count rate monitoring 78−29718
curve fitting to data with low statistics 80−9471
cutting fluids testing rel. to tool wear, thin layer activation technique 80−55619
Danube River, distrib. of artificial radionuclides at mile 34, 1976 79−39323
decay time coincidence spectra, anal. 77−38575
determ. of bulk α and β radioactivity *(Rumanian)* 79−88346
determ. of levels of ^{54}Mn, ^{59}Fe, ^{58}Co and ^{60}Co 78−85608
digital leaky integrator 79−22560
distribution in extended medium, qualitative and quantitative anal., mathematical modelling 80−71985
education, nuclear fallout radioactivity γ-ray detection and anal., Chinese fission bomb anal. 78−49596
effluent monitoring, symposium, Portoroz (1977) 78−89985
electronic measurement apparatus development at ATOMKI *(Hungarian)* 80−18768
environmental, NBS mixed-radionuclide gamma sources for Ge(Li) detector calibration 77−38541
environmental measurements and US regulatory responsibilities 77−38430
environmental radioactivity, methods for determ. of radionuclides in environmental samples 79−48202
environmental radioactivity meas. in the EEC, 1977, for air, deposition, water and milk 79−62162
environmental radioactivity near a radioactive waste disposal site 80−98148
environmental radioactivity prior to the Kori nuclear power plant operation 79−6773
environmental radioactivity standards, USA 77−38431
exponential distrib. parameter estimates under poor statistics, computer program 78−57863
fallout nuclides determ., 19th Chinese test 78−82520
fallout of highly radioactive particles originating from the Chinese nuclear explosions *(Japanese)* 79−63813
filter testing, Winfrith, double automatic Pollak counter 78−33301
fission product and actinide adsorption on silica gel, for urinary gross α activity determ. 79−88155
fossil bones from N. Greece, conc. of U and daughter prods., γ-spectroscopy, activation anal. 77−60161
French nuclear power plant occupational radiation exposure meas. and prediction 79−9900
gamma radiation interaction with air, using ionisation chamber *(Czech)* 79−67967
gamma-emitters, mixed energy, meas. using radionuclide calibrator 77−14319
gamma-radiating radionuclide activity, comparison of standards within COMECON framework 80−42899
geological samples, large volume, absolute activity determs. independ. of self-absorpt. effects 80−56643
geometry factors, for teaching expts. 78−12471
heavy element quantitative sample preparation 79−9936

radioactivity measurement continued
hospital radioisotope release to environment, model and meas. 78−96105
hot fuel examination facility, air sampling system 79−13541
hot particle physical props. determ. 79−3251
hybrid spark chamber for radioisotope distrib. meas. 78−46227
inert gas analysis, calibration of Ge(Li) gamma-ray spectrometer 77−83442
inhaled heavy elements deposited in vivo, external counting, review 80−36152
instant working level meter methods, mathematical evaluation 79−9918
internal-gas radioactivity-counting with pure H_2S as counting gas 78−854
ionising radiation, traceability in meas. systems 80−5355
IR spectroscopy appl. to charged part. dose meas. in cellulose triacetate 78−94145
Kodak LR 115 dielec. track detect., applicability as α-particle detector *(Czech)* 79−8711
large-volume proportional gas counter for measuring low concentrations of tritium 79−26822
leakage radiation charcts., 18 MeV, clinical linear acceleration 79−5379
leukocyte uptake of radiolabelled compounds in whole blood, liq. scintillation method 77−90882
liquid activity meas. instrumentation in Czechoslovakia 79−49873
liquid column chromatography, scintillation counters, review *(Czech)* 80−27885
liquid contamination measurement using $CaSO_4$:Dy TLD 77−38574
liquid scintillation counting, ^{3}H meas. 79−22554
liquid scintillation counting, single and double labels, absolute activity analyser vs. on-line computer 77−83470
liquid scintillation counting, single and double labels, quench correction with on-line computer 77−79520
low activities, definition of detection limit for non-selective determ. *(German)* 77−61668
low-level, statistical interpretation of counting data 77−23387
lung monitor for assessment of low energy photon emitters 79−25067
LWR waste, leach tests of cement containers under high hydrostatic press. *(Japanese)* 79−63761
marine gamma-spectrometric surveying problems 79−2390
marine sediments, radioactivity uptake, rel. to metal pollutants monitoring 79−12145
mass spectrom., movable dynode elec. multiplier 79−716
medical, absloute measurement technique using a gamma camera and a computer 79−25087
metallic sample, specific activity determ., by mathematical modelling *(Rumanian)* 79−63881
mineral prospecting, thermoluminescence radiation dosimetry appl. 78−32244
monitoring nuclear plants discharges, state of art *(German)* 77−42174
moving tape apparatus for $T_{1/2}$ determ. of short-lived neutron deficient isotopes 77−65411
Muller statistics for counting systems for non-extending dead time, exptl. test 78−94173
natural fracture water identification by radiological parameters 77−78245
natural soil radioactivity monitoring with portable gamma ray spectrum 80−31148
natural substances *(Rumanian)* 77−49067
nondestructive assay of highly enriched spent fuel, using Ge(Li) detector and ^{235}U fission chambers 79−89522
nosetip recession meas. using implanted radioactive sources, error analysis 78−16272
NRX and process effluents, gamma ray spectrometric anal. 78−29656
nuclear explosion, time distrib. and anal. fallout particles from 1977 Sept. 18 Chinese detonation 79−25796
nuclear fission aerosol products, bioindication using needles of common pine tree 79−100550
nuclear installations, radioactivity release, air monitoring, emergency procedures 78−70610
nuclear power plant radioactive liquid direct meas. instrument design *(Russian)* 79−3250
nuclear power stations, γ emission in heat transfer *(Hungarian)* 77−26833
nuclear reaction thresholds and half-life meas., computer controlled system 78−55114
nucleon stability testing, radiochemical and geochemical method limits 79−22093
on-line radiation monitoring at fuel reprocessing plant 79−85731
Ontario Hydro nuclear power plant stack effluent monitoring 79−3254
optimum conditions in radioactive measurements with the statistic accuracy taken into account 79−41083
Oregon, meas. of natural radioactivity 80−37638
parent activity determ. by daughter decay after separation with different radiochem. yields 78−78596
pharmaceutical preparations, standardization of control of physical charcts. 79−81139
phosphate fertilizer, specific activity of U and Th rel. to particle size 80−106244
photon irradiator calibration, compensation for geometry induced errors 80−18702
power station ashes, Th, U, and K conc. meas., dose rates in Poland 79−100754
power station fly-ash, environmental protection *(Polish)* 77−14318
PWR, T sources, releases, monitoring, management and environmental impact 80−18690
radiation monitor for nuclear power station radioactivity meas. *(German)* 79−67876
radioactive emission meas. and control *(German)* 77−79484
radioisotope densitometers, electronic threshold device 79−26849
radioisotopes, identification, possible problems *(Chinese)* 79−89506
radiometric exploration meas. standardisation advantages and methods 78−28325
radionuclide, half-life meas. by ion implantation 78−70713
radionuclide calorimeter for liquid He range 4.2 to 8K 79−18093
radionuclide concentration determ. in ground level air 79−24927
radionuclide distribution, selective determ., mathematical modelling *(Rumanian)* 79−81098
radionuclide migration at US ERDA Nevada test site 77−57752
radionuclides, short-lived, meas., counting statistics 80−58098
radiopharmaceutical dose calibrator performance and quality control 77−56470

radioactivity measurement continued
radiopharmaceutical industry, Atomic Industrial Forum-NBS quality assurance programme 77−40769
random summing in multi-detector counting system meas. radionuclide mixtures 80−36097
reactor containment air contamination, sampling and measurement techniques *(French)* 78−89997
release from Institution of Nuclear Research, instruments and expt. results *(Czech)* 77−6568
remote monitoring system for radioactive emissions of nuclear reactors 77−50307
river bottom sediments, in situ neutron activation anal., pollution, mapping and prospecting appl. 77−87115
river water, field sampling unit using ion exchange resin to concentrate radioactive ions 77−9532
rocks and soils, Ge(Li) detectors for γ-radioactivity meas. 80−67418
scintillation β-spectra, nucleus identification 79−26805
scintillation counters, use of miniature glass vials in multi-functional standards 77−70370
sea water, radioactivity of advected water masses calc. *(Russian)* 78−77275
shadow-shield background reduction method 80−108999
shielded syringes, radioactivity checking instrument 80−94325
SI units in radiological protection 78−86235
soil and vegetation, surface β-activity caused by nuclear explosion products, depend. on isotope vertical migration 78−86700
soil samples, meas. trace radionuclide L X-ray detection 78−49020
solid sample activity meas., use of plastic scintillator in liq. scintillation counter 77−88333
source activity calculation from counting rates in single and coincidence photopeaks 78−13371
specific activity determination, procedure optimisation and error anal. 77−6645
spectral radiation detectors, calibration and error anal. 78−46177
spectrometer user interface to computer systems 79−9986
stack release radioactivity monitoring with digital processing 79−3253
standards, American National Standards Institute quality assurance programme 77−38585
standards program of the NBS, USA 80−18700
statistical distribs. accumulation in real time 78−94178
subterranean gamma-ray in situ spectroscopy 77−57806
superheavy elements, synthesis and identification 78−46239
tackishade sampling to measure airborne radioactivity *(Hungarian)* 80−94136
terrestrial radioactivity, natural, estimates of ground concentration from airborne data 79−53575
transuranic element meas. in vivo at CRNL 77−77993
transuranic waste assay instrumentation, Los Alamos Scientific Laboratory developments 79−85692
underground cavities, natural radioactivity, Rn conc. and exposure levels *(Spanish)* 79−39322
units, definitions and interrelations 80−17914
waste, low-level, shallow land disposal, microbiological aspects 79−85630
waste, low-level commercial disposal sites, trench water survey 79−85629
water, sensitive sampling method in alum coagulation unit 79−39768
water pollution by reactor organic coolant, environmental effects 79−66425
wave packet reduction as medium of communication 77−74242
wear measurement by thin layer activation technique 78−72945
whole-body counter for meas. of radionuclides in large dogs 78−11786
whole-body counting, effects of changes in relative organ position 77−66847
whole-body sections, ^{14}C and ^{3}H determ. by liq. scintillation counting *(German)* 77−5114
α-particle detectors, two layer proportional counter for measuring U content in solid-waste mats. *(Russian)* 80−27904
γ-emitting radioelements, meas. of weak doses *(French)* 80−91410
$^{242}Am^{m}$ activity measurement by ^{242}Cm daughter decay meas. after separation with different radiochem. yields 78−78596
^{41}Ar release from TRIGA reactor, comparison of γ-ray detectors 78−57309
CO_2-^{14}C animal exhalation meas. by liquid scintillation counting *(French)* 79−48384
^{14}C activity and distrib. in gaseous effluents from PWRs 79−85829
^{14}C beam prod. from natural sample, radioactive dating 79−25352
^{14}C, detect. via small van de Graaff accelerator 79−11844
^{14}C, influence of quenching on the background of liquid scintillation counters 79−18082
^{14}C, low level activity measurement, comparison of proportional counters *(Czech)* 80−52818
^{14}C, low level counting in multielement proportional counters 79−76287
^{14}C meas. in proportional counter, continuous examination of counting efficiency 78−58548
^{14}C, meas. using Cherenkov liquid scintillator counter 79−26817
^{14}C-$NaHCO_3$ solution liq. scintillation counting, prevention of radiocarbon loss 78−21811
$^{14}CO_2$ meas. in Karlsruhe Reprocessing Plant exhaust air 79−3231
$^{14}CO_2$ trapped in solns. of NaOH, reliable scintillation counting method 79−62410
^{45}Ca, liquid scintillation counting in plant and soil material 77−44536
Ce in marine sediments, determination method 80−104543
$^{139}Ce \rightarrow ^{139}La$, internat. comparison of activity meas. March 1976 79−13613
^{242}Cm decay meas., determ. of $^{242}Am^{m}$ activity after separation with different radiochem. yields 78−78596
^{56}Co activity loss, erosive wear from steel surface meas. 79−57166
Cs, in seawater, rapid determ. using Cs selective resin 78−85609
^{137}Cs $T_{1/2}$ determ. using new specific activity meas. 78−70714
^{18}F, meas. using Cherenkov liquid scintillator counter 79−26817
$^{59}Fe/^{51}Cr$ in blood, simultaneous meas. by liq. scintillation counting 77−29195
$^{59}Fe/^{55}Fe$ activity ratio of blood, meas. using semicond. detector 80−17062
Ge detectors in space, computer spectral anal. of cosmic ray proton induced radioactivity 79−12413
Ge(Li) anticoincidence shielded spectrom. for environmental radionuclide meas. 79−6791
HCN, gaseous, radioactivity meas. by internal counting method 79−36483
HT-HTO in air meas. system 80−21433

radioactivity measurement continued
^{3}H assay by liq. scintillation counting, use of Aquasol in plastic Mini-Vials 77−26934
^{3}H conc. meas., scintillation detector appl., bremsstrahlung from β-rays 78−55042
^{3}H, environmental levels, detection with liquid scintillation spectrometers 77−9489
^{3}H in aqueous samples, single solvent cocktail for liq. scintillation counting 78−856
^{3}H in water, low-level meas., inter-laboratory comparison 78−44888
^{3}H, influence of quenching on the background of liquid scintillation counters 79−18082
^{3}H, low level activity measurement, comparison of proportional counters *(Czech)* 80−52818
^{3}H, low level counting in multielement proportional counters 79−76287
^{3}H, multiwire proportional counter for low-level counting 79−6800
^{3}H personnel exposure, rapid evaluation using surface monitor 77−56485
^{3}H urine analysis, liq. scintillation solns. 77−9273
He jet system for radioactivity studies 79−93855
^{123}I, coincidence-counting assays 77−14320
^{123}I uptake in thyroid, correction for thyroid depth 78−11728
^{125}I airborne vapour detection 80−51027
^{125}I worker thyroid meas. 80−36151
^{129}I and organic compound determ. in LWR irradiated fuel solns. *(French)* 79−3230
^{129}I coincidence counting, efficiency extrapolation technique, methane 4π counter efficiency 77−88354
^{129}I measurement rel. to ^{131}I accumulation in thyroids of pasture animals *(German)* 77−52891
^{131}I determination in vegetation, ashing procedure 78−15930
^{131}I in milk, extreme low level determ. 78−92703
^{131}I in nuclear power plant gaseous discharge, cumulative meas. *(Russian)* 79−3224
^{131}I, low level detection in milk rel. to population dose 78−31911
^{131}I transport from pasture to milk, modelling Dresden-Monticello data 79−88203
^{42}K, whole-body content, sex-dependent calibration factor of NaI scintillation counter 79−29593
Kr atmospheric activity meas. using ^{85}Kr 77−78454
^{85}Kr monitoring system with permselective membranes 79−3260
^{85}Kr, radioactive pollution in atmos., Warsaw 1975 to 1977, meas. methods 79−34458
NaI:Tl spectrometer meas. of activity of radioisotope emitting two gammas in cascade, geometrical effect 77−88320
^{14}O, half life determ., precision meas. 78−90043
^{212}Pb inhaled body burden calibration, general phantom procedure 77−64138
^{147}Pm, in-vivo measurement by phoswich detector 78−28087
Pu, alpha-energy and mass analyses, using single sample mount 78−15744
Pu dosimetry, calibration of whole-body counters 80−21547
Pu in waste, anal. of enhanced variance and twin gate methods 80−5454
Pu inventory verification at ANL, IAEA safeguards 78−821
Pu low-background assay using modified commercial liq. scintillation detector and sample changer 77−54474
Pu skeletal level estimation based on DTPA induced excretion in faeces 78−85390
PuO_2 heat sources, ave. total decay power meas. using Bunsen ice calorimeter 77−6547
^{239}Pu, lung burden X-ray counting efficiency, from inhaled ^{103}Pd studies 78−85391
^{239}Pu, prep. and chem. charact. for half-life meas. 79−26404
^{240}Pu passive assay by neutron detection, theoretical response of counters 79−22570
^{226}Ra, alpha scintillation counter for determ. of low natural conc. 80−9456
^{226}Ra body burden determ., postprandial changes in exhalation rate of Rn prod. in vivo 78−69224
^{226}Ra determination in water, sampling and meas. methods 77−9278
^{226}Ra, emulsion scintillation counting of biological samples 78−81089
^{226}Ra leaching from fossil bones 78−58562
^{87}Rb, absolute counting technique appl. to half-life determ. 77−26943
Re isotopes, $T_{1/2}$ determ. for β-decay using moving tape apparatus 77−65411
Rn aerosols in uranium mine *(French)* 78−32195
Rn conc. in underground waters and soil-air around Asama Volcano, Japan *(Japanese)* 79−70813
Rn concentration measurement in groundwater and springs for earthquake prediction 78−88924
Rn daughter airborne conc. meas. in atmosphere 80−37636
Rn daughters in air, precision alpha counting methods 77−57841
Rn detection, effect of humidity 77−6647
Rn dosimetry using plastic nuclear track detectors 78−33298
Rn in groundwater, continuous meas. method for earthquake prediction 77−44935
Rn mapping in U exploration, exclusion of ^{220}Rn signal 80−61916
Rn, meas. with electronic cups, U exploration appl. 78−7781
Rn, moisture insensitive monitoring using solid detectors 79−31228
Rn/Tn daughter air conc. meas. by filter method, general formula 78−70711
^{222}Rn, alpha scintillation counter for determ. of low natural conc. 80−9456
^{222}Rn alpha-scintillation counting, statistical counting error calc. 77−3211
^{222}Rn conc. monitoring by proportional counter, study of thermal diffusion in Rn-CO_2 mixture 79−50839
^{222}Rn concentration in water, meas. by gamma counting 78−53733
^{222}Rn concentrations in water, rapid meas. with commercial liq. scintillation counter 78−28339
^{222}Rn daughter conc., meas. sensitivity computer optimisation 78−49126
^{222}Rn daughters, meas. of low conc. in air 78−28308
^{222}Rn daughters emission and enrichments from Etna volcanic magma 77−21736
^{222}Rn determination in air and water, sampling and meas. methods 77−9278
^{222}Rn, emulsion scintillation counting of biological samples 78−81089
^{222}Rn flux measurement using charcoal canister 77−6646
^{222}Rn low conc. meas. in air, α-scintillation method 78−92970
^{222}Rn, meas. of concs. in Earth using nuclear track technique 79−53574
^{222}Rn release from U ore crushing, grinding and leaching 78−89970
^{222}Rn scintillation counting, standard deviation estimation 77−79519

radioactivity measurement continued
^{222}Rn short lived decay products in air, collection efficiency of Whatman GF/A filter 78−20526
^{222}Rn very low conc. meas. with proportional counter 80−27907
$^{106}RuO_4$ in lung, in vivo meas. and dosimetry 78−53515
^{90}Sr body content determination, ^{90}Sr body content determination, ^{90}Sr+^{90}Y bremsstrahlung efficiency for humans 77−2061
T determination in biological samples, field instrument 77−9306
T enrichment in water by electrolysis for low-level T activity meas. 78−17536
T in air, scintillation detection using liquid adsorbent 79−76291
T in water, flow cell type detector for continuous monitoring in high γ-background 78−82524
T in water, meas. with electrolytic enrichment cell and reduction system 78−20128
T monitoring at nuclear power stations 80−18691
T monitoring methodology using SiO_2 desiccant, appl. to research reactor facility 80−21434
T monitoring with proportional counters 80−27874
T species, sources and reactions 80−21432
U activity, liquid scintillation counting 80−27873
U analysis in phosphate fertilisers and other materials using liq. scintillation spectrometry 78−53280
U in vivo chest survey confirmation by autopsy specimen anal. 77−66859
U, mineral analysis using alpha particle absorption by cellulose nitrate *(Spanish)* 77−70358
U ore bodies ground level radiometric surveys, overburden effects correction techniques 79−88485
U prospecting, ^{222}Rn and ^{210}Pb meas. 79−53573
U stored in lung, meas. using NaI and solid-state detectors 78−28090
U^{235} in pegmatites, homogenised fission track anal. using solid state track detector 80−97719
U- and Th-series, secular equilib. investigation method 79−2381
U-bearing rocks, radioactive disequilib. determ., isotopes relative abundance meas. 78−57330
U_3O_8, ^{235}U enriched aerosol, characterisation by solid state track recorders 78−17538
^{235}U thermal fission product long-term activity meas. and calc. 79−9644
^{236}U activity meas. in UO_2 mineral deposit *(Spanish)* 78−44822

radioactivity measuring apparatus
ARS-1 attachment, for radiometry of samples containing alpha-radioactive isotopes 77−75022
body radioactivity measurement, SABRE 3 computer system 78−85425
continuous radiogauges, transient characteristics 79−31328
detector immersed in extensive liquid, sensitivity determ. *(Rumanian)* 77−26950
double cylindrical 4π ionisation chamber for γ source nuclide activity 77−10536
eight-channel unit, automatic, for recording tracer activity 78−86751
flow device to measure γ radioactivity uptake and size of microparticles 77−5074
FUNGI, radon meas. with fast response 78−46216
gas radiometer, portable, for noble gases and gaseous tritium meas., by ionisation method 80−32570
geophysical radiometric field instruments, experiences with concrete calibration sources 79−5633
lung counter system, improvements to overcome interference from neighbouring compartments 79−2132
MAS-1 multichannel amplitude selector, for dense pulse flow anal. 77−75029
monitoring nuclear plants discharges, state of art *(German)* 77−42174
nitrocellulose, radiography of geological specimens for determ. of α- and fission-activity 78−20540
nuclear power stations, γ emission in heat transfer *(Hungarian)* 77−26833
on-line monitor for α-emitting aerosols 78−46236
Pollak counter, aerosol leakage, filter testing 78−33301
proportional flow counter, for high-temp. gas radiochromatography 78−44420
pulse processing technique, pulse shaping *(Japanese)* 79−81138
radiation monitor for nuclear power station radioactivity meas. *(German)* 79−67876
reactor coolant, automated system for radioiodine anal. 78−35768
release from Institution of Nuclear Research meas. *(Czech)* 77−6568
Rn emanation rate measuring apparatus consisting of sealed chamber and scintillation cell, rock samples appl. 80−63494
scanning ultra-low-level radiochromatograms, multicounter system 77−88335
scintillation detector, gain stabilising scheme, gated radioactive source and broad digital window 80−63453
seawater γ-ray field, meas. system *(Russian)* 80−109268
short lifetime meas., β-spectrometer, plastic scintillator, effects of light guide and mag. field *(Japanese)* 78−90016
student laboratory radioactivity detector, lengthened time consts. 79−44686
thoron content in exhaled air, meas. apparatus 79−34672
Whatman GF/A filter, collection efficiency for ^{222}Rn short lived decay products in air 78−20526
γ-ray detector system for determ. of internal radiation exposure dose 79−5378
Ge planar detector array for Pu detect. in lungs 77−17004
^{125}I surface contamination meas., due to medical use of ^{125}I sources, detectors sensitivity comparison *(Czech)* 79−34673
Pu-Am survey instrument, β-α-γ-X-ray scintillation detect. probe 78−33376

radioactivity protection *see radiation protection*

radioaltimeters
see also aircraft instrumentation; radionavigation
on automatic lunar stations, radar expts. 77−53438
Geos 3 altimeter, biases from comparison with other tracking systems 80−4227
ocean surface wind obs., SeaSat scatterometer/scanning radiometer/altimeter comparison 80−46249
ocean wave height statistics, dual frequency correlation radar measurements 77−17236
ocean wave heights, meas. by high resolution pulse-limited radar altimeter 78−81172
radar altimeter height and timing bias report 80−46326

radioaltimeters continued
rough surface average impulse response, appl. to satellite radar altimetry 77−17235
satellite, average impulse response of rough surface, appls. 77−25791
sea wave profile meas. by radar altimeter, computer simulation 77−5367
Seasat, altimeter sensor file algorithms 80−94680
Seasat, initial performance assessment 80−94679
SEASAT altimeter wave height comparisons 80−46201
SEASAT radar altimeter, resolution capability preliminary estimates 80−72645
SEASAT radar altimeter 80−56613
SEASAT-A satellite radar altimeter design 77−5415
SEASAT-A satellite radar altimeter spaceborne microcomputer 79−75073
short-pulse radar altimeter, on experimental oceanographic satellite Seasat-A 78−77455

radioastronomical observations
see also radiosources (astronomical)
1.35 cm radiogranulation, optical identification with chromospheric network pattern *(Russian)* 78−40897
5 GHz galactic plane sources, catalogue 80−4269
6 cm sources, survey by Westerbork Synthesis Radio Telescope, data 79−88604
10 MHz map of northern sky 77−13485
22 GHz observations with resurfaced Parkes radiotelescope 77−33347
30 MHz all-sky map, galactic features study 79−21469
0241+62, nearby quasar, radio props. 79−25752
0816+526, cD galaxy, classical double radiosource, 4885 MHz obs. 80−109545
0816+526, classical double source in direction of rich galaxy cluster, interferometric obs. 78−57662
0915+320, wide-angle-tail radio source in group of galaxies, 4.9 GHz map 78−93441
1232+414, classical double source in direction of rich galaxy cluster, interferometric obs. 78−57662
1331+170, quasi-stellar object, 21 cm absorpt. detect. at Z≈1.8 79−75292
1401−33, radio structure and spectrum 77−29942
1633+38, quasar, very high resolution obs. 77−33663
2033+59, appl. of Clean and Restore technique to Northern Cross radiotelescope obs. *(Italian)* 80−98563
8550 MHz sky survey, appl. of computer data processing techniques 77−17708
2A 1219+305, high latit. X-ray source identification with BL Lacertae object 79−48960
A 1710−34, X-ray, optical and radio obs. 79−71158
Abell 1367, 17 W list from 610 and 1415 MHz obs. of rich cluster of galaxies 79−35401
Abell 1367 central region, peculiar radio sources Westerbork obs. 79−2574
Abell 2029 galaxy cluster, radio and SAS 3 X-ray obs. 80−82519
Abell 2118 cluster, extent of hot intergalactic gas 78−86021
Abell 2197 and 2199, Westerbork survey at 610 MHz, 18W catalogue 80−67883
Abell 2218, complex radiosource in centre, 2.7 GHz obs. 79−30137
Abell 2256, rich cluster, steep-spectrum radiosource obs. 79−9016
Abell 2256, X-ray cluster of galaxies, radio props. 80−36726
Abell 2319, cluster of galaxies, X-ray and radio obs. 77−53692
Abell 2634, radiosources around 3C 465, continuum maps 78−73764
Abell 401, X-ray cluster of galaxies, radio emission distrib. 80−98731
Abell 478, cluster of galaxies, X-ray and radio obs. 78−8133
Abell 754, cluster of galaxies, radio and optical obs. 79−25737
Abell cluster, lunar occultation obs. at 327 MHz, survey 80−73052
Abell cluster radio sources, spectra and optical identification, SHF obs. 80−98729
Abell clusters, radio survey at 11.1 cm wavelength 79−58432
Abell clusters, search for radio sources 78−12379
Abell clusters of galaxies, 4C radiosources 79−88756
Abell clusters of galaxies, complex radio sources obs. at 2.7 GHz 79−92881
Abell clusters of galaxies, interferometric obs. of radiosources 78−4380
Abell clusters of galaxies, radio survey at 11.1 cm wavelength 78−20897
Abell clusters of galaxies, Westerbork 610 MHz survey of extended radio emission 80−36727
Abell clusters of galaxies, Westerbork obs. of fields 78−96549
Abell clusters of galaxies containing tailed radio galaxies, Westerbork synthesis obs. 80−56957
AFCRL 618, thermal radio emission from young planetary nebula 78−12343
AFGL IR sources, mol. line obs. 80−51856
amateurs' contributions, solar activities obs. *(Italian)* 78−7887
λ Andromedae, radio emission detect. from giant binary 77−22248
anticentre anomalous-vel. streams, 21 cm. line obs. 79−40257
AO 0235, mapping with uncalibrated visibility data, 5011 MHz obs. 80−77295
AO 0235+16.4, BL Lacertae object, another source exceeding the speed limit 77−2482
AO 0235+164, BL Lacertae object, radio halo obs. 78−4386
AO 0235+164, BL Lacertae object, radio study of z=0.524 absorpt. system 78−65680
AO 0235+164, BL Lacertae-type object, VBLI obs. of redshifted H I absorpt. 80−46658
AO 0235+164, Lacertid, optical and radio absorption line systems 78−16520
AO 0235+164, radio polarisation, evidence for rot. in variable radiosource 79−48917
aperture synthesis observations, tropospheric H_2O vapour irregularities effects on seeing 78−24339
R Aquarii, 43 and 86 GHz obs. of SiO maser 79−71036
R Aquarii, Mira variable, 14.9 GHz obs. 79−75210
R Aquarii, symbiotic star, radio mol. maser line obs. 80−72960
R Aquilae Mira variable, 14.9 GHz obs. 79−75210
Ariel 0535+26, flaring X-ray source, 2 cm obs. 78−54081
UX Arietis, binary star, radio obs. 77−64793
UX Arietis, RS Canum Venaticorum binary, two-freq. radio polarimetry 79−21335
Arp 205 (NGC 3448 and UGC 6016), aperture synthesis obs. of H I 79−53916
AS 501, compact H II region, OH main-line maser emission obs. 80−67716

radioastronomical observations continued
asteroids, radar detectability, opportunities for 1977-87 period 77−82149
B2 0055+26 (NGC 326), radio galaxy with precessing beam model 79−17118
B2 1308+326, BL Lacertae object, photometry and polarization during 1978 outburst 79−25718
B2 1502+28, head-tail galaxy in Abell 2022, Westerbork obs. of spectral index and polarisation distrib. 80−36727
B2 1506+34, peculiar radiogalaxy, H I absorption detection 78−54048
B2 catalogue radio sources, optical identifications and 5 GHz flux meas. 79−40283
B2 catalogue sources, high resolution obs. at 408 MHz 77−45589
B2 quasars, radio spectral props. 79−44632
B2 radiogalaxies of low luminosity, polarization at 1.4 GHz 79−71141
B335, mol. cloud, continuum emission mapping at 89.6 GHz 80−94842
B361, rotating dust globule, CO obs. 77−33582
B 0844+31, extended radio galaxy, multifreq. obs. 80−56963
B 35, bright rimmed molecular cloud, CH obs. 80−62238
B-type stars embedded in R-associations, free-free emission obs. 80−26851
background radiation, meas. at 2 mm *(French)* 77−13503
background radiation fluctuations at 1394 MHz 79−53941
background radiation spectrum, cosmological significance of obs. *(Italian)* 79−48972
Barnard 213 NW, rotation and vel. structure rel. to parent nebula 78−41007
Be-stars, radio emission 77−56984
1580 Betulia, radar obs. and radius of Amor-type object 80−36544
binary galaxies, dynamics and masses from 21 cm obs. 80−105332
blackbody radiation at 3.2 cm wavelength, linear polarization 79−97106
Bok globules, search for neutral H 77−29904
bright galaxies, Arecibo 2380 MHz, survey 78−57470
bright galaxies, radio obs. of lunar occultations, spectra and struct. 79−9005
bright galaxy nuclei, optical and radio survey, sample selection and obs. 80−73039
bright southern galaxies, H I obs. 77−57084
3C111, new very large radioenergy source in core of radio galaxy *(German)* 78−16558
5C9 survey of radiosources, 214 objects 78−16312
4C 03.59, BL Lacertae object, radio halo obs. 78−4386
3C 105, struct. and identification with galaxy 79−35413
3C 10, 3C 58, H I distrib. small scale struct. 78−45383
3C 10, Tycho's SNR, 10.7 GHz obs. 79−75264
3C 111, 3C 236, radio galaxies, 150 GHz obs. 80−41908
3C 111, optical and radio positions 79−48948
3C 111, radio galaxy, obs. at 1.38 cm wavelength with resolutions up to 8″ *(Russian)* 80−109558
3C 111, radio nucleus struct. 77−5581
3C 119, 286, 345, 454.3, quasars, 5 milliarcsecond resolution maps at 1.67 GHz 80−82531
3C 120, 273 and 345, structure from hybrid maps of quasars 79−92883
3C 120, 273 and 345, superluminal vars. of quasars 79−92882
3C 120, radio galaxy, linear polarisation and flux density vars. 77−9805
3C 123, brightness and polarisation distrib. at 3.7 and 6 cm wavelength 78−4340
3C 123, radio struct. at 2.7 and 15 GHz 78−54050
3C 129 and 129.1, in situ particle accel. and energy supply 80−46691
4C 13.17A, B, in X-ray cluster of galaxies Abell 401, radio emission distrib. 80−98731
3C 147, 3C 286, quasars, VLBI obs. at 329 MHz 80−67898
3C 147, 3C 380, quasars, milli-arcsecond struct. determined by hybrid mapping with five-station array 80−46694
3C 147, hybrid mapping on Very Large Array, SHF obs. 80−82534
3C 147, quasar, radio struct. determ. by multi-element very long baseline interferometry 78−4391
3C 178, H I absorption within radiogalaxy 79−5910
5 C 1 to 5 survey areas sources, 1421 MHz obs. 79−84864
3C 219, double radio galaxy, high-resolution 80−77500
3C 225.0, UHF and EHF obs. of foreground cold diffuse cloud 80−105311
3C 236, high resolution VLBI obs. of compact central component 79−92878
3C 236, radio galaxy, 6-49 cm obs. of double source 80−82528
3C 236, VLA obs. of extended radio core of giant radiogalaxy 79−75288
3C 264 (NGC 3862), radio galaxy, high resolution radio maps 77−5582
3C 270.1 and 3C 275.1, radio maps at 15 GHz 78−93452
3C 273, 3C 454.3, quasars, very high resolution obs. 77−33663
3C 273, rapid fluctuations of radio flux and circular polarisation and optical linear polarisation 77−91663
3C 273 B, small-scale structure and variability, 2.8 cm obs. 77−33672
3C 279, interplanetary scintillations and solar wind vel., SHF obs. *(Russian)* 80−77248
3C 279, superluminal expansion 79−53922
3C 27 area sources, 2695 MHz continuum obs. 80−46688
3C 286, quasar, radio absorpt. line obs. and appl. to cosmological deceleration mea. 78−20902
3C 293, radio galaxy, radio and optical obs. 78−93418
3C 303, double radiosource, radio struct. and optical field 78−16519
3C 310, extended radio galaxy, multifreq. obs. 80−51890
3C 315, radio galaxy, high resolution radio maps 77−5582
3C 319, radio struct. and optical identification with elliptical galaxy 80−31377
3C 31, linear polarization obs. of radio galaxy at 1.4 and 2.7 GHz 79−48925
3C 31, multifreq. radio obs. of galaxy with jets and peculiar spectra 78−16533
3C 31, radio emission obs. at 2.7, 4.8, and 10.7 GHz 79−35375
3C 31, radio galaxy, mag. field struct. in radio jets 80−82526
4C 32.69, quasar with radio jet, high resolution radio obs. 80−105375
3C 326, very large radio galaxy, multifreq. obs. 78−28810
3C 345, 418, 371, compact radio sources, arcsecond struct. 80−4450
3C 345, quasar, compact radiosource obs. 78−12399
3C 345, quasar, time dependent radio fine structure 77−17711
3C 345, quasar, VLBI obs. at 1.67 GHz 80−94885
3C 345, quasar relation between optical and radio VLBI 77−64876
3C 345 and 3C 454.3, D2-type QSOs 77−64875
3C 345 and 454.3, quasars, 102 MHz obs. of interplanetary scintillations *(Russian)* 80−94889

radioastronomical observations continued
3C 345 and NRAO 512, relative position to submilliarcsecond accuracy via VLBI 80−22097
3C 351, quasar, VLA maps and outer lobe optical emission search 80−105376
3C 382, 3C 386, radio galaxies, two-freq. high resolution obs. 78−86031
3C 388, galaxy in Abell 643, classical double radiosource, 4885 MHz obs. 80−109545
4C 39.04, powerful giant radio galaxy, multifreq. obs. 80−17682
3C 391, supernova remnant, obs. at 1.4 and 10.7 GHz 80−4417
4 C 39.25, compact radio source, search for time-depend. radio fine struct. 80−90552
4C 39.25, quasar, compact radiosource obs. 78−12399
3C 395, compact radio source, high resolution obs. at 1671 MHz 80−56960
4C 39-08, appl. of Clean and Restore technique to WSRT obs. *(Italian)* 80−98563
3C 405 (Cygnus A), radio galaxy, obs. at 1.38 cm wavelength with resolutions up to 8″ *(Russian)* 80−109558
3C 427.1, brightness and polarisation distrib. at 3.7 and 6 cm wavelength 78−4340
3C 449, radio jet structure at 1465 and 4885 MHz 80−12823
3C 452, spectral index variation 77−82309
3C 454.3, flat-spectrum source, variability at 962 MHz 77−82317
3C 465, extended radio galaxy, multifrequency UHF and SHF obs. 80−105338
4C 47.51, complex radiogalaxy, aperture synthesis obs. 80−94883
3C 48, 3C 273, 3C 295, scintillation at 25 MHz rel. to ang. struct. 78−65711
3C 48, QSO, search for variability at 408 MHz *(Russian)* 77−17710
4C 53.37 (1638+538), tailed radiogalaxy, dual curved jets 80−62265
3C 61.1, 3C 33, 1.4 GHz aperture synthesis obs. of circular polarisation 77−29656
5C 6 survey of 292 radiosources 78−24471
4C 73.08, multifreq. obs. of giant source assoc. with compact Zwicky galaxy 79−25745
5C 7 survey of 271 radiosources 78−24471
3C 84, 3C 273, quasars, vars. in circular polarisation at 8 GHz 77−33673
3C 84 (NGC 1275), Seyfert galaxy, search for variability at 408 MHz *(Russian)* 77−17710
3C 84 (Perseus A, NGC 1275), Seyfert galaxy, 5′ halo SHF obs. 80−105372
4C radio galaxies, structs. and optical identifications 79−71137
4C radio sources in Abell clusters, struct. and props. in declination ranges 10 to 20° and >50° 79−25743
4C radiosources, brightness and polarisation distrib. 77−26076
3C sources, lunar occultation obs. at 327 MHz 77−45588
3C sources, possible giant radio structure discovery at 11 cm 80−67895
4C sources 20°<δ<40°, 318 MHz flux density meas. 79−71140
4C sources in Zwicky galaxy clusters, detailed interferometer obs. and anal. 80−22099
4C sources with steep radio spectra, Westerbork obs. 79−35414
6C survey at 151 MHz, prospects 78−28813
Calar Alto IR objects, search for continuum radio emission 77−41418
calibration radio sources, flux density at 8420 MHz rel. to Virgo A 80−86004
calibration sources, precision flux-density meas. at 2295 MHz 77−37663
Callisto, brightness temp. at 1.3 cm wavelength 77−67062
Cancer cluster, Westerbork survey at 610 MHz 80−67884
Canes Venatici I galaxy group, neutral H obs. of NGC 4136, 4144, 4190, IC 4182 and (DDO 133) 79−84853
YZ Canis Majoris, flare star, coordinated X-ray, optical and radio obs. 78−8012
VY Canis Majoris, OH and H_2O microwave maser emission obs. 78−53949
VY Canis Majoris, OH masers very long baseline interferometric obs. 78−36712
VY Canis Majoris, OH/IR star, 1612 MHz OH maser multibaseline VLBI obs. 80−12766
YZ Canis Minoris, red dwarf star, weak radio flares interferometric obs. 78−65633
RS Canum Venaticorum, radio flare obs., (1979, February 6) 79−40220
RS Canum Venaticorum binary stars, radio luminosities and spectra 79−21333
Carafe group of galaxies, spectroscopic and photographic obs. of peculiar galaxies 79−35387
Cassiopeia A, 90 GHz map of young SNR 79−2561
Cassiopeia A, ^{14}N radioemission at 26 MHz 80−41886
Cassiopeia A, absolute radio spectrum 78−8090
Cassiopeia A, HF obs. using interference-excising correlator 79−75110
Cassiopeia A, intensity and polarisation at 9 mm wavelength 80−36732
Cassiopeia A, proper motions and temporal flux changes of compact features 77−60818
Cassiopeia A, radio emission evolution, freq. dependence *(Russian)* 78−4387
Cassiopeia A, radio emission evolution 79−67074
Cassiopeia A, secular decrease in 927 MHz flux, radio flux density obs. 80−67840
Cassiopeia A, secular decrease in radio emission flux density at 437 and 510 MHz *(Russian)* 80−8702
Cassiopeia A, spectral intensity variations *(Russian)* 77−91661
Cassiopeia A, supernova remnant, 38 MHz flux density meas. 78−12344
Cassiopeia A, supernova remnant, 927 MHz emission secular decrease 79−75255
Cassiopeia A, supernova remnant, flux density meas. and confirmation of 38 MHz anomaly 77−45531
Cassiopeia A, young SNR, radio emission evolution according to observational data 79−75256
R Cassiopeiae, Mira variable, vel. struct. in SiO maser spectrum 78−12248
R Cassiopeiae, VLBI obs. of SiO maser in Mira variable 79−92779
cD and related galaxies in poor clusters, pencil beam obs. of radio emission at 6 cm 80−62293
cD galaxies and related objects in poor clusters, 1400 MHz pencil beam obs. 80−62263
Proxima=V645 Centauri, coordinated X-ray, optical and microwave study 79−5830
Centaurus A, giant quasiperiodic mm wavelength bursts in nucleus 79−48928

radioastronomical observations continued
Centaurus A (NGC 5128), fast var. of nucleus at 13.5 mm wavelength 77−87564
Centaurus A (NGC 5128), radio and X-ray var. of nucleus 78−36711
Centaurus A (NGC 5128), radio galaxy, obs. at 1.38 cm wavelength with resolutions up to 8″ *(Russian)* 80−109558
Centaurus A (NGC 5128), slowly varying flux component, 22 GHz confirmation 80−36939
Cepheids between l=294° and 331°, UBV and 21 cm obs. 79−12478
Cepheus A mol. cloud, OH maser lines obs., star form. region 80−36691
Cepheus OB3 association, star form. in mol. cloud complex 78−28750
Cepheus OB3 association molecular cloud, mol. obs. rel. to star form. 80−12798
Ceres, radar obs. at 12.6 cm wavelength, surface roughness 80−36545
o Ceti, SiO maser variability at 86 GHz 80−41839
o Ceti (Mira), variable 2.6 mm CO emission obs. 78−12241
UV Ceti-type flare stars, simultaneous 1420 MHz and optical obs. of flares 78−49464
CG195.5+4.5, upper limit to 59.35 s periodic radio emission at 18 cm 80−86018
CG 135+1, γ-ray source, new highly variable radio source as possible counterpart 78−54095
CG 195+4, pulsating γ-ray source, no pulsed ratio emission at 325 MHz 78−65717
Circinus galaxy, H I 21 cm line obs. 77−33652
Circinus X-1, binary model, orbital eccentricity from X-ray and radio obs. 80−98735
Circinus X-1, distance from H I absorpt. obs. 78−12413
Circinus X-1, radio flare obs. at 2.1 cm wavelength 79−9035
Circinus X-1, radio flare phenomena Dec. 1979 and Jan. 1980 obs. 80−36731
Circinus X-1, radio source obs. at 408 MHz 79−53940
Circinus X-1, X-ray and radio flux meas. 77−2498
Circinus X-1 (3U 1516−56), obs. of optical and radio counterpart 78−12414
circumsolar plasma, d.m. propag., Venera 10 meas. 80−21886
circumsolar plasma, Venera 10 radio signal spectral meas. 80−109326
circumstellar shells of long-period variables, weak maser emission pedestal assoc. with SiO maser 78−93256
Cirinus X-1, simultaneous radio and optical obs. during outbursts 79−17137
CIT 6 (IRC+30219), IR C star, CO obs. of mass outflow 80−12761
CL 4, H I absorption from compact source 79−48944
CL 4, H I emission-absorption meas. at 1420 MHz 79−62922
CL 4, high-resolution 8450 MHz obs. of compact radiosource 79−44629
close binary stars, radio survey at 6 cm wavelength 78−32510
Cloud 2, mol. cloud, detect. of HC_5N (cyanodiacetylene) and HC_7N (cyanohexatriyne), SHF obs. 80−101627
clusters of galaxies, distances from X-ray and microwave obs. 79−71134
clusters of galaxies, gas content meas. by obs. of microwave background at 10.6 GHz 78−96551
clusters of galaxies, H I broad band emission search 80−46667
clusters of galaxies, H I content of intracluster medium 79−5896
clusters of galaxies, interferometer obs. of 77−53693
clusters of galaxies, microwave search for ionised gas 80−82477
clusters of galaxies, obs. of radio sources 78−12397
clusters of galaxies, rich X-ray emitting clusters, VHF obs. 80−62294
clusters of galaxies, X-ray and microwave obs., cosmological deceleration parameter determ. 79−21476
Coma cluster, H I emission search, gas content determ. of elliptical galaxies 80−46657
Coma cluster, Westerbork survey at 610 MHz, radio data and identifications 77−60628
Coma cluster of galaxies, diffuse radio emission obs. 79−88750
Coma cluster of galaxies, intergalactic intracluster H I, improved limits 79−75276
Coma galaxy cluster, halo radio source meas. by Westerbork survey 78−86027
Comet Bradfield (1978c), search for mm wave emission from HCN, CO and methyl cyanide 79−75157
Comet Kohler (1977m), OH 1667 MHz line absorption detection 78−4152
Comet Kohoutek (1973 XII=f), HF obs. 79−8883
Comet Meier (1978f) OH emission at 1665 and 1667 MHz 78−61800
comet plasma tails electron density deduced from refr. of occulted radiosources 79−53773
Comet West (1975n), microwave continuum radiation obs. 78−16349
Comet West (1975n), search for CH RF emission 78−20735
communication with extraterrestrial intelligence, international conference discussion and conclusions *(German)* 77−56845
compact central components in 17 extended radiosources, VLBI detect. 77−17703
compact extragalactic radio sources, interpretation of spectra 80−62299
compact extragalactic sources, flux density and linear polarisation at 3.7 and 11.1 cm wavelength 77−49490
compact H II regions, review of radio obs. 78−16507
compact H II regions near Type I OH maser sources, obs. 78−8094
compact nonthermal sources, polarisation at cm., mm., IR and visual wavelengths 79−5913
compact radio sources, vars. in intensities and sizes at 13 cm wavelength 77−78876
compact radiosources, high declination search at 8 GHz 78−69896
compact radiosources at 609 MHz, VLBI obs. 79−101209
compact radiosources in and near bright galaxies 78−49548
compact radiosources positions from VLBI obs. 78−81698
compact source in supernova remnant G78.1+1.8, props. from interstellar scintillation obs. 79−101213
compact sources, phase stability, ang. struct. and position meas. by radio-link interferometer 77−5452
compact sources high-resolution obs. at 1.35 cm wavelength high-resolution obs. at 1.35 cm wavelength *(Russian)* 78−69902
compact sources in bright galaxies, very long baseline interferometry 79−48943
compact sources in directions of SNRs, 2.8 and 3.7 cm obs. *(Italian)* 79−53925
compact unresolved sources, aperture synthesis obs. of circular polarisation, techniques and appl. 77−9670
Cone nebula, formaldehyde kinematics and distrib. 80−4418
cool gaseous nebulae, electron temps. from radio recomb. lines obs. 79−88726
coronal hole, radio and EUV obs. 77−78753
radioastronomical observations continued
coronal hole structrue from UV and radio obs. 77−53513
cosmic background, vars. in freq. spectrum along declination (+50° 30′) 77−17723
cosmic blackbody radiation, anisotropy detect. 78−4415
cosmic gamma burst, possible obs. at radio freqs. 77−9819
cosmic glack body radiation meas. using low temp. optical techniques, 2-40 cm^{-1} 79−71161
cosmic microwave background, no anisotropies at 31 GHz 80−51922
cosmic microwave background radiation, anisotropy meas. 80−41918
cosmic radio bursts with microsecond time scales, limits 79−17119
cosmological information from new types of radio obs. 78−28872
couble galaxies, H I 21 cm. line obs. 80−51886
3CR sources, multifreq. obs., results and interpretation 79−35416
3CR sources, multifreq. obs. 79−30141
3CR sources, VLBI obs. of hot spots in lobes 79−40286
Crab Nebula, 2695 MHz high-resolution maps *(Italian)* 79−53891
Crab Nebula, 2.7 GHz study with 3.7×10 arcsec ang. resolution 79−40248
Crab Nebula, compact source flux density meas. by interferometer 80−62252
Crab Nebula, emission region size, electron transport and mag. field models 77−17650
Crab Nebula, Faraday rot. obs. during solar control occultations 77−45593
Crab Nebula, flux density at 1.8 mm *(Russian)* 78−32558
Crab Nebula, lunar occultation obs. at 114 and 26.3 MHz, small-scale struct. 80−46627
Crab Nebula, lunar occultation obs. at decametre wavelengths 80−62248
Crab Nebula, millimetre and submillimetre meas. 79−75267
Crab Nebula, obs. of linear polarisation during occultation by solar corona 77−60837
Crab nebula, polarised radioemission occultation by solar corona during weak solar activity *(Russian)* 78−77527
Crab Nebula, radio emission from compact source, HF meas. with URAN-1 interferometer 80−31343
Crab Nebula, short-wave millimetric obs. with wide-band radiometer 79−96916
Crab Nebula, struct. at 327 MHz from occultation obs. 78−12339
Crab Nebula occultation by Moon, 1974, Sept., 180 and 1646 MHz obs. 77−26043
CRL 2591, IR source rel. to radio and H_2O counterparts 77−22330
CRL 2688, bipolar nebula, search for OH emission 78−41016
CRL 437, microwave spectral line profiles, rotation effects 78−45426
CTA1, continuum obs. of supernova remnant at 2695 MHz 79−62890
CTA 102, quasar, 5 milliarcsecond resolution maps at 1.67 GHz 80−82531
CTB 1, UHF emission and radio shell of SNR 80−77461
CTB 80, peculiar supernova remnant, central radio source optical and H I obs. 80−56896
CTD 93, compact radio source, high resolution obs. at 1671 MHz 80−56960
Culgoora-3 list of 2045 radiosources, obs. at 160 MHz 78−20655
cyanoacetylene, and ^{13}C substituted species, in Sagittarius B2 and Orion A, relative isotope fractionation 79−21374
cyanoacetylene, cyanodiacetylene in interstellar clouds, obs. 80−46634
cyanodiacetylene (HC_5N), obs. in (Heiles's cloud 2) 80−22054
cyanohexatriyne, detect. at 14.7 GHz in Heiles Cloud 2 and Sagittarius B2 78−73745
V Cygni, C star, 1-4 mm continuum emission obs. 79−88670
V1057 Cygni, CH radio emission obs. 77−87512
V1057 Cygni, FU Orionis-type star, flare up in 1720 MHz OH line 79−62843
χ Cygni, Mira variable star, variable 2.6 mm CO emission obs. 78−12241
V1057 Cygni, OH obs. 80−36629
NML=V1489 Cygni, OH/IR star, 1612 MHz OH maser multibaseline VLBI obs. 80−12766
V645 Cygni (CRL 2789), bipolar nebula, O-type exciting star 78−4392
V645 Cygni (GL 2789), IR and EHF spectroscopy 80−72956
V1500 Cygni (Nova 1975), radio emission from expanding shell 80−26868
V1500 Cygni (Nova 1975), radio obs. and analysis 80−67726
γ Cygni SNR, ang. diameter from 1.4 GHz aperture synthesis obs. 78−4328
Cygnus A, 99 GHz obs. of components and central source 78−41069
Cygnus A, digital hologram reconstruction of radio obs. 77−64653
Cygnus A, polarization maps at 23 GHz 79−71109
Cygnus A, radio galaxy, 150 GHz obs. 80−41908
Cygnus A, radiogalaxy structure at 150 MHz 80−101646
Cygnus Loop, radio struct. at 25 MHz 78−54027
Cygnus Loop, UHF emission and filamentary structure of SNR 80−77461
Cygnus Loop H I distrib. rel. to high-vel. gas 79−71083
Cygnus OB 2 association, H content, radio continuum emission search 77−64809
Cygnus X, H I 21 cm line emission maps of field containing G78.2+2.1 SNR 80−56917
Cygnus X region, 10.6 GHz survey 77−74153
Cygnus X region, riddle of γ Cygni radio source resolved 78−28809
Cygnus X region, visual extinction map and radio brightness temp. 78−61929
Cygnus X-1, correlated X-ray-radio transition, 1976 February 77−17719
Cygnus X-1, X-ray binary, variable star, SHF obs. 80−73071
Cygnus X-3, high-resolution 8450 MHz obs. of compact radiosource 79−44629
DA 267, compact radio source, arcsecond struct.. 80−4450
DA 406 (1611+343), broad-band flux density vars. 79−40282
dark and molecular clouds, 30 GHz obs. in 1_0-0_1 transition of SO 80−46639
dark clouds, $^{13}C^{16}O/^{12}C^{18}O$ double ratio, isotopic fractionation evidence 80−73017
dark clouds, C recombination line obs. 79−75260
dark clouds, formaldehyde obs., 5 GHz survey 80−73028
dark clouds, H I 21 cm line obs. 79−21393
dark clouds, H I 21 cm Zeeman effect obs., magnetic fields 79−8977
dark clouds, HCO^+ isotopes, anomalous line intensities 79−17054
dark clouds, $HN^{13}C$ and HNC, hyperfine structure at 87 and 90 GHz 79−101182
dark clouds, NH_3 survey 78−49507
dark clouds, search for radio continuum radiation 77−33585

radioastronomical observations continued
dark clouds, unsuccessful search for formaldehyde-d_1 79−12500
dark dust clouds in southern hemisphere, formaldehyde obs. 77−13434
decameter wavelength spectrum of quiet Sun 78−7966
decametric storm burst source positions, UTR-2 obs. at 25 MHz 80−90403
decametric survey of discrete northern sources, catalogue of 329 objects, 10-20° declinations 78−57471
decametric survey of discrete northern sources, LF absolute flux scale 78−57663
decametric survey of discrete northern sources, spectra of 266 sources in 10-1400 MHz range 78−57664
decametric survey of discrete northern sources, UTR-2 radiotelescope, expt. techniques, data processing 78−57461
deflection of polarized microwave radiation, relative phase delay technique 78−53818
HR Delphini (Nova 1967), radio emission from expanding shell 80−26868
diffuse nebulae, formaldehyde and H110α recomb. lines obs. towards bright rims 77−87510
discrete sources, flux densities meas. at 14.9 GHz (2 cm) 77−37664
30 Doradus, absorpt. by foreground H I in LMC 78−24541
30 Doradus region, in LMC, radio model 78−96523
double galaxies, observational data on well-defined sample 80−17674
double quasar 0957+561A, B, radio study rel. to gravit. lens hypothesis 79−88762
double radio sources, hot spots behaviour 80−94882
double radiosource near NGC 2823 elliptical galaxy 78−24562
DR15, galactic H II region, obs. at 408, 1407 and 2695 MHz 80−94881
DR21(OH) obs. of J=1→0 emission from $H^{15}NC$ 77−82299
DR 21, anomalous NH_3 absorpt. obs. 77−53669
DR 21, H II region CO J=2-1 isotopic line obs. at 230 GHz 77−33590
DR 21, HF calibration source, flux density obs. at 8420 MHz 80−86004
DR 21 (W75), continuum obs. at 3.9 mm 79−35333
DR 21 OH, relationships of N_2H^+, HCO^+, HCN and CN 77−33587
dust cloud complex in Taurus, radio obs. of fragmentation and localised multiple vel. components 78−4308
dust cloud in Corona Austrina, mm wavelength obs., nonhomologous collapse, rel. to star form. 79−30102
DW 1548+05, intensity variations at 2.7, 6.6 and 10.6 GHz 77−60834
dwarf galaxies, nearby, 6 cm continuum emission limits from compact components 79−30126
dwarf galaxies in Nilson's Uppsala General Catalogue, H I 21 cm line survey 79−92846
dwarf nearby galaxies, search for intergalactic H I clouds 79−71126
dwarf spheroidal galaxies, H I content upper limits 78−57633
early-type galaxies, in Virgo cluster, H I survey 79−30123
early-type stars, mass loss from radio obs. at 6 cm 80−82347
early-type stars with large IR excess, OH emission 79−71035
Effelsburg 100 m radiotelescope, first obs. at 7 mm wavelength, props. and performance 80−62013
electron temperature gradients with distance from galactic centre 79−88744
elliptical and S0 galaxies, H I obs. 77−64838
elliptical galaxies, H I detect., upper limits 77−53685
elliptical galaxies, H I emission search, gas content determ. 80−46657
elliptical galaxies, search for H I emission 78−65681
40 Eridani, multiple star system undetected at 4885 MHz 80−105282
expanding molecular envelopes around evolved stars, CO emission line obs. 77−22219
extended extragalactic radiosources, compact structure, freq. depend. 78−69895
extended radio sources, VLBI obs. of compact components 80−17680
extended radiosource 1400+162, BL Lacertae object in group of galaxies 78−4339
extended radiosources and elliptical galaxies, search for radio cores using Very Large Array 78−81700
extended radiosources and elliptical galaxies, small-diameter components in extended structs. 78−81699
extended radiosources catalogue, 408 MHz fan-beam survey at low galactic latits. 77−26078
external galaxy spiral arms, CO emission detect. 77−33641
extragalactic 3C sources, polarization and total intensity at 2695 and 8085 MHz 79−35411
extragalactic CO emission obs. at 2.6 mm 77−45543
extragalactic compact sources with faint components, VHF and SHF obs. 80−90547
extragalactic continuum sources, EHF of interstellar spectra 79−35319
extragalactic decimeter sources flux variability 79−62924
extragalactic flat spectrum sources, VLBI UHF and SHF obs. 80−90549
extragalactic objects, 1 mm continuum obs. 78−36720
extragalactic powerful radiosources, compact and extended components spectra 77−41415
extragalactic radio sources, confusion-limited survey at 4.755 GHz, source list and areal distribs. 80−98577
extragalactic radio sources, search for compact sources at low freqs. (81.5 MHz) 80−90553
extragalactic radio sources, Texas Interferometer radio positions and optical identifications 79−88753
extragalactic radio sources, variable radio emission temporal charact. *(Russian)* 80−62307
extragalactic radio sources (>1 arcsecond), large-scale struct. 78−57668
extragalactic radio sources study of emission variability in millimeter wave range *(Russian)* 80−90559
extragalactic radiosource variability at 2.7 GHz, 2 yr monitoring 77−17702
extragalactic radiosources, integrated linear polarisation meas. 78−4381
extragalactic radiosources, mag. field orientation evidence 80−46690
extragalactic radiosources, variability at 408 MHz, 3-yr. monitoring program 79−71142
extragalactic radiosources, variable with flat spectra, 90 GHx flux density 80−73056
extragalactic sources, 318 MHz variability of complete sample 79−30139
extragalactic sources, astrometric obs. rel. to lunisolar precession determ. 77−5129
extragalactic sources, deep survey of selected regions at 4.85 GHz 80−77502
extragalactic sources, evidence on origin of rot. measures 77−5584
radioastronomical observations continued
extragalactic sources, flux densities, and variability at 2.7 GHz 77−53694
extragalactic sources, obs. with Cambridge 5 km telescope at 5 GHz 78−12391
extragalactic sources, QSOs and galaxies, linear polarisation meas., SHF obs. 80−73058
extragalactic sources, rot. measure, linear polarisation obs. at 7.2 cm 80−82530
extragalactic sources, statistical props. of compact features as function of flux density 78−41071
extragalactic sources, vars. at 7.9 GHz 77−37661
extragalactic sources, very high resolution obs. 77−33663
extragalactic sources at 10.5 GHz, linear polarization meas. 79−12533
extragalactic sources from NRAO-MPIfR 6 cm surveys, 21 cm flux density meas. 79−88754
extragalactic sources suspected of decimetric flux density vars., 610 MHz VLBI obs. 77−78879
extragalactic sources with short wave radio emission excess, flux densities and variability at 1.35 cm *(Russian)* 78−57666
extragalactic sources with strong millimetre wave emission, 90 GHz obs. 78−16548
extragalactic sources with strong mm components, simultaneous radio obs. 80−73055
extragalactic variable radiosources, linear polarisation obs. at 7.2 cm wavelength 77−64870
extragalactic variable sources, ten-year study at centimetre wavelengths 78−89267
extraterrestrial radio emission detection, Jansky's original 1932 data 79−17144
faint extragalactic radio sources, counts estimate at 5 GHz 78−32588
faint radio sources, statistical study of mean ang. size and sky density at 81.5 MHz 80−51893
faint radiosources statistical counts at 2380 MHz 78−65706
FJM 3, 100 micron source, radio and IR studies 77−26082
FJM 6, molecular cloud, far IR, near IR radio mol. line studies 80−26929
flare stars, combined optical and radio obs., long-duration events 79−53827
flare stars, nature of nearby radiosources 78−12388
flat-spectrum radio sources, variability at 96 MHz 77−82317
formaldehyde, ^{18}O isotope, 4389 MHz obs. 79−44591
formaldehyde, survey in Orion dust cloud L1641 79−71099
formaldehyde absorption and visual extinction in several dark clouds near NGC 2264 79−88715
formaldehyde as probe to investigate dark cloud struct. EHF and SHF obs. 80−105317
formaldehyde-d_1, detect. in interstellar clouds 80−8670
Fornax A, obs. of central region of double radiosource at 4.9 GHz 79−5912
G0.7-0.0 (Sagittarius B2), struct. and He abundance 78−45380
G120.1+1.4, Tycho's SNR, rot. measure and turbulent struct. 79−88718
G12.2−0.1, radio and IR obs. of OH/H_2O source 78−57620
G126.2+1.6 SNR near 4U 0115+63 X-ray transient 80−8668
G127.1+0.5, remarkable supernova remnant centred on very compact radiosource 78−16555
G127.1+0.5, supernova remnant, VLBI obs. of assoc. compact radiosource 78−86029
G127.3+0.7, possible supernova remnant in open cluster, 1.4 GHz obs. 77−64826
G127+0.5, continuum obs. at 2695 MHz of supernova remnant 78−61903
G292.0+1.8, unusual SNR, synthesis map at 1415 MHz 77−49454
G309.81+0.07, point radio source and possible stellar remnant of supernova, obs. 80−51849
G326.3−1.8, G348.5+0.1, G348.7+0.3, unusual supernova remnants, radio obs. 79−84841
G339.2−0.4, radio recombination line obs. of low-excitation H II region 80−46650
G339.2−0.4, supernova remnant or planetary nebula, radio and optical obs. 80−22104
G35.6−0,0 and G35.6−0.4, kinematic distance estimates 78−73769
G37.7+0.1, double recombination line galactic thermal source, obs. at 1400 and 2371 MHz 78−69897
G46.8−0.3, galactic supernova remnant, kinematic distance estimate 79−84833
G48.6+0.0, galactic H II region, direction, H I, OH and H_2CO absorpt. line meas. 78−85996
G49.5−0.4 (W51), high resolution obs. at 5 and 15 GHz of giant H II complex 78−54065
G55.7+3.4, shell source, high resolution obs. at 610 and 1415 MHz 78−8140
G65.2+5.7, 1420 MHz continuum obs. of new SNR 79−44587
G65.2+5.7, 1420 MHz continuum obs. of supernova remnant *(Italian)* 79−53886
G74.9+1.2, continuum obs. at 2695 MHz of SNR 80−67830
G74.9+1.2, supernova remnant, distance 77−64864
G74.9+1.2, supernova remnant, distance estimate from H I absorpt. line meas. 78−28765
G74.9+1.2, supernova remnant, VLBI obs. of assoc. compact radiosource 78−86029
G78.2+2.1 in Cygnus X region, H I 21 cm line emission maps 80−56917
G 0.7−0.0 (Sagittarius B2), interpretation of radio recomb. line emission 77−17651
G 109.7+2.2, type I OH maser source near Herbig-Haro object *(Russian)* 80−17684
G 21.5−0.9, supernova remnant resembling Crab Nebula, obs. 77−5553
G 261.9+5.5, H I 21 cm obs., H I clouds in SNR 80−62229
G 339.6−0.1, high resolution map at 1415 MHz, possible assoc. with 4U 1642−45 79−71143
G 74.9+1.2, supernova remnant, total intensity and polarization struct. 79−8980
G 84.2−0.8, high resolution 1415 and 2695 MHz obs. of SNR 80−98702
G 84.2−0.8, new supernova remnant in Cygnus 77−29906
galactic, nonthermal emission in 0.25-9.18 MHz range, RAE 2 lunar satellite obs. 78−45398
galactic 21 cm line obs. in 348°≤l≤360°, −22°≤b≤−1° region 77−60824

radioastronomical observations continued
galactic anticentre, 21 cm obs. of H I stream 80−90524
galactic background, linear polarisation between 408 and 1411 MHz, reductions 77−2500
galactic centre, ang. size for compact radio source 78−28779
galactic centre, extended thermal component, broad-line H94α emission 78−77598
galactic centre, H radio recombination line obs. of arc-like source 80−82498
Galactic Centre, H recomb. lines obs. at decimetric wavelengths 77−82310
galactic centre, high-resolution 8450 MHz obs. 79−44629
galactic centre, OH absorpt. struct. determ. using regularisation method 80−17505
galactic centre, radio recomb. lines obs. rel. to extended thermal emission ionising agent 79−97059
galactic centre, spectrum of compact radiosource 79−21422
Galactic Centre direction, 252α recomb. line emission 77−45587
galactic centre direction, 327 MHz obs. upper limit for D/H ratio 80−26949
galactic centre direction, H200β line detect. 77−78868
galactic centre direction, low-freq. radio recomb. lines studies 78−32589
galactic centre region, 5 GHz formaldehyde absorpt. obs. 79−84855
galactic centre region, compact radio continuum sources obs. 79−21430
galactic centre region, compact radiosource interferometry 77−53686
galactic centre region, H I 21 cm line survey 78−12361
galactic centre region, H I absorpt. obs. 77−45560
galactic disc, thickness from H I 21 cm obs. rel. to mass models 79−75273
galactic disc emission at 4 cm wavelength, large-scale and small-scale cloud structs. 78−28795
galactic dust globules, microwave spectral lines obs. 78−57609
galactic equator, H I recomb. line emission, 408 MHz obs. 77−13451
galactic gas-to-dust ratio determ. from globular cluster obs. 79−88747
galactic H_2O vapour sources, maser phase duration galactic distrib. 79−35343
galactic H I, combined northern and southern survey, photographic presentation 80−62241
galactic H I 21 cm emission-absorpt. survey, two component interstellar medium model 79−40256
galactic H I 21 cm line obs. for southern hemisphere 80−85987
galactic H I 21 cm obs., possible four-arm spiral pattern 77−60821
galactic H I absorption, obs. of struct. on small ang. scales 80−22051
galactic H I absorption spectra in direction of extragalactic radiosources 78−24541
galactic H I at $|b| \geq 10°$, southern sky survey 77−64830
galactic H I cloud struct. in interarm region 79−21445
galactic H I distrib. outside solar circle 79−21421
galactic H I shells and supershells 79−53861
galactic H II large scale distrib., recomb. line surveys 78−16539
galactic H II regions, aperture synthesis obs., quick look survey 78−12329
galactic H II regions, H I and He I ratio recomb. line survey at 10.2 GHz 79−48874
galactic halo, radio obs. 78−96544
galactic large-scale magnetic features 79−58418
galactic LF background radiation, spectra and absorpt. 77−33707
galactic linearly polarised radio emission, bright spot obs. at 1 m wavelength 77−17709
galactic magnetic field from radio polarisation obs. 78−24547
galactic magnetic field from radioastronomy obs. 78−24548
galactic magnetic field scale and strength from pulsar data 78−28752
galactic nebulae, obs. at 5 GHz 78−4327
galactic non-thermal radio radiation from polar regions, spectra 80−22082
galactic nucleus, 6 cm recomb. line emission vels. 78−69885
galactic nucleus, H I contour maps 79−35386
galactic nucleus radio source, obs. 77−5572
galactic OH clouds in direction of extragalactic radiosources, survey 77−64822
galactic plane, S hemisphere survey at 5 GHz 78−81686
galactic plane radio survey at 4.875 GHz, list of 1186 sources 79−21431
galactic plane towards PSR 1858+03, obs. rel. to pulsar distance 77−64785
galactic radiation, distributed, linear polarization obs. results processing optimal algorithm selection *(Russian)* 77−91441
galactic radio emission, 151.5 to 408 MHz, spectral index ang. and freq. var. 79−21446
galactic radio halo shape and size 79−12521
galactic radio sources, OH radio lines absorpt. obs. 78−54068
galactic sources, H110α line and formaldehyde absorption line obs., SHF obs. 80−77472
galactic southern H II regions, mapping at 1415 MHz 79−53899
galactic spiral structure from H I 21 cm obs., linear theory, nonreson. region 79−88738
galactic structure from H I 21 cm surveys 79−44611
galactic supernova remnants, 5 GHz obs. 77−29907
galaxies, 21 cm. line obs. and integrated Brandt masses 78−93398
galaxies, 21 cm line obs. of H I large-scale distrib. in early type objects 80−8685
galaxies, 3 cm obs. of 141 optically bright objects 80−73040
galaxies, 408 MHz obs. of 91 spirals 80−98720
galaxies, active nuclei, radio obs., future prospects 78−57652
galaxies, blue compact, with emission lines, H I content 77−87542
galaxies, bright, 1415 MHz continuum survey 80−94869
galaxies, bright, distrib. and density of neighbouring background radio sources 80−56964
galaxies, detection of extragalactic ammonia 79−48886
galaxies, distance scale from IR magnitude/H I vel.-width relation 80−82480
galaxies, early type disks, H I distrib. and vel. structure, 21 cm line obs. 79−35357
galaxies, early-type, H I obs. 78−45401
galaxies, elliptical, extended radio sources, partial synthesis maps at 2.7 and 8.1 GHz 80−105330
galaxies, flat spectrum, in 5 GHz S4 survey, Westerbork obs. 79−58435
galaxies, H I 21 cm line obs. 79−67091
galaxies, H I 21 cm line obs. of 14 edge-on spirals 79−97075
galaxies, H I 21 cm line widths correl. with absolute magnitude and type 79−5900
galaxies, H I extent from centre, 21 cm line study 79−97067
radioastronomical observations continued
galaxies, H I vel. widths and IR magnitudes rel. to distance scale and expansion rate outside Local Supercluster 80−105325
galaxies, HI content, 21 cm obs. of elliptical and 10 objects 79−97066
galaxies, isolated, continuum survey at 5 GHz 80−105333
galaxies, large, H I mapping survey obs. 80−94870
galaxies, late-type H I obs. rel. to integral props. derivation 78−86015
galaxies, low luminosity, radio struct. and fluxes, Westerbork obs. 77−82306
galaxies, nearby, H I profiles obs. 80−41895
galaxies, nearby, radio continuum obs. *(German)* 80−109544
galaxies, new complete sample, struct., redshifts 79−17096
galaxies, optically bright, radio survey at 1400 MHz, 248 radiosources detect. 77−60627
galaxies, quasars and galactic radiosources, flux densities at 1.35 cm wavelength *(Russian)* 77−64868
galaxies, radio brightness distrib. obs. with RATAN-600 telescope 78−65698
galaxies, radio continuum obs. at 11 cm 80−94872
galaxies, radio recombination line studies of nearby objects 78−93397
galaxies, rich Abell clusters, survey at 408 and 1407 MHz 78−81694
galaxies, Sc I type, 21 cm. vels. rel. to motion of Galaxy and Local Group, data 77−5560
galaxies, small, accurate 21 cm H I spectra 79−35382
galaxies, unseen, H I obs. rel. to limits on space density 77−29925
galaxies, warped H I discs obs. 77−5567
galaxies, warped H I layers 78−16543
galaxies and Milky Way obs. *(Spanish)* 79−40275
galaxies in Abell clusters, Westerbork aperture synthesis obs. 78−12360
galaxies isolated pairs, radio continuum survey 78−57657
galaxies primordial protoclusters, search for H I emission at Z=3.33 and (4.92) 78−41066
galaxies with radio jets, 5 GHz obs. 77−29945
galaxies with tail-bridge struct., spectral index, radio polarisation, mag. field 79−58416
Galaxy, rot. curve from H I 21 cm obs. accounting for interstellar gas expansion *(Russian)* 79−48938
Galaxy, rot. curve to R=16 kiloparsecs 79−97081
Galaxy central region, improved H I data rel. to barlike model of inner Galaxy gas distrib. 80−67845
galaxy clusters, central regions, 3.5 and 4.0 mm obs. *(Russian)* 80−82525
galaxy clusters, radio halos, 610 MHz obs. 80−17673
galaxy clusters, scattering of microwave background, 9 mm obs. 80−105366
galaxy clusters, scattering of microwave background radiation 80−105367
galaxy clusters, Sunyaev-Zeldovich effect at 9 mm wavelength 80−41919
Galilean satellites, 12.6 cm radar obs. 77−71057
Galilean satellites, radar obs. during 1976, results 78−61788
Ganymede, brightness temp. at 1.3 cm wavelength 77−67062
Ganymede, surface model and characts. from radar obs. 80−90359
GB2 1400 MHz survey, radio spectra of flat-spectrum sources 79−44628
GB2 sky survey at 1400 MHz, differential radiosource counts 78−54063
GB sky survey at 1400 MHz, rel. to isotropy of radio source population 77−45584
Geminid meteor stream, struct. from radar obs. 80−82310
giant molecular cloud near M17, H I abundance, 21 cm obs., chem. evolution 79−21383
giant molecular cloud near M17, structure and extent from CO 115 GHz obs. 79−71084
giant molecular clouds, H_2 densities and $^{12}C/^{13}C$ ratio 80−51837
giant molecular clouds, turbulent cores, CS obs. 80−51822
giant planets, 1.4 nm obs., effective temps. 77−87312
giant radio galaxies, 26-100 MHz obs. of four objects 80−56961
globular cluster fields, radio continuum obs. at 2.7, 4.8 and 10.7 GHz 80−101619
globular cluster fields, radiosources detect. 79−17114
globular clusters, $^{12}C^{16}O$ emission, unsuccessful search at 2.6 mm wavelength 78−41000
globular clusters, H_2 mass upper limit from CO 2.6 mm transition obs. 79−17029
globular clusters, H_2O maser emission search 79−30094
globular clusters, high sensitivity search for main-line OH emission 80−62207
globular clusters, obs. of assoc. radiosources 77−87484
globular clusters, search of OH and H_2O lines for extraterrestrial intelligence 80−56725
globular clusters, southern, gas content upper limits 80−22047
Green Bank second survey of extragalactic radiosources of 1400 MHz, catalogue of 2022 sources 79−62761
Green Bank surveys at 1400 MHz 78−28543
GT 0236+610, position and LS I +61°303 as optical counterpart 78−36568
GT 0236+610 (LS I+61°303), radio, optical, X-ray, gamma-ray Be star, obs. 79−88755
GT 0236+610 radio counterpart for γ-ray source CG 135+1 78−24560
GX 13+1 (3U 1811-17), search for radio emission 78−41081
GX 17+2 (3U 1813-14), radio and optical identification 78−45428
GX 17+2 (3U 1813-14), search for radio emission 78−41081
H1-36 (3U 1746-37), emission line object, radio spectrum 77−82239
H 2155−304, X-ray source, Very Large Array obs., radio source discovery 79−44643
H I regions, 42 cm absorpt. search rel. to protons mag. monopole struct. limits 79−53717
H II regions, aperture synthesis obs. 77−87507
HB13, radio galaxy with jets, 151 MHz obs. 79−48926
HD 118216=HR 5110, radio outburst and UV spectra of RS Canum Venaticorum-type binary 79−62844
HD 192163, Wolf-Rayet star in ring nebula HGC 6888, SHF obs. 80−82386
HD 26676, radio emission at 6 and 21 cm wavelengths 77−91532
head-tail radio galaxies, intrinsic parameters distrib. 80−17653
head-tail radio galaxies, VLA obs. 79−48945
head-tail radio galaxies in poor clusters, radio and optical obs. 78−96530
head-tail radio galaxies velocities with respect to intracluster medium 78−49516
Heile's Cloud 2 at SHF cyanohexatriyne detection 78−41018

radioastronomical observations continued
Heiles 2 cloud collision, assoc. cyanodiacetylene emission at 24 GHz 78−65675
Heiles 2 dust cloud, NH_3, and cyanobutadiyne emission relative distrib. 80−17641
Heiles 2 interstellar dark cloud, NH_3 hyperfine struct. 77−78852
Heiles Cloud 2, obs. of H I self absorpt. 77−29901
Herbig-Haro objects, radio obs. and nearby compact H II regions 80−51756
Herbig-Haro objects 7-11, compact H II region and H_2O maser sources 80−73019
Herbig-Haro objects and surrounding dark clouds, NH_3 23 GHz obs. 80−72934
Hercules supercluster, evidence for intracluster medium 80−22092
Hercules supercluster, radio luminosity function at 610 MHz 79−44625
YY Herculis, symbiotic star, radio continuum detect. 79−25615
YY Herculis region, stellar radio emission refuted and new source discovery 79−35274
HFE 2,3, molecular cloud, for IR radio mol. line studies 80−26929
HFE 2, 100 micron source, radio and IR studies 77−26082
HIA 0255+574, characts. of radiosource near HD 18391 supergiant star 78−81701
HIA 2344+092, HIA 2344+094, sources near quasar PKS 2344+09, obs. 77−37659
high positive velocity H I clouds, spatial and vel. struct. 77−13442
high velocity H I clouds, fine struct. 77−29898
high-velocity H I cloud near M33, obs. rel. to M33 H I tail 80−12815
high-velocity H I clouds, map 80−26923
Holmberg II, irregular galaxy, aperture synthesis obs. 77−2475
HR 1099, 10 GHz radio emission from RS Canum Venaticorum binary 80−82427
HR 1099, binary stars, radio obs. 77−64793
HR 1099, flare activity observed at 2.8 cm wavelength 78−36590
HR 1099, flare emission at 2.8 cm (1978 February) 78−32476
HR 1099, noneclipsing RS Canum Venaticorum binary, radio flare obs. 77−17632
HR 1099, radio flux vars. obs. and optical ephemeris 78−36641
HR 1099, RS Canum Venaticorum binary, nonthermal flare emission during February 1978 outburst 79−21332
HR 1099, RS Canum Venaticorum binary, rapidly variable polarisation obs. at radio freqs. 79−21336
HR 1099, RS Canum Venaticorum binary, strong radio flaring discovery 79−21330
HR 1099, RS Canum Venaticorum binary, two-freq. radio polarimetry 79−21335
HR 1099, RS Canum Venaticorum binary, VLA radio obs. during 1977 international campaign 79−21334
HR 1099, RS Canum Venaticorum binary star, radio obs. at 8.0 GHz 79−21331
HR 1099, RS Canum Venaticorum type binary, radio emission detect. 77−9772
HR 1099, RS Canum Venaticorum type binary, strong radio flaring obs. 79−84821
HR 5110 (HD 118216), RS Canum Venaticorum binary, radio flaring obs. 79−67053
HR 8752, G-type supergiant, obs. of associated radio source 78−40942
HVC 132+23−211, small high-velocity cloud, detailed struct. 78−89241
W Hydrae, long-period variable, suspected Zeeman splitting in OH masers 80−36632
W Hydrae, long-period variable star, cyanodiacetylene detect. 77−82238
IC239, H I distrib. determ. 79−53910
IC 10, H I emission obs., unusual kinematics 79−67098
IC 10, irregular galaxy, giant H I envelope obs. 79−67094
IC 1318 b and c, H_2CO absorpt. 78−16484
IC 1396, bright rims, high resolution 1415 and 4830 MHz obs. 79−71092
IC 1396, H II region three dimens. model from 2695 MHz high resolution map 80−105316
IC 1396 (Sharpless 131), 2695 MHz continuum map of H II region 80−105310
IC 1795, HF C I recomb. line emission obs. 78−28748
IC 1795/1805, radio obs. rel. to exciting star total luminosity and H II regions IR luminosity 78−96519
IC 1795/1805/1848 extended H II region, 2695 MHz map 77−17658
IC 1805, 1848, giant H II regions, physical anal. from radio obs. 80−36695
IC 1848 A, bright-rimmed mol. cloud, mol. and IR obs. rel. to star form. 79−5810
IC 2149, planetary nebula, extinction and radio struct. 77−41402
IC 342, Scd galaxy, central regions IR and radio emission rel. to star form. 80−62256
IC 342, Scd galaxy, discovery of companion 80−36712
IC 342, Scd galaxy, H I large-scale struct. obs. 80−67857
IC 342, Scd galaxy, struct. from H I obs. 80−73045
IC 342, spiral galaxy radio continuum obs. 77−74132
IC 4296, double-double radio galaxy 1415 MHz obs. 77−41412
IC 443, H I distrib. rel. to high-vel. gas 79−71083
IC 443, shocked clouds of subthermally excited OH in SNR 79−35349
IC 443, supernova remnant, CO emission from dense cloud 77−29897
IC 443, supernova remnant, H I cloud and jet obs. 77−33592
IC 443, supernova remnant, negative vel. H I condensations obs. 78−54016
IC 443, supernova remnant, shocked CO discovery 80−8669
IC 5146, young open cluster, CO obs. of assoc. dark cloud 79−48881
IC 708, Papillon radio galaxy, morphology, polarization 79−92855
IC 708 and 711, head-tail radiogalaxies in Abell 1314, 1.4 GHz obs. 77−60833
II Zw 70/II Zw 71, compact galaxies, H I maps, tidal interactions 78−96531
interarm region and gas layer parameters, 21 cm line obs. 79−9007
interferometric obs., data storage requirements 77−78651
interferometric obs. for Earth precession and nutation precision estimation 77−73623
interferometry, atmospheric delay fluctuations with scale sizes >1 km 79−8675
intergalactic cloud in Sculptor, 21 cm obs. 77−64843
intergalactic H I clouds, search in NGC 1023 and Canes Venatici II 79−35389
intergalactic H I clouds search in Sculptor group of galaxies 79−30122
intergalactic H I search in nearby groups of galaxies 79−30121
radioastronomical observations continued
intergalactic high velocity H I clouds, high sensitivity survey 78−65686
intergalactic hot gas in distant richness class 4 clusters of galaxies, detection 78−12369
interplanetary magnetic field structures out of the ecliptic 77−78592
interplanetary plasma, scintillation obs. of solar wind 78−49279
interplanetary radiowave phase scintillation rel. to search for VLF gravit. radiation. 79−70995
interplanetary scintillation, m wavelength, bispectral anal. 78−12153
interplanetary scintillation, obs. rel. to solar wind plasma irregularities anisotropic struct. 80−67489
interplanetary scintillation, obs. ref. to solar wind speed latit. and longit. struct. 79−40049
interplanetary scintillation, obs. using fully automatic system 79−101064
interplanetary scintillation, synoptic anal., rel. to solar wind turbulence 79−2460
interplanetary scintillation, theory and appl. 79−8880
interplanetary scintillation enhancements due to solar flare assoc. shock waves 77−2318
interplanetary scintillation meas. of electron density power spectrum in solar wind 78−77448
interplanetary scintillation obs. and solar wind vel. meas. 78−49278
interplanetary scintillation observations, solar wind vel. determ. *(Russian)* 79−80185
interplanetary scintillation of radio sources in August (1972) 77−25901
interplanetary scintillation response to solar wind density struct. var. 79−2455
interplanetary scintillation spectra, radio spectrograph obs. 80−72741
interplanetary scintillations, dispersion anal. of solar wind vel. 78−7852
interplanetary scintillations, freq. correlation *(Russian)* 77−17427
interplanetary scintillations spectra, influence of source sizes, obs. 80−46361
interplanetary shock waves, flare-generated, scintillation obs., 1977 Sept. 79−48638
interplanetary shock waves, generated emission in 100-700 kHz range, Prognoz obs. 78−69636
interplanetary shock waves during second STIP interval (1976, March 15-May 15), scintillation obs. 78−81514
interplanetary turbulent plasma, radio imagery 79−92645
interstellar, SO, millimetre wave emission obs. 78−24535
interstellar *(Russian)* 80−36698
interstellar $^{12}C/^{13}C$ ratios from radioastronomical obs. 77−87530
interstellar ^{13}CO emission distrib. in galactic plane, rel. to giant mol. clouds distrib. in Galaxy 79−101183
interstellar ^{30}SiO detect. in Orion Nebula and Sagittarius B2 78−8097
interstellar CH, obs. of 3.3 GHz ground state transitions 78−77592
interstellar clouds, HCN dimer, abundance, upper limit 78−54004
interstellar clouds, search for DNC 79−44578
interstellar CO^+, HCN^+, HNC^+, and CN^+ ions, radio search 78−24534
interstellar CO, out-of-plane survey at 115 GHz 78−12334
interstellar CO clouds, blister model for assoc. H II regions 79−25681
interstellar CO obs. at 115 GHz in southern H II regions 77−87506
interstellar cyanoacetylene, 36.4 GHz rotational transition detect. 77−87515
interstellar cyanoacetylene, vibrationally excited state detect. in Orion molecular cloud 77−13436
interstellar cyanoacetylene in Sagittarius B2, evidence for chemical fractionation, ^{13}C isotopes 77−87532
interstellar cyanodiacetylene, detect. of J=9 to 8 transition 77−91603
interstellar cyanodiacetylene (HC_5N), J=2-1 transition detect. 79−25692
interstellar cyanodiacetylene weak maser action in Sagittarius B2 77−5555
interstellar D, galactic radial gradient, from $DCN/H^{13}CN$ and $DCO^+/HC^{18}O^+$ ratios 79−40232
interstellar dark clouds, CO obs. and CO/H_2 ratio 78−96513
interstellar dark clouds, radio continuum interferometric search for newly formed H II regions 80−98699
interstellar dark clouds, radio continuum interferometry rel. to newly formed H II regions physical props. 80−105301
interstellar dark clouds with assoc. young stellar objects, radio obs. of mol. lines 79−58390
interstellar DCO^+, detect. in NGC 2264, L134 and DR 21(OH) 77−2460
interstellar DCO^+ and electron density in dark clouds 78−12336
interstellar dense molecular clouds, distrib., phys. conditions, origin *(Polish)* 79−101187
interstellar dense molecular clouds, mag. field upper limit from SO obs. 79−21375
interstellar deuterated molecules, obs. and implications for interstellar chemistry 79−5891
interstellar DNC, detect. at 152.6 GHz in NGC 1333, 2264, Orion A and L134 dark cloud 78−4334
interstellar DNC detection, difficulties of chemical equilibrium hypothesis for D enrichment 77−82298
interstellar ethyl cyanide, mm wave emission line detect. in OMC-1 and Sagittarius B2 78−12317
interstellar ethylene oxide, possible detect. in Kleinmann-Low IR nebula 77−53662
interstellar ethynyl radical abundance and distrib. 78−65664
interstellar excited H, decametric-range radio lines search *(Russian)* 80−12822
interstellar formaldehyde, detect. at 1.3 mm in mol. clouds 79−25683
interstellar formaldehyde, obs. along galactic plane 79−48893
interstellar formaldehyde absorpt. in four small dust clouds 77−5558
interstellar formaldehyde detect. in M31 79−48929
interstellar formamide, ^{13}C isotope detect. in galactic centre 79−25680
interstellar formyl ion ($HC^{18}O^+$), detect. in Sagittarius B2 79−35346
interstellar gas, local, in southern sky, single 21 cm component study 79−84834
interstellar glycine, 22-83 GHz search in mol. clouds 79−30115
interstellar $H_2{}^{18}O$, detect. in Orion mol. cloud and DR 21(OH), H_2O abundance estimate 78−57621
interstellar H_2 densities from CO obs. 79−25687
interstellar H_2O maser emission, new sources detect. 80−62298
interstellar H_2O masers, survey in southern hemisphere 77−91599
interstellar H_2O masers in H II regions, time vars. obs. 79−88725
interstellar H_2O masers in NGC 6334, positions and spectra rel. to star form. 80−73025

radioastronomical observations continued
interstellar H_2O vapour sources struct. and kinematics in OB star form. regions 78−61901
interstellar H I clouds in distant galaxies, colour pictures of Doppler shifts 77−17383
interstellar H I temp. distrib. at high galactic latits. 77−22293
interstellar HC_5N, HC_7N, obs. in dark dust clouds 78−54023
interstellar HCN, absorpt. lines obs. towards Cassiopeia A 80−101624
interstellar HCN, isotopic abundance vars. meas. 77−53657
interstellar HCO^+, shock enhancement of abundance in supernova remnant (IC 443) 80−82464
interstellar high-velocity clouds, fine struct., H I 21 cm obs. 79−30113
interstellar HNO, radio detect. in Sagittarius B2 and NGC 2024 78−8098
interstellar ketene, microwave detect. in Sagittarius B2 77−37638
interstellar low-velocity molecular cloud obs. near Sagittarius A 79−53898
interstellar medium, radio emission at l=31.2° and (31.9°) 77−17724
interstellar medium, struct., pictorial analysis of radio signals 78−54026
interstellar methanol, 84.5 GHz and 96.7 GHz lines obs. in Sagittarius B2 and Orion A 80−62245
interstellar methanol in Orion A, two new transitions obs. 79−25667
interstellar methanol masers, search for microwave emission 78−32543
interstellar methyl alcohol, obs. 79−25666
interstellar methylamine-d_1, probable detect. 77−33610
interstellar methylamine-d_1, unconfirmed from 10 GHz obs. 79−92822
interstellar microwave spectrum lines, review 77−71138
interstellar mol. clouds, relationship of submillimetre optical depth to ^{13}CO column density 77−45508
interstellar mol. isotopic abundance ratio $H_2{}^{13}CO/H_2C^{18}O$ determ. from 6.8 cm obs. 79−35347
interstellar molecular cloud complex near M17, detailed obs. 77−33603
interstellar molecular cloud near RCW 36, H_2CO and OH obs. 78−69862
interstellar molecular cloud near S106, NH_3 obs. 79−84840
interstellar molecular cloud struct. from 2 cm formaldehyde and 2.6 mm CO lines 79−80341
interstellar molecular clouds, CO(J=2-1) emission obs. 79−92827
interstellar molecular clouds, CO rot. transitions obs. 77−33612
interstellar molecular clouds, detect. of new transitions of H, OCS and CH_2O, search for F 77−60808
interstellar molecular clouds, relative distribs. of N_2H^+, HCO^+, HCN and CN 77−33587
interstellar molecular clouds containing Herbig-Haro objects, mol. obs. and physical props. 80−36689
interstellar molecular complexes in Orion 78−4310
interstellar molecules, review 77−33616
interstellar molecules, RF emission spectra obs. towards ζ Ophiuchi 80−26958
interstellar N_2D^+, radio detect. 78−16492
interstellar NH_2D, detect. in Kleinmann-Low Nebula 78−20881
interstellar NH_2D, microwave detect. in Sagittarius B2 78−20880
interstellar NH_3, nonmetastable levels obs. 79−25665
interstellar NH_3, obs. in DR 21, NGC 1333 and NGC 6334 N 79−17044
interstellar NH_3 absorpt. in Sagittarius B2 direction 79−35341
interstellar OH, $^{16}OH/^{18}OH$ abundance ratio obs. in three H II regions 78−54024
interstellar OH and formaldehyde absorpt. in Cassiopeia A direction, obs. 78−45381
interstellar radio recombination line obs., review *(Russian)* 77−57080
interstellar S_2, upper limits on abundance in mol. clouds 78−28738
interstellar southern molecular clouds, $^{12}C/^{13}C$ abundance ratio derived from H_2CO obs. 79−84838
interstellar thioformaldehyde (H_2CS), 3 GHz absorpt. transition obs. 80−67837
interstellar type I OH masers, positions, polarisation, nearby H_2O masers, radio and IR props. 79−25671
intersteller CH, radio obs. 78−28751
intracluster Faraday rotation of radio sources, obs. 79−75285
Io, SHF radioemission and radiation belts *(Russian)* 80−36565
Io plasma torus, auroral hiss obs. (by Voyager 1) 79−92709
IR 12.4+0.5, compact far IR source discovery 79−40234
IR object assoc. with passage of interstellar shock front, radio identification 78−93369
IR sources, 5 GHz survey 78−69906
IR sources and CO emission from late-type giants, molecular envelopes and planetary nebula origin 78−40940
IR stars, 43 and 86 GHz obs. of SiO masers 79−71036
IR stars, search for 18 cm OH emission 78−8026
IR stars, search for OH 18 cm emission 78−40949
IR stars, survey for circumstellar OH emission 79−48787
IRC+10216, butadiynyl N=12→11 doublet study 80−51829
IRC+10216, C star, HC_5N and HC_7N detect. 79−17126
IRC+10216, isotope abundance anomalies in C star 79−5814
IRC+10216, luminous C star, ^{14}C search 77−53662
IRC+10216 and related objects, CO obs. at 230 GHz 79−62931
IRC+10374, IRC+10523, IR stars, H_2O maser emission detect. 80−62298
IRC+10420, high-resolution OH maser obs. at 1612 MHz 79−44471
IRC+10420, stellar OH maser VLBI obs. rel. to mag. field 79−25742
IRC+10420, supergiant star, new OH maser feature spatial struct. 79−48946
IRC +10216, detection of vibrationally excited CO at 114 GHz from C star 78−40941
IRC-10442 (GL5268S), near IR and radio obs. 80−4412
isothiocyanic acid, interstellar detect. in Sagittarius B2, mm wave spectrum 80−41878
joint source near supernova remnant G74.9+1.2, distance 77−64864
JP 1953+29, timing data anal., spinup/spindown 78−24522
Jupiter, 11 cm radiation Stokes parameters meas. 78−12141
Jupiter, brightness distrib., 1.3 cm wavelength, interferometric obs. 79−12424
Jupiter, circular polarisation of 1.4 GHz emission from radiation belts 77−37556
Jupiter, circular polarisation of 1.4 GHz radio emission 77−64692
Jupiter, decametric and hectometer radio emission obs. 80−67644
Jupiter, decametric emission features and vars. *(Russian)* 78−65546
Jupiter, decametric emissions, freq. and time depend. 78−89113
Jupiter, decametric emissions, obs. by spaced receiver network 79−48730
Jupiter, decametric noise and solar activity effects *(Russian)* 77−64694

radioastronomical observations continued
Jupiter, decametric obs. using facility at Mt. Zao, Japan 80−51656
Jupiter, decametric radiation, bandlike emissions 77−37558
Jupiter, decametric radiation, burst morphology and drift rates 77−37557
Jupiter, decametric radio bursts, modulation lanes in dynamic spectra 80−17535
Jupiter, decametric radio bursts hyperfine polarisation struct. 77−33400
Jupiter, decametric radio emission, dynamic spectra *(Japanese)* 79−8877
Jupiter, decimetric radio spectrum, 1975 December 77−60718
Jupiter, drift rates of S-bursts 78−36492
Jupiter, electron density profiles, Voyager 1 radio occultation meas. 79−96953
Jupiter, electrons pitch angle distrib. in radiation belt from radio obs. 77−33402
Jupiter, EM noise and radiowave propag. below 100 kHz in atm., equatorial region 80−26782
Jupiter, hectometric radiation, Voyager spacecraft radio obs. 79−84732
Jupiter, HF obs. using interference-excising correlator 79−75110
Jupiter, kilometric radiation, 10-56 kHz, Voyager obs. 80−26781
Jupiter, L-burst origin in decametric radio emission, observational study *(Japanese)* 79−70988
Jupiter, L-bursts in decametric radio spectra 78−96424
Jupiter, linear polarisation obs. at 6, 11 and 21 cm wavelengths 77−87313
Jupiter, magnetosphere HF and LF events from Voyager 2 obs. 80−77344
Jupiter, methane emission at 76 GHz correl. with decameter activity 78−4140
Jupiter, MF radio emissions latitudinal beaming 80−31246
Jupiter, microwave spectrum of atmosphere 78−85889
Jupiter, non-Io decametric radiation obs. at freqs. above 30 MHz 80−85886
Jupiter, obs. at 327 and 1410 MHz during Pioneer 11 fly-by 77−13280
Jupiter, Pioneer 10 and 11 obs. of magnetic field orientation in ionosphere 79−25540
Jupiter, radiation belts, 21 cm maps from all rot. aspects 80−105195
Jupiter, radiation belts and atmosphere, Pioneer 10 ratio obs. 79−35179
Jupiter, radio brightness distrib. across disc. 77−87319
Jupiter, radio emission in decimetre range, Pioneer 10 data 77−45355
Jupiter, radio S-bursts, source of 2.5-35 MHz radiation 80−36562
Jupiter, radioemission at 100 kHz, from magnetosphere 80−85891
Jupiter, rotation period, decametric radio meas. 80−17541
Jupiter, S-burst drift rates 79−75146
Jupiter, S-burst drift rates from 26-33 MHz obs. 80−12705
Jupiter, short-wave millimetric obs. with wide-band radiometer 79−96916
Jupiter, study at 2.7 GHz with Cambridge 5 km telescope 80−82272
Jupiter, Voyager 1 planetary radio astronomy obs. 80−26796
Jupiter, whistler mode chorus obs. and Io torus implications 80−72862
Jupiter, whistler obs. by Voyager 1, lightning detect. 79−84733
Jupiter atmosphere and ionosphere, Voyager 1 preliminary radio profiles 80−26791
Jupiter bursts, obs. with student-designed radiotelescope, multidisciplinary teaching exercise 80−17759
Jupiter decametric radiation beaming, first direct meas. 78−89114
Jupiter decametric radio bursts, polarisation patterns in dynamic spectra 77−5490
Jupiter decametric radio emission, S-bursts dynamic spectra 78−20722
Jupiter ionosphere, spectral broadening meas. by Pioneers 10 and (11) 80−109391
Jupiter ionosphere, Voyager 2 occultation, radio obs. 80−77337
Jupiter magnetosphere, plasma waves from Voyager 2, radio obs. 80−77343
Jupiter radio emission, Stokes parameters obs. at 11 and 18 cm wavelength 80−67637
Jupiter S-bursts, freq. drift meas. at different freqs. throughout several storms 80−85888
Jupiter S-bursts, obs., assoc. with Io, and origin 78−36499
Jupiter S-bursts, occurrence with L-bursts and freq. upper limit 80−85887
Kepler's supernova remnant, struct. at 327 MHz from occultation obs. 78−12339
Kleinmann-Low i.r. nebula in Orion, high-vel. gas obs., CO 115 GHz line 77−5554
Kleinmann-Low nebula, ^{12}CO line profile rel. to radially moving cloud model 78−20865
Kleinmann-Low nebula, nature of broad molecular line emission 77−5556
Kleinmann-Low Nebula, NH_3 obs. 77−13440
Kleinmann-Low nebula, NH_3 obs. and hot core source 80−73016
Klemola 44, cluster of galaxies, X-ray, optical and radio obs. 77−74150
L134 dark cloud, DCO^+ and HCO^+ obs. 78−65673
L134 dust cloud, formaldehyde excitation temp. 77−5552
L134 N interstellar dark cloud, NH_3 hyperfine struct. 77−78852
L1544, L1521B, interstellar clouds in Taurus, HC_5N detect. 80−26957
L 183 (L 134 N) dust cloud, NH_3 and cyanoacetylene mapping at 23 GHz 80−105307
L 43, CO mm wave and near IR obs. of filamentary cloud 79−62886
BL Lacertae, flat-spectrum radio source, variability at 962 MHz 77−82317
BL Lacertae, major radio outburst, (1980 April 17 to May 6) 80−73043
BL Lacertae, polarisation and flux density data, prolonged particle generation at single location 79−35376
RT Lacertae, RS Canum Venaticorum binary, radio emission obs. 79−58379
AR Lacertae, RS Canum Venaticorum type star, VLA obs. 78−8054
BL Lacertae, very high resolution radio obs. 77−33663
BL Lacertae object 0109+22, optical and radio props. 78−32567
BL Lacertae objects, radio structure and spectral index, reviews 80−46672
late-type giant stars, CO emission lines obs. from expanding molecular envelopes 77−22219
late-type stars, OH emission time var., correl. with visual magnitude 77−60764
late-type supergiants, radio emission search 77−87392
lenticular galaxies, H I 21 cm line obs. 79−67090
Leo A, H I 21 cm. line survey of dwarf irregular galaxy 78−81688
Leo galaxy triplet (NGC 3623/7/8), H I distrib., 21 cm line obs. 79−44623

radioastronomical observations continued
R Leonis, SiO maser variability at 86 GHz 80−41839
LF variable radiosource survey 77−22324
LGS 3 in Local Group, 21 cm line obs. of new dwarf galaxy 79−101195
linear polarisation of 78 small diameter radio sources at 2695 MHz 78−77611
LMC, radiosources at 3.4 cm, catalogue and spectral indices 78−65695
LMC, space orientation and translational motion *(German)* 77−53684
LMC X-1 region (MC76 and 77), 2 cm obs. 80−51875
Local Group, H I 21 cm obs. of newly discovered dwarf galaxies 79−30133
local radio luminosity function of elliptical galaxies 77−57086
long-period variable and IR stars, discovery of new 1665/1667 MHz OH/IR sources 77−64763
long-period variable stars, OH maser lines struct. and saturation 78−93264
long-period variables, CO and SiO millimetre line emission obs. rel. to circumstellar shell props. 78−49423
Loop III, linear polarization of 920 MHz galactic background 79−97087
low-frequency variable radio sources, search for microarcsecond struct. 78−16550
low-frequency variable sources, interstellar scintillation evidence for relativistic expansion 79−9018
LSI+61°303, supergiant Be star, radio emission and radial vel. periodic vars. 80−62149
lunar heat flow and regolith struct. from radio interferometric obs. 77−5469
lunar radio transmitters, orbital dynamics and selenodetic results from VLBI 77−29672
lunar surface bistatic radar surveillance with FM signal 79−5758
lunar surface mapping from side looking orbital radar images 77−37520
lunar total eclipse, 1978 March 24, 3.4 mm obs. 80−31220
lunar total eclipse, 1978 March 24, 3.4 mm wavelength obs. *(Japanese)* 79−101095
Lynds 134, dust cloud, isotope ratios and CO chemical fractionation 77−87531
Lynds 134, OH emission obs. in dark nebula 80−22062
Lynds 134 dust cloud turbulence, formaldehyde obs. at 6 cm. 80−94845
Lynds 134 N, CO isotope, mapping 79−30108
Lynds 1551, CO obs. of dark cloud and stellar wind driven shocks 80−105318
Lynds 1778/1780, H I and OH emission obs. in dark nebula 80−17628
Lynds 673 nebula, radiosource obs. at 3.5 and 4 mm *(Russian)* 78−32557
M101, extended H I envelope obs. 79−62904
M101, H I distrib. and motions in giant spiral galaxy 79−44613
M101 companion galaxies, integral props. from H I meas. 78−49532
inner M101 galaxy group, H I obs. 80−67885
M13, search for faint nearby radiosources 78−32531
M15, globular cluster, search for radio emission from ionized H 77−13410
M16, emission nebula assoc. with open cluster NGC 6611, 85α recomb. lines obs. 79−35330
M17, aperture synthesis obs. at 5 GHz 79−35342
M17, discovery of extended mol. cloud assoc. with star forming complex 77−37635
M17, high resolution radio and far IR maps compared 79−75263
M17, radio brightness distrib. at 3.5 mm wavelength 77−64837
M17 (NGC 6618), 21 cm obs. of components and structure of H II region 78−49508
M1-78, emission nebula, 15.4 GHz struct. 78−41025
M1-92, bipolar nebula, OH emission obs. 78−41016
M31, aperture synthesis obs. complemented by short spacing data fron single dish obs. 79−66928
M31, CO partial radial distrib. meas. 78−8117
M31, gas-to-dust ratio determ. 78−8120
M31, H I emission in NE.region, 21cm obs. 80−90537
M31, H I emission in SW region 80−51873
M31, H I in outer regions 78−16532
M31, high-resolution H I obs., spectra and major axis rel. plots 78−41057
M31, line intensity distrib., contour maps, vel. profiles, 21 cm HI line survey 80−73038
M31, M51, M81, spiral galaxies, polarisation detect. at radio wavelengths 77−5575
M31, new Bonn 21-cm survey, first results 77−91645
M31, polarised radio emission detect. 78−86017
M31, polarised radio emission distrib. rel. to large-scale mag. field 80−41899
M31, radio continuum survey at 2695 MHg comparison with optical data 77−57085
M31, radio emission obs. at 102.5 MHz *(Russian)* 78−49512
M33, density wave motion obs. evidence from star form. and evolution 77−45552
M33, detect. of H_2O maser emission 77−29926
M33, H I distrib. obs. and spiral struct. 80−56948
M33, H I large-scale struct. 78−96539
M33, radio and optical obs. of supernova remnants *(Italian)* 79−53890
M33, radiocontinuum emission obs. at 14850 MHz 78−28783
M33 direction, H I 21 cm emission/absorpt. obs. 80−62262
M33 H I tail, obs. rel. to adjacent high-vel. H I cloud 80−12815
M3-99, bipolar nebula, search for OH emission 78−41016
M43, emission nebula around NU Orionis, radio and IR obs. 78−54012
M51, high resolution obs. at 21 and 49 cm 77−29921
M51, radio continuum obs. 77−74135
M51, spiral galaxy, mag. fields config. from Faraday rot. data 79−48934
M51 system, extended H I obs. 78−89253
M53, search for faint nearby radiosources 78−32531
M81 and 82 interacting galaxies, H I 21 cm obs. 77−45561
M81 nucleus, small radiosource obs. 77−13484
M81-82 system, 2.7 GHz continuum survey of intergalactic gas stream 78−36691
M82, 87.2 GHz continuum obs., Ne abundance 78−41042
M82, compact radio source 41.9+58 in nucleus 78−93442
M82, galaxy, interstellar HCN and CS search 77−53661
M82, H125α recomb. line, SHF obs. 80−82486
M82, H 102α radio recomb. line detect. 77−49476
M82, HCO^+ detection and HCN confirmation, 89 GHz obs. 79−44582
M82, Irr II galaxy, high angular resolution H I study 77−33626
radioastronomical observations continued
M82, irregular galaxy, aperture synthesis obs. of H I emission 79−17077
M82, irregular galaxy, OH absorption and emission obs. 77−5565
M82, M104, VLBI obs. of galactic nuclei at 18 centimetres 80−22078
M82, nature of radio recomb. lines in extragalactic sources 78−45418
M82, radio recomb. line emission detect. from irregular galaxy 77−57093
M82, radio structure at 23 GHz 79−71119
M82, stimulated recomb. line emission obs. 77−41408
M82 nucleus, λ6 cm formaldehyde absorpt. detect. 79−17088
M82 nucleus, obs. of compact radio source 77−78869
M87, 2 and 6 cm VLA obs. of jet 80−105345
M87, millisecond radio bursts discovery 80−73034
M87, very high resolution radio obs. of nucleus 77−33663
M87 jet, radiation from knots rel. to model *(Russian)* 80−36719
M8, large-beam near IR and 24 GHz obs. 79−48882
M8, new IR-CO source obs. 77−64818
M8, radio recomb. line obs. at 5 and 10 GHz 79−84832
M 81, CO emission upper limits 78−36693
M 81, spiral galaxy, aperture synthesis obs. at 1415 and 610 MHz 77−33639
M 87, radio continuum halo at 2.7, 4.8 and 10.7 GHz 79−48915
M- and S-type stars, detect. of 7 mm SiO maser sources 78−4215
M-type supergiants in southern hemisphere, search for OH 1612 MHz emission 78−69792
Maffei 2, CO emission obs. 78−16530
Magellanic dwarf irregular galaxies, gas distrib., motions and dynamics 78−36690
Magellanic Stream, high sensitivity obs., small-scale struct. 79−35385
Magellanic Stream, turbuelnt wake of Magellanic Clouds in galactic halo 78−69884
Magellanic Stream, vel. structure from H I obs. 79−97078
Magellanic Stream and adjacent HVCs, Jodreel Bank 21-cm obs. 77−91650
Magellanic Stream H I regions, fine struct., 21 cm obs. 80−90523
Markarian 205, weak radio emission and Seyfert-like props. 79−48912
Markarian 348, Seyfert galaxy, H I envelope, 21 cm obs. 80−82504
Markarian 3, Seyfert galaxy radio maps, 5HF obs. 80−82501
Markarian 421, BL Lacertae-type object, radio variability 77−49483
Markarian 421, optical and radio obs., identification with 2A 1102+384 X-ray source 79−5899
Markarian 668, Seyfert galaxy, radio emission in 2.3-14.4 GHz range 79−88740
Markarian 668 (=OQ 208), Seyfert, H83α and H99α radio recomb. lines detect. 80−94864
Markarian galaxies, 3.2 mm and IR continuum obs. 77−22317
Markarian galaxies, obs. with RATAN-600 radiotelescope 79−88737
Markarian galaxies, radio continuum obs. at 1410, 2380 and 5000 MHz 80−46668
Markarian galaxies, radio continuum obs. at 1410 MHz and 2700 MHz 77−87548
Markarian galaxies, radio spectra 77−37647
Mars, atmospheric parameters from Mars 6 descent module radio data 77−33386
Mars, dynamics, atmospheric and surface props. from Viking radio tracking data 77−56865
Mars, dynamics obs. from Viking lander tracking data anal. 80−77314
Mars, Hellas basin, Viking bistatic radar observations 79−84723
Mars, microwave detect. of atm. CO 77−74000
Mars, orbit determination on basis of radar and visible observations 80−90323
Mars, radar altimetry of S.Tharsis 80−98591
Mars, radar characts. of rough planar surfaces 80−98589
Mars, radio brightness longit. depend. confirmation 80−21937
Mars, radio emission meas. by Mars 5 spacecraft 77−29689
Mars, radio occultation meas. of surface atmospheric pressure, Viking 1 lander verification 77−22129
Mars, rot. vars. in radio brightness 77−45340
Mars, soil density and dielectric permittivity, Mars probe radio obs. 78−69722
Mars, soil density from 3 cm meas. 79−88614
Mars, spin axis orientation and Viking 1 lander posn. from radio tracking data 77−13269
Mars, surface characts. in N. hemisphere, Arecibo obs. at 2380 MHz 79−25533
Mars, surface props. obs. by Earth-based radar at 70, 12.5, and 3.8 cm wavelengths 77−91457
Mars, surface roughness from Arecibo radar obs. 78−28565
Mars, surface slopes, roughness and reflectivity, radar obs. during 1975 opposition 78−45254
Mars, Viking 1 landing sites, radar obs. rel. to site choice 77−13272
Mars, Viking radio occultation meas. of atmosphere and topography 78−20687
Mars atmosphere and topography, Viking orbiters radio occultation meas. during one Martian year 80−72836
MC2 1210+121 and 1620+103, radio-quiet BL Lacertae-type objects 80−101641
MC2 and MC3 sources, radio spectra and optical identification 77−33670
MC5 1307+121, BL Lacertae object, radio spectrum shape, VHF and SHF obs. 80−67866
Mercury, right ascension determ. from radio obs. *(Russian)* 79−21213
Mercury radius and atmosphere data from Mariner 10 occultation obs. 77−37535
meteor bursts, forward scatt. technique, obs. over India 78−89132
meteor ionisation trails, characts. from radar obs. 77−71069
meteor radar obs. at Ondrejov and Dushanbe 78−20760
meteor rate depend. on geomag. activity and coronal activity 80−67662
meteor trails, radio echoes rel. to thermal diffusion 77−21955
meteor wind automatic meas. set, drift obs. accuracy *(Russian)* 77−41248
meteors, forward scatter, amplitude distrib. index, D-region absorpt. effect 78−65552
meteors, head echo heights 78−36537
meteors, heights obtained from decay rates of 18000 radar echoes 77−82175
meteors, optical brightness rel. to ionised trail props. 80−77354
meteors, radar echo drift deceleration 78−36538
meteors, radio echo characteristics rel. to deionisation processes and meteoroid props. 80−17550

radioastronomical observations continued
meteors ionisation columns, initial radii meas. 80−94762
methane, first detection in interstellar medium at 76 GHz 78−16503
methyl formate, microwave spectra, rot. consts., moments and struct., radio astronomy appl., review 80−17637
methyl mercaptan, interstellar detect. in Sagittarius B2, mm wave spectrum 80−41877
methylamine-d_1, interstellar, probable detect. 77−33610
methylidyne, obs. in Sagittarius B2 direction 78−65671
microwave background anisotropy, galactic dust emission 80−77524
microwave background fluctuations, search for Universe primeval perturbs. *(Russian)* 78−36734
microwave background radiation large-scale anisotropy meas. 80−8718
microwave background radiation polarisation, 0.5 to 3 mm survey 78−73779
microwave radar obs. of the Sun 79−88635
Milky Way companion galaxy, synthesis obs. at 0.610 GHz rel. to identification 77−29941
Milky Way sources, obs. at 8.87 GHz near (l=333°) 80−22102
millimetre obs., calibration, effect of Earth's atmosphere, two-layer model 78−53691
millimetre region cosmic background radiation, large scale anisotropy meas. 80−82553
millimetre temps. of planets, galactic and extragalactic sources 78−28556
Mira and semiregular variables, microwave and IR obs. of H_2O vapour maser emission 79−67037
Mira envelopes, OH maser luminosity and expansion vel. gradient 79−71043
Mira variables, discovery of 7 new SiO maser sources 78−32467
Mira variables, OH emission high-sensitivity search 78−89203
mm emission from extragalactic objects, luminosities, spectra, microwave background contrib. 77−17677
mm wave telescope, Epping, Australia, test obs. 79−53719
MO758+120, extended radiosource identification with quasar 77−87563
molecular cloud assoc. with NGC 7023, CO obs. at 2.7 mm wavelength 78−41008
molecular cloud complex assoc. with bright rim near VY Canis Majoris, CO obs. 78−24536
molecular cloud in NGC 2264, NH_3 and OH line emission mapping, SHF and UHF 80−94847
molecular clouds, H I and CO obs. comparison 78−24538
molecular clouds as galaxy spiral struct. tracer, 2.6 mm CO survey 80−105346
molecular clouds associated with refl. nebulae, CO emission, EHF obs. 80−82447
Molonglo catalogue sources selected at 408 MHz, radio spectra 77−5583
Molonglo Deep Sky Survey, 373 radiosources in declination zone −20° 77−56840
Molonglo Deep Sky Survey, source counts 77−56842
Molonglo deep sky surveys 77−33358
Molonglo Deep Survey sources, radio spectra 78−69900
Molonglo radio source surveys at 408 MHz 78−28541
Monoceros R1 molecular clouds ring struct., CO obs. 80−12784
Monoceros R2 cloud, near IR and mol. obs. of rot. collapsing cloud 77−78840
Mononglo Deep Sky survey, 95 radiosources in declination zone −62° 77−56841
monopulse signals, omnidirectional search, probable origin 78−24563
Moon, 3 cm radar obs. from Luna 16 to 24 spacecraft 80−77302
Moon, brightness at 2 and 6 cm wavelength, centre to limb var. 78−81572
Moon, brightness distrib. over disc at 6 cm 77−37518
Moon, Earth-based radar mapping, review 80−12694
Moon, high-resolution radar map at 7.5 m wavelength 79−25523
Moon, plasma near surface, radiosource occultation obs. 80−8559
Moon, radar scatter data rel. to surface parameters from images 79−40100
Moon, selenographic coords. determ. of ALSEPs using RATAN-600 equipment *(Russian)* 79−25517
Moon, surface radio reflection, Luna 23 meas. at 3.1 cm wavelength 80−8560
Moon, surface structure forecast, based on thermal conditions 78−77502
MWC 349, Be star, spectral EHF obs. 80−105262
MXB 1636−53, simultaneous radio and X-ray obs. of X-ray burst source 79−48961
MXB 1730−335, 4100 MHz obs. of microwave bursting pattern 80−46705
MXB 1730−335, microwave bursts detect. from rapid X-ray burster 79−48957
MXB 1730−335 (Rapid Burster), microwave bursts obs. 80−62320
MXB 1837+05 (Serpens X-1) simultaneous radio and X-ray obs. 79−21467
narrowband radio radiation near H I 21 cm line, all-sky search 77−29661
narrowband signals of extraterrestrial origin, search at 21 cm wavelength 79−25521
nearby galaxy in Orion, H I 21 cm obs. 79−30131
NGC1023, H I distrib. determ. 79−53910
NGC2805, 2814, 2820 and IC2458, H I 21 cm obs. of close galaxy group 79−53917
NGC 1023 galaxy group, H I obs. and possible intergalactic H I cloud discovery 80−67886
NGC 1023 galaxy group, H I radial vels. rel. to group membership and mass/light ratio 80−82521
NGC 1052, 4278, VLBI obs. of galactic nuclei at 18 centimetres 80−22078
NGC 1052, active elliptical galaxy, radio and optical study 78−65693
NGC 1052, elliptical galaxy, field, H I emission mapping and line profiles 80−98719
NGC 1052, elliptical galaxy, H I obs. 78−69873
NGC 1052, H I detect. in elliptical galaxy 78−41041
NGC 1068, 87.2 GHz continuum obs., Ne abundance 78−41042
NGC 1167, S0 galaxy, extended core radio source 14.8 GHz mapping 79−25727
NGC 1265, 1275, in Perseus cluster, low-resolution aperture synthesis map at 408 MHz 80−56958
NGC 1265, VLA obs. at 4886 MHz of head-tail radiogalaxy 79−21428
NGC 1275, double nucleus, radio and emission line obs. *(Russian)* 79−21439
radioastronomical observations continued
NGC 1275, Seyfert galaxy, nucleus struct. *(Russian)* 80−62288
NGC 1275, Seyfert galaxy, radio and optical variability of nucleus 78−28793
NGC 1275 (3C 84), Seyfert galaxy, optical and 3 mm radio vars. similar struct. 79−67102
NGC 1275 (Perseus A), correl. between optical and radio variability *(Russian)* 80−77505
NGC 1275 nucleus, structural changes at 2.8 cm wavelength 80−31359
NGC 1291 and 1326, kinematics of lenticular galaxies from 21 cm line obs. 79−53908
NGC 1499, California Nebula, decametric radio emission 79−21385
NGC 1499 (California Nebula), CO obs. along ionisation front 78−24537
NGC 1512 and 1510, interacting galaxies, optical and H I study 79−80348
NGC 1569, dwarf irregular galaxy, H I obs. 80−90538
NGC 1851, globular cluster, H I detect., 21 cm line obs. 78−45368
NGC 1851, globular cluster, unsuccessful search for H I 79−5873
NGC 1851, NGC 1904, globular clusters, radio and X-ray obs. 77−26028
NGC 1961, rotation curve for massive spiral 79−62898
NGC 2024, H II region, study of nearby partially ionised interstellar medium 77−57077
NGC 2024, HF C I recomb. line emission obs. 78−28748
NGC 2024, search for linear polarisation in radio recomb. lines of H II region 80−41872
NGC 2024 (W12), 21 cm obs. of components and structure of H II region 78−49508
NGC 2146, peculiar spiral galaxy, extensive H I obs. 77−17676
NGC 2175 (S252), galactic H II region, aperture synthesis obs. 77−64828
NGC 2237, Rosette Nebula, decametric obs., brightness temp. contours 78−57615
NGC 2237 (Rosette Nebula), H II region obs. in absorption at 12.6 and 25 MHz *(Russian)* 78−41024
NGC 2264, H II region, classification of optical, IR and radio obs. data 80−67818
NGC 2264, mol. cloud, continuum emission mapping at 89.6 GHz 80−94842
NGC 2264, open cluster, CH radio obs. 78−28751
NGC 2264, open cluster, CO obs. of mol. cloud 79−21363
NGC 2264 and other Bok globules, formaldehyde absorpt. obs. at 6 cm 77−45511
NGC 2366 H II region visible and radio obs. 80−77475
NGC 253, 87.2 GHz continuum obs., Ne abundance 78−41042
NGC 253, galaxy, interstellar HCN and CS search 77−53661
NGC 253, H_2O emission detection at 22.235 GHz 78−16534
NGC 253, HCN confirmation 79−44582
NGC 253, radio continuum obs. at 8.7 GHz 79−92853
NGC 253, radio recombination line obs. of galaxy 80−56941
NGC 253, Sc galaxy, aperture synthesis obs. of H I distrib. 77−74131
NGC 253, spiral galaxy, H102 alpha recomb. line detect. 77−87540
NGC 2623, interacting galaxy, H I absorpt. and emission obs. 79−17087
NGC 2685, H I 21 cm line survey of galaxy 80−56943
NGC 281, H II region, CO and H_2O obs. 78−28740
NGC 281, H II region, obs. of shock in region of shock-induced star form. 79−25688
NGC 2974, 4105, 5846, elliptical galaxies, H I contents 79−62906
NGC 300, spiral galaxy, aperture synthesis obs. of H I, outer plane warping 79−53905
NGC 3031 (M81)/3077 H I bridge, structure and kinematics, 21 cm obs. 79−67093
NGC 3079, peculiar edge-on spiral galaxy, 2.7 and 8.1 GHz obs. 78−36692
NGC 315, giant radio galaxy, jet structure and polarization 79−35379
NGC 315, NGC 6251, very large radio galaxies, 11.1 cm obs. 78−86014
NGC 315, radio galaxy, mag. field struct. in radio jets 80−82526
NGC 3310, peculiar spiral galaxy, 2.7 and 8.1 GHz obs. 77−29929
NGC 3448, optical and H I 21 cm line obs., peculiar nucleus 78−36696
NGC 3556, edge-on galaxy, multi-freq. radio continuum study 79−44607
NGC 3628, detection of emerging H I plume at 21 cm wavelength 78−54038
NGC 3665, elliptical galaxy with dust lane, radio obs. 79−58414
NGC 3718, peculiar early-type galaxy, H I survey, interaction with NGC 3729 79−35383
NGC 3904, elliptical galaxy, H I content from 21 cm line 77−87545
NGC 3962, elliptical galaxy, large scale H I distrib. 79−80347
NGC 4038/39, interacting galaxy pair, H I kinematics and distrib. 79−35365
NGC 4151, Seyfert galaxy, 21 cm line obs. 77−57087
NGC 4214, barred Im galaxy in Canes Venatici I group, H I obs. 79−92862
NGC 4248, galaxy, H I obs. 78−4358
NGC 4258, aperture synthesis obs. complemented by short spacing data fron single dish obs. 79−66928
NGC 4258, high resolution 21 cm, line obs. of active galaxy 80−56946
NGC 4278, elliptical galaxy, H I content meas. 77−22312
NGC 4278, elliptical galaxy, H I detect. 78−4342
NGC 4319, weak radio emission 79−48912
NGC 4472, very weak radio galaxy, struct. and radio power 78−65708
NGC 4485/90 interacting galaxies, radio continuum and H I obs. 80−62274
NGC 4490/4485, interacting galaxy pair, 2.7 and 8.1 GHz obs. 78−36692
NGC 4565, warped Sb galaxy, H I distrib. 21 cm obs. 80−109542
NGC 4631, edge-on spiral galaxy, high freq. radiocontinuum obs. 77−74129
NGC 4631, edge-on spiral galaxy, radio continuum halo obs. 77−26054
NGC 4631/NGC 4656, interacting pair of galaxies, neutral H aperture synthesis obs. 78−54043
NGC 4636, elliptical galaxy, H I content from 21 cm line 77−87545
NGC 4636, elliptical galaxy, H I emission detect. 78−32570
NGC 4636, elliptical galaxy, H I large-scale distrib. 78−45400
NGC 4725/47 interacting galaxy pair, 21 cm line obs. of H I distrib. 80−46662
NGC 4736, spiral galaxy, H I study 77−57090

radioastronomical observations continued
NGC 4736, spiral galaxy, multifrequency radio continuum study 77−17683
NGC 4945, galaxy, water vapour emission obs. 78−93427
NGC 4945, spiral galaxy, H I absorpt. obs. 77−33651
NGC 4945, strong H_2O maser emission from edge-on spiral galaxy 79−40271
NGC 5128, H I, OH and formaldehyde absorpt. line obs. in lenticular galaxy 77−33649
NGC 5128 (Centaurus A), formaldehyde absorpt. obs. at 14 GHz 80−17657
NGC 5236 (M83), Sc galaxy, CO obs. 78−65689
NGC 5291, massive gas-rich peculiar lenticular galaxy in IC 4329 cluster 79−71127
NGC 5296/7, galaxy pair with nearby quasar, radio obs. 78−93419
NGC 5363, radiosource and compact core 77−49468
NGC 5383, barred spiral galaxy, radio continuum emission obs. at 1415 MHz 78−73753
NGC 5383, H I 21 cm line obs. of barred spiral galaxy 80−8687
NGC 5474, peculiar Scd galaxy, H I distrib. and kinematics 80−8683
NGC 6034 radio tail galaxy in Hercules cluster, Westerbork obs. at 0.6, 1.4 and 5 GHz 78−36706
NGC 6240, unusual radio galaxy, radio and optical, obs. 80−4440
NGC 6251, elliptical galaxy, nuclear jet radio obs. 78−41059
NGC 6251, extended radio galaxy, polarisation at 610 MHz 78−61918
NGC 6251, radio galaxy, radio jets misalignment, VLBI obs. 80−27001
NGC 6251, very large radio galaxy with exceptional jet 78−12394
NGC 6334, CO detailed struct. in mol. cloud complex 78−4324
NGC 6334, relationships of N_2H^+, HCO^+, HCN and CN 77−33587
NGC 672 and IC 1727, interacting galaxies, H I obs. and computer modeling 2 km line obs. 80−67853
NGC 6822, galaxy, CO emission upper limits 78−36693
NGC 6822, irregular galaxy, interferometer study of H I assoc. with optical core 78−20889
NGC 6946, galaxy, radio continuum emission from H II complexes and nonthermal disc 77−41407
NGC 7023, refl. nebula, radio continuum obs. 79−17048
NGC 7027, planetary nebula, radio recomb. line obs. 77−9780
NGC 7129, refl. nebula, star form., CO mol. line and far IR obs. 79−17043
NGC 7217, spiral galaxy, extended rot. curve, mass distrib. 79−21414
NGC 7331/Stephan's Quintet area, obs. at 1421 MHz 78−12392
NGC 7385, optical-radio knot obs. in elliptical galaxy 79−35362
NGC 7538, IRS 1, formaldehyde maser, SHF band obs. 80−67822
NGC 7538 and Sherpless 159, H II region/mol. cloud complex, H I aperture synthesis obs. 80−90510
NGC 7822, bright-rimmed mol. cloud, CO obs., heat sources 78−36664
NGC 7822, NGC 281, bright rimmed mol. clouds, CH obs. 80−62238
NGC 7822 (W 1), supernova remnant, 2.8 and 6 cm wavelength obs. 78−4383
NGC 891, edge-on disc galaxy, radio continuum obs. 78−28786
NGC 891, HI 21 cm. obs. of edge-on Sb galaxy 79−48914
NGC 891, radio continuum obs. at 8.7 GHz 79−92853
NGC 891, radiogalaxy halo, Westerbork obs., electron propag. and magnetic fields 78−61920
NGC 925, barred spiral galaxy, high-resolution H I obs. 80−105329
nighttime ionosphere, two-freq. radioscopy results from Venera 9 and (Venera 10) 77−91454
noise storms and bursts, preliminary results from Mark II Nancay radioheliograph 78−28517
North Celestial Pole region, deep survey at 4.85 GHz 79−12536
North Polar Spur, radio continuum obs. at 1420 MHz 80−22100
Nova Centauri 1979, radio detect. of novalike object 79−67026
nova shells, radio emission obs. 80−26868
NP 0532, Crab Nebula, pulsar, radiofrequency, pulse arrival times 77−71123
NP 0532, Crab Nebula pulsar, variability of dispersion and scatt. 77−49409
NP 0532, Crab pulsar, ang. size at 74 MHz 78−12260
NP 0532, Crab pulsar, lunar occultation obs. at decametre wavelengths 80−62248
NRAO 150, compact radio source, search for time-depend. radio fine struct. 80−90552
OB associations, 22 GHz obs. of nearby H_2O masers 79−25649
OE323 (4C 34.13), extended radiosource identification with quasar 77−87563
OH 205.1−14.1, unusual OH maser, new flare report and 1667 MHz line obs. 80−98734
OH 351.78−0.54, UHF obs. of brightest OH maser (1980 August) 80−101644
OH masers, interstellar, obs. near Orion population stars 80−67716
OH near galactic plane, 18 cm lines survey 79−75265
Ohio Sky Survey and other radio surveys, review 77−45325
Ohio sources, optical identification using radio and optical positions meas. by Texas interferometers 78−28808
OJ 287, flat-spectrum source, variability at 962 MHz 77−82317
OMC-1, methane-d_1 abundance upper limits from rot. spectrum obs. 80−56705
Ooty occultation extragalactic sources radio spectrum obs. in SHF 80−105371
open clusters, H I upper limits 79−30095
ρ Ophiuchi dark cloud, ^{13}CO self absorpt., EHF obs. 80−90500
ρ Ophiuchi dark cloud, atomic and mol. obs. 78−41013
ρ Ophiuchi dark cloud, C II and S II regions obs. 78−49500
ρ Ophiuchi dark cloud, new S II and C II regions, recombination line obs. 78−57617
ρ Ophiuchi mol. cloud, continuum emission mapping at 89.6 GHz 80−94842
optical quasars, radio and optical obs., redshifts, luminosity function 78−49552
OQ 208 (Markarian 668), radio spectrum 79−12531
Orion, NH_3 interstellar emission line obs. at 23 GHz 79−30109
Orion, shock chemistry and molecular line emission 79−21391
Orion A, 22 GHz water line giant outburst 80−8703
Orion A, C recomb. lines and H I clouds obs. 78−57605
Orion A, confirmation of H_2O 22 GHz line outburst 80−8704
Orion A, methane detect. 79−17060
Orion A, methanol source ang. size lower limit from VLBI obs. 77−13429
Orion A, mm emission lines from organic molecules 77−2477
Orion A, probable detect. of methylamine-d_3 77−33610

radioastronomical observations continued
Orion A, radio brightness distrib. at 3.5 mm wavelength 77−64837
Orion A, radio meas. of electron temp. distrib. at 22 GHz 77−87558
Orion A, relationships of N_2H^+, HCO^+, HCN and CN 77−33587
Orion A, SiO and H_2O maser obs. 78−8085
Orion A, SiO maser variability at 86 GHz 80−41839
Orion A, struct., radio obs., partially ionized gas 79−21379
Orion B (NGC 2024), recomb. line obs. 77−29895
Orion H_2O masers, matter outflow in star formation last stages 78−8091
Orion methanol masers, interferometric and multitransitional study 80−67891
Orion Molecular Cloud, $^{15}NH_3$ detection at 23 GHz 79−44590
Orion Molecular cloud, CO vel. features rel. to shock fronts and expansion of Orion H II region 80−41880
Orion Molecular Cloud, HCN, HNC and HCO^+ J=3-2 lines detect. 79−25669
Orion Molecular Cloud, NH_3 emission obs. 80−36687
Orion Molecular Cloud, NH_3 spectrum and new dynamical model 78−93373
Orion Molecular Cloud, S0 obs. rel. to rotational explanation of high-vel. mol. emission 80−36688
Orion Molecular Cloud 1, cyanoacetylene emission obs. 78−4322
Orion Molecular Cloud 2, relationships of N_2H^+, HCO^+, HCN and CN 77−33587
Orion molecular cloud/H II region NGC 1977 interface, radio recombination line obs. 79−25658
Orion molecular source, CO J=2-1 isotopic line obs. at 230 GHz 77−33590
Orion Nebula, C recomb. line mapping 78−20866
Orion Nebula, dimethyl ether emission detect. 79−53862
Orion Nebula, H 76α recombination line obs. and ionized gas structure 79−67073
Orion Nebula, physical conditions from optical and radio lines obs. 77−45524
Orion Nebula, radio obs. of nearby H I distrib. and vels. 80−105322
Orion Nebula, SO 36 GHz emission line detect., rel. to mag. fields 80−46642
Orion Nebula, temp. gradients, obs. and model 78−8077
Orion Nebula molecular cloud, anomalous var. of $N_2H^+/HCO^+/SO_2$ rel. to ion-molecule reactions 77−26034
Orion population stars, OH emission survey 80−67716
Orion region, struct. in radiocontinuum 78−49549
Orion-KL nebula, VLBI obs. at 43 GHz of SiO maser 79−92836
Orionid meteor shower 1975, radar echo rates, long-baseline obs. 80−36576
α Orionis, 14.9 GHz obs. 79−75210
V380 Orionis, B8-A2e star, assoc. interstellar CH emission obs. 80−51856
α Orionis, CO and SiO millimetre line emission search rel. to circumstellar shell props. 78−49423
U Orionis, outbursts in main line OH emission 79−101158
U Orionis, stellar OH maser VLBI obs. rel. to mag. field 79−25742
α Orionis (Betelgeuse), radio emission 79−48788
U Orionis OH maser flare detect. 79−40197
OS210 (4C 28.40), extended radiosource identification with quasar 77−87563
OTL radio sources, position and struct. determ. from 327 MHz lunar occultation obs. 80−73061
OTL radio sources, position and struct. determ. from 327 MHz obs. 80−73060
OTL radiosources, position and struct. determ. from 327 MHz lunar occultation obs. 80−73062
OV-236 (1921−29), radio outburst obs. of quasar 80−51906
Parkes 2700 MHz survey, catalogue for Declinations −4° to −15°, Right Ascensions 10^h to 15^h 79−75121
Parkes 2700 MHz survey, part twelve 77−49315
Parkes 2700 MHz survey of radiosources, 13th part, 404 objects 78−20656
Parkes 2700 MHz survey sources, 408 MHz obs. 80−86008
Parsamyan 21, bipolar nebula, search for OH emission 78−41016
peculiar galaxies radio emission detect. 77−17674
peculiar H II regions with nonthermal radioemission, supernova shell interaction *(Russian)* 77−91610
AG Pegasi, symbiotic nova, radio emission obs. 77−22232
Periodic Comet d'Arrest (1976e), radio OH lines obs. 77−49333
periodicity investigation in special objects at 21 cm 80−82529
S Persei, M-type supergiant, OH emission rel. to circumstellar envelope struct. 77−22218
S Persei, supergiant 22 GHz H_2O maser emission temporal var. 78−49461
Perseus cluster, WSRT 610 MHz obs. and catalogue of sources 79−75283
Perseus galaxy cluster, low-resolution aperture synthesis map at 408 MHz 80−56958
Perseus OB2 association molecular cloud, mol. obs. rel. to star form. 80−12798
Phobos, mass from Viking Orbiter radio tracking data, density estimate 78−32380
Phobos, mass from Viking Orbiter radio tracking data 78−32379
Pioneer 11 at Saturn, trajectory var., carrier freq. Doppler shift, Saturn mass determ. 80−82294
Pioneer Venus occultation experiment, radio science data generation 80−67492
Pioneers 10 and 11, tracking data rel. to gravity field of Jupiter and satellites 77−37554
PKS 0131−36 (NGC 612), radio galaxy with disc, struct. 79−2568
PKS 0211−47 and 0634−20, giant radiogalaxies, optical and radio obs. 78−81702
PKS 0438−43, high radio luminosity quasar, identification 79−17124
PKS 0521−36, BL Lacertae object, radio and optical props. 79−84854
PKS 0735+178, flat radio spectrum, 0.3-90 GHz obs. 80−94880
PKS 0735+178, search for redshifted H I 21 cm absorpt. line 77−49478
PKS 1510−08, large radio outburst at 2.8 cm 79−30144
PKS 1718−649, galaxy, radio and optical study 77−45564
planetary atmosphere composition anal. by radiowave transmission by space probes 79−21204
planetary atmospheres, turbulence effects on profiles from Doppler meas. of occultations 79−2498

radioastronomical observations continued
planetary atmospheres, turbulence effects on profiles from intensity meas. of occultations 79−2499
planetary nebulae, advances in radio obs. 80−109526
planetary nebulae, electron temps. from radio continuum obs. 78−41027
planetary nebulae, interstellar extinction determ. 77−22295
planetary nebulae, OH emission search 79−48787
planetary nebulae, radio and optical structure, comparison using 6 cm data 79−75262
planetary nebulae, radio flux densities at 2.7 GHz 79−58394
planetary nebulae, radio mapping with Very Large Array 79−21196
planetary nebulae, southern, radio obs. at 5 GHz 79−58396
planetary nebulae, stellar, VLA obs. 80−22056
planetary nebulae-galactic centre distribution radio obs. 77−17667
planetary nebulae in southern hemisphere, IR and SHF obs. 80−90496
planetary nebulae near galactic centre, 1415 MHz obs. 79−71096
planets, astrometric and radiometric methods, tests of general relativity 78−45552
planets, H_2O 1.35 cm line obs. 78−20664
planets, radar studies of surfaces 78−73663
planets, surface structure forecast, based on thermal conditions 78−77502
planets LF radio survey by RAE 2 77−49321
Population I objects, location with respect to galactic plane 77−74127
powerful radiosources low freq. struct. and departures from equipartition 77−82316
primordial black holes and distant supernovae, search for radio pulses 79−25626
PSR 0031−07, drifting subpulses obs. and implications for pulsar models 80−67763
PSR 0239+54, four-freq. study of single-pulse structure 78−53972
PSR 0329+54 and 1133+16, obs. of single pulses at 327 and 2695 MHz 79−8939
PSR 0355+54, pulse shape change, 11 cm obs. 80−67761
PSR 0525+21 occulted by solar corona, Faraday rot. at 1720 MHz 80−46526
PSR 0531+21, interplanetary scintillations at 74 MHz 78−36625
PSR 0611+22, short time scale integrated pulse shape vars. 80−105267
PSR 0809+74, pulsar, phase stability in drifting subpulse pattern 78−40980
PSR 0820+02, long-period binary pulsar, discovery from timing obs. 80−56867
PSR 0826−34, 408 MHz obs. of unusual profile and sporadicity 79−40207
PSR 0833−45 (Vela pulsar), period change (1978 June-July) 78−89215
PSR 0833-45, Vela pulsar, position determ. 77−49416
PSR 0833-45, Vela pulsar, radio and γ-ray pulses, relative phases 78−85966
PSR 0950+08, ghost SNR, 327 MHz obs. 79−12506
PSR 0950+08, pulsar, micropulses freq. struct. 80−22030
PSR 0950+08, submicrosecond time resolution obs. 79−8941
PSR 1133+16, high time resolution obs. of high freq. radio emission microstruct. 78−45348
PSR 1133+16, pulse microstruct. direct. obs. at timescales down to 6 μs 78−28711
PSR 1641−45, large period discontinuity in long period pulsar 78−77570
PSR 1913+16, binary pulsar, confirmation of existence of gravit. waves *(French)* 79−80495
PSR 1913+16, binary pulsar, general relativistic effects meas. 79−35286
PSR 1913+16, binary pulsar, report 79−75234
PSR 1913+16, binary pulsar, test of new dispersion-removing radiometer 79−35142
PSR 1913+16, binary pulsar obs. at 327, 408, 610 and 1420 MHz 77−78810
PSR 1919+21, interpulse radio emission at freqs. 16.7-38 MHz 78−16447
PSR 1919+21, P_3 period temporal variability 78−36626
PSR 1919+21, pulsed radiation at 16.7, 20 and 25 MHz 77−87466
PSR 2020+28, pulsar, orthogonal polarisation modes obs. 78−93291
PSR 2045−16, multiple-ring struct. in hollow-cone emission 78−12259
pulsar acceleration by asymmetric radiation, observational evidence 77−60783
pulsar proper motions from timing obs. 77−33540
pulsar radiation patterns, obs. of objects with synchronised drift across window 77−57005
pulsar scintillation decorrel. bandwidth for interstellar electron density determ. 77−78850
pulsar signal microstructure, periodicities, polarisation and pulsar magnetospheres probing 79−75232
pulsars, 102.5 MHz obs. of three new pulsars *(Russian)* 80−67764
pulsars, detection at 22.7 GHz 77−33539
pulsars, discovery story 78−65644
pulsars, energy spectra and pulse shapes at metre wavelengths 79−75233
pulsars, flux obs., long-term intensity and spectral vars. 78−4268
pulsars, integrated pulse profiles and mean fluxes at 2.388 GHz 79−92791
pulsars, intensity vars. and timing irregularities 79−12485
pulsars, interpulse emission struct. 80−36652
pulsars, interpulses and other off-pulse emission 77−87467
pulsars, low latitude, H I absorption in spectra, interstellar electron density determ. 79−92792
pulsars, low-latit., H I absorpt. spectra meas. 80−101606
pulsars, obs. at 14.8 and 22.7 GHz 78−81645
pulsars, periods, positions and proper motion determ. from pulse arrival times, UHF, obs. 80−77431
pulsars, polarisation characts. at 400 MHz 77−64787
pulsars, polarisation characts. at 640 MHz for 43 southern pulsars objects 78−65642
pulsars, polarised radiation at 430 MHz, statistical summary 80−67760
pulsars, polarization, intrinsic posn. angles for 40 objects 79−44517
pulsars, polarization at 3.5 m wavelength 78−28713
pulsars, proper motions from timing obs. 79−17003
pulsars, pulse structure obs. at 102.5 MHz with 10 μsec time resolution 79−62862
pulsars, radio emission, millisecond intensity var. 80−98682
pulsars, radio emission spectra, 17-1420 MHz 79−62863
pulsars, radio flux density and pulse profile at 102.5 and 61 MHz 80−17601
pulsars, search for radio halos 77−5539

radioastronomical observations continued
pulsars, second Molonglo survey, 155 discoveries 79−12486
pulsars, southern sky survey, progress report 78−69821
pulsars, spectra and flux densities in 61-1420 MHz range for 9 objects 79−12487
pulsars, subpulse widths lower bound 77−17607
pulsars, suggested educational expts. 78−61982
pulsars, timing obs. at NASA Deep Space Station, Tidbinbilla 77−33542
pulsars, timing obs. from Arecibo Observatory 79−8938
pulsars, trigonometric parallax meas., electron density determ. in solar neighbourhood 79−88694
pulsars in northern sky, 17 new discoveries at 400 MHz 79−5853
pulsars in southern hemisphere, polarisation obs. at 1612 MHz 80−90462
RR Puppis, peculiar emission-line star, cm wavelength radio emission detect. 77−17573
ζ Puppis, radio emission obs. at 2 cm 78−40969
Puppis A supernova remnant, optical and radio comparison 78−28760
Q0000−398, angular size of high-redshift quasar 79−44634
Q0000−398, high redshift, large angular size, 2695 MHz obs. 77−45601
QSO 0241+622, nearby X-ray quasar, extended radio emission search 80−31382
QSO 0957+561, double quasar, 6 cm wavelength obs. 80−62312
QSO 0957+561, double quasar as gravitational lens, 6 cm VLA obs. 80−101647
QSO 0957+561, H I 21 cm radio absorpt. line redshifted to 594 MHz 80−36735
QSO 0957+561 A, B, 1.666 GHz VLBI meas. and gravitational lens hypothesis 80−27007
QSO 1038+528 A,D, close pair of radio-emitting quasi-stellar objects, radio and optical obs. 80−51902
QSO 3C273, using VLBI *(Japanese)* 80−17503
QSO redshifted 21 cm absorption line clouds 80−62310
QSO spectra, H I 21 cm absorption 78−93448
QSOs, catalogue of 403 objects 77−26080
QSOs, high-redshift, radio emission search 77−64874
QSOs, optically selected, radio study 80−82536
QSOs, radio obs. of 70 optically selected MCS objects 80−105377
QSOs, redshifted clouds, 21 cm line studies 80−105389
QSOs from 4C and Parkes catalogues, complete samples, radio structs. 79−62927
QSOs near S.Galactic Pole, photometry and 5000 MHz emission 79−88761
Quadrantids, overdense radio meteors, stream maxima position var. with meteor magnitude 78−12161
quasar 0241+622, very high resolution radio obs. 79−88758
quasar 0420−01, correlated time-delayed radio-optical outburst 79−25750
quasar 0957+561, radioastron. obs. of assumed double quasars 80−105381
quasar 1229−021, H I 21 cm absorpt. at redshift z=0.395 79−62928
quasar radio emission, from quasar group selected for optical brightness 80−41910
quasar radio var. timescale, redshift effect 77−29947
quasar-galaxy associations, search using Jodrell Bank 966 Hz survey 78−24566
quasars, bright optical PG objects, radio emission at 2.7 and 8.1 GHz 78−45424
quasars, flux meas. of OH 471, PKS 0735+178, 3CR 216 and TON 490 78−81703
quasars, optically discovered, search for radio emission 80−90561
quasars, optically selected, search for radio emission 78−20904
quasars, radio intensity and polarisation distribs. at three freqs. 78−96560
quasars, radio structs. at 6-cm wavelength 77−60845
quasars 3C 345 and NRAO 512, VLBI obs. of circular polarizations at 8 GHz 78−41075
quasars from 5C2 survey, struct. 78−28837
quasars from B2 catalogue, radio structs. at 1415 MHz 79−35422
quasars from Jodrell Bank 966 MHz survey, interferometer obs. 79−5915
quasars from Parkes survey, high resolution obs., spectra 79−75295
quasars of 3CR and 4C catalogues, comparative study of props. 77−67136
quasars of 4C catalogue, radio structs. of complete sample 79−75293
quasars of high redshift, search for 21 cm absorpt. 80−4453
quasars with double radio components, separation vel. *(Chinese)* 78−69903
quasistellar objects, radio quiet, obs. at 3.3 mm wavelength 78−81703
quiet Sun, fine struct. and time var. at 1.3 cm wavelength 79−30043
quiet Sun, high-resolution obs. at 6 cm using Westerbork Synthesis Radio Telescope 80−36601
quiet Sun, obs. at metre and decametre wavelengths 78−4184
radar meteor echo rates, correl. with zonal winds at 95 km altitude 80−56775
radio burst correlated with gamma-ray event 77−33668
radio galaxies components, fly away velocities upper limits *(Russian)* 80−62306
radio galaxy 1159+583, wide-angle tailed, radio obs. and models 80−31352
radio recombination line obs. 79−101193
radio sources in North Polar Spur region, 1420 MHz obs. and catalogue 80−22100
radio star obs. at 3.3 mm 77−74065
radio stars, positions for extragalactic reference frame 78−16278
radiogalaxies, polarized brightness distrib. at 2695 and 8085 MHz 79−35410
radiogalaxies from B2 Catalogue, optical identification, radio positions and redshifts 80−86005
radiometeors characts. assessment; statistical analysis of time-dependent series *(Russian)* 80−56777
radiosource catalogue S4 5 GHz survey between +35° and +70° declination 78−69893
radiosource linear and circular polarisation at 49 cm 77−60835
radiosource position meas. and optical identifications for 538 sources at 966 MHz 77−87561
radiosources, catalogue of 347 sources obs. at 610 MHz, source parameters, identifications 78−40838

radioastronomical observations continued
radiosources, circular polarisation obs. conflict with magnetic dipole model 79−53926
radiosources, coordinated photometric and spectroscopic observations of strong extragalactic 90 GHz sources 78−93440
radiosources, flat spectrum, optical identification of complete sample 79−5911
radiosources, in fields of five unidentified high latit. X-ray sources, list of 249 objects 77−87281
radiosources, linear polarisation meas. at 99 GHz 78−93439
radiosources, positions and optical identifications, 966 MHz survey 80−73059
radiosources in Zwicky clusters of galaxies, pencil beam and interferometer obs. 79−9019
radiosources near North Celestial Pole, 1421 MHz survey 77−45590
radiosources of intermediate strength, statistical props. 80−62303
radiosources with flat or inverted spectra, optical and radio props. 78−81697
radiosources with peculiar optical features, structure 79−12532
RCW 48-49, H II region complex, discovery of strong H_2O maser emission 77−57102
recombination line emission from galactic plane, obs. 77−13433
resolved sources, 1.4 GHz aperture synthesis obs. of circular polarisation 77−29656
ring galaxies, H I survey 79−5901
ring galaxies, radio continuum emission 80−67846
ring galaxy A0035 (Cartwheel), H I 27 cm line obs. 77−64852
ring galaxy discovery in Bootes on Palomar Sky Survey prints, radio flux meas. 80−26985
Rosette Nebula (NGC 2237/2246), new physical parameters from 6.5 GHz obs. 80−4414
S0 galaxies, H I obs. 77−2466
S0 galaxies, radio continuum and H I obs. 77−87549
S104, 609 MHz aperture synthesis obs. of H II region 78−57618
S106, H II region, radio obs. of assoc. mol. cloud, CO, HCO^+ HCN, OH and formaldehyde lines 78−61906
S106 and S235, aperture synthesis of H II regions, star form. regions 78−36672
S132, radio continuum emission from giant H II region 79−8974
S140, mol. cloud, continuum emission mapping at 89.6 GHz 80−94842
S140 molecular cloud, energetics, mol. line data, temp., density, abundances 78−36650
S159, H II region, CH obs. 78−28751
S187, H109α recomb. line obs., core envelope type struct. 79−8965
S232, H II region, mag. field strength meas. 80−51840
S252 (NGC 2175), mol. line obs. of star-forming complex 80−4411
S255, H II region, CO emission small-scale struct. from lunar occultation obs. 80−46637
S255, molecular cloud, molecular line, radio continuum and IR data 78−8087
S4 sources, flux density meas. at 9.5 mm wavelength 78−69894
S88B, Hα knot, optical radio and IR obs. of vicinity 77−74115
S-bursts, obs. at 32 MHz 78−36498
Sa spiral galaxies, H I study 80−98714
Sa type spiral galaxies, redshifted 21 cm line profiles, radio obs. 80−73041
HM Sagittae, emission variable as embryonic planetary nebulae 77−56950
HM Sagittae, emission-line variable star, radio emission detect. 78−28706
HM Sagittae, radio emission flux density 77−60770
HM Sagittae, young planetary nebula, 2.8 cm flux density secular increase 79−67025
VX Sagittarii, VLBI obs. of SiO maser in supergiant 79−92779
Sagittarius A, aperture synthesis obs. of H I absorpt. 77−26037
Sagittarius A, H200β line detect. 77−78868
Sagittarius A, H recomb. lines obs. at decimetric wavelengths 77−82310
Sagittarius A, multifrequency radio image *(Russian)* 77−2478
Sagittarius A, Sagittarius B2, probable detect. of methylamine-d_1 77−33610
Sagittarius A region, 8.2 mm obs. 78−28794
Sagittarius A West, temp. and dynamics of ionized gas from radio recombination line obs. 79−44595
Sagittarius B2, 5 and 7 GHz obs. of cyanodiacetylene 79−92817
Sagittarius B2, acetonitrile emission obs. 77−64835
Sagittarius B2, cyanodiacetylene 2663 MHz transition obs. 77−33669
Sagittarius B2, dimethyl ether emission detect. 79−53862
Sagittarius B2, microwave detection of NO 78−93378
Sagittarius B2, mol. cloud, detect. of HC_5N (cyanodiacetylene) and HC_7N (cyanohexatriyne), SHF obs. 80−101627
Sagittarius B2, recomb. lines obs. rel. to He abundance problem 78−49496
Sagittarius B2 molecular cloud, chemical fractionation of ^{13}C isotopes of cyanoacetylene 77−29900
Sagittarius dwarf irregular galaxy, H I obs. 78−20887
Saturn, decimetric radio obs., brightness temp. 80−46474
Saturn, ionosphere electron density from Pioneer II radio occultations 80−94751
Saturn, limb darkening and brightness temp., 1.30 cm interferometry obs. 80−82279
Saturn, radio emission flux density at 102.5 MHz, upper limit meas. *(Russian)* 78−4146
Saturn, ring brightness temp. meas. at 8 mm wavelength 78−36502
Saturn, ring particle composition and size distrib. from radar obs. 78−36501
Saturn, short-wave millimetric obs. with wide-band radiometer 79−96916
Saturn, upper neutral atm. and ionosphere, vertical struct., Pioneer 11 radius occultation obs. 80−82293
Saturn's rings, two-freq. radar obs. 77−33404
Saturn and its rings, aperture synthesis study at 3.71 cm wavelength 79−96963
Saturn and its rings, interferometric obs. at 3.71 cm wavelength 79−96962
Saturn ionosphere, spectral broadening meas. by Pioneer (11) 80−109391
Saturn rings, 3 mm obs. and props. 80−46470
Saturn rings, model constraints from radar obs. of polarisation and albedo 80−82277
scintillating background, determ. of mean ang. size of sources at low flux densities 77−5453

radioastronomical observations continued
AH Scorpii, M-type supergiant, OH emission rel. to circumstellar envelopes struct. 77−22218
Scorpius X-1, high energy X-ray and SHF radio obs. 80−73067
Sculptor dwarf irregular galaxy, 21 cm obs. 77−64843
RY Scuti, β Lyrae system, optical and radio spectra 79−30090
RT Serpentis, symbiotic star/nova, possible H_2O maser obs. 79−8932
FH Serpentis (Nova 1970), radio emission from expanding shell 80−26868
SETI at 18 cm, high sensitivity search 80−82229
Seyfert and related galaxies, 1415 MHz survey 77−9800
Seyfert galaxies, H I survey 79−8988
Seyfert galaxies, obs. at 1.3 and 2.8 cm wavelength, spectra 78−69866
Sharpless 115, evolved H II region, struct. from UHF obs. 80−105313
Sharpless 155 nebula and Cepheus OB3 association, thermal radio emission obs. 78−96514
Sharpless 159 and NGC 7538, H II region/mol. cloud complex, H I aperture synthesis obs. 80−90510
Sharpless 235A, optical, radio and IR obs. of H II region 80−4415
Sharpless H II regions, small-scale struct. at 4.995 GHz, high-resolution catalogue 78−61755
Sharpless small H II regions, radio line and continuum obs. 77−87509
Shostak high-velocity cloud, H I obs. 78−32575
sky background, microwave emission spectra 79−48967
sky survey, large beam, at millimetre and submillimetre wavelengths made from balloon altitudes 79−97045
sky survey at 8085 MHz of 0.181 steradians, 64 sources, identifications, spectral indices 78−40836
SN 1572 (Tycho's supernova), small dia. radio source discovery and precise position 80−98680
SN 1979c in NGC 4321 (M100), detect. at 60 nm wavelength 80−82402
SO -alaxies, radio and IR photometry 78−16531
soil, surface refl. characts. for radar, obs. from Luna spacecraft 80−72798
solar 3.5 mm depression features assoc. with Hα disparitions brusques 77−78756
solar 810 MHz bursts in 1957-67 period, obs. data 77−33446
solar 'spike' type radio bursts, morphological characts. 78−65599
solar active region, comparison of 9.1 cm and soft X-ray emission 77−22180
solar active region and bursts, 6 cm obs. with 6″ resolution 80−62096
solar active region flare rates and 8.6 mm brightness temps. 77−29769
solar active regions, 6 cm obs. with 6 arc seconds resolution 77−33444
solar active regions, magnetic and microwave struct. 77−49361
solar active regions, VLA synthesis maps at 6 cm wavelength 79−40157
solar atmosphere differential rotation, from mm wave obs. 77−2378
solar brightness distrib. at 8.6 mm wavelength, interferometer obs. 77−2388
solar burst intensity fluctuations at metre wavelengths *(Russian)* 77−64733
solar bursts at 30 and 60 MHz, STEREO-5 obs., ionospheric scintillation evidence 78−61822
solar chromosphere, brightness distrib. at 3 mm wavelength, obs. at 1976 October 23 eclipse 79−30042
solar chromosphere, periodic brightness fluctuations at 2.8 cm wavelength, rel. to photospheric vel. oscills. 79−35216
solar chromosphere, ubiquitous structs. observed in quiet Sun at mm and cm wavelengths 79−12456
solar chromospheric structure from brightness distrib. at mm wavelengths 79−53799
solar corona, Helios 1 Faraday rot. expt. results 78−20790
solar corona, plasma radiowave fluctuations and turbulence, Venus 10 radio transmission expt. 79−80295
solar corona, radio emission fluctuations 78−45311
solar corona, stereo obs. 78−49419
solar corona, Viking radio occultation obs. at 1976 Mars solar conjunction 78−20789
solar corona above active regions, soft X-ray and cm wavelength obs. 79−44431
solar corona probing, Helios 1 and 2 occultations, S-band time delay meas. 78−20791
solar coronal hole, obs. with λ 8-cm radioheliograph 80−4326
solar coronal hole obs. at 85 GHz 77−17521
solar coronal holes, radio and EUV meas. of temp. distrib. and electron density *(Russian)* 78−16378
solar coronal source regions of U-type bursts 78−77543
solar coronal transient, 1973 August 21, radio and white light obs. 79−71010
solar coronal transient, massive slow-moving, radio obs. 79−53796
solar coronal transient event, 1973 Sept. 14-15, material motions and mag. field 77−17529
solar decametric noise storms and coronal irregularities, microscopic spectral features 77−45392
solar drifting spikes, new species of solar radio bursts obs. 79−48753
solar emission, harmonic generation and mm waves mixing for receiver *(Italian)* 77−49292
solar fibre bursts concurrent with weak noise storm 77−2399
solar filament, study of transition sheath from radio obs. 78−28619
solar filament, synthesized map at 6 cm with about 15″ resolution 80−90380
solar filament eruptions and nonflaring coronal transients assoc. with nonthermal electrons 78−65595
solar filaments, multifreq. obs. at centimetre wavelengths 78−28602
solar fine structure radio emission in 20-30 MHz range *(Russian)* 78−16383
solar flare, 1971 January 14, radio emission position and polarisation 77−2393
solar flare, 1973 September 5, radio data and theoretical model for fast-mode MHD shock wave 79−92734
solar flare, 1978 February 11, Hα, Hβ and VHF obs. 78−93187
solar flare continuum events, m wavelength obs., emission mechanism 79−21248
solar flare localisation in Sun's atmosphere, radio observations 79−88641
solar flare magnetic fields and microwave burst spectra 78−7970
solar flare spatial structure in soft X-rays and cm wavelengths 77−17524
solar flares, Hα, hard X-ray and microwave emissions in impulsive phase 78−77540
solar flares, microwave and optical emissions comparison 80−31284
solar flares, millisecond microwave spikes obs. 78−96464

radioastronomical observations continued
solar flares, nonthermal particle prod. during buildup and in absence of flares 77−17492
solar flares, observation by optical and radio techniques 79−48765
solar flares, radio brightness distrib. processing in one-dimensional synthesis *(Italian)* 80−98628
solar flares, VLA obs. interpreted with optical X-ray and other microwave data 79−44428
solar flares and type I sources, evolutionary relation from 146 MHz obs. *(Chinese)* 80−8609
solar flares in 1972 August radio scintillation obs. of shock wave form and energy 78−57534
solar flux quasiperiodic variations at 10.7 GHz 77−17516
solar impulsive microwave bursts, superimposed fast time structs. with slowly varying polarisation 79−40173
solar metre-wave emission, source positions determ. rel. to wave ducting 80−21978
solar metre-wave radio bursts positions, correl. with X-ray emission 78−69774
solar metric radiobursts polarisation and location rel. to new mag. field emergence 78−61824
solar microbursts at 22.2 GHz rel. to lower freq. events 77−2398
solar microwave absolute flux, spectra of individual components 77−5461
solar microwave activities associated with McMath regions 14943 and 14979, 1977 Sept.-Oct. 79−48767
solar microwave burst, 1976 March 28, superimposed 4.7 s periodic oscills. 78−7972
solar microwave burst, polarisation obs. 77−29773
solar microwave bursts, spike, rise, fall and absorpt. types, obs. 79−88636
solar microwave bursts fast structs., negligible large-scale mag. field changes 79−2536
solar microwave radio emission, sudden decreases obs. 79−101134
solar microwaves, lower intensity limit *(Portuguese)* 77−78729
solar moving type IV burst, associated pulsating struct. radioheliograph obs. 79−40171
solar moving type IV bursts, gyro-synchrotron modulation obs. 80−26833
solar moving type IV radio bursts, obs. and interpretation 79−40174
solar multiply impulsive bursts, hard X-ray and microwave spectral evolution 80−26828
solar noise storm, 1972 May 21, m wavelength pulsating bursts, model 79−25569
solar noise storm, drifting pulsations obs. 80−62105
solar noise storms, correl. with particular photospheric mag. structs. 78−4185
solar noise storms, spectrum and position at decametre wavelengths 78−28622
solar noise storms and radio bursts during cycle 20, statistical anal. 80−56794
solar partial eclipse, 1977 April 18, obs. at 590 MHz 77−87362
solar plasma EM wave propag., observations using Mars-2 and Mars-7 probes 78−49345
solar plasma inhomogeneous structure, Venera-9, 10 dispersion-interferometer meas. 79−8789
solar plasma inhomogeneous structure, Venera-9 and 10 radio sounding meas. 79−8788
solar prominences, cm and mm wavelength obs., size and spectrum of radio filaments 79−66988
solar proton flare, 1971 January 14, assoc. complex radio emission event 79−40175
solar quasiperiodic oscillations at 3 cm 77−29768
solar quiescent prominence, obs. at 8 mm during 1975 May 11 eclipse 78−7977
solar radio and X-ray bursts positions and sizes 77−33459
solar radio bursts, 6 cm obs. with 6″ resolution 78−53897
solar radio bursts, evidence for dense non-potential magnetic flux tubes in corona 78−28615
solar radio bursts, synchronous obs. in Crimea and Cuba *(Russian)* 77−64718
solar radio bursts at 100-9500 MHz, obs. during 1977 Sept.-Oct. 79−48770
solar radio bursts at 26.4 MHz, struct. and evolution 78−65596
solar radio bursts at 3.7 and 11.1 cm wavelength, interferometric obs. 80−31285
solar radio bursts in 0.2-1.4 GHz range, ms fine struct. 77−53499
solar radio bursts obs. at 1.9, 2.5 and 3.5 cm wavelength during 1972 Aug. 3-6 period *(Russian)* 77−64719
solar radio bursts of drifting pairs type, results of obs. near 25 and 12.5 MHz 78−24502
solar radio emission, from McMath regions 14943 and 14979, interferometric obs. at 8.6 mm wavelength 79−48768
solar radio emission, m and dm wavelength obs. during 1977 Sept.-Oct. 79−48769
solar radio emission, S-component spectrum fine struct. in 5.0 to 7.0 GHz freq. range 80−21977
solar radio emission obs. at 1.9, 2.5 and 3.5 cm wavelength, assoc. with 1974 July sunspots *(Russian)* 78−65585
solar radio emission polarisation in 1.9-3.5 cm wavelength region, obs. method *(Russian)* 78−65587
solar radio emission S-component, statistical anal. 79−40172
solar radio radiation, spectral polarisation obs. of local sources during March (1970) 77−53535
solar radioflux, 1970 absolute calibration at 2800 MHz 80−17570
solar radiowaves diffraction and refl. from lunar limb during solar eclipses *(Russian)* 78−65586
solar S-component, local sources emission directivity, spectral study 78−24500
solar SHF flux fluctuations from limited areas, rel. to coronal wave propag. 79−35222
solar sporadic radiation, Interkosmos-Copernicus 500 satellite obs. 77−53503
solar stria burst sources ang. sizes, 24-26 MHz range 78−65597
solar total flux obs. at 3.2 cm wavelength at Peking Obs., 1965-75 period *(Chinese)* 78−69763
solar total intensity and circular polarization struct. at 21 cm 78−7957
solar type I and III m wavelength bursts source heights meas. 77−33460
solar type I burst, 1972 August, m wavelength charact. *(Chinese)* 77−22156
solar type I stormburst chains, radio spectra 77−22192
radioastronomical observations continued
solar type II bursts with reverse frequency drift 78−7978
solar type II decameter wave burst assoc. with behind-limb flare 77−22194
solar type II radio burst, 1973, May 3, fine struct. 78−24501
solar type II radio burst with reverse freq. drift against noise storm background, obs. 80−17567
solar type II-IV bursts, 1971 Dec. 14, rel. to compact and diffuse white-light clouds in corona 77−22193
solar type III and type J-like decametric emission in coronal mag. arch 78−12179
solar type III and type IV bursts from source above solar limb, heliograph obs. 79−53798
solar type III burst, stereoscopic direction finding meas., second harmonic emission 78−45312
solar type III bursts, conf., Berkeley, California, USA (May 1975) 77−2406
solar type III bursts, direction finding meas. out of ecliptic plane 77−22195
solar type III bursts, enhancements assoc. with interplanetary shocks 77−2409
solar type III bursts, flaming struct. 77−74031
solar type III bursts, fundamental and harmonic radiation 77−2413
solar type III bursts, high time resolution obs., instrumentation, data reduction *(Italian)* 78−96458
solar type III bursts, LF, directivity 77−2410
solar type III bursts, LF obs., fast electrons interplanetary scatt. 77−2411
solar type III bursts, LF obs. apparent source sizes 77−2412
solar type III bursts, LF spectra 79−30048
solar type III bursts, radio intensity and fast electron flux at 1 AU 77−2407
solar type III bursts, tracking in elevation and elongation, apparent source sizes 77−2408
solar type III bursts at decameter wavelengths, longit. depend. of duration 78−81596
solar type III radio bursts, 1972 May-Aug., obs. in interplanetary space 79−62805
solar type III radio bursts, fundamental and harmonic, circular polarisation, 24-220 MHz *(Russian)* 78−16384
solar type III radio bursts, interplanetary baseline obs. 78−20808
solar type III U-shaped radiobursts, circular polarisation 77−45379
solar type IIIb radio bursts, polarisation meas. 77−22161
solar type IV meter burst, continuous radiation microstruct. and source model 77−53534
solar type IV radio burst quasiperiodic struct., anal. and interpretation 80−62097
solar type IV radio events, pulsating structs. 78−96455
solar type U radio bursts, polarisation evolution 80−26834
solar type V radio bursts, dynamic spectra distinctive struct. 80−46527
solar type V radio bursts, VHF obs. 78−28639
solar VHF noise registrations at Oslo Solar Obs. (1965-74) 77−53541
solar wind, electron density fluctuations obs. by radioscintillation 80−61978
solar wind, electron density small-scale fluctuations, interplanetary scintillation obs. 78−96376
solar wind, low freq. continuum from ISEE 3, thermal electrostatic noise, LF obs. 80−101519
solar wind, meas. of second moment field 78−16369
solar wind, plasma turbulence, Venera 10 radiowave spectral width meas. 79−88560
solar wind, radial depend. of props. from Helios 1/2 and Pioneer 10/11 scatt. expts. 78−28595
solar wind, vel. estimation from multi-station interplanetary scintillation 78−73601
solar wind, velocity out of ecliptic from interplanetary scintillation obs. 77−5409
solar wind 74 MHz interplanetary scintillation and IMP 7 obs. during 1973 78−89033
solar wind density fluctuations near Sun from Pioneer 6 spectral broadening meas. 77−13199
solar wind electron content, Pioneer 6, 8 and 9 obs., graphical summary 79−53699
solar wind large-scale density fluctuations, meas. using dual freq. phase scintillations 77−13198
solar wind turbulent plasma, radio wave propag. meas. using three satellites 80−101518
solar X-ray bright point flares, search for microwave emission 77−45384
souce surveys at 5 GHz at NRAO and MPIfR 78−28817
source posns. using transatlantic long base line interferometry at 10680 MHz 79−48390
source survey with WSFT at 6 cm, analysis 79−75287
southern bright elliptical and S0 galaxies, 5 GHz survey 77−49479
Southern Coalsack, CO emission obs. 77−29902
southern extragalactic radio sources of large ang. extent, emission spectrum vars. 80−17683
southern extragalactic sources, obs. with Fleurs synthesis telescope 78−4385
southern H II regions models from radio recomb. line data 77−33620
southern molecular clouds, CS J=1-0 transition at 49 GHz 78−65674
southern open clusters, search for interstellar H I 80−46619
southern sky, obs. in 2-20 MHz range 77−45563
southern X-ray sources, radio continuum obs. 77−17573
spectroscopic observations by Jodrell Bank 1024 channel digital autocorrelation spectrometer 77−73970
spiral galaxies, 21 cm line studies rel. to local mass-to-light ratio 80−31361
spiral galaxies, in Coma cluster, nuclear radio emission upper limits 78−8107
spiral galaxies, radial vels. from H I 21 cm line obs. 79−21419
spiral galaxies, radio continuum morphology, review 77−26071
spiral galaxies, redshifted 21 cm absorption line clouds 80−62310
spiral galaxies, rot. curves, mass distrib. and total masses 77−49477
spiral galaxies with unusual radio morphology, radio continuum obs. 77−60822
spiral struct. of galactic inner parts from 21 cm line and stellar data 77−82304
sporadic meteors, ionisation height meas., VHF obs. 80−82312
sporadic meteors, sunrise effect on persistent radar echoes 78−20759
SS 433, 180 mm interferometric obs. of triple structure 80−105259
SS 433, 1979 May-June radio flare, 3.24 GHz obs. 80−46567

radioastronomical observations continued
SS 433, change in radio struct., 1980 January to June, from VLBI obs. 80−109557
SS 433, Hα emission object, 21.6 and 43 GHz obs. 79−92783
SS 433, H I absorption obs. and distance 80−56848
SS 433, radio and optical obs. 79−88661
SS 433, radio and optical positions coincidence 80−56840
SS 433, radio jet discovery 80−31381
SS 433, search for radio spectral lines in UHF 80−109556
SS 433, UV spectral search and 8 GHz linear polarization 79−71048
SS 433, VLBI detect. and ang. struct. 80−31304
star clusters, OH 18 cm line obs. of young groups 79−25655
star formation 78−32565
stars, OH maser emission from late-type objects, UHF obs. 80−56826
stars in Pleiades region, radio and optical obs. of flares *(Russian)* 78−93245
steep spectrum radiosources, spectral index dependent props. 80−36730
steep-spectrum sources, possible LF variables, 410 MHz fine struct., interplanetary scintillation obs. 78−41068
stellar H_2O maser emission, circumstellar shell model 77−60765
stellar H_2O masers, detect. of new sources 78−32466
stellar H_2O masers, time vars., 22 GHz obs. 79−30077
stellar OH masers, struct. 77−53583
stellar radio emission monitoring at 10.6 GHz 77−60763
stellar SiO masers, $J=1\rightarrow0$ $v=1$ and 2 masers relative intensity and vel. 80−4339
Stephan's Quintet, H I emission search 79−30136
Stephan's Quintet, radio continuum maps at 2695 MHz 77−57099
Stephan's Quintet, redshifted H I associations 80−67882
Stephen's Quintet, broadband 21 cm H I emission 80−109554
Stephenson's planetary nebula, optical, near IR and radio obs., position 79−67086
Stephenson-Sanduleak 433, Hα emission object, nonthermal radio emission obs. 78−86033
Stephenson-Sanduleak 433, Hα emission object, variable radio emission obs. 78−86034
Sun, 1978 May 7 events, radio, optical and geophysical manifestations *(French)* 80−8611
Sun, 2800 MHz radio minimum (1976 February) 80−4324
Sun, active prominences at cm. wavelengths, RATAN-600 obs. *(Russian)* 79−16926
Sun, active region coronal loops, gyroresonance absorption evidence 80−56792
Sun, active region McMath 15403, 5 minute oscills., SHF obs. 80−98639
Sun, active regions, 3 cm radio emission spectral slope, flare-associated variations 80−98630
Sun, anal. of solar radio obs. at 3.2 and 10 cm at Purple Mountain Observatory *(Chinese)* 80−105223
Sun, bright active regions at 2.8 cm, development and structure 78−53910
Sun, brightness at 8 and 13.5 mm rel. to magnetic fields and Hα activity *(Russian)* 77−64724
Sun, brightness distrib. at 33 and 37 GHz 77−53524
Sun, brightness distrib. at 8.6 mm, interferometer obs. 80−56800
Sun, brightness temp. at millimetre wavelengths 77−22171
Sun, bursts at m wavelength, 169 MHz radioheliograph obs. 79−30033
Sun, centimetre-wave bursts space-time relation to impulsive chromospheric flares *(Russian)* 79−16924
Sun, corona, radio obs. at Culgoora Observatory 79−48754
Sun, coronal holes, Arecibo obs. at 11.5 and 21 cm wavelength 78−61834
Sun, coronal holes, EUV and radio spectrum 80−56802
Sun, coronal holes and arches, brightness temps. at 169 and 408 MHz rel. to UV obs. 79−8893
Sun, decametric emsemission, quasi-periodic fluctuations *(Russian)* 79−25561
Sun, decametric obs. of corona at high resolution 80−31288
Sun, decimetre fluctuations, quasiperiodic components *(Russian)* 77−74034
Sun, decimetric type IV narrow-band burst with fine structure 78−36546
Sun, drift pair bursts, polarisation obs., position and freq. characts. 80−85925
Sun, emission preceding proton flares, pulsation instability 78−53911
Sun, emission pulsations in 1.9-3.5 cm wavelengths *(Russian)* 80−17563
Sun, equatorial brightness distrib. at 2.8 cm, one dimensional aperture synthesis obs. 77−22173
Sun, flux level distrib. and oscillatory bursts 77−33451
Sun, ground-based obs. of August 1972 flare events, review 77−25993
Sun, Hα-flares rel. to radio bursts and sunspots 80−41803
Sun, hectometric and kilometric radio emission in August 1972, satellite obs. 77−25994
Sun, high angular resolution obs. at 8.5 mm wavelength 79−25578
Sun, high resolution polarimetry at 3.7 and 11.1 cm wavelengths 77−71089
Sun, impulsive mm-wave bursts, quasi-quantization 80−94770
Sun, impulsive X-ray and radio bursts obs. 78−93174
Sun, local source radioemission fluctuations rel. to sunspot group development *(Russian)* 79−30035
Sun, microwave flux decreases rel. to assoc. activity complex 77−25989
Sun, moving type IV bursts, brightness temps. 79−48760
Sun, moving type IV bursts, circular polarisation rel. to photospheric magnetism 78−53915
Sun, moving type IV bursts, Culgoora radioheliograph obs., statistical study 79−44456
Sun, obs. by RATAN 600 telescope, preliminary results 77−78760
Sun, proton region of McMath 13043 active region, radio burst obs. 78−89142
Sun, quiescent and active states, radio emission obs. *(Spanish)* 79−40160
Sun, quiet, interferometric obs at 8 millimetre wavelength 79−40149
sun, quiet, obs. with student-designed radiotelescope, multidisciplinary teaching exercise 80−17759
Sun, quiet 2.8 cm emission, small-scale sources 79−5794
Sun, quiet spatial structure during 1977 October eclipse, VLA 6 cm obs. 80−72895
Sun, radio spectrum to 10 km wavelength 79−92748
Sun, radius at 35 GHz 77−22174

radioastronomical observations continued
Sun, radius at centimetre wavelengths and brightness distrib. across disc 80−21968
Sun, rapid var. of centimetre-wave sources above McMath region 13043 rel. to optical phenomena 80−67688
Sun, relation between type I (metre wave) radio sources and proton events *(Chinese)* 80−105222
Sun, S-component, fine spectral structure in 4.5-7 GHz range *(Russian)* 77−33457
Sun, S-component source spectra, correl. with flare occurrence, EHF obs. 80−101579
Sun, short millimetre wave radiation obs. by wide-band radiometer 79−62750
Sun, short-wave millimetric obs. with wide-band radiometer 79−96916
Sun, spectral index of local radio sources in 1.9-3.5 cm range *(Russian)* 77−64732
Sun, three freq. obs. of moving type IV burst at limb 78−69776
Sun, Torun Observatory 127 MHz data since 1958, survey *(Polish)* 78−36549
Sun, two dimens. maps at 408 MHz 80−85922
Sun, type II radiobursts and shock waves in interplanetary medium 80−56690
Sun, type III bursts, assoc. with flaring X-ray bright points 80−67681
Sun, type III bursts, drift rate rel. to polarization at 237 MHz 78−36545
Sun, type III bursts, fundamental emission in 25-200 kHz range 80−56789
Sun, type III bursts, position and polarisation, VHF and HF obs. 80−105214
Sun, type III bursts, radio spectra obs., effect of interactions in ionospheric plasma 80−72904
Sun, type III bursts during decametric storm 80−90399
Sun, type III-like bursts, UHF obs. 80−56793
Sun, type IIIb bursts, 25 MHz obs. and theoretical model 80−90400
Sun, type V radio bursts, position and polarisation, HF and VHF obs. 80−105215
Sun, type-II bursts, LF and MF obs. by Prognoz satellites 78−16375
Sun, types I and III storm radiation, obs. and cut-off freq. interpretation 79−21249
Sun, VHF activity and auroral effects 77−67004
Sun, X-ray and 2.8 cm coordinated obs. of active regions *(Italian)* 79−21254
Sun total microwave flux, search at Toyokawa for five minute oscillations 80−4327
Sun under quiet conditions, SHF brightness temp. distrib., RATAN-600 obs. *(Russian)* 80−94776
sunspot group, local radiosource fine structure *(Russian)* 79−21260
sunspots bipolar groups, circularly polarised radioemission obs. at 1.35 cm *(Russian)* 78−57532
superluminal radiosources, structure monitoring 79−44626
supernova remnant, radio maps 77−37642
supernova remnant in irregular galaxy NGC 4449, radio emission obs. 79−17056
supernova remnant W44, expansion into surrounding interstellar medium, dense cloud encounter 77−22298
supernova remnants, CO emission obs. 78−8071
supernova remnants, low surface brightness, optical and radio obs. 79−88717
supernova remnants, mag. field distribs., Faraday rot. and depolarisation 77−13428
supernova remnants, radio struct. obs. 77−13435
supernova remnants, southern, high resolution radio obs. 80−51849
supernova remnants in LMC, SHF obs. 80−67864
supernova remnants in young objects NGC 6946, search for radio emission from four young objects 80−77473
supernovae in clusters of galaxies, microwave pulsed emission upper limit 78−69890
symbiotic stars, 2 cm emission obs. 78−93274
symbiotic stars, survey at 1612 MHz 80−12774
V711 Tauri, radio flare on 1978 Nov. 6 at 15.5 GHz 79−5836
T Tauri stars, OH and NH_3 emission line obs. 79−25662
T Tauri stars, props. of assoc. ionized regions 80−36624
Taurus A, decametric emission, quasi-periodic fluctuations *(Russian)* 79−25561
Taurus A, intensity and polarisation at 9 mm wavelength 80−36732
Taurus A, secular decrease in 927 MHz flux, radio flux density obs. 80−67840
Taurus A, sporadic radio flux increases and decreases 77−78877
Taurus A (Crab Nebula), supernova remnant, 927 MHz emission secular decrease 79−75255
Taurus dark cloud, gas temps. and motion 77−78851
Taurus HL-1, small H I velocity bridge, 21 cm obs. 78−28755
Taurus Molecular Cloud 1 in Heiles' cloud 2, molecular radio obs. 78−69858
Taurus Molecular Cloud 2 (TMC-2), HC_5N and NH_3 obs. 80−26957
RR Telescopii, cm wavelength radio emission detect. 77−17573
terrestrial kilometric radiation polarization, Voyager 1 and 2 direct meas. 79−12373
Titan, brightness temp. at 6 cm wavelength 79−101114
Tololo list of emission line galaxies, spectroscopic and radio survey 77−64851
Tycho's SNR (3C 10), distance, Westerbork H I obs. 80−101633
Tycho's supernova remnant, radio flux density meas. separated by 15-year interval 80−26955
Tycho supernova remnant, radio struct. 80−56919
type II radio burst, coronal mag. struct. in source region 78−69775
4U 0241+61, optical and radio identification, luminous low-redshift QSO 78−61940
3U 0901-09 radio counterpart, 2695 MHz obs. 77−26089
UKS 1927−177 and 2323−326, 21 cm. obs. of new dwarf irregular galaxies 78−65697
ultracold molecular gas toward galactic centre, CO isotopic rotational transitions 80−51826
Uranus, 34.3 MHz synchrotron flux upper limit 77−60724
Uranus, decimetric radio obs., brightness temp. 80−46474
Uranus, microwave brightness temp. increase 78−93150
Uranus, microwave radiometry and interferometry 80−56766
Uranus, NH_3 depletion in atmosphere, theory and obs. 78−53870
UTR-2 survey, sources in $0°<\delta<+10°$ range 79−97091
UTR-2 survey, spectra of sources in 10-1400 MHz range 79−97092
UTRAO 335-380 MHz survey, interim report 78−28815

radioastronomical observations continued
variable and peculiar stars, search for radio emission 77−22248
variable extragalactic radiosources, 90 GHz obs. 77−71152
variable extragalactic sources with flat spectra, structure 78−28811
variable extragalactic sources with steep spectrum, VHF and SHF obs. 80−90548
variable radio sources, obs. at 0.95 and 1.65 cm wavelength 78−16552
variable radio sources search at 18 cm wavelength, complete sample obs. 78−89268
variable radiosource obs. at 13 cm *(Russian)* 78−32591
variable radiosources, search at 408 MHz 77−33671
variable radiosources, spectra, RATAN-600 radiotelescope obs. *(Russian)* 78−61927
variable sources, 18 cm obs. 77−37662
variable stars, long-period, SiO maser emission obs. 78−4225
variable stars with long periods, radial and expansion vels. from SiO line at 86.8 GHz 78−40956
Vela pulsar, detect. of change in rot. measure 77−29867
Vela supernova remnant, rot. measure and turbulent struct. 80−51836
Vela X supernova remnant, radio polarisation maps 80−56909
γ^2 Velorum, radio emission obs. at 2 cm 78−40969
Venera-10 occultation by Sun, plasma turbulence and vel. *(Russian)* 77−91504
Venus, astrometric radar meas. in 1977, results 80−17522
Venus, atmosphere, diffr. effects in radio transmission 77−64682
Venus, atmosphere, turbulence from Pioneer multiprobe radio scintillations 80−46437
Venus, atmosphere radio occultation obs. and surface bistatic radiolocation by Venera-9 and (Venera-10) 79−48698
Venus, delay time and Doppler freq. correction in radar obs. 78−7897
Venus, electrical discharges in atmosphere *(Russian)* 79−66950
Venus, equatorial zone surface topography, radar obs. from USSR 77−87303
Venus, impact cratering and tectonic activity, evidence from radar obs. 80−46426
Venus, ionosphere, day and nighttime radio sounding meas. from Venera 9, 10 spacecraft 79−8867
Venus, lightning discharges, frequency of occurrence 80−56743
Venus, liquid content of lower clouds, Mariner 10 radio occultation data 79−40106
Venus, Mariner 10 radio occultation obs., pressure-temp. profiles 78−28563
Venus, microrelief irregularites mean height, determination from radio transillumination data 80−72807
Venus, neutral atmosphere, radio sounding meas., Venera-9, 10 spacecraft 79−8868
Venus, nightside ionosphere, Pioneer orbiter radio occultations 80−46441
Venus, nighttime atm. radioscopy by Venera 9 and 10 probes 79−62777
Venus, nighttime atmosphere, radiowave fluctuation and turbulence, Venera radioscopy data 79−80254
Venus, nighttime ionosphere, two freq. radioscopy by Venera 9 and 10 probes 79−62778
Venus, orbit and radius determ. from radar obs. in 1962-1977 period 79−88570
Venus, phase effect at 3.4 mm wavelength *(Japanese)* 78−89095
Venus, Pioneer radar data, planet's topography *(German)* 80−105190
Venus, polar heating and shape of planet, 6 cm wavelength obs. 79−70981
Venus, polar ionosphere, Pioneer orbiter radio occultations, electron density 79−48706
Venus, radar image, 46 to 75° latit., 290 to 10° longit. 77−5474
Venus, radar mapping by Pioneer Venus orbiter 79−48723
Venus, radar obs. of atmos., soil and relief 80−36537
Venus, radio interferometric meas. of retrograde zonal winds below clouds 80−46436
Venus, S-band radar imagery and surface lava flow features 77−64685
Venus, short-wave millimetric obs. with wide-band radiometer 79−96916
Venus, spin vector determ. by radar obs. 80−105185
Venus, surface, evidence of diverse landforms from radar obs. 77−78705
Venus, surface bistatic radar survey, using Venera 9 and 10 satellites 77−87304
Venus, surface charact., radioaltimeter meas. in Venera 8 descent vehicle landing area 77−29677
Venus, surface features, Pioneer orbiter topographic and surface imaging 80−46438
Venus, surface reflections of Pioneer Venus descent vehicles radio emission, atm. data 80−105187
Venus, surface reflectivity in equatorial region, radar obs. 77−17394
Venus, surface relief meas. using bistatic radar on Venera 10 satellite 77−64684
Venus, wind vel. and turbulence, Venera 9 and 10 Doppler meas. 77−78693
Venus atmosphere, model from radio, radar and occultation obs. 80−46420
Venus atmosphere, radio waves attenuation investigation by bistatic radar method 80−62061
Venus atmosphere, Venera 9 and 10 radio transmissions near limb 77−78694
Venus atmosphere and surface, investigation by radiosounding from Venera 9 and 10 satellites 80−101543
Venus atmosphere profile from Mariner 10 radio occultation, statistical and computational uncertainties 79−96938
Venus daytime atmosphere, density, press. and temp., Venera radio probing results 79−80253
Venus daytime ionosphere, two freq. radioscopy results from Venera 9 and (Venera 10) 78−4129
Venus daytime ionosphere, two-freq. radio transillumination data using Venera-9, 10 probes 80−21936
Venus daytime ionosphere, Veneras 9 to 10 dual-freq. radio occultation expts. studies 79−96939
Venus motion, numerical theory using radar, optical and Venera satellite obs. data 78−16325
Venus radar brightness and altitude images from 12.6 cm obs. 79−35163
Venus surface, geologic interpretation of new radar obs. 78−20666
Venus surface relief, Venera 9 and 10 bistatic radar obs. results 77−78689
Venus wind velocities, vector determ. by radio interferometry 79−48722
Viking landers radio tracking data, lander location, Mars ephemeris and solar system parameters 78−20685
Viking mission, radio science investigations 78−20684

radioastronomical observations continued
Viking relativity experiment: verification of signal retardation by solar gravity 80−36933
Viking spacecraft, Doppler and range data rel. to geocentric gravit. const. evaluation 80−3891
Virgo A (M87), 1.3 cm obs. 78−49550
Virgo A (M87), Westerbork map at 610 MHz 80−62302
Virgo cluster core, membership and vel. distrib. 79−35402
Virgo cluster galaxies, 1.4 GHz continuum survey 80−98721
Virgo cluster of galaxies, radio luminosity v volume emissivity diag. 77−17696
Virgo cluster spiral galaxies, H I deficiency from 21 cm obs. 80−62277
VLBI expt. with mobile equipment, 5 GHz operation 80−31217
VLBI observations at 430 MHz for 108 radiosources 77−41416
Voyager 2, obs. of solar coronal occultation, 1979 August 80−51639
NQ Vulpeculae (Nova 1976), CO emission and η Carinae stage 79−25609
14W12, in X-ray cluster of galaxies Abell 401, radio emission distrib. 80−98731
0846+51W1, eruptive BL Lae object with high z, visible and radio obs. 79−62899
W28 A_2 H II region, RATAN-600 2-13 cm wavelength obs. *(Russian)* 80−17642
W31 region, compact far IR source assoc. with G10.6−0.4, early stage of stellar evolution 78−49504
19 W32, 43 and 109, galactic centre planetary nebulae search 80−90506
W33, H I shell obs. 77−64871
W33, H II complex, high resolution obs. at 2.8, 6, 18 and 21 cm wavelength 78−57619
W33, OH radio emission sources obs. *(Russian)* 80−62247
W33, recomb. lines as evidence for cool H II region with mass flow 78−49501
W35, W43, H II regions, low-freq. radio recomb. lines studies 78−32589
W3, 10.5 GHz recombination line map 77−60817
W3(OH), 49N and 51, OH and H_2O maser spatial distrib. 78−93355
W3(OH), H_2O emission vars. *(Russian)* 78−16556
W3(OH), H_2O maser emission increase 77−53672
W3(OH), H_2O vapour maser turn-on in H II region 78−36677
W3(OH), interstellar OH maser, struct. from VLBI synthesis obs. 80−105368
W3(OH), NH_3 emission and absorption at 23 GHz 78−36714
W3(OH) and surrounding diffuse ionised gas, radio recomb. line obs. 78−93371
W3 (OH), non-metastable NH_3 absorption at 23.1 GHz, first obs. 78−65677
W3 (OH), Zeeman effect in OH maser emission 78−93377
W3 H II region, CO, CS and HCN obs. LF obs. 80−82446
W3-W4-W5 complex, CO emission mapping 79−17059
W3/W4/W5 region, 1420 MHz continuum survey 78−16497
W3/W4/W5 region, heavy optical obscuration obs. 80−62301
W40 and W48, near IR and CO mm wavelength obs. 78−65667
W43, radio emission obs. 77−17724
W44, supernova remnant, associated molecular cloud obs. 78−8079
W48, 18 cm obs. of OH source 78−28812
W48, H II region, H 85α recomb. lines obs. 78−28762
W48, OH emission and absorption, spatial distrib. in H II region *(Russian)* 80−36733
W49 A, H_2O masers and H II regions obs. at 23 GHz 79−71136
W49 A, struct. deduced from mol. and recomb. line obs. 77−33665
W49 H_2O vapour maser source, correlated variability 79−35352
W49 N, VLBI obs. of high vel. H_2O maser emission 77−26038
W49A, H I and C I radio recomb. lines obs. 77−64821
W49A, high sensitivity Hnα radio recomb. line obs. 80−26998
W49A, W51A, compact H II regions, H109α recomb. line, aperture synthesis obs. 80−105314
W49A, W51A, W51B, Arecibo obs. of H166α and C166α recomb. lines 77−22300
W50, continuum obs. at 2695 MHz of SNR 80−67830
W51, detect. of impact broadening of recomb. line 78−28741
W51, H II region, CO J=2-1 isotopic line obs. at 230 GHz 77−33590
W51, H II region-molecular cloud complex, cold gas flow 79−97048
W51, probable detect. of methylamine-d_1 77−33610
W51, radio recomb. line obs., confirmation of impact broadening theory 78−54019
W51, structure and vel. charact. of H II regions 79−71139
W51 H_2O source obs. with Crimea-Haystack interferometer *(Russian)* 78−69865
W51 Main, H_2O maser emission 80−8701
W51A, W3 (Main), W49A, continuum obs. at 3.9 mm 79−35333
W51B, H I and C I radio recomb. lines obs. 77−64821
W58, galactic star-forming region, CO obs. 80−67810
W75 maser sources, 1667 MHz line profile features 79−5914
W80 (Pelican Nebula), CO obs. of expanding mol. shell surrounding H II region 80−105296
W 3, H II region, study of nearby partially ionised interstellar medium 77−57077
W 51 region, possible detect. of Na I 17 cm hyperfine emission 78−8139
28 W sources and catalogue in NGC 7000 IC 5070 H II region complex 80−105308
weak point sources, aggregate flux at 1404 MHz 77−13480
weak radio nuclei in galaxies and quasars 77−17680
weak radio sources scintillation, low freq. obs. 79−53921
Westerbork observations of deep 5 GHz NRAO survey, positions, optical identifications 77−87560
Westerbork radiosource surveys at 610 and 1415 MHz 78−28542
wide spectrum H_2O source detect. at 22 GHz 77−74120
X-ray burst sources, search for correlated X-ray and radio emission 78−57695
X-ray clusters of galaxies, radio limits on ionised gas 78−89243
X-ray sources, extragalactic, positional and spectral data, HF obs. 80−86019
X-ray sources, radio identifications at 2 cm wavelength 79−53939
X-ray sources in galactic bulge, radio continuum obs. at 2.7, 4.8, and 10.7 GHz 80−101619
young SNRs, search for radio emission at 3.7 and 11 cm 78−40972
young stars, high-freq. radio continuum obs. 80−51766
young supernova remnants, radio emission evolution according to observational data 79−75256
Zw 1400+0949 cluster (NGC 5416 group), 21 cm obs. 80−22090
III Zw 2, compact galaxy, radio outburst obs. 79−75277

radioastronomical observations continued
III Zw 2, radio outburst, 14.5 GHz flux density increase of type I Seyfert compact galaxy 78−12373
III Zw 2, X-ray and radio emission from compact galaxy 78−65691
III Zw 2, X-ray emitting Seyfert galaxy, VLBI obs. 79−5903
II Zw 40, 70, 71, CO emission upper limits 78−36693
II Zw 40, dwarf galaxy, radio obs. 79−8992
II Zw 70, optical and radio obs., evidence for star form. 79−16935
C II regions assoc. with reflection nebulae, recombination line spectra 78−69857
C stars, search for HCN and CH maser emissions 80−51856
CH, detect. in NGC 4945, NGC 5128 and LMC 80−46673
CH in diffuse interstellar medium, optical and radio obs. 78−93356
CH, interstellar, radio obs. towards various galactic objects 77−87512
CH, interstellar excitation temps. and abundance rel. to H_2CO 79−48883
CH, radio emission obs. towards W49 region 77−87511
C_4H (butadiynyl) radical, detect. towards (IRC+10216) 78−93374
CN towards interstellar clouds, EHF emission obs. 79−17037
C_3N, tentative detect. in IRC +10216 77−29913
CNO isotope abundances in interstellar clouds 77−87527
CO distrib. in central region of Galaxy 79−21416
CO distribution in galactic equatorial plane, 115 GHz obs. 78−36689
CO emission, obs. in galactic refl. nebulae 77−53658
CO emission and visual extinction in dark cloud L134 77−13425
CO in interstellar dark clouds, evidence for isotopic fractionation 80−46638
CO in nearby galaxies, survey 80−62276
CO in the inner Galaxy 78−8072
CO, interstellar, distrib. around (l=30°, b=0°) 80−41868
CO, interstellar, isotope fractionation in Lynds 134 dust cloud 80−26924
CO, interstellar, obs. in Perseus OB2 dark cloud and W44 mol. cloud 77−64836
CO kinematics within 1° of galactic centre 77−33597
CO obs. of southern H II regions, RCW 38, RCW 122 and G316.8−0.1, star form. regions 79−35353
CO observations in compact H II regions assoc. with OH masers 77−57078
$(CO)_2$, RF lab. meas. and interstellar search 80−43035
^{13}CO in external galaxies, $^{12}CO/^{13}CO$ intensity ratios 80−4416
CaO, J=4-3 106 GHz undetected transition in stars and molecular clouds 79−71090
Co emission in Markarian and Seyfert galaxies, unsuccessful search 80−26975
Cygnus A, intensity and polarisation at 9 mm wavelength 80−36732
D absorption line at 327 MHz, search towards galactic centre 78−77599
DCN in the Galaxy mm line obs. 77−33580
H I, column density as function of position in southern sky 80−4420
H I, galactic, high angular resolution emission spectra, self absorpt. and other characts. 79−35350
H I, galactic subsystem, 21 cm line profile rel. to galactic rot. curve *(Russian)* 80−36724
H I, nonplanar, assoc. with Perseus spiral arm, 21 cm obs. 78−16489
H I 21 cm absorption towards extragalactic radiosources, catalogues of 819 sources 78−57638
H I 21 cm line radial vel. contour maps 80−17626
H I 21 cm line survey, low latits. 20-42° galactic longit. 78−57637
H I absorpt. by high vel. clouds at low galactic latits. 78−49506
H I absorption at intermediate galactic latit., aperture synthesis obs. 79−12503
H I absorption lines high-resolution mapping in direction of NGC 2024, M17, W49 and Orion A 78−81667
H I and Mg II absorpt. lines obs. in QSOs and BL Lacertae objects 78−28838
H I at high galactic latitudes, time variable 21 cm line profiles correction 80−51844
H I clouds, search in radio galaxies and intergalactic space 78−12316
H I clouds in solar vicinity, kinematics from Nancay 21 cm absorpt. survey 79−8971
H I cool clouds, kinematics and distrib. from 21 cm. obs. towards H II regions 79−44577
H I deficient spiral galaxies in Abell 1367 and coma cluster 79−17072
H I emission in direction of quasar PHL 957, upper limits 77−91659
H I envelopes round spiral galaxies, 21 cm obs. 80−90520
H I in galactic centre region, survey 79−88722
H I in region 348°≤l≤12°, +3°≤b≤+17°, 21 cm obs. 78−45377
H I low-latitude negative velocity clouds in galactic anticentre, distance 77−45506
H I radio recombination lines obs. in direction of pulsars 77−74155
H I regions, comparison of 21 cm obs. with UV and optical absorpt. line meas. 78−24532
H I regions, galactic, emission absorpt. obs. from Arecibo 78−57610
H I regions, high-latit., obs. in OH 18 cm lines 80−67841
H I regions, new feature discovery in Vulpecula-Delphinus *(Russian)* 80−46654
H I regions and assoc. H II regions, H and C radio recomb. lines obs. 77−17659
H I regions towards extragalactic radio sources, 21 cm emission, and absorpt. obs. 80−94854
H I search in galaxy clusters 78−49544
H I survey, contour maps, 21 cm obs. 80−85986
H I survey of 500 southern galaxies 77−33650
H I within 10° of galactic centre direction, broadband obs. 77−78853
H II regions, $^{12}C^{16}O$ and $^{12}C^{18}O$ J=2→1 transitions obs. 80−73022
H II regions, electron temps. determ. from radio recomb. line obs. at 22 GHz 79−35334
H II regions, galactic, comparative study of high-radiofrequency and far IR obs. 78−49497
H II regions, gradient of electron temps. and He abundance from radio recombination line obs. 79−21389
H II regions, H I absorption profiles towards 11 galactic sources 79−12499
H II regions, H radio recombination line obs. from Arecibo 79−48880
H II regions, H166α recomb. line obs. at 1425 MHz 80−90512
H II regions, He abundance from 15 and 22 GHz recombination line obs. 80−98703
H II regions, He II abundance and IR excess 78−86000
H II regions, radio recombination line obs. of C and H from 10 areas 78−93360
H II regions, search for Zeeman effect in RF recomb. lines 77−60809
H II regions, small, with exciting stars, radio maps 80−62224
radioastronomical observations continued
H II regions around l=111°, aperture synthesis obs. 77−64827
H II regions assoc. with optical nebula K3-50, 15 GHz obs. 78−16554
H II regions in Perseus Arm, high-resolution radio maps 78−32549
H II regions near OH 43.79-0.13 and OH 48.61+0.02, radio obs. 78−36669
H II regions relationship to CO clouds, blister model 79−25681
HCN emission detect. in Sagittarius A mol. cloud 78−73750
HCN, J=1-0 transition obs. in southern interstellar mol. clouds 79−8983
$H^{13}CN$ in the Galaxy mm line obs. 77−33580
HC_3N, detect. in interstellar space 78−93370
H_2D^+, interstellar and circumstellar search, upper limit determ. 79−2562
H_2O, interstellar, 183 GHz line emission obs. 80−41869
H_2O maser emission from external galaxies, detects. 78−45417
H_2O maser emission in W49N, W51 and Sagittarius B2, high vel. features 77−9779
H_2O maser features, high-velocity, in W3(OH), obs. 80−31339
H_2O maser source in Orion A, obs. of outburst *(Russian)* 80−105320
H_2O maser source near NGC 2071, discovery 78−73768
H_2O maser sources, W 49N and 51 global radiotelescope obs. *(Russian)* 77−22072
H_2O maser sources in different stages of evolution, new VLBI maps 80−26954
H_2O maser sources in galactic plane, southern hemisphere survey 80−73054
H_2O maser sources in W3, accurate positions 78−4332
H_2O masers, 22 GHz galactic plane survey, 14 new sources 80−77464
H_2O masers, 22 GHz obs. with resurfaced Parkes radiotelescope 77−33347
H_2O masers, accurate interferometric positions at 1.35 cm 78−45374
H_2O masers, in dense interstellar mol. clouds, high sensitivity survey 78−85988
H_2O masers, in mol. clouds assoc. with small Hα emission regions 79−17042
H_2O masers, interstellar obs. with resolution of 0.0008 arcsec 77−74154
H_2O masers assoc. with late-type variable stars, structure 79−71037
H_2O masers assoc. with mol. clouds, VLBI aperture synthesis obs. 79−21368
H_2O masers associated with compact H II regions in Sagittarius B2 77−13486
H_2O masers in H II regions, time variability 77−82296
H_2O masers located near Herbig-Haro objects, discoveries 79−21369
H_2O sources, linear polarisation of 22 GHz line emission 78−77612
H_2O sources, spectra and autocorrel. anal. 78−65713
H_2O sources in Galaxy, sites of newly formed OB stars 78−12390
H300 α recombination line obs. towards galactic centre 78−20873
H56α radio recomb. line anomalous emission from galactic plane 79−80361
$^3He^+$, interstellar, probable detect. and significance 79−25689
NGC 1499, H II region nebula parameters determ. from decametre wavelength obs. *(Ukrainian)* 79−40243
NH_3 emission obs. from galactic regions 78−28780
NH_3, obs. in southern H II regions 78−69863
^{14}N interstellar neutral gas, search for radioemission 80−41886
O/H abundance ratio determ. in Galaxy from H II regions radio obs. 80−36692
OH 1612 MHz survey at high declinations 80−4452
OH 18 cm emission sources, fluxes and circular polarisation (1965-1972) 77−13441
OH 18 cm lines obs. towards interstellar dust clouds 78−4318
OH 205.1-14.1, unusual OH maser source, 1667 MHz emission monitoring 77−64819
OH and H_2O masers, radial vel. struct. 77−33617
OH astronomical maser sources OH 231.8+4.2, CY Canis Majoris, M1−92, UHF obs. 80−90550
OH emission sources, 13 GHz OH features obs. 77−33619
OH emission sources, low latitude search at 1612 MHz 77−49452
OH in interstellar dust clouds, nonthermal main lines obs. and OH abundance 80−36683
OH, interstellar, new main line maser obs. with probable Zeeman pattern 80−56908
OH, interstellar, radio obs. towards ζ Ophiuchi and evidence for interstellar shock 79−97052
OH, J=9/2 Λ-doublet line detect. in W3(OH) 78−65670
OH large-scale sky survey at 1612 MHz 78−32358
OH maser clouds, saturation effects 77−91657
OH maser sources, accurate position meas. 80−46646
OH maser sources, search at 1612 MHz, large-scale survey 79−58395
OH maser sources near galactic centre, systematic search at 1612 MHz 79−35415
OH masers assoc. with IR stars, very long baseline interferometric obs. 77−53699
OH masers in direction of H_2O masers, new discoveries 78−12393
OH masers in Orion Nebula, obs. 78−16493
OH Mira variables, light curve shapes rel. to mass loss 77−56944
OH sources, 1720 MHz transition survey, comparisons with 1612, 1665, and 1667 MHz obs. 77−45586
OH sources in CRL objects and late-type stars, 18 cm obs. 79−35427
OH type II stars, unidentified, search for H_2O emission 79−75286
OH weak masers detect. in H_2O masers direction 77−33618
OH/IR stars, new SiO transition detect. 78−53954
OH/IR Type II sources, radial diameters from 1612 MHz OH line obs. 78−36713
OH/IR unidentified Type II sources, 1612 MHz obs. at low galactic latits. 77−17704
OH/IR unidentified Type II stars, galactic distrib. and kinematics from 1612 MHz survey 78−49450
rho Ophiuchi dark cloud, o-formaldehyde excitation temp. and optical depths 80−51846
SO_2 in Orion Molecular Cloud-1 (OMC-1), rot. temp. 79−25670
SiO 86.2 GHz maser sources, polarisation props. 80−4449
SiO maser obs. in late-type stars at 43 GHz 77−74067
SiO maser sources, 43 GHz obs. 79−16942

radioastronomical techniques
3K blackbody cosmic background radiation meas. 77−41422
acousto-optic spectrograph, design, testing *(Russian)* 79−25506
acousto-optical high-resolution radiospectrometer, mm wave astronomy appls. 78−4109

radioastronomical techniques continued
acousto-optical spectrometer for processing of MM-wave signals 80−4253
acousto-optical spectrum analyser *(Russian)* 77−29652
algorithm selection for galactic radiation linear polarization processing *(Russian)* 77−91441
ALSEP-quasar differential very long baseline interferometry, for lunar position meas. 78−45245
antenna calibration, radioastronomical methods, standard sources *(Russian)* 78−4103
antenna meas. technique and recording system using punched tape *(Russian)* 78−65501
aperture synthesis, appl. to large-scale struct. of extra-galactic radio sources (>1 arcsecond) 78−57668
aperture synthesis, appl. to obs. of Saturn and rings at 3.71 cm wavelength 79−96963
aperture synthesis imagery data optical reconstruction 78−69702
aperture synthesis meas. processing, tangent-plane aberration, new transform 79−8847
aperture synthesis obs. of circular polarisation, techniques and appl. 77−9670
aperture synthesis radio data, complementing by short spacing data from single dish obs. 79−66928
aperture synthesis radioastronomy *(French)* 80−46410
arc measurement procedure, optimisation using radiointerferometer *(Russian)* 79−101082
Arecibo Observatory, radiotelescope and instrumentation description 80−4249
artificially created hole in F-layer, convergent lens for radiotelescope 77−78571
asteroids, radar detectability, opportunities for 1977-87 period 77−82149
astrometry, influence of troposphere on radio-interferometric meas. of coordinates 80−67581
astrometry, tropospheric limitations on meas. accuracy *(Russian)* 77−22092
astrometry, using interferometers, principles and accuracy *(French)* 80−46411
astrometry for rotating radiosources, VLBI response freq. technique *(Russian)* 77−22093
astrometry using differential VLBI, accuracy estimation *(Russian)* 77−22091
astrometry using radio interferometers *(Danish)* 77−22087
automated system for detect. of cosmic radio bursts at VHF and UHF 78−77489
background deflection analysis, appl. to faint radio sources statistical study at 81.5 MHz 80−51893
background radiation spectrum meas. in near-mm region 80−62327
baseline ripple reduction by quasi-optical phase modulation, mm radio spectra 80−56710
black hole explosions, detect. via radio pulses, emission rate upper limit 77−87469
brightness distribution recovery, artificial eclipse method *(Russian)* 77−22099
broad-band multifunctional recording system for radioastronomical interferometer *(Russian)* 77−29650
CETI call signals, mutual search strategy 80−56723
circular polarisation, aperture synthesis obs. technique, appl. to resolved sources 77−29656
clean and restore technique, appl. to WSRT and Northern Cross radiotelescope obs. *(Italian)* 80−98563
CLEAN deconvolution algorithm appl. 79−8844
CLEAN method, iterative beam removal, mathematical-statistical description 78−57464
comet plasma tails electron density deduced from refr. of occulted radiosources 79−53773
communication with extraterrestrial intelligence, international conference discussion and conclusions *(German)* 77−56845
computer controlled receivers, RT-22 radiotelescope for spectral meas. *(Russian)* 77−9674
computer modelling of radioastronomical systems and radioastronomical information processing methods *(Russian)* 77−22097
cosmic MW background radiation, radioastronomical meas. techniques, history of detection and identification 79−97109
cross-correlators, incoherent optical 1-bit for radio antenna arrays 80−98555
data output device using narrow tape recorder for radio receivers 79−29993
data processing of radiosource rotation measures 80−86006
decametric survey of discrete northern sources, UTR-2 radiotelescope, expt. techniques, data processing 78−57461
density reconstruction using arbitrary ray-sampling schemes 78−80954
digital hologram reconstruction of telescope data 77−64653
direction finding with short electric antennas on spacecraft 79−21184
dispersion-removing radiometer, obs. tests on PSR 1913+16 binary pulsar 79−35142
display techniques, radiographs 77−9672
double radiosources, polarization moments appl. to investigation of component polarizations 79−53923
Effelsburg 100 m radiotelescope, large dynamic range obs. 78−96391
ETI signals search, obs. program using existing facilities 80−4266
extragalactic radio sources modelling, appl. to complex source (3C 288) 80−90558
extraterrestrial intelligence, microwave observational approach 78−61759
extraterrestrial intelligent radio signal search 77−17386
frequency-scanning interferometry for fast-proceeding solar phenomena investigation *(Russian)* 77−22094
fringe visibility intensities, uniquely related to brightness distribs. 79−8842
geodynamic monitoring and earthquake research, radiointerferometry appl. 80−31151
gravitational background radiation, possible detection by Doppler tracking interplanetary spacecraft 80−67914
gravitational radiation stochastic background detection using Doppler tracking of spacecraft 80−67913
HELIOS command antenna, correction factors for main transmission axis determining *(German)* 78−4116
high resolution solar astronomy, obs. by RATAN 600 telescope 77−78760
historical account and development trends *(Italian)* 78−12095
holographic radio data aperture synthesis reconstruction 79−21191
image reconstruction 80−56718
radioastronomical techniques continued
image synthesis from projections 80−67579
image two-dimensional reconstruction algorithms 77−82379
interferometer signal processing by acoustooptic correlation devices, radio astronomy applications 80−8543
interferometric meas., atm. turbulence effects *(French)* 80−46402
interferometric meas. of Haystack-Westford base line vector 80−89929
interferometric obs. for Earth precession and nutation precision estimation 77−73623
interferometry, appl. to obs. of Saturn and rings at 3.71 cm wavelength 79−96962
interferometry, theoretical review 80−12676
interferometry and aperture synthesis, review 77−9671
interplanetary scintillation meas. in conditions of strong radio interference 80−46413
interplanetary scintillation method, appl. to faint radio sources statistical study at 81.5 MHz 80−51893
interplanetary scintillation observations, fully automatic system 79−101064
interstellar communication, signalling strategy 78−61757
interstellar H I clouds in distant galaxies, colour pictures of Doppler shifts 77−17383
interstellar molecules, microwave spectrosc. obs. 79−41160
J^2 supersynthesis of circular aperture 78−40835
Jodrell Bank 1024 channel digital autocorrelation spectrometer 77−73970
Josephson point contact detector, high-sensitivity, for 1.5 to 2 mm waves 78−4106
linear restoration using Hermite polynomials 80−82217
maser, low-noise 4-stage K-band, for receivers, 18.3 to 26.5 GHz 79−2481
meteor modelling with radar observations, adaptation techniques *(Russian)* 80−67664
meteor radar, logarithmic, operating at 37.5 MHz *(Czech)* 79−21188
meteor trail studies using large-aperture radio system 80−85870
meteors, simultaneous visible and radar obs. technique 80−77354
microwave burst data rel. to solar proton fluxes 78−73591
million channel 300 MHz bandwidth digital spectrum analyser for Deep Space Network and SETI 78−73642
mm radioheliograph, design *(Chinese)* 80−12661
mm wavelength spectral lines detectability from planetary atms. 79−5769
mm-wave, review and future developments 77−5454
modulation radiometer, two-channel, simultaneous meas. in 6 and 8 mm wave ranges *(Russian)* 77−29647
Moon located station, for extraterrestrial civilisations communication *(Czech)* 77−9677
multichannel system for data recording and processing in real time *(Russian)* 78−65507
multielement radio interferometer, baseline coordinate vector measurement, maximum-likelihood method 80−26753
optical image-forming system for T-type correlation antennas 79−27180
optical modelling of antenna systems with complex aperture form *(Russian)* 77−22095
parallaxes of objects at cosmological distances, meas. via radiointerferometric techniques 78−53796
pencil beam formation by fan beam rotation 80−4262
phase tracking meteor radar ambiguity elimination algorithm *(Russian)* 77−41311
phaseless aperture synthesis, technique 78−32353
Pioneer Venus occultation experiment, radio science data generation 80−67492
planetary atmosphere composition anal. by radiowave transmission by space probes 79−21204
planetary nebulae radio search near galactic centre, implications of flux density distrib. 80−56913
plasma wave instrument on Pioneer Venus Orbiter, design and performance 80−67497
polarisation map interp., discontinuities 77−64661
polarisation patterns in dynamic spectra, colour representation, appl. to Jupiter 77−5490
power spectral analysis, multidimensional rel. to aperture synthesis 79−12406
power spectrum estimation using maximum entropy method, data analysis appl. 80−37006
precession, lunisolar, determ. via obs. of extragalactic radiosources 77−5129
quantum amplifiers and their application in space research, review 80−36503
radar interferometry, linear phase detect. *(Italian)* 78−85855
radar signal reflection from Sun, efficiency of four-plasmon interactions 80−101582
λ 8-cm radioheliograph at Toyokawa, sensitivity and phase stability improvement project 79−101066
radioheliograph phase error meas. and correction 77−87269
radiointerferometric frequency and coordinate meas. accuracy, tropospheric fluctuation constraints 79−8848
radiointerferometric phase meas. ambiguity detection, recurrence relationship *(Russian)* 79−25513
radiometeors characts. assessment, statistical analysis of time-dependent series *(Russian)* 80−56777
radiometer, wide-band, based on superconducting point contact, for short-wave millimetric radioastronomical obs. 79−96916
radiometer instability influence on meas. results, reduction by computer *(Russian)* 78−65506
radiospectroscopy, MM-wave klystron appl., phase-locking system 77−5456
radiotelescope gravitational astigmatism meas. 78−45222
radiotelescope linking by satellite Hermes for VLBI 77−70977
radiotelescope optical modelling using coherent optics and holographic methods, expt. *(Russian)* 77−22096
real-time very-long-baseline interferometry using communications satellite 78−24469
refracting radiotelescope using chemically modified ionosphere as lens 77−45312
regularisation method, appl. to radio telescope resolving power increase 80−17505
resolution improvements for a phase switching interferometer *(Italian)* 79−58271
rotational synthesis data processing, direct transform hardware techniques 78−85856

radioastronomical techniques continued
rotational synthesis data processing, direct transform hardware techniques 78−85857
satellite, LF, source localization and polarization determination *(French)* 79−70940
satellite radiosounding, appl. to Venus atmosphere and surface investigation by (Venera 9 and 10) 80−101543
scintillating radio sources at low flux densities, mean ang. size determ. 77−5453
search for extraterrestrial intelligence, implications for telecommunication 77−33361
search for radio emissions from extraterrestrial civilizations 80−4273
SETI strategy in microwaves 80−4265
solar corona, magnetic field determ. using type II burst obs. and theory 80−41785
solar flares rich in ^{3}He, 8666 MHz superfine structure line detection 80−109417
solar flux calibration in 1970, at 2800 MHz 80−17570
Solar Radio Data Acquisition and Communication System (SORDACS) of Toyokawa Observatory 79−101074
solar radio emission centre displacement measurement using alignment of antennas *(Russian)* 77−22089
solar sporadic radiation, Interkosmos-Copernicus 500 obs., expt. methods 77−53503
solar wind vel. meas. from scintillation obs. of H_2O and OH maser sources *(Russian)* 78−69704
source, mapping with uncalibrated visibility data 80−77295
source mapping by fixed base interferometry *(Russian)* 80−17499
source parametric determ. method from spinning satellite obs. 80−85871
source structure mapping using VLBI obs. 79−96921
source structure meas., scintillation effects 79−96922
sources angular diameters meas., errors 79−12534
sources Faraday rotation measures, computation method 80−4263
sources two-dimensional radio brightness reconstruction, maximum entropy technique 78−28534
spacecraft deep radio occultations and evolute flashes, planetary atms. struct. determ. 79−53731
spacecraft radio-occultation concept origin and implementation for planetary atmospheres obs. 77−45316
spectral baseline ripple reduction on Parkes radiotelescope 78−69703
spectral index determ. of radio emission of individual solar regions 80−94723
spectrum analyser, 32-channel filtering type *(Russian)* 77−29653
spectrum expander for multichannel filter spectromers 79−35790
submilliarcsecond astrometry via VLBI, relative position of radio sources 3C 345 and (NRAO 512) 80−22097
submillimetric wave astronomy techniques, instruments, and trends 77−41315
Sun activity and radiocommunication implications, historical account and predictions *(Italian)* 78−24496
Sun tracking, by fully-automatic radiopolarimeters for solar patrol at microwave freqs. 79−101065
superheterodyne mm wave spectrometers, intensity calibration 77−33353
supernova radio pulses, searches and possible sensitivity improvements 78−40975
synchronous dispersion reception method for detecting signals from ETI 80−4264
three dimensional spatial autocorrelation function meas. reduction 80−67576
two-channel recording system for punched tape *(Russian)* 77−29651
two-dimensional radio images, optimal discretisation and interpolation *(Russian)* 77−22098
two-frequency dispersion interferometers for space plasma nonuniformity 79−70964
UHF, antenna direction patterns recovering, improved optical simulator appl. 80−26742
UHF radiospectrometer, double-comparison, quasi-zero, neutral hydrogen lines investigation appl. *(Russian)* 77−29658
uncooled millimeter wave receiver charact. *(Swedish)* 78−24461
velocity meas. rel. to microwave background for clusters of galaxies 80−46686
Venus atmospheric precipitation detect., remote sensing radar and radio techniques 80−56741
Venus microrelief irregularites mean height, determination from radio transillumination data 80−72807
Venus nighttime ionosphere, two-freq. sounding by Venera-9 and Venera-10 probes 77−37543
Venus radar mapping, Pioneer Venus Orbiter mapper design and operation 80−67495
Venus wind velocities, vector determ. by radio interferometry 79−48722
very long baseline interferometry appl. to geodesy and geodynamics 77−56767
VHF/UHF polarisation measurement, radiowave irradiators with switching of polarisation *(Russian)* 77−22090
VLBI, appl. to astrometry *(Japanese)* 80−21930
VLBI, appl. to determ. of struct. of flat spectrum radio sources 78−16549
VLBI, clock synchronisation, influence of relativity theory *(Russian)* 77−5664
VLBI, correction for effects of troposphere, ionosphere and Earth crustal tide *(Japanese)* 80−21926
VLBI, first expt. in Japan during 1977 80−4268
VLBI, general considerations of international systems *(Japanese)* 80−17501
VLBI, improvement of freq. stability of local oscillators *(Japanese)* 80−17504
VLBI, Japanese domestic system, general aspects *(Japanese)* 80−17502
VLBI, Japanese domestic system, receiver and local oscillator *(Japanese)* 80−21923
VLBI, Japanese domestic system, recording signal generator *(Japanese)* 80−21924
VLBI, Japanese domestic system, selection of radio sources and experimental procedure *(Japanese)* 80−21922
VLBI, mapping of planetary radio sources *(Japanese)* 80−21927
VLBI, orbit determ. of geostationary satellites 80−4238
VLBI, orbit determination of geosynchronous satellites using computer program *(Japanese)* 80−21925
VLBI, principles of measurement *(Japanese)* 80−21921
VLBI, resolution of celestial radio sources *(Japanese)* 80−26754
VLBI, results of observations of radio source QSO 3C273 *(Japanese)* 80−17503

radioastronomical techniques continued
VLBI, time synchronization *(Japanese)* 80−26755
VLBI applications to geodynamics and astrometry *(Russian)* 78−32357
VLBI between geostationary satellites for hectometric observations of radio stars *(Japanese)* 80−21928
VLBI hybrid mapping of nuclei of radio galaxies and quasars 80−105356
VLBI using geostationary satellite link 79−29968
Voyager radio science experiment 78−24430
Voyager spacecraft, receiver for measuring LF planetary radio emissions 78−4075
H II regions, clumping factor meas. technique 78−20870
OH maser sources, accurate position meas. 80−46646

radioastronomy
see also pulsars; quasars; radiofrequency cosmic radiation; radiosources (astronomical); radiotelescopes; solar radiofrequency radiation
absolute flux density scale in 10-180 MHz range 78−28814
AKAIHOSHI flexible real time software system 80−82214
angular coordinate accuracy of multi-frequency interferometer, noise effects *(Russian)* 77−78644
aperture synthesis observations, tropospheric H_2O vapour irregularities effects on seeing 78−24339
array detectors for mm line astronomy 79−44364
astrometry, review 77−25952
atmospheric phase path corrections for very long baseline radio interferometry, mathematical modelling techniques 77−78637
atmospheric thermal radiation fluctuations, influence on radiotelescope sensitivity, expt. *(Russian)* 77−21832
Australian Astronomical Society, conf. Melbourne, Australia (May-June '77) 78−69655
bandpass interference filters for 1-3 mm window 80−109368
Bologna survey at 408 MHz, statistical analysis 78−28816
brief survey *(Swedish)* 78−24589
6C survey at 151 MHz, prospects 78−28813
calibration radio sources precision flux-density meas. at 2295 MHz 77−37663
calibration sources, flux density at 8420 MHz rel. to Virgo A 80−86004
Canadian developments, review 80−8542
CETI, 1.5 mm as optimum wavelength region 79−40094
CETI failure possibilities 77−49316
CETI from Earth satellite orbit 78−61758
CETI from Earth satellite orbit 80−4275
circular waveguide system for large antenna array 78−24465
communication with civilisation around other stars 78−16314
communication with extraterrestrial civilisations, call signals struct. 77−13257
coordinate measurements using phase and fringe freq., tropospheric limitations 79−44375
Cosmic Background Explorer, satellite instrumentation 80−61988
Cosmic Background Explorer Satellite, IR and mm wave techniques 78−49344
cosmological aspects, IAU Symposium 74 (Cambridge, England, 16-20 Aug. 1976) 78−28871
cyanoacetylene, microwave spectrum, mol. consts. 78−74647
data reduction, via digital electronic integrator *(Russian)* 78−57465
EM radiation, from line sources interacting with moving uniaxial dielectric or plasma half-space 79−92661
EM spectrum, overcrowding and use by radio astronomy 80−85874
equipment, techniques and observations, review *(German)* 77−56827
extraterrestrial civilisation radiocommunication, efficiency of signals associated with natural phenomena *(Russian)* 78−40842
extraterrestrial civilisations, problems of radio contact attempts 78−69707
extraterrestrial intelligence, antenna concepts for interstellar search systems 78−28545
extraterrestrial intelligence, search of OH and H_2O lines 80−56725
extraterrestrial life communication problems *(Czech)* 77−9678
fast transient phenomena, physical mechanisms affecting observations *(Italian)* 78−93105
flicker noises, stochastic prop. 78−57473
for extragalactic radioastronomy, recent advances 77−17706
formaldehyde substituted with ^{17}O and ^{18}O, microwave spectra of ground vibr. states, rot. and distortion const. determ. 80−83349
formic acid (-d), microwave spectra and rot. consts., astrophysical appl. 80−91550
free radicals, high resolution spectroscopy *(Japanese)* 79−79355
frequency-agile phase lock system for mm wave klystron 77−5446
fundamental astrometry rel. to celestial mechanics and radioastronomy *(German)* 78−45200
galaxies, active nuclei, radio obs., future prospects 78−57652
galaxies and Milky Way obs. *(Spanish)* 79−40275
Green Bank surveys at 1400 MHz 78−28543
heterodyne 0.9 mm receiver 78−93116
historical account and development trends *(Italian)* 78−12095
history of its evolution and Cygnus A *(French)* 79−40287
image reconstruction, from incomplete and noisy data 78−53837
image restoration appls., conf., Bordeaux, France (Mar. 1979) 80−41935
images iterative reconstruction, non-negativity constraint 79−101081
IMPATT source, frequency-stabilised, 115 GHz 80−67573
interference-excising correlator, for HF radio astronomy 79−75110
interferometry, atmospheric delay fluctuations with scale sizes >1 km 79−8675
intergalactic graphite whiskers, RF adsorpt. props. rel. to microwave background radiation 80−31357
interstellar communication, review of theory 80−4271
interstellar communication, timing strategy 78−16313
interstellar communication rel. to molecular column densities 79−84836
interstellar communications, preferred freq., 4.8 GHz formaldehyde line 79−16845
interstellar molecular spectra frequencies prediction, accuracy determ. from OH spectrum 79−48666
interstellar molecular transitions, rest freqs. 80−62218
interstellar molecules, microwave astronomy, modern aspects, book contrib. 80−56921
inverse problem, regularisation method appl. to radio telescope resolving power increase 80−17505
ionospheric daytime effect on radioastronomical intensity meas. and interferometry 80−67450
ionospheric irregularities effects on HF and VHF radio waves, ray tracing study 77−91362

radioastronomy continued
Jansky, Karl Guthe, 1932 original data 79−17144
Jupiter, beaming model of Io-independent decametric radiation 79−53755
lunar surface bistatic radar surveillance with FM signal 79−5758
meteor radar research, growth and decline 77−78722
meteor recording freq., influence of form and orientation of antenna directivity diagram *(Russian)* 80−67665
microwave detection of interstellar methane, SiH_4 and GeH_4, possibilities 78−41020
millimetre obs., calibration, effect of Earth's atmosphere, two-layer model 78−53691
millimetre wave, review 79−29992
millimetre-wave astronomy, advances and prospects *(French)* 80−36502
MM wave space applications and technology in 100-1000 GHz range 79−92650
mm-wave, review and future developments 77−5454
mm-wave technology applic. 77−5450
Molonglo radio source surveys at 408 MHz 78−28541
Moon, radar contact in 1946 80−85866
multidimensional power spectral anal., new method, radioastron. appl. 77−17378
mutual coherence function in radio astronomy 79−75115
narrowband signals of extraterrestrial origin, search at 21 cm wavelength 79−25521
National Radio Astronomy Observatory, W.Virginia 79−80216
Nova Cygni 1975, synchrosignal for extraterrestrial civilizations 78−28546
on-line and real-time processing in radio astronomy 79−16838
optical reconstruction from projections via circular harmonic expansion 78−42286
parametric amplifiers for radioastronomy at 18 and 1.35 cm wavelengths, characts. *(Russian)* 77−9658
Pioneer Venus Differential Long Baseline Interferometry expt. 80−67578
pioneering work by Jansky, and Penzias and Wilson 79−44655
planetary atmosphere, occulting spacecraft signal, turbulence determin. 80−94734
planetary atmosphere HF radio occultation meas., phase screen concept 80−56735
planetary atmosphere radio spectroscopy by automatic interplanetary stations *(Russian)* 77−91442
planetary nebulae radio search near galactic centre, implications of flux density distrib. 80−56913
polarization of quasars with optical absorption spectra 78−12405
pulsars radio emission, mag. field, energisation, comparison with Jupiter 80−46466
radar astronomy 77−25947
radio image of Universe *(Japanese)* 78−73637
radiometer instability influence on meas. results, reduction by computer *(Russian)* 78−65506
radiometer with InSb detector, radioastronomical appl. in 0.2-5 mm wavelength range 77−13241
Rao Observatory in Sweden, history and current research *(Swedish)* 78−28513
receiver design, 408 MHz band, 30 MHz IF freq., amplifier noise disc *(Italian)* 78−45234
scattering cross section of radiowaves reflected from planet with spherically symmetrical atmosphere 80−21935
SETI, systems analysis 80−4274
SETI strategies 80−4270
signal processing equipment, improved 78−69709
solar power satellites, effect of transmissions on radio-astronomical research 80−61291
solar stereo radioastronomy 78−49419
sources of EM radiation and terrestrial effects *(Japanese)* 80−51600
spectroscopy *(Japanese)* 80−62031
stray radiation problem and time variable 21 cm lines 80−56708
submillimetric wave astronomy techniques, instruments, and trends 77−41315
superheterodyne receiver of solar emission obs. at 220 GHz *(Italian)* 77−49292
transatlantic long base line interferometry at 10680 MHz 79−48390
transillumination of planetary atmospheres 78−96413
UTRAO 335-380 MHz survey, interim report 78−28815
Very Large Array, phase switching, Walsh function appl. 78−81539
Viking landers radio tracking data, lander location, Mars ephemeris and solar system parameters 78−20685
Viking mission, radio science investigations 78−20684
VLBI expt. with mobile equipment, 5 GHz operation 80−31217
Voyager planetary radioastronomy experiment 78−24433
WARC 1979 regulations, impact on space appl. and research 80−105147
water hole (1400-1700 MHz), rationale for SETI 80−4272
Westerbork radiosource surveys at 610 and 1415 MHz 78−28542
wideband carcinotron tunable submillimetric source 77−41304
Hnα radio recombination lines, profile in static ion field 77−78629
Hnβ radio lines profiles in static ion field 79−62740
NH^+, interstellar radioastronomical freq. prediction at 13625 MHz 78−24544
$OHX^2\Pi$ radical, ground and vibr.-excited ($\nu \leq 6$) levels, microwave spectrum 79−63985

radiocarbon dating *see radioactive dating*

radiochemistry
see also radioactive chemical analysis; radioactive tracers
actinide solutions, differential alpha radiography using solid state track detectors 80−71932
alkanes, tritiated, fragmentation by β-decay, dissoc. of daughter species 78−31669
alpha-particle sources, thin, prep. from solns. at low temps. 80−27843
anodic electrolysis of radioactive isotopes *(Hungarian)* 80−93765
aromatics, halogen substituted, as positronium inhibitor 80−93783
astatotyronine and astato-iodotyronine, prep. and stability 80−55687
automated radiochemical separation systems use in destructive neutron activation analysis 77−90691
beta-decay, chem. and biological consequences 78−28018
beta-decay in labelled molecule, chem. and biological consequences 78−11541
BWR, design and operation, review of water chemistry, in feed water, coolant and steam systems 79−36311
chemical behavior associated with tritium decay *(Japanese)* 79−20452

radiochemistry continued
cyclobutane-t_1, recoil hot reaction product, unimol. behaviour 79−16024
cyclobutane-t, chem. activated by nucl. recoil reaction, energy transfer interpret. 80−25985
cyclobutane-t, chemically activated by nuclear recoil, vibr. energy transfer 77−66763
diamond, sub-surface contamination by hot-atom recoil in neutron activation anal. 77−60144
diatomic molecule, dissoc. due to gamma quantum recoil momentum 77−1941
difluorodichloromethane+^{38}Cl, reactions due to $^{37}Cl(n,\gamma)^{38}Cl$ 77−86342
1,1-difluoroethane, nucl. recoil ^{18}F chemistry at high press. 80−89510
DNA costacking nucleotides, γ-irrad., charge-migration phenomena, EPR obs. 80−36015
ethylene+Cl, nuclear recoil, addition and abstraction reactions, kinetics 77−86340
fission, discovery, research of 1930's, '40's, Otto Hahn 80−57063
fission products, short-lived, rapid paper electrophoretic separation, γ-rays and half-lives determ. 77−44498
fission reactor fuel reprocessing, technical status review 77−34420
fission recoils, chem. effects, energy deposition efficiencies, surface conditions depend. 78−80776
geological samples, multielement anal. by sequential instrumental and radiochem. neutron activation 78−7798
halobenzenes, benzene solns., positronium form., additive effects 79−43610
halocarbons, benzene solns., positronium form., additive effects 79−43610
history, early research 80−86067
hot atom+mol. reaction, steady state vel. distrib., Boltzmann eqn. with BGK elastic collision model 80−66856
hot atom chemistry, general variational principles 80−11941
hot atom chemistry of fast ions in gas phase 77−25290
hot atom reactions, hydrodynamic steady states 79−34342
hot atom reactions, nonequilib. vel. distrib. and reaction rate, Monte Carlo anal. 77−16855
hot cell for synthesis of labeled organic compounds 80−68970
hot H atom reactions and mechanisms of liq. n-alkanes radiolysis 77−36771
hot laboratories, post irrad. work, trends and prospects 78−41844
hot-atom collisional energy density function, stochastic calc. 79−29342
hot-atom reactions, photolytically-driven, kinetic theory, appl. to DI 79−74408
improved labelling with 99mTc by stannous tartrate reduction of pertechnetate 80−72324
intermolecular energy transfer following kinetically controlled chem. activation, multistep deactivation processes 80−25985
ion exchange chromatography significance 77−25343
isotope production at LAMPF, hot cell chemistry 80−18674
isovaline radioracemization, cosmochemical implications 80−62087
lanthanides (III), extraction with di-isodecyl phosphoric acid from HNO_3 soln. 79−22398
layers, intermediate thickness, radionuclides activity calc. 80−21311
marine ^{242}Cm conc. supported by ^{242m}Am 77−49091
metal tritide, ^3He detrapping and release after ^3H decay, strain model 77−60101
metal tritide, ^3He outgassing after ^3He decay, ^3H conc. effects 77−60100
methyl chloride+T* reaction, methyl abstraction to substitution ratio 78−85187
methylamine-t_1-NH_3, β^- decay effect on H-bond, ab initio LCAO SCF MO calc. 78−76894
Miller-Urey reaction, N isotope fractionations, appl. to carbonaceous chondrites 80−46496
multicurie radiochemical separations, remote system 80−71933
muon spin rotation, review of recent advances 79−24252
muonic radicals formation 79−57277
muonium atom reaction dynamics using surface muons in gas phase 79−57274
muonium chemistry, isotope effects and collision theory 79−57273
muonium kinetics in liqs., coherent diamag. fraction obs. 79−57278
muonium reaction in soln., rate const. and effective charge 79−57275
muonium reactions, tunnelling effect 79−57276
neutron activation analysis course experiments with 14 MeV neutron generator 77−82353
nuclear reactor chop-leach fuel hulls, chemical decontamination and melt densification 77−65319
nuclear reactor fuel particle failure, chemical aspects 77−42099
nuclear reactor irradiated fuel, anal. of α-emitting isotopes through laser micro-boring 80−37444
nucleon stability testing, radiochemical and geochemical method limits 79−22093
orchard leaf, multielement anal. by sequential instrumental and radiochem. neutron activation 78−7798
perhalo-compounds, labelled, high yields from ^{18}F and ^{38}Cl reactions with CCl_xF_{4-x} and C_3F_6 80−109025
α-phthalocyanine target, reactor-irrad., extraction rate and mechanism of ^{64}Cu 80−35563
positronium formation, quenching and inhibition in Ag and Cd salt solns. 78−15690
positronium formation inhibition by solvated electron precursor scavenging, line shape Doppler broadening, lifetime spectroscopy 80−93784
propene+$^{38}Cl \rightarrow CH_3CHCH_2{}^{38}Cl(CH_3CH^{38}ClCH_2)$, thermal, terminal and central addition 77−86341
pulsed proton radioluminescence in binary liquid scintillators 79−52731
pyrrole, free radicals produced by X-irrad. and decay of tritium atom, EPR study 78−48676
radioactive waste, chem. treatment prior to evaporation 77−54327
radioactive waste, phosphate vitrification, KS-KT-100 plant *(Russian)* 77−61552
radioactive waste calcination and vitrification 77−61546
radioactive waste calcining at Idaho Chemical Reprocessing plant, design criteria 77−61549
radioactive waste solidification, Sandia process 77−61551
radioactive waste vitrification without precalcination, radionuclide behaviour *(Russian)* 77−61553
radioimmunoassay for thromboxane B_2 with thromboxane B_2-^{125}I-tyramide 79−88222
radioisotope excited X-ray analysis of environmental samples, calibration procedure and applications 79−20491

radiochemistry continued
radiopharmaceuticals preparation by Szilard-Chalmers labelling and radioprotection in ice lattice 80−51259
rapid automated nuclear chemistry, short lived fission products, reactor safety 80−81353
recoil hot reactions, average energy calc. 78−68906
recoil hot reactions, average energy of reaction rel. to system composition 77−73457
recoil tritium reactions with cis- and trans-1, 2-dichloroethylene 78−3360
SI units in radiochem. and radiology 78−81939
solar neutrino radiochemical detectors, internal contamination backgrounds 79−16827
solvent extraction device using radioactive tracers 77−32819
spiral ion exchanger for rapid radiochem. separations 77−25296
sulphonated cool, gamma radiation breakdown 78−693
superheavy element prod. in ^{48}Ca ion+^{248}Cm, spontaneous fission 78−74390
symmetrical implosion system, charged reaction products, electrostatic field effects 80−32499
teaching, undergraduate, courses, facilities 80−27086
technologically enhanced natural radiation, chemical problems, human exposure 79−96346
tetrahydro-2-methylfuran glass, γ-irrad., spin trapping of radicals by BNB, EPR obs. 78−10776
transuranium cpds. in aq. soln., electrochem. 77−29040
transuranium processing plant, chem. process engng. 77−54338
transuranium processing plant, remote processing practices, equipment changing and modification facilities 77−54339
tributyl phosphate, fuel reprocessing solvent 77−65320
trifluorethane, nuclear recoil ^{18}F atoms, high press. study 77−86339
trifluorochloromethane+^{38}Cl, reactions due to $^{37}Cl(n,\gamma)^{38}Cl$ 77−86342
uranyl acetate solns., radiocolloidal and pseudoradiocolloidal state 78−44390
waste decontaminability, low level long lived radioactive liquids, chem. treatments 77−54351
$^{32,33}P$ incorporated in DNA, transmutation effects 80−26283
Ag/CN, coverage meas. using surface enhanced Raman scatt. and radioisotope meas., electrochemical treatments 80−29260
Am cpds., prep. and stability of highest oxidation states in phosphoric acid. soln. 77−29029
Am, production by US irrad. in reactor, chem. separation, yield 77−63986
Am(VI) formation in molten salts 77−29039
Ar, muonium formation by positive muons 79−57272
^{211}At protein labelling technique using an acylation reaction 80−36130
Au, ^{18}F recoil ranges by irradiation of O_2 with ^3He and ^4He particles 80−71931
$^{209}Bi(^{12}C,f)$, mass distrib. of fission fragments determ. *(Chinese)* 78−86558
Br_2, muon stopping, diamag. shielding of muon-substituted cpds. 79−57279
^{87}Br, prod. by radiochem. separation, for neutron decay obs. 78−70951
^{80m}Br labelling of tyrosine, uracil and cytosine 80−51248
CF_3Cl, ^{18}F-recoil labelling 80−23203
^{11}C-acetylene, production by methane pyrolysis and irrad. 80−36129
^{11}C-l-lactic acid, enzymatic synthesis 80−61695
^{11}C-lactic acid synthesis and scintigraphic evaluation of in vivo distrib. in dog 78−80965
^{11}C-lactonitrile synthesis and scintigraphic evaluation of in vivo distrib. in dog 78−80965
^{11}C-pyruvic acid, enzymatic synthesis 80−61695
^{14}C labelled compounds synthesis, technological aspects 78−76895
^{250}Cf, spontaneous fission, mass distrib., radiochem. and γ-ray spectrometric meas. 77−67775
^{252}Cf fission source, undergraduate laboratory expts. 77−382
$^{38}Cl+H_2(D_2)$ reactions, characterisation, effect of ethylene-I_2 scavenger 78−73071
^{38}Cl+ethylene+HI(H_2S), thermal, mechanisms and rate consts., fluoroethane decomp. 77−86343
Cm, production by US irrad. in reactor, chem. separation, yield 77−63986
^{248}Cm, spontaneous fission, mass distrib., radiochem. and γ-spectrometric meas. 77−67775
^{60}Co, in radioactive waste water, improved removal using diethyldithiocarbamate 78−37415
$^{51}Cr_2O_7^{2-}$ tracer solution preparation *(French)* 79−29385
D_2-DT-T_2 system, quadrupole mass filter sensitivities and β-particle induced exchange kinetics 78−58090
$ErT_{1.8}$, ^3He thermal desorption, comparison of aged and ^4He implanted samples 77−60102
^{253}Es, separation and α-spectra identification following neutron irradiation of Cf 78−17435
FHe^+, fragmentation and potential energy curves from FT β-decay 78−56910
^{18}F-F_3COF-^{18}F radiopharmaceutical synthesis procedure 79−29619
$^{18}F+H_2$, hot-atom reaction, nonequilib. vel. distrib. and reaction rate calcs. 77−63942
$^{18}F+H_2$, nuclear recoil reaction, steady state hot atom kinetic theory calc., rate coeffs. 78−35712
Fe, proton bombardment, stable nuclide form. and separation 78−20045
H_2, solid, storage of atomic H, rate process theory 77−32770
H_2-HT-T_2 system, quadrupole mass filter sensitivities and β-particle induced exchange kinetics 78−58090
$H_2(D_2)(T_2)$, ortho-para transition, catalytic-, radiation-, and self-induced conversion, review 77−90633
HF+T hot atoms, energy loss 78−15691
H_2O, muon stopping, diamag. shielding of muon-substituted cpds. 79−57279
H_2O, muonium atoms and intraspur reactions 79−70358
HT, dissociation by T beta-decay 77−63941
^3H-impregnated solid H_2, equilib. conc. of stored atomic H 77−46510
H^*+chloroform-d_1→HD+CCl_3, hot atom reaction, threshold energy meas. 78−44356
He, muonium formation by positive muons 79−57272
^{177}Hf production, recovery and purification for nucl. medicine use as ^{177}Lu generator 78−48893
^{181}Hf, decay, perturbed γγ directional correlations, complex chem. 77−36774
^{121}I labelling of radiographic contrast media 80−26350
radiochemistry continued
^{123}I, carrier-free iodide generated from ^{123}Xe, kit prep. and quality control 77−29205
^{123}I labelled compounds, synthesis by $^{123}Xe(\beta^+,EC)^{123}I$ 79−63676
^{123}I labelling of radiographic contrast media 80−26350
^{123}I production by ^{124}Te (p,2n) reaction, new approach to target chem. 77−60250
^{123}I production in cyclotron by $^{124}Te(p,2n)^{123}I$, improved targetry and radiochem. 78−28064
^{123}I, production in LASL radiochemistry hot cells 80−72326
^{123}I, radiochemically pure, prep. as iodide for synthesis of radiodiagnostic agents 77−21627
^{124}I production in cyclotron by $^{124}Te(p,n)^{124}I$, improved targetry and radiochem. 78−28064
^{125}I+methane, γ irrad. effects on organic iodide form. and decomp. *(Japanese)* 77−81418
^{131}I production by TeO_2 irrad., determ. of Se in TeO_2 by neutron activation 77−86400
^{131}I, separation from water by ion exchange *(Japanese)* 77−60099
^{131}I-tetracycline, prep. and stability 77−29204
$^{115}In(\gamma,\gamma')^{115m}In$, appearance energies of In complex cpds. determ. 78−8794
^{99}Mo fission product, sequential cation-exchange separation from neutron irrad., U_3O_8 77−90898
^{99}Mo separation from ^{131}I and ^{103}Ru uranium fission products 77−25297
Mu+F_2→MuF+F, 300 to 400K in N_2 moderator, reaction rate determ., tunnelling 78−48682
N_2, muonium formation by positive muons 79−57272
NH_2TNH_3, β^-decay effect on H-bond, ab initio LCAO SCF MO calc. 78−76894
$Na^{99m}TcO_4$ solution, special chambers for production *(Hungarian)* 80−93785
^{97}Nb, independent yields from thermal neutron induced fission, radiochem. obs. 78−54807
^{98}Nb, 51 min, independent yields from thermal neutron induced fission, radiochem. obs. 78−54807
Ne, muonium formation by positive muons 79−57272
^{63}Ni applications in biological research 80−12321
$Np^{4+/3+}$ in fused salts, redox and chem. props. 77−29038
Np(V)/Np(IV) catalytic redox reactions, kinetics and mechanisms 77−29006
Np(VII) formation in molten salts 77−29039
OH radical participation in terminal muon spur for muonium prod. 79−57271
^{15}O, recoils from $^{16}O(n,2n)^{15}O$, labelled mol. O_2 form. 78−3359
^{233}Pa removal from ^{237}Np by coprecipitation with MnO_2 or sorption on silica gel 79−52733
Pu, production by U_3S_y irrad. in reactor, chem. separation, yield 77−63986
$Pu^{4+/3+}$ in fused salts, redox and chem. props. 77−29038
Pu(IV) catalytic redox reactions, kinetics and mechanisms 77−29006
Pu(VII) formation in molten salts 77−29039
Ra, annual rate of release to atmosphere as result of coal combustion in UK 80−93787
^{228}Ra, separation from thorium oxalate 80−45600
^{186}Re labelled EHDP preparation and possible use in osseous neoplasms treatment 80−56215
Ru, hazards and control in nuclear fuel cycle, review 79−36392
^{97}Ru preparation investigation 80−30891
T decay in solid H_2 matrix to produce H atoms 77−29028
T recoil replacement reactions in alkane systems moderated with inert gases 78−68906
T+H_2O, energetic reactions, hard sphere excitation functions 79−1963
T+HD hot atom exchange reactions, trajectory calcs. 80−26037
T+O_2 high energy reaction, excitation function 78−68907
^{181}Ta, 133-482 keV cascade, effect of source preparation technique on differential ang. correl. 77−71711
Tc, radiochemical characts. and role in nuclear fuel reprocessing, review *(Czech)* 78−82496
^{99}Tc, reduction and sorption in granitic bedrock, biological hazard estimation 79−79415
$^{99}Tc^m$ decay constant, chemical state effect 80−42591
^{99m}Tc glucoheptonate, prep. using formamidine sulfinic acid 80−51252
^{99m}Tc labelled 2,3-dimercaptopropansulphonate, prep. and distrib. in the rat 80−51244
^{99m}Tc radiopharmaceuticals, radiation decomposition 79−83907
^{99m}Tc radiopharmaceuticals evaluation, miniaturised chromatography systems 79−96391
^{99m}Tc-pertechnetate labelling of human plasma proteins, rapid chemical method 79−29618
^{132}Te, fission product, sequential cation-exchange separation from neutron irrad. U_3O_8 77−90898
Th sulphito complex ion precipitation with hexammine Co(III) chloride cation 78−92495
^{232}Th, induced fission in natural systems, radiochem. obs. 78−4966
Ti film, deuteriding inhibition by surface contamination, rel. to Ti sublimation pump operation 77−57335
U natural reactor in Oklo, isotopic composition 77−56628
U ores, estimation of ratio of induced to spontaneous fission 78−53234
U production by U_xS_y irrad. in reactor, chem. separation, yield 77−63986
U^{235} in pegmatites, homogenised fission track anal. using solid state track detector 80−97719
$U^{4+/3+}$ in fused salts, redox and chem. props. 77−29038
U/Pu separation, use of carboxylic acids 77−38377
UO_{2+x}, C coated particles, variation of O/U ratio and CO+CO_2 press. 77−61504
^{238}U (μ^-,f), fission product mass distrib., fission probability, radiochem. investigation 78−29514
$^{238}U(^{12}C,f)$, mass distrib. of fission fragments determ. *(Chinese)* 78−86558
U(n,f), heavier rare earths separation by radiochem. method 79−67785
^{90}Y extraction and determ. in acidic media 79−16025
^{88}Zr, spallogenic, radiochem. separation for photoneutron source 77−14296

radiocommunication
see also mobile radio systems; radio links; radio reception; radiotelegraphy
auroral propagation condition anticipation for radio amateurs 77−64529

radiocommunication continued
broadband systems, tropospheric scatt. mechanisms and channel characterization 79−29837
CETI call signals, mutual search strategy 80−56723
CETI from Earth satellite orbit 80−4275
conference on electromagnetic wave scattering in radiocommunication, Cambridge, MA, USA (Oct. 1977) 79−29836
electrodynamics and electrostatic problems, solns. 80−1105
extraterrestrial civilisation, efficiency of signals associated with natural phenomena *(Russian)* 78−40842
extraterrestrial civilisations, call signals struct. 77−13257
interstellar communication, theory 80−4271
interstellar link using Sun as gravitational lens antenna 80−62040
interstellar travel and communication, bibliography 80−101677
ionosphere, UHF and VHF scintillation, signals from geostationary satellite 80−56674
ionosphere transmission of L-band signals coded by phase reversal, signal degradation 80−41632
ionospheric propagation forecast chart, high solar activity period appl. 80−26664
microwave Earth-space link, rain cell attenuation 80−94586
propagation aspects in planning of services 80−12613
propagation problems connected with special source structs., review 80−87272
quantum-information theory, expressions for Shannon quantity of information 79−55075
radiowave propagation above 30 MHz, role of sporadic-E layer and troposphere 80−41636
scatter communications, review 79−34935
SHF signal attenuation by rain, monitored by radar 80−51567
transhorizon radiocommunication by short-wave ionospheric refraction 79−84567
VHF noise field strength at 95 MHz over India, meas. techniques and obs. 80−109294

radiocrystallography *see X-ray crystallography*

radiofrequency amplifiers
see also preamplifiers
3 kW solid-state amplifier for pulsed NMR, 1 to 22 MHz 79−54162
common anode high power amp., particle accelerator appl. 79−68051
gyrocon, computer modeling, electron eqns. of motion, beam losses 79−68100
gyrocon, microwave oscillator for charged particle accel. 79−72176
high power, accelerator appls., recent advances 79−68082
linac cavities, microprocessor based control 79−71996
linear accelerator, Chalk River, 100% duty factor Alvarez linac high power supply 77−38487
pulsed NMR, extremely fast recovery time receiver-amplifier 77−26376
Tokamak plasma power coupling by 500 KW RF amplifier 80−13877
trirotron, RF vacuum tube amplifier, electron accel. appl. 79−68086
VHF, UHF and microwave radiation effect on human body 80−8101

radiofrequency and microwave spectra of diatomic inorganic molecules
see also nuclear magnetic resonance; paramagnetic resonance
atmospheric pollutants and constituents, microwave absorp. coeffs. 77−64378
CO isotope mapping of L 134 N 79−30108
diatomic mil., hyperfine struct. transitions, quantum theory for undergraduate demonstration 80−17762
diatomic mols., RF excited inductively coupled Ar plasma spectroscopy 80−86358
free radicals, spectroscopy, review, book contrib. 77−38653
interstellar molecular transitions, rest freqs. 80−62218
microwave radiation, kinetic theory of interaction with diatomic gas, j=0, j=1 transitions 78−9750
OH main lines, IR pumping in Mira variable stars and OH-IR sources 80−46632
Ar-Xe gaseous mixtures, collision-induced microwave absorpt. 78−78680
BaO, mm wave spectrum, spectroscopic consts. 78−37629
BiCl, form., microwave spectrum, hyperfine struct., mol. rot. vibr. consts., bonding 77−14418
BiF, mm spectrum, HFS struct., HFS, vibr. and rot. consts. and equilib. distance 77−79604
^{79}BrF, (^{81}BrF), hyperfine struct., elec. dipole moment, rot. transitions, microwave spectral obs. 80−32695
CN, radical, $X^2\Sigma^+$ ground state, microwave absorpt. spectrum 78−17657
CN towards interstellar clouds, EHF emission obs. 79−17037
CN^+, interstellar, rot. transitions rest freqs. and radio search 78−24534
CO isotopic rotational transitions in ultracold molecular gas 80−51826
CO, microwave detect. in Martian atm. 77−74000
CO, microwave spectral line profiles, rotation effects in CRL 437 peculiar IR source 78−45426
CO submillimetric high-resolution Fourier transform spectra 79−31509
CO^+, interstellar, rot. transitions rest. freqs. and radio search 78−24534
$^{13}CO^+$+CO, charge-exchange detection of $^{13}CO^+$ electronic absorption spectrum, hyperfine consts. calc. 78−70822
CS J=1-0 transition at 49 GHz in southern molecular clouds 78−65674
CS, vibr. states in RF discharge plasma, microwave spectrosc. obs. 80−14133
$^{12}C^{16}O$ and $^{12}C^{18}O$ J=2→1 transitions obs. towards galactic H II regions 80−73022
CaO, J=4-3 106 GHz undetected transition in stars and molecular clouds 79−71090
CaO, millimetre wave spectrum, spectrosc. consts. 77−61737
ClO, aircraft search for 3 mm emission in stratosphere 80−41510
ClO, rot. spectrum, mol. parameters in v=0, v=1 states 78−70821
^{35}ClO, microwave spectrum in excited vibr. state, centrifugal distortion const. 77−83580
CsCl, hyperfine spectrum, mol. beam elec. reson. meas. 77−71797
CuBr, rot. spectrum hyperfine struct., coupling consts., microwave spectroscopy study 80−18844
CuCl, hyperfine struct., microwave rot. spectrum obs. 78−21917
CuI, hyperfine struct., quadrupole coupling const., rot. spectrum 77−88447
GaBr, rot. analysis of $^3\Pi_{0,1}$-$X^1\Sigma^+$ transition 80−69129
GaBr, rot. spectrum hyperfine struct. 79−13838
GaI, rot. spectrum, EHF spectra obs. 80−58245
GeS, rot. spectra, Born-Oppenheimer approx., adiabatic corrections *(German)* 77−57994
$^{72}Ge^{32}S$, $^{74}Ge^{80}Se$, $^{74}Ge^{130}Te$, rot. g_J-factor meas., $^1\Sigma$ ground state *(German)* 77−30865

radiofrequency and microwave spectra of diatomic inorganic molecules continued
GeSe, rot. spectra, Born-Oppenheimer approx., adiabatic corrections *(German)* 77−57994
o-H_2 pairs, in solid H_2, microwave absorpt. 77−68034
H_2, $S_0(3)$ pure rot. quadrupole transition, obs. using tunable diode laser 78−82723
HCl+methane, pure rot. line broadening obs., transition cross sections 77−75134
$H_2{}^{17}O$ and $H_2{}^{18}O$, centrifugal distortion anal. of ground vibr. states 78−70834
I_2, B-X transitions, rot.-vibr. hyperfine coupling consts., extension to other levels 80−63625
I_2 vapour, absorpt. lines meas. using FM spectrosc. 80−42262
$^{115}In^{79}Br$, $^{115}In^{81}Br$, rot. J=1→2 hyperfine struct., quadrupole coupling consts. *(German)* 77−30866
LiF, RF spectra, spin interactions and moments, mol. beam elec. reson. meas. 77−18912
N_2, gas, liq., collision-induced microwave absorpt. 77−42312
N_2, spectroscopic data review 77−38680
NO, interstellar microwave detection in Sagittarius B2 direction 78−93378
NO_2, v=0,1 states, spectroscopic data calc. 78−86851
NO^+, interstellar transitions in mm and IR wavelengths 80−56906
NS, spontaneous radiation transitions theory rel. to interstellar line emission 78−54031
$^{14}NH^+$($^{15}NH^+$)($^{14}ND^+$), ab initio CI calc. Λ type doubling in $X^2\Pi$ states 78−82714
N_2O+OCS 80−48063
Ne-Xe gaseous mixtures, collision-induced microwave absorpt. 78−78680
O_2, 60 GHz absorpt. spectra for atmos. remote sensing 80−77172
O_2, gas, intermol. pot. for spectra, acoustic absorpt., rot. relax., etc. 79−68224
O_2, microwave absorpt. at high-press., 9, 23 and 60 GHz 78−13490
O_2, microwave absorption, spectral line press. broadening theory 77−30864
O_2, microwave absorption meas. by Fabry-Perot spectrometer 77−46558
O_2, microwave spectrum, press. broadening 80−23412
O_2^+, $b^4\Sigma_g^-$ state, laser-induced predissoc. in ion beam 78−70886
O_2^+, rotational analysis of $A^2\Pi_u$-$X^2\Pi_g$ band system of $(^{16}O\ ^{18}O)^+$ 78−58678
O_2+Ar, gas, intermol. pot. for spectral props. and rot. energy transfer 79−68224
O_2+$O_2(N_2)(H_2O)$(Ar)(He), 118750 GHz transition, press. broadening 77−75136
OH, 13.4 GHz absorpt. line width *(French)* 77−61801
OH 1.6 GHz maser emission from W3(OH), 49 N and 51, spatial distrib. 78−93355
OH emission from Comet Meier (1978f) at 1665 and 1667 MHz 78−61800
OH excited states, satellite lines anomalies 77−42315
OH, J=9/2 Λ-doublet line detect. in W3(OH) 78−65670
OH, Λ-doublet splitting calc. rel. to predicted radioastronomical freqs. accuracy 79−48666
OH, maser emission from OH/IR sources 78−16432
OH maser emission from W3 (OH), Zeeman effect 78−93377
OH, microwave spectral line breadth in NH_3, H_2O, NO_2, SO_2, O_2, H_2, He, N_2, chloromethane 79−45806
OH, mol. beam electric reson., hyperfine Λ-doubling transitions 79−36628
OH, nonthermal main lines in interstellar dust clouds and OH abundance 80−36683
OH, prod. by photolysis, Λ-doublets, population, rot. states, hyperfine struct., microwave spectra 80−32694
OH, radical $v=1^2\Pi_{3/2}$ state, microwave spectrum 79−26972
OH radicals, microwave spectra data tables 78−50542
OH, vibr. ground-state, MFS, rot. spectra and electronic band anal. 78−5206
OH, vibrationally excited, high-resolution hyperfine Λ-doubling spectrum 78−90153
OH, $X^2\Pi$ state, microwave spectrum calcs. 77−30858
OH+$H_2O(NO_2)(CH_3Cl)(N_2)(H_2)$(He), mean collision cross sections from microwave spectroscopy 80−1046
$OH(^2\Pi_{3/2}, v=1)$, population inversion of Λ doublets in microwave spectrum 80−974
$OHX^2\Pi$ radical, ground and vibr.-excited ($v\leq6$) levels, microwave spectrum 79−63985
PbBr, $b^1\Sigma^+$-$X^1\Sigma^-$ band system, microwave discharge obs., mol. consts. 79−81203
PbCl, rot. analysis of A-X_1 system 80−32703
$^{208}Pb^{32}S$, $^{208}Pb^{80}Se$, rot. g_J-factor meas., $^1\Sigma$ ground state *(German)* 77−30865
RbI, ground vibr. state rot. transition, quadrupole HFS and coupling consts. *(German)* 77−57990
S_2, microwave spectra 79-150 GHz, rot. and fine struct. parameters 79−63987
SO 1_0-0_1 transition in dark and molecular clouds, 30 GHz obs. 80−46639
S0 in Orion Molecular Cloud, line profile rel. to rotational explanation of high-vel. mol. emission 80−36688
$^{32}S_2$, magnetic-dipole transitions and upper limits in interstellar mol. clouds 78−28738
SeO, mol., mm wave spectra, $X^3\Sigma^-$ state 79−85959
SiH, optically derived lambda splitting rel. to interstellar existence 77−17657
SiO interstellar line emission from Orion, shock chemistry 79−21391
SiO, maser emission from OH/IR sources 78−16432
SiO maser line evidence for circumstellar ring systems in supergiant stars 78−89195
SiO, rot. and vibr. consts., millimetre-wave spectrum 77−34619
SiS, and isotopes, microwave spectra and consts., review 77−23493
$^{120}Sn^{32}S$, $^{120}Sn^{80}Se$, $^{120}Sn^{130}Te$, rot. g_J-factor meas., $^1\Sigma$ ground state *(German)* 77−30865
SrO, mm wave spectrum, spectroscopic consts. 78−37629

radiofrequency and microwave spectra of organic molecules and substances
see also nuclear magnetic resonance; paramagnetic resonance
1,3-butadiene-1-one, spectroscopic consts., IR and microwave spectra, prep. 80−18859
absorption by water in heterogeneous organic materials 80−15998
acetaldehyde, microwave spectra, low-freq. 79−81305

radiofrequency and microwave spectra of organic molecules and substances continued
acetaldehyde, T_2-relax. meas. press. depend. for rot. transitions, pulse spectrometer 80−78612
acetaldehyde photolysis, HCO product microwave spectra 79−5163
acetic acid-d_1(-d_2), equilib. config. from microwave spectrum 79−59442
acetonitrile, ^{13}C mag. shielding from beam maser meas. of spin-rot. interaction 79−45707
acetonitrile, sub mm laser, generation lines identification *(Russian)* 78−82952
acetyl cyanide, (^{15}N), microwave spectrum, rot. consts., internal rot. barrier 77−75141
acetyl cyanide, rot. spectrum, rot.-torsion-vibr. interaction, A-E rot. splittings 77−10667
acetyl cyanide-d_1, microwave spectra, r_s, r_0-struct. 78−13491
acetylene-d_2, microwave spectrum, P-branch transitions, Stark shifts 77−27057
aliphatic, in dil. solns., dielectric relax. dipole reorientation, rot., microwave obs. 77−28516
allylamine, N-cis lone-pair gauche rotamer ground state microwave spectrum anal. 78−82720
allylamine, NGLT, rot. and centrifugal distortion consts. 78−74644
aminoacetonitrile, microwave rot. spectrum, quadrupole hyperfine struct. 78−17658
3-aminopropanol, and deuterated forms microwave spectrum, dipole moment, struct. 79−59441
atmospheric pollutants and constituents, microwave absorp. coeffs. 77−64378
atmospheric submillimetric-wave interferometric spectrometry 79−34979
1-aziridineethanol, mol. spectrum and hydrogen bonding 78−70820
benzene+bromomethane, microwave line width and quadrupole moments, perturbation theory 80−69190
benzene+OCS, microwave line width and quadrupole moments, perturbation theory 80−69190
benzenes, nitrohalide substituted, microwave absorpt., mol. struct. 78−75522
bicyclo[3.1.0]hex-2-ene, microwave spectra, rot. consts., ring struct. and config. 78−42041
bicyclo[3.1.0]hexane, zero-point average struct., microwave spectra and electron diffraction 78−25738
Δ^6-bicyclo[3.2.0]heptene, microwave spectrum and dipole moment 80−9591
2-bromo-2,3-dimethylbutane, low resolution 79−54846
bromoacetic acid, microwave spectrum, rot. consts., nucl. quadrupole coupling, conform. 79−13702
bromoacetonitrile, ground state microwave spectrum assignments, mol. struct., rot. consts., quadrupole coupling 77−6763
bromoacetylene, microwave spectrum, dipole moment 78−17660
bromoallene, microwave spectra in vibr. ground state, rotational consts., nuclear quad. coupling consts. *(French)* 77−10664
bromomethane, and isotopic forms, self-broadening and self-shifting of rot. spectra 78−13551
bromomethane, microwave spectra, isotope substitution, Br quadrupole coupling, J=0←1 transitions 79−45709
bromomethane, microwave spectrum obs., B rot. and centrifugal distortion consts. 77−75135
bromomethane, rotational spectrum in ground state of vibr., 18 to 350 Hz *(French)* 77−57980
bromomethyl methyl ether, microwave spectra, quadrupole computing effect 80−18848
bromomethyl methyl ether, microwave spectra, quadrupole coupling effect 80−14135
bromomethyl oxirane, conformation, microwave spectrum in ranges 12.5-18 and 26.6-40 GHz 79−98076
bromomethylsilane, microwave spectra, quadrupole computing effect 80−18848
bromomethylsilane, microwave spectra, quadrupole coupling effect 80−14135
3-bromopropene, $^{79,81}Br$, microwave spectrum, mol. struct., nucl. quadrupole coupling consts., rot. consts. 77−6767
3-bromopropene, microwave spectra, torsionally excited mol., HFS and rot. consts. 79−63988
bromotrifluoromethane, mol. struct., electron diffr., microwave spectra, CNDO/2 calcs. 78−37766
1-1-d_2-but-1-ene skew form, microwave spectra, rot. const. and centrifugal distortion coefficients determ. 80−83351
butadiynyl in IRC+10216, N=12→11 doublet study 80−51829
butadiynyl radical, interstellar, detect. towards (IRC+10216) 78−93374
1-butene oxide, gas, microwave spectrum 79−13703
cis-butene-1, microwave rot. spectrum, centrifugal distortion effects, rot. consts. 78−9137
t-butyl bromide, bond lengths, nucl. quadrupole coupling, microwave spectrum 79−31512
t-butyl cyanide-HF, hydrogen bonded heterodimer, spectroscopic consts. from IR and microwave spectra 80−43039
t-butylphosphine, microwave spectrum, meas., determ. 78−58675
caesium perfluoro-octanoate/D_2O system, ^2H NMR quantum orders, RF pulses 80−103892
carbonyl chlorofluoride, rot. Zeeman effect, g-factors and mag. suscept. anisotropies, microwave meas. *(German)* 77−57993
2-chloro-2-nitropropane, far IR-microwave estimation of binary collision approx. 80−55095
chlorobenzene-d_5, and isotopic forms, microwave spectrum, rot. consts. 78−58667
chloromethane, microwave spectrum, width and shift parameters 77−18985
chloromethane-d_2, microwave spectrum, rot. consts. 78−9140
chloromethyl cyclopropane, microwave spectra and struct. 79−36625
chloromethyl oxirane, microwave spectra and conformations of cis and gauche-2 forms 80−5534
chloromethylethyl ether, GT isomer, microwave spectra and geom. config. 79−59444
chlorotrifluoromethane, mol. struct., electron diffr., microwave spectra, CNDO/2 calcs. 78−37766
cholesterol+water, interaction in organic media, dielec. and NMR spectroscopy 78−76979
cis-1-cholobutadiene-1,3, microwave spectrum, struct., nuclear quadrupole coupling, distortion const., thermodynamic functions calc. 80−99500
trans-crotonaldehyde, rot. Zeeman effect, microwave spectra, mol. parameters 79−3491

radiofrequency and microwave spectra of organic molecules and substances continued
1-cyano-1,3-cyclopentadiene, microwave spectrum, rot. consts., dipole moment 78−42043
4-cyano-4′-octylbiphenyl, dielec. props., 1 Hz-1 GHz, in smectic, nematic and liq. phases *(French)* 77−40168
cyanoacetylene, ^{13}C and ^{15}N isotopic species, rot. transitions, 8-220 GHz 77−61740
cyanoacetylene, and deuterate, microwave spectrum, ground and excited vibr. states 78−90157
cyanoacetylene, microwave spectrum, mol. consts. 78−74647
2-cyanoaziridine, microwave rot. spectrum, assignments 80−91546
cyanobutadiyne-d_0,d_1, microwave spectrum, substitution struct., dipole moment 77−3348
cyanocyclopentane, microwave spectral study of axial and equatorial conformers 80−95604
cyanodiacetylene, interstellar, J=2-1 transition detect. and hyperfine splitting const. 79−25692
cyanodiacetylene in Sagittarius B2, 5 and 7 GHz obs. of J=2→1 and 3→2 rotational transitions 79−92817
N-cyanoformimine, stability, identification by microwave spectroscopy 79−10095
N-cyanoformimine-d_2, struct., microwave transitions 80−973
2-cyanofurane, rot. consts., dipole moments, nuclear quadrupole coupling, spectral obs. 77−34620
cyanohexatriyne detection in Heile's Cloud 2 at SHF 78−41018
cyanomethane, collisional rot.-line widths and shifts, microwave region 78−25619
cyanomethane-HF, hydrogen bonded heterodimer, spectroscopic consts. from microwave spectrum 80−43038
cyanooctatetrayne, line freqs. prediction and detect. in interstellar space 78−93370
2-cyanothiophene, rot. consts., dipole moments, nuclear quadrupole coupling, microwave spectra 77−34620
3-cyanothiophene, rot. spectrum and consts., elec. dipole moment, quadrupole coupling, r_0-struct., 77−79607
3-cyanothiophene-^{34}S(-^{15}N), partial r_0-struct., microwave spectra 80−91552
cyclobutanol-d_0,-d_1, conformation, microwave spectrum 78−86852
1,3-cycloheptadiene, microwave spectrum, conform. 79−98074
2-cycloheptene-1-one, microwave spectrum, dipole moment and mol. conform. 79−72303
cyclohexane$_{(e)}$ solns., positive ion-solute mol. reaction rate consts. in radiolysis 77−9091
cyclohexanecarbonitrile, rot. consts., conformers, struct., microwave spectrum 77−42314
cyclooctanone, vibr., rot. spectra and conformations, pot. function 78−78707
cyclopentene-3,5-dione(-d_1) microwave spectrum assignments, rot. consts., dipole moment, config. 78−55168
cyclopentyl chloride, microwave spectrum, conformation, quadrupole coupling consts. 79−3434
cyclopopane, conformations, rot. consts., microwave spectrum 79−98075
cyclopropyl cyanide, high-resolution microwave spectra, quadrupole hyperfine struct. of rot. transitions anal. 80−95601
cyclopropylamine struct., microwave spectrum 79−10096
trans-decalin, liq., irrad., positive charge mobility meas. by microwave absorpt. 77−20100
di thioformic acid, cis and trans isomers, rot. microwave spectra and config. 79−63989
p,p′-di-n-alkoxyazoxybenzene series, C_1-C_7, submillimetre wave absorpt. investig. 80−34910
m-dichlorobenzene, nucl. quadrupole coupling consts., hyperfine struct., bonding 77−14422
dichlorodifluoromethane, microwave rot. absorpt. spectra, nuclear quadrupole coupling, hyperfine splitting 77−30861
1,1′-dicyanoethene(-d_2), microwave spectrum, Coriolis interaction, rot. assignments 78−82721
N,N-diethyl formamide, dipole moment, dielectric relax., internal rot., microwave absorpt. 79−56716
diethylcarbonate, liq., alkoxy group internal torsion, extended microwave/far IR anal. 78−19457
difluoramine, up to J=19, centrifugal distortion anal., microwave rot. spectrum 78−58650
1,1 difluoroethylene, -d_1, -d_2, mol. struct., rot. consts., gas phase electron diffr., microwave data 77−65542
cis-1,2-difluoroethylene oxide, substituent and isotope effects, microwave assignments 78−78682
difluoromethane, microwave spectral line widths 78−70816
difluoromethane, microwave spectral lines, line-width parameters 77−68077
difluoromethylborane, microwave spectra and struct. obs. 80−43036
dimethyl ether, review of microwave spectrum, tabulated data 80−51965
dimethyl ether-d_0,d_3,-d_6, microwave spectra, torsional splittings 77−3347
dimethyl selenide-d_6, microwave spectrum in ground and excited torsional states *(German)* 77−57992
dimethylallene, excited states, microwave spectrum and strong Coriolis coupling 78−9141
2-dimethylaminoethanol(-d_1), microwave spectrum, hydrogen bonding, rot. consts., struct., dipole moment 77−6764
dimethylcarbonate, liq., alkoxy group internal torsion, extended microwave/far IR anal. 78−19457
3,3-dimethylcyclopropene, microwave spectrum, dipole and quadrupole moments calcs. 79−59440
dimethyldichlorosilane, microwave spectrum, rot., centrifugal distortion and quadrupole coupling consts. 80−91547
dimethylphosphine, microwave spectra, internal rot. barrier 78−5205
dioxirane, form. in O_3+ethylene reaction, identification by microwave spectra 78−15659
disilylmethane, microwave spectrum, struct., dipole moment and internal rot. 79−13699
dithioformic acid, prod. and microwave spectra 78−58671
divinyl ether, microwave spectrum, doublet splitting, vinyl group internal rot. 78−86849
DPPH-benzene, organic radical, pressure induced mag. ordering *(Russian)* 78−88120
epichlorohydrin, microwave spectra and struct. 79−36626
ethane, $^{13}CH_3{}^{12}CD_3$, $^{12}CH_3{}^{13}CD_3$, microwave spectra, Stark effect, C-C bond length and mol. consts. 77−50428
ethane, d_2, microwave spectra for internal rot. barrier 79−93986

radiofrequency and microwave spectra of organic molecules and substances continued
ethaneselenol, IR, Raman and microwave spectra, barriers to internal rot. 77−38666
ethyl alcohol-d_0(-d_1)(-d_1)(-d_2), internal rot. and microwave rot. spectra 80−69128
ethyl cyanide, isotopic species, rot.-torsion-vibr. interaction in rot. spectra 77−458
ethyl cyanoformate, conformers, dipole moments, rel. energies, microwave spectra 78−55164
ethyl fluoroformate, microwave spectra of rot. isomers 79−10097
ethyl formate, microwave rot. spectrum, centrifugal distortion effects 80−52979
ethyl hyoochloride, microwave spectrum, dipole moment, quadrupole coupling consts. 78−58673
ethyl iodide, microwave spectra and internal rot. anal. 80−69130
ethyl nitrite, microwave spectra, rot. isomerism and dipole moments 79−93990
ethylchloride, d_0-d_5, microwave spectra, elec. field gradient tensor at Cl nucleus *(German)* 78−46325
ethyldifluoroborane, microwave, Raman, IR spectra, conform., dipole moments, vibr. assignment 78−90155
ethylene oxide, ^{13}C and D variants, T_2-relax., 2_{20}-2_{11} rot. transition by microwave pulse spectrometer 80−47976
ethylene ozonide-d_4, isotopic species, microwave rot. spectrum assignments, struct. 77−57982
ethylgermane, microwave, IR and Raman spectra, struct., internal rot., dipole moments 77−79605
ethylidenimine, pyrolysis product, microwave spectra, rot. distortion and electric quadrupole const. and rot. barriers determ. 80−78608
ethynyl radical, mm wave emission obs. of interstellar clouds 80−90503
fluorene crystal, doped, photochemical hydrogen abstraction, proton hyperfine structure via optical nuclear polarisation 80−63659
fluoroacetylene-d_0,-d_1, microwave spectrum, laser enhancement effects 79−41161
o-fluoroaniline, conformation by microwave spectroscopy, rot. consts. 78−9144
fluoromethane, in interstellar mol. clouds, search for $J_K=1_0$-0_0 transition 77−60808
fluoromethane, microwave spectrum, and 2nd order Coriolis reson., mol. consts. 77−18915
fluoronitrobenzene, equilib. config. and barriers, microwave spectra 80−95606
formaldehyde, ^{18}O isotope, 4389 MHz obs. 79−44591
formaldehyde, hyperfine interactions, mol. beam elec. reson. spectra 77−88445
formaldehyde, interstellar, collisional excitation and lines pressure-broadening widths 78−89237
formaldehyde, interstellar, excitation, effects of microwave background radiation observed spectrum 80−36681
formaldehyde, microwave spectra, low-freq. 79−81305
formaldehyde, microwave-microwave double resonance 80−53029
formaldehyde, mol. beam, vel. meas. by Doppler effect on RF spectrum splitting *(French)* 78−13627
formaldehyde, pressure-broadened linewidths in microwave region, temp. depend. 77−34694
formaldehyde, T_2-relax., rot. transitions, time resolved spectra, microwave pulsed spectrometer study 80−18846
formaldehyde, vibr. excited states, RF spectrum *(French)* 77−30863
formaldehyde+He, rot. excitation, coupled-channel calcs., microwave doublets cooling 77−3436
formaldehyde(-d_1, d_2), and isotopic forms, microwave spectrum, ν_4-ν_6 vibr. states Coriolis reson. 78−82719
formaldehyde in giant molecular clouds, H_2 densities and $^{12}C/^{13}C$ ratio 80−51837
o-formaldehyde in rho Ophiuchi dark cloud, excitation temp. and optical depths 80−51846
formaldehyde substituted with ^{17}O and ^{18}O, microwave spectra of ground vibr. states, rot. and distortion const. determ. 80−83349
formaldehyde-d_1, ν_5 and ν_6 vibr. excited states, microwave spectrum obs. 79−72304
formaldehyde-d_1, rot. transitions, millimetre wave spectrum 77−34617
formaldoxime, centrifugal distortion effects, microwave rotational spectrum 79−22699
formic acid, ^{16}C, ^{18}O, microwave spectra and centrifugal distortion consts. 80−83352
formic acid, microwave spectrum, 10-200 GHz, vibrational excited states, ν_6, ν_8 79−93987
cis-formic acid (-d_2,d_2), and isotopic forms, bond lengths and angs., microwave spectrum obs. 78−55169
formic acid (-d), microwave spectra and rot. consts., astrophysical appl. 80−91550
formic acid and isotopic species, microwave spectra, Coriolis reson. between vibr. excited states 79−13700
formyl chloride, rot. Zeeman effect of low-J transitions 78−25519
formyl fluoride, and isotopic forms, mol. struct., from electron diffr. and microwave data 80−23570
formyl radical ion, mm wave emission obs. of interstellar clouds 80−90503
formyl radical-d_0,-d_1, microwave spectroscopy, high field Zeeman effect 78−37631
free radicals, spectroscopy, review, book contrib. 77−38653
glycine, mm wave spectrum 79−3435
1-haloalkanes, microwave spectra, conformation 78−21913
heptafulvene, microwave spectrum and dipole moment 77−14421
hexa-deutero dimethyl selenide, microwave spectrum, first excited torsional states, top-top interaction 77−10668
hydrazine-1,2-d_2, microwave spectra, mol. structural parameters 77−27056
indene, microwave spectrum, assignments, rot. consts. and config. 79−31510
interstellar molecular transitions, rest freqs. 80−62218
interstellar molecules, microwave spectrosc. obs. 79−41160
2-iodo-2,3-dimethylbutane, low resolution 79−54846
iodomethane, and isotopic forms, self-broadening and self-shifting of rot. spectra 78−13551
iodomethane, collisional rot.-line widths and shifts, microwave region 78−25619
3-iodopropene, microwave spectra, rot. consts. and HFS 78−975
3-iodopropene, microwave spectra, torsionally excited, rot. consts. 79−63986

radiofrequency and microwave spectra of organic molecules and substances continued
2-iodopropene, microwave spectrum, quadrupole coupling consts., internal rot. barrier 79−45710
iodotrifluoromethane, mol. struct., electron diffr., microwave spectra, CNDO/2 calcs. 78−37766
isocyanic acid, molecular structure and centrifugal distortion constants 80−47974
isoproplyiodide, microwave spectrum, quadrupole coupling 78−86848
isopropyl fluoroformate, microwave spectrum and conformation 79−10098
isopropylamine-d_0,-d_1,-d_2, microwave spectra, struct., dipole moments and quadrupole coupling consts. 77−34613
isopropylphosphine, gauche form, microwave spectrum, identification 78−58674
isothiocyanic acid, $H^{15}NCS$, $HN^{13}CS$ and $HNC^{34}S$, ground state spect. constants and molecular struct. 80−47973
isoxazole-4D, microwave spectrum, ^{14}N nucl. quadrupole coupling tensor 78−90154
ketene, hyperfine interactions, mol. beam elec. reson. spectra 77−88445
ketene-d_1(d_2), microwave and millimetre spectra, rot. transition, centrifugal distortion anal. 77−57991
maleic anhydride, struct., DRM microwave spectra, isotope shifts 78−21918
methane, ν_3=1 state, dipole moment and IR-radiofrequency double reson. spectra 80−14161
methane, gas, liq., collision-induced microwave absorpt. 77−42312
methane, microwave Q branch distortion moment Stark spectrum, rot. transitions, C isotope shifts 77−455
methane-d_1, laboratory rotational spectrum and upper limits on abundance in (OMC-1) 80−56705
methanol, interstellar, two new transitions obs. in Orion A 79−25667
methanol, vap., rot. spectrum, 8-50 cm^{-1}, 293K 79−72305
methanol mol., microwave linewidth parameter 79−31508
methanol-d_1, (CH_2DOH), microwave torsional-rot. spectrum, rel. to interstellar search 80−99498
methanol-d_1, laboratory freqs. of J=2-1, a-type transitions 80−63624
methoxy free radical, laser mag. reson. submillimetre spectrum, linear Zeeman effect 77−46579
2-methoxyethylomine, microwave spectra, H-bond, torsional motion and mol. vibr. obs., rot. isomerism, mol. moments determ. 80−95603
3-methoxypropionitrile, microwave spectrum, rot. conformer, rot. consts., vibr. state 77−14419
methyl acetate, microwave spectra and internal rot. 80−87100
methyl alcohol submillimetric high-resolution Fourier transform spectra 79−31509
methyl azidoformate, microwave rot. spectrum, satellite transitions 80−69127
methyl bromide, NQR and A_1-A_2 splitting, RF spectrosc. inside laser cavity 80−91579
methyl bromide, pressure-broadened linewidths in microwave region, temp. depend. 77−34694
methyl bromide, rot. spectrum, microwave region *(Russian)* 78−70823
methyl bromide, sub mm laser, generation lines identification *(Russian)* 78−82952
methyl chloride, microwave spectrum of excited vibr. states, Coriolis coupling, rot. consts. 77−14420
methyl chloride, pressure-induced shift of the J=0→1 transition, 193 to 366K 77−14497
methyl chloride submillimetric high-resolution Fourier transform spectra 79−31509
methyl chloroformate, struct., microwave, Raman, far IR and NMR spectra 77−34614
methyl cyanide, microwave rot. spectra, mol. consts. 77−34615
methyl cyanide and isocyanide, microwave spectra, harmonic force field and r_z struct. 79−36627
methyl cyanide submillimetric high-resolution Fourier transform spectra 79−31509
methyl fluoride, second-order Coriolis resonance between ν_2 and ν_5 states, microwave spectra 78−74646
methyl formate, microwave spectra, rot. consts., moments and struct., radio astronomy appl., review 80−17637
methyl hypochlorite-d_0, -d_3, microwave Zeeman spectra, dipole moment, nuclear quadrupole tensor 77−459
methyl iodide, mag. hyperfine struct. of quadrupole spectra *(Russian)* 77−34622
methyl iodide, rot. microwave spectra, nucl. quadrupole, spin-rot. and nucl. shielding tensors 78−42040
methyl iodide mol. nonlinear resonant interaction with pulsed subMM radiation *(Russian)* 80−99523
methyl isocyanide, and ^{15}N derivative, microwave spectra in $4\nu_8$ state 77−83582
methyl isocyanide, microwave spectrum, anal., N isotope effects 77−50430
5-methyl isoxazole, microwave spectrum internal rot. barrier 78−58665
N-methyl m-fluoroaniline, conformational anal., microwave spectra obs. 80−58247
methyl oxirane, centrifugal distortion consts. and struct. parameters calcs. 77−34616
methyl selenocyanate, and isotopic forms, microwave spectrum 79−13705
methyl vinyl ether, microwave spectrum, quartic centrifugal distortion and rot. consts. 79−10099
methyl vinyl ether, rot. Zeeman effect, g-values, mag. susceptibility, quadrupole moments 77−490
methyl vinyl sulphide, syn-gauche equilib., force field and ab initio calcs., microwave and Raman spectra 80−23573
2-methyl-pyrimidine, microwave spectrum, V_6 barrier, dipole moment, rot. consts. 77−3345
methylacetylene, ν_5 band, microwave and IR laser Stark spectrosc. 80−91558
methylamine-d_1, unconfirmed from interstellar 10 GHz obs. 79−92822
7-methylbicyclo[2.2.1]-hept-2-ene-5-one, config., microwave spectrosc. obs. 80−9593
methylchloride, high resoln. rot spectrum, spin-rotation and nucl. mag. shielding tensors 77−27054
methyldiborane, microwave spectra, bond lengths, dipole moments, rot. consts. 77−83579
methyldichlorosilane, Stark effect and microwave-microwave double reson., struct. *(German)* 80−47975

radiofrequency and microwave spectra of organic molecules and substances continued
methylene chloride, microwave spectra, rot. consts. and geometric struct. 79−63990
methylene fluoride, excited vibr. state, microwave spectrum 78−58672
methylene ketene, microwave spectrum, rot. and centrifugal distortion consts., dipole moment 78−17659
methylidyne, search for maser emission in C stars 80−51856
methylidyne in diffuse interstellar medium, optical and radio obs. 78−93356
methylpropylether, trans-trans isomer, microwave spectra, struct., dipole moment and rot. barriers calcs. 80−83348
N-methylpyrazole, microwave spectrum, internal rot. barrier 78−58666
monothioformic acid, cis-, trans-rotamers, rot. spectrum, force consts. and isotopically substituted struct. 78−9145
morpholine, centrifugal distortion consts., microwave spectrum 80−5531
N-methylhydroxylamine, microwave spectra, struct., moments, internal rot., HFS and rot. consts. 79−45708
natural rubber latex ^{13}C NMR spectra 80−15816
N-nitroso-dimethylamine-d_0, -d_3, -d_6, struct., microwave spectra 79−59446
nitrosomethane, microwave spectrum, structure, dipole moment and centrifugal distortion 78−66540
3-nitrothiophene, rot. transitions, torsion, microwave spectra 77−42313
norbornane, microwave spectrum and dipole moments 80−78606
7-oxabicyclo (4.1.0) hept-3-ene, conformation, dipole moment, microwave spectrum 78−66539
oxazole(-d_1), dipole moment, quadrupole coupling tensor, from microwave spectrum 78−55166
oxiranecarboxaldehyde, microwave spectrum, torsional excitation energy, partial struct., dipole moment 77−38655
phenols, ^{13}C and D substituted, microwave spectra, substitution struct. and absolute dipole moment 79−31511
phenyl isocyanate, microwave spectrum, rot. consts., dipole moment 77−61739
1-phosphapropyne, microwave spectrum, vibration-rotation analysis, dipole moment, structural parameters 79−93989
polyacetylenes, symm. top, microwave spectra 78−58676
polyatomic mol. gas phase spectra, struct., review and tabulation 80−14136
propane, gaseous, dielectric losses, absorpt. of 8 and 12 mm radiation under pressure *(French)* 79−93991
propargyl mercaptan (−d_1), microwave spectra, struct., rot. anal. 77−18916
2-propene-1-imine, rot. isomers, microwave spectra 78−58670
propiolamide(-d_2, d_3), microwave spectrum, struct., dipole moment 78−78685
propionitrile, quartic and sextic centrifugal distortion consts., microwave spectrum 78−94236
propynal-d, IR microwave double reson. spectroscopy 80−69172
propyne, ^{13}C isotopic species, microwave spectra, rot. consts. 78−86850
propyne, microwave spectra and mol. consts., rot. anal. 79−76411
pyridine, and -d_1, microwave spectra, mol. struct., rot. consts. 78−25517
4-pyridine carbaldehyde, microwave spectrum, rot. assignments, quadrupole coupling consts. 80−91548
s-trans-3-pyridinecarbaldehyde, microwave spectrum, assignments 78−21912
selenoacetaldehyde, microwave spectrum, struct. internal rot. barrier 78−74645
selenoketene, formation, microwave spectrum, struct. determ. 78−25515
selenoketene, microwave spectra, 26.5-40 GHz, mol. config., bond angle and length 78−46322
1-silabicyclo 2,2,2 octane, double-min. skeletal torsion, microwave spectroscopy 80−47972
silyl acetylene, microwave spectra in ground and ν_{10} vibr. state 80−78610
stibabenzene, struct., microwave spectrum and nucl. quadrupole coupling consts. 78−70817
structural energy characteristics, rotational isomerism, mol. motion *(Russian)* 79−56602
N-sulphinylaniline, microwave rot. spectra, torsional freq., dipole moment and internal rot. barrier 78−973
symmetric top mol., overlapping press. broadening, nonreson. microwave absorpt. line radii 78−17662
tertiarybutylisocyanide-borane, vibr., rot. consts., moment of inertia, microwave spectra obs. 80−32706
tetracyclo[3.2.0.$0^{2,7}$.$0^{4,6}$]heptan-3-one, microwave spectrum and effect of cyclopropyl-carbonyl group interactions on dipole moment 78−9138
tetrafluorobenzene, microwave spectra, dipole moment, centrifugal distortion consts. 77−75133
1,1,2,2-tetrafluorocyclobutane, microwave spectrum, dipole moment, rot. and vibr. modes assignments 77−18914
tetrafluoromethane, gas, liq., collision-induced microwave absorpt. 77−42312
tetrahydrothiophene, microwave spectrum, centrifugal perturbation effects 77−3350
1,2,4-thiadiazole, struct., double reson. modulation microwave spectra 77−14424
thioacetaldehyde (-d_1), microwave spectrum, substitution struct. internal rot. barrier, dipole moment 77−6762
thioacetic acid, −d_1, principle axis method anal. of microwave spectra 78−9139
thioformaldehyde, hyperfine interactions, mol. beam elec. reson. spectra 77−88445
thioformaldehyde, interstellar, 2_{11}-2_{12} transition obs. and rest freq. 80−67837
thioformic acid, g-values, mag. susceptibility, quadrupole moments, rot. Zeeman effect, isomer effects 78−25520
thioketen, microwave spectrum, substitution structure and dipole moment 80−975
o(m)-toluidine+o-chlorophenol, H-bonded mol. complex, microwave absorpt., dipole moment and relax. times 80−14134
trans-propargyl amine, microwave spectra, dipole moments and struct., isotopic species 78−974
1,2,3-triazole, nucl. quad. coupling in microwave spectrum 77−57987
trifluorobenzene, equilib. config. and barriers, microwave spectra 80−95606
1,2,4-trifluorobenzene, microwave spectrum, dipole moment and centrifugal distortion constants 78−37630
trifluorodimethylmercury, gas phase mol. struct., electron diffr. and microwave spectra obs. 80−78609

radiofrequency and microwave spectra of organic molecules and substances continued
trifluoroiodomethane, laser microwave double reson. spectroscopy with CO_2 laser lines 80−87156
trifluoromethane, and -d_1, microwave spectra in ν_6=1 state, accidental degeneracy, mol. struct. 79−3436
trifluoromethyl bromide, mol. rot. and isotopic variation in bond lengths, Stark meas., dipole moment determ. 80−74165
trifluoromethyl iodide, microwave spectra, mol. rot., isotopic variation in bond lengths, Stark meas., dipole moments determ. 80−74165
trimethylamine, and analogues, struc. struct. and vibr. force fields, electron diffr. and microwave spectra 77−54609
trimethylaminegallane, microwave, IR and Raman spectra, struct., vibr. assignment 80−95600
trimethylbromosilane, microwave spectra, struct., chemical bonding 80−95602
trimethylene sulphoxide, microwave spectrum, mol. struct., methylene group, bends, tilts, twists 77−50431
trinitromethane, microwave and rot. spectra, effect of twist of NO_2 groups, rot. and centrifugal distortion const. determ. 80−95605
trioxane, $\nu_{19}(E)=\nu_{20}(E)=1$ state, rot. spectrum assignment, microwave obs. 80−58248
vinyl alcohol-d_0, -d_1, microwave spectrum, centrifugal distortion 77−71796
vinyl azide, microwave spectrum 77−57985
vinyl bromide, mol. struct., from gas-phase electron diffr. and microwave data 80−23571
vinyl chloride+O_3 reaction, IR matrix and microwave spectroscopy 77−90587
vinyl cyanide, microwave spectra data tables 79−59445
vinyl isocyanate, conformers, geometrical and electronic structures, microwave spectra 78−9142
vinyl isocyanate, microwave and photoelectron study of cis- and transforms 78−70819
vinyl mercaptan -d_0, -d_1, anti rotamer, conform., microwave spectrum 80−9592
vinyl mercaptan -d_0, -d_1, synrotamer, conform., microwave spectrum 80−5535
vinylchloride, mol. struct., gas-phase electron diffraction and microwave spectra, vibr. amplitudes 79−76421
vinylfluoride, gas phase electron diffr. and microwave spectra, rot. consts., struct., isotope shifts 79−31686
2-aminoethanol(-d_2)(-d_3), microwave spectra, hydrogen bonding, rot. const. 77−6765
CD, Λ-type doubling in excited rot. levels 77−57979
CH, interstellar excitation temps. and abundance rel. to H_2CO 79−48883
CH, Λ-type doubling in excited rot. levels 77−57979
$CH_3C^{15}N$, rot. relax. time meas., self- and foreign-gas collisions, Stark-switched microwave, obs. 79−86048
CSFCl, vibr. excited states, microwave spectra *(German)* 78−55167
C_3O_2, vibr.-rot. band, microwave, spectrum obs. 80−5536
^{13}CH, predicted Λ-doubling spectrum 77−30857
chloromethane, collisional rot.-line widths and shifts, microwave region 78−25619
$Fe(CO)_5$, microwave dielec. relax., fluxional mechanism 78−94235
HF-cyanomethane, microwave spectroscopic investigations of hydrogen-bonded complexes 78−62794
HNCS, a-type rot. spectrum in excited bending vibr. states 79−3437
OCS, collisional rot.-line widths and shifts, microwave region 78−25619
OCS+nonpolar perturbation, J=1→2 microwave line press. broadening 80−9644
cis-vinylisocyanate, dipole moment from microwave spectra 79−98078

radiofrequency and microwave spectra of polyatomic inorganic molecules *see also nuclear magnetic resonance; paramagnetic resonance*
atmospheric pollutants and constituents, microwave absorp. coeffs. 77−64378
atmospheric submillimetric-wave interferometric spectrometry 79−34979
collisional line broadening of microwave spectra, semiclassical theory 78−29776
gas microwave absorption Fourier spectrometer for 300 GHz to 1.2 THz 77−5935
interstellar molecular transitions, rest freqs. 80−62218
methylenimine, mol. struct., microwave spectra, isotope effects 77−61738
nonrigid molecules, rot.-vibr. study, rigid core with nearly-free atoms 78−62789
OCS, submillimetre rot. lines, press. shifts 80−23463
polyatomic mol. gas phase spectra, struct., review and tabulation 80−14136
symmetric top mol., overlapping press. broadening, nonreson. microwave absorpt. line radii 78−17662
water vapour, absorpt. at 7.1 cm^{-1}, temp. depend. 78−82722
Ar-O_3 Van der Waals complex, struct. and props., RF and microwave obs. 80−32704
$ArBF_3$, microwave spectrum and struct. 79−76420
$ArCO_2$, struct. determ. by mol. beam elec. reson. spectrosc. 79−64019
ArHBr, ArHCl, and isotopic forms, rot. spectra, mol. struct., mol. consts. 80−58246
Ar.HBr(DBr), van der Waals complexes, rot. spectra and struct. 80−48055
$AsBr_3$, microwave spectra, rot. consts., mol. struct. 77−3485
$AsCl_3$, 100 to 200 GHz spectra, mol. struct., harmonic force field 78−42042
AsF_3, millimetre rot. spectra, vibr. excited states, anharmonic force field 78−33502
AsH_3, forbidden millimetre-wave transitions 78−55165
$BClF_2$, microwave spectrum, struct., quadrupole coupling consts. 77−57986
BF_2CO, microwave spectrum and struct. 79−76420
BFHOH, transient mol. form., microwave spectroscopic obs. 78−74643
$BF(OH)_2$, identification, rot. and centrifugal consts., mol. struct., microwave spectra obs. 80−32705
BH_3CO, struct., quadrupole coupling consts., dipole moment, microwave spectra 77−54557
BH_2NH_2, microwave spectra, rot. consts., dipole moment, mol. struct. 79−85957
$BH(OH)_2$, transient mol. form., microwave spectroscopic obs. 78−74643
BrCN, pressure-broadened linewidths in microwave region, temp. depend. 77−34694

radiofrequency and microwave spectra of polyatomic inorganic molecules continued
$BrCN+N_2^*$, vibr. energy transfer, α_3 vibr.-rot. const., microwave meas. 77−83578
BrF_5, excited vibr. states, microwave spectrum, rot. const. determ. 78−94237
BrF_5, gas phase electron diffraction and microwave rot. consts. data anal., mol. struct. 79−76363
BrF_5, microwave spectrum, Coriolis interaction, A_1-A_2 splitting of kl levels 77−38657
CO-HBr, weakly bound, rot. spectra 80−91544
CO-HCl, weakly bound, rot. spectra 80−91544
CO-HF, weakly bound, rot. spectra 80−91544
CO_2, collision-induced absorpt. at 4.6 cm^{-1} 78−78679
$(CO)_2$, RF lab. meas. and interstellar search 80−43035
$COCl_2$, microwave spectra, 24-154 GHz, rot. and centrifugal distortion consts. 78−46324
$COCl_2$, phosgene, Cl_2 nuclear quadrupole coupling tensor, microwave spectra 80−52982
CSFCl, sextic centrifugal distortion consts., microwave spectra *(German)* 77−75140
ClBS, form., photoelectron and microwave spectra 78−90214
$ClCN+N_2^*$, vibr. energy transfer, α_3 vibr.-rot. const., microwave meas. 77−83578
ClF_5, microwave spectrum, rot. transitions, dipole moment, struct., nuclear quadrupole coupling consts. 77−14423
$ClNO_3$, microwave spectrum 77−57984
cis-ClONO, microwave spectrum, rot. consts., inertial defects and config. 79−59439
$ClONO_2$, laboratory microwave spectrum, atm. chem. appl. 77−6760
CsOH, quadrupole hyperfine struct., Δ-level splitting, microwave spectra 77−88446
DN_3, microwave spectra, 8-340 GHz, spectrosc. consts. for ^{13}N isotope 79−85958
DNC in HNC interstellar clouds, temp. effects and D fractionation 79−44578
DNCS, ground state spectroscopic constants and elec. dipole moment, from microwave and millimetre wave spectra 79−804
D_2O, isotopic species, far IR spectra, assignments, moments 77−6761
D_2O, sub mm beam maser spectrum, D hyperfine splitting 77−61874
FCN, in interstellar mol. clouds, search for J=2-1 transition 77−60808
FCP, microwave spectrum, struct., dipole moment and vibr.-rot. props. obs. 80−91549
GeH_4, microwave spectra of Q-branch, rot. consts. 79−54845
GeH_3NCS, mol., IR, Raman and microwave spectra, $^{70,72,74}Ge$ and $^{1,2}H$ isotopes 79−89663
HCN 88.6 GHz transition obs. in galaxy 79−44582
HCN and HNC, mm wave emission obs. of interstellar clouds 80−90503
HCN, and isotopic forms, l-type doublet transitions 79−13704
HCN, and stable isotopic species, mol. struct., ground vibr. rot. transitions and consts. 77−10666
HCN, J=1-0 transition obs. in southern interstellar mol. clouds 79−8983
HCN, laser plasma, microwave spectra of excited vibr. states 78−17656
HCN laser processes, mm. and submm. microwave spectroscopy 78−13685
HCN, microwave-microwave double resonance 80−53029
HCN, search for maser emission in C stars 80−51856
HCN^+, interstellar, rot. transitions rest. freqs. and radio search 78−24534
$HC^{14,13}N$ dimer, and $(DCN)_2$, microwave rot. spectrum identification and struct. 77−50427
HCN-HF, dimer, rot. transition intensity, dissoc. energy determ. 78−46323
HCN-HF, elect. dipole moment, Stark effect of linear mols. 78−70818
HCN+HCN, collisional line broadening of microwave spectra, semiclassical theory, calcs. 78−25516
$(HCN)_2$, and isotopic forms, microwave spectroscopic investigations of hydrogen-bonded complexes 78−62794
HCN...HF, hydrogen bonded heterodimer, spectroscopic consts. from microwave spectrum 80−43037
HCO, microwave spectra, hyperfine struct. 77−75139
HCO^+ 89.2 GHz transition obs. in galaxies 79−44582
HCO^+ isotopes, interstellar anomalous line intensities towards dark clouds 79−17054
$HCO^+ + H_2$, J=0-1 transition press. broadening, microwave absorpt. 80−52981
HDO, T_1 and T_2 relax. cross sections meas. 77−34733
HF-ClF complex, and isotopic forms., mol. beam elec. reson. spectra, config., bonding, spectroscopic consts. 77−30860
HF-HCN, microwave spectroscopic investigations of hydrogen-bonded complexes 78−62794
HF-HCl, H bonding , struct., mol. beam-elec. reson. spectra 78−29777
HNC, and stable isotopic species, mol. struct., ground vibr. rot. transitions and consts. 77−10666
HNC, millimetre spectrum, rot. consts., force consts., U90.7 interstellar line, struct. parameters 77−57989
HNC^+, interstellar, rot. transitions rest freqs. and radio search 78−24534
$HN^{13}C$ and HNC, hyperfine structure in dark interstellar clouds 79−101182
$H^{15}NC$, J=1→0 transition, freq. meas. and interstellar detect. 77−82299
HNCO, a-type rot. spectrum in excited bending states, rot. consts. 78−21915
HNCO, microwave and RF spectra, b-type rot. transitions 78−21914
HNCS, ground state spectroscopic const., microwave, millimeter and IR spectra 80−28010
HNCS, microwave spectrum, K_a=0 and 1 rot. levels inversion 77−38656
HNCS, microwave transitions 78−9143
HNCSe, struct., microwave spectrum 79−18178
HNO_3, centrifugal perturbation in microwave spectrum 77−57981
HNO_3, microwave spectra, centrifugal distortion effect 77−34621
HNSO, centrifugal distortion anal. 79−59438
HNSi, structures and microwave freqs. calcs. rel. to interstellar emission lines 78−36648
HO_2 free radical, dipole moments and Stark effects from microwave spectra 80−63623
HO_2 radical, microwave spectrum 77−57983

radiofrequency and microwave spectra of polyatomic inorganic molecules continued
H_2O 22 GHz maser emission from W3(OH), 49N and 51, spatial distrib. 78−93355
H_2O, 22 GHz rot. transition relax. rate consts. 79−18180
H_2O dimer, partially deuterated, microwave spectra and struct. 80−74212
H_2O emission detection in galaxy NGC 253 at 22.235 GHz 78−16534
H_2O gas submillimetric high-resolution Fourier transform spectra 79−31509
H_2O, isotopic species, far IR spectra, assignments, moments 77−6761
H_2O, maser emission from OH/IR sources 78−16432
H_2O, maser emission from stellar sources, bright IR star monitoring at 2.7 μm 78−16433
H_2O maser emission from supergiant star S Persei, 22 GHz variability 78−49461
H_2O maser emission from W51 Main 80−8701
H_2O maser line evidence for circumstellar ring systems in supergiant stars 78−89195
H_2O mesospheric vapour line at 22.2351 GHz, hyperfine structure 79−8666
H_2O, microwave absorption, spectral line press. broadening theory 77−30864
H_2O^+, electronic spectrum, predicted IR and microwave lines, comet tail bands 77−473
H_2O-HF, microwave spectroscopic investigations of hydrogen-bonded complexes 78−62794
H_2O-HF heterodimer, H bonding, microwave rot. spectrum, mol. geometry and moment 80−99501
$(H_2O)_2$, struct. from mol. beam elec. reson. spectra 77−54555
$(H_2O)_3$, electric-dipole selection rules 77−54549
H_2S dipole moments, submillimetric Stark cell meas. 77−38694
H_2S, rot. transitions, press. broadening, microwave spectra 77−50429
HSiN, structures and microwave freqs. calcs. rel. to interstellar emission lines 78−36648
$HSiO^+$, $HOSi^+$, rot. consts. and rot. transition freqs. 78−37541
H_2Te, mol., submm. rot. microwave spectrum 79−59443
ICN, microwave spectrum, mag. hyperfine struct., I nucl. shielding tensor 78−17661
ICN, microwave spectrum, vibr.-rot. const., equilib. struct. 78−58677
IF_5, microwave spectra obs., rot. assignments, mol. parameters *(French)* 78−55163
KOD, mm wave spectrum, rot. transitions in excited vibr. states 77−3351
KOH, mm wave spectrum, rot. transitions in excited vibr. states 77−3351
KOH, quadrupole hyperfine struct., Δ-level splitting, microwave spectra 77−88446
KrHBr, KrCHl, and isotopic forms, rot. spectra, mol. struct., mol. consts. 80−58246
KrHCl, van der Waals complex, prod. and rot. spectra assignments 80−5532
KrHCl, van der Waals complexes, struct., RF and microwave spectra, isotope effects 80−37806
KrHCl, weak complex, rot. spectra 80−52980
N_2, collision-induced absorpt. at 4.6 cm^{-1} 78−78679
N_3, spectroscopic data review 77−38680
N_2BF_3, microwave spectrum and struct. 79−76420
ND_3, sub mm beam maser spectrum, D hyperfine splitting 77−61874
N_2D^+, lab. rest frequencies 78−1102
N_2D_4, ^{14}N quadrupole coupling consts., inversion barrier, microwave spectrum 77−54556
N_2D_4, microwave spectrum, barrier to inversion determ. 78−62793
N_2F_4, centrifugal distortion effect in microwave rot. spectrum 77−30859
NF_2H, centrifugal distortion anal., microwave rot. spectrum 78−58650
NH_3, dynamic Stark shift, microwave obs. 79−72352
NH_3 in interstellar dark clouds, hyperfine struct. 77−78852
NH_3 in Taurus dark cloud, mag. hyperfine struct. rel. to gas temp. and motion 77−78851
NH_3, interstellar, nonmetastable levels obs. 79−25665
NH_3, interstellar emission line in Orion, 23 GHz obs. 79−30109
NH_3 inverscon lines from nonmetastable rotational levels, SHF obs. of Kleinmann-Low nebula 80−73016
NH_3, inversion splitting calc., variable pot. barrier 79−18177
NH_3, linewidth parameter $\Delta\nu/p$ for the J=13, K=13 inversion line *(French)* 78−42131
NH_3, magnetic relaxation rates for microwave spectrum and contributions to linewidth 80−5564
NH_3, microwave spectrum, width and shift parameters 77−18985
NH_3, microwave-microwave double resonance 80−53029
NH_3, mol. beam state selection and focusing, hyperfine spectrum 80−28119
NH_3, non-metastable absorption at 23.1 GHz, first obs. towards compact H II region W3 (OH) 78−65677
NH_3, press. shift of inversion lines 79−31615
$^{14}NH_3$, $^{15}NH_3$, submm-wave rot.-inversion transition, ν_2 state 77−75138
$^{14}NH_3$, inversion spectrum 79−3438
$^{14}NH_3$, J=13, K=13 inversion line displacement as function of pressure *(French)* 78−70815
$^{15}NH_3$, inversion doublets, T_1 and T_2 M depend. 78−13489
NH_3+H_2, NH_3 inversion transition, linewidths and T_1/T_2 ratio 80−99499
NHD, rotational transitions, microwave optical double resonance obs. 80−58293
NO_2, rot. spectra at 93 GHz, press. broadened hyperfine multiplet 78−90156
NO_2^-, microwave transition probability in zero field, spin-orbit interaction 78−25518
N_2O, submillimetre rot. lines, press. shifts 80−23463
N_2O submillimetric high-resolution Fourier transform spectra 79−31509
N_2O, submm wave spectra, 375-565 GHz, isotopic species, mol. consts. 77−3346
$^{14}N_2{}^{16}O$, elec. and mag. props., hyperfine struct., mol. beam elec. reson. obs. 78−62792
NOCN, struct., dipole moment, quadrupole coupling, microwave spectra 78−94238
NSF_3, microwave spectra in vibr. excited states, mol. consts. 79−50009
NSF_3, RF-mm wave double reson. of vibr. excited state 79−50054
$^{15}NH_3$, interstellar detection at 23 GHz 79−44590
$^{15}NH_3$, T_2/T_1 determ. for inversion transitions, power-broadened line shape 77−38654

radiofrequency and microwave spectra of polyatomic inorganic molecules continued
O_3, (010) and (020) states, 14 μm diode laser spectra, assignments 79−98079
O_3, and isotopic substitutions, rot. spectra calcs. 77−38659*
O_3, IR and microwave spectra, ν_3 vibr.-rot. band 77−38663
O_3, microwave and IR spectra, ν_2 state, $(\nu_3+\nu_2)-\nu_2$ band, 10 micron lines 78−82718
O_3, mol. beam electric resonance, electric and mag. props. determ. 77−27055
OCS interstellar transition in Orion, shock chemistry 79−21391
OCS, MM wave spectrum, centrifugal distortion const. 77−34618
OCS, microwave rot. lines, self-broadening 78−58668
OCS, microwave rot. transitions, phase shift effect, collisional effects 79−98073
OCS, microwave spectrum, width and shift parameters 77−18985
OCS, microwave spectra, rot. Q-band *(Polish)* 78−29866
OCS, microwave spectral lineshape of J 1→2 line 79−68225
OCS, microwave spectra, Ku-band Fourier transform spectrometer appl. 80−68265
OCS, microwave-microwave double resonance 80−53029
OCS, millimeter wave rot. spectra, isotope shifts, freqs. and mol. consts. 80−78611
OCS, pressure-broadened linewidths in microwave region, temp. depend. 77−34694
OCS, T_2 relax. meas. using budge-type superhet. microwave spectrometer 80−91551
OCS+CO_2, collisional line broadening of microwave spectra, semiclassical theory 78−29776
OCS+CO_2(H$_2$)(N$_2$)(OCS), collisional line broadening of microwave spectra, semiclassical theory, calcs. 78−25516
OCS+$H_2(CO_2)$(fluoromethane) rot. relax. parameters, microwave spectra linewidth parameters 80−28009
OCS+N_2* 80−48063
OCSe, isotopic species, microwave and IR spectra 77−38658
OH, maser emission from stellar sources, bright IR star monitoring at 2.7 μm 78−16433
ON^{81}Br, anharmonic force field from IR and microwave data 78−82809
ON^{35}Cl, anharmonic force field from IR and microwave data 78−82809
OPF_3, distortion moment microwave obs., rot. consts., mol. config. 77−50426
$^{16}OPF_3$, microwave centrifugal distortion moment spectrum 78−78684
OSC, N_2O, submillimetre rot. lines, press. shifts 80−23463
$^{16}O_3$ and ^{18}O isotopic species, rot. spectra 18 to 382 GHz, force and Coriolis coupling consts. 77−75137
$P^{35}Cl_3$, microwave, rotational spectra, excited vibrational states 79−98080
PD_3, forbidden rot. spectra, spectal consts., bond lengths and angles 77−83581
PF_3, anharmonic force field from mm wave spectra of vibr. excited states 79−13701
PF_3, microwave l-type reson. transitions in v_4=1 state 77−57988
PH_3, forbidden rot. spectra, spectal consts., bond lengths and angles 77−83581
PH_3, millimeter spectra, ν_2=1, ν_4=1 excited vibr. states, J=0→1 rot. transition 79−6936
RbOH, quadrupole hyperfine struct., Δ-level splitting, microwave spectra 77−88446
$S_2{}^{35}Cl_2$, microwave spectra and double reson., assignments, distortion consts. and struct. 79−89664
SCl_2, microwave spectrum, quadratic pot. function, average struct. 77−65456
SF_2, microwave spectrum inertia defects, ν_1, ν_3, ν_2, equilibrium structure, vibration rotation constants, anharmonic potential functions 79−93988
SF_6, microwave absorpt. 2.3 cm^{-1} region 77−46557
SF_5Cl, pure rot. spectra, 300 GHz, isotope effects 80−5533
SO_2, microwave spectra, Ku-band Fourier transform spectrometer appl. 80−68265
SO_2, T_2 relax. meas. using budge-type superhet. microwave spectrometer 80−91551
SO_2, T_2 relax. time meas. by microwave transient nutation 77−30862
SO_2, T_2-relax., rot. transitions, time resolved spectra, microwave pulsed spectrometer study 80−18846
SO_2-H_2O microwave absorption, 94 GHz by mol. interaction 79−31507
$SO_2+H_2O(N_2)(SO_2)$, linewidths, intensities, isotope shifts, 91.5-95.5 GHz 78−42044
SPF_3, isotopic forms, microwave spectra, centrifugal distortion consts., vibr. and rot. states, IR matrix spectra 77−10665
$^{32}SF_5{}^{35}Cl$, microwave rot. spectra, mol. parameters *(French)* 77−456
SiD_3F, microwave spectrum, rot.-vibr. interaction consts., Coriolis reson., E1 moment 77−6766
SiH, rot. transition freqs. calc., rel. to search in interstellar space 78−93100
SiH^+, rot. transition freqs. calc., rel. to search in interstellar space 78−93100
$SiH_3{}^{81}Br$, high resolution rot. microwave spectrum, 8-40 GHz, mol. consts. 78−21916
SiH_2DF, $SiHD_2F$, microwave spectra, harmonic force field, mol. struct. 77−18913
SiH_3F, microwave spectrum, rot.-vibr. interaction consts., Coriolis reson., E1 moment 77−6766
SiH_3NCS, microwave spectrum, mol. consts., isotope effects 77−46559
SiH_3NCS, microwave spectrum, struct., dipole moment, ^{14}N quadrupole coupling const. 77−46560
SiH_3NCS, microwave spectrum, rot. Zeeman effects 79−54847
$(SiH_3)_2S$, rot. consts., internal rot. parameters, anal. of microwave spectra 78−46316
$(SiH_3)_2S$, microwave spectrum, r_0-struct., elec. dipole moment, internal rot. barrier 79−3439
SiO, maser emission from stellar sources, bright IR star monitoring at 2.7 μm 78−16433
XeHCl, microwave and RF spectra, mol. beam elec. reson. meas. 79−72302

radiofrequency cosmic radiation
see also pulsars; quasars; radioastronomy
3K background, Large Numbers Hypothesis and scale-covariant cosmology 78−93480
3K background, rel. to Dirac cosmology 77−22334
3K blackbody cosmic background radiation meas. 77−41422

radiofrequency cosmic radiation continued
21 cm emission from non-uniform gas at high z, spectral freq. struct. 79−92898
30 MHz all-sky map, galactic features study 79−21469
absolute motion of Earth rel. to relict radiation *(Czech)* 80−31394
airborne 33 GHz radiometer system for 3K background anisotropy mapping 78−61735
anisotropy on large angular scale 80−105407
automated system for detect. of cosmic radio bursts at VHF and UHF 78−77489
background, microwave emission spectra 79−48967
background 2.7K radiation coherence rel. to black body 79−97108
background 3K radiation, cosmological implications 79−97117
background anisotropy, galactic dust emission 80−77524
background meas. with Cosmic Background Explorer, satellite instrumentation 80−61988
background microwave radiation, cosmological explanation *(Polish)* 80−41920
background radiation, ang. momentum 79−80374
background radiation, meas. at 2 mm *(French)* 77−13503
background radiation, ray aberration large-scale anisotropy 78−24576
background radiation, vars. in freq. spectrum along declination (+50° 30′) 77−17723
background radiation fluctuations at 1394 MHz 79−53941
background radiation fluctuations produced by evolving hierarchical cosmologies 80−101655
background radiation nonequilib. distrib., radiation flux spectrum source 80−46710
background spectrum, cosmological significance of obs. *(Italian)* 79−48972
background spectrum meas. in near-mm region 80−62327
black body radiation meas. using low temp. optical techniques, 2-40 cm^{-1} 79−71161
blackbody radiation at 3.2 cm wavelength, linear polarization 79−97106
clusters of galaxies, gas content meas. by obs. of microwave background at 10.6 GHz 78−96551
cosmic background radiation, isotropy and Planck spectrum rel. to generalised cosmological principle, in Newtonian and relativistic theories *(Polish)* 80−27025
cosmic blackbody radiation, anisotropy detect. 78−4415
cosmic microwave background, pregalactic fluctuations visibility and upper limit on q_0 80−8717
cosmic microwave background, Sunyaev-Zel'dovich effect in millimetric region 79−25765
cosmic microwave background, temp. diminution distrib. by Coma cluster X-ray source 79−92896
cosmic microwave background, translational anisotropy and galactic dust clouds far IR emission 77−33706
cosmic microwave background, ultrahigh energy electrons and photons penetration distance 79−5742
cosmic microwave background isotropy, role of asymptotic freedom in early big bang 80−46712
cosmic microwave background radiation, polarisation in anisotropic universe 80−82552
cosmic microwave background spectrum, distortion by intercluster medium 80−4426
cosmic radio bursts with microsecond time scales, limits 79−17119
cosmological background radiation *(Italian)* 79−48966
cosmological constant, broken gauge theories and 3K black-body radiation 78−28870
cosmological microwave black body radiation spectrum, implications for Population III stars 80−67915
deflection by Sun, General Relativity test 77−70994
detection, identification and properties, review 79−97109
detection in 1932, Jansky's original data 79−17144
discovery of microwave background, history 80−57074
double radio sources, struct. and evolution, plasma and twin exhaust models *(Chinese)* 79−40284
dust in clusters of galaxies, IR and radio radiation *(Russian)* 79−21449
EAS radio emission, electric field strength *(Russian)* 78−93061
EAS radio emission spectra, Cherenkov and synchrotron radiation mechanisms 77−64566
electron spectrum determ. from galactic radio background 78−93056
fine-scale anisotropy of microwave background, long-wavelength gravitational wave effects 78−81535
G-varying cosmology, thermodynamic relations and 3K background radiation 80−56979
galactic, nonthermal emission in 0.25-9.18 MHz range, RAE 2 lunar satellite obs. 78−45398
galactic 21 cm line obs. in 348°≤l≤360°, −22°≤b≤−1° region 77−60824
galactic background, linear polarisation between 408 and 1411 MHz, reductions 77−2500
galactic background radio emission fine struct. correl. with discrete radio-sources 79−21457
galactic centre direction, H200β line detect. 77−78868
galactic diffuse background, distrib. and model 77−5602
galactic disc emission at 4 cm wavelength, large-scale and small-scale cloud structs. 78−28795
galactic equator, H I recomb. line emission, 408 MHz obs. 77−13451
galactic H I 21 cm line obs. for southern hemisphere 80−85987
galactic halo low-frequency radio emission, diffusion models 78−12433
galactic LF background radiation, spectra and absorpt. 77−33707
galactic non-thermal radio radiation from polar regions, spectra 80−22082
galactic nonthermal emission, rel. to cosmic ray electron distrib. 77−33299
galactic nonthermal radio spectrum, rel. to cosmic ray electrons spectrum and gamma-rays prod. 80−62257
galactic radiation, distributed, linear polarization obs. results processing optimal algorithm selection *(Russian)* 77−91441
galactic radiation belts, trapped electrons as radiowave source 80−26982
galactic radio emission, rel. to interstellar gas hydrostatic equilib. and cosmic ray confinement 77−29919
galactic radio emissivity, three-dimens. model 78−77604
galactic radio spectrum, influence of primordial black holes 80−62179
galactic synchrotron radiation, distrib. from cosmic ray electrons propag. diffusion model 79−53679
galactic synchrotron radiation, rel. to cosmic ray electrons source spectrum and diffusion 79−53677

radiofrequency cosmic radiation continued
galactic synchrotron radiation, rel. to mag. field configurations 78−20884
galactic synchrotron radio emission, rel. to Galaxy cosmic rays and mag. field distrib. 80−4207
Galaxy, radio-emitting electrons and cosmic ray confinement 77−73910
Galaxy, synchrotron radiation in inhomogeneous mag. field 77−67127
Galaxy radio halo, implications for cosmic rays origin 79−44314
gravitational cyclotron instability, mechanism for cosmic radio emission 78−65724
homogeneous cosmologies, dipole and quadrupole anisotropies 80−109572
intergalactic graphite whiskers, RF adsorpt. props. rel. to microwave background radiation 80−31357
interstellar medium, radio emission at l=31.2° and (31.9°) 77−17724
inverse-Compton emission from radiosource electrons and microwave background photons, prospects for X-ray detect. 79−71144
ionosphere radionoise absorpt., impulsive quasi-periodic variations 80−105116
IR limit on fine-scale anisotropy 78−28863
isotropy of relict radiation, coherence of Universe *(Russian)* 79−85024
linear polarisation measurement, VHF/UHF irradiators with polarisation switching *(Russian)* 77−22090
longitudinal relict radiation, from photons condensation in hot Universe *(Russian)* 78−65734
Loop III, linear polarization of 920 MHz galactic background 79−97087
magnetosphere cosmic noise absorption during substorms 80−72727
microwave 3K background, in Hoyle-Narlikar conformal gravitation theory 80−56698
microwave background, anisotropy rel. to early universe density-temp. fluctuations observability 80−82554
microwave background, Compton drag rel. to pregalactic evolution 79−92863
microwave background, contrib. of Hawking process in steady state universe 79−80380
microwave background, diminution towards X-ray clusters of galaxies rel. to ionised gas limits 78−89243
microwave background, effects of unborn clusters of galaxies 78−8131
microwave background, flux rel. to metagalactic diffuse IR radiation 77−29964
microwave background, generation by intergalactic pyrolitic graphite whiskers 80−94866
microwave background, generation in tepid early universe 78−20919
3K microwave background, in Universe expansion model 80−98746
microwave background, influence on interstellar clouds radio spectral lines widths 79−12398
microwave background, no anisotropies at 31 GHz 80−51922
microwave background, pseudoscalar bosons rule *(French)* 79−44361
microwave background, rel. to cosmology and element origin 80−62359
microwave background, rel. to Dirac cosmology 78−8176
microwave background, residual fluctuations, gravitational effects 80−62332
microwave background, review 80−62336
microwave background, search for temp. change produced by ionised gas in clusters of galaxies 80−82477
microwave background, temp. dips due to X-ray clusters of galaxies from sources large-scale struct. 80−82524
microwave background, universal anisotropy limits and He production 78−36737
microwave background, upper limit to temp. fluctuations at 4.755 GHz 80−98577
microwave background, Zel'dovich effect rel. to intergalactic dust in galaxy clusters 78−54041
microwave background angular distrib., large scale fluctuations 80−62328
microwave background angular distrib., small scale fluctuations 80−62329
microwave background anisotropy rel. to Friedmann universe long wavelength perturbs. 79−21478
microwave background at z=40, transparency of dust grains 78−28869
microwave background dipole anisotropy, dynamical inferences 80−62330
microwave background distortion by hot intergalactic medium 79−97107
microwave background distortions in baryon-symmetric cosmologies 78−65727
microwave background fluctuations, recombination epoch effects 80−62333
microwave background fluctuations, search for Universe primeval perturbs. *(Russian)* 78−36734
microwave background fluctuations, universal anisotropy and gravit. waves 78−28866
microwave background fluctuations due to intergalactic gas secondary ionization *(Russian)* 78−36736
microwave background fluctuations rel. to galaxy and cluster formation 78−28865
microwave background fluctuations rel. to Universe entropy perturbs. *(Russian)* 78−36735
microwave background in Bianchi type V universe 80−98744
microwave background in direction of clusters of galaxies *(Russian)* 80−94899
microwave background intensity and velocity meas. of clusters of galaxies 80−46686
microwave background obs. in direction of clusters of galaxies, cool ionized gas mass limit 78−41098
microwave background radiation, anisotropy meas. 80−41918
microwave background radiation, Compton scatt. by gas in galaxy clusters 78−24575
microwave background radiation, influence of observed spectrum on interstellar formaldehyde excitation 80−36681
microwave background radiation, search for linear polarisation 79−21470
microwave background radiation, temp. and spectrum rel. to universe origin 79−25770
microwave background radiation density, accreting blackholes contrib. 80−4461
microwave background radiation fluctuations, in adiabatic and entropic theories of galaxy form. 79−62942
microwave background radiation isotropy and spectral distrib. as test of Dirac cosmologies 78−49570
microwave background radiation large-scale anisotropy meas. 80−8718
microwave background radiation rel. to big bang cosmologies 77−49508
radiofrequency cosmic radiation continued
microwave background radiation spectrum, effect of interstellar dust and molecules *(Russian)* 80−8719
microwave background radiation spectrum, statistical anal. of data 78−86039
microwave background radiation spectrum deform. by lasting recomb. 77−9824
microwave background rel. to big bang cosmology 77−9830
microwave background small-scale fluctuations, consequences of neutrino rest mass *(Russian)* 80−109576
microwave background spectrum, distortion by pregalactic dust 80−67916
microwave background spectrum, survey of results 78−28864
microwave background spectrum 80−105406
microwave background spectrum and G-varying cosmology 80−86020
microwave background spectrum and isotropy rel. to cosmic turbulence 80−98747
microwave background spectrum distortion by dust 80−27022
microwave background temp. fluctuation, constraints on primordial evolution in hot Universe 80−105411
microwave pulsed emission upper limit for supernovae in clusters of galaxies 78−69890
millimetre obs., calibration, effect of Earth's atmosphere, two-layer model 78−53691
millimetre region cosmic background radiation, large scale anisotropy meas. 80−82553
monopulse signals, omnidirectional search, probable origin 78−24563
noise absorption events meas. on riometers, due to backscatt. by E-region irregularities 77−25831
nonthermal galactic radio background rel. to secondary electrons and positrons in interstellar clouds 78−49527
photon-tachyon interactions and the isotropic photon flux 80−446
pioneering work by Jansky, and Penzias and Wilson 79−44655
Planck's constant cosmological var. upper limit from microwave background radiation spectrum 78−12434
polarisation, anisotropic cosmological expansion 78−73778
polarisation of microwave background radiation, IR survey 78−73779
pregalactic microwave background, origin 78−86040
primordial background radiation, temp. fluctuations due to gravit. waves 78−65728
primordial microwave radiation, recomb. lines calc. 78−54097
QCD black body radiation, big bang universe hadron era 80−62341
recombination line obs., review *(Russian)* 77−57080
recombination lines from H^+ regions, interstellar clouds, planetary nebulae, b_n factors computation 77−64832
relic radiation, as possible product of quantum era in universe expansion *(Russian)* 78−81717
relict black-body radiation temp. fluctuations prod. by cosmological turbulence *(Russian, English)* 78−77630
relict radiation in anisotropic universe, polarisation and anisotropy 80−67917
relict radiation temp. fluctuations rel. to universal structure evolution 80−105360
review, cosmic gamma radiation, sources and detection 78−12059
scattering of microwave background in clusters of galaxies, 9 mm obs. 80−105366
scattering of microwave background radiation in clusters of galaxies 80−105367
spectral distortions in microwave background longward of 3 mm 80−62326
spectral lines of prestellar origin, prediction in cosmic relic radiation *(Russian)* 78−77628
spectrum distortions in background 80−62334
sudden cosmic noise absorpt., solar Zenith angle depend. 78−12047
Sunyaev-Zeldovich effect at 9 mm wavelength 80−41919
universal microwave radiation and extragalactic γ radiation 80−22121
universe with variable G and c, initial conditions 79−48977
H56α radio recomb. line anomalous emission from galactic plane 79−80361

radiofrequency filters
frequency to voltage convertor using SAW linear FM chirp filter 80−19182
SAW filters, low insertion loss, using multiphased unidirectional transducers 80−28397
SAW TV IF filter, temp. stable ZnO/Pyrex glass substrate 80−43566
VHF SAW delay line filters, wideband, low insertion loss 80−28398

radiofrequency heaters *see radiofrequency heating*

radiofrequency heating
27.12 MHz selective heating of cutaneous tumours 78−24179
baking yeasts, survival rate, obs. *(Russian)* 79−2100
biological effects and dosimetric data useful for RF safety standards development, review 80−67154
biological effects of radiowaves and microwaves 80−98011
biological models, induction of focal hyperthermia by RF radiation and EM fields 78−40244
biological specimens, meas. of power absorpt., 10 to 100 MHz 77−90916
biomedical microwave hyperthermia treatment and thermometry system 80−72280
brain tumour destruction by 8 MHz implanted metal powder eddy currents *(German)* 79−16337
brain tumour therapy by RF field controlled temp. gradients 77−25522
breast cancers, microwave irradiation, EM energy and temp. distrib., numerical calculations 79−100697
calorimetric measurements of microwave energy absorption. of mice, equipment and obs. 80−55996
cancer therapy, invasive microwave system localised hyperthermia 79−100700
cancer therapy, review of 4 years use of microwaves 80−56162
cancer treatment appl. of microwave arrays for localised tumour heating 80−94308
cancer treatment by local microwave hyperthermia system 79−83893
choke-earthed surgical diathermy circuit analysis 79−20705
combined microwave heating and radiometry methods 80−85465
conformal applicators, therapeutic potential for hyperthermia induction 79−100696
corneal curvature alteration appl. 77−40665
corrosive liquid flowmeter with UHF heater *(Russian)* 78−59523
cranial structure exposed to RF radiation, thermal response model 80−94285

radiofrequency heating continued
cutaneous human tumours, selective RF heating at 27.12 MHz 79−2123
cylindrical component temperature field computation for quench control 78−90632
defective dielectrics, EM heating with time depend. param., WKB calcs. 80−71367
diathermic heating, 27.12 SW, biological effect in expt. tumours 79−2102
diathermy, shortwave and microwave, for deep-tissue heating 80−17050
diathermy 2.45 GHz microwave direct-contact applicator 79−2122
diathermy 915 MHz microwave applicator for deep tissues in humans 79−2121
diathermy 915 MHz microwave direct-contact applicator for tissues 79−2120
diathermy applicator for irrad. of rat brain 80−94425
diathermy equipment and power indicator 77−40901
dielectric, heating by high-power EM fields 77−14640
dosimetric measurements of far-fields in full-scale man model 80−67255
effects of microwave energy on Acacia longifolia 79−53190
electrosurgical instrumentation review 78−44680
energy deposition in simulated human operators of 800-MHz portable transmitters 79−8525
eye lens thermal stresses induced by microwaves 78−80914
fibreglass/epoxy laminate curing by microwave heating 77−77457
furnace, electric with RF coil, for NMR measurements up to 2000K 79−63214
furnace with RF coil, high temperature ^{1}H NMR probe 79−49234
fusion plasma *(Japanese)* 80−92338
fusion reactor, ELMO Bumpy Torus, microwave coupling 80−99328
fusion reactor, ISX-B, electron cyclotron microwave heating 80−99329
fusion reactor, TNS, electron cyclotron heating startup system, design 80−99330
geophysical research appl. of microwaves, oil composition analysis by means of cracking, permittivity thermal dependences obs. *(Czech)* 80−46289
glioma cells, cultured, influence of microwave irradiation 79−100661
heat potential distrib. in cranial structure model exposed to microwaves 79−2105
HF tumor therapy, slotted cylinder antenna for selective heating inside human body 79−34629
hyperthermia, deep local, induction by US and EM fields, problems and choices 80−94283
hyperthermia, localised, comparison of EM and US diathermy 80−104725
hyperthermia by local EM heating and conductivity change, cancer treatment appl. 77−86578
hyperthermia dosage definition form in vitro thermal cytotoxicity data 78−24178
hyperthermia in tissue-like substances, EM and US induction 80−98012
hyperthermia induced by microwaves, dose definition 79−2135
hyperthermia induction in small animals using microwave system 79−2118
hyperthermia of expt. mouse cancers using 2450 MHz microwaves 79−2119
hyperthermia research with dual-beam microwave applicator 80−17052
hyperthermia techniques in cancer management, clinical appls. 78−44682
immune system, RF induced alterations due to hyperthermia, mouse obs. 80−35975
industrial and food processing appls., conf., London, England (Nov. 1979) 80−21520
ionosphere, heating by powerful radio emission with random modulation of carrier freq. 80−109310
ionosphere, heating due to parametrically excited Langmuir waves, short-scale field-aligned density striations form. 79−8766
ionosphere heating by radio waves, predictions for Arecibo and satellite power station 78−77403
ionosphere modification rel. to nightglow intensity vars. 78−77401
labelled microspheres, localised embedding by microwave heating of tissues of hypothermic dogs 80−61640
microstrip antenna for biomedical applications 80−89826
microstrip slot radiator for medical appls. 80−108994
microwave, alfalfa seed germination improvement 77−2023
microwave, effect on dog thyroid gland at 2.45 GHz 78−31854
microwave, treatment of cancer by hyperthermia 77−52859
microwave absorbing ferrite-dielectric composite 77−7880
microwave and HF thawing, of cryogenically preserved canine kidneys 77−5059
microwave and RF radiation protection, American and European standards 78−80973
microwave antenna, invasive, for locally-induced hyperthermia for cancer therapy 80−67193
microwave applicator, broad band, for heating tumours 80−30830
microwave bulk biomaterial thawing, electric field uniformity requirements *(Russian)* 79−83852
microwave diathermy, circularly polarised direct contact applicator design and performance 78−7531
microwave diathermy direct-contact applicators, comparative heating patterns 78−40286
microwave diathermy direct-contact circular aperture applicator with corrugated flange, design 80−67190
microwave enzyme inactivation system, electronic control to reduce dose variability 78−40285
microwave enzyme inactivation system with electronic dose control 77−81762
microwave heating combined with radiation therapy, skin and tumor thermal enhancement ratios 80−67192
microwave heating system for improving temperature uniformity in heated tissue 79−100795
microwave heating with mass transfer using Luikov's system equations 80−106715
microwave hyperthermia, 3000 MHz, tumour growth inhibition in mice 79−2101
microwave hyperthermia, localised, biomedical devices 80−104724
microwave hyperthermia applicators, development of 79−25059
microwave hyperthermia for hamster melanoma treatment expt. 77−77931
microwave induced hyperthermal therapy of tumours in mice, bolusing technique 77−77934
microwave induced hyperthermia in cancer treatment, apparatus and preliminary results 79−62296
radiofrequency heating continued
microwave induced thermal stresses, stomatal response of leaves 77−2021
microwave irrad., heat dissipation rate determ., mice 77−81472
microwave irradiated breast tumour thermal pattern calc. *(French)* 80−3759
microwave irradiation of dielectric, near-field theory 79−41288
microwave oven, Intern. Microwave Power Symposium, Minneapolis, Minn., USA May 1977 77−70492
microwave power absorption differences between normal and malignant tissue 80−104640
microwave power symposium, Monaco (1979) 80−3758
microwave radiation, 2450 MHz, and γ-radiation effects on flour beetle 79−2103
microwave radiation appls. in surgery and cancer therapy 79−5336
microwave radiation of biologically active microorganisms, coherent elec. vibrs. 79−2106
microwave radiation of Ehrlich ascites carcinoma cells, metabolism 79−2104
microwave surface wave plasma at atmospheric press. 79−50868
microwave system for controlled production of local tumour hyperthermia in animals 79−34624
microwave temperature-jump apparatus, with spectrophotometric detection, biological appl. 79−20733
microwave therapy, multimode square waveguide applicator 79−34630
microwave thermography and local heating by same system, clinical applications 79−100695
microwave transmission through normal and tumour cells, standing waves 79−2107
microwave whole-body dosimetry in small animals, effect of body mass and exposure geometry 78−40348
microwave-enhanced thermographic turnover detection, sweep-freq. illum. investigation 78−73194
microwave-induced chronotropic effects in isolated rat heart 78−69137
microwave-induced non linear thermoelastic vibrations of human eye lens 79−83853
microwaves, direct-contact heating of dielec. encapsulated mouse tumour using dual-beam TEM applicator 78−40245
microwaves, meas. of energy absorbed by biological systems by anal. of heating and cooling data 78−40343
microwaves, meas. of energy absorbed by biological systems by Dewar-flask calorimetry 78−40344
model mouse cancer response to 2.45 GHz free-field hyperthermia 79−70584
mouse foetal body weight effects of 148 MHz irradiation 80−3726
mouse lung tumour growth delay by bleomycin with 2.45 GHz local hyperthermia 79−83894
multibeam microwave therapy with computer control 80−3766
multiple murine tumours, simultaneous microwave irradiation bolusing technique 78−7422
neck node metastases, effectiveness of microwave hyperthermia combined with ionising radiation 80−94307
open-ended waveguide probe/applicator combination *(French)* 80−3820
paramagnetism of plasma in RF field 79−46490
plasma, magnetized rarefied 80−24195
plasma production appl. using surfatron 77−80321
prostate, dog, microwave localised heat treatment, new applicator 79−100698
radioresistant malignant tumours, HF hyperthermia and γ-rays therapy results 79−100699
rat embryo acute viral infection inhibition by whole-body microwave heating 80−3769
rat embryo localised microwave heating effect 80−3728
semiconductor, UHF heating of charge carriers using lumped-capacitance resonators 80−20203
skin, pig, combined effects of X-irrad. and microwave heating 80−94290
skin, pig, response to combined X-irrad. and microwave heating 80−61653
small-animal microwave induced hyperthermia development system 78−11715
sporadic-E layer inhomogeneous structure influence of RF heating *(Russian)* 78−61653
steel, C, hardened by HF current, mech. testing method 80−61053
thermographic observability of tumours with microwave heating 78−73193
tissue, microwave heating, effect of surface cooling and blood flow 78−57038
tissue heating system for hyperthermia research 80−30829
tissue microwave heating models, surface cooling and blood flow effects 78−7388
tissue microwave heating patterns in spherical models 77−86537
tissue-equivalent medium, heating patterns produced by 434 MHz Erbotherm UHF^{69} 80−98013
tumor irradiation using focused microwave array system, feasibility 79−100689
tumour eradication by RF diathermy 77−70516
tumour microwave heating for thermographic detection enhancement 79−2124
tumour microwave heating with automatic temperature control 77−77963
tumour oncolysis, mouse, local HF hyperthermia, X-irradiation and apathogenic clostridia 79−100662
tumours, solid, destruction by RF heating 80−61637
vasodilation, peripheral, induced in squirrel monkeys by microwaves 80−104682
VHF and UHF signals, biological tissue 77−73541
VHF radiowave induction heating of biological tissue from portable transmitter, expt. 78−57039
water, complex permittivity meas. and microwave heating for specific purities and salt. soln. 80−60480
Wega tokamak, HF heating at low hybrid freq. 77−76136
Al radioactive liquid waste calcination 77−81594
Ar inductively-coupled RF plasma torch, computer model 78−71559
C high-frequency of C, position regulator 79−80612
Fe-Ni-Mn, Invar, collapse and thermal effects, Mossbauer study 80−100624
Si monocrystal peripheral fusion channelling under HF heating *(Russian)* 80−59627

radiofrequency heating continued
Si solar cells, junction formation techniques using spray-on polymer dopants, cost effective, high throughput 80−94014
UO_2, UO_3, U_3O_8, microwave heating in nuclear fuel preparation 80−37556
radiofrequency interference
see also atmospherics; jamming; radar interference; whistlers
AC power line radio and TV interference control 77−75745
amplitude scintillations of radio beacon signals in equatorial electrojet region 77−29578
atmospheric noise data for tropical regions 80−61875
atmospheric noise field in VLF band, observation time limits *(Spanish)* 79−16758
automobile ignition RFI suppression at distributor rotor gap 79−55586
cardiac pacemaker RF susceptibility tests 78−48935
coherent radiation from modulated electron beam in residual gas 77−594
discharges for sputter deposition and sputter etching, RFI/EMI 78−71566
Doppler phase meas. of interfering reflections from interfering objects 79−81340
Earth-ionosphere waveguide channel parameters, influence of geomagnetic activity and statistical props. of VLF signals 79−88452
energy coupling into cylindrical enclosure 78−87000
ground wave atmospherics generated by lightning return strokes, initial peaks, model 80−61876
implanted cardiac pacemakers, microwave interference effects 79−92421
industrial RF heaters, measurements of elec. and mag. field strengths 80−52175
interplanetary scintillation meas. in conditions of strong radio interference 80−46413
ionospheric scintillation, model review 77−21995
isotropic RF electric/magnetic field strength meter, design 80−82751
LF band, noise field and skywave propag. 79−5708
magnetic field strength meter calibration system *(Polish)* 80−51311
medium wave broadcasting, interference fading *(Russian)* 79−40018
microwave power transmission from solar power satellite, environmental aspects 79−52896
million channel 300 MHz bandwidth digital spectrum analyser for Deep Space Network and SETI 78−73642
near-space radio noise environment characteristics and sources 78−89034
nuclear power plant equipment electromagnetic interference and RFI effects 80−57880
particle beam, RF fields due to Schottky noise 77−88632
radiotelescope observations, sporadic pulses originating in Earth's atmosphere *(Russian)* 78−24411
radiowave above uneven Earth's surface, field calc. 78−57275
screening enclosure for Coulter Counter, design and construction 79−96721
SEASAT-A satellite intersystem interference minimisation 78−49294
sweepers in HF and VHF bands 78−16231
thermal noise, zero point energy noise term presence 80−68213
tropospheric effects on radio communication, book 80−62400
UHF atmospherics, emissions from lightning discharge considered as plasma 78−61497
radiofrequency oscillators
butterfly, for detectors of NQR signals, 200 to 650 MHz 79−54163
limiting oscillator circuit for metallic NMR meas., with S/N improvement 79−26096
local oscillator system for λ 8-cm radioheliograph at Toyokawa, phase stability 79−101073
NMR detector, transistorised marginal oscillator, for student lab. 80−27078
radiofrequency spectra of diatomic inorganic molecules *see radiofrequency and microwave spectra of diatomic inorganic molecules*
radiofrequency spectra of inorganic solids
see also nuclear magnetic resonance; paramagnetic resonance
crystals, NMR quadrupolar effects, RF energy absorpt., relaxation times *(Russian)* 80−71235
oxide semiconducting glass, structural energy characteristics, rotational isomerism, mol. motion *(Russian)* 79−56602
B-C system, struct. of paramag. centres 80−20460
$CaF_2:Eu^{++}$, dielec. spectrum 77−36171
$CeVO_4$, monazite struct., IR and NMR spectra 79−78534
$CrBr_3$, HF spectra, susceptibility, spin waves in domain walls *(Russian)* 80−80909
$LaVO_4$, monazite struct., IR and NMR spectra 79−78534
$Li_{0.5}Fe_{2.5}O_4$, neutron-irrad., mag. spectra *(Russian)* 77−44092
$NdVO_4$, monazite struct., IR and NMR spectra 79−78534
$PrVO_4$, monazite struct., IR and NMR spectra 79−78534
radiofrequency spectra of organic molecules and substances *see radiofrequency and microwave spectra of organic molecules and substances*
radiofrequency spectra of polyatomic inorganic molecules *see radiofrequency and microwave spectra of polyatomic inorganic molecules*
radiofrequency spectrometers
see also magnetic resonance spectrometers
acousto-optical high-resolution radiospectrometer, mm wave astronomy appls. 78−4109
acousto-optical spectral analyser at RATAN-600 radio telescope, first test *(Russian)* 80−51668
deep level transient spectrometer, automatic calibration cct 80−37067
dielectric spectrometer for 20 Hz to 80 kHz range, automatic 77−13768
digital lock-in amplifier simulation 77−151
grating spectrometer for mm waves 78−12768
Jodrell Bank 1024 channel digital autocorrelation spectrometer 77−73970
magnetic field modulator, EPR radiospectrometer having discrete set of modulation frequencies 80−52285
magnetic flux stabiliser, resonance conditions stabilisation 80−52286
millimetre-wave astronomical, intensity calibration error evaluation 78−53821
NMR meas. of transient species and effects in flowing systems 77−150
NMR radio spectrometers, meas. of field uniformities in gap of precision magnets 80−105683
NMR radiospectrometer electromagnet field uniformity rel. to pole piece shape and material 78−86309
NMR radiospectrometers, calc. of optimal configuration of shims 80−73398
NMR spectrometers, SQUID-based, sensitivity limit 80−98961
NQR, pulsed panoramic spectrometer 77−10074
radiofrequency spectrometers continued
NQR, pulsed spectrometer for metre and decimetre ranges 77−10076
NQR coherent pulsed apparatus for studying hexamethylenetetramine complexes 77−10075
NQR temperature meas. and regulation system 77−10020
NQR thermometer, capture effect 77−10018
NQR thermometer, pulsed, for up to 870K 77−13749
NQR thermometer circuit 77−10019
NQR thermometer with high precision 77−10017
photoelectric spectrometer giving integrated parameters in real time *(French)* 78−53730
program controlled heterodynes for radiotelescope *(Russian)* 77−9659
pulsed NMR transmitter, for relaxation time meas. in biological samples, construction and operational details 78−93745
pulsed NQR-FFT radiofrequency spectrometer for ^{14}N, description and operation 80−17982
quasi-zero double-comparison spectrometer for 21 cm wavelength, UHF channel *(Russian)* 77−29658
radioastronomy, RATAN-600 radiotelescope, acousto-optic spectrograph 80−46398
radiotelescope RT-22, computer controlled receivers *(Russian)* 77−9674
RE-1306 radiospectrometer for crystals obs., using LF modulation of magnetic field 80−57350
resonator uniaxial crystal deformation unit 80−31822
RYa-2308 radiospectrometer, attachment for obs. of DNMR in ^{31}P 80−98957
solar radiospectrographs complex for frequency range 100-1000 MHz *(Russian)* 77−29648
spectrum analyser, 40-channel quartz filter *(Russian)* 77−22566
spectrum expander for multichannel filter spectromers 79−35790
superheterodyne mm wave spectrometers, intensity calibration 77−33353
superheterodyne UHF ESR spectrometer for 0.04-4.2K operation 78−257
Varytemp NMR for pulse spectrometers, applic. to lineshape determ. 77−2674
radiofrequency spectroscopy
see also magnetic resonance spectroscopy; nuclear magnetic resonance; radiofrequency spectrometers
air lubricated sample turbine for applications in solid body multipulse spectroscopy *(German)* 80−52284
antenna calibration, radioastronomical methods, standard sources *(Russian)* 78−4103
chemical exchanges, rate parameters, NMR determ. method *(French)* 77−21383
coupled spin systems, NMR correlation spectroscopy, interference effects 77−13789
dielectric relaxation spectroscopy, liquids, frequency and time domain expt. methods 80−40044
dielectric spectroscopy, combined total reflection-transmission method 78−86295
difference NMR spectroscopy, reference lineshape adjusted, expts. 78−17693
difference NMR spectroscopy, reference lineshape adjusted, theory 78−25561
dispersion-absorption plots, for spectral line shape anal. 78−89511
double-quantum saturation spectroscopy, laser and RF, appl. to H 80−77880
ENDOR, negative enhancement and phase shift 78−39445
EPR spectroscopy, absorption curve, spin concentration, numerical double integration, computer subtraction *(German)* 77−37954
EPR standard samples, precision meas. of g-factor 77−26370
EPR techniques, developments 78−74045
inductively coupled Ar plasma spectroscopy, RF excited, for diatomic mol. spectra 80−86358
in laser cavity, pure nucl. quadrupole spectra 78−90320
light-beating spectroscopy, collisionless sources, Forrester effect 77−34034
metal, RF size effect meas. via optimised marginal oscillator 77−26377
microwave polarimeter, for 8 mm (35 GHz) band, MnF_2 Cotton-Mouton-Voigt effect *(French)* 78−74040
MM-wave klystron appl., phase-locking system 77−5456
molecular beam maser spectroscopy, extsn. to sub mm wave region 77−61874
NMR, frequency sweep nonlinearity, meas. and correction 78−24836
NMR, signal to noise ratio, reciprocity principle calcs. 77−13792
NMR, two-dimens., state-of-the-art 78−74044
NMR meas. of transient species and effects in flowing systems 77−150
NMR spectroscopy, ^1H, automatic PMR spectra interpretation system 78−32840
NQR signal envelope, automatic detection apparatus 77−13785
parametric resonance in transverse disturbing RF fields *(Russian)* 77−3624
positive ions, RF spectroscopy, using optical pumping, review 78−1107
recent advances *(Chinese)* 79−71504
saturation transfer EPR spectroscopy, source modulation, mol. reorientation effects 78−41339
spin-$^1/_2$ RF spectroscopy, saturation effects, semiclassical calcs. 77−67998
subMM laser spectroscopy of solids 80−31895
time domain spectroscopy of dielectrics, survey 80−68212
time-domain, methods, appl. to dielectrics 80−52310
transient EPR phenomena, wide-band detect. method 77−13793
Ar-acetylene van der Waals molecule, radiofreq. spectroscopy and Stark effect meas., equilib. struct. and props. 80−91543
Hg ions, relaxation two constants meas. of optically pumped stored Hg ions 80−106287
radiofrequency sputtering
alumina film, RF sputtered, stability 78−22993
apparatus for cleaning electron microscope components 77−54022
asymmetric diode system design for RF sputtering device, vac. system *(German)* 77−12527
automatic RF sputtering system for multicomponent film production 78−52672
bias voltage, maintenance via press. control 77−28720
boride RF sputtered wear-resistant coatings, XPS study of adherence 79−34191
butane plasma, initial etching prior to deposition of C 79−66224
carbide RF sputtered wear-resistant coatings, XPS study of adherence 79−34191

radiofrequency sputtering continued
carbonaceous insulating films, RF diode sputtering growth, IR absorpt. and Rutherford backscatt. meas. 79−99458
chalcogenide glass films, weak field behaviour 77−36004
cleaning, substrate surface contamination from dark-space shielding 77−8968
coating techniques, for SEM and X-ray microanalysis 79−12783
discharges for sputter deposition and sputter etching, RFI/EMI 78−71566
electrodeless discharge sputtering system *(Japanese)* 80−16183
ferrite film, reactive RF sputtering prep., high mag. recording density 77−12528
ferroelectric film, vacuum deposition method using RF sputtering technique 78−84712
film deposition with sputter gun 77−44162
fluorocarbon polymer film, prep. by RF sputtering and plasma polymerisation, props. 77−55890
getter pumping for economical sputtering with Xe 77−40371
glass film, roughness parameters 77−69202
glass waveguide, refr. index rel. to deposition 77−11046
glow discharge, Langmuir probe study at various freqs. 80−55294
glow discharge sputtering model 77−44154
high-rate vapour quenching techniques and use in amorphous phase prep. 80−80977
impedance matching networks, experimental and design information 80−50555
inline production magnetron sputtering 78−3048
insulator film contouring over substrate topography 77−8752
ion plating, RF plasma excitation 79−69995
Josephson junction, fabricated by RF plasma oxidation, IV characts. *(Japanese)* 80−84564
Langmuir probe technique, plasma characts. in sputtering 80−80929
low pressure plasma system, design and operating characteristics 79−64880
magnetic bubble device fabrication, appl. of sputter etching in Ar-O plasma 79−83347
magnetic bubble film prep., multiple target method 77−16493
magnetic bubble materials, props. and preparation models, review *(Rumanian)* 80−93149
magnetically enhanced sputter sources, high-rate, basic physics and operational characts. 77−44159
magnetron sputter coating of microspherical substrates, appl. to laser fusion targets 79−78883
magnetron sputtering, appl. to sputtered thin compound films, review *(Japanese)* 80−25561
magnetron sputtering equipment and application status 79−83124
mass spectometric analysis of RF reactive sputtering reaction mechanism *(Japanese)* 78−19665
metal film, deposition by ion beam sputtering, composition and stress state 77−89674
moving deposition mode of magnetron sputtering *(German)* 78−39690
multitarget sputtering using decoupled plasmas, appl. to semicond. alloys 77−12529
obsidian, hydration profiles meas. by sputter-induced optical emission, rel. to dating technique 79−24871
optical coatings of TiO_2, ZrO_2 and SiO_2, deposition by high freq. cathodic method 79−76900
optical film, production by RF cosputtering of dielectrics, and optical props. 78−6849
optical waveguide, trapezoidal cross-section ridge design, propag. characts. 78−55436
oxide, tracer diffusion obs., RF sputtering as microsectioning technique 78−14499
Permalloy film preparation 78−3044
permalloy films, O effects on mag. and elec. props. 80−100603
Permalloy RF sputtered films, struct.-sensitive mag. props. 80−34705
piezoelectric gas admission valves, discharge suppression 80−100110
planar magnetron sputtering 78−72725
planar magnetron sputtering developments and applications 77−77379
plasma etching, ion energy 79−73049
plasma utilisation in sputtering and surface reactions 78−84714
rare earth compound vaporisation by cathode ray and HF ion-plasma methods 77−77380
rare earth-Au alloys, negative ions origin and effects 78−60574
redeposition, problem in RF sputter etching of structures of micron dimensions 77−44388
refractory compounds, RF sputtered, comp. by XPS 78−51839
sapphire, RF sputtering of Hf, high stress in graded interfacial layers, AES meas. 77−43446
selective-black absorbers and transparent heat mirrors for solar collector 77−54812
semiconductor, RF etch sputtering under controlled atmosphere 77−44397
silicide RF sputtered wear-resistant coatings, XPS study of adherence 79−34191
sputtering device, pressure regulation *(French)* 77−81217
substrate biased, steady-state mass balance approach 77−20204
substrate surface damage induced by RF-diode sputtering 77−90274
system electrical characterisation theory 79−87578
thin film evaporator with cooled rotatable RF cathode 79−78876
thin film optical circuit fabrication using CO_2 laser 80−99881
transition metal-Ge, RF cosputtered system, supercond. props. 77−51835
Ag, by 10 keV inert gas ions, angular distrib. 79−52061
Al, by 10 keV inert gas ions, angular distrib. 79−52061
Al film, nucleation-grown, RF sputtered, Mayadas-Shatzkes cond. 77−1498
Al, magnetron sputtering in Ar and Ar/O_2 mixtures, discharge characts. 80−89145
Al magnetron sputtering target, oxidation in Ar/O_2 mixtures 80−55291
Al metallisation for VLSI 80−66429
Al, planar magnetron sputtering, H_2 effect on Ar discharge 80−80970
Al-Cu alloy metallisation sputter deposition for VLSI 80−66429
Al-Si alloy metallisation sputter deposition for VLSI 80−66429
Al-Si-Cu alloy metallisation sputter deposition for VLSI 80−66429
Al-Si-Mg alloy metallisation sputter deposition for VLSI 80−66429
Al-ZnS-Au structure, coulombic centres, thermal ageing, cond. and photovoltaic characts. *(French)* 77−43741
AlF_3 film, RF sputtered, dielec. props. meas. 77−36173
AlN, piezoelectric film, low temp. growth by RF reactive planar magnetron sputtering method 80−76175
Al_2O_3 film, RF sputtered by planar magnetron, phys. props. 77−43448

radiofrequency sputtering continued
Al_2O_3, film form. by reactive HF sputtering with voltage bias 78−3045
Al_2O_3, sputter deposited, struct. and heat treatment charact. 78−15307
Au, polycryst., RF bias-diode and triode sputtered, resist. and microstruct. 78−80072
Au, vapour deposition, improvement of adhesion, line definition, contact resistance and semiconductor properties by sputter-etching 79−43145
$Au\text{-}Ti_{0.3}W_{0.7}$, thermal annealing study of metallisation on Si 80−80134
Au-TiC, multilayer struct., microhardness and elec. resist. 80−2950
BN films, optical and electrophysical props. *(Russian)* 77−20941
$BaFe_2O_4$ amorphous film, prep. by RF sputtering, crystallisation 80−76183
$BaPb_{1-x}Bi_xO_3$, superconducting thin films, RF sputtering prep. 80−76181
$Ba_xSr_{1-x}TiO_3$, ferroelec. film, heteroepitaxial growth in cathode sputtering 80−93486
$BaTiO_3$, ferroelec. thin films, r.f. sputtering, X-ray and microprobe obs. 79−47627
$BaTiO_3$, RF sputtered amorphous films, phys. and elec. characterisation 79−83119
$BaTiO_3$, RF-sputtered tetragonal films on Si, ferroelec. and insulating props. 79−78888
Be, RF sputtered film, props. rel. to deposition conditions 77−39965
Bi_2O_3 compound films for SAW devices and filters *(Japanese)* 77−73116
$Bi_{12}TiO_{20}$, RF sputtered epitaxial film on $Bi_{12}GeO_{20}$, for optical waveguiding 78−9462
Bi_2WO_6 film, sputtering from powdered target 77−15705
C film, sputtered glassy, prep., mech. and struct. props. 77−66588
C, reactive RF sputtering in N_2, paracyanogenlike film deposition 79−78886
Cd-Co(-Mo), amorphous films, thermal stability of mag. props. *(Japanese)* 79−47307
CdO-SnO_2 film, prep. by RF sputtering, elec. cond. and transparency 80−7492
CdS films, photosensitive, growth by reactive RF sputtering, props. *(French)* 78−35308
CdS-Cu_xS heterojunctions produced by RF sputtering, for thin film solar cells 79−100053
Cd_2SnO_4 film, RF sputtered from powder targets, props. 77−43759
Cd_2SnO_4 film, sputter deposition and characterisation 79−43146
$Cd_{1-x}Zn_xS$, electro-optical multilayer film, for data storage and display 78−71176
CeO_2:Y_2O_3, bias sputtering, film growth and characts. 77−40366
Cr-Si, amorphous sputtered film, material for kilo-ohm sheet resistances, prep. and props 79−78227
Cr-SiO film, substrate bias effect obs. 78−60573
Cr-SiO_2 cermet film, deposition by RF sputtering of powder target, elec. resist. and TCR 79−78890
Cr_2O_3, RF sputtered coating for wear appls., on Inconel X-750 foil, prep. and props. 80−40605
Cu film deposition, reactive sputtering in RF discharge, glow discharge mass spectrometry 77−44155
Cu-Zr, vapour quenching prod. (thermal evaporation and r.f. sputtering), amorphous film for electron microscopy 78−6851
$CuInS_2$ films prod. by RF sputtered Cu-In films exposure to H_2S 79−95926
$CuInS_2$ thin films, growth, struct., and elec. props. 79−38729
$CuInSe_2$ thin film fabrication for solar cell appls. 80−100786
$CuInSe_2$ thin films for solar cells, radiofrequency sputtering technique, elec. props. 80−93487
Cu_xS, layers produced by reactive RF sputtering, struct., elec. and optical props. 79−90908
Fe-Co-Cr film RF sputtering for magnetic recording 80−2947
Fe-O noncrystalline RF sputtered film, vapour species control 78−60575
Fe_xN_y, prep. by reactive sputtering, struct. and props. *(Japanese)* 78−92190
Fe_2O_3 sputtered films, optical transmission and reflection spectra depend. on substrate temp. 79−91517
Fe_xO_y, prep. by reactive sputtering, struct. and props. *(Japanese)* 78−92190
GaAs amorphous film/GaAs crystal junction, optical and elec. props. 79−99611
GaAs-Al,$Ga_{1-x}As$ integrated optics structs., dry processing 77−27383
n-GaAs-Au-Mo, RF sputtering, elec. props. of contacts, compensating damage centres form. 80−34507
GaP, effects of hydrogen incorporation during deposition by sputtering 79−69981
GaP film, struct. and elec. props. obs. *(Czech)* 78−52667
GaP films, RF sputtering on glass and Au film substrates, struct. and elec. props. 80−2311
GaP:H/GaAs, amorphous film/crystal junction, optical and elec. props. 79−99611
GaP-GaAs, amorphous film/crystal junction, optical and elec. props. 79−99611
GaSb film, ion bombard. effects on elemental Sb incorporation probability during sputter deposition 79−83120
Gd-Co, amorphous film, RF sputtering, DC bias role 77−16494
Gd-Co alloy, sputtered film, mag. props. determ. *(Chinese)* 78−2714
Gd-Co amorphous film, DC or RF sputtered, mag. props., He^+-backscatt. investig. 77−20650
Gd-Co amorphous films, uniaxial perp. anisotropy induced by resputtering effect, expt. *(Japanese)* 77−55885
Gd-Co based amorphous sputtered films, microstruct. variability and mag. anisotropy, implanted ion effects 80−88459
Gd-Co film, amorphous, RF sputtered, prep. and props. 79−1693
Gd-Co film, amorphous, selective resputtering-induced anisotropy 78−72376
GdCo film, sputtered amorphous, incorporation of Ne, Ar and Kr 77−44163
$Gd_{0.27}Co_{0.64}Kr_{0.09}$, amorphous film, thermal release of Kr and H, meas. using UHV mass spectrometric technique 80−3439
GdCoMo film, sputtered amorphous, incorporation of Ne, Ar and Kr 77−44163
GdFe, amorphous films, thermal stability of mag. props. *(Japanese)* 79−47307
Ge, amorphous, doping, Schottky barrier and p-n junction form. by RF sputtering 77−8187
Ge, black, solar selective absorber characterisation 80−80112
$Ge_{15}Te_{81}X_4$ amorphous semicond. switches, fabrication technology *(German)* 80−7493

radiofrequency sputtering continued
Hf, RF sputter deposition, ion bombardment and ion implanation 80−25564
HfC, reactive RF sputtering in N_2, HfN film deposition 79−78886
HfN, RF sputter deposition, ion bombardment and ion implanation 80−25564
$Hg_{0.74}Cd_{0.25}Te$ thin film deposition on Si substrates by RF triode-sputtering, large-area photodetector arrays 80−80965
HgS film, RF sputtered, effect of K on cryst. modification 77−62773
HgS, on NaCl, growth and struct., electron diffr. and TEM obs. 77−90271
IN_2O_3:Sn, RF magnetron sputtered film, elec. and optical props. 80−104065
$In_{1-x}Ga_xSb$ film, epitaxial growth by multitarget RF sputtering 77−44157
n-In_2O_3 film, RF sputter grown, substrate bias effect on elec. and optical props. 78−64150
In_2O_3, transparent electrode deposition on PLZT ceramic 78−74848
In_2O_3:Sn, coating on polyester film, elec. and optical props. 79−99959
In_2O_3:Sn, film, HF sputtered, cond., Hall mobility, oxidation, charge carrier density 78−72287
In_2O_3:Sn, sputtered films for selective transparent films, prep., elec. and opt. props. *(Japanese)* 77−68247
In_2O_3:Sn film, RF sputtered, effect of O_2 press. during deposition on props. 78−19664
In_2O_3-SnO_2 electro-optical film, for data storage and display 78−71176
In_2O_3-SnO_2/GaAs, solar cell, fabrication, characts. and interfacial chemistry 80−21401
In_2O_3-SnO_2/InP, solar cell, fabrication, characts. and interfacial chemistry 80−21401
p-InP, RF sputtering on CdS and other substrates, and grain size obs. 77−90272
InSb film, ion bombard. effects on elemental Sb incorporation probability during sputter deposition 79−83120
InSb-GaSb superlattice, interlayer diffusion 77−85086
$InSb_{1-x}Bi_x$, multitarget RF sputtering, metastable phase, conductivity transition 80−76178
$K_3Li_2Nb_5O_{15}$ optical waveguides fabricated on sapphire by RF sputtering 79−98488
$K_xLi_{1-x}NbO_3$, epitaxial growth of single-cryst. films on $K_2BiNb_5O_{15}$ substrate by RF sputtering 79−15041
$KTa_{1-x}Nb_xO_3$ film, structural and electrical properties obs. 78−88426
Kr.2SiO_2, props. of vitreous deposits 78−22664
$LiNbO_3$, heteroepitaxial growth on MgO by RF sputtering, SHG 79−27323
$LiNbO_3$ sputtered layers, on $LiTaO_3$, optical waveguide props. 77−11012
MnCuBi film, for mag. storage appl., prep. and props. 77−8369
MnPt, disordered film produced by RF sputtering, ferromag. behaviour 78−68310
Mo sputtering for laser mirror refurbishment 80−14498
MoS_2, RF sputtered layers with variable stoichiometry, lubrication props. 80−40557
MoS_2, RF sputtered lubricant, wear life, sputtering parameter effects 80−40558
Nb, by 10 keV inert gas ions, angular distrib. 79−52061
Nb-NbO_x-Al/Pb supercond. proximity function, production by RF sputtering and photolytographic techniques 77−43787
Nb-Ni, amorphous, synthesis by vapour quenching, and struct. 78−11111
$Nb_3Al_{1-x}Ge_x$, RF sputtering synthesis, supercond. transition temp. variation 77−81216
Nb_3Ga film, RF sputtered, supercond. and struct. props. 77−28274
Nb_3Ge, RF and DC sputtered films comparison, O content effect 78−72022
Nb_3Ge, RF sputtered film, high superconducting transition temp. 77−59346
Nb_3Ge(Si), RF sputtered films, amorphous atomic scale struct. 80−84064
Nd:glass films for integrated optics, RF sputtering and optical characts. 79−46087
Ni film, RF sputtered on $LiNbO_3$, SAW delay variation obs. 79−56102
Ni films on Si single cyrstal, pseudodiffusion of Ni in Si 78−2396
Ni-Cr thin film production by HF cathode sputtering *(Bulgarian)* 79−19992
PLZT film, epitaxial growth by RF sputtering, and characterisation 77−85937
PLZT film, growth by RF sputtering, struct. and ferroelec. props. 77−48340
PLZT, RF sputtered thin film, ferroelectric props. 79−69780
PLZT, thin film epitaxial growth and characteris. 79−28918
PLZT, thin film prep. by RF sputtering, struct. and ferroelec. props. *(Japanese)* 77−69992
PLZT, transparent ferroelec., RF sputtering and film characterisation 78−72727
Pb, by 10 keV inert gas ions, angular distrib. 79−52061
Pb, Josephson junction, oxide formation process, ellipsomesric meas. *(Japanese)* 80−11561
Pb/Au/Pb, Josephson junction, oxide formation process, ellipsomesric meas. *(Japanese)* 80−11561
Pb-In and Pb-In/Au, Josephson junction, oxide formation process, ellipsomesric meas. *(Japanese)* 80−11561
Pb-In film, RF sputter anodisation, Josephson junction form., ellipsometry anal. 79−29258
$Pb_xSn_{1-x}Te$, RF sputtered films, struct., lattice parameter, stoichiometric comp., RHEED 78−38975
$PbTiO_3$ ferroelec. thin film, prep. by RF sputtering and dielec. props. 79−100052
$PbTiO_3$ ferroelectric thin films, characts. 80−40261
$Pb(Zr,Ti)O_3$ film, by RF sputtering in PbO vapour 78−39689
$Pb(Zr,Ti)O_3$ thin film, ferroelec., fabrication by RF sputtering *(Japanese)* 80−25560
Pd-Au-Si amorphous films, composition and thermal behaviour 80−55292
Pd-Si amorphous films, compositions and thermal behaviour 80−55292
Pt film resistance thermometer, fabrication, appls. 77−37890
Pt-GaAs contacts, sintered, eval. of W, Ti, Mo and Hf barrier metals 77−8193
Si, amorphous, control of dihydride bond density using RF sputtering 80−34327

radiofrequency sputtering continued
Si, amorphous, doping, Schottky barrier and p-n junction form. by RF sputtering 77−8187
Si, amorphous, prep. by RF sputtering, photoconductivity determ. 77−73231
Si, amorphous, prep. by reactive RF sputtering in Ar-silane mixtures, undoped, n-type and p-type targets 80−76182
Si, amorphous, Schottky barrier solar cell, large-area RF sputtered, contact form, scaling and optimisation 80−45679
Si, amorphous, sputtered, Auger surface spectroscopy 80−50472
Si, amorphous co-sputtered doped, photovoltaic material appl. 80−93488
Si, amorphous film, RF-sputtered, influence of O_2 and deposition conditions, elec. cond., IR absorpt. and ESR 80−2949
Si amorphous film, sputter-deposited, elec., optical, and photoelectronic props. 79−24433
Si amorphous films, RF sputtered, appl. as Schottky barrier solar cells 79−34434
Si, amorphous films, RF sputtering prep. at high Ar press., props. obs. 80−80418
Si, amorphous layers, RF-sputtered on sapphire, crystallisation by CW ion laser annealing 80−80109
Si films, RF sputtered, Ar conc. as function of operation frequency and discharge pressure 80−65393
Si, fine pattern etching by RF sputtering *(Japanese)* 77−70196
Si, minority carrier lifetime, effect of SiO_2 coating deposited by RF diode sputtering 80−11003
Si:B, RF glow discharge sputtering damage centres, barrier formation 79−33329
Si:F, amorphous alloys, RF sputtering prep. in SiF_4-Ar gas mixture, spectra 80−80772
Si:H, amorphous, RF sputtered, suitability as solar cell material 80−40864
Si:H, amorphous, RF sputtered, Schottky barrier solar cells, photovoltaic props. and capacitance-voltage charact. 80−45678
Si:H, amorphous, sputtered Schottky barrier solar cells, conduction mechanism 80−104506
Si:N, amorphous, prep. by RF sputtering and props. 80−44229
Si:P, RF sputtered polycryst. film, MOS compatibility 78−6455
Si-H, RF sputtered amorphous alloy, influence of Ar press. on elec. props. and photoluminesc. 79−91585
Si-SiO_2 interfaces, thin film homogeneity improvement using mag. quadrupole field, expt. *(Croatian)* 78−48316
SiC coatings for first-wall candidate materials by RF sputtering 80−25563
β-SiC, film prep. 77−44164
SiC, reactive RF sputtering in N_2, Si_3N_4 film deposition 79−78886
SiC thin film, RF-sputtered, highly reliable temp. sensor 80−224
$Si_{1-x}H_x$ film, amorphous, RF sputtered, pure and P(B) doped, optical consts. 79−95866
Si_3N_4 film production, by HF plasma *(German)* 80−7507
Si_3N_4, RF-sputtered thin-film optical waveguide, effect of deposition parameters on optical loss 79−76881
SiO_2 controlled electrode area ratio sputtering system operation and film props. 77−77382
SiO_2 deposition on InP by RF sputtering, surface damage 79−78879
SiO_2, film form. by reactive HF sputtering with voltage bias 78−3045
SiO_2 films sputtered in H-Ar mixed gas, enhanced step coverage 80−75470
SiO_2 HF plasma sputtered dielectric layer thickness and refractive index obs. 79−56931
SiO_2, magnetron sputtering, compared with CVD 77−77381
SiO_2, planarised sputter deposition 78−75959
SiO_2 quartz glass sputtering by high frequency plasma, deposition products study *(Russian)* 77−21023
SiO_2 RF magnetron sputtered coatings for laser fusion targets 80−35089
SiO_2 RF sputtered film, Na^+ motion, small-voltage elec. response 79−90822
SiO_2-Ta_2O_5 film, refr.-index-adjustable, for integrated optical ccts., prep. and props. 78−63203
SnO_2 thin films, solid state gas sensor 80−40790
SnO_2, transparent conductive film, prep. by magnetron sputtering and elec., optical and structural props. *(Japanese)* 79−8247
SnO_2, transparent electrode deposition on PLZT ceramic 78−74848
SnO_2:Eu film, RF cosputtering, cryst. site of Eu, cathodolum. obs. 77−7987
$Sr_2Nb_2O_7$, sputtered films, amorphous, dielec. props. 80−54573
Ta_2O_5, film form. by reactive HF sputtering with voltage bias 78−3045
Ta_2O_5, RF-sputtered thin-film optical waveguide, effect of deposition parameters on optical loss 79−76881
Ta_2O_5, sputtering conditions rel. to electronic cond. 77−40365
Te-As-Ge, temp. and bias effects on comp. 77−40367
Ti, in Ar-O plasma, effect of oxidation on reactive sputtering rate 77−24955
Ti, RF sputter deposition, ion bombardment and ion implanation 80−25564
Ti, sputtered film, energetic neutrals rel. to impurities 79−69980
Ti-W, bias-sputtered, resist. and comp. 80−25023
Ti-W magnetron sputtered films metallisation 80−45231
Ti-W/Au, metallisation on Al by RF sputtering, temp. stability, barrier props. 79−23868
TiC coating, activated reactive evaporation and sputter deposition, ancillary props. 77−44395
TiC coatings, RF sputtered, on 440-C steel, adherence, friction, and wear props. 79−47823
TiC, reactive RF sputtering in N_2, TiN film deposition 79−78886
TiC, TiVC, on steel, sputter deposited, adhesive quality 77−12531
TiN, RF sputter deposition, ion bombardment and ion implanation 80−25564
TiO_2 film, RF sputtering, dielec. props. and X-ray phase analysis 78−80288
TiO_2, reactive- and chemical-sputter deposition from Ti and TiC target 79−100051
TiO_2-SiO_2 multilayered film striped optical filters, optical props. and fabrication of RF sputtering 80−10030
TiO_x, reactive sputtering, film prep. conditions rel. to stoichiometry 77−40370
W-SiO_2 cermet film, deposition by RF sputtering of powder target, elec. resist. and TCR 79−78890
WC-Co sputter deposited film, struct. and comp. 78−72023
WC-Co sputter deposited film, friction and wear 78−72918

radiofrequency sputtering continued
ZnO deposition for metal-ZnO-SiO_2-Si struct., SAW appl., fabrication related deterioration 78−14829
ZnO, film, reactively RF sputtered, anal. of texture 78−67921
ZnO, films for SAW devices and filters *(Japanese)* 77−73116
ZnO, high rate epitaxy on sapphire by planar magnetron RF sputtering 79−28916
ZnO monocrystal and RF sputtered heteroepitaxial film, SAW attenuation comparison 79−56063
ZnO piezoelec. film, fabrication and appl. *(Japanese)* 78−23616
ZnO, RF sputtered epitaxial film, appl. to integrated optics 77−14821
ZnO sputtered films, undoped and Ga doped, props. rel. to deposition conditions 80−107935
ZnO thin film SAW device manufacture, sputtering system and film characterisation 78−95692
ZnO/Si using magnetron discharge sputtering, acoustoelectric device appls. 80−80332
ZnO-Cu_2O heterojunction solar cells, prop. by RF sputtering 80−93945
ZnO-SiO_2-Si layered films for SAW devices and filters *(Japanese)* 77−73116
ZnS, RF sputtered film, stoichiometry, chem. comp. 78−34727
ZnSe, RF bias-sputtered CVD films on CaF_2 79−14060
Zr, RF sputter deposition, ion bombardment and ion implanation 80−25564
ZrN, RF sputter deposition, ion bombardment and ion implanation 80−25564
ZrO_2:Y_2O_3, bias sputtering, film growth and characts. 77−40366

radiogalaxies *see galaxies; radiosources (astronomical)*

radiogoniometers *see goniometers*

radiographs (x-ray photography) *see radiography*

radiography
see also electrophotography; neutron radiography; nondestructive testing; radioisotope scanning and imaging; scanning radiography
3D picture processing use 79−100736
abdominal arteriography, super selective, technics and indications in children *(French)* 80−36092
abdominal surgery, role of rapid-sequence image intensifier fluorography 79−92340
absorption-edge fluoroscopy, spectral considerations 77−21618
absorption-edge transmission technique using ^{139}Ce for stable I conc. meas. 80−56194
alloys, oxidation mech., exam. using autoradiography 79−20326
alloys, segregating phases identification, single crysts., radiographs computer calc. 80−84934
analytical X-ray photogrammetry, use for patellar tracking patterns meas. 80−30864
angio processing, left ventricular, using Contouromat hard-wired system 79−16325
angio processing, left ventricular, using Contouromat hard-wired system 79−16326
angiocardiogram computer analysis, pot. energy distrib. rel. to left ventricular efficiency 77−40757
angiocardiogram objective quantitative processing, Cardiac Image Analysis System 79−70629
angiocardiographic image computer quantitation 80−36118
angiocardiography, digital multiprocessor system 80−94362
angiocinedensitometry, blood flow values in iliac artery, conscious humans 79−25022
angiograms, augmentation of computed tomograms 80−8150
angiograms, digital, comparison of methods of meas. blood flow *(German)* 79−39468
angiographic computerised evaluation of left ventricular wall motion 79−70634
angiographic definition and quantification of regional left ventricular contraction 79−70637
angiographic I imaging using spectral anal. 80−36122
angiographic image processing in multiprocessor, blood flow meas. *(German)* 78−92690
angiographic images, simulated, blood vessel detection, evaluation of observer performance 79−5357
angiographic images of left ventricle, system for off-line anal. using minicomputer 78−80964
angiographic information visualisation correl. with measured system MTFs 78−73230
angiographic methods for the diagnosis and therapy of liver diseases *(German)* 80−56211
angiographic pelvis-leg programming, using test injection to determine contrast medium flow time 77−70523
angiographic universal setups for general hospital with vascular surgery facility 79−92336
angiography, comparison of convolution and ray tracing computations of small blood vessel images 77−48863
angiography, computerised, anal. and visualisation of blood dynamics and motion of organs 80−8170
angiography, effects of asymm. focal spots 77−21617
angiography, free arc, with film changer and image intensifier mounted on U-arm 77−86601
angiography, indocyanine green fluoresc. spectrum in blood and other solvents 78−28057
angiography, pelvis and legs, programming of injection and table-top movement 79−34646
angiography, selective, renal and peri-renal inflammatory lesions, correl. with histopathology 79−74740
angiography, standardised general and cerebral under automatic exposure control 78−24121
angiography, validity of computer simulation of blood vessel imaging 78−3594
angiography, visual perception limits 78−85313
angiography and scintigraphy, equipment for quant. evaluation and off-line operation *(German)* 78−88736
angiography installation, first experiences 80−17080
angiography of head and neck region, selective and superselective 77−73560
angiography visual perception limits 78−73231
angiography-pathology correlations with meningioma scintigraphy 77−56453
Angioskop multidirectional examination unit 78−28039
antiscatter grid exptl. evaluation method 78−53485
apparatus optimal operating conditions 80−30847
area exposure product monitor, DQ-20 *(Japanese)* 77−73578

radiography continued
arterial pathology discrimination from angiograms 79−16274
arthrographic equipment for double contrast knee exam. 79−48320
arthrotomographic diagnosis of meniscus perforations in the temporomandibular joint 80−56170
atherosclerosis detection, computerised electronic radiographs appl. 80−8169
automated screening image processing laboratory 77−13004
automatic processing of radiographs 79−66242
automatic reading systems, radiography, automatic reading systems, estimation of performance time 78−40005
backscatter X-ray technique, medical appls. 80−98096
bi-layer struct., radiation attenuation technique for simultaneous layer thickness determ. 77−12758
biological objects, using soft X-ray emission of laser plasma mirror 79−43983
biological volume reproduction by foreshortening roentgenograms, compound hologram method 79−57748
biomedical image enhancement using 2-dimens. digital filters *(Italian)* 78−53539
biomedical image processing and understanding 79−100737
biomedical mobile X-ray unit, Mobil XR 78−24122
biomedical pictures, digital processing and enchancement techniques 77−40815
bladder pressure noninvasive determ. from micturition cinecystourethrogram 79−92370
blood flow meas., instantaneous, X-ray imaging using cine/video densitometric data 79−34598
bone, disease diagnosis, automatic texture anal. methods 80−8156
bone, meas. of LiF powder packing density in trabecular bone cavities for dosimetry 77−66855
bone, mineral content, coherent scatt. of photons 80−67238
bone and bone marrow involvement in malignant lymphoma, detect. obs. 80−36086
bone biopsy, automatic image anal., var. in rib architecture 78−61253
bone density and cortical thickness, meas. by photon absorptiometry 79−8535
bone density and irregularity meas. in normal hands 80−30839
bone density measurement by ^{125}I photon absorptiometric anal., dialysis patients 80−36075
bone distribution profile, healing process obs. appl. 78−15890
bone mass measurement, effect of rot. on radiographic dimens. 77−5062
bone mineral measurement using EMI scanner vs. densitometry 78−24119
bone mineral measurement using X-ray (low energy γ-ray) transmission, positioning errors 78−96084
bone strength determination, data on compressive strength rel. to density and strain rate 77−36976
bone structure, anal. by X-ray pictures *(German)* 80−89828
breast dose and cancer risk due to fluoroscopic chest exams. of women with tuberculosis 78−65128
breast examination, recent techniques *(French)* 77−81564
breast examination by radiography, thermography and US, reviews *(French)* 78−7472
breast examination methods including radiography, thermography and cytology, review 78−3656
breast parenchymal patterns meas. 80−8155
breast radiography, foreign body diagnosis *(French)* 78−7432
breast radiography with Mammomat, skin exposure and absorbed dose 78−73245
bremsstrahlung, filtered spectra, equivalent half-value thicknesses and mean energies 80−46011
bremsstrahlung X-ray spectra stripping up to 300 kVp on desk type computer 79−83846
bronchial angiography in the staging of bronchogenic carcinoma 80−46007
capacitor discharge mobile X-ray apparatus *(Japanese)* 79−88165
cardiac, wall motion abnormality detect. using regional changes in ventricular shape and vol. 79−70633
cardiac catheterization laboratory sensitometric system application and clinical evaluation 78−20263
cardiac circumferential fibre shortening vel. determ. from meas. left ventricular dimensions 77−48867
cardiac diagnosis, analysis of signals from pulsating arteries 77−48831
cardiac insufficiency, criteria in X-radiology *(German)* 79−53237
cardiac left ventricle regional wall motion, spatial resolution and correl. between segments 79−62359
cardiac left ventricular wall motion assessment from computer-processed fluoroscopy 79−62358
cardiac performance mechanics from computer anal. of circumferential fibre shortening vel. 77−37095
cardiac radiographic image sequence analysis and recording 78−57069
cardiac right ventricular angiogram computer quantification 79−62360
cardiac work, practical aspects of X-ray apparatus 79−96659
cardiology, varifocal imaging 79−70631
cardiovascular measurements, conf., Bellingham, USA (Sept. '78) 80−31419
cardiovascular radiopaque marker tracking algorithm 78−40329
carotid angiography, eye shield 78−44615
cassette for autoradiography 79−52535
cast steel, heat treatment, effects of explosive loads, radiographic anal. 77−25072
cast turbine blade microporosity tests 77−86276
$CaWO_4$ intensifying screen, meas. of X-ray induced light photons emitted 80−41218
cellular logic techniques in radiological image analysis 80−8171
cellulose nitrate emulsion for α-particle track relocalisation 78−17480
cellulose nitrate layer, α-particle autoradiography 78−17499
cerebral angiography, brain O_2 tension response, using animal model 77−52872
cerebral angiography, cortical pO_2 and K^+ dynamics rel. to contrast agent neurotoxicity 78−35954
cerebral angiography, evaluation of Contrac injector 78−40293
cerebral angiography in stereoscopic magnification *(Japanese)* 77−73574
cerebral angiography routine enlargement system, Poly Diagnost N 77−86602
cervical spinal cord injuries, metrizamide myelography 79−92362
cervico-thoracic boundary, method for obtaining clear radiograms *(German)* 79−39499
charge transfer electroradiography, physical processes 79−17594

radiography continued
charged particle detection by photographic recording systems, appls. 78−17527
chest film, pre-operative, rel. to post-operative management 80−51207
chest images, recognition of feature points by sequential decision process model *(Japanese)* 79−39480
chest photofluorograms, computer anal. and appl. to automated screening 80−72282
chest photofluorograms, recognition of vessel shadows *(Japanese)* 79−57761
chest photofluorograms, recognition of vessel shadows for automated meas. and classification 77−81566
chest photofluorograms automated interpretation using AISCR-V3 software system 79−88183
chest radiograms, rib image recognition using octagonal distance transformation of digitised binary pictures 80−89842
chest radiograph nodule detection system 80−8140
chest radiograph optoelectronic processing for pulmonary venous hypertension detect. 79−74754
chest radiograph texture anal. model 78−40323
chest radiographs, algorithms for finding rib cage 77−44804
chest radiographs, computed detection of nodules 80−8172
chest radiographs, model-directed detection of ribs 79−88179
chest radiographs, processing of large numbers, problems 80−8138
chest radiography, comparison of 350 kV and 120 kV techniques 78−73238
chest radiography screening for employees in nuclear industry 80−26342
chest radiology, introduction to physiological aspects 79−25071
chest X-ray automated anal. 80−98098
chest X-ray automated screening, texture anal. of lung fields 80−41228
chest X-ray lung region subimage automated extraction for pneumoconiosis opacities detection 79−88182
chest X-ray rib extraction algorithm for pneumoconiosis detect. 78−31904
chest X-rays, coal miners, small opacities computer anal. 78−40324
chest X-rays automated screening, image segmentation and cardiac silhouette anal. 79−88178
cholangiography, intravenous, child obs. 79−62333
cine-radiography in peripheral arteriography 78−24123
cineangiocardiography, accuracy of ventricular models and localisation of contraction anomalies 80−89845
cineangiocardiography, analogue method for automated left ventricular boundary determ. 77−60281
cineangiograms, computerised anal. system 80−72284
cineangiography, automatic detect. of apex of heart 80−89847
cineangiography, left ventricular contour segmentation from anatomical landmark trajectories and its application to wall motion analysis 80−94363
cineangiography, physiological event marking using ECG R-wave triggering 77−52873
cineanigiocardiogram of left ventricle, automatic processing and cardiac function display techniques *(Japanese)* 80−72311
cinefluorographic units, protection survey results of four X-ray units. 79−20618
cineradiography, with continuous X-ray source 78−44341
cineroentgenography, quantitative biplane method, error propag. 78−73224
cineurethrocystography, gonad dose 78−35956
cisterna magna, unusually large, plain film, angiographic and computerised tomography indications 79−66549
coded aperture imaging: the modulation transfer function for uniformly redundant arrays 80−99019
coded aperture imaging, review 80−101914
collimators, semi-automatic and automatic, manufactured by Medicor Works 80−85475
collimators, wire-wound multi-aperture 79−35911
colon, rational and practical X-ray diagnosis *(German)* 79−83922
colonic diverticular disease population survey, patient X-ray dose 78−61259
compton scatter densitometry determ. of bone density in living patients 80−17102
computed, low-dose X-ray imaging system 80−98092
computed radiography, contrast-detail-dose evaluation 80−41221
computer angiography, new tool for X-ray functional diagnostics 79−79640
computer generated radiographs filing and retrieval system 79−16289
computer system SYSCORMORAM for haemodynamic and cineangiographic data treatment 78−81030
computer-aided analysis of radiographs 79−16290
computer-aided diagnosis of medical images, conf., Coronado, USA, (Nov. 1976) 77−78018
computer-assisted X-ray reporting in German language 78−73284
computerised electronic radiography 80−8162
computerised fluoroscopy for non-invasive cardiovascular imaging 80−17121
computerised image processing of US and radiographic images 79−79195
computerised image smoothing and edge enhancement 80−109015
concrete, density meas. by back-scattered gamma radiation 77−36699
conference, international congress of radiology, Rio de Janeiro, Brazil (Oct. 1977) 79−16284
conference on nuclear power systems, Washington, USA (1978) 79−41045
congenital intracranial vascular malformation detect., scintigraphy vs. tomography and angiography 78−77104
contour extraction *(Japanese)* 80−81702
contrast enhancement of high-energy radiotherapy films 80−8126
contrast improvement using fore-and-aft rotating aperture wheel device 80−41227
contrast media labelling with ^{121}I and ^{123}I 80−26350
convergent wide-angle beam, for polycrystals 80−40634
coronary angiogram computer quantitation 80−41233
coronary arteriography, current techniques and equipment 78−35940
coronary artery disease, abnormal left ventricular contraction pattern cineangiography 79−83930
cortical bone diameter meas., manual and computer-aided methods comparison 78−85376
cost-effectiveness considerations in evaluation of new technology 78−69192
couch-cover, heatable, use in X-ray exams. *(German)* 80−104751
crack detection, effect of stress 80−40653
radiography continued
cross section imaging for treatment planning, using radiotherapy simulator 77−13030
cylindrical ceramics-metal laminated components, X-radiography 79−5123
decision making and phys. image props. 78−69189
defect depth determ. by radiographic inspection 79−66241
defect radiographs, method and apparatus for automatic decoding 78−40002
defect size measurement by radiography 79−91858
defect thickness determ., visual comparative method 79−11737
delphinid porpoises, sound production and air recycling, cineradiography 79−48275
dental, reduction of patient exposure 79−25106
dental patients, X-ray exposure obs. 80−104761
dental radiography, pantomographic and conventional, doses to patients 79−92375
dental radiography, phantom meas. of absorbed doses 77−81576
dental radiological safety, pilot survey 79−43993
dental X-ray photographs, comparative study of patient exposure to radiation 78−92702
dental X-ray tubes, improvements 78−65129
dental X-ray unit kVp meas. 77−40767
desmodontal gap evaluation with data-processing system, mandible X-ray image changes 79−62337
detection of bars and discs in quantum noise [radiography] 80−41042
Diagnost C, localisation of intracavity Rn applicators 79−48331
diagnostic, anal. of making, reading and reporting films, rel. to equipment design 80−17123
diagnostic, analytical stereo system 80−67231
diagnostic, detector sensitivity and image conversion improvement 77−25546
diagnostic, electro-optical imaging 77−21651
diagnostic, foetal vs. parenteral radiosensitivity 80−51271
diagnostic, high-resolution low light level video systems 77−40759
diagnostic, X-ray spectra determ., high intensity 80−41217
diagnostic facilities, quality assurance programme, proposed recommendation 78−73235
diagnostic imaging systems, image quality assessments 77−90890
diagnostic imaging systems, non-silver halide, recent developments and pot. 80−41223
diagnostic instrument calibration, energy depend. of correction factors for Victoreen 666 Survey System 78−3596
diagnostic isocon imaging system 77−40760
diagnostic machine X-ray quality and output determ. by TLD 77−60241
diagnostic performance of radiologists, decision making and physical image props. 78−85367
diagnostic radiographic video system psychophysical evaluation 79−74751
diagnostic radiological digital image processing facility 80−36127
diagnostic radiology, mean active bone marrow dose to USA adult population 78−85382
diagnostic system compatible with DHEW standards 78−7445
diagnostic table, remote-controlled, clinical experiences 79−43987
diagnostic X-ray exposure meas., energy depend. of correction factors for Victoreen 570 Condenser R-meters 78−3597
diagnostic X-ray rooms, simplified shielding 79−16313
diagnostic X-rays, principles of design of assemblies 78−57065
diamond, synthetic monocrystals, inclusions phase comp., radiographic method 80−100978
diazotype duplicating system with appl. as diagnostic aid 78−69249
diazotype imaging film, continuous tone, for duplicating of radiographs 78−32911
diazotype radiographic duplicating system as diagnostic aid 80−8137
differential energy absorpt. X-ray cassette, radiographic image contrast enhancement 78−20264
diffraction phenomena on using Al attenuation-equalising filters 79−39486
digestive tract, using Sircam cameras and X-ray image intensifier 78−92694
digestive tract diagnosis, X-ray dose to patient and radiologist *(German)* 78−28086
digital picture analysis, book 77−17962
digital picture coding techniques, redundancy reduction 77−40850
digital signal processing for vessel edge detection in angiograms, appl. of Wiener filter, book contrib. 79−92357
digital transmission over voice-grade telephone channels, laser scanning system 78−80953
digital video acquisition system for extraction of subvisual information 78−69208
digital video image processor for real-time X-ray subtraction imaging 79−25080
direct recording and reconstruction of 3D X-ray images 79−6242
discography, diagnosis of posterior annulus fibrosus in the lumbar spine 79−53213
dose compensation filter design using megavoltage radiography 80−3785
dose distribution calculation method for bone- and lung-equivalent material *(German)* 80−61704
dose distribution description by X-ray quality monitoring *(German)* 80−41251
dose reduction in medical diagnosis 80−98087
dose to children from examinations 79−16308
dose-rate measurement, response time consts. of two dosimeters 77−13006
doses from X-ray units used outside radiology 80−89856
double contrast meal, new high density $BaSO_4$ powders 79−74745
double-contrast, rel. to endoscopy in upper gastrointestinal tract haemorrhage 80−98063
double-contrast technique for individual small intestine sections *(German)* 80−61694
Dynalyzer II, application to X-ray quality control 78−77896
dynamic cardiac imagery, gross and segmental motion analysis 79−25093
dynamic using image intensifier 79−24685
ear, radiological anatomy of the round window, review 79−62332
ECG-gated radiography 80−26344
electrobronchogram fringe effects 77−25542
Electrochemical Society Meeting, Boston, USA, (May, 1979) 79−91959
electrokymographic pick-up, external device 77−21606
electron, feasibility for microcrack detection 78−72967

radiography continued
electron microscope autoradiographs, iterative anal., sample sizes and confidence limits 79−35896
electron microscope autoradiographs, iterative anal. method 79−35895
electron microscope autoradiography of isolated mols. 80−85564
electronic radiography, computerised, for early detect. of vacular disease 80−41226
electronic recording of X-ray images 80−62815
electronic scanning of X-ray images 80−8161
electrophoretic radiographic device 80−22501
electrophotetic X-ray imager, self-contained instant display erasable 80−22491
electrophotographic and electroradiographic image convertors with electronic readout 79−71554
electrophotographic imaging using high purity Al_2O_3 78−35936
electroradiographic image laser readout 80−41225
electroradiography, image quality, charge transport random fluctuations influence 78−66015
electroradiography, phys. fundamentals *(German)* 78−73228
electrostatic X-ray imaging, book 80−31426
electrostatic X-ray imaging, book contrib. 80−36112
electrostatic X-ray imaging techniques for medical and industrial appl. 79−79645
Emergency Response Planning and Preparedness Training Programmes, USA 78−57079
endocardium motion during contraction, anal. method 80−109072
endoscopic retrograde cholangio-pancreaticography 77−73559
endoscopic roentgenography appliance users' experience 77−25544
enlarged photofluorography using 12 inch image intensifier *(Japanese)* 78−96087
enlargement system, for viewing radiographs, description 78−53043
epoxy resin based tissue substitutes for radiography studies 78−7424
equipment, computer-assisted quality assurance 80−89838
equipment, idealised, for routine chest exams., specifications and requirements 80−46034
equipment, method and algorithm for adjusting 80−30852
equipment, state of the art 80−81688
equipment acceptance testing, systems approach 78−69203
equipment and layout in up-to-date working places 79−62352
equipment for production line inspection 79−29320
equipment planning, systems approach 78−57064
equipment safety and preventative maintenance in rural community hospitals 77−40758
equipment safety in diagnostic X-ray departments 79−48346
equipment servicing by hospital-based group 78−69247
exposure, influence of cassette front 79−25105
exposure measurement during exams. using phototiming techniques, attenuation phantoms 77−40766
extra-fast shutter, for soft X-ray photography *(French)* 78−41397
eye protection shield for the fluoroscopist 79−92398
eyeglasses, conventional, value for X-ray protection 79−88202
falling load technique, performance evaluation 78−69201
fatigue crack detection, improved 77−86262
femoral angiography, ioxaglate, a new low osmolar contrast medium 79−48319
femoral neck fractures, meas. of fissure, X-ray picture anal. *(Croatian)* 80−109023
fetal exposure in diagnostic radiology 80−8133
fibre reinforced composite, fatigue damage, early detection by NDT 77−28951
fibre reinforced composite, opaque fibres, inspection aid for NDT by B fibre addition 78−95880
field characteristics of geometric unsharpness due to X-ray tube focal spot 77−21616
film characteristics for X-rays, heuristic model 77−195
film development by machine, risk of faults *(German)* 80−90972
film quality, CAA 80−8158
film-screen characteristics effects on threshold detectability of small low-contrast objects 78−53487
film-screen characteristics effects on threshold detectability of small low-contrast objects 78−53488
film/intensifying screen system, contrast detail from Wiener spectrum *(German)* 80−73559
film/intensifying screen system, MTF and Wiener spectrum, film and screen quality effect *(German)* 80−73560
film/screen combinations and patient exposure, Nationwide Survey of X-ray Trends 78−73233
film/screen system noise 79−21841
films, selected, response to ^{14}C-β-radiation 80−90937
films sensitive to green light, reciprocity law failure 78−69199
fine puncture and biopsy, efficiency and technique in tumour diagnosis *(German)* 80−41212
finger doses received by radiologists during Chiba needle percutaneous cholangiography 80−81737
fingerprints, radiographic and physicochem. techniques, for detect. 78−78055
flash, high energy 79−91860
flash radiography, high energy, for dynamic NDT 78−15624
flashing tomosynthesis 80−67243
flaw detection, correction of shadow images 80−89456
flaw detection systems based on semicond. detectors and scintillation crysts. for hard bremsstrahlung 79−11748
flaw dimensions in direction of irradiation determ. from radiographs with aid of defectometer 80−71863
fluorescent screens, new approach to line spread function meas. 79−20665
fluorescent X-ray intensifying screen, efficiency determ., standard method 80−37140
fluorescent X-ray intensifying screen efficiency determ., standard method 78−69198
fluoro-arteriography and -phlebography by the middle format technique *(German)* 80−56212
fluorography with image intensifier, apparatus for mass stomach survey *(Japanese)* 77−73575
fluorometallic intensifying screens suitability in X- and gamma-radiography *(German)* 77−180
fluorometallic radiographic intensifying screens 79−61809
fluoroscopic cardiac imaging, real-time computerised system 80−36123
fluoroscopic examinations, multi-image camera for spot radiography 80−109020
fluoroscopic filtration systems, half-value-layer meas. method 79−35903
radiography continued
fluoroscopic image recording using multiformat camera 80−51234
fluoroscopic installations, diagnostic X-ray survey procedures, automatic brightness controlled units 77−25560
fluoroscopic installations with undertable X-ray tubes, survey form and techniques 77−73597
fluoroscopic spot film system image quality evaluation and optimisation 78−69205
fluoroscopic system, alignment checking device 77−86604
fluoroscopic unit, variable aperture, reduced patient exposure 79−92368
fluoroscopy, absolute efficiency of (ZnCd)S:Ag phosphor 78−73203
fluoroscopy, acute radiation injury caused by faulty use during cardiac procedures 77−9272
fluoroscopy, automatic brightness control operating protocols and effect on image quality 80−17120
fluoroscopy, kVp variable, with automatic brightness stabilisation, X-ray tube pot. var. 78−69202
fluoroscopy, organ dose per unit exposure, estimation method for artificial pneumothorax 78−96097
fluoroscopy without the grid, dose reduction method 80−41240
focal spot measurements for quality control, using random object distrib. 77−2047
focal spot size determ. from pinhole camera images 79−79627
focal spot size measurement, optical simulation, for correction factor determ. 77−26449
focal spots of X-ray tubes, effective size of transverse dimension 77−71414
free-focus, using conventional films, exposures in a simulated clinical study 80−89835
fundamentals 78−95875
gallbladder images obtained by radiographic magnification technique 78−69186
gallstone vol. meas. system, computerised 79−62348
gamma ray source, choice for welded joint monitoring 80−104396
gamma-ray radiography, use of Se electroradiographic plates 78−72978
gastric Ba-filled X-ray films, computer screening *(Japanese)* 78−73211
gastric ulcers, shallow, comparison of radiographic techniques 79−92358
gastric X-ray image, multi-contour detection by organising before identification 79−88177
gastric X-ray image using Ba, feature point extraction method 80−101259
gastro-enterological X-ray diagnosis using Diagnost C by Philips 77−86599
gastrointestinal tract exam., automatic radiographic system and HT generator *(Japanese)* 79−88167
glass fibre reinforced epoxy pipe, radiometric inspection by image analysing system 77−90532
glass fibre reinforced polypropylene, effect of injection speed on fibre orientation 79−4944
gonadal dose determ. in Turkish diagnostic radiology 79−79655
gonadal doses to 78070 patients undergoing diagnostic X-ray exam. 78−53503
gradient pattern coding−an application to the measurement of pneumoconiosis in chest X-rays 79−34632
granularity of screen-film systems, assessment by entropy method 80−98070
graphite composite aircraft structures, flaw detection by US methods 78−44288
grid control X-ray tube, diagnostic quality improvements 78−11733
grid for elimination of scatter, zig-zag design 78−3598
gypsum wallboard, use as protective barrier 79−70650
gypsum wallboard, X-ray attenuation characts. 79−70651
gyroscopic X-ray television apparatus for clinical studies 78−15883
hand radiographs, congenital abnormalities classification 80−30870
heart, internal image display *(Dutch)* 79−70623
heart radiographic images, automatic extraction of location of surgically implanted markers 79−88175
heart volume determination by angiography, X-ray magnification estimation 78−73197
heavy ion radiography 80−17122
heavy-ion radiography and autoactivation techniques 79−20624
held radiograph technique and radiation protection 78−73199
high energy flash radiography applications 79−71581
high potential X-ray generator, PD150L, standardisation of exposure factors *(Japanese)* 77−73577
high tension unit, HD150G-40, for X-ray diagnosis *(Japanese)* 77−73576
high-resolution X-ray TV system and video recorder for medical work 78−24120
high-sensitivity autoionography, detection of radioactive spots on thin-layer chromatograms 78−86960
high-speed cassette film fogging and shielding 78−8460
high-speed cineradiography, of projectiles 78−41395
hillslope hydrology appl. 79−74910
hip dislocations, possibilities of diagnostic error *(German)* 79−83923
hip joint diseases from radiological and pathological-anatomical view points *(German)* 79−83920
hip lameness, bull, skin and gonadal dose reduction, Pb sheeting and Cu filtration 79−100743
Hiroshima mass radiologic gastric surveys, examinees' doses 80−89858
history, X-ray engineering, development in the operating theatre 80−101703
holographic 3-D synthesis of X-ray pictures 80−67245
holographic methods of 3-D representation from no. of plane images 80−67244
holographically stored X-ray images, grey-tone reproduction 78−65120
holography applications 80−67242
hybrid optical-digital radiography system for lung disease detection 78−11753
hydrogen entrapment, direct obs. 78−48585
hysterosalpingography, appraisal of current indications 80−56169
ICRP new concept of person dose, related to film badge exposure 79−29631
IEEE statement on technology development 80−41199
image amplifier, 14 inch, clinical appls. *(Japanese)* 79−92355
image amplifiers, high performance for clinical use *(Japanese)* 77−73579
image anal., computer aided, patient diagnosis appl. 78−61256
image anal. 80−8163
image analogue processing by photographic spatial filtering 78−57070
image analysis by computer 77−21624

radiography continued
image analysis by LEITZ-TAS with process computer 80−68773
image computer-controlled subtraction procedures 80−109014
image display, medically significant features 77−78020
image enhancement and anal. system, digital computer eval. 78−27708
image evaluation by entropy, appl. to development process 79−12914
image formation, perceptual eval. of phys. parameters, computer-simulated images 80−41222
image information content and patient exposure 78−35935
image intensification in medical and industrial radiology *(French)* 77−30223
image intensifier, fibre-optic coupled large-area contrast 77−70534
image intensifier closed circuit TV system 80−3775
image intensifier fluorography, image quality rel. to patient dose 80−17081
image intensifier fluorography, low-dose studies of infant hip dysplasia 79−48343
image intensifier fluorography in paediatric radiology 80−41201
image intensifier fluorography with fast exposure technique 78−31900
image intensifier noise evaluation, digital method 80−98097
image intensifier video system, design charact. 78−69209
image intensifier video system, psychophys. evaluation rel. to system measures 78−73234
image intensifier with 14 inch input field, clinical experience 78−31899
image intensifiers, biomedical appl. and limitations 79−79644
image intensifiers, design and future possibilities 79−74756
image performance, comparison with computed radiography 80−12250
image processing techniques 78−87022
image quality, effect of inadequate screen-film contact *(German)* 80−61057
image quality and patient exposure 78−28060
image quality assessment using standardised step/hole IQIs 77−66724
image quality comparison for different screen/film combinations by subjective judgments 78−73229
image quality evaluation, visual and objective methods 77−25543
image quality in photon imaging 80−81687
image quantitative analysis by TV image analyser 80−109008
image receptor, large area, with electrophoretic display 80−98091
image recording system choice in mammography, tomography and angiography 78−69180
image segmentation and texture unit cell size determ. 80−95817
image series encoding and anal. 79−83928
image storing equipment of Medicor Works 80−85476
image transmission system response rel. to X-ray diagnosis 78−35941
image transmission systems of Medicor Works 79−100725
image understanding systems, seminar, San Diego, CA, USA (Aug. 79) 80−94918
image-forming systems, reciprocity-law failure 79−53229
imaging properties of X-ray focal spots 77−21596
imaging system, new, in computed radiography 80−8147
imaging systems, unified view using Schade aperture theory, noisy images 77−73563
imaging techniques, developments, review 80−26324
Industrex Instant 600 paper system evaluation 77−52592
industrial, accidental over-exposure to ^{192}Ir source 77−56472
industrial, basic physical principles, survey 77−38067
industrial, discontinuous registration using profile analysis and piecewise correlation techniques 80−102645
industrial, present role of radiological methods in engineering 79−79191
industrial, recent improvement of techniques in gas industry *(French)* 77−38073
industrial, X-ray emulsions *(French)* 77−38069
industrial, X-ray generation equipment 77−38068
industrial equipment, thick-walled parts study via stereomicrotron 77−65064
industrial hard X-ray channel-plate image intensifier 78−54517
industrial innovation 77−63840
industrial X-ray defectoscopy, devices to improve X-raying conditions 77−73405
industrial X-ray film information processing methods *(German)* 78−15637
inferior colliculus of immature mouse, plastic reinnervation, autoradiography with ^{14}C-deoxyglucose 79−92233
information capacity of viewbox, improvements 79−74746
inspection, improved effectiveness of differential circuits used to suppress low-frequency noise 79−52608
inspection algorithm speedup by array processor 80−108659
instructional program in X-ray science, survey of former students 79−9
intensifying screen, relationship between resolution and speed 78−65124
intensifying screen, role of reflective layer 80−62816
intensifying screen equivalent blur 78−69197
intensifying screen information content and contrast, comparison of rare earth with $CaWO_4$ 78−73232
intensifying screen MTF, empirical eqn. 78−65123
intensifying screens, role of reflective layers 79−25090
intensifying screens, sensitivity to scattered radiation 77−77970
intensifying screens made of rare earth oxysulphide, resolution and dose 77−21597
internal corrosion and wall thickness meas. 77−32737
intervertebral joints, painful, meas. of movement by biplanar radiography 80−98079
intraoperative angiography in cardiac, thoracic and vascular surgery 77−90880
intraoperative coronary arteriography for graft patency prediction 79−92343
intraoperative X-ray diagnosis, exposure reduction by magnetic disc store 79−92345
intravenous angiography, digital video subtraction system 80−41234
intravenous angiography, digital video subtraction system 80−98089
intravenous angiography using computerised fluoroscopy 80−81689
intravenous contrast angiography, improved digital real-time processing and storage 79−70624
intravenous fluid overload, cardiopulmonary effects, radiologic manifestations 79−92259
ion microradiography, of hydrated cells with SEM imaging 79−16360
ionographic imaging, saturation curve for Freon 13-B1 and mixtures with Xe and Kr, 1 to 8 atm. 77−12997
ionography, closed-system, image transfer to outside chamber, for diagnostic radiology 77−9242
ionography, edge contrast, effect of Mylar foil thickness 79−8532

radiography continued
ionography, high-press. gas, amplification and resolution degradation 77−70532
ionography, optimisation of design parameters 78−31888
ionography, powder cloud development technique 77−56462
ionography, resolution and sensitivity dependents 77−86616
ionography, sensitivity and edge enhancement determ., theory and expt. 80−89833
ionography on thick dielectric sheets 79−57759
ionography sealed chamber system, optically projected X-ray charge images 78−4748
isodose curves in water phantom due to diagnostic quality X-rays 78−15892
K-edge tomography rel. to K-edge imaging and tomography 77−70538
Keithley diagnostic ion chambers, energy depend. of correction factors 78−53507
kidney, conf., Brussels, Belgium (Oct. 1978) 80−31409
kidney, intra-operative X-ray diagnostics in detection and localization of residual concretions 80−41202
kidney distension during urography, rat. obs. 79−62334
kidney function studies following radiation therapy of spleen 79−20615
knee ligament disorder diagnosis, radiological meas. of laxity *(French)* 80−8136
kVp indirect determ. using digital readout device 78−53486
laser fusion pellets, microradiographic characterization 78−745
laser fusion target microradiographs, wall thickness meas., 2D modelling 79−63804
laser fusion targets, X-ray meas. using least squares fitting 80−32425
laser fusion targets, X-ray microradiographs, improved image analysis techniques 80−79562
laser scanner for densitometric anal. 79−70619
left ventricle dynamic geometry in intact unanaesthetised man, midwall motion 80−85491
left ventricular cineangiograms, computing appl. for numerical information, wall movement obs. 77−90891
left ventricular ejection fraction determ., comparison of three radionuclide techniques with contrast angiography 78−31889
left ventricular function, effects of intracoronary nitroglycerin, computer anal. 79−70575
left ventricular localised wall motion abnormality assessment, usefulness of quantitative parameters 80−89848
left ventricular pressure volume anal. in eval. of heart diseases 79−70628
left ventricular regional function anal. from cineangiogram, computer system appl. 78−80963
left ventricular wall motion anal., externally referenced polar coord. system 80−89846
leg long bone growth meas. in children from radiogram, error reduction using computer processing 78−77103
lesion contrast and photon count density rel. to D-log E curve 78−69195
Lexiscope, portable pocket size X-ray imaging system for medical/dental radiography 78−92701
light radiography, strengthening covers, rare earth oxysulphides *(French)* 78−41396
line spread function meas. 79−88161
linear infiltration of three dimensional image 79−66243
low dose, intensified minification camera 78−20262
low temperature, possibilities 77−81348
lumbar spine, lateral flexion, plane kinematic anal. 79−8522
lumbar spine, mech. and kinematic anal., orthogonal radiography 79−74708
lung, effects of body position and respiration on regional differences 79−25073
lung, effects of smoking on regional differences 79−25075
lung, roentgenfilm densitometry and linear lung expansion relationship 79−25074
lung physiology and chest radiology 79−25072
lung regional differences, effects of left heart failure 79−25076
lung structure visibility and sharpness at 90, 140 and 350 kV 80−98124
lung translation, rot. and strain calc. from roentgen-videographically recorded marker displacements 78−31843
lung volume determination, interactive graphics 77−77985
lung volume measurement from supine portable chest radiographs 80−81703
macroradiographic X-ray diagnostic table *(Japanese)* 79−88166
magnification angiography, routine 80−21527
magnification angiography, usefulness in the field of pneumology 80−89829
magnification mammography evaluation 80−17124
magnification skeletal radiography, imaging parameters and clinical relevance 78−69185
maintenance of 300°F temp. 77−66723
mammogram densitometric distinction between cancer and fibrocystic lesions 77−25551
mammogram inspection, computer-assisted microcalcification outlining 79−16291
mammogram inspection by computer 79−57757
mammographic dose reduction, Kodak Definix Medical rel. to Kodak Min R film *(German)* 80−12243
mammographic film and film/screen combinations, quantitative evaluation 79−88151
mammographic image quality comparison phantom 78−85357
mammographic image quality improvement by scattered radiation grids 79−92332
mammographic imaging, historical review in terms of image quality and reduced radiation dose 80−41229
mammographic imaging, new modalities, comparison of techniques 79−48335
mammographic screen-film system image props., laboratory and clinical evaluations 79−29616
mammographic screen-film systems, comparison of laboratory and clinical evaluations 78−69187
mammographic screen-film systems, laboratory and clinical evaluations of image props. 78−85365
mammographic X-ray screen sensitivity and resolution 78−7449
mammographs, high quality low-radiation, tone reproduction system 80−41198
mammography, absorbed dose evaluation, Monte Carlo simulation studies 80−98143
mammography, backscatt. factors, var. with field diameter and half-value layer 78−3593

radiography continued
mammography, breast cancer determinants rel. to radiographic features 80−41170
mammography, comparison of film and xerography methods in early diagnosis *(German)* 78−35946
mammography, detective quantum efficiency anal. of electrostatic imaging and screen-film imaging 80−41232
mammography, dose meas. with high-sensitivity coated-film system *(German)* 79−53257
mammography, effective modelling of diagnostic examinations 78−85366
mammography, experience with 153 breast carcinoma cases *(German)* 80−12244
mammography, exposure timing by use of film/screen systems 80−17059
mammography, image quality and dose requirements *(German)* 79−79646
mammography, method for reducing radiation exposure and improving image quality 78−31901
mammography, model to analyse radiographic factors 80−76828
mammography, most reliable method for early breast cancer detect. 80−21528
mammography, optimum radiographic image conditions 77−90879
mammography, picture quality test *(German)* 78−20270
mammography, reduced dose, anal. of significance of scatt. radiation 79−62346
mammography, relative carcinogenic effects of different techniques 79−70617
mammography, simulation of X-ray spectra 80−76826
mammography, survey of patient skin dose, New Zealand 77−90901
mammography, test object for assessing image quality 80−56171
mammography, use for early cancer diagnosis 79−100724
mammography, use of phosphor X-ray screens, speed and resolution 77−90883
mammography, utility of modelling 78−69188
mammography film/screen combination, reciprocity law failure 78−65103
mammography modalities, advantages and limitations *(French)* 78−7430
mammography radiation dosage in different examination systems *(German)* 79−100750
mammography rel. to grey-scale echoscopy in breast exam. 79−62313
mammography reliability for early breast cancer detection 80−8127
mammography techniques, appl. to bird skull struct. anal. 80−36209
mammography techniques comparison, in vitro studies of breast microcalcification detectability 80−41230
mammography with magnification and grids: detail visibility and dose measurements 80−41231
mammography X-ray beam filtration 78−69207
mammography X-ray exposure meas., Baldwin-Farmer chamber response 78−28040
mamography, risks, radiation dosage and picture quality, review *(German)* 80−36103
mass prophylactic examinations, electroroentgenography advantages 77−25545
mass testing of hollow cylindrical parts, radiation field use 78−48597
medical, photon path visualisation by Monte Carlo simulation 77−66848
medical, solns. for film and data handling in large diagnostic departments 78−40294
medical, US Nationwide Evaluation of X-ray Trends and state radiation meas. 77−40779
medical diagnosis, appl. and limitations of the use of X-rays 79−79643
medical diagnosis, information storage requirements 80−98086
medical diagnosis, problems anal. 78−31903
medical diagnosis, sensitometry, review 78−20260
medical diagnosis, stochastic late effects after partial body irrad. 78−69152
medical diagnosis, working places incorporating Medicor equipment 78−35942
medical diagnostic decision making and image quality 78−28059
medical diagnostic equipment needs for radiology department, math. model 78−65107
medical diagnostic radiation exposure of Italian population in 1974, genetically significant dose 77−66850
medical diagnostic X-rays, effects, risks and protection, review 78−3591
medical images, formation, perception and measurement, conference, Leeds, England (Mar. 1976) 77−86561
medical imaging, conf., San Diego, USA, (Aug 1978) 80−17025
medical imaging, conference, San Diego, USA (Aug. 1979) 80−94919
medical imaging overview 80−98082
medical imaging system evaluation by contrast-detail-dose analysis 80−98140
medical imaging system evaluation using contrast-detail-dose anal. 80−98108
medical physics conference, Ottawa, Canada (Jul. 1976) 77−16897
medical X-ray and fluorographic film sensitometry 77−48858
medical X-ray diagnostics, NDT impetus, novel techniques *(German)* 78−7146
medical X-ray exposure survey, performance characts. of integrating ion chambers 78−853
megavoltage imaging, influence of metal screens on contrast 80−30866
metabolic bone diseases in childhood *(German)* 80−17091
metal fatigue crack detection using nondestructive evaluation (NDE) methods 80−71826
metal screen-film detector MTF at megavoltage X-ray energies 80−30868
metals, oxidation mech., exam. using autoradiography 79−20326
micro-dose system 80−51233
microchannel plate image intensifier, quantum detection efficiency 77−83462
microchannel plate X-ray image intensifier, image resolution 78−35937
microchannel plate X-ray image intensifier, noise characts. 78−53483
microcoded, aperture imaging, appl. to laser plasma diagnosis 80−24251
microdensitometer computer interface design and construction, for X-ray image anal. 77−44821
microdensitometer temporal reponse, MTF determ. 78−32904
microdosimetry, conf., Brussels, Belgium (May 1978) 80−4472
microfocus projection, scattering effect on contrast 80−100973
microfocus rod anode system, 150 kV, for nondestructive testing 78−95881
microphotodensitometry in traumatology and orthopaedic surgery *(Croatian)* 80−109022
radiography continued
microprocessor-based teleradiology system 80−26343
microscopy using ultrasoft X-rays, potential operating region for biological materials 77−90972
minerals, radiography of geological specimens for determ. of α- and fission-activity 78−20540
miniaturisation, comparison of two methods 77−81560
MIRA series of impulse X-ray apparatus 79−34252
modulation transfer data for X-ray film screen combinations 78−66016
modulation transfer function of screen film systems 79−100712
motion picture filming of moving objects with aid of pulsed and continuous X-rays 78−57057
motor-tilted diagnostic examination device Model UV-5B 80−85479
MTF concept, use and abuse for various X-ray imaging systems 77−86623
mucociliary tracheal clearance vel., radiological method for determ. 80−104727
multiple radiography overexposures anal. 79−49877
multiply-exposed radiograph digital image restoration improvement 78−78054
multispectral X-ray imaging, nonlinear techniques 80−72293
muscle single fibres, Rb^+, Cs^+ and Na^+ localisation, autoradiographic demonstration at 77K 79−96726
MWPC, appl. to radiation localisation problems in medicine and biology, review 79−5432
myelographic device based on concentric principle 79−92369
myelographic technique for cysts in spinal canal and cord 79−92363
myelography, contrast agents evaluation 79−92361
myocardial contrast accumulation, densitometric evaluation 78−69216
myocardial performance index from left ventricular area ratios 77−56465
nasal mucociliary transport, mucous velocity meas. using roentgenographic method 79−29600
NDT, gamma-ray flaw detector with analogue data processing, param. optimisation 77−81374
NDT betatron flaw detection, signal processing algorithm 77−81375
negatoscope, 0D-10N, for scanning radiograph 80−35494
neuroradiology, radiation dose to critical organs of staff and patients 80−8184
Neuroscope, for multiprojectional isocentric fluoroscopy and angiography 78−40292
neurosurgical intraoperative X-ray equipment use 79−92344
neutron beam characterisation by radioactivation image transfer technique 79−88196
noise equivalent parameters, in general medical radiography 78−28058
nondestructive materials testing, review of radiographic principles and methods 78−53065
nuclear emulsions, recording possibilities in electron microscopic autoradiography conditions 78−17489
nuclear fuel element assembly NDT 78−72940
nuclear reactor fuel inventory, autoradiographic techniques 78−82066
nuclear scattering radiography, progress in 79−48330
nuclear scattering radiography using 500 to 1000 MeV protons 77−9244
nucleonics history, record of lost opportunities 78−65986
object and film rotating rel. to X-ray beam 77−66716
observer performance meas. and characterisation, free response approach 78−69200
observer performance meas. and characterisation, free-response approach 79−74752
obstetric radiography, fetal radiation dose 79−92376
one-sided cardiac failure differentiation by planimetric electrokymography 79−43990
operating theatre X-ray installation planning 79−92339
optical and digital image processing 77−70241
optical centreing systems, operation 80−30831
optical density difference measurement on X-ray film by analog measurer 79−39099
optical density variation, characterisation of radiographic edge-blurring effect 80−13176
optical fibre preform core diameter and Ge doping profile meas., X-ray nondestructive method 80−64231
optical instrumentation appl. in medicine, conf., Boston, USA (Sept. 1977) 78−69184
optical instrumentation in medicine, conf., Toronto, Canada, (Mar. '79) 80−36777
Optiplanimat clinical experience, ear ob. examples 79−62339
Optiplanimat X-ray planigraphic unit, use in daily routine 79−62340
OTF as means of evaluation of image charact. *(German)* 80−35450
OTF of radiographic imaging systems 80−17085
paediatric chest stand, working procedure and radiation exposure 79−48337
paediatric patient, radiation exposure from cardiac catheterisation and angiography 80−41241
paediatric radiology, the Diagnost 73 P, universal diagnostic system 79−48334
paediatric radioluscent bone length meas. 78−48891
paediatric X-ray examination equipment assessment, point system 77−21603
pancreas, scintigraphy rel. to endoscopic retrograde parenchymography *(Japanese)* 80−81725
panoramic magnification technique, diagnosis of facial skull tumours 79−34645
panoramic tomograph users' experience in exam. of teeth and jaws 77−21605
patient dose estimation, quantitative meas. *(German)* 78−57073
patient exposure, anal. of 1972-1975 NEXT data 79−39505
patient exposure 80−46066
patient exposure and radiation risks, Swedish diagnostic radiology 79−53248
pediatric cardiac catheterisation, absorbed dose in presence of contrast agents 80−30897
pelvimetry, low radiation dose gridless method 80−46010
penetrameter cassette, multiple exposure, for meas. of effective kilovoltage of diagnostic X-ray beams 80−61662
penetrameter cassette calibration to 400 kV and extra-focal radiation effects in X-ray tube filtration meas. 78−20242
penetrameter for measuring peak kilovoltage of dental X-ray sets 80−41171
percutaneous cricothyroid bronchography *(Dutch)* 80−85471
percutaneous transhepatic cholangiography and endoscopic retrograde cholangiopancreaticography 79−92333

radiography continued
perforating rods, length reduction at high impact velocities, X-ray studies 78−40016
person dose, ICRP concept, related to exposure in industrial radiography 79−5370
Petri dish autoradiographed cell counter 79−70723
phantoms for testing X-ray imaging performance 80−51229
phosphates, U content, α-ray autoradiography, fluorimetry, estimation 78−20414
photofluorographic camera with electro-optical image intensifier 80−36128
photogrammetry use in absorbed dose determ. in radiation therapy 80−12222
photographic film response to 25 MV X-rays, sensitometric curves, relative dosimetry 80−52376
photographic images, quantitative anal. of autoradiographic image intensification using Thiourea-^{35}S 80−90343
photographic noise in data processing by coherent light *(Italian)* 78−22088
photography of medical X-ray plates, audio-visual presentations for physicians 80−37103
photon energy distribution of diagnostic X-ray beams 77−70530
phototimers, acceptance testing and performance monitoring 77−5071
picture coding, closed orthogonal functions, X-ray pictures appl. 77−77965
picture examination TV equipment 77−21607
picture-display systems, developments and limitations *(German)* 79−100705
pinhole camera, hole size required for no distortion 80−46028
pipeline inspection, welding flaw detect., NDT 78−19984
planar defect depth determ. 77−81350
plasma X-ray photography using quartz analyser crystal 77−35403
plasmas, laser produced, as X-ray source for microradiography 80−320
pneumoconiosis, small lesions, computer aided identification 80−30887
pneumoconiosis of coal-workers, optical-digital system for pattern recognition 78−40389
pneumoconiosis opacities in chest X-rays, improved detection algorithm 78−73242
polycrystalline solids, radiographic determ. of dispersion of disordered and ordered dislocation distribs. 77−51373
polycrystals, deformed, particle sizes and mean square strains *(German)* 78−3284
polyurethane supportive dressing, radiolucency and mechanical properties 77−73561
portable, high energy source 79−47849
portable low-dose X-ray imaging system 78−85375
postero-anterior radiography, method for eye dose reduction 79−92388
power supply design 77−21608
prenatal X-ray examination frequency and radiation risks in Japan 77−5070
prescription lenses, attenuation of diagnostic X-rays 79−92395
pressure vessels weld quality assessment, NDT methods and equipment 78−56871
processing radiographs, computer appl. 80−3259
processor control using preexposed control strips and visual comparative densitometry 78−69210
productivity of radiographic inspection method 80−71861
projection microradiography, historical development and applications 80−37138
projection radiography in medicine, future trends 80−98083
proportional counter for radiographic investigation of objects 79−67449
proton, beam line establishment at Fermi National Accelerator Laboratory 78−65121
proton, fluorescent intensification screen+photographic film combination, response, radiography appl. 78−20268
proton, medical application *(French)* 79−2128
proton, review 79−91896
proton (heavy ion) radiography in medical diagnosis 79−57753
proton radiography, solid state detectors 78−92424
proximity X-ray image intensifier tube 78−69206
pseudo-colour images, microprocessor controlled method for electronic image processing *(German)* 78−92724
pulmonary arterial occlusion, comparison of methods in detect., dog expts. 80−56191
pulmonary infiltration interactive analysis 77−21625
pulmonary radiograph interpretation, review of models used 80−36089
pulmonary selective angiography in dogs with pulmonary embolism, radioisotope comparison 78−65113
pulmonary vascularity automated diagnosis from chest roentgenograms 77−60248
pulmonary vascularity computerised texture features rel. to catherisation parameters 80−8154
pulmonary venous pressure estimation from routine chest radiographs using hybrid optical-electronic system 78−44657
pulsating potential X-ray machines, filter method for peak volt. and inherent filtration meas. 78−73201
pulsed X-ray radiography, precise control of linear electron accelerator *(Japanese)* 78−35944
quality assurance meas. for diagnostic X-ray systems 77−40763
quality control programme, economic analysis 78−73236
quality health care and cost containment, conf., Washington, USA (Mar.-Apr. 1978) 79−39333
quantum mottle anal., fast Fourier digital technique appl. to rare earth intensifiers 77−52868
radiation output constancy during diagnostic exposures 79−5340
radiation protection survey of mobile mass-miniature radiography unit, TLD obs. 79−62375
radioactive uniform sources of extended area using radiotoned photographic 78−78537
radiochromatograms, thin-layer, anal. by proportional chamber 78−77174
radiographic quality, tube potential, and patient dose 79−62349
radioisotope X-radiation sources in defectoscopy 77−56176
radiological-endoscopic combined setups for gastrointestinal organ exam., experience 77−90947
radiology conference, London, England (Apr. 1979) 80−30838
radiopaque marker clinical usefulness in left ventricular function 80−36119
radius, human, compact bone mineral density meas. 79−74739
random pulse train processing by linear filter *(Russian)* 78−46518
rare earth phosphor intensifying screen speed gain 78−7447
radiography continued
rare-earth screens, effect of P X-rays 80−30867
reactor fuel rod radiography, feature extraction via least squares fit to model 77−14229
reactor vessels, thin-walled, radiographic testing, sensitivity using 10 MeV microtron 78−70603
receiver operating characteristics curves and their use in diagnostics *(German)* 80−98109
reconstruction of objects from their projections, measurement error effects 77−67550
reduced radiation dose with electroradiography *(Swedish)* 77−9259
reduced scatter, effect on information content and patient exposure 80−51225
regional left ventricular wall motion in coronary heart disease 80−85490
relief-exposure charact. of radiographs in relief 78−49945
renal and ureteral calculi, surgical treatment under fluoroscopic control 79−92342
renal angiography, renal vascular resistance and I washout 77−77927
renal arteriography, magnification selective obs. 79−53209
renal diagnosis by blood circulation angiocinedensitometry *(German)* 79−2127
renal length measurement, importance of renal inclination as meas. by US 78−77092
reoentgenokymographic unit, physical and operational charact., plate thickness optimisation 79−57747
resolution, falling load principle, focal spot performance 77−2045
resolution and contrast reduction 79−20663
review of X-ray imaging, image intensification systems and techniques 80−51236
RMS focal spot, validity considerations 80−81691
Roentgen cinefilms, circuit for densitometric evaluation *(German)* 79−53214
roentgen densitometer for detect. of congenital heart defects, patient dose 77−9239
roentgen stereophotogrammetric methods for human knee joint evaluation 80−30952
roentgenocardiograph with photoelectronic sensors, calibration device 78−57061
roentgenokymographic image formation, rel. to optimal grid slit width 78−57058
rotating aperture wheel device for radiographic contrast improvement 80−56202
rotating disk device for slit radiography of the chest 80−98116
rotating-anode X-ray tube apparatus 78−58100
routine diagnostics, effect of automation 79−16292
RUM-20 apparatus, obs. on improving roentgenogram quality 80−30850
safety training for radiographers 78−81961
safety training program for radiographers 80−17141
sandwich technique for hot objects 79−96251
scanning multiple slit assembly, design and performance 79−70616
scatter to primary radiation ratio variation obs. 80−81722
scattered radiation grids, method for testing 80−81717
scattered X-rays, effect on diagnostic image quality 79−8533
scoliotic spine, anal. of changes using 3D technique 80−94346
screen characteristic X-ray reabsorption calc. 79−74753
screen sharpness quantum noise depend. 78−20261
screen-film combination selection 80−46047
screen-film detectors, megavoltage OTF meas. technique 79−80736
screen-film processing sensitometry standard developed by ANSI 78−69196
screen-film system, determination of charact. curve and its gradient 79−5362
screen-film system comparisons, fluoresc. X-ray source 78−24132
screen-film system evaluation, intensity vs. time scale sensitometry 80−41219
screen-film system evaluation, sensitometric method 80−41220
screen-film systems, H and D curves, factors affecting X-ray energy dependence 79−39484
screen-film systems, quantum fluctuations 79−58857
sensitivity and detail visibility 78−44286
sensitivity calc. and scale parameters of radioisotope meas. instruments 79−11747
sensitometers, for radiographic processing quality assurance, performance evaluation 79−29617
sensitometry, conference, Binghamton, N.Y., USA (Sep. 1976) 77−30214
sensitometry in medical imaging applied in diagnosis and therapy 78−69193
shape descriptors, Fourier-Walsh, radiographic image processing appls. 80−8153
sheet material surface density nonuniformity using beta radiation 77−77717
shielding calculations below 100 kVp in concrete-equivalent materials 79−29637
shielding device, Pb glass, for use with ceiling mounted tube 79−92397
shielding windows, improvement in optical charact. by antirefl. surfaces 77−21601
Shroud of Turin, scientific investigation 80−87576
Siemens star X-ray image artifacts, computer simulation 77−21615
signal detection in visible noise, threshold mechanisms 77−86624
signal to noise ratio improvement *(German)* 79−39078
signals and relationship 80−95808
site training 78−25329
skeletal diagnostics, direct magnification, exposure technique and timing 80−104747
skeletal maturity determination system *(French)* 80−41209
skeletal metastases detect., radiographs vs. scans 77−44746
skeletal radiographic imaging, computer/scanner approach 77−77989
skull, frontal diagnostics of injuries *(German)* 80−36104
skull, struct. changes due to Recklinghausen's disease, X-ray and nuclear medicine diagnosis *(German)* 80−76831
small diameter pipe weld, gamma radiography using enriched ^{169}Yb source 79−83399
small intestine, babies, X-ray exam. technique 80−104739
small intestine diagnosis *(German)* 79−100726
small-grain development of emulsion monofilms for electron-microscope autoradiography *(Russian)* 80−297
solid state electrophotographic imaging with ionic dielectric X-ray receptors 78−16899
somatic dose index, human, typical beam quantities and exposures 79−16306

radiography continued
source coding of X-ray pictures for compact storage or fast transmission 78−40310
spectra and angular distrib. meas. of scattered X-radiation *(German)* 78−7148
speed-granularity relations for X-ray and γ-ray exposures 79−21828
spinal radiograph standardisation for scoliosis assessment, computer method 78−57066
spot-camera of Medicor Works 80−85477
star test pattern image interpretation 77−21614
steel, austenitic stainless, mottling on radiographs of weldments and castings 80−16614
steel, austentic stainless, butt welds, US exam., comparison with radiographic techniques 80−93710
steel, C martensite, electron irrad., reversible C at. redistrib. 77−65991
steel, castings for use at high temp., correlation between US and radiographic inspection *(German)* 78−88599
steel, Cr-Ni, microstructural distrib. of cathodic H_2, autoradiography *(French)* 79−99234
steel, crack detectability by radiography 79−91857
steel, interpretation of weld radiographs 79−91861
steel, N determ. by track autoradiography 80−100979
steel, Ni-C, martensitic, microstructural distrib. of cathodic H_2, autoradiography *(French)* 79−99234
steel, pressing die X45 CrNiWMoVCo 9.9, test results *(German)* 80−50785
steel, radiography with the 25000 R/min Linac 80−97656
steel, stainless, austenitic, microstructural distrib. of cathodic H_2, autoradiography *(French)* 79−99234
steel, tempered martensitic, type AISI 410, role of C in embrittlement phenomena 80−93652
steel, welded joint, standardization of radiographic flaw detection 79−91900
steel 40 KhSN2MVF, chemical micro-inhomogeneity recovery during thermal working *(Russian)* 78−15442
steel fibre reinforced cementitious material, radiographic anal. of fibre distribs. 78−52747
steel slab, scattered radiation intensity of ^{192}Ir gamma rays 77−30673
stenosis densitometric analysis from remote terminal 79−83900
stereo X-ray comparator, Zeiss StR 1-3, analytic system for 3D X-ray picture meas. *(German)* 78−92691
stereography, method of precision position determ. 80−56314
stereoradiography, exam. of discontinuities in welds 78−53178
stereoradiology, single monitor systems using PLZT electro-optic shutters 77−60247
stereoscopic image evaluating device, Medicor Model SZRK 80−85478
stereoscopic X-ray unit for medical diagnostic sets 80−85467
stomach, postoperative, double-contrast exam. 79−92359
stomach contour extraction *(Japanese)* 78−53482
stomach double-contrast exam. using Orbiskop 78−73200
stomach examination, quality improvement by use of fine-focus tubes 80−85468
stomach radiograms, pattern anal. system *(Japanese)* 79−39481
stomach radiograms image anal. 79−88176
subtraction, wax phantom simulating flat tumour with diffuse edges for film evaluation 77−70536
subtraction device for daily practice and vascular procedures 80−36090
subtraction radiography, characts. and limitations of photographic films 77−2046
Super Rotalix Ceramic, new type of X-ray tube 80−104749
supervoltage beam films for radiotherapy 78−3580
surface dose product meas., for official ionising radiation practice *(German)* 79−2137
surface imaging, with backscatt. beta-rays 78−48588
technological and philosophical changes over a decade of X-ray tubes 80−37136
test objects for systems performance evaluation 80−46022
test phantom for meas. of phys. parameters of diagnostic apparatus *(German)* 78−57068
testing equipment, device characts. *(German)* 80−76438
TEXAC image processing computer for radiographic feature enhancement 80−12251
texture, multicomponent axial, quantitative evaluation 80−85100
texture analysis and EPQ of radiographic images 79−34643
thermal, prep. of cholesteryl oleyl carbonate for IR detection 77−15311
thermoluminescent, improved resolution image storage panel 78−16898
thermoplastic structural foams, charact. by equidensitometry and radiography 77−44417
thickness meas., destructive and nondestructive methods compared *(French)* 78−15611
thoracic X-ray image comparison automation *(Japanese)* 79−29615
Thoramat automatic thoracic radiography unit experience 80−12212
three dimensional, X-ray microscopy provides 10 nm resolution *(German)* 77−38077
three dimensional image recording and reconstruction 80−31953
three-dimensional imaging 80−85486
thrombophlebitis patients, venographic, impedance and Doppler US findings 78−48919
thrombosis detection by US, plethysmography and phlebography 78−7435
thyroid, simultaneous emission and fluorescent scanning 79−16275
thyroid nodules, attenuation of monoenergetic photons from ^{125}I 79−5346
tibia, human, simplified method of radiographic anal. of its cross-section, anthropometric correls. 80−89827
timer for processing 79−5125
tissue section imaging by α and thermal neutrons 79−29591
tomofluorographic camera with lens objective and angular tube 79−57750
tomogram reconstruction by holographic methods 80−67246
tomography, X-ray resolution by finite field transforms 77−67549
total unsharpness analysis 78−11730
track density, device for determ. in solid-state particle detector 79−85859
transmission image reconstruction from projections, max. likelihood meth. 77−86690
transmission of X-ray pictures over voice grade telephone channels 78−44607
transmission wedge for anatomical localisation, prior to radiopharmaceutical injection 79−16333
transmission X-radiographic development trends *(German)* 78−15636
radiography continued
transthoracic punch biopsy, X-ray locator 79−92331
transvenous xeroarteriography, peripheral blood vessel angiography *(German)* 79−2126
traumatised patient diagnostic radiology requirements 80−8128
tube current fall-off during an exposure, investigation and explanation 80−56203
tube to tubesheet welds, X-ray and isotropic techniques for boroside radiography 77−86261
TV installation for projection of high-resolution X-ray images *(German)* 79−57751
TV picture transfer of X-ray image intensifier output screens 77−5077
TV radioscopic system, for 400 kV X-rays, using microchannel plate image intensifier *(French)* 77−38071
TV system, camera and picture monitor 77−9251
unsharpness, total, integral formulation 77−16978
unsharpness additivity 77−52871
upper airways in newborn and infants, X-ray physiological exam. using Orbiskop 80−8130
urodynamic combination EMG and functional X-ray exam. technique 80−8131
urography, double-dose, image clarity and contrast range obs. *(German)* 80−30875
urology, universal room using Uro Diagnost 78−31902
uterine venography, value in diagnosis of pelvic pain in women *(French)* 80−17079
valvular regurgitant fraction meas. by radionuclide angiocardiography, iterative estimation 79−34668
venography, contrast, correl. with dynamic radionuclide venogram 79−96655
venography in management of proximal venous occlusion 79−53210
venous system visualisation combined with press. meas., technique and equipment 80−36094
ventricle, left, boundary detection from cineangiocardiograms 80−8168
ventricle, left, cineangiographic images automatic processing 79−83927
ventricle, left, human, geometric modelling, using biplane cineangiograms 80−35955
ventricle regional wall motion parameters, angiography vs. echocardiography 79−62392
ventricular function evaluation, comparison of systolic and diastolic parameters 79−70636
ventricular wall regional motion extent and sequence, clinical study 79−70635
ventriculography, algorithm for automatic selection of end diastolic and end systolic cine frames 78−88757
vesico-ureteric reflux detect., nuclear rel. to radiographic technique 79−100703
video images, enhancement 80−94353
video processor for computer calc. of press.-vol. indices from left ventriculograms 78−53495
video subtraction procedures, computer-controlled 80−98102
video-angiocardiographic image series storage improvement by digital signal processing *(German)* 78−92723
videodensitometric camera and video disc system 77−40761
videodensitometry and image analysis, minimum computer system 79−34664
videodensitometry in angiography 80−104745
vidicon tube for low level X-ray and γ-ray imaging 77−81561
weld joint of high-pressure vessel 79−100313
weld joint shape fluctuations effects on errors 78−53145
weld testing between tubes and tube-plates in heat exchangers *(German)* 78−7151
welded joint, radiographic inspection, standardization of sensitivity and flaw size 80−89455
welded joint inspection by X-ray TV intrascope, photographic recording of images 80−86485
welded joints, radiographic inspection, real flaws detectability evaluation 80−81266
welded joints inspection, effectiveness investigation 78−56872
welds, interpretation 79−91861
welds and castings, differential method of balancing out thickness-variation effects in radiography 80−66748
Wisconsin mammographic kVp cassettes, evaluation of spectral response 80−81715
X-radiography image, contrast improvement by use of filter between specimen and film 77−5968
X-ray attenuation measurements, effects of meas. apparatus 77−38587
X-ray beam, high-energy, contamination by electrons 79−8534
X-ray beam characteristic time vars. meas. using solid state devices 80−46048
X-ray camera attachment for aimed investigation of fractures 80−85102
X-ray coded mask telescope, appls. to radiography 77−13239
X-ray departments, General Hospitals, planning standards 78−92741
X-ray diagnostic department dimensioning problems in university hospitals 77−90946
X-ray diagnostic sets with automatic exposure relays, switching delays 77−48903
X-ray diagnostics appl. to laser induced fusion, review 77−55176
X-ray equipment, scattered-radiation exposure 79−34670
X-ray equipment, STATUS X, for canine teeth localisation 77−90881
X-ray equipment selection for intensive care unit 79−92346
X-ray equipment survey in hospital and preventive medicine establishments 77−21602
X-ray film, reversal-developed, image quality with reference to density 79−100713
X-ray film processing 78−27707
X-ray film with reduced crossover, evaluation 79−70621
X-ray films, reciprocity law failure in reversal processing 79−97483
X-ray flaw detection, electroluminescent storage screens, expt. results 77−77722
X-ray focal spot, MTF, modified meas. method 80−37149
X-ray generators, acceptable latitudes in the specifications 80−37137
X-ray image convertor with video signal output 80−36125
X-ray image intensifier freq.-contrast charact. curves determ. 78−7427
X-ray image intensifier performance, image quality, and development trends 80−36124
X-ray image intensifier tube, 14 in 79−16285
X-ray image intensifiers, design aspects 77−38070
X-ray image intensifiers, quantum noise meas. 80−46033
X-ray image magnification technique 80−18054

radiography continued
X-ray image quality, MTF anal. of influencing factors *(Japanese)* 77−73580
X-ray image reconstruction, iterative scheme 78−66014
X-ray imaging scope, low-intensity, principle, appls. 79−30637
X-ray imaging system, MTF 77−38815
X-ray incoherent holography *(Korean)* 79−6250
X-ray installation, for rapid process frame-by-frame registration 80−47159
X-ray magnifier for image magnification 79−17592
X-ray microscopy and X-ray lithography, techniques, appls. 77−34059
X-ray paper use in radiographic control of MTR fuel production 78−5001
X-ray photograph comparator with sliding calliper 78−86397
X-ray photographs, CCTV transmission, TV camera operation *(Hungarian)* 78−21306
X-ray portable unit, RAPS-1, for quality control, defectoscopy 79−44998
X-ray powder diffraction camera, absorpt. attachment, appl. to gallstone study 77−41744
X-ray production equipment, USA safety standard 78−29223
X-ray quantum statistics limited electrostatic imaging 78−7451
X-ray residual stress anal. theory 77−84200
X-ray rotating anodes, comparison, w.r.t. temperature distribution 79−2901
X-ray stress anal., recent German activities 77−81359
X-ray television system, based on vidicons, used for defectoscopy 78−72977
X-ray tomography, transaxial simple rotational photographic method 79−93242
X-ray tube anode voltage compensation under dropping power condition, digital compensation system *(Bulgarian)* 79−35902
X-ray tube current, effect of electron evaporation 78−69204
X-ray tube performance characteristic rel. to radiologic image quality 80−17125
X-ray tube single- and three-phase generator performance comparison *(Japanese)* 79−92354
X-ray tube thermal monitoring system, LOADIX, features 78−3658
X-ray tube voltage error effects on image quality of roentgenograms 78−57060
X-ray tubes, focal spot size meas., systematic error 79−75666
X-ray tubes, meas. of focal spot size 80−89831
X-ray tubes, rotating anode, increased loadability 79−12915
X-ray tubes, rotating anode, upper limitation of output 79−30631
X-ray tubes, vacuum technology *(German)* 79−30634
X-ray tubes and generators, calibration system 79−17583
X-ray TV chain MTF and image quality determ. factors 80−36126
X-ray TV display system, transmission characts. *(German)* 79−53215
X-ray TV of gas turbines, problems 78−95861
X-ray TV systems, parameter estimation 77−73404
X-rays, spatially modulated, pattern recognition 78−45761
xerography and mammary microcalcifications *(French)* 80−51224
xeromammography, absorbed dose obs. 80−41242
xeromammography, dose to patient and image quality 79−100741
xeromammography, image optimisation, detailed systems-based anal. 79−39483
xeromammography, image quality 80−89834
xeromammography, Monte Carlo calc. of integral radiation dose 80−41248
xeromammography, technique and advantages *(French)* 78−7431
xeromammography exposure timing 78−40291
xeroradiographic image accuracy rel. to X-ray dose 77−77966
xeroradiographic imaging linearity and MTF applicability 80−4825
xeroradiography, for teaching 78−45449
xeroradiography, high kV techniques and optimal filtration 77−21598
xeroradiography, imaging factors for the extremities 79−20614
xeroradiography, negative development, doses and clinical indications in breast exams. 80−56217
xeroradiography, physical theory and photon noise obs. 77−5072
xeroradiography, reduction of patient dose 79−16303
xeroradiography, sensitivity and edge enhancement determ., theory and expt. 80−89833
xeroradiography, sensitivity of Se plates 77−45909
xeroradiography for direct field control in radiotherapy 77−81551
xeroradiography of frontal skull and nasopharynx *(German)* 80−30873
xeroradiomammography, positive rel. to negative mode considerations *(French)* 80−51223
Al parts, radiographic testing *(German)* 77−1900
Al-Cu, type 1100, synchrotron radiation microradiography 80−85121
Al-Cu-Mn, type 2219, synchrotron radiation microradiography 80−85121
Al-PMMA laminated composites, shock wave propag., flash radiographi obs. 79−4370
BaFCl:Eu X-ray intensifying screen 78−11735
$Ba_5SiO_4Br_6$:Eu, blue emitting X-ray luminescent material for intensifying screens *(French)* 80−66260
^{209}Bi spatial distrib. on microscopic scale, ^{4}He 40 MeV ion beam 77−12859
$CaWO_4$ and rare-earth X-ray intensifying screen sensitivity to scattered radiation 78−7450
$CaWO_4$ X-ray intensifying screens, absorbed-energy const. 77−70537
^{252}Cf wire neutron source distrib., meas. by autoradiography 77−61643
Co-based eutectic alloy, autoradiographic investig. of struct. defects *(Russian)* 77−25038
^{60}Co 20 Ci source, site radiography incident 78−53523
^{51}Cr-labelled lymphocyte autoradiographic detection problems 79−29592
CsI based powdered phosphors and screens possible appl. in X-ray radiography and fluorography 79−6245
Cu conductors in reinforced concrete, radiographic method of inspection 79−15936
Cu hollow charge jet, density meas. by light radiography *(French)* 78−44344
Cu-Al (14.3 wt.%), ^{110}Ag diffusion in β/γ_2 interphase boundary 80−79989
^{159}Dy evaluation for transmission imaging and bone mineral anal. 77−48861
Fe, cast, Mg, despheroidising effect of Bi, Sn on graphite in alloy 78−56670
Fe, pure, Sn and Cr diffusion, effect of boundary struct., autoradiography study *(Japanese)* 80−49419
radiography continued
α-Fe-Cr alloys, recrystallised, C segreg. effects, TEM *(French)* 77- 28828
Fe-Ni-C martensite, autoradiographic evidence of C clustering 79−83203
Fe-Ti (0.15 wt.%), H trapping obs. by high resolution autoradiography 79−73205
I isolated images using spatial-frequency encoding 79−39485
I meas. in tissue, separation of bone and water, appl. of filtered bremsstrahlung spectra 79−74747
I, stable, tissue determ. by X-ray photographic method 77−70540
I, stable tissue content, meas. by coherently and Compton scatt. photons 79−88220
^{192}Ir gamma-ray source development, high-intensity 77−2715
^{192}Ir radioactive sources, field determ. of output and effective size 80−30193
^{192}Ir radiographic source, radiation accident 78−53514
LaOBr:Tb phosphor X-ray mottle reduction by multilayer screen construction 78−4756
N determinaiton by track autoradiography 80−100979
NaH_2PO_4-NH_4Cl-$NiCl_2$, soln., Ni yield, factors affecting, pot. use as radiographic media 79−52702
PbO, binder layer, properties of radiographic system 78−21238
PbS-base photodetectors, proton radiography 80−104388
^{208}Pb spatial distrib. on microscopic scale, ^{4}He 30 MeV ion beam 77−12859
^{35}S radioisotope, study of Fe oxidation in SO_2 atmospheres 77−52550
Se, electroradiographic layer, radiographic contrast 80−12241
Se layers, latent electrophotographic image, formation mechanism *(Russian)* 79−26157
Se, X-ray sensitivity, induced photocurrents, xeroradiographic meas., pair creation energy 80−22490
Se, xeroradiography films, photosensitivity recovery from X-ray induced fatigue 77−2709
Si:P, neutron irrad. crysts., qualitative distrib. of P using autoradiography 80−24486
$(U,Pu)O_2$, autoradiographic anal. of PU distrib. 79−49811

radioisotope scanning and imaging
see also computerised tomography; scanning radiography
140 keV γ position-sensitive multiwire proportional chamber characteristics 79−54749
abdominal abscesses detection, role of ^{67}Ga-scintigraphy, ultrasonography and computerised tomography 80−17096
abdominal disease, ^{67}Ga imaging 79−57772
abdominal infection evaluation, complementary role of ^{67}Ga-citrate imaging and computed tomography 78−73207
abnormality detection, influence of size and radiopharmaceutical concentration ratio 79−16272
abscess scanning, comparison of ^{111}In-labelled agents 80−94328
abscess-localising agents, tissue distrib. of ^{203}Pb-acetate, comparison with ^{67}Ga-citrate 77−5064
acoustic neuroma diagnosis, contrib. of radioisotope axial tomography 78−28045
activity absolute measurement techniques using a gamma camera and a computer 79−25087
adrenal absorbed dose, human, from ^{131}I-iodomethylnorcholesterol 79−79660
adrenal gland, associated high thyroid dose in ^{131}I scanning 79−29629
adrenal gland imaging with radiolabelled inhibitors of enzymes 78−65118
adrenal glands, using ^{131}I-19-iodocholesterol 77−48853
adrenal imaging, radiopharmaceutical distribution and dosimetry 79−29632
adrenal imaging agents, rationale, synthesis, formulation, metabolism 78−85370
adrenal imaging in primary aldosteronism using ^{131}I-iodomethylnoncholesterol 79−79634
adrenal medulla imaging with an ^{131}I-labeled antiadrenergic agent 79−83910
adrenal scintigraphy using ^{131}I labelled radiocholesterol, diagnosis 78−85371
adrenal scintigraphy with ^{131}I-19-iodocholesterol, Cushing's syndrome diagnosis 80−72289
adrenal uptake measurements, operator-independ. background subtraction method 78−7429
aerosol lung clearance studies, adjustable response detector 77−56451
aerosol particle size meas. by scintillation counting, inhalation technique development *(Slovak)* 79−74750
albumin macroaggregates labelled with radioisotopes for clot detect. 78−7438
albumin microspheres, rapid method for labelling with ^{111}In, ^{113m}In 79−34669
Anger, Hal O., work at the Donner Lab. 80−42027
Anger camera, dual head system for imaging of positron-emitting radionuclides 79−29598
Anger camera dead-time, effect of window fraction 77−86598
Anger camera field-uniformity correct., effect of spatial distortion 79−100721
Anger camera image digital filtering 77−9256
Anger camera/computer system using seven pinhole collimator for myocardial perfusion tomography 80−61663
Anger rectilinear tomographic scanner 78−20257
Anger scintillation camera, development since 1958 80−12234
Anger scintillation cameras, state-of-the-art in suitable photomultiplier tubes 78−40304
Anger tomographic scanner, comparison with 15 in. scintillation camera for Ga imaging 79−34658
angiocardiogram anal. program for radiology trainees 80−8143
angiocardiograms, image enhancement and left ventricular contour extraction techniques appl. 80−72283
angiocardiography, computerised, ECG-gated, automatically generated LV regions of interest 79−70626
angiocardiography, exercise techniques 79−57762
angiocardiography, first pass technique, automation during anal. 79−70625
angiocardiography, quantitative radionuclide, in dogs with atrial septal defects 78−85362
angiography, gated, use of computer-generated functional images to define ventricular boundaries 80−85487

radioisotope scanning and imaging continued
angiography of the left ventricle using the first-pass technique *(German)* 80−109019
angiography technique for assessment of regional wall motion abnormalities 80−85488
annular coded-aperture images, decoding techniques 78−37818
appls. of nuclear reactors *(Japanese)* 79−83913
Auger camera collimator selection for ^{67}Ga imaging 79−57764
Auger camera performance, effects of a reduction in crystal thickness 80−41187
autoionography of beta-emitting radionuclides distrib. on thin-layer chromatograms 78−20126
automated interpretation of nuclear medicine studies 80−8164
autoradiograms of serial sections, preparation for electron microscopy 80−67312
autoradiographic and cytophotometric simultaneous anal. device 78−77172
autoradiographic image intensification, medical appls. 78−61255
autoradiographic whole-body sections, ^{14}C and ^{3}H determ. by liq. scintillation counting *(German)* 77−5114
autoradiography, criterion for classifying radioactive cells 77−37041
autoradiography, direct deposition method, radioactivity detect. 78−77167
autoradiography, double radionuclide methods for tissue sections or cell smears, using light microscopy 77−5113
autoradiography, increasing detect. power of type M nucl. emulsion gel 78−20269
autoradiography and soft laser scanning in radioisotope work, appl. to metabolic studies 78−3576
autoradiography combined with SEM for cell topography obs. 78−24212
autoradiography of serial sections, method for holding electron microscope grids 78−20331
axial tomography by half back-projection 78−28056
bar-phantom image distortion by collimator 79−100722
basic radionuclide imaging techniques, book contrib. 80−36113
benzodiazepine receptors in brains of humans and animals, autoradiographic localisation 79−83752
biliary tract disorders, evaluation by cholescintigraphy, ultrasonography and computerised tomography 80−17093
biofocal diverging collimator for equilibrium radionuclide ventriculography 80−72310
blood flow, regional, assessment by intravenous injection of ^{99m}Tc pertechnetate 80−104732
blood flow, rel. to brain function 79−43988
blood flow and tracer uptake in normal and abnormal canine bone 80−17072
blood flow measurement in dynamic phantom using ^{81}Rb-^{81m}Kr and NaI detector 77−66843
blood pool imaging by in vivo labelling of red cells with ^{99m}Tc 77−37052
blood-pool imaging in ^{99m}Tc myocardial scintigraphy 80−12228
bolus-injection system for dynamic time-function studies 80−41194
bone, diffuse alterations, quantitative assessment of ^{99m}Tc-MDP scans 80−72287
bone, healing fracture, blood flow rel. to ^{85}Sr uptake 80−72187
bone, normal, uptake of bone-seeking radioisotopes rel. to blood flow 80−94320
bone, X-irradiated, changes in ^{99m}Tc pyrophosphate imaging 80−72239
bone blood flow, meas. with a ^{133}Xe washout method 80−72288
bone blood flow determ., comparative study of $^{99m}TcO_4$ and ^{131}I-iodoantipyrine 78−28046
bone density determination in vivo, computed tomography vs. mineral analyser 77−73567
bone diseases, benign, the particular usefulness of radioisotope methods 80−51209
bone fracture healing, evaluation, rabbit obs. 79−70613
bone fracture healing, significance of scintigraphy *(German)* 80−76833
bone imaging, comparison of ^{99m}Tc-labelled P-based agents 77−66842
bone imaging, evaluation of ^{113m}I-EDTMP 77−56455
bone imaging in infants and children, review 78−77107
bone imaging radiopharmaceutical local accumulation model 78−24127
bone marrow haemopoietic activity assessment in normal subjects 80−36073
bone marrow scanning in pediatric oncology, evaluation of ^{99M}TcS colloid 80−17067
bone metastases detect., clinical comparison of ^{99m}Tc HEDP and ^{99m}Tc MDP 79−83904
bone rectilinear scanning, differentiation between metastases and degenerative spinal disease 78−44585
bone revascularisation processes study method, local blood flow dynamic anal. using ^{85}Sr 80−81684
bone scan, whole body, value in breast carcinoma pre-operative assessment 80−51210
bone scan quality vs. time between dose and scan 78−3585
bone scanning, historical survey 80−42029
bone scanning, improved quantitative method 78−24125
bone scanning in osteomalacia 78−73204
bone scans, appearance following fractures 80−56189
bone scintigraphy, importance in pretherapeutic development of mammary neoplasms *(French)* 80−8135
bone scintigraphy, use in uremic pulmonary calcification detect., ^{99m}Tc HEDP obs. 80−3788
bone scintigraphy as detect. method for bone and bone marrow involvement in malignant lymphoma 80−36086
bone scintigraphy clinical comparison of ^{99}Tc^{m}-diphosphonate and -pyrophosphate 78−65112
bone scintigraphy obs. in renal osteodystrophy 79−70611
bone tumours, human, scintigraphic assessment of ^{99m}Tc-diphosphonate 79−20613
bone-scan interpretation, implications of skeletal blood flow 80−72199
book, basic radionuclide imaging techniques 80−31426
brain, artifact in supine posterior projection 79−34661
brain, baboon, ^{11}C-flunitrazepam displacement visualisation 79−83730
brain, combined static and circulation imaging 80−51211
brain, complementary role with computerised axial transmission tomography 77−77975
brain, imaging, comparative study with γ-camera, single-photon emission CT, and transmission CT 80−109004
brain, positron imaging device for dynamic studies 79−48327
brain, radioisotopic activity, 4-dimens. reconstruction using 200-element detector array of Ge 78−11732
radioisotope scanning and imaging continued
brain, role and relation of computerised tomography 79−34637
brain activity concentration after administration of ^{11}C-α-p-iodoanilinophenylacetonitrile 80−3776
brain angioscintigraphy in posterior view, clinical value 80−72290
brain autoradiographs, rapid semiautomatic quantification, microprocessor appl. 80−41332
brain capillary, microkinematic obs. of blood velocity *(Russian)* 79−5366
brain diagnosis, comparative study of radionuclides and computerised tomography 80−72320
brain gamma-angiograph images, enhancement, reduction of statistical fluctuations, by computer *(French)* 79−5345
brain imager, transverse-section, for single-gamma emitters 80−3794
brain isotope distribution reconstruction, error anal. for instrument design 80−3772
brain lesions, compensative value of ^{99m}Tc labelled DTPA and MDP *(Japanese)* 80−67235
brain scan vs. cranial computed tomography, clinical efficacy and cost anal. 77−77974
brain scanning utility, patterns of diagnostic clues 77−77988
brain scans hard-copy image display systems comparison 79−74744
brain scintigraphy, early and delayed image evaluation using ^{99m}Tc glucoheptonate 80−3790
brain tumour detection using ^{99m}Tc-glucoheptonate radiotracer 78−20253
bronchial epithelium tissue, technique for high sensitivity α autoradiography 80−17210
bronchoscopic tumour localisation, small radiation detector probes, scintillation and semiconductor detectors 80−61676
camera, optical imaging device 77−5056
camera aperture for data collection optimisation 80−67221
cameras, γ-ray detect., quantitative assessment field procedure 79−29611
cameras, resolution, sensitivity and efficiency *(Spanish)* 78−7428
cardiac, wall motion abnormality detect. using regional changes in ventricular shape and vol. 79−70633
cardiac blood pool, dynamic images, time-motion display 79−5347
cardiac blood pool, ECG-gated emission computerised tomography 80−98117
cardiac blood pool imaging, evaluation of ^{99m}Tc labelled human serum albumin kits 80−17130
cardiac blood pool imaging over complete cardiac cycle using multiformat imager 77−40737
cardiac blood pool visualisation, ^{99m}Tc labeled red blood cells and serum albumin 79−29601
cardiac chamber imaging, comparison of red blood cells labelled with ^{99}Tc^{m} in vitro and in vivo 78−65109
cardiac cineangiography, clinical utility of real-time computer-based system 78−80957
cardiac function and anatomy evaluation, complementary role of echocardiography and radionuclide imaging, book contrib. 80−101241
cardiac function scintigraphy using Bonn System III 78−73198
cardiac functional imaging, clinical experience 78−80958
cardiac imaging, ECG-gated, motion phantom for computerised tomography 80−98115
cardiac left ventricle function, nucl. medicine equilib. meas. 79−62357
cardiac left ventricular ejection fraction from gated images count rate 79−29605
cardiac left ventricular ejection fraction meas., scintigraphic count-volume and geometric methods compared 79−83896
cardiac left ventricular function obs. 79−74749
cardiac motion study, computer-processed, ECG gating device 78−73210
cardiac nuclear medicine for clinicians, book 80−98765
cardiac nuclear medicine instrumentation, review, book contrib. 80−101260
cardiac output determination, automated computer program 80−56196
cardiac output regional distrib., non-invasive determ. using ^{201}Tl 78−31890
cardiac probe, microprocessor-based, for gated equilib. and beat-by-beat left ventricle function 79−62396
cardiac scan computer-aided anal., using ECG gate 78−40328
cardiac scintigrams, time gated, analysis by digital boundary detect. techniques 80−98081
cardiac scintigraphic cineangiography with ECG gating 77−9255
cardiac scintigraphic image handling using microprocessor system 80−85489
cardiac scintigraphy-radiocardiography left ventricular ejection fraction and regurgitation meas. *(French)* 77−29194
cardiac shunt detection with the short-lived radioactive gases 80−94357
cardiac shunts, left-to-right, deconvolution anal. in radionuclide quantitation 80−12229
cardiac trauma evaluation 80−94361
cardiac US and nuclear medicine, complementary roles 80−98051
cardiological noninvasive techniques, using minicomputers, ischemic heart disease diagnosis appl. 79−96661
cardiology, beat-by-beat validation of ECG gating [nuclear medicine] 80−98071
cardiology, clinical nuclear, computer system 79−25094
cardiology, conf., London, England (June 1979) 80−36759
cardiology, noninvasive meas. by radiocardiography 77−40754
cardiology, nuclear, automated chest parsing algorithm 80−61678
cardiology, performance characts. of a commercial ECG gate 80−98073
cardiology, sequential meas. of ventricular vols. and cardiac output 80−94319
cardiology, varifocal imaging 79−70631
cardiomyopathy scintigraphic diagnosis by ^{99m}Tc-labelled pyrophosphate, method sensitivity 80−17061
cardiovascular applications 77−40746
cardiovascular measurements, conf., Bellingham, USA (Sept. '78) 80−31419
cardiovascular nuclear medicine, an overview 80−85480
cardiovascular nuclear medicine, instrumentation and data processing, ventricular function evaluation 80−85481
cardiovascular shunts, detection and quantitation with commonly available radioisotopes 80−94356
CdTe detectors in nuclear medicine, capabilities, limitations 77−44748
cellular radiation dose of labeled neutrophils and platelets 79−100749
α-cellulose iodination for dietary fibre analogue tracing 79−48339
cerebral blood flow, atraumatic meas. by ^{133}Xe *(French)* 77−37039
cerebral blood flow, colour functional imaging 77−5067

radioisotope scanning and imaging continued
cerebral blood flow, linear computer model 79−92288
cerebral blood flow automated analyser for ^{133}Xe studies 77−86597
cerebral blood flow meas., lateral counting corrections 79−8536
cerebral blood flow meas., use of ^{133}Xe and computer calc. 77−5098
cerebral blood flow noninvasive meas., analytical problems 80−41208
cerebral blood flow parameterisation, scintiangiography meas. 79−25025
cerebral blood flow regional meas., cyclotron prod. of ^{77}Kr 77−56468
cerebral blood volume meas. by ^{11}C-labelled carboxyhaemoglobin 80−8134
cerebral perfusion image processing, minicomputer system 77−29200
cerebral radiographic scintillation detection unit fixture 79−57749
cerebral regional blood flow, computerised monitoring system for stroke patients 79−79626
cerebral regional blood flow and vol. meas., intravenous isotope method 77−86610
cerebral regional blood flow assessment by continuous carotid infusion of ^{81m}Kr 78−20254
cerebral regional blood flow meas., ^{133}Xe inhalation method with on-line computer 77−40734
cerebral regional blood flow meas. by ^{133}Xe clearance 79−83912
cerebral regional O_2 distrib. model during continuous inhalation of $^{15}O_2$, $C^{15}O$ and $C^{15}O_2$ 78−65108
cerebral tissue perfusion rate determ. from ^{15}O activity decay after photon activation 80−26341
cerebral vascular disease, experience with radionuclide imaging and computed tomography 77−77977
chest radiology, introduction to physiological aspects 79−25071
cholescintigraphic possible agent, ^{99m}Tc labelled complex 79−79653
choroidal blood flow meas., theoretical basis using radioactive inert gas 79−92349
chromosome autoradiograph analysis by computer 78−57071
cinepneumography, flow-vol. imaging of the respiratory cycle 80−94343
cisternography, transverse section radionuclide scanning 77−2038
Cleon imager, clinical evaluation 78−24128
clinical quality assessment, image processing 77−86626
clinical realisation and engineering pot. 80−98084
coded aperture γ-ray imaging, multiplex noise *(French)* 77−90887
coded aperture imaging, analogical deconvolution *(French)* 78−35943
coded aperture imaging, predicted performance of uniformly redundant arrays 79−18351
coded aperture imaging, signal to quantum noise ratio 78−37122
coded aperture imaging of gamma-ray sources, class of near perfect coded apertures 78−40300
coded aperture imaging with uniformly redundant arrays 78−37812
coded-aperture configuration, gamma-ray imaging in Fourier space 79−17588
coded-aperture imaging of the heart, improved aperture 80−98072
coherent coded imaging without side lobes 79−25079
collimator design and fabrication, Pb hexagonal multihole type 78−11717
collimator evaluation, multi-slice fan beam system 79−44993
collimator optimal design parameters for dynamic spatial resolution 80−17087
colour scintiphotographic radionuclide angiography, aide to isotope ventriculography 80−12239
colour TV imaging computer peripheral 79−20667
comparison at rest and during isometric exercise 80−30857
complementary use with B-scan US 77−37043
compuerised tomographic section, synthesis and enhancement 80−109003
computed axial tomograph, design and performance characts. for positron emission 79−48328
computed tomography, review 80−56213
computer aided processing of diagnostic information 77−9253
computer application to rapid dynamic studies 79−16297
computer applications 80−3801
computer applications in nuclear medicine, history 80−42037
computer applications in nuclear medicine, review *(German)* 80−41214
computer applications to gamma-ray imaging 77−56452
computer assisted data processing and display methods, intercomparison using math. tumour 78−15886
computer definition of regions of interest, double-cursor method 79−29612
computer processing of static gamma camera images 80−36095
computer reconstruction of scintigraphic images 80−30846
computer software package for internal dose calc. 80−98139
computer system for acquisition and processing of data, Janus III 78−80948
computer systems, buyer's guide to current performance and future promise 78−48883
computer-aided diagnosis of medical images, conf., Coronado, USA, (Nov. 1976) 77−78018
computer-assisted cardiology, off-line viewing using videotape 78−65119
computer-scintillation camera interface 77−21613
computerised axial tomography, transmission and emission techniques review 77−77973
computerised axial tomography from multiple γ-camera views using freq. filtering 80−94321
computerised data processing *(Hungarian)* 78−35933
computerised emission transaxial tomography, effect of Compton scatt. photons 79−66530
computerised gamma transaxial tomography, focused collimator scanner 79−66519
computerised internal mammary lymphoscintigraphy in radiation treatment planning 80−12223
computerised multiple image object detection techniques 77−37087
computerised positron emission tomography for assessment of myocardial integrity 80−36120
computerised rotating laminar radionuclide camera 80−3796
computerised scanning system control 77−9254
computerised tomographic scanner potential resolution using ^{137}Cs, radiotherapy planning 79−48323
computerised tomography, 3-D object reconstruction 79−66535
computerised tomography, display instrumentation *(Japanese)* 79−70688
computerised tomography, double-tracer, multiple-organ, transaxial, radiotracer distribs. localisation and characterisation 80−98128
computerised tomography, engineering aspects of PETT V 79−66517
computerised tomography, fundamental limitations in radionuclide imaging 80−30882
radioisotope scanning and imaging continued
computerised tomography, longitudinal reconstruct. using calligraphic CRT graphics system 80−8173
computerised tomography, new system for positron-emitting radiopharmaceuticals 79−16280
computerised tomography, positron emission, crystal size optimisation 80−61681
computerised tomography, positron emission, data acquisition and processing electronics 80−61690
computerised tomography, positron emission CT device with continuously rotating detector ring 80−81697
computerised tomography, single photon emission, current status 79−66526
computerised tomography, single photon emission, review 80−81698
computerised tomography, single photon ring system 79−53220
computerised tomography, single photon system, initial performance of SPRINT 79−66523
computerised tomography, single-photon, physical attributes 80−109007
computerised tomography, single-photon emission, imaging capabilities of Ge camera 80−61668
computerised tomography, time-coded, appl. of algebraic reconstruction technique 79−92348
computerised tomography, transverse section imaging with the MGH positron camera 79−66516
computerised tomography of the body, clinical appls. 79−83906
computerised tomography of the body using routine radiopharmaceuticals 79−83905
computerised tomography system, expt. meas. of impulse response and noise 80−56182
computers and quality control in nuclear medicine 79−16295
computers in nuclear medicine, image and data processing 79−16294
computers in nuclear medicine 79−25096
conference, Detroit, USA (June 1980) 80−105418
conference, Karlovy Vary, Czechoslovakia (May, 1979) 80−12840
conference on cyclotrons and their appl., Bloomington, USA (Sept. 1978) 79−54626
conference on nuclear power systems, Washington, USA (1978) 79−41045
congenital intracranial vascular malformation detect., scintigraphy vs. tomography and angiography 78−77104
constant infusion of short-lived isotopes, theoretical study of quantitative flow meas. 80−17088
controllable parameters affecting number of false positives and negatives 78−69191
coronary artery disease, clinical value of ^{201}Tl stress test compared to ECG 79−29595
coronary artery disease, sensitivity and specificity of ^{201}Tl perfusion scintigrams 79−25069
coronary artery disease, significance of abnormal rest ^{201}Tl myocardial image 80−17060
coronary artery disease extent prediction by ^{201}Tl myocardial images 80−26336
coronary blood flow meas., precordial counting collimator 77−77967
cranial scintigraphy, value of adding emission CT sections to conventional pertechnetate images 80−56187
Crohn's disease, value of ^{67}Ga-citrate scanning 79−100719
culture device for cell growth, quantitative microscopy and autoradiography 78−65163
cyclotron produced medical radioisotope yields 79−57776
cyclotron produced short lived radionuclides, medical appl. 79−57774
cystography, technical aspects and pitfalls 79−96656
Cytocomputer biomedical image analysis 79−92419
data collection station, based on autonomous CAMAC crate 80−61689
data evaluation system, for use with gamma cameras in nuclear medicine 78−92732
depth discrimination γ-γ coincidence methods in scintigraphy, contribs. to 79−53235
detectors, Ge rel. to Na(Tl), imaging efficiency and scatter rejection 79−83915
diagnostic imaging systems, image quality assessments 77−90890
diagnostic techniques in nuclear medicine, review, book contrib. 80−72322
diffusion of $^{241}Am^{3+}$ ions in ion-exchange membrane, autoradiographic method 78−35721
digital data collection system, portable, cost-effective 80−41195
digital filter, dynamic nuclear medicine imagery data smoothing 79−25070
digital image change detection 80−102637
digital image processing appl. to scintillation images 77−81559
digital image superposition algorithm, accuracy and reproducibility 78−73209
digital images, math. models and physiological parameters 80−98107
digital low-pass filtering, random noise removal 77−5065
digital scan resolution enhancement, processing algorithm 78−15887
digital technique for accurate change detect. in images 79−48326
digitised images display, minimisation of data transfer losses 80−56206
display algorithms evaluations 80−8144
display systems, minimum detectable grey-scale differences 78−61249
dose calculation from remaining body activity 79−83941
dose to children from examinations 79−16308
dose to embryo due to radiopharmaceuticals 77−5083
dosimetry, cumulative dose calcs., graphical representation 77−66852
dosimetry of radiopharmaceuticals 78−35967
dynamic phantom for radionuclide cardiology 80−12232
dynamic scintigraphy with high temporal resolution 80−94322
ear middle, and sinuses, ventilation and clearance using ^{133}Xe 80−98075
ECG gated acquisition cardiac imaging, quantification of left ventricular function 79−70638
ECG gated radionuclide cardiac imaging system 79−70639
ECG-gated scintigraphy, appl. to studies of heart 78−7440
ECG-gated scintillation probe meas. of left ventricular vol. 78−31891
ECG-triggered scintigraphy of intracardiac space 78−28033
eight-sensor low-energy γ topograph *(Russian)* 78−35932
ejection fraction determ. from left ventricular time-activity curves, noise effects 77−40741
electron microscope, fluoro-autoradiography, improvement of efficiency 78−65162
elementary particle interactions, radiological imaging appls. 80−61675
embryo, radiation absorbed dose estimates from some nuclear medicine procedures 80−104760

radioisotope scanning and imaging continued
emission computerised tomography using positron-emitting isotope, review 80−17083
emission tomography, attenuation correction and incomplete projection 79−66532
emission tomography, comparison of scanner and camera systems 79−66529
emission tomography, improved coded-aperture system 79−66534
emission tomography, simultaneous calcs. of attenuation and activity coeffs. 79−66531
encephalic exploration, clinical value of single photon emission CT 80−51216
equipment and methods in nucl. medicine *(French)* 78−48888
erythropoietic bone marrow, recovery of Fe uptake following large field radiation therapy 79−20616
European nuclear medicine, present status and future trends 80−94331
Ewing's sarcoma, place of bone scanning 80−72308
excitation functions for neutron deficient isotope form. via high-energy d-Br reactions 78−44609
exercise-radionuclide ventriculograms, methods for eliminating motion 80−41193
external counting procedures, history 80−42033
extrapulmonary tuberculosis, use of ^{67}Ga citrate in detect. and follow-up 80−46012
facial bone scanning by emission tomography 78−31892
femoral head activity in Perthes' disease, ^{99m}Tc tracer uptake estimation 79−29606
femoral head disease radionuclide uptake patterns 78−28042
films for nuclear medicine, sensitometry 80−72292
flood field nonuniformity 78−48885
focal-plane tomography, image reconstruction using digital computer 80−61674
focusing collimator coincidence scanning, three-dimensional imaging of cold lesions 77−37083
Fourier multiaperture emission tomography 80−41188
fourier reconstruction with a distortion function 80−8174
Fresnel zone plate aperture for γ-ray imaging system, digital modelling 78−7442
Fresnel zone plate images, optical decoding 77−86621
gamma, Anger-type, time resolution *(German)* 77−13000
gamma camera, line spread function meas., practical considerations 79−17585
gamma camera, multidetector Ge 79−49353
gamma camera, multiple multiwire proportional chamber, improving the spatial resolution 79−49361
gamma camera, using Compton interactions, 3-D particle track chamber 77−86622
gamma camera dynamic studies, use of principal components in quantitative anal. 80−56207
gamma camera image processing *(French)* 77−37038
gamma camera imaging, recent advances 80−17127
gamma camera low loss data acquisition with subsequent computer anal. 79−49358
Gamma Camera ON 110, physical properties, clinical applications 77−44739
gamma camera oscilloscope display, performance meas., computer simulation 78−7425
gamma camera performance comparison 78−44595
gamma camera pulse quantitative reproduction from video tape recordings 78−53496
gamma camera transfer function, statistical study 77−70541
gamma camera using CdTe detectors, medical appls. 79−49351
gamma camera visual outcome units comparison, use of MTF 80−94323
gamma camera with brightness amplifier *(French)* 77−37036
gamma camera-computer systems for rapid dynamic imaging studies 78−44598
gamma camera/computer pulse-stretching interface 78−40380
gamma cameras, appl. of orthogonal light propag. 77−16979
gamma cameras, performances under high counting rates 79−16277
gamma cameras, state of art 80−3802
gamma cameras, use of coded apertures with digital decoding 77−86620
gamma computerised camera for medical diagnosis *(Swedish)* 79−70607
gamma detector, gaseous, good low-energy resolution for ≤50 keV imaging 80−3795
gamma emitting organs, 2 and 3-dimens. digital Fourier reconstruction 80−101705
gamma ray image intensifier camera, using Si posn. sensitive strip detector 77−81565
gamma scintillation camera, GSG-2 twin-transducer, colour shading, grey-scale photographic recording 79−34631
gamma scintillation chamber, operating model 80−30848
gamma topograph, GSG-2 twin-sensor, functional and clinical qualities 80−56172
gamma-camera adaptive gating device for heart synchronisation 78−31898
gamma-camera for gated cardiovascular imaging 79−5367
gamma-camera image information prob., methods of checking, use of scintigram *(German)* 78−88734
gamma-camera used in nuclear medical examinations, developments in photographic recording *(German)* 78−88733
gamma-ray tomographic imaging by scintillation camera, algorithm 79−57773
gammagraphy, 3-dimens. image processing appl. to coded aperture imaging *(French)* 78−57067
gas-filled channel convertor for fast coincidence cameras 77−60276
gastric emptying measurement by scintigraphy, techniques and errors 78−73206
gastrointestinal bleeding, evaluation by ^{99m}Tc labelled red blood cells 80−51219
gated blood pool scan, radioisotope evaluation of ventricular performance 80−85483
gated cardiac scintigram anal., digital boundary detect. techniques 80−98106
gated cardiac studies, data processing system 79−25091
gated regional spirometry (GRS) 79−25097
genetically significant dose due to medical diagnostic exposure of Italian population, (1974) 77−66850
graphic code generation for black and white scintigrams *(French)* 80−104743
gray scale optimisation for photoscanners 79−79555
radioisotope scanning and imaging continued
greyshade scale optimisation, use of dedicated minicomputer 77−21609
Grigg, Emanuel Radu Newman, (1916-1976) radiologist and historian, biography 80−42026
GT-2 gamma scanner, improvement, neurosurgery appl. 78−11719
haematocrit determination in dog using radionuclides 79−62411
hazards to personnel, protection problems 77−81587
heart, anal. of high speed multicrystal gamma camera recording 79−25077
heart, computerised tomography of normal and infarcted patients 80−30859
heart, equilibrium left ventricular ejection fraction determ., background noise estimation 80−94365
heart, real-time system for multi-image ECG gated studies 77−21611
heart and circulation evaluation by nuclear medicine 79−70605
heart imaging, left side, following inhalation of $C^{15}O^2$ 77−9240
heart shunt diagnostics by radioisotope angiography, anal. by PASD computer program 78−20250
heart synchronized gamma-camera gating for haemodynamic status evaluation 79−53232
heart wall motion cine display using ^{99}Tc^m-labelled red blood cells 80−17129
hepatic effective blood flow, meas. by fractional clearance of ^{198}Au-colloids 79−66547
hepatic lesion visualisation improvement with upright views 78−24129
hepatic mass evaluation, relationship of ultrasonography, nuclear medicine and computerised tomography 80−17092
hepatic metastases, γ-scan accuracy for detect., comparative study with grey scale ultrasonography *(French)* 80−104741
hepatic scintiangiography, patient positioning techniques 78−20259
hepatic scintigraphy, motion-corrected, objective clinical evaluation 78−65111
hepatic scintiphotography, clinical value optimisation 79−88169
hepatic steatosis, ^{133}Xe retention rel. to biopsy 80−17069
hepatobiliary disorder scintiscanning, evaluation of ^{131}I labelled ioglycamic acid 80−36072
hepatobiliary dynamic flow study using ^{99m}Tc 79−53217
hepatobiliary functional scintillation recording, review *(German)* 80−30874
hepatobiliary imaging, jaundiced adults, infants, using ^{99}Tc^m-pyridoxylidene glutamate scans 79−5339
hepatobiliary imaging agent assessment, importance of uptake and retention indices 79−83911
hepatobiliary imaging agents in rats, pharmocokinetics 79−79637
hepatobiliary imaging in non-jaundiced patients, comparison of ^{99}Tc^m imaging agents 79−5338
hepatobiliary reagent, evaluation of ^{99}Tc-diethyl-acetanilido-iminodiacetate 77−90874
hepatobiliary scintigraphy, characts. of ^{99m}Tc-E-HIDA *(Japanese)* 80−81729
hepatobiliary study of liver-transplant patients, ^{99m}Tc diethyl-iminodiacetic acid rel. to ^{131}I rose bengal 80−3793
hepatocellular disease diagnosis, computer quantification of spleen/liver ratio 79−83909
high density proportional counter, medical imaging of e^+ radioisotope distrib. 79−5399
high voltage electron microscope autoradiography, HeLa cells 78−36077
Hippuran plasma clearance meas. using gamma camera and cardiac background subtraction 77−52870
Hippuran renograms, application of transform methods 79−8540
Hodgkin's disease and lymphomas, ^{67}Ga substraction scanning 79−74738
Hodgkin's disease and other malignant lymphomas, ^{67}Ga imaging 79−57769
human body tomography using computerised pattern recnogition *(Japanese)* 78−3603
human dietary absorption of Zn, radionuclide study technique 79−5349
hybrid MWPC gamma ray detecting system for applications in nuclear medicine 79−5397
hybrid scanner, design of detector and collimators 78−7423
hydrocephalus, role of computed cranial tomography and radionuclide cisternography 77−77978
hyperthyroidism, computer diagnosis, in vitro and radioisotope uptake tests compared 77−9252
image artifacts at high photon fluence rates, using single-cryst. NaI(Tl) scintillation camera 78−85364
image formation, perception and measurement, conference, Leeds, England (Mar. 1976) 77−86561
image intensifier scintillation cameras for nuclear medicine 77−40732
image linear filtering, optimal compromise 80−36071
image processing, tracer kinetics, nuclear medicine, cardiology appls. 78−48873
image processing and display methods, computer assisted, multicentre comparison 79−53233
image processing and synthesis in radiology and nucl. medicine *(German)* 78−40325
image processing in clinical nuclear medicine 79−92371
image processing in nuclear medicine, review 80−81694
image processing system for display and anal., computerised 80−41174
image reconstruction, projection completion methods 78−42285
image reconstruction from hollow and truncated projections, theory 78−24912
image restoration, 2D coded Poisson process, appl. to nuclear imaging *(French)* 79−57767
image restoring filter, appl. of constrained optimization 79−39494
image understanding systems, seminar, San Diego, CA, USA (Aug. 79) 80−94918
imaging device performance assessment, psychophysical approach 77−86625
imaging principles, concepts and equipment 80−17113
imaging techniques, book 80−12861
imaging techniques, developments, review 80−26324
incremental deconvolution, possible method 80−56208
Indian nuclear medicine, review 80−36082
infection diagnosis in total hip joint replacements, ^{99m}Tc-diphosphonate scanning 77−73558
inflammatory disease, role of ^{67}Ga 79−57770
inflammatory diseases, computerised double-tracer subtraction scanning 79−70612
instrumentation, recent developments 80−81692
instrumentation manufacture in India 79−96653
instrumentation trends in nucl. medicine 78−44594

radioisotope scanning and imaging continued
instruments and radiopharmaceutical production, review *(French)* 80−17056
interaction in vacuum percussion welding 79−29061
intracoronary radiolabelled particulate imaging 80−94360
intracranial disorder diagnosis by cerebral sequence scintigraphy 79−92335
intracranial mass lesion detection, computerised cranial tomography and radionuclide imaging 77−77976
intrahepatic lithiasis detection, sequential scintiphotography with ^{99m}Tc pyridoxylideneglutamate 80−72309
intraocular fluid dynamics meas. by minicomputer-based system 78−24130
intravascular radioactive tracers, calc. of residence time distribs. in fields of external registration 80−72291
ion beam injection, positron emitting, imaging instrument 79−48329
ischaemia index using peak diastolic dV/dt of heart chambers from ECG-gated radiocardiogram 78−44602
joint imaging, technical aspects 80−56197
kidney, ^{99m}Tc methylene diphosphonate, immediate renal imaging and renography, clinical evaluation 80−98126
kidney, allografted, normally functioning, ^{67}Ga localisation 79−100717
kidney, deconvolution anal. of scintillation camera renogram 77−21599
kidney, quantitative anal. in bilateral renal scintigraphy 79−34662
kidney filtration fraction, noninvasive determ. by dual tracer technique 77−86596
kidney function studies following radiation therapy of spleen, ^{197}Hg, ^{99m}Tc, ^{131}I 79−20615
kidney transplants, dynamic imaging with ^{99m}Tc DTPA (Sn), transplant perfusion index 79−34653
Laguerre functions, appl. to washout curves 80−81521
large field scintillation gamma cameras, performance charcts. 78−7441
left heart imaging following $C^{11}O_2$ inhalation 77−64126
left venticular ejection fraction meas. in equilib. radionuclide angiography 80−46009
left ventricle, 3D image expression 80−104731
left ventricle ejection fraction meas., scintillation camera deadtime 79−62355
left ventricular boundary extraction from radioisotope angiocardiogram *(Japanese)* 77−81562
left ventricular edges detect. methods 80−98132
left ventricular ejection fraction determ., comparison of three radionuclide techniques with contrast angiography 78−31889
left ventricular ejection fraction determ. 78−80962
left ventricular ejection fraction determ. by equilib. radionuclide angiography 80−12227
left ventricular ejection fraction determ. using multicryst. scintillation camera 78−73213
left ventricular equilib. radionuclide angiography, arrhythmia effects correction method 80−17089
left ventricular function, radioisotope evaluation with nonimaging probes 80−85484
left ventricular function assessment using radionuclide techniques, technical considerations, review, book contrib. 80−101261
left ventricular function evaluation by myocardial scintigraphy and radionuclide angiocardiography *(Japanese)* 80−81724
left ventricular function evaluation using ECG synchronised scintillation camera 78−65110
left ventricular parameter meas., noninvasive radioisotope images with digital prefiltering and boundary detection 78−48887
left-ventricular aneurysm, reliability of gated scintigrams in detect. 80−30856
left-ventricular ejection fraction and segmental wall motion by peripheral first-pass radionuclide angiography 78−61246
left-ventricular ejection fractions meas. by equilib. radionuclide angiography 80−12226
lesion contrast and photon count density rel. to D-log E curve 78−69195
lesion detectability, cold, effects of scintillation camera nonuniformity 79−5352
leucocytes, radioactive-labelled, appl. for proof of inflammations 80−67218
leukocyte migratory patterns, use of ^{99m}Tc as radioactive label for study 80−51222
LeVeen shunt, patency testing technique 79−57763
liposome-entrapped tracers, organ distrib. of liposome [^{99m}Tc-DTPA] in mice and dogs 77−16969
liposomes labelled with ^{111}In oxine or ^{99m}Tc DTPA, metabolic and scanning tracers, mouse 80−17073
liquid scintillation counting, apparent and actual ^{14}C retention 80−36080
liquid scintillation vial system, new container geometry for better sensitivity 80−46021
liquid-scintillation vial system, biphasic, for radiometry, modifications 80−101253
liver, comparison of radionuclide imaging, computer tomography and grey-scale US 77−52864
liver, comparison of scintigraphy, US and computerised tomography scanning 80−17105
liver, dynamic studies with ^{99m}Tc labelled S colloid, processing 80−41169
liver, gamma-camera image improvement using physiological gating mechanism 80−98065
liver, nuclear imaging, comparison of conventional rectilinear and multiplane tomographic scanning 80−17106
liver, perfusion, normal and partially hepatectomized rat, in vivo meas. using ^{99m}Tc S colloid 79−79636
liver, pharmacokinetic and imaging studies of hepatobiliary agent ^{99m}Tc-pyridoxal leucine 79−29597
liver, respiratory motion in supine and upright positions 80−30858
liver cirrhosis, evaluation of 1D profile scans with a whole body counter 80−51213
liver disease, diffuse, computerised diagnosis by scintigram pattern characterisation 79−83926
liver disease diagnosis, microprocessor-based radioisotope image processing system 79−83925
liver gamma camera scans, clinical evaluation of computer processing 79−29579
liver hepatoma, dog, evaluation of 3 imaging instruments 80−17074
liver imaging, ^{178}Ta radiopharmaceuticals rat expts. 80−51254
liver mass estimation from γ-camera images, computer assisted method 79−83908
radioisotope scanning and imaging continued
liver scanning agents, comparison of ^{113m}In-phytate, ^{99m}Tc-phytate and ^{113m}In-colloid 79−96650
liver scintigraphy, intercomparison of computerised image processing and display methods 79−53234
liver scintigraphy, optimisation of analogue-circuit motion correct. 79−39472
liver scintigraphy, pattern recognition 80−8157
liver visualisation and ^{125}I-toluene azonaphthol excretion, rat 77−56456
liver volume measurement by emission computerised tomography 80−12230
longitudinal radioisotope tomograph 77−81556
lung, Bayer map evaluation in ^{57}Co-bleomycin scintigraphy *(Japanese)* 80−72319
lung, estimates of radiation absorbed doses from radioxenons 80−101269
lung, gated and cinematic perfusion imaging, dogs with expt. pulmonary embolism 80−17071
lung, quantitative assessment of ventilation-perfusion mismatch using ^{133}Xe 79−16279
lung, regional distrib. of tracer bolus inhaled from residual volume, using scintigraphy 77−12950
lung, regional function, short-life radionuclides, review 79−53211
lung function assess., ^{99m}Tc labelled aerosol particles rel. to ^{81m}Kr ventilation imaging 79−100716
lung function examination using ^{13}N *(French)* 77−70521
lung imaging, ^{178}Ta radiopharmaceuticals rat expts. 80−51254
lung imaging, history 80−42035
lung imaging, technique for contralateral subtraction 80−41207
lung monitor for assessment of low energy photon emitters 79−25067
lung perfusion, effect of particle number 77−37049
lung perfusion image sensitivity, lateral vs. oblique views 77−16965
lung phantom, dynamic, use as educational tool 80−8757
lung physiology and chest radiology 79−25072
lung regional ventilation and perfusion, dynamic meas. with ^{133}Xe 77−86595
lung scan automatic classification 77−29201
lung scanning and radionuclide venography 80−3791
lung scintiphotography with dry aerosol, generation and delivery system 78−24126
lung tumour diagnosis, use of ^{197}Hg and ^{67}Cu *(French)* 77−70519
lung ventilation and perfusion scintigrams, computer aided diagnosis 79−88181
lung ventilation model, radioactive tracer tidal breathing 80−56095
lung ventilation regional and whole, math. model for radioactive tracer studies 78−20249
lung ventilation studies with ^{133}Xe, patient dose 78−24146
lymph node imaging agent, ^{99m}Tc labelled liposomes 79−96649
lymph node scanning in sheep with ^{111}In labelled lymphocytes 79−62343
lymphography in prostatic carcinoma, implications for metastases diagnosis 80−41168
lymphography using ^{99m}Tc-MDP *(Japanese)* 80−94352
lymphoscintigraphy, comparison of 2 ^{99m}Tc labelled radiopharmaceuticals 80−41185
lymphoscintigraphy, comparison of ^{99m}Tc colloids 79−29580
lymphoscintigraphy, quantitative, mammary metastases detect. using ^{99m}Tc 79−16266
lymphoscintigraphy, radiocolloid optimal uptake in rabbit parasternal nodes 80−46018
lymphoscintigraphy using ^{99m}TcS colloid 80−36114
magnifier/rotator for enhanced image visualisation 78−15889
mandibular bone graft fate determ., quantitative radionuclide imaging 80−3792
MDS computer systems, improvement of pulse-mode photographic images 80−30862
mean clearance time transverse section imaging 78−73222
mediastinal lymphoscintigraphy, use in observing cell kinetics of developing malignant ascites 79−92176
medical gamma-ray cameras of Anger type, optimisation *(French)* 80−26328
medical imaging, conf., San Diego, USA, (Aug 1978) 80−17025
medical imaging, conference, San Diego, USA (Aug. 1979) 80−94919
medical imaging overview 80−98082
medical physics conference, Ottawa, Canada (Jul. 1976) 77−16897
meningioma scintigraphy, correl. with angiography and pathology 77−56453
merits rel. to US imaging and computerised tomography 79−48324
metabolic bone disease diagnosis using whole-body retention of ^{99m}Tc-diphosphonate 78−73208
metabolic substrate regional utilisation rate meas. by emission tomography 78−69183
metastatic calcification, role of bone scanning 79−92366
metastatic survey using ^{131}I as aid in determ. functional thyroid metastases 79−96657
metrology of ionising radiations and nuclear medicine *(French)* 80−17057
microprocessor systems for data acquisition, image processing, RIA anal., patient data retrieval 80−61670
minicomputerized automatic radiocardiogram analysis *(Japanese)* 79−29614
mobile nuclear medical instrumentation, review 80−101262
motion blurring in scintigraphic images, improved means of correcting 79−39493
MTF calculation, improved FORTRAN II program 77−21612
MTF calculation, modified FORTRAN program 78−25807
muco-ciliary transport monitoring method using ^{99m}TcS colloid, bronchiectatic patient appl. 80−30840
Muehllehner's tomographic camera, quantitative evaluation of depth effect 77−86609
multi-element band display performance 77−56448
multidimensional space and time signal processing in biology and medicine 80−85493
multiplanar emission tomography, new method using a 7 pinhole collimator and Anger scintillation camera 79−16281
multiplane γ source image reconstruction using Fresnel zone plate aperture 77−52874
multiplane tomographic scanner, simulated, correct. for out-of-focal-plane blurring 80−51221
multiple counters using RAMs, nuclear medicine appl. 79−85870
multiwire proportional chambers, adaptions and appls. 77−86618
multiwire proportional gamma camera for imaging ^{99m}Tc radionuclide distribs. 78−53493

radioisotope scanning and imaging continued
muscular hyperemia, study technique using ^{133}Xe 79−5351
MWPC positron camera, 3-D iterative reconstruction method 78−40302
MWPC positron camera, two detector, appl. medical imaging 79−5398
myocardial ^{201}Tl imaging, redistrib. rel. to rest images 80−12225
myocardial ^{201}Tl perfusion images, computer anal. method 80−30860
myocardial ^{201}Tl perfusion scintigrams in the evaluation of aortocoronary sapheneous bypass surgery 80−12235
myocardial ^{201}Tl scintigram anal., nonredundant coded aperture tomographic method 80−94364
myocardial ^{201}Tl scintigram anal. by coded aperture imaging 79−79647
myocardial ^{201}Tl scintigraphy, effect of gate width 80−41172
myocardial blood flow, meas. by fractional uptake of ^{84}Rb and microspheres 79−34656
myocardial dosimetry of ^{99m}Tc-pyrophosphate used in infarct imaging 77−40771
myocardial function studies, exptl. approaches using $C^{15}O_2$ and ^{81m}Kr 77−40755
myocardial imaging, rationale and radiopharmaceuticals 77−40747
myocardial imaging agents, comparison of ^{201}Tl, ^{129}Cs, ^{43}K, ^{81}Rb 77−2037
myocardial imaging in humans with ^{134m}Cs 77−16964
myocardial imaging using ^{201}Tl, characterization of ECG-synchronized images 79−39473
myocardial imaging using ^{201}Tl, eval. of right-ventricular overloading 79−53230
myocardial imaging with ^{123}I-hexadecenoic acid, distrib. in animals 77−16970
myocardial imaging with $^{13}NH_4^+$, prod., distrib. and imaging 77−40752
myocardial imaging with ^{201}Tl, clinical usefulness analysis based on Bayes theorem 79−88170
myocardial imaging with ^{201}Tl, exptl. model for anal. of myocardial and background components 78−11727
myocardial imaging with ^{201}Tl, subtraction imaging using $^{201}TlCl$ and $^{99m}TcO_4^-$ 80−72318
myocardial imaging with ^{201}Tl 77−40751
myocardial imaging with time-modulated coded aperture, results with ^{201}Tl 79−92372
myocardial infarct imaging with ^{43}K and analogues 77−40750
myocardial infarct imaging with ^{99m}Tc complexes 77−40749
myocardial infarct imaging with ^{99m}Tc-phosphates 77−40748
myocardial infarct scintigraphy, inexpensive rib phantom 77−56461
myocardial infarct size computerised quantification from ^{201}Tl scintigrams 78−44601
myocardial infarct sizing, comparison of noninvasive methods, dog expt. 77−66869
myocardial infarct sizing using computer programming and 3-dimens. model 77−90888
myocardial infarction, ^{99m}Tc pyrophosphate scintigrams for diagnosis, localisation 79−5350
myocardial infarction, acute, ^{99m}Tc imaging in dogs, emission-computed tomography appl. 79−79638
myocardial infarction, acute, ^{99M}Tc pyrophosphate rel. to ^{99M}Tc methylene diphosphonate 80−17070
myocardial infarction, acute, comparison of ^{99M}Tc pyrophosphate with ^{99M}Tc hydroxymethylene diphosphonate 80−94342
myocardial infarction, nontraumatic radionuclide assessment of ventricular wall motion and stroke vol. 77−52865
myocardial infarction, perioperative, comparison of ECG, scintigraphy and enzyme diagnosis 80−30855
myocardial infarction, topographic relation between myocardial ^{201}Tl uptake and left ventricular kinetics 78−61243
myocardial infarcts, acute modified ^{99M}Tc heparin for imaging, dog expts. 80−81733
myocardial left lateral images using ^{201}Tl, effect of patient positioning 79−100714
myocardial perfusion evaluation by coded aperture tomographic technique 80−21537
myocardial perfusion images using ^{201}Tl, quantitative evaluation methods 79−39479
myocardial perfusion imaging, quantitative aspects, review 80−94358
myocardial perfusion imaging using ^{201}Tl, algorithm for background activity calc. 80−56195
myocardial perfusion imaging using ^{201}Tl, computer processing 79−62356
myocardial perfusion imaging with ^{201}Tl, single photon emission computerised tomography *(Japanese)* 80−98114
myocardial perfusion scan interpretation, computer technique 78−80960
myocardial perfusion scintigrams using ^{201}Tl, aorto-coronary saphenous bypass surgery 79−25068
myocardial regional blood flow from dynamic anal. of ^{201}Tl 79−70627
myocardial regional perfusion, tomographic scintigraphy 78−3584
myocardial scans and wall motion studies using ^{99m}Tc pyrophosphate 79−96654
myocardial scintigrams, specificity of ^{99M}TC pyrophosphate in prior infarction cases 79−39476
myocardial scintigraphy, computerised extraction of organ contours *(German)* 78−88735
myocardial scintigraphy, sequential, following myocardial infarction, using ^{99M}Tc stannous pyrophosphate 79−39474
myocardial scintigraphy in stressed state using ^{201}Tl, segmental anal. 77−66840
myocardial scintigraphy using ^{99M}TC pyrophosphate, correls. with coronary-artery bypass surgery 79−39475
myocardial studies, prod. and characts. of ^{81}Rb 79−29628
myocardial uptake of ^{201}Tl, correl. with local perfusion, dog expts. *(French)* 80−104740
myocardial uptake of ^{99m}Tc stannous pyrophosphate in expt. viral myopericarditis, mouse obs. 80−46019
myocardial-stress perfusion scintigraphy, predictive value in patients without previous infarction 78−73205
myocardium, collimator evaluation for ^{201}Tl 79−34657
myocardium, regional wall motion, assessment by radionuclide kymography 79−39478
myocardium, transverse computerised axial tomography with ^{201}Tl 80−67222
neoplasm localisation with radionuclides, review 80−67215
neoplastic disease, serial ^{67}Ga-citrate imaging in children 79−100718
neuroradiology, radiation dose to critical organs of staff and patients 80−8184
new imaging methods, conf., London, England (Feb. 1979) 79−83897

radioisotope scanning and imaging continued
nMTCB task analysis of nuclear medicine technology 80−8753
nonlinear digital filtering *(Japanese)* 78−35930
nonlinear image processing methods 78−48874
nuclear cardiography, deadtime meas. in scintillation cameras 79−16276
nuclear counting, method to reduce cosmic background 80−897
nuclear medicine, trends *(French)* 80−26327
nuclear medicine display systems 79−16298
nuclear medicine growth, contribution of research reactors 79−11998
nuclear medicine imaging, computer display system 78−61275
nuclear-medicine image display system, dynamic physiological function visualisation 79−5396
oesophagus dynamic study, modified scintigraphic technique 78−28044
oncology, role of radionuclides, review 77−9248
optical instrumentation appl. in medicine, conf., Boston, USA (Sept. 1977) 78−69184
optimum detector spatial resolution, comparison of statistical theory and observer performance 78−73223
organ blood flow measurements, effect of instantaneous partition coeff. of Xe 80−101256
organ depth estimation by gamma-ray spectral comparison 77−86612
organ radionuclide uptake, quantitative meas. by a γ-camera 80−51212
osteomyelitis, suspected, in children, value of radioisotope bone scanning 80−67216
OTF in evaluation of γ-camera data in moving organ exam. 80−30845
ovarian imaging, use of ^{131}I labelled chorionic gonadotropin, rat expts. 80−41186
paediatric nuclear medicine, conf., Edinburgh, Scotland (Oct. 1978) 79−88150
pancreas, ^{11}C-labelled amino acids for rectilinear and positron tomographic imaging 80−12258
pancreas, multiplane tomographic imaging 80−98076
pancreas, scintigraphy rel. to endoscopic retrograde parenchymography *(Japanese)* 80−81725
pancreas disorders, integrated nucleus medical diagnosis *(German)* 79−16293
pancreas scanning, extension of the subtraction technique 79−66506
pancreas scanning by coldspot method 78−73214
pancreatic disease, study by multiple imaging modalities 80−17094
pancreatic scanning agents, comparison of four ^{75}Se-labelled amino acids 78−35921
pancreatic scanning review 77−9237
pancreatic scanning with ^{11}C methionine positron emission computerised tomography 80−30861
parasternal lymphoscintigraphy, radiation treatment planning implications, breast cancer 80−72299
parathyroid, possible imaging with ^{67}Ga and other Al analogues 80−101252
particulate myocardial perfusion scintigraphy in eval. of coronary artery disease 77−40753
pattern recognition for lesion detectability in medical scintigraphic images 79−62354
pericardial effusion, malignant, myocardial accumulation of labelled phosphate 80−17068
peritoneum and retroperitoneum, anatomic correls. in ^{67}Ga imaging 80−17097
personnel doses anal. from nuclear medicine procedures 79−70645
phantom, perspex, for assessment of imaging equipment 79−25089
phantom for clinical evaluation of total system resolution 80−41197
phantom for simulating fast dynamic studies on gamma camera 77−16980
phlebography, appl. to lower extremity venous thrombosis 80−94330
photodocumentation, improvement rel. to other methods 79−83898
photographic image intensification by autoradiography 77−5937
photographic recording from oscilloscope screen, 10×10 cm photographic cassette 77−25574
photomultiplier tube balance assessment 80−41196
photomultiplier tube instability, consequences for radioactivity meas. accuracy 79−76272
physiologic tomography, noninvasive meas. of myocardial metabolism, blood flow and function 80−104730
physiological compartment tracer flow modelling and digital imaging 80−101257
physiological processes, radionuclide dynamic studies 79−62353
picture-display systems, developments and limitations *(German)* 79−100705
pinhole and continuous projections, limited angle 3-D reconstruction 80−61667
planar positron cameras, 3-D reconstruction using Fourier deconvolution of generalised tomograms 78−40295
plasminogen, ^{123}I or ^{131}I labelled, evaluation as imaging agent for preexisting thrombi 77−21610
point source depth, meas. from γ-ray spectra 79−39492
polar reference texture in radiocolloid liver images 78−73241
Polaroid film artifacts 77−18115
polyacrylamide gel, automated scanning of ^{14}C 80−17221
positron annihilation detectors ring, wobbling mathematics 79−63867
positron camera, 3-dimens., for nucl. medicine 78−73225
positron camera, 3-dimens. imaging using Fourier techniques 77−32951
positron camera, $Bi_4Ge_3O_{12}$ as potential scintillation detector 78−3586
positron camera, circular ring transverse axial, performance and evaluation 77−64124
positron camera for brain imaging, appl. and charact. *(Swedish)* 78−28032
positron camera proportional chamber, Fourier deconvolution technique 78−40297
positron camera using ring detector system, for emission tomography of brain 80−30880
positron camera-computer system for various section images 79−66528
positron circular ring cameras for computerised tomography, trends and prospects 79−66524
positron circular ring transverse axial camera system, efficiency optimisation 77−12994
positron computerised tomography, system design considerations 79−66525
positron computerised tomography *(Japanese)* 80−94347
positron computerised transaxial tomography, physical aspects 77−12993
positron emission computed tomograph, POSITOLOGICA 80−104753
positron emission computer-assisted tomographic scanner 80−36116
positron emission computerised tomography, 3-D image reconstruction, Fourier deconvolution method 80−61669

radioisotope scanning and imaging continued
positron emission computerised tomography, detect. system 79−66522
positron emission computerised tomography, optimisation of system design parameters 80−26347
positron emission computerised tomography, review *(Japanese)* 79−70610
positron emission tomography, appl. to meas. of cerebral metabolic rate 80−3799
positron emission tomography, fully 3D considerations 80−36098
positron emission tomography, sampling requirements and detector motion 79−66527
positron emission tomography and its applications 79−11996
positron emission transverse tomograph, PETT IV 78−40299
positron emission-computed tomography, multi-slice, design criteria, shielding 80−61673
positron emitters, high resolution computed tomography 77−66837
positron emitters, liq. Xe scintillators 77−2042
positron emitters, short-lived, use in lung function studies 77−25552
positron focused tomogram object reconstruction 78−40314
positron image reconstruction in nuclear medicine, three-dimens., fast iterative method 78−7443
positron imaging, positron sensitive detectors 80−61687
positron imaging device resolution limit 77−60243
positron imaging instrumentation for physiological functions 78−24196
positron imaging system using annihilation coincidence detection, model, design, performance 78−40303
positron ring, 280-crystal, design and construction for 3D imaging 78−28063
positron ring camera scanning and an exact subdivision of the Radon transform 80−81721
positron tomograph, Donner 280-crystal, data acquisition, image reconstruct. and display 80−61671
positron tomographic system, single slice, physical performances and preliminary clinical results 80−56181
positron tomography, Donner 280-crystal high resolution system 79−66533
positron tomography, evaluation of semiconductor detectors 79−53221
positron tomography, regional cerebral glucose utilisation rates 79−53222
positron-emitting blood pool imaging agents compared 80−12213
precision computer display techniques 80−98100
precision computer display techniques in nuclear medicine 80−109011
pressurised Xe-filled multiwire proportional chamber for radionuclide imaging 78−48871
proportional chamber, multiwire, low energy radionuclide distrib. 80−61679
proportional counter, Xe-filled multiwire chamber 79−49901
proportional multidetector for lung function study *(French)* 77−37035
prostate scanning with ^{75}Se labelled adenosyl selenomethionine, rat distrib. obs. 80−17132
prostrate, rat, rel. to ^{77}Br-bromide 80−51247
prostrate imaging, comparison of ^{18}F and ^{123}I labelled compounds in the rat 80−51215
pulmonary and recirculation parameter identifiability following sequential bolus inputs of ^{133}Xe 78−44605
pulmonary arterial occlusion, comparison of methods in detect., dog expts. 80−56191
pulmonary arterial pressure, noninvasive estimation in dogs using ^{133}Xe images 80−41184
pulmonary blood flow, spatial distribution in dogs in increased force environments 78−92664
pulmonary disorders, review of use of ^{67}Ga 79−57771
pulmonary embolism patients, usefulness of ^{99m}Tc-fibrinogen phlebography 80−36093
pulmonary embolism resolution rates assessed by serial positron imaging 80−3789
pulmonary function using ^{133}Xe, camera-computer system *(German)* 77−21600
pulmonary ischaemic lesions, after ^{11}CO inhalation 77−2035
pulmonary ischemic lesions, after inhalation of diffusible radioaerosol 77−37047
pulmonary lesions evaluation, comparison of ^{67}Ga-citrate, ^{111}In-bleomycin and ^{99m}Tc-citrate 80−94327
pulmonary physiology, pathology, and ventilation-perfusion studies 79−29613
pulmonary regional perfusion, comparison of ^{81M}Kr continuous intravenous infusion, ^{99M}Tc macroaggregates 79−39477
pyrophosphate myocardial imaging, review 80−94359
quality assurance in in vitro and in vivo meas. 77−40764
quantitation of infarct size using radionuclides 80−85492
radioaerosol delivery, US nebuliser system 77−2050
radioassays, historical development 80−42034
radiocardiogram parameter identification *(Slovene)* 78−44586
radiocardiograph equipment TESLA NRG 724, description 78−28062
radiocardiography, parameter estimation for left ventricular ejection and valvular regurgitant fraction determ. 78−48886
radiographic transmission wedge for anatomical localisation, prior to radiopharmaceutical injection 79−16333
radioiodine-labelled pharmaceutical administration, optimal thyroid radiation protection, computer simulation 78−44616
radioisotope angiocardiographic image, left ventricular contour extraction and vol. computation *(Japanese)* 80−3798
radioisotope measuring convertor, parameter calc., thickness monitoring appl. *(Russian)* 78−25403
radioligand assays, in vitro diagnostic use *(Korean)* 79−39482
radiology conference, London, England (Apr. 1979) 80−30838
radionuclide, left ventricular systolic ejection rate assessment of cardiac function 79−79633
radionuclide appls. in medicine, props. and use in radiopharmaceuticals and organ imaging 78−61241
radionuclide tomographic section synthesis and enhancement 79−25103
radiopharmaceuticals for tumour detection, review 79−48318
radiopharmaceuticals newly developed, conf., London, England (Feb. 1979) 79−92329
random summing in multi-detector counting system meas. radionuclide mixtures 80−36097
receiver operating characteristic anal., generalisation to detect. and localisation tasks 77−40745
rectilinear bone scanning techniques 77−56460
rectilinear scanner, large crystal, improved focused uptake probe 78−28053
radioisotope scanning and imaging continued
rectilinear scanner, multichannel analyser interface 80−101254
rectilinear scanner, multiple window, modification of 79−70620
rectilinear scanning, direct recording of images on 4×5 in. film 77−5066
rectilinear scanning, error due to radionuclide decay 78−3590
refractory products, apparent density determination, using surface γ densimeter 80−35464
regional left-ventricular dyskinesis, paradox nuclear image as noninvasive index 80−56190
regional myocardial function quantitative parameters 79−25095
regional ventilatory clearance, estimation by Xe scintigraphy 80−30854
regulatory controls over use 79−96660
renal, thyroid and hepatic clearance, automatic meas. 79−34644
renal accumulation of ^{99}Tc^{m}-pencillamine as index of differential renal function 78−65115
renal blood flow measurement using externally monitored ^{131}I-hippurate uptake 77−2036
renal cortical imaging and renal mass lesion detect. 80−46016
renal differential function in dogs using ^{99m}Tc-dimercaptosuccinic acid 79−79639
renal function, identification techniques 79−96658
renal function, labelling of o-iodohippuric acid with ^{123}I 79−39503
renal function in rat, use of gamma camera system for radiation effects monitoring 77−56454
renal function measurement with ^{111}In-DTPA in dogs 77−66838
renal function studies, combined in vitro-in vivo radionuclide procedure, technical aspects 77−90884
renal graft evaluation with pertechnetate and ^{131}I Hippuran 80−46017
renal imaging with radionuclides, US and computerised tomography 80−17095
renal scintigraphy, value of additional lateral scans 80−36074
renal uptake measurements using $^{197}HgCl_2$, single tracer method for background subtraction 80−67217
renogram, comparison of techniques for filtering of noise 77−32952
renogram curves, quantitative evaluation and imaging of functions 79−39495
renograms, single injection technique for subtraction of blood background 79−29581
renography, comparative study in hydration and dehydration *(Japanese)* 80−81726
renography, role of midi-maxi computer interaction 78−7476
renography, using ^{99m}Tc-DTPA and scintillation camera 78−20256
renography using scintillation camera and ^{99m}Tc-DTPA, single-kidney function estimation 77−40736
renography with electronically assisted kidney localisation 78−11716
renovascular hypertension, computer-assisted static/dynamic imaging evaluation as screening test 79−79635
replicon autoradiograms, computer-assisted measurement 78−92692
resolution loss at depth, elimination technique 79−49352
review of apparatus, techniques and performance 80−51237
review of diagnostic nucl. medicine, for teaching 78−49618
review of nucl. medicine 1977 78−85459
rheumatoid arthritic activity quantitative evaluation with ^{99m}Tc-HEDP 78−20255
rI image processing with a microprocess 80−8175
right-to-left shunting determ., suitability of radiopharmaceuticals 77−37048
ring pseudorandom aperture for transverse section radioisotope tomography 77−64129
sacroiliac scintigraphy, ^{99m}Tc-EHDP uptake quantification, comparative study 80−94326
scan-rescan process anal. using dynamic programming *(Japanese)* 78−3602
scanner performance improvement, subtraction of Compton scattering 79−16273
scanner performance to overcome efficiency problems in 3 dimensional scintigraphy 79−92351
scatter reduction in nuclear medicine and computed axial tomography 79−5368
scintiallation camera collimators, point spread function study 79−35910
scintigram change obs. by crosscorrelation 78−80961
scintigram improvement by computer processing 79−16296
scintigram preprocessing and display by microcomputer *(Hungarian)* 78−15881
scintigrams, influence of digital representation on image quality *(German)* 78−88738
scintigrams, investig. and appl. of pattern recognition technique 78−61252
scintigrams recorded on X-ray films, simple method for copying and photographic data processing 79−16283
scintigraphic camera systems and their assessment by computer 78−57063
scintigraphic diagnosis of hypothyroidism, sealed radioactive sources appl. *(French)* 78−53497
scintigraphic images, acquisition and processing system, simultaneous use of several radioisotopes *(French)* 77−70520
scintigraphic imaging with ^{178}Ta and the Anger scintillation camera 80−12231
scintigraphic investigations in neuroradiology *(German)* 80−12242
scintigraphy, application of deconvolution method 79−53236
scintigraphy, medical, digital image processing methods 78−80947
scintigraphy, multichannel, collimated, Compton effect on spatial resolution, digital spatial filtering 78−69182
scintigraphy and angiography, equipment for quant. evaluation and off-line operation *(German)* 78−88736
scintigraphy in paediatrics *(French)* 78−44590
scintigraphy of human organs, digital image anal. 78−20251
scintillation γ-cameras, wide field, performance evaluations 79−29609
scintillation camera, investigation of contribution functions 79−29603
scintillation camera, multidetector design with 254 channels 77−40739
scintillation camera, with 2 mm intrinsic resolution 77−70525
scintillation camera 70 mm photographic camera with roll film *(Japanese)* 77−70546
scintillation camera based on image intensifier tubes 77−5069
scintillation camera collimator image form. 80−89844
scintillation camera control, Pilotix module *(French)* 77−37040
scintillation camera data, recording method for low and moderate count rates 79−8539
scintillation camera dead time with and without computer 80−3777

radioisotope scanning and imaging continued
scintillation camera device for labelling film with patient identification number 77−60242
scintillation camera electronics capable of high processing rates, clinical significance 77−40740
scintillation camera field uniformity, global and local, statistical features 80−61677
scintillation camera imaging of ^{125}I 79−49359
scintillation camera performance monitoring, equally-spaced parallel-bar phantom 77−2041
scintillation camera systems, importance of correct photopeak setting 79−34660
scintillation camera upgrading, comparative study 80−12236
scintillation camera whole-body single-photon emission computerized tomography system 80−17086
scintillation camera/high energy collimator system, misleading results with a bar phantom image 80−12237
scintillation cameras, automatic field uniformity corrections 80−17128
scintillation cameras, effect of photon energy on field uniformity tests 79−16278
scintillation cameras, large-field-of-view 78−44596
scintillation cameras using liq. and solid Xe detectors *(French)* 77−37034
scintillation detector MTF calc. on programmable pocket calculator 77−66844
scintillation gamma camera, anal. of basic charact. 78−57059
scintillation probe detector in assessment of cardiovascular disease 80−3800
scintillation probe pulse multiplexing device 79−92347
screen for radiation dose minimisation to nursing staff 79−53259
Searle Pho/Con tomographic multiplane scanner, tomographic plane separation and detector distance determ. 78−20258
semiconductor gamma-cameras in nuclear medicine 80−81693
sensitometry, review 78−20260
septum visualisation and random collimator movement in γ-camera work 79−34648
sequential method for high 3D resolution imaging 78−53489
shadow casting of volume objects 78−48872
short-lived radionuclide potentials and props. 77−52863
Sigma cameras, development since 1960 79−63328
sigma scan, method for enhancement of statistically significant differences 80−36096
single-channel γ-spectrometer transformation to computer controlled multichannel analyser 79−57765
skeletal disease, profile scanning, ^{47}Ca rel. to ^{32}P 80−51218
skeletal metastases detect., radiographs vs. scans 77−44746
skeletal scintigraphy benefits in metastatic and primary bone tumor patients 79−88168
skeletal tracer kinetics, ^{99m}Tc(Sn)methylenediphosphonate uptake in canine tibia rel. to blood flow 80−56192
skeleton, uptake of ^{95m}Tc, ^{96}Tc pyrophosphate evaluated by autoradiography 79−29608
skin, perfusion, quantitative meas. with ^{133}Xe 80−81707
skull, struct. changes due to Recklinghausen's disease, X-ray and nuclear medicine diagnosis *(German)* 80−76831
source dependent imaging system 77−77983
spleen and liver colloid take up ratio in diagnosis and treatment of diffuse hepatic disease 80−41203
spleen scanning in humans using ^{99m}Tc-labelled erythrocytes 80−67230
splenic sequestration measurement by external scanning, calibration methods 77−2043
splenomegaly, comparative values of ^{99m}Tc-Sn-phytate and ^{99m}Tc-S colloids 79−62342
statistics, understanding and using 80−12233
stereoscopic images with gamma ray cameras 79−5365
stress ^{201}Tl scintigram anal. methods comparison 80−89851
subtraction scintigraphy with ^{67}Ga-citrate and ^{99m}Tc-colloid in the diagnosis of intrahepatic masses 80−104752
subtraction technique in diagnosis of abdominal abscesses 78−73212
superconducting gamma camera, for clinical utilisation 79−63330
technology conference, Louisville, USA (Feb. 1980) 80−51949
telemetric system, with external storage, for detect. of radionuclide tracers in humans 77−12995
testicular perfusion imaging, [^{99m}Tc] sodium pertechnetate study, method and obs. 80−12238
therapy monitoring using $C^{15}O$ and $^{15}O_2$ steady state imaging 78−40298
three dimensional gamma-ray imaging using scintillation camera, expt. 78−11734
three-dimensional imaging by coded aperture and shadow casting techniques 79−74757
three-dimensional imaging using source-depend. time-modulated apertures 77−29202
three-dimensional imaging with circular ring transverse axial positron camera 77−77982
three-dimensional scintigram processing algorithm 78−7446
thromboembolic disease diagnosis, review 78−7434
thrombosis, deep-vein, comparative imaging of ^{111}In platelets and ^{131}I fibrinogen 79−29607
thrombosis diagnosis in deep veins with $Na^{99m}TcO_4$ 77−16971
thrombus detection radiopharmaceuticals, selection, prep. and evaluation 78−11731
thyroid, accumulation curve of radioiodine and its role in diagnostics *(Hungarian)* 80−94341
thyroid, comparison of 4 and 24 hr scans 77−16968
thyroid, radionuclide in vivo studies, technical considerations, developments, review 78−85372
thyroid, simultaneous emission and fluorescent scanning 79−16275
thyroid, volume and dose estimation by ^{131}I scintigraphy 79−16302
thyroid ^{123}I uptake meas., correction for thyroid depth 78−11728
thyroid ^{131}I uptake determination *(Hungarian)* 80−94339
thyroid $^{99m}TcO_2$ uptake meas., gamma camera method 78−20244
thyroid 'cold' areas scintigraphic evaluation using ^{201}Tl 80−36078
thyroid cancer, diagnostic rel. to thyroablative ^{131}I distrib. 79−83903
thyroid gland, vol. estimation by US in addition to scintigraphy 79−74730
thyroid gland $^{131,132}I$ concentration diagnostic counter 77−81557
thyroid imaging, ^{125}I rel. to ^{99m}Tc 80−36077
thyroid irradiation and 1977 ICRP dose limits for medical radioisotopes 78−65135
thyroid nodules, attenuation of monoenergetic photons from ^{125}I 79−5346

radioisotope scanning and imaging continued
thyroid scan with ^{99m}Tc-bleomycin, evaluation of cold areas 80−56183
thyroid scintigraphy, clinical comparative study of $^{99m}TcO_4^-$ and ^{123}I-Na *(Japanese)* 80−81728
thyroid scintigraphy, pinhole images rel. to rectilinear scans 79−88173
thyroid scintigraphy with time-coded aperture 80−3797
tibia fractures, ^{99m}Tc-pyrophosphate scans, algorithm for automatic computer anal. 79−88171
time modulated apertures for tomography 77−64127
tissue section imaging by α and thermal neutrons 79−29591
tomograph, positron emission, ring detector, attenuation, scatt. radiation and random coincidences 80−61684
tomographic image reconstruction, optical processing 77−73572
tomographic imaging, historical review 80−42038
tomography, 3-dimens., with circular ring positron camera 77−73566
tomography, computerised, longitudinal, bilateral collimator, gamma camera and minicomputer 80−61666
tomography, emission, compensation of tissue absorption 79−70686
tomography, emission computed, Compton scatter correction, integral transport method 80−61683
tomography, Fourier multi-aperture 80−61685
tomography, positron emission, CSF detector 80−61688
tomography, single photon emission, camera configs., performance anal. 80−61686
tomography, single photon emission, nuclear medicine computer interfaced to Anger multiplane scanner 80−61665
tomography, X-ray fluorescence techniques, I distrib. in thyroid gland 80−61664
tomography machine uses radioisotopes for patient diagnosis 77−56464
tomography simulator, emission computed, design 80−61672
tomoscanner, low cost 78−40313
tracer kinetics, a method of study 79−70609
transmission densitometry, modified method 80−36091
transverse axial emission tomography of brain, clinical results 77−73557
transverse section picture reconstruction, correction functions and statistical noise 77−12989
transverse section reconstruction, statistical errors, effects of projection angle number and projection sampling 77−52869
transverse-section emission tomography, description and potential of technique 77−86619
transverse-sectional imaging with $Na^{18}F$ in myocardial infarction 80−46015
tumour and organ affinity of ^{201}Tl 80−67234
tumour concentrating properties studies using ^{18}F-5-fluorouracil 80−109000
tumour detection status of ^{67}Ga 80−98074
tumour localisation agent evaluation, animal tumour models, review 77−9249
tumour localisation expts. using heat-denatured radioiodinated calf thymus DNA 79−96651
tumour localisation studies and method for labelling DNA with ^{125}I 80−51249
tumour scintigraphy by intraarterial injection of $^{201}TlCl$ *(Japanese)* 80−98111
tumour-localising radionuclides in retrospect and prospect 80−42036
tumours, autoradiographic study of tracer accumulation, experimental infectious lesions 79−5348
TV displays, 4 standard types, comparative study 80−109005
two way scanning method for total body in vivo neutron activation anal. 78−92697
valvular regurgitant fraction meas. by radionuclide angiocardiography, iterative estimation 79−34668
vascular permeability in rat ears after X-irradiation 79−5330
vascular space visualisation using ^{99m}Tc-labelled red blood cells 79−11999
Vena cava, superior, optimum radiation schedule in obstruction treatment, importance of ^{99m}Tc scintiangiograms 80−72334
venogram, dynamic, correl. with radiographic contrast venography 79−96655
venography, features of inferior vena cava obstruction using ^{99m}Tc pertechnetate 79−34655
venography, large vol. ^{99m}Tc pertechnetate injection without tourniquet, lower extremities 79−34654
venography, lower extremity, recognition of systemic portal shunts 80−94329
venography, using scintillation camera and synchronised whole-body scanning bed 77−5068
venography for investigation of thromboembolic phenomena 78−7439
venography in management of proximal venous occlusion 79−53210
venous blood flow visualisation using dynamic leg scintigraphy with large field-of-view scintillation camera 78−73215
venous thrombosis, deep, detection by ^{125}I fibrinogen testing 79−16282
ventilation abnormalities detection using ^{133}Xe, washout rel. to single-breath imaging 80−41183
ventilation regional measurement using ^{81m}Kr, math. lung model 77−86611
ventilation scintigraphy, comparative analysis of ^{81m}Kr and ^{133}Xe 78−85360
ventilation studies, ^{127}Xe distrib. in lungs 78−44606
ventilation studies, ^{127}Xe vs. ^{133}Xe 77−37044
ventilation studies, clinical comparison of ^{127}Xe and ^{133}Xe 77−86594
ventilation-perfusion lung imaging in dogs with pulmonary embolism, angiography comparison 78−65113
ventilation-perfusion scintigraphy on pulmonary disease, artefact suppression 80−17082
ventrical, left, haemodynamical parameters meas., frame rate requirements 79−100715
ventricle, left, contour extraction from radioisotope angiocardiograms, and wall motion classification 79−88180
ventricle volume characts., nuclear medical determ., appl. of computer system *(German)* 78−88737
ventricular ejection fraction determ. by radionuclide angiocardiography, correction of noisy data 77−48868
ventricular function, left, dual-probe system for rapid bedside assessment using radionuclide 77−2039
ventricular function monitor, ambulatory, CdTe detector, cardiac ejection fraction meas. 80−61680
ventricular mean transit time, right, using radiocardiography 77−2040
ventricular performance, 1st pass radioisotope assess. 80−85482
ventriculograms, processing and display 77−86627

radioisotope scanning and imaging continued
ventriculography, computerised, assessment of LV wall motion and regional kinetics 80−89850
ventriculography with slant hole collimator 78−3588
vertebrae, abnormal accumulations found in the bone scintigram of cancer patients 80−67233
vesico-ureteric reflux detect., nuclear rel. to radiographic technique 79−100703
video output signal, composite, from GAMMA-11 computing system 79−29610
video-sync mixer for cassette videotape recording of computer images 79−29604
vidicon tube for low level X-ray and γ-ray imaging 77−81561
vitamin B_{12}, ^{57}Co-labelled, meas. using liquid-scintillator whole-body counter 79−96648
whole body autoradiography of bumetanide-^{14}C in dogs by round saw method 80−72399
whole-body counter, shadow-shielded, for detection, identification, and localisation of incorporated radionuclides *(German, English)* 78−20266
whole-body counter in vivo calibrations for quantitative retention estimation 78−3579
whole-body counting, comparison of Buddha posture with other geometries 77−66839
whole-body counting of ^{67}Cu, ^{32}P and ^{51}Cr retention in man 79−62378
whole-body imaging methods and devices, comparison 78−44597
whole-body K content, ^{42}K calibration of whole-body counters 79−25086
X-ray imaging gas scintillating proportional counters, performance in medical appl. 79−2153
zero summation filter optimisation in scintigraphy 77−16963
zone plate camera longit. tomogram digital processing, computer simulation 78−40311
zone plate coded aperture imaging 77−40762
α-autoradiography of irrad. nuclear fuel, effect of β radiation *(German)* 78−78466
β-ray quantitative microautoradiograhy, by X-ray emission microanal. 78−20545
B_4C absorber rods, nondestructive exam. with dual-energy gamma gauge and multigauge scanners 79−93721
$Bi_4Ge_3O_{12}$, low-temp. scintillation props. and appl. to high-energy γ-imaging devices 80−55191
^{76}Br production, excitation functions for neutron deficient isotope form. via high-energy d-Br reactions 78−44609
^{77}Br production, excitation functions for neutron deficient isotope form. via high-energy d-Br reactions 78−44609
C^{15}O, steady state imaging as therapy monitor 78−40298
^{11}C, scintigraphy, labelled thymidine, thymidylate, in vivo distrib. in rabbits 79−5344
^{11}C-1-aminocyclopentane carboxylic acid, tumour location, clinical trials with single photon detect. 78−31895
^{11}C-lactic acid synthesis and scintigraphic evaluation of in vivo distrib. in dog 78−80965
^{11}C-lactonitrile synthesis and scintigraphic evaluation of in vivo distrib. in dog 78−80965
CdTe detectors, international workshop 78−41887
CdTe detectors, small, props. uses in biotelemetry 77−44747
CdTe detectors in nuclear medicine, capabilities, limitations 77−44748
^{165}Er decay parameters and whole-body dose 77−70529
^{18}F production and yield from ^{16}O(^{3}He,p)^{18}F reaction in water 78−28065
Fe, water sorption visualisation using THO and autoradiography 78−26761
Ga radionuclides, history of medical use 79−53955
^{66}Ga tumour uptake in rats after whole-body ^{60}Co irrad. 78−65081
^{67}Ga scanning in eval. of therapy of malignant tumours of head and neck 77−37046
^{67}Ga tumour scanning, review 77−9250
^{67}Ga-citrate images obtained with rectilinear scanner and large-field Anger camera 77−66841
Ge camera, 2-detector, 512 element high purity prototype 78−40301
Ge detectors array, collimated, computer-driven scanning bed, clinical appls., tomography 78−40309
Ge γ-ray camera, calc. of picture element efficiency and side scatt. fraction 77−77968
H embrittlement in metals, local detection by T autoradiography 78−3439
HgI_2 detectors, international workshop 78−41887
HgI_2, energy response to ^{137}Cs photons, appl. to medical imaging 78−44592
HgI_2 probe with charge sensitive preamplifier 79−66555
^{197}Hg fixation test, new kidney physiopathology concepts *(French)* 77−70518
^{123}I imaging with scintillation camera, detect. performance and quality factor 77−40743
^{123}I preparation as iodide for synthesis of radiodiagnostic agents, use of compact cyclotron 77−21627
^{123}I, prod. and use in nucl. medicine diagnosis *(German)* 78−28061
^{123}I production by ^{124}Te(p,2n) reaction, new approach to target chem. 77−60250
^{125}I-fibrinogen scintigraphy for thrombosis detect. 78−7437
^{131}I-fibrinogen for clot detect. in canine model of cervical carotid thrombosis 78−85363
^{131}I-tetracycline, prep. and stability 77−29204
^{113m}In-labelled transferrin, use in meas. of blood vols. in rat, rabbit 80−3878
^{43}K evaluation for rectilinear scanner imaging using performance index technique 78−73226
^{79}Kr for pulmonary ventilation and blood flow studies, prod. and imaging 77−16966
^{81m}Kr dosimetry for various source organ-target organ pairs 77−16989
^{81m}Kr, lung, regional distrib. of (dV/dt)A/(dQ/dt) in man, at rest and with exercise 79−16232
^{177}Lu organ distribution in mouse 78−48879
NaI(Tl) scintillation cameras, image artifacts and counting losses 80−94345
Na(Tl), circular ring transaxial positron camera, coinc. electronics 78−31953
^{63}Ni applications in biological research 80−12321
$^{A}O_2$ A=14,15 imaging of cerebral metabolism, long range transmission of short-lived gases in tuned pipeline 79−53239
$^{15}O_2$, steady state imaging as therapy monitor 78−40298
radioisotope scanning and imaging continued
$^{239}PuO_2$, size charact., Rocky Flats soil, autoradiographic technique 78−96102
^{81,82m}Rb production for positron emission tomography 80−98068
^{81}Rb evaluation for rectilinear scanner imaging using performance index technique 78−73226
^{82}Rb generators for imaging studies, ion exchange resin comparison 77−21626
^{97}Ru, preparation, separation from TC isotopes 77−37054
^{47}Sc preparation in carrier-free state by ^{48}Ti(γ,p) reaction for radiopharmaceutical appls. 77−90892
^{75}Se-Na-selenite distrib. in human body, and organ doses 78−48880
Si(Li) detector probe with RFT radiation meas. unit for diagnosis of intraocular tumours *(German, English)* 78−20265
SiO_2, insulating films, neutron activation anal. and autoradiography 78−92574
Tc-labelled bone imaging agent, biological half-life determ. using ^{95m}Tc 77−16961
^{99}Tc^m-dimercaptosuccinic acid evaluation as static renal imaging agent 78−77102
^{99m}Tc detection by scintillation camera, effect of small amounts of ^{131}I 77−16972
^{99m}Tc labelled lung imaging agent quality control, labelling of macroaggregated albumin 78−28069
^{99m}Tc lung imaging kit, radiochem. impurities 77−56469
^{99m}Tc radiopharmaceuticals evaluation, miniaturised chromatography systems 79−96391
^{99m}Tc-EHDP accumulation in canine tibia, meas. method 78−20245
^{99m}Tc-bleomycin selective labelling for tumour imaging 79−53228
^{99m}Tc-pyridoxal-phenylalanine evaluation as hepatobiliary imaging agent 78−31893
^{99m}Tc-pyridoxal-phenylalanine evaluation as hepatobiliary imaging agent 78−31894
^{99m}Tc-stannous glucoheptonate and ^{99m}Tc-stannous dimercaptosuccinate, renal localisation in rat 77−56463
^{201}Tl distribution in stressed rats, imaging, organ uptake and myocardial kinetics 78−65114
^{201}Tl, human distrib. and phys. imaging props. 77−37042
^{201}Tl myocardial imaging, interinstitutional study of observer variability 78−85361
UO_2 compact, density distrib. determ. using autoradioagraphy 77−25234
^{127}Xe, handling and dispensing technique 78−85378
^{127}Xe, simple device for efficient transfer and unit dose packaging 78−85377
^{133}Xe gas dispenser for lung ventilation studies 78−28068
^{133}Xe trapping and re-use system for nucl. medicine 78−28051
Zn radionuclide dosimetry and permissible body burden ^{65}Zn and ^{69m}Zn 77−56474
^{62}Zn production and bleomycin labelling, excitation function for ^{60}Ni(α,2n)^{62}Zn 78−28067

radioisotope separation *see isotope separation*

radioisotopes
see also radioisotope scanning and imaging
^{123}Xe, production in ^{127}I(p,5n)^{123}Xe 79−79651
^{222}Rn concentration distribution under ground, effect on natural γ-ray flux density and exposure rate 80−36300
^{222}Rn flux through multilayered covers cover U mill tailings 80−95487
actinide element movement through food chain 78−61264
activity evaluation and statistical accuracy in activation determ. of low element conc. 79−87928
AECL commercial products, contrib. to nuclear medicine and radiation processing 80−81736
aerosol particle charging using beta sources, elect. and mag. fields 79−36429
air monitoring systems for radioiodine and inert gases, evaluation 80−95480
alkali metal radioisotopes, hyperfine spectroscopy, nucl. props. 80−57677
analysis, quantitative, using gamma-ray spectrometry 77−18734
analytical and industrial applications of sealed sources 79−85847
anodic electrolysis of radioactive isotopes *(Hungarian)* 80−93765
application to solid phase synthesis mechanism in $LaMnO_3$ and $YMnO_3$ 80−21268
applications in agriculture, hydrology, medicine industry etc., booklet 78−35947
applications in industry and science *(Czech)* 80−32554
artificial, 25 years of use and production in Hungary *(Hungarian)* 80−94340
artificial, initial stages of use in Hungary *(Hungarian)* 80−90643
artificial and natural, tracers of large-scale ocean circulation *(Russian)* 79−39742
artificial radionuclides, depositional history in Ross Ice Shelf, Antarctica 79−88027
atmospheric pollution, nature and extent of unplanned releases from nuclear power stations, review 79−57530
automatic radioisotope production devices adapted to a medical cyclotron 80−12260
beta-emitters, activity meas. of low radiators using Cherenkov radiation *(Czech)* 77−46450
beta-emitting volume-seeking radionuclides in human bone, mean skeletal dose factors 78−77115
biological effects of inhaled radionuclides 80−94288
biological samples, neutron-activated, radiochem. determ. of short-lived radionuclides 80−109067
blood-organ transfer kinetics of radioisotopes 80−109044
bone-seeking, dosimetry, comparative study in man, rhesus monkey, beagle and miniature pig 80−72338
calibrator analysis, ionisation chamber sensitivity 77−18738
charact., natural occurrences, technological enhancement and health effects 80−46071
Chinese 19th nuclear test explosion, fractionation effect of hot particles 79−45424
clinical nuclear medicine, internal dosimetry of ^{99m}Tc labelled radiopharmaceuticals 79−12007
coastal marine sediments and seawater, ^{134}Cs, ^{137}Cs, ^{210}Pb, ^{226}Ra and ^{228}Ra concs. determ. 79−88370
collective dose commitments from the release of radioactive nuclides to the atmosphere 80−3556
committed effective dose equivalent conversion factors for intake of selected radionuclides 80−67256

radioisotopes continued
computer-based radionuclide analyzer system for nuclear power stations 79−81100
concentration determ. in ground level air 79−24927
conference on cyclotrons and their appl., Bloomington, USA (Sept. 1978) 79−54626
contaminated groundwater zone control by underground impermeable wall, radioactive waste site *(Japanese)* 79−34446
cosmic rays, two-zone propag. model 79−66891
cosmogenic, in Dhajala chondrite, rel. to interplanetary cosmic ray vars. 79−35207
cosmogenic and artificial, distrib. in ocean, turbulent exchange intensity determ. *(Russian)* 79−39744
cosmogenic isotope concs., data on galactic cosmic ray anomalous behaviour (1971-4) from Gorlovka meteorite 78−61695
cosmogenic radioisotope flux onto Earth's surface and atm., magnitude and time var. 78−61634
crustal fracture water, radioisotope long-term vars. rel. to earthquake prediction 79−62451
cyclotron applications, radiation damage, radioisotope dating, and large-scale radioisotope prod. 79−54692
cyclotron produced medical radioisotope yields 79−57776
cyclotron produced short lived radionuclides, medical appl. 79−57774
cyclotron production, ^{122}Te on Au target fabrication 77−83406
cyclotron production for diagnostic medical research appls. *(French)* 78−48895
cyclotron production of radiodiagnostic isotopes 80−51255
cyclotron production of radioisotopes for medical appl. 80−51256
cyclotron production of radionuclei for medical appl., UC-Davis program 80−51257
Danube water and sediments, radionuclides detec. during 1977 79−12158
decontamination of radioactive isotopes 80−13950
depositions, shallow, on body surfaces, meas. using M X-rays 80−67223
detection using accelerators 80−63468
development trends and appl. 78−55041
direct detection method for radioisotope dating with accelerators 79−34990
dose calculations for inhaled natural radioactive nuclides 80−26354
dose rates to human thorax, low energy photon attenuation theory-expt. discrepancies 79−5373
dosimetric data tables 80−105438
effluent gases from nuclear power industry, ambient contamination *(Spanish)* 78−61540
Egypt's technological experience in radioisotope production 77−65358
environmental pathway anal. calcs., RAMM system of computer programs 77−13015
environmental radioactivity, methods for determ. of radionuclides in environmental samples 79−48202
excitation functions for neutron deficient isotope form. via high-energy d-Br reactions 78−44609
fallout, radionuclide composition and activity over Bulgaria in 1976 79−88018
fallout nuclide determination for 19th Chinese nuclear test 79−54601
food products, radionuclide concs., FOOD II interactive code calc. 79−48348
fracture water radioisotope abundances for earthquake prediction 79−44124
fracture water radioisotope vars. and earthquake prediction 79−44204
fuel reprocessing waste ^{137}Cs, ^{90}Sr and rare earth radioisotope separation by cation exchange 78−78486
gamma-emitters, mixed energy, meas. using radionuclide calibrator 77−14319
gamma-ray spectrum analysis program SAMPO, radioisotope identification subroutine IDENT 79−9953
gamma-rays, half-life vs. energy map, photon activation anal. appl. 77−16883
haematologic disorders, radionuclide therapy 80−36109
half-lives measurements for 35 radioisotopes 80−83070
hospital radioisotope release to environment, model and meas. 78−96105
Hudson River estuary, man-made radionuclides and sedimentation 77−2183
human body radiation monitoring, radioisotopes direct determination 79−54602
Hungarian development in the use of radioisotopes *(Hungarian)* 80−90646
identification, possible problems *(Chinese)* 79−89506
identification and mass determination, using SAMPO programme with IDENT subroutine 78−48731
identification by coincidence methods *(German)* 78−90038
industrial gauging applications, cross section needs 77−23312
industrial uses, role in national economy of USSR 77−23314
inhalation exposure of miniature swine 79−11976
intake by man through terrestrial pathways, TERMOD II interactive code analysis 79−48349
internal radionuclide point source microdosimetry, specific energy density calc. 80−26373
isobar nuclear reaction products separation in on-line separators *(German)* 78−33291
JEN nuclear power industry, uses of isotopes *(Spanish)* 77−50313
labelling of materials with short-lived radioisotopes produced at the place of application *(German)* 79−89503
lake sediments, radionuclide geochronology and pollution history 78−61451
laser spectroscopy of unstable isotopes, nucl. props. determ. from atomic spectra using fast beams 80−9720
life-expired LWR, neutron activation product density and dose rate calc. 79−9908
liquid activity meas. instrumentation in Czechoslovakia 79−49873
low-level radioactive waste, impact of decay daughters 79−52964
low-level waste, radionuclide migration in soil 79−54610
low-toxicity, calc. methods of derived working limits for surface contamination 79−66562
lunar soil samples from Luna 24 and Apollo 16, natural radioactivity meas. 80−67595
lung histological sections, techniques for studying radionuclides 80−56315
malignant thyroid disease treatment 80−36108
marine organism concentration, temp. effect 77−90920
marine sediments, radioactivity uptake, rel. to metal pollutants monitoring 79−12145
radioisotopes continued
marine sediments, radionuclide conc. rel. to residence time near Maine Nuclear Power Reactor 78−49021
mass flow measurements of single-phase and multi-phase flows using radionuclide methods *(German)* 79−86532
mass spectrometric detection using tandem electrostatic accelerators 79−52806
material location technique, rat small intestine 80−8226
medical application of a compact cyclotron, isotope production *(Japanese)* 80−104757
medical cyclotrons for fast neutron radiotherapy and radioisotope prod. 79−53244
medical diagnosis appls. *(French)* 78−48888
medicine, nuclear, production of useful radioisotopes, Los Alamos Meson Physics Facility 80−67251
methylradioiodide, catalytic trapping by beds of impregnated charcoal 78−21681
movement through soil *(Japanese)* 77−81593
multicompartment systems, analytical techniques 79−83689
natural radioisotopes in phosphate fertilizers, occupational dose 79−100751
naturally occurring radionuclides in building materials, estimation and control of population dose 78−9000
nondisplacement chromatography for chromatographic isotope separation 79−50146
nuclear and atomic data sources 79−25081
nuclear experiments performed with intense radioactive ion beams, review 79−97922
nuclear fuel, irradiated, shipping cask design 77−79483
nuclear isotopes far off stability line, production, props., review *(Hungarian)* 79−9927
nuclear radwaste geologic disposal, modelling of radionuclide transport and decay products 80−78415
nuclear weapons testing, radionuclide distributions in oceans and marine sediments 78−13344
ocean photic layer, organic matter studies, radioisotopic methods appl. *(Russian)* 77−60427
optical waveguide materials, radioisotope methods and neutron activation anal. appls. 78−7286
Pecs University Biophsyics Unit, Hungary, 25 years of radioisotope appls. *(Hungarian)* 80−90647
pharmaceuticals, suitability in right-to-left shunting determ. 77−37048
pharmaceuticals in cardiovascular nucl. medicine 77−40746
pharmaceuticals in myocardial imaging 77−40747
preparation at variable energy cyclotron of Frederic Joliot Hospital Service *(French)* 77−65361
production, appl. of compact cyclotrons *(Hungarian)* 78−74517
production, bremsstrahlung beams rel. to proton beams 80−63424
production, for medical use, at TRIUMF 80−72325
production, remote flow system, connecting target and purification systems 80−69004
production by chemical reactions in heterogeneous systems *(Spanish)* 79−45490
production by cyclotron for medical use 79−53245
production by medical cyclotrons 79−53238
production cross sections in Al, Si, Ti, Cr and stainless steel by 12-45 MeV protons 77−17310
production of radionuclides and radiopharmaceuticals using proton and deuteron accelerators 79−53240
production technology transfer to developing countries 77−65357
production using 14 MeV neutron generators 80−3811
production using electron accelerators, terms used 80−91347
production using proton beam at LAMPF 79−53216
protective coating thickness meas. using radioisotope method 77−90520
proton cyclotron targets for prod. of e^+-emitting radionuclides for medical appl. 79−53241
pulmonary effects of radionuclide and chemical pollutants *(French)* 80−8102
PWR primary coolant after fuel failure, dynamic behaviour of tag gas isotopes 77−46363
quantum radiation, data handbook 80−94933
radiation protection, development in use of radioisotopes in Hungary *(Hungarian)* 80−90644
radiation therapy, pot. future appl. of radioisotopes 80−36031
radio-nuclide transport in soil, conc. profile in groundwater, waste storage problems *(German)* 79−74556
radioactive material migration in soil, hydrologic transport model 80−16848
radioactive transport in the aquatic ecosystem, foodweb model 80−104777
radioactive waste, geochemical aspects of radionuclide migration from waste repositories 80−13711
radioactive waste, leach-migration experiments to determine the mobility of radionuclides in geologic media 80−18487
radiochemical purity quality control by rapid feedback system 77−90900
radioiodination, microelectrolytic, of polypeptide hormone, using Pt microcell 79−48340
radioisotope power generation, radiation techniques and technology development in the Soviet Union 79−685
radioisotopic energy dispersive X-ray fluorescence spectrometry, determination of fuel oil S content 78−61122
radionuclide accumulation in marine organisms, computer kinetic modelling 79−53261
radionuclide chain migration in groundwater 78−85616
radionuclide migration from repository sites, stochastic anal. 80−37486
radionuclide migration in groundwater from accelerator earth shields 79−48194
radionuclide radiation precision spectrometry using semiconductor detectors *(Russian)* 79−31305
radionuclide transport through heterogeneous media 80−32382
radionuclides in reactor circuits, continuous meas. techniques *(French)* 79−97857
radiopharmaceutical dose calibrator performance and quality control 77−56470
radiopharmaceutical patient diagnosis, absorbed dose derivation techniques 79−12006
radiopharmaceutical preparation and injection, dose to hands 78−20276
radiopharmaceutical purity determ., adaptation of multichannel scalar device for radiochromatogram scanning 78−48894
radiopharmaceuticals, γ-emitting, in rat blood, continuous monitoring technique 79−2129

radioisotopes continued
radiopharmaceuticals, cyclotron prod. for nuclear medicine appls. 77−44753
radiopharmacy optimisation by redesign 77−90899
rapid automated nuclear chemistry facility for the study of short lived fission products 79−71978
reactor cooling system, radioisotopes prod., transfer, life cycle, radiation calcs. using program system TIBSO 78−54821
receptor binding radiotracer preparation 80−51258
resuspended, possible importance of short-term exposure 80−85501
review of the development in the use of radioisotopes *(Hungarian)* 80−90645
risk anal. of transport using Monte Carlo and probability methods *(Norwegian)* 79−13437
River Periyar, S.India, pollution profile 79−57510
secondary system fission product transport study at the Oconee Nuclear Station 79−49781
short life isotopes, props. and prep. for medical appl. *(Danish)* 79−83933
short lived, Soviet medical diagnosis appl. 77−37032
short-lived, meas., counting statistics 80−58098
short-lived radionuclide potentials and props. 77−52863
short-lived radiopharmaceuticals, radiochem. quality control 77−52876
soluble radioisotopes, meas. of activities and their origin in reactor steam generator leakage water 80−693
spectral unfolding method to determine source depth distribution 80−81719
steady gas flowmeter design 79−32721
testing and measurements on industrial plant, appls. *(German)* 77−70522
thermoelectric generator cooling in spacecraft 80−40881
thermoelectric generator shock and vibration test program for MB-M75(A) 80−35711
thermoelectric generators, design optimisation for Solar-Polar Mission 80−40880
thermoelectric generators, power degradation predictions 80−40879
thermoelectric generators, SNAP 19 performance update for Pioneer and Viking missions 80−40883
thickness and surface layer density meas., contactless, appl. *(German)* 79−71414
thoron content in exhaled air, meas. apparatus 79−34672
thrombus detection radiopharmaceuticals, selection, prep. and evaluation 78−11731
trace element analysis of radiological effluents from coal-burning power plants 80−21426
transuranic production for medical use, chemical treatment of targets *(French)* 77−42203
transuranics for industrial and medical appl. *(French)* 77−42206
transuranics production by irradiation in expt. reactors, medical *(French)* 77−42202
transuranium nuclides, production in reactor, yields, nuclide fractional concs. determ. 77−63986
transuranium radionuclides in the foodchains 79−74554
tube wall thickness gauge, radioisotopic, description 78−44310
two phase flow continuity measurement by radioisotope method, error 79−32723
ultrasonographers, pot. hazard from previously administered radionuclides 80−98120
waste disposal in geologic media, radionuclide migration model 80−37499
X-ray characteristics in neutron activation anal. at 14 MeV 80−93827
γ-emitting radioelements, meas. of weak doses *(French)* 80−91410
(p, spallation) cross sections for medial isotope preparation 77−23052
^{133}Xe custom trapping and holding system for animal research, design and evaluation 80−30950
^{135}Cs, conc. variations in Baltic Sea 1973 to 1975 79−92100
^{222}Rn daughters exposure, electronic dosimeter 80−46054
^{108}Ag^{m}, neutron cross-section for production from ^{107}Ag 79−29625
^{108}Ag^{m}, prod. in nuclear reactors by thermal neutron capture in stainless-steel structure 80−42747
^{26}Al and partial ionization of solar nebula 79−58282
^{26}Al content of Dalgety Downs meteorite 79−75167
^{26}Al in Fe meteorites and past cosmic ray intensity 79−44422
^{26}Al in primordial comet interiors, contrib. to radiogenic melting 80−67659
^{26}Al, use in meas. Mn nodule growth rate 78−40537
^{28}Al radioisotope source, activation expt. 79−31
Am contaminated wound, surgical treatment after glove box accident *(French)* 78−53521
Am determination in biological samples by solvent extraction and liquid scintillation counting 79−53260
Am release into estuarine-coastal sea ecosystem, assessment methodology 79−70471
Am, transport through skin, role of diffusion 78−20158
^{241}Am 60 keV γ backscatter meas. of solid powder mixture composition 77−52695
^{241}Am, biological availability, influence of DTPA at soil-plant and plant-animal interfaces 78−73264
^{241}Am, conc. in thermonuclear test debris, collected near Bikini Atoll 78−96103
^{241}Am, environmental pollution, biophysical aspects 79−39530
^{241}Am III retention and distrib. in neonatal beagle 78−28094
^{241}Am removal, Ca-DTPA vs. Zn-DTPA in beagles 77−73599
^{241}Am sorption on USA subsoils from differing weathering intensity areas, ^{241}Am, ^{237}Np and ^{99}Tc 78−16014
^{A}Ar, A=37,39, simultaneous activity meas. 80−23270
^{37}Ar form. from Ca in fission reactors 77−83048
^{37}Ar method for in vivo Ca meas., inert gas elimination in humans 78−61247
^{40}Ar(γ,2p)^{38}S production on recirculatory, Ar gas target 79−88185
^{40}Ar(γ,p)^{39}Cl production on recirculatory, Ar gas target 79−88185
^{41}Ar, near-stack reactor effluent dispersion studies by SF_6 tracer method 78−11992
As neutron deficient isotopes (A=68,69,70,71), production in heavy ion reactions 77−38292
^{A}At, A=209, 210, production by photospallation of ^{232}Th and ^{238}U 80−52797
Au plated layer thickness meas., ^{195}Au nondestructive method 79−96244
^{198}Au, hepatic fractional clearance of colloids as meas. of effective blood flow 79−66547
^{198}Au, use in ovarian carcinoma treatment 80−36087
^{199}Au, carrier-free extraction from neutron-irradiated ^{198}Pt, medical appls. 79−2130
Ba, radioisotopes, at. beam laser spectroscopy, hyperfine struct., nucl. moments and radii 80−57678
^{140}Ba, airborne short-lived radionuclides of unknown origin in Sweden (1976) 78−32219
^{133m}Ba production for medical purposes by ^{133}Cs(d,2n)^{133m}Ba 77−60251
^{7}Be, atmospheric conc. at South Pole 79−84382
^{7}Be, cosmic-ray-produced, mean tropospheric residence time at north temperate latits. 78−85633
^{7}Be production in atm. and transport from Sun, tracer for terrestrial-solar relationship 80−98525
^{10}Be conc. vars. search in marine sediment core during geomag. reversal 80−26511
^{10}Be, distrib. in geophysical samples meas. using tandem van de Graaff accelerator 80−61924
^{10}Be in marine sediments rel. to geophysical events and cosmic ray var. 79−29748
^{10}Be in Mn nodules, meas. using tandem Van de Graaff accelerators 79−74967
^{10}Be in ocean surface layer, conc. and residence time 79−66714
^{10}Be, mass spectrometric meas. with cyclotron, geochronological appl. 79−57338
^{10}Be survival and cosmic ray age distribs. in galactic convective halo 80−51625
^{10}Be, use in meas. Mn nodule growth rate 78−40537
^{210}Bi, determ. in human urine by direct extraction by Ni foil 79−100707
^{75}Br, excitation functions for production, pot. nuclear medicine appls. 80−98135
^{76}Br, ^{77}Br, production from decay of cyclotron produced ^{76}Kr and ^{77}Kr 80−52799
^{76}Br production, excitation functions for neutron deficient isotope form. via high-energy d-Br reactions 78−44609
^{77}Br production, excitation functions for neutron deficient isotope form. via high-energy d-Br reactions 78−44609
^{77}Br, production excitation curves 79−85468
^{79}Br(p,3N)^{77}Kr→^{77}Br^{-} production, separation and radiopharmaceutical labelling 79−79649
^{80}Br-bromohippuric acid preparation 79−88187
$^{14}CO_2$, respiratory, determ. by $Ba^{14}CO_3$ decomposition in sample oxidiser 79−88153
$C^{15}O_2$, exptl. approaches to myocardial function studies 77−40755
CO_2-^{14}C animal exhalation meas. by liquid scintillation counting *(French)* 79−48384
^{11}C, absorbed dose comparison rel. to γ-ray emitters 79−70647
^{11}C, clinical results using short-lived radioisotopes prod. by medical cyclotron 79−57775
^{11}C, production by cyclotron, biomedical appls. *(French)* 80−56216
^{11}C production for nuclear medicine use 80−30889
^{11}C, racemic [1-^{11}C]-alanine and partially resolved [3-^{11}C]-alanine synthesis 79−88186
^{11}C, radionuclide prod. for medical appl., by Groningen 280 cm AVF cyclotron 79−54696
^{11}C-glucose, meas. of brain glucose utilisation by emission tomography 78−69183
^{11}C-iodomethane remotely controlled synthesis 79−88192
^{11}C-labelled radiopharmaceuticals, automated synthesis 80−17133
^{14}C, bomb-produced, distrib. in equatorial Atlantic, upwelling rate estimation 79−39726
^{14}C β-rays, biological hazards, cell killing effects, E. coli expts. 80−89805
^{14}C dating, thermal diffusion enrichment, N. American glacial history extended to 75000 yrs ago 78−77284
^{14}C dating, time scale extension by thermal diffusion enrichment, appl. to NW. Europe climatology 78−77314
^{14}C dating method using 20 keV Kr ion beam for objects <65000 yrs. *(Danish)* 80−8440
^{14}C dating of CO_2 sample with accelerator, blind meas. 79−25362
^{14}C dating of coastal marine sediments, fossil C effect 80−98308
^{14}C dating of geological and archaeological samples 78−92993
^{14}C dating of mg geological samples with electrostatic accelerators 79−25361
^{14}C dating technique using cyclotrons, or Van de Graaff as mass spectrometer 80−5414
^{14}C detection, $NaH^{14}CO_3$ liquid and $Ba^{14}CO_3$ gel suspension, scintillation cocktails efficiencies 79−3283
^{14}C, determ. of low radiocarbon activity by CO_2 absorpt. 78−74550
^{14}C direct detection at natural concs. by mass spectrometry, for dating 78−32916
^{14}C, dissolved in groundwater initial activity determ., new model and review 80−8458
^{14}C, dosimetry and metabolism of low energy β-emitters 79−8551
^{14}C, dosimetry of labelled diethylenetriamine pentaacetic acid in the rat 79−62366
^{14}C fallout from nucl. weapons testing, human radiation burden 77−64091
^{14}C, formation, distrib. in nuclear fuel cycle *(Russian)* 80−5316
^{14}C formation by solar flare particles in terrestrial atmosphere 78−92886
^{14}C, high accuracy meas. by gas proportional and liq., scintillation counting 78−74544
^{14}C labelled amino acids, optimisation factors in liquid scintillation counting 80−30951
^{14}C labelled compounds synthesis, technological aspects 78−76895
^{14}C liquid scintillation counting using thick-walled vials 78−857
^{14}C, liquid scintillation counting efficiency, volume and quenching effects 79−76270
^{14}C low level liq. scintillation counting using small vol. teflon-Cu vial 80−16887
^{14}C measurements on floating tree-ring chronology from NE.Scotland 78−70236
^{14}C natural var. in atmosphere, Suess effect determ. accuracy 79−96801
^{14}C, organic, activity in abyssal marine sediment 79−16434
^{14}C radioactive fallout damping coefficients 78−92961
^{14}C, radioactivity meas. using Cherenkov liquid scintillator counter 79−26817
^{14}C released to atmosphere, dynamic model for estimating radiation dose to world population 80−89852
^{14}C released to atmosphere as CO_2, population dosimetry 78−35958
^{14}C time scale changes and Late Pleistocene geomagnetic var. 79−62433

radioisotopes continued
^{14}C, use in dating, review of technique 79−49922
^{14}C variations in terrestrial atmosphere rel. to 11-year solar cycle 78−92885
^{14}C-$NaHCO_3$ solution liq. scintillation counting, prevention of radiocarbon loss 78−21811
$^{14}CO_2$, photosynthesis rate of wheat meas. using Geiger counters *(German)* 77−70436
$^{14}CO_2$ meas. in Karlsruhe Reprocessing Plant exhaust air 79−3231
Ca, stable and radioisotopes, hfs, isotope shifts, dye laser saturation spectroscopy, beam expt. 80−58169
^{41}Ca, possible use for radioactive dating 79−21063
^{45}Ca and ^{32}P determination in biological samples by Cherenkov and liq. scintillation counting 80−98183
^{45}Ca, effect on spleen and thymus of Indian desert gerbil 80−8106
^{45}Ca, effects on bone marrow of Indian desert gerbil 80−45971
^{45}Ca, giant liver cell formation after administration to desert gerbil 79−92299
^{45}Ca tracer diffusion in silicate melt 79−90809
^{47}Ca, bone imaging radiopharmaceutical local accumulation model 78−24127
^{252}Cb, polyethylene pellets in design, construction of storage safe, transport vessel, portable shield 79−5380
^{109}Cd, production in nuclear reactors by neutron irrad. of ^{107}Ag 80−52798
^{144}Ce absorption through damaged and undamaged skins of guinea pigs 80−26383
^{144}Ce, anodic deposition on Pt anode, electrochem. separation 79−91958
^{144}Ce, effects of repeated inhalation exposure of mice to $^{144}CeO_2$ 80−104676
^{144}Ce gastrointestinal absorpt. and distrib. in suckling pig 78−15942
^{144}Ce, inhalation exposed mice, toxicity, dosimetry and ^{144}Ce retention 80−89874
^{144}Ce, intravenous injection, wound site absorption, comparison of metabolic behaviours in rats 79−8545
^{144}Ce, radiation dose-response curves, hazard function method of resolution 79−66556
^{144}Ce, removal rate in lower stratosphere, seasonal vars. 80−55957
^{144}Ce repeated inhalation exposure of $^{144}CeO_2$, retention and dosimetry 80−109034
$^{144}Ce/^{144}Pr$ miniature radioisotope generator 79−49885
Cf determination in biological samples by solvent extraction and liquid scintillation counting 79−53260
^{252}Cf fission-neutron spectrum unfolding experiment 80−13514
^{252}Cf, human lymphocyte chromosome aberrations induced by neutron radiation 79−16169
^{252}Cf, measured neutron and γ spectra in a tissue equivalent medium 80−3805
^{252}Cf, medical appl., fast neutron therapy *(Japanese)* 80−98112
^{252}Cf, optimum design for subcritical neutron multiplier 79−59290
^{252}Cf, use for brachytherapy 78−20272
$^{252}CfCl_3$, metabolism in rat and effect of in vivo DTPA chelation therapy 78−85387
^{36}Cl, Cherenkov counting using Teflon vials 78−858
^{36}Cl in environmental water samples, anal. using electrostatic accelerator 79−20895
^{36}Cl in meteorites from Antarctic, cosmic irrad. histories 80−21950
$^{34m}Cl^-$ production, inorganic yields 80−23202
Cm determination in biological samples by solvent extraction and liquid scintillation counting 79−53260
^{244}Cm, biological availability, influence of DTPA at soil-plant and plant-animal interfaces 78−73264
^{244}Cm, inhalation carcinogenesis of high-fired $^{244}CmO_2$ in rats 80−21502
^{244}Cm, mobility in bronchially intubated rat 80−30967
Co, A=58, 60, accumulation by oysters in reactor effluent, math. model 77−81589
Co isotopes, thick-target yields in Ni due to proton bombardment up to 100 MeV 77−88312
Co^{2+} ion removal in high temp. water using TiO_2 79−89376
^{55}Co, carrier-free positron-emitting label for bleomycin from $^{56}Fe(p,2n)^{55}Co$ 79−79648
^{55}Co, cyclotron prod. by ^3He bombardment of natural Fe, bleomycin complex synthesis 77−86629
^{57}Co, radionuclide prod. for medical appl., by Groningen 280 cm AVF cyclotron 79−54696
^{60}Co absorption through damaged and undamaged skins of guinea pigs 80−26383
^{60}Co beams, cylindrical ion chamber A_c and A_{eq} factors exam. 79−81121
^{60}Co behaviour in sediments in laboratory-scale aquatic ecosystem 78−3831
^{60}Co, distrib. and behaviour in Urazoko Bay sediment 80−97825
^{60}Co distribution in N_2O_4 condensate cooling circuit *(Russian)* 79−13491
^{60}Co, fixation on natural sorbents from phenol-polluted water 79−57506
^{60}Co γ-rays, dose assignment criteria, beagles, bilateral exposure 79−16305
^{60}Co, in radioactive waste water, improved removal using diethyldithiocarbamate 78−37415
^{60}Co, inhaled, long-term clearance 79−79663
^{60}Co ion removal in waste water by oxine impregnated activated charcoal 79−26558
^{60}Co irradiation sterilisation processing, nonstandard double carton simulation 79−26760
^{60}Co irradiation sterilisation processing unequal mass interchange model verification 79−26759
^{60}Co irradiation sterilisation processing, unequal mass interchange model 79−26758
^{60}Co, long-term retention in Indian workers, dose commitment 78−35960
^{60}Co radiation therapy, eval. of dosimetric accuracy and uniformity 80−12269
^{60}Co, radioactive waste migration by complexing agent ethylenediaminetetraacetic acid 79−20687
^{60}Co radionuclide distribution among green alga, marine sediments and sea water 78−53534
^{60}Co, radionuclide leaching from hardened cement grout, container dimension depend. 79−13439
^{60}Co, sediment-bound, absorpt. through digestive tract of marine demersal fish 79−92400

radioisotopes continued
^{60}Co source irradiation of 2 media, absorbed dose in vicinity of an interface 80−30894
^{60}Co, teletherapy dosimetry, USA survey (1974-77) 79−12011
^{60}Co teletherapy installations calibrations, US national evaluation 79−5360
^{60}Co, transfer from irrigation water to crops and agricultural products *(French)* 78−8996
^{51}Cr, lung burdens of low-energy photon-emitters, interlaboratory comparison of meas. techniques 79−20671
^{51}Cr, whole-body counting of retention in man 79−62378
^{57}Cr, new isotopes of interest to explosive nucleosynthesis, β-decay scheme and mass determ. 79−45208
Cs, A=134, 137, accumulation by oysters in reactor effluent, math. model 77−81589
Cs dynamics in herons inhabiting contaminated reservoir system 78−28092
Cs, liquid effluents, aquatic radiological impact anal., radiocaesium transport in sediment 80−95486
Cs, transport in soil, evaluation of combined sorption model 79−8554
Cs, transport through skin, role of diffusion 78−20158
^{127}Cs production for radiopharmaceutical appls., high energy alpha reactions 77−37053
^{127}Cs, yield in I irrad. by α-particles 79−67760
^{129}Cs, yield in I irrad. by α-particles 79−67760
^{134}Cs, activity meas. 79−59292
^{134}Cs and ^{137}Cs at Atlantic nuclear waste disposal site, radionuclide redistrib. 80−85309
^{134}Cs and ^{137}Cs in Clyde Sea Area 80−3541
^{134}Cs, as potential radiotherapy radionuclide, prod. and decay scheme 77−90875
^{134}Cs behaviour in sediments in laboratory-scale aquatic ecosystem 78−3831
^{134}Cs, defective fuel rods ultra sensitive detection with low core burn-up, method 79−45374
^{134}Cs, for treatment of cervical cancer, isodose curves 77−90876
^{137}Cs absorption through damaged and undamaged skins of guinea pigs 80−26383
^{137}Cs accumulation by marine organisms, sediment and sea water influences 78−80981
^{137}Cs accumulation in fruitbodies of Basidiomycetes 78−80977
^{137}Cs accumulation in rat liver, effects of altered thyroid states 78−24136
^{137}Cs and K contents in low-teens in areas of different fallout level in Japan 77−90922
^{137}Cs body burden in Japanese, biological half-life meas. 79−57795
^{137}Cs, conc. in wet and dry deposition samples, USA, 1976 Jun.-1977 Dec. 79−29807
^{137}Cs conc. meas. in ocean, sorbent props. *(Russian)* 79−39763
^{137}Cs, contents in coastal sediments 79−57974
^{137}Cs, contents in fish flesh 79−79718
^{137}Cs, coyote scats, Hanford Reservation, radioactive waste distrib. 79−25120
^{137}Cs, defective fuel rods ultra sensitive detection with low core burn-up, method 79−45374
^{137}Cs deposition on plate glass surface, contamination *(Japanese)* 78−29654
^{137}Cs, distrib. and behaviour in Urazoko Bay sediment 80−97825
^{137}Cs excretion in urine vs. total excreta following continuous intake of ^{137}Cs in fall-out 78−20294
^{137}Cs, fallout effects of Nagasaki atomic bomb 78−85393
^{137}Cs fallout in arid watersheds, phys. and chem. parameters affecting transport 78−61461
^{137}Cs, fixation on natural sorbents from phenol-polluted water 79−57506
^{137}Cs gynecologic insertions, expt. derived algorithm for computer calc. dose rates 80−101264
^{137}Cs immobilisation in cement-waste composites 78−82466
^{137}Cs, intake by Bikini Island residents, model using bioassay data 80−109043
^{137}Cs, K, model for turnover in pike 79−8553
^{137}Cs levels in soils and vegetation of W.Malaysia 78−73263
^{137}Cs, long-term retention in Indian workers, dose commitment 78−35960
^{137}Cs, migration in Magenta dolomite, effect on radioactive waste storage 80−13718
^{137}Cs movement and loss in small lake 78−24317
^{137}Cs radiation effect on Chinese hamster cells, marker phenotype rescue 80−17005
^{137}Cs radioactive fallout and lacustrine sedimentation rates 80−4048
^{137}Cs radionuclide distribution among green alga, marine sediments and sea water 78−53534
^{137}Cs, radionuclide leaching from hardened cement grout, container dimension depend. 79−13439
^{137}Cs, radiotracer studies in equatorial Indian Ocean *(Russian)* 79−39743
^{137}Cs removal from ocean waters, adsorpt. on hydrated MnO 78−3822
^{137}Cs, runoff coeff. from surfaces of river basin soils 79−44212
^{137}Cs source for computerised tomography 77−60239
^{137}Cs, study of absorpt. by Lemna minor 80−30677
^{137}Cs, time variation of low concentrations in rain water 79−43994
^{137}Cs transfer coefficient into cows milk rel. to level of milk prod. 78−80978
^{137}Cs, transfer from irrigation water to crops and agricultural products *(French)* 78−8996
^{137}Cs, uptake by cotton rats inhabiting banks of radioactive liquid waste pond 79−25121
^{137}Cs whole-body content in a normal New Mexico population 1956-1977 80−26382
$^{137}Cs/^{134}Cs$ radioisotopes in seawater, Cs-selective resin determ. 80−94137
^{137}Cs-irradiation, response of pig skin, various schedules of irrad. 80−72237
Cu, metabolic model and dosimetric data 78−65130
^{62}Cu, whole-body counting of retention in man 79−62378
^{64}Cu, simultaneous prod. with ^{67}Cu and ^{67}Ga, and bleomycin labelling with ^{67}Cu or ^{64}Cu 78−28066
^{67}Cu, simultaneous prod. with ^{64}Cu and ^{67}Ga, and bleomycin labelling with ^{67}Cu or ^{64}Cu 78−28066
^{144}e inhalation effect of influenza virus infection on pulmonary retention and mouse survival 78−85340

radioisotopes continued
^{165}Er decay parameters and whole-body dose, for radioisotope scanning 77−70529
^{152,154}Eu fixation in solid/liquid systems 79−13530
^{18}F, bone imaging radiopharmaceutical local accumulation model 78−24127
^{18}F labelled anhydrous fluorinating reagent preparation using cyclotron accelerated p, d, ^{3}He, or α 79−2131
^{18}F, prep. with an electron linear accelerator, medical and biological appls. 80−98136
^{18}F production and yield from ^{16}O(^{3}He,p)^{18}F reaction in water 78−28065
^{18}F, production by α bombard. of SiO_2 target 79−79650
^{18}F, production from ^{18}Ne, carrier free H^{18}F acid 79−29626
^{18}F, radioactivity meas. using Cherenkov liquid scintillator counter 79−26817
^{18}F recoil labelling of CF_3Cl 80−23203
^{18}F recovery during transport from reactor 78−78821
^{18}F-F_3COF-^{18}F radiopharmaceutical synthesis procedure 79−29619
^{18}F-5-fluorouracil, synthesis and purification by fractional sublimation 80−17134
^{18}F-5-fluorouracil distrib. in tumour-bearing mice and rats 78−48878
^{52}Fe and contaminant ^{55}Fe, combined use in bone marrow studies 77−56447
^{52}Fe and stable Fe forms and availability in oceanic aerosols 79−12241
^{55}Fe as contaminant in ^{52}Fe, use in bone marrow studies 77−56447
^{55}Fe, susceptibility of haematopoietic stem cells to radiation damage 79−11975
^{55}Fe, thick-target yields in Co due to proton bombardment up to 100 MeV 77−88312
^{55}Fe fixation in solid/liquid systems 79−13530
^{59}Fe, sediment-bound, absorpt. through digestive tract of marine demersal fish 79−92400
^{59}Fe, self-diffusion in Fe-V *(Czech)* 80−88352
^{59}Fe, uptake in human melanoma cells 79−62217
^{59}Fe uptake in marrow, rel. to ^{239}Pu deposition in bone, mouse 78−85395
^{59}Fe uptake in normal and splenectomised rats, marrow dose estimation, 1000 kVp X-irrad. 78−15894
^{59}Fe/^{55}Fe activity ratio of blood, meas. using semicond. detector 80−17062
^{66}Ga tumour uptake in rats after whole-body ^{60}Co irrad. 78−65081
^{67}Ga, mechanism of localisation in tumours 79−57768
^{67}Ga, prod. for medical uses using Ruder Boskovic Institute cyclotron 78−20273
^{67}Ga, simultaneous prod. with ^{64}Cu and ^{67}Cu 78−28066
^{67}Ga, subtraction technique in diagnosis of abdominal abscesses 78−73212
^{67}Ga, uptake in human melanoma cells 79−62217
^{68}Ga, new generator, medical appls. 80−76834
^{68}Ge/^{68}Ga radioisotope generator system 78−78536
HT-HTO in air meas. system 80−21433
^{3}H biological half-life estimation in man, model 79−20689
^{3}H, conc. and distrib. in N.Atlantic surface water 78−65345
^{3}H distribution between gas and liquid in isotope equilibrium in H_2O-H_2S and D_2O-D_2S systems 79−45376
^{3}H experimental reactor loop, hazard and protection 79−36420
^{3}H formation by solar flare particles in terrestrial atmosphere 78−92886
^{3}H, incorporation of HTO in maize and barley 79−25107
^{3}H intake during various processes in industrial, academic and medical institutions 77−73600
^{3}H labelled amino acids, optimisation factors in liquid scintillation counting 80−30951
^{3}H levels in urine of occupational exposed persons, working environment effects 79−83947
^{3}H, mouse liver, effects of tritiated water rel. to age 79−43967
^{3}H radioactive fallout damping coefficients 78−92961
^{172}Hf production, recovery and purification for nucl. medicine use as ^{172}Lu generator 78−48893
^{175}Hf, thick-target yields in Ta due to proton bombardment up to 100 MeV 77−88312
^{197}Hg, radionuclide prod. for medical appl., by Groningen 280 cm AVF cyclotron 79−54696
^{203}Hg separation from chlormerodrin-203, electrophoretic method 77−56283
^{203}Hg, tracer for Hg conc. in seawater expts., ^{75}Se tracer 80−21420
^{166}Ho electrosorption on anodically polarised Pt surface 79−52684
I, A=123 to 135, derived air concs. annual limits 78−31909
I, adsorption in soils, concentration depend. obs. *(Czech)* 80−12031
I, adsorption on charcoal filter, safety evaluation *(Japanese)* 78−33267
I behaviour during PWR steam generator tube rupture accident 79−59230
I increased release from defective fuel rods during PWR shutdown 79−49710
I isotopes, history of use in medicine 80−42032
I, radioactive, air sampling system, separation into gaseous and particulate fractions 80−57962
I, radioisotopes, environmental and biological effects from nuclear fuel cycle *(Russian)* 80−52768
I radioisotopes, high efficiency mixed species air sampling, readout and dose assessment system 78−57074
I radioisotopes, meas. of crit. environmental exposure for reactor accidents 78−57081
I spiking in LWR, release mechanism and its verification in plant operation 79−59229
I spiking in PRW fuel rods, general model of origin and behaviour 79−59228
I spiking in PWR fuel rods, cause and effects 79−59227
I volatilisation problem, soln. using plexiglas iodination box 77−56484
I-labelled pharmaceutical administration, thyroid protection, computer simulation 78−44616
I_2 adsorption on steel in HTGR He environment 80−44233
^{A}I, A=121, 123 and 125, cyclotron prod. by ^{127}I(p,xn)Xe→(β)→I reactions, yield curves 78−44611
^{A}I, A=131-2, comparative effects in rat thyroid glands 80−104670
^{121}I labelling of radiographic contrast media 80−26350
^{121}I, production on Heidelberg compact cyclotron, dosimetry studies 80−21539
^{123}I, absorbed dose to thyroid from radioiodine impurities 77−29207
^{123}I, carrier-free, prod. from ^{127}I(p,5n)^{123}Xe using in-beam collection of ^{123}Xe 78−44610
radioisotopes continued
^{123}I, carrier-free iodide generated from ^{123}Xe, kit prep. and quality control 77−29205
^{123}I labelling of radiographic contrast media 80−26350
^{123}I, large scale prod. from flowing liq. target using ^{127}I(p,5n)^{123}Xe reaction 77−29203
^{123}I, prep. from gaseous TeF_6, nuclear medicine appl. *(French)* 80−98137
^{123}I, prod. and use in nucl. medicine diagnosis *(German)* 78−28061
^{123}I, prod. at Manitoba Univ. using ^{124}Te(p,2n) 79−54695
^{123}I prod. from ^{127}(p,5n)^{123}Xe→^{123}I, at 58 MeV 80−94369
^{123}I, prod. using 6 MeV Van de Graaff accelerator 79−53243
^{123}I, prod. via ^{124}Xe(n,2n)^{123}Xe reaction in nucl. reactor, for nucl. medicine 77−2051
^{123}I, prod. via ^{127}I(p,5n)^{123}Xe reaction, excitation function 77−2981
^{123}I product radionuclidic purity using ^{124}Te(p,2n), reply 79−29622
^{123}I product radionuclidic purity and quality, comments from ^{124}Te(p,2n) 79−29621
^{123}I production by ^{124}Te(p,2n) reaction, new approach to target chem. 77−60250
^{123}I production for radiopharmaceuticals, excitation functions and target enrichment vs. radionuclidic purity 77−60252
^{123}I production from ^{123}Xe formed in spallation reactions by 660 MeV protons, medical appls. 80−85494
^{123}I production in cyclotron by ^{124}Te(p,2n)^{123}I, improved targetry and radiochem. 78−28064
^{123}I, production in LASL radiochemistry hot cells 80−72326
^{123}I, routine prod. of ^{123}I at Karlsruhe isochronous cyclotron using ^{124}Te(p,2n) at 26 MeV 79−54694
^{123}I, simultaneous prod. of ^{123}I, ^{62}Zn and $^{13}NH_3$, multitarget assembly for high energy irrad. 77−90896
^{123}I uptake in thyroid, correction for thyroid depth 78−11728
^{123}I-fibrinogen scintigraphy for thrombosis detect. 78−7437
^{124}I production in cyclotron by ^{124}Te(p,n)^{124}I, improved targetry and radiochem. 78−28064
^{125}I accidental inhalation, bioassay and thyroid monitoring results 78−24151
^{125}I airborne vapour detection 80−51027
^{125}I contamination monitoring using portable scintillation camera 78−85388
^{125}I, counting device with automatic efficiency correction 80−42897
^{125}I, determ. of exposure rate constant using a scintillation detector 80−89863
^{125}I gamma ray effects on Vicia faba roots, comparison with ^{182}Ta 78−48832
^{125}I in partially blocked thyroid of rats, testis damage 78−3565
^{125}I in the thyroid, 2-probe meas. method 80−81718
^{125}I, insulin radioiodine labelling using dimethylsulphoxide as labelling agent *(Korean)* 78−88746
^{125}I interstitial seed implants, new afterloading technique 79−34652
^{125}I, intramol. effects of decay in o-iodotyrosine 80−108973
^{125}I, intranuclear atoms not bound to DNA, radiotoxicity 80−104655
^{125}I labelling hazards, recommended code of practice 80−51270
^{125}I microelectrolytic labelling of polypeptide hormones 80−12255
^{125}I, oxytocin radioimmunoassay, human plasma 79−5353
^{125}I photons, absorbed fractions in the thyroid 80−109032
^{125}I, procedures for safe working in labs. 79−35698
^{125}I, release in autoclave sterilization of radioimmunoassay kit *(Japanese)* 80−81727
^{125}I response of LiF and $CaSO_4$ TLD discs, influence of thyroid geometry 78−73250
^{125}I seed implants in prostatic cancer, preoperative extended field radiation 80−72303
^{125}I, shielding of *(Japanese)* 80−63404
^{125}I, spleen damage after partial thyroid blockage, rat expt. 79−96631
^{125}I surface contamination meas., sensitivity comparison with other detectors *(Czech)* 79−34673
^{125}I thyroid dose calc., air and water conc. limits 79−88195
^{125}I uptake minimisation and thyroid monitoring 77−40796
^{125}I, use of screened low energy radiation sources for moulds in mouth carcinoma treatment 77−48855
^{125}I, variation of γ-counting efficiency with sample composition 80−83238
^{125}I worker thyroid meas. 80−36151
^{125}I-fibrinogen uptake test for detect. of deep vein thrombosis, review of current practice 78−7436
^{125}I-toluene azonaphthol excretion and liver visualisation, rat 77−56456
^{127}I(p,5n)^{123}Xe→^{123}I statistical model based computation 79−26416
^{127}I(p,5n)^{123}Xe→^{123}I^{-} production, separation and radiopharmaceutical labelling 79−79649
^{127}I(p,n)^{127}Xe statistical model based computation 79−26416
^{129}I and organic compound determ. in LWR irradiated fuel solns. *(French)* 79−3230
^{129}I coincidence counting, efficiency extrapolation technique, methane 4π counter efficiency 77−88354
^{129}I, dose to world population from nucl. power industry 80−47619
^{129}I in man, cow and deer 78−80975
^{129}I, in reactor waste, sorption by minerals 79−49721
^{129}I, limits to radiological dose, dog retention data 77−60253
^{129}I, long-lived, immobilization by fixation of $Bn(IO_3)_2$ in Portland cement 79−59208
^{129}I measurement rel. to ^{131}I accumulation in thyroids of pasture animals *(German)* 77−52891
^{129}I photons, absorbed fractions in the thyroid 80−109032
^{129}I radioactive waste, fixation with Portland cement, radiation stability tests 80−83200
^{129}I storage, IO_3^- adsorption by hematite 80−22992
^{129}I, tandem accelerator mass spectrometry 80−86494
^{129}I, thyroidal burdens from dietary sources 77−44755
$^{129}I_2$ detection in nuclear fuel cycle, intracavity selective absorpt. analysis 78−46182
^{131}I accumulation in thyroids of pasture animals, rel. to ^{129}I meas. *(German)* 77−52891
^{131}I, adsorption by minerals 80−83203
^{131}I, age-related radiosensitivity obs. of guinea pig thyroid glands 80−104671
^{131}I, air concs. during thyroid therapies 79−25122
^{131}I, airborne conc. in nuclear medicine lab. 79−34674
^{131}I, airborne release from operating BWRs 80−23033
^{131}I airborne release from PWR, determ. of sources 80−17138

radioisotopes continued
^{131}I, airborne short-lived radionuclides of unknown origin in Sweden (1976) 78−32219
^{131}I and antithyroid drugs, simultaneous treatment of toxic diffuse goiter 80−56193
^{131}I, behaviour during rinsing in in-pile loop after fission product release expt. 80−73879
^{131}I concentrations in air, milk and antelope thyroids in southeastern Idaho 80−89871
^{131}I, defective fuel rods ultra sensitive detection with low core burn-up, method 79−45374
^{131}I determination in vegetation, ashing procedure 78−15930
^{131}I dosimetry of the rat thyroid, accurate method 80−46063
^{131}I, estimation of γ dose to gastric wall after administration of isotope *(Japanese)* 80−98141
^{131}I fixation in solid/liquid systems 79−13530
^{131}I in human thyroid gland, rapid monitoring using Ge(Li) detector 79−2134
^{131}I in milk, extreme low level determ. 78−92703
^{131}I in nuclear power plant gaseous discharge, cumulative meas. *(Russian)* 79−3224
^{131}I, in vivo whole-body counter calibration for quantiative retention estimation 78−3579
^{131}I, long-term retention in Indian workers, dose commitment 78−35960
^{131}I, low level detection in milk rel. to population dose 78−31911
^{131}I manipulated in syringes, radiation exposure obs. 80−67252
^{131}I measurement in human thyroid gland, use of NaI(Tl) scintillation survey meter 78−80970
^{131}I metabolism in amphibian and reptile thyroid *(Italian)* 79−20579
^{131}I, milk transfer coeff., review of meas. values 79−2141
^{131}I population thyroid dose in USA after Chinese atm. nucl. weapons tests 78−77116
^{131}I produced radiation, low-dose, somatic mutations induction in Tradescantia 80−72266
^{131}I production by TeO_2 irrad., determ. of Se in TeO_2 by neutron activation 77−86400
^{131}I radionuclide pollution, protection of thyroid gland 79−66560
^{131}I recovery and trapping, in sublimation separation of ^{99}Mo from neutron irrad. 77−9257
^{131}I response of LiF and $CaSO_4$ TLD discs, influence of thyroid geometry 78−73250
^{131}I, separation from water by ion exchange *(Japanese)* 77−60099
^{131}I therapy, absorbed doses to marrow and blood 77−48869
^{131}I therapy, review of contamination and exposure hazards 80−41257
^{131}I therapy, role in childhood hyperthyroidism treatment 80−41182
^{131}I therapy for toxic diffuse goitre, incidence of hypothyroidism within 1 year 78−65116
^{131}I, thyroid dose eval. following accidental release from reactor spent fuel 80−26366
^{131}I thyroid therapy, estimating doses recorded by personnel dosimeters 78−15891
^{131}I treated patients, monitoring of I excretions and used materials 80−89873
^{131}I, treatment of benign thyroid disease, review 80−36107
^{131}I, use in hyperthyroidism treatment of children and adolescents 80−46013
^{131}I, use in the treatment of metastatic thyroid cancer 80−36084
$^{131}I_2$, $CH_3{}^{131}I$, airborne, diffusion coeffs. 79−2142
$^{131}I_2$ transport via pasture-cow-milk pathway, stat. anal., thyroid dose uncertainty 79−83950
^{131}I-19-iodocholesterol in adrenal gland imaging 77−48853
^{131}I-4-iodoantipyrine preparation from ^{131}I-iodide 80−12256
^{131}I-iodo-antipyrine in bone blood flow determ., comparison with $^{99m}TcO_4$ 78−28046
^{131}I+propane, U_3O_8 released radioiodine relative reactivity in O and He atmospheres 79−52644
^{113m}I-EDTMP, evaluation as bone imaging agent 77−56455
^{111}In, human lymphocyte labelling 79−5354
^{111}In metabolic fate in rat 78−48881
^{111}In-DTPA, renal function meas. in dogs 77−66838
^{113m}In eluates from ^{113}Sn generator, monitoring Zr and ^{113}Sn breakthrough 77−5078
^{113m}In generator with modified silica gel column 77−90897
^{113m}In intravenous injection meas. of placental blood flow 78−28043
^{192}Ir afterloaded implant in retreatment of head and neck cancers 78−96083
^{192}Ir, estimation of long-term biological elimination 79−70642
^{40}K, isotope relative abundance, radioactivity expt. for schools 79−21511
^{40}K, contents in fish flesh 79−79718
^{40}K, natural content and internal radiation burden of Hungarian adult population 80−26355
^{40}K, natural radiation exposure in New Zealand 78−88747
^{40}K, pressure-induced changes in electron-capture decay const., theory 80−22771
^{40}K, terrestrial beta radiation field in natural environment, numerical evaluation 78−81161
^{43}K and analogues in myocardial infarct imaging 77−40750
^{43}K evaluation for rectilinear scanner imaging using performance index technique 78−73226
^{43}K, prod. by V target bombard. with medium energy protons, separation medical appls. 77−81572
^{77}K, cyclotron prod. for regional cerebral blood flow meas. 77−56468
Kr ion implantation using Lublin separator 79−82251
^{76}Kr, ^{77}Kr production, excitation function meas. 79−88191
^{77}Kr carrier-free isotope prod. by (p,xn) reactions on natural Br 78−29678
^{79}Kr, kinetics after inhalation in man, rel. to internal dosimetry calcs. 78−28073
^{79}Kr, kinetics of total body retention and clearance after inhalation 77−37121
$^{81}Kr^m$ generator for lung ventilation studies, test for free Br in carrier gas 79−79642
^{85}Kr, air pollution, seasonal and annual concs. at 30-150 km from point source 79−20994
^{85}Kr atmospheric concentration in North and South Hemisphere 80−93756
^{85}Kr, beta dose to crit. human tumour sites 78−28074
^{85}Kr concentration in atmosphere over USSR (1971-1975) 78−37453
^{85}Kr extraction, occupational doses in gas liquefaction industry 78−15905
^{85}Kr immobilization, evaluation of methods 79−26578
radioisotopes continued
^{85}Kr, latitudinal distrib. in atm. surface layer over ocean *(Russian)* 79−39813
^{85}Kr, radioactive pollution in atmos., Warsaw 1975 to 1977, meas. methods 79−34458
^{85}Kr radioisotope, estimation of radiation safety 80−5346
^{85}Kr, removal from gaseous wastes by cryogenic rectification process 78−50268
^{81m}Kr dosimetry, internal conversion electrons, error in previous work 79−12005
^{81m}Kr, exptl. approaches to myocardial function studies 77−40755
^{81m}Kr regional ventilation scintigraphy, comparative analysis with ^{133}Xe 78−85360
^{172}Lu generator, ^{172}Hf production, recovery and purification for nucl. medicine use 78−48893
^{177}Lu organ distribution in mouse 78−48879
^{28}Mg carrier-free production by 50-180 MeV protons on Si, P, S, Cl, Ar and K 79−83934
^{28}Mg, intestinal absorpt. obs. in man 80−36217
^{28}Mg, prod. by high-energy α-induced nucl. reactions on ^{27}Al and ^{26}Mg 77−3021
^{28}Mg producting using compact cyclotron 77−90894
^{28}Mg production with 50 MeV neutrons 77−90895
^{28}Mg radionuclide yield from ^{27}Al(α,3p) and ^{26}Mg(α,2p) 80−32290
^{54}Mg, removal from waste water by oxine-impregnated activated charcoal 80−9344
^{53}Mn, chondrite exposure ages study using longlived spallogenic isotope 79−53776
^{54}Mn, accumulation by oysters in reactor effluent, math. model 77−81589
^{54}Mn distribution in N_2O_4 condensate cooling circuit *(Russian)* 79−13491
^{54}Mn, sediment-bound, absorpt. through digestive tract of marine demersal fish 79−92400
^{54}Mn, transfer from irrigation water to crops and agricultural products *(French)* 78−8996
^{59}Mn, new isotopes of interest to explosive nucleosynthesis β-decay scheme and mass determ. 79−45208
^{60}Mn, new isotopes of interest to explosive nucleosynthesis, β decay scheme and mass determ. 79−45208
^{52m}Mn, new short-lived, generator-produced radionuclide, positron tomography appl. 80−109006
^{99}Mo, airborne short-lived radionuclides of unknown origin in Sweden (1976) 78−32219
^{99}Mo fission product, sequential cation-exchange separation from neutron irrad., U_3O_8 77−90898
^{99}Mo separation from neutron irrad. UO_2 by vacuum sublimation 77−90893
^{99}Mo separation in $^{99}Tc^m$ generator of higher activity 80−17136
^{99}Mo, sublimation separation from neutron irrad. UO_2 77−9257
^{13}N, absorbed dose comparison rel. to γ-ray emitters 79−70647
^{13}N, clinical results using short-lived radioisotopes prod. by medical cyclotron 79−57775
^{13}N labelled NH_3 production for medical appl. 80−72327
^{13}N prod. by accelerators for nitrosourea-^{13}N prep. 79−53242
^{13}N, production by cyclotron, biomedical appls. *(French)* 80−56216
^{13}N production for nuclear medicine use 80−30889
^{13}N production in cyclotron by $^{16}O(p,\alpha)^{13}N$, water loop target 80−23201
^{13}N, radionuclide prod. for medical appl., by Groningen 280 cm AVF cyclotron 79−54696
^{13}N species formed by proton irradiation of water 80−45532
$^{13}NH_3$, simultaneous prod. of ^{123}I, ^{62}Zn and $^{13}NH_3$, multitarget assembly for high energy irrad. 77−90896
$^{13}NH_4^+$ for myocardial imaging, prod., distrib. and imaging charact. 77−40752
^{15}N-NH_4, absorpt. and transfer to amino-N, rat small intestinal sac 80−16909
^{16}N γ-rays for activation of elements in (γ, γ') reaction 78−88689
^{16}N tagging for two-phase mass flow measurement 79−93793
^{22}Na injection, testis mass loss obs., mouse 80−67156
^{22}Na injection or X-irrad. of mice, sperm count reduction and abnormal sperm increase 80−108961
^{22}Na, thick-target yields in Mg due to proton bombardment up to 100 MeV 77−88312
^{23}Na, transfer from irrigation water to crops and agricultural products *(French)* 78−8996
^{24}Na, carrier-free production by 50-180 MeV protons on Si, P, S, Cl, Ar and K 79−83934
Nb foils, polycryst., proton irrad., diffusion of nuclear react. products *(German)* 77−35756
Nd isotopes, determ. in nuclear fuels as burnup indicator, separation, mass spectrometric method 77−44553
^{147}Nd, anodic deposition on Pt anode, electrochem. separation 79−91958
^{57}Ni, cyclotron prod. by ^{3}He bombardment of natural Fe, bleomycin complex synthesis 77−86629
^{63}Ni applications in biological research 80−12321
^{237}Np in invertebrate tissues, uptake from water 79−74765
^{237}Np migration potential in radioactive waste 80−3537
^{237}Np, sorption on USA subsoils from differing weathering intensity areas 78−16014
^{239}Np, airborne short-lived radionuclides of unknown origin in Sweden (1976) 78−32219
$^{A}O_2$ A=14,15 imaging of cerebral metabolism, long range transmission of short-lived gases in tuned pipeline 79−53239
^{15}O, absorbed dose comparison rel. to γ-ray emitters 79−70647
^{15}O, clinical results using short-lived radioisotopes prod. by medical cyclotron 79−57775
^{15}O production, non-linear behaviour of gas targets 78−25361
^{15}O, production by cyclotron, biomedical appls. *(French)* 80−56216
^{15}O production for nuclear medicine use 80−30889
^{18}O, palaeoclimatic features, based on stable isotope compositions, Lake Biwa, central Japan 79−12230
P ion implantation using Lublin separator 79−82251
^{30}P, short lived positron emitter, cyclotron production 79−76236
^{32}P and ^{45}Ca determination in biological samples by Cherenkov and liq. scintillation counting 80−98183
^{32}P, Cherenkov counting using Teflon vials 78−858
^{32}P Cherenkov effect detect. efficiency determ. by ^{60}Co external source on liq. scintillation system 78−25387
^{32}P, radioactive interference with neutron activation anal. of biosamples 79−12059

radioisotopes continued
^{32}P radioassay by Cherenkov counting, prep. of plant samples 78−81088
^{32}P secondary radiation, effects of extremely low doses on synchronised cultures of Chlorella pyrenoidosa 78−73176
^{32}P, whole-body counting of retention in man 79−62378
^{203}Pb production by proton reactions on natural Tl 79−88184
^{204}Pb/^{207}Pb ratio rel. to Earth age and chemical evolution 79−88315
^{210}Pb, ^{210}Po, concs., physico-chem. states and residence times in marine and estuarine waters 78−11913
^{210}Pb and ^{210}Po concs. in liver and kidneys of cattle 80−30904
^{210}Pb, atmospheric conc. at South Pole 79−84382
^{210}Pb chronology of Long Island Sound sediment core, biological mixing effects 79−66672
^{210}Pb dating of annually laminated Finnish lake sediments 79−74916
^{210}Pb determination in lake and marine sediments 79−48582
^{210}Pb determination in U ores, dusts and mill tailings 78−15736
^{210}Pb, external γ-counting and bioassay meas. on retired U miners 80−26332
^{210}Pb, time variation of low concentrations in rain water 79−43994
^{212}Pb ion clearance from rabbit bronchial epithelium to blood 77−86641
^{103}Pd inhalation studies, derivation of X-ray counting efficiencies for lung Pu 78−85391
^{103}Pd, lung burdens of low-energy photon-emitters, interlaboratory comparison of meas. techniques 79−20671
^{109}Pd, ^{238}U fission product, gamma-ray spectra, half-life determ. 77−50084
^{112}Pd, ^{238}U fission product, gamma-ray spectra, half-life determ. 77−50084
^{147}Pm, acute toxicity in rats and dogs 78−65082
^{147}Pm fuelled betavoltaic pacemaker system status 77−81733
Po metabolic model, dosimetry appls. 79−79657
^{210}Po contamination of surfaces, removal coeff. determ. 79−26769
^{210}Po, determ. in human urine by direct extraction by Ni foil 79−100707
^{210}Po, expt. lung cancer, Syrian hamster, effect of dose distrib. 79−16254
^{210}Po in Bombay diet 77−81592
^{210}Po/^{210}Pb atmospheric ratio, modification by volcanic emissions 80−41507
^{218}Po, ^{214}Po, dosimetry in Syrian golden hamster lung 79−16304
^{218}Po, airborne Rn daughter concs. in dwellings in Great Britain 78−77118
^{143}Pr, anodic deposition on Pt anode, electrochem. separation 79−91958
^{144}Pr, effect of maximum β energy on colour quenching of Cherenkov radiation *(Spanish)* 79−76268
^{239,240}Pu, conc. in thermonuclear test debris, collected near Bikini Atoll 78−96103
^{238,239,240}Pu, concs. in arthropods at a nuclear facility 80−30905
Pu aerosols, charge distribution from mixed-oxide reactor fuel fabrication lab. 79−5181
Pu, air concs. near Rocky Flats, $^{239+240}$Pu 78−16150
Pu air monitor with background compensation system 80−27824
Pu assay, in vivo methods for humans 79−20674
Pu body burden estimation from urine data influenced by DTPA therapy 78−73259
Pu distribution in Ohio soils, local and stratospheric sources 78−16015
Pu distribution in Rocky Flats soil 78−73265
Pu dose to lung and bone from contaminated soils, statistical uncertainties 80−109028
Pu dynamics in deciduous forest ecosystem, linear compartment donor-controlled model 78−85392
Pu ecological export from reprocessing waste pond 78−53533
Pu, fume aerosols, aerodynamic and dissolution behaviour of laser-ignited droplets 79−13438
Pu in biota from E. Tennessee floodplain forest 78−85394
Pu in lungs of pronghorn antelope near a nuclear fuel reprocessing plant 80−30906
Pu, industrial effluent, behaviour and transport in Great Miami River, Ohio 78−16061
Pu isotopes, maximum permissible inhalation values 79−70640
Pu isotopes in Antarctic snow layers, deposition and accumulation 79−70820
Pu, Manhattan project workers, 32-year medical follow-up 80−26379
Pu measurement in Japanese human organs 78−80980
Pu, nuclear fuel workers management 79−74763
Pu release into estuarine-coastal sea ecosystem, assessment methodology 79−70471
Pu, remote contamination and total inventory from Rocky Flats, mass spectroscopic anal. 77−73739
Pu skeletal level estimation based on DTPA induced excretion in faeces 78−85390
PuO_2 multiple low level exposure, case study 78−80967
$^{238}PuO_2$ particle inhalation, pulmonary tissue local dose computation 79−92385
$^{239}PuO_2$ inhalation, rat pulmonary connective tissue modification by internal α-irrad. 79−92302
^{A}Pu, A=238,239,240, contents in coastal sediments 79−57974
^{A}Pu, A=239,240, distrib. of fallout Pu in southern Finns 80−109045
^{236}Pu, ^{239}Pu, ^{242}Pu, ^{244}Pu, distrib. in mice after injection 79−12001
^{237}Pu, ^{239}Pu, citrate, early retention in mature beagles 78−96095
^{237}Pu, bioaccumulation in inland water and marine algae *(German)* 80−108820
^{237}Pu gamma-emitting isotope, prep. of tracer by ^{238}U(^{3}He,4n) 77−34497
^{237}Pu IV and VI oxidation states, relative uptake from water by bush beans 78−73266
^{237}Pu, intracardially injected in channel catfish, distrib. kinetics 79−20673
^{238}Pu, ^{239}Pu, ^{240}Pu, content in deer from integrated nuclear fuel cycle facility 79−57778
^{238}Pu, conc. in wet and dry deposition samples, USA, 1976 Jun.-1977 Dec. 79−29807
^{238}Pu, factors affecting particle mobility in rats 79−12003
^{238}Pu for cardiac pacemakers, radioactive controls *(French)* 77−44752
^{238}Pu fuelled cardiac pacemaker, evaluation *(French)* 77−44833
^{238}Pu IV citrate chronic exposure effect on embryonic development of fish eggs 78−53447
^{238}Pu isotopic pacemakers, 2 to 4 years' follow-up 77−81695
^{238}Pu power units for artificial hearts and auxiliary circulation systems 77−78052
^{238}Pu production, chemical treatment of Np targets *(French)* 77−42201
radioisotopes continued
^{238}Pu production from target elements based on MgO and NpO_2 *(French)* 77−42199
^{238}Pu production from targets in Celestin reactors, medical use *(French)* 77−42200
^{238}Pu, sources for cardiac pacemakers, manufacture and safety tests *(French)* 77−44751
$^{238}PuO_2$, uptake by plants in polluted soil 79−5381
^{239}Pu, ^{240}Pu, Danish cereal grains, variation of direct contamination 79−5382
^{239}Pu aerosol, characterisation inside safety enclosures of mixed oxide fuel fabrication facility 79−13501
^{239}Pu alpha particle tracks on polycarbonate foils 79−76310
^{239}Pu alpha particles, internal source microdosimetry 78−3615
^{239}Pu, aquatic microscosms, trophic transfer by Chironomoids 79−5383
^{239}Pu, biological availability, influence of DTPA at soil-plant and plant-animal interfaces 78−73264
^{239}Pu, bone dosimetry model, surface and volume 79−8550
^{239}Pu, bone model for calc. of annual limits of intake in man 79−53252
^{239}Pu, cancer risk from $^{239}PuO_2$, max. permissible conc. in air 79−25108
^{239}Pu, carcinogenicity of inhaled dioxide, rat obs. 79−66492
^{239}Pu, comparison of early mortality in baboons and dogs after inhalation of $^{239}PuO_2$ 80−108977
^{239}Pu, conc. in wet and dry deposition samples, USA, 1976 Jun.-1977 Dec. 79−29807
^{239}Pu contaminated wound, surgical treatment after glove box accident *(French)* 78−53521
^{239}Pu contamination in snakes inhabiting Rocky Flats plant site 77−81591
^{239}Pu deposition in bone, rel. to ^{59}Fe uptake in marrow, mouse 78−85395
^{239}Pu, distrib. and behaviour in Urazoko Bay sediment 80−97825
^{239}Pu, distribution in mouse skeleton 79−12002
^{239}Pu distribution in mouse testis, significance of interstitial tissue ultrastruct. 79−57610
^{239}Pu, effect on mouse haemopoietic stem cells 80−51174
^{239}Pu, endosteal cell dose and relative distrib. factors compared to ^{226}Ra 78−96091
^{239}Pu in plankton, upper limit calc. method for α-dose rates 79−2133
^{239}Pu, influence of administered mass of cross-placental transfer in mice 79−20672
^{239}Pu, inhalation of $^{239}PuO_2$ by rhesus monkeys, cytogenetic and other biological effects 80−108968
^{239}Pu, isolation and characterisation of particles in atm. effluent 79−63757
^{239}Pu, lung burden, assessment of tissue substitutes for calibration purposes 79−16307
^{239}Pu, lung burden X-ray counting efficiency, from inhaled ^{103}Pd studies 78−85391
^{239}Pu, lymphoid tumours and leukaemia induced in mice by bone-seeking radionuclides 78−69141
^{239}Pu, nanocurie amounts, lesions in CBA mice 80−81657
^{239}Pu, polymeric, effects on erythrocyte survival in mice 80−45973
^{239}Pu, radiation dose-response curves, hazard function method of resolution 79−66556
^{239}Pu, study of non-uniform distrib. in mouse testis 79−39507
^{239}Pu, subparticle formation expt. by α-decay 79−6520
^{239}Pu, toxicity and translocation of inhaled $^{239}PuO_2$ in baboons 79−2109
$^{239}PuO_2$, in vivo solubility in rat lung 78−28093
$^{239}PuO_2$ alpha-particle freq. in lung cells 78−69151
^{241}Pu bone distribution, high resolution autoradiography 78−7399
^{241}Pu concentrations in Swedish reindeer lichens, radiochem. anal. 78−15912
^{241}Pu, environmental pollution, biophysical aspects 79−39530
^{241}Pu, uptake and redistribution within the gonads, hamster, rabbit 79−12004
^{242}Pu, isotope form. calc., effect of reactor charact. 79−26489
^{242}Pu preparation by EM isotope separation, for use as α-spectrometry and mass spectrometry tracer 78−9011
^{226,228}Ra in humans, radiation induced malignancies 78−96075
Ra storage safe, design, safety, ease of use 78−92736
^{A}Ra, A=226, 228, content in groundwater of Fall Line aquifers 80−89682
^{222}Ra short lived daughter disequilibrium in a mixed maritime and continental atmosphere 80−108822
^{224}Ra and daughters, radioactive props. and biological behaviour 78−96090
^{224}Ra and thorotrast radiobiological significance 78−96076
^{224}Ra biological effects, conf., Alta, USA (July 1974) 78−96068
^{224}Ra, endosteal cell dose and relative distrib. factors compared to ^{226}Ra 78−96091
^{224}Ra injections into humans, soft-tissue effects 78−96070
^{224}Ra injections into humans, skeletal effects 78−96071
^{224}Ra preparation, for ankylosing spondylitis therapy 78−96089
^{224}Ra, short-lived α-emitter, late effects after incorporation in mice 78−96069
^{224}Ra usage in radiotherapy and radiobiology, brief history 78−96085
^{224}Ra use in treatment of ankylosing spondylitis and rheumatoid synovitis 78−96086
^{226}Ra, ^{228}Ra, dose-response relationships for female dial painters 80−21545
^{226}Ra body burden determ., postprandial changes in exhalation rate of Rn prod. in vivo 78−69224
^{226}Ra, conc. in Florida phosphate materials 80−30615
^{226}Ra daughters, natural radiation gxposure in New Zealand 78−88747
^{226}Ra, desorption from river-borne sediments in Hudson estuary 79−79877
^{226}Ra, determ. of tap water pollution *(Czech)* 79−34675
^{226}Ra determination in U ores, dusts and mill tailings 78−15736
^{226}Ra, emulsion scintillation counting of biological samples 78−81089
^{226}Ra, fractional retention by the bluegill 79−39506
^{226}Ra in public water supplies, conc. determ. *(German)* 80−94138
^{226}Ra in Taiwan buffalo bone and environmental samples of N. Taiwan power reactor site 77−64142
^{226}Ra long-term retention in contaminated dial painters 77−90917
^{226}Ra, lymphoid tumours and leukaemia induced in mice by bone-seeking radionuclides 78−69141
^{226}Ra, radiation-induced carcinogenesis, beagle dog obs. 79−66487
^{226}Ra, radioactivity of thermal and mineral springs in Slovenia 80−7963
^{226}Ra-burdened dog skeleton, Rn retention rel. to age and dosage 78−65092

radioisotopes continued
^{81,82m}Rb production for positron emission tomography 80−98068
Rb neutron deficient radioisotope selective production in (α,xn) reacts. *(Croatian)* 78−44608
^{81}Rb evaluation for rectilinear scanner imaging using performance index technique 78−73226
^{81}Rb, excitation functions of proton induced nuclear reactions on ^{85}Rb, medical appls. 80−78286
^{81}Rb production, non-linear behaviour of gas targets 78−25361
^{81}Rb/^{81m}Kr, prod. for medical uses using Ruder Boskovic Institute cyclotron 78−20273
^{81}Rb/^{81m}Kr ratio as radioactive tracer study of organic bleeding *(Dutch)* 80−3807
^{81}Rb-^{81m}Kr, blood flow meas. in dynamic phantom using NaI detector 77−66843
^{81}Rb-^{81m}Kr, production in (α,2n) and (^{3}He,3n) reactions on KBr 80−12253
^{82}Rb generator with alumina column, radioactive Sr adsorption 80−12257
^{84}Rb, prod. at Manitoba Univ. using ^{84}Kr(p,n) 79−54695
^{86}Rb, countercurrent fluxes through bilayer lipid membranes 79−70528
^{86}Rb radioassay by Cherenkov counting, prep. of plant samples 78−81088
^{87}Rb dose-rate contrib. in thermolum. dating of pottery 78−70242
^{186}Re labelled EHDP preparation and possible use in osseous neoplasms treatment 80−56215
^{106}Rh, radioactive decontamination methods, effectiveness for different terrains 78−96104
^{101m}Rh, cyclotron prod. through natural precursor ^{101}Pd 77−52875
^{220,222}Rn daughters, 2-count filter method for meas. in air 80−63480
Rn air concs. in certain houses 79−79662
Rn and Rn daughters, background concs. in Canadian homes 80−104546
Rn and Rn daughters in Howe Caverns, USA, doses to employees and public 80−89859
Rn, atmospheric, accumulation in calcite caves 80−104531
Rn barrier, interior of building structs. foundations built on U mill tailings material 79−2138
Rn barrier to reduce indoor airborne Rn progeny 78−73262
Rn concentration in dwellings and influencing factors 80−108832
Rn concentration in Norwegian dwellings 79−70485
Rn, continuous monitoring system 79−76150
Rn daughter concentrations in different atmospheres 80−85316
Rn daughter time-integrating environmental TLD dosimeter 79−67962
Rn daughters, dose conversion factors 79−70641
Rn daughters, influence of room ventilation rate variations on respiratory, dose 79−92381
Rn daughters in atmospheric air, efficiency of HV-70 filters for sampling 80−108827
Rn decay products, influence of elec. charge and humidity on diffusion coeff. 80−6192
Rn diffusion, effectiveness of U mill tailing covers 79−93838
Rn, diffusion coefficient and exhalation rate from building materials, meas. technique 80−4694
Rn dose calculations, for inhalation of ^{222}Rn, ^{220}Rn and daughters 77−64133
Rn, evolution in neutral atmospheres *(Spanish)* 80−4058
Rn monitoring instrumentation 80−106204
Rn/Tn daughter air conc. meas. by filter method, general formula 78−70711
^{211}Rn production by ^{209}Bi(^{7}Li,5n), excitation function 80−95323
^{211}Rn, production by photospallation of ^{232}Th and ^{238}U 80−52797
^{222}Rn, and decay products, vertical distrib. in atmosphere, time-dependent calc. 79−84383
^{222}Rn, atmospheric, in calcite caves at Akiyoshi Karst Plateau *(Japanese)* 79−83671
^{222}Rn, atmospheric conc. at South Pole 79−84382
^{222}Rn, conc. in air, absolute determ. using cellulose nitrate track detector 80−63492
^{222}Rn, conc. in free air *(Hungarian)* 80−94128
^{222}Rn conc. over intertropical convergence zone of Atlantic 80−26648
^{222}Rn concentration in N.Carolina groundwater supplies rel. to stomach dose and conc. standards 78−85612
^{222}Rn concentration in tunnel air, atmospheric press. and precipitation effects *(Japanese)* 80−97845
^{222}Rn concentration in water, meas. by gamma counting 78−53733
^{222}Rn daughters, meas. of low conc. in air 78−28308
^{222}Rn emanation from building materials, plastic α-track detectors study 80−101144
^{222}Rn emanation into air of dwellings in Great Britain 78−77118
^{222}Rn, emulsion scintillation counting of biological samples 78−81089
^{222}Rn enhancements and gas upflow possibility in Earth 79−74893
^{222}Rn evasion rates in Atlantic and Pacific, Geosecs determ. 79−79875
^{222}Rn exhalation meas., soil and meteorological effects *(Spanish)* 80−31082
^{222}Rn, fractional retention by the bluegill 79−39506
^{222}Rn in biologically produced gas from reactor cooling pond 78−80976
^{222}Rn, instant working level meter methods, mathematical evaluation 79−9918
^{222}Rn meas. in geothermal fluids, steam reservoirs characts. determ. 79−74918
^{222}Rn potential appl. as tracer in ocean hydrophys. studies *(Russian)* 79−39745
^{222}Rn progeny, air conc. meas. by α-particle spectrometric counting 79−68171
^{222}Rn, props. and behaviour of short lived daughter nuclides in the atmos. *(Japanese)* 80−72339
^{222}Rn, radioactivity of thermal and mineral springs in Slovenia 80−7963
^{222}Rn release from U ore crushing, grinding and leaching 78−89970
^{222}Rn rich water, chromosome aberrations in peripheral blood lymphocytes 79−70587
^{222}Rn short-lived daughter population exposure in Great Britain 78−35970
^{222}Rn, theoretical, evaluation of emanation under a variety of conditions 80−104545
^{97}Ru, preparation, separation from TC isotopes 77−37054
^{103}Ru, ^{106}Ru, radioactive decontamination methods, effectiveness for different terrains 78−96104
^{103}Ru, in sublimation separation of ^{99}Mo from neutron irrad. UO_2 77−9257

radioisotopes continued
^{106}Ru-^{106}Rh, accumulation by marine organisms, sediment and sea water influences 78−80981
^{106}Ru-^{106}Rh, acute toxicity in rats and dogs 78−65082
^{106}Ru-^{106}Rh radionuclide distribution among green alga, marine sediments and sea water 78−53534
$^{106}RuO_4$ in lung, in vivo meas. and dosimetry 78−53515
^{38}S, for meas. SO_2 atm. removal rate *(German)* 79−53411
^{38}S producting using compact cyclotron 77−90894
^{125}Sb, in HCl solns., valency states investig., radioanal. tracer preparation, stability 77−63943
^{47}Sc carrier-free radiopharmaceutical prep. with epithermal neutrons in ^{47}Ti(n,p) reaction 79−79652
^{47}Sc preparation in carrier-free state by ^{48}Ti(γ,p) reaction for radiopharmaceutical appls. 77−90892
Se neutron deficient isotopes (A=68,69,70,71), production in heavy-ion reactions 77−38292
^{73}Se, excitation functions for production using ^{72}Ge(^{3}He,Zn)^{73}Se reaction 79−39501
^{73}Se, yield for various reactions and chem. processing 80−36131
^{75}Se, tracer for Se conc. in seawater expts., ^{203}Hg tracer 80−21420
^{75}Se, whole body retention following intravenous injection as selenomethionine 77−90904
^{75}Se-Na-selenite distrib. in human body, and organ doses 78−48880
^{75}Se-amino acids, comparison of four pancreatic scanning agents 78−35921
Sn, photoactivation by 42 MeV bremsstrahlung, gamma transition energies and line intensities 78−13057
Sr isotope excretion in man, comparison of stable Sr, ^{85}Sr and ^{90}Sr 78−24153
Sr, transport through skin, role of diffusion 78−20158
^{82}Sr-^{82}Rb generator improvement using inorganic exchangers 80−17135
^{85}Sr assay in aqueous solutions by Cerenkov radiation 79−87895
^{89}Sr behaviour in sediments in laboratory-scale aquatic ecosystem 78−3831
^{89}Sr distribution between bound and free forms, in vitro meas. of rat soft tissue 78−28095
^{89}Sr therapy of bone metastases of prostatic gland carcinoma 80−36076
^{90}Sr, balance in man, effect of P intake 78−15911
^{90}Sr, conc. and distrib. in N.Atlantic surface water 78−65345
^{90}Sr, conc. in wet and dry deposition samples, USA, 1976 Jun.-1977 Dec. 79−29807
^{90}Sr, conc. meas. in Caribbean Sea, vertical transport of admixtures determ. 79−53362
^{90}Sr, conc. variations in Baltic Sea 1973 to 1975 79−92100
^{90}Sr concentration in freshwaters of USSR 79−39770
^{90}Sr concentrations in pronghorn antelope bones near a nuclear fuel reprocessing plant 80−89875
^{90}Sr, coyote scats, Hanford Reservation, radioactive waste distrib. 79−25120
^{90}Sr diffusion from instantaneous point source in ocean, numerical calc. *(Russian)* 78−69372
^{90}Sr, effect on fetal mouse ovary rel. to time administered during pregnancy 80−51163
^{90}Sr heat source, from $SrTiO_3$, synthesis process *(Japanese)* 77−54319
^{90}Sr, in atmosphere, bioindication using needles of common pine tree 79−100550
^{90}Sr in human bone, Yugoslavia 77−56490
^{90}Sr in milk and composite diet samples in India 77−86650
^{90}Sr in W Gulf of Mexico 77−81590
^{90}Sr, leaching behaviour in cement composites 78−37416
^{90}Sr, lymphoid tumours and leukaemia induced in mice by bone-seeking radionuclides 78−69141
^{90}Sr migration in aerated zones, theoretical estimation *(Japanese)* 79−9896
^{90}Sr, pollution in N.Pacific surface water during 1974, conc. meas. 80−26181
^{90}Sr, radiation dose-response curves, hazard function method of resolution 79−66556
^{90}Sr, radiation-induced carcinogenesis, beagle dog obs. 79−66487
^{90}Sr radioactive fallout damping coefficients 78−92961
^{90}Sr radionuclide leaching from hardened cement grout, container dimension depend. 79−13439
^{90}Sr removal from ocean waters, adsorpt. on hydrated MnO 78−3822
^{90}Sr, runoff coeff. from surfaces of river basin soils 79−44212
^{90}Sr, time variation of low concentrations in rain water 79−43994
^{90}Sr, transfer from irrigation water to crops and agricultural products *(French)* 78−8996
^{90}Sr/^{90}Y radioisotope generator, educational aid 78−78535
T concentration reduction for aquifer 80−21423
T, concentrations in Caspian Sea 79−34858
T, in PWR, sources, releases, monitoring, management and environmental impact 80−18690
T monitoring at nuclear power stations 80−18691
T monitoring methodology using SiO_2 desiccant, appl. to research reactor facility 80−21434
T release from nuclear power stations 80−23032
T species, sources and reactions 80−21432
^{178}Ta, chemical separation from parent ^{178}W, applications to nuclear medicine 79−16301
^{178}Ta, short lived nuclide for nuclear medicine, production of the parent ^{178}W 79−16300
^{182}Ta gamma ray effects on Vicia faba roots, comparison with ^{125}I 78−48832
^{99}Tc accumulation by plants 77−56489
^{99}Tc accumulation by tumbleweed and cheatgrass grown on arid soils 78−80974
^{99}Tc in reactor waste, sorption by minerals 79−49721
^{99}Tc lifetime in generator-produced ^{99m}Tc, calc. 79−88188
^{99}Tc migration potential in radioactive waste 80−3537
^{99}Tc sorption on USA subsoils from differing weathering intensity areas 78−16014
^{99}Tc^m, in vitro and in vivo labelled red blood cells, comparison for cardiac imaging 78−65109
^{99}Tc^m-dimercaptosuccinic acid evaluation as static renal imaging agent 78−77102
^{99}Tc^m-hydroxyethylidene diphosphonate whole-body retention in metabolic bone disease diagnosis 78−73208
^{99}Tc^m-penicillamine relative renal accumulation as index of differential renal function 78−65115
^{95m}Tc, adsorption by minerals 80−83203

radioisotopes continued
^{99m}Tc, atmospheric release, dose evaluation 79−25119
^{99m}Tc, automatic dispensing system, radiation exposure evaluation 79−96663
^{99m}Tc, beta-decay and dose calcs. 80−91154
^{99m}Tc complexes in myocardial infarct imaging 77−40749
^{99m}Tc contamination of laboratory personnel, its degree and routes 80−98147
^{99m}Tc, generation from ^{99}Mo, influence of radiation dose on elution yield 79−29624
^{99m}Tc generators, operational assessment by performance indices 80−94332
^{99m}Tc intravenous isotope method for regional cerebral blood flow and vol. meas. 77−86610
^{99m}Tc labelled lung imaging agent quality control, labelling of macroaggregated albumin 78−28069
^{99m}Tc labelled possible cholescintigraphic agent, formed from 3-hydroxy-4-formylpyridine, glutamic acid 79−79653
^{99m}Tc lung imaging kit, radiochem. impurities 77−56469
^{99m}Tc manipulated in syringes, radiation exposure obs. 80−67252
^{99m}Tc radiolabelling of mouse spleen leucocytes 79−100739
^{99m}Tc radiopharmaceutical kits, rapid colour spot test for stannous Sn levels 77−86630
^{99m}Tc radiopharmaceuticals, rapid miniaturised chromatographic quality control procedures 78−28070
^{99m}Tc, subtraction technique in diagnosis of abdominal abscesses 78−73212
^{99m}Tc-DTPA scintillation camera renography 78−20256
^{99m}Tc-EDTA complex production method and renal retention obs. 80−12254
^{99m}Tc-HEDP, quantitative evaluation of rheumatoid arthritic activity 78−20255
^{99m}Tc-S colloid uptake patterns in femoral head disease 78−28042
^{99m}Tc-1-hydroxy-ethylidene-1,1-disodium phosphonate labelling using Sn(II) reductant 79−88190
^{99m}Tc-diethyl-acetanilido-iminodiacetate, evaluation as hepatobiliary reagent 77−90874
^{99m}Tc-diethylentriaminepentaacetic acid freeze-dried kit prep. 79−88189
^{99m}Tc-labelled red blood cells, kit preparations 79−11999
^{99m}Tc-macroaggregated albumin particles, effect of particle number on lung perfusion images 77−37049
^{99m}Tc-pertechnetate labelling of human plasma proteins, rapid chemical method 79−29618
^{99m}Tc-phosphates in myocardial infarct imaging 77−40748
^{99m}Tc-pyrophosphate uptake patterns in femoral head disease 78−28042
^{99m}Tc-red blood cells, in vivo labelling for blood pool imaging 77−37052
^{99m}Tc-stannous glucoheptonate and ^{99m}Tc-stannous dimercaptosuccinate, renal localisation in rat 77−56463
$^{99m}TcO_4$ in bone blood flow determ., comparison with ^{131}I-iodo-antipyrine 78−28046
^{124}Te(p,2n)^{123}I statistical model based computation 79−26416
^{132}Te, fission product, sequential cation-exchange separation from neutron irrad. U_3O_8 77−90898
^{132}Te in lower troposphere, airborne levels and lifetime 79−12242
^{132}Te, in sublimation separation of ^{99}Mo from neutron irrad. UO_2 77−9257
Th, stability index measurement by natural radioactive tracers *(Spanish)* 80−51448
^{227}Th, short-lived α-emitter, late effects after incorporation in mice 78−96069
^{230}Th determination in U ores, dusts and mill tailings 78−15736
^{232}Th daughters, natural radiation exposure in New Zealand 78−88747
^{232}Th, radioactivity in Straits of Malacca marine environment 79−12135
^{232}Th, reevaluation of dose unit per unit intake 80−26356
^{232}Th, terrestrial beta radiation field in natural environment, numerical evaluation 78−81161
^{232}Th, Thorotrast kinetics and radiation dose 79−39523
^{45}Ti production by proton bombardment of Sc in cyclotron 78−80966
^{53}Ti, new isotopes of interest to explosive nucleosynthesis, β-decay scheme and mass determ. 79−45208
^{201}Tl as myocardial imaging agent 77−40751
^{201}Tl distribution in stressed rats, imaging, organ uptake and myocardial kinetics 78−65114
^{201}Tl from Tl(p,xn)^{201}Pb→^{201}Tl, E_p=15 to 60 MeV, yields and excitation functions 79−5369
^{201}Tl myocardial imaging, exptl. model for anal. of myocardial and background components 78−11727
^{201}Tl, myocardial perfusion evaluation by coded aperture tomographic technique 80−21537
^{201}Tl, non-invasive determ. of regional distrib. of cardiac output 78−31890
^{201}Tl production by proton reactions on natural Tl 79−88184
^{201}Tl, production in neutron therapy cyclotron idle beam using Tl(d,xn) 79−20669
^{201}Tl, transverse computerised axial tomography of the myocardium 80−67222
^{201}Tl, tumour and organ affinity 80−67234
^{204}Tl, effect of maximum β energy on colour quenching of Cherenkov radiation *(Spanish)* 79−76268
^{205}Tl(p,5n)^{201}Pb→^{201}Tl, yields and excitation functions for Pb radioactivities, medical appls. 80−67249
Tn alpha particle etch pits in CA80-15 and LR-115 cellulose nitrate track detectors 78−855
Tn and Rn, air concentration in dwelling places *(Hungarian)* 77−78409
Tn decay products, ats. and ions, adsorption probability on submicron particles 79−39803
U, determ. of content in dental porcelains and dose to oral mucosa 80−89830
U, determ. of content in some Indian coal and flyash samples 80−104547
U ore, radioisotopic X-ray anal. by K-shell fluorescence 79−79353
U personnel monitoring, 16 yrs. experience 79−76149
U, radioactivity of thermal and mineral springs in Slovenia 80−7963
U, separation, gas centrifuge 79−3227
U, simultaneous determ. of ^{238}U, ^{234}U, ^{230}Th, ^{226}Ra and ^{210}Pb in U ores, dusts and mill tailings 78−15736
U, specific α radioactivity meas. rel. to size using aerosol centrifuge 79−76255
U, urine analysis by delayed neutrons 80−26331
UO_2, equilib. conc. of fission products, ^{235}U induced fission and ^{238}U spontaneous fission *(Spanish)* 78−44823
UO_2, equilib. conc. of fission products, calc. comparison with expt. values *(Spanish)* 78−44824
^{234}U→^{230}Th→^{226} Ra, superposition soln. of transport of decay chain through sorbing medium 80−37500
^{234}U→^{230}Th→^{226}Ra decay chain, hydrogeological migration anal. 80−37501
^{235}U, conc. in $UO_2(NO_3)_2$ aq. soln., pulsed NMR determination 80−2658
^{235}U, determ. of amount in urine by delayed-neutron counting 79−25118
^{236}U activity meas. in UO_2 mineral deposit *(Spanish)* 78−44822
^{238}U, conc. in Florida phosphate materials 80−30615
^{238}U, determ. of time since arrival in matrix existing at time of discovery in Pakistan 79−34822
^{238}U, terrestrial beta radiation field in natural environment, numerical evaluation 78−81161
^{55}V, new isotopes of interest to explosive nucleosynthesis, β-decay scheme and mass determ. 79−45208
^{178}W, productions in ^{181}Ta(p,4n), purification procedure 80−12252
^{133}X calibration of environmental and personal dosimeters 80−86992
Xe, for ventilation studies, ^{127}Xe vs. ^{133}Xe 77−37044
Xe in radionuclide ventilation studies, clinical comparison of ^{127}Xe and ^{133}Xe 77−86594
Xe ion implantation using Lublin separator 79−82251
Xe prod. cross sections with protons of 320-590 MeV, nuclear medicine appl. 80−36133
Xe whole-body counting and dose determs. 80−89853
^{A}Xe, A=133,135, interference with low-energy meas. systems 80−89872
^{122}Xe-^{122}I short-lived positron emitter generator 79−100740
^{123}Xe production by 1 GeV proton spallation on Cs, Ba, La 79−63676
^{123}Xe production for radiopharmaceutical appls., high energy alpha reactions 77−37053
^{123}Xe production in ^{127}I(p,xn) and ^{127}I(p,pxn) reactions 78−594
^{125}Xe production by 1 GeV proton spallation on Cs, Ba, La 79−63676
^{125}Xe production for medical use by ^{3}He bombardment of natural Te 78−3604
^{127}Xe distribution in lungs during ventilation studies 78−44606
^{127}Xe, handling and dispensing technique 78−85378
^{127}Xe, health physics, dose calcs. 80−98142
^{127}Xe, kinetics of total body retention and clearance after inhalation 77−37121
^{127}Xe maximum permissible conc. in air 78−61262
^{127}Xe, production in ^{127}I(d,2N)^{127}Xe 79−79651
^{127}Xe, simple device for efficient transfer and unit dose packaging 78−85377
^{127}Xe whole-body retention for dosimetry calcs. 77−60257
^{133}Xe air contamination, meas. technique 80−41255
^{133}Xe charcoal traps, simple leak tests, nuclear medicine appl. 80−104734
^{133}Xe gas dispenser for lung ventilation studies 78−28068
^{133}Xe in a plastic catheter, diffusion dynamics obs. 80−79973
^{133}Xe intravenous injection meas. of placental blood flow 78−28043
^{133}Xe intravenous isotope method for regional cerebral blood flow and vol. meas. 77−86610
^{133}Xe regional ventilation scintigraphy, comparative analysis with ^{81m}Kr 78−85360
^{133}Xe, removal from gaseous wastes by cryogenic rectification process 78−50268
^{133}Xe, simple method of air monitoring 79−83949
^{133}Xe solubility coefficients in water, saline, dog blood and organs 80−56331
^{133}Xe storage and dispensing device for nuclear medicine *(Czech)* 79−43986
^{133}Xe trapping and re-use system for nucl. medicine 78−28051
^{133}Xe waste storage and retrieval, clinical use 77−86649
^{90}Y, appl. to cancer therapy of liver 80−17098
^{90}Y electrosorption on anodically polarised Pt surface 79−52684
^{90}Y extraction and determ. in acidic media 79−16025
^{90}Y, radiation dose-response curves, hazard function method of resolution 79−66556
^{91}Y, radiation dose-response curves, hazard function method of resolution 79−66556
^{91}Y, removal rate in lower stratosphere, seasonal vars. 80−55957
^{169,175}Yb electrosorption on anodically polarised Pt surface 79−52684
Zn radionuclide dosimetry and permissible body burden ^{65}Zn and ^{69m}Zn 77−56474
Zn radionuclide dosimetry standards and crit. organs 78−35961
^{62}Zn production and bleomycin labelling, excitation function for ^{60}Ni(α,2n)^{62}Zn 78−28067
^{62}Zn, simultaneous prod. of ^{123}I, ^{62}Zn and $^{13}NH_3$, multitarget assembly for high energy irrad. 77−90896
^{65}Zn behaviour in sediments in laboratory-scale aquatic ecosystem 78−3831
^{65}Zn, sediment-bound, absorpt. through digestive tract of marine demersal fish 79−92400
^{65}Zn, transfer from irrigation water to crops and agricultural products *(French)* 78−8996
^{65}Zn whole-body retention in pregnant mice, and secretion into milk 79−88200
^{95}Zr-^{95}Nb radionuclide distribution among green alga, marine sediments and sea water 78−53534

radiology
see also patient diagnosis; patient treatment; radiation therapy; radioisotope scanning and imaging
biotelemetry of glomerular filtration rate in man by external detection of DTPA-(Sn)-^{99m}Tc with CdTe 78−44591
bone mineral concentration estimation by beta-ray backscatt. *(German)* 78−69179
bone mineral measurement using polychromatic X-rays, correls. 78−53478
bremsstrahlung, accounted for by kerma partition 79−66482
calibration of instruments used in radiology and radiotherapy, metrological problems *(Spanish)* 79−92377
calibration of radiological instrumentation by British Calibration Service 80−8186
cardiac dynamic imagery, gross and segmental motion anal. 79−70632
cerebral blood flow meas. by radioisotope clearance, radiation scattering effect 78−3600
cerebral regional blood flow meas. by ^{133}Xe inhalation, anal. method comparison 78−44604

radiology continued
cerebral regional blood flow meas. with ^{133}Xe, functional landscapes in brain 78−85356
Compton scatter tissue densitometry, calc. of single and multiple scatter photon fluences 78−28048
computer appls., conf. Newport Beach, CA, USA (June 1979) 80−8141
computer monitoring system appl. 78−7466
computer systems in diagnosis 79−34663
computer use 80−8142
conference, international congress of radiology, Rio de Janeiro, Brazil (Oct. 1977) 79−16284
conference, London, England (Apr 1979) 80−51938
conference, nuclear cross sections and technology, Washington, USA (March 1975) 77−22826
development trends in isotope and radiation appls. 78−55041
diagnostic equipment, ergonomic design problems *(German)* 79−74729
diagnostic methods, non-invasive, seminary, Brno, Czechoslovakia (Sept. 1976) *(Czech)* 77−17001
diagnostic radiology efficacy study 80−8167
diagnostic techniques *(Slovenian)* 80−30863
diagnostic visualisation by nuclear medicine cross-modality techniques 79−79612
digital image change detection 80−102637
education program in medical radiological physics based on nucl. engineering 80−31448
elementary particle interactions, radiological imaging appls. 80−61675
film, cassettes, automatic handling 77−45907
functional imaging, appls. in three radiological modalities 80−8139
Gevamatic 240 developing machine, constancy testing by test film strips in a radiological practice *(German)* 80−95206
hazards of ionising radiations *(Italian)* 77−77942
herpes simplex virus radiometric detect. 78−65117
history of applications of nucl. physics to medicine *(French)* 78−45453
history of the early years 79−80410
hospital radioisotope release to environment, model and meas. 78−96105
image processing and synthesis in radiology and nucl. medicine *(German)* 78−40325
image processing in diagnostic radiology 80−81690
image reconstruction, projection completions methods, computational examples 78−46524
image texture anal. using pattern recognition 77−21643
imaging at Bureau of Radiological Health 80−8160
imaging system line spread function and MTF determ., effect of finite slit 78−24118
instrumentation, new industrial contributions, review 78−31924
insulin, radioimmunoassay, improvement in precision and accuracy of commercial kit 78−48884
left ventricular images digital processing *(Japanese)* 80−12224
liquid scintillation, counting technique, review 78−82586
liver fat content determ. by photon scatt. technique 78−24124
liver metastases diagnosis, conf., Brussels, Belgium (Nov.-Dec. 78) 80−82568
lymphocyte carbohydrate metabolism in response to mitogens, liq. scintillation vial for radiometric assay 78−61248
medical engineering, review of present state 80−17023
mixed-oxide fuel fabrication plant, large commercial, accident radiological risk assessment 78−17401
mobile testing laboratory PPLII-3 for ionizing radiation 79−74761
Monte Carlo simulations using minicomputers, random number generation 79−81122
muscle blood flow meas. by ^{133}Xe clearance, CdTe semicond. detector system 78−40305
nuclear data requirements 77−25553
nuclear installations, environmental surveillance programme, Spanish experience 77−65336
nuclear medicine, diagnosis appls., equipment and methods *(French)* 78−48888
nuclear medicine computer systems, buyer's guide to current performance and future promise 78−48883
nuclear medicine diagnostics, for teaching 78−49618
nuclear medicine instrumentation trends 78−44594
nuclear medicine measurements, quality assurance 77−40764
nuclear medicine procedures, radiation dose to embryo due to radiopharmaceuticals 77−5083
nuclear physics appl. to life sciences 78−15882
nuclear science, nuclear power systems, confs., San Francisco, USA, 19-21 Oct. 1977 78−33304
optical reconstructions from projections via deconvolution 80−63962
organ depth estimation by gamma-ray spectral comparison 77−86612
photon absorptiometry of soft tissue and fluid content, method, precision and accuracy 78−73221
photon dosimetry, practical problems 77−60261
placental blood flow evaluation, comparison of ^{113m}In and ^{133}Xe intravenous injection methods 78−28043
proton imaging for medical applications 80−98129
public health aspects of radiation 78−35895
radiation exposure of UK population, review 79−62373
radiochemical purity quality control by rapid feedback system 77−90900
radioimmunoassay, hypergeometric theory of competitive binding 77−77980
radioimmunoassay, instrumentation developments 77−86614
radioimmunoassay, probe for fine struct. of biological systems, review 78−73217
radioimmunoassay, statistical evaluation of normal range data 77−90885
radioimmunoassay computer-assisted analysis 79−25100
radioimmunoassay of insulin receptor, receptor structure and function 79−88164
Radioimmunoassay Total System *(Japanese)* 79−92356
radioiodine-labelled pharmaceutical administration, optimal thyroid radiation protection, computer simulation 78−44616
radioisotope applications in agriculture, hydrology, medicine industry etc., booklet 78−35947
radioisotope production, non-linear behaviour of gas targets 78−25361
radioisotope production in cyclotron for diagnostic medical research appls. *(French)* 78−48895
radioisotopes, simultaneous prod. of ^{67}Cu, ^{64}Cu and ^{67}Ga and bleomycin labelling with ^{67}Cu or ^{64}Cu 78−28066
radionuclide tracer telemetry, semicond. memory systems for data storage 77−90877
radiopharmaceutical investigations, appl. of ten-day rule 77−21633
radiopharmaceutical preparation and injection, dose to hands 78−20276
radiology continued
radiopharmaceutical purity determ., adaptation of multichannel scalar device for radiochromatogram scanning 78−48894
radiopharmaceuticals in diagnosis, patient dose 78−35967
radiopharmacy optimisation by redesign 77−90899
radioprotection, medical regulations and standards in France *(French)* 78−48897
radiotelemetry pill for biomedical meas. of ionising radiation using HgI_2 detector 78−40318
renal function studies, combined in vitro-in vivo radionuclide procedure, technical aspects 77−90884
renogram deconvolution, Hippuran transit times in kidney 78−40317
reporting system based on individualised list of diagnostic possibilities 79−83860
review of past and future diagnostic and therapeutic radiology 77−12984
sealed radioactive sources, medical appls. *(French)* 78−53497
sequential coherent optical reconstruction from projections using a ROACH filter 80−63961
SI units 77−12980
SI units *(Spanish)* 79−62365
SI units in radiochem. and radiology 78−81939
spectral radiation detectors, calibration and error anal. 78−46177
standardisation of apparatus *(French)* 77−73602
sterilisation facility, in Medicor Works' Debrecen Factory of Surgical Instruments, test dosimetry 78−40336
teaching, slide console 78−4435
thyroid $^{99m}TcO_2$ uptake meas., gamma camera method 78−20244
thyroid I measurement by X-ray fluoresc. scanning, effect of background radiation change 78−73216
tumour blood flow, meas. by photon activation, ^{15}O decay technique 80−104755
US state and federal regulatory meas. responsibilities around medical facilities 77−40765
X-ray apparatus electrical circuit fault classification 77−21604
X-ray bremsstrahlung filtered spectral source for radiological studies 77−77969
X-ray image intensifier freq.-contrast charact. curves determ. 78−7427
^{11}C labelled molecules, examples of use in medical research *(French)* 77−66833
Ca in vivo measurement by ^{37}Ar method, inert gas elimination in humans 78−61247
CdTe detector for radionuclide tracer telemetry 77−86587
HgI_2 in vivo medical probe, DC and pulse counting meas. 78−44593
HgI_2 miniature probes for in-vivo medical appls., fabrication, spectroscopic evaluation 78−40308
^{123}I production in cyclotron by $^{124}Te(p,2n)^{123}I$, improved targetry and radiochem. 78−28064
^{124}I production in cyclotron by $^{124}Te(p,n)^{124}I$, improved targetry and radiochem. 78−28064
^{125}I-fibrinogen uptake test for detect. of deep vein thrombosis, review of current practice 78−7436
^{111}In metabolic fate in rat 78−48881
$^{81}Kr^m$, new type generator using cellulose chromatography paper, for hospital use 79−8541
$Na^{125}I$ tracer telemetric detection for biological rhythms in renal function study 77−86586
Pu recycling in LWRs and environmental impact 78−89969
T_2O, injectable soln., radionuclidic purity using liquid scintillation counter *(French)* 78−73118
^{99m}Tc radiopharmaceutical kits, rapid colour spot test for stannous Sn levels 77−86630
^{99m}Tc-EHDP accumulation in canine tibia, meas. method 78−20245
U mill tailings, radiological criteria 78−82480
^{133}Xe gas dispenser for lung ventilation studies 78−28068
^{133}Xe radio-spirometric measuring system for regional respiration function testing 77−90889

radiolysis
acetaldehyde formation on radiolysis of ethanol formaldehyde systems *(Russian)* 80−55684
acetate ion radicals, solns., pulse radiolysis, CIDEP, viscosity depend. 77−75189
acyloxy radical ion, in irrad. Rochelle salt, decarboxylation, pulse radiolysis and EPR obs. 78−70854
adrenaline, acid aq. solns., pulse radiolysis, H., OH. react. kinetics, UV spectra 77−16841
albumin, pulsed laser study of adsorbed aromatic mol. excited states 77−86448
alcohol galsses, tunnelling reactions of trapped electrons with electron acceptors 78−76887
alcohols, glass, electron trapping, pulse radiolysis obs. 80−30264
alkali halides, F^--centres, thermal and photolytic decay processes 78−95053
alkali halides, radiolysis, growth of colloidal metal inclusions 78−92493
alkali metal halides, irradiated, annealing 78−92494
alkaline frozen solutions, polycryst. and glassy, photocond. and radiometric obs. 80−45531
alkane:toluene, radiolysis at 77K, luminesc., excited singlet toluene form., energy transfer mechanism 77−16846
alkane glass, γ-irradiated, charge trapping, isotope and mol. struct. effects 79−5164
In-alkanes, liq., radiolysis mechanisms rel. to hot H atom reactions 77−36771
n-alkanes, single cryst., γ-irrad., ESR, energy deposition rel. to alkyl radical form. 77−16844
D-amino acid oxidase, crit. residues, pulse radiolysis and inactivation study 78−27897
α-amino acids, γ-irradiated, primary oxidation products, ESR and ENDOR 77−48754
amino acids, aq. solns. EPR of spin-trapped radicals, hydrated electron reactions 78−27796
amino acids, high energy radiation effects and chemical evolution 77−63937
amino acids and their complexes, corrected G-values 79−20516
aminoacridines, interaction with nucleic acids 78−85186
ammoniated electron+R^{3+}, reaction kinetics meas. by ns. pulse radiolysis 79−52638
aqueous glass, γ-radiolysis, photolysis of trapped electrons, quasi-free electron IR absorpt., luminesc. 77−21401
aqueous solutions radiolysis by recoil particles from $^{10}B(n,\alpha)^7Li$, intratrajectory reacts. *(French)* 77−12812

radiolysis continued
aromatic ethers, comparative study of X-ray and γ-induced photolysis and radiolysis *(German)* 78−64854
aromatic hydrocarbons, oxygen quenching of triplet states, charge-transfer interactions 77−23516
aromatic hydrocarbons, singlet energies, correlation with anion radical protonation 78−40064
ascorbic acid, action with perhydroxyl radicals 80−35523
L-asparagine.H_2O, X-irrad. at room temp., ESR and ENDOR 77−40131
atmospheric aerosol, produced by α-particles, evolution of <0.02 micron particles *(French)* 79−43640
B-group vitamins in aqueous systems, decomposition by γ-rays in presence and absence of protective additives 79−2006
benzene, γ-radiolysis, phenyl radical intermediate, spin trapping, EPR 78−7218
benzene, lowest triplet state, pulse radiolysis obs. 79−39168
benzophenone, aqueous system, LET depend. of transient yields in deuteron and alpha pulse radiolysis 77−63940
benzyl halides, in matrix, UV-, γ-irrad., benzyl radical-halide ion form., charge transfer bands 77−16854
bilirubin, aq. soln., pulse radiolysis 78−48761
bremsstrahlung yield produced by 4 MeV linear electron accelerator calc. rel. to hazard in radiolysis 79−76181
brom phenol blue aqueous soln., irradiation induced discolouring as dose meas. 78−41866
n-butane formation by fission fragment radiolysis in ethane-ammonia system 77−56236
t-butanol, aqueous system, LET depend. of transient yields in deuteron and alpha pulse radiolysis 77−63940
carotenoid pigments, radical ions, radiolysis generation, absorpt. spectra, MO calcs. 77−65488
cellular radiation damage model, radiation chemistry approach for direct and indirect effects 79−11974
cellulose fibre, gamma-irrad., and storage effects on props. *(Russian)* 80−61121
chemical processes induced radiolytically in well defined aqueous systems 80−66823
Cherenkov radiation light source in pulse radiolysis 80−42267
chloroform-n-hexane, liq. mixture, radiolysis, mechanism, rate consts. 78−20039
chloroform-paraffin system chem. changes after ^{60}Co γ-irradiation, dosimetry appl. 80−30258
chlorophyll a, cation radical formation by pulse radiolysis, oxidation and demetalation rate consts. 80−61505
1-chloropropane, formation of chlorohexanes by ion-mol. reactions in radiolysis 78−27802
chlorotrifluoromethane, matrix radiolysis, photoionis., IR spectra of CF_2Cl^+ and parent cations 78−80767
cholesteric esters, effect of nature of organic solvent on gamma radiolysis 80−7835
cholesteric liquid crystals, gamma-ray irrad. effects, dosimetry, thermography appls. *(Spanish)* 80−92457
cholesteric products, gamma irradiation, effect of presence of organic solvents 79−24777
cholesteryl decanoate organic solns., γ radiolysis, colour transition temp. 79−57266
cholesteryl nonanoate organic solns., γ radiolysis, colour transition temp. 79−57266
chromatin extracted from cultured mammalian cells, gamma radiolysis, DNA alkali-labile strand damage 78−77003
chromatin from cultured mammalian cells, DNA-protein cross-links formation 80−81655
chromatographic support materials decomposition by ionising radiation *(German)* 78−92587
CIDEP, examples of $S\text{-}T_{\pm1}$ polarisation 78−86891
CIDEP, $S\text{-}T_{\pm1}$ polarisation in H radical reactions 77−48656
citric acid, single cryst., X-irrad., EPR and ENDOR, 4.2K radical identification 79−65764
computerised pulse radiolysis system 78−64862
computerised pulse radiolysis system using Biomation recorder and PDP 11/40 computer 77−40560
concanavalin A-carbohydrate interactions, implication of protein aromatic amino acids, radiolysis 78−40110
coumarin in aqueous soln., fluorescent prod. form. on γ-irrad. 77−60094
crystal, electron-irradiated, free radical stabilisation, filler content effects *(Russian)* 77−56241
cyclohexane$_{(c)}$ solns., positive ion-solute mol. reaction rate consts. in − radiolysis 77−9091
cyclohexane, liq., ps time-resolved energy transfer, ultra-fast process, ps single pulse radiolysis 79−79267
cyclohexane+toluene, energy transfer, pulse radiolysis obs. 80−16714
cytidine-5′-monophosphate, γ-irrad. aq. soln., spin-trapped radicals, liq. chromatography and EPR spectroscopy 78−53340
cytochrome c and related metalloproteins, fast electron transfer processes 79−8478
cytochrome c conformationally-nonequilibrium state reactivity obs. by pulse radiolysis 79−43816
cytochrome c-phospholipid interaction, studied by pulse radiolysis 78−48746
2′-deoxyadenosine in aq. deaerated soln., new radiolysis mechanism 80−81350
di(2-ethylhexyl) phosphoric acid, organic extractant in liquid radwaste, gamma radiolysis 79−67879
dichlorodifluoromethane, matrix radiolysis, photoionis., IR spectra of CF_2Cl^+ and parent cations 78−80767
dichloromethane, in liq. hexane, radiolysis 78−80769
dihalogenated benzene derivatives, 77K, gamma radialysis radical pair formation, EPR 79−29334
4,6-dihydroxypyrimidine, aq. soln., reaction with OH, short-lived radicals, ESR 80−101031
2,2-dimethylbutane, fluid phases, electron mobility, density effects meas. 77−7619
9,10-diphenyl anthracene, cyclohexane soln., solute excited state form. kinetics in pulse radiolysis 79−79263
diphenylamine, in nitrobenzene soln., dry hole capture in pulse radiolysis expt. 79−79266
DNA, cytosine ^{14}C-2 labelled, gamma radiolysis products from N-glycosidic bond rupture 77−9171
DNA and other biopolymers 80−67163

radiolysis continued
DNA kinetics in soln., electron pulse radiolysis using light scatt. detect. 77−16910
dodecane-tributyl phosphate solns., radiolysis, liquid products 80−40723
dodecane-tributylphosphate solns. 78−74459
dulcitol, X-irrad., 4.2K, electron traps, alkoxy hyperfine coupling, ENDOR obs. 80−50863
electro-optical multichannel spectrommeter for transient resonance Raman and absorption spectroscopy 80−31890
electrochemical behaviour of metals in nucl. reactor radiation field, depend. on radiolysis products of solns. 77−52650
electron beam pulse radiolysis, appl. to chemical research 79−52730
electron linac for pulse radiolysis, correl. between radiation absorbed dose and elec. parameters 77−34482
electron pulse, field emission tube, electron pulse duration reduction 77−3530
electron sensitive materials, electron microscopy and diffr. 78−83701
electron source, for pulse radiolysis, Febetron 708 type 77−88319
endosseous implant material, radiation processed alumina-polyacrylic acid composite 77−60308
EPR, ns time-resolved, in pulse radiolysis, via spin echo method 80−43075
ethane, gas-phase radiolysis, inhibition of free radical prod. by H_2O, ethylene and SF_6 79−39178
ethane, X-irradiated, 4.2K, pairwise radical trapping mechanism, EPR obs. 79−100412
ethanethiol, rare gas sensitised radiolysis and charge exchange mass spectra 77−48664
ethanol, electron solvation, ps laser study 80−101032
ethanol, pulse radiolysis, solvated electrons decay kinetics 79−66319
ethyl carbazole, in nitrobenzene soln., dry hole capture in pulse radiolysis expt. 79−79266
ethylamine formation by fission fragment radiolysis in ethane-ammonia system 77−56236
ethylene-butane matrix, D atom bombardment, ethyl radical proton exchange reaction, indirect ESR obs. 80−16700
ethylenimine, gas phase γ radiolysis and mass spectra of products 77−29022
ferredoxin, pulse-radiolysis study of conformationally nonequilibrium states 79−70506
ferrous sulphamate radiolytic instability in nuclear process solns. 77−70314
fibrinogen solution, effect of scavengers on radiation-susceptible sites 78−11701
fission reactor cooling water chemical reagent pyrogallic acid, radiation effects *(Russian)* 79−43603
fluorobromomethanes, matrix photoionisation and radiolysis, IR spectra of free radicals 79−24765
Freon, matrix radiolysis, photoionis., IR spectra of CF_2Cl^+ and parent cations 78−80767
frozen media, electron transfer reactions and multiphonon transition theory 80−7812
glass, alcoholic and aq., 4.2K, trapped electron photocond. and optical spectra following radiolysis 79−29378
glasses, aqueous soln., stabilising excess electrons, DTA at cryogenic temps. 78−76889
glyceraldehyde-3-phosphate dehydrogenase radiolysis, active-site and SH loss 78−77000
α-glycine, irradiated, oxidation prod. N-centred π radical ERR 77−14459
glycine-d_5, pulse radiolysis, primary reaction product optical and EPR spectra 79−79265
graphite, nucl. grade, neutron small angle scatt., thermal and radiolytic oxidation effect, porosity size distrib. 79−17977
graphite moderator structure design and manufacturing specification 80−23110
haemoglobin, dynamic characts. of conformational nonequilib. states, radiolysis investig. 78−58877
haemoglobin+CO reaction kinetics, using various regimes of photolytic illum. 78−48753
heterogeneous inanimate systems, radiobiology appl. 80−66824
hexafluorobenzene, γ-radiolysis, matrix isolation spectra of radical anions 79−52704
high-level liquid radwaste partitioning, radiation damage of organic extractant 79−67879
high-level liquid waste, damage to organic extractant in positioning process 80−9345
L-histidine HCl, X-irrad., $=C\text{-}^{+}NH_3$ radical form., exchangeable H^+ hyperfine coupling 79−36669
hydrocarbon solutions, scavenging yield from initial electron distribution 79−87860
hydrocarbons, γ-radiolysis in glassy and polycryst. states, EPR spectra 77−52658
hydrocarbons, electron energy influence on radiolysis yields 79−43602
hydrocarbons, liq., competitive reactions in radiolysis 79−39179
hydrocarbons, soln. radiolysis, electron scavenging, Warman-Asmus-Schuler parameter 79−70354
ice, electron-irrad., cluster-ion prod., lattice and fragmentation energies 77−4911
ice, pure and acidic, electron irrad., ESR of H atoms, motional narrowing and spin polarisation 77−20706
ice, X-irradiated, EPR spectra, obs. of thermally reversible radical, g-value 79−5144
indole, in water-ethanol soln., radiolysis *(Russian)* 77−86338
iodoform in cyclohexane soln., γ-radiolysis, G-values 79−52705
ion beam pulse radiolysis, LET dependence of transient yields 80−30260
ion-pair clusters and excited-state yields in organic solns. 77−29024
kinetic data acquisition, and anal., by computer based system 79−39180
lactate dehydrogenase, O_2 effect in radiolysis obs. 80−72223
lactate dehydrogenase+free radicals, reactions, pulse radiolysis 78−7214
lithium acetate dihydrate, γ-irrad., methyl radical, ENDOR, line-shape model appl. 79−73853
lithium acetate dihydrate, γ-irradiated single crystal, $CH_3...CO_2$ pairs, e.s.r. 77−9100
matrix radiolysis, photoionis., IR spectra of CF_2Cl^+ and parent cations 78−80767
metalloporphyrin, cation radical formation by pulse radiolysis, oxidation and demetalation rate consts. 80−61505
methane, adsorbed on γ-Al_2O_3, γ-radiolysis, reaction kinetics 78−95940
methane, simulated, with low energy electrons 3.5 to 17.5 eV 79−43602

radiolysis continued
methane, X-irradiated, 4.2K, pairwise radical trapping mechanism, EPR obs. 79−100412
methane adsorbed on γ-Al_2O_3, γ-radiolysis 80−3375
methanol, aq., radiolysis, CIDNP, methoxy radical involvement 78−53223
methanol, electron solvation, ps laser study 80−101032
methanol, high temp. n, γ-radiolysis *(Russian)* 79−61890
methanol-2-methyltetrahydrofuran glasses, electron solvation conversion, pulse radiolysis obs. 77−77795
methanol-methyltetrahydrofuran glass:β-naphtholate, electron solvation, laser flash photoionis. compared with pulse radiolysis 79−74405
methyl iodide, in 3-methyl pentane glassy matrix, γ-radiolysis and effects caused by aggregation 78−64864
2-methyl tetrahydrofuran radical formation on liq. phase γ-radiolysis 77−60080
methylcyclohexane glass, γ-radiolysis, electron tunnelling from matrix trapped biphenyl ions 79−29379
methylene diiodide, in 3-methyl pentane, γ-radiolysis 79−24776
3- methylhexane, glass, γ-irradiated, trapped electron-radical mag. energy transfer, ELDOR, cross relax. 77−16209
6-methylmercaptopurine riboside, S-substituted nucleoside, ESR and ENDOR obs. 77−36766
3-methylpentane glass, γ-radiolysis, electron tunnelling from matrix trapped biphenyl ions 79−29379
2-methyltetrahydrofuran, glass, γ-irradiated, trapped electron-radical mag. energy transfer, ELDOR, cross relax. 77−16209
micelle solns., aq., pulse radiolysis, CIDEP in time-resolved EPR 77−30891
modeling of elementary step of chemical transform. of crysts., appl. to decomp. 79−15985
molecular excited states, prod. by electron pulse radiolysis 79−50142
molecular solid, electron tunnelling, long-range electron transfer processes, orbital overlap model 80−7813
monophenyl phosphate in aq. soln., pulse radiolysis obs. 80−30261
muonium chemistry, radiolysis effects 78−88653
muonium interaction with radiolysis products in pure water, OH. scavenging by tert-butyl alcohol 79−24806
myoglobin conformationally-nonequilibrium state reactivity obs. by pulse radiolysis 79−39353
naphthalene (-d_8), gamma irradiated soln., fluoresc. mag. field depend., spin correls. 77−44492
nitro compounds in cyclohexane, electron attachment reaction rates from pulse radiolysis 78−31663
nitroaniline, pulse radiolysis in aq. soln., intermediates form. and decay 77−60096
nitrobenzene, pulse radiolysis in aq. soln., intermediates form. and decay 77−60096
nitromethyluracil, radiation-induced oxidation and reduction 77−32816
nitrophenol, pulse radiolysis in aq. soln., intermediates form. and decay 77−60096
β-nitrostyrene free anionic polymerisation during electron radiolysis, primary reactions 78−44378
nonpolar liquids, cavitation threshold under ionising acoustic radiation 79−37074
nucleotide sugar-phosphate region, γ-irradiated, deoxycytidine 5′-phosphate alkoxy radical EPR 79−5249
octafluorotoluene, γ-radiolysis, matrix isolation spectra of radical anions 79−52704
Penning collision processes, review *(Japanese)* 79−64092
pentafluoromethyl iodide, ion-molecule reactions, amongst radiolysis products, reaction rates, mechanisms, mass spectra 79−5136
perfluorocarbons, γ-irrad. solns., mag. field effect on fluoresc. 80−55677
peroxidase, low-temperature radioreduction, MCD and absorpt. spectra 78−31763
PET fibre, irrad., radical yields 79−96343
phosphorylation in simple lipid and chloroplast ATP synthetase system 79−92298
photochemistry, appl. of electron pulse radiolysis 79−52698
photoreceptor membrane viscosity and component dynamics, recombination kinetics method 79−39366
PMMA, reactor irrad., growth of macroscopic radiolytic gas bubbles, diffusion model 80−65058
PMMA, visoelastic props., γ-irrad. influence *(Russian)* 78−88492
polar glass, UV and γ-prod. electrons geminate recombination, radical yield 77−9094
poly-2-vinylnaphthalene, soln., lowest triplet props., flash photolysis and radiolysis obs. 80−32861
poly-N-vinylcarbazole, soln., picosecond time-resolved fluoresc. by pulse radiolysis 80−28122
polychlorinated biphenyls, pollutants, radiation degradation in organic solvents, H_2O 80−30262
polydextran, γ-irrad. frozen gel, electron trapping, EPR and optical obs. 78−20030
polyethylene, linear, irrad. crosslinking and chain scission in extended chain and bulk films 77−60095
polyethylene prostheses, radiation crosslinking improvement of shock- and abrasion-resistance 77−60307
polyethylene terephthalate fibre, radiation grafting 79−96342
polymer, photoradiative processes in free radical form. *(Russian)* 79−57269
polymers, synthetic, radiative degradation, chem., phys., environmental, technological effects, review 80−40948
polymethylpentene, visoelastic props., γ-irrad. influence *(Russian)* 78−88492
polynucleotides, single-stranded, reaction of O_2 with radiation-induced free radicals 78−48759
polynucleotides poly(A+U), double-stranded, radiolysis in presence of O_2 78−48760
potassium antimonyl tartrate, neutral aq. soln., gamma radiolysis 80−101030
potassium hydrogen malonate, γ-irrad. cryst., ESR and ENDOR of trapped radical 79−78524
product detection by Pt electrode rest potential 80−11973
propane-d_8, liq., solvated electron optical absorpt. band 78−72544
1propanol, glassy, electron trapping, pulse radiolysis obs. 80−30264
1-propanol, low temp. pulse radiolysis, solvated electrons, absorpt. spectral changes 77−12813
n-propanol-3-methylpentane mixtures, pulse radiolysis, solvated electrons 79−66321
radiolysis continued
propene, triplet states, electron impact and photosensitised dissoc., chem. effects 77−14592
proteins, study by pulse radiolysis 79−8480
pulse, composite optical spectra, synthesis, anal., computerised 77−12810
pulse, fast chemical reactions obs. *(Czech)* 80−81325
pulse radiolysis, applic. of NMR and CIDNP 77−32814
pulse radiolysis, var. temp. cell housing 78−27794
pulse radiolysis appl. to biomolecule reactions and struct., review 78−61145
pulsed electron accelerator giving 20 ps 300 A electron pulses *(Japanese)* 78−80754
pulsed radiolysis, nonlinear radiation-acoustic phenomena 80−79029
pulsed radiolysis acoustic wave generation in liquids 79−8446
Purex process, radiolytic degradation of extractant-diluent systems 77−70313
purine and pyrimidine, γ-irrad. investig. by diffuse refl. spectrophotometry 77−48756
PVC, radiation destruction, automatic control *(Polish)* 77−29025
PVC, structural studies by Raman spectroscopy 79−7044
PVC+$Br_2(I_2)$, reaction in surface-modified film subject to thermal-radiative and photochem. action *(Russian)* 77−21385
pyrene solutions, radical ion pairs, pulse radiolysis, time resolved EPR spectra meas. by ODMR of fluoresc. 80−83395
pyrimidine N_2O aq. solns., dimer formation in γ-radiolysis, chromatographic obs. 80−7785
quantum mechanical kinetics problems, averaging principle appls. 78−19995
α-quartz, electron irrad., defect struct. and radiolysis 80−107321
radiation sensitivity, conf., Rome, Italy (Sept. 1978) 80−62368
radicals, radiolytically produced, CIDEP 78−13534
radioactive waste solidification products, radiolysis gases generation, mass spectrometric anal. 79−85626
radiochemical decomposition in aqueous soln., use of revised MIRD eqn. for dosimetry calcs. 77−66851
radiolytically formed chelating agents, corrosion prevention appls. 78−64745
recombination of atoms or ions in radiolytic spur reaction 77−1940
DL-serine, X-irrad., $=C-^+NH_3$ radical form., exchangeable H^+ hyperfine coupling 79−36669
sodium aluminium tartrate, β-particle effects on crystallisation from aq. solns. 77−36387
sorbitol, X-irrad., 4.2K, electron traps, alkoxy hyperfine coupling, ENDOR obs. 80−50863
steel, low-alloy hydrogenation and embrittlement under neutron irrad. in contact with water *(Russian)* 77−52529
stereoselective rearrangement reaction, electron impact induced, temp. depend. 77−25288
stilbene, radiolysis, electron transfer and protonation, vis. spectra, isomer effects 77−60085
sucrose, single cryst., absorption spectrum of electron traps, pulse radiolysis obs. 80−93369
supercrit. hydrocarbons radiolysis, electron reaction rate const./diffusion coeff. ratio 80−101033
synthetic fuel prod. by direct radiolysis using fusion radiation sources 80−61227
synthetic fuel production from fusion, economic prod. pot. 77−34467
TBP-n-paraffin extractant for Th reactor fuel reprocessing, degradation 77−70316
p-terphenyl, cyclohexane soln., solute excited state form. kinetics in pulse radiolysis 79−79263
2,2,3,3-tetramethylbutane, radiolysis, radical prods., EPR obs. 80−32747
tetraphenylcyclobutane, in hexamethylphosphoric triamide soln., pulse radiolysis, optical absorption decay obs. 79−16019
thiamine, radiolysis, one electron redox pot. 79−53048
thymidine, frozen aq. solns., final products of gamma radiolysis 78−77001
thymidine-5-monophosphate, γ-irrad. aq. soln., spin-trapped radicals, liq. chromatography and EPR spectroscopy 78−53340
thymine, γ-irradiated, EPR study of post-radiolysis growth of spin-trapped radicals 79−16155
thymine aq., and N_2O solns., radiolysis products anal. 80−30257
toluene-1-hexene(1-pentene), radiolysis at 77K, fluoresc., energy transfer processes 78−20037
toluene-9,10-diphenylanthracene, soln., electron beam pulse radiolysis, energy transfer 80−7808
trichlorofluoromethane, matrix radiolysis and photoionis. at 15K,IR spectrochem. anal. 78−76893
trifluoromethyl iodide, ion-molecule reactions, amongst radiolysis products, reaction rates, mechanisms, mass spectra 79−5136
trifluoromethylhalide radical anions, formation, ESR and struct. 77−32809
triphenylamine in 3-methylpentane and ethanol glasses, γ-radiolysis, IR spectra, trapped electron 77−16842
tritiated radioactive waste, gas generation by autoradiolysis 80−32384
tritiated waste materials, gas generation by self-radiolysis, container suitability 79−26579
tryptophyl peptides, pulse radiolysis, hydrated electron reaction 78−48679
vitamins, B group, γ-irrad. resist. 78−76890
waste water of sulphate cellulose prod., radiation treatment *(Russian)* 80−55688
water, and effects upon in-reactor zircaloy corrosion 77−12817
water, decomposition by fusion energy, H_2 prod., synthetic fuel 78−50335
water, mathematical modelling for kinetics in operating reactors 78−61036
water, pulse radiolysis OH ($C^2\Sigma^+$) time resolved emission 79−10138
water vapour, Xe sensitized radiolysis, primary product yield 79−57265
xylitol, X-irrad., 4.2K, electron traps, alkoxy hyperfine coupling, ENDOR obs. 80−50863
Ag, and Ag^+, solvation in deuterated-ice matrices, electron spin echo obs. 80−15780
AgBr colloidal suspension radiolytic reduction obs. 79−91979
Ar, electron pulse radiolysis, 2p levels formation and decay kinetics 78−31665
AsF_6^-, AsF_5^- form., ESR spectrum 77−16845
BeF_2, aq. glass, 76K, solvated electron spectrum evolution, following ns radiolysis 78−88295
$Bn(IO_3)_2$, radiolysis in Portland cement, rel. to immobilisation of long lived ^{129}I 79−59208

radiolysis continued
CO III-EDTA solution, radiolysis by charged particles through $^6Li(n,\alpha)^3H$ reaction 80−93788
CO, nonequilib. dissoc. induced by electron-vibr. and IR laser pumping 79−86016
CO_2 decomposition, plasma radiolysis by high current relativistic electron beam 79−91947
CO_2, Febetron radiolysis in the presence of O_2 and CO 80−35557
CO_2, γ-radiolysis in glass packed vessels, CO yields rel. to packing, baking 77−12811
CO_2-$H_2O(D_2O)$-mineral oils, radiolysis products form. in nucl. reactor 78−689
CO_2-propane system, radiolysis by fission fragments, CO form., G-values 77−48657
$CO_2^- + O_2$, nanosec. pulse radiolysis, react. rate const. meas. 77−16843
^{13}C, CIDNP, obs. in reactions of organic and inorganic radicals during pulse radiolysis 80−63660
$CoSeO_4$, electron capture and γ-radiolysis, radn. damage 80−16705
Cu(II) iminodiacetates in aqueous solution, gamma-ray radiolysis 80−35560
$Cu(ethylenediamine)_2^{2+}$, electron tunnelling probability as function of distance for chem. reactions 78−80759
D_2O, effect of phase density on ionisation process and electron localisation 77−89731
D_2O ice, crystalline, irrad., temp. depend. of trapped electrons, 77 to 6K 79−83474
D_2O, ice cryst., electron traps, electron irrad. effects, EPR 77−1939
D_2O, positronium form. inhibition by NO_3^- electron scavenger 79−66325
Fe^{3+}/Fe^{2+} in frozen solns., stabilisation on ^{57}Co decay, electron scavenger effects, Mossbauer obs. 77−40562
$Fe(H_2PO_2)_2$, γ-ray and electron radiolysis, Mossbauer study 80−7816
$FeSO_4$ aq. soln., oxidation by high-energy electrons 79−52700
$FeSeO_4$, electron capture and γ-radiolysis, radn. damage 80−16705
H_2, radiolytic/thermal cycles 80−51011
$H^+ + O_2^-$, nanosec. pulse radiolysis, rate consts. meas. 77−16843
H_2, solid, electron-irrad., cluster-ion prod., lattice and fragmentation energies 77−4911
$HO_2 \rightarrow H^+ + O_2^-$ nanosec. pulse radiolysis, react. rate const. meas. 77−16843
$HO_2 + NO_2$ form. and react. in aq. soln., pulse radiolysis 79−24805
H_2O, positronium form. inhibition by NO_3^- electron scavenger 79−66325
H_2O, pulse radiolysis, hydrated electron absorbance, spur overlap 77−86328
H_2O, radiolysis, excitation, ionisation processes *(Rumanian)* 77−48666
H_2O vapour, H_2 production by thermoradiation dehydrogenation using nuclear power, kinetic anal. 80−67010
$H_2O + H(n=3)$, $O(3p^3P)$, radiation quenching in pulse radiolytically excited water vap. 79−89738
$H_2O_2 + HO_2(O_2^-)$ Haber-Weiss reaction kinetics, chain mechanism 79−83444
H_2S, liq., optical absorption transients produced by ns pulse radiolysis 79−11803
H_2SO_4, frozen soln., EPR of trapped H-atoms produced by UV and X-irrad. 80−3369
H_2SO_4:Fe^{2+}, frozen soln., photo- and radiation-produced H-atoms obs. 79−39162
He-N_2, de excitation rate consts., energy transfer, pulse radiolysis obs. 80−30303
Hg halides in aq. soln., pulse radiolysis, emission species 79−24764
HgI_2, aq. soln., luminesc. after high energy electron pulse radiolysis 77−32793
I^--$S_2O_8^{2-}$ aqueous redox mixtures, γ-radiolysis 79−16017
KBr, pulse radiolysis of metastable interstitial centre of high temp. 80−20658
KBr, V- and X-centres accumulation *(Russian)* 80−54228
KCl, irradiated, determ. of molar extinction coeff. and oscillator strength of V_2-centre *(Russian)* 78−80384
KCl, V- and X-centres accumulation *(Russian)* 80−54228
$KClO_4$, ClO_3^- detection by EPR of ClO_3 radicals created by X-irrad. 78−76311
KNO_3-$Ca(NO_3)_2$ glasses, radiation products and recombination 79−57261
KOH-O_2-N_2O-t-butane pulse radiolysis, kinetics of transient O compound form. meas. from Cherenkov emission 77−70321
KOH.xH_2O, pulse radiolysis, absorpt. spectra of electrons 79−16013
Kr, electron pulse radiolysis, 2p levels formation and decay kinetics 78−31665
$LiBrO_3$, radiation damage, XPS obs. 80−29844
LiCl aqueous glass, X-irradiated, localised electron optical, IR and photoconductivity spectra 78−73064
LiCl, deuterated aq. glasses, pulse radiolysis, trapped electron reactions 79−24804
LiCl, deuterated aqueous glasses, pulse irrad., trapped electron yield 79−20385
LiCl-D_2O, aq. 10 M glass, optical absorpt. spectra after X-irrad., electron scavenging efficiency 79−83476
$LiClO_4$, radiation damage, XPS obs. 80−29844
$LiIO_4$, radiation damage, XPS obs. 80−29844
^{24}Mg, removal from waste water by oxine-impregnated activated charcoal 80−9344
MnF_2, radiation damage, energy transfer, radiolysis, effect of defect centres 78−2161
N+alkene (1,3-butadiene)(acetylene), reaction rate consts., pulse radiolysis obs. 80−35508
N_2, ($C^3\Pi_u$) state, radiative lifetime, collisional quenching, pulse radiolysis meas. 78−29813
ND_3, effect of phase density on ionisation process and electron localisation 77−89731
NH_3, cluster-ion prod. in electron-irrad. solid, lattice, and fragmentation energies 77−4911
NH_3, cryst., radiolysis yield, temp. effects, Arrhenius depend. 77−48662
NH_3+olefin gas mixtures, γ-radiolysis over whole composition range *(Japanese)* 79−5172
NH_4ClO_4, photothermochemical process, influence of phase transition 79−24770
$(NH_4)_2SO_4$:MnO_4^-, X-ray irrad. damage, optical absorpt. spectra study 80−66246
NO_2^--IO_4^- aqueous redox mixtures, γ-radiolysis 79−20392
N_2O, pure and in mixtures, electron attachment near 1 atm., microwave cond. meas. 80−1063
$N_2O^- \rightarrow N_2 + O^-$, nanosec. pulse radiolysis, rate consts. meas., N_2O^- lifetime 77−16843
NaCl, irradiated, determ. of molar extinction coeff. and oscillator strength of V_2-centre *(Russian)* 78−80384
NaCl, V- and X-centres accumulation *(Russian)* 80−54228
NaCl-O^{2-} X-ray irrad., defect generation during radiolysis 80−7831
$NaClO_3$, γ-irradiated, metastable O_2 reson. Raman scatt.., excitation profile, polarisation meas. and decay kinetics 77−14437
$NaClO_3$, radiation damage, XPS obs. 80−29844
$NaClO_3$ trapped O species in irradiated samples, low-temp. X-ray photoelectron spectroscopy 78−27799
$NaClO_4$, frozen soln., acidic, X-irrad., H atom scavenger effects 79−39163
$NaClO_4$, frozen soln., EPR of trapped H-atoms produced by UV and X-irrad. 80−3369
$NaClO_4$ glass, radiation induced trapped electrons, photobleaching, H form. 77−44494
$NaClO_4$:Fe^{2+}, frozen soln., photo- and radiation-produced H-atoms obs. 79−39162
NaOH aqueous glassy systems, 77K, γ-irrad., struct. stabilisation 79−91976
NaOH, aqueous system, LET depend. of transient yields in deuteron and alpha pulse radiolysis 77−63940
NaOH, frozen soln., EPR of trapped H-atoms produced by UV and X-irrad. 80−3369
NaOH glass, radiation induced trapped electrons, photobleaching, H form. 77−44494
$NaOH:CrO_4^{2-}(NO_2^-)$, electron tunnelling, pulse radiolysis 80−108722
$NaOH:Fe(Cn)_6^{4-}$, electron tunnelling, pulse radiolysis 80−108722
Ne, electron pulse radiolysis, 2p levels formation and decay kinetics 78−31665
$Ne+SF_6(N_2)$, metastable state de-excitation, rate consts., radiolysis obs. 80−40709
O_2, thermal electron attachment with various compounds present, microwave cavity-radiolysis 77−42422
O_2-CO_2 (ethylene)(neopentane), thermal electron attachment meas., microwave cond., pulse radiolysis 80−28592
$O(^3P)$ atom yield in radiolysis of water by $^2H^+$ and $^4He^{2+}$ 80−35556
$RbMnF_3$, radiation damage, energy transfer, radiolysis, effect of defect centres 78−2161
SeO_2, free radicals, pulse radiolysis obs. 78−20040
$SrCl_2$, F-centre production mechanism, radiolysis exam. 79−23602
Tb^{3+}, aqueous soln., radioluminescence intensity conc. depend. 80−87055
tetrafluoromethane+C react. in ionising radiation of nuclear reactor 77−63934
UO_2 interaction with water, in-pile meas. 77−42097
Xe, electron pulse radiolysis, 2p levels formation and decay kinetics 78−31665
ZnO, polycryst., γ-radiolysis, O_2 radiation yield, mechanism 77−36772

radiometers
see also infrared detectors; microwave detectors
3 cm band with 3 GHz tuning range for radiotelescopes *(Russian)* 77−56828
absolute differential radiometer, compensation circuit, features 78−65956
absolute radiometer instrumental correction theory improvement 77−82585
absolute radiometer with uniform response, fabrication, characts. and anal. 80−268
absolute radiometer with uniform sensitivity over receiver surface 79−49289
acoustic emission from coherent structures in turbulent jet *(French)* 77−65775
actinometric radiosondes comparison during GATE-74 period 79−29906
airborne, for ocean chlorophyll content remote meas. under cloudy sky 79−25359
array antennas, radiometric earth and atmospheric sensing systems for large structure 77−41281
atmosphere precipitable water, dual-channel microwave method 80−51564
atmospheric attenuation meas. for satellite link system *(Czech)* 78−36351
atmospheric far IR laser radiation absorption, theory and expt. 77−41250
atmospheric IR emission meas. using versatile sensitive radiometer 77−70887
atmospheric O_3 monitoring with IR heterodyne radiometer 78−16216
atmospheric remote sensing, four band mm-wave radiometer design 78−96324
atmospheric transmissometer/radiometer for electro-optical sensor evaluation 77−70884
automatic nulling radiometer for the 3-4-mm band 80−18016
autotracking solar radiometer for atmospheric water vapour and aerosol optical depth determ. by remote sensing 78−65389
ball radiometer, calib. of radiant flux sensors 78−282
Balloon Altitude Mosaic Measurements Program 78−81455
biomedical temp. measurements, radiation balance microwave thermograph, simultaneous independent temp. and emissivity measurements 79−100692
blackbody for energy calibration of infrared equipment 80−86377
brightness temps. estimates from scanning radiometer data 78−85716
calibration, for atm. temp. remote sounding 77−41174
calibration blackbody, radiation methods, ChT-2R oven (USSR) 80−62722
calibration for radiant flux meas. of arbitrary source 77−34022
cavity, spherical, computation of errors 79−35829
cavity pyrheliometer, total solar optical irradiance meas. 79−35130
cavity pyrheliometers, appl. to solar const. accurate determs. 79−2341
chemical actinometer for UV solar radiation intensity meas. 77−45163
cm-wave radiometer, with enhanced long-term stability, for solar radio emission obs. 80−109361
Crookes, teaching, N_2 laser power investig. appls. 79−62978
Crookes radiometer, physics anal., for teaching 79−35504
cryogenically cooled two-channel paramp radiometer for 47 GHz 77−37982
design for total and net exchange solar radiation meas. 79−54190

radiometers continued
detector type, commercial devices survey and classification 78−16830
Dicke-type, 50 GHz band solar radiation attenuation meas. 78−73494
Dicke-type microwave radiometer, for atmos. temp. profile meas. *(Chinese)* 79−80188
digital radiometer/photometer (Tektronix) optical transmission charact. meas. *(French)* 79−89000
directional radiometer, for atm. longwave radiation meas. at ground 78−73537
dispersion-removing radiometer, obs. tests on PSR 1913+16 binary pulsar 79−35142
dual-detector radiometer, in far IR photometer for Kuiper Airborne Observatory 79−66926
Earth radiation budget data collection and interpretation model 77−37497
Earth resources, remote sensing by Skylab microwave radiometer 78−16273
electric apparatus and power lines, temp. rise meas. by infrared radiometer *(Russian)* 78−89537
electrically calibrated, using thin film thermopile 79−6176
emissometers, refl. errors elimination by use of alternate instruments 77−10089
energy calibration, geometrical relationships 77−74482
errors due to circular aperture diffr. edge effects 77−34023
evapotranspiration remote sensing Nimbus 5 satellite IR radiometer, evaluation *(French)* 77−17156
filter radiometer using selective interferometer 77−5880
forward looking IR system, radiometric accuracy 77−82604
Fourier transform spectrometer performance, instrumentation for assessment 80−95165
functional elements of spectroradiometer, accuracy optimisation in light and colour 79−12836
Funk net pyrradiometers for shipboard net radiation meas. 79−21055
general theory for wideband radiometers *(Russian)* 77−21926
heat transfer rate meas. by light fibre-photomultiplier combination 77−2658
heterodyne, high sensitivity, using diode laser, spectroscopy of ethylene 77−91300
heterodyne receiver, meas. of electron cyclotron emission from hot plasmas 79−90463
HF radiometer random process dynamic simulation models 79−80686
high-energy carbon arc, radiation loss measurement 77−7613
high-speed spectral radiometer with full electronic control *(German)* 79−54169
industrial precision filter radiometer development and applications 79−21814
instability effect of varistor frequency transducers on radiometer sensitivity, anal. *(Russian)* 77−22598
IR, distant-focused system, thin film thermal-profile meas. 77−169
IR, passbands for clear-air-turbulence detect. 78−96318
IR, thermopiles appl. 80−47104
IR, two-stage solid cryogen cooler development, orbital operation, spacecraft appl. 78−89040
IR and mm wave techniques, for Cosmic Background Explorer Satellite 78−49344
IR emission meas. of atm. and targets 78−4681
IR emissivity meas. method and equipment 79−35812
IR heterodyne, airborne dual-channel, for atm. meas. 78−57369
IR heterodyne radiometer for atmospheric temp. profiling 77−49200
IR heterodyne radiometer using tunable diode laser local oscillator 78−267
IR modulation radiometer using Zn-doped Si S-diode 78−4694
IR optical system input diffr. effects and use of spatial apodisation 78−79113
IR radiometer objective lens, optimal refr. index 78−29137
IR radiometer optical head thermostabilisation structure 78−86316
IR radiometer with pyroelectric radiation receptor 80−101842
IR radiometers, on Viking orbiters 78−20612
IR scanning radiometer data interpretation 79−30541
IR space sensors, low-background large-aperture, meas. facility for evaluation 79−21126
IR space sensors, low-background large-aperture, meas. facility for evaluation 79−21125
IR spectroradiometer, ground-based, for atm. vertical temp. profile meas. *(Japanese)* 77−29499
Josephson point contact detector, high-sensitivity, for 1.5 to 2 mm band, radioastronomical obs. appl. 78−4106
laser energy meas., by optical calorimetry, hollow graphite cone appl., absorption charact. *(Slovak)* 79−40572
laser intensity, chem. photooxygenation actinometric meas. 77−30193
laser power meas., radiometric and calorimetric scales' equivalence 77−7115
laser power meas., scale comparison for calorimeter and radiometer systems 79−76729
Limb Infrared Monitor of Stratosphere, radiometer spatial frequency response 79−101048
Limb Infrared Monitor of Stratosphere (LIMS) radiometer, design and performance, expt. goals 78−61601
liquid-scintillation vial system, biphasic, for radiometry, modifications 80−101253
low-temperature, with conical light pipe, IC manufacture appl. 80−47105
luminescence quantum counter comparator 79−49295
Meteosat imaging payload, functional aspects 78−36424
Meteosat spacecraft, elec./mech. configurations 78−36423
microwave, atmospheric water vapour studies at 22.235 GHz 80−72610
microwave, for indirect determ. of atmospheric boundary layer temp. profile 79−25369
microwave, gain stability improvement for remote sensing 79−25367
microwave, ground-based, regional precipitation meas. *(Chinese)* 79−84547
microwave, microprocessor-based signal processing unit 80−77874
microwave, multichannel scanning, for Nimbus-G and SeaSat-A 77−29625
microwave, passive, airborne imaging for soil moisture meas. 78−36310
microwave, rain attenuation measurement at X, K bands appl. 80−68254
microwave, stepped frequency, 4.5 to 7.2 GHz, airborne remote sensing 79−80062
microwave radiometer, on experimental oceanographic satellite Seasat-A 78−77455
radiometers continued
microwave radiometer blackbody calibration standard for MM wavelengths 80−269
microwave radiometer calibration standard with Brewster angle impedance matching 77−5918
microwave radiometers, ice movement measurement *(Danish)* 80−26624
microwave radiometry for avalanche victim detection 77−2652
millimeter-wave, airborne, multi-channel, dual frequency, high altitude obs. of atmospheric water vapour 79−80061
MM wavelength band, Josephson superconducting point contact as detector 80−21918
mm-wave imaging system 77−2271
modulation radiometer, limiting pulse noise *(Russian)* 77−67497
modulation radiometer, portable instrum. for SHF atmospheric sounding *(Russian)* 78−49159
modulation radiometer, two-channel, simultaneous meas. in 6 and 8 mm wave ranges *(Russian)* 77−29647
MTF shape effect on stratified layer microwave radiation detection 77−18069
multi-frequency microwave radiometer system for oceanography, performance evaluation 78−81417
multiband radiometer for field research 80−90250
multichannel, AGC using digital control *(Russian)* 77−26399
multichannel radiometer, programmable, for Earth remote sensing 80−77253
multichannel scanning, for spatially-resolved radiance measurements of short-duration rocket plumes 80−13164
multiple-filter, design, for solar radiation meas. 78−93004
multiple-frequency heterodyne correlation radiometer, min. detectable power 77−74508
multipurpose, history of development for thermal-vacuum testing at Johnson Space Center 80−90894
multipurpose, large thermal vacuum chambers, Johnson Space Centre 80−31875
narrow beam spectral radiometer for 4-14.5 μm atm. radiance meas. 78−61596
narrow-field radiometer response in quasi-isotropic atmosphere 80−90345
neutron, testing techniques standardisation, in Soviet Union 80−99405
nuclear multichannel, automatic channel separating system *(Russian)* 80−58094
null radiometer scheme for photodetector noise power spectrum density meas. 78−21197
ocean surface wind obs., SeaSat scatterometer/scanning radiometer/altimeter comparison 80−46249
optical baffling system for radiometric instruments 77−70888
with optical fibre as optical lens, principles and appl. 78−49828
optical sensor system simulation and evaluation 80−96030
optical sensor system simulation elements and techniques 79−76851
orthomode type mixer, radioastron. appls., 1.35 cm range 79−2817
passive microwave radiometers for remote sensing 77−56775
photoelectric radiation flux density meas. technique 78−89521
photoelectric transducers with astatic characteristics, statistical error determ. 78−93760
Pioneer Venus Orbiter radiometer (VORTEX) 80−67504
Pioneer Venus small probes net flux radiometer experiment 80−67512
Pioneer Venus Sounder Probe IR radiometer 80−67509
Pioneer Venus Sounder Probe Solar Flux Radiometer 80−67508
Pioneer-Venus large probe infrared radiometer optical system 78−81543
Pioneer-Venus large probe IR radiometer optical system 78−61715
planetary radiometers for space probes 77−49299
polarisation effects meas. using partially polarized light 79−49266
polarisation sensitive spectroradiometer, methods for overcoming refl. spectra meas. problems 79−40623
polarising radiometer, data reduction technique 77−78472
portable, with Cu_2S-CdS photo-cell, solar radiation meas. appl. 78−53763
PP-8 (USSR), monitoring of transmission electron microscope foil thinning by jet electropolishing 80−73525
pressure modulator radiometer for atm. gas emission meas. 78−81457
pyranometer, inclination depend. of sensitivity 80−8465
pyranometers for mesoscale solar irradiance network, test and calibration experience report 79−74499
pyrgeometer performance improvement 77−70860
pyrheliometers, solar aureole contribution to radiation meas. 77−2284
pyroelectric detectors appl., principle, materials and charact. *(Czech)* 79−40611
quasi-optical radiometer receiver design 78−8447
quasioptical superheterodyne radiometer for upper atmosphere 77−41241
radiation balance microwave thermograph for industrial and medical appls. 78−45621
radioastronomical, instability influence on meas. results, reduction by computer *(Russian)* 78−65506
radiometers, hemispherical soft dome net type, recirculating purging system 78−3984
rain attenuation measurement at microwave freq. compared with radar and distrometer results 79−62542
reference averaging radiometer using microprocessor 78−70176
relative spectral detector response meas., 350 to 1200 nm using monochromator based spectral comparator 79−67374
remote sensing, spectral reflectance, scene composition, instrument for simultaneous recording 78−81443
remote sensing of atmosphere, land and sea props. 78−93015
remote sensing of rivers and lakes, spectral response field meas. 77−78469
replicated light weight wave flats for scanning radiometer 78−66889
RNB-76 monitor for low energy beta-emitter contamination 79−36486
satellite IR radiometer, calibration 80−101440
satellite-borne IR scanning radiometer obs. of stratosphere, optimum field view and spacing 78−16201
scanning, improvement by digital reference averaging 79−35824
scanning radiometer images, electronic conversion to stereographic projection 79−21056
Seasat scanning multichannel microwave, calibration algorithm development 80−94682
Seasat scanning multichannel microwave, description and performance 80−94681
Seasat scanning multichannel microwave antenna pattern corrections 80−94683
SeaSat scanning multichannel microwave radiometer 80−46248
Seasat visible and IR radiometer 80−94687

radiometers continued
SEASAT-A satellite scanning multichannel microwave radiometer 77−5416
selective modulation radiometer for gaseous pollutant remote sensing *(French)* 78−20550
semiconductor radiometer-spectrometer for meas. of surface contamination by α-radioactive materials 77−38423
sensitivity normalisation 78−86335
six-channel for spectral investigations of terrestrial and planetary atmospheres *(Russian)* 77−29468
solar aureole almucantar radiance meas., comparison between photographic and photoelec. methods 78−77321
solar aureole radiometer for atmospheric aerosol studies 77−53240
solar radiation meas., field instrument calibration standard 78−88946
solar radiation measurement, survey 77−5348
solar spectral distribution monitoring, broadband filter radiometry error anal. 77−53163
spatial responsivity variations in absolute radiometers, instrumental corrections 79−97434
spectral radiometer for determ. of solar radiation spectral distrib. for solar cell appls. 80−61369
spectroradiometer, display colour meas. appl. 79−40605
spectroradiometer, lone wavelength Exotech model 20C, Earth resource remote sensing appl. 79−88474
spectroradiometer for airborne remote sensing 78−88943
spectroradiometer for reflectance measurements 80−56658
spectroradiometer for whole sky coverage *(French)* 77−53243
spectroradiometers, for atm. meas. 77−9568
spherical radiometer, theoretical anal. 80−62721
square-wave modulation radiometer limiting sensitivity formula correction *(Russian)* 78−58030
standard apparatus to measure the radiant thermal flux density 80−62674
stratospheric composition, IR meas. radiometer, H_2O vapour profile 79−8718
submillimetric wire grid array Fabry-Perot interferometers 77−37974
superconducting point contact, LF fluctuations, cond. and voltage *(Russian)* 77−20500
system design, mathematical modelling of relevant physical processes *(Rumanian)* 79−59313
temperature difference recording, heat radiation flux 78−49836
tethered float radiometer for US therapy equipment output power meas. 80−104691
thermal radiation detector design with uniform surface response 80−27345
thermal radiation sources, high-temp., for calibrating radiometers 80−17946
thermal receiver with temp. readout by laser beam 77−82605
thermal sighter-radiometer for temp. meas., signal drift compensation unit 79−35830
thermocouple output signal calc. for cylindrical receiver *(German)* 78−41305
thermopile type, for UV spectrum appl. *(Japanese)* 78−54422
thermovision system, AGA 680, calibration procedure to extend versatility 78−4680
TIROS N microwave sounder unit, blackbody calibration 78−93016
TIROS-N microwave sounder unit for global temp. distribution meas. 80−90265
UHF radiometer with superconducting detector 79−71526
underwater radiance scanner, design and implementation 78−61609
US elastic sphere radiometer, appl. to US intensity determ. 77−68342
UV, Spectroline DM series, UV appl. 80−77854
UV radiation meas. using ferrioxalate actinometer 80−41731
vane radiometers, elementary model 77−64901
visible and infrared imaging radiometers for ocean observations 78−69536
Visible and Infrared Radiometer evaluation from SeaSat-A surface temp. obs. 80−46325
visible IR spin-scan radiometer, fibre optics 78−59160
wide-band radiometer based on superconducting point contact, for short-wave millimetric radioastronomical obs. 79−96916
wide-band radiometer for short millimetre range wavelengths, based on superconducting point contact 79−62750
X-ray radiometric analyser, appl. of expt. planning 80−61186
GaAs injection photodiode IR radiometer 79−75597
GaAs single-cell, for artificial satellite measurement system 80−13147
Ge optical windows, contaminated by NH_3, CO_2, CO, HCl, methane, cryocooled, IR transmission 79−32007
InSb detector, liquid He cooled, radioastronomical appl. in 0.2-5 mm wavelength range 77−13241
Si detector based radiometer for measuring absolute spectral response of detectors 78−54461
Si radiometer for meas. of synchrotron flux from SURF II storage ring 80−90895
Si radiometer for storage ring synchrotron radiation 80−86411
Si ring photodiode reflectometer for cavity reflectance 80−86376
SiO_2, fused, filter in wide field-of-view SW radiometer for Earth radiation meas. 80−87473

radiometry
see also radiometers
3 mm wavelength scattering and emission characteristics of natural media 78−3770
9 GHz radiometry of tumours *(French)* 80−3767
20 and 30 GHz radiometer calibration using ATS-6 satellite beacons 77−74500
22.75 GHz microwave attenuation charcts. at high elevation *(Japanese)* 80−27346
absolute luminescence quantum yields, actinometric meas. 77−41691
aerial radiometric data modelling program 78−46237
airborne spectroradiometric data, and LANDSAT data, hydrothermal alteration mapping appl. 79−34973
asteroids, radiometric and polarimetric sizes and albedos, review 77−60708
atmosphere, ground-based radiometry in O_2 5 mm absorpt. band for temp. inversion detect. *(Russian)* 78−11963
atmosphere, IR system for radiating source meas. 77−70891
atmosphere boundary layer temp. profile determ. from ground-based 60 GHz radiometry *(German)* 80−82097
atmosphere ground-based radiometry, atmospheric variables spectra deduction 79−92567
radiometry continued
atmosphere parameters, retrieval from scanning multichannel microwave radiometer obs. 80−90261
atmosphere radiances meas. from TIROS-N processing for temp. sounding 80−77133
atmosphere temperature, impact of satellite sounding data on weather forecasts 80−77028
atmospheric boundary layer, vertical temp. profile determ. by ground-based microwave radiometry 79−79915
atmospheric constituents, spectral radiometric meas. 77−70883
atmospheric H_2O vapour and cloud liquid determ. by dual freq. ground-based microwave radiometry 78−93007
atmospheric noise measurement at 30 GHz, ATS-6 satellite link appl. *(Dutch)* 78−7742
atmospheric radiometry methods (Soc. Photo-Optical Instrum. Engrs., Proc. vol.91, San Diego, 26-27 Aug. 1976) 77−70880
atmospheric turbidity, skylight at South Pole station, Antarctica, polarising radiometer meas. 78−57320
atmospheric UV radiation detection, space appls. 77−70881
atmospheric water vapour, IR, clear air turbulence detect. 77−73890
atmospheric water vapour and liquid monitoring using radiometry at 21 and 32 GHz 80−26628
atmospheric water vapour and temperature profiles, ground-based microwave radiometric sensing 79−84392
automatic radiometric flaw detection with X-rays on series production parts *(German)* 80−21240
bidirectional reflectance and transmission for optical diffusers use in space projects 78−36438
biological systems, microwave radiometry applications 77−81770
biomedical temp. measurements, radiation balance microwave thermograph, simultaneous independent temp. and emissivity measurements 79−100692
broadband, using spectrally selective detectors 80−68255
BRV source, emission at 34 nm, absolute radiometric meas. 77−75636
calibrated imagery for thermography 77−40893
calibration, theory and methods 77−45878
Candela, radiometric definition appraisal *(German)* 78−32845
capillary porous body, drying, X-ray absorption obs., radiometry, temp. control 78−67023
cavity emissivity meas. in thermophysical investigation 78−74005
centimeter- and millimeter-wave thermography−a survey on tumor detection 79−100690
chemical actinometric measurement of absolute luminescence quantum yields 78−32892
chimney plume particulate and gaseous pollutant conc. and mass flow, IR radiometry 77−37393
cirrostratus clouds, IR emissivity meas. by remote sounding 80−82061
cloud microwave radiation emission meas. 80−17351
cloudy atm., long distance meas. by radiometry 80−90196
cloudy atmosphere moisture content determ., long-range, by thermal radioemission meas. *(Russian)* 79−5637
coherence and radiometry, basic concepts 78−66745
combined microwave heating and radiometry methods 80−85465
comparison of parametric data content of radiation beam 79−31342
computerised rapid-scan spectroscopy, at NAVWPNSUPPCEN Crane 78−41362
conformal applicators, therapeutic potential for hyperthermia induction 79−100696
contactless temp. meas. by EM radiation *(German)* 77−79099
continuous radiogauges, transient characteristics 79−31328
conversion factor to photometric data, international standard 78−86315
cylindrical gradient index lens and array radiometric props. 80−14421
defectoscope with feedback, charact. of operation 78−44321
density of materials on supply line, neutron radiometric inspection 80−21205
designations of photometric and radiometric equipment *(German)* 79−75570
development trends 77−61105
diffraction error reduction in radiometry by toothed apertures 79−9232
domestic coal, radiometric method for determ. of heating value, rel. to moisture content 78−20111
Earth's surface in presence of vegetation cover, microwave radiation spectra 80−68239
Earth resources survey sensor, calibration linear photodiode array, satellite appl. 80−56693
Earth surface, Heat Capacity Mapping Mission 79−5640
electro-optical technological, review 78−29140
electron optics, isoplanatic image formation 78−9312
electron optics, partially coherent sources, radiometric quantities 77−38797
emissivity, measurement for low temp. sources, flux double modulation method 78−45634
energy irradiance from pulsed source, curve fitting problems 77−71377
equipment for production line inspection 79−29320
433 Eros, thermal props. from radiometric and refl. light obs. 80−31231
far IR technology and applications, conf., Reston, USA, (Apr. 1977) 78−45711
far UV, comparison of standards, photodiodes, ion chambers and thermocouples 77−5912
far-IR heterodyne radiometric measurements with quasioptical Schottky diode mixers 78−77958
far-zone angular coherence and intensity calc. 78−8435
fibre lens, gradient index, radiometric props. 80−69481
fibre solid matter content radiometric meas. experience *(German)* 77−67488
finite planar sources of arbitrary coherence states, radiance function existence 79−50208
flat finite wave tank, three-dimensional vector modelling and restoration of meas. 77−22599
flat finite wave tank radiometric measurements, 3-dimensional vector modelling and restoration 77−17238
flaw-detector, performance evaluation and parameter choice for smoothing filter 79−15945
fluctuating sources and second-order radiometry 78−50879
flue gas dust monitoring *(German)* 77−29452
forest fire sources, microwave radiation spectra 80−52314
forest fire survey application of microwave radiometry 77−87127
fundamental quantities and partial coherence effects 80−77838
generalised radiance uniqueness theorem 78−94365
geophysical environment sensing by radiophysical methods *(Russian)* 77−78435

radiometry continued
glass, thin layer thermal conductivity meas., radiometric method 79−94475
ground mapping resolution accuracy of scanning radiometer from geostationary satellite 77−73858
heat flux transducer calibration *(Russian)* 77−82505
heterodyne correlation radiometry 78−77980
high power continuous laser emission meas. appls., pyroelectric ceramic appl. *(Russian)* 78−16845
incandescent lamp calibration for spectral irradiance by absolute radiometers 80−102788
inverse problem for scalar planar sources radiometry and coherence, book contrib. 79−31797
IR radiometric microscope technique for melt growth kinetics determ. 78−34453
IR technology fundamentals 77−61120
irradiance dynamic meas., using Kalman filter 77−5914
irradiance scales intercomparison, 90 to 250 nm wavelength range 80−98963
isotope radiometry, counting algorithm for information processing 78−44323
isotope radiometry, nonlinear information processing in random signal detection *(Russian)* 80−22428
Jupiter and satellites, IR obs. from (Voyager 1) 80−26790
Knudsen manometer based on radiometric forces 77−26320
lake ice, microwave radar and radiometric remote sensing meas. 80−85691
LANDSAT digital thematic maps, radiometric interpretive legend 77−78468
laser rangefinder radiometric efficiency, optomechanical tolerance analysis 79−21705
lock-in amplifier, for measurements when signal-to-noise ratio is less than unity 78−29134
material continuous monitoring, with fluctuating parameters, smoothing filter synthesis 77−90553
medical appls., radiation balance microwave thermograph 80−26315
microwave, for determination of cloud atmospheric parameters 80−67435
microwave, passive, remote sensing of Earth physical parameters, from satellite 79−80060
microwave, X-band, natural emission detection, biological, medical appl. 77−32949
microwave brightness temp. distrib. over Bay of Bengal using SAMIR Satellite Microwave Radiometer data at 19 and 22 GHz 80−104980
microwave brightness temperature measurements *(Danish)* 80−26625
microwave heating system for improving temperature uniformity in heated tissue 79−100795
microwave radiometric determ. of ocean surface wind speed during BESEX 77−29479
microwave radiometric methods and the problem of forest and peat fires 80−31877
microwave radiometry, advances generated by progress in mm-wave region 79−25366
microwave radiometry from satellites 77−70882
microwave radiometry in detect. of breast cancer 78−40384
microwave scanning radiometry, appls. 78−73551
microwave scanning radiometry, passive, for ocean surveillance 78−73550
microwave thermography: principles, methods and clinical applications 79−100691
microwave thermography, for breast cancer detection 79−29655
microwave thermography, principle and biomedical appls. *(French)* 80−30957
microwave thermography and local heating by same system, clinical applications 79−100695
MM wave, influence of atmosphere in 10 to 1000 GHz range 79−88465
MM wave radiometry conducted at Appleton Laboratory 80−67442
MM wave radiometry for atmospheric sounding 79−84551
MM wave sensors, conf., London (Apr. 1980) 80−67441
mm-wave thermography, application to breast cancer 79−100693
mobile testing laboratory PPLII-3 for ionizing radiation 79−74761
multiple graybody resolution from spectrally sampled optical systems 79−76615
multiplicative comparator of spectral radiances, systematic errors *(Japanese)* 78−29139
NDT flaw detector, relay-type with time delay signal smoothing, prob. anal. 77−81377
neutron absorption radiometric testing of materials, review 80−71860
nuclear materials, safeguards applications of far infrared radiometric techniques for the detection of contraband 80−83156
nuclear materials safeguards applications of far infrared radiometric techniques for the detection of contraband 80−73925
ocean, appl. of radio obs. of polar regions 78−81419
ocean, microwave radiometry appls. review 78−81415
ocean, microwave radiometry contribs. to large-scale oceanography 78−77337
ocean passive radiometry, radio meteorology colloquium, Victoria, British Columbia, Canada (1978 June 14 to 21) 80−46724
ocean surface, microwave radiometry remote sensing 80−36428
ocean surface parameters, retrieval from scanning multichannel microwave radiometer obs. 80−90261
ocean temp. and salinity meas. by microwave radiometry 78−81416
oceans remote sensing, utility of polarised visible radiation 79−5498
open-ended waveguide probe/applicator combination *(French)* 80−3820
optical coherence, review 80−48140
optical coherence applications, seminar, San Diego, CA, USA (Aug. 1979) 80−77542
optical radiation measurement, practical considerations, rel. to enforcement of Federal standards 77−38012
optical system aperture, effect on measurements in thermophysical research 80−17992
optimal relation between geometric charact. of flaw and radiator optical focus 79−34246
p-n junction, quantum efficiency as absolute radiometric standard 79−49284
Pacific Ocean, box cores from Ontong-Java Plateau, radiometric obs. 80−61793
partially coherent fields, generalised laws 77−2676
partially coherent fields, generalised radiant intensity 77−2677
passive microwave radiometry as a tool for investigating phase transitions 79−23729
radiometry continued
photochemistry appls. 79−49294
photodiode detector calibration using synchrotron radiation 80−90810
photoelectric spectrometer, drift correction procedure 78−29178
photometric radiation equivalent and meas. units *(German)* 79−54166
photophoretic spectroscopy, broadband 80−86469
photothermal radiometry, contact-free condensed matter anal., K_2SO_4 powder appl. 80−26088
pipe, transverse oscillation effect on measurement accuracy in radiometric inspection 79−34245
plant and soil monitoring, from tethered balloon, multispectral radiometry 78−3958
pyroelectric radiometry, optical calibration system 77−61106
quasihomogeneous planar source, coherence and radiometry 78−9421
radiation detector calibration in VUV, using wall-stabilised Ar cascade arc 79−80679
radiation standards for source spectral emission and detector spectral sensitivity 77−39007
radiation temperature, reflectivity, emissivity meas. of room temp. materials *(Chinese)* 80−101814
radioactive element conc. from γ-ray intensity meas., numerical method 79−18059
radioactive ores, effective γ-ray attenuation coeffs. 77−25680
radiochromic-based monitoring system 77−70264
radiometric flaw detectors, results of practical appl. 78−40004
radionuclide survey of USA, ERDA aerial radiometric and magnetic survey 78−12027
rain attenuation, radiometric determ. at millimetre wavelengths, multiple-scatt. effects metric determ. at millimetre wavelengths, multiple-scatt. effect 80−90260
rain attenuation at 10 and 11 GHz, radiometric measurements 80−67397
rain attenuation meas. on Earth-space paths at 37 GHz by passive radiometry 77−41109
rain attenuation on satellite-Earth path at 11.4 and 14 GHz by radiometric meas. *(French)* 78−49066
rainfall rate detect over ocean and land by spaceborne microwave radiometry 80−101423
Raman spectra, radiometric correction 80−90899
reference averaging techniques, algorithm to extend Dicke technique 77−74509
reference source radiation, temp. instability and compensation methods 79−14071
reflected sunlight polarisation, meas. from high-altitude balloon 78−61561
remote sensing and profiling of lower atmosphere using radiowaves, ground-based 80−56628
remote sensing of cloudy atmospheres by microwave radiometry *(Chinese)* 80−51549
remote sensing of ocean surface currents, recent progress 77−87114
remote sensing using solid-state linear array technology 80−4150
remote sounding of high clouds, visible and LR optical props. from lidar and radiometer meas. 80−82060
review, applied radiation *(Japanese)* 77−33984
Schottky diode concepts, heterodyne radiometry 78−45713
scintillation radiometric path automatic stabilisation 77−23372
sea ice, low-salinity, radiometer studies 78−81175
sea ice, microwave remote sensing in AIDJEX main expt. 78−81173
sea ice age category differentiation through location and temp. observations using microwaves 80−67380
sea ice in Arctic Basin, time depend. of ice conc. and multiyear ice fraction 78−81174
sea surface temp. meas. using IR radiometry and visible spectrometry 78−69535
sea surface temperature, Noaa 4 satellite and Aries airborne radiometer meas. comparison 79−62517
sea surface temperature, radiometric observations at 2.65 GHz, atmospheric and surface corrections, Chesapeake Bay 77−17114
sea temperature, microwave radiometric obs. at 2.65 GHz at Chesapeake Bay 77−29314
seawater, microwave freqs., improved model 77−17113
second order, radiant noise, coherence 78−287
seminar, optical radiation meas., San Diego, CA, USA (Aug. 1979) 80−86036
sensitometric sources, photometric and radiometric calibration, tutorial 77−34044
sensitometry, use of photographic film in radiometric meas. 78−269
SI unit proposition 78−93644
slot method, radiometric determ. of concentration profile during zone melting *(Czech)* 80−55289
snow, parameters investigation by radiometry in 3 to 60 mm wavelength region 80−72561
soil moisture content, microwave radiometer meas. over bare and vegetated surfaces, comparison 78−88851
soil moisture content measurement by microwave radiometry, review 80−17425
solar cell spectral response characterisation, 400 to 1000 nm 80−35675
solar constants, radiometric scales 77−78737
solar flux in Venus atmosphere, meas. by Pioneer Venus multiprobe mission radiometer expt. 79−48718
solar irradiance, multispectral measurements, atm. total ozone determ. 79−53401
solar radiation measurement requirements for energy conversion 79−57400
solar radiometry correction for diffuse atmospheric scatt. 79−80015
solar receiver radiative loss and eye hazard evaluation by Net-Radiometer 80−89673
spectral irradiance scale, 1973 NBS standard 77−83942
spectral radiance calibrations, 165-300 nm, interlab. comparison 77−74478
spectroradiometry, principles *(Japanese)* 78−4678
spectroradiometry automation and applications 78−12740
spectroradiometry of daylight at sea level in Durban. 79−100955
specular reflection, use for radiation thermometry *(Japanese)* 80−101795
standards development, calibration 79−6161
statistical image anal., 3 parameter probability distrib. density function 80−43266
steel, stainless, thin layer thermal conductivity meas., radiometric method 79−94475

radiometry continued
steel articles thickness and continuity monitoring by neutron radiometry 79−93100
stratosphere, radiometry and spectroscopy from aircraft 77−70890
stratosphere observations with balloons 80−85763
submillimetre wave mixers, review 78−45712
surface temperature meas., emissivity effect elimination 77−5840
suspensions, colloidal, radiometric method for particulate processes characterisation, theory 80−45578
synchrotron radiation as an absolute standard source 80−90879
system design, mathematical modelling of relevant physical processes *(Rumanian)* 79−59313
telemetry, automation of information input and processing 77−78429
temperature measurement of object using IR radiometer 77−57326
terminology and units 77−61108
terrestrial surface temperature sensing, emissivity correction for thermal radiation interpretation 80−82092
thematic mapper, time-delay and integration CCD imager appl. 79−35098
thermal radiation, coherence recognition 77−74505
thermal radio emission from inhomogeneous medium 79−80667
thermal radio emission polarimetry, loss matrix 79−21069
thermography, mm-wave, head and neck diseases, preliminary findings 79−100694
thunderstorms, microwave radiometric detect. of corona from chaff 78−16106
total luminous flux meas. on radiometric base, goniophotometer 80−42250
transfer standard radiometric sources and detectors, calibration using synchrotron radiation 78−65967
transfer standards calibration in UV and VUV by electron synchrotron radiation 79−12847
tritium water, small samples, radiometry with gas-flow counter 80−17989
troposphere, IR fluxes meas. by radiometric soundings, parametric law derivation *(French)* 79−25358
units, new candela and lumen definitions 79−6162
upper atmosphere, constituents detection, using submillimetre wave heterodyne radiometry 78−49183
upper atmosphere, irregular motions from radiometric meas. *(Russian)* 78−96333
UV radiation meas. using ferrioxalate actinometer 80−41731
UV radiometric standards 79−49193
UV radiometric standards at NBS 77−38011
vacuum UV, Ar mini-arc as spectral radiance secondary standard 77−34921
vacuum UV radiation scales, plasma blackbody lines and synchrotron radiation 78−1309
Venus middle atmosphere, IR remote sounding from Pioneer orbiter 79−48712
wideband acousto-optic radiometry 78−77983
X-ray radiometric fluorescence analysis using Ge detector 77−52701
X-ray radiometric methods applic. in geochem. haloes analysis 77−53231
yeast cells in suspension, vacuole detect. by transmittance radiometry 80−26418
zenith brightness radiometry, absorption altitude profile determ. at 2.53 mm 77−81979
K determ. in NPK and GVM fertilisers *(Czech)* 80−22427
Pu in irradiated reactor fuel, microamounts meas. by radiometric method *(Czech)* 77−42111
SO_2 molecules in air, remote sensing methods assessment using mm-waves *(Japanese)* 78−96288
n-Si, hot-electron diffusion noise, meas. using radiometric method in X-band region 77−39905
Si photodiode internal quantum efficiency basis for absolute radiometric standard 80−86410
Si, photovoltaic cell, absolute spectral sensitivity calibration, radiometry, photometry *(Chinese)* 80−86367
p-Si:P semiconductor detector in radiometric inspection problems 80−62819
U at Oklo natural fission reactors, radiometric meas. and isotopic anal. *(French)* 80−21754
U content determ. using liquid scintillation spectroms. *(Czech)* 78−69487
U, National Uranium Resource Evaluation (NURE) aerial radiometric survey data interpretation via principal components anal. 80−101438
W incandescent lamp, thermostatic control 79−36970

radiometry, ultraviolet *see photometry*

radionavigation
see also radio direction-finding
communication satellites, orbital perturbation and stationkeeping, literature survey 78−89039
Global Positioning System, computationally efficient modelling for long-term prediction of orbits 79−80198
Global Positioning System NAVSTAR connection to World geodetic system of DOD 79−25378
gravimetric estimation technique using FFT 79−25376
inertial navigation system, error analysis using spatial Gauss-Markov models of ocean currents 80−36411
interferometric systems appls. in spacecraft guidance, geodesy, satellite navigation 79−25375
Loran signal comparator at Kagoshima Space Center *(Japanese)* 77−73963
Loran-C, progress report update 77−70875
Loran-C signal, ground wave propag. theory 80−94580
Loran-C systems, propagation in polar regions, full wave analysis 78−7834
marine and hydrographic surveys appl., available systems survey, modes and accuracy 80−36408
Mini Range III positioning system, meas. range improvements, technical details and characts. *(Italian)* 80−56611
NAVSTAR, satellite Global Positioning System 79−101042
NAVSTAR, satellite navigation system 78−61711
Navstar global positioning system, meteorological appl. 80−17396
NAVSTAR Global Positioning System, sea trials results 80−12645
NAVSTAR Global Positioning System satellite clock, H maser design 78−58969
NAVSTAR Global Positioning System satellites Doppler meas., geodetic solutions accuracy 79−100803

radionavigation continued
NAVSTAR satellite system plans 77−70978
Navstar system for US satellite survey *(Norwegian)* 79−62723
Navy navigation satellite system TRANSIT, on-board computer 79−29978
NTS-1, propagation effects near mag. equator 78−7839
ocean dumping surveillance and data recording system 77−5247
oceanographic research problems *(Russian)* 80−17286
offshore surveys, accurate positioning at distances to 400 km 80−12328
OMEGA, polar region ionospheric disturbance, propagation effects 78−7835
Omega system, hydrophysical research appls. *(Russian)* 80−17418
plasmaspheric time delay effects, observations, satellite navigation appl. 78−7831
position location and navigation, conf., San Diego, CA, USA, Nov. (1978) 79−25374
radio methods, quasi-single freq. Doppler-Faraday technique 80−77128
satellite navigation systems, ionospheric and plasmaspheric effects 77−82100
satellite onboard orbit determ., algorithm 79−25450
satellite solar cell power plant, operating experience 80−94055
time deviation and prediction error for clock specification 79−21719
transionospheric radio signal time delay spatial correlation 78−45117
TRANSIT Navigation satellite, phase fluctuation and ionospheric irregularities observations 78−7832
VLF nighttime propagation anomalies, obs. at 10.2 and 13.6 kHz 78−28414

radios *see radio receivers*

radiosondes
see also meteorological instruments
actinometric radiosondes comparison during GATE-74 period 79−29906
atmospheric turbulence, radiosonde meas. and spectral anal. of LOS fading 80−56568
BASORA secondary radar, sounding ballon tracking appl. 80−17357
cloud altitude measurements 79−88444
free air press. estimation from radio sonde data 79−88508
intracranial pressure monitoring by passive radiosonde 79−57798
meteorological instruments development in Finland, by Vaisala Oy manufacturer 79−12310
precipitation forecasts using a single radiosonde 79−88397
propagation research appl., computerised data analysis 79−2350
radio meteorology in Switzerland *(French)* 79−25319
radio refractive index variations over Arabian Sea during MONEX 1973 77−2281
systematic temperature sensing anomalies 79−70864
tropical constant-level balloon system 80−17395
troposphere, radio refr. index and potential refr. index, S.England 79−34928
UK Mark 3, brief introduction 79−84548
windfinding, NCAR aircraft dropwindsonde system 80−17393

radiosources (astronomical)
see also BL Lacertae-type objects; pulsars; quasars
5 GHz galactic plane sources, catalogue 80−4269
6 cm sources, survey by Westerbork Synthesis Radio Telescope, data 79−88604
6 cm survey with WSRT, analysis 79−75287
10 MHz sources, map of northern sky 77−13485
30 MHz all-sky map, galactic features study 79−21469
0406+121, optical spectra 4950-7950 Å, of possible BL Lacertae object 80−51895
0816+526, cD galaxy, classical double source, 4885 MHz obs. 80−109545
0816+526, classical double source in direction of rich galaxy cluster, interferometric obs. 78−57662
0915+320, wide-angle-tail radio source in group of galaxies, 4.9 GHz map 78−93441
1159+583, wide-angle tailed radio galaxy, radio obs. and models 80−31352
1232+414, classical double source in direction of rich galaxy cluster, interferometric obs. 78−57662
1308+32, BL Lacertae object, rapid optical outburst, 1980 June to July 80−98733
1401−33, radio structure and spectrum 77−29942
1610−771, radio QSO with steep optical spectrum, obs. 80−94887
1909+048 (Stephenson-Sanduleak 433), new type of radio star, possibly supernova stellar remnant 79−17117
2033+59, appl. of Clean and Restore technique to Northern Cross radiotelescope obs. *(Italian)* 80−98563
8550 MHz sky survey, appl. of computer data processing techniques 77−17708
HR 1099, RS Canum Venaticorum type binary, light and colour curve meas. 80−73004
2 A 1052+606, X-ray and optical variability of RS CVn star 80−31331
Abell 1367 central region, peculiar radio sources Westerbork obs. 79−2574
Abell 2029 galaxy cluster, radio and SAS 3 X-ray obs. 80−82519
Abell 2218, complex radiosource in centre, 2.7 GHz obs. 79−30137
Abell 2256, X-ray cluster of galaxies, radio props. 80−36726
Abell 2634, radiosources around 3C 465, continuum maps 78−73764
Abell 401, X-ray cluster of galaxies, radio emission distrib. 80−98731
Abell 478, cluster of galaxies, X-ray and radio obs. 78−8133
Abell 754, cluster of galaxies, radio sources obs. 79−25737
Abell cluster, lunar occultation obs. at 327 MHz, survey 80−73052
Abell clusters, search for radio sources 78−12379
Abell clusters of galaxies, complex radio sources obs. at 2.7 GHz 79−92881
Abell clusters of galaxies, interferometric obs. of radiosources 78−4380
in Abell clusters of galaxies, spectra and optical identification, SHF obs. 80−98729
Abell clusters of galaxies, Westerbork 610 MHz survey of extended radio emission 80−36727
Abell clusters of galaxies, Westerbork obs. of fields 78−96549
absolute flux density scale in 10-180 MHz range 78−28814
acceleration processes in extended extragalactic sources 79−101210
accretion disk model, gas flow above alpha disk 80−62161
accurate optical positions 77−29943
active galaxies, forbidden lines theory 78−93408
active radio galaxies, dust lane origin, explosion model 79−62910
activity, scheme for quasars, radio galaxies, N galaxies and Seyferts 77−45541

radiosources continued
AFGL IR sources, mol. line obs. 80−51856
angular broadening of distant compact radio sources seen through ionized gas in rich clusters of galaxies 79−35380
angular diameter-redshift relation for scintillating sources 78−28824
angular diameters of H II regions, meas. errors 79−12534
angular size-flux density relation rel. to evolution 78−28822
angular sizes and cosmological tests 78−28821
angular struct. determ., lunar occultation technique 77−13249
angular structure, investigation via lunar occultations, resolving power 78−65712
anticorrelation rel. to dark intergalactic matter in galactic haloes 79−2567
AO 0235, mapping with uncalibrated visibility data, 5011 MHz obs. 80−77295
AO 0235+164, BL Lacertae object, possible correlated optical-radio outburst 80−56924
AO 0235+164, nonthermal emission spectral break development 77−57092
R Aquarii, Mira variable, 14.9 GHz obs. 79−75210
R Aquarii, UV, visible and 85 GHz continuum obs. 80−85946
R Aquilae Mira variable, 14.9 GHz obs. 79−75210
arc-like source, H radio recombination line obs. of galactic centre 80−82498
UX Arietis, binary star, radio obs. 77−64793
UX Arietis, RS Canum Venaticorum binary, two-freq. radio polarimetry 79−21335
AS 501, compact H II region, OH main-line maser emission obs. 80−67716
astometric determinations using VLBI *(Japanese)* 80−21930
astrometric catalogues 80−105180
astrometry, precise, positions meas. on 35 km baseline 78−16551
astrometry, VLBI response freq. technique *(Russian)* 77−22093
astrometry using differential VLBI, accuracy estimation *(Russian)* 77−22091
B2 0055+26 (NGC 326), radio galaxy with precessing beam model 79−17118
B2 1308+326, optical and IR variability during 1978 outburst 80−51888
B2 1502+28, head-tail galaxy in Abell 2022, Westerbork obs. of spectral index and polarisation distrib. 80−36727
B2 1506+34, peculiar radiogalaxy, H I absorption detection 78−54048
B2 catalogue radio sources, optical identifications and 5 GHz flux meas. 79−40283
B2 catalogue sources, high resolution obs. at 408 MHz 77−45589
B2 quasars, radio spectral props. 79−44632
B2 radiogalaxies of low luminosity, polarization at 1.4 GHz 79−71141
B2 source counts and isotropy of faint sources 80−105374
B2 sources assoc. with elliptical galaxies, orientation 80−77501
B 0844+31, extended radio galaxy, multifreq. obs. 80−56963
B 35, bright rimmed molecular cloud, CH obs. 80−62238
B-type stars embedded in R-associations, free-free emission obs. 80−26851
background sources, Westerbork survey, angular size distrib. and source count 78−96553
Be stars, radio meas. set to circumstellar shells charact. 79−84809
Becklin-Neugebauer source in Orion, high resolution 1.5 to 5 micron spectroscopy 78−93368
big bang cosmology, evidence from radiosource obs. 77−2503
black hole explosions, upper limit of radio pulse emission rate 77−87469
black holes, theory of radio detect. of explosions 77−53622
Bologna survey at 408 MHz, statistical analysis 78−28816
bright galaxies, Arecibo 2380 MHz, survey 78−57470
bright galaxy nuclei, optical and radio survey, sample selection and obs. 80−73039
brightness distribution, determ. via phaseless aperture synthesis 78−32353
burst correlated with gamma-ray event 77−33668
bursting sources, search for 2-60 keV emission 80−17679
3C111, new very large radioenergy source in core of radio galaxy *(German)* 78−16558
5C1 sources, optical identification by photographic photometry and spectra 80−77503
3C273, HEAO 1 (A4) obs. of 13-120 keV X-rays 79−44633
3C273, spectroscopic obs. and redshift of associated galaxy 78−77606
5C2 survey revised distances of optical objects from radiosources 78−57472
5C3 sources, optical idents., spectroscopic results 80−46689
5C4 survey, search for optical identifications 78−73767
5C9 survey of radiosources, 214 objects 78−16312
4C+36.11, extragalactic source, Faraday rot. in S232 rel. to mag. field strength 80−51840
3C 105, struct. and identification with galaxy 79−35413
3C 10, 3C 58, H I distrib. small scale struct. 78−45383
3C 10, Tycho's SNR, 10.7 GHz obs. 79−75264
3C 10 (Tycho's SNR), distance, Westerbork H I obs. 80−101633
3C 111, 3C 236, radio galaxies, 150 GHz obs. 80−41908
3C 111, optical and radio positions 79−48948
3C 111, radio galaxy, obs. at 1.38 cm wavelength with resolutions up to 8″ *(Russian)* 80−109558
3C 111, radio nucleus struct. 77−5581
3C 111, spectrum and redshift of luminous N-type galaxy 77−33666
3C 120, emission-line nebulosity morphology 79−80363
3 C 120, galaxy and nucleus, UBV photoelectric obs. 79−44601
3C 120, radio galaxy, linear polarisation and flux density vars. 77−9805
3C 120, radio galaxy, vars. in optical spectrum *(Russian)* 80−90540
3C 120, Seyfert galaxy, IUE and visual spectrophotometry 79−92856
3C 120, Seyfert galaxy, spectrophotometric obs. of assoc. nebulosity 80−67890
3C 120, Seyfert galaxy, X-ray emission detect. 77−78890
3C 120, Seyfert galaxy nuclei, optical variability, UBV obs. 80−73049
3C 123, OH 18 cm lines obs. 78−4318
3C 129, orbital dynamics of head-tail radio galaxy around nearby supergiant galaxy 78−49518
3C 129 and 129.1, in situ particle accel. and energy supply 80−46691
4C 13.17A, B, in X-ray cluster of galaxies Abell 401, radio emission distrib. 80−98731
3C 132, 3C 192, radio galaxies, study of bridges metre and centimetre wavelengths 77−91658
3C 178, H I absorption within radiogalaxy 79−5910
5 C 1 to 5 survey areas sources, 1421 MHz obs. 79−84864

radiosources continued
3C 219, double radio galaxy, high-resolution 80−77500
3C 225.0, UHF and EHF obs. of foreground cold diffuse cloud 80−105311
3C 227 and 382 radiogalaxies, spectral-flux distrib. in 0.36-3.5 μ range 78−36710
3C 236, high resolution VLBI obs. of compact central component 79−92878
3C 236, radio galaxy, 6-49 cm obs. of double source 80−82528
3C 236, VLA obs. of extended radio core of giant radiogalaxy 79−75288
3C 264 (NGC 3862), radio galaxy, high resolution radio maps 77−5582
3C 270.1 and 3C 275.1, radio maps at 15 GHz 78−93452
3C 273, 345 and 454.3, D2 quasars, alignment of radio structure and magnetic field 79−12540
3C 273, field, QSO-galaxy group assoc. 80−105385
3C 273, high-resolution obs. at 1.35 cm wavelength *(Russian)* 78−69902
3C 273, quasar containing dust, IR spectra obs. 80−56970
3C 273 B, small-scale structure and variability, 2.8 cm obs. 77−33672
3C 279, interplanetary scintillations and solar wind vel., SHF obs. *(Russian)* 80−77248
3C 279, superluminal expansion 79−53922
3C 27 area sources, 2695 MHz continuum obs. 80−46688
3C 285, 3C 265, 3C 390.3, optical emission in radio lobes 78−57630
3C 285, double radio galaxy, discovery of optical emission in radio lobes 77−64866
3C 288, complex extragalactic radio source, radio brightness distrib. model 80−90558
4C 29.03, towards M33, H I 21 cm emission/absorpt. obs. 80−62262
3C 293, radio galaxy, radio and optical obs. 78−93418
3C 303, double radiosource, radio struct. and optical field 78−16519
3C 303, QSO group in cluster, gravit. lens effect 77−78878
3C 310, 326, relaxed double radio sources, implications of fine scale struct. 80−51891
3C 310, extended radio galaxy, multifreq. obs. 80−51890
3C 315, radio galaxy, high resolution radio maps 77−5582
3C 318.1 (NGC 5920), poor cluster cD galaxy, extended X-ray emission obs. 80−51884
3C 319, radio struct. and optical identification with elliptical galaxy 80−31377
3C 31, radio galaxy, mag. field struct. in radio jets 80−82526
3 C 31, radio jet brightness and shape rel. to beam and slingshot models 79−25741
3C 31 (NGC 383), dynamical interpretation of radio jet, galaxy interactions 79−9020
4C 32.69, quasar with radio jet, high resolution radio obs. 80−105375
3C 326, very large radio galaxy, multifreq. obs. 78−28810
4C 33.56, search for radio emission bridge to Stephan's Quintet 77−57099
3C 33, 98, 184.1 and 218, rotation axes 80−26997
3C 33, optical emission detect. in SW radio lobe 78−57665
3C 33, optical line emission rel. to physical conditions in compact head 80−51892
3C 33, rot. axis. of assoc. optical galaxy 78−4355
3C 33 and 327, double radiogalaxies, spectrophotometry 78−54066
3C 345, 418, 371, compact radio sources, arcsecond struct. 80−4450
3C 345, high-resolution obs. at 1.35 cm wavelength *(Russian)* 78−69902
3C 345, quasar, compact radiosource obs. 78−12399
3C 345, quasar, VLBI obs. at 1.67 GHz 80−94885
3C 345 and NRAO 512, relative position to submilliarcsecond accuracy via VLBI 80−22097
3C 382, 3C 386, radio galaxies, two-freq. high resolution obs. 78−86031
3C 388, galaxy in Abell 643, classical double source, 4885 MHz obs. 80−109545
3C 390.3, 3C 273, 3C 111, 3C 129, extragalactic sources, search for hard X-ray emission 77−29939
4C 39.04, powerful giant radio galaxy, multifreq. obs. 80−17682
4C 39.11, N galaxy, radio and optical obs. 78−16553
3C 391, supernova remnant, obs. at 1.4 and 10.7 GHz 80−4417
4 C 39.25, compact radio source, search for time-depend. radio fine struct. 80−90552
4C 39.25, quasar, compact radiosource obs. 78−12399
3C 395, compact radio source, high resolution obs. at 1671 MHz 80−56960
4C 39-08, appl. of Clean and Restore technique to WSRT obs. *(Italian)* 80−98563
3C 405 (Cygnus A), radio galaxy, obs. at 1.38 cm wavelength with resolutions up to 8″ *(Russian)* 80−109558
3C 449, radio jet structure at 1465 and 4885 MHz 80−12823
3C 452, spectral index variation 77−82309
3C 454.3, flat-spectrum source, variability at 962 MHz 77−82317
3C 465, extended radio galaxy, multifrequency UHF and SHF obs. 80−105338
4C 47.51, complex radiogalaxy, aperture synthesis obs. 80−94883
3C 48, 3C 273, 3C 295, scintillation at 25 MHz rel. to ang. struct. 78−65711
3C 48, interplanetary scintillations obs. rel. to solar wind plasma irregularities anisotropic struct. 80−67489
4C 53.37 (1638+538), tailed radiogalaxy, dual curved jets 80−62265
3C 58, Crab-type supernova remnant, comparison of optical and radio emission 80−73023
3C 58, optical remnant of SN 1181 discovered 78−65678
3C 58, spectra of faint knots in SNR 78−93375
3C 58, supernova remnant, soft X-ray flux upper limits 80−56915
3C 58 (SN 1181), discovery of optical counterpart 78−32546
3C 58 (SN 1181), plerionic supernova remnant, supernova absolute magnitude and type classification 80−56862
3C 61.1, 3C 33, 1.4 GHz aperture synthesis obs. of circular polarisation 77−29656
4 C 61.20, optically active extragalactic radiosource 77−17712
3C 6.1, 265 and 352, spectrophotometry of high-redshift radio galaxies 79−92876
5C 6 survey, optical identifications 79−48949
5C 6 survey of 292 radiosources 78−24471
4C 73.08, multifreq. obs. of giant source assoc. with compact Zwicky galaxy 79−25745
5C 7 survey, optical identifications 79−67111
5C 7 survey of 271 radiosources 78−24471
3C 84, high-resolution obs. at 1.35 cm wavelength *(Russian)* 78−69902

radiosources continued
3C 84 (NGC 1275), Seyfert galaxy, search for variability at 408 MHz *(Russian)* 77−17710
3C 84 (Perseus A, NGC 1275), Seyfert galaxy, 5′ halo SHF obs. 80−105372
3C 98, 3C 178, 3C 192, 3C 327, narrow-line radio galaxies, optical spectra 77−33664
4C −05.93, properties and relevance to spectrum of PHL 5200 QSO 79−88760
5C areas, optical identifications 77−37665
3C catalogue faint red QSO candidates, spectrophotometry and red shifts 80−67897
3C quasars, depolarization parameter and H II mass 79−35420
4C radio galaxies, structs. and optical identifications 79−71137
4C radio sources in Abell clusters, struct. and props. in declination ranges 10 to 20° and >50° 79−25743
4C radiosources, search for variable quasars by image tube photography 77−22326
4C radiosources clustering, statistical analysis 79−5761
4C radiosources clustering 78−96556
3C sources, lunar occultation obs. at 327 MHz 77−45588
4C sources, optical identifications 77−26077
3C sources, possible giant radio structure discovery at 11 cm 80−67895
4C sources, radio brightness and polarisation distrib. 77−26076
5C sources, spectrographic obs. of optical counterparts 79−101212
3C sources, systematic optical identification 78−36709
4C sources $20° < \delta < 40°$, 318 MHz flux density meas. 79−71140
4C sources between declinations 20° and 40°, samples 80−73057
4C sources in Abell clusters of galaxies 79−88756
4C sources in Zwicky clusters of galaxies, pencil beam and interferometer obs. 79−9019
4C sources in Zwicky galaxy clusters, detailed interferometer obs. and anal. 80−22099
4C sources with steep radio spectra, Westerbork obs. 79−35414
6C survey at 151 MHz, prospects 78−28813
CA 0340−538, rich cluster of galaxies, X-ray emission 77−5599
calibration sources, flux density at 8420 MHz rel. to Virgo A 80−86004
calibration sources, precision flux-density meas. at 2295 MHz 77−37663
Cancer cluster, Westerbork survey at 610 MHz 80−67884
Canes Venatici I galaxy group, neutral H obs. of NGC 4136, 4144, 4190, IC 4182 and (DDO 133) 79−84853
VY Canis Majoris, OH and H_2O microwave maser emission obs. 78−53949
VY Canis Majoris, OH masers very long baseline interferometric obs. 78−36712
VY Canis Majoris, OH/IR star, 1612 MHz OH maser multibaseline VLBI obs. 80−12766
YZ Canis Minoris, red dwarf star, weak radio flares interferometric obs. 78−65633
RS Canum Venaticorum, radio flare obs., (1979, February 6) 79−40220
RS Canum Venaticorum binary stars, introduction to series of papers 79−21329
RS Canum Venaticorum binary stars, mag. starspot model for photometric and spectroscopic behaviour 80−109488
RS Canum Venaticorum binary stars, radio luminosities and spectra 79−21333
RS Canum Venaticorum stars, Hα line variability, visible spectra obs. 80−105277
RS Canum Venaticorum systems, candidate list for southern HD stars 80−4395
RS Canum Venaticorum systems, X-ray obs. and coronal model development 80−56873
Carina I and II H II regions, far IR obs. 79−25657
Cassiopeia, A, weak X-ray source, ANS meas. 80−46701
Cassiopeia A, ^{14}N radioemission at 26 MHz 80−41886
Cassiopeia A, absolute radio spectrum 78−8090
Cassiopeia A, diffraction of radiowaves by artificial ionospheric irregularities *(Russian)* 77−29552
Cassiopeia A, foreground interstellar HCN absorpt. obs. 80−101624
Cassiopeia A, HF obs. using interference-excising correlator 79−75110
Cassiopeia A, intensity and polarisation at 9 mm wavelength 80−36732
Cassiopeia A, numerical model of SNR 80−12790
Cassiopeia A, possible binary pulsar 80−56868
Cassiopeia A, proper motions and temporal flux changes of compact features 77−60818
Cassiopeia A, radio emission evolution, freq. dependence *(Russian)* 78−4387
Cassiopeia A, radio emission evolution 79−67074
Cassiopeia A, radio spectrum evolution 79−30104
Cassiopeia A, radio spectrum rel. to cosmic ray electrons spectrum and diffusion 79−53677
Cassiopeia A, secular decrease in 927 MHz flux, radio flux density obs. 80−67840
Cassiopeia A, secular decrease in radio emission flux density at 437 and 510 MHz *(Russian)* 80−8702
Cassiopeia A, spectral intensity variations *(Russian)* 77−91661
Cassiopeia A, supernova remnant, 927 MHz emission secular decrease 79−75255
Cassiopeia A, supernova remnant, anal. of motion of details in thin shell model *(Russian)* 80−56920
Cassiopeia A, supernova remnant, continuous particle injection model for radio flux var. 77−13426
Cassiopeia A, supernova remnant, explanation of secular flattening of radio spectrum 80−101637
Cassiopeia A, supernova remnant, flux density meas. and confirmation of 38 MHz anomaly 77−45531
Cassiopeia A, supernova remnant, progenitor evolution involving supergiant mass loss 78−36623
Cassiopeia A, supernova remnant, search for X-ray line emission 78−57607
Cassiopeia A, supernova remnant, statistical particle accel. models 78−57606
Cassiopeia A, young SNR, radio emission evolution according to observational data 79−75256
Cassiopeia A direction, OH and formaldehyde absorpt. obs. 78−45381
Cassiopeia A historical records 80−77430
Cassiopeia A supernova remnant, abundance inhomogeneities 80−12797
V509 Cassiopeiae (HR 8752), no emission at Hβ (1979 July 31) 79−92782
V509 Cassiopeiae (HR 8752), spectrum variable supergiant, Hα emission obs. 79−88672

radiosources continued
Cassiopeiae A, supernova remnant, historical records 80−72792
Cassiopeiae A, supernova remnant, mag. field origin 80−85989
Cassiopeid A used to study ionosphere inhomogeneities 80−36454
catalogue of 347 sources obs. at 610 MHz, source parameters, identifications 78−40838
catalogue of positions, reference sources 80−105176
cD and related galaxies in poor clusters, pencil beam obs. of radio emission at 6 cm 80−62293
cD galaxies and related objects in poor clusters, 1400 MHz pencil beam obs. 80−62263
celestial masers physics, review 79−21455
celestral, resolution using VLBI *(Japanese)* 80−26754
Centaurus A, gamma-ray emission from Penrose powered black hole 80−56925
Centaurus A, giant quasiperiodic mm wavelength bursts in nucleus 79−48928
Centaurus A, NGC 5128, stellar population and dust lane 78−20890
Centaurus A, nuclear γ-rays detect. 77−13482
Centaurus A, nuclear gamma-ray lines, origin in relativistic plasma 80−41890
Centaurus A, X-ray struct., radio-lobe energy source evidence 80−26978
Centaurus A, X-ray variability, OSO-8 obs. 78−41082
Centaurus A (NGC 5128), dark lane, extended 10 μ emission 79−21429
Centaurus A (NGC 5128), detect. of X-ray emission from giant radio lobes 78−41055
Centaurus A (NGC 5128), fast var. of nucleus at 13.5 mm wavelength 77−87564
Centaurus A (NGC 5128), high-resolution spectroscopy and tubelike model of dust band 80−56945
Centaurus A (NGC 5128), nucleus, radio and X-ray variability model 80−90522
Centaurus A (NGC 5128), optical struct., picture processing anal. 79−53907
Centaurus A (NGC 5128), radio and X-ray var. of nucleus 78−36711
Centaurus A (NGC 5128), radio galaxy, obs. at 1.38 cm wavelength with resolutions up to 8″ *(Russian)* 80−109558
Centaurus A (NGC 5128), slowly varying flux component, 22 GHz confirmation 80−56939
Centaurus A (NGC 5128), struct. and evolution from multicolour photography 79−53913
Centaurus A (NGC 5128), X-ray and gamma-ray lines prod. by nonthermal ions 78−36725
Centaurus A as source of ultra-high energy cosmic rays 78−61941
Cepheus IV star formation region, continuum and recomb. lines, SHF obs. 80−90501
Cepheus OB3 association molecular cloud, mol. obs. rel. to star form. 80−12798
o Ceti (Mira), variable 2.6 mm CO emission obs. 78−12241
Circinus galaxy, optical and radio obs. 77−41409
Circinus X-1, changes in optical, IR and radio emission 80−67910
Circinus X-1, distance from H I absorpt. obs. 78−12413
Circinus X-1, nature and binary star model 79−75296
Circinus X-1, radio flare phenomena Dec. 1979 and Jan. 1980 obs. 80−36731
Circinus X-1 (3U 1516−56), obs. of optical and radio counterpart 78−12414
circumstellar masers, assoc. with IR objects and compact dust-bounded H II regions 77−26032
CIT 6 (IRC+30219), IR C star, CO obs. of mass outflow 80−12761
CL4, optical counterpart accurate position 79−17116
CL 4, H I absorption from compact source 79−48944
CL 4, H I emission-absorption meas. at 1420 MHz 79−62922
CL 4, high-resolution 8450 MHz obs. of compact radiosource 79−44629
CL 4, optical detect. 79−71138
CL 4, optical identification and optical position 79−21453
close binary stars, radio survey at 6 cm wavelength 78−32510
clustering, statistical analysis of source surveys 78−28818
clustering of extragalactic radiosources, power spectrum anal. of Parkes and Bologna catalogues 77−60838
clustering of extragalactic radiosources, power spectrum anal. of 5C surveys 77−60839
clustering test in 0.16 sr of 6C survey 79−71145
clusters of galaxies, H I broad band emission search 80−46667
in clusters of galaxies, interferometer obs. 77−53693
clusters of galaxies, intracluster gas heating by relativistic electrons rel. to X-ray and radio emission 78−57655
clusters of galaxies, props. of radio sources 78−12398
clusters of galaxies, radio and X-ray emission, review 77−64862
in clusters of galaxies, review of obs. 78−12397
clusters of galaxies, spatial distribs. of radio and X-ray fluxes 77−33686
clusters of galaxies, unborn, microwave and X-ray emission 78−8131
clusters of galaxies with LF radio emission, dynamical evolution 78−24558
Coma cluster field, accurate positions of faint optical objects in fields of radiosources 79−9015
Coma cluster of galaxies, diffuse radio emission obs. 79−88750
Coma cluster of galaxies, origin and transport of electrons in halo radio source 77−26073
Coma cluster of galaxies, spatial distribs. of X-ray and radio fluxes, theory 77−33686
Coma galaxy cluster, halo radio source meas. by Westerbork survey 78−86027
compact central components in 17 extended radiosources, VLBI detect. 77−17703
compact double radio sources, relativistic blast-wave model for superlight motion 78−28807
compact extragalactic radio sources, apparent superluminal motion, models, review 80−77504
compact extragalactic radio sources, electron-positron pair prod. rel. to Faraday rot. 78−73770
compact extragalactic radio sources, relativistic jets model 80−4448
compact extragalactic source model, stellar collisions near Kerr black hole 79−12490
compact extragalactic sources, anisotropic radio emission model 80−62304
compact extragalactic sources, flux density and linear polarisation at 3.7 and 11.1 cm wavelength 77−49490
compact extragalactic sources, radio spectra interpretation 80−62299
compact extragalactic sources, relativistic blast-wave model for rapid flux vars. 79−9017

radiosources continued
compact extragalactic sources, super-luminal expansion 77−53695
compact features in extragalactic sources, statistical props. as function of flux density 78−41071
compact H II regions, fine struct. IR line emission 78−16482
compact H II regions assoc. with OH masers, CO obs. 77−57078
compact H II regions near Type I OH maser sources, obs. 78−8094
compact nonthermal sources, polarisation at cm., mm., IR and visual wavelengths 79−5913
compact radio quasars, apparent magnitude-redshift relations for resolved and unresolved sources *(Chinese)* 80−105380
compact radio sources, energetics 78−57671
compact radio sources, mapping from VLBI data 78−89266
compact radio sources, strong mag. dipole model 79−17115
compact radio sources in galaxies and quasars, struct. and time vars. 78−57669
compact source in supernova remnant G78.1+1.8, props. from interstellar scintillation obs. 79−101213
compact sources, absorption models for low freq. var. 79−35409
compact sources, apparent superluminal expansion velocities in the dipole magnetic field model 78−77614
compact sources, high declination search at 8 GHz 78−69896
compact sources, particle accel. and flux vars. 77−13479
compact sources, phase stability, ang. struct. and position meas. by radio-link interferometer 77−5452
compact sources, vars. in intensities and sizes at 13 cm wavelength 77−78876
compact sources at 609 MHz, VLBI obs. 79−101209
compact sources high-resolution obs. at 1.35 cm wavelength high-resolution obs. at 1.35 cm wavelength *(Russian)* 78−69902
compact sources in and near bright galaxies 78−49548
compact sources in bright galaxies, very long baseline interferometry 79−48943
compact sources in directions of SNRs, 2.8 and 3.7 cm obs. *(Italian)* 79−53925
compact sources positions from VLBI obs. 78−81698
compact synchrotron sources variability, model of knots spontaneous form. in relativistic flows 80−105369
compact unresolved sources, aperture synthesis obs. of circular polarisation, techniques and appl. 77−9670
compact variable radiosources, small-pitch-angle synchrotron radiation model 79−53919
complex structured radiosources in clusters of galaxies 78−93443
component separation, apparent superluminal vels. investigation 79−67110
Compton and synchrotron processes in spherically-symmetric non-thermal sources 79−88583
Compton scattering at nonzero particle fluxes, radiation and relativistic electrons spectra 79−8825
continuous beam model, numerical study 77−60841
coordinate measurements using phase and fringe freq., tropospheric limitations 79−44375
cosmic radio bursts with microsecond time scales, limits 79−17119
cosmological distance determination, new method, appl. to weighing of Universe 79−9003
cosmological evolution, free-form anal. method 78−41070
cosmological evolution, free-form analysis, self-consistent luminosity function 80−46716
cosmological evolution of extragalactic radiosources 77−17728
cosmological evolution of extragalactic radiosources 78−28799
cosmological information interpretation 78−28831
couble galaxies, H I 21 cm. line obs. 80−51886
3CR, radio galaxies, spectrophotometry spectral energy distrib. 79−21413
3CR identifications 78−28825
3CR radio galaxies, optical spectra 79−71124
3CR radio galaxies, redshifts, strong emission line spectra 77−33666
3CR radio sources, optical fields investigations to faint limiting magnitudes 78−54067
3 Cr radio sources, spectral index breaks 79−67108
3CR radiosources, photographic obs., optical identifications 77−13481
3CR sources, multifreq. obs., results and interpretation 79−35416
3CR sources, multifreq. obs. 79−30141
3CR sources, quasars and galaxies, optical identification 80−90555
3CR sources, source counts and V/V_{max} tests for complete sample 78−77613
3CR sources, VLBI obs. of hot spots in lobes 79−40286
3Cr sources in directions of Zwicky clusters of galaxies, statistical investigation 78−4378
Crab Nebula, 2.7 GHz study with 3.7×10 arcsec ang. resolution 79−40248
Crab Nebula, compact source flux density meas. by interferometer 80−62252
Crab Nebula, continuous particle injection model for radio flux var. 77−13426
Crab Nebula, Faraday rot. obs. during solar control occultations 77−45593
Crab Nebula, lunar occultation obs. at decametre wavelengths 80−62248
Crab Nebula, millimetre and submillimetre meas. 79−75267
Crab Nebula, obs. of linear polarisation during occultation by solar corona 77−60837
Crab nebula, polarised radioemission occultation by solar corona during weak solar activity *(Russian)* 78−77527
Crab Nebula, short-wave millimetric obs. with wide-band radiometer 79−96916
Crab Nebula, struct. at 327 MHz from occultation obs. 78−12339
Crab Nebula occultation by Moon, 1974, Sept., 180 and 1646 MHz obs. 77−26043
Crab Nebula radio struct. 79−75257
Crab-like supernova remnants, radio props. of plerions *(Italian)* 79−53888
CTB 1, UHF emission and radio shell of SNR 80−77461
CTB 80, peculiar supernova remnant, central radio source optical and H I obs. 80−56896
CTB 80, supernova remnant, optical emission and historical evidence 80−51853
CTD 93, compact radio source, high resolution obs. at 1671 MHz 80−56960
CUL sources in ZA catalogue, positional and spectral data, HF obs. 80−86019
Culgoora-3 list of 2045 sources, obs. at 160 MHz 78−20655

radiosources continued
V1057 Cygni, CH radio emission obs. 77−87512
V1057 Cygni, FU Orionis-type star, flare up in 1720 MHz OH line 79−62843
χ Cygni, Mira variable star, variable 2.6 mm CO emission obs. 78−12241
V1057 Cygni, OH obs. 80−36629
NML=V1489 Cygni, OH/IR star, 1612 MHz OH maser multibaseline VLBI obs. 80−12766
V1500 Cygni (Nova 1975), radio emission from expanding shell 80−26868
Cygnus A, 99 GHz obs. of components and central source 78−41069
Cygnus A, giant cD radio galaxy, extended X-ray source 79−67109
Cygnus A, HEAO-1 pointed obs. 78−7856
Cygnus A, models for central compact radiosource 79−17073
Cygnus A, optical struct. 77−9802
Cygnus A, polarization maps at 23 GHz 79−71109
Cygnus A, radio galaxy, 150 GHz obs. 80−41908
Cygnus A, radio obs., digital hologram reconstruction 77−64653
Cygnus A, radiogalaxy structure at 150 MHz 80−101646
Cygnus A, rot. axis of assoc. optical galaxy 78−4355
Cygnus A and the evolution of radioastronomy *(French)* 79−40287
Cygnus A compact radiosource, astrometric obs. 77−74152
Cygnus A model, radio source powered by M87 type knots 78−57661
Cygnus A region, X-ray obs. of 3U 1957+40 with ANS 77−53700
Cygnus Loop, radio struct. at 25 MHz 78−54027
Cygnus X, connection with Cygnus X-ray superbubble 80−90575
Cygnus X, H I 21 cm line emission maps of field containing G78.2+2.1 SNR 80−56917
Cygnus X region, 10.6 GHz survey 77−74153
Cygnus X region, far IR survey 80−82538
Cygnus X region, mapping and physical parameters 77−9783
Cygnus X region, riddle of γ Cygni radio source resolved 78−28809
Cygnus X region, visual extinction map and radio brightness temp. 78−61929
Cygnus X-1, correlated X-ray-radio transition, 1976 February 77−17719
Cygnus X-1, X-ray binary, variable star, SHF obs. 80−73071
Cygnus X-3, cocooned X-ray binary pulsar model 78−36723
Cygnus X-3, efficient particle acceleration 80−31391
Cygnus X-3, gamma radiation during radio outburst 77−64884
Cygnus X-3, high-resolution 8450 MHz obs. of compact radiosource 79−44629
Cygnus-X region, embedded IR source GL 2636, visible and IR obs. 80−105302
DA 240, radio galaxy, high-vel. gas in jet 78−28773
DA 267, compact radio source, arcsecond struct. 80−4450
DA 406 (1611+343), broad-band flux density vars. 79−40282
dark clouds, search for radio continuum radiation 77−33585
decametric survey of discrete northern sources, catalogue of 329 objects, 10-20° declinations 78−57471
decametric survey of discrete northern sources, LF absolute flux scale 78−57663
decametric survey of discrete northern sources, spectra of 266 sources in 10-1400 MHz range 78−57664
decametric survey of discrete northern sources, UTR-2 radiotelescope, expt. techniques, data processing 78−57461
decay excitation of plasma turbulence and nonlinear radiative transfer 77−17707
decimetric variability of extragalactic sources *(Russian)* 79−21454
HR Delphini (Nova 1967), radio emission from expanding shell 80−26868
dense radio H II regions distrib. in inner Galaxy, kinematic models 80−12813
diffuse nebulae, formaldehyde and H110α recomb. lines obs. towards bright rims 77−87510
direction finding with short electric antennas on spacecraft 79−21184
discrete sources, flux densities meas. at 14.9 GHz (2 cm) 77−37664
discrete sources correl. with galactic background radio emission fine struct. 79−21457
Dopplers, Hα line freq. depend. general relativistic formula, appl. to (SS 433) 79−97010
double extragalactic radio sources, central radio component 78−77617
double extragalactic radio sources, collimation 80−22098
double quasar 0957+561A, B, radio study rel. to gravit. lens hypothesis 79−88762
double radio galaxies, symmetry rel. to dressed slingshot effect 78−12359
double radio source structures, form. and superluminal expansion 78−8141
double radio sources, hot spots behaviour 80−94882
double radiosource near NGC 2823 elliptical galaxy 78−24562
double radiosources, compact hot-spots correl. with galaxy cluster membership 79−48947
double sources, angular size-redshift test 77−57100
double sources, beam and cloud stability, shear layers, two dimens. computations 80−67893
double sources, compact struct. 79−17113
double sources, galaxies, evolutionary charact. *(Chinese)* 80−86007
double sources, polarization moments appl. to investigation of component polarizations 79−53923
double sources, review 77−33667
double sources, statistical props. 79−92877
double sources, steady-state configs., Cygnus A models 78−45416
double sources, twin beam models, dynamical calcs. 78−49547
double sources and cosmic plasma physics 78−69898
double sources and jets, models and current-carrying beams 78−49313
double sources statistical props., asymmetry and components flux ratio 80−67892
DR15, galactic H II region, obs. at 408, 1407 and 2695 MHz 80−94881
DR21(OH) obs. of J=1→0 emission from $H^{15}NC$ 77−82299
DR 21, anomalous NH_3 absorpt. obs. 77−53669
DR 21, HF calibration source, flux density obs. at 8420 MHz 80−86004
DR 21 (W75), continuum obs. at 3.9 mm 79−35333
DR 21 OH, relationships of N_2H^+, HCO^+, HCN and CN 77−33587
DW 1548+05, intensity variations at 2.7, 6.6 and 10.6 GHz 77−60834
dwarf galaxies, H I redshifts rel. to absolute solar motion and discrete redshift 78−49530
E/S0 radio galaxies, ionized gas obs. 79−17105
electrons acceleration by weak MHD turbulence, energy spectrum, radiosources appl. 79−88582

radiosources continued
elliptical and S0 galaxies, H I obs. 77−64838
elliptical galaxies, extended sources, partial synthesis maps at 2.7 and 8.1 GHz 80−105330
elliptical galaxies, optical posns. for identified radiogalaxies 79−97074
elliptical galaxies, radio sources orientation rel. to galaxies minor axes 80−82527
EM radiation, from line sources interacting with moving uniaxial dielectric or plasma half-space 79−92661
evolved stars expanding envelopes, CO thermal and maser emission 80−82334
expanding nonthermal sources, evolution, nonrelativistic expansion 78−4376
expanding synchrotron sources theory, relativistic corrections 80−12821
exploding black hole, radio pulse spectrum calc. 78−12271
extended, particle accel. and radiative losses effects on source dynamics 80−46687
extended and compact sources *(German)* 78−45420
extended double sources and central radio cores, symm. 80−86003
extended extragalactic double radio sources, expansion speeds from ang. struct. 80−67894
extended extragalactic radio sources, MHD instabilities and electron accel. 80−27000
extended extragalactic radio sources, relation between radio luminosity and spectrum 80−51894
extended extragalactic radio sources, relativistic parametric instabilities 78−24561
extended extragalactic radio sources, statistical evidence on dynamical evolution 79−88757
extended extragalactic sources, compact structure, freq. depend. 78−69895
extended extragalactic sources, models, review 77−26079
extended radio galaxies, multiple ejection theory 77−45592
extended radio galaxies, multiple explosion model 80−41894
extended radio sources, VLBI obs. of compact components 80−17680
extended radiosources and elliptical galaxies, search for radio cores using Very Large Array 78−81700
extended radiosources and elliptical galaxies, small-diameter components in extended structs. 78−81699
extended radiosources catalogue, 408 MHz fan-beam survey at low galactic latits. 77−26078
extended radiosources obs. in galaxy clusters 77−64861
extended sources, non-linear propagation effects of relativistically strong plasma waves 79−10698
extragalactic, 408 MHz obs. of Parkes 2700 MHz survey sources 80−86008
extragalactic, in fields of five unidentified high latit. X-ray sources, list of 249 objects 77−87281
extragalactic, integrated linear polarisation meas. 78−4381
extragalactic, luminosity functions 78−28827
extragalactic, method for distance determ. 80−109559
extragalactic, optical identification, astrometry using Palomar Sky Survey prints 77−87274
extragalactic, optical variability 78−12396
extragalactic, optically violent variables, monitoring of long-term vars. optically violent variables, monitoring of long-term vars. 80−31376
extragalactic, problems and advantages *(German)* 77−67134
extragalactic, rot. measures interpretation 77−60836
extragalactic, small angular size, probable number, for radio astrometry 77−78883
extragalactic, statistical tests on angular size-flux density relation 77−82315
extragalactic, struct. and luminosity relationship 77−64869
extragalactic 3C sources, polarization and total intensity at 2695 and 8085 MHz 79−35411
extragalactic background between 0.5 and 400 MHz 77−74166
extragalactic compact sources, ripple radiation rel. to low-freq. variability 79−21450
extragalactic compact sources with faint components, VHF and SHF obs. 80−90547
extragalactic decimeter sources flux variability 79−62924
extragalactic double radio sources, gas dynamical calcs. 79−67107
extragalactic double radio sources separation, depend. on redshift 80−22096
extragalactic double sources, axially symm. explosion, thermal radiation effects 77−87249
extragalactic double sources, beam models, relativistic fluid flow 78−69668
extragalactic extended sources models, internal dynamics and brightness distribs. 77−22323
extragalactic flat spectrum sources, VLBI UHF and SHF obs. 80−90549
extragalactic high-latitude sources, search for OH 18 cm absorpt. lines in projected H I clouds 80−67841
extragalactic index of catalogues 77−60629
extragalactic large radiosources, preferred orientation rel. to parent elliptical galaxies 79−92880
extragalactic nonthermal sources, spectral flux var. in 0.36-3.5 μ range 79−35412
extragalactic objects, 1 mm continuum obs. 78−36720
extragalactic objects with active nuclei, distance determ. method *(Russian)* 80−51880
extragalactic optically variable objects, calibration of photoelec. comparison sequences 77−87537
extragalactic powerful sources, compact and extended components spectra 77−41415
extragalactic radio recombination lines, stimulated emission 78−86030
extragalactic radio sources, ang. size-redshift diagram interpretation 80−22101
extragalactic radio sources, beaming and double struct. rel. to gravity power model 78−57667
extragalactic radio sources, jets configuration and propag. 80−31374
extragalactic radio sources, obs. of galactic H I absorpt. struct. on small ang. scales 80−22051
extragalactic radio sources, polarisation props. 79−53920
extragalactic radio sources, radio emission from intense EM beam-plasma system 79−84663
extragalactic radio sources, relativistic electrons in situ accel. by shock waves 78−49241
extragalactic radio sources, relativistic Kelvin-Helmholtz instabilities 78−45419
radiosources continued
extragalactic radio sources, search for compact sources at low freqs. (81.5 MHz) 80−90553
extragalactic radio sources, variable radio emission temporal characts. *(Russian)* 80−62307
extragalactic radio sources (>1 arcsecond), large-scale struct. 78−57668
extragalactic radio sources in vicinity of bright galaxies, distrib. and density 80−56964
extragalactic radio sources study of emission variability in millimeter wave range *(Russian)* 80−90559
extragalactic radio sources with speeds exceeding speed of light, geometric models *(Danish)* 78−36715
extragalactic radiosource counts rel. to big bang model 78−69920
extragalactic radiosources, interpretation and theory of extended and compact components 78−57670
extragalactic radiosources, synchrotron radiation, contour maps and energy source *(French)* 79−75291
extragalactic source based positional reference frame, finding charts and optical identification 80−101645
extragalactic source variability at 2.7 GHz, 2 yr monitoring 77−17702
extragalactic source variability at 408 MHz, 3-yr. monitoring program 79−71142
extragalactic sources, 318 MHz variability of complete sample 79−30139
extragalactic sources, astrometric obs. rel. to lunisolar precession determ. 77−5129
extragalactic sources, bent beams and overall size 79−21452
extragalactic sources, confusion-limited survey at 4.755 GHz, source list and areal distribs. 80−98577
extragalactic sources, deep survey of selected regions at 4.85 GHz 80−77502
extragalactic sources, evidence on origin of rot. measures 77−5584
extragalactic sources, Faraday rot. rel. to Galaxy turbulent struct. 78−20885
extragalactic sources, flux densities, and variability at 2.7 GHz 77−53694
extragalactic sources, intracluster Faraday rot. obs. 79−75285
extragalactic sources, line of sight galactic H I emission and absorpt. obs. 80−94854
extragalactic sources, model for superlight vels. 77−29944
extragalactic sources, obs. of optically misidentified nearby stars 78−73708
extragalactic sources, obs. with Cambridge 5 km telescope at 5 GHz 78−12391
extragalactic sources, optical and radio props. 78−28829
extragalactic sources, optical positions 77−78881
extragalactic sources, origin of aligned inner and outer double struct. 77−45582
extragalactic sources, photoelectric UBV sequences of comparison stars 77−5562
extragalactic sources, precise optical positions in FK 4 system, pilot programme results 78−65709
extragalactic sources, QSOs and galaxies, linear polarisation meas., SHF obs. 80−73058
extragalactic sources, radio jets brightness and shape rel. to beam and slingshot models 79−25741
extragalactic sources, redshift-apparent dia. relation 77−87559
extragalactic sources, rot. measure, linear polarisation obs. at 7.2 cm 80−82530
extragalactic sources, spectroscopic obs. in 3200-5700 Å range 78−86032
extragalactic sources, statistical investigation of compact emitting regions 78−32590
extragalactic sources, survey of galactic OH clouds absorpt. 77−64822
extragalactic sources, vars. at 7.9 GHz 77−37661
extragalactic sources, very high resolution obs. 77−33663
extragalactic sources at 10.5 GHz, linear polarization meas. 79−12533
extragalactic sources from NRAO-Bonn 5 GHz survey, optical identifications 77−78880
extragalactic sources from NRAO-MPIfR 6 cm surveys, 21 cm flux density meas. 79−88754
extragalactic sources suspected of decimetric flux density vars., 610 MHz VLBI obs. 77−78879
extragalactic sources variability at 2.7 GHz, depend. on spectral class 78−4379
extragalactic sources with short wave radio emission excess, flux densities and variability at 1.35 cm *(Russian)* 78−57666
extragalactic sources with strong millimetre wave emission, 90 GHz obs. 78−16548
extragalactic sources with strong mm components, simultaneous radio obs. 80−73055
extragalactic sources with superluminal vels. review 77−78882
extragalactic strong 90 GHz sources, radio, IR and optical obs. 78−93440
extragalactic variable radiosources, linear polarisation obs. at 7.2 cm wavelength 77−64870
extragalactic variable sources, ten-year study at centimetre wavelengths 78−89267
extragalactic variable sources with flat spectra, 90 GHz flux density 80−73056
extragalactic X-ray sources, radio emission problems *(Dutch)* 77−67133
extragalactic X-ray sources correl. with radiosources from 26.3 MHz survey 78−65707
faint extragalactic radio sources, counts estimate at 5 GHz 78−32588
faint extragalactic sources with radio jets 77−29945
faint radio sources, statistical study of mean ang. size and sky density at 81.5 MHz 80−51893
faint radio sources statistics, interpretation of interplanetary scintillation meas. at 81.5 MHz 80−90554
faint sources statistical counts at 2380 MHz 78−65706
Faraday rotation in variable sources, upper limits 77−91660
Faraday rotation measures, computation method 80−4263
Faraday rotation of extragalactic radiosources, measure of galactic magnetic field 79−58430
Faraday rotation of extragalactic sources and intergalactic magnetic fields 80−22086
Faraday rotation of polarization plane for extragalactic radiosources 77−26066
filamentary and diffuse nebulosity near giant nonthermal radio loop 78−93445
FJM 3, 100 micron source, radio and IR studies 77−26082

radiosources continued
FJM 6, molecular cloud, far IR, near IR radio mol. line studies 80−26929
flare stars, nature of nearby radiosources 78−12388
flat or inverted radio spectra sources, optical and radio props. 78−81697
flat spectrum optically variable quasars, distrib. of ang. distances from bright galaxies 79−58438
flat spectrum sources, optical identification of complete sample 79−5911
flat-spectrum radio sources, variability at 96 MHz 77−82317
fluctuating sources, size limits 77−45585
flux densities at 1.35 cm wavelength *(Russian)* 77−64868
flux density-angular size distrib. for extragalactic sources 78−28823
formaldehyde near Cone nebulae and NGC 2264 IR source, kinematics and distrib. 80−4418
Fornax A, obs. of central region of double radiosource at 4.9 GHz 79−5912
Fornax A (NGC 1316), optical study of giant radiogalaxy 80−77479
frequency dependence of source counts, rel. to spectral index distrib. with flux density 78−96554
FXP 0520−66, flaring X-ray pulsar, nature and optical identification *(Russian)* 80−77521
G0.7-0.0 (Sagittarius B2), struct. and He abundance 78−45380
G120.1+1.4, Tycho's SNR, rot. measure and turbulent struct. 79−88718
G12.2−0.1, radio and IR obs. of OH/H_2O source 78−57620
G126.2+1.6 SNR near 4U 0115+63 X-ray transient 80−8668
G127.11+0.54, optical spectroscopy and photometry of assoc. luminous obscured galaxy 80−31371
G127.1+0.5, remarkable supernova remnant centred on very compact radiosource 78−16555
G127.1+0.5, supernova remnant, VLBI obs. of assoc. compact radiosource 78−86029
G127.3+0.7, possible supernova remnant in open cluster, 1.4 GHz obs. 77−64826
G127+0.5, continuum obs. at 2695 MHz of supernova remnant 78−61903
G206.9+2.3 (=PKS 0646+06), supernova remnant, optical identification 78−36660
G206.9+2.3 (PKS 0646+06), optical supernova remnant discovery 78−96518
G219.3-0.7, OH excited states, satellite lines anomalies 77−42315
G286.8−0.5, nonthermal radiosource in front of Carina Nebula, SNR 79−35355
G287.8−0.5, possible supernova remnant in Carina *(Italian)* 79−53924
G290.1−0.8, optical SNR photographed 79−40249
G292.0+1.8, supernova remnant, optical identification and spectrum 79−84839
G292.0+1.8, young supernova remnant, high vel. material obs. 80−22064
G309.81+0.07, point radio source and possible stellar remnant of supernova, obs. 80−51849
G321.9-0.3 rel. to Cirinus X-1, simultaneous radio and optical obs. 79−17137
G326.3−1.8, G348.5+0.1, G348.7+0.3, unusual supernova remnants, radio obs. 79−84841
G326.3−1.8, peculiar supernova remnant, optical identification 79−25675
G333.6−0.2, G298.2−0.3, southern compact H II regions, IR emission lines obs. 78−96522
G333.6−0.2, powerful H II region, 2 μm line emission detect. 78−54017
G334.9−0.3, G339.6−0.1, identification with X-ray sources 4U 1624−49 and (4U 1624−45) 78−28860
G339.2−0.4, radio recombination line obs. of low-excitation H II region 80−46650
G339.2−0.4, supernova remnant or planetary nebula, radio and optical obs. 80−22104
G35.6−0.0 and G35.6−0.4, kinematic distance estimates 78−73769
G37.7+0.1, double recombination line galactic thermal source, obs. at 1400 and 2371 MHz 78−69897
G45.1+0.1, 8-13 μm spectrophotometry of compact H II region 78−65672
G46.8−0.3, galactic supernova remnant, kinematic distance estimate 79−84833
G48.6+0.0, galactic H II region, direction, H I, OH and H_2CO absorpt. line meas. 78−85996
G49.5−0.4, giant H II region, $^3He^+$, probable detect. and significance 79−25689
G49.5−0.4 (W51), high resolution obs. at 5 and 15 GHz of giant H II complex 78−54065
G55.7+3.4, shell source, high resolution obs. at 610 and 1415 MHz 78−8140
G65.2+5.7, 1420 MHz continuum obs. of new SNR 79−44587
G65.2+5.7, 1420 MHz continuum obs. of supernova remnant *(Italian)* 79−53886
G74.9+1.2, continuum obs. at 2695 MHz of SNR 80−67830
G74.9+1.2, supernova remnant, distance 77−64864
G74.9+1.2, supernova remnant, VLBI obs. of assoc. compact radiosource 78−86029
G 0.7−0.0 (Sagittarius B2), giant H II region, radio maps interpretation 78−85994
G 0.7−0.0 (Sagittarius B2), interpretation of radio recomb. line emission 77−17651
G 109.7+2.2, type I OH maser source near Herbig-Haro object *(Russian)* 80−17684
G 21.5−0.9, supernova remnant resembling Crab Nebula, obs. 77−5553
G 307.1+1.2, G 309.7+1.7, low-latit. radio galaxies, optical and radio obs. 79−12535
G 339.6−0.1, high resolution map at 1415 MHz, possible assoc. with 4U 1642−45 79−71143
G 84.2−0.8, high resolution 1415 and 2695 MHz obs. of SNR 80−98702
G 84.2−0.8, new supernova remnant in Cygnus 77−29906
G-varying cosmology, radio source counts and models 80−56981
galactic, anticorrelation with soft X-ray sources, plasma cloud interpretation 80−82514
galactic centre, ang. size for compact radio source 78−28779
Galactic Centre, H recomb. lines obs. at decimetric wavelengths 77−82310
galactic centre, ionising agent of extended thermal radio emission 79−97059
radiosources continued
galactic centre, OH absorpt. struct. determ. using regularisation method 80−17505
galactic centre, point radiosource size determ. *(Russian)* 79−58427
galactic centre, radio emitting features rel. to eruptive phenomena 78−57647
galactic centre, size and struct., radiation scatt. and scintillation *(Russian)* 78−16535
Galactic Centre direction, 252α recomb. line emission 77−45587
galactic centre direction, low-freq. radio recomb. lines studies 78−32589
galactic centre region, 5 GHz formaldehyde absorpt. obs. 79−84855
galactic centre region, compact radio continuum sources obs. 79−21430
galactic centre region, compact radiosource interferometry 77−53686
galactic centre region, sources and obscuration 80−77487
galactic diffuse background, distrib. and model 77−5602
galactic dust globules, microwave spectral lines obs. 78−57609
galactic halo, radio obs. 78−96544
galactic halo low-frequency radio emission, diffusion models 78−12433
galactic linearly polarised radio emission, bright spot obs. at 1 m wavelength 77−17709
galactic masers, role of plasma effects in generating high-vel. and symmetric spectral features 80−31378
galactic nonthermal radio spectrum, rel. to cosmic ray electrons spectrum and gamma-rays prod. 80−62257
galactic nuclei, radio sources expansion rel. to compact X-ray sources model 78−28847
galactic nuclei, rotating supermassive magnetized disc model 79−84849
galactic nucleus, 6 cm recomb. line emission vels. 78−69885
galactic nucleus source, radio obs. 77−5572
galactic plane, recomb. line and continuum emission obs. 77−13433
galactic plane, S hemisphere survey at 5 GHz 78−81686
galactic plane radio survey at 4.875 GHz, list of 1186 sources 79−21431
galactic polar regions, non-thermal radio radiation spectra 80−22082
galactic radiation belts, trapped electrons as radiowave source 80−26982
galactic radio emission, rel. to interstellar gas hydrostatic equilib. and cosmic ray confinement 77−29919
galactic radio sources, OH radio lines absorpt. obs. 78−54068
galactic sources, H110α line and formaldehyde absorption line obs., SHF obs. 80−77472
galactic supernova remnants, radio brightness depend. on galactic height, implications 79−48894
galactic synchrotron radio emission, rel. to Galaxy cosmic rays and mag. field distrib. 80−4207
galaxies, 3 cm obs. of 141 optically bright objects 80−73040
galaxies, accretion wake model of radio jets *(Japanese)* 79−84857
galaxies, bivariate size-luminosity function determ. 78−65687
galaxies, bright, 1415 MHz continuum survey 80−94869
galaxies, continuous optical spectra of active nuclei 78−57644
galaxies, distance scale from IR magnitude/H I vel.-width relation 80−82480
galaxies, early-type, H I obs. 78−45401
galaxies, early-type accretion from gas-rich dwarf galaxies 80−31349
galaxies, elliptical, extended radio sources, optical positions 80−105331
galaxies, flat spectrum, in 5 GHz S4 survey, Westerbork obs. 79−58435
galaxies, late-type H I obs. rel. to integral props. derivation 78−86015
galaxies, log N-log S relation rel. to Dirac cosmology 77−22334
galaxies, Markarian and Seyfert types, search for CO emission 80−26975
galaxies, models, rel. to solar flare physical mechanisms 77−17499
galaxies, nearby, H I profiles obs. 80−41895
galaxies, nearby, interstellar CO survey 80−62276
galaxies, nearby, radio continuum obs. *(German)* 80−109544
galaxies, new complete sample, struct., redshifts 79−17096
galaxies, optical counterparts, astrometry 80−90551
galaxies, optical emission in rad o lobes 78−57630
galaxies, optical emission-line spectra 78−57643
galaxies, optical spectra, morphological classification rel. to spectroscopic classification 78−41038
galaxies, optically bright, radio survey at 1400 MHz, 248 radiosources detect. 77−60627
galaxies, orientations 79−53911
galaxies, possible high energy neutrinos emission and detect. techniques 79−2484
galaxies, radio brightness distrib. obs. with RATAN-600 telescope 78−65698
galaxies, radio components fly away velocities *(Russian)* 80−62306
galaxies, radio continuum obs. at 11 cm 80−94872
galaxies, radio emission of active and normal nuclei 78−57646
galaxies, radio emission rel. to galactic dynamo numerical models 79−40262
galaxies, radio emission rel. to mean surface brightness *(Russian)* 77−91615
galaxies, radio luminosity and source size rel. to cluster membership 79−25729
galaxies, red shift dependence of proper densities and colours 80−62286
galaxies, relativistic and nonrelativistic gas flows, low press. limit 77−9655
galaxies, relativistic fluids flow through channels, self-similar solns. and stability 80−62006
galaxies, relativistic jets and beams 78−96541
galaxies, search for H I clouds 78−12316
galaxies, small, accurate 21 cm H I spectra 79−35382
galaxies, warped H I discs obs. 77−5567
galaxies, X-ray emission 78−57701
galaxies active nuclei, emission line spectra rel. to ionised gas and dust 79−88730
galaxies active nuclei, massive black hole binaries model rel. to radio jets struct. 80−109546
galaxies and quasars, energy supply and press. balance 77−41417
galaxies and quasars, VLBI hybrid mapping of nuclei 80−105356
galaxies close pairs, excess radio emission 78−57658
galaxies clustering about extragalactic radio sources, cross-correl. anal. 80−22103
galaxies from B2 Catalogue, optical identification, radio positions and redshifts 80−86005
galaxies in Virgo cluster radio luminosity v volume emissivity diag. 77−17696
galaxies isolated pairs, radio continuum survey 78−57657
galaxies primordial protoclusters, search for H I emission at Z=3.33 and (4.92) 78−41066
galaxies with dust lanes, radio morphology 79−44604

radiosources continued
galaxies with radio jets, 5 GHz obs. 77−29945
galaxies with radio jets, Hα and 450 nm obs. 80−51889
galaxies with radio jets, optical spectra of nuclei 79−84859
galaxies with radio tails, review *(French)* 78−41054
galaxies with tail-bridge struct., spectral index, radio polarisation, mag. field 79−58416
Galaxy, H I 21 cm obs. rel. to rot. curve accounting for interstellar gas expansion *(Russian)* 79−48938
Galaxy, synchrotron radiation in inhomogeneous mag. field 77−67127
Galaxy, synchrotron radiation rel. to mag. field configurations 78−20884
Galaxy central region, improved H I data rel. to barlike model of inner Galaxy gas distrib. 80−67845
galaxy clusters, central regions, 3.5 and 4.0 mm obs. *(Russian)* 80−82525
galaxy clusters, intergalactic dust thermal emission rel. to Zel'dovich effect 78−54041
Galaxy H I subsystem, rot. curve *(Russian)* 80−36724
Galaxy nucleus, compact radiosource struct. 78−57669
gas poor disc galaxies, radio and optical props. 77−22310
GB2 1400 MHz survey, optical identifications of flat-spectrum sources 79−40281
GB2 1400 MHz survey, radio spectra of flat-spectrum sources 79−44628
GB2 1400 MHz survey sources, spectral index depend. counts 80−98732
GB2 sky survey at 1400 MHz, differential radiosource counts 78−54063
GB sky survey at 1400 MHz, rel. to isotropy of radio source population 77−45584
giant radio galaxies, 26-100 MHz obs. of four objects 80−56961
globular cluster fields, radio continuum obs. at 2.7, 4.8 and 10.7 GHz 80−101619
globular cluster fields, radiosources detect. 79−17114
globular clusters, obs. of assoc. radiosources 77−87484
in globular clusters, optical identifications 79−62923
gravitational cyclotron instability, mechanism for cosmic radio emission 78−65724
Green Bank second survey of extragalactic radiosources of 1400 MHz, catalogue of 2022 sources 79−62761
Green Bank surveys at 1400 MHz 78−28543
GT 0236+610, absence of variability in optical counterpart (LSI+61°303) 78−49438
GT 0236+610, highly variable source, as possible counterpart of γ-ray source (CG 135+1) 78−54095
GT 0236+610, position and LS I +61°303 as optical counterpart 78−36568
GT 0236+610, possible identification with LS I +61°303 (OB star) 78−32473
GT 0236+610 (LS I+61°303), radio, optical, X-ray, gamma-ray Be star, obs. 79−88755
GT 0236+610 radio counterpart for γ-ray source CG 135+1 78−24560
GX 17+2 (3U 1813-14), radio and optical identification 78−45428
gyrosynchrotron emissivity peak freq. of weakly relativistic electrons in isotropic plasma 77−64633
H1-36 (3U 1746-37), emission line object, radio spectrum 77−82239
H 2155−304, X-ray source, Very Large Array obs., radio source discovery 79−44643
HB13, radio galaxy with jets, 151 MHz obs. 79−48926
HB3, supernova remnant, X-ray emission obs. 78−81679
HB 3, supernova remnant, soft X-ray obs. 80−56915
HB 9, soft X-ray emission obs. from old SNR 80−36697
HD 26676, radio emission at 6 and 21 cm wavelengths 77−91532
HD 26676, unusual radio star, not close binary 78−73707
HD 26676 (HR 1307), UV spectrum, possible radio star 79−101150
head-tail radio galaxies, galaxy counts in surrounding region rel. to tail orientation 78−54060
head-tail radio galaxies, intrinsic parameters distrib. 80−17653
head-tail radio galaxies, VLA obs. 79−48945
head-tail radio galaxies in clusters, radial vels. 79−9014
head-tail radio galaxies in poor clusters, radio and optical obs. 78−96530
head-tail radio galaxies velocities with respect to intracluster medium 78−49516
head-tail radio sources formation, role of hot gas in elliptical galaxies 80−36703
Heiles's cloud 2, cyanodiacetylene (HC_5N) obs. 80−22054
Heiles's Cloud 2, HC_9N detect. 78−93370
Heiles 2, interstellar dark dust cloud, HC_5N and HC_7N obs. 78−54023
Heiles 2 dust cloud, detect. of cyanodiacetylene J=9 to 8 transition 77−91603
Heiles 2 dust cloud, NH_3, and cyanobutadiyne emission relative distrib. 80−17641
Heiles 2 interstellar dark cloud, NH_3 hyperfine struct. 77−78852
YY Herculis, symbiotic star, radio continuum detect. 79−25615
YY Herculis region, stellar radio emission refuted and new source discovery 79−35274
HFE 2,3, molecular cloud, for IR radio mol. line studies 80−26929
HFE 2, 100 micron source, radio and IR studies 77−26082
HFE 64-70, 100 μm objects in Cygnus X, identifications with H II regions 77−17663
HIA 0255+574, characts. of radiosource near HD 18391 supergiant star 78−81701
HIA 2344+092, HIA 2344+094, sources near quasar PKS 2344+09, obs. 77−37659
high positive velocity H I clouds, spatial and vel. struct. 77−13442
high velocity clouds, evidence against intergalactic interpretation 77−41399
high-velocity H I clouds, map 80−26923
hot spots in radiosources as cosmological probes 77−13483
hot stars, effect of winds and coronae on IR and radio continua 77−29817
HR 1099, 10 GHz radio emission from RS Canum Venaticorum binary 80−82427
HR 1099, binary stars, radio obs. 77−64793
HR 1099, Ca II H and K emission enhancement during February 1978 radio flare 79−21341
HR 1099, flare emission at 2.8 cm (1978 February) 78−32476
HR 1099, Hα region spectrophotometry during February 1978 radio flare 79−21344
HR 1099, H and Ca II, emission during February 1978 radio outburst 79−21340
HR 1099, radio flux vars. obs. and optical ephemeris 78−36641

radiosources continued
HR 1099, RS Canum Venaticorum binary, February 1978 radio flare obs. 80−26911
HR 1099, RS Canum Venaticorum binary, nonthermal flare emission during February 1978 outburst 79−21332
HR 1099, RS Canum Venaticorum binary, optical spectrophotometry during major flare outburst 79−21342
HR 1099, RS Canum Venaticorum binary, rapidly variable polarisation obs. at radio freqs. 79−21336
HR 1099, RS Canum Venaticorum binary, strong radio flaring discovery 79−21330
HR 1099, RS Canum Venaticorum binary, two-freq. radio polarimetry 79−21335
HR 1099, RS Canum Venaticorum binary, VLA radio obs. during 1977 international campaign 79−21334
HR 1099, RS Canum Venaticorum binary star, radio obs. at 8.0 GHz 79−21331
HR 1099, RS Canum Venaticorum star, 4U 0336+01 optical counterpart 78−32475
HR 1099, RS Canum Venaticorum type binary, strong radio flaring obs. 79−84821
HR 1099, RS Canum Venaticorum variable, photoelectric photometry 77−53602
HR 1099 (V711 Tauri), RS Canum Venaticorum star, Hα line variability, visible spectra obs. 80−105277
HR 5110, Algol type RS Canum Venaticorum star, Hα, yu photometry obs. 80−105276
HR 5110, RS Canam Venaticorum binary, V photometry near radio outburst time 80−90469
HR 5110 (HD 118216), RS Canum Venaticorum binary, radio flaring obs. 79−67053
HR 8752, G-type supergiant, obs. of associated radio source 78−40942
HR 8752, radio emitting G-type supergiant, search for light vars. 79−88657
HR 8752, superluminous star, hot companion discovery by IUE 79−16947
Hubble constant determ. from super-luminal radiosources 78−12439
HVC 132+23−211, small high-velocity cloud, detailed struct. 78−89241
W Hydrae, long-period variable, suspected Zeeman splitting in OH masers 80−36632
W Hydrae, long-period variable star, cyanodiacetylene detect. 77−82238
hydrodynamic expansion of relativistic gas, Euler eqns. 77−33331
hydrodynamical acceleration of particles in supernovae and extragalactic radio sources 80−31313
IAU 13S6A, strong southern radiosource, optical identification 77−64865
IC 10, irregular galaxy, giant H I envelope obs. 79−67094
IC 1805, 1848, giant H II regions, physical anal. from radio obs. 80−36695
IC 1848 A, bright-rimmed mol. cloud, mol. and IR obs. rel. to star form. 79−5810
IC 342, Scd galaxy, central regions IR and radio emission rel. to star form. 80−62256
IC 342, Scd galaxy, discovery of companion 80−36712
IC 4296, double-double radio galaxy 1415 MHz obs. 77−41412
IC 5146, young open cluster, CO obs. of assoc. dark cloud 79−48881
IC 708, Papillon radio galaxy, morphology, polarization 79−92855
IC 708 and 711, head-tail radiogalaxies in Abell 1314, 1.4 GHz obs. 77−60833
identification and spectroscopy of distant radiosources 77−17705
inhomogeneous cosmic masers, numerical calcs. of saturation behaviour 78−20898
inhomogeneous magnetic fields in extragalactic radio sources 79−40285
intergalactic cloud in Sculptor, 21 cm obs. 77−64843
intergalactic H I clouds, search for 21 cm emission 78−12316
intermediate strength sources, statistical props. 80−62303
interplanetary scintillation, appl. to detect. of solar wind whistler turbulence 78−45173
interplanetary scintillation, joint Gaussian statistics appl. 77−2316
interplanetary scintillation, mathematical anal. in weak scatt. approximation 77−9706
interplanetary scintillation, multi-station obs. and solar wind vel. estimation 78−73601
interplanetary scintillation, obs. for turbulent plasma radio imagery 79−92645
interplanetary scintillation, obs. rel. to solar wind speed latit. and longit. struct. 79−40049
interplanetary scintillation, theory and appl. 79−8880
interplanetary scintillation during August (1972) 77−25901
interplanetary scintillation pattern, rearrangments 79−96879
interplanetary scintillations spectra, influence of source sizes, obs. 80−46361
interstellar, SO, millimetre wave emission obs. 78−24535
interstellar *(Russian)* 80−36698
interstellar ^{13}CO emission distrib. in galactic plane, rel. to giant mol. clouds distrib. in Galaxy 79−101183
interstellar C II region, narrow radio recomb. lines prod. around X-ray source 79−8972
interstellar clouds, cyanoacetylene and cyanodiacetylene obs. 80−46634
interstellar clouds, emission from energetic secondary electrons, contrib. to galactic background 77−33593
interstellar clouds, strongly deuterated mols. obs. and implications for interstellar chemistry 79−5891
interstellar clouds spectral line widths, influence of extended continuum source 79−12398
interstellar CO clouds, blister model for assoc. H II regions 79−25681
interstellar dark clouds, CH obs. 78−28751
interstellar dark clouds, CO/H_2 ratio meas. 78−96513
interstellar DNC detection, difficulties of chemical equilibrium hypothesis for D enrichment 77−82298
interstellar excited H, decametric range radio lines search *(Russian)* 80−12822
interstellar formaldehyde absorpt. in four small dust clouds 77−5558
interstellar gas, local, in southern sky, single 21 cm component study 79−84834
interstellar H_2O maser emission, new sources detect. 80−62298
interstellar H_2O masers in H II regions, time vars. obs. 79−88725
interstellar H_2O masers in NGC 6334, positions and spectra rel. to star form. 80−73025
interstellar H II/OH maser regions, heating by ion streams 80−56912

radiosources continued
interstellar HCN, isotopic abundance vars. meas. 77−53657
interstellar HCO^+, shock enhancement of abundance in supernova remnant (IC 443) 80−82464
interstellar ionisation fronts, narrow radio recomb. lines emission 77−29940
interstellar masers, Λ-doublet population inversion in OH, OD, CH, CD and NH^+ collisions 80−22065
interstellar masers, assoc. with isentropic instabilities 77−17644
interstellar masers membership in star form. regions rel. to population categories 80−17645
interstellar medium, radio emission at l=31.2° and (31.9°) 77−17724
interstellar methyl alcohol, obs. 79−25666
interstellar mol. clouds, relationship of submillimetre optical depth to ^{13}CO column density 77−45508
interstellar molecular cloud near RCW 36, H_2CO and OH obs. 78−69862
interstellar molecular cloud near S106, NH_3 obs. 79−84840
interstellar molecular clouds, CO(J=2-1) emission obs. 79−92827
interstellar molecular clouds, detect. of new transitions of H, OCS and CH_2O, search for F 77−60808
interstellar molecular clouds, microturbulence, systematic motions and spectral line form. 77−33586
interstellar molecular clouds, radio search for CO^+, HCN^+, HNC^+ and CN^+ 78−24534
interstellar molecular clouds, relative distribs. of N_2H^+, HCO^+, HCN and CN 77−33587
interstellar molecular clouds containing Herbig-Haro objects, mol. obs. and physical props. 80−36689
interstellar molecular line and IR sources, 9400 Å photography 77−45602
interstellar molecules, RF emission spectra obs. towards ζ Ophiuchi 80−26958
interstellar OH and H_2O masers, form. by thermal instability of radiative shock 80−67821
interstellar OH masers, 18 cm lines pumping by H+OH collisions 79−48892
interstellar OH masers, role of $H+OH(^2\Pi)$ collisions 79−101186
interstellar S_2, upper limits on abundance in mol. clouds 78−28738
interstellar southern molecular clouds, $^{12}C/^{13}C$ abundance ratio derived from H_2CO obs. 79−84838
inverse-Compton emission from radiosource electrons and microwave background photons, prospects for X-ray detect. 79−71144
IR object assoc. with passage of interstellar shock front, radio identification 78−93369
IR stars, survey for circumstellar OH emission 79−48787
IRC+10216, C_4H (butadiynyl) radical detect. 78−93374
IRC+10216, C star, HC_5N and HC_7N detect. 79−17126
IRC+10216, C star, possibility of detecting cyanoacetylene-d_1 (DC_3N) 78−69901
IRC+10374, IRC+10523, IR stars, H_2O maser emission detect. 80−62298
IRC+10420, stellar OH maser VLBI obs. rel. to mag. field 79−25742
IRC+10420, supergiant star, new OH maser feature spatial struct. 79−48946
IRC-10442 (GL5268S), near IR and radio obs. 80−4412
isotropy in B2 catalogue 78−73766
jets inextragalactic radio sources, particle acceleration 80−31379
joint source near supernova remnant G74.9+1.2, distance 77−64864
Jupiter, Io-related decametric radiation, geometrical beaming model 79−101112
Kepler's supernova remnant, struct. at 327 MHz from occultation obs. 78−12339
Kleinmann-Low nebula, ^{12}CO line profile rel. to radially moving cloud model 78−20865
Kleinmann-Low nebula, NH_3 nonmetastable levels obs. 79−25665
L134 N interstellar dark cloud, NH_3 hyperfine struct. 77−78852
L1544, L1521B, interstellar clouds in Taurus, HC_5N detect. 80−26957
AR Lacertae, Hα spectrogram following radio outburst, results 77−49432
BL Lacertae, major radio outburst, (1980 April 17 to May 6) 80−73043
RT Lacertae, RS Canum Venaticorum binary, radio emission obs. 79−58379
AR Lacertae, RS Canum Venaticorum type star, VLA obs. 78−8054
BL Lacertae object 0109+22, optical and radio props. 78−32567
BL Lacertae objects, review 77−26069
Leo A, H I 21 cm. line survey of dwarf irregular galaxy 78−81688
LF variable radiosource survey 77−22324
linear and circular polarisation at 49 cm 77−60835
linear polarisation, catalogue 80−51671
linear polarisation meas. at 99 GHz 78−93439
linear polarisation of 78 small diameter radio sources at 2695 MHz 78−77611
LMC, radiosources at 3.4 cm, catalogue and spectral indices 78−65695
long-period variable and IR stars, discovery of new 1665/1667 MHz OH/IR sources 77−64763
long-period variable stars, maser activity rel. to Hδ emission, obs. 79−88685
long-period variable stars, OH maser lines struct. and saturation 78−93264
long-period variables, CO and SiO millimetre line emission obs. rel. to circumstellar shell props. 78−49423
Loop I, X-ray features, SNR model 80−22066
low freq. struct. and departures from equipartition 77−82316
low-frequency variable radio sources, search for microarcsecond struct. 78−16550
low-frequency variable sources, interstellar scintillation evidence for relativistic expansion 79−9018
LS I+61°303, variable binary radio star (B1 Ib), X-ray emission detect. 80−105400
LS I +61°303, radio variable Be star, UV spectrum, stellar models 80−26879
LSI+61°303, supergiant Be star, radio emission and radial vel. periodic vars. 80−62149
Lynds 673 nebula, radiosource obs. at 3.5 and 4 mm *(Russian)* 78−32557
β Lyrae, nature of secondary component from radio emission 78−36638
M101, extended H I envelope obs. 79−62904
M101 companion galaxies, integral props. from H I meas. 78−49532
M17, discovery of extended mol. cloud assoc. with star forming complex 77−37635
radiosources continued
M17 diffuse cloud, density distrib. from mol. lines intensities 79−97056
M1-78, emission nebula, 15.4 GHz struct. 78−41025
M1-92, bipolar nebula, OH emission obs. 78−41016
M31, aperture synthesis obs. complemented by short spacing data fron single dish obs. 79−66928
M31, CO partial radial distrib. meas. 78−8117
M31, high-resolution H I obs., spectra and major axis rel. plots 78−41057
M31, M51, M81, spiral galaxies, polarisation detect. at radio wavelengths 77−5575
M31, polarised radio emission detect. 78−86017
M31, polarised radio emission distrib. rel. to large-scale mag. field 80−41899
M33, detect. of H_2O maser emission 77−29926
M33, H I distrib. obs. and spiral struct. 80−56948
M33, radiocontinuum emission obs. at 14850 MHz 78−28783
M33 H I tail, obs. rel. to adjacent high-vel. H I cloud 80−12815
M51, high resolution obs. at 21 and 49 cm 77−29921
M51, radio spectral index distrib. 78−8119
M51 system, extended H I obs. 78−89253
M81, M51, spiral galaxies, 21 cm emission rel. to phase shifts between gaseous and stellar arms *(Chinese)* 79−17098
M81 nucleus, small radiosource obs. 77−13484
M82, compact radio source 41.9+58 in nucleus 78−93442
M82, M104, VLBI obs. of galactic nuclei at 18 centimetres 80−22078
M82, model with galaxy drifting through dust 77−33632
M82, nature of radio recomb. lines in extragalactic sources 78−45418
M82, stimulated recomb. line emission obs. 77−41408
M82 as exploding radiogalaxy, image tube spectrogram evidence 78−69880
M82 nucleus, λ6 cm formaldehyde absorpt. detect. 79−17088
M82 nucleus, obs. of compact radio source 77−78869
M87, 2 and 6 cm VLA obs. of jet 80−105345
M87, Faraday rot. in radio/X-ray halo 80−67844
M87, giant elliptical galaxy, appl. of black hole theory *(French)* 79−92866
M87, millisecond radio bursts discovery 80−73034
M87, nature of jet, rel. to elongated radiosource feeding 78−54055
M87, polarised radio emission rel. to galaxy mass and extended X-ray source model 78−28775
M87, search for hard X-ray emission 77−29939
M87, spectroscopic evidence for large central mass 80−94873
M87, UV spectrum, IUE obs. 80−82502
M87 galaxy, jet, nonlinear Poynting flux for radio emission 80−26736
M87 jet, internal shocks in plasma beam 78−93416
M87 jet, synchrotron optical and radio emission origin *(Russian)* 80−8694
M87 jet knots, polarisation, spectroscopic and radio props. 80−12817
M89, elliptical galaxy, associated optical jet discovery 79−25731
M8, large-beam near IR and 24 GHz obs. 79−48882
M8, new IR-CO source obs. 77−64818
M8, radio recomb. line obs. at 5 and 10 GHz 79−84832
M 81, CO emission upper limits 78−36693
Maffei 2, CO emission obs. 78−16530
magnetic dipole model, circular polarization obs. conflict 79−53926
magnetic field orientation evidence 80−46690
magnetized spheroids, anisotropic explosions 80−67532
magnetogasdynamics of double sources 80−26999
mapping with uncalibrated visibility data 80−77295
Markarian 296, clumpy irregular galaxy, spectroscopic and 21 cm line investigations 79−44608
Markarian 3, Seyfert galaxy radio maps, 5HF obs. 80−82501
Markarian 421 (2A 1102+384), BL Lacertae object, low-energy X-rays detect. 78−54083
Markarian 501, UV and X-ray obs. of BL Lacertae-type object 80−36717
Markarian 79, Seyfert galaxy, IUE and visual spectrophotometry 79−92856
Markarian galaxies, radio continuum obs. at 1410, 2380 and 5000 MHz 80−46668
Markarian galaxies, radio continuum obs. at 1410 MHz and 2700 MHz 77−87548
maser sources, role of dust in pumping 78−36716
masers, collision-collisional pumping model collisions *(Russian)* 80−90560
Maxwellian synchrotron sources, spectral characts., model for 3C 273 radio and X-ray spectra 79−35107
MC2(3) radio sources, optical positions from Palomar Sky Survey 80−31375
MC2 and MC3 sources, radio spectra and optical identification 77−33670
MC5 1307+121, BL Lacertae object, radio spectrum shape, VHF and SHF obs. 80−67866
MC76, MC77 (LMC X-1 region), 2 cm obs. 80−51875
Milky Way companion galaxy, synthesis obs. at 0.610 GHz rel. to identification 77−29941
Milky Way sources, obs. at 8.87 GHz near (l=333°) 80−22102
millimetre wavelength sources, large beam sky survey from balloon altitudes 79−97045
Mira variables, OH emission high-sensitivity search 78−89203
MO758+120, extended radiosource identification with quasar 77−87563
molecular cloud complex assoc. with bright rim near VY Canis Majoris, CO obs. 78−24536
Molonglo catalogue sources selected at 408 MHz, radio spectra 77−5583
Molonglo catalogues MC2 and MC3, optical identifications, 11^h28^m to 17^h00^m right ascensions 78−20900
Molonglo catalogues sources, optical obs. 77−60840
Molonglo Deep Sky Survey, 373 radiosources in declination zone −20° 77−56840
Molonglo Deep Sky Survey, source counts 77−56842
Molonglo Deep Survey sources, radio and optical spectra 78−69900
Molonglo radio source surveys at 408 MHz 78−28541
Molonglo sources optical counterparts, spectrophotometric obs. 78−4375
Molonglo survey and QSO identifications 78−28842
Monoceros R2 cloud, near IR and mol. obs. of rot. collapsing cloud 77−78840
Mononglo Deep Sky survey, 95 radiosources in declination zone −62° 77−56841

radiosources continued
morphology distortion and clusters of galaxies assoc. with QSOs 78−93434
morphology of extended extragalactic sources rel. to gaseous halos 80−17675
MSH 11-54 (H1122−59), supernova remnant, X-ray obs. 80−82463
MSH 14−63, probable remnant of A.D. 185 supernova, X-ray emission obs. 78−45427
MWC 349, Be star, spectral EHF obs. 80−105262
MXB 1730−335 (Rapid Burster), microwave bursts obs. 80−62320
N49, supernova remnant in LMC, possible assoc. with gamma ray burst (1979, March 5) 79−58441
narrow line radio galaxies, spectrophotometry 78−93391
narrowband radio radiation near H I 21 cm line, all-sky search 77−29661
nebular complexes, props. of thermal and non-thermal components 77−57101
NGC 1052, 4278, VLBI obs. of galactic nuclei at 18 centimetres 80−22078
NGC 1052, elliptical galaxy, H I obs. 78−69873
NGC 1167, S0 galaxy, extended core radio source 14.8 GHz mapping 79−25727
NGC 1265, 1275, in Perseus cluster, low-resolution aperture synthesis map at 408 MHz 80−56958
NGC 1275, galaxy, radio emission rel. to model for compact X-ray source 77−29961
NGC 1275, possibly BL Lacertae object 78−45406
NGC 1275, Seyfert galaxy, nucleus, ralation between gas and radio source structs. *(Russian)* 79−48936
NGC 1275, Seyfert galaxy, nucleus struct. *(Russian)* 80−62288
NGC 1275 nucleus, structural changes at 2.8 cm wavelength 80−31359
NGC 1499 (California Nebula), CO obs. along ionisation front 78−24537
NGC 1851, NGC 1904, globular clusters, radio and X-ray obs. 77−26028
NGC 2024, H II region, interstellar $^{16}OH/^{18}OH$ abundance ratio obs. 78−54024
NGC 2024, H II region, study of nearby partially ionised interstellar medium 77−57077
NGC 2110, Seyfert 2 X-ray galaxy, optical studies 80−22071
NGC 2175 (S252), galactic H II region, aperture synthesis obs. 77−64828
NGC 2264, continuum source 6 cm map and formaldehyde kinematics and distrib. 80−4418
NGC 2623, interacting galaxy, H I absorpt. and emission obs. 79−17087
NGC 281, H II region, CO and H_2O obs. 78−28740
NGC 281, H II region, obs. of shock in region of shock-induced star form. 79−25688
NGC 2915, southern galaxy, optical and H I obs. 77−67126
NGC 2974, 4105, 5846, elliptical galaxies, H I contents 79−62906
NGC 3079, peculiar edge-on spiral galaxy, 2.7 and 8.1 GHz obs. 78−36692
NGC 315, giant radio galaxy, jet structure and polarization 79−35379
NGC 315, NGC 6251, very large radio galaxies, 11.1 cm obs. 78−86014
NGC 315, radio galaxy, mag. field struct. in radio jets 80−82526
NGC 3556, edge-on galaxy, multi-freq. radio continuum study 79−44607
NGC 3665, elliptical galaxy with dust lane, radio obs. 79−58414
NGC 4038/39, interacting galaxy pair, H I kinematics and distrib. 79−35365
NGC 4151, galaxy, radio emission rel. to model for compact X-ray source 77−29961
NGC 4214, barred Im galaxy in Canes Venatici I group, H I obs. 79−92862
NGC 4248, galaxy, H I obs. 78−4358
NGC 4258, aperture synthesis obs. complemented by short spacing data fron single dish obs. 79−66928
NGC 4278, elliptical galaxy, H I content meas. 77−22312
NGC 4472, very weak radio galaxy, struct. and radio power 78−65708
NGC 4490/4485, interacting galaxy pair, 2.7 and 8.1 GHz obs. 78−36692
NGC 4631, edge-on spiral galaxy, radio continuum halo obs. 77−26054
NGC 4631/NGC 4656, interacting pair of galaxies, neutral H aperture synthesis obs. 78−54043
NGC 4636, elliptical galaxy, H I large-scale distrib. 78−45400
NGC 4736, spiral galaxy, H I study 77−57090
NGC 4945, galaxy, water vapour emission obs. 78−93427
NGC 5128, southern radio galaxy, OAO UV photometry, energy distrib. 79−40255
NGC 5128 (Centaurus A), formaldehyde absorpt. obs. at 14 GHz 80−17657
NGC 5128 (Centaurus A), narrow band photography 79−92854
NGC 5128 (Centaurus A), struct. and evolution from photographic and spectroscopic obs. 80−4429
NGC 5128 (Centaurus A), X-ray structure 78−24569
NGC 5236 (M83), Sc galaxy, CO obs. 78−65689
NGC 5363, radiosource and compact core 77−49468
NGC 5474, peculiar Scd galaxy, H I distrib. and kinematics 80−8683
NGC 612, rotation of lenticular radio galaxy 80−51874
NGC 6240, unusual radio galaxy, radio and optical, obs. 80−4440
NGC 6251, elliptical galaxy, nuclear jet radio obs. 78−41059
NGC 6251, extended radio galaxy, polarisation at 610 MHz 78−61918
NGC 6251, radio galaxy, CCD photometry rel. to central supermassive object 80−26966
NGC 6251, radio galaxy, radio jets misalignment, VLBI obs. 80−27001
NGC 6251, radio jet brightness and shape rel. to beam and slingshot models 79−25741
NGC 6251, very large radio galaxy with exceptional jet 78−12394
NGC 6334, CO detailed struct. in mol. cloud complex 78−4324
NGC 6334, relationships of N_2H^+, HCO^+, HCN and CN 77−33587
NGC 6624, globular cluster, radio, optical and X-ray obs. 77−45498
NGC 6822, galaxy, CO emission upper limits 78−36693
NGC 6822, irregular galaxy, interferometer study of H I assoc. with optical core 78−20889
NGC 6946, galaxy, radio continuum emission from H II complexes and nonthermal disc 77−41407
NGC 7000/IC 5070 (North American/Pelican) nebular complex, thermal radio emission rel. to obscuration and excitation 78−36667
NGC 7023, refl. nebula, region, radio continuum obs. 79−17048
NGC 7027, planetary nebula, optical position meas. with small Schmidt telescope 78−73749
NGC 7331/Stephan's Quintet area, obs. at 1421 MHz 78−12392
NGC 741, 1316, 7626, radio galaxies, dynamics 80−94871
NGC 7538, IRS 1, formaldehyde maser, SHF band obs. 80−67822
NGC 7538 and Sherpless 159, H II region/mol. cloud complex, H I aperture synthesis obs. 80−90510
NGC 7714−7715, peculiar interacting galaxies, discovery of two nearby quasars 78−28835
NGC 7822, NGC 281, bright rimmed mol. clouds, CH obs. 80−62238
NGC 7822 (W 1), supernova remnant, 2.8 and 6 cm wavelength obs. 78−4383
NGC 891, edge-on disc galaxy, radio continuum obs. 78−28786
NGC 891, radiogalaxy halo, Westerbork obs., electron propag. and magnetic fields 78−61920
NGC 925, barred spiral galaxy, high-resolution H I obs. 80−105329
nonthermal radiosource posns. near SN 393, no optical nebulosity 79−58366
nonthermal sources, contrib. to cosmic background spectrum along declination (+50° 30′) 77−17723
nonthermal sources, evolution, relativistic expansion 78−41067
North Celestial Pole, 1421 MHz radiosource survey 77−45590
North Celestial Pole region, deep survey at 4.85 GHz 79−12536
North Polar Spur, origin rel. to MHD waves propag. from galactic centre 77−87547
North Polar Spur, possibly supernova remnant *(Russian)* 78−41072
North Polar Spur, radio continuum obs. at 1420 MHz 80−22100
North Polar Spur (Radio Loop 1), X-ray obs. 80−105370
nova shells, radio emission obs. 80−26868
novalike object in Centaurus, variable radio counterpart detect. 79−67026
NRAO 150, compact radio source, search for time-depend. radio fine struct. 80−90552
NRAO 150, high-resolution obs. at 1.35 cm wavelength *(Russian)* 78−69902
NRAO 5 GHz S2 and I surveys, radiosource identifications 78−54062
number-flux density counts of unidentified radiosources 78−12395
OA 33, variability of optical counterpart 78−45421
OC, 253, towards M33, H I 21 cm emission/absorpt. obs. 80−62262
occultation by comet tails, refr., comet plasma density determ. 79−53773
OE323 (4C 34.13), extended radiosource identification with quasar 77−87563
OF-024 optically active extragalactic radiosource 77−17712
OH 0739−14, IR polarization obs. 79−48901
OH 0739−14, M-type giant in reflection nebula, IR obs. 80−46692
OH 205.1−14.1, unusual OH maser, new flare report and 1667 MHz line obs. 80−98734
OH 205.1−14.1 in Lynds 1630 dark cloud, coincident IR source obs. 80−101630
OH 231.8+4.2, OH maser source, UHF spectra obs. 80−90550
OH 351.78−0.54, UHF obs. of brightest OH maser (1980 August) 80−101644
OH masers, interstellar, obs. near Orion population stars 80−67716
Ohio Sky Survey sources, data reduction and statistics 77−45325
Ohio sources, optical identification using radio and optical positions meas. by Texas interferometers 78−28808
OJ 287, BL Lacertae object, case for synchronous optical-radio outbursts 80−8679
OJ 287, flat-spectrum source, variability at 962 MHz 77−82317
OMC-1, methane-d_1 abundance upper limits from rot. spectrum obs. 80−56705
Ooty occultation extragalactic sources radio spectrum obs. in SHF 80−105371
OP 313, CSVS 6997 as counterpart 77−33515
ρ Ophiuchi dark cloud, atomic and mol. obs. 78−41013
ρ Ophiuchi dark cloud, C II and S II regions obs. 78−49500
optical and radio props. rel. to identifications of 3CR sources 78−28830
optical counterparts of extended radiosources, improved optical positions 78−93444
optical identification of 3rd Westerbork survey sources 79−58436
optical identification of sources in 5C3 field *(German)* 79−30140
optical identification of sources south of declination −75° 77−64863
optical identifications, from position coincidences, using Texas Interferometer radio positions 79−88753
optical identifications, spectrophotometric obs. 79−92879
optical identifications, statistical anal., data selection 78−61928
optical identifications of extragalactic radio sources 80−105373
optical identifications using accurate radio and optical positions 77−37660
OQ 208, red shift difference between broad and narrow emission lines 79−67100
OQ 208 (=Markarian 668), Seyfert galaxy, H83α and H99α radio recomb. lines detect. 80−94864
OQ 208 (Markarian 668), radio spectrum 79−12531
Orion A, 22 GHz water line giant outburst 80−8703
Orion A, C recomb. lines and H I clouds obs. 78−57605
Orion A, confirmation of H_2O 22 GHz line outburst 80−8704
Orion A, detect. of DNC at 152.6 GHz 78−4334
Orion A, first detection of methane at 76 GHz 78−16503
Orion A, H_2O maser source outburst obs. *(Russian)* 80−105320
Orion A, H I absorpt. lines high resolution mapping 78−81667
Orion A, methanol 84.5 GHz and 96.7 GHz lines obs. 80−62245
Orion A, methanol source ang. size lower limit from VLBI obs. 77−13429
Orion A, mm emission lines from organic molecules 77−2477
Orion A, probable detect. of methylamine-d_1 77−33610
Orion A, radio brightness distrib. at 3.5 mm wavelength 77−64837
Orion A, radio meas. of electron temp. distrib. at 22 GHz 77−87558
Orion A, relationships of N_2H^+, HCO^+, HCN and CN 77−33587
Orion A, SiO and H_2O maser obs. 78−8085
Orion A, SiO maser variability at 86 GHz 80−41839
Orion A, struct., radio obs., partially ionized gas 79−21379
Orion A, two new methanol transitions obs. 79−25667
Orion A diffusion cloud, density distrib. from mol. lines intensities 79−97056
Orion A SiO maser intensity vars. 78−93256
Orion B (NGC 2024), recomb. line obs. 77−29895
Orion methanol masers, interferometric and multitransitional study 80−67891

radiosources continued
Orion Molecular Cloud, HCN, HNC and HCO^+ J=3-2 lines detect. 79−25669
Orion Molecular Cloud, NH_3 emission obs. 80−36687
Orion Molecular Cloud, NH_3 spectrum and new dynamical model 78−93373
Orion Molecular Cloud, rotational explanation of high-vel. mol. emission 80−36688
Orion Molecular Cloud 1, cyanoacetylene emission obs. 78−4322
Orion Molecular Cloud 2, relationships of N_2H^+, HCO^+, HCN and CN 77−33587
Orion Molecular Cloud-1 (OMC-1), SO_2 rot. temp. 79−25670
Orion Nebula, C recomb. line mapping 78−20866
Orion Nebula, H_2O 183 GHz line emission obs. 80−41869
Orion Nebula, OH masers obs. 78−16493
Orion Nebula, radio obs. of nearby H I distrib. and vels. 80−105322
α Orionis, 14.9 GHz obs. 79−75210
Orion Nebula molecular cloud, anomalous var. of $N_2H^+/HCO^+/SO_2$ rel. to ion-molecule reactions 77−26034
Orion region, struct. in radiocontinuum 78−49549
U Orionis, Mira variable, relation between 1612 MHz flare and light curve 80−56844
U Orionis, stellar OH maser VLBI obs. rel. to mag. field 79−25742
OS210 (4C 28.40), extended radiosource identification with quasar 77−87563
OTL sources, position and struct. determ. from 327 MHz lunar occultation obs. 80−73061
OTL sources, position and struct. determ. from 327 MHz lunar occultations obs. 80−73062
OTL sources, position and struct. determ. from 327 MHz obs. 80−73060
OV-236 (1921−29), radio outburst obs. of quasar 80−51906
OX+029, nearby extended variable object 79−67096
pairs of radiosources near spiral galaxies 77−26074
parameter determ. method from spinning satellite obs. 80−85871
Parkes 2700 MHz survey, catalogue for Declinations −4° to −15°, Right Ascensions 10^h to 15^h 79−75121
Parkes 2700 MHz survey, optical identifications 77−49489
Parkes 2700 MHz survey, part twelve 77−49315
Parkes 2700 MHz survey, source counts and distrib. 78−28544
Parkes 2700 MHz survey of radiosources, 13th part, 404 objects 78−20656
Parkes 2700 MHz survey of radiosources, 13th part, optical identifications 78−20901
Parkes 2700 MHz survey sources, new optical identifications 79−75289
Parkes 2.7 GHz selected area survey sources optical identifications 77−17701
Parkes sources with flat spectra, optical identifications 78−4382
particle acceleration and radio emission above pulsar polar caps 80−51794
particle acceleration in double sources 80−31380
particle reacceleration in radio galaxies 79−71104
particles accelerated by Alfven waves, distrib. function self-similar solns. 79−32757
peculiar galaxies radio emission detect. 77−17674
AG Pegasi, symbiotic nova, radio emission obs. 77−22232
periodicity investigation at 21 cm 80−82529
S Persei, supergiant 22 GHz H_2O maser emission temporal var. 78−49461
S Persei, supergiant OH star, conditions for circumstellar OH emission 77−22218
β Persei (Algol), orbital period, 1964 to 1978, rel. to radio and X-ray activity 79−58377
β Persei (Algol), radio outbursts and possible period change 80−26907
β Persei (Algol), X-rays detect. 77−9773
Perseus A (NGC 1275), correl. between optical and radio variability *(Russian)* 80−77505
Perseus cluster field, accurate positions of faint optical objects in fields of radiosources 79−12527
Perseus galaxy cluster, low-resolution aperture synthesis map at 408 MHz 80−56958
Perseus OB2 association molecular cloud, mol. obs. rel. to star form. 80−12798
Pictor A, powerful radio galaxy, photographic and spectrophotometric obs. 77−49481
UV Piscium, RS Canum Venaticorum star, identification with X-ray source H0118+067, X-ray obs. 80−101654
PKS 0131−36 (NGC 612), radio galaxy with disc, struct. 79−2568
PKS 0211−47 and 0634−20, giant radiogalaxies, optical and radio obs. 78−81702
PKS 0502-696, no connection with NGC 1809 galaxy 79−30129
PKS 0528−250, neutral stellar object with no emission and rich absorption 78−49551
PKS 0548-322, possible BL Lacertae object, low-energy X-rays detect. 78−89270
PKS 0735+178, B mag. brightening of BL Lacertae object 77−37654
PKS 0735+178, BL Lacertae object, spectrum, multiple components in z=0.424 absorpt. system 79−25707
PKS 1144−379 BL Lacertae object, radio, IR and optical obs. 80−4451
PKS 1345+12, radio galaxy, optical spectrum 78−4341
PKS 1402+044, dissector scanner obs. of red object with 3.20 redshift 78−65710
PKS 1718−649, galaxy, radio and optical study 77−45564
PKS 1934−63, spectrophotometry of radiogalaxy 78−54066
PKS 2126−15, QSO (z=3.27), JHK photometric obs. 80−94888
PKS 2155-304 (H2155−304), newly discovered BL Lacertae object, optical and X-ray props. 80−36702
PKS 2201+04, compact galaxy, optical variability 77−26051
PKS 2322-12, narrow-line radio galaxy, optical spectrum 77−33664
planetary, mapping using VLBI *(Japanese)* 80−21927
planetary and stellar magnetospheres, conf., Snowmass, Colorado, USA (Aug. 1978) 80−41939
planetary nebulae, 6630 MHz brightness rel. to electron density evolutionary changes 77−78861
planetary nebulae, advances in radio obs. 80−109526
planetary nebulae, electron temps. from radio continuum obs. 78−41027
planetary nebulae, radio emission flux density distrib. rel. to radio search near galactic 80−56913
planetary nebulae, radio fluxes rel. to distances determined from ionised mass/radius relation 80−101625
planetary nebulae, southern, SHF obs. 80−90496

radiosources continued
planetary nebulae, stellar, VLA obs. 80−22056
plasma turbulent reactor, relativistic electrons spectrum, synchrotron radio emission 79−40071
plasma turbulent reactor model, Comptonisation process and spectra of relativistic electrons *(Russian)* 77−19760
plasma turbulent reactor power distrib., energy and particle flux directions *(Ukrainian)* 78−93104
plasma turbulent reactors, effect of Compton scattering of transverse waves by relativistic electrons 80−51644
plasma turbulent reactors, relativistic electrons accel. and cosmic radiosources nonlinear spectra 79−8824
polarisation angle, variance rel. to vel. field in turbulent cosmic plasmas 77−17358
polarisation map interp., discontinuities 77−64661
polarised compact radio sources, physical conditions 78−4384
polarization meas. of distant double sources 78−28834
Population I objects, location with respect to galactic plane 77−74127
position meas. and optical identifications for 538 sources at 966 MHz 77−87561
primaeval giant elliptical galaxies, observable props. 78−89260
protostellar H_2O maser sources, disc struct. 79−48784
ζ Puppis, radio emission obs. at 2 cm 78−40969
Puppis A, Fe XIV coronal line and filamentary emission 79−84843
Puppis A, X-ray images of SNR 79−48889
Puppis A supernova remnant, X-ray spectra var. with position 80−82472
Q 0420−388, QSO (z=3.13), JHK photometric obs. 80−94888
QSO 0241+622, nearby X-ray quasar, extended radio emission search 80−31382
QSO 1038+528 A,D, close pair of radio-emitting quasi-stellar objects, radio and optical obs. 80−51902
QSOs, detection of ten MCS objects in SHF 80−105377
QSOs, new type, identified through IR meas. 80−8708
QSOs, optical polarisation alignment with radio struct. 79−25751
QSOs, optically selected, radio study 80−82536
QSOs from Molonglo Deep Survey, optical spectra 80−94884
quasar 0957+561, radioastron. obs. of assumed double quasars 80−105381
quasar radio emission, from quasar group selected for optical brightness 80−41910
quasars, optically selected, search for radio emission 78−20904
quasars, redshift and 3 GHz radio magnitude correl. 78−45422
quasars and galaxies active nuclei, conference, Copenhagen, Denmark, (1977 June 27 to July 2) 78−57675
quasars with radio structure, statistical analysis and redshift-magnitude relation *(Chinese)* 77−67135
radio and Seyfert galaxies, optical spectra 77−17686
radio galaxies, anisotropic explosion of rotating, self-gravitating uniform spheroids 79−8822
radio galaxies, book 78−24564
radio galaxies, local space density 78−57676
radio galaxies, optical catalogue 80−21931
radio galaxies in Coma cluster, optical obs. 78−12358
radio galaxies nuclei, gamma-ray source model 79−25747
radio star obs. at 3.3 mm 77−74065
radio tail galaxy in Abell 2634 cluster, spectrum and radial vel. 77−64857
radio tail galaxy in Abell 401 cluster, evidence for in situ particle accel. 77−26072
radio-galaxies with $13.0 \leq m_{corr} \leq 15.5$, peculiar radial rel. distrib. 77−9798
radioastronomical equipment, techniques and observations, review *(German)* 77−56827
radiogalaxies, accel. of supermassive compact objects by emission of asymmetric radiation 77−45481
radiogalaxies, colour and space density, redshift dependence 79−75278
radiogalaxies, faint southern objects, identification and spectrophotometry 80−56935
radiogalaxies, hot spots in outer lobes 78−69899
radiogalaxies, optical spectroscopy and redshifts for 18 objects 80−56966
radiogalaxies, polarized brightness distrib. at 2695 and 8085 MHz 79−35410
radiogalaxies, redshift-magnitude relation and cosmological test 78−28798
radiogalaxies and quasars, models of extended and double sources 78−16557
radiogalaxies and quasars, spectrophotometric survey 78−28828
radiogalaxies and supermassive black holes 78−61882
radiogalaxies in clusters 78−28806
radiogalaxy interaction with intergalactic medium *(Italian)* 77−87562
radiogalaxy luminosity function and past population evolution 79−44597
radiogalaxy matter and energy ejection *(Italian)* 77−87552
radiogalaxy models, relativistic channel flow, soliton soln. stability 80−56962
rapidly varying radio sources, relativistic plasmoids dynamics theory 78−93438
RCW 38, RCW 57, H II regions, interstellar $^{16}OH/^{18}OH$ abundance ratio obs. 78−54024
RCW 48-49, H II region complex, discovery of strong H_2O maser emission 77−57102
recombination line source model, electron temp. and density inhomogeneity 79−92830
recombination lines, high-n, Zeeman splitting 80−58210
red shifts and rot. measures, Universe isotropy test 77−2502
red shifts for 32 Parkes southern radiosources 79−44627
relativistic blast waves in two dimensions, adiabatic case solns. 80−22108
relativistic blast waves that accelerate 80−67534
relativistically expanding spherical radiosources, flux vars. 79−17112
resolved sources, 1.4 GHz aperture synthesis obs. of circular polarisation 77−29656
revised 3C catalogue of radiosources, optical identifications and spectroscopy 77−22114
revised 3C catalogue sources, study of confusion and resolution 78−12105
rich galaxy cluster, morphology and peculiar vels. of radiosources 78−77610
ring galaxies, H I survey 79−5901
ring galaxies, radio continuum emission 80−67846
RMB 56 (1216+141), compact blueshifted galaxy, H I emission obs. 78−16527

radiosources continued
Roberts 22, bipolar nebula with OH emission, visual, radio and IR obs. 80−94859
Rosette Nebula (NGC 2237/2246), new physical parameters from 6.5 GHz obs. 80−4414
rotation measures and data processing 80−86006
S0 galaxies, radio continuum and H I obs. 77−87549
S252 (NGC 2175), H II region, mol. line obs. of star-forming complex 80−4411
S255, H II region, CO emission small-scale struct. from lunar occultation obs. 80−46637
S255, molecular cloud, molecular line, radio continuum and IR data 78−8087
S4 5 GHz survey between +35° and +70° declination, catalogue 78−69893
S4 sources, flux density meas. at 9.5 mm wavelength 78−69894
Sa spiral galaxies, H I study 80−98714
Sa type spiral galaxies, redshifted 21 cm line profiles, radio obs. 80−73041
HM Sagittae, emission-line variable star, radio emission detect. 78−28706
HM Sagittae, young planetary nebula, 2.8 cm flux density secular increase 79−67025
Sagittarius A, 540 μ obs. of galactic centre 78−36699
Sagittarius A, far IR obs., luminosity, colour temp., optical depth 78−41012
Sagittarius A, H200β line detect. 77−78868
Sagittarius A, H recomb. lines obs. at decimetric wavelengths 77−82310
Sagittarius A, multifrequency radio image *(Russian)* 77−2478
Sagittarius A, radio emission scattering from compact object 78−54049
Sagittarius A, Sagittarius B2, probable detect. of methylamine-d_1 77−33610
Sagittarius A (galactic centre), forbidden O III 88 μm line emission obs. 78−49503
Sagittarius A region, 8.2 mm obs. 78−28794
Sagittarius A W(N), galactic centre, 4 to 8 micron spectrum 79−48922
Sagittarius A West, radial vel. rel. to expansion of Galaxy 77−5574
Sagittarius A West, temp. and dynamics of ionized gas in nucleus 79−44595
Sagittarius B2, 5 and 7 GHz obs. of cyanodiacetylene 79−92817
Sagittarius B2, cyanodiacetylene 2663 MHz transition obs. 77−33669
Sagittarius B2, dimethyl ether emission detect. 79−53862
Sagittarius B2, evidence for chemical fractionation, ^{13}C isotopes 77−87532
Sagittarius B2, far IR obs., luminosity, colour temp., optical depth 78−41012
Sagittarius B2, far IR spectrum obs. 78−8073
Sagittarius B2, galactic centre region, formamide ^{13}C isotope detect. 79−25680
Sagittarius B2, He abundance problem 78−49496
Sagittarius B2, He recombination line obs. interpretation 80−62300
Sagittarius B2, high vel. H_2O maser features obs. 77−9779
Sagittarius B2, interstellar cyanodiacetylene (HC_5N) J=2-1 transition detect. 79−25692
Sagittarius B2, methanol 84.5 GHz and 96.7 GHz lines obs. 80−62245
Sagittarius B2, microwave detect. of interstellar ketene 77−37638
Sagittarius B2, microwave detection of NO 78−93378
Sagittarius B2, mm wave detect. of isothiocyanic acid 80−41878
Sagittarius B2, mm wave detect. of methyl mercaptan 80−41877
Sagittarius B2, NH_3 nonmetastable levels obs. 79−25665
Sagittarius B2, NS radio emission lines detectability 78−54031
Sagittarius B2 molecular cloud, chemical fractionation of ^{13}C isotopes of cyanoacetylene 77−29900
Sagittarius C, far IR obs., luminosity, colour temp., optical depth 78−41012
Sagittarius dwarf irregular galaxy, H I obs. 78−20887
scintars rel. to interplanetary scintillation in N.Polar Spur 79−44579
scintillating radio sources at low flux densities, mean ang. size determ. 77−5453
scintillation, space-freq. correl. function 77−13444
scintillation enhancements due to solar flare assoc. interplanetary shock waves 77−2318
AH Scorpii, supergiant OH star, conditions for circumstellar OH emission 77−22218
Scorpius X-1, review of X-ray, optical and radio emission 78−16576
Sculptor dwarf irregular galaxy, 21 cm obs. 77−64843
RY Scuti, β Lyrae system, optical and radio spectra 79−30090
FH Serpentis (Nova 1970), radio emission from expanding shell 80−26868
FH Serpentis (Nova 1970), thick inhomogeneous shell model for radio emission 78−12236
Seyfert 1 galaxies, H I Balmer lines correl. with disk struct. 80−82503
Seyfert and radio-galaxy nuclei, optical spectra of ionis. gas region, model 78−93420
Seyfert and related galaxies, 1415 MHz survey 77−9800
Seyfert galaxies, H I survey 79−8988
Seyfert galaxies, radio props. 78−49535
Seyfert galaxies, type 1, nuclei props., UV emission, colour index *(French)* 79−48923
Sharpless 159 and NGC 7538, H II region/mol. cloud complex, H I aperture synthesis obs. 80−90510
Sharpless 88A-B and 106, compact H II regions, optical obs. 79−8969
Sharpless H II regions, small-scale struct. at 4.995 GHz, high-resolution catalogue 78−61755
Sharpless small H II regions, radio line and continuum obs. 77−87509
Shostak high-velocity cloud, H I obs. 78−32575
sky survey at 8085 MHz of 0.181 steradians, 64 sources, identifications, spectral indices 78−40836
small diameter sources, catalogue of 23 objects in field of CTA1 SNR 79−62890
small-diameter sources, microwaves deflection by Sun gravit. field, polarisation depend. upper limits 77−2596
SN 1572 (Tycho's supernova), small dia. radio source discovery and precise position 80−98680
SN 1979c in NGC 4321 (M100), detect. at 60 nm wavelength 80−82402
SNR radio shells, spectral index distrib. 80−77462
source count and redshift interpretation in evolutionary use 78−28832
source counts and spectral index distrib. for Westerbork 610 MHz sources 79−44630
source posns. using transatlantic long base line interferometry at 10680 MHz 79−48390
source structure meas., scintillation effects 79−96922
south polar cap sources, optical identifications 79−75284
Southern Coalsack, CO emission obs. 77−29902
southern extragalactic radio sources of large ang. extent, emission spectrum vars. 80−17683
southern extragalactic sources, obs. with Fleurs synthesis telescope 78−4385
southern Molonglo radio sources, optical spectra 78−96555
southern Parkes radiosources, redshift obs. 78−20899
southern PKS sources, spectroscopic identification 79−25744
southern radiosource identifications 77−45591
southern radiosources, redshift meas. 77−26075
southern radiosources, redshifts for 19 QSOs and three galaxies 79−97060
southern sources, spectral indices 78−28819
southern sources with steep radio spectra, identification, assoc. with clusters of galaxies 78−32587
space distrib. from short wavelength surveys 80−62305
space distribution of extragalactic sources, comparison with clusters of galaxies *(Chinese)* 79−17111
spatial distribution, statistical method of multiple binning 80−8698
spectral index of extragalactic sources selected at 1.4 GHz 78−28820
spectral index rel. to synchrotron reactor particle energy distrib. function *(Russian)* 78−4098
spectroscopy *(Japanese)* 80−62031
spiral galaxies, local mass-to-light ratio radial var. 80−31361
spiral galaxies, radio continuum flux from discs, theory 77−13460
spiral galaxies, radio continuum morphology, review 77−26071
SS 433, 10 GHz variability and thermal radio emission hypothesis 80−31307
SS 433, 164^d period as precessional motion, massive black hole and pulsar models 80−62138
SS 433, 180 mm interferometric obs. of triple structure 80−105259
SS 433, 1979 May-June radio flare, 3.24 GHz obs. 80−46567
SS 433, 6.55 day periodicity in emission line wavelengths 80−51784
SS 433, accreting black hole model 80−85958
SS 433, accretion disc viscosity determ. using slaved disc model 80−62110
SS 433, associated filamentary optical nebulosity detect. 79−88723
SS 433, B V photometry and short-term light vars. (1979 July 23 to September 17) 79−101165
SS 433, beam acceleration, radiation and precession theory 80−72971
SS 433, beam models, energetics anal., possible triple system 80−90433
SS 433, binary star model including mag. white dwarf 80−4385
SS 433, change in radio struct., 1980 January to June, from VLBI obs. 80−109557
SS 433, deviations from standard model 80−98669
SS 433, discrepancy between optical and radio positions 80−31303
SS 433, disk-driven precession 80−94803
SS 433, dissipative infall model 80−67749
SS 433, early-type binary model 80−56843
SS 433, emission line radical vels. and no periodic signals 79−80327
SS 433, emission line wavelength changes 79−48816
SS 433, emission regions and black hole accretion disk 80−67746
SS 433, enormous periodic Doppler shifts obs. 80−17593
SS 433, evidence for association with supernova remnant (W50) 80−51851
SS 433, general spectral features 80−77421
SS 433, Hα blue component wavelength obs. and weak lines interpretations 79−67023
SS 433, Hα emission object, 21.6 and 43 GHz obs. 79−92783
SS 433, Hα radial vel. obs. (1979 July) 79−88674
SS 433, H I absorption obs. and distance 80−56848
SS 433, IR and visible obs., IR excess and emission processes 80−4387
SS 433, IR energy distrib. obs. 80−31312
SS 433, IR light curves from BVIJHK photometry, period and ephemeris 80−8642
SS 433, IR photometry, and search for short period variability 79−58346
SS 433, IR spectral obs., reddening and emission 80−4388
SS 433, IR variability obs. 80−98676
SS 433, light curves, double peak and binary-like period, photometry 80−94804
SS 433, light minimum epoch and period 80−26886
SS 433, line posn. vars. interpretation 79−75218
SS 433, magnetic X-ray binary model 80−109447
SS 433, mass accel. and collimation mechanisms 80−4368
SS 433, mass loss rates and lifetime from W50 optical filaments 80−12804
SS 433, models of supercritical accretion discs around black holes 80−105272
SS 433, nature and evolutionary state *(Russian)* 80−36647
SS 433, near IR (600 to 1100 nm) spectra, 1979 June and September 79−97009
SS 433, near IR spectrum obs. 79−84803
SS 433, nearby faint, highly-contorted nebular filament discovery 80−94855
SS 433, no 6-day periodicity in 1978 June-1980 Feb. obs. period 80−62150
SS 433, Of star orbited by neutron star, model 80−22025
SS 433, photometric and astrometric obs. 79−84801
SS 433, photometry, 1979 July to October, and 6.5 day period identification 80−8643
SS 433, precessing ring model, test by spectral line obs. 79−101152
SS 433, radial vel. curve low amplitude section, visible spectra anal. 80−67737
SS 433, radio and optical obs. 79−88661
SS 433, radio and optical positions coincidence 80−56840
SS 433, radio jet discovery 80−31381
SS 433, reality of 6-day periodicity in spectral lines wavelengths var. 80−67743
SS 433, relativistic beam interaction with interstellar matter, mass loss rate, visible obs. 80−101629
SS 433, review of obs. and theories 80−72987
SS 433, search for radio spectral lines in UHF 80−109556
SS 433, short term Hα central intensity increases 80−4375
SS 433, spectral features interpreted a precessing neutron star with jets, possible binary 80−90447

radiosources continued
SS 433, spectroscopic obs. and probable binary nature 80−51780
SS 433, UV spectral search and 8 GHz linear polarization 79−71048
SS 433, V band photometry and broad min. prediction (1980 April-May) 80−82390
SS 433, visible and IR photometric and polarisation obs. 79−80321
SS 433, visible and JHKL photometry and light vars. periodicity 79−53821
SS 433, VLBI detect. and ang. struct. 80−31304
SS 433 (H 1908+050), X-ray obs. 79−71153
SS 433 (W50), assoc. optical supernova remnant discovery 80−56916
SS 433 (W50X), kinematic model for line wavelengths vars. 79−75226
SS 433 as veiled pulsar 80−41842
SS 433 inside SNR, unique spectrum 80−82381
SS 433 model, precessing jets in ultra-close binary system 80−4384
stars in Pleiades region, radio and optical obs. of flares *(Russian)* 78−93245
stars with mass loss, polytropic models 79−2544
statistical properties temporal vars. of complete samples of radiosources at cm wavelengths 79−2575
statistical test on complete sample of identified sources 78−89269
steep LF radio spectra search among quasars and clusters of galaxies 77−45583
steep spectrum radiosources, spectral index dependent props. 80−36730
steep-spectrum sources, possible LF variables, 410 MHz fine struct., interplanetary scintillation obs. 78−41068
stellar OH masers, struct. 77−53583
stellar SiO masers, $J=1\rightarrow0$ $v=1$ and 2 masers relative intensity and vel. 80−4339
Stephan's Quintet, radio continuum maps at 2695 MHz 77−57099
Stephenson-Sanduleak 433, 1.2-2.5 μm spectroscopy, photometry and polarimetry 80−41838
Stephenson-Sanduleak 433, anomalous emission lines, gas around central massive black hole 79−53831
Stephenson-Sanduleak 433, emission-line star/X-ray source/radiosource assoc. with W50 SNR 79−8930
Stephenson-Sanduleak 433, Hα emission object, hot spot detect., rot. vel. and spectrum vars. 79−8933
Stephenson-Sanduleak 433, Hα emission object, nonthermal radio emission obs. 78−86033
Stephenson-Sanduleak 433, Hα emission object, variable radio emission obs. 78−86034
Stephenson-Sanduleak 433, massive black hole hypothesis 79−71057
Stephenson-Sanduleak 433, model, precessing ring around massive black hole 79−88678
Stephenson-Sanduleak 433, moving emission features, dynamical models 79−67034
Stephenson-Sanduleak 433, nature, special relativistic effects, binary model 79−88679
Stephenson-Sanduleak 433, possible double jet struct. 79−48827
Stephenson-Sanduleak 433, spectral variability 79−62839
Stephenson-Sanduleak 433, Thomson scatt. lines in spectrum, relativistic gas motions 80−22019
Stephenson-Sanduleak 433, unusual optical spectrum changes of Hα-emission object 79−5838
Stephenson-Sanduleak 433, X-ray emission obs. 79−12480
stimulated linear acceleration bremsstrahlung 79−92658
strong EM waves in collisionless homogeneous plasma, waveform, polarisation and nonlinear effects 78−53809
structure and intergalactic medium 79−62921
structure dependence on freq., 81.5 MHz-5 GHz data 77−49491
structure mapping using VLBI obs. 79−96921
structures of 18 radio sources with peculiar optical features 79−12532
superlight flux variations in relativistically expanding sources, models 78−4377
superluminal expansion velocities, rel. to doubling of Hubble's const. 78−81722
superluminal expansion vels. and redshifts, kinematic model 77−26050
superluminal radio sources, cosmological proper motion-redshift relation 80−22095
superluminal radio sources, mag. dipole model 80−56959
superluminal sources, structure monitoring 79−44626
superluminally expanding radiosources and radio-quiet QSOs 79−30142
supernova radio pulses, searches and possible sensitivity improvements 78−40975
supernova remnant in irregular galaxy NGC 4449, radio emission obs. 79−17056
supernova remnant with broad optical emission lines near NGC 4449 irregular galaxy 79−17057
supernova remnant/pulsar associations, possible origin in close binary systems 78−85965
supernova remnants, compact, positional coincidences with COS-B γ-ray sources 78−45435
supernova remnants, cosmic rays accel. in shock fronts rel. to synchrotron emission 78−32302
supernova remnants, electron acceleration mechanism 80−85988
supernova remnants, galactic, new catalogue corrected for distance from galactic plane 79−75120
supernova remnants, galactic, new optical obs. 80−17636
supernova remnants, galactic, radio evolution and population characts. 79−75254
supernova remnants, galactic, systematic search for optical nebulosity 79−29998
supernova remnants, physical parameters from radio emission characts. 77−13431
supernova remnants, radio dynamical evolution of young objects 78−93365
supernova remnants, radio evolution, generalized theoretical approach 80−85990
supernova remnants, radio struct. obs. 77−13435
supernova remnants, radio surface brightness-diam. correl. 77−29899
supernova remnants, source counts rel. to galactic supernova outbursts frequency 80−62168
supernova remnants, southern, high resolution radio obs. 80−51849
supernova remnants, X-ray obs. by ANS 79−92833
supernova remnants in LMC, SHF OBS. 80−67864
supernovae long-lived remnants, number rel. to supernovae occurrence freq. 77−64784
supernovae stellar remnants, identified with new class of radio star 79−17117
radiosources continued
superrelativistic velocities, apparent, redeterm. in chronometric cosmology 79−25768
surveys at 5 GHz at NRAO and MPIfR 78−28817
symmetric struct. in slingshot theory of radiogalaxies 77−45542
synchrotron radiation, sources, discovery, spectra, review 77−5585
synchrotron self-absorbed sources, polarized radiation transfer 77−53413
synchrotron sources, form. of universal and diffusion regions of relativistic electrons non-linear spectra 80−109555
synchrotron sources, nonuniform struct. effects on physical parameters 78−8138
synchrotron sources with internal absorpt., radio spectra 77−5580
V711 Tauri, radio flare on 1978 Nov. 6 at 15.5 GHz 79−5836
V711 Tauri (HR 1099), 1977-1978 photometry before radio outburst 79−21337
V711 Tauri (HR 1099), 1978 photometry during radio outburst 79−21338
V711 Tauri (HR 1099), Lyman α H I and D I interstellar absorption 80−8658
V711 Tauri (HR 1099), RS Canum Venaticorum star, BV light curve during (1978-79) 80−105279
Taurus A, decametric emission, quasi-periodic fluctuations *(Russian)* 79−25561
Taurus A, intensity and polarisation at 9 mm wavelength 80−36732
Taurus A, sporadic radio flux increases and decreases 77−78877
Taurus A (Crab Nebula), supernova remnant, 927 MHz emission secular decrease 79−75255
Taurus dark cloud, gas temps. and motion 77−78851
Taurus HL-1, small H I velocity bridge, 21 cm obs. 78−28755
Taurus Molecular Cloud 1, interstellar cyanodiacetylene (HC_5N) J=2-1 transition detect. 79−25692
Taurus Molecular Cloud 2 (TMC-2), HC_5N and NH_3 obs. 80−26957
The Galaxy, continuum radiation interpretation using new model of spiral struct. 77−13465
thermal radiation sources, polarisation theory *(Russian)* 77−91656
thermal radio emission from explosion in stellar atm. 77−53580
TMC2, interstellar dark dust clouds, HC_5N and HC_7N obs. 78−54023
transparent synchrotron astronomical sources, internal Faraday rot. effect 80−72760
Turner-Gott galaxy groups, virial mass/galaxy mass ratio from galaxy H I profiles 80−56937
twin jet model for radio trails 79−75290
two-dimensional radio brightness reconstruction, maximum entropy technique 78−28534
Tycho's supernova (SN 1572), unsuccessful search for optical stellar remnant 80−101603
Tycho's supernova remnant, radio flux density meas. separated by 15-year interval 80−26955
Tycho supernova remnant, radio struct. 80−56919
Type I OH maser sources, obs. of nearby compact H II regions 78−8094
type II OH/IR sources in AFCRL catalogue, optical, IR and radio sources 78−4393
4U 0241+61, optical and radio identification, luminous low-redshift QSO 78−61940
3U 0901-09 radio counterpart, 2695 MHz obs. 77−26089
UHF survey, positions and optical identifications, for sources selected at 966 MHz 80−73059
unidentified high latitude sources likely to be radio galaxies and quasars 78−57672
UTR-2 survey, sources in $0°<\delta<+10°$ range 79−97091
UTR-2 survey, spectra of sources in 10-1400 MHz range 79−97092
UTRAO 335-380 MHz survey, interim report 78−28815
variable extragalactic radiosources, 90 GHz obs. 77−71152
variable extragalactic sources with flat spectra, structure 78−28811
variable extragalactic sources with steep spectrum, VHF and SHF obs. 80−90548
variable radio sources, obs. at 0.95 and 1.65 cm wavelength 78−16552
variable radio sources search at 18 cm wavelength, complete sample obs. 78−89268
variable radiosource obs. at 13 cm *(Russian)* 78−32591
variable sources, 18 cm obs. 77−37662
variable sources, nature of cm radiation quasisteady component 79−21456
variable sources, search at 408 MHz 77−33671
variable sources, spectra, RATAN-600 radiotelescope obs. *(Russian)* 78−61927
Vela supernova remnant, rot. measure and turbulent struct. 80−51836
Vela supernova remnant, X-ray maps comparison with radio and optical features 80−51838
Vela X supernova remnant, radio polarisation maps 80−56909
γ^2 Velorum, radio emission obs. at 2 cm 78−40969
Virgo A, core object, comparison of 5 and 23 GHz maps 80−82488
Virgo A (M87), 1.3 cm obs. 78−49550
Virgo A (M87), Westerbork map at 610 MHz 80−62302
Virgo cluster galaxies, 1.4 GHz continuum survey 80−98721
Virgo cluster spiral galaxies, H I deficiency from 21 cm obs. 80−62277
VLBI observations at 430 MHz for 108 radiosources 77−41416
VRO 42.05.01, Hα inteferometric obs. of fast filaments and high vel. gas 79−75258
14W12, in X-ray cluster of galaxies Abell 401, radio emission distrib. 80−98731
W12 (NGC 2024), H I absorpt. lines high resolution mapping 78−81667
0846+51W1, eruptive BL Lae object with high z, visible and radio obs. 79−62899
1601+17W1 (NGC 6034), radio tail galaxy in Hercules cluster, Westerbork obs. 78−36706
W1 (NGC 7822), optical studies of kinematics rel. to supernova remnant struct. 78−54028
W1 (S171), optical supernova remnant radial vel. field 80−62250
W28 A_2 H II region, RATAN-600 2-13 cm wavelength obs. *(Russian)* 80−17642
W31 region, compact far IR source assoc. with G10.6−0.4, early stage of stellar evolution 78−49504
W31 region, high resolution far IR survey 78−12389
19 W32, 43 and 109, galactic centre planetary nebulae search 80−90506
W33, compact H II region, 3.4 to 33 microns obs. 77−22287
W33, H I shell obs. 77−64871
W33, H II complex, high resolution obs. at 2.8, 6, 18 and 21 cm wavelength 78−57619

radiosources continued
W33, OH radio emission sources obs. *(Russian)* 80−62247
W33, recomb. lines as evidence for cool H II region with mass flow 78−49501
W33 A, OH source, IR spectrophotometric and polarimetric obs. 79−21451
W35, W43, H II regions, low-freq. radio recomb. lines studies 78−32589
W3, 8 to 13 micron spectrophotometry of compact sources 77−57070
W3, dusty H II region, stellar optical polarisation meas. 78−45379
W3, IR line emission, airborne obs. 78−93353
W3, IR maps from 4.9 μm to 20 μm 78−49495
W3(OH), 49N and 51, OH and H_2O maser spatial distrib. 78−93355
W3(OH), H_2O emission vars. *(Russian)* 78−16556
W3(OH), H_2O maser emission increase 77−53672
W3(OH), high vel. water maser features obs. 80−31339
W3(OH), interstellar OH maser, struct. from VLBI synthesis obs. 80−105368
W3(OH), NH_3 emission and absorption at 23 GHz 78−36714
W3(OH), production by moving compact object 78−54064
W3(OH), rapid time vars. of H_2O maser source, models 79−17058
W3(OH) and surrounding diffuse ionised gas, radio recomb. line obs. 78−93371
W3 (OH), Zeeman effect in OH maser emission 78−93377
W3 H II complex, mapping of source parameters 79−58392
W3 H II region, CO, CS and HCN obs. LF obs. 80−82446
W3 region, near IR obs. of far IR sources G133.8+1.4 (W3N) and G133.982+1.14 (BS4) 80−22058
W3/W4/W5 region, 1420 MHz continuum survey 78−16497
W3/W4/W5 region, heavy optical obscuration obs. 80−62301
W40 and W48, near IR and CO mm wavelength obs. 78−65667
W43, radio emission obs. 77−17724
W44, ANS obs. of X-ray emission from SNR 78−54010
W48, 18 cm obs. of OH source 78−28812
W48, H II region, H 85α recomb. lines obs. 78−28762
W48, OH emission and absorption, spatial distrib. in H II region *(Russian)* 80−36733
W49, H I absorpt. lines high resolution mapping 78−81667
W49, stimulated Raman scatt. and high vel. H_2O maser features 77−49463
W49 A, H_2O masers and H II regions obs. at 23 GHz 79−71136
W49 A, struct. deduced from mol. and recomb. line obs. 77−33665
W49 H_2O vapour maser source, correlated variability 79−35352
W49 region, CH radio emission obs. 77−87511
W49A, high sensitivity Hnα radio recomb. line obs. 80−26998
W49A, W51A, compact H II regions, H109α recomb. line, aperture synthesis obs. 80−105314
W49A, W51A, W51B, Arecibo obs. of H166α and C166α recomb. lines 77−22300
W50, conditions for assoc. with SS 433, models 80−67737
W50, continuum obs. at 2695 MHz of SNR 80−67830
W50, probable supernova remnant, relation to (SS 433) 80−72987
W50, supernova remnant, N II emission enhancement and distance rel. to assoc. with (SS 433) 79−92783
W50, supernova remnant, optical filaments spectra rel. to SS 433 mass loss rates and lifetime 80−12804
W50, supernova remnant, optical spectrum 80−90557
W50, supernova remnant, spectrum of optical nebulosity 80−51851
W50, supernovae remnant, associated filamentary optical nebulosity detect. 79−88723
W50 (SS 433), supernova remnant, optical filamentary nebulosity discovery 80−56916
W51, detect. of impact broadening of recomb. line 78−28741
W51, first optical detection, rel. to galactic spiral struct. 78−61900
W51, H II region-molecular cloud complex, cold gas flow 79−97048
W51, high vel. H_2O maser features obs. 77−9779
W51, probable detect. of methylamine-d_1 77−33610
W51, radio recomb. line obs., confirmation of impact broadening theory 78−54019
W51, structure and vel. characts. of H II regions 79−71139
W51, W49, airborne for IR spectroscopic obs. rel. to dust cloud model 80−36684
W51 H_2O source obs. with Crimea-Haystack interferometer *(Russian)* 78−69865
W51 Main, H_2O maser emission 80−8701
W51A, W3 (Main), W49A, continuum obs. at 3.9 mm 79−35333
W58, galactic star-forming region, CO obs. 80−67810
W58, IR obs. of H II regions and dust clouds near K3-50 77−49457
W75 maser sources, 1667 MHz line profile features 79−5914
W80 (Pelican Nebula), CO obs. of expanding mol. shell surrounding H II region 80−105296
W 3, H II region, study of nearby partially ionised interstellar medium 77−57077
W 51 region, possible detect. of Na I 17 cm hyperfine emission 78−8139
18W catalogue of radiosources in Abell 2197 and 2199, Westerbork survey at 610 MHz 80−67883
29, 30 and 31W catalogues, Virgo cluster galaxies 80−98721
17W list from 610 and 1415 MHz obs. of Abell 1367 cluster of galaxies 79−35401
28 W sources and catalogue in NGC 7000 IC 5070 H II region complex 80−105308
20W sources in Hercules supercluster 79−44625
22W sources in Perseus cluster, WSRT 610 MHz obs. 79−75283
weak point sources, aggregate flux at 1404 MHz 77−13480
weak radio galaxies, relationship between radio power and enhanced emission regions separation 79−25726
weak radio nuclei in galaxies and quasars 77−17680
weak radio sources scintillation, low freq. obs. 79−53921
weak sources with components, flux densities and source parameters 78−28833
Westerbork 1415 MHz survey of background radiosources, optical identifications 77−49488
Westerbork 1415 MHz survey of background radiosources, optical identifications 77−64867
Westerbork observations of deep 5 GHz NRAO survey, positions, optical identifications 77−87560
Westerbork radiosource surveys at 610 and 1415 MHz 78−28542
WSRT deep surveys, identifications 78−28826
X-ray burst sources, search for correlated X-ray and radio emission 78−57695
X-ray sources, compact, radio emission origin 80−62317

radiosources continued
X-rays from radio binary systems 77−33700
young SNRs, search for radio emission at 3.7 and 11 cm 78−40972
young stars, high-freq. radio continuum obs. 80−51766
young supernova remnants, radio emission evolution according to observational data 79−75256
Zw 1400+0949 cluster (NGC 5416 group), 21 cm obs. 80−22090
III Zw 2, compact galaxy, radio outburst obs. 79−75277
III Zw 2, X-ray emitting Seyfert galaxy, VLBI obs. 79−5903
II Zw 40, 70, 71, CO emission upper limits 78−36693
II Zw 40, dwarf galaxy, radio obs. 79−8992
3C 348, 3C 111, multiple radio galaxies, intermediate latit. H I absorpt. obs. 79−12503
CH, interstellar, radio obs. towards various galactic objects 77−87512
CO emission, obs. in galactic refl. nebulae 77−53658
CO in interstellar dark clouds, evidence for isotopic fractionation 80−46638
CO, in molecular clouds, obs. rel. to Galaxy rot. curve to R=16 kiloparsecs 79−97081
CO, interstellar, distrib. around (l=30°, b=0°) 80−41868
CO, interstellar, isotope fractionation in Lynds 134 dust cloud 80−26924
CO, interstellar, radio emission rel. to cold mol. clouds in inner Milky Way 80−4425
^{13}CO in external galaxies, $^{12}CO/^{13}CO$ intensity ratios 80−4416
Cygnus A, intensity and polarisation at 9 mm wavelength 80−36732
H I, column density as function of position in southern sky 80−4420
H I, galactic, high angular resolution emission spectra, self absorpt. and other characts. 79−35350
H I, nonplanar, assoc. with Perseus spiral arm, 21 cm obs. 78−16489
H I at high galactic latitudes, time variable 21 cm line profiles correction 80−51844
H I emission in direction of quasar PHL 957, upper limits 77−91659
H I in field of elliptical galaxy NGC 1052, 21 cm emission mapping and line profiles 80−98719
H I in galactic centre region, survey 79−88722
H I in region 348°≤l≤12°, +3°≤b≤+17°, 21 cm obs. 78−45377
H I low-latitude negative velocity clouds in galactic anticentre, distance 77−45506
H I of local spiral arm, fine struct. 77−57091
H I profiles classification system for dwarf galaxies, discrete redshift and asymm. 78−49517
H I regions, 21 cm spectra rel. to galactic shocks 78−54042
H I regions, comparison of 21 cm obs. with UV and optical absorpt. line meas. 78−24532
H I regions, galactic, emission absorpt. obs. from Arecibo 78−57610
H I regions, new feature discovery in Vulpecula-Delphinus *(Russian)* 80−46654
H I within 10° of galactic centre direction, broadband obs. 77−78853
H II blisters, dusty, appearance at radio and IR wavelengths 80−85979
H II regions, anisotropic, with axial symmetry, models rel. to radio brightness distribs. 78−85993
H II regions, clumping factor meas. technique 78−20870
H II regions, compact, in interstellar dark clouds, radio continuum interferometry 80−98699
H II regions, compact inhomogeneous, radio recomb. line and continuum emission theory 79−62885
H II regions, effects of dust on radio emission 77−33588
H II regions, electron temps. determ. from radio recomb. line obs. at 22 GHz 79−35334
H II regions, forbidden O III 88 μm line emission obs. 78−49503
H II regions, galactic, comparative study of high-radiofrequency and far IR obs. 78−49497
H II regions, galactic, radio continuum fluxes rel. to forbidden S III 18.71 micron emission 79−97046
H II regions, H137β/109α intensity ratio interpretation 80−31344
H II regions, multiple-component, radio recomb. lines press. broadening 80−4419
H II regions, newly formed, in interstellar dark clouds, physical props. from radio continuum interferometry 80−105301
H II regions, origin from supernovae explosions 80−67877
H II regions, profile of Hnα radio recomb. lines in static ion field 77−78629
H II regions, search for Zeeman effect in RF recomb. lines 77−60809
H II regions, southern, 1 mm continuum obs. 79−8968
H II regions, southern, NH_3 obs. 78−69863
H II regions around l=111°, aperture synthesis obs. 77−64827
H II regions assoc. with optical nebula K3-50, 15 GHz obs. 78−16554
H II regions in Perseus Arm, high-resolution radio maps 78−32549
H II regions is IC 1795/1805, IR luminosity compared with exciting star total luminosity 78−96519
H II regions near OH 43.79-0.13 and OH 48.61+0.02, radio obs. 78−36669
H II regions radio emission analysis, consequences of improper analytic methods 78−54000
H II regions relationship to CO clouds, blister model 79−25681
H I+molecular/H II shells from 1 to 2000 pc dia., wind-driven or supernova remnants 79−25678
H-like ions, departure coeffs. from thermodynamic equilib., rel. to radiosources recomb. lines 79−76369
H_2D^+, interstellar and circumstellar search, upper limit determ. 79−2562
H_2O cosmic masers, influence of dust on collisional pumping 78−54030
H_2O maser emission from external galaxies, detects. 78−45417
H_2O maser near RT Serpentis, obs. 79−8932
H_2O maser source near NGC 2071, discovery 78−73768
H_2O maser sources, near IR pumping 77−78862
H_2O maser sources, W 49N and 51 global radiotelescope obs. *(Russian)* 77−22072
H_2O maser sources in different stages of evolution, new VLBI maps 80−26954
H_2O maser sources in galactic plane, southern hemisphere survey 80−73054
H_2O maser sources in W3, accurate positions 78−4332
H_2O masers, 22 GHz galactic plane survey, 14 new sources 80−77464
H_2O masers, accurate interferometric positions at 1.35 cm 78−45374
H_2O masers, interstellar obs. with resolution of 0.0008 arcsec 77−74154
H_2O masers assoc. with mol. clouds, VLBI aperture synthesis obs. 79−21368
H_2O masers located near Herbig-Haro objects, discoveries 79−21369
H_2O sources, linear polarisation of 22 GHz line emission 78−77612
H_2O sources in Galaxy, sites of newly formed OB stars 78−12390

radiosources continued
H_2O sources spectra, autocorrel. anal. 78−65713
N_2D^+, interstellar, radio detect. in L134 N 78−16492
NGC 1499, H II region nebula parameters determ. from decametre wavelength obs. *(Ukrainian)* 79−40243
OH 1612 MHz survey at high declinations 80−4452
OH 18 cm emission sources, fluxes and circular polarisation (1965-1972) 77−13441
OH astronomical sources OH 231.8+4.2, CY Canis Majoris, M1−92, UHF obs. 80−90550
OH emission sources, low latitude search at 1612 MHz 77−49452
OH in interstellar dust clouds, nonthermal main lines obs. and OH abundance 80−36683
OH, interstellar, new main line maser obs. with probable Zeeman pattern 80−56908
OH, interstellar, radio obs. towards ζ Ophiuchi and evidence for interstellar shock 79−97052
OH maser clouds, saturation effects 77−91657
OH maser emission, rot. excitation by H_2 at interstellar temps. 80−62232
OH maser source OH 0739−14, IR polarization obs. 79−48901
OH maser sources, accurate position meas. 80−46646
OH maser sources, interstellar, radiative transport effects on inversion 80−17681
OH maser sources near galactic centre, systematic search at 1612 MHz 79−35415
OH masers, ground state Λ doublet emission as result of overlapping far IR transitions 77−45533
OH masers, obs. of new assoc. IR objects 78−12407
OH masers, type I, positions, polarisation, nearby H_2O masers, radio and IR props. 79−25671
OH masers assoc. with IR stars, very long baseline interferometric obs. 77−53699
OH masers in direction of H_2O masers, new discoveries 78−12393
OH Mira variables, light curve shapes rel. to mass loss 77−56944
OH molecules, detection of monopoles by nonlinear effects in interstellar masers 77−91609
OH radio emission sources, type IIc, in W33, obs. *(Russian)* 80−62247
OH sources, 1720 MHz transition survey, comparisons with 1612, 1665, and 1667 MHz obs. 77−45586
OH type I maser sources, model 80−90556
OH type II stars, unidentified, search for H_2O emission 79−75286
OH/IR source in compact H II region G45.5+0.1, IR photometry 78−4396
OH/IR stars, IR search and identifications 78−24510
OH/IR stars, new SiO transition detect. 78−53954
OH/IR stars, OH main lines masers inversion 78−28664
OH/IR Type II sources, radial diameters from 1612 MHz OH line obs. 78−36713
OH/IR unidentified Type II sources, 1612 MHz obs. at low galactic latits. 77−17704
OH/IR unidentified Type II stars, galactic distrib. and kinematics from 1612 MHz survey 78−49450
SiO 86.2 GHz maser sources, polarisation props. 80−4449

radiostars *see radiosources (astronomical)*

radiotelegraphy
INMARSAT marine system, satellite radio teletype communication 80−26614

radiotelescopes
see also radioastronomy
3 cm band radiometer with 3 GHz tuning *(Russian)* 77−56828
7 m Cassegrain antenna, quasioptical feed system for millimetre wavelengths 78−32343
5120-channel digital cross-correlator for Westerbork radiotelescope 77−64650
amateur, intermediate freq. amplifier, phase-switching radiomater, power supply, chart recorder, construction 79−21189
amateur equipment, site choice and obs. techniques 79−40076
amateur equipment, testing equipment 79−16830
amateur radio telescope, design 78−81541
amateur radio telescope, design 78−85849
N.American observatories, VLBI meas. rel. to intra-plate crustal deformation 80−51379
antenna arrays, direct transform hardware processing of rot. synthesis data 78−85857
antenna arrays, incoherent optical 1-bit cross-correlators for digital signal processing 80−98555
antenna calibration, radioastronomical methods, standard sources *(Russian)* 78−4103
antenna concepts, for interstellar search systems for extraterrestrial intelligence 78−28545
antenna design for amateur radio interferometer 79−88597
antenna meas. technique and recording system using punched tape *(Russian)* 78−65501
antenna multi-beam system, fully automatic, for interplanetary scintillation obs. 79−101064
aperture efficiency of 6m mm-wave antenna *(Japanese)* 78−89061
aperture synthesis, electronic technique for two dimensional Fourier transformation *(Dutch)* 77−67042
aperture synthesis telescope, data complementing by short spacing data from single dish obs. 79−66928
aperture synthesis using very long baseline interferometry 80−46414
Arecibo Observatory, ionospheric props. meas. without rockets 78−81488
Arecibo Observatory, radiotelescope and instrumentation description 80−4249
array detectors for mm line astronomy 79−44364
Australian synthesis telescope, design, array config. 78−69690
Australian Synthesis Telescope, design plans 77−33345
basic, construct., perform., and testing 78−40828
beam size, rel. to radio source meas. ang. dias. 79−12534
C-band p-i-n diode integrated switch matrix, cryogenically cooled 78−96392
chromatism due to blocking and feed scatt. 78−73630
cm-wave radiometer, with enhanced long-term stability, for solar radio emission obs. 80−109361
coherence theory 77−5428
coherent microwave imaging of limited fields of view, angular and aperture noise, optimum procedure 77−67045
Columbia GISS 4 ft telescope, low-noise 115 GHz receiver 79−53718
compound spherical mirror for space telescope 80−41720

radiotelescopes continued
contour maps of reflector surface errors, rapid meas. method 77−41301
correlator interferometer antenna arrays, theory 80−12670
cost-scaling laws applicable to very large optical telescopes and radiotelescopes 80−41722
Crimea-Haystack VLBI instrument operation *(Russian)* 78−69693
Croce del Nord, new front-end receiver with 30 to 408 MHz amplifier-convertor *(Italian)* 79−2478
cryogenically cooled mixer for 80 to 120 GHz, improvements 79−40073
Culgoora, correlator back-end, advantages and disadvantages 80−85865
decametre radiotelescope facility at Mt. Zao Observatory, Japan 80−51656
decametric range radio telescope, for interstellar excited H lines searching *(Russian)* 80−12822
design, multidisciplinary teaching exercise, Jupiter bursts and quiet Sun obs. 80−17759
development survey *(Japanese)* 80−12664
diplexer, quasi-optical, for mm wavelength 79−21187
DKR-1000, T-shaped alignment results *(Russian)* 77−22068
Effelsburg 100 m radiotelescope, first obs. at 7 mm wavelength, props. and performance 80−62013
Effelsburg 100 m radiotelescope, large dynamic range obs. 78−96391
error correction computation, due to temperature differences of mechanical structure *(German)* 79−84669
far-field of blocked circular aperture, example of 100 m radiotelescope, Effelsberg *(German)* 77−2341
feeds, compact dual-hybrid-mode feeds with low crosspolar radiation 80−12662
Five College Radio Astronomy Observatory facilities 77−73948
Fleurs Synthesis Telescope extensions 77−33346
global radio solar telescope network, solar activity monitoring appl. 80−82202
gravitational astigmatism meas. 78−45222
hectametric cross-shaped radiotelescope for 2.8 to 10 MHz obs., design *(Russian)* 80−12660
heterodyne freq. analyzer, detection of 200 to 400 GHz weak microwave signals 80−94716
historical account and development trends *(Italian)* 78−12095
interferometer, tropospheric influence in differential meas. of astrometric coordinates 80−67581
interferometer, two antennae, phase-switched between 160 and 190 MHz *(Italian)* 79−12402
interferometer, two telescope, principles, effect of atmospheric disturbances *(Dutch)* 77−67041
interferometer signal processing by acoustooptic correlation devices, radio astronomy applications 80−8543
interferometer with long baseline, classical response 78−61733
interferometry and aperture synthesis, review 77−9671
Jodrell Bank, Multi Telescope Radio Linked Interferometer (MTRLI) system 80−12676
Jodrell Bank radio-link interferometer, sources phase stability, ang. struct. and position meas. 77−5452
large reflector antenna structural design for gravity and wind loading 78−57448
large telescopes, RATAN 600 and VLA *(German)* 78−4108
large-aperture radio system for meteor studies 80−85870
Lebedev Physical Institute 22 m radiotelescope, parameters at 8.2 mm, meas. *(Russian)* 77−22069
millimetre-wave astronomy, advances and prospects *(French)* 80−36502
millimetric and sub-millimetric facility, European cooperation *(German)* 79−44369
Mills' cross array antenna, digital baseband processing 80−36500
minimum noise, maximum gain by iterative relaxation for shaped asymmetric surfaces 78−65498
MM range receiver using powdered superconductor 80−21919
mm wave telescope, Epping, Australia, test obs. 79−53719
mm wavelength aperture synthesis interferometer 77−73950
MM wavelength band radiometer, Josephson superconducting point contact as detector 80−21918
mm-wave, radioastronomical observations and techniques review 77−5454
mm-wave annular synthesis telescope with fully steerable structure 78−61731
mm-wave receiver, travelling-wave maser for 85-90 GHz, using slot-fed guide slow wave cct. 77−5429
mm-wave receiver, travelling-wave maser using Fe doped rutile 77−3562
MM-wave spectral line receiver, low noise 77−41300
Molonglo Radio Observatory synthesis telescope 77−41302
multichannel reflector, factors affecting noise interference, anal. *(Russian)* 77−22067
multiple beam technique for overcoming atmospheric limitations to single-dish observations of extended radio sources 79−75113
multiple-beam array antenna for supernova radio pulse searches, sensitivity 78−40975
Nancay radioheliograph, Mark II, preliminary results 78−28517
NIRFI reflector of light construction with prestressed guyed rod 80−109360
Northern Cross radiotelescope, appl. of Clean and Restore technique to obs. of 2033+59 *(Italian)* 80−98563
Northern Cross radiotelescope, data acquisition system *(Italian)* 77−5426
observation techniques, basic principles *(Dutch)* 77−67039
Onsala 20-m. telescope 77−9662
optical modelling of antenna systems with complex aperture form *(Russian)* 77−22095
optical modelling using coherent optics and holographic methods, expt. *(Russian)* 77−22096
Parkes, efficiency improvement by resurfacing, 22 GHz obs. 77−33347
Parkes, mm wavelength performance of new 16.7 m surface 78−69691
phase switched interferometer for amateurs, construction details 80−12663
portable two aerial system, for detecting the Sun, Milky Way, and remote sources 78−28524
principal properties *(Swedish)* 78−24589
prism beamswitch for Cassegrain radiotelescope 79−21186
radio receivers, oxide-barrier-tunnel junctions, low-noise 115 GHz mixing 79−51722
radioastronomical equipment, techniques and observations, review *(German)* 77−56827
radioheliograph control system, 8 cm instrument at Toyokawa, Japan 80−98549

radiotelescopes continued
radiometer, wide-band, based on superconducting point contact, for short-wave millimetric radioastronomical obs. 79−96916
radiometer design with orthomode type mixer, radioastron. appls. and 1.35 cm range 79−2817
radiopolarimeters, fully automatic, for solar patrol at microwave freqs. 79−101065
radiospectrograph for solar emission S-component in 4-7 GHz range *(Russian)* 78−49320
radome and backstructure design improvements 78−57449
at Rao Observatory in Sweden, features *(Swedish)* 78−28513
RATAN 600, program controlled heterodynes for radiospectrometers *(Russian)* 77−9659
RATAN-600, operation and investigation of first sector *(Russian)* 77−22064
RATAN-600, Soviet Union 79−88596
RATAN-600 (Soviet), basic features and appl. *(Czech)* 78−53824
RATAN-600 radiation charact. investigated by optical modelling method 78−96395
RATAN-600 radio telescope, acousto-optical spectral analyser first test *(Russian)* 80−51668
RATAN-600 radiotelescope, acousto-optic spectrograph 80−46398
RATAN-600 solar telescope, preliminary obs. 77−78760
RATAN-600 telescope, variable-profile reflector antenna design, 0.8 to 30 cm 79−2480
reflector antenna design millimetre range *(German)* 77−53427
reflector phased array aberration effects, optical modelling *(Russian)* 78−16290
reflector surface meas. with two feeds 79−12403
refracting radiotelescope using chemically modified ionosphere as lens 77−45312
resolving power, increase using regularisation method 80−17505
review, rel. to cosmic microwave background radiation obs. 79−97109
rotational synthesis data processing, direct transform hardware techniques 78−85856
RT-22, automatic obs. by computer 80−109359
RT-22 spectrometer, computer controlled receivers *(Russian)* 77−9674
Salyut 6 submm. telescope with InSb receiver 80−67566
sensitivity, influence of atmospheric thermal radiation fluctuations *(Russian)* 77−21832
sensitivity optimisation, deterioration coeff. *(Italian)* 78−85845
solar, numerical control *(Czech)* 79−44371
Soviet 6 m diam. optical and RATAN 600 radio telescopes *(German)* 77−78639
space antenna, self-deploying large parabolic antenna and array design 78−57450
space radiotelescope, modular design proposal 80−51655
spectral resolving power, 5000 channel digital correlation receiver *(Dutch)* 77−67040
spherical wide angle mirror under oblique illumination, diffraction in focal region 80−1108
stray radiation problem and time variable 21 cm lines 80−56708
super synthesis telescope, Japan, 10-mϕ 5-element array performance 80−98548
supersynthesis interferometer, resolution solid angle rel. to point sources aggregate flux 77−13480
surface contour control of radio reflector surface of radiotelescope antennae 79−80221
Table Mountain 8 mm wavelength interferometer 80−26741
Tidbinbilla two-element interferometer system design 78−69692
tiltable radio telescopes, design and improvement 77−45313
Toyokawa λ 8-cm radioheliograph, new local oscillator system phase stability new local oscillator system phase stability 79−101073
Toyokawa λ 8-cm radioheliograph, project to improve sensitivity and phase stability 79−101066
Toyokawa Observatory, Solar Radio Data Acquisition and Communication System (SORDACS) 79−101074
tracking correlation receiver with feedback for radio astronomical interferometry 78−57445
transmission lines, antenna arrays and impedance transformation 78−96399
two-element radiointerferometer, arc meas. procedure optimisation *(Russian)* 79−101082
Ude-Yagi array operating at 1.37 m, Cuba *(Spanish)* 79−96909
uncooled millimeter wave receiver for radioastronomical observations uncooled millimeter wave receiver charact. *(Swedish)* 78−24461
UTR-2 based heliograph, 25 MHz obs. of solar storm burst source positions 80−90403
UTR-2 radiotelescope, expt. techniques, data processing, for decametric survey of discrete northern sources 78−57461
Very Large Array, New Mexico, pilot programme, planetary nebulae radio mapping 79−21196
Very Large Array, phase switching, Walsh function appl. 78−81539
Very Large Array, Plains of San Augustin, New Mexico, construction progress 77−17373
Very Large Array multiband low-noise receivers 77−41299
Very Large Array waveguide transmission system 77−5444
vibration behaviour, anal. of large adjustable parabolic antennas using dynamic equivalent models *(German)* 77−2342
VLA, TE_{on}-mode filters for circular waveguide system 79−66922
VLPA FIAN, antenna phased array equipment, charcts. *(Russian)* 77−22065
VLPA FIAN, antenna systems, charcts. *(Russian)* 77−22066
Westerbork Synthesis Radio Telescope, standardized data formats 77−78641
wideband carcinotron tunable submillimetric source 77−41304
WSRT, appl. of Clean and Restore technique to obs. of (4C 39.08) *(Italian)* 80−98563
X-band planetary radar, Goldstone 77−37503

radiotherapy *see radiation therapy*

radiowave propagation
see also electromagnetic wave propagation
11 GHz forward scattering due to rain, 9 km line of sight link 77−86995
11 GHz rain attenuation distribution, from 5-min. rain rate statistics, calc. 78−24326
12 GHz statistical propag. params. meas., effect of rain *(German)* 77−17183
15 GHz, losses on long-range air-to-ground transmission, statistics 77−17218
20 and 30 GHz radiometer calibration using ATS-6 satellite beacons 77−74500
20 GHz multi relay links, simultaneous probability of rain attenuation 78−3898
22.75 GHz microwave attenuation charcts. at high elevation *(Japanese)* 80−27346
140 GHz atmospheric attenuation by rain, obs. 78−3914
absorbing medium having dispersion relations with repeated solns., quasi-ioptical approx. 77−75377
absorption by atmospheric water vapour, 10 cm-0.27 mm wavelengths, temp. dependence 77−2235
accelerating atomic clock synchronisation by radiowave propag., one-way Doppler effects 80−13044
acoustic signal processing, influence of time- and space-varying random filters 78−5615
aerospace propag. environment, user requirements for modelling and forecasting 79−58169
aerospace propagation environment operational modelling conf., Ottawa, Canada, 1978, April 79−53651
air, vertical struct. of refr. index for ultrashort radio waves at subfreezing temps. 78−16128
AM/FM radio signal diffraction in homogeneous dispersive medium, space time geometric theory 79−4149
amplitude distributions, appl. in practical data assessment problems 80−27107
amplitude scintillations of mm waves, wind vel. effects 78−61496
Amsat-Oscar 7 subhorizon ratio signals beacon, above F2 layer, 30 MHz 77−70937
angular scattering of water drops and ice particles [electromagnetic interference], freq. above 10 GHz appl. 80−109183
anomalous propagation, meteorological aspects 78−57277
antennas, horizontal, above infinite plane Earth, input impedance and current distrib. 80−90259
antennas and interferometers, troposphere random inhomogeneities, effect on operation, statistical anal. 77−13111
Arctic ice cover, attenuation of 8 and 20 cm EM waves 80−67379
atmosphere, absorption meas., O_2 band, at 5.6 mm *(Russian)* 77−91210
atmosphere, amplitude spectrum rel. to fluctuation frequency in absorption region 77−21878
atmosphere, attenuation of 1.25 and 2.0 mm waves, radiotelescopic obs. 79−34897
atmosphere, conf., Oslo, Norway (May 1978) 78−93044
atmosphere, differential attenuation at 13 GHz and 20 GHz on 53 km link *(French)* 78−53684
atmosphere, field intensity vertical pattern on one-hop path 79−58156
atmosphere, ITCZ, 13.9 GHz radar altimeter obs. of total attenuation 77−29355
atmosphere, microwave dispersion appl. in multi-wavelength distance meas. instrument 77−29484
atmosphere, microwave refraction coeff. rel. to humidity 78−69398
atmosphere, modulation instability saturation in magnetised plasma *(Russian)* 77−47203
atmosphere, propag. of microwaves, refr. and absorpt. coeffs., optimal orthogonal expansion props. 80−98414
atmosphere, pulse propagation, scatt. and diffusion in scatterers and turbulence 79−66775
atmosphere, radar reflectivity gradients 77−91229
atmosphere, radio noise vars. at Ping-Cheng, Taiwan 77−45246
atmosphere, radio propag. in natural waveguides 77−78328
atmosphere, recent progress in duct propagation predictions 79−84374
atmosphere, refraction of MM-wave radio noise from cosmic sources near horizon, meas. 80−21813
atmosphere, refractive index structure in transitional boundary layer 78−57268
atmosphere, water vapour absorpt. in transparent window at 0.869 mm *(Russian)* 77−5277
atmosphere radio refractivity gradient analysis over S.E.Asia 77−91244
atmospheric absorpt. by water vapour in 0.8-20 mm range 80−4086
atmospheric amplitude scintillation temporal spectra at 10 and 36 GHz 79−12192
atmospheric amplitude spectra in absorption region 78−44920
atmospheric attenuation at 225 GHz meas., correlation with surface water vapour density 78−85624
atmospheric attenuation meas. using radiometer *(Czech)* 78−36351
atmospheric attenuation of 230 GHz, meas. 78−73425
atmospheric attenuation of solar 50 GHz band radiation 78−73494
atmospheric boundary layer, ultrashort wave refr. index derivation 80−36380
atmospheric delay fluctuations with scale sizes >1 km, obs. with radio interferometer array 79−8675
atmospheric inhomogeneity transfer velocity meas. by 10 cm radiowave propagation correlation *(Russian)* 78−77297
atmospheric noise data for tropical regions 80−61875
atmospheric propag. expts. in 19 and 28 GHz range using COMSTAR beacon 78−73420
atmospheric radiowave refractive index meas. using digital refractometer 78−86321
atmospheric refractive effect, ducting phenomena 80−94557
atmospheric submillimetre spectrum meas. with high resolution Fourier spectroscopy 77−87133
atmospheric water vapour meas. over 10 years for microwave radio link planning 78−3857
atmospherics, sweepers modulation struct. in HF and VHF bands 79−5707
atmospherics noise variation with sunspot number during 1600-2000 hours at Delhi 78−49083
ATS-6 30 GHz propag. meas. during heavy thunderstorms 77−64377
ATS-6 radio beacon experiment, ground refls. effects 77−53144
attenuation and bistatic scatter in rain at mm wavelengths, simultaneous meas. tech. 77−9554
attenuation and cross polarisation meas. at 20 GHz, ATS-6 satellite and radar system caused by hydrometeors 79−20912
attenuation and rainfall rates dual-polarisation radar meas. technique, precision 79−25371
attenuation caused by rain above 10 GHz freq. *(French)* 78−53686
attenuation due to precipitation, atmospheric gases, 22.75 GHz *(German)* 78−20465
attenuation due to water vapour, microwave radiometer study at 22.235 GHz 80−72610

radiowave propagation continued
attenuation in atmosphere of Venus by bistatic radar method 80−62061
attenuation meas., satellite Earth path, in the freq., bands 20 and 30 GHz 78−7822
attenuation meas. for radio delay system design *(French)* 78−53685
attenuation statistics influenced by rain cell orientation 77−5278
aurora, radio emissions in 2.5-6 MHz range 79−70906
aurora, small scale absorpt. events assoc. with substorms 77−56791
auroral ionosphere, radio turbidity coeff. 78−45112
auroral radio absorption, spike events 80−12589
auroral radio echo, ion-acoustic, short term characts. 78−45080
auroral scattering anisotropy, from 42 MHz polarisation investig. 77−21968
auroral zone activity coupled to mid-latitude radiowave absorpt. 80−61945
auroral zone riometer meas., day/night absorpt. ratio 77−91365
axisymmetric scattering by conical bodies 80−18971
backscatter, from scatt. cells located in random medium 77−39428
backscatter from vegetation, water cloud model 78−57274
backscattered pulse shape, small-angle multiple scatt. in random media 80−77079
bandwidth limitations in turbulent atmosphere using coherency and differential amplitude spectra *(French)* 78−49070
beacon signals from ATS-6 satellite, ground refl. effects on polarization 78−40612
biotelemetry antenna and propagation requirements for appl. for fresh water fish 77−78074
birefringent medium, propag. and polarisation, appl. to ice sheet sounding 77−56755
bistatic radar signals, scattering by planetary surfaces 80−41743
bounded inhomogeneous isotropic media, generalized charact. functions appl. to propag. 79−72462
Bremmer, H., contrib. to atmospheric propag. 79−62984
broad-band wave meas. in ARAKS expt. 79−21072
chorus and power line harmonics, effect on magnetosphere 79−101028
circumglobal signals in Atlantic equatorial zone *(Russian)* 78−69585
circumsolar plasma, d.m. propag., Venera 10 meas. 80−21886
circumsolar plasma, radio signal spectral lines formation 80−92330
circumsolar plasma, Venera 10 radio signal spectral meas. 80−109326
classical propagation criteria and effect of atmospheric anomalies 80−67390
cloud liquid H_2O obs. from 28 GHz satellite signal absorpt. 80−94623
collisional plasma, nonlinear energy pump between radio waves *(Russian)* 77−62365
combination frequency radiation generation in region of auroral electrojet *(Russian)* 77−41268
Communications Technology Satellite beacon, 12 GHz meas. of Earth-space propag. 78−73422
complex representation of polarised signal rel. to ULF wave anal. 77−53236
Comstar beacon cumulative slant path rain attenuation statistics, 28.56 GHz 80−26582
copolar and cross-polar signals rain attenuation meas. at 30 GHz using ATS-6 satellite *(French)* 78−49064
correlation bandwidth, empirical evaluation over troposcatter paths *(French)* 80−41527
corrugated reflector model for one-hop oblique propagation 79−35041
cosmic noise absorption, F-lacuna and slant-E condition rel. to E-region Farley-Buneman instability 78−73563
cosmic radio noise absorpt. events meas. on riometers, due to backscatt. by E-region irregularities 77−25831
cosmic radio noise absorpt. rel. to mag. storms at Delhi 78−69589
cosmic radio waves, depolarisation in turbulent cosmic plasma 77−17358
in critical coupling media, comparison of generalised WKB and Katsenelenbaum's methods 80−91728
cross-modulation of radio cosmic noise 77−70936
cross-polarisation comparison with circular and linear polarisation at 11.6 GHz 79−16633
crosspolarisation, raindrop canting angle as function of wind velocity 78−3855
crosspolarisation and attenuation meas. at 11-6 GHz using theoretical rain model, canting angle distrib. 80−4070
over curved anisotropic surfaces, study *(Japanese)* 78−42266
D-region, absorpt. diurnal var. at high latit., riometer data 77−53294
D-region, anomalous absorpt., during sudden disturbances, solar zenith angle depend., electron loss coeff. 78−69568
D-region, electron density profiles from gyrowave interaction expt., error anal. 79−5705
D-region, irregularities responsible for partial reflection 80−41629
D-region, mid-latit., energetic particles precip. during baylike absorpt. disturbance 79−12333
D-region, partially refl. radiowaves ang. distrib. meas. 78−49204
D-region, radiowave absorpt. rel. to interplanetary mag. field polarity changes 77−33272
D-region, radiowave absorption during solar minimum, 2.5-4.1 MHz 80−41628
D-region, radiowave heating at HF, consequent MF absorpt. effects 80−94646
D-region, radiowave propag. results during Western European Winter Anomaly Campaign (1975/76) 78−45123
D-region, radiowaves self-action effect *(Russian)* 77−41254
D-region, relationship betw-en VLF phase deviatios and 1-8 Å solar X-ray fluxes during flares 77−87170
D-region, southern hemisphere, radio wave scatt. obs. 78−36363
D-region absorption, effect on forward scatter radiometeor amplitude distrib. index 78−65552
D-region absorption, winter anomaly 79−58176
d-region absorption and forward-scatter radio-meteor data 79−75033
D-region HF wintertime absorption, O I airglow emission as precursor 79−58148
D-region short-wave radio absorpt. vars., transient coupling with tropospheric planetary press. waves 77−33162
daytime sky wave component in Calcutta-C MF signals 78−16239
decametric wave propagation, ionosphere conditions forecasting by CNET, in France *(French)* 80−85790
deflection by Sun, General Relativity test 77−70994
depolarisation by rain, thermal emission Stokes spectral vector 77−66976
depolarisation due to snow at 11.6 GHz 78−57239
depolarization at 11.6 GHz on a terrestrial radio link *(French)* 78−53687
radiowave propagation continued
differential attenuation and phase shift meas. for 36.5 GHz polarised waves rel. to raindrops 78−3856
differential rain attenuation prediction, adjacent microwave and mm-wave links 77−87048
dipole field diffraction by perfectly conducting thick half-plate 78−46488
direct attenuation function and field strength calc., computer aided anal. 79−25373
dispersion by plasma ejected from BL Lacertae objects 80−82516
distortion characterisation of tropospherical channel for digital transmission *(French)* 79−58065
Doppler freq., quasi-specular beam effect of Earth's surface elec. props. *(Russian)* 79−45890
Doppler processing of HF backscatter radar and mode structures of ionospheric propagation 79−16753
Doppler radar probing of clear atmosphere 79−66811
Doppler scattering by ocean ripples due to acoustic and capillary waves 78−3807
E_s-layer, critical freq. integral distrib. patterns 77−60524
E_s-layer, mid-latit., effect of strong radio waves on form. 77−60514
E_s-layer, oblique incidence propag. and ionospheric attenuation 78−73578
E_s-layer, temperate zone, maps of $f_0E_s>7$ MHz 78−73579
E_s-layer parameters determ. from refl. coeffs. 79−53626
E-region, critical freq. computation 78−45109
E-region, quasi-periodic artificial inhomogeneities formation *(Russian)* 79−21093
E-region, solar radioburst night-time reception 77−56790
E-region, unstable polar cap, rocket-borne wave, field and plasma obs. 77−21978
E-region, vertical drift effect on absorpt. and phase height change of refl. 79−101003
E-region drift and anisotropy parameters of small-scale irregularities at Waltair, India 77−13176
Earth, using parabolic equations and transformation operators method 79−36816
Earth-ionosphere cavity, resonance phenomena *(Russian)* 77−73801
Earth-ionosphere duct, radiowave propag. parameters at ELF 77−45067
Earth-ionosphere waveguide, concise theory 79−48616
Earth-ionosphere waveguide, mode conversion coeffs. for VLF propag. below stratified anisotropic ionosphere 77−53143
Earth-ionosphere waveguide, program to compute EM fields in irreg. spheroidal model 80−94638
Earth-ionosphere waveguide, VLF propag., multimode nature effects on correlation factors *(Russian)* 77−70745
Earth-ionosphere waveguide, VLF radio signal refl. from day-night transition region 79−96859
Earth-ionosphere waveguide channel parameters, influence of geomagnetic activity and statistical props. of VLF signals 79−88452
Earth-ionosphere waveguide parameter determ. by VLF transitional route meas. 77−91234
Earth-satellite paths, 11.5 GHz, annual and annual-worst-month statistics of fading 78−57238
Earth-sounding radar obs. of EM lateral waves 77−44909
Earth-space communication links, path diversity performance 78−69424
Earth-space path rain attenuation at 11 and 14 GHz, Darwin, Australia, satellite communications appl. 79−62541
Earth-space paths, rel. between rain depolarisation and attenuation 78−3858
Earth-space paths, tropical rain attenuation at 11 GHz, radiometric meas. in Australia 77−33165
Earth-space signals, at 19 and 28 GHz, depolarisation by ice particles 78−73492
echo signals propag. characts., 10 and 15 MHz 78−69574
EHF clear air refractivity calc. procedure 78−57266
EHF propag. in air, atmospheric medium characterization and modelling 79−53504
EHF propag. in clear air, modelling 79−58075
ELF Earth-ionosphere waveguide daytime propag. parameters, 5 to 2000 Hz 79−92637
ELF eigenvalues approx. determ. in Earth-ionosphere waveguide 79−8763
ELF mode theory for Earth-ionosphere cavity 78−45131
ELF normal mode reflection and absorption, nighttime ionosphere effects 79−8754
ELF propag. in nonstratified Earth-ionosphere waveguide, integral eqn. method 80−61959
ELF propagation and midlatit. localized nighttime D-region disturbances 77−21989
ELF propagation in Earth-ionosphere cavity, flat Earth approx. 77−13178
ELF propagation in Earth-ionosphere transmission line, rel. to ionospheric profiles 78−36234
ELF propagation in Earth-ionosphere waveguide 80−41634
ELF radiation, from New Zealand power system, in Earth-ionosphere waveguide 79−48609
ELF radio waves, effect of sporadic-E on nocturnal propag. 78−36392
ELF resonance mode splitting in Earth-ionosphere cavity during high solar activity 78−77416
ELF transmission anomalies and energetic particle precip. in ionosphere 78−93040
ELF waves in Earth-ionosphere cavity, field eqn. for inhomogeneous ionosphere 80−61950
ELF-LF radiowave reflection from lower ionosphere, mechanism 78−49224
ELF/VLF ground-based obs. at high latits. during GEOS-1 and ISEE-1 and -2 passes 79−29949
elliptical tunnel with contained axial conductor, radio transmission 79−55030
EM pulse propagation, in weakly nonlinear plasma, numerical calc. 77−58863
EMF air refractivity, variability w.r.t. temp. pressure and freq. 77−41112
EMF properties of air 77−17182
equatorial ionosphere, phase scintillation of 40 MHz signals rel. to ionisation irregularities 79−44303
equatorial spread-F irregularities from spaced fading records, Thumba, India 79−88543
ETS-II, radiowave propag. expt. facility *(Japanese)* 79−2471

radiowave propagation continued
ETS-II satellite, 1.7 GHz, 11.5 GHz, 34.5 GHz wave propag. rel. to rain precipitation strength *(Japanese)* 78−85669
exosphere, global model using optical and incoherent scatter meas. 78−36343
extended path with single obstacle, attenuation factor calc. 80−95775
external dielectric reflection, beam sideways displacement 77−61896
extinction cross section for single particles at 100 GHz 80−82116
F2 critical frequency, solar influence 79−2423
f_0F_2 monthly median values, verification of long-range forecast 77−60513
F_2-layer, peak electron densities in main trough region rel. to radiowave propag. 78−28417
F_2-layer ionisation through a solar cycle, SW communications appl. 80−41626
F_2-layer vertical sounding, radio signal Doppler spectrum and arrival angle meas. *(Russian)* 78−61651
F_2-peak altitude determination using global model based on M3000 values 79−101020
F-region, absorpt. separation from cosmic radio noise absorpt. 78−85769
F-region, electron density disturbances nonlinear saturation, strong radiowave effects 78−28378
F-region, generalized magnetoionic formulae 80−61963
F-region, HF backscatter curtains rel. to plasmapause location 79−58165
F-region, irregularities rel. to backscatter obs. at 3 m wavelength 79−12338
F-region, modulation instability 77−25814
F-region, pulse spreading as cause of unresolved spread-F 77−78557
F-region, radiowave influence on nonhomogeneity appearance connected with current instability *(Russian)* 78−49200
F-region, scintillation rel. to aurora 77−87158
F-region critical frequency small scale fluctuations at Kodaikanal 79−16745
F-region equatorial scintillations model from in situ meas. 77−13180
F-region heating, caused by powerful radiowaves, calc. *(Russian)* 78−32278
F-region HF phase path records, anomalous var. over daytime Waltair 77−70924
F-region irregularities and scintillations in equatorial region, VHF radar maps 78−36382
fading from spaced receiver obs. at Thumba 80−109296
Faraday tarotion, effects of pulsewidth 78−71540
field aligned radiowave scattering, artificial small scale irregularities, field aligned scattering *(Russian)* 78−32274
field intensity and propagation mode of JJY signal at Okinawa *(Japanese)* 77−81980
field strength variation for WWV, 15 MHz SW oct. at Hiraiso, Japan, rel. to mag. storms 79−53650
fluctuating component of scattered field in far-field zone 80−36456
FM-CW radar signal propag. in lower atoms. 80−90186
forward scatter and cross polarisation, due to ice spheroids 78−3853
forward scatter and cross-polarisation from spheroidal ice particles 77−25733
forward/backward scattering from liquid/solid hydrometeors, Rayleigh approx. 79−25321
frequency depend. of ang. wave fluctuations in plane-stratified isotropic medium 79−53627
frequency scaling of attenuation above 10 GHz due to rain, use of COMSAT satellites 79−5595
frequency-time filtering of ULF signals and magnetospheric channel characterisation *(French)* 79−70920
giant planets, atmospheric radiowave refraction 80−98608
global model for rain attenuation prediction 79−5594
gravitational focusing in interstellar medium, model *(Russian)* 78−81905
ground diffraction pattern parameters assoc. with D-region partial reflections 77−60534
ground screening factor evaluation to protect systems from interference *(French)* 78−49071
ground wave atmospherics generated by lightning return strokes, initial peaks, model 80−61876
ground wave attenuation function for a spherical Earth with arbitrary surface impedance 80−94585
guiding properties of a smoothly inhomogeneous layer and diffraction excitation of ionospheric waveguides 80−36449
gyrowave interaction expt., diurnal var. of impressed modulation 79−5706
hail, Doppler radar spectra at vertical incidence 78−65368
hail, radio emission characts. in cm waves 79−96802
HF, absorption variation in ionosphere *(Spanish)* 79−16735
HF, in horizontally inhomogeneous ionosphere, anal. *(Russian)* 77−5391
HF, ionospheric recurrent storms causes, effects and occurrence probability 78−4028
HF, nonlinear interaction in ionosphere 77−13175
HF and MF signals refl. from spread-F, fading anal. 79−101005
HF and VHF refl. from E_s-layer on 1050 km path, M factor determ. 77−17281
HF and VHF signals amplitude fluctuations due to ionospheric scatt. and E_s-layer refl. 78−45105
HF and VLF propag. in magnetosphere, expt. results 77−25861
HF at high latitudes, geomagnetic activity influence *(Russian)* 77−29551
HF communication at low latitudes, problems and solns. 77−70921
HF Doppler ground-wave radar for off-shore wind meas. 78−77295
HF Doppler method studies of high-latitude ionospheric dynamics 78−73569
HF Doppler obs., realtime display system 77−73887
HF Doppler obs. over S.E. Australia during 1976 Oct. 23 total eclipse 78−61662
HF Doppler observations associated with spread-F 79−70918
HF excited plasma instabilities in ionosphere 78−45130
HF fading ionospheric reflection channel, delay and Doppler power spectra 79−8765
HF ground wave propag. over seawater, basic transmission loss meas. 77−78353
HF induced plasma waves in ionosphere, time vars. 78−45119
HF ionospheric absorption at low latits., solar particle effects 78−69594
HF long-range propag. in ionospheric ducts 77−78569
radiowave propagation continued
HF max. usable freq. prediction along foF2 line, MINIMUF-3 algorithm 79−25372
HF mode predictions using simple method with approximation 79−16754
HF oblique radar obs. of plasma instabilities in equatorial electrojet over Africa 78−49205
HF oscillating echoes from polar E-region 78−57390
HF peculiar lunar echoes, guided wave propag. in ionosphere and magnetosphere 78−93032
HF propag. in ionosphere in minimum sunspot cycle, records 79−25397
HF radar obs. of horizontal plasma waves, in equatorial ionosphere 79−29930
HF radio meteor echoes duration rel. to dense trains deionisation 79−5697
HF radioemission during ARAKS expt., ground-based obs. 79−21078
HF range, noise intensity distrib., empirical laws approx. 77−9603
HF reflection and transmission coeffs. for horiz. polarised waves, sporadic-E layer 78−32290
HF short-term field-strength predictions, real-time 79−58180
HF signal envelopes, spatial correlation coeff. 79−62663
HF signal fluctuation spectra in auroral zone, geophys. conditions effects 77−25821
HF signal fluctuations energy spectra in auroral zone 77−17284
HF signal reflection obliquely from ionosphere, trajectories 77−21996
HF signal strength, triangular enhancements rel. to TIDs 78−16236
HF signal trajectory parameters for single-hop path in auroral zone 77−25823
HF signals, allowance for fadings in computation of single-hop paths 77−91352
HF signals, arrival angles meas. on paths between Moscow and Indian and Atlantic Oceans 77−91351
HF signals, freq. shift during solar eclipse (1976, April 29) 78−45111
HF signals, magnetospheric propag. mechanism 80−4196
HF signals magnetospheric propag. on Earth-Earth path, exptl. investigations 80−4195
HF signals statistical characts. during auroral substorms 78−69583
HF signals statistical characts. on auroral radio paths during equinox 77−60526
HF sky wave radar remote sensing of sea state, minimisation of ionospheric disturbance 80−21857
HF sky-wave received signal level determination for communication link 78−85758
HF surface fields excited by point source on concave perfectly conducting cylindrical boundary 79−64146
HF time signal bilateral transmission propagation time error anal. 77−87740
HF transionospheric long range propag. from satellite, obs. at Florence 78−36396
HF wave at Arecibo, induced plasma line shifts in ionosphere 79−101012
HF wave propagation with lateral deflection from great circle arc, investigation 78−45096
HF waves reflected from ionosphere, freq. var. *(Chinese)* 80−56665
HF-enhanced plasma line height in ionosphere above Arecibo 78−28392
HF/VHF absorption in disturbed D-region, meas. 77−53286
horizontally inhomogeneous ionosphere, adiabatic mode constriction *(Russian)* 77−78553
IEE antennas and propag. international conf., London, England, 1978, Nov. 79−12342
incoherent backscatter from rough surfaces, two-scale model re-examined 78−71013
incoherent energy and coherent time of depolarised microwaves, interferometric analysers 78−96277
incoherent scatter radar, correlation function meas. 77−73888
incoherent scatter results for co-ordinated special intervals at St. Santin (France) 79−2416
incoherent scattering by plasma, Nyquist theorem appl. 79−75024
inhomogeneous media, horizontally polarized wave transmission and trapped waveguide modes 78−9297
inhomogeneous scattering media, characterisation via space-variant transfer functions 78−71012
inhomogeneous stratified atmosphere, normal-wave soln. 78−53710
Intelsat transmissions, determ. of electron content and slab thickness near equatorial anomaly 79−84574
interference factor above uneven Earth's surface, field calc. 78−57275
International time and freq. comparison using Loran-C radio waves *(Japanese)* 78−81951
interplanetary density discontinuities rel. to radiosource scintillations 77−17314
interplanetary plasma meas. by modulation method, amplifiers sensitivity increase 79−92676
interplanetary plasma meas. by satellite to Earth signals, radio interferometers oscillator stability 77−60571
interplanetary scintillation, appl. for solar wind probing 78−45178
ionograms, vertical incidence, simulation by ray tracing with replacement layer and ionospheric trough 77−78559
ionosphere, A1 absorption measurements at 2.4 and 5.6 MHz 80−82132
ionosphere, absorpt. events at high latits. 77−21987
ionosphere, absorpt. freq. var. in model D- and E-regions 77−13169
ionosphere, absorpt. meas., differences between sporadic-E and normal E-layer refls. 78−40734
ionosphere, absorpt. meas. at Waltair, India, D- and E-region models 77−13173
ionosphere, absorpt. rel. to solar activity 78−69591
ionosphere, absorpt. vars. at 2.5 MHz at Ahmedabad, India 77−13165
ionosphere, absorption azimuthal patterns for circumterrestrial signals 77−49222
ionosphere, absorption meas. using sweep freq. technique 79−75029
ionosphere, anomalous absorpt. during disturbance due to strong radio emission 79−53624
ionosphere, anomalous absorption during SID rel. to solar X-ray radiation intensity 79−96857
ionosphere, anomalous radiowave absorpt. due to heating effects 77−25857
ionosphere, artificial disturbances effects on HF propag. *(Russian)* 77−56789
ionosphere, artificial quasiperiodic inhomogeneities formation due to powerful radiowave 79−84585
ionosphere, asymptotic distrib. law of scatt. field amplitude and phase 77−29548

radiowave propagation continued
ionosphere, ATS-6 radio beacon expt. results 78−69592
ionosphere, ATS-6 signals diffr. by isolated irregularities 79−35049
ionosphere, ATS-6 signals equatorial scintillations, freq. depend. 79−35050
ionosphere, attenuation meas. by oblique pulsed sounding method 78−28380
ionosphere, auroral, field-normal plasma-line scatt. detect. expt. 78−73580
ionosphere, backscatter inversion is spherically asymm. ionosphere 80−36446
ionosphere, backscatter radar data rel. to O I 6300 Å nightglow intensity 78−77401
ionosphere, backscatter sounding method using spatial and spectral sampling, for investigation of plasma inhomogeneities *(French)* 79−29911
ionosphere, backscatter sounding technique *(Spanish)* 79−100998
ionosphere, closely-spaced receiver technique for horizontal drift meas. 78−40743
ionosphere, condition forecasting and prediction, long- and short-terms 78−93046
ionosphere, correlation ellipse physical significance in drift anal. 77−13179
ionosphere, cosmic radio noise absorpt. over Delhi, calc. and obs. 77−64521
ionosphere, cosmic ray layer, electron density distrib., radiowave absorpt. 77−22024
ionosphere, cross-modulation phenomenon for MF waves 77−13167
ionosphere, day to night absorpt. ratio in auroral zone riometer meas. 78−20580
ionosphere, daytime satellite radio scintillation rel. to sporadic-E layer near mag. equator 77−45225
ionosphere, daytime scintillation assoc. with geomagnetic storm 77−78563
ionosphere, decametric freq. shift of magnetoionic component 80−105104
ionosphere, derivation of WKB soln. for coupled eqns. 77−13177
ionosphere, diffr. from discrete and homogeneously structured irregularities 79−48612
ionosphere, diffraction trapping of HF waves by waveguide 78−53772
ionosphere, disturbance effects and their predictability 79−58171
ionosphere, disturbance forecasting through solar radiation measurements from NRL SOLRAD satellites 79−58134
ionosphere, diurnal radiowave absorption variation asymmetry, seasonal variation 77−87175
ionosphere, DNA Wideband satellite expt., complex signal scintillation 78−45133
ionosphere, Doppler fluctuations and angle-of-arrival var. caused by scintillation 78−77411
ionosphere, E-region reflections at 2.2 MHz rel. to phase height var. and vertical drift 78−40747
ionosphere, echo signals, between Khabarovsk and Irkutsk, 14-17 MHz band *(Russian)* 78−32281
ionosphere, effects of induced and combination scatt. on propag. of strong radio waves 77−91345
ionosphere, effects of solar X-ray and Lyman α radiation on absorpt. 78−40737
ionosphere, equatorial scintillation at 40, 140, 360 and 860 MHz, simultaneous obs. 78−57393
ionosphere, equatorial scintillation rel. to irregularities, review 78−36380
ionosphere, equatorial spread-F, VHF scattering 78−61661
ionosphere, equatorial spread-F artificial control 78−69602
ionosphere, f_0F_2 determ. from satellite obs. of HF noise 77−53292
ionosphere, f_{min} coherence with 30 mb temp., five-day wave 77−33275
ionosphere, Faraday rotation measurements at Ootacamund 79−88533
ionosphere, fluctuations during multiple refl. 78−45104
ionosphere, focusing at boundary of zone of silence 77−13158
ionosphere, forecast chart for periods of high solar activity, amateur radio appl. 80−26664
ionosphere, foreshortened scatt. by auroral inhomogeneities *(Russian)* 77−64519
ionosphere, frequency method of signal averaging 79−53628
ionosphere, Fresnel diffraction patterns for ionospheric irregularity modelling 77−9614
ionosphere, global MF absorpt. variations, empirical formula 80−77204
ionosphere, gravity waves due to total solar eclipse, detect. by radio technique 77−91364
ionosphere, group delay var. at oblique incidence rel. to travelling disturbances 78−45132
ionosphere, group refr. index for propag. over Rio de Janeiro 77−13171
ionosphere, H_E scatter signals power calc. 77−60520
ionosphere, heating by strong radiowave, geomag. pulsations artificial generation 77−29541
ionosphere, heating due to parametrically excited Langmuir waves, short-scale field-aligned density striations form. 79−8766
ionosphere, height determ. from VLF signal phase fluctuations *(Russian)* 77−91358
ionosphere, HF, at oblique incidence, anal. 78−93045
ionosphere, HF Doppler observations at Chubu Inst. Tech. (Japan) *(Japanese)* 80−31165
ionosphere, HF freq. standard utilisation 78−93027
ionosphere, HF propagation calculation of max. usable freq. in presence of steep electron density distrib. gradients *(French)* 79−58177
ionosphere, HF signal, group path variations from modulation envelope measurements 80−51597
ionosphere, HF signals and oblique sounding characts. 79−62658
ionosphere, HF signals transmitted along high-latitude radio path 80−41609
ionosphere, incoherent scatt. radar for correl. meas. of electron and ion temps. 77−25820
ionosphere, incoherent scatter technique development 78−81503
ionosphere, inhomogeneous anisotropic, reflection and transmission coeffs. determ. at low freqs. using 4×4 matrices 78−53769
ionosphere, inhomogeneous isotropic, propag. parameters of VLF radio waves during sunrise period 80−31166
ionosphere, ionisation irregularity drift motion from spaced fading and scintillation obs. 80−82133
ionosphere, irregular struct. in field of strong obliquely incident radiowave 79−62648
ionosphere, irregularities characts. from Faraday fading of 40 MHz signals 77−13166
radiowave propagation continued
ionosphere, irregularities drift vels. from ATS-6 140 MHz Faraday rot. records 78−69599
ionosphere, irregularities effects on group path 77−53291
ionosphere, isotropic, field strength near caustic and cusp 77−21986
ionosphere, L-band signals coded by phase reversal, signal degradation 80−41632
ionosphere, LF and MF absorpt. following enhanced geomag. activity 77−53332
ionosphere, LF and MF very strong radiowaves cross-modulation 77−17285
ionosphere, LF transmission, electrons effective collision freq. determ. 78−40683
ionosphere, LF waves, contrib. of low level meteors to ionization, obs. system 79−84514
ionosphere, limited beam diffusion due to scatt. on random inhomogeneities 77−91349
ionosphere, limited height resolution effect in differential-phase partial-refl. expt. 77−21991
ionosphere, maximum usable frequency predictions, real-time updating 79−58179
ionosphere, metallic ions of meteor origin effect in VHF forward scattering, contribution to sporadic-E formation 80−67461
ionosphere, meteor trail ionization effects 79−101001
ionosphere, MF absorpt. nocturnal var. and nighttime E-region 77−29563
ionosphere, MF waves generated by 8-40 keV electron beam 78−40750
ionosphere, mid-latit. absorpt. rel. to zero and maximal vel. contours in equatorial ionosphere 80−12597
ionosphere, midlatit. sporadic-E obs. using HF Doppler technique 79−66867
ionosphere, midlatitude, VLF radio waves anomalies assoc. with geomag. disturbances 80−56671
ionosphere, model computations of scintillation caused by equatorial bubbles 80−94641
ionosphere, mol. rot. amplification of intersecting radiowave modulation *(Russian)* 77−41255
ionosphere, morphological features of winter absorpt. anomaly at middle latits. 80−67459
ionosphere, multifreq. scintillation data from ATS-6 radio beacon expt. 77−45250
ionosphere, multifreq. spectra of amplitude scintillations 77−87161
ionosphere, multiray HF propag. during equinoctial periods 77−49220
ionosphere, natural noise, Interkosmos-Copernicus 500 satellite obs. 77−53503
ionosphere, nonlinear effects during partial radio wave refls. 77−60516
ionosphere, nonlinear effects influence on incoherent scatt. 78−40729
ionosphere, nonlinear phase distortion of partially refl. signal 78−69573
ionosphere, O_2^- effects 79−8762
ionosphere, oblique scattering from magneto-oriented irregularities *(Russian)* 77−64518
ionosphere, oblique sounding signals Doppler freq. shift in disturbed region 79−53630
ionosphere, oblique-backscatter sounding signal fluctuations and accumulation method of reception 77−60521
ionosphere, operational physical models 79−58172
ionosphere, parametric generation of plasma waves by extraordinary RF wave 77−13153
ionosphere, partial ref. expt., quasi-longit. approx. to generalized magnetoionic formula 77−13170
ionosphere, partially reflected radio signals *(Russian)* 79−48603
ionosphere, Pederson ray effect on direction finding accuracy 77−91355
ionosphere, penetration of quasi-parabolic layer, path integrals calc. 78−49208
ionosphere, persistent subauroral scintillation enhancement obs. in Alaska 78−20573
ionosphere, perturbation of collisional plasma by opposing EM wave, anal. *(Russian)* 77−9605
ionosphere, phase and dispersion signal blurring of monochromatic reflected wave *(Russian)* 77−17293
ionosphere, phase fluctuations meas. by radio-link interferometer 77−5452
ionosphere, physical model and profile reconstruction, for inhomogeneous ionised regions 80−1109
ionosphere, plasma and ion-acoustic waves parametric excitation by strong radiowave 77−17283
ionosphere, plasma disturbance by extraordinary wave 77−29542
ionosphere, plasma interactions, instability growth rates and threshold powers *(Russian)* 78−32277
ionosphere, polarisation coupling loss and sea gain effects in MF band 79−5709
ionosphere, polarisation fading records, spectra interpretation 77−60527
ionosphere, prediction and extrapolation 79−58168
ionosphere, PROPHET, real-time propagation assessment system, operational environmental models 79−58170
ionosphere, pulse delay and distortion by random scattering 79−29934
ionosphere, pulse time dispersion, Earth's mag. field effects 78−45116
ionosphere, quadrature components of narrowband signal, statistical props. 79−75038
ionosphere, radio lens, UHF and VHF fading patterns 77−53299
ionosphere, radio noise propag. through sporadic-E layer in equatorial region 79−84575
ionosphere, radio pulse dispersion and virtual height determ. 80−61954
ionosphere, radio window theory, transmission coeff. 80−61953
ionosphere, radiowave phase and amplitude meas. interpretation *(Russian)* 78−77394
ionosphere, radiowave refl., large-scale screen speed determ. 77−9602
ionosphere, randomly dispersive and absorbing, HF pulse reflection 79−84568
ionosphere, ray path eqns., multisegment quasi-parabolic ionosphere 80−41633
ionosphere, ray-tracing calc. through Bradley/ Dudeney ionospheric model 78−7826
ionosphere, refl. freqs. during vertical and oblique sounding 78−45099
ionosphere, refl. or scatt. waves, automatic processing device 77−49179
ionosphere, reflection drift data, internal consistency analyses 79−53539
ionosphere, refr. index determ. using GEOS-3/ATS-6 satellite-to-satellite tracking data 78−93039
ionosphere, rel. to Pc 1 source regions 77−25881
ionosphere, satellite expt. using Doppler effect in presence of wave perturbs., modelling 79−8744

radiowave propagation continued
ionosphere, satellite-referenced propagation correction for USAF SPACE-TRACK radar systems 79−58131
ionosphere, scatt. amplitude distrib. and focusing effect of large-scale inhomogeneities 77−91354
ionosphere, scatt. on artificial inhomogeneities, trapped energy escape from interlayer duct 77−9601
ionosphere, scintillation, power law phase screen model, strong scatt. 80−61962
ionosphere, scintillation, power law phase screen model, weak scatt. 80−61961
ionosphere, scintillation, signal-statistical and morphological model 79−58185
ionosphere, scintillation calc. by thin phase screen approx. 77−53298
ionosphere, scintillation meas. at 1.5 and 4 GHz 77−29581
ionosphere, scintillation studies using ATS-6 radio beacons at Delhi 78−69600
ionosphere, scintillations induced by cloud of sporadic-E layer 77−37477
ionosphere, scintillations of ISIS-1 VHF beacon signals 79−8752
ionosphere, scintillations of phase and quadrature components 79−80077
ionosphere, seasonal and daily vars. of multiple rays on short radio waves 77−21972
ionosphere, seasonal pattern of freq. depend. of absorpt. 77−49221
ionosphere, self-focusing instability during oblique incidence 77−49218
ionosphere, self-focusing instability in oblique ionosonde meas. 80−105101
ionosphere, short radiowaves ducted propag., large-scale inhomogeneities effects 79−62657
ionosphere, short wave radio absorpt. in winter, rel. to O airglow 80−77184
ionosphere, shortwave drift-dissipative instability, caused by EM wave *(Russian)* 77−47179
ionosphere, singly scatt. wavefields, angle depend. 77−87174
ionosphere, soundings during 1973, June 30 solar eclipse rel. to atmospheric waves 77−53302
ionosphere, spatial and temporal variation meas., differential Doppler technique using satellite 79−12311
ionosphere, spatial dependencies of props. of wavelike inhomogeneities, anal. of diffraction patterns 80−36448
ionosphere, spread-F obs. rel. to plasma density profile 78−36383
ionosphere, spread-F parameters, related to geomag. disturbance index 80−8471
ionosphere, stimulated Brillouin scatt. and incoherent backscatter 77−78552
ionosphere, stimulated Brillouin scatt. theory 77−37478
ionosphere, strong radio waves self-focusing instability near caustic 78−45107
ionosphere, struct. from satellite radio beacon signals 78−12050
ionosphere, structure prediction techniques 79−58178
ionosphere, subauroral, strong signal demodulation *(Russian)* 77−41267
ionosphere, sudden freq. deviations during solar flares, depend. on operating freq. 78−28373
ionosphere, SW radio noise level variation obs., as function of ionospheric perturbations, in auroral zone *(Russian)* 77−91359
ionosphere, SW radio propag., inhomogeneities effect in auroral regions 79−101017
ionosphere, sweepers in HF and VHF bands 78−16231
ionosphere, temporal amplitude and phase spectra from ATS-6 radio beacon expt. 77−45251
ionosphere, theoretical soln. of Helmholtz eqn. in statistically inhomogeneous medium 79−92638
ionosphere, time dispersion of EM pulses 80−94645
ionosphere, topside HF noise meas. for F_2 critical freq. determ. 79−8756
ionosphere, topside sounder extp. rel. to lab. excitation of electron cyclotron harmonic waves 78−93042
ionosphere, topside sounding and determination of electron profiles 80−56669
ionosphere, total electron content determ. from Faraday rot. 77−33249
ionosphere, total electron content meas. at Gauhati, using ATS-6 140 MHz transmissions 78−69598
ionosphere, total electron content obs. at Kurukshetra, suing ATS-6 140 MHz transmissions 78−69597
ionosphere, travelling disturbances effect on radio noise from discrete sources 77−91353
ionosphere, travelling disturbances effect on statistical charact. of refl. signals 78−45092
ionosphere, upper, disturbance by strong radio wave with amplitude modulation 79−12330
ionosphere, upper and lower rays signal levels ratio on single-hop high-latit. 79−8748
ionosphere, valley problem in bottomside ionogram anal. 77−33268
ionosphere, VHF absorpt. winter anomaly over Delhi 77−64522
ionosphere, VHF and L-band scintillation over Huancayo 78−36381
ionosphere, v.h.f. and u.h.f. ATS-6 total electron content meas. 77−2303
ionosphere, VHF periodic fadings from satellites during solar eclipse 77−33277
ionosphere, VHF scintillation, assoc. with reversal of horiz. elec. field 80−101489
ionosphere, VHF scintillation rel. to peculiar Faraday rotation fluctuations 78−61663
ionosphere, VHF scintillations, equatorial, nature and dynamics of irregularities 79−48601
ionosphere, VHF system for spaced-receiver meas. of scintillation irregularities 80−56639
ionosphere, VLF, over Greenland Ice Cap, mode conversion coeff. calc. 79−25398
ionosphere, VLF amplitude-phase vars. and AA-type absorpt. 77−60519
ionosphere, VLF and LF propagation and eigenmode scatt. relations 80−61944
ionosphere, VLF focusing during solar eclipse 80−61965
ionosphere, VLF propag., X-ray star effects 79−53649
ionosphere, VLF waves self-interaction 78−28382
ionosphere, waves interaction nonstationary processes *(Russian)* 78−93028
ionosphere, whistler-mode pulse propag. between two satellite at medium freqs. 78−69605
ionosphere, winter absorpt. correl. with Na nightglow 77−33239
ionosphere, winter absorpt. obs., 1975/76, at about 52°N, 9°E 78−45124
ionosphere, winter absorption anomaly rel. to D-region electron density 77−21990
radiowave propagation continued
ionosphere, winter anomaly absorpt. events and E_s layer form. due to metallic ion drifts 77−9599
ionosphere absorption, general formulae 79−58166
ionosphere artificial irregularity spectra disturbed by SW transmission *(Russian)* 78−32275
ionosphere D- and E-regions, electron densities vars. from radiowave propag. 77−33267
ionosphere D-region, partial refls. ang. and temporal characts. 79−66858
ionosphere distant HP propagation, role of near-critical rays 79−53619
ionosphere ducts, trapping of radio waves scattered by meteor trails 80−4172
ionosphere E_s-layer, meteors propag. 77−25837
ionosphere E_s-layer, relationship of class 1 E_m to meteors 77−29572
ionosphere E-layer, prediction methods, accuracy *(Japanese)* 79−40017
ionosphere EM wave absorpt. rel. to wind and temp. struct., winter 1975/6 obs. 80−36438
ionosphere EM wave propagation, backscatter echo spectral analysis and radio transmission forecasts *(French)* 79−29912
ionosphere equatorial region, UHF and VHF signal scintillation 80−56674
ionosphere heating by radio waves, predictions for Arecibo and satellite power station 78−77403
ionosphere HF sky-wave field strengths, developments in prediction techniques 79−58132
ionosphere incoherent scatter measurement complex, Kharkov Poly. Inst. 77−9555
ionosphere ionization var. caused by powerful radiowaves in lower region *(Russian)* 78−32273
ionosphere LF propagation, refl. coefficient determ. via modulation method 78−45114
ionosphere LF radiowave absorpt., variation during solar cycle 80−77193
ionosphere luminesc. amplification by radiowave anomalous absorpt. *(Russian)* 79−29925
ionosphere MF wave propagation expts. between two satellites, Z-mode pulses 79−53646
ionosphere mid-latitude trough, scintillation of extraterrestrial radio noise sources signals 78−73574
ionosphere modelling, for use in administration of HF radio transmission networks *(French)* 79−58175
ionosphere radio drift meas. simulation and analysis by correlation methods 78−45033
ionosphere radiowave scintillation, nighttime equatorial F-region 80−26681
ionosphere regular absorption, differences in daily vars. and annual pattern in N.hemisphere 78−45091
ionosphere scintillation, calcs. based on in situ irregularity spectra 78−28415
ionosphere scintillations at 4 and 6 GHz using INTELSAT programs 79−5715
ionosphere SHF scintillations, refr. scatt. explanation 79−48615
ionosphere sporadic-E layer behaviour in EM field during oblique irradiation by radio waves 78−73566
ionosphere upper layers, drift instability generation by action of strong radio wave 77−91344
ionosphere vertical sounding, electron densities meas. by artificial plasma inhomogeneities *(Russian)* 79−5636
ionosphere vertical sounding by radiowaves, magnetoionic components lateral deviations 79−8747
ionosphere waveguide propagation, excitation by ground based sources *(Russian)* 78−32283
ionosphere waveguides, excitation of electromagnetic modes, using Lorentz lemma method *(Russian)* 78−32284
ionosphere waveguides, excitation problem, using asymptotic method *(Russian)* 78−32285
ionospheric, electron density profile determ. from rocket-based 40 kHz propag. obs. *(Japanese)* 78−24403
ionospheric, nonlinear effects 77−60544
ionospheric, scattering from artificial plasma inhomogeneities, ionospheric electron density meas. appl. 79−75074
ionospheric absorption, Gauhati, India 77−41261
ionospheric absorption measurement, peak amplitude recording system 78−3979
ionospheric absorption studies by riometer technique at magnetic equator 77−53275
ionospheric cross-modulation of radio signals between two nearby stations 78−93048
ionospheric ducting at high-frequency, review 80−21872
ionospheric effects, engineering problems in VLF to VHF bands 79−16751
ionospheric effects on Doppler frequency for SARSAT search and rescue satellite 79−58183
ionospheric effects on radio communication and ranging pulses 80−26667
ionospheric equatorial absorption, lunar tides 79−44286
ionospheric HF radio wave absorpt. temporal variations 77−53305
ionospheric irregularities and associated VHF/UHF scintillations 80−46345
ionospheric irregularities effects on HF and VHF radio waves, ray tracing study 77−91362
ionospheric LF radiation generation by HF transmitter, nonlinear currents height meas. *(Russian)* 77−41256
ionospheric modification and parametric instabilities 79−101019
ionospheric oblique HF pulsed signals propag. dispersion coeffs. calc. 77−13181
ionospheric plasma, hysteresis effect on artificial excitation of inhomogeneities 80−36450
ionospheric plasma, radiowave scattering by superexcited atoms, quantum model 80−32677
ionospheric propagation conditions at decimetre wavelength 78−45136
ionospheric reflection, multimode signal operation, propag. direction fluctuations 77−53309
ionospheric reflection height estimation from Doppler measurements 77−21979
ionospheric reflections, meas. of fluctuations in angle of arrival and amplitude 80−17439
ionospheric refractive influence on geodetic measurements using artificial satellites *(French)* 79−58133
ionospheric scintillation, critical prop. freq. up to 1 GHz 78−7827
ionospheric scintillation, effects on received signal level 78−93047
ionospheric scintillation, model review 77−21995

radiowave propagation continued
ionospheric scintillation meas. at 1.7 GHz at midlatitude 79−2434
ionospheric scintillation of solar bursts at 30 and 60 MHz, STEREO-5 obs. 78−61822
ionospheric scintillation theory, mini-review 77−5393
ionospheric scintillations at GHz freqs. power spectra model comp. 77−45233
ionospheric travelling disturbances, medium-scale, diurnal and seasonal var. modelling 79−58181
in isotropic inhomogeneous atmosphere with refractive index arbitrary profile, mode theory anal. *(Japanese)* 78−44968
jet stream winds, mesoscale var., Sunset 40 MHz Doppler radar obs. 79−53477
Kanpur-Nainital troposcatter link, radio signal charcts., simulation and obs. 78−40614
land-to-seafloor EM transmissions in 0.1-15 Hz band 78−93008
LF, Earth-ionosphere waveguide, model *(Russian)* 77−41257
LF, in ionosphere, electrostatic wave generation near lower hybrid reson. 77−29557
LF absorption events during meteor showers, rel. to meteoric constituents ionization 78−40736
LF absorption in midlatit. ionosphere, interplanetary mag. field sector struct. effects 77−29546
LF and MF ground waves in realistic terrain, elec./mag. field ratios 78−88795
LF band, noise field and skywave propag. 79−5708
LF broadcasting, sky-wave propag. in daytime 78−61648
LF field strength meas. on single-hop path 77−29547
LF radio propag. at high altitudes 79−16752
LF radio wave absorpt. temp., seasonal variation 79−48602
LF radio waves, signal vars. over sunspot cycle 77−78560
LF signals attenuation due to meteor trains 78−40726
LF signals knife-edge type field strength depression during mag. storms 78−40740
LF signals nocturnal amplitude correl. with neutron monitor count 78−40741
LF sky wave, atm. refr. effects *(Chinese)* 80−4165
LF/VLF, ionospheric, propag. charcts. anal. 78−93049
LF/VLF links for time-freq. secondary standard comparison 77−87737
LF/VLF propag. below nonuniform isotropic ionosphere 79−44224
lightning, VLF spectral charcts. of K-field changes, expt. 77−2217
lightning cross polarisation model, for satellite links, 78−11961
lightning radio emission, Maxwell's eqns. soln. 77−29403
line-of-sight radio link, experimental investigation by direct meas. of impulse response *(Italian)* 79−70867
line-of-sight radio link propag. charcts. eval. using impulse analysis *(Italian)* 79−70868
linear interaction of EM waves in inhomogeneous magnetoactive plasma 79−94802
long-delay echoes, 28 MHz amateur band obs. 80−90277
long-delay echoes generation, models 80−26670
long-distance, relationship with processes in Earth's crust 80−26682
Loran-A (1.85 MHz) radio wave backscatter from ocean waves, Doppler spectra *(Japanese)* 78−85737
Loran-C in polar regions, amplitude and time-delay computations, full wave analysis 78−7834
Loran-C signal, ground wave propag. theory 80−94580
low latitude whistlers, lower and upper freq. cut-off explanation 80−82131
low-frequency radiation, from elec. dipole in isotropic plasma 79−46436
lower atmosphere, remote sensing and profiling using ground-based measurements 80−56628
lower atmosphere remotely sensed by two satellites, radio illumination method 80−51550
lower daytime ionosphere, model for VLF field forecasting 77−49216
lower ionosphere, excitation of sound waves, heating effect investigation *(Russian)* 77−78554
lower ionosphere, Hollingworth patterns in VLF range rel. to electron density profile estimates 77−64516
lower ionosphere, nonlinear thermal focusing of radio waves 77−60511
along lunar surface of waves in 0.1 to 100 MHz freq. range 79−5768
magnetic equator observations, amplitude and differential propagation delay data 78−7839
magnetoplasma, refr. index profiles in layered media, extraordinary mode 80−77223
magnetosheath and kilometric radiation scattering at very high altitudes 79−101025
magnetosphere, controlled VLF phase reversal expt. 77−25866
magnetosphere, discrete VLF line radiation obs. within transmitter-induced amplification bands 78−96360
magnetosphere, echo induced suppression of coherent VLF transmitter signals 77−87191
magnetosphere, ELF emissions, geographic control search 80−12615
magnetosphere, HF and VLF propag. between mag. conjugate pts. on Earth surface 80−41639
magnetosphere, linear and nonlinear amplification during 6.6 kHz transmission 78−40771
magnetosphere, morning sector, eastward movement of auroral radio absorption events 77−56792
magnetosphere, radio window theory, transmission coeff. 80−61953
magnetosphere, side-band mutual interaction of whistler-mode waves 80−82148
magnetosphere, VLF injected wave obs. by Explorer 45 and Imp 6 77−53321
magnetosphere, VLF power line radiation effects on trapped electrons 79−12357
magnetosphere, VLF pulse propagation and distortion, fast Fourier transform investig. 80−56679
magnetosphere, VLF transmission induced slot electron precip. 78−32296
magnetosphere, VLF wave propag., bouncing period, plasma inhomogeneity effect 77−53319
magnetospheric waves, digital techniques for ULF wave polarisation analysis *(French)* 79−70923
man-made VLF waves, effects on radiation belts struct. 78−45150
Marconi's scientific activity, role of his discoveries in radio research 79−17172
Mars, microwave absorption in atmosphere 77−71045
maximum usable frequency for distant radio lines, comparison of calc. methods *(Russian)* 78−32282
Maxwell's eqns. for wave propag. 79−76558
mesosphere VHF radar signal scattering, tropical latitude 80−90193
meteor burst data communication system 78−69608
meteor rate seasonal var., atmos. ionisation effect on LF radio navigational signals 80−82309
meteor wind meas. over Atlanta 79−2411
meteorological radar performance as device for propagation studies at Spino d'Adda 79−84342
MF broadcasting waves, long-distance propag. charcts., round-Pacific mobile expt. *(Japanese)* 77−21997
MF pulsed transmissions, method for separating D- and E-region contribs. to toal absorpt. 78−69593
MF radiowave propag. between two ionospheric satellites, results 78−69604
MF sky wave, combined terrestrial diffraction/ionospheric reflection effects 78−28410
MF skywave field strength prediction, North America new method 77−73904
microwave, in troposphere, amplitude/phase fluctuations, statistical charcts. 79−12225
microwave, rain attenuation study on terrestrial link, weather radar appl. 77−41130
microwave absorption coefficient and refractive index, optimal orthogonal functions 80−36379
microwave absorption in atmosphere of giant planets induced by collisions of H molecules 80−90350
microwave attenuation at 36.8 GHz in sea ice, freshwater ice and snow, meas. *(Russian)* 77−5209
microwave attenuation by salt water droplets 78−7725
microwave attenuation due to precip. of water vapour in atmosphere, meteorological data, raindrop spectral distrib. *(German)* 80−90176
microwave attenuation in 1-3 cm band, path- and area-integrated rainfall meas. 78−65414
microwave attenuation in rain, UK rainfall studies 78−11965
microwave attenuation under adverse dust-storm conditions 80−46247
microwave backscatter modulation by shoaling ocean waves 78−57212
microwave birefringence at gyrotropic boundary by inclined plane wave *(Slovak)* 78−55281
microwave cross polarization discrimination statistics for spatially non-uniform rain 80−12534
microwave crosspolarization, effects of sizes of nonspherical raindrops 80−21790
microwave crosspolarization on satellite to Earth path, effect of rain 80−21789
microwave depolarisation, rain and imperfect antennas combined effects 78−92936
microwave dielectric constant logging, EM wave propag. method 80−12558
microwave diffraction around Earth, bilinear model of troposphere *(Russian)* 77−64367
microwave ducting in inhomogeneous troposphere, anal. 79−39818
microwave Earth-space link rain cell attenuation 80−94586
microwave link, 680 m vertically polarised attenuation by rainfall at 60 GHz 78−36238
microwave link, cross-polarisation on terrestrial path, wind, raindrop size and canting angle effects 79−66736
microwave link, scintillation fading meas. at 100 and 36 GHz, wavelength depend. 77−41110
microwave link at 19 GHz over 35 km, attenuation meas., effects of rain and multipath propag. 79−88453
microwave links, 11 GHz, fading due to rain, snow and multipath propag. 77−91206
microwave links, rain attenuation estimation in UK at freqs. 10 to 100 GHz 78−73426
microwave links, rain attenuation in 10-40 GHz range, from rainfall rates 78−40607
microwave links, short and long term rainfall rates, link design implications *(German)* 78−49082
microwave propag. in 1 to 300 GHz band, computer model for atmospheric propag. conditions 79−53505
microwave propagation in standard atmosphere, ducting, subrefraction effects, radio links appl. *(Norwegian)* 79−29835
microwave propagation under multipath conditions, expt. investigation *(Russian)* 77−5392
microwave radiation from solar power satellite, theoretical anal. of nonlinear interaction with ionosphere *(Japanese)* 80−94634
microwave radiometer for rain attenuation measurement at X, K bands 80−68254
microwave rain attenuation, 11.6 GHz, diversity meas. at Etam and Lenox, West Virginia 79−79922
microwave rain attenuation distributions on Earth-satellite paths, empirical calc. 79−5592
microwave remote sensing, radiative transfer eqns. 80−21855
microwave satellite paths, crosspolarisation phase due to ice crysts. 78−7684
microwave scatt. and depolarization by spheroidal raindrops 77−9480
microwave scatter and sea state estimation, ocean wave models 78−77244
microwave scatterometer, backscatter optimisation using complex charact. polarisation concept 79−100966
microwave slant-path attenuation prediction from rainfall rate meas. 77−70741
microwave solar radiation, forward scattering from water surface 78−44872
microwave transmission charcts. *(Norwegian)* 79−29834
microwaves anomalous depolarisation on 19 and 12 GHz Earth-space paths 77−78354
microwaves at 11 GHz, rain outage performance of tandem and route diversity systems 77−41131
microwaves in troposphere, satellite-borne monitoring of atmospheric and surface characteristics 78−24353
microwaves near horizon meas. over water at 30 GHz, ATS-6 to ground link 78−24345
middle atmosphere, 50 MHz radiowave depolarisation on backscattering 80−85729
millimetre-wave link amplitude scintillation in town environment, observations 77−78302
mm wave atmospheric slant path propag., 15 to 40 GHz 79−84465
mm wave attenuation in rain 78−96280
mm wave propag., rain attenuation meas. at 35 GHz over two sites at different altitudes 79−8667

radiowave propagation continued
MM wave propag. in 100-1000 GHz range 79−92578
mm wave propagation and atmospheric influences 79−84466
MM wave systems, atmospheric attenuation factors 80−67405
mm waves, attenuation due to rain at 74 GHz 79−80002
MM waves, conf., London (Apr. 1980) 80−67441
MM waves, influence of atmosphere on passive radiometric measurements in 10 to 1000 GHz range 79−88465
mm waves, measurements of effective sea reflectivity and attenuation due to rain at 81 GHz 79−80001
MM waves, propag. expts. using Kiku-2 satellite-to-Earth link 79−79909
mm waves, rain attenuation measurements at 94 GHz 79−80000
mm- and sub-mm-wave absorption by atmospheric water vapour 77−49144
MM-wave, Earth's sphericity and radiowave refraction influence on atmospheric radio emission 80−56589
modulation in turbulent shearing plasma, pulsar microstructure 80−94822
Moon, radar scatter data rel. to surface parameters from images 79−40100
multicomponent HF skywave arrival elevation angle meas. 78−24408
multicomponent time-varying signals, unambiguous determ. of fine structures *(French)* 79−70921
multipath fading and radio refractivity meas. at 11, 19 and 36 GHz on 7.5 km path 77−41111
multipath fading and rain attenuation on terrestrial radio links, 7 to 15 GHz 79−16630
multiple scattering, iterative treatment method 79−8709
MW broadcast field strength meas., sunset, night, ionospheric radiowave propagation appl. 77−67010
navigation systems, ionospheric and plasmaspheric effects 77−82100
nonlinear refl. from inhomogeneous plasma bodies 80−1806
North Sea, surface film, 13.9 GHz radar backscatter cross section meas. 79−39764
NWC VLF signal in magnetosphere, Doppler shift meas. by JIKIKEN (EXOS-B) satellite *(Japanese)* 80−94651
ocean surface, radar backscatter rel. to wind speed and fetch 78−77247
ocean surface, radar echoes of second order from waves, first inversion 78−49032
ocean surface wave imaging, synthetic aperture radar mechanism 79−5651
ocean waves travelling against wind, HF radar obs. 78−77242
oceanography, HF radio obs. of wave height, surface winds and currents 78−77241
oil pollution on sea surface, effect on radio location signals *(Russian)* 77−78230
OMEGA, navigational transmission, polar region ionospheric disturbance 78−7835
over-the-sea propag. hops in Republic of Indonesia 80−46245
partial reflection experiment using FM-CW technique 77−29580
partial reflection wind obs. of waves during 1976 over Saskatoon 79−79935
partially polarised waves, polarimetry, accuracy 77−46666
path diversity and baseline orientation [rain cell effects], geometrical approach for circular cylindrical rain cells 79−20913
Pc 1 stimulation by controlled VLF transmissions 77−49239
periodically nonstationary process, envelope distrib. functions and phase 80−4173
phase fluctuations in anisotropic turbulent atmosphere when emitted by moving source 80−17352
planetary atm., refraction attenuation of radio waves 80−4280
planetary atmosphere, diffr. effects in radio transmission 77−64682
planetary atmosphere, occulting spacecraft signal, turbulence determin. 80−94734
planetary atmosphere HF radio occultation meas., phase screen concept 80−56735
planetary atmospheres, complex geometric optics under superrefraction *(Russian)* 78−49353
planetary occultations, turbulence effects 78−85871
plasma with layered struct., use of Fuchsian differential eqns. 80−75060
plasmapause, radio sounding by geostationary satellite *(Japanese)* 78−85770
plasmapause, sounder design using ray tracing studies from geostationary satellite 80−4191
plasmapause, spectra peculiarities of VLF emission 77−25852
plasmapause afternoon sector, simultaneous ULF and strong riometer absorption events 77−25849
plasmapause as a VLF waveguide 77−87193
plasmasphere, ATS-6 radio beacon signals, study of electron content and scintillations *(French)* 79−58184
plasmasphere, v.h.f. and u.h.f. ATS-6 total electron content meas. 77−2303
plasmasphere, VLF ducts modelling 79−58202
plasmaspheric effects, satellite navigation systems 78−7831
power line radiation, propag. rel. to magnetospheric VLF wave activity Sunday decreases 79−66883
power line radiation effects on magnetosphere, transmitter simulation 79−12348
precipitation, attenuation and cross-polarization due to various drop size distribution functions 79−84373
precipitation attenuation studies from meas. of ATS-6 20/30 GHz beacon signals 79−20911
probing at dm wavelengths, aspect depend. characts. 79−88547
propagation problems connected with infinitesimal point source, review 80−90194
pulsation excitation by 4.61 MHz transmitter action on ionosphere *(Russian)* 78−4026
pulse propagation over smooth irregular terrain 78−20458
pulse-long distance propagation measurements in HF region, results *(German)* 80−41637
pulsed EM radiation, from line source in two-media configuration 79−64153
pulsed radar method for river and lake ice-cover thickness meas. 78−92862
quasi-static range propagation within conducting slab, expressions for horizontal elec. dipole 79−48515
radar attenuation and detection of boreholes in advance of mining 78−96305
radar aurora, per-unit-vol. RF scatt. cross section calc. 78−45079
radar backscatter from ocean surface, friction vel. depend. 78−77246
radiowave propagation continued
radar cloud meas., comparison of simultaneous studies by satellite 79−58077
radar echoes from clear air, mechanisms 80−90181
radar for mm wave propag. expt. *(Japanese)* 78−16208
radar impulse reflection from nonlinear random sea 80−12416
radar meas. of surface roughness, soil moisture and texture with vegetation cover 79−62534
radar propag. through turbulence, scintillation detection using monopulse techniques 78−85717
radar reflection from lunar surface, Luna 23 meas. at 3.1 cm wavelength 80−8560
radar reflections in rock salt 78−96215
radar reflectivity calibration using ground return targets 79−53471
radar reflectivity of ground-level hail in Colorado hailstorms 79−53470
radar reflectivity profile classified by rain types 80−101420
radar reflectivity/rainfall rate relation, effect of vertical air motions 77−45098
radar reflectivity/rainfall rate relation for seeded and nonseeded clouds 77−45099
radar return from radar-acoustic sounding system, refractive turbulence effect 79−39821
radar signal scatt. from turbulent air, VHF and UHF 80−85728
radio oceanography, colloquium (Hamburg 1976 Sept.29-Oct. 6) 78−77239
radio pulse reflection from ionospheric model, distortion, compression, approximate theoretical solution 77−21969
radioastrometry, tropospheric limitations on meas. accuracy *(Russian)* 77−22092
radiocommunication services, propagation aspects in planning 80−12613
radiointerferometric frequency and coordinate meas. accuracy, tropospheric fluctuation constraints 79−8848
radiometeorological characteristics, statistical structure *(Russian)* 79−84376
radiosonde data computing 79−2350
rain, SHF scatt. props. of Pruppacher-Pitter form drops and cross polarisation, 11 to 34.8 GHz 77−41129
rain attenation at 11 GHz *(French)* 78−77292
rain attenuation, frequency scaling 77−45071
rain attenuation, microwave link, freq. range 10 to 40 GHz calcs., meas. 77−70771
rain attenuation, rapid response rain gauge 77−87128
rain attenuation, year and worst-month rain rate distrib. estimation method 79−5648
rain attenuation above 10 GHz, regression curves for tropical areas 80−90111
rain attenuation above 11 GHz, radio links appl. 80−98410
rain attenuation and depolarization of Earth-satellite transmissions at freq. greater than 10 GHz *(French)* 78−53689
rain attenuation at 10 and 11 GHz, radiometric measurements 80−67397
rain attenuation at 11 GHz on radio links *(French)* 78−53683
rain attenuation at 13 GHz on Earth-space paths, depend. on elevation angle 77−70742
rain attenuation calc. 78−44919
rain attenuation data, appl. to path engineering 78−24327
rain attenuation distribution estimation *(French)* 78−53688
rain attenuation distribution estimation method *(Japanese)* 79−100891
rain attenuation effect on Earth to satellite radio link, statistical study *(Japanese)* 79−5555
rain attenuation estimation formulae, worst-month, worst-year, satellite communications in Japan appl. *(Japanese)* 79−100890
rain attenuation for Earth-satellite path, correlation with predicted values using radar 77−5279
rain attenuation for Earth-space links, comparison between radar- and radiometer-derived data 78−24343
rain attenuation in microwave and MM wavebands, estimation of duration time distribution *(Japanese)* 80−21788
rain attenuation meas., microwave radio link projected design appls. *(Slovenian)* 80−46217
rain attenuation meas. on Earth-space paths at 37 GHz by passive radiometry 77−41109
rain attenuation model for Earth-satellite paths 79−62561
rain attenuation of 19 GHz COMSTAR satellite beacon signals 79−5593
rain attenuation on microwave link slant path 79−66737
rain attenuation on parallel, series, and convergent terrestrial paths 79−66735
rain attenuation on satellite-Earth path at 11.4 and 14 GHz by radiometric meas. *(French)* 78−49066
rain attenuation on terrestrial and Earth-space propag. paths, joint statistics 78−73490
rain attenuation on terrestrial path 79−66734
rain attenuation prediction methods comparative analysis, radiowave propagation appl. 80−109182
rain attenuation prediction on terrestrial radio links from rainfall data 79−16636
rain attenuation prediction using radar and in situ meas., 28 GHz Comstar beacon signal 79−70839
rain attenuation ratios and path diversity gains of mm waves at 11, 20 and 36 GHz 79−16631
rain attenuation results, expt. and theoretical, propag. meas. at 94 GHz 79−16632
rain attenuation studies, raingauge data selection 77−45048
rain attenuation study at 11 GHz, statistical properties of single attenuative events 79−34885
rain depolarisation and attenuation meas. at 11.7, 19.04 and 28.56 GHz *(French)* 78−49067
rain depolarisation using INTELSAT-IV satellite in 4 GHz band at low elevation angle *(French)* 78−49068
rain effects on 18 GHz dual-polarised propagation link 77−29404
rain effects on multiple access transmission of data via satellite 78−77313
rain rate distrib. study, Japan, attenuation in telecommun. systems 78−92934
rain rate statistics, approx. method for use in signal attenuation estimating 79−70840
rain scatter interference in medium scale broadcasting satellite for experimental purposes 79−8668
rain scattering of microwaves, drop-size and temp. effects on forward and backward scattering 80−17317

radiowave propagation continued
rain slant path attenuation statistics prediction at various locations 78−24344
rain-cell modelling for earth-space links using SIRIO satellite radiowave propagation data 80−36352
rain-induced attenuation, expt. results and calcs. *(French)* 79−12164
raindrop induced forward and backward scattering amplitudes, tabulations 79−34884
raindrop sizes in mm radio attenuation, lognormal distribution 79−16635
raindrops, spreading of ellipsoidal raindrops orientation during intense rainfall, expt. results 79−16634
rainfall characteristics across Europe 79−66733
rainfall intensity data for radio-relay system design above 10 GHz *(French)* 78−53690
random media causing pulse spreading and wandering 80−37942
ray trajectories in ionospheric waveguide, influence of inhomogeneities 80−61966
ray trajectory props. in irregular ionospheric waveguide 80−90284
reflectivity meas. by radar and disdrometer, comparison for rain 79−53546
refraction corrections for exponential atmosphere, real-time computational method 80−98432
refraction in atmospheric boundary layers 80−36400
refraction values in troposphere in air temp. inversion 80−4087
refractive index microstructure and scintillation fading meas. in tropical region 79−16629
refractivity and temp.-humidity cospectrum 79−39819
refractivity diurnal variation up to 3 km over India 78−40627
refractivity gradient variation in atmosphere, statistical distrib. and max. critical value 80−12522
remote sensing, scatter model for leafy vegetation 79−12193
remote sensing of atmosphere, land and sea props. 78−93015
round-the-world echo signals, height factor estimate from expt. results 77−13159
round-the-world signal group delay, frequency dependence calc. *(Russian)* 78−61654
sandstorms effect on microwave propagation 79−70834
sandy and clay soils, microwave absorption *(Russian)* 78−81162
satellite 35 GHz wave attenuation along slant path by rain *(Japanese)* 78−85671
satellite communication systems, rain effects on propag. 77−41126
satellite communications above 10 GHz, rain effects 80−8410
satellite link, ionospheric radio lenses causing fading 78−7833
satellite link, space diversity improvement, squall line direction effects 77−91205
satellite links, ionospheric wave disturbances effect on polarisation fading freq., simulation 78−69572
satellite links, seasonal var. of attenuation statistics due to bright-band height 79−100889
satellite links at 20 and 30 GHz, crosspolar phase variations on satellite-Earth path, meas. 77−81957
satellite links rain attenuation and site diversity effect, statistical studies 78−88892
satellite low angle transmission effects, VHF and UHF 78−7747
satellite radio signals amplitude scintillations rel. to spread-F and sporadic-E over Brisbane 78−49209
satellite relay signals, 30 GHz, attenuation due to weather *(Dutch)* 78−7741
satellite signals, phase shifts due to plasma shock waves and solitons 77−45273
satellite transionospheric signals, group delays rel. to electron density profiles determ. 78−28371
satellite transmissions, morphological and ionospheric aspects of quasiperiodic scintillations 77−91361
satellite VHF/UHF communications, effect of ionospheric scintillation 77−41264
satellite-to-ground radio path, 12 GHz, low elevation-angle space-diversity expt. 77−70914
scalar microwaves propagation in medium with severe random nonuniformities, Green's function 80−69297
scatter communications, review 79−34935
scattering amplitudes and crosspolarisation of spheroidal ice particles, calc. 77−70740
scattering by 1-D power law phase screen 80−77220
scattering by E-region anisotropic inhomogeneities oriented along geomag. field 78−53771
scattering by plasma cylinder, numerical anal. *(Russian)* 77−39424
scattering by rain, COMSTAR beacon receiver diversity experiment 78−73421
scattering cross section of radiowaves reflected from planet with spherically symmetrical atmosphere 80−21935
scattering from acoustic atmospheric formations 79−92579
scattering from rough surfaces, full wave and physical optics solns. 78−66717
scattering from semi-infinite plate, linear algebraic eqns. infinite system soln. 78−55286
scattering from uneven surface and law of conservation of energy 78−46492
scattering in presence of background slab, algorithm for profile reconstruction 80−94644
scattering of microwave background in clusters of galaxies, 9 mm obs. 80−105366
scattering of microwave background radiation in clusters of galaxies 80−105367
scattering on acoustical formations of atmosphere in field of moving point source of sound 78−32210
Schumann resonance in ionosphere-Earth waveguide, line splitting detection, chirp-z transform 78−3861
scientific background to studio by International Radio Consultative Committee 78−77311
scintillation, thin screen theory for spherical wave 78−13645
scintillation by ionosphere, statistical study 80−109306
scintillation effects at 30 GHz on ATS-6 geostationary satellite *(French)* 78−49065
scintillation enhancements rel. to sheet-like auroral ionospheric irregularities 79−35033
scintillation levels of synchronous satellite beacons at equatorial and high latitudes, empirical models 79−58182
scintillation of VHF, UHF and SHF in equatorial ionosphere, theory 80−61946
radiowave propagation continued
sea echo radar spectra resolution limitation inferred from ionospheric Doppler broadening 78−81489
sea surface scattering theory for large incident angles 77−86911
semi-arid region radio climate and tropospheric model 77−21844
SHF, ATS-6 satellite 20 GHz carrier, attenuation and depopolarisation meas. *(French)* 78−49063
SHF beyond-the-horizon signals, evaporation duct influences 78−92935
SHF differential phase shift method for total electron content meas. of ionosphere-plasmasphere 78−36304
SHF radar altimetry from Geos 3, backscatter characts. 80−3915
SHF signal attenuation by rain, monitored by radar 80−51567
SHF waves for satellite broadcasting, rainfall attenuation characts. *(Japanese)* 80−12501
short-wave echo azimuthal variation obs. over 2300 km *(Russian)* 78−4027
signal and atmospheric noise mixture statistical characts. in HF band 78−57276
signal level fluctuations on long-distance radio paths, energy spectra 79−53629
sinusoidal surfaces, scatt. patterns 80−58448
SIRIO, fade statistics for 11.6 and 17.8 GHz *(Italian)* 80−4095
SIRIO 1 experimental satellite circular polarisation on satellite-Earth path 79−84334
SIRIO satellite, 11.6 and 17.8 GHz cumulative attenuation statistics 79−84339
SIRIO satellite down link propagation expts. in Finland 79−84338
SIRIO satellite link, 11.6 and 17.8 GHz attenuations relationship 79−84340
SIRIO satellite link, 11.6 GHz, propag. meas. in Munich 79−84337
SIRIO satellite link, propag. meas. in Eastern USA 79−84343
SIRIO satellite link 11.6 GHz attenuation, meas. and estimated from sky noise temp. 79−84341
SIRIO satellite reception, atten. meas. during first year at Deutsche Bundespost Earth station at Leeheim 79−84335
SIRIO satellite signal propag. meas. by Netherlands PTT ground station, and equipment 79−84344
SIRIO satellite to Earth propagation path, precipitation scatter meas. 79−84336
SIRIO satellite transmissions near 11.6 GHz at Slough UK, meas. 79−84333
SIRIO-1 satellite link, analysis of oblique propag. measurements made at Gometz-la-Ville Earth station *(French)* 80−56504
skywave field strength prediction, MF propag. in North America 77−78350
slant path rain attenuation, satellite relay broadcasts 77−86988
slant path rain attenuation characteristics in 20 and 30 GHz bands 79−8678
snow, microwave signatures rel. to state and wetness 78−57235
solar activity implications, historical account and predictions *(Italian)* 78−24496
Solar Cycle 21, radio communication effect 79−75181
solar EM radiation and terrestrial effects *(Japanese)* 80−51600
solar plasma, observations using Mars-2 and Mars-7 probes 78−49345
solar radio bursts at 26 MHz, obs. brightness distrib., possible ionospheric effects 80−41806
solar system investigation by radiowave transmission by space probes 79−21204
solar wind, radial depend. of props. from Helios 1/2 and Pioneer 10/11 scatt. expts. 78−28595
solar wind radio scattering, meas. of spacecraft signals 78−49277
solar wind turbulent plasma, radio wave propag. meas. using three satellites 80−101518
solar-terrestrial environment monitoring and forecasting system, SELDADS, for radiocommunication appls. 79−58097
Sommerfeld integral, numerical approximations for fast convergence 78−66727
source radiation in presence of smooth convex bodies, theory 79−64151
space plasma front parameter determ. by noncoherent response 77−45274
space sciences, conf., Trivandrum, India (Jan. 1977) 78−69586
space sciences, conf., Waltair, India (Jan. 1978) 79−101000
space-time distribution of refractive index of air in Mongolia 78−81335
spaced receiver drift experiments, triangle size effect 79−53635
spaced receiver drift expt., triangle size effect, ground diffr. pattern estimation errors 79−88525
spaced receiver fading records, nature of ionospheric irregularities determ. 79−88532
spatial phase structure meas. of ionospherically reflected waves using HF array 79−84505
specific attenuation and phase shift due to rain in freq. range 10 to 30 GHz *(Italian)* 78−96261
sporadic-E affecting ELF wave propag. at nighttime 80−77202
sporadic-E and troposphere effects on radiowave propag. above 30 MHz 80−41636
sporadic-E layer behaviour in EM field of strong decametric waves 78−69569
sporadic-E layer inhomogeneous structure influence of RF heating *(Russian)* 78−61653
sporadic-E layer radiowave reflection, full-wave anal. 77−87176
sporadic-E modes, directional dispersion between 9 and 14 MHz 78−28412
spread-F, lunar tidal effect 79−80070
spread-F and magnetic activity at Kodaikanal, India 79−88542
standard transmissions stability on transionospheric paths 79−84577
STARE: a new radar auroral backscatter experiment in northern Scandinavia 79−39977
stochastic waves, temporal moments, mutual coherence function 78−20979
strato-mesosphere dynamics, rel. to medium and short radiowaves seasonal absorpt. courses 79−58149
stratosphere and troposphere, VHF radar scatt. and refl. 80−90182
subsurface-to-subsurface and subsurface-to-air propag., horizontal electric dipole fields 78−73375
sudden commencement absorpt. events at polar cap edge 77−70935
sudden ionospheric disturbance, VLF phase shifts and amplitude variations 77−91363
sunspot cycle effects on amateur radio communication 79−58308
super distant trajectories, 10-15 MHz signal transmission, amplitude characts. *(Russian)* 78−32280
superposed plane waves, complex angles of arrival 77−71908

radiowave propagation continued
surface and interface aspects, Conf. Istanbul, Turkey (Oct. 1976) 78−22075
surface geology sensed by ground mode radiowave propag., glaciated area of USA 80−76979
SW ionosphere-Earth waveguide, through polar and subpolar night ionosphere *(Russian)* 78−32279
SW ionospheric scattering by periodic artificial irregularities *(Russian)* 78−32276
SW propag. over long distances, predictions and observations 79−70919
SW radio waves, polarisation on slant path 78−73573
SW transmission, proportional effect of ionospheric damping, solar activity *(Hungarian)* 80−56675
synoptic windfinding using Omega VLF navaid, atmos. radiowave propag. 80−17309
thermal radio emission from exponential slab, sea ice appl. 78−28244
thermosphere, incoherent scatter meas. of props. 79−53597
thermosphere, lower, echo from ionospheric sublayers 80−61956
Thomson scattering, collision-dominated, negative ions effect, ionospheric D-region appl. 78−45118
thunderstorm location by single station techniques, improved method, radiowave propag. effects 80−67438
thunderstorms, depolarisation at millimetre wavelengths 78−3854
time signal from Loran-S station, propagation path effect on locking error 77−87742
time signals, Tokyo reception accuracy 78−69606
time signals transmission times meas., dynamics of seasonal variations obs., in SW and VLW ranges 77−79061
time varying medium, transmission and refl. of EM wave 79−81341
time-varying medium, EM wave reflection anal. 79−25385
TM mode-conversion at terminator for anisotropic ionosphere, param. study *(German)* 80−46333
trajectories in horizontally inhomogeneous ionosphere, angular characts. 78−73571
trans-horizon propagation path over sea, transmission loss due to ducting at 1.8 GHz 80−105041
trans-ionospheric, evolution and effects of scatt. equatorial F-region irregularities 79−29933
transequatorial propag. in 144 MHz amateur radio band, forward scattering at rising plasma bubbles 79−35057
transequatorial radiowave propag. in freq. range 28 to 432MHz, amateur bands, obs. and expts. 80−101491
transequatorial radiowave propag. over 21 year period, VHF/UHF signals, theories 80−109311
transhorizon radiowave propag. in lower troposphere, refractivity effects 77−70747
transillumination of planetary atmospheres, radiowave refraction 78−96413
transionospheric radio signal time delay spatial correlation 78−45117
transionospheric radio wave scintillation, time struct. 80−90281
transionospheric signal time delays at widely separated locations 79−58186
TRANSIT, satellite observations, phase fluctuations, and ionospheric irregularities 78−7832
tree-covered surface scattered radio signal spectral density obs. 77−87049
triggered VLF emissions and detrapped electrons 78−77421
troposcatter aperture-medium coupling loss 79−29840
troposcatter channels and appls. of adaptive equalization techniques, statistical anal. 79−29841
troposcatter developments in North Sea 80−46246
troposhere, Danish experimental line-of-sight propag. path, 13.5-15.0 GHz 79−48555
troposphere, angular depend. of rain scatt. at freqs. below 30 GHz 80−8416
troposphere, attenuation statistics at 15 and 35 GHz for very low elevation angles 79−8674
troposphere, ducting of HF radiowaves, numerical study 80−36378
troposphere, fading at low elevation angles, meas. of satellite signals *(French)* 78−49069
troposphere, investigation using modelling technique 79−29838
troposphere, lower, over S.England, 6-year study of RRI and PRI 79−39823
troposphere, lower, vertical distribs. of Radio Refractive Index and Potential Refractive Index 79−12228
troposphere, microwave propag. during 1974, Dec. 17-21 disturbance 77−70736
troposphere, nonuniform wave guide, coupled mode anal. 80−94587
troposphere, over sea, refr. index statistical characts. *(Russian)* 78−65363
troposphere, radio beam curvature effect on phase meas. 78−49118
troposphere, radio propag. characts. prediction using FORTRAN computer programs *(Italian)* 78−85666
troposphere, radio refr. index and potential refr. index, S.England 79−34928
troposphere, radio refractive index, calc. from temp., press. and humidity data *(Czech)* 80−36351
troposphere, radiowave propag. problems, URSI and CCIR collaboration 78−57322
troposphere, refr. index struct. parameter height distrib. with lower boundary spatial transition 78−73491
troposphere, refr. index variance and its height distrib. in different air masses 77−41133
troposphere, refr. theories of radio wave propag., review 78−69425
troposphere, refractive index gradients study, new approach 79−25322
troposphere, refractive struct. using Rake probing 77−91231
troposphere, refractivity turbulence struct. const., Sunset Radar obs. comparison with theoretical model 79−8673
troposphere, RF refractive index, synthetic properties, over Japan 77−87047
troposphere, signal strength and surface radio refractivity, sea breeze circulation effects 79−20919
troposphere, transhorizon propag. paths in Indian subcontinent, transmission loss prediction 77−13105
troposphere, transhorizon radiowave propag. rel. to remote sensing 78−44921
troposphere, VHF propag. over diffr. paths 77−13108
troposphere and ionosphere, effects on communication systems 78−92954
troposphere and ionosphere, propag. errors during geomag. storms 80−4077
radiowave propagation continued
troposphere and stratosphere, decametric radiowaves emitted by dipole 78−69399
troposphere communication, effect of beam with on energy spectrum of delays *(Russian)* 79−2329
troposphere communication channel, energy spectrum of delays 79−84442
troposphere scatter path loss, new formulas 79−48556
troposphere waveguide, effect of elevated M-inversion 80−90195
troposphere waveguide, propag. of atmosphere radiothermal radiation *(Russian)* 79−88406
tropospheric, spot dancing in inhomogeneous random media 78−46496
tropospheric and precipitation scatter, rel. importance in interference and coordination calcs. 78−73423
tropospheric ducting environments, case studies of beyond horizon propag. 77−41132
tropospheric ducts used for line-of-sight links, protection against signal cancellations *(French)* 80−17303
tropospheric effects on radio communication, book 80−62400
tropospheric links, refractive index gradient layers effects 77−13107
tropospheric long-distance propag., multiple scatt. effect 80−109229
tropospheric range correction algorithm 78−61591
tropospheric reflection of differently polarized transient signals 79−29839
tropospheric scatt. mechanisms and channel characterization 79−29837
tropospheric stratification and anomalous propagation 79−29842
tropospheric transhorizon propag. at freqs. >1 GHz on transmission paths set up in CSSR and GDR *(German)* 80−17364
tropospheric waveguide, numerical comparison of ray method and normal wave method 80−21858
turbulence and wavelength effect on scintillation fading at mm. wavelengths 78−85623
turbulent atmosphere, phase difference and derivative fluctuations 78−92951
turbulent layer propagation, phase and amplitude scintillation freqs. 78−24405
turbulent troposphere, complex RI, temporal RF spectra of multifreq. waves 77−21834
TV picture 'ghosts', used to locate offending building, for teachers 78−81764
tweek atmospherics propag. mechanism 78−49213
UHF diffraction field, mountain ridge snow cover effect 77−64395
UHF diffuse radar aurora, rapid scan Doppler vel. maps 78−77388
UHF meas. of atm. O_3 absorpt. spectrum, O_3 conc. and distrib. determ. *(Russian)* 79−100897
UHF/SHF tropospheric scatter radio links, scanning beams 78−81276
ULF, field strength meas., ionospheric C-layer props. determ. 77−25816
ULF signal conversion coeffs. seasonal depend. on ionospheric height in sunrise zone 77−25817
ULF wave-particle interactions, dynamic cross correlation studies *(French)* 79−70926
ULF waves, magnetospheric, conjugated ground-satellite relationships 79−29947
ULF waves detected on GEOS-1 satellite, amplitude and polarisation anal. *(French)* 79−70924
ultrashort wave, long-range propagation, climate effects 77−56716
ultrashort-wave diffraction field in shadow of ridge-crests, simulation using dielectric prism 78−86995
unified wave propagation theory, tenuous random medium 78−4491
upper atmosphere, meteor wind study at Kyoto University 79−48595
upper atmosphere, scatt. theory appl. to radio meteor obs. 79−5696
Urbana Meteor Radar observations during GRMWSP/CTOP periods 79−2412
URSI Commission F, First Open Symposium (La Baule, France, 1977 April 28-May 6) 78−57321
USA rainfall variability rel. to microwave attenuation 79−62562
variation during low solar activity *(Japanese)* 79−40032
Venus atmosphere, microwave absorption in 21-117 GHz range 77−71040
Venus atmosphere, Venera 9 and 10 radio transmissions near limb 77−78694
vertical profiles of rain rates rel. to Earth-satellite radio attenuation modelling 79−70841
VHF, meas. in Rajasthan area, India, rel. to climate 77−13106
VHF, UHF and SHF equatorial scintillations calc. using disturbed ionosphere model 77−17289
VHF amplitude scintillation in auroral oval 78−71660
VHF and SHF scintillations and F-region irregularities correl. meas. 77−21977
VHF and UHF terrestrial propag., influence of polarisation on transmission quality *(German)* 78−61518
VHF backscatt. from blanketing E_s-layers in equatorial electrojet, gradient instabilities 77−29577
VHF backscattering from E/region irregularities near mag. equator 77−33248
VHF daytime scintillations and electrojet irregularities 78−28406
VHF double-peaked spectra at negative Doppler shifts in the morning sector of radio aurora 79−40014
VHF duty cycle diurnal and seasonal vars. due to meteor forward scatt. 79−88534
VHF Faraday rotation meas. of total electron content at low latitudes 79−16749
VHF ionospheric forward scattering, effect of meteors *(Japanese)* 78−81504
VHF multi-satellite scintillations correl. with spread-F and sporadic-E increase over Brisbane 77−53297
VHF propagation through ionosphere equatorial plasma bubbles, transequatorially 80−41635
VHF radar aurora and strong HF backscatt. comparison 80−61960
VHF radar echoes from equatorial E-region irregularities, sudden disappearance 78−40738
VHF radar obs. of stratosphere, specular reflection 79−39822
VHF radar partial reflections from equatorial E-region plasma density gradients 77−25828
VHF radar signals, partial refl. and scatt. from clear atmosphere 78−81278
VHF radar signals partial refl. from troposphere 78−85656
VHF satellite signals, 40 MHz, ionospheric characts. determ. 79−88529
VHF satellite signals, 40 MHz, scintillations obs. at Kurukshetra 79−88527
VHF scintillation at high-latitude, analytical formulas 80−77224

radiowave propagation continued
VHF scintillation at high-latitude near 70°W 80−77221
VHF scintillation late evening enhancements at low latits. 79−75031
VHF signal scintillation, from ETS-2 satellite, obs. of Waltair and Calcutta 80−109295
VHF signals, ionospheric radio fluctuation obs. from geostationary satellite 79−21091
VHF signals from satellite radio beacons, ionospheric scintillations 79−53634
VHF technique for space-time mapping of lightning discharge processes 78−85721
VLF, at sunrise and sunset, spatial phase-difference vars. *(Russian)* 77−5390
VLF, between Earth and ionosphere, anisotropic 3-layer model *(German)* 78−36358
VLF, ionospheric density gradients effects at low latits. 79−88530
VLF, multi-mode, signal and communication channel parameters calc. *(Russian)* 79−5702
VLF, signal variations spectral anal. in Earth-ionosphere waveguide *(Russian)* 77−78305
VLF, sunrise modal interference over west-east paths 77−53296
VLF absorpt. seasonal variations, geopot. field 79−66766
VLF bursts, daily vars. in number, synchronous obs. 77−29549
VLF bursts synchronous obs. in Schumann reson. freq. range 77−17286
VLF direction-finding techniques comparison for determ. whistlers exit point at ionosphere 80−26631
VLF Doppler signatures theory rel. to magnetospheric density struct. 77−87202
VLF ducts in magnetosphere, protonospheric-ionospheric modelling 78−28446
VLF emission and radiation belt electron lifetime 79−62682
VLF emission modulation freq. shift relative to geomagnetic pulsation freq. 80−77229
VLF emissions, mid-latitude obs. at Yakutsk 79−62683
VLF hiss, convective beam amplification 79−40029
VLF hiss propag. characts. obs. at low latit. ground stations 78−69561
VLF nighttime propagation anomalies, comparison at 10.2 and 13.6 kHz 78−28414
VLF noise storms rel. to magnetospheric ring current 77−91376
VLF non-ducted whistler-mode signals at low latitudes 78−61658
VLF phase disturbances and energetic electron precip. following 1971 Dec. 16 mag. storm 77−53284
VLF plane wave airborne survey of ground resistivity, resolution studies 80−12333
VLF propag. during sunrise 78−93030
VLF propagation in auroral zone, essential height determ. 79−53631
VLF scattering by perfectly conducting half plane below stratified overburden 78−57167
VLF sferics from Union City, Oklahoma tornadic storm 78−85639
VLF signal phase and amplitude vars. over transequatorial path, Australia-New Delhi 79−5703
VLF signal phase velocity calc., curvature correction/frequency relationship 77−60543
VLF signals, differences in diurnal phase and amplitude vars. 78−49212
VLF signals, numerical study of satellite reception using waveguide concepts 80−90282
VLF signals, time-varying, determination of wave normal directions *(French)* 79−70927
VLF signals in ionosphere-Earth waveguide, geomag. activity effects *(Russian)* 79−2426
VLF subionospheric propag., whistler-induced anomalies 80−26668
VLF sudden phase anomalies correl. with solar microwave burst energies 78−77418
VLF sudden phase anomalies during 1972 Aug. 2-4 solar flares 78−40739
VLF transmitter, ground-based, obs. on GEOS-1 of 10.2-13.6 kHz signals 79−25411
VLF transmitter, ground-based, reception of signals on GEOS-1 79−29948
VLF wave activity during mag. storm, stimulated by power line radiation 77−87199
VLF waves, magnetospheric, conjugated ground-satellite relationships 79−29946
VLF waves in Earth-ionosphere waveguide near eigenvalues degeneration points 77−49219
VLF waves in ionosphere generated by ground transmitter, mag. field intensity world wide mapping 77−78567
VLF waves polar disturbances obs. at Inubo, Japan *(Japanese)* 77−21998
VLF whistler-mode transmissions, Pc 3 micropulsation obs. 79−8781
VLF-EM modelling of conductors 79−79736
VLF/RLF atmospheric noise, amplitude-probability distribution model 78−32288
water vapour dielectric constant, rotational part, engineering method of calc. 78−40717
wavy water surface thermal radioemission obs. at 3.5 and 14.5 MHz *(Russian)* 78−61425
whistler mode, obs. of plasma drift and ionosphere-magnetosphere coupling 80−77239
whistler mode signals, initial results from tracking receiver direction finder 78−77429
whistler range in plasma, wave radiation *(Russian)* 78−36400
whistler-mode signals, spacecraft obs. near electron gyrofrequency 78−28418
whistlers, effect of Earth-ionosphere waveguide propagation on polarisation and arrival angles 80−36457
wireless transmission, 1900-1935, early ionospheric research 79−9070
X-band, dielectric constant of dust, effect of moisture content 80−72578
Yugoslav soil medium-wave conductivity chart computation *(Slovenian)* 79−39718
Zenneck surface wave, excitation by vertical aperture 79−39820

radium
see also nuclei with .....
accumulation, in animal thyroid glands, U and Th prospecting appls. 78−27853
atom, Rydberg series, ionisation limit derivation from multichannel quantum defect theory, UV absorpt. spectra 80−52918
content in natural samples, γ spectrometric determ. *(Russian)* 78−92562
electrical resistivity; 1-1000K, data tables 79−78073
radium continued
groundwater in Grants Mineral Belt, New Mexico, effects of U mining and milling 77−56657
isotope abundances in E.Pacific surface waters 78−96234
osteosarcomogenic effectiveness of ^{224}Ra and ^{226}Ra in mice 77−86560
N.E.Pacific Ocean, deep water ^{226}Ra maximum 77−5221
radiotherapy of cervical carcinoma, external irradiation and 1 Ra appl. 79−88158
radiotherapy source leakage testing 77−16977
retinal stimulation by Ra 79−71213
separation from thorium oxalate of ^{228}Ra 80−45600
storage safe, design, safety, ease of use 78−92736
water baseline radioactivity in Arizona 78−81230
^{228}Pa, near-surface temporal var. in Gulf of Mexico 79−66713
^{226,228}Ra in humans, radiation induced malignancies 78−96075
^{A}Ra, A=226, 228, content in groundwater of Fall Line aquifers 80−89682
^{222}Ra short lived daughter disequilibrium in a mixed maritime and continental atmosphere 80−108822
^{223}Ra,^{229}Ra, activity ratio and separation from Indian spring water 78−86962
^{224}Ra and daughters, radioactive props. and biological behaviour 78−96090
^{224}Ra and thorotrast radiobiological significance 78−96076
^{224}Ra biological effects, conf., Alta, USA (July 1974) 78−96068
^{224}Ra, endosteal cell dose and relative distrib. factors compared to ^{226}Ra 78−96091
^{224}Ra injections into humans, soft-tissue effects 78−96070
^{224}Ra injections into humans, skeletal effects 78−96071
^{224}Ra preparation, for ankylosing spondylitis therapy 78−96089
^{224}Ra, short-lived α-emitter, late effects after incorporation in mice 78−96069
^{224}Ra usage in radiotherapy and radiobiology, brief history 78−96085
^{224}Ra use in treatment of ankylosing spondylitis and rheumatoid synovitis 78−96086
^{226}Ra, ^{210}Pb and ^{210}Po disequilibria in western N.Pacific 77−5227
^{226}Ra, ^{228}Ra, dose-response relationships for female dial painters 80−21545
^{226}Ra, alpha scintillation counter for determ. of low natural conc. 80−9456
^{226}Ra, assessment of quantities in North Carolina drinking water supplies 80−45826
^{226}Ra, behaviour in Pee Dee River−Winyah Bay estuary, S.Carolina 80−98360
^{226}Ra body burden determ., postprandial changes in exhalation rate of Rn prod. in vivo 78−69224
^{226}Ra, conc. in Florida phosphate materials 80−30615
^{226}Ra, conc. in New Zealand soils 77−53057
^{226}Ra, conc. in water near a phosphate facility 80−45827
^{226}Ra, desorption from river-borne sediments in Hudson estuary 79−79877
^{226}Ra, determ. in environmental samples by ^{222}Rn separation, integral counting methods 77−63988
^{226}Ra, determ. of tap water pollution *(Czech)* 79−34675
^{226}Ra determination in U ores, dusts and mill tailings 78−15736
^{226}Ra determination in water, sampling and meas. methods 77−9278
^{226}Ra, distrib. in Antarctic Ocean 77−5220
^{226}Ra, distrib. in Atlantic Ocean 77−5219
^{226}Ra, effect on proliferative and differentiative ability of mouse haemopoietic stem cells 79−79611
^{226}Ra, emulsion scintillation counting of biological samples 78−81089
^{226}Ra, exposure rates from gamma sources in dwelling room walls, Monte Carlo calc. 78−73260
^{226}Ra, flux from estuarine and continental shelf sediments 78−32061
^{226}Ra, fractional retention by the bluegill 79−39506
^{226}Ra in public water supplies, conc. determ. *(German)* 80−94138
^{226}Ra in Taiwan buffalo bone and environmental samples of N. Taiwan power reactor site 77−64142
^{226}Ra leaching from contaminated soils, investigation of Ra bearing soils from Port Hope, Ontario 79−20900
^{226}Ra leaching from fossil bones 78−58562
^{226}Ra long-term retention in contaminated dial painters 77−90917
^{226}Ra, meas. in U mill tailings pile rel. to ^{222}Rn diffusion and exhalation 79−92109
^{226}Ra paint, effect of occupational exposure, chromosomal aberrations in lymphocytes 77−37011
^{226}Ra, radiation-induced carcinogenesis, beagle dog obs. 79−66487
^{226}Ra, radioactivity of thermal and mineral springs in Slovenia 80−7963
^{226}Ra, seawater content in Atlantic and Pacific Oceans, comparison with Ba 77−5222
^{226}Ra/^{222}Rn/^{238}U ratios in fracture zone water of N.Kirgizia 77−33108
^{226}Ra/^{238}U dating of quaternary corals by γ-spectrometry 79−88221
^{226}Ra-^{222}Rn disequilib. and pumice radioactivity, Sakurajima volcano 77−33033
^{226}Ra-burdened dog skeleton, Rn retention rel. to age and dosage 78−65092
^{228}Ra-^{228}Th radioactive disequilib. rel. to coastal pollution in New York Bight 79−29784
^{234}U→^{230}Th→^{226} Ra, superposition soln. of transport of decay chain through sorbing medium 80−37500
^{234}U→^{230}Th→^{226}Ra decay chain, hydrogeological migration anal. 80−37501

radium compounds
No entries

radium emanation *see radon*

radius measurement *see diameter measurement*

radius of curvature measurement *see curvature measurement*

radon
see also nuclei with .....
^{222}Rn, disssolved in Boisson spring water, physiological props. 79−48292
^{222}Rn concentration distribution under ground, effect on natural γ-ray flux density and exposure rate 80−36300
^{222}Rn flux through multilayered covers cover U mill tailings 80−95487
adsorption, on surface of elastically deformed body 80−10775
aerosol particle size distrib. in uranium mine *(French)* 78−32195
air concentration in dwelling places *(Hungarian)* 77−78409
air concs. in certain houses 79−79662
alpha activity meas. with electronic cups, U exploration appl. 78−7781
alpha particle etch pits in CA80-15 and LR-115 cellulose nitrate track detectors 78−855

radon continued
atmosphere, ^{222}Rn daughter products, measurement using diffusion sampler 80−81510
atmosphere, automatic counter for continual unattended operation 78−73539
atmosphere, diffusion props. determ. over urban site using Th(B) and Rn decay products 79−84347
atmosphere, diffusion props. determ. over urban site using Th(B) and Rn decay products 79−84348
atmosphere, estimation of short lived daughter conc. by least squares anal. 78−7728
atmosphere, induced radioactivity increase rel. to geomag. perturbations biotropicity 79−96621
atmosphere, Rn daughter's radioactivity levels over Arabian Sea, air mass mixing ratio 77−91227
atmosphere, Rn series disequilib. in S. California coastal air 79−58041
atmosphere boundary layer, diurnal var. for USA Gulf Coast 80−101404
atmospheric, accumulation in calcite caves 80−104531
atmospheric, use in determination of vertical stability of lower atmosphere, influence of air flow on Rn content *(Spanish)* 79−92560
atmospheric concentrations, influence of meteorological parameters *(Spanish)* 79−92562
atmospheric concentrations, statistical analysis of stability indexes *(Spanish)* 79−92561
atomic structure, Thomas-Fermi model with Fermi-Amaldi correction 79−81156
automated Rn-Th monitor for earthquake prediction research 78−73532
background concentrations of Rn and Rn daughters in Canadian homes 80−104546
barrier, interior of building structs. foundations built on U mill tailings material 79−2138
barrier to reduce indoor airborne Rn progeny 78−73262
carcinogenic effects of low level exposure 80−41142
cellulose nitrate α-particle detector for Rn short lived daughters, results and calibration *(Czech)* 78−62663
concentration in dwellings and influencing factors 80−108832
concentration in Norwegian dwellings 79−70485
concentration in underground waters and soil-air around Asama Volcano, Japan *(Japanese)* 79−70813
concentration in underground waters from landslide zone, Narao district, Japan 78−11918
concentration measurement in groundwater and springs for earthquake prediction 78−88924
concentrations in geothermal reservoirs 78−69381
continuous monitoring system 79−76150
daughter concentrations in different atmospheres 80−85316
daughter products, airborne reduction by plateout on air mixing fan 79−57529
daughter products in lung, pulmonary filtering capability measuring instrument 79−100729
daughter products in S.California coastal air 78−49087
daughters, dose conversion factors 79−70641
daughters, influence of room ventilation rate variations on respiratory dose 79−92381
daughters as atmospheric tracers *(Spanish)* 77−9553
daughters in atmospheric air, efficiency of HV-70 filters for sampling 80−108827
daughters in mine air, equilib. factor rel. to relative conc. 80−7977
decay products, concs. in mine air 77−9280
decay products, influence of elec. charge and humidity on diffusion coeff. 80−6192
decay products as tracers for atmospheric stability *(Spanish)* 80−51448
detection methods in underground and free atmosphere air 80−57987
diffusion, effectiveness of U mill tailing covers 79−93838
diffusion coefficient and exhalation rate from building materials, meas. technique 80−4694
diffusion coeffs., wash-out and deposition effects 77−68726
diffusion in soil, moisture effects 80−37491
diffusion through inactive rock sections 77−5194
disequilibrium ratio in the atmosphere, Rn decay products/Rn *(Spanish)* 80−31083
dose calculations for inhalation of ^{222}Rn, ^{220}Rn and daughters 77−64133
doses to employees and public from Rn and Rn daughters in Howe Caverns, USA 80−89859
dosimetry by plastic solid state nuclear track detectors 78−20556
dosimetry of Rn using plastic nuclear track detectors 78−33298
earthquake, precursory soil Rn changes, San Jacinto, California 80−94468
earthquake precursory changes of groundwater Rn content 80−94467
earthquake precursory Rn changes, California active faults 80−94465
earthquake precursory Rn changes, in shallow subsurface of New York State 80−94463
earthquake precursory Rn changes, Izu-Oshima-kinkai earthquake (1978) 80−94472
earthquake precursory Rn changes in California Transverse Ranges 80−94464
emanation from ground, statistical anal. 80−41259
emanation from rock specimens and powders, apparatus for measurement of rates 80−63494
emulsion scintillation counting of biological samples 78−81089
environmental sources in contiguous United States 80−41258
evolution in neutral atmospheres *(Spanish)* 80−4058
exhalation rate of Rn prod. in vivo, postprandial changes 78−69224
exposure standards for U mining 80−46055
flow in porous medium, temporal (spatial) conc. variation, rel. to Earth crust 80−33671
flux from U mill tailings, attenuation by consolidation 79−66563
FUNGI, radon meas. with fast response 78−46216
gamma spectrometry of Ra daughters in air 80−30628
gas concentration meas. using alpha sensitive plastic detectors 80−94617
gas concentration measurement using alpha sensitive plastic films for U exploration 80−94618
geophysical exploration by Rn mapping in U exploration, exclusion of ^{220}Rn signal 80−61916
geothermal resources, Rn release 80−41263
in groundwater, continuous concentration monitoring using ionisation chamber 79−21068
in groundwater, continuous meas. method for earthquake prediction 77−44935
Hawaii, ground Rn survey of Puna geothermal area 80−85657
radon continued
human exposure due to Ra bearing residues 80−41260
inhalation of Rn daughters, health hazards of Canadian U mining 79−88140
isotope separation by barrier technique, U prospecting appl. 78−21770
leakage from Ra radiotherapy sources 77−16977
liquid, calc. of critical density 80−59547
long-distance migration in Earth, subterrestrial fluid convection hypothesis 77−37246
lunar ^{222}Rn emanation as indicator of current activity 77−71032
lung cancer rel. to Rn in dwellings 80−89870
moisture insensitive monitoring using solid detectors 79−31228
monitor, continuous, response to transient Rn concs. 80−32519
monitoring for earthquake prediction *(Japanese)* 78−28181
monitoring instrumentation 80−106204
pollution and human disease, impact of energy conservation in residential buildings 80−56225
radiation exposure assoc. with surface U mining 77−64140
radiation exposure in energy efficient buildings 80−41261
radioactivity of Bulgarian spring waters *(Russian)* 77−41098
radioactivity releases fron nucl. power phosphate mining and coal burning 80−46072
radiochemical analysis for Rn in groundwaters appl. to Christchurch artesian wells 77−82039
reactor cooling pond, ^{222}Rn in biologically prod. gas 78−80976
retention for ^{226}Ra-burdened dog skeleton, rel. to age and dosage 78−65092
room air concentration of ^{222}Rn, ^{220}Rn and decay products, exhalation, ventilation and deposition effects 78−73261
San Andreas fault, Rn emanation vars. rel. to local seismicity 78−32022
seismicity near Lake Jocassee, S.Carolina, precursory changes of groundwater Rn 80−94466
short lived daughters, detection method *(Chinese)* 80−42889
short lived daughters meas., modification of three interval method 79−26754
soil, integrated Rn emanation mapping for gases long-distance migration detect. 78−85560
soil, Rn lognormal distrib. 77−5205
sources, distrib., exposure in residential buildings 80−41262
thermal conductivity, law of corresponding states *(Russian)* 78−87426
tracer measurement in aqueous samples by decay product filtration 77−60476
underground cavities, natural radioactivity, Rn conc. and exposure levels *(Spanish)* 79−39322
^{222}Rn daughters exposure, electronic dosimeter 80−46054
Fe:^{220}Rn(^{222}Rn), combined elec. quad. and mag. interaction, PAC 77−16214
Ra, annual rate of release to atmosphere as result of coal combustion in UK 80−93787
^{226}Ra-^{222}Rn disequilib. and pumice radioactivity, Sakurajima volcano 77−33033
^{220,222}Rn daughters, 2-count filter method for meas. in air 80−63480
Rn daughter time-integrating environmental TLD dosimeter 79−67962
Rn daughters in air, precision alpha counting methods 77−57841
^{222}Rn, atmospheric, two-filter continuous monitor 80−58097
^{A}Rn A=220, 222, decay products attachment to polystyrene aerosols 80−41256
^{211}Rn production by ^{209}Bi(^{7}Li,5n), excitation function 80−95323
^{220}Rn decay products attachment to flowing aerosols using centrifuge 80−61167
^{220}Rn integrated meas. of long-distance transport for U ore detection 80−98476
^{220}Rn, thoron, decay products, diffusion coeffs. in air and Ar 79−90366
^{220}Rn unattached decay products, diffusion coeff. depend. on ventilation and rel. humidity 77−9279
^{222}Rn, accumulation and circulation between lunar fines 77−60668
^{222}Rn, alpha scintillation counter for determ. of low natural conc. 80−9456
^{222}Rn alpha-scintillation counting, statistical counting error calc. 77−3211
^{222}Rn as tracer for sediment-water chem. exchange in coastal zone 80−101386
^{222}Rn, atmospheric, in calcite caves at Akiyoshi Karst Plateau *(Japanese)* 79−83671
^{222}Rn characts., natural occurrences, technological enhancement and health effects, review 80−46071
^{222}Rn, conc. in free air *(Hungarian)* 80−94128
^{222}Rn, conc. in water near a phosphate facility 80−45827
^{222}Rn conc. over intertropical convergence zone of Atlantic 80−26648
^{222}Rn concentration in N.Carolina groundwater supplies rel. to stomach dose and conc. standards 78−85612
^{222}Rn concentration in tunnel air, atmospheric press. and precipitation effects *(Japanese)* 80−97845
^{222}Rn concentration in water, meas. by gamma counting 78−53733
^{222}Rn concentration meas. by plastic detectors to determ. environmental α-emitters from natural sources 80−91292
^{222}Rn concentrations in water, rapid meas. with commercial liq. scintillation counter 78−28339
^{222}Rn content in air, diffusion in lower atm., U deposits prospecting appl. *(Spanish)* 77−78303
^{222}Rn continuous meas. for air-sea gas exchange field determ. 78−73534
^{222}Rn curved plesiotherapy applicators, dosimetry 80−51261
^{222}Rn daughter conc., meas. sensitivity computer optimisation 78−49126
^{222}Rn daughters emission and enrichments from Etna volcanic magma 77−21736
^{222}Rn determination in air and water, sampling and meas. methods 77−9278
^{222}Rn, diffusion and exhalation meas. from U mill tailings pile 79−92109
^{222}Rn diffusion through U mill tailings covers, coeff. meas., lab. techniques 80−95387
^{222}Rn emanation from building materials, plastic α-track detectors study 80−101144
^{222}Rn emanation from uraniferous materials, influence of variability on prospecting 79−62498
^{222}Rn emanation into air of dwellings in Great Britain 78−77118
^{222}Rn enhancements and gas upflow possibility 79−74893
^{222}Rn evasion rates in Atlantic and Pacific, Geosecs determ. 79−79875
^{222}Rn, excess bottom distrib. in deep ocean passages 79−16514
^{222}Rn exhalation meas., soil and meteorological effects *(Spanish)* 80−31082

radon continued
^{222}Rn external plesiotherapy, dosimetry obs. 80−36135
^{222}Rn, fractional retention by the bluegill 79−39506
^{222}Rn gas detection using Track Etch system for U exploration 80−98488
^{222}Rn in Hudson River estuary, distrib. and transport across sediment-water interface 78−16064
^{222}Rn, instant working level meter methods, mathematical evaluation 79−9918
^{222}Rn low conc. meas. in air, α-scintillation method 78−92970
^{222}Rn meas. during marine fog off Nova Scotia 78−40624
^{222}Rn meas. in geothermal fluids, steam reservoirs characts. determ. 79−74918
^{222}Rn, passive environmental monitor based on exoelectron dosimeter 78−82523
^{222}Rn progeny, air conc. meas. by α-particle spectrometric counting 79−68171
^{222}Rn, props. and behaviour of short lived daughter nuclides in the atmos. *(Japanese)* 80−72339
^{222}Rn, radioactivity of thermal and mineral springs in Slovenia 80−7963
^{222}Rn release from U ore crushing, grinding and leaching 78−89970
^{222}Rn released by uranium tailings piles, potential population dose 79−85824
^{222}Rn releases associated with cultivation of agricultural land 80−16850
^{222}Rn rich water, chromosome aberrations in peripheral blood lymphocytes 79−70587
^{222}Rn scintillation counting, standard deviation estimation 77−79519
^{222}Rn, theoretical, evaluation of emanation under a variety of conditions 80−104545
^{222}Rn very low conc. meas. with proportional counter 80−27907
^{222}Rn/^{226}Ra ratio in fracture zone water of N.Kirgizia 77−33108
^{222}Rn-CO_2, thermal diffusion, expt. method for study 80−5922
Tn decay products, ats. and ions, adsorption probability on submicron particles 79−39803
U mill tailings, diffusion consts. for soil covers 80−42807
U mills, radioactivity release meas. 78−82479
U mine radon control research 78−82525
U, miners Rn daughter inhalation and pulmonary cancer incidence 78−96080
U mines, radiological evaluation 80−42806
U mines and mills, Rn emission and control 80−41264

radon compounds
No entries

rail traffic
see also railways; traffic control
acoustic noise, conf. Oct. 1978, Lyon, France 80−48495
acoustic noise propagation models 80−48500
acoustic requirements and testing, standard light rail vehicle for mass transportation 78−87191
aerodynamic noise generated by high-speed trains 80−48512
coaches, noise generation expts. 80−48498
Deutsche Bundesbahn, noise caused by trains with and without sound protection screen 77−68316
Deutsche Bundesbahn exptl. line, vibration and structure borne noise 77−68320
environmental railway noise impact assessment, high speed trains in AMTRAK Northeast corridor 80−48507
ground noise, underground systems 80−48490
ground vibration, propagation pathway modelling 80−48491
ground vibration measurement 80−48494
high speed trains, noise annoyance 77−68313
infrasound, effect on people, exptl. study of levels 78−88726
internal noise, sources and mechanisms 77−68318
noise, annoyance in residential areas 80−48503
noise, attenuation by tree belts, pilot study 80−48501
noise, conf., Derby, England, 1976, March 77−68309
noise, diesel electric locomotives, SD40-2 noise under various operating conditions 80−102924
noise, Dutch study 80−48511
noise, effect on sleeping subjects 80−48509
noise, effects on nearby residents, survey 78−18114
noise, environmental controls for new housing sites 80−48505
noise, environmental impact in Britain 80−48508
noise, importance in France 80−48510
noise, service evaluation tests on locomotives, AMTRAK Northeast corridor 80−48506
noise, survey *(German)* 77−821
noise, wheel/rail mechanisms 80−48496
noise annoyance in residential areas 77−68311
noise duration relations *(German)* 77−27423
noise emission of passing trains 77−68310
noise levels in residential areas 77−68317
noise produced by passage of trains, investigation *(German)* 77−822
noise propagation 77−68315
reprocessed nuclear fuel transportation 79−30918
spent-fuel rail cask system, high-speed impact and fire test 79−59206
subway trains, retrofit noise control of rapid transit cars 80−48502
train generated ground vibrations, propagation and wayside effects 80−48489
tramway noise in city traffic 77−68312
Viennese Subway stations, noise control problems 77−68314
wave reflections from slotted tunnel portals 78−18108
wayside noise, high-speed trains 80−48497

railroads *see railways*

railways
see also locomotives; signalling; traction
acoustic noise, conf. Oct. 1978, Lyon, France 80−48495
acoustic noise propagation models 80−48500
automated rail flaw detection, US wheel probe variation problems 79−47862
coaches, noise generation expts. 80−48498
environmental noise impact assessment, high speed trains in AMTRAK Northeast corridor 80−48507
floating track slab resolution for noise and vibration reduction 77−68321
ground noise, underground systems 80−48490
ground vibration, propagation pathway modelling 80−48491
high speed ground transportation vehicles gas-flow-controlled arcs for power collection 80−70054
materials testing using X-ray 77−11436
noise, annoyance and activity interference patterns 80−48504
noise, Dutch study 80−48511
noise, effect on sleeping subjects 80−48509
noise, effects on nearby residents, survey 78−18114
noise, environmental controls for new housing sites 80−48505
noise, environmental impact in Britain 80−48508
noise, importance in France 80−48510
noise, service evaluation tests on locomotives, AMTRAK Northeast corridor 80−48506
noise and its estimation, for newly established line in Japan *(Japanese)* 79−10428
noise and vibration, annoyance in residential areas 80−48503
noise prediction and control from bridges and elevated structures 77−68319
noise protection screens, meas. *(German)* 80−102916
passenger coaches, structure-borne noise suppression *(German)* 80−91957
rail joint, thermit-welded, US flaw detection probe 78−56852
sound meas. standards 80−14531
steel wheel/steel rail vehicles using steerable steel wheel system for noise reduction 78−26005
subway trains, retrofit noise control of rapid transit cars 80−48502
train generated ground vibrations, propagation and wayside effects 80−48489
train noise, attenuation by tree belts, pilot study 80−48501
tunnels, reflection of step-wavefronts from perforated and flared tube extensions 79−14426
underground, natural rubber for vibration insulation 80−96099
underground, tunnel structure-borne sound levels and spectra 80−48499
underground transit systems, noise control for fan and vent shafts in subways 79−18589
urban railway vehicles with sound absorbing wheel systems, noise emission reductions *(German)* 79−50508
US rail-inspection transducers lateral position automatic control 79−57200
US track rail testing using defectoscope car, acoustic contact stability 77−77710
vehicle internal design and wayside noise abatement 78−55514
wayside noise, high-speed trains 80−48497
wheel/rail noise research 80−48496
H-fuelled railway motive power systems 80−40923
Na/S cells appl., dimensions optimisation 79−48112

rain
11 GHz forward scattering due to rain, 9 km line of sight link 77−86995
11 GHz rain attenuation distribution, from 5-min. rain rate statistics, calc. 78−24326
12 GHz statistical propag. params. meas. *(German)* 77−17183
20 GHz multi relay links, simultaneous probability of rain attenuation 78−3898
30-day periodicity in sunspot activity and rainfall 79−84765
140 GHz atmospheric attenuation by rain, obs. 78−3914
acid content vars. of rainwater during single precip. event 79−57990
acid rain, neutralization in Hubbard Brook ecosystem 79−74922
acid rain, Pittsburgh (Pennsylvania) area 80−94129
acid rain and interactions with dust 77−37326
acid rain rel. to S compounds long range transport, chem. aspects 78−81391
acidic rain interacting with rock partially covered by lichen 80−17302
acidity, contrib. of SO_4^{2-}, NO_3^- and NH_4^+ ions 79−2327
acidity, natural variance of pH time dependence 80−61840
acidity, release of S and nitrogen oxides by burning fossil fuels 80−26590
aerosol, scavenging of particles by cloud drops and small rain drops, elec. field effect 80−82001
aerosol particle scavenging, effects of elec. fields and charges on collision efficiency 77−25748
aerosol particles scavenging by clouds and raindrops, elec. charge effect 79−53459
aerosol particles scavenging by falling water drop, lab. expt. 79−5572
aerosols, characts. over India, role in warm rain process 79−92573
W.Africa, criterion for locating subtropical high, rel. to Sahelian drought 78−7718
E.Africa, evidence, for dramatic decreases during Pleistocene 77−56723
Africa, rainfall over Sahel rel. to upper air circulation 77−87038
Africa, southern east coast rainfall rel. to southern oscill. and subtropical high press. belt 80−12518
SE.central Africa, wind flow patterns in relation to rainfall 79−84460
Afro-Asian monsoon, numerical index for monitoring during northern summers 77−78400
agricultural land urbanisation hydrologic impact, distributed watershed model 77−37277
air pollutant deposition research using rain gauges *(Dutch)* 78−81367
Amazon Basin, water recycling, ^{18}O conc. study 80−81955
Andhra coast, India, unusual rainfall during 1974 October 77−53129
Andhra Pradesh, rainfall rel. to fluctuations in aridity 77−56661
annual rainfall, stochastic anal. rel. to effects of urbanisation 80−98407
annual rainfall records, comparison methods for climatology 80−51587
annual totals rel. meridional interactions with surface pressure 77−2214
areal rainfall amount assessment, two techniques compared 79−62612
areal rainfall averages processes synthesis, multidimensional model 77−91176
arroyo cutting near Santa Fe, New Mexico 77−70698
Asia, change in sign of relation between sunspots and press., rainfall and monsoons 77−45123
S.Asia, monsoon circulation, role of mountains 77−49121
Asian summer monsoon, simulation by general circulation models 78−40637
Asiatic monsoon area, drought 77−53170
Asiatic monsoon area, summer monsoon failures 77−53173
Asiatic monsoon area, synoptic aspects of droughts 77−56703
tropical Atlantic surface atm. and oceanic circulation patterns assoc. with Subsaharan weather anomalies 79−5587
Atlantic tropical belt, rainfall field *(Russian)* 77−21851
attenuation, effect on Earth to satellite radio links, statistical study *(Japanese)* 79−5555
attenuation caused by rain above 10 GHz freq. *(French)* 78−53686
attenuation characts. of SHF waves for satellite broadcasting *(Japanese)* 80−12501
attenuation distribution estimation, new method *(Japanese)* 79−100891

rain continued
attenuation distribution estimation *(French)* 78−53688
attenuation distribution in satellite communications, estimation formulae for worst-month, worst-year distribution, Japan *(Japanese)* 79−100890
attenuation effect on 11 GHz radiowave propagation 79−34885
attenuation effects on multiple access transmission of data via satellite 78−77313
attenuation in radiowave propagation above 11 GHz, radio links appl. 80−98410
attenuation meas. at 11 GHz on radio links *(French)* 78−53683
attenuation meas. for radio delay system design *(French)* 78−53685
attenuation measurements of microwave freq., radar and distrometer results compared with radiometer readings 79−62542
attenuation of 19 GHz COMSTAR satellite beacon signals 79−5593
attenuation of radiowaves at X, K bands, microwave radiometer design 80−68254
attenuation on satellite-Earth path at 11.4 and 14 GHz by radiometric meas. *(French)* 78−49066
attenuation on terrestrial radio links, 7 to 15 GHz 79−16630
attenuation prediction on terrestrial radio links from rainfall data 79−16636
attenuation ratios and path diversity gains of mm waves at 11, 20 and 36 GHz 79−16631
attenuation study on 11 GHz radiowave propagation *(French)* 78−77292
W.Australia, rainfall rate meas. during tropical cyclone by satellite microwave sensing 80−98485
S.Australia, T fallout in rainfall and wine samples 78−11960
automatic sequential rain sampler 78−73545
automatic telemetering raingauge system 79−21038
average over W.India during summer monsoon from H_2O vapour continuity eqn. 79−79990
banded rainfall distrib. over S.England, wintertime 80−82023
Bangladesh, regional variations in seasonality of precipitation 77−53176
Bay of Bengal and Arabian Sea, cyclones and depressions during 1975 78−32148
Bedford Ouse River, rainfall-runoff behaviour rel. to stream flow and water quality models 80−81956
Belgium, annual maximum intensity distribs. *(French)* 77−64392
Belgium, monthly rainfall maps *(French, Flemish)* 80−94583
Belgium, weather in 1975, review 77−25747
NE Brazil, large scale circulation rel. to extreme drought and floods 77−45134
Brazil, precipitable water, distrib. maps 80−77075
N.E.Brazil, rainfall forecasting using sea surface temp. data 77−29398
British Isles, 1975-76 drought 77−17201
NW British Isles, dust fall on 1977 March 6 assoc. with short rain shower 78−57287
British Isles, October weather recent trends 77−17210
British Isles, regular rainfall meas. since 1677, historical review 78−36248
British Isles, systematic rainfall recording since 1677, tercentenary 78−44950
British Isles, wet spell of September to October (1976) 77−45124
British spring weather, survey (1950 to 1979) 80−98427
British winters (1659 to 1979), study of temp. correl. with precipitation 80−98444
Burma during southwest monsoon, drought 77−53174
California, rainfall rel. to N.Pacific sea surface temp. 77−91239
California, spring rains correl. with Pacific Ocean December sea surface temps. 80−77064
catalogues of rainfall and temp. anomalies, 1891-1975, for European USSR, N.Kazakhstan, and W.Siberia 79−39826
catchment model parameters sensitivity anal. 78−77288
chain-dependent process, daily precip. amounts calc. 78−7712
chemical composition of precipitation, Trinidad, West Indies, meteorological parameters effects 79−79945
chemistry and multiple H ion donor systems, obs. in Minnesota 77−37335
chrysotile asbestos determ. in rainwater 78−44895
climate, soil and vegetation, annual precip. distrib. from storm sequences 79−84314
climate, soil and vegetation, annual water balance dynamics 79−79896
climate, soil and vegetation, annual water yield distrib. 79−84316
climate, soil and vegetation, storm surface runoff distrib. 79−84315
climate, soil and vegetation, water balance dynamics 79−79893
cloud, warm cumulus, three-dimens. numerical model with microphysical processes *(Russian)* 78−88884
cloud condensation nuclei from paper mill, calc. effects on rainfall 78−11970
cloud seeding, num. simulation technique 79−84519
cloud seeding, radar reflectivity/rainfall rate relation 77−45099
cloud seeding with AgI and metaldehyde, Fujian province, China *(Chinese)* 80−46235
clouds, water droplets size, density distrib. meas., laser remote sensing technique *(Japanese)* 78−49175
Clutha Lakes catchment area, water inflow rel. to rainfall and atm. circulation 78−11926
coagulation processes, Monte Carlo simulation *(Russian)* 79−84377
coastal areas, frictional and orographic effects on precip. 77−60442
cold front, obs. of 3-D circulation, precipitation and wave motions 80−90142
cold front of midlatitude cyclone, cloud and precipitation struct. 80−109192
cold-frontal rainband, cellular struct. obs. 80−51512
collection and chemical anal. 78−57368
collision-induced breakup effect on drop size distrib. in steady state rainshafts 79−92574
composition and SO_2 washout, model 78−28253
Comstar beacon cumulative slant path rain attenuation statistics, 28.56 GHz 80−26582
conference, Rochester, NY, USA (May 1979), polluted rain 80−82585
convection model, three dimensional *(French)* 79−84413
convective clouds, dry ice appls. for on-top seeding 78−73531
convective clouds and rain showers form. over Indian Ocean 78−7735
convective day precipitation, correl. with atmos. parameters observed by radar 80−109205
convective mean rainfall, meas. over small areas using high-density raingauges and radar 80−77157
convective rainfall, storm life cycle, model 79−16589
convective rainfall, surface vel. fields, obs. in S.Florida 79−16588

rain continued
convective shallow cloud model, precip. mechanisms 78−81311
cooling towers affecting rainfall, statistical study 80−109202
W.Cornwall, heavy rainfall, 1977 October 5 event 79−100935
cumulonimbus clouds, elec. field strength and raindrop spectra, study from mobile ground station 78−92943
cumulus clouds, warm rain and salt seeding, numerical simulation 80−90201
cup anemometer meas. of mean wind speed at sea, rain-induced errors 78−61485
cyclonic storm, 1974 Aug. 14-16, Calcutta, rainfall estimate using S-band radar 78−32157
cyclonic storm, Arabian Sea, 1976 June, diurnal var. and secondary vortices form. 79−20915
cyclonic storm, rainbands, precip. cores and generating cells 78−81307
cyclonic storms, mesoscale and microscale organization and struct. of clouds and precip. 79−74946
daily occurrence process, Markov chain modelling 78−61464
dangerous weather phenomena prediction, research prospects 79−34932
Darling River system floods, chronological evolution, Nimbus-5 radiometry obs. 80−94543
Deer-Sloan Creek watershed, rainfall vars., wind and topography influence 77−2212
degradation of cross-polarization isolation due to rain 78−69417
Delhi rainfall, recursive prediction model 79−79998
depolarisation and attenuation meas. at 11.7, 19.04 and 28.56 GHz *(French)* 78−49067
depolarisation meas. using INTELSAT-IV satellite in 4 GHz band at low elevation angle *(French)* 78−49068
depolarization at 11.6 GHz on a terrestrial radio link *(French)* 78−53687
depolarization statistical distribution for microwave signal propag. *(French)* 78−53673
desert region, surface albedo and vertical vel. relations 78−11953
design storm selection for stormwater management simulation 77−37278
differential attenuation at 13 GHz and 20 GHz on 53 km link *(French)* 78−53684
differential rain attenuation prediction, adjacent microwave and mm-wave links 77−87048
digital raingauge recording system 77−70862
dipole scattering of EM waves 80−36388
disdrometer measurement of terminal velocity *(French)* 79−88448
diurnal variation of rain and low cloud over Ozar airfield rel. to forecasting 79−100904
Diyala catchment, Iraq, water balance between Derbendikhan and Himrin dams 80−12462
drainage density changes during rainfall 79−20881
drizzle drop collision coalescence in presence of elec. field 80−51516
drop, single, growth by condensation and droplet capture, props. 79−12208
drop charge and assoc. electric field for different rain types 78−44933
drop formation at cloud top, effect on charge separation 80−81999
drop representation by use of bubbles in wind tunnel for flow visualisation 77−80238
drop sise distributions parameterisation 78−77301
drop size distrib. expressions 77−25744
drop size distrib. in hilly region of N.Wales 77−29390
drop size distrib. with collision breakup in axisymmetric warm cloud model 79−34918
drop size spectra, in Buenos Aires 79−53485
drop size spectra and growth in cumulus cells, model 80−21800
drop size spectra and intensities at Praia, Santiago, Cape Verde Is. during 1973-74 period *(German)* 77−5306
drop spectra and fine structure on different time bases *(French)* 78−53681
drop spectra evolution with collision-induced breakup 77−33152
droplet collisions, satellite drop production expts. 80−12492
droplet size and falling velocity meas. using laser Doppler velocimeter 80−68185
drops, charged, interaction energy 77−567
drops, coalescence, theoretical model of approaching drops 78−32207
drops, coalescence problem, efficiency 78−32208
drops, collisions, coalescence efficiency, expt. evaluation 78−32206
drops accel. to terminal vel. 77−78334
drought, classification and study of droughts at Kew 77−41121
drought, forecasting in subcontinent of India 77−56710
drought, S.England, 1976, water quality and stream networks anal. 78−73409
drought and weather modification in India, review 77−56715
drought effects on agriculture in United Kingdom, 1975-76 period 78−57298
drought in California and western Europe, 1976, atm. and oceanographic factors 79−48560
drought in England and Wales, 1975-6, development of water resources 78−88869
drought in England and Wales, 1975-6, effect on agriculture 78−88890
drought in England and Wales, 1975-6, effects on groundwater and aquifers 78−88866
drought in England and Wales, 1975-6, effects on the river systems 78−88867
drought in England and Wales, 1975-6, meteorological aspects and numerical expts. 78−88889
drought in England and Wales, 1975-6, pollution problems 78−88868
drought in India, agricultural and hydrological aspects 77−56707
drought in semi-arid regions, effects of albedo change 78−32128
drought in streamflow series, statistical charact. 80−105009
drought years at Masulipatam (Andhra Pradesh), water balances 77−56663
droughts, continental, study *(French)* 77−37344
droughts, diagnostic study by quasi-geostrophic diabatic four level model 77−56713
droughts, in Himalayan region of Uttar Pradesh, influence on ground water supplies 77−56708
droughts in the Asiatic monsoon area, symposium, Poona, India (Dec. 1972) 77−56701
dry and wet days occurrences, Markov chain model 78−7698
dual-polarisation radar for rain targets, rel. of diff. reflectivity to correl. 79−62556
dustfall from isolated cement works, implications for residential development 77−37403

rain continued
Earth-satellite transmission depolarization of freq. greater than 10 GHz *(French)* 78−53689
Earth-space path rain attenuation at 11 and 14 GHz, Darwin, Australia, satellite communications appl. 79−62541
Earth-space paths, rel. between rain depolarisation and attenuation 78−3858
Earth-space paths, tropical rain attenuation at 11 GHz, radiometric meas. in Australia 77−33165
earthquake precursory rainfall, S.California 80−85615
earthquake prediction, rel. to temp., rainfall and soil tilt 77−91058
effective rainfall analysis at Parbhani, India, rel. to irrigation planning 79−96794
electric rainfall intensity sensor 79−39888
electronic high-resolution rainfall intensity recorder and totaliser 78−7793
EM pulsed beam wave propag. 78−12000
EM radiation scattering by dielectric spheroids and ellipsoids, integral eqn. soln. 78−85622
EM sensor window materials, particulate erosion 80−38080
EM wave attenuation and rainfall rates dual-polarisation radar meas. technique, precision 79−25371
S.England, 1968, September 14-16, mesoscale and small scale motions revealed by hourly rainfall maps 77−45122
England, annual rainfall totals for 1725-1973 period 77−17207
England, decreasing wetness in 1969-77 period 78−65377
S.E.England, rainfall, medium term fluctuations 77−21861
England and Wales, 1975-6, water balance investigations 78−88865
England and Wales, 1975-76, zonal winds assoc. with dry period 77−56700
SE England dry years since 1698 77−29420
environmental γ radiation, variation during rainfall *(Japanese)* 78−36240
equatorial vortices over South China Sea and Malaysia during winter monsoon 78−40633
erosion of sandy soils, field study 79−20879
Europe, characts., microwave links appl. 79−66733
evaporating downdraught model comparison with obs. behind squall lines 78−92913
evaporation from nimbostratus, effect on mesoscale unsaturated downdraughts, numerical anal. 80−8400
evaporation rate of large water drops falling at terminal vel. in air, wind tunnel investig. 80−56541
extreme floods, rainfall rel. to runoff, nonlinear analysis 78−81247
falling drops, boundary layer theory for internal circulation 77−66964
fine structure meas. and microwave attenuation due to rainfall *(French)* 78−53680
flash floods, synoptic and mesoscale mechanisms for heavy rainfalls 80−8385
flood estimation, critical duration of rainfall 77−41084
flood event real-time predictors, stochastic model 80−67383
flood forecasting in river, by unit hydrograph method 77−5254
flood forecasting model from rainfall catchment and evaporation data, retention hysteresis 80−81951
flood freq., analysis of storm prediction techniques 78−11976
floods, 1975 August, in Orissa, India 79−20886
floods, severe, in River Burhi Gandak, 1974 and 1975 79−20891
S. Florida, description and field testing of digital recording system for tipping bucket raingauges 80−77161
Florida Area Cumulus Experiment, rainfall results 1970-75 77−45113
Florida Area Cumulus Experiment (FACE) rainfall results, seeding effect or natural variability 80−82002
Florida Area Cumulus Expt., natural and seeded rainfall 78−3872
Florida convective rainfall aspects 79−88455
forecast accuracy for rain, limit due to spatial variability of rainfall 80−56510
forecasting, use of wet bulb pot. temp. charts 77−91232
forecasting quantitative precipitation, prediction formula using Spanish data *(Spanish)* 80−36374
forest canopy, evaporation of intercepted rain, comments 77−25727
formaldehyde, in marine air and rainwater, wet season obs. 80−85703
formaldehyde content, meas. and contrib. from atmospheric aerosol 78−57243
formation, drop breakup modelling 79−2352
freezing level during rainfall over British Isles 77−29391
frequency relationships study for Karnataka region, India 80−31094
frequency scaling of attenuation above 10 GHz using COMSAT satellites 79−5595
frequency values, air pollution effects 78−7697
frontal rainband, conditional symm. instability explanation 80−56584
gamma ray exposure rates due to rainfall, in situ Ge(Li) spectrum 80−42873
Gangetic West Bengal (India) drought incidence 77−53172
GATE mean rainfall patterns, isohyet maps from radar maps 80−90172
gauge, quick response, water drop counting type 79−5647
gauge, simplified optical path-averaged, based on scintillation detect. 78−40674
Gaul, drought in 54 BC rel. to northward extension of Azores high 77−49149
Genoa, Italy, 1976, scarcity *(Italian)* 77−78291
geomorphological processes, conf., Louvain, Belgium (Apr. 1976) 77−81923
SW.Germany, heavy rainfall from May 22 to 24 (1978) *(German)* 80−61869
Ghaggar River catchment area, India, hydrometeorological study of rainfall trend 77−56660
global model for rain attenuation prediction 79−5594
Gujarat, India, short period rainfall characts. rel. to crop planning 79−96791
hailstone nuclei formation, role of giant aerosols *(Russian)* 80−56530
Hampstead storm, London, numerical simulation of quasistationary cumulonimbus system 78−77308
Haryana State, India, cumulative periods of rainfall statistical distrib. rel. to crop planning 79−96792
Haryana State, India, rainfall patterns rel. to crop planning 79−100902
Hawaiian rainfall normals, ridge regression-time extrapolation 80−51489
Hawaiian warm rain showers, aircraft obs. below cloud base 78−44932
Heatree, Devon, England, 1976 June 27 isolated heavy storm 78−57288
heavy rain, anal. by potential pseudoequivalent temp. field *(Chinese)* 79−48532
rain continued
heavy rain, dynamical anal., potential pseudoequivalent temp. condition conservation *(Chinese)* 79−48533
heavy rainfall over S.China, meson-anal. *(Chinese)* 79−53402
heavy rains basic characts. determ., max. runoff calc. 79−29802
heavy rainstorms in Britain, diurnal var. in occurrence 77−64402
Hudson Valley, New York, tree ring-drought relationships 78−28299
S.Humberside, 1949-76 summer months, evaporation and rainfall 77−73819
Hunan and Zhejiang Provinces, rainy season, long range forecasting 80−90204
Hurricane Agnes storm and flood, geomorphic effects, SE.Pennsylvania 78−77280
hurricane over Arabian Sea, surface wind and sea waves 77−53159
hurricane rainbands, possible form. mechanism 79−8658
hurricane rainbands, vertical struct., interaction with mean vortex 79−8659
hydrologic behaviour of forested mountian soil, coastal British Columbia 79−84320
hydrologic data set distribution functions, extremes and confidence intervals 78−24313
hydrologic records analysis and comparison, statistical program suite 77−21819
hydrological prediction models, adaptive algorithm 79−53381
hydrometeor backscattering cross sections, meas. at 6328 Å 78−49135
immature cyclonic storm struct. in Bay of Bengal revealed by radar 78−85628
incoherent effects in EM propag. through rain *(French)* 78−53679
India, area-depth relations for freq. values of rainfall 77−53116
India, climatic water balance 77−64408
NE India, higher seismicity related to lower premonsoon rainfall 79−79742
India, moisture flux across west coast and rainfall during SW monsoon 77−70783
India, rainfall characts. within 200 km of steel industry 77−56714
N India, rainfall deficiency due to absence of tropical disturbances 77−53178
India, rainfall rel. to overall assessment of surface water resources, water balance calc. 77−56662
India, SW monsoon, normal period of large-scale break 77−53175
India and other countries, droughts and floods 77−56702
Indian monsoon rel. to equatorial stratospheric westerlies 77−29370
Indian subcontinent summer monsoon, causes of 1899 drought 77−56705
Indian summer monsoon, Arabian Sea surface temp. anomaly effects 77−49120
Indian summer monsoon, influence of Arabian Sea 78−81333
Indian summer monsoon cyclogenesis and variability 78−81319
Indian summer monsoon meteorology 79−74938
Indian summer monsoon rainfall rel. to Eurasian winter snow cover 77−41076
Indian summer monsoon rel. to tropospheric flow patterns over southern hemisphere 78−81334
Indian SW monsoon field mesoscale accentuations, very heavy rainfall 78−85629
infiltration during an unsteady rain 79−16538
infiltration into bare soils, theoretical model and expts. 78−49058
insecticide, DDT and DDE in New York rain following Pacific N.W. spraying 77−29425
instantaneous rainfall rate, technique and influence on high-voltage transmission lines 80−98471
instantaneous rainfall rates, climatology 79−39841
intensity characts. of rainfall, possibility of using monthly averages in calcs. 80−105040
intensity distribution, conversion to shorter or longer integration times 78−61520
intensity effect on storm flow and peak discharge from forest land 77−78271
interception by forests, analytical model, evaporation 79−79966
intertropical convergence zone struct. over GATE area 78−57283
ionic composition of rain during sixteen convective showers 79−58003
ionic stability of precipitation samples 79−70828
IR broadband transmission rel. to meteorological events 80−85744
IR window rain erosion resistant antireflective coatings 78−83050
Israel and Jordan, rainfall fields, cloud seeding effects 78−73452
Israeli rainfall stimulation expt., 1961-67 period, anal. 78−92926
Israeli rainfall stimulation expt., 1961-67 period, reply to criticisms 78−92927
Jerusalem, seasonal precip. temporal fluctuations 80−72618
Joss-Waldvogel rainfall disdrometer, obs., comments and reply 77−64386
Kalahari, evidence for widespread late Pleistocene humid period 79−58083
Kalahari desert, widespread heavy rainfall (October 1973) *(German)* 78−16119
Kansas City flash flood (1977, September 12), events and causes 79−25291
Kerala (S.India), weak monsoon rel. to satellite-determined cloudiness and large-scale flow 77−56706
Kew, monthly mean temp. and rainfall in August 1973-July 1976 period 77−73820
Lahontan Basin, Nevada, pluvial lake level fluctuations 79−2310
Lake Biwa basin, hydrological cycle, system theoretic study *(Japanese)* 77−81951
Lake Leman area, precipitation trends, evidence for 50 year cycle *(French)* 77−21824
land-lake precip. relationships, using Lake Michigan data 78−44942
landslides, relationship to rainfall, Kitakyushu City, Japan *(Japanese)* 78−88848
landslides due to rainwater permeation, residual strength and frictional resist. of sliding soil masses *(Japanese)* 78−11919
large scale rain systems, vertical vels. and precipitation patterns, model 80−85727
laser beam propagation, intensity fluctuations during precip. *(Russian)* 77−29432
laser radiation transmission meas. at 10.6 μm 78−92977
laser techniques for rain impact and erosion recording 79−62610
laser-radiation-intensity fluctuations in rainfall, statistical characts. 80−101433
lidar observations of high plains thunderstorm precipitation 78−32167
Lithuania, karst lake replenishment *(Russian)* 79−8643

rain continued
Lithuania, river flood durations rel. to rainfall (1946-72) *(Russian)* 79−5516
local climatic anomalies, causes, rel. to precip. in Washington State 77−78399
loess erosion and redeposition by water, expt., micromorphology 77−81925
lognormal distribution of raindrop sizes in mm radio attenuation 79−16635
London area rainstorm of 16-17th Aug. 1977 80−77093
long-period rainfall records in England and Wales, spectral and filter anal. 80−4080
long-term rain rate distribution estimation, extremal statistical method 77−13096
Madhya Pradesh (India), rainfall trends and periodicities 77−53177
Madras, India, periodicity in rainfall 79−84426
Mahanadi basin, India, climatic study of river regime 80−81941
central Mali, rainfall comparison between Kabara and Tombouctou 80−4092
mapping of rainfall by radar 78−24397
March rainfall in one day, record for St. Mawgan, Cornwall 78−44971
marine atmosphere, rain detect. via microwave radiometry 78−81415
Markov chain modelling of weather data 77−49124
maximum possible in Great Britain−time limited, determ. methods 80−4091
maximum precipitation, 1900-1977, Great Britain 78−85672
maximum rain runoff calc. for USSR far eastern rivers 78−81238
maximum rate rel. to mesoscale parameters 79−53469
measurement by dual-polarisation radar, drop size and fall rate 80−72650
measurement by optical scintillation, correl. method simulation 78−36290
measurement of rain rate and dropsize distribution, with fast-response optical sensor 80−31135
medium scale broadcasting satellite for experimental purposes, rain-scatter interference 79−8668
melting ice particles producing rainfall, radar obs. 78−3873
mesoscale precipitation areas persistence and orographic modulation 79−79967
mesoscale rainbands in extratropical cyclones, assoc. cloud microphysics and dynamics 80−82030
mesoscale structure of line convection at surface cold fronts 80−12514
microwave absorption, rel. to pollutant gases monitoring from space using passive sensing techniques 80−76690
microwave attenuation, terrestrial radio link, freq. range 10 to 40 GHz, calcs., meas. 77−70771
microwave attenuation at 10, 11 GHz, radiometric measurements 80−67397
microwave attenuation due to precip. of water vapour in atmosphere, meteorological data, raindrop spectral distrib. *(German)* 80−90176
microwave attenuation for SIRIO link, fade statistics for 11.6 and 17.8 GHz *(Italian)* 80−4095
microwave attenuation from rainfall rates, 10-40 GHz 78−40607
microwave attenuation in 1-3 cm band, path- and area-integrated rainfall meas. 78−65414
microwave attenuation in rain, UK rainfall studies 78−11965
microwave attenuation on terrestrial link, radar study 77−41130
microwave attenuation statistics influenced by rain cell orientation 77−5278
microwave cross polarization discrimination statistics for spatially non-uniform rain 80−12534
microwave crosspolarization, effects of sizes of nonspherical raindrops 80−21790
microwave crosspolarization on satellite to Earth path 80−21789
microwave depolarisation, rain and imperfect antennas combined effects 78−92936
microwave link, rain attenuation on terrestrial path 79−66734
microwave link at 19 GHz over 35 km, attenuation meas., effects of rain and multipath propag. 79−88453
microwave link attenuation on parallel, series, and convergent terrestrial paths 79−66735
microwave link attenuation on slant path 79−66737
microwave link cross-polarisation effects 79−66736
microwave link rain attenuation, year and worst-month rain rate distrib. estimation method 79−5648
microwave links, 11 GHz, fading due to rain, snow and multipath propag. 77−91206
microwave links, rain attenuation estimation in UK at freqs. 10 to 100 GHz 78−73426
microwave links, short and long term rainfall rates, link design implications *(German)* 78−49082
microwave outage at 11 GHz, performance of tandem and route diversity systems 77−41131
microwave propag. numerical calcs. *(French)* 78−53675
microwave radiation from clouds meas. by Nimbus 6 for rainfall distrib. determ. 78−3981
microwave radiometry by Nimbus 6 for rainfall over land 80−56635
microwave rain attenuation, 11.6 GHz, diversity meas. at Etam and Lenox, West Virginia 79−79922
microwave rain attenuation distributions on Earth-satellite paths, empirical calc. 79−5592
microwave rainfall attenuation, 680 m vertically polarized link invest. 78−36238
microwave scatt. and depolarization by spheroidal raindrops 77−9480
microwave signal attenuation by rain cell, Earth-satellite link 80−94586
microwave slant-path attenuation prediction from rainfall rate meas. 77−70741
microwave thermal emission, EM scattering effect 77−91211
microwave transmission, attenuation and cross-polarization 79−84373
microwaves attenuation for Earth-space links, comparison between radar- and radiometer-derived data 78−24343
microwaves scattering, drop-size and temp. effects on forward and backward scattering 80−17317
microwaves slant path attenuation statistics prediction at various locations 78−24344
Middle East, monthly temps./rainfall relation appl. to palaeoclimates evaluation 80−31091
Middle Europe, 1708-54 precipitation record for Zurich *(German)* 78−85661
mixing with near-surface water 79−53371
rain continued
mm wave attenuation and bistatic scatter simultaneous meas. tech. 77−9554
mm wave attenuation in rain 78−96280
mm wave propag., rain attenuation meas. at 35 GHz over two sites at different altitudes 79−8667
mm wave propagation and atmospheric influences 79−84466
mm wave radar, measurements of effective sea reflectivity and attenuation due to rain at 81 GHz 79−80001
mm waves, attenuation due to rain at 74 GHz 79−80002
mm waves, rain attenuation measurements at 94 GHz 79−80000
modification of rainfall by topographical vars. 79−100888
Moisie River, Quebec, gully flow development after heavy rainfall 77−5249
monitoring, using dual freq. radar *(Japanese)* 78−57358
monsoon, West Coast of India, rainfall features 80−61874
monsoon breaks, effects of surface press. 10 to 20-day westward propag. mode 80−94592
monsoon circulation and rainfall S.Asia 78−44958
monsoon circulations numerical simulation 80−21812
monsoon depression, Bay of Bengal, intensifying into cyclonic storm over land 79−20916
Monsoon Experiment, Monex, GARP subprogram 80−8428
monsoon monthly activity, Western Ghats region, major climatological discontinuities 79−96790
monsoon over Calcutta, rel. to VLF atmospherics anomalies 80−82127
SW.monsoon over India, onset and northern limit 78−49102
monsoon over India during Aug. 1977, tropospheric structure 80−56570
monsoon over Indian region, energy anal. by baroclinic model 80−77073
monsoon rain over tropical W.Africa 77−37321
monsoon rainfall rel. to summer solar radiation and temperature 78−32154
monsoon rainwater, India, halogen and sea-salt conc. 80−51517
monsoon system oscillations, spectral anal. of obs. records 77−33148
monsoon trough typical config. at 850 mbar, assoc. rainfall patterns 79−96795
monthly expected rainfall, confidence limits for Peninsular Malaysia 78−81300
monthly rainfall forecasting and synthetic generation, stochastic models 79−70861
monthly rainfall in NW.Georgia, spatial correls. rel. to climatology and weather modification expts. 80−51479
monthly rainfall totals, East Midlands, England, 1726-1975 period 77−64411
Montreal, rain estimation using geostationary satellite data 80−90244
mountain station, heavy rain rel. to atmospheric electrode effect 79−25307
mudslide potential situations, meteorological parameters critical values, Caucasus mountains 79−39782
multielement analyiss of rainwater 78−69512
Negev rainfall diurnal variation, climatological and meteorological implications 80−17344
network design for estimation of areal mean of rainfall events 77−41082
network design for runoff prediction 77−41083
New Zealand, rainfall short-period fluctuations 77−25746
Neyveli thermal power station, India, rainfall vars. 77−37286
Norwich, homogeneous record of monthly rainfall totals for years (1836 to 1976) 78−3886
oceanic rainfall estimates, temp. correction 79−12220
oceanic rainfall maps, global climatic features 78−65379
optical materials rain erosion mechanisms 78−83049
optical scintillation, rain parameters meas. 77−82015
optimal raingauge densities and accumulation times, decision making precedure 77−29485
optimal sampling and anal. method 78−73530
organic micropollutants in precipitation in Norway 78−36262
organochlorine residues 78−73495
orographic rainfall in warm sectors of depressions 77−70776
orographically enhanced accumulations, forecasting with 10-level model data 78−69420
overland flow model, infiltration and rainfall effects 77−25720
Oxford, 1682 May 31, point deluge and tornado 80−51521
Oxford, England, private records of rainfall in 1767-1814 period 78−44948
central Pacific, persistence of rainfall anomalies 79−34926
Palmdale, California, long raining period correl. with crustal resist. changes 79−16373
particulate conc. in raindrops, electron microscopy study 77−81971
passive microwave obs. from Nimbus satellites 80−101422
path diversity and baseline orientation [rain cell effects], geometrical approach for circular cylindrical rain cells 79−20913
perennial grasses potential yield and yield shortfall due to water deficit, agroclimatic estimate 78−61450
persistence, runs and recurrence characts. of precip. 78−3865
pH and amount of rainfall in Michigan 77−37332
pH and S content in rural areas of England and Wales 79−16562
pH var. in convective storms over St. Louis 77−37333
photoelectric spectrometer giving integrated parameters in real time *(French)* 78−53730
plum rains in Shanghai, mid-range forecasting *(Chinese)* 80−109232
plume models, application of rainfall statistics 79−84355
PMMA, rain erosion behaviour, exam. 78−53001
point discharge current meas. during different types of rainfall 79−84379
pollution from coal-fired power plants, effects on cloud and precip. processes 79−20933
Port Moresby, Papua New Guinea, rainfall trend, (1945 to 1976) 80−98430
power spectrum anal. of time series 79−16705
precipitation probability forecasts, nonparametric technique based on pattern recognition algorithm 78−44946
precipitation strength obs. by radar rel. to ETS-II satellite wave propag. *(Japanese)* 78−85669
probability distrib. of rainfall of various intensities 79−25318
probability estimation 77−78347
process dynamics investigation using time-varying models 77−41099
propagation meas. at 94 GHz, expt. and theoretical rain attenuation results 79−16632
radar and radiometry techniques combined use for rainfall meas. *(Chinese)* 80−109272
radar attenuation, rel. to rain-rate estimates 78−73540

rain continued
radar attenuation in rain, iterative correction 78−92923
radar derived statistics on precip. patterns struct. 78−57260
radar measurement of clouds and precipitation, correl. and spectral anal. 80−12529
radar measurement of rainfall, methods and interpretation of data 80−81969
radar observation of rainfall, differential refl. method 80−46221
radar observations of rainfall, appl. to hydrology 80−90263
radar polarisation techniques for precip. props. determ. 80−61925
radar precipitation maps as lightning indicators 78−85652
radar rainfall meas. system, weather radar and real-time data processor combination 77−91326
radar reflectivity profile classified by rain types 80−101420
radar reflectivity variations with height due to wind shear on rain cells *(French)* 78−53682
radar reflectivity/precipitation relation variations *(German)* 77−17180
radar reflectivity/rainfall rate relation, effect of vertical air motions 77−45098
radars calibration with raindrop disdrometers, field expt. 77−91311
radio attenuation and depolarisation at 18 GHz 77−29404
radio attenuation model for Earth-satellite paths 79−62561
radio attenuation on Earth-space communication links, rel. to path diversity performance 78−69424
radio attenuation on terrestrial and Earth-space propag. paths, joint statistics 78−73490
radioactive fallout in air and rain over United Kingdom 77−73847
radioactive fallout in atmospheric dust, results to end of (1978) 79−79997
radioactive fallout investigations, 1973 to 1975, beta activity meas. *(German)* 77−64420
radioactive fission products, washout by rain *(Spanish)* 79−92399
radionuclide ratios in wet and dry deposition samples, USA, 1976 Jun.-1977 Dec. 79−29807
radiowave attenuation, radiometric determ. at millimetre wavelengths, multiple-scatt. effects 80−90260
radiowave attenuation at 13 GHz on Earth-space paths, depend. on elevation angle 77−70742
radiowave attenuation calc. 78−44919
radiowave attenuation in microwave and MM wavebands, estimation of duration time distribution *(Japanese)* 80−21788
radiowave attenuation meas., microwave radio link projected design appls. *(Slovenian)* 80−46217
radiowave attenuation meas. on Earth-space paths at 37 GHz by passive radiometry 77−41109
radiowave attenuation on SIRIO-1 Earth-satellite link *(French)* 80−56504
radiowave attenuation prediction using radar and in situ meas., 28 GHz Comstar beacon signal 79−70839
radiowave depolarisation by rain, thermal emission Stokes spectral vector 77−66976
radiowave forward/backward scattering from liquid/solid hydrometeors, Rayleigh approx. 79−25321
radiowave propag., angular depend. of rain scatt. at freqs. below 30 GHz 80−8416
radiowave propag., crosspolarisation and attenuation meas. at 11.6 GHz using theoretical rain model, canting angle distrib. 80−4070
radiowave propag., rain-induced attenuation, expt. results and calcs. *(French)* 79−12164
radiowave propag. at 10 to 30 GHz, specific attenuation and phase shift *(Italian)* 78−96261
radiowave propagation, differential attenuation and phase shift meas. for 36.5 GHz polarised waves rel. to raindrops 78−3856
radiowave propagation, rain attenuation, frequency scaling 77−45071
radiowave propagation, raindrop canting angle as function of wind velocity, crosspolarization 78−3855
radiowave propagation, raingauge data selection for rain attenuation studies 77−45048
radiowave propagation, tropospheric and precipitation scatter, rel. importance in interference and coordination calcs. 78−73423
radiowave propagation data from SIRIO satellite for earth-space rain-cell modelling 80−36352
radiowave scattering, COMSTAR beacon receiver diversity experiment 78−73421
rain attenuation data, appl. to path engineering 78−24327
rain attenuation prediction methods comparative analysis, radiowave propagation appl. 80−109182
rain cloud effect on diversity reception at 13/18 GHz range, satellite relay systems *(Italian)* 78−49072
rain-gauges, dual-gauge and Wyoming shield systems 80−61928
rain-scatter interference between satellite, terrestrial communications systems *(Japanese)* 79−16612
rainband dynamics and cloud microphysics in occluded frontal system 77−33147
rainbow, anomalous arc due to refl. image of Sun from water surface 80−77114
rainbow, physics, historical review 77−73854
rainbow formation in pendant drops, angular scattering 79−96816
rainbow polarisation rel. to droplet size and scatt. angle 79−80017
raindrop growth physics, for teaching 79−35502
raindrop induced forward and backward scattering amplitudes, tabulations 79−34884
raindrop interactions effect on drop size distrib. obs. at ground 78−44945
raindrop sizes and related parameters for GATE 80−41521
rainfall frequencies correl. with lunar phases 77−13112
rainfall intensity data for radio-relay system design above 10 GHz *(French)* 78−53690
rainfall parameter diagram, methods and appls. 78−57349
rainfall prediction for attenuation prediction in Earth-space paths *(French)* 78−49062
rainfall prediction for short response time hydrological basins 80−98491
rainfall rate determ., derivatives computation from equally spaced data 77−49125
rainfall rate meas. from weighing raingauge records 77−49126
rainfall record in elm tree rings 78−65381
rainfall variation in historical and contemporary epochs 80−36390
rainfall-runoff relation, deterministic nonlinear model 78−85615
raingauge station network for flood forecasting, Yamuna and Damodar rivers, India 78−32126

rain continued
rainwater chemical composition 30 km downwind from industrial complex 77−37395
Rajasthan (India) drought and scarcity survey 77−53171
rapid response rain gauge 77−87128
rate detect over ocean and land by spaceborne microwave radiometry 80−101423
rate distrib. by theory of extreme value statistics 78−77293
rate distrib. study, Japan, attenuation in telecommun. systems above 10 GHz appl. 78−92934
rate distribution estimation technique *(Japanese)* 79−66827
rate statistics, approx. method for use in signal attenuation estimating 79−70840
recording of rainfall at Oxford, England, since 18th century 79−29810
rectangular catchment basin downflow and infiltration, kinematic wave models 78−81235
reflectivity meas. by radar and disdrometer, comparison 79−53546
regression curves for tropical rain attenuation above 10 GHz, terrestrial and satellite telecommunication, broadcasting systems appl. 80−90111
reliability in Ethiopia 77−33172
remote sensing techniques from satellite borne microwave radiometry 80−105085
reversible washout of SO_2, NH_3 and CO_2 from polluted atm. and acid rain prod. 79−83657
rill and gully erosion of loamy sand, Flanders hilly region 77−81936
runoff-rainfall process, Semois river appl. 79−5537
Sahel, West Africa drought conditions *(French)* 77−37345
Sahel drought, Africa, 1967 to 1974, Earth surface albedo vars. investigation 80−76981
sampling errors in parameter meas. 78−28279
sand deserts, extent during glacial maximum and climatic optimum 78−36259
satellite communication systems, rain effects on propag. 77−41126
satellite communications above 10 GHz, rain effects 80−8410
satellite communications wideband polarisation separation network with adaptive control 77−78394
satellite link, space diversity improvement, squall line direction effects 77−91205
satellite links, seasonal var. of attenuation statistics due to bright-band height 79−100889
satellite links at 20 and 30 GHz, crosspolar phase variations on satellite-Earth path, meas. 77−81957
satellite links rain attenuation and site diversity effect, statistical studies 78−88892
satellite mapping technique for use over oceans 78−3982
scavenging of HTO 79−16563
scavenging of urban pollutants, inorganic nonmetallic species, convective storm systems 80−12039
scavenging rates of background aerosol 78−85648
S.E.Scotland, potential moisture deficit, 200-year series 78−7746
sea surface temperature and rainfall correls. during GATE 79−79864
seasonal forecasts and northern hemisphere circulation anomalies 77−2237
seeding studies application of lidar remote sensing 80−109203
sequential sampler, design, construction and operation 80−105090
severe local storms, St. Louis region, urban effects 79−12199
severe rainstorm in Honan province, China, 1975 August, case study *(Chinese)* 79−84448
shadow mapping to study rain attenuation on satellite microwave links 77−29505
sheet flow on smooth surface, hydraulics, simulated rainfall effects 77−81926
Shetland weather during 1975 77−56718
SHF meas. using 12 GHz Communications Technology Satellite beacon 78−73422
SHF scattering and cross polarisation by Pruppachev-Pitter form raindrops, 11 to 34.8 GHz 77−41129
SHF signal attenuation by rain, monitored by radar 80−51567
shipboard measurements of rainfall, comparison with weather reports 78−57258
Shirburn Castle, Oxfordshire, an 18th C. rainfall record 79−84419
short-duration rainfall, runoff calc. method *(French)* 80−77143
shower intensity, sudden increase rel. to electrification in thunderclouds 78−20491
showers and simultaneous floods in Alps, meteorological study *(French)* 79−66721
Sierra Leone, monsoon characts. 78−7693
simulated, for evaluation of surface mine area restoration, Wyoming 77−49094
simulation for lab. water erosion expts. 77−81931
simulation for surface coal mine spoils area restoration 77−33120
simulator, portable, for soil erosion studies in difficult terrain 78−20537
SIRIO satellite link, 11.6 and 17.8 GHz attenuations relationship 79−84340
SIRIO satellite link, 11.6 GHz, propag. meas. in Munich 79−84337
SIRIO satellite reception, atten. meas. during first year at Deutsche Bundespost Earth station at Leeheim 79−84335
SIRIO satellite to Earth propagation path, precipitation scatter meas. 79−84336
slant path attenuation, satellite relay broadcasts 77−86988
slant path attenuation of 35 GHz waves in satellite-Earth communications *(Japanese)* 78−85671
slant path rain attenuation characteristics in 20 and 30 GHz bands 79−8678
slopewash and wind action, Quaternary morphogenesis in Belgium 77−81924
small watersheds, rain gravit. pot. energy and runoff kinetic energy, urbanisation effects 79−25275
snow balance used as rain gauge *(German)* 77−33207
soil erosion prior to overland flow, time and aggregate size rel. to crusting process 79−20876
soil erosion processes meas. in German area of Moselle river valley 77−81937
soil loss factors rel. to flow, runoff creep and rainwash 77−45028
soil moisture, effect on circulation and rainfall in a tropical model 77−45133
soil moisture vars. under bare conditions rel. to rainfall at Pune and Delhi, India 79−96777
solar activity-weather correlation, anal. 78−40628
solar activity-weather relationship, study of temp. and rainfall at Oxford 78−85674

rain continued
sound measurement affected by rain and wind in trees 79−76926
South Africa, above and below normal rainfall periods estimation, 1972-2000 period 77−66980
South Africa, statistical modelling rel. to precipitation forecasting 77−45109
Southern Hemisphere, moisture conditions and precipitation efficiency 80−98424
Spalding, Lincolnshire, rainfall series discontinuities 80−105026
spatial distrib. in small catchment, influence on storm runoff 80−8357
spectra, evolution in warm-based convective storms 79−88417
spiral bands in linear model of cyclonic vortex 77−25736
spiral rainbands in hurricanes, inertia-buoyancy waves 78−7705
splash erosion, animal activity and sediment supply in forested catchment 77−81928
splash erosion and colluvium form. beneath deciduous woodland, Luxembourg Ardennes 77−81929
spreading of ellipsoidal raindrops orientation during intense rainfall, expt. results 79−16634
Sri Lanka, anal. of droughts 77−56704
St. Louis, Missouri, pollutant source strength-rainfall relationships investigation 80−77059
St. Louis metropolitan area, rainfall correl. with traffic accidents 79−16604
St. Louis urban precip. anomaly rel. to synoptic weather factors 79−39806
statistics over paths from 1 to 50 km 79−70827
stochastic dynamic model of rain attenuation 79−53506
storm and tornado watches compared to observed tornadoes, rel. to weather modifications 80−12505
storm depth, optimal estimation of total area, network analysis 78−49059
storm type effect on precipitation in small mountain watershed, theoretical study 80−8355
Storm Water Management Model for runoff prediction 77−37275
submillimetric wave noise interaction with rainy atmospheres 77−41138
sulphate washout from stack plumes 77−37327
summer droughtand autumn rainfall, England, 1976, effects on stream solute levels 79−48523
summer monsoon over S. Asia, break and active phases 78−3912
summer monsoonal rainwater comp. over India, geochemistry 79−53473
summer monsoons over Africa and India, comparison 78−32149
summer rainfall, St. Louis region, urban, topographic and diurnal effects 79−12198
summer rainshowers statistical models from fine-scale radar obs. 78−85650
supercooled drops, hydrodynamic behaviour, interaction with columnar ice crystals 78−32205
surface rainfall calc., model grid length and orographic rainfall efficiency effects 77−70774
Sutlej catchment annual rainfall and Bhakra dam site annual runoff statistics 77−53082
Switzerland, 1975 August rainfall at Vitznau on Lake Lucerne 78−7743
Tamil Nadu, N.E. monsoon rainfall singularities 77−70746
Tamil Nadu, rainfall pattern during N.E. monsoon rel. to solar activity 77−70749
Tasmania, rainfall increase accompanying cloud-seeding expt. 80−51485
Tehran area, Ivan, precipitation climatology, 1894-1974 period 77−9483
Thambraparani river, Tamil Nadu, India, large floods 77−53081
thermodynamics of nucleation on charged centres 79−20955
throughfall under a forest, estimation methods 79−2307
thunderstorm, precipitation obs. immediately after lightning stroke 80−77055
thunderstorms, severe, nature and effects on society 79−5560
thunderstorms near Langmuir Laboratory, airborne and ground based studies 80−85725
time series models, evaluation of practicality and complexity 77−29341
time-averaged areal mean of precipitation, estimation and network design 79−79901
trace constituents in Indian west coast SW monsoon rainwater 80−81967
trace elements in rainwater, determ. by neutron activation analysis 78−3944
Transcaucasia rainless periods, 1966-75 obs. 80−26603
Trinidad, conc. determ. 80−82045
Tromso, Norway, intensive precip., 1965-73 period *(German)* 79−16609
tropical cloud clusters, temp., moisture and precipitation 77−29406
tropical coastal region, lower troposphere features during rainfall 78−81332
tropical cyclones simultaneous occurrence on either side of equator, Indian Ocean area 78−81301
tropical open-ocean rainfall estimation from satellite obs. 77−29486
tropical rainstorm over Queensland, 6-min. intensity data 79−100937
tropical regions, rainfall during ice age, simulation 78−16144
typhoons rainfall intensity, effects of extratropical circulation 78−3908
ungauged urban watershed flood frequency model parameter estimation 77−37269
unit hydrographs for Barakar and Yamuna catchments, flood forecasting 79−20887
United Kingdom, regional units, wet and dry periods defined 80−51522
United Kingdom, trace elements concs. meas., 1975 results 77−25759
United Kingdom, use of radar as part of integrated system for rain meas. and forecasting 80−98490
United States west coast, rainfall rel. to Nimbus 6 liq. water data over NE.Pacific Ocean 80−82005
unusual weather frequency variability over last century 78−73479
urban catchment flow and water quality model predictive accuracies 77−37279
urban effects on precipitation, metropolitan Detroit-Windsor example 78−92917
urban effects on precipitation initiation in convective clouds, radar first echoes appl. 79−16601
urban hydrology and sediment control, symposium, Lexington (1976) 77−37266
urban influence on rainfall, obs. at St. Louis, USA 80−51513
urban pollutants scavenging by thunderstorm rainfall, numerical expt. 79−12261
urban runoff, effects of storm freq. on pollution 78−53667
urban storm water drainage system design, rainfall criteria 77−64336
urban storm water in Sydney, Australia, quality charects. 77−64357
urban storm water management, flood vol. distrib. 80−8361
rain continued
USA rainfall variability rel. to microwave attenuation 79−62562
variable rainfall infiltration, eqns. 79−53379
variations in rainfall around thermal power station 78−3846
Venice, Italy, air pollution indicated by isotopic anal. of rainwater and stonework 79−79992
vertical precipitation structure recording, meteorological radar appl. *(German)* 80−17358
vertical profiles of rain rates rel. to Earth-satellite radio attenuation modelling 79−70841
Vizcaya, Spain, B, Mg, Cr, Mn, Fe, Co, Ni, Pb, Ga, Ge and Si conc. in atm. and rainwater *(Spanish)* 78−57264
central Wales, large, summer storm 1971, June 77−56717
S.Wales floods of late December 1979, meteorological anal. 80−98429
warm cloud showers, initiation, efficient nuclei mass range 79−58029
warm frontal clouds in midlatitude cyclones, air motion and precipitation 80−109193
water drops collision efficiency in atmosphere 77−29378
waterdrop interaction extps., review 78−11974
watershed geomorphology, relative scales of time and effectiveness of climate 78−81229
watershed stream network, model of rainfall-runoff process 77−29347
watersheds, multiple, rainfall runoff computer model 79−29805
weather forecasting processing of radar and satellite imagery data 80−109252
weather modification in USSR 77−64362
weather radar calibration, correl. with rain gauge data *(Japanese)* 78−85670
westerly trough unusual SE. movement over India, 1974 December 78−32161
wind gust effects on rain-induced polarization, theoretical model *(French)* 78−53678
winter, predictive relationship with summer O_3, San Francisco Bay Area 79−12224
year-to-year rainfall prediction model, microwave appl. 78−88885
Zambia, weather during rainy system rel. to upper westerly waves interaction with intertropical convergence zone 80−90175
zero cross-polarisation mode for orthogonally polarised signals in rain 77−81991
Ag cloud seeding of Florida cumuli, rainwater conc. obs. 80−56563
Ag content from seeded and nonseeded Florida cumuli 77−29387
B concs. in coastal N. Florida rainfall 77−21838
Be conc. in rainfall, Katowice, Poland *(Polish)* 79−16558
Ca excess in snow and rain samples, Japan, from calcite source 79−39766
Ca, Mg, Na, K, supply from rainfall to NE.Rhodesia 79−57988
Cl^- ion concentrations in river, spring waters in Okinawa Honto, origin *(Japanese)* 79−39324
^{137}Cs levels in soils and vegetation of W.Malaysia 78−73263
D areal distribution in California and Nevada precipitation, 1968-1969 period 79−100918
Hg in S.New England coastal rain 80−41508
Hg, neutron activation anal. for low levels in water 79−70503
IO_3^-, determ. in rainwater by neutron activation anal. 78−76953
Mn determination in environmental waters by neutron activation anal. 79−74584
NH_4^+, NO_3^-, in rain water collected at Julich, Germany, N isotope comp. 78−57284
$^{15}N/^{14}N$ ratios in gaseous NH_3, NO_2 and NO_3^- in aerosols and precip. 78−44896
^{210}Pb tropospheric residence time 78−85396
$^{87}Rb/^{87}Sr$ studies of waters in geothermal area, Cantal, France 78−61443
S compounds wet removal from atmosphere 79−2363
S content, sources in rain collected below wheat canopy 77−56698
S isotopic composition in precipitation within Great Lakes Basin 79−16625
S pollutant removal from atmosphere by rain, modeling method 80−85318
SO_2 and SO_4^{2-}, dry and wet removal from atmosphere 79−2361
SO_2 and sulphates in rain, urban and rural Norfolk, England 80−55955
SO_2 oxidation in clouds and rain, O_2, O_3 and H_2O_2 role 79−84351
SO_2 oxidation in stored rainwater samples, rel. to Mn content 79−84352
SO_2 pollution washout coeff., data from ground level monitoring network 79−74926
SO_2, reversible washout by rain, improved model 79−2364
SO_2, vertical distrib., influence of clouds and rain, one-dimens. model 79−20982
SO_4^{2-}, conc. in rainwater, obs. by European Atmospheric Chemistry Network 79−2365
SO_4^{2-} content, isotopic tracing of pollution *(Italian)* 77−53078
SO_4^{2-} production in rain and raindrops in polluted atm. 79−88388
soil, surface moisture content parametrization, use in atm. prediction models 78−49052
^{90}Sr tropospheric residence time 78−85396
U determination in environmental waters by epithermal neutron activation 79−53010

rainfall *see rain*

Raman effect *see Raman spectra*

Raman lasers
atomic vapours, stimulated electronic Raman scatt., saturation of tunable IR lasers 78−37941
backward Raman amplifier for excimer laser pulse compression, parasitic superfluoresc. suppression 80−69453
benzene, Raman laser as efficient excitation source for stimulated Raman scatt. 79−18480
coherence effects in multiply pumped spin-flip Raman laser 80−87398
cryogenic active media, stray transverse stimulated emission 78−25927
double resonance Raman amplifier, theory 80−87434
energy storage and nonstoring advanced lasers for fusion appls. 78−79027
ethylene, off-reson. IR laser action without population inversion, Raman type transition 77−10891
external resonator CW spin-flip laser, output charects., spectroscopic appls. 79−72571
external-resonator controlled, pumped by CW CO laser, mol. spectroscopy uses 80−9624
Faraday rotators in fibre Raman lasers 80−58775
fibre optic, tunable 77−14721

Raman lasers continued
fibre optic CW Raman laser, freq. spectrum and temporal behaviour 77−61965
fibre optical CW Raman oscillator, using two-mirror resonator config. 79−7152
fibre Raman and Brillouin laser gains, polarisation effects 80−9887
fibre Raman laser, CW, bandwidth reduction using prisms, gratings and etalons 80−53366
fibre Raman lasers 80−102767
fibre Raman oscillator, pulse synchronisation for fibre dispersion meas. 80−48410
fibre Raman oscillator, two-mode, group velocity matching 78−25925
fibre Raman ring laser 79−22981
fluoromethane, $^{12}CH_3F$, far IR Raman laser line obs., CO_2 laser pumping 80−69381
fluoromethane high-power laser, tuning behaviour 80−63994
frequency conversion, via stimulated Raman scattering 80−69451
frequency measurement with MIM diode, spectroscopy in 5.3 μm region 77−10935
gain, influence of polarisation degree 79−89965
gain enhancement in Raman amplifiers with broadband pumping 80−43398
gas concentration meas. using Raman intensity depend. on giant pulse laser polarization 80−98986
glass fibere, 1-1.3 μm source 77−42568
higher modes and saturation effects, theory 78−71106
n-InSb, intraband processes exam. by stimulated spin-flip Raman scatt. 77−19362
intracavity Raman laser theory 79−27296
IR, for 16 μm range, review *(Rumanian)* 80−87408
IR, high-power tunable, review 79−7140
IR, tunable, review 78−13724
IR and far IR source, powerful and tunable 80−5787
IR frequency synthesis with MIM diode 77−19277
IR spin flip laser, matrix isolated photochemistry, isotopic, stereochemical and lattice site selectivity 78−92492
laser amplifier and monomode optical fibre system *(German)* 79−81454
methane, backward Raman amplifier, large-signal gain and intensity enhancement 78−90450
methane backward Raman amplifier, KrF laser driven, high-efficiency energy extraction 80−106533
methyl fluoride Raman FIR laser, high-intensity CO_2 laser pumping, new emission lines 80−23675
molecular spectroscopy and atmospheric constituents detection uses, review 80−55762
multiple-pass Raman gain cell 80−48334
narrow-linewidth high-efficiency Raman amplification and spectral compression 80−102770
near-IR fibre Raman oscillator, 1.07-1.32 μm tunable 79−72622
nitrobenzene, Raman laser as efficient excitation source for stimulated Raman scatt. 79−18480
nitromethane, Raman laser as efficient excitation source for stimulated Raman scatt. 79−18480
noncrystalline materials, optical spectroscopic anal. *(French)* 77−77284
optical fibre laser oscillators, theory 79−81439
optical fibres, Raman scatt., guiding structs. effects on spontaneous and stimulated emission 80−58636
quartz multimode lightguide in pulsed Nd^{3+}:YAG laser resonator, intense Raman generation 80−99735
relativistic electron beam Raman laser 78−74877
scalable tunable IR laser operating characteristics and limitations 77−54713
solid, methods for increasing efficiency, optical damage avoidance 77−79853
spin flip Raman laser, IR source, physical processes, theory 78−17943
spin flip Raman laser absorption spectrometer sensitivity enhancement 78−29173
spin-flip, laser beam propag. through inhomogeneous media 77−79883
spin-flip, multiline output by multiline operation of CO pump laser 79−7132
spin-flip Raman laser spectrometer as source for high resolution mol. spectroscopy and photochem. review 78−32894
time-dispersion-tuned fibre Raman oscillator 77−42562
tunable 1.1 μm fibre Raman oscillator 78−1242
tunable coherent light sources, nonlinear freq. mixing, Raman, and semicond. lasers 77−7131
tunable coherent middle IR sources, review 77−38991
tunable high power systems and appls. 77−27302
tunable IR lasers, principles and operating characts., review 79−98376
tunable IR solid-state laser characteristics and principles 80−87406
tunable multiple Stokes CW fibre Raman oscillator 77−88786
tunable source, near IR to submillimetric waves, stimulated Raman scatt. in mol. fluids *(French)* 79−31993
tunable spin-flip, adaptation for structural chemists use 77−65597
two-mode optical resonator mode mutual quenching in stimulated Raman emission 79−36960
vitreous oxides, Raman cross sections, rel. to appl. in fibre Raman lasers 78−31176
wide-band pump radiation conversion efficiency, possibility of brightness increase 77−75532
Br_2+CO_2 mixture, Raman laser optical excitation, electron phototransition theory *(Russian)* 80−99711
CO_2, optical pumping in stimulated Raman scatt., tunable laser emitting at 14,16 μm, theory 78−46568
CO_2+COS mixture, Raman laser optical excitation, electron phototransition theory *(Russian)* 80−99711
CO_2+monobromomethane mixture, Raman laser optical excitation, electron phototransition theory *(Russian)* 80−99711
CS_2, Raman laser as efficient excitation source for stimulated Raman scatt. 79−18480
$CaCO_3$, calcite, methods for increasing efficiency, optical damage avoidance 77−79853
Cl_2+N_2 mixture, Raman laser optical excitation, electron phototransition theory *(Russian)* 80−99711
D_2O far IR laser pulses, real-time spectral anal. using SAW dispersive delay line 79−45983
D_2O tunable vapour laser, optically pumped with single-mode CO_2 TEA laser 79−55145
GaAs, tunable stimulated Raman scatt. in far IR, laser feasibility 79−50344
GaP semiconductor Raman laser 80−78864

Raman lasers continued
n-Ge, possibility of tunable impurity Raman laser action 77−46759
H_2, compressed, axial mode self-locking 79−94223
H_2, compressed, tunable high power systems and appls. 77−27302
H_2, compressed, tunable i.r. emission 77−668
H_2, compressed, tunable laser, isotope separation by SF_6 selective dissociation 77−34708
H_2 compressed high-power tunable Raman lasers and applications 77−54709
H_2, efficient tunable Raman laser 80−28245
H_2, for efficient coherent summation of Nd laser nanosecond pulses 80−23718
H_2 gas, 2Z 79−81483
H_2 gas, efficient higher-Stokes-order Raman conversion 80−33082
H_2 high power tunable IR compressed laser, for spectroscopy 80−48277
H_2, improvement using up to 10 m path length 77−72033
H_2 laser, stimulated Raman scatt., appl. to holography 80−91782
H_2 laser, tunable IR waveguide Raman type pumped by dye laser, 0.7-7 μm range 79−45959
H_2 Raman laser, multiple-pass-cell, controllable pulse compression 80−91825
H_2, stimulated Raman scatt. gain of Nd laser radiation by rot. levels 80−69464
H_2, use of waveguide for improved conversion efficiency 77−658
$Hg_{0.77}Cd_{0.23}Te$ nonlinear optical IR generation 80−58642
$Hg_{0.77}Cd_{0.23}Te$, spin flip, high conversion efficiency 77−79832
$Hg_{1-x}Cd_xTe$, nonlinear optical effects 80−14389
n-InSb, electron spin-flip relax. time meas. 77−3631
InSb, pulsed, external cavity operation at 10.6 μm 77−71990
InSb pulsed spin-flip Raman laser, external cavity, low field operation at 10.6 μm 79−41394
n-InSb Raman spin-flip laser, hot electron effect distrib. calc. 80−23743
n-InSb, spin flip Raman scatt. from electrons in localised donor states 77−3630
InSb, spin flip Raman scattering, gain, linewidth, effective g-value 78−22167
InSb spin-flip, characts. *(Japanese)* 78−25883
InSb, spin-flip, pumping by IR multiline NH_3 laser 79−94216
InSb, spin-flip Raman laser, cond. electron T_1 meas. 77−3593
InSb spin-flip Raman laser, pumped by TE CO_2 laser, fund. characts. *(Japanese)* 77−42542
InSb spin-flip Raman laser 77−50674
InSb, spin-flip Raman laser, Stokes output mag. field depend. 77−61959
InSb spin-flip Raman laser, external cavity CO_2-pumped, with intracavity etalon 78−42345
InSb spin-flip Raman laser external-cavity system, oscill. characts. 78−55383
InSb, spin-flip Raman laser, charact. and phys. props., review *(Japanese)* 80−39576
InSb, stimulated spin-flip Raman scatt. and stimulated recomb. radn. 79−72623
InSb, with two photon pumping by CO_2 laser radiation 79−86182
$LiNbO_3$, tunable parametric Raman laser utilizing polaritons 79−41418
N_2 high power tunable liq. Raman laser, for spectroscopy 80−48277
N_2, liq., delay of broadband-pumped stimulated Raman gain 79−50351
N_2, liq., laser action due to stimulated Raman scatt., nonmonochromatic pump radiation 79−64284
N_2, liq., possible active media in high-power Raman lasers 80−19028
N_2, liq., tunable high power systems and appls. 77−27302
N_2, liq., tunable Raman laser based on third Stokes component 78−50859
N_2, liquid, output radiation divergence 79−98352
N_2 liquid high-power tunable Raman lasers and applications 77−54709
N_2 liquid IR Raman laser with unstable resonator 79−31957
NH_3, far IR CW Raman lasing 80−83595
NH_3, off-reson. IR laser action without population inversion, Raman type transition 77−10891
NH_3, stimulated hyper-Raman scatt. via 3-photon process to obtain IR and far IR radiation 80−58633
NO, Zeeman modulation IR spectroscopy using spin-flip Raman laser 79−18181
Nd^{3+}:YAG, Raman laser with optical-fibre resonator, expt. investigation 79−31913
O_2, liq., possible active media in high-power Raman lasers 80−19028
OCS, 5.3 μm vibr.-rot. bands, rot. consts., spin-flip Raman laser obs. 77−34631
n-$Pb_{0.88}Sn_{0.12}Te$ spin flip Raman laser pumped by TE CO_2 laser, characts. 80−87397
S_2+N_2 *(Russian)* 80−99711
SiO_2 fibre, CW tunable near IR Raman oscillator 78−1235
SiO_2 fibre near IR Raman laser, as universal fibre optic meas. system 79−23070
SiO_2, fibre waveguide, backward Raman amplification and pulse steepening 77−23740
SiO_2, fused, fibre Raman laser emitting over very large spectral region *(French)* 78−55405
Sn vapour, Raman emission at 285 nm 79−3748

Raman scattering *see Raman spectra*

Raman spectra
see also molecular rotation; molecular vibration; Raman spectra of diatomic inorganic molecules; Raman spectra of inorganic liquids and solutions; Raman spectra of inorganic solids; Raman spectra of organic molecules and substances; Raman spectra of polyatomic inorganic molecules; Raman spectroscopy; stimulated Raman scattering
AB_2 and AB_4 molecules Raman overtone and combination transition intensities, bond-polaris. approach 78−42034
absolute Raman cross section determ. from inverse Raman effect 79−3447
adsorbates, on metals, enhanced Raman scatt., including nonlocal metal response, nonradiative modes excitation 80−88994
adsorbed molecule, classical theory of light scatt. 79−51944
adsorbed molecule, in electrochem. systems, Raman scattering 80−60563
adsorbed molecule near solid surface, light scatt. calcs. 79−56069
adsorbed molecules, on metallic surface, reson. Raman scatt. 79−45729
adsorbed molecules, Raman and fluoresc. enhancement by surface roughness 80−102511
adsorbed molecules, surface induced ıeson. Raman scatt., theory 80−54518
adsorbed molecules on bumpy metal surface, Raman intensity 79−15448
adsorbed molecules on metal surface, theory 79−37922

Raman spectra continued
adsorbed molecules on metal surfaces, enhanced Raman scattering, calc. 79−99882
adsorbed molecules on metal surfaces, giant Raman effect 80−65374
adsorbed mols., effective reson. Raman spectra 80−97730
air, temp. meas. using rot. Raman spectra 78−62200
air pollution detection appl. *(Czech)* 78−81359
amorphous solids, electron-phonon interactions, fluoresc. line broadening and spectral diffusion 78−84655
amorphous solids, Raman intensities, connection with EXAFS Debye-Waller factors 80−108214
anharmonically coupled oscills., time depend. Hartree theory, susceptibility, absorpt. and Raman spectrum 80−58241
anticorrelation effects in Raman scattering by phonons, Heisenberg eqns. of motion 79−95747
antiferromagnet, two-dimensional, with easy-plane anisotropy, mag. excitations and two-magnon Raman scatt. 80−65839
antiferromagnet, two-magnon Raman scatt., temp. effects 77−48178
antiferromagnet, two-magnon Raman scatt., temp. effects 77−48179
antiferromagnetic insulator, light scatt. in strong mag. field 78−72523
antiferromagnetic semiconductor, magnon-plasmon interaction and its effect on Raman scatt., theory 78−56302
antiferromagnetic semiconductor, theory of Raman scatt. due to magnon-spin flip excitation 77−36209
antisymmetric light scattering of molecules with non-degenerate electronic state 79−18192
assembly of partially oriented scatterers 77−16295
asymmetric top molecules, Raman spectra, vibr.-rot. selection rules and general band contours 77−58020
atmosphere, Raman/aerosol signal ratio obs. for visibility meas. 79−100953
atmosphere at twilight, Raman scattering spectrum 79−92596
atmospheric aerosol particles characterisation by Raman spectroscopy 77−49188
atom, collision and Doppler broadening of fluorescence and Raman scatt. 78−13465
atom, excitation by coherent pumping, induced Raman scatt. 78−66519
atom, multiphoton transition amplitudes, exact summation of higher-order terms 77−18878
atom, near-reson. scatt. with collisional perturbation, time and freq. depends. 79−72281
atom, reson. Raman X-ray scatt., K-vacancy excited state widths, appl. to Zr, Mo, Rh, Ag and Sn 79−45661
atom, resonance Raman scatt. modification in intense laser fields 77−27002
atomic gases, active reson. spectroscopy 77−27003
atomic level field splitting, resonant cooperative light scatt. *(Russian)* 80−74148
atomic system, time depend. spectra after two-photon excitation 79−13664
atoms, laser cooling, Raman mechanism 80−23371
atoms, Raman scatt. in presence of two-photon reson., coherence effects 79−45679
atoms, two photon excitation, time depend. emitted light spectra, perturbation theory 80−63605
bacterial cells, active, reson. between 10^{11} and 10^{12} Hz obs. by laser Raman spectroscopy 77−36893
bound polaron and phonon states, optical charact's. *(Russian)* 78−39556
C_{3v} molecules, Placzek-Teller coeffs. for normal ^{3}Raman transitions 78−86914
carotenoid molecules in living cells of chlorella, vibrational state population 80−97861
coherent hyper-Raman scattering from isotropic material, quantum theory 80−106327
coherent optical spectroscopy 78−1112
coherent three-level beats, in Doppler broadened mol. system, theory 77−23526
combinational scatt. of light, discovery and history 80−27101
combinational scatt. of light, history 80−27100
combustion, turbulent, averaging of pulsed laser Raman signals 78−70839
complex molecules, reson. Raman spectra, vibr. scatt., review 78−37644
condensed matter, effect of inter- or intramol. energy exchange on vibr. dephasing times 77−66506
condensed media, effective field method for mol. interaction 77−52081
condensed media, effective light field effect 77−52079
condensed media, internal field concept 77−52080
condensed media, vibrational relaxation studied by picosecond or Raman spectros., review 80−80797
condensed phase, reson. Raman and reson. fluoresc. spectra, density matrix approach 78−80323
conference, Moscow, USSR (Mar. 1978) 80−62377
cooperative Raman scattering, effect of phase self-modulation of light 80−91855
crystal, noncylindrical, 90° Raman scatt., cryst. principal axis rot. depend. 79−73938
crystal impurity librational relax., phonon assisted transitions, direct, Orbach and Raman processes 78−83887
crystal impurity mols., orientational tunnelling on polarisation of Raman spectra 77−77208
crystal not cut parallel to principal axes, Raman spectrum birefringence effect 79−69836
crystal point groups, basis functions for irreducible representation, appl. to morphic effects on IR and Raman spectra *(Japanese)* 79−4265
crystal point groups, electric and magnetic field-induced Raman tensors, effective charges 78−43848
crystal powders, absolute Raman scatt. cross sections, determ. method 77−77199
crystals, book 80−2774
crystals of C_{4h}, D_{2d} and D_4 symmetry at second-order structural transform., spectroscopic props. 78−22845
cubic crystals, Raman scatt. from tunnelling of substitutional molecules 80−40107
cyclohexane, plastic and liquid crystal phase, rot. correl. func. by Raman spectroscopy 80−23403
degenerate electronic state, vibronic coupling between nucl. vibr. and electronic motion 77−83568
delta function equation, bond order rel. to bond polarisability 77−61693
dense media, Q-branch, impact thoery, collisional rotational relaxation, line broadening 79−98104
dense media, Q-branch Raman line width, rotational relaxation, reorientation, collision strength 79−98106
dense optically transparent media, third-order optical susceptibilities 77−38981
dephasing, in gases, liquids and solids, molecular mechanism 79−36654
depolarising dipole-induced-dipole effect *(French)* 77−61751
diatom+diatom, effect on depolarised light scatt. linewidths 80−58321
diatomic gas, transient flow, temp. and conc. profiles, by rot. Raman scatt. 77−75995
diatomic molecule, continuum reson. Raman scatt. 77−71809
diatomic molecule, overtone intensities in reson. Raman scatt. 80−48001
diatomic molecule, resonant and near-resonant Rayleigh and Raman scatt. 78−78705
dielectric cylinder embedded mols., Raman and fluoresc. scatt. 80−37949
discovery, historical reminiscences 78−73819
discovery of Raman effect 78−49627
disordered media, LF spectrum study from Raman scattering cross section 80−25363
disordered semiconductors, resonance Raman scatt. 79−11419
disordered solid reson. Raman scatt., smooth random field model 78−6676
disordered solids, harmonic approx. for vibr. spectra 78−51635
disordered solids, rel. between simple analytic models 78−76473
disordered system, reson. Raman scatt. 80−2772
disordered systems, phononless Raman scattering 80−76031
doped semiconductor plasma, inelastic light scatt., spin diffusion 77−36241
Doppler-free Raman spectroscopy and suppression of laser-induced mol. Doppler broadened transitions 80−9638
doubly degenerate mode systems, excitation profiles, depolarisation ratios, reson, Raman scatt. 79−98108
electric dipole susceptibility, third order, rel. to mol. spectra 79−36624
electrolyte solutions, strong, at high concs., collective vibrational modes 77−81105
electron+phonon system, weakly coupled, reson. light scatt. and luminesc. 77−12374
electron-phonon interaction effects on polarisation 80−55088
electron-phonon system, weakly coupled, resonant light scatt. and luminescence 80−40100
electronic Raman scatt. in polaron gas 79−95753
electronically degenerate states, asymmetric scattering tensors of normal modes, selection rules 77−12381
evanescent field excitation of homogeneous Raman scattering closed to a dielectric 79−99864
excitation profiles and mol. spectra synthesis, vibronic and exciton-in-mol. theory 78−42076
excitation profiles by vibronic theory, preresonance scatt. 77−79619
excited electronic states, ultrashort T_1 and T_2 relax., reson. Raman spectrosc. obs. 79−36554
excitonic molecule, Bose condensation, optical response 77−43512
excitonic molecule, reson. Raman scatt. and luminesc. 79−95763
excitons, condensation effects, review 78−2427
faint Raman scatt. recording by interference contrast system 79−67393
Fermi resonance theory 77−1666
ferroelectric, susceptibility, Raman line shape of overdamped mode 79−91426
ferromagnetic film, shift of ant. temp. as result of Raman scatt. 80−54909
ferromagnetic polariton linewidths, theory 78−87918
flame temperature meas. by Raman scattering 77−16822
flames, temperature and conc. meas. by rot. Raman scatt. 79−31530
fluctuations effect on emission spectra 77−58055
fluid, dense, isotropic Raman polaris., correlation function, kinetic eqn. 77−28567
fluid, molecular, multiphoton Raman scatt. spectra 77−63404
fluid, of isotropic mols., DID Rayleigh and Raman depolarised scatt., lattice-gas model 80−10356
fluids, atomic and molecular, collision induced light scatt. *(German)* 79−27057
forbidden rotational and vibr.-rot. transitions in strong optical field, spontaneous and stimulated Raman scatt. 80−74174
Fourier analysis of Raman signals nonintrusive technique for measuring concentration fluctuations in turbulent combustion processes 78−92564
Franck-Condon effects in resonance Raman spectra and excitation profiles, appl. to CrO_4^{2-} and β-carotene 80−14129
gas matrix sample, electronic and reson. Raman spectra, simultaneous meas. 78−66554
gas mixture concentration and temp. meas. techniques *(French)* 79−17425
gas temperature meas., 300-1200K, choice of informative parts of rot. spontaneous Raman spectrum *(Russian)* 77−31416
gaseous mixtures, equilib. at high temp., Raman scatt. obs. 80−45619
gases, high resolution rotational Raman spectra, review 80−23425
gases, rot.-vibr. Raman spectrosc., high resolution, review 80−22442
gases and vapours, degree of depolarisation of scattered light, meas. accuracy, Raman-lines effect 80−1737
Hanle effect, influence on Raman scattered light 80−83323
Heisenberg antiferromagnet, magnon renormalisation, two-magnon Raman scatt., kinematic interaction 78−23228
Heisenberg paramagnet, two-spin Raman scatt. at high temp. 77−40225
high intensity Raman interactions, review 79−76759
high magnetic field behaviour of solids and plasmas, conference, Cambridge, MA, USA (Sept. 1978) 79−60667
high pressure optical cell for Raman studies of gases, liquids and molecular solids 78−12767
high pressure Raman cell, press. determ. at 42K 78−49850
history of discovery *(Polish)* 79−75314
hydrogenic atoms, metastable, Raman-like two-photon scatt., calc. 80−47953
hyper Raman effect, quantum statistics 80−23754
hyper-Raman effect, master eqn. approach, quantum statistical treatment 78−82736
hyper-Raman effect, scatt. intensity enhancement, light source statistical props. 77−42572
hyper-Raman effect, vibr. mode classification and spectral line assignment, QED method 78−58703
hyper-Raman scattering by chiral molecules 79−45727
impurities in crysts., dynamics 79−60442
impurity centre pairs, possibility of cooperative effects 78−60449

Raman spectra continued
impurity centres, theory of time depend. of resonant secondary emission specta 78−92082
incommensurate crystals, first order Raman scatt. from unbounded phonons 80−88990
inelastic light scattering conference, Santa Monica, CA, USA (Jan. 1979) 79−95762
inert gas, laser induced translational absorpt. *(Russian)* 78−31197
inhomogeneous Airy function, Gi(3) and Hi(3) 80−43259
inhomogeneous high temperature plasmas, Raman scatt. simulations 80−92268
intensities, rel. to IR instensities 78−94290
intensity analysis, electrooptical parameters transferability 78−29820
interatomic correlation effect on spontaneous Raman light scatt. *(Russian)* 77−46711
intermediately coupled localised electron-phonon system, transient reson. Raman scatt. Franck-Condon-like excitation 79−8141
intermolecular forces Raman scatt. obs., review 80−23427
intermolecular spectroscopy and dynamical properties of dense systems, conf., Varenna, Italy (1978) 80−82581
internal Raman scattering, effect on cryst. luminesc. *(Russian)* 78−60518
ionic equilibria in water and mol. dynamics of pure liqs. using high-press. Raman spectroscopy 79−24301
ionic solvation, spectroscopic data comparison for methanolic and aqueous solns. 80−26099
irreducible scattering tensor operator for 32 cryst. point groups 77−8572
Jahn-Teller (E×e) system, resonant Raman scatt. 79−28736
Jahn-Teller multimode effect for E-term with strong vibronic coupling, IR and Raman spectra band shapes 80−20139
Kerr effect, Raman-induced, line shape calc. *(German)* 79−50358
kramers-Kronig relations and resonance Raman scattering 80−97267
large molecules, reson. Raman scatt. cross-section calcs. 79−31532
laser near-reson. scatt. from collisionally perturbed mol. 78−1033
layer or thin slice at solid interface, Raman spectrum 77−48261
lidar-Raman method of air pollution detect. 77−9569
light hyper-Raman scatt. by polaritons, active spectroscopy *(Russian)* 80−60623
line broadening, rotational structure, vibrational relaxation 79−98105
linear atomic susceptibility role 78−55142
linear molecules in inert solvent, collapse of rot. struct. of scatt. spectra *(Russian)* 77−3371
liquid, band shape, rot.-vibr. coupling effect for reorientation 78−72491
liquid, induced Raman scatt., anomalous line broadening 78−56490
liquid, inverse Raman scatt. in optical fibre scatt. cell 79−9249
liquid, Raman band profile, vibr. dephasing and intermolecular interactions 80−60556
liquid, vibr. relax., line widths, intermol. forces dephasing 77−47315
liquid (isotope) mixture, isotropic Raman spectra, intermol. vibr. mode coupling 79−31535
liquid drop, Raman scattering by forced surface oscills. 80−92763
liquid drop in EM field, Raman line splitting 77−69826
liquid droplets, forced vibr., Raman scatt. obs. 80−34929
liquid mixture, anomalous broadening of excited Raman scatt. lines *(Russian)* 77−52103
liquid phase band contours, data processing, band shape corrections 78−27215
liquid structure and dynamics from light scatt. spectra 80−55105
liquids, H-bonded, IR and Raman spectra, elec. anharmonicity on H-stretching bands 78−48167
liquids, inverse electro-optical problem 78−2845
liquids, Kerr effect induced by Raman scatt. *(German)* 78−60427
liquids, vibrational relaxation studied by picosecond or Raman spectros. 80−80797
liquids, with weak H-bonds, short range order and anharmonicity effects 78−64357
living cells, laser Raman spectra, review 80−56113
local void fraction in two phase flow, Raman effect measurement technique 79−64813
localised centres, reson. scatt. and absorpt. *(German)* 79−65848
localised electron-phonon system, linearly coupled, reson. Raman scatt. polaris. effects 79−91428
localised electron-phonon system, second order optical processes, stationary response 78−43916
localised electron-phonon system, second order optical processes, transient response 78−43917
magnetised plasma, Brillouin and Raman scatt. by extraordinary mode 80−92269
many-level atoms, Raman scatt. resons. in separated fields 79−31449
metal-solution interface with adsorbed molecules, enhanced light scatt. 79−82989
methane backward Raman amplifier, KrF laser driven, high-efficiency energy extraction 80−106533
methane-N_2-isobutane gas mixture composition by Raman spectra 80−87124
methyl iodide, vibrational dephasing by translational collision 80−87202
microprobe analysis, laser, principles and appl. 80−57390
mixed crystal, line profile of absorpt. and Raman spectra, calc. 78−48183
molecular band intensities, use in force const. calcs. 77−27120
molecular charge transfer complex, Raman scatt. intensity enhancement model 79−13720
molecular coupling parameters, determ. in two interacting C_{3v} rotor systems 78−42074
molecular crystal, intermolecular interactions, correlation with absolute Raman intensities of lattice modes 77−66502
molecular crystal, Raman scatt. by external vibrs. 77−85711
molecular crystal, Raman scatt. on nondipole vibrs. 79−95751
molecular crystals, low freq. Raman spectra, defects and lattice vibr. 78−31194
molecular crystals, polarised Raman scatt. from lattice modes 78−43845
molecular crystals, Raman scatt. from external orientation vibrations 79−95776
molecular dynamics, allotropy, solid-state phase transitions effects, Raman spectra *(French)* 77−42372
molecular electronic continuum, reson. Raman scatt., anal. model 77−65475
molecular fluid, optical props., intermol. forces effects, theory, appls. 77−28535
molecular line intensities, modified CNDO/2/INDO calc. 78−25621
molecular liqs., anisometric, Raman spectra components, vibr. reson. coupling and noncoincidence effect 80−69149
molecular liquid, hot bands, vibr. correlations, dephasing 79−85966
molecular multilevel thermally relaxing system, reson. Raman scattering 77−50440
molecular near-resonant fluoresc. and Raman scatt. theory 79−3446
molecular predissociation, spectroscopic interferences, unified description 77−23524
molecular Raman excitation profiles, vibronic theory 77−23501
molecular Raman scatt. theory, vibr. state summation, polarisability tensor upper and lower bounds 80−48000
molecular Raman selection rules, spin degeneracy and vibronic states 78−987
molecular reorientation of symmetric top molecules, in liquid state, book contrib. 78−22623
molecular resonant Raman scatt., strong vibronic coupling limit, Green's function 77−83605
molecular resonant Raman scatt., strong vibronic coupling limit, overtones, hot bands 77−83606
molecular scattering of light, spatial dispersion, distributed dipole and local multipole approx. 80−80796
molecular single crystal, librational-Raman spectra polaris., temp. depend. 79−1760
molecular solids, Raman, fluoresc. and nonlinear props. 79−33702
molecular system in weak field limit, Raman damping const. and its effect on reson. light scatt. 79−94005
molecular vibrational Raman spectrum, dispersion of depolaris. and conversion factors 79−72323
molecular vibrational relax. in liqs. *(Russian)* 79−59476
molecular vibrational relax. in liqs. *(Russian)* 79−64012
molecule, C_{3v} and T_d, forbidden pure rot. Raman spectra 77−58019
molecule, chiral, circular intensity differential, ang. relationship depend. 77−34639
molecule, collision-induced rot. Raman scatt. in low, high freq. Rayleigh tails 78−25546
molecule, correlation with vibronic coupling and adiabatic potential 77−71804
molecule, degenerate Jahn-Teller active mode, depolaris. dispersion in resonance Raman scatt. 77−58012
molecule, forbidden Raman scatt. theory, including two-photon operators 79−54814
molecule, intensities dipolaris. ratios, polarisability, matrix rotation, isotopic rules 78−5288
molecule, intensity calc., efficient ab initio computation method 79−45698
molecule, ordinary Raman scatt., two-photon saturation effect 78−82738
molecule, polarised line widths (intensities) in Raman scatt., conc. depend. 78−70879
molecule, pre-reson. Raman scatt. by t-type mode near A→T electronic transition 80−58261
molecule, Raman and IR intensities relation 77−65514
molecule, reson. Raman spectra, Dushinsky effect 79−45726
molecule adsorbed on electrode, enhanced Raman scatt. 79−95767
molecule embedded in dielec. spheroid, Raman and fluoresc. scatt. 80−99507
molecule embedded in dielectric sphere, fluoresc. and Raman scatt. 79−76435
molecule near solid surface, light scatt., classical theory 79−18247
molecule with double minimum pots., resonance Raman scatt. 77−58011
molecules, chemisorbed on metal surface, spectrosc., electron gas effects 80−54504
molecules, excited state, vibronically coupled, reson. Raman scatt. calcs. 79−54858
molecules, intensity modified CNDO/2/INDO method 79−825
molecules, optically active, coherent Raman scatt., quantum theory 80−69150
molecules, Rayleigh and Raman optical activity, scatt. angle anal. 80−69151
molecules, spherical top, with electronic degeneracy, rot. Raman spectrum 79−72322
molecules adsorbed on electrode surfaces, Raman scatt. theory 79−13724
molecules adsorbed on metal surface, giant Raman scatt. mechanisms 79−51960
molecules adsorbed on rough surfaces, Rayleigh, Mie and Raman scatt. 80−83378
molecules embedded in particles 77−23618
molecules embedded in small particles, Raman and fluoresc. scatt., coherent results 79−41338
molecules embedded in small particles, Raman and fluoresc. scatt., incoherent results 79−41337
molecules with vibronically coupled excited states, resonance Raman spectra 77−6784
monolayer in inelastic electron tunnelling spectroscopy junctions, surface enhanced Raman scatt. 80−93344
monolayer on metal surface, giant Raman scatt., review 80−93343
monolayer on metal surface, giant Raman scatt. theory 80−93345
n-type semiconductor, inelastic light scatt. from magnetoplasma oscills. 77−12385
naphthalene-$SbCl_3$ system, phonon bands in π-electron charge transfer complex 77−39644
nonlocality effects on optical phenomena in bounded solids, developments 80−93328
nonstationary Raman scattering, by polaritons, correlation spectroscopy *(Russian)* 78−23450
nonstationary Raman scattering, of light, by vibration and polariton excitations *(Russian)* 78−23449
nuclear-gamma ray scatt. using (n,γ) photons 80−18288
opaque semi-infinite crysts., dynamical light scatt. from dielec. bulk waves, phenomenological theory, appl. to n-InSb 79−69829
optical activity parameters, circular intensity differentials comput. by atom-dipole interaction model 79−76407
optical dephasing in condensed phases, coherent spectrosc. obs., theory 79−36693
optically active mol. light scatt., elliptical polaris. production 77−58089
optically isotropic molecules, collision-induced scatt., many-body correls. 80−87127
optically unstable electronic defect-states, reson. Raman studies by double laser beam excitation 77−77220

Raman spectra continued
organic surface contaminants, anal. by plasma chromatography-mass spectroscopy, and Raman microprobe technique 80−108773
oriented atoms, electronic Raman reson. scatt., statistical theory 80−102467
oriented molecules, angle resolved, group theory 79−47425
oriented molecules, hyper-Raman scatt. 79−36650
outer planets, probing using Raman effect 77−87277
overlapping lines in band, separation *(French)* 79−3499
PAA, light scatt. near cryst. to nematic transition 80−16046
paramagnet, Heisenberg, two-spin Raman scatt. 77−85715
paramagnetic crystal, magnetisation change by light pulse 80−70932
partially orientated symmetrical molecules, polarised Raman scatt. expressions 80−988
partially oriented molecules, uniaxial, two-photon processes, polarised spectrosc. 80−74209
particles with embedded molecules, Raman and fluoresc. scatt. 79−64177
photographic plates, meas. by computer-controlled photometer 77−65051
photosynthetic systems, discovery of phase transitions, Stokes Raman scatt. 80−81539
picosecond interactions in liquids and solids, book contrib. 77−65057
piezocrystals, uniaxial, Kerr effect induced by Raman scatt. *(German)* 78−60427
plasma, collisionless, enhanced Raman backscatt. of Gaussian laser beam from plasma wave 79−86566
plasma, laser amplitude calibration from Raman spectra, for diagnostics *(Russian)* 80−38702
plasma, plasmon prod. by laser light Raman conversion 78−47125
plasma, Raman and Brillouin backscatt., nonlinear theory 78−47127
plasma devices, calibration of laser light scatt. expt. 77−35399
plasma laser pulse amplifier using induced Raman or Brillouin processes 80−1279
polar molecules, vibr. relax., Raman overtone band obs. 77−14436
polar phonons in crysts., Raman scatt. theory 79−47447
polar semiconductor, electron-phonon and electron Raman scatt. in mag. field 79−91438
polar semiconductor, Raman spectra of coupled LO phonon-plasmon mode, de Haas-Shubnikov like quantum oscills. 78−43863
polar semiconductors, resonant secondary radiation 78−31242
polar semiconductors, secondary cyclotron emission giant oscillations of intensity and line shape 80−66192
polar semiconductors, two-phonon resonance Raman scattering 80−108204
polarisation effects in nonlinear scatt., hyper-Rayleigh (Raman) scatt. 77−88858
polarisation reduced Raman light scatt., review 80−34928
polariton and phonon scatterers, freq.-angle spectra 79−4805
polariton Fermi resonance, Raman spectra in band of many-particle states 80−25374
polariton investigation in solids 77−40238
polaritons, appl. of IR reflectivity and Raman scatt. expt. 77−40237
polaritons, Raman scattering, photoelec. recording method *(Russian)* 78−23468
polyatomic molecules, vibr. energy transfer and relax., picosec. time-resolved spectra 79−50028
polyatomic molecules in condensed phases, origin of vibr. dephasing 79−27069
potential modulation Raman spectroscopy, appl. to pyridine on Ag electrode 79−63310
powdered samples, pressed discs. Raman versus Rayleigh light scatt. 79−91437
premixed H_2-O_2-N_2 laminar flames, temp. profiles, Raman, absorpt. and line reversal obs. 80−42227
propane-air flame, chem. anal. of reaction zone by Raman spectra 78−64837
protein-water interactions in aq. solns., Raman spectroscopy 77−6792
pyridine, adsorbed on Ag surface, Raman active librational modes 80−65359
quasiequilibrium sample, light scatt. and thermal radiation, phenomenological approach 80−91840
Raman-luminescence problem, interference analogy and expt. discrimination by polarisation correl. 79−95764
rare earth impurities in crystals, magneto-Raman effect 78−43864
recent developments and historical review 78−73821
redistribution of scattered radiation by collisions in nonimpact region of spectral line profile 79−35109
reflection symmetry violation for crysts. and mols. 78−48184
relative Raman line intensities, extended Huckel valence basis sets 80−106329
relativistic electrons in strong mag. field, Raman scatt., pulsar radiation *(Chinese)* 77−53418
representation of scatt. tensors by ellipsoids and by hyperboloids 79−91452
resonance coherent Raman scattering, excitation profile, inhomogeneous broadening effects 79−35840
resonance hyper-Raman effect induced by realistic coherent pulses, theory 77−58010
resonance interactions of atomic and molecular systems driven by strong laser field, theory 80−14097
resonance light scattering, spectral props. and photon correls. 80−91510
resonance light scattering and hot luminesc. of self-trapping excitons 80−93336
resonance Raman cross-section, theory 80−5551
resonance Raman effect, theory and appls. 80−23428
resonance Raman effect and hot luminesc. of impurity centres 77−81149
resonance Raman lineshapes and fluorescence in strong radiation fields 80−87074
resonance Raman profile with consideration for quadratic vibronic coupling 80−55099
resonance Raman scatt., duality 77−59568
resonance Raman scatt. cross sections, forbidden electronic transitions, depolaris. ratios 78−42075
resonance Raman scatt. from mols., temp. effect, displaced harmonic oscillator model 80−23424
resonance Raman scattering, appl. to ultrafast dephasing and relax. obs., phonon scatt. effects 80−7337
resonance Raman scattering, first and second order, in mag. field, theory 77−36242
resonance Raman scattering, in strong elec. field 77−16305
Raman spectra continued
resonance Raman scattering, of totally symmetric vibr., depolarisation dispersion, vibronic coupling 77−65472
resonance Raman scattering, polarisation dispersion, inhomogeneous broadening effects 77−6787
resonance Raman scattering, polariton theory, book contrib. 79−38551
resonance Raman scattering, second-order, theory for case of strong excitonic effects 78−76460
resonance Raman scattering and luminescence of excitons in self-trapping process 80−20689
resonance Raman scattering and resonance fluoresc., time and freq. resolved 77−75624
resonance Raman scattering in systems with localised carriers 80−7356
resonance Raman scattering polariton theory, book 79−37966
resonance Raman spectra, optimum sample concs. 78−66555
resonance Raman spectra, saturation effects, coherent pulse calcs. 77−6785
resonance Raman spectra lineshapes, first order, rel. to optical absorpt. lineshapes 80−5548
resonance Raman spectroscopy, inorg. chem. appls., book contrib. 80−972
resonance scattering, electronic and vibrational intensities 77−77186
resonance scattering, time and spectral resolution 77−58305
resonance-preresonance interference effects, theory 77−68047
resonant coherent Raman scatt. spectra of excited molecules 80−87129
resonant light scattering from magnetic excitations, review 80−97290
resonant localised impurity vibrs. at finite temps., spectral distrib. 77−7814
resonant Raman effect, appls. and theories, review, book contrib. 77−38676
resonant Raman scattering, intense optical waves, quantum mechanical theory 79−89958
resonant Raman scattering by LO phonons 78−39551
resonant Raman scattering in laser fields of arbitrary strength, antibunching effects 80−23653
resonant Raman scattering in systems with localised electron states, theory 79−15455
resonant Raman spectra, overtone intensity distrib., effect of excited electronic state 80−87128
resonant scattering, resonant secondary emission theory 79−38615
resonant scattering of light by slowly fluctuating localized electrons 80−7365
resonant secondary emission components classification, theory applic. to expt. 80−93339
resonant secondary emissions by impurities in crysts. 80−93335
resonant secondary radiation of excitons weakly interacting with phonons, theory 78−31241
resonant X-ray Raman scattering, IR divergence of Compton effect 78−21873
scattering cross-sections in gases and liquids 80−23426
scattering surface polaritons and compensation effect 78−10374
second order optical processes, intermediate state interaction stochastic models 77−48243
second order optical processes, stochastic models of intermediate state interaction, stationary response 77−85770
second order optical processes, stochastic theory 79−94201
semiconductor, deep impurity centres, elastic light scattering 80−97315
semiconductor, direct band gap, electronic Raman scatt. of polarised light on donor levels 80−93309
semiconductor, influence of impurities on Raman scatt. by Landau levels 77−1668
semiconductor, optical non-locality phenomena near exciton reson. 79−95794
semiconductor, optical props. under intense laser field 79−43040
semiconductor, p-type, determ., g-values, spin temp., from Raman spectra 78−43856
semiconductor, phonon spectrum in mag. field, renormalisation 79−28060
semiconductor, polar, longwave secondary radiation *(Russian)* 78−80343
semiconductor, quasi-one-dimensional, light absorpt. and Raman scatt., large exciton form. 77−16272
semiconductor, Raman scatt., one-phonon final states and many-body effects 80−34913
semiconductor, reson. Raman scatt. at indirect gap 79−73931
semiconductor, resonance secondary radiation emission, theory 78−60452
semiconductor, resonant Raman scatt., book contrib. 77−36251
semiconductor, scattering by light by phonon zero sound 79−56145
semiconductor, two-phonon Raman scatt. by longitudinal optical phonons, double reson. 77−24852
semiconductor, zero-phonon Haman scatt. of light 79−69843
semiconductor resonant Raman scattering book 77−36250
semiconductors, degenerate, resonance Raman scatt., Green's function approach 80−80781
semiconductors, free carrier optical props., book contrib. 80−80738
simple liquids, vibrational Raman bands, electric field induced changes, in short-time spectroscopy *(German)* 79−28715
simple solid, scatt. cross sections determ. 80−93334
small volume flames, temp., temporal meas., two line at. fluoresc. technique, Raman scatt. 80−42226
solid, disordered, IR and Raman spectra, analytic models 80−7336
solid, spectral line shape, quantum field theoretic formulation 78−31187
solids, interacting elementary excitations, review 78−43846
solutions, resonance Raman lineshape studies of vibrational and rotational relaxation 80−60560
solvated electrons, Raman spectrum modification, polarisation CARS obs. 80−5549
spherical liquid particle, Raman scatt. of light by random thermal oscill. in shape 78−13662
spherical particle, surface enhanced Raman scatt. by molecules 80−95629
spherical top type molecules, rot. spectra, CARS *(Russian)* 77−75168
spin system, optical-acoustic two-phonon relax. 80−11244
spontaneously modulated materials, Raman scatt. 79−95739
stable molecules, matrix isolation spectroscopy obs., appls. 78−46320
Stark quantisation effects on scatt. cross section, calcs. 77−16314
stimulated Raman scatt. Dewar cell for biomedical appls. 80−99799
stimulated Raman scattering, review of appls. 77−735
stress-induced Raman tensors and effective charges for 32 point groups 79−33667

Raman spectra continued
subsurface water temperature and salinity remote sensing by Raman scatt. 79−80036
surface analysis, atomic beam scatt., SIMS, and vibr. spectra, book contrib. 79−42357
surface enhanced Raman scattering surface plasmon model 80−108211
surface enhanced Raman spectra, image dipole description, critical review 80−87125
surface polaritons, effect of surface roughness 79−73451
surface polaritons, nonlinear fluctuation-dissipation theorem 77−12391
surface roughness effect on surface enhanced Raman scatt. 80−83377
temperature of gas or plasma, Raman Q-branch intensity 79−37545
tetrahedral mol. fluids, collision induced light scatt. intensity 80−103955
tetrahedral molecular fluids, collision-induced light scatt. 79−68237
thin film sample, electronic and reson. Raman spectra, simultaneous meas. 78−66554
three-level system, intense laser field spontaneous Raman effect 78−86802
three-level system, reson. Raman, superposition of adiabatic state theory 78−78734
time dependent theory, vibr. Raman scatt. in weak field limit 80−28023
time-dependent excitation profiles for continuum Raman scattering 79−41175
time-reversal symmetry in light scatt. theory, Stokes-anti-Stokes connection formula 78−56479
transient resonance Raman scattering, excitation, relaxation and observation, semiclassical theory *(Japanese)* 78−42078
transition quasilinear spectra of resonant secondary emission *(Russian)* 80−16102
transparent solids, review *(Chinese)* 79−33714
trigonal symmetry doubly degenerate mode systems, excitation profiles, depolarisation ratios, reson, Raman scatt. 79−98108
triply degenerate singlet electronic states, reson. Raman scatt. 78−78714
two level atom, coherent and Raman scatt. spectra, secondary emissions 80−69449
two-level system coupled to thermal bath, quantum dynamics of relax. 77−3437
two-phonon, morphic effects, appl. of irreducible representations in symmorphic space groups *(Japanese)* 79−77541
two-phonon Raman scattering, double reson. 77−40226
two-photon resonant processes, conserved quantity 79−45688
two-photon saturation effect on ordinary Raman scatt. 80−9967
two-spin light scattering, disordered phase rutile antiferromags., MnF_2, NiF_2 78−80336
very thin films, improvement in Raman spectrometry 80−31911
vibrational dephasing by translational collision 80−87202
vibrational intensity changes due to long-range interactions 80−53084
vibrational interference in reson. Raman scatt. 77−42328
vibrational Raman optical activity spectra, perpendicular polarisation recording method 79−21821
vibrational relaxation of molecules in condensed media, survey, book contrib. 77−36295
vibronic state short lifetime, determ. from reson. Raman excitation profiles 79−98103
vibronic systems with localised electrons, reson. Raman scatt., hot luminesc. 79−38616
vibronically coupled excited states, reson. Raman scatt. and depolarisation ratio 78−94249
VUV and soft X-ray source, using anti-Stokes emission 79−46024
weak ferromagnet, single-ion anisotropy, one-magnon Raman processes 78−27234
X-ray and synchrotron radiation inelastic scattering in crystals 78−39625
X-ray Raman scattering edge, atomic struct. and extended modulation 79−99031
XY_4 tetrahedral mol., hyper-Raman scatt. intensities calc., tensor method *(French)* 79−22712
78−18749
Ag, adsorbed pyridine, 210-243 cm^{-1} mode in surface enhanced Raman scatt. 80−89003
Ag-electrolyte interface, enhanced Raman scatt. of adsorbed molecules, background continuum obs. 79−73926
Ar atom, Raman scatt. of light, HF approx. *(Russian)* 77−30808
Ar, Raman scatt., single particle HF approx. and RPA many-electron correlations calcs. 80−23374
$(C_2H_5)_2Fe^+$ complexes, vibrational electronic (Franck-Condon) Raman transitions 78−42070
CN monolayer on Ag, picosecond Raman gain spectroscopy 80−25351
CN^-, on Ag surface, Raman active librational modes 80−65359
D_2+D_2, collision effect on depolarised light scatt. linewidths 80−53059
F, Raman scatt. cross section for transitions between ground fine-struct. electronic states 80−23349
$GeAs+Cl_2(Br_2)(I_2)$, high temp. Raman spectra, cryst. growth mechanism *(French)* 79−26999
H_2 flame in air, laminar diffusion flame, Raman spectra diagnostics 79−47928
H_2+H_2, collision effect on depolarised light scatt. linewidths 80−53059
H_2O, resonance Raman spectra for detection bacteria and algae 80−94418
H_2O+Li^+, ab initio GTO calc. of vibr. intensity changes of spectroscopic parameters 78−58583
H_3PO_4, aq. soln., elec. cond. and Raman spectra at high-press., 25°C 79−56220
^4He, liquid, fourth order struct. and Raman scatt. 79−56801
^4He, superfluid, Raman expts., interpretation 79−73362
$InX(X_2)(X_3)$, $InAlX_4$, X=Cl,Br, Raman spectra, up to 1200K 80−48003
KH_2PO_4, aq. soln., elec. cond. and Raman spectra at high-press., 25°C 79−56220
$LiNO_3$ in N,N-dimethylacetamide, Raman, IR and US relaxation studies 80−50315
$LiNO_3$, soln. in organic liq. or D_2O, Raman lineshape, solvent-solute interaction 78−76448
LiSCN in N,N-dimethylacetamide, Raman, IR and US relaxation studies 80−50315
LiX-alcohol mixtures, (X=Cl, Br, ClO_4), OH(OD) vibr. bands in sat. solns. and crysts. 77−8564
Mg, atom, forbidden Raman scatt. theory, including two-photon operators 79−54814
Mo, reson. Raman X-ray scatt., evidence for K-M scatt. 79−61466

Raman spectra continued
NO_3^-, in aq. nitrate solns., vibr. dephasing process, Raman obs. 79−51936
Na, atoms, in presence of two-photon reson. 79−45679
$NaNO_3$ in N,N-dimethylacetamide, Raman, IR and US relaxation studies 80−50315
Na_3PO_4, aq. soln., elec. cond. and Raman spectra at high-press., 25°C 79−56220
NaSCN in N,N-dimethylacetamide, Raman, IR and US relaxation studies 80−50315
O_2, gas, temp. meas., vibr. Raman intensity, 500-2000K 79−37436
PCl_5-$SnCl_4$, mixtures, liq. and solid, Raman spectra study *(German)* 79−91451
Pd and Pt mixed valance complex, $[Pd(ethylenediamine)_2Pt(ethylenediamine)_2Cl_2](ClO_4)_4$, Raman spectra 80−84734
$SiAs+Cl_2(Br_2)(I_2)$, high temp. Raman spectra, cryst. growth mechanism *(French)* 79−26999
Sm^{3+} in cubic environment, importance of T^{-5} and T^{-7} terms in spin-lattice relax. time 80−25192
Tl, line shape in Ar gas, collisional redistrib. of near-reson. rad. 79−31469
Tl, spontaneous to stimulated regions obs., collisional and radiative effects 78−87103
Yb^{3+}, in dessicated (nondessicated) and protonated (deuterated) solvents, photoluminesc. energy degredation 78−19544

Raman spectra of diatomic inorganic molecules
air pollutant gases and vapours, relative Raman scatt. cross section 80−100061
diatomic molecule, reson. Raman scatt. amplitudes, semi-classical estimate 79−36649
dilute solutions, IR and Raman spectra temp. depend. anal. model *(French)* 77−88456
homopolar, light scatt. *(Hungarian)* 77−50442
intensity relation, IR to Raman intensity, matrix notation 78−62853
Lennard-Jones fluids, orientational and collision induced light scatt. 80−63644
polarisability anisotropy derivative determ. from relative Raman intensities 78−55177
resonance Raman scatt. amplitude, coupled channel eqns., collision theory 78−94248
resonance Raman scattering with tunable lasers, review, appls. 78−94247
rotational Ramam intensities and polarisability anisotropy change meas. with internuclear distance 80−63641
scattering amplitude calculations, role of radiative crossings between potentials of dressed mol. 80−63642
Ag_2, Raman spectra, matrix isolated in Kr 78−46347
Ar_2, collision-induced Raman spectrum, absolute cross sections 78−46349
Ar_2, collision-induced Raman scatt., polarisability anisotropy 78−46350
Ar_2, Raman spectra, press. broadened transitions, calc. 79−64009
Br_2, adsorbed layer on zeolites, Raman spectra, aromatic bromination catalysis 80−3408
Br_2, Ar matrix reson. Raman excitation profile, red shift rel. absorption spectrum 77−14440
Br_2, $B^3\Pi(O^+)$ and $^1\Pi(1)$ states, reson. Raman spectra 79−59470
Br_2, chemisorbed on zeolites, Raman spectra 80−93301
Br_2, condensed phases, spontaneous and stimulated Raman scatt., weak and strong radiation fields 79−3450
Br_2, continuum reson. Raman scatt., interference effects 79−6946
Br_2 in Ar matrix, reson. Raman scattering amplitude damping in discrete reson. limit 80−58262
Br_2, organic solvent effects on Raman parameters 79−26998
Br_2, Q branches of $\Delta n=1$ profiles, calcs., rotation effect on scatt. amplitudes 80−63643
Br_2, reson. Raman scatt. *(German)* 79−26983
Br_2, reson. Raman scatt. obs., excited-state interference 77−79618
Br_2, reson. Raman spectrum, vibr.-rot. struct. 78−17674
CN, monolayer on Ag surface, vibr. spectra, picosec. Raman gain technique 80−91859
CN^-, adsorbed on Ag, giant Raman scatt. 79−95768
CN^-, chemisorbed on AG (110), Raman scatt. 80−45075
CO adsorbed on Ag, Au films, enhanced Raman scatt. mechanism in ultrahigh vacuum 80−107645
CO, adsorbed on Ag films, Raman scatt. study 79−78672
CO, adsorbed on Ni, high press., low temp. Raman spectra 78−6219
CO, chemisorbed on Al_2O_3-supported Rh-Cu catalysts, IR spectra *(French)* 80−60559
CO flame, background-free CARS technique 79−94288
CO, line broadening, short range force effects, semiclassical calcs. 79−98085
CO, solid and matrix isolated, IR and Raman spectra 78−48156
Ca_2, in Kr matrix, 1- and 2-photon fluoresc. excitation 78−50567
Ca_2, in solid Kr, discrete reson. Raman scatt. and vibr. relax. 79−18188
Cd_2, matrix isolated, Raman spectra 79−50024
CdO, formed by matrix reactions, IR, Raman and visible spectra 80−87110
Cl_2, Ar ion laser excited, normal and reson. Raman spectra 79−26993
Cl_2, liq., mol. reorientation, Raman spectra obs. *(French)* 78−31192
Cl_2, resonance Raman spectrum, Q-branches of $^{35}Cl_2$ and $^{35}Cl^{37}Cl$ 78−25542
Cl_2^-, near Ag electrode, intense Raman spectra, free radical form. 80−55076
$^{37}Cl_2$, pure rot. Raman spectrum 78−94252
$Cs_2NaCe(III)Cl_6$ high symmetry complex, low temp. Raman spectrum CF splitting, paramag. susceptibility temp. depend. *(German)* 77−12380
D_2, electric discharge, vibr. excitation spontaneous Raman scatt. obs. 78−5234
D_2, matrix rot. and vibr.-rot. spectra, free and hindered rot. 77−83607
D_2, Q(2) line, absolute Raman freq. meas. using CW CARS 78−29794
D_2, Raman spectra, vibr. freq. press. shifts 78−78703
DBr, spin-flip Raman laser double-beam spectrum, SFRL multiline output 79−7132
DCl and $(DCl)_2$, matrix isolated Raman spectra 78−42063
DT, vibr. rot. Raman anal. 80−87126
H bonding molecules, self assoc., intermolecular interactions, matrix isolation vibr. spectra obs. Raman and IR spectra 80−52995
H_2, D_2 and HD, intermol. collision process obs. using light scatt. expts. 80−53001

Raman spectra of diatomic inorganic molecules continued
H_2, electric discharge, vibr. excitation, spontaneous Raman scatt. obs. 78−5234
H_2, fluid, Raman meas., 0.2-630 kbar, at room temp. 80−58269
H_2 isotope mols. in laser fusion microsphere targets, nondestructive anal. using rot. Raman spectroscopy 80−50896
H_2 molecule, high resolution CW stimulated Raman spectroscopy 78−70973
H_2, polarisability anisotropy derivative determ. from relative Raman intensities 78−55177
H_2, Raman scattering, cooperative effect observations *(Russian)* 80−5553
H_2, Raman spectra, vibr. freq. press. shifts 78−78703
H_2, rot. Raman linewidths, self-broadening calcs. 77−42356
H_2, two-photon enhanced third harmonic generation and Raman scatt. 77−88843
H_2^+, Raman and Rayleigh scatt. tensors 79−50027
H_2+A, vibr.-vibr. energy transfer, stimulated Raman excitation obs. 79−64086
HCl and $(HCl)_2$, matrix isolated Raman spectra 78−42063
HCl, anhydrous conc. solns. in methanol, Raman and IR spectra 78−82724
HCl, Raman spectra in various solvents, depolaris. ratio and profiles 79−59464
HCl+HCl(Ar), pure rot. Raman lines, press. broadening cross sections 78−74702
HD, Q-branch band shapes, motional narrowing and overlapping effects 78−29785
HD+inert gas, isotropic Raman Q branch, vibr. dephasing effects and motional narrowing 78−74738
$H_2(D_2)$, dissolved in vitreous SiO_2, Raman spectra 79−33707
HF-DF, CW chem. laser, specie conc. and temp. 78−58999
$H_2(HD)(D_2)$, matrix rot. and vibr.-rot. spectra, free and hindered rot. 77−83607
$^1H^3H$ and $^2H^3H$, pure rot. and vibr.-rot. Raman spectra 80−14145
He_2, collision induced Raman spectrum, polarisability anisotropy 79−72320
He_2, polarisability and collrision induced Raman spectra 80−48005
He_2, Raman spectra, collision-induced, diatom polarisability 79−64011
I_2, adsorbed on silica, reson. Raman spectrum 78−42066
I_2, chemisorbed on zeolites, Raman spectra 80−93301
I_2, continuum reson. Raman scatt. 77−71809
I_2, dissociative mol. pot. functions from continuum reson. Raman spectra 77−38673
I_2, in CCl_4 (cyclohexane) soln., ps dye laser excitation, fluoresc. and resonance Raman emission 80−28021
I_2, in CCl_4 and cyclohexane solns., higher vibr. levels, dephasing lifetimes, from reson. Raman spectrum 78−42068
I_2, matrix samples, laser spectroscopy, evidence for $(I_2)_2$ species 78−58735
I_2, photodissociating, theory of resonant Raman scattering *(Russian)* 78−55180
I_2, reson. Raman lines, Stokes-antiStokes intensity ratio meas. 77−6786
I_2, reson. Raman scatt., time delay 77−34641
I_2, reson. Raman scatt. *(German)* 79−26983
I_2, resonance Raman scatt. and collision-induced redistrib. scatt. 77−14439
I_2 solutions, vibr. and rot. relax., reson. Raman lineshape meas. 79−31616
I_2, time-resolved reson. Raman and reson. fluoresc., hyperfine splitting effects 77−30874
$InX(X_2)(X_3)$, $InAlX_4$, X=Cl,Br, Raman spectra, up to 1200K 80−48003
Kr:Mg_n, matrix isolated Raman spectra 78−90170
Kr_2, collision-induced Raman spectra, absolute cross sections 78−46351
LiH, finite-field method calcs., dipole moment gradients, polarisability gradients and elec. field effects 77−88589
MnO_4^-, reson. Raman lines, Stokes-antiStokes intensity ratio meas. 77−6786
N_2 discharge, non-Boltzmann vibr. level populations, CARS determ. 78−5968
N_2 dissolved in Ar, mol. orientation, Raman spectrosc. obs. 80−52994
N_2, excited kinetic investigation of vibr. distrib. function, Raman scatt. *(Russian)* 78−66557
N_2 fluid, light scatt. orientational memory function at moderate density 80−102521
N_2, gas, picosec. pulse CARS obs. 79−6942
N_2, high-speed Raman spectroscopy, condensed discharge vibr. excitation, vibr. temp. 78−82740
N_2 in nonequilibrium gas-dynamic current, vibr.-level populations determ. by Raman scatt. 80−99509
N_2 in premixed laminar methane-air flame, Raman scatt. meas. of vibr. temp. 79−80622
N_2, in turbulent flame, Raman scatt. diagnostics 77−72368
N_2, light polarisability parameters, Raman scatt. ang. meas. 80−37814
N_2, line broadening, short range force effects, semiclassical calcs. 79−98085
N_2, matrix isolated, fundamental vibr. Raman spectra 80−272
N_2, polarisability anisotropy derivative determ. from relative Raman intensities 78−55177
N_2, polarisability tensor anisotropy, Raman spectra differential scatt. cross section 80−18860
N_2, pure rot. CARS obs. 80−99511
N_2, Q-branches, high resolution pulsed CARS 78−17676
N_2, Raman intensities calcs., ab initio method 80−52993
N_2, Raman intensity, ab initio calc. 80−1028
N_2, Raman spectra, intermol. torques and orientational correlation times 80−48006
N_2, Rayleigh and Raman depolarised light scatt., density evolution 78−58706
N_2, rot. Raman and elastic scatt. for atm. temp. profiles 77−9515
N_2, rot. Raman linewidths, self-broadening calcs. 77−42356
N_2, rot. Raman scatt. of Thomson scatt. 80−1844
N_2, single and multiple free jets, CW laser Raman spectroscopy 80−32727
N_2, spectroscopic data review 77−38680
N_2 stimulated scattering investigation, 1-4 atm press. range 80−91568
N_2-Ar, liq. mixture, isotropic Raman line shape theory 78−88298
N_2-Ar liq. mixtures, coherently excited mol. vibrs., dephasing time 78−62813
$^{14}N^{14}N$, direct determ. of rotation-vibration coupling coeff. α_e 77−38675

Raman spectra of diatomic inorganic molecules continued
NO, press. broadening coeffs., spin-flip Raman laser spectrosc. 80−43147
NO, spontaneous vibr.-rot. Raman scatt. from $X^2\Pi$ state 79−36646
NO, vibr.-rot. bands of Raman spectra 78−29173
$NO_2(N_2O_4)$ surface decomposition, resonance and spontaneous Raman spectra 80−61144
Ne_2, collision induced Raman spectra and diatom polarisability 80−63647
Ne_2, Raman spectra and polarisability 79−98107
O_2, anharmonicity const., Raman meas. 77−34637
O_2, coherent anti-Stokes Raman scattering in hollow dielec. waveguide 77−50721
O_2 dissolved in Ar, mol. orientation, Raman spectrosc. obs. 80−52994
O_2, gas, intermol. pot. for spectra, acoustic absorpt., rot. relax., etc. 79−68224
O_2, gas, vibr. Raman spectrum, anomalous behaviour near crit. point 78−55179
O_2 isotopes, $^{17}O_2$, $^{16}O^{17}O$, $^{17}O^{18}O$, pure rot. Raman spectra, bond lengths 78−42071
O_2, light polarisability parameters, Raman scatt. ang. meas. 80−37814
O_2, polarisability tensor anisotropy, Raman spectra differential scatt. cross section 80−18860
O_2, pure rot. CARS obs. 80−99511
O_2, Q-branches, high resolution pulsed CARS 78−17676
O_2, Raman spectra of fundamental vibr. band, rot. consts. 78−21932
O_2, rot. Raman and elastic scatt. for atm. temp. profiles 77−9515
O_2 rot. Raman spectra fine struct., press. broadening *(French)* 79−94003
O_2, vibr.-rot. Raman spectrum, Q-branch resolution, direct recording spectrometry *(German)* 79−85967
$^{18}O_2$, Raman spectrum and mol. parameter 77−46565
OH, spontaneous vibr.-rot. Raman scatt. from $X^2\Pi$ state 79−36646
$^{16}O^{16}O$, direct determ. of rotation-vibration coupling coeff. α_e 77−38675
$^{18}O^{18}O$, direct determ. of rotation-vibration coupling coeff. α_e 77−38675
Rb_2, $X^1\Sigma_g^+$ state, Raman spectra, fluoresc., vibr. energy 78−46345
S_n, (n=2-12), vibr. spectra and thermodynamic functions *(German)* 78−82742
SO_2 surface reaction and decomposition on zeolites, resonance Raman study 80−61145
Sn_2, matrix isolation Raman spectrum, overtone bands breadth 78−33515
$^3T_2$, pure rot. and rot.-vibr. Raman spectrum 78−94253
Xe_2, collision-induced Raman spectra, absolute cross sections 78−46351
Zn_2, matrix isolated, Raman spectra 79−50024
ZnO, formed by matrix reactions, IR, Raman and visible spectra 80−87110

Raman spectra of inorganic liquids and solutions
alkali bisulphites, and disulphites, and isotopic forms, solid and soln., Raman spectra assignments 79−42968
alkali halide solutions, tetrahedral hydration of ions from Raman bands obs. 78−55804
alkali nitrites, molten, combination scatt. spectra, freq. shifts, jumps at melting, line widths *(Russian)* 77−40241
alkaline earth nitrites, molten, combination scatt. spectra, freq. shifts, jumps at melting, line widths *(Russian)* 77−40241
alkaline nitrates, Raman and Brillouin scattering, temp. influence on freq. of NO_3^- ion *(French)* 79−69833
dilute solutions, IR and Raman spectra temp. depend. anal. model *(French)* 77−88456
electrolyte, soln. and cryst. *(German)* 80−80804
metal chloride aqueous solns. with NO_2^- impurities, luminesc., absorpt. and Raman spectra *(Russian)* 77−36291
metal-electrolyte interface, optical methods of study *(French)* 80−7318
molecular liquids, vibr. line broadening, Zwanzig-Mori theory and quasi-elastic processes 78−27221
molecular rotation, model for IR and Raman studies in liqs. and gases 80−11390
molten salts, IR, Raman, EPR and NMR spectroscopy, review *(French)* 79−69832
nitrates, aq. solns., high resolution AC coupled Raman spectra 79−40619
nonaqueous solutions, Raman spectrosc. obs. techniques 78−72514
polyatomic fluid, local dynamics, spectroscopic studies, summer school lecture series 80−6343
resonance Raman scattering with tunable lasers, review, appls. 78−94247
solid-liquid interface, optical methods of study *(French)* 80−7318
succinic acid and its alkaline salts in aqueous soln., Raman and IR spectra *(French)* 80−32723
water, coherent Raman ellipsometry, vibr. stretching region and liq. struct. obs. 80−93341
water, high-pressure Raman spectra, bending and librational bands 78−68499
water, Raman and IR spectrum in overtone OH stretching region 80−58263
water, Raman bands, influence of paramag. rare earth cations 78−15157
water, Raman spectra, liq. state, depolarisation ratios, libration and translational spectra 79−4797
water-HF(HBr)(HCl) complex, in supersat. soln., Raman spectra assignments 78−70840
AgBr melt, Raman spectra, rel. to sublattice melting in α-AgI 78−10882
AgCl melt, Raman spectra, rel. to sublattice melting in α-AgI 78−10882
$AgNO_3$, cryst. and molten salt, Raman and IR spectra, vibr. anal. 77−16311
Ar, liq., low temp. Raman spectra 78−84580
AsD_3, solid and liq., vibr. relax., Raman ν_1 band, 54, 160K 78−27198
B_2O_3, molten, BO_3 triangles in boroxyl rings and random networks, Raman intensity investig. 80−45058
Bi complexes, Bi(III) halide complexes, Raman spectra in aq. soln. 80−25354
CO, liq., pure vibr. Raman spectra 80−97262
CO liq. and CO-O_2 (N_2)(Ar) mixtures, polarised vibr. Raman scatt. lineshapes 78−27199
CO_2, in H_2O, D_2O soln., Raman spectra 77−65467
CS_2, liquid, Raman spectra, effects of intermolecular forces 79−41177
CS_2 liquid, Rayleigh and Raman bands, intensities of interaction induced components 80−63645

Raman spectra of inorganic liquids and solutions continued
CS_2, vibrational dephasing meas. with CW mode-locked dye lasers 79−65846
$CdCl_2$, aq. soln., Raman spectrum, local order 78−84563
Cl_2, liq., dynamics, depolarised Raman and Rayleigh scatt. 79−99867
Cl_2, liq., mol. motion, Raman spectrum 78−5236
Cl_2, liq., mol. reorientation, Raman spectra obs. *(French)* 78−31192
$CoCl_2$, saturated soln., jet flow Raman spectroscopy for highly absorbing liq. systems 80−52323
Cr complex, tris(2,2′-bipyridine)Cr(III), excited states, Raman spectra 80−97263
$CuCl_2$, aq. soln., Raman spectrum, local order 78−84563
$CuCl_2$, saturated soln., jet flow Raman spectroscopy for highly absorbing liq. systems 80−52323
$Cu(NO_3)_2$, aq. soln., Raman spectrum, local order 78−84563
DCl, liquid, on coexistence line, light scatt., orientational correlation function 80−20632
D_2SO_4, pure, IR and Raman spectra in liq. state, assignments and cryst. spectra comparison *(French)* 79−33699
F_3SiAsH_2, liq. Raman, gas phase IR spectra, normal coord. anal., assignments *(German)* 77−6778
$FeBr_4^-$, in various solvents, $^4A_1$ ^4E d-d band reson. Raman spectra, solvent depend. 80−55085
$GaCl_3$, Raman spectral differences from liquid to glassy state, ionic equilib. interpretation 80−20619
GeH_3NCS, liq. and solid, IR and Raman spectra 79−89663
GeO_2 melts, density, viscosity, struct., at high and low press. 79−87431
H_2, fluid, Raman meas., 0.2-630 kbar, at room temp. 80−58269
HBr, liquid, on coexistence line, light scatt., orientational correlation function 80−20632
HCl, liq., IR spectral intensity and Raman cross-section meas. 80−2742
HCl, liquid, on coexistence line, light scatt., orientational correlation function 80−20632
HNO_3-H_2O, liq. and glass, mol. assoc., ion pairs, Raman obs. 79−28749
H_2O, $H_2{}^{18}O$, D_2O, low freq. Raman spectra, isotope shifts, ice-like struct. 79−28732
H_2O, liq., intermol. coupling, isotope and salt effects, Raman spectra 78−90169
H_2O, liq. and gas, Raman scatt. of ν, vibr. transverse cross-section 78−82739
H_2O, Raman spectra, liq. state, depolarisation ratios, libration and translational spectra 79−4797
$H_3(PMo_{12}O_{40})$, decomp., in aq. soln., Raman spectra obs. 79−13719
H_3PO_4, broad-band picosecond light generation by mode-locked ruby laser 79−31989
H_2SO_4, pure, IR and Raman spectra in liq. state, assignments and cryst. spectra comparison *(French)* 79−33699
$H_4(SiMo_{12}O_{40})$, decomp., in aq. soln., Raman spectra obs. 79−13719
He, superfluid 78−59991
^{4}He, liquid, integrated polarised Raman scatt. intensity calcs., Jastrow ground state 80−50342
HgI_2, Raman spectra, in high-temp. $CsNO_3$, metaterphenyl, and paraterphenyl solns. 78−86876
I_2 solutions, vibr. and rot. relax., reson. Raman lineshape meas. 79−31616
$_xI_{1-x}$ mixtures, high-temp. solids and melts, struct., thermodynamic props., Raman spectra obs. 80−66174
K_2CO_3-SiO_2-As_2O_3, laser Raman spectrosc. study of ions in quenched reaction mixtures 80−25357
K_2MoO_3S, aq. soln., Raman spectrum, MoO_3S^{2-} force consts. 78−74668
KNO_3 soln., Raman spectral studies of NO_3^- motion and interaction 78−92067
$3KNO_3-2Ca(NO_3)_2$, glass form. from liq., struct. transform., Raman spectrum obs. 80−64916
$3KNO_3-2ZnCl_2$, glass form. from liq., struct. transform., Raman spectrum obs. 80−64916
$K_2[RuCl_5NO]$, polarised Raman and IR spectra, vibr. anal. 77−69819
$K_2[B_{12}D_{12}]$, in aqueous soln., laser Raman spectra 78−15158
$K_2[B_{12}H_{12}]$, in aqueous soln., laser Raman spectra 78−15158
$LiClO_4$-$CsNO_3(RbNO_3)(KNO_3)(KClO_4)(RbClO_4)(CsClO_4)$, binary melt, Raman spectra, polarised line width, temp. depend. 78−84578
$LiNO_3$ soln., Raman spectral studies of NO_3^- motion and interaction 78−92067
$LiNO_3$, soln. in organic liq. or D_2O, Raman lineshape, solvent-solute interaction 78−76448
$MgCl_2$, molten Raman spectrum, $MgCl_4^{2-}$ and polynuclear complexes equilib. 77−1669
$MgCl_2$-alkali metal chloride system, solid and molten states, struct. props., Raman spectra 80−76011
$MnCl_2.2ACl$, (A=Li, Na, K, Rb, Cs), melts, Raman spectra of $MnCl_4^{2-}$ ion 79−24310
N_2 dissolved in Ar, mol. orientation, Raman spectrosc. obs. 80−52994
N_2, liq., near BP, vibr. reson. energy transfer and dephasing, Raman spectra 77−6790
N_2, liq., parametric generation 77−741
N_2, liq., pure vibr. Raman spectra 80−97262
N_2, liq., Raman Q branch temp. depend., interferometric obs. 77−43987
N_2, liq. spontaneous Raman scatt., vibr. dephasing, review 77−28568
N_2, liquid, in Kr, methane, and CO, Raman scatt. parameters, high-resolution coherent active spectroscopy 80−66207
N_2, liquid, vibrational dephasing, computer simulation, pair potential effect 80−63863
N_2, Raman lineshape 80−11384
N_2, vibr. line broadening, Zwanzig-Mori theory and quasi-elastic processes 78−27221
N_2:$CO_2(N_2O)$(methane-d_4), liq., vibr. relax., Raman scatt. obs. 78−92061
N_2-Ar, liq. mixture, isotropic Raman line shape theory 78−88298
N_2-Ar liq. mixtures, coherently excited mol. vibrs., dephasing time 78−62813
N_2-Kr(Kr)(O_2)(CO)(CH_4), liquid, high resolution CW CARS spectra 80−63635
NF_3, liq., plastic cryst., gas, Raman spectra, Coriolis coupling and transition dipole 78−39533
$(NH_4)_2MoS_4$, aq. soln., Raman intensity, scatt. frequency depend. 79−28747
NH_4NO_3 soln., Raman spectral studies of NO_3^- motion and interaction 78−92067
$(NH_4)_2(RuCl_5NO)$, polarised Raman and IR spectra, vibr. anal. 77−69819

Raman spectra of inorganic liquids and solutions continued
N_2O, in soln., IR and Raman band shapes, mol. dynamics, ν_3 band 77−36238
N_2O, in soln., Raman and IR ν_1 and ν_2 band shapes, mol. motion dynamics 78−64352
N_2O, pure liq., mol. motion, anisotropic interaction 80−24345
Na_2, liq., vibr. line broadening, Zwanzig-Mori theory and quasi-elastic processes 78−27221
$NaNO_3$, aq. soln., Raman spectra, vibr., orient. relaxation *(French)* 78−62808
$NaNO_3$, in liq. NH_3, Raman spectra, curve resolution anal. 77−82610
$NaNO_3$ soln., Raman spectral studies of NO_3^- motion and interaction 78−92067
Na_2O-SiO_2, aqueous solns., Raman and IR spectra, pH depend., species at equilib. identification 79−87866
NaOH water solution, struct. props. of disordered systems, Raman spectral study 77−4631
$NbCl_5$ in chloroaluminate melts, Raman spectral study 80−34915
$NiCl_2$, aq. soln., Raman spectrum, local order 78−84563
O_2 dissolved in Ar, mol. orientation, Raman spectrosc. obs. 80−52994
O_2, liq., pure vibr. Raman spectra 80−97262
O_2, liq., Raman Q branch temp. depend., interferometric obs. 77−43987
O_2, liq. spontaneous Raman scatt., vibr. dephasing, review 77−28568
O_2, phase equilibria near 298K, Raman spectral study of solid and fluid 80−19937
PD_3, liq. and plastic cryst. states, vibr. dephasing and correl. functions 79−69036
PHD_2, vibr. dephasing in liq. and solid PD_3, calcs. 80−19884
$(PMo_{11}O_{39})_7$ decomp., in aq. soln., Raman spectra obs. 79−13719
Pt complexes, $Pt(NH_3)_4Cl_2$, $Pt(ND_3)_4Cl_2$, Raman spectra in solid state and aq. soln. *(French)* 79−19876
$3RbNO_3-2Ca(NO_3)_2$, glass form. from liq., struct. transform., Raman spectrum obs. 80−64916
SCN^-, associated with metallic cations in aq. soln., press. effect, Raman spectra *(French)* 78−80333
SF_6, dissolved in O_2 and Kr, cryogenic liqs., mol. motions, IR and Raman spectra 79−69823
SF_6-N_2O solution, IR and Raman rot. correl. functions, expt. and theory 79−46541
S_4N_4, solid and soln., IR and Raman spectra, vibr. assignment 78−74659
$S_3N_3Cl_3$, solid and soln., IR and Raman spectra, vibr. assignment 78−74659
$S_4N_4H_4$, and -d_4, solid and soln., IR and Raman spectra, vibr. assignment 78−74659
$S_{8-x}(NH)_x$, (x=1,2,3,4), and deuterates, IR and Raman spectra, isotope shifts, mol. vibr. assignment 79−10110
SO_2 liquid, short range orientation effects, vibr. Raman spectra 80−2759
$SO_3^{2-}+BrO_3^-$, fast oxidation in acid medium, laser Raman multichannel spectroscopy 78−27754
SO_4^{2-}, ν_1 linewidth, in acidic aq. soln. 77−65481
$S(SiD_3)_2$, gaseous, liquid, solid phases, molecular vibr. exam. 78−25547
$S(SiH_3)_2$, gaseous, liquid, solid phases, molecular vibr. exam. 78−25547
$SbCl_3/AlCl_3$ molten mixtures, Raman spectra 80−93305
$SbCl_5$-$NbCl_5$, melt and solid-soln. Raman spectra, $SbNbCl_{10}$ dimer *(German)* 77−4645
Se, Raman scatt. meas., comparison with amorphous Se spectra 80−50328
Se, Raman spectra, crystn. processes 80−60608
$SeCl_4$-$SbCl_5$ systems, Raman spectra *(German)* 80−93324
SeO_4^{2-} ions in aqueous solns. of halides at 4.2-290K *(Russian)* 77−28624
$SiH_3PH_2BD_3$, liquid, vibr. analysis, spectra and structure of P-B compounds 78−84586
$SiH_3PH_2BH_3$, liquid, vibr. analysis, spectra and structure of P-B compounds 78−84586
$SnCl_2$-AlkAlCl$_4$ melts (Alk=Li, Na or Cs) 79−99874
$SrCl_2$, aq. soln., Raman spectrum, local order 78−84563
Te, Raman spectra, crystn. processes 80−60608
$TlNO_3$, molten and aqueous soln., Raman spectra 79−78673
YCl_3-MCl melt, M=Cs, K, Li, Raman spectra 77−59567
$ZnCl_2$, aq. soln., Raman spectrum, local order 78−84563
$ZnCl_2$-$CdCl_2$ melt, Raman spectra, struct. anal. 79−38549
$ZnCl_2$-$ZnBr_2$ melt, Raman spectra, struct. anal. 79−38549
$ZnCl_2(Br_2)(I_2)$ glassy aqueous solutions, Raman spectral study 80−84738
$ZrCl_4$, cryst., melt, gas, Raman spectra interpretation *(German)* 79−28753

Raman spectra of inorganic solids
adamantane, plastic cryst. lattice vibr. study of phase transition 80−7355
adsorbed diatomic on electrode, reson. Raman scatt. 79−51421
alkali bisulphites, and disulphites, and isotopic forms, solid and soln., Raman spectra assignments 79−42968
alkali borates, vitreous and cryst., vibr. spectra and struct. comparison 78−23470
alkali germanate glasses, struct., Raman scatt. obs. 80−1936
alkali halates, NQR freq. temp. depend., phonon spectra interpretation 77−12226
alkali halide: S_2^-, laser-excited spectra and reorientation of S_2^- 77−28563
alkali halide, lattice dynamics calc., extended three body force shell model 78−47491
alkali halide, lattice vibrs., effect of NO_2^- impurity molecule, theory 77−35654
alkali halides, F-centres, first order Raman scatt. *(French)* 78−2828
alkali halides, localised vibration of interstitial H atom 80−88998
alkali halides, resonance Raman scattering, electron-phonon interaction for F centres 78−68519
alkali metal hexachlorotellurates, $A_2(TeCl_6)$, (A=Cs, Rb, K), IR and Raman spectra, lattice and internal modes, phase transition 78−6659
alkali metal tetrafluoroborates, intramol. force fields and mean vibr. amplitudes 80−2743
alkali metaphosphate glasses, low frequency Raman scattering and glass transitions 79−95745
alkali sulphates, SO_4^{2-} optical and spectroscopic props., cryst. environment effect 77−40224
alkali-alkaline earth ceramic solid solutions, with tetragonal tungsten bronze struct., low freq. optical modes 78−76477
alkaline nitrates, Raman and Brillouin scattering, temp. influence on freq. of NO_3^- ion *(French)* 79−69833

Raman spectra of inorganic solids continued
alkaline trihydrogen selenites, ferroelec. phase transitions, Raman spectra 77−8525
alunite-jarosite, spcae group refinement by means of vibr. spectroscopy 79−94981
amorphous semiconductor, local order as determined by electronic and vibrational spectroscopy 79−37627
antiferromagnetic polaritons, inelastic light scatt., theory 77−73144
antiferromagnetic semiconductor, magnon-spin flip excitations in Raman scatt., g-factors 77−66494
arsenates, $M^{II}M^{IV}(AsO_4)_2$, (M^{II}=Ba,Sr; M^{IV}=Ge,Ti,Sn,Zr,Hf), vibr. spectra, cryst. struct., bonding 77−36225
B_2O_3-Li_2O-LiCl, ionic conductor, IR refl. Raman study 80−66173
benzene, liq. and adsorbed mol., Raman spectra using pulsed laser and gated detection 77−74529
binary alloys, three mode, long wavelength optical vibr., appl. to Ge_xSi_{1-x} 78−6135
binary oxides fluorite related struct., order-disorder phenomena, Raman spectra 77−65960
borate glass:Cr, Raman spectra of Cr^{VI} 77−52076
boroxyl ring breakdown in vitreous B_2O_3, Raman intensity investig. 80−45058
butoxybenzylidene-aminobenzonitrile, crystalline and liq. cryst. states, low freq. spectra 78−34437
carbon tetrachloride, solid, phase transition, Raman study 78−80345
carbons, in 2600-3300 cm^{-1} region, heat treatment temp. effect 79−42955
$CdSiP_2$, one- and two-phonon Raman scatt. 79−78681
chalcogenide magnetic semiconductors, spinal-type, closed tube vapour transport method *(Japanese)* 80−25539
cloud rotational Raman and double scatt., lidar meas. 78−77318
cokes, graphitised, Raman spectra, effective Debye parameter, magnetoresist. 78−44231
cryolite, hydrothermal synthesis of large synthetic single crystal, props. 78−19654
cryst., vibr. spectrosc. *(French)* 78−6667
crystal, first order Raman effect, polariton, exciton *(Rumanian)* 77−48172
crystal optics and Raman intensities 79−4795
cubic crystal, Klebsch-Gordon coefficients and two-phonon resonance Raman scatt. *(Russian)* 79−1755
diamond, coherent nonlinear two-phonon Raman spectra 79−19878
diamond, Gruneisen spectroscopic mode parameters via Raman spectra 77−7876
diamond, light coupling prism, Raman spectra for thin film props. study 80−88978
diamond, resonant Raman scatt., first and second order 78−60471
diamond, resonant Raman scattering 78−48176
diamond, two-phonon bound state, Raman freq. 80−65179
diamond, two-phonon Raman peak linewidth, bond polarisability model 77−77212
diamond, two-phonon Raman spectrum, harmonic pot. and bond polarisability model 77−77213
diamond-type crystal, lattice dynamics from Keating's valence force field 78−79687
electrolyte, soln. and cryst. *(German)* 80−80804
ferroelectrics, critical hyper-Raman scattering 78−76466
ferromagnetic semiconductor, Raman scatt. due to magnon-spin flip of cond. electrons 77−20839
ferromagnetic semiconductors, Raman scattering of light on plasmon excitations 80−2738
fluorides with rutile struct., exptl. determ. by Raman absolute cross section 78−56471
fluorite structure solids, long wavelength behaviour, elastic consts. 79−87441
fluorite type crystal, effects of anharmonicity and disorder on Raman scatt. at high temp. 78−80349
four-wave mixing spectroscopy in crysts., nonlinear spectroscopy developments 80−91861
gemstones, light coupling prism, Raman spectra for thin film props. study 80−88978
glass:Nd^{3+}, $^4I_{11/2}$ level population enhanced by Raman scatt. 77−36290
glass, alkali-alkaline earth nitrates, Raman spectra, vibr. perturbations effect 79−8132
glass, localised acoustic phonons, effects on thermal cond. and Raman spectra 77−81092
glass, low freq. Raman scattering by defects 77−8580
glass, low-freq. Raman scatt., 6-700K, excess scatt. 78−23473
glass, porous Vycor, surface phonons, Raman and IR reflectivity spectra meas. 78−38931
glass, relaxation phenomena and Raman spectroscopy, review of developments 78−22665
glass fibre waveguide, polymer cladding effect 78−30073
glass structure, vibr. spectroscopy studies 80−84732
glasses, elec., mag., and optical props., conference, Troy, NY, USA (Aug. 1979) 80−105417
graphite, E_{2g} mode splitting, two-phonon spectrum 78−92077
graphite, finite-size crysts. first- and second-order Raman scatt. 79−95759
graphite, ground natural, grinding influence 79−42956
graphite, H^+, D^+, He^+ ion bombardment, Raman scatt. and SEM anal. 77−35609
graphite, long wavelength lattice vibrations, Raman and IR reflectivity spectra 78−75746
graphite, obs. of anomalously sharp feature in second order Raman spectra 77−81103
graphite, optical probe of lattice dynamics 78−35131
graphite, pyrolytic, neutron irrad., Raman spectra, point defects 77−69834
graphite and graphitic intercalation compounds, lattice dynamics 78−34574
graphite and luminesc. 78−23460
graphite intercalated with AsF_5, HNO_3 and $SbCl_5$, Raman scatt. in low stage cpds. 80−20638
graphite intercalated with Cs(K) donor atoms, Raman scatt. 78−10890
graphite intercalation compounds, C_8M, (M=K, Rb, Cs), Breit-Wigner line shape anal., Raman spectra 80−50336
graphite intercalation compounds with Rb Raman scattering 78−35130
graphite intercalation cpds., Raman scatt. and IR refl., review 80−45066
graphite interclation with Li, Raman scatt. study 80−88999
graphite-$AlCl_3$, well-staged, Raman and IR spectra 80−50339
graphite-Br_2, in-plane intercalate lattice modes, Raman scatt. 79−42163
graphite-Br_2 stage 2 intercalation cpds., Raman spectra 80−80787
graphite-$FeCl_3$ intercalation complex, IR and Raman spectra study of optical modes 79−56797
graphite-$FeCl_3$ layered compound, lattice modes, Raman spectra 79−95785
graphite-halogen intercalation compounds 77−12390
graphite-HSO_3F intercalation compound, Raman spectral study *(French)* 80−60581
graphite-Rb intercalation compounds, Raman scatt. from in-plane lattice modes 78−15168
gypsum, struct., vibr. spectroscopic obs. *(Russian)* 78−15175
heavily doped, Raman phonons, interband excitation effects 78−52501
hot electron distribution functions, expts., review 78−27231
ice, amorphous, 2500-4000 cm^{-1} Raman and IR spectra, vibr. anal. 77−59562
ice, hexagonal, Raman spectra of temp. depend., 80 to 250K, translational vibr. modes 77−36221
ice, hexagonal, Raman spectrum of translational lattice vibrs., press. effects 79−24304
ice, Ih, polycryst., vibr. spectrum anal., OH stretching region 79−11412
ice, Ih-phase, oriented single cryst., proton distrib., light scatt. obs. 77−16318
ice, isotopic, I_H, single crystal Raman intensities, OH bond polarisability, librational modes 78−27208
ice, O-H and O-D bond stretching vibrs., Raman spectra at atmospheric press. 80−66166
ice, press. effects on Raman spectrum 78−95582
ice I, assignment of O-H stretching bands in disordered state 78−19454
ice I, OH stretching region anal. of vibr. spectra 77−59563
ice I, polycryst., 2500-4000 cm^{-1} Raman and IR spectra, vibr. anal. 77−59562
ice VI, high-pressure Raman spectra, bending and librational bands 78−68499
ice VI, OH stretching peak freq. press. depend., Raman spectra using diamond anvil cell 80−16023
ice VI, VII and VIII, press. up to 35 kbar 77−87839
II-VI semiconductor, resonant secondary emission spectra, relax. of energy and polarisation 80−93331
III-V semiconductors, electronic Raman scatt. on donor levels, transition matrix element determ. 79−56792
incommensurate structure, IR and Raman activity of soft modes, appl. to K_2SeO_4 79−28738
inert gas, self-consistent phonon theory, book contrib. 77−51460
inert gas solid, two-phonon Raman light scatt. 79−56783
interband electronic Raman scattering, three band semiconductor, resonant EM field 78−23452
ionic crystals, dispersion calcs. of cubic nonlinear susceptibility near Raman resonance 79−94292
ionic crystals incorporating S-state ions, expt. exam. 79−28326
layered compound, anisotropy of lattice vibrs., polarisable ion model 77−35642
Lennard-Jones, glass, Raman spectrum calc. 78−48165
linear conductor, dynamical aspects of fluctuations 79−33715
lithium ammonium tartrate monohydrate, struct. phase transitions, light scatt. meas. 79−95774
$M^IM^{IV}IO_6$, vibr. spectra (M^I=Na,K,Rb,Cs,NH_4; M^{IV}=Ge,Sn,Pb) 77−42325
metal, electronic X-ray Raman scattering, many-body suppression 77−20953
metal oxide metaphosphate glasses, vibr. study of metal cation reduction at surface 78−56797
metal oxides, cation ordering effect on Raman spectra 78−43850
metal surface, rough, anomalous low-freq. Raman scatt. from localised acoustic vibrs. 80−93307
metal surface molecule enhanced Raman scatt., rough surface spheroidal model 80−84744
mixed alkali glasses, Raman and far IR spectra, vib. at cation site, struct. 78−60435
mixed crystals, reson. Raman scatt. of light by longitudinal optical phonons 77−28577
molecular crystal, lattice vibr., Raman and IR obs., review 78−43079
molecular crystals, non-dipole vibr., Raman effect *(Russian)* 78−76471
molecular optical laser examiner appl. 80−62737
molecular reorientation barrier, from LF lattice vibr. spectra 77−69824
niobates, columbite struct., IR and Raman spectra *(French)* 78−19485
nitrate salts, Raman spectra, thermally disordered energy states 78−35122
non-crystalline materials of low atomic number, X-ray Raman edge extended modulation for struct. study 80−49111
noncentrosymmetric crystals, anti-Stokes stimulated Raman scatt. by polaritons 79−36962
nonmetals, Raman scatt. from impurities, phonon effects 79−24299
nonmetals, Raman scatt. of impurities, anharmonic effects 79−24300
optical fibres, Raman scatt., guiding structs. effects on spontaneous and stimulated emission 80−58636
optical glass, Raman scatt. and nonlinear refr. index 80−2749
oxide semiconductor crystals, with forbidden energy gap, review of spectroscopic props. 78−2876
oxyanions, in nuclear waste materials, laser Raman spectrometric determ. 78−35743
parametric Raman scatt. in crystals *(Russian)* 79−18476
perovskites, ordered cubic, cationic effect on intramolecular forces, stretching force const. 80−88979
perovskites, Raman scatt. and ferroelec. soft modes 77−16300
phosphate glasses, cation-site interactions 80−2744
phosphate glasses, non-alkaline, transition states, phys. effects of fluors, phase diagrams and optical effects *(German)* 80−88045
phosphates, $M^{II}M^{IV}(PO_4)_2$, (M^{II}=Ba,Sr; M^{IV}=Ge,Ti,Sn,Zr,Hf), vibr. spectra, cryst. struct., bonding 77−36225
picosecond interactions for vibr. relax. meas., book contrib. 77−65057
point defects in crystals, book 77−47442
polar crystal, vibronic levels for Jahn-Teller impurities 78−68520
polar crystals, vibrational Raman scatt. induced by Jahn-Teller systems 79−69830
polar semicond., secondary radiation intensity oscills., effect of high mag. field 79−19880
polar semiconductor, secondary emission, multiphonon cascade process *(Russian)* 78−2850

Raman spectra of inorganic solids continued
polar semiconductor crystalline thin films, surface vibr. states, IR absorpt. spectra obs. *(Russian)* 80−60606
polar semiconductors, resonant magneto-Raman scatt. 79−51958
polycrystalline samples, Raman intensities and Raman tensor invariants 77−85696
polycrystalline specimens, effect of cryst. size on parameters of LF Raman spectrum *(Russian)* 77−28581
polysulphur nitride:bromine, struct. and phase transition 80−24382
α-quartz, anharmonic effects *(Russian)* 77−32382
quartz, fused, hyper-Raman scatt. and longit.-transverse splitting of vibrs. 79−73953
α-quartz, laser Raman line polarisation meas. 77−4641
quartz, neutron irradiated, annealing effect on optical props. *(Russian)* 77−32381
α-quartz, Raman FTIR spectra, surface layer and vol. spectra comparison 78−52491
α-quartz, Raman spectral lines, radiation and temp.-induced changes in width and intensity 78−2859
α- quartz, Raman spectrum, piezospectroscopic behaviour 78−35138
α-quartz, Raman spectrum of optical phonon mode, stress splitting and wave-vector depend. 77−77214
quartz glass, $Si^{+}O^{-}$ defect bands, Raman intensities, thermal treatment effects 79−15444
Raman spectra, vibr. anal. 80−93312
rare earth chlorides, doubly degenerate E-phonons, mag. field splitting 77−43297
rare earth compounds, Raman light scatt., phonons and valence fluctuations, review 77−63415
rare earth double orthophosphates with alkali metals, spectroscopic obs., struct. and chem. nature 80−100674
rare earth orthoferrites, Raman scatt. from magnons, anisotropy consts. determ. 80−66178
rare earth orthophosphates, RPO_4 (R=Tb, Dy, Ho, Er, Tu, Yb, Lu), IR and Raman spectra 80−34904
rare earth oxyphosphates, IR and Raman spectra, vibr. assignments, cryst. struct. charcts. 80−97258
rare earth perrhenates, $(ReO_4)^-$ ion vibrs. rel. to static field, Raman investig. *(Russian)* 78−76470
rare earth perrhenates, Raman spectra, $(ReO_4)^-$ ion normal vibrs. rel. to static field 79−65858
rare earth phosphors, Ln_2O_2S:Eu, Raman spectra, lattice vibrs. 79−78669
rare earth sulphides-1.8 Ga_2S_3 glasses, vibr. spectra, electronic transitions, short range order 77−69820
rare earth thiosulphate, $R_2(S_2O_3)_3.4H_2O$, possible evidence for nonexistence of cpd. of given formula *(French)* 77−24279
rare earth titanates, $R_2Ti_2O_7$, synthesis and phys. props. 79−43128
rare earth trichlorides, mag. phonon splitting 77−52099
rare earth trihydroxides, cryst., Raman spectra, vibr. assignments 78−76455
rare earth zirconate, $R_2Zr_2O_7$, Raman spectra, anion disorder characterization 80−25358
rare earth-gallium sulphide glass, R_2S_3-1.8Ga_2S_3, vibr. and electronic spectra, short-range order 78−27228
resonance Raman scatt. singularities *(Russian)* 80−89007
resonance Raman scattering, influence of mass defect disorder 78−35133
resonance Raman scattering with tunable lasers, review, appls. 78−94247
resonant Raman scattering via virtual exciton 80−71412
Rochelle salt, ferroelectric, Raman and IR study 80−71406
ruby, 29 cm^{-1} phonon propag. and lifetime, reson. scatt. *(Russian)* 78−34581
ruby, optically-pumped, excited-state Raman processes 79−4798
ruby, Raman ^2E and phosphorescence transitions, line widths, time correl. study 80−20621
β-Sb_2O_3, Raman spectra, vibr. anal. 80−93312
semiconducting crystal, opaque, inelastic dynamical light diffraction 80−25399
semiconductor, direct band gap type, polariton theory of reson. electronic Raman scatt. on neutral donor levels 80−108194
semiconductor, excitons, exciton-phonon interaction, review, book contrib. 80−49624
semiconductor, ferromagnet, light scatt. from magnons under strong fields, appl. to $CdCr_2Se_4$ 78−84554
semiconductor, light scatt. spectra, interference effects 79−82977
semiconductor, optical props. under intense laser fields 78−72513
semiconductor, radiative spectra from hot photocarriers 78−31249
semiconductor, Raman scattering from impurities 78−56468
semiconductor, Raman scattering from impurities 78−56469
semiconductor, resonant Raman scatt. *(Japanese)* 78−76459
semiconductor, saturated, dielectric response 78−10384
semiconductor, sound absorption at very low temps. 79−95089
semiconductor, vibr. IR excitons, spectra *(Russian)* 78−15173
semiconductor, zinc-blende struct., shallow acceptor contribution to near-resonance spin-flip Raman scatt. 79−95754
semiconductor alloys, reson. light scatt., luminesc. and Raman spectra 79−38615
semiconductor with complex band struct., free carriers effect 77−44001
semiconductors, elemental amorphous, vibr. props., review 77−84873
semiconductors, exciton effect in interband electronic Raman scattering 80−103946
semiconductors, extrinsic covalent, Raman scatt. of light by phonons 77−73147
semiconductors, light induced electron drift, two-photon transitions *(Russian)* 80−107853
semiconductors, optical props. due to phonons, book contrib. 80−80805
semiconductors, polar, resonance electron-phonon Raman scatt., cross-section oscills. 80−60598
semiconductors, resonant Raman scatt. from exciton-polaritons *(Japanese)* 80−50349
semiconductors, spin orientation by optical pumping, review 79−38410
semiconductors *(German)* 79−28729
semiconductors with direct band gaps, exciton-polariton interactions, Green's function approach 80−92831
silicate glass:Cr, Raman spectra of Cr^{VI} 77−52076
silicate glasses containing AsO_4^{3-} ions, fining mechanism 77−12379
silicate glasses containing sulphate, Raman scatt. meas. 77−69818
silicate minerals, thermodynamics and lattice vibr. props. 79−100830
space group refinement by vibr. spectroscopy methods, possibility 78−79507

Raman spectra of inorganic solids continued
steel, stainless, surface oxide characterisation by Raman spectroscopy 80−50308
superconducting alloy containing paramag. impurities, Raman scatt. of light 79−73634
superconductor and normal metal, Raman sound scattering *(Russian)* 78−23199
superconductors, phonon Raman scatt. 80−100657
superionic conductor, model taking account of polarizability changes due to ionic motions 78−2855
superionic conductors, light scatt. and IR absorpt. book contrib. 80−25382
superionic conductors, phase transitions and dynamics 78−59924
superionic conductors, Raman scattering from mobile ions, theory 78−80352
talc, vibr. mode assignments, Raman microprobe spectra 80−88977
tetracyanoplatinate conductors, IR and Raman spectra, cyanide stretching vibrs. 79−11415
tetrahedral glass AX_2, band limits and vibrational spectra 79−73935
tetramethylammonium hexabromotellurate, far IR and Raman spectra and phase transitions 80−11376
TGS, ferroelec., phonon contributions to anomalous sp. ht. near phase transition temp. 77−52023
TGS(Se), optical phonons near T_c, IR refl. and Raman spectra 77−48136
TGS(Se), optical phonons near T_c, nonlinear pseudospin-phonon interaction 77−48137
thiourea, ferroelectric, Raman and IR study 80−71406
tourmaline, Raman spectra 79−4801
transition metal complex anion, vibr. spectra in solid and soln., struct. and fundamental mode assignment 78−62803
transition metal hexafluorides, density of exciton states, two-particle and mixed cryst. spectra 78−2829
trissarcosine calcium chloride, ferroelec. phase transition, Raman and Brillouin scatt. studies 80−71340
two-photon reson. Raman scatt. by excitons via intermediate excitonic mol., polarisation and polariton effects 78−10880
two-photon reson. scatt. by excitons via intermediate excitonic mol. 77−52086
vibrational dynamics of liquids and solids, Raman scatt. of picosecond light pulses 78−94414
water, low-density amorphous solid, OH stretching spectrum 79−11413
water, low-density amorphous solid, Raman spectra, OH stretching region 79−11410
zero-gap semiconductors, reson. two phonon absorpt. 79−55847
Ag electrode, adsorbed cyanide, enhanced Raman effect 80−50348
Ag, sorption of pyridine, surface enhanced Raman scatt., mol.-surface separation depend. 80−92775
Ag surface, electrochemically roughened, nature and role in promoting anomalous Raman scatt. intensity 78−84587
Ag, surface roughness induced electronic Raman scatt. 80−50347
Ag, with adsorbed Cl monolayer, enhanced Raman intensity 79−95766
Ag/CN, coverage meas. using surface enhanced Raman scatt. and radioisotope meas., electrochemical treatments 80−29260
Ag_3AsS_3, and Ag_3SbS_3, Raman spectra obs. of low-temp. phases 80−93327
Ag_3AsS_3, proustite, cryst., vibr. spectra 78−48172
Ag_3AsS_3, proustite, phonons and soft modes at ferroelec. transition 80−60524
AgBr, dispersive phonon modes, reson. Raman scatt. obs. 78−10896
AgBr, exciton relax. by intervalley scatt., reson. Raman meas. 79−33713
AgBr, exciton relaxation by intervalley scattering 80−20644
AgBr, lattice dynamics, 295K, three-body-force shell model 77−15517
AgBr:AgCl, mixed crystals, first order reson. Raman scatt., momentum conservation relax. 79−56790
AgBr:Cl, exciton-phonon interaction, reson. Raman scatt. vs photolum. 80−29798
$AgClO_3$, γ-irradiated, resonant Raman effect of O_3^- centres 78−48178
$AgGaS_2$, degenerate mods, temp. depend. 78−35150
Ag_2HgI_4, ordered and disordered phases Raman spectra temp. depend., ion hopping 78−23438
Ag_2HgI_4, polycryst., Raman spectra, press. depend. 77−73137
Ag_2HgI_4, Raman line shape and ionic cond., coupled mode model 80−66171
AgI, α and melt phases, light scatt. from correl. ion fluctuations 79−95771
AgI, density of states, IR cond., and Raman scatt., lattice dynamics calc. 78−30709
α-AgI, ionic motion, low freq. Raman scatt. 78−80354
β-AgI, polariton dispersion curves, Raman spectra 80−29338
α-AgI, superionic, continuous order-disorder transition, Raman spectroscopic evidence 80−45070
α-AgI, superionic cond., compared to liquid like model 78−2855
α-AgI, superionic cond., sublattice melting, Raman spectra, rel. to AgBr(Cl) melts 78−10882
α-AgI, superionic conductor, Raman spectra, freq. depend. cond. exam. 78−10883
α-AgI, superionic conductor, Raman scattering evidence for sublattice melting 78−80350
AgI, superionic conductor, Raman study 78−80353
AgI, superionic conductor, lattice dynamics 79−95111
α-AgI, superionic. liquid-like Raman scatt. 79−95769
β-AgI, temp. depend. of anomalous and ordinary Raman scatt. 79−19890
$Ag_{26}I_{18}W_4O_{16}$, struct. phase transition, dielectric, cond. and Raman obs. 79−19368
Ag_2MI_4 (M=Cd, Zn), fast ionic cond. and order-disorder transition 79−99363
$AgNO_3$, cryst. and molten salt, Raman and IR spectra, vibr. anal. 77−16311
$AgNO_3$, differences between diffr. and vibr. spectroscopic results 79−69818
$AgNa(NO_2)_2$, ferroelectric phase transition, theory 79−24272
$AgNa(NO_2)_2$, ferroelectric transitions, group theoretic comparison with $NaNO_2$ 80−7311
$AgNa(NO_2)_2$, ferroelec., Raman scatt. and phase transitions 80−71349
$AgNa(NO_2)_2$, ferroelec. cryst., Raman spectrum, phase transition, comparative anal. with $NaNO_2$ 80−88935
$AgNa(NO_2)_2$, Raman spectrum, NO_2^- bending vibr. 79−28737
$AgPO_3$-Ag_2SO_4, new Ag^+ and Li^+ ion glass conductors, glass transition, Raman spectra *(French)* 79−47094

Raman spectra of inorganic solids continued
$AgPO_3$-CdI_2 glasses, ionic conductivity and structure *(French)* 78−67854
$AgPO_3$-$HgI_2(CdI_2)(PbI_2)$ glass, elec. cond. and Raman. spectra rel. to struct. *(French)* 79−10979
Ag_xTiS_2, intercalation cpd., Raman scatt. and electron diffr. meas. 79−24321
$Ag_xV_2O_5$, metallic, Raman scatt. 78−80358
$Ag_8W_4O_{16}$, high temp. Raman spectra exam. 77−36236
$AlBr_3$, Raman IR spectra, organic solvent effect *(German)* 77−3370
AlF_3 based glasses, chem., thermal and optical props. *(French)* 80−70139
AlF_3-M_2F glasses, M=alkaline earth, density-of-states and structural forms, Raman spectra study 80−97255
$Al_{0.5}Ga_{0.5}As$, first order phonon spectrum replicas 78−60467
$Al_xGa_{1-x}As$, Raman spectroscopy, characterisation of thin films and heterostructures 78−76439
$Al_xGa_{1-x}Sb$, vibr. spectra, Raman light scatt. study 80−45080
β-AlO_3-$(Na,Li)_2O$, NMR, Raman and IR spectra, and X-ray diffr., heat treatment induced changes 80−107508
Al_2O_3, Raman spectroscopy study of adsorbed molecules 80−65358
β-Al_2O_3, stoichiometric, Raman and IR spectra, Frenkel defects, order-disorder transition and cation cond. 80−55086
η-Al_2O_3, surface, laser Raman fluoresc. background, OH^- excitation 78−10875
α-Al_2O_3:Cr^{3+}, electronic Raman transition from optically pumped excited state 78−39531
α-Al_2O_3:Cr^{3+}, Raman effect to probe dynamical processes of Cr^{3+} photoexcited states 80−2740
Al_2O_3:Mn^{3+}, electronic and vibronic Raman scatt. 78−2839
β-Al_2O_3:NH_4^+(Nd_4^+), polarised Raman scatt. 80−103947
α-Al_2O_3:V^{4+}, emission spectrum, Jahn-Teller effect in $^2T_{2g}$ and ^2E_g states 79−83007
β-Al_2O_3-$(Na,Li)_2O$, β-Al_2O_3-$(K,Li)_2O$ and β-Al_2O_3-$(K,Sn)_2O$, ionic cond. and Raman spectra 80−107509
β''-Al_2O_3-Ag_2O, Raman scatt. from mobile cations 80−11394
β''-Al_2O_3-$Ag_2O(K_2O)(Li_2O)(Na_2O)(Rb_2O)$, single cryst. Raman scatt., cond. mechanism and cryst. struct. 80−66209
β-Al_2O_3-H_3O^+ protonic cond., struct. investig. 79−19213
β-Al_2O_3-$H^+(H_2O)_n$, IR and Raman spectra, OH stretching freqs., struct. and cond. 78−27210
β''-Al_2O_3-K_2O 80−11394
β-Al_2O_3-Li_2O, Raman scatt. from $^6Li^+$ and $^7Li^+$ ions 79−28766
β-Al_2O_3-NH_4^+, protonic cond., struct. investig. 79−19213
β-Al_2O_3-Na_2O, cation vibrations, disorder and hydration, IR and Raman spectra *(French)* 80−7343
β-Al_2O_3-Na_2O, low freq. Raman scatt. from NH_4^+ ions 78−43878
β''-Al_2O_3-Na_2O, Raman scatt. from mobile cations 80−11394
β-Al_2O_3-Na_2O-K_2O, cation interstitial pair modes in vibr. spectra 79−37788
β-Al_2O_3-Na_2O-Rb_2O, cation interstitial pair modes in vibr. spectra 79−37788
β-Al_2O_3-$Na_2O(Ag_2O)$, Raman scatt., 12-400K, 2nd order phase transition 77−81091
β-Al_2O_3-X_2O, (X=Na,K,Rb,Ag,Tl), infrared and Raman spectra 79−1761
Al_xO_y, Raman spectra using pulsed laser and gated detection 77−74529
$Al_x(OH)_y$, Raman spectra using pulsed laser and gated detection 77−74529
γ-AlOOH and γ-AlOOD, struct. and D_{2h}^{17} space group anal. 80−89000
$AlPO_4$, α-β cristobalite phase transition, Raman meas. 79−4799
α-$AlPO_4$, berlinite, H_2O conc. determ. by Raman scatt. 80−76572
α-$AlPO_4$ crystal, totally symm. high-freq. fund. vibrs., identification refinement 80−100656
α-$AlPO_4$, IR and Raman spectra, optical phonons 80−2767
Al_2SiO_5, andalusite, phonon spectra and rigid-ion model calcs. 80−11391
amorphous, Raman scatt. investig. of irreversible thermostruct. transform. 77−48163
Ar crystals, first order Raman scattering, evidence for HCP phase 78−23454
Ar, low temp. Raman spectra 78−84580
Ar:NO_2, Raman spectra, high press., low temp. effects 78−52479
Ar:O_2 (6%) cryst., vibr. Raman spectra 80−60558
As, amorphous, bonding coordination defects, Raman scatt. and IR absorption meas. 78−60498
As, amorphous, intermediate range order from polarised features of Raman spectrum 80−49113
As, amorphous, optical, vibr., transport and defect-related props., review 79−51935
As, amorphous, vibr. excitations at defect sites, IR and Raman spectra calc. 80−49329
As, amorphous, vibrational excitations of defect sites 80−49332
As amorphous films, interference enhanced Raman scatt. 80−50326
As, black phosphorous struct., Raman vibr. spectra and bonding 80−11411
As, bulk and sputter-deposited amorphous, vibr. props., Raman spectra meas. 77−63411
As-S glasses, resonance Raman scatt. 80−50325
As-S-I system, glasses, Raman spectra, struct. 79−65857
As-Se amorphous system, Raman scatt. 80−88984
AsD_3, solid and liq., vibr. relax., Raman ν_1 band, 54, 160K 78−27198
As_2O_3, glassy, intermediate range order from polarised features of Raman spectrum 80−49113
As_2O_3, vitreous, local struct. and vibrational spectra 80−55091
As_2O_3, vitreous, Raman and IR spectra 79−73933
As_2O_3-SO_3, polarised Raman and IR spectra, force field calc. *(French)* 78−6674
$(As_2O_3)_n$, claudetite I, vibr. spectra, force field calc. *(French)* 78−60447
As_2S_3, amorphous thin films resonant Raman scattering 78−68505
As_2S_3 crystal, polarisation anal. of Raman spectrum 79−47461
As_2S_3, crystalline, two phonon vibrational spectra 78−35142
As_2S_3 glass, press. effect on optical props. 80−50363
As_2S_3, LF inelastic light scatt. meas. 78−15181
As_2S_3, two-phonon vibrational spectra, crystalline and amorphous forms, Raman and IR spectra 78−39537
As_2S_3-$AsBr_3$, glass, exam. of combination scatter spectra in IR 78−88315
As_2S_5, amorphous, struct., vibr. and electronic spectra 80−64908
As_2S_5-AsSI glasses, IR and Raman spectra, struct. rel. to comp. *(Russian)* 77−81107
Raman spectra of inorganic solids continued
As_2S_x glass, Raman and IR spectra, struct. model 78−80330
As_4S_4, effects of pressure and temp. on phonons, Raman scattering study 80−7360
As_4S_4 polymorphs, Raman spectra, structural implications for As_2S_3 amorphous films 79−61385
As_4S_4, vibrational spectra, effect of temp. and press. on phonons 79−37776
As_xS_{1-x} glass, Raman spectra, chem. struct. *(Russian)* 78−76469
As_xS_{100-x} glasses, Raman spectrum and structure 80−60593
$(As_2S_3)_{1-x}(AsBr_3)_x$ glass, struct. interpretation of Raman spectra 79−65856
$(As_2S_3)_x(AsI_3)_{1-x}$, glass, Raman spectra, chem. struct. *(Russian)* 78−76469
$(As_2S_3)_{1-x}(As_2Se_3)_x$ and $(As_2Se_3)_{1-x}(As_2Te_3)_x$ pseudobinary glasses, comp. depend. of opt. props. 77−90157
$As_2S_3Ge_x$ glasses, vibr. props. and struct., IR refl. and Raman scatt. 79−78682
$(As_2S_3)_{1-x}(GeS_2)_x$ and $As_2S_3Ge_x$ glasses, struct. and vibr. spectra 79−91440
$(As_2S_3)_{1-x}(GeS_2)_x$, LF inelastic light scatt. meas. 78−15181
$(AsSI)_x(GeS_2)_{1-x}$ glasses, Raman and long-wave IR spectra obs. of struct. 79−51964
$As_2S_3(Se_3)$ evaporated films, struct. and thermally induced effects 79−41963
$As_{0.2}Sb_{0.8}SI$ cryst., ferroelec., soft mode Raman and IR spectroscopy 80−76016
$As_xSb_{1-x}SI$ mixed crystals, phonon coupling, ferroelectric phase transition, Raman study 80−108165
As_2Se_3, glossy, Cu, Ag and O impurities influence on electronic energy spectrum and mol. vibr. spectrum 77−90181
As_2Se_3, LF inelastic light scatt. meas. 78−15181
As_2Se_3, photodarkening and photostructural effects, Raman, IR and NQR studies 80−16036
$AuSb_2$, pyrite structure, Raman scatt., phonon frequencies 77−40235
B, amorphous, X-ray Raman edge extended modulation for struct. study 80−49111
B, amorphous, X-ray Raman scatt. 78−48157
B amorphous film, interference enhanced Raman scatt. 80−50326
B, amorphous film, Raman scatt. exam. 78−39545
BN, hexagonal, low freq. Raman active vibr. 78−43880
BN, Raman scatt. exam. of high press. effects on force const. anisotropy 79−38542
B_2O_3 and alkali borate glasses, Raman study at high temps. 80−93306
B_2O_3 glass, struct. and phonon spectra 80−50324
B_2O_3, vitreous, Raman cross sections, rel. to appl. in fibre Raman lasers 78−31176
B_2O_3, vitreous and crystalline, Raman spectra exam. 77−66491
B_2O_3-NaF-$NaBF_4$, crystalline compounds and glasses 78−11210
B_2O_3-V_2O_5-P_2O_5, glass, mech. and elec. props 80−84228
$(B_2O_3)_x$-$(SiO_2)_{1-x}$, spontaneous Raman scattering *(French)* 79−78674
Ba hexafluorometallates, $BaMF_6$, (M=Si,Ge,Sn,Ti), press. up to 25 kbar, anion libration obs. 78−6670
$BaBr_2.2H_2O$, pure and deuterated, low temp. IR and Raman spectra *(German)* 79−19874
$BaCl_2$ film, non-cryst., very-low-freq. inelastic light scatt. 80−25367
$BaCl_2$, non-crystalline film, disorder-induced Raman scatt. 80−11387
$Ba(ClO_3)_2H_2O$, γ-irradiated, resonant Raman effect of O_3^- centres 78−48178
$BaCl_2.2H_2O(D_2O)$, lattice vibr., IR and Raman spectra 79−15443
Ba_2EuNbO_6, luminescence Raman spectra, means for localisation of binding energy levels *(German)* 78−88304
Ba_2EuTaO_6, luminescence Raman spectra, means for localisation of binding energy levels *(German)* 78−88304
BaF_2, polarised Raman scatt. in fluorite crysts., anharmonicity, high-temp. disorder 78−35132
BaF_2, Raman spectra, 15 to 1300K, anharmonic vibr. effects 77−43990
BaF_2, superionic conductor, theoretical investigation of Raman scatt. 78−80351
BaFCl film, non-cryst., very-low-freq. inelastic light scatt. 80−25367
BaFCl, non-crystalline film, disorder-induced Raman scatt. 80−11387
BaFCl, thin film, in vacuo Raman spectra using prism-film coupler 78−24873
$Ba_2KNb_5O_{15}$, Raman scatt. experiments in tetragonal tungsten bronze compounds 80−40113
$BaMnF_4$, phase transitions review 79−78378
$BaMnF_4$, spectroscopy near ferroelec. transition, dielec. anomalies near mag. ordering temp. 80−75965
$BaNB_2O_6$, IR and Raman spectra, vibr. anal. *(French)* 79−91446
$Ba(NO_3)_2$, Raman spectra temp. depend. anomalies in symmetric stretch region 79−61361
$Ba(NO_3)_2$, vibrations of isotopic impurities, IR-reflection and Raman spectra meas. 77−51465
$Ba_2NaNb_5O_{15}$, struct. phase transitions, light scatt. meas. 79−95774
$Ba_2NaNb_5O_{15}$, high press. phase transitions, Raman scatt. studies 80−71402
$Ba_2NaNb_5O_{15}$, optical mode softenings, Raman scatt. meas., 1.5 to 600K 79−33631
$Ba_2NaNb_5O_{15}$, phase transition at high press., Raman scatt. obs. 79−55884
$Ba_2NaNb_5O_{15}$, Raman spectra, soft oscillations, temp. depend. 78−31203
$Ba_2NaNb_5O_{15}$, Raman spectra in elec. field 79−1763
$Ba_2NaNb_5O_{15}$, Raman scatt. experiments in tetragonal tungsten bronze compounds 80−40113
BaO, lattice dynamics, sp.ht., Debye temp. and Raman spectra calc. 77−1195
α-$Ba_2P_2O_7$, Raman, IR spectra, factor group anal. and band assignment 78−35126
$BaSO_4$, polarised IR refl., absorpt. and laser Raman spectra 77−43997
$BaSO_4$, single cryst., SO_4^{2-} vibr. levels, cryst. field effects, laser Raman spectroscopy 78−43847
$Ba_{0.25}Sr_{0.75}Nb_2O_6$, ferroelec., influence of temp. on Raman scatt. spectra 77−69842
$Ba_{0.50}Sr_{0.50}Nb_2O_6$:$La_2O_3(Tm_2O_3)(Y_2O_3)$, Raman spectra 79−78678
$Ba_{0.5}Sr_{0.5}Nb_2O_6$, temp. depend. of Raman spectra 78−72524
$BaTa_2O_6$, structural study X-ray diffr., IR absorpt. and Raman spectra *(French)* 80−107173
$BaTiO_3$, A_1 and E optical phonons obs. in temp. range 10 to 132°C 77−27963

Raman spectra of inorganic solids continued
$BaTiO_3$, A_1(TO) phonon spectrum, ferroelectric phase transition, Raman scatt. meas. 78−56478
$BaTiO_3$, ferroelec. cryst., IR and Raman spectra, mode coupling 80−66194
$BaTiO_3$, ferroelec. phase transition, soft phonons, Raman scatt. obs. *(Japanese)* 79−65880
$BaTiO_3$, ferroelec. temp. depend. of broad A_1 (TO) phonon Raman linewidth 78−2857
$BaTiO_3$, polariton freq. meas. by Raman scattering and permittivity 78−76006
$BaTiO_3$ polymorph, hexagonal, low temp. and surface CO_3 adsorption and desorption, Raman spectra obs. 80−80713
$BaTiO_3$, Raman intensity analysis, symmetry coords., optical modes, electro-opt. consts. 79−95740
$BaTiO_3$, soft mode exam. 79−37799
$BaTiO_3$, struct. phase transitions, light scatt. meas. 79−95774
$Ba_2TiSi_2O_8$, luminescence of TiO_5 group, decay time, IR and Raman spectrosc. 80−2819
$Be_3Al_2(SiO_3)_6:Cr^{3+}$, Raman effect to probe dynamical processes of Cr^{3+} photoexcited states 80−2740
$BeCl_2.4H_2O$, IR and Raman spectra *(French)* 80−20618
BeF_2, vitreous, band limits and vibrational spectra 79−73935
BeF_2, vitreous, IR and reduced Raman spectra, weak Raman bands 78−68498
BeF_2, vitreous, Raman and IR spectra 78−39549
BeF_2, vitreous, Raman spectra meas. 77−20858
$BeSO_4.4H_2O$, IR and Raman spectra *(French)* 80−20618
Bi, k=0 optical phonon temp. depend., Raman scatt. meas. 77−76509
$BiCl_3$, Raman scatt. spectrum, librational and translational vibr. *(Russian)* 77−54562
$Bi_{12}GeO_{20}$, optical phonon freq. in vicinity of Brillouin zone, linear wave-vector depend. 79−19892
$Bi_{2-x}La_xWO_6$, synthesis and crystallography 80−66459
Bi_2O_3 and sillenite struct. derivatives, $MO_x.6Bi_2O_3$, IR and Raman spectra, vibr. anal. 78−76464
BiOCl, cryst. growth, Raman and IR spectra *(German)* 77−21012
$Bi_{1-x}Sb_x$, crystalline, vibrational, spectra, second order Raman scattering 79−47455
$Bi_{1-x}Sb_x$, sputtered thin films, first order Raman scatt. 79−69831
$Bi_xSb_{1-x}SI$, atomic substitution and ferroelec. phase transition 78−68464
$Bi_xSb_{1-x}SI$, low freq. Raman spectroscopy 78−15162
Bi_2Se_3, Raman spectra, Raman and IR-active modes 79−56776
$Bi_{12}SiO_{20}:Sn(Mo)$, Raman scatt. spectra, impurity effect 80−80795
Bi_2Te_3, Bi_2Se_3, $Bi_2(Te_{1-x}Se_x)_3$, Raman and far infrared investigation of phonons 78−23453
Bi_2Te_3, Raman spectra, Raman and IR-active modes 79−56776
$Bi_2Ti_4O_{11}$, anomalous temp. depend. of phonon modes, Raman spectra 78−10893
$Bi_2Ti_4O_{11}:PbO$, anomalous temp. depend. of phonon modes, Raman spectra 78−10893
$BiVO_4$, ferroelastic, observation of soft optical phonon 78−2856
Br_2, condensed phases, spontaneous and stimulated Raman scatt., weak and strong radiation fields 79−3450
C, amorphous, diamond-like 3-fold coord. 80−50323
C, amorphous film, struct. props., Raman scatt. study 80−11417
C, in various forms including graphite, new lines, exam. 78−48169
C_8K(Rb), graphite intercalated, phonon dispersion relations and Raman spectra 80−44272
$(CN)^-$, monolayer on Ag, Raman spectra 78−72520
α-CO, IR and Raman spectra, vibron band, vibron-phonon combination bands 78−68495
CO, solid and matrix isolated, IR and Raman spectra 78−48156
$^{12}C^{16}O$:CO isotopes, IR and Raman spectra, vibron band, vibron-phonon combination bands 78−68495
CO_2, $\nu_2+\nu_2$ biexciton transition in Raman spectra 77−48158
CO_2, solid, Fermi reson. press. tuning, Raman spectra 80−93293
CO_2-N_2O, mixed cryst., librational motion, Raman obs. 78−6661
C_3O_2, ν_2, $\nu_2+2\nu_7^0$ and $2\nu_7^0$ Raman band-accumulations 79−3449
CS_2, liq., two-photon absorpt. meas., using nonlinear light-mixing spectroscopy 77−79620
CS_2, second order Raman spectrum in condensed phase 80−93299
$CaCO_3$, aragonite, split ν_4 mode of CO_3^{2-} ions 80−45077
$CaCO_3$, calcite, A_{1g} Raman mode obs., new technique appl. 79−61354
$CaCO_3$, calcite, coherent excitation of vibr., dephasing time meas. 78−35120
$CaCO_3$, calcite, laser Raman line polarisation meas. 77−4641
$CaCO_3$, calcite crystal, higher-order CARS spectra 79−14035
$CaCO_3$, hyper Raman scatt. of light by optical phonons 79−69844
$CaCl_2(Br_2)(I_2)$, glassy aqueous soln., LF region Raman spectra 80−84729
CaF_2, polarised Raman scatt. in fluorite crysts., anharmonicity, high-temp. disorder 78−35132
CaF_2, Raman spectra, 15 to 1300K, anharmonic vibr. effects 77−43990
CaF_2, superionic conductor, theoretical investigation of Raman scatt. 78−80351
$CaF_2:Dy^{3+}$, cubic cryst. field effects 80−2368
$CaHPO_4.2H_2O$ powder and crystals, vibrational spectra, factor group anal. 80−45076
$Ca_8La_2(PO_4)_6O_2$, IR and Raman spectra 79−78671
$Ca_8La_2(PO_4)_5(VO_4)O_2$, IR and Raman spectra 79−78671
$Ca_8La_2(VO_4)_6O_2$, IR and Raman spectra 79−78671
$CaMgSi_2O_6$, single cryst., IR reflection spectra, vibr. spectrum calc. 77−73142
$Ca(NO_3)_2$, Raman spectra temp. depend. anomalies in symmetric stretch region 79−61361
$CaNb_2O_6$, columbite, polarised Raman and IR spectra, normal coord. anal. 77−76500
$CaO-Al_2O_3-SiO_2$ glasses, density-of-states and structural forms, Raman spectra study 80−97255
$CaO-Na_2O-B_2O_3$, Raman scatt. studies of glass struct. 77−90147
$Ca(OH)_2$ and $Ca(OD)_2$, molecular and lattice dynamics by IR[2] and Raman spectra 77−73134
β- and γ-$Ca_2P_2O_7$, IR and Raman vibr. spectra 80−25355
α-$Ca_2P_2O_7$, Raman, IR spectra, factor group anal. and band assignment 78−35126
$Ca_{10}(PO_4)_6(OH_2)$, polarised Raman and LF IR spectra, lattice vibr. 77−77192
CaR_2S_4, R=rare earth, ternary sulphide with Th_3P_4 struct., vib. spectra 78−2844

Raman spectra of inorganic solids continued
$CaSO_4$, anhydrite and gypsum, phonon spectroscopy, lattice dynamical calc. 80−19889
$CaSO_4(.2H_2O)$, single cryst., SO_4^{2-} vibr. levels, cryst. field effects, laser Raman spectroscopy 78−43847
β-Ca_2SiO_4, stabilisation, IR and Raman spectra 79−42265
$Ca(UO_2PO_4)_2.6H_2O$, calc. and meas. of vibr. spectrum 77−76499
$CaWO_4:Nd^{3+}$, thermal behaviour of shape and width of 9145 Å laser line 78−6755
$Ca(WO_4)_x(MoO_4)_{1-x}$, Raman scatt. line shape 78−10898
CdA_2X_4 (A=Ga,In; X=S,Se), Fourier IR and Raman spectra, cryst. struct. and symm. *(German)* 79−24313
$Cd(ClO_3)_2$ single crystals, Raman scatt. 80−55106
$CdCr_2S_4$, magnetic semicond., resonance Raman scatt., mag. circular polarisation props. 80−50341
$CdCr_2S_4$, phonon Raman scatt., mag. circular polarization effects 79−8134
$CdCr_2S_4$, spin dependent phonon Raman scatt., resonance effects 77−73145
$CdCr_2S_4(Se_4)$, ferromagnetic semiconductors, spinel-type, resonance Raman scattering and electronic structure *(Japanese)* 79−47421
$CdCr_2S_4(Se_4)$, spin depend. phonon Raman scatt., band struct. 78−68491
$CdCr_2S_4(Se_4)$, thermoreflectance, photoconductance, Raman scatt. near mag. phase transition 80−97298
$CdCr_2Se_4$, ferromag. semiconductor, light scatt. from magnons under strong fields 78−84554
$CdCr_2Se_4$, influence of ferromag. ordering on phonon Raman scatt. 78−2853
$CdCr_2Se_4$, resonant Raman scatt. 79−4802
$CdCr_2Se_4$, spin dependent phonon Raman scat., resonance effects 77−73145
$CdGa_2S_4$, Raman scatt. anal., optical phonons 79−73951
$CdGa_2S_4$, vibr. spectra, 33-400 cm^{-1}, symm. transform. *(Russian)* 78−23465
$CdGa_2Se_4$, ordered vacancy compound, Raman scatt. 79−95749
$CdGa_2Se_4$ ordered vacancy compound, Raman scatt. 79−99870
CdI_2, interlayer interactions estimate from Raman and Brillouin scatt. 79−99884
$CdI_2:Fe^{2+}$, polarised electronic Raman scatt. 80−29733
CdI_2-$CdBr_2$ mixed layer cpds., rigid layer modes and van der Waals interactions, Raman spectra obs. 79−33700
$CdInGaS_4$, crystal, Raman scattering spectra, polarisation meas. *(Russian)* 80−71410
$CdIn_2S_4$, photoluminesc., reson. Raman scatt. 78−48179
$CdIn_2S_4$, Raman and IR spectra 78−48181
$Cd_{1-x}Mn_xTe$ mixed crystals, Raman spectra 80−103961
$Cd(NH_3)_6Cl_2(Br_2)(I_2)$, crit. behaviour of light scatt. intensity at phase transitions 77−90141
$Cd(NH_3)_6X_2$, X=Br, Cl, I, orientational phase transitions 80−11382
$Cd_2Nb_2O_7$, Raman-scattering investigation of vibrational structure 78−76441
CdP_2, Raman light scatt. efficiency for He-Ne laser light *(Russian)* 77−52104
CdP_2, Raman spectra, mode symmetry 79−91441
CdP_2, reson. interaction of vibr. states, polarised Raman spectra meas. 77−15521
CdP_2, tetragonal, one and two phonon states using second order Raman spectra 78−43874
CdR_2S_4, (R=Sc, Yb, Tm), IR and Raman spectra, force consts. 78−68503
CdS, doped, amorphous antiferromagnet model, susceptibility and spin-flip Raman scatt. meas. 80−97057
CdS electronic two- and one-photon Raman scatt. via biexcitons, stimulated config. obs. mag. field shift 80−103963
CdS, exciton resonant secondary emission spectrum temporal evolution 79−51499
CdS, pure spin diffusion without charge transport, spin flip Raman scatt. obs. 80−93329
CdS, Raman shift dispersion near exciton reson., two-phonon cascade processes 80−11405
CdS, reson. Raman Scatt. under two-photon excitation of excitonic mols. 78−52486
CdS, resonant Raman scattering by LO phonons 78−39551
CdS, resonant scatt. of exciton polaritons by LO and acoustic phonons 79−95760
CdS, second order polaritons associated with van Hove singularities, light scatt. expt. 77−90146
CdS, spin flip Raman scatt. linear k term 78−19475
CdS, spin-flip line shape 78−88307
CdS, study of electron dynamics by spin flip Raman scatt. 79−95789
CdS, two photon Raman scatt. at high excitation levels *(Russian)* 80−16032
CdS, two-photon absorpt. effect on hyper-Raman scatt. 80−74441
CdS, two-photon absorption coefficient rel. to inverse Raman cross section 78−6678
CdS, two-photon Raman scatt. via biexcitons, angle- and polarisation depend. 79−87446
CdS, virtually excited biexcitons polaritons dispersion, two photon Raman scatt. 80−45067
CdS:Cl, resonant Raman scatt. exam. 78−39546
CdS:F(Cl), shallow donors electronic Raman scatt., reson. enhancement 80−45068
CdS:In, spin flip Raman scatt., electron dynamics 78−80342
$3CdSO_4.8H_2O$, cryst., phonon assisted indirect transitions 78−72559
$CdS_{1-x}Se_x$, zone edge phonon, IR absorpt. and Raman scatt. meas. 77−76508
CdSe, fundamental vibrs., Raman scatt. and IR refl. obs. 78−60451
CdSe, polarisation correl. of resonant Raman scatt. or hot luminesc. 80−25384
CdSe:Li, pure and doped, reson. Raman and Brillouin scatt., elastic exciton-defect scatt. 80−80788
CdTe, excitation spectra, resonant Raman scatt. versus hot electron effects 79−38645
CdTe, reson. Raman scatt. by excitonic polaritons 80−11396
$CdTe_{1-x}S_x$, long-wavelength optical phonons, composition depend., IR and Raman spectra 78−67788
$CdTe_{1-x}Se_x$, Raman scatt. spectra, two-mode behaviour 78−60450
$Cd_{1-x}Zn_xTe$, solid soln., vibr. spectra restructuring anomalies 79−4803
CeB_6, Raman spectra of phonons 79−82972

Raman spectra of inorganic solids continued
$CeCl_3$, doubly degenerate phonon states, mag. field dependent splitting 77−16320
$CeCl_3$, Raman spectra circ. polaris., Faraday effect phonon state splitting 78−43855
CeH_x, phonon features in IR and Raman spectra 80−93310
$Ce_cLa_{1-c}F_3$, Raman spectra circ. polaris., Faraday effect phonon state splitting 78−43855
$Ce_xLa_{1-x}F_3$, paramag. mixed crystal, scattering of optical phonons by rare earth ions 78−68518
$Ce_2(SO_4)_3.9H_2O$, grown from solution, exam. of Raman spectra and physical props. 79−52104
$Ce_2(SO_4)_3.9H_2O(D_2O)$, polarised Raman spectra, vibr. props. and role of lattice H_2O 80−66201
ClF_5, condensed phases, structural study by vibr. spectroscopy and X-ray and neutron diffr. 79−1405
ClO_2F, cryst. struct., X-ray and neutron diffr., Raman spectra *(French)* 78−83788
$CoBr_2$, magnon Raman scatt. 79−15462
$CoBr_2$, paramag. and antiferromag., Raman scatt. from electronic excitations and phonons 79−69826
$CoCO_3$, antiferromag., Raman spectra, 2-300K 77−32380
$CoCO_3$, exciton and magnon excitation spectra *(Russian)* 78−23467
$CoCO_3$, LF exciton and Raman spectra, one-magnon and two-magnon scatt. 80−93333
$CoCO_3$, light scatt. by thermal magnons and magnons excited by antiferromag. reson. 79−82965
$CoCO_3$, spin wave excitation by uniform precession of magnetisation due to two magnon scatt. 78−68207
$CoCl_2$, antiferromag., elementary excitations 77−69519
$CoCl_2$, antiferromag. elementary-excitations, electronic Raman scatt. meas. 77−80922
$CoCl_2$, interlayer force constants 78−14406
$CoCl_2$, one-magnon Raman scatt. 78−43877
$CoCl_2.2H_2O$, antiferromag., light scatt. from phonons and magnons 80−40104
$CoCl_2.2H_2O$, magnon-phonon interactions and two-magnon Raman scatt., magnetoelastic waves and selection rules 80−34917
$CoCl_2.2H_2O$, phonons and electronic transitions, Raman spectra 79−28761
$CoCs_2(SO_4)_2.6H_2O$, obs. of H^2T^7 Raman spin-lattice relax. process 77−51459
$CoK_2(SO_4)_2.6H_2O$, obs. of H^2T^7 Raman spin-lattice relax. process. 77−51459
$Co(NH_3)_6FeF_6$, anomalous Raman intensities, due to interionic coupling by H bonding 78−27230
$Co(NH_4)_2(SO_4)_2.6H_2O$, obs. of H^2T^7 Raman spin-lattice relax. process 77−51459
CoO-MoO_3, catalyst pellets, Raman spectra 77−40216
$Co(OH_2)_6(SiF_6)$, phase transitions, spectrometric exam. *(French)* 78−88291
$Co_cZn_{1-c}F_2$, Raman scatt. from Zeeman split levels 77−66243
Cr, antiferromagnetic, surface Raman scatt., calc. 80−45069
$CrBr_4$, $CrCl_4$, Raman spectra, struct. and thermodynamic functions 78−60443
$Cr(CO)_6$, solid and matrix isolated, Raman spectra 79−28755
Cs halides, F-centres, first excited degenerate states, props. of electron-phonon interaction 78−63824
Cs salts, Raman and IR spectra of the dicyanoiodate (I) ion 80−60572
Cs-Graphite, interaction ordered and disordered cpd., Raman spectra 80−11393
$CsAlCl_4$, solid state Raman spectra, 298-80K, vibr., struct. 79−28745
$CsAl_xFe_{(1-x)}(SO_4)_2$, solid soln., Raman and IR spectrum study *(French)* 79−47453
CsB_3H_8, IR, Raman and inelastic neutron scatt. spectra 79−42966
CsBr, electron-phonon interactions of F-centres, first-order Raman scatt. 78−64370
CsBr, first-order Raman off- and on-reson. scatt. induced by F-centres 78−92073
CsBr, hyper-Raman spectra by single channel method 78−84591
CsBr:Tl^+, impurity induced Raman spectra, breathing shell model 78−39541
CsBr:Tl^+, perturbed lattice dynamics, breathing shell model calculation 78−75744
CsBr(I), single crysts., polarisation of luminesc. and reorientation of NO_2^- centres 79−95823
$CsCdCl_3$:Co^{2+}, Zeeman Raman scatt. and Zeeman IR absorpt. spectra 79−56782
CsCl, electron-phonon interactions of F-centres, first-order Raman scatt. 78−64370
CsCl, first-order Raman off- and on-reson. scatt. induced by F-centres 78−92073
CsCl(Br)(I):NO_2^-, vibronic and reson. Raman spectra of BCC cryst. 79−87468
$CsCoBr_3$, ID Ising antiferromagnet, spin dependent Raman scattering from phonons and electronic excitations 80−103948
$CsCoBr_3$, quasi ID Ising antiferromag., polarised Raman scatt. from mag. excitations 80−66182
$CsCoBr_3$, quasi one dimensional antiferromag., magnon Raman scatt. 80−11395
$CsCoCl_3$, 1-D Ising antiferromag., mag. phase transitions 79−51779
$CsCoCl_3$, 10 Ising antiferromag., mag. excitations, electronic Raman and IR absorption spectra 78−2668
$CsCoCl_3$, Ising antiferromagnet, electronic Raman scatt. on Co^{2+} 78−10878
$Cs_3CoCl_5(Br_5)$, polarised single cryst. spectra 78−39535
$CsCr_xFe_{(1-x)}(SO_4)_2$, solid soln., Raman and IR spectrum study *(French)* 79−47453
CsF, doped with F-centres, first order Raman scatt. 78−52492
CsF, electron-phonon interactions of F-centres, first-order Raman scatt. 78−64370
CsF, second-order Raman spectra and phonon spectrum 77−90148
CsH_2AsO_4, and deuterated isomorph, E-mode splitting in ferroelec. phase, Raman scatt. meas. 77−16296
CsH_2AsO_4, and deuterated isomorph., ferroelectric mode and molecular vibr. press. depend. 78−19424
CsH_2AsO_4, pres. depend., LF dielec. response, ferroelec. props. 78−15120
CsH_2PO_4, Raman scatt. and high temp. props. 80−16024
$CsHSeO_3$, and deuterated analog, vibr. spectra 79−24311

Raman spectra of inorganic solids continued
$CsHg(CN)_3$, CN and HgC stretching vibrations and HgCN bending vibration assignments 80−69140
CsI, hyper-Raman spectrum, optical phonons, nonlinear processes 77−4640
CsI, hyper-Raman spectra by single channel method 78−84591
CsI:MnO_4^{2-}, multiple-order Raman scatt., and absorpt. spectra 77−40229
CsI(Br), IR active and silent modes, hyper-Raman scatt. obs. 79−61376
Cs_2KPrF_6, Raman spectrum and cryst. field *(German)* 79−51940
$Cs_2LiCo(CN)_6$, mol. vibr. in cryst., normal mode anal., Raman and IR obs. 77−76494
$Cs_2LiFe(CN)_6$, struct., phase transformations, temp. depend. Raman spectra 79−11416
$Cs_2MFe(CN)_6$, M=Ba, Mg, Ca, Sr, lattice instabilities 77−72668
$Cs^+M^{III}(SO_4)_2$, M=Al^{3+}, Cr^{3+}, Fe^{3+}, Raman and IR spectrum study *(French)* 79−47453
$CsMgCl_3$, Cs_3MgCl_5, Raman spectrosc. investigation of struct. 80−49202
$CsMgCl_3$:Co^{2+}, Zeeman Raman scatt. and Zeeman IR absorpt. spectra 79−56782
CsNCS, vibr. spectra, multiphonon modes 77−40230
$CsNO_3$, Raman spectra temp. depend., NO_3^- ion external librational modes, I→II transition, Raman spectra temp. depend., NO_3^- ion external librational modes 79−78662
$Cs_2NaErCl_6$, mag. susceptibility and IR and Raman spectra meas., crystal field splitting determ. 80−100652
$Cs_2NaEuCl_6$, luminescence Raman spectra, means for localisation of binding energy levels *(German)* 78−88304
$Cs_2NaFe(CN)_6$, structural phase transformations 79−19178
Cs_2NaMCl_6, M=Eu, Tb, Er, Tm, Raman spectra 77−77205
Cs_2NaRCl_6 (R=rare earth), low-temp. Raman spectra meas., cryst. field parameters calc. *(German)* 77−36228
Cs_2NaYCl_6, Raman spectrum 77−59567
$Cs_2NaYbCl_6$, electronic struct., paramag. susceptibility and electronic Raman spectrum, cryst. field parameters *(German)* 77−63072
$Cs_{11}O_3$, ionic clusters in alkali metal suboxide cryst., struct., vibr. freqs., Raman spectra 79−37772
Cs_2ReF_6(-Cs_2GeF_6) cryst., $ReF^{-2}{}_6$ ion electronic absorpt. spectra, Raman, visible, IR and UV, liq. H and room temps. 77−77193
Cs_2SO_4, cryst., coord. and Raman intensity anal. 78−2831
$CsSbF_6$, high press. phase relations, vibr. spectra, and cryst. chemistry 80−108200
$CsSbF_4(OH)_2$, solid, IR and Raman spectra 80−40114
$CsSbF_5OH$, solid, IR and Raman spectra 80−40114
Cs_2SeO_4, single cryst., orthorhombic, Raman spectra 77−73140
Cs_2SiF_6, lattice dynamics from neutron scatt., Raman and IR absorpt. meas. 79−60449
$Cs_2(TeBr_6)$, far IR and Raman spectra and phase transitions 80−11376
Cs_2TiF_6, Raman spectra, internal and lattice vibrs. 77−8569
$Cs_4(UO_2)_2F_8.2H_2O$, IR absorpt. and Raman spectra, normal coordinate anal. *(French)* 78−52509
$Cs_2Zn(N_3)_4$, IR and Raman spectra 77−43999
$Cs_2[ZnCl_4]$, Raman-active phonons, $[ZnCl_4]^{2-}$ distortion, press. effects 77−52073
Cu complex, $[(CH_3)_2NH_2]_3CuCl_5$, single cryst. Raman spectra 78−39535
Cu halides, phonon anomalies for Cu^+ at off-centre sites, dynamical model and Raman meas. 80−10618
Cu I, press.-induced phase transitions, Raman scatt. obs. 77−43995
Cu-halides, phonon anomalies, dynamical model 79−73272
$Cu_3B_7O_{13}Cl$, Raman study of ferroelec. phase transition 79−38529
CuBr, dispersion of multicomponent exciton polaritons, hyper-Raman emission spectra 80−20096
CuBr, emission spectra after two-photon excitation, Raman scatt. 79−47518
CuBr, excitonic mols., two photon generation 77−43511
CuBr, press. depend. of Raman scatt. meas., Gruneisen parameters determ. 77−24845
CuBr(Cl)(I), LF light scatt. spectra in superionic cond. phases, ion motion obs. 80−108217
CuBr(Cl)(I), polariton Raman spectra, oscillator strengths, temp. depend. 80−66197
$CuBr_xI_{1-x}$, disorder-induced TA Raman lines 79−73929
CuCl, anomalous Raman spectrum in transverse optic phonon region 77−24846
CuCl, biexciton luminescence and two photon Raman emission, polarisation props. 78−80406
CuCl crystal resonant Raman scatt. and luminescence competition *(Japanese)* 80−80770
CuCl, emission spectra after two-photon excitation, Raman scatt. 79−47518
CuCl, exciton spatial dispersion determ., two-photon Raman scatt. via excitonic mol. state 80−60595
CuCl, excitonic mols., two photon generation 77−43511
CuCl, excitonic polariton-polariton resonance scattering 79−24306
CuCl, fission of relaxed excitonic mols. into upper and lower branch polaritons induced by M_L emission 80−11380
CuCl, forward scattering by excitonic molecule 78−2838
CuCl, giant two-photon absorption into excitonic mol., anomalous dispersion of excitonic polariton 78−27211
CuCl, luminesc. and Raman processes under reson. two-photon excitation 79−33796
CuCl, luminesc. and reson. Raman scatt. of excitonic mols. 79−33814
CuCl, phonon interaction of excitonic molecule 80−50316
CuCl, picosecond spectroscopy of secondary radiation from resonantly excited excitonic molecules 79−15461
CuCl, polariton effects in resonant Raman scatt. 78−10881
CuCl, press. depend. of Raman scatt. meas., Gruneisen parameters determ. 77−24845
CuCl, Raman and luminesc. processes under reson. two-photon excitation of excitonic mol. 79−8143
CuCl, reson. Raman scatt. and luminesc. of biexcitons 79−38618
CuCl, reson. Raman scatt. and luminesc. due to excitonic mols. 79−91425
CuCl, reson. Raman scatt. and luminesc. under two-photon excitation 79−95765
CuCl, reson. two-photon Raman scatt., excitonic polariton dispersion 78−72509
CuCl, reson. two-photon excitation of excitonic mol. using circ. polarised light 78−84566

Raman spectra of inorganic solids continued
CuCl, resonantly excited excitonic molecules, time resolved spectroscopy 78−92109
CuCl, two-photon reson. Raman scatt. with recoiling excitonic polariton 77−36223
CuCl, two-photon reson. Raman scatt., recoil of upper-branch excitonic polariton 78−27212
CuCl, two-photon reson. Raman scatt. and luminesc. of excitonic mols. 79−28819
CuCl, two-photon resonant Raman scatt. via biexcitons 78−43302
CuCl, zincblende struct., high press. Raman scatt., 77K 78−60463
$CuCl_xBr_{1-x}$, disorder-induced TA Raman lines 79−73929
CuCl(Br)(I), Raman spectra, Cu ions vibr. and diffractive motions 80−11412
$CuGaS_2$, lattice vibr. modes, Fourier transform spectroscopy 79−33701
$CuGaS_2$, reson. Raman scatt. by extraordinary phonons obs. 77−85704
Cu_2HgI_4, ordered and disordered phases Raman spectra temp. depend., ion hopping 78−23438
Cu_2HgI_4, polycryst., Raman spectra, press. depend. 77−73137
CuI, α and melt phases, light scatt. from correl. ion fluctuations 79−95771
CuI, press. depend. of Raman scatt. meas., Gruneisen parameters determ. 77−24845
CuI, superionic cond., Raman spectra in all 3 phases 78−19486
CuI, superionic conductor, Raman study 78−80353
CuI, superionic conductor, lattice dynamics 79−95111
CuI, superionic conductor, lattice dynamic meas. and calcs. 79−99880
$CuInS_2$ crystals, growth, struct., and elec. props. 79−38729
CuO_2, width of reson. Raman scatt. enhancement profiles, phenon-lifetime contrib. 79−19883
Cu_2O, 1s yellow exciton, lineshape studies by reson. Raman scatt. 78−76465
Cu_2O, exciton-phonon dynamics, reson. Raman scatt. 80−11406
Cu_2O, fine struct. of exciton spectrum 78−18972
Cu_2O, reson. Raman scatt., yellow and green excitonic series 78−72511
Cu_2O, reson. Raman scatt. from stress-split forbidden excitons 80−93332
Cu_2O, uniaxial stress effects on excitons 80−60589
Cu_2O, yellow exciton states investig. by forbidden resonant Raman scatt. 77−48165
$Cu_2O:Cd^{2+}$ implanted, reson. Raman scatt., annealing effect 77−24838
Cu_2O:He(Na)(Cd), ion-implanted, resonance Raman studies of annealing 79−55765
Cu_3PS_4, solid, reson. Raman spectra at low temp. 79−8129
$CuSO_4.5H_2O$ and $CuSO_4.5D_2O$, Raman and IR spectra, mode assignments 77−66493
$CuSeO_4.5H_2O$, Raman and IR spectra, mode assignments 77−66493
$Cu_xV_2O_5$, metallic, Raman scatt. 78−80358
Cu_3VS_4, Raman active modes 80−11414
Cu_3VS_4, Raman linewidth of A_1 mode under high press., reson. effects 80−108210
D_2, Raman active optical phonon, density depend. 79−87432
D_2, Raman scatt. meas of rotational spectrum under press. 77−69814
p-D_2, solid, bound libron state form., Raman scatt. data 77−80600
D_2, solid, libron spectra and conversion as function of ortho-para conc., Raman scatt. spectra 78−84570
o-D_2, solid, up to 150 kbar, 5K, Raman spectrum 80−50332
DBr(DCl), solid, ferroelec. and paraelec. phases, transitions, Raman scatt. 77−43980
DF, cryst., Raman spectra 80−55075
DI, crystalline, Raman and IR spectra, mol. vibr., libration and translation 80−2757
D_2S, solid, low-temp. phase, IR, far IR and Raman spectra 78−27218
D_3SiNCS, IR and Raman spectra, vibr. anal., LF bending mode 78−70842
Dy_2S_3, vibr. spectra, factor-group anal. 80−80793
$DyVO_4$, Jahn-Teller distortion, mag. field depend. 78−79733
$ErCrO_3$, phonon Raman spectra rel. to mag. ordering 77−52100
Er_2O_3 sesquioxide, Raman spectra 78−19478
Eu chalcogenide, spin-disorder Raman scatt., mag. phase depend., theory 78−10887
Eu chalcogenides, magnetic semiconductor, light scatt. exam. 79−61372
Eu chalcogenides, multiphonon inelastic light scatt., hot recomb. 77−8559
Eu chalcogenides, paramag., spin-disorder-induced Raman scatt. 78−19474
Eu chalcogenides, resonant Raman scatt. 77−55787
Eu chalcogenides, resonant Raman scattering model via magnetic exciton in ferromagnetic phase 80−93326
Eu chalcogenides, spin-dependent Raman scatt. from phonons 80−97274
Eu complex, $(Et_4N)_3$ [$Eu(NCS)_6$], Eu^{3+} ion site symm. 78−84656
Eu_x monochalcogenides, multiphonon inelastic light scatt. 77−90144
Eu^{3+} fluoresc. lineshape in glass, temp., time and conc. depend., two-phonon Raman scatt. 78−64406
Eu-As-S, glass forming region, Raman and IR obs. *(French)* 79−99080
EuO, Raman scatt. and phonon dispersion 77−55786
EuO, spin-dependent Raman scattering 79−95782
Eu_3O_4, inelastic light scatt. 77−55788
$Eu_3O_4(S_4)$, mixed valence system, inelastic light scatt., photoluminesc. 77−90145
EuO(S)(Se), spin assisted Raman scatt. theory 78−43866
EuO(S)(Se)(Te), cryst. and electronic struct., mag., elec., and optical props., book contrib. 80−39760
EuO(S)(Se)(Te), spin order and fluctuations, Raman scatt. study 80−97273
EuO(S)(Se)(Te), spin-disorder induced phonon Raman scatt. 78−60457
EuS, Raman scatt. and phonon dispersion 77−55786
EuS-Ga_2S_3-GeS_2, chalcogenide glasses, conditions of form. of glassy prod. *(French)* 80−100325
Eu_3S_4, inelastic light scatt. 77−55788
EuS(Se), mag. phase depend. Raman scatt. 78−10886
EuS(Se)(Te), spin-assisted phonon Raman scatt., mag. phase depend. 80−71413
EuS(Se)(Te)(O), Raman scatt. near mag. phase transitions 79−47458
EuSe, first- and second-order Raman scatt. near T_N 79−61374
EuSe, mag. ordered phase, first order Raman scatt. theory 77−85723
EuSe, Raman scatt. and phonon dispersion 77−55786
EuSe, Raman scatt. near mag. phase transitions 79−61373
EuTe 79−61373
EuTe, antiferromag. semicond., Raman scatt., spin-phonon interactions 80−66185
Raman spectra of inorganic solids continued
EuTe, antiferromagnet, phonon Raman scatt. from spin superstructures 80−16030
EuTe, field depend. correl. function theory of Raman scatt. near antiferromag.-paramag. transition 78−68490
EuTe, mag. 'Bragg' scatt. obs. through Raman scatt. 80−66179
EuTe, mag. ordered phase, first order Raman scatt. theory 77−85723
EuTe, Raman scatt. and phonon dispersion 77−55786
EuTe, Raman scatt. exam. 79−61375
EuTe, spin-dependent Raman scattering 79−95782
$Eu_{1-y}X_yS$ (X=Sr,Gd), spin-disorder-induced Raman scatt. from phonons, expt. investigation 80−20635
$Eu_{1-y}X_yS$ (X=Sr,Gd), spin-disorder-induced Raman scatt. from phonons, theory 80−20636
EuX(X=0,S,Se) 80−20635
EuX(X=0,S,Se), spin-disorder-induced Raman scatt. from phonons, theory 80−20636
Fe complex, Fe(II), 2,2′-bipyridyl complexes, reson. Raman spectra, vibr. anal. 79−61363
Fe corrosion products, Raman spectroscopic detect. 79−16063
Fe-Cr-Ni based alloys, surface oxides at high temps., backscattering Raman spectroscopy 80−93291
$FeBO_3$, antiferromag., two magnon reson. Raman scatt. 79−33703
$FeBr_2$, dynamic Jahn-Teller system, Raman scatt. from electronic excitations and phonons 78−56474
$FeCO_3$, antiferromag., siderite, Raman spectra obs. 77−85708
$Fe(CO)_4^{2-}$, Raman spectra 77−59571
$Fe_2(CO)_9$, solid, Raman and IR spectra, vibr. exam. 78−27214
$Fe(CO)_2(NO)_2$, vib. assignment ^{15}N isotopic substitution 77−48152
$FeCl_2$, dynamic Jahn-Teller system, Raman scatt. from electronic excitations and phonons 78−56474
$FeCl_2$, electron-phonon coupling, temp. depend. Raman scatt. obs. 79−15451
$FeCl_2$, interlayer force constants 78−14406
$FeCl_2$, one-magnon Raman scatt. 78−43877
$FeCl_2$, vibrational excitations, polarised Raman spectra 79−19888
$FeCl_3$ intercalated with graphite, vibrational excitations, polarised Raman spectra 79−19888
$FeCl_2.2D_2O$, magnon-phonon coupling 78−72530
$FeCl_2.2D_2O$, metamagnetic, excitonic Davydov splitting in Raman spectrum 79−33704
$FeCl_2.2H_2O$, also deuterated, electronic transitions in Raman spectra 78−80337
$FeCl_2.2H_2O$, and $FeCl_2.2D_2O$, Raman scatt. at metamagnetic phase transitions, mag. hysteresis 78−14958
$FeCl_2.2H_2O$, magnon-phonon interactions and two-magnon Raman scatt., magnetoelastic waves and selection rules 80−34917
$FeCl_2.2H_2O$, metamagnetic, resonant magnon-optical phonon coupling 79−28773
$FeCl_2.2H_2O(2D_2O)$, phonons and electronic transitions, Raman spectra 79−28761
FeF_2, absolute first order Raman polarisabilities 78−64369
FeF_2 antiferromag., anomalous anti-Stokes/Stokes Raman scatt. intensity ratio 80−66177
FeF_2, interacting phonon-magnon states, theory of Raman scattering and IR obs. 80−71426
FeF_2, one-magnon Raman scatt., anomalous behaviour of anti-Stokes-Stokes intensity ratio 80−40115
FeF_2, Raman spectra, cross section determ. 78−56471
FeF_2, theory of Raman scattering, coupled phonon-magnon excitations 78−72531
$Fe(H_2O)_6SiF_6$, Raman spectra, vibr. modes 79−61369
$Fe_{1-x}Mn_xCl_2$, disordered, Raman scatt. from Fe^{2+} and Neel temp. 80−60579
$Fe_{1-x}Mn_xCl_2$, low-lying electronic excitations in antiferromag. and paramag. phases Raman scatt. study 80−71414
α-Fe_2O_3, antiferromag., reson. two magnon Raman scatt. obs. 77−63417
α-Fe_2O_3, antiferromag., two magnon reson. Raman scatt. 79−33703
$Fe(OH_2)_6(SiF_6)$, phase transitions, spectrometric exam. *(French)* 78−88291
$Fe_{1-x}Zn_xF_2$, dil. antiferromag., Raman scatt. expts. 79−78666
$Fe_{1-x}Zn_xF_2$, dil. antiferromag., electronic and mag. props., Raman scatt. and optical absorpt. study 80−108207
$Fe_{1-x}Zn_xF_2$, electronic Raman scatt., mag. anisotropy 80−66184
$Ga_x In_{1-x}P$, localised exciton-phonon complex as intermediate state in light scatt. 78−39543
$Ga_{1-x}Al_xAs$, IR refl. spectra and Raman spectra 80−20623
$Ga_{1-x}Al_xAs$, solid solution, synthesized by ion implantation, Raman scattering 79−42972
$Ga_{1-x}Al_xSb$, second order Raman spectra, photon combinations *(French)* 80−34912
$Ga_{1-x}Al_xSb$, surface oxidation, Raman spectra, residual Sb layers 80−71419
GaAs, anodised, interfacial reactions, Raman scatt. obs. 80−49544
n-GaAs, coupled plasmon-LO phonon modes, Raman scatt. meas. 78−60472
n-GaAs, coupled plasmon-LO phonon modes and Lindhard-Mermin dielec. function 79−82540
GaAs, effective mass, Raman spectrum determ. 80−24797
GaAs, electronic Raman scatt. of polarised light on donor levels 80−93309
GaAs, excited, LO phonon effective temp., Raman meas. 80−20639
GaAs, forbidden Raman scatt. by LO phonons 78−64367
p- GaAs, heavily doped, self energy of phonons 80−44277
GaAs, highly excited, LO phonon Raman lineshape 79−78683
GaAs, insulating, optically pumped electron-hole plasma, Raman scatt. 77−40236
GaAs, ion implanted, laser induced damage and recrystallisation by freq.-doubled Nd:YAG laser 79−73197
GaAs, ion implanted, laser induced recrystn. and damage, ion backscatt. and Raman scatt. obs. 80−49248
GaAs, laser-induced recrystallisation and damage of ion-implanted amorphous samples 79−47557
GaAs, light scatt. spectra, interference effects 79−82977
GaAs oxide film growth in As_2O_3 vapour, As incorporation 79−77928
GaAs oxidised surface, detection of excess crystalline As by Raman scatt. 78−19453
GaAs, photoluminescence and resonant Raman spectra, press. depend. 78−31251
GaAs, polar modes, light scatt. intensities, wave vector depend. 77−77219

Raman spectra of inorganic solids continued
GaAs, Raman scatt., electron-phonon deformation potential coupling 78−52502
n-GaAs, Raman scatt. by coupled phonon-plasmon mode, nonlocal theory 77−36222
n-GaAs, Raman scatt. by wavevector depend. coupled plasmon-LO phonons 77−40232
GaAs, Raman scattering absolute cross section band struct. model calcs. 80−7349
GaAs, Raman scattering from nonequilibrium LO phonons with picosecond resolution 80−80779
n-GaAs, Raman spectra of coupled LO phonon-plasmon mode, de Haas-Shubnikov like quantum oscills. 78−43863
GaAs, Raman spectroscopy, characterisation of thin films and heterostructures 78−76439
GaAs, reson. Raman scatt. at indirect gap 79−73931
n-GaAs, resonance enhancement of Raman scatt. by electron gas excitations 79−65878
GaAs, resonance Raman scattering by 2 TO phonons and cond. band minima ordering 77−20854
GaAs, surface segregation of implanted alkali metals, photoemitter prep. and characts. *(French)* 78−60544
GaAs, surface studies during MBE growth 79−90899
GaAs, two-phonon Raman scatt. meas. 77−81097
p-GaAs:Zn, Raman scatt. by LO phonon-plasmon coupled modes, wave vector non-conservation 80−16033
p-GaAs-$Al_{0.3}Ga_{0.7}As$, cladded dielec. waveguide, loss meas. using Raman scatt. 79−81539
GaAs-$Al_xGa_{1-x}As$ heterojunctions, inelastic light scatt. 79−65867
GaAs-AlAs alternating epitaxial monolayers, Raman scatt. and zone-folding effects 77−90208
GaAs-AlAs alternating monolayers, zone folding effects on phonons 78−72510
GaAs-AlAs superlattice, folded acoustic phonons obs., Raman scatt. 80−88996
GaAs-anodic oxide interfaces, struct. and chem. props., Raman scatt. obs. 79−47168
GaAs-$Ga_{1-x}Al_xAl$ superlattice, reson. Raman scatt., 2-D quantum states 77−8577
GaAs-$Ga_{1-x}Al_xAs$, superlattice umklapp processes in resonant Raman scattering 78−64362
GaAs-$Ga_{1-x}Al_xAs$ superlattices, resonance enhanced Umklapp Raman process 78−39547
GaAs-$Ga_{1-x}Al_xAs$ superlattice, Raman scatt., polar phonon anisotropy 80−45052
GaAs-native oxide interface, vibr. modes 77−85709
$GaAs_{1-x}H_x$, amorphous, vib. props., Raman and IR meas. 80−50322
$GaAs_{1-x}P_x$, localised exciton-phonon complex as intermediate state in light scatt. 78−39543
$GaAs_{1-x}P_x$, solid solution, synthesized by ion implantation, Raman scattering 79−42972
$GaCl_3$, Raman spectral differences from liquid to glassy state, ionic equilib. interpretation 80−20619
$GaCl_3(I_3)$, gaseous, Raman spectra, struct., Fermi reson. and thermodynamic functions 77−18929
GaI_3-$SbCl_3$, total exchange of halogens, Raman spectra and phase equilibrium *(French)* 79−65874
$Ga_xIn_{1-x}As_yP_{1-y}$, conduction band and phonons, Shubnikov-de Haas effect, magnetophonon resonance, Raman scattering 80−24795
$Ga_xIn_{1-x}Sb$ LO phonon obs. using Raman scatt. 78−35152
$Ga_{1-x}In_xSe$, Raman scatt. spectra, optical phonon freq., cryst. vibr. freq. types 80−29744
Ga_2O_3-Na_2O, β- and β''-phases, superionic conductors, Raman results 77−40234
GaP, complex form of donor energy levels, optical spectra anal. 78−23045
GaP, dispersion of vibrational excitations, Raman scatt. 78−84588
GaP, double reson. in two-phonon Raman scatt. by longitudinal optical phonons 77−24852
GaP, high-order Raman spectra, polariton scatt. 78−56483
GaP, light scatt. by LO phonons, high-resolution study 80−80798
GaP, light scatt. spectra of guided wave polaritons 79−15101
GaP, obs. of Raman scatt. by Cu vapour laser 78−95586
GaP, photoexcited, Raman scatt. from plasmons 79−38541
GaP, polariton linewidth in k-space, anharmonicity and permittivity 77−85155
p-GaP, Raman scatt. by coupled plasmon-phonon oscills. 78−6687
GaP, Raman scatt. from plasmon-phonon coupled modes 80−93337
GaP, Raman scatt. from surface polaritons, selection rules 77−52083
GaP, Raman scattering selection rules for surface polaritons 78−72091
GaP, Raman spectra, press. depend. optical phonon anharmonicity 77−8586
GaP second order Raman spectrum, polarisation meas. 78−64368
GaP, single cryst., Raman scatt., effective cross-section rel. to nonlinear coeffs. *(Russian)* 78−71152
GaP single cryst., Raman scatt. cross section, nonlinear optical coeffs. 79−56784
p-GaP, spin-flip Raman scattering, review 80−108209
GaP, surface polaritons, light scattering studies, effect of surface roughness 80−6753
GaP, two-photon absorption coefficient rel. to inverse Raman cross section 78−6678
GaP:Cu, Raman scatt. from acceptor state 80−11408
GaP:Zn, Raman spectra of Zn acceptor 77−77187
GaS, Davydov splitting of degenerate lattice modes 79−61382
αGa_2S_3, single crystal, lattice phonon exam., Raman and IR spectra of polycrystalline samples *(French)* 78−27229
GaS(Se), absorpt. edge, exciton levels and Raman scatt., press. effects above 40 kbar 77−48187
GaS(Se), layered, optical phonons, IR and Raman scatt. meas. 78−59903
GaS_xSe_{1-x} layered system, neutron diffr., IR and Raman scatt. 79−87443
GaSb, accumulation layer localised carriers interaction with LO phonons, Raman interference lineshapes 80−93338
n-GaSb, coupled LO-phonon-plasmon modes, Raman spectrum 80−11409
p-GaSb, heavily doped, LO phonon-carrier interaction, Raman interf. lineshapes 80−93319
p-GaSb, hot exciton luminesc., LO phonon Raman scatt. 80−11474
GaSb, interaction of exciton recombination with LO phonons 79−38647

Raman spectra of inorganic solids continued
GaSb oxidised surface, detection of excess crystalline Sb by Raman scatt. 78−19453
GaSb, reson. two phonon Raman scatt. near E_1 and $E_1+\Delta_1$ gaps 78−60470
GaSb, second order Raman scatt. meas., comparison with photon density of states calc. 77−8579
GaSe and GaS_xSe_{1-x}, multiphonon reson. Raman scatt., excitonic transition 77−59574
GaSe, cascade resonant Raman processes 80−25385
GaSe films, optical props. at lattice vibr. freqs., IR and Raman spectra 80−60696
GaSe, multiple-phonon reson. Raman scatt. processes 77−4634
ε-GaSe, Raman scatt., hydrostatic press. effect 80−84745
GaSe, reson. light scatt., luminesc. and Raman spectra 79−38615
GaSe, zone-centre optical phonons, Raman scatt. meas. 78−10141
$GaSe_{1-x}S_x$, struct. transition, Raman scatt. obs. 79−99888
$GaSe_{1-x}Te_x$, Raman scatt., optical phonons and phase transition 80−66202
$GaSe_{1-x}Te_x$, Raman spectra, phonon freq. 80−97286
$GaSe_{1-x}Te_x$, zone-centre optical phonons, Raman scatt. meas. 78−10141
GaTe, long wavelength phonons, Raman and far IR spectra obs. 79−69210
α-GaTe, single cryst., Raman scatt. 80−60599
α-GaTe single crystals, Raman spectra 79−99883
GaTe, zone-centre optical phonons, Raman scatt. meas. 78−10141
$Gd_2(MoO_4)$, ferroelec., Raman scatt. from soft modes 77−85706
$Gd_2(MoO_4)_3$, ferroelec., anomalous damping of phonons, Raman spectra, stress and temp. effects 79−38503
$Gd_2(MoO_4)_3$, uniaxial stress effect on ferroelec. transition, Raman scatt. 78−80360
B-Gd_2O_3, monoclinic single cryst., Raman spectrum 80−103953
$Gd(OH)_3$, dynamical effects of interaction between 4f electrons and optical phonons 80−108196
GdS, FCC metallic phase, Raman scatt., phonon density of states 78−19480
GdS, metallic FCC antiferromag., phonon Raman scatt. 78−60458
GdS(Se)(Te), metallic, phonon density of states, Raman scatt. expt. 78−23451
Ge, amorphous, growth rate of crystallisation, Raman spectroscopy study 80−44227
Ge, amorphous, pure and hydrogenated, Raman spectra 79−61358
Ge and Ge III, effect of pressure on the Raman shift 78−92064
p-Ge, heavily doped, self energy of phonons 80−44277
Ge, impurity modes due to point defects, comparison with IR and Raman meas. 79−4386
Ge, reson. Raman scatt. under uniaxial stress near E_1 gaps 79−42960
Ge:As, uniaxially stressed, electronic Raman scatt. from valley-orbit transitions 78−15166
n-Ge:P(As), nonlinear optical susceptibility, Raman scatt. cross-sections for impurities 77−46759
Ge-Se glass, vibr. props., Raman and IR spectra obs. *(Japanese)* 77−43989
Ge-Si, dil. alloy, IR absorpt. and first-order Raman scatt. due to single and paired impurity atoms 79−82976
Ge-Si alloys, defect modes and optical spectra 80−11413
Ge-type semiconductor, light scatt. from zero-sound 78−43857
$GeBr_4$, fine struct. resolution in Raman-active fundamentals 79−42967
GeF_4, Raman spectra at 77K, scatt. angle, polaritons and space group 78−23439
GeH_3NCS, liq. and solid, IR and Raman spectra 79−89663
GeO_2, glassy high freq. vibr. bands, central force model 80−49330
GeO_2, tetrahedral glass, Raman studies 78−71823
GeO_2, vitreous, band limits and vibrational spectra 79−73935
GeO_2, vitreous, LO vibrational modes, Raman and IR spectra 77−7819
GeO_2, vitreous, Raman cross sections, rel. to appl. in fibre Raman lasers 78−31176
GeO_2-$K_2O(Na_2O)(Li_2O)$, glass, Raman spectra, struct. and crystn. 80−92463
$Ge(S,Se)_2$ glasses, comparison A_1 Raman line, microscopic origin 80−29740
GeS_2, cryst. and glass, Raman spectra, struct. *(Russian)* 79−51966
GeS_2, glass, structure correlation range, Raman Brillouin light scatt. determ. 77−20857
GeS_2, glassy, high freq. vibr. bands, central force model 80−49330
GeS_2, LF inelastic light scatt. meas. 78−15181
GeS_2, single cryst., IR polarised reflectivity spectra, 79−56775
GeS(Se), layer cpds., Raman spectra, press. coeffs. and mode Gruneisen parameters 78−10891
$GeSe_2$, cryst. and glass, Raman spectra, struct. *(Russian)* 79−51966
$GeSe_2$ evaporated films, struct. and thermally induced effects 79−41963
$GeSe_2$, IR and Raman spectra 78−95585
$GeSe_2$, LF inelastic light scatt. meas. 78−15181
$GeSe_2$, single cryst., IR polarised reflectivity spectra, 79−56775
$GeSe_2$, single crysts., 3 polymorphic forms, DTA, photolum., IR and Raman sepctroscopy 80−33923
Ge_xSe_{1-x} glass, $1/3 \leq x \leq 1/2$, Raman scatt., local order 78−23442
$(GeSe_2)_x(As_2Se_3)_{1-x}$, vibr. excitations of large atomic clusters, Raman and depolarisation spectra 77−20856
$GeSe_xS_{1-x}$ solid solutions, long-wavelength optical phonons, Raman spectra 80−25378
$Ge_{1-x}Si_x$, vibrational and Raman-scattering props. 78−10884
H_2, ortho-para mixtures, 10 to 23K, rot. Raman spectra, quantum calcs. 77−6700
H_2, Raman active optical phonon, density depend. 79−87432
H_2, Raman scatt. meas of rotational spectrum under press. 77−69814
o-H_2, solid, bound libron state form., Raman scatt. data 77−80600
H_2, solid, compressed, vibr. Raman spectrum 79−47422
H_2, solid, libron spectra and conversion as function of ortho-para conc., Raman scatt. spectra 78−84570
H_2 solid, localised excitations due to p-H_2 impurity 79−65288
H_2, solid, Raman active phonons, freq. depend. on ortho-para conc. and temp. 79−73918
p-H_2, solid, time-resolved CARS, disorder effects on coherent vibr. states 80−93342
HBO_2, cubic, monoclinic and orthorhombic forms, H bonding, IR and Raman spectra 80−76029
HBr(HCl), solid, ferroelec. and paraelec. phases, transitions, Raman scatt. 77−43980
$HEu(PO_3)_4$, vibr. spectra 80−34905
HF, cryst., Raman spectra 80−55075

Raman spectra of inorganic solids continued
HI, crystalline, Raman and IR spectra, mol. vibr., libration and translation 80−2757
HIO_3 crystals, anharmonicity effects in Raman spectra 80−25379
HIO_3, polariton Fermi-resonance and dissociated phonon states *(Russian)* 80−20634
HIO_3, single crystal, ang. depend. of Raman spectra 78−72518
$HNO_3.H_2O$, devitrification crystallisation, fast Raman and wide-line NMR obs. *(French)* 79−73915
H_2S, solid, low-temp. phase, IR, far IR and Raman spectra 78−27218
HSO_3F crystal, indication of molecules existing as infinite chains *(French)* 80−989
H_2SeO_3, and deuterated analog, vibr. spectra 79−24311
H_2SeO_3, cryst., vibr. spectra in O-H stretching region 79−51949
H_3SiNCS, IR and Raman spectra, vibr. anal., LF bending mode 78−70842
HfO_2, Y_2O_3-stabilised, solid soln., Raman scatt. anal. of struct. transform. 78−88312
HfS_3, one-dimensional semicond., Raman spectra meas. 80−50345
$HfS_3(Se_3)$, phonon study of chemical bonding 80−20645
HgA_2X_4 (A=Ga,In; X=S,Se), Fourier IR and Raman spectra, cryst. struct. and symm. *(German)* 79−24313
Hg_2Br_2, ferroelastic, Brillouin and Raman scatt. spectra 79−95770
Hg_2Br_2, improper ferroelastic, soft mode props. in Raman spectra 77−36246
Hg_2Br_2, powder, Raman spectra, press. effects 78−2837
$Hg_2Br(Cl_2)$, paraphase, Raman scatt. spectra, soft mode from Brillouin zone boundary *(Russian)* 78−2851
$Hg_2(BrO_3)_2$, Raman and IR spectra, vibr. anal. 77−66492
$Hg(CN)_2$, phonon freq. anomalous press. depend., mol. struct. distortion 80−88981
$Hg_{0.77}Cd_{0.23}Te$, near reson. spin-flip Raman scatt. 79−82983
Hg_2Cl_2, calomel, press. depend. optical soft mode 79−55859
Hg_2Cl_2, improper ferroelastic, soft mode props. in Raman spectra 77−36246
Hg_2Cl_2, low temp. phase transition, X-ray diffr., Raman spectra 78−22849
Hg_2Cl_2, neutron and Raman scatt. studies, ferroelastic transitions 80−76015
Hg_2Cl_2, powder, Raman spectra, press. effects 78−2837
Hg_2Cl_2 prototype phase, soft mode, inelastic neutron scattering, Raman effect 78−91411
$HgCr_2Se_4$, ferromag. semicond., Raman spectra 78−52496
$HgCr_2Se_4$, Raman scattering, as function of temp. and incident photon energy 79−95781
$HgCr_2Se_4$, thermoreflectance, photoconductance, Raman scatt. near mag. phase transition 80−97298
α-HgI_2, Raman scatt. at room temp., improved polarisation spectra 80−25368
HgI_2, Raman spectrum 114 cm^{-1} line, differential analysis using covalence bonds modulation 79−24315
HgI_2, red, luminesc. and Raman scatt., biexcitons and exciton-phonon interactions 79−61424
HgI_2, red, reson. Raman scatt. and luminesc. 78−84579
HgI_2, red, resonant Raman scatt. in B-exciton and band to band transition regions 79−61381
Hg_2I_2, thermal softening of mode on Brillouin zone boundary in Raman scatt. spectra 79−73948
$Hg_3In_2Te_6$, complex ordered-vacancy cpd., struct. and lattice dynamics 78−34496
$Hg_2(NO_3)_2.2H_2O$, Raman and IR spectra, vibr. anal. 77−66492
α-HgS, cinnabar, reson. Raman effect and luminesc. meas. 80−50338
Hg_2SO_4, Raman and IR spectra, vibr. anal. 77−66492
I_2, reson. Raman lines, Stokes-antiStokes intensity ratio meas. 77−6786
$_xI_{1-x}$ mixtures, high-temp. solids and melts, struct., thermodynamic props., Raman spectra obs. 80−66174
In pnictides, mixed, impurity induced Raman scatt. spectra 80−88983
InAs, oxidised surface, detection of excess crystalline As by Raman scatt. 78−19453
InAs, Raman scatt. by LO phonons 77−20852
InAs, second order Raman scatt., electron-two phonon deform. pots. determ. 78−60473
InAs, surface space charge investig., reson. enhanced Raman scatt. 77−20849
In_4CdI_6, ionic conductivity, Raman spectra 77−69113
InCl$_3$, aqueous soln., factor analysis and band contour resolution applications, book contrib. 78−21931
$In_{1-x}Ga_xAs_yP_{1-y}$, lattice vibrs., Raman study 78−91391
$In_{1-x}Ga_xP$, non-isodisplacement of P atoms in long-wavelength optical phonons 79−47444
$In_{1-x}Ga_xP$, phonon density of states, cluster Bethe lattice treatment 80−6475
InI, photoluminesc., Raman scatt. 79−38593
InP, depend. of phonon spectrum on hydrostatic press., Raman spectra 80−93315
InP, reson. Raman scatt., deformation pots. 78−52495
InP, surface space charge layers and Schottky barrier form., Raman scatt. study 80−50319
$InP_{1-x}As_x$, long wave and short wave phonons, Raman spectra obs. 80−50317
InS, layer semicond., Raman scatt. meas. 78−35134
InS, layer single cryst., Raman scatt. meas. 78−76478
InS, Raman scatt. spectra and interpacket interaction 79−8146
InSb, accumulation layer localised carriers interaction with LO phonons, Raman interference lineshapes 80−93338
n-InSb, effective g-value of electrons determ. by spin flip Raman scatt. and electric-dipole-excited ESR 78−52494
InSb, electronic interband Raman scatt. 80−11407
p-InSb, heavily doped, LO phonon-carrier interaction, Raman interf. lineshapes 80−93319
InSb, interaction of exciton recombination with LO phonons 79−38647
InSb oxidised surface, detection of excess crystalline Sb by Raman scatt. 78−19453
InSb, polar semicond., resonant magneto-Raman scatt. 79−51958
InSb, Raman scattering study of unoxidised Sb in anodic oxide films 80−88985
InSb, reson. Raman scatt. under uniaxial stress near E_1 gaps 79−42960
InSb, spin flip Raman scattering, gain, linewidth, effective g-value 78−22167
p-InSb, spin-flip Raman scattering, review 80−108209
InSe, directional dispersion of extraordinary phonons 79−65154

Raman spectra of inorganic solids continued
InSe, exciton and polaron anisotropies, reson. Raman scatt. study 80−76033
InSe, layer cpd., reson. Raman scatt. at higher Mo exciton edge 79−28764
InSe, layer cryst., Raman and IR refl. spectra meas. 79−95777
InSe, layer semicond., Raman scatt. meas. 78−35134
InSe, layer single cryst., Raman scatt. meas. 78−76478
InSe, layer single crystal, infrared and Raman spectra 78−92070
InSe, layer type, Raman spectrum exam. 78−23461
InSe, Raman scatt. spectra 79−69846
InSe, Raman scatt. spectra, optical phonon freq., cryst. vibr. freq. types 80−29744
InSe, Raman spectra, inter-, intra-layer interaction estimates 78−88313
InSe, second order Raman spectrum and phase transition 79−38545
InTe, Raman spectra, phonon modes 80−40109
In_2ZnI_4, ionic conductivity, Raman spectra 77−69113
$IrBr_6^{2-}$, resonance spectra, vibrational and electronic Raman effects 79−47437
$IrCl_6^{2-}$, resonance spectra, vibrational and electronic Raman effects 79−47437
IrF_6, neat and mixed cryst., Raman scatt., Jahn-Teller interaction in ground state 79−38540
K halide solids, lattice dynamics, three body force shell model studies 79−55841
KAg_4I_5, solid electrolyte, Raman spectra 79−73934
$KAlCl_4$, cryst., Raman spectra, orthorhombic space group, Cl splitting of $AlCl_4^-$ 77−85700
$KAl(SO_4)_2.12H_2O$, single cryst., Raman spectra, temp. depend., SO_4^{2-} site dynamic disorder 77−40219
K_3AsO_4-$KAsO_3$, glass and cryst., Raman and IR spectra 79−99862
$KB_5O_8.4H_2O$, polariton Fermi reson., spontaneous parametric light scatt. 78−87923
$K_2Ba(NO_2)_4$, ferroelastic, Raman spectra and phase transition 79−56800
KBr, doped with F-centres, Raman spectra meas. excitation in F and K bands 80−16027
KBr:MnO_4^-, many-phonon impurity reson. Raman scatt. 80−60603
KBr:MnO_4^-, model system, reson. Raman spectra, general behaviour obs. 80−60592
KBr:MnO_4^- (MnO_4^{2-}) Raman scatt. spectra, freq. and type of symm. of internal vibr. of impurity centres 79−15466
KBr:Tl, impurity-induced first-order Raman scatt., critical-point and critical-line anal. 79−19884
KBr(I), absolute cross sections of second order Raman scatt. 78−39548
$KBrO_3$, near-forward Raman scatt. by polaritons 78−43842
$KBrO_2F_2$, struct. data, vibr. spectra 77−39563
KCN, cryst. phases at press. up to 55 kbar, Raman spectra obs. 79−82975
KCN, disordered ordinary and metastable phases, light scatt., press. depend. 78−95151
KCN, dynamics of CN^- ions near phase transitions at 83K 80−80717
KCN, order-disorder transition, light scatt., Raman obs. 77−1672
KCN, plastic phase, Raman scatt. spectra *(French)* 80−11379
KCN, polymorphism, high pressure, Raman spectra 78−88302
KCN, Raman diffusion spectra, IR absorpt. in phases II and III *(French)* 80−84741
KCN, Raman spectra, at very high press. 79−1759
KCN-KCl mixed system, order-disorder transition, Raman spectra obs. 78−15113
KCNS, librational modes in phase transition, Raman spectra obs. 79−55885
KCNS, single cryst., IR and Raman multiphonon bands, factor group anal. 77−4644
K_2CO_3-SiO_2 glass forming batch, Raman spectroscopy 78−64519
K_2CO_3-SiO_2-As_2O_3, laser Raman spectrosc. study of ions in quenched reaction mixtures 80−25357
$K_2(Cd(CN)_4)$, vibr. spectra, isotope substitutions, force consts. determ. *(German)* 77−61750
$KCdCl_3:Co^{2+}$, Zeeman Raman scatt. and Zeeman IR absorpt. spectra 79−56782
KCl, F-centre first order reson. Raman spectra, line shape freq. depend. 77−32370
KCl, Raman spectra and vibrational modes of V_K centre meas. 78−80338
KCl, TSM study of lattice statics and dynamics 79−82292
KCl:CN^-, Raman scatt. from tunnelling and hindered rotational sites 77−66507
KCl:MnO_4^{2-}, Raman scatt. spectra, bands due to ν_1, vibr. of MnO_4^{2-} 79−15466
KCl:Tl, impurity-induced first-order Raman scatt., critical-point and critical-line anal. 79−19884
$KClO_4$:MnO_4^-, reson. Raman excitation profiles for totally symmetric mode, vibronic struct. 80−50309
$K_3Co(CN)_6$, Raman scatt. and electronically-induced phase transition at 130K 77−90142
K_2CoF_4, 2-dimens. Ising antiferromag., mag. excitons, Raman scatt. obs. 80−66181
K_2CoF_4, pseudo Ising antiferromag., inelastic light scatt. by mag. excitons 80−11377
K_2CoF_4, two-dimensional antiferromag., one- and two-magnon Raman scatt. 79−51945
$K_xCs_{(1-x)}Al(SO_4)_2$, solid soln., Raman and IR spectrum study *(French)* 79−47453
$K_3Cu(CN)_4$, isotopic mixed crystal with ^{12}C and ^{13}C, Raman scattering 78−76476
$K_2Cu(H_2O)_6(SO_4)_2$, IR and Raman vibr. spectra 79−28743
$K_2Cu(H_2O)_6(SeO_4)_2$, IR and Raman vibr. spectra 79−28743
KD_2AsO_4, ferroelec., high temp. phase transition, Raman spectra 80−71338
KD_2AsO_4, ferroelectric, high temp. phase transitions, proton dynamics 80−76023
KD_2AsO_4, phase transition and centre-area-wing-scattering 78−84540
KDP-type cryst., Raman scattering and phase transitions, deuteration effects 78−76400
KD_2PO_4, IR and Raman polarised spectra, rel. to crystal struct. 78−56489
$KDy(MoO_4)_2$, polarised IR and Raman struct., $^{92}Mo/^{100}Mo$ isotope effect 80−108198
αKEu$(PO_3)_4$, vibr. spectra 80−34905
$K_3Fe(CN)_6$, pressure induced reduction, Raman spectra 80−66776

Raman spectra of inorganic solids continued
$K_3Fe(CN)_6$, Raman scatt. and electronically-induced phase transition at 130K 77−90142
$K_4Fe(CN)_6.3H_2O$, C-N vibrs., Raman study 80−40106
$K_4Fe(CN)_6.3H_2O$, dynamic disorder and ferroelec. transition, Raman spectra obs. 77−81069
$K_4Fe(CN)_6.3H_2O$, effect of ordering on OH Raman bands 79−51959
$K_4Fe(CN)_6.3H_2O$ ferroelectric cryst., vibrational spectrum of $[Fe(CN)_6]^{4-}$ anion 77−69839
$K_4Fe(CN)_6.3H_2O$, Raman spectrum and dielec. relax. 78−19476
K_2FeF_4, Raman scatt. in two dimens. antiferromagnet 78−19488
K_2FeF_4, two dimensional planar antiferromag., mag. excitations, Raman and far IR spectra obs. 78−72343
K_2FeF_4, two-dimensional antiferromag., with easy-plane anisotropy, mag. excitations and two-magnon Raman scatt. 80−65839
$KFe(MoO_4)_2$, phase transitions at 312 and 139K 80−70396
KH_2AsO_4, and deuterated isomorph, E-mode splitting in ferroelec. phase, Raman scatt. meas. 77−16296
KH_2AsO_4, and deuterated isomorph, ferroelectric mode and molecular vibr. press. depend. 78−19424
KH_2AsO_4, ferroelec. modes, polariton lineshape calc. 77−8585
KH_2AsO_4, ferroelec., temp. broadening of hard mode Raman lines near Tc 78−88296
KH_2AsO_4, ferroelec., high temp. phase transition, Raman spectra 80−71338
KH_2AsO_4, ferroelectric, high temp. phase transitions, proton dynamics 80−76023
KH_2AsO_4, pres. depend., LF dielec. response, ferroelec. props. 78−15120
KH_2AsO_4, Raman linewidth, isotope effect 77−8565
$K(H_{1-x}D_x)_2PO_4$, ferroelec., Raman scatt. intensity, pseudo-spin model calc. 77−52024
$KH_{2(1-x)}D_{2x}PO_4$, Raman spectra, effects of deuteration on proton tunnelling modes and coupled optic modes 77−59570
$KH_{2(1-x)}D_{2x}PO_4$, Raman spectra of overdamped mode 79−91427
KH_2PO_4, anharmonic phonons and central peaks at struct. phase transitions 79−95775
KH_2PO_4, E-mode splitting in ferroelec. phase, Raman scatt. meas. 77−16296
KH_2PO_4, E-symmetry Raman spectra 79−38535
KH_2PO_4, ferroelec., Raman internal-mode line broadening by proton jumps 77−43981
KH_2PO_4, ferroelec., temp. broadening of hard mode Raman lines near Tc 78−88296
KH_2PO_4, ferroelec. phase transition, soft phonons, Raman scatt. obs. *(Japanese)* 79−65880
KH_2PO_4, laser light scatt. spectroscopy 78−10156
KH_2PO_4, paraelec., Raman scatt. spectra of B_2-polariton and B_2(LO) modes 79−28762
KH_2PO_4, paraelectric phase, forward and backward Raman scatt. 79−33681
KH_2PO_4, Raman scatt. near T_c, search for soft modes 78−15114
KH_2PO_4, Raman scatt. for polaritons of mixed B_2-E symm. 79−56795
KH_2PO_4 type crysts., evidence of non-linear behaviour of soft modes, Raman spectra 79−33639
KH_2PO_4 type ferroelectrics, coupled tunnel-phonon modes, isotope effect 79−69205
$KHSeO_3$, and deuterated analog, vibr. spectra 79−24311
$KH_3(SeO_3)_2$, and $KD_3(SeO_3)_2$, anharmonic phonons and central peaks at struct. phase transitions 79−95775
KI, containing F-centres, calc. 77−16306
KI doped with F-centres, mag. vibr. Raman scatt. 77−4636
KI, X-irrad., V-centres 79−91429
$KI:NO_2^-$, first-order Raman scatt. meas. 77−52085
$KI:NO_3^-$, Raman spectra, high press., low temp. effects 78−52479
$KI:S_2$, Raman spectra, orientational dynamics 78−56482
$KI:Se_2^-$, reson. secondary emission, total spectrum *(Russian)* 78−19551
$KI:Tl^+$, pre-resonant enhancement of Raman scatt. 80−7354
KIO_3, temp. depend. Raman spectra and phase transitions *(Russian)* 78−15171
$K_2InCl_5.H_2O$, crystal structure and H-bonding 80−64978
$KLa(PO_3)_4$ (α and β forms), vibr. spectra 80−34905
$K_{0.75}Li_{0.25}TaO_3$, press. depend. of impurity soft modes, low energy Raman scatt. meas. 78−2852
$K^+M^{III}(SO_4)_2$, M=Al^{3+}, Cr^{3+}, Fe^{3+}, Raman and IR spectrum study *(French)* 79−47453
$K_2Mg(S_2O_3)_2.6H_2O$, isolation, struct., decomposition *(French)* 78−52506
$KMn_{1-x}Co_xF_3$, Raman scatt. by mag. excitations 77−55775
$KMnF_3$, precursor order and Raman scatt. near displacive phase transitions 80−45061
K_2MnF_4 and K_2NiF_4, two-dimens. antiferromag., two-magnon Raman scatt. linewidth, finite temp. 77−66508
K_2MnF_4, perovskite type layer struct., far IR reflectivity and Raman spectra 77−15511
$K_2MnF_4:Co^{2+}$, Raman spectra meas. 77−12389
$K_2MnF_4:Ni^{2+}$, and undoped, magnon spectra, Raman and far IR spectra meas. 77−20573
$K_3Mn_2F_7$, antiferromagnet, two magnon Raman scatt. 78−15164
$K_3Mn_2F_7$, quadratic double layer antiferromag., two-magnon Raman scatt. 80−66183
$K_3Mn_2F_7$, two magnon Raman scatt., magnon dispersion, susceptibility, Green's function methods 80−50340
KN_2AsO_4, phase transition and centre-area-wing-scattering 78−84540
KNCO, polycryst., IR and Raman spectra, lattice and internal modes 77−32369
KNCSe, IR and Raman spectra, internal and external modes 77−16312
KNO_2 polymorphs, high press. vibr. spectra 77−85725
KNO_3 (II), struct. props., disordered groups 77−66486
KNO_3, antiferroelec., press. induced II to IV phase transition, Raman scatt. 78−15161
KNO_3 polycrystalline specimens, effect of cryst. size on parameters of LF Raman spectrum *(Russian)* 77−28581
KNO_3, Raman and IR spectra and lattice vibrs. 80−60565
KNO_3, Raman spectroscopic study of NO_3^- component with temp. 78−76458
KNO_3, vibrations of isotopic impurities, IR reflection and Raman spectra meas. 77−51465
KNO_3-urea solid eutectic mixtures, Raman, IR spectra, line shifts, width 77−55793
$K_3N(SO_3)_3.2H_2O$ and ^{15}N derivative, Raman and IR spectra, $N(SO_3)_3^{3-}$ normal coord. anal. 79−91433

Raman spectra of inorganic solids continued
$K_2NaGaF_6:Cr^{3+}$, magneto-optical study of $^2T_{1g}$, $^4T_{2g}$, ^2E_g-$^4A_{2g}$ transitions 80−71384
$K_xNa_{1-x}TaO_3$, press. depend. of impurity soft modes, low energy Raman scatt. meas. 78−2852
$KNbO_3$, anomalous scatt. and asymmetrical line shape in Raman spectra 77−20853
$KNbO_3$, ferroelec. cryst., IR and Raman spectra, mode coupling 80−66194
$KNbO_3$, ferroelectric soft modes and order-disorder transition 77−47534
β-$KNd(PO_3)_4$, vibr. spectra 80−34905
$KNiF_3$, electronic UV laser excited Raman, scatt. by mag. excitons 78−68492
K_2NiF_4, electronic UV laser excited Raman, scatt. by mag. excitons 78−68492
$K_3Ni_2F_7$, quadratic double layer antiferromag., two-magnon Raman scatt. 80−66183
$KNi_xMn_{1-x}F_3$, mixed antiferromagnet, light scatt. meas. 80−16025
$KNi_xMn_{1-x}F_3$, two-magnon Raman scatt. 77−66509
K_2O-MgO-B_2O_3:Cu^{2+}, micro-inhomogeneities, EPR and Raman study 80−84080
K_2O-PbO-SiO_2, structural units, Raman spectroscopy 77−20847
K_2O-SiO_2 glass, Raman scattering of dissolved CO_3^{2-} ions 78−27848
K_2O-SiO_2-Al_2O_3 glasses, Raman spectra 79−73925
K_2O-SiO_2-GeO_2 digermanosilicate glass, Raman study of structure 79−77524
K_2O-SiO_2-GeO_2 metagermanosilicate glass, Raman study of structure 79−77523
$(K_2O)_x(SiO_2)_{1-x}$ glass, pure and with As_2O_3, Raman study of As 80−84733
$K_2O.2GeO_2$, powder Raman spectra, compared with digermanosilicate glass 79−77524
$K_2Pt(CN)_4Br_{0.3}3.2H_2O$, linear conductor, dynamical aspects of fluctuations 79−33715
$K_2Pt(CN)_4Br_{0.3}.3.2H_2O$, deuterated, coupling of charge density wave and water mode 77−4646
$K_{1.75}Pt(CN)_4.1.5H_2O$, Raman scatt. and luminesc. studies 80−25394
$KReO_4$, vibr. spectrum, Raman and IR spectra obs. 80−55104
K_2SO_4, α-β phase transition, Raman scatt. study *(French)* 80−55096
K_2SO_4, D_{2h}^{16} and C_{2v}^9 phases, internal and external vibrs. 79−47446
KSO_3F, disordered cryst., IR and Raman spectra, internal modes assignment, space group *(French)* 79−95742
$KSc(MoO_4)_2$, soft modes and Raman spectrum at ferroelastic phase transitions 79−47450
K_2SeO_4, 77-300K, soft mode and phase transitions obs. *(Japanese)* 77−43988
K_2SeO_4, anharmonic phonons and central peaks at struct. phase transitions 79−95775
K_2SeO_4, ferroelec., incommensurate struct., dynamic props. *(Russian)* 80−11373
K_2SeO_4, improved Raman spectra at room temp. 78−56487
K_2SeO_4, incommensurate phase transition, stress depend. of T_c 79−4391
K_2SeO_4, incommensurate phase transitions under existence of Lifshitz invariant, Raman scatt. 79−15416
K_2SeO_4, incommensurate structure, IR and Raman activity of soft mode 79−28738
K_2SeO_4, lower freq. soft-mode in ferroelec. phase 77−81065
K_2SeO_4, phase mode in incommensurate phase, Raman scatt. obs. 80−80766
K_2SeO_4, Raman scatt. and dielec. props. 80−11313
K_2SeO_4, Raman scattering spectra and discovery of soft mode 78−76442
K_2SeO_4, Raman spectra, effects of temp., substitutional cations, and stress 80−71405
K_2SeO_4, single cryst., orthorhombic, Raman spectra 77−73140
K_2SeO_4, soft modes below incommensurate transition Raman and Brillouin scatt. meas. 79−91387
K_2SeO_4, structural transition, polarised Raman spectra 80−75349
K_2SnBr_6, transform. dynamics probed by Raman scatt. and microscopy 78−63832
K_2SnCl_6, structural phase transitions, Raman spectra 77−73143
K(TCNQ), Raman spectra from 30 to 2300 cm^{-1} 80−11392
$KTa_{1-x}Nb_xO_3$, paraelectric phase, defect induced fluctuations, Raman meas. 79−15423
$KTaO_3$, Raman scatt. and ferroelec. soft modes 77−16300
$KTaO_3$, stress-induced ferroelectricity, Raman scatt. obs. 77−40190
$KTaO_3$:Li(Na)(Nb), microscopic distortions in paraelec. phase 78−75793
$K_2(TeBr_6)$, far IR and Raman spectra and phase transitions 80−11376
$K_5(UO_2)F_9$, optical spectra, vibr. freqs. calcs. *(Russian)* 78−31205
$K_3(UO_2)_2F_7.2H_20$, single cryst., polarised Raman spectra, vibr. modes assignment *(French)* 80−29728
$K_2(UO_2)_3F_8.4H_2O$ and $K_3(UO_2)_2F_7.2H_2O$, IR and Raman vibr. spectra *(French)* 79−51937
K_2XY_6 (X=Sn, Te, Y=Cl, Br), low temp. vibr. spectra, lattice dynamics and phase transitions 79−73917
$K_2(Zn(CN)_4)$, vibr. spectra, isotope substitutions, force consts. determ. *(German)* 77−61750
$K_2Zn(H_2O)_6(SO_4)_2$, IR and Raman vibr. spectra 79−28743
$K[Ag(CN)_2]$, Raman scatt., press.-induced phase transitions and phonons 79−33698
La-B, amorphous, B-rich, low freq. modes, Raman scatt. obs. 80−108202
LaB_6, synthesis and props. *(Japanese)* 80−40255
$LaBO_3$, single cryst., not cut parallel to principal axes, Raman spectra birefringence effect 79−69837
$La(BrO_3)_3.9H_2O$, IR and Raman spectra, vibr. asignments 78−84569
$LaCl_3$, Raman intensity anal. 79−33710
LaF_3, zone centre optical phonon stress dependence, point group symm., Raman spectra meas. 79−78686
$La(NO_3)_3.6H_2O$ single cryst. polarised Raman spectra *(French)* 77−1670
$LaNbO_4$, Raman scatt. and fluoresc. spectra 80−20625
$LaNbO_4$, room temp. phase exam. 78−26536
$LaNbO_4:Eu^{3+}$, single cryst., photoluminesc. obs., vibronic transition dichroism 77−69890
La_2O_3, Raman spectra, lattice vibrs. 79−87440
LaP_5O_{14}, ferroelastic transition, polarised Raman study 80−16035
La_2S_3, vibr. spectra, factor-group anal. 80−80793
$La_2(SO_4)_2.9H_2O$, Raman spectra meas. *(French)* 77−20855
$La_2(SO_4)_3.9H_2O$, and isotopic forms, water librations, Raman obs. *(French)* 79−28754

Raman spectra of inorganic solids continued
$La_2(SO_4)_3.9H_2O(D_2O)$, cryst., polarised Raman spectra, phase transition *(French)* 77−66497
LaTe, metallic, phonon density of states, Raman scatt. expt. 78−23451
$LiBaPO_4$, vibrational spectra and cryst. struct. 78−39536
LiC_6, Raman spectrum, rigid band model anal. 79−4800
$^7Li_2CO_3$, and $^6Li_2CO_3$, polycryst., Li-O Raman bands 79−42969
$^7Li_2CO_3$, and $^6Li_2CO_3$, polycryst., low freq. IR and Raman bands assignments 79−42970
LiCl, and LiBr, glassy aq. solns., Raman spectra, rel. to amorphous ice and liq. water 79−47423
LiCl:Ni^{2+}, first order induced Raman scatt. from Ni^{2+} and cation vacancies 77−48169
LiCl-Li_2O-P_2O_5 glass system, vitreous domain, struct., elec. cond. *(French)* 80−70135
LiCl(Br)(I), glassy aqueous soln., LF region Raman spectra 80−84729
LiD, resonance Raman scatt. *(Russian)* 78−52503
$LiEu(PO_3)_4$, vibr. spectra 80−34905
LiF, Raman spectra and vibrational modes of V_K centre meas. 78−80338
$LiGaO_2$, light scatt. *(German)* 79−28730
$LiGaO_2$, Raman scatt., optical modes determ. 79−15463
LiH, resonance Raman scatt. *(Russian)* 78−52503
LiH(D), resonant Raman scattering in crystals with self-trapping excitons 80−7344
LiH(D), second-order Raman spectra 79−47443
$Li_{1-x}H_xIO_3$, dielec. behaviour, Raman and IR spectra 77−32357
LiH_2PO_3, Raman and IR spectra of transverse and longitudinal modes *(French)* 80−60573
$LiHSeO_3$, and deuterated analog, vibr. spectra 79−24311
$LiH_3(SeO_3)_2$, IR and Raman spectra, internal modes, intra- and inter-H-bond tunnelling 78−43853
$LiIO_3$ crystal, coherent antiStokes Raman scatt. by polaritons 79−36961
$LiIO_3$ crystal, noncollinear stimulated Raman scatt. using parallel pump beam 80−78912
α-$LiIO_3$, hexagonal cryst., vibrs. and force consts. 79−69220
$LiIO_3$, possible separation of direct and cascade processes in active combination scatt. Raman spectroscopy 78−13764
$LiIO_3$, Raman induced Kerr effect with elliptical polarisation 78−42392
$LiIO_3$, Raman spectra and phase transitions 77−16316
α-$LiIO_3$, Raman spectra behaviour in electrostatic field *(Chinese)* 80−7333
$LiIO_3$, Raman-induced Kerr effect 77−40227
$LiIO_3$, Stokes and antiStokes scatt. by LF polaritons 77−77202
α-$LiIO_3$, temp. depend. studies of Raman spectra of polaritons in region of phase transition 78−76467
$LiKSO_4$, polarised Raman and IR reflection spectra, internal and external mode assignments 77−16293
LiN_3, evidence for N_3^- from static and dynamic props. 78−60465
Li_3N, IR and Raman spectra and lattice dynamics 78−48177
Li_3N phonon spectra and lattice dynamics 77−59580
Li_3N, superionic conductor, cryst. growth and struct., phys. props., book contrib. 79−42308
β-$LiNH_4SO_4$, lattice modes and phase transition, polarised Raman meas. 77−20859
$LiNH_4SO_4$, phase transitions and phys. props. 78−76399
$LiNO_2$, Raman spectra, 18-493K, polycryst., comparison with other nitrites 79−87425
$LiNO_3$, Raman spectroscopic study of NO_3^- component with temp. 78−76458
$^{6,7}LiNO_3$, cryst. vibr., Raman and IR spectra 79−15445
$LiNO_3$-$NaNO_3(KNO_3)$ solid eutectic mixtures, Raman, IR spectra, line shifts, widths 77−55793
$LiNbO_3$, comparative frustrated total refl. and Raman scatt., fundamental mode freq. and phonon dispersion 77−28579
$LiNbO_3$, dispersion law of polaritons, refr. index in IR, and Raman spectra meas. 78−27232
$LiNbO_3$, dispersion law and temp. depend. of polariton damping constant 79−95779
$LiNbO_3$, hyper-Raman scatt. *(Russian)* 78−87102
$LiNbO_3$, inverse Raman scatt. by polaritons 78−23434
$LiNbO_3$, low freq. Raman scatt. spectra of polaritons, photographic recording 79−73952
$LiNbO_3$, non-centrosymm. crystal, hyper-Raman scatt. obs. 78−94409
$LiNbO_3$, Raman line phonon relative intensities *(German)* 77−59582
$LiNbO_3$, Raman scatt. intensities, photorefractive index change effects 78−84590
$LiNbO_3$, Raman spectra temp. depend. 77−40239
$LiNbO_3$, Raman spectra and dielec. props. near Curie point 79−38530
$LiNbO_3$, spontaneous parametric scatt. line profile, IR absorpt. coeffs. 80−25377
$LiNbO_3$, temp. dependence of Raman scattering 77−16297
$LiNbO_4$, dispersion of vibrational excitations, Raman scatt. 78−84588
Li_2O-Al_2O_3-SiO_2-TiO_2 system glasses, Raman spectra obs. of glass-ceramics form. 80−60825
Li_2O-B_2O_3-P_2O_5, glass, mech. and elec. props 80−84228
Li_2O-Fe_2O_3-siO_2 glass, struct. and crystallisation behaviour 78−83738
Li_2O-Li_2SO_4-B_2O_3 vitreous electrolytes, ionic cond. and Raman spectra *(French)* 80−24656
Li_2O-LiX-B_2O_3 glass, X=halogen, high anionic cond. of new solid electrolytes 80−107546
Li_2O-SiO_2-GeO_2 digermanosilicate glass, Raman study of structure 79−77524
$^{6,7}LiOH$, LiOD, polycryst., Raman active modes and isotopic effects 79−87424
$Li_2O.2GeO_2$, powder Raman spectra, compared with digermanosilicate glass 79−77524
$LiPO_3$-Li_2SO_4, new Ag^+ and Li^+ ion glass conductors, glass transition, Raman spectra *(French)* 79−47094
$LiPO_3$-LiX(X=I, Br, Cl) glass, ionic cond. *(French)* 79−99365
$LiPbPO_4$, vibrational spectra and cryst. struct. 78−39536
Li_2S-GeS_2, glass forming region, struct. and ionic cond. 80−88358
$Li_2SO_4.H_2O$, $^6Li/^7Li$ and H/D substituted, IR and Raman spectra, vibr. and librational modes 77−85716
$Li_2SO_4.H_2O$, X-ray diffr., IR and Raman spectra, internal optic modes, mol. dipole model 77−76493
Li_2SiO_3, IR and Raman spectra, normal coord. anal. of unit cell vibrs. 77−81090
$Li_2Si_2O_5$-Li_2SO_4 glasses, electrical cond. and Raman study of struct. *(French)* 79−65482

Raman spectra of inorganic solids continued
$Li_2Si_2O_5$-TiO_2 glasses, struct. and crystn. investigation using Raman spectra 80−38918
$LiSrPO_4$, vibrational spectra and cryst. struct. 78−39536
$LiTaO_3$, low freq. Raman scatt. spectra of polaritons, photographic recording 79−73952
$LiTaO_3$, Raman spectra and dielec. props. near Curie point 79−38530
Li_4WO_5, IR, Raman, luminesc. spectra meas., cryst. struct. investig. 77−52074
$LiZnVO_4$, high press. spinel modification, vibr. spectra 78−35124
$Lu_{2-x}Si_2O_7$:Eu_x, synthesis and spectroscopic study 80−84846
$Lu_2Si_2O_7$, IR and Raman spectra, internal and external modes 79−61365
$MgAl_2O_4$, lattice dynamics, rel. to space group of spinel 78−59898
$MgCl_2$:Co^{2+}, Zeeman electronic Raman scatt. spectra 79−42962
$MgCl_2$-alkali metal chloride system, solid and molten states, struct. props., Raman spectra 80−76011
MgF_2, absolute first order Raman polarisabilities 78−64369
MgF_2, Raman spectra, cross section determ. 78−56471
MgF_2, rutile structure, dielectric props., neutron and Raman scatt. exam. 78−79684
Mg_2Ge, semicond., electronic band struct., reson. Raman scatt. meas. 77−12384
$Mg(H_2O)_6SiF_6$, Raman spectra, vibr. modes 79−61369
$Mg(NH_3)_6(ClO_4)_2$, solid, mol. rot., Raman contour, quasielastic neutron scatt., and PMR obs. 79−87444
MgO film, graphitic C detected by surface Raman spectra 80−2297
MgO, second-order Raman scatt. 78−10894
MgO, surface, laser Raman fluoresc. background, OH^- excitation 78−10875
MgO:Co^{2+}, electronic and impurity-induced Raman scatt. 80−100659
MgO-Na_2O-B_2O_3, Raman scatt. studies of glass struct. 77−90147
$Mg(OH_2)_6(SiF_6)$, phase transitions, spectrometric exam. *(French)* 78−88291
$Mg_2P_2O_7$, α- and β-phase, vibr. spectra, Raman and IR spectra 78−19467
MgR_2S_4, (R=Sc, Yb, Tm), IR and Raman spectra, force consts. 78−68503
Mg_2Si, semicond., electronic band struct., reson. Raman scatt. meas. 77−12384
Mg_2Si, stress effects on Raman spectra 77−20851
Mg_2SiO_4, fosterite, lattice dynamics, IR and Raman spectra meas. 79−65153
Mg_2Sn, semicond., electronic band struct., reson. Raman scatt. meas. 77−12384
Mg_2Sn, stress effects on Raman spectra 77−20851
$Mg_xZn_{1-x}Te$, long wavelength optical phonon replica 78−60468
Mn^{++}, in nearly tetrahedral clusters, ^4E levels, orbit-lattice interaction and Jahn-Teller effect, spectra obs. 80−24860
$Mn_3B_7O_{13}Cl$ improper ferroelec., orthorhombic phase, Raman spectrum, lattice vibrs. 78−43849
$MnBr_2$, vibr. struct. in cryst. field electronic transitions 78−59895
$Mn(C0)_5$ Br-Re$(C0)_5$Br, polycryst., ν(C0) vibr. intermol. Raman intensity transfer 80−60564
$Mn_xCd_{1-x}Te$, lattice vibrs., Raman and IR spectra meas. 80−93311
$Mn_xCd_{1-x}Te$, phonons, Raman scatt. and IR absorpt. meas. *(French)* 80−97275
$MnCl_2$, vibr. struct. in cryst. field electronic transitions 78−59895
$MnCl_2.2H_2O$, phonons and electronic transitions, Raman spectra 79−28761
$MnCl_2.2H_2O$, Raman spectra and lattice dynamics 79−28742
$Mn_3(Co(CN)_6)_2.xH_2O$, mol. vibr. in cryst., normal mode anal., Raman and IR obs. 77−76494
$Mn_{1-x}Co_xF_2$, Raman scatt. by mag. excitations 77−55775
MnF_2, absolute first order Raman polarisabilities 78−64369
MnF_2, inelastic light scatt. from antiferromag. polaritons, theory 77−73144
MnF_2, Raman spectra, cross section determ. 78−56471
MnF_2, two-magnon Raman scatt., temp. effects 77−48179
MnF_2:Fe^{2+}, temp. depend. of magnon pair-mode energies, Raman scatt. meas. 77−20577
MnF_6^{2-}, $A_2{}^IM^{IV}F_6$ hosts, luminesc., IR and Raman spectra, 5K, assignments 77−20904
MnO_4^-, reson. Raman lines, Stokes-antiStokes intensity ratio meas. 77−6786
$Mn(OH_2)_6(SiF_6)$, phase transitions, spectrometric exam. *(French)* 78−88291
$(Mn_xRe_{1-x})_2(CO)_{10}$, Raman spectra, intramol. vibr. coupling, ^{13}C substitution 79−47431
$Mn_xRe_{1-x}(CO)_5X$(X=Cl, Br), 0<x<5, vibr. spectra in the 2000 cm^{-1} region of mixed and isotopic crystals 78−84585
$MnTa_2O_6$, columbite struct., X-ray diffr., IR and Raman spectra *(French)* 78−63727
Mo complex, $MoOCl_3.2Ph_2SO$, prep. and characterisation 78−30592
Mo complexes, dinuclear, chem. and spectroscopic props. 77−77239
MoF_6, cryst., overall vibr. band struct., excitons 77−90136
MoF_6 crysts., density of exciton states, two-particle and mixed cryst. spectra 78−2829
MoF_6, orthorhombic crysts., Raman spectra, int./external mode separation and factor group anal. 77−90135
MoO_3, catalysts, supported on aluminas, Raman obs. of struct. 79−28734
MoO_3, Raman scatt. and struct. props. 77−55780
MoS_4^{2-}, anharmonicity consts., reson. Raman spectra 77−61754
MoS_2(2H), Raman spectra, phonon modes, high press. effects 80−40111
$MoSe_4^{2-}$, anharmonicity consts., reson. Raman spectra 77−61754
$MoSe_2(Te_2)$, IR and Raman spectra, lattice vibrs. interlayer bonding 80−40110
β-N_2 cryst., vibr. Raman spectra 80−60558
N_2, solid, α- and γ-forms, Raman spectra, vibron and lattice freq. shifts, libration 80−16020
N_2, solid, α- and γ-phases, Raman intensities of internal and external modes 79−33706
N_2, solid, gamma-phase, anharmonic lattice vibr. 79−33705
N_2, solid, Raman spectra vibron and lattice freq. shifts, librational force consts., α- and γ-phases 78−19460
α-N_2, solid, Raman spectra vibron bands, a priori calcs. 78−31181
N_2, solid, Raman spectroscopy up to 374 kbar 80−7353
α-N_2 solid, time-resolved CARS, disorder effects on coherent vibr. states 80−93342

Raman spectra of inorganic solids continued
N_2:CO, IR and Raman spectra, vibron band, vibron-phonon combination bands 78−68495
N_2-CO mixed cryst., librational motion, Raman obs. 78−6661
$(ND_4)_2BeF_4$, ferroelec. transition, Raman spectra obs. *(Russian)* 78−23408
ND_4Cl, ordered phase, Raman spectrum, dipole and polarisability derivatives 77−52072
$(ND_4)_2Cu(OD_2)_2Cl_4$, Raman spectra, order-disorder transition *(French)* 79−91436
ND_4DS, polycryst., vibr. spectrum, lattice dynamics 77−90138
ND_4I, Raman spectrum, press. effects 80−97261
ND_4IO_4, Raman spectra, libration lattice modes 80−60575
ND_4NO_3, low temp. phase, Raman scatt. meas. 78−84568
ND_4NO_3, Raman spectra meas., 250-420K 77−20845
$(ND_4)_2(SO_4)_3$, ferroelec. langbeinites, Raman scattering 80−34926
NF_3, plastic cryst., Raman spectra, Coriolis coupling and transition dipole 78−39533
NH_3, IR and Raman intensity of lattice vibrs., theory 80−11381
$NH_4Ag_4I_5$, Raman spectra, internal vibrs. of NH_4^+ ions 78−72497
$NH_4Ag_4I_5$, solid electrolyte, Raman spectra 79−73934
NH_4AlCl_4, crystal struct., X-ray, Raman, IR and NMR 78−63720
$(NH_4)_2BeF_4$, ferroelec. transition, Raman spectra obs. 77−85705
$(NH_4)_2BeF_4$, ferroelec., incommensurate struct., dynamic props. *(Russian)* 80−11373
NH_4Br and NH_4I, Raman scatt., 1 bar-7 kbar, 86-295 K 80−34909
NH_4Br, partially disordered, librational modes below 235K, Raman scatt. obs. 78−72500
NH_4Br, partially disordered, librational modes below disorder-order phase transition temp. 78−79680
NH_4Br, phase diagrams, from Raman meas. under high press. 78−52776
$(NH_4)_2Cd_2(SO_4)_3$, ferroelec. langbeinites, Raman scattering 80−34926
NH_4Cl crystal, polariton light scattering spectra in zone of dissociated states 79−47029
NH_4Cl, dispersion of vibrational excitations, Raman scatt. 78−84588
NH_4Cl, obs. of Raman scatt. by Cu vapour laser 78−95586
NH_4Cl, ordered phase, press. depend. of Raman scatt. meas. 77−12388
NH_4Cl, ordered phase Raman spectrum, dipole and polarisability derivatives 77−52072
NH_4Cl, orientational disorder, Raman and far IR spectra 78−23447
NH_4Cl, polariton Raman spectra, bound and many particle states 77−32372
NH_4Cl, Raman scatt. at polarons near intramol. vibrs. 77−44003
NH_4Cl, Raman scatt. of light on limiting and nonlimiting dipole vibr. 80−11402
NH_4Cl Raman spectra, pressure effects 80−97268
NH_4Cl, vibrations of isotopic impurities, IR reflection and Raman spectra meas. 77−51465
$(NH_4)_2CuCl_4.2\ H_2O$, lattice dynamics, anal. of Raman scatt. measurements 80−34149
$(NH_4)_2CuCl_4.2H_2O$, Raman sepctra, dynamics, struct., phase transition 79−47434
$(NH_4)_2CuCl_4.2H_2O$, order-disorder transition, Raman spectra obs. 79−61357
$(NH_4)_2H_3IO_6$, Raman spectra and phase transition 77−77196
NH_4HS, polycryst., vibr. spectrum, lattice dynamics 77−90138
$NH_4H_3(SeO_3)_2$, Raman spectra meas. 78−10899
α-NH_4HgCl_3, Raman study of phase transition *(French)* 80−11378
NH_4I, orientational disorder, Raman and far IR spectra 78−23447
NH_4I, phase diagram from Raman meas. under high press. 78−52776
NH_4I, Raman spectra at high press. 79−47459
NH_4I, Raman spectrum, press. effects 80−97261
NH_4IO_4, Raman spectra, libration lattice modes 80−60575
$((NH_4)_{1-x}K_x)_2\ CuCl_4.2H_2O$, Raman scatt. spectra 79−15459
$((NH_4)_xK_{1-x})_2SnCl_6$, mixed cryst., spectroscopic study 79−33712
$(NH_4)_5Mo_2Cl_9.H_2O$, resonance Raman spectra, $MO_2Cl_8^{4-}$ vibrs. 78−64350
NH_4NO_3 crystals, NH_4^+ ion symmetry in phases II-V, Raman spectra obs. 80−66200
NH_4NO_3, low temp. phase, Raman scatt. meas. 78−84568
NH_4NO_3, Raman scatt. in region of extended IV-V phase transition 79−99887
NH_4NO_3, Raman spectra meas., 250-420K 77−20845
NH_4NO_3, Raman spectra of low temp. phases 78−92081
NH_2O_2, long-lived radical prod. by photolysis of ammoniacal KO_3 soln. 77−16838
$(NH_4)_2PO_3F$, H_2O, X-ray diffraction and Raman spectra struct. determ., external mode temp. depend. *(French)* 78−52507
NH_4ReO_4, ND_4ReO_4, Raman spectrum, temp. depend. 78−80335
$(NH_4)_2SO_4$, phase transition mechanisms by optical spectroscopy 79−15411
$(NH_4)_2SO_4$, pure and Rb doped, ferroelec. transition, light scatt. meas., dielec. and elastic props. 78−43822
$N_2H_6SO_4$, orthorhombic, low-temp. phase transition, Raman spectra meas. 77−24849
$(NH_4)_2SiF_6$, cryst. phases, Raman obs. 20-290K 77−66495
$(NH_4)_2SnBr_6$, structural phase transitions study by Raman scatt. 80−93318
$(NH_4)_2SnCl_6$, $^{35,37}Cl$ NQR, Raman spectra and spin lattice relax., hindered rot. 80−54974
$(NH_4)_2(TeBr_6)$, far IR and Raman spectra and phase transitions 80−11376
$(NH_4)_2(TeCl_6)$, IR and Raman spectra, lattice and internal modes, phase transition 78−6659
$(NH_4)_2TiF_6$, vibr. spectra 77−8569
$NH_4UO_2(NO_3)_3$, Raman spectra 6-293K, phase transition 78−27220
$NH_4[TcO_4]$, powder, Raman spectrum 80−39016
N_2O_2, IR spectra of solid, Raman spectra of solid and liq., vibr. anal. 77−81093
$(^{14}NO)_2$ and $(^{15}NO)_2$ solids, Raman spectra at 20K 77−73139
$NOClBCl_3$, solid, Raman spectroscopy study *(French)* 79−69834
Na, Raman transients obs. in Doppler free two-photon excitation 77−61728
Na_2S-S-GeS_2 system, glass formation, struct. and ionic conduction 80−54138
$NaAlCl_4$, Raman spectra, cryst. struct. *(French)* 80−60578
$NaBrO_3$, IR and Raman spectra, vibrs., dipolar coupling effect 78−43852
$NaBrO_3$, Raman spectra, intramolecular vibrs. and lattice vibrs. *(Russian)* 77−1683

Raman spectra of inorganic solids continued
$NaBrO_3$, temp. depend., 77-400K *(Russian)* 78−23466
NaCN, cryst. phases at press. up to 55 kbar, Raman spectra obs. 79−82975
NaCN, FCC, orientational anisotropy of CN^- ions, Raman spectra meas. 77−36247
NaCN, plastic phase, Raman scatt. spectra *(French)* 80−11379
NaCN, Raman diffusion spectra, IR absorpt. in phases II and III *(French)* 80−84741
NaCN, Raman spectra, at very high press. 79−1759
NaCN, Raman spectrum, hydrostatic press. effects 78−6663
NaCl, containing Na colloids, first-order Raman spectra 79−73943
NaCl, F-centre aggregation, initial stage study by Raman scatt. 79−56791
NaCl(Br) (F) (I), lattice dynamics and statics, three-body-force shell model 80−49323
$NaClO_3$, γ-irradiated, metastable O_2 reson. Raman scatt.,, excitation profile, polarisation meas. and decay kinetics 77−14437
$NaClO_3$, IR and Raman spectra, vibrs., dipolar coupling effect 78−43852
$NaClO_3$, reson. Raman scatt. from metastable O_2 produced by γ-irrad. 78−60432
$NaClO_3$:O_3^-, form. by γ-irrad., reson. Raman scatt., temp. depend. 78−92062
$NaClO_3$-$NaBrO_3$, Raman spectra, mode coupling and ^{79}Br-^{81}Br isotope effects 79−19873
$NaClO_3$-$NaBrO_3$ mixed crystals, internal optic modes, Raman and IR spectra meas. 79−95746
$NaClO_4$, anhydrous, Raman, IR and FIR spectra, 90 to 600K *(German)* 79−78687
$NaClO_4$, Raman spectra temp. depend. near 581K phase transition 78−56477
$NaCrS_2$, antiferromag. semicond., Raman and far-IR spectra 79−47454
$Na(D_xH_{1-x})_3(SeO_3)_2$, Raman spectra and nature of phase transitions 78−80341
$NaD_2PO_4.2D_2O$, Raman spectra, phonon freqs. 79−61370
$NaD_3(SeO_3)_2$, polarised Raman spectra, lattice vibrs., ferroelec. transition 77−24851
$NaH_2PO_4.2H_2O$, Raman spectra, phonon freqs. 79−61370
$NaHSeO_3$, and deuterated analog, vibr. spectra 79−24311
$NaH_3(SeO_3)_2$, β to δ ferroelec. transition under press. Raman spectra study 80−80725
$NaH_3(SeO_3)_2$, IR and Raman spectra, internal modes, intra- and inter-H-bond tunnelling 78−43853
$NaH_3(SeO_3)_2$, $NaD_3(SeO_3)_2$, IR and Raman spectral interpretation of ferroelectric phases 79−24312
NaI, resonant Raman scattering in crystals with self-trapping excitons 80−7344
NaI:F, electron-lattice coupling of F-centres, optical props. 80−60641
$NaIO_4$, normal coord. anal., internal and external modes 79−23684
$NaLO_3$, disorder of NO_3 ions, rel. to Raman spectrum temp. depend. *(Russian)* 78−2099
$NaNH_4SeO_4.2H_2O$, ferroelectric phase transition mechanism 78−31162
$Na^{15}N_x{}^{14}N_{1-x}O_3$ mixed crystal, Raman spectra determ. of phonon density of states *(Russian)* 80−93313
$NaNO_2$, ferroelec., ang. dispersion of internal phonon modes, Raman meas. 79−51211
$NaNO_2$, ferroelec., lattice dynamics, two-phonon Raman scatt. and IR absorpt. 79−33684
$NaNO_2$, ferroelectric, second-order vibr. spectra and dispersion of phonon branches 79−69847
$NaNO_2$, ferroelectric transitions, group theoretic comparison with $AgNaNO_2$ 80−7311
$NaNO_2$, mechanism of ordering type ferroelec. transition, vibr. spectroscopy 78−76402
$NaNO_2$, ν_1 Raman linewidth and reorientation of NO_2^-, temp. depend. 78−72522
$NaNO_2$, Raman and IR spectra, destructive Fermi reson. 77−16309
$NaNO_3$, disordered, temp. depend. of Raman spectra, Rayleigh wing scatt. 78−31209
$NaNO_3$, isotopically mixed, vibr. spectra, IR and Raman spectra 79−28770
$NaNO_3$, press. induced ferroelec. transition, soft mode dynamics, Raman scatt. meas. 78−72475
$NaNO_3$, Raman scatt. band lineshape, orientational disorder of NO_3^- ion in pre-transition region 77−8589
$NaNO_3$, Raman spectroscopic study of NO_3^- component with temp. 78−76458
$NaNO_3$, soft mode dynamics at ferroelec. transition 78−80308
$NaNO_3$, vibrations of isotopic impurities, IR reflection and Raman spectra meas. 77−51465
$NaNO_3$-urea solid eutectic mixtures, Raman, IR spectra, line shifts, width 77−55793
$Na_2N_2O_3$, vibr. spectra, assignments 77−38670
$NaN0_3$, fine structure changes on interaction with weak shock waves *(Russian)* 80−54313
$NaNiF_3$, electronic UV laser excited Raman, scatt. by mag. excitons 78−68492
Na_2O-B_2O_3-P_2O_5, glass, mech. and elec. props 80−84228
Na_2O-CaO-MgO-Al_2O_3-SiO_2 glasses, ternary and quaternary, struct., Raman spectra obs. 77−36229
Na_2O-Li_2O-β-$Al_2O_3.H_2O$, water mol. vibrs., IR and Raman spectra 80−89006
Na_2O-MgO-B_2O_3:Cu^{2+}, micro-inhomogeneities, EPR and Raman study 80−84080
Na_2O-SiO_2-Al_2O_3 glasses, Raman spectra 79−73925
Na_2O-SiO_2-GeO_2 digermanosilicate glass, Raman study of structure 79−77524
Na_2O-SiO_2-GeO_2 metagermanosilicate glass, Raman study of structure 79−77523
Na_2O-TiO_2-SiO_2 glass, IR refl., Raman and EPR spectra, struct. *(Russian)* 78−2860
$NaPF_6$, high press. phase diagram, vibr. spectra 78−60446
$NaPF_6.H_2O$, IR and Raman spectra 77−61749
$NaPF_6.H_2O$, Raman spectra 79−19875
Na_2S, dielectric const., transverse and longitudinal optical mode, static dielectric const., effective charge 79−73892
Na_2S-GeS_2, glass, synthesis, elec. cond., Raman spectra, temp. and composition depends. *(French)* 79−14962
Na_2S-P_2S_5, glass forming region, struct. and ionic cond. 80−88358

Raman spectra of inorganic solids continued
Na_2S-XS_2, X=Si, Ge, glass forming region, struct. and ionic cond. 80−88358
NaSCN, cryst., Raman spectral lines, temp. depend., anion disorientation *(German)* 78−52514
$Na_2S.9H_2O$-NaOH-H_3BO_2, glass, IR and Raman spectra of boro-ultramarine, exam. of S_3^- presence 78−68502
Na_3SbS_4, vibrational spectra, internal SbS_4 vibr. assignments 80−66199
$Na_3SbS_4.9H_2O(D_2O)$, vibrational spectra, internal SbS_4 and $H_2O(D_2O)$ vibr. assignments 80−66199
$Na_3UO_2F_5$, IR and Raman spectra, struct. *(French)* 79−11409
$Na_xV_2O_5$, metallic, Raman scatt. 78−80358
$Na_2W_2O_7$, Raman and IR spectra 80−25356
Na_xWO_3, metallic, light-scatt. studies 80−45071
Na_xWO_3, X>0.5, temp. depend. of Raman active soft modes, tetragonal-tetragonal transition 78−48180
$Na_4[UO_2(CO_3)_3]$, vibr. and low temp. optical spectra, rel. to U recovery from oceans 79−73939
Nb complex, $NbOCl_3.2L$ (L=Ph_2SO, Ph_3PO and $(Me_2N)_3PO$), prep. and characterisation 78−30592
Nb complex, prep. by halide reaction with tetramethylurea and tetramethylthiourea, and characterisation 79−15972
$NbCl_5.CD_3CN$, Raman spectra and Teller-Redlich product rule 79−69817
$NbCl_5.CH_3CN$, Raman spectra and Teller-Redlich product rule 79−69817
$NbCl_5.POCl_3$, Raman spectra, normal coordinate treatment 77−46568
NbN, Raman spectra and superconductivity of various phases 78−68506
$NbOPO_4$, cation ordering effect on Raman spectra 78−43850
NbS_2 (3R), Raman spectra, vibr. modes 79−87449
$NbSe_2$, 2H polytype, effect of incipient CDW on second-order Raman spectra 78−80357
$NbSe_2$ (2H), effect of CDW fluctuations on Raman active optic phonon freq. 78−87750
$NbSe_2$ (2H), Raman scatt. from supercond. gap excitations 80−93340
$NbSe_2$ (2H), Raman scatt. by supercond. gap excitations, coupling to CDWs 80−103956
$NbSe_3$, phonon study of chemical bonding 80−20645
$NbSe_2$(2H), Raman spectra of soft modes at CDW transition 77−16301
$Nb_nW_{6-n}O^{(n+2)-}$, config., IR and Raman spectra 77−42324
$Nd(BrO_3)_3.9H_2O$, IR and Raman spectra, vibr. asignments 78−84569
Nd_2O_3, Raman spectra, lattice vibrs. 79−87440
$Nd(OH)_3$, dynamical effects of interaction between 4f electrons and optical phonons 80−108196
NdP_5O_{14}, ferroelastic, Raman scatt. from soft phonons, 4.2-600K, monoclinic-orthorhombic transition temp. 79−51962
Nd_2S_3, vibr. spectra, factor-group anal. 80−80793
Ni (111) surface with adsorbed CO, H_2 and O_2 79−28769
Ni, chemisorption of H_2, Raman spectra, vibr. bands 79−61368
Ni complexes, $[Ni(NH_3)_6](ClO_4)_2$ and $[Ni(ND_3)_6](ClO_4)_2$, phase transitions, Raman spectra meas. 77−66501
Ni, with chemisorbed CO 80−2755
Ni-Cr, surface oxide characterisation by Raman spectroscopy 80−50308
$Ni^{2+}+MoO_3$ catalyst on Al_2O_3, Raman spectrum 80−108742
$Ni_3B_7O_{13}I$, cubic, Raman spectrum, 88-295K, vibr. anomalies 78−76479
$Ni_3B_7O_{13}I$, dynamics of ferroelec. phase transition, Raman spectra obs. 79−33630
$Ni_3B_7O_{13}I$, Raman spectra in paraelec. phase 78−60434
$Ni_3B_7O_{13}I$, struct. and mag. transitions, light scatt. study 79−24308
$NiBr_2$, vibr. struct. in cryst. field electronic transitions 78−59895
$NiBr_2(Cl_2)$ two-phonon vibronic progressions, Raman obs. 80−29742
$NiCl_2$, Raman spectrum at and below antiferromagnetic ordering temp. 79−99871
$NiCl_2$, vibr. struct. in cryst. field electronic transitions 78−59895
$Ni_{1-x}Co_xF_2$, Raman scatt. by mag. excitations 77−55775
NiF_2, electronic UV laser excited Raman, scatt. by mag. excitons 78−68492
$Ni(H_2O)_6SiF_6$, $Ni(D_2O)_6SiF_6$, Raman spectra, vibr. modes 79−61369
$Ni(NH_3)_6(NO_3)_2$, Raman spectra exam. of orientational phase transitions 78−31184
$Ni(NH_3)_6X_2$, (X=Cl, Br, I, ClO_4, BF_4) and d, far IR, Raman spectra, 80-300K 78−31190
NiO, antiferromag., two magnon reson. Raman scatt. 79−33703
NiO-Cr_2O_3-$MgSiO_3$ methanation catalyst, S-resistant, IR and Raman spectra 80−93290
$Ni(OH_2)_6(SiF_6)$, phase transitions, spectrometric exam. *(French)* 78−88291
NiS_2, Raman scatt., optical phonon peaks obs. 77−85728
$NiS_{2-x}Se_x$, first-order Raman scattering 80−108206
$NiSiF_6.6H_2O$, dynamical props. of H_2O below 300K, Raman spectroscopic obs. 79−8140
$(Ni[NH_3]_6)(ClO_4)_2$, reorient. correlation times of NH_3 and ClO_4 groups, Raman obs. 79−28748
γ-O_2 cryst., vibr. Raman spectra 80−60558
O_2, mol. dynamics, solid-state phase transitions effects, Raman spectra *(French)* 77−42372
O_2, phase equilibria near 298K, Raman spectral study of solid and fluid 80−19937
O_2, solid, lattice dynamics 79−95095
$OsBr_6^{2-}$, resonance spectra, vibrational and electronic Raman effects 79−47437
P, amorphous, vibrational excitations of defect sites 80−49332
P, amorphous red, Raman scattering 80−11416
P, black phosphorous struct., Raman vibr. spectra and bonding 80−11411
P, bulk red amorphous, Raman scatt. and IR absorption 79−24323
PBr_3, Raman scatt. spectra in gas, liq. and solid states, mol. dynamics *(Russian)* 77−55779
PCl_5 III, Raman spectra of phase formed by high-press., PCl_6^- ionising dissoc. 79−82968
PCl_5, sublimed phase studied by ^{31}P NMR, Raman spectra and X-ray diffr. 80−100209
PCl_5-HCl_2, Raman spectra, solid and melt, species identification *(German)* 80−45083
PCl_5-$SnCl_4$, mixtures, liq. and solid, Raman spectra study *(German)* 79−91451
PCl_5-$TiCl_4$, gas, melt, and solid, dimer-monomer conversion, Raman spectra obs. *(German)* 79−70320
PD_3, liq. and plastic cryst. states, vibr. dephasing and correl. functions 79−69036
PF_2D, normal coordinate analysis of vibrational spectra 79−68233
PF_2H, normal coordinate analysis of vibrational spectra 79−68233
$PF_2H(D)$, Raman and IR spectra 80−14147
γ-$PH_{3-x}D_x$, Raman and IR spectra, phase transition, internal and external modes 77−77191
PHD_2, vibr. dephasing in liq. and solid PD_3, calcs. 80−19884
$PMo_{12}O_{40}$, vibr. anal., symmetry coords. and force field anal., IR and Raman spectra 77−15522
P_2O_5, glassy, high freq. vibr. bands, central force model 80−49330
P_2O_5, pure vitreous, Raman spectra and struct. 79−69838
P_2O_5 vitreous, Raman cross sections, rel. to appl. in fibre Raman lasers 78−31176
$(P_2O_5)_x$-$(SiO_2)_{1-x}$, spontaneous Raman scattering *(French)* 79−78674
(Pb,La)TiO_3, soft E(TO) phonons, and phase transitions, Raman spectra, −200 to 400°C 78−15109
Pb, aq. corrosion film, IR and Raman spectroscopy 80−55567
Pb electrode, in situ surface phase study by laser Raman spectroscopy 80−103542
Pb-As-S semiconductor glasses, far IR transmission and Raman scattering 77−63419
$Pb_5(AsO_4)_3Cl$, mimetite, vibr. spectra, normal coord. anal. 78−88305
$(Pb_{1-x}Ba_x)_5Ge_3O_{11}$, ferroelec. phase transition, dielec. const. and quasi-elastic light scatt. 80−71289
$Pb_{5-x}Ba_xGe_3O_{11}$, Raman spectra, temp. depend. of ferroelec. soft A-mode 79−33682
$PbCO_3.PbX_2$ (X=Cl,Br), vibr. props. 79−24319
$PbCl_2$, evidence for diffuse transition, elec. cond. and Raman spectra meas. 79−73552
$PbCl_2$, Raman spectra, phonon modes 80−2754
PbF_2, polarised Raman scatt. in fluorite crysts., anharmonicity, high-temp. disorder 78−35132
PbF_2, Raman scatt. exam. at high temp. 77−32367
PbF_2, superionic conductor, theoretical investigation of Raman scatt. 78−80351
$Pb_5Ge_3O_{11}$, anharmonic phonons and central peaks at struct. phase transitions 79−95775
$Pb_5Ge_3O_{11}$, factor group anal., external and librational modes 77−36240
$Pb_5Ge_3O_{11}$, ferroelectric transition exam. by Raman scatt. 78−56439
$Pb_5Ge_3O_{11}$, ferroelectric soft mode exam., Raman spectra 79−42202
$Pb_5Ge_3O_{11}$, ferroelectric, anharmonic effects in low freq. symm. modes, Raman study 80−25365
$Pb_5Ge_3O_{11}$, light scatt. obs. of unresolved central peak 77−4649
$Pb_5Ge_3O_{11}$, paraelectric and ferroelectric, Raman spectra near ferroelectric transition 80−55090
$Pb_5Ge_3O_{11}$, Raman scatt., soft modes and damping near structural phase transition 79−28739
$Pb_5Ge_3O_{11}$, temp. depend. of A_{LO}-modes, Raman spectra meas. 78−2213
$Pb_5Ge_3O_{11}$:Ba,O, impurities, static central peak 78−92079
$PbGeS_3$, vitreous and cryst., IR and Raman spectra *(Russian)* 78−72527
$Pb_5(Ge_{1-x}Si_x)_3O_{11}$, ferroelec. soft mode, temp. and Si impurity, effects Raman scatt. 79−1762
$Pb_5Ge_{3-x}Si_xO_{11}$, ferroelec. soft mode, temp., press. and comp. depend. 78−80304
$Pb_{1-x}Ge_xTe$, electron-phonon interaction effect on ferroelec. transition 78−76416
$Pb_{1-x}Ge_xTe$, Raman scatt. from soft TO-phonon modes 79−95773
$Pb_{1-x}Ge_xTe$, TO phonon interaction with acoustic phonons near phase transition temp. 79−90776
$PbHAsO_4$, ($PbDAsO_4$), Raman spectra of ferroelec. transition proton tunnelling 78−23410
$PbHPO_4$, ferroelec. phase transition, Brillouin and Raman spectra obs. 79−33683
$PbHPO_4$, Raman spectra study of ferroelec. transition, proton tunnelling 78−23410
PbI_2, 2H polytype, anisotropy of lattice vibrs., optical modes analysis 77−7807
PbI_2 (2H), multi-phonon scatt. near direct absorpt. edge, resonant Raman obs. 79−87448
PbI_2 direct gap polar semicond., electron hole liquid phase diagram *(Russian)* 80−93314
PbI_2, high-pressure phase transition, optical props. meas., 300K and 78K 77−51495
PbI_2, Raman spectra, phonon dispersion curves, vibrational props., lattice parameters 79−69211
PbI_2 single crysts., resonant and nonresonant Raman spectra 77−69823
$Pb_2M_2^{III}Ge_2O_9$, (M^{III}=Fe,Mn,Sc,In), synthesis, X-ray diffr. and vibr. anal. 79−61360
$Pb_2M^{II}M^{IV}Si_2O_9$, (M^{II}=Mg,Ni,Co,Cu for M^{IV}=Sn; M^{II}=Co, Ni for M^{IV}=Ti), synthesis, X-ray diffr. and vibr. anal. 79−61360
$PbMoO_4$, Raman scatt. obs. of external and internal modes 79−69842
$PbMoO_4$, vibr. props. and struct., effect of hydrostatic press. 77−28571
$Pb(NO_3)_2$, Raman spectra temp. depend. anomalies in symmetric stretch region 79−61361
$PbNb_2O_6$, IR absorpt. spectra and diffuse Raman scatt., normal coord. anal. *(French)* 80−66198
$Pb_2Nb_2O_7$, Raman-scattering investigation of vibrational structure 78−76441
PbO-B_2O_3, glass exam. of Raman spectra *(Japanese)* 79−19894
PbO-GeO_2, glass, exam. of Raman spectra *(Japanese)* 79−19894
PbO-SiO_2, glass IR and Raman spectra, heat treatment conditions effect 79−66088
PbO-SiO_2 glass, IR and Raman spectra interpreted in terms of struct. 78−27213
PbO-SiO_2 glasses, density-of-states and structural forms, Raman spectra study 80−97255
Pb_3O_4, IR and Raman study of structural phase transitions *(French)* 78−84582
$(PbO)_x(SiO_2)_y$ glass, vibrational spectroscpic exam. 79−11417
PbO.$2B_2O_3$, vitreous, structural aspects studied by Raman scattering 77−8575
12PbO.6SiO_2.$PbSO_4$, crystn. from 2PbO-SiO_2-xSO_3 melts, struct. and vibr. spectra 80−59400
$Pb_3(PO_4)_2$, ferroelastic, Raman scatt. by soft vibr. involved in ferroelastic phase transition 80−16040
$Pb_3(PO_4)_2$-$Pb_3(VO_4)_2$, direct obs. of ferroelasticity 77−21203
$Pb_5(PO_4)_3Cl$, pyromorphite, vibr. spectra, normal coord. anal. 78−88305
$Pb_3(P_{1-x}V_xO_4)_2$, x=0.1, 0.2, Raman scatt. by low freq. vibrs. 80−55111
$Pb_3(P_xV_{1-x}O_4)_2$, ferroelastic phase transitions, lattice dynamics, dielec. and optical props. meas. 77−55334
Pb_2SiO_4-$PbSiO_3$, Raman and IR spectra of crystalline phases 80−3013

Raman spectra of inorganic solids continued
$Pb_{1-x}Sn_xTe$, soft-phonon-induced Raman scatt. 77−77209
$Pb_xSn_{1-x}Te$, oxide and Te monolayer films, Raman backscattering spectra 77−48211
$PbTa_2O_6$, IR absorpt. spectra and diffuse Raman scatt., normal coord. anal. *(French)* 80−66198
Pb(Ti,Zr)O_3, soft E(TO) phonons, and phase transitions, Raman spectra, −200 to 400°C 78−15109
$PbTiO_3$, amorphous, crystallisation process, DTA and Raman spectroscopy meas. 80−75161
$PbTiO_3$, damping of soft E-symmetry phonon, Raman scatt. meas. 78−67799
$PbTiO_3$, laser light scatt. spectroscopy 78−10156
$Pb_5(VO_4)_3Cl$, vanadinite, vibr. spectra, normal coord. anal. 78−88305
$PbWO_2$, IR and Raman multiphonon spectra, struct. 77−90143
$PbWO_4$, reflectivity, dispersion parameters and optical const. temp. depend. 77−28575
Pb(Zr,Ti)O_3, temp. and hydrostatic press. depend of vibr. modes, rel. to phase transforms 77−89510
Pd complex, linear ionic mixed valence cpd., IR and resonance Raman spectra rel. to lattice modes 80−25393
Pd mixed valence-mixed metal compounds, ionic crystals, longitudinal lattice modes, Raman spectroscopy 80−40099
Pd-H(D), vibr. modes Raman study 77−85713
Pr_2O_3, Raman spectra, lattice vibrs. 79−87440
$PrVO_4$, energy levels, opt. and NMR measurements 78−80226
Pt complex, $[Pt(en)_2][Pt(en)_2Cl_2](ClO_4)_4$, reson. Raman spectra 80−2760
Pt complex, linear ionic mixed valence cpd., IR and resonance Raman spectra rel. to lattice modes 80−25393
Pt complex, $PtCl_2$ (9-methyladeninium), laser Raman spectra 77−66499
Pt complex, $Pt(NH_3)_4Cl_2.H_2O$, Raman spectrum *(French)* 79−19876
Pt complexes, $Pt(NH_3)_4Cl_2$, $Pt(ND_3)_4Cl_2$, Raman spectra in solid state and aq. soln. *(French)* 79−19876
Pt, electrode, unroughened, I_2, I_3^- adsorbed from H_2SO_4-KI, Raman spectra 78−31689
Pt, mixed valence-mixed metal compounds, ionic crystals, longitudinal lattice modes, Raman spectroscopy 80−40099
Rb halides, role of quantum effects in lattice dynamics, Debye temp., shell model calcs. 80−70336
$RbAg_4I_5$, solid electrolyte, polarised Raman scatt. meas. 77−12376
$RbAg_4I_5$, solid electrolyte, Rayleigh-Brillouin and low-frequency Raman spectra 79−33720
$RbAg_4I_5$, solid electrolyte, Raman spectra 79−73934
Rb_2AgI_3, cryst. struct. and polarised Raman spectrum 77−69813
$RbAlCl_4$, solid state Raman spectra, 298-80K, vibr., struct. 79−28745
RbCN, molecular motion and ordering from dielec. and Raman techniques 79−73932
RbCNS, single cryst. factor group anal. of IR and Raman multiphonon bands 77−4644
$RbCaCl_3$, Raman scatt. study of phase transitions 80−71411
$RbCaF_3$, precursor order and Raman scatt. near displacive phase transitions 80−45061
$RbCdBr_3$, polarised Raman spectra 78−76443
$RbCdCl_3$, crystal struct., polarised Raman spectra and X-ray diffraction obs. 78−76443
RbCl, Raman spectra and vibrational modes of V_K centre meas. 78−80338
RbCl:Ag^+, first-order impurity-induced Raman scatt. 77−77216
RbCl:H^-, defect pairs of F-centres and U-centres, Raman meas. 79−7599
RbCl:NO_2^-, first-order Raman scatt. meas. 77−52085
$RbClO_3$/$RbBrO_3$ mixed crystals, internal optic modes obs., Raman and IR reflectance spectra 80−76024
$RbCoF_3$, mag. space group and Raman tensors in antiferromag. phase 79−82760
$RbCoF_3$, single oriented antiferromag. domain, polarised Raman scatt. under uniaxial stress 78−23463
$RbCoF_4$, 2-dimens. Ising antiferromag., mag. excitons, Raman scatt. obs. 80−66181
Rb_2CoF_4, pseudo Ising antiferromag., inelastic light scatt. by mag. excitons 80−11377
$RbEu(PO_3)_4$, vibr. spectra 80−34905
Rb_2FeF_4, two dimensional planar antiferromag., mag. excitations, Raman and far IR spectra obs. 78−72343
Rb_2FeF_4, two-dimensional antiferromag., with easy plane anisotropy, mag. excitations and two-magnon Raman scatt. 80−65839
$RbGa_3Br_{10}$, cryst., vibr. spectrosc. *(French)* 78−6667
RbH_2AsO_4, and deuterated isomorph, E-mode splitting in ferroelec. phase, Raman scatt. meas. 77−16296
RbH_2AsO_4, and deuterated isomorph, ferroelectric mode and molecular vibr. press. depend. 78−19424
RbH_2AsO_4, pres. depend., LF dielec. response, ferroelec. props. 78−15120
RbH_2AsO_4, Raman scatt. near T_c, search for soft modes 78−15114
RbH_2PO_4, Raman scatt. near T_c, search for soft modes 78−15114
$RbH_3(SeO_3)$, ferroelectric phase transition, Raman spectra meas. 79−19871
$RbH_3(SeO_3)_2$, Raman spectra meas. 78−10899
RbI, hyper-Raman spectra by single channel method 78−84591
RbI, IR active and silent modes, hyper-Raman scatt. obs. 79−61376
RbI, temp. depend. of second order Raman spectra 78−68512
$Rb^+M^{III}(SO_4)_2$, M=Al^{3+}, Cr^{3+}, Fe^{3+}, Raman and IR spectrum study *(French)* 79−47453
$RbMnCl_3$ crystal, structural phase transition, birefringence, elastic moduli and Raman spectra 80−15243
Rb_2MnCl_4, perovskite type layer struct., far IR reflectivity and Raman spectra 77−15511
$RbMn_{1-x}Co_xF_3$, Raman scatt. by mag. excitations 77−55775
$RbMnF_3$, two-spin Raman scatt. at high temp. 77−40225
$RbMnF_3$, zone-boundary magnon energy and damping, Raman scatt. meas. 78−31202
RbN_3, lattice vibration Raman study, tetragonal-cubic phase transitions 79−77743
RbNCO, polycryst., IR and Raman spectra, lattice and internal modes 77−32369
$RbNO_2$, Raman spectra temp. depend., NO_3^- ion external librational modes, IV→III transition, Raman spectra temp. depend., NO_3^- ion external librational modes 79−78662
RbO_2-Na_2O-P_2O_5 glasses, Raman and far IR spectra, vib. at cation site, struct. 78−60435
Raman spectra of inorganic solids continued
Rb_2O-Li_2O-P_2O_5 glasses, Raman and far IR spectra, vib. at cation site, struct. 78−60435
Rb_9O_2, ionic clusters in alkali metal suboxide cryst., struct., vibr. freqs., Raman spectra 79−37772
Rb_2PtI_6, cryst., role of ordinary and harmonic Raman processes, ^{127}I nucl., spin-lattice relax., obs. 79−8063
Rb_2SeO_4, single cryst., orthorhombic, Raman spectra 77−73140
$Rb_2(TeBr_6)$, far IR and Raman spectra and phase transitions 80−11376
$Rb_4(UO_2)_2F_8$-$2H_2O$, IR absorpt. and Raman spectra, normal coordinate anal. *(French)* 78−52509
Rb_2ZnBr_4, Raman scatt., normal-incommensurate-commensurate phase transitions, soft modes 80−40071
Rb_2ZnBr_4, soft modes obs. by Raman scatt. 80−97283
$Rb_2ZnBr_4(Cl_4)$, Raman spectra near incommensurate phase transitions 80−76013
Rb_2ZnCl_4, phase transitions, soft mode, Raman scatt. meas. 79−4389
Rb_2ZnCl_4, phase transition, Raman scatt. evidence 80−40116
Rb_2ZnCl_4, single crystals, Raman scatt. spectra, temp. range covering two phase transitions 80−7340
Re, Raman scattering spectrum at room temp. 80−25373
$Re(^{12}CO)_{5-y}(^{13}CO)_yX$(X=Cl, Br), 0<y<5, vibr. spectra in the 2000 cm^{-1} region of mixed and isotopic crystals 78−84585
ReF_6, cryst., Raman and absorpt. spectra, Jahn-Teller effect 78−6675
ReO_3 type lattice, group-theoretical symmetry anal. of vibr. *(Russian)* 80−10610
Ru complexes, carbonyl hydrides, pre-reson. Raman spectra, Ru-Ru and Ru-C modes 78−43854
S, mol. dynamics, solid-state phase transitions effects, Raman spectra *(French)* 77−42372
SF_6, cryst., IR and Raman spectra at 9 and 97K, cryst. struct. 79−87427
S_2F_{10} 77−6775
SF_5Br, Ar matrix and solid phase Raman and IR spectra, vibr. assignments 77−6775
SF_5Br, vibr. spectrum and normal coord. anal. 77−18926
SF_5Cl AR matrix and solid phase Raman and IR spectra, vibr. assignments 77−6775
SF_4O, vibr. spectra, struct. and thermodynamic props. 77−63416
$(SN)_x$, brominated, Raman spectra meas. 78−72519
$(SN)_x$ film and crystal, acoustic and optical phonons, Raman, i.r. and transmission spectra 77−4642
$(SN)_x$, phonon spectra, four-parameter valence force model rel. to Raman spectra 77−20027
S_2N_2, cryst. and partly polymerised films, Raman scatt., optical absorption 77−8673
S_4N_4, effects of pressure and temp. on phonons, Raman scattering study 80−7360
S_4N_4, press. and temp. depend., 0-10 kbar, 10-295K 78−15160
S_4N_4, Raman scatt. and opt. absorpt., press. and temp. depend. 77−36227
S_4N_4, solid and soln., IR and Raman spectra, vibr. assignment 78−74659
S_4N_4, vibrational spectra, effect of temp. and press. on phonons 79−37776
$(SNBr_{0.}$, Raman scatt. exam. 78−39550
$S_3N_3Cl_3$, solid and soln., IR and Raman spectra, vibr. assignment 78−74659
$S_4N_4H_4$, and -d_4, solid and soln., IR and Raman spectra, vibr. assignment 78−74659
$S_{8-x}(NH)_x$, (x=1,2,3,4), and deuterates, IR and Raman spectra, isotope shifts, mol. vibr. assignment 79−10110
$(SNI_x)_x$ crystals, reson. Raman scatt. meas. 80−66203
SO_2, IR and Raman spectra, mol. and lattice vibrs. 78−19464
$S(SiD_3)_2$, gaseous, liquid, solid phases, molecular vibr. exam. 78−25547
$S(SiH_3)_2$, gaseous, liquid, solid phases, molecular vibr. exam. 78−25547
Sb, amorphous, vibrational excitations of defect sites 80−49332
Sb, amorphous sputter-deposited film, vibr. props., Raman spectra meas. 77−63411
Sb, k=0 optical phonon temp. depend., Raman scatt. meas. 77−76509
$SbBr_x^{-y}(I_x^{-y})$, low freq. Raman and IR spectra, force consts. 80−55097
$SbCl_3$ and $SbBr_3$ mixture in CS_2, factor analysis and band contour resolution applications, book contrib. 78−21931
$SbCl_5$-$NbCl_5$, melt and solid-soln. Raman spectra, $SbNbCl_{10}$ dimer *(German)* 77−4645
$SbCl_5.CD_3CN$, Raman spectra and Teller-Redlich product rule 79−69817
$SbCl_5.CH_3CN$, Raman spectra and Teller-Redlich product rule 79−69817
$SbCl_5.POCl_3$, Raman spectra, normal coordinate treatment 77−46568
Sb_5O_7I, ferroelastic, Raman scatt. and symm. aspects of phase transition 77−8578
Sb_5O_7I, polytype 2MA, ferroelectric, ferroelastic, Raman scattering and symmetry anal. 79−38550
SbSBr, electronic and optical props. 78−34763
SbSI, electronic and optical props. 78−34763
SbSI, near tricritical point 78−15159
Sb_2Se_3, Raman spectra, Raman and IR-active modes 79−56776
SbSeI, electronic and optical props. 78−34763
Sb_2Te_3, $(Bi_{1-y}Sb_y)_2Te_3$, Raman and far infrared investigation of phonons 78−23453
$Sc_2Si_2O_7$, IR and Raman spectra, internal and external modes 79−61365
Se, amorphous, bulk, Raman scatt. near Tg 80−60596
Se, amorphous, bulk, reson. Raman scatt. 80−60597
Se, amorphous, Raman scatt. meas., comparison with liq. spectra 80−50328
Se, amorphous, Raman spectra, crystn. processes 80−60608
Se amorphous film, interference enhanced Raman scatt. 80−50326
Se film, resonance Raman spectrum 79−28760
Se, trigonal, Raman scatt. at very high press. 80−60566
Se-Ge, amorphous, Raman spectra and average band gap 80−50327
Se-Ge, chalcogenide glass, Raman scatt. and bond struct. 79−95772
Se-Ge glass, lattice vibr. spectra, photostruct. change, far IR absorpt. 78−72494
$SeCl_4$-$SbCl_5$ systems, Raman spectra *(German)* 80−93324
Si, amorphous, pure and hydrogenated, Raman spectra 79−61358
Si, amorphous, Raman spectra, vibrational properties 79−99881
Si, amorphous film, IR and Raman spectra of Si-H bonds 78−19482
Si, amorphous layers, RF-sputtered on sapphire, crystallisation by CW ion laser annealing 80−80109

Raman spectra of inorganic solids continued
Si, elasto-optic constants, real and imaginary, direct absorpt. and Raman scatt. meas. 80−97234
Si films, polycryst., glow discharge deposited below 250°C, struct. and morphology 80−49535
p-Si, heavily doped, intra- and interband Raman scatt. 79−95788
p-Si, heavily doped, intra- and interband Raman scatt. by free carriers 80−108208
n-Si, heavily doped, intraband Raman scatt. by free carriers 78−19483
n-Si, heavily doped, self energy of phonons interacting with free electrons, Raman scatt. 78−64366
Si, ion implanted, pulsed-laser annealed, Raman obs. 79−73189
Si, laser pulsed heating, lattice temp., Raman meas. 80−80780
Si, p-i-n structures, pinch effect expt. obs. 79−90971
Si, photoexcited, highly stressed, electronic Raman scatt. and antireson. 80−29737
Si, piezo-optical consts., Raman meas. 78−65951
Si, piezobirefringence above fundamental edge, Raman scatt. meas. 79−42941
Si, Raman cross section and its press. depend., theoretical study 79−91448
Si, Raman scattering absolute cross-section 80−11410
p-Si, Raman scattering by phonons and electrons, interference effects 78−60469
p-Si, Raman spectra, pseudopot. calc. of discrete-continuum interference 80−2747
Si, Raman spectrum, two-dimens. tensile stress effects 78−48173
Si, reson. Raman scatt. at indirect gap 79−73931
Si, stretched, lattice vibr. anharmonicity, influence of stress on elastic moduli, Raman spectra 80−80791
Si, temperature during CW laser heating, Raman scatt. meas. 80−76109
Si, thin slabs, vibr. freq. calcs., dimens. effect 80−60585
Si, X-ray resonance Raman scattering, solid target, proton bombarded 79−61465
Si:As, ion-implanted, laser recrystallisation by freq.-doubled Nd:YAG laser 79−77613
Si:B, As, first and second order Raman scatt. by pair modes 79−65869
Si:B, implanted, free carrier conc. and impurity location, Raman scatt. obs. 77−55295
Si:B, ion implanted, laser annealed, IR and Raman spectra 79−73914
Si:B, ion implanted, laser annealed, Raman scatt., Fano interactions, lattice damage 79−78711
Si:B, P, first and second order Raman scatt. by pair modes 79−65869
Si:F, amorphous, pure and doped, vibr. excitations at defect sites, IR and Raman spectra calc. 80−49329
a-Si:H, structural interpretation of vibr. spectra 79−69864
Si:H amorphous films, interference enhanced Raman scatt. 80−50326
Si-F-H:P, film, dark cond., struct., Raman scatt. 80−88588
Si-H (up to 15 at.%), amorphous, ion implanted, laser annealing obs. 79−69133
Si-H:P amorphous film, dark cond., struct., Raman scatt. 80−88588
Si-H(-D), film, IR and Raman spectra, H bonding effects 78−72515
$SiBr_4$, fine struct. resolution in Raman-active fundamentals 79−42967
SiC, amorphisation induced by ion bombardment, Raman spectroscopy 77−80551
SiC, H^+, D^+, He^+ ion bombardment, Raman scatt. and SEM anal. 77−35609
SiC, H^+, D^+ and He^+ ion implanted, Raman scatt. obs. of localised vibr. modes 78−6689
SiC, laser Raman spin-flip scatt. from excitons, luminesc. 80−80786
SiC, radiation damage, review 77−80553
p-SiC, spin-flip Raman scattering, review 80−108209
SiC, spin-flip scatt. of laser light from photoexcited excitons 80−93330
α-SiC, wurtzite type cryst., temp. depend. of one phonon Raman spectra, Gruneisen parameters 77−66500
SiC:Al, g-values, spin temp., determ. from Raman spectra 78−43856
SiF_4, mol. cryst., giant anomaly of intensity of vibrs. of isotopic impurity, Raman spectrum 79−73276
SiF_4, Raman spectra at 77K, scatt. angle, polaritons and space group 78−23439
Si_xGe_{1-x}, amorphous, vibr. props. 79−23693
$SiH_3PH_2BD_3$, vibr. analysis, spectra and structure of P-B compounds 78−84586
$SiH_3PH_2BH_3$, vibr. analysis, spectra and structure of P-B compounds 78−84586
α-Si_3N_4, Raman active modes, spectra 78−80326
Si_3N_4:Fe, α- and β-phases, Mossbauer and Raman obs. of state of Fe 79−33572
SiO_2, amorphous, intrinsic surface phonons, Raman scatt. and IR refl. 80−24728
SiO_2, amorphous, phonons, neutron, IR and Raman spectra calcs. 78−10150
SiO_2 and SiO_2-B_2O_3 glasses, struct. and phonon spectra 80−50324
SiO_2 fibres, LF optical phonons, Raman spectra 80−80789
SiO_2 films, Si-rich, amorphous Si region obs. 80−84400
SiO_2 glass, Raman spectra of dissolved molecular H_2 and D_2 79−33707
SiO_2, OH group interactions, IR and Raman spectra 78−80383
SiO_2, tetrahedral glass, Raman studies 78−71823
SiO_2, vitreous, band limits and vibrational spectra 79−73935
SiO_2, vitreous, H impregnated, Raman spectroscopy 77−36230
SiO_2, vitreous, LO vibrational modes, Raman and IR spectra 77−7819
SiO_2, vitreous, Raman active defects, thermal equilibration 80−55092
SiO_2, vitreous, Raman cross sections, rel. to appl. in fibre Raman lasers 78−31176
SiO_2 vitreous, Raman spectrum, bound OH, Si-O stretch vibr. 78−19462
SiO_2, vitreous, valence-attenuation pair defect, states, IR and Raman spectra 79−91442
SiO_2:H(D), γ-irrad., hydroxyls and hydrides form., detect. by Raman scatt. 77−32817
SiO_2:P_2O_5, optical fibre, stimulated Raman scattering *(French)* 79−27324
SiO_2-Al_2O_3 glass, Raman spectra and refr. index meas. 77−24836
SiO_2-Li_2O-Li_2SO_4, glass-forming region, struct. and ionic cond. 80−84320
SiO_2-TiO_2 glass phonons, IR and Raman spectra meas. 79−91447
SiO_x, amorphous and recrystallised layer, optical props. 80−25474
Si_2Te_3, cryst., IR reflection, Raman spectra 77−12393
SmB_6, f-d hybridisation, optic phonon anomalies 78−92080
$Sm_{0.8}La_{0.2}AlO_3$, high temp. Raman spectra, phase transition 79−61367

Raman spectra of inorganic solids continued
SmS, f-d hybridisation, valence fluctuation and phonon spectrum, Raman scatt. expts. 78−60464
SmS, f-d hybridisation, optic phonon anomalies 78−92080
Sm_3S_4, inelastic light scatt. 77−55788
Sm_3S_4, mixed valence system, inelastic light scatt., photoluminesc. 77−90145
α-Sn, reson. first and second order Raman scatt. 78−35144
Sn tetrahedral molecular solids, ^{119}Sn Mossbauer and Raman spectra 78−15070
$SnBr_4$, fine struct. resolution in Raman-active fundamentals 79−42967
$SnCl_2.2H_2O$, protonic order-disorder transition, H-bond vibr. Raman spectra temp. depend. 78−23437
$SnCl_2.2H_2O$, protonic order-disorder transition, inelastic light scatt. obs. 78−68497
SnI_2 single crysts., Raman scatt. of light 79−73950
SnI_4, mol. solid, dynamics, press. and temp. depend. 78−79691
SnI_4, Raman spectra, temp. and press. meas. and lattice dynamical calcs. 78−56472
$Sn_2P_2S_6$, ferroelec., IR and Raman spectra, photocond., edge absorpt. spectra, spontaneous polarisation, forbidden gap 78−68514
$Sn_2P_2S_6$, ferroelec. semicond., phase transition and lattice dynamics 80−60526
$Sn_2P_2S_6$ ferroelectric semicond., polarisation Raman scatt. spectra, X-ray struct. study 79−95778
$Sn_2P_2S_6$, soft mode, interaction of modes and crit. Rayleigh scatt. 79−99836
$Sn_2P_2S_6$, soft mode, temp. depend. of Raman spectra near phase transition 78−88263
$Sn_2P_2S_6$, soft mode props., Raman scatt. study 80−60525
$Sn_2P_2(S_{1-x}Se_x)_6$, solid solutions, ferroelectric soft mode freq., displacive transformations 80−29701
$(Sn_{1-x}Pb_x)_2P_2S_6$, solid solutions, ferroelectric soft mode freq., displacive transformations 80−29701
SnS, splitting and coupling of lattice modes 77−76503
SnS_2, Raman active mode assignments 77−12387
Sn_2S_3, mixed valence semicond., long wavelength phonons, full space group theoretical anal. 79−65873
$SnS_{2(1-x)}S_{2x}$ solid soln. system, long-wavelength optical phonons, Raman scatt. study 80−80794
SnS(Se), IR reflectivity and Raman spectra, phonon frequencies and dielec. const. 77−48166
SnS(Se), layer crystals, optical phonons, Is and Raman spectra 77−73148
$SnS_{2-x}Se_x$, layer cryst., Raman active modes 80−80767
$SnS_{2-x}Se_x$, Raman spectra 79−28763
SnS_2(2H and 4H), Raman scatt. and phonon frequencies 77−48159
SnSe, Raman scatt., zone centre optical phonons, layer-like struct. 78−48158
$SnSe_2$ (6Hb), Raman scatt. and phonon frequencies 77−48159
$SnSe_2$, Raman active mode assignments 77−12387
SnTe, carrier density depend. of soft TO-phonon, Raman scatt. meas. 78−6684
SnTe, electron-phonon interaction effect on ferroelec. transition 78−76416
SnTe, light scatt. from soft modes, theory above and below displacive transform. temp. 79−95791
SnTe, obs. of soft TO-phonon by Raman scatt. 77−69838
SnTe, Raman scatt. from soft TO-phonon modes 79−95773
SnX_6^{2+}, (X=Cl,Br,I), spectroscopic consts., environmental cation effects 79−56779
$SrAg_2I_4$, Raman and autocorrelation spectra, solid and soln. 79−38532
$Sr_xBa_{1-x}Nb_2O_6$, high press. phase transitions, Raman scatt. studies 80−71402
$Sr_{1-x}Cd_xF_2$, lattice dynamics 78−75763
$SrCl_2$ film, non-cryst., very-low-freq. inelastic light scatt. 80−25367
$SrCl_2$, non-crystalline film, disorder-induced Raman scatt. 80−11387
$SrCl_2$, single cryst., second order Raman spectrum *(French)* 78−80327
$SrCl_2$:S, S_2^- and S_3^- mol. paramag. centres, investigation using EPR, Raman and optical spectroscopy 79−51855
SrClF, cryst., Raman intensity anal., normal coord. anal. 78−72493
$SrCl_2.2(H,D)_2O$, IR and Raman spectra, force fields 80−2753
$SrCl_2.2H_2O$, IR and Raman spectra, force fields 80−2753
SrF_2, doped, Raman spectra using pulsed laser and gated detection 77−74529
$SrF_2(Cl_2)$, Raman spectra, 15 to 1300K, anharmonic vibr. effects 77−43990
$SrF_2(Cl_2)$, superionic conductor, theoretical investigation of Raman scatt. 78−80351
$SrF_2(Cl_3)$, polarised Raman scatt. in fluorite crysts., anharmonicity, high-temp. disorder 78−35132
$Sr_2KNb_5O_{15}$, Raman scatt. experiments in tetragonal tungsten bronze compounds 80−40113
$SrNO_3$, single cryst., normal Raman modes, temp. effects *(French)* 77−43998
$Sr(NO_3)_2$, Raman and infrared spectra, structure of nitrate ion from space groups 78−43002
$Sr(NO_3)_2$, Raman spectra temp. depend. anomalies in symmetric stretch region 79−61361
$Sr_2NaNb_5O_{15}$, Raman scatt. experiments in tetragonal tungsten bronze compounds 80−40113
$Sr_2Nb_2O_7$, high press. phase transitions, Raman scatt. studies 80−71402
$Sr_2Nb_2O_7$, optical mode softening in incommensurate phase 80−7352
α-$Sr_2P_2O_7$, Raman, IR spectra, factor group anal. and band assignment 78−35126
SrR_2S_4, R=rare earth, ternary sulphide with Th_3P_4 struct., vib. spectra 78−2844
$SrTa_2O_6$, structural study X-ray diffr., IR absorpt. and Raman spectra *(French)* 80−107173
$Sr_2Ta_2O_7$, soft optic phonon responsible for structural phase transition, Raman scatt. meas. 80−96618
$SrTiO_3$ 78−6678
$SrTiO_3$, absolute cross sections of second order Raman scatt. 78−39548
$SrTiO_3$, anharmonic phonons and central peaks at struct. phase transitions 79−95775
$SrTiO_3$, central peak in spectrum of ferroelec. mode fluctuations and dielec. losses, 4.2K 78−19432
$SrTiO_3$, centrosymmetric crystal, phonon polariton hyper-Raman scatt. obs. 80−76028
$SrTiO_3$, disorder manifestation, light scatt. spectra, high temp. 80−76017

Raman spectra of inorganic solids continued
$SrTiO_3$ ferroelectric modes, Raman spectra, neutron scatt. meas. 80−80727
$SrTiO_3$, heavily reduced, soft mode behaviour 80−71409
$SrTiO_3$, hyper Raman scatt. on polaritons, polariton branches *(Russian)* 80−50334
$SrTiO_3$, hyper-Raman scatt. spectra due to lattice vibr. 80−29732
$SrTiO_3$, IR active and silent modes, hyper-Raman scatt. obs. 79−61376
$SrTiO_3$, Raman scatt. and ferroelec. soft modes 77−16300
$SrTiO_3$, tetragonal, effect of impurities on Raman spectrum 80−2770
$SrWO_4$, vibr. props. and struct., effect of hydrostatic press. 77−28571
Ta complex, prep. by halide reaction with tetramethylurea and tetramethylthiourea, and characterisation 79−15972
$TaCl_5.CD_3CN$, Raman spectra and Teller-Redlich product rule 79−69817
$TaCl_5.CH_3CN$, Raman spectra and Teller-Redlich product rule 79−69817
TaS_2, 1T polytype, charge density waves effects on phonon modes, Raman spectra meas. 77−36245
TaS_2 (2H), Raman scatt. 77−1679
TaS_3, CDW state, Raman spectroscopy obs. 78−60439
TaS_3, Raman spectra, CDW induced metal-semicond. transition 80−11404
$TaS_2(Se_2)$, 2H polytype, effect of incipient CDW on second-order Raman spectra 78−80357
$TaS_2(Se_2)$, intercalated with ethylenediamine, Raman spectra 78−48182
$TaSe_2$ (2H), effect of CDW fluctuations on Raman active optic phonon freq. 78−87750
$TaSe_2$ (2H), Raman scatt. from CDW 80−93340
$TaSe_2$ (2H) and (1T), Raman spectroscopy of CDW state 78−35141
2H-$TaSe_2$, commensurate superlattice vibr., Raman spectra 77−16299
$TaSe_2$(2H), Raman scatt., charge density wave mode softening at superstruct. transition 77−8584
$TaSe_2$(2H), Raman spectra of soft modes at CDW transition 77−16301
TbAG, reson. electronic Raman effect, interferences, lifetime meas. 80−93294
$Tb_2(MoO_4)_3$, mode softening near ferroelec. transition, Raman and Brillouin spectra 79−33685
$Tb(OH)_3$, dynamical effects of interaction between 4f electrons and optical phonons 80−108196
TbP_5O_{14}, Raman scatt. at monoclinic to orthorhombic phase transition, soft mode behaviour 78−56486
$TbVO_4$, Jahn-Teller distortion, mag. field depend. 78−79733
Te, amorphous, Raman spectra, crystn. processes 80−60608
Te film, interference enhanced Raman scatt. 80−42273
Te, trigonal, Raman scatt. at very high press. 80−60566
Te_8 ring in zeolites, identification by Raman scatt. *(Russian)* 79−61378
TeO_2, glass, phonon density of states, Raman spectra *(French)* 77−20841
TeO_2, paratellurite, atomic motions corresponding to zone centre phonons 78−76461
TeO_2, paratellurite, lattice dynamics, IR refl. and Raman scatt. expts. 77−15518
TeO_2, paratellurite, phase transition at high-press., Raman and far IR spectra 78−80328
TeO_2, paratellurite, stress induced changes in Raman spectrum 78−39540
TeO_2, zone centre optical phonons under uniaxial stress 78−79700
TeX_6^{2-}, (X=Cl,Br,I), spectroscopic consts., environmental cation effects 79−56779
$ThSiO_4$, synthetic, Raman spectrum and lattice vibrs. 77−48160
Ti complex, $Ti_2Cl_8(CH_3NO_2)_2$, single cryst., struct., IR and Raman spectra, X-ray diffr. 78−43000
Ti film, interference enhanced Raman scatt. 80−40105
TiC, Raman scatt., phonon density of states 78−52499
TiC_x (x=0.97, 0.90, 0.80), Raman scatt. induced by C vacancies 78−52500
$TiCl_3$, vib. spectra 77−40231
$(TiCl_4.POCl_3)_2$, solid, IR and Raman spectra, vibr. assignments 78−43868
TiN, Raman scatt. supercond. transition temp., phonon density of states, Debye temp. 78−52499
TiO_2, anatase, effect of hydrostatic press. on Raman spectrum 79−61384
TiO_2, anatase, natural and synthetic crysts., Raman spectra and assignments 79−28752
TiO_2 anatase, Raman spectrum, temp. depend. 80−76027
TiO_2 devitrified glass, Raman spectra 79−78677
TiO_2, diffusivity of T and Raman scatt. meas. 79−86927
TiO_2, Raman spectra and struct. at high press. 79−87442
TiO_2, rutile, first order Raman spectrum, uniaxial stress effects 80−66196
TiO_2, rutile, first-order Raman spectrum, uniaxial-stress depend. 80−60586
TiO_2, rutile, Raman study at high press. 80−89002
TiO_2, second order Raman spectrum 79−61364
TiO_2, two-photon absorption coefficient rel. to inverse Raman cross section 78−6678
TiO_2-SiO_2 glass system, Raman and hyper-Raman light scatt. spectra 80−66187
Ti_xO_x film, interference enhanced Raman scatt. 80−40105
TiS_3, linear chain compound, lattice props., Raman spectral study 80−71421
$TiSe_2$ (1T), Raman studies of lattice dynamics 80−103962
$TiSe_2$, superlattice formation, Raman and far IR spectra 78−35135
$TlAsS_2$, Tl_3AsS_3, and Tl_3AsS_4, Raman and IR spectra *(Russian)* 77−66512
Tl_3AsS_4, optical phonons, Raman and refl. spectra 80−11400
TlBr, reson. Raman scatt., forbidden one phonon and intervalley scatt. at direct exciton 80−45073
TlBr, second order Raman scatt., reson. behaviour rel. to phonon bands 80−40101
$TlBrO_3$, polycryst., Raman and IR spectral assignments, room temp. 78−15156
Tl_4CdI_6, ionic conductivity, Raman spectra 77−69113
$Tl_2Cd_2(SO_4)_3$, ferroelec. langbeinites, Raman scattering 80−34926
TlCl, Raman spectra in melting region 78−27224
TlCl, second order Raman scatt., reson. behaviour rel. to phonon bands 80−40101
$TlClO_3$, polycryst., Raman and IR spectral assignments, room temp. 78−15156

Raman spectra of inorganic solids continued
$TlGaS_2$, layer ternary semicond., polarised Raman, IR reflect. spectra 78−68513
$TlGaS_2(Se_2)$, intralayer and interlayer modes 78−43876
$TlGaS_2(Se_2)$, optical phonons, IR and Raman scatt. meas. 78−59903
$TlGaS_2(Se_2)$, phase transforms. under hydrostatic press., Raman scatt. study 80−25366
$TlGaS_{2x}Se_{2(1-x)}$, layer solid soln., mixed one- and two-mode behaviour of optical phonons 79−47445
$TlGaSe_2$, layer ternary semicond., polarised Raman, IR reflect. spectra 78−68513
$TlGaSe_2$, Raman and IR spectra, zone centre optical phonons 78−76462
$TlGaTe_2$, IR refl. and Raman scatt. spectra, lattice vibrs. 80−40108
$TlGaTe_2$, multilayer cryst., lattice vibr. symm., IR absorpt. and Raman scatt. selection rules 80−39231
$Tl_6I_6M_{2/n}^{n+}(I_4)^{2-}$, (M=Pb, Ag, Au, $(Bi_{0.5}Tl_{0.5})$), struct., rel. to phonon spectra 80−71425
$TlIO_3$, polycryst., Raman and IR spectral assignments, room temp. 78−15156
β-$TlInS_2$, intralayer and interlayer modes 78−43876
β-$TlInS_2$, layer ternary semicond., polarised Raman, IR reflect. spectra 78−68513
$TlInS_2$, optical phonons, IR and Raman scatt. meas. 78−59903
$TlInS_2$, optical phonons, IR and Raman spectra *(Russian)* 79−10903
$TlInS_{2x}Se_{2(1-x)}$, layer solid soln., mixed one- and two-mode behaviour of optical phonons 79−47445
$TlInSe_2$, single crystals, optical phonons, Raman and infrared spectra studies 79−55842
$TlInSe_2(Te_2)$, multilayer cryst., lattice vibr. symm., IR absorpt. and Raman scatt. selection rules 80−39231
$TlInTe_2(Se_2)$, IR refl. and Raman scatt. spectra, lattice vibrs. 80−40108
TlN_3, lattice vibration Raman study, tetragonal-cubic phase transitions 79−77743
TlN_3, press. induced phase transition, Raman scatt. meas. 78−19468
TlN_3, press. induced transition dynamics, light scatt. 78−80362
$Tl_3Na(SO_3)_2$, α-phase, IR and Raman spectra, order of cryst. struct. *(French)* 77−85718
$TlSbF_6$, press. up to 25 kbar, anion libration obs. 78−6670
TlSe, optical phonons, IR and Raman scatt. meas. 78−59903
TlSe, Raman spectra, phonon modes 80−40109
TlSe, vibr. props., Raman and far IR spectra meas. 78−71800
Tl_2SeO_4, structural transition, polarised Raman spectra 80−75349
Tl_3TaS_4 and Tl_3PS_4, optical phonons, Raman spectra study 80−80790
$Tl_2(TeCl_6)$, IR and Raman spectra, lattice and internal modes, phase transition 78−6659
$Tl_2ZnBr_4(I_4)$, fast ionic cond. and order-disorder transition 79−99363
Tl_2ZnI_4, ionic conductivity, Raman spectra 77−69113
TmSe, intermediate valent, Raman scatt. 80−16038
UF_6, cryst., overall vibr. band struct., excitons 77−90136
UF_6 crysts., density of exciton states, two-particle and mixed cryst. spectra 78−2829
UF_6, orthorhombic crysts., Raman spectra, int./external mode separation and factor group anal. 77−90135
$UO_2(NH_2O)_2(H_2O)_2.H_2O$, cryst., Raman and IR spectra 77−63409
$UO_2S_2O_3.H_2O$, possible evidence for nonexistence of cpd. of given formula *(French)* 77−24279
$(V_{1-x}Cr_x)_2O_3$, Raman scatt. and phase transitions 80−71420
VI_2, antiferromag., zone-boundary phonon Raman scattering, modulation of exchange interaction 80−11386
VI_2, antiferromagnet, phonon Raman scatt. from spin superstructures 80−16030
VI_2, mag. 'Bragg' scatt. obs. through Raman scatt. 80−66179
VI_2, spin-dependent Raman scatt. from phonons 80−97274
VO_2, $V_{1-x}Nb_xO_2$, crysts. and polycryst. films, metal-semicond. transition, polarised Raman scatt. 77−90151
V_2O_3, phase transitions, Raman scatt. expts., 20-300K 78−39538
V_2O_3, polarised Raman scatt. in metallic and semicond. phases 77−90152
V_2O_3, Raman scatt. and phase transitions 80−71420
V_2O_5-P_2O_5 glasses, Raman spectra 79−78667
VPO_5, cryst., vibr. spectra 77−52064
V_3Si, A 15 compound, Raman scatt. and phonon density of states 79−28768
V_3Si, E_g optical phonon, Raman scatt. meas. 79−24316
W, chemisorbed H_2, vibr. spectra charact., adsorption sites 80−70535
W-complex, $WOCl_4.Ph_3PO$, prep. and characterisation 78−30592
WF_6, cryst., overall vibr. band struct., excitons 77−90136
WF_6 crysts., density of exciton states, two-particle and mixed cryst. spectra 78−2829
WF_6, orthorhombic crysts., Raman spectra, int./external mode separation and factor group anal. 77−90135
$W_xMo_{1-x}O_3$, mixed cryst., structural phase transition, Raman and IR spectra 78−79766
WO_3, ceramic, Raman spectra, 80-300K, inhibited ferroelectric phase transition 77−32378
WS_2 (2H), layered cpd., Raman scatt. 80−103960
WSE_2, Raman spectrum, long wavelength optical phonons 77−40218
WSe_4^{2-}, anharmonicity consts., reson. Raman spectra 77−61754
Xe, two-phonon difference scatt. 80−60588
Y-B, amorphous, B-rich, low freq. modes, Raman scatt. obs. 80−108202
YAG:Cr^{3+} 80−2740
YCl_3, Raman spectrum 77−59567
YIG, one-magnon Raman scatt., Faraday rot. 80−66156
$Y(OH)_3$, dynamical effects of interaction between 4f electrons and optical phonons 80−108196
Yb chalcogenides, multiphonon inelastic light scatt., hot recomb. 77−8559
Yb monochalcogenides, multiphonon inelastic light scatt. 77−90144
YbS, multiphonon processes and exciton-LO phonon interaction 79−95784
YbS, Raman spectra reson., reflectance spectra, multiphonon processes 78−84581
$Yb_2Si_2O_7$, IR and Raman spectra, internal and external modes 79−61365
Zn, TO optical phonon, anharmonicity 77−15520
ZnA_2X_4 (A=Ga,In; X=S,Se), Fourier IR and Raman spectra, cryst. struct. and symm. *(German)* 79−24313
$ZnAl_2O_4:Cr^{3+}$, Raman effect to probe dynamical processes of Cr^{3+} photoexcited states 80−2740
$ZnAs_2(P_2)$, monoclinic, lattice vibr. symm., IR and Raman active frequencies *(Russian)* 77−69055

Raman spectra of inorganic solids continued
$Zn_{1-x}Cd_xS$ mixed crystals, frequency internal between LO(Γ) to TO(Γ) 78−2854
$Zn_xCd_{1-x}S$, resonance Raman scatt. involving exciton complexes 80−16039
$Zn_{1-x}Cd_xSe$, mixed crystals, antireson. in phonon spectrum, Raman spectroscopy 80−88992
$Zn_xCd_{1-x}Te$, reson. Raman scatt. of light by longitudinal optical phonons 77−28577
$ZnCl_2$, polymorphism 78−80332
$ZnCl_2(Br_2)(I_2)$ glassy aqueous solutions, Raman spectral study 80−84738
$Zn_{1-x}Co_xF_2$, Raman scatt. by mag. excitations 77−55775
$ZnF_2:Co^{2+}$, Raman tensor calcs. of isolated impurity in diamagnetic matrix 80−76025
$ZnGeP_2$, one- and two-phonon Raman scatt. 79−78681
$ZnIn_2S_4$, lattice dynamics, IR and Raman spectra 77−81106
$ZnIn_2S_4$, photoluminesc., reson. Raman scatt. 78−48179
$ZnIn_2S_4$, Raman and IR spectra 78−48181
$ZnIn_2S_4$, Raman scatt., hydrostatic press. effect 80−84745
$ZnIn_2S_4$, vibr. spectrum, Raman study 80−97278
$Zn_{1-x}Mg_xTe$, long wavelength optical phonons, IR ref. and Raman obs. *(French)* 78−60433
ZnO, existence of biexcitons, reson. two-photon Raman scatt. 79−19889
ZnO, near-forward Raman scatt. intensity of E_1(TO) polariton mode 78−23462
ZnO, reson. Raman scatt. 78−35137
ZnO, wurtzite type cryst., temp. depend. of one phonon Raman spectra, Gruneisen parameters 77−66500
$Zn_4O(BO_2)_6$, phonon coupling exam. by Raman spectroscopy 78−30719
$Zn(OH_2)_6(SiF_6)$, phase transitions, spectrometric exam. *(French)* 78−88291
ZnP_2, Raman light scatt. efficiency for He-Ne laser light *(Russian)* 77−52104
ZnP_2, reson. interaction of vibr. states, polarised Raman spectra meas. 77−15521
ZnP_2, resonance Raman scatt. singularities *(Russian)* 80−89007
ZnP_2, second-order vibr. spectra and dispersion of phonon branches 80−25376
ZnP_2, tetragonal, one and two phonon states using second order Raman spectra 78−43874
ZnP_2:As, local vibrs. of impurity ions, Raman study 80−29745
ZnS, phonon dispersion under extreme press. and metallic transform., Raman spectra meas. 78−10895
ZnS, Raman scatt. by phonon polaritons 80−103959
ZnS with cation impurity, first order transitions 78−88310
ZnS, wurtzite type cryst., temp. depend. of one phonon Raman spectra, Gruneisen parameters 77−66500
ZnS:Co(Fe)(Mn)(Ni), impurity-induced Raman scatt., central force const. reduction 77−32379
ZnS:Cr(Mn)(Fe)(CoXVi), vibr. modes of transition element impurities 78−76472
ZnS:Mn, luminesc. rejection 77−18100
ZnS-Mn crystal, polarisation meas., luminesc. and Raman spectra 79−8138
ZnS(Se)(Te), second order Raman scatt., lattice dynamical calc. and expt. 80−25370
$ZnSc_2S_4$, IR and Raman spectra, force consts. 78−68503
ZnSe films, reson. Raman spectra 80−80888
ZnSe, linear electro-optic coeff. dispersion, relation to reson. Raman scatt. 78−56459
ZnSe, luminesc., reson. Raman scatt. due to excitonic mols. 79−33816
ZnSe, phonon dispersion under extreme press. and metallic transform., Raman spectra meas. 78−10895
ZnSe, relaxation processes in Raman scattering and exciton luminescence under resonant excitation 80−25386
ZnSe, reson. Raman scatt. meas. 77−66510
ZnSe, resonance Raman scatt., exciton-polariton luminescence *(Russian)* 80−97287
ZnSe:Mg, local vibrations of impurities, IR absorpt. spectra exam. 77−7815
ZnSe(Te), Raman-luminescence problem, interference analogy and expt. discrimination by polarisation correl. 79−95764
$ZnSiP_2$, first- and second-order Raman scatt. 78−35151
$ZnSiP_2$, one- and two-phonon Raman scatt. 79−78681
ZnTE, relaxation processes in Raman scattering and exciton luminescence under resonant excitation 80−25386
ZnTe crystals, secondary radiation polarization and relaxation of optical excitation 80−11399
ZnTe, phonon dispersion under extreme press. and metallic transform., Raman spectra meas. 78−10895
ZnTe, Raman scatt. and exciton luminesc. under reson. excitation 79−38617
ZnTe, relax. times of secondary radiations, circular polarisation correlation 79−28816
ZnTe, reson. secondary radiation 79−99886
ZnTe, resonance Raman scatt. of excitonic polaritons by LO and acoustic phonons 79−65879
ZnTe, resonance Raman scatt. at high excitation levels *(Russian)* 80−55109
p-ZnTe, spin-flip Raman scattering, review 80−108209
ZnTe, temp. depend. of Raman scatt. and exciton luminesc. spectra 78−39586
ZnTe:As(P), spin flip acceptor scatt. 78−92072
ZnTe:As(P)(Li), electronic Raman scatt. and IR absorpt. spectra of shallow acceptors 79−73978
ZnTe:Li, electron-phonon interactions in Raman scatt. 80−60594
ZnTe:Li(As), electronic Raman scatt., mag. field depend. 79−73928
ZnTe:Na(Li), spin flip acceptor scatt., transition selection rules, gyromagnetic ratios 79−61380
ZnTe:P, spin flip scatt., shallow acceptor states 77−8587
ZnTe:P(As), g-values, spin temp., determ. from Raman spectra 78−43856
ZnTe(Se), optical circular polarisation correl. in secondary radiation, resonant light excitation 77−69885
$ZnTe_xSe_{1-x}$, Raman phonon spectra, resonance interaction effect 80−25375
Zr, two-phonon Raman scatt. at low temps. 79−87433
$ZrCl_4$, cryst., melt, gas, Raman spectra interpretation *(German)* 79−28753

Raman spectra of inorganic solids continued
ZrO_2, R_2O_3-stabilised (R=La, Gd, Y or Yb), solid soln., Raman scatt. anal. of struct. transform. 78−88312
ZrO_2, Raman spectra, temp. depend. 78−6668
ZrO_2-Sc_2O_3-Yb_2O_3 system, order-disorder phenomena, Raman spectra study 80−97254
ZrO_2-Y_2O_3, stabilised, light scatt. spectrum 79−73954
$ZrOS_2O_3.8H_2O$, possible evidence for nonexistence of cpd. of given formula *(French)* 77−24279
ZrS_3, excitonic transition, reson. Raman spectra, Franck-Condon factors 80−97252
ZrS_3, one-dimensional semicond., Raman spectra 79−87447
ZrS_3, Raman spectra and cryst. symm. 80−34922
$ZrS_3(Se_3)(Te_3)$, phonon study of chemical bonding 80−20645
$ZrSe_3$, long wavelength optical phonons, Raman scatt. and IR refl. 80−34921
$ZrSiO_4$, synthetic Raman spectrum and lattice vibrs. 77−48160
$ZrSiO_4$, zircon, resonance splitting of internal vibr. freq. of complex anion 80−55080

Raman spectra of organic molecules and substances
1,1-dimethyl-1-silacyclopentane, IR and Raman spectra 80−60577
1,4-dithiane-1-oxide, cryst., IR and Raman spectra 79−69839
2-chloronaphthalene, vibr. and calorimetric investigation of polymorphism 78−87641
2-fluoronaphthalene, vibr. and calorimetric investigation of polymorphism 78−87641
3,3,3-trifluoropropene, struct. and vibr. spectra, IR, Raman polarisation study 80−18845
acenaphthalene, mol. and cryst., vibr. anal., normal coord. calcs. 79−47428
acenaphthene, vibr. spectra, mol. crystal dynamics, librational modes 78−64356
acenaphthylene, orientational disorder, spectroscopic exam. 78−14670
acetanilide, cryst., low-freq. polarised Raman spectra 78−84574
acetate ions adsorbed on Ag particles in aqueous soln. Raman spectra 80−69148
acetic acid, in cyclohexane soln., Raman scatt. near crit. stratification, temp. depend. *(Russian)* 79−11420
acetic acid, protonated complexes, IR and Raman spectra *(French)* 78−78691
acetone, liq., C-C stretching mode relax., Fermi reson. influence 80−25352
acetone, Raman scatt., intermol. vibr. coupling effects 77−58026
acetonitrile, ν_2, ν_3 and $2\nu_3$ bands, vibr. relax., Raman spectra of liq. and dil. soln. 78−9154
acetonitrile, adsorpt. on Ag colloids, surface enhanced Raman spectra obs. 80−97251
acetonitrile, electrolyte solns., IR and Raman spectra interpretation, CN-stretching region 79−73941
acetonitrile, in liq. phase, Ramon band profiles, calc. using IR intensities 80−2741
acetonitrile, Raman spectra, vibr. and reorientational and energy transfer width separation, rot. const. determ. 80−87131
acetonitrile, Raman spectral study of aq. soln. struct., H-bond effects 77−88454
acetonitrile, soln., vibr. relax., isotropic Raman spectrosc. obs. 79−50025
acetonitrile-carbon tetrachloride solns., rot. and vibr. relax., Rayleigh and Raman scatt. 77−66513
p-acetotoluidide, cryst., low-freq. polarised Raman spectra 78−84574
acetyl cyanide, IR and Raman spectra, vibr. spectrum and vibr. anal. 77−10676
acetyl halide-titanium tetrahalide adducts, coordination, IR and Raman spectra 78−42050
acetylcholine, nonenzymatic hydrolysis, Raman obs. 79−29505
acetylene, ν_2 band, Q-branch, high resolution CW CARS 77−42329
acetylene, pure rot. Raman spectra of ground and vibr. II states, intensity distrib. 77−65476
acetylene, Q-branches, high resolution pulsed CARS 78−17676
acetylene, Raman spectra, high resolution using laser source 78−42072
acetylene, rot. vibr. anal., Raman spectra obs. 80−69146
acetylene-cumulene dehydro annulenes, anomalous polarisation in resonance Raman spectra 80−60574
acetylene-d_2(d_1), rot.-vibr. Raman spectra 80−83372
acetylenic compound, 1,5-hexadiyne, hydrogen bonding effects on Raman line ν(≡C-H) *(French)* 77−75167
acetylenic compounds, 1- and 4-octyne, hydrogen bonding effects on Raman line ν(≡C-H), solvents effects *(French)* 77−71805
acetylpyridines, vibr., IR and Raman spectra 78−74653
acid oxalate ion in aq. soln., vibr. studies, IR and Raman spectra 80−95589
acrylic, Raman spectra using pulsed laser and gated detection 77−74529
adamantane, plastic and solid-solid transitions, Raman study 80−60590
adenosine 5'-monophosphate, UV resonant Raman spectra 78−48756
adenylyl 3'-5' adenosine, conform. equilib., Raman temp. jump obs. 78−8450
air pollutant gases and vapours, relative Raman scatt. cross section 80−100061
DL-alanine, cryst., Raman spectra and lattice dynamics 79−28741
L-alanine and DL-alanine, cryst., Raman band intensities of local group modes 80−93298
DL-alanine-α,β-d_4, Raman spectra, intermol. pot. 79−91432
alcohols, monohydric saturated, vibrational bandshapes 78−90226
alicyclic ring compounds, vibrational spectra and structure, book 78−78700
alicyclic ring cpds., vibr. spectra, conformational props., book contrib. 78−78702
alkanes, $\nu(CH_2)$ and (CH_3) Raman bands, global integrated intensity, dilution effects *(French)* 77−61755
n-alkanes, liq., Raman spectra, longit. acoustic modes and gauche-trans energy difference 80−93295
n-alkanes, longitudinal acoustic modes, Raman intensities 80−32718
alkoxy-benzoic-acids, temp. depend. of Raman spectra of homologous series 77−81098
n-alkyl carboxylic acids, vibr. spectra, C-H stretching mode assignments 79−47429
alkyl metal carbonyls, phosphine monosubstituted, LF vibrs., IR and Raman spectra 80−95585
4-n-alkyl-4'-cyanobiphenyls, Raman spectra in solid state, polymorphism of mesogenics 79−82964

Raman spectra of organic molecules and substances continued
alkylammonium tetrachloromanganate (II) IR and Raman spectroscopic exam. 78−31189
alkynes, $\nu(CH_2)$ and (CH_3) Raman bands, global integrated intensity, dilution effects *(French)* 77−61755
allene, liq., orientational dynamics, Raman obs. *(French)* 79−28746
allene-1,1-d_2, rot.-vibr. Raman spectra 77−65477
allene-d_4, Raman and IR spectra, rot.-vibr. bands, ground state constants 78−25545
amaranth, reson. Raman spectra, sample conc. optimisation 78−66555
amaranth, trace amount determ., by reson. Raman spectroscopy *(Japanese)* 79−48017
amide group in soln., interactions, IR, Raman spectral investigs., peptide, protein struct., review 78−90330
amines, Raman bands and H bonding in liq. phase *(French)* 77−65479
γ-aminobutyric acid, aq. soln., low freq. vibrs. Raman spectra obs. 80−987
ammonium hydrogen glutarate, H bonding, vibr. spectra 78−43860
ammonium oxalate monohydrate, IR refl. and Raman spectra, internal and external modes *(French)* 77−36231
ammonium oxalate monohydrate, Raman spectrum, internal and external vibrs. 79−73924
all-trans anhydrovitamin A, resonance enhanced Raman spectrum 79−43815
aniline, prereson. Raman effects, intensity enhancement mechanism 78−42069
aniline hydrobromide, ferroelastic phase transition, Raman scatt. study 80−108195
anisole and -d_3, Raman spectra, low freq. vibrs., torsional barrier 78−25543
anthracene, isotopically mixed cryst., exciton dynamics 80−29329
anthracene, Raman intensities rel. to vibronic coupling and excited electron state geometries 77−27075
anthracene, Raman spectra, in-plane vibr. force fields, five-parameter approx. calcs. 79−59436
anthracene, reson. Raman emission and hot luminesc. *(Russian)* 79−61377
anthracene, resonance Raman effect in pre-resonance region 77−77201
anthracene, single cryst., CARS and CSRS, two-photon reson. effect 80−95946
anthracene crystal, dynamical matrix eigenvectors from Raman scatt. 80−100315
anthracene crystal, resonance secondary emission, Raman scatt. in exciton absorpt. region *(Russian)* 80−40120
anthracene crystal, stimulated emission and Raman scatt. 78−1303
anthracene crystals, pre-reson. Raman scatt., 4.2-30K 80−60571
anthracene crystals, resonance Raman spectra sensitivity to exciting light intensity *(Russian)* 78−52504
anthracene-phenanthrene-tetracyanobenzene, CT-cryst., mini-excitons and lattice dynamics, ESR, optical and Raman spectra 80−60406
anthracene-PMDA, charge transfer cryst., 2K, zero-phonon lines, singlet spectra 78−23484
anthracene-pyromellitic dianhydride, mol. charge transfer cryst., Raman scatt. meas. 80−29743
anthracene-TCNB, charge transfer cryst., Raman study of phase transition 79−19885
anthracene-TCNB charge transfer crystal, orientational phase transition, EPR, Raman spectroscopy exam. 78−26817
anthracene-tetracyanobenzene, charge transfer complex, phase transitions, deuteration effect, mag. reson., spectral and thermal meas. 79−4412
anthracene-trinitrobenzene complex, neat and mixed cryst. and glass opt. spectra 77−40274
antimony ethyl derivative, Et_3Sb, IR and Raman spectra, rot. isomerism 79−41167
aromatic molecules in clathrates, Raman and phosphoresc. spectra 79−36647
arsenic ethyl derivative, Et_3As, IR and Raman spectra, rot. isomerism 79−41167
astaxanthin, aq. soln., aggregate, reson. Raman spectra, and IR spectra, exciton interactions 78−31770
azo dyes, tautomerisation, structs., laser Raman spectra 77−38672
azobenzene, parasubstituted derivatives, reson. Raman spectra *(French)* 79−59472
azulene, resonance Raman spectrum 77−10677
azulene in naphthalene, reson. Raman and reson. fluoresc. spectra, 30K 78−80323
bacteriorhodopsin, photosynthetic cycle, time-resolved Raman spectra 78−85294
bacteriorhodopsin, reson. CARS spectrosc. 80−8014
bacteriorhodopsin, reson. Raman evidence for secondary protein-Schiff base interactions, primary excitation mechanism 80−55981
bacteriorhodopsin, time-resolved resonance Raman characterisation 79−83705
bacteriorhodopsin, time-resolved resonance Raman spectroscopy 77−29103
bacteriorhodopsin Schiff base deprotonation dynamics using kintic reson. Raman spectroscopy 77−48981
barium formate, cryst., Raman scatt. 79−4804
BBOA, smectic B phase, fluidlike mol. dynamics, Raman scatt. study 80−20630
benzaldehyde, prereson. Raman effects, intensity enhancement mechanism 78−42069
benzaldehyde derivatives, Raman intensities obs., phenyl ring-carbonyl group conjugation 78−29792
benzaldehydes, para-halogenated, IR and Ramam spectra, vibr. assignments, thermodynamic functions 80−14139
1,2-benzanthracene, secondary reson. radiation and hot energy transfer, soln. luminesc. 80−87167
benzene, absolute Raman intensities determ. 77−68046
benzene, absolute Raman scatt. cross-sections for totally symm. modes 80−102510
benzene, bromination on zeolite adsorption complex, Raman spectroscopic anal. 80−16670
benzene, coherent anti-Stokes Raman spectra in UV 77−46567
benzene, cryst., IR and Raman intensity of lattice vibrs., theory 80−11381
benzene, crysts., Raman and two-photon reson. in three wave mixing 79−38538
benzene, deuterated and chemisorbed on glass, vibr. bands, Raman scatt. study 80−84737
Raman spectra of organic molecules and substances continued
benzene, doubly degenerate high-resolution rot.-vibr. Raman bands 79−6941
benzene, high order stimulated Raman scatt. *(Chinese)* 79−81206
benzene, high resolution AC coupled Raman spectra 79−40619
benzene, in benzene-d_6 soln., IR and Raman spectra, line breadths, rot. diffusion consts. 79−56772
benzene, low lying $^1A_{2u}(\sigma,\pi^*)$ and $^1E_{2g}(\pi,\pi^*)$ states, Raman line intensities 78−78709
benzene, mol. cryst., reson. four-wave mixing, third order susceptibilities 80−100654
benzene, molecule translational mobility in depolarised Raman spectra 80−14150
benzene, prereson. Raman scatt. of overtones in μV 79−59471
benzene, Raman and IR intensity anal. 78−70829
benzene, Raman and IR spectra at high press. 78−35127
benzene, Raman scatt. cross sections 79−6945
benzene, reson. Raman cross sections, forbidden electronic transitions, depolaris. ratios 78−42075
benzene, reson. Raman effect in gas, liq., and solid phases 79−31531
benzene, stimulated Raman scatt., anti-Stokes components, class II radiation cones 80−28276
benzene, totally symm. bands, high resolution rot.-vibr. Raman spectra 78−70838
benzene, totally symmetric rot.-vibr. Raman bands 79−59474
benzene, ultrahigh sensitivity stimulated Raman gain spectroscopy 80−48337
benzene, vib. relax. and Raman line widths 77−32359
benzene, vibr. relax. in soln., ν_1 C-H stretching band Raman spectra 78−25540
benzene($-d_6$), prereson. Raman effects, intensity enhancement mechanism 78−42069
benzene (deuterobenzene) adsorpt. on Ag colloids, surface enhanced Raman spectra obs. 80−97251
benzene adsorbed on metal surface, obs. of vibrational modes 80−6649
benzene in solution, CW coherent Raman gain spectrum 78−58057
benzene in solution, rotational motion, Raman study 80−44104
benzene liquid-filled waveguide, generation of enhanced CARS signals 79−89961
benzene soln., UV Raman scatt., forbidden states 78−9155
benzene-^{13}C, liq., vibr. spectra, band assignments 78−13500
benzene-acridine orange, Raman spectra using pulsed laser and gated detection 77−74529
benzene-$Br_2(Cl_2)$ π-σ complexes, low freq. spectra 78−78713
benzene-Br_2 charge transfer complex, Raman spectra, bending modes, electronic excited states 78−56485
benzene-carbon tetrachloride, mixture, mol. and Raman scatt., profile shape, conc. depend. 77−58025
benzene-chloroform mixture, reorientational motion and intermolecular interaction by Raman spectroscopy 77−24839
benzene-cyclohexane mixture, interference between Raman resonances in four-wave difference mixing 77−23712
benzene-d_0-d_6, pre-reson. Raman effect and vibronic coupling 77−83604
benzene-d_3, gas phase Raman spectrum, E′ and E″ species, Coriolis consts. *(French)* 78−5235
benzene-d_6, high resolution rot.-vibr. Raman spectra 79−64006
benzene-d_6, liq., Raman spectra vibr. relax. and band widths 78−23440
benzene-d_6, liq., reorientational motion, Raman obs. 78−70841
benzene-fluorobenzene system, phase transitions, Raman spectra 79−91449
benzene-p-dioxan, mixtures, mol. reorientation and assoc., depolarised Raman scatt. obs. 80−7341
benzil, phase transition study be simultaneous Raman-scatt. and domain-struct. investigations 79−60504
n-benzoates, MP and rot. mobility of struct. groups *(Russian)* 77−69074
benzoic acid, dimer, cryst., IR and Raman spectra, vibr. assignments 78−31191
benzonitrile, IR absorpt. and Raman bands, half-band width conc.-depend. 80−74171
benzonitrile, transverse sound wave and mol. motion, light scatt. obs. 77−79621
benzotrifluoride, and mono-substituted derivatives, vibr. spectra, internal rot. 77−83598
bicyclic ring compounds, Raman circular intensity differential spectra obs., mol. struct. 80−87130
bicyclo(3.2.0)hept-6-ene, LF vib. spectra, conformations 78−58685
bicyclopropyl, Raman study of rotational isomers 79−18194
biological macromolecules, conformational dynamics subnanosecond T jump and Raman spectroscopy appl. 79−66445
biological molecules, chem. reactions, Raman difference spectroscopic obs. 78−44368
biomolecules, struct. and vibr. Raman spectra 77−52939
biopolymer, local mode resonance enhancement in Raman spectra 77−77204
biopolymer motions, nonsteady hydrodynamics, damping effects 77−36861
biphenyl, crysts., Raman and two-photon reson. in three wave mixing 79−38538
biphenyl, mol. cryst., reson. four-wave mixing, third order susceptibilities 80−100654
biphenyl, second order phase transition at 40K, Raman spectral obs. 77−32361
biphenyl glutarate polymer, resonant Raman spectra and fluoresc. 77−24830
bis(methylthio)alkanes, model compounds of polythioethers, vibr. spectra 80−58430
bis(p-toluene sulfonate) diacetylene polymer cryst., second order phase transition 79−73922
bis(tetrathiotetracene)triiodide, struct., reson. Raman spectra 78−66556
bis(trifluoromethyl)peroxide, gas and solid, Raman, IR spectra, internal rot. barrier of CF_3 78−29789
bromanil and radical anion, Raman and IR freq. shifts 78−33516
1-bromo-1-chloroethylene, vibr. assignment, IR and Raman spectra 77−18925
1-bromo-2,2-dimethylpropane, Raman and IR spectra, vibr. anal. 78−90173
1-bromo-2,4-dimethylbenzene, liq., IR and Raman spectra 78−42049
1-bromo-2,6-dimethyl benzene, IR and Raman spectra, vibr. anal. 77−57997
bromobenzene-d_0, -d_1, -d_4, vibr. spectra and force fields 77−65463

Raman spectra of organic molecules and substances continued
p-bromochlorobenzene, vibr. relax., Raman active phonons temp. depend. 80−29139
bromochlorofluoromethane, and d_1, Raman optical activity atom dipole interaction model 79−82033
bromochlorofluoromethane, Raman optical activity parameters, circular intensity differentials comput. 79−85950
bromocyanoacetylene, cryst., IR, far-IR and Raman spectra, vibr., struct. 77−63407
bromoform, liq., orientational motion, Raman spectra 77−50443
bromoform, Raman spectra, intermol. interactions 79−76436
1-butanol, IR and Raman spectra, vibr., conformers 78−25532
trans-2-butene, Raman and IR spectra, torsional mode pot. function 79−89676
t-butyl acetate, rot. isomerism, dielect. and Raman spectra 80−106328
t-butyl alcohol, and deuterates, gaseous and matrix IR spectra, liq. Raman spectra, vibr. assignment 79−10113
t-butyl bromide, vibr. relax. in pure liq. and soln., Raman spectra 80−66167
n-butyl bromide conformers, IR and Raman spectra, vibr. anal. *(German)* 77−88451
t-butyl chloride, vibr. relax. in pure liq. and soln., Raman spectra 80−66167
t-butyl chloride-d_0 and -d_9, polymorphism, Raman spectra 80−20617
t-butyl derivatives, liq., reorientational correlation times, Hubbard model 79−61353
t-butyl formate, deuteration effects, IR and Raman spectra 79−50016
t-butyl formate, rot. isomerism, dielect. and Raman spectra 80−106328
butylsilane-d_0,($-d_n$), vibr. spectra, normal vibrs. and rot. isomerism 79−31523
p-t-butyltoluene, selective deuteration, proton spin-lattice relax. 79−1721
3-butyn-1-ol, vibr. spectra, assignments, rot. isomerism 80−58257
calcium dipicolinate trihydrate, IR and Raman spectra, isotopic frequency shift, mol. vibr. obs., point groups determ. 80−89001
calcium oxalate, anhydrous, IR and Raman spectra, vibrational studies 80−69139
calcium oxalate monohydrate, IR and Raman spectra, vibrational studes 80−69139
d-camphor systems, mol. reorientation dynamics, Raman spectra 78−31178
carbon tetrabromide, solid, Raman spectrum, temp. depend. 78−52488
carbon tetrabromide, vapour deposition for optical studies, Raman spectra 78−64451
carbon tetrachloride, adsorbed on silica, laser Raman spectrum 77−3367
carbon tetrachloride, intense ps pulse excitation, multiple stimulated Raman spectra 78−66867
carbon tetrachloride, isotropy, mol. interactions, effects, Raman scatt. obs. 78−58697
carbon tetrachloride, solid, Raman and far IR spectra 79−33680
carbon tetrachloride, solid, Raman study of phase transition and dynamic struct. 80−34916
carbon tetrafluoride, compressed gas, ν_1 vibr. Raman line 78−32884
carbon tetrafluoride, liq. and plastic crystn., Raman spectra 77−59565
carbonium ions, adsorbed on porous Vycor glass, reson. Raman spectra 78−84571
carbonyl compounds, interpretation of Raman spectra 79−18193
β-carotene, ν_1 line shape, CARS and CSRS 78−82727
trans-β-carotene, coherent anti-Stokes Raman spectra 77−79169
β-carotene, coherent anti-Stokes reson. Raman spectrum excitation profiles 77−56342
β-carotene, excitation profile of ν_2 line in resonance Raman spectrum, solvent effects 80−74173
β-carotene, Franck-Condon effects in resonance Raman spectra and excitation profiles 80−14129
β-carotene, in CS_2, reson. Raman spectra, room temp. 78−35803
trans-β-carotene, Raman excitation profile spectra, prereson. region 78−33514
β-carotene, resonance CARS results 79−6189
β-carotin, resonance Raman effect *(Hungarian)* 78−74666
cell, living, of C. pyrenoidosa, enhanced anti-Stokes Raman scatt. 79−16171
cetyl orange monolayers on water surface, reson. Raman spectra 79−91434
cetyltrimethylammonium bromide, aq. soln., mol. conform., laser Raman spectra 78−21934
charge-transfer complex, mixed-stack crystalline, phonon bands 78−75767
chloranil and radical anion, Raman and IR freq. shifts 78−33516
p- chloraniline cryst., lattice vibr., IR and Raman spectra, lattice energy 78−56481
chloro(ethyl)silanes and its C derivatives, Raman spectra, mol. vibr. and rot. isomerism 80−87134
3-chloro-1-butene, rot. isomerism, vibr. spectra assignments 78−58702
1-chloro-2,2-dimethylpropane, IR and Raman spectra, vibr. assignment 80−74169
1-chloro-2-methylbutane, conformer depend. C-Cl stretching vibrs., Raman optical activity spectrum simulation 80−14146
1-chloro-2-methylpropane, IR and Raman spectra, vibr. assignment 80−74169
p-chlorobenzaldehyde and deuterated derivs., vibrational spectra 79−3441
p-chlorobenzylidene-p-n-pentylaniline, metastable phases formed by rapid cooling of mesophase, IR and Raman spectra and DSC obs. 80−34919
o-chlorobromobenzene, phase transition evidence from far IR absorption and Raman spectra 79−33693
p-chlorobromobenzene, single cryst., polarised Raman and IR spectra, assignments 78−60431
trans-1,4-chlorobromocyclohexane, liquid, crystalline and amorphous state, conformation and vibr. spectra, IR obs. 80−60568
2-chlorobuta-1,3-diene, far IR and Raman spectra, internal rot. 79−89668
4-chlorobutyrylchloride, Raman and vibr. IR spectra of solid and liq., rot. isomerism 78−62810
chlorocyanoacetylene, cryst., IR, far-IR and Raman spectra, vibr., struct. 77−63407
chloroethanes, electro-optical parameters, Raman spectra absolute intensities and depolaris. 77−10678
2-chloroethanol, IR and Raman spectra, normal coord. anal., isomerism 78−74661
chloroethylene, adsorbed on silica, laser Raman spectra 77−3367
chloroform, adsorbed on silica, laser Raman spectrum 77−3367
Raman spectra of organic molecules and substances continued
chloroform, and d, polar soln., Raman line shape of ν, band 78−74705
chloroform., liq., two-photon absorpt. meas., using nonlinear light mixing spectroscopy 77−79620
D-chloroform, soln., Raman scattering tensor components 80−99508
chloroform, solns., vibr. dephasing and reorientational relax., solvent depend., Raman spectra 79−85968
chloroform $-d_0$, $-d_1$, absolute Raman intensities and force fields 77−71808
chloroform and -d, Raman spectra study of mol. reorientation 79−24303
chloroform-d_0(-d_1), Raman and IR intensity anal. 80−18857
chloroform-d_1, isotropy, mol. interactions, effects, Raman scatt. obs. 78−58697
chloroform-d_1, Raman scatt., intermol. vibr. coupling effects 77−58026
chloroform-d in soln., vibr. and reorientational relax., Raman study 80−63636
D-chloroform-dimethylsulphoxide, soln., Raman scattering tensor components 80−99508
chloroform-He(Ar)(N_2) gaseous compressed mixture, mol. reorientation, Raman spectra 80−23422
chloroform-p-dioxan and chloroform-benzene mixtures, mol. reorientation and assoc., depolarised Raman scatt. obs. 80−7341
chloromethane, and $-d_3$, cryst., IR and Raman spectra of lattice vibrs. 79−95741
chloromethane-d_3, A_0 determ. from ν_4 Raman band obs. 78−82737
m-chloronitrobenzene, cryst., low freq. vibrs., polarised Raman and IR spectra study *(French)* 80−16029
m-chloronitrobenzene, molecular crystals, translational and orientational vibr. determ. 80−55103
chlorophyll, -a and -b in cyclohexane soln., far IR and reson. Raman spectra 77−48753
chromium tetraphenylporphyrin, reson. Raman spectra, excitation profiles, nucl. distortion and Jahn-Teller effects 77−58018
chromium tri(bipyridyl)tri-perchlorate, aq. soln., Raman scatt. from electronically excited state 79−94001
chromocene, solid, Raman transition assignments, mag. susceptibility, mag. moment 78−43861
cinnoline, prereson. Raman spectra, vibr. band intensities obs. 80−102515
coal, Raman scatt. and luminesc. 78−23460
coccine, new, trace amount determ. by reson. Raman spectroscopy *(Japanese)* 79−48017
combustion products, Raman scatt., fluoresc. interference 78−15728
conjugated molecules, resonance Raman spectra calc. 78−984
COOB, solid state dimorphism and cryst.-smectic transition, Raman study 80−45063
copper porphins, vibr. spectra, planar vibrs., normal coord. anal. 77−65474
copper tetraphenylporphyrin, reson. Raman spectra, vibronic coupling 79−26985
copper-porphin-d_4, reson. Raman and IR spectra 77−75164
coronene, mono- and dianions, reson. spontaneous Raman spectra, vibronic interactions 79−3451
Creutz-Taube complex, mixed valence, reson. Raman calcs. using vibronic coupling model 80−97249
croconate ion, Jahn-Teller coupled vibrs., reson. Raman profiles 77−83602
crystal violet, prereson. Raman spectra 80−32721
crystals, first order Raman effect, polariton, exciton *(Rumanian)* 77−48172
cyanide, on Ag, at electrolyte interface, enhanced Raman effect 79−28767
cyanoacetylene, and-d_1, cryst., IR, far-IR and Raman spectra, vibr., struct. 77−63407
cyanopyridine, isomeric forms, adsorbed of Ag electrodes, Raman scatt., orientational specificity 79−69822
1,1-cyclobutane dicarboxylic acids and K salts, IR and Raman vibr. spectra *(French)* 80−2758
cyclobutane-d_0(d_8), cryst. modifications, low. freq. Raman and IR spectra 80−7342
cyclobutylmethylether, IR and Raman spectra, config. 79−31525
1,3-cycloheptadiene, Raman and IR spectra, normal coord. analysis, conform. 77−77203
cycloheptane, cyclooctane, high resoln. rot. Raman spectra 77−75163
cycloheptanone, vibr. spectra, pot. functions and conformers 77−83569
cyclohexane, adsorbed on silica, laser Raman spectra 77−3367
cyclohexane, liq., absolute Raman intensities determ. 77−68046
cyclohexane, liq., two-photon absorpt. meas., using nonlinear light-mixing spectroscopy 77−79620
cyclohexane, liq., vibr. relax. at high press., Raman obs. 79−50026
cyclohexane, liq. and soln., Raman scatt. for vibr. and rot. relax. 79−82969
cyclohexane, rot. correl., Raman scatt. 77−83603
cyclohexane, solid, Raman spectra near 186K phase transition 78−56480
cyclohexane-d_0(d_{12}), plastic crystal phase transition, mol. reorientation, Raman scatt. phonon spectra 80−20631
cyclohexane-d_{12}, Raman linewidth and molecular diameter meas. 80−69153
cyclohexanol, polymorphism, Raman spectroscopy 77−73138
2-cyclohexene-1-one, planarity barrier, from LF Raman spectrum 79−54859
cyclohexene-Br_2 (Cl_2) π-σ complexes, low freq. spectra 78−78713
cyclohexyl halide-thiourea clathrate, conform., Raman spectra 77−77200
1,5-cyclooctadiene, gas, high resolution Raman spectroscopy with laser sources, rot. spectra 79−27000
1,5-cyclooctadiene, liq. and solid phases, IR and Raman spectra 79−19877
cyclooctanone, vibr., rot. spectra and conformations, pot. function 78−78707
1,3,5,7-cyclooctateraene, gas, high resolution Raman spectroscopy with laser sources, rot. spectra 79−27000
cyclopentadienylhafniumdichloride, gaseous, far IR and Raman spectra 80−95624
cyclopentadienyltitanium dichloride, gaseous, far IR and Raman spectra 80−95624
cyclopentadienyltitaniumtrichloride, gaseous, far IR and Raman spectra 80−95624
cyclopentadienylzirconiumdichloride, gaseous, far IR and Raman spectra 80−95624
cyclopentylamine, vibr. spectra and struct. 80−102516
cyclopropane, lattice vibrs., IR and Raman spectra, 4 to 78K 78−27209

Raman spectra of organic molecules and substances continued
cyclopropane, liq., mol. dynamics, Raman and NMR studies of orientational motion 80−93296
cyclopropane, rot. Raman spectrum 78−86873
cyclopropane-d_0, -d_6, force fields, Raman spectra 77−71806
cyclopropyl bromide, IR absorption, Raman scatt., assignments, thermodynamic functions 80−984
cytochrome c, dilute soln., reson. Raman spectra, pulsed laser excitation; optical multichannel detection 78−76999
cytochrome c, fast Raman spectroscopy using dye laser intracavity reson. Raman amplification 77−66794
cytochrome c, ferric- and ferro-, reson. Raman excitation profile, Soret excited 79−92147
cytochrome c, low freq. modes and excitation profiles, reson. Raman spectra 80−94428
cytochrome c, protein influence on haeme, Raman difference spectroscopy 80−72125
cytochrome C, vibronic theory of reson. Raman scatt. 79−94004
cytochrome-c, CARS near one-photon reson. 77−65466
cytochrome-c, coherent reson. Raman scatt. and incoherently broadened reson. fluoresc., condensed phase 78−60429
decacyclene, mono- and dianions, reson. spontaneous Raman spectra, vibronic interactions 79−3451
deoxyhaemoglobin, Fe(II)-N_ϵ(His-F8) stretching freq. rel. to quaternary struct. 80−94160
deuteriochloroform, Raman spectra, mol. orientational relax. 79−65865
deuterochloroform, solns., vibr. dephasing and reorientational relax., solvent depend., Raman spectra 79−85968
di(methylammonium) manganese tetrachloride, LF Raman spectra and phase transitions 77−63414
1,6-di-p-methoxybenzene sulphonyloxy-2,4-hexadiyne, thermal polymerization, Raman spectra 80−103952
dialkyl tartrates, Raman circular intensity differential spectra obs., mol. struct. 80−87130
dialkylammonium metal chlorides, soft modes, phase transitions 78−79723
diamantane, LF light scattering temp. depend., 40 to 340K 79−24307
diamantane, low temp. soft librational mode, Raman spectra exam. 78−30730
diamantane, plastic and solid-solid transitions, Raman study 80−60590
diamantane, Raman study of three solid-state phase transition 79−51946
4,10-diazachrysene, absorpt. spectra and luminesc. in cryst. and glassy matrices, 77K 78−37650
meso-2,3-dibromo-1,4-dichlorobutane, rot. isomerism, IR and Raman spectra 80−981
1,3-dibromobutane, IR and Raman spectra, normal coord. anal., C-halogen stretch bands and conformers 79−31522
dicalcium lead propionate, Raman scatt., order-disorder type transform 77−12373
dicalcium strontium propionate, Raman scatt., order-disorder type transform. 77−12373
1,12-dicarbaclosododecaborane, plastic solid, phase transitions, 10-320K, Raman and IR obs. 79−28744
dichloroanilines, vibr. assignments, Raman spectra obs., thermodynamic functions 80−52992
p-dichlorobenzene, cryst., Raman spectra , intensity of low freq. line 78−2846
m-dichlorobenzene, phase transition evidence from far IR absorption and Raman spectra 79−33693
p-dichlorobenzene, Raman spectra, P-T diagram for α,β and γ-phases 78−68515
p-dichlorobenzene, vibr. relax., Raman active phonons temp. depend. 80−29139
p-dichlorobenzene(−d_4), mixed cryst. phases, mol. reorientations and intermol. interactions, Raman obs. 79−28751
4,4′-dichlorobenzophenone, phase changes, Raman spectra *(French)* 80−2756
3,4-dichlorobromobenzene, liq., laser Raman spectrum, LF band assignments 80−48002
1,3-dichlorobutane, IR and Raman spectra, normal coord. anal., C-halogen stretch bands and conformers 79−31522
2,2-dichlorobutane, liquid and solid., vibr. spectra, IR and Raman obs. 80−60567
1,1-dibromo-2,2-dichlorocyclopropane, IR and Raman spectra 79−41170
2,2-dichloroethanol, vibr. spectra, normal coordinate anal. 79−22694
dichloromethane, $d_{0\text{-}3}$, Raman intensity, force consts. and electro-optical parameters 79−36651
dichloromethane, Raman line intensities, modified CNDO/2/INDO calc. 78−25621
dichloromethane, vibr. population lifetimes in liqs. anti-Stokes Raman scatt. 78−74665
1,1-dichroethane and d, IR and Raman spectra, βCH stretching interaction force consts. 77−79616
dicyanobenzene, deuterated isomers, vibr. spectra 79−31521
dicyclopentadienyl Ti^{3+}-N_2 compound complexes, reson. Raman scatt. 80−99510
diethylamine, liq., Raman scatt. following optical excitation, vibr. relax. 79−26984
diethylcyanine, reson. Raman spectra *(French)* 77−65484
diethylcyanine, vibrational Raman bands, excitation profiles *(French)* 80−83380
diethylsilane-d_0(−d_n), vibr. spectra, normal vibrs. and rot. isomerism 79−31524
diethynylbenzenes, vibrational spectra, deuterated isomers 78−58705
1,2-difluoroethane, gauche-trans conformers, IR and Raman spectra, vibr. 78−17667
2,2-difluoroethanol, vibr. spectra, normal coordinate anal. 79−22694
1,5-difluoronaphthalene, IR and Raman study of crystal dynamics 78−80346
diglycine, cyclic, solid phase laser Raman spectrum 77−85695
p-dihalobenzene, mixed cryst., Raman spectra, phonons and vibr. excitons, criteria for solid solns. 78−43840
p-dihalobenzene series, cryst., chem. perturbation and lattice instability, X-ray and Raman scatt. 77−39654
dihalobenzenes, IR and Raman spectra, phase transitions *(French)* 78−84557
2,2-dihalohexafluoropropane, IR and Raman spectra, gas, liq. and solid, normal coord. anal. 79−72314
1,4-dihalonaphthalene: octafluoronaphthalene, Raman spectra, phonon band mass coeff. tuning 79−8131

Raman spectra of organic molecules and substances continued
1,4-dihalonaphthalenes, binary solid solns. lattice stability, mol. motions 78−31182
p-diiodobenzene, far IR single cryst. transmission spectrum, temp. and polaris. depends., assignments 78−72498
1,2-diiodotetrafluoroethane, Raman and far IR spectra, conformation 78−78715
dimethoxymethane, vibr. spectra and rot. isomerism 80−106325
N,N-dimethyl acrylamide (−d_3,d_6,d_9), force field, IR and Raman spectra obs. 80−47979
dimethyl ammonium cadmium tetrachloride, dynamics of structural phase transitions 79−73309
N,N-dimethyl aniline, adsorpt. on Ag colloids, surface enhanced Raman spectra obs. 80−97251
dimethyl di(trifluoromethyl) germanium, and perdeuterated analogues, vibr. spectra, normal coord. anals. *(German)* 80−5547
dimethyl ether -d_0, -d_3, -d_6, internal rot., far IR and Raman spectra 77−79612
dimethyl ether-d_0,(-d_6), solid solns., vibr. Raman spectra and intermol. pot. function 78−68494
dimethyl ether.HCl, gas-phase Raman spectra, profile of stretching vibr. 79−45728
dimethyl sulphoxide, 1:1 and 1:2 complexes with H_2O and D_2O, H-bonding, IR and Raman vibr. spectra 77−34633
dimethyl sulphoxide-d_6, intensities in inelastic electron tunnelling, IR, and Raman spectroscopy *(French)* 79−822
N,N-dimethyl-p-nitrosoaniline, coherent anti-Stokes Raman spectra, negative peak intensities 77−72805
N,N-dimethyl-p-nitrosoaniline, coherent anti-Stokes Raman spectra, negative peak intensities 77−75161
dimethylacetylene, laser Raman spectra, pure rot. anal. 79−59468
N,N-dimethylbenzamide+$POCl_3$ reaction products 78−7199
dimethylboric anhydride, IR and Raman spectra, vibr. and struct. 78−25531
2,3-dimethylbuta-1,3-diene, IR, Raman spectra, torsional pot. function, thermodynamic function 80−43046
cis-3,4-dimethylcyclopentanone, conformational analysis, vib. spectra 77−75325
1,1-dimethylcyclopropane-d_0,-d_6, internal rot., Raman spectra 78−985
dimethyldiacetylene, laser Raman spectra, pure rot. anal. 79−59468
trans-dimethyldiazene-1, 1, 1-d_3, IR and Raman spectra, vibr. assignments and pot. functions 78−33507
trans-dimethyldiazene-d_0,d_6, IR and Raman spectra, vibr. assignments and pot. functions 78−33507
1,2-dimethyldiborane, IR and Raman spectra of cis and trans isomers 78−86868
dimethylether, ab initio SCF calcs., force field, IR and Raman intensities 77−79601
N,N-dimethylformamide+$POCl_3$ reaction products 78−7199
dimethylnitrosamine, in aq. soln., detect. and meas. by laser Raman spectroscopy 78−15725
dimethylsolphoxide, effects on water struct., Raman and IR spectral study 80−14143
dimethylsulphide, Raman spectra, torsional pot. consts. and kinetic coeffs. 78−5233
dimethylsulphide-d_3, two interacting C_{3v} rotor system, mol. coupling parameters, Raman spectra 78−42074
dimethylsulphite(-d_6), cryst., liq., and oriented film, vibr. spectra, force fields 79−91443
m-dinitrobenzene, cryst., low-freq. polarised Raman spectra 78−84574
4,4′-dinitrobiphenyl complexes, intermol. interacts. and geometry of non-rigid mols., vibr. spectra 78−88294
2,2-dinitropropane-d_0(-d_6), phase polymorphism, vibrational assignments, IR and Raman study 80−16031
dinucleoside monophosphates, struct. and conform. in aq. soln., Raman spectra 78−78847
dioxane, 1:1 and 1:2 complexes with H_2O and D_2O, H-bonding, IR and Raman vibr. spectra 77−34633
1,4-dioxane, liq., reorientational correl. times from light scatt. 77−32385
dioxane, Raman spectral study of aq. soln. struct., H-bond effects 77−88454
dioxane-$HgCl_2$ complexes, IR and Raman vibr. spectra, inter- and intramol. forces 77−66489
dipalmitoyl phosphatidylcholine, conformational nonequivalence of chains 1 and 2 79−16133
dipalmitoylphosphatidylcholine/glucagon (cardiolipin/insulin) systems, Raman spectra study 80−16903
diphenyl.2$SbCl_3$ 77−16291
1,1-diphenylethylene, adsorbed on porous Vycor glass, reson. Raman spectrum, surface species identification 78−42066
diphenylpolyene, oriented in polymer film, polaris. reson. Raman spectra 79−59466
all-trans-diphenyltetradecaheptaene, oriented, photochem. reaction production and monitoring, reson. Raman spectroscopy 77−29020
dipicolinic acid, IR and Raman spectra, isotopic frequency shift, mol. vibr. obs., point groups determ. 80−89001
dipotassium malonate, aq. soln., IR and Raman vibr. spectra *(French)* 79−26989
1,4-disilabutane, rot. isomerism, Raman and IR spectra 80−74168
1,3-disilacyclobutane, ring-puckering combination band spectra in SiH_2 stretching region 78−70836
2,5-distyrylpyrazine, absorpt., Raman and fluoresc. spectrosc. 80−28049
1,2-disubstituted imidazole compounds, IR and Raman spectra, vibr. anal. *(French)* 79−45713
DOBAMBC, polarized Raman scatt. and elec. field effects in aligned smectic phases 79−94873
dyes, absorption edge struct. in stimulated fluorescence spectra, Raman scatt. 78−55350
dyes, stimulated reson. Raman scatt. at transverse pumping, mol. vibrs. 77−88453
E. coli B, active, evidence for non-thermal excitation of energy levels 78−15800
EBBA, liq. cryst., Raman and calorimetric evidences for existence of three solid modifications 77−77207
EBBA, metastable phases formed by rapid cooling of mesophase, IR and Raman spectra and DSC obs. 80−34919
EBBA, NMR and Raman scatt. studies in nematic phase 80−100619
electron donor-acceptor complex formation, equilib. const. determ., reson. Raman spectroscopy 78−3329
EOBC, liquid crystal phase transforms., Raman obs. 78−87774
epifluorohydrin, IR and Raman spectra and conformations 80−60576

Raman spectra of organic molecules and substances continued
erythrocyte membrane, cooperative pH-sensitive state transition, Raman spectroscopy 77−36881
ethane, liq., correl. function modelling, third order memory function method 80−7339
ethane, ordered cryst., Raman spectra, 74K 79−73942
ethanedithiol, mol. vibr., conformational anal., Raman spectra 79−31534
ethaneselenol, IR, Raman and microwave spectra, barriers to internal rot. 77−38666
ethanol, effect of hydrogen bonding on Raman spectrum 79−18197
ethanol, picosecond stimulated Raman effect, time-resolved spectra 77−3369
ethanol, vibr. population lifetimes in liqs. anti-Stokes Raman scatt. 78−74665
ethanol in CCl_4, vibr. energy redistrib. after ultrashort IR excitation 77−6894
ethanol mols. reorientation in ethanol-water mixtures, Raman and Rayleigh spectra 78−76449
ethanol-CS_2 mixture, Rayleigh and depolarised Raman scatt. lines near crit. temp. 77−20863
ethene, general valence force field, ab initio calcs., IR and Raman intensities 77−71746
ethers, Raman spectra, interpretation 77−65483
ethoxy-hexyltolane, orientation-statistical props. studies by optical methods *(Russian)* 79−77518
ethoxy-octyltolane, orientation-statistical props. studies by optical methods *(Russian)* 79−77518
ethoxyhexyltolan, Raman spectra, molecular conformational instability, internal field effects 80−54127
ethoxyoctyltolan, Raman spectra, molecular conformational instability, internal field effects 80−54127
ethyl iodide, microwave spectra and internal rot. anal. 80−69130
ethyl methyl sulphide, low freq. vibr. spectra, methyl torsional pot. functions and internal rot. 80−5543
ethyl-p-azoxybenzoate, far IR and Raman spectra, smectic polymorphism 80−76022
ethylamines, torsional Raman spectra 77−77195
ethylcyclopropane, solid, liquid, vapour phase, IR and Raman vibr. spectra 80−84740
ethyldifluoroborane, microwave, Raman, IR spectra, conform., dipole moments, vibr. assignment 78−90155
ethylene, IR and Raman intensities calc., efficient ab initio computation method 79−45698
ethylene, isotopically mixed, crystal, dilute guest probe orientational energy, IR, Raman spectra 78−68496
ethylene, Raman intensities, CNDO approximation, polarization functions 79−93925
ethylene, Raman line intensities, modified CNDO/2/INDO calc. 78−25621
ethylene, Raman spectra, ν_1, ν_3 and ν_5 bands, polarisability 77−58021
ethylene, Raman spectra, ν_3 and ν_5 band centres 78−74669
ethylene, Raman spectra, vibr.-rot. selection rules and general band contours 77−58020
ethylene, Raman spectra of ν_3 band, rot. consts. 79−26988
ethylene crystal, partially deuterated, Raman phonon spectra 78−56470
ethylene oxide, cryst. symmetry, X-ray diffr., far IR and Raman spectra 78−35123
ethylene-$Br_2(Cl_2)$ π-σ complexes, low freq. spectra 78−78713
trans-1,2-ethylene-d_2, Raman spectra, vibr.-rot. selection rules and general band contours 77−58020
ethylene-d_4, Raman spectrum, fundamental bands 79−59473
ethylenediammonium metal chlorides, $(NH_3CH_2CH_2NH_3)MCl_4$, M=Ni,Pd,Cu,Cd,Mn, struct. and mag. props., vibr. spectra 79−10842
ethylgermane, microwave, IR and Raman spectra, struct., internal rot., dipole moments 77−79605
ethylmethylamine, low freq., vibr. spectra, methyl torsional pot. functions, mol. struct. 80−43045
ethylmethylether($-d_3$), low freq. vibr. spectra, methyl torsional pot. functions, internal rot. 79−26978
ethylmethylsilane-$d_0(-d_n)$, vibr. spectra, normal vibrs. and rot. isomerism 79−31524
ethyloxirane, solid, liquid, vapour phase, IR and Raman vibr. spectra 80−84740
eye, intact bovine lens protein, Raman spectroscopy with intensified Vidicon detectors 79−29525
fatty acids, LF Raman spectra, accordion vibrs. *(French)* 77−27074
ferric cytochrome c, reson. Raman spectra, Fe^{3+} low-lying electronic levels 78−53335
ferrocytochrome c, mag. reson. Raman opt. activity at different laser wavelengths 77−38681
ferrous porphyrin, intermediate spin, reson. Raman spectra 79−69820
flavins, reson. Raman spectra avoiding fluoresc. interference 79−10114
fluorene, cryst., low-freq. polarised Raman spectra 78−84574
fluorescent molecules, stimulated spectra, excited state intramol. vibrs. 80−32717
1-fluoro 2:4-dinitrobenzene, laser Raman and infrared spectra 79−22711
3-fluoro-4-chloroaniline, Raman and IR spectra, vibr. anal. 79−81198
2-fluoro-5-bromotoluene, IR and Raman spectra 78−70830
m-fluoroaniline, vap. (liq)., Raman and IR spectra, vibr. assignments 78−58699
fluoroaromatics, CH stretching, vibr. force fields, substitution pattern effects 77−54550
fluorobenzene, lattice vibs. *(French)* 77−32366
fluorobenzene, mol., UV prereson. Raman scatt., interference effects 79−64008
fluorobenzene, mol., UV prereson. Raman scatt. intensity 79−64007
fluoromethane ν_2, ν_5 rot.-vibr. Raman bands, anisotropic components, ^{13}C shifts 78−74667
fluoromethyl methyl mercury-d_0, -d_3, vibr. spectra, normal coord. anal. 79−50017
2-fluoropyridine, IR and Raman spectra, vibr. assignments 78−25534
fluorostyrene, UV Raman spectra, reson. effect in photoreactive states 80−106326
formamide, intermol. H bonding, vibr. spectrosc. obs. 79−50018
formamide($-d_2$), vibr. spectra NH_2 stretching modes assignment 79−89675
formate ions adsorbed on Ag particles in aqueous soln. Raman spectra 80−69148
fungicides, in water, detect. by laser excited reson. Raman spectroscopy 78−31732

Raman spectra of organic molecules and substances continued
furane, cryst., low freq. vibr. spectrum, temp. depend., 12 to 253K 80−84743
glycerol($-d_3$), single cryst., glassy, and supercooled, polarised Raman spectra, anharmonic multiphonon interactions 79−91419
X-glycine, cryst., Raman band intensities of local group modes 80−93298
α-glycine, natural and ^{15}N-substituted, solid, Raman spectra, normal vibrs. 77−63408
α-glycine-C-d_2, Raman spectra, intermol. pot. 79−91432
glycylglycines, isotope substituted, IR and Raman vibr. spectra 78−42051
guanine, ^{15}N and D substituted, in acid and base solutions, vibr. anal. 79−26994
guanine nucleotides, purinic 8-CH exchange kinetic isotope effect, Raman spectral study 80−83381
haeme protein, reson. Raman line intensity formulae applicability 77−83609
haeme protein, resonance Raman effect *(Hungarian)* 78−74666
haeme protein solns., resonance Raman spectra at low temp. 77−23588
haeme proteins, inversely polarized modes in reson. Raman scatt., depolarisation dispersion curves, vibronic interactions 78−78676
haemoglobin, low freq. modes and excitation profiles, reson. Raman spectra 80−94428
haemoglobin, nanosec. probe of dynamics using time resolved reson. Raman scatt. 80−94162
haemoglobin haem structure after photo-deligation, Raman spectra 80−61510
haemoproteins, fluoresc., reson. Raman and radiationless decay 77−30916
2-haloethanols, Raman spectra, rot. isomerism and conform. energies 79−10117
2-haloethyl ethers, relative conformational energies 79−27002
halogenated propanes, IR and Raman spectra, LF vibrs. 79−10105
halomethanes, Raman spectra, totally symmetric vibr. bands depolaris. ratios 79−89677
heptafluoroiodopropane, cross-sections, implications for large-scale atomic I laser 79−23022
heptane, liq., Raman scatt. at high-press., chain kinking 79−87429
hexa(trifluoromethyl) germanium, gas and liq., IR and Raman spectra, normal coord. anal. *(German)* 79−72315
hexabromobenzene, cryst., IR and Raman spectra, vibr. normal coordinate anal. 77−79602
hexachlorobenzene, Raman intensities, polarised scatt. from lattice rot. modes. 78−43845
hexadecane, liq., Raman scatt. at high-press., chain kinking 79−87429
cis-2,trans-4-hexadiene, addition kinetics of HCl, Raman spectra meas. *(French)* 79−91940
hexafluorobenzene-benzene, liq., mol. interactions, IR and Raman lineshape obs. 80−28907
hexafluorobutene, vibrational broadening, dense fluid region, Raman and NMR study 80−43056
hexafluorohalopropanes, gas and solid, IR and Raman spectra, normal coord. anal. *(German)* 79−72317
hexafluoropropane($-d_2$), IR and Raman spectra, gas and liq., normal coord. anal. 79−68235
hexafluoropropene, struct. and vibr. spectra, IR, Raman polarisation study 80−18845
hexaidobenzene, cryst., IR and Raman spectra, vibr. normal coordinate anal. 77−79602
hexamethyl benzene, high press., variable temp. Raman spectra 78−56488
hexamethylbenzene, cryst., Raman spectra, intensity of low freq. line 78−2846
hexamethylbenzene, mol. dynamics, allotropy, solid-state phase transitions effects, Raman spectra *(French)* 77−42372
P-hexamethylcyclotriborophosphanes, substituted, struct., vibr. spectra 77−65460
hexane, liq., Raman scatt. at high-press., chain kinking 79−87429
n-hexatriacontane, cryst., orthorhombic modification, vibr. spectra 80−50314
4-n-hexyloxybenzylidene-4′-n-propylanilene, smectic S_H and S_m phase structs. 79−14673
highly fluorescent compounds coherent antiStokes reson. Raman spectra 79−36655
HxBPA smectic phases, X-ray diffr. and Raman spectra 78−6012
hyaluronic acid, Raman spectrum, primary and secondary structs. 79−59467
hydrocarbons, mol. Raman intensities calcs. 80−52993
p-hydroxyazobenzene, acidic soln., reson. Raman spectra, ring deuterated derivatives 79−26987
imidazole, single cryst. Raman spectrum, ν(NH) region temp. depend. 77−8561
imidazole, vibr. spectra, mol. crystal dynamics, librational modes 78−64356
indigoid dyes, Raman, IR and Shpolskii spectra 79−65866
intensity relation, IR to Raman intensity, matrix notation 78−62853
iodocyanoacetylene, cryst., IR, far-IR and Raman spectra, vibr., struct. 77−63407
iodomethane, liq. (liq. mixtures), vibr. relax. and reorientation, symmetric C-H bending mode 1st overtone 78−62884
iodomethane, Raman band shapes, mol. oscill. bands *(German)* 80−69154
iodomethane, vibr. population lifetimes in liqs. anti-Stokes Raman scatt. 78−74665
iodomethane, vibr. relax., Raman overtone band obs. 77−14436
2- and 3-iodopyridine, IR and Raman spectra, vibr. assignments 78−25534
isobutene-d_0, -d_6, torsional pot. functions, spectra anal. 78−25528
isobutylene, liq., vibr. phase relax. and freq. shifts, density and temp. effects 80−74235
isopropylcyclopropane, solid, liquid, vapour phase, IR and Raman vibr. spectra 80−84740
isoquinoline, adsorbed on Ag, surface enhanced Raman spectrum 80−100400
isorhodpsin, resonance Raman spectra 79−92148
Kevlar 49 fibre, poly p-phenylene terephthalate, Raman spectroscopy, heat, stress, radiation effects 79−65871
large molecules, condensed phase, reson. Raman effect, review, book contrib. 77−38676

Raman spectra of organic molecules and substances continued
lecithin-cholesterol interaction, hydrocarbon chain length and unsaturation effects, Raman spectra 77−64012
liquid, absolute Raman intensities determ. 77−68046
liquid, photoacoustic Raman gain spectroscopy 79−75606
liquid crystal orientation mol. ordering determ. by Raman scatt. *(Russian)* 79−19153
liquid crystals, solid state polymorphism, differential scanning calorimetry and IR and Raman spectra obs. 80−55094
liquid crystals, uniaxial, polarized Raman scatt., orientational order 77−76296
liquid-liquid interface, adsorbed monolayer mol. orientation, electrolyte effects, reson. Raman obs. 78−60430
liquids, H-bonded, IR and Raman spectra, elec. anharmonicity on H-stretching bands 78−48167
lithium ammonium tartrate monohydrate, Raman spectra, anomalous low-lying response 80−2746
lithium formate, and deuterated, polaritons, spontaneous parametric light scatt. 77−90150
lithium formate, optical phonons, small oscillator strength meas. from frequency-angular polariton spectra 80−92629
lithium formate monohydrate, temp. depend. Raman spectra, H bonds 78−6673
lutein, aq. soln., aggregate, reson. Raman spectra, and IR spectra, exciton interactions 78−31770
lysozyme, aq., Raman intensities, interac. 78−58704
malonic acid, aq. soln., IR and Raman vibr. spectra *(French)* 79−26989
malononitrile, cryst., phase transitions, Raman and IR obs. 80−88980
malononitrile, displacive phase transition, 294.7K, Raman and Brillouin-Rayleigh scatt. obs. 80−16047
malononitrile, solid phases I-IV, vib. spectra 77−20840
MBBA, dye activated, isotropic phase, induced Raman emission *(Russian)* 78−13766
MBBA, metastable phases formed by rapid cooling of mesophase, IR and Raman spectra and DSC obs. 80−34919
MBBA, nematic, order parameters meas. by Raman scatt. 78−6011
MBBA, NMR and Raman scatt. studies in nematic phase 80−100619
MBBA, Raman spectra in cryst., frozen glassy, and liq. cryst. states 80−60601
MBBA, solid phase polymorphism, IR and Raman spectra study *(French)* 79−87438
MBBA liquid crystals, meas. of nonlinear optical susceptibilities in isotropic and nematic phases *(Russian)* 78−74945
Menshutkin complexes 77−16291
menthane ring compounds, Raman circular intensity differential spectra obs., mol. struct. 80−87130
mesophase pitches, Raman spectroscopy 79−91416
metallo-octaethyl porphyrins, I oxidation products, metallic cond., EPR and reson. Raman spectra 80−29610
metallomacrocytes, mixed valent, cofacial assembly, cond. polymeric material 80−70143
metallooctaethylporphyrin, ^{15}N-enriched, reson. Raman spectra, haemoprotein oxidation state marker bands 77−58008
metalloporphins, deuterated, resonance Raman spectra, vibr. and vibronic levels 78−62812
metalloporphyrin, low symmetry environment, Raman excitation spectra and absorpt. spectrum 80−74172
metalloporphyrin, vibronic coupling, Raman scatt. 78−21933
metalloporphyrins, mol. origin of anomalous polarisation in reson. Raman spectra 77−3368
metalloporphyrins, reson. Raman specta, intra- and inter-manifold couplings interference 80−28020
metalloporphyrins, Soret excited, reson. Raman excitation profiles, Jahn-Teller distortion and vibronic anal. 78−58698
methaemoglobin, struct. change on addition of inositol hexaphosphate 80−72130
methane, $\nu_1(a_1)$ vibrational state rotational structure, CARS obs. 79−98109
^{13}C-methane, ν_1 fund., quasi-CW inverse Raman spectra 80−48004
methane, ν_1 fundamental, CW stimulated Raman gain spectroscopy 79−6943
methane, and d_1-d_4, absolute Raman intensities of fundamental, overtone and combination bands 77−65468
methane, and d_4, Raman scatt. activity and IR intensity, finite field method 79−59462
methane, and deuterates, absolute Raman intensities, depolaris. ratios, bond polaris. theory 77−10705
methane, collision induced rot. Raman scatt., polarisability effects 78−86874
methane, concentration along line in jet, spatially resolved coherent anti-Stokes Raman spectra 79−74476
methane, CW coherent antiStokes Raman spectrum, ν_1 band, press. depend. 78−42377
methane, high density fluid, LF Raman spectra, dimer formation 77−46566
methane, high resolution coherent anti-Stokes Raman scatt. *(Russian)* 77−75168
methane, high-resolution coherent Stokes Raman scattering, of ν_1 and ν_3 bands 79−31981
methane, intradoppler CARS saturation spectroscopy 80−43057
methane, liq., pure vibr. Raman spectra 80−97262
methane, liq. and solns., Raman spectra, vibr. anal. 79−27001
methane, phase II, IR and Raman spectra of ν_3 and ν_4 modes 78−2834
methane, photoacoustic Raman spectroscopy using CW laser sources 79−44947
methane, pulsed photoacoustic Raman spectrosc., gaseous trace anal. 80−40769
methane, pure rot. Raman scatt. 78−86875
methane, $Q(\nu_1)$ Raman line, CW high-resoln. CAR spectra 77−27076
methane, Raman intensity from electro-optical parameters 79−36645
methane, Raman spectra, 2850-3100 cm^{-1}, ν_3 band anal. 77−75162
methane, solid, orientational order of molecules in phase III 79−51042
methane, solid, phase II, Raman spectrum, vol. and temp. depend. 80−97260
methane, solid, phase III, Raman spectra 79−65849
methane, solid, Raman spectra and II-III phase transition 80−2745
beta-methane, solid, Raman spectrum in intramol. and lattice region 79−33697
methane, solid phase II Raman spectrum, lattice vibr. and ν bands 78−19456
methane, stimulated Raman scatt. obs. 80−53003

Raman spectra of organic molecules and substances continued
methane, vibration-rotation energies, $2\nu_2$ and $\nu_2+\nu_4$ bands 80−47963
methane ($-d_1,d_2,d_3,d_4$) Raman electro-optical parameters, overlay least squares calcs. 78−42105
methane and halogen derivatives Raman scatt. parameters at.-dipole interaction model calcs. 77−65465
methane jet flow, average conc. meas. by Raman scatt. 79−98827
methane molecular pair, polarisability tensor anisotropy 79−31725
methane-air flame, stimulated Raman scatt. obs. 80−53003
methane-d_1, A_0 determ. from ν_4 Raman band 77−83608
methane-d_4, ν_2 Raman band anal. 79−31536
methane-d_4, B_0 determ., from ν_3 Raman band and IR spectrum 77−88455
methanol, aqueous, damped coupled oscillator model used to study Fermi resonance 80−69152
methanol, C-O-H bending mode in α- and β-forms at 85K 77−8588
methanol, coherent anti-Stokes Raman spectra in UV 77−46567
methanol, effect of hydrogen bonding on Raman spectrum 79−18197
methanol, pure liq. and soln., Raman and IR intensity, polymerisation degree *(French)* 79−28740
methanol-acetonitrile, solns., H bonding, IR and Raman band profiles 77−42320
methanol-carbon tetrachloride, soln., Raman spectra in OH(OD) stretching region *(French)* 79−26986
methotrexate-dihydrofolate reductase complex form., conform., laser Raman obs. 80−104553
methoxy-amyltolane, orientation-statistical props. studies by optical methods *(Russian)* 79−77518
p-methoxy-p′-alkyl tolanes, Raman scatt. in isotropic, nematic, and solid phases *(French)* 77−15309
α,ω-methoxy-poly(ethylene oxide) effect of swelling on longitudinal acoustic mode 80−29739
methoxyamyltolane, nematic phase orientation mol. ordering determ. by Raman scatt. *(Russian)* 79−19153
p-methoxybenzylidene-p′-alkyl anilines, Raman scatt. in isotropic, nematic and solid phases *(French)* 77−15309
methoxydifluorophosphine-d_0 and -d_3, IR and Raman spectra, mol. vibr. and struct. obs. 80−87103
methoxytrifluorosilane and -d_3, IR and Raman spectra, vibr. anal., barrier to internal rot. 79−18185
methoxytrimethylsilane-d_0,($-d_3$) 78−86853
methyl 2-bromopropionate, IR and Raman liq. phase spectra, rot. isomerism 78−58680
methyl 2-chloropropionate, IR and Raman liq. phase spectra, rot. isomerism 78−58680
methyl ammonium chloride, Raman spectra, 70 to 300K, H stretching vibrs. 80−20628
methyl chloride, cryst., Raman band anomalous splitting, isotope effects 77−8562
methyl chloroformate, struct., microwave, Raman, far IR and NMR spectra 77−34614
methyl cyanide, vibr. relax., Raman overtone band obs. 77−14436
methyl cyanide ($-d_3$), vib. dephasing, Raman obs. 77−59566
methyl fluoride, solid, IR and Raman spectra, cryst. struct., and deutero deriv. 77−36218
methyl halides, Raman spectra and lattice motions 77−77197
methyl iodide, liq., A_1 modes, vibr. relax., temp. depend. Raman spectra obs. 80−32806
methyl iodide, liq., Raman meas. of transversal angular velocity correlation function 79−87422
methyl iodide, liq., vib. relax., A_1 Raman bands 77−40220
methyl iodide, vib. relax. and Raman line widths 77−32359
methyl iodide in CCl_4, vibr. energy redistrib. after ultrashort IR excitation 77−6894
3-methyl 1-butanethiol, Raman and vibr. IR spectra of solid and liq., rot. isomerism 78−62810
methyl mercapto acetate, Raman and vibr. IR spectra of solid and liq., rot. isomerism 78−62810
methyl orange, aq. soln., reson. Raman spectra of D and ^{14}N isotopes 80−91566
methyl orange, trace amount determ. by reson. Raman spectroscopy *(Japanese)* 79−48017
methyl symmetric stretching vibr. bandwidths, vibr. and reorientational effects, IR and Raman spectra 78−78686
methyl thionine chloride, intramol. vibr. spectra 80−977
methyl torsion modes, vibrational optical activity, inertial contrib. 80−5524
methyl tri(trifluoromethyl) germanium, and perdeuterated analogues, vibr. spectra, normal coord. anals. *(German)* 80−5547
methyl vinyl ether, and -d_3, IR and Raman spectra, vibr., torsion and internal rot. 78−94250
methyl vinyl sulphide, syn-gauche equilib., force field and ab initio calcs., microwave and Raman spectra 80−23573
1-methyl-2-thiomethyl imidazole, IR and Raman spectra, vibr. anal. *(French)* 79−45713
N-methylacetamide, and isotopic forms, low-freq. Raman spectra, internal torsional mode 79−26992
N-methylacetamide, structure *(French)* 80−7343
α-methylammonium chloride, disordered, lattice vibrs. Raman spectra 77−85699
methylborodichloride-d_0($-d_3$), vibr. spectra and force constants *(German)* 79−26982
methylcyclohexane, and d_{14}, evidence for two crystalline phases, low-temp. Raman spectra 79−56771
(+)-(3R)-methylcyclohexanone, vibr. optical activity, Raman obs. 80−102499
methyldisilylamine, and -d_3, vibr. assignment and barriers to internal rot., IR and Raman spectra 78−13496
methylene glycol($-d_4$)=formaldeyhyde($-d_2$)+H_2O(D_2O) Raman spectra and normal vibr. 80−58271
methylphosphinosilane, IR and Raman spectra, vibr. assignment and asymmetric potential function 79−85962
methylpropylsilane, vibr. spectra, normal vibrs. and rot. isomerism 79−31524
methylpyridine adsorbed on Ag, surface enhanced Raman spectra 80−83376
N-methylthioacetamide($-d_1$), reson. Raman spectra obs. and mechanism 78−17672
molecular crystals, intermolecular interactions, spectroscopic studies, review 80−103958

Raman spectra of organic molecules and substances continued
molecular crystals, mol. orientation defects, effect on polarised IR and Raman spectra 80−88989
molecular crystals, non-dipole vibr., Raman effect *(Russian)* 78−76471
molecular monolayer in MIM tunnel junction, anomalous surface enhanced mol. Raman scatt. 79−72324
molecular rotation, model for IR and Raman studies in liqs. and gases 80−11390
molecular shape determination, of high temp. species 80−52233
molecular vibr. freq. tables, up to 13 atom mols., and Raman and IR values 77−79614
molecules, Raman spectra intensities, electronic polarisabilities, quantum mech. calc. 79−27041
molecules D_{6h}, D_{3h} and D_{3d}, appln. of Aliev-Watson maxima-minima criteria for quartic centrifugal distortion const. 80−87132
monochlorobenzene, overlapping Raman lines resolution by coherent ellipsometry 79−98110
monochlorobenzene, prereson. Raman effects, intensity enhancement mechanism 78−42069
monohalobenzenes, circularly polaris. Raman spectra, vibr. symmetries assignment 78−29787
mucochloric acid-d_0, -d_1, vibr. spectra, struct. 78−46326
N-(4-alkoxybenzylidene)-4′-n-alkylanilines, Raman spectra in solid state, polymorphism of mesogenics 79−82964
naphthalene.2$SbCl_3$ 77−16291
naphthalene:azulene, reson. fluoresc., Raman spectra, single vibronic level relax. 79−38588
naphthalene:octafluoronaphthalene, cryst., interactions, Raman spectra 77−43982
naphthalene, cryst., laser reson. Raman effect, near 3200 Å, B_{3g} vibr. enhancement 77−52067
naphthalene, cryst., low freq. Raman spectra, defects and lattice vibr., 80-320K 78−31194
naphthalene, crystal optics and Raman intensities 79−4795
naphthalene, crysts., Raman and two-photon reson. in three wave mixing 79−38538
naphthalene, external mode one-density states, low freq. Raman scatt. spectra *(French)* 80−76012
naphthalene, melting of rotational degrees of freedom near cryst.-liq. transition 80−54352
naphthalene, mol. cryst., reson. four-wave mixing, third order susceptibilities 80−100654
naphthalene, nontotally symmetric Raman lines, destructive interference effects 77−6789
naphthalene, prereson. Raman spectra, vibr. band intensities obs. 80−102515
naphthalene, Raman active phonon freqs., linewidths and line shapes, temp. depend. 79−47432
naphthalene, Raman intensities, polarised scatt. from lattice rot. modes. 78−43845
naphthalene, Raman intensities rel. to vibronic coupling and excited electron state geometries 77−27075
naphthalene, reson. Raman scatt. from non-totally symm. mode 78−37641
naphthalene, solns., two-photon absorpt. meas., using nonlinear light-mixing spectroscopy 77−79620
naphthalene, vibr. dephasing and Raman active localised internal mode temp. depend. 80−45060
naphthalene, vibr. relax. studied by four wave mixing (CARS), spectral lineshapes obs. 80−80762
naphthalene charge transfer complexes, cryst., vibr., factor group splittings 79−7658
naphthalene crystal, dynamical matrix eigenvectors from Raman scatt. 80−100315
naphthalene in nonpolar solvent, vibr. and reorientational relax., correl. function 80−45065
naphthalene radical cation, in organic glass, 77K, reson. Raman spectra 78−78704
naphthalene-β-naphthol mixed mol. cryst., multiplet struct. of electron absorption spectra 77−1706
naphthalene-d_8, powdered 70 and 293K polarisation spectra of melt 77−32358
naphthalene-d_8 and -h_8, Davydov splitting of Raman-active vibr. levels 77−36210
naphthalene-octafluoronaphthalene complex, Raman spectrum, intermol. vibrs. 77−66004
naphthalene-TCNB (PMDA), Raman spectra orientational disorder, charge transfer cryst. 78−19459
naphthalene-tetracyanobenzene, charge transfer complex, phase transitions, deuteration effect, mag. reson., spectral and thermal meas. 79−4412
naphthalene-tetracyanobenzene, Raman spectra, phase transition and isotopic substitution 78−80364
nearly tetrahedral cpds., Mn^{2+}, ^4E levels, orbit-lattice interaction and Jahn Teller effect 80−24860
nematic liquid crystal, vibrational IR and Raman spectra 79−73913
neopentane, diamond force const., rel. to crystal elastic consts., Raman freq., bulk compressibility and freq. assignments 80−65183
nickel etioporphyrin, reson. Raman spectra, excitation profiles, nucl. distortion and Jahn-Teller effects 77−58018
nickel-porphin, reson. Raman spectra 77−75164
nicotinamide adenine dinucleotide, and reduced form, pH induced modification, Raman spectra 80−85343
nitriles, intermolecular interaction, band contour exam. *(Russian)* 79−808
m-nitroaniline, cryst., low-freq. polarised Raman spectra 78−84574
n-nitroaniline, IR and Raman spectra, internal modes 79−61366
p-nitroaniline, Raman spectra, mol. struct. in molten state 79−91435
nitrobenzene, absolute Raman cross section determ. from inverse Raman effect 79−3447
nitrobenzene, intensities in inelastic electron tunnelling, IR, and Raman spectroscopy *(French)* 79−822
nitrobenzene, IR absorpt. and Raman bands, half-band width conc.-depend. 80−74171
nitrobenzene, liq., induced Raman scatt., anomalous line broadening 78−56490
nitrobenzene-d_0(p-d)(d_5), vibr. spectra 79−26966
nitrobenzene-d_5, vibr. spectra 79−22695
nitrocyclopropane, vibr. spectra struct. and bonding 80−102520
N-nitrodimethylamine-do,(-d_6), structural phase transition, Raman study 80−34911

Raman spectra of organic molecules and substances continued
nitroethane-3-methylpentane, binary liq., depolarised light scatt. at crit. point 78−39558
nitromethane, vibr. relax., Raman overtone band obs. 77−14436
nitromethane in carbon tetrachloride, polarised line widths (intensities) in Raman scatt., conc. depend. 78−70879
nitromethane-d_0,-d_3, polycryst., methyl torsion, Raman spectra 79−82970
nitrosobenzene, fluoresc. quantum yields, determ. from Raman scatt. 80−58294
p-nitrosodimethylaniline, solid and CCl_4, H_2O solns., Raman and IR absorpt. spectra 77−79615
p-nitrotoluene, low-freq. vibr. spectrum, Raman and IR spectra 78−56484
p-nitrotoluene, vibr. spectra, normal mode calcs. 77−65482
p-nitrotoluene crystal film, exciton spectrum, IR absorpt. and Raman scatt. 80−80771
nonafluorobutane(-d_1), and halo-substituted forms, gas and liq., IR and Raman spectra, normal coord. anal. *(German)* 79−72318
nonaqueous solutions, Raman spectrosc. obs. techniques 78−72514
nucleic acid bases, excited state geometry distortion, normal modes reson. Raman intensity anal. 79−68236
nucleic acid components, UV resonant Raman spectra 78−48756
nucleic acid constituents, reson. Raman spectra using synchronously pumped dye laser 79−12869
nucleic acids, Raman spectroscopy obs. *(German)* 79−27119
nucleoside cyclic monophosphates, phosphodiester stretching vibrs., IR and Raman spectra 77−65461
nylon, Raman spectra using pulsed laser and gated detection 77−74529
octafluoronaphthalene, phase transitions at elevated press., Raman and mid-IR spectroscopy obs. 80−45062
octafluoronaphthalene, struct. phase transition exam. 77−47572
octafluoronaphthalene crystals, phase transition, Raman spectra 77−24829
octamethylcyclotetrasilazane, gas, liq., cryst., CCl_4 soln. IR and Raman spectra, assignments, struct. *(French)* 78−29790
octane, liq., Raman scatt. at high-press., chain kinking 79−87429
p-octoxybenzoic acid:cholesteric nonanoate, mag. field induced cholesteric→nematic transition Raman spectra 77−27988
4-octyloxy-4′-cyanobiphenyl, CN stretching in liq. cryst. phases, vibr. spectra 78−80325
one-dimensional conductor, IR and Raman activity 78−60441
optically active molecules, differential Raman scatt. of right and left circularly polarized light *(Japanese)* 78−17675
organic compounds, low freq. anharmonic vibr., pot. function determ., Raman and IR spectra obs. 80−52997
organic molecules, C-H Raman stretching bands in soln., vibr. freqs. and linewidth 80−78622
organic mols., relative Raman intensities, CNDO/2 INDO param. effect 80−95633
organic solids, vibr. relax. and dephasing Raman spectra, review 80−88987
organo-arsenic compounds, $(CF_3)_2AsSCH_3$ and $(CF_3)_2AsSeCH_3$, gas phase IR and liq. Raman spectra, normal coord. anal. *(German)* 80−32725
organometallic amines, Raman spectra, band intensity and assignment, force const. determ., vibr. props. *(German)* 80−87133
organometallic compounds, vibr. spectra, book 77−38671
organophosphorus compounds, $(CF_3)_2PSCH_3$ and $(CF_3)_2PSeCH_3$, gas phase IR and liq. Raman spectra, normal coord. anal. *(German)* 80−32725
organosilane coupling agent interphase of glass-fibre reinforced plastics, molecular organisation 80−44195
oxalate ion in aq. soln., vibr. study and Raman bands 80−95588
oxalic acid in aq. soln., vibr. studies, IR and Raman spectra 80−95589
oxanilide, IR and Raman spectra, cryst. struct. and vibr. 79−42954
oxocarbon ions, reson. Raman scatt., Jahn-Teller effect 79−18190
2-oxybicyclo(3.2.0)hept-6-ene, LF vib. spectra, conformations 78−58685
oxyhaemoglobin, dilute soln., reson. Raman spectra, pulsed laser excitation; optical multichannel detection 78−76999
oxyhaemoglobin, normal and sickle cell, Raman spectra, polarisability difference 79−62191
PAA, cryst. phase transitions, intermolecular motion, Raman and inelastic neutron scatt. spectra 80−2164
palladium bis-β-diketonates, IR and Raman spectra 78−46327
PAP, cryst. phase transitions, intermolecular motion, Raman and inelastic neutron scatt. spectra 80−2164
2,2 paracyclophane, dimer vibration influence on emission spectrum 80−69133
n-paraffin, longitudinal acoustic mode, perturbing forces 80−70348
n-paraffins, Raman spectra obs. of longitudinal acoustic modes intensities 78−84584
n-paraffins, solid and liq., Raman spectra, longitudinal acoustic vibr. mode 78−31183
pattern recognition anal. of IR and Raman spectra for cpd. classification 77−75158
pentachloronitrobenzene crystal, anomalous microwave permittivity, IR absorption and Raman spectra *(Japanese)* 78−15169
p-n-pentyl-p′-cyanobiphenyl, nematic liq. cryst., Raman depolaris. ratios, order parameters 79−28733
perchloro-[4]-radialene, IR and Raman spectra 77−77198
perdeuteropolyethylene, IR and Raman intensities by electro-optical parameters, single chain 78−1115
perfluoro-1,3-butadiene, vibr. spectra, struct. and barrier to planarity 78−9147
perfluorocyclobutane, matrix isolation Raman and IR spectra, pot. function 77−3352
perfluorocyclobutanone, IR and Raman spectra, vibr. anal. 77−38661
perylene crystal, molecular exciton system, resonance Raman and fluorescence studies, dynamical effects 80−66169
perylene-TCNQ complexes, Raman spectra intensities, freq. depend. 79−61362
pesticides, in water, detect. by laser excited reson. Raman spectroscopy 78−31732
PET, biaxial orientation, refr. index meas. by Raman and IR spectrosc. 80−60583
PET, uniaxially drawn, comparison of polarised fluorescence, polarised Raman and IR dichroism measurements 79−99084
phenanthrene.2$SbCl_3$ 77−16291
phenanthrene, cryst., Raman spectra, intensity of low freq. line 78−2846
phenanthrene, crystalline, Raman band intensity temp. depend. 77−59564

Raman spectra of organic molecules and substances continued
phenanthrene, IR and Raman spectra, lattice and internal mode coupling 77−20843
phenanthrene, low freq. Raman spectra intensity temp. depend., phase transition, conformation change 77−36211
phenanthrene, phase transition, Raman spectral obs. 77−59112
phenanthrene, vibr. spectra, mol. crystal dynamics, librational modes 78−64356
phenazine, prereson. Raman spectra, vibr. band intensities obs. 80−102515
phenol, cryst., mol. vibrs., factor group splittings 80−16021
phenyl acetylene, liq., phase relax., vibr. dephasing, Raman spectra obs. 80−91567
phenyl propargyl ether, dimerised, H getter 77−18001
p-phenylenediamine, reson. Raman spectra 77−58009
phenylsilanetriol-d_0,(-d_3), cryst. and liq. vibr., IR and Raman spectra 78−86855
phosphatidylcholine bilayer endothermic transitions, Raman difference spectroscopy 78−40119
phospholipid bilayer, Gramicidin antibiotics effect on Raman spectra 77−66798
phospholipid-d, as nonperturbing components, for Raman studies of biomembranes 78−53330
phthalazine, prereson. Raman spectra, vibr. band intensities 80−102514
phthalic anhydride, vibr. excitons reson. interaction in IR and Raman spectra *(Russian)* 79−61386
phthalic anhydride crystal, Raman spectra, overlapping spectral bonds separation by computer *(Russian)* 79−51968
picosecond interactions for vibr. relax. meas., book contrib. 77−65057
pivalic acid(-d_1, d_9), liq. and soln., Raman assignments, CH_3 rot. barrier, dimerisation 79−26991
pivalic anhydride, liq. and soln., Raman assignments, CH_3 rot. barrier, dimerisation 79−26991
PMMA, amorphous, LF Raman modes, strain and temp. effects 77−36219
PMMA, C-H stretching and bending vibrs. in Raman spectra 80−93300
Polaroid K, oriented analogue of polyacetylene, reson. Raman spectroscopy 80−66208
poly(m-methylene terephthalate) polymers, IR and Raman spectra 77−52088
poly-1,6-di-p-toluenesulphonyloxy-2,4-hexadiyne, thermal polymerisation, Raman spectra 80−35531
poly-β-ethynylnaphthalene, insoluble, reson. Raman spectrum, struct. models 78−70981
polyacetylene:I, pure and doped, reson. Raman spectroscopy 80−66208
polyacetylene:I charge transfer complex, struct. 79−74052
polyacetylene, doped and neutral, resonance Raman scatt. 80−55107
polyacetylene, doping with AsF_5, mechanism, effect on elec. cond. and spectra 80−24473
polyacetylene, polymerisation and Raman spectra on zeolite and alumina surfaces 79−13721
polyacetylene films, pure and Br and I doped, Raman scatt. 79−47457
trans-polyacetylene obtained by polymerisation on TiO_2, Raman spectrum *(Spanish)* 80−88988
polyacetylene-I_2, highly conducting, Raman, XPS and X-ray diffr. obs. 78−80454
polyalkenamers, longitudinal accordion mode, low frequency Raman spectroscopy 80−25369
polyatomic fluid, local dynamics, spectroscopic studies, summer school lecture series 80−6343
polyatomic liquids, vibr. relax. and energy transfer, ultrafast dynamics obs. 77−50506
polybutene-1 glass, Raman spectra, low temp. crystallisation *(French)* 79−99875
polybutylene terephthalate, hysteresis of stress-induced cryst. phase transition 78−31404
trans-1,4-polychloroprenes, prep. and struct., Raman spectra 77−66496
polydeoxyribonucleotides, poly(dA).poly(dT) and poly(dAT).poly(dAT), HF vibr. modes, Raman and IR spectra 80−32698
polydiacetylene, monocrystal, vibr. freq. stress depend., Raman obs. 77−50574
polydiacetylene cryst., electronic struct. change at phase transition, Raman spectra 78−2833
polydiacetylene crystals, electronic spectra and struct. 79−73923
polydiacetylene fibre resonance Raman spectrum meas. 79−17507
polydiacetylene polymer crystals, one dimensional conjugated, optical props. 77−43993
polyethyl ethylene and deuterated derivatives, modification I, vibrational spectra and normal coordinate anal. 79−87434
polyethylene:NaCl, internal field strength, Raman spectra obs. 80−40061
polyethylene, CH_2 Raman scissor modes *(French)* 79−69825
polyethylene, crystal split fundamentals, resolution by Raman difference spectroscopy 79−95373
polyethylene, crystallinity, Raman spectral investig. 79−14696
polyethylene, crystn. under high pressure 80−38946
polyethylene, direct ram extrusion, correl. between chain folding and tensile modulus 77−44209
polyethylene, H bonding effects on skeletal optical and longitudinal acoustical modes 80−34914
polyethylene, IR and Raman intensities by electro-optical parameters, single chain 78−1115
polyethylene, linear, bulk-crystallised, morphology study 79−32918
polyethylene, linear, glass transition temp. 80−15225
polyethylene, oriented, Raman active modes 78−23457
polyethylene, phase characterisation, Raman spectra study *(French)* 80−93303
polyethylene, phase orientation by stretching, Raman study *(French)* 80−93304
polyethylene, polarised Raman studies of crystalline and amorphous orientation 78−67660
polyethylene, quenched melt, factors controlling lamellar thickness 77−62484
polyethylene, Raman spectra, drawing effect on longit. acoustic mode *(French)* 77−24828
polyethylene, Raman spectra obs. of longitudinal acoustic modes intensities 78−84584
polyethylene, rapid crystn. from melt rel. to struct. 80−44152
polyethylene, second order Raman scatt. 78−72504
polyethylene, single crystal texture, polarised Raman spectra 77−61888
Raman spectra of organic molecules and substances continued
polyethylene, straight chain segment length distrib., from Raman LAM-1 band 79−41981
polyethylene, two phonon Raman spectrum, final state interactions 78−76457
polyethylene (orthorhombic), intermol. pot. functions, force consts., vibr. assignments, thermodynamic props. 77−39639
polyethylene electret, internal pot. topography, Raman and IR spectra 80−7362
polyethylene oxide, cryst., lowest laser Raman active accordion oscillations, elastic moduli effect 80−29734
polyethylene oxide, Raman scatt. from longitudinal acoustic modes of crysts. swollen by oligomers 78−27226
polyethylene oxide 2000-200 mixtures, Raman scatt., small-angle X-ray scatt. 77−52089
polyethylene oxide aqueous solns., spectroscopic obs. of structural variability WRT turbulent resistance reduction 77−7356
polymer, amorphous, bulk, structure models and exptl. methods, review 78−22671
polymer, amorphous, translational motion and lattice vibr. obs. by Raman scatt., T_g phenomena 78−23469
polymer, light and Raman scattering obs. of high press. phases *(Japanese)* 80−2773
polymer, longitudinal acoustic mode, perturbing forces 80−70348
polymer, Raman spectra, cryst. morphology, longitudinal acoustic mode 78−43859
polymer, Raman spectra, longitudinal acoustic mode 78−43858
polymer orientation measurement, in solid, by spectroscopic techniques, mech. anisotropy 78−75558
polymer viscoelasticity and strength characterisation, advanced light scatt. techniques 80−11857
polymers, Raman active longitudinal-acoustical mode spectra interpretation 80−103950
polymers, zigzag chain, second order Raman scatt. theory, appl. to polyethylene 78−72504
polymethine dyes, mol. struct., lasing props. 79−3693
polymethylene, extended chain, C-H stretching band struct., Fermi reson., Raman spectrum 80−5552
polymethylene chain, vibr. spectra, CH stretching region, struct. and assignments 78−70991
polynuclear aromatic hydrocarbons, synchronous excitation spectrofluorometry *(Japanese)* 80−86452
polynucleotide soln., order-disorder transition, Raman spectra 78−41360
polyoxymethylene, melt-crystallised, longit. acoustic mode obs. 77−59572
polyoxymethylene, rapid crystn. from melt rel. to struct. 80−44153
polyperdeuteroethylene, IR and Raman spectra, 77K and room temp., vibr. anal. 78−72517
polyphenylacetylene, cryst., resonant Raman scatt., opt. absorpt. 77−4630
polypropyl ethylene and deuterated derivatives, modification I, vibrational spectra and normal coord. anal. 79−87435
polypropylene, extruded, chain orientation, polarised Raman scatt. 79−1756
polypropylene, helical syndiotactic, laser Raman spectrum 77−79719
polypropylene, isostatic, uniaxially oriented, Raman spectra *(French)* 80−60557
polypropylene, isotactic, melt-crystallised, longit. acoustic mode obs. 77−59572
polypropylenes, iso- and syndio-tactic, Raman tacticity bands, vibr. spectrum 80−66193
polyriboadenylic acid, soln., Raman spectra, struct. and conformation 77−71899
polystyrene, amorphous, LF Raman modes, strain and temp. effects 77−36219
polystyrene, isotactic, normal vibrational anal. 78−43869
polystyrene, solid, low freq. Raman scatt., vibr. density of states, 29-300K 78−72516
polystyrene, substituted, Raman, IR and neutron spectra of LF vibs. 78−2848
polystyrene, total reflection Raman spectroscopy study 80−80784
polystyrene, uniaxially oriented atactic, laser Raman scattering 79−73920
polystyrene, uniaxially stretched atactic thin film, mol. orientation, polarized Raman study 80−103951
polystyrene and model cpds., conformational struct. influence on normal modes of benzene ring, Raman study 80−14144
polystyrene coated Ag holographic grating, Raman spectra enhancement by plasmon surface polaritons 80−80885
polytetrafluoroethylene copolymers and oligomers, melt and solid, Raman active longit. acoustic modes 78−19484
polytetrahydrofuran, H bonding effects on skeletal optical and longitudinal acoustical modes 80−34914
polythylene, and perdeuteropolyethylene, crysts., IR and Raman intensities, factor group splittings 79−65851
polyvinyl alcohol, absorption of H_2O mols. from liq., Raman spectrosc. technique 79−42364
polyvinyl alcohol, doubly orientated, polarized Raman spectra 79−65872
polyvinylidene chloride, vibr. spectra, amorphous and cryst. state conforms. 79−27930
polyvinylidene electrets, IR and Raman spectra 80−7359
polyvinylidene fluoride-PTFE copolymer, local electrostatic field determ. *(French)* 77−12305
porphins, and deuterated derivatives, resonance Raman spectra 79−64010
porphins, reson. Raman spectra, selection rules, normal coord. treatment 80−53175
porphyrins, complex Raman tensors, irreducible tensor method, antisymmetric scatt. 78−37623
porphyrins, reson. Raman scatt. by degenerate mode, Renner-Teller coupling 79−59461
potassium acid phthalate, Raman spectra and lattice vibr., 77, 300K 78−27219
potassium hydrogen glutarate, H bonding, vibr. spectra 78−43860
potassium hydrogen malonate, aq. soln., IR and Raman vibr. spectra *(French)* 79−26989
potassium hydrogen malonate single cryst., IR and Raman spectra 78−60444
potassium hydrogen oxalate, oriented single cryst., Raman spectra with very strong H-bonding 80−25359
potassium oxalate, anhydrous, phase II, vibr. spectra and cryst. struct. 80−34901

Raman spectra of organic molecules and substances continued
potassium tetrachlorophthalimide, polycrystalline, IR and Raman band assignments 79−50015
propanal, methyl torsional pot. functions, LF Raman and IR vibr. spectra 80−95612
propane-d_0 and -d_3, Raman spectra, torsional pot. function 77−58015
propenoyl chloride, far IR and Raman spectra, internal rot. 79−89668
propenoyl fluoride, far IR and Raman spectra, internal rot. 79−89668
propiolyl chloride(-d), 357-333 nm absorpt. system 80−69161
isopropyl chloride, torsional pot. function, far IR and Raman obs. 80−28022
1,3-propylenediammonium manganese tetrachloride, vibr. study of phase transitions, IR and Raman spectra 80−40103
propylsilane-d_0(−d_n), vibr. spectra, normal vibrs. and rot. isomerism 79−31523
protein, secondary structure determ. by laser Raman spectroscopy 77−23587
PTFE, Raman spectra obs. of high press. phase conformal deform. 79−1757
purine, single cryst., Raman spectra and lattice vibr. 77−66498
PVA, swollen crystallinity determ. by laser Raman spectroscopy 80−38953
PVC, filled, drawn, mol. orientation study by Raman spectroscopy 79−73919
PVC, Raman spectrum, C-Cl stretching region 78−84583
PVC, structural studies by Raman spectroscopy 79−7044
PVC particles, Raman spectra, conform. during polymerisation 79−33709
pyrazine, cryst., 3300 Å reson. Raman band, vibr. assignments 77−1684
pyrazine, phase transitions, sp. ht., X-ray diffr., LF vibr. spectra 78−43122
pyrazine, prereson. Raman spectra, vibr. band intensities obs. 80−102515
pyrazine, Raman spectrum, correlation with vibronic coupling and adiabatic potential 77−71804
pyrazine, reson. Raman and absorpt. spectra to $S_2(\pi,\pi^*)$ state, excited state geometry 79−76433
pyrazine, reson. Raman spectra, vibronic theory of Raman intensity 78−37643
pyrazine, reson. to the $S_2(\pi,\pi^*)$ state, Raman spectra calcs. 80−69147
pyrazine absorbed on electrode, surface enhanced Raman spectra, symmetry and polarisability changes 80−50310
pyrazole and deuterated species, CH stretching vibrs., anharmonicity, pseudo-symm. 78−78710
pyrene, appl. of new force field for condensed aromatics, inplane vibrs. 79−81201
pyrene-tetracyanobenzene, charge transfer complex, phase transitions, deuteration effect, mag. reson., spectral and thermal meas. 79−4412
pyridazine, prereson. Raman spectra, vibr. band intensities 80−102514
pyridine, adsorbed on Ag, giant Raman scatt. 79−95768
pyridine, adsorbed on Ag, Raman intensity enhancement using surface plasmons 80−7334
pyridine, adsorbed on Ag electrode with graphitic C overlayer, Raman spectra obs. 80−103954
pyridine, adsorbed on Ag electrodes, ang. resolved Raman spectra 80−16017
pyridine, adsorbed on Ag surface, enhanced Raman scatt., ultrahigh vac. study 80−88993
pyridine, adsorbed on Cu(Au) electrode, angle-resolved Raman spectroscopy 80−52991
pyridine, adsorpt. on Ag colloids, surface enhanced Raman spectra obs. 80−97251
pyridine, deuterium substituted, Raman and IR vibr. spectra 80−84739
pyridine, in carboxylic acid soln., stimulated Raman scatt., H-bonded complex effects *(Russian)* 77−3625
pyridine, near Ag electrode, intense Raman spectra, free radical form. 80−55076
pyridine, on Au substrate with Ag monolayer, giant Raman effect 80−63637
pyridine, sorbed on Ag, surface enhanced Raman scatt., mol.-surface separation depend. 80−92775
pyridine adsorbed on Ag, reson. Raman scatt. 80−25380
pyridine adsorbed on Ag (100), (111), and polycryst. electrode surfaces, intense Raman spectra 78−72492
pyridine adsorbed onto roughened Ag electrode, Raman band intensity 78−48160
4-pyridine carboxaldehyde-doped Al-Al_2O_3-Ag tunnel junction, surface enhanced Raman spectra, surface plasmons 79−98111
pyridine iodine complexes, charge transfer complexes, vibr. spectra, laser Raman obs. 80−52990
pyridine on Ag electrode, appl. of pot. modulation Raman spectroscopy 79−63310
pyridine-2,3,5,6-d_4, vibr. spectra, IR and Raman, assignment 80−102519
pyridine-3,4,5-d_3, vibr. spectra, IR and Raman, H exchange rates meas. 80−102518
pyridine-3,5-d_2, vibr. spectra, IR and Raman, H exchange rates meas. 80−102518
pyridine-bromine charge transfer complexes, Raman spectra 77−6788
pyridine-d_0-d_5, nπ^* excited state vibronic coupling, vis. and Raman spectra 77−14438
pyridine-d_5, physisorbed thin film on Ag surface, enhanced Raman scatt. study 80−20620
pyridine-d_5, vibr. spectra, IR and Raman, assignment 80−102519
pyridine-I_2(Br_2) charge transfer complexes, vibr. spectra, vibronic contrib., intensity enhancement 80−53048
4-pyridinecarboxaldehyde monolayer in inelastic electron tunnelling spectroscopy junctions 80−93344
pyridines and water complex, Raman spectra, Fermi reson. in ν_8 region 79−89679
pyridinium iodide, order-disorder phase transition and reorientation fluctuations studied by Raman spectra 80−80764
pyrimidine nucleotides, UV reson. Raman excitation profiles 80−58265
pyrometallic dianhydride radical anion, MTHF glass, 77K, reson. Raman spectra 78−78704
pyronine, reson. Raman scatt., normal and excited mol. struct. determ. 77−58024
QED theory of differential scatt., Raman scatt. of circularly polarised light, two chromophores model 78−9158
QED theory of differential scatt., Rayleigh scatt. of circularly polarised light, two chromophores model 78−9157
p-quaterphenyl, Raman spectra, struct. transitions 79−19870

Raman spectra of organic molecules and substances continued
quinazoline, prereson. Raman spectra, vibr. band intensities obs. 80−102515
quinoxaline, prereson. Raman spectra, vibr. band intensities 80−102514
Raman spectra in OH(OD) stretching region *(French)* 79−26986
reson. spontaneous Raman spectra, vibronic interactions 79−3451
resonance Raman scattering from small molecule, vibronic theory 79−94004
resonance Raman scattering with tunable lasers, review, appls. 78−94247
resonance scattering by doubly degenerate vibr., Jahn-Teller effect 79−59460
resorcin, Raman line intensity as function of mol. orientation 80−11383
retinal, all-trans, reson. Raman excitation profile 78−73137
retinal chromophore, reson. Raman spectra obs. of struct. 80−94168
retinal Schiff bases, Raman spectra modelling of rhodopsin and bacteriorhodopsin chromophores 79−62190
rhodamine 6G, in glycerine-water solns., anti-Stokes fluoresc., conc. quenching 79−24349
rhodamine 6G soln., stimulated reson. Raman scatt., first excited and ground electronic states contrib. 79−89968
rhodamine B, 6G, resonance CARS line shape, scatt. processes in ground or excited states 80−48043
rhodamines, reson. Raman scatt., normal and excited mol. struct. determ. 77−58024
rhodopsin, bovine, photochem. cis-trans isomerisation at liq. He temps. 78−64939
rhodopsin, resonance Raman effect *(Hungarian)* 78−74666
rhodopsin, resonance Raman spectra 79−92148
ring compounds, three-membered, vibr. spectra and struct., book control 78−78701
RNA, laser Raman spectra, cloverleaf secondary struct. 79−100569
Rochelle salt, ferroelec. phase transition, Raman scatt. study 80−97211
Rochelle salt, phase transition mechanisms by optical spectroscopy 79−15411
rose bengal, adsorbed on ZnO electrode, reson. Raman spectra 78−76446
rubidium hydrogen glutarate, H bonding, vibr. spectra 78−43860
rubidium tetramethylborate, vibr. spectra and force constants *(German)* 79−26981
salicylic acid, Raman active external modes *(French)* 78−23458
samarium oxalate, IR and Raman spectra exam. *(French)* 78−48159
sandwich compound, electronically degenerate ground state, depolarisation ratio of fundamental modes 77−75165
scandium oxalate, IR and Raman spectra exam. *(French)* 78−48159
selenocyclopentane, interconversion barrier, spectra and struct. 79−10115
semiconductor, vibr. IR excitons, spectra *(Russian)* 78−15173
L-serines-d_0 and -d_4, IR and Raman spectra, rot. isomers *(French)* 79−45714
silacyclopentane, Raman spectra, pot. energy surface, barrier to interconversion 78−25541
simple liquids under influence of quasi-static elec. fields 79−8139
smectic liquid crystal, vibrational IR and Raman spectra 79−73913
sodium formate, vibr. spectrum, lattice modes 79−28759
sodium hydrogen oxalate monohydrate, oriented single cryst., Raman spectra with very strong H-bonding 80−25359
solids, Raman phonon spectra, mol. motions 79−73921
solution, of polar mols., local order and vibr. coupling, Raman bands, dielec. const. 79−99868
solutions, Raman line intensity conc. depend. 79−56786
squaric acid, 2-dimens., phase transition studied by Raman scatt. 79−82330
squaric acid, struct. and Raman spectra 78−47311
squaric acid, two-dimens. phase transition, Raman scatt. study 80−71401
squaric acid and deuterated derivative, vibrational study, IR and Raman spectra 78−92076
squaric acid thin films, Raman and IR spectra, Davydov splitting rel. to interlayer interaction 79−99878
stearyl alcohol, H bonding effects on skeletal optical and longitudinal acoustical modes 80−34914
trans-stilbene dianion, photolysis, intermediate struct., time-resolved reson. Raman spectra obs. 79−52695
strong H bonded systems, vibr., Raman, IR spectra, biology appls. 78−82735
styrene, and isotopic forms, IR and Raman spectra, normal vibr. assignments 77−18930
styrene, UV Raman spectra, reson. effect in photoreactive states 80−106326
styrene-β-d_2, IR and Raman spectra, vibr. assignments 79−13711
styrene-sodium methacrylate copolymers, Raman spectra, ion clustering 80−71416
succinic acid and its alkaline salts in aqueous soln., Raman and IR spectra *(French)* 80−32723
succinonitrile, phase transition, Raman spectrosc. obs. using low-temp. sample holder 78−86342
sulphonyl compounds, H-bonding by methyl groups, Raman spectra obs. 79−24320
sulphophthalein dyes in aq. soln., reson. Raman spectra 79−89678
sultams, characteristic band in IR region, Raman obs. 78−29784
sym-trioxane, phase transition, polarised Raman spectra obs. 80−84742
TBAA, smectic B phase, deform. vibrs. of alkyl chains 77−39531
TBBA, smectic liq. cryst., polarised Raman spectra, 90-300K, 0-400 cm^{-1} 77−12383
TCND, IR and Raman spectra, vibr. anal. 79−36630
TCNE, Raman active fundamental vibrations, revised assignment 77−68049
TCNE aromatic donor/acceptor complexes, reson. Raman excitation and absorpt. profiles, model theory 77−18982
TCNQ, anions, screened INDO model, appl. to resonance Raman spectra 79−765
TCNQ, resonance Raman spectra 79−56787
TCNQ alkaline salts, in dimethylsulphoxide, and aq. solns., Raman and IR spectra 78−46344
TCNQ salts, conducting, Raman spectra, estimation of degree of charge transfer from vibrational frequencies 80−50344
TCNQ salts, quasi-one-dimensional organic crystals, charge transfer, Raman scatt. *(German)* 79−28731
tellurophene(-d_4), cryst., struct., phonon spectrum, exciton splittings, assignments 77−81088
p-terphenyl, Raman scatt., order-disorder phase transition 78−43841

Raman spectra of organic molecules and substances continued
p-terphenyl, Raman spectra, struct. transitions 79−19870
p-terphenyl in benzene, triplet state resonance Raman spectroscopy 79−6944
tetra(trifluoromethyl) germanium, gas and liq., IR and Raman spectra, normal coord. anal. *(German)* 79−72315
tetraalkylammonium bromide, solid and liq., Raman spectra, longitudinal acoustic vibr. mode, mol. dimensions of ions 78−31183
1,2,4,5-tetrabromobenzene, lattice vibrs., Raman and far IR spectra 78−76444
1,2,4,5-tetrabromobenzene, structural phase transition, Raman and IR spectra meas. *(French)* 77−66503
meso-1,2,3,4-tetrabromobutane, IR and Raman spectral studies 80−32722
1,1,2,2-tetrabromocyclopropane, IR and Raman spectra 79−41170
tetrabromomethane, fine struct. resolution in Raman-active fundamentals 79−42967
tetrabromomethane, in disordered phases, IR active mode Raman line shape, dipole-dipole interaction 80−9603
tetrabromomethane, monoclinic monocryst., polarised Raman spectra *(French)* 80−93302
tetracene, cryst., solid-state transitions, Raman spectra, prompt fluoresc. in mag. field 79−99865
1,1,4,4-tetrachloro-1,3-butadiene, reson. Raman intensities, mol. struct., excited states, vibr. anal. 77−65470
tetrachloro-p-benzoquineone, IR and Raman spectra of phase transition *(French)* 78−60445
1,2,3,5-tetrachlorobenzene, chemical perturbation of cryst. structs., Raman phonon spectra 78−26559
sym-tetrachlorobenzene, LF Raman bands and space symmetries 77−66504
1,2,4,5-tetrachlorobenzene, structural phase transition, Raman and IR spectra *(French)* 77−66503
meso-1,2,3,4-tetrachlorobutane, IR and Raman spectral studies 80−32722
2,2,3,3-tetrachlorobutane, vibr. spectra, liq. and solid-state, conform. struct. 79−73936
tetrachlorocyclopropene, A_1 vibrs., laser Raman obs. 79−76437
tetrachloroethylene, liquid, twisting vibration, direct obs. via hyper-Raman effect 77−28559
tetrachloroethylene, Raman line intensities, modified CNDO/2/INDO calc. 78−25621
tetrachloromethane, fluid, collision induced light scatt. intensity 80−103955
tetrachloromethane isotopic liq., Rayleigh and Raman depolaris. components *(French)* 79−99895
tetrachlorophthalic anhydride, polycrystalline, IR and Raman band assignments 79−50015
tetrachlorophthalimide, polycrystalline, IR and Raman band assignments 79−50015
1,1,1,3-tetrachloropropane, Raman and IR obs. of rot. isomerism, entropy difference between vapour and liq. phase isomer *(Russian)* 79−31529
1, 2, 4, 5-tetracyanobenzene and -d_2, IR and Raman spectra, vibr. anal. 79−36629
tetracyanoethylene-hexamethylbenzene, electron-donor/acceptor complex, reson. Raman scatt. 77−24831
1,1,2,2-tetrafluoroethane, anti- and gauche-rotamers, struct., spectra, electron diffr. 77−50439
tetrafluoroethylene, Raman line intensities, modified CNDO/2/INDO calc. 78−25621
tetrafluoromethane, collision induced rot. Raman scatt., polarisability effects 78−86874
tetrafluoromethane, collision-induced scatt., many-body correls. 80−87127
tetrafluoromethane, collision-induced scattering at a vibrational Raman frequency 78−62814
tetrafluoromethane, in disordered phases, IR active mode Raman line shape, dipole-dipole interaction 80−9603
tetrafluoromethane, liq., pure vibr. Raman spectra 80−97262
tetramethyl germanium(-d_{12}), vibr. spectra, normal coord. calcs. 79−22717
tetramethyl lead(-d_{12}), vibr. spectra, normal coord. calcs. 79−22717
tetramethyl silicon(-d_{12}), vibr. spectra, normal coord. calcs. 79−22717
tetramethyl tin(-d_{12}), vibr. spectra, normal coord. calcs. 79−22717
2,3,5,6-tetramethyl-p-phenylenediamine, reson. Raman spectra 77−58009
tetramethylammonium cation(-d_{12}) aqueous solution, Raman and IR spectra 78−82741
tetramethylammonium chloride in HCl, Cl^- solvation no., Raman spectra 79−96410
tetramethylammonium chloride solns., aq. and methanolic, Raman spectra 79−28750
tetramethylammonium cobalt tetrachloride, Raman spectra near incommensurate phase transitions 80−76013
tetramethylammonium hexachloroplatinate, order-disorder transition, IR and Raman spectra 78−92060
tetramethylammonium hexachlorotellurate, IR and Raman spectra, lattice and internal modes, phase transition 78−6659
tetramethylammonium zinc tetrachloride, Raman spectra near incommensurate phase transitions 80−76013
tetramethylethylene, adsorbed on silica, laser Raman spectra 77−3367
tetraphenylarsonium, Raman and IR spectra of the dicyanoiodate (I) ion 80−60572
tetraphenyldithiapyranylidene mixed valence polyiodides, crystalline struct. and optical props. 80−92516
tetraphenylphosphonium, Raman and IR spectra of the dicyanoiodate (I) ion 80−60572
tetrathiofulvalene, Raman spectra 77−24832
tetrohydrofuran-$HgBr_2$ complexes, IR and Raman vibr. spectra, inter- and intramol. forces 77−66489
tetrolyl fluoride, IR and Raman spectra 79−41171
1,3,5,7-tetroxocane, vibr. spectra and intermol. forces 77−36216
thiazolidine, mol., vibr. anal., IR and Raman spectra *(French)* 79−26964
Δ-2 thiazoline and alkyl derivatives, IR and Raman vibr. spectra, conformation *(French)* 79−10104
thieno(3,2-b)thiophene, electronic and vibr. spectra, vapour phase and cryst. 77−34654
2-thio alkyl (allyl, benzyl) pyrimidines, IR and Raman spectra anal., mol. vibr. and symmetry *(French)* 80−87123
thioamides, characteristic pattern in IR and Raman spectra 78−29818
Raman spectra of organic molecules and substances continued
thiocarbonyl bromide, IR spectra, gas, liq. and matrix isolated, mol. force consts. *(German)* 79−36640
thiocyanate complexes at Ag electrode surface, Raman spectroscopic study 80−37813
thiophosgene, IR spectra, gas, liq. and matrix isolated, mol. force consts. *(German)* 79−36640
thiophosgene, laser Raman spectra, vibr. anal., Cl isotope splitting 77−65486
thiourea, phonon modes near order-disorder transforms., hard-core modes due to pseudospin-phonon coupling 80−44285
thiourea, phonon modes near phase transitions, IR and Raman spectra 80−45084
thiourea, Raman scattering spectra, soft mode frequency 79−24305
thiourea, Raman spectra of external frequencies 77−24840
thymine monoanions in soln., tautomer identification by laser Raman spectroscopy 80−14148
tin tetrahedral molecular solids, ^{119}Sn Mossbauer and Raman spectra 78−15070
TMCC chain compounds, Raman spectra and struct. phase transitions 79−56794
TMMC(-d) chain compounds, Raman spectra and struct. phase transitions 79−56794
toluene, asymmetric bending vibrs. 79−13696
toluene, mol., UV prereson. Raman scatt., interference effects 79−64008
toluene, mol., UV prereson. Raman scatt. intensity 79−64007
toluene, molecule translational mobility in depolarised Raman spectra 80−14150
toluene sulphonate diacetylene polymer, electronic and vibr. excitations, press. and temp. depend. 78−31188
toluene sulphonate diacetylene polymer, vibr. modes, strain depend. using Raman spectra 80−20626
toluene-d_0-d_8, polycryst., methyl torsion, Raman spectra 79−82970
toluene-d_3, liq., vibr.-vibr. near resonant energy transfer, Raman spectra 77−61836
p-toluidine, cryst., low-freq. polarised Raman spectra 78−84574
p-toluidine, vibr. spectra, normal mode calcs. 77−65482
toxic organic substances detection in water using matrix isolation Raman spectroscopy 80−30616
trans-polyacetylene, intrinsic, electron-phonon coupling 80−79901
transition metal complex anions, ligand-bridged, binucl., reson. Raman spectra 78−42067
tri(trifluoromethyl) germanium halides, gas, liq. and solid, IR and Raman spectra, normal coord. anal. 79−72316
tri-i-propygermylamine, and isotopomers, IR and Raman spectra, normal coord. anal. *(German)* 80−32716
tri-t-butylstannylamine, and isotopomers, IR and Raman spectra, normal coord. anal., Mossbauer spectrum *(German)* 80−32716
triamantane, plastic and solid-solid transitions, Raman study 80−60590
s-triazine, Raman spectrum, lattice vibrs. 78−19465
tribromobenzene, Raman spectra line intensities 79−65863
2,4,6-tribromophenol, Raman and IR spectra, hydrogen bonds 80−84735
tribromotrifluoroethane, IR and Raman spectra, normal coord. anal. *(German)* 80−32726
1,3,5-trichloro-2-bromobenzene, chemical perturbation of cryst. structs., Raman phonon spectra 78−26559
1,2,3-trichloro-5-bromobenzene, chemical perturbation of cryst. structs., Raman phonon spectra 78−26559
1,3,5-trichlorobenzene, lattice vibr., Raman spectra line intensities calc. 77−69825
1,2,3-trichlorobenzene, low freq. vibs. 77−32365
1,2,4-trichlorobenzene liq., mol. reorientation, translation and vibr. relax., Rayleigh and Raman spectra 80−95632
trichloroethane, CH_3-stretching modes, Raman spectra reson. energy transfer obs. 78−48162
1,1,1-trichloroethane, Raman spectra, vibr. dephasing 79−59465
trichloroethane, vibr. population lifetimes in liqs. anti-Stokes Raman scatt. 78−74665
2,2,2-trichloroethanol(-d_2), vibr. spectra and normal coord. anal. 79−72319
trichloromethane, and -d_1, depol. Raman scatt. line shapes in liq., density effects 79−4796
trichloromethane, and -d_1, liq., vibr. relax., Raman spectra 78−19471
trichloromethane, vibr. population lifetimes in liqs. anti-Stokes Raman scatt. 78−74665
trichloromethane(-d_1), electrooptical parameters and Raman intensities obs., bond polaris. calcs., vibr. force field 77−50441
trichloromethane-d_1, in nonpolar solvents, vibrational and rotational relax. 79−10182
trichloromethane-d, Raman band shapes, mol. oscill. bands *(German)* 80−69154
2,4,6-trichlorophenol, Raman and IR spectra, hydrogen bonds 80−84735
trichlorosilane liquid, Si-H stretching mode vibr. dephasing, Raman study 80−84736
1,3,5-trichlorotrifluorobenzene, IR and Raman vibr. spectra 77−3356
trichlorotrifluoroethane, IR and Raman spectra, normal coord. anal. *(German)* 80−32726
tricosane, single cryst., polarised Raman spectra 77−61888
tricyclo(3.3.0.$0^{2,6}$)octane, liq., Raman spectrum, vibr. assignments 77−61753
triethylenediamine, aq. soln., stimulated Raman scatt., struct. enhancing solute 78−27222
triethylenediamine, Raman spectra study *(French)* 80−80768
triethylsilylamine, and isotopomers, IR and Raman spectra, normal coord. anal. *(German)* 80−32716
1,1,1-trifluoro-3-chloropropane, Raman and IR obs. of rot. isomerism, entropy difference between vapour and liq. phase isomer *(Russian)* 79−31529
trifluorochloromethane, Raman and IR spectra, $^{35/37}Cl$ isotope splitting and mol. constants *(German)* 77−83595
trifluoroethane(-d_3), IR and Raman spectra, normal coord. anal. *(German)* 80−32726
2,2,2-trifluoroethanol(-d_2), vibr. spectra and normal coord. anal. 79−72319
1,1,1-trifluoroethyl halides, internal rot. barriers and LF Raman spectra 77−65478
trifluoromethyl hydroperoxide(-d), CF_3 torsional vibrs., low freq. Raman spectra 80−91565
trifluoromethyl hypochlorite, vibr. spectra and normal coord. anal. 80−102517

Raman spectra of organic molecules and substances continued
trifluoromethyl hypofluorite, vibr. spectra and normal coord. anal. 80−102517
trifluoromethyl hypofluorite (hypochlorite), CF_3 torsional vibrs., low freq. Raman spectra 80−91565
trifluoromethyl peroxyfluoride (peroxychloride), CF_3 torsional vibrs., low freq. Raman spectra 80−91565
trifluoromethyl trimethyl germanium (tin)(lead), and perdeuterated analogues, vibr. spectra, normal coord. anals. *(German)* 80−5547
trifluorotriiodoethane, IR and Raman spectra, normal coord. anal. *(German)* 80−32726
1,1,1-trimethoxyethane, mol. struct., electron diffr., vibr. spectra 78−37765
trimethyl-d_9-vinylsilane, IR spectra, struct., vibr. assignment, barriers to internal rot. calc. 80−87102
trimethyl-d_9-vinylsilane, Raman spectra, struct., vibr. assignment, barriers to internal rot. calc. 80−87102
trimethylaminegallane, microwave, IR and Raman spectra, struct., vibr. assignment 80−95600
α-trimethylammonium chloride, disordered, lattice vibrs. Raman spectra 77−85699
trimethylammonium chloride in HCl, Cl^- solvation no., Raman spectra 79−96410
trimethylborane, vibr. spectra and force constants *(German)* 79−26981
trimethylgermylisocyanate, IR and Raman spectra, struct. 78−37637
trimethylgermylisothiocyanate, IR and Raman spectra, struct. 78−37637
trimethylsilyl azide, vibr. spectra, normal mode assignment 78−86867
trimethylsilyl isocyanate, vibr. spectra, normal mode assignment 78−86867
trimethylsilyl isothiocyanate 78−86867
trimethylvinylsilane, Raman spectra, struct., vibr. assignment, barriers to internal rot. calc. 80−87102
trimethyoxybenzenes, liq. and solid, IR and Raman spectra, vibr. assignments 78−58701
S-trioxane, lattice vibrs. from Raman spectra 78−6672
s-trioxane, Raman spectra of single crystal, liquid and chloroform-d solution 79−94000
1,3,5-trioxane, vibr. spectra and intermol. forces 77−36216
triphenylene, mono- and diamons, reson. spontaneous Raman spectra, vibronic interactions 79−3451
triphenylmethane dyes, IR and Raman vibr., spectra, vibr. anal., vibronic theory of Raman scatt. 77−68048
triphenylphosphine compounds, $(C_6H_5)_3PM_xM'_{1-x}(CO)_5$, M,M′=Cr, Mo, W, mixed cryst., CO vibr. spectra, modal anal. 78−35128
tris-sarcosine calcium chloride, ferroelec. transitions, soft modes, Raman scatt. spectra obs. 80−80763
S-trithiane, lattice vibrs. from Raman spectra 78−6672
trithiane, Raman spectrum, press. effect on internal rot. angle 78−37642
tryptophan, Raman line characterisation 79−26996
TSet, resonance Raman spectra 79−56787
(TTF^+) radical cation, optical props. in mixed-valence and monovalent halide salts and solns. 79−61399
TTF, origin of Raman spectrum instability 79−15456
TTF, TTF-TCNQ, $(TTF)_7I_5$ and TCNQ, Raman scatt. and charge transfer 77−69817
TTF and derived cpds., intramolecular vibrs. and vibronic effects, IR and Raman spectra 80−25387
TTF crystals, polarised Raman spectra meas. 78−6681
TTF halides, charge transfer effect on internal modes, Raman scatt. 80−25392
TTF salts, mixed valent, Raman spectra, formal charge rel. to Raman freq. 80−93317
TTF salts, quasi-one-dimensional organic crystals, charge transfer, Raman scatt. *(German)* 79−28731
TTF-d_0, -d_4, IR and Raman spectra, vibr. assignments 78−23436
TTF-TCNQ, ^{15}N, ^2H isotope labelled, IR, Raman spectra, mol. vibrs., electron-phonon interactions 77−69835
TTF-TCNQ, charge transfer, mode shift study, Raman scatt. *(German)* 79−28731
TTF-TCNQ, charge transfer determ. from spectral line shift using Raman scatt. 80−25392
TTF-TCNQ, crystal, Raman scattering 78−80356
TTF-TCNQ, one-dimensional conductor, Raman scatt. 78−80355
TTF-TCNQ, origin of Raman spectrum instability 79−15456
TTF-TCNQ, Raman spectra, formal charge rel. to Raman freq. 80−93317
TTT, neutral, cation and conducting complex reson. Raman spectra, vibr. lines, charge transfer 79−4794
TTT, resonance Raman spectra 79−56787
uracil monoanions in soln., tautomer identification by laser Raman spectroscopy 80−14148
uranocene, reson. Raman spectra, anomalously polarised electronic band, energy level assignment 79−59451
urea, aqueous soln., mol. reorientation, Raman spectra 78−64354
urea in NaI aq. soln., Raman scatt., mol. reorientation relax. time 79−8136
urea-$NaNO_3(KNO_3)$ solid eutectic mixtures, Raman, IR spectra, line shifts, widths 77−55793
uridine monophosphate, excited state geometry distortion, normal modes reson. Raman intensity anal. 79−68236
vanadyl porphyrins, anion radicals and dianions, reson. Raman spectra 77−471
vibrational dephasing in liquids and solids 79−38552
vibrational dynamics of liquids and solids, Raman scatt. of picosecond light pulses 78−94414
vinyl acetate, monomer and polymer, Raman and IR spectra, liq. and solid 78−58700
vinyl sulphides, divalent S linking with multiple bonds, spectrosc. obs. *(Russian)* 78−21929
vinylcyclopropane, Raman study of rotational isomers 79−18194
vinyloxirane, Raman and IR vibr. spectra and conformations 80−83379
vinylsilanetriol-d_0,(-d_3), soln., vibr., IR and Raman spectra 78−86854
visual pigments, reson. Raman studies, review 77−90729
vitamin B_{12}, CARS near one-photon reson. 77−65466
vitamin B_{12} derivatives, vis. and UV reson. Raman spectra, rapid flow method 77−66796
Wolffram's red salt, mixed valence, reson. Raman calcs. using vibronic coupling model 80−97249
Wurster's cation dimers, reson. Raman spectra 77−58009
XH_2 molecules 1:2 complexes, H-bonding fluctuation hypothesis, IR and Raman vibr. spectra 77−34632

Raman spectra of organic molecules and substances continued
m-xylene, mol., UV prereson. Raman scatt., interference effects 79−64008
m-xylene, mol., UV prereson. Raman scatt. intensity 79−64007
zeaxanthin, aq. soln., aggregate, reson. Raman spectra, and IR spectra, exciton interactions 78−31770
zinc porphyrins, anion radicals and dianions, reson. Raman spectra 77−471
acetone-d_0, d_6, Raman spectral study of aq. soln. struct., H-bond effects 77−88454
BCl_2NCO, soln., force fields and normal modes, vibr. spectra, IR and Raman obs. *(French)* 80−58266
$BX_2{}^{14}NCS$ (X=Cl, Br, I), soln., force fields and normal modes, vibr. spectra, IR and Raman obs. *(French)* 80−58266
Br_2-pyridines, charge transfer complexes, $\nu_{Br\text{-}Br}$ vibr., Raman intensity obs. 79−36644
1-bromo-1-chloro-1-fluoroethane(-2-d_1), IR and Raman spectra, vibr. assignments, normal coord. anal. 78−42053
CO-haemoprotein photolysis, transient Raman study, quantum yield origin 80−67155
Cd complexes, Cd(II) mixed halide complex anions, Raman spectra 80−58270
chloroform, absolute Raman intensities determ. 77−68046
ClH-dimethyl ether, H bonded complex, IR and Raman spectra, mech. and elec. anharmonicity 79−89672
Co complex, octaethylporphinato cobalt (II), electronic and reson. Raman spectra, simultaneous meas. 78−66554
Co complex, tris(ethylenediamine) cobalt(III) chloride, Raman scatt., interference effects 77−68047
CoIII salen complexes, O binding, reson. Raman obs. 80−58267
Cu complex, bis(1,5-cyclooctadiene)copper(I) perchlorate, IR and Raman spectra 79−19877
Cu complex, di-μ-chlorobis[(1,5-cyclooctadiene)copper(I)], IR and Raman spectra 79−19877
Cu complex, glycylglycine, isotope substituted, IR and Raman vibr. spectra 78−42051
p-dichlorobenzene, mol. dynamics, allotropy, solid-state phase transitions effects, Raman spectra *(French)* 77−42372
Di(methylammonium) cadmium tetrachloride, LF Raman spectra and phase transitions 77−63414
$K^+CF_3SeO_2^-$, IR and Raman spectra, normal coordinate anal. for $CF_3SeO_2^-$ anion 80−87122
KNO_3(II), Raman spectral study of struct. props., disordered groups 77−66486
Mn III chloro complexes, IR and Raman vibr. spectra 77−68038
N-containing organic compounds, Raman spectra, systematic interpretation 79−26995
N_2:methane-d_4, liq., vibr. relax., Raman scatt. obs. 78−92061
$NH_4{}^+CF_3SeO_2^-$, IR and Raman spectra, normal coordinate anal. for $CF_3SeO_2^-$ anion 80−87122
$NbCl_5.CD_3CN$, Raman spectra and Teller-Redlich product rule 79−69817
$NbCl_5.CH_3CN$, Raman spectra and Teller-Redlich product rule 79−69817
Ni catalyst, chemisorption of ethylene-(d), Raman and vibr. spectra 80−108747
Ni porphin, reson. Raman excitation profiles, simulation, vibronic coupling consts. 77−65471
trans-$Ni(S_2N_2CH_3)_2$, IR and Raman spectra, normal coord. anal. 80−28019
Pd complex, tetrabenzo tetra-azacyclohexadecine, I_2 oxidation product, synthesis and characterization 79−47900
Pt complex, ethylenediamine trihalide, reson. Raman spectra, dissoc. energy 79−26990
Pt phthalocyanine, reson. Raman excitation profiles, solvent effects 80−102512
Pt-nucleoside complexes, Raman spectra, vibr. anal. 77−65473
$Rb^+CF_3SeO_2^-$, IR and Raman spectra, normal coordinate anal. for $CF_3SeO_2^-$ anion 80−87122
Re complex, $((C_2H_5)_4N)_2$ [ReI_6], electronic resonance Raman spectrum, 80K *(German)* 79−82982
Rh complex, di-μ-chlorobis[(1,5-cyclooctadiene)rhodium (I)], IR and Raman spectra 79−19877
SCF_2, IR, Raman and matrix isolation spectra, isotopic shifts, anharmonicity consts. *(German)* 77−83600
SF_6, collision induced rot. Raman scatt., polarisability effects 78−86874
$SbCl_5.CD_3CN$, Raman spectra and Teller-Redlich product rule 79−69817
$SbCl_5.CH_3CN$, Raman spectra and Teller-Redlich product rule 79−69817
$SeCF_2$, IR, Raman and matrix isolation spectra, isotopic shifts, anharmonicity consts. *(German)* 77−83600
$Si_2O(Cl_3)_2$, IR and Raman spectra, vibr. anal. 78−66552
SrF_2, F-centres, single-phonon Raman scatt. meas. 77−20844
TGSe, Raman and far IR spectra, lattice vibrs. in para- and ferroelec. phases 77−77190
$TaCl_5.CD_3CN$, Raman spectra and Teller-Redlich product rule 79−69817
$TaCl_5.CH_3CN$, Raman spectra and Teller-Redlich product rule 79−69817
1,2,4,5-tetramethylbenzene, liq. and solid, vibr. dephasing, intermol. energy exchange mechanism 78−74737
tetraselenatetracene, neutral, cation and conducting complex reson. Raman spectra, vibr. lines, charge transfer 79−4794

Raman spectra of polyatomic inorganic molecules
actinide (VI) ions, AnO_2^{2+}, in CO_3^{2-} media, Raman scatt. 79−13718
air pollutant gases and vapours, relative Raman scatt. cross section 80−100061
alkali metal nitrates, Raman spectra, interionic interactions effect on bond lengths, dissoc. energies and vibr. 79−36653
arsenides, group III, chem. transport equilib. with I_2 *(French)* 77−55876
bromochlorofluoromethane, and d_1, Raman optical activity atom dipole interaction model 79−82033
hexafluoride molecule selective excitation via Doppler free multiphoton process 78−55178
high temperature, review 80−52234
inorganic and coordinated cpds., IR and Raman spectra, book 79−807
inorganic species, vibr. and electronic props., reson. Raman spectra appl. 80−52996

Raman spectra of polyatomic inorganic molecules continued
intensity relation, IR to Raman intensity, matrix notation 78−62853
IR multiple-photon excited molecules 80−74207
liquid polyatomic molecule vibrational mode obs. with picosecond laser pulses 77−58007
methane, photoacoustic Raman spectroscopy under pulsed laser excitation 80−82825
molecular shape determination, of high temp. species 80−52233
molecular vibr. freq. tables, up to 13 atom mols., and Raman and IR values 77−79614
nitrates, aq. solns., high resolution AC coupled Raman spectra 79−40619
α-quartz, laser Raman line polarisation meas. 77−4641
quasi-linear molecules, low frequency anharmonic vibrations, pot. function determ., Raman and IR spectra obs. 80−52997
rare earth oxalates, struct., IR absorpt. and Raman spectra *(French)* 80−32714
resonance Raman scattering with tunable lasers, review, appls. 78−94247
resonance Raman spectra intensity distribs. in soln. 79−22763
resonance scattering by doubly degenerate vibr., Jahn-Teller effect 79−59460
strong H bonded systems, vibr., Raman, IR spectra, biology appls. 78−82735
transition metal complex anion, vibr. spectra in solid and soln., struct. and fundamental mode assignment 78−62803
transition metal complexes, of 4-methylpyridine, IR and Raman spectra, vibr. anal. 78−25536
transition metal hexahalide complex, polarised reson. vibr. Raman spectra, electronic degeneracy effects 78−78708
trifluoroiodomethane, IR multi-photon excited mols. 80−74207
vibrational dephasing, polyat. mols. in condensed phases, intermol. energy exchange mechanism 78−74737
water media, remote determ. of impurity conc. by laser spectroscopy, calibration by Raman scatt. 79−16090
water vapour, Raman lidear meas., daytime atmosphere 80−85718
water-HF(HBr)(HCl) complex, in supersat. soln., Raman spectra assignments 78−70840
Ag_3, Raman spectra, matrix isolated in Kr, linear config. 78−46347
$Ag(CO)_2^+$, laser Raman spectra, CO stretching region 79−59469
Al_2Br_6, Br_2Al-Br-$AlBr_3$, vibr. obs., normal coordinate anal. *(German)* 79−26967
Al_2Cl_6, matrix isolated, vibr. spectra, isotopic fine struct. and valence force field calcs. 80−58258
$AsBr_3(AsCl_3)$, Raman scatt. spectrum, intermol. interaction and dimeric assoc. *(Russian)* 77−54562
AsH_3, vibr. relax. in dense media, memory functions approach 78−37722
As_4O_6, high temp. Raman band contours, vibr. anal. 79−10116
As_4O_6, IR and Raman spectra vibr. spectra, valence force field calc., pot. function *(French)* 78−50549
BCl_2SH, BCl_2SD, Raman and IR spectra, barrier to internal rot. 78−5223
$^{10,11}B_5H_9$ gas (liq.) phase, vibr. dephasing and Raman spectra 80−48101
$B_3N_3H_6$, isotopic variants, pure rot. Raman spectra 77−71803
$Ba(ClO_4)_2$, solutions in amides and esters, structure *(French)* 80−7343
BaF_2, Raman spectra, 15 to 1300K, anharmonic vibr. effects 77−43990
BaO_3, visible absorpt. and reson. Raman spectra in Ar and N_2 matrices 77−65487
$BrCl(H_2O)_n$, mean vibr. amplitudes, Raman spectra, isotope effects 77−58014
BrO_3^- in $NaClO_3$, Raman spectra, fundamental vibr. modes 78−78711
C_2N_2, $2\nu_4$ band overtones, Raman intensities, bond polarisability theory 80−63639
C_2N_2, gas, high resolution Raman spectra 78−17673
C_2N_2, gas phase 79−18191
CO_2, collision induced Raman scatt. at ν_2 and ν_3 inactive vibrs. 78−90175
CO_2, collision-induced Raman spectrum, theoretical studies 80−63646
CO_2 conc. and temp. in flames, Raman spectroscopy 80−32720
CO_2, in H_2O, D_2O soln., Raman spectra 77−65467
CO_2, isotropic Raman scatt., Fermi reson. vibr.-rot. spectra 77−38741
CO_2, line broadening, short range force effects, semiclassical calcs. 79−98085
CO_2, matrix isolated Raman and IR spectra, fundamental freqs., isotope effects 77−88457
CO_2, near critical point Rayleigh and Raman scatt., Fermi diad 80−80765
CO_2, photoacoustic Raman spectroscopy under pulsed laser excitation 80−82825
CO_2, pulsed photoacoustic Raman spectrosc., gaseous trace anal. 80−40769
CO_2, pure rotational stimulated Raman photoacoustic spectroscopy 80−32724
CO_2, rarefied jet beam, Raman scatt., for rot. temp. and density 80−6185
CO_2, rot. Raman and IR lines, self-broadened linewidths 77−42357
CO_2, rot. Raman spectra, 01^10 state effects on intensity distrib. *(German)* 77−10679
CO_2, single and multiple free jets, CW laser Raman spectroscopy 80−32727
CO_2, Σ-diads, Raman spectra, O isotope effects 77−83610
CO_2, vibr.-rot. transition overtones, active Raman spectra obs. 78−50550
$^{12}C^{18}O_2$, vibr.-rot. Raman spectrum, in Fermi reson. region 78−42073
$C^{18}O_2$, Raman spectra in Fermi reson. region 78−74664
CO_2+He(Ar), dipole and Raman line press. broadening temp. depend. 79−68265
C_3O_2, far IR and Raman spectra, vibr. mode and quasilinear config. 78−62940
C_3O_2, Raman bands, vibr. assignments 79−59463
$COCl_2$, Raman line intensities, modified CNDO/2/INDO calc. 78−25621
CS_2, fundamental vibr. bands in liq. phase 79−54856
CS_2, in carbon tetrachloride soln., Raman scatt. 79−65850
CS_2, liq., props. from allowed light scatt. spectra 80−25364
CS_2, liquid, Raman spectra, effects of intermolecular forces 79−41177
CS_2 liquid, Rayleigh and Raman bands, intensities of interaction induced components 80−63645
CS_2, matrix isolated Raman and IR spectra, fundamental freqs., isotope effects 77−88457
$CaCO_3$, calcite, laser Raman line polarisation meas. 77−4641

Raman spectra of polyatomic inorganic molecules continued
CaF_2, Raman spectra, 15 to 1300K, anharmonic vibr. effects 77−43990
$CaMg(CO_3)_2$, dolomite, Raman spectra calc. 77−24848
$Ca(MoO_4)_{1-x}(WO_4)_x$, Raman scatt. meas. 77−28578
CaO_3, visible and absorpt, and reson. Raman spectra in Ar and N_2 matrices 77−65487
CdFCl, CdFBr, existence and vibr. characterisation, IR and Raman matrix isolation obs. 78−78706
CdF_2(FCl)(FBr), matrix isolated IR and Raman spectra, assignments, force consts., isotope effects and thermodynamic props. 80−63631
$CdFe(CO)_4$, IR and Raman spectra, vibr. anal. 78−66553
CdO_3, formed by matrix reactions, IR, Raman and visible spectra 80−87110
CdP_2, reson. interaction of vibr. states, polarised Raman spectra meas. 77−15521
CdS, LO phonons, size effect reson., first order forbidden light scatt. 77−44002
CdS, multiphonon reson. Raman scatt. and exciton-phonon luminesc. 77−16319
CdS, reson. Raman scatt., temp. depend. polarisation, A-exciton 77−12386
$CdSiP_2$, polarised Raman spectra 77−24853
CdX_2, CdXY, (X,Y=Cl,Br,I), matrix isolated vibr. spectra, isotopic effects, force consts. 77−3358
$CeCl_3$, complex Raman tensors, irreducible tensor method, antisymmetric scatt. 78−37623
ClF_5, condensed phases, structural study by vibr. spectroscopy and X-ray and neutron diffr. 79−1405
$Cl_2(H_2O)_n$, mean vibr. amplitudes, Raman spectra, isotope effects 77−58014
ClO_2, solns., reson. Raman spectra, appl. of Morse pots. 77−65485
ClO_2, solns., reson. Raman effect and absorption spectra 77−71807
ClO_3^- in $NaBrO_3$, Raman spectra, fundamental vibr. modes 78−78711
ClO_3F, vap. phase Raman spectrum, single isotopic species bands 78−78712
$Co_4(CO)_{12}$, heptane soln. Co-Co force consts., prereson. Raman spectra, rel. to solid IR spectra *(French)* 78−31193
$Cr(CO)_6$, ν(CO) region, IR and Raman spectra in organic solvents 79−41169
$Cr(CO)_6$, relative intensities of ν(CO) and ν(MC) Raman bands 78−55176
$Cr(CO)_6$, solid and matrix isolated, Raman spectra 79−28755
CrO_4^{2-}, Franck-Condon effects in resonance Raman spectra and excitation profiles 80−14129
CsBrICN, Raman and IR vibr. spectra, struct. 80−102513
CsClICN, Raman and IR vibr. spectra, struct. 80−102513
CsI_2CN, Raman and IR vibr. spectra, struct. 80−102513
CsN_3, Raman spectra, weaker features obs. 77−68045
$CuAl_2Cl_8$, resonance spectra of vapour 78−94251
$CuBr_4^{2-}$, ground state Zeeman splittings, reson. Raman spectra and mag.-optical activity 80−5579
$Cu(CO)_4^+$, laser Raman spectra, CO stretching region 79−59469
D_2, high resolution CW CARS spectra of Q-branch 77−58023
DCl and $(DCl)_2$, matrix isolated Raman spectra 78−42063
D_2O, mol., Raman scatt. activity and IR intensity, finite field method 79−59462
D_2O, pulsed opto-acoustic spectroscopy 80−62743
D_2SO_4, pure, IR and Raman spectra in liq. state, assignments and cryst. spectra comparison *(French)* 79−33699
D_3SiNCO, low freq. bending mode, pot. function 78−82728
D_3SiNCS, IR and Raman spectra, vibr. anal., LF bending mode 78−70842
$F_3SiOSiF_3$, vibr. anal., normal coordinates, siloxane bridge vibr. band struct. 79−50003
$FeBr_4^-$, circularly polarised Raman spectra, spin-orbit induced vibr. antisymmetry 78−5232
$FeBr_4^-$, ground state Zeeman splittings, reson. Raman spectra and mag.-optical activity 80−5579
$Fe(CO)_2(NO)_2$, vib. assignment using ^{15}N isotopic substitution, solid, liq. and soln. spectra 77−48152
$FeCl_3$, Fe_2Cl_6, matrix isolation Raman spectra 77−65480
$FeCl_3$, matrix isolation Raman spectra, mol. config., thermodynamic props. 78−46346
$FeCl_4^-$, effective charge, from IR and Raman scatt. intensity obs. 78−62809
Fe_2Cl_6, matrix isolation Raman spectra, mol. config., thermodynamic props. 78−46346
GeH_3NCS, mol., IR, Raman and microwave spectra, $^{70,72,74}Ge$ and $^{1,2}H$ isotopes 79−89663
HCN, IR and Raman vibr. intensity changes due to Li^+ interaction 79−45712
HCl and $(HCl)_2$, matrix isolated Raman spectra 78−42063
$HClO_4$-H_2O, aq. soln., IR and Raman spectra, conc. depend. *(Russian)* 80−53002
HN_3, and DN_3 pure rot. Raman spectra, rot. consts., K-depend. parameters 78−29791
$H^{14}N_3$, rotational-vibrational Raman spectrum of ν_2 band 80−91564
HNO_3, overlapping Raman lines resolution by coherent ellipsometry 79−98110
H_2O, IR and Raman spectra, bonding, vibr., band shapes 79−6938
H_2O, in D_2O ice I_c, decoupled vibr. spectra 80−52984
H_2O in flames, CARS spectrum 79−36652
H_2O, liq., broad band vibr. struct., polarisation CARS obs. 79−85963
H_2O, liq., intermol. coupling, isotope and salt effects, Raman spectra 78−90169
H_2O, liq. and gas, Raman scatt. of ν, vibr. transverse cross-section 78−82739
H_2O, mol., Raman scatt. activity and IR intensity, finite field method 79−59462
H_2O, pulsed opto-acoustic spectroscopy 80−62743
H_2O, Raman and IR spectrum in overtone OH stretching region 80−58263
H_2O, Raman spectra, liq. state, depolarisation ratios, libration and translational spectra 79−4797
H_2O, sum rule props., SCF optimizations of MO and VB calcs. 78−5156
H_2O, vap., depolarised Rayleigh scatt., rot. Raman spectra, mol. polarisability 78−33513
H_2O vapour, rovibrational Raman spectrum 78−90174
H_2O, vibr. Raman scatt. signature in flames 78−25539

Raman spectra of polyatomic inorganic molecules continued
$H_2O_2(D_2O_2)$, vibr. consts rot. struct. doubling, Raman spectra assignment 77−54563
$H_3(PMo_{12}O_{40})$, decomp., in aq. soln., Raman spectra obs. 79−13719
HPO_3, overlapping Raman lines resolution by coherent ellipsometry 79−98110
HPO_3^{2-}, in NaH_2PO_2-Na_2HPO_3, quantitative anal. by relative Raman intensities obs. *(Japanese)* 78−23991
$H_2PO_2^-$, in NaH_2PO_2-Na_2HPO_3, quantitative anal. by relative Raman intensities obs. *(Japanese)* 78−23991
H_3PO_4, aq. soln., laser Raman spectra, 0.005-15.6 M 78−46348
H_2SO_4, pure, IR and Raman spectra in liq. state, assignments and cryst. spectra comparison *(French)* 79−33699
HSO_3F, gas, indication of molecules existing as cyclic dimers *(French)* 80−989
HSO_3F, liquid, indication of molecules existing as mixture of cyclic dimers and infinite chains *(French)* 80−989
$HSiCl_3(DSiCl_3)$, Raman and IR spectra, mol. motion 78−64353
$H_4(SiMo_{12}O_{40})$, decomp., in aq. soln., Raman spectra obs. 79−13719
H_3SiNCO, low freq. bending mode, pot. function 78−82728
H_3SiNCS, far IR and Raman spectra, vibr. mode and quasilinear config. 78−62940
H_3SiNCS, IR and Raman spectra, vibr. anal., LF bending mode 78−70842
$H_3SiOSiH_3$, pot. function governing low freq. bending mode 77−58016
Hg complex, methylethynylmercury(II)(-d_1,-d_3,-d_4), vibr. spectra and normal coord. calcs. 80−58259
Hg complex, trihalogenomercurate II ions in amide solvents, config. equilib. 79−26997
$Hg(CN)_2$, solvation by NH_3 and ND_3, Raman spectroscopic study 78−90172
$Hg(CN)_3^-$ ion, CN and HgC stretching vibrations and HgCN bending vibration assignments 80−69140
$Hg(CNS)_2$, solvation by NH_3 and ND_3, Raman spectroscopic study 78−90172
HgFCl, HgFBr, HgFI, existence and vibr. characterisation, IR and Raman matrix isolation obs. 78−78706
$HgF_2(FCl)(FBr)$, matrix isolated IR and Raman spectra, assignments, force consts., isotope effects and thermodynamic props. 80−63631
$HgFe(CO)_4$, IR and Raman spectra, vibr. anal. 78−66553
HgI_2, in $CsNO_3$ at 703K, in meta and para terphenyl at 508K and 513K 78−29796
HgI_2, Raman spectra, in high-temp. $CsNO_3$, metaterphenyl, and paraterphenyl solns. 78−86876
$Hg(NO_3)_2$, solvation by NH_3 and ND_3, Raman spectroscopic study 78−90172
HgX_2 (X=Cl,Br), aprotic donor solns., Raman spectra, mol. vibr. and solvent strength 78−29788
HgX_3^- (X=Cl,Br), aprotic donor solns., Raman spectra, mol. vibr. and solvent strength 78−29788
HgX_4^{--} (X=Cl,Br), aprotic donor solns., Raman spectra, mol. vibr. and solvent strength 78−29788
$HgX_2(HgXY)$, (X,Y=Cl, Br, I), IR and Raman matrix isolation spectra, bending force consts. 77−465
IO_3^- in $NaClO_3$, Raman spectra, fundamental vibr. modes 78−78711
In complexes, chlorocomplexes, digitised Raman band profiles 77−71802
$InCl_3$ in Kr lattice, Raman and IR spectra, vibr. assignments, force consts., isotope shift and config. 79−89671
$InX(X_2)(X_3)$, $InAlX_4$, X=Cl,Br, Raman spectra, up to 1200K 80−48003
$IrBr_6^{2-}$, complex Raman tensors, irreducible tensor method, antisymmetric scatt. 78−37623
$IrBr_6^{2-}$, Raman tensor patterns, vibr. reson. Raman scatt., group theoretical calcs. 78−986
$IrCl_6^{2-}$, circularly polarised Raman spectra, spin-orbit induced vibr. antisymmetry 78−5232
$IrCl_6^{2-}$, complex Raman tensors, irreducible tensor method, antisymmetric scatt. 78−37623
$(IrCl_6)^{2-}$, electronic Raman spectra, spin-orbit components of ground state, vibr. 78−5231
$IrCl_6^{2-}$, ground state Zeeman splittings, reson. Raman spectra and mag.-optical activity 80−5579
IrF 6, $\Gamma_{8g}(^2T_{1g})$ state, electronic Raman scatt. and absorption spectra at 1.6 μ, resolution of Jahn-Teller problem 79−36648
K_2MoO_3S, aq. soln., Raman spectrum, MoO_3S^{2-} force consts. 78−74668
KN_3, Raman spectra, weaker features obs. 77−68045
$K_2(RuCl_5NO)$, polarised Raman and IR spectra, vibr. anal. 77−69819
K_2SO_4, IR and Raman spectra of vap. over heated matrices 78−25525
$K_2[B_{12}D_{12}]$, in aqueous soln., laser Raman spectra 78−15158
$K_2[B_{12}H_{12}]$, in aqueous soln., laser Raman spectra 78−15158
Kr:Mg_n, matrix isolated Raman spectra 78−90170
LiCNS, ether solns., dimer struct. and force consts., IR and Raman spectra 79−72442
$LiClO_4$, solutions in amides and esters, structure *(French)* 80−7343
MgO_3, visible absorpt. and reson. Raman spectra in Ar and N_2 matrices 77−65487
$Mn(CO)_5Br$, ν(CO) region, IR and Raman spectra in organic solvents 79−41169
Mo complexes, dinuclear, chem. and spectroscopic props. 77−77239
$Mo_2Br_8^{4-}$, electronic and reson. Raman spectra, Mo-Mo band 78−82745
$Mo(CO)_6$, relative intensities of ν(CO) and ν(MC) Raman bands 78−55176
$MoCl_n^{n-}$, n=1,2,3, vibr. Raman spectra obs. 79−68234
N_2:$CO_2(N_2O)$(methane-d_4), liq., vibr. relax., Raman scatt. obs. 78−92061
N_3, spectroscopic data review 77−38680
NF_3, Raman spectra, Coriolis coupling and transition dipole 78−39533
NH_3, adsorbed on amorphous silica 80−11948
NH_3 in benzene(CCl_4)(pentane) Fermi resonance, solvent and phase depend. 80−47960
NH_3, pure, Raman scatt., high press., high temp. 77−27077
NH_3, rot.-inversion Raman spectra, K-splitting 80−9611
NH_3, stimulated hyper-Raman scatt. via 3-photon process to obtain IR and far IR radiation 80−58633
NH_3, symmetric bending mode, Raman intensity, electrolyte solvent effects 77−34638
$^{15}NH_3$, modulated coherent Raman beats 80−23464
$NH_4Ag_4I_5$, Raman spectra, internal vibrs. of NH_4^+ ions 78−72497
Raman spectra of polyatomic inorganic molecules continued
$NH_4I(ND_4I)$.dioxane complexes, Raman spectra, vibrs., H-bonding 78−25544
$(NH_4)_2MoS_4$, aq. soln., Raman intensity, scatt. frequency depend. 79−28747
$(NH_4)_2(RuCl_5NO)$, polarised Raman and IR spectra, vibr. anal. 77−69819
$(NH_4)_2S_5$, Raman spectra, vibrs. and rot. isomers of Sn^{2-} (n=4-8) *(German)* 78−13504
NO dimer, asymmetric, characterisation, Raman, IR spectroscopy 79−41176
NO_2, high-press. Raman matrix isolation spectra 78−45721
NO_2, in Ar matrix, Raman spectra, high press., low temp. effects 78−52479
NO_2, reson. coherent antiStokes Raman and absorpt. spectra 79−54860
NO_2, reson. Raman spectra, vibr.-rot. scatt. Q branch enhancement 78−989
NO_2^-, in KI matrix, Raman spectra, high press., low temp. effects 78−52479
NO_3^-, aq. soln., vibr. width and dephasing, conc. depend. 80−43029
NO_3^-, determ. in waste and treated waters by laser Raman spectroscopy 79−92113
NO_3^-, in aq. nitrate solns., vibr. dephasing process, Raman obs. 79−51936
NO_3^-, Raman spectrum of ν_1 mode in soln., reorientation 78−92067
N_2O, in soln., Raman and IR ν_1 and ν_2 band shapes, mol. motion dynamics 78−64352
N_2O, pulsed photoacoustic Raman spectrosc., gaseous trace anal. 80−40769
N_2O, pure rotational stimulated Raman photoacoustic spectroscopy 80−32724
N_2O, rot. Raman spectra, 01^10 state effects on intensity distrib. *(German)* 77−10679
N_2O, rot. Raman spectrum, meas. using Fabry-Perot interferometers with 20 cm^{-1} free spectral range *(Japanese)* 77−87847
$NO_2(N_2O_4)$ surface decomposition, resonance and spontaneous Raman spectra 80−61144
$NaNO_3$, in liq. NH_3, Raman spectra, curve resolution anal. 77−82610
Na_2SO_4, IR and Raman spectra of vap. over heated matrices 78−25525
Ni complex, octaethylporphyrinato-Ni(II), meso-deuterated and ^{15}N substituted derivs., reson. Raman spectra 79−13725
Ni complex, octaethylporphyrinato-Ni(II), meso-deuterated and ^{15}N substituted derivs., reson. Raman spectra 79−13726
Ni_3, in solid Ar, reson. Raman spectra 80−63638
$O_2^+AsF_6^-$, thermal decomposition, Raman spectra study, free radical mechanism 80−55652
OCS in n-alkane, rot. relax., solvent hydrodynamic props., Raman and IR spectra 80−45055
OCS, vibr.-rot. bands of Raman spectra 78−29173
$OsBr_6^{2-}$, complex Raman tensors, irreducible tensor method, antisymmetric scatt. 78−37623
OsO_3F_2, OsO_4 matrix-isolated IR and Raman spectra 77−75166
PBr_3, mol. dynamics 77−55779
PBr_3, Raman scatt. spectrum, intermol. interaction and dimeric assoc. *(Russian)* 77−54562
PCl_5-$TiCl_4$, gas, melt, and solid, dimer-monomer conversion, Raman spectra obs. *(German)* 79−70320
PF_2D, liq., normal coordinate analysis of vibrational spectra 79−68233
PF_2H, liq., normal coordinate analysis of vibrational spectra 79−68233
$PF_2H(D)$, vibr. spectra and normal coordinate anal., Raman and IR spectra 80−14147
$(PF_2)_2O$, IR and Raman spectra, vibr. assignment 78−50544
$(PMo_{11}O_{39})_n^{7-}$ decomp., in aq. soln., Raman spectra obs. 79−13719
P_4O_6, IR and Raman spectra vibr. spectra, valence force field calc., pot. function *(French)* 78−50549
P_4S_{10}, gas, vaporisation and thermal dissoc. obs. *(French)* 78−47511
P_4S_3, gas, vaporisation and thermal dissoc. obs. *(French)* 78−47511
P_4S_7, gas, vaporisation and thermal dissoc. obs. *(French)* 78−47511
Pd complex, $Pd^IPt^I(CNCH_3)_6(PF_6)_2$, vibr. spectra, M-M bonds. *(French)* 80−47997
$PdAl_2Cl_8$, resonance spectra of vapour 78−94251
$PdBr_4^{2-}$, Raman scatt., interference effects 77−68047
$Pd(S_3N)_2$, IR and Raman spectra, normal coord. anal. 80−28019
Pt complex, $Pt^{II}(CNCH_3)_4(PF_6)_2$, $Pt_2^I(CNCH_3)_6(PF_6)_2$, and $Pt^IPd^I(CNCH_3)_6(PF_6)_2$, vibr. spectra, M-M bonds. *(French)* 80−47997
Pt complexes, $Pt(NH_3)_4Cl_2$, $Pt(ND_3)_4Cl_2$, Raman spectra in solid state and aq. soln. *(French)* 79−19876
$PtCl_4^-$, effective charge, from IR and Raman scatt. intensity obs. 78−62809
RbN_3, Raman spectra, weaker features obs. 77−68045
RuO_4^{2-}, antireson. Raman effect, excitation profile 79−50019
$(Ru_2OCl_{10})^{4-}$, reson. Raman, IR and electronic spectral studies 79−10118
S_7, Raman and IR spectra, vibr. anal., force consts., thermodynamic functions 78−50545
S_8 rings, vibr. spectra and thermodynamic functions *(German)* 78−82742
S_n, (n=2-12), vibr. spectra and thermodynamic functions *(German)* 78−82742
SCN^-, associated with metallic cations in aq. soln., press. effect, Raman spectra *(French)* 78−80333
$(SCN)_2^-$, reson. Raman spectrum, vibr. freqs. 79−18189
S_4Cl_2, Raman spectra, vibrs. and rot. isomers of S_n^{2-} (n=4-8) *(German)* 78−13504
SF_6, collision-induced forbidden Raman transitions 77−6791
SF_6, ground state, mol. consts., ν_2 Raman band calcs. *(French)* 78−9156
SF_6, IR multi-photon excited mols. 80−74207
SF_6, vibr. coupling in collision-induced Raman scatt. 80−83373
SF_6, vibr. Raman spectrum, Q branches shapes 78−42077
SF_6, vibr. spectra, rot. consts., IR spectra, Raman spectra obs. 80−32719
S_2F_{10} 77−6775
SF_5Br, Ar matrix and solid phase Raman and IR spectra, vibr. assignments 77−6775
SF_5Br, vibr. spectrum and normal coord. anal. 77−18926
SF_5Cl AR matrix and solid phase Raman and IR spectra, vibr. assignments 77−6775
S_4N_4, solid and soln., IR and Raman spectra, vibr. assignment 78−74659

Raman spectra of polyatomic inorganic molecules continued
$S_3N_3Cl_3$, solid and soln., IR and Raman spectra, vibr. assignment 78−74659
$S_4N_4H_4$ ($S_4N_4D_4$), vibr. spectra, force consts. *(German)* 78−13499
$S_4N_4H_4$, and -d_4, solid and soln., IR and Raman spectra, vibr. assignment 78−74659
S_7NH, solid and solns. vibr. spectra, force consts. isotope effects 77−66490
SO_2, force field determ. from first and second order Raman spectra *(Russian)* 77−14441
SO_3, rotational Raman spectrum, rot. consts. and bond lengths 79−18195
SO_4^{2-}, ν_1 linewidth, in acidic aq. soln. 77−65481
SSF_2, FSSF, and ^{34}S isotropic forms, matrix IR and Raman spectra *(German)* 79−89674
$S_{12}(S_{12}.CS_2)$, vibr. spectra and thermodynamic functions *(German)* 78−82742
$S(SiD_3)_2$, gaseous, liquid, solid phases, molecular vibr. exam. 78−25547
$S(SiH_3)_2$, gaseous, liquid, solid phases, molecular vibr. exam. 78−25547
$SbCl_5$, nitrile addition compounds, mol. vibr., IR and Raman spectra *(French)* 77−23499
Sb_4O_6, IR and Raman spectra vibr. spectra, valence force field calc., pot. function *(French)* 78−50549
SeO_3, rotational Raman spectrum, rot. consts. and bond lengths 79−18196
Si_6Br_{12}, and Si_6Cl_{12}, vibrational spectra and force constants, rel. to Si_5Cl_{10} and Si_5Br_{10} *(German)* 79−22716
Si_5Cl_{10}, and Si_5Br_{10}, vibrational spectra and force constants, rel. to Si_6Cl_{12} and Si_6Br_{12} *(German)* 79−22716
$(SiCl_3)_2O$, IR matrix isolation spectrum, Raman spectrum 78−82730
SiH_4, ν_3 band assignment in IR and Raman spectra, ν_1-ν_3 coupling 77−75124
Si_6H_{12}, and Si_6D_{12}, Raman and IR spectra, vibr. force consts., config. *(German)* 79−22715
$(SiH_3)_2O$, and d_6, Raman spectra, vibr. mode and config. 78−62940
$SrAg_2I_4$, Raman and autocorrelation spectra, solid and soln. 79−38532
$SrF_2(Cl_2)$, Raman spectra, 15 to 1300K, anharmonic vibr. effects 77−43990
SrO_3, visible absorpt. and reson. Raman spectra in Ar and N_2 matrices 77−65487
Ti complex, Ti(IV)-H_2O_2, H_2SO_4-aq. soln., reson. Raman spectrum, vibr. assignments, molar absorptivity 77−65469
$TiBr_4$, reson. Raman spectrum, vibr. analysis, Jahn-Teller coupling 79−85965
Tl_2Cl_2, mol. consts., IR and Raman freqs. assignments 78−17648
Tl_2F_2, mol. consts., IR and Raman freqs. assignments 78−17648
$Tl_2F_2(Cl_2)$, assignment of vibr. Raman and IR spectra bands 80−58268
$TlNO_3$, molten and aqueous soln., Raman spectra 79−78673
U complexes, tetranuclear halogenocomplexes, preparation, vibr. spectra *(French)* 77−83596
UF_5, monomer struct. and pot. consts., IR and Raman spectra in inert gas matrices 78−5215
UF_6 in Ar matrices, fluoresc. and Raman spectra, vibr. anal. 78−66585
UF_6, Raman scatt. cross section and density meas. 77−75160
VCl_4, Raman spectra and selection rules, Jahn-Teller splitting 78−988
$W(CO)_6$, relative intensities of ν(CO) and ν(MC) Raman bands 78−55176
WCl_6^{n-}, n=1,2, vibr. Raman spectra obs. 79−68234
XeF_2, pure rot. Raman spectrum 78−94254
ZnFCl, existence and vibr. characterisation, IR and Raman matrix isolation obs. 78−78706
$ZnF_2(FCl)(FBr)$, matrix isolated IR and Raman spectra, assignments, force consts., isotope effects and thermodynamic props. 80−63631
ZnO_3, formed by matrix reactions, IR, Raman and visible spectra 80−87110
ZnP_2, reson. interaction of vibr. states, polarised Raman spectra meas. 77−15521
ZnX_2, ZnXY, X and Y=halogen, matrix isolation IR and Raman spectra 78−55171
ZnXY, (X,Y=Cl,Br or I), matrix isolation, vibr. spectra, isotope effects, force consts. and geometry 78−46337
$ZrCl_4$, cryst., melt, gas, Raman spectra interpretation *(German)* 79−28753

Raman spectroscopy
see also Raman lasers; Raman spectra
absorbed molecules from medium, Raman spectrosc. technique 79−42364
AC-coupled inverse Raman spectrometry 79−40619
active Raman spectroscopy, high resolution molecular methods 80−52998
adenylyl 3'-5' adenosine, conform. equilib., Raman temp. jump obs. 78−8450
air pollutant emission and emission meas. by laser *(German)* 78−40665
air pollution, laser-Raman microprobe anal. of suspended particulates 80−76687
air pollution, stationary source, quantitative meas. using Raman lidar 78−36291
air pollution chem. anal., particulate C and SO_4^{2-} species identification 79−5625
air pollution detection, optical methods *(Czech)* 78−69444
analytical techniques using tunable lasers 78−61134
angularly resolved coherent Raman spectroscopy, crossed beam config., 79−30570
anti-Stokes spectrometer, microcomputer-controlled 80−24111
atmosphere, minor constituents detection using tunable spin flip Raman laser, review 80−55762
augmented CARS spectroscopy linewidth parameter from laser mode structure 80−33083
background rejection method, for remote sensing using Fabry-Perot interferometers 77−71384
band shape characterisation 78−86920
benzene liquid-filled waveguide, generation of enhanced CARS signals 79−89961
biological applications of laser Raman spectroscopy 77−52940
biological macromolecules, conformational dynamics subnanosecond T jump and Raman spectroscopy appl. 79−66445
biological tissue, laser Raman probe microanalysis 78−88773
biomolecules, Fe-containing, appl. of spectroscopy 79−24956
biomolecules, resonance Raman spectra interpretation, review 77−90976
biophysics, laser techniques, reviews 77−90975

Raman spectroscopy continued
book 80−22155
CARS, background suppression, polarisation techniques 77−5924
CARS, reson.-enhanced, and coherent anti-Stokes hyper-Raman spectroscopy 78−86980
CARS, resonance, quasiresonant pumping 79−6190
CARS, theory and appls., review 77−71378
CARS development for molecular parameter meas. 77−57405
CARS resonance spectrometer, results for β-carotene band 79−6189
CARS spectroscopy, laser linewidth effects 79−89012
CARS techniques and applications 77−57404
Cassegrain mirror system with high light grasp 78−78000
catalysts, laser Raman spectroscopy in controlled atm. rot. cell 80−86437
catalytic surface phenomena, Raman spectroscopy using rot. vacuum cell 78−16852
chemical identification of substances fixed on silica gel, using Raman spectroscopy *(French)* 78−88664
chemical species anal. in conjunction with liq. phase chromatography *(French)* 80−93823
chemical spectroscopy and dynamics, higher-order susceptibility effects, laser appls. 79−40625
chiral molecules in mag. fields 80−102532
chromatograph, liquid, coupled with Raman spectroscopy for anal. of mixtures *(French)* 80−45595
coherent, molecular shape determination, of high temp. species 80−52233
coherent, using optical heterodyne detect. 78−21223
coherent anti-Stokes Raman scatt. for mol. homogeneous linewidth meas. 77−71810
coherent anti-Stokes Raman scattering, for quantitative gas anal. 78−68968
coherent anti-Stokes Raman scattering for local and continuous density meas. in gas flow *(French)* 77−35281
coherent anti-Stokes Raman scattering integrated power, press. depend. 78−59081
coherent anti-Stokes Raman scattering with counterpropagating laser beams, appl. to CS_2 79−72626
coherent anti-Stokes Raman spectrometry, micro sampling cell 77−79169
coherent anti-Stokes Raman spectroscopy, anal. capabilities, rel. to other methods 77−40589
coherent anti-Stokes Raman spectroscopy, appls. 77−87844
coherent anti-Stokes Raman spectroscopy, negative peak form. 77−75161
coherent anti-Stokes Raman spectroscopy, polarisation sensitive 79−75605
coherent anti-Stokes Raman spectroscopy, selection rules, depolarisation ratios, rot. struct. 77−34640
coherent anti-Stokes Raman spectroscopy, with focused laser beam, power generation 78−4701
coherent anti-Stokes Raman spectroscopy adjustable angle beam-crossing system 77−82613
coherent anti-Stokes Raman spectroscopy system, using freq. doubled Nd+YAG laser 78−64906
coherent ellipsometry of Raman light scatt., four-photon spectroscopy *(Russian)* 77−58387
coherent polarisation spectroscopy of Raman scatt. 78−13758
coherent Raman gain spectroscopy using CW laser sources 78−37076
coherent Raman loss spectroscopy, appl. to conc. meas. and fundamental spectrosc. 80−89580
coherent Raman spectroscopy, high resolution *(French)* 77−57394
coherent Raman spectroscopy techniques, review 80−22440
coherent Raman spectroscopy using powerful tunable lasers 77−53985
coherent signals, heterodyne detect. methods 78−82055
coloured solids, line focus method for recording laser Raman spectra 80−90897
combinatorial Raman scattering, coherent active spectroscopy using tunable lasers 77−49782
combustion, coherent Raman spectrosc. obs. 80−16691
combustion diagnostics, laser appls. 80−16688
combustion diagnostics, laser Raman and fluoresc. techniques 78−88635
combustion diagnostics, space- and time-resolved coherent anti-Stokes Raman spectroscopy 79−76757
complete resonance Raman polarisation spectroscopy, linear and circular, modulation techniques 77−61130
compressed gas, small depolarisation factor meas. method 78−32884
computer acquisition, simultaneous, of IR, microwave and Raman spectral data *(Japanese)* 80−4776
computer controlled scanning spectrometer, for study of gases 79−26148
concentration fluctuations, chem. species in unsteady flow, Raman spectrosc. obs. 79−66379
continuously tunable filter for reson. Raman spectroscopy 77−22604
crystal absorption spectroscopy, new expt. method, appl. to calcite 79−61354
crystals, book 80−2774
curve resolution analysis, minicomputer-computer appl. 77−82610
CW coherent Raman gain spectroscopy 78−58057
CW stimulated, sensitivity limitations 77−87848
CW stimulated Raman gain spectroscopy, coherent detect. of Raman modes 77−87845
cytochrome c, fast Raman spectroscopy using dye laser intracavity reson. Raman amplification 77−66794
dephasing dynamics, of Raman active ground state mol. vibr. 79−44942
detector systems, for near IR Raman spectroscopy *(German)* 77−65059
diamond anvil cell method, weak Raman signals obs. 77−71383
diamond selection for anvils in high press. devices for Raman spectroscopy 77−57413
dielectric film, excitation using diffr. grating *(French)* 77−41694
digital control of spectrometer, appl. to soft mode spectroscopy 78−86345
digital processing of spectra, numerical method 77−61131
Doppler broadening at electronic resonance 80−38065
double beam difference spectroscopy 77−82627
double resonance Raman amplifier, theory 80−87434
electro-optical multichannel spectrommeter for transient resonance Raman and absorption spectroscopy 80−31890
electrocrystallisation, recent progress in electrochem. and physical methods *(French)* 80−7510
electrode-electrolyte interfaces 77−77777

Raman spectroscopy continued
electron donor-acceptor complex formation, equilib. const. determ., reson. Raman spectroscopy 78−3329
evanescent waves in total reflection, Raman scatt. direct recording, boundary layer obs. 80−52317
eye, intact bovine lens protein, Raman spectroscopy with intensified Vidicon detectors 79−29525
Fabry-Perot prefilter for Raman spectroscopy 79−71532
Febry-Perot interferometer, with automated data acquisition and stabilisation system 78−70180
fiftieth anniversary, review 79−49003
films, very thin absorbing, interference enhanced Raman scatt. 80−42273
flame, bluff-body stabilised diffusion, CARS meas. 79−85964
flame, temp. meas. *(German)* 78−32900
flame diagnosis, laser modulated particulate incandescence effects 78−20117
flame diagnostics using multichannel pulsed Raman spectroscopy 80−30237
flavins, reson. Raman spectra avoiding fluoresc. interference 79−10114
flowing gas He cryostat for Raman spectroscopy 79−67312
fluorescence interference, theory 77−71382
FM technique for luminescing sample 77−57412
Fourier transform, signal modulation within elec. bandpass 78−82041
frequency shifts, determ. by Raman difference spectrosc. 80−78654
frequency-modulated shot noise limited stimulated Raman gain laser system for monolayer vibr. spectroscopy 80−62744
gas, angularly resolved CARS config. 80−22453
gas analysis by polarised coherent active Raman scatt. spectroscopy *(Russian)* 77−56295
gas chromatography-vibr. spectroscopy, method of trapping fractions 77−4960
gas concentration meas. using Raman intensity depend. on giant pulse laser polarization 80−98986
gases, interferometric investigations of rotational Raman spectra 77−73494
gases, vibr.-rot. transitions, conf., USSR Acad. of Science, (June 1977) 79−18062
gases, vibr.-rot. transitions 79−18198
glass He cryostat for Raman scattering meas. 78−290
grating double monochromator, GDM 1000, spectral anal. of low intensity emissions 79−80701
high local resolution Raman spectroscopy with giant pulse lasers, optical energy and spatial filter 79−35838
high pressure cell for matrix isolation Raman spectroscopy 80−272
high resolution CW stimulated Raman spectroscopy, mol. H_2 appl. 78−70973
high resolution scanning resonant Raman spectrometer 79−6185
high temperature chemistry, review 80−52234
high-pressure optical cell for Raman scattering at low temps. 79−49247
high-pressure Raman matrix isolation spectroscopy 78−45721
high-resolution, using tunable spin flip Raman laser, review 80−55762
high-resolution molecular spectroscopy, rot. and rot.-vibr. spectra, review 78−42064
high-speed Raman spectroscopy, condensed discharge vibr. excitation of N_2, vibr. temp. 78−82740
industrial atmospheric pollutant remote analysis by Raman lidar 80−12047
intensities, CNDO approximation, polarization functions 79−93925
interface total reflection and surface wave obs. 80−108292
interference enhanced Raman scatt., app. to amorphous semicond. thin films 80−50326
interferometric accessory, for resolution enhancement 78−74063
internal combustion engine, CARS noninvasive temp. and species meas. 80−30293
intracavity laser Raman spectrometer, appls. 78−65973
intradoppler CARS saturation spectroscopy 80−43057
inverse Raman AC coupled spectroscopy, detection limits 80−86454
inverse Raman scattering, highly fluorescent substances 78−4702
inverse Raman scattering spectroscopy and chem. appls. 80−37094
inverse Raman spectrometer for absolute Raman cross section determ. from inverse Raman effect 79−3447
IR and Raman spectroscopy, molecular structural anal. appls. 79−35859
isotropic scattered light, direct scanning method 77−38741
jet flow technique for highly absorbing liq. systems 80−52323
Kerr effect, background suppression, polarisation techniques 77−5924
kinetic resonance Raman spectroscopy, bacteriorhodopsin Schiff base deprotonation dynamics 77−48981
laser, implications of 5062Å Ar ion laser line CW oscillation 80−1186
laser measurement of optical, thermal and mech. props. of materials 77−74513
laser microprobe analysis principles and appl. 80−57390
laser microprobe appl. to molecular analysis, particle characts. determ. 80−57391
laser nonlinear spectroscopy polaris. selective optical heterodyne detection 79−58798
laser optical microprobe, MOLE 77−60141
laser Raman diagnostics of aerodynamic flows and flames *(French)* 77−35280
laser Raman optical multichannel analyser, for gas conc. profile and temp. determ. 78−73098
laser Raman spectrometer, 180° microscope sampling and viewing attachment 80−13150
laser Raman spectrometer, Chinese WFL model design *(Chinese)* 79−30573
laser Raman temp. jump apparatus 78−41360
laser spectroscopy, appls., conf., Graz, Austria, (Jun. 1978) 79−26137
laser spectroscopy, review 77−5927
laser spectroscopy, review of progress 78−82867
laser-heated miniature oven, for prop. of matrix isolation samples for Raman studies 78−45737
laser-Raman spectroscopy, for ambient sulphate aerosols monitoring 78−69532
laser-Raman spectroscopy with AC differential analysis 77−38031
lasers application in Raman spectroscopy, review 78−65979
lidar Raman spectroscopy of atmosphere *(Russian)* 78−24387
light hyper-Raman scatt. by polaritons, active spectroscopy *(Russian)* 80−60623
liquid media, comparison of inverse Raman scatt. and CARS 79−7178
liquid sample cell, thermostatted, for Raman spectrometer 77−38016
living cell metabolism, laser Raman spectrosc. obs. *(German)* 79−29577
Raman spectroscopy continued
low temperature spectroscopy of crystals, sample holder systems 78−86342
luminescence rejection 77−18100
matrix isolation, toxic organic substances detection in water 80−30616
matrix isolation Raman spectroscopy, water pollution detect. appl. 80−108829
matrix isolation vibr. spectroscopy, complex form. studies 78−62952
micro-Raman spectrometer, for individual aerosol microparticles identification 78−68970
microcomputer-controlled Raman spectrometer 80−27352
microprobe for micron size particle anal. and cryst. state determ. 77−86421
Microprobe Mole/plasma chromatograph system, for anal. of compounds on micron scale 80−101049
microprobe studies of mineralizing tissues 80−76884
microscope using laser beam *(French)* 77−56290
mole (molecular optical laser examiner) appl. 80−62737
molecular microprobe, microscope system 78−45686
molecular spectroscopy book 80−27051
molecular spectroscopy book 80−27052
molecular structure and properties from high-resolution spectra of gases 80−53000
molecules, stimulated Raman and two-photon absorpt. 80−52999
molecules and crystals, recent applications *(French)* 80−7343
monochromator adjustable intermediate slit, Zeiss GDM 1000 *(German)* 79−9245
monomode fibre dispersion and bandwidth meas. by mode-locked Q-switched Nd:YAG laser 80−91933
multichannel detection of Raman spectra with vidicon spectiograph analyser 77−74518
multipass-systems for Raman spectroscopic gas analysis *(German)* 80−81393
multiple atmospheric parameter meas. laser radar system 78−4009
near reson. Raman lines, relative intensities, A-term method 79−81205
noncrystalline materials, optical spectroscopic anal. *(French)* 77−77284
nonlinear optical methods of active Raman Rayleigh scatt. spectroscopy, review 79−991
oil spills remote detection using laser-excited Raman backscatt. and backscatt. fluoresc. 78−32242
opaque material, stress-induced birefr., Raman meas. 78−65951
optical fibre, use in remote inelastic light scatt. probe 80−58769
optical vacuum furnace for Raman and Brillouin spectroscopy 78−58062
optically active molecules, differential Raman scatt. of right and left circularly polarized light *(Japanese)* 78−17675
organic surface contaminants, anal. by plasma chromatography-mass spectroscopy, and Raman microprobe technique 80−108773
overlapping Raman lines resolution by coherent ellipsometry 79−98110
particles with embedded molecules, Raman and fluoresc. scatt. 79−64177
photoacoustic Raman spectroscopy using CW laser sources 79−44947
photoionisation, quantum beats, origin 80−52954
picosecond laser techniques for obs. of vibr. modes in liqs. 80−5800
picosecond Raman techniques, vibr. dynamics in liqs. 80−52325
picosecond resonance Raman spectroscopy of highly dilute solns., appl. to β-carotene and cytochrome c 79−98102
picosecond spontaneous Raman spectra recording 79−89011
polarisation scrambling device, for Raman spectroscopy 77−82612
polarised coherent active Raman spectroscopy *(Russian)* 78−55414
polaritons, Raman scattering, photoelec. recording method *(Russian)* 78−23468
polyacrylamide, conversion to poly-N-dimethylaminomethacrylate, Raman method meas. 79−74460
polyatomic vapour phase mols., medium resolution, appls. review 78−42065
polydiacetylene fibre resonance Raman spectrum meas. 79−17507
polyethylene melt, cryst. kinetics during cooling, nucleation density effect 80−100181
polymers, Raman, spectroscopy of thin films, integrated optical techniques 80−22432
powder, optimum conditions for laser Raman spectra *(Russian)* 77−28580
premonochromator for stray light rejection in Raman spectroscopy 77−58438
pulse-sequenced CARS spectroscopy, method for nonreson. background suppression 80−53375
pulsed laser and gated detection, repetitive vs. burst mode 77−74529
pulsed photoacoustic Raman spectrosc., gaseous trace anal. 80−40769
pulsed Raman spectroscopy, using Nd-YAG lasers photon counting compression effects 78−74086
pulsed spontaneous Raman scattering technique for luminous environments 78−89549
pure rot. spectra of CO_2, H_2, dry-lab expt. for undergraduates 78−32634
radiometric correction of spectra 80−90899
Raman induced Kerr effect spectroscopy 77−87843
rapid intramolecular radiationless transitions, decay rate by time resolved reson. Raman spectra 79−76434
rapid scanning expts. and appls. 78−62242
recent advances, review 78−41359
remote detection of CARS employing fibre optic guides 80−9984
remote spontaneous, new trends in recording of signals 80−73485
residual carbonaceous material, in urban airborne particulates, Raman microprobe obs. 78−69441
resolution enhancement, using polarisation data 78−74062
resonance coherent Raman scattering, excitation profile, inhomogeneous broadening effects 79−35840
resonance four-wave mixing spectroscopy, recent developments 80−53383
resonance Raman cross-section, theory 80−5551
resonance Raman effect, biological appl. *(Hungarian)* 78−74666
resonance Raman kinetic spectroscopy of bacteriorhodopsin on μsec time scale 78−20320
resonance Raman spectra, optimum sample concs. 78−66555
resonance Raman spectroscopy, uses in analytical chem., review 79−92014
resonance Raman spectroscopy 78−4425
resonance scattering methods in atomic spectroscopy 80−53167
retroreflecting multipass cell 77−74510
reversal coefficient, direct scanning meas. 77−38017
rotational Raman studies, folded BOXCARS 80−101846
sample heating apparatus, for laser Raman spectroscopy 80−22439

Raman spectroscopy continued
scattering spectrometer, multiple transmission attachment 77−38036
single and multiple free jet conc. meas., CW laser Raman spectroscopy 79−97447
single crystal impurity luminesc. attenuation in Raman spectra using Cu vapour laser 79−15467
slitless optical fibre laser Raman spectrometer, with concave holographic grating 77−71380
spatial resolution enhancement in coaxial light scatt. geometries 77−57393
spectral sensitivity calibration 77−5930
spectrochemical analysis in hydrocarbon flames, computer processed laser Raman spectra 79−43652
spectrometer calibration using Ar ion laser lines 79−97446
spectrometer calibration using Kr^+ laser plasma lines 80−57394
spin flip Raman laser absorption spectrometer sensitivity enhancement 78−29173
spin-flip Raman laser spectrometer as source for high resolution mol. spectroscopy and photochem. review 78−32894
stimulated Raman gain spectroscopy, ultrahigh sensitivity, S/N ratio meas. 80−48337
stimulated Raman gain spectroscopy, using two pulsed dye lasers 78−93769
stimulated Raman scattering, sensitivity enhancement by quasi CW laser scheme 80−53003
stimulated Raman scattering under resonance illumination conditions 80−64105
stimulated Raman spectroscopy using low power CW lasers 78−29172
sub-nanosecond time-resolved background rejection, fluoresc. enhancement 77−18109
surface analysis techniques and appls., symposium, Dayton, USA (Jun. 1979) 80−62363
surface picosecond Raman gain spectroscopy 80−25351
surface polaritons, Raman scatt., active spectroscopy theory 77−59576
surface vibrational spectroscopy using stimulated Raman scatt. 80−38062
synchronous excitation spectrofluorometry *(Japanese)* 80−86452
synchronously pumped dye laser, freq. doubled, appl. to reson. Raman spectroscopy 79−12869
temperature jump apparatus, with pulse spectrometric detection 78−8450
temperature jump kinetics, Raman laser technique 79−2831
thin films condensed onto cold substrate, prism-film coupler for in vacuo investigation 78−24873
time-resolved Raman spectra, fluoresc. suppression 77−53984
time-resolved resonance Raman spectroscopy and vidicon Raman spectrography, vibr. spectra on nsec scale 80−37095
transparent substances, system optimisation *(German)* 77−65055
triple monochromator a spectrometer in Raman scatt. *(French)* 80−96007
turbulent flow field investigation techniques 78−34224
ultrahigh vacuum chamber for Raman studies of gases adsorbed on metals 78−81991
ultrasmall samples in diamond anvil cell 77−87839
very high resolution CARS spectroscopy in mol. beam 79−30568
vibrational Raman optical activity spectra, perpendicular polarisation recording method 79−21821
vibrational spectroscopy, high pressure, and conformational analysis 80−9758
vibrational spectroscopy, modern trends, book 78−13503
vidicon Raman spectrometer, appl. to heme protein study 80−94428
visual excitation, mol. mechanisms exam. by tunable laser resonance Raman spectroscopy 77−56378
visual pigments, reson. Raman studies, review 77−90729
water pollution hazardous chemicals, detection using resonance Raman spectroscopy 79−74581
wavelength-modulation Raman spectroscopy 79−12863
CO flame, background-free CARS technique 79−94288
I_2 absorption lines removal from 514 nm excited Raman spectra 78−70200
N_2 single and multiple free jet conc. meas., CW laser Raman spectroscopy 79−97447
Nd:YAG laser multipass cell for Raman scatt. diagnostics 80−1231
Nd:YAG pumped tunable sources, appl. to spectroscopy 80−58576

ramp generators
drive system for Mossbauer spectroscopy, low cost, using μA747 ICs 79−89049
linear scanning circuit, for piezoelectrically controlled Fabry-Perot etalon 78−4704
MIS integrated stepped-sawtooth waveform generator 78−86376
temperature controllers, time-linear, used in analysis of thermoluminescence glow curves 79−63202

Ramsauer effect *see collision processes*

random-access storage
electronic delay, dynamically variable, for real-time US imaging 79−46142
Josephson nondestructive readout RAM cells, design criteria 80−50000
magneto-optic memories, state of the art 77−42494
magneto-optical photoconductor sandwich 77−40213
MOS, influence of point like and extended defects 79−82679
multiple counters using RAMs, nuclear medicine appl. 79−85870
neurophysiological Random-Access Memory-Interval Timer and buffered storage system 79−84066
optical disc, large capacity (ten billion bits), using diode laser, Philips development 79−81369
optoelectronic, with data record in bits, information capacity anal. 79−41342
RAM, use as α-particle detector 80−37701
rhythm analysis, long-term ECG data storage and multipass scanning 79−39578
superconducting film, memory device storage of Abrikosov vortices 79−28487
touch-sensitive audio tablet for blind access to digital memory 79−76916

random functions
see also random processes
acoustic imaging systems using random signal analyses 78−42499
asymptotic sufficiency in non-regular cases, for independent identically distributed random variables 77−41462
convergence to stable distribution laws in limiting theorem *(Russian)* 78−28920

random functions continued
differential inequalities and stochastic differential eqns. 77−5641
estimation aided by instrumental variables, regression model *(German)* 78−29080
exponential random variables sum, probability density function 78−12537
fluctuations generation with arbitrary power spectrum, algorithm 78−73927
functional random walk model, asymptotic steady state soln. 78−62143
generation of rough surfaces, numerical procedure 78−62060
Gibbs random field, integral central limit theorem, equivalence of ensembles 77−53826
independent random sine waves in additive Gaussian noise 79−68497
linear dynamic system with many fluctuating parameters, single group approx. *(Russian)* 78−62154
linear stochastic diffusion equations, two-dimens. system, asymptotic behaviour of functional for distribs. from argument of soln. *(Russian)* 78−21083
macrovariable, statistical behaviour in terms of Langevin eqns. within general random force 79−21653
microinhomogeneous media, appl. of random functions theory *(Russian)* 78−63280
nonstationary Poisson train intensity meas. error analysis 79−67246
orthogonalization of random variables, weather forecasting appl. 77−74203
random moires processes, densities of Minkowski measures *(German)* 77−64932
randomly-inhomogeneous conducting media, generalised charac. computation using random function theory *(Russian)* 80−75535
reaction of continuous dynamic systems with complex form under time-space random fields 78−65767
sequence of series of one-dimensional random variables with arbitrary depend. character, limit theorems *(Russian)* 77−49571
signal mean power meas. error *(Polish)* 78−89425
stationary Gaussian sequences, spectral function estimation 79−75324
sums of random variables, independent, Gram-Charlier-Edgeworth expansion 77−41461
sums of random variables, independently and identically distributed, Gram-Charlier-Edgeworth expansion 77−41460
with time correlation 77−17788
two-time correlation functions 79−46428

random noise
see also thermal noise
1/f, biological and synthetic membranes 79−24969
1/f, conductance noise, with four arbitrarily shaped and placed electrodes 77−85275
1/f, from singularities in fluctuation weighting function 77−62969
1/f and 1/Δf noise, relationship between magnitudes 79−78143
1/f current noise, random walk model 77−8162
1/f fluctuations *(Japanese)* 78−43448
1/f noise, amplitude distribution 79−24042
1/f noise, nonlinear mechanism 80−96955
1/f noise, quantum theory 80−100491
1/f noise, review 79−24038
1/f noise, theoretical analysis *(Polish)* 78−91737
1/f noise in barrier layers, expt. and analytical dependences *(Russian)* 79−19648
1/f noise in electrical conductors, survey 80−107878
1/f noise in variance of Johnson noise 78−68059
1/f noise mechanism, review of experimental investigations 78−64076
1/f noise mechanisms, linearity 78−45568
1/f-noise in Hall voltage 79−24039
acoustic array gain, sampling error effect anal., Bryn processor 78−66975
acoustic waveguide, active noise suppression 78−5613
amplifying system, distributed feedback due to meeting of oppositely propag. noise waves, beats *(Russian)* 77−71965
astronomical data, effect of noise on accuracy of max. entropy method 80−56712
astronomical hard X-ray telescope, balloon borne, background noise calc. 77−5427
atomic collisions and radiation trapping, analysis using charact. noise of strong EM wave 80−99492
Bayesian deconvolution, convergent props. 78−57861
Bayesian deconvolution, noise props. 78−57862
biological system with diffusion, noise-induced phase transition 79−100560
biomembranes, mechanism for 1/f noise in diffusing ion channels 78−27911
bolometers, superconducting, effect of LF noise on threshold sensitivity 79−89005
burst noise, physical sources 79−24033
BWR neutron noise local component meas., two phase flow study 78−94059
catastrophe and fractal regimes in random waves 80−8811
charge sensitive preamplifiers, signal and noise response 78−33404
coherent Raman spectroscopy techniques, review 80−22440
computerised tomography, noise factor of a polyenergetic X-ray beam 80−56204
conductor, four-probe investigation, theory 77−85276
conference, Bad Nauheim, West Germany (Mar. 1978) 79−24031
current fluctuations in strong elec. field, interelectron collisions, drifted Maxwellian distribs. *(Russian)* 80−2436
Cygnus X-1, short-term time variability, shot noise model 78−36721
Cygnus X-1, shot noise model for short-term variability 78−93474
Cygnus X-1, X-ray flux time variability struct. *(Russian)* 80−51921
Cygnus X-1 short term time variability, shot noise model 78−93466
Cygnus X-1 X-ray emission, shot noise rel. to physical reality of millisecond bursts 78−45429
Cygnus X-2 optical emission, shot noise variability upper limit 78−96564
deep ocean, low freq. noise prod. by surface waves 78−81184
diffusion noise, VHF extension of Einstein relation 80−17901
digital fibre optical communication system, average error probability calc. 80−53228
digital fibre-optic transmission system average error probability 77−27380
digital frequency meter, probability distribution function, effect on accuracy *(Russian)* 77−41575

random noise continued
disordered systems, spontaneous echoes, spectral diffusion decay 80−84270
ECG signals, diagnostical functions, effect of random noise *(Croatian)* 80−98169
ECG signals, random noise influence quantitative assessment of program accuracy *(Slovenian)* 79−25143
education, Poisson statistics demonstration using X-ray tube, electronic 'shot noise' 80−73129
EEG techniques for averaging noise, improving signal to noise ratio 77−81609
electrical fluctuations, quasiequilib. conditions, fluctuation-dissipation theorem 79−11191
electrical noise in equilibrium conditions 79−56274
electrodes, ellipsoidal, embedded in conductor, spreading resist. and 1/f cond. fluctuations 80−2435
electrolytic resistors and conc. cells, 1/f noise theory 79−47940
electron micrograph, image processing systems, random noise removal 78−12791
EM radiation, noncoherent polarimetry anal. 80−1111
equilibrium system, temp. fluctuations and 1/f noise 78−23143
extremal levels *(Rumanian)* 78−21070
fibre optic systems, digital, error probability with inter-symbol interference and additive noise 79−89855
fibre-optic digital transmission, shot noise probability distribution function 78−50717
fibre-optic interferometer gyro, thermally induced nonreciprocity 80−58665
field emission cathode, film, with Mo cones, phys. props. 77−24931
finite realisation, phase prop. and influence on deconvolution 79−44254
fission reactors, coupled core system, noise sources in coupling medium, stochastic study 80−22962
flicker noises in astronomy, stochastic prop. 78−57473
FM-CW acoustic sounder resolution rel. to modulation noise *(Japanese)* 78−30137
forward biased junctions, excess noise sources due to defects 79−38154
gas, thermal fluctuations of optical absorpt., noise *(Russian)* 77−31423
Gaussian field optical heterodyne detection, S/N ratio 79−13912
Gaussian noise, simple models 78−32763
Gaussian noise hypotheses testing 78−58551
gear noise, real-time bispectral anal. appl. to contactless diagnosis 77−84066
geophysical data analysis, random values separation *(Russian)* 79−74983
hair cell voltage noise during mech. stimulation 77−90817
Hall effect, 1/f noise, mobility fluctuations 80−92950
Hall effect noise, explained as carrier mobility fluctuations 77−62949
HF ECG, origin and characts. 77−44797
holographically stored X-ray images, grey-tone reproduction 78−65120
homogeneous electron irradiation *(German)* 80−102603
III-V semiconductors, noise calc. using Monte-Carlo method 80−75575
imaging systems, statistical anal. characterisation, measurement 77−86562
independent random sine waves in additive Gaussian noise 79−68497
inhomogeneous Boltzmann gas, lumped phase space, non-linear diffusion approx., stochastic hydrodynamic theory 80−64666
n-InSb Corbino disc, acoustic noise effect on I-V characts. *(Russian)* 80−100492
interaction of determinate packet with random noise, in Burgers' equation 80−106650
Josephson tunnel junction, flicker (1/f) noise 77−1520
junction devices, generation recombination current, noise reduction, SRH centres in space-charge layer 77−76905
K-distributed noise, statistics 80−27220
laser beam scattering, 1/f noise in model systems 79−98290
laser heterodyne signals from moving object, bandpass filtering by finite apertures 78−55306
laser radar system, mobile computerised meteorological phenomena observation 80−56644
laser Raman signals, pulsed, from turbulent combustion media, averaging considerations 78−70839
lattice scattering as origin of 1/f noise, confirmed from expts. on p-Ge and n-GaAs 78−64074
LF fluctuation, dissipation and relaxation properties, universality 80−84687
light intensity fluctuations, higher-order correls. and photoelectron time-interval distrib. 77−61932
limiting oscillator circuit for metallic NMR meas., with S/N improvement 79−26096
linear system, mean square response to nonstationary random excitation 80−57085
magnetic thin films influence of external random fields *(Russian)* 78−64229
magnetometer, induction-coil, optimisation theory for min. equivalent mag. field noise 79−85156
Mandelstam-Brillouin stimulated scatt., amplitude and phase time oscills. noise *(Russian)* 80−87435
maser amplifier, zero point energy noise effect 79−72546
MBBA, nematic, EHD transitions, white noise effects 80−6159
mechanical Nyquist noise in cryogenic gravitational wave antenna 77−30078
medical US imaging, stochastic noise influence on perceived image 80−98053
metal, with impurities, quaternary correlation function calc. 79−24041
metal film and whiskers, 1/f noise 79−38193
metal film resistor, resistance fluctuations from spontaneous enthalpy fluctuations 78−72217
metal films and whiskers, 1/f noise theory 78−34872
metal-oxide-metal photodetector, noise, ultimate sensitivity 77−5915
metals, excess noise energy scales 79−95458
metals, resistivity, temp. fluctuations and 1/f noise effects 77−20373
MIM cathodes, LF noise sources and reduction 80−108328
mode coupled fluctuations and 1/f noise 77−79035
MOSFET, flicker noise theory 80−11100
multimode fibre link, modal noise 80−87536
multiturn fibre Sagnac interferometer, shot-noise-limited inertial rotation meas. 80−1349
neutron microscopy, vel. distrib. rel. to fluctuation theory *(Hungarian)* 77−49679
neutron noise analysis techniques 77−3069
NMR, 1/f noise in direct and lock-in recording 77−6[illegible]049

random noise continued
noise voltage in film structures, two-dimensional analysis 78−6420
nonequilibrium phase transitions in presence of external non-white noise 80−42182
nonlinear noisy sine wave oscillator, optimal control 80−27218
nonlinear stochastic differential eqns. excited by Gaussian noise and harmonic disturbances 77−87631
nuclear reactor, reactivity and neutron density noise excited by random rod vibr. 77−50203
nuclear reactor identification, test inputs review 78−41819
nuclear reactor temperature sensors, response time testing by noise anal. 78−13300
optical, Schade detail S/N ratio derived from decision theory 78−63022
optical fibre communication systems, computer design aids 80−28350
optical fibre magnetostrictive perturbation for possible mag. field detect., shot noise 80−53450
optical fibre system, timing error tolerant waveforms 80−14293
optical fibres, modal noise, dependence on source coherence and fibre length 80−48402
optical PCM communication system, Poisson and Gaussian analysis *(Italian)* 77−50759
optical problems, statistical reversal methods of linear transforms. *(Russian)* 78−1179
optical quantum amplifiers, spatially modulated optical signal noise performance *(Russian)* 77−38850
p-n junction, low freq. noise 78−6419
p-n junction diode, surface flicker noise at high injection level 77−47892
p-n junctions, 1/f noise 79−82666
p-n junctions, inhomogeneous, theory of LF noise 78−2559
p-n junctions, microplasma noise, stochastic model, breakdown voltage of microplasma 78−47854
particle beam, RF fields due to Schottky noise 77−88632
particle flux noise in reduction, multiplication and branching processes 79−21667
pattern generation using coherent optical spatial filtering 79−98462
period analysis at high noise level 80−73263
Photographic Zenith Tube at Tokyo Astron. Observatory, observational errors anal. 80−98547
physical aspects of electrical noise in solids and semiconductor devices *(French)* 78−19111
physical models of 1/f noise 77−71272
plasma probe, digitised random signal analysis method, power spectrum, phase vel. 77−84509
point reactor kinetic eqn. with Gaussian reactivity fluctuation, exact soln. 80−68735
polarography, differential pulse, improved signal to noise ratio 77−29072
polyethylene film, 1/f noise, 10^{-4}-1 Hz, 20-80°C 79−51643
polyethylene terephthalate film, 1/f noise, 10^{-4}-1 Hz, 20-80°C 79−51643
polystyrene film, 1/f noise, 10^{-4}-1 Hz, 20-80°C 79−51643
preamplifier, low noise, for gravit. research 78−243
probability density, time dependent, for nonlinear non-Markovian stochastic process, coloured noise effect 80−22281
pseudo-Gaussian noise signals, for hydrophone calibration 77−84045
pseudo-random noise dielectric spectrometry *(Japanese)* 79−17445
pseudo-random noise generator, for sound absorption and buildings, insulation testing *(Spanish)* 78−13861
pseudorandom noise method, review *(Japanese)* 78−77688
pulsar radiation, polarised shot noise model 77−13374
quasi-stellar objects historical light curves, shot-noise interpretation 77−37666
radiation spectra unfolding code COOLC 78−5090
radiographic mottle, screen sharpness quantum noise depend. 78−20261
radioisotope imaging, digital low-pass filtering 77−5065
radiotelescope sensitivity optimisation, deterioration coeff. *(Italian)* 78−85845
reach-through photodiodes, Si, avalanche buildup time 77−15892
relaxation spectra, superposition, 1/f noise 80−105575
respiratory impedance and derived parameters in young children by forced random noise 80−30745
retarding field energy analyser in electron spectrometry, noise meas. 80−27377
satellite Fourier spectroscopy methods and problems *(German)* 80−36477
Schottky barriers, 1/f noise 79−82666
seismic data, noise-resistance of optically generated correlograms *(Russian)* 78−40699
seismic recordings, information quality and data processing techniques efficiency *(Russian)* 79−39666
seismograms, noise effects on meas. accuracy 77−45181
semiconductor, 1/f noise origin 80−11060
semiconductor, current and voltage fluctuation determ. by noise spectral density meas. 80−15577
semiconductor, highly doped, flicker noise in terms of number fluctuation model, surface effects 79−60882
semiconductor, homogeneous, Hall effect noise 78−39173
semiconductor, homogeneous, nondegenerate, single-level Schockley-Read-Hall recomb. centres, flicker noise 80−70779
semiconductor, new look at 1/f noise 79−24030
semiconductor, nonohmic transport fluctuations 79−24034
semiconductor, theory of carrier multiplication and noise due to avalanche processes 80−6865
semiconductor, with transition to metallic state, low freq. current fluctuations 77−66189
semiconductor DH lasers, effect of impurities on quantum shot noise reson. 78−22132
semiconductor generation-recombination noise 79−24032
semiconductor materials, noise models for investigation of defects *(German)* 78−87661
semiconductors, flicker noise, not true bulk effect 79−24028
semiconductors, lightly doped, 1/f noise for hopping conduction, theory 80−44683
semiconductors, mobility-fluctuation description of 1/f noise 80−84496
semiconductors, nondegenerate, flicker noise, mobility fluctuation possibility 79−91108
semiconductors, resistivity, temp. fluctuations and 1/f noise effect 77−20373
shot noise, extended class, inverse problems 79−17199
single injection diodes, 1/f noise 78−60204
sound Gaussian noise and its transformation by moving boundary condition effect 80−33281

random noise continued
spatial correlation theory for noise field, evaluation of integral 77−88981
spectrochemical analysis, noise and signal-to-noise ratios 79−43671
spectrochemical analysis, noise and signal-to-noise ratios 79−43672
spectrometric sources, signal flicker, shot noise, noise power spectra 77−53980
spectroscopic light source fluctuations, automatic correction, split beam system 77−10115
spectroscopic measurement, convergence of iterative deconvolution technique, effect of errors 77−53849
speech enhancement by frequency-domain spectral weighting 79−94416
spin wave parametric excitation by noise pumping *(Russian)* 80−34617
SQUID, RF, LF noise expt. exam. 80−98947
SQUID, thermodynamic equilibrium fluctuations generation by Josephson junction, Werthamer theory 80−100564
SQUID magnetometer, AC-biased 80−98948
SQUID magnetometers, signal detection of 1/f noise 79−26091
Stark effect in Gaussian noise field, three-level system 78−41266
stochastic characteristics of the burst noise 80−98855
stochastic evolution eqns. with general white noise disturbance 78−16734
stochastic inverse problem in the radiation of noise 79−49168
stopping and sojourn time asymptotic evolution *(French)* 77−45683
streamflow, skewed annual flows generation using fast fractional Gaussian noise generator 79−53395
submillimetre astronomy, sky emission and absorpt. noise reduction 77−41308
superconducting foil, flux flow noise cross-correl. functions 77−36034
superfluorescence, phase-wave fluctuations 80−23652
superfluorescence-initiating noise source, average strength meas. 80−58492
symmetry principles and 1/f noise 80−68136
teaching, Campbell's theorem, use in elec. noise formulae derivation 78−24602
tectonomagnetic experiments, noise reduction by multivariate linear regression 79−84515
time convolution Master equation and generalised Langevin equation equivalence 78−93610
transducer flow noise, rejection using coherence function method 77−84067
transport noise, Green's function procedures 80−17902
tunnel-effects in junctions generating burst-noise *(Rumanian)* 80−6960
turbulent jet, particle conc. meas., laser scatt. technique 77−39372
two-dimensional isotropic conductor, transverse and longitudinal noise 79−51642
two-level system in resonant multifrequency field with structureless noise *(Russian)* 80−91766
type II superconductor, induced flux-flow noise 77−4476
US blood flow meas. using random noise, target model and optimal receiver 77−21589
vision, fly, movement discrimination rel. to S/N ratio 77−48801
vision, stereomovement from interocular delay, random spatial disparity hypothesis 78−24074
visual detection, effect of photon noise 80−61559
Ag, excess noise energy scales 79−95458
Ag film, 1/f noise, role of substrate 79−28388
Ag film, 1/f noise and its temp. depend. 79−60939
Ag film, 1/f noise and its temp. depend. 79−60940
Ag film, continuous, 1/f noise, temp. and substrate depend. 79−24086
Ag film, temp. depend. of 1/f noise meas. 77−85277
Ag films, excess (1/f) voltage noise 79−42598
Al granular films, vortex noise at supercond. transition 80−84530
Al thin conducting film, electromigration under superimposed DC and noise powers 80−107879
Al thin films 1/f noise, depend. on internal mech. stresses 80−65711
Al-Si_3N_4-Al cathode, fluctuation noise 78−2998
Al_2O_3 supermicrogrid preparation and props. use in electron microscopy, noise reduction 80−99010
Au films, excess (1/f) voltage noise 79−42598
$BaSrTiO_3$, model for 1/f excess noise 79−99591
$BaSrTiO_3$, semiconducting, excess noise characts. exam. 78−19110
Bi film, carrier conc., mobility and 1/f noise 80−44748
Bi, thin film, 1/f noise, boundary scatt. effect 80−49836
Bi whiskers, excess 1/f noise, 50 to 350K 80−92951
$Cd_{0.1}Hg_{0.9}Te$, polycrystalline thin film, correlation between structure and 1/f noise 78−39234
n-$Cd_xHg_{1-x}Te$, single crystal, scattering mechanism on intensity of 1/f noise 80−39642
CdS plates, noise amplification as function of drift field intensity, conductivity and freq. *(Russian)* 79−73556
CdSe film, current noise due to thermal field ionisation 79−91110
CdSe, single crystal, low-frequency current noise, effect of temperature quenching of photoconductivity 78−34874
Cr film, 1/f type noise, spatial correlation 79−38194
Cu film, 1/f noise, role of substrate 79−28388
Cu film, 1/f noise and its temp. depend. 79−60939
Cu film, 1/f noise and its temp. depend. 79−60940
Cu film, continuous, 1/f noise, temp. and substrate depend. 79−24086
Cu film, temp. depend. of 1/f noise meas. 77−85277
Cu films, excess (1/f) voltage noise 79−42598
Cu whiskers, current induced 1/f noise 77−32058
Fe-Ni alloy toroidal core, magnetic noise *(Russian)* 78−60308
Ga, solid and liq. phases, 1/f noise 78−64073
GaAlAs CW DH diode lasers, 1/f noise behaviour 78−1226
GaAs, epitaxial layers, low freq. current noise between 4.4 and 300K 78−95388
GaAs injection lasers, direct modulation enhancement effect of HF noise 80−83608
GaAs, photocapacitive MIS IR detector, spectral response, noise characts. 80−75644
Gd, coil noise due to permeability fluctuations at phase transition temp. 80−84598
n-Ge, deformed, 1/f noise, resist., mobility, and carrier density 77−8161
Ge, magnetic field influence on 1/f noise, surface origin evidence 79−99592
He-Ne laser, 6328 Å power fluctuations due to striation noise 80−78834
n-$Hg_{0.61}Cd_{0.39}Te$ single crystals, flicker noise due to grain boundaries, meas. 79−1611
$Hg_{1-x}Cd_xTe$, Hooge's flicker noise MIS expt. 78−56233
InGaAsP avalanche photodiodes, leakage current, shot noise, quantum efficiency, gain saturation 79−67381
random noise continued
InGaAsP avalanche photodiode, 1.3 μm, noise performance, −190°C 80−57370
InP, hot carrier noise, Monte Carlo simulation 77−51792
InSb, 1/f noise, Hooge's parameter 79−24040
InSb, film, transverse 1/f noise and signal-to-noise ratio of related Hall elements, comment 79−99593
InSb, film, transverse 1/f noise and signal-to-noise ratio of related Hall element 79−99594
InSb films, transverse 1/f noise and S/N ratio of related Hall elements 79−42597
n-InSb, flicker-noise power spectrum, 0.1 Hz to 10 kHz 79−73555
K adsorbed on W(112) planes, temp. depend. of noise spectral density functions 78−2992
$La_{1-x}Sr_xVO_3$, semiconductor-metal transition, Anderson localisation, Hall mobility and 1/f noise meas. 79−78142
n^+-n-pGe avalanche photodiode, noise factors, internal quantum efficiency 80−70803
Nb superconducting point contact, singularities of I-V curve and voltage fluctuations 80−93044
$NbSe_3$, CDW noise, temp. and freq. depend. 80−103681
$NbSe_3$ interference effects of CDW motions 80−88544
Ni films, excess (1/f) voltage noise 79−42598
PbTe, semiconductor polycrystalline thin films, low-frequency 1/f noise meas. 80−15629
Pt, elec. cond. and current noise 78−72286
p-Si, deformed, 1/f noise, resist., mobility, and carrier density 77−8161
Si, electron-beam-evaporated amorphous thin films, noise meas. 79−24091
Si, inversion layer, 1/f noise and percolation in impurity bands 79−24029
Si p-n diode, 1/f noise calc., free carrier mobility interpretation 80−54774
Si, photocapacitive MIS IR detector, spectral response, noise characts. 80−75644
n^+nn^+Si planar device, hot electron flicker noise at 78K 80−103732
V_2O_5-P_2O_5 glass, electrical 1/f noise and DC cond. 79−91109
W, adsorbed K, field emission flicker noise, coverage depend. 78−35262
W, adsorbed layers of K on (112) planes, flicker noise field emission obs. 78−26774
W surface, adsorbed K, field emission flicker noise power 80−59795
ZnS, low resistivity, ohmic contact noise characts. and contact resistance 78−14827
ZnSe, with wurtzite-sphalerite boundaries, LF photofluctuations 79−69560
ZnSe-GaAs heterojunction, LF noise, I-V and C-V characts., illumination effects *(Russian)* 77−66200

random number generation
Cebysev mixing transformations, use in random process digital simulation 79−80510
congruential pseudorandom number generators uniformity, number sequence length, resolution effects 78−41147
core operating limit supervisory system stochastic simulation 79−630
digital scene generation with specified statistics 80−99666
fluctuations generation with arbitrary power spectrum, algorithm 78−73927
Monte Carlo simulations using minicomputers 79−81122
physics experiment design 79−89577
pseudo-random number generators, statistical test 78−86125

random phase approximation *see RPA calculations*

random processes
see also Brownian motion; fluctuations; Markov processes; probability; queueing theory; stochastic processes
absorption time by a random trap distribution 80−86209
acceleration through random classical radiation, thermal effects 80−73191
acoustic discontinuous waves in nonlinear media, characts. 78−5601
acoustic Doppler effect for randomly moving scatterers and platforms 77−62093
acoustic emission, random signal parameters, computer calc. 77−44454
acoustic signal processing, influence of time- and space-varying random filters 78−5615
acoustic wave propag., product of matrices and random transfer *(French)* 78−5596
acoustics, average field attenuation in irregular waveguide 78−1459
algebraic models for probability measures assoc. with solns. of random eqns. 77−67236
anisotropic random medium, scatt. in depth direction 79−2635
anisotropic system, random field conjugate to non-crit. variable, effect on phase transition 80−13022
arbitrary random noise and vibration waves, statistical consideration of peak distribution 80−23836
astronomical X-ray burster phenomenon, mathematical simulacrum 77−87570
atmosphere boundary layer, similarity theory for random fields *(Polish)* 77−25753
atmosphere pollutants dispersion, completely Lagrangian random-walk model 78−81380
atmospheric boundary layer and upper ocean layer, fluctuations, linear filtration errors 80−12425
atomic migration on disordered surfaces, theory 80−54516
attractors in the non Morse-Smale dissipative dynamical systems 79−75447
autocorrelation coefficients, unknown, estimation 79−49021
background ensembles, nonlinear modeling 80−95037
basin hydrology, tests of random network model 77−45029
BCC lattice, probability of visiting new site in random walk 79−88891
Bethe lattice, displacement correl. function, random walk 78−41247
bias meas. lessening of dispersion of non-centred and nonstationary random processes *(Russian)* 78−12645
bidimensional surface waves, periodic correlational random field model *(Russian)* 78−20430
binary galaxies, random optical pairs in Turner's (1976) sample 80−67849
biomedical flow systems effects 78−44445
boundary-value problem, two point, statistical version anal. 79−63154
broadband sound radiation from randomly vibrating pipe walls, power efficiency estimation charts 77−62104
Brownian functionals, analysis 77−33949

random processes continued
cavitation noise emission from marine propellor, random pulse anal. 77−14853
Cebysev mixing transformations, use in random process digital simulation 79−80510
cell membrane particles, max. density of random placing 79−44862
cell mixture sorting, random walk model 77−44606
chaos, external noise and Fredholm theory 80−86216
chaos, reinjection principle, folded and cut chaotic flows 80−12996
chaotic behaviour of physical and biological systems 78−62158
chaotic processes, time correl. functions, in one-dimens. 79−25985
chaotic states of anharmonic systems in periodic fields 80−22288
chaotic turbulent flows, scaling behaviour, Lyapunov characteristic exponent 80−86217
chaotization based diagnostic algorithm for handling small samples 79−39568
chemical reactions, diffusion-controlled, continuous-time random walk modelling 80−3297
chloroplast conformational vars., auto-correl. anal. 80−30680
classical, with arbitrary preparation, perturbation theory 79−54057
classical statistical mechanics, random-walk theory and correl. functions 77−5768
classical stochastic electrodynamics, positive temp. random EM field 79−40382
climate predictability 79−16645
clock random perturbations, absolute continuity theorem *(French)* 78−62150
cluster size, pair connectedness for fluid and lattice systems, percolation and condensation 77−61019
coaxial electron and atomic beams sequential multiple scatterings, random walk approach 80−99574
cocktail parties, acoustical aspects 77−80008
coherence and randomness in quantum theory, uncertainty relations 80−22231
colloid stabilisation by polymers, excluded volume effects 77−60129
column with nonlinear restraints and random initial displacement, buckling 80−79192
comets neutral atmospheres, average random walk model for mol. phot. dissociation 80−77351
conditioned random walk, absorpt. time moments 79−62165
correlated particle migration in cryst. struct. *(Russian)* 80−96683
correlated walk on lattice, correl. of successive steps, absorbing walls 79−44863
correlated walks theory, exact results 80−27214
correlation coefficient sign determ. 79−71232
correlation function of statistical functional of system of interacting particles *(Ukrainian)* 78−54285
cosmic ray muons, time distribution, random and nonrandom components of arrival times 80−72732
cosmic rays propagation, non-field-aligned diffusion effects on neutral monitor diurnal anisotropy 78−32304
coupled oscillatory-reaction system exhibiting bifurcation scheme leading to a chaos 79−80517
coupled random walk process, spatial structure, regression to steady states 79−25986
coupled random walk process specified by Hamiltonian in pot. field 80−42169
coupled random walk process theory, Fokker-Planck eqn. calcs. 80−77710
crack propagation considered as random walk process 80−43666
critical behavior of random resistor networks near the percolation threshold 78−87956
cross-spectrum inequality proof for pair of stationary random processes 77−67380
crystal growth rates, random processes theory to study fluctuations 79−55689
crystal lattice sites, many-particle random motion 80−92703
Curie-Weiss model, random magnetisation, statistics, asymptotic behaviour 79−4639
Cygnus X-1 shot-noise variability, extended-bandwidth X-ray obs. vel. to energy depend. 80−17689
demonstration, for student lab., showing time distrib. 78−41124
density perturbations in expanding universe, three-point correl. function and higher order functions prediction 78−65730
deterministic orbits, chaotic behaviour, turbulent phase problems 79−80518
deterministic systems with multiple steady states, small fluctuations effects 79−80526
diamond and HCP lattices, random walks 78−71876
diffractals (wave interaction with fractals) 79−58549
diffusion in presence of high diffusivity paths, random walk model 80−24640
diffusion in random networks near percolation threshold, ant in labyrinth problem 80−77732
diffusion in solids, random walk model with correlated jumps, appl. to H in metals 80−24639
diffusion processes with two-point boundary conditions, probability distribs. 80−42144
diffusion product *(French)* 80−8909
direct renormalisation soln. 1D random walk problem 80−4512
discrete random walk, differential equations for transport in two or more dimensions 79−85073
discrete systems with random excitations, random excitations 77−41537
disordered systems, random walks and AC cond. 80−70661
dispersion of equal spheres, random, average nearest-neighbour spacing 79−58639
dissipative dynamical systems, ergodic problem, numerical approach 79−88878
dissipative structures, non-equilibrium systems, self organisation *(Chinese)* 80−42168
distribution function for random walks without self-intersection 78−8350
distribution functions, oscillographic measurement 78−4607
drainage basin composition, random model appl. 77−45030
Earth surface height variation, Fourier transform. of altitude obs. *(German)* 78−61312
earthquakes, acceleration simulation 79−2186
echoes scattered by random fluctuating surface, statistical model *(French)* 77−11066
education, random walk approx., theory of generating function and method of steepest descent 78−36744
elastic wave scatt. by random distrib. of inclusions 77−886
random processes continued
electron relax. time in metals, waiting time paradox, for teaching 78−36771
EM field in unstable medium, estimation of dyadic Green's function using random current source 79−94129
EM irradiance distribution function in turbulent media, theoretical review 79−64155
EM wave propagation, in one-dimensional, randomly inhomogeneous medium, with specularly reflecting walls 80−105514
EM wave strong scatt. in random media, operator and diagram techniques for intensity moment eqns. 79−64154
EM waves backscattering, multiple, from randomly fluctuating media 77−50593
EM waves in medium with ellipsoidal inhomogeneities and regular refr., ray statistics 78−25773
empirical relationships for random self-avoiding walks on lattices 79−9190
ensembles for random matrices of Hamiltonians with small time reversal noninvariant part 80−77694
equilibrium statistical mechanics models investigation, book 77−22485
ergodic flows, set catching 79−63147
ergodic properties of an operator obtained from a continuous representation 78−89305
ergodic theory, classification of certain real transformations *(French)* 79−63146
errors, in active noise-suppression, influence on sound fields compensation 77−14852
errors of meas. instrument analysis, under transient conditions, based on instantaneous frequency response 80−77741
escape probability of random walker on lattice doped with impurities 79−17353
Euler's finite difference scheme and chaos 79−80523
European air temperature band-pass filtered series, random phase displacements 80−26579
evolution systems, meas., rel. to master eqn., Bayesian anal. 80−90782
excitons, coherent and incoherent motion in continuous time random walk framework 80−59882
fields solution using transmission line matrix, random walks appl. 79−53991
film deposition, adatom diffusion and capture by clusters, random-walk problem 78−2385
flood levees, failure rel. to reliability anal. 77−91182
flood sequences, apparent regional skew 77−64355
fluctuations, random, moment behaviour of soln. processes for nonlinear stochastic differential eqns. *(Japanese)* 80−95039
fluctuations, wave-number spectrum moments, correlation method for estimation 78−16732
fluidised bed, two-dimens. gas fluidised, mixing characts. of large particles 79−86503
FM signal modulation by smoothed random telegraph signal, appl. to underwater acoustic meas. 78−18130
Fokker-Planck eqn. eigenfunction expansion soln. extension, first order system 80−31668
Fokker-Planck equation, for random process of nonlinear system, nonstationary soln. 77−88
frequency meas., using automatic electronic meter *(Bulgarian)* 80−27283
functional equations, random, stochastic approx. in Banach space *(Japanese)* 80−95038
fuzzy boundary dividing the attraction domains of two attractors *(French)* 79−63149
galaxies, distrib. of ang. momenta 78−20886
galaxies and clusters, large-scale distrib. and random motion 78−54056
Gaussian beam wave scatt. from perfectly conducting column 78−1135
Gaussian Markov random fields, discrete parameter, generalised potential theory 80−57185
Gaussian process testing method 79−1993
Gaussian random fields 78−36934
Gaussian random surfaces, umbilic points 78−4467
general matrix approach to residual spectra 80−94947
generalised Gram-Charlier series with application to the sum of log-normal variates 77−37736
generalised random walks, transform. of recursion relations 80−101757
genetic systems, dynamics of neutral mutation 78−86220
geological materials and processes, models 77−81890
geophysical data, detrending and smoothing techniques 80−67425
geophysical fields, covariance function definition rel. to correl. anal. input conditions *(German)* 79−35014
geophysical interpretation problems, soln., correl. theory of homogeneous random fields appl. 79−100986
geophysics, probabilistic model for oil and gas forms. pre-drilling prediction *(Russian)* 79−39970
glass, electron migration and spectral relax., random-walk model 80−80280
grains in random arrays, spectral properties 80−12727
Hajek-Renyi type inequalities for random elements in Hilbert space 80−17784
harmonic chain with random masses, transmission coeff. and heat conduction 79−80547
harmonic oscillators, randomly disordered linear chain, normal frequencies 78−36818
heat conduction in random medium, method of time ordered cumulants 78−54320
heat eqn. soln. by iterative scheme 79−9195
Henon mapping, topological horseshoe, chaotic behaviour 80−73257
HF radiometer random process dynamic simulation models 79−80686
HF random process statistical characteristics meas. 77−18045
homogeneous random fields, modelling realisations 80−8911
hopping conduction, AC conductivity in random structs., renewal theory 78−141
hopping conduction in disordered insulator, continuous-time random walk model 80−96863
hopping conductivity, one-dimensional bond percolation model 80−103655
Husimi-Temperley model under a random field 79−97313
hysteretic systems under random excitation, equivalent linearisation 80−79210
infinitely thick slab subject to random surface temps., frequency response function, temp. variations 77−19511
innovation process theory in Hilbert space *(French)* 79−17349

random processes continued
instabilities and fluctuations in systems far from thermodynamic equilibrium 79−21671
interacting particle diffusion in periodic pots., two particle model, random motion 79−46828
internal system states, random walks and generalized master eqns. 77−82461
intersection characteristics *(Russian)* 80−90660
interstellar clouds, turbulence effects on collapse, three-dimensional numerical models 80−56910
interstellar dust, grains random vels. and collisions in turbulent gas 80−77470
interstellar polarisation in irregularly fluctuating medium, statistical anal. 80−26926
inverse problem for random sources 79−97214
ionosphere reflected signal, sum phase random props. investigation 79−53615
Ising model, thermodynamic limit 80−17885
Ising model simulation, random mixture critical props. 77−69573
Ising systems of different spin values, random system 80−11144
Ising two-dimens. model, cluster shape and size 77−61024
isotope separation cascade, random walk model 77−58190
jump time determ. algorithm for equation parameters 77−17785
kinetic theory of systems in random fields 79−21652
Kirchhoff approximation in horizontally polarized backscatt. from random surface 79−7061
kit of instruments for statistical research 78−87215
Lagrangian and Eulerian characteristics of random field, rel. between *(Russian)* 77−5761
laminated composites, mechanics of homogenisation and random evolutions 80−28423
Landau-Zener problem, random nature of motion role in intersecting terms problem 80−8937
laser beam scatt. by diffusing surfaces *(Chinese)* 80−1128
lattice random walks, average number of steps to trapping 77−17912
lattice random walks, occupation times 80−42162
lattice-gas system, random-walk theory and ordered phases 77−5769
lattices, finite, with traps, random walks, Monte Carlo simulations 80−52131
level crossing time interval fluctuations 79−21534
limit cycle, symmetric bifurcation to asymmetric limit cycle, simple model 80−57080
linear dynamic mol. system, correlated radiation impulse sequence interaction 80−38058
linear dynamic systems, response to product random processes 78−34054
linear randomly perturbed systems, mean-square stability 77−9870
linear system, external parametric random perturbations, oscillations *(Russian)* 79−17207
linear systems acted upon by Poisson processes 80−57196
liquids, electron scavenging and ion recomb. processes, 3-dimens. continuous time random walk model 78−7216
local limit theorem for Gibbs random fields of particles and unbounded spins 79−97296
localization of eigenstates in one-dimensional infinite disordered systems with off-diagonal randomness 80−17876
Lorentz model, simplest limit cycle analytic form 79−86405
Lorenz attractor, origin and struct., appl. to specific model systems 78−29054
Lorenz model, intermittency, first limit cycle-second strange attractor transition 80−31674
Lorenz model, transient behaviour in periodic regions 79−17346
lunar soil electrostatic transport, terminator configuration model 79−35157
macromolecule, flexible, modelling by length distrib. projection of self-avoiding random walks 77−75352
many-particle system, generalised diffusion processes 78−73942
marginal local instability of quasi-periodic motion, separation distance effects 80−82633
Markov, linear operators conditional averaging 79−71233
Markovian nature of the two-dimensional self-avoiding random walk problem 80−4648
martingales, set function processes, vector lattices, Riesz decomposition and characts. *(French)* 80−8908
measurement errors, random, simulation (Monte Carlo) method, teaching appl. 78−86062
memory effects in random walk process 80−27232
metastable chaos, transition to sustained chaotic behavior in Lorentz turbulent convection model 80−4643
metastable state relaxation, critical point region nucleation in thermodynamic systems *(Russian)* 80−13026
MHD turbulent diffusion, root mean square mag. field calc. 78−36449
mixing flow and Palm measures *(French)* 78−89307
molecular crystals, disordered, incoherent, electronic energy transfer in impurity band 80−75525
molecular flow through cylindrical channel, Monte Carlo calc. 77−55042
Monte Carlo simulation, random walks with residence time dependent transition probability rates 79−2722
motion, roller device appls. 78−16600
multidimensional wave radiation from source with Gaussian time variation and Gaussian approx. distrib. about spherical sheet 78−45487
multifrequency mth order coherence function, path integral approach 79−89836
multistate diffusion in perfect and defective system, stochastic theory 79−93066
multistate diffusion in perfect and defective systems, stochastic theory 79−93067
multivariate, consequences of non-negative definiteness of spectral density matrix 79−80511
multivariate response relationships, appl. matrices to treatment of residual spectra 80−68132
neural networks with random topology randomness of generated eigenvalues 80−22291
neutron scatt., random sampling technique for choosing scatt. angle from ang. distrib. 77−61619
NGC 4151, Seyfert galaxy, shot noise model for repeated X-ray flaring 80−90534
noise waves, low-frequency, parametric excitation in nonlinear medium 78−9472
noiselike optical signals, photoelectron counting statistics and error rate characteristics 78−1178
non-Gaussian, average number of trajectory overshoots over given level calc. 79−71234
non-negative matrix, random evolutions and spectral radius 79−93042
nonlinear differential equations, random behaviour 80−77706
nonlinear Mathieu eqn., chaos and successive subharmonic bifurcations 79−63153
nonlinear oscillators, random excitation, response envelope statistics 79−6052
nonlinear stochastic functional, correlation depend. *(Russian)* 77−67235
nonparametric forecasting method for stationary processes, appl. to random meas. *(French)* 80−90780
nonstationary random vibrations of multiple-mass systems 80−69728
nuclear decay, γ-decay of coherent rotational states, random quantum meas. 80−73855
Nyquist formula, quadratic generalisations 80−57198
ocean, weak turbulence of random internal wave field *(Russian)* 77−33089
ocean and atm. waves, adaptive spectral anal. *(Russian)* 77−29475
ocean current flow and drifter motion, random walk model 77−66923
ocean internal waves, damping by rough bottom *(Russian)* 78−24293
ocean internal waves, influence on sound propag. 77−14837
ocean random gravity wave mathematical representation 80−46198
ocean random hydrophysical processes, quantification *(Russian)* 78−77359
oceanic crust random magnetisation, effect on coherence of short-wavelength marine mag. anomalies 80−36225
oceanographic nonstationary random processes, simulation and prediction *(Russian)* 77−60408
one-body approx., disordered system spectral props., Schrodinger eqn., random fields 80−90696
optical experiments, autocovariance functions and power spectra 78−63018
organic compounds, complex, nuclear relaxation influence on stimulated emission 80−48019
Ornstein-Zernike lattice system, random-walk theory and pair correl. 77−5770
oscillator, linear, excitation by stationary random force *(Russian)* 80−27116
oscillator with dry friction, forced vibrs., response random process treatment *(Russian)* 80−36841
oscillators, nonlinear stochastic, triangular wave, optimally controlled, Weiner process and Poisson process, numerical studies 80−52128
packing of spheres, computer simulation 80−77705
palaeoclimatology, abrupt events time scales and causes 80−51531
parametric vibr. of hollow cylindrical shells *(Russian)* 79−27572
parking problem, asymptotic estimates, jammed state density 80−86206
particle transport with multiplication, math. expectation of symm. functionals *(Russian)* 77−82469
particles from oil-fired burners, size distrib. characterisation using Beta distrib. 78−81384
path integrals for waves in random media 79−63049
percolation lattice, diffusion, random walk method, Monte Carlo method 78−60098
percolation theory, review 80−98868
percolation theory and related topics 77−61022
period analysis at high noise level 80−73263
periodic lattices, random walkers, multiple trapping 79−2732
petroleum, two phase flow in underground reservoirs, soln. of nonlinear eqn. by random choice method 79−50773
phase statistics in coherently superposed Gaussian speckle patterns 80−102626
point defect trapping by extended sinks, model of cloud random walk of lattice pts. 79−82199
point defects short term annealing, in α-Fe, computer simulation 80−54282
Poisson processes subset selection procedures, binomial and multinomial problem appls. 78−36802
Poisson-sampled random process, moments estimation 77−37738
polar liquid, IR absorpt. spectra and hydrodynamic model *(Russian)* 79−78689
pollutants in urban atmosphere, prediction of long-term mean and mean square concs. 77−2226
polymer adsorption at interface, self-avoiding random walk anal. 77−1085
polymer network, Riemann's metric degeneration to graph metric demonstration, chain entanglement problems 80−38963
polymer network formation, struct. and mech. props., computer simulation 80−38965
polymer random flight chain, surface adsorbed, end-to-end mean value 78−22060
power spectrum of a random process, computing using data segmentation 77−60912
probabilistic bond percolation in random arrays 79−2729
PSR 0950+08, pulsar, micropulses freq. struct. 80−22030
pulsar microstructure shot-noise model, propag. effects in shearing field-free plasma 80−17483
pulse train processing by linear filter *(Russian)* 78−46518
pulsed, of nth order of complexity 77−64931
quantification of stochastic process, principles of quantification noise *(Spanish)* 80−57190
quantum system, nonintegrable, irregular part of discrete energy spectrum, statistical theory 80−82667
quantum system subject to random pulses, Blume's integration of Schrodinger's eqn. 79−97232
quasar red shifts, anal. for randomness 78−12400
quasar redshifts, evidence for random distrib. 78−54070
quasars red shifts, anal. for randomness rel. to Earth-centred universe 78−16563
quasi-maximum likelihood method appl., to systems with complete connections *(Rumanian)* 80−57183
quasistationary processes and universal codes 80−91994
quenched random system, statistical mechanics 79−63155
radio sources distribution in vicinity of bright galaxies, evidence for random population 80−56964
radiowaves in ionosphere, limited beam diffusion due to scatt. on random inhomogeneities 77−91349
rainfall areal averages, multidimensional model for synthesis of processes 77−91176
random beadsets, substitute for self avoiding random walk, proof of conjectures *(French)* 79−21663

random processes continued
random binary Ising system with transverse field, Curie temp., paramagnetic susceptibility 80−65938
random sampling of scattering angle in neutron transport 79−85574
random walk on homogeneous spaces of certain rigid type groups *(French)* 79−75320
random walk problem, history, in consideration of interdisciplinarity 78−16618
random walk problems, weighted uniform sampling technique 79−49165
random walk properties on periodic and random lattices via generating function 80−42157
random walks, spatial structure and stability 79−49169
random walks on simply connected nilpotent Lie group homogeneous spaces *(French)* 79−25977
randomly transitional phenomena in the system governed by Duffing's equation 79−54055
reacting gas flow, time-depend., one dimens., random choice method anal. 78−9726
reactor neutron noise theory, role of factorial cumulants 79−63711
receiver operating characteristic curves for Poisson signals 79−83778
resonance transfer rate of electron excitation, model of convergent terms, effect of diffusional motion of particles 80−8936
retinal neuron interspike intervals variability, model dynamics 79−24984
river meanders, disturbed periodic model 77−45034
saltating solid particles in turbulent flow, accel. and forces *(Russian)* 80−1675
scalar field theory in lattice space, analogy to random walk 78−21325
scalar wave propagation, coherent scalar field in pair correlated random distribs. of aligned scatterers 78−32690
Schrodinger equation, random walk calcs., method of successive corrections 79−68180
Schrodinger equation, randomly fluctuating interaction term, uncertainty in nature 80−62499
seismic signals, amplitude and phase jitter rel. to optimal multichannel filtering evaluation *(Russian)* 78−40697
seismic waves propag. in medium with randomly distrib. inhomogeneities, attenuation and scatt. *(Hungarian)* 77−86791
self avoiding random walks, exactly soluble lattices 78−32767
self avoiding walk and supersymmetry 80−101756
self avoiding walk attached to a surface, tests of scaling theory 78−81927
self-avoiding lattice walks with high coordination and small excluded volume 80−77718
self-avoiding random walk, real-space renormalisation group approach 79−63167
self-avoiding random walk, renormalisation group eqn. 80−36947
self-avoiding random walks, exact enumeration method and Monte Carlo sampling 79−67228
self-avoiding random walks on lattice strips 80−17875
self-avoiding walk, asymptotic behaviour in continuous space 77−13700
self-avoiding walks of macromolecules confined to strips and capillaries 78−94345
self-avoiding walks on the face-centred cubic lattice 79−93048
self-avoiding walks with nearest- and next-nearest-neighbour steps 80−86222
selfavoiding random walk problem, direct renormalisation method 80−77703
semiclassical wave functions, regular and irregular 78−20998
signal detection, random phase modulated signals, nonlinear medium *(Russian)* 77−75606
signal processing method for circular arrays 80−4123
single mass vibroimpact system, response to white noise random excitation 80−64454
Smoluchowski process, number fluctuation anal. of random locomotion 78−54318
solar spectrum, statistics of intensities 77−53537
sonar, deterministic and random error model of multibeam hydrographic system 79−3873
sound wave propagation in two-phase random media, coarse grained eqns. 79−86280
space-time random speckle pattern optical analysis 80−102682
span-constrained random walks, on cubic lattice, internal configs. 80−68148
sparsely periodic and random lattices, random walk props., lattice bond enumeration 79−21675
spatial spectrum of random field, use of reference sensor in autoregression evaluations *(Russian)* 78−61578
spectral analysis, method of moments 80−68137
spectral density relationships, harmonic response characts. effect, random excitations 80−62582
spins, block, defined by random field, convergence 80−101759
stationary, correlation between level-crossing time interval lengths 80−22292
stationary, spectral density structure estimation *(Russian)* 78−24736
stationary behaviour testing, comparison of actual and predicted fluctuations 77−37817
stationary random fields, statistical inference 77−64930
stationary with non-Gaussian distribution, number of excursions 78−86221
statistical and classical fields, quantum aspects 79−58585
statistical geophysics, appl. of two-timing methods 77−73879
statistics, use of stochastic occupation densities and local times *(French)* 80−46972
steady-state process, probability characts. error calcs. 80−42145
stellar systems dynamics, purely discontinuous random processes in field of irregular forces *(Polish)* 78−16465
stellar turbulent convection equations, ensemble averaging 80−67698
stirred fluids, long distance behaviour 79−77082
stringers, discrete and random, polymer molecule shape modeling appl. *(French)* 79−21662
strong coupling expansion for classical statistical dynamics, randomly driven system 80−105568
surface profiles reference line selection and fitting 78−45594
surface topography as nonstationary random process 78−24739
synthetic aperture radar imagery for oceanography, random phase changes effects 77−25793
system acted upon by non-delta-correlated random forces *(Russian)* 77−74323
thermal radiation from randomly inhomogeneous stratified media, appl. to Earth surface *(Russian)* 78−96312
random processes continued
thermal radio emission from random layered media, appl. to Antarctic glaciers *(Russian)* 77−33106
thermometer errors analysis, thermoelectric, Pt-Rh 80−77783
thin walled elements, unbound quasistatic random thermoelastic fields, oscillations 80−69673
three-dimensional cubic lattice, random walk of particle, polymer chain config. approach 80−22294
three-dimensional lattices, random walks, probability of eventual return calc. by matrix method 78−6172
three-dimensional lattices with coord. number 4, random walk calcs., tracer diffusion 80−13001
tight-binding Green's functions for surfaces, thin films, and solid interfaces using random-walk theory 80−54753
time ordered operator cumulants, statistical independence and noncommutativity 80−31670
time series analysis and forecasting for ANL TREAT expts. on fast reactors 78−13289
track length type estimators, general formulation 78−37401
troposphere EM wave propagation, limitations on astronomical co-ordinate meas. via phase and fringe freq. 79−44375
truncated exponential density sequence, estimator asymptotic variance comparison 78−12539
turbulence in systems with small parameters 80−105571
turbulent hydrodynamically unsteady flow, unsteady random contact time distrib. 77−51036
two dimensional walks 80−95034
two-layer plate, random temp. fields and heat conduction, Monte Carlo method 80−33417
two-level system, kinetics at diffusion modulated local interactions *(Russian)* 79−2716
underwater ambient acoustic noise, compound random process 80−83699
underwater sound, amplitude and phase fluctuation periods for long-range propag. 77−50808
underwater sound, background ambient noise estimation from spectral anal. of time series 77−84046
underwater sound, random ocean current effects on acoustic transmission in isospeed channel 78−13840
universal time, random function determ. 80−46120
vibrating mechanical system, random parametric excitation, internal and combination resonances 77−72230
vibrations, statistical data digital processing method *(Japanese)* 80−64430
vibratory system, nonstationary, nonlinear, with arbit. random input, effect of feedback operation on probability distrib. 79−14316
viscoelastic cylinder with elastic shell, vibration when subjected to random forces 79−59941
viscoelasticity, stress/strain relationships, fluctuations 80−17802
walk, with arbitrary pausing time distrib., master eqns. 78−16736
walks with Markovian steps *(French)* 80−17868
wave propag., mean power transmission determ. by using cumulant expsn. 78−36841
wave propagation, probability distrib. at large depth in extended random medium 78−28959
wave propagation, random periodic structure, statistical properties 77−75392
wave propagation in random linear systems and temporal homogeneity 78−32691
wave propagation in random media, oceanic appls. 79−5987
wave propagation in random stratified media, statistical theory *(Russian)* 78−1157
wave propagation in randomly inhomogeneous media, quasi-optical parabolic approx., validity analysis 80−106422
wave reflected from randomly inhomogeneous layer description, by series satisfying causality condition 80−106420
wavefront dislocations, incoherent Gaussian random waves 78−16660
waves multiple scatter problems, use of physical concepts 79−21561
weak spherical shock waves, propagation from arbitrary piston motions 80−22204
Weiner-Einstein processes, Markov, maxima and first-passage-time statistics 80−68134
Yong Shan-Da Guan, Yunnan earthquake (May 19, 1974), main shock source multiplicity *(Chinese)* 79−12075
zero crossing time intervals, determ. via statistical analyser with visual display 77−37850
range finding *see distance measurement*
range of particles *see energy loss of particles*
ranging (sonar) *see sonar*
rapid transit systems
noise, conf., Derby, England, 1976, March 77−68309
rare earth alloys
see also cerium alloys; dysprosium alloys; erbium alloys; europium alloys; gadolinium alloys; holmium alloys; lanthanum alloys; lutetium alloys; neodymium alloys; praseodymium alloys; promethium alloys; rare earth compounds; samarium alloys; terbium alloys; thulium alloys; ytterbium alloys
amorphous, antiferromagnetism, mol. field approx. 78−80142
amorphous, cryst. field, nonaxial elec. field gradient 80−20138
amorphous, exhibiting Mossbauer spectra, mean mag. props. *(French)* 80−80489
amorphous, ferromag. state, non-axial elec. field gradient effect 80−75728
amorphous, high field magnetisation and magnetoresistance 78−72136
amorphous, mag. props., Mossbauer spectra 80−7225
amorphous, magnetoresistivity 78−95287
amorphous, random anisotropy antiferromag. model 78−95428
amorphous, random anisotropy antiferromag. model 80−20399
amorphous, random mag. anisotropy 80−20398
amorphous, study of hysteresis effects using Monte Carlo technique 79−1686
amorphous, transport props. 80−20152
amorphous, with random anisotropy axes, spin excitations in paramag. phase 80−80476
amorphous alloys, at. order effects on mag. props. 77−73006
amorphous alloys, mag. props. rel. to struct., review 79−15298
amorphous alloys, random anisotropy magnetism 80−65853
amorphous alloys, random mag. anisotropy, antiferromag., Monte Carlo calcs. 79−33471
amorphous random anisotropy ferromagnetism in pair approx. 79−47276
Anderson model susceptibility for high mag. impurity conc. 77−63069

rare earth alloys continued
compensation-point Hall effect temperature sensor 78−93679
conference, St. Pierre-de-Chartreuse, France (Sept. 1978) 80−12844
conference on rare earths and actinides, Durham, England (July 1977) 78−84115
configuration entropy and stability of intermetallic hydrides 77−84949
CPA calc. of mag. moments and transition temps. 78−84423
crystal field effects 78−67987
crystal field effects rel. to mag. props. 80−59933
crystal field excitations, linewidth 78−67988
crystal field interactions, book contrib. 80−39540
crystal field splitting in alloys with Cu_3Au struct. 80−54663
crystal field theory 78−84177
crystal-field excitations, line width 77−85183
cubic, direct coulombic contrib. of cond. electrons to cryst. elec. field 79−91005
cubic, exchange coulombic contrib. of cond. electrons to cryst. elec. field 79−95376
cubic, third-order mag. susceptibility, quadrupolar effects 79−99674
cubic intermetallics, mag. order effects on cryst. field parameter 77−40019
cubic intermetallics, self polarisation field at rare earth nuclei 80−15487
cubic rare earth intermetallics, direct Coulomb contrib. of cond. electrons to crystalline elec. field 77−76784
Curie temperature, high press. effects *(Japanese)* 80−20444
cylindrical rare-earth magnet repulsion dynamic characteristics *(Japanese)* 79−22878
diagrammatic Green function technique appl. to cryst. field systems with exchange 78−68130
dihydride epitaxial films, growth and struct. 79−37936
dilute metal-rare earth alloys US attenuation in mag. field, absorpt. mechanisms 79−15336
electrical resistance alloys, effect of lanthanide additions on oxidation *(Polish)* 79−79143
ferrimagnetic, magnetic torque near compensation point 79−33472
ferromagnetic properties, book contrib. 80−75725
germanides, X-ray emission, absorption and photoelectron spectra *(Russian)* 80−11509
heavy, mag. anisotropy *(Japanese)* 77−85444
heavy alloys, mag. ordering temps., Heisenberg exchange 79−61103
heavy binary alloys, press. effect on mag. props. *(Japanese)* 77−43835
high pressure studies, review 79−69193
high-energy magnetic materials, development, props., treatment procedures and testing *(Italian)* 80−54914
hydrides, magnetic properties, effect of hydrogenation 78−68210
hyperfine interaction, static and dynamical aspects, NMR investigation, review 79−91299
indirect magnetic interactions, NMR anal. 80−71193
intermediate valence, models for anomalous alloys 80−96827
intermediate valence systems, neutron scatt., review 80−49674
intermetallic compounds, containing d-transition metal, hydrogenated, magnetism 80−34609
intermetallic compounds, ferromagnetic properties, book contrib. 80−75726
intermetallic compounds, RM_5, low temp. sp. ht. 80−15259
intermetallic compounds of rare earths and non-mag. metals, struct. and mag. props., review 79−95377
intermetallic compounds of rare-earth and 3d transition metals, struct., props., review 78−10668
intermetallic cpds., cryst. chemistry, book contrib. 80−39010
intermetallics, mag. struct. 80−15698
intermetallics, neutron scatt., induced moment magnetism, high press. 80−15699
intermetallics, quadrupole interactions, magnetoelasticity 80−15489
ion exchange chromotography for Co and rare earth determ. in alloys for high energy magnets *(Polish)* 80−35606
iron intermetallic, O-stabilised, $R_{12}Fe_{32}O_2$, prep., struct. and mag. props. 77−8956
Kondo effect, review 79−69506
Kondo singularity, Anderson-Smith model 80−80479
Laves phase compounds, $R_xR_{1-x}Fe_2$, magnetostriction, anisotropy energy 80−25177
light-heavy alloys, resistivity, mag. contrib. to resist. and Neel temp. 78−51971
liquid, elec. resist. meas. 77−51718
liquid, electron charge transfer 77−1388
liquid alloys of actinides and lanthanides, thermodynamic props. 77−55366
magnetic, low frequency modes 78−88087
magnetic amorphous, nonaxial elec. field gradients 78−39285
magnetic and electronic phase transitions 79−87254
magnetic excitations, review of neutron scatt. data 80−60227
magnetic moments of rare earths in metallic environment 78−6515
magnetic phase diagram, mean field random alloy model 78−10684
magnetic properties, impurity effects, CPA calc. 80−44784
magnetic properties 78−84380
magnetic props., book contrib. 80−39759
magnetic structures and inelastic neutron scattering, review 79−69654
magnetic symmetry in alloys with $CaZn_5$ type struct. 79−24143
magnetically concentrated cubic Laves phase cpds., ESR 80−71174
magnetically hard materials, review 77−73051
magnetically hard materials, technology, development *(Polish)* 77−89973
magnetocrystalline anisotropy of rare earth intermetallics 77−8299
magnetoelastic waves, LF, theory 78−64250
magnetostrictive underwater sound transducers 80−19204
magnets, cylindrical, dynamic characts. of repelling force system, forced vibrations of one-degree-of-freedom system *(Japanese)* 80−4744
metallurgical appl. 77−12639
misch metal, improvement of Al alloy 51S, for space appl. 80−55466
mischmetal-based magnets, $MM_{1-x}Sm_xCo_5$, demagnetisation, temp. depend., 175 to 425K 79−78440
mischmetal-Co system, thermomagnetic analysis of intermediate phases 80−93115
mischmetal-Co-Cu-Fe-Mg, mag. props. 80−35353
mischmetal-Co-Cu-Mg, mag. props. 80−35353
mischmetal-cobalt, $MMCo_5$, polished, domain wall grooving, optical microscopy and SEM obs. 77−8334
mischmetal-Mg, appl. to H_2 storage 80−72093
mischmetal-$Ni_{5-x}Al_x$, ternary alloys, Al addition effects on structural and H_2 absorpt. props. 79−52761
Mischmetal-Ni, $MMNi_5$ substituted hydrides for H storage appls. 80−45791
mischmetal-Ni-Al alloys, H_2 absorpt.-desorpt. characts. 79−95168
mixed-valence effect, dilute limit model of impurity in d-band metal 77−47768
Mossbauer isomer shifts, book contrib. 79−87361
NMR, EPR, and Mossbauer effect, book contribs. 80−39883
NMR and EPR, cryst. field effects 78−56391
noble metal-rare earth, dil., magnetotransport props., theory 78−39097
parastriction, magnetoelastic and quadrupolar exchange coeffs. 79−19758
permanent magnets, physics and technology 80−20433
permanent magnets appl., development, properties, manufacture and appl. 77−8331
permanent magnets flux stability enhancement by thermomechanical treatments, gyroscope-based guidance systems performance improvement 80−50144
phase diagram, infra-rare earth systems, Kaufman approach 80−25657
phase structure, dimens. anal. 80−96470
phonons in systems with valence transitions 80−96611
photoemission, rel. to electronic struct., book contrib. 80−16157
quadrupolar interactions, parastriction 80−60400
$R^1_xR^2_{1-x}H_2$-H_3 systems, phase transitions 78−18767
R-Al_2, mag. coupling mechanism 79−4655
R-Co amorphous alloys, mag. compensation temp. 77−66277
R-transition metal, amorphous film, microstruct. 77−51619
R-Y, Neel temps., mag. susceptibility meas. 77−73025
random anisotropic magnetic alloys, multicrit. points 77−16091
rare earth alloys, phase transitions in complex mag. struct. *(Russian)* 78−72361
rare earth cobalt oriented materials as permanent multipole magnets 80−37925
rare earth-3d transition metal amorphous alloys, crystallisation behaviour 80−49116
rare earth-Co permanent magnet EM acoustic transducer design 77−19508
rare earth-Co system, spin reorientation and sp. ht. anomaly *(Japanese)* 79−47287
rare earth-Fe, intermetallic compounds, mag. props. *(Rumanian)* 78−92007
rare earth-transition metal (4f-3d) intermetallic cpds., mag. moment and mag. anisotropy 80−25107
rare earth-transition metal alloys, amorphous, anomalous low-temp. props. 78−91872
rare earth-transition metal alloys, H_2 absorption, effect on mag. props. 78−68231
rare earth-transition metal amorphous thin films, mag. potential distribution and wall velocity meas. 80−34725
rare earth-transition metal amorphous thin films for thermomag. recording 80−20403
rare earth-transition metal Laves phase, thermodynamic exam. of formation 77−1241
rare-earth-transition metal amorphous films, domain structure, technique for observation 78−91914
resistivity anomalies 78−19018
RMn_{12}, mag. interactions, mag. meas. and neutron diffr. 77−63103
singlet ground states, low freq. modes 78−68131
spin glass alloys, low field susceptibilities 78−84446
spin glasses, bulk mag. props. in amorphous and cryst. systems 80−20415
spin waves and excitations 78−84407
spin-reorientation transitions in rare-earth magnets, review 77−36073
stacking faults and magnetism, transform. effects 80−75840
steel, influence of rare earth additions on low-temp. fracture toughness *(Russian)* 79−52346
steel, low-alloy, fracture toughness and brittle fracture, S and rare earth additions effect 79−87720
steel, rare earth addition effects and behaviour, review *(Chinese)* 79−43257
steel, rare earth additions review 78−72786
steel, rare earth metal additions effects on mech. props. 78−52829
steel, stainless knife line attack phenomena, addition of rare earth metals 79−20289
steel, structural, effect of rare earth metals on cold temper brittleness 79−29202
steel creep resistant, rare earth metal effect on inclusion charact. *(Czech)* 77−86134
structural, electronic, and mag. props., book 80−36785
structural instabilities in alloys with CsCl struct. 80−24587
superconducting alloys with Cu_3Au lattice, cryst. chemistry and supercond. crit. temp. 79−86744
superconductivity, review 79−69621
surface effects on valence 78−91746
thermal properties, cryst. field effects 77−12072
Ticonal, effect of rare earth metals on mag. props., struct., and phase transformations 79−99732
transition metal alloy amorphous film, magnetostriction, dipolar mechanism 78−95502
transition metal alloys, amorphous, electronic and mag. props. 80−93093
transition metal alloys, amorphous, mag. anisotropy 77−66295
transition metal alloys, amorphous, mag. props., mean field anal. 79−4701
transition metal alloys, amorphous, struct. and mag. props., book contrib. 80−39818
transition metal alloys, amorphous films, radiation damage of domain struct. 77−66398
transition metal alloys, amorphous mag. props. 77−72985
transition metal alloys, binary system constitution diagram interrelations *(Russian)* 80−7535
transition metal alloys, cryst. and amorphous, mag. props. 77−73008
transition metal alloys, magnetic amorphous films for mag. bubble memories, materials review *(Polish)* 80−34715
transition metal alloys, RM_2, magnetostriction and struct. distortion 77−63248
transition metal alloys, $RM_2Si_{2-x}Ge_x$ and $RM_{4+x}Al_{8-x}$, magnetism and hyperfine interactions, magnetisation and Mossbauer effect studies 80−75892
transition metal alloys, RM_5, intermetallic compound $CaCu_5$ struct. crystal field pots. 78−43339

rare earth alloys continued
transition metal intermetallic permanent magnets, props. and technology, book contrib. 79−65696
transition metal intermetallics, H absorpt., Mossbauer studies 80−39987
transition metal-rare earth alloy, dilute limit model of mixed-valence effect 77−47768
transition metal-rare earth alloy, disordered, saturation mag. moment using CPA 77−20515
transition metal-rare earth alloy, H_2 absorpt. 77−35812
transition metal-rare earth alloys, amorphous, ferrimag., spin arrangements in large fields 80−75718
transition metal-rare earth alloys, CPA calcs., moments and transition temps. 78−52252
transition metal-rare earth alloys, disordered, magnetisation behaviour 80−71099
transition metal-rare earth amorphous alloy film, magneto-elastic tensors, pair model calcs. 78−80185
transition metal-rare earth film, amorphous, microstruct., TEM obs. 78−72018
transition metal-rare earth film, amorphous, microstruct. and magnetism 78−64230
transition metal-rare earth intermetallics, two sublattice system with high competing single ion anisotropies, model 80−39767
transition metal-rare earth alloy, dil., hyperfine fields, theory 78−68226
unstable valence, model for thermodynamic props. 77−69487
US attenuation, temp. and mag. field depend. 80−15195
valence, coordination no., polyhedral at. vols. 80−19742
volume magnetostriction, point charge cryst. field model 77−63254
widths of 5d energy bands in the heavy rare-earth metals 78−63971
Ag-R, dil., single and polycrystal, low temp. magnetostriction meas. 79−78501
Ag-rare earth alloys, Ag-rich, phase equilib. 80−45276
Al, thin film resistor, rare earth alloying effects *(Russian)* 79−78211
Al-Nb-R system, R=rare earth, X-ray diffr. obs. of phase equil. *(Ukrainian)* 77−32560
Al-rare earth alloys, granules, rolling to form foil, exam. 80−20825
Au-R, dil., magnetoresist., quadrupole scatt. effects 78−39096
Co-mishmetal-rare earth alloys for high energy permanent magnets, manufacture technology *(Polish)* 80−35132
Co-R, permanent magnet material development 78−91895
Co-R dilute alloys, mag. annealing, conc. depend. 78−35011
Co-R permanent magnet, grain alignment, metallographic method using eutectoid transform, of Co_5R 77−9003
Co-R permanent magnets, microstruct., TEM obs., magnetisation 78−91901
Co-R permanent magnets, processing and props., review *(Japanese)* 77−73049
Co-rare earth magnets testing method for mag. parameters 79−49260
Cr, thin film resistor, rare earth alloying effects *(Russian)* 79−78211
Cr-M, optimum alloying with rare earth metals, Ti, Zr, Hf, Nb, Ta 78−68651
Cr-R, dil., oxidation of Cr, effect of rare earth impurities 79−79160
Cr-rare earth alloy, calc. of phase diagrams, with immiscibility in liquid state, using thermodynamics *(Russian)* 79−20029
Cr-rare earth alloys, liquid phase, topology in diagrams of state *(Russian)* 80−54121
Cr-rare earth phase diagrams, model of ideal solns. *(Russian)* 77−55946
Fe, cast, cast Fe, spheroidal graphite, rare earth treated, nodularizing element distrib. *(Chinese)* 80−11653
Fe, cast, nodularization efficiency of rare earth alloy treatment, charging effect 79−91714
Fe, cast, rare earth-Mg, metallurgical and technological features, appl. in China *(Chinese)* 78−84851
Fe, magnetoelasticity and moment rot., US vel. calc. and neutron scatt. meas. 80−65992
Fe-Cr-Al, elec. heating alloy, effect of rare earth additives on quality *(Chinese)* 78−84825
Fe-R, dil., contact contribution to mag. hyperfine interaction of R impurities 77−80932
Fe-R alloys, mag. elastic properties 78−52331
Ga/rare earth systems, direct calorimetric exam. 78−84775
GaNiR, (R=Ce, Pr, Nd, Sm, Gd, Tb, Dy, Ho, Er, Tm, Yb, Lu, Y), struct. by X-ray powder method *(Ukrainian)* 80−10529
Gd-R alloys, phase diagram determ. 78−15366
Gd-rare earth metal, dil. resist. anisotropy due to impurities 77−62902
$(Gd_{1-x}R_x)(Co_{1-y}M_y)_5$, R=rare earth, M=Cu, Ni, Pt, origin of hyperfine fields acting on Gd, Mossbauer study 80−44967
Ge-rare earth alloys, nature of chemical interaction, X-ray emission, absorpt. and photoelectron study *(Russian)* 80−55261
H storage props. and characts. 80−21416
La-Gd(Tb,Dy,Ho,Er,Tm) alloys, FCC, supercond. transition temp. 79−4614
$(LaR)Sn_3$, dil., rare earth impurities, press. depend. of supercond. transition temp. 79−47184
Lu-R, dil., cryst. fields 78−80127
Lu-R, dil., elec. resist. 79−82578
Mg-R, dil., mag. susceptibility and magnetisation 80−15689
Mg-R dil. alloys, anisotropic magnetoresist. 77−62905
Mg-Zn-Zr rare earth alloy, mech. props., effect of microshrinkage during solidifaction 79−43234
Ni, thin film resistor, rare earth alloying effects *(Russian)* 79−78211
Ni-Cr-Co-R, oxidation depend. on alloying element, cohesion strength *(Russian)* 80−40587
Pr-R dilute alloy, low field magnetic props. 78−84443
R-3d alloys (3d=Mn,Fe,Co,Ni), magnetic properties 78−52231
R-Ag alloys amorphous, model calcs. of mag. props. 80−84616
$R-Al_2$ (R=Gd, Dy, Tb, Ho), cubic Laves phase compounds, exchange striction determ. 80−44895
R-Au, amorphous, mag. and transport props. 80−34605
R-Au, dil., Mossbauer exam. of mag. hyperfine field at ^{197}Au impurity 78−88244
R-Au, sputtering, negative ions origin and effects 78−60574
R-Au-In, Fe_2P type phases 77−70033
R-Co, 2-17 comp., permanent magnet props. 77−8348
R-Co, Curie temp. determ. 79−65672
R-Co, electron microscopy exam. 78−67722
R-Co, fault struct. and shear transform., stacking sequence notation 77−35571
R-Co, ferromagnet, first and second order transitions 80−34631
R-Co, permanent magnet production and props. 78−52309
rare earth alloys continued
R-Co, plastic magnet appl., anisotropic, based on moulding ferromagnetic powder material with plastics *(Japanese)* 80−60829
R-Co, powdered, fine grinding in gastight attrition mill 79−33967
R-Co films, extraordinary Hall effect meas. 78−6459
R-Co permanent magnets, generation mechanism of high coercive force *(Japanese)* 79−100269
R-Co systems, anomalous Hall effect and Kerr rotation obs. 77−11897
R-Cu, amorphous, mag. and transport props. 80−34605
R-Fe, amorphous, random anisotropy model, generalised mol. field calcs. 77−28345
R-Fe, amorphous thin film, crystallisation, TEM obs. 79−19483
R-Fe alloys, magnetoelastic props. *(Japanese)* 78−23316
R-Fe Laves phase alloys, sintering, magnetostrictive props. 77−16139
R-Fe rod, US resonance with large eddy currents 80−54933
$R-Fe_2$, Laves phase intermetallics, mag. ordering temps. by DTA 79−47283
R-Ga, phase diagrams 79−78932
R-Ga-Ni (R=rare earth), cryst. struct. investigation 80−33930
R-Pt, chem. shifts of L_3-absorpt. edge of Pt 79−78789
R-Pt alloys, cryst. struct. determ. 78−26491
R-transition metal, amorphous, mag. props. 77−16054
R-transition metal alloy, R_xT, cryst. struct. 77−55265
R-X-Sn, X=Rh, Ir, Ru, Co, cryst. growth and cryst.-chem. invest, supercond./mag. ternary cpds. 80−100777
R-Zn, ferromag., parastriction and magnetoelastic coeffs. 80−65996
R-Zn(Cd)(Hg), existence and cryst. struct. 79−77555
$R_{50}Ag_{50}$, amorphous, bulk mag. props., field, time and temp. depends. 77−89932
RAl_2, anisotropic magnetostriction, temp. depend. 80−39841
RAl_2, cryst. field volume magnetostriction calc. 79−8029
RAl_2, cubic Laves phases, prep. and phys. props. *(German)* 78−23075
RAl_2, exchange modification of cond. bands 79−82568
RAl_2 Laves phases, spontaneous cell distortion due to cryst. field, magnetoelastic consts. 77−63255
RAl_2, orbital and spin polarisations of cond. electrons 80−65791
RAl_2, ordered, NMR determ. of hyperfine fields 78−84180
RAl_3, long period polytypes, electron diffr., high resolution imaging 78−83781
R_2Al, mag. characts. 78−68183
RAu_3 (R=Gd, Tb, Dy, Ho, Er, Tm), mag. props. *(German)* 79−51761
$RAu_{3.6}$, ordering temps. and effective moments 78−60283
R_2Au, mag. characts. 78−68183
R_2Au, mag. props., 4.2-300K 79−7972
R_4Au heavy-rare-earth based alloys, anisotropy versus exchange 80−34624
$R_3Au_3Sb_4$ (R=Tb, Ho, Er, Tm), mag. suscept. meas., 4 to 300K 79−51742
RB_2, thermochemistry and stability 80−97723
RBe_{13}, ESR studies 80−108064
RBe_{13}, XPS, resist. and susceptibility study 80−71565
RBi, LCAO calc., electronic struct. *(Russian)* 77−39777
RCd_2, binding props. 77−58969
R(Co,M)$_5$, magnetisation reversal and high coercive force, domain boundary pinning *(Russian)* 77−8345
RCo_2, 'as cast', fibre texture, neutron diffr. exam. 78−3117
RCo_2 amorphous alloys, atomic order, mag. behaviour 78−19221
RCo_2, elastic moduli, 4.2-300K 78−52332
RCo_2, elec. resistivity, thermopower, X-ray struct. meas. 80−24874
RCo_2, H_2 reaction, thermal anal. 79−100434
RCo_2, Invar props. 79−56593
RCo_2, itinerant ferromag., magnetovolume effects 79−8038
RCo_2, itinerant metamagnetism, Van Vleck model 79−78297
RCo_2, itinerant system weak ferromagnetism 78−52191
RCo_2, Laves phase cmpds., elastic props. rel. to temp., mag. field 79−51834
RCo_2 metamagnetic transitions in internal fields 80−60272
RCo_2, spin wave spectra 78−56304
RCo_2, spontaneous vol. magnetostriction and thermal expansion meas. 77−12183
RCo_2: ^{57}Fe Laves compounds, easy magnetisation directions, Mossbauer meas. and cryst. field calc. 77−63168
RCo_2-Al, dil., nonmag. impurities effect on ordering temp. 78−84427
RCo_3 (R=Gd, Dy and Ho), effect of absorbed H_2 on mag. behaviour 79−33483
RCo_3, hydride phase synthesis, thermal stability and struct. 80−59438
RCo_5 and R_2Co_{17}, ferromagnetic intermetallic compounds, comminution charact. 77−12564
RCo_5, ferromag., thermomag. charact. in mag. field *(Russian)* 78−23273
RCo_5, high anisotropy origin, cryst. field contrib. 77−73020
RCo_5, mag. anisotropy, individual Co site contribution 79−78366
RCo_5, mag. moment orientation, anisotropic mol. field model 77−89950
RCo_5, magnetocryst. anisotropy 77−8299
RCo_5, R=Mischmetall, absorpt.-desorpt. charcts for H_2 77−89640
RCo_5 sintered magnets, texture determ. 79−100085
RCo_5, X-ray absorpt. spectra, electronic struct. 80−16122
RCo_5, X-ray chemical shift and atomic charges 77−44085
RCo_5-H(D) system, mag. orientation aftereffect 80−50148
$R_{1-x}Co_5$, amorphous alloys, thermal stability, elec. cond. enthalpy 80−100172
R_2Co_{17}, ^{59}Co NMR obs. of hyperfine fields and mag. moments 77−20726
R_2Co_{17}, formation of mag. anisotropy role of rare earth ions *(Russian)* 78−76238
R_2Co_{17}, mag. anisotropy 78−84414
R_2Co_7, polymorphism of Ce subgroup alloys, eutectic decomposition *(Russian)* 80−66504
$R_{69}Co_{31}$, amorphous, mag. props. 80−84590
RCoAl, mag. props. 78−2659
$RCo_{5x}Cu_{5-5x}(Ni_{5-5x})$, narrow Bloch walls, magnetisation, 4.2K 77−8333
$R(Co_{1-x}Ni_x)_5$, single cryst., mag. props., mag. reversal 77−85489
RCo_2(R=Ho,Tb,Pr,Nd), sublattice magnetisation, powder neutron diffr. meas. 79−19725
$RCo_2Si_2(Ge_2)$, $ThCu_2Si_2$ type, lattice parameters 78−51469
RCu_2 intermetallic compds., single crysts., mag. props. 80−54892
RCu_2, metamag., mag. props. 79−87242
RCu_2, metamag., mag. props. 79−87243
RCu_x, mag. props., 4.2 to 200K 79−87233
RCu_4Ag, mag. props. and cryst. struct. 77−20562

rare earth alloys continued
RCu_4Ag, struct. study 78−30587
RCu_4Al, struct. study 78−30587
RCu_4Al_8, mag. struct. and interactions 80−25092
RFe_2 (R=Tb, Dy, Ho and Y) crit. phenomena, Mossbauer exam. 78−52403
RFe_2, elastic vs. magnetoelastic anisotropy 78−68347
RFe_2, electronic heat capacity coeffs. 80−39787
RFe_2, H_2 reaction, thermal anal. 79−100434
RFe_2, highly magnetostrictive, isotropy breaking magnetoelastic behaviour 78−72386
RFe_2, Laves phase compounds, magnetostriction anisotropy 77−63250
RFe_2, Laves phase intermetallics, ordered and paramagnetic phases, mean field exchange consts. 80−50084
RFe_2, mag. props. changes due to H_2 absorption, unit cell vol. 77−63178
RFe_2, magnetomech. coupling and Young's modulus 78−84472
RFe_2, magnetostriction in polycryst. samples 77−73065
RFe_2, magnetostriction studies, book contrib. 80−39846
RFe_2, magnetostrictive, elastic props. 78−84469
RFe_2, magnetostrictive, magnetoelast. props, book contrib. 80−75838
RFe_2, spontaneous magnetoelastic distortion, X-ray diffr. expts. 77−63253
RFe_2, temp. depend of coercivity 79−61185
RFe_x, amorphous alloys, atomic order, mag. behaviour 78−19221
R_2Fe_{17}, and $R_2Fe_{17-x}Ni_x(Co_x)$, mag. anisotropy and hyperfine interactions 77−8298
R_2Fe_{17}, Invar props. 79−56593
R_xFe_{1-x}, amorphous film, cosputtered, struct. and mag. props. 78−60323
R_xFe_{1-x} amorphous film, crystn., TEM obs. 79−87019
R_xFe_y, conc. depend. of Fe moments 78−56413
RFeAl, scatter order cpds., mag. props. 77−51891
RFe_4Al_8, mag. props., Mossbauer spectra, ordering effects 77−63179
RFe_2Ge_2, magnetisation and Neel temp. 77−8310
$R(Fe_{1-x}Mn_x)_2$, phase struct., mag. and Mossbauer meas. 77−20563
$R(Fe_xRh_{1-x})_2$, mag. props., Mossbauer spectra 80−25108
RFe_2Si_2, mag. props. 4.2 to 950K 77−20544
$R_2Fe_4Si_9$ and $RFeSi_3$, cryst. struct. and mag. suscept., temp. depend. *(Russian)* 78−34957
$RFe_2Si_2(Ge_2)$, $ThCu_2Si_2$ type, lattice parameters 78−51469
RGa, mag. props., 4.2-350K 77−63230
RGa_2, AlB_2-type struct., electron transfer, bonding, heat of form. theory 78−92499
RGa_2 intermetallics, mag. structs. 78−84394
RGa_2, mag susceptibility, 1.5-300K and Neel temp. 78−68184
RGa_2, magnetic ordering and exchange interactions 80−39779
$RGe_{2-x}Ni_x$ phases with AlB_2-type struct., lattice parameters 77−24292
RIn_3, ^{111}Cd quadrupole coupling consts. and valence states, PAC meas. 77−48102
R_2In, R_3In, R=Gd, Tb, Dy, Ho, Nd, mag. props. 80−108009
$R_{0.2}La_{0.8}Ni_5$ (R=Er,Y,Gd,Nd,La,Th,Zr), H_2 storage appl., desorption isotherms depend. on d-bandfilling 78−18912
RM_2, (M=Fe, Co, Ni), magnetism, review 80−20365
RM_4Al_8 (M=Cr, Mn, Fe, Cu), magnetism and hyperfine interactions 80−25256
RM_2X_2 (M=Rh,Pd,Ag,Ir,Pt,Au; X=Si,Ge), cryst. struct. 80−1964
RMg, magnetisation and neutron diffr. meas. 77−63105
RMg_2, cryst. and mag. props., ordering 78−68185
$RMnGe_2$, magnetisation, 4.2-1200K 77−8285
RMn_2Ge_2, cryst. struct. 78−59782
$RMnSi_2$, magnetisation, 4.2-1200K 77−8285
RMn_2Si_2, cryst. struct. 78−59782
RNi_2 (R=Gd, Tb, Dy, Ho or Er), Mossbauer effect of ^{57}Fe 77−69743
RNi_2, H_2 reaction, thermal anal. 79−100434
RNi_3 amorphous alloys, mag. and transport props. 79−42513
RNi_4Al, Hz absorpt. and cryst. struct. of hydride 78−34487
$RNiSi_3$, mag. susceptibility, 80-1200K *(Russian)* 77−66281
R_3Os, cryst. struct. 80−96475
R_3Pd_4, mag. props. 77−47980
RPt, (R=Gd, Tb, Dy, Ho, Er, Tm), structs. and mag. props. 80−50069
R_2Pt, mag. susceptibility meas., mag. transitions obs. 80−60222
R_3Pt_4, cryst. struct. and lattice const. determ. 77−55266
RPt_2Si_2, struct. determ. 77−89407
RRh_xSn_y, synthesis, supercond. and mag. props. 80−100547
R_3Ru and R_5Ru_2, cryst. struct. 80−1965
RSb, (R=Er, Ho, Dy, Tb, Nd, Gd), mag. props., hydrostatic press. depend. 77−80918
RSn_3, ^{111}Cd quadrupole coupling consts. and valence states, PAC meas. 77−48102
RT_6Al_6, T=Cr, Mn, Fe, Cu, cryst. struct. 80−107110
$R_xTb_{1-x}Fe_2$ (R=Gd, Sm, Dy, Ho), props. of near magnetostrictive materials 77−51934
$R_xTb_{1-x}Fe_2$, Laves phase alloys, magnetostriction *(Russian)* 77−51932
$R_xY_{1-x}Pd_3$, magnetostriction due to rare earth impurities 79−4714
RZn, ordered, NMR determ. of hyperfine fields 78−84180
RZn_{12}, mag. props. and structs. 78−84393
RZn_{12}, mag. struct. and interactions 80−25092
Sn-R, dil. liq., elec. resist. and mag. susceptibility 78−43350
Y-R, dil., cryst. fields 78−80127
Zn-R, cubic ferromag. single crysts., mag. and magnetoelastic props. 79−15332
$ZnY_{0.95}R_{0.05}$ resist. anisotropy due to impurities 77−62902

rare earth compounds
see also under the individual compounds e.g. cerium compounds
see also rare earth alloys
actinide oxide/rare earth oxide system, high temp. vaporization, valence effects 79−99309
activated orthovanadates, spectroscopic props. 77−16363
alkali metal rare earth double metaphosphates, vibr. spectra, rel. to struct. 80−34905
aluminate film coatings, electrophys. props. w.r.t. prep. technology 80−60781
aluminates, effects of roasting in reducing and oxidizing media on elec. props. 78−52736
aluminates with perovskite structure, elasticity meas. to 6 kbar 77−51428
amorphous films for mag. bubble memories, materials review *(Polish)* 80−34715
Anderson model susceptibility for high mag. impurity conc. 77−63069
arsenides, chemical bonding and structural features, coherent alloying theory 80−107101
beryllogallates with melilite struct., synthesis 77−81236
binary, regression eqns., for calc. props. from electron struct. 80−39498
binary insulating compounds, exchange interactions, paramag. susceptibility expts. 80−60177
bismuthides, chemical bonding and structural features, coherent alloying theory 80−107101
bond lengths in oxygen and halogen compounds of d and f elements 79−37653
borides, higher types, phys. props. and electronic struct., group orbitals-LCAO calcs. 80−20077
borides, mag. props., book contrib. 78−47978
carbonates, determ. by mass spectrometric complexometric method 80−3442
carbonates, standard ht. of formation determ. 78−53239
chalcogenide, charge transfer, influence of cryst. field 79−99516
chalcogenides, compositions, props., computer prediction 79−42429
chalcogenides, cond. mechanism and thermoelec. efficiency 79−38110
chalcogenides, cryst. field splitting, press. depend. 80−24852
chalcogenides, resonant Raman scattering via virtual exciton 80−71412
chlorides, doubly degenerate E-phonons, mag. field splitting 77−43297
chlorides, glass transition temp. meas., inner-sphere coordination number change effect on soln. props. 80−83239
chromates (lanthanide series), paramag. state, crystalline elec. field calcs. 78−39074
chromite based electrode material development for MHD generators 80−84893
complex, $R(DMMP)_6(ClO_4)_3$ and $R(TBPO)_4(ClO_4)_3$, synthesis and characterisation 77−23498
conference, St. Pierre-de-Chartreuse, France (Sept. 1978) 80−12844
coordination polyhedra classification 77−4088
crystal field effects 78−67987
crystal field effects on EPR and NMR 79−4736
crystal field interactions, book contrib. 80−39540
Curie constant rel. to valence bond strength 80−60251
dicarbides, solid solns., phase transformation, strain energy 78−51672
dielectric thin films from vaporisation by cathode ray and HF ion-plasma methods 77−77380
dihalides, rare earth valence changes, rel. to stability and enthalpy of formation 79−91000
dihydrides and dideuterides, electronic and mag. props. 80−25260
dodecaborides, magnetic susceptibility temp. depend., 90-1200K 80−20374
double nitrate, Van Vleck temp. independent suscept. 78−43555
double orthophosphates with alkali metals, conc. depend. of luminesc. props. 80−100673
double orthophosphates with alkali metals, spectroscopic obs., struct. and chem. nature 80−100674
double tungstates with Cd, scheelite struct. 78−44103
electron-phonon interaction influence on electronic phase transitions *(Russian)* 78−47743
electronic phase transitions, f-level broadening 77−47773
enneaaquo rare-earth ethyl sulphates, cryst. field parameters, angular overlap model 79−56171
ESCA spectra, intense shake-up satellites, model 78−50589
ethyl sulphate nonahydrate:Gd^{3+}, high-precision EPR of cryst. 79−69717
ethyl sulphate nonahydrates:Gd^{3+}, $g_{\parallel}$, EPR obs. 78−35031
ethyl sulphates:Ce^{3+}, Kramers ions, virtual phonon exchange, field theoretic formalism 80−20137
ethyl sulphates, sp. ht., susceptibility 79−24129
exchange field and Fe and Co moments 77−1551
ferrite aluminates, prep. 77−85970
ferrite garnets, phase transitions, field-induced spin-orientational 80−75767
ferrite-garnets, compensation temp., rare earth ion influence 79−51775
fluoride doped ZnSe film, electrolum, meas. 77−16397
fluorides, antirefl. laser window coatings at 10.6 μm 77−61963
fluorides, interband, collective and atomic (p,d) excitations, Z-160 eV, fast EELS 80−93443
formates, second optical harmonic generation 80−43403
garnet, RIG, Faraday rotation from empirical scaling model 77−81083
garnet, RIG, spectra calc. using exact microscopic Hamiltonian 77−8553
garnet preparation, novel Li_2MoO_4-$R_2(MoO_4)_3$ flux system 77−48359
garnet single crystal films, synthesis and props., reviews 78−48013
garnet substrate crystals, substituted, and LPE films, for magneto-optic appls. 78−31351
garnet thin films, macroscopic mag. props., magneto-optical expts. 80−46764
garnets, chemical site preference of rare earth ions 77−68936
garnets, cryst. field depend. on coordination of dodecahedron 79−73475
garnets, Debye charact. temp. and reciprocal lattice consts. 80−29144
garnets, field depend. magnetocryst. anisotropy 77−69543
garnets, prep. and props. book contrib. 80−44193
garnets, preparation, substrate and epitaxial layer surface quality control, X-ray topography *(German)* 77−55432
geochemistry and mineralogy, book contrib. 80−46157
germanates, flux-grown, X-ray topography 80−64939
germanates, R_2O_3-GeO_2 system cpds., physicochem. characts. 80−97469
germanides, X-ray emission, absorption and photoelectron spectra *(Russian)* 80−11509
group IIIa dihydrides, structs. and stabilities 80−107146
gyromagnetic resonance, study of magnetism *(Danish)* 79−15359
halide vapour, discharge, potential fusion laser systems 78−63074
halide vapours, discharge spectra, fluoresc. lifetimes meas. 79−27025
halides, prep. and props., book contrib. 80−54211
halides and oxides, stability study, energy difference between trivalent and tetravalent metal states 78−79553
handbook 80−41957
heavy lanthanide perchlorator, aq. solns., US vel. and solvation numbers meas. 79−19319
hexaboride single crystals, microhardness meas. 80−21087
hexaborides, electron fractography 77−8906
hexaborides, low work function thermionic electron emitters, props. 79−33884
hexaborides, obtained by melting, micromech. props., rel. to bonding 80−21082
hexaborides, powders, evaporation 77−89535

rare earth compounds continued
hexaborides, thermoelectronic props. rel. to surface state *(French)* 79−69950
hexagonal, cryst. field effect in thermal expansion 80−49390
hexahalometallate (IV) complexes, A_2MX_6, A=alkali metal or ammonium, M=lanthanide or actinide, X=F or Cl, lattice energies and thermochem. 79−60307
high pressure studies, review 79−69193
high temperature paramagnetic-supercond. phase transitions, mag. cell symm. *(Russian)* 79−78255
hydride films, prep., struct. and props., general review 80−54556
hydrides, form. by rare earth reaction with H_2O vapour 80−76504
hydrides, magnetic properties, effect of hydrogenation 78−68210
hydrides, magnetic props., book contrib. 79−82754
hydrides, Mossbauer studies, book contrib. 79−82906
hydrides, props., book contrib. 80−45291
hydrides, rare earth and intermetallic, electronic and mag. props., Mossbauer study 80−34830
hydroxides, cryst. field parameters, ang. overlap model calcs. 77−89738
hydroxides, heat capacity from near 5 to 350K, lattice and Schottky contribs. 80−49374
intermediate valence, models for anomalous cpds. 80−96827
intermediate valence compounds, mag. susceptibility and sp. ht., mean-field theory of periodic Anderson model 78−47937
intermediate valence induced by alloying, CPA calculations 78−67986
intermediate valence systems, neutron scatt., review 80−49674
intermediate valency, review 79−91001
iodates, crystallographic and nonlinear optic data 78−6044
ions, 4f photoelectron spectral intensity, relativistic calc. 79−54816
ions in soln. radiationless energy transfer and complexation processes 79−10144
kaolinite rare-earth complexes, relax., molar free energy of activation for dipole relax. 80−88919
Kondo effect, review 79−69506
Kramers light rare earth compounds, temp. renormalised spectrum of mag. excitations, cryst. field level ordering 77−20516
lanthanide(III) complexes, f-f transition intensities, general theory of solvent effect 80−18811
lanthanide complex, struct. and equilib. by time resolved Eu(III) spectrosc. 80−78736
lanthanide ion bound to macromol., struct. and equilib. by time resolved Eu(III) spectrosc. 80−78736
lanthanide ion complexes, lanthanide-induced NMR shifts, temp. depend. 77−68061
lanthanide ion complexes, octahedral, f-f transition intensities, vibronic coupling model 78−58659
laser channels, 3μm, in inorg. materials with R^{3+} ions 80−97306
laser materials, linear conc. quenching of luminesc. 79−31908
lead apatites, $Pb_{10-2x}R_xM_x(PO_4)_6Z_2$, M=Na or K and Z=F or Cl, cryst. struct. and IR spectra 80−107167
ligand fields calcs., strong and intermediate fields, tensor algebra 80−42922
ligand ordering parameters, nephelauxetic and spectrochem. series 77−76777
mag. field depend. of polaritons 79−33246
magnetic, low frequency modes 78−88087
magnetic moment and valence fluctuations 78−23244
magnetic octupole scatt. of neutrons, quadrupole excitation creation 77−47977
magnetic properties, cryst. field theory 78−27006
magnetic properties, cryst. field theory 78−27007
magnetic structures and inelastic neutron scattering, review 79−69654
magnetic superconductor, appl. of reformulated boson theory to mixed state 80−7050
magnetic susceptibility in intermediate valence state 78−14928
magneto-optical effects rel. to 4f electron excitation energies, XPS 77−52222
metal-rich compounds, struct. and props. 78−95045
metallic, indirect multipole interactions 77−4308
metaphosphates, glasslike, spectral intensity, effect of number of 4f electrons 78−84602
Mischmetal-Ni, $MMNi_5$ substituted hydrides for H storage appls. 80−45791
mixed ferrite-chromites, mechanism of polarisation of rare earth ions 79−42740
mixed valence compounds, charge dominated fluctuation props. comparison, mag. moments and ordering 80−54659
mixed valence compounds, spin dynamics, mag. neutron scatt., Mossbauer effect, XPS studies 80−39786
mixed valence state, conduction band struct. 80−103624
mixed valence systems, spatial correlations in simple model 79−60770
mixed valence systems, spatial correlations of rare-earth ions 79−19560
mixed valent, renormalisation of transversal phonons 79−90749
mixed valent compounds, lattice dynamics 79−73268
molybdates, cryst. growth, cryst. chem., and phys. props., book contrib. 80−44194
molybdates, isotope exchange with $C^{18}O_2$, 300-500°C 77−63884
molybdenum chalcogenides, Chevrel phase correlation between struct. and supercond. transition temp. 80−7023
monazites, search for superheavy elements 80−36297
monobismuthides, thermal expansion, thermal cond., 300-900K 78−91453
monochalcogenides, 4f-6s excitation energy, metallic and insulating elec. props. 80−44603
monochalcogenides, electronic transitions 77−43496
mononitrides, heat of vaporisation and standard heat of form. 77−52664
monophosphides, K-emission bands, electronic struct. 78−15250
monopnictides, Knight shift systematics 78−43661
monosulphides, vaporisation thermodynamics and dissoc. energy obs. 78−67822
monoxide, flame absorption spectra, dye laser amplified absorption method 77−29075
Mossbauer isomer shifts, book contrib. 79−87361
multipolar interactions, evidence and origins 80−59935
mutual solubility of LaN, CeN, NdN and GdN *(German)* 79−19374
neutron scatt. cross-section, mag. inelastic, rel. to cryst. field splitting 77−55659
nickelates, form. conditions and props. 80−21270
niobate based ceramics, synthesis, struct., elec. cond., mag. props. *(Czech)* 80−45259
niobates, pyrochlore structure, synthesis and props., 79−11533
rare earth compounds continued
NMR, EPR, and Mossbauer effect, book contribs. 80−39883
non-metallic compounds, handbook 80−51972
nonmetallic compounds, indirect spin-spin coupling, models 80−80238
optical side-bands, theory in cryst. with cooperative Jahn-Teller phase transition 77−1398
orbit-lattice interaction empirical parameter determ. 78−38799
organic molecules, complexes with rare earth ions, energy transfer in strong donor solvents 79−54930
orthoferrite, domain wall crit. vel. 79−38354
orthoferrite, phonon slowing down of domain wall *(Russian)* 79−33503
orthoferrite, second-order reorientation transition, NMR signal relax. 77−90066
orthoferrite, stripe domain struct. near spin-reorientation points, Landau phase transition theory 77−24707
orthoferrites, domain wall dynamics 80−65957
orthoferrites, hyperfine interaction anisotropy, NMR study *(Russian)* 80−66052
orthoferrites, mag. anisotropy in cryst. field approx. 80−60241
orthoferrites, muon states, local mag. fields 80−75911
orthoferrites slow neutron elastic scattering, domain boundary observation *(Russian)* 79−82811
orthophosphates, gas transport reactions 79−1819
orthophosphates, high-temp. treatment and formation of oxyphosphates *(French)* 77−44199
orthotitanates and orthovanadates, interrelationship between cryst. struct., IR spectra and physiochem. props. 77−24835
orthovanadates, magnetic insulators, indirect exchange interactions, polar model study 78−88110
orthovanadites, X-ray diffraction investig., unit cell parameters 77−27859
oxalates, struct., IR absorpt. and Raman spectra *(French)* 80−32714
oxide cermets with Re, prep. and props. 78−27466
oxide containing systems, highly refractive, phase equilib. and metastable phases 80−97467
oxide film, transmission of refl. spectra, opt. consts. and parameters 79−95864
oxide films, non-stoichiometric phases 79−7755
oxide films, optical absorpt., refractive index, band gap and zone struct. *(Russian)* 78−76544
oxide mixtures, determ. of individual rare earths using ion microanalyser *(Japanese)* 78−88683
oxide powders and mixtures, hydrostatic pressing, density and hardness variation 79−70029
oxides, absorption spectra and energy levels of trivalent ions 77−63420
oxides, binary, struct. and props., book contrib. 80−45292
oxides, catalysts for reduction of NO by CO 77−81422
oxides, core electron binding energies, XPS study 77−48309
oxides, Cu and Fe impurities at. absorpt. determ. 79−87905
oxides, determ. by mass spectrometric complexometric method 80−3442
oxides, determ. using ion microanalyzer *(Japanese)* 78−23987
oxides, dielec. const. and loss at low temp. 80−93229
oxides, electron beam evap., optical and mech. props. 77−79907
oxides, electronic structure rel. to valence, chem. bonding 80−54601
oxides, electronic transitions, obs. by inelastic electron tunnelling spectroscopy 79−3511
oxides, energy levels of trivalent ions 77−62874
oxides, from reactive evaporation, struct. and polymorphic transform. 79−51441
oxides, interband, collective and atomic (p,d) excitations, Z-160 eV, fast EELS 80−93443
oxides, microhardness anisotropy of single cryst. *(French)* 77−52489
oxides, mixed, phase relations and struct., book contrib. 80−45293
oxides, occurrence in sunspots and cool stars 78−85933
oxides, phase transition hysteresis, thermodynamic model 77−76570
oxides, polyatomic gaseous atomisation energies and stand. ht. of formation determ. 77−54622
oxides, segregation study by electron energy-loss spectroscopy 80−79953
oxides, TEM lattice images *(French)* 78−26397
oxides, thermodynamic props. and high temp. chem. behaviour, comparison with actinide oxides 79−100127
oxides, thin films, in MOS struct., elec. props. and band struct. 80−7013
oxides, very-short-lived radiation effects following Coulomb excitation 79−60411
oxides, XPES final state struct., 4d electron ionis. 78−25616
oxides, XPS, 4f-electron ionisation 77−14493
oxides, XPS 80−87170
oxides and fluorides, thermal expansion and MP correl. 77−47605
oxides films, crystallisation, electron microscope obs. 79−15034
oxides in binary system with WO_3, phase relations 79−8290
oxydiacetate, spectra, energy level patterns 79−38561
oxydiacetate crystal, opt. rot. dispersion 77−36193
oxyfluorides, mag. susceptibility, 2-1000K *(Russian)* 79−82750
oxyhalides, thermochromic luminescent mats. *(Russian)* 78−48230
oxymolybdates, growth from soln., struct., props. 77−28705
oxymolybdates and oxytungstates, R_2MO_6, spectroscopic props. and crystallochem. laws 77−36215
oxyphosphates, IR and Raman spectra, vibr. assignments, cryst. struct. characts. 80−97258
oxyphosphates, x Ln_2O_3.y P_2O_5, synthesis, characterisation and thermal stability 80−16256
oxysulphides, strengthening covers in light radiography *(French)* 78−41396
oxysulphides, thermochromic luminescent mats. *(Russian)* 78−48230
oxysulphides and oxyhalides, Tm^{3+}, Tb^{3+}, Eu^{3+} activated, thermochromatic luminophors, lumines. spectra rel. to temp. 79−56849
paramagnetic, Faraday and Cotton-Mouton effects for acoustic phonons 78−52476
paramagnetic phase, mag. dynamics of singlet-triplet system 79−91203
parvalbumins, Ca-binding, lanthamide-substituted, of muscle, ^{13}C NMR obs. 79−96516
perchlorates, glass transition temp. meas., inner-sphere coordination number change effect on soln. props. 80−83239
perchlorates, in solvents with high dielectric const., spectra and struct. 79−65860
periodicity of atom props. and inorganic cpd. props. 80−96586
perovskite type compounds, electrode catalysts for cathodic reduction of O_2 79−29371
perovskite-like oxides, high-pressure series, rel. between structure and physical properties 78−51493
perovskite-like oxides, synthesis, struct., elec. props. 80−65554

rare earth compounds continued
perovskites, prep. and props. book contrib. 80−44193
phonons in systems with valence transitions 80−96611
phosphates, penta-, tetra-, ortho-, Eu activated, electronic-vibr. spectra rel. to struct. 79−56850
phosphor development survey 78−6781
phosphor intensifying screen speed gain 78−7447
phosphors, Ho^{3+} and Er^{3+} doped, active layer effective thickness calc. *(Russian)* 79−43039
photoemission, Fano-resonances, surface and bulk effects 80−97405
photoemission, rel. to electronic struct., book contrib. 80−16157
phthalocyanine solutions, bleaching by ruby laser beam 78−30030
pnictide, effective cryst. field 77−63050
pnictides, Ab_2X_2, A=rare earth, B=Fe, Co, Ni, X=P, As, Sb, cryst. struct. 78−51502
pnictides, charge transfer, influence of cryst. field 79−99516
pnictides, cryst. field splitting, press. depend. 80−24852
pnictides, cubic Van Vleck compounds, paramag. fluctuations, ESR or NMR relax. 77−66420
pnictides, mag. props. 78−72325
pnictides, phase diagram for cubic model in Kikuchi cluster variational method 79−35639
pnictides, prep. and props., book contrib. 80−54212
polisher powders, comparative analysis 79−50453
polymorphic phase diagrams, as function of pressure exam. 79−8289
porphyrin complexes, intramol. energy migration, mol. luminesc. 77−3412
pressure effect on mag. ordering temp. 80−100584
R complex, 1,2-naphthalocyanine-rare earth ion, electronic excitation deactivation mechanism 79−85988
R-Fe garnets, solubility model in PbO/B_2O soln. 79−46807
radiographic intensifying screens, sensitivity to scattered radiation 77−77970
Raman light scatt., phonons and valence fluctuations, review 77−63415
rare earth complexes, paramag., and shift reagents, NMR, book contrib. 80−53023
rare earth molybdates, mag. susceptibility meas. 79−69650
rare earth titanates, $R_2Ti_2O_7$, synthesis and phys. props. 79−43128
reaction processes in solid phase *(French)* 78−30756
reduction in molten halides 77−29088
RIG, garnets, contribution of Fe ions in noncubic magnetostriction from crystal field model 78−43622
salts, phonon field contrib. to g-shift, symm. restrictions 77−55500
scandate film coatings, electrophys. props. w.r.t. prep. technology 80−60781
selenides, cryst. struct., book contrib. 80−54210
selenides of yttrium subgroup, paramag. props. *(Ukrainian)* 77−32153
selenides of yttrium subgroup, powder prep. conditions and energy of optical transitions 77−63581
semiconductors, studies in Soviet Union, review 80−96875
sesquioxide films, prep., struct. and props., general review 80−54556
sesquioxides, exchange interactions, paramag. susceptibility expts. 80−60177
short-arc lamp for Super 8 cinefilm projector using rare-earth halogens 80−62747
singlet ground states, low freq. modes 78−68131
Slater-Koster tables for f electrons 80−44461
solutions, absorpt. and fluoresc. spectra, book contrib. 80−45112
spin glasses 80−50132
spin-reorientation transitions in rare-earth magnets, review 77−36073
spinless periodic Anderson model with phonons, appl. to mixed valence systems 78−84153
Sternheimer antiscreening and finite ligand size, in lanthanide ions 79−19561
stoichiometric, reson. energy transfer 79−99930
structural, electronic, and mag. props., book 80−36785
sulphate:Gd^{3+}, hydrated, EPR spectra, host lattice effects 78−95516
sulphide, polymorphic transforms. on impact compression 77−47575
sulphides, cryst. struct., book contrib. 80−54210
superconducting pairing, mag. ordering effect 80−15641
superconducting phases, phase stratification *(Russian)* 79−42685
superconductivity, phenomenological study 78−43512
superconductivity, review 79−69621
superconductors, upper crit. fields in the dirty limit, depend. on intra- and interaction exchange interactions 79−56461
tellurate perovskites, $M_2^{2+}Y^{2+}TeO_6$, M=Ba,Sr,Ca,Cd, Y=Ba,Sr,Ca,Cd,Zn,Mg, luminesc. on activation by Eu^{3+}, Tb^{3+}, Dy^{3+}, Er^{3+} 79−4838
tellurides, cryst. struct., book contrib. 80−54210
tellurides, electron density distrib. from Mossbauer spectra 78−23374
ternary, superconductivity and ferromagnetism 79−69617
ternary, theory of superconductivity 79−73628
ternary borides, coexistence of magnetism and superconductivity 79−73630
ternary compounds, supercond. and antiferromag. coexistence 80−25030
tetraborides, electronic structure and bonding determ. from X-ray spectra 77−59646
tetraborides, theory of metamagnetic transitions *(Russian)* 78−95436
theoretical chemistry, book contrib. 80−42919
thiohafnates, thermal stability and oxidation products in air 79−83346
titanates, $R_2Ti_2O_7$, synthesis and phys. props. 79−43128
titanoniobates, $RTiNbO_6$, physicochem. investig. 77−47422
titanotantalates, mag. susceptibility, temp. depend., 78-293K 77−36050
transition metal-rare earth hydrides, magnetic props., book contrib. 79−82754
trichloride hexahydrates, Tb to Yb, EPR of Gd^{3+}, spin Hamiltonian parameters 77−36128
trifluoride film, optical props., 5 to 34 eV 79−38687
trifluorides, bomb calorimetric determ. of enthalpy of formation 80−50879
trifluorides, MS Xα electronic struct. calc., inner shell photoelectron spectra 77−10594
tris-dipivaloylmethide chelates, XPS, 4f-electron ionisation 77−14493
trivalent, hypersensitive transitions, intensity parameters, charge transfer mixing 77−55498
tungstates, elec. cond. and thermoelec. power meas., band theory 80−20191
tungstates, mag. susceptibility determ. 77−4495
tungstates and molybdates, A_2BO_6 type, elec. cond. and Meyer-Neldel rule 78−72157

rare earth compounds continued
tungsten bronzes, search for coexistence of superconductivity and long range mag. order 79−38226
unstable valence, model for thermodynamic props. 77−69487
valence changes, book contrib. 80−39533
valence changes of rare earth elements 79−91000
valence fluctuation type, replicate core level XPS probe 80−25521
valence fluctuations, electron-phonon coupling effect 80−20134
valence instabilities, rel. to electronic structure of $GaMn_3(C_{1-x}N_x)$ *(French)* 80−34596
valence transitions and intermediate valence states 79−42496
valency transition, pseudospin model 77−72819
vanadites, X-ray fluoresc., IR and UV spectra 77−77206
vitreous dielectric, electronic energy transfer to impurity OH^-, luminesc. kinetics *(Russian)* 79−47509
X-ray intensifying screens for pulsed X-ray sources, calibration in 15-70 keV energy range 77−26446
X-ray lines, K-series, shift associated with valency change and with isomorphous phase transitions 79−47553
XPS, intermediate valence states 79−33887
XPS satellites, screening of 3d holes 78−76586
Y-type zeolites, ion exchanged, XPES obs. 80−83421
zirconate film coatings, electrophys. props. w.r.t. prep. technology 80−60781
zircons, Jahn-Teller cooperative phase transition, crossover effects 80−88316
$AgR(WO_4)_2$, polymorphism, struct. of α,β and β' phases 77−31627
BaF_2:RF_3, cryst., absorpt. spectra, γ-ray effects 77−12409
Ba_2RF_7, (R=Dy, Ho, Er, Tm, Yb, Lu, Y), superstructure phases, prep., thermal characterisation and X-ray powder diffr. 80−96494
BaR_2O_4, luminesc. on activation by Eu^{3+}, Nd^{3+}, Eu^{3+}-Tb^{3+} 77−52156
CaF_2-(Y,R)F_3 (R=any lanthanide except Pm, Eu), phase diagrams 78−84783
CaF_2-(Y,R)F_3 systems, phase diagrams, limiting solubilities and non-stoichiometry 79−47665
CaF_2-RF_3, characts. of ordering of solid solns. 79−14725
CaR_2S_4, R=rare earth, ternary sulphide with Th_3P_4 struct., vib. spectra 78−2844
CdF_2:rare earth fluorides, elec. cond. and electroluminesc. 79−87508
$CdLn(TiNb)O_7$, Ln=La-Lu, synthesis physicochem. props. 77−43186
Cs_2NaMCl_6, M=Eu, Tb, Er, Tm, Raman spectra 77−77205
Cs_2NaRCl_6, low-temp. Raman spectra meas., cryst. field parameters calc. *(German)* 77−36228
Cu-rare earth oxide-Y composite coatings, oxide and Y effect on coating precipitation 80−55554
$EuRs_4$, R=La, Ce, Pr, Nd, Sm, Gd, elec. cond. meas. 80−65555
Fe-R-O systems, thermodynamic props., cpd. formation 78−31390
Ga_2O_3-R_2O_3:Nd^{3+} glass, prep., characts., X-ray diffr., absorpt. and thermal anal. obs. *(French)* 78−19704
$KR(SO_4)_2$, R=La to Tb, unit cell parameters, thermal stability and decomposition 78−18613
$K_{6+3n}R_{4-n}(SO_4)_9$, (n≈0.4), cryst. struct. 80−28985
Li_2O-Fe_2O_3-R_xO_y, Hall effect and magnetoresist. 78−34849
$LiRF_4$, R=rare earth, laser matrices prep. and characterisation 77−24945
$(Li_{0.5}R_{0.5})TiO_3$, distorted perovskite struct. 78−83791
Lu_2O_3-K_2O_3 (K=Ho, Er, Tm, Yb, Y), crystn. by Verneuil method 80−40254
Mo-Y(La)(Ce)-B, X-ray diffr., reciprocal lattice, crystal struct., phase equilibria 77−21122
$Na_5RSi_4O_{12}$ (R=Sm to Lu, Y, Sc), solid electrolytes, struct. characts. 80−1997
$Na_5RSi_4O_{12}$, superionic conductors, Na conductivity paths 78−91482
OH^- vibr. dipole field and ion-pair processes with rare earth ions 79−38624
$Pb_{1-nx}R_xTiO_{3+x(1.5-n)}$, ceramic, ferroelec. Curie temp. comp. depend. 77−16258
(R, Pb)MnO_3 (R=La, Nd, Eu), flux growth 79−83113
R (III) complex, octahedral, f-f transitions, mag. dipole intensities, vibronic coupling model 80−25404
R complex, formation and props., book contrib. 80−43204
R halide-Al halide system, potential R ion laser, spectroscopic props. 78−66812
R^{3+} ions, coord. in aq. Cl^- soln., X-ray diffr. obs. 80−92445
R-B systems, phase equilibria, phase diagrams, book contrib. 78−48389
R-M-B systems (M=transition metal), phase diagrams and struct. considerations 80−16286
R-O systems, exam. of phase diagrams and crystal structure 79−8291
$RAlO_3$, effects of Co and Ti ions on cryst. growth 77−28711
RAs, R=Dy, Gd, Er, microwave resist. meas. 77−4383
$RAsO_4$, ferroelectricity, dielec. meas. 80−60515
$RAsO_4$, flux growth and characterisation by X-ray topography 78−48311
RAsS, struct. determ. *(French)* 77−51361
RB_{12} (R=Dy, Ho, Er, Tm, Lu, Yb), exam. of electronic structure, using X-ray emission spectra *(Russian)* 79−33865
RB_{12}, nature of magnetism *(Russian)* 78−31049
RB_2, mag. props. 78−84401
RB_4, mag. and elec. props., metallic character 80−20386
$R_4Ba_6(BO_3)_9$, flux growth and chem. characts. 78−23595
RBi, R=La, Ce, Pr, Nd, Sm, thermal expansion, 20-800°C 79−14942
RCl_3, magnetic phonon splitting, Raman spectra 77−52099
$RCl_3.6H_2O$ Gd^{3+}, R=Nd, Sm, Eu, Tb, Dy, Ho, Er, Tm, Yb, EPR obs., 9.4 GHz, 297K 78−15017
$RCl_3.6H_2O$, Gd^{3+} EPR, linear point charge model predictions 80−25200
$R(Co(CN)_6)n.H_2O$, (R=La to Ly), optical spectra 78−39566
$RCoO_3$, ^{59}Co NMR, quadrupolar and hyperfine interactions 79−15366
$RCoO_3$, catalytic props. 80−66875
$RCrO_3$, elec. transport 80−70700
$RCrO_3$, mag. interactions and weak ferromagnetism 78−52220
$RCrO_3$:Sn^{4+}, indirect Sn^{4+}-O^{2-}-Cr^{3+} interactions 77−11887
$RCu_3Mn_4O_{12}$, R=La to Lu, synthesis and mag. props. 80−75717
R_2CuO_4, catalytic props., mag. props., elec. conductivity 79−66350
RCu_2Si_2, interconfiguration fluctuation system, NMR meas. 80−15817
RF_3, struct. changes in series 78−26548
RFX mixed halides, synthesis and lattice parameters 78−30594
RFe_4Al_8, cryst. struct. mag. props. and hyperfine interactions 78−87648
RFe_4Al_8, mag. props. 78−52250
$RFe_3(BO_3)_4$, cryst. growth from soln.-melt, props. 80−108337
$RFe_{5-x}Ni_x$, giant intrinsic mag. hardness 78−56354
$RFeO_3$ and $RCrO_3$, exchange interactions 78−60279

rare earth compounds continued
$RFeO_3$, cubic anisotropy consts. 80−11190
$RFeO_3$, linear dichroism influence on Faraday effect 80−2737
$RFeO_3$, mag. dipole anisotropy and magnetostriction 79−73710
$RFeO_3$, parameters of interaction between rare earth and Fe ions, theory and expt. 79−73705
$RFeO_3$, Raman scatt. from magnons, anisotropy consts. determ. 80−66178
$RFeO_3$, spin reorientation and magneto-optical effects *(Japanese)* 79−47414
$RFeO_3$, struct. changes in series 78−26548
$RFe^{3+}O_3$, Neel point, cation depend. *(Japanese)* 77−43834
$RFeO_3:Sn^{4+}$, indirect Sn^{4+}-O^{2-}-Fe^{3+} interactions 77−11887
RFe_5O_{12}, sputtered layer comp. rel. to target comp. 78−6848
$R_3Fe_0O_x$-H, TGA-DTA meas., H absorption characts. 80−24600
$R_3Fe_5O_{12}$, mol. field coeffs. 77−1544
$R_2Fe_3Si_5$, superconductivity 80−49968
RGa garnet, growth of crystals from $50PbO.40PbF_2.10B_2O_3$ flux 77−21014
$RGa_3(BO_3)_4$, high temperature crystallisation, composition, struct., props. 80−40253
$R_{2x}Gd_{2(1-x)}(MoO_4)_3$, R=Nd,Sm,Gd,Tb,Ho,Yb, ferroic, linear and non-linear optical susceptibility 78−22164
R_5Ge_3, thermal expansion, phase transition effects 80−70433
RH_2, latrice thermal expansion and point defect form. energy 77−51524
RIG, (Ca,Ge)-substituted, flux growth in regular soln. approx. 79−78907
RIG, anisotropic, mag. props., high field and low temp. 80−75801
RIG, crystal and static mag. props. 79−99166
RIG, level intersection and instability of mag. struct. *(Russian)* 77−43816
RIG, magnetic relaxation phenomena 79−99776
RIG, site ordering and magnetostriction 77−90007
RIG, two-sublattice ferrimags., mag. polaritons 80−65845
R(III) complexes, cysteinates, thermodynamics of form. 80−89515
R_3Ir, lattice constants 79−69057
RIr_4B_4, $NdCo_4B_4$ type struct., mag. behaviour 80−20375
RIr_4B_4, supercond., magnetism and metastability 80−29501
$RKMo_2O_8$, flux growth in R_2O_3-K_2O-MoO_3 system, and cryst. struct. 78−35289
$R_4Lu_{11}S_{22}$, cryst. struct. *(French)* 79−77575
$RM_3(BO_3)_4$, (R=Y,Nd,Er, M=Fe,Ga), quantitative X-ray 79−46635
R_3MO_7, (M=Nb, Sb or Ta), struct. determ. 79−46620
R_3MO_7, (M=Nb, Sb or Ta), cryst. chem. 79−46619
$R_2M_{12}P_7$ (M=Fe, Co, Ni), crystal. struct., X-ray diffr. obs. 79−1411
$RMnO_3$, (R=Sm, Dy, Y, Er, Yb), thermogravimetric study of phase stability 79−100121
$RMnO_3$, R=La-Eu, catalytic activity 80−71941
$R_{12}Mo_6O_{35}$, R=La to Tb, synthesis and characterisation 79−1419
$R_2(MoO_4)_3$, cryst. growth and crystallographic data, Curie temp. determ. 79−43132
R_2MoO_5, preparation, exam. of higher oxygen pressure limit, mag. susceptibility *(French)* 78−76618
R_2MoO_5, preparation and struct. 79−46624
R_2MoO_6, flux growth in R_2O_3-K_2O-MoO_3 system 78−35289
R_6MoO_{12}, flux growth in R_2O_3-K_2O-MoO_3 system 78−35289
$R(MoO_4)(ReO_4)$, synthesis and props., cryst. struct., IR spectra *(French)* 79−32976
RMo_6S_8 ($Se)_8$, supercond. and long range mag. order coexistence 80−15642
RMo_6S_8, supercond. and magnetism coexistence *(Japanese)* 80−7025
$R_{1.2}Mo_6S_8$, low temp. magnetisation meas., and supercond. props. 79−8018
$R_xMo_6S_8$, high crit. field Chevrel phase 79−61003
$R_xMo_6S_8$, mag. susceptibility meas., 1.3-300K 78−14936
RMo_6S_8(Se_8), coexistence of supercond. and mag. ordering *(Russian)* 80−84542
$R_xMo_6Se_8$, coexistence of superconductivity and long-range magnetic order 79−11264
$R_xMo_6Se_8$, supercond., mag. props., 0.7 to 295K 77−32113
RMo_6X_8, X=S,Se, coexistence of supercond. and antiferromag. order 79−65579
$R(NO_3)_3.6H_2O$:Gd^{3+}, EPR spectral parameters 79−4720
$RNaMTa_5O_{15}$ (R=rare earth, M=K, Rb, Tl, Cs), relative stability of struct. types, and piezoelec. props. *(French)* 80−49206
$RNbO_4$, luminescence, model of energy transfer processes 77−4670
$RNbO_4$-$CaWO_4$, phase transitions of fergusonite-scheelite *(French)* 80−19942
RNb_3O_9, synthesis and phys. props. 77−90304
R_3NbO_7, mag. susceptibility, 77-300K 79−87226
RNi_4AlH_x, Hz absorpt. and cryst. struct. of hydride 78−34487
R_2NiTiO_6, perovskites, preparation, struct. *(French)* 79−46629
RO_x, film, short-range order to long-range order transition 78−10288
R_2O_3, 300 to 900K, mag. susceptibility and Curie temp. meas. 78−56288
R_2O_3, (R=Dy,Ho,Tm,Yb,Lu), EXAFS and chemical shift 77−81176
R_2O_3, cathode material, influence of surface and bulk effects 78−11065
R_2O_3, cubic, covalency, overlap integrals calc. 77−89401
R_2O_3, cubic, indirect exchange interactions Anderson model 79−95585
R_2O_3, reaction with liq. Li and liq. Li-N 79−66276
R_2O_3-H_2O, hydrothermal phase equilibria studies 80−104132
R_2O_3-M_xO_y glassy systems (M=Ti,Nb,Tm), rapid quenching by laser beam, exam. of composition and crystallization 78−52856
R_2O_3-MoO_3, solid-state chem., review 77−24288
R_2O_3-P_2O_5-$M_2O(M'O)$, (M=alkali metal, M'=alkaline earth), metaphosphate glass phosphors, fluoresc. props., activation conc. effect 80−89058
R_2O_3-ZrO_2 (HfO_2,) cubic solid soln., lattice parameters 79−82186
R_xO_y film, struct., electron microscope and diffr. obs. 79−11028
$R(OH)_3$, cryst., Raman spectra, vibr. assignments 78−76455
$R(OH)_3$, cryst. structs., trends 77−35529
$R(OH)_3$, R=La, Ce, Pr, Nd, Pm, Sm, Eu, Gd, Tb, Dy, Ho, Er, Tm, Y, Am, Cm, single cryst. X-ray lattice constants determ. 80−19766
R_2O_2S:Eu, Raman spectra, lattice vibrs. 79−78669
$R_2O_2S:Eu^{3+}(Tb^{3+})(Pr^{3+})$, branching ratios for fluoresc. 79−33807
$R_2O_2S:Yb^{3+}$, (R=Y, La, Lu), charge transfer type luminesc. 79−33797
R_2O_2S-Ga_2S_3, (R=La to Nd), exam. of prep. and props. *(French)* 78−80504
R_2O_2S-La_2O_2S, solid solubility, differences in ionic radii 77−15593
$ROsB_4$, R=Y, Gd, Tb, Dy, Ho, Er, Tm, struct. and mag. props. 78−79584

rare earth compounds continued
ROs_4B_4, $NdCo_4B_4$ type struct., mag. behaviour 80−20375
RPO_4, ^{31}P NMR exam. of transferred hyperfine effects 79−61241
$RPO_4:Yb^{3+}$, (R=Y, La, Lu), charge transfer type luminesc. 79−33797
RPO_4-$Pb_2P_2O_7$, R=Tb-Lu, solubility curves for high temp.-melts for growth of single crysts. 78−95687
RPO_4+3PBr_3, exam. of diffusion coefficients of gas mixture resulting, using chemical transport theory 79−1945
RP_5O_{14}, spectroscopy, ferroelastic/ferroelectric coupling, soft mode frequencies, phase diagram 79−19845
$RP_5O_{14}:Ce^{3+},Tb^{3+}$, energy transfer between dopants, excitation spectra, laser appls. 78−10961
R_3Pt, lattice constants 79−69057
$R_2(Pt(CN)_4)_3.nH_3O$, energy transfer from linear stacks of donors 78−68546
RPt_2Si_2, crystallographic study *(French)* 78−47286
$R_{2(1-x)}R'_{2x}(MoO_4)_3$, cryst. growth and crystallographic data, Curie temp. determ. 79−43132
RR'_2S_6, R,R'=rare earth, Sc or Y, structural organisation *(French)* 77−11519
$R_2Re_3Si_5$, RRe_4Si_2, crystal structs. 79−38806
RRh_3B_2, supercond. and mag. props. 80−97028
RRh_4B_4 and RMo_6X_8 (X=S, Se), mag. order and supercond., neutron scatt. studies 80−44807
RRh_4B_4, coexistence of supercond. and ferromag. order 79−65579
RRh_4B_4, coexistence of supercond. and mag. ordering *(Russian)* 80−84542
RRh_4B_4, ferromag. Curie temp., high supercond. transition temp. 77−89893
RRh_4B_4, NMR and sp. ht. in supercond. and mag. ordered phases 80−7037
RRh_4B_4, R=Y, Nd, Sm, Gd, Tb, Dy, Ho, Er, Tm, Lu, Th, cryst. struct., X-ray diffr. 77−89423
RRh_4B_4, supercond. and ferromagnetism, Sc substitution 78−95438
RRh_4B_4, supercond. and long range mag. order coexistence 80−15642
RRh_4B_4, supercond. re-entrant magnetism, energy band calcs. 78−52140
$R(Rh_{0.85}Ru_{0.15})_4B_4$, mag. ordering and supercond. 78−14861
$RRuB_4$, R=Y, Cd, Tb, Dy, Ho, Er, Tm, struct. and mag. props. 78−79584
RRu_3B_2, supercond. and mag. props. 80−97028
RRu_2Si_2, crystallographic study *(French)* 78−47286
$RS_{1.5}$ (R=La,Ce,Pr,Nd,Gd,Tb,Dy,Ho,Er,Tm,Lu), sp. ht. between 2 and 20K 79−60518
R_2S_2-Ga_2S_3 glasses *(French)* 77−19877
R_2S_3 condensates, struct. and optical transmittance 80−20727
R_2S_3-1.8GaS_3, chalcogenide glasses, (R=La, Ce, Pr, Nd, Gd), vibr. and electronic spectra, short-range order 78−27228
R_2S_3-In_2S_3, intermediate combinations, description of crystal types *(French)* 78−75648
$R_2(S_2O_3)_3.4H_2O$, IR and Raman spectra, possibility of nonexistence of cpd. of given formula *(French)* 77−24279
$R_2(SO_4)_3.8H_2O$:Gd^{3+}, EPR 80−20458
RSb, cubic ferromag. single crysts., mag. and magnetoelastic props. 79−15332
$RSbO_4$ (R=Nd-Lu or Y), high temp. modifications, cryst. chem. identification X-ray anal. 79−65059
$RSbO_4$, low temp. form, prep., cryst. chem. identification 78−47300
$RScO_3$ synthesis and lattice constant reevaluation 78−30593
$R_{10}Si_6O_{24}N_2Q_{24}$, CC apatites, replacement by La, Nd, Sm, Gd by Ti, Ge, Mn^{V}, V^{V} *(French)* 79−69093
$R_2(SiO_3)_3$, mag. susceptibility, temp. depend., 77-800K 80−20372
R_2SnS_5, cryst. struct., intermediate compounds *(French)* 77−1104
$R_{1-x}Sr_xCoO_3$, R=La, Pr, Sm, Nd, Gd, ferromag. reson., Lande g-factor 80−25215
$R_{1-x}Sr_xVO_{3-0.1x}$, elec. cond. and mag. susceptibility, temp. depend., 77-300K 77−47816
$RThNbTiO_8$, synthesis and cryst. struct. *(French)* 78−83799
$RTiNbO_6$, electrophys. props. 78−23388
$RTiO_3$, bulk mag. and struct. props., ferrimag. order 80−107993
$RTiO_3$, elec. and mag. props. 79−38068
$RTiO_3$, R=La, Nd, Sm, Gd, Y, cryst. struct. and cryst. chem. 80−1984
$RTiO_3$, unusual mag. props., role of mag. moments 78−84400
R_2TiO_5, crystallochem. classification 80−107142
$R_2Ti_2O_7$ (R=Tm, Er, Dy, Tb, Pr), flux growth 79−83113
$R_2Ti_2O_7$, crystal synthesis and SHG, solid laser freq. manipulation 79−41421
$R_2Ti_2O_7$, pseudoperovskite struct., nonlinear spectral and luminesc. characts. 80−29771
RVO_3, electrical conductivity, extrinsic p-type semicond. behaviour 77−11919
RVO_3, indirect exchange 78−34977
RVO_3, mag. ordering, susceptibility meas., 60-300K 77−32190
RVO_3, magnetic and cryst. struct. by X-ray and neutron diffr., Jahn-Teller effect 77−32169
RVO_4, covalency, chemical bonding and opt. spectra 77−80442
RVO_4, transferred hyperfine effects, ^{51}V NMR studies 79−82893
$RVO_4:Eu^{3+}$, ligand field parameters, computed from fluoresc. and absorption data 78−2453
$R_2V_2O_7$, (R=Tm, Yb, Lu), physical props. 78−39320
$R_2(V_{4/3}W_{3/3})O_7$, (R=Gd, Tb, Dy, Ho, Er, Tm, Xb, Lu), synthesis and elec. props. 80−29914
R_2WO_6, growth from soln. in melt 77−1806
R_xWO_3, metallic, elec. props. meas. 78−30906
$R_2Zr_2O_7$ (R=Nd, Sm, Gd, Dy, Er, Yb), Raman spectra, anion disorder characterization 80−25358
$R_xZr_{1-x}O_{2-x/2}$, growth from skull melting, directional solidification 78−60567
rare earth oxide-Nb_2O_5 system, phase formation thermodynamics 77−86348
Sc_2O_3-R_2O_3, regular soln. approx. of solidification diagram *(French)* 79−24505
Sc_2O_3-R_2O_3 (R = rare earth or Y), phases and phase transitions at high temp. *(French)* 79−100126
SiO_2-Al_2O_3-R_2O_3-MgO-TiO_2, T=rare earth of Ce group, glass-ceramic permittivity comp. depend. 77−43928
SiO_2-RO-Na_2O-Li_2O (RO=MgO, CaO, SrO) glass-ceramic coating, optimisation of props. by selective oxide action 80−55552
$Sm_{1-x}R_xS_y$, stability of Sm^{2+} 80−65508
$Sm_{1-x}R_x^{3+}S$, (R is rare earth metal), semicond.-metal phase transition 79−47017
SrF_2-(Y,R)F_3, phase equilibria, X-ray characts. of phases 79−61570

rare earth compounds continued
Sr_2RAlO_5 (R=La, Pr, Nd, Sm, Eu, Ga, Tb), monocrystals growth by flux method 80−20776
SrRFeO$_4$, R=La, Pr, Nd, Sm, Eu, Gd, Mossbauer effect, Neel temp. and internal mag. field 77−12284
$SrR_2Fe_2O_7$, (R=Pr,Nd,Sm,Eu,Gd or Tb), Mossbauer exam. of mag. struct. 77−40157
$SrR_2Fe_2O_7$ series, mag. struct. and spin reorientation, neutron diffr. and Mossbauer meas. 77−69503
Sr_2RFeO_5 (R=Nd, Sm, Eu, Gd), monocrystal growth by flux method 80−20776
SrRMnO$_4$, (R=La,Nd,Sm,Gd), cryst. struct. determ. *(French)* 78−6042
$Sr_2R_2O_4$ luminesc. on activation by Eu^{3+}, Nd^{3+}, Eu^{3+}-Tb^{3+} 77−52156
SrR_2S_4, R=rare earth, ternary sulphide with Th_3P_4 struct., vib. spectra 78−2844
ThN-rare earth nitride mixed system, quasibinary existence *(German)* 80−91221
$TlR(MoO_4)_2$ (R=La to Ho), polymorphism, X-ray diffr., thermographic anal. 78−47269
$TlR(MoO_4)_2$ (where R=Er, Tm, Yb, Lu, Y), polymorphic transition charcts., temp. regions of stability 79−14785
W-Y(La)(Ce)-B, phase equilib., struct. of crysts. 77−21122
YIG-RIG solid solns., magnetisation temp. depend. calcs. 80−20388
Y_2O_3-R_2O_3, (R=La,Nd,Sm,Gd and Dy to Yb), cryst. growth by Verneuil method 77−1803
$Y_{1-x-y}R_xEr_yAlO_3$, $Y_{1-x-y}R_xEr_yScO_3$, stimulated emission of Er^{3+} ions 78−6705
$(Y_{1-x}R_x)_3Fe_5O_{12}$, photoinduced decrease in permeability, 77K 77−85497
ZnS:RF$_3$ film, AC electrolum., memory effects 79−38673
ZrF_4-BaF_2-ThF_4-NaF(RF$_3$) (R=rare-earth) glass system, anion cond. 80−70460
ZrO_2-Y_2O_3-Nd_2O_3(CeO_2), solid solns., form. by coprecipitation, struct., X-ray, electron diffr. anal. 77−12583

rare earth elements *see rare earth metals*

rare earth metals
see also the individual metals e.g. cerium
4f, electron impact excited soft X-ray spectra, resonances and many body effects 80−50468
4f levels, obs. by bremsstrahlung isochromat and XPS spectroscopy 79−24411
abundance in Ap and Am stars 77−33505
abundance in Archean sedimentary rocks, rel. to crustal evolution 77−60374
abundance in chert, indication of form. in marine environment 77−37200
abundance peak, fission origin implications for astrophysical r-process 78−93204
abundances in layered Komatiite lava flow, Ontario, Canada 79−29764
abundances in Melrose-b howardite 80−101566
adsorption of $H_2(D_2)$ 77−4257
alkaline earth fluoride:R^{2+}, photoionis. thresholds 79−78132
amorphous mag. substance with rare earth ions, low temp. specific heat, elec. resistance and US absorpt. *(Russian)* 79−19734
Anderson model susceptibility for high mag. impurity conc. 77−63069
anisotropy of magnetic component of electrical resistivity 79−69494
anorthosite complexes, Marcy (New York) and Morin (Quebec), rare earth element abundances 77−78177
APS, position of unoccupied 4f levels 80−16125
Archaean granite composition in Yellowknife, Northwest Territories, Canada 80−4007
Archaean metasedimentary rocks from Kambalda, Western Australia, rare earth element geochemistry 80−109143
atom, extended orbital calculation method, refinement of ordinary method 77−6667
atom, photoionisation thresholds and Rydberg spectra 78−66522
atom, Rydberg spectra and ionisation thresholds, time resolved resonant multistep technique 78−82701
atom, Yb II, III to Bi XV, XVI isoelectronic sequences, wavelengths and ionisation energies 77−429
atom on transition metal, effects of changes in valence state due to adsorption 79−69367
atom properties periodicity and inorganic cpd. props. 80−96586
atomic and ionic hyperfine interactions, relativistic effects on core-polarisation contrib. 77−67990
atomic energy levels, data tables 78−86805
atomic partition functions, Chebyshev approximations 80−67544
atomic spectra analysis, present state and trends 78−62749
atoms, Gaussian basis sets calcs. 80−63541
Azorean lavas, REE and LIL element compositions 77−25669
band structure calcs. 80−15441
band structure Fermi surface, magnetisation density 78−84140
basalt isotopic and element composition, Reykjanes Peninsula, Iceland 80−21725
basaltic achondrite meteorites, rare earth element abundance patterns rel. to origin 80−36581
bone uptake, Mossbauer study 80−8019
E.Carpathians volcanic rocks, rare earth elements concs. 77−5151
cations in aqueous chloride soln., effect on Raman bands of water 78−15157
ceramics, rare earth elements use as dopants *(Polish)* 80−97455
chemical analysis by selective excitation of probe ion luminesc. 80−40797
N.Chilean ignimbrites, REE data and Sr isotopes rel. to petrogenesis 79−44146
chondritic meteorites, rare-earth abundances 79−21234
composite dike geochemistry, light rare earths partitioning between co-existing acidic and basic melts 79−2233
conduction electron interactions, anisotropic 80−15492
conference, St. Pierre-de-Chartreuse, France (Sept. 1978) 80−12844
conference on rare earths and actinides, Durham, England (July 1977) 78−84115
core electron binding energies, XPS study 77−48309
3d core electron XPS spectra, low-binding-energy satellites, exception of Eu 80−104040
core-hole screening, 3-d XPS, multiplet splitting 79−43095
Coulomb excitation, very-short-lived radiation effects 79−60411
Cretaceous mid-ocean ridge basalt (MORB), Nd and Sr isotopic comps. and rare earth element abundances 80−94520

rare earth metals continued
crustal evolution and Australian post-Archaean sedimentary rocks 77−41015
crystal field parameters, variation of $\langle r^4 \rangle$ and $\langle r^6 \rangle$ across rare earth series 78−72122
crystal field theory 78−84177
crystal structure rel. to d-band occupancy 77−35510
density of 4f states below and above Fermi level, XPS and bremsstrahlung isochromat spectroscopy 80−76140
determination, in flux-grown magnetic garnets, by AAS 78−92585
determination, in rocks, by neutron activation anal. 78−27870
determination in geological materials, using thermal and epithermal neutron activation 78−7797
determination in PuO_2, PuO_2-UO_2, by chem. separation, at. emission anal. 77−52723
diffusion, review 79−69281
doubly ionised, f-d interaction 78−90102
Earth upper mantle, partitioning between hydrous silicate melt, amphibole and garnet peridotite 79−20775
EFG produced by conduction electrons, mag. ordering effects 77−40020
elastic and mechanical properties, review 79−70132
elastic properties, connection with electron struct. *(Russian)* 80−19895
electrical resistivity, 80-1000K 77−43572
electrical resistivity, anisotropy, scatt. mechanism 78−72134
electrical resistivity, high temp., scatt. mechanisms 80−39553
electron affinity semi-empirical calcs. 77−6955
electron interactions rel. to lattice props. *(Russian)* 77−35901
electron transfer of impurities in liq. Ga *(Russian)* 77−59132
electron work function by contact pot. difference method *(Russian)* 79−60913
electronic excitation energies calcs. 80−54592
electronic phase transitions, f-level broadening 77−47773
electronic sound attenuation anomalies at transition to helical phase, Fermi surface topology *(Russian)* 80−92807
electronic struct. and magnetism, review 80−70573
electronic structure, calc. methods, review 79−69405
electronic structure, Hubbard's alloy approx. 79−73665
electronic structure rel. to valence, chem. bonding 80−54601
electrotransport of solutes 77−51548
energy transfer and two-centre optical transitions in OH^- and rare earth double-doped solid 80−7398
in eucrite meteorites, abundances rel. to parent body comp. and evolution 78−20766
excitation energies, 3d electrons, relativistic calcs. 80−20109
excitation energies for 4f electrons, relativistic calc. 78−72117
excitation energies for 5s electrons 78−10408
4f level energy position relative to Fermi energy 80−6764
ferromagnet, mag. hyperfine field interaction, ^{197}Au Mossbauer effect 77−8463
ferromagnet, polarisation in external mag. fields TDPAC 77−8462
ferromagnet-simple helix transition, cond. electron spin polarisation *(Russian)* 79−7995
ferromagnetic, RKKY interaction and conduction electron polarisation 78−91859
ferromagnetic, spin polarisation of field-emitted electrons 77−40337
ferromagnetic, spin polarised electron tunnelling 78−68094
ferromagnetic, theory of low-temp. and freq. depend. of extraordinary kinetic effects *(Russian)* 79−91408
ferromagnetic metal-rare earth, dil., hyperfine fields 78−87947
ferromagnetic ordering *(Russian)* 78−60262
ferromagnetic properties, book contrib. 80−75725
ferromagnetism, boson field anal. of crit. temp. region 77−51911
film, anomalous crystal structures 79−28222
film, i.r. conductivity, room temp., free electron contrib., rel. to mag. transitions 77−1745
film, O_2 and H_2 contamination effect on elec. resist. 77−80856
film, optical cond., rel. to cryst. struct. and electronic config. 77−36303
film, reactions with O_2 and water, XPS obs. 77−31888
films, prep., struct. and props., general review 80−54556
fission product isotopes, separation in thin-layer chromatography *(German)* 80−37635
flame absorption spectra dye laser, amplified absorption method 77−29075
fluorite:R, natural, colour centres, associated rare earth ions and origin of coloration 79−61408
fluorophosphate glasses, rare-earth activated, luminesc., bonding 78−64415
free atoms, atomic props. and electronic struct., review 79−68204
fuel reprocessing waste ^{137}Cs, ^{90}Sr and rare earth radioisotope separation by cation exchange 78−78486
geochemistry and mineralogy, book contrib. 80−46157
geochemistry of Late Cainozoic alkaline lavas from Antarctica 77−41030
glass:R, photoacoustic spectrosc. 80−92611
glass, rare earth elements use as dopants *(Polish)* 80−97455
grains, submicron size, in Earth's atm., solar vs. terrestrial origin 78−12180
Hall constant, 80-1000K 77−43572
Hall effect, 80-1000K 80−15504
HCP, lattice dynamics, microscopic theory 77−43292
heat capacity near melting pt., vacancy mechanism of melting 80−15221
heats of vaporisation and valence band energies, theory 78−91431
heavy, mag. anisotropy *(Japanese)* 77−85444
heavy, NMR exam. of electric field gradient 78−52363
heavy lanthanides, second order phase transition, nonvalidity of Lifshitz condition *(Chinese)* 78−51643
heavy rare earths, X-ray absorption spectra, $L\alpha$ and $L\beta$ satellites, explained using EXAFS data 79−52045
high pressure studies, review 79−69193
hyperfine interaction, static and dynamical aspects, NMR investigation, review 79−91299
identifications in HD 187473, Si star 80−98671
impurities in Ba silicate and phosphate glasses, quenching of Nd^{3+} luminesc. 80−25449
impurities in Cr, effect on oxidation resist. 80−66703
impurities in crystals, magneto-Raman effect 78−43864
impurities in fluorophosphate glasses, magneto-opt. characts. 80−64126
impurities in s-band metals, Kondo anomaly 78−52208
impurities in s-p metals, isomer shifts 80−15839
industry review 80−25537

rare earth metals continued
interband, collective and atomic (p,d) excitations, Z-160 eV, fast EELS 80−93443
ion, crystal field, spin correlation effect calc. 78−23058
ion, tripositive, relativistic mag. form factors, Dirac-Fock calc. 77−40037
ion energy separation, $4f^N$-$4f^{N-1}$ nl, host depend. 80−49676
ion potential laser system, using R halide-Al halide complex, spectroscopic props. 78−66812
ion source using surface ionisation process 80−68999
ion spectra, crystal field integral parameters, spin-orbit interaction 80−100447
ionic crystal:R, intra- and inter-ionic multiphonon transitions 80−34973
ionic transition, hypersensitivity to environment, mechanism 79−72255
ions, 4f photoelectron spectral intensity, relativistic calc. 79−54816
ions, aquo complex form., in aq. chloride soln., coord., X-ray diffr. obs. 79−64975
ions, Dirac-Fock exam. of electronic props. 79−56106
ions, EPR in solids, review of 1973 literature 77−69675
ions, in crystal hosts, effects of coordination polyhedron struct. on spectra 77−55807
ions, in ionic crysts., optical props., review 79−15492
ions, ligand-induced pseudoquadrupole absorpt., vibronic contribs. 80−52978
ions, nonreson., energy transfer interactions, randomly distrib. mols. in lattice, numerical anal. 77−8626
ions, optically excited states, EPR, ENDOR 78−43637
ions in $4F^N$ electronic config., correlation cryst. fields 77−76785
ions in aq. solns., optoacoustic spectroscopy using pulsed dye laser for micron thick film 80−42265
ions in crystals, corrections to cryst. field Hamiltonian 79−33268
ions in crystals, electric dipole transitions intensities 79−78062
ions in cubic field, anal. of absorption spectra $4f^{N+1}$→$4f^N5d$-6s 80−7382
ions in solids, indirect exchange between localised moments *(Russian)* 79−87237
ions in soln., absorpt. and fluoresc. spectra, book contrib. 80−45112
isotopic analysis, Oklo natural fission reactor fluence distrib. meas. *(French)* 80−21759
isotopic analysis at Oklo natural fission reactor *(French)* 80−21761
Kimmeridgian black shales, N Atlantic region, rare earth elements distrib. 79−44187
lanthanide ion fluorescent probes, spectroscopic obs. system 78−11573
lanthanide ions, tripositive nucl. hexadecapole antishielding factors 79−26909
lanthanide series properties, double peaks effect *(Chinese)* 78−29740
lanthanides, 4d spectra in atoms rel. to solids 79−31450
lanthanides, 4f-screening, ionisation pots. by modified Slater method *(Chinese)* 79−97977
lanthanides' ionisation pot. calc., T-value and number of 4f electrons linear correlation *(Chinese)* 80−63850
lanthanides in Si Ap-star HD 192913, spectral identifications and abundances 78−45345
laser line prediction in solid and vapour lasers 79−3700
laser using R in organic soln., nuclear pumping 78−5470
lasers, solid, gas and liq., book contrib. 80−53306
lasers and excited states of rare earths, book 78−29958
lattice dynamics and scatt. reson. 78−59872
liquid, elec. resist. meas. 77−51718
liquid, entropies 77−69100
liquid, mag. susceptibility rel. to theories of electronic struct. 77−1536
liquid, resistivity 80−24865
liquid, strong-scatt. theory of elec. resist. 77−59274
liquid, struct. factors, high temp. X-ray diffr. obs. 79−7544
liquid, structure factors, calc. of temp. coeff. of resistivity, one component plasma model 79−32881
liquid, varying d-band occupancy 78−39083
liquid heavy rare earths, mag. susceptibility meas. 80−75740
liquid structure 77−76294
low temperature heat capacity, review 79−69263
luminescence from intensity meas. on powdered phosphor screens, self-concentration quenching mech. determ. 79−69880
luminescence of R activated materials, relaxation phenomena, book contrib. 77−32439
magnetic and transport properties 79−69658
magnetic excitations, neutron inelastic scatt., review 79−47265
magnetic excitations, review of neutron scatt. data 80−60227
magnetic heavy elements and alloys, electronic struct., book 78−60259
magnetic impurities in s-p hosts, self-polarization hyperfine fields 79−33456
magnetic phase transitions in heavy rare earth metals *(Russian)* 79−7993
magnetic properties, nonlinear s-f exchange interaction effect 80−15711
magnetic structs., nonspherical Fermi surface in RKKY theory 77−63227
magnetic structures and inelastic neutron scattering, review 79−69654
magnetic-anisotropy, two- and single-ion 77−63164
magnetically hard materials, review 77−73051
magnetically hard materials, technology, development *(Polish)* 77−89973
magnetism, review 77−63123
magneto-optical Kerr effect spectra in UV region using synchrotron radiation 77−52127
magnon dispersions in ferromag. and screw structs., nonlinear s-f exchange interaction effect 80−75746
metal:rare earth, effective exchange interaction model 80−25127
metallurgical appl. 77−12639
meteoritic spherules in oceanic sediments, trace element concentrations 79−84755
mobility and fractionation during granodiorite weathering 79−62512
monazites, nuclear waste, synthesis, ideal actinide hosts for geologic disposal 79−22406
Mossbauer isomer shifts, book contrib. 79−87361
multiplet splittings of s-core levels, exchange correl. 78−10407
muon spin relax. meas. of Neel temp. and antiferromag. transitions *(Russian)* 79−87369
neutron activation anal., geochem. of genesis of ore deposits *(German)* 80−30301
neutron activation anal., interference by neutron induced 2nd order nuclear reacts. 77−81444
p-nitrobenzoic acid:rare earth laser materials, vibr. spectra, wavelength 125 to 500 mm 80−2769
NMR, EPR, and Mossbauer effect, book contribs. 80−39483
rare earth metals continued
NMR shift induction, temp. depend. 77−28464
nuclei, validity of pseudo SU(3) model 77−34240
Oklo natural reactor, elemental and isotropic abundances rel. to rare earths behaviour 78−49019
Oklo natural reactors, data on stability and remobilisation, summary *(French)* 80−21771
optical properties, review 77−40259
orbital radii, quantum-mech. calcs. rel. to inner series contraction 77−83514
oxidation potential 80−5495
paramagnetic, elastic consts., c_{11}, c_{33}, mag. field depend. 77−16143
paramagnetic metals, polarised neutron studies of field induced magnetisation 80−25084
partitioning in clinopyroxene-orthopyroxene pairs from spinal peridotite xenoliths 79−62488
in peridotite partial melts, fractionation patterns rel. to upper mantle rock form. 77−37198
Periodic Table subclassification 77−26109
phosphor, rare earth activated, cathodolum., use of internal reference 77−44071
phosphor, rare-earth-doped up-conversion and excited state energy transfer, book contrib. 77−36296
photoemission, rel. to electronic struct., book contrib. 80−16157
physics and chemistry (book) 79−69384
plasma, absorpt. spectra continua, 40 to 2000 Å 78−54471
preparation and refining 78−84705
preparation methods and properties 79−69969
purification, laser induced photochem. separation methods, review 79−61883
purification, laser methods 80−16712
radioactive waste, high-level, oxalate precipitation for separation of Am, Cm, and trivalent lanthanides 80−83202
radwaste partitioning, separation of transplutonium and rare earth elements 79−97881
rare earth:YAG crystal, laser freq. conversion by reson. pumping *(Russian)* 79−10314
refining, production of pure metals *(Russian)* 77−59687
research developments since 1950 78−84116
resistivity anomalies 78−19018
RKKY interactions, anisotropic effects from spin-split bands 80−15712
RKKY theory of magnetism, electron-electron interactions 79−73667
rocks, neutron activation analysis, optimum method 79−88491
rocks and minerals, neutron activation analysis 79−88492
screening effects on cryst. electric fields 79−78058
sea-floor basalt, rare earth elements behavior during weathering 79−57910
sedimentary rocks, Huronian sequence 79−92511
semi-infinite surface with magnetic structure, density of states calc. 80−10851
separation from clays, complexation method 80−3442
solar nebula, rare earth element condensation and fractionation 80−72796
sound attenuation anomaly near mag. transition temp. 78−15004
spectral determ. in luminescent materials 77−73485
spectral determination using hollow cathode discharge in mag. field *(Russian)* 79−52859
spilitic rocks, rare earth element mobility and geochem. charact. 77−86887
spin waves and excitations 78−84407
stacking faults and magnetism, transform. effects 80−75840
structural, electronic, and mag. props., book 80−36785
structural properties rel. to F electrons 78−83951
submonolayer films, electronic phase transitions, heat of absorption 80−24736
superconductivity, review 79−69621
surface, continuous emission spectra of particles ejected by ion beams *(Russian)* 78−55140
surface atoms, photoionisation of 4f electrons, photoelectron spectra 78−11077
surface valence state from surface tension props. 79−95462
SXAPS with sealed-off analyser tube 80−80908
systematics, rel. to the long periodic table 79−37649
thermodynamic props. determ. from US vel. meas. 78−55912
thermodynamics in steelmaking 77−4782
thermoelectric power, 80-1000K 77−43572
tholeiitic basalts, rare earth elements behaviour during submarine weathering 78−73369
Ticonal, effect of rare earth metals on mag. props., struct., and phase transformations 79−99732
in titanite, lanthanides, relative concs. rel. to host rock type 79−62492
trace diffusion of nuclear reaction products, lanthanides, in polycryst. Ta 78−22896
transition metal-rare earth dil. alloy, hyperfine field of rare earth impurity 79−1588
trivalent, 5d states, charge transfer and intershell spectra, separation and overlap 78−10966
US attenuation, exchange striction, and spin-phonon interaction 79−33518
US attenuation in applied fields 77−51933
valence transitions and intermediate valence states 79−42496
valency, ionicity and electronic config. 80−18775
widths of 5d energy bands in the heavy rare-earth metals 78−63971
X-ray 3d spectra, 4f and 5f states 78−84681
X-ray 5p emission bands, valence energy band 80−104016
X-ray chemical shift and atomic charges 77−44085
X-ray diffraction obs. of magnetostriction and phase transitions 77−73068
X-ray emission spectra, atomic interaction effects *(Russian)* 79−69905
X-ray $N_{IV,V}$ emisison spectra in region of 5p→4d transitions *(Russian)* 78−6815
XPS and bremsstrahlung isochromat spectra of f^{n+1}, f^{n-1} states 80−40220
XPS satellites, screening of 3d holes 78−76586
yttrium ethylsulphate, rare earth doped, NMR of protons adjacent to impurity 77−85589
BaF_2:R, dopant effect on superionic state transition 79−60547
BaF_2:R, far IR electronic transitions 77−4657
BaF_2:R^{3+} (R=rare earth) dipole reorientation, ionic thermocurrents obs. 79−95705

rare earth metals continued
$BaY_2F_8:Eu^{2+}$, R^{3+}, energy transfer from Eu^{2+} to trivalent rare earth ion 79−91490
CaF_2:defect model for nonlocally compensated trivalent impurities 77−72629
CaF_2:Eu,R, thermolum. meas. 80−2870
CaF_2:R, cluster-associated relax., 5.5-400K 78−31153
CaF_2:R, dopant effect on superionic state transition 79−60547
CaF_2:R, natural fluorite colouring, effect of impurities on absorpt. spectra 79−56822
CaF_2:R_1R', doubly doped, elec. dipole relax. of mixed clusters 79−82924
CaF_2:R^{3+}, dichroism, elec. field effects *(Russian)* 77−24823
CaF_2:R^{3+}, dipole reorientation of charge compensation centres, ionic thermocurrents meas. 79−73880
CaF_2:R^{3+}, elec. dipole-dipole interaction, ionic thermocurrent and EPR study 80−108060
CaF_2:R^{3+}, force const. changes near impurity site, calc. 77−47529
CaF_2:R^{3+}, props. of ionic thermocurrents 77−7897
CaF_2:rare earth ion, hydrogenated, local lattice modes, spectroscopy 80−50375
CaF_2:rare earth metal, thermal cond., 80 to 300K, defect centre struct. 77−15638
$CaSO_4$:R, ESR, thermolum. correlation studies following gamma irradiation 77−59628
$CaWO_4$:R^{3+}, X=rare earth, cryst. field parameters, ang. overlap model 79−60772
CdF_2: rare earth, electronic props., compared to CaF_2 *(French)* 80−49662
CdF_2:R, multicoloured electrolum. 79−78755
CdF_2:R^{3+}, cooperative luminescence influenced by symmetry of centres 78−6791
CeO_2:R, ionic cond. meas. 79−60543
$CsMnCl_3(Br_3)$:R^{3+}, rare earth doped, energy transfer, emission spectra obs. 80−20684
Dy, magnetocrystalline anisotropy, perturbation theory 78−2675
Fe formations, REE data rel. to seawater 79−66715
Fe-Cr (20 wt.%), role of rare earths and reactive elements in high-temp. oxidation 79−79178
Ga-Ge-Se:R chalcogenide glasses, elec. props. 80−96885
GaP:R, photolum. and elec. props. *(Russian)* 78−52545
H, and He, stopping powers meas. 80−42904
$KAlSi_3O_8$:R^{3+}, glass, nonradiative energy transfer and fluoresc. quenching 77−20905
$KGd(WO_4)_2$:R^{3+}, stimulated emission 78−23496
$KMnCl_3$:R^{3+}, rare earth doped, energy transfer, emission spectra obs. 80−20684
K_2O-BaO-SiO_2:R glass, spectral intensity, effect of number of 4f electrons 78−84602
$KY(WO_4)_2$:R^{3+}, stimulated emission 78−23496
$LaCl_3$:R^{3+}, cryst. field parameters, angular overlap model calcs. 78−26830
LaF_3:R^{3+}, crystal field anal., intensity calcs. 80−100670
$LiTmF_4$:rare earth, EPR spectra, elec. field effects, cryst. field interactions 80−71176
$LiYF_4$:rare earth, EPR spectra, elec. field effects, cryst. field interactions 80−71176
MgO:R, single cryst., grown with modified plasma torch furnace *(Japanese)* 79−95923
Na_2ZrSiO_5:Ln^1,Ln_2, scintillation, α-excited *(Russian)* 79−28841
Nd_2O_3, and oxalate, X-ray fluoresc. spectrometric anal. of trace rare earth impurities 79−24853
R doped crystals, nonradiative processes, book contrib. 80−55188
R^{3+}, in O-dominated host, high energy states, reflectance spectra 77−69849
R/p-Si(p-GaAs) contacts, surface pot. barrier 80−60086
R-activated phosphors, chemistry and physics, book contrib. 80−55187
R^{3+}+ammoniated electron, reaction kinetics meas. by ns. pulse radiolysis 79−52638
Rb_2MnCl_4:R^{3+}, rare earth doped, energy transfer, emission spectra obs. 80−20684
in Si, reaction of rare earth impurities with carbon during cryst. growth 79−38733
SnO_2:R^{3+}, luminesc. and charge compensation 78−76532
$SrCl_2$:R, dopant effect on superionic state transition 79−60547
SrF:R^{3+}, reorientation of dipoles 77−8494
SrF_2:R^{3+}, elec. dipole-dipole interaction, ionic thermocurrent and EPR study 80−108060
SrF_2:R^{3+}, IR and EPR spectra meas. 77−69865
SrF_2:rare earth, electric dipoles, relaxation parameters and dipole-dipole interaction 79−24255
YAG:R, phonon impurity scatt., lattice thermal cond. and US attenuation meas. 78−87748
YAG:rare earth metal, US absorpt. meas., relax. model 80−24539
$Y_3Ga_5O_{12}$:R, high temp, mag. susceptibility 79−78347
Y_2O_3, rare earth activated, cathodolum., use of internal reference 77−44071
ZnO:R, photo- and electrolum. 79−28803
ZnO:rare earth metals varistors, microstructure-prop. relations 80−100249
ZnS:R^{3+} in Ta-Ta_2O_5-ZnS:RF_3-Au struct., electrolum. and cathodolum. meas. *(French)* 77−16398

rare gases *see inert gases*

rarefied fluid dynamics
see also atomic beams; Knudsen flow; molecular beams
acoustic dispersion hydrodynamic soln. 77−68630
aerosol beam instruments, nozzle inlet design 80−6183
atomic beam, produced by laser-metal surface impact 80−5637
atomic beam, produced from He nozzle flow, high speed ratio 80−5636
atomic beam production, He skimmed from freejet zone of silence 80−5635
attenuated gas energy flux, rot. degrees of freedom effect 79−64705
attenuated gas flow round plate, Monte Carlo soln. of Boltzmann eqn. 79−68754
binary gas mixture, free expansion through channel, composition change 79−64709
binary gas mixture, isothermal creep along flat surface, half-space moments method 77−42873
binary gas mixtures, separation and isotope separation in curved shock wave 79−94753
rarefied fluid dynamics continued
binary mixture, two-dimens. channel flow, separation phenomena, num. soln. 77−58740
blunt body, in hyperthermal flow, near free mol. heating 79−94671
Boltzmann equation, continuous nonnegative equilib. soln. 78−41250
Boltzmann equation, steady-state solns. for rarefied gas 77−35172
Boltzmann equation collision integral, relax. problem soln. 79−64706
Boltzmann linearised eqn. with long range pots., numerical anal. 77−35168
boundary conditions in rarefied gas dynamics, phase shift formulation 78−1694
n-butane, freejet flow, vibr. relax. time 79−98760
n-butane-CO_2, freejet flow, vibr. relax. time 79−98760
centrifuged flow with recirculation, book contrib. 80−1604
channel, annular, long, free-mol. and radiative transport, approx. analytical soln. 80−6165
channel 2-D flow in presence of condensation 79−32577
chemically reactive gas, wave structures, kinetic theory of gases calcs. 79−94678
cluster formation, in rarefied nozzle flowfield 80−5639
compressible and incompressible flows, recent theoretical and expt. developments, book 80−1620
condensable rarefied gas flow through porous media, heat and mass transfer 78−59473
conductance for the gas flow of an accelerating tube 80−102359
conductance of long inclined tubes in collisionless flow 79−94661
conference, Snowmass-at-Aspen, Colorado, USA, July 1976 79−98754
conical gas flows, two-dimens. unsteady problems 77−51085
convective heat transfer coeff. and surface emissivity, effect of degree of vac. 78−1693
convective heating of concave bodies in high speed rarefied gases 79−1214
convex body aerodynamics in rarefied mol. flow, kinetic theory 78−59424
Couette flow, BGK scatt. model, by Boltzmann eqn. soln. 79−97327
Couette flow, half-range expansions soln., for arbitrary Knudsen nos. 77−51088
Couette flow along surface, isothermal slip 78−67220
cylindrical capillary, mass transfer kinetics during evaporation, BGK eqn. basis 77−47044
diffusion slip velocity, binary gas mixture, along curved surface 78−83432
diffusophoresis of nonspherical aerosol particles in a free molecular flow 80−43765
dilute monatomic gas flow round macroscopic object, kinetic theory 77−965
discrete kinetic theory, maths. and numerical aspects, Couette flow appls. 80−19413
disparate mass mixture flows, phys. mechanisms, shock wave struct. 79−94657
disparate-mass gas mixtures, effect of cross-sectional mass depend. 78−71371
disparate-mass gases description, generalised Navier-Stokes eqns. 77−51086
electrically conducting rarefied gas, oscill. flow, past vertical porous plate, free convection 78−90830
electrically conducting rarefied gas near accelerated porous plate, MHD flow 80−14836
evaporation, quasisteady half-space problem, gas kinetics theory and expt. 80−6106
evaporation, quasisteady one-dimens. problem, entropy-balance relation 80−6168
evaporation-condensation two-surface problem, in presence of noncondensable gas 80−6169
evaporation-effusion problem, rarefied regime, nonlinear numerical soln. 80−6167
finite length plate in supersonic low density flow, surface pressures and corrections 80−14741
flat plate flow, direct simulation and expt. 79−94667
flat plate skin friction, between hypersonic continuum and free mol. flow 79−94668
flat plate trailing edge in rarefied supersonic airflow, boundary layer 80−24046
flow in narrow slit channel with sublimation from one wall and heat inflow from other 77−15064
flow induced by thermal stress, imperfect accommodation at boundary 78−87362
flow over body with small accomodation coeff. 79−90286
flow over plane wall, slip coeffs. 79−90287
flow through finite length slots, kinetic theory 77−72331
free jet, N_2^+ UV spectra for rot. temp. 80−6184
free molecular channel flow, complementary variational principles 79−64708
free molecular flow, impact pressure probe 79−41716
free molecular flow, recovery factor, accommodation coeffs. 77−15065
free molecular flow, rot. degrees of freedom effect *(Russian)* 78−9657
free molecular flow analysis over slightly waved wall 77−51087
free molecular flow fields near plate leading and trailing edges 79−86463
free molecular flows, Monte Carlo functional expansion calc. 79−72912
free molecular gas flow in capillary, effect of absorption time differences 77−89164
free molecular vapour flow, mass transfer during condensation in channel 78−51198
free molecule flows through circular tubes with orifices, enlargements or contractions, numerical solns. 79−94660
free molecule heating of micron size particles at hypersonic speeds 80−19442
free-molecule flow, through circular tube with sudden enlargement or contraction 78−14047
gas, flow through aperture into vacuum 78−9621
gas, nonisothermal flow in cylindrical capillary, calc. of vel. profile and flux 80−6098
gas, nonsteady flow through semipermeable screen to vacuum 80−100029
gas, terminal speed ratio in spherical source expansion 77−84285
gas clouds released at satellite orbital velocity, dynamics expts. 80−14748
gas diffusion in supersonic jet 79−32604
gas flow, full solns. for Burnett eqns. c.f N-S eqns. 80−69876

rarefied fluid dynamics continued
gas flow characteristics through fibrous filter with supercrit. press. drops 78−1738
gas flow over a flat plate, influence of internal degrees of freedom 80−6099
gas jet expsn. into vacuum, rot. relax. 79−32625
gas mixture Poiseuille flow 79−14438
gas mixtures, background gas penetration into underexpanded jets, densitometric obs. 79−94655
gas mixtures, velocity slip in free jet expansions 79−94656
gas mxitures, velocity slip in free jet expansions 78−90951
gas with rot. degrees of freedom macroscopic description of motion 79−86465
gas-liquid film interface stability behind slipping shock wave front *(Russian)* 78−55630
gasdynamic laser flow, vibr. wall accomm. for CO_2-N_2-H_2O 79−98340
gravitational collapse, finite-particle scheme for three-dimens. gas dynamics 78−67218
H-matrix calculations, incorporation of linear constraints 79−30394
H-matrix for time depend. problems in rarefied gas dynamics 80−43739
heat transfer, cylinders, between continuum and free mol. flow limits 79−98756
heat transfer, temp. jump problem in BGK model 77−53841
heat transfer between coaxial circular cylinders, with large temp. difference 79−94664
heat transfer between parallel surfaces, collisional models 79−86464
heat transfer equation, mol.-kinetic generalisation 78−67219
heat transfer for gas between parallel plates *(Russian)* 78−46961
heat transfer in plane Couette flow, ellipsoidal model 77−72330
heat transfer in rarefied MHD laminar channel flow 80−48687
heavy species velocity, in low density supersonic free jet 79−94754
heterogeneous liquid stream, stress diffusion effect, molar diffusion coeff. 78−79338
highly attenuated gas flow around body, surface interactions, free molecular conditions 79−90285
hydrodynamic theory, ang. vel. correlation function with slip boundary conditions 77−47043
hypersonic cavitation of high and low gas mixtures at low density *(German)* 80−1651
hypersonic flat-plate problem, numerical simulation 77−19626
hypersonic flow on wedge, numerical anal. *(Japanese)* 79−32580
hypersonic flow over blunt wedge, cooling 77−35169
hypersonic flow past forward facing step 77−42872
hypersonic free molecular flow, momentum transport to surfaces 79−64704
hypersonic free molecular flow, pulse transmission coeffs. for surfaces *(Russian)* 77−89163
hypersonic free-molecular heating of micron size particulate 79−4058
hypersonic laminar boundary layer at stagnation pt., slip, mass transfer 77−19625
ideal monatomic gases, rarefied flow statistical modelling, computer simulation 79−98753
incompressible Kramers problem, direct simulation 79−94666
inert gases, weak shock wave struct. investig. 79−94679
initial shock parameters for explosion in rarefied gas 80−53815
inlet flow with slip, laminar in incompressible Newtonian fluid 79−94659
intermolecular interaction, Boltzmann eqn., Monte Carlo simulation *(German)* 78−34165
ionospheric rocket-borne mass spectrometer, Monte Carlo prediction of +ve ion collection 80−8459
isotope separation, by probe in supersonic flow, Monte Carlo simulation 79−94098
isotope separation techniques based on vel. slip in freejet expansions 80−19441
jet, free, streamlines and local velocities in rarefied atm. 77−42884
jet flow, free expansion of N_2, expt. tests of energy balance eqn. 79−98777
jets, free expsn. and interference 79−46353
jets, issuing into rarefied chamber *(French)* 79−7395
kinetic theory, Boltzmann eqn. generalisations for relatively dense systems 79−98851
kinetic theory of rarefied flow, closure relations 79−98757
laminar boundary layers with swirl in slip regime 77−31336
linear rarefied gas dynamics, integral transport equation functional anal. 79−50756
linearised plane Couette flow, rarefied gas with infinite range molecular interactions, asymptotic anal. 79−23340
low density supersonic gas flow, temp. meas. probe 80−74913
low density wind tunnel for rarefied gas dynamics 80−96285
low-density flows through tubes and nozzles 79−94658
low-density hypersonic wedge flow, numerical soln. 79−94665
low-speed flow over sphere, convergence of integral methods 78−22375
mass dependent molecular beam focusing by cross-jet deflection 79−93257
mass transfer in cylindrical channel with evaporation and condensation at walls 80−6101
mass transfer in highly rarefied gas 77−11222
Maxwell gas, shock struct., numerical integration of Burnett eqns. 79−94677
MHD channel flow, effects of external cct. 80−33630
MHD channel flow of rarefied gas, external circuit effects on heat transfer 80−83860
MHD flow near time-varying accelerated plate 77−11271
MHD slip flow regime over porous plate, skin friction and heat transfer 77−31392
moderate density gas, isothermal creep along planar surface 79−82022
molecular beam generator for investigating gas flow 79−32717
molecular beam parameters meas. in presence of residual gas 79−27727
molecular beams, intensity dependence on stagnation temp. 77−68629
molecular flow, approx. calc. of transmission probability for conductance of tabulations 79−68756
molecular flow, in tubes, effect of cross-sectional shape 79−64710
molecular flow, structure with arbitrary geometry, kinetic anal. method 80−79355
molecular flow conductance of long tube, cross section depend. 78−34167
molecular flow in vacuum, kinetic method analysis, flux in elementary structs. 78−55663
molecular flow in vacuum kinetic method for analysis basic formulation 78−51201
rarefied fluid dynamics continued
molecular flow through cylindrical channel, Monte Carlo calc. 77−55042
molecular gas radiation in the thermal entrance region of a duct 80−6051
molecular hydrodynamics of inhomogeneous systems, slip boundary conditions 77−89165
molecular shield for Shuttle Orbiter, effect of expts. on density distrib., model 78−22374
molecular velocity distribution function between differentially heated parallel plates 79−94663
monatomic gas, rarefied flows in axisymmetric expansion nozzle 80−92182
monodimensional Poiseuille and thermal creep flows, rigorous constructive soln. 78−30319
Monte Carlo simulation of homogeneous dissociating diatomic gas 77−51128
multicomponent isothermal diffusion and forced flow of gases in capillaries 79−18914
n-incompressible and immiscible rarefied gases, pulsating flow between two plates 80−10306
Navier-Stokes equations solutions for flow in rectangular groove facing moving wall 77−42874
nonequilibrium free jet expansion, translational temp. meas. in N_2 80−64600
nonlinear Boltzmann eqn., rarefied gas, fluid dynamical limit 78−79336
nozzle, gas mixture in quasi-one-dimens. flow, vel. slip and temp. difference 79−64735
nozzle beam expansion, Monte Carlo simulation 79−94675
nozzle flow formation of cluster beam, high energy beam 80−5638
nozzle of molecular beam mass spectrometer, sampling nozzle 79−49330
nozzle profile for free molecules flow simulation of air-intakes and cascades 79−94652
nuclear reactor fuel element gap conductance, heat transfer over range of Knudsen number 78−13213
optical interferometry, gas dynamic meas., review 77−35286
outgas flow from spherical spacecraft, Bhatnagar-Gross-Krook model 79−94676
parallel plate flow of polyatomic gas, theory, and thermal transpiration effect 79−86466
particle slip, temp. depend. in gaseous medium, free mol. regime 77−11249
plasma, nonisothermal, transport processes and Lenard-Balescu eqn. 80−6222
plasma rarefied flow around body, electrostatic field struct. in wake 77−91402
Poiseuille flow, thermal creep and slip at boundary wall 79−68753
Poiseuille slip and thermal creep at boundary surface *(Russian)* 78−38371
polyatomic gas, thermomag. press. difference, ang. depend. 78−51199
polyatomic gases, ang. momentum polarisations, boundary layer behaviour 78−51200
profiling pressure pulse by rarified gas layer 77−68631
propane, freejet flow, vibr. relax. time 79−98760
propane-CO_2, freejet flow, vibr. relax. time 79−98760
relaxing low-density flow, nonequilib. flow expts. at Novosibirsk 79−98824
scattering index from rough surface, meas. in high speed molecular flow 79−94653
scattering of gas stream by rough surface, spectral expansion method *(Russian)* 77−58739
separated supersonic gas flow at low Reynolds no., heat transfer 79−98713
sharp flat plate, drag reduction in rarefied hypersonic flow 79−94669
shock wave structure, model eqns. for nonlinear Boltzmann eqn. 79−98758
shock wave structure close to wall, book contrib. 80−1650
shock wave visualisation, at few torr, holographic technique 77−55038
shock waves in monatomic gas, ionising large Mach numbers 80−6096
shock-shock interaction in hypersonic flow 79−94673
shockless near free molecular flow, drag reduction calc., profile optimisation 79−14435
Shuttle/Spacelab platform in near Earth ionospheric plasma, aerodynamics 80−8517
slightly rarefied gas, unsteady motion about rotating cylinder, slip effects 77−39312
slip boundary condition, rough sphere ang. vel. correlations, hydrodynamic anal. 77−51286
slip boundary condition for rough sphere rotation 77−31335
slip flow, developing, vel. distrib. and press. drop, Navier-Stokes analysis 77−55039
slip flow, MHD, over porous plate, with variable suction, heat transfer 78−79337
slip flow in porous medium, effective diffusion coeff., variational method 79−90325
slip flow over surface due to temp. difference 77−932
slip flow past tangential flat plate at low Reynolds numbers 78−47000
slip flow with suction or injection, Rayleigh problem 77−19627
slip flows, analogy for viscous incomp. flows 79−64707
slow viscous flow, slip-plane and slip-cylinder theorems 78−14046
small channels, gas flow, graph and nomograph for anal. eval. 80−106848
sound wave propagation, in rarefied gas, linearised BGK model calcs. 79−64369
source flow expsn., distrib. function model 79−27667
Spacelab pallet, meas. of mol. streaming fields 80−82173
sphere, drag in low velocity rarefied gas flow 80−48752
sphere drag coeff. correlation method, continuum and rarefied flows 77−84349
sphere in gas slip flow, vel. field, heat exchange, friction dissipation *(German)* 78−34138
sphere rotation in rarefied gas *(Russian)* 79−14436
sphere slow rotation in confined vol. of dilute gas 79−77187
spherical condensed phase, motion in uniform vapour gas flow, kinetic theory 78−1725
spherical particle in slightly rarefied gas, forces calcs. 79−94672
statistical particle-in-cell method for num. investig. of rarefied gas flows 77−55043
stochastic stationary Gaussian processes, rarefied gas theory *(Russian)* 77−35173
Stokes problem, free convection effects, rarefied gas flow past plate 79−32581

rarefied fluid dynamics continued
subsonic gas flow over convex corner, density jump *(Russian)* 77−65755
supersonic CO_2 flow, fluctuations in intensity of radiation excited by electron beam in jet core 77−55104
supersonic expansion of Ar, non-Maxwellian vel. distrib. function 79−98762
supersonic laminar flow over backward facing step, numerical soln. at high Reynolds number 77−47040
surface flow of dilute gas in model pores, free mol. flow calc. in adsorbent force field 80−6100
temperature-jump problem with arbitrary accommodation 78−67221
test particle diffusion, in conservative field, integral Boltzmann eqn. solns. 79−97324
test particle diffusion under conservative field, integral Boltzmann eqn. soln. 79−97325
test particle slowing down, rarefied gas added to host, with external conservative force 79−97326
thermal accommodation coefficients from heat transfer data for low-density gases 77−35167
thermal creep for gas flow in flat channel, accommodation coeff. 77−11264
thermal gas slip coeff., using Onsager symm. principle 77−58737
thermal transpiration, theory and expt. comparison using He, Ar, CO_2 and air 79−32579
thermal transpiration, thermal and friction forces, generalised hydrodynamics 77−35171
thermomagnetic force kinetic theory *(Russian)* 79−94765
thermophoreses velocity and coeff. of thermal slip of gases 77−7416
thermophoresis, photophoresis *(Russian)* 77−27560
transition flow, macroscopic theory *(Japanese)* 80−1647
transition flow, past bluff faced cylinder, Monte Carlo calcs. 79−94670
transition regime, rot. temp. and density distrib. meas. 79−98755
translational temp. determ. from mol. beam transverse density profiles 79−27726
transmission probabilities tubulation conductance, molecular flow regime 78−83433
transmission probability for mol. gas flow through tube 77−7417
transmission probability of free molecular flow through a tube 79−94662
two-dimensional long slots, rarefied gas transition flow 80−43738
underexpanded jet interaction with flat plate 79−94674
unsteady heat transfer from suddenly heated infinite plate in rarefied gas 78−34166
unsteady state slip of gas near infinite plane with diffusion-mirror refl. of mols. 77−35170
vapour distribution between parallel plates, condensation, evaporation 77−3847
vehicle hypersonic wake, radiation from injected small particles, free molecular regime 80−64650
vibrational nonequilibrium flow, transport coeffs. and relax. phenomena 79−98825
visco-magnetic heat flux, in Brunett regime 79−98844
viscomagnetic heat flux, in a Burnett regime, gas kinetic theory 78−71400
Ar, clusters in supersonic beam, electron diffr. study 80−5655
Ar-He rarefied mixture in supersonic nozzle and jet, longit. translational nonequilib. 79−27678
CO_2, beam molecules capture probability on surface 79−32578
CO_2, free expsn. of jet, nonequilib. effect 79−27676
CO_2, free jet, homogeneous condensation scaling law 80−6121
CO_2, rarefied jet beam, Raman scatt., for rot. temp. and density 80−6185
H_2 cluster beam formation, from nozzle flow, isotope effect 80−6127
H_2O vapour, shock waves, in pure vap. vibr. relax. time at low density 79−98761
N_2, flow meas. by electron beam-body interactions 80−6186
N_2 jet, mixing zone in continuous to free mol. transition 79−32605
N_2, rot. relax. in viscous shock layer *(Russian)* 77−89162
N_2, rot. temp. meas., rocketborne electron beam fluoresc. meas., reflected mol. effects 77−29519
N_2, rotational relax. in shock layer 79−64703
Na vapour jet target, gating and pumping action 80−10281
Ne isotope separation by gaseous diffusion transport in regular geometries 79−94099
UF_6, U isotope separation by velocity slip process, calcs. 79−94100
^{235}U, large scale enrichment using separation nozzle 79−94654
rarefied gas dynamics *see rarefied fluid dynamics*
rarefied gas flow *see rarefied fluid dynamics*
Rayleigh-Benard instability *see flow instability*
Rayleigh law *see Rayleigh scattering*
Rayleigh limit *see Rayleigh scattering*
Rayleigh scattering
acetic acid, Rayleigh-Brillouin scatt., 20-115°C, viscoelastic theory anal. 79−28774
acetonitrile, Rayleigh linewidth, in crit. region 79−24329
acetonitrile, soln., high press., mol. reorientation, correl. times, depolarised Rayleigh scatt. obs. 80−29748
acetonitrile-carbon tetrachloride solns., rot. and vibr. relax., Rayleigh and Raman scatt. 77−66513
acoustical waves, approximate formula for second-order scattering from N acoustical scatterers 79−81589
adsorbed molecule, classical theory of light scatt. 79−51944
adsorbed molecule near solid surface, light scatt. calcs. 79−56069
agglomerates of small spheres, scatt. efficiency factors 80−1131
air, absolute Rayleigh cross section 79−1342
aliphatic chains, mol. orientation correls. with squalane in soln., depolarised Rayleigh scatt. *(French)* 79−65885
alkanes, bonding, optical anisotropy and polarisability 79−22713
n-alkanes, depolarised Rayleigh spectroscopy 79−4808
n-alkanes, obs. and anal. of depolarised Rayleigh doublet 78−35154
alkenes, bonding, optical anisotropy and polarisability 79−22713
amorphous polymer, Rayleigh-Brillouin spectroscopy 79−38556
amphotericin B in H_2O and hydroalcoholic solns., circular dichroism, Rayleigh scatt., absorpt. spectra, temp. depend. *(French)* 78−62807
aniline-cyclohexane solution, depolarised mol. light scatt. near critical exfoliation temp. *(Russian)* 80−108222
antisymmetric light scattering of molecules with non-degenerate electronic state 79−18192
atmosphere, aerosol effects on polarisation of scatt. light from point source *(Russian)* 80−4106
Rayleigh scattering continued
atmosphere, luminance and colour temperature of clear sky *(Japanese)* 79−92594
atmosphere, Rayleigh scattering, optical thickness values 80−90216
atmosphere, scatt. of middle UV radiation from an internal source, Monte Carlo model 79−12263
atmosphere, sunlight scattering, Rayleigh and Mie theory 80−56605
atmosphere model, scatt. light intensity and polarisation degree, mol. anisotropy effect 80−77104
atmosphere optics, mol. and particles scatt., book 77−5323
atmospheric, estimation up to fourth order *(Japanese)* 77−13124
atom, K-shell electron elastic photon scatt., high-energy calcs. 77−431
atom, near-reson. scatt. with collisional perturbation, time and freq. depends. 79−72281
atom, photon scatt. by bound electrons, form factor predictions for amplitude, numerical method calc. 78−33474
atomic form factors, relativistic Hartree-Fock, tables for Z=1-100 79−59381
atomic Rayleigh scattering, 0-10 mc 80−9536
atomic system, magnetoelec. susceptibility in static mag. field 78−55143
bacteria, diffusing and motile, light scatt. props. calc., RGD approx. accuracy 79−92193
BBOA, thermal diffusivity meas. by forced Rayleigh scatt. 78−76483
benzene, depolaris. Rayleigh scatt., optical anisotropy 78−27245
benzene, in polar solvent, excess thermodynamic props., Rayleigh scatt. meas. 78−52523
benzene, laser wavefront reconstruction by stimulated scatts. in picosecond range 79−986
benzene+cyclohexane (hexafluorobenzene), isotropic light scattering, excess Gibbs function 79−8150
benzene(substituted)-n-alkane mixtures, mol. orientation correls., depolarised Rayleigh scatt. 79−22714
benzene depolarisation ratios 77−32387
benzene-n-alkane mixtures, mol. orientation correls., depolarised Rayleigh scatt. 79−22714
benzenes, substituted, optical bond anisotropies, by depolarised Rayleigh scatt. 78−90171
n-benzoates, MP and rot. mobility of struct. groups *(Russian)* 77−69074
benzocondensed five-membered heterocycles continuing S and O, optical anisotropy, depolarised Rayleigh scatt. obs. *(French)* 79−31533
benzonitrile, depolarised Rayleigh scatt. 78−68522
benzonitrile, transverse sound wave and mol. motion, light scatt. obs. 77−79621
bidirectional optical fibre, Rayleigh scattering freq. depend. meas. 79−64317
bidirectional optical systems, Rayleigh backscatt. freq. depend. 80−69511
binary fluid mixture, thermal diffusion ratio determ. by forced Rayleigh scatt. 78−75858
binary mixtures and simple fluids near crit. point, Rayleigh and Brillouin scatt. 77−36256
biophysics, laser techniques, reviews 77−90975
2,4-biphenylpentane, depolaris. Rayleigh scatt., optical anisotropy 78−27245
p-bis-octyloxyazoxybenzene, liq. cryst., thermal diffusivity, Rayleigh scatt. obs. 78−94977
bisphenol A-phthallic anhydride epoxy resin, diglycidyl ether, Rayleigh scatt., Brillouin and IR spectra 80−66211
bistability and anomalies in absorption and resonance scattering of intense light 79−95803
borosilicate glass, phase separated, depolarised light scatt. in terms of Rayleigh-Gans theory 79−87452
t-butylbenzene, depolaris. Rayleigh scatt., optical anisotropy 78−27245
p-butyloxybenzylidene-p'-octylaniline, liq. cryst., thermal diffusivity, Rayleigh scatt. obs. 78−94977
calcium alginate gels, Raleigh scatt., spectral broadening, density fluctuations 79−1776
carbon tetrachloride, depolarisation ratios 77−32387
carbon tetrachloride, Rayleigh scatt. from liq. near solidification temp. 79−4807
CBOOA, isotropic, nematic, smectic-A phases, Brillouin scatt. 80−11421
cellulose trinitrate, in soln., gel-like aggregate form. rel. to configuration 77−31036
central rigid cores, mesogenic power, depolarised Rayleigh scatt. study 80−89012
chloroform-ethanol solns., light scatt. spectra, conc. fluctuations, assoc. complex form. 77−40254
2-chloropropane, separation of collision-induced from intrinsic mol. depolaris. Rayleigh scatt., C-Cl bond optical anisotropy 78−27244
classical and wave mechanical theory 77−31067
clouds, optically thick medium, asymptotic radiance and polarisation 77−21776
coherent four photon Rayleigh scattering *(Russian)* 78−48191
coherent radiation scattering, calc. of diameter distrib. function of long hollow cylinders 77−70569
collision-induced spectrum, intermediate density, second freq. moment, appl. to Ar 80−24125
collisional and radiative damping effects in Rayleigh and reson. fluorescence scatt. at high intensities 80−102478
colloidal dispersions, birefringence in Rayleigh and anomalous diffr. approximations 80−29710
compressed gas, small depolarisation factor meas. method 78−32884
critical fluid, Rayleigh linewidth, simulation using emulsion 77−16324
critical fluid, Rayleigh linewidth meas., double scatt. effect 77−20865
cross-section measurement, momentum transfer effect 79−85969
crystal defect, Rayleigh and hyper-Rayleigh light scatt. 78−60478
crystals, book 80−2774
cumene, depolaris. Rayleigh scatt., optical anisotropy 78−27245
cyanobiphenyls, liq. cryst., thermal diffusivity, Rayleigh scatt. obs. 78−94977
cyclohexane, depolarisation ratios 77−32387
cyclohexane, dynamic props. investig. by Rayleigh scatt. of Mossbauer radiation *(Russian)* 77−69760
cyclohexane, laser wavefront reconstruction by stimulated scatts. in picosecond range 79−986
cyclohexane-methanol, crit. opalescence, AC elec. field effect 78−35159
cyclohexane-methanol, crit. opalescence, elec. field effect 79−28775
cyclohexane-tetrachloromethane, heteromolecular vibr. relax. time, Rayleigh-Brillouin spectra 78−59731

Rayleigh scattering continued
cis-dekalin, dynamic props. investig. by Rayleigh scatt. of Mossbauer radiation *(Russian)* 77−69760
Delbruck and Rayleigh scattering below 5 MeV 80−13456
depolarised Rayleigh bands, permanent series expansion for correl. functions 77−61752
depolarised Rayleigh scatt. and Kerr effect, dipole-induced dipole model 79−72321
depolarising dipole-induced-dipole effect *(French)* 77−61751
depolarized double scattering, spatial and temporal coherence coupling 78−1164
depolarized Rayleigh scattering from fluids of spherical molecules 78−88319
diatom+diatom, effect on depolarised light scatt. linewidths 80−58321
diatomic homopolar molecules, light scatt. *(Hungarian)* 77−50442
diatomic molecule, resonant and near-resonant Rayleigh and Raman scatt. 78−78705
dichloromethane, liq. and dil. CCl_4 soln., far IR spectra and Rayleigh scatt. for planar itinerant oscillator 78−47229
dielectric cylinder, infinite, randomly oriented, radiation press. 80−58454
dielectric needle and disc, light scatt. using Rayleigh-Gans and Rayleigh scatt. method 79−76591
1,1′-diethyl-4,4′-quinocyanine iodide, S_0-S_1 transition, relax. time meas. by reson. Rayleigh technique 78−42374
1,2-difluorotetrachloroethane, orientationally disordered, mol. reorientation, depolarised Rayleigh scatt. obs. 78−88316
1,4-dioxane, liq., reorientational correl. times from light scatt. 77−32385
disperse system, dilute, orientationally induced conservative dichroism 80−102623
disperse systems, light scatt., decay in orientationally induced var., Rayleigh approx. 80−45576
n-dodecane-β,β′-dichlorodiethyl ether crit. mixture, Rayleigh line wing 77−20864
n-dodecane-dichlordiethyl ether, stratified solns., depolarisation of scatt. light 78−10910
dust, soil derived atmospheric, IR spectra, Christiansen effect, Rayleigh limit 80−105046
dynamical properties of solid surfaces, analytic approach 78−71929
electrolytes, Rayleigh anisotropic light scatt. *(Russian)* 79−91459
electron+phonon system, weakly coupled, reson. light scatt. and luminesc. 77−12374
electron-phonon system, weakly coupled, resonant light scatt. and luminescence 80−40100
entropy and LA fluctuations in solids, polarisation of scattered light 77−81113
epoxy material, filled, US props. for sonar transducers 78−59867
ethane, gas-liquid crit. pt. region, depolarised light scatt. 78−34612
ethane-propane, binary mixture near crit. point, conc. fluctuation decay rate, spectrosc. obs. 77−81108
ethanol, picosecond stimulated Raman effect, time-resolved spectra 77−3369
ethanol mols. reorientation in ethanol-water mixtures, Raman and Rayleigh spectra 78−76449
ethylene, gas-liquid crit. pt. region, depolarised light scatt. 78−34612
external transverse resonator, spectral and time characts. of stimulated scatt. *(Russian)* 77−85738
Fabry-Perot expt. for lines in presence of elastic scatt. 78−4703
fibre optical ring interferometer, Sagnac-effect, sensitivity 79−50379
fibre waveguide, Brillouin and Rayleigh scatt. meas. 78−30085
fluid, near crit. pt., nonzero beam diameter and gravity effect 77−85737
fluid, near crit. pt., nonzero beam diameter effect 77−85736
fluid, of isotropic mols., DID Rayleigh and Raman depolarised scatt., lattice-gas model 80−10356
fluid, relaxing, thermally induced light scatt. 77−32388
fluids, polarisation state of light scatt. in elec. and mag. fields, symmetry indications 80−29751
fluids, Rayleigh-Brillouin scatt., nonlinear spectroscopy 77−50731
focused laser beams, Rayleigh-Debye scatt. 78−71030
forced, appl. in method to determ. thermal diffusion ratio *(French)* 78−2271
forced, for anal. of light-induced grating structs., review 80−20646
forced scattering, principle techniques and expts., review 80−34938
Freon-12(22), gas, Rayleigh vol. scatt. coeffs., spectronephelometric meas. 78−14127
gamma ray coherent scatt., semiempirical formulation 77−55846
gamma-rays, circ. polarised, magnetised Fe-Co scatt., spin depend. 77−59637
gas molecules, meas. of depolarisation rates and polarisability anisotropies 79−45770
gases, depolarisation ratio, molecular polarisability anisotropy 79−45730
gases and vapours, degree of depolarisation of scattered light, meas. accuracy, Raman-lines effect 80−1737
Gaussian light, partially polarised, photon statistics 80−19012
gaussian-lorentzian light, photoelec. pulses, two-fold time interval distrib. 77−41683
Gaussian-Lorentzian light, photon counting distrib. factorial moment, spatial coherence 80−83571
glass, Schott BG20 and FG18, forced Rayleigh scatt. anomalies 79−82988
glycerol, liq. and glass, thermal diffusivity meas. 79−82394
glycerol, supercooled liq., mol. motion, Mossbauer effect, Rayleigh scatt. obs. 77−73099
n-hexadecane-β,β′-dichlordiethyl ether exfoliating mixture, light scatt. and hypersound vel. 77−28586
ice-water interface, dynamic light scatt. during freezing 79−33074
imperfect Rayleigh scattering in semi-infinite atmosphere, transport eqn. soln. 79−75094
inert gas, dense, depolarised Rayleigh scatt. 79−69851
interstellar grains, unusual extinction profiles 77−45527
inverse scattering problem in Rayleigh-Debye approx., diameter distrib. functions of helical structs. 80−27182
ionic conductor, quasielastic scatt. of light, neutrons and electrons, Debye-Huckel eqn. *(Chinese)* 78−68521
ionic solution, light scatt., hydrodynamic theory 78−6692
isobutyric acid-water binary fluid system, crit. props. 77−76563
isotropic medium, 3-photon scatt. by density fluctuations *(Russian)* 78−74841
ketones, bonding, optical anisotropy and polarisability 79−22713
laser Rayleigh scatt., forward direction, spatial coherence deterioration, polaris. interferometry technique 77−10838
Rayleigh scattering continued
Lennard-Jones fluids, orientational and collision induced light scatt. 80−63644
light wave propagation in randomly inhomogeneous media, moments of field calc. in limit of saturated fluctuations 79−72497
linear atomic susceptibility role 78−55142
linewidth near crit. pt., simple fluid, gravity effect 77−85735
lipid-water smectic phase, forced Rayleigh scatt. 78−14278
liquid, depolarised light scatt., mol. motion and orientational correl. time *(French)* 77−1687
liquid, induced Raman scatt., anomalous line broadening 78−56490
liquid, mol. reorientation, autocorrelation functions 77−80400
liquid binary mixtures of optically anisotropic molecules, depolarized Rayleigh scatt. 80−40122
liquid crystal, Rayleigh scatt. in isotropic phase, mol. orientational correl., mesophase possibilities 77−84637
liquid crystals, thermal conductivity anistropy, forced Rayleigh light scatt. meas. 78−94991
liquid structure and dynamics from light scatt. spectra 80−55105
liquids, depolarised Rayleigh scatt., nonlorentzian behaviour, 3-variable theories *(French)* 80−25395
liquids, depolarised Rayleigh scatt., review 77−40256
liquids, molecular, depolarised light scatt., flow birefringence and local order 80−45094
localised electron nonequilibrium vibration interaction secondary radiation spectrum 80−2778
localised electron-phonon system, second order optical processes, transient response 78−43917
Lorenz-Mie scattering, range of validity of Rayleigh and Thomson limits 78−66755
low temp. plasma diagnostics by reson. Rayleigh scatt. 80−48980
low-frequency props. from scattering meas., flaws in solids appls 80−76475
2,6-lutidine-water critical mixture, spinodal decomposition, Rayleigh scatt. 80−70416
lycopene, soln., depolarised Rayleigh light scatt. in absorpt. bands 79−87451
macromolecular, solutions, Rayleigh scatt., elec. induced variations, spectral width and intensity meas., review 78−48187
macromolecule, rigid, in soln., depolarised Rayleigh spectroscopy 79−94119
macromolecules in soln., Rayleigh scatt., elec. reorient. rel. to spectral line rot. broadening 79−1774
macroparticles; charged spherical, dilute soln., Rayleigh scatt. 80−84748
malononitrile, displacive phase transition, 294.7K, Raman and Brillouin-Rayleigh scatt. obs. 80−16047
Markovian polymeric systems, Rayleigh scatt. and fluctuation correls. *(Russian)* 79−65890
MBBA, Frank elastic const. ratio determ. by Rayleigh scatt. 79−99059
MBBA, isotropic, depolarised doublet, de Gennes viscosity coeffs. 78−31207
MBBA, isotropic, obs. and anal. of depolarised Rayleigh doublet 78−35154
MBBA, nematic liq. cryst., thermal diffusivity, Rayleigh scatt. obs. 78−94977
MBBA, thermal diffusivity meas. by forced Rayleigh scatt. 78−76483
methane, collision-induced Rayleigh scatt. intensity calcs. 77−46569
methane, gas, Rayleigh-Brillouin scatt., hydrodynamic effects calcs. 77−470
methane, spontaneous thermal fluctuations, Rayleigh scatt. obs. 78−88317
methane, Stokes collision-induced Rayleigh scatt. 78−25546
methane, thermal diffusivity within 0.001K of critical temp., Rayleigh scatt. obs. 78−34607
methanol, Rayleigh linewidth, in crit. region 79−24329
methanol-cyclohexane, crit. mixture, single and multiple light scatt., autocorrel. spectroscopy 77−85734
3-methylpentane-nitroethane, binary fluid, Rayleigh linewidth meas. near crit. point 78−48190
metmyoglobin, dynamics study using Rayleigh scatt. of Mossbauer radiation 80−40963
mirror, dielectric, Rayleigh scatt. at 441.6 nm 80−97367
mixtures, Rayleigh line narrowing near critical mixing pt. 79−56803
molecular crystal, dipole plasma oscillations, scattering of light 79−33723
molecular crystal with point and linear defects 77−44011
molecular liquid, anisometric, light scatt. obs. of orientational pair correlations 77−36252
molecular liquid, depolarised Rayleigh-Brillouin spectra, theory 79−69850
molecular liquid, dynamical Rayleigh light scatt. 79−51970
molecular liquid, Rayleigh scattered light, spectral and intensity distrib., mol. statistical theory, Racah algebra approach 79−99890
molecular liquids, depolarised Rayleigh-wing scatt. and far IR absorpt. spectra 78−39532
molecular relaxation, statistical treatment, review 77−51284
molecular scattering of light, spatial dispersion, distributed dipole and local multipole approx. 80−80796
molecular solid, depolarised Rayleigh-Brillouin spectra, theory 79−69850
molecular spectroscopy book 80−27052
molecule, chiral, circular intensity differential, ang. relationship depend. 77−34639
molecule, collision-induced rot. Raman scatt. in low, high freq. Rayleigh tails 78−25546
molecule near solid surface, light scatt., classical theory 79−18247
molecules, nonrigid, orientational correlation times, tensor correlations 79−4220
molecules, Rayleigh and Raman optical activity, scatt. angle anal. 80−69151
molecules adsorbed on rough surfaces, Rayleigh, Mie and Raman scatt. 80−83378
monodisperse polymer solution, thermodynamic fluctuations, light scattering 77−52107
Mossbauer scattered radiation, perturbed ang. correl., hyperfine field determ. 77−81032
myoglobin, atomic vibr. mean square displacement, Rayleigh scatt. of Mossbauer radiation meas. *(Russian)* 80−100665
N-particle second order Rayleigh scatt., approximate formula 79−905
narrow gap semiconductors, magnetoplasma resonance, mag. dipole resonance, microwave effect 79−95437
nematic liquid crystal, narrow linewidth meas. 77−26408

Rayleigh scattering continued
nematic liquid crystal solutions, isotropic phase, orientational pair correl. obs. using depolarised Rayleigh light scatt. *(Russian)* 79−90552
nematic liquid crystals, viscoelastic props. 77−39538
nephelometer meas. of aerosols and gases 79−29865
nitrobenzene:n-hexane, depolarised Rayleigh scatt., crit. anomalies 78−68524
nitrobenzene, in acetone-isopropanol soln., Rayleigh scatt. and viscosity 80−5550
nitrobenzene, liq., induced Raman scatt., anomalous line broadening 78−56490
nitrobenzene, liquid and CCl_4 soln. shear waves and translation-rotation coupling obs. by depolarised Rayleigh scattering 80−71432
nitrobenzene-n-hexane, crit. mixtures, reorientation spectra, linewidths and intensities 79−28777
nitrobenzene-n-hexane crit. mixture, depolarised Rayleigh linewidth meas. 77−81112
nitrobenzene-n-hexane crit. mixture, Rayleigh line and depolarised scatt. 77−20864
nitroethane-3-methylpentane, binary liq., depolarised light scatt. at crit. point 78−39558
nitroethane-isooctane mixture, depolarised Rayleigh scatt. near crit. point 80−45089
nondipolar liquids, axially-symm., diamag. mols., Kerr effect and Cotton-Mouton effect meas. 78−39524
nonlinear optical methods of active Raman Rayleigh scatt. spectroscopy, review 79−991
nonspherical particles, Rayleigh-Gans-Debye scatt. theory 78−46510
nonunitarity of scattering approx. 79−64175
p-nonyloxy benzoate p-butyloxyphenol, smectic A to smectic C transition, crit. ang. fluctuations, Rayleigh scatt. obs. 79−95131
p-nonyloxybenzoate p-butyloxyphenol, smectic A to smectic C transition, crit. fluctuations, Rayleigh scatt. obs. 78−95140
nuclear-gamma ray scatt. using (n,γ) photons 80−18288
8OCB, nematic-smectic A transition, impurity effects 78−47507
7-8-OCB mixture, nematic-smectic A transition, impurity effects 78−47507
ocean, optically thick medium, asymptotic radiance and polarisation 77−21776
octylcyanobiphenyl, second sound propag. and smectic response function, forced Rayleigh scatt. obs. 79−86693
opt. freq. shifting of light and laser beams for Rayleigh scatt. spectroscopy 78−79392
optical fibre loss mechanisms, separation by graphical method 77−14806
optical fibres, bandwidth and backscatter measurements, review 79−64356
optical fibres attenuation, drawing conditions influence, expt. 78−68667
optical film, 441.6 nm, scatt. losses correl. with deposition parameters 79−78782
optical waveguide, Rayleigh scatt. of stimulated Raman scatt. Stokes component 80−106569
optically active mol. light scatt., elliptical polaris. production 77−58089
optically isotropic molecules, collision-induced Rayleigh scatt. intensity calcs. 77−46569
optically isotropic molecules, collision-induced scatt., many-body correls. 80−87127
organic liquid, Rayleigh factor absolute meas., 79−99896
organic tensio-active compounds, mol. orientation correlations in hydrophobic groups *(French)* 79−73957
Orientational optic effects from above Rayleigh particles 80−106453
particle shape effect on low freq. absorpt. 80−99626
particles in colloidal state, refr. index, theory 78−95567
PBLG, cholesteric, exam. of Rayleigh line reveals low freq. modes, scatt. via orientational fluctuations 78−19496
periodic hard corrugated surface, wave scatt., formalism and numerical solns. 78−81876
perovskites, crit. dynamics at struct. transition 77−12396
4-phenyl n-pentyl ester, Nematel 105, nematogen, isotropic phase, Rayleigh scatt. and mol. reorientation 78−34429
plane parallel atmospheres, radiative transfer eqn. soln. 80−67409
planetary atmosphere, polarisation state, aerosol and Rayleigh scatt. 77−49171
planetary atmospheres, Rayleigh scattering in spherical shells 78−85872
in planetary plane-parallel optically thick atmosphere 77−73947
plasma, excited atoms, near-reson. Rayleigh scatt. obs. 77−3992
plasma diagnostic technique, CW Ar laser, radiation scatt. 78−38536
plastic crystal, k-independent Rayleigh diffuse line and orientational order 77−36253
plastic crystal, Rayleigh scatt. of Mossbauer radiation 78−27125
PMMA, amorphous polymer, Rayleigh scattering of Mossbauer γ-rays 80−39926
PMMA, Rayleigh scatt. of Mossbauer γ-rays 79−73864
PMMA aqueous colloid, coagulation kinetics, light scatt. determ. 79−39215
polarisation effects in nonlinear scatt., hyper-Rayleigh (Raman) scatt. 77−88858
polyacrylamide-water gels, copolymerised with N,N-methylene bisacrylamide, dynamic light scatt. 78−60477
polyatomic fluid, local dynamics, spectroscopic studies, summer school lecture series 80−6343
polyatomic gas, in non-hydrodynamic domain, Rayleigh-Brillouin scatt. *(French)* 78−86872
polybutadiene-n-hexane-n-heptane soln., Rayleigh scatt., diffusion coeff., viscosity 78−15179
polycrystalline materials, freq. and grain size dependency of US attenuation 80−50783
polydisperse aerosols, Rayleigh-Gans approx. appl. 79−44249
polyethylene glycol, depolarised Rayleigh scatt., orientational motion, pure and soln. 77−44008
polyethylmethacrylate, Rayleigh-Brillouin light scatt. study 79−11425
polymer, amorphous, light scatt. and local struct. 77−81111
polymer, total integrated light scatt. intensity 80−45092
polymer films, low-angle apparatus, calibration 79−58803
polymer solns., supermol. struct. determ. from scattered light spectrum *(Russian)* 79−32880
polymer solution, depolarised Rayleigh scatt., time correlation function 78−2862
polymer solution, Rayleigh scattering, intermolecular correlations effect 80−75146
polymer solutions, dilute, depolarized Rayleigh scatt. 78−35155

Rayleigh scattering continued
polymer system, two-phase, transparency conditions, interparticle interference effects 78−23428
polymers, soln. props. by low angle laser light scatt. photometry 78−35156
polypropylene glycol, depolarised Rayleigh relax. times, backbone motion 77−566
polysaccharide gels, spectral broadening 78−31771
polystyrene, atactic, Rayleigh-Brillouin scatt. 77−4648
polystyrene, benzene soln., self-diffusion, test for scaling and reptation 79−77789
polystyrene, conc. soln., friction const., Rayleigh scatt. 77−35737
polystyrene, depolaris. Rayleigh scatt., optical anisotropy 78−27245
polystyrene, moderately conc. solns. in cyclohexane, polymer diffusion and dimensions 77−62462
polystyrene, photon correlation spectroscopy near glass-rubber relaxation 79−47464
polystyrene, polarised Rayleigh scatt. near glass-rubber relax., photon correl. spectroscopy 80−40124
polystyrene, soln., laser light scatt. Rayleigh linewidths anal., intramol. motion 77−3500
polystyrene, thermal polymerisation, kinetics, Rayleigh scatt. 79−57228
polystyrene in cyclohexane, dil. theta soln., translational diffusion coeffs., conc. depend., Rayleigh scatt. meas. 79−90812
polystyrene latex particle size by electron microscopy and light scattering 79−66365
polystyrene networks swollen in cyclohexane, swelling equil. and light scatt. at theta conditions 80−107036
polystyrene solns. at theta conditions, Rayleigh scatt. determ. of conc. depend. of diffusion coeff. 79−77790
polystyrene-cyclohexane mixture, Rayleigh and Brillouin scatt. and struct. relaxation 80−63640
polystyrenes, p-halogenated, optical anisotropies, Kerr consts. 78−27246
powdered samples, pressed discs. Raman versus Rayleigh light scatt. 79−91437
pyridine, cyclohexane soln., depolarised Rayleigh scatt. 79−47467
pyridine, liq. and in CCl_4 soln., depolarised Rayleigh scatt. 79−51973
pyridine-water soln., reorientational relax. and activation energy of pyridine, depolarised Rayleigh scattering 80−76037
QED theory of differential scatt., Rayleigh scatt. of circularly polarised light, two chromophores model 78−9157
quartz crystal, opalescence near α-β transition, static model rel. to domain wall form. 80−11420
quartz synthetic crystals, observation of growth defects by light scatt. tomography 78−71743
radiation field polarized, asymptotic characts. for low absorpt., appl. to nonconservative Rayleigh scatt. 80−5686
radiation transport, multidimensional, in plane-parallel atmosphere, appl. to 4.3 μm auroral arc 78−88917
radiative transfer in isothermal slab with Rayleigh scatt. 77−46896
redistribution of scattered radiation by collisions in nonimpact region of spectral line profile 79−35109
reflected light from Earth's surface, estimation *(Japanese)* 78−40663
representation of scatt. tensors by ellipsoids and by hyperboloids 79−91452
resonance enhancement in absorbing media, fluctuation theory 78−72533
resonance scattering, time and spectral resolution 77−58305
resonant Rayleigh type optical mixing, appl. to ultrafast relax. process obs. 78−42373
resonant Rayleigh type optical mixing, appl. to ultrafast relax. in dye solns. 78−42374
resonant Rayleigh-type mixing spectroscopy using picosec. dye laser system 79−44944
resonant Rayleigh-type mixing spectroscopy using ps light pulses, ultrafast relax. study 80−91834
resonant scattering of light by slowly fluctuating localized electrons 80−7365
rough surface, convergence limit of Rayleigh method for surface scatt. 78−56495
rough surfaces, general theory and small roughness limit 77−75423
ruby, forced Rayleigh scatt., 50 to 300K 77−42564
SAWs, propag. along corrugated solid boundary 80−87600
scalar wave scattering by periodic surfaces, general modal theory 80−87271
second order optical processes, stochastic theory 79−94201
semiconductor, deep impurity centres, elastic light scattering 80−97315
semiconductor, sound absorption at very low temps. 79−95089
SHG, parametric amplification and stimulated scatt. phenomena 77−38994
solar radiation reaching Earth's surface directly, turbid ideal Rayleigh atm. 78−36274
spectronephelometer, automatic scanning integrating, visible and IR spectra 77−79165
spheroidal particles, colloidal dispersions, refractive index 80−106454
stably stratified fluid layer under thermal constraint, propagating thermal modes, force Rayleigh scatt. 79−76943
stimulated Rayleigh wing scatt. line, anomalous shift in external transverse resonator containing CS_2, CS_2-ethanol, o-xylene 78−13763
stratified fluid layer, propagative thermal excitations, Rayleigh scatt. meas. *(French)* 80−33590
styrene, thermal polymerization, Rayleigh-Brillouin light scatt. study 78−53206
succinonitrile, plastic cryst., orientational order, depolarised Rayleigh scatt. method 78−75612
temporal characteristics of single-scatter radiation 79−59634
tenuous particles, generalisation of Rayleigh-Gans-Rocard approach 77−7006
terphenyl, liq. cryst., thermal diffusivity, Rayleigh scatt. obs. 78−94977
tert-butyl chloride, separation of collision-induced from intrinsic mol. depolaris. Rayleigh scatt., C-Cl bond optical anisotropy 78−27244
tetrachloromethane, separation of collision-induced from intrinsic mol. depolaris. Rayleigh scatt., C-Cl bond optical anisotropy 78−27244
tetrachloromethane isotopic liq., Rayleigh and Raman depolaris. components *(French)* 79−99895
tetrafluoromethane, collision-induced Rayleigh scatt. intensity calcs. 77−46569
tetrafluoromethane, collision-induced scatt., many-body correls. 80−87127
1,2,5-thiadiazole, liq., light scatt. from orientational and density fluctuations, hypersonic vel. 77−81110

Rayleigh scattering continued
tobacco mosaic virus, solutions, Rayleigh scatt., elec. induced variations, spectral width and intensity meas. 78−48187
toluene, depolaris. Rayleigh scatt., optical anisotropy 78−27245
toluene, in polar solvent, excess thermodynamic props., Rayleigh scatt. meas. 78−52523
transition quasilinear spectra of resonant secondary emission *(Russian)* 80−16102
transparent medium, linear birefringence meas. turning birefr. method *(French)* 79−8112
transport eqn. exact soln. by Laplace transform and Wiener-Hopf technique 79−8827
1,2,4-trichlorobenzene liq., mol. reorientation, translation and vibr. relax., Rayleigh and Raman spectra 80−95632
trichloroethane, separation of collision-induced from intrinsic mol. depolaris. Rayleigh scatt., C-Cl bond optical anisotropy 78−27244
trichloromethane, separation of collision-induced from intrinsic mol. depolaris. Rayleigh scatt., C-Cl bond optical anisotropy 78−27244
triethylamine, Rayleigh line and acoustic spectra, fine struct. 77−39629
2,4,6-triphenylheptane, depolaris. Rayleigh scatt., optical anisotropy 78−27245
two component reacting fluid, density fluctuations, light scatt. spectrum 80−25397
undecylazoxymethylcinnamate, crit. angular fluctuations above second order smectic-A to smectic-C transition 77−4190
Venus atmosphere, spectral line profiles and phase curves for Rayleigh scatt. 77−29684
vibrational relaxation of molecules in condensed media, survey, book contrib. 77−36295
virtual nematic-isotropic transitions, depolarised Rayleigh scatt. 78−51652
viscoelastic liquids, structural relax., fast and slow relax. limits 79−47465
viscous liquid, acoustic and thermal props., phenomenological models 79−82393
water, collision-induced far IR absorpt., depolarised Rayleigh scatt. 77−81100
water, Rayleigh-Brillouin scattering and compressibility 79−91455
water dodecane potassium oleate hexanol, micro emulsion, Rayleigh scatt., micellisation *(French)* 80−43055
water toluene sodium dodecylsulfate butanol, micro emulsion, Rayleigh scatt., micellisation *(French)* 80−43055
water-oil microemulsion, thermal diffusion coeff. *(French)* 79−87880
water-oil microemulsions, optical matching 80−61157
Ag electrode, enhanced inelastic light scatt. caused by adatoms 80−89013
Ar, cluster formation and homogeneous nucleation, comparison of expt. and theory 80−79925
Ar, depolarised Rayleigh scatt., mol. dynamics calcs., fluid density effects 80−24123
Ar, gas, compressed, Rayleigh-Buillouin spectrum, scaling 80−100062
Ar, gas, compressed, Rayleigh-Brillouin spectrum, hydrodynamic region 80−100063
Ar, liq., depolarised scatt. lineshape correlation function theory 77−40253
Ar, liquid, depolarized Rayleigh scatt. at triple point, mol. dynamics simulation 80−60617
Ar, triple point, depolarized Rayleigh scattering from fluids of spherical molecules 78−88319
Au, at 59.54 keV through 60° to 150° 77−83547
$BaMnF_4$, spectroscopy near ferroelec. transition, dielec. anomalies near mag. ordering temp. 80−75965
$Ba_{0.54}Sr_{0.46}Nb_2O_6$, line broadening effect in Rayleigh scatt. of Mossbauer radiation 80−50238
$BaTiO_3$, dynamic Rayleigh light scatt. in region of ferroelectric-paraelectric transition 78−64371
$BaTiO_3$, line broadening effect in Rayleigh scatt. of Mossbauer radiation 80−50238
$BaTiO_3$, para to ferroelec. transition, strong Rayleigh scatt. 78−76486
$BaTiO_3$:Fe, photoinduced Rayleigh scatt. and bulk photovoltaic effect 79−38554
$BaTiO_3:Fe^{3+}$ bulk photovoltaic effect and photoinduced Rayleigh scatt. 77−77226
Bi, liquid, elec. cond. and assoc. optical scattering 78−76040
CO_2, gas-liquid crit. pt. region, depolarised light scatt. 78−34612
CO_2, liq., 100 to 3000 atm., depolarised Rayleigh spectra, orientation dynamics, wings 78−92084
CO_2, near critical point Rayleigh and Raman scatt., Fermi diad 80−80765
CO_2, Rayleigh linewidth, vap. near crit. pt., gravitationally induced effects 79−82035
CS_2, in CCl_4, orientational fluctuations, depolarised Rayleigh relax. time obs., temp. and conc. depends. 79−4809
CS_2, in carbon tetrachloride soln., Raman scatt. 79−65850
CS_2, liq., props. from allowed light scatt. spectra 80−25364
CS_2 liquid, Rayleigh and Raman bands, intensities of interaction induced components 80−63645
CS_2, radiation self synchronisation on Rayleigh edge time stimulated scatt. in external resonator *(Russian)* 80−69461
CS_2-ethanol mixture, Rayleigh and depolarised Raman scatt. lines near crit. temp. 77−20863
CS_2-ethanol mixture, thermal diffusion ratio determ. by forced Rayleigh scatt. 78−75858
Cl_2, liq., dynamics, depolarised Raman and Rayleigh scatt. 79−99867
Co^+, Rayleigh and Compton scatt., differential cross section determ. 80−52912
D_2+D_2, collision effect on depolarised light scatt. linewidths 80−53059
Fe, $3d^64s^2$ and $3d^74s$ configs., Rayleigh and Compton scatt., differential cross sections 80−52912
Fe^+ (Fe^{2+}), Rayleigh and Compton scatt., differential cross section determ. 80−52912
α−Fe_2O_3 colloids, absorpt. index and colour 79−92009
Ge reflectivity changes due to illumination by beams of unequal frequency 79−76749
H atoms, Rayleigh scatt. from n=2 states, fusion plasma diagnostics appls. 80−43002
H_2, compressed, Rayleigh-Brillouin spectrum rel. to translational hydrodynamics 77−24856
H_2, D_2 and HD, intermol. collision process obs. using light scatt. expts. 80−53001
H_2 diffusion flame, Rayleigh temp. profiles meas. 80−16692

Rayleigh scattering continued
H_2, Rayleigh-Brillouin spectrum at high densities 78−90189
H_2^+, Raman and Rayleigh scatt. tensors 79−50027
H_2+H_2, collision effect on depolarised light scatt. linewidths 80−53059
H_2O, sum rule props., SCF optimizations of MO and VB calcs. 78−5156
H_2O, vap., depolarised Rayleigh scatt., rot. Raman spectra, mol. polarisability 78−33513
He, gas, compressed, Rayleigh-Buillouin spectrum, scaling 80−100062
He, gas, compressed, Rayleigh-Brillouin spectrum, hydrodynamic region 80−100063
He I, plasma, excited atoms, near-reson. Rayleigh scatt. obs. 77−3992
^{4}He, liq., dynamical behaviour to λ-line, light scattering review 79−7717
^{4}He, liq., Rayleigh linewidth meas. 78−14522
KCl:Pb, impurity distrib., light scatt. and microhardness study, heat treatment 80−96562
KD_2PO_4, acoustic phonon dispersion, elastic stiffness, light scatt. obs. 80−103966
KD_2PO_4, Brillouin spectrum and broad central component, depend. on scatt. wave vector direction 80−34931
KD_2PO_4, Rayleigh scatt. and narrow central component, depend. on scatt. wave vector direction 80−29747
KH_2PO_4, Brillouin-Rayleigh scatt. studies near ferroelec. transition temp. 80−76036
KH_2PO_4, crystal nonequilibrium thermodynamics, quasielastic light scatt., systematic anal. 79−61391
KH_2PO_4, D_2-impurities effect on Rayleigh central peak 77−81068
K_2O-GeO_2:tb^{3+}, Yb^{3+} glass, luminesc, cooperative sensitization correlated with Rayleigh scatt. intensity 78−52573
KOH, amorphous and aqueous soln., depolarised Rayleigh scatt., phonon-like excitations 77−81109
α-$LiIO_3$, Raman spectra behaviour in electrostatic field *(Chinese)* 80−7333
$LiNbO_3$:Fe, photoinduced Rayleigh scatt. and bulk photovoltaic effect 79−38554
Mo, at 59.54 keV through 60° to 150° 77−83547
N_2, absolute Rayleigh scatt. cross section at 10.6 μm 77−38674
N_2, Rayleigh and Raman depolarised light scatt., density evolution 78−58706
Na arc plasma, dense, high-temp., near-reson. Rayleigh scatt. 77−1019
Na atom, Rayleigh scatt. near $A^2P_{3/2,1/2}$-$^2S_{1/2}$ reson. doublet, polarisation reversal 77−10616
Na, near-resonant Rayleigh scattering and atomic flame fluorescence spectroscopy 79−92033
Na, Rayleigh scatt. from vap. in flames with N_2 and Ar diluents 79−22627
Na, reson. line, laser excitation, combustion Rayleigh scatt., at. flame fluoresc. spectroscopy 80−42972
NaCl, containing Na colloids, first-order Raman spectra 79−73943
$NaNO_3$, disordered, temp. depend. of Raman spectra, Rayleigh wing scatt. 78−31209
$NaNO_3$, order-disorder transition point, hyper-Rayleigh scatt. due to rotation of NO_3^- 78−52520
Na_2O-B_2O_3-SiO_2 glass, Rayleigh scattering losses 79−99893
Na_2O-CaO-SiO_2, glass, light scatt. rel. to heat treatment *(German)* 78−84598
Ne, gas, compressed, Rayleigh-Buillouin spectrum, scaling 80−100062
Ne, gas, compressed, Rayleigh-Brillouin spectrum, hydrodynamic region 80−100063
Ni^{2+}, Rayleigh and Compton scatt., differential cross section determ. 80−52912
$Ni_3B_7O_{13}I$, struct. and mag. transitions, light scatt. study 79−24308
O (O^+) (O^{2+}), Rayleigh and Compton X-ray scatt. cross sections in plasma 80−43884
PLZT type ceramics, variation of light scatt. during field induced AF→F transition *(French)* 77−90158
Pb, at 59.54 keV through 60° to 150° 77−83547
Pb, Rayleigh scatt., expt. and form factor approx. 78−33474
$Pb_5Ge_3O_{11}$, dynamic central peaks and phonon interactions near structural phase transitions 78−83903
$RbAg_4I_5$, crystal nonequilibrium thermodynamics, quasielastic light scatt., systematic anal. 79−61391
$RbAg_4I_5$, solid electrolyte, Rayleigh-Brillouin and low-frequency Raman spectra 79−33720
SF_6, collision-induced Rayleigh scatt. intensity calcs. 77−46569
SF_6, gas, Rayleigh vol. scatt. coeffs., spectronephelometric meas. 78−14127
SF_6, gas-liquid crit. pt. region, depolarised light scatt. 78−34612
SF_6, liq., depolarised light scatt., dipole-induced dipole effect 77−12395
SF_6, long-range correlation length near liquid-vapour transition, Rayleigh scatt. 77−8593
Sb, Mossbauer radiation, Rayleigh scatt., Debye-Waller factor determ., annealing effect 80−39963
Sb_2Te_3, Mossbauer radiation, Rayleigh scatt., Debye-Waller factor determ., annealing effect 80−39963
Sn, at 59.54 keV through 60° to 150° 77−83547
$Sn_2P_2S_6$, soft mode, interaction of modes and crit. Rayleigh scatt. 79−99836
Sr, near reson. laser beam Rayleigh scatt., collisional redistrib. and saturation 77−57938
$Sr_xBa_{1-x}Nb_2O_6$, neutron and light scatt. in phase transition region 78−64336
$SrTiO_3$, dynamic central peaks and phonon interactions near structural phase transitions 78−83903
$SrTiO_3$, forced thermal scattering 78−80371
Ta (γ,γ), 2.754 MeV, elastic scatt. diffr. cross section, Rayleigh, Thomson, Delbruck scatt. interference 79−528
Ta, at 59.54 keV through 60° to 150° 77−83547
Te, amorphous, Rayleigh scatt. of Mossbauer radn., lattice dynamics 80−15845
Xe, fluid, near crit. point, correl. range and Rayleigh linewidth 80−93352
Xe, gas-liquid crit. pt. region, depolarised light scatt. 78−34612
Xe, ortho-positron quenching rate critical slowing down near gas-liquid transition 77−24907
Zn, at 59.54 keV through 60° to 150° 77−83547

Rayleigh-Taylor instability *see flow instability*

Rayleigh waves
see also surface acoustic waves
acoustic microscope, ray interpretation of material signature 80−1386

Rayleigh waves continued
amorphous film, tunnelling states, at low temps., thermal and acoustical props. 77−24500
amplitude-distance relation 77−73651
anisotropic, elastic crystals, Rayleigh wave speed, secular eqn. 79−77889
anisotropic attenuation of mean-period seismic waves 79−88259
anisotropic elastic half space, existence 79−27575
anomalous Eurasian earthquakes, spectral and magnitude charact. 77−73656
anomalous generation from underground nucl. explosion 80−81833
E.Antarctica, age from Rayleigh wave dispersion meas., Precambrian shield 79−92513
antifrictional materials, propag. along rough surface 77−68505
N. Atlantic, 1972 May 13, focal parameters from Rayleigh wave study *(Spanish)* 77−86823
attenuation across Pacific Ocean, 15-110 s periods 77−9353
attenuation by point defects 79−73251
attenuation of elastic waves by surface inhomogeneities 79−23822
backscattered echoes rel. to circumferential waves impinging on submerged Al cylinders 79−86276
Black Sea basin, crustal struct. from Love and Rayleigh waves dispersion *(Russian)* 78−28192
brass/water interface leaky Rayleigh wave reflectivity loss meas. 78−59187
channel waves propag. in coal seams, model seismic expt. *(German)* 78−40513
China, seismic surface wave study of crust and mantle 80−104916
couple stress effects on wave prop. in elastic layer immersed in infinite liquid 79−1126
critical surface wave velocity near phase transitions 77−35803
cylinder on elastic support, excitation by harmonic Rayleigh waves, free surface effects *(German)* 78−87296
cylindrical cavity in elastic half-space, Rayleigh wave loading, stress spectral representation 80−64453
defectoscopy, development of and problems in theory of normal waves, review 80−81265
dispersion, rel. to mantle structure under north central Italy 80−3977
dispersion, subsurface struct., estimation, dense data 77−39730
dispersion and damping of Rayleigh wave propagating along rough surface 80−102892
dispersion function computations for unlimited freq. values 80−21837
dispersion in upper mantle of W.Europe 77−73693
dispersion in visco-elastic solid *(Japanese)* 77−17035
dispersion on rough surface, model of surface layer 77−39727
dispersion relations for surface waves in cubic crysts. 80−102906
Earth crust and upper mantle, inversions of high freq. $Q_\gamma^{-1}(f)$ 77−33000
earth mantle, regional differences in phase velocity and Q-factor 79−16413
Earth upper mantle, inversion of surface wave dispersion data with random errors 77−73681
earthquake magnitudes from ultralong period seismometer records 77−44928
elastic isotropic half space interaction with periodic surface corrugation 79−50484
elastic surface waves propag., charact. for SAW filters, book contrib. 80−1378
energy flux for trains of inhomogeneous plane waves 80−46817
excitation and detection using piezoelectric polymer sheet transducers *(French)* 79−14182
ferroelectric crystal with piezoeffect, Rayleigh wave propag. near Curie temp. 77−89630
ferromagnetic metal, EM generation of US guided waves, model 78−22236
ferrous material, wave vel. and attenuation 80−2258
film coated materials, Rayleigh wave dispersion, approx. solution 77−39731
frequency-filter anal. of surface waves, fast method, west Pacific region appl. 79−48573
global and regional phase vels. of long-period fund. mode waves 77−73680
Great Basin of Nevada and W Utah, struct. from seismic surface waves 78−73336
great circle waves attenuation and group vel. 79−2192
group vel. distribs. and upper mantle models, Pacific Ocean *(Japanese)* 79−70747
heterogeneous material, effective elastic props. of finite media, integro-differential eqns. *(German)* 78−22291
hexagonal crystal, surface contrib. to low temp. sp. ht., and Rayleigh wave velocity 77−1233
hexagonal crystals, semiinfinite, surface waves charact. 79−60614
inelastic particle reflection 79−74022
interfacial waves launched by an explosive line-source in a submerged elastic half-space 78−75088
isotropic materials, third-order elastic moduli meas. using Rayleigh waves *(Russian)* 80−50786
isotropic solid half-space, Rayleigh and leaky surface waves 77−50974
Japan area, surface wave group vels. 77−56603
laminar crystal, surface waves *(Russian)* 78−84041
leaky Rayleigh waves, restrictions on the existence 79−82429
liquid-filled crack, Rayleigh wave reflection and transmission calc. 77−32762
lossy liquid-lossless isotropic solid interface, reflection coeff. acoustic wave reflection coeff. 79−72733
magneto-thermoelastic solids with thermal relaxation 79−28581
magnetothermoelastic Rayleigh waves with thermal relaxation, theory 79−62
magnetothermoelastic Rayleigh waves with thermal relaxation in uniform magnetostatic field 80−2617
magnetoviscoelastic solids under initial stress, surface waves 79−84140
mantle of Europe and Eurasia, inferences from higher mode seismic data 80−72436
Mediterranean area, surface wave and seismotectonic studies 77−37151
metal, detect. via electrostatic transducer, NDT appls. 77−19498
metal, Rayleigh sound absorption *(Russian)* 78−43233
metal, SAW mode conversion, by EM generation of US 80−84357
metal surface, resonant absorpt. of sound *(Russian)* 78−95216
metal-dielectric contact, surface barrier Rayleigh wave transducer 79−98578
microcracks, Rayleigh waves interaction, and extension 80−39214
microseisms, geological control on three-component spectra 79−84122
Rayleigh waves continued
microseisms meas. on Isle of Sylt *(German)* 77−86808
microseisms obs. at New York Rayleigh and Love wave charact., geologic control 80−26462
mode conversion, shear, Lamb and Rayleigh waves, demonstration 80−101687
Mountain Crimea region, surface seismic Rayleigh waves, amplitude spectra 80−89969
multilayered half space solutions, computer algorithms 80−98260
multiple surface waves on viscoelastic half-space 78−79254
New Hebrides earthquake, dispersion of first and second Rayleigh modes, periods greater than 50 s *(French)* 77−64212
nonellipsoidal sample, demagnetising factor meas., magnetoelastic Rayleigh wave convolution 77−10072
nonlinear interaction in $LiNbO_3$-CdS system, expt. investigation 80−102946
North Sea region upper mantle struct. from Rayleigh wave dispersion 78−36122
Novaya Zemlya crust and upper mantle model from Rayleigh wave dispersion data 79−84187
oceanic long-period Rayleigh group vel. dispersion curve from HF Doppler sounding of ionosphere 79−70756
oceanic upper mantle intrinsic heterogeneity effect on Rayleigh wave phase vels. 77−49022
Oroville earthquake, California, 1975 August 1, surface wave constraints on source parameters 77−56579
P-wave to Rayleigh-wave conversion coefficients for wedge corners: model experiments 79−14309
Pacific crust surface wave dispersion 77−56604
Pacific upper mantle regionalized shear vel. models from Love and Rayleigh wave dispersion 79−53321
phase vel. determ. of fundamental Love and Rayleigh waves 77−37148
physics of elastic surface waves 77−50981
piezoelectric crystals, elastic surface waves 80−103558
piezoelectric medium, semibounded, body waves and quasi-body surface waves 80−107367
piezoelectric semiconductor film, Rayleigh wave amplification, quantum theory approach 77−69158
piezoelectric surface waves on cubic crystals, energy propagation props. 78−51811
piezoelectric surface waves on semiinfinite crystal, asymptotic expressions 78−51812
pink westerly granite, wave propag. study by holographic interferometry 78−20536
polymers, corrugated surface, Rayleigh wave excitation, modified wedge method 79−37261
polymers, mech. props. testing 79−70249
prism couplers for Rayleigh and Lamb waves, anal. 80−69619
propagation, isotropic elastic material with homog. strain 78−94460
propagation in layer sandwiched between two semi-infinite media 77−68480
propagation over liquid and crystalline layers, effect of crysts. elastic consts. 80−76924
propagation over liquid and crystalline layers, theory 80−76925
Pyrex, stress intensity factors of surface cracks and fracture stress, acoustic meas. 79−47845
quasistationary Rayleigh waves on inhomogeneous anisotropic elastic body surface 80−69721
Rayleigh waves, surface topography effects on propagation 77−37154
real-time US imaging with shear, Rayleigh, and Lamb waves 77−32759
reflection acoustic microscopy, acoustic material signatures 79−46139
reflection and transmission coeffs. in media with lateral inhomogeneities 77−37156
reflection from periodic corrugations of surface in oblique incidence 80−58850
Reykjanes Ridge, Rayleigh wave dispersion rel. to lithosphere age 79−88267
roughness effects on dynamical props. 78−75923
S-wave velocity, lateral var. in upper mantle, Rayleigh mode data 79−66643
San Fernando earthquake, strong ground motion, ray models 80−61762
scattering by surface breaking crack, ray analysis 80−69575
scattering from hard corrugated surfaces, ill conditioned matrices 79−35572
scattering from topographical irregularities at oblique incidence 78−38927
scattering of normally incident waves by thin surface strip 77−11773
seismic, fundamental mode and harmonic waves, appl. to distant earthquakes focal depths determ. 80−21654
seismic amplitude attenuation across Eurasia 77−91028
seismic attenuation in volcanic area of Massif Central, France 80−98264
seismic channel waves for reflection method, dipping coal seam discontinuity obs. 78−69471
seismic dispersion over Canadian Shield 77−91029
seismic higher mode phase vels., regional var., spatial filtering 78−77187
seismic higher mode Rayleigh waves, study as individual seismic phases 79−62440
seismic interference waves (F-waves), appl. in coal forms. seismic tracing *(Russian)* 79−74858
seismic long period, obs. phase vels. across Canadian shield 78−61346
seismic long-period waves dispersion obs., shield-like upper mantle struct. 77−56608
seismic phase velocity and attenuation, simultaneous inversion over continental and oceanic paths 79−92488
seismic Rayleigh surface waves, interaction with structures 78−81109
seismic Rayleigh wave signatures from Nevada Test Site (NTS) explosions, inferred crustal structs. 79−66632
seismic Rayleigh waves, dispersion function computations for unlimited freq. values 79−74848
seismic Rayleigh waves, first and second modes dispersion meas. 79−39974
seismic Rayleigh waves, phase vel. investigations in middle Europe 79−44136
seismic Rayleigh waves, possible mode conversion at continental margin 78−73314
seismic Rayleigh waves, scatt. by ridge 77−78125
seismic Rayleigh waves in mantle, phase vel. and Q 79−74846
seismic Rayleigh waves of period 50 seconds, group vel. distrib. in Pacific Ocean 78−65197
seismic study of crustal and upper mantle structure beneath Apennines 80−46153

Rayleigh waves continued
seismic surface wave data inversion in source mechanism studies 77−33204
seismic surface waves, principal mode and harmonics obs. for earthquakes focal depth determ. 78−61351
seismic surface-wave ray tracing, appls. 79−66630
seismic wave amplitude meas. from earthquakes in distance range 0-150° 78−48979
seismic wave anelastic attenuation lateral var. across Pacific 79−84123
seismic wave dispersion and rifting in Tyrrhenian Sea 80−56445
seismic wave flattening corrections 77−40987
seismic wave phase vels. rel. to upper mantle struct. in Apennines 78−53618
seismic waves, great circle attenuation and group vel. for 150-600 s periods 77−49030
seismic waves, phase-matched filters appl. 78−45010
seismic waves azimuthal anisotropy, physical model 78−65186
seismic waves dispsersion, Baltic shield and Barents Sea, crust and upper mantle struct. 78−77204
seismic waves from point source in spherical medium with homogeneous layers 78−92790
seismic waves group vel. in Cap Vert and Canarian Basins *(French)* 77−32999
seismic waves refr. and refl. in Tibet 77−78120
seismic waves under Pacific Ocean, group vels. and response 80−41398
semi-infinite isotropic elastic medium, reson. scatt. of Rayleigh waves by mass defect 80−20025
shell, cylindrical, Rayleigh wave propag. using elasticity theory *(Russian)* 80−38307
small earthquake mechanism and depth from radiation patterns 80−61764
smooth surfaces of arbitrary shape, propag. of waves 80−64272
solid surface, Rayleigh wave scatt. from mass defect 77−20177
steel, round bar inspection, EM-acoustic techniques 78−60973
steel, US critical angle reflectivity, near-surface metallic prop. gradient effect 80−70516
stressed anisotropic solid, Rayleigh wave vel., third-order elastic constants 77−11772
superconductor, Rayleigh sound absorption *(Russian)* 78−43233
surface layer structure, from Rayleigh wave dispersion, anal. theory for sparse data case 78−38928
surface layer structure estimation from Rayleigh wave dispersion, sparse data case 79−14995
surface polariton interaction with periodic surface struct. 77−47879
surface Rayleigh waves, magnitude MLV depend. on travel paths 77−21681
and surface thermodynamics 78−6207
surface wave generated at Rayleigh angle, velocity determ. by graphic method *(French)* 77−4253
surface waves anomalous propagation in Barents Sea, from NORSAR data 79−25202
surface waves in vertically inhomogeneous elastic halfspace with horizontal inhomogeneity 77−52998
surface waves propag. in crystalline media 78−2350
surface-tension dispersion of Rayleigh waves 80−14513
teleseismic Rayleigh waves, anal. for S.California regional S-wave struct. determ. 79−92510
thermoelastic half space under initial stresses, Rayleigh waves 79−94545
thermoelastic layer, gravity influence on wave propag. 79−94544
thermoelastic Rayleigh-type surface waves, retrograde modes 79−77888
thermoelastic surface waves in micropolar elastic solid medium 77−72206
thermoelasticity, coupled problems, wave propags., effect of second order time derivatives 77−42772
Thomson-Haskell method extension to non-homogeneous spherical layers 77−9362
transducer, pick-up efficiency of wedge-type 77−77708
transmission and reflection through a step 78−44775
transmission coeffs. in trench 80−98266
transmission coeffs. through vertical interface 80−46144
transmission prevention, trench performance, seismic model experiments 80−24727
upper mantle S-wave velocity model, based on great circle Rayleigh waves 80−109107
upper mantle structure, probed by use of higher wave modes 80−104890
US leaky-waves, interaction with subsurface flaws 77−63868
USA Midwest, ellipticity of Rayleigh waves 77−73648
velocity measurement, pulse technique 78−5618
viscoelastic media, surface wave propagation 78−42555
viscoelastic Rayleigh waves over isotropic half-space 77−68499
Vladivostok earthquake 1973 September 29, seismic moment from P-waves and mantle Rayleigh waves 78−61354
Walvis Ridge, lithospheric struct. from Rayleigh wave dispersion 80−41412
weakly nonlinear medium, wave propagation anal. 78−67897
YIG, convolution with magnetoelastic Rayleigh waves 79−64404
Al, plastic deform. effect on third-order elastic moduli, dislocation anharmonism *(Russian)* 80−50786
Al-alloys, laser-induced, Rayleigh waves 79−51407
$BaTiO_3$, nonpiezoelec. dielec., light-sensitive Rayleigh wave generation by surface piezoelectricity 78−43228
$BaTiO_3$, Rayleigh wave generation by surface piezoelectricity 78−71925
$BaTiO_3$-metal contact, surface barrier Rayleigh wave transducer 79−98578
CdS, surface acoustoelec. current due to Rayleigh wave, ambient medium effects and surface state changes 77−69383
Fe, cast, with uniaxial loading, changes in ultrasonic waves vel. and attenuation 79−15756
KCl, irrad. with intense nanosecond electron beam, super-Rayleigh vel. of brittle fracture front 80−6458
$KTaO_3$, nonpiezoelec. dielec., light-sensitive Rayleigh wave generation by surface piezoelectricity 78−43228
$KTaO_3$, Rayleigh wave generation by surface piezoelectricity 78−71925
$KTaO_3$-metal contact, surface barrier Rayleigh wave transducer 79−98578
$LiNbO_3$, light scatt. by Rayleigh waves on refl. and transmission 79−24288
$LiNbO_3$-CdS, layered structure, transverse acousto-electric current 80−44669
$LiTaO_2$ and $SiO_2/LiTaO_3$ struct., Rayleigh waves, piezoelectric leaky surface waves, temp. depend. 79−46905
Rayleigh waves continued
NiZn ferrite, magnetic field effect on Rayleigh wave attenuation 78−6557
Si amorphous film, acoustic study using Rayleigh waves 80−75312
SiO_x amorphous films, acoustic study using Rayleigh waves 80−75312
$SrTiO_3$-metal contact, surface barrier Rayleigh wave transducer 79−98578
YIG, anisotropic elastic waveguide normal-mode anal., appl. to Rayleigh-Love wave mode converter 79−23113
YIG, ferromag. film on nonmag. substrate, magnetoelastic wave propag. 79−99744
YIG, nonreciprocal attenuation of elastic surface waves 77−55696
YIG, nonreciprocal attenuation of magnetoelastic Rayleigh waves 80−60399
YIG:Gd, Ga, optical probing of magnetoelastic Rayleigh waves 79−78495

reactance, electric *see electric reactance*

reaction kinetics
see also catalysis; chemical exchanges; chemical reactions; explosions; potential energy surfaces for collision processes; reaction kinetics theory; reaction rate constants
abstract 3-variable systems, toroidal oscills. 77−44462
acetalehyde decomposition reaction, intracavity laser spectroscopy obs. 79−61858
acetone, adsorbed on ZnO, decomp., IR and kinetic obs. 80−59780
acetylenic material, solid, on Pd-$CaCO_3$ catalyst, H getter, hydrogenation rates 77−44510
activated chemisorption, kinetics, adsorbate distrib., temp. and press. depend. 78−35720
activated chemisorption kinetics, differential heat of adsorption meas. 78−84062
activated processes in condensed phases, general kinetic models 80−81281
activation energies and rate constants, optical absorbance meas. method 77−81387
activation of kinetic processes in condensed media 77−55368
actomyosin kinetic anal., review 80−21441
alcohol galsses, tunnelling reactions of trapped electrons with electron acceptors 78−76887
alkali halide adsorbate motions and reactions at surface defects, mol. beams 77−59205
alkali metals, liq., soln. chemistry as elucidated from elec. resist. studies 77−52636
alkali silicate glasses in aqueous solutions, leaching kinetics rel. to surface pot. 80−11803
alkenes, π bond dissoc. energies, derivation from isomerisation kinetics, for teaching 79−58498
alloys, binary, selective oxidation with quasiparabolic kinetics, fixed alloy-scale boundary soln. 78−72930
allyl chain free radical, decay kinetics in γ-irrad. polyethylene state depend. 78−76855
ammoniated electron+R^{3+}, reaction kinetics meas. by ns. pulse radiolysis 79−52638
analysis method, kinetic method insensitive to variables affecting rate const. 79−34374
analysis methods, effect of reaction extent, uncertainty of rate parameters 79−34373
analytical chemistry, kinetic aspects, review 1975-1977 78−85216
anisothermal oxidation kinetics, model 78−44375
aqueous soln. reaction kinetics meas. microwave apparatus 80−3470
atom+diatom, prior statistical distribs., collinear reactions, theory review 78−35670
auto-catalytic systems, kinetics rel. to symbiosis and origin of life 77−90979
axially irradiated cylindrical photoreactor, plug flow model 79−47942
7-azaindole dimers, photoautomerisation by double proton transfer, fluoresc. kinetics 80−11880
barium oxalate, lacunary phase form., morphological and kinetic charcts. 79−60299
Belousov-Zhabotruskii reaction, existence of solitary travelling wave solns. 80−35525
benzene peroxide+dibenzylsulphide in atactic polymeric medium, reaction kinetics *(Russian)* 77−21362
bimolecular autocatalytic reaction-diffusion system with Michaelis-Menten saturation law, multiple steady states 78−40045
bimolecular reactions, minimum state density criterion in transition state theory 79−52645
binary systems containing one chemical cmpd., reaction kinetics and diffusion *(Russian)* 79−87014
biological, temporal oscillations in chemically reacting system 77−25359
biomembrane non-enzymatic influence, modelling 78−64945
Bray reaction, kinetics obs. *(French)* 80−7788
burning rate in engine cylinder, swirl and turbulence effects 80−89492
2-butene ion, fragmentation, angular momentum in ion-mol. reacts., RRKM calc. 80−66773
calcium oxalate hydrates, crystn. kinetics, comparison for mono-, di-, and trihydrates 80−81528
calorimetry, ballistic meas. with batch microcalorimeter 77−5843
carbonaceous chondrites, reduction kinetics, Mossbauer obs. 80−41777
carboxylic acid-ethanol systems, proton exchange process kinetics, effect of H bond strength in intermediate state *(Russian)* 79−96306
catalysis, advances in TEM obs. 80−85214
catalysis, heterogeneous, kinetic transport, deactivation rate interactions on steady state and transient response 78−68914
catalytic gaseous heterogeneous reactions, interpretation of power kinetic eqns. 77−60117
catalytic processes and stochastic processes of chem. kinetics, historical review 80−105483
chaos source in distributed kinetic systems 79−47890
charge transfer reactions in biological systems, mech. of coupling 80−76889
charge-transfer, excited, ps. kinetics, geometrical and solvent polarity effects 77−30986
chemical bond thermal energy storage feasibility 79−57495
chemical kinetic data, evaluation and computation 79−74345
chemical kinetics, connection to chemical thermodynamics *(Chinese)* 79−96352
chemical reactions, fluctuations, irreversible thermodynamics 77−52616
chemical reactions, oscillatory systems, weak coupling 80−66775

reaction kinetics continued
chemical system, nonlinear, open, information, critical fluctuations and phase-transition-like phenomena 79−24720
chemical turbulence, expt. 79−47891
chemiluminescence, beam-gas, kinetics of metastable excited state products 77−56231
chromatophores of Rhodospirillum rubrum, kinetic characts. of dark reduction 79−53067
coal gasification, catalytic, predevelopment research 79−52870
combustible flow, stiff boundary valued problems in kinetics and diffusion, numerical methods 79−86525
comet comae, gas-phase chemistry in one dimension 78−93154
concrete, thermal decomposition, empirical model for kinetics and stoichiometry 78−17386
condensed adsorption layers, effect on electrode reaction rates 80−93769
condensed media, rate processes, anharmonicity effects 79−19349
conductivity meas. for high press. chem. kinetics in soln. 79−93161
copolymer cooperative reactions, sequential anal. 77−36752
copolymer cooperative reactions sequential anal., Markov chain structure 77−36753
copolymerisation, alternate random and block, role of temperature 78−76859
corrosion, polarisation resistances method of study 77−28930
corrosion pit, convective diffusion 80−40601
counterdiffusion of two substances, stationary boundary and precipitate form. 79−1933
coupled chemical reactions, stochastic time evolution, Monte Carlo simulation procedure 77−9047
crystalline solid, decomposition, kinetic parameters 79−15984
CVD process, flow-graph model 79−78893
1-cyano-2-methyl-3-(cis-propenyl) cyclopropanes, rotational propensities and bond rupture identity 80−104437
cyclobutane-t, chem. activated by nucl. recoil reaction, energy transfer interpret. 80−25985
data acquisition system using stopped-flow spectrometry *(French)* 77−12779
DC plasma jet, NO synthesis, chem. kinetics obs. 80−38728
detonation cell model, geometry, kinematics, mixture kinetics 79−66296
diacetylene, photopolymerisation, optical absorpt. spectra, time depend., reaction kinetics 80−85174
dialkylanilines, p-substituted, twisted internal charge transfer excited state form. 79−22683
3,3′-diethyloxadicarbocyanine iodide, lasing and photoisomerisation, conc. and temp. effects 77−7081
diffusion controlled reaction kinetic studies, light scatt. obs., for one-step reaction case 78−35659
diffusion equation, nearly degenerate bifurcations, mode interactions 80−85149
diffusion saturation of commercial iron and steel with Cr in closed reaction space, kinetics and mechanism 79−52458
diffusion system, two chemical species reacting at boundary 80−93733
diffusion systems, Chapman-Enskog development of multivariable master eqn. 80−81283
diffusion-controlled reaction rates, competitive effects 77−28981
dimers, dissociating, in nonisothermal ideal gas phase, stationary state anal. 78−76848
N,N-dimethylcarbomoylchloride, chem. exchange rate by NMR method, temp. depend. 79−79243
2,6-diphenyl-1,4-benzoquinone+aromatic amine, triplet exciplex quenching, H-transfer mechanism 79−79228
dissipative structures, nonlinear reaction-diffusion model, stability of secondary multiple steady states 80−76485
droplets, kinetics of processes controlled by diffusion 79−11828
DTA and thermal analysis, nonisothermal kinetics, for teachers 79−40335
dual microcomputer-controlled stopped-flow spectrometer 80−57379
dynamics, Markov chains for simulation 77−60035
electrocatalysis, surfaces modified by metal adatoms, review 80−61110
electrochemical coupled homogeneous chem. reacts., kinetics, modified double pulse technique, appls. 77−25280
electrochemical electrode processes, kinetics from transitional sections of polarisation curves 77−25283
electrochemical electron transfer at electrodes in soln., review, in book, for teaching 78−8203
electrochemical passage reaction, kinetic parameters meas. *(German)* 79−52690
electrochemical reaction kinetics, discreteness-of-charge effect, electroreduction in double layer 77−32803
electrochemical surface reacts. driven by linear pot. sweep, kinetics 77−25275
electrochemical surface reacts. driven by linear pot. sweep, sequential reactions, kinetics 77−25276
electrochemistry, double-layer capacity and kinetic parameters, simultaneous meas. instrument 80−40704
electrode MHD phenomena in electrolytes heterogeneous processes *(Russian)* 78−27768
electrode reaction kinetic parameters, programs for computer retrieval, in FORTRAN 78−31654
electrodeposition, film growth kinetics and mechanism 79−52685
electron attachment to O_2 and H_2O in flames, kinetics 80−3349
electron transfer, in rigid medium, exothermic rate restrictions 80−30224
electropolishing of horizontal surfaces, role of natural convection mass transfer 79−57143
elimination reaction, D kinetic isotope effects, tunnelling, zero-point energy effects 78−56889
emulsion polymerisation, ideal, first-stage kinetics calcs. *(Russian)* 79−66295
emulsion polymerisation in unsteady state 79−47923
endothermic gas phase reactions, kinetic parameters meas. method *(German)* 79−39122
enzyme activity, kinetic assay, progress curve algorithm for spectrophotometric meas. 78−20083
enzyme catalyzed reactions with positive feedback, existence of stable limit stables 79−96289
enzyme kinetics simulation 79−15961
enzyme mechanisms, multiple pathway, computer-aided analysis and modelling 77−81388
epoxy resin, curing investigation by polarisation current method 80−3345
equilibrium distrib. functions *(Russian)* 79−11765
esterification kinetic study by monitoring pitch changes in cholesteric liq. cryst. solvent 80−7786
ethane, pyrolysis, thermodynamics and kinetics 79−43577
ethane hydrogenolysis mechanism and kinetics on evap. Ir film 79−100436
ethyl cyanide, pyrolysis kinetics and mechanism 79−24728
ethyl radical decomposition, mol. dynamics, trajectory studies 80−7780
ethylene, adsorption on Ni, Pd and Pt films, reactivity with adsorbed H, surface pot. meas. 79−86995
ethylene, polymerisation kinetics, heterogeneous Ziegler-Natta catalysts, polyethylene struct. and morphology 79−96307
ethylene+Cl, nuclear recoil, addition and abstraction reactions, kinetics 77−86340
ethylene+F(CH_3), transition state, ab initio calc. 78−48640
excited atoms, absorption spectrophotometry of fast reactions, optical laws 79−52667
exothermic fluid phase flow reacts., mechanisms, apparatus *(Russian)* 77−9042
explosion detonation, similarity and differences between conditions for initiation and failure 80−103038
explosives, secondary, thermal decomp., solid-state kinetics, differential scanning calorimetry 78−92449
fast chemical reaction obs., by pulse radiolysis *(Czech)* 80−81325
fast electrode reactions, kinetics meas., galvanostatic double-pulse method 77−25268
fast kinetics studied by NMR, review 80−55662
fast reaction kinetics meas. by ESR of free radicals 80−21286
field theory modification for solvent polarities 79−91913
fixed bed reactor catalyst decay, dynamic phenomena study *(German)* 78−7201
flame, counterflow diffusion, struct. in elec. field, interferometric obs. 80−16685
flame, laser excitation, rate eqns. 77−86327
flame, turbulent mixed gases, thermal exchange effect on reaction rate 78−7205
flames, effects of finite reaction rate and molecular transport on premixed turbulent combustion 80−3348
flames, laminar, premixed, non-adiabatic, nonlinear theory 80−93757
flow through porous barrier of reactive gas, exit flux, composition depend. 77−31383
flow tubes, kinetic measurements 79−74386
fluid, dense, chem. reacting, Enskog theory 78−35667
fluoresceindiacetate conversion to fluorescein, in living cells and in vitro, kinetics 77−56332
fluoresceindiacetate hydrolysis and transport in mammalian cells after UV and gamma-irrad. 77−56333
fog and sensitivity centre form. kinetics and activation energies during chem. sensitisation 77−44495
formation kinetics of solid layer on surface in reaction diffusion 78−63938
Fourier transform ion reson. spectroscopy of ions undergoing collisions with mols. 80−35598
free radical copolymerisation kinetics, monomer reactivity ratios under high press. conditions, meas. methods 79−91950
free radical reactions, photolytically initiated, high temp. kinetics meas. technique 80−61085
fusion chain reactions, kinetics, high electron temps., interactions with D-T plasma 80−68945
gas, dilute, reacting, mass and momentum transport, DIPR model extension 78−35666
gas mixture, kinetic coeffs. determ. by Enskog-Chapman method *(Russian)* 77−36733
gas phase chemical reactions in atmosphere, evaluated kinetic and photochemical data 80−101671
gas phase reaction systems, sound interaction 77−84024
gas-phase reactions, spectral-kinetic investig. rel. to chemical laser development *(Russian)* 77−90604
gas-solid interactions, controlled atmosphere electron microscopy obs. 77−29042
glass reactions with aq. solns., influence of surface pot. on kinetics 80−108612
global sulphur cycle study, atmospheric pollution modelling appl. 78−92902
glow curves and desorption spectra anal. method 80−80053
glyoxal-photoreduction-product-radicals, kinetics and intramol. dynamics 77−32808
graphite, desorption of CO, CO_2 78−60025
graphite-$FeCl_3$ intercalation compounds, form. kinetics and microstruct. *(German)* 79−43560
graphitisation kinetics within first min. of heat treatment 77−66596
groundwater, confined, form. rate of chem. composition 80−46207
group VIb, oxides, oxysalts, reduction kinetics and mechanism 77−77733
haemoglobin+CO reaction kinetics, using various regimes of photolytic illum. 78−48753
haemoglobin macroporous particle study, photoacoustic spectrometry 80−85543
haemoglobin-CO reaction kinetics, relax. meas. on photolytic illum. 77−70405
hard chemical instabilities, stationary distribs., unimodality 79−5129
heat and mass transfer, simultaneous, chemically reactive flow characts. *(Japanese)* 78−22431
heavy particle shock-radiational recombination, chemiluminesc., kinetics, reversed predissoc. 77−1924
heterogeneous atom recombination on surface sites, kinetics of Langmuir-Rideal mechanism 79−87876
heterogeneous catalysis, basic eqns. and examples *(Dutch)* 78−80788
heterogeneous charge transfer kinetic effects, deconvolution by FFT faradaic admittance meas. 78−20091
heterogeneous chemical kinetics by modulated mol. beam mass spectrometry 77−25305
heterogeneous reaction kinetics, convective mass transfer of cone, in nonlinear viscous field 77−55103
heterogeneous reaction kinetics, microcalorimetric and thermogravimetric curve comparison 77−21359
heterogeneous reactions, modified entrainment method appls. 79−23551
hexaborates of group II metals, thermal dehydration 78−43132
cis-2,trans-4-hexadiene, addition kinetics of HCl, Raman spectra meas. *(French)* 79−91940
2,4-hexadiynyl-1,6-bis(p-toluenesulphonate), programmed temp. and DSC obs., cryst. forms and polymerisation kinetics 79−43583

reaction kinetics continued
high pressure equipment for reaction kinetic meas. *(German)* 79−49244
high temperature, model *(Russian)* 79−29360
high temperature metallic species, absorpt. and fluoresc., high-temp. fast flow reactor technique 80−42231
high temperature system characterisation, models, phys. and chem. reference data sources 80−41958
high-pressure stopped-flow apparatus up to 3 kbar 80−3350
II-VI semiconductors, thin epitaxial layer, direct synthesis *(German)* 80−104070
information content of mol. beam scatt. vs. resolved product state distrib. expts. 77−28980
inorganic solid, interfacial endothermic reaction, abnormal thermal decomp. rate 78−76852
instabilities, stochastic approach, anomalous fluctuation and transient behaviour 80−89465
instability, mol. dynamics model, computer soln. 77−4892
instrument for quenching studies on rare gas and metal halide excited complexes 79−17511
interactive simulator, teaching appls. 79−48992
interstellar dense molecular clouds, chem. evolution 78−28749
interstellar dust condensation in clouds, importance of reaction kinetics 80−26939
interstellar molecules prod. on oxide grains, form. rates 79−25690
ion+molecule, electronic states, kinetic energy, molecular beams obs. 80−30230
ion+molecule reactions, kinetics, conf., La Baule, France (1978) 80−27043
ion-molecule equilibria in solvolysis, secondary β ^{2}H isotope effects, hyperconjugation 80−50874
ion-molecule reactions, anisotropic molecular polarisability, effects on rates 79−15967
ion-molecule reactions, vibr. energy effects on kinetics, phase space model 78−11508
ionospheres, ionic reactions in lab. and planetary atmospheres 80−59168
IR laser chemistry research using mol. beam *(German)* 80−55683
IR laser photolysis of polyat. mols. photochem. appls. 80−66835
isopropanol, decomp. on α- and β-V_2O_5 bronzes, 186-300°C, kinetics and mechanism 78−11553
isopropyl alcohol, adsorbed on ZnO, decomp., IR and kinetic obs. 80−59780
isotope separation, by selective laser-induced mol. vibr. excitation effect on reaction kinetics 78−33627
labile species, electron photoejection, reaction kinetics characterisation 80−26089
Lagrange-Hamilton formalism, concept of chemical inertia 80−7756
Landau-Zener problem, random nature of motion role in intersecting terms problem 80−8937
laser photochemical reaction kinetics, holography use 79−29383
laser-chemical reaction kinetic mechanism *(Russian)* 80−101007
lattice model, coupling of translational and reactive dynamics 78−55696
liquid phase reaction systems, combination rates of steady state processes and transient phase process *(Chinese)* 77−77764
liquid solutions, reaction rates, mol. mobility effects, review, book contrib. 77−40526
lithium formate monohydrate, dehydration, kinetic parameters from thermogravimetric data 79−61859
low temperature reactions, mechanisms and rates, review, book contrib. 77−40542
macromolecule functional groups, reaction kinetics and statistics, review *(Russian)* 79−87825
masked antifoggants, hydrolysis stability, photographic process depend. *(German)* 80−45530
measurement and control using laser technology, free electron laser appl. 80−81349
measurement over many orders of magnitude in time, using minicomputer 78−7200
membrane surfaces, antibody association kinetics with spin-label haptens 80−66787
metal, H_2-diffusion-rate-limited hydriding and dehydriding kinetics 80−35764
metal extraction kinetics, from deep-sea Mn nodules, pore diffusion controlling case 77−28984
metal extraction kinetics, from deep-sea Mn nodules, pore diffusion with chemical reaction 77−28985
metal interaction with gases and C, conf., Stuttgart, Germany (Sept 1977) *(Russian)* 79−57134
metal-gas interactions, kinetics and mechanisms, book contrib. 78−11558
metal-gas reactions, surface chemiluminesc. study 80−55708
metal-gas systems, surface reaction rate meas., resist. relax. method 79−66355
metal-polymer deposit, simultaneous electrophoretic deposition and electrochemical precipitation 79−56938
metal-slag interface, interaction under diffusion conditions, impurity oxidation *(Russian)* 80−35390
metals and alloys, chemicothermal treatment, process kinetics 80−35415
metals and alloys, sulphidation, high-temp., thermobalance for studying kinetics 78−23876
methane, adsorbed on γ-Al_2O_3, γ-radiolysis, reaction kinetics 78−95940
methane formation, CO hydrogenation kinetics, using polycryst. Ni ribbon catalyst 78−40078
methane gas→C(dissolved)+2H_2 (gas), kinetics on Fe and Fe-Ni surface 80−55712
methyl iodide, dissolution into aqueous NaOH solns., fission reactor accident conditions 77−88236
methylundecanhydride hardened phenol formaldehyde resin, hardening kinetics and mech. losses 80−66520
micelle dissociation-recombination kinetics, stochastic model 80−30291
micelles, organic reaction kinetics 79−29416
microcomputer interfaced spectrophotometer studies 80−62726
mineral, dissolution under Earth surface conditions, rate control 79−20817
model optimization of detonation-wave description on consideration of combustion kinetics 79−91955
molecular chemical tunnelling, facts and hypotheses 79−59520
molecular system dissociating in laser radiation mass action law 77−70298
molecular tunnelling in chemical reactions *(Russian)* 77−52615
molecule+molecule, enhancement by collision induced absorpt. of IR laser radiation 80−66798
reaction kinetics continued
molten carbonate fuel cell, electrolyte comp. effect on electrode kinetics 80−101092
molten metals, reaction rates, interface phenomena *(French)* 79−43632
monomethylamine, dilute mixtures, decomposition, shock tube studies, IR emission obs. 79−96301
montmorillonite, dehydration kinetics 78−76857
multiphonon relaxation, statistical anal. 79−79223
multiquantum deactivation reactions, simplified modelling 77−25266
multispecies Tani transorm., kinematical props. 79−17333
multistep reaction rate eqn. integration, interactive computer program system 80−31469
muonium kinetics in liqs., coherent diamag. fraction obs. 79−57278
myosin kinetic anal., review 80−21441
naphthalene:β-chloronaphthalene, reaction rate constants of triplet excitons 78−80407
network thermodynamics with entropy stripping 78−7223
nitriding process, monitoring systems 79−52556
NMR line-shape anal. of peaks broadened by hidden exchange partner 79−43554
nonequilibrium chemical phase transition, kinetic potential and Maxwell construction 77−87716
nonequilibrium molecular system, time-depend. kinetic-thermodynamic description 80−9877
optical image phase recording using sensitised photooxidation reactions 80−87350
organic reactions in solid state 80−21309
oscillating chemical reaction, entrainment by periodic light pulses of variable freq. *(French)* 80−35551
oscillations, chemical and thermokinetic, feedback *(French)* 79−57205
oscillators responding frequency switch 80−108837
oscillatory chemical reactions, dynamical theory of pattern formation 77−9048
2′-oxaindan (dihydroisobenzofuran) spiropyrans, photochromic transforms, spectrokinetic study 80−30259
Pb/Ag-Pd, sequentially deposited, thin film reaction kinetics, X-ray diffr. expts. 77−89594
peroxidase, photo-induced reduction, reaction with indole acetic acid 79−79452
Petrovic equation of chemical kinetics, kinetics of solid state processes 80−97685
photochemical smog, rate parameters and computer simulation 78−48677
photographic, film development kinetics of viscous solutions *(German)* 79−83482
photolysis and radiolysis, kinetic data acquisition, and anal., by computer based system 79−39180
photoresists, photochemical reaction rates, intensity depend., kinetic model 80−104452
photosynthesis, redox conversion kinetics in the electron transport chain 80−40950
photosynthetic redox conversions, electron transport, EPR obs. 79−92179
picosecond spectroscopy using ultrashort laser pulses, appls. 79−54195
plasma, nonideal, elem. excitations and macroscopic props., review 80−43842
plasma chemistry, appl. to IC fabrication 79−79252
polarography, pulse, chronoamperometric, chronocoulometric techniques, kinetic, mass transport effects 77−25334
polarography, pulse time scanning, limiting current diagnostic differentiation technique 77−25339
poly(m-xylylene adipamide), molten, gel form. kinetics *(Japanese)* 80−108757
poly(trans-1,4-butadiene), crystals in suspension, epoxidation kinetics 79−61861
polyamide-Cu(Ni) oxalate, oxalate decomposition kinetics, in polymeric medium, thermogravimetry and DTA 78−52749
polybutadiene networks, cis-trans isomerisation, γ-ray induced 79−74374
polycarbonate, turning yellow during oxidation, kinetic regularities *(Russian)* 79−24644
polyelectrolyte 'catalysis' of chem. reactions 79−57217
polyesterification reactions, uncatalysed, comments on Flory's work 79−96309
polyether-urethane elastomers, crosslinked, three dimensional polymerisation, kinetics, gel. form., mech. props. *(Russian)* 80−7792
polyethylene, polymerisation kinetics math. model, mol. wt. evaluation *(Russian)* 79−52661
polyethylenepolyamine hardened epoxy resin, hardening kinetics and mech. losses 80−66520
polyketo cpds., oxidation, Mo complex formation mechanism 77−77732
polymer, ageing and stabilisation, struct.-kinetic aspects *(Russian)* 79−52660
polymer, kinetic study of random scission *(Japanese)* 77−66754
polymer materials, chem. reacting, kinetic characts. of thermal effects determ. using Calve type microcalorimeter 77−57328
polymeric crosslinked compositions formation, structural kinetic method *(Russian)* 79−34303
polymerisation, multicomponent, differential and integral rate eqn. 78−23944
polymerisation, nonisothermal, in spherical reactor, temp. distrib., and reaction kinetics 79−87844
polymerisation, unterminated reactions, kinetics of intermediates 79−91949
polypropylene, oriented, thermooxidative degradation kinetics, durability, influence of mech. initiated processes *(Russian)* 79−24591
polystyrene, thermal degradation, kinetic study *(Japanese)* 79−39139
polystyrene, thermal polymerisation, kinetics, Rayleigh scatt. 79−57228
power reactor noise analysis, nonlinear kinetics effects and new techniques 79−13454
precursor intermediates in adsorption, desorption and reaction 80−108731
pressure jump method for fast kinetics using optical rotation and circular dichroism 78−77175
primitive Earth, chemical evolution and energetics of reactions in aqueous solns. 77−33189
product state distribs., uniform phase space representation 77−28979
propellant decomposition kinetics, eqns. 79−91941
propene soft oxidation, gas-solid catalytic reaction, kinetics, automatic meas. *(French)* 77−1912
protein isomerisation kinetic consts. determ. by gel permeation chromatography of interacting multicomponent systems 78−68951
proton transfer photoreaction kinetics, in singlet excited state 78−48671

reaction kinetics continued
proton transfer reactions, excited state, laser pH jump analysis method 79−47922
proton-transfer reactions, potential energy curves and Bronsted exponents 77−32784
pulsed differential reactors for kinetic study of the H_2S-alkaline minerals reaction in coal 79−20465
Purex kinetics, U extraction with tributylphosphate *(German)* 80−57937
pyrolysis, of single solid particle accompanied by consecutive reactions, vol. reaction model 79−47896
quantum mechanical, trajectory and transition-state theory calcs. 77−25249
quartz, mechanically activated, reactivity *(German)* 79−29395
quinone electrochemical reduction at packed, fluidised bed electrodes, kinetic behaviour 79−57235
radiation decontamination of surface, influence of carrier on efficiency *(Czech)* 79−31222
radiation induced exchange reaction kinetics of H_2, D_2 and T_2, review 78−61005
radiation-induced trapped electron yields, close effects, tunnelling processes 79−39161
radical+radical reactions, reaction path calc. using perturbation expansion *(German)* 79−34300
radical pair recombination kinetics, low conc. in solid matrix, 1, 2 and 3 dimens. 78−27793
rapid scanning wavelength kinetics experiments, statistically weighted principal component anal. 77−77826
reacting polymer system, convergence to equilibrium, free energy 79−52624
reaction rate constants, modified collision theory expression, comparison with exact expression 79−74370
reaction-diffusion equation solutions, Lotka scheme 79−34280
recombination, in steady supersonic flow, in devices for laser isotope separation 79−31717
rhodopsin, bovine, kinetics of intermediate photolysis processes 79−43608
rhodopsin bovine, interaction with Ca^{2+} 79−100563
Rochelle salt, dehydration kinetics in ferroelec. and paraelec. phases, surface acoustic waves influence 80−97204
rock metamorphism, rate laws 79−16467
roughness fluctuation in layer between two phases 80−85147
salicylamide, excited state proton transfer, kinetics, picosec. fluoresc. 79−59502
second-order kinetics, student experiment 77−26117
semiconductor catalytic kinetics, complex mech. of excitation, constant state problems 80−85213
semiconductors, recombination enhanced defect reactions 79−38094
sequential fast kinetics, relaxation methods obs. 79−43575
shock initiation, vol. of activation determ. 80−16683
shock wavefront molecular process kinetics, IR absorption meas. installation 79−70389
silicate+$Ca(OH)_2$, reaction rates 80−26006
silicate+Portland cement, reaction rates 80−26006
solid phase reactions induced by scanning CW laser, reaction rates, analytical model 80−66334
solid reactions with solid, liq. or gas phase, electrochem. methods for kinetics determ., book contrib. 79−65251
solid state reactions, elementary chemical step, activated complex theory 79−11763
solid-phase reaction kinetics, intercrystallite diffusion role 79−33106
solid-solid pellet systems, diffusion and reaction 78−85139
solids, reactivity control, review 80−50853
solvent effects, semiempirical model 80−25986
spatially homogeneous simple reaction systems, indefinite second time derivatives of thermodynamic pots. 78−85126
sphalerite, kinetic study on press. leaching 77−4893
spiropyrans, polymer matrix effect on photochromism, thermal decolouration kinetics 80−76537
stacking reactions, temperature jump kinetics, Raman laser technique 79−2831
steady state of stiff linear kinetic systems, Markov matrix method 77−52613
steel, Cr-Mo (2.25,1 wt.%), exposed to H_2-H_2O-H_2S environment, fatigue crack growth 80−40623
steel, mild, electrodes, in H_2SO_4, H evolution reaction kinetics 80−97630
steel, mixed alloy, sintering, reaction kinetics of Fe and graphite powders 77−55907
steel, stainless, liq. Li corrosion rate expressions, 600-1000°C 80−93682
steel, stainless, stabilised with Cr-Ni-Nb, reaction with Te vapour 77−8986
stiff differential equations, numerical soln. 79−15960
trans-stilbene photoisomerisation, ps dynamics under collision-free conditions 79−91975
stirred tank reactor, homogeneous p-order reactions, mixing effects, two parameters model 80−14843
stopped flow temperature jump apparatus with spectrophotometric detection of fast chem. reactions 77−3892
stopped-flow apparatus, data acquisition and processing using minicomputer *(German)* 78−53190
stopped-flow spectrometry for kinetic meas. of fast chem. reaction 78−56925
stopped-flow system, computer controlled, for fundamental studies 79−15953
stopped-flow systems, automated, for fast react. rate anal. methods, review 78−95971
student laboratory, appl. of simplified recording manometer 79−58502
styrene-maleic anhydride copolymerisation, alternate random and block, role of temperature 78−76859
superconducting composites, bronze process, metallurgy 80−3004
surface reactions, kinetics and dynamics, conf., La Jolla, CA, USA (Aug 1979) 80−105415
surface transport and reaction, stochastic calcs. 80−108736
teaching, clarification oversimplifications 78−69928
teaching, Faraday balance for studying strong mag. field effects on react. rates 80−57043
teaching, Monte Carlo method, computer program 77−24
temperature jump kinetics, Raman laser technique 79−2831
temperature-jump apparatus, data acquisition and processing using minicomputer *(German)* 78−53190

reaction kinetics continued
temporal oscillations in kinetic model of Belousov-Zhabotinskii reaction 78−85132
tetramethyldioxetane, multiphoton dissoc., collisional vibr. relax., rate eqns. model 80−63729
thermal boundary layer interactions in shock tube sampling for kinetic obs. 80−104420
thermal fluctuation of self oscillating reaction system under periodic external force 80−50828
thermal instability of vibr.-excited mol. gas, appl. to surface ignition *(Russian)* 78−56895
thermal kinetics meas. using modified commercial stopped flow apparatus 80−86291
thermochemical instability in optically heated condensed medium 79−66282
thermostimulated effects, correlations and invariants 78−31619
thionine coated electrode for photogalvanic cells, kinetics 80−35696
thymine+muonium, radical form. in aq. soln., spin reson. obs. 78−74679
transition metal complexes, reaction mechanisms and solvent effects 80−26012
travelling waves for a model non-linear reaction-diffusion system 80−89476
trickle bed, packed, gas-liq. reactions, extended crossflow model implications 79−46399
troposphere, lower, modelling, chemical kinetic data needs, conference, Reston, Virginia (1978 May 15 to 17) 80−62383
troposphere, photochemical mechanisms, computational methods 78−49084
turbulent diffusion, flames, high Reynolds number, rocket exhaust appl., chem. processes theory 80−45504
turbulent mixing with react. of miscible reactant streams, simulation 80−64651
unimolecular dissociation, master eqns., analytic theory of extrema 80−50841
unimolecular IR multiphoton decomp., energy grained master eqn., approx. model and exact soln. 80−66829
upper atmosphere, odd N prod. by meteoroids 79−2404
urban kinetic chemical calculations with altered source conditions 79−16560
water radiolysis, mathematical modelling for kinetics in operating reactors 78−61036
water thermolysis, solar furnace, thermodynamic analysis 79−83625
weak neutral currents displayed in biological isomerism, L- and D-mol. reaction rates 78−415
Zircaloy, hydriding reaction kinetics, oxidised specimens 78−26728
Na leakage in reactor steam generators, solution kinetics of solid NaOH in Na 79−36365
AgBr sols, kinetic exam. of halide conversion 77−82636
AgI/RbI quasibinary system, solid state reactions and transport props. 80−96700
AgI-type crystallising agents, kinetic parameters *(Russian)* 77−81963
Al dissolution in HCl soln., inhibition by hydrazine derivatives 80−50759
Al magnetron sputtering target, oxidation in Ar/O_2 mixtures 80−55291
Al, reaction with H_2, influence of surface reactions on rate *(Russian)* 80−66863
$Al_2Ge_2O_7$, reduction processes by C, kinetic analysis, reaction products *(Russian)* 80−55644
AlH_3, photoelectric effect spectra and kinetics, photochem. mechanism colour centres 78−56506
$Ar+NO^+$, reaction product ratios, 300K 80−7783
Ar^++NO, reaction product ratios, 300K 80−7783
$Ar(^3P_{2,0})$+F-containing mols., rate consts. for ArF^* formation 79−24731
Ar^*+CO_2, CO* prod., use in laser systems 80−63824
$Au(CN)_2^-$, electrochemical reduction kinetics 78−73052
B_4C, kinetics of high temp. oxidation in oxygen, chromatography method 77−21305
B_4C, reaction kinetics with liq. Al, Si, Ni and Fe 80−84344
BCl_3+methane reaction, laser-induced, vibr. excitation influence on reactivity, isotope selectivity 80−11921
Ba getter film, initial reaction probability with O_2, water, CO and CO_2, AES obs. 80−61153
$Ba+CO_2(O_2)$, crossed beam kinetics, BaO recoil velocity spectra 80−76500
$Ba+N_2O$, crossed mol. beams, BaO recoil vel. spectra 78−7184
$BaBr_2.H_2O$, dehydration, kinetic parameters from thermogravimetric data 79−61859
BaF_2+BCl_3, crossed beam metathesis, total cross sections 77−21354
BaI_2+Cl_2(HCl)(1,1-dichloroethane)(chloroethene), crossed beam metathesis, total cross sections 77−21354
$Ba(PO_3)_2$, hydrolytic decomp. 80−21271
$BaTiO_3$, synthesis by solid-solid reactions 79−38776
$BeAl_2O_4$, chrysoberyl, kinetics and mechanism of formation, in presence of V_2O_5 79−11535
$BeO+SiO_2+V_2O_5$, reaction kinetics and mechanism, phenakite formation 78−23608
Bi_2O_3-CdO system, solid-state reaction, kinetics and mechanism 77−90303
$Br_2+H(d)\rightarrow HBr(DBr)+Br$, reactive cross-section, collision energy depend. obs. 79−11784
C gases, position regulator for high-frequency heating 79−80612
C particle formation,C_2+C_3 as possible first step 78−68876
$C+CO_2$ reaction, kinetics at low press. and hydrogen inhibition 77−63950
$C+CO_2$ reaction, Langmuir-Hinshelwood kinetics at intermed. press. 77−66766
$C_3+NO(O_2)$, reaction kinetics, laser induced fluoresc. obs. of allene photolysis 80−66820
$C_4H_6^+$, fragmentation, kinetic energy release 77−77737
CO, oscill. oxidation on Pt surface, kinetic model 77−4926
CO, oxidation over Ir, tracer studies on reaction path and kinetics of CO oxidation 80−7857
CO oxidation over Pt, kinetics determ. using ^{13}C tracer 79−29400
CO_2 reaction with adsorbed O_2 on Pd, kinetic behaviour, AES obs. 77−90640
CO, reaction with O_2 adsorbed on Cu (111), AES, LEED and ellipsometric meas. 79−65317
CO, titration of pre-adsorbed O on Ir (111), XPS investigation 79−91994

reaction kinetics continued
CO-N_2O gasdynamic laser, CO_2 vibr. level superequilibrium chem. pumping, mixture composition, He effects 79−76666
CO+CO_2, exchange rates behind reflected shock waves for $C^{18}O$ and ^{13}CO 79−29363
CO+H_2, interaction on Ni (100), reaction rate, AES and UPS obs. 79−79290
CO+N_2O catalytic reaction on Sc_2O_3 and MgO, kinetic obs. 79−29389
CO_2, photoelectrocatalytic reduction in aq. suspensions of semicond. powders 79−39141
CS+O→CO+S, shock tube reaction, chemiluminescence and lasing 77−16824
CS_2, aerosol form. by laser, kinetics study and photoreaction products chem. nature study 80−21324
$CaCO_3$ crystallisation from aqueous solutions, kinetic study 80−59419
$CaEuGa_3O_7$, synthesis, mechanism and kinetics, cryst. props. 77−52268
CaF_2:Eu, oxidation and reduction of Eu, EPR and optical studies 80−25199
$CaGeO_3$, reduction processes by C, kinetic analysis, reaction products *(Russian)* 80−55644
CaO-Al_2O_3, binary slag, reduction of Al_2O_3 by C saturated Fe *(Japanese)* 79−24733
$Ca_{10}(PO_4)_6(OH)_2$ dissolution kinetics, nucleation-controlled 80−59659
$C_2(a^3\Pi_u)$+NO(vinyl cyanide)(ethylene), laser-generated radical kinetics 79−100352
β-Ca_2SiO_2, reaction kinetics with CO_2 and water vapour 80−76484
Ca_3SiO_2, reaction kinetics with CO_2 and water vapour 80−76484
$Ca^*+Cl_2(HCl)$, luminesc. reactive collisions 77−16816
$CdFe_2O_4$, ferrite, synthesis 77−16523
CdO-WO_3-H_2O, interconnection between kinetics of structure formation and chem. reactions 78−53198
CdS, dry process formation from CdO and S *(Spanish)* 78−56607
CdS, thermal decomp. kinetics, in vacuo, free electron density depend. 77−59111
Ce^{2+}, oxidation kinetics in X zeolite on O_2 adsorpt. 78−3373
CeO_n, redox reactions, quasiisothermal thermogravimetric obs. 79−15980
Cl+HD, reactions, branching ratio, energy partitioning and ang. distrib. 79−70312
Cl+$O_3(H_2O_2)$(methane), reaction kinetics, temp. depend., reson. fluoresc. obs. 77−4903
Cl_2+$H_2(H_2S)$(methanethiol), laser-initiated chain reactions, rates, mechanisms, chemiluminesc. obs. 80−55651
Cl_2+HI, pulsed chem. laser, rot. distrib. time evolution, kinetic master eq. calc. 77−65593
$ClCO_3NO_2$, synthesis by UV irrad. of Cl_2, NO_2, CO in air, decomp. kinetics 78−76880
$ClONO_2$, form., reaction with OH, kinetics 77−86303
Co, oxidation kinetics, effect of Curie temp. 77−48592
CoO, high temperature physico-chemical interactions with oxygen under pressure *(French)* 78−31549
$Co_4TeMo_3O_{16}$, synthesis, mechanism and kinetics 77−32782
Cr_2O_3, reduction rate by C and C in liquid Fe-Cr-C 78−6877
Cs sorption in nuclear graphite, sorption kinetics modelling 80−102244
Cu (111) surface, room-temp. oxidation, press. effects 79−79283
Cu, corrosion, use in reaction kinetic investigation 79−70213
Cu, electrode potential, transient response to elastic straining rel. to reaction kinetics 79−70212
Cu wire, corrosion in $AgNO_3$, effective corrosion time, resistance variation 78−11404
Cu-Al_2O_3 disperse phase alloy oxidation kinetics 77−48584
Cu-CaO concentrate pellet, oxidation kinetics 77−4894
CuCr alloys, supersaturated solid soln. dissociation *(Russian)* 79−52201
$CuFeS_2$, chalcopyrite, electrode surface reduction kinetics 78−56897
Cu_2S, solid, oxidation mechanism, kinetic factors 78−85133
$CuSO_4.5H_2O$ dehydration kinetics depend. on water vapour press. 79−15986
D_2-DT-T_2 system, quadrupole mass filter sensitivities and β-particle induced exchange kinetics 78−58090
DF-CO_2 chemical laser, photon branching in chain reactions, IR radiation initiation 80−91785
F+H_2, in pulsed HF chem. laser evolution, irreversible thermodynamic anal. 79−31887
F_2+Mg(Ca)(Sr)(Ba), crossed beam chemilum., kinetics and mechanisms 80−21264
F_2+UO_2, reaction kinetics, molecular beam study 78−46157
Fe, adsorbed S effects on surface reaction kinetics and surface self-diffusion 78−7234
α-Fe, carburisation and decarburisation kinetics in methane/H_2 mixture *(German)* 79−1949
Fe diagenesis in sulphide rich sediments, reaction rates from Mossbauer spectral studies 79−74917
γ-Fe, kinetics of carburisation in CO-He and CO-H_2 atmospheres at 920°C *(German)* 78−85024
Fe ore, cold bound pellets, reduction using H_2 gas, 700 to 900°C *(Japanese)* 80−71907
Fe, oxidation kinetics near Curie temp. 79−66218
Fe surface, adsorbed O_2 effect on chem. reaction kinetics 80−55572
Fe/Cu_2O displacement reaction kinetics at temps. between 800 and 1050°C 80−21278
Fe-Al (up to 7.2%), oxidation process 78−85022
Fe-C, levitated drops, carburisation and decarburisation in CO-CO_2 gas mixture, exam. of reaction kinetics 78−85053
Fe-C-(P)(S), drops, oxidation kinetics in oxidizing slags 78−11153
Fe-Co-C(0.8 wt.%), unidirectional transformation, eutectoid reaction kinetics 77−70029
Fe-Cr (24 wt.%), low temperature oxidation, kinetics, oxide morphology 80−11838
Fe-Ni (19wt.%) alloy, oxidation in CO_2, 700 to 1000°C, kinetics study 78−72931
Fe-Ni alloy, fluorination kinetics and fluoride film form., chem. nature obs. 80−101035
Fe-Zn couple, Zn electrodeposited on polished Fe, reaction rate in solid state *(Japanese)* 78−15322
$(Fe^{2+}Fe_{2-x}^{3+}M_x^{3+})O_4^{2-}$ ($M^{3+}=Al^{3+}$, Cr^{3+}), oxidation to γ lacunar spinels, rate law vs. O_2 press. 80−50849
Fe(III)+SCN^-, reaction kinetics, computer-controlled stopped-flow system 79−15953
FeO surface, water-gas shift reaction kinetics 80−11949
$Fe_{0.925}O$, wustite, kinetics of reduction at moderate temps. 79−83154
Fe_2O_3, direct reduction by H_2 reaction kinetics 80−40689
Fe_2O_3, reduction by H_2, kinetics and mechanism 77−48619

reaction kinetics continued
Fe_3O_4, substituted magnetite, oxidation kinetics 77−1889
FeS_2, pyrite, magnetokinetics of oxidation, appl. to mag. separation from coal 77−12161
GaAs, heterogeneous reactions in chemical transport by water vapour, growth kinetics of epitaxial layers 77−16500
GaAs hydrothermal oxidation kinetics, exam. 80−40566
GaN, epitaxial growth kinetics in Ga-HCl-NH_3 77−80710
Ge, formation of sulphide layers on surface in S vapour 79−7757
Ge, monocryst., with S vapour, applicability of Kossel's crystal model 79−87833
Ge+Br_2, surface reaction, rate-limiting step, ellipsometric and photochem. meas. 80−16730
Ge+S (vapour) reaction kinetics 78−35718
GeO formation from Ge-GeO_2 mixtures, gasification kinetics *(Russian)* 80−21273
GeO_2, reduction processes by C, kinetic analysis, reaction products *(Russian)* 80−55644
GeP, dissociation kinetics rel. to volatile component sublattice 77−84917
H isotope interphase exchange in H-Pd system 77−50551
H, thermochemical prod. by H_2O decomposition, impact of thermal burdens and kinetics 80−35787
H, thermochemical production by steam reforming of methane, kinetic anal. 80−35788
H-air, laminar diffusion flames, chem. nonequilib. effects model 78−48654
H+CN(NC)(NSi), bimolecular exchange reactions, dynamical-statistical method calcs. 80−104435
H+O_3→HO_2+$O(^3P)$, yields 80−71900
H_2 formation, reaction rates and chemical kinetics 79−17070
H_2 production by steam reforming of natural gas, chemical kinetics 80−97815
H_2 production from coal, water and electrons, reaction rates 79−61962
H_2 sorption/desorption by ternary $LaNi_5$ type alloys, reaction kinetics 80−45813
H_2-HT-T_2 system, quadrupole mass filter sensitivities and β-particle induced exchange kinetics 78−58090
H_2+F, in pulsed HF chem. laser, kinetic modelling, rot. nonequilib. 79−36888
H_2+F_2 reaction, coherent emission efficiency 78−17928
H_2+H_2O^+→H+H_3O^+, reaction kinematics 78−31625
H_2+O_2, adsorbed on Pt (111), reaction kinetics 77−55461
H_2+O_2, combustion, kinetic modeling and sensitivity anal. 80−89490
H_2^++D_2→$_2$H++H, product angular and vel. vector distributions meas. by crossed beam expt. 80−101012
H_2^++H_2→H_3^++H, reaction dynamics, isotopic variations 78−27745
H_3, form. and dissoc., kinetics, historical review, book contrib. 77−40527
H_3AsO_4, reduction with aqu. SO_2 77−4901
HBr, laser emission at 4 μm based on chem. generation of Br atoms 80−9878
H_2CO_3, dissoc. reaction rate meas. using reference electrode liq. junction 77−4906
HCl, in nonequilib. plasma, electron energy distrib. function and dissoc. kinetics 80−11882
HF chemical laser, time-depend. kinetic-thermodynamic description 80−9877
HF laser with flow-through chem. active medium, pulsed-periodic regime realisation 80−106513
HF, pulsed laser numerical modelling, rot. relax. 80−87388
$H_{1.6}MoO_3$ bronze, form., kinetic, thermodynamic investig. *(French)* 80−45247
HO_2+NO, reaction kinetics meas. 78−31624
H_2O_2+catalase ($[Fe^{3+}(EDTA)]_2$), effect of mag. field on decomposition rate 79−52631
HO_2NO_2, thermal decay kinetics 79−5135
H_2SO_4 formation in urban atmosphere, flame photometric obs. *(French)* 77−41136
H_2SO_4, secondary particles form. and growth, kinetic aerosol model 79−29492
H_2SO_4-$KBrO_3$-KBr-Mn^{2+} system, chem. automat with three steady states 80−7769
H_2SO_4+atmospheric species, collisional reaction probabilities rel. to H_2SO_4 aerosols as tropospheric sinks 80−72612
He^*+D, Penning and assoc. ionis. with metastable He, 0.01 to 10 eV beams 79−27074
Hf-Fe alloys, oxidation 79−52460
$HgBr_2$+AgI, solid state reaction, kinetics and mechanisms 77−16790
I laser, photolytically pumped, chem. kinetics 80−48235
I photodissociation Q-switched laser, optically thick active medium, chemical kinetics and gasdynamics 79−64218
I_2, photolytic cage effect in gas phase 80−81345
$I^*(5^2P_{1/2})$+HF(HCl)(HBr)(HI), collisional quenching rate consts. meas. 77−3299
InCl disproportionation under influence of high pressure 80−16660
InP hydrothermal oxidation kinetics, exam. 80−40566
Ir (110), adsorption of CO and reaction with O_2, transient study 80−30284
KO_2, non-isothermal decomp. kinetics 80−16649
KO_2, thermal decomp. macrokinetics, differential thermal anal. 80−16650
K_2O-Al_2O_3-P_2O_5-TiO_2, structural role of Ti, kinetic study of chem. destruction 80−88055
Kr^++F^- and Kr_2^++F^-, ionic recomb. rates in buffer rare gases 79−8425
Kr^++HD, kinetic isotope effect, cross sections, rot. transfer 77−9041
LaN, form. conditions 80−101019
$LaNi_5$+$3H_2$⇄$LaNi_5H_6$ reaction, absorpt. capacity and reaction kinetics 79−43626
Li/SO_2 cells, safety studies, kinetics of Li-organic solvent exothermic reactions 80−72030
Li+$CH_3I(CCl_4)(CH_3NO_2)$, mol. beam kinetics 77−28978
Li+$SnCl_4(PCl_3)(SF_6)$, product mag. deflection slotted disc vel. anal. mol. beam kinetics 77−25250
LiH, form. on polycryst. Mo membrane, from diffusing gases, mass spectrometric obs. 77−66771
LiH+Te exothermic solid-state reaction, ion backscatt. obs. 78−20064
LiOH(D)(T), thermal decomposition rates 530-690K, activation energy and enthalpy meas. 80−3321
Li_2ZnSiO_4, tetahedral struct., polymorphic α-β transform. kinetic obs. and method 79−90778
Mg nitridation in HF discharge, temp. effect 80−3399

reaction kinetics continued
Mg/Mg_2Cu eutectic, hydriding and dehydriding kinetics obs. by press. sweep method 80−35765
$Mg\text{-}In+H_2 \rightarrow HgH_2$ reaction, catalytic effect of In 78−76851
$Mg+O_2 \rightleftharpoons MgO+O$, shock-tube study of evap. and oxidation kinetics 80−16651
$MgCO_3^0$, in solution, ion-pair relaxation rel. to acoustic absorpt. 79−74914
$MgCr_2O_7.6H_2O$, dehydration, thermal decomposition, kinetics 79−11777
Mg_2GeO_4, reduction processes by C, kinetic analysis, reaction products *(Russian)* 80−55644
MgH_2 formation kinetics, electron microscope obs. of H_2 reaction with Mg metal 77−52553
$MgI_2+Cl_2(HCl)$, crossed beam metathesis, total cross sections 77−21354
MgO:Fe, Fe^{2+} oxidation and Fe^{3+} reduction kinetics, EPR obs. 79−70399
Mo complex, halogenoxomolybdenum (V), cryst. and electronic struct., reactivity 77−76369
Mo complex, nitrate reductase, reduction mechanism and kinetics in dimethylformamide 77−86366
Mo, nitriding kinetics 80−35415
Mo oxides, oxysalts, reduction kinetics and mechanism 77−77733
Mo, thin film on Si, stress effects 78−43261
Mo_2C, corrosion and electrochem. props. in aq. H_2SO_4, HCl, HNO_3 and KOH solns. 80−11813
MoF_6 reduction by H, chemical kinetics eqn., adsorbed component interactions *(Russian)* 80−35569
MoO_2 powder bed, H_2 reduction kinetics 80−16230
MoS_2 on Mo, sulphate coating growth kinetics and mechanism 77−86220
N heterogeneous atom recomb. on glass, Langmuir-Rideal mechanism 80−7853
N_2^+, electron impact dissociative recomb. coeffs. inferred from Atmosphere Explorer meas., objections 78−86957
N_2-Ar plasma, coupled thermal-chem. relax., thermodynamic nonequilib. 78−34265
N_2+methane, N_2 fixation, catalytic processes in non-equilibrium plasma chemical reactors *(French)* 80−89483
N_2+O_2, N_2 fixation, catalytic processes in non-equilibrium plasma chemical reactors *(French)* 80−89484
NF_3, disappearance and appearance in excimer lasers, reaction kinetics 77−38860
N_2F_4, collisionless dissociation kinetics in highpower IR radiation field 80−66853
NH_2 free radical recombination meas. using intraresonator laser spectroscopy 77−86292
NH_2+propylene, reaction kinetics, laser reson. absorpt. obs. 77−9096
NH_3, decomposition, on supported FE catalyst, kinetics, IR obs. 79−11792
NH_3, flow in steel tubes, wall heat transfer with catalytic dissoc. 78−14099
NH_3 oxidation leaching of chalcopyrite, surface deposit effects 77−48643
NH_3 oxidation leaching of chalcopyrite, reaction kinetics 77−52639
NO, chemisorption on Rh, reactions with CO over Rh, flash desorption spectra, titration, reaction kinetics calcs. 78−61045
NO, interstellar, ion-molecule reactions rel. to candidate mols. form. 78−28739
NO synthesis, reactions of vibr. excited N_2 in nonequilib. plasmachem. system 77−86310
$NO+O_3$, chemilum. reaction, NO_2 light amplification *(Russian)* 77−88717
N_2O, dissoc. in alternating elec. field, kinetic and energetic data *(French)* 78−13620
N_2O, interaction with Cu (111), kinetics using AES, LED and ellipsometry 79−65317
N_2O+CO, nonequilibrium reaction in shock waves *(Russian)* 78−76845
N_2O_4 dissociating coolant, chemical reaction kinetics in transient regimes *(Russian)* 78−58344
N_2O_4 dissociating coolant, O_2 generation time constant, enthalpy change *(Russian)* 78−58345
NaO_2, non-isothermal decomp. kinetics 80−16649
NaO_2, thermal decomp. macrokinetics, differential thermal anal. 80−16650
$Na_2O\text{-}SiO_2\text{-}Ga_2O_3\text{-}Al_2O_3$ glasses in mixed $AgNO_3\text{-}NaNO_3$ melts, ion exchange 80−21282
Na_xWO_3 bronzes, reaction with Fe powder, reaction mechanism and reactivity 80−108712
Nb, corrosion kinetics in sulphidizing atm. 80−35396
Nb, kinetics and thermodynamics of reaction with N_2 *(German)* 79−74415
Nb, nitriding kinetics 80−35415
Nb-Mo(Ru)(Re), kinetics and thermodynamics of reaction with N_2 *(German)* 79−74415
$Nb+O_2$, high temp. interaction kinetics and mechanism 79−100432
$Nd_2O_3\text{-}HfO_2$ system, phase relationships 80−35169
Ni (100), kinetics of C deposition from adsorbed CO 80−76553
Ni, corrosion, high temp., SO_4 induced, studied at 900°C in O_2+4.2% SO_2 80−97639
Ni electrodeposition in sodium thiocyanate soln., kinetics study using rotating disc electrode method *(Spanish)* 78−92486
Ni, oxidation, diffusion enthalpy and entropy 78−7084
Ni, oxidation kinetics near Curie temperature 78−88578
Ni, pack aluminisation process kinetics 77−32718
Ni, reaction with CO_2 interfacial kinetics, $^{14}CO_2$-CO exchange reaction, S effect 79−47978
Ni, sulphidation kinetics, in $H_2S\text{-}H_2$ 550 to 600°C 78−64780
Ni-Fe alloy, oxidation, diffusion enthalpy and entropy 78−7084
Ni-Mn, hydrogenation kinetics, magnetisation, interstitial H influence 80−35528
$NiFe_2O_4$, solid state formation, exam. of kinetics for formation at 700 to 1400 degrees C 78−48648
NiO-ZnO, solid solution, exam. of mechanism and kinetics of reaction with Fe_2O_3 ferrite formation 80−3309
$NiTiO_3$, synthesis from products of soln. spray drying, kinetics 77−16519
$Ni_{0.71}Zn_{0.29}Fe_2O_4$ and $Ni_{0.57}Zn_{0.43}Fe_2O_4$, form. kinetics 79−83159
Np(V)/Np(IV) catalytic redox reactions, kinetics and mechanisms 77−29006

reaction kinetics continued
O atom production and removal rates in current modulated O_2 glow discharges 79−90477
O+methane→OH+methyl reaction, photolytically initiated, high temp. kinetics meas. technique 80−61085
O_3 yield, rel. to discharge field strength and gas pressure 79−19116
$O(^3P)$, translationally hot, in Earth atmosphere, energy distrib. function 80−21811
$O(^3P)$+1-butyne (2-butyne), CO pro dynamics, mechanisms 78−11510
$O(^3P)+CH_3CN(CF_3CN)$, reaction mechanisms and kinetics 77−36728
$O(^3P)$+dimethyl disulphide, absolute reaction rate const. determ. 80−89472
$O(^3P)+H_2S(D_2S)$, reaction rate, flash photolysis-reson. fluoresc. obs. 77−4918
$O(^3P)$+tetrafluoroethylene, time-resolved absorpt. spectra, triplet CF_2 formation 77−44472
$O_2^+.O_2$, reactions with CO_2, O_3 and methane in flowing afterglow, stratospheric appls. 79−2343
$O_2^+.O_3$, reactions with H_2O and methane in flowing afterglow, stratospheric appls. 79−2343
PF_5 dopant for polyacetylene 80−88171
$Pb+N_2O \rightarrow PbO+N_2$, chemiluminesc. reaction, vel. depend. 78−27762
PbI_2, thin films, photolysis kinetics 77−36769
PbO_2, thermal decomposition, heating rate effect, kinetics, mechanism, struct. 78−92473
$Pb(SCN)_2$, thermal decomposition, kinetic parameters from thermogravimetric data 79−61859
PbSe(Te), single cryst. growth, reaction kinetics in binary melts of KCl, NaCl and $PbCl_2$ 77−16486
$Pb(Ti,Zr)O_3$, kinetics of initial stage of sintering 77−85973
^{147}Pm, deposition on anodically polarised Pt surface 78−27424
$PrO_{1.714}$, oxidation, kinetic study 80−108707
Pt electrode O_2 reduction kinetics in conc. H_3PO_4, H_2SO_4 and $HClO_4$ 78−23952
PtO_2, sputtered film, optical props. under H_2 reduction 80−20728
Pu-Ga (1 wt.%), alloy powder, hydriding kinetics 80−76503
Pu(IV) catalytic redox reactions, kinetics and mechanisms 77−29006
Ru (110), kinetics of C deposition from adsorbed CO 80−76553
Ru complex, (2,2′-bipyridyl)$_3$ruthenium^{2+}, excited-state redox processes, electron transfer theory 79−39126
S_2 polymerisation, kinetics obs. by pulsed field ionis. time-of-flight mass spectrometer 77−63890
SF_5Cl, laser induced reactions, yields, product distrib. and isotropic selectivity 78−53225
SO_2, homogeneous oxidation mechanism in troposphere 78−96257
$SO_3^- + BrO_3^-$, fast oxidation in acid medium, laser Raman multichannel spectroscopy 78−27754
$S(^2P)+N(^4S)$, $NS(B^2\Pi)$ form. kinetics, chemilum. obs. 79−39151
$\beta\text{-}Sb_2O_3$ reduction to Sb powder, atomic H effect 80−2978
Si, dissolution rates in KOH, orientation effect 77−36674
Si, nitridation kinetics, combined effect of Fe and H_2 78−95722
Si, oxidation, thermal growth kinetics, SiO_2 profile meas. 78−88551
Si oxidation mechanism and kinetics 78−95833
Si, thermal oxidation in O_2/N_2 mixture, 950-1100°C 77−86202
Si thermal oxidation kinetics in O_2/HCl mixtures 77−77617
Si:P(As)(B)-SiO_2 interface oxidation kinetics, high doping levels, experiment 80−11828
Si-H, amorphous, thermal stability and decomp. kinetics 80−24758
Si-SiO_2, bonding at (111) interface, stoichiometry and kinetics, synchrotron radiation photoemission spectroscopy 80−24744
Si-SiO_2 interface oxidation kinetics, high doping levels, theory 80−11827
Si-SiO_2 system, structural defect formation rel. to thermal oxidation kinetics *(Russian)* 78−43478
$3Si+2N_2=Si_3N_4$, synthesis and props. of silicon nitride shapes 79−47650
$Si+HF_{(g)}$, reaction kinetics 77−86288
SiC, fibre growth kinetics in laser-heated system 77−81203
SiC-fission product reaction kinetics in HTGR TRISO UC_2 and UC_xO_y fuel in thermal gradient 80−47570
$SiH_4\text{-}CO_2\text{-}NH_3\text{-}H_2$ system, SiO_xN_y deposition kinetics 77−48346
Si_3N_4 reaction bonded, microstructure, formation, properties, phase composition 79−56947
SiO_2 fibre reinforced Al, thermal degradation kinetics 77−44194
SiO_2 polymerisation and deposition from dil. solns., kinetics, 5-180°C 80−7790
SiO_2, vaporisation in steam atmosphere 80−44306
SiO_2, vitreous, hydroxyl free, reaction with H, diffusion, absorpt. spectra 80−85210
SiO_2-water system, inorg. polymer struct. form., globular crystn. 80−101042
SiO_x deposition by reactive sputtering of Si in magnetron sputtering system, reaction kinetics 80−49553
$SmCo_5$ hydriding kinetics, inverse over-pressure effect 80−55944
$SmCo_5$ thin film, hydride form., kinetics, mag. monitoring 80−35571
SmN, form. conditions 80−101019
$Sm_2Ti_2O_7$ form. kinetics rel. to TiO_2, Sm_2O_3 polymorphic transitions 79−11606
Sn, oxidation kinetics, in high-temp. fast flow reactor, chemiluminesc. titration meas. 77−48623
$Sn+CH_3I(n\text{-}C_3H_7I)(CCl_4)$, crossed beam mol. kinetics, SnI and SnCl recoil vel. spectra 79−1947
$Sn+N_2O$, oxidation chemiluminesc., quenching kinetics 79−52672
$Sn+O_2$, crossed mol. beam kinetics, SnO time of flight recoil vel. spectra 78−68883
$SrBr_2(SrI_2)+Cl_2$, crossed beam metathesis, total cross sections 77−21354
$SrFe_{12}O_{19}$, exam. of factors affecting reaction kinetics, thermal analysis *(German)* 79−24471
T+HD hot atom exchange reactions, trajectory calcs. 80−26037
Ta, kinetics and thermodynamics of reaction with N_2 *(German)* 79−74415
Ta, sputtered layer, thermal oxidation, reaction kinetics 78−39959
Ta-8W-2Hf wt.% (t-111) alloy, dissolution kinetics of small amounts oxygen, internal oxide disp. reactions, annealing 77−16612
Ta-Nb(W)(Re), kinetics and thermodynamics of reaction with N_2 *(German)* 79−74415
$Ta+F_2$, reaction, 690-930K modulated mol. beam mass spectrometry expts. 77−70341
$Ta+F_2$ reaction, modulated molecular beam mass spectrometry 78−15678

reaction kinetics continued
Ta_2N film, high temp. nitriding kinetics depend. on press. *(Russian)* 80−50838
Ta_2N, sputtered layer, thermal oxidation, reaction kinetics 78−39959
TaS_2, 2H polytype, Li intercolation kinetics PAC hyperfine spectrosc. 79−87337
TaS_2-2H electrodes, topotactic reduction nechanism, neutron diffr. obs. and intercalation cpd. form. 80−108748
Ti, $\alpha \rightarrow \omega$ transform., pressure-induced, impurity effects and reaction kinetics 78−11220
Ti, oxidation kinetics in water vapour-Ar ambient mixtures 77−90498
Ti, reaction with P, at high temp. 78−44260
Ti, sulphurisation kinetics, 450-550°C, thermogravimetric determ. 77−25197
Ti-Al(Cr), interaction with N_2 at elevated temp., nitridation behaviour 77−12742
Ti-Mo alloys, boronizing, reaction kinetics 79−61797
Ti-O system, nonstoichiometry between Ti_3O_5 and TiO_2 comps. at high temps. 77−15594
$Ti+N_2$ at elevated temp., kinetics and mechanism of reaction 77−12741
$TiB_2+Ti \rightarrow 2TiB$ react., kinetics, X-ray diffr. anal. using internal standard, dilution methods 77−70393
TiC-Ni, reaction kinetics under simulated liq.-phase sintering 78−52746
TiN-Al_2O_3, exam. of sintering and densification kinetics, and physical props. 79−95986
Ti_xN_y, synthesis by nitriding Ti and TiH_2 77−44200
TiO_2:$TeCl_4$ system, chem. vapour transport, matrix isolation IR studies 80−93755
TlCl+KI, solid state displacement reaction, kinetics and mechanism 79−11788
$TlCl_3.(TlCl)_3$, labelled, exchange of Tl ats. rel. to γ-irrad., heat treatment, grinding 78−92470
$U+H_2$, surface reaction, temp. depend. 79−91996
UO_2-zircaloy-4, reaction kinetics at high temps., O_2 diffusion 80−16667
$U_{0.75}Pu_{0.25}O_{2-x}$, variation in O_2 potential with simulated burnup 78−70597
V_2O_5-$AlNbO_4(GaNbO_4)(TiNb_2O_7)$ systems, interfacial reactions, efficient boundary conditions and solid state reactivity 80−76542
W, CVD by reaction of WF_6 and H_2, kinetics 79−19995
W, carburisation by methane, initial kinetics 79−47824
W, desorption of D_2, meas. of fast desorption kinetics by laser heating technique 79−23837
W siliciding, in vacuum, diffusion saturation, effect of NaCl, kinetics 79−15859
W-O-Br system, appl. of mass transfer model of halogen doped incandescent lamps 77−32832
$W+SO_2$, reaction kinetics, 1600-2100K 79−20266
WF_6, mechanism of heterogeneous reduction by H_2 *(Russian)* 80−21265
WO_3 electrochromic reaction kinetics 77−77176
WO_3 reduction with H, starting specific surface effect on kinetics 80−11599
$Xe(^3P_{0,2})+Br_2 \rightarrow Xe^*+Br$, excitation function 78−40028
Zn electrodeposit dendritic growth control using impedance meas. 78−84721
Zn+P reaction mechanism and kinetics, effect of Ag and Mn impurities 77−21416
ZnS, oxidation in fluidised bed 77−4929
ZnS-CdS, equimolar solid soln. formation kinetics 80−39289
ZnSe-HCl-H_2, vapour phase chemical kinetics in open tube horizontal furnace *(French)* 77−63909
Zr, interaction kinetics with graphite, reactive diffusion 79−42318
α-Zr, oxidation in O_2-N_2 atmospheres 80−104353
ZrC layers grown on graphite via activated cementation *(French)* 77−52552
ZrC_xN_{1-x} coating, on Zr, oxidation kinetics, 450-600°C 50-400 Torr O_2 press. *(French)* 77−25171
ZrN coating, on Zr, oxidation kinetics, 550-700°C, 50-500 Torr O_2 press. *(French)* 77−25170
ZrN, form. in RF discharge 77−86222
ZrN-Al_2O_3, exam. of sintering and densification kinetics, and physical props. 79−95986

reaction kinetics models and mechanisms *see reaction kinetics theory*

reaction kinetics theory
$A+A_n \rightleftarrows A_{n+1}^*$, cluster dynamics, classical trajectory study 80−3316
A+B→C+D overall reaction types, a priori possible mechanisms derivation 79−91914
A-factor, temperature dependence, in thermal unimolecular reactions 79−74347
absolute rate theory, ab initio calcs., elementary gas phase reaction 80−7757
absolute rate theory, symmetry numbers and statistical factors, Bronsted relations 78−85123
absolute rate theory, use of statistical factors and chirality effects 78−85124
acetaldehyde, carbonyl addition, model transition states, vibr. anal. 80−71898
acetic acid-formic acid, 'dimer', tritium β^--decay causing H^+ transfer, ab initio MO calc. 80−3391
Acree relation, re-evaluation of its conceptual foundations *(French)* 78−7172
activation energy, bond energy-bond order method 78−60981
adiabatic nuclear group transfer processes in condensed media, electronic energy hypersurfaces 80−25982
aluminisation in Al packs, for protective coating form., kinetic diffusion theory 77−32727
aqueous solution reactions, surface constrained soft sphere dipoles model 78−60980
aromatic compounds, oxidative bromination, chem. oscills. 80−3335
Arrhenius A and E interconversion algorithms 79−15957
Arrhenius activation energy, derivation using collision theory 78−93495
Arrhenius equation, pre-exponential factor temp. depend., thermogravimetric data calcs. 78−15654
atom+diatom, complex formation in collinear collision, trajectory study using pot. surface 79−87821
atom+diatom, microcanonical reaction probability, classical transition state theory 80−50842
atom+diatom collinear collisions, exponentiating trajectories and statistical behaviour, variational eqns. 78−27742

reaction kinetics theory continued
atom+diatom reactions, semiclassical tunnelling probabilities, trajectory calc. 80−71886
atom+diatom reactive collision, three dimens., exact classical formulation in natural coords. 80−50835
atom+molecule, dissoc. and exchange, classical and near classical rates 79−11778
atom transfer processes, tunnelling at low-temp. Gamov formula 79−66263
atom transfer reaction in gas phase, reaction rate computing, tunnelling corrections 79−79237
atom transfer reactions, reaction rate computing, trajectory calcs. 79−74371
autocatalytic reaction system, sustained oscills., deterministic and stochastic theories 78−95922
autocatalytic reactions, symmetry breaking, spatial struct. striation theory 77−12778
autocatalytic system, concentration waves, multiplicity and stability 79−16037
azoethane, pyrolysis, master eqn. for rate coeff. 78−48612
backward differentiation method, extrapolant formulation, appls. to chem. kinetics eqns. 78−48628
BEBO method calculations 77−19007
Belousov Zhabotinskii reactions, model, computation of travelling wave solns. 79−70318
Belousov-Zhabotinski reaction, chem. oscill. mechanisms 80−3304
Belousov-Zhabotinski reaction, oscill., thermal props. 80−7762
Belousov-Zhabotinskii reaction, Field-Noyes model, threshold phenomenon 77−70284
Belousov-Zhabotinsky reaction, chem. turbulence, strange attractor representation 80−85148
Belousov-Zhabotinsky reaction, excitable, Winfree meandering 79−58660
Belusov-Zaikin-Zhabotinsky reaction, chem. wave equation 78−15653
Belusov-Zhabotinski reaction, nonlinear effects 80−3302
Belusov-Zhabotinskii reaction, chaotic states obs. 78−20006
bifurcation and reaction-diffusion spectroscopy 78−95910
bifurcation and stability of systems far from equilibrium 77−73461
bifurcation diagram of model chemical reactions 80−3303
bimolecular endoergic reactions, threshold behaviour, statistical phase space approach 78−48615
bimolecular exchange reactions, dynamical-statistical method calcs. 80−104435
bimolecular gas phase reactions, collision theory, quantum corrections 79−8433
bimolecular isomerisation in liq., kinetic theory, spatial nonequilib. effects 79−5138
bimolecular reaction, partly diffusion-controlled, physical and chem. kinetics competition 79−43566
bimolecular reaction kinetics, role of density fluctuations 78−44351
bimolecular reactions, almost diffusion-controlled, Arrhenius activation energy calcs. 77−63893
biological electron transfer kinetics models 79−39339
biological tissue, O_2 diffusion and chem. reaction 77−44615
biology, reaction rate theory in bioluminesc. and other life phenomena, review 77−90716
biomaterial growth phenomena and behaviour, math. theory 77−81458
bistable reaction system, stochastic dynamics investig. of discrete trimolecular chemical model 80−16645
branched chain reactions, thermal nonequilib. effects 80−76507
Briggs-Rauscher reaction, chem. oscill. obs. 80−3336
Brownian motion theory of transition rates 77−36731
Brusselator, dynamic correl. functions, Mori-Zwanzig formalism 80−25988
Brusselator, two-box model, multiple stable steady states, chem. hysteresis 79−100428
burning droplet, finite reaction rate model rel. to flame sheet model 79−34306
cage reaction in solid state, model 79−87820
calorimetric methods 78−27733
catalysis, heterogeneous, kinetic model depend. of reaction rate 77−90583
catalysis, heterogeneous, vibr. excitation, classical trajectory calcs. 80−26045
catalysis of reversible flow reaction by oligomeric enzyme 77−36859
catalysis on single cryst. surface in UHV system, limitations 77−9126
catalytic heterogeneous, bimolecular surface reactions, defect renormalised propagator stochastic theory 78−95955
catalytic pellet, isothermal n-order decomposition reaction, steady state stability anal., topological degree and Lypunov method 80−30280
catalytic reaction rate, influential factors, new definition of catalysis 79−1943
catastrophe theory in chem. reactions, study and classification of propagating phenomena 78−7170
catastrophe theory of nth order reactions, uniqueness and multiplicity criteria 79−70296
cell adhesion models, reaction kinetics and forces 78−80844
chaos and strange attractors 80−7760
chaotic behaviour in simple system, continuous Euclidean dynamics 77−60046
chemical 'birth' and 'death' processes, absorbing zero boundary problem 78−95911
chemical centre waves, dynamic Pade approx. 80−76486
chemical composition centre waves, periodic chaotic, Pade approximant scheme 78−80716
chemical evolution far from equilibrium, concepts *(French)* 80−7761
chemical instability with diffusion, nonlinear rate eqns. 78−31615
chemical instability with diffusion 78−73014
chemical kinetics, first-order model, optimal design of expts. to estimate parameters 78−15650
chemical mechanism struct. and coincidence of stoichiometric and kinetic subspaces 78−56877
chemical reactions, Brownian dynamics simulation in soln. 80−104422
chemical reactions and reactive collision phenomena, props. of stochastic process description 78−60991
chemical rectifiers, one-way catalysis 80−71901
chemical system, multiple steady state, phase transform. stochastic theory, nucleation 78−53187
chemical systems, single variable, master eqn. approximation by Fokker-Planck type eqns. 80−77702
chemically assisted fracture, general reaction rate theory and thermodynamics 80−64465

reaction kinetics theory continued
chemically reacting quantum gases, kinetic eqns. 78−40024
chemically reactive flow, kinetics, stiff ordinary differential eqns. numerical soln. 78−48631
chemiluminescence, charge-pair recombination kinetics, nonGaussian diffusion 79−34312
chemiluminescence reactions, electron exchange initiated, kinetics correl. with free energy changes 80−50856
chemisorption kinetics, heterogeneity effects *(German)* 78−85202
chromatographic reaction and separation in pulse-fed catalytic reactor 78−64880
circulation reactions, stochastic model 79−15955
classical dynamics of triatomics appl. to energized harmonic molecules 77−60039
collective quantum states in model chem. systems 78−48634
collinear asymmetric model reaction probabilities quantum and quasiclassical calcs. 80−85145
collinear reaction prob. and thermal rate constant for pot. energy surface with middle barrier, classical dynamics. theory 79−91916
collinear reaction prob. and thermal rate constant for pot.-energy surface with early barrier, classical dynamics theory 79−91917
compartmentalised free radical polymerisation reactions 79−24748
competitive decomposition and stabilisation models for collisional efficiency in external activation systems 80−25989
complex chemical systems, chemical process and rate models, computer simulation appls. 78−48620
complex chemical systems, kinetic mechanisms simulation method 78−48622
complex reaction interphase boundary kinetics, appl. to water-zeolite desorption 79−57203
concerted reaction, rate depend. on degrees of freedom in transition 77−70285
condensed phase chemical dynamics, many-body problems, generalised Langevin theory, modeling 80−76482
condensed phase microscopic theory, configuration space eqns. 80−61067
condensed phase microscopic theory, pair phase space kinetic eqn. 80−61066
condensed phase reacts. at low temps., at.-mol. transforms. 77−25253
conference on nonlinear nonequilibrium statistical mechanics, Kyoto, Japan, (Jul. 78) 79−75441
consistency between kinetics and thermodynamics 77−44460
copolymers, cooperative reactions, sequential anal. of 2nd order Markovian chains 78−7204
copolymers, cooperative reactions, sequential anal. of binary copolymer with protecting monomer 78−7203
coupled chemical reactions, exact stochastic simulation, using digital computer algorithm 78−48625
curve-crossing, two-state and reactive, DWBA and Landau-Zener approx. 79−24719
cyclobutane, dissoc., frontier orbitals and activation energy, HAM/3 method 78−92452
decomposition, reaction rate calc. by differential quotient 80−25990
decomposition of isolated mols., transition state theory 77−16786
decomposition reactions, endothermic, kinetics 79−52646
definition of terms related to reaction rate, order 79−52625
dense fluid chem. kinetics, correlated binary collisions, solvent effects 78−44347
dense fluid systems, spatial correls. effect on steady state nucleation kinetics 78−11500
desorption, relaxation time approach limitations 80−93795
diamond powder, rapid oxidation development, kinetic model *(French)* 78−68917
diatom+atom, cross section, translational excitation features, dynamical model 80−16655
diatomic dissociation equilibrium, isotopic mass depend. theory 79−74372
diatomic molecules, vibr. relax. distrib. rate, rel. to nonequilib. vibr. levels and dissoc. 77−54596
3,3'-diethyloxadicarbocyanine iodide, kinetic model and expt. results of picosecond photobleaching 78−53226
diffusion controlled processes, nonequilibrium decay effects 80−66764
diffusion controlled rate, pair of reacting sinks 77−86289
diffusion controlled reaction, passage time approach 80−71903
diffusion controlled reactions, correlated and uncorrelated particle pairs 80−45477
diffusion controlled reactions, kinetics 78−40022
diffusion controlled reactions, particle fates; Onsager and Monchick methods unification 79−52621
diffusion processes, nonlinear, oscillations 77−73440
diffusion reaction nonlinear eqns., secondary bifurcation 77−9860
diffusion theory of reaction rates, rate consts. and transmission coeffs. calcs. 80−89464
diffusion-controlled chemical reactions modeled by continuous-time random walks 80−3297
diffusion-controlled processes among partially absorbing stationary sinks 79−54074
diffusion-controlled reaction kinetics 80−16643
diffusion-controlled reactions, freq. depend. rate coeff. theory 77−66746
diffusion-reaction equations for semilinear parabolic systems, soln. existence and stability 79−47889
diffusion-reaction problem, nonlinear, dissipative structs., stability anal. 79−1938
diffusion-reaction system, bistable, stationary solns. bifurcation 79−79224
diffusion-reaction systems, effect of gravity on pattern formation 79−70302
diffusional barrier crossing processes, trajectory simulation for kinetics of reacting soln. 80−81280
diradical+singlet reaction, SCF calc. involving orbital symm. forbidden reaction pathway 79−98004
discrete simulation methods, appl. 78−48627
disordered system, donor-acceptor energy transfer, diffusion modulated 80−71888
dissipative structures, bifurcation, symmetry and influence of elec. field 80−81289
dissipative structures, fluctuation effects, appearance of optically active states 79−83442
dissipative structures, fluctuation effects on chem. oscill. systems 79−83441
dissipative structures in chemical systems, nonlinear effects 80−3302
reaction kinetics theory continued
dissociation, A+BC→A+B+C, statistical classical trajectory theory 77−28977
dissociation, diffusion-controlled reaction, theory 78−64820
dissociation reaction, shift of chem. equilib. in laser reson. IR radiation field 77−56224
dissociatively chemisorbed molecules, desorption kinetics 79−86977
dissolution kinetics 78−63686
double well potential, transfer and tunnelling rates, density matrix calcs. 80−30209
droplet formation in supersaturated systems, reaction kinetics 77−66748
Eckart barrier tunnelling, Arrhenium plot curvature 80−3298
education, unimolecular gas reactions, Lindemann theory 78−27753
electric field effects on thermodynamic equilib., and field chem. consequences 78−7224
electrochemical corrosion, kinetics anal. 79−96335
electrochemical kinetics at interface with space charge layer, appls. *(German)* 77−32807
electrochemical reaction, metal surface adsorbed surfactant effect 80−40703
electrochemical reaction kinetics, in presence of surface-active substances, eqn. selection 79−34322
electrochemical reaction rate in presence of surface-active substances on electrodes 79−43597
electrochemical reactions, mechanisms studied by parameter sensitivity functions and zone diagrams *(French)* 78−88638
electron kinetics in nonpolar liquids 78−95918
elementary reactions on single crystal surfaces, kinetics 80−108729
endoergic reactions, reagent internal excitation effects on rates 80−93731
energy disposal specificity on magnitude of thermal rate const. 78−44350
enzymatic catalysis, dynamic theory, conform. rearrangements 77−36858
enzymatic charge transfer across oil-water interface, effect of dielec. const. 77−70419
enzymatic open reaction, mathematical model 79−53024
enzyme activity rate reduction by EM fields *(Russian)* 78−61142
enzyme catalysis, electron pairing in thermodynamically consistent pathways 79−5179
enzyme-catalysed reactions, network thermodynamic modelling 80−89463
enzymes, modelling 77−4979
epoxy cure, autocatalytic reaction, kinetic parameter estimation 79−70327
1,2-epoxypropane, photopolymerisation by arenediazonium salts, obs. 79−24747
equations of chemical kinetics, numerical solns., stiffness 78−48624
equilibrium fluctuations, deviations from Poisson behaviour, molecular dynamics 80−86211
equilibrium fluctuations in conc. for reversible reaction *(Russian)* 78−11501
escape probability calc. for diffusion controlled reactions 79−1934
estuary and river sited power plants, water discharge and chlorination, simulation 78−96250
ethane, photolytic decomp. to ethylene via triplet ethylidene, MINDO/2 calcs. 78−64869
exchange reaction, phenomenological rate eqn. model 79−87824
excitation functions, dynamical content, linearisation methods 77−63886
exothermic reactions, Marcus eqn., Born approx., strong vibr. nonadiabatic transitions 77−56214
exothermic triatomic exchange reactions, dynamics, anal. theory 78−3322
explosions, thermal homogeneous, influence of reactant consumption on critical conditions 78−92483
Faddeev equations and Franck-Condon models for chemical reactions, appl. to $H+Cl_2$ 80−35507
first order, localisation of roots in complex plane *(German)* 79−66257
first order reaction in catalyst particle, conc. depend. diffusion coeff., effectiveness factors 78−48693
first-order rate equations, coupled, closed system, symmetry theory 78−40021
fluctuation, equiv. of stochastic diffusion process with fluctuation dissipation theory 77−77734
fluid mixture, BBGKY hierarchy in arrangement channel quantum mechanics 79−70299
fluid-solid reactions, exam. of law of additive reaction times 78−53189
Fokker-Planck model, reactive and translational dynamics coupling 78−60988
formamide dimer, tritium β^--decay causing H^+ transfer, ab initio MO calc. 80−3391
formic acid dimer, tritium β^--decay causing H^+ transfer, ab initio MO calc. 80−3391
Fourier sensitivity analysis, improved freq. sets 78−31628
Franck-Condon factors rel. to information theory for vib.rot. distribs. and isotopic branching ratios 77−60041
free radical reaction, mechanisms, mathematical theory 78−48647
gas absorption by liquid, exothermicity altering solubility and reaction rate 79−74341
gas mixture, physical and chemical process modelling 80−71892
gas mixtures, kinetic eqn. 80−25983
gas-solid reaction, grain model for porous solids 79−70297
gas-solid reactions solid catalysed, effectiveness factors 79−47966
gases, chem. reacting, kinetic fluctuations *(Russian)* 78−59552
glassy polymers double NMR, appl. of cross relaxation dynamics in modulated systems 80−71242
graphite, chem. rate theory applic. to fast neutron irrad. damage 77−27913
Green's function method of sensitivity anal. 79−20343
growth, self-reproduction and autoregulation model, anal. of reactions with stretchable semi-perm. walls 77−81460
growth and patterns of spatial organisation 80−81287
Hafke-Gilles reaction, oscill., thermal props. 80−7762
hard sphere dynamics, Liouville eqn. for condensed media 79−70298
heterogeneous, statistical interpret. 78−60987
heterogeneous reactions *(Russian)* 78−53191
heterogeneously catalysed reactions, kinetic instabilities, oscill. instabilities 79−24717
heterogeneously catalysed reactions, kinetic instabilities rate multiplicity 79−20341
heterogeneously catalyzed oscillatory reactions 80−108732

reaction kinetics theory continued
hot atom+mol. reaction, steady state vel. distrib., Boltzmann eqn. with BGK elastic collision model 80−66856
hot atom reactions, hydrodynamic steady states 79−34342*
hot atom reactions, nonequilib. time-depend. theory, model calcs. 80−61125
hot atom reactions, nonequilib. vel. distrib. and reaction rate, Monte Carlo anal. 77−16855
hot-atom reactions, Boltzmann eqn. for hot-atom relax. 79−100423
hot-atom reactions, photolytically-driven, kinetic theory, appl. to DI 79−74408
hydrocarbon diffusional combustion in air, finite activation energy anal. 78−95930
information contained in open systems by example of chemical reaction systems 79−91915
intermicellar kinetics theory, stochastic approach, master equation for, irreversible reactions 80−76561
intermolecular energy transfer following kinetically controlled chem. activation, multistep deactivation processes 80−25985
intermolecular reaction dynamics, pot. barrier crossing in high friction limit 79−29343
interstellar molecules, collision-induced dissociation 80−17632
intramolecular reaction, transient initial conditions for diffusive barrier crossing 79−29344
intrinsic field theory, intrinsic reaction coordinate approach 80−11877
ion+molecule reactive collisions, models of dipole capture, energy depend. 79−91911
ion+polar molecule collisions, average dipole orientation theory, ang. momentum conservation 78−92466
ion pairs, in dilute soln., Debye-Smoluchowski eqn. soln. 79−66259
ion-molecule association rate calc. 80−81282
ion-molecule association reacts., gas phase, statistical phase space theory approach 80−50839
ion-molecule reaction, exothermic, rate coefficient, transition state method 80−40688
ionic systems, chemical wave equation 78−15653
isolated pairs in condensed media, partially diffusion controlled reaction 78−92441
isomerisation, model reaction, SCF-SI theory calcs. 80−23399
isomerisation, thermal, rate theory 79−34291
isomerisation dynamics in condensed phases, kinetic theory, trajectory anal. 79−66273
kinetic systems, determ. of number of independ. variables by correlation function meas. 78−31614
Kramer's theory, eigenvalue and eigenfunction anal. 79−29330
Kramers' theory, accuracy anal. 80−7758
Kramers theory of friction and vel. in chemical kinetics 80−50826
Langevin equations, stochastic source term 77−28982
Langevin theory, generalised, for many-body problems, formulation and equiv. harmonic chain representation 80−35504
large chemical kinetic systems, functional group anal. 78−48626
large mol. reaction with intermediate complex, vibr., translational distrib., pot. hypersurface calc. 77−52612
large mol. reaction with intermediate complex, vibr. distrib., R-matrix, hybrid quantum statistical mechanics 77−52611
linear free energy slopes and curvatures, rel. to barrier shape 78−80713
linear Onsager relation, mol. kinetics basis 79−67242
linearised reaction diffusion equations solutions 77−74331
liquid phases interface, hydrochemical stability 78−22933
liquid-solid reactions, shrinking core model application 79−47887
liquids, hydrodynamic interactions and pair correl. functions on reaction kinetics, dynamic effect 80−97684
liquids, reactive pair dynamics, kinetic theory 79−11761
liquids, with chemical relax., generalised Langevin eqn. 79−91908
local fluctuations in chemical reactions, nonlinear master eqn., dimensionality expansions, augmented mean field theory 78−73019
looped reactions in dissipative chem. kinetics 79−15959
Lotka-Volterra model, effect of fluctuations far from equilibrium 77−28983
lumped system Arrhenius reaction, exact uniqueness and multiplicity criteria 79−47888
magnitude and variation, with energy, structural modifications of reactants 79−74349
maser equation near nonequilibrium transition, stationary solns. 80−89466
mass action kinetics, closed and open, μ-molar representation 78−85129
mass action kinetics, second order, dynamic props. 78−85130
mass action kinetics, second order, enumeration 78−73018
measurements of reaction rate consts., reliability criterion 79−8423
metal, oxidation, Rosenburg kinetic method applied to determ. of parabolic rate const. 78−64774
metal, oxidation kinetics, effects of control of scale structure 77−16751
metals, electrocrystallisation and passivation kinetics, multiple stationary states and dissipative structs. theory *(French)* 80−7804
metastable and unstable states relax., analytical theory of extrema 80−50829
methyl group internal rot., pot. barrier and activation energy, absolute rate theory 79−79220
methylene+H_2→CH_3+H, triplet methylene abstraction, partial open shell FSGO calc. 78−80719
methylene*+H_2→CH_3+H, barrier height, CI with double zeta polarisation basis 78−64812
micellar diffusion-controlled reaction kinetics 80−30213
micellar interface, reaction kinetics, rotamer population, fast proton transfer 80−26050
micellar phase dissoc.-recombination kinetics, stochastic model 80−55628
micellar system, photoinduced redox processes kinetics, intramicellar electron transfer 78−92603
Michaelis Menten mechanism, modified, global asymptotic stability of soln. 79−79456
microcanonical sampling method, simulation appls. 78−73917
minimum energy reaction paths, virial theory implications 80−97686
mixture, kinetic behaviour, first order reactions 77−52609
mixtures of reacting gases, extension of Chapman Enskog method *(Russian)* 78−57878
modelling, numerical method based on Taylor series expansion 78−48629
modulated mol. beam mass spectrometry, reaction prod. vector, surface reaction 77−63952
molecular beam reactions, transient complex form., product mol. translational energy distrib., theory 77−90602
reaction kinetics theory continued
molecular collisions, joint products' state distribs. 78−64807
molecular dynamics simulation of chemical reactions in solution 80−40673
molecular models of condensed systems and interfaces *(German)* 80−20062
molecular transition states locations and reaction pathways, synchronous transit method calcs. 77−77730
monotonic time laws, kinetic process anal. *(German)* 80−11875
multi-component one dimensional chemical kinetics calculations, new algorithm development 80−45479
multiple stationary point in reacting systems, minimal requirement 80−85146
multiple stationary states systems, meas. of stability and relative stability 80−3338
multiroute systems, optimum characts. 79−39124
multistable chemical reaction systems, separatrices calc. 79−16033
multivariate master eqn. diffusion operator, reaction diffusion system eigenfunctions 78−29077
multivariate master equation for reaction-diffusion system 80−95045
muonium atom reaction dynamics using surface muons in gas phase 79−57274
muonium reaction in soln., rate const. and effective charge 79−57275
network, nonlinear oscills., transformation group symmetry treatment 77−32771
network structures of a system coded by groups 80−81286
NMR chemical shift between two sites in rapid exhange limit, Fourier transform method 79−24743
noise analysis for differentiation between equilib. and nonequilib. kinetic systems 78−44439
noise power spectrum matrix 78−48617
non-ideal mixtures, birth and death formalism 80−101006
non-ionic reactions, temp. and press. effect on kinetic and thermodynamic parameters 80−3300
nonadiabatic cage reactions, relaxation hindrance 80−93740
nonequilibrium kinetics, linear mixture formula, eigenvalue approx. 77−63895
nonequilibrium phase transition, exact results, stochastic anal. 78−29076
nonequilibrium phase transitions and chemical reactions 79−79221
nonequilibrium plasma chemical reaction kinetics 78−76863
nonequilibrium reacting systems, critical bifurcations, scaling and Ginzburg criteria 80−81290
nonequilibrium steady state fluctuations, stability and generalised state functions 77−28987
nonequilibrium steady-states in chemical systems, fluctuations 77−28988
nonequilibrium systems, with multiple stationary states, kinetic anal. 78−27735
nonequilibrium systems, with multiple stationary states, stability, thermodynamic anal. 78−27734
nonisothermal ideal gas mixture, stationary state, inert and dissoc.-assoc. components 77−60042
nonlinear chemical rate processes with multiple stationary states, stochastic theory 77−90582
nonlinear eqns. for reacting system with physical interactions 80−81288
nonlinear master equation, asymptotic expansion 77−49682
nonlinear reaction diffusion model, dissipative structures 79−66279
nonlinear reaction diffusion systems, bifurcation anal., dissipative structs. in a sphere 79−11767
nonlinear reaction-diffusion equations, pattern selection at the bifurcation point 80−50827
nonlinear system, networks induced by symmetries of transformation groups 79−43556
nonradiative transition rates integral eqn. method 78−76827
oil-water interface, chem. and hydrodynamic instabilities *(French)* 80−7789
open chemical reaction system with exactly evaluable limit cycle oscillations 80−21260
open chemical system, noise-induced transitions 80−3337
open systems, arbitrary dynamic behaviour 77−73438
oscillating chemical reactions, kinetic model based on catastrophe theory 79−43557
oscillating reactions, thermal props. 80−7762
oscillations, reaction systems with exactly evaluable limit cycles 79−66262
oscillations in chemical systems, Oregonator concept 77−16784
oscillations in chemical systems, Oregonator concept 77−16785
outer sphere electron transfer reactions: a generalized Landau-Zener model 79−34278
packed bed reactor, diffusion controlled mass transfer coeff. 79−43555
parameter estimates, correl. reduction 79−39121
partial and differential eqn. parameters, estimation using Galerkin's method 79−66258
partial differential equations, time-varying, numerical solns. 78−45463
phase transition probability, system size depend., consequences for stochastic eqns. 78−41258
phase transitions, nonequilibrium transient behaviour 80−93732
photobleaching of large mols., kinetic model 78−53226
photochemical reaction, avoided crossings in excited states potential energy surfaces 78−76881
photochemical reaction kinetics, in absence of diffusion, small conversion approx. 77−36768
photochemistry, reversible excited-state electron-transfer reactions 78−76885
photochemistry, unimolecular reactions, kinetics, monochromatic IR radiation 79−47949
photochemistry of powder, conc. and radiation intensity reaction time and depth depend. 77−29023
photodissociation of molecules, application of inverted triangle mol. pot. 79−74400
photographic process, reaction tensor analytical treatment *(German)* 79−83481
photoinduced radical pair recombination in high mag. field, Monte Carlo method 79−87861
photorecombination laser theory thermally induced behind a shock wavefront 79−76682
photosynthesis primary processes kinetics, influence of certain back reactions 79−79491
phototropy, kinetic investig. *(German)* 78−64868
plastic flow, consecutive energy barriers system, reaction kinetics theory 80−106730

reaction kinetics theory continued
polyatomic molecule reacting with heat bath molecules, collisional energy transfer, statistical theory 78−60983
polyatomic molecules, energised, mean lifetime *(German)* 78−85131
polyatomic species, application of statistical theories, phase space theory 79−74369
polymer network formation, relaxational props. variation 80−38961
polymerisation, from emulsion, homogeneous nucleation 79−29354
polymerisation, single-phase, solid-state reaction kinetics 78−61006
porous medium during gas blow through, exothermal reaction wave propagation 79−79222
positive photoresist film exposure, formal kinetics *(German)* 80−104454
powder reactions, isothermic kinetic eqn. *(Czech)* 79−70301
preferential solvation, effects on reaction kinetics 78−73017
propane pyrolysis, model, kinetics *(French)* 79−52649
protein-ligand equilibrium binding, mathematical models 78−48688
proteins with memory, relax. expts. 77−70406
proton transfer reactions, kinetic isotope effects, quantum theory 80−3301
pseudothermodynamic activation parameters, empirical extended Arrhenius eqn. calcs. 78−85127
pumped chemical system, stationary states, relative dynamic stability, model calc. 80−30211
pyrolysis, mean first-passage time, steady-state and equilib. rate consts. 78−35673
quadratic programming, appl. to kinetic rate const. determ. 78−53185
quantum gases, kinetic eqns. 78−19997
quantum mechanical kinetics problems, averaging principle, degenerate states and reson. effects 78−19996
quantum mechanical kinetics problems, averaging principle appls. 78−19995
quantum mechanical reaction coordinates, point transformation calcs. 77−36730
quantum reactive scatt. theory, 3-dimens. 80−55637
quantum statistical mechanics of relaxation phenomena, non-exp. decay 79−44850
quantum statistical theory, dense systems 78−73016
quantum tunnelling of proton and activated complex theory 78−17586
quasi-stationary complex-energy states, fundamental quantum mech. relationships 79−72374
quasiclassical trajectory calculations, Monte Carlo method, reactivity functions and product distrib. 79−15958
radial solid spread factors in gas-solid packed column at trickle flow, evaluation 79−46363
radical+radical, mag. field effects on rates, theory, projection rule 77−86312
rapid reaction of two chemical species in the presence of weak random advection and molecular diffusion 79−66261
rate equations, soln. by CAKE program 78−48630
rate measurement computational processing iterative optimisation techniques 77−32765
rate process theory, role of coherent mechanical vibr. 77−509
Rayleigh-Benard instability, n-component reactive fluids 80−69945
Rayleigh-Benard instability, reactive binary fluids 80−69944
reactant concentrations in oscillatory chem. reactions, turbulence-like behaviour 77−4895
reacting-diffusing system, turbulent spatio-temporal dynamics 78−56880
reaction mechanisms, deduction from rate laws, computer appls. 78−48623
reaction mechanisms, models, computer method appls., conf., New Orleans, USA (1977) 78−48645
reaction zone propagation, combustion wave structure inversion in porous media 80−89494
reaction-diffusion eqns., slowly varying waves and shock structures 77−66747
reaction-diffusion phenomena, singularity theory, calcs., nonlinear partial differential eqns. appls. 80−4510
reaction-diffusion problem, nth order, asymptotic anal. 79−11764
reaction-diffusion system, nonlinear, multiscale propag. phenomena 79−91910
reaction-diffusion system with one degree of freedom, stability anal. of dissipative structs. 79−87826
reaction-diffusion systems, bifurcation theory, classification 80−108713
reaction-diffusion systems, dissipative struct., sphere bifurcation numerical determ. 80−76483
reactive scattering, infinite order sudden approx., l labeled formulation 79−91912
reactive scattering, trajectory calcs., Monte Carlo sampling method for initial values 78−41147
reactive scattering of polyatomic molecules, Franck-Condon theory 78−60984
reactive-diffuse systems with Arrhenius kinetics, multiple solns., ignition and extinction 79−66260
reactivity-selectivity, bounds derivation 80−66763
recombination probability, reactivity depend., scavenger effects 80−76494
Reggeon field theory and Markov processes 78−77774
relaxation process determination of activated event rates 78−95909
relaxation pulses and waves, lowest order multiple time scale expsn. 78−68874
relaxation spectrometry, injected white noise as soln. of phase problem 78−76830
resonant transfer of electronic excitation, eqns. of classical system interacting with quantum system 79−76498
reversible chemical reactions involving H atoms, formation rates and lifetimes of intermediate complexes 79−15956
reversible isomerisation, rate consts. and kernels 78−40020
reversible small bimolecular systems, numerical anal. of statistical functions 78−64831
Schlogl model, transition time statistics 80−89467
second-order chemical reactions, stochastic theory 78−73015
self-oscillating reaction system under periodic external force, thermal fluctuations 79−66338
sensitivity analysis, numerical Green's function procedure 79−100334
shock waves, starvation kinetics 78−64841
shock-wave-initiated photorecombination kinetics and lower mode waveguide amplification *(Russian)* 79−96313
simulation, teaching approach 77−13555
simultaneous reactions, kinetic eqns. optimisation anal., appl. to dissolution problem *(French)* 78−19994
slime mould mitotic cycle lengthening by ELF waves 79−25032
reaction kinetics theory continued
slurry catalyst with particle size distrib., internal effectiveness factor 79−34355
solid pellet, reaction kinetics 79−39123
solid-gas heterogeneous reaction, general kinetic eqn. *(French)* 78−92444
solid-gas reactions, existence of instabilities 80−7861
solution, escape probability and time-depend. reactivity 79−96287
solution, short-range caging effects 79−96286
sphalerite, kinetic study of pressure leaching for Zn prep. 78−44050
spherical particle, parabolic kinetics, Ginzburg-Brounshtein eqn. modification 79−34279
spherical reaction diffusion systems, steady state spatial patterns, mitosis secondary bifurcation theory 80−40672
stability and relative stability in systems with multiple stationary states 79−79280
stability diagram and nonlinear structures, reaction with inhibition forward 77−21360
starvation kinetics, thermally activated processes and vibr. relax. rate consts. temp. depend. 78−95908
stationary states, pumped, model for mixing 80−71887
steady state approximation, validity 79−83439
stochastic formulation, physical validity anal. 77−60044
stochastic model, for nonequilib. coexistence of three phases *(German)* 77−21351
stochastic model, one variable system, birth and death processes 77−49681
stochastic model, with autocatalysis and saturation law 79−52623
strange attractors in 3-variable reaction systems 79−1939
stratospheric photochemistry and kinetics, modelling 79−53495
sudden rotational approximation, reactive and inelastic, body-fixed frame, exchange reaction extension 80−61073
supersaturated gas condensation kinetic model, cluster nucleation assoc. and dissoc. 78−85151
surface processes, nonequilib. distribs. on lattice, operator formalism 79−4468
surface reaction with orientational selectivity, diffusion controlled effective reaction rate 79−16040
surface reactions and mass transport, in Leveque's approx. 78−76907
surface thermodynamics, equilib. and nonequilib. processes, review 77−44505
surfactant inhibition of electrochem. reaction rate, random error effect on characteristic parameters 80−40705
synergetics, chemical processes far from equilib., conf. Bordeaux, France (Sept. 78) 80−3334
system far from equilibrium, stochastic simulation 80−3339
systems with parallel reaction paths, relax. times 77−86285
teaching, complex chem. reacts., kinetics, Markov chain appl. 80−27085
temperature integral approximating eqns. accuracy 78−92445
termolecular rate calcs. for differing 3-particle collision pathways 77−9045
thermal decomposition, rotational effects, analytical model 79−24741
thermal explosion, critical condits., step function reaction rate approx. 78−92480
thermal explosions, heat balance and reactant consumption 77−90601
thermal rate constants, quasiclassical trajectory calcs., detailed balance 79−87822
thermal unimolecular reactions, rate calcs., weak collisions centrifugal barrier effects, adiabatic channel calcs. 79−74348
thermal vibr. relaxation times, exponential transition probabilities 78−64810
thermodynamic density fluctuations effect on low of mass action and kinetics *(Russian)* 78−60990
thermodynamic theory of solvent-jump relax. method, coupled equilibria 79−39186
thermodynamic-like relations, mixing entropy for activation barrier 78−19993
thermodynamics at nonequilib. steady states 79−6068
thermodynamics of internal variables, rel. to absolute reaction rate theory 78−18696
three-body ion-molecule reaction, statistical theory 79−57204
topochemical reaction input mechanism, statistical approach applicability, using model process 78−92446
transition state structure, charge development calc. using Bronsted eqn. 79−83438
transition state theory, absolute rate theory and variational formulations, Porter Karplus pot. surface 80−16642
transition state theory generalisations, classical mech. theory, applics. to collinear reactions of H_2 80−26002
transition state theory generalisations, quantum effects for collinear reactions of H_2 80−26003
translationally driven reactions, transition state theory, cross section curve 80−26000
trapped electrons in rigid matrix, two-step tunnelling to scavenging 79−96288
triatomic molecular systems, unimol. decomp., exit-channel coupling effects 80−25984
triatomic negative ions, dissoc. product kinetic energy, classical trajectory method 78−64809
trifluoroacetyl iodide, UV photodissoc. into three fragments, expt. and trajectory calc. 79−70356
trimer formation from chemical capable of reacting with itself 80−71889
troposphere, urban photochemistry, computer simulation 78−49085
turbulence state, chem. reaction and diffusion, reduced model 77−4896
two time correlation functions for Poisson representation, nonequilib. and equilib. chemical reactions 79−1936
two-component bimolecular reaction system, stable limit cycles 79−47907
unimolecular decay dynamics, pole approx. calcs. 80−35501
unimolecular decomp. kinetics, rot. effects 80−81319
unimolecular dynamics, classical trajectory calcs. 80−108692
unimolecular reaction, intramolecular energy transfer and stability of mol. motion 79−45779
unimolecular reaction, Lindemann fall-off by master eqn. 79−20342
unimolecular reaction, RRKM formula correction by non Boltzmann character factors, Markov eqns. 80−71891
unimolecular reaction rate theory, nonequilib. quantum statistical mechanics 77−44463
unimolecular reaction rates, RRKM calcs., exact state counting methods 77−73437
unimolecular reaction theory, master eqn. basis 77−44457

reaction kinetics theory continued
unimolecular reaction theory, transition probabilities, relax. matrix, commutative properties 80−25991
unimolecular reaction theory mean first passage time and reaction rates 78−60986
unimolecular reactions, in one dimension, theory 78−44364
unimolecular reactions, induced by monochromatic IR radiation 78−88645
unimolecular reactions, master eqn. for rate coeff. Nesbet's algorithm 78−48612
unimolecular reactions, nonequil. time-depend., model calc., single collision approx. 80−25987
unimolecular reactions, pot. energy surfaces, SCF perturbation theory 79−91918
unimolecular reactions, RRKM theory using effective strong collision freq. 78−44365
unimolecular reactions, vibrational collisional energy transfer efficiencies 78−80714
unsteady heat conduction accompanied by an endothermic solid reaction *(Japanese)* 79−76939
urban atmospheric photochemistry, O group anal. and O_3 prod., theory 78−48626
variance matrix construction system 78−56878
vector representations for constructing stochiometric equations 77−21361
vibrational adiabaticity, quantum mechanical derivation of transition state theory 79−74350
vibrational disequilibrium, in bulk reaction system 77−75119
vibrational state distribution from classical trajectory calcs. 77−32773
walking-stick maps, syncope, rel. to chaos 77−63894
$Ba^+ + D_2 \rightarrow D + BaD^+$, sequential impulse model, prod. bond dissoc. energy and cross section 80−81295
$Br + Br_2$, atom-exchange, rate and activation energy, trajectory model and pot. energy surface 78−64811
$Br_2 + Ar$, collision de-energisation of highly vibr. excited Br_2, mol. dynamics simulation 77−42378
$Br_2 + Ar$, ergodic deactivation, anharmonic effects on transfer rate 78−82818
C, impregnated, reaction steps in gas sorption 78−68916
C, porous particle, internal combustion, model 78−92481
$CH_2 + H_2 \rightarrow CH_4$, MINDO/3-FORCES calc., acativation energy and enthalpy of reaction 78−66472
$CH_4^+ \rightarrow CH_3^+ + H$, MINDO/3-FORCES calc., activation energy and reaction enthalpy 78−66472
Ca+NaCl, crossed beam reaction, collision complex lifetime internal state depend. fluoresc. 77−56217
$Cl + H_2 \rightarrow HCl + H$, quasiclassical trajectory calcs. 77−60040
$Cl_2 + F$, reaction kinetics, pot. energy surface and Franck-Condon integrals 79−61855
$D + HI \rightarrow H + DI$, Franck-Condon theory 78−60984
D_2-Ar, thermal dissoc. of dilute mols., vibr. bias mechanism 79−61854
$D_2 + F$, reaction kinetics, pot. energy surface and Franck-Condon integrals 79−61855
$F + CH_4 \rightarrow HF + CH_3$, cross section and rate const. calc. using kinetic trajectory model 77−29010
F+chlorobenzene→fluorobenzene+Cl, statistical theory, phase space theory 79−74369
$F + H_2$, collinear trajectories, reaction dynamics calcs. 79−70311
$F + H_2$, reactivity, multiple electronic surface effects 77−21363
$F + H_2$ dynamics, Franck-Condon factors rel. to information theory for vib.-rot distribs. and isotopic branching ratios 77−60041
$F + H_2 \rightarrow HF + H$, reson. struct., quantum scatt. calc. 79−61847
$F + HD \rightarrow FD + H$, multiple scatt. theory, knockout-pickup mech. 79−66265
$F + HD \rightarrow HF + D(DF + H)$, branching ratios, information theory test by classical trajectory calcs. 78−64822
F+muonium (H)(D)(T), exothermic triatomic exchange reactions, dynamics, anal. theory 78−3322
$^{18}F + H_2$, hot atom reaction, nonequilib. time-depend. theory 80−61126
$^{18}F + H_2$, nuclear recoil reaction, steady state hot atom kinetic theory calc., rate coeffs. 78−35712
Fe_2O_3, reduction, double reaction, reaction kinetics exam., expt. verification *(French)* 78−31705
Fe_3O_4, reduction, double reaction, reaction kinetics exam., expt. verification *(French)* 78−31705
H atom recombination, Morse oscillator model 78−20001
$H + Cl_2$ dynamics, Franck-Condon factors rel. to information theory for vib.-rot. distribs. and isotopic branching ratios 77−60041
$H + Cl_2 \rightarrow HCl + Cl$, quantum mech. reaction coords., point transformation calcs. 77−36730
$H + H_2$, collinear exchange reaction, unified statistical model 79−34295
$H + H_2$, exchange reaction, three-dimens., dynamical S matrix method 79−91930
$H + H_2$ dynamics, Franck-Condon factors rel. to information theory for vib.-rot. distribs. and isotopic branching ratios 77−60041
$H + O_2 \rightarrow OH + O$, kinetic study, pot. energy surface of HO_2, MO theory 79−74353
$H^- +$methane→methane$+ H^-$, nucleophilic substitution, ab initio pot. energy classical trajectory anal. 78−68886
H_2 oxidation, thermodynamic model appl. *(German)* 79−5130
H_2, solid, storage of atomic H, rate process theory 77−32770
H_2-Ar, relaxation rates, thermal dissociation, decomposition, master equation theory 79−74368
H_2-Ar, thermal dissoc. of dilute mols., vibr. bias mechanism 79−61854
$H_2 + F$, collinear trajectories, statistical behaviour and detailed dynamics 80−16664
$H_2 + F$, reaction kinetics, pot. energy surface and Franck-Condon integrals 79−61855
$H_2 + F \rightarrow FH + H$, collinear probability, quantum calc. using pot. energy surface 78−64829
HO_2, pot. energy surface for $H + O_2 \rightarrow HO_2^* \rightarrow OH + O$ reaction, MC SCF CI method 79−74353
$HO_2NO_2 + N_2 \rightleftarrows HO_2 + NO_2 + N_2$ react., kinetics, RRKM theory appl. 78−73032
HeI_2, vibr. excited mol., dissoc., predissoc., quasiclassical trajectory obs. 79−87839
$N_3 +$NCl, reaction rate consts. calc. 79−74342
NH_3, inversion, transfer reaction theory calcs. 78−44364
$Ne + He_2^+ \rightarrow$He+products, surface-hopping trajectory calc. 79−52637
O_2-Ar, thermal dissoc. of dilute mols., vibr. bias mechanism 79−61854
O_3, UV photodissoc. rate, expt. and theory 80−40722
reaction kinetics theory continued
$O(^3P) + CS_2 \rightarrow CS + SO$, reaction rate enhancement, triat. mol. symmetric vs. asymmetric stretch excitation 79−91927
SF_6, IR multiphoton photolysis, master eqn. anal. 79−47945
$SO_2 + O_2(O_3)$, in aq. soln., kinetics, rel. to atm. rate processes 79−20905
$SO_3 + H_2O \rightarrow H_2SO_4$, gas phase kinetics, CNDO/2 calc. of H_2SO_4 and $SO_3.H_2O$ struct. 78−76840

reaction rate coefficients *see reaction rate constants*

reaction rate constants
2-methylcyclopentadiene dimer dissoc., kinetics, multicolumn chromatographic reactor appl. 78−92590
A-factor, temperature dependence, in thermal unimolecular reactions 79−74347
absolute rate theory, ab initio calcs., elementary gas phase reaction 80−7757
acetanilide, bromination, fast reaction kinetics, rot. Pt. electrode meas. 77−16821
acetone, photochem. and photophysics, 330-250 nm, 0-1000 torr 78−17706
acetone, thermal energy charge transfer reactions 79−87828
acetone-d_6, multiphoton dissoc., recomb. to ethane 80−3371
o,m-acetotoluidide, bromination, fast reaction kinetics, rot. Pt electrode meas. 77−16821
acetyl radical, absorpt. spectrum obtained by flash photolysis and kinetic spectroscopy 79−13731
acetylcholine, nonenzymatic hydrolysis, Raman obs. 79−29505
acetylene$+ XH^+(X^-)$, proton transfer reactions, rate consts. meas., Average Quadrupole Orientation Theory 77−63887
acetylperoxy radicals, absorpt. spectrum and reaction kinetics 80−91571
acid, weak, ionisation in aq. soln., rate const. meas., elec. field jump method errors 79−43611
Acree relation, re-evaluation of its conceptual foundations *(French)* 78−7172
acridine, excited state proton transfer reactions, ns fluorometry obs. 79−5132
adiabatic liquid-phase dynamic controlled reaction calorimeter, design and use 77−82519
adrenaline, acid aq. solns., pulse radiolysis, H., OH. react. kinetics, UV spectra 77−16841
aerodynamic levitation flow reactor and applics. 77−29046
alcohols, electrochem. oxidation, kinetic isotope effect *(German)* 78−15681
alkaline ice, trapped electrons, photostimulated decay, time-depend. rate const. 79−52692
1-alkynes$+ O(^3P)$, CO prod., vibr. population distrib., rate consts., laser reson. absorpt. technique 80−40676
allene$+ O(^3P)$, absolute rate consts. meas., 297-439K 78−7196
allyl free radical decay, in irrad. polyethylene, const. diffusion controlled rate const. 78−15651
allyl isocyanide, state-selected, visible absorption spectra and photoisomerisation kinetics 80−11879
allylmethylether, thermal and IR laser induced unimol. decompositions 78−20012
aminophenols, photographic development, comparison with 1-phenyl-3-pyrazolidone 78−64825
ammoniated electrons, reaction rate consts. with hydroquinone, phenol, propionamide 77−9043
anthracene-aliphatic amine, photochemically induced H isotope exchange 79−11771
anthracenes, exciplex form. with amines, form. kinetics and luminesc. props. 80−66792
bis(9-anthryloxy)polyoxaalkanes,, intramolecular excimer form. and photodimerisation, kinetic anal., rate constants determ. 80−66800
aromatic hydrocarbons, singlet energies, correlation with anion radical protonation 78−40064
ascorbic acid, action with perhydroxyl radicals, radiolytic study 80−35523
atmosphere photooxidation reactions, rates, reactivity and mechanism for organic compounds reaction with OH radicals 80−72104
atmospheric chemistry, laboratory kinetic studies 79−53409
atmospheric chemistry, reaction rates and photochemical data 78−77312
atmospheric rate chemistry calculations, algorithmic approach 77−13095
atom+diatom, collinear exchange reaction rates and probabilities, threshold behaviour 78−27738
atom+molecule, dissoc. and exchange, classical and near classical rates 79−11778
atom+molecule reaction rate meas. 80−16676
atom+vibrationally excited molecule reactions, rel. to high power lasers 79−5155
atom transfer reaction in gas phase, reaction rate computing, tunnelling corrections 79−79237
atom transfer reactions, reaction rate computing, trajectory calcs. 79−74371
atomic to molecular ion conversion, rate constant calc. 78−64835
ATPase kinetics in E. coli cells, ^{31}P NMR meas. 78−77022
azoethane, pyrolysis, master eqn. for rate coeff. 78−48612
bacteriochlorophyll, photochem. oxidised, kinetics of dark reduction, R. rubrum chromatophores 77−25390
benzene, and substituted forms, thermodynamic ionis. energy, rel. photoionis. energy 77−16858
benzene cation+benzene, trapped ion mass spectra 80−89470
benzil triplet-anisole, reversible exciplex form., phosphorescence, photostationary and transient obs., simulation 78−9182
2-benzyl-5-benzylidenecyclopentanone, and substituted form, topochem. single-cryst.-to-single-cryst. photodimerisation 80−66819
biacetyl, thermal energy charge transfer reactions 79−87828
bilirubin, aq. soln., pulse radiolysis 78−48761
bimolecular beam-gas single collision chemiluminesc., kinetics temp. depend., theory 77−63914
bimolecular beam-gas single collision chemiluminesc., kinetics temp. depend., expt. 77−63915
bimolecular isomerisation in liq., kinetic theory, spatial nonequilib. effects 79−5138
bimolecular positive ion reactions in interstellar clouds, comets and reducing planetary atmospheres 77−63896
bimolecular rate constant ionic strength dependence, effect of a molecular dipole 80−55977
bimolecular reactions, diffusion-controlled reaction kinetics 79−79226
bimolecular thermal rate coefficients, Monte Carlo calcs. 77−16789

reaction rate constants continued
biradical, triplet state, S-T_0 CIDNP, biradical scavenging rate const. from mag. field depend. CIDNP 79−3461
bromomethyl radical+alkane, rate constants 77−25248
bromomethyne radical+paraffins (olefins)(O_2)(NO), absolute reaction rate parameters 77−1909
1,3-butadiene, absolute rate consts. meas., 297-439K 78−7196
n-butane, decomposition in RF discharges, 10-40 torr 78−3318
n-butyl acetate, alkaline hydrolysis in water-alcohol mixture, solvent polarity effects 77−48639
butyl radical+O_2, reaction rate consts. meas. 80−45490
carbazole, excited state, dissociation rate, normal isotope effect 77−32767
carbohydrates, reactions with hydrated electrons and hydroxyl radicals, rate constants obs. 80−50825
carbonitriding steel, high-temp., saturation kinetics *(Russian)* 79−52450
catalysis, heterogeneous, kinetic model depend. of reaction rate 77−90583
catalyst surface mag. field effect on mol. dissoc. rate 80−16721
charge transfer reactions, empirical rate coeffs. status and astrophysical appls. 80−56701
chemical equilibrium rate coefficient derivation, using scatt. theory 78−15697
chemical exchanges, rate parameters, NMR determ. method *(French)* 77−21383
chemical kinetic data, evaluation and computation 79−74345
chemical reactions, Brownian dynamics simulation in soln. 80−104422
chemical viscosity effects on rate consts. 77−86286
chloroacetylene dissoc. and predissoc., state selected unimolecular reaction dynamics 77−36744
chlorodifluoroethane, CW laser-induced reaction, vibr. rate enhancement obs. 80−11922
chlorodifluoromethane, unimol. reaction by IR radiation, rate consts. and prod. yield, fluence and intensity depend. 80−97713
chloroform-n-hexane, liq. mixture, radiolysis, mechanism, rate consts. 78−20039
chloropentafluoroethane, multiphoton dissoc., crossed laser and mol. beam obs. 80−11908
chlorophyll a, cation radical formation by pulse radiolysis, oxidation and demetalation rate consts. 80−61505
chlorophyll a, photo-oxidation by p-benzoquinone, nature of electron-excited state 78−76991
chlorophyll-a radical cation lifetime in water-acetonitrile soln. 80−72136
circulation reactions, stochastic model 79−15955
collinear reaction prob. and thermal rate constant for pot. energy surface with middle barrier, classical dynamics. theory 79−91916
collinear reaction prob. and thermal rate constant for pot.-energy surface with early barrier, classical dynamics theory 79−91917
complex reaction, evaluation of first order rate constant 79−1937
complixity and time in physics *(Chinese)* 80−81285
computational processing iterative optimisation techniques 77−32765
computer modelling derivation of elementary reaction rate constants 79−74343
condensed media, rate processes, master eqns. 80−77687
consecutive reactions, reaction rate constants, absorbance meas. using isosbectic points 77−73433
coumarin 102, excited state protonation kinetics, laser pH jump and picosecond spectroscopy 80−25992
coupled multistep chemical reactions, rate const. determ., relax. spectroscopy 80−66766
crossed beam studies, gas kinetics 79−74388
crystal growth coefficient, determ. of individual rate constants of reaction 78−59773
cyanoacetylene, rate coeffs. for reactions with ions of interstellar significance 79−57221
cycloheptatriene, and substituted forms, vibr. highly excited, steady-state photoisomerisation 80−16704
cycloheptatrienes, highly vibr.-excited thermal isomerisation in shock waves 79−79236
cycloheptatrienes, substituted, photoisomerisation, rate consts. 78−35708
cyclohexane$_{(g)}$ solns., positive ion-solute mol. reaction rate consts. in radiolysis 77−9091
cyclopropane, thermal unimol. isomerisation, vibr. energy transfer, diffusion cloud method 80−26001
cyclopropane+inert gas, reactant decomp., rot.-vibr. energy transfer, relax. analytic soln. 80−55650
1,1-cyclopropane(-d_2), isomerisation in He bath, vibr. transfer, temp. depend. 79−24723
cytochrome c_3−hydrogenase, reduction kinetics, Mossbauer spectra 80−67031
cytochrome c, trifluoroacetylated, electron transfer reactions 79−20505
cytochrome c conformationally-nonequilibrium state reactivity obs. by pulse radiolysis 79−43816
data evaluation and compilation, simulation and models 78−48621
decomposition, reaction rate calc. by differential quotient 80−25990
defect interactions, Monte Carlo simulation 78−71754
dextran, activation of acid hydrolysis by ultrasound, mech. stress effect on reactivity 79−74375
diatomic mol., vibr. relaxation, nonequilibrial dissoc. rate consts. 77−52632
diatomic molecule, gaseous, dissociation rate const. eqn. 77−32769
diatomics, master eqn. theory, dissoc. rate consts. 77−77742
diazonium, amplifying material, kinetic and sensitometric props. *(German)* 79−43607
dichloromethane, in liq. hexane, radiolysis 78−80769
1,2-dicyanocyclopropane, stereomutations, isomerizations, reaction rate consts., extended Huckel calcs. *(Italian)* 79−20348
dicyclopentadiene dissoc., kinetics, multicolumn chromatographic reactor appl. 78−92590
Diels-Alder reaction, benzogenic, of polycyclic aromatic hydrocarbons, PMO treatment *(German)* 79−15994
diffusion systems, quantum statistical theory, multi-channel reactive scatt. 80−81284
diffusion theory of reaction rates, rate cónsts. and transmission coeffs. calcs. 80−89464
diffusion-controlled reactions on a two-dimensional lattice 80−71940
difluorodiazine, cis-trans isomerisation, mechanism and kinetics, CNDO/2 study 77−90589
1,1-difluoroethane, unimol. decomposition, direct meas. via IR laser photolysis, collision effects 79−57254
reaction rate constants continued
dimethyl sulphide+O(^{3}P), fast flow reson. fluoresc. obs. of absolute rate consts. 80−61077
dimethylamine proton-bound dimers, form. in ion-mol. assoc. reactions, rates analysis 77−60054
dimethylamino radical+O_2(NO)(NO_2), reaction rate constants, FTIR obs. 80−16652
p-dimethylaminoacetophenone, ps reversible isomerisation kinetics, O_2 quenching obs. 79−5133
2,3-dioxogulonic acid, reversible transformation to enol, kinetics, pH effects 79−5152
direct chemical reactions in fast molecule collisions, eikonal approx. calcs. *(Russian)* 80−3332
dissociation-recombination, collision induced, exactly soluble model 78−7191
DNA-Au (III) interaction, rate consts., activation energies, pH, spectrophotometric obs. 80−30228
drift tube studies, buffer gas mixture choice, for ion-neutral reactions 79−57232
drift tube with hollow cathode ion source, for reaction rate consts. meas. 78−64834
electrochemical reaction rate in presence of surface-active substances on electrodes 79−43597
electrochemical redox reactions, Franck-Condon approx. 77−1929
electrode processes possessing charge transfer mechanism, overvoltage theory, in book, for teachers 78−8204
electron reaction with scavengers in nonpolar liquids, rate const. 77−52654
endothermic reaction rate enhancement in EM field 80−66852
energy disposal specificity on magnitude of thermal rate const. 78−44350
energy requirements vibr. and translational energy depends. 79−57206
energy transfer effects, nonsteady state solns., weak collisions 79−74351
enzyme reaction rate determ. by capacitance meas. 78−31997
enzyme-substrate interaction forces influence on reaction rates 78−31765
enzymic kinetics, rate constants estimation 79−70505
epoxy cure, autocatalytic reaction, kinetic parameter estimation 79−70327
ester+amine, consecutive reactions, reaction rate constants, absorbance meas. using isosbectic points 77−73433
ethane, decomposition in RF discharges, 10-40 torr 78−3318
ethanol-d_0,-d_1, solvated electrons reacting with scavengers, inverse isotope effects 78−31751
ethyl acetate, CW laser induced reactions, activation energies, temps. and rate consts. 80−40710
ethyl acetate, gas, radiatively heated by CO_2 laser, cooling mechanism investig. 80−75021
ethyl cation+alkane reaction, temp. and kinetic energy relative rate consts. determ. 80−81299
ethylacetate, CW laser induced reactions, activation energies, temps. and rate consts. 80−40710
ethylacetate, thermal and IR laser induced unimol. decompositions 78−20012
ethylene, decomposition in RF discharges, 10-40 torr 78−3318
ethylene+H→C_2H_5*, rate const., 198-320K, high press. 78−48618
ethylene+HBr, low temp. chain hydrobromination, kinetics and mechanism 80−93735
ethylene oxide-d_0, -d_4, ion chemistry, photoionisation and ion cyclotron reson. obs. 77−21373
ethylperoxy radical+NO_2, reaction rate const. meas. 80−21262
ethylperoxy radicals+NO reaction, flash photolysis and kinetic spectroscopy obs. of rate consts. 79−83470
exponential transition probilities for collision induced dissoc. and vibr.-rot. relax. 78−27749
fast chemical transformations dynamics, study via time-of-flight mass spectrometer 77−74547
fast reactions, pulsed selective photoexcitation, rate determ., spectral method 77−86336
fire plume, turbulent, reaction rate, air entrainment, radiation 78−35682
first order kinetic data anal., optimisation method 78−12500
first order reaction in catalyst particle, conc. depend. diffusion coeff., effectiveness factors 78−48693
first-ordr electrochemical analysis, reversible pot. and rate const., chronoamperometric determ. 78−61086
flame, rate constants for A+X⇄A^++X^- and AX+M⇄A^++X^-+M (A=metal, X=halogen, M=flame species) 79−34310
flame calculations, list of rate coeffs. 78−85160
flames, diffusion, reaction rates 78−35637
flow tubes, kinetic measurements 79−74386
fluctuation spectroscopy, determ. of chemical reaction rates based on optical density fluctuation 78−27730
fluid-solid reactions, exam. of law of additive reaction times 78−53189
fluorobenzene in liq. NH_3, solvated electrons reaction kinetics 77−73434
fluoromethane+Br($^2P_{3/2}$)($^2P_{1/2}$), photobromination 78−11535
fluoromethanes+Ne^+(He^+)(Ar^+)(Kr^+)(Xe^+)(N_2^+)(CO^+)(CO_2^+)(N_2O^+), thermal energy charge transfer reactions mechanism 77−63889
fog and sensitivity centre form. kinetics and activation energies during chem. sensitisation 77−44495
formaldehyde+Br reactions, rate consts. by EPR 80−93736
formaldehyde+Cl, rate const. 78−85136
formaldehyde+ClO radical, expt. showing no reactivity, stratospheric implications 80−90119
formaldehyde+F reactions, rate consts. by EPR 80−93736
formaldehyde+H_3O^+(H_3S^+)(HCNH$^+$)(HCHO.H$^+$), proton transfer, rate and equilib. consts. 78−48636
formaldehyde+O, absolute rate consts., discharge flow and flash photolysis reson. fluoresc. meas. 80−55648
formic acid, decomposition, using Ni (110) catalyst, reaction kinetics and mechanism, mol. beam relax. spectroscopy 77−70340
formyl fluorides, gas phase ion-mol. reactions, comparison with H_2CO+F_2CO, H_2CO+Cl_2CO 77−63900
free radical recombination, rate consts. meas., student expt. 79−48996
free radical recombination reaction kinetics in atm. chem. 79−53410
fuel, liq. droplet, combustion, quasi-steady analytical model predictions 78−35681
fuel cell electrocatalytic O_2 reduction mechanism with metal chelate coating 78−23951
gallium transferrin, formation constant, nuclear medicine appls. 79−96285
gas, dilute, reacting, mass and momentum transport, DIPR model extension 78−35666

reaction rate constants continued
gas phase chemical reactions in atmosphere, evaluated kinetic and photochemical data 80−101671
gas phase reaction consts. for electronically excited species, relax. processes, data tables 80−16644
gases, radiatively heated by CO_2 laser, cooling mechanism investig. 80−75021
glasses, electron scavenging kinetics, random walk hopping model 79−74401
graphite, oxidation kinetics near 1000K 77−48616
H+FH(FD), low barrier quantum model, vibr. deactivation 80−69216
haemoglobin, modulated excitation meas. of quaternary conformation struct. change rate 77−44589
halocarbons, decomp. by natural tropospheric ions 77−21889
halosodalites, synthesis, cathodochromism, reflectivity spectra 77−40399
hematite pellet, reduction with CO-H_2 mixture 77−4935
heterogeneous reactions, bimolecular, following Langmuir-Hinshelwood mechanism, rates 79−84907
hexane, liq., burning rate in small vessel, convection effect 78−35680
hot atom chemistry, general variational principles 80−11941
hydrated electrons, photochem. generated in solns., decay kinetics 77−52656
hydrocarbon ions+H_2(methane), rate coeffs., ionised product. distribs. 77−44471
hydrocarbons, pulsed irrad. electron mobilities and reaction rate consts. for electron-solute reactions 79−91112
hydrocarbons, reactions, rate consts., temp. depend., photolysis, high temp. fast flow reactor technique 80−42231
hydrogen halide+unsaturated hydrocarbon, vibr. stimulated addition reaction 79−91928
8-hydroxy, 1,3,6-pyrene trisulphonate, picosec. proton ejection, ultrafast pH jump 79−83475
hydroxymethyl radical +0_2, rate coefficient meas. by laser magnetic resonance flow tube method 80−66767
8-hydroxyquinoline+phthalic anhydride, solid-state reaction kinetics 77−36746
indium transferrin, formation constant, nuclear medicine appls. 79−96285
inerg gas excited molecules formation, rate const. determ. 80−9859
inert gas afterglow, excimer form., VUV emission obs. at low press. 80−38755
inert gas atom+$Ne^{2+}(Ar^{2+})(Kr^{2+})(Xe^{2+})$, low energy reactions, SIFT and drift tube obs. 80−97705
inert gas dimer formation, free-jet expansions, rate coeffs. 77−66745
inert gas mixtures, high-press., collisional radiative recomb. 80−63595
iodoheptafluoropropane, photolysis, reaction rate consts. meas., photodissociation I laser characts. 79−52671
1-iodopropane, pyrolysis, intermol. energy transfer in two-channel unimol. reaction 79−11769
iodotrifluoromethane, photolysis, reaction rate consts. meas., photodissociation I laser characts. 79−52671
ion+ion mutual neutralisation rate coefficient parametrisation 80−81301
ion+mol. reactions, ion vel. distribs. in high field swarms, Boltzmann eqn. soln. 77−70283
ion+molecule, association, temp. depend., rate coeffs. calc. 80−16661
ion+molecule, slow reactions, carbonyl addition rate consts. rel. to struct. 80−30232
ion+molecule, slow reactions, nucleophilic displacement, rate consts. rel. to struct. 80−30232
ion+molecule, slow reactions, proton transfer, rate consts. rel. to struct. 80−30232
ion+molecule, slow reactions, three body assoc., rate consts. rel. to struct. 80−30232
ion+molecule association density of quantum states and temp. depend. of rate coeff. 80−101015
ion+molecule reaction rate coeffs., ions containing C and H, review 77−25260
ion+molecule reactions, atmospheric ion chemistry 80−61885
ion+molecule reactions, low energy, dipole interaction influence 80−89475
ion+neutral atom, reactant internal energy, rate constants, drift tube 80−30231
ion+neutral molecule, reactant internal energy, rate constants, drift tube 80−30231
ion+neutral reaction, ion speed distribution effects in flow-drift tubes 77−56219
ion+neutral reaction, ion speed effects in flow-drift tubes, statistical mechanical theory 77−56220
ion kinetics in high-pressure laser plasmas 80−64002
ion photodissociation, kinetics meas. using time of flight mass spectrometer 77−75240
ion-atom reactions related to interstellar mol. synthesis, rate coeffs. and product ions 80−67812
ion-molecule, from mass spectroscopy using selected-ion flow tube 77−188
ion-molecule association rate calc. 80−81282
ion-molecule association reacts., gas phase, statistical phase space theory approach 80−50839
ion-molecule reaction rate consts., time resolved meas. in mass spectrometry 78−48614
ion-molecule reactions, anisotropic molecular polarisability, effect on rate const. 79−15968
ion-molecule reactions, in drift tube, reaction rates and cross-section determ. 77−60052
ion-molecule reactions, rate consts. meas. by ion cyclotron resonance 77−86287
ion-molecule reactions in dilute gases and solutions, electric field effect 80−81315
ion-molecule reactions in interstellar gas clouds, lab. meas. 78−12314
ion-molecule thermochemistry, flames and diagnostic techniques 80−55664
ion-selective electrodes, liq. membrane, free and supported, ion transport, interfacial kinetics, time depend. phenomena 79−83535
ionic reaction rate increase in US cavitation, diffusion model 79−96312
ionic reactions rate coeffs. in thermosphere, AE satellite meas. 79−48594
isobutane+HO→H_2O+iso(or t-)C_4H_9, 700 and 100 torr, 25°C, FT-IR anal. 77−25247
isopropyl vinyl ether, chem. initiated soln. polymerisation and radiation-initiated bulk polymerisation 79−91952
reaction rate constants continued
isopropylbromide, thermal and IR laser induced unimol. decompositions 78−20012
ketene+H, reaction rate consts., lab. meas., rel. to interstellar cloud processes 79−74359
kinetic theory of reacting systems, transport processes, rate coeffs. 77−86284
Kramer's chemical reaction model, barrier mediated diffusion, generalisation to include viscosity term 80−71890
Kramers theory of friction and vel. in chemical kinetics 80−50826
lactate dehydrogenase+free radicals, reactions, pulse radiolysis 78−7214
laser induced reactions, activation energies, temps. and rate consts. 80−40710
laser specific and thermal reactions classifications 80−11919
laser studies of relaxation and reaction of species in defined quantum states 80−11918
laser system, trimer form. rates 80−50831
laser-based methods for transient chem. events meas. 80−40801
laser-controlled unimolecular and bimolecular processes, field-depend. rate const. 80−11906
laser-induced predissociation, diatomic and polyatomic mols., photocatalytic effect 80−11907
measurement using fluorometric instrument 77−79157
measurements of reaction rate consts., reliability criterion 79−8423
metal halide (oxide) dissociation energies, calc. from chemiluminesc. reactions, temp. depend. rate const. correction 77−40524
metal ions, in unusual valency states, reaction rate consts. 79−47921
metal surface oxidation study, vacuum microbalance investigation 80−76552
metalloporphyrin, cation radical formation by pulse radiolysis, oxidation and demetalation rate consts. 80−61505
methane, decomposition in RF discharges, 10-40 torr 78−3318
methane+Cl, rate const., discharge flow-reson. fluoresc. meas. 78−7178
methane+O_2^+, reaction rate const. kinetic energy depend., 300K, 0.125-0.450 torr 78−76850
methane+$O^+_4(O_2^+)$, products, rate consts., rel. to stratosphere 77−9040
methane +$O_2^+(a^4\Pi_u)$, 0.04-1.2 eV, reaction rate consts. 79−47911
methane-air flame, reactions, radical overshoot 79−34308
methanethiol+OH radical, reaction rate const., 299-426K 77−40525
methanol, catalytic decomp. on NiO, mol. beam relax. spectrometry using surface temp. modulation 79−29401
methanol (dimethyl ether)+Cl, absolute rate consts., 200-500K, stratospheric chem. appl. 79−66271
methanol glass, H atom abstraction by methyl radicals, 15-100K, limiting rate const. rel. to tunnelling 77−60037
methoxy+NO, reaction rate upper limit, laser induced fluoresc. 80−85200
methoxy radical+NO, reaction rate meas. 80−76534
3-methoxybenzanthrone in ethanol, photoprotolytic reactions, spectra, rate consts. and lasing thresholds 80−43327
methyl(-d) radical recombination rate const. calcs. in low press. limit 77−4891
methyl cation+$H_2(N_2)(O_2)(CO)(CO_2)$, ternary assoc. reaction, rate coeffs., 100-300K 79−61845
methyl cation+NH_3, reaction kinetics, 0.04-1 eV. *{French}* 80−66768
methyl ion+H_2O(He) ternary association reaction in energy range 0.04-0.1 eV 80−71896
methyl isocyanide, intracavity CW dye laser state-selective activation of isomerisation 78−11533
methyl radical decay in methanol glass, accumulation and dark decay kinetics 79−74352
cis-3-methyl-1,3-pentadiene-1,2-d_2, nonrandom isomerisation, internal energy relax. 79−70313
m-methyl-p-cyanodimethylaniline, ps reversible isomerisation kinetics, O_2 quenching obs. 79−5133
methylamine, proton-bound dimers, form. in ion-mol. assoc. reactions, rates analysis 77−60054
methylamine+OH radical, reaction rate const. 299-426K 77−40525
4-methylumbelliferone, excited state reaction rate, fluoresc. and decay time 77−63919
MHD generator, supersonic, working body thermodynamic props., chem. kinetics effect 78−91163
modified collision theory expression, comparison with exact expression 79−74370
molecular dynamics simulation of chemical reactions in solution 80−40673
Monte Carlo quasi-classical trajectory calculations 79−74366
multiphoton dissociation, collisionless, laser pulse shape effect on product yield 80−78667
muonium, bimol. rate consts., Larmor precession relax., kinetic isotope effect rel. to H 77−38752
muonium, reaction with DNA and its constituents in water soln., rate constants 79−57210
muonium+Cl_2, gas-phase reaction, muonium spin rot. rate meas. 77−58207
muonium atoms reactivity in aq. soln. 78−80774
muonium reaction in soln., rate const. and effective charge 79−57275
myoglobin conformationally-nonequilibrium state reactivity obs. by pulse radiolysis 79−39353
2-naphthol-3,6-disulphonate, picosec. proton ejection, ultrafast pH jump 79−83475
naphthylamines, abnormal fluorimetric titration behaviour, kinetic anal., fluoresc. quantum yields and lifetime meas. 80−89560
neopentane, steady state in flow pyrolysis, determ. individual rate consts. 78−35650
neopentylcyclobutane, $^1CH_2$-activated, decomposition rate const., press. depend., internal vibr. relax. 78−64819
nitro compounds in cyclohexane, electron attachment reaction rates from pulse radiolysis 78−31663
NMR spectral lineshape analysis of two-site exchange kinetics, student expt. 77−26118
non-ionic reactions, temp. and press. effect on kinetic and thermodynamic parameters 80−3300
nonequilibrium corrections, effects on stability 77−25254
nonsolvated electron reactions, positron annihilation method 77−81417
Norrish type II reaction biradicals+O_2, diffusion controlled rate const. 77−90617
nth-order reactions, reaction kinetics, DTA obs. 77−81386
organic compounds, hydrolysis in water, rate consts. 78−76856

reaction rate constants continued
organic ion, excited electronic state correlation with mass-spectral fragmentation pattern 80−45482
pentafluoromethyl iodide, ion-molecule reactions, amongst radiolysis products, reaction rates, mechanisms, mass spectra 79−5136
peroxymethyl radical+NO, reaction rate const. 79−61848
peroxymethyl radical+peroxymethyl radical, reaction kinetics, H_2O vap. depend 79−61844
phase transitions, Schlogl's chemical model, critical fluctuations near non-equilib. critical point 80−85150
phenylalanine, hydrated electron impact dissoc., laser flash photolytic investig. 80−58396
photoelectrochemical cells, metal, electrodes in contact with fluoresent dye solns., photovoltage generation, comprehensive model 80−40871
photographic development rate, effect of developer ion charge 79−24753
photographic dye, colour coupling in soln., kinetic anal., appl. of flash-light photolysis *(German)* 79−39173
photographic stabiliser reactions with colloidal Ag, decoloration reaction kinetics *(German)* 77−40563
plasma, chemical reactions, rate coeffs., database creation, DATSTOR 80−48846
plasma, nonequilib., diat. mols. vibr. excited state population, rel. to plasma chem. 80−19553
plasma of given chemical content, chemical reactions, computer generation, REACS 80−48844
polyatomic molecule under nonequilibrium conditions, dissoc. kinetics, unimol. decomp. rates 80−11886
polyatomic species, application of statistical theories, phase space theory 79−74369
polycaprolactam, after polycondensation, falling film evaporator system *(Japanese)* 79−70325
polydiacetylene, single cryst., polymerisation under hydrostatic press. 79−20367
polyethylene, chlorination, rate const. determ. using NMR spectra of chain sequence *(German)* 79−100366
polymer, accelerated ageing data processing using linear regression analysis 78−39815
positive ions+H_2O, reaction rate consts., product distrib., ICR obs. 79−8428
prereaction effects on laser-initiated reaction rate meas. by chemilum. obs. 78−44386
propane pyrolysis, model, kinetics *(French)* 79−52649
proteins, kinetic constants of association and dissociation, theoretical determ. 80−51033
PVC granule morphology during polymerisation, kinetic parameters influence *(German)* 80−85176
quadratic programming, appl. to kinetic rate const. determ. 78−53185
quantum mechanical, trajectory and transition-state theory calcs. 77−25249
racemization, relative and absolute rate consts., kinetic isotope effects 79−43558
radiative association reactions in dense interstellar clouds, rate coeffs. calcs. 80−82441
radical addition, rate consts. calc. 78−40023
radical species, tube electrode generation, laminar flow through EPR cavity, decomp., convection 77−24746
rapid reaction of two chemical species in the presence of weak random advection and molecular diffusion 79−66261
reactive diffusion in silicides with small homogeneity region, kinetics and mechanisms 77−35751
reactive-diffuse systems with Arrhenius kinetics, multiple solns., ignition and extinction 79−66260
resistivity relaxation measuring system, for surface reaction meas. 80−55718
reversible chemical reactions involving H atoms, formation rates and lifetimes of intermediate complexes 79−15956
reversible isomerisation, rate consts. and kernels 78−40020
ruthenium tris-bipyridyl, excited state electron transfer quenching, H_2O photoreduction mediators effects 80−102536
sampling of rapidly reacting gases, mol. vel. distrib. effect on time resolved spectra 77−63888
scattering experiments, deconvolution of thermal averaging using integral transform methods 78−92442
secondar free radicals, primary reacting with substrated, CIDEP relax. time, theory 78−25573
semiconductors, multiply doped, donor-acceptor complexes and interactions, physicochem. nature 80−15472
shock tube measurements of elem. gas reaction rate coeffs., review 80−3299
silylene, decomp. kinetics under shock tube conditions 79−34292
solid phase chemical reactions, low temp. and fast, mol. motion effect 80−97681
solvated electron reaction rates in alcohols and water 77−25259
sonochemical reactions, cavitation induced, rate dependence on US intensity 77−36732
specific equilib. recombination rate coeffs., Laplace transform calcs. of temp. depend. 78−60989
statistical models characterisation, prior distribs., appl. to at.-diat. exchanges 77−66744
stilbene, cis→trans photoisomerisation rate const., direct meas. 80−30250
trans-stilbene, fluoresc. decay, picosecond anal. 79−31569
stilbene, radiolysis, electron transfer and protonation, vis. spectra, isomer effects 77−60085
stratosphere, NO_x catalytic O_3 destruction, sensitivity to rate coeffs. 77−37472
stratospheric chemistry, reaction rate coeffs. and product distribs. 78−81305
styrene, thermal polymerization, PMR obs. 80−3342
supercrit. hydrocarbons radiolysis, electron reaction rate const./diffusion coeff. ratio 80−101033
surface layer thickness measurement by kinetic method 77−24503
synergism of PQ developers 79−24732
teaching, rate consts. rel. to equilib. consts., student demonstration 79−58501
temperature coefficients, evaluation of mean values, and standard errors 79−74346
temperature dependence analysis 79−74344
terbium salicylate, fast reactions, pulsed selective photoexcitations, rate determ., spectral method 77−86336
reaction rate constants continued
termolecular rate calcs. for differing 3-particle collision pathways 77−9045
1,1,2,2-tetrafluorocyclobutane, ion-mol. reactions, reaction pathways, mass spectra 77−21368
tetrafluoroethylene, high temp. oxidation behind refl. shock waves 77−36743
thermal dissociation, vibrational relaxation at high temps., ab initio calcs. 79−74367
thermal unimolecular reactions, rate calcs., weak collisions centrifugal barrier effects, adiabatic channel calcs. 79−74348
thermal unimolecular reactions, strong collision rate consts, in low press. limit 77−56215
thin-layer cell, fast reaction, kinetic consts., diffusion and conc. impedance 78−73053
thioindigo, in nonpolar solvent, photoisomerisation mechanism, fluoresc. obs. 77−63933
time independent diffusion controlled rate consts. anal., second order solid state reactions 78−15651
toluene+OH, rate constant under simulated atmospheric conditions 80−50846
transient species, form., quantitative anal. by extrapolation method 78−15685
trichloroethane+OH→H_2O+CH_2CCl_3, rate const. and tropospheric chem. 80−16658
1,1,1-trifluoroacetone, photochem. and photophysics, 330-250 nm, 0-1000 torr 78−17706
trifluoroiodomethane, vap. phase photolysis, UV irrad. 78−73070
trifluoromethyl iodide, ion-molecule reactions, amongst radiolysis products, reaction rates, mechanisms, mass spectra 79−5136
trifluoromethyl radical reactions, prod. and meas. by IR multiphoton dissoc. of iodotrifluoromethane 80−26036
trimer formation from chemical capable of reacting with itself 80−71889
tryptophyl peptides, pulse radiolysis, hydrated electron reaction 78−48679
tubular flow reactors with first-order kinetics 79−4088
turbulent gas, reaction rate distortion, applic. of Tsuge kinetic theory 79−7418
unimolecular reaction, thermal, expressions for deriving rate const. 80−85164
unimolecular reactions, master eqn. for rate coeff. Nesbet's algorithm 78−48612
unimolecular reactions, master eqn. solns. 77−70291
unimolecular reactions, monochromatic IR radiation induced, rate const. intensity depend. 79−87857
unimolecular reactions, strong collision rate consts. 77−73446
unimolecular reactions, vibrational collisional energy transfer efficiencies 78−80714
unimolecular reactions induced by monochromatic IR radiation, intensity and laser energy fluence influence 80−11903
upper atmosphere, rate coeffs. for 557.7 nm line and Herzberg bands excitation 79−75008
van der Waals force, effect on diffusion controlled reaction rate, Smoluchowski's formula 79−100335
vibrational adiabaticity, quantum mechanical derivation of transition state theory 79−74350
vinyl methyl ether+$O(^3P)$, absolute rate consts. meas., 297-439K 78−7196
water cluster ions form. in ionospheric D-region rel. to mesospheric temp. 77−21842
water-cetyltrimethylammonium bromide-haxanol system, ^{13}C NMR, catalysis in micellar and liq. cryst. phases 79−61909
Zircaloy-4, oxidation in steam, 900-1500°C, kinetics 80−3241
Zircaloy-4, oxidation in steam, 900-1500°C, O diffusion in oxide and α-phases 79−100288
Zirconium-4, oxidation reaction kinetics in unlimited steam environment 77−8988
$3NO \rightarrow N_2O+NO_2$, irreversible thermal decomposition, rate consts., 440 to 650°C *(Russian)* 79−70322
$A^+ + 2A \rightarrow A_2^+ + A$, gas phase reaction rate const. calc. 78−92457
$Ag_2S + Ln_2S_3$, powdered mixtures, reaction rate, production of ionic semiconductors 80−93741
Al-SiO_2, film system, kinetics of interaction 77−44459
$Al + CO_2 \rightarrow AlO + CO$, HTFFR kinetics obs., 300 to 1900C 77−90596
$Al + NO + Ar \rightarrow AlNO + Ar$, rate coeff., 600K, fluoresc. and absorption spectrum obs. 77−40521
$Al + SO_2$, high temp. fast flow reactor obs. of kinetics 80−30226
Ar, stationary afterglow obs. of singly charged atomic ions, three-body rate coeffs. 80−38757
$2Ar + Ar^+(Kr^+)$, three body reaction, rate coeffs., temp. depend., 100 to 300K 80−108703
$Ar + Ar(^3P_2)(^3P_0)$, flowing afterglow metastable decay rates, diffusion, two- and three-body rate consts. 78−73027
$Ar + H_2$, 4500K dissoc. collision vibr. selectivity, Monte Carlo trajectory method 79−70307
$Ar + He_2(^3\Sigma)$, press. depend. reactions, rate coeffs. 78−64823
$Ar + He^+$, (Ne^+), charge transfer reaction rate coefficient 79−91932
$Ar + Kr(^3P_2)$, flowing afterglow metastable decay rates, diffusion, two- and three-body rate consts. 78−73027
$Ar + Xe^+$, $XeAr^+$ form., dissoc. energy, reaction equilib. and rate consts. 80−61071
$Ar + Xe(^3P_2)$, flowing afterglow metastable decay rates, diffusion, two- and three-body rate consts. 78−73027
$Ar^+ + (N_2)(H_2)(O_2)$, charge exchange reaction rates 77−86295
$Ar^+ + Ar$, quasi-resonant charge transfer at thermal energies 80−48082
$Ar^+ + H_2(O_2)(CO_2)$, reactions in flow-drift tube, rate consts. 78−15664
$Ar^+ + Kr(Xe)$, thermal energy charge transfer reaction rates, mass spectrometric obs. 78−61000
Ar^++molecule (atom), dissociative reaction rate coeffs., in high-press. afterglow 79−87837
$Ar^{2+} + Kr(Xe)$, thermal energy charge transfer reaction rates, mass spectrometric obs. 78−61000
$Ar^{2+} + O_2(CO_2)(C_2H_2)$, reactions in flow-drift tube, rate consts. 78−15664
$Ar^+(Ar^{2+}) + N_2$, reaction rate consts. 78−48613
$Ar^+(Ar^{2+}) + O_2$, reaction rate consts. 78−48613
ArCl*, excimer formation rate consts., B state radiative lifetimes, quenching, VUV excitation 80−55631
$Ar(^3P_2)$+fluorine containing molecules, quenching rate consts. 77−9072
Ar*+formaldehyde thermal collisions, $CH(A^2\Delta \rightarrow X^2\Pi)$ emission 77−86304

reaction rate constants continued
B+$O_2(SO_2)(CO_2)(N_2O)$, gas phase rate consts., 300K, at. absorption obs. 79−83445
BCl_3, vibr. excited states distrib. in reson. radiation, photodissoc. rate 78−50603
Ba+HF→BaF+H, dual mol. beam excitation difference spectroscopy, state-to-state vibr. resolved dynamics 80−89474
Ba+SO_2→BaO+SO, reaction kinetics, BaO recoil velocity spectra 79−74361
Bi_2Te_3-based solid solns., decomp. kinetics under flux layer 77−81205
$Bi(6^4S_{3/2})$+acetylene(ethylene), absolute rate consts., time-resolved reson. fluoresc. meas. 78−27731
Br, recomb., in presence of inert gas atoms and mols. 80−45496
Br+Br_2, atom-exchange, rate and activation energy, trajectory model and pot. energy surface 78−64811
Br+Br+Ar⇄Br_2+Ar recombinations rate const. calcs. 80−40685
Br+F_2, reaction kinetics, mass spectroscopic obs. 77−77743
Br+H_2O_2, rate constant upper limit 80−30216
Br+HI→HBr+I, thermal rate const., 220-400K, H/D isotope effect 79−47906
Br+NOBr, primary and secondary photochemistry, vibrationally excited NO, IR fluoresc. obs. 80−48030
Br+NO→Br+NO_2, reaction rate const., mass spectrometric determ. 79−34288
Br+O_3→BrO+O_2, rate consts., mass spectrometric obs. 77−63897
Br+O_3→BrO+O_2, reaction rate constant, 200-360K 78−73024
Br+OClO, reaction rate consts., mass spectrometry meas. 78−3316
Br_2, dissoc. and recomb. rate consts. meas., 1200-3000K, techniques comparison 77−63892
Br_2, thermal electron dissoc. attachment rate consts., meas., in flowing afterglow 77−10773
Br_2+Ar→2Br+Ar, 3500K trajectory anal., rate const. 77−52617
Br_2+O_2, reaction with W surface, rate of reaction meas., gas flow experiment 78−92510
BrO+ClO, reaction rate consts., mass spectrometry meas. 78−3316
BrO+O→Br+O_2, reaction rate constant, 200-360K 78−73024
C oxidation kinetics, in Fe-C melts by CO_2 *(Russian)* 80−40680
C, oxidation kinetics on Ni (110), AES meas. 79−79291
C+CO_2 Boudouard reaction, catalysed by Li_2O and Li_2CO_3, reaction rates 839-1050°C 79−16035
C+CO_2 reaction, kinetics at low press. and hydrogen inhibition 77−63950
C+CO_2 reaction, Langmuir-Hinshelwood kinetics at intermed. press. 77−66766
C^{2+}+$H_2(N_2)(O_2)$ (inert gas), charge transfer reaction rate consts. 80−7779
C_3+O_2→C_2*+CO+O, chemiluminesc., rate consts. 77−44466
CCl, reaction rate const. determ. using laser-induced fluoresc. technique 80−97682
CCl+alkynes, absolute reaction rate consts. 78−27728
CCl_2, reaction rate const. determ. using laser-induced fluoresc. technique 80−97682
CClF, reaction rate const. determ. using laser-induced fluoresc. technique 80−97682
CCl($\tilde{X}^2\Pi$)+methylhalosilanes, reaction rate const. determ. by kinetic absorpt. spectroscopy 80−97683
CD_n^++$H_2(HD)(D_2)$, isotopic exchange, interstellar implications 80−61087
CF_x, exam. of graphite fluorination kinetics, meas. of activation energy, reaction rate 79−96284
CH^+ $X\,^1\Sigma^+$, dissoc. recomb. rate coeff., rel. to interstellar mol. form. 78−56884
CH+O reaction, absolute rate const. 80−97690
$CH_{2(triplet)}$+CO_2, reaction rate constant determ. 77−36727
CH_3^++small molecules, binary and ternary reactions at thermal energies, rate coeffs., product distribs. 78−44358
CH_4^++CH_4→CH_5^++CH_3, ion cylcotron resonance technique for absolute rate constants determ. 79−8462
CH_n^++COS(H_2S)(formamide)(methanol)(methylamine), (n=Q-4), reactions at 300K 78−44357
CH_n^++$H_2(HD)(D_2)$, isotopic exchange, interstellar implications 80−61087
CH_2N_2+triplet CH_2→CH_3, reaction rate constant determ. 77−36727
CH_3O_2, radical, form. and decay rates, UV absorpt. spectra 77−48631
CH_3O_2+NO, rate const., flash photolysis and kinetic spectroscopy 79−70305
CH($X^2\Pi$) radical, prod., detect. and reactions 79−61842
CN+NO, reaction rate constants 79−1935
CN+O(^3P)(O_2) reacts., prod. energy distribs. meas., CO vibr. level population *(German)* 78−76833
CO, catalytic oxidation over NiO, activated complex struct., rate consts. 78−80786
CO oxidation on Pt, AC pulsing technique 79−100439
CO+$^{13}C^+$(HCO^+), isotopic exchange, interstellar implications 80−61087
CO+Ar, shock heated steady state dissoc. rate consts. calc. 78−40039
CO+chemisorbed O_2, on Pt surface, transient kinetics obs. 78−7229
CO+OH(+isobutane), reaction rate consts., press. depend. 78−35654
CO+O+M→CO_2+M, time-resolved and flame-band emissions in shock tube expts. 77−36729
CO^++2CO_2→2CO_3^+, reactions of electronically excited CO^+ 77−1915
CO_2, dissoc. in shock tube, interferometric meas. 77−9071
CO_2 glow discharge chemical processes and rate coefficients 78−63626
CO_2, primary ionis. coeff., electron attachment coeff. rate coeff. 77−4900
$C^{18}O_2$, isotope exchange with $CeMoO_4$, $LaMoO_4$, $PrMO_4$, $NdMoO_4$, 300-500°C 77−63884
CO_2-Cs-He discharge, CO_2+Cs reaction rate meas. by IR absorption, press. depend. 78−44367
CO_2+C^+(N_2H^+), rate coeffs. meas. at 300 and 100K in flowing afterglow 79−20346
CO_2+inert gas, reactant decomp., rot.-vibr. energy transfer, relax. analytic soln. 80−55650
CO_2^-+O_2, nanosec. pulse radiolysis, react. rate const. meas. 77−16843
CO_2^++2CO_2⇌$(CO_2.CO_2)^+$+CO_2, reaction rates 77−36745
CO_2^++ethylene, rate coeffs. and product distribution determ. 80−97693
$(CO_2)_2^+$, ion-mol. reaction product distribs. and rate coeffs. 80−50852
CO_3^-, formation and dissociation in CO_2 77−60058
C_2O+$NO(O_2)$(isobutene), absolute reaction rate consts. meas. by laser induced fluoresc. 80−93738

reaction rate constants continued
CO(1)+CO(v)→CO(0)+CO(v+1), vibr. energy accumulation, reaction rate anal. 80−78692
$(CO_2.CO_2)^+$+CO→$(CO_2.CO)^+$+CO_2, reaction rates 77−36745
$CO_2.CO_2^+$+ethylene, rate coeffs. and product distribution determ., dissoc. energy and heat of form. 80−97693
$CO_2.CO_2^+$+SO_2, reaction rate coeff. and product distrib. 80−3305
$C(^3P)$+$O_2(^3\Sigma_g^-)$→$CO(^3\Sigma^+)$+$O(^1D)$, pot. energy surface, vibr. population inversion, classical dynamics 77−52630
CS+O→CO+S, rate const. temp. depend., ESR-mass spectrometer obs. 78−20013
CS_2, photodissoc. below 1600 Å, CS($a^3\Pi$) production, quantum yield, rate const. 77−48658
C^-(4S)+molecule, spin angular momentum conservation in proton transfer 77−16805
Ca+NH_4^+($CH_3NH_3^+$)(PH_4^+), proton transfer reaction cross sections, 1-6 eV 78−20003
CaO+CO_2→$CaCO_3$, reaction kinetics, effect of temp. and CO_2 press. 80−45552
$C_2(a^3\Pi_u)$+methane(acetylene)(ethylene)(ethane)(O_2), reaction rate consts. and quenching, multiphoton UV photolysis, fluoresc. obs. 79−74355
$CaWO_4$, cryst. growth from solns. in melts, kinetics parameters and thermodynamic props. 80−59424
$Cd(^3P_1)(^1P_1)$+$H_2(HD)(D_2)$ reacts., CdH(CdD) yields, quenching cross sections 79−1948
Cl, recomb., in presence of inert gas atoms and mols. 80−45496
Cl+C_2H_2, reaction kinetics, stratospheric implication 78−31618
Cl+D_2→DCl+Cl, LEPS pot. energy surface, rate consts., isotope effect, quasiclassical trajectory calc. 78−56887
Cl+DI→DCl+I, thermal rate const., 220-400K, H/D isotope effect 79−47906
Cl+fluoromethane, photochlorination electron and oscill. energy 80−81320
Cl+formaldehyde, rate const., 200-500K 79−39133
Cl+formaldehyde→HCl+HCO, stratospheric O_3 decreased sensitivity to Cl perturbations 79−12190
Cl+H_2, absolute reaction rate consts., 200-500K 78−15655
Cl+H_2O_2, absolute rate const., 265-400K 78−15652
Cl+H_2S→HCl+HS, laser-initiated chain reactions, rate consts., product energy distrib. 78−85144
Cl+HI→HCl+I, Monte Carlo quasiclassical trajectory anal., product distribs. 77−16783
Cl+HNO(H_2O_2)(HO_2), rate consts., stratospheric appl. 78−85125
Cl+HO_2 react. rate const. determ. at 298K *(French)* 78−64817
Cl+M+NO_2, reaction rate constants 79−100350
Cl+methane, reaction rate const., stratospheric modelling appl. 79−20345
Cl+methane→HCl+CH_3, absolute reaction rate, flash photolysis-reson. fluoresc. obs. 77−56222
Cl+NH_3, reaction rate consts., flash photolysis-reson. fluoresc. obs. 78−3327
Cl+NOCl, primary and secondary photochemistry, vibrationally excited NO, IR fluoresc. obs. 80−48030
Cl+NO+N_2→NOCl+N_2, rate const. temp. depend. 78−76828
Cl+O_3→ClO+O_2, rate consts. meas. 77−60059
Cl+OH*→HCl*+O, reaction dynamics, vibr. excited reagent and product 77−81392
Cl+SO_2, rate const. rel. to stratospheric Cl chemistry and Venus atm. 79−84353
Cl^++molecule, reactions at room temp. 80−93749
^{38}Cl+ethane (methane)(vinyl bromide), rate consts., stratospheric temps., radiotracer meas. 77−48632
Cl_2 absorption in acetic acid, kinetics in presence of homogeneous catalysts 80−11876
Cl_2, thermal electron dissoc. attachment rate consts., meas., in flowing afterglow 77−10773
Cl_2-O_3-H_2 dilute mixtures, photolysis products, Fourier Transform IR kinetic obs. 80−26033
Cl_2+2Br^-→Br_2+2Cl^-, aqueous soln., specific rate determ., competition technique 78−44348
Cl_2+muonium (H)(D), pot. energy surfaces, inversion calcs. 80−93734
ClNO+Cl_2O→ClONO+Cl, reaction kinetics, IR spectra 78−35641
$ClNO_2$, kinetics of thermal decomposition *(German)* 78−95924
ClO+NO_2+M, reaction rate constants 79−100350
ClO+NO_2→$ClNO_3$, reaction rate consts., stratospheric appl. 77−78306
ClO+NO_2→$ClONO_2$, fall-off curves, N inclusion effects 77−63910
ClO+O(NO)→Cl+O_2(NO_2) rate consts. meas. 77−60059
ClO+O→Cl+O_2, rate consts. calc. 220-1000K 79−79233
ClO+O→Cl+O_2, reaction kinetics, 220 to 426K, at. fluoresc. obs. 77−21380
ClO^-+NO(NO_2)(SO_2)(CO_2), rate consts. at 300K 78−76829
ClO_x, atmospheric gas phase reactions, review 77−81390
$ClONO_2$+NO(ClNO) react., gas phase, kinetics, mechanism, IR photometric investig. *(German)* 78−76834
$ClONO_2$+O(^3P), fast flow reaction, rate const. 77−12777
$ClONO_2$+O(^3P), photolytic gas phase kinetics at 245K 79−52719
$ClONO_2$+O(^3P), rate consts., flash photolysis-reson. fluoresc. obs. 77−77796
$ClONO_2$+O(OH), in stratosphere 77−33134
Cl(^2P)+CH_4→CH_3+HCl, reaction rate const., laser flash photolysis-resonance fluoresc.-kinetic study 80−45485
Cl(^2P)+$ClONO_2$, rate consts., flash photolysis resonance fluoresc. meas. 77−60038
Cl(^2P)+methane, absolute rate and temp. depend. 78−80731
^{38}Cl+ethylene+HI(H_2S), thermal, mechanisms and rate consts., fluoroethane decomp. 77−86343
$CoCl_4$ formation kinetics, in nonaqueous systems, rate constants and temp. change determ. *(German)* 79−70300
$CoFe_2O_4$ formation rate consts. meas. by Mossbauer effect 78−68875
CoO, and Co_3O_4, surface reequilibration kinetics 77−55449
Cr corrosion, high-temp., in Cl_2 and Cl_2-O_2 mixtures 78−15601
Cr, corrosion in SO_2, 700-1000°C 80−97642
Cr, oxidation kinetics, 300 to 600°C, struct. and morphology of oxide film 77−59982
Cr, oxidation kinetics, 300 to 600°C, O_2 press. effects 77−59983
CrO_3 reduction by powdered graphite, mechanism 77−4748
Cr_2O_3 corrosion, high-temp., in Cl_2 and Cl_2-O_2 mixtures 78−15601
Cr_2O_3, reduction by H_2, reaction kinetics 80−11950
Cs+O_2, reaction kinetics, time-resolved meas. 77−90588
Cu and Cu-S, liquid, oxidation kinetics, by CO_2 77−28986
Cu, cementation, on Fe, deposit struct., reaction rates, SEM 80−104421

reaction rate constants continued
Cu corrosion, by COS, kinetic and morphological study *(French)* 79−43488
Cu-O (0.05 to 0.1 wt.%) liquid alloy, deoxidation kinetics by rotating graphite cylinders 80−61084
$CuFeO_2$, oxidation, thermogravimetric obs. 77−86203
Cu(I) complex, oxidation, fast reactions meas. by pulsed-flow instrument 80−66890
$Cu_2S+Ln_2S_3$, powdered mixtures, reaction rate, production of ionic semiconductors 80−93741
$CuSO_4.5H_2O$ monocryst. platelets, dehydration into trihydrate, displacement rate modulation of reaction front 80−108711
$D+Cl_2$, collinear reaction rate consts., quantum and semiclassical calcs. 77−12782
$D+D_2$, collinear reaction, transmission coeff. isotope depend., statistical theory, invariance 77−36748
D+FD(FM), low barrier quantum model, vibr. deactivation on chemically reactive potential surfaces 80−69216
$D+H_2$ reaction, transition state theory calculations, kinetic isotope effect explanation 80−66784
$D+H_2$ rearrangement collision, vibr. excitation effects 80−71910
D+HCl→DCl+H, rate consts., EPR 77−9059
DF+H, reaction rate, DF fluoresc., shock tube obs. 77−12784
DO_2+NO, reaction kinetics, near IR chemiluminesc. determ. 80−21261
D_2O+Ar, energy transfer isotope effect, rate consts. 79−8422
$D_3O^+(D_2O)_n+H_2O(NH_3)$, binary reactions, rate coeffs. and product ion distributions determ. 80−81305
Eu complex, fast reactions, pulsed selective photoexcitation, rate determ., spectral method 77−86336
$F+CH_4→HF+CH_3$, calc. using kinetic trajectory model 77−29010
F+chlorobenzene→fluorobenzene+Cl, statistical theory, phase space theory 79−74369
F+DX, (X=I, Br, Cl), H abstraction, absolute reaction rate, H/D isotope effect 78−80721
F+F, homogeneous recombination, room temp. rate consts. 77−32766
$F+H_2$, reactive collision, semiclassical dynamics on multiple electronic surfaces, 3-dimens. calcs. 78−27746
$F+H_2(Cl_2)(HCl)$(methane), delay and decay times of stimulated emission 78−3317
$F+H_2(D_2)$, absolute reaction rate coeffs., time resolved IR emission meas. 79−68258
F+HBr(HI)→HF+Br(I), electronic and vibr. energy transfer 77−63899
F+HCl(HBr)(DBr)(HI), H abstraction reactions, temp. depend., laser photolysis IR fluoresc. obs. 80−93744
F+HCl→HF+Cl, time resolved vibr. chemiluminesc. and rate consts. 80−61069
F+HX, (X=I, Br, Cl), H abstraction, absolute reaction rate, H/D isotope effect 78−80721
F+hydrocarbon (substituted methane)(inorganic hydride), HF IR chemiluminesc., H abstraction rel. rate consts. 77−86319
F+iodobistrifluoromethylphosphine, reaction mechanism and kinetics, ESR 77−86294
$F+O_2$, quantum reactive scatt. theory, 3-dimens. 80−55637
$F+O_2+M→FO_2+M$, flash photolysis IR chemiluminesc., rate const. 78−3311
$F+T_2→TF+T$, rate meas. using TF-molecule chemical laser 77−86291
F_2, thermal electron dissoc. attachment rate consts., meas., in flowing afterglow 77−10773
$F_2+X→XF+F$ (X=Mu,H,D,T), isotope effects, quantum mech. and information theoretic calcs. 78−44360
$^{18}F+H_2$, hot-atom reaction, nonequilib. vel. distrib. and reaction rate calcs. 77−63942
$^{18}F+H_2$, nuclear recoil reaction, steady state hot atom kinetic theory calc., rate coeffs. 78−35712
Fe, sponge, oxidation kinetics by nuclear γ-resonance method *(Russian)* 80−40681
Fe-Cr-Ni alloys, oxidation-sulphidation in gas mixture, parabolic kinetics, thermochem. diagram 78−72932
$Fe_{2-x}M_xO_4$, M=Al,Cr, time dependence of oxidation, elec. cond. obs. *(French)* 77−66710
FeO_2 nucleation, kinetics of formation of H_2O and C_2O 79−83449
Fe_3O_4 (magnetite), effects of mag. field on reduction rate 77−44461
Fe_3O_4, magnetite, oxidation rate anomaly at Curie temp. 79−96298
$F_2(v=0)+Mu→MuF(v'\leq 3)+F$, (Mu=muonium), quantum mech. calcs. 77−21366
GaAs {100} surface, interaction kinetics of As_2 and Ga 77−60115
GaAs thermal oxidation rate and activation energy obs., 470° to 830°C *(Japanese)* 77−52517
Ge gas phase reactions with oxidisers, visible chem. laser development 79−948
$Ge+Br_2$, heterogeneous photochem. reaction kinetics, laser radiation intensity effect 79−66326
$Ge+GeBr_4$, single crystal+vapour system, reaction kinetics and laws of soln., heat of adsorption 79−39196
$Ge+N_2O$, chemiluminesc. reaction, HTFFR kinetics study 80−76496
$Ge+N_2O→GeO+N_2$, rate coeff. meas. 78−63110
$Ge+O_2(NO)(N_2O)$, reaction rate consts. at 350K 78−53186
$GeCl_4$ hydrolysis and oxidation kinetics for graded-index fibre vapour phase axial deposition 80−48477
$Ge(^3P_0)+N_2O$, reaction rate const. meas., in flowing afterglow 77−77731
GeTe, oxidation kinetics 77−44380
$Ge(3^3P_0)+O_2(Cl_2)(COS)(N_2O)(NO_2)(NO+Ar)$ oxidation reacts., gas phase, kinetics 78−92468
H+acetaldehyde, absolute reaction rate consts., 298-500K 77−16788
H+BrF(1F)→HF+Br(I), reaction product energy distrib. 80−30219
H+bromotrifluoromethane, reaction rate consts., flash photolysis-reson. fluoresc. obs. 78−3327
H+chlorotrifluoromethane, reaction kinetics, ESP obs. 77−21358
$H+Cl_2$, collinear reaction rate consts., quantum and semiclassical calcs. 77−12782
$H+Cl_2$(organic molecule), rate const., discharge flow-reson. fluoresc. meas. 78−7178
$H+Cl_2→HCl+Cl$, rate consts. meas., Lyman-α fluoresc. technique 77−16780
H+ClBr→HCl+Br(HBr+Cl), product energy distrib., rate const., IR chemilum. obs. 77−81391
H+ClF→HCl*+F, stimulated emission meas. 77−71980
$H+D_2$ reaction, transition state theory calculations, kinetic isotope effect explanation 80−66784

reaction rate constants continued
H+ethane, chemical reaction, 357-544K 78−7198
H+ethylene episulfide→HS+ethylene, absolute rate parameters, flash photolysis reson. fluoresc. 78−3312
$H+F_2$, vibr. prod. distrib., Einstein coeffs. 78−92448
H+formaldehyde, reaction, absolute rate coeffs., 250-500K 79−100349
H+H, recombination, orbiting reson. theory, rate consts. meas. 77−83681
$H+H_2$, collinear reaction, isotope depend. transmission coeff., transition state theory 77−36747
$H+H_2$, collinear reaction, transmission coeff. isotope depend., statistical theory, invariance 77−36748
$H+H_2$, three dimens. reaction, Porter-Karplus pot. energy surface, rot. distribs., rate consts. 77−21378
$H+H_2(HD)(D_2)$, exchange reaction rate consts. meas., vibr. effects 79−5134
$H+H_2(O_2)$, quantum reactive scatt. theory, 3-dimens. 80−55637
$H+H_2(v=1)→H_2+H$, exchange reaction, classical trajectory method, vibr. excitation, partial rate consts. 78−60993
$H+H^+$, vibr. excited H_2^+ form. by stimulated radiative association 79−100346
$H+HCO→H_2+CO$, classical trajectory study 80−93750
H+HCl, reaction kinetics, ESR and mass spectrometric obs. 77−21357
H+ICl→HCl+I, IR chemiluminesc., product energy distrib. 78−23926
H+ICl→HCl+I, product energy distrib., rate const., IR chemilum. obs. 77−81391
$H+N_2O→N_2+OH$, rate const., 2000-2850K, combustion of $H_2/N_2O/CO/Ar$ 78−85162
$H+N^{3+}$, charge exchange, assoc. reaction, rel. to interstellar gas 80−7763
$H+NO_2→NO+OH$ and $H+O_3→O_2+OH$ by atomic resonance fluorescence 77−48618
$H+NO_2→OH+NO$, H+NOCl→HCl+NO, rate meas. by Lyman-α fluoresc. 77−21353
$H+NO+H_2→HNO+H_2$, rate of reaction, temp. depend., third body efficiencies 78−23933
H+NO+M→HNO+M, HgH+NO→HNO+Hg, rate consts. of photosensitised reactions 77−36757
$H+O_2+Ar$, HO_2 free radical prod., rate const. calc. 80−101026
$H+O_2→OH+O$, combustion, quasiclassical trajectory calcs. 78−53201
$H+O_3$, absolute reaction rate const., 219-360K 78−80734
H+OCS→HS+CO, absolute rate parameters, flash photolysis reson. fluoresc. 78−3312
$H+PH_3$, abstraction rate consts., 209-495K, time-resolved fluoresc. 77−16807
$H^++O_2^-$, nanosec. pulse radiolysis, rate consts. meas. 77−16843
H_2 formation, reaction rates and chemical kinetics 79−17070
H_2-Ar, relaxation rates, thermal dissociation, decomposition, master equation theory 79−74368
H_2+Ar, 4500K shock wave expt. simulation, vibr. state changes and dissoc. 79−61850
$H_2+Cl(Br)(I)(F)$, gas phase H-atom transfer reactions, struct.-reactivity correl., pot. energy surfaces 80−104433
H_2+F_2, chain reaction pulsed laser, single rate eqn. model 77−3572
$H_2+H(F)(Cl)$, collision induced IR laser absorpt., rate enhancement, theory 79−66275
$H_2+I→H+HI$, quasiclassical tragectory vs. quantum cals., vibr. state depend., kinetics 78−80733
H_2+O_2, combustion, kinetic modeling and sensitivity anal. 80−89490
H_2+O_2+CO, 500°C, rate consts. involving OH and HO_2 radicals 78−35646
H_3^++XCN, flowing afterglow, rate const. meas. 77−40533
H_n^++e, electron-ion dissoc. recomb., rate const., electron beam sustained discharge 78−50652
HBr+Cl→HCl+I, rate const. temp. depend., laser-initiated reaction 78−23929
HBr+OH→H_2O+Br, absolute rate const., 249-416K 79−70303
HBr*+I, reaction rate, vibr. excitation effect, isotope enrichment 77−90581
$HCN+H_3O^+(H_3S^+)(HCNH^+)(HCHO.H^+)$, proton transfer, rate and equilib. consts. 78−48636
HCN(DCN), photodissoc. dynamics, rot. (vibr.) energy disposal 78−48672
HCO, prod. by formaldehyde photolysis, vibr. relax., chem. kinetics and spectra 79−11808
$HCO+NO(O_2)$, reaction rate consts. 78−31617
$H_3CO^++H_2S⇌H_3S^++HCHO$, chemical equilib. consts., proton affinity of HCHO and H_2S 78−85189
$H_3CO^++HCN⇌H_2CN^++HCHO$, chemical equilib. consts., proton affinity of HCHO and HCN 78−85189
HCl, dissoc. electron attachment kinetics in flame, mass spectra obs. 78−68872
HCl-N_2 mixture, electron swarm, Cl^-.HCl cluster formation, dissoc. attachment, drift tube mass spectra 78−68884
HCl+Ar, shock heated steady state dissoc. rate consts. calc. 78−40039
HCl+Cl(Br)(H), vibr. relaxation and reaction rates determ. 80−108698
$HCl+O^-(O_2^-)(NO_2^-)(CO_3^-)(CO_4^-)$, rate consts. at 300K 78−76829
HCl+O(OH), reaction rate const. temp. depend., stratospheric implications 78−31616
$HCl(v=1,2)+O(^3P_g)$, reaction and deactivation, laser-induced fluoresc. obs. 78−35669
HCl(v=1)+H(D)(Cl)(Br) reactions, selective vibr. excitation effects, kinetics *(German)* 77−21364
HF+Ar, shock heated steady state dissoc. rate consts. calc. 78−40039
HF+H(D), kinetic isotope effect and temp. depend. 78−53202
HI+Cl→HCl+I, rate const. temp. depend., laser-initiated reaction 78−23929
HN_3, UV photolysis 80−101027
HN_3+F, production of $NF^*(a^1\Delta$ and $b^1\Sigma^+)$ 79−11770
$HN_3+NH(NH_2)$, rate consts. from HN_3 UV photolysis data 80−101027
HNCO, 193 nm photolysis, photodissoc. products, $NH(a^1\Delta)$ internal energy distrib. reaction rate with O_3 79−83489
HNO_2+O_3, rate consts. determ. with diode laser 79−70310
HNO_2+O_3 reaction kinetics under stratospheric conditions 78−11499
$HNO_2+OH→H_2O+NO_2$ react. kinetics, at high temps. behind shock waves 77−44477
HNO_3-HNO_2, aq. soln., N isotope exchange in presence of NO 80−16662
HNO_3+NO, rate consts. determ. with diode laser 79−70310
HO+CO→H+CO_2, 700 and 100 torr, 25°C, FT-IR anal. 77−25247

reaction rate constants continued
$HO_2 \rightarrow H^+ + O_2^-$ nanosec. pulse radiolysis, react. rate const. meas. 77−16843
HO_2 radical, atmospheric reactions studied by laser mag. reson. spectroscopy 80−12511
HO_2+ClO, free radical reaction rate consts. and products at 298K, discharge flow mass spectra 80−67391
HO_2+ClO→HOCl+O_2, reaction rate consts. 79−5140
HO_2+HO_2, reaction rate, press. depend. 80−7766
HO_2+HO→H_2O+O_2, rate coeff. meas. by laser mag. reson., atm. chem. appl. 77−52614
HO_2+NO, reaction kinetics, near IR chemiluminesc. determ. 80−21261
HO_2+NO reaction rate constant effects on O_3 perturbations, model of stratosphere 78−73474
HO_2+NO_2, reaction rate consts. by laser mag. reson. 78−27748
HO_2+NO_2, UV irradiated, kinetics and mechanism, peroxynitric acid form., smog 77−63885
HO_2+NO→OH+NO_2, kinetics temp. depend. 80−3313
HO_2+NO→OH+NO_2, rate constant determination in Arrhenius form 79−47904
HO_2+O_3, reaction kinetics, laser mag. reson. obs. 80−102528
HO_2+O_3→OH+$2O_2$, rate coeff., effects on stratospheric O_3 78−96275
HO_2+O→HO+O_2, rate coeff. meas. by laser mag. reson., atm. chem. appl. 77−52614
H_2O+Ar^+, thermal-energy charge transfer, H_2O^+ product internal and kinetic energy 80−16654
H_2O+$H_3O^+H(H_3S^+)(HCNH^+)$(HCNO.H^+), proton transfer, rate and equilib. consts. 78−48636
H_2O^++diatomic (polyatomic) molecule, reaction, ICR obs. 79−8429
H_2O^++$NO_2(O_2)$(NO)(CO)(H_2)(ethylene)(methane), rate constants determ. as function of relative kinetic energy 80−81292
H_2O_2 80−34826
H_2O_2 decomposition, IO_3^- catalysed, oscillatory Bray-Liebhafsky reaction 79−91931
H_2O_2+$HO_2(O_2^-)$ Haber-Weiss reaction kinetics, chain mechanism 79−83444
$H_3O^+(H_2O)_n$, ion clustering, diffusion, flowing afterglow obs. 77−12799
$H_3O^+(H_2O)_n$+$D_2O(NH_3)$, binary reactions, rate coeffs. and product ion distributions determ. 80−81305
HO_2NO, unimol. dissoc., rate consts., temp. depend., atmospheric implications 78−7175
HO_2NO_2, unimol. decomp., press. and temp. depend. 78−68887
HO_2NO_2+N_2⇄HO+NO_2+N_2 react., kinetics, RRKM theory appl. 78−73032
$H_3O^+.H_2O$, cluster ion form. mech., rate coeffs. 78−25764
$H_3O^+.nH_2O$ cluster ions, stability, assoc. and dissoc. 77−60055
$HPO_4^-(H_2PO_4)$ radicals + organic compounds, reaction rate consts. 78−15669
H_2S+D_2 homogeneous exchange reacts., kinetics 77−48633
H_2S+$H_3O^+(H_2S^+)$(HCNH$^+$)(HCHO.H^+), proton transfer, rate and equilib. consts. 78−48636
H_3S^++HCN⇄H_2CN^++H_2S, equilib., rate coeffs. and proton affinity, flowing afterglow 78−56885
$H_3S^+.H_2O$ cluster ions, stability, assoc. and dissoc. 77−60055
$H_3S^+.nH_2S$ cluster ions, stability, assoc. and dissoc. 77−60055
HX (X=Cl,Br,I) dissoc. attachment, negative ion form. and removal kinetics in flame 77−52642
Hbr+Cl_2(BrCl), four-centre reaction, quasiclassical trajectory study 79−57213
He-CO_2-Cs mixture in rapidly circulating laser, interaction rate of Cs and CO_2, gasdynamic parameters 79−86173
He+He, (2^3S) and (2^1S) metastable states, direct and assoc. ionisation rate consts. in afterglow, electron energy spectra 79−13812
2He+$He^+(Ne^+)$, three body reaction, rate coeffs., temp. depend., 100 to 300K 80−108703
He+water (cyanomethane), afterglow, excitation and quenching reactions, optical pumping 78−35690
He^++$H_2(D_2)$, dissociative charge transfer, 78-330K 80−61079
He^++N_2O, rate coeffs. meas. at 300 and 100K in flowing afterglow 79−20346
He_2^+, rate coeffs. for bimol. and termol. ion-mol. reactions 78−53188
He_2^++Ne(Ar)(N_2)(CO)$(CO_2)(CH_4)$, bimol. and termol. charge transfer reactions, rate coeffs. 77−1910
HeH^++H_2→H_3^++He, reaction rate. coeff. 78−18371
He^*_2 diatom, optical absorpt. spectra and kinetic behaviour 80−95635
He^*_2 inert gas atoms, optical absorpt. spectra and kinetic behaviour 80−95635
$He_2(2^3\Sigma_u^+)$+He_2(Ne), reaction rate consts. meas. in afterglow 78−7173
Hg-Cl_2-Ar, photochem. reactions, producing HgCl($B^2\Sigma^+$) 79−39154
$HgCl_2$, reaction on metallic Cu, reaction velocities, effect of neutral salt addition 78−64887
HgH+M→Hg+H+M, reaction rate temp. depend., chemiluminescence 78−68885
HgH+NO→HNO+Hg, reaction rate temp. depend., chemiluminescence 78−68885
$Hg_2(Hg_3)$, violet emission, formation and decay kinetics, luminesc. time resolved spectra 79−76464
Hg(6^3P_0)+Cl_2 reaction, reactive quenching metastable states 79−57208
Hg(6^3P_0)+t-butylamine, attachment mechanism, kinetics, dimer emission, luminesc. spectra 77−73442
I ($5^2P_{1/2}$)+HBr, reactive and inelastic channels rate, temp. depend., AAS obs. 78−35657
I, recombination in inert gas buffer, computer simulation, rate const., press. depend. 77−25261
I+I+O_2→I_2+O_2, photolysis, rate const. obs., mechanism 77−63883
I+I±I_2, termolecular chemiluminesc. reaction, rate const. for interaction with n-C_3F_7I 79−96291
I_2, hydrolysis, reaction rate const. 80−11883
I_2, recomb. shock heating in unsteady Ar expansion, vibr. relax. effect 77−16794
I*+$I_2(Br_2)(Cl_2)$(IBr)(ICl)(BrCl), collisional deactivation and reaction rate consts., obs. 78−80738
I*($^2P_{1/2}$)+Br_2→IBr+Br*($^2P_{1/2}$), rate const., chemiluminesc. obs. 77−40520
I($5^2P_{1/2}$)+HBr(DBr)(methane)(propane), collisional deactivation, rate consts. meas. 77−86300
K+Cl⇄K^++Cl^-, KCl+M⇄K^++Cl^-+M, rate consts. in at. press. flames 77−60036
$K_4(MoCl_4)_2$+acetic acid, reaction kinetics and mechanism 77−86305
Kr, stationary afterglow obs. of singly charged atomic ions, three-body rate coeffs. 80−38757

reaction rate constants continued
Kr+ArF*→KrF*+Ar, in gas cell pumped by 150 keV electrons 78−33730
Kr+N_2, in afterglow 77−427
Kr^++2Kr→Kr_2^++Kr, reaction rate const. in afterglow period 77−9044
Kr^++Kr, quasi-resonant charge transfer at thermal energies 80−48082
Kr^++molecule, $^2P_{3/2}(^2P_{1/2})$ doublet ground state reactions at 300K 80−108702
Kr^{2+}+$H_2(N_2)(O_2)$ (inert gas), charge transfer reaction rate consts. 80−7779
Kr^{2+}+$H_2(N_2)(O_2)$(CO)(CO_2)(methane), charge transfer reactions, rate coeffs. and product-ion distributions meas. 80−104431
KrCl*, excimer formation rate consts., B state radiative lifetimes, quenching, VUV excitation 80−55631
KrF, laser, e-beam pumped Kr-F_2 mixtures, form. and quenching processes 78−42322
KrF+He(Ne)(Xe)(NF_3), quenching rate consts. meas. 79−24718
KrF*+Ar(Kr)+Ar(Kr), recomb. rate consts., 300 to 800K, appl. to KrF* laser efficiency 79−45930
KrF*+Ar(Kr)+Ar(Kr)→Ar(Kr)KrF*+Ar(Kr) recombination rate consts. calc. 77−75488
KrF*+inert gas, three body collision rate consts., trimer form. rates 80−50831
Kr($^3P_2$)+fluorine containing molecules, quenching rate consts., KrF* formation branching ratios 77−9072
Kr^+.+$H_2(D_2)$(HD) reactions, temp. depend., isotope effect 78−31630
Li^+, mobility and clustering in Ar gas 77−84389
$Li_2(B^1\Pi_u)$+inert gas, laser-excited collision-induced dissoc. 79−79232
Li_2CO_3, decomp. and ferritisation, effect of initial Fe_2O_3 content 77−52269
Mg+$N_2O(O_2)$(acetylene), ($^3P_1$)metastable atom afterglow quenching rate consts. 77−6720
$MgBr_2$-ABr (A=Cs, Rb, K, Na, Tl), thermochemical and struct. investigation *(German)* 79−1423
$Mg(NO_3)_2$-RNO_3 (R=Li, Na, K), thermogravimetric anal. of dehydration processes *(Japanese)* 80−66791
MgO, rate of reduction by C 77−28743
MgO-Nd_2O_3-Al$(Cr)_2O_3$, reactions kinetics in mixtures of components and phases 77−40523
Mg$(OH)_2$, decomposition to MgO, mechanism, product crystallite size rel. to reaction rate 78−85152
$MgSO_4$, rate constant of reaction, determ. from overall crystal growth coeff. 78−59773
Mn_xN_y, prep., rate of formation, chem. stability 78−11185
MoF_6, reduction by H in the presence of HF *(Russian)* 80−61076
$MoSi_2$, reactive diffusion of Si, kinetics and mechanism 77−35751
$MoSi_3$ crystalline layers, diffusion growth kinetics at 1700°C under influence of direct elec. current 79−52112
Mu+F_2→MuF+F, 300 to 400K in N_2 moderator, reaction rate determ., tunnelling 78−48682
N+alkene (1,3-butadiene)(acetylene), reaction rate consts., pulse radiolysis obs. 80−35508
N+NO, $^4(S)$ state reaction rate, discharge flow and photolysis reson. fluoresc. method 79−5142
N+organic molecule, rate const., discharge flow-reson. fluoresc. meas. 78−7178
N^++CO(CO_2) (methane)(NO), product distribs., rate consts., ion cyclotron reson. obs. 77−52618
N^++O_2, branching ratio kinetic energy depend. 80−97703
N^++O_2, drift tube mass spectra, rate coeffs. and prod. distrib. 77−77746
N_2, nonequilibrium dissociation rates in electrical discharges, temp. depend. 78−33447
N_2^+, dissociative recombination in ionosphere, rate cont. 80−17435
N_2+HgX_2 (X=halide), $A^3\Sigma_u^+$-state quenching obs. 80−108693
N_2+methylmercury halides, $A^3\Sigma_u^+$-state quenching obs. 80−108693
N_2^++$2N_2$→$2N_3^+$, reactions of electronically excited N_2^+ 77−1915
N_2^++O→NO^++N, aeronomical determ. of rate coeff. 79−75000
N_3+NCl, reaction rate consts. calc. 79−74342
N_3^++O_2, drift tube mass spectra, rate coeffs. and prod. distrib. 77−77746
N_4^++$O_2(CO_2)(H_2)(D_2)$ reactions, flow-drift tube obs. 78−60985
N(^{2}D)+O_2, chemiexcited NO form., 90-180K IR obs. 78−90163
ND*+DN_3→ND_2*+N_3, chemiluminesc. reaction of electronically excited species, rate const. 78−80771
NF+H(NF), electronically-excited free radical reactions 80−97707
NF_2+H(O)(N), electronically-excited free radical reactions 80−97707
NF_3, dissoc. electron attachment, rate consts. meas. 78−3326
NF_3, thermal decomp. in shock waves, rate consts. meas. 77−16810
NF_3, thermal dissoc. behind shock waves, rate meas. 78−61002
N_2F_4, mol. photodissoc. using CO_2-laserradiation, rate const. meas., mol. fluoresc. and time-resolved UV spectra obs. *(German)* 80−83434
NH, ND, ($b^1\Sigma^+$) states quenching by deuterated cpds., kinetic isotope effects 77−63891
NH, photofragment, energy distrib., chemiluminesc. reaction rates 77−90618
NH_2+HO_2, rate const., in NH_3+O_2 flash photolysis 79−47943
NH_2+NO_2, reaction rate const. meas. 80−7772
NH_2+O_3, reaction mechanism, flash photolysis obs. 80−104425
NH_2+O_3, reaction rate const., rel. to atmospheric processes 80−85155
NH_2^++H_2O, bimolecular reactions, product. distrib., rate consts. 78−11513
NH_3, decomposition kinetics on single cryst. planes of Pt 77−1948
NH_3→NH_4^+ conversion, in atmosphere, pseudo first-order reaction rate const. 80−94132
NH_3 proton-bound dimers, form. in ion-mol. assoc. reactions, rates analysis 77−60054
NH_3+$C^+(CH_n^+)$, rate coeffs., ionised product distribs. 77−40522
NH_3+$OH^+(H_2O^+)(H_3O^+)$, bimolecular reactions, product. distrib., rate consts. 78−11513
NH_3+radical ion, thermal energy charge transfer, reaction mechanism 77−16796
NH_3^++H_2O, bimolecular reactions, product. distrib., rate consts. 78−11513
NH_4^+, mutual neutralisation, with simple and clustered positive (negative) ions 78−44372
NH_n^++molecule (n=0 to 4), reactions, selected ion flow tube obs. 80−45489
NH*+HCl(methane)(ethylene)(cyclopropane) (cyclohexane), rate const., time resolved chemiluminesc. 78−60982

reaction rate constants continued
$NH^*+HN_3 \rightarrow NH_2^*+N_3^*$, rate const., time resolved chemiluminesc. 78−60982
NO, electrocatalytic decomp. on electrochem. reduced zirconia surface 80−61113
NO^+ +molecule, reaction rate consts. meas. 80−7782
NO^+, three-body reactions, rate coeffs. rel. to cluster ion form. in D-region 77−53308
NO+BrO, temp. depend. kinetic study, stratospheric Br photochemistry implication 80−50866
NO+O, chemiluminesc., O_3 effect 80−45507
NO+O, chemiluminesc., rate const., optical comparison method meas. 77−90603
$NO+O_3^*$, laser excitation effects, fluoresc. meas. 77−21372
$NO+O_3(001)$, laser-enhanced reaction, rates, temp. depend. 78−48675
$NO+O_3(001) \rightarrow NO_2(^2B_{1,2})+O_2$, laser enhanced reaction, temp. depend. 77−81397
$NO+O_3 \rightarrow NO_2+O_2$, rate const., 203-361K, fast flow method 77−33143
$NO+O_4$, IR laser enhanced reaction rate. vibr. excitation 77−1911
$NO^+ + 2N_2 \rightleftharpoons NO^+.N_2+N_2$, rate const., enthalpy and bond strength 77−16809
NO^+ +atmospheric gases, thermal energy reaction rates 78−92443
$NO^+ + e^- \rightarrow N+O$, recombination rate const. determ. in flames 78−48632
$NO^+ + X^- \rightarrow NO+X$ (X=Cl, Br, I), rate const. determ. in flames 78−48633
NO_2, thermal decomposition, kinetics in medium pressure region *(Russian)* 79−70321
NO_2, thermal decomposition kinetics *(Russian)* 80−3329
$NO_2+OH+M \rightarrow HNO_3+M$, rate constant under simulated atmospheric conditions 80−50846
$NO_2^+ + O \rightarrow NO^+ + O_2$, rate constant rel. to atm. ion chem. 77−41245
N_2O photodissociation, CC $O(^1S)$, prod. and props. in liq. Ar and N_2 80−43063
$N_2O^- \rightarrow N_2+O^-$, nanosec. pulse radiolysis, rate consts. meas., N_2O^- lifetime 77−16843
N_2O+inert gas, reactant decomp., rot.-vibr. energy transfer, relax. analytic soln. 80−55650
N_2O+OH. reaction, rate const. meas., N_2O atmospheric residence time appl. 77−21352
$N_2O_5+CO_3^-(NO_2^-)(F^-)(Cl^-)(Br^-)(I^-) = NO_3^- + XNO_2$, rate consts. 78−56879
$N_2O_5+H_3O^+$, rate consts. 78−56879
$N_2O_5+NO^+ = 3NO_2^+$, $N_2O_5+NO_2^+$, rate consts. 78−56879
$N_2O_5+O_2^+ = NO_2^+ + NO_3+O_2$, rate const. 78−56879
$NO^+(NO)+SO_2$, cluster form., equilib. const. and rate coeffs., UV irrad. effects 77−60060
$NO_2^*+CO \rightarrow CO_2+NO$, laser-stimulated reaction 77−9075
$NO_2^*+CO \rightarrow NO+CO_2$, laser stimulated reaction, rate const. 78−40044
$NO^+.H_2O+O \rightarrow NO_2^+ + H_2O$, rate constant rel. to atm. ion chem. 77−41245
$N(^4S)$ recombination rate in Lewis-Rayleigh afterglow 79−68968
$N(^4S)+O_3$, rate const. at 298K, upper limit determ. 79−74360
$Na+HX(J;v) \rightarrow NaX+H$, (X=F,Cl), reaction rate, rot. excitation depend. 78−64818
$NaAsO_2$ aq. solns., O exchange between $AsO_2(OH_2)^-$, and water 78−92459
NaCl+Ar, dissoc.-ionis. process rates in shock tube 78−35674
Nd_2O_3-HfO_2, kinetics of initial stages of formation of cpds. 77−48617
$Ne^+ + 2Ne \rightleftharpoons Ne_2^+ + Ne$ processes in Townsend discharges 80−38747
$Ne^+ + H_2(N_2)(CO)(CO_2)(N_2O)(O_2)(NO)(NH_3)(SO_2)(COS)(H_2O)$, thermal energy, reaction rate coeffs. and product distrib. 79−29333
$Ne^+ + Kr(Xe)$, thermal energy charge transfer reaction rates, mass spectrometric obs. 78−61000
Ne^+ +methane(chloromethane)(ethylene), thermal energy, reaction rate coeffs. and product distrib. 79−29333
$Ne^+ + Ne$, quasi-resonant charge transfer at thermal energies 80−48082
$Ne^{2+} + H_2(N_2)(O_2)(CO)(CO_2)$(methane), charge transfer reactions, rate coeffs. and product-ion distributions meas. 80−104431
$Ne_2^+ + Kr(Xe)$, thermal energy charge transfer reaction rates, mass spectrometric obs. 78−61000
Ne*+Xe, chemiionis. in metastable state collisions 79−68306
Ni (110), oxidation, initial stage kinetics, RHEED and X-ray emission 78−15588
Ni, chemisorption of CO, carbonylation rate mag. field depend. 79−24828
Ni-Cr alloy, phosphidation in P vapour, 700°C, phosphide layer struct. and kinetics 80−25906
Ni-Cr-M alloys, M=minor alloying addition Y, La, Ce, Sm, Th, U, Zr, V, corrosion rates 77−16750
Ni_3C films, on graphite, thermal decomp., AES lineshape study 79−79293
$Ni(CO)_4$, form. reaction rate, substrate mag. phase depend. 80−108737
NiO disc, reduction with CO 77−4936
NiO, undoped and Li_2O doped, surface reequilibration kinetics 77−55449
$NiO+Cr_2O_3 \rightarrow NiCr_2O_4$, kinetic parameters calcs. using anal. soln. of Fick's second law 78−34644
$Ni_xZn_{1-x}Fe_2O_4$, catalytic oxidation of CO, mag. props., kinetic parameters and composition depend. 80−16723
O atoms and potential photosmog inhibitors 79−12185
O^{2+} collisions with O_2 and N_2, reaction rates 79−16726
O^{2+} reactions with atoms or molecules of ionospheric importance, lab. meas. 80−26004
O+acetaldehyde(propylene), rate const., discharge flow-reson. fluoresc. meas. 78−7178
O+acetylene reaction, kinetics, flash photolysis-reson. fluoresc. meas. 77−73439
O+chloroethylene reaction, kinetics, flash photolysis-reson. fluoresc. meas. 77−73439
$O+Cl_2O$, reaction rate const. 79−20344
O+ethylene, OH chemiluminesc., mechanism, rate const., mathematical model calcs. 78−48655
O+formaldehyde, reaction, absolute rate coeffs., 250-500K 79−100349
$O+H_2$, classical trajectory calcs., ab initio surface, singlet state, rate consts. 80−66786
$O+H_2$, pot. energy surfaces and reaction rates, ab initio calcs. 80−63531
$O+H_2S$, ^3P-state, absolute reaction rate, flash photolysis reson. fluoresc. obs. 79−66283
reaction rate constants continued
O+HCl, vibr. excited, laser enhanced reaction rate, OH vibr. distrib. obs. 78−95912
O+methane, photochem. reaction, high temp., rate coeff. meas. 80−16699
$O+N_2O_5$, rate const., 220K, 300K, discharge-flow method 78−44352
O+NO+M, rate const., 217-500K 79−52626
$O+NO+M \rightarrow NO_2+M$, (M=He, Ne, Ar, Kr), 217-500K, absolute rate consts. 77−16787
O+nitroethane (nitromethane), H atom abstraction in discharge flow system 78−35671
O+OCS (ethylene), reaction dynamics, IR laser excitation, vibr. effects 77−12788
O+olifin, relative rate consts., N_2O photolysis obs. 79−83472
$O^- + N_2 \rightarrow N_2O+e$, rate studies 78−40036
$O^- + O_2 \rightarrow O_2^- + O$, cross section kinetic energy depend., rate consts. meas. and Monte Carlo calcs. 80−78701
O^+ +atmospheric gases, thermal energy reaction rates 78−92443
$O^+ + N_2$, atom transfer, reaction rates and cross-section determ. 77−60052
$O^+ + N_2$, reaction rate coeff. in ionosphere 77−87167
$O^+ + N_2(O_2)$, reaction rates, 300-900K 79−8434
$O^+ + NO$, charge transfer, reaction rates and cross-section determ. 77−60052
O_2 dissociation relaxation behind regular reflected and stationary oblique shocks 78−85159
$O_2+Be(Mg)(Ca)(Sr)(Ba)$, reaction kinetics in diffusion flame 77−90579
$O_2+CH_3 \rightarrow OH+H_2CO$, 368K, rate const. upper limit 80−7771
O_2+hydrated electron, rate const., Arrhenius parameters 78−20041
O_2+inert gas, reactant decomp., rot.-vibr. energy transfer, relax. analytic soln. 80−55650
$O_2+La(Y)(Sc)$, crossed beam chemiluminescence reaction, spectral simulation, hyperthermal energy meas. 78−80732
O_2+muonium, aq. soln., reaction rate const., spin-conversion 79−100422
$O_2+N^+(O^+)(C^+)$, rate coeffs. meas. at 300 and 100K in flowing afterglow 79−20346
O_2^+ +atmospheric gases, thermal energy reaction rates 78−92443
$O_2^+ + N \rightarrow NO^+ + O$, rate constant rel. to atm. ion chem. 77−41245
O_3, laser flash photolysis, $O(^1D)$ quantum yields in fall-off region 80−45524
O_3, laser-induced photolysis, reactions of $O(^3P)$, $O(^1D)$ and $O_2(^1\Delta)$ 80−11928
O_3 photolysis by sunlight, rate constants at ground level 80−61836
O_3, UV photodissoc. rate, expt. and theory 80−40722
$O_3+O_2(^1\Delta_g)(O_2^*)$, UV photolysis, $O(^3P)$ prod., rate consts. determ. 80−55636
$O_3+O^-(OH^-)(S^-)(SH^-)$, associative detachment, rate coeffs. 78−3325
$O_3+OH \rightarrow HO_2+O_2$, reaction rate const., 238-357K 79−47902
$O_3+O(^1D)$, UV photolysis, $O(^3P)$ prod., rate consts. determ. 80−55636
O_3+thiirane, autocatalytic reaction, stopped-flow study, reaction rate meas. 80−85152
$O_3^- + CO_2 \rightleftharpoons CO_3^- + O_2$, rate const., 200-600K in flowing afterglow 78−7193
O_3^- +molecule reactions, thermochemistry, electron affinity and rate consts. 78−40040
OCS photodissociation, $S(^1S)$ prod. and props. in liq. Ar and N_2 80−43064
$O(^1D)$, chemical reactions of stratospheric importance, temp. depend. 79−53494
$O^+(^2D)+e \rightarrow O^+(^4S)+e$ in thermosphere, rate coeff. meas. 80−94630
$O^+(^2D)+N_2$, charge exchange rate coefficient, effect of N_2^+ recomb. on aeronomic determ. 78−88954
$O^+(^2D)+N_2$, thermal rate coeff., products and branching ratios in ionosphere 80−82117
$O^+(^2D)+N_2$ charge exchange, rate coeff. temp. depend. 80−77179
$O(^1D)+H_2O$, rate coeff., atm. OH prod. 79−58009
$O(^1D)+H_2(HCl)(NH_3)(N_2O)$(methane), rate consts., temp. depend. 78−27747
$O(^1D)$+haloalkanes, deactivation reactions, absolute rate consts. determ. 79−11783
$O(^1D)+O_2(N_2)(CO_2)(O_3)(H_2O)$, 100-350K, reaction rate consts. 77−21355
$O(^1D)+Xe(Kr)(Ar)$, deactivation rate consts., 110-330K 78−88628
$O(^1D_2)+N_2O$, chemical-ionisation mass spectrometry branching ratio measurements in N_2O/He mixtures 79−47905
$O_2(^1\Delta_g)+O_2$, deactivation rate const. meas. 78−5262
OH radical, reactions with ester vapours, reaction rate consts. determ. at 292K 78−27729
OH radicals vibrationally excited in stratosphere, instantaneous rate model 77−5273
OH+2-methyl-2-butene, reaction rate consts. meas. 78−61001
OH+acetylene (CO), reaction rate consts. meas. 78−35663
OH+alkanes (alkenes), photooxidation, 305K, absolute and rel. rate consts. 77−16782
OH+alkene, absolute rate consts., 297K 79−100353
OH+allene (1,3-butadiene)(3-methyl-1-butene), absolute rate consts. 78−23927
OH+CO, reaction mechanism, HOCO radical stability 77−73436
OH+CO, reaction rate consts. at 296K, press. effect 77−73435
OH+COS(CS_2)(dimethyl thioether), reaction rate consts., 299-430K 78−35653
OH+CO(trichloroethane), reaction rate consts. and quenching kinetics, reson. fluoresc. obs. 79−72349
$OH+ClO(Cl_2)(Cl_2O)$, rate const. at 298K, rel. to stratospheric O_3 depletion 79−87831
OH+dimethyl ether (vinyl methyl ether) reaction rate consts., 299-427K 77−86301
OH+dimethylamine, rate const., 298-426K, Arrhenius expressions and activation energy 78−48619
OH+ethylamine, rate const., 298-426K, Arrhenius expressions and activation energy 78−48619
OH+ethylene, reaction rate consts., 229-425K 77−40535
OH+ethylene (and halogenated derivatives), reaction rate consts. 77−21356
OH+formaldehyde (acetaldehyde), rate consts., 299-426K, UV flash photolysis, reson. fluoresc. obs. 78−68873
$OH+H_2O_2$, reaction rate const., 298K, flash photolysis-reson. fluoresc. obs. 79−57215
$OH+H_2O_2 \rightarrow HO_2+H_2O$, reaction rate consts., laser induced fluoresc. 80−101017
$OH+H_2 \rightarrow H_2O+H$, rate constant, ab initio calc. 80−45478

reaction rate constants continued
OH+HO_2→H_2O+O_2, rate const. meas. *(German)* 79−52629
OH+HO_2→H_2O+O_2 gas flow reaction, upper bound and probable value of rate const. 79−24730
OH+haloalkanes (haloalkenes), reaction kinetics in microwave discharge, reson. fluoresc. obs. 77−77744
OH+halocarbons rate consts., appl. to tropospheric degradation 79−52622
OH+halomethane(haloethane), reaction rate consts., reson. fluoresc. meas. in discharge-flow system 79−72350
OH+methane+M, absolute rate consts., 296K, flash-photolysis reson. absorpt. technique 77−86290
OH+N_2O (CF_2Cl_2) ($CFCl_3$), upper limits, tropospheric lifetimes 77−64366
OH+n-propyl acetate (sec-butyl acetate) (tetrahydrofuran) (peroxyacetyl nitrate), raction rate consts., in irrad. NO_x mixture 78−7171
OH+NO_2+M→HNO_3+M, reaction kinetics, temp. and press. depend. 79−66284
OH+OCS(CS_2), lower atmosphere chem. 80−61870
OH+OH→H_2O+O, rate meas. by UV absorpt., 1200 to 1800K 78−35642
OH+trichloroethane, 1,1,1- and 1,1,2-isomers, reaction kinetics, 298-460K, lower atmos. chem. 80−16657
OH+trimethylamine, rate const., 298-426K, Arrhenius expressions and activation energy 78−48619
OH+vinyl halides, reaction rate consts., 299-426K 77−81389
OH^-+methoxybenzene (o-cresol), gas phase reaction, 299-435 K, kinetics and mechanism 78−11515
OH+CO(N_2O), rate consts. 77−16781
OH+O, OH+CO, reaction rates, mechanism, flow discharge chemilum. obs. 77−52610
OH(ν=0, 1)+H_2(ν=1), rate consts., 298K 79−11768
ON+azomethane, rate const. meas. 80−7771
$O(^3P)$+2-methyl-2-butene, reaction rate consts. meas. 78−61001
$O(^3P)$+alkenes, absolute reaction rate consts., 298-439K, photolysis-chemiluminesc. determ. 77−77747
$O(^3P)$+amines, rate consts. temp. depend., 298-440K 78−48616
$O(^3P)$+benzene (toluene), absolute reaction rate consts., 299-440K 79−70304
$O(^3P)$+CH_3CN(CF_3CN), reaction mechanisms and kinetics 77−36728
$O(^3P)$+CO($X^1\Sigma^+$), vibr. deactivation and atom exchange, rate. consts., Monte Carlo anal. 77−48627
$O(^3P)$+dimethyl disulphide, absolute reaction rate const. determ. 80−89472
$O(^3P)$+HCl(HBr)(HI), rate consts. temp. depend. 79−52627
$O(^3P)$+mercaptans, reaction rate consts., O_2 effect 79−52630
$O(^3P)$+n-butane ($NO(M=Ar)$), reaction rate constants using flash photolysis-NO_2 chemiluminesc, method 77−44458
$O(^3P)$+O_3, bimolecular reaction rate coeff. reactant vibr. excitation depend., reson. fluoresc. obs. 78−76837
$O(^3P)$+vinyl halides, reaction rate consts. 298-442K flash photolysis obs. 78−7195
$O(^1S)$ in afterglow, prod. rate coeff. meas., appl. to $O(^1S)$ airglow 79−53604
$^{18}O^{16}O$, atmospheric photodissoc. rates 80−94559
O^*+H_2→OH*+H, rate const. and vibr. energy distrib. in OH*, for $O(^3P)$ 78−60998
$O(2^1D_2)$+Cl_2, reaction kinetics, vac. UV at. spectra 77−21365
$O(2^1D_2)$+$N_2(O_2)(N_2O)(CO_2)(H_2O)$(methane), collisional deactivation meas., 295K, rel. to atmospheric processes 80−16663
$O_2(b^1\Sigma_g^+)$ quenching by $O(^3P)$ and O_3, rate coeffs. 79−70309
P, ground state $3p^3(^4S_{3/2})$, time-resolved reson. fluoresc. obs. 79−34333
PH_3, photolysis and abstraction reactions, rel. to Jovian atmosphere 79−66327
PH_3+radical ion, thermal energy charge transfer, reaction mechanism 77−16796
PO_4^{2-} anion radicals + organic compounds, reaction rate consts. 78−15669
PbI_2, thin films, photolysis kinetics 77−36769
Pt electrode, multilayer oxides, electrochem. reduction mechanism, kinetics 78−61019
Rb, radiatively excited states, ionis. rate coeffs. in two atom collisions 80−43160
Ru bipyridine ion, electron transfer limiting efficiency and rate constant meas., step excitation method expt. 79−91929
Ru dimers, mixed-valence, electron transfer rate consts. calc. from intervalence transfer absorpt. bands 79−81164
S+OCS→S_2+CO, reaction kinetics of $S(^1D_2)$ reactions 79−79274
S^++NO→NO^++S+1.1 eV, rate consts. kinetic energy depend., drift tube meas. 80−7778
S^++O_2→SO^++O+0.26 eV, rate consts. kinetic energy depend., drift tube meas. 80−7778
SF_6, collisionless multiphoton dissoc. rate, statistical thermodynamic process 77−50482
SF_6, laser-induced isotope separation, threshold intensity 77−4898
SF_6, multiple-photon dissoc. rate determ. 77−60079
SF_6, unimolecular reaction model 78−7189
SO_2, gas, photooxidation, cloud chamber obs. 79−1961
SO_2 oxidation rate, CO effect, smog chamber expt. 79−74925
SO_2+Ar, dissoc. rate meas. behind shock wave, laser Schlieren method 80−81296
SO_2+CO(C_2H_2), photochem. reactions, rate consts. 78−23956
SO_2+O_2(O_3), in aq. soln., kinetics, rel. to atm. rate processes 79−20905
SO_2+O_2=SO+O_2, gas phase reaction, rate coeffs. meas. 80−97704
SO_2+OH, role for stratospheric HSO_3 layer 78−32202
SO_3+Ar→SO_2+O+Ar, rate const. of spin forbidden dissoc. in shock wave 79−57214
$^{32}SF_6$, multiphoton dissoc., temp. depend. 79−89722
SbF_5+benzyl chloride, chemi-ionis. reaction, temp. depend., flow tube investig. 80−108701
$Sb(5^4S_{3/2})$+NO(O_2), rate consts., time-resolved reson. fluoresc. meas. 78−27732
$Sc_2(SO_4)_3$+$Al_2(SO_4)_3$ aq. solns., complex form. reacts., kinetics, US relax. investig. 79−1942
Si, epitaxial growth kinetics in damp H_2 77−44171
Si, nitridation, effect of Fe_2O_3 addition *(Japanese)* 77−60123
Si, oxidation, solubility and transport behaviour of water, dissolution 80−93801
Si, oxidation in high-press. steam, 800 to 1000°C, rate consts. 77−48565
Si oxidation rate constants and role of H_2O 78−7072
reaction rate constants continued
Si, thermal oxidation in O_2-trichloroethylene mixture, 900, 1000 and 1100°C 80−3221
Si, thermal oxidation kinetics in O_2/HCl mixture, rate consts. 77−59953
Si+F_2, fast flow reactor, second order rate coeff. determ. 78−80723
Si+O_2(NO)(N_2O), reaction rate consts. at 350K 78−53186
$SiCl_4$ hydrolysis and oxidation kinetics for graded-index fibre vapour phase axial deposition 80−48477
SiH_4, silane, decomp. kinetics under shock tube conditions 79−34292
SiO_2+H_2 reactions, rate controlling processes for H_2 transport in vitreous silica 78−26733
Sm_2O_3-HfO_2, kinetics of initial stages of formation of cpds. 77−48617
Sn $5p^2(^3P_0)$, kinetic studies of ground state atoms, by resonance line absorpt. 78−85128
Sn gas phase reactions with oxidisers, visible chem. laser development 79−948
Sn+N_2O, chemiluminesc., high temp. fast flow reactor kinetics obs. 78−88636
Sn(4^3P_0)+O_2(Cl_2)(COS)(N_2O)(NO_2)(NO+Ar) oxidation reacts., gas phase, kinetics 78−92468
T+HD, variational transition field theory and unified statistical model 80−97700
Ti alloys, hydrogenation at 200-600°C and up to 10000 kPa 80−107435
Ti, nitriding kinetics in RF discharge, surface hardening 77−36684
Ti, sulphurisation kinetics, 450-550°C, thermogravimetric determ. 77−25197
$TiN_{0.91}$ plates, oxidation kinetics *(French)* 78−85199
TiO_2 reaction with C/Cl_2, high temperature chlorination 79−83450
U powder, hydriding kinetics, 13.3 and 26.6 kPa, 50-250°C 80−16725
UF_6, gas phase thermal decomp., dissoc. energy of U-F bond *(German)* 79−29353
Xe+Ne, quenching of excited $Xe^*(^3P_2, ^3P_1, ^1P_1)$ states 80−63578
Xe^++molecules, $^2P_{3/2}(^2P_{1/2})$ doublet ground state reactions at 300K 80−108702
Xe_2^++Xe, quasi-resonant charge transfer at thermal energies 80−48082
Xe^{2+}+$H_2(N_2)(O_2)$ (inert gas), charge transfer reaction rate consts. 80−7779
XeF, transfer and quenching rate constants for (III, 1/2) and (II, 3/2) states 79−16003
XeF_2, dissociative electron attachment, rate const., flowing afterglow obs. 77−6946
XeF_2 photolysis with VUV radiation, XeF (B,C) state prod. and kinetics 80−32975
XeF_2+Ar(Kr)(Xe) metastable atoms→XeF*, mechanisms 77−30897
XeF*+inert gas, three body collision rate consts., trimer form. rates 80−50831
Xe($^3P_2$)+fluorine containing molecules, quenching rate consts., XeF* formation branching ratios 77−9072
Zn (0001), oxide film growth, at. and electronic struct. 78−15587
Zn, phosphidation in P vapour, kinetics and associated diffusion coeffs. 80−3405
Zn surface oxidation, 78-493K, kinetics 78−64886
$ZnSO_4$, rate constant of reaction, determ. from overall crystal growth coeff. 78−59773
ZnSb, orientated crystn. conditions during reaction diffusion *(Russian)* 80−70558
$Zr(HPO_4)_2.H_2O$, Na^+ transport, gas-solid and solid-solid reaction kinetics 80−61086

reactions (chemical) *see chemical reactions*

reactions (nuclear) *see nuclear reactions and scattering*

reactive power
see also power factor correction
control by thyristor, KEK 12 GeV proton synchrotron, voltage flicker suppression 77−83230
ferromagnetic medium with variable permeability and hysteresis loss, plane EM wave *(Polish)* 77−79722
meter for periodical signals in range 50 Hz to 5 kHz *(Spanish)* 80−86339
phasemeter test measuring transducers 78−77894
three-phase two wattmeters, meas errors *(Croatian)* 80−105677
three-phase two-element VAr meter inaccuracies 77−13774

reactive sputtering
cathode, ion generation by O low pressure reactive sputtering *(Japanese)* 80−50494
ceramics coating by physical vapour deposition processes *(Japanese)* 80−55306
coating techniques, for SEM and X-ray microanalysis 79−12783
detonation, exp. determ. of dynamic charact. of two-phase flow *(Russian)* 78−94852
dielectric films, low temp. epitaxy in laser sputtering 80−34335
Fe-SiO_2 cermet film, solar absorbing, production by dual cathode DC magnetron sputtering 80−16186
ferrite film, reactive RF sputtering prep., high mag. recording density 77−12528
fused silicon substrate, directional reactive ion etching at oblique angles 80−66428
fusion reactor material, chem. interaction with H plasma discharge impurity ions 77−35357
fusion reactors, sputtering erosion in inertial confinement reactors 79−22462
graphite, reactive sputtering by H^+ ions, target temp. depend. *(Russian)* 77−4707
ion beam, plasma and reactive ion etching, review 80−108621
low-Z materials, H_n^+ sputtering expts., rel. to plasma-wall interactions, review 77−48297
magnetron sputtering, Cu_2S for solar cell appl. 79−11258
magnetron-plasmatron processing and instrumentation, review 80−35090
mass spectometric analysis of RF reactive sputtering reaction mechanism *(Japanese)* 78−19665
metal oxide ultrathin layers by reactive sputtering, controlled deposition and characterisation 79−78887
metal-semiconductor system, interfacial reaction, dynamical obs. at room temp. using AES 80−10798
metallic thin film, multilayered, depth profiling, improved depth resolution by reactive ion sputtering 79−91557
optical filters, diffractive, prepared by reactive sputter etching, microfabrication and evaluation 79−90008
PTFE film, reactive sputtering in Ar-CF_4 mixture, MSCA 78−92191
refractory carbides, adhesion to metal substrates, improved 80−76481

reactive sputtering continued
steel, stainless, vacuum components, sputtering and reactive effects during glow discharge treatment 78−70141
Al magnetron sputtering target, oxidation in Ar/O_2 mixtures 80−55291
Al-Cu, film, prep. by planar magnetron sputtering *(Japanese)* 80−16184
AlN film, oriented c-axis, low temp. deposition by reactive magnetron sputtering 80−76180
AlN films on glass substrate, prep. by reactive DC magnetron sputtering technique, c-axis orientation 80−89146
Al_2O_3 films, DC reactive sputtering prep., IR spectra characterization 79−11513
Al_2O_3 optical waveguide, fabrication by reactive Al sputtering in O_2-Ar atm. 80−33262
Al_2O_3-based ceramics, high rate reactive ion etching 80−85070
Au, DC reactive sputtering, glow discharge mass spectrometry and X-ray diffr. 79−38701
BN, thin film prep. and I-V charcts. of Al-BN-Au device *(Japanese)* 77−73230
C, reactive RF sputtering in N_2, paracyanogenlike film deposition 79−78886
CdO-SnO_2 film, DC sputtering prep., visible and near IR transmission, resist. 78−88049
CdS films, photosensitive, growth by reactive RF sputtering, props. *(French)* 78−35308
Co, DC reactive sputtering, glow discharge mass spectrometry and X-ray diffr. 79−38701
Co, X-ray diffr. exam. of chem. struct. *(French)* 77−63519
Cu, SIMS depth profiling, surface roughening by low energy ion irrad. 80−60727
Cu-Al_2O_3 cermet film, solar absorbing, production by dual cathode DC magnetron sputtering 80−16186
Cu_2O film, for solar cell applic. 79−7914
Cu_xO, film, thermoelec. power, activation energy variation with electrode spacing in DC sputtering 78−76099
Cu_2S epitaxial films, reactive sputtering prep. and electronic props. 79−78885
Cu_xS film, for Cu_xS-CdS heterojunction solar cell 79−11256
Cu_xS, layers produced by reactive RF sputtering, struct., elec. and optical props. 79−90908
FeC_x-CrC_y-NiC_z, stainless steel carbide, graded solar selective surface, magnetron sputtered 80−81485
FeC_x-CrC_y-NiC_z, stainless steel carbide, sputtered solar selective surface, grading profile 80−81486
Fe_xN_y, prep. by reactive sputtering, struct. and props. *(Japanese)* 78−92190
Fe_2O_3, film, increased capacity deposition system *(Bulgarian)* 78−60572
Fe_xO_y, prep. by reactive sputtering, struct. and props. *(Japanese)* 78−92190
GaAs, sputtered-etched surface, Schottky contact characterisation and its recovery by annealing 79−99603
GaAs thin films, reactively sputtered, ESCA/XPS study 80−97430
GaN, GaAs MIS struct. fabrication and props. 78−39686
Ge-Si alloy, epitaxial growth by getter sputtering, charcts. 79−28915
HfC, reactive RF sputtering in N_2, HfN film deposition 79−78886
In, reactive sputtering in DC triode config. 78−23618
In, reactive sputtering in Ar-N_2, N_2-O_2 discharges, mechanism, model 80−89109
InN film growth by reactive sputtering in Ar-N_2 discharge, mechanism 80−89107
In_2O_3 film reactive sputtering gas composition and film growth rate *(Russian)* 80−50554
In_2O_3, thin film, sputter deposition form., optical and elec. props. 80−60123
In_2O_3-InN film growth by reactive sputtering in N_2-O_2 discharge, mechanism 80−89108
In_2O_3-SnO_2 film, reactive DC diode sputtering, using large scale system 78−72723
InP cylindrical magnetron reactive sputtering, for solar cell appl. 78−39693
IrO_2, electrochromic film, prep. by reactive sputtering 80−29876
Mo, film, cc preparation by H_2 reactive sputtering *(Japanese)* 79−95929
Mo, ion bombarded, sputtering yield in presence of reactive gas 77−66566
Mo, product identification by absorpt. spectra 80−28027
Mo-Si, film deposition by reactive sputtering, characteris. *(Japanese)* 80−93485
MoO_3-Si photodiode, fabrication as function of O_2 partial press. 80−29464
MoS_2, RF sputtered layers with variable stoichiometry, lubrication props. 80−40557
Mo_xSi_y films, magnetron DC reactive sputtering, struct. and props. 80−80966
Ni/Fe interfaces sputter profiling, by AES 79−15572
Ni-Pd-H, film, struct. and phases formed, when Ni, Pd are sputtered in H 80−29289
Ni_xO, film, thermoelec. power, activation energy variation with electrode spacing in DC sputtering 78−76099
Pb film, reactive ion beam sputtering 78−19666
Pt, DC reactive sputtering, glow discharge mass spectrometry and X-ray diffr. 79−38701
Pt, reactive sputtering in Ar-O_2 mixtures, glow discharge mass spectrometric meas. 79−91552
PtO_x, thin film, sputtering deposition, XPS and X-ray diffr. chracterisation 79−78878
Si, amorphous, prep. by reactive RF sputtering in Ar-silane mixtures, undoped, n-type and p-type targets 80−76182
Si, high rate reactive ion etching 80−85070
Si, N^+ and N_2^+ ions, photon emission studies of mol. synthesis, interstellar process simulation 77−70297
Si, reactive sputtering, current-voltage charact. 79−95888
Si:H, amorphous, control and anal. of deposition, using plasma spectroscopy 80−45230
Si-Ag-Si heat mirror on plastic sheet for radiation insulation of visible windows 80−95985
Si-H amorphous film, reactively sputtered, prep. and props. 79−78889
SiC, coating on graphite, by reactive magnetron sputter deposition *(Japanese)* 80−16185
SiC, reactive RF sputtering in N_2, Si_3N_4 film deposition 79−78886

reactive sputtering continued
Si_xC_{1-x}:H reactive sputtering deposition, compositional and structural props. 79−99077
SiN_x, film by magnetron sputtering, composition, hardness and optical props. 78−3047
Si_3N_3, film growth by reactive sputtering, influence of electron-ion bombard. *(Russian)* 77−28717
Si_3N_4 amorphous film deposition by high rate DC reactive sputtering, passivation appl. 80−100784
Si_3N_4 films, reactive plasma sputtering prep. 79−43147
Si_3N_4 layers, on GaAs, encapsulation, low-energy ion beam sputtering 79−78882
SiO_2, fabrication of surface relief struct. with linewidth below 2000 Å 78−42478
SiO_2, reactive ion etching damage, electron trapping charcts. in MOS struct. 79−90704
SiO_x deposition by reactive sputtering of Si in magnetron sputtering system, reaction kinetics 80−49553
Sn, DC reactive sputtering, glow discharge mass spectrometry and X-ray diffr. 79−38701
SnO_2 film, reactive ion-plasma sputtered, elec. and opt. props. 79−42677
SnO_x films reactive DC sputtering prep., phase comp., X-ray diffr. and Mossbauer meas. 79−90914
Ta, ion bombarded, sputtering yield in presence of reactive gas 77−66566
TaN film, prep., comp. anal., and supercond. T_c 79−15605
Ta_2O_5, plane optical waveguide, fabrication by reactive sputtering 78−71221
Ta_2O_5-SiO_2, plane optical waveguide, fabrication by reactive sputtering 78−71221
Te-Se-CdO struct., fabrication and charcts. 78−76106
Ti, D bombarded surface, ion fraction and energy anal. of sputtered particles 77−36345
Ti, film, reactive ion beam sputtering 78−19666
Ti, in Ar-O plasma, effect of oxidation on reactive sputtering rate 77−24955
Ti, ion bombarded, sputtering yield in presence of reactive gas 77−66566
Ti, sputtered ion fraction meas. using matrix isolation spectroscopy 80−60738
Ti-$C_x(N_x)(O_x)$, solid soln. film prep. by reactive sputtering, solubility and effect on props. 79−28231
TiC, reactive RF sputtering in N_2, TiN film deposition 79−78886
TiN thin films, elec. props. 80−15638
TiO_2 and Dy_2O_3-TiO_2, high refractive index film growth by sputtering, waveguide appl. 77−48341
TiO_2, reactive- and chemical-sputter deposition from Ti and TiC target 79−100051
TiO_2, reactively sputtered optical coating for inertial confinement fusion laser components 80−23705
TiO_2-Ag-TiO_2 heat mirror on plastic sheet for radiation insulation of visible windows 80−95985
TiO_x, film prep. conditions rel. to stoichiometry 77−40370
V, D bombarded surface, sputtered particles, ion fraction and energy anal. 77−36345
VO_2:Al(W), thin layer prep. by reactive DC sputtering doping effectiveness *(German)* 78−6847
W, ion bombarded, sputtering yield in presence of reactive gas 77−66566
Y, D bombarded surface, ion fraction and energy anal. of sputtered particles 77−36345
$Zn_{1-x}Cd_xS$ films, polycryst., reactively sputtered, MSM struct. obs. of dielec. props. and cond. mechanism *(French)* 78−14841
ZnO, film, reactively RF sputtered, anal. of texture 78−67921
ZnO film on glass substrate, high-rate deposition using DC reactive magnetron sputtering 80−80978
ZnO films, DC reactive magnetron sputtering technique, quality study 79−78877
Zr film, reactive ion beam sputtering 78−19666
Zr, O_2 press. depend. 77−12530
Zr, sputtered ion fraction meas. using matrix isolation spectroscopy 80−60738

reactive voltamperes *see reactive power*

reactively sputtered coatings
biological solar cells, photosynthetic bacterial reaction centres on sputtered C and SnO_2 electrodes 80−66981
borosilicate glass films, phys. and chem. props., B diffusion into Si, SiO_2 80−29040
closed loop control of deposition using glow discharge mass spectroscopy 80−80973
DC reactive sputtering system for coating tubes 78−35307
ferrite film, reactive RF sputtering prep., high mag. recording density 77−12528
metal carbide, magnetron-sputtered, solar selective absorbing surfaces 79−92079
metal silicide solar selective absorbing surfaces 78−52671
solar collector DC reactively sputtered metal carbide and silicide selective surface props. 79−62029
steel, stainless, carbide reactively sputtered solar selective absorbers for all-glass tubular evacuated collectors, absorptance and emittance 80−101132
transition metal carbides and silicides, solar absorbing surface, struct. and optical props. 79−79407
Al-Cu, film, prep. by planar magnetron sputtering *(Japanese)* 80−16184
AlN, formation and characterisation 80−44452
AlN, piezoelectric film, low temp. growth by RF reactive planar magnetron sputtering method 80−76175
AlN, protection on GaAs, $Ga_{1-x}Al_xAs$ and $GaAs_{1-x}P_x$ *(French)* 78−23849
AlO_x, obtained by oxidation of Al magnetron sputtering target in Ar/O_2 mixtures 80−55291
Al_2O_3, DC reactively sputtered, in MIS structs., effects of annealing on C-V charcts. 77−51822
Al_2O_3, DC reactively sputtered, in MIS structs. optical and elec. props. 79−19486
Al_2O_3 films, DC reactively sputtered, struct. 80−96764
Al_2O_3, form. and behaviour under particle bombard. 80−35029
Al_2O_3 optical waveguide, fabrication by reactive Al sputtering in O_2-Ar atm. 80−33262

reactively sputtered coatings continued
$Ba_{0.4}Sr_{0.6}TiO_3$, ferroelec. thin film, fabrication, props. 77−28521
BiF_3 thin films, optical props. 79−32005
CdO-SnO_2, transparent electrode props., optimum sputtering conditions 80−11116
CdO-SnO_2 DC reactively sputtered films, elec. and optical props. 80−103763
CdS films, photosensitive, growth by reactive RF sputtering, props. *(French)* 78−35308
$CdSn_xO_y$ DC reactively sputtered film, elec. and optical props. 79−87022
$Cd_{1-x}Zn_xS$ reactively sputtered phtoconductive films for high field applications *(German)* 78−39154
Cr_2C_3, reactively sputtered solar selective absorbers for all-glass tubular evacuated collectors, absorptance and emittance 80−101132
CuI, film, prep. on NaCl by reactive sputtering, struct. and composition investigation 79−90900
CuI films, reactively sputtered, epitaxial growth on rocksalt substrates 79−4918
Cu_2O, phase comp., resist. and optical consts. 79−95534
Cu_2S, Hall effect meas., 90-300K 80−15541
Cu_2S-CdS solar cell fabrication by magnetron reactive sputtering deposition 80−61363
Cu_xS films, magnetron reactive sputtering deposition and elec. props. 79−78884
Cu_xS, layers produced by reactive RF sputtering, struct., elec. and optical props. 79−90908
Dy_2O_3-TiO_3 sputtered film, optical waveguide with high refractive index 79−3797
Fe-C, solar absorbing surface, struct. and optical props. 79−79407
$Fe_x(C,N)$, obtained by ion bombardment thermochemical treatment of Armco Fe *(French)* 77−86229
FeC_x-CrC_y-NiC_z, stainless steel carbide, graded solar selective surface, magnetron sputtered 80−81485
Fe_xN_y, prep. by reactive sputtering, struct. and props. *(Japanese)* 78−92190
Fe_2O_3 films, DC reactively sputtered, for selectively semitransparent photomasks, struct., mech. and chem. props. 80−59835
Fe_2O_3 films, DC reactively sputtered, for selectively semitransparent photomasks, deposition conditions and optical props. 80−60782
Fe_2O_3 thin films, reactively sputtered, mechanical stresses rel. to deposition conditions 80−80146
Fe_xO_y, prep. by reactive sputtering, struct. and props. *(Japanese)* 78−92190
Ge:H, amorphous, H content determ. by IR absorpt., gas evolution and nuclear reaction methods 80−44130
InN film, refl. and transmission spectra, band struct. 78−72625
InN film growth by reactive sputtering in Ar-N_2 discharge, mechanism 80−89107
InN, thin film, characterisation using XPS electron energy loss spectra 79−87561
In_2O_3, conductive, transparent, optimal reactive sputtering conditions for prep. 79−95295
In_2O_3, thin film, characterisation using XPS electron energy loss spectra 79−87561
In_2O_3, thin film, sputter deposition form., optical and elec. props. 80−60123
In_2O_3:Sn films, RF reactive sputtered, optical props. rel. to band struct. 79−91515
In_2O_3-InN film growth by reactive sputtering in N_2-O_2 discharge, mechanism 80−89108
In_2O_3-SnO_2, stress, and elec. and optical props. 78−51861
InO_xN_y, thin film, characterisation using XPS electron energy loss spectra 79−87561
$In_xSi_yO_z$, thin film, sputter deposition form., optical and elec. props. 80−60123
$In_{1.9}Sn_{0.1}O_3$ laser-damage-resistant transparent conductive coatings, appl. in Pockels cells 79−50333
$In_{2-x}Sn_xO_{3-y}$ thin films, optical transmission and elec. resist. 77−69926
IrO reactively sputtered electrochromic films, electrocatalytic O_2 evolution 80−26125
$MnCo_2O_4$ DC sputtered films, struct. and elec. props. 80−54812
MoS_2, RF sputtered layers with variable stoichiometry, lubrication props. 80−40557
MoS_x RF reactively sputtered film, struct. and comp. 78−60038
Nb-Ge film, CVD and sputter deposited, critical current density and stability 77−28327
Nb-Ta-N films and their anodic-oxides, elec. props. of resist. and dielec. films 80−11126
NbN, supercond. props., SQUID behaviour 78−72311
NbN, supercond. RF reactively sputtered films, deposition parameter effects on props. 80−80972
Ni-Pd-H, film, struct. and phases formed, when Ni, Pd are sputtered in H 80−29289
$Pb_5Ge_3O_{11}$, sputtered ferroelec. films, prep. struct. and dielec. props. 80−75452
PtO, existence 78−18923
PtO_x, thin film, sputtering deposition, XPS and X-ray diffr. chracterisation 79−78878
Si, etching by CF_4, plasma deposition reactor gas phase characts., mass spectra 80−70566
Si:H, amorphous, H content determ. by IR absorpt., gas evolution and nuclear reaction methods 80−44130
Si:H, amorphous, H content effect on props. 80−49714
Si:H, amorphous, image pickup devices 80−100481
Si:H, amorphous, sputter deposited, O_2 incorporation during and after fabrication 80−49541
Si:H, amorphous Schottky solar cells, prep. and characts. of diode RF reactive cathodic sputtered films *(French)* 80−61347
Si:H,Li, amorphous, DC electrical conductivity, absorption edge and IR meas., role of H 80−54694
Si:H amorphous film, sputtered IR vibr. spectra and photolum., effects of partial evolution of H 80−44413
Si:H amorphous films, reactively sputtered, prep. and characterisation 80−100785
Si:H amorphous films, role of Ar in deposition process, IR absorpt. and photocond. meas. 80−50321
Si-H, amorphous, on Nb or W, spectrally selective absorber, IR spectra 80−26164
Si-H, amorphous, sputtered, photolum. obs. 80−80856
Si-H, amorphous, thermal stability and decomp. kinetics 80−24758
reactively sputtered coatings continued
Si-H amorphous film, reactively sputtered, prep. and props. 79−78889
SiC, amorphous, effects of S/C ratio and H content on elec. and optical props. 79−90906
SiC, comp. and struct. props., effect of target materials 80−54549
SiC, on graphite, by reactive magnetron sputter deposition *(Japanese)* 80−16185
α-SiC:H, prepared by reactive sputtering, layer props. *(Japanese)* 80−60695
SiC:H amorphous reactively sputtered film, H content effect on film props. 80−75459
Si_xC_{1-x}:H reactive sputtering deposition, compositional and structural props. 79−99077
SiH_x amorphous reactively sputtered films, optical props. 80−50444
SiN_x, film by magnetron sputtering, composition, hardness and optical props. 78−3047
Si_3N_4, formation and characterisation 80−44452
Si_3N_4, MNS struct. hysteresis elimination 79−99633
Si_3N_4 on Si and GaAs, Ga and As concentration measurement by CAMECA probe *(French)* 77−86411
Si_3N_4 thin film, reactively sputtered, struct. and elec. props. 80−88656
SiO_2 film, form. by reactive sputtering, effect of defects in Si wafer 77−89676
$Si_xO_yN_2$ film, opt. props. rel. to reactive sputter prep. conditions 77−81165
Sn, discharge produce evaluation, mass spectrometer obs. 80−6668
SnO_2 film, reactive ion-plasma sputtered, elec. and opt. props. 79−42677
SnO_x films, non-stoichiometric, DC reactively sputtered, elec. props. 80−80415
$SrTiO_3$ film, polycrystn., dielec. props. and struct. 77−81057
Ta, N content determ. from Fourier anal. of X-ray diffr. profile 77−76693
Ta-Al-N thin film resistors with improved elec. props. 80−100544
TaN, prep., comp. anal., and supercond. T_c 79−15605
Ta_2O_5 on Si, in two-electrode magnetron system, dielectric and optical props. obs. *(Bulgarian)* 80−89144
Ta_2O_5, reactive DC sputtering deposited films with magnetron-plasmatron, mechanical elec., optical props. 80−25566
Ta_2O_5 thin film protection of unstable OF-type glass components 79−14079
$Ta_2O_5N_x$, sputtered birefr. film, deposition conditions effect on refr. index 77−39118
TiC reactively sputtered coatings on Ni-Cr-Mo-Ti (19,11,3 wt.%), adherence, XPES and wear study 80−25565
TiC sputtered coatings on Ti-Al-V (6,4 wt.%), adherence, XPES and wear study 80−25565
TiN films, reactively RF sputtered, struct. and elec. props., substrate bias effects 80−96763
TiN layers investigation for solar-cell contacts 80−81461
TiN thin films, elec. props. 80−15638
TiN_x, sputtered in Ar-N_2 atm., elec. and struct. props. 80−15636
TiO_2, reactive DC sputtering deposited films with magnetron-plasmatron, mechanical elec., optical props. 80−25566
TiO_2, reactively sputtered optical coating for inertial confinement fusion laser components 80−23705
TiO_2-SiO_2 interference filters, narrow band, 0.7 to 1.5 μm spectral region, from cathodic sputtering 79−7221
VO_2, influence of manufacturing parameters on film struct. and props. *(French)* 77−81218
WO_3 solar absorber surface spectral selectivity rel. to temp. and UV ageing 79−62027
$Zn_{1-x}Cd_xS$, polycrystalline, cond. mechanism and grain boundary barriers *(French)* 77−76972
$Zn_xCd_{1-x}S$ solid soln. films, reactive cosputtering, struct., comp. and opt. absorpt. edge *(French)* 78−6237
ZnO, film, reactively RF sputtered, anal. of texture 78−67921
ZnO RF sputtered films, post deposition annealing behaviour 80−100416
ZrC, solar selective surface *(Japanese)* 78−90465

reactors (electric)
see also capacitors; inductors; saturable core reactors
EHV choke coil measuring bridge *(German)* 77−18047
electron beam heated solenoid reactors for fusion power and fissile fuel breeding 78−8992

reactors (nuclear) *see fission reactors*

Read diodes *see IMPATT diodes*

read-only storage
14th Annual Reliability Physics Symposium, Las Vegas (1976) 77−40514
electrically erasable and programmable read only memory writer *(Japanese)* 79−101072
ferroelectric memory, matrix-addressed analogue, on $Gd_2(MoO_4)_3$ cryst. 80−103926
hologram memory using one dimensional Fourier transform image hologram 78−87032
holographic ROM recording with stationary reference beam 79−81396
holographic storage system, laser apparatus for recording transparencies of ROM 80−28177
image analyser control, diode matrix replacement by PROMs 77−22539
microscopically rough substrate local smoothing for optical storage 80−14288
modular arithmetic inner product processor optical implementation 80−48170
photosensor spectral responsivity calibration microprocessor system 80−86409
radiometric system design, mathematical modelling of relevant physical processes *(Rumanian)* 79−59313
seven segment display, for oscilloscopes 77−37933
single channel pulse height analyser, control and meas. system contruction appl. 79−93891
single-beam spectrophotometer, EPROM for automatic baseline control 79−35691
VMOS dynamic memory, 65536-bit, investigation of alpha-particle induced soft errors 80−88223

readout, digital *see digital readout*
readout, nondestructive *see nondestructive readout*
real time computer systems *see real-time systems*
real-time systems
see also online operation
acoustic holography system, Sonoscan using microprocessor 80−38184
acousto-optical snapshot Pockels Readout Optical Modulator 77−19193
air pollution data, real-time meas. transformation and statistical processing 78−24365
air pollution episodes in Venetian region, real-time forecasting via advection-diffusion model 80−77096
air pollution episodes in Venetian region, real-time forecasting via Kalman predictor 80−82046
astronomical telescopes, stellar image sharpening, phase correction 79−12410
audiometer, screening, and real-time computer techniques 78−81009
controllable real-time data collection system for coastal oceanography 77−5329
cutaneous receptors, on-line receptive field mapping technique 79−74797
data acquisition system for online analysis of large bubble chamber pictures CDC 1700 computer *(French)* 77−42223
data buoy wideband wave directional spectra, real-time telemetry 80−46305
data management systems, remotely sensed data from space 79−92600
design appl. of formal logic 78−33247
display techniques, for neurophysiology 77−2071
distributed exptl. facility 77−54486
distribution function parameters determ. in real time, instrument description 80−202
ECG detection, foetus, using near-orthogonal basis functions 77−21638
ECG real-time analyser with digital readout, portable device 80−56234
ECG slow wave real-time anal., hardware implementation of selective Bouilland transform. 80−56233
edge detection, numerical, optical and hybrid methods compared 80−102662
EEG analysis, real-time programming system 79−100767
environmental α-β-γ radiation monitoring system 78−94152
eye movement research, data collection using on-line computers 80−41329
fluoroscopic cardiac imaging, real-time computerised system 80−36123
forecasting precipitation, evaluation of real time operation 79−88443
frequency analysers for acoustic noise control 78−83192
geophysical data, real-time processing using DGU-2 curve plotter 80−36422
HF Doppler obs. display system 77−73887
high-speed correlometer based on US delay line 77−75757
holographic viewing in moving fog 80−102676
HTR spent fuel reprocessing facility, real-time data acquisition and processing system *(German)* 80−106148
hydrophysical nonstationary processes, real time digital filtration *(Russian)* 78−65425
image contrast enhancement, local area histogram equalisation and gain control 77−50636
image edge enhancement 80−43273
ionosphere, Dynasonde software, real-time data acquisition and display 80−36405
ionosphere soundings using small spaced receiving system 80−36406
ionospheric radiowave propag., maximum usable frequency predictions, real-time updating 79−58179
kinoform synthesis using chalcogenide glass films *(Russian)* 78−13669
LF real-time spectral analyser design and operation *(French)* 78−20538
magnetic torque curve analysis, online microprocessor system 78−254
magnetometer data transmission via telephone lines 77−13126
meteorological real-time data acquisition and anal. 78−69466
microprocessor in real-time Fourier analysis *(German)* 79−67266
minicomputer, portable, for dynamic ocean data acquisition and display 80−12552
minicomputer high-level languages and real-time operating systems for scientific instrumentation 79−12778
minicomputer-aided ECG diagnostic system 79−44024
moire topograms, real-time, video electronic generation 80−67198
moonlit object real-time optical matched filtering 77−19192
multichannel system for radioastronomical data recording and processing *(Russian)* 78−65507
multispectral feature classification by analogue CCD 78−24438
neuronal spike activity discriminator 77−48966
nuclear material control and accountability system (DYMCAS), prototype terminal 79−89485
nuclear materials control system, generalised concept 79−89449
ocean oil spill trajectory modelling, advancements 79−5509
oceanographic data acquisition and processing system, microprocessor based, real-time 79−16676
oceanography, data anal. by Naval Coastal Systems Center (NCSC) environmental measuring system 80−12570
one-arm magnetic spectrometer, Alfa facility, description and charact. 79−26809
online real-time data acquisition system design 78−35994
optical data processing operations achievable, real-time devices, systems and applications 80−9816
optical mixing spectra, real-time analysis system 79−67392
optical wavefront distortion compensation 77−17219
phased array US imaging, real-time digital scan conversion and multi-dimensional processing 79−48363
photon correl. laser anemometry, on-line data reduction system 79−60080
physiological stimulator, programmable, real-time numerical simulation appl. to laboratory instrumentation 77−44873
Pioneer Venus occultation expt., bandwidth reduction for radio science data generation 80−67492
plasma diagnostic real-time spectral analysis methods, applicability and constraints *(Russian)* 77−31525
plethysmography, whole-body, automated real-time anal. system 78−28112
polarising radiometer, data reduction and live time printout 77−78472
real-space US scanning principle 79−70594
real-time and frequency-domain processor simulation 79−81643
remote programming, real time computers, space flight on-board expts. *(German)* 78−53791
river management operational system development using weather radar 78−40718
real-time systems continued
satellite location by tone-code trilateration 77−9653
scintigraphy, multi-image gated cardiac studies 77−21611
sea surface contour airborne radar as remote sensing instrument 80−51562
side-entry surface acousto-optic interaction signal processor 80−48174
signal processing, appl. to underwater acoustic imaging 79−90089
signal processing activities of United States Army 80−48172
solar spectrometric research, automation system for on-line signal processing *(Russian)* 80−12659
solar thermal test facility, 5 MW, real-time computer control 80−72075
spectrum analyser, with on-line definition of confidence levels 77−73959
speech high-performance processor design 80−96144
SPS, real-time control system, operating system principles 80−875
still-picture real-time Hadamard transform coding quantiser design 77−27263
systolic time interval meas. microprocessor system for heart malfunction detect 79−79681
Tokamak Fusion Test Reactor, conceptual digital computer control systems 77−23281
two-beam interference pattern monitoring by phase modulation 80−77844
two-phase flow meas., digital signal processor 77−80235
underwater real-time communications, non-acoustic long-distance system appl. 79−5667
US diagnostic system, for dynamic and still images 79−92309
US imaging, dynamically variable electronic delays 79−46142
US imaging with shear, Rayleigh, and Lamb waves 77−32759
US real-time B-scan machine attachment for three-dimensional display 78−61229
US real-time diagnostic system 80−30819
reboilers *see boilers*
receivers
see also acoustic receivers; radar receivers; radio receivers; telephone receivers; television receivers; transceivers; transponders
acousto-optic parallel channel wideband receiver 80−48447
broadband transmit/receive circuit for NMR 78−89520
fibre-optic communication receiver designs 77−68281
heat receivers with moving heat carrier, freq. charact. 80−4733
heterodyne 0.9 mm, for astronomical observations 78−93116
heterodyne receivers of CO_2 laser emitters, antenna charact. meas. 77−67498
high signal density, SAW filters for signal sorting, identification, military communications appl. 79−18615
ionosphere soundings using small spaced receiving system 80−36406
Josephson junctions, applications in plasma physics 80−103194
Josephson receivers, mm- and submm-wave, close-cycle cooling 78−93709
laser digital communication system, 100 Mb/s, optical receiver and pulse generator *(Russian)* 79−94170
multichannel IR receiver performance 79−76596
optical, optimisation in terms of excess noise factors dependence on avalanche gains 77−792
optical communication, components development *(German)* 79−81563
optical communication, phase compensation type 78−1329
optical communication receiver, direct detection, performance for intensity subcarrier FSK 77−39033
optical fibre communication, cabling, light source and receiver technology, review 78−59125
optical fibre communication for military appls., review and assessment 78−42438
optical fibre communications development and need for standardisation *(Italian)* 79−23066
optical fibres, 0.95 Gbit/s PRS signals regeneration after transmission over 0.91 km of fibre, regeneration cct. 79−59807
optical heterodyne receiver arrays in turbulent atm., joint signal current probability distrib. 79−81368
optical receiver noise analysis, time-domain impulse response technique 77−68280
optical receivers, transmission error investigation *(Italian)* 77−54775
optical signal receivers, optimal and nonoptimal, logical structs. efficiency comparison, simulation *(Russian)* 78−71041
radioastronomical, 408 MHz band, design details HF transistor amp., ring modulator LO, 30 MHz IF amp. *(Italian)* 78−45234
sound production receiver for radiomicrophones, film, TV studios, theatres appl. *(German)* 80−4787
standard frequency, electronic clock control appl. *(German)* 78−57902
vertical ionosonde, interference suppression *(Polish)* 78−88950
receiving antennas
see also reception
acoustic arrays, underwater acoustics, review 79−64467
coherent microwave imaging of limited fields of view, angular and aperture noise, optimum procedure 77−67045
diffraction by semi-infinite parallel-plane waveguide in anisotropic plasma 78−1845
embedded bare and insulated receiving antennas, design for biotelemetry appls. 77−40947
heterodyne receivers of CO_2 laser emitters, antenna charact. meas. 77−67498
Ionospheric Sounding Satellite control, tracking system *(Japanese)* 77−78608
multi-beam antenna system, fully automatic, for interplanetary scintillation obs. 79−101064
optical, angle-distance sensitivity variation anal. 78−33841
optical antenna, sensitivity to scatt. aerosol particle, laser location of atm. aerosols 77−70847
optical antennas focused at finite distances, angle-distance pattern 78−33842
parabolic aerial with monopulse exciter for meteorological satellite S-band reception *(German)* 79−92628
submillimetre planar sandwich receiving antenna 79−40609
tuned loop, 100 MHz, for indoor biotelemetry 77−90925
reception
see also diversity reception; radio reception; television reception
RF frequency standard transmission, phase instability due to effect of ionosphere 78−41279
reception quality *see reception*
recombination, electron-hole *see electron-hole recombination*
recombination, ion *see ion recombination*

reconnaissance satellites *see artificial satellites*

record players *see gramophones*

recorders
see also recording; tape recorders
AC electrical load information recorder utilising standard multi-point chart recorder 80−42238
acousto-optic photorecorder, 1 GHz bandwidth 77−57365
adaptation to varying operating conditions *(Polish)* 77−67423
analogue, guide to different techniques 77−41583
atomic probe, field ion microscope with time-of-flight mass spectrometer 80−73520
automatic, for DC Josephson current meas. 79−17444
automatic crack growth recording using PSR-1-19 potentiometer 78−39971
automatic deformation recording instrument 78−7122
automatic device for thermomechanical and linear dilatometric testing of polymers 80−11858
automatic digital equipment for recording acoustic emission signals 80−102948
automatic pressure recording method, 5 to 10^{-2} torr 79−85148
automatic quantum efficiency yields, recording system 77−67489
automatic recording system of probe meas. for plasma parameters *(Japanese)* 79−41870
biological impedance automatic recording system 78−44625
Biomation 8100, DMA interface for Intel MDS-800 microcomputer system 80−203
Biomation 8100 recorder interfaced to remote computer, data acquisition in photolysis expts. 78−21107
blast noise measurement, recording system 77−88984
blind person's rocking motion sensor and recorder 77−52921
boxcar integrator/US recording unit using sample-and-hold circ., for student lab. 80−27083
chart recorder, for amateur radiotelescope 79−21189
chart recorder, multichannel sequential switcher, for teachers 78−81754
chart recorder, pen-holder design 78−16611
chart recorder and plotter assimilation 79−93128
chart recorder information translation into digital form 77−22537
chart recorder specification and selection, voltmeter type 77−37931
chart recorder timer control, pen overload protection systems, at. absorpt. appl. 77−73481
chart recorders, for school use 78−12503
contraction recorders for animal nictitating membrane and skeletal muscle 77−48969
crack measurement, recording instrument 80−100984
CRO visual trend display, an elecqronic equivalent to the chart recorder 77−37930
data, rack-mounted and portable, state of art and appl. 79−40555
decrepitometric recorder with electronic filter *(French)* 79−48571
densitometer for electron micrographs 79−49343
differential optical spectra recorder using wavelength modulation method 79−2832
differential pressure recorder for breeder reactor liquid Na cooling pressure monitoring *(German)* 77−88270
digital automatic blood pressure recorder *(Japanese)* 78−24168
digital colour recording system for digital-analogue hybrid image processing 78−16880
digital instrument for astronomical meas. recording *(Polish)* 79−88598
digital register for astronomical elec. photometer *(Russian)* 78−93117
digital scanning and recording system for spot electron diffr. patterns 77−13825
digital temperature recorders, advantages over analogue instruments 80−210
digital transient recorders, enhancement of signal averaging using microcomputer 78−57930
Digitron fast multichannel time recorder 77−67949
direct-writing analogue type, features, appls. 77−30137
DNA derivate melting curves, automatic recorder using real time processing *(French)* 80−104833
driven-sweep generator scan velocity transducer 78−57925
Earth tide registering stations, electronic time basis *(Rumanian)* 77−33216
ECG, low cost modification for multi-channel use 77−44813
ECG, with statistical pulse train interval digital analyser *(German)* 77−78007
ECG long-term recording and analysis sytem, Siretape C 79−92407
ECG recorder and printer with fixed writing heads 80−3854
electric dichroism measurement instrument with digital processing 80−82800
electrical instruments in photometric laboratory, selection, care, and use 80−86283
electrolytic cell resistance meas., differential recorder 78−86297
electromyographic analyser and recorder 79−57785
electronic high-resolution rainfall intensity recorder and totaliser 78−7793
electronic transient, use in quarrying for control of noise and vibration emission from explosions 80−67023
exponential decays analogue anal. using transient recorder 78−86244
eye movement recording system for clinical appl. 78−3623
fast transient recording, by analogue storage register 77−45827
fibre optic chart recorders using UV recording papers 77−18006
fibre optic recorders for traces and images 79−67292
flexible high-resolution film recorder system 80−102827
frequency marking for an x-t chart recorder 77−53947
hard copy imagery from remote sensing systems, laser beam recorder appl. 79−80715.
high-speed physical process parameter measurement by means of time-scale conversion 80−8968
hysteresigraph with data printout 79−58760
induction profilometer for surface irregularity recording 77−74358
ink recorder pen moisture maintenance device 77−17964
ink-writing recorder, warning device indicating stoppage of paper 77−5111
integrating recorder of a slowly varying voltage 79−93124
internal friction in semicond., simple recording system using digital electronic counting timer 79−37260
IR, nanosecond recorder of 10.6 μ wavelength radiation 77−37990
IR line scanner, Reconofax XIII A, improved recording system using LED 79−25335
Landsat imagery laser film recorder and processor 80−105084

recorders continued
laser recorder of video signals, on dry-developed photosensitive paper *(French)* 78−92998
light flux recording system, multichannel 79−35809
lightning counter, multichannel, with digital display 80−51570
lightning flash counter and interval recorder 78−88928
lightning peak current meas. and recording device results *(Japanese)* 80−46288
logarithmic convertors and amplifiers appl. *(German)* 79−9233
long-term continuous ECG recorder *(Japanese)* 77−66871
magnetic circular dichroism recorder calibration at 10.6 μm 80−90876
magnetic field sweeper and recorder drive for de Haas-van Alphen type phenomena 77−67474
mass spectra registration system for digital recording 79−93252
metal secondary electron emission coefficient recorder 78−58094
metallography, semiautomatic recording apparatus 79−87767
meteor wind radar, semiautomatic display and photographic recording system 79−8712
metrological balance automatic recorder and printer 77−22530
molecular weight measurement using recording thermistor cryoscope based on standard components 77−50572
monolithic timers form capacitive transducer-to-recorder interfaces 77−87781
Mossbauer spectra recording apparatus, effect of gate setting on spectral parameters 80−90938
movement-activated recording monitor for motor activity 77−25565
Multi-Scan 2100 series, electronic potentiometric recorders with variable characteristics 77−18008
multichannel Cerenkov mass spectrometer, electronic recording apparatus 79−26174
multichannel UV chart recorders, interface, GT8 galvanometer drive amplifier system 79−63204
multifunctional broad-band recording system for radioastronomical interferometer *(Russian)* 77−29650
multipen, features and operation principles 78−49815
muscle isometrical contraction maximum and standby tension, additional equipment *(Hungarian)* 80−41342
one, two, three or four channel indicating recorder 77−18007
optometer recorder of human eye microfluctuations, IR *(French)* 78−7463
oscillograph, eight-channel, for recording one-shot processes 77−37872
paper charts, electro-sensitive, pressure sensitive, heat sensitive, photo sensitive 77−17965
peak amplitude, ionospheric absorption of radio waves appl. 78−3979
pen control, for chart recorders 77−79121
pen type, vertical, with improved performance and long life, using DC servo system 79−40552
photoelectric, for kinematics obs. of artifical heart valve closing elements 79−48370
photoelectric spectrographic detection, direct reading attachment 80−275
photographic immunogram recording apparatus, self-contained, modified version using Polaroid film 80−17209
piston core behaviour recording device 78−20532
point recording device realisable operations *(Polish)* 78−29099
polygraph for simultaneous recording of diagnostic parameters 78−36011
potentiometer type, Servogor, features, appls. *(German)* 78−12681
potentiometric strip chart recorder calibrator/performance evaluator 77−87752
pressure meas. in pipes supplying collant to nuclear reactor *(German)* 77−88218
pulse continuous RF signal amplitude and phase difference measuring device 78−12719
pulse rate recorder providing printed record 78−3644
pulsed electron accelerator current density distrib. multichannel recorder 78−58520
punched tape data recorder for F5080 freq. meter, oceanological appl. 77−49175
radiation detectors, effects of averaging within field of view on recording equipment 78−53098
recorders, direct-writing analogue type, biomedical appls., techniques and maintenance, review 78−69241
respiratory rate and ventilation digital recorder 78−81005
rock elastic wave absorption meas. and recording instrument *(Russian)* 79−29891
sampling instrum. for recording/meas. instantaneous values of periodic events, oscilloscope appl. *(German)* 77−53876
satellite cloud picture recorder for reception of APT pictures 78−81434
scanning laser beam direct picture printers on photographic paper, appl. in life sciences *(French)* 80−72119
seismic recording channel, input cct. parameters matching *(Russian)* 79−39920
seismic recording equipment, digital automatic amplitude control unit parameters choice *(Russian)* 79−39964
seismic wide-band recorders specification 79−39908
shadow instrument with photoelec. recording, signal charact. rel. to turbulence spectrum charact. 77−35267
shock wavefront molecular process kinetics, IR absorption meas. installation 79−70389
signal peak recorded profile, influence of integration time const., appl. to crystallography *(French)* 77−5798
single-sweep waveform recorder with automatic range selection 78−77889
six colour, six channel recorder synchronised by a microprocessor *(French)* 78−77885
snowfall detectors and automatic depth recorder *(Japanese)* 79−8700
spectra registration system for spectrophotometers, graphical and digital forms 80−47113
stance stability of man, investigation using vectorstabilograph 77−44772
strength and deformation testing, ceramics, wide temp. range, universal apparatus 79−57177
strip chart recorder future in laboratory 80−57279
submarine quantum irradiance and photoperiod meter, with digital recording 80−98474
surface meas. instrument, modular *(German)* 80−57283
surface temperature contactless meas. instrument 78−57946
system for recording the activation times of pulsed light sources 80−73488
temperature monitor using thermistor sensor 78−209
temperature recorder, long-term, geophys. appl. *(Japanese)* 77−82035
tensile test diagram remote recording device 78−7139

recorders continued
thousandfold pulse duration convertor for automatic pen recorders 77−56521
torsion pendulum oscillations recording equipment for internal friction meas. 78−36998
toxic gas microconcentration determ. by automatic belt photometer *(Russian)* 78−28347
transient, for natural and induced phenomena 80−27284
transient 8 bit recorder using proportional step size tracking A/D convertor 80−57269
transient recorder, with digitised O/P, for biomedical applic. 77−40943
transient recorder for signal averaging, microcomputer-controlled 80−31723
transient recorders, multichannel *(German)* 78−235
transient recorders for acoustic emission studies 80−83717
transient signal recorder, Transcribe 10 uses A/D and D/A conversion 77−71340
two-channel system for punched tape, recording radioastronomical obs. *(Russian)* 77−29651
unit to record and reproduce acoustic emission signals 80−79039
UV recording, latest trends 79−54117
Viking Ground Reconstruction Equipment for facsimile picture recording 77−38051
voltage recording potentiometer, 2-coordinate, method for accomplishing time scanning 77−61080
waveform, features 79−12788
waveform, functions and appls. 80−57278
waveform distortion anal. due to recording and playback speed instability 78−73981
X-ray tube for recording rapid processes, type RTR-1 80−9080
X-Y, development progress 78−49816
X-Y, inkless, using thermosensitive paper 79−40553
X-Y, market review *(Norwegian)* 77−37869
X-Y recorder for Auger spectrometer using pulse height analyser, computer interfaces 78−49942
X-Y recorder use in LF function generator/controller 78−21108
zero position recording interferometer 77−71368
C materials, bend strength testing, bench assembly with strain recording 79−57176
Hg manometer, student apparatus 77−26119

recording
see also audio recording; magnetic recording; video recording
analogue signals, simultaneous recording using multichannel data acquisition system 79−26045
astronomy, data recording system for KSC 60 cm reflecting telescope *(Japanese)* 80−94717
auxiliary information recording with B3-15 digital printers 79−26044
blood coagulation parameter selection for automatic digital recording 77−21543
blood pressure Hg manometer contactless readout and recording cct. 77−81603
captured nerve fibre multiple single-unit recording by tubular electrode array 77−60321
coercivity meter, attachment for heat treatment monitoring 77−87795
contactless electropneumatic transducer parameter determ. *(Bulgarian)* 80−47045
crack growth recording, automatic, elec. resist. method 79−39070
creep curves, multicycle, device for recording at elevated temps. 79−43512
determination of complete dynamic characts. of recording systems, multifrequency dynamic charact. method 80−62651
dichromated PVA specific wavelength sensitisation for laser beam recording 78−5531
digital LF micro-holograms on photographic film 77−34845
Earth tides, tilts, parallel recording through digital print-out and photorecording channels *(Russian)* 78−88785
ECG recording system simplification *(Russian)* 78−40379
ECG skin artifact reduction by skin puncture method 78−44672
electrical resistance changes, continuous recording apparatus 77−53931
electrochemistry, recording coulometer for controlled atmosphere reactions of metals in molten salts 78−3344
electrooculargrams, single channel method for vertical and lateral eye movements 79−16205
electrophotography, bit capacity limitation, toner size and deposition 80−62762
face-voice synchrony for videotape speech dubbing 79−68503
fast processes, photographic and cine methods 80−57413
flexible high-resolution film recording system design 80−102828
fluorescence de-excitation function recording, one-quantum method, error anal. *(Russian)* 77−65925
galvanometric UV recording techniques 79−93129
hologram electronic heterodyne recording and self-interference term rejection 80−91756
holographic recording, using photopolymer material, redox sensitized 78−13674
horizontal pendulum tiltmeters, recording device 78−40679
human eye movements using opto-television method *(Russian)* 77−12909
implanted cardiostimulator pulse recording 77−78041
interference fringe fractions, meas. by means of time intervals method 79−17478
laser beam threshold recording energy density meas. method 78−5520
laser recording and information handling, seminar, San Diego, CA, USA (Aug. 1979) 80−101663
laser speckle pattern obs. through finite-size scanning apertures, extreme-value statistics 78−66759
luminescence spectrum recording monochromator wavelength reference marker generator 78−58050
luminous pointlike object, three-dimensional trajectory recording 78−12671
lustre quality meas., recording and evaluation 80−98967
magnetocardiography recording, props. of ideal system, appl. of ECG theory 80−104700
Multi-Scan 2100 series, electronic potentiometric recorders with variable characteristics 77−18008
ocean dumping surveillance and data recording system 77−5247
oceanic temperature-depth profiles, recording via solid-state memories 78−24383
oil and gas well profiles, appl. of combined well-logging techniques *(Russian)* 78−40705

recording continued
optical, on disc using diode laser 80−19001
optical and strain gauge methods comparison for split Hopkinson press. bar test on C fibre composites 80−85132
organic compound luminescence spectrometer attachment for recording at liquid N_2 temp. 79−67394
oscilloscope add-on cct. for stochastic instantaneous signal recording *(German)* 78−74031
parallel recording system for magnetostrictive spark chambers 78−867
pattern recognition by one-dimensional projection recording and processing *(Russian)* 78−42291
phonocephalography, passive noninvasive technique, normal tracing 77−81618
photoconductivity recording at UHF, simple method 77−41642
rain, description and field testing of digital recording system for tipping bucket raingauges 80−77161
real time laser recording, plastic versus metal coatings 77−74536
respiratory data, using XY recorder with data storage 78−7474
sea waves motion *(Italian)* 77−29458
seismic recordings, information quality and data processing techniques efficiency *(Russian)* 79−39666
SIMS, recording, optimisation 79−43683
sinoatrial node activity, intracardiac recording by prememorised averaging 77−81621
sleep EEG ambulatory monitoring and anal. 78−44650
soil reflection, polarised visible light photographic recording for surface moisture indications 79−53557
spectral line recording in presence of intense background, techniques, appls. *(Russian)* 77−40613
spectrometer automatic control unit for discrete recording 78−58049
SQUID, appl. to cardiac recording, phase and amplitude relationships of elec. and mag. events 80−104695
star transit instants, photoelec., automatic 77−91435
star transits, grating inclination effect 77−91436
text information micro-recording using laser beam *(Russian)* 77−54750
theodolite microprocessor selection, development, and programming 78−24218
thermal analysis data transfer to single recording instrument using multichannel commutator 79−52821
thermal contours, pulsating, using film structures, spatial resolution determ. *(Russian)* 77−74395
thermoplastic recording, theoretical problems 79−24803
thermoplastic recording with homogeneous mixture of thermoplastic and organic photoconductors 78−63161
thermoplastic sheet local fusion image recording and erasure *(Russian)* 77−57416
time-freq. secondary standards automatic recording/processing system 77−87738
vidicon based apparatus for spectral line contours investig. 79−93226
water run off at Syr Darya hydroelectric power station, aspects *(Russian)* 77−86942
welded joint inspection by X-ray TV intrascope, photographic recording of images 80−86485
well mud logging, online data processing *(Russian)* 78−40706
X-ray apparatus electrical circuit fault classification 77−21604

recording instruments *see recorders*

recovering *see recovery*

recovery
see also recovery-creep
A15 compounds, disordered, reordering kinetics, recovery of supercond. transition temp. 80−96678
anisotropic reinforced resin laminate, cyclically reversing load, strain behaviour determ., approx. method *(German)* 79−5096
anthracene, single cryst., X-radiation damage recovery, using triplet state exciton probe 78−75694
$\alpha+\beta$ brass, plastic deform., recovery and recrystn., positron annihilation 79−57003
brass, recovery and recrystallisation of plastically deformed α-phase, comparison of positron annihilation, elec. resist. and microhardness 79−52240
brass positron annihilation in α and $\alpha+\beta$ phase, short-range order, clustering and lattice defects influence 79−29107
brass single crystal, intracrystalline slip bands in high temp. creep *(Czech)* 79−77604
brittle abrasive material, rating capability for elastic deformation 78−56680
cell wall and lattice misorientation origin during deform. 80−71712
cellulose acetate films, light scatt., tensile creep, desalination 80−16050
cement paste, heat-cured, recoverable and irrecoverable deform. 77−63732
colloids, nonlinear rheological behaviour and shear dependent struct. 79−7358
creep deformation model incorporating recovery and thermally activated glide 79−64534
cyclic plasticity, creep recovery unified approach to interaction prediction 79−8329
diamond, B doped, electron irradiated, defects at low temps., elec. resist. meas. 77−11593
dislocations, in 9ubgrains and subgrain coalescence 77−76398
ductile fracture, strain hardening and damage relationship 80−108564
FCC metals, high dose neutron irrad. effects, 4.6K 78−34548
FCC metals, props. of vacancies and divacancies 80−10545
ferritic alloy, reinforced by dispersed oxide, mech. props., modification by recovery heat treatment *(French)* 77−59837
graphite, polycryst., reactor-grade, neutron irradiated, isothermal annealing obs., by ESR *(Japanese)* 77−43254
graphite, pyrolytic, neutron irrad. at low temp., thermal cond. recovery *(French)* 77−62566
grinding, role of elastic and plastic behaviours *(Japanese)* 80−100868
internal stress, stochastic model for dip test in steady-state creep 80−58915
interstitials, mobility and interactions 78−47328
lubricated elastomers in contact with regularly spaced sliders, frictional dynamics 79−20213
martensite ageing, influence of neutron irradiation *(Czech)* 78−84859
metal, electron irrad., selfinterstitial atomic defect interaction radii, recovery expts. and error sources 80−65049
metal, HCP, long-range interstitial migration rel. to c/a ratio 79−28125
metal, ion and neutron irrad., low temp. defect prod. and stage 1 recovery 78−79637

recovery continued
metal, irradiated, determ. of time threshold energy for Frenkel pair creation 77−47444
metal, low temp. neutron irrad., dose depend. of recovery peaks 78−71767
metal, polycrystalline, strain hardening, dislocation link length model 80−84953
metal, recovered dislocation substructure, prod. and utility, review 77−84749
metal sheet, recovery strain during unloading in tensile test, roll-forming appl. *(Japanese)* 79−100182
metals, radiation damage production in stage II, temp. and impurity effects 77−68997
muscovite mica, annealing of latent tracks of heavy ions *(French)* 79−19290
optical fibre, γ-ray irrad., damage recovery by annealing 79−23078
oxides, interaction between point defects and dislocations, cryst. plasticity 80−15149
polycarbonate, compressive recovery behaviour 79−38919
polyethylene, linear, strain rate effects on ratio of recoverable to nonrecoverable strain 78−27566
polyethylene, linear role of recovery forces in deformation 78−48459
polyethylene, low density, melt elongation, stress and recovery maxima 79−90209
polyethylene films, two-layer, elongation, recovery rates meas., relaxational props. *(Russian)* 77−32663
polymeric systems, rheology, review 78−87317
polystyrene, atactic, indentation recovery, defect struct. produced by deformation 79−43275
polystyrene, atactic, indentation recovery 80−84988
polyurethane, segmented, time depend. struct. changes on annealing, X-ray meas. 77−4052
PVC, amorphous, orientation study by creep thermomechanical method, computer anal. 78−75561
PVC, mech. behaviour in nonlinear viscoelasticity range 79−4996
PVC, plasticised, history-independent recovery, creep, stress relaxation 78−80607
Pyrex glass, indentation recovery, defect struct. produced by deformation 79−43275
recrystallisation *(Czech)* 79−70081
recrystallisation and grain growth in materials, conf., Chicago, USA (Oct. 1977). 79−97122
RF receiver with extremely fast recovery for pulsed NMR 77−26376
sapphire, work hardening 77−16604
shape memory alloy, recovery stress determ. 79−15665
spark gap electric strength recovery after impulse current passage 78−67565
steel, Al-stabilised, texture formation in continuous annealing, effect of coiling temp. of hot strip 79−91688
steel, austenitic, 45Kh2N12GS, post deformation holding at deform. temp. effect on struct. and strength of austenite and martensite *(Russian)* 79−1880
steel, austenitic, dislocation structural changes on hot rolling *(Russian)* 77−59805
steel, austenitic stainless, AISI 316 L, viscoplastic deformation under hot working conditions, struct. model 79−83278
steel, austenitic stainless, creep deform. effect on struct. of twin boundaries 79−8332
steel, austenitic stainless, stress relaxation model, experimental confirmation of model 78−92293
steel, cold-rolled, recovery of lattice defects in cementite 77−90370
steel, Cr (3.51, 3.74, 3.56 wt.%), bainite transform. of deformed austenite 77−32574
steel, deformation at large plastic strains, work hardening rate 79−20065
steel, high strength, thermally strengthened by rolling heat, H_2 embrittlement *(Russian)* 77−77562
steel, HSLA, V and N effect on recovery and recrystn. during and after hot working 80−84973
steel, law-C, hot deform., austenite strengthening and weakening 80−76282
steel, low alloy, hot deform. behaviour and modified ausforming *(Japanese)* 78−11244
steel, low C, instability obs. by large strain compression 80−35253
steel, low C, Mn-Nb, quenched and tempered, microstruct. and props. 77−36549
steel, low C, rolling deform., effect on NbC particle size distrib. 79−47717
steel, martensitic, ageing, thermal recovery 77−56011
steel, plastic loosening and deform. defect healing during recovery annealing of 12Kh18N10T *(Russian)* 80−66530
steel, quenched, martensite, tensile and compressive deform. resist. *(Russian)* 78−19819
steel, Si-P-C, low C, varying Si content, cold rolled annealing 80−3090
steel, stainless, 304, deformed in torsion, annealed, static recrystallization and restoration after hot deform. 79−47735
steel, stainless 304, crack propagation under intermittent overloading at elevated temperatures *(Japanese)* 79−38947
steel, stainless 316, recovery by annealing of creep produced dislocations 80−11702
steel, strain hardening and dynamic recovery, weakening factor in range 1273-1473K *(Russian)* 79−78990
steel 15Kh1M1F, microstruct. changes rel. to creep and fracture *(Russian)* 79−24572
steel 40 KhSN2MVF, chemical micro-inhomogeneity recovery during thermal working *(Russian)* 78−15442
stress relaxation, experimental data, analysis methods 77−84822
superconductor, fast neutron irrad. effects on T_c, comparison for C-15 Laves phase, A-15 and Chevrel phases 77−55633
superconductor, neutron effects 78−52121
thermoplastic polymer, linear viscoelasticity, rel. to orientation, recoverable strain and mech. props. 77−56041
unsaturable trap model for defect accumulation in recovery stage II 77−47481
wood, vibratory cutting, behaviour of chip and effect on cutting force *(Japanese)* 77−77540
work hardening-recovery type constitutive eqns., numerical integration, improved method 78−6949
Zircaloy, post irradiation recovery of growth 79−46711
Zircaloy-2, recoverable plastic strain 77−63708
Zircaloy-4, stress relaxation specimens, thermally induced strain recovery causing microstruct. changes 77−25057
recovery continued
Zircaloy-4-O alloys, rapidly heated and quenched, transform. charact. 79−20041
Ag, Ag-Cd(In) dil. alloys, electron irrad., stage I_E recovery 77−39616
Ag, cascade energy density effect on isochronal recovery 78−47431
Ag, dislocation recovery *(Russian)* 77−65980
Ag, polygonisation, impurity effects rel. to stacking fault energy 77−63685
Ag, production and annealing of radiation defects 78−47362
Ag, proton irrad., radiation-annealing effects in energetic displacement cascades, film resist. meas. 78−26603
Ag, recovery and formation of mixed dumbbells after thermal neutron irradiation 79−69161
Ag, rolled, dislocation struct. and recovery during annealing *(Russian)* 79−29084
Ag, surfaces, dislocation climbing, etch pit investig. 79−19260
Ag-Zn(Cd), production and annealing of radiation defects 78−47362
AgAu, recovery and formation of mixed dumbbells after thermal neutron irradiation 79−69161
AgCl, single crystal, recovery controlled transient creep, substructural obs., phenomenological anal. 77−77526
Al, Al-Ag(Mg) dil. alloys, electron irrad., stage I_E recovery, interstitial trapping 77−15405
Al alloy, 2024, shock-loaded, recovery of Young's modulus 78−23751
Al alloy, deformation at large plastic strains, work hardening rate 79−20065
Al alloy 2618, creep and recovery under combined stress, viscous-viscoelastic model representation 79−34117
Al, annihilation spectrum, narrow component, Fermi impulse of electrons, plastic deform. recovery *(Czech)* 78−64591
Al bronze, BA 1032, deformation at high temp., dynamic recovery *(Polish)* 79−79023
Al cell structures produced by cycling and monotonic creep 80−55452
Al, deformed, thermal recovery, microstruct. and stress-strain relations 80−16325
Al, FCC, strain hardening and recovery by pure metal mode, high temp. deform. *(Japanese)* 78−52843
Al, high purity, cyclic torsional deform., factors influencing ductility 77−56031
Al, interstitial trapping configuration study by ion channelling 78−47455
Al, pure, creep, grain size effect on rate at 408K 77−52428
Al, recovery and recrystallisation during temperature strain *(Czech)* 77−73287
Al, recovery annealing, exam. using in situ high voltage electron microscopy 80−7596
Al, recovery during stress relaxation testing at 298K 77−8872
Al, recovery features, TEM and positron lifetime meas. examination 78−80611
Al, recrystallisation and recovery during temperature strain *(Czech)* 77−70071
Al single crystal, polygonisation at high press. kinetic regularities, dislocation struct. at 140°C 79−66070
Al-Ag(Ge)(Mg)(Zn) alloy, dil., electron-irradiated, impurity-interstitial interaction 77−15449
Al-Al_6Fe, fibre reinforced eutectic, deformation behaviour by rolling, TEM and SEM study 79−29129
Al-Cr(V)(Ti), dil., electron irradiated, interaction of self interstitials with undersized solute atoms 78−63789
Al-Ga, dil., neutron irrad., 4.2K, defect prod., recovery 77−1155
Al-Li alloy, annealing of vacancies and ageing, resist. and TEM obs. 77−21172
Al-Li alloy, dil., quenched and irrad., recovery, resist. and internal friction obs. 78−52848
Al-Mg, dil., neutron irrad., 4.2K, defect prod., recovery 77−1155
Al-Mg, Mg effect on ductility, 25 to 250°C 79−100214
Al-Mg (2.2 at.%), creep at 573K 79−20145
Al-Mg (4 wt.%), enhanced ductility at elevated temps. 77−63740
Al-Mg (5 wt.%), recovered dislocation substruct. during plastic flow 79−83273
Al-Mg alloys, initial decomposition exam. by X-ray diffr. *(Russian)* 77−77482
Al-Mg-Si, heavily rolled, electron microscope obs. of cube oriented region, rolling texture 79−29093
α-Al_2O_3:Pb, implantation, lattice disorder 77−80525
As_2Se_3, film, amorphous, fatigue and recovery of electrophotographic props. 78−21253
Au, deformed, annealing kinetics of vacancies *(Japanese)* 80−88139
Au film, adatom surface diffusion at low temps., elec. resist. study *(French)* 80−65376
Au film sandwiches, recovery kinetics and early stages of diffusion, DC resist. expts. 79−77971
Au, proton irrad., radiation-annealing effects in energetic displacement cascades, film resist. meas. 78−26603
Au, work hardened, Hasiguti peaks, spectrum and recovery, impurity effects *(French)* 77−66670
Au-Fe, polygonisation, recrystallisation, precipitation microstruct. without external plastic deform. 79−43276
Be bronze BrB2, quenched deformed, substruct. and props., effect of prerecrystallisation annealing *(Russian)* 78−60677
Bi film, adatom surface diffusion at low temps., elec. resist. study *(French)* 80−65376
Cd, recovery after 6.1 MeV α-particle irradiation at 4.2K 78−47441
Cd, stage III recovery, after α-particle irradiation 77−27924
Cd-Ag, polycryst. quenched foil, the influence of Ag on the recovery spectrum 78−76661
CdO, influence of initial compacting press. on elec. resis. Hall coeff. 80−20872
CdS, 200 keV electron induced defects, low temp. annealing 77−80796
Co, low temp. electron irrad., elec. resist. recovery 77−35588
Cr, atomic displacements in electron irrad. cryst. 79−46705
Cu, cascade energy density effect on isochronal recovery 78−47431
Cu crystals, two-phase, recrystn. retardation, particle size, spacing effects 80−89242
Cu, defect annealing around stage III, γγ ang. correlation expt. 79−14846
Cu, deformed and annealed, positron lifetime investig. of recovery and recrystn. 77−70064
Cu, electron irrad. at 130K, positron lifetime investig. of stage III recovery mechanism 77−47484
Cu, electron irrad., positron lifetime exam. of annealing recovery 78−47354

recovery continued
Cu, electron irrad. at 4.7K, recovery of Frenkel defects, defect-agglomerate effects *(German)* 77−84797
Cu, electron irradiated, additional recovery around 200K 78−38755
Cu, electron irradiated, small-angle X-ray scatt. investig. of stage III recovery 77−7763
Cu, electron-irrad., stage III recovery kinetics 78−63792
Cu foi.foil, interstitial impurity interaction investigation by stage II isochronal recovery expts. 78−47423
Cu, heavily rolled, electron microscope obs. of cube oriented region, rolling texture 79−29093
Cu, high purity crystal, resistivity changes with deform., subsequent recovery 77−52397
Cu, interstitial trapping configuration study by ion channelling 78−47455
Cu, irradiation with O_2 ions, defect production and annealing 80−88214
Cu, isochronal recovery of high energy d-Be neutron damage 78−51592
Cu, plastically deformed, recovery, isochronal annealing, positron lifetime meas. 77−59807
Cu, polycryst., low temp., plastic deform., structural defects, elec. resist. meas. *(Russian)* 78−39844
Cu, polycrystalline, intracrystalline slip bands in high temp. creep, comparison with brass single crystal *(Czech)* 79−77604
Cu, polycrystalline, recovery and recrystallization after hot working 79−91661
Cu, polycrystalline, recovery and recrystn. kinetics 80−81081
Cu, polygonisation, impurity effects, rel. to stacking fault energy 77−63685
Cu, proton irrad., radiation-annealing effects in energetic displacement cascades, film resist. meas. 78−26603
Cu, recrystallisation and recovery during temperature strain *(Czech)* 77−70071
Cu, recrystallisation and recovery during temperature strain *(Czech)* 77−73287
Cu, rolled, dislocation struct. and recovery during annealing *(Russian)* 79−29084
Cu single crystal, weakly deformed, elec. resist. recovery, annealing effect 77−81304
Cu, strengthening by dislocation substructures 77−36538
Cu, thermal neutron irrad., stage II recovery 77−31695
Cu, thermal neutron irradiated, isochronal resist. recovery, 30-400K 79−19287
Cu, thermal-neutron damaged, I_D and I_E recovery substages 77−35590
Cu, very low atomic displacement threshold energy obs. 78−95078
Cu-Au, dil., thermal neutron irradiated, isochronal resist. recovery, 30-400K 79−19287
Cu-Au, dose depend. of recovery after thermal neutron irrad. 77−69011
Cu-Cr, dil. alloys, Frenkel defects, effects on anomalous resistivity and thermopower 77−8084
Cu-Nb multifilamentary composite, dislocation resistivity 80−70671
Cu-Zn-Si, deform. close to martensitic transform. temp. 77−63714
CuAu, thermal-neutron damaged, I_D and I_E recovery substages 77−35590
Dy, electron irradiated, defect annealing, recovery spectra 79−23648
Er, electron irradiated, defect annealing, recovery spectra 79−23648
Fe, BCC, strain hardening and recovery by pure metal mode, high temp. deform. *(Japanese)* 78−52843
α-Fe, high purity, neutron and electron-irrad., interstitial migration at 200K 79−55920
Fe, high-purity, H_2 charged, resist. recovery at low temps. 78−26729
α-Fe, internal friction for low temp. deform. 80−40420
Fe, irradiated with electrons then annealed, magnetoresistance at 20K *(French)* 80−103677
Fe vacancy form. by positron annihilation in thermal equilibrium 78−10041
Fe, vacancy recovery stage, radiation doping, elec. resistivity meas. 79−51102
Fe:^{133}Xe, heavy ion implantation, recovery, Mossbauer effect meas. 78−52393
Fe-Al, deformed, low temp. recovery of elec. resist. *(Russian)* 80−7697
Fe-Al (38.5-47 at.%), type B_2 ordered alloys, elec. resist. recovery stages after neutron irrad. *(French)* 77−69010
Fe-Al (40 at.%), ordered, plastically deformed, neutron irrad. damage and recovery, resist. meas. 77−19993
Fe-Al (40 at.%) and Fe-Al (50.5 at.%) ordered alloys, 20K neutron irrad. effects, stoichiometry depend., resist. obs. *(French)* 80−84215
Fe-Al (50.5 at.%), ordered, neutron irrad. enhanced defect diffusion, resist. meas. 77−11598
Fe-Al alloys, cold-worked, Mossbauer study of recovery 80−7593
Fe-Co(-V) alloys, neutron irradiated, influence of dislocation doping on recovery 79−46715
Fe-H, recovery of hydrogenated and quenched alloy, solute diffusion 77−77510
Fe-Ni, alloy 20N24, martensitic, exam. of structure after laser treatment, and recrystallisation *(Russian)* 79−11608
Fe-Ni-C (24, 0.5 wt.%), recovery and recrystallisation of stable austenite after hot rolling *(German)* 77−32591
Fe-Ni-Ti, shape recovery depend. on hardening *(Russian)* 79−83259
Fe-Si alloy, deformed by slip, polygonal boundary form. *(Russian)* 79−24534
γ-Fe_2O_3, vibro-milled, energy storage and liberation 78−83941
GaAs, ion damage, TEM study of laser annealing 80−88215
GaAs shallow junction solar cells damaged by electron irrad., recovery of short cct. current 79−29471
GaAs, Si ion implantation and annealing, damage recovery, surface carrier profile 77−4119
GaAs, sputtered-etched surface, Schottky contact characterisation and its recovery by annealing 79−99603
GaAs:Be, ion implanted, elec. profiling and optical activation expts. 77−89457
p-GaAs:Be, ion implanted, annealing characts., defect cond. profiling, electron diffr. obs. 79−4318
n-GaP:S, Hall effect and resistivity meas. *(Japanese)* 77−39840
Gd, electron irradiated, defect annealing, recovery spectra 79−23648
Ge (111) surface, 500 eV Ar^+ bombard., high temp. annealing, recovery, RHEED obs. 78−87723
Ge, dynamical recovery and self-diffusion 79−82379
Ho, electron irradiated, defect annealing, recovery spectra 79−23648
InSb, high-purity, electron irradiation effects on transport props. 79−23650
KCl:Pb^{2+}, γ-irrad., rel. to props. 78−31262

recovery continued
LiF crystal, gamma irradiated, shear stress depend. on oriented dipoles conc. 79−28013
Lu, electron irradiated, defect annealing, recovery spectra 79−23648
Lu, low-temp. electron-irradiated, recovery 78−6102
Mg-Ag, ion implanted, recovery stage characterisation by electron irrad. 80−107295
Mg-Al-Zn, anelastic creep and recovery 77−63709
MgO, plastically deformed, recovery of internal friction at room temp. *(French)* 78−80577
Mn-Al alloy, vacuum codeposited, disorder of $MnAl_6$ phase in recovery process 78−51854
Mo, desorption of He, during stage III annealing, vacancy model 77−1123
Mo, dislocation structure inhomogeneity in electromachining crater zone, rel. to plastic deform., dynamic recovery *(Russian)* 80−16326
Mo, electron irradiated, recovery studies of pure and radiation doped crystals 79−19280
Mo, neutron irradiated extended low temp. annealing 79−79014
Mo, point defect migration, stage III annealing 77−80548
Mo, rolled single cryst., polygonisation and recrystn., strain depend. *(Russian)* 77−81270
Mo, vacancy recovery stage, radiation doping, elec. resistivity meas. 79−51102
Mo:Xe, BCC, heavy ion implanted, vacancy recovery, Mossbauer spectroscopy 79−82896
Mo-Re(Os)(Ru), recovery after deform. and annealing, destrengthening mechanism *(Russian)* 80−97546
Mo-Zr-B-C, dil. alloy, struct. changes under prolonged high temp. annealing *(Russian)* 78−6944
Mo-Zr-C (0.63, 0.06 wt.%), quenched and deformed, structural changes during heating to ageing temp. *(Russian)* 79−1879
NaCl, plastically deformed, recovery of work hardening *(German)* 77−35626
NaCl, pure and doped, 20K X-ray irradiation, thermolum. and recovery processes 80−93412
NaCl, single crystal, recovery controlled transient creep, substructural obs., phenomenological anal. 77−77526
Nb, dislocation substruct. in deformed and recovered single crystal 77−8897
Nb, high-purity, resistivity recovery following low temp. electron irrad. 77−27909
Nb, isochronal recovery of high energy d-Be neutron damage 78−51592
Nb, mobile interstitials after electron irrad., resistivity recovery meas. 79−55783
Nb, neutron irrad., microvoid form., ang. correl. and yield strength meas., TEM obs. 78−88381
Nb, recovery and recrystallisation, fast neutron irradiation effects 77−70069
Nb, superconductor, neutron irradiation, low temp., effect on critical current 78−52180
Nb-O, Snoek mechanism and long distance diffusion under strain ageing *(French)* 77−81279
Nb-Zr(Nf)(Mo)(W)(Rh), dil., neutron irradiation at 4.6K, influence of impurities on defect prod. 79−55790
NbC_x, reactor irrad. effects on elec. resist. and supercond. props. *(Russian)* 78−47895
Nb_3Ge, neutron irradiated, A15 compound, recovery of T_c by annealing 78−52132
NbO, single cryst. with 25% vacancies, neutron damage 77−15459
Nb_3Sn, highly disordered, elec. resist. and supercond. T_c 78−52142
Nb_3Sn(Al), neutron irradiated, A15 compound, recovery of T_c by annealing 78−52132
Ni alloy IN-738, Y_2O_3 (1.5 wt.%) addition, mechanical alloying 77−40427
Ni and Ni-Co, recovery of single crystal after varying amounts of cold work 79−100162
Ni, cold rolled, influence of impurities on recovery and recrystallisation, positron annihilation meas. 79−15696
Ni, H diffusion in H_2 quenched sample, elec. resist. recovery 78−2299
Ni, laser irrad., elec. cond. recovery *(Russian)* 77−55512
Ni, plastically deformed, recovery stages III and IV investig. by positron annihilation 77−31715
Ni, push-pull fatigued polycrystals, point defects, elec. excess resist. meas. 80−100910
Ni, rolled, dislocation struct. and recovery during annealing *(Russian)* 79−29084
Ni, shock loaded, work softening 78−27537
Ni, thermal softening, influence of alternating mag. field *(Russian)* 78−23312
Ni, US deformation at low temps., elec. resistivity recovery *(Russian)* 79−11656
Ni-Cr-Fe alloy, recovery behaviour after electron irradiation 79−83054
Ni-Cr-W-Mo-Ti-Al, heat-resist., recovery and recrystn. 80−76268
Ni-ZrO_2, dispersed inclusions, effect on recovery and recrystallisation 77−25064
Pb, charged particle irrad., damage and recovery processes 77−69002
Pb, electron irradiation at 4.7K and below 3K, annealing expts. 77−11595
Pb, strain hardening and recovery during primary creep 78−39799
Pb-Cu, charged particle irrad., damage and recovery processes 77−69002
Pb-Sn, directionally solidified lamellar eutectic, deform. induced microstruct. instability 77−32623
Pd-Fe, dil., plastically deformed, positron annihilation study of recovery of crystal, imperfections *(German)* 77−85835
$Pd_{77.5}Si_{16.5}Cu_6$ amorphous, indentation recovery, defect struct. produced by deformation 79−43275
Pt, deuteron irrad., energy release and resist. recovery, self-interstitial-atom interaction energies 79−95002
Pt, electron and deuteron irrad., close Frenkel pair recomb. during annealing 78−87716
Pt, isochronal recovery of high energy d-Be neutron damage 78−51592
Pt, point defect properties, damage curve anal. 78−47359
Pt, radiation damage, recovery of elec. resist., interstitial migration and clustering 77−11604
Pt, radiation damage recovery curves, evidence for two self-interstitial configs. 77−7773
Pt, recovery of thermal-neutron-irradiated samples 78−95081
Pt, recovery spectrum after thermal neutron irrad., resist. obs., Au addition effect and defect conc. depend. 80−65057

recovery continued
Pt wire, cold worked, recovery of elec. resist. 77−12643
Pt-Au, ion-irradiated, self-interstitial migration in stage II recovery, FIM obs. 77−59140
Pt(Au), ion irradiated alloys, stage II recovery 78−47440
Se, single crystals, fast neutron irradiated, annealing expts., dark conductance, reflectivity spectra 77−85266
Si (111) surface, 500 eV Ar^+ bombard., high temp. annealing, recovery, RHEED obs. 78−87723
Si, B implanted layers, damage obs. by X-ray double refl. 77−15463
Si, dynamical recovery and self-diffusion 79−82379
n-Si, influence of deform. on capture of electrons by divacancies 77−1449
Si, ion damage TEM study of laser annealing 80−88215
Si, laser pulse train shaping for polycrystal recovery in self-ion implanted samples 79−47555
p-Si radiation defects due to 30 MeV proton irrad., rel. to solar energy convertors 78−71776
Si:As, laser annealing, channelling, optical obs., and resist. meas. 79−1444
Si:Bi, ion implanted, channelling obs. of pulsed Q-switched ruby laser annealing 80−59542
p-Si:P, annealing behaviour, recovery, surface carrier density and Hall mobility meas. 77−32012
Si:P, implantation damage of channelled P ions, elec. activity recovery stages 77−59034
Sn plate, quality evaluation method using elasticity characts. 77−52582
steel, 36NKhTYu, aged, rate of discontinuous precipitation of γ'-phase, short high-temp. treatments *(Russian)* 78−11226
steel, Nb, deform., recrystn. and precip. interaction 80−97515
Ta, deformed at 4.2K, electrical resistivity recovery spectrum, stage III 77−8895
Ta, rolled single crystal, recovery and recrystallization 80−3093
Ta, vacancy formation and migration energies, positron annihilation meas. 77−84739
Ta:H, recovery after cold working at 4.2K, resist. meas. 79−4977
Ta:Xe, BCC, heavy ion implanted, vacancy recovery, Mossbauer spectroscopy 79−82896
Ta-T(D), diffusion and resistivity at low temps. 78−14511
Tb, electron irradiated, defect annealing, recovery spectra 79−23648
Te, electron irrad., mobility increase due to defect prod. 80−24501
Ti, industrial grade structural changes during polygonization *(Russian)* 78−19779
Ti, neutron irradiated, relation between microstructure and recovery behaviour 77−15456
Ti, rolling and recrystallisation texture formation *(Russian)* 77−59802
Ti sheet, anisotropy and texture, effect of plastic deform., recovery and recrystallisation *(Russian)* 77−8850
Ti-Mo-Zr-Sn (11.5, 6, 4.5 wt.%), metastable beta III phase, recrystallization and grain growth 80−3091
Ti-Mo-Zr-Sn-Fe-C-Si alloy, β-III, cold deform. and annealing, effect on struct. and mech. props. *(Russian)* 79−24533
Ti-Ni, effect of alloying on crit. points and martensitic transform. hysteresis 80−20935
Ti-Ni-Cu (44.5, 10 wt%), opposing stress effect on shape memory and martensitic reversion 78−44185
Tm, electron irradiated, defect annealing, recovery spectra 79−23648
UC, quenched-in defects, formation, migration and resistivity 80−64990
UCN, quenched-in defects, formation, migration and resistivity 80−64990
UO_2, irradiation induced lattice defects 78−33251
UO_2, isothermal crack healing and strength recovery, thermal shock effects 77−36625
UO_2, neutron irradiated, thermal recovery of defects 79−45348
UO_2, quenched and neutron irrad., recovery processes, vacancy migration 77−28048
UO_2, strength recovery and crack healing 77−8918
V, superconductor, neutron irradiation, low temp., effect on critical current 78−52180
V_3Si, neutron irradiated, A15 compound, recovery of T_c by annealing 78−52132
W and W alloys, ion-irradiated, recovery behaviour studied by field ion microscope 80−29074
W, defect recovery following neutron irrad., annealing effect 79−77642
W, electron irradiated, recovery of resistivity, 4.5-380K *(German)* 78−87714
W, Frenkel pair creation and stage I recovery of electron irrad. cryst. near threshold 79−1463
W, neutron irrad., at thermal energies, annealing exam. of recovery 78−47355
W, neutron irrad., recovery of defects, isochronal and isothermal annealing 79−46712
W, polygonisation critical stage in single crystals deformed in compression 79−4979
W, structural defect recovery after irradiation and cold work 78−47429
W, thermal neutron irradiated, recovery processes 80−19848
W, vacancy recovery stage, radiation doping, elec. resistivity meas. 79−51102
W, vacancy-defect clustering, due to annealing and quenching, TEM and elec. cond. exam. 78−47344
W:Xe, BCC, heavy ion implanted, vacancy recovery, Mossbauer spectroscopy 79−82896
Zn, 6.1 MeV α-particle irrad., stage III and IV recovery kinetics, defect diffusion 77−76474
Zn, defect recovery after low temp. electron irrad. 78−10090
Zn, neutron irradiated, recovery of c-axis spacing and elec. resist. 80−34081
Zn, recovery after 6.1 MeV α-particle irradiation at 4.2K 78−47441
Zn, thermal recovery and stress-strain relations 78−11266
Zr, rolling and recrystallisation texture formation *(Russian)* 77−59802
α-Zr, vacancy recovery following 1.5 MeV electron irrad., positron annihilation meas. 77−47485
Zr-Al(8.6 wt.%), neutron irradiated, irradiation growth and recovery, annealing 80−15162
Zr-O-N system, struct. and plastic deform. *(Russian)* 78−80588

recovery-creep
concrete, creep during drying and wetting 79−52319
cyclic heating and loading, recovery-creep theory 77−19551
dispersion-strengthened alloys, threshold stress for creep 80−93626

recovery-creep continued
high temperature, screw dislocation cross-slip and edge dislocation climb processes 77−19965
ice, dislocation creep, creep deform. predictions 78−19815
LDPE melt, nonlinear shear creep and constrained elastic recovery 78−87318
metal creep, deform. struct. modeling, compatibility conditions *(Russian)* 78−13924
microscopic models, stress drop test interpretation during creep 77−75814
non-metallic materials dislocation creep, creep deform. predictions 78−19815
PMMA, modified with dibutyl phthalate, mech. and optical props. *(Polish)* 77−52423
polyethylenes, linear, ultra-high modulus, tensile creep, recovery 78−95784
polymers, structural, creep and recovery under hydrostatic compression in programmed loading 80−100881
polyolefins, ultra-high modulus, production by tensile drawing and hydrostatic extrusion 80−81022
polypropylene, nonlinear viscoelastic effects 77−90401
polystyrene-tricresyl phosphate solns., viscoelastic props., conc. depend. 80−76299
polythene, ultraoriented, microhardness, extrusion conditions effect 80−50704
pure materials, model 77−75815
steel, austenitic, creep exposure, partial recovery of mech. props. by subsequent annealing *(German)* 77−59886
steel, stainless, creep test at elevated temps., based on state variable theory 79−61687
steel, stainless, Kh18N10T, creep strain recovery during cyclic stress changes 79−43354
Al-Zn(11 wt.%), dynamic recovery during and after steady state deform. 77−1842
$Al_{20}Cu_{25}Zr_{55}$ metallic glass, inelastic deform., free energy spectra 80−71699
Al_2O_3, dislocation creep, creep deform. predictions 78−19815
Cu, creep stimulated by interrupted loading 79−74213
Cu single crystals, dispersion strengthened, low temp. recovery of work-hardening and creep 79−83211
Cu-Cd (1 wt.%), creep stimulated by interrupted loading 79−74213
Cu-Ni (10 at.%), hardening, recovery, and struct. changes during high temp. creep *(Russian)* 80−89288
Cu-SiO_2, low-temp. recovery creep, Orowan loop accumulation 80−81126
Cu_2O, high-temperature investig. of recovery creep, 700 to 1000°C *(French)* 77−72650
$Cu_{40}Z_{60}$, $Cu_{56}Zr_{44}$, and $Cu_{60}Zr_{40}$ metallic glass, inelastic deform., free energy spectra 80−71699
Fe-Mo (1.8 at.%), recovery creep theory estimation using high temp. creep data 79−15747
LiF, dislocation creep, creep deform. predictions 78−19815
MgO, dislocation creep, creep deform. deformations 78−19815
Ni alloys, creep transients, friction stress and recovery, dislocation substruct. 80−60933
Pb, work hardening, and recovery rates during steady state deformation, temp. and stress effect 80−45319
$Pd_{80}Si_{20}$ metallic glass, inelastic deform., free energy spectra 80−71699
α-Pu, internal stresses during deform. of fine and coarse grained specimens 77−28880
Si, self-diffusion and dynamical recovery at high temps. 79−69284
Si, single crystals, dynamical recovery and self-diffusion 78−87816
Si_3N_4, hot-pressed, creep and strain recovery 80−100874
Si_3N_4, hot-pressed, viscoelastic strain recovery obs. 79−79042
Si_3N_4-MgO, compressive creep, source of viscoelastic effect 80−50675
UO_2, dislocation creep, creep deform. predictions 78−19815
V_3Si single cryst., creep deform. 80−71695
Zn, creep in temp. range of dynamic recovery *(Russian)* 77−81294
Zr-Nb (1 wt.%), stress drop expt. during creep 79−29152

recrystallisation
microstructural processes and features only
see also recrystallisation annealing; recrystallisation texture
alloy, austenitic, mechanical changes after electrolytic quenching *(Russian)* 80−50653
alloy, two-phase, recrystallisation mechanisms 79−47708
annealing twin form., statistical anal. *(French)* 77−81281
Astroloy, grain coarsening by critical strain annealing 79−47711
austenitic stainless steel, recrystallisation transformation energies, α' to γ, effect of Si content and deformation by rolling *(French)* 77−48433
austenitic steel, 45G17Yu3, structure and loss of strength after hot deform. by rolling *(Russian)* 78−39794
austenitic steel, mechanical properties, effect of high temp. thermomechanical treatment and post-deform. ageing *(Russian)* 78−39809
Babbitt grade Bk-2Sh, improvement in antifriction layer props. by impulse discharge *(Russian)* 79−1917
biotite, deform. and recrystallisation in Woodroffe Thrust mylonite zone 80−21739
bone tissue crystals, effect of compression 77−25492
brass, α and $\alpha+\beta$ type, positron annihilation, short-range order, clustering and lattice defects influence 79−29107
brass, plastic props., room temp. to recrystallization temp., stress-strain relations, computer program 77−1865
brass, recrystallization during induction heating 80−97511
α-brass, texture, recrystallised orientation distrib. function comparison with 40°⟨111⟩ rolling texture 80−25723
α-brass sheet, shear bands and recrystallisation 79−91680
camphor, rhombohedral, polycryst., compressive deform. and dynamic recrystn. 80−71698
cell wall and lattice misorientation origin during deform. 80−71712
conference, Leeds, England, (April 1978) 79−47706
crack tip, plastic deform., metallographic anal. by recrystn. 80−85029
crack tip strain distribution measurement by recrystn. *(German, English)* 77−56203
disilicate, piezoelectric glass ceramic, recrystallisation, pyroelectric response, permittivity 80−80703
dislocation behaviour at advancing grain boundary during recrystallisation 77−7734
dislocation elimination by recrystallisation *(German)* 78−51559
disperse particles concentration and spacings between them in Poisson point field model 78−39963

recrystallisation continued
dry sliding wear, role of dynamic recrystallisation 80−108599
Duralumin 2017, superplasticity *(Korean)* 79−38902
dynamic recrystallisation diagrams *(German)* 80−25729
dynamic recrystallisation model *(German)* 77−4792
electron microscopic observation of recrystallisation *(Hungarian)* 79−56987
feldspars, chemical changes and recrystallisation rel. to superplastic flow 79−79831
films, vac. deposited two-layer, thermal strength, recrystn. influence 79−87748
foil, recrystn. during heating in column of electron microscope *(Russian)* 78−48421
glassy materials in steep, thermal gradients, apparatus for phase transform. 78−84767
grain boundary motion 80−103449
grain size and orientation, appl. of X-ray synchrotron topography to recrystallisation studies 78−35610
heat-resisting alloys, VM-1 and VX-4, thermal fatigue rel. to struct. changes *(Russian)* 78−11302
induced, in thin metal plates *(German)* 78−19783
kinetics, system of eqns. 78−22650
low C steel, explosive-thermal treatment, sulphide cracking decrease, hydrogen embrittlement *(Russian)* 80−108477
martensite, rel. to struct. transforms. during deform. *(Russian)* 77−16606
metal, FCC, low stacking fault energy, nucleation phenomena 79−90681
metal, oxidation kinetics, effects of control of scale structure 77−16751
metals, FCC, deformed single crysts., struct. evolution at heating 80−103337
metals, grain struct. form. during two-dimensional recrystallisation, simulation on electronic calc. machine *(Russian)* 79−87666
metals, recrystallisation during hot deform. 78−68714
mylonites, grainsize reduction and grain boundary sliding rel. to flow strength 80−21721
notched flat tensile specimens, deform. zone *(German, English)* 78−64603
nucleation, criterion for dynamic recrystallisation during hot working 78−52852
nucleation, finely dispersed second-phase particles effect 77−8845
nucleation, model for strain induced grain boundary migration 79−46675
olivine dynamic recrystallisation, applicability limits of grain size geopiezometer 78−85715
photographic emulsion grains, latent image distrib., etching and recrystn. effects of solns. 80−77890
plastically deformed metal, positron annihilation *(German)* 77−70252
1,4-cis-polybutadiene, stereoregular, recrystn. in partial melting temp. region *(Russian)* 80−6495
polycrystalline film, singularities of recrystallisation *(Russian)* 78−2382
polycrystalline film couples, diffusion during recrystn., numerical simulation 79−77844
polyethylene, high press. phase, US, DTA, and X-ray diffr. study 80−75188
polyethylene, highly oriented fibre composite, self-hardening, tensile props. 77−55939
polyethylene, mol. conformations after recrystallisation or annealing at high press. 77−88612
polyethylene terephthalate, mech. props., influence of cryst. arrangement and noncryst. region struct. 78−76707
polymer, recrystallisation during drawing 78−76658
polymeric cryoprotectants in preservation of biological ultrastruct., aq. soln. low temp. states 78−65157
polytetramethylene terephthalate, injection-moulded, struct. depend. of fracture behaviour 77−8912
porous materials and ceramics, survey 78−76660
positron annihilation, appl. to determ. of volume fraction of recrystallised material 77−1760
primary, one dimension, model considerations, nuclei start to grow simultaneously, with same rate *(German)* 79−29094
quartz, twinned crystals, after Japan Law, investigation of regrowth 80−54162
quartz in Moine thrust zone, recrystallisation rel. to differential stress 80−85652
recovery *(Czech)* 79−70081
recovery recrystallisation and grain growth in materials, conf., Chicago, USA (Oct. 1977) 79−97122
review 77−4790
rolling, critical reduction, effect on chemicothermal treatment processes 77−70073
steel; low alloy, high strength, hot compression dynamic precip. and coarsening of Nb(CN) 80−97514
steel, 45G17Yu3, deformed, influence of hot rolling on struct. *(Russian)* 77−25073
steel, Al killed, cold rolled and recrystallised grain shape anisotropy 79−34064
steel, alloy, high speed, type R18, hot deformation and recrystn. 80−16391
steel, alloy type 25KhN3MFA, tempering of bainitic structure 80−20983
steel, austenite hot deformation influence on phase transformations 80−7606
steel, austenitic, 45Kh2N12GS, post deformation holding at deform. temp. effect on struct. and strength of austenite and martensite *(Russian)* 79−1880
steel, austenitic, Cr-Ni (18,12 wt.%), containing coarse grain boundary precipitates, thermomechanical treatment 78−27545
steel, austenitic, Cr-Ni (25, 20 wt.%) recrystallisation and sigma phase formation 80−35211
steel, austenitic, dislocation structural changes on hot rolling *(Russian)* 77−59805
steel, austenitic, explosive-thermal treatment, sulphide cracking decrease, hydrogen embrittlement *(Russian)* 80−108477
steel, austenitic, high-speed, austenite grain growth, W addition effects 79−20085
steel, austenitic, low C, struct. charact. of dynamic recrystallisation *(Czech)* 77−59813
steel, austenitic, Nb modified, HSLA, interaction between recrystallisation and precipitation during high temp. determ. 79−100187
steel, austenitic stainless, 08Kh18N10T, hot-worked precipitation kinetics and struct. of dispersed phases, Ti effect 80−29964
recrystallisation continued
steel, austenitic stainless, AISI 316 L, viscoplastic deformation under hot working conditions, struct. model 79−83278
steel, austenitic stainless, dynamic recrystallization kinetics 79−47731
steel, austenitic stainless, ferritic, prep. with fine grains by cold rolling and recrystallisation, superplasticity *(French)* 78−35406
steel, austenitic stainless, grain boundary struct. changes during initial stages of recrystallisation 77−36559
steel, austenitic stainless, grain boundary struct. during recrystn. and grain growth 80−76270
steel, austenitic stainless, plastically deformed, TEM obs. *(French)* 77−44302
steel, austenitic stainless, recrystallisation, TEM obs. *(Japanese)* 79−52269
steel, austenitic stainless, recrystallization after hot rolling 79−47734
steel, austenitic stainless, supersaturated, recrystallisation 77−77506
steel, austenitic stainless *(Japanese)* 77−52346
steel, B-Si, grain-oriented, high induction, Cu impurity effects 80−89366
steel, C, austenitic, recrystallisation and grain growth obs. with photoelectron microscope 79−47730
steel, C-Mn-Nb, Nb microalloying, weldable, structural, recrystallization and precipitation induced by high temp. deform. *(French)* 79−61632
steel, cold-formed, low pearlite, Nb alloyed, Nb effects, precipitation, recrystallisation *(German)* 77−8832
steel, comp. and processing effects on microstruct. and props. rel. to low temp. applic. 77−52365
steel, Cr, phase transform., effect of high temp. plastic deform. *(Slovak)* 78−19837
steel, Cr-Mo and Cr-Ni-Mo, V effects on recrystallisation *(Russian)* 77−66654
steel, Cr-Ni (16,14 wt.%), Si effect on texture, grain growth after rolling or recrystallisation *(French)* 77−55986
steel, Cr-Ni-Mo-V, austenite form. during heating, influence of recrystn. during tempering *(Russian)* 80−104188
steel, deformation under modified ausforming *(Japanese)* 79−11673
steel, electric sheet, hot-rolled, recrystallization and texture formation during ht. treatment 77−44271
steel, extra-mild rimming, thin sheet, grain growth in the recrystallisation *(French)* 79−70074
steel, Hadfield, cast and crystallised, deform. resist. of grain boundaries *(Russian)* 77−21216
steel, high speed R6M5, secondary inheritance investigation by austenite recrystallisation 77−90367
steel, HSLA, V and N effect on recovery and recrystn. during and after hot working 80−84973
steel, hypoeutectoid, C22, recrystn., influence of carbides distrib. *(German)* 79−38850
steel, hypoeutectoid, recrystn. initiation, carbide particle size effect 77−12641
steel, law-C, hot deform., austenite strengthening and weakening 80−76282
steel, low alloy, hot deform. behaviour and modified ausforming *(Japanese)* 78−11244
steel, low C, capped, cold rolled sheet, deep drawability, effect of carbide size, cold reduction annealing 78−64559
steel, low C, cold rolled and recrystallised, containing Nb(CN) dispersion, struct. and textural aspect of deform. 79−47712
steel, low C, cold rolled sheet, Cu effect on recrystallization texture *(Chinese)* 79−74173
steel, low C, Mn, recrystallisation and grain growth in hot rolling 79−47714
steel, low C, Mn effect on recrystallisation and texture *(French)* 80−3110
steel, low C, quenched, struct. and props. after plastic deform. and tempering 78−23734
steel, low C, rolling deform., effect on NbC particle size distrib. 79−47717
steel, low-alloy, recrystallisation after hot deformation 77−44268
steel, low-C, Cr, ferritic, optimal heat treatment development 79−38869
steel, low-C, with Nb-B addition, transform. characts. and mech. props. *(French)* 79−43253
steel, maraging, structural recrystallisation, alloying element effects 77−70080
steel, martensitic, Cr-Ni, grain refining and phase transforms. effect on plasticity *(Russian)* 78−39837
steel, microalloy V-Nb, V, Nb effects on strength and formability of cold rolled sheets 77−55979
steel, microalloyed, hot-rolled, Nb(C,N) precip. and austenite recrystn. 80−97513
steel, microalloyed, recrystallisation, precipitation effect 79−47695
steel, mild, plastic deform. around fatigue cracks, X-ray microbeam and recrystn. studies 80−35258
steel, mild, sheet, with low Al content, annealing, AlN recrystn., precipitation kinetics *(French)* 79−20083
steel, multilayered with types St2kp and 10Kh18N10T, secondary recrystallisation props. *(Russian)* 80−66533
steel, N_2 effect on grain boundary migration rate during secondary recrystallisation *(Czech)* 77−59812
steel, Nb,(V),(Al), hot-rolling, laboratory simulation, recrystn. of austenite 80−97512
steel, Nb-V, cold rolled, HSLA, prod. by precipitation hardening, annealing 78−88471
steel, Ni and W, recrystallisation mech. during laser treatment 80−50658
steel, Ni-Co-Mo-Ti, hot formed, recrystallization and grain boundary precipitation effect on mech. props. *(German)* 79−66073
steel, pearlitic, struct. variations under plastic strain and subsequent heating, cementite decomp. *(Russian)* 80−84954
steel, plastic props., room temp. to recrystallisation temp., stress-strain relations, computer program 77−1865
steel, ShKh15, carbide particle size and pearlite grain size changes *(Russian)* 78−6946
steel, Si, textured, alloying addition inhibition effects on grain orientation and growth *(Japanese)* 79−43270
steel, Si (3 wt.%), hot rolled, effect of initial texture on secondary recrystallisation *(Czech)* 79−91711
steel, Si (3 wt.%), struct. and preferred orientation, annealing parameters influence *(Czech)* 80−89248
steel, Si (3 wt.%), textured, secondary recrystn., precip. annealing effect *(Japanese)* 80−71662
steel, Si-P-C, low C, varying Si content, cold rolled annealing 80−3090

recrystallisation continued
steel, stainless, 304, deformed in torsion, annealed, static recrystallization and restoration after hot deform. 79−47735
steel, stainless, ferritic, corrosion resistance improvement by Mo and Ti additions 77−90505
steel, stainless, ferritic Ti stabilised, changes in structure and mech. props., after alkali bath etching *(Russian)* 79−29271
steel, stainless, hot rolled texture, effect on cold rolled and annealed textures *(Japanese)* 78−48425
steel, stainless, Kh18N10T, substructure after high-temp. thermomechanical treatment with high deformation rates *(Russian)* 78−76657
steel, stainless, microduplex, austenite/ferrite, recrystallisation, annealing and cold work effects 79−47713
steel, stainless 304, recrystallisation, effect of dislocation structure 77−32595
steel, stainless recrystallisation of thin bands, heating time investig. 79−38848
steel, stainless type XM-19, influence of recrystn. behaviour on mech. props. 79−83213
steel, structural, CrN-modified, tempering and quenching effects on struct. and props. 77−59835
steel, structural inheritance characts., X-ray and internal friction obs. 79−57017
steel, structural mechanism of recrystallisation during ht. treatment 78−84847
steel, structural recrystallisation, phase and struct. transformations during heating 77−55990
steel, tempering effect on struct. and mech. props. of types 70, U8, and U12 *(Russian)* 80−50655
steel, thermomechanical treatment effect on mech. props. and microstruct. *(French, German)* 79−66090
steel, type 20Kh deformed, austenite grain size, inheritance effect with quenching and tempering 80−60881
steel, type 34Cr4, post-hotforming recrystallisation condition, use of NEOPHOT 2 and EPIQUANT 80−84949
steel austenite, recrystallisation diagrams, heating, plastic deform. rel. to struct. 79−20067
steel austenitic Cr-Ni-Be, cellular precipitation *(Japanese)* 78−11229
steel fibre reinforced Ag, exam. of recrystallisation behaviour *(German)* 78−84849
steels, C, cold worked and recrystallised, attenuation behaviour *(German)* 78−48445
steels, hot forming property and struct. *(German)* 80−25730
steels 4Kh4VMFSSh and 45Kh3V3MFSSh, grain size, hot deform. and austenitising effects 80−76286
structural changes in single crystal under single electric impulse discharge *(Russian)* 79−65086
supercooled, struct. refinement mech. *(Russian)* 80−20975
TCNQ complex formed from cation (methyl-l-N-ethyl benzimidazolium)$^+$ conductivity transition 80−10954
textured sheet, grain orientation during secondary recrystallisation 79−34063
TGS:Cr single cryst., lattice defect influence on critical behaviour 80−25315
thermally induced structural changes, specimen surface influence 80−103559
thermoelectric recrystallisation, epitaxial film growth rate 80−100424
TNT, creamed, dimensional stability, irreversible thermal expansion 79−73316
vacancy adsorption on internal boundaries, rel. to recrystalln. and precip. 78−10084
weightless zone recrystallization, stability of a singly connected molten zone 79−78874
zinc oxalate, isothermal crystallisation from soln. 80−108336
AG, wear, recrystallisation as controlling process, FCC metal 77−56117
Ag, Bordoni effect during recrystallisation 77−90388
Ag contacts on InP, TEM obs. of struct. 77−62765
Ag epitaxial films, grain boundary struct. evolution during recrystn., interface energy effect *(Russian)* 80−15387
Ag epitaxial growth, on W-ribbon substrate, in UHV, cryst. orientation determ. by etching *(German)* 79−65994
Ag, FCC, low stacking fault energy, nucleation phenomena 79−90681
Ag, grain growth in strained {110}<112> low stacking fault FCC crystals after artificial nucleation 79−91722
Ag, high purity, nucleation and twinning during recrystallization, TEM study 79−29082
Ag, rolled single crystal with defined solute content, stored energy and recrystallization temp. 79−96037
Ag, tensile deformed, dynamic recrystn. *(German)* 80−84959
Ag vacuum condensates, on Cu substrate, struct. and substruct *(Russian)* 79−73412
Ag, vacuum deposited on Al substrate, recrystallisation 78−60044
Ag, vacuum-condensed film, structural changes under glow discharge *(Russian)* 79−15852
Ag-Ni, two ductile phase alloy, exam. of softening behaviour after cold rolling 78−72847
Ag-Pd alloy, investigation of recrystallisation process, for use as wire-spring relay contact material 79−52278
Ag-Sn, dil., high perfection single cryst. growth, strain-anneal technique 78−44010
Al alloy, dil., recrystallisation during hot rolling 79−47732
Al alloy, recrystallisation during hot deform. and after cold working 79−47715
Al alloys, thermomech. treatments, effects on microstruct. 80−100858
Al, annealing of lightly deformed samples, effect of press. *(Russian)* 78−39795
Al bronze, O free, annealing in photoemission electron microscope, twin density recrystallised grain size relation *(German)* 78−52850
Al, cold rolled, commercial purity, initial stages of recrystallisation, TEM obs. 79−56999
Al, compressed, nucleation and recrystallisation study by electron microscopy and Kikuchi diffr. 79−52236
Al, deformed, nucleation and recrystallisation at second phase particles 78−6941
Al, deformed, struct. and recrystallisation transmission Kossel diffr. obs. 77−52340
Al, elongated, deformation and recrystallisation, Rowland transform. model *(French)* 77−77498
Al, elongated, deformed, recrystallisation, orientation relations, hard-sphere model for Rowland transform. *(French)* 77−77497

recrystallisation continued
Al epitaxial films, grain boundary struct. evolution during recrystn., interface energy effect *(Russian)* 80−15387
Al, high purity, development of rolling and recrystallisation textures 77−25070
Al, large perfect single crystal preparation by isothermic recrystallisation after small deform. *(Czech)* 77−63688
Al, plastic props., room temp. to recrystallisation temp., stress/strain relations, computer program 77−1865
Al, polycrystalline, synchrotron X-ray topography dynamic expts. 78−67621
Al, pure, Bordoni effect during recrystallisation 77−90388
Al, recovery and recrystallisation during temperature strain *(Czech)* 77−73287
Al, recrystallisation and recovery during temperature strain *(Czech)* 77−70071
Al, recrystallisation kinetics after small deform. and grain growth *(Czechoslovakian)* 77−32592
Al, recrystallisation nuclei form. and well defined deform. band struct. 79−20136
Al, rolled single crystal, annealing texture 79−91678
Al sheet, recrystallization, DSC eval. 80−3105
Al, single crysts., misfit recrystn. dislocations formation study during recrystn. by X-ray synchrotron topography 79−38849
Al, subgrain coalescence, grain boundary recrystallisation nucleation 80−3094
Al substitutional solid solution alloys, volumetric effect and props. *(Russian)* 80−39293
Al, substruct. developed during recrystallisation, exam. *(Japanese)* 78−64566
Al, tensile deformed single crystal, form. of recrystallisation textures 77−12647
Al, thermal desorption of oxide film, influence of grain boundaries and recrystn. 80−61023
Al, vacuum-condensed film, structural changes under glow discharge *(Russian)* 79−15852
Al, wear, recrystallisation as controlling process, FCC metals 77−56117
Al wire, hot and cold deformation drawing strengthened, thermal EMF study *(Russian)* 80−54674
Al-(Mg)(Fe), pure (dilute), large wire drawing plastic deform. 80−108508
Al-Al_2O_3, recrystallisation nucleation in drawn wires, optical and TEM obs. 79−47709
Al-Cr(Zr), simultaneous recrystallisation and precipitation *(French)* 80−16313
Al-Cu, stir cast microstructure, turbulent flow and solidification 79−20036
Al-Cu-Zr, superplastic alloy Supral, solidification and recrystallisation 80−7550
Al-Cu-Zr (6, 0.3 wt.%), superplastic, texture studies 79−83210
Al-Li, dil. alloy, cold-worked, annealing spectrum 78−39801
Al-Li-Mn (2.8, 0.3 wt.%), recrystallised sheet, fracture behaviour, SEM and TEM study 80−97566
Al-Mg-Li-Zr alloys, struct., mech. props. 79−24498
Al-Mg-Si, deformed, orientation of recrystallisation nuclei 79−91681
Al-Mg-Si, effect of quenching on recrystn. after hot working 79−43289
Al-Mg-Si rod, extruded and cold drawn, annealing *(German)* 78−39804
Al-Mn, cooling after recrystallisation, phase transform., X-ray and thermal anal. *(Russian)* 77−66663
Al-Mn (1 wt.%), commercial, recrystallisation 79−47710
Al-Mn (1.8 wt.%), cold-rolled, precipitation and recrystallisation 78−27540
Al-Mn-Si, recrystallisation and precipitation 78−52824
Al-Mn-Zr (0.9, 0.4%), strain induced continuous recrystn., rel. to superplastic behaviour 78−84915
Al-Mn(Cr), quenched, thermal stability *(Russian)* 80−20976
Al-Pb alloys, with isolated liq. phase inclusions, recrystn. *(Russian)* 80−20970
Al-Sn dil. alloy, cube orientation texture development 79−96040
Al-Zn, plastic deform. effect on struct. transform. at elev. temp. *(Czech)* 79−79044
Al-Zn alloys, recrystallisation and superplasticity, HVEM straining 80−39207
Al-Zn-Mg, polygonized struct. in extrusions, thermal stability and mech. props. 80−50659
Al-Zn-Mg-Cu (6,2, xwt.%) type alloy, fatigue crack propag., Cu content and recryst. effect 80−60960
Al-Zn-Mg-Cu type 7XXX, Cu effect and recrystallisation, low cycle corrosion fatigue 79−91852
$Al_xGa_{1-x}As$ DH laser material, Ar laser induced catastrophic damage 79−86178
AlN powder, plasma synthesized, sintering behaviour, props. and struct. 79−100097
$As_x(S,Se)_{1-x}$, chalcogenide, covalent non crystalline topology, short range order 80−15009
Au epitaxial films, grain boundary struct. evolution during recrystn., interface energy effect *(Russian)* 80−15387
Au on oxidised Si with metal adhesion layer, ageing props. 77−11820
Au-Cu-Zn-Ni (13, 3.4, 8.5 wt.%), white gold, metallographic structure after cold rolling, effect of heat treatment, recrystallisation *(French)* 79−52238
Au-Fe, polygonisation, recrystallisation, precipitation microstruct. without external plastic deform. 79−43276
BC, sintered, struct. and props. 80−104181
BaO-Fe_2O_3 system, splat cooled phases struct., magnetisation and susceptibility 300-1100K *(French)* 77−48017
BaO.$2SiO_2$, glass, spherulitic growth and recrystallisation 77−4046
Be bronze BrB2, quenched deformed, substruct. and props., effect of prerecrystallisation annealing *(Russian)* 78−60677
Be, phase struct. *(Russian)* 78−15401
Be, rolled ingot, with duplex microstruct., basal texture of two grain size distrib. 77−36556
Be, ultra fine-grained, recrystn. after deform. 79−52239
$Bi_3B_5O_{12}$, crystal growth from melt, exam. of growth kinetics 78−72717
α-brass, defect removal, obs. by positron annihilation 78−84677
C fibre, Ni coated, high-temp. compatibility 78−19829
CaF_2, hot forged, laser window material, fabrication, props. 77−46773
CaF_2, laser windows, intermediate temp. forging 77−46775
$Ca_{10}(PO_4)_6(OH)_2$, hydroxyapatite, prep. by hydrotherm. recrystn. 79−33913
$CdGeAs_2$, amorphous, thermal gradient expts., recrystn. 80−55438

recrystallisation continued
CdGeAsMn$_x$ glass, recrystallisation 80−44133
$Cd_{0.2}Hg_{0.8}Te$ recrystallisation for supercooled IR detector production *(German)* 80−86403
$Cd_xHg_{1-x}Te$, cast-recrystallise-anneal growth 79−91578
CdS, effect of halide (NaCl, $CdCl_2$, $CdBr_2$, CdI_2) and polysulphide (Na_2S_x, K_2S_x) on recrystn. 78−11171
CdS film, cryst. and electronic surface struct., stimulated recrystn. effects 79−78151
CdS film, doping and recrystn. effect on photocurrent relax. time. 77−4409
CdS thin layers, recryst. from CdS-Cr_2O_3 mixtures, phys. and photoelec. props. 80−96935
CdS:Ag, vacuum deposited film, recrystn. by H_2S heat treatment 80−34328
CdS:Cu(Cl), thin layer, electron pulse induced cond. relax. 80−2501
CdS-based phosphor, microstruct. and luminesc. efficiency 78−10959
CdS_xTe_{1-x}, recryst. from CdS_xTe_{1-x}-Cr_2O_3 mixtures, photocond. props. 80−96936
CdSb single crystals, surface layer melting and recrystallisation due to laser irradiation *(Ukrainian)* 79−46699
CdSe, effect of halide (NaCl, $CdCl_2$, $CdBr_2$, CdI_2) and polysulphide (Na_2S_x, K_2S_x) on recrystn. 78−11171
CdSe film, as-deposited and recrystallised, struct. and fund. optical absorpt. 77−1753
CdSe film, stimulated recrystallisation 77−4272
CdSe film, stimulated recrystn. influence on photocond. 77−43754
CdTe film formation on glass substrates, influence of sublayers of recrystn. stimulators 77−43455
Co, recrystallisation kinetics, deform. degree effects *(Russian)* 78−6943
Co-W alloy electrolytic coatings, heat treatment effects on coercivity, hysteresis and structure *(Russian)* 80−60381
Cu alloy, mobility of boundaries, transition metal addition effects *(Russian)* 77−21160
Cu, annealing of lightly deformed samples, effect of press. *(Russian)* 78−39795
Cu, cold rolling, mechanical props., ageing, annealing, recrystallisation, plastic strain *(Russian)* 80−35202
Cu, cold work, P effect on annealing 79−47707
Cu, continuously cast, O free, effect of nonmetallic inclusion on microstruct. and props. 77−81280
Cu crystals, two-phase, recrystn. retardation, particle size, spacing effects 80−89242
Cu, cyclic torsional deform. at high deform. amplitudes *(German)* 79−87701
Cu, defect removal, obs. by positron annihilation 78−84677
Cu, deformed by rolling and torsion, stored energy *(German)* 79−29160
Cu film, electrodeposited, recrystallisation kinetics, X-ray scatt. *(Russian)* 78−60045
Cu film, oxidised, recrystn. during vac. annealing 77−12738
Cu, foil recrystallisation during annealing in high voltage electron microscope, grain growth *(Russian)* 79−100159
Cu, foils, faulted defect formation by moving boundaries 80−107281
Cu, fragmentation and dynamic recrystallisation after heavy and very heavy deform. *(Russian)* 78−39793
Cu, grain growth in strained {110}<112> low stacking fault FCC crystals after artificial nucleation 79−91722
Cu, grain growth rate, 520-970°C *(Russian)* 80−29972
Cu, grain refinement of dynamic recrystallisation during hot working *(Japanese)* 77−52345
Cu, heavily drawn ETP wire, secondary recrystallisation 77−36537
Cu, high purity, recrystallisation kinetics *(Russian)* 78−11238
Cu, hot forged powder compact 77−24981
Cu, O free, annealing in photoemission electron microscope, twin density recrystallised grain size relation *(German)* 78−52850
Cu pin against steel ring, dry sliding wear, role of dynamic recrystallisation 80−108599
Cu, plastic props., room temp. to recrystallisation temp., stress/strain relations, computer program 77−1865
Cu, polycryst., grain size and high-temp. yield strength 80−7641
Cu, polycrystalline, recovery and recrystallization after hot working 79−91661
Cu, polycrystalline, recovery and recrystn. kinetics 80−81081
Cu, polycrystn., strain localisation during hot deform. 80−104195
Cu, recrystallisation and recovery during temperature strain *(Czech)* 77−70071
Cu, recrystallisation and recovery during temperature strain *(Czech)* 77−73287
Cu, recrystallisation kinetics after small deform. and grain growth *(Czechoslovakian)* 77−32592
Cu, recrystallisation of cold rolled samples *(French)* 79−43269
Cu, recrystallisation of room-temp. deformed torsion samples, microcalorimetry 77−28827
Cu, recrystallization diagram for fine grained metal in region of small deform. *(Czech)* 77−59811
Cu, recrystn. centre growth kinetics, impurity effects *(Russian)* 80−89253
Cu, rolled single crystal with defined solute content, stored energy and recrystallization temp. 79−96037
Cu, tensile deformed ⟨110⟩ orientated single cryst., recrystn., high voltage electron microscopy study 80−84958
Cu, tension deformed single crystal, dynamic recrystallisation 79−47716
Cu, thin film, recrystallisation during Ar^+ bombardment 79−65969
Cu, types MOb and M1, primary recrystallisation kinetics depend. on state of impurities *(Russian)* 79−66069
Cu, vacuum deposited on Al substrate, recrystallisation 78−60044
Cu, vacuum-condensed film, structural changes under glow discharge *(Russian)* 79−15852
Cu wire, mech. props. and struct. after high-speed recrystallisation *(Russian)* 79−47704
Cu, wire, recrystallisation *(German)* 77−86055
Cu, wires, effect of heat treatment during drawing 78−56659
Cu-Al-Fe, strength increase from intermediate annealing determ. of annealing temp. by recrystallisation 78−44136
Cu-Mn(Fe)(Ni)(Zn)(Ge), dilute solid soln., exam. of recrystallisation and stored energy 78−52836
Cu-Pb thin film couple, interdiffusion and recrystallisation, grain size effects 77−76625
Cu-Sb, dil., grain growth rate, 520-970°C *(Russian)* 80−29972
Cu-Si-Ni, undercooled, grain refinement 79−34079
recrystallisation continued
Cu-Ti, deform. effect on precipitation and recrystallisation, electron microscope study 77−70115
Cu-Ti (4 wt.%), combined recrystallization and precipitation 79−29072
Cu-Zn (30 wt.%), rolled, electron microscope exam. of recrystallisation 78−76663
α-Cu-Zn(Al) fracture behaviour, effect of deform. temp. and alloying content *(Japanese)* 79−20159
CuZn32 bands, mechanical props. anisotropy after annealing at variable heating rates 77−90364
Fe, (100) [001], texture development by recrystallisation and normal grain growth 78−27539
Fe alloy, (110) [001] texture development by recrystallization and normal grain growth 77−32594
Fe alloy, low, (110)[001] oriented, mag. charact. 77−1879
γ-Fe alloy, supersat. solid soln., recrystn. inhibition by cold rolling 77−73286
Fe, Armco, dislocation struct. after hot and cold rolling *(Russian)* 77−8847
Fe, Armco, structural inheritance characts., X-ray and internal friction obs. 79−57017
Fe atomised powder, sintering effect on recrystn., mech. props. 80−40292
Fe, compressed, recrystallisation, transmission Kossel study of struct. 78−19776
Fe, high purity, prep. and recrystallisation temp. 77−55911
Fe, pure, grain growth, abnormal, kinetics 79−24537
Fe, purification, recrystn. temp. and elec. resistivity *(Japanese)* 80−100780
Fe, recrystallisation kinetics, deform. degree effects *(Russian)* 78−6943
Fe, single cryst. growth by recrystn., twinning, growth length *(French)* 77−12523
Fe, sintered, produced by dynamic hot pressing, recrystn. diagram 79−70017
Fe, thin foil, extrinsic grain boundary dislocations, low C content influence 80−107273
Fe-Cr (9 wt.%), extrinsic grain boundary dislocations, low C content influence 80−107273
α-Fe-Cr alloys, recrystallised, C segreg. effects, TEM *(French)* 77−28828
Fe-Cr-Al-Y (Y-Al_2O_3)(Y_2O_3), preparation and exam. of mech. props. 78−52720
Fe-Cr-Co ductile magnet, with high $(BH)_{max}$, processing, mag. props., and microstruct. 77−8957
Fe-Cu (1.2 wt.%) effect of precipitation on recrystallisation, texture 78−88476
Fe-Mo alloy, TZM, doped, Ni activated recrystallisation, ion probe mass spectrometer obs. 77−44280
Fe-Ni, alloy 20N24, martensitic, exam. of structure after laser treatment, and recrystallisation *(Russian)* 79−11608
Fe-Ni, austenite formed from martensite during annealing in (α+γ) region, crystallographic study 78−19782
Fe-Ni, secondary recrystallisation singularities *(Russian)* 80−66528
Fe-Ni (32.86, 30.65 wt.%), characts. of quenched struct. formed in textured sheets, TEM and optical microscopy study 79−34084
Fe-Ni (4 wt.%), extrinsic grain boundary dislocations, low C content influence 80−107273
Fe-Ni alloys, graim growth texture 79−91687
Fe-Ni-C, C effect on recrystallisation and reversion *(French)* 77−81282
Fe-Ni-C, single crystal, form. and strength of strain-induced martensite 79−100225
Fe-Ni-C (24, 0.5 wt.%), recovery and recrystallisation of stable austenite after hot rolling *(German)* 77−32591
Fe-Ni-Co, texture form. after cold working and annealing *(German)* 80−3089
Fe-Ni-Ti, undeformed metastable alloy, cellular decomposition of austenite during ageing *(Russian)* 79−100178
Fe-Si, grain oriented, with unique inhibition system for texture development 77−90366
Fe-Si, recrystallisation study 79−91275
Fe-Si (3 wt.%), behaviour of disperse inclusions, influence of recrystn. processes *(Russian)* 80−66519
Fe-Si (3 wt.%), grain oriented, MnS precipitate distribution, electron microscope observation *(Chinese)* 78−95751
Fe-Si (3 wt.%), grain oriented, mag. props., effect of decarburizing *(Chinese)* 80−103821
Fe-Si (3 wt.%), high induction grain oriented, metallurgical treatment and mag. props. 77−86044
Fe-Si (3 wt.%), orientation development during secondary recrystallisation, primary matrix effect, magnetic props. *(Czech)* 78−60679
Fe-Si (3 wt.%), recrystallisation along grain boundaries *(Russian)* 78−6942
Fe-Si (3 wt.%), secondary recrystn., role of solutes 77−86043
Fe-Si (3 wt.%), secondary recrystallisation, effect of composition and original orientation 78−68707
Fe-Si (3 wt.%), temp. depend. of migration rate of secondary recrystallisation grain boundaries *(Russian)* 79−1436
Fe-Si (3wt.%), grain-oriented, secondary recryst., grain growth inhibition 80−89245
Fe-Si (3wt.%), quantitative determ. of grain orientation and textile by etch figure method *(Chinese)* 78−11233
Fe-Si alloys, recrystn. while carburising, interphase boundaries movement 79−52208
Fe-Si as grown crystal, dislocation study by etching and X-ray topography 78−47377
Fe-Si-B-S, grain-oriented, high induction, B and S addition effect on magnetic props. *(Slovak)* 79−4697
Fe-Si-MnS-Al, Al effect on hot rolling struct., recrystallization, texture magnetic props. *(Chinese)* 78−11237
Fe-V(Cr)(Mn)(Ni), unlimited component solubility, intercrystallite internal adsorption *(Russian)* 80−39294
Fe-W(Ni), recrystallisation under laser irradiation *(Russian)* 78−35396
$Fe_{80}B_{20}$, metallic glass, Doppler broadening of positron annihilation γ-radiation and elec. resist. 80−66321
$Fe_{78}Mo_2B_{20}$, metallic glass, Doppler broadening of positron annihilation γ-radiation and elec. resist. 80−66321
$Fe_{32}Ni_{36}Cr_{14}P_{12}B_6$, metallic glass, Doppler broadening of positron annihilation γ-radiation and elec. resist. 80−66321
Fe_xO_y colloid prep., thermal decomposition of metal chelates 80−71953
GaAs large-grained solar cell film recrystallisation 79−38737

recrystallisation continued
GaAs, laser-induced recrystallisation and damage of ion-implanted amorphous samples 79−47557
GaAs:Cr pulsed electron beam induced recrystallisation and damage, amorphous layer formation 80−34052
GaAs:Te, laser annealing of implanted Te 78−35400
GaAs:Zn(Se), recrystn. of implanted amorphous layers, TEM and channelling obs. 77−89459
GaSb film, gamma-irradiated, struct., TEM and SEM obs. 79−15033
Gd-Co, amorphous films, mag. props. ferromag. reson. meas., 20-520°C *(Russian)* 80−97144
Ge, amorphous film, ion-implanted, regrowth 79−15043
Ge, amorphous layer, epitaxial recrystn. by electron irrad., solar cell appl. 78−84079
Ge, amorphous layer, on single cryst. Si, heteroepitaxy by laser annealing 79−77952
Ge film recrystallised by unidirectional solidification, GaAs film deposition 78−19671
Ge, regrowth under laser irrad. 80−24481
Ge-S-Sb glasses, microgravity effect on recrystn., optical and elec. props. 80−49127
Ge-Si-Sb solid soln., struct. peculiarities and mech. props. under weightlessness *(Russian)* 78−23693
$Ge_x(S,Se)_{1-x}$ chalcogenide covalent non crystalline topology, short range order 80−15009
In, recrystallisation of films prep. by vacuum evap. 79−4488
InP recrystallisation, and grain growth in p-InP film grown by close vapour transport 79−28944
InSb film, gamma-irradiated, struct., TEM and SEM obs. 79−15033
KCl:TlCl, lattice defects, X-ray line profile obs. 80−24455
Li_2GeO_3 piezoelectric glass ceramic, recrystallisation, pyroelectric response, permittivity 80−80703
Li_2SiO_4, piezoelectric glass ceramic, recrystallisation, pyroelectric response, permittivity 80−80703
Mg, recrystallisation after straining by rolling, −25 to 100°C *(French)* 77−59815
Mg, recrystallisation after cold rolling 78−72790
MgF_2, hot pressing in vacuum, compaction kinetics, selective recryst. 77−16517
Mo container for leucosapphire synthesis, recrystallisation 78−2151
Mo, dislocation structure of diffusional welding zone *(Russian)* 80−96531
Mo, electron beam melted with C additions, mech. props. *(Japanese)* 77−48449
Mo, recrystallisation kinetics, deform. degree effects *(Russian)* 78−6943
Mo, rolled single cryst., polygonisation and recrystn., strain depend. *(Russian)* 77−81270
Mo, secondary recrystallisation grain structure, effect of conditions of annealing *(Russian)* 78−6945
Mo sheet, 45° brittleness due to partial recrystallisation, 45° crack formation and propagation *(Russian)* 79−100238
Mo, single crystals, recrystn. textures, effect of fine precipitates 78−88480
Mo wire, struct. and high-temp. creep, dopant elements influence 80−66603
Mo-Zr-B-C, dil. alloy, struct. changes under prolonged high temp. annealing *(Russian)* 78−6944
Mo-Zr-Ti-C(0.1, 0.15, 0.004 wt.%), alloy TsM2A, cavitation failure mechanism 77−70169
$MoSi_2$, ceramic additives effect on sintering, recrystallisation 80−40306
NaCl, halite, dynamic recrystn. during compression creep, geophys. appl. 80−25772
NaCl:Ca crystals, surface recrystn., moisture effect 80−84950
Na_2O-SiO_2, recrystn. to form US transducer bond 79−83437
Na_2O-SiO_2-H_2O-FeO system, 'heavy phase', recrystallisation and struct. 78−2089
Nb alloy SVMTs, high-temp. ageing, struct. and morphology of hardening phases *(Russian)* 80−40390
Nb, recovery and recrystallisation, fast neutron irradiation effects 77−70069
Nb-Zr-C alloys, plastic deform. and annealing, dislocation struct. *(Russian)* 80−20951
Nb-Zr-N, deformed and annealed, internal friction, rel. to structural state *(Russian)* 78−6957
NbC, recrystallisation 78−11251
Ni alloy, recryst. after hot deform. *(German)* 80−25716
Ni alloy IN-738, Y_2O_3 (1.5 wt.%) addition, mechanical alloying 77−40427
Ni, alloying, influence on recrystn. and grain growth *(Russian)* 80−81071
Ni and Ni-Cr(Mo), wear tracks, TEM obs., tested in simulated face seal 77−52508
Ni base superalloy, γ'-precipitation influence on recrystallisation 80−29955
Ni base superalloys, recrystallisation 77−16616
Ni, cold rolled, influence of impurities on recovery and recrystallisation, positron annihilation meas. 79−15696
Ni, cold swaged, unidirectional recrystallisation over range of temp. gradients *(Japanese)* 78−48424
Ni, cold-worked, impurity-induced vacancy clustering 79−99972
Ni, defect removal, obs. by positron annihilation 78−84677
Ni, deformed, struct. form. during annealing, Ni_3Al type ordered phase precipitation *(Russian)* 80−45325
Ni electrodeposit on Cu, growth and microstruct. 77−11823
Ni film, electrodeposited, recrystallisation kinetics, X-ray scatt. *(Russian)* 78−60045
Ni, grain boundaries, mobility, effect of impurities *(Polish)* 79−96073
Ni, grain boundary migration during recrystallisation after cold drawing 77−73289
Ni, O free, annealing in photoemission electron microscope, twin density recrystallised grain size relation *(German)* 78−52850
Ni, plastically deformed, volume fraction of recrystallised material determ. from positron annihilation 77−1760
Ni, polycryst., recrystn. kinetics, high press. effects *(Russian)* 77−48453
Ni, powder, recrystallisation, effect of sintering atmosphere 77−12573
Ni, powder, subjected to vibratory milling, exam. of plastic deformation, recrystallisation, sintering 80−16234
Ni, recrystallisation kinetics, deform. degree effects *(Russian)* 78−6943
Ni, supercooled, struct. refinement mech. *(Russian)* 80−20975

recrystallisation continued
Ni, thermal softening, influence of alternating mag. field *(Russian)* 78−23312
Ni, vacuum-condensed film, structural changes under glow discharge *(Russian)* 79−15852
Ni, wear, recrystallisation as controlling process, FCC metal 77−56117
Ni-A-Ti (6,1 wt.%), γ' phase precip., deform. effects *(Russian)* 78−48404
Ni-based superalloys, TEM obs. of cellular transformation products 80−3045
Ni-Co-Cr superalloy, powder produced, necklace struct. development 80−40395
Ni-Co-Cr-Mo-Al, Astroloy, extruded powder metallurgy superalloy, recrystallisation study 79−4976
Ni-Cr, deformed, struct. form. during annealing, Ni_3Al type ordered phase precipitation *(Russian)* 80−45325
Ni-Cr alloy KhN70MVYu wire, recrystn., optimum heat treatment 80−76278
Ni-Cr-W-Mo-Ti-Al, heat-resist., recovery and recrystn. 80−76268
Ni-Cu (30 wt.%), cast cold- and warm-worked, recrystallization 79−29092
Ni-ThO_2(HfO_2) dispersion hardened alloys, recrystallisation during annealing, O_2 partical press. effects *(Russian)* 78−3140
Ni-W-Co-Cr, superalloy MAR 200, with Hf, cellular composite prod. by isothermal dendrite ripening 78−44150
Ni-ZrO_2, dispersed inclusions, effect on recovery and recrystallisation 77−25064
Ni_3Al, Mossbauer spectra, exam. of struct., superlattice population anal. 78−88240
NiSb, dilute alloy, impurity-induced vacancy clustering 79−99972
Pb, deformed by torsion, stored energy and recrystallization 79−34069
Pb-Ca-Sn alloys for battery grids, proposed phase diagram, grain struct. development, corrosion phenomena 77−16546
Pb-Sb, improvement in antifriction layer props. by impulse discharge, impulse discharge treatment *(Russian)* 79−1917
Pd, H phase hardened, recrystallisation study 80−60883
$Pd_{1-x}Ag_xH_n$, positron annihilation examination of electronic structure *(German)* 77−69931
SbSBr glass, IR reflectivity spectra 80−71403
Si, amorphous, epitaxial regrowth, structure and impurities effect 80−84401
Si, amorphous, ion implanted, laser annealing, reflectivity meas. 80−29039
Si, amorphous, laser-induced epitaxial regrowth, substrate and doping effects 79−56082
Si, amorphous film, epitaxial laser crystallisation 78−84078
Si amorphous film, ion-implanted, regrowth 79−15043
Si, amorphous laser effects 79−69921
Si, amorphous layer, ion-implanted, spatially controlled cryst. regrowth by laser irradiation 78−55810
Si, amorphous-implanted, laser irrad., stress assisted recrystallisation mechanism 79−69123
Si CVD grown polycrystal recrystallisation 78−64560
Si, crucible grown, virgin and implanted, laser irradiation effects on surface structure 80−92768
Si, dislocation structure, effect of induction heating *(Russian)* 77−21180
Si film, growth on SiO_2 substrate by pyrolysis of SiH_4 77−89678
Si, implanted crystal, laser induced annealing and diffusion behaviour 80−88202
Si, ion implanted, difference between ruby and Nd:YAG laser annealing 79−37723
Si, joining and recrystallisation using thermomigration process 80−65298
a-Si, laser induced crystallisation mechanism, epitaxial regrowth 80−84962
Si, photoacoustic signal changes assoc. with crystallinity, recrystallisation after laser annealing 80−16127
Si, plasma effects during pulsed laser annealing 80−84480
Si, polycryst, CVD, electron beam recrystn. 80−24759
Si, polycryst., CVD, recrystn. on heating 80−80107
Si, polycrystalline, recrystn. after plastic deform. and annealing 80−3145
Si, pulsed laser annealing, nonthermal, plasma annealing 80−25498
Si, recrystallisation of CVD-grown polycryst. Si and influence of B, Al dopants on grain growth 80−54575
Si, recrystallised amorphous layer, self-ion irradiated, defect structures, TEM obs. 78−75688
Si, regrowth under laser irrad. 80−24481
Si solar cells, polycrystalline, from recrystallized plasma deposited thin films 80−104509
Si, thin slabs, vibr. freq. calcs., dimens. effect 80−60585
Si:Ar, ion implanted, amorphous, epitaxial regrowth 79−10868
Si:As, implanted, spatially varied activation during regrowth of amorphous layers, sheet resist. and backscatt. obs. 78−71749
Si:As, ion implanted, amorphous-cryst. transition induced by multiple-pulsed ruby laser 79−90555
Si:As, melting by high power ns laser pulsing, As diffusion 78−79789
Si:As^+, implanted layers recrystn., ellipsometry meas. 79−73190
Si:As(Sb), implanted, pulsed ruby-laser annealing, Rutherford backscatt., TEM and ion channelling study 79−86805
Si:BF_2^+(Si^+,B^+), recrystallisation of implanted amorphous layers, elec. props. 79−55762
Si:B(P), ion implanted, polycryst. annealing characts. 77−24324
Si:In(Sb), incorporation of implanted impurities during amorphous layer regrowth 79−55761
Si:Ne(Ar)(Kr), amorphous, implanted and sputtered, epitaxial regrowth, influence of noble gas atoms 80−2289
Si:Ne(Ar)(Kr), ion implantation damage, annealing, comparative study 79−10867
Si:Ne(Kr), ion implanted, amorphous, epitaxial regrowth 79−10869
Si:P, heavily ion implanted, polycrystalline, grain growth 79−19477
Si:P, polycrystalline laser recrystallised film on Si substrate, cryst. struct., thermal oxidation 80−65391
Si:Sb, epitaxial regrowth of amorphous layers created by high-dose Sb implantation 78−30654
Si/Al and Si/Al-Si(Cu), Si regrowth minimisation through overlying Al or Al alloy film 80−70569
p-Si-Al, ohmic contacts, Si dissoln. and recrystn. effects, computer calc. 80−103749
Si-Al system, Si regrowth minimisation methods in Al films 80−15384
SiC, reaction sintered, TEM exam. of recrystallisation, phase transformation 78−80567

recrystallisation continued
β-SiC, thermodynamic props., temp. depend., 5 to 300K 80−96666
Si_3N_4, consolidation by hot isostatic pressing 80−11605
Si_3N_4, recrystallisation during hot pressing 77−12587
SiO_x, amorphous and recrystallised layer, optical props. 80−25474
Si(111):Pb ion implanted amorphous layers, recrystallisation, impurity out-diffusion model *(Chinese)* 80−88363
steel, Nb, deform., recrystn. and precip. interaction 80−97515
Ta, rolled single crystal, recovery and recrystallization 80−3093
Ta-C-B system, mech. and physical props. 77−59731
Te film condensed on mica, struct. and electrophysical props. 80−39688
β-IIITi alloy, anal. 80−108470
Ti alloy, hot deform. *(French)* 77−52371
Ti, heating and cooling rate effects on α to β phase transform. and recrystallisation 77−90379
Ti, oxidation by water vapour *(French)* 78−76787
Ti, recrystallised, dislocation obs. and characterisation by X-ray topography *(French)* 78−22722
Ti sheet, anisotropy and texture, effect of plastic deform., recovery and recrystallisation *(Russian)* 77−8850
Ti-Al, structural and phase changes due to annealing *(Russian)* 80−55440
Ti-Al-Cr-Mo-V alloy VT-22, effect of heating rate on phase recrystallisation *(Russian)* 79−34077
Ti-Al-V, oxidation by water vapour *(French)* 78−76787
Ti-Al-V (6,4 wt.%) alloy foil, substrate temp. effect on struct. 80−7497
Ti-Al(Mo), swaged and recrystallized, grain growth 80−3092
Ti-Mo-Zr-Sn (11.5, 6, 4.5 wt.%), metastable beta III phase, recrystallization and grain growth 80−3091
TiN-AlN composites, struct. and props. 77−40413
Tm_2O_3 film, between Al electrodes, prep. and elec. props. 80−60103
VO_2(:Al,W), layers, liq. phase prep., resist.-temp. behaviour *(German)* 77−77435
W alloy wire reinforced stainless steel, fibre/matrix interaction, fabrication and heat treatment effect 79−91607
W alloys, alloying effects of ThO_2, Mo-Re, HfC, NbC 77−70083
W alloys, deformed, vacuum technology appl., mech. props. *(German)* 79−57046
W, doped, Ni activated recrystallisation, ion probe mass spectrometer obs. 77−44280
W, doped wire, secondary recrystallisation temp., bubble parameter effects 77−32596
W fibre, KSiAl doped, recrystallisation, Li diffusion effects, hardness, strength, microstructure meas. *(German)* 78−64644
W fibre reinforced, Co powder alloys, reactions and recryst. 80−11603
W heater for leucosapphire synthesis, recrystallisation 78−2151
W, hot emitter, surface struct. change during baking above 2000K 79−65971
W, polygonisation critical stage in single crystals deformed in compression 79−4979
W, powder, subjected to vibratory milling, exam. of plastic deformation, recrystallisation, sintering 80−16234
W, recrystallisation of commercially pure and doped wire drawn to high strain 79−100165
W, wire, doped, heavily drawn, recrystallisation 77−16609
W wire, struct. and high-temp. creep, dopant elements influence 80−66603
W-C(0.01 to 0.2 wt.%), C effect on high temp. strength 77−16614
W-Ni powder compacts and wires, recrystallisation, influence of omnidirectional press. *(Russian)* 77−8849
YAG, production of densely sintered ceramic, exam. of recrystallisation during sintering 80−11609
ZnS-based phosphor, microstruct. and luminesc. efficiency 78−10959
ZnSe, recrystallisation during hot pressing 77−85952
ZnSe-Ge(GaAs)(mica) epitaxial heterostructs., growth struct. 78−43257
Zr-Nb microduplex alloys, struct. and props. 78−3170
Zr_3Al, cold worked, annealing effects 77−36535
ZrC, recrystallisation 78−11251
ZrC, sintering shrinkage, effect of struct. vacancies in interstitial phases 78−60630
ZrN-AlN composites, struct. and props. 77−40413

recrystallisation annealing
alloy, two-phase, deform. struct. and recrystallisation, review 79−34061
annealing twins density, photoemission microscopy 80−35208
$\alpha+\beta$ brass, plastic deform., recovery and recrystn., positron annihilation 79−57003
brass, recovery and recrystallisation of plastically deformed α-phase, comparison of positron annihilation, elec. resist. and microhardness 79−52240
brass, tubular parts induction apparatus for vacuum annealing 79−57021
dose depend. in laser annealing 78−91354
Fe, Armco, electron microscope object prep. method 80−50789
laser annealing, optical constants, ellipsometry observation 80−34024
metal, deformed struct. role in recrystallisation nucleation, review 79−34060
metal, heavily deformed recrystallisation 79−34062
metal filings and wires, thermal processing encapsulated under vac. in metal tubulations 77−59810
Nimonic PE16, abnormal grain growth after cold working and annealing 79−74176
segregation, nonequilibrium, during pulsed laser annealing, model 80−108451
semiconductor, ion implanted, epitaxial regrowth, laser annealing dynamics 80−92548
semiconductor, ion implanted, ruby laser pulse effects 79−69125
semiconductor, ion-implanted, laser annealing dynamics 79−69121
semiconductor epitaxial regrowth, ion implantation induced defects, annealing 80−24479
semiconductor laser annealing, review and anal. 80−25741
semiconductor laser annealing to round edges of Si structures 80−25742
semiconductors, ion-implanted, laser pulse annealing, TEM and channelling study 80−100264
steel, C, recrystallization annealing, grain growth, effect of type of deform. 80−100847
steel, Cr (17 wt.%), stainless, hot-rolled texture, effect on cold-rolled and annealed textures 80−55425
steel, low-C, Al-stabilised, texturing during annealing *(Russian)* 78−19777
steel, phase separation, effect of plastic deform. and heat treatment *(Polish)* 78−92295

recrystallisation annealing continued
steel, stainless, Cr-Cu (17, 0.6 to 1.1 wt.%), texture 80−84957
steel, stainless, recrystallisation texture, effect of Cu, Ti additions on development *(Japanese)* 78−80558
steel, unkilled deep drawing sheets, influence of N content on recrystn. *(German)* 80−40376
thermoelectric materials, extruded from ceramic blanks, recrystn. and elec. props. 79−43267
thermoelectric materials, extruded materials with tetradymite struct., primary and in situ recrystn., elec. props. 79−43266
Ag, rolled, dislocation struct. and recovery during annealing *(Russian)* 79−29084
Al, exoelectron emission under recrystallisation annealing 77−90412
Al, recrystallised, substructure strengthened, long-term strength 77−21173
Al, secondary recrystallization *(Czech)* 79−70080
Al sheet, texture evolution, effect of rolling or tensile deform., rel. to strain ratio 79−91672
Al, single crysts., misfit recrystn. dislocations formation study during recrystn. by X-ray synchrotron topography 79−38849
Al wire, grain boundary internal friction after recrystn. annealing *(Russian)* 80−66561
Al-Cu(Si)(Zn)(Mg)(Cr), recrystallization texture 79−91679
Al-Mg_2Si (1 wt.%) secondary recrystallisation by grain boundary unsewing 79−1886
Al-Ni (6 wt.%) alloy, misorientation between subgrains, second-phase particles role, STEM microdiffr. obs. 80−104415
$B_{12}C_3$, sintering and subsequent high temp. annealing, struct. and props. 80−20858
Bi, effect of Sb, Sn and Pb 78−52841
Bi film, surface defects and struct., electron microscopy and elec. props. *(French)* 80−15415
C steel, strain hardening parameters, determination from stress-strain curves 78−80562
C steel, type 45, inelasticity under cyclic strain in active media 78−80613
CdS, evaporated film, effects of heat treatment on photosensitivity *(Japanese)* 78−39237
CdS, polycrystn. films, recrystn. accompanying annealing *(Russian)* 80−20948
CdS:Cu, Cl films, photocond. growth and decay time 80−60041
Cr bronze Sn, recrystn. props., hot rolling, annealing, polygonisation *(Russian)* 80−55419
Cu *(Russian)* 78−15430
Cu, anisothermal annealing, effect on props. of MOOB bands 78−23719
Cu, annealing twins, density, effect of recrystallisation temp. and electron microscope resolution *(French)* 78−31423
Cu, deformed and annealed, positron lifetime investig. of recovery and recrystn. 77−70064
Cu film, on Ni, recrystallisation and interdiffusion, electron microscope obs., 450-600°C 80−39363
Cu, grain growth during isothermal annealing *(Russian)* 79−52259
Cu, polycrystalline, recovery and recrystn. kinetics 80−81081
Cu, porous, sintering, cold working, recrystn. annealing, mech. props. and microstruct. 78−76660
Cu, recrystallization annealing, grain growth, effect of type of deform. 80−100847
Cu, rolled, dislocation struct. and recovery during annealing *(Russian)* 79−29084
Cu, rolled sheet, texture transform. during primary recrystallisation as function of annealing time 79−91683
Cu, types MOb and M1, primary recrystallisation kinetics depend. on state of impurities *(Russian)* 79−66069
Cu-Ag, deformed, recrystallization nucleation at second phase particles, electron microscope obs. 79−34059
Cu-Ag(Se)(Sn)(Ag-Se-Sn), Ag, Se, and Sn effects, singly and together, on recrystallisation 79−100164
Cu-Al (3 wt.%), annealing twins density, photoemission microscopy 80−35208
Cu-Ni-Fe (26,8 wt.%), microduplex struct. form., recrystn. annealing *(Japanese)* 78−76659
Fe, Armco, inelasticity when under cyclic strain, in active media 78−80613
Fe, commercial, deformability, containing H_2 77−90411
Fe powder, recryst. annealing effect on struct. and technological props. *(Czech)* 80−89250
Fe spherical single crystals, recrystallisation annealing 79−74086
Fe, texture, recryst. annealing effect *(Czech)* 80−89249
Fe, zone refined, strained, substructural changes during annealing *(Slovenian)* 78−84845
Fe-Co-Cr (50, 0.4 wt.%), ordering and recrystallisation 79−34029
Fe-Mn-C-Si alloy G20, effect of Si and Mn additions on phase composition in multiple $\gamma \rightleftarrows \varepsilon$ transitions *(Russian)* 78−95743
Fe-Ni, secondary recrystallization *(Czech)* 79−70080
Fe-Ni-Ti (25.9, 2.15 wt.%), exam. of effect of inhomogeneous solid soln., on martensitic transformation *(Russian)* 79−34034
Fe-Si, twinned annealing, plastic deform., and recrystallisation *(Russian)* 77−28829
Fe-Si (3 wt.%), cold rolled, effect of primary recrystallisation texture, on behaviour of secondary recrystallisation 78−39802
Fe-Si (3 wt.%), texture form., plastic strain effect, hot rolled 79−79002
Fe-Si-B, high induction alloy, improving mag. props. by adding B to coating 79−83338
Fe-Si-B, melt C content effect on grain growth and induction 80−35351
GaAs, amorphous layers, ion-implanted, low-temp. epitaxial regrowth 80−92790
GaAs, ion implanted, laser induced damage and recrystallisation by freq.-doubled Nd:YAG laser 79−73197
GaAs, ion implanted, laser induced recrystn. and damage, ion backscatt. and Raman scatt. obs. 80−49248
GaAs, ion implanted, mode-locked Nd:YAG laser annealing, recrystn. 80−19817
GaAs, ion implanted and laser-annealed, photoacoustic meas. 80−47117
GaAs, ion-implantation induced damage profile, ellipsometric study, annealing 80−103400
GaAs, ion-implanted, laser pulse annealing of amorphous surface layer, TEM 80−55436
GaAs:$p^+(N^+)$, struct. characts. of radiation damage produced by high energy ion implantation 79−4340
GaAs:Te, ion implanted, ohmic contacts produced by laser-annealing 79−73585

recrystallisation annealing continued
GaP, ion implanted, mode-locked Nd:YAG laser annealing, recrystn. 80−19817
GaP, ion-implanted, form. and annealing of radiation damage 78−91363
Ge, strained crystal, annealing effect, recrystn. and struct. *(Russian)* 80−89252
Ge:B(P), ion implanted, laser-induced regrowth 79−69130
InSb, ion implanted layers, amorphisation, recrystallisation 78−63782
InSb, micron size Hall probe for precision mag. field mapping 79−75558
Mo, powder, defective structure and activated sintering, exam. 80−16240
Mo-Ti-Zr, alloy TZM, polycrystalline, anal. of elastic anisotropy and microyielding 80−30050
Mo-W (30 wt.%), wrought, fracture, characteristic features 80−104278
Nb base alloy, high temp. creep estimation and long term strength charact. 78−3195
Nb-W-Mo-Zr (5, 2, 1 wt.%), surface-layer struct. and mech. props., effect of O_2 diffusion saturation 79−5087
Nb-Zr-C, (1, 0.1 wt.%) alloy, mech. charcts. structral sensitivity in strained state *(Russian)* 79−52301
Nb-Zr-N biphase alloy, recrystallization annealing 80−104180
Nb_3Si, high press. phase, prod. by recrystn. of metastable sputter deposits, struct. and supercond. props. 78−60571
Ni, (99 wt.%), annealing twins density, photoemission microscopy 80−35208
Ni alloys, recrystallised, grain boundary inheritance and props. 77−59816
Ni, annealing twins, density, effect of recrystallisation temp. and electron microscope resolution *(French)* 78−31423
Ni, pure, anomalous grain growth 80−20984
Ni, rolled, dislocation struct. and recovery during annealing *(Russian)* 79−29084
Ni-Dy, annealing behaviour of implantation damage, Dy outdiffusion, TEM obs. 77−77505
Si, amorphous, epitaxial regrowth by pulsed laser beam 78−91554
Si, amorphous, implanted, recrystn. induced by scanning CW laser, reaction rates, analytical model 80−66334
Si, amorphous film, selective laser recrystn. over heavily doped lines 80−84947
Si, amorphous layer, epitaxial growth by laser annealing 78−79899
Si amorphous layer, solar furnace annealing to induce solid-phase epitaxy 80−2277
Si amorphous layer recrystallisation by laser beam 80−93566
Si, amorphous layers, recrystallisation, pulsed laser annealing 80−65404
Si CVD film on amorphous substrate, CW laser recryst. 79−90894
Si, deep amorphous layer implantation, laser effects, channelling diffr. study 80−25494
Si, defect annihilation depth by pulse laser annealing 80−16128
Si, deformed, annealed and recrystallized, struct., implications for solar cells 80−60922
Si, furnace preannealed (111) ion implanted, laser irrad. 80−65015
Si, implanted with low solubility dopants, laser annealing, TEM study 80−70233
Si, ion implantation, high dose, solid phase epitaxial regrowth 80−103380
Si, ion implantation and pulsed laser annealing of group III and group V dopants, supersat. alloy form. 80−54267
Si, ion implanted, CW laser annealing 80−92550
Si, ion implanted, complex annealing behaviour of amorphous layers, TEM obs. of defect struct. 80−107299
Si, ion implanted, electron beam annealing, surface struct. study using SEM 80−70235
Si, ion implanted, laser annealed microstructure 79−74027
Si, ion implanted, mode-locked Nd:YAG laser annealing, recrystn. 80−19817
Si, ion implanted, pulsed-laser annealed, Raman obs. 79−73189
Si, ion implanted, scanning electron beam annealing 80−6420
Si, ion implanted, transient optical reflectivity study of laser annealing, thresholds and kinetics 79−60390
Si, ion implanted layers, laser annealing 78−67732
Si, ion-implantation damage, annealing using pulsed-electron-beam 79−55768
Si, ion-implanted, annealing using scanning CW laser system 80−100265
Si, ion-implanted amorphous, laser epitaxial recrystallisation threshold energy 80−70571
Si, ion-implanted layers, crystn. by ns laser pulses, TEM and RHEED 80−100421
Si, ion-implanted layers, epitaxial regrowth by laser beam and flash annealing 80−100420
Si, laser induced cryst. regrowth 79−69913
Si, melting and resolidification, laser-induced, surface morphology 79−87529
Si on sapphire, stress-relieved regrowth by laser annealing 80−65389
Si p-n homoepitaxial junctions, elec. and struct. charcts. 80−6662
Si polycrystalline films, texture formation study 79−87662
Si, post-annealed amorphous layer, twinning struct. by transmission electron diffr. 77−76685
Si, self implanted, and additional impurity implanted laser induced recrystn., threshold power density 79−69131
Si, strained crystal, annealing effect, recrystn. and struct. *(Russian)* 80−89252
Si wafer, thin surface layers, amorphous to cryst. transform., obs. technique 80−107288
Si:Ar, ion-implanted, epitaxial regrowth by laser annealing, microstruct. 80−84404
Si:As, ion implanted, pulsed laser annealing, partial solid-state regrowth 80−103591
Si:As, ion implanted, recrystallisation by free running ruby laser 79−73185
Si:As, ion-implanted, laser recrystallisation by freq.-doubled Nd:YAG laser 79−77613
Si:As, time-resolved reflectivity during laser annealing 78−92086
Si:As,Sb, amorphous, damage depend. of epitaxial regrowth during annealing 78−47679
Si:As laser annealing, heat and mass transport model 80−92546
Si:As^+, annealing by scanning Ar ion laser, dislocation loop density comparison 78−47438
Si:As^+(P^+)(Sb^+), annealing misfit dislocations removal by laser irradiation 79−74024

recrystallisation annealing continued
Si:As(B), ion-implanted, scanned laser and electron beam annealing 79−73182
Si:As(Pb), ion-implanted, impurity redistrib. during laser irrad. 80−100280
Si:B, lattice location of implanted ions after laser annealing 78−30660
Si:B implanted wafers, ionis. assisted annealing and effects 80−100257
Si:BF_2^+, recrystallisation of implanted amorphous layers, F migration 79−55763
Si:Bi, ion-implanted, solid phase epitaxial growth during annealing, supersaturated solid soln. form. 80−103384
Si:Fe(Cu)(Pt), implant redistrib. and enhanced solubility following laser irrad. 79−69129
Si:Ga^+, influence of recrystallisation of amorphous layers on impurity distrib. during annealing 79−69152
Si:Ge, recryst. after implantation using different temp. and energy sequences 80−84196
Si:P, annealing after ion implantation, ellipsometric study 80−65018
Si:P, ion implanted, selective annealing of amorphous layers by Nd^{3+}:YAG laser irrad. 79−14823
Si:Pb, He^+ Rutherford backscatt. and TEM exam., implant species effect on recrystn. 78−47452
Si:Pb, low-solid solubility ion-implanted, pulsed and continuous laser annealing and furnace annealing comparison 79−73184
Si:Pb implanted layers, recrystn. on annealing, backscatt. and TEM obs. 77−51421
Si:Pt, implanted and laser annealed, segregation and increased dopant solubility 80−65016
Si-B, diffusion-free annealing, use of scanning CW Kr laser 78−91345
Si-H (up to 15 at.%), amorphous, ion implanted, laser annealing obs. 79−69133
SiC(6H), ion-implanted, laser-induced recrystallization and defects 80−44221
SiO_2 layers, crystallisation, structural props. rel. to annealing 78−34724
α-Ti, cold rolled, primary recrystn., in situ investig. in HVEM 80−104185
Ti, crystalline orientation distribution analysis of texture development 79−91669
Ti lamellar single cryst. formation by heat treatment *(Russian)* 77−59800
α-Ti, primary recrystallization study by three dimensional anal. of textures and annealing, HVEM obs. 79−91677
α-Ti, recrystallised commercial purity, Fe-rich precipitates obs. *(French)* 80−50637
Ti-Al-V, (6.7, 4.3 wt.%), fatigue crack growth and fracture resistance enhancement, due to annealing 78−35510
Ti-Al-V (6, 4 wt.%), α-β anneal, recrystn. anneal, β-anneal, room temp. creep 79−61662
Ti-Al-V-Sn (5.5, 5.3, 2.3 wt.%) fatigue crack growth and fracture resistance enhancement, due to annealing 78−35510
U, γ- and β-hardened, recrystallisation, effect of impurity distrib. 78−70602
W, deformed, surface layer struct. effect on polygonisation and recryst., X-ray diffr. anal. and metallographic exam. *(Russian)* 80−84948
W, powders, defective structure and activated sintering, exam. 80−16240
Zn-Al-Mg alloy, annealed, recrystallised, influence of strain and purity on orientation *(Russian)* 79−52234
Zr_3Al, deformed and irrad., lattice defects obs., superlattice dislocations and defect clusters 80−107261

recrystallisation texture
brass, orientation distribution function anal. by superposition of Gauss type scattering functions 79−86735
α-brass, rel. to rolling temp. 80−11664
brass, rolling and recrystallization texture as function of Zn-content 79−91676
brass 63, recrystallisation textures, and deformation formed by dry sliding against steel 79−91698
development, recent aspects of understanding 79−87654
grain growth in textured matrix, theory *(Russian)* 77−81273
growth selection theory proof by growth selection expt. 79−91684
low C, deep-drawing, mechanism of recrystn. texture formation 79−87658
materials texture, conf., Aachen, Germany, (March 1978) 79−83217
metals, plant deform. and recrystallisation textures 78−68708
orientation distribution functions, rel. between recrystn. texture and deformation texture 79−83222
quartz, naturally deformed, dynamic recrystn. during creep, dislocation substruct., Mg alloy comparison 80−109142
quartz, plant deform. and recrystallisation textures 78−68708
rolling texture, determ. by three-dimens. anal. 77−86049
steel, Al-stabilised, texture formation in continuous annealing, effect of coiling temp. of hot strip 79−91688
steel, Cr (25 wt.%) surface structure investigation in polarised light 77−28947
steel, Cr-Mn type, martensite struct. after quenching and HTMT, X-ray diffr. obs. 80−84975
steel, deep drawing, texture control as affected by processing variables 79−91689
steel, electric sheet, hot-rolled, recrystallization and texture formation during ht. treatment 77−44271
steel, high strength, treatment effect on ductility and strength 80−60880
steel, low C, Ti-stabilized, recrystn. texture development 79−83231
steel, low C sheets, effect of N_2 content on recrystn. texture 79−83233
steel, low-C, Al-stabilised, texturing during annealing *(Russian)* 78−19777
steel, low-C contaning Ti, sheets, recrystn. texture effects on plastic strain ratio and deep-drawing *(Chinese)* 80−66527
steel, mild, cold rolled, texture and plastic anisotropy rel. to alloying and precipitation *(French)* 80−108475
steel, mild, solderability, annealing effect *(Japanese)* 80−89244
steel, Nb-stabilised, orientation depend. of cell size and recrystallisation texture development 79−91682
steel, stainless, Cr (17 wt.%), recrystallisation texture, effect of N *(Japanese)* 79−4978
steel, stainless, recrystallisation texture, effect of Cu, Ti additions on development *(Japanese)* 78−80558
steel, transformer, formation of perfect cubic texture in thin sheets *(Russian)* 78−80557
thermoelectric materials, extruded from ceramic blanks, recrystn. and elec. props. 79−43267

recrystallisation texture continued
thermoelectric materials, extruded materials with tetradymite struct., primary and in situ recrystn., elec. props. 79−43266
Ag, development after plane-strain deform. 77−48448
Ag expitaxial film, twin boundaries of recrystn. type, electron microscope obs. *(Russian)* 79−4484
Ag, rel. to rolling temp. 80−11664
Ag, tensile deformed single crystal, recrystallisation texture 79−91685
Al alloy, AK4-1, hot-worked, struct. states and recrystn. *(Russian)* 78−19778
Al-Cu(Si)(Zn)(Mg)(Cr), recrystallization texture 79−91679
Al-Mn (1 wt.%), single crysts., rolled to (123)[41$\bar{2}$], recrystn. textures 80−104183
Al-Ni (6 wt.%) alloy, misorientation between subgrains, second-phase particles role, STEM microdiffr. obs. 80−104415
CdTe film formation on glass substrates, influence of sublayers of recrystn. stimulators 77−43455
Cu -Sn (0.05 at.%), grain boundary relax., misalignment angle effect *(Russian)* 78−3159
Cu, recrystallisation textures, and deformation formed by dry sliding against steel 79−91698
Cu, rel. to rolling temp. 80−11664
Cu, single crysts., ⟨110⟩ oriented, tensile deformed, HVEM of recrystn., recrystallised state 80−89256
Cu single crysts., deformed, HVEM study of recrystn. texture 80−104179
Cu, solderability, annealing effect *(Japanese)* 80−89244
Fe, pure, initial grain boundaries effect on cold-rolling and annealing textures *(Japanese)* 80−35205
Fe-C single crystals, effect of heat treatment prior to cold rolling on recrystn. texture 79−83232
Fe-Co-Si (4,1.5 wt.%), textured, mag. props. 80−35200
Fe-Co-V alloy, Remendur, heat treatment effects on mech. and struct. props. 77−8846
Fe-Ni, crystallization texture, rolling, effect of impurities 78−15425
Fe-Ni, secondary recrystn. and mag. props. 80−89247
Fe-Ni (50 wt.%), secondary recrystallization 78−23723
Fe-Si (3 wt.%), (110)[001] oriented single crystal, form. of rolling and annealing texture 77−16608
Fe-Si (3 wt.%), AlN-inhibited, Se effect on primary grain recrystallisation 77−12715
Fe-Si (3 wt.%), cold rolled, effect of primary recrystallisation texture, on behaviour of secondary recrystallisation 78−39802
Fe-Si (3 wt.%), effect of heating rate during primary recrystn. on props. after secondary recrystn. 78−84837
Fe-Si (3 wt.%), grain oriented, MnS-AlN-inhibited, precipitate morphology 77−12648
Fe-Si (3 wt.%), orientation distrib. in primary recrystallised textures, mag. permeability 77−12712
Fe-Si (3 wt.%), secondary recrystn., struct. inhibition, permeability improvement 77−12713
Fe-Si (3 wt.%), secondary recrystallisation, effect of composition and original orientation 78−68707
Fe-Si (3 wt.%) high-permeability grain-oriented steel, quenching effect on primary recrystn. texture development 80−84956
Fe-Si (3 wt.%) struct. and texture changes during repeated deform.-recrystn. *(Russian)* 78−88474
Fe-Si steel, high permeability, processing effect on recrystn. and deform. 77−12716
Ge, strained crystal, annealing effect, recrystn. and struct. *(Russian)* 80−89252
Mg alloy, dil., dynamic recrystn. during creep, dislocation substruct., quartz comparison 80−109142
Mo alloy with dispersed HfN phase, recrystallisation, crystallographic and structure texture *(Ukrainian)* 80−71668
Mo filament, coated with thin Ni film, creep and recrystn. *(Russian)* 78−19822
Mo, rolled and annealed, zone-refining effect on recryst. grain orient. 77−36532
Mo-Ti-Zr, alloy TZM, polycrystalline, anal. of elastic anisotropy and microyielding 80−30050
Ni-Cr-Al-Y_2O_3 superalloy, recrystn. and texture development 80−16328
Ni-Fe-Co, alloy with step hysteresis loops *(German)* 79−42806
$Ni_{65}Mo_2Fe$, O_2 effect on secondary recrystallisation and mag. props. 80−35201
Pb, recrystallisation textures, and deformation formed by dry sliding against steel 79−91698
Si, compressed, polycrystalline, deform. and recrystallisation texture 78−27538
Si, strained crystal, annealing effect, recrystn. and struct. *(Russian)* 80−89252
Sn, recrystallisation textures, and deformation formed by dry sliding against steel 79−91698
Ta, rolled and annealed, zone-refining effect on recryst. grain orient. 77−36532
α-Ti alloy, VT1-1, cold rolled, recrystn. texture and prop. anisotropy 78−52846
α-Ti, cold rolled, primary recrystn., in situ investig. in HVEM 80−104185
Ti, rolling and recrystallisation texture formation *(Russian)* 77−59802
Ti thin sheet, texture and mechanism of primary recrystallisation 78−23721
Ti, Ti recrystallisation texture from neutron diffr., cf X-ray diffr. *(French)* 77−84593
W, doped wire, textural aspects of recrystallization 78−11239
W filament, coated with thin Ni film, creep and recrystn. *(Russian)* 78−19822
Zn-Al(Mg) alloys, cold-rolled, texture formation rel. to Zn purity *(Russian)* 77−59804
Zr, rolling and recrystallisation texture formation *(Russian)* 77−59802
Zr-O-N system, struct. and plastic deform. *(Russian)* 78−80588

rectangular waveguides
air, microwave breakdown field calc., resonator and rectangular waveguide expt. 79−41789
anisotropic media, gyroelectric or gyromagnetic, EM wave propag. *(French)* 77−10813
arbitrarily shaped dielectric body inside waveguide, three-dimensional anal. 78−71005
blackbody radiation, EM fluctuations 79−41309
Cherenkov radiation source 80−99373

rectangular waveguides continued
dielectric, exact analytical soln. for waveguide modes 79−98490
dielectric loss measurements at microwave frequencies *(Russian)* 79−2788
dielectric waveguides for integrated optics, bending losses 78−63205
diffraction at inclined dividing boundary between dielectric materials in rectangular waveguide 79−885
EM field calc. in dielectric medium *(Russian)* 78−82884
EM wave scatt. by ideally conducting bodies in rectangular waveguide 79−81336
far IR waveguide laser Stark effect obs. 77−38875
flexible hollow waveguide, IR light propag., optical losses 77−19389
gas DFB laser waveguide precision calc. and pulse energy obs. 80−58577
H_{10} mode scatt., in rectangular waveguide, by cylinder with longitudinal slot 80−43238
hollow rectangular anisotropic dielec. guide, wave propag. 78−83084
inhomogeneous semiconductor plasma filled rectangular waveguide propagation 79−68928
IR flexible hollow metallic rectangular pipes, beamshaping and polarisation control props. 79−76856
laser, construction and operation characteristics *(Rumanian)* 78−59049
light pipes of different dimens., coupling efficiency 77−7186
liquid and solid complex permittivity meas., rectangular waveguide method 80−15941
optical, propagation losses at 10.6 μm for distributed feedback appl. 80−38101
plasma-filled, nonlinear mixing of microwaves 79−77394
pulsating sphere in acoustic waveguide, field suppression 77−68287
radiation generated by charged beam near plane flanged waveguide 79−13880
relativistic sheet electron beam interaction with slow-wave structure 77−38795
singularity extraction in kernel function rel. to rectangular cavity dyad 78−66728
subMM and MM detection by Josephson junctions mounted in a waveguide 80−4767
symmetrical rib optical waveguide fundamental modes 77−23744
total reflection by small slotted capacitive cylinder 80−5662
trifurcated parallel-plane plasma waveguide 77−84448
twisted IR metal waveguide, low-loss propag. and polarisation rotation 79−41435
two-dimensional object imaging *(Japanese)* 78−87146
undulator radiation anal. 78−71021
uniaxial anisotropic relativistic warm plasma, EM wave propag. and attenuation 80−59246
unit power standard for 53.57 to 78.33 GHz 80−90808
visualization of microwave EM fields using thermooptical effects in liquid crystals 80−62723
wave scattering by ideally conducting bodies in rectangular waveguide *(Russian)* 79−884
waveguide-dielectric resonances for UHF meas. of dielectric parameters 77−55760
weakly anisotropic rectangular dielec. optical waveguides, wave propag. anal. using coupled modes 80−64154
X-band ENDOR cavity 79−80653
CO_2 waveguide laser amplifier with strong discharge tube 80−74398
Ge waveguide, nonlinear third harmonic generation of submillemetre waves 80−44632
n-InSb, optical SHG in rectang. waveguide 80−43401
InSb waveguide, nonlinear third harmonic generation of submillemetre waves 80−44632
$LiNbO_3$ microwave laser beam electro-optic modulators using rectangular waveguides, 1.0 to 10 GHz 80−43381
$LiNbO_3$, Nd laser radiation, difference frequency generation in mm waveguides 79−18479
$LiNdP_4O_{12}$ glass-clad rectangular waveguide, laser performance 80−32996
n-Si, rod, in rectangular waveguide, microwave field distribution 80−39622

rectification
alternating current electrode processes, review 80−61107
full wave, demonstration 80−77598
IR point-contact diode tunnelling and rectification rel. to electrode geometry 80−57378
metal whisker diode, thermal field emission, nonlinearity, response time and polarity reversal 78−2579
metal whisker point contact junctions, tunnelling and rectification characts. 80−6955
metal-vacuum-metal point contact junction characts., Green's function calc. 80−103744
metallic point contact diodes, tunnelling props., geometrical asymmetry effects 78−10576
nonlinear wave rectification, quantum limit 80−83634
point contact IR detector tunnelling and rectification characteristics, geometrical and multiple image interactions 80−57376
point contacts between identical metals, HF rectification at low temp. 80−105706
polymer p-n junction, rectification effects in dark and photocurrents 77−69407
Schottkey barrier, high freq. rectification, transport theory 79−82660
Schottky barrier diode, CdS, with evaporated Au-Ti blocking contact 77−85319
thermoplastic-photoconductor media, charge carrier behaviour, microscopic response 79−28370
two-layer baths, dynamic rectification effect calcs. 78−95934
$Al/As_2SeTe_2/Sb$ structures, rectifying effects 80−75654
$Al_xGa_{1-x}As$-GaAs n-n heterojunction, LPE, Auger profiling and absence of rectification 78−95349
Al|chlorophyll-a|Hg/In, sandwich cell, photovoltaic, rectifying and tunnelling effects 79−1628
p-GaAs-Al interface, produced by diffusion method using heavily doped GaAs, rectifying props. 79−28409
$GaAs-Ga_{0.7}Al_{0.3}As$ n-n heterojunction, LPE, rectification 80−49888
GaAs-GaAlAs-GaAs rectifying semicond. struct., prep. by MBE and charcts. 80−65657
GaInAsP, rectifying and ohmic contacts 80−80376
n-GaP, optical rectification due to free carriers, detector appl. 77−10967
Ge, thermal rectification and negative differential cond. 79−42554

rectification continued
$Ge_{20}Te_xSe_{80-x}$-Si, amorphous-cryst. heterojunction form. of abrupt rectifying contact and depletion layer 79−65546
In_2O_3-Si(Ge)(GaAs)(InP) heterostructure solar cells, photovoltaic and rectifying props., electron affinity determ. 79−1618
KH_2PO_4,(KD_2PO_4), photoelectric phenomena, nonlinear optical rectification *(Russian)* 79−19628
Ni-Nichrome, MOM diode, breakdown effect in visible and near-IR regions 80−6999
$Pb_xSn_{1-x}Te$-PbTe p-n junction, epitaxial, elec. props. and photoresponse 78−56225
PbTe surfaces, Te coating, struct. and junction charact. 80−50743
$Se_{1-x1}Te_{x1}$-$Se_{1-x2}Te_{x2}$ heterostructure, amorphous, rectification phenomena and photovoltaic effects 79−99610
$Se_{1-x}Te_x$-$Se_{1-y}Te_y$ junctions, photovoltaic effects and rectification phenomena 80−84506
Si p-n junction, compressed by shock wave, rectifying props. 77−4429
a-Si-metal Schottky barrier, I-V charact., barrier heights 77−8191
n-Si-Ni surface barrier junction, rectifying, struct. and elec. charact., effect of low temp. annealing 78−14821
SnO_2-Si heterojunction solar cell, elec. props. *(Korean)* 80−45665
Te-Se-Cd, sandwich structure, fabrication and characteristics 80−60089
W-Ni, MOM diode, breakdown effect in visible and near-IR regions 80−6999
W-Ni point contact diode, rectifying props. in CO_2 laser radiation 77−76942
n-ZnS based heterojunctions, epitaxial, elec. props. *(Russian)* 78−88023
ZnS-$CuGaS_2$ n-p heterojunction, for LED appl., prep. and characterisation 79−1831

rectifier tubes
thermionic emission triode, with auxiliary discharge, rectifying parameters 79−64925

rectifier valves *see rectifier tubes*

rectifiers
see also electrolytic rectifiers; mercury arc rectifiers; solid-state rectifiers
corona gaps, asymmetrical, as high-voltage rectifiers 77−57352
electrolysis installation, circuit description *(Dutch)* 77−63925
fusion reactor, Doublet-III, frequency generator-rectifier system performance 80−102326
solar power satellites microwave power transmission system rectennas, Yagi-Uda receiving elements design, characteristics and economics 80−66938
As electroplating technique of manufacture, expt. *(Bulgarian)* 77−4744

rectifying circuits
see also rectification; rectifiers
burn period plasma current maintenance, rectifying first wall, cct. anal. 80−102307
current supply modules, parallel ferroresonance circuit anal. *(Russian)* 77−55708
electropolishing rectifier, thyristor current control, quick-acting electronic protection from short circuits 77−74377
glow discharge electrolysis, power supply unit, current regulator 77−39489
MIS structure wideband admittance meas. by phase-selective rectifier *(German)* 77−61089
phase controlled, in pulsed power supplies, charact. 77−83223
precision full-wave rectifier/integrator for physiological signals 79−83988
spectrometer LF module reference signal shaper 78−57924
stabilised rectifier unit 78−4643
start control device for ultrahigh press. short-arc lamp, current stabilisation 77−57362
three-phase frequency meas. transducers with saturating transformers 78−77893
transformer rectifier flux pump power supply using inductive current transfer 78−12704
transformer-rectifier flux pump power supplies performance anal. 78−12703

recursive functions
3j and 6j coeffs., recursive computation 77−5687
Anderson localisation problem, cond. numerical studies 80−49673
astronomy, J-integrals assoc. with close eclipsing binary stars, recursion formulae 77−9666
astronomy, J-integrals assoc. with close eclipsing binary stars, numerical evaluation 77−9668
atmospheric diffusion model for short distances and complex topography 77−37386
atomic spectra, two-electron matrix elements in Hylleraas coords., ang. integrals, radial recurrence relations 79−3386
eclipsing variables, light curves linear analysis, fractional light loss anal. 80−82416
education, Fibonacci numbers, recurrence relation soln., combinatorics function anal. 80−51988
education, recursive method for partition function calc., average energy calc., APL program 79−9050
Gaussian integrals, evaluation by backwards recursion or Taylor expansion 80−31488
Ising spin glass, three-dimensional mag. correlations 80−103849
linear differential equation with two strong singularities, second order, iterative numerical soln. method *(German)* 77−30000
linear recursion relns., discrete path approach 78−24678
molecule, modified Sharma formula for STO Lowdin alpha functions, coeff. matrix recurrence relations 79−31364
multiterm linear recursion relations 77−29992
octahedral group, symmetry-adapted functions, calc. of rotation matrices using recursion relation 80−31482
percolation problem, recursion eqn. *(Russian)* 79−38038
phonocardiogram classification, linear prediction analysis appl. *(Japanese)* 78−36010
radiative transfer exponential integrals, Λ-transform determ. via recursive anal. 79−35114
sound synthesis by continuous spectral transformation *(French)* 80−79100
SU_n C-G coeffs., contiguous relns., derivation method 78−74171
transition metal, de Haas van Alphen signal anal. by linearly recursive approx. 78−91603
transmission coeff. for 1-D potential barrier, discretisation of Schrodinger eqn. 80−57123

red giants *see stars*

red shift
see also cosmology; Doppler effect; gravitational red shift
0254+334/2, high-redshift QSO without Lyman α emission or absorpt., spectroscopic obs. 79−92886
0957+561 A, B, twin QSOs, absorpt.-line redshifts from multiple-mirror telescope obs. 80−12827
1008−3814, southern ring galaxy in Vela, struct., spectrum and redshift 79−58413
1309−216, probable BL Lacertae object with absorpt. red shift 1.49, optical spectrum 80−67856
1331+170, quasi-stellar object, 21 cm absorpt. detect. at $Z \approx 1.8$ 79−75292
1610−771, QSO with steep optical spectrum red shift 80−94887
A0035, large southern ring galaxy, radial vel., distance and dynamics 77−45559
Abell 2241, candidate X-ray cluster of galaxies 77−17699
Abell 2255, X-ray luminosity/vel. dispersion correl. for one and two cluster models 78−49553
Abell 2319, X-ray luminosity/vel. dispersion correl. for one and two cluster models 78−49553
Abell 262 cluster of galaxies, redshifts meas. 77−45579
Abell 2634 galaxy cluster, spectroscopic study and radial vels. 77−64857
Abell 399/Abell 401, X-ray binary galaxy cluster, radial vels. and mass 80−90546
Abell 401 cluster of galaxies, red shifts and vel. dispersion 77−26072
Abell 478, X-ray cluster of galaxies, redshift and optical struct. 78−8134
Abell 754, cluster of galaxies, radio galaxies redshifts 79−25737
Abell clusters, mean mass from Hubble diagram scatter 77−13474
abnormal galaxies and stars, discrete states of redshift 77−22307
anharmonic molecules, multiple photon absorption in CW laser beams 78−58755
8-anilinenaphthalene-1-sulphonic acid, edge excitation red shift, temp. depend. 77−6849
anomalous Hubble expansion and inhomogeneous cosmological models 77−13513
anomalous red shifts in galaxies compact groups, statistical anal. 77−22320
anomalous redshifts in galaxies and quasars, examples 79−25722
anomalous redshifts mechanism, possible measurable effects on shape of symmetrical spectral lines 77−13458
anthracene, fluorescence spectra in aq. and surfactant solns. 77−83639
AO 0235+164, BL Lacertae-type object, VBLI obs. of redshifted H I absorpt. 80−46658
AO 0235+164, Lacertid, optical and radio absorption line systems 78−16520
AO 0235+164, nature of nebulosity assoc. with BL Lacertae object 78−28778
AWM 4, redshifts for five galaxies in poor cluster 78−45415
bacteriorhodopsin, reson. Raman evidence for secondary protein-Schiff base interactions, primary excitation mechanism 80−55981
Bianchi V type universe, red shift and anisotropic microwave background 80−98744
binary galaxies, radial vel. separation rel. to dynamics 78−4354
bright galaxies, optical redshifts 78−89252
bright quasars discovery program, preliminary results 77−17715
3C273, spectroscopic obs. and redshift of associated galaxy 78−77606
3C 111, spectrum and redshift of luminous N-type galaxy 77−33666
3C 120, underlying galaxy red shift from spectrum of assoc. nebulosity 80−67890
3C 232, quasar, redshifts of quasar lines and NGC 3067 CaII absorpt. lines 78−36719
3C 249.1, quasar, spectroscopic obs. of assoc. nebulosity 77−33677
4C 25.05, H_2 lines identification in spectrum of quasar *(Russian)* 78−69905
3C 286, quasar, optical absorpt. lines detect., redshift 80−4454
3C 286 radio absorpt. line, red shift rel. to cosmological deceleration meas. 78−20902
3C 303, QSO group in cluster, gravit. lens effect rel. to red shift 77−78878
3C 33, red shifts and rot. axis of assoc. optical galaxy 78−4355
3C 343.1, distant radio galaxy, spectroscopy and photometry, redshift 78−8123
4C 39.11, N galaxy, radio and optical obs. and red shift 78−16553
4C 55.27, quasar, redshift and spectrum 77−45596
CA 0340−538 (3U 0328−523), southern cluster of galaxies, redshift, vel. dispersion and global parameters 78−36705
α Carinae (Canopus), generalised Compton effect in spectrum 78−53938
catalogue of galaxy redshifts rel. to local mean mass density and galaxy clustering 78−45436
cD galaxies in poor clusters, photometry, spectra and redshifts 79−48907
cD galaxies in poor clusters, radial vel. meas. 79−8994
Centaurus cluster (HMS 1247−4102), galaxies redshifts meas. 77−45578
Centaurus I cluster of galaxies, redshift meas. and resolution into two vel. systems 80−77499
charged sphere, freq. shift of radiation from moving surface 77−57260
chronometric redshift theory, erroneous presentation correction 78−85839
cluster galaxies, redshift determ. using Image Dissector Scanner, visible spectra 80−90544
cluster of galaxies 0122−688, spectrographic obs., redshift 80−41906
clusters of E and S0 galaxies, colour distribution rel. to redshift 80−105361
clusters of galaxies, ang. size-red shift relation as test for deceleration parameter 78−12437
clusters of galaxies, ang. size-redshift relation for nearby clusters 78−4372
Coma Berenices supercluster, appl. of nonisotropic Newtonian cosmological model *(Spanish)* 79−48978
Coma cluster, two-dimens. struct., Zel'dovich disc model 78−41062
Coma I galaxy cloud, redshifts and struct. 77−45575
Coma/A1367 supercluster of galaxies and environment 78−65700
compact galaxies in systems of galaxies, redshifts 77−71143
conference on high redshift objects, IAU Symposium 92, Los Angeles (August 1979) 80−101669
conformally invariant gravit. theory, astrophysical appl. 77−82428
Corona Borealis cluster of galaxies, vel. dispersion 77−49487

red shift continued
S Coronae Austrinae, a bright southern YY Orionis star, absorpt. line red shifts 77−29818
correctionless observational cosmology 79−53946
cosmological, critical anal. of explanation by new field 77−9828
cosmological constant and data reduction 80−41923
cosmological distance determination, new method, appl. to weighing of Universe 79−9003
cosmological models with Hoyle's hypothesis 78−86045
cosmological objects in nonradial motion, redshifts, special and general relativistic anal. 79−80212
cosmological red shift, Doppler and gravitational components using Birkhoff's theorem 78−86041
cosmological red shift, nonexpanding universe models 78−57705
3CR radio galaxies, redshifts, strong emission line spectra 77−33666
Cygnus A, red shift and rot. axis of assoc. optical galaxy 78−4355
DA 240, radio galaxy, jet, high-vel. gas obs. 78−28773
de Vaucouleurs' groups of galaxies, type-redshift relation 77−17693
deceleration parameter, determ. from struct. of galaxy superclusters 77−64889
Dirac cosmology Hubble-Sandage diagram for first ranked galaxies 77−57110
discrepant red shift associations, QSO-galaxy and QSO-QSO pairs statistical anal. 79−8999
distance relation, square law 79−67095
distant cluster of galaxies, photometry and red shift 78−12377
distant objects, magnitude-redshift and ang. dia.-redshift relations for matter and radiation filled universes 78−20917
Doppler redshifts in oblique approach of source and observer, for teaching 79−58475
double radio sources, ang. size-redshift test 77−57100
dwarf galaxies, H I redshifts rel. to absolute solar motion and discrete redshift 78−49530
emission line objects from Curtis Schmidt thin prism survey, redshifts 78−28537
emission line redshift, and true redshift differences 77−64853
emission-line galaxies with IR excesses, red shifts from 8000-11000 Å spectra 77−67124
emission-line objects in Curtis Schmidt thin prism survey, redshifts 78−28538
ESO 012-G21, Seyfert 1 galaxy, spectrum, redshift, UBV photometry and X-ray identification 80−8695
ESO 113-IG45, galaxy and/or quasar, red shift 78−28782
ESO 140-G43 (Fairall-51), new southern Seyfert 1 galaxy, discovery and red shift 78−54044
excited mols. that have undergone radiationless transitions, optical probing 77−27106
extragalactic objects, redshift distrib. and luminosity function *(Chinese)* 80−4437
extragalactic objects, redshift distrib. rel. to evolution of galaxies 80−90527
extragalactic redshifts, interpretation 80−4427
faint galaxies radial vel. meas. from objective prism plates 77−45562
faint quasars, spectroscopy and props. of CTIO 4 metre survey 78−32592
Fairall 9=ESO 113-IG45, companion galaxy to Seyfert 79−44616
Fairall 9 and Fairall 51, spectrophotometry, Seyfert 1 class galaxies 79−17076
field galaxies space distrib., redshifts and photometry of complete sample 79−21418
Fourcade-Figueroa galaxy near NGC 5128, resolution, redshift and distance 78−73758
Friedman universe, parallax depend. on redshift 78−12438
G-varying cosmology, galaxy and QSO magnitude/red shift relations 80−56980
galaxies, absolute mag.-redshift var. in magnitude-limited sample 79−101189
galaxies, angular redshift anisotropy, additional evidence and interpretation 77−2472
galaxies, bright, nearby, vel. field and Local Group peculiar motion rel. to Virgo cluster 80−36699
galaxies, bright with low red shift, red shift-magnitude relation 80−101639
galaxies, colour-redshift relations as probe of cosmology and galactic evolution 77−33627
galaxies, compact and bright-nucleus, in S.hemisphere, spectra, redshifts and blueshift 80−94725
galaxies, Doppler shift meas. technique without spectrograph 78−20646
galaxies, Doppler shifts distrib. for relativistic gas 78−65492
galaxies, double, redshift intervals periodicity 80−56923
galaxies, early-type, in NGC 7331 field, distances rel. to red shifts 80−4435
galaxies, early-type, redshift distance moduli rel. to distances from relative luminosities 80−31363
galaxies, elliptical, red shifts and vel. dispersions rel. to mass to light ratios 80−98707
galaxies, homogeneity of sample used to determine Hubble parameter 77−13506
galaxies, Hubble's law as laboratory exercise in astronomy 78−65740
galaxies, interacting, radial vels. rel. to luminosities and diameters 80−17677
galaxies, Kirshner, Oemler, Schechter redshift sample rel. to universe mean mass density 79−75298
galaxies, late-type, red shifts from H I obs. 78−86015
galaxies, luminosity evolution from 2.2 μm of giant ellipticals 80−105358
galaxies, nearby, H I profiles and redshifts 80−41895
galaxies, optical redshifts 80−56936
galaxies, radial vels. distortion by night sky spectrum 77−41406
galaxies, redshift discrete states, systems of galaxies 77−37643
galaxies, redshift-distance square law statistical scrutiny 78−81683
galaxies, redshift-magnitude bands and evolution from Perseus and A1367 clusters obs. 78−54033
galaxies, redshifts, vel. dispersions and line strengths meas. 77−29916
galaxies, redshifts and superluminal expansion vels., kinematic model 77−26050
galaxies, redshifts for 196 bright objects 80−46661
galaxies, reshift-distance relation and evidence for linearly expanding Universe 80−31354
galaxies, Simkin effect and Hg I 4047 Å night sky contamination 78−41032

red shift continued
galaxies, statistical method for determ. of cosmological density parameter 77−29965
galaxies, surface brightness-redshift relation and evolution 77−13462
galaxies, V−K colours and IR Hubble diagram for giant ellipticals 80−105359
galaxies and quasars, composite Hubble diagram 77−22333
galaxies and quasars paradoxical redshifts compatibility with gravitation theory 78−73757
galaxies evolution and redshift-magnitude bands, data anal. 78−57629
galaxies form ESO/Uppsala list, spectroscopic obs. and radial vels. 77−22113
galaxies in Abell 2255, red shifts 79−40276
galaxies in rich clusters 80−85872
galaxies in Yerks poor clusters 80−51858
galaxies near late-type spiral NGC 4945, radial vels. and BV photometry 80−109547
galaxies of high surface brightness, spectra, redshifts absolute magnitudes *(Russian)* 77−49467
galaxies of high surface brightness, spectral obs. *(Russian)* 77−49466
galaxies red shifts, evolution free test for non-zero cosmological const. 80−4465
galaxies redshift-magnitude bands, internal struct. and galaxies morphological evolution 80−22070
galaxies with double and multiple nuclei, radial vels. of nuclei components 80−67848
galaxy cluster found by Einstein Observatory, CCD camera study and redshift 80−62315
galaxy clusters, LF gravitational radiation and redshift discrepancies 77−71148
galaxy clusters, radial vel. dispersions of real and spurious clusters 80−101643
galaxy clusters with known galaxy number-density distrib., redshifts and other data 79−80362
galaxy group in Cetus with redshift discrepancy 78−36708
galaxy groups, radial vel. meas., membership, mass/light ratios and distances 77−33660
galaxy groups, radial vels. distribs. and virial props. 79−9010
galaxy quintets, statistical anal. of discrepant redshifts 78−65701
galaxy redshifts rel. to photon damping in discrete space-time *(Chinese)* 77−67145
galaxy redshifts survey, data reduction techniques 80−22074
galaxy vel.-distance relations and Local Supercluster Hubble ratio 80−17698
geometry of the space of events hypothesis 77−53713
Hercules supercluster, basic redshift data 80−36725
Hercules supercluster, cosmography 80−51883
Hubble's constant, doubling rel. to superluminal radio sources model 78−81722
Hubble's law, appl. to inverse square law deduction from Newtonian cosmology *(Italian)* 80−8722
Hubble's law, galaxies recession and quasar redshifts *(Swedish)* 77−71144
Hubble constant, implications for discrete source models of diffuse X-ray background 79−101226
Hubble constant and Virgo I cluster distance 79−62917
Hubble constant determ., large turbulent Universe model 78−96578
Hubble constant determ., large turbulent Universe model 79−58453
Hubble constant value limits from obs. of galaxy clusters 79−67099
Hubble diagram curvature, from redshifts and photometry of distant galaxy clusters 78−49515
Hubble diagram for QSOs 78−77616
Hubble diagram statistics, form of luminosity function and density vars. with appl. to quasars 79−97093
Hubble diagram statistics, q_0 determ. and luminosity evolution rel. to quasars 79−71102
Hubble Law, rel. to Newtonian mechanics and gravitational theory *(Italian)* 80−12835
Hubble law isotropy test on quasars 79−97111
Hubble Modulus, numerical simulation test of cluster effect 79−2569
Hubble modulus increase behind clusters of galaxies 77−78872
Hubble parameter, anisotropy rel. to large-scale cosmological inhomogeneity 77−91675
hydrogenic ion lines, red shift in plasma 80−103128
IC 342, Scd galaxy, companion galaxy discovery and systemic velocity difference 80−36712
IC 5152, low-luminosity barred galaxy, struct., rot. curve and redshift 80−56950
interacting glaxies, radial vels. and luminosities 77−78874
intergalactic medium, shock waves generated by galaxies and quasars at large redshifts 79−21442
Klemola 44, X-ray cluster of galaxies, redshifts and vels. 78−45414
BL Lacertae, spectrum and redshift 77−26055
BL Lacertae objects, redshifts upper limits from absence of redshifted C IV absorpt. lines 80−62267
AP Librae, BL Lacertae object, emission lines obs. and red shifts 77−29932
light having traversed moving prism, freq. shifts *(Spanish)* 77−88638
line broadening by photon interaction with new field 79−48663
local cluster, satellite galaxies and globular clusters, radial vels. and galactic mass 78−49522
Local Group galaxies, 21 cm red shifts and solar motion rel. to centroid 78−12376
Local Group galaxies, possible new members from solar motion solns. 77−22321
Local Supercluster, redshift anisotropy, luminosity selection effects 77−74147
local supercluster and red shift anisotropy *(Russian)* 79−92875
Longuet-Higgins-Pople theory extension using isotropic polarisability 79−31617
M82, Ne II 12.8 micron emission obs. and red shift 79−17082
M83 and Centaurus galaxy group, redshifts rel. to distance 80−4434
M87, red shifts and dynamical evidence for central mass concentration 78−49529
Markarian 132, spectrum and redshift systems 78−89248
Markarian 205, spectrum and redshift of nearby condensation rel. to distance 79−97058
Markarian 231, Seyfert galaxy, emission and absorpt. line redshifts 77−45558
Markarian 295, 297, radial vels. from optical and 21 cm obs. 79−44608

red shift continued
Markarian 296, clumpy irregular galaxy, radial vel. from optical and 21 cm obs. 79−44608
Markarian 374, Seyfert galaxy, double nucleus components red shifts 78−69882
Markarian galaxies, Hubble modulus 78−49538
massive black hole accretion disc, red and blue shifts rel. to X-ray spectrum 78−40985
MCG-5-9-22, galaxy, red shift rel. to supernova absolute magnitude 78−81644
MKW 3s, poor galaxy cluster, redshifts obs. rel. to cD galaxy extended X-ray emission 80−51884
MR 2251−178, X-ray QSO, spectrophotometric obs. 79−17122
multiphoton absorption induced reactions, appl. of effective photon concept 78−88651
neutron stars, redshift determ. of X- and γ-ray lines rel. to strong principle of equivalence 78−40814
neutron stars, rotating, max. surface redshifts in bi-metric theory of gravitation 80−90466
NGC 1023 galaxy group, H I radial vels. rel. to group membership and mass/light ratio 80−82521
NGC 1023 galaxy group, H I redshifts of subgroups and possible intergalactic H I cloud 80−67886
NGC 1275, spectrum and vel. systems 77−33630
NGC 128, S0 galaxy, red shift and rot. curve 77−33631
NGC 1313, barred spiral galaxy, red shift from interferometric study 77−49474
NGC 2639 companion galaxy, redshift and assoc. UV excess objects 80−56965
NGC 2915, southern galaxy, red shift from optical and H I obs. 77−67126
NGC 2997, late-type galaxy, rot., mass and systemic vel. 79−21409
NGC 3227, Seyfert galaxy, photoelectric photometry, spectrum and redshift 80−98724
NGC 3256, peculiar galaxy, radial vels. and kinematics 78−96537
NGC 3379, elliptical galaxy, red shifts, rot. and vel. dispersions 78−49529
NGC 4235, Seyfert galaxy, spectrum and radial. vel. 78−49536
NGC 4248, radial vel. from H I obs. 78−4358
NGC 4945, galaxy, water vapour emission redshifts 78−93427
NGC 5128 (Centaurus A), heliocentric rel., struct. and evolution 80−4429
NGC 5416 cluster, redshifts, morphologies and photometry 79−58434
NGC 6240 unusual radio galaxy, optical redshifts 80−4440
NGC 628, evidence against discrete states of redshift 77−60820
NGC 6872, remarkable barred spiral, redshift distance and linear extent 80−31358
NGC 931, interacting Seyfert galaxy, struct. and redshifts 79−25716
NGC 935-IC 1801, close pair of spiral galaxies, systemic vel. and rot. curves 77−45556
non-Dopplerian nature, static Euclidean model 80−73081
nonstatic universe, generalised Doppler formula 77−78900
NRAO 5 GHz and 4C catalogues, optical spectra and redshifts 78−8145
objects at the highest redshift 80−105360
OH 471, QSO, gravit. and cosmological redshifts 77−13229
optical quasars, radio and optical obs., redshifts, luminosity function 78−49552
OQ 172, H_2 lines identification in spectrum of quasar *(Russian)* 78−69905
OQ 172, quasar, H_2 absorpt. lines identifications and redshifts 80−36734
OQ 208, red shift difference between broad and narrow emission lines 79−67100
parallactic distances in locally inhomogeneous Universe 79−97120
parent galaxies of supernovae 79−44612
peculiar extragalactic sources, red shifts from mutliaperture UBV photometry 78−28772
PG 1115+08, triple QSO, spectroscopic obs. and gravit. lens model 80−86012
PHL 1070, quasar spectrum and redshift of surrounding halo 78−28771
PHL 957, quasar, H_2 and CO absorpt. lines redshift *(Russian)* 79−101216
photon decay in curved space-time, Hubble red shift and solar limb effect explanation 79−35606
photon splitting into 3, cosomological limits, spectral broadening, frequency-dependent and multiple red-shifts 80−77284
photon-scalar boson scatt., impact on Planck's radiation law and Hubble effect 78−54212
Pisces group of galaxies, redshifts meas. 77−45579
PKS 0237−23, absorpt. spectrum obs., absorpt. lines origin 78−41074
PKS 0237−23, absorption redshift of QSO 79−35417
PKS 0521−36, BL Lacertae object, optical spectrum and redshift 79−84854
PKS 0528−250, neutral stellar object with no emission and rich absorption 78−49551
PKS 0537−286, high-z QSO with extreme Lyman continuum cutoff 79−12538
PKS 0735+178, BL Lacertae object, spectrum, multiple components in z=0.424 absorpt. system 79−25707
PKS 1157+014, spectral obs., of QSO with no Lα emission 80−31384
PKS 1158+007, redshift from QSO spectrum 79−58440
PKS 1402+044, dissector scanner obs. of red object with 3.20 redshift 78−65710
PKS 2126−15, bright quasi-stellar object with neutral colour and redshift of (3.27) 78−93450
PKS 2155-304, BL Lacertae object, no evidence for redshifted forbidden O III emission 80−73035
polyatomic organic molecules, electronic excitation transport in inhomogeneity broadened 79−54884
Population II stars at distortion∼10, rel. to distortion of cosmological microwave black body radiation spectrum 80−67915
primeval galaxies, investigation of red shift 80−31372
profile of lines emitted by massive body or bodies behind it *(French)* 80−46670
protogalaxy formation age and γ-ray background 80−62325
pseudoscalar bosons rule *(French)* 79−44361
pyrene, fluorescence spectra in aq. and surfactant solns. 77−83639
Q0000−398, high redshift, large angular size, 2695 MHz obs. 77−45601
red shift continued
Q2227.6−3928, highest redshift quasar from Tololo deep survey 78−12403
Q2228.1−4033, high redshift quasar from Tololo deep survey 78−12403
Q 0002−422, QSO with $z_{abs} \ll z_{em}$ 78−16565
Q 0957+561, double quasar, red shift of galaxy component of spectrum 80−27005
Q 1246−057, absorpt. line spectrum, presence of outflowing material 78−93453
Q 2240.9-3702, Q 2238.9-4115, optically selected QSOs with broad-lined absorpt. systems, redshifts 80−4456
QSO 0242+622, spectrum and luminosity of low redshift object 78−93451
QSO 1038+528 A,D, close pair of radio-emitting quasi-stellar objects, optical redshifts 80−51902
QSO absorption line spectra for six high-redshift objects 78−93449
QSO candidates, redshifts for 38 objects 80−56966
QSO candidates, spectroscopic obs., indentifications 80−31385
QSO pairs, spectroscopic obs. 77−5587
QSO redshift $(1+z_i)/(1+z_j)$ distrib. 78−65715
QSO redshift data, statistical 78−32598
QSO redshifts and field galaxies 78−89271
QSO/galaxy associations, redshifts and distances 80−31369
QSOs, absorpt. line redshift distrib. 80−90563
QSOs, absorpt. line redshifts rel. to absorbing regions physics 78−57680
QSOs, absorption lines shortward of Lα emission, redshifts, origin in moving H I clouds 79−9025
QSOs, absorption systems in high redshift objects 78−28843
QSOs, emission-line spectra and redshift distrib. 78−57677
QSOs, high-redshift, Image Dissector Scanner (IDS) spectrometry and redshifts 80−22111
QSOs, optically selected, redshift inverse correl. with radio detectability 80−82536
QSOs, profiles and redshifts of broad lines 78−16566
QSOs, redshift doublets in absorpt. spectra, model 77−22325
QSOs, redshifted clouds, 21 cm line studies 80−105389
QSOs, redshifts for 24 optically selected objects 78−54073
QSOs, selection effects in redshift distrib. 78−57674
QSOs, super-luminal velocities and chronometric redshift theory 79−9023
QSOs from Molonglo Deep Survey, optical spectra 80−94884
QSOs in Tololo deep survey, apparent red shift cut-off unreal 79−12539
QSOs lying in spiral arms of NGC 1073, spectrophotometric obs. and redshifts 80−22110
QSOs near bright galaxies, non-cosmological redshifts 80−105386
QSOs number density excess and initially inhomogeneous cosmologies 79−2576
QSOs of small and intermediate emission redshift, absorpt. lines homogeneous survey results 80−31218
quasar, strong emission line, with redshift z=0.189, spectrum and photometry 80−8710
quasar 0933+733, redshift determ. from low dispersion objective prism plates 79−2485
quasar 1229−021, H I 21 cm absorpt. at redshift z=0.395 79−62928
quasar absorption, origin of redshift splittings and large absorpt. redshifts 78−57684
quasar absorption line systems, lack of dust 77−49493
quasar absorption lines due to intervening interacting galaxies 77−17714
quasar Hubble diagrams, nonparametric statistics 79−40289
quasar near companion galaxy NGC 5296, spectrum and redshift 77−13489
quasar radio var. timescale, redshift effect 77−29947
quasar red shifts, anal. for randomness 78−12400
quasar redshift data, cosmological interpretation using V/V_{max} test 78−28844
quasar redshift determ. from low dispersion objective prism plates 79−2485
quasar redshifts, teaching consideration 80−90621
quasar redshifts cosmological nature, new test 77−17713
quasar redshifts distributions, periodicity 80−62313
quasar spectra, statistical tests for line-locking evidence 77−33675
quasar-galaxy associations, search using Jodrell Bank 966 Hz survey 78−24566
quasars, absolute magnitudes and Hubble plot 77−91662
quasars, absorpt. line spectra and redshift systems 77−13488
quasars, absorption line spectra, accidental redshift system estimation 78−16562
quasars, absorption red shift systems origin in galactic coronae 77−13448
quasars, angular diameter−redshift test for large redshift objects 78−28841
quasars, colours in near IR, interpretation 78−69904
quasars, CTIO surveys of large redshift objects 78−57692
quasars, cyclic depend. of brightness on parameter ln (1+z) 80−105382
quasars, discovery and theories, review 77−60847
quasars, Doppler shifts distrib. for relativistic gas 78−65492
quasars, emission line redshift distrib. 77−53698
quasars, emission line redshift distrib. gaps, trend analysis 78−45423
quasars, emission line redshifts random distrib. 78−54070
quasars, emission-line, new candidates redshifts and faint quasars number limits 79−92884
quasars, faint red 3C QSO candidates spectrophotometry and red shifts 80−67897
quasars, gravit. and Doppler redshifts, interpreted as massive black holes ejected from galaxies 80−46695
quasars, high-redshift, from CTIO survey 78−4389
quasars, Hubble diagrams 78−57691
quasars, Hubble diagrams and optical luminosity functions 78−61930
quasars, line identifications, red shifted UV lines or violet shifted IR lines 80−8707
quasars, ln(1+z) periodicity 78−12406
quasars, nonuniform radial distrib. regardless of redshift 78−32593
quasars, optical and radio Hubble diagrams 78−28845
quasars, periodicity in ln(1+z) distrib. 77−22327
quasars, props. of $Z_{abs} > Z_{em}$ systems rel. to origins of QSO absorpt. line systems 78−57682
quasars, red-shift hypothesis implies Earth-centred universe 78−16563
quasars, redshift and 3 GHz radio magnitude correl. 78−45422
quasars, redshift distrib. periodicity, selection effects 78−57690
quasars, redshift-magnitude relation, statistical study and chronometric cosmology 78−93455

red shift continued
quasars, redshifts and Hubble diagrams 78−96559
quasars, redshifts and superluminal expansion vels., kinematic model 77−26050
quasars, redshifts clumping and geocentric universe 77−87565
quasars, redshifts of 24 southern objects 77−13491
quasars, rejection of photon-photon interaction explanation 79−35423
quasars, selection effect in absorption line redshifts 79−92885
quasars, slitless spectroscopy of large redshift objects 78−96562
quasars, spectral characts. of three high redshift objects 80−4455
quasars, z=1.95 peak rel. to line-locking and intervening galaxies models for absorpt. lines 78−57685
quasars 0957+561 A, B, twin quasistellar objects or gravit. lens theories 79−67114
quasars absorption line redshifts, limits to past variability of proton/electron mass ratio 77−61338
quasars absorption lines, red shifts statistics and line-locking effects 78−57681
quasars absorption redshifts, evidence for large-scale uniformity of physical laws 80−73079
quasars aligned across galaxy NGC 3384 79−53927
quasars and rich clusters of galaxies, two-point ang. correl. function 79−80364
quasars assoc. with compact radio sources, apparent magnitude-redshift relations for resolved and unresolved sources *(Chinese)* 80−105380
quasars emission line redshifts distribution periodicities 77−60842
quasars from Molonglo Deep Survey, spectra and red shifts 78−69900
quasars greatest redshifts rel. to parent galaxies masses 77−49480
quasars in region of NGC 1629 companion galaxy, spectra and redshifts 80−56965
quasars in southern hemisphere, spectra and redshifts 77−67137
quasars in spiral arms of galaxy NGC 1073 79−53904
quasars near peculiar pair of galaxies NGC 7714−7715, spectra and redshifts 78−28835
quasars of Michigan-Tololo survey, spectrophotometry and redshift distrib. 80−22105
quasars redshifts, relativistic Doppler formula rel. to transverse vels. and distances *(Chinese)* 80−105379
quasars with absorption redshifts greater than emission redshifts, spectroscopic study 77−45595
quasars with radio structure, statistical analysis and redshift-magnitude relation *(Chinese)* 77−67135
quasars with strong interplanetary scintillation, magnitude-red shift link *(Chinese)* 80−12828
quaser red shift parameter ln (1+z), periodicity 80−17687
quasi-stellar objects, absorpt. line spectra review 78−57679
quasi-stellar objects, low-redshift, absorpt. lines obs. and redshifts 79−21459
quasi-stellar objects, red shifts correl. with element abundance ratios 78−20903
quasi-stellar radio sources from 4C and Parkes catalogues, redshifts and magnitudes 78−65714
quasi-stellar radio sources with large redshifts, angular dia.-redshift test 78−24565
quasistellar objects possible assoc. with radio galaxies and rich clusters of galaxies 78−8142
radio galaxies, new complete sample, struct., redshifts 79−17096
radio galaxies, optical catalogue 80−21931
radio galaxies, red shift dependence of proper densities and colours 80−62286
radio galaxies in Coma cluster, red shift distrib. 78−12358
radio sources, cosmological evolution rel. to predicted redshifts 78−41070
radio sources, double, redshifts rel. to hot spots behaviour 80−94882
radio sources, double, separation depend. on redshift 80−22096
radio sources, extragalactic, ang. size-redshift diagram interpretation 80−22101
radio sources, extragalactic, redshift-apparent dia. relation 77−87559
radio tail galaxies in clusters 78−69889
radio-galaxies with $13.0 \leq m_{corr} \leq 15.5$, peculiar radial rel. distrib. 77−9798
radio-quiet quasars, Hubble diagram, luminosity function and density evolution 80−51903
radiogalaxies, colour and space density, redshift dependence 79−75278
radiogalaxies, optical spectroscopy and redshifts for 18 objects 80−56966
radiogalaxies, redshift-magnitude relation and cosmological test 78−28798
radiogalaxies from B2 Catalogue, optical identification, radio positions and redshifts 80−86005
radiosource populations and redshift interpretation in evolutionary use 78−28832
radiosources, angular diameter-redshift relation for scintillating sources 78−28824
radiosources, cosmological information interpretation 78−28831
radiosources, optical identifications, spectrophotometric obs. 79−92879
radiosources, red shifts and rot. measures, Universe isotropy test 77−2502
radiosources cosmological evolution, free-form analysis, self-consistent luminosity function 80−46716
recession vels. greater than light 77−87585
relativistic interpretation of redshift related to light crossing clusters of galaxies 77−17685
relativistic radiation temperature of moving bodies 78−57775
RMB 56 (1216+141), compact galaxy, blue shift 78−16527
Sa type spiral galaxies, redshifted 21 cm line profiles, radio obs. 80−73041
SC galaxies, space distrib., large-scale struct. 79−71106
Sc I galaxies, vel. anisotropy rel. to motion of Galaxy and Local Group, data 77−5560
Sc I galaxies, vel. anisotropy rel. to motion of Galaxy and Local Group 77−9796
Sc-type galaxies of Rubin et al. sample, Milky Way galactic absorpt. study 78−49533
Segal chronogeometric redshift, classical anal. 77−45618
Seyfert galaxies, H I redshifts 79−8988
Seyfert galaxies, profiles and redshifts of broad lines 78−16566
Seyfert-like galaxies, medium-redshift, redshift-magnitude-ang. dia. data statistical anal. 78−86016
Seyferts, quasars and red shift controversy 77−2476
Shahbazian I group of galaxies, dynamics from spectroscopic, obs. 80−67878
short-pulse laser backscatter from gas target 80−79454
solar limb effect, Fe I line contours and shifts 77−13309
solar Lyman α line, wavelength and profile meas. 79−8896
southern groups and clusters of galaxies, redshift data 79−84861
southern Molonglo radio sources, optical spectra and redshifts 78−96555
southern Parkes radiosources, redshift obs. 78−20899
southern peculiar galaxies and galaxy pairs, morphologies, spectra and redshifts 78−32579
southern radiosources, red shifts for 32 Parkes objects 79−44627
southern radiosources, redshift meas. 77−26075
southern radiosources, redshifts for 19 QSOs and three galaxies 79−97060
spacetime, extended conformal, interactions and dynamical groups of elementary particles 78−8290
spherically symmetric self-similar universe, redshifts and blueshifts 80−8727
spiral and elliptical galaxies in Virgo cluster, redshift differences 77−17694
spiral galaxies with large redshifts, optical obs. 77−29933
star clusters, isotropic relativistic, stability rel. to centrel redshifts 78−73742
star clusters, relativistic, with high central redshift 80−105293
steady state Universe using stochastic electrodynamics, cosmic background radiation and red shift 78−77631
steep spectrum radiosources, spectral index dependent props. 80−36730
Stephan's Quintet, H I emission search 79−30136
Stephan's Quintet, redshifted H I associations 80−67882
Sun, limb effect of redshift rel. to solar activity 77−53553
superluminal radio sources, cosmological proper motion-redshift relation 80−22095
Tautenburg objective prism survey objects, high-resolution spectra and redshifts 80−4436
TCNE aromatic donor/acceptor complexes, reson. Raman excitation and absorpt. profiles, model theory 77−18982
4U 0241+61, optical and radio identification, luminous low-redshift QSO 78−61940
Universe and general field clumpy structure 78−45443
universe expansion law, effect of cosmological turbulence 78−77629
velocity-distance relation, history 80−12880
Virgo cluster, distance and redshift rel. to Hubble's const. 78−89265
Virgo cluster area, study from taxonomy and redshifts *(French)* 79−35400
Virgo cluster redshift controversy, evidence from Centaurus cluster 78−54061
VV 150, galaxy chain, photoelectric photometry, spectrum and redshift 80−98724
VV 8, galaxy, red shift, rot., mass and surface brightness obs. *(Russian)* 79−48937
white holes, blueshifted light rays emission rel. to ang. appearance 78−45352
Zw 1400+0949 cluster (NGC 5416 group), radial vels. rel. to group dynamics 80−22090
I Zw 1727+5015, redshift and spectra of BL Lacertae-type object 78−41044
III Zw 2, quasar, spectrophotometry of assoc. galaxies and nebulosity, redshifts 79−21460
H I in field of elliptical galaxy NGC 1052, line profiles and systematic vel. shift 80−98719
H I profiles classification system for dwarf galaxies, discrete redshift and asymm. 78−49517
H, line spectrum, relativistic red shift phenomenon 80−32675
Hγ energy levels and Debye screening, no evidence for red shift 79−31369
NaKr, red wing radiation and pot. 80−87180
S_4N_4, Raman scatt. and opt. absorpt., press. and temp. depend. 77−36227

reduction (chemical)
see also oxidation
actinide oxides, preparation of metals and refractory cpds. 80−16229
actinides, in molten halides 77−29088
air-acetylene flame, atom form., theory 78−7208
N-alkylpyridinium salts, electrochem. reduction, radical form., INDO calcs., EPR obs. 77−71821
alumina reduction cells, electrolytic, instabilities of metal surface, computer simulation 78−39720
aromatic compounds, by KC_{24} intercalation compound 80−3306
bacteria, photosynthesis, primary electron acceptor, EPR, ENDOR investigs. 78−77004
bacteriochlorophyll, photochem. oxidised, kinetics of dark reduction, R. rubrum chromatophores 77−25390
bacteriochlorophyll *b* and pheophytin pair redox potential obs. 79−39338
bacteriochlorophyll P870, photo-oxidised, dark reduction kinetics, temp. depend. 77−36888
bacteriochlorophyll-800, implication in picosec. electron transfer to bacteriopheophytin in R.rubrum reaction centres 80−35844
basaltic magmas, O_2 fugacity, role of gas forming elements 78−77218
basalts, terrestrial, lunar and planetary, redox state 78−77217
bauxite reduction at 800-1800°C, corundum recrystallization 77−86296
Bering Sea shelf sediments, denitrification estimates 80−12433
bilirubin, aq. soln., pulse radiolysis 78−48761
butadiene, effect of redox initiation in emulsion polymerisation *(German)* 78−85158
carbonaceous chondrites, reduction kinetics, Mossbauer obs. 80−41777
carbothermic process for production of pure highly reactive metals from oxides 80−3311
carboxyhaemoglobin, redox investig. using reson. Raman, visible absorption and electrochem. methods 78−76832
cassiterite, reduction by H_2 *(Korean)* 79−39201
chlorophyll, aq. solns. of detergents, polarographic obs. 79−57565
chlorophyll, electron transfer across octane-water interface 77−81474
chlorophyll analogues, mechanism of activation of photosensitising action 79−57583
chlorophyll excited stated, redox pots. 77−25372
chlorophyll in aqueous solns., electrochem. behaviour, cathodic reduction 79−29373
chlorophyll pigments of photosynthetising organisms redox pots. rel. to evolutionary development 77−56337
chlorophyllide fluorescence quantum yield during photochlorophyllide reduction in etiolated leaves 80−81542

reduction continued
chloroplast suspension, photoinduced changes in oxidation-reduction pot. rel. to photosystem II activity 77−25399
chromatophores of Rhodospirillum rubrum, kinetic characts. of dark reduction 79−53067
chromite, carbothermic reduction 79−61900
chromites, reduction to ferrochromium in methane-H_2 gas mixtures 77−60109
clay, Al_2O_3 and SiC recovery by C reduction 80−108704
coal, new catalysts for CO-H_2O induced liquefaction 80−30335
copper molybdates, oxidation, reduction and thermal decomp. mechanisms 80−50847
corundum, behaviour in reducing conditions at temps. above 1700°C 77−16522
corundum, spinel formation during reducing heating 77−36427
2-cyclohexenone, reduction by hydride ions, delocalised model, CNDO/2 calc. 79−79231
cytochrome c_3−hydrogenase, reduction kinetics, Mossbauer spectra 80−67031
cytochrome c, electron reactions in ethylene glycol/water glass at −196°C 79−62194
cytochrome C, immobilised, investigs. using magnetic micromixer attachment for SPECORD UV VIS spectrophotometer 80−56302
cytochrome c, redox investig. using reson. Raman, visible absorption and electrochem. methods 78−76832
cytochrome c and related metalloproteins, fast electron transfer processes 79−8478
cytochrome c complexes, reduction by Mo cysteine complexes 77−86371
cytochrome c interaction with bilayer phospholipid membranes 78−69001
cytochrome c oxidase, oxidised and reduced, X-ray absorpt., edges, using synchrotron radiation 78−48758
cytochrome P-450, non-equilib. states formed by low-temp-reduction, absorpt. spectra 80−35837
diazo materials, system aspects of spectral sensitization 79−20434
distillation deoxidation during electron beam melting *(Russian)* 79−70306
duroquinone, soln., electrochem. props. obs. *(French)* 79−66301
Earth interior, undifferentiated, thermal effects of reduction reactions 79−25218
electrocatalysis, surfaces modified by metal adatoms, review 80−61110
electrochemical reaction kinetics, discreteness-of-charge effect, electroreduction in double layer 77−32803
electrochemical redox reactions, Franck-Condon approx. 77−1929
electrode surface, covalently bound molecules, redox reactions, steric effects 78−73077
electrolyte, ionic mass transfer in narrow rectangular conduits 80−61105
electrolytic, of aromatic nitro compounds, using $Ti(SO_4)_2$ addition 79−57248
emulsions, reduction sensitised by dyes, redox potentials, quantitative correls. 79−34298
ethylene+diimide, reduction, reaction tree algorithm, using pot. surfaces 77−70286
ferricyanide reduction on Au electrodes partially covered with photoreist. layer 78−85236
ferricyanide reduction using pyrolytic C film electrode 78−92487
ferricytochrome, photoreduction in presence and absence of electron donor 78−53337
ferricytochrome c photoreduction, transient absorpts. in indole aq. solns., 600 to 800 nm 78−53228
ferrite reduction using plasma methods *(Russian)* 80−7700
ferrous alloy melting, chromatogravimetric equipment for redox studies 78−40097
flame spectrometry, analyte reduction by heterogeneous reactions 79−48026
fluid-solid reactions, law of additive reaction times 79−83452
fluorenone, in DMF, galvanostatic reduction, chronopotentiometry convolution procedures 77−25278
fluorenone photoreduction by DABCO, ion-radical yield enhanced by mag. field, cage recomb. region 79−79268
fuel cell electrocatalytic O_2 reduction mechanism with metal chelate coating 78−23951
furil, photochem. reduction by pentachlorophenol, zero-field CIDNP study 77−90625
furil + pentachlorophenol, photochem. reduction, cross-relax. and CIDNP, PMR relax. obs. 79−52694
gabbro-anorthosite, reduction of Fe, Ti, Si in H atm., X-ray photoelectron spectra 79−25527
geikielite, solid soln., phase transform. during reduction *(Russian)* 78−44042
glass, alkali silicate, oxidation reduction equilibria and optical absorption of Cu ions *(Japanese)* 77−12824
glass, redox number 79−29392
glass fibres, types E and A, surface composition, effect of ageing, reduction, exam. using X-ray photoelectron spectroscopy 79−20223
glyoxal-photoreduction-product-radicals, kinetics and intramol. dynamics 77−32808
graphite, intercalation compound with $AuCl_3$, reduction by H_2 *(French)* 78−27820
graphite-metal chloride intercalation compound, reduction 78−27821
groundwater flow systems, oxidation-reduction sequences 79−84303
group VIb, oxides, oxysalts, reduction kinetics and mechanism 77−77733
haematite, degree of reduction, potential relaxation due to cracks *(Russian)* 80−66770
haematite, importance of convective mass transfer during reduction 79−52769
haematite, reduction to magnetite, HVEM 78−6892
haematite, reduction to magnetite under natural and laboratory conditions 78−65277
haematite reduction to magnetite, stress development mechanism *(Russian)* 80−93553
haeme proteins and metalloporphytins, redox chem. and oxygen binding 80−3573
haemoglobin, dynamic characts. of conformational nonequilib. states, radiolysis investig. 78−58877
hematite, by C 77−48687
hematite pellet, reduction with CO-H_2 mixture 77−4935
ilmenite, solid soln., phase transform. during reduction *(Russian)* 78−44042
ilmenite ore, liquid, behaviour above 1500°C, X-ray obs. *(French)* 79−70100
reduction continued
iron(II)-A-zeolites, reduction, mag. and Mossbauer study 80−71115
iron oxide in V slag enrichment during plasma melting *(Russian)* 78−52716
iron phthalate, prep. of Fe powder 77−40090
isotope compounds, conversion to metals by reduction-distallation methods 80−23223
kaolinite:C, high temp. reduction reactions, thermodynamic anal. 80−104426
lake sediments, E_h meas. reliability conditions 79−48528
leaf $P700^+$ reaction centre reduction in higher plants 78−64954
lunar regolite, Fe reduction on heating in vacuum, XPES spectra 80−41740
lunar regolith, reduction of Fe, Ti, Si in H atm., X-ray photoelectron spectra 79−25527
lung gas analysis using redox gas sensors *(German)* 78−85440
magnetite nodules, from superconcentrates, strengthening annealing and reduction *(Russian)* 80−16333
membranes, artificial, light-driven carrier-mediated electron transfer 77−29110
metal ion electroreduction, ion-induced adsorpt. 80−21297
metal oxide, by H_2-CO mixture 78−44404
metal oxide metaphosphate glasses, vibr. study of metal cation reduction at surface 78−56797
metal oxide reduction by electron cyclotron reson. plasma of H, model study on discharge cleaning 80−76548
metal oxide reduction using plasma methods *(Russian)* 80−7700
metal oxides, chemical dissoc. under pressure as alternative to metallisation, feasibility study *(Russian)* 78−48553
metal oxides by H_2 78−61053
metal powders manufacture by CaH method, $Ca(OH)_2$ separation 80−84878
metal sulphates, thermochem. approach to gas-phase reduction by H_2 79−5147
metallic oxides reduction, mechanism and intrinsic rates 79−83153
methyl viologen, chlorophyll a sensitised reduction in non-ionic micelles 79−1962
methylviologen, photosensitised electron transport across phospholipid vesicle walls 78−80787
mixed-gas reduction, diffusion 79−61902
Nb, pure, production by carbothermic reduction-electron beam melting combination method 80−89177
nitrobenzene, reduction, radical generation in tube electrode, laminar flow, convective diffusion, EPR 77−24746
nitromethyluracil, radiation-induced oxidation and reduction 77−32816
nitroxyl radical reduction kinetics, modelling non-enzymatic influence of membranes 78−64945
organic fluid charge carrier generation, role of molecular electroinduction effects *(Russian)* 79−96321
oxaxine-1, laser dye, electrochem. reduction, EPR spectra 77−70304
oxidant impurities elimination, in viologens electrochromic solutions, using Pd catalyst 80−78922
oxiphenol, oxidation-reduction interaction with metal ions *(Russian)* 79−39138
pentlandite, prep., H_2 reduction with lime, to yield Fe-Ni alloy 78−85018
perovskite type compounds, electrode catalysts for cathodic reduction of O_2 79−29371
peroxidase, low-temperature radioreduction, MCD and absorpt. spectra 78−31763
peroxidase, photo-induced reduction, reaction with indole acetic acid 79−79452
pheophytin reduction obs. in higher plant photosystem II 79−43817
photochemical diode using p-n heterojunction or Schottky barrier immersed in electrolyte 77−66201
photoelectrochemical cells, semiconductor based, interaction of light and transport control 80−12020
photographic emulsion, redox potential evolution during development, potentiometric anal. 78−16865
photosynthetic reaction centres, primary electron transfer rate 79−8481
picrate anion active transport through organic liq. membrane 78−11556
plasma reduction technology, low temp., present state and future prospects *(Russian)* 78−18462
polymeric reducing agent design 80−26050
polyuranate gels, changes in pore structure during reduction and sintering 77−71685
porous oxide pellet, spherical, reduction by gas flow *(French)* 79−27713
porous solid, reaction with mixed gases 78−44404
porphyrin light-activated reduction, rapid spot test for stannous Sn levels in ^{99}m Tc kits 77−86630
PTFE, anisotropic electrochemical attack 79−39004
PtO, irrad., black form., adsorpt., props. 77−11796
quinone electrochemical reduction at packed, fluidised bed electrodes, kinetic behaviour 79−57235
quinones-Zn porphyrin, quinones sensitised reduction in vesicle systems 80−71897
rare earth aluminates, effects of roasting in reducing and oxidizing media on elec. props. 78−52736
rare earth metals, in molten halides 77−29088
rare earth metals, preparation methods and properties, review 79−69969
rare earth niobates, pyrochlore structure, synthesis and props., 79−11533
rare earth oxides, R_2MoO_5, preparation and struct. of R_2MoO_5 79−46624
rare earths, purification, laser methods 80−16712
redox pot, determ. by semicond. electrodes in N,N-dimethylformamide solns. 79−96322
reducing agents, spectrophotometric determ. by $K_2Cr_2O_7$ and H_2SO_4 79−39234
refractory chlorides→refractory metals, prep. of Ti-Nb-Na alloys *(Russian)* 77−28747
refractory metals and oxides, reactions of liq. alkali metals, relevance to reactor technology 80−85173
refractory oxide development for fusion reactor first walls, chem. environment effects 80−83221
reversible photoredox system, thionine type and I_2 type, chem. equilibria *(German)* 77−90630
rhodopsin, bovine, kinetics of $NaBH_3CN$ reduction 78−64926
rubrene radical cation reduction at n-ZnO electrode, triplet state formation, luminesc. 77−16825
ruthenium tris-bipyridyl, excited state electron transfer quenching, H_2O photoreduction mediators effects 80−102536

reduction continued
saturation of Ti alloys with A and Cr, powder method 77−21052
semiconductor-electrolyte solar cells for photochemical reduction of CO_2 to organic fuel 80−55880
SL/RN direct reduction process, mathematical model 78−6876
solid-fluid reactions, law of additive reaction times 79−83453
solid-state redox reaction, electron tunnelling rate, transfer model 78−76844
stainless steel, reduction of H by Ar glow discharge, rel. to ultra cold neutron storage 80−104459
steel, Al semikilled, $(Fe,Mn_{1-x})O.Al_2O_3$ inclusions, deoxidation, thermodynamic conditions 80−60830
steel, Al-Cr, $FeO.(Al_xCr_{1-x})_2O_3$ inclusions, thermodynamics 80−60831
steel, deoxidation by Ca-Si alloy, thermodynamics *(Russian)* 80−16268
steel, ferritic stainless (26 wt.% Cr) passivation, cathodic reduction and AES anal. 77−90500
steel, oxidation-reduction processes on surface during heating in vacuum *(Russian)* 78−11403
steel, stainless, reduction of oxide layer by H atoms 80−40738
steel 35KhN2VL, deoxidation effect on fatigue and endurance limit in wear tests varying P and S content *(Russian)* 78−35523
steel electroslag refining, O_2 removal *(Russian)* 77−55903
steel powder, high speed, S and O reduction in a H_2 gas stream 80−61015
stubnite, H_2 reduction, Sb production 79−66023
styrene, effect of redox initiation in emulsion polymerisation *(German)* 78−85158
succinamic acid, X-irrad., primitive radn. damage, ESR, ENDOR 78−3352
TCNQ salts with heterocyclic amines and hydroquinone form. via redox reaction 80−26013
tetrazolium salt, catalytic reduction to formazan dye 79−39170
thermal energy, electrochem. conversion using cells with reversal of pot. with temp. 80−26124
thermochemical H prod. from water based on mordenite-hosted redox reactions 80−55939
tolusafranine-EDTA, photoredox reaction, photopot. and photocurrent generation 77−81420
transition metal oxide and hydroxide surfaces, chem. changes induced by Ar^+ bombardment, XPS obs. 79−83084
transition metal oxide catalysts, reduction, cryst. defects influence, in-situ electron microscopy 80−81322
vitamin B_{12}, electrochemical reduction of methylcobalamin and methylcobinamide, one electron intermediates 78−85286
wood, hybrid poplar, direct hydrogenation to liq. and gaseous fuels 79−87945
zinc etioporphyrin I anion radical, photoreduction obs. *(Russian)* 78−23958
Zn-salt, molten system, separation of Hf and Zr 80−11884
$3Al_2O_3$-GeO_2-SiO_2, reduction by C, mixed diffusional-kinetic regime *(Russian)* 80−66771
Ag halide, exposed and unexposed grains, discrimination in photographic development 79−83447
Ag^+ reduction in aqueous solns. 80−69148
AgBr colloidal suspension radiolytic reduction obs. 79−91979
Ag(I) reduction by tartrate in HN_3 solns. *(Russian)* 79−47976
Al film+vitreous silica substrate, reaction 77−86380
Al-Mg (7 wt.%), bare surface reaction rates in aq. solns. 80−101022
$Al+NO_3^-$, reactions between metal and aq. nitrate solns., XPS 77−12825
$Al_2Ge_2O_7$ reduction by C, gaseous and metallic Ge yields *(Russian)* 80−40737
$Al_2Ge_2O_7$, reduction processes by C, kinetic analysis, reaction products *(Russian)* 80−55644
Al_2O_3 layer prep. by reduction by carbon in vacuum 77−8757
Al_2O_3, refractory, chemical reduction by atomic hydrogen 79−93830
Al_2O_3, surface microstructural changes due to reduction by C *(Russian)* 80−100378
Al_2O_3, thermodynamics 77−90595
$Al_2O_3+W(WO_2)$ reacts. in H_2, vacuum, high temps., reduction, oxidation conditions 77−16518
β-$Al_2O_3Na_2O$, H-exchanged, effect of moisture, on H_2 activity changes and thermal stability 78−47580
Al_2SiO_5, kyanite, sillimanite, mullitisation, effect of gaseous atm. 79−11604
As(III) and As(V), redox stability in aq. soln. 80−61068
$Au(CN)_2^-$, electrochemical reduction kinetics 78−73052
B compounds, prep. of amorphous B, review, book contrib. 78−48358
B films, prep. by H reduction of BCl_3, struct. and hardness 80−54543
BBr_3-PCl_3-H_2, gas phase equilib. comp. 80−35166
BCl_3, endothermic reduction in H_2 thermal plasma and nonequil. H_2 plasma discharge 78−15671
(Ba,La)TiO_3, redox reactions, defect chemistry and elec. cond., thermogravimetric meas. 77−39580
BaO, reduction by C, kinetics and mechanism *(Russian)* 80−93743
BaO-Al_2O_3-B_2O_3-V_2O_5 glass, spectra, oxidation-reduction behaviour, DC cond. 77−76814
BaO-B_2O_3-V_2O_5 glass, oxidation-reduction of V, thermodynamics 80−85169
$BaSc_2O_4$, synthesis, thermal stability, emissivity, reduction processes 77−8791
$Ba_3Sc_4O_9$, synthesis, thermal stability, emissivity, reduction processes 77−8791
$BaTiO_3$, oxygen vacancies and partial pressures 77−84938
$BaTiO_3$, reduction inhibition by impurity ions 80−101018
$BaTiO_3$-$Ba_{1/2}NbO_3$, defective solid solns., reduction 77−81395
BeO, reduction by C, kinetics and mechanism *(Russian)* 80−93743
C gas-diffusion O_2 electrode in acid, electrochem. performance 78−31652
C, in nonequilibrium plasma, effect of non-Boltzman population vibrationally excited states 79−20362
C polymeric chains, reduced from poly(tetrafluoroethylene), reactivity 80−89488
C, prod. from solid-state reduction of carbonate ions, X-ray diffr. 78−56594
$C+CO_2$ Boudouard reaction, catalysed by Li_2O and Li_2CO_3, reaction rates 839-1050°C 79−16035
$CN^-.H_2O$, redox processes, MINDO/3 calcs. 79−47895
CO, hydrogenation to methane and higher mol. wt. compounds on Rh(Fe) surface 78−73034

reduction continued
CO_2, aqueous solution, photoelectrochemical reduction on p-type GaP in liq. junction solar cells 78−88649
CO_2, electrochem. reduction for use in energy storage 78−92490
CO_2 electrochemical reduction for H storage 80−7934
CO_2, photoelectrocatalytic reduction in aq. suspensions of semicond. powders 79−39141
CO_2, thermochem. reduction using solar energy to provide C-based fuels 80−76610
$CaF_2:M^{3+}$ M=activator ion, redox processes during growth 77−85924
$CaF_2:Mn^{2+}$, fluorite, radiation and thermal redox processes 80−55678
$CaGeO_3$, reduction processes by C, kinetic analysis, reaction products *(Russian)* 80−55644
CaO, reduction by C, kinetics and mechanism *(Russian)* 80−93743
CaO, thermal reduction with Al under reducing atmosphere 77−16864
CaO-Al_2O_3, binary slag, reduction of Al_2O_3 by C saturated Fe *(Japanese)* 79−24733
$CaO.V_2O_5$, reduction by Al powder for V production 78−44049
Cd, electrodeposition on solid Cd or CdHg amalgam, rate, impedance meas. 78−52693
CdS, dry process formation from CdO and S *(Spanish)* 78−56607
Cd_2SnO_4 and Cd_2SnO_4:CdO, thin film electrodes in H_2SO_4 electrolytes, reduction, AES and SEM 80−65674
CdTe electrode, redox reaction due to complex $M(CN)_6^{3-/4-}$ *(French)* 80−89482
$CdUO_4$, phase transforms., anomalous oxidation state change 80−54369
Ce-S-O equilibrium in molten Fe *(Chinese)* 80−104423
$CeNbO_{4+x}$, oxidation-reduction reactions 78−39930
CeO_2 doped electrolyte cell, polarisation phenomena associated with CeO_2 reduction 80−55827
CeO_{2-x} ($0<x<0.3$), oxidation-reduction study, Cahn electrobalance appl. 77−79084
CeO_n, redox reactions, quasiisothermal thermogravimetric obs. 79−15980
$CeTaO_{4+x}$, oxidation-reduction reactions, phase equilibrium, thermogravimetry and magnetic susceptibility meas. 78−39930
$^{249}CfCl_2$, prep. by reduction of $CfCl_3$, spectrochem. anal. 78−27756
CfO_x-O_2 system, for $1.50<O/Cf<1.72$, temp., press. and stoichiometry depends. 77−28009
Co based alloys, distillation deoxidation during electron beam melting *(Russian)* 79−70306
Co-Al_2O_3 catalysts, reducing and sulphiding treatments, XPS obs. 78−85196
Co-O thin films, exam. of oxide phase reduction, by electron photographic analysis *(Russian)* 79−34359
$CoCl_2$, purification by H_2 reduction, of Co, exam. of conductivity *(Russian)* 79−28981
$(Co_{1-x}Mg_x)_2SiO_2$, reduction to Co *(Russian)* 78−44043
CoO, plasma reduction melting *(Russian)* 78−31359
CoO, reduction, magnetic field effects 79−52764
$CoWO_4$, reduction in H_2 77−4931
$CoWO_4$, reduction in H_2 77−4932
Cr_3C_2, form. from Cr_2O_3/graphite mixture in H_2 atmos. *(Japanese)* 78−92225
$CrMoO_4$, ESCA on H_2 reduction *(French)* 77−36365
CrO, reduction by powdered graphite, mechanism 77−4748
Cr_2O_3, by C, mechanism 7573-2073K *(Russian)* 80−45483
Cr_2O_3, carbothermic reduction to metallic Cr, effect of oxide additions (Al_2O_3, SiO_2, MgO, and CaO) *(Japanese)* 78−48651
Cr_2O_3 dissociation in presence of C in Ar, CO and vac. atm., Cr_3C_2 form. *(Russian)* 80−35570
Cr_2O_3, reduction by H_2, reaction kinetics 80−11950
Cr_2O_3, reduction rate by C and C in liquid Fe-Cr-C 78−6877
Cu, electroless deposition, electrochemistry 79−61520
Cu, liquid, deoxidation kinetics using CO 78−44403
Cu, liquid, deoxidation mechanism by reducing gas mixture *(Japanese)* 77−52638
Cu melts, induction stirred, electrochemical deoxidation 78−39718
Cu^+, in LiCl-KCl fused eutectic, diffusion and surface effects, chronopotentiometry *(French)* 78−11524
Cu-Ni crystals, growth, H_2 reduction of CuI-$NiBr_2$ mixture, habit study by X-ray difr., optical and SEM 79−60665
Cu-O (0.05 to 0.1 wt.%) liquid alloy, deoxidation kinetics by rotating graphite cylinders 80−61084
Cu-W composite powder, prod. by H_2 reduction of $CuWO_4$ 79−20006
$CuFeS_2$, chalcopyrite, electrode surface reduction kinetics 78−56897
CuI, H_2 reduction, Cu whisker growth mechanism 78−30853
$Cu_xMo_6S_8$, prep. by topotactic electrode reactions, struct., supercond. 79−99158
Cu_2O, and CuO, reaction with solid K_2O and liq. K 79−66277
Cu_xO_y ore, recovery of Cu by segregation roasting *(Japanese)* 79−52136
$CuWO_4$, controlled reduction in H_2O/H_2 mixture 79−24458
D_xTaS_2, struct., form. by cathodic reduction, neutron diffr. obs. 79−73150
Dy_2O_3 reduction by B, DyB_6 form. mechanism, DTA appl 80−55643
$EsCl_2(Br_2)(I_2)$, prep., characterisation and decay of Es(II) 80−16727
Eu(III) complexes with gluconate ions, reduction, polarographic behaviour 78−92568
α-F_2O_3:alkali metal hydroxides, reduction, Mossbauer spectra 80−16672
Fe, cast, atomised powder, reduction-decarburisation annealing with converted gas, optimum conditions 79−24465
Fe, cast, atomised powder, reduction and decarburisation annealing in converted gas 79−24463
Fe, cast powder, exam. of reaction between C and O, before and after annealing in converted gas 79−33973
Fe, deoxidation by H_2 during plasma arc heating *(Russian)* 78−15703
Fe, deoxidation by V, phase equilibrium with V_2O_3 *(Russian)* 80−16275
Fe, metallised pellet, factors influencing crushing strength after H_2 reduction 79−11531
Fe ore, cold bound pellets, reduction using H_2 gas, 700 to 900°C *(Japanese)* 80−71907
Fe ore, reduction degree, chemical anal. calcs. *(Russian)* 80−66769
Fe, oxide reduction processes by gases, mathematical modelling *(Russian)* 80−93742
Fe oxides, disperse, reduction in electrical arc discharges *(Russian)* 78−95915
Fe oxides, haematite and wustite, structural changes during reduction by CO-CO_2 mixtures 77−60110
Fe, passive film form. in phosphate soln., intensity-following ellipsometry study 80−104345

reduction continued
Fe, powder, reduction annealing, thermodynamic anal. 78−60597
Fe powder, reduction annealing, comminution of sintered cakes 80−66456
Fe powder manufacture, collision speed effect 80−84884
Fe sheet, cyclic oxidation and reduction kinetics in O_2-H_2 atmosphere *(Korean)* 80−71906
α-Fe single crystal whiskers, controlled growth by H reduction of ferrous halides, X-ray and SEM exam. of crystals 78−60554
Fe whisker growth, on wustite, Wagner's mechanism 80−10847
Fe^{3+} solute in MgO, oxidation reduction behaviour in defect model 79−99181
Fe-Al-Ni-Co-Cu alloys, Ti alloying and deoxidising addition *(Russian)* 78−80181
Fe-C-O alloys, deoxidation when cooled and frozen, appl. of quasiequilib. two-phase zone model *(Russian)* 80−16222
Fe-Cl_3-graphite intercalate, slow electrochem. reduction, Fe-graphite intercalate production *(French)* 78−27437
Fe-Co-Ni-Al-Zr magnetically hard alloys, reduction *(Russian)* 78−43614
Fe-Co-Ni-O, mag. powder prod. by reduction of oxalates 77−63582
Fe-Ni-C, atomized, O/C ratio effect, particle size on annealing kinetics, physicotechnological props. 80−20832
Fe-Si (3 wt.%), tertiary products from deoxidation, electron emission microscope study *(Russian)* 78−11214
$Fe_{0.394}$-$Ti_{0.606}$-O-S subsystem, equil. phase data under reducing conditions rel. to ilmenite upgrading 80−76240
$Fe(CN)_6^{4-}$−$Fe(CN)_6^{3-}$, redox reactions, mass transfer at vibr. spheres 80−57220
$Fe(CN)_6^{4-}$⇌$Fe(CN)_6^{3-}$, redox pot. in nonaqueous-water mixtures 79−52654
$FeCl_2$-graphite, intercalation compound, formation by reduction of Fe(III) compounds with $Fe(CO)_5$ 78−63721
$FeCr_2O_4$, reduction by C *(Japanese)* 77−48682
$Fe(H_2PO_2)_2$, γ-ray and electron radiolysis, Mossbauer study 80−7816
FeO, molten, reduction mechanism by solid C 77−48636
FeO, reduction rate by C 77−73468
FeO surface, water-gas shift reaction kinetics 80−11949
FeO_2 nucleation, kinetics of formation of H_2O and C_2O 79−83449
$Fe_{0.925}O$, wustite, kinetics of reduction at moderate temps. 79−83154
$Fe_{1-x}O$, wustite disc reduction with CO, 573 to 845°C 78−53253
Fe_2O_3 (haematite) reduction to Fe_3O_4 (magnetite) during thermomag. anal. 77−56622
Fe_2O_3, direct reduction by H_2 reaction kinetics 80−40689
α-Fe_2O_3, haematite, reduction by H_2, mag. field effect 77−12827
Fe_2O_3, hematite, reduction, exam. of role of convective mass transfer 78−52724
Fe_2O_3, reduction, double reaction, reaction kinetics exam., expt. verification *(French)* 78−31705
Fe_2O_3, reduction by H_2, kinetics and mechanism 77−48619
Fe_2O_3, reduction rate by C 77−73468
α-Fe_2O_3, reduction to active magnetite and direct air oxidation to α-Fe_3O_4 *(German)* 78−7060
Fe_2O_3-FeO, sinter, heating and reduction effect of phase transform. and fracture *(Russian)* 78−15375
Fe_2O_3-FeO, sintered and pellets, reduction in H_2 *(Russian)* 78−15705
Fe_3O_4 briquettes, porous, struct. changes during reduction 77−21064
Fe_3O_4, FeO, effect of mag. field on reduction rates 77−44461
Fe_3O_4, orientation on α-Fe_2O_3 after low-temp. reduction, X-ray texture analysis *(French)* 77−39738
Fe_3O_4, reduction, double reaction, reaction kinetics exam., expt. verification *(French)* 78−31705
Fe_3O_4-Cr_2O_3-Ni_2O mixture, reduction by gases heated by electric arc discharge *(Russian)* 78−15704
Fe_xO_y, adsorption of H_2O, oxidation and reduction effects on adsorption 78−43237
FeOCl, cathodic reduction in organic electrolytes, intercalation complex production 79−1833
α-FeOOH, to γ-Fe_2O_3 via Fe_3O_4, influence of reduction temp. on mag. props. 79−69698
FeS_2-$CaCO_3$-C, reaction on heating, dissociation, reduction to Fe *(Russian)* 78−44041
FeS_x, reduction by H_2 78−61053
Ga, gaseous reduction and extraction from mica 78−92216
p-GaAs, electrodes in acetonitrile soln., photoassisted reduction, development of under-potential 79−70341
GaAs-Sn-H_2-HCl, thermodynamic calcs., reduction of $SnCl_2$ by H_2 79−86903
GeO_2, reduction processes by C, kinetic analysis, reaction products *(Russian)* 80−55644
GeO_2-SiO_2, reduction by C, mixed diffusional-kinetic regime *(Russian)* 80−66771
H production by thermochemical cycles using fusion energy source 80−51010
H production from coal using steam-Fe process, development status 80−55942
H reduction reaction with Fe substrate 78−95700
H_2, production by solar energy, homogeneous photoredox system 80−3387
H_2, reducing agent in natural U ore deposits 78−36169
H_xNbS_2, struct., form. by cathodic reduction, neutron diffr. obs. 79−73150
H_2O_3, vac. thermal reduction with Th, for Ho prod. *(Russian)* 80−16226
H_2SeO_3, reduction, reaction sequence and CdSe film deposition 80−71603
HfC+Ta_2O_5 reaction for direct prep. of Hf-Ta alloy 77−12554
HfO_2 reduction by Ca 80−18746
I^--$S_2O_8^{2-}$ aqueous redox mixtures, γ-radiolysis 79−16017
In(III) complexes with gluconate ions, reduction, polarographic behaviour 78−92568
$IrCl_6$, reduction by BH_4^- 78−76854
$K_3Fe(CN)_6$, pressure induced reduction, Raman spectra 80−66776
$K_3Fe(CN)_6$-KCl, press. induced reduction, IR spectra after pressurization 80−66776
K_2TiF_6 in LiCl-KCl eutectic mixture, analysis of reduction waves of Ti ion in chronopotentiometry *(Japanese)* 78−20025
$K_{0.27}WO_{(3+y)}$, struct. analysis 77−11510
LaB_6-SmB_6(YbB_6), exam. of secondary ion-ion emission, due to bombardment with 8 keV Ar ions 79−33882

reduction continued
$La_{0.9}Ca_{0.7}CrO_3$ polar semiconductor, elec. props., slight reduction effect 80−20183
$LaCoO_3$, reduction, direct obs. using high voltage TEM 77−63817
$LaMnO_3$, stoichiometric manganite form. reaction, thermodynamic characts. 80−108727
La_2O_3, reduction by Si in solar furnace *(French)* 80−16784
Li ferrite, reduction, phase transitions 80−55642
Li/$SOCl_2$ primary cells, $SOCl_2$ reduction mech. in supporting electrolyte 80−108792
Li_2CrO_4, electron irrad., reduced species form., XPS 79−11498
$LiNbO_3$, reduced cryst., photovoltaic effect, appl. to holographic recording *(Russian)* 79−51635
$LiNbO_3$:Fe, origin of photoelectrons and conc. of point defects 77−43645
$MgCr_2O_4$, reduction with graphite powder *(Japanese)* 77−56225
Mg_2GeO_4, reduction processes by C, kinetic analysis, reaction products *(Russian)* 80−55644
MgO, filamentary crysts., synthesis and props. 77−52267
MgO, rate of reduction by C 77−28743
MgO, reduction by C, kinetics and mechanism *(Russian)* 80−93743
MgO:Fe, Fe^{2+} oxidation and Fe^{3+} reduction kinetics, EPR obs. 79−70399
MgO:Fe cryst., reduced, optical absorpt. spectra at low temps. 77−63436
MgO:Li, oxidation and reduction up to 1700K, defect prod. 79−39013
MgO:Mn^{2+}(Fe^{2+})(Cr^{2+}), redox behaviour of ions, ESR and X-ray diffr. 78−52341
$MgTi_2O_5$, formation of solid solutions, on chemical reduction, X-ray analysis of phases *(Russian)* 79−33072
MnO, reduction by C, surface reactions, CO regeneration *(Russian)* 80−66772
Mn_3O_4, reduction by C and CO, exam. by thermogravimetric methods 78−80743
Mo complex, dithiocarbamate, model for molybdoenzymes, thermochem. meas. 77−86365
Mo complex, nitrate reductase, reduction mechanism and kinetics in dimethylformamide 77−86366
Mo complexes, oxo- and sulphido-bridged, binuclear, in aprotic media, electrochem. and redox mechanisms 77−86324
Mo oxides, oxysalts, reduction kinetics and mechanism 77−77733
Mo oxycyano complex, reaction with reducible substrates, biological N_2 fixation 77−86369
Mo, substitution and redox reactions in oxidation states III to VI, role in enzymes 77−86364
Mo-Al_2O_3, catalysts, reducing and sulphiding treatments, XPS obs. 78−85196
Mo-RE-O system, Mo-Re alloys prep. *(Russian)* 80−16225
$MoCl_5$, by H_2, influence of electric field on Mo film deposition 80−93491
MoF_6, reduction as method for synthesis of MoF_3 77−86307
MoF_6 reduction by H, chemical kinetics eqn., adsorbed component interactions *(Russian)* 80−35569
MoF_6, reduction by H in the presence of HF *(Russian)* 80−61076
MoF_6, reduction by H_2 at 500-1200°C to Mo, exam. of Mo props. and MoF_6 props. *(Russian)* 80−7516
MoO_2 powder bed, H_2 reduction kinetics 80−16230
MoO_3, ESCA of surface composition changes under ion bombardment 77−20974
MoO_3, ESCA on H_2 reduction *(French)* 77−36365
MoO_3, reduction at low temps., surface defects obs. in HV electron microscope 77−35564
MoO_3, reduction at low temp., role of defects, electron microscope obs. 77−77755
MoO_3 reduction to MoO_2 by electron beam, electron difrr., microscope investigs. *(French)* 78−95945
MoO_3 topotactic transform into MoO_2, electron microscopy, X-ray anal. 80−107417
MoO_3, ultrafine crystals, exam. of reduction using electron microscopy *(Russian)* 79−29394
MoO_3-Fe_2O_3 coreduction kinetics, thermodynamic equilib. in Mo-Fe-O-H system 78−60657
MoO_3-TiO_2, reduction, Mo^{5+} and O_2^- form. 77−90590
$Mo_3S_4(Se_4)$, channel-type, topotactic redox reactions 77−90598
Mo(ZrO_2.La_2O_3) structural changes during reduction and sintering 80−25636
N_2, photoreduction, to NH_3, by desert sand 79−83483
NH_3 synthesis using Fe catalysts, XPS obs. 79−70370
NO, catalytic reduction with CO by rare earth oxides 77−81422
NO, reduction with NH_3 and laterite catalyst 79−91993
NO_2, reduction by electron beam irrad., appl. to exhaust gas treatment 78−80765
NO_2^--IO_4^- aqueous redox mixtures, γ-radiolysis 79−20392
NO_x reduction on Fe-based catalysts containing V 79−12285
Na_4 $Fe(CN)_6.10H_2O$, single cryst., X-irradiated product ESR, 4.2K 77−48659
Na_2O-CaO-Bi_2O_3-SiO_2, electro-conducting glass-ceramic production by ion-exchange and reduction treatment 79−1616
Na_2O-SiO_2(-CaO) glass, molten, metal ion diffusion and redox behaviour, electrochemical studies 80−81332
NaRhY zeolite, Rh complexes with CO and methyl iodide ligands, spectrosc. obs. 80−85159
Na_xWO_3 bronzes, reaction with Fe powder, reaction mechanism and reactivity 80−108712
Nb-Mo, prod. by simultaneous carbothermic reduction of oxides/electron beam melting method *(Japanese)* 80−11590
Nb_2O_5 and Al_2O_3 by CaH_2, Nb_3Al prep., thermodynamic calc. 80−100809
Nb_2O_5, carbothermal reduction in N_2 intermediate phases 79−11773
α-Nb_2O_5, reduction in H_2 discharge, AES and SEM anal. 77−59708
Ni (100), adsorption of O_2 and reduction of surface oxide by H_2 80−108741
Ni electrodeposition cathode polarisation, influence of unsaturated sulphates *(Russian)* 79−91963
Ni^{2+}, in zeolites, reduction, UV spectroscopic obs. 77−77738
Ni-O system, oxidized polycryst. Ni films, H_2 reduction, AES 77−12472
Ni-P, electroless deposition on Al, X-ray and SEM obs. 79−90907
$(Ni_{1-x}Mg_x)_2SiO_2$, reduction to Ni *(Russian)* 78−44043
NiO disc, reduction with CO 77−4936
NiO ore in segregation roasting process *(Japanese)* 80−71908
NiO, plasma reduction melting *(Russian)* 78−31359

reduction continued
NiO powder, mixed with graphite, reduction mechanism *(Korean)* 78−11555
NiO_4, strong mag. field effect on reduction 77−4868
$Np^{4+/3+}$ in fused salts, redox and chem. props. 77−29038
Np(V)/Np(IV) catalytic redox reactions, kinetics and mechanisms 77−29006
O_2 molecule reduction flow probe for cerebrospinal fluid 79−100777
O_2 sensing electrode stability 77−60268
PLZT, reduced, exam. of ageing phenomena, using dielectric hysteresis *(German)* 79−33647
$PaCl_2$, thin films, reduction to Pd by Ne^+ ion irrad., 2 MeV He^+ ion backscatt. anal. 79−4493
Pb ore in blast furnaces, gas composition, temp. and pressure meas., O_2 potential diagram, reduction mechanisms 78−85118
Pb-Zn-SiO melt, mathematical model of thermal C reduction *(Russian)* 78−15663
$Pb_3Fe_2WO_9$, perovskite ferroelec., characts. of dielec. polarisation, influence of oxidation and reduction 77−8496
PbO glass, mechanochemical reduction 77−52628
$PbO-B_2O_3$, solder glass, thermal reduction of Cu^{2+} and Cu^+:Cu^{2+} effect on thermal props. 78−15350
PbO_2, corrosion in HBF_4, redox mediator effects 77−90480
PdO, irrad., black form., adsorpt. props. 77−11796
Pt complex, $PtCl_4^{2-}$, in chloride-sulphate soln., Pt electrodeposition, galvanostatic transients *(Russian)* 78−31655
Pt electrode, multilayer oxides, electrochem. reduction mechanism, kinetics 78−61019
Pt electrode O_2 reduction kinetics in conc. H_3PO_4, H_2SO_4 and $HClO_4$ 78−23952
Pt, low index surface, struct. sensitivity of O_2 reduction in acid electrolyte 79−70343
Pt surface, electrochem. oxidation and reduction, XPS obs. 78−95653
Pt(IV), reduction to Pt(II), X-ray irrad., Ar ion bombardment, XPS obs. 80−35573
PtO_2, finely divided, reduction 77−90643
PtO_2, sputtered film, optical props. under H_2 reduction 80−20728
$Pu^{4+/3+}$ in fused salts, redox and chem. props. 77−29038
Pu(IV) catalytic redox reactions, kinetics and mechanisms 77−29006
PuO_2, conversion to $PuC_{0.88}$, thermodynamic assessment 77−70293
Pu(VI) reduction to Pu (IV) with NO_2 and NO gases 79−31108
Ru complex, (2,2'-bipyridyl)$_3$ruthenium^{2+}, excited-state redox processes, electron transfer theory 79−39126
RuO_4, catalytic reduction in radioactive liquid waste processing 79−76092
SO_2, reduction by CO in presence of H_2O and O_2, catalyst effects 79−24819
$SOCl_2$, in Li/$SOCl_2$ cell discharge reaction, cyclic voltammetric and coulometric obs. 80−30440
SO_2ClF, reduction by anhydrous HI 79−5150
$Sb_{0.2(0.4)}MoO_{3.1}$, synthesis by H_2/H_2O reduction of Sb_2MoO_6-MoO_3 *(French)* 80−64971
β-Sb_2O_3 reduction to Sb powder, atomic H effect 80−2978
Sc_2O_3, reduction in Li vapour, 1800-2500K, thermodynamics 77−90595
Se gravimetric determ. by reduction of H_2SeO_3 77−90683
Si production from rice husk ash for solar cells 79−62008
Si surface, reduction growth, autoepitaxy *(Russian)* 80−107672
Si-O-C system, product quenching, mol. dynamics 78−39711
$SiCl_4$, conversion to $SiCl_3$ in unipolar HF discharge 80−1855
SiO_2, by Mg vapour, reaction mechanism, SEM obs. 77−1944
SiO_2 decomposition and reduction, in low temp. plasma jet *(German)* 80−45499
SiO_2 fibre reinforced Al, thermal degradation kinetics 77−44194
SiO_2, on Si, reduction by heating in Ga mol. beam at 800°C 80−50730
SiO_2 reduction, with C and SiC, forming SiO vap. 79−79240
SiO_2, reduction by C using a plasma, thermodynamic computer anal. 77−40530
SiO_2, reduction by RF induction plasma torch., Si form. 78−11186
SiO_2, reduction with C black in plasma reactor, feasibility of Si production 78−27426
SiO_2/InP interface formation, thermodynamic considerations 80−100529
SiO_2-Al_2O_3 glass, nitrides formed by reduction with C *(Japanese)* 78−68929
SiO_2-MgO-CaO-Al_2O_3:Ce,Fe, redox equilib., expt. 80−85171
SnO_2 by C 79−61901
SrO, reduction by C, kinetics and mechanism *(Russian)* 80−93743
$SrTiO_3$ and $SrTiO_3$:Nb, reduced samples, optical absorpt., effect of impurity-O vacancy complex *(Korean)* 79−8163
$SrTiO_3$ semicond. electrodes, electroreduction process kinetics, cathodic dark current meas. 80−66807
$SrTiO_3$ surface, oxidation and reduction by D_2O, $H_2{}^{18}O$, D_2, isotope exchange study 80−104461
Ta_2O_5, preferential sputtering by Ar^+ ions, XPS obs. 79−83083
Ta_xO_y on Ta, anodic film, electrochem. reactions by tunnel current 77−81340
TaS_2-2H electrodes, topotactic reduction nechanism, neutron diffr. obs. and intercalation cpd. form. 80−108748
^{99}Tc, reduction and sorption in granitic bedrock, biological hazard estimation 79−79415
^{99m}Tc-1-hydroxy-ethylidene-1,1-disodium phosphonate labelling using Sn(II) reductant 79−88190
$(Th,U)O_2$ fuel conversion to $(Th,U)C_2$ for reprocessing 79−54579
Ti-O system, nonstoichiometry between Ti_3O_5 and TiO_2 comps. at high temps. 77−15594
TiC_xN_y, powder preparation, physical, chemical props. *(Russian)* 80−76212
$TiCl_4$, electrochemical behaviour in alkali chloride baths 80−30243
$TiCl_4$, electrolytic reduction *(French)* 78−23644
$TiCl_4$, reduction in steady beam-plasma discharge 80−100099
TiO_2, reduction with CaH_2, preparation of rolled Ti foils 80−18744
TiO_2, rutile, reduction by C, thermodynamic and struct. study, 1400 to 1600K 79−52650
TiO_2:Nb semicond. electrodes, electroreduction process kinetics, cathodic dark current meas. 80−66807
TiO_{2-x} reduced, crystallographic shear planes, dislocation struct. 80−107175
$(U,Pu)O_{2-x}$, fuel, particle cavitation during reduction by H_2 78−8958
$U^{4+/3+}$ in fused salts, redox and chem. props. 77−29038
UO_2, ionisation potential, cohesive, electronic and redox props. 79−47916
UO_2 reduction by H_2, modulated mol. beam mass spectra 77−25305
reduction continued
UO_2, refractory, chemical reduction by atomic hydrogen 79−93830
V (III) complex, alcoholic VCl_3 soln., fluoresc. and photoreduction 78−85177
V_2O_3, to VO_xC_y carbothermic reduction, rel. to steel prep. 78−40049
V_2O_5 and lower oxides, defect structures and related props., review 80−59454
V_2O_5, electron beam induced decomposition, appearance pot. spectroscopy 80−85203
V_2O_5, reduction in butyllithium, ESR study 80−100611
V_2O_5-$AlNbO_4(GaNbO_4)(TiNb_2O_7)$ systems, interfacial reactions, efficient boundary conditions and solid state reactivity 80−76542
V_2O_5-TiO_2 interface, role of struct. props. in interfacial reactions 78−31688
V_2O_5-water, EPR of VO_{aq}^{2+} formed by solar light photoreduction, electrolysis appl. 78−11540
$(V_2O_5)_{0.93}(MoO_3)_{0.07}$ solid soln., struct. transform. in oxidizing and reducing gas atm. 79−23740
W surface wetting by liquid Cu depend. on preliminary surface treatment *(Russian)* 80−35388
WC, fine powder prod. from $WO_3+C+Co_3O_4$ *(Japanese)* 78−92226
WC, powder form. from WO_3-Co_3O_4-C powder mixture *(Japanese)* 78−92227
WF_6, mechanism of heterogeneous reduction by H_2 *(Russian)* 80−21265
$W_xMo_{1-x}O_3$, reduction and temp. effect on electronic core levels, XPES 79−91564
$WO_{2.96}$, reduction to W 77−28744
WO_3, electron spectroscopic exam. of reduction 77−4714
WO_3, reduction, defect role, in situ HVEM obs. 80−81323
WO_3 reduction, in H plasma jet, W powder prep. *(Russian)* 80−76211
WO_3, reduction and temp. effect on electronic core levels, XPES 79−91564
WO_3 reduction in hydrogen, electron microscopic obs. of solid phases formed *(Hungarian)* 77−48635
WO_3, vap. deposited, W particle and whisker growth by reduction 77−52249
WO_3, with H, starting specific surface effect on kinetics 80−11599
WO_3-$NiCO_3$-Fe_2O_3, reduction alloy form. 80−60801
W_xO_y, carburisation/reduction with CO, morphological study 79−47977
$W(ZrO_2.La_2O_3)$, structural changes during reduction and sintering 80−25636
Y_2O_3, reduction in Li vapour, 1800-2500K, thermodynamics 77−90595
Zn(II) complexes with gluconate ions, reduction, polarographic behaviour 78−92568
ZnTe electrode, redox reaction due to complex $M(CN)_6^{3-/4-}$ *(French)* 80−89482
ZrO_2-CeO_2, semiconducting ceramics, electronic conductivity and oxidoreduction *(French)* 78−26919
ZrO_2-Y_2O_3-Nd_2O_3, high-temp. thermophys. props. 78−26663

redundancy
see also bandwidth compression; data compression; logic design
cosmic ray variation spectrograph, redundancy and hardware monitoring rel. to data reliability 79−84610
exercise ECG analysis, noise-impervious pattern recognition approach 78−7515
gyros appl. to angular velocity meas., precision increase using structural redundancy *(Russian)* 78−49804
hologram memory redundancy evaluation by spatial and defect permittance 78−1197
noncoherent optical processing, two-pupil hybrid systems 78−74858
optical coherent processing system, modification to achieve some redundancy 80−106468
optical parallel processing 80−95831
optoelectronic system, symmetrical input, direction-finding sensitivity control 79−50401
radiographic pictures, digital encoding, redundancy reduction 77−40850
solid body motion parameters, determination reliability improvement using redundancy methods 79−30431
spacecraft attitude control and navigation systems, instruments reliability enhancement 77−29623
vector ECG meas., bandwidth limitation effects 78−36001
H time and frequency standards with redundancy 77−79065

redundancy theory *see redundancy*

reed relays
modulated backscatter from reed switch loaded dipole 77−75386
optical multimode fibre routeing reed switch improvement 80−53463
RMS digital voltmeter, description and application *(German)* 77−18048
routing switch for multimode optical fibres, features 79−72704
temperature measurement, using magnetically controlled reed switches *(French)* 80−57291
Hg wetted, heat treatment variations effects on Fe-Ni alloys surface conditions and on switch behaviour 80−66547
Ni-Fe reed contact, Au-plated, submicron Auger spectroscopy exam. 79−15027

reeling *see winding (process)*

reference circuits
comparator with auto reference level, used in physiological research 78−31992
luminescence spectrum recording monochromator wavelength reference marker generator 78−58050
primary meas. transducer error twin-circuit correction *(Russian)* 79−71404
resistive voltage-ratio standard for 10 kV DC meas. 77−5873
RF signal level reference, for instrument calibration 77−115
spectrometer LF module reference signal shaper 78−57924
time interval reproduction device 78−77869
voltage reference cct. with adjustable temp. coeff. 79−30407

references (standards) *see standards*

refining, oil *see oil refining*

reflectance *see reflectivity*

reflection
see also acoustic wave reflection; electromagnetic wave reflection; neutron reflection; reflectivity
Alfven waves in solar photosphere, refl. rel. to sunspots cooling 79−5799
anisotropic crystal, additional light waves and boundary conditions 77−73121
elastic reflections of particle in expanding sphere, rebound function 78−86196

reflection continued
elastic wave, transverse, reflection from cylindrical defect 78−47472
elastic waves, reflection and refraction in presence of separation at solids interface 77−75848
elastic waves at frictional boundary, transmission (reflection), approx. anal. method 78−63371
electron beam, relativistic, refl. and transmission by strong mag. field *(Japanese)* 80−91737
fundamental symmetric Lamb wave, refl. at edge of semi-infinite plate, variational anal. 77−78987
glass, surface treatment, improvement in mech. and optical props. recent progress *(Japanese)* 79−79141
glass plane layer, thermal radiation spatial distrib. rel. to temp. field, internal reflect. 79−59913
hydromagnetic-inertial-gravity waves in mag.-vel. shear, refl. by finite shear layer 79−55422
laminated composite, nonlinear transient pulse propag., interface reflection effect 78−63222
linear transport operator, spectrum with diffuse reflection 77−17930
liquid waves, obliquely incident on permeable quaywall with reservoir *(Japanese)* 79−32546
Love waves in infinite strip with surface step, transmission, reflection and diffraction 79−88260
Mach reflection of solitary wave 80−79340
magnetothermoviscoelastic waves reflection at semi-infinite solid boundary 80−48633
ocean propagating inertial and internal waves, refl. at rigid boundary rel. to induced drift currents 80−51403
P-wave reflection at non-vertical incidence, synthetic seismograms 80−56401
phase transitions and reflection positivity, Peierl contour probabilities, long range lattice models 78−89398
plane nonuniform waves of general form *(Russian)* 77−54668
plane obstacles, weak shock wave reflection in air 80−48751
plane wave motions, energy partition in refl. and refr. 78−77727
plane wave reflection and refraction at elastic interface, initial stress effects 79−62445
plane wave reflection under initial stresses at free surface 78−55581
probabilistic model for the reflection of waves from a rough surface 79−40380
quantal particle, inverted Morse pot. barrier, transmission, reflection coeffs., phase-integral approx. 77−53801
Schottky barrier, excitonic refl. of light 80−10885
seismic body waves in anisotropic media, refl. and refr. at plane interface 77−49019
seismic reflection coefficients, determ. from waves 79−44115
seismic surveys, residual static and crossdip corrections simultaneous estimation 79−92500
seismic waves, admissibility of soln. to multilayered dynamic problem without consideration of multiples 77−73668
seismic waves, attenuation by intrabed multiple refls. 79−16393
seismic waves, CDP effective vels. critical values for stratified homogeneous forms. *(Russian)* 79−39668
seismic waves, deep refl. profiling for oceanic crust studies *(Russian)* 79−39966
seismic waves, effect of partial multiple refl. on primary signal form. *(Russian)* 78−85484
seismic waves, interpretation of travel-time curves as head wave curves 77−9371
seismic waves, multiple reflections and head waves in Gulf of Suez 80−56400
seismic waves, nature of arc-shaped line-ups on common depth point profiles *(Russian)* 79−44134
seismic waves, refl. and transmission coeffs. in ellipsoidally anisotropic media 79−84136
seismic waves, refl. coeffs. rel. to multi-segment traces deconvolution and synthesis 80−77162
seismic waves, refl. refr. and diffr. in media with elliptical vel. depend. 79−5454
seismic waves, reflection coeffs. identification from noisy data 79−29718
seismic waves, spectral characts. in region of bright spot anomalies *(Russian)* 79−53319
seismic waves, suppression of long-decay long-delay multiple reflections by predictive deconvolution 79−84133
seismic waves, tool for energy resource exploration, book 78−96162
seismic waves deep reflections, unravelling via seismic stripping 79−34970
seismic waves reflecting/refracting plane surface image, form. using two-point eikonal *(Russian)* 79−96740
seismic waves two-dimensional refl. time-delay curve, approximation for arbitrary refl. surface *(Russian)* 79−44132
seismic waves upercritical refl. from essentially nonplane seismic boundary, peculiarities of record *(Russian)* 79−8606
seismology, reflected wave method for cross seismic sounding data interpretation *(Russian)* 78−92796
shock waves, termination of regular reflection 79−81910
shock waves diffraction and reflection from shock tube, numerical computation *(Chinese)* 80−43735
spinless particles through one dimens. pot. barrier, formal series method, refl. coeff. 78−32700
transient waves in fluid-filled porous media, refl. and refr. 77−49604
transversely isotropic layered media, reflection and transmission of seismic waves 77−91025
tsunami simulation, Hawaii, open boundary reflection interference 80−17232
water wave, partial reflection by nonuniform adverse currents 79−64681
wave reflection from an asymmetric inhomogeneous medium 79−44753
wave reflection in slowly varying medium 78−81856
Ar^+ ion, polycrystal bombardment, sputtering efficiency 77−85869
Kr^+ ion, polycrystal bombardment, sputtering efficiency 77−85869
Xe^+ ion, polycrystal bombardment, sputtering efficiency 77−85869

reflection high energy electron diffraction
amorphous surface, refr. correction by RHEED patterns 78−71646
Bragg diffraction imaging of cryst. surface defects 78−9920
computer simulation for FCC platelets using kinematic theory *(French)* 77−62450
diamond, epitaxial synthesis by C-ion deposition at low energy, and struct. 79−1559
diamond surface, polished, RHEED pattern 80−65345
epitaxial growth, vapour phase, growth mode characterisation 78−87885

reflection high energy electron diffraction continued
ferrite bubble film struct., EM and RHEED, Mn and Mn-Cu ferrites 77−11801
fluorescent screen, metal-backed, appl. to high temp. RHEED obs. 80−75126
graphite, highly oriented, pyrolytic surface, polish-induced damage, RHEED obs. 79−15481
I-III-VI_2 semiconductor epitaxial layers, lattice parameters meas. using RHEED 79−90913
paragonite, $2M_1$, cryst. struct. refinement by HV electron diffr. 78−67696
paragonite, 3T, cryst. struct., oblique texture electron diffr. 78−67697
quartz, amorphous layer on mech. treated single crysts. electron microscope and RHEED obs. 80−24721
quartz, surface structural modification by high temp. gases, computer simulation of RHEED patterns *(German)* 79−95251
RHEED-AES combined system, simultaneous struct. and comp. information 78−47216
SEM, ultra-high, vac., diffr. unit 78−83699
SEM with ultrahigh vacuum system for surface physics expts. 78−38925
semiclassical analysis of HEED by stacking faults, classical limit 79−46523
semiconductor, electron spectroscopy techniques, review *(Japanese)* 80−49061
specimen transfer device for combined AES/RHEED and TEM obs. 80−70093
stepped surface exam. of LEED 77−72762
stepped surfaces, surface geometry, RHEED study 79−77881
streaked intensity distrib. origins in RHEED 78−47215
surface analysis, RHEED scatt. intensities 79−42354
surface analysis, theory of RHEED 79−42353
surface chemical anal. using RHEED-solid state detector method 80−108760
surface microstructure determ. and microanalysis by ultrahigh vacuum field emission gun SEM 80−96423
surface research developments *(Japanese)* 78−22607
surface state resonance effect, obs. by convergent beam RHEED 80−107622
surface structure appls. of new techniques 77−62452
surfaces with hexagonal symm., anal. of two-dimens. superstructs. obs. by LEED and RHEED 79−23817
ternary semiconductors, measurement of lattice parameters of thin heteroepitaxial layers, RHEED technique 80−15406
Ag, adsorbed on Si (111), electronic and cryst. struct., Schottky barrier form. obs. 78−84091
Ag, Cl adsorption, AgCl epitaxial layer form. 78−14642
Ag, cluster growth and nucleation on Mo (100), UHV-SEM, AES/(RHEED or LEED) obs. comparison 78−63956
Ag, epitaxial growth on electron bombard. NaCl(111) surfaces, RHEED and AES 80−15419
Ag film, MBE deposited on InP(001), struct. using TEM and RHEED 79−82492
Ag film, vacuum deposition on Pb (111), substrate diffusion effects, RHEED, LEED, AES 80−65410
Ag thin film, X-ray fluoresc. spectroscopy of surface using RHEED-solid state detector method 80−108760
Al film, MBE and field emission deposition on III-V semiconductors, comparative study 79−87016
Al, specimen transfer device for combined AES/RHEED and TEM obs. 80−70093
$Al_xGa_{1-x}As$, MBE grown film, in situ surface characterisation by RHEED, SIMS and AES 77−43410
AlN, epitaxial film growth by MBE, physical and optical props. 80−2293
AlN films, RF reactive ion-plating, struct. and morphology 80−104074
Au film, MBE and field emission deposition on III-V semiconductors, comparative study 79−87016
Au, spherical crystal, drop grown from melt, RHEED obs., superstructs. 78−43225
Bi film, structure and electronic props. 80−70562
$BiF_2Si_2O_8OH$, crystal struct., space groups by RHEED 78−47297
Cd epitaxial monolayer, nucleation and growth on Ge (111), RHEED and mol. beam study 77−43447
$CdIn_2S_4$ film, vac. deposited, growth, struct., optical and photoelectronic props. 80−10831
CdS film, prep. by hot wall technique, morphology and semicond. props. 79−95292
CdS/InP epitaxial thin films on NaCl, HEED and TEM study 80−88446
CdS(Se)(Te), evap. onto electron bombarded NaCl substrates, epitaxial growth and characts. 79−28948
CdSe evaporated films, struct. and epitaxy, TEM, RHEED, and X-ray diffr. obs. 79−77939
Cr (111) face, oxidation, LEED and RHEED meas. *(French)* 78−39955
$CrCl_2$, epitaxial relationships studied by RHEED and Auger emission spectra *(French)* 78−22990
Cu (111), vicinal stepped surface obs., LEED vs. RHEED 77−72762
Cu deposition on Au electrode in underpotential region, RHEED investig. 80−54539
Cu evaporated layer on Ge, RHEED Kikuchi bands, anomalous contrast 78−87597
Cu film, vacuum deposition on Pb (111), substrate diffusion effects, RHEED, LEED, AES 80−65410
$CuGaSe_2$, epitaxial layers, lattice parameters meas. using RHEED 79−90913
$CuGaSe_2$ on GaAs, epitaxy grown RHEED exam. of epitaxial overgrowth *(German)* 79−11042
$CuGaSe_2$ thin films, on GaAs substrates, structural and elec. props., photoluminesc. meas. 79−65564
$CuInSe_2$, heteroepitaxy on {111} oriented Ge by flash evaporation, struct. 80−108333
Cu_2O(111) growth modes, on (111)Cu surfaces, UHV-RHEED and TEM study 79−19481
Cu_2S, epitaxial layers grown from liq. soln. RHEED obs. 78−91558
Cu_2S, epitaxial overgrowths on Cu films, characts., TEM and RHEED obs. 78−84101
Cu_2S, epitaxial overgrowths on Cu(111), struct. and morphology 79−82494
Fe oxide films, anodically formed, compositions 79−90898

reflection high energy electron diffraction continued
$Ga_{1-x}Al_xN$, VPE growth on sapphire, RHEED obs.of orientation rels. 77−20208
GaAs (001) surface, thermal treatment before MBE growth, RHEED-AES meas. 79−61754
GaAs, (001) vicinal stepped surface obs., LEED vs. RHEED 77−72762
GaAs, (100) surfaces, struct. and stoichiometry during molecular beam epitaxy, RHEED anal. 79−4921
GaAs, adsorpt.-desorpt. of Zn, thermal desorpt., at. beam adsorpt., AES, SEM, RHEED 78−14591
GaAs epitaxial layers, non-doped, from Ga-$AsCl_3$-H_2 system, TEM and RHEED study of micromorphology and defects 79−65340
GaAs, homoepitaxy and epitaxy, surface anal. during growth, using RHEED and Auger spectroscopy 80−66433
GaAs, ion implanted, encapsulation surface effects 77−1883
GaAs, MBE grown film, in situ surface characterisation by RHEED, SIMS and AES 77−43410
GaAs, MBE of autoepitaxial films, temp. range for growth, RHEED monitoring 78−44025
GaAs, substrate for homoepitaxy, vicinal surfaces characterisation 77−20207
GaAs, surface studies during MBE growth 79−90899
GaAs VPE growth, in situ surface anal. 79−95937
GaAs:Sn films, MBE grown, doping profiles, carrier mobilities, RHEED and AES obs. 79−1447
$GaAs_{1-x}P_x$, MBE growth on GaP, and crystallographic evaluation 77−8762
$GaAs_{1-x}P_x$, mol. beam epitaxial growth, cryst. quality, composition investig. *(Japanese)* 77−55895
$Ga_xIn_{1-x}As$, alloy film surface processes controlling growth by MBE RHEED and AES exam. 78−84084
$Ga_xIn_{1-x}P$ alloy films, surface processes controlling growth by MBE, RHEED and AES exam. 78−84084
GaN, initial growth, on Al_2O_3 and spinel *(German)* 80−107664
GaN on Si, form. with GaCl-NH_3-H_2(He), ESCA and RHEED meas. 79−90909
GaP, heteroepitaxial growth on Si substrate by MBE 78−64481
GaP, MBE growth on GaP, and crystallographic evaluation 77−8762
GaP, mol. beam epitaxial growth, cryst. quality composition investig. *(Japanese)* 77−55895
$GaSb_{1-x}As_x$, MBE RHEED meas. 78−18916
$Gd_3Ga_5O_{12}$, garnet substrate surfaces, working damage, electron microscope investig. 77−77605
Ge (111), Cd adsorption, combined RHEED-mol. beam obs. 77−4255
Ge (111), epitaxial growth of Cd, simultaneous RHEED-mol. beam obs. 77−7986
Ge (111) Cd adsorption, struct. and surface coverage, RHEED-mol. beam obs. 77−4265
Ge (111) surface, 500 eV Ar^+ bombard., high temp. annealing, recovery, RHEED obs. 78−87723
Ge, (111) surface, clean, double diffr. spots in RHEED patterns 79−90855
Ge-$Ga_{1-x}Al_xAs$, MBE of ultra thin film superlattices on GaAs substrates, TEM study 79−37932
Ge(111) surface, diffuse scatt. at high temp., RHEED study 80−80043
Ge(111) surface, Sn monolayer, induced 7×7 superlattice struct., RHEED obs. 78−91521
In film, $\sqrt{3}$ and $\sqrt{31}$ submonolayer superstructures on Si (111) isothermal desorption, RHEED meas. 79−86992
In film, MBE deposited, struct. by RHEED obs. 79−82491
InAs, MBE growth, SEM, RHEED, optical microscopy and elec. meas. 78−18925
$In_{1-x}GaxAs$, MBE, RHEED meas. 78−18916
InP, MBE, substrate temp. related degradation mechanisms 80−65385
InSb (110), clean, O_2 adsorption, AES, LEED, RHEED and field effect meas. 80−49501
InSb (110), ion bombard. effect on surface struct. and electronic props. 80−6923
InSb (110) surface, struct. and electronic props., RHEED and field effect meas. 80−11068
InSb film, grown by MBE, RHEED study 80−100415
MgO epitaxy on alkali halides with NaCl-type struct., RHEED meas. 78−67920
MgO film, IR spectroscopy and RHEED analysis 77−89664
MgO film, vacuum deposited on NaCl-type alkali halides, struct. characterisation 79−82490
Na (111) surface, epitaxial film, electron induced dissociation 80−6646
Nb-Nb_2O_5-Pb(In) Josephson junctions, props. of Nb_2O_5 thermally grown tunnel barriers 80−100568
Ni (001) surface, initial oxidation, RHEED and X-ray emission meas. 77−31885
Ni (100)-c(2×2)-O system, adsorbed monolayer, RHEED study 79−77912
Ni (110), oxidation, initial stage kinetics, RHEED and X-ray emission 78−15588
Ni, epitaxial growth, on NiO(100), by low pressure hydrogen reduction *(French)* 80−11578
Ni/GaAs film contact system, alloying reaction 80−96747
NiO (100) surface, sulphurisation by H_2S, AES, LEED, RHEED structural study *(French)* 78−64888
NiO, (100) surface interaction with SO_2, electron diffr. and Auger spectrosc. obs. *(French)* 80−97728
NiO film, formed by Ni galvanic oxidation in borate buffer soln., struct. 80−100948
$NiSi_2$, epitaxial film on Si, ^4He ion channelling meas. and RHEED anal. 80−10834
Pb, epitaxial growth on Ag (111) and Cu (111) LEED, RHEED, AES study 78−84090
PbS-Si heterojunction, PbS film growth and struct. 80−96762
$Pb_xSn_{1-x}Te$, RF sputtered films, struct., lattice parameter, stoichiometric comp., RHEED 78−38975
PbTe (111), lattice vibr. amplitude anisotropy, RHEED study 80−39408
PbTe, VPE, on $LiNbO_3$, struct. and morphology obs. 80−54561
Pd_2Si, epitaxial film on Si, ^4He ion channelling meas. and RHEED anal. 80−10834
PtSi, epitaxial film, cryst. perfection and thermal stability, channelling and backscatt. meas. 79−99255
PtSi, epitaxial film on Si, ^4He ion channelling meas. and RHEED anal. 80−10834
Sb, epitaxial growth, of electrodeposits on oriented single cryst. surfaces of CU, electron diffr. study 79−66016
reflection high energy electron diffraction continued
Sb film, MBE deposited, struct. by RHEED obs. 79−82491
$SbFe_2Si_2O_8OH$, crystal struct., space groups by RHEED 78−47297
Se film, epitaxially grown on Te substrates, crystallinity, RHEED and SEM meas. 77−40373
Si, (001), clean, double diffr. spots in RHEED patterns 79−90855
Si (001), RHEED, expt. compared with calcs. 78−91523
Si (001), surface Debye temp. meas. by HEED 77−89633
Si (111), surface structure, high temp. RHEED obs. using metal-backed fluoresc. screen 80−75126
Si (111) 7×7 surface, structure model from anal. of RHEED patterns 80−49471
Si (111) 7×7 surface structure investigation, RHEED 80−96723
Si (111) surface, 500 eV Ar^+ bombard., high temp. annealing, recovery, RHEED obs. 78−87723
Si (111) surface, clean, new diffr. phenomena in RHEED 78−63910
Si (111) surface structs., induced by Ag evaporation, RHEED obs. 79−23814
Si (111) surface structure induced by Ag evaporation, RHEED meas. 78−22942
Si (111)($\sqrt{31}\times\sqrt{31}$)R ±9°-In struct., RHEED obs. 79−60612
Si, amorphous laser effects 79−69921
Si amorphous layers, glow-discharge, laser-annealed, elec. props. 80−75661
Si, CVD, surface anal. during growth, using RHEED and Auger spectroscopy 80−66433
Si, epitaxial film growth on Si(111) and sapphire ($1\bar{1}02$), simultaneous RHEED/AES study 80−10833
Si, epitaxial growth on sapphire by partially ionised vapour deposition, RHEED-AES obs. 80−80985
Si film, amorphous, plasma-deposited, H_2 evolution, mass spectrometry and RHEED obs. 78−72050
Si film, epitaxial growth by partially ionised vapour deposition, RHEED-AES-QMS study 79−83136
Si, glow discharge film decomposed from silane, on amorphous substrate, elec. cond., RHEED study 80−20044
Si, ion bombard. effect on surface struct., RHEED and Au decoration 80−2096
Si ion implanted, amorphous to crystalline transition due to laser irrad. 80−103451
Si, ion-implanted layers, crystn. by ns laser pulses, TEM and RHEED 80−100421
Si, laser annealed layers, reflection electron diffr. obs. 79−73190
Si, laser pulse induced amorphous to cryst. transition, thickness depend. 78−47678
Si, MBE growth and surface struct. 80−10816
Si, Pb implantation, channelling and RHEED anals. 78−30657
Si, polycrystalline layer, laser-induced single cryst. transition, RHEED and backscatt. obs 78−87704
Si, self-ion implanted, amorphous to polycrystalline transition induced by laser beam, RHEED meas. 77−84771
Si surface structure, Si (111)7×7, Si (111)$\sqrt{19}\times\sqrt{19}$ Ni, Si (111)5×1 Au, RHEED 77−62452
Si:O, CVD layer, RHEED study of surface crystallinity, annealing effect on structure 79−69371
Si-Pb heterojunction, RHEED, Mossbauer spectroscopy and I-V characts. 80−70828
Si-Sn heterojunction, RHEED, Mossbauer spectroscopy and I-V characts. 80−70828
SiC, 102R polytype struct, and localisation, by RHEED *(French)* 77−65966
SiC, film, synthesized by RF reactive ion plating, struct. 77−40391
SiC film synthesis by plasma deposition process 78−11127
SiC, polytypism, reflection electron diffr. 78−83694
Te film growth on KBr (111) on mica *(Japanese)* 78−79903
Te-Se-CdO struct., fabrication and characts. 78−76106
TiC, CVD coating on Co-bonded multicarbide substrate, SEM, RHEED, AES interface study 79−77927
Tl, epitaxial growth on Ag (111) and Cu (111), LEED, RHEED, AES study 78−84090
W_6Co_6C cemented carbide substrate, TiC CVD coating, structure, composition and hardness exam. 78−11425
ZnO piezoelectric films, RF planar-magnetron sputtered, characterisation 80−96751
ZnSe, evap. onto electron bombarded NaCl substrates, epitaxial growth and characts. 79−28948
ZnSe:In films, MBE growth, doping effect on photoluminesc. 80−10818

reflection nebulae *see nebulae*

reflection spectra *see reflectivity; spectra*

reflectivity
see also electroreflectance; magnetoreflectance; piezoreflectance; thermoreflectance
actinide compounds, spectroscopic techniques for electronic props. meas. 80−11427
adsorbed molecules, surface plasmon enhanced light absorption 80−40176
adsorbed species, IR ellipsometric spectroscopy 80−39434
airborne laser scanner, modulation techniques 80−5770
alcohols, opt. consts. in IR, stretch band obs. 79−91421
alkali halides, far IR reststrahlen spectra, γ-induced changes 77−40244
alkali halides, microcryst. powders, colour centres, refl. spectra 78−23493
alkali metal suboxides, thermal and struct. anal., elec. and optical props., photoelectron spectra 79−47587
alkali sulphates, SO_4^{2-} optical and spectroscopic props., cryst. environment effect 77−40224
alkali-alkaline earth silicate glasses, IR refl. spectra *(Japanese)* 78−52505
alkaline earth oxide with adsorbed CO, reflectance spectra obs. 79−28781
ammonium oxalate monohydrate, IR refl. and Raman spectra, internal and external modes *(French)* 77−36231
anisotropic crystal, refl. spectra, phase difference determ., Fresnel formula validity 77−43956
anisotropic medium, optical wave reflectance, general formula *(Japanese)* 78−87012
anisotropic nonconservative media, diffuse reflectance 77−7002
anthracene, fluoresc. from (001) surface and sub-surface excitons 79−33763
anthracene, polarised refl., surface excitons, Davydov splitting 77−16327

reflectivity continued
anthracene, polarised reflection spectra, surface and vol. exciton coupling, vibronic states 78−72543
anthracene, reflectivity and fluoresc. of (001) surfaces, sub-surface exciton states 79−15508
anthracene, surface polaritons, attenuated total refl. 77−63423
anthracene, thin film vacuum deposited, exciton reflection spectra *(Russian)* 78−15194
anthracene, total reflection spectra, site shift surface exciton dispersion 77−77233
anthracene isotopic mixed crystals, exciton spectra 79−38602
anthracene single cryst., Frenkel exciton spectra at dielectric and conducting layer interfaces 80−44510
antireflection coating, multilayer achromatic, extended region of low reflection coeff. values 80−95982
antireflection coating evaluation by attenuated total refl. 77−50783
antireflection films, on alkali-borosilicate glasses produced by chem. treatment 80−66677
Arctic summertime stratus clouds, solar radiation pyranometric meas. 78−32165
astronomical mirror reflection coefficient checking against control samples 79−75106
astronomical mirror testing, portable visible-IR reflectometer 77−62033
ATIR spectra, Davydov splitting 77−24865
ATR spectroscopy, Goos-Hanchen shift and effective sample thickness 77−49791
attenuated total reflection minima, correlation with surface polariton modes, computational study 78−31265
automatic concentric shaft reflectometer for use in vacuum UV 77−2684
B_2O_3-Li_2O-LiCl, ionic conductor, IR refl. Raman study 80−66173
beam incidence angle determ. from refl. meas. *(French)* 80−37072
beamsplitter using ultrathin metal grids, polishing technique to improve reflectivity 78−55459
bidirectional reflectance and transmission for optical diffusers use in space projects 78−36438
bidirectional reflectance and transmission for space appl. 77−56809
bidirectional reflectance distribution function meas., mirror surface contamination assessment 79−59790
binary composites, percolation effects and sum rules in optical props. 79−69801
biphenyl, cryst., electronic absorpt. and refl. spectra 78−64377
bis(p-toluene sulfonate) diacetylene polymer cryst., second order phase transition 79−73922
bis(p-toluene sulphonate)diacetylene, fully and partially polymerised, optical props. 77−1696
black chrome solar selective absorber, microstruct., chemical comp. and reflective props. 80−7959
blackbody cavities, directional emissivity calc., Monte Carlo method 80−83729
borosilicate glass, IR refl. spectra resulting from phase separation *(Japanese)* 78−39542
Bragg reflector statistical analysis 78−66882
brain reflectance, mapping technique using optical fibres 80−72381
cadmium arachidate monolayer, Ag(Au) substrate, reson. surface plasmon reflection 78−56536
Ceres, broadband IR reflectance rel. to carbonaceous chondrite mineralogies remote spectral identification 79−96946
cermet film, as solar selective absorbers, production, struct. and optical props. 79−29485
Chesapeake Bay, water surface laser radar refl. as function of wind speed 77−41034
cholesteric helix surface, elec. field-induced high-order ref. 78−35115
cholesteric liquid crystal, influence of orientational order 78−42900
cholesteric liquid crystal, stabilisation, multicomponent mixtures, refl. spectra, clarification temp. and melting point meas. 78−9951
cholesteric liquid crystal, thermosensitive, props. *(Hungarian)* 78−59755
cholesteric liquid crystal coatings, superimposed left- and right-handed, peak refl. and colour gamut 80−74472
cholesteric mixtures, optical props., temp. meas. *(German)* 77−44013
cholesteryl esters, isotropic mesophase, optical props. 79−65891
cholesteryl myristate, two blue phases demonstrated by selective refl., 300-400 nm 79−90553
cholesteryl nonanoate, polymorphism of blue phase, optical rot. and refl. 79−37820
cholesteryl propionate-acetate mixture, light refl., twisting power 77−84641
cloud diffuse reflectance, semiempirical model 79−80014
cloud reflectance with laser beam illumination, multiple scatt. contrib. 78−85686
clouds, horizontally inhomogeneous, albedo and refl. radiance 77−78417
clouds, particle size distrib. from spaceborne line spectrum imagery, theory 79−5613
clouds, radar reflectivity rel. to cloud dynamics and microphysics 80−61877
coal, considerations involved in automation of reflectance microscopy 80−18001
coated substrate, transmittance and reflectance, film refr. index meas. 78−56534
coating, low reflection, continuously varying refr. index, transmission curves 78−25947
complex contours interpretation of IR refl. bands, dispersional analysis 78−72508
complex reflection amplitudes of photons, sum rules 78−63006
conjugate interfaces: interfaces between transparent media of the same reflection coefficient for the parallel polarization at the same angle of incidence 80−87299
copper (II) carboxylates, magnetic and spectroscopic props. 79−91204
corundum, complex reflection spectra, dispersional anal. 77−36239
crop and soil bidirectional reflectance factor calibration, remote sensing field research 80−86382
CTIP, exciton surface polaritons at room temp. 79−47476
p-$CuInTe_2$, single cryst., IR study of lattice and free carrier effects 80−45074
cumulus clouds, size and particles effects on satellite-observed reflected brightness 78−73510
cyanine dye, crysts., extraordinary exciton polaritons in refl. spectra, macroscopic dielec. theory 77−89715
4-cyano-4′-n-pentylbiphenyl, refr. index meas. and isotropic-nematic phase transition study, surface plasmon technique 80−84282
9-cyanoanthracene, cryst., polarised refl. spectra at 2K, 360-460 nm, dielec. function 79−91461
reflectivity continued
γ-cyclopropyl-bis (1,3,3-trimethylindolenine-2-yl)pentamethinium fluoroborate, exciton surface polaritons, reflecting faces obs. 80−65645
cylindrical dielectric array, multiple scatt. effects in photon diffraction 80−1905
dense scattering media, anisotropy factor 80−87307
N,N′-di(methyloctadecyl) squarylium monolayers on Ag surface, attenuated total refl. 79−11480
p-dibromodiphenylether surface, normal and ultra-Brewster refl. spectra 80−25400
9,10-dichloroanthracene, quasi 1D α-cryst., exciton transitions, optical refl. spectra obs. 77−81116
dichroic beam splitters, high-performance, for DF chem. lasers 80−95932
dielectric, complex reflection spectra, dispersional anal. 77−36239
dielectric film, reflectivity, polariton standing-wave struct. as test of boundary conditions for spatial dispersion theories 79−4865
dielectric half space, spatially dispersive exact microscopic theory of polaritons 77−4301
dielectric material, reson. method of meas. complex refl. coeffs. 79−56756
dielectric multilayer coating, optical phase shift at boundary, reflection coeffs. 77−34926
dielectric slab, spatial theory of dispersion, models 79−73891
dielectric surface, reflectances, undergraduate exptl. meas. 78−73809
dielectric thin films, refractive index variation for given reflectivity, analytic soln. to synthesis problem 80−34996
dielectric-vacuum interface, spatial dispersion in optical props. 77−4613
diethylammonium manganese tetrachloride, IR active modes, interlayer and intralayer forces 77−59575
diffuse reflect. spect., standards and calibration rel. to chromatography 77−56278
diffuse reflectance, FT IR spectrometric meas. 79−35858
diffuse reflectance, in near IR, spectrophotometric method 77−82625
diffuse reflectance meas. for buildings 80−27334
diffuse reflectance spectra, model interprets., review 78−32859
diffuse reflectance spectra interpretation 77−53982
diffuse reflectance spectrometry, continuum models 77−21430
diffuse reflectance spectroscopy, applics., standards and calibration 78−32848
diffuse reflectance spectroscopy, calibration of reflectance standards, review 78−32860
diffuse spectral reflectance, calibration of standards 77−53983
diffuse surface, in situ laser refl. meas. 78−82022
1,5-bis dimethylamino pentamethinium perchlorate, refl. spectra calcs. 77−85154
dimethylammonium manganese tetrachloride, IR active modes, interlayer and intralayer forces 77−59575
directional-hemispheric reflectance factor scale establishment, Van den Akker method 78−77967
dispersion relations for complex reflectivities 77−65572
DODCI, saturable absorber, picosecond phase-conjugate refl. 80−95960
dual-polarisation radar for rain targets, rel. of diff. reflectivity to correl. 79−62556
dye crystal, CTIP, exciton surface polaritons detect. by ATR spectra at 295K 79−4818
dye in contact with Ag film, enhanced total refl. with surface plasmons 79−59694
dye saturable absorbers, picosecond phase-conjugate refl. 80−95960
Earth's surface, radiance of natural formations 79−62515
Earth seismic reflectivity function, extraction via data deconvolution, book contrib. 79−92635
education, Fourier transform interferometry, visible reflectivity spectra 77−33765
electrolyte, solid film, size-selective photochromism 79−99968
electronic elementary excitations in far UV, core level exciton and core hole polarisation 78−39032
ellipsoidal lens for sub keV X-ray imaging 77−26444
ellipsometry method, sensitivity threshold, sample polaris. reflectance and inhomogeneity effects 78−24846
EM waves, parallel polarised, equal reflectance at normal and oblique incidence, dielec. const. meas. 80−1119
epoxy films, in polished metal mirrors, refl.-absorpt. IR spectrosc. and ellipsometry obs. 79−78765
N-p-ethoxybenzylidene-p′-cyanoaniline, nematic, mol. reorientation in DC elec. field, IR ATR spectra study 80−45064
ethylammonium cadmium tetrachloride, order-disorder transition, far IR reflectivity obs. 79−65870
exciton reflection of light for arbitrary surface pot. 79−38568
exciton resonances, interacting, dielec. theory 78−14673
excitons in semi-infinite crystals, microscopic calc. of optical refl. 79−69430
excitons internal structure, review, book contrib. 80−44518
Fabry-Perot cavity, dispersive optical bistability 80−78889
far IR absorbent solid dispersive reflection meas., using Fourier spectrometer and cryostat 79−30580
far IR complex reflectivity meas., automated asymmetric interferometer 79−30534
far IR diagnostic quartz beam splitters 77−39470
far IR surface polariton obs. by attenuated total reflection 77−39790
film, computational algorithm for optical consts. determ. 78−72617
film, optical and elec. props. in situ determ. during deposition 77−59341
film, optical const. determ. from meas. of normal incidence reflectance and transmittance 77−85825
film, optical consts. determ. 80−2883
film inhomogeneity characterisation by refl. and refractive index changes *(French)* 77−73180
film pulsed laser damage determ., optical techniques 80−33060
film refractive index determ. using reflectance extrema 78−70178
film with exponential refr. index distrib., refl. coeff. *(Russian)* 79−56877
films, in situ meas. in ultrahigh vac. at low temp., optical reflectivity and transmissivity, DC resistivity, Au appl. *(French)* 78−39617
films, optical constants, reflection spectra by Kramers Kronig method 80−76099
fluorescence spectrometry, beam splitter and cell window errors 80−31897
fluoride coating materials, refractive index, spectroreflectometry meas. 250 to 2000 nm 79−32006
formamide, liq., vac. UV optical and dielec. meas. 80−25329
Fourier series algorithm 77−85679

reflectivity continued
Fresnel formula for dielectric multilayer mirrors 80−33118
frosts, Na and K doped, reflectance spectra and implications for Io surface 78−84561
Fuchs-Muller-Kennett reflectivity program, causal absorption, effect on synthetic seismograms 79−92486
Galilean satellites, water ice existence, IR spectral reflectance obs. 80−82263
garnets, IR refl., ATR, Voigt and Faraday expts. 80−66180
gas/glass interface, used in measurement of gas pressure transients due to weak shock waves 79−63297
geometric reflecting props. and nomenclature 78−29146
Georgian Bay, chlorophyll conc. from airborne spectral refl. meas. 78−16202
glass:Nd, surface struct., laser beam effects, IR spectra appl. 79−95250
glass, IR emissivity calc., strongly absorbing media surface refl. 80−107452
glass, IR total internal refl. spectrum, surface polaritons *(Russian)* 77−20861
glass, irrad. with laser beam, damage accumulation kinetics 79−99991
glass, laser induced surface damage, free electron density meas. 77−40309
glass, porous Vycor, surface phonons, Raman and IR reflectivity spectra meas. 78−38931
glass, transmission, reflection, absorption factors, solar radiation, calc. method 77−34918
glass, white-surface, spectral reflection coeffs. and colour coordinate comparison 77−71358
glass laser disc interface with edge cladding glass, reflection meas. 79−27300
glasses, high vol. low cost, as solar reflectors, compositions and weathering effects 80−106589
glazed ceramic insulators, surface quality monitoring 79−61813
gloss measurements, polarisation effects 79−80662
gloss paints, reference glossmeter 80−82805
glossiness of curved surface, physical and psychological, meas. method 80−37074
glycerol, liq., reflectivity, in VUV region, for optical and dielec. functions 79−15475
graphite, highly oriented, pyrolytic surface, polarised reflectivity spectra at near normal incidence, surface prop. effects 79−15481
graphite, IR active optical vibrations, IR reflecting meas. 77−69837
graphite, IR optical properties, refl. data and complex dielec. function 78−10889
graphite, pyrolytic, IR reflectance, dielec. props. 77−55781
graphite, reflectance meas. in visible spectrum 77−77241
graphite, reflectivity in near IR and hydrostatic press. 79−91423
graphite, reflectivity in near IR under hydrostatic press., lineshape anal. 79−91424
graphite intercalation compounds, alkali and halogen, electronic props., conductivity and optical reflect. *(German)* 80−49837
graphite intercalation compounds, band struct. model, dynamical dielec. function, reflectivity 80−34348
graphite intercalation compounds, galvanomagnetic and optical data, electronic structure 77−51634
graphite intercalation compounds, props. and appls. 78−71711
graphite intercalation cpds., Raman scatt. and IR refl., review 80−45066
graphite nitrate, $(C_{3.24})^{+}(NO_3)^{-}3HNO_3$, DTA, NMR and refl. meas., dynamical and electronic props. 77−59478
graphite-alkali metal intercalation cpds., electronic props. 80−45202
graphite-SbF_5 intercalation compounds, elec. cond. and opt. reflectance 77−62970
grass canopy spectral reflectance, 500-1000 nm, asymptotic value 77−64442
halosodalites, synthesis, cathodochromism, reflectivity spectra 77−40399
heavy water, optical consts., absorpt. and refr. index 0.1 Å-1 m 78−48139
heavy water, VUV reflectance, refr. index, absorpt. coeff., isotope effects 78−6695
hemicylinder-air-quartz system, semi-infinite crystal, dispersion of surface phonon polaritons 78−71939
high temperature specular refl. meas., Fourier transform spectrometer alignment 79−17498
highly absorbing solid, dispersive refl. meas. using modular interferometer 78−89568
I-III-VI_2 chalcopyrite compounds, d-level struct. and p-d coupling 79−42451
Iapetus, relative reflectance meas. at 1.6 and 2.2 μm 80−98607
II-VI and III-V cryst., excitons detect., precision method 79−19906
II-VI semiconductors, photoreflection exciton spectra *(Russian)* 77−20874
illumination and reflection edges, recognition by human visual system 80−94209
immersed multilayers, optimum reflectance attainment for TM polarised flux 79−59627
inert gas, solid, dead layer effects in UV reflectance of excitons 78−72553
inhomogeneous diffuse media, reflectances and transmittances, charact. matrices 80−32915
inhomogeneous layer synthesis with given spectral charact. 78−52588
insulating thin film, thickness meas. by IR refl. spectroscopy *(German)* 79−58671
insulator, semiinfinite, spatial dispersion influence on EM props. 77−24814
integrating spheres for absolute refl. meas., goniophotometric corrections 78−21202
interface between transparent media, *p* and *s* polarisation amplitude reflectances and phase shifts 79−76578
interference filters, multilayer, design method 80−48396
interference microscope, VELOMET interphako, for optical path difference measurement 78−37054
inverse scatt. problem of lossy dielectrics, exact soln. 77−79732
ion bombarded surfaces, spectral refl. 77−55308
IR diffuse reflectance, Fourier transform spectrophotometer 77−5929
IR imaging systems, sensibility equation modification *(Chinese)* 80−102806
IR metallic film reflectivity rel. to thickness less than penetration depth 77−39018
IR reflection spectroscopy cross section rel. to electron energy loss spectroscopy 77−85729
reflectivity continued
IR reflection spectrum, dispersion formula fitting, Kramers-Kronig anal. 80−50311
IR scanning by SAW modulation 79−80687
IR spectroscopy of adsorbed layer systems, review, book contrib. 80−84747
IR specular reflectance meas., spectrometer accessory 77−2702
IR thermography, reflectance errors 80−62661
Jupiter, methane band photometry, absolute reflectivity, centre-to-limb vars. 79−53759
Jupiter, methane band photometry, SEB and STrZ reflectivity, atm. models 79−53760
Kapton, optical, elec. props., struct., ion textured surface 78−72904
Kramers-Kronig anal. with preliminary dispersion anal. 78−49915
Kramers-Kronig analysis, reflectivity extrapolation 78−19438
Kramers-Kronig transformation, validity 77−66468
Lake Kainji, W.Africa, water columns movement, LANDSAT data 79−25284
lakes, volume reflectance rel. to suspended solids anal. via Landsat multispectral data 79−16523
laser cavity resonator, photon lifetime and reflectance meas., phase-shift method 80−38039
laser mirror, low-loss, precision meas. technique 78−17947
laser mirrors, high precision reflectivity meas. technique 77−23698
laser plasma, reflectivity and temp., scaling laws 80−87913
latex, monodisperse, order-disorder phase transitions, short-range order 77−29056
latex, monodisperse, reflectivity obs. of phase separation into ordered and disordered phases 77−70345
latex, monodisperse particle size determ., spectroscopic method 77−29055
layer surfaces, reflectivity at 3.39 μm, meas. method, relevance to pipelines 80−52340
layered compounds, book contrib. 77−44023
leucosapphire, electronic band struct., optical props. 79−95329
LiH, cubic, vibronic struct. and anisotropy of excitons, refl. and edge luminesc. spectra 78−23523
liquid, reflectivity meas. by gas ionisation, vac. UV 78−294
liquid semiconductors, data and model densities of states 80−50364
liquid-liquid moving boundary, reflected freq. conversion *(Russian)* 77−7152
liquid-solid interfaces, measurements of voltage-induced reflectance changes 79−58804
lunar, soils, mineral comp. determ. from spectral behaviour of albedo 79−21207
lunar regional basalt types from remote spectral refl. meas. 77−22118
lunar surface, TiO_2 distrib. from anal. of Mikhail's photometric catalogue *(Russian)* 78−73661
lustre quality meas., recording and evaluation 80−98967
Mars, cloud formations, reflectivity time var., visible photometry obs. 80−72840
Mars, near IR spectral reflectance, surface comp. determ. 79−21216
matching methods determ. 77−85682
MBBA, nematic liq. cryst. isotropic phase, phase-conjugate refl. by degenerate four-wave mixing 80−43389
measurement at diffuse incidence *(German)* 78−21201
measurement attachment for type SF-16 spectrophotometer 79−85160
measurement of reflectance and transmittance, arrangement for integrating sphere *(German)* 80−31844
mechanical surface excitons, interaction with radiation, refl. and transmission spectra 79−15098
Mercury, IR and vacuum UV reflectivity rel. to surface material props. 78−12130
metal, change in refl. on adsorption of molecular monolayer 79−65877
metal, laser irrad., time-resolved specular reflectivity 79−69819
metal, O_2 diffusion and dissolution effects on optical props. in radiative heating, appl. to Ti 79−65884
metal, struct. induced surface plasmon polariton modes using ATR, theory 79−60890
metal, surface-plasmon dispersion relation from reflectivity of parallel-polarised light 79−78030
metal carbide, magnetron-sputtered, solar selective absorbing surfaces 79−92079
metal drilling with Nd lasers, absorption phenomena 78−30002
metal film, carrier relax. time, optical determ. by surface plasmon excitation 77−1499
metal film mirror prep. by ultraclean DC sputtering, optical props. 77−50748
metal island film, two-dimens. distrib. system, optical refl. and transmission calcs. 79−4862
metal mirrors, diamond turned, evaporated and sputtered, surface and optical studies 78−79098
metal optical elements, diamond turned 77−27400
metal reflectance changes during laser irrad. 80−93261
metal surface, optics by reflectance of p-polarised light 79−78706
metal surface, perturbative calc. of elec. field 80−45108
metal surface, reflectivity, single laser pulses, plasma burst effect 78−19609
metal surface oxidation, refl. spectra obs. 78−39958
metal surfaces, adsorbate spectra, vac. UV differential reflectivity obs. 79−28783
metal-dielectric bilayer system, optical, mechanical and corrosion props. 77−32707
metal-dielectric codeposited film, optical, elec., mechanical and corrosion props. 77−32708
metal-electrolyte boundary, electrodynamics in visible and near UV range, microscopic effects 80−45521
metal-electrolyte interfaces, optical reflectance specta, interpretation 80−93263
metal-insulator composite solar selective absorbers optical props. 79−52037
metal-insulator layers on transparent substrates for making scales 77−798
metal-metal bilayer system, optical, mechanical and corrosion props. 77−32707
metal-metal interface, EM wave propag., plasmon polaritons, computer simulation 78−84276
metallic film, IR reflectivity, mirror appl. 78−5536
metallic glass, bulk and surface properties, review 80−44147
metallic mirror coatings, protected and unprotected specular reflectance 79−76792

reflectivity continued
metallic rough surface, reflection loss for s and p polarised waves near surface plasmon freq. *(French)* 80−97225
metallic thin films, free-electron, optical props., theory including electron surface scatt. 80−29817
metallic thin layered structures, coupled surface plasmons 79−56873
metals, specular refl. anomalous behaviour after 10.6 μ pulsed laser irrad. 80−93260
methane, liq., optical consts. meas. in IR, possible planetary cloud cover component 78−64341
microscope photometry in studies of molecular struct. of carbonized bitumens and pyrobitumens 80−18011
microwave thermophotoindicators, analysis of diffuse light spectra 80−73457
mirror, highly reflective, reflectivity meas. 78−54444
mirror reflectance meas. using multipath optical cavity *(French)* 77−13797
mirror reflectance meas. using multiple wave interferometer *(French)* 77−42585
mirror reflection coefficient meas. instrument 78−18036
mirror reflectivities from 50-150 eV 80−90966
mirror surface of gyroscope rotor, reflectivity, statistical characts. 77−10996
mirror surface reflectances, expt. investigation 78−83066
mirror surfaces for solar power stations, specular reflectance obs. 78−13786
mirrors, dielectric mutltilayer, reflectance under slight absorpt. conditions 80−83655
modulation spectroscopy, anal. of Kramers-Kronig relations 78−23423
molecular crystal, surface exciton levels, radiation corrections 80−34962
molecular crysts., extraordinary exciton polaritons in refl. spectra, macroscopic dielec. theory 77−89715
molecular monolayers, IR absorpt. enhancement by thin metal overlayers, ATR technique 80−88995
monoclinic crystal, refl. spectra dispersion anal. 79−99877
monoclinic crystals, IR refl. spectra 79−78676
Moon, IR and vacuum UV reflectivity rel. to surface material props. 78−12130
multilayer dielectric coating producing 90° phase change 79−76788
multilayer dielectric enhanced mirrors for 2 to 6 μm 79−14086
multilayer dielectric mirrors, exam. of reflectance, optical thickness and refractive index 78−59106
multilayer dielectric reflectors, optical props. calc. 78−30041
multilayer highly reflective coating design for wideband 90° phase shift 80−74464
multilayer mirrors, high refl. at fundamental, second and third harmonic laser wavelengths 78−90490
multilayer nonabsorbent coating reflectivity computation program 80−28293
multilayer optical film thickness analyser 78−32785
multilayer stack reflectance derivatives, fast computation method 78−46508
multilayer structure, multiple internal reflections effect on Faraday rot. 78−48148
multilayer superlattice stacks, very thin nonideal, wavelength variation of transmissivity, refl. 80−100701
multilayer systems, neutron optical props. 79−55044
multipole surface plasmons, attenuated total refl. spectra 79−78149
multiwavelength radiation pyrometry where reflectance is measured to estimate emissivity 80−31757
near IR diffuse reflectance analysis anomalies 80−86383
nematic liquid crystal, tilt angles, total refl. meas. *(French)* 78−79528
Neptune, evidence for optically thin high-altitude cloud form. 77−53469
Neptune, IR refl. spectrum, evidence for weather 77−53468
nitromethane, far IR reflection meas. and plasmon model relevance 79−33687
nonabsorbing film with randomly rough boundaries, refr. index and thickness meas. 77−82589
noninvasive beam-wave reflectometer for complex permittivity meas. at microwave freqs. 78−74030
nonlocality effects on optical phenomena in bounded solids, developments 80−93328
normal, superconvergent sum rules 77−85678
normal reflectance of conductors and insulators, dispersion relations and sum rules 80−29706
oblique selective Fabry-Perot etalon fabrication tolerances 79−68424
ocean, continuously stratified, remote sensing of optical props. 78−77331
ocean, flat, reflectance in zero water depth limit 77−41032
ocean chlorophyll content airborne meas. under cloudy sky, Gulf of Guinea appl. 79−25359
ocean diffuse reflectance, effects of chlorophyll a fluorescence at 685 nm 79−66700
oil traces, on water surface, continuous detect. system *(German)* 80−72115
olivine irradiated by heavy ions, IR reflectance and extinction rel. to interstellar dust 79−53873
opaque layered system, complete absorpt. of transverse mag. waves 78−39615
opaque microrough radiative surfaces, behaviour modification *(French)* 78−94366
optical apparatus for reflectivity meas. by changing incident angle 80−18000
optical coating refl. spectroscopy 79−61448
optical coatings, algorithms for determ. of reflectance and transmittance 79−98271
optical component, surface evaluation techniques 79−46094
optical consts. determ. as func. of wavelength, causality calcs. in reflection spectroscopy 78−32887
optical glass, spottability determ. 78−30102
optical system, cryogenic and contamination effects 80−38113
optical thin film, reflection coefficient partial derivatives, matrix calc. *(French)* 80−89080
optical thin film, Smith chart and charact. matrix for reflectance computation 79−45904
ore minerals, recent developments in microscopic meas. of spectral reflectance *(French)* 79−5627
organic charge transfer complexes, refl. spectra, excitons 79−47477
orthovanadates, rare earth activated, spectroscopic props. 77−16363
Osterberg problem and wave propag. in inhomogeneous plasma, numerical study 80−63925
reflectivity continued
oxide coating materials, refractive index, spectroreflectometry meas. 250 to 2000 nm 79−32006
oxide layers on high-temp. alloys, for central-receiver, solar-thermal power systems 78−18071
oxide surfaces, adsorbate spectra, vac. UV differential reflectivity obs. 79−28783
Pallas, broadband IR reflectance rel. to carbonaceous chondrite mineralogies remote spectral identification 79−96946
paper, coating type and extent, attenuated total refl. spectrosc. obs. 79−79329
parallel surfaces, absorptance, reflectance and transmittance, generalised eqns. for calc. 78−42273
particulate material, spectral reflectance, Monte Carlo model with asperity scatt. 78−37804
pentacene, ATIR spectra, Davydov splitting 77−24865
perylene, α- and β-crysts. and soln., polarised reflection and absorption spectra 77−8598
PET film interatomic bond determ. by IR transmission and reflection spectroscopy 77−65958
petrographic characterization of coal using automatic image analysis 80−18002
phase boundary, Fresnel refl. coeffs., optical thickness *(German)* 77−69794
phenanthrene, cryst., refl. spectra of first singlet transition 78−88323
phenothiazine derivatives, semicond. elec. props., optical spectra, and EPR 80−103693
Phobos, composition, evidence for carbonaceous chondrite surface from spectral anal. 78−49365
Phobos, evidence for carbonaceous chondritic composition from multicolour obs. with Viking lander cameras 78−49366
photometric etalons, scatt. matrix and brightness coeffs. of MS-20, MS-14 reflectors 78−82020
photometric standards and coatings, retrofefl. meas. 78−25940
photothermal absorber stacks on Ag, stabilisation 77−32459
pitch weathering processes, IR multiple internal refl. obs. 79−74461
planar waveguide, index profiles determ. from angular depend. of refl. 78−71210
planetary reflectance meas. in thermal emission region, thermal component removal 80−17497
plant canopies reflectance meas. using spectroradiometer 80−56658
plant canopy reflectance models, theory and expt. tests for wheat and cotton 77−34822
plasma prod. by laser, reflection losses from plane target, optical calorimetry 78−9809
plasma target, underdense, Brillouin backscatt. saturation 80−14886
plasmon surface polariton dispersion curve, optical obs., demonstration 80−101690
plastic films, IR reflectance of aluminised thermal screens for energy conservation in greenhouses 80−64351
plastic optics, design patterns 79−32009
polar semiconductor, electron-hole liquid, electron-phonon interactions 80−6739
polarised specular reflectance spectra meas., microspecular apparatus for Cary spectrophotometer 77−5926
polaritons, appl. of IR reflectivity and Raman scatt. expt. 77−40237
polaritons, molecular thin plate, with near-surface polariton transition layer, reflection and transmission spectra *(Russian)* 78−14677
polaritons, multi-component, reflectance spectrum 78−87921
poly(5,7-dodecadiyne-1, 12-diol-bis phenylurethane), visible refl. spectra, photocond., excitons 77−81117
poly-1,2-bis 4-isopropylcarbamoyloxy-n-butyl-1-buten-3-ynylene, cryst., UV refl. spectra, 25-160°C 79−82991
poly-2,4-hexadiyne-1,6-diol bis (p-toluene sulfonate), exciton surface polaritons, reflecting faces obs. 80−65645
poly-2,4-hexadiyne-1,6-diol bis (p-toluene sulphonate), cryst., exciton surface polaritons, reflectivity of (100) face, 295K 78−80372
poly-2-vinylpyridine, electron energy loss spectra, for optical and dielec. props. 79−15569
polyacetylene, pure and heavily doped, optical and IR studies, electronic struct. calcs. 80−7347
polyacetylene films, doping effect on elec. cond., chem. and optical props. 80−65572
polyacetylene pure and doped films, anisotropic optical properties 78−92137
polyamide fibres, differently matted, meas. of diffuse reflectance spectra, using SPEKOL spectrocolorimeter 80−77836
polybutadiene, C black filled, struct., Fourier transform IR obs. 77−50571
polydiacetylene, cryst., refl. spectra, Kramers-Kronig transforms 78−43889
polydiacetylene, reflection spectra, thermochromism, temp. hysteresis and phase transformation 78−19452
polydiacetylene, single cryst. piezomodulated and specular refl. spectra 77−20869
polydiacetylene crystals, electronic spectra and struct. 79−73923
polydiacetylene PTS crystal, Davydov splitting in spectra at 15000 to 19000 cm^{-1}, at low temp. 78−31212
polydiacetylene-bis(toluenesulphonate), refl. spectra, 0-15 kbar, doublet press. shift 78−43891
polydiacetylenes substituted with urethane, solid and film, visible spectra, refl. and absorpt. 79−87460
polydimethylsiloxane film, formed by RF discharge plasma polymerisation, optical props. 78−80479
polyethylene, surface fluorination effects, internal refl. spectroscopy obs. 78−86340
polyethylene terephthalate, film, optical consts., frustrated total internal refl. obs. 77−55763
polymethinium dye, cryst. metallic refl., damping theory 77−16294
polypropylene, surface fluorination effects, internal refl. spectroscopy obs. 78−86340
polystyrene, electron energy loss spectra, for optical and dielec. props. 79−15569
powder mixtures, diffuse reflectance, quantitative anal. 80−87308
power reflection spectroscopy, analytical techniques 80−62714
print contrast measurement 77−34045
proustites, natural and synthetic, refl., refr. indices and colour parameters, genetic interpretation 78−95566
PTFE, surface layer optical consts. in 1000-1300 cm^{-1} region 79−51957
PTS, exciton surface polaritons at room temp. 79−47476

reflectivity continued
PTS polydiacetylene single cryst. reflection spectra, exciton site splitting 78−31211
pyrargyrites, natural and synthetic, refl., refr. indices and colour parameters, genetic interpretation 78−95566
pyromellitic dianhydride-anthracene, cryst., charge transfer exciton transitions, refl. spectra obs. 78−72540
quartz, fused, IR total internal refl. spectrum, surface polaritons *(Russian)* 77−20861
quartz, IR reflection spectra of rough surfaces *(Russian)* 77−48175
quartz beach sand, spectral reflectance/grain size relationship 78−16005
radiation temperature, reflectivity, emissivity meas. of room temp. materials *(Chinese)* 80−101814
radiative transfer between surfaces in diathermal medium, radiation anisotropy modelling 80−33435
rare earth ions, trivalent, in O-dominated host, high energy states, reflectance spectra 77−69849
rare earth trifluoride film, optical props., 5 to 34 eV 79−38687
rare gas adsorbates on simple metals, optical excitation, configurational switching, charge transfer 80−107643
real thin films, optical consts. determ. 78−35213
reference materials 79−49190
refl. depend. on angle of incidence, 8 to 12 μm 78−37960
reflectometer, for laser mirrors, high accuracy 78−87118
reflectometer, versatile high-precision multiple-pass 78−93754
refractory metal films, evaporated, optical props., rel. to struct. 80−55211
resonance scattering on 1-D cryst. and thin film *(Russian)* 78−31268
reststrahlen bands, bulk phonon polariton dispersion 77−35647
retinal photocoagulation by laser beam, temp. and bleaching dynamic meas. *(German)* 79−2098
retroreflectors and retroreflective materials meas., luminous intensity, photometry accuracy assessment *(Dutch)* 79−85159
ribbon growth using scanned focused CO_2 laser beams 80−66417
Rochelle salt, cryst., oriented intrinsic absorpt. edge shape 77−66505
rocks, metamorphic, visible and near IR spectra rel. to comp. 77−17087
rocks, sedimentary, visible and near IR spectra rel. to comp. 77−17086
rocks and minerals, colour values from diffuse reflectance spectra *(French)* 78−11881
rocks and minerals spectral refl. data, lab. and remote obs. comparison 77−17251
rocks from Cr-rich areas, visible and near IR spectra, remote sensing appls. 80−4000
rough surface, random, reflectance derived with Fresnel approx. 80−87309
rough surfaces, anisotropic, light scatt. 79−60606
rough surfaces, general theory and small roughness limit 77−75423
rough surfaces, reflection light, division into specular and diffuse components *(Japanese)* 80−106457
roughened spheres, ang. distrib. of reflected radiation, models analysis 77−42479
roughness measurement using laser scanning analyser 80−36992
saline environmental waters, IR relative reflectance and complex refr. index 77−45013
sapphire and Si surfaces quality determ., using IR and UV specular reflectance meas. 80−108684
scattering layers, reflectance 79−99962
scattering matrix polaris. props., multiplicity effect, transmission and reflection 77−83807
Schottky barrier field, exciton reflection band burning *(Russian)* 79−47479
Schumann UV spectrophotometer system for absorpt. and refl. meas. on thin films and solids 78−12772
sea reflectivity for mm waves at 81 GHz 79−80001
seawater and ice meas., at 100, 140 and 180 GHz 79−84552
selective solar absorbers, reflectance calcs. for inhomogeneous surfaces 80−12029
semi-infinite crystals, linear wave vector effects on optical props. 77−85721
semiconducting alloys, comp. profile, second derivative wavelength modulation 80−103967
semiconducting film, exciton oscillator strength, EM wave-polaritan propagation, reflective power *(Russian)* 79−99491
semiconductor, carrier intrinsic conc. and effective mass determ. by IR refl. 79−51580
semiconductor, excitons and nonlocal optical props. 79−95345
semiconductor, inhomogeneously doped, computed IR refl. spectra 78−27205
semiconductor, IR plasma reflectivity spectra analysis 78−52480
semiconductor, optical absorpt. coeff. and minority-carrier diffusion length, differential photocurrent method of meas. 80−96896
semiconductor, p-type, infrared absorption and plasma reflection 80−97284
semiconductor, struct. induced surface plasmon polariton modes using ATR, theory 79−60890
semiconductor, surface electronic props., optical spectroscopic techniques, review 80−11070
semiconductor, time resolved reflectivity of ps pulses 78−31217
semiconductor dopant surface concentration determ. by IR reflectance 80−34036
semiconductor surface electron states, optical methods of detection 77−66191
semiconductor with wurtzite structure, natural optical activity *(Russian)* 79−78647
semiconductor-insulator structure, light refl. and absorpt. control, boundary state population rearrangement 77−69795
semiconductors, appl. to optical props. determ. via Kramers-Kronig transform. 77−8537
semiconductors, free electron scattering and dynamical cond. 78−2476
semiconductors, optical props. under press., book contrib. 80−84715
semiconductors, photoexciton waves, restrictions imposed on nature of additional boundary conditions 79−28789
seminar, optical radiation meas., San Diego, CA, USA (Aug. 1979) 80−86036
Shroud of Turin, IR reflectance spectrosc. and thermographic investigations 80−87578
Shroud of Turin, spectral props. 80−87577
Shroud of Turin, UV-visible reflectance and fluoresc. spectra 80−87579
silicate glass, IR refl. spectra resulting from phase separation *(Japanese)* 78−39542

reflectivity continued
silicate glass corroded by moisture, IR refl. spectra change *(Japanese)* 78−53013
single layer gradient refr. index film, ang. refl. 78−5538
skin reflectance rel. to serum bilirubin conc., neonatal jaundice screening 79−92328
small particle composite, optical properties from periodic multiple scatt. theory 78−56444
small particle spectral diffuse IR reflectivity meas. 80−68276
snow spectral reflectance, two-stream theory 79−88376
soil, ultrashort radio waves reflectance rel. to moisture content determ. 78−16075
solar collector selective coating microstructure rel. to processing parameters and optical props. 79−62033
solar collector stainless steel selective absorption surface props. 79−62030
solar energy collection augmentation by planar refle-tive surfaces, calc. and expt. 79−83574
solar photothermal non-selective and energy control films coatings 80−26157
solar reflectivity of common building materials, effect on roof heat gain 80−55810
solar selective absorber coatings, reflectance, emittance, and thermal stability 80−12027
solid dielectric complex and power reflectivity determ., 100 GHz to 3 THz 80−15999
solid spectra, phase correction in Kramers-Kronig anal. 79−56815
solid surfaces, non-ideal, optical props., phenomenological models 80−88950
solid-liquid transition, optical reflectance spectra 80−24569
solids, effect of angular aperture and radiation polarisation of instrument on reflection coeff. 80−9020
spatial dispersion, boundary conditions in crystal optics with spatial dispersion 78−92040
spatially dispersive crystal, reflectivity and transmittivity 80−99604
spatially dispersive crystal, reflectivity calc. 78−48140
spatially dispersive semi-infinite media, polariton Green's functions, refl. spectra 77−85154
spectra, correction for spectrometer polarisation 77−22603
spectra of diffuse reflection and photoluminesc. *(Russian)* 79−11447
spectral bidirection refl. props. meas., at 0.52 μm, for savannah, bog, pasture, and coniferous forest vegetation 78−40649
spectral reflectance and transmittance measuring apparatus for variable angle of incidence 80−250
spectral reflectance curves estimation from multispectral image data 78−32886
spectral reflectometry of 0.1 mm surface elements *(Japanese)* 78−89527
Spectrofloat glass, theoretical anal. of optical transmission and refl. props. 77−90120
spectrophotometer, Brewster's angle refined absolute refl. technique for film thickness meas. 79−21820
spectrophotometer attachment for absolute refl. meas. 77−174
spectroradiometer, polarisation sensitive, methods for overcoming refl. spectra meas. problems 79−40623
specular reflectance meas. with double-beam spectrophotometers 78−45674
specular reflectance standards for visible and infrared region using thin Al film vacuum deposited on optical flats *(Japanese)* 80−102789
specular reflection coeff. meas. on SF-4A spectrophotometer, 0.5% accuracy 77−13804
specular reflection coefficient comparison, sample materials 79−71512
sphalerite, hydrothermal single crysts., feasibility of optical methods for quality control 80−89065
spherical specimen glossiness meas. 79−54175
stearic acid salts, pseudocryst. integral X-ray reflectance coeff., cation depend. 77−11437
steel, multiple crater refl., effect on refl. props. 78−52596
steel, reflectivity at 10.6 μm, calorimeter meas. 78−55393
steel, stainless, hard, and mild, optical constant dispersion and emissivity, up to 900K 78−52464
steel, stainless, mirror acted on by laser radiation, reflectivity meas. 79−10342
structural colours of beetles, analysis using reflectance measurements from macro- and microspectrophotometers 80−18023
submillimetre wave surface reflectivity of common materials 77−36191
submillimetric reflectivity of common materials 77−39005
substrate, surface quality determ. by optical reflectance methods 78−43862
subsurface layers, attenuated total refl. Fourier transform spectra 77−71379
superconducting-normal metal interface and applications 78−91822
superposition photometer for material absorptivity meas. 78−89522
surface analysis, atomic beam scatt., SIMS, and vibr. spectra, book contrib. 79−42357
surface bidirectional refl.-distrib. function, reflectance map calc. 79−75568
surface contaminant generation and bidirectional reflectance distrib. function meas. 80−14493
surface diffuse reflection optoelectronic meters 77−79135
surface exciton polaritons, attenuated total reflection spectra 77−24867
surface phonon-polaritons on semi-infinite crystals, attenuated total reflection spectroscopy, review 77−89827
surface ripples, role of reflectivity in light scatt. 80−20653
$TCNQ_2$-TEA, quasi 1-D cryst., interaction between electronic and vibr. states 77−52102
$TCNQ^0$, crysts., extraordinary exciton polaritons in refl. spectra, macroscopic dielec. theory 77−89715
TCNQ, cryst., metallic refl., damping theory 77−16294
TCNQ, exciton surface polaritons at room temp. 79−47476
TCNQ, metallic reflection band, vibronic struct. 78−19502
TCNQ, salt, $(NMe_3H)(I)(TCNQ)$, semicond. 'metal-like' complex, optical props. 79−95761
TCNQ, single crystal, exciton surface polaritons, attenuated total reflection spectra 79−91460
TCNQ charge transfer complexes, elec. cond. 79−38058
TCNQ complexes with pyridine, polarised IR refl. spectra, evidence for electron-vibr. coupling 79−47448
TCNQ donor-acceptor complexes, refl. and absorpt. spectra 79−73965
TCNQ salt, $(NMe_3H)(I)(TCNQ)$, one-dimens. semicond. with metal-like cond. 80−24909

reflectivity continued
TCNQ salt, decamethylferrocenium, monomeric and dimeric, optical and EELS study 80−100660
TCNQ salt, HMTTF-TCNQ, electron-electron interactions, mag. susceptibility and optical reflectivity 77−81104
TCNQ salt, K^+TCNQ^- particles, light scatt., absorpt. spectra 79−24332
TCNQ salt, K-TCNQ, single crystal, charge transfer band interpretation, refl. spectrum obs. 80−25353
TCNQ salt, MTPA $(TCNQ)_2$, IR refl., dielec. function and cond. 80−34924
TCNQ salt, n-methyl-n-ethylmorpholinium, unpaired electron states, IR refl. study 80−75491
TCNQ salts, anomalous infra-red activity and the determination of electron-molecular vibration coupling constants 80−25389
TCNQ salts, IR, X-ray electron spectra, tetrathiotetracene $(TCNQ)_2$ cond. investig. 77−44005
TCNQ-HMTSeF, polarised single cryst. reflectance obs. and one-dimens. behaviour interpret. 78−6690
Teflon, optical, elec. props., struct., ion textured surface 78−72904
tetracene single crystals, exciton refl. spectra, 4.2 to 300K 79−47478
tetracene surface states, electric field effects, exciton-charge carrier interactions *(Russian)* 80−24989
tetracyanoplatinates, energy band calcs. 77−39780
tetramethyltetraphenyltrisiloxane film, DC-704, on Ge, Al and KRS-5, IR refl. spectra anal. 77−59630
tetraselenatetracene bromide complex, optical props. 78−6680
tetrathiotetracene salts, IR, X-ray electron spectra, tetrathiotetracene $(TCNQ)_2$ cond. investig. 77−44005
textured surface, reflectance and transmission props. 78−1165
TGFB, IR spectra and optical consts. *(French)* 79−95748
TGFB, optical props. in 5 to 22 eV region, reflectance spectra 79−33652
TGFB, refl. spectra 4-22 eV, optical consts. 79−4821
TGS, optical props. in 5 to 22 eV region, reflectance spectra 79−33652
TGS, refl. spectra 4-22 eV, optical consts. 79−4821
thermal radiation property meas. of materials 80−96181
thermoregulative coatings, radiation effects on reflectivity, space vehicle appl. *(Russian)* 78−76542
thin film, magnetoresistance, specular reflectivity angular depend. *(Russian)* 80−100453
thin films, optical constant volume and surface change separation, reflection, transmission *(Russian)* 80−66320
thin films, optical transmittance and reflectance, bulk optical props. determ. 80−88954
thin films, vac. deposited, mass change, optical transmittance, and reflectance, simultaneous meas. apparatus 79−75501
thiourea, ferroelec., soft mode and Debye relax., IR reflection spectra 77−90111
thiourea, IR reflectivity study of ferroelec. and antiferroelec. phases, dielec. function model 79−33686
thiourea, order-disorder transitions, soft modes 78−80361
thiourea, phonon modes near phase transitions, IR and Raman spectra 80−45084
thiourea, soft mode and Debye relaxations 78−80347
three-layer dielectric reflectivity standard error analysis 77−79727
three-phase system, determ. of complex Fresnel reflection coeff. by modulated reflectance spectroscopy and modulated interferometry 77−82621
tissue model, two-layer, theoretical anal. of diffuse reflectance 80−35956
tissue reflectance oximetry, exptl. and theoretical models 79−79624
$(TMTSF)_2X$, $(X=PF_6^-, AsF_6^-, SbF_6^-, BF_4^-, NO_3^-)$ highly conducting salts, props. 80−59969
TMTTF salts, $(TMTTF)_2$-X, $(X=BF_4^-, ClO_4^-, SCN^-, PF_6^-, Br^-)$, physical props. 79−47085
toned paper reflectance 79−2855
topogram sensitivity, wavefront correl. effect 80−69345
total, meas. technique using specular-reflectance and diffuse reflectance references 80−73421
transition metal, normal total emittance at 400 to 850K and normal spectral reflectance at room temp. 77−20813
transition metal complex, MX_2.b(hexamethylenetetramine).nH_2O, optical reflection spectra, mag. suscept. 79−56810
transition metal complexes, acetylacetonates, mag. susceptibility and optical reflection spectra 77−59381
transition metal dichalcogenides, layer type cpd., reflectivity meas., 6-40 eV 77−55801
transition metal dichalcogenides, optical phonon modes and localised effective charges, reflection spectra 78−76453
transition metal oxides, refractive index and extinction coeff. 79−78643
transition metals, BCC, films, vac. evaporated, optical cond. 80−76100
transparent film thickness and refr. index meas., polarisation-independ. reflectance matching 77−65052
Triton, narrow band spectrophotometry 79−16879
(TTF^+) radical cation, optical props. in mixed-valence and monovalent halide salts and solns. 79−61399
$(TTF)_{12}(SCN)_7$ and $(TTF)_{12}(SeCN)_7$, charge-transfer salts, elec., mag. and optical props. 77−43575
TTF-I_n, single cryst. optical props., polarised specular reflectance meas. 77−12400
TTF-TCNQ, electron-molecular distortion coupling near Peierls transition, IR spectra obs. 80−25390
TTF-TCNQ, IR reflectance in conducting phase 80−25388
TTF-TCNQ, irradiated, IR reflectance, optical and low-freq. transport comparison 79−51961
TTF-TCNQ, reflectance meas. press. to 70 kbar by micro-optic system 77−61133
TTF-TCNQ derivatives, transport props., refelctance spectra 78−91683
$TTT_2(I_3)_{1+x}$, physical props., elec., mag. and optical meas. 80−24908
$TTT_2I_xBr_{3-x}$, charge transfer complex, optical and elec. props. 79−4554
$(TTT)_2I_3$, optical, spin-reson., magnetoresist. study, nature of ground state 78−68023
TTT-I_n, charge transfer salt, electronic spectra in soln. and solid state 78−2878
undergraduate laboratory experiment, reflectivity, quantitative meas. 78−49624
uniaxial crystal, dispersion of bulk phonon polaritons meas. by IR refl. 78−59902
Uranus satellites, narrow band spectrophotometry of Ariel, Umbriel, Titania and Oberon 79−16879
vacuum UV coatings reflectance and transmission, depend. on wavelength 79−46030
reflectivity continued
vegetation changes with maturity, solar elevation effects on sequential LANDSAT imagery 77−45159
vegetation reflectivity, effect on atmospheric radiance and polarisation 78−40650
veiling reflections and reflected glare from glossy paper, lighting conditions for visual comfort 80−76733
Venus, UV markings contrast spectral depend. 79−62783
visual acuity screens, reflectance obs. 80−67178
walls, floors and ceilings, reflection factor determination *(German)* 79−27165
water, diffuse irradiance refl., two flow model 77−29301
water, IR spectrum, influence of Cu^{++} ions 78−72501
water, optical consts., absorpt. and refr. index 0.1 Å-1 m 78−48139
water, VUV reflectance, refr. index, absorpt. coeff., isotope effects 78−6695
water bodies, natural, volume reflectance, rel. to suspended sediment remote sensing 79−53558
water cryofilm, on specular and diffusing surfaces, bidirectional reflectance 78−88274
waveguide grating, diffraction efficiency, Brewster's law 80−91935
wavelength modulated spectrometer for reflectivity meas. in 150-900 nm range 77−13807
weather radar echo, receiver bandwidth effect on refl. and Doppler vel. estimates 79−53549
wheat canopy reflectance, Suits' spectral model appls. 78−7811
X-ray photoabsorption of solids by specular reflection 79−15561
xerographic images on paper, optical model 79−17549
Ag chemically deposited layer, reflectivity rel. to heat treatment 79−27366
Ag film, chemisorption effects on optical reflectance and elec. resistance 79−33361
Ag film, evaporated, chemisorption effects on reflectance and elec. resist. 80−11495
Ag film, evaporated, sulphide formation, attenuated total reflection surface plasma wave reson. 79−15874
Ag film, granular, transmission and reflection spectra, validity of sum rule 80−97358
Ag films, underlayer effect on surface roughness, surface plasmon excitation meas. 79−51456
Ag foil, interface with liq., oxide props., refl. and scatt. light spectroscopy 80−60702
Ag foil, surface-plasmon resonance, roughness-induced wavelength corrections 80−108288
Ag foil-electrolyte boundary reactively formed oxide layers, differential reflectance 79−69856
Ag foils, surface plasma-wave reflectance and roughness-induced scatt. 80−66228
Ag, intraband optical conductivity, electron-electron scatt. 78−35166
Ag mirror, Y_2O_3 coated, for the 0.5 to 14 μm region 80−87456
Ag mirror IR reflectance at 45° incidence, obs. 79−14074
Ag surface layers, reflectivity, contrib. of longit. polarisation waves 79−83046
Ag surface layers on Au and Al substrates, reflectance spectroscopy 79−78780
Ag, surface plasma oscills., sinusoidal surface 77−73179
Ag, surface plasma waves 79−47151
Ag surfaces, Cs and Cs-O covered, surface plasma waves, ATR study 80−39451
Ag thin layered structures, coupled surface plasmons 79−56873
Ag-Cu, metastable alloy film, optical props. 77−12460
Ag-LiF, alternating plasma-dielec. five layer system, ATR angular spectra 79−19943
Ag-MgF_2-Ag layered system bounding dielec., ATR ang. spectra, assoc. reson. EM oscills. 79−15541
Ag-Sb alloy, reflectivity, effect of electrodeposition conditions 78−13784
Ag-Zr(Nb)(Mo) film, dielec. const., optical props., DC resist. and thermoelec. power 77−85824
Ag_3AsS_3, proustite, reflectivity and optical constants at 80K and 300K from 18 to 700 μm *(French)* 77−36235
AgBr, far IR spectra, cond., cation local motion 79−1754
AgBr, molten, freq. depend. ionic cond. 77−7882
AgCl, molten, freq. depend. ionic cond. 77−7882
$Ag_{0.85}Cu_{0.15}Br$, far IR spectra, cond., cation local motion 79−1754
$AgGaSe_2$, optical phonons, IR reflectance meas. *(French)* 77−81095
$AgGaSe_2$, polarised IR refl. spectra, optical phonon modes 77−16304
$AgGaSe_2$ wavelength-modulated reflectance, optical electronic transitions, 1.5-5.5 eV 78−35170
$AgGaTe_2$, optical phonons, IR reflectance meas. *(French)* 77−81095
Ag_8GeTe_6, optical props. and polymorphism 80−45082
Ag_2HgI_4, preparation, optical and luminescence spectra 80−104064
β-AgI, 2H and 4H polytypes, exciton refl. spectra at 4.2K 79−69860
β-AgI (4H), visible spectra, reflected light phase and amplitude, exciton resonance 80−45110
β-AgI, exciton refl. spectra, optical activity *(Russian)* 78−64380
AgI, molten, freq. depend. ionic cond. 77−7882
p-$AgInSe_2$, far IR props. 79−42976
$AgInSe_2$, far IR refl. spectra, polarised light 78−43870
$AgInSe_2$, far IR refl. spectra, ionic bonds 79−55695
$AgInTe_2$, far IR refl. spectra, polarised light 78−43870
$AgInTe_2$, far IR refl. spectra, ionic bonds 79−55695
AgPd, dil. alloys, electronic states, virtual bound states model test *(French)* 77−62809
Ag_3SbS_3, IR refl. spectra, permittivity, lattice vibrs. 79−65862
Al, anodised, cryogenic material, IR reflectance 79−71458
Al, anodized, as cryogenic material, IR reflectance 79−61387
Al coating reflectivity in vacuum UV, heating effect 80−95981
Al, diamond-turned, surface reflectivity meas. 1 to 12 μm 80−1298
Al, electron beam evaporation, on Kapton laminates, and characterisation 78−11373
Al film, dispersion curve of surface plasma waves, rel. to refl. power minimum curve *(French)* 78−88372
Al film, enhanced mirror, high-rate sputtering, reflectance and dispersion 77−42636
Al, film, reflection coeff., effects of plasma bursts prod. 78−56547
Al films, anodisation rate and augmentation factor, oxidation in ammonium tartrate 79−79152
Al, IR laser reflectance, anomalous absorpt., plasma ignition 80−7439
Al, low vacuum condensates, struct., IR refl. obs. *(Russian)* 78−30850
Al mirror, with MgF_2 overcoating, reflective scatt. and reflectance meas. in vac. UV, moisture and oil vapour influence *(German)* 79−86227

reflectivity continued
Al mirror IR reflectance at 45° incidence, obs. 79−14074
Al, multiple crater refl., effect on refl. props. 78−52596
Al oxide anodic film, colloidal metal, origin of colour, optical props. meas. 78−68571
Al plasma, laser produced, reflectance meas. 80−79568
Al, refl. coeffs., changes at high temps. 78−19440
Al reflective coating, reflectance in UV and visible 80−28307
Al, reflectivity at high temps. pulsed laser heating 77−63388
Al, surfaces, Au-coated and diamond turned, EUV reflection efficiencies 79−14073
Al thin film evaporated on quartz substrate, surface irregularities 79−90920
Al, transient reflectivity at 10.6 μm 79−11408
Al-As_2Se_3-Al layers, photoelectrochem. process 77−76953
Al-Cu alloy, deposition from RF induction source, onto laminated polyimide substrates and characterisation 80−16535
Al-Ge-SiO solar selective absorber surfaces, optical behaviour at high temp. 80−101130
Al-Si, DC magnetron-sputtered, residual gas influence on props. 80−80968
Al-SiO_2 layered system, complete absorpt. of transverse mag. waves 78−39615
$Al_{1-x}Ga_xP$, IR phonons, lattice reflection spectra 78−51626
AlN:O, UV spectra of deep impurity centres, radiative recombination 79−87490
Al_2O_3 anodic films, formed on Al, optical reflectance method anal. 80−37073
Al_2O_3, anodic films, influence of substrate orientation 78−88581
Al_2O_3, films on Al, photoacoustic refl.-absorption spectroscopy 78−31264
Al_2O_3, hyperfine film on metal, IR refl.-absorpt. spectra *(Russian)* 78−11014
α-Al_2O_3, single crystal transmission and reflectance IR phonon spectra, polariton dispersion 80−66170
Al_2O_3:Ni anodised films, electrolytically coloured, spectrally selective surface 80−11490
Al_2O_3:Si, Ti, pure and doped, luminescence, optical absorpt. and colour centres 79−87501
β-Al_2O_3-X_2O, (X=Na,K,Rb,Ag,Tl), infrared and Raman spectra 79−1761
anthracene, polycrystalline, optical props., 3.2-9.3 eV 80−76097
Ar, adsorbed on Al, differential refl. spectroscopy, local field effect 80−80811
AsF_5-graphite intercalation compound, metallic. optical reflectance meas. 78−6683
As_2O_3, vitreous, local struct. and vibrational spectra 80−55091
$As_2S_3Ge_x$ glasses, vibr. props. and struct., IR refl. and Raman scatt. 79−78682
$(As_2S_3)_{1-x}(GeS_2)_x$ and $As_2S_3Ge_x$ glasses, struct. and vibr. spectra 79−91440
$As_{1-x}S_x(Se_x)$, bulk-quenched glasses, opt. freq. dielec. const., chem. ordering effects 78−23472
$As_{0.2}Sb_{0.8}SI$ cryst., ferroelec., soft mode Raman and IR spectroscopy 80−76016
As_2Se_3, polarised light reflectance spectra, band struct. 78−63979
Au coated surface, reflectivity in soft X-ray range 78−45221
Au, dielectric const. by multiangle reflection meas., optical props. 79−95723
Au electrodes, adsorpt. of Br^-, specular reflect. investig. 78−61047
Au film, granular, transmission and reflection spectra, validity of sum rule 80−97358
Au film, modifications of optical and elec. props. as function of struct. during deposition 79−78777
Au film growth, optical and elec. prop. meas. during deposition *(French)* 77−70007
Au films, on Al, Ni, EUV reflection efficiencies 79−14073
Au, films, optical props. meas. rel. to electron surface scatt. theory 80−29818
Au, intraband optical conductivity, electron-electron scatt. 78−35166
Au, ion implanted, ellipsometry, 1.8-5.5 eV, dielec. function 78−6697
Au, optical consts. direct determ., d absorpt., reflectivity 77−69791
Au, optical props., dielec. function, void model, sample effects 80−76048
Au, surface plasma waves 79−47151
Au thermal modulation reflectance spectrum, temp.-dependent shift 77−81121
Au, with cadmium arachidate monolayer, surface plasma reson. 77−90210
Au, Xe physisorption, electronically excited atoms coupling to cond. states 77−89642
Au/Al thin film, Al diffusion studied by attenuated total reflection method 80−92722
Au-Cr, cosputtered films, optical props. 0.2 to 6.1 eV 77−32454
Au-Cu, dielectric const. by multiangle reflection meas., optical props. 79−95723
Au-Pd dil. alloys, electronic states, virtual bound states model *(French)* 77−62809
Au(Ag)(Cu)-Sn liquid, optical reflectivity spectra of virtual bound states 80−89021
AuCu, optical constants direct determination, d absorpt., reflectivity 77−69791
$Au_{1-x}Si$ amorphous metallic films, optical props. as function of composition 79−95865
$Au_{1-x}Si_x$, amorphous film, spectra 0.01-6.2 eV, $0.13 \leq x \leq 0.5$ 78−68574
Au_8Si_{19}, optical refl., 0.5 to 6 eV, hall coeff. and elec. resist. 80−29755
B, β-rhombohedral, optical absorption band in 8 μm region, anomaly of temp. dependence 80−29735
B, IR-active phonons, reflectivity and absorption spectra 79−82294
BC_x, IR-active phonons, reflectivity and absorption spectra 79−82294
$B_{12}C_x$, phonon energies and electronic props., x depend., refl. spectra and thermoelec. power meas. 80−16052
BaFX, X=Cl, Br, I, absorpt. and refl. spectra 79−82994
$Ba(NO_3)_2$, IR reflection spectra, dynamical props. 77−16303
$Ba(NO_3)_2$, vibrations of isotopic impurities, IR reflection and Raman spectra meas. 77−51465
BaO, logarithmic derivative reflectance spectra 80−11429
BaO, surface states, reflectance spectra, impurity effects 77−20873
$BaSO_4$, polarised IR refl., absorpt. and laser Raman spectra 77−43997
$BaSO_4$, pressed powder Eastman White reflectance standard, absolute refl. meas. 78−25939
reflectivity continued
$BaSO_4$ white reflectance standard, Kubelka-Munk optical props. 77−42581
$BaSO_4$ white reflectance standard, Kubelka-Munk optical props. 78−4675
$(Ba_xSb_{1-x})TiO_3$, ferroelectric films, dielectric and semicond. props. 79−91388
$BaTiO_3$, ferroelec. cryst., IR and Raman spectra, mode coupling 80−66194
$BaTiO_3$, ferroelectric mechanisms, anharmonic couplings by scanning IR interferometry 80−75978
$BaTiO_3$, paraelec. phase, stabilisation of soft mode 80−75985
$BaTiO_3$, photoelectron and optical spectra derived from self-consistent charge MO and band calcs. 80−96785
$BaTiO_3$, soft mode spectroscopy IR refl. meas. 80−88982
$BaTiO_3$, UV refl. spectra, optical consts. 0 to 32 eV Kramer-Kronig anal., band struct. calcs. 78−43903
BaX_2, X=Cl, Br, I, absorpt. and refl. spectra 79−82994
(Be, Al)B_{12}, wide-gap semicond., elec. cond., refl. and absorpt. spectra 80−20188
Be, normal total emittance at 400 to 850K and normal spectral reflectance at room temp. 77−20813
Be substrate for lightweight mirror, surface quality and thermal props. 80−23762
BeO film, amorphous or polycryst., dielec. function, refl., from electron energy loss meas. 78−43947
BeO reactively evaporated film, elec. and optical props. 77−32512
$Bi_{12}GeO_{20}$, $Bi_{12}SiO_{20}$, IR reflection spectra studies of lattice vibrations 79−99879
$Bi_{12}GeO_{20}$, reflectivity spectrum and band struct. 79−47474
$Bi_4Ge_3O_{12}$, fluoresc., absorption emission, excitation and decay time meas. 77−20910
BiI_3, layered compound, exciton spectra, surface and stacking fault effects 80−40134
BiI_3, layered single crystal, band-edge excitons, optical constant meas. *(Russian)* 77−90171
BiI_3 single crystals, refl., absorpt. and photoluminesc. spectra, exciton transitions 77−52164
$(Bi_{0.25}Sb_{0.75})_2Te_3$, opt. props. of bulk and films 78−27206
BiSe, reflection spectra 77−16325
n-Bi_2Se_3, cryst. nonparabolic cond. band., IR refl. and Hall voltage meas. 77−31940
n-Bi_2Se_3, IR, reflectance, Seebeck coeff. and Hall voltage meas. 79−60692
Bi_2Se_3, Raman spectra, Raman and IR-active modes 79−56776
Bi_2Se_3:Hg point defects in crystal lattice, Hall coefficient and IR spectra determ. 80−55129
$Bi_{12}SiO_{20}$, film and single cryst., optical absorpt. edge and optical transitions 79−33730
BiTe, reflection spectra 77−16325
Bi_2Te_3, Raman spectra, Raman and IR-active modes 79−56776
BiTeI, melt and vapour grown, optical props. 80−84746
$Bi_8Te_7S_5$, anisotropic dielec. const., oblique incidence reflectivity data 77−73124
CC GaAs, n- and p-types, optical consts., 2.5-3.5 eV, normal incidence reflectance meas. 79−15428
CO, adsorption on Pt (111), adsorption site investigation by IR reflection spectra 78−14565
CO chemisorbed on Pt, IR refl.-absorpt. spectra, absorbate island struct. 80−84385
CO, chemisorobed on Ni(111), surface optical excitations, reflectance spectra, electron energy loss meas. 78−84064
CO_2 laser cavity and Ge phase-conjugate 10 μm reflection expts. 80−78894
Ca film, optical absorption and plasma reson. 77−40296
Ca, optical props., 2-11 eV 78−15191
$CaCO_3$, IR reflectivity, oblique phonons 78−60440
$CaCl_2(Br_2)$, aq. solns., IR spectral reflectance meas., Kramers-Kronig anal. 77−4633
$CaCo_2(PO_4)_2$, reflection spectrum and mag. susceptibility meas. 77−59586
CaF_2, adsorbed water film internal reflection spectroscopy 79−15549
CaF_2 trapezoid, ThF_4 and ZnSe coated, IR characterisation by internal-refl. spectra 78−71161
CaF_2-Ge(Si), cosputtered composite semiconductors, selective solar energy absorbers 79−56876
$CaMgSi_2O_6$, single cryst., IR reflection spectra, vibr. spectrum calc. 77−73142
CaO-Ga_2O_3, vitrification, spectroscopic and petrographic anal. 77−15556
$Ca_5(PO_4)_3$, fluorapatite, far IR reflectivity to polarised light 79−56778
CaS, single crystal, reflectance and absorption spectra, at edge of fundamental absorption *(Russian)* 78−56499
CaS:Pb^{2+} phosphors, luminesc., refl., emission, and excitation spectra 79−11456
$CaSO_4$, anhydrite, resonance splitting of complex anion internal vibrs. 80−55081
$CaSO_4$, anhydrite and gypsum, phonon spectroscopy, lattice dynamical calc. 80−19889
Cd, film, freshly deposited, 77K, refl., annealing effect, thickness depend. 77−16413
Cd films, nucleation and growth, props. 80−29878
$CdBr_2$ crystal, transverse and longitudinal lattice mode freq., IR reflection spectra meas. 78−27227
$CdBr_2$, optical refl. spectra, exciton bands obs. around optical gap 78−15192
$CdCl_2$ crystal, transverse and longitudinal lattice mode freq., IR reflection spectra meas. 78−27227
$CdCl_2$, optical refl. spectra, exciton bands obs. around optical gap 78−15192
$CdCr_2S_4$, $Cd_{1-x}X_xCr_2Se_4$, (X=Zn, Hg), optical and magneto-optical surface effects 79−82953
$CdCr_2S_4$, ferromag. semicond., IR refl. spectra, phonon props. and dielec. function 80−66191
$CdCr_2Se_4$, magnetic red shift origin, specular reflectivity, band struct. 80−40127
$CdCr_2Se_4$, optical reflectivity, dielectric const. by expt. data Kramers-Kronig anal., spinel struct. 79−99903
$CdCr_2Se_4$, reflectance magneto-circular dichroism 77−81120
CdF_2, UPS and XPS spectra, rel. to optical props. 80−66386
$CdGa_2S_4$, direct excitons, refl. spectra 79−90972

reflectivity continued
$CdGa_2S_4$, IR light transmission, IR refl. spectra and cryst. struct. 79−56777
$CdGa_2S_4$, IR refl. spectra 80−60604
$CdGaS_4(Se_4)$, absorption and refl. spectra anisotropy, band struct. 77−69840
$CdGa_2Se_4$, IR refl. spectra and cryst. struct. 79−56777
$CdGa_2Se_4$, IR refl. spectra, optical phonon dispersion 80−29746
$CdGa_2Se_4$, struct. of valence band, photocond. and reflection spectra meas. 80−6719
$CdGa_2Te_4$, IR refl. spectra and cryst. struct. 79−56777
$CdGeAs_2$, polarised IR reflectivity, optical modes, optical phonons 77−69836
$Cd_xHg_{1-x}Te$, band struct. and optical props. 80−15450
n-$Cd_xHg_{1-x}Te$, conduction band struct., IR refl. spectra obs. 80−39502
CdI_2 crystal, transverse and longitudinal lattice mode freq., IR reflection spectra meas. 78−27227
CdI_2, layered cryst., photoluminesc., and reflection spectra obs. 78−6726
CdI_2, optical phonon anisotropies and intralayer bonding forces from IR refl. 77−59573
$(CdI_2)_x(PbI_2)_{1-x}$, layered cryst., photoluminesc., and reflection spectra obs. 78−6726
CdInGaS4, far IR refl. and transmission spectra, lattice vibrs. 79−91439
$CdIn_2S_4$, fund. reflectivity, 2 to 6 eV, band struct. implications 78−39574
$CdIn_2S_4$, fundamental optical constants 78−84549
$Cd_{1-x}Mn_xSe$, fundamental optical props. 80−84751
$Cd_{1-x}Mn_xTe$, magneto-optical props. of free excitons rel. Mn^{2+} ions spin alignment 79−47419
CdO, elec. cond. and IR refl. spectra after sintering and compaction 79−56945
CdS, $A_{n=1}$-exciton, reflectance and thermoreflectance spectra, spatial dispersion and angle of incidence effects 80−25409
CdS, absorpt. spectra, 400-650 nm, electron irrad. defects and absorpt. edge shift 78−64382
CdS active surface, exciton stimulated emission and superradiance refl. spectra, props. 80−25411
CdS, additional waves and polariton dispersion, reflectivity, transmittivity spectra 80−71443
CdS, chemically precipitated film, optical spectra, annealing effects *(Russian)* 79−11424
CdS, electron-hole plasma, gain and refl. spectra study 80−66227
CdS, exciton-contrib. to reflection spectrum at high excitation intensities 78−43900
CdS, excitonic polariton reflectance, quantitative anal. in spectral range of A-exciton 79−15480
CdS, excitonic polariton reflectance, B-exciton and k-linear term 80−7369
CdS, gain spectroscopy and plasma recomb. 78−88327
CdS, group velocity of light and polaritons, refl. and luminesc. spectra 77−24863
CdS, high intensity excited, exciton reflection spectra, reflection struct. 80−20692
CdS, highly excited semicond., linear optical response, electron-hole liq. 79−51980
CdS, influence of Lamb US waves on exciton spectra *(Russian)* 80−7374
CdS, irrad. with high doses of fast reactor neutrons, exciton reflection spectra 79−73221
CdS, optical activity in exciton spectra region, reflectance spectra 79−28707
CdS, optical props., spatial dispersion effect *(Russian)* 79−61404
CdS, photoexciton waves, restrictions imposed on nature of additional boundary conditions 79−28789
CdS, plastically deformed, optical and electronic transport anisotropies 77−8611
CdS, reflectance, transmittance and luminesc. spectra, light group vel. near exciton reson. *(Russian)* 77−69857
CdS, spectra of refl. and transmission coeffs. near exciton absorpt. line 80−88951
CdS, spontaneous optical activity in exciton spectrum *(Russian)* 78−35167
CdS, surface props., photoreflectance spectra in the exciton region 78−95324
CdS, wurtzite structure, natural optical activity *(Russian)* 79−78647
CdS:Cu,Pb reflectivity of Ni-salt coated powder, pre-irrad. effect on defect form. 79−27973
CdS/Cu_2S, polycryst. thin film photovoltaic materials, photon loss anal., expt. determ. 80−93888
$CdS_{1-x}Se_x$ film, resonance between Se atom dipole vibr. and interference modes, IR spectra obs. *(Russian)* 80−2888
CdS_xSe_{1-x} mixed crystals, exciton spectra 78−92131
CdSe, high intensity excited, exciton reflection spectra, reflection struct. 80−20692
CdSe, undoped and Cr doped, far IR transmission and reflectance spectra 80−71429
$CdSiP_2$, reflectance spectra at 300K 80−25407
$CdSnP_2$, optical props., band struct. calcs., real space atomic potential parameters 79−95325
CdTe, energy bands and optical props. calc., tight-binding model with spin-orbit interaction 80−65448
CdTe, lattice mode, dispersive refl. meas. using modular interferometer 78−89568
n-CdTe, single crystal, photoreflectance, temp. depend. of exciton spectra *(Russian)* 78−23488
CdTe, spatial dispersion rel. to exciton reflection spectra *(Russian)* 80−40126
CdTe:Fe(Ni), luminesc. and refl. spectra, high temp. annealing effects 80−24472
$CdTe:Mn^{2+}$, exciton refl. spectra and mag. susceptibility 80−66253
CdTe:V,Cr, optical props. meas. 79−73969
$CdTiO_3$, refl. and absorpt. coeffs. 3-3.5 eV, and refr. index dispersion *(Russian)* 78−39561
(CdZn)S-Cu_2S solar cell, film form. and charact. 78−68080
Ce_2ASe_5, A=Ge, Sn, diffuse refl. spectra and band gaps 79−51963
CeB_6, mag. and electronic props. 80−71048
CeH_x, phonon features in IR and Raman spectra 80−93310
CeN, optical props. and valence mixture 78−56450
CeSb, forbidden band gap and electrotransfer parameters 80−39497
Co film, optical props. by self-consistent photometric technique 80−55217

reflectivity continued
$CoAl_tFe_{2-t}O_4$, Kerr effect, magneto-optical refl. spectra 79−82954
$CoBr_2$, UV reflectivity spectra for band struct. calc. 77−20878
$CoCl_2$, UV reflectivity spectra for band struct. calc. 77−20878
$CoCl_2.6H_2O$ solution in ethanol, thin absorbing film, nonlinear optical props., Q-switch appl. 80−91836
$CoFe_{2-x}Ga_xO_4$, IR reflection spectra, permittivity spectra and effective ionic charges 79−69841
$Co_{1-x}Fe_xSi$, elec. and optical props. 80−49740
$Co_xMg_{1-x}Al_2O_4$, struct., catalytic activity, Co^{2+} ion distrib. 78−30595
$Co_{1-x}Ni_xSi$, IR refl. spectra in plasma refl. region 78−27233
CoO-MgO-Cr_2O_3-Fe_2O_3-TiO_2, form. and colour of spinel solid soln. *(Japanese)* 80−16059
CoO-ZnO-MgO ternary systems, solid solns., struct. charact. 80−60629
CoSi, IR refl. spectra in plasma refl. region 78−27233
CoSi, thermoelectric and optical props. 78−91714
Cr black, coating on Cu substrate, selective solar energy absorpt., model calcs. 79−57440
Cr black films, electrodeposited, visible and IR reflectance 77−81168
Cr, emissitivty and reflectivity, oxide film thickness effect 79−82364
Cr, evap. film, refl. and struct. 78−72021
Cr film, evaporated, black selective solar absorbers, optical props. 77−34956
Cr film, evaporated, concurrent ion bombard. effects 80−80142
Cr-Cr_2O_3, black chrome films, surface microstruct. rel. to optical props. in solar absorbers 79−52036
Cr-Cr_2O_3, black chrome solar selective absorber, microstruct. 79−56875
Cr-Cr_2O_3, black chrome electroplating for solar energy photothermal conversion, optical props. 79−74545
Cr-Cr_2O_3 black chrome, commercial, solar absorber coating characterisation 80−80111
Cr-Ni-Ti alloy and steel, emissitivty and reflectivity, oxide film thickness effect 79−82364
$CrBr_3$, reflectance and thermoreflectance meas. 77−24866
$CrBr_3$, reflectance and thermoreflectance spectra in paramag. and ferromag. phases 79−56770
$CrCl_3$, reflectance and thermoreflectance meas. 77−24866
CrO_n, mag. and optical obs., prep. by calcination of $CrCl_3$ 79−24736
Cr_2O_3 films, black, microstruct. depend. of optical props., SEM, XPS, and sputter depth-profiling 79−43049
Cr_2O_3, IR active phonons 78−34578
Cr_2O_3, UV absorption spectra from reflectivity meas. 78−2879
Cr_2O_3-Cr black, selective coating, optical and topographical props. 80−26165
CrSb, optical props., 0.05 to 5 eV 77−48194
CrTe, film, attenuated total refl., magneto-optical effects 77−52196
$Cs_3BiSbBr_9(Cl_9)$, ^{121}Sb Mossbauer chem. shifts, optical reflectance spectra, solid state band populations 77−40162
$CsCd(NO_2)_3$, pure and metal ion doped, cryst. struct., reflectance spectra and thermal decomp. 79−51081
$CsDy(MoO_4)_2$, effect of 38K phase transition on phonon spectrum, IR reflection spectra *(Russian)* 79−10902
CsI, far-IR optical props., shell-model calcs. 77−28557
CsI(Br)(Cl), electronic struct. anal. by reflectance and thermoreflectance studies 79−69855
CsN_3, polycryst., IR active lattice vibr., optical consts. 77−77185
$CsPbBr_3$, $CsPbCl_3$, ionic semiconductors, electronic and optical props. 79−38594
$CsPbBr_3$, electronic and optical props. 80−25414
$CsPbBr_3$, optical props. and electronic struct. 78−48198
$CsPbCl_3$, electronic and optical props. 80−25414
$CsPbCl_3$, electronic struct. and optical props. in fundamental absorpt. region 80−93367
$CsPbCl_3$, optical props. and electronic struct. 78−48198
$CsPbCl_xBr_{3-x}$, optical meas., LCAO band scheme 80−25437
Cu adsorbed atoms on Pt electrode, optical props., electronic struct. 77−69855
Cu, dielectric const. by multiangle reflection meas., optical props. 79−95723
Cu film, EXAFS meas. by total refl. 80−55228
Cu, fine interaction of surface electrons, IR spectra 80−16041
Cu halides, reflection spectra, 4.5-7.5 eV, bond struct. scheme 79−61402
Cu, intraband optical conductivity, electron-electron scatt. 78−35166
cu, laser light absorpt. by plasma with very steep density gradient 80−96348
Cu light pipe, submm. wave transmission, and refl. of surfaces 50-10 cm^{-1} 78−18050
Cu mirror, microstruct. effect on Ag overlayer deposition, 10.6 μm reflectivity 77−42543
Cu, multiple crater refl., effect on refl. props. 78−52596
Cu, optical consts. direct determ., d absorpt., reflectivity 77−69791
Cu, polished mirror, optical props. ageing 77−79912
Cu, refl. coeffs., changes at high temps. 78−19440
Cu, reflectivity at high temps., pulsed laser heating 77−63388
Cu, surface plasma waves 79−47151
Cu-Al, optical composition modulation spectra, dielec. const. var., Fermi surface and electronic level shifts 80−6707
Cu-Au film, optical props. of ordered and disordered alloys 77−20945
Cu-Cu_2O film, numerical anal. of normal reflect. data 79−99457
Cu-Ni, dil. alloy, optical reflectivity meas. virtual bound state model analysis 78−2873
Cu-Pd dil. alloys, electronic states, virtual bound states model test *(French)* 77−62809
Cu-Zn, optical composition modulation spectra, dielec. const. var., Fermi surface and electronic level shifts 80−6707
$CuAl_{1-x}Fe_xS_2$ system, delocalisation of d-electrons, mag., elec. and optical obs. 78−34804
β-CuBr, far IR spectra, cond., cation local motion 79−1754
CuBr, surface exciton polariton, ATR meas. 77−77236
CuBr(I), reflectance and thermoreflectance spectra, electronic struct. 80−71444
CuCl, refl. spectra, 4.5-30 eV, vel. to band struct. 80−103969
CuCl, surface exciton polariton, ATR meas. 77−77236
$CuCl_2$, aq. solns., IR spectral reflectance meas., Kramers-Kronig anal. 77−4633
$CuFeS_2$ single crystal, optical reflectivity spectrum 80−40129
$CuGaS_2$, IR lattice reflectivity spectra obs. 78−19477
$CuGaS_2$-CuGaSe, solid solutions, IR lattice reflectivity spectra obs. 78−19477
$CuGa(S_xSe_{1-x})_2$, refl. spectra, comp. depend. 78−39570
$CuGaSe_2$, IR lattice reflectivity spectra obs. 78−19477

reflectivity continued
CuGaTe$_2$, IR lattice vibr. spectra 79−28765
CuI, single crysts., growth and optical props. 80−93470
CuInS$_2$, fund. reflectivity, 2 to 6 eV, band struct. implications 78−39574
CuInSe$_2$, far IR refl. spectra, ionic bonds 79−55695
CuInSe$_2$, IR lattice vibr. spectra 79−28765
CuInSe$_2$, influence of impurities and free carriers on optical props. 80−108225
CuInTe$_2$, far IR refl. spectra, ionic bonds 79−55695
CuInTe$_2$, infrared optical properties 79−82974
$Cu_xMg_{1-x}Al_2O_4$, spinel solid solns., solid-state and surface props. 77−66415
CuO-MgO system, Cu ions valence states, electronic refl. spectra 78−35168
Cu$_2$O, refl.-absorpt. IR spectroscopy 78−84555
Cu$_2$O:He(Na)(Cd), ion-implanted, resonance Raman studies of annealing 79−55765
Cu$_2$S, optical and calorimetric meas. of thin films for Cu$_2$S-CdS solar cells 80−55863
Cu$_2$S:Cd(Zn), effects of doping on elec. and optical props. 78−38743
Cu$_2$S-CdS thin film planar junction devices, quantitative photon loss anal. 80−61362
Cu$_x$S, layers produced by reactive RF sputtering, struct., elec. and optical props. 79−90908
D$_2$O, IR spectral refl. and complex index of refr. 78−68501
Dy$_2$S$_3$, optical props. and electronic struct. in fund. absorpt. region 80−80817
Dy$_2$S$_3$, vibr. spectra, factor-group anal. 80−80793
Eu chalcogenides, resonant Raman scatt. 77−55787
EuO, mag. semicond., dielec. and optical props. 78−10824
EuO, reflectivity spectra near absorpt. edge 79−47471
EuO:Gd, pure and doped, elec., mag., and optical props. rel. to electronic conc. 80−96880
EuS films, ferromag., optical spectra and light scatt. from spin waves 80−16116
EuS, pure and Gd doped, electronic struct., mag. exchange and elec. transport props. 78−87974
EuSe, mag. semicond., dielec. and optical props. 78−10824
$Eu_{1-x}Sr_xS$, exciton refl. spectra 80−2782
$Eu_{1-x}Yb_xTe$, (0<x<1), mag. semicond., elec., mag. and optical props. 80−97070
Fe complex, Fe(II) and Fe(III) cyanides-3d transition metal, mag. suscept., reflectivity spectra, cryst. field 79−56808
Fe complex, $K_3[Fe(SCN)_6].4H_2O$, optical reflection spectrum, mag. suscept., permittivity, dehydration temp. 79−56809
Fe complexes, cycanides, mag. susceptibility and optical reflection spectra 77−59382
Fe film bounded by dielec. layers, surface polariton in ATR angular spectra 79−15545
Fe granular deposits, plasma reson., rel. to interstellar dust extinction curve 79−21387
Fe, optical constant dispersion and emissivity, up to 900K 78−52464
Fe-Cr alloys, passivation films, modulation spectroscopy study 80−3244
FeF$_2$, dielectric properties, IR spectra, lattice dynamics *(French)* 80−76026
FeF$_2$, IR reflectivity spectrum 79−51952
$Fe_{1-x}O$, IR reflectivity obs. 77−43996
Fe$_2$O$_3$, haematite, anal. of refl. spectrum by Kramers-Kronig relations 80−16058
Fe$_2$O$_3$ sputtered films, optical transmission and reflection spectra depend. on substrate temp. 79−91517
Fe$_3$O$_4$, IR refl., ATR, Voigt and Faraday expts. 80−66180
Fe$_3$O$_4$, magnetite, optical props. in IR 80−97271
Fe$_3$O$_4$, optical props. in spectral range 0.03 to 12 eV 79−51977
$xFe_2O_3.(1-x)[3B_2O_3.PbO]$ glasses, diffuse refl. spectra 79−51982
FeSi$_2$ films, structural and Anderson transitions, cond. and IR reflectance meas. 79−15200
Ga, film, freshly deposited, 77K, refl., annealing effect, thickness depend. 77−16413
Ga film, optical props., 2-15 eV 77−77308
Ga, optical properties in 0.3 to 5 eV range 78−31196
Ga, optical props. in 0.5-60 eV range, dielectric const. and loss functions *(French)* 77−12353
Ga-Te, liq., reflectance, 0.65-3 eV, comp.-depend. 78−72549
GaAS, anodic oxide film growth, in situ differential refl. obs. 77−73354
$GaAl_xAs$, epitaxial layers, reflectivity meas. by wavelength modulation spectroscopy *(French)* 77−59632
$GaAl_xAs$, IR refl. spectra and Raman spectra 80−20623
$GaAl_xSb$, surface oxidation, Raman spectra, residual Sb layers 80−71419
GaAs (110), surface states, optical techniques 80−6939
GaAs anodic oxide film, ellipsometric and IR spectroscopic studies 80−11493
GaAs anodic oxide films, optical studies using rot. light-pipe reflectometer 80−76096
GaAs, anodisation obs. by in situ differential refl. 80−50732
n-GaAs, bulk and epitaxial film, IR reflectance meas. 77−32364
GaAs, CC Ga-3d-excitation, high resolution reflectivity down to 15K 80−25415
n-GaAs, conduction band nonparabolicity and coupled plasmon-phonon modes, IR refl. spectra 80−55110
GaAs epitaxial film on GaAs substrate, IR characterisation 78−23544
n-GaAs epitaxial wafers, IR reflectance and elec. characts. 79−56293
GaAs, exciton parameters near absorption edge 79−73448
p-GaAs, IR plasma reflectivity spectra calc. 78−52511
n-GaAs, implanted, IR refl. meas. of free carrier parameters 77−36244
GaAs, ion implanted, mode-locked Nd:YAG laser annealing, recrystn., optical reflectivity meas. 80−19817
GaAs, laser, transverse modes, mirror reflectivity dependence 79−68404
GaAs, laser annealing, optical refl. meas. of melted layer 79−78796
GaAs laser convex micromirror mode control 79−36920
GaAs, lower conduction band minima, ordering and props. 77−28114
n-GaAs, mechanical polishing damage effect on IR refl. and ATR spectra 77−20848
GaAs, oxide film growth, thermal oxidation, optical obs., model 77−56120
GaAs, plasmon-phonon coupling, and IR refl. spectra of impure crysts. 79−56150
GaAs, reflection spectra, optical consts. *(Russian)* 79−38571
GaAs, Schottky barrier ellipsometric electroreflectance spectra, energy band parameters 79−99853

reflectivity continued
GaAs:Se, ion implanted, surface state study from photoreflectance 79−91465
GaAs:Te, amorphous, ion implanted layers, optical refl., 1.5-7.0 eV 79−8152
GaAs:Te, implanted and laser annealed, surface crystallinity, refl. and channelling meas. 79−95036
GaAs:Te, ion implanted optical transitions in modulated reflectivity spectrum 79−73972
GaAs(P)(Sb), fine struct. in energy derivative reflectance spectra 79−78705
e-GaAse, optical consts. for ⊥ and ∥ light polarisation, reflectivity, interf. meas. 77−52077
$Ga_{1-x}In_xAs$, IR reflectivity, cluster effect on optical phonons 80−97259
$Ga_{1-x}In_xAs$, VPE grown, refractive index, reflectance meas. 79−4780
$Ga_xIn_{1-x}As$, far IR reflectivity spectrum, damped harmonic oscill. model 77−52070
$Ga_{0.08}In_{0.92}As_{0.18}P_{0.82}$, band struct., optical studies 79−47013
$Ga_xIn_{1-x}As_{1-y}P_y$:Ge(Sn)(Te), epitaxial film, elec. and optical props. 79−11251
$Ga_xIn_{1-x}As_yP_{1-y}$, IR refl. spectra 80−60602
$Ga_{1-x}In_xSe$ solid solution, IR spectra of static reflectivity 79−69849
GaP, impurity-containing single crysts., refl. spectra 80−80823
GaP, ion implanted, mode-locked Nd:YAG laser annealing, recrystn., optical reflectivity meas. 80−19817
GaP, polariton dispersion, IR reflection spectroscopy 80−11415
GaP, upper polariton branch obs. by ATR 78−68510
GaP:N(Te), ion implanted at 40 keV, refl. spectra, 210-2000 nm, annealing *(Russian)* 78−80386
GaS, infrared optical props., polarisation depend., vibr. modes 80−100658
GaS, reflectivity from 4 to 32 eV, Kramers-Kronig anal. 80−34943
Ga$_2$S$_3$, IR refl. spectra, linear chain model for lattice vibrs. 78−27235
GaS(Se), polar optical phonon ang. behaviour, IR refl. meas. 80−20633
$GaS_{1-x}Se_x$, mixed crystals, IR reflectivity spectra 80−66204
GaS_xSe_{1-x}, IR reflectivity and transmission spectra, stacking transform. 77−32371
GaS_xSe_{1-x} solid solutions, two-mode behaviour of optical phonons, IR reflect spectra 79−78680
GaSb, bulk and epitaxial, IR reflect. meas., carrier conc. and mobility determ. 80−80769
p-GaSe, back wall Schottky barrier cells, diffusion length, RT spectral response meas. 80−107806
GaSe excitonic spectra fine struct., reflection and transmission spectra *(Russian)* 80−55126
GaSe films, optical props. at lattice vibr. freqs., IR and Raman spectra 80−60696
GaSe, reflectivity from 4 to 32 eV, Kramers-Kronig anal. 80−34943
GaSe, refr. index 0.45 to 330 μm, interf. and refl. meas. methods 77−63387
GaSe, single cryst., dispersion of refr. indices and exciton absorption 79−73947
Ga$_2$Se$_3$, IR refl. spectra, linear chain model for lattice vibrs. 78−27235
Ga_2Se_3-Ga_2S_3 solid solutions, IR refl. spectra, linear chain model for lattice vibrs. 78−27235
GaTe, 1-35 eV, electron props. determ. 77−20872
GaTe, exciton polariton effect on absorpt. edge, absorpt. and refl. spectra, 4.2 to 300K 80−20664
GaTe, excitonic absorpt. edge, transmission and refl. meas. 80−40133
GaTe, laser modulated reflectance meas. 77−63424
GaTe, layer cryst., polarised IR refl. spectra 80−97279
GaTe, long wavelength phonons, Raman and far IR spectra obs. 79−69210
GaTe monocrystal, far IR polarised complex reflectivity obs. 80−60609
Gd, optical constants, reflectance meas. *(French)* 78−2869
Gd, optical consts. polarimetric meas., mag. ordering effects 78−15184
Gd-Co amorphous thin film, mag. and optical props., conc. depend 79−19748
Gd-Fe amorphous films with CeO_2 coatings, Kerr magneto-optical effect enhancement 79−19866
Gd$_2$ASe$_5$, A=Ge, Sn, diffuse refl. spectra and band gaps 79−51963
GdFeBi, amorphous ferrimag. films, magneto-optical props., optical spectra 80−76008
Gd$_3$Ga$_5$O$_{12}$, IR refl., ATR, Voigt and Faraday expts. 80−66180
GdIG, IR refl., ATR, Voigt and Faraday expts. 80−66180
GdN, and $GdN_{1-x}O_x$, mag. interactions 80−60218
GdP, electronic struct., mag. exchange and elec. transport props. 78−87974
GdS, electronic struct., mag. exchange and elec. transport props. 78−87974
Ge, black, solar selective absorber characterisation 80−80112
Ge film, A1-type and amorphous, complex refractive index and reflectance 77−52121
Ge, free-carrier plasma edge, fast transient spectroscopy 77−8558
Ge, high refl. phase conjugation at 10 μm, intracavity CO_2 laser techniques 80−78894
Ge, laser annealing, optical refl. meas. of melted layer 79−78796
Ge, nonlinear refl., picosec. laser pulses and electron-hole plasma 79−47463
Ge, nonlinear reflection props. rel. to thermal effects 78−42371
Ge optical props. in 2.5-15 micron region 80−80775
Ge, picosecond pulses from Nd:glass laser 79−18469
Ge reflectivity changes due to illumination by beams of unequal frequency 79−76749
Ge, refr. index and refl. changes due to intense laser irrad., surface heating effect 78−42372
Ge surface reflectivity changes and moving diffr. grating efficiency 80−58662
GeO_2, ultrathin layers on Ge substrate, ATR spectra, thickness depend., struct. obs. 80−55214
GeO_2, vitreous, LO vibrational modes, Raman and IR spectra 77−7819
GeS, far IR reflectivity spectra, lattice vibr. and dielec. const. 77−52068
GeS, IR reflectivity meas. 77−8570
GeS, orthorhombic single cryst., fine struct. in reflectivity 79−19903
GeS$_2$, energy gap and optical props. in IR region 79−51948
GeS$_2$, single cryst., IR polarised reflectivity spectra, 79−56775
$Ge_{1-x}S_x(Se_x)$, bulk-quenched glasses, opt. freq. dielec. const., chem. ordering effects 78−23472
GeSe, amorphous film, optical properties 78−39620
GeSe$_2$ amorphous film, laser induced light absorpt. oscillation, exciton model 80−50446

reflectivity continued
$GeSe_2$ amorphous film, laser induced oscillatory phenomena 80−84711
$GeSe_2$, far IR reflectivity meas. 77−28565
$GeSe_2$, far IR reflectivity spectrum, dielec. const. and lattice vibrs. 77−52069
$GeSe_2$, IR and Raman spectra 78−95585
$GeSe_2$ multimode layer cryst., far IR transmission and reflection spectrosc., comparative merits 80−76019
$GeSe_2$, single cryst., IR polarised reflectivity spectra, 79−56775
GeTe, heterophase state, plasma refl. spectra, twinning domain distrib. study 79−69845
γ-GeTe, investigation by elec. resist., latent heat of phase transform. and plasma refl. of light 79−99317
p-GeTe, reflectance, and thermorefl. spectra 80−80814
Ge(111)2×1, oxide layer, surface states detect optical reflectivity obs. 80−50368
Ge(111)2×1, surface electron states detected by external reflectivity 78−80036
α-HIO_3, dispersion anal. of IR reflection spectrum *(Russian)* 78−56493
HNO_3, aqueous soln., reflectance and complex refractive index, IR spectra, vibr. modes 80−66168
H_2O, liquid, far IR optical consts. meas. with optically pumped laser 80−40082
$H_3PO_4(MoO_3)_{12}.29H_2O$, electrochromic solid-state cells 80−2724
$(H_3PO_4)(WO_3)_{12}29H_2O$, electrochromic solid-state cells 80−2724
H_2S frost, near IR reflectance spectra, tetragonal to cubic phase transition 77−81094
H_2SeO_3, cryst., vibr. spectra in O-H stretching region 79−51949
HfS_3, quasi one-dimens., optical phonon anisotropy, IR spectra study 80−40112
$HfS_2(Se_2)$, vacuum UV reflectivity spectra, cond. band model 77−44012
Hg, expanded fluid, optical props. 79−19902
Hg, reflection spectra, electronic density of states, calc. 80−66229
Hg, surface, use in surface temp. meas. 77−2653
Hg_2 vapour, high-press., selective refl. meas. up to 700 bar 80−28031
$Hg_{2.86}AsF_6$, anisotropic linear-chain conductor, optical reflectance meas. 77−77247
$Hg_{0.75}Cd_{0.25}Te$, single crystal, reflection spectra 80−40140
$Hg_{1-x}Cd_xTe$, props. and appls., book contrib. 77−39834
Hg_2Cl_2, cryst., birefringence and dichroism, 200-500 nm and far IR 78−27257
Hg_2Cl_2 single crysts., IR refl. spectra and ferroelasticity 79−99889
n-$HgCr_2Se_4$, ferromagnetic semiconductor, plasmon refl., 86 to 320K 80−50346
$HgCr_2Se_4$, optical and magneto-optical surface effects 79−82953
HgI_2, exciton study by wave length modulated reflectivity, band parameters 77−51667
HgI_2, excitons, spectral obs. 78−23492
HgI_2, IR lattice vibr. and dielec. dispersion 80−76018
$HgIn_2Se_4$, IR refl. spectra and cryst. struct. 79−56777
$Hg_3In_2Te_6$, complex ordered-vacancy cpd., struct. and lattice dynamics 78−34496
$Hg_{1-x}Mn_xTe$, 1.7 to 3.5 eV, reflectivity spectra 78−43899
$Hg_{1-x}Mn_xTe$, far IR interband absorption obs. 79−33696
$Hg_{1-x}Mn_xTe$, far IR studies of lattice and free carrier effects 78−39544
α-HgS, polarised reflectance spectra, 2-5 eV, 77 and 293K 77−77243
$Hg_{2.91}SbF_6$, anisotropic visible and IR refl. rel. to metallic cond. 77−8602
HgSe, dielec. function at 2, 95, and 300K, reflectivity spectra meas. 79−15458
HgSe, two-phonon resonant effect, far-infrared reflectivity 80−108203
HgTe, energy bands and optical props. calcs., tight-bonding model with spin-orbit interaction 80−65448
p-HgTe, far IR reflectivity spectra, experimental and theoretical study of the dynamic dielectric function 78−92069
In, film, freshly deposited, 77K, refl., annealing effect, thickness depend. 77−16413
In, film, vac. deposited, influence of ion bombardment during condensation 79−82483
In-Bi, single crystal, vacuum UV optical props. 77−1697
In-Te, liq., reflectance, 0.65-3 eV, comp. depend. 78−72549
InAs, plasmon-phonon coupling, and IR refl. spectra of impure crysts. 79−56150
InAs, temporary diffr. grating form. on surface 79−59801
InAs:Zn, optical absorpt. and refl. spectra 79−91479
$(InAs)_x(CdTe)_{1-x}$, band gap and effective mass, IR spectra obs. 78−56491
InAs(P)(Sb), fine struct. in energy derivative reflectance spectra 79−78705
InAs(Sb), IR reflectivity, longitudinal optical phonon-plasmon coupling 77−59578
$In_{1-x}Ga_xAs_yP_{1-y}$ epitaxial layer, far IR refl. spectra, lattice vibrs. 80−97282
InI, orthorhombic, reflection spectra, exciton transition 79−24333
InN film, refl. and transmission spectra, band struct. 78−72625
InN film, specular reflection spectra, lattice parameters 80−7428
In_2O_3:Sn, coating on polyester film, elec. and optical props. 79−99959
In_2O_3:Sn coated Si, temp. depend. of 10.6 μm refl., solar selective absorber appl. 77−58398
In_2O_3:Sn films, prep. at low deposition temps. by ion-beam sputtering, elec. and optical props. 79−66004
InP, free carriers, freq. depend. relax. time 80−2385
InP, reflection spectra, optical functions, exciton peaks *(Russian)* 80−50372
InP, surface phonon polariton dispersion and damping, frustrated total internal refl. meas. 80−80792
InS, IR reflection spectra 80−11389
InSb-GaSb solid solution ingots, orientation, twinning and orientation depend. reflectance 79−28001
$InSb_{1-x}As_x$, cryst. struct. and far IR reflectivity 79−56752
$InSb_{1-x}As_xBi_y$, far IR reflectivity 79−56752
InSe, energy band structure, chem. bond polarity, photoemission, semiempirical tight binding method 80−44504
InSe, layer cryst., Raman and IR refl. spectra meas. 79−95777
InSe, optical props. from 2-25 eV 80−29760
InSe, optical props. near fundamental absorption edge 77−12434
n-InSe, optical spectra, photocond. and resistivity 78−88321
InSe, polar optical phonon ang. behaviour, IR refl. meas. 80−20633
InSe, reflectivity and low energy absorption 80−34944
InSe, reflectivity from 4 to 32 eV, Kramers-Kronig anal. 80− 34943

reflectivity continued
α-In_2Se_3, far infrared optical study of ordered and disordered forms 78−84572
K double fluorides, IR refl. spectra, vibr. modes, optical vibr. freq., Kramers Kronig anal. 80−66190
K, Mayer-El Naby optical absorption anomaly 77−4643
K salts, spectral refl. changes and luminesc. during 2-10 keV proton bombardment, implications for Io 79−96950
KBr, colour centres isothermal decay 79−51975
KBr, m-crocryst. powders coloured in electrodeless discharge, reflectance spectra, thermolum. 78−15238
KBr:Na(Rb)(Cs), microcrystalline powders, isothermal decay of colour centres 80−2804
$KBrO_3$, polarised IR reflection spectra, surface damage effects 79−19872
KCN_xCl_{1-x}, finite field local field catastrophe phenomena in spectra 80−92830
$K^+CN_x^-Cl^-_{1-x}$, influence of structural disorder on exciton spectra 80−108224
KCl and KCl:KBr, colour centres isothermal decay 79−51975
KCl, m-crocryst. powders coloured in electrodeless discharge, reflectance spectra, thermolum. 78−15238
KCl surface, vacuum UV radiation damage, spectroscopic study 78−71758
KCl:Ca(Ba)(Mg)(Sr), microcrystalline powders role of Z centres in stabilising coloration, optical absorption 80−54227
KCl-Al composite, optical and IR reflectance 78−56465
KCl(Br)(I) with alkali and halogen impurities, colour centre deformation induced nonradiative decay 80−7387
KD_2PO_4, electronic struct., UV reflection spectra 79−38558
KF(Br)(Cl)(I), K^+3p core excitons, refl. spectra study, low temp. 80−29759
KH_2AsO_4, electronic struct., UV reflection spectra 79−38558
KH_2AsO_4, ferroelec., electronic struct. study *(Japanese)* 79−87463
$K(H_{1-x}D_x)_2PO_4$, for IR response exam. by asymmetric Fourier spectroscopy 77−28570
KHF_2, IR refl. spectra 78−80324
KH_2PO_4 and related substances, electronic structures study *(Japanese)* 79−87463
KH_2PO_4, electronic struct., UV reflection spectra and XPS 79−38558
KH_2PO_4, far IR dispersive reflection spectra 77−36213
KMF_3, M=Mg, Ni, Co, Mn, reflectivity, 8-60 eV, excitonic struct. 77−20871
K_2MnF_4, IR active modes, interlayer and intralayer forces 77−59575
KN_3, IR refl. spectra, fundamental lattice modes, azide ion dipole derivatives 78−48166
KN_3, mono- and polycrysts., IR active lattice vibr., optical consts. 77−77185
KNO_3, far IR study of dielec. function by asymmetric Fourier spectroscopy 79−51947
KNO_3, Raman and IR spectra and lattice vibrs. 80−60565
KNO_3, vibrations of isotopic impurities, IR reflection and Raman spectra meas. 77−51465
$KNbO_3$, ferroelec. cryst., IR and Raman spectra, mode coupling 80−66194
K_2O-SiO_2 glasses, IR reflection spectra, computer resolution *(Japanese)* 77−69832
$K_2Pt(CN)_4Br_{0.3}.xH_2O$, conductivity and optical refl. depend. on water content 77−39828
K_2PtCl_4, far IR reflection spectra, assignments, effective ionic charges, force consts. 77−66488
$K_xRb_{1-x}Cl_yBr_{1-y}$, IR reflection spectra 78−76474
K_2SO_4:XO_4^{2-}, X=Cr, Se, Mo, W, lattice-impurity interactions, IR spectra 78−19522
K_2SeO_4, incommensurate and ferroelec., far IR and mm dielectric response 79−73955
Kr, solid, reflectivity, Kromers-Kronig anal. 77−73122
La compounds, plasma light reflection by free charge carriers 80−11403
La_2ASe_5, A=Ge, Sn, diffuse refl. spectra and band gaps 79−51963
LaOF, features of formation of band structure 79−33232
La_2S_3, optical props. and electronic struct. in fund. absorpt. region 80−80817
La_2S_3, vibr. spectra, factor-group anal. 80−80793
Li aggregated deposits, optical props., 1-6 eV 77−66549
Li-graphite intercalation compounds, synthesis, elec. and optical props. 79−74108
$Li_2Ag_{2-x}In_x$, optical props., struct., energy bands, interband transitions 78−72539
β-LiAl, optical dispersion, room temp. reflectance spectra 80−66195
$LiAlSi_2O_6$, IR refl. spectra dispersion anal. 79−99877
LiC_6 intercalation cpd., synthesis method and reflectivity spectrum 79−15600
$Li_2Cd_{2-x}In_x$, optical props., struct., energy bands, interband transitions 78−72539
LiD, cubic cryst., exciton-phonon interaction and exciton anisotropy 78−72083
LiF, ATR IR spectrum from rough surfaces 77−20850
LiF film, ATR spectrum, reson. between longit. phonons and substrate surface polaritons *(Russian)* 77−32384
LiF film, refractive index as function of time, ATR meas. 79−65940
LiF, molten, charge fluctuations, collective dynamics, from IR reflectivity 78−67841
$Li_{0.5}Fe_{2.5}O_4$, magneto-optical Kerr effect, reflectivity spectra 80−66157
$Li_{0.5}Fe_{2.5}O_4$, magnetooptical spectra, polar Kerr rotation, dielectric tensor elements spectra 80−40091
LiH (D), single crystals, electronic excitations, review *(Russian)* 78−72574
LiH, cubic cryst., exciton-phonon interaction and exciton anisotropy 78−72083
LiH, excitons, reflection, cathodolum. and photocond.-excitation spectra 78−10989
LiH(D), isotope effect on Wannier-Mott exciton levels 80−103633
α-$LiIO_3$, attenuated total reflection spectra of anisotropic surface polaritons 78−87919
$LiKSO_4$, polarised Raman and IR reflection spectra, internal and external mode assignments 77−16293
LiN_3, polycryst., IR active lattice vibr., optical consts. 77−77185
Li_3N phonon spectra and lattice dynamics 77−59580
$LiNbO_3$ and $LiTaO_3$, IR reflectivity spectra and phonon self-energy effect 77−63413
$LiNbO_3$, asymm. phononlines, IR refl. analysis 78−27197

reflectivity continued
$LiNbO_3$, ferroelec., displacive type phase transition, far IR reflection spectra 80−71339
$LiNbO_3$, ferroelec. phase, soft vibr. modes, far IR refl. meas. 79−87407
$LiNbO_3$, IR reflectivity temp. depend. 78−27202
$LiNbO_3$, luminesc. props., Li/Nb ratio effect 80−97323
Li_2O-Al_2O_3-SiO_2, kinetics of glass-ceramic formation, by modified broken total internal reflection method 77−36444
Li_2O-TeO_2 glasses, struct., IR reflection spectra 78−68516
Li_2SO_4·H_2O, far IR spectra, H_2O flipping motion, lattice modes 80−84258
Li_2SO_4·H_2O, X-ray diffr., IR and Raman spectra, internal optic modes, mol. dipole model 77−76493
$LiTaO_3$, asymm. phonon lines, IR refl. analysis in paraelec., ferroelec. phases 78−27197
$LiTaO_3$, far IR complex refl. coeff. and refr. index, dispersive Fourier transform meas. 79−2841
$LiTaO_3$, ferroelec., displacive type phase transition, far IR reflection spectra 80−71339
$LiTaO_3$ high-temp. ferroelec. transition, soft mode IR reflectivity spectroscopy 79−33692
$LiTaO_3$, paraelectric phase, soft vibr. modes, far IR refl. meas. 79−87407
Mg, deposits of different roughness, refl. drops and surface plasmons 77−20392
Mg-Bi alloy, Eq., far IR reflectivity rel. to possible transport processes 78−2827
Mg-Bi alloys, liq., far IR reflectivity meas. 77−52105
$MgAl_2O_4$ spinel, optic frequencies, evidence for membership of F43m space group 78−48168
$MgCl_2$, aq. solns., IR spectral reflectance meas., Kramers-Kronig anal. 77−4633
MgF_2/In/MgF_2 struct. surface plasma wave optical excitation in In 79−91516
MgO-MgF_2 multilayer stack selective mirror with high reflectivity *(French)* 80−64131
Mg_2SiO_4, fosterite, lattice dynamics, IR and Raman spectra meas. 79−65153
$Mg_xZn_{1-x}Te$, band struct. refl. spectra meas. 80−80813
$Mg_xZn_{1-x}Te$, high purity, luminesc. and band gap 78−68553
$Mg_xZn_{1-x}Te$, temp. depend. of energy gap, near band gap reflectivity spectra 79−28786
MnAs, optical props., 0.3-14 eV 77−52122
$MnAs_{0.85}P_{0.15}$, optical props., 0.3-14 eV 77−52122
$MnAs_{0.88}P_{0.12}$, excitonic absorpt., derivative refl. spectra 80−25406
$Mn_xCd_{1-x}Te$, far IR refl. spectra, phonon spectra 78−52497
MnCuBi film, optical and magneto-optical props. 77−4695
MnF_2, ATR spectra and surface EM wave dispersion anisotropic case 77−77215
$Mn_xFe_{3-x}O_4$, optical props. 80−20606
MnSb, optical props., 0.05 to 5 eV 77−48194
$MnSe_2$, IR lattice vibrs., dielectric dispersion 79−28735
$MnSi_x$, X=1.72 to 1.75, IR absorpt., transmission, refl., spectra 80−60600
Mn_nSi_{2n-m}, thermoelectric and optical props. 78−91714
MnTe, optical props. and electronic struct. 78−6682
MnZn ferrite, optical refl. and electroreflection spectra obs. 78−27262
Mo, CVD films of high IR reflectance 79−52119
Mo, evap. film, refl. and struct. 78−72021
Mo film, CVD, with high IR refl. and large solar absorpt., prep. and props. 80−26163
Mo film, deposited by cylindrical magnetron sputtering, internal stresses, optical reflectance and elec. resist. 77−43449
Mo film, polycryst., energy loss function, Kramers-Kronig anal., reflectivity, optical props., EELS 80−40194
MoS_2, excitons, mag. circular dichroism and wavelength modulated reflectance meas. 79−23900
MoS_2-(Se_2)-(Te_2)(2H) polytypes, Kramers-Kronig anal. of reflectivity spectra, 0-30 eV, band model 79−51976
$MoSe_2$, exciton spectra 80−97296
$MoSe_2$, excitons, mag. circular dichroism and wavelength modulated reflectance meas. 79−23900
$MoSe_2$-(Te_2), IR and Raman spectra, lattice vibrs. interlayer bonding 80−40110
N_2 solid, refl. spectra, 500-1300 Å 79−33724
NH_3 frost, near IR refl. spectra, appl. to Saturn upper clouds 79−8135
$(NH_4)_2BeF_4$, far-infrared and submillimetre dielectric response 80−80782
NH_4Cl, vibrations of isotopic impurities, IR reflection and Raman spectra meas. 77−51465
$NH_4H_2PO_4$, electronic struct., UV reflection spectra and XPS 79−38558
$NH_4H_2PO_4$, ferroelec., electronic struct. study *(Japanese)* 79−87463
NH_4X, X=OH, Cl, Br, aq. soln., IR reflectivity spectra, Kramers-Kronig anal. 78−68500
Na salts, spectral refl. changes and luminesc. during 2-10 keV proton bombardment, implications for Io 79−96950
$Na_4Al_3Si_3O_{12}Cl$:Br,Ge, sodalite, reflectance and luminescence obs. 79−4839
$Na_8Al_6Si_6O_{24}NaX_{2-6x}$ (X=Cl, Br, I), X-ray irrad., thermal-erase cathodochromism and dihalide mol. centres *(Russian)* 80−66236
NaAr, ground and excited state pot. curves, dispersed fluoresc. spectrum 79−98140
NaBr powder coloured in electrodeless discharge, reflectance spectra, thermoluminescence props. 78−6796
NaCN, aq. solns., IR spectral reflectance meas., Kramers-Kronig anal. 77−4633
NaCl, far IR dispersive-reflection meas. at room temp., comparison with calc. 78−35139
NaCl, m-crocryst. powders coloured in electrodeless discharge, reflectance spectra, thermolum. 78−15238
NaCl, single cryst., for IR dispersive refl. meas., low temp., rel. to anharmonicity calcs. 80−11371
$NaClO_3$-$NaBrO_3$ mixed crystals, internal optic modes, Raman and IR spectra meas. 79−95746
$NaClO_4$, Brewster type surface mode dispersion, IR refl. meas. 80−11415
NaF:LiF, γ-irrad., colour centre form., reflectance and thermolum. meas. 79−55739
$NaHF_2$, IR refl. spectra 78−80324
Na_2KSb(Cs), photocathode, optical props. 79−78827
NaN_3, polycryst., IR active lattice vibr., optical consts. 77−77185
reflectivity continued
$Na^{14}N_x{}^{15}N_{1-x}O_3$, reflection spectra, Kramers-Kronig anal. with preliminary dispersion anal. 78−49915
$NaNO_3$, lattice vibrs., order-disorder transform., IR spectra study 80−65176
$NaNO_3$, vibrations of isotopic impurities, IR reflection and Raman spectra meas. 77−51465
$Na^{14}NO_3$, $Na^{15}NO_3$, polarised IR reflection spectra, surface damage effects 79−19872
$Na^{15}NO_3$, $Na^{14}NO_3$, multiphonon transitions in microcryst. reflectivity 78−72399
Na^ANO_3, (A=14,15), anomalous IR reflectivity min. in transverse-longitudinal band gap 79−56796
Na_2O-SiO_2 glasses, elementary electronic excitations, refl., luminesc., and photoemission meas. 80−84778
Na_2O-TiO_2-SiO_2 glass, IR refl., Raman and EPR spectra, struct. *(Russian)* 78−2860
Na_2SO_4:XO_4^{2-}, X=Cr, Se, Mo, W, lattice-impurity interactions, IR spectra 78−19522
$NaSbSe_2$ films, struct., photoelec. and opt. props. 78−51834
Nb, bulk, optical props., 6.6 to 23 eV 79−4815
Nb, electronic and optical properties 78−91612
Nb film, far IR reflection and transmission spectra, room temp. 77−55792
Nb, optical properties and electronic props. 79−42439
Nb_3Ge film, far IR reflection and transmission spectra, room temp. 77−55792
NbO_2, IR dispersion 79−65854
Nb_2O_5 anodic coatings, refr. index and spectral phase change, reflectance meas. 79−43052
Nd_2ASe_5, A=Ge, Sn, diffuse refl. spectra and band gaps 79−51963
NdP_5O_{14}, fluoresc. lifetime meas., IR and photoacoustic spectroscopy 80−60652
Nd_2S_3, optical props. and electronic struct. in fund. absorpt. region 80−80817
Nd_2S_3, vibr. spectra, factor-group anal. 80−80793
NdSb, forbidden band gap and electrotransfer parameters 80−39497
Ni (110), chemisorption of N_2, mol. and dissociative mechanisms 80−39431
Ni, anodic passive film form. in NaOH soln., refl. and ellipsometric study 80−104447
Ni, black, solar collector selective coatings, optical and thermal props. 79−62028
Ni complex, Ni-hexamethylenetetramine, reflectance spectra 78−31218
Ni, emissitivty and reflectivity, oxide film thickness effect 79−82364
Ni film, deposited by cylindrical magnetron sputtering, internal stresses, optical reflectance and elec. resist. 77−43449
Ni film, evaporated hydrocarbon chemisorption, IR refl. study 79−69343
Ni film, surface magnetoplasma waves, ATR meas. 77−69639
Ni, surfaces, Au-coated and polished, EUV reflection efficiencies 79−14073
Ni-Co(Fe)(V)(Ti), dil., optical absorpt., electronic struct. 80−108227
Ni-Ge-SiO, solar selective absorber surfaces, optical behaviour at high temp. 80−101130
$NiAl_xFe_{2-x}O_4$, Kerr effect, magneto-optical refl. spectra 79−82954
NiAs, optical props., 0.05-5 eV 77−48194
$Ni_{1-x}Co_xS_2$, elec. cond., thermoelec. power and optical meas. 80−59986
NiI_2, far IR study of lattice dynamics 78−80359
NiO-MgO, ESR and refl. spectra, Ni^{2+} distrib. 79−33745
NiSb, optical props., 0.05 to 5 eV 77−48194
Ni(100) platelet surface optical and magneto-optic consts. 78−15151
Pb film, vacuum deposited, reflectance spectra, structural rearrangement effects 77−24905
Pb, superconducting, phonon density of states determ. 77−20493
$PbBr_2$, reflectance spectra, exciton peaks 77−24870
$PbCl_2$, single cryst., far IR refl. spectra, effective ionic charges 79−87430
$PbCl_{2-2x}Br_{2x}$, luminesc. and reflection spectra *(Russian)* 80−84762
$PbCo_2(PO_4)_2$, mag. susceptibility, elec. cond. and optical refl. 79−56495
PbF_2 optical props. 77−32394
PbFBr(Cl), reflectance spectra, exciton peaks 77−24870
$Pb_{1-x}Ge_xTe$ epitaxial layers, phase transition obs. by far IR reflectivity spectroscopy 79−33691
$Pb_{1-x}Ge_xTe$, ferroelec. phase transition, IR refl. and resist. meas. 80−11353
$Pb_{1-x}Ge_xTe$ magnetoplasma reflectivity and transmission spectra 80−71428
$PbHAsO_4$, ferroelec., far IR and submillimetre dielec. dispersion 79−38528
$PbHPO_4$, ferroelec., far IR and submillimetre dielec. dispersion 79−38528
$PbHPO_4$, microwave permitt. and far IR refl. spectra in paraelec. and ferroelec. phases 80−40033
PbI_2, exciton spectra depend. on strong excitation, crystal transmission 79−69433
PbI_2, film, reflectance meas., optical consts., humidity effects 80−34994
PbI_2, first-order 2H-4H polytype transition, exciton spectroscopic study 80−59647
PbI_2 laminar semicond., phase transition of first kind by exciton spectroscopy *(Russian)* 79−82334
PbI_2, layered compound, exciton spectra, surface and stacking fault effects 80−40134
PbI_2, layered cryst., photoluminesc., and reflection spectra obs. 78−6726
PbI_2, optical phonon anisotropies and intralayer bonding forces from IR refl. 77−59573
PbI_2, optical props. 77−32394
PbI_2, photoexciton interaction, luminescence spectra, polariton dispersion diagram 80−93397
PbI_2, photolum. and reflectivity temp. depend., cryst. anisotropy effect on electron-phonon interaction *(Russian)* 78−15225
PbI_2, single cryst., far IR refl. spectra, effective ionic charges 79−87430
$Pb(NO_3)_2$, IR reflection spectra, dynamical props. 77−16303
PbO glass, reflection spectra 78−88325
$Pb_3(PO_4)_2$, crit. behaviour of polar modes near ferroelastic phase transition 79−95750
PbS epitaxial film, struct., optical and elec. props. 78−19583
PbS film, vac. deposited, optical and phys. props. 80−2315
n-PbS, natural galenite, function of wavelength in range 10 to 40 μm 79−42975
n-PbSe, polar semicond., mag. field influence on high-freq. relaxation time 79−95438

reflectivity continued
p-PbSe, valence band structure, IR refl. and absorpt. meas. 77−55791
$PbSe_{1-x}Te_x$, symmetry change in cond. levels, photovoltaic effect and reflectivity obs. 78−34766
$Pb_xSn_{1-x}I_2$, thin films, photosensitivity, ageing and annealing effects *(Russian)* 78−6804
$Pb_{1-x}Sn_xSe$, plasma reflection spectra, carrier effective masses and relax. times determ. 78−2858
$Pb_{1-x}Sn_xTe$, heteroepitaxial film, fundamental absorpt. edge and Shubnikov-de Haas effect 79−24381
$Pb_{1-x}Sn_xTe$, hole effective mass near zero bandgap, IR refl. study 80−108205
$Pb_{1-x}Sn_xTe$, reststrahlen band, reflection spectra 79−8162
$Pb_2Ta_{2-x}M_{2x}O_{7-x}$, (M=Ti, Sn Zr), oxygen deficient, form., IR spectra, dielec. const. *(Japanese)* 77−48171
PbTe epitaxial layers, submillimetre spectroscopy 79−83048
PbTe film, characts. of photocond. spectra and reflectivity 77−55624
p-PbTe, IR reflection and Faraday rotation angle meas. 77−1680
PbTe, index matching far i.r. method for static dielectric const. meas. 77−1678
PbTe, TO phonon mode softening, sub mm spectra 78−6665
PbTe very thin epitaxial films, transmission and refl. spectra, 1 to 5 eV 80−7430
PbTe:As, hole conc. control, in LPE layers, plasma reflectivity and thermoelec. probe meas. 79−99640
$PbWO_2$, IR and Raman multiphonon spectra, struct. 77−90143
$PbWO_4$, reflectivity, dispersion parameters and optical const. temp. depend. 77−28575
Pd film, evaporated, hydrocarbon chemisorption, IR refl. study 79−69343
PdIn, refractive index, reflectivity and band struct., APW calcs. 80−40139
$Pd_{81}S_{19}$ and $Pd_{84}Si_{16}$, metallic glasses, optical refl. spectra and optical consts. 79−87464
Pr compounds, plasma light reflection by free charge carriers 80−11403
Pr_2ASe_5, A=Ge, Sn, diffuse refl. spectra and band gaps 79−51963
PrSb, forbidden band gap and electrotransfer parameters 80−39497
Pt (100), (110), and (111), form. of Cu monolayer, optical and electrochem. studies 79−99419
Pt, adsorbed CO, IR reflection absorpt. spectra, 1875 cm^{-1} band 79−65852
Pt electrodes, chemisorbed H, anion effects on multiple states, reflection spectra obs. 79−43634
Pt evaporated film, optical props. meas. in VUV, 220 to 150 Å 80−45159
PtO film, electrochemically formed, anisotropy of optical constants, reflection spectroscopy and Kramers-Kronig analysis 77−32456
α-quartz, reflection and surface polariton spectra, ion implantation effect *(Russian)* 79−47451
$RbClO_3/RbBrO_3$ mixed crystals, internal optic modes obs., Raman and IR reflectance spectra 80−76024
$RbHSeO_4$, ferroelec., far IR spectra 80−71404
Rb_2MnCl_4, IR active modes, interlayer and intralayer forces 77−59575
$RbMnF_3$, reflectivity, 8-60 eV, excitonic struct. 77−20871
RbN_3, polycryst., IR-active lattice vibr., optical consts. 77−77185
Ru (001), adsorption of CO, IR spectra, LEED, and thermal desorption meas. 80−70533
α-$RuCl_3$, reflectivity and absorpt. spectra, thermo-reflectance 79−47438
S, orthorhombic, photogeneration of charge carriers 80−107844
S powdered pressings proposed near IR reflectance standard 78−90464
$(SN)_x$, electronic struct. and opt. props. 78−6256
$(SN)_x$, epitaxial, optical props. and plasmon dispersion, from electron energy loss spectra 77−35882
$(SN)_x$, reflectivity calc. taking account of fibrous struct. 79−87462
$(SN)_x$, reflectivity spectra meas. by synchrotron radn. 79−91513
$(SN)_x$, single cryst., elec. anisotropy, polarised refl. spectra 77−36264
$(SN)_x$, temp. depend. of reflectance spectrum 77−85744
$(SNBr_{0.4})_x$, metallic, transport and optical props. 77−85724
$(SNBr_{0.4})_x$, polarised reflectance 77−59349
SbI_3, layered compound, exciton spectra, surface and stacking fault effects 80−40134
SbI_3, refl. spectra of cryst., 300-800nm, and derived optical consts. 79−87456
SbSBr, electronic and optical props. 78−34763
SbSBr glass, IR reflectivity spectra 80−71403
SbSI, band gap photoreflectance spectra near ferroelec. transition 79−38559
SbSI, electronic and optical props. 78−34763
SbSI, ferroelec. semicond., laser-modulated reflectance near T_c 78−72552
SbSI-SbSBr system, ferroelec., anharmonic effects in far IR reflectivity spectra 80−76014
Sb_2Se_3, Raman spectra, Raman and IR-active modes 79−56776
SbSeI, electronic and optical props. 78−34763
SbTe, reflection spectra 77−16325
Sc, HCP, optical examination of electronic struct. 77−89694
Se, A1 type metallic phase, optical consts. and refl. 77−32455
Se, electronic struct. of cryst. phases and hydrostatic press. effects 80−59865
Se film, vacuum deposited, struct. asymmetry, reflectivity elec. cond. 79−23855
Se films, Ag diffusion, effect on interferometric thickness meas. 80−96695
Se formed in chiral polymer matrix, circular dichroism 77−85685
Se, single crystals, fast neutron irradiated, annealing expts., dark conductance, reflectivity spectra 77−85266
Se, trigonal reflectivity and density of states press. depend., self-consistent pseudopotential calc. 77−31931
Se-Te-As-Ge glasses, absorpt. spectra, diffuse reflectivity loss correction 79−82995
Si (111)7×7, dangling-bond surface states and O_2 adsorption, reflectometric study 79−99600
Si, absorpt. spectrum red shift, spectrum temp. depend. 79−78699
Si, amorphous, ion implanted, laser annealing, reflectivity meas. 80−29039
Si amorphous film, film, glow discharge deposited, refl. spectra and dielec. function 80−50360
Si, amorphous film, glow-discharge, optical props. *(Japanese)* 79−65946
Si amorphous film, optical props., electronic states 80−25475
Si, CVD amorphous films, effect of surface characts. on visible and UV optical props. 80−60698
reflectivity continued
Si complex reflectivity determ., absolute method 79−30584
Si, epitaxial film on sapphire, optical absorption and interface comp. profiles 77−12459
Si film, amorphous and crystalline, optical properties 77−24906
Si film, polariton resonance obs. from reflectivity meas. 77−69251
Si film thickness meas. from visible refl. spectra 79−99960
Si, free carrier and interband absorpt. at 1.06 μm, temp. depend. 80−2783
Si, glow discharge amorphous film, reflectance and transmittance *(Japanese)* 80−34995
Si, glow discharge deposited, optical spectra, reflectance, dielectric function and oscillator strength 80−11492
Si, high-dose implantation damage, reflectivity, Rutherford backscatt. and TEM obs. 77−7743
Si, interband and free carrier absorpt. consts. at high-level photoinjection 79−38514
Si, ion implanted, dynamic behaviour of pulsed-laser annealing, time depend. optical reflectance meas. 79−60393
Si, ion implanted, mode-locked Nd:YAG laser annealing, recrystn., optical reflectivity meas. 80−19817
Si, ion implanted, transient optical reflectivity study of laser annealing, thresholds and kinetics 79−60390
Si, ion implanted amorphous layers, free carrier plasma effects 77−73133
Si, ion irrad., temp. and dose depend. of defect profiles 80−29097
Si, ion-implanted, pulsed-laser annealing, dynamic behaviour by optical reflectance meas. 79−69122
Si, laser annealing, optical refl. meas. of melted layer 79−78796
Si, light reflection, effect of repeated oxidation 79−52402
Si on sapphire, laser annealing dynamics epitaxial regrowth, optical reflectivity 80−29285
Si, optical constants, heavily doped crystals, Kramers-Kronig analysis 77−85676
Si, optical consts. by unpolarised incident radiation 80−76044
Si, optical reflectance rel. to surface damage 79−14985
Si photodiode, refl. and external quantum efficiency change after surface cleaning 79−93212
Si photovoltaic detector, quantum efficiency rel. to position and wavelength 79−75593
Si, polycrystalline, film thickness meas., visible spectral reflectance analysis 78−32786
Si polycrystalline CVD film optical props. 77−77315
Si, reflectivity time dependence during pulsed laser annealing 80−66214
Si ring photodiode reflectometer for cavity reflectance 80−86376
Si, surface roughness evaluation by UV refl. 80−39393
Si, thinly oxidised wafer reflectance at normal incidence, calc. 79−78641
$Si:^{31}P^+$, implanted layers, characterisation by ellipsometry 79−90683
Si:As, annealed, dopant profile parameter contactless probing by IR spectroscopy 79−77629
Si:As, laser annealing, channelling, optical obs., and resist. meas. 79−1444
$Si:As^+$, implanted layers, refractive index and reflectivity calcs. from ellipsometry meas. 79−73190
Si:N(P), ion implanted, IR transmission and rel. spectra study 80−108244
Si:O film, near IR reflectivity at high temps. 78−56532
Si:P, characterisation by IR reflectivity 78−56501
Si:P, high fluence ion implantation, layer thickness and refr. indices, IR refl. meas. 79−82248
Si:P, ion-implanted, optical refl. obs. of damage 78−55883
$Si-Si_3N_4-SiO_2$ non absorbing double layers, optical parameters reflectivity by liquid immersion method 80−71503
SiC diffraction grating for vac. UV, fabrication 77−79920
SiC ion implanted, laser induced ordering and defects 80−84754
α-SiC, lattice absorpt. bands in IR spectra, surface treatment effects 77−52071
Si_3N_4, CVD films, chemically trapped H reflection spectrometry 78−10081
Si_3N_4 film in MNOS memory struct., distrib. and role of N-H and Si-H bonds 79−33358
Si_3N_4 thin film, multiple internal refl. IR spectroscopy 80−11499
SiNH films, thickness and refractive index meas., comparison of techniques 80−8957
SiO amorphous film, optical transmittance and reflectance, bulk optical props. determ. 80−88954
SiO evaporated film, dielec. function 8 to 33 μm, spectrophotometric and refl. meas. 80−80883
SiO film on Al, radiative cooling surface 80−50439
SiO_2, amorphous, and layers on Si substrate, IR optical props. 79−56780
SiO_2 film, attenuated total reflectance study, impurity spectra 80−97311
SiO_2 film, on GaP substrate, N ion implantation, optical refl. and EPR meas. 80−84197
SiO_2 film on Cu substrate, surface EM wave absorpt., optical consts. *(Russian)* 80−108216
SiO_2 film on Si substrate, reflectance and absorptance obs. 79−15542
SiO_2 films, microporous, sintering effects, IR ATR, transmission investigs. 79−66031
SiO_2 films, thickness and refractive index meas., comparison of techniques 80−8957
SiO_2, fused, surface crystn. by Li^+ ion implantation and annealing 80−89383
SiO_2, ion implanted, fused, refr. index profiles 80−54272
SiO_2, ultrathin layers on Ge substrate, ATR spectra, thickness depend., struct. obs. 80−55214
SiO_2, vitreous, LO vibrational modes, Raman and IR spectra 77−7819
SiO_2-PbO-K_2O glass, reflection spectra 78−88325
SiO_2-Si system, implanted with N, P, and Te ions, reflectance spectra and interference fringes 79−23629
SiO_x protected Al mirror, far UV refl., UV irrad. effect 79−7191
Si_2Te_3, cryst., IR reflection, Raman spectra 77−12393
Si(111)2×1, oxide layer, surface states detec., optical reflectivity obs. 80−50368
Si(111)2×1, surface electron states detected by external reflectivity 78−80036
Sm_2ASe_5, A=Ge, Sn, diffuse refl. spectra and band gaps 79−51963
SmS, metallic, optical refl. investig. of valence fluctuations 77−63428
SmS, optical props. and electronic struct., Kramers-Kronig model anal. 79−69859

reflectivity continued
SmS, press. effect on lattice parameter, mag. susceptibility, and reflectivity 79−56272
SmS, semicond. thin film, absorpt. and refl. spectra, fine struct., cond. band extremum 79−69897
Sm_2S_3 films, refl. and transmission spectra at 300K 80−80889
SmSb, forbidden band gap and electrotransfer parameters 80−39497
SmSe, pressure-induced reflectivity changes and semiconductor-metal transition 79−56763
Sn, film, vac. deposited, influence of ion bombardment during condensation 79−82483
Sn film, vacuum deposited, reflectance spectra, structural rearrangement effects 77−24905
Sn film, white, optical props. between 2-15 eV 78−19584
Sn, globular film, interf. and diffr., solar selective props. 79−4860
Sn globular film, solar selective props., effect of dielec. layer addition 79−4861
SnI_2, layered cryst., photoluminesc., and reflection spectra obs. 78−6726
SnI_2, single crysts. and film, optical props. 77−32437
$Sn_{1-x}Mn_xTe$, IR reflectivity, elec. susceptibility mag. order effects 79−47433
SnO_2 doped films for spectral-selective surfaces, refl. and elec. props. meas. 79−74013
SnO_2 films, selective, optical characterisation by thermodynamical method 80−84796
SnS, coupling of plasma waves with optical phonons 78−31204
SnS, far IR optical props. 77−12375
SnS_2, crystal growth and optical props. in visible and IR regions 77−52114
SnS_2, optical props. and band struct. 78−2880
SnS_2, refl. using Kramers-Kronig anal., optical functions 79−95798
SnS_2, single cryst., far IR reflectivity 79−56774
Sn_2S_3 mixed valence semiconductor, far IR refl. spectra 80−108191
SnS(Se), IR reflectivity and Raman spectra, phonon frequencies and dielec. const. 77−48166
$SnS_2(Se_2)$, optical phonon anisotropies and intralayer bonding forces from IR refl. 77−59573
$SnS_2(Se_2)$, optical transitions from d core levels 80−45105
SnSe, far IR reflectivity spectra, lattice vibr. and dielec. const. 77−52068
SnSe, lattice refl. spectra in long-wavelength IR range 78−27236
$SnSe_2$, optical props. and band struct. 78−2880
$SnSe_2$, refl. using Kramers-Kronig anal., optical functions 79−95798
$SnSe_2$, single crystal, reflectivity, XPS, UPS, and band struct. 78−6701
SrF_2, UPS and XPS spectra, rel. to optical props. 80−66386
SrFX, X=Cl, Br, absorpt. and refl. spectra 79−82994
$Sr(NO_3)_2$, IR reflection spectra, dynamical props. and phase transition 77−16303
SrO, logarithmic derivative reflectance spectra 80−11429
SrO, surface states, reflectance spectra, impurity effects 77−20873
$SrO-Ga_2O_3$, vitrification, spectroscopic and petrographic anal. 77−15556
$SrTiO_3$, absorption coeff., reflectivity, 293-853K 78−64342
$SrTiO_3$, plasmon-phonon reson., IR reflection spectra 78−56093
$SrTiO_3$, surface EM wave propag., IR refl. expts. 78−39553
$SrTiO_3$, UV refl. spectra, optical consts. 0 to 32 eV Kramer-Kronig anal., band struct. calcs. 78−43903
SrX_2, X=Br, Cl, absorpt. and refl. spectra 79−82994
TGS-TGSe solid solution, temp. depend. of fundamental reflection spectra meas. 77−16337
Ta, electronic props. and reflectivity, iterative empirical pseudopot. calc. 77−76745
Ta film, deposited by cylindrical magnetron sputtering, internal stresses, optical reflectance and elec. resist. 77−43449
Ta, optical properties and electronic props. 79−42439
Ta_2O_5 antireflection coatings for Au-GaAs solar cells parameters determ. 77−763
TaS_2 (1T), commensurate and incommensurate CDW state, far IR reflection spectra 79−95755
TaS_2 mixed coordination polytypes, optical props. 0.5-6.0 eV range, reflectivity spectra 79−15476
$TaSe_2$ (1T), commensurate and incommensurate CDW state, far IR reflection spectra 79−95755
Te, electronic struct. of cryst. phases and hydrostatic press. effects 80−59865
Te, synthetic, optical props. in visible spectrum and microhardness meas. *(French)* 77−28590
TeO_2, paratellurite, optical absorpt. and refl. spectra, 80-500K, optical consts. determ. 80−50359
Th, interband structure and role of 5f electronic states, optical reflectivity meas. 77−76744
Th, optical reflectivity 80−16054
Ti anodic film, growth kinetics, determ. *(French)* 78−76788
Ti, clean and oxidised surfaces, refl., 2-25 eV 80−55123
Ti, electropolished, optical props. from 1.8 to 3 eV 80−85088
Ti film, deposited by cylindrical magnetron sputtering, internal stresses, optical reflectance and elec. resist. 77−43449
Ti, oxidation kinetics, refl. interf. meas. of film thickness 77−90498
Ti, oxide layer form. in acid soln., electrochem. and optical props. 78−48560
Ti, Xe physisorption, electronically excited atoms coupling to cond. states 77−89642
TiN, optical props. at 300K 78−19466
TiN_x, film, non-stoichiometry rel. to optical characts. 77−12456
TiO_2 film on Ti, simultaneous determ. of optical indices of film and substrate by statistical anal. 77−20946
TiO_2, rutile, optoelectronic props., band struct., theory 80−80175
TiO_2 single cryst., refl. and electrorefl. spectra 78−2870
TiO_2 single cryst., refl. and electrorefl., energy levels 78−2871
TiO_2-SiO_2 multilayer vacuum coatings, optical props. 80−97361
TiO_x antireflection coatings for solar cells, optical, struct., and compositional characts. 80−55852
Ti_2O_3, IR refl. spectra, IR active phonons, Ti 3d electronic effects 78−35145
Ti_2O_3, metal-semicond. transition, refl. spectra study 80−10880
Ti_2O_3, optical consts., polarisation dependent reflectivity 78−52531
TiS_2, electron energy loss spectra, dielectric function, absorption coeff. 79−69937
TiS_2, evidence for semicond. props., Hall coeff., refl., cond., thermoelec. power 80−20220
TiS_2, transport props. and semicond. nature 80−44598
$TiS_2(Se_2)$, vacuum UV reflectivity spectra, cond. band model 77−44012
reflectivity continued
$TiSe_2$, IR reflectivity, phonons and free carriers 79−61379
$TiSe_2$, optical refl. spectra obs., suppression of antiferroelectricity by excess carriers 77−59536
$Ti_{1+x}Se_2$, superlattice form., phase transform., IR reflectivity meas. 77−15383
$Ti_{1+x}Se_2$, superlattice form. and phase transition, IR reflectivity meas. 79−24322
$TiSe_2(S_2)$ (1T), electronic and vibronic struct. 80−44500
Tl-Te, liq., reflectance, 0.65-3 eV, comp. depend. 78−72549
Tl_3AsS_4, optical phonons, Raman and refl. spectra 80−11400
TlBr, resonant polaron coupling and excitons under mag. field 80−71383
TlCl-TlBr mixed crystal, reflectivity spectra meas. 77−85743
$TlGaS_2$, IR refl. spectrum., LO phonons *(Russian)* 77−40221
$TlGaS_2(Se_2)$, IR reflection spectra, lattice vibrs. *(Russian)* 77−85701
$TlGaS_{2x}Se_{2(1-x)}$ layer solid soln., long wave lattice vibrs., IR reflection spectra 80−11388
$TlGaTe_2$, IR refl. and Raman scatt. spectra, lattice vibrs. 80−40108
$TlGaTe_2$, $TlInTe_2$, and $TlInSe_2$, IR refl. spectra 80−60605
$TlInS_2(Se_2)$, IR reflection spectra, lattice vibrs. *(Russian)* 77−85701
$TlInS_{2x}Se_{2(1-x)}$ layer solid soln., long wave lattice vibrs., IR reflection spectra 80−11388
$TlInSe_2$, single crystals, optical phonons, Raman and infrared spectra studies 79−55842
$TlInTe_2(Se_2)$, IR refl. and Raman scatt. spectra, lattice vibrs. 80−40108
TlS_2, amorphous semiconductor, optical consts. 79−11400
TlSe, refl. spectrum in 4.2 to 8.0 eV range 79−51984
TlSe, vibrational spectrum, IR spectra meas. 78−35146
TmSe, metallic, optical refl. investig. of valence fluctuations 77−63428
U complex, $[UO_2(CO_3)_3]^{4-}$, vibr. and low-temp. optical spectra, rel. to U recovery from oceans 79−73939
UO_2, 5f-magnetic semiconductor, spectroscopic data, review 80−97299
UO_2 and U_4O_9 single crysts., optical props. rel. to chem. bonding 77−28598
UO_2, electronic transitions, crystal field effects and phonons, phase transition 80−97303
UO_2, localised versus itinerant 5f electrons exam., reflectivity meas. 79−19905
UO_2, optical props. and electronic struct. 78−68527
US, ferromagnet, electronic structure, reflectivity *(German)* 80−49567
US, optical props. and electronic struct. 80−25410
US(Se)(Te), electronic struct. and exchange band splitting, optical refl. meas. 80−66226
USb, localised versus itinerant 5f electrons exam., reflectivity meas. 79−19905
USb, reflectivity spectrum, band struct. 80−7368
USe (s) 80−16053
V, film, vac. deposited, influence of ion bombardment during condensation 79−82483
V, optical properties and electronic props. 79−42439
VO_2 film, metal-dielec. transition, refl. after 40 keV ion bombardment 79−23899
VO_2, film, metastable metallic phase due to laser and electron beam irrad., refl. spectra 79−19944
VO_2 film, optical and elec. props., 0.8 to 4.2 mm, near metal-semicond. transition 77−32473
VO_2, nonstoichiometry influence on electron struct. and metal-insulator phase transition 80−44507
VO_2 single cryst. film, ion-irrad., 'splitting' of semicond.-metal transition 80−11053
VO_2 variable-reflectance mirror for CO_2-N_2-He 10.6 μm scan laser 80−38026
V_2O_5 cathode, used in Li-V_2O_5 reserve cells, microstruct. optical reflectance, elec. cond. meas., chem. anal., SEM obs. 79−43752
V_2O_5 film, amorphous, thickness, density and refr. index determ. from reflectance interference spectra 80−55206
V_6O_{13}, optical props. in metallic and semicond. phase 80−40135
V_6O_{13}, semicond., IR vibration spectra 80−88997
V_3Si, complex refr. index and reflectivity of thin film, microscopic characts. and superconductivity 78−31267
V_3Si film, far IR reflection and transmission spectra, room temp. 77−55792
W (110) surface, adsorption of H, band struct. and adsorbate geometry, surface-reflectance-spectroscopy 80−44416
W, adsorption of $CO(H_2)(O_2)$, surface reflectance spectroscopy on low index planes 78−71965
W, chemisorbed H, surface cond. and intrinsic surface states, surface refl. spectra 80−15378
W, dendritic, solar absorbing surfaces anodised interference coatings 78−13815
W surface, (110), chemisorpt. effects on dielec. function, refl. spectra 80−75616
W-Fe spin glass, optical props. and electronic states 80−20412
WO_3, antireflection coating on W dendritic surfaces, reflectance, geometrical study 79−91511
WO_x, powders, coarseness meas. using powder surface reflectance 79−96246
WS_2, excitons, mag. circular dichroism and wavelength modulated reflectance meas. 79−23900
WSe_2, excitons, mag. circular dichroism and wavelength modulated reflectance meas. 79−23900
WSe_2, refl. spectra and photovoltaic effect, 1.5-3.2 eV, 4.1-300K 79−47470
Xe, crystalline, polariton effects, reflectivity, absorpt., and resonant luminesc. spectra calcs. 80−20095
Xe, liq., UV reflection spectra, density depend., excitonic band evolution 77−77246
Xe-Ar system, band formation exam. by photoelectron spectroscopy 77−66116
Y film prepared in ultrahigh vac., optical meas. 6 to 14 eV 79−78767
Y, reflectivity spectrum, 3.5 to 30 eV dielectric function and plasmons 77−44014
Y-Er, surface, high-freq. elec. cond. dispersion function, effects of polishing and annealing 78−19506
$YAlO_3$, reflection spectra, Kramers-Kronig anal. of optical characts. 79−8161
YIG, magneto-optical Kerr effect, reflectivity spectra 80−66157
YIG, magnetooptical spectra, polar Kerr rotation, dielectric tensor elements spectra 80−40091
YIG:Ga(Sc), magneto-optical Kerr effect, reflectivity spectra 80−66157
Y_3Se_4 powder, prep. and optical props. 77−28771

reflectivity continued
YVO_4, pure and Bi^{3+} doped, absorpt. and emission props., excitons 79−38592
YbS, multiphonon processes and exciton-LO phonon interaction 79−95784
YbS, Raman spectra reson., reflectance spectra, multiphonon processes 78−84581
YbSb, forbidden band gap and electrotransfer parameters 80−39497
Zn-In-S thin layers, ternary phases, optical props. near long-wavelength intrinsic absorpt. edge 80−80887
$Zn_xCd_{1-x}S$, forbidden band width, exciton refl. and luminesc. meas. 78−10947
$Zn_xCd_{1-x}S$, reflectivity spectrum, excitons and energy band struct. 77−55804
$Zn_xCd_{1-x}Se$, exciton reflection spectra anomalies *(Russian)* 80−97304
$Zn_xCd_{1-x}Te$, reflection spectra, energy band struct. comp. depend. *(Russian)* 78−56500
$ZnCl_2$, aq. solns., complex IR refr. indices, IR spectra, mechanisms, spectrometer system 78−43831
(ZnFe)S, marmatite, optical properties 78−39555
$ZnIn_2S_4$, fund. optical consts., Kramers-Kronig analysis, reflectivity spectra 78−39573
$ZnIn_2S_4$, fund. reflectivity, 2 to 6 eV, band struct. implications 78−39574
$ZnIn_2S_4$, IR refl. spectra and cryst. struct. 79−56777
$ZnIn_2S_4$, layered semicond., dielec. function and electronic density of states 79−8155
$ZnIn_2S_4$ layered semiconductor, fundamental optical constants, comparison with band structure calcs. and PES 79−56757
$Zn_{1-x}Mg_xTe$, variation of fundamental edge, wavelength modulated reflectivity meas. *(French)* 77−81124
ZnO, ang. depend. of reflection spectra and directional dispersion of anisotropic exciton polaritons 78−31216
ZnO, electron-hole plasma, gain and refl. spectra study 80−66227
ZnO, electronic struct. calc., appl. of O nonlocal ionic pseudopot. 77−51659
ZnO, polariton dispersion, IR reflection spectroscopy 80−11415
ZnO, reflection spectra, exciton reflection at high excitation levels 77−69853
ZnO, surface exciton polaritons, ATR obs., book contrib. 79−42620
Zn_3P_2 bulk and thin film, UV reflectivity spectra, photovoltaic effects, optical consts. 80−25472
Zn_3P_2, optical props., transition energies from transmission and refl. meas. 80−60532
ZnS, cubic, direct and modulated refl. spectra, 165-360 nm 77−13807
ZnS evaporated film, refl. loss on UV irrad., ZnO form. 80−99813
ZnS evaporated film optical props. 160 to 2000 A 79−15544
ZnS, plastically deformed, anisotropic cond. 78−56143
ZnS, temp. coeffs. of charact. reflectivity struct. 77−85745
ZnS:Cu,Cl, exciton refl. spectra, hexagonal struct. 77−44021
ZnS:Mn^{2+}, heavily doped, anomalies in reflectivity 77−20891
ZnS-Ag, broad band visible heat reflecting mirror 77−39017
ZnS-O, single cryst., fast neutron irrad., optical props. 78−27331
ZnS-ZnO, solid solns., edge emission and exciton spectra *(Russian)* 77−24899
ZnS(Se), wavelength-modulated refl. spectra, 2.5 to 8 eV 77−20877
ZnSe, attenuated total refl. spectra of surface exciton polariton 77−36262
ZnSe crystal, exciton reflection spectra, control of exciton-free surface layer thickness 80−7373
ZnSe, exciton refl. spectra, temp. depend. 80−59886
ZnSe, single crysts., opt. band gap and Mn^{2+} EPR, effects of prep. conditions 77−47730
ZnSe, temp. coeffs. of charact. reflectivity struct. 77−85745
$Zn_4Si_2O_7(OH)_2H_2O$, hemimorphite, polarised IR refl., vibr. modes *(French)* 77−85698
$ZnSiP_2$, reflectance spectra at 300K 80−25407
ZnTe, reflectivity meas., double beam wavelength modulated technique *(Korean)* 80−50365
ZnTe, shape of reflectance and thermoreflectance spectra 79−11430
ZnTe, single cryst., anomalous struct. of exciton refl. spectra 77−44020
p-ZnTe, single crystal *(Russian)* 78−23488
ZnTe, wavelength-modulated reflectance spectrum, electron-phonon and exciton-phonon interactions 79−11434
ZnTe:Bi, laser annealing, channelling, reflectivity spectra 80−66215
ZrB_2, self-consistent band struct., XPS, reflectance, NQR, Hall effect and density of states meas. 80−107689
ZrC, film, solar selective surface *(Japanese)* 78−90465
ZrN, optical props. at 300K 78−19466
ZrO_2 thin film, optical props. rel. to cryst. struct. 80−97357
ZrO_2:Y_2O_3, cryst., IR refl., refr., absorpt. 77−12382
$ZrS_2(Se_2)$, vacuum UV reflectivity spectra, cond. band model 77−44012
$ZrS_3(Se_3)$, quasi one-dimens., optical phonon anisotropy, IR spectra study 80−40112
$ZrSiO_4$, zircon, resonance splitting of internal vibr. freq. of complex anion 80−55080

reflector antennas
see also antenna reflectors
7 m Cassegrain radiotelescope, quasioptical feed system for millimetre wavelengths 78−32343
140 GHz atmospheric attenuation by rain, obs. 78−3914
Cassegrain, double knife-edge diffraction for curved screens 80−14273
Cassegrain radiotelescope prism beamswitch 79−21186
far IR antennas for 0.1 to 3.0 mm range, review 80−69553
far-field of blocked circular aperture, example of 100 m radiotelescope, Effelsberg *(German)* 77−2341
feeds, compact dual-hybrid-mode feeds with low crosspolar radiation 80−12662
large adjustable parabolic antennas, vibr. behaviour anal. using dynamic equivalent models *(German)* 77−2342
large reflector antenna structural design for gravity and wind loading 78−57448
millimetre range design, radiotelescope appl. *(German)* 77−53427
multichannel radiotelescope, factors affecting noise interference, anal. *(Russian)* 77−22067
parabolic aerial with monopulse exciter for meteorological satellite S-band reception *(German)* 79−92628
paraboloidal reflector backward diffraction suppression by corrugated cylinder 77−75383
phased array aberration effects, optical modelling *(Russian)* 78−16290

reflector antennas continued
radiotelescope, RATAN-600, variable-profile reflector antenna design, 0.8 to 30 cm 79−2480
radiotelescope construction, light-weight, with prestressed guyed rod 80−109360
radome and backstructure design improvements 78−57449
rainfall monitoring, dual freq. radar appl. *(Japanese)* 78−57358
space antenna, self-deploying large parabolic antenna and array design 78−57450
suppression of diffracted waves by corrugated cylinder 79−81342
transform-pair relationship between incident and scatt. fields from arbitrary reflector 79−7058

reflex klystrons
No entries

refraction
see also acoustic wave refraction; electromagnetic wave refraction; refractive index
auroral electron beam, electrostatic noise generation and refr. 78−85759
S.China Sea, satellite obs. of internal wave refr. 77−64298
coastal surface gravity wave refraction for flat inclined ocean bottom *(Russian)* 77−33084
Dirac equation derivation, inhomogeneous media electrodynamics refraction *(German)* 79−13005
elastic waves, reflection and refraction in presence of separation at solids interface 77−75848
inelastic neutron scattering, influence of refraction 78−87592
interstellar H II regions, ionization front, oblique refraction 78−54025
metallic surface state, influence of refr. of p-polarised light on photoemission 80−20772
microseisms at Palisades, source location and propag., refr. effects 78−85495
ocean wave groups, vels. and refr. laws verification 78−85575
ocean wave refraction by circular island, model 80−36316
plane wave motions, energy partition in refl. and refr. 78−77727
plane wave reflection and refraction at elastic interface, initial stress effects 79−62445
sea surface waves, structures loading calc., using finite and infinite elements 77−81910
seismic body waves in anisotropic media, refl. and refr. at plane interface 77−49019
seismic longit. wave by inclined media interface, refr. effect on ground surface displacements *(Russian)* 78−85485
seismic refraction method appl. to faults prospecting, model expt. and features of seismograms *(Chinese)* 79−12286
seismic waves, nature of errors in refractor vel. determ. 80−56621
seismic waves, refl. refr. and diffr. in media with elliptical vel. depend. 79−5454
seismic waves, refr. delay time appl. to weathering correction 79−44255
seismic waves, refr. index distrib. image reconstruction via iterative ray tracing between boreholes 80−98466
seismic waves reflecting/refracting plane surface image, form. using two-point eikonal *(Russian)* 79−96740
tetragonal media, elliptical conical refraction of elastic waves 80−5976
transient waves in fluid-filled porous media, refl. and refr. 77−49604
tsunamis, refr. and wave height distrib. in coastal zone 78−77192
$SbO_{3/2}$-$BO_{3/2}$, glass, props. and struct. *(Japanese)* 77−27836

refractive index
see also photorefractive effect; refractometers
acetic acid-acetone mixture, physical parameters 80−2716
acetic acid-H_2O, assoc. liq., struct. props., static and dynamic phys. props. meas. 79−70316
acetone, refr. index. temp. depend., deviation from Lorentz-Lorenz formula 77−40200
achromatism of optical wedge of holographic elements *(Russian)* 78−13787
acoustic, allowance for temporal variablity of random inhomogeneities of a medium in connection with the local method 79−32144
acrylic moulding formulations, optical and mech. props. 80−106582
additive-orbital scheme for calculating atomic and molecular polarizabilities 77−3273
aerosol optical extinction coefficients, practical upper limits 79−72486
air, meas. with improved Rayleigh interferometer *(Chinese)* 77−57383
air, Schlieren photography, detection of abnormal nasal escape 80−64145
air, vertical struct. of refr. index for ultrashort radio waves at subfreezing temps. 78−16128
air-moving arc interface, optical anal. at atm. press. 79−90482
alcohols, opt. consts. in IR, stretch band obs. 79−91421
alkali and alkaline earth metal metaphosphate glasses exam. of thermooptical and photoelastic props. 78−88287
alkali boroaluminosilicate system, self-focusing fibres with aperture of 0.18 80−87548
alkali halide, optoelectronic props. 80−25330
alkali halide, rel. to optical breakdown, damage threshold calcs. 79−95708
alkali halides, refractive index calculation 80−88949
alkali lime germanosilicate GRIN fibre prep., losses and geometrical props. 80−69560
alkali metal halide, laser damage morphology simulation 80−35015
alkali metal ternary chlorides, $ABCl_3$ type, optical props. 78−35111
alkaline earth halides, refractive index, wavelength and temp. derivatives 80−88948
alkaline earth silicate glasses, morphology effects on props. 80−49118
alkoxyazoxybenzenes, isotropic-nematic transitions, RI, orientational relax. times 77−24390
p-n-alkoxybenzoic acid, homologs, principal mol. polarisabilities calc., refr. indices of nematic mesophase meas. 78−2004
4′-n-alkyl-4-cyanobiphenyls, nematic, elastic and optical props. 77−11613
alloy, expt. methods, review 79−33655
aluminate glasses, new families, light transmission, 0.4 to 6 μm 77−24843
ammonium bioxalate monohydrate, refractive indices in IR region 78−52512
ammonium malate, SHG, 492-640 nm, phase matching, refr. index and nonlinear susceptibility 77−72031
ammonium malate, single cryst., optical SHG, refr. index, susceptibility 78−63152
amplitude-phase holograms, optical parameter dispersion 80−58481
p-n-amyloxybenzoic acid, refr. index and orientational order parameter, temp. depend. 79−90537

refractive index continued
anilines, substituted, in benzene soln., dielectric relax. time, dipole moment 80—50259
anisotropic inhomogeneous guiding media, rel. between phase and group indices 78—9320
anisylidene-p-aminophenyl acetate, nematic liq. cryst., refractive index, density, orientational order 78—76419
anisylidene-p-aminophenyl butyrate, nematic liq. cryst., refractive index, density, orientational order 78—76419
anodic film, automated interpretation of ellipsometer obs. 78—56902
anthracene, polariton effects in transmission and absorpt. spectra in thin crysts. 77—20886
antireflection coating, three-layer, refractive index optimum combination 80—28306
antireflection coatings on metals, conditions on refractive index and film thickness for zero refl. 79—65951
aqueous electrolyte solutions, refr. index, Tamman-Tait-Gibson model 78—10863
aqueous solution fluorescence spectra, refr. correction 78—93766
arachidate monolayers, optical props. integrated optics meas. 78—35214
Araldite CT200/HT907, 263 to 343K, mechanical, physical and optical props. 78—56682
asymmetric three-layer optical waveguide, radiation losses due to discontinuities 80—53446
asymmetric-slab optical waveguide losses due to refractive index inhomogeneities 78—1381
atmosphere, boundary layer temp. profile from inferior mirage obs., simple soln. 79—80035
atmosphere, micrometeorological temp. profile from optical data inversion 79—80034
atmosphere, propagation calcs., use of average complex refr. index 78—57314
atmosphere, refr. angles accuracy obtained by statistical orthogonal expansion of refr. index *(Russian)* 77—70829
atmosphere, refr. index profiles, upper and lower atm. contribs. 77—87070
atmosphere, refractive turbulence profiles, meas. by spatial filtering of scintillation 77—5331
atmosphere radio refractivity gradient analysis over S.E.Asia 77—91244
atmospheres of giant planets VHF refraction 80—98608
atmospheric aerosol constituents, absorpt. coeff. rel. to imaginary refr. index 79—74956
atmospheric dust, imaginary refr. index rel. to particle size 78—7763
atmospheric extinction and absorpt., effects of particulate complex refr. index and size distribs. 79—29849
atmospheric haze microstruct. and refr. index from scatt. light polarisation characts. *(Russian)* 79—29852
atmospheric particulates, index of absorption, determination by remote sensing, theory 79—88438
atmospheric refractive index temp. struct. parameter estimation over ocean 77—41033
atmospheric scintillation, optical and IR waves, simulation 77—82005
atmospheric vertical profile of refr. index turbulence, stellar scintillation meas. 77—45126
azoxy compound, liquid cryst. mixture, nematic, elec., optical and viscoelastic props. 79—55803
azoxy-4,4′(di-undecyl α-methyl cinnamate), refr. index at 2nd order smectic A to C phase transition 79—19357
4,4′-azoxyanisole, temp. depend. of refractive indices in nematic phase 79—47410
azoxybenzenes, nematic, refr. index, birefringence, internal field 78—34427
bacteria, scattering pattern analysis 78—80946
beer, lecture room demonstration 78—54128
benzene, magneto-optic rotatory dispersion curves 80—45040
benzene, refr. index temp. depend., deviation from Lorentz-Lorenz formula 77—40200
benzene liqs., refractive index, pressure effect 80—71375
benzene refractive index temp. depend., differential photoelectro-optical refractometer 77—40202
benzene-d_6, C-H vibr. states, thermal lensing spectra, local mode model test 77—71812
binary fluid, coexistence curve from refractive index obs. 77—32823
biological cells, light scatt., backscatter depend. on membrane thickness and refr. index 79—48225
4,4′-bis(heptyloxy)azoxybenzene, nematic liq. cryst., refractive index, density, orientational order 78—76419
4,4′-bis(hexyloxy)azoxybenzene, nematic liq. cryst., refractive index, density, orientational order 78—76419
bis(p-toluene sulphonate)diacetylene, fully and partially polymerised, optical props. 77—1696
borosilicate glass, phase-separated, refr. index. and density changes 77—66025
borosilicate glasses, gamma irradiation effect on density, refractive index, thermal expansion 80—79838
bromoform, refr. index, temp. depend., deviation from Lorentz-Lorenz formula 77—40200
buried 2D waveguide with asymm. graded refr. index profile, modal solns. 79—41431
p-n-butoxybenzoic acid, refr. index and orientational order parameter, temp. depend. 79—90537
N-(p-butoxybenzylidene)-p-pentylaniline, refr. index and density in nematic and isotropic phases 79—90538
t-butyl acetate, rot. isomerism, dielect. and Raman spectra 80—106328
tert-butyl alcohol in nonpolar solvents, liq. struct. from dielectric studies 80—38894
t-butyl formate, rot. isomerism, dielect. and Raman spectra 80—106328
butyloxybenzylidene octylaniline film, freely suspended, smectic A layer spacing, optical determ. 80—64883
cadmium arachidate monolayer, surface plasmon spectra, refractive index dispersion 78—64424
carbon disulphide, refr. index, temp. depend., deviation from Lorentz-Lorenz. formula 77—40200
carbon tetrachloride, optical props. under press., molecular polarisability depend. on thermodynamical state 78—80312
carbon tetrachloride, refr. index temp. depend., deviation from Lorentz-Lorenz formula 77—40200
carbonaceous hard insulating film, phys. props. 77—39752
carbonized bitumen, refractive index and absorpt. coeff. as measures of structural organization 79—35811

refractive index continued
CBOOA film, freely suspended, smectic A layer spacing, optical determ. 80—64883
CdS film, polycryst, optical spectra, 0.5-6.5 eV 80—55212
cellulose acetate, conc. soln., light scatt. studies 80—16050
ceramic, KO1, optical homogeneity in terms of refr. index 80—64125
chalcogenide glass, O free, refr. index, temp. coeff. 77—58403
chalcogenide glass Z 79—14063
chalcogenide glasses, atomic refractions determ. using optimum polynomial method 79—65828
chalcogenide glasses, O-free, cooling rate influence on optical consts. 80—88952
chalcopyrite crystal acousto-optical props. 79—46054
chalcopyrite crystals, refractive index, temp. depend., appl. to nonlinear devices 80—60555
chalcopyrite crystals, temp. depend. Sellmeier coeffs. and coherence lengths 79—76752
chalcopyrites, refr. index dispersion 80—55057
charged particle self-reson. motion in EM wave with varying propag. vel. 77—75399
chemical laser, low pressure, line-shape flattening resulting from hypersonic nozzle wedge flow 80—91783
Cherenkov radiation, variation of colour attenuation due to refr. index modifications *(Spanish)* 80—7432
chloroform, refr. index, temp. depend., deviation from Lorentz-Lorenz formula 77—40200
chloroplasts, in suspension, near IR radiation dispersion *(Russian)* 78—24045
cholesteric binary mixtures, composition and temp. depend. of pitch 78—1984
cholesteric films, absorpt. and contrast in dichroic liq. cryst. displays 80—75155
cholesteric liquid crystal, molecular polarisability, arrangement order calc. *(Polish)* 80—10495
cholesteric liquid crystal, normal incidence, boundaries effect 77—32345
cholesteric mixtures, optical props., temp. meas. *(German)* 77—44013
cholesteric-nematic mixture, striped domain structure, refr. index distrib. 77—24261
cholesterol esters, molecular-optical, and structural anisotropy 80—84056
cholesteryl esters, blue phase, model 80—88030
cholesteryl esters, isotropic mesophase, optical props. 79—65891
cholesteryl nonanoate, cyclohexanone admixture effect on mesophase order parameter, refr. index meas. 80—100165
cholesteryl pelargonate, optical dispersion 79—64990
coating, low reflection, three layer, spectral characts. computed 77—759
coating, refr. index calc. method refl. and transmission coeffs. 77—5890
complex, for Lorentzian-type absorption band 80—50291
complex diamond like crystals, optical nonlinearity and average refractive index 78—30011
COOB film, freely suspended, smectic A layer spacing, optical determ. 80—64883
corundum, growth of large crystals of high opt. quality 77—34916
critical binary mixtures, dielec. props., droplet model 79—69762
crystal density, liquid mixture, comment on simple method of measuring by determ. of refractive index 79—51014
crystal optical characteristics, relax. processes exciton dispersion 80—107709
crystal optics, spectral expansions of refr. index tensors 80—34873
crystalline optical material props., symmetries and tensorial relationships 80—108174
crystals, nonlinear refractive index coefficient at 1064 nm, meas. methods 79—3737
cubic symmetry cryst., quadrupole exciton theory 80—103632
curved graded index medium, aberration analysis 80—14295
CVD fabricated fibres, abrupt central dip 78—22217
4-cyan-phenyl esters of 4′-N-alkoxycinnamic acids, liq. cryst., refr. indices, optical anisotropy 79—28704
4-cyano-4′-n-pentylbiphenyl, refr. index meas. and isotropic-nematic phase transition study, surface plasmon technique 80—84282
cyanobiphenyl, nematic liq. cryst., refr. index, crit. angle meas. 78—60413
cyanobiphenyl nematic homologous series, Kerr consts., relax. times, refr. index, dielectric const. 79—19863
4-cyanophenyl esters, of 4′-n-alkylcinnamic acids, birefringence 79—64991
p-cyanophenyl p-n-alkylobenzoates, nematic, birefringence, polarisability and order parameter 80—100642
cyclohexane, refr. index, temp. depend., deviation from Lorentz-Lorenz formula 77—40200
cylindrical fibre with symmetric index distrib., matrix analysis 77—84001
cylindrical gradient index lens and array radiometric props. 80—14421
degenerate four-wave mixing, hysteresis and optical bistability 80—69446
degenerate four-wave mixing, refr. index changes 80—9936
demonstrations, refr. index-matching soln. for Pyrex 78—12519
density stratified turbulent liquid flows, refractive index variation elimination 79—77215
DH diode lasers, appl. of equivalent-index method 80—23772
DH lasers, phase and group indices 80—64016
di-(4-n-alkyloxy) benzoic esters, of hydroquinone series, effect of polar substituents on electro optical props. 79—46569
p,p′-di-n-alkoxy-azoxybenzenes, homologous cpds., nematic, refr. indices and opt. anisotropy, temp. depend., order parameters 77—16278
diallyl isophthalate-methyl methacrylate copolymer, light focusing rod prep. by copolymerisation, refractive index distrib. const. *(Japanese)* 79—46042
diamond, temp. and press. var. 78—27174
dichlorophenol isomers, elec. dipole moments determ. *(Spanish)* 77—69762
dielectic-semiconductor systems, immersion ellipsometric obs. *(Russian)* 79—15548
dielectric fibres, transversely incident beam wave scatt. 80—96004
dielectric films, refractive index and structure, deposition temp. depend. 79—4857
dielectric inhomogeneous medium, refractive index profile determ. from inverse scattering 78—58914
dielectric interference film, with equal optical thicknesses of layers, theoretical design *(Russian)* 80—43471
dielectric liquid, charge generation and transport from contacting surface, Mach-Zehnder and Schlieren obs. 80—20589
dielectric plate index profile determ. 79—7081

refractive index continued
dielectric response function, Kohn singularities near gapless state 80−59904
dielectric slab, spatial theory of dispersion, models 79−73891
dielectric slab waveguide, radiation pattern determ. due to refractive index fluctuations 78−22216
dielectric thin film stack, control by stationary ratio method, refractive index dispersion influence *(French)* 80−60693
dielectric thin films, refractive index variation for given reflectivity, analytic soln. to synthesis problem 80−34996
diethyl ether, refr. index, temp. depend., deviation from Lorentz-Lorenz formula 77−40200
diethylcarbonate, liq., alkoxy group internal torsion, extended microwave/far IR anal. 78−19457
differential mode delay rel. to refr. index profile, geometrical optics treatment 80−69529
diffused channel waveguides, mode dispersion by effective index method 77−27334
diffused optical waveguides, refractive-index profiles 79−7204
diffused waveguide, refractive index profile determ. by inverse scatt. theory 80−5838
p,p′-diheptylazobenzene, nematic, physical props. 78−79524
p-diiodobenzene, phase transition obs. using interferometry 78−34616
dimethylammonium cadmium tetrachloride, far IR refractive index, extinction coeff. and dichroism obs. 80−66144
dimethylcarbonate, liq., alkoxy group internal torsion, extended microwave/far IR anal. 78−19457
1,2-dimyristoyl-sn-glycero-3-phosphoserine multilayers, phase transitions, temp. depend., ellipsometric study 80−108846
1,4-dioxane, refr. index, temp. depend., deviation from Lorentz-Lorenz formula 77−40200
1,2-dipalmitoyl-sn-glycero-3-phosphocholine multilayers, phase transitions, temp. depend., ellipsometric study 80−108846
dispersion, possibility of highly transparent dielectrics 79−72635
dispersion energy consts., dipole oscill. strength sums, refractivity, for Li, N, O, H_2, N_2, O_2, NH_3, H_2O, NO, N_2O 77−50492
dispersion of opt. characts. in amplification range, freq. spectrum of stimulated emission, calcs. *(Russian)* 77−54757
dispersion staining, in IR and UV 80−76874
distributed Bragg reflector laser, tunability by modulating refractive index in corrugated waveguide 77−79866
DNA-cetavlate crystal growth and morphology 77−66583
n-dodecane liqs., refractive index, pressure effect 80−71375
Doppler-free two-photon dispersion problem 80−106562
double Gauss basic lenses, design *(German)* 80−53398
EBBA, nematic liq. cryst., refr. indices, densities, polarisabilities and mol. order 77−28536
education, refractive index, spatially varying, demonstration and theory 80−62425
elastooptical constants and refractive index, thermo-optical method for meas. 80−7327
electrolysis, solid-liquid mass transfer, meas. by holographic interferometry 79−87852
electrolyte containing $CuSO_4$ and H_2SO_4, cathodic diffusion layer, profile of refr. index 77−77774
electromagnetic wave scattering, physical model and profile reconstruction, for inhomogeneous ionised regions 80−1109
electrooptic deflectors, end effects rel. to operating quality 79−55223
elliptical fibres, near-field correction factor 80−87490
elliptical multimode fibres, leaky ray correction factors 80−87487
EM wave propagation in ionosphere, generalised differential eqn. 78−53770
EM wave propagation in stochastically stratified medium, transmission coeff. 80−32887
EMF air refractivity, variability w.r.t. temp. pressure and freq. 77−41112
emittance, directional, of semi-infinite scattering medium with refr. index >1 79−94471
empirical relationship for a nonlinear index coefficient 80−74445
empty space and scalar gravit. fields, Fresnel formula 77−30082
epoxy, clear, refr. index and extinction coeff. meas. 79−18492
ethane, gas, up to 50 atm, refr. index, 328, 3103 MHz *(French)* 78−14129
p(p-ethoxyphenyazo)phenyl undecylenate, nematic liq. cryst., refractive index, density, orientational order 78−76419
p(p-ethoxyphenylazo)phenyl heptanoate, nematic liq. cryst., refractive index, density, orientational order 78−76419
p(p-ethoxyphenylazo)phenyl hexanoate, nematic liq. cryst., refractive index, density, orientational order 78−76419
p(p-ethoxyphenylazo)phenyl valerate, nematic liq. cryst., refractive index, density, orientational order 78−76419
ethylene, imperfect gas contrib. to refractive index and quadrupole moment 78−55253
eye, role of spectacle in visual optics of snake eye 77−36917
famatinite crystals, optical nonlinearity 77−61996
Faraday rotation, intensity depend., nonlinear refr. index effect 77−77181
ferroelectric, photoinduced changes in refractive index and spontaneous polarisation 78−43804
ferroelectric crystal., optically induced refr. index changes, holography appls. 77−50742
ferroelectric material properties study, LF HV generator applic. *(French)* 77−41647
ferroelectric materials, refractive index variation, fluctuative mechanism *(Russian)* 79−56755
ferroelectric oxide crystals for electrooptics and nonlinear optics, optical inhomogeneities, review *(Japanese)* 77−65613
ferromagnet, refractive index, magnetic contribution 79−28727
ferromagnetic semiconductor, refr. index variation in strong alternating mag. field 80−23741
fibre, doubly clad, excitation by misaligned Gaussian beams 78−74972
fibre, gradient index, refr. index profile influence on transmission quality 78−42453
fibre, refractive profile distortion and dispersion, group delay calc. 78−55433
fibre, single-mode, effect of dip in refractive index on cut-off freq. 77−39029
fibre cable transmission performance in operational ducts *(German)* 78−33864
fibre lens, gradient index, radiometric props. 80−69481
refractive index continued
fibre lens, plastic focusing, change of ref. index profile during heat treatment process in fabricating 78−83091
fibre minimal dispersion refractive index profiles 79−98469
fibre with arbitrary refr. index profile, mode cutoff freqs. formula 79−55244
fibre-optic index-difference dispersion and bending loss/wavelength relationships 78−1367
film, optical consts. determ. 80−2883
film, optical inhomogeneity, rel. to struct. 79−83047
film inhomogeneity characterisation by refl. and refractive index changes *(French)* 77−73180
film pulsed laser damage determ., optical techniques 80−33060
filter, interference type, transmission band splitting elimination, oblique incidence 77−765
fingerprint deposit refractive index 78−78056
fluctuation spectrum in region of convection above heated surface *(Russian)* 77−9497
fluids, low gravity expts. on phase transition and critical phenomena 77−39658
fluoride coating materials, refractive index, spectroreflectometry meas. 250 to 2000 nm 79−32006
fluoride crystals, nonlinear refr. index, 1064 nm 78−30005
fluorocarbon polymer film, prep. by RF sputtering and plasma polymerisation, props. 77−55890
fluorophosphate glasses, rare-earth activated, luminesc., bonding 78−64415
fluorophosphate glasses with silicofluorides, optical props. 77−72040
fluorophosphate laser glasses, low nonlinear refr. index, development 78−50870
fly ash particles, water accretion, refract. index and accreted layer thickness 80−58462
formamide, liq., vac. UV optical and dielec. meas. 80−25329
1-formyl 2(4-nitrophenyl) hydrazine, preparation, optical and electrooptical props. 77−36201
freon 12, gas, up to 50 atm, refr. index, 328, 3103 MHz *(French)* 78−14129
Freon-113, correlative and optical props. near critical pt. 79−65822
Fresnel's relations in IR, verification and determ. of emissivity and compound index *(French)* 80−84309
garnet double layer prod. for magneto-optical devices, LPE 77−21043
garnet epitaxial film, physical thickness and refr. index meas. 77−77309
garnets films, containing Ca and Ge refr. index meas., 0.56-0.97 microns 77−52192
gas, mol. double resonance expts., off-reson. dispersion 77−58052
gas, up to 50 atm, refr. index, 328, 3103 MHz *(French)* 78−14129
gas, virial expansions for dielec. and refr. indices, rel. to collision-induced absorption bands 79−86547
gas complex refractive indices, dispersive Fourier transform spectrometry using modular interferometer 78−89567
gas parameter determ. using total internal reflection 77−58839
gases, compressed, refractive index meas. using Fabry-Perot interferometer *(French)* 80−14878
geodesic aspherical perfect lens, general sol. for integrated optics 80−10049
geodesic lenses, aberration-corrected rounded edge, profile calcs. 80−10048
glass:Nd, laser material, linear expansion coeff. and r.i., temp. depend. 77−733
glass, chem. tempered, surface stress meas. using opt. waveguide effect *(Japanese)* 80−45473
glass, equilib. thermodynamics, sp. ht., refr. index and glass transition *(German)* 78−83745
glass, freq. depend., use of dispersion formulae 79−65825
glass, homogeneity by Christiansen filter method 80−84066
glass, index inhomogeneity, rapid interferometric determ. 79−93207
glass, laser induced surface damage, free electron density meas. 77−40309
glass, optical, refractive index, oscillator strength effect *(Japanese)* 77−28538
glass, optical grade, refractive index-density relationship changes assoc. with reannealing 78−27175
glass, plate 79−28713
glass, refractive index during annealing, nonlinear structural relaxation model 78−44234
glass, refractive index freq. depend., dispersion enq. calc. 80−40083
glass, refractive index gradient, chromatic variation 80−74471
glass, refractive index gradients, form. using ion exchange diffusion 80−64227
glass, sheet, laminated struct., effect of prod. method 79−61555
glass, sheet, striation form. mechanism, luminous point method meas. 79−61751
glass, tempered, density and refractive index variation 78−64564
glass, thermally tempered sheet and plate, surface stress meas. using optical waveguide effect 80−25967
glass characteristics, electromagnetic, mechanical and thermal props. 80−106587
glass CVD fibres with axial refractive index dip, dispersion meas. *(German)* 78−33857
glass cylinder refractive index variation by field-assisted ion exchange 80−14500
glass fibres of graded index, optical communication light propag. props. 78−83106
glass film, SiO_2 rich, prepared by modified CVD, refr. index behaviour 78−60526
glass laser disc interface with edge cladding glass, reflection meas. 79−27300
glass optical waveguide fabrication by effusion 80−5850
glass planar optical waveguide fabricated by ion exchange, refr. index profile 80−14460
glass waveguide, ion-exchanged, r.i. profile 77−772
glasses, gradient composition, optical props. 80−88947
glasses, nonlinear refractive index coefficient at 1064 nm, meas. methods 79−3737
L(+) glutamic acid halogen acid salts, crystallographic, optical and calorimetric meas., halide effect 78−34505
glycerine, refractive index at X-ray wavelengths *(Russian)* 79−47409
graded fibres with non-circular index contours, core fields 80−14455
graded glass fibre, effect of shape of refractive index profile, on distortion 80−33197

refractive index continued
graded index fibre, low-loss, produced by double crucible technique 80−48449
graded index fibres made by vapour phase axial deposition, refr. index profile 80−48477
graded index planar lightguide, electrooptical diffraction 80−78995
graded index rod lens applications in optical fibre communications 80−14485
graded index single-mode fibres, spot size profile independent representation, determ. 79−50380
graded refractive index optical fibre process 79−76836
graded-index curved media, generalised Fresnel power transmission coefficients 80−102815
graded-index fibre differential mode attenuation meas. 78−1403
graded-index fibre transmission characteristic computation 80−1321
graded-index fibres, near-optimum, pulse broadening 79−7213
graded-index non-circular fibres, ray theory 79−55229
graded-index noncircular fibres, geometric optics analysis 79−55231
graded-index optical fibre, with near parabolic-index profiles, mode dispersion 79−76873
graded-index slab waveguide TE mode analysis 77−72087
gradient index fibre array, illumination intensity unevenness, theory and expt. 80−14480
gradient index fibre array, transmittance analysis 80−14478
gradient index fibre array development and imaging props. 80−14483
gradient index fibre array for photocopying machine 80−14482
gradient index fibre image intensifier system 80−14484
gradient index imaging lens and system status 80−14420
gradient index imaging system theory 80−14294
gradient index lens array fabrication for office photocopier 80−13178
gradient index lens fabrication by molecular stuffing 80−14499
gradient index material models and exptl. verification 80−16002
gradient index optical elements and system design 80−106594
gradient index optical imaging systems, topical meeting, Rochester, USA (May 1979) 80−12851
gradient index SELFOC lens, aberration improvement 80−14425
gradient index spherical lens design for selfcoupled optical pickup system 80−14427
gradient refractive index fibres, optical characts. 77−787
gradient-index imaging, theory 80−69331
gradient-index optics: a review 80−69478
graphite, reflectance meas. in visible spectrum 77−77241
gravitational waves, interaction with elastic body, RI *(Russian)* 77−2584
guided electro-optic structures, distributions 77−72068
gyrotropic media, artificial, EM scattering 80−106423
Hartmann interpolation equation for refractive index, TI-59 calculator program 79−98451
heavy water, 6-450 cm^{-1}, 19°C 78−6649
heavy water, optical consts., absorpt. and refr. index 0.1 Å-1 m 78−48139
heavy water, piezo- and elasto-optic props. under high press. 80−50296
heavy water, VUV reflectance, refr. index, absorpt. coeff., isotope effects 78−6695
heptafluoroiodopropane light amplifier, wave-front distortion due to photolysis-gas dynamic effects 79−18412
n-heptane, refractive index at X-ray wavelengths *(Russian)* 79−47409
n-heptane liqs., refractive index, pressure effect 80−71375
p-heptyl-p'-cyanobiphenyl, refractive index, dielec. const., mag. susceptibility, orientational ordering *(Dutch)* 80−33884
heptylcyanobiphenyl, nematic, surface and bulk order parameters, refr. index anisotropy 79−90522
n-hexane, high-press optical interferometric meas. to 14 kilobars 77−49764
n-hexane, optical props. under press., molecular polarisability depend. on thermodynamical state 78−80312
n-hexane, refractive index at X-ray wavelengths *(Russian)* 79−47409
n-hexane liqs., refractive index, pressure effect 80−71375
N-p-hexyloxybenzylidene-p-toluidine, optical props., density, and order parameter in liq. cryst. phases 79−55657
holographic storage, electro-optic crystals *(German)* 79−27198
ice, O-H and O-D bond stretching vibrs., Raman spectra at atmospheric press. 80−66166
II-VI semiconductors, mag. susceptibility, effect of physical parameters 80−44793
imaging plastic focusing fibre with parabolic refractive index distribution 77−19437
indandione-1,3 derivative, layer, electrooptical effect *(Russian)* 79−73900
index-matching fluids for long wavelength (1.2-1.6 micron) fibre-optic appls. 80−99841
inhomogeneous and randomly distributed media, diffracted amplitude and intensity, statistical models *(Spanish)* 80−48151
inhomogeneous dielectric material, light refl. by refr. index distrib. gradient 78−25800
inhomogeneous layer synthesis with given spectral characts. 78−52588
insulating film for semicond. devices, props., rel. to deposition conditions 78−23612
interference coating, theoretical design, with two narrow spectral transmission bands *(Russian)* 79−72666
interference coating, with narrow reflection bands, design *(Russian)* 80−43472
interpolation of data, collection of program library 80−55056
ion bombarded surfaces, rel. to spectral refl. changes 77−55308
ion exchange, field assisted, for production of graded-index optical materials 80−74447
ion implanted layers, complex refr. index profile, ellipsometric meas. 80−93262
ionosphere, refr. index determ. using GEOS-3/ATS-6 satellite-to-satellite tracking data 78−93039
IR laser window material refractive props., temp. depend. 79−14052
IR radiometer objective lens, optimal refr. index 78−29137
IR window materials, optical phenomena, book contrib. 78−9420
irradiated spheres, absorption centre distribution refractive index and size parameter dependence 79−50221
iso-octane, refr. index, temp. depend., deviation from Lorentz-Lorenz formula 77−40200
isobutyric-acid-H_2O, crit. fluid, refr. index, α and Δ components 79−82940
isotropic dielectric mirror theory 80−102797
refractive index continued
isotropic medium, nonlinear refr. index, self-induced polarisation rot. 80−5802
Langmuir-Blodgett films, lightguiding 80−79006
laser amplifier system, small-scale self-focusing 80−106580
laser beam, high power, focusing props., influence of nonlinear refractive index medium *(French)* 78−46696
laser beam refraction at spherical surface, distortion, geometrical optics calc. 80−95929
laser glass cladding composition and design criteria 79−18450
laser glasses, figures of merit and physical/optical property correlations 79−13970
laser window materials, optical suitability 77−58361
laser window materials, temp. and stress effects 77−46771
laser with inhomogeneous active medium, emission asymmetry 80−28191
layer with exponentially varying refr. index, oblique incidence of light, interf. matrix 78−55296
layergram iterative method for 3D ref. index distrib. reconstruction 79−54172
lens, graded index, design using refr. index reconstruction method 77−39013
lens, gradient-index rod, aberrations in multimode optical fibre devices 80−69487
lens, gradient-index rod, appl. in optical fibre communication systems 80−69488
lens, gradient-index rod, evaluation by imaging 80−69485
lens, gradient-index spherical, design for optical pickup systems 80−69483
lens, photographic gradient singlet, design techniques based on total aberrations 80−69479
lens, radial gradient-index, with zero Petzval aberration, third-order aberrations 80−69484
lenslike medium, mode degeneracy removal by x^2y^2 term in index distrib. 77−83812
Lexan, optical and phys. parameters 79−32004
lightguides, Maxwell's eqn., numerical soln., refractive indices 80−87520
lightpipe, helical, const. cross section, varying refr. index, radiation transport 77−65640
limestone, complete refr. index meas. in visible and IR 78−40541
$LiNbO_3$, stoichiometry effects 77−59549
linear optical transfer, three-dimensional, by holographic depth selection 77−10867
lipid bilayers, calc. from bond polarisabilities 77−29105
liquic crystals, orientational order parameter, optical birefr. meas., polarisation field problems 80−79688
liquid, cavity model, refr. index and density, permittivity *(French)* 79−78642
liquid, determ. from Raman-induced Kerr effect meas., 5500 Å 77−88874
liquid, of chiral mols., magnetorefractive effect, linear 80−25343
liquid, under high press., refr. index vs. density 79−28712
liquid, under high press., refr. index vs. press. and strain 79−33668
liquid binary acid+base mixtures, excess vol. and viscosity 77−21408
liquid complex refractive index, 5 to 500 cm^{-1}, Fourier transform interferometric determ. 77−13798
liquid crystal, refr. index anisotropy, meas. using different methods *(French)* 77−16274
liquid crystal, refractive index near smectic-A/smectic-C transition, orientational order 80−24572
liquid crystal cells, twisted, mol. orientation, refr. index and birefringence meas. 77−27818
liquid crystals, cylindrically aligned, optical characts., interferometric analysis 79−73897
liquid crystals, prep. and phys. props., book 80−105444
liquid crystals, pretransitional behaviour, nonlinear optical obs. 77−51483
liquid with absorbing particles, laser beam illum., refr. index change, bubbles form. 80−25334
liquids, anisotropic, light propag., intermol. correlation technique for mol. susceptibility tensor 77−58251
liquids, cargille PCB-free, refractive index 80−80741
liquids for cooling and index matching of Nd:glass laser systems 80−33015
lithium ammonium tartrate monohydrate, in paraelec. phase, Brillouin scatt. 78−64373
lithium formate, and deuterated parametric light scatt., refr. index dispersion 77−90150
low-aberration focusing fibre, optimum diffusion exchange and heat treatment 78−1378
low-V optical fibre with dip in refractive index, perturbation theory 79−37012
luminescence spectroscopy, refractive index correction, quantum efficiencies calc. 80−86444
2,6-lutidine-water, fluid film, crit. phenomena, scaling, law of corresponding states 79−90787
2,6-lutidine-water, fluid film, crit. temp. shift, crossover temp., coexistence curve amplitude, fluid-boundary interaction 79−90788
2,6-lutidine-water thick films, interferometric obs. of crit. behaviour 80−93266
magnetic dynamic susceptibility and refractive index under change of origin *(French)* 77−61890
magnetic gyrotropic absorbing crystals, refr. index tensors 77−8539
magneto-nonlocal fluids, optical properties 77−58840
magneto-optical linear and nonlinear effects, general system 77−52058
magnetosphere, VLF wave propag., bouncing period, plasma inhomogeneity effect 77−53319
matching fluids for long wavelength fibre-optic appl. 80−69470
MBAB, liq. cryst., Brillouin-Mandelshtam light scatt. and refr. index 80−55119
MBBA, anisotropic refr. indices from optical interference meas. 77−8538
MBBA, nematic liq. crys., refractive index distrib. and mol. alignment in electro-optical effect *(Japanese)* 80−20613
MBBA, nematic liq. cryst., ultrasound produced rolls, spatial coherence props. of scatt. light 78−75534
MBBA, refr. index, high press. meas. 78−26428
MBBA, refractive index, dielec. const., mag. susceptibility, orientational ordering *(Dutch)* 80−33884
medium-particle correlation effects in single scattering from particles in fluctuating medium 80−32917

refractive index continued
meta-toluylene-diamine, equal-deflection method, UV laser rad. 78−29145
metal, expt. methods, review 79−33655
metal, optical props., high-temp., from emissivity ang. depend. data 78−39519
metal film, optical props. as function of wavelength *(Russian)* 78−52591
metal oxide layers, obtained by cathode and HF sputtering, light scatt. and refr. index reduction 80−29877
metal-clad diffused optical waveguide propagation losses 77−84000
metallic thin film, refr. index for X-rays, elec. current density influence *(Spanish)* 79−78784
methane, gas, up to 50 atm, refr. index, 328, 3103 MHz *(French)* 78−14129
methane, liq., optical consts. meas. in IR, possible planetary cloud cover component 78−64341
methane, second refractivity virial coeff. direct determ. 77−15158
methane($-d_4$), liq., Brillouin scatt. and refr. index measurements 80−76035
methanol, refr. index, temp. depend., deviation from Lorentz-Lorenz formula 77−40200
methylene blue in methanol, concentrated solutions, calculation from dispersion of Nd laser radiation *(Russian)* 77−54753
3-methylpentane, refr. index, temp. depend. deviation from Lorentz-Lorenz formula 77−40200
microwave absorption coefficient and refractive index, optimal orthogonal functions 80−36379
mixed metal chloride acousto-optical props. *(Russian)* 78−60419
MNOS device, high temperature annealing, effect on Si_3N_4 stress, interface charge density and memory props. 79−87158
molecular polarizability, anisotropic, optical study *(Rumanian)* 80−74256
molecule embedded in dielec. spheroid, Raman and fluoresc. scatt. 80−99507
monochromatic coherent plane wave scatt. by living cell *(Russian)* 78−48765
Monsanto X-500 aromatic polyamide hydrazide soln., light scatt. study 80−76038
multi-layer optical system, reflection and transmission coeffs. calcs., computer program 80−66316
multicomponent optical glass fibre, profile synthesis 77−27333
multilayer, electric field distrib. and laser damage reduction 80−87420
multilayer dielectric mirrors, exam. of reflectance, optical thickness and refractive index 78−59106
multilayer dielectric waveguide, effective index nonlinearity 78−9446
multilayer multimode optical fibre, ray theory, optimal distrib. of refractive index 80−87489
multilayer oxide correcting coatings, u.v. transmission cutoff 77−760
multilayer superlattice stacks, very thin nonideal, wavelength variation of transmissivity, refl. 80−100701
multilayer synthesis computations, use of Fourier coeffs. 78−90509
multimode fibre bandwidth, calc. from refr. index profile meas. 80−5817
multimode fibre bandwidth spectrum, depend. on refr. index profile 80−9985
multimode optical fibres, optimum refr. index distrib., vector wave anal. 78−63183
multiple-α index profile analysis 79−50371
mutual diffusion coeff. determ. from refractive index gradient profile 77−30198
negative photoresist, KMR-747, transmission and refr. index 2 to 10 μm, interferometric meas. *(French)* 79−76780
nematic liquid crystal, diamagnetic susceptibility, refractive index, density and polarisability 77−15315
nematic liquid crystal, ZLI-207, electro-opt. props. *(Russian)* 77−43967
nematic liquid crystalline mixture, orientational order parameter calc. 77−24259
nematic liquid crystals, light transmission exam., positive and negative dielectric anisotropy 77−43141
nematic liquid crystals, refr. index, appl. to MBBA 77−51313
nematic liquid crystals, refractive index, order parameter, density 79−38513
nematic liquid crystals, refractive index and birefringence by interference method 80−96440
nematic liquid crystals, temp. dependent props., twisted nematic displays 79−32901
nematic liquid crysts. of mols. containing nitrile groups, dipole moments determ. 77−19872
nitrobenzene, oscill. optically induced Kerr kinetics 80−1286
nitrobenzene, refr. index, temp. depend., deviation from Lorentz-Lorenz. formula 77−40200
nitroethane, refr. index, temp. depend., deviation from Lorentz-Lorenz formula 77−40200
nitroethane-isooctane, crit. fluid, refr. index, α and Δ components 79−82940
nitroethane/iso-octane, crit. mixture, refractive index 79−87413
nitromethane-isooctane, liq. mixture, coexistence curve, refr. index meas. 80−10655
nonhomogeneous media, Fuchsian differential equations, aspects 78−9302
nonlinear optical crystals, SHG, absorpt. coeffs. and temp. variation of refr. index difference 80−14390
nonlinear optical uniaxial crystals, review and summary of data 77−75615
nonlinear refractive index n_2 of transparent dielectric crystals *(Chinese)* 80−45028
Novaya Zemlya effect, arctic mirage 79−80022
objectives, tolerancing of refr. index heterogeneity 80−78948
ocean, internal waves, acoustic refractive index modulation, parabolic moment eqns. 80−83698
ocean refractive index microstruct. from diffusive and turbulent ocean mixing 80−56486
oceanic hydrosols, refr. index and turbidity effects on solar radn. flux in atm.-ocean system 77−64303
n-octane, refractive index at X-ray wavelengths *(Russian)* 79−47409
n-octane liqs., refractive index, pressure effect 80−71375
4-n-octyl-4′-cyanobiphenyl, smectic A and nematic liq. cryst., refr. indices and order parameters 78−22644
N-p-octyloxybenzylidene-p-toluidine, optical props., density, and order parameter in liq. cryst. phases 79−55657
oligoethylene glycols, ref. index meas. 79−34375
refractive index continued
one-dimensional medium, propagation in periodic structs., theory 79−45892
optical coating, low reflection, continuously varying refr. index, transmission curves 78−25947
optical elements, refractive index gradient tolerance 78−71179
optical fibre, arbitrary index profile, formula for TE_{01} cutoff freq. 80−48418
optical fibre, elliptical step-index, tunnelling-radiating effect 80−58714
optical fibre, gamma irradiated, radii and refr. index changes 80−1338
optical fibre, graded index, intermodal dispersion meas. 80−38115
optical fibre, high bandwidth graded-index, propag. consts. meas. related to material props. 80−38103
optical fibre, low V-number, secondary maxima in far-field radiation pattern 80−33182
optical fibre, microbending eqns., exact time-dependent, soins. 80−87530
optical fibre, modal dispersion of power-law profiles with tails 80−95991
optical fibre, multimode, graded index, mode conversion coeff. meas. method 80−99820
optical fibre, parabolic index, selective excitation by Gaussian beams 80−95992
optical fibre, power-law graded-index, core/cladding power distrib., propag. const. and group delay 80−48420
optical fibre, power-law refractive index profile, scalar modal eigenvalues and group delays 80−28322
optical fibre, quasiparabolic index profile, propag. characts., perturbation anal. *(French)* 80−33189
optical fibre, rapid Δ meas. by refr. index tuning 78−13792
optical fibre, refractive index and radius ratio determ. from backscatt. light 78−30049
optical fibre, refractive index profile distortion, stress-induced 80−91889
optical fibre, single mode, dispersion characts., correlation between numerical prediction and meas. 80−91890
optical fibre, soliton pulse propag. 80−58759
optical fibre, step-index, nearly elliptical, with high eccentricity, fabrication for studying modes 80−95989
optical fibre, vapour-oxidation fabricated, refractive index modulation, pulse dispersion 80−58756
optical fibre, W-type, range of monomode operation, inner cladding refr. index effects 79−7212
optical fibre, weakly guiding, modes calc. by integral representation technique 80−58758
optical fibre array, gradient-index, appl. in copying machine 80−69500
optical fibre array, gradient-index, unevenness of illuminance 80−69482
optical fibre bandwidth change under production process and splicing *(German)* 78−33858
optical fibre coupling using graded-index rod lenses 80−91891
optical fibre refractive index change due to external forces 78−74971
optical fibre refractive index profile distortion due to thermal stresses 80−58726
optical fibre refractive index profile models 80−14453
optical fibre single mode characterisation by LP_{11} mode radiation pattern 80−23790
optical fibre waveguide, photosensitivity, appl. to refr. filter fabrication 78−63171
optical fibre with profile distortion, multimode delay compensation 80−33143
optical fibres, differential delay time relationship with propagation mode number study by effecting selective mode excitation *(Japanese)* 80−87504
optical fibres, graded-index, partially excited, pulse dispersion 77−11033
optical fibres, graded-index, propag. consts. and group delays 80−23770
optical fibres, leaky mode behaviour, with non-circularly refractive index profile 77−62045
optical fibres, multiple-α index profiles 79−46078
optical fibres, parallel-beam excitation method for estimating refractive-index profile 79−23062
optical fibres, piezo-optical effects due to thermal stresses 80−87519
optical fibres, profile synthesis using algorithm for inverse Sturm-Liouville problem 80−28351
optical fibres, refractive index profile, effect on fibre bandwidth 80−23773
optical fibres and preforms, modified CVD, axial refr. index depression, interf. microscopy obs. 80−1319
optical film, layered coating synthesis, optimisation formulae 78−25946
optical film, M-like refractive index distrib., light pulse dispersion 78−71225
optical film, non-homogeneous, oblique light incidence *(Russian)* 79−13905
optical film, production by RF cosputtering of dielectrics, and optical props. 78−6849
optical films, optical, struct. and mechanical properties 79−76772
optical glass, long range fluctuations, before and after annealing, light scatt. exam. 78−13772
optical glass, Raman scatt. and nonlinear refr. index 80−2749
optical glass, refr. index tables and calcs. for optical designer 80−83650
optical glass, refraction coeff., photothermal effects *(Polish)* 78−52465
optical glass, refractive index, effects of alkali oxide comp. changes *(Russian)* 78−22182
optical glass, thermally tempered, surface stress meas. by crit. ray method 80−106766
optical glass, TI-20, IR transmitting semicond., dn/dT, wavelength depend. 77−77163
optical glass homogeneity determ. using holographic interferometer 78−90401
optical glass under stress, refr. index based upon polarisation characts. *(Japanese)* 79−4781
optical glasses, development and manufacturing processes 80−53393
optical materials, at laser wavelengths, calc. methods 77−58400
optical solids, nonlinear refr. index, empirical relationships 78−83025
optical surface wave at a nonlinear interface 80−91867
optical system, cryogenic and contamination effects 80−38113
optical thin film, thickness monitoring 79−97358
optical waveguide, asymmetric dielectric-slab, beam mode scatt. characts. 80−38114
optical waveguide, diffused, refr. index profile determ., quick method 77−31130
optical waveguide, planar, refractive index distrib., fabrication methods 79−27429
optical waveguide, plane, form. by K^+ diffusion 79−90043

refractive index continued
optical waveguide, refractive index profile calc. from measured coupling angles 80−78954
optical waveguide, stress induced (embossed), refractive index profile obs. 77−14799
optical waveguides, multimode, step index limit of power law refr. index profiles 79−10387
optical waveguides with var. refr. index 78−46837
organic bases, biologically important, and derivatives, optical crystallographic props. 78−3449
organic compounds usable as solvents in laser saturable absorber, nonlinear refr. index meas. 80−102758
organic liquid, optical anisotropy, determ. from refr. index, Rayleigh's const. and depolarisation *(French)* 77−59548
organic liquid and branched-chain, temp. coeff. of refr. index *(Japanese)* 77−28537
organic liquids, relation between density and refractive index *(Japanese)* 79−24279
organic molecular crystals, optical anisotropies 80−50287
organic thin film refractive index adjustment by absorbing dyes 80−43413
oriented polyethylene film, deformation band studies 77−52420
orthorhombic crystal, birefr. and refr. index determ., refl. method 80−86380
oxide, porous transparent films as antirefl. coatings for glass surfaces, low refr. index 80−74448
oxide coating materials, refractive index, spectroreflectometry meas. 250 to 2000 nm 79−32006
oxide film, on Ti, optical consts. and thickness determ., ellipsometric method *(Russian)* 77−81164
PAA, refractive index, dielec. const., mag. susceptibility, orientational ordering *(Dutch)* 80−33884
PAA-PAP, nematic orientational order parameter calc. 77−24259
palmitic acid monolayer on water, characterisation by multiple wavelength ellipsometry 78−92136
parabolic gradient index lens, SELFOC, chromatic aberration in imaging system 80−14422
parathymol, negative uniaxial cryst., linear and nonlinear optical and dielec. props. 77−75602
particles in colloidal state, refr. index, theory 78−95567
PCB, nematic, smectic phases, dielec. and optical props. 78−60377
pentafluorobenzene, C-H vibr. states, thermal lensing spectra, local mode model test 77−71812
n-pentane, high-press. optical interferometric meas. to 14 kilobars 77−49764
n-pentane, optical props. under press., molecular polarisability depend. on thermodynamical state 78−80312
n-pentane, refractive index at X-ray wavelengths *(Russian)* 79−47409
4-n-pentyl-4′-cyanobiphenyl, nematic liq. cryst., refr. indices and order parameters 78−22644
4-n-pentyl-4′-cyanobiphenyl, refr. index, high press. meas. 78−26428
permalloy film, Fe-overcoated, optical and magneto-optical charact., mag. preps. 79−82956
perovskite and tungsten bronze cryst. struct. types, ionic grouping theory, electrooptical, nonlinear optical effects *(Chinese)* 78−52472
PET, biaxial orientation, refr. index meas. by Raman and IR spectrosc. 80−60583
petroleum samples, extinction coeff., refractive index meas., 0.25-25 microns 79−65818
petrols, optical consts. in 0.25 to 25 micron region, sea pollution detection appl. *(Russian)* 78−76976
phase form. and relations, phys. props. 79−43218
phase objects, refractive index distrib., holographic interferometry meas. 78−37846
phase transitions, ferroelectric and structural refractive indices and electro-optics 79−19850
phase velocity matching method *(Russian)* 78−30406
phosphate glasses, opt. and thermo-opt. props., calc. from chem. comp. 79−65826
phosphatidylcholine dispersion, phase transitions obs. with interference refractometer 78−44459
phosphosilicate films, deposited, P conc. meas. 79−69014
photocopier lens array design, Wood lens and gradient index fibre comparison 80−14479
photographic gradient singlet, total aberrations 80−13177
photoreceptor form dichroism in vertebrates 78−56969
photorefractive process sensitivity *(French)* 77−31124
planar diffused waveguides, refr. index distrib. function 79−55227
planar waveguide structure for integrated optics, props. *(Czech)* 80−96018
planar waveguides prepared by solid-state diffusion, refr. index distrib. function 79−10404
plane parallel optical layer interference props. for radiation parameters control 80−83547
plano-cylindrical Fresnel plastic lens, design and performance analysis as solar collector 80−53403
plasma, laser-induced modulation of refr. index 79−10668
plasma (fluid), hydrogenic, transverse dielec. function, excitation spectrum 78−67311
plasma polymerised ethane for laser window coatings 77−50737
plastic gradient index lens fabrication and image evaluation 80−14426
plastic rods, light focusing, prep. by two step copolymerisation of diallyl phthalate with methyl methacrylate *(Japanese)* 79−37064
Plexiglas 55, optical and phys. parameters 79−32004
PMMA, optical waveguide, direct writing of gratings by electron beam 79−46091
PMMA, piezobirefringence, optical and mech. relaxations, temp. depend. 80−34885
poly(p-phenylene terephthalamide) fibres, optical anisotropy determ. 79−4786
poly (alkyl cyano acrylate), sensitised with parabenzoquinone, holographic storage mechanism exam. 78−37850
poly-2-vinylpyridine, electron energy loss spectra, for optical and dielec. props. 79−15569
polydimethylsiloxane film, formed by RF discharge plasma polymerisation, optical props. 78−80479
polyethylene glycols, size exclusion chromatography, response correction of differential refractometer 79−34375
polyethylene terephthalate, isotropic and oriented, refr. index meas. 40 to 300 cm^{-1} 78−52482
polyethylene terephthalate film, deformation band studies 77−52420

refractive index continued
polyisoprene, in cyclohexane soln., conform. transition *(French)* 79−7542
polymer, total integrated light scatt. intensity 80−45092
polymer antireflection coatings of TiCl components 79−27346
polymer crystalline structure stability *(Russian)* 77−19880
polymer gel, quasielastic laser light scatt. theory 79−82986
polymer glasses, thermodynamics of densification process, refr. index, changes estimated 78−95723
polymeric films, solvent cast, optical anisotropy origin 80−20610
polystyrene, crazed, orientation and struct., optical meas. 80−30121
polystyrene, electron energy loss spectra, for optical and dielec. props. 79−15569
polystyrene, film, optical props. from near IR to X-ray, sum rules 77−48195
polystyrene, in trans-decalin soln. refr. index, temp. and conc. depend. 78−84547
polystyrene, n-heptane and methanol crazes, structure 77−12681
polystyrene, refr. index at 5461 angstroms, 30 to 260K 77−55764
polystyrene-collodion, tunable multilayer-film distributed-Bragg-reflector filter 79−76838
polystyrene-polyvinyl alcohol, tunable multilayer-film distributed-Bragg-reflector filter 79−76838
polysulfonamide, optically active, synthesised by interfacial polycondensation, mol. wt. determ. 80−99595
POPOP solution dye lasers, multiplate reflectors 80−83606
porous glass preform optical waveguide props. 79−94375
precision objectives, high resolution, image-forming quality *(German)* 78−87120
propane, refr. index and Lorentz-Lorenz functions, 944 cm^{-1} and 15803 to 22002 cm^{-1} 78−59543
N-(p-propoxybenzylidene)-p-pentylaniline, refr. index and density in nematic and isotropic phases 79−90538
proustites, natural and synthetic, refl., refr. indices and colour parameters, genetic interpretation 78−95566
PTFE, surface layer optical consts. in 1000-1300 cm^{-1} region 79−51957
PVC, magneto-electrets, refr. index, temp. and mag. field effects 78−6655
PVC, uniaxially stretched, mol. orientation, birefringence, effect of plasticizers, draw ratio 77−48500
pyrargyrites, natural and synthetic, refl., refr. indices and colour parameters, genetic interpretation 78−95566
pyrrhotite, complex refractive indices rel. to comp. of Saturn's rings 77−29716
quartz, cryst., far IR complex refr. index spectra determ., new method, for transparent solids 77−28566
quartz, cryst. and fused, far UV 77−81078
quartz, natural and synthetic, α-β transition, impurities effect, refr. index meas. 80−20928
quartz, pure, fused, optical consts. in far IR, 20 to 120 cm^{-1} 78−79080
quartz, synthetic, Ge doped, refr. index and α-β phase transition 78−83945
quartz, synthetic Fe-doped prisms, refr. index study of α-β transition 77−1225
quartz fused, refractive index distrib. normal to polished surface, ellipsometric meas. 79−86965
quartz glass, Ge and B dopants, OH impurities, preform material and fibre optic waveguide struct. 80−64173
radial refractive index gradient optical element, off-axis aberrations 80−14423
radiative source function, isotropically scatt. medium, refr. index effect 77−83805
radio refractivity diurnal variation up to 3 km over India 78−40627
radiowave propagation in troposphere waveguide, effect of elevated M-inversion 80−90195
rare earth aluminium borates, thermal stability, X-ray struct. anal., refractive indices 79−4297
rare earth germanates, R_2O_3-GeO_2 system cpds., physicochem. characts. 80−97469
rare earth molybdates, cryst. growth, cryst. chem., and phys. props., book contrib. 80−44194
rare earth oxide film, transmission of refl. spectra, opt. consts. and parameters 79−95864
rare earth oxide films, optical absorpt., refractive index, band gap and zone struct. *(Russian)* 78−76544
rare earth oxides, electron beam evap., optical and mech. props. 77−79907
rare earth oxyorthotitanates, crystallochem. classification 80−107142
rare earth RNb_3O_9, synthesis and physicochem. props. 77−90304
rare earth titanates, $R_2Ti_2O_7$, synthesis and phys. props. 79−43128
rare earth titanoniobates, $RTiNbO_6$, physicochem. investig. 77−47422
(rare-earth) $Fe_3(BO_3)_4$, cryst. growth from soln.-melt, props. 80−108337
ray paths, prescribed, rel. to refr. index distrib. 79−59633
ray paths in nonuniform axially symmetric medium 79−7076
ray tracing in general index distributions 80−14279
Rayleigh scattering, reson. enhancement in absorbing media, fluctuation theory 78−72533
reflectivity, quantitative meas., undergrad. lab. expt. 78−49624
refr. index calcs., 0.365-2.6μm spectral region 80−87444
refracted beam formation during light ray motion along optically homogeneous media interface 80−74298
RF sputtered glass optical waveguide, reduced SYNCANG method 77−11046
rhodamine 6G laser soln., freq. shift due to RI changes 77−7078
ring laser, rotating, medium refr. index effect on eigenfreq. splitting 79−98414
Rochelle salt, refractive index, dispersion and temp. depend. 77−16275
Rochelle salt, refractive index, X-ray radn. effect on dispersion and temp. depend. 78−72480
rod, tapered gradient-index, geometrical optics 80−69322
rod outer segment and interstitial matrix of rat, refr. index difference determ. using waveguide parameter 79−5277
rough interfaces, light reflection, scattering in homogeneous media *(French)* 79−50211
ruby cryst. R-line absorpt. and dispersion spectra, mag. field effects *(Russian)* 78−92056
saline environmental waters, IR relative reflectance and complex refr. index 77−45013
sapphire, shock compressed, refractive index, density, and polarisability behaviour 80−50295

refractive index continued
schlieren method for the determination of electric field distributions in dielectrics 80−31720
sea ice, initial forms, microwave refr. index and absorpt. 78−49036
seawater, optical anisotropy coeff., temp. fluctuation, optical meas. method 78−69488
seignette salt, refractive index temp. depend., differential photoelectro-optical refractometer 77−40202
self-filtering multilayer S-waveguides with absorption and radiation losses 80−38102
Selfoc lens, aberration improvement by glass composition and ion exchange process parameter choice 80−69486
Selfoc lens as imaging system, chromatic aberration 80−69480
semi-transparent film, optical cond., complex index and thickness, photometric meas. *(French)* 77−52193
semiconductor, Moss formula, refr. index rel. to energy gap 80−108173
semiconductor, nonlinear refractive index under many-photon resonance conditions 78−90449
semiconductor film, two-photon absorpt., optically induced diffr. 77−7154
semiconductors, forbidden gap width, relation to refractive index, single oscillator calcs. *(Russian)* 80−71372
semiconductors, mixed and binary, nonlinear polarisability, self-action effects 80−99786
semiconductors, Moss relation between refr. index and energy gap 80−11357
semiconductors, nonlinear effects, induced by lasers 79−94300
semiconductors with diamond and zinc-blende struct., refractive index dispersion 79−24280
semitransparent solids, approx. band model for radiative transfer 79−37136
silica binary comp. fibres, refr. index and profile dispersion meas. 77−19388
silicate glass, Li_2O and Na_2O effect on thermo-optic props. 78−18029
single mode and graded-index multimode fibre cable random bend losses 80−58741
single mode fibre near- and far-field characteristics, profile-independent representation 80−58739
single mode optical fibres, microbending loss evaluation, core index profile effects 80−48412
single-mode fibre with refr. index dip, wave propag. 78−63194
single-mode fibres, axial refr. index dip effect on zero total dispersion wavelength 80−78962
single-mode optical fibres with different B_2O_3-SiO_2 compositions 78−1392
six-level atomic medium, self-focusing of two intense monochromatic waves *(Russian)* 78−25932
slab waveguide, inhomogeneous step-index and WKB anal. 78−66923
smectic liquid crystal, C-phase, optical props. *(French)* 77−43959
smoke aerosol microstruct. and refr. index, optical determ., inversion method 80−36399
smoke aerosols, optical absorption to extinction ratio, photoacoustic determ. 80−58459
soda lime glass gradient index variation by ion exchange and migration 80−14412
solar selective film absorber, design improvements by refr. index grading 78−25976
solid, absorption band struct. resolution by using complex dielectric const. 78−72546
solid laser thermo-optic lens temp. distrib. and focal length calc. 79−72575
solid solns., phase equilibria, cryst. optical, X-ray struct. charact. 79−11577
space-time distribution of refractive index of air in Mongolia 78−81335
spheroidal particles, colloidal dispersions, refractive index 80−106454
sputtered films, optical props. and appls. 78−72623
stannite crystals, optical nonlinearity 77−61996
step index waveguide, effective index calc. method 78−50916
step-index fibres, multimode silicone-clad, mode dispersion 80−33142
structural phase transition induced refractive index changes in cryst. 80−16000
structure const., height depend., turbulent atmosphere 80−36397
submerged diffused waveguide prep., refr. index distrib. determ. 78−18068
surface anisotropy measurement by ellipsometry 78−56452
surface tension temp. dependence from triple point to critical point *(German)* 80−100376
tapered gradient index rod, geometrical optics and imaging props. 80−14280
teacing, lens object-image relations 78−36780
tellurite glasses, binary, struct. and props. *(Japanese)* 79−32917
ternary chalcopyrite bond orbital theories 77−55761
tetrachloromethane liqs., refractive index, pressure effect 80−71375
TGFB, dispersion and temp. depend. of refr. index *(Russian)* 77−66472
TGFB, refractive dispersion, absorpt. spectra characteristics 78−68469
TGS, dispersion and temp. depend. of refr. index *(Russian)* 77−66472
TGS, refractive dispersion, absorpt. spectra characteristics 78−68469
TGSe, refractive dispersion, absorpt. spectra characteristics 78−68469
thin films, optical constant volume and surface change separation, reflection, transmission *(Russian)* 80−66320
thin films, unbacked, optical constants by transmission interferometry 79−78778
thin layer, weakly absorbing, radiant absorption/transmittance ratio 79−11481
thin pigment films, by perturbed total internal refl. spectroscopy *(Russian)* 77−52197
thin-film multimode waveguides, higher order mode amplification 80−96012
three-level system, adiabatic following in two-photon transitions refr. index, line asymmetry 77−57956
toluene, refr. index temp. depend., deviation from Lorentz-Lorenz formula 77−40200
TOPOT vapour dye lasers with multiplate reflectors 80−83606
transients, laser-induced, low-temp. solns., excited triplet state polarisabilities role 79−87411
transition metal oxides, refractive index and extinction coeff. 79−78643
transparent optical material surfaces and films, pulsed laser induced damage 79−89948
trichloracetonitrile, IR dispersion, complex refractive index and permittivity, time correl. function 80−45057
refractive index continued
triethylamine-H_2O, crit. fluid, refr. index, α and Δ components 79−82940
trifluoroethyl methacrylate vinyl chlorobenzoate copolymer light focusing rod, photocopolymerisation temp. effect *(Japanese)* 79−46043
troilite, complex refractive indices rel. to comp. of Saturn's rings 77−29716
troposphere, over sea, refr. index statistical charact. *(Russian)* 78−65363
turbulence, Kolmogoroff's theory, high Reynold's no. model, laser beam atmospheric propag. 79−7368
turbulent water optical propag., refr. index spectrum of temp. or salinity fluctuations 79−5487
underground optical waveguide air refractive index thermal fluctuation obs. 78−9452
uniaxial crystals, refl. ellipsometry nonlinear eqn. inversion 80−95120
uniaxial film on nonabsorbing substrates, characterisation by multiple wavelength ellipsometry 78−92136
urea, single cryst., optical SHG, refr. index, susceptibility 78−63152
UV high-power laser material, refractive props. and optical constants 80−106555
van der Waals parameters determ. from liq. and soln. refractive indices 77−44609
vapour, radiatively cooled resonant, 3rd-order nonlinear optics processes 79−81477
Venus cloud particles, refr. indices from Pioneer Venus nephelometer expt. 79−48716
volume holograms in electrooptic crysts., dynamically produced refr. index variations 77−19195
water, 400-5000 cm^{-1}, 1, 16, 27, 39 and 50°C, rel. to intermol. struct. 77−66469
water, 6-450 cm^{-1}, 19°C 78−6649
water, IR spectrum, influence of Cu^{2+} ions 78−72501
water, low-density amorphous solid, IR spectrum, OH stretching region 79−11411
water, optical consts., absorpt. and refr. index 0.1 Å-1 m 78−48139
water, optical props. under press., molecular polarisability depend. on thermodynamical state 78−80312
water, refractive index, temp. depend., relationship to mol. polarisability 78−56448
water, transmittance in laser radiation field, effect of thermal defocusing *(Russian)* 79−1745
water, VUV reflectance, refr. index, absorpt. coeff., isotope effects 78−6695
water droplet aerosol interaction with EM radiation, temp. field and refractive index distrib. model 78−3899
waveguide, clad parabolic-index square-law dielectric, perturbation anal. 80−33190
waveguide, curved, with parabolic refr. index profile over cross section, light propag. 80−19104
waveguide, graded-index surface or buried, realized by ion exchange in glass 80−69499
waveguide, refractive index smoothly graded, near and far fields 79−72705
waveguide, variable refractive index, self-focusing 79−7208
waveguide, with refr. index varying over cross section, curved, light propag. 80−19103
waveguides, diffused glass, graded refractive index, anisotropy 80−33210
WKBJ method, deductions from artificial RI profiles, based on elementary functions 77−38778
zero Petzval curvature radial gradient index lens, third-order aberrations 80−14424
Ag, aggregated film, optical props., 0.35-1 μm 77−66548
Ag film, optical props., inverse problem of phenomenological theory 79−43053
Ag film, optical props. as function of wavelength *(Russian)* 78−52591
Ag_8GeTe_6, optical props. and polymorphism 80−45082
AgI large single crysts., gel and soln. growth and props. 80−35071
$AgNO_3$, molten, refr. index and molar refractivity 80−93265
(Al,Ga)As:Zn planar stripe lasers with deep Zn diffusion, guiding mechanisms controlled by impurity concs. 80−78853
AlAs-GaAs monolayered periodic cryst., optical props. 77−81079
AlF_3 based glasses, chem., thermal and optical props. *(French)* 80−70139
$Al_xGa_{1-x}As$ CSP laser, analytical waveguide study, effective refr. index differences 79−10302
$Al_xGa_{1-x}As$-GaAs multilayer heterostructures, optical birefringence 78−64422
$Al_xGa_{1-x}P$, solid solutions, refr. index dispersion charact. *(Russian)* 77−81080
AlN film, chemical and plasmachem. vapour deposition, optical and other props. 77−28727
AlN-Si_3N_4 CVD film preparation and props. 77−77408
Al_2O_3 anodic layer formation in H_3PO_4 solns., surface charact. 78−15603
Al_2O_3, composite film, barrier layer, ellipsometric meas. 78−67918
Al_2O_3, DC reactively sputtered, in MIS structs. optical and elec. props. 79−19486
Al_2O_3, film, CVD, props. rel. to deposition parameters 78−92197
Al_2O_3 film, determ. by Nomarski differential interference contrast microscopy 78−24849
Al_2O_3 film, RF sputtered by planar magnetron, phys. props. 77−43448
Al_2O_3, film form. by reactive HF sputtering with voltage bias 78−3045
Al_2O_3, molten particles, complex refractive index *(Russian)* 77−55766
Al_2O_3 optical waveguide, fabrication by reactive Al sputtering in O_2-Ar atm. 80−33262
Al_2O_3 porous transparent films as antirefl. coatings for glass surfaces, low refr. index 80−74448
Al_2O_3, transparent films on Al refr. index, thickness, ellipsometric meas. 77−52195
Al_2O_3-Al, multiphase thin films, correlation between optical props. and chemical/metallurgical constitution 78−19588
Al_2O_3-B_2O_3-P_2O_5 glasses, formation and props. 78−83737
Al_2O_3-Y_2O_3-SiO_2 containing TiO_2, La_2O_3, exam. of elastic moduli and refractive indices 78−80502
$Al(PO_3)_3$-BaF_2-Al_3 glasses, opt. props., group I-III fluorides effect 80−66143
$Al(PO_3)_3$-NaF-LiF glasses, mixed-alkali effect 80−19715
anthracene, polycrystalline, optical props., 3.2-9.3 eV 80−76097
Ar, dense plasma, complex refractive index 79−23397

refractive index continued
Ar, gas, liquid, solid, refractive index, density and dielectric const. 80−66138
Ar, meas. using low temp. refractometer 77−57382
As, amorphous, refr. index meas. near absorpt. edge 78−2819
As-Ge-Se based glasses, refr. index, 1-11 μm 78−39520
As-S, amorphous film, photoinduced RI changes, heterodyne interferometry 77−3639
As-S, melt struct., orientation birefr., viscosity, refr. index, and density 80−84713
As-S film, amorphous, photo-induced dynamical changes in refr. index 79−28705
As-S system glasses, photostruct. transforms. under laser radiation, use in holographic recording 77−76316
As-S-Se-Ge semiconducting glasses, IR characts. *(Czech)* 80−25332
As-Se and As_2S_3 films, electron-stimulated changes in optical props. and dissolution rate 80−29709
As-Se based glasses, refr. index, 1-11 μm 78−39520
As-Se chalcogenide glass, semicond. film, laser stimulated refr. index change, writing/erase cycle 77−50677
As-Se chalcogenide glass, optical const. photoinduced changes mechanism 80−7321
AsGe amorphous film, far IR absorpt. spectra, refractive index 80−80785
As_2O_5-$Rb_2O(Rb_2CO_3)$ system, phase diagram, polymorphic transform. 79−83181
As_2S_3 amorphous films, meas. of photoinduced transformations by optical waveguiding 79−43050
As_2S_3 evaporated film, optical props., depend. on light exposure and heat cycling 78−68572
As_2S_3 film, amorphous, opt. const. changes under illumination 77−77316
As_2S_3 film, amorphous, photo-induced dynamical changes 80−66142
As_2S_3 film optical constants, wedged-film meas. 79−14066
As_2S_3 glass, press. effect on optical props. 80−50363
As_xS_{100-x} amorphous film, composition depend. of photo-induced refr. index changes 79−78644
As_xS_{100-x} amorphous film, photoinduced changes in optical props. 80−50445
As_xS_{100-x} amorphous films, optical props. and photoinduced changes 80−60700
$As_2S_3(Se_3)$, film on KCl, strain-induced refractivity anisotropy, 10.6 μ ellipsometric obs. 79−14064
AsSe, relaxation of photoinduced refr. index changes *(Russian)* 78−23426
$As_{1-x}Se_x$, ave. energy gap, optical freq. dielec. const. and refr. index 77−76739
$As_{1-x}Se_x$ glass, refr. index comp. depend. and photo-induced variation 79−91398
As_2Se_3, IR window coating, prep. and optical props. 77−50736
$(As_2Se_3)_{1-x}(As_2Te_3)_x$ amorphous films, changes in optical props. under elec. fields and optical excitation 79−61455
Au, aggregated film, optical props., 0.35-1 μm 77−66548
Au film, obs. using automated Fourier-Stokes analyser ellipsometer system 78−49886
Au film, unsupported, simultaneous meas. of refractive index and thickness *(French)* 77−55842
Au, transmission interferometry, refr. index and extinction coeff. 77−69790
Au-Cu alloy, refr. index and absorpt. coeff., 1-5 eV *(Russian)* 78−60484
B films, amorphous, prep., struct., props., review, book contrib. 78−48321
B:H amorphous CVD films, IR, visible, and near UV optical props. 80−50442
BN film, undoped and P-doped, effect of CVD parameters on props. 80−25571
B_2O_3 glass, nonlinear structural relaxation model for glassy state 78−26448
$(Ba,Sr)Nb_2O_6$ monocrystal optical homogeneity requirement for light beam control 79−82952
Ba film, semitransparent, opt. props. in 2-5.6 eV range, electronic transitions, thickness depend. *(French)* 80−108289
$BaAl_{12}O_{19}$, refr. index and optical absorpt. 80−66139
BaB_2O_4-RF_2, R=Mg, Ca, Sr, Ba, glass form., struct. and props. 80−84077
$BaCa_2Mg[SiO_4]_2$, synthesis and struct. characterization 78−22698
$Ba_{15}Ca_{27-x}Nd_xAl_{31}Be_{27}F_{231+x}$, $0 \leq x < 8$, optical props. and vitreous domain 79−65820
BaF_2, 20-85°C, temp. depend. 77−8536
BaF_2 crystal, refr. index temp. increments meas. 80−33098
BaF_2, vol. depend. of refr. index 78−88275
$BaGeO_3$-(0.25MgF_2.0.75YF_3)-Ga_2O_3 glass, synthesis and props. 80−25648
$Ba(NO_2)_2.H_2O$, nonlinear optical props. and polariton scatt. spectra 77−75616
$Ba_2NaNb_5O_{15}$, electrooptic coeffs. and refractive indices 79−33673
$Ba_2NaNb_5O_{15}$, equal-deflection method, UV laser rad. 78−29145
$Ba_2NaNb_5O_{15}$, growth layer form., crystallization conditions effect, light diffr., Curie temp. 80−100778
BaO-Al_2O_3-GeO_2-MF_2 (M=0.45CaF_2+0.55MgF_2), MgF_2 and CaF_2 effect on physicochem. props. 80−34876
BaO-B_2O_3, composition effects on mean dispersion 78−80313
BaO-B_2O_3 glass, refraction, refractive index from 0.365 to 2.50 μm 80−88953
BaO-B_2O_3-GeO_2, exam. of glass formation and physicochemical props. 79−4959
BaO-La_2O_3-B_2O_3, glass, refraction, refractive index from 0.365 to 2.50 μm 80−88953
BaO-PbO-GeO_2-MF_2 (M=0.45CaF_2+0.55MgF_2), MgF_2 and CaF_2 effect on physicochem. props. 80−34876
$BaPO_3F$-Al_2O_3-B_2O_3 glasses, phys. props. 78−63676
$BaR_2(MoO_4)_4$, R=rare-earth, struct., optical, mech., spectral and physicochem. props. 80−84161
$BaTiO_3$, dielec. and optical props. using shell model 79−33654
$BaTiO_3$ film, sputtered, refr. index, 0.3-1.0 μm, substrate temp. effects 77−55840
$BaTiO_3$ type vibronic ferroelectric, light induced refractive index change *(Russian)* 79−91399
$Ba_2TiSi_2O_8$, fresnoite, Czochralski growth and phys. props. 78−3026
$BaWO_4$, single crystals having scheelite struct. 78−79082
refractive index continued
BeF_2 glass, nonlinear refr. index, meas. of electronic and nucl. contribs. 78−50866
Bi film, optical props., inverse problem of phenomenological theory 79−43053
Bi film, optical props. as function of wavelength *(Russian)* 78−52591
Bi film, refractive index determ. using Rayleigh-Lowe refractometer 80−7427
$Bi_{12}GeO_{20}$ monocrystal optical homogeneity requirement for light beam control 79−82952
BiI_3 film, exciton-phonon interaction, optical consts., Faraday effect., permitt. 80−59884
Bi_2O_3 film, wavelength depend., transmission spectra obs. 78−76440
α-Bi_2O_3, single cryst. growth and refractive indices 77−21018
$Bi_{1-x}Sb_x$, far IR transmittance meas. *(Russian)* 77−44006
Bi_2Si_3, cryst., RI anisotropy obs., polarised light effects 77−12354
$Bi_{12}SiO_{20}$ monocrystal optical homogeneity requirement for light beam control 79−82952
$Bi_xSi_yO_z$ films on Si, form. kinetics and props. 80−35358
$Bi_2(Te_{1-x}S_x)_3$ film, optical consts. meas., Shamir-Graff method evaluation 80−11489
C, arc evap. film, optical props., 0.6-3.8 eV 77−81166
C, colloidal, refractive index determ. 79−66363
C, film with random struct. growth from ion impact damage in butane plasma 79−83139
C films with high conductivity, prep. and props. 80−80983
C sphere aerosol, black smoke opacity, calc. variation with particle size and refr. index 79−72488
C, vapour-deposited, transparent and hard insulating layer, struct. and props. 80−10830
CC GaAs, n- and p-types, optical consts., 2.5-3.5 eV, normal incidence reflectance meas. 79−15428
CO, liq., refr. index meas. by interferommetric technique 79−65816
CO_2 CW laser radiation, freq. conversion in Tl-Cs vapour mixture 80−74438
CO_2 ice spheres, IR scatt. and absorpt. props. 80−97269
CO_2, refr. index and Lorentz-Lorenz functions, 944 cm^{-1} and 15803 to 22002 cm^{-1} 78−59543
CO_2 refractive index meas., intermolecular interaction effects 80−33728
CO_2, solid, IR spectra and refr. index, Martian implications 80−72821
COS, density and refractive index, volumetric meas. by Burnett method 80−29707
CS_2, intensity dependent total refl., ps pulses 77−14781
CS_2, liq., struct. and equilib. optical props. 80−45026
CS_2-glass boundary, optical bistability at nonlinear interface 80−33094
Ca, optical props., 2-11 eV 78−15191
$Ca_2Al_2GeO_7$, gehlenite struct., synthesis and physicochem. props. 79−43181
$CaCO_3$, Iceland spar natural crystals, optical characts. 77−10988
$CaCeAl_3O_7$, melilite struct., prep. and props. 80−93524
$CaEuGa_3O_7$, synthesis, mechanism and kinetics, cryst. props. 77−52268
CaF_2, 20-85°C, temp. depend. 77−8536
CaF_2, hot forged, refr. index, temp. coeff. 77−46772
CaF_2, surface, adsorption of water, IR internal reflection spectra 79−77920
CaF_2, vol. depend. of refr. index 78−88275
CaF_2-Ge(Si), cosputtered composite semiconductors, selective solar energy absorbers 79−56876
$CaLn_4(SiO_4)_3O$ silicate oxyapatites, prep. and props. of single crystals 77−28704
$CaMoO_4$, single crystals having scheelite struct. 78−79082
CaO-B_2O_3-GeO_2 system glass, physicochem. props., alkaline earth oxides effect 79−65827
CaO-Ga_2O_3-Bi_2O_3, vitrification regions 77−15557
Ca_2SiO_4-MgO, conditions and mechanism in cryst.-chemical stabilisation of unstable phases 80−39302
$CaTaRO_6$, (R=La, Nd, Gd, Sm, Er, Lu), synthesis and physicochem. props. 79−52139
$Ca_3(VO_4)_2$, linear and nonlinear optical props. 79−23010
$CaWO_4$, single crystals having scheelite struct. 78−79082
$CaZrO_3$-$CaHfO_3$, solid soln. formation obs. 77−86003
Cd, gas, refraction, determ. by phase vel. matching method *(Russian)* 78−30406
Cd_3As_2 film, cryst. and amorphous 78−11013
$CdCl_2$:Cu, optical props. 78−43918
$CdCr_2Se_4$, refr. index variation in strong alternating mag. field 80−23741
$CdGeP_2$ thermo-optic coefficient, dispersion 80−71396
$CdInGaS_4$, layered structure crystals, refractive index meas. method 80−98966
CdLn(TiNb)O_7, Ln=La-Lu, synthesis physicochem. props. 77−43186
$CdMoO_4$, single crystals having scheelite struct. 78−79082
CdS, exciton condensation effects on refr. index 77−20818
CdS, excitonic polariton reflectance, quantitative anal. in spectral range of A-exciton 79−15480
CdS film, ellipsometry of natural boundaries *(Russian)* 79−4866
CdS, nonlinear refr. index coeffs. meas. by nonlinear refraction method *(Russian)* 78−79066
CdS, nonlinear refr. index meas. by nonlinear lens method *(Russian)* 79−26111
CdS, optical props., spatial dispersion effect *(Russian)* 79−61404
CdS, optically controlled range of refr. index 78−6650
CdS plane parallel slab, optical const. determ. methods 80−60531
CdS, spatial dispersion effects, exciton decay const. depend. *(Russian)* 78−72086
CdS, temp. coeffs. meas. of refr. index and birefr. 77−55762
CdS thermo-optic coefficient, dispersion 80−71396
CdS, thermoreflectance spectra, additional boundary conditions in terms of optical constants 79−15478
CdS, vol. depend. of refr. index 78−88275
CdS:Li film, optical props. 80−2886
$CdS_{1-x}Se_x$ gradient cryst., pseudointersection of dispersion curves n_o (λ) and n_e (λ) 79−15487
CdSe, temp. depend. phase-matched nonlinear optical devices 80−99794
CdSe thermo-optic coefficient, dispersion 80−71396
CdSe, undoped and Cr doped, far IR transmission and reflectance spectra 80−71429
CdTe, cryogenic refractive indices and temp. coeffs. meas. 80−7319
CdTe crystal, 10.6 μm ellipsometric meas. 78−24847
CdTe, IR transmitting semicond., dn/dT, wavelength depend. 77−77163
CdTe, temp. depend. Sellmeier coeffs. SHG coherence length 77−69789

refractive index continued
$CdTiO_3$, refl. and absorpt. coeffs. 3-3.5 eV, and refr. index dispersion *(Russian)* 78−39561
$Ce_2(SO_4)_3.9H_2O$, grown from solution, exam. of Raman spectra and physical props. 79−52104
CeSb, forbidden band gap and electrotransfer parameters 80−39497
Co-Gd(Tb)(Sm) film, magneto-optic coeff. and refr. index, ellipsometric determ. 80−71501
Co-Si interface, glassy layer, ellipsometric charact. 80−103589
$Co_{1-x}Ni_xSi$, IR refl. spectra in plasma refl. region 78−27233
CoSi, IR refl. spectra in plasma refl. region 78−27233
CsBr, cryogenic temp. IR refractive index obs. 80−7320
$CsCaCl_3$, optical charact. over wide spectral range 80−34875
$CsCuCl_3$, optical props. rel. to IR electro-optical modulator appl. 78−42393
$CsCuCl_3$, phase transition, refr. index, electrooptic coeff., pyroelec. signal, and NQR meas. 80−70386
$CsCuCl_3$, phys. props. 77−62511
CsI, cryogenic temp. IR refractive index obs. 80−7320
CsI, far-IR optical props., shell-model calcs. 77−28557
CsI, optical props. in vacuum UV 77−24861
CsN_3, polycryst., IR active lattice vibr., optical consts. 77−77185
$Cs_2NaBiCl_6$, optical, photoelastic, acoustooptic props. 80−55064
$Cs_8Nb_{22}O_{59}$, melt growth and struct., dielec. and optical characterisation 78−35294
$CsPbCl_3$, refr. index and birefr., struct. transition effects 77−90126
$CsSrCl_3$, refr. index and birefr., struct. transition effects 77−90126
Cu, aggregated film, optical props., 0.35-1 μm 77−66548
Cu film, electron energy loss spectra meas., optical functions calc. 78−19618
Cu, nearly ideal surface, optical consts., 5461 and 6328 Å 77−36192
Cu-Al film, electron energy loss spectra meas., optical functions calc. 78−19618
$Cu-Cu_xO$ film, numerical anal. of normal reflect. data 79−99457
$CuGaS_2$ thermo-optic coefficient, dispersion 80−71396
$CuGaTe_2$, refr. indices meas. 80−93259
$CuInSe_2$, influence of impurities and free carriers on optical props. 80−108225
$CuInSe_2$, refr. indices meas. 80−93259
$CuInTe_2$, refr. indices meas. 80−93259
CuO film, electron energy loss spectra meas., optical functions calc. 78−19618
Cu_2O film, electron energy loss spectra meas., optical functions calc. 78−19618
Cu_2O film, reactively-sputtered, phase comp., resist. and optical consts. 79−95534
Cu_2S, polycryst. thin films, struct., optical and elect. props. for solar energy appl. 80−10837
Cu_xS, layers produced by reactive RF sputtering, struct., elec. and optical props. 79−90908
$CuSO_4$, single cryst., IR optical consts., comparison with soln. 77−66470
DF laser, refr. index changes during stimulated emission 78−17929
D_2O, IR spectral refl. and complex index of refr. 78−68501
$DyAsO_4$, cooperative Jahn-Teller transition, optical study 80−15240
$DyAsO_4$, first order Jahn-Teller phase transition, sp. ht. and refr. index meas. 80−59645
$DyAsO_4$, phase transitions obs. 80−70412
$Dy_2(MoO_4)_3$, cryst. growth and props. 79−55727
$DyVO_4$, cooperative Jahn-Teller transition, optical study 80−15240
$DyVO_4$, phase transitions obs. 80−70412
$Er_2O_3-TiO_2-WO_3-PbO$, glass form., refr. indices and density meas. 77−90312
Eu complex, benzoyltrifluoro-acetone-chelate, refr. index determ. of fluoresc. films 80−40175
$EuS-Ga_2S_3-GeS_2$, chalcogenide glasses, conditions of form. of glassy prod. *(French)* 80−100325
Fe-Al (45%), ordered and disordered states, optical and elec. props. 77−85826
Fe-Gd(Tb) film, magneto-optic coeff. and refr. index, ellipsometric determ. 80−71501
Fe-Ni alloy, optical and electronic charact., 20-1750°C, comp. depend. *(Russian)* 78−84601
Fe-Si alloys, liq., refractive index, absorpt. coeff., elec. cond. 78−43830
$Fe_{1-x}B_x$ film, optical and magneto-optical charact., mag. preps. 79−82956
Fe_3BO_6, orthorhombic cryst., birefr. and refr. index determ., refl. method 80−86380
$FeCl_2$, antiferromag. and paramag. states, rel. to light scatt. in mixed state 77−40069
Fe_2O_3 sputtered films, optical transmission and reflection spectra depend. on substrate temp. 79−91517
$Fe_2O_3-B2O_3-PbO$ glasses, visible and UV optical props. *(Rumanian)* 78−48196
$Fe_{1-x}Si_x$ film, optical and magneto-optical charact., mag. preps. 79−82956
$Ga_{1-x}Al_xAs$, anodic oxide films, ellipsometric anal. 79−20234
$Ga_{1-x}Al_xAs$ LPE layers, comp. and refr. index, ellipsometry meas. 79−87011
GaAs amorphous film, EXAFS, optical and elec. props. 80−49547
GaAs anodic oxide, refl. and transmission, 0.01-6 eV 78−95613
GaAs anodic oxide, refr. index meas., Sellmeier eqn. 77−12454
GaAs anodic oxide film, optical props. 78−72626
GaAs anodic oxide film growth obs. by in situ differential refl. 80−50732
GaAs, anodisation at low substrate temp. by low pressure O_2 plasma 80−104314
n-GaAs, crystal growth by Czochralski method kinetics, total emittance determ. 80−75193
GaAs, electron beam pumped laser, far-field radiation pattern, optical confinement effects 79−86181
GaAs, high-energy ion layer implanted, layer thickness and refr. indices meas. 77−24837
GaAs, ion-implantation induced damage profile, ellipsometric study, annealing 80−103400
GaAs laser, refractive-index profile and resonant modes 79−86179
GaAs, nonlinear refractive index dispersion at helium temp. 78−2820
GaAs, optical conductivity, constants, refractivity from IR absorption spectra 78−43873
GaAs, optical inhomogeneity, physical basis 79−15430
GaAs oxide, anodic, 1.5-6.0 eV 77−90209
refractive index continued
GaAs oxide, anodic, heat treatment temp. effects, optical props. obs. 78−27658
GaAs oxide, anodic, optical props., 1.5-6.0 eV 77−90209
GaAs, refr. index and induced birefringence dispersion 80−2717
GaAs:Cr, ion implanted, implantation damage profiles, laser annealing, ellipsometry study 80−79819
$GaAs:P^+$, ion-implanted, refr. index, IR reflection and transmission meas. 77−1671
$GaAs-Ga_{1-x}Al_xAs$ stripe geometry lasers 79−94245
$GaAs_{1-x}P_x$, anodic oxide films, ellipsometric anal. 79−20234
GaInAs, electron-pumped laser, far-field radiation pattern, optical confinement effects 79−86181
$Ga_{1-x}In_xAs$, VPE grown, refractive index, reflectance meas. 79−4780
GaInAsP DH laser emitting at 1.55 μm, threshold currents 80−83609
$Ga_xIn_{1-x}P$, refractive index comp. depend., nonlinearity parameter *(German)* 77−32344
GaP amorphous film, EXAFS, optical and elec. props. 80−49547
GaP, dispersion of refr. index and permittivity 77−55765
GaP, effects of hydrogen incorporation during deposition by sputtering 79−69981
GaP, high-energy ion-implanted, layer thickness and refr. indices meas. 77−24837
GaP, ion-implanted, radiation damage, ellipsometry expts. 78−38735
GaP, optical inhomogeneity, physical basis 79−15430
GaP oxide, anodic, 1.5-6.0 eV 77−90209
GaP oxide, anodic, optical props., 1.5-6.0 eV 77−90209
GaP, refr. index, 100 to 420K, permittivity calcs. *(Russian)* 77−90156
GaP_xAs_{1-x}, refractive index comp. depend., nonlinearity parameter *(German)* 77−32344
GaS, refr. index in far IR, permitt. meas. 78−64360
GaS, refr. index meas. 78−10864
Ga_2S_3 glass *(French)* 80−71369
GaS(Se), birefringent layer cryst., indices of refraction 77−20815
GaSb oxide, anodic, 1.5-6.0 eV 77−90209
GaSb oxide, anodic, optical props., 1.5-6.0 eV 77−90209
GaSe, optical consts. at fundamental absorpt. edge 77−66471
GaSe, refr. index 0.45 to 330 μm, interf. and refl. meas. methods 77−63387
GaSe, refr. index meas., temp. variation 300 to 75K 80−25328
GaSe, refr. index meas. 78−10864
GaSe, single cryst., dispersion of refr. indices and exciton absorption 79−73947
GaSe, thin layers, far IR refractive index 80−80799
Gd, optical consts. polarimetric meas., mag. ordering effects 78−15184
$Gd_3Ga_5O_{12}$ monocrystal optical homogeneity requirement for light beam control 79−82952
$Gd_3Ga_5O_{12}$, opt. dispersion 78−64343
$Gd_2(MoO_4)_3$, effect of ferroelec. ordering on refractive index 79−33653
$Gd_2(MoO_4)_3$, ferroic, linear and nonlinear optical susceptibility 78−22164
Ge, 95-298K, 2.5-12 μ 77−8535
Ge, anisotropic oxidation ellipsometry meas. *(Russian)* 79−43451
Ge, far IR photon drag and radiation pressure in refractive media 80−60048
Ge film, A1-type and amorphous, complex refractive index and reflectance 77−52121
Ge, monocryst., for IR optics, prod. techniques and charact. 78−50873
Ge, photoelastic consts. determ. 78−68474
Ge, refr. index and refl. changes due to intense laser irrad., surface heating effect 78−42372
Ge, Sellmeier coeffs. temp. depend., nonlinear optics average power limit 79−50349
Ge single cryst. prism, refr. index meas., interlaboratory comparison 78−54443
Ge surface, atomically pure, optical consts. and temp. depends. 79−65823
Ge-As-Se IR transmitting glass composition, prep. and props. 80−69474
Ge-S-In, chalcogenide glass, refractive index using immersion method 79−23526
Ge-S-Se system, glass-forming, struct. and props. 80−19713
Ge-Se based glasses, refr. index, 1-11 μm 78−39520
Ge-Se glass system, effect of changes in local surrounding of atoms on optical props. *(Russian)* 78−80414
Ge-Te alloy films, amorphous, semicond. props., refr. index, struct. study 78−26978
GeH_4, Lorenz-Lorentz coeff., refr. index, crit. consts. and density depend. 78−92041
GeO amorphous semicond. films, photostructural changes by photomodulation ellipsometry 79−71510
GeO film, optical props., rel. to possible appl. in holography 80−29816
$GeO_2.B_2O_3.SiO_2$ glasses, material and mode dispersion 77−19415
GeS, thin layer cryst., far IR transmission spectra 79−56870
GeS_x glass, chem. struct. effects 77−63460
$GeSe_2$ amorphous film, laser induced oscillatory phenomena 80−84711
$Ge_{1-x}Se_x$, ave. energy gap, optical freq. dielec. const. and refr. index 77−76739
$Ge_{1-x}Se_x$ glass, refr. index comp. depend. and photo-induced variation 79−91398
GeSi alloy, composition determ. by ellipsometry 79−83537
$Ge_{0.5}Sn_{0.5}Te$ film, elec. and optical props. 77−12028
H_2, gas, refractivity and dispersion in visible and IR regions 78−34258
H_2, refractive props. due to SRS *(Russian)* 77−88865
H_2, solid, high pressure phase, 57 kbar, 25°C, transparent crystalline mass 79−55870
HF, IR dispersion, refractive index meas., vibr.-rot. fundamental intensities, dipole moment 79−37441
HFO_2, vacuum deposited film, use in multilayer reflector for near UV 77−34924
HFO_2-SiO_2, layer for dielectric mirror, for KrF excimer laser *(Japanese)* 79−72588
H_2I_2, crysts., growth, optical props. *(German)* 77−77167
HNO_3, aqueous soln., reflectance and complex refractive index, IR spectra, vibr. modes 80−66168
H_2O, liquid, far IR optical consts. meas. with optically pumped laser 80−40082
H_2O, vap., optical refractivity, comparison of expt. with sum rule moment calcs. 78−5156
H_2O vapour, refr. index calc. and dispersive Fourier transform spectrometry 79−32736
H_2O vapour and liquid far IR spectroscopy 80−60610

refractive index continued
H_2O+HDO, isotope exchange in liq.-vapour system, r.i. and thermal cond. obs. *(German)* 77−4902
H_2SO_4 soln., opt. consts. in far IR 77−8574
He, liq. and vapour phases, thermodynamic and thermophysical props. calc. using HEPROP computer program 80−6529
HfO_2 film, CVD growth, struct., elec. and optical prop. characterisation 77−55891
HfO_2 single crystals, Y_2O_3 stabilised, optical props., impurities and annealing conditions influence 79−52399
HfO_2, vac. deposited, near UV multilayer reflector 77−39014
HfO_2-CeO_2, solid solutions 77−16549
HfO_2-La_2O_3 system, phase form. and relations, phys. props. 79−43218
Hg drop, optical consts. meas. from Hg-air interface, ellipsometry at spherical object 79−61326
Hg-As-S-I system, glasses, optical and acousto-optical props. 78−83053
Hg_2Br_2, crysts., growth, optical props. *(German)* 77−77167
$Hg_{1-x}Cd_xSe$, IR absorpt. spectra, band struct., refr. index 80−50337
$Hg_{1-x}Cd_xTe$, anodic oxide films, formation and props. 80−3212
$Hg_{1-x}Cd_xTe$, IR optical absorpt. and refr. index, 80 to 300K 79−91418
Hg_2Cl_2, cryst., birefringence and dichroism, 200-500 nm and far IR 78−27257
Hg_2Cl_2, ferroelastic transition, refr. index, 80 to 300K 79−82941
$HgGa_2S_4$, melt growth, optical props. and SHG, HgS-$HgGa_2S_4$ phase diagram 80−50548
HgSe(Te), dynamic dielectric function, IR absorpt. meas. 78−68508
$Ho_{2x}Gd_{2(1-x)}(MoO_4)_3$, ferroic, linear and nonlinear optical susceptibility 78−22164
I flashlamp pumped photodissociation laser characts., local optical inhomogeneities 80−53284
I, iodoseptofluoropropane photodissoc. laser, refr. index distrib. fields, double exposure holography 80−9873
InGaAsP, anodic oxidation, refractive indices 80−97601
InGaAsP-InP DH lasers, threshold characteristic 79−81430
InGaAsP-InP DH laser with self-aligned struct., oscillation characts. 80−38017
$In_{0.84}Ga_{0.16}As_{0.46}P_{0.54}$, at laser oscillating wavelength of 1.2 μm 79−64224
$In_{1-x}Ga_xP_{1-z}As_z$ DH laser, effective index of refr., wavelength depend. 77−61954
In_2O_3, elec. conducting film on glass substrate, measurement of optical constants and thickness 78−60525
In_2O_3, thin film, sputter deposition form., optical and elec. props. 80−60123
In_2O_3:Sn films, RF reactive sputtered, optical props. rel. to band struct. 79−91515
In_2O_3-SnO_2 film, stress, and elec. and optical props. 78−51861
InSb, anode oxide film coated, ellipsometric and interferential study, optical parameters *(Russian)* 80−50449
InSb, low-power nonlinear refraction effect on laser beam propagation 80−5801
InSb, magnetoacoustic wave excitation by acoustic wave propagation 80−88597
InSb, optical bistability, signal amplification, low power nonlinear effect applications 80−19066
InSb, optical constants and oxidation with various surface treatment *(Russian)* 80−88955
InSb, refractive index and absorpt. coeff., cryst. orientation depend. 80−60536
n-InSb, transparency, DC field induced enhancement 79−91407
$In_xSi_yO_z$, thin film, sputter deposition form., optical and elec. props. 80−60123
$InVO_4.2H_2O$, $In_4(V_2O_7)_3.14H_2O$, physicochem. props. 77−85702
$KB_5O_8.4H_2O$, freq. doubling, angle tuning, mol. appl. 77−3632
KBr, additively dyed, amplitude-phase holograms *(Russian)* 80−1152
KCl, crystal, 10.6 μm ellipsometric meas. 78−24847
KCl IR window material, polish layer effect, ellipsometric meas. 78−55419
KCl laser windows at 10.6 μm, optical distortion parameter 78−79036
KCl:Ca, vol. holographic grating, modulation characts. 79−94197
KCl(Br)(I), far IR complex refr. indices, dispersive Fourier transform 78−80322
$KD_{2x}H_{2(1-x)}PO_4$ crystals, $0<x<0.98$, light scatt. by polaritons 80−96802
$KD_{2x}H_{2(1-x)}PO_4$, deuteration effects 77−59550
$K_2(F,O)$-B_2O_3-SiO_2, effect of replacing B_2O_3 by Al_2O_3 or Ga_2O_3 78−63677
KH_2PO_4, ferroelectric phase transition exam. by spontaneous parametric light scatt. 78−19427
KH_2PO_4, spontaneous electrooptic effect in far IR 79−95734
$K_3Li_2Nb_5O_{15}$ films for optical waveguides epitaxial growth and characterisation 80−79016
KN_3, mono- and polycrysts., IR active lattice vibr., optical consts. 77−77185
$KNbO_3$, dielec. and optical props. using shell model 79−33654
$KNbO_3$:Fe, optically induced refractive index changes 77−4612
$KNiF_3$, isotropic exchange contrib., from comparison with expts. on diamag. $KMgF_3$ 77−69808
K_2O-CaO-BaO-B_2O_3, glass, refraction, refractive index from 0.365 to 2.50 μm 80−88953
K_2O-CaO-BaO-SiO_2 (B_2O_3) (GeO_2), calc. of network refraction and exam. of glass structure 79−4783
K_2O-PbO-SiO_2, glass, mech. and optical props. *(Russian)* 77−20860
K_2O-SiO_2 glass 80−33897
K_2SO_4-$ZnSO_4$ system, glass formation and phase diagram study, physical props. 78−27500
K_3Sb, optical and dielectric props., energy spectra, density of states calcs. 80−20083
$KTaO_3$, complex refr. index meas. in far IR, by dispersive Fourier transform spectroscopy 78−92042
KTb_3F_{10}, Faraday rotation, optical absorpt. spectra and refr. index 78−72542
Kr, gas, liquid, solid, refractive index, density and dielectric const. 80−66138
Kr, meas. using low temp. refractometer 77−57382
La, $(SO_4)_3.9D_2O$, soln. growth, struct., props. 77−77363
LaF_3-BaF_2-ZrF_4(-MF), M=Na, Li, glassy transition, refr. index, density and molar refr. 80−1937
La_2S_3 glass *(French)* 80−71369
La_2S_3 single crystals, optical props. 79−87458
refractive index continued
Li aluminosilicate glasses, variation of refractive index during ion-exchange diffusion from molten salts *(Russian)* 77−28539
$LiBi_xNd_{1-x}P_4O_{12}$ waveguide laser layer epitaxially grown on $LiNdP_4O_{12}$ substrate 80−23709
LiCl, 300-700 nm., temp. coeff., 100-580K *(Russian)* 78−15142
LiF film, refractive index as function of time, ATR meas. 79−65940
LiF, refractive index, effect of ageing, wavelength range 460-1000 nm 80−84707
$Li_2Gd_4(MoO_4)_7$, Czochralski growth, struct. and optical props. 78−27397
α-$LiIO_3$, single crysts., light diffr. under DC field 80−11367
α-$LiIO_3$, temp. coeff., 285-700 nm, 320-500K *(Russian)* 77−66473
$LiIO_3$, visible and UV refr. indices 78−19439
LiN_3, polycryst., IR active lattice vibr., optical consts. 77−77185
$LiN_2H_5SO_4$, single cryst., refr. indices, birefringence, optic axes orientation 77−90125
$LiNbO_3$, acousto-photorefractive effect 77−88878
$LiNbO_3$ diffused waveguide, with exponential profile, metal-clad and dielec. overlay effects 78−46755
$LiNbO_3$, dispersion law of polaritons, refr. index in IR, and Raman spectra meas. 78−27232
$LiNbO_3$, electro-optical modulator, light propag. close to optic axis 79−42947
$LiNbO_3$, equal-deflection method, UV laser rad. 78−29145
$LiNbO_3$, light induced ultrasonic wave velocity change, refractive index 80−97236
$LiNbO_3$, OH^- groups effect on dielec. and optical props. of single crysts. 77−12327
$LiNbO_3$, optical damage induced by X-irradiation 77−20814
$LiNbO_3$, optical damage effects 77−40186
$LiNbO_3$, optical diffusive waveguide, profile determ. *(Russian)* 77−42622
$LiNbO_3$ optical waveguides, Ag-Li and Tl-Li ion exchange effects 80−58791
$LiNbO_3$, optical waveguides by ion implantation 80−106622
$LiNbO_3$, photorefractive process sensitivity *(French)* 77−31124
$LiNbO_3$, photorefractive medium, hologram form. theory 77−68185
$LiNbO_3$ planar waveguide, refractive index rel. to Ti diffusion *(Russian)* 78−59120
$LiNbO_3$, refractive index, temp. depend. over 300 to 620 nm *(Russian)* 78−56451
$LiNbO_3$, SHG, refr. index induced optical inhomogeneity effect 80−9951
$LiNbO_3$ sputtered layers, on $LiTaO_3$, optical waveguide props. 77−11012
$LiNbO_3$, Ti diffused planar waveguide, WKB approx. for refr. index profile determ. 78−30086
$LiNbO_3$, Ti diffused waveguide, refr. index and thickness precise determ. 79−41446
$LiNbO_3$ waveguide, diffusion of Ti, exam. by electron probe anal. and X-ray diffr. 78−47588
$LiNbO_3$, waveguide and modulator form. by ion implantation 80−48469
$LiNbO_3$, Y-cut, waveguide form. by Ti diffusion, refr. index and electrooptic coeffs. 79−14114
$LiNbO_3$:Fe, induced optical inhomogeneity, refr. index and short-circuit photocurrent meas. 79−69806
$LiNbO_3$:Fe, optical damage induced by laser light, X-ray irrad., carrier mobility effects 79−33657
$LiNbO_3$:Fe, optical damage depend. on temp., press., and applied elec. field *(Japanese)* 79−81498
$LiNbO_3$:Fe, photorefraction, γ-irrad. influence, polarisation-optic and holographic obs. 80−11359
$LiNbO_3$:Fe, refractive index change induced by light irrad. *(Japanese)* 79−65824
$LiNbO_3$:Fe(Cu), photorefractive centres, optical absorption, EPR and Mossbauer spectra meas. 77−32403
$LiNbO_3$:He, ion implantation, optical waveguide form., refr. index changes 78−46762
$LiNbO_3$:Mn, photorefractive sensitivity, holographic and photocurrent investig. 77−24581
$LiNbO_3$:Ti, diffused strip waveguide, refractive index changes, two-dimensional distrib. 79−86254
$LiNbO_3$:Ti, dopant conc., refr. index profile rel. to integrated optics 78−5583
$LiNbO_3$:Ti diffused optical waveguide, guided light scatt. sources 80−78966
$LiNbO_3$:Ti diffused optical waveguide, efficient tapered gap prism coupling 80−78967
$LiNbO_3$:Ti waveguide, diffused, Mg diffusion effects on characts. 78−66905
$LiNbO_3$:Ti waveguide, precise determ. of refr. index 78−94442
$LiNbO_3$:Ti waveguide, in-plane scatt. obs. and countermeasures 80−33215
$LiNbO_3$:transition metal, photorefr. effect, 1.5-4.0 eV 77−28213
$LiNb_{1-y}Ta_yO_3$, Czochralski grown, refr. index, 5893-10600 Å, and zero birefr. 78−31166
LiNd phosphate glass, spectral and generation props. 77−1700
$LiNd(PO_3)_4$, crystallisation from $LiPO_3$ flux, exam. of optical props. *(German)* 79−11401
Li_2O-Al_2O_3-SiO_2, with refractive index gradient, produced by ion exchange diffusion, exam. of refractive index and concentration changes 79−4782
Li_2O-Al_2O_3-SiO_2 glasses, viscosity, thermal expansion, glass transform. temp., and refr. index 79−42282
Li_2O-GeO_2 glass, synthesis, Ge coordination state 77−24271
$LiRF_4$, R=rare earth, laser matrices prep. and characterisation 77−24945
Li_2SO_4 based solid electrolytes, FCC phase transport mechanism studies and uses 80−107525
Li_2SO_4, fast ion conductors, X-ray diffr., neutron diffr., and Brillouin scatt. study 80−107170
Li_2SO_4, molten, Brillouin spectra, refr. index meas., hypersonic vel. 78−68523
$LiTaO_3$, equal-deflection method, UV laser rad. 78−29145
$LiTaO_3$, far IR complex refl. coeff. and refr. index, dispersive Fourier transform meas. 79−2841
$LiTaO_3$ optical waveguides, Ag-Li and Tl-Li ion exchange effects 80−58791
$LiTaO_3$ optical waveguide, Ag-Li ion exchange 80−91888

refractive index continued
$LiTaO_3$, photorefractive sensitivity, holographic and photocurrent investig. 77−24581
$LiTaO_3$, refr. index distrib. after surface lapping, theory 78−72479
$LiTb_4$, $LiTb_{0.5}Y_{0.5}F_4$ and $LiTb_{0.25}Gd_{0.75}F_4$, Faraday rotation, optical absorpt. spectra and refr. index 78−72542
$LuAlO_3$, single crysts., prep. and phys. props., X-ray struct. anal. 79−4298
$MNbO_3$, tetragonal, electronic struct., optical anisotropy 80−70599
Mg-cordierites, synthetic end member, variation of refractive index with water content 80−80739
MgF_2 film, 1064 nm 150 ps laser pulse damage rel. to OH^- content and refr. index 79−14016
MgF_2 refractive index and extinction coefficient meas., 115 to 400 nm 79−78640
$MgGeO_3$-$Ca_{0.5}Fe_{0.5}GeO_3$, solid solns., physicochem. props. 77−44223
MgO, liq., imaginary part of complex refr. index, suspension meas. *(Russian)* 79−33659
MgO:Cu, dopant conc., refr. index profile rel. to integrated optics 78−5583
Mg_2TiO_4 single crystals, growth by floating zone method, refractive index 79−78873
Mn film, refractive index determ. using Rayleigh-Lowe refractometer 80−7427
MnCuBi film, optical and magneto-optical props. 77−4695
MnF_2, magnetic, thermal, elastic refraction of light, mag. order influence on refractive index *(Russian)* 80−34880
$Mn_xFe_{3-x}O_4$, optical props. 80−20606
MoS_2, 2H phase, far IR magnetoabsorption and refr. index meas. 77−24847
2H-MoS_2, far IR optical and magneto-optical absorpt. 77−52078
N_2 gas, up to 50 atm, refr. index, 328, 3103 MHz *(French)* 78−14129
N_2, liq., high repetition rate stimulated Raman scatt., thermal blooming 80−91865
N_2, refr. index and Lorentz-Lorenz functions, 944 cm^{-1} and 15803 to 22002 cm^{-1} 78−59543
$(NH_4)_2BeF_4$, linear and nonlinear optical props. in incommensurate phase 80−69452
$NH_4H_2PO_4$, 90° phase matching temp., refr. index freq. and temp. depend. 78−46720
$(NH_4)_2SO_4$, aqueous solns. and cryst., optical consts. meas. rel. to atm. aerosol props. 77−52034
NH_4X, X=OH, Cl, Br, aq. soln., IR reflectivity spectra, Kramers-Kronig anal. 78−68500
N_2O, gas, up to 50 atm, refr. index, 328, 3103 MHz *(French)* 78−14129
Na, radiatively cooled vapour, 3rd order nonlinear optics processes 79−81477
Na vapour, reson. refr. and dispersion, appl. to flow visualisation 79−41790
Na_3AlF_6, film on Si, fused quartz substrates, H_2O absorpt., IR anal. 80−75446
$NaAlSi_2O_6.H_2O$, synthetic analcite, optical and crystallographic props. *(French)* 77−43183
$NaBrO_3$, temp. coeff., 285-700 nm, 320-500K *(Russian)* 77−66473
NaCl, amplitude phase hologram recording on colloid type centres *(Russian)* 80−69347
NaF, IR window coating, prep. and optical props. 77−50736
NaF(Cl), far IR complex refr. indices, dispersive Fourier transform 78−80322
NaI, 300-700 nm., temp. coeff., 100-580K *(Russian)* 78−15142
NaN_3, polycryst., IR active lattice vibr., optical consts. 77−77185
NaO-SiO_2, glass, distrib. of different O ions, molar refractivity meas. 80−33897
Na_2O-B_2O_3-SiO_2 glass, low-loss GRIN fibres, double-crucible prod., loss and bandwidth meas. 80−69559
Na_2O-B_2O_3-SiO_2 low-loss optical fibre prep. by double crucible technique *(German)* 78−33929
Na_2O-B_2O_3-SiO_2:GeO_2 medium-loss graded-index preform fabrication by phase separation and leaching *(German)* 78−33930
Na_2O-GeO_2(TiO_2)(SnO_2)(ZrO_2)(ThO_2)-SiO_2 glass, density, refractive index, thermal expansion, hardness IR spectra, DTA *(Japanese)* 78−15535
Na_2O-SiO_2 glass, bridging to non-bridging ratio and correl. to glass density and refr. index, ESCA study 80−84832
$NaPO_3$-AlF_3(-NH_4HF_2) glasses, synthesis, chem. thermal and optical anal. *(French)* 79−100104
$NaSbSe_2$ films, struct., photoelec. and opt. props. 78−51834
Nb anodic oxide films, reversible optical changes 78−35580
Nb, BCC lattice, optical prop. in range λ=0.265−18 μ, polarimetric meas. 79−15075
Nb_3Al, complex refractive index meas. 80−93264
Nb_2O_5 anodic coatings, refr. index and spectral phase change, reflectance meas. 79−43052
Nb_2O_5-ZrO_2 sputtered thin layer structure and optical props. 79−28851
Nd^{3+}:glass, nonlinear refractive index, two-photon resonant absorption by Nd^{3+} *(Chinese)* 80−43387
$Nd_{2x}Gd_{2(1-x)}(MoO_4)_3$, ferroic, linear and nonlinear optical susceptibility 78−22164
NdSb, forbidden band gap and electrotransfer parameters 80−39497
Ni, anodic passive film form. in NaOH soln., refl. and ellipsometric study 80−104447
Ni, nearly ideal surface, optical consts., 5461 and 6328 Å 77−36192
Ni, optical constants at high temp. 79−24281
Ni-Cr, interband absorpt. and refractive index, photoconductivity dispersion function 77−36263
$Ni(NH_4)_2(SO_4)_2.10H_2O$, precipitation, supersaturation, cryst. size distrib. changes 77−72573
Ni(100) platelet surface optical and magneto-optic consts. 78−15151
O_2 solid film, optical and structural props. 78−56052
P-As-Se glasses, mag. susceptibility, dielec. const., opt. props. 78−64184
P-Se-Te system glasses, mag. susceptibility and opt. props. 80−25079
P-Se-Tl system glasses, polarisation, refr. index and dielec. const. meas. 80−20608
PLZT ceramic, optical gate, dielec., optical props., electro-optical effect meas. 78−42418
PLZT ceramics, optical recording *(French)* 77−31078
PLZT ferroelectric thin films, epitaxial growth and optical props. 80−70543
PLZT, refr. index, 405-764 nm, surface layer 78−35110
PLZT, thin film epitaxial growth and characteris. 79−28918

refractive index continued
Pb bismuthate glass, IR transmission props., density 79−74127
$Pb_{1-x}Ba_xMoO_4$, refr. index. and photoelastic consts. 77−63393
$Pb_{1-x}Cd_xS$ epitaxial layer, metastable, optical props. and electronic struct. 79−15543
PbF_2-AlF_3 glass, optical props., crystn. and thermal expansion 80−48367
$PbGeO_3$, cryst. struct., dielec. and optical props. 77−1118
Pb_3GeO_5, cryst. struct. dielec. and optical props. 77−1118
$PbHPO_4$, single cryst., growth, optical props., ferroelec. transition 78−35285
PbI_2, film, fundamental absorption edge, complex dielec. const. *(Russian)* 77−40266
PbI_2 film, photolyzed, refr. index change 78−11010
PbI_2, film, reflectance meas., optical consts., humidity effects 80−34994
$PbMg_{1/3}Nb_{2/3}O_3$ single cryst., electro-optical hysteresis curves and phase transitions *(German)* 79−28717
$PbMg_{1/3}Nb_{2/3}O_3$, vibr. spectrum and dispersion of optical consts., coexisting ferro- and paraelec. phases 77−63422
$PbMoO_4$, single crystals having scheelite struct. 78−79082
PbO thin layers on PbO-SiO_2 glass, reaction behaviour 78−34660
PbO-Bi_2O_3-GeO_2, exam. of glass forming and liquid phase separation regions, and optical props. 78−88453
PbO-containing binary systems, acoustooptic props. from comp. and density 80−76000
PbO-GeO_2 glass, synthesis, Ge coordination state 77−24271
PbO-SiO_2 glass, distrib. of different O ions, molar refractivity meas. 80−33897
PbO-SiO_2 glass, leaching behaviour in dil. HNO_3, ellipsometry and AES obs. 78−23846
PbS, colloidal, light scatt. and electron microscopy 78−3379
$Pb_xSi_yO_z$ films on Si, form. kinetics and props. 80−35358
$Pb_{1-x}Sn_xSe$, thin film, opt. props. *(Japanese)* 77−1750
PbSnTe, optical dielectric const. variation with carrier conc. 80−84709
$Pb_{1-x}Sn_xTe$, heteroepitaxial film, fundamental absorpt. edge and Shubnikov-de Haas effect 79−24381
Pb_xTe_{1-x} film, highly absorbant, complex index of refr. determ. method 78−54445
$PbWO_4$, single crystals having scheelite struct. 78−79082
$Pb(Zr,Ti)O_3$ film, ferroelec. and optical props. 77−85674
$Pd_{0.775}Cu_{0.06}Si_{0.165}$ glass, optical props. in energy range 0.67 to 5.6 eV 80−34872
PdIn, refractive index, reflectivity and band struct., APW calcs. 80−40139
PdO, optical props., 0.5-5.4 eV 79−56813
phosphate glass, Li_2O and Na_2O effect on thermo-optic props. 78−18029
PrSb, forbidden band gap and electrotransfer parameters 80−39497
RbCl(Br)(I), far IR complex refr. indices, dispersive Fourier transform 78−80322
$RbD_{2x}H_{2(1-x)}PO_4$, deuteration effect 77−59550
RbN_3, polycryst., IR-active lattice vibr., optical consts. 77−77185
Ru (1120), complex RI meas. in visible region 77−1650
Ru, optical props. 79−24282
S-Se-Te semicond. glasses, mag. suscept. meas., refractive index 78−34952
SF_6, liq., near crit. point, optical props. meas. 77−72673
SF_6, refractive index meas., intermolecular interaction effects 80−33728
Sb_2S_3, amorphous and crystalline thin films, optical consts. 79−91518
SbSI-GeS_2 system glasses with and without antireflection coatings, optical props. 77−8595
$Sb_xSi_yO_z$ films on Si, form. kinetics and props. 80−35358
Se, A1 type metallic phase, optical consts. and refl. 77−32455
Si, 95-298K, 2.5-12 μm 77−8535
Si amorphous film, anisotropic etching phenomenon, appl. as solar selective absorber surfaces 80−72054
Si, amorphous film prepared by CVD, optical props. and struct., solar absorber appl. 79−52035
Si, anodisation at low substrate temp. by low pressure O_2 plasma 80−104314
Si, CVD, amorphous and polycryst., solar thermal absorber, temp. variation of absorpt. edge 80−12028
Si, CVD films, polycryst., elec. and optical props., electronic density of states model 79−56332
Si, diamag. and dielec. susceptibility, temp. depend. 78−10646
Si, far IR complex refr. index spectra determ., new method, for transparent solids 77−28566
Si, far IR photon drag and radiation pressure in refractive media 80−60048
Si film, amorphous and polycrystallised, localised states, elec. and optical props. 78−64008
Si film, low press. CVD prep., struct., elec. and optical props. 80−70548
Si, ion implanted, radiation defect production at different temps. 80−103398
Si, optical constants, heavily doped crystals, Kramers-Kronig analysis 77−85676
Si, optical constants at 5461 Å 78−92043
Si, optical consts. by unpolarised incident radiation 80−76044
Si oxide, photoresist residual film, ellipsometric characterisation 77−48266
Si oxides, steam grown, index of refr. ellipsometric meas. 80−75995
Si plasma deposited amorphous hydrogenated film, optical props., annealing effect 79−56874
Si RF sputter-etched surface, cryst. damage, spectroscopic ellipsometry obs. 80−103538
Si rubber as electro-optic material for optical hydrophones 80−43412
Si surface, atomically pure, optical consts. and temp. depends. 79−65823
Si:$^{31}P^+$, implanted layers, characterisation by ellipsometry 79−90683
Si:As^+, implanted layers, refractive index and reflectivity calcs. from ellipsometry meas. 79−73190
Si:B, ion implanted, ellipsometric study for low doses, cryst. damage parameter 79−65105
Si:B ion implanted layers, light refl. and transmission coeffs., computer program 80−66316
Si:H, amorphous, refr. index, temp. depend., implications for thermoreflectance and electroreflectance 80−50290
Si:H, amorphous film, prep. by plasma decomp. of SiH_4 under mag. field, and characterisation 80−45239
Si:H, amorphous films, plasma-deposited, defect states, IR, ESR, and refractive index meas. 79−65944
a-Si:H, influence of H on optical props., H conc. and H bonds 80−76098

refractive index continued
a-Si:H alloys, sputter deposited thin film coatings, property-comp. relationships 80−80975
Si:H amorphous film, prep. by RF glow discharge decomp. of SiH_4, optical props. and H conc. 80−15416
Si:H amorphous film, prop. by glow discharge deposition, and plasma parameter effects on props. 80−45240
Si:H amorphous films for solar cells, optical and elec. props. of RF glow discharge deposited films 80−54576
Si:H amorphous glow discharge film, optical absorpt., near IR region 79−87518
Si:N, ion implantation, refractive index, IR spectra, ion range and straggling meas. 80−34020
Si:N(P), ion implanted, IR transmission and rel. spectra study 80−108244
Si:P, high fluence ion implantation, layer thickness and refr. indices, IR refl. meas. 79−82248
Si:P, IR absorpt. and D^--band 78−52533
Si-N film, passivation layer, density comp., and ref. index, Lorentz-Lorenz correl. 78−39697
Si-Si_3N_4-SiO_2 non absorbing double layers, optical parameters reflectivity by liquid immersion method 80−71503
Si-SiO_2 interface, props. variation in SiO_x region 80−49548
Si-SiO_2 interface, thermally grown oxide, spectroscopic ellipsometric anal. 80−107659
Si-SiO_2 interlayer, optical evidence 79−69800
Si-SiO_2-$Si_xO_yN_z$ waveguide model *(Russian)* 79−10374
SiC, dielectric coating effect on surface polaritons, optical consts. *(Russian)* 80−88489
SiC, ellipsometric exam. of polytypes 78−92044
SiC film, amorphous, reactively sputtered, effects of S/C ratio and H content on elec. and optical props. 79−90906
SiC, nonlinear refr. index meas. by nonlinear lens method *(Russian)* 79−26111
SiC, refractive index dispersion, 0.4-50 μm, 105-297K 78−84548
SiC:H amorphous reactively sputtered film, H content effect on film props. 80−75459
$Si_xC_yH_z$ films, reactive plasma deposited, comp., IR anal., and optical props. 79−95945
$SiH_{0.16}$ amorphous films, optical props. and photocond. near optical gap 80−50443
SiH_x amorphous reactively sputtered films, optical props. 80−50444
$Si_{1-x}H_x$ film, amorphous, RF sputtered, pure and P(B) doped, optical consts. 79−95866
SiN_x film, plasma deposited, comp. and characterisation, optical and elec. props. 80−15401
SiN_x, film by magnetron sputtering, composition, hardness and optical props. 78−3047
SiN_x film reactive plasma deposition and characterisation 77−77406
SiN_x films, plasma-deposited, radial wafer-to-wafer uniformity 80−104073
Si_3N_4, CVD, chem. bound H, NH_3/SiH_4 ratio and annealing depend. 77−76680
Si_3N_4, film, absorption, refr. index, freq. dispersion 78−48248
Si_3N_4 film, amorphous, optical props., band gap and surface roughness 77−32396
Si_3N_4 film, CVD, high-field dark currents 80−54791
Si_3N_4 film, ion beam effects on opt. props. *(Russian)* 77−48265
Si_3N_4 film, plasma-activated CVD, optical prop. depend. on growth conditions 77−55892
Si_3N_4 film, with varying refr. index, AES and XPS 78−72029
Si_3N_4 layers, on GaAs, encapsulation, low-energy ion beam sputtering 79−78882
Si_3N_4 layers, RF plasma deposition and props. 79−43155
$Si_xN_yO_z$ film, band diagram, optical props. and elec. cond. meas. 78−84333
SiO, film, effect of ion implanted O_2 on optical props. 80−45027
SiO_2 (silicalite), hydrophobic crystalline mol. sieve, refr. index and density 78−30598
SiO_2, amorphous, and layers on Si substrate, IR optical props. 79−56780
SiO_2 anodised layers on clean and ion bombardment Si surfaces ellipsometry meas. *(Russian)* 79−24382
SiO_2 based glass fibres, refr. index and comp. data 77−79950
SiO_2, chem. bond and rel. props. 77−43199
SiO_2 film, 1064 nm 150 ps laser pulse damage rel. to OH^- content and refr. index 79−14016
SiO_2, film, formation from tetraalkoxysilanes in O_2 current, props. 77−44170
SiO_2 film, ion beam effects on opt. props. *(Russian)* 77−48265
SiO_2 film, prep. using high press. O_2, residual stress, chemical etch rate, refr. index and density meas. 80−71768
SiO_2, film form. by reactive HF sputtering with voltage bias 78−3045
SiO_2 film on 6H-SiC substrate, ellipsometric meas., accuracy and sensitivity 80−77840
SiO_2 films, CVD at reduced press., optical props. 80−2957
SiO_2, fused, refractive index dispersion, thermal history depend. 80−25331
SiO_2, fused, shock compressed, refractive index, density, and polarisability behaviour 80−50295
SiO_2, fused, stress optical coeff. 79−28713
SiO_2, fused silica, continuous inhomogeneities, refusing effect in H_2 77−50734
SiO_2, glass, ion implanted, radiation effect on chem. stability 77−1158
SiO_2 glasses, opt. consts. in IR and vacuum UV 78−27238
SiO_2 grown anodically over Si, optical and electrophys. props. 77−72934
SiO_2, ion implanted, fused, refr. index profiles 80−54272
SiO_2 ion implanted, radiation defects and optical props. 80−107293
SiO_2, optical constants at 5461 Å 78−92043
SiO_2, oxide growth in HCl-O_2 mixture, ellipsometric meas. 78−7073
SiO_2 thin films, comparison of RI and IR spectra 80−11497
SiO_2, thin films on rough polycryst. Si surfaces, oxide thickness and refractive index meas. 80−93422
SiO_2, transparent film on Al, refr. index, thickness, ellipsometric meas. 77−52195
SiO_2 ultrathin layers, refr. index meas. 80−103936
SiO_2, uniform film prep. by pyrolysis of tetraethoxysilane 77−40379
SiO_2, vitreous, electron irrad., vol., refr. index and stress changes 77−47482
SiO_2, vitreous, radiation behaviour of optical props. 78−21655

refractive index continued
SiO_2:GeO_2 graded-index fibres, without index dip, fabrication by CVD method 78−9431
SiO_2-Al_2O_3 glass, Raman spectra and refr. index meas. 77−24836
SiO_2-Al_2O_3-B_2O_3-LiO_2 (LiO_2.Na_2O) (Na_2O) glass exam. of optical props. 78−88277
SiO_2-B_2O_3 glass system, gel hot pressing synthesis and characterisation *(French)* 80−66468
SiO_2-B_2O_3(P_2O_5)(GeO_2), optical fibres, double Sellmeier oscillator model 78−33793
SiO_2-GeO_2 glass, refr. index and density, comp. depend. 78−23424
SiO_2-GeO_2-Li_2O(Na_2O)(K_2O), refractive index and density 79−51926
SiO_2-K_2O-Na_2O-BaO-SrO-ZnO glass, props. optimisation 79−91611
SiO_2-P_2O_5 glass, refr. index behaviour, optical fibre appl. 77−46777
SiO_2-Ta_2O_5, plane optical waveguide, fabrication by reactive sputtering 78−71221
SiO_2-Ta_2O_5 film, refr.-index-adjustable, for integrated optical ccts., prep. and props. 78−63203
SiO_2-TiO_2 films, obtained from $Si(OC_2H_5)_4$ and $TiCl_4$, exam. of props. 79−95934
SiO_x, amorphous and recrystallised layer, optical props. 80−25474
SiO_x amorphous film, dispersion of refr. index and chem. comp. 80−7429
SiO_x film, durable optical, ion plating onto plastics, optical and mech. props. 80−38141
SiO_x film, reactively evaporated, substrate temp. depend. of optical props. 77−70006
SiO_xN_y film, ion beam effects on opt. props. *(Russian)* 77−48265
$Si_xO_yN_z$ film, opt. props. rel. to reactive sputter prep. conditions 77−81165
Si_2Te_3, fundamental absorption and Franz-Keldysh effect meas. 77−1694
$Sm_{2x}Gd_{2(1-x)}(MoO_4)_3$, ferroic, linear and nonlinear optical susceptibility 78−22164
SmSb, forbidden band gap and electrotransfer parameters 80−39497
SnO-GeO_2 system, glass form., compound anal. 77−35486
SnO_2, elec. conducting film on glass substrate, measurement of optical constants and thickness 78−60525
SnS_2, crystal growth and optical props. in visible and IR regions 77−52114
SnS_2 thin layer, far IR refractive index 80−93421
SnS_xSe_{2-x}, thermal changes in optical props. 78−19504
$SrAg(PO_3)_3$, physicochem. characts. 77−52302
$Sr_2Al_2GeO_7$, gehlenite struct., synthesis and physicochem. props. 79−43181
$Sr_{0.75}Ba_{0.25}Nb_2O_6$ single cryst., electro-optical hysteresis curves and phase transitions *(German)* 79−28717
SrF_2, 20-85°C, temp. depend. 77−8536
SrF_2 fusion-cast prism refractive index obs., 0.2138 to 11.475 μm 80−34882
SrF_2, IR window coating, prep. and optical props. 77−50736
SrF_2, thin film, optical props., spectral dependence, 460-1000 nm 80−76094
SrF_2, vol. depend. of refr. index 78−88275
$SrMoO_4$, single crystals having scheelite struct. 78−79082
SrO-B_2O_3-GeO_2 glass system, physicochem. props., alkaline earth oxides effect 79−65827
$SrTiO_3$, complex refr. index meas. in far IR, by dispersive Fourier transform spectroscopy 78−92042
$SrTiO_3$, fabrication damage characterisation by internal and external meas. 80−102782
$SrTiO_3$ film, sputtered, refr. index, 0.3-1.0 μm, substrate temp. effects 77−55840
$SrWO_4$, single crystals having scheelite struct. 78−79082
Ta film, oxidation in ambient conditions, resist. and ellipsometric meas. 79−34209
Ta_2O_5, anodised film, nonuniformities, optical props., spectrophotometric obs. 78−2933
Ta_2O_5 antireflection coatings for Au-GaAs solar cells parameters determ. 77−763
Ta_2O_5 film, for MIS device, CVD and characterisation 77−4742
Ta_2O_5 film, reactively sputtered on SI, dielectric and optical props. obs *(Bulgarian)* 80−89144
Ta_2O_5 film, refractive index 80−84792
Ta_2O_5, film form. by reactive HF sputtering with voltage bias 78−3045
Ta_2O_5, plane optical waveguide, fabrication by reactive sputtering 78−71221
Ta_2O_5, reactive DC sputtering deposited films with magnetron-plasmatron, mechanical elec., optical props. 80−25566
$Ta_2O_5N_x$, sputtered birefr. film, deposition conditions effect on refr. index 77−39118
$Tb_{2x}Gd_{2(1-x)}(MoO_4)_3$, ferroic, linear and nonlinear optical susceptibility 78−22164
TbIG, higher-order anisotropic mag. contrib. 77−69808
TeO_2, paratellurite, equal-deflection method, UV laser rad. 78−29145
TeO_2, paratellurite cryst., polariton Raman scatt., refr. index dispersion 78−25928
TeO_2, visible and UV refr. indices 78−19439
ThF_4 film, 1064 nm 150 ps laser pulse damage rel. to OH^- content and refr. index 79−14016
ThF_4 film, 10.6 μm ellipsometric meas. 78−24847
Ti anodic oxide films, reversible optical changes 78−35580
TiN_x, film, non-stoichiometry rel. to optical characts. 77−12456
TiO_2 amorphous film, alkali resistance, refractive index, IR spectra *(Japanese)* 78−23546
TiO_2 and Dy_2O_3-TiO_2, high refractive index film growth by sputtering, waveguide appl. 77−48341
TiO_2, film, prepared by reactive evap. 77−19372
TiO_2 films, deposition by electron beam evap. chem. comp., refr. index, struct. *(Japanese)* 77−62777
TiO_2 layers, activated reactive evaporation and absorpt. indices 80−97363
TiO_2 optical coatings, deposition, performance 77−88896
TiO_2 particles in suspension, light scatt. phenomena and abs. *(German)* 77−10835
TiO_2, reactive DC sputtering deposited films with magnetron-plasmatron, mechanical elec., optical props. 80−25566
TiO_2, rutile, vol. depend. of refr. indices under hydrostatic press. 77−52036
TiO_2 transparent film thickness and refractive index calc. 79−15547
TiO_2-Nb_2O_5 sputtered thin layer structure and optical props. 79−28851

refractive index continued
TiO_2-SiO_2, semicond. glass, optical props. 78−60412
TiO_2-SiO_2 multilayer vacuum coatings, optical props. 80−97361
TiO_2-ZrO_2 sputtered thin layer structure and optical props. 79−28851
TiO_2-ZrO_2-SiO_2 amorphous film, alkali resistance, refractive index, IR spectra *(Japanese)* 78−23546
TiO_x antireflection coatings for solar cells, optical, struct., and compositional characts. 80−55852
TiO_x film, durable optical, ion plating onto plastics, optical and mech. props. 80−38141
Tl_3AsSe_3, refractive index, thermal expansion temp. depend. 80−97223
TlBS, synthesis, struct., optical, spectral props. 79−15631
TlBr, complex refr. index meas. in far IR, by dispersive Fourier transform spectroscopy 78−92042
TlBr-TlI, TlCl-TlBr, KRS-5 and KRS-6 crystals, refr. index temp. increments meas. 80−33098
TlCl-TlBr mixed crystal, reflectivity spectra meas. 77−85743
$TlGaS_2(Se_2)$ film, elec. and photoelec. props. *(Russian)* 78−52109
$TlGaSe_2$, electrooptic effect and refr. index anisotropy 77−16281
TlI-PbF_2 graded-index film coating technique and results 80−33265
$TlInS_2$, layered structure crystals, refractive index meas. method 80−98966
$TlMnCl_3$, optical props. 78−35111
$TlMnCl_3$, refr. index and birefr., struct. transition effects 77−90126
TlS_2, amorphous, spectral depend. of absorpt. and refr. indices 77−77222
TlS_2, amorphous semiconductor, optical consts. 79−11400
$TlSbS_2$, single cryst., spectral transmission distrib., polaris. effect, refractivity, dispersion 77−59551
VO_2 film, optical and elec. props., 0.8 to 4.2 mm, near metal-semicond. transition 77−32473
VO_2, film, optical consts. and electrical props. near phase transition *(Russian)* 77−59631
VO_2 interference films, colour valencies as function of thickness and phase change *(German)* 78−56533
V_2O_5 film, amorphous, thickness, density and refr. index determ. from reflectance interference spectra 80−55206
V_2O_5, optical characts., far IR transmission spectra 78−72525
V_3Si, complex refr. index and reflectivity of thin film, microscopic characts. and superconductivity 78−31267
V_3Si film, optical props. *(Russian)* 80−93418
WO_x, anodic oxide films, quadratic electro-optic and electrostrictive effects, ellipsometry 80−108184
WS_2-oxide layer formation and props. 79−50359
WSe_2-oxide layer formation and props. 79−50359
Xe, gas, liquid, solid, refractive index, density and dielectric const. 80−66138
Xe, meas. using low temp. refractometer 77−57382
Xe, refraction, determ. by phase vel. matching method *(Russian)* 78−30406
Y film prepared in ultrahigh vac., optical meas. 6 to 14 eV 79−78767
YAG:Nd, laser material, linear expansion coeff. and r.i., temp. depend. 77−733
$YAlO_3$:Nd, refractive index determ. 78−80311
$Y_3Fe_{5-x}Ga_xO_{12}$, refr. index spectrum, visible region 79−73894
YIG, isotropic exchange and higher-order anisotropic mag. contribs. 77−69808
Y_2O_3-SiO_2-Al_2O_3 system, composition depend. of refractive index in vitrification region 77−24812
$(YSmCa)_3$ $(FeGe)_5O_{12}$ mag. bubble garnets, ion implantation induced stress influence on props. 79−91274
$(YSmLuCa)_3(GeFe)_5O_{12}$, garnet film, refractive index dispersion 78−88273
$YbAlO_3$, single crysts., prep. and phys. props., X-ray struct. anal. 79−4298
$Yb_{2x}Gd_{2(1-x)}(MoO_4)_3$, ferroic, linear and nonlinear optical susceptibility 78−22164
Yb_2O_3 thin film on Cr substrate, refr. index depend. on thin film thickness 80−108290
YbSb, forbidden band gap and electrotransfer parameters 80−39497
ZnB_2O_4-MF_2 (M=Mg, Ca, Sr, Ba) glass system, physicochem. props. 80−34877
ZnB_2O_4-RF, R=Mg, Ca, Sr, Ba, glass form., struct. and props. 80−84077
$ZnCl_2$, aq. solns., complex IR refr. indices, IR spectra, mechanisms, spectrometer system 78−43831
$Zn_2Fe(PO_4)_2.4H_2O$, phosphophyllite, chem., optical and X-ray data 77−15366
$ZnGeP_2$, temp. depend. phase-matched nonlinear optical devices 80−99794
$ZnGeP_2$ thermo-optic coefficient, dispersion 80−71396
ZnO, vol. depend. of refr. index 78−88275
ZnO-B_2O_3, glass, refraction, refractive index from 0.365 to 2.50 μm 80−88953
ZnO-La_2O_3-B_2O_3, glass, refraction, refractive index from 0.365 to 2.50 μm 80−88953
ZnP_2, birefringence, circ. dichroism, temp. depend. *(Russian)* 79−1748
ZnP_2, birefringence dispersion *(Russian)* 77−85686
Zn_3P_2 bulk and thin film, UV reflectivity spectra, photovoltaic effects, optical consts. 80−25472
Zn_3P_2, optical props., transition energies from transmission and refl. meas. 80−60532
Zn_3P_2 photovoltaic material and Schottky diode characteristics 78−64066
$Zn_3(PO_4)_2.4H_2O$, thermal transitions, thermographic investig. 77−9063
ZnS antireflection coatings on solar cells 80−43414
ZnS, CVD sample, refractive index var. with temp., 22° and 34°C 79−14053
ZnS, current and refractive index oscills. in electric fields due to barrier instability 79−91372
ZnS film on Si, fused quartz substrates, H_2O absorpt., IR anal. 80−75446
ZnS hot pressed microcryst. compact, Irtran 2, refr. index meas. 78−66877
ZnS, refr. index oscills, in strong. elec. field 79−28720
ZnS, vol. depend. of refr. index 78−88275
ZnS-Na_3AlF_6 multilayer films, thermally evaporated, dispersion characts. 77−59629
ZnS(Se), IR transmitting semicond., dn/dT, wavelength depend. 77−77163
ZnSe crystal, refr. index temp. increments meas. 80−3309f

refractive index continued
ZnSe crystal and film, 10.6 μm ellipsometric meas. 78−24847
ZnSe, magnetoreflectance of exciton-polaritons, semiclassical treatment 79−99857
ZnSe, refr. index meas. and nonlinear moment parameters 77−85681
ZnSe, refr. index meas. at 3.8 μm, 10.6 μm, 80 to 300K 79−82938
ZnTe ion implanted planar waveguides, refr. index profiles 77−62039
ZrF_4-BaF_2-NdF_3 glass, vitreous domain, prep. and optical props. 78−27304
ZrF_4ThF_4-BaF_2 system, new fluoride glass, optical props. *(French)* 77−36443
ZrO_2 amorphous film, alkali resistance, refractive index, IR spectra *(Japanese)* 78−23546
ZrO_2 film, 1064 nm 150 ps laser pulse damage rel. to OH^- content and refr. index 79−14016
ZrO_2 film, CVD from organometallic cpds. and characterisation 78−23626
ZrO_2 film, electron beam deposition, refr. index and microporosity 78−90467
ZrO_2 single crystals, Y_2O_3 stabilised, optical props., impurities and annealing conditions influence 79−52399
ZrO_2 thin film, optical props. rel. to cryst. struct. 80−97357
ZrO_2 transparent film thickness and refractive index calc. 79−15547
ZrO_2:Y_2O_3, cryst., IR refl., refr., absorpt. 77−12382
ZrO_2-SiO_2, layer for dielectric mirror, for KrF excimer laser *(Japanese)* 79−72588
ZrO_2-$ZrTiO_4$, optical film material 77−753

refractive index measurement
see also refractometers
absolute interference method for solids 77−41674
absorbent liquid media, refractometry errors 79−67377
absorbing material optical consts., transmission interferometry meas. on medium-thickness films 79−78768
absorbing media using frustrated total internal reflection refractometer 80−9021
air, meas. with improved Rayleigh interferometer *(Chinese)* 77−57383
apparent thickness method, student expt. 77−41445
atmosphere, pulse spectrum from optical meas. *(Russian)* 77−29439
atmosphere, refr. index struct. parameter from refractivity and amplitude scintillation meas. at 36 GHz 78−81316
atmospheric, microwaves non-conventional appl. survey *(Italian)* 80−13093
atmospheric radiowave refractive index using digital refractometer 78−86321
attenuated total reflection, optical consts. determ. *(Spanish)* 77−69788
axially symmetric object, refr. index determ. from emerging ray directions 77−87809
axially symmetric r.i. distrib. determ., using eikonal approx. 77−2686
Brewster's angle method, for teachers 79−71202
Brewster angle determ. by dithered laser beam synchronous detection 80−73422
bubble film, ellipsometric meas. of thickness and refr. index 79−78463
calibration substrate for Abeles equipment 78−77965
Cargille liquids, eqn. for evaluating refractometer readings 79−58772
chromatography refractive index detector for monitoring model dialysis expts. 79−96724
coated substrate, transmittance and reflectance, film refr. index meas. 78−56534
coating technique and refractive index meas. 80−43488
colloidal dispersion, spherical particle, optical turbidity and refr., particle size and relative refr. index meas. 79−92012
complex, of liquid dielec., at mm and sub-mm wavelength 77−82595
computer-controlled heterodyne interferometer for index gradient meas. 80−13131
condensed media, temp. depend. of refr. index, meas. tech. *(Russian)* 78−54446
continuous wavelength interferometry for measuring dispersion of complex refractive index 80−22423
crystals, meas. installation 78−4673
demonstration methods 80−77577
dielectric film, refr. index, film thickness, phase shift and order of interference, interferometric method 78−276
dielectric film, refractive index and thickness meas. by optical method 80−82806
dielectric film, spectroscopy, using Lummer-Gehrcke interferometer 77−5898
dielectric film or membrane, optical thickness meas. using Fabry-Perot interferometer 77−71367
dielectric film refractive index meas., synchronous angle integrated optical method 80−15976
dielectric films, thickness and refractive index meas. by photoelectric scanning 80−105606
dielectric layers, ellipsometry for semicond. process control 78−49887
dielectric thin film refractive index and thickness, algorithm for determ. on basis of ellipsometric meas. 80−34881
dielectric thin films, accurate meas. by symmetric prism wave couplers *(Chinese)* 80−2885
dielectric thin films, refractive index and thickness, spectrophotometric determ. 78−29144
diffused channel waveguides, direct index meas. 80−87562
diffused microwaveguide, refr. index profile determ. 77−23764
diffused optical waveguide numerical analysis and applications 78−1377
diffused waveguide index profile determ. from expt. mode spectra 77−23745
dispersed system, simultaneous determ. of refr. index and particle size from scattered radiation characts. 80−27335
dispersive Fourier transform spectroscopy, mode of operation of polarising interferometer 78−78003
ellipsometric method 79−26108
ellipsometric method for IR materials 78−24847
ellipsometry data analysis aided by derivative plots in n,κ-space 80−86378
elliptical optical fibre or preform, nondestructive method 79−64322
equal-deflection method, IR and UV determinations 78−29145
erythrocytes, determ. of relative refractive index, dimensions and conc. from turbidity spectrum 79−79698
Fabry-Perot interferometer, effect of zero points in light modulation *(Russian)* 79−58781
far IR complex refr. index spectra determ., new method, for transparent solids 77−28566

refractive index measurement continued
fibre, single-mode, cutoff wavelength meas., using refracted power technique 80−99844
fibre automatic refr. index profiling using video-based system 78−79104
fibre index near-field profiling methods, detail resolution 78−42451
fibre index profile data assessment method 78−71205
fibre index profile meas. technique 78−42452
fibre index profile measurement using transverse interferogram, accuracy 78−66931
fibre index profiling methods 78−79118
fibre mode analyser using refraction from oblique section 77−88952
fibre preforms, nondestructive struct. meas. with photoelastic effect 79−86255
fibre refractive index profile calc. from transverse interf. patterns 78−74967
fibre refractive index profile nondestructive determ., backward light scatt. method 79−64306
fibre refractive index profile nondestructive determ., fast Fourier transform method 79−64307
fibre refractometry by interference microscopy, simplified method 79−18504
fibre waveguide and cable parameter meas. techniques *(German)* 78−33860
fibre waveguides characteristics 78−59143
film, by Nomarski differential interference contrast microscopy 78−24849
film, nearly transparent, refractive index meas. method 80−68242
film, optical characts., computer inversion method 78−11008
film, refr. index and thickness determ. using guided optical waves 78−74049
film, unsupported, simultaneous meas. of refractive index and thickness *(French)* 77−55842
film optical consts. meas., Shamir-Graff method evaluation 80−11489
film optical parameters meas. method, reevaluation 80−104004
film refractive index and thickness meas., error anal. of SYNCANG and SYNCWANG methods 78−8439
film refractive index dispersion meas. by optical waveguiding 79−85162
film thickness and optical consts., spectrophotometer meas., computer program evaluation *(French)* 77−13808
films, by light intensity ratios 77−2678
films, electrically conducting on transparent ceramic, ellipsometry determ. of optical consts. 79−67376
films, highly absorbant, complex index determ., appl. to Pb_xTe_{1-x} 78−54445
Fizeau interferometry, for refr. index and thickness meas. of nearly transparent films 79−17469
fluids in microscopic tubes, refractometry, focal position observation 79−49273
fluorescent film, method for refr. index and thickness determ. 80−40175
focusing method for fibre or preform 79−27374
Fourier transform interferometric determ. of liq. complex refr. index, 5 to 500 cm^{-1} 77−13798
frozen gas matrix, refr. index determ. by emission spectrosc. 80−90884
frustrated total internal reflection technique, foreign and Soviet refractometers 79−6165
gas in boundary layer, refractive index meas. by light refl. 78−8438
gas refractive index meas., 150 GHz to 6 THz 77−5892
gases, compressed, refractive index meas. using Fabry-Perot interferometer *(French)* 80−14878
glass disc, laser beam path 80−46779
glass fibre refractive index profile meas. using interf. microscope with freq. shift 80−64175
glass surface, ellipsometric study of zone of optical contact 80−4754
graded index fibre profile determ., interferometric method 80−14481
graded index materials, optical props. meas. 79−9237
graded-index optical waveguide characteristics meas. 79−14108
graded-index preform refr. index ratio and gradient profile determ. from laser beam refr. 79−81519
gradient index material profiles and chromatic props. 80−14409
gradient index optical lenses, use, design, fabrication and refr. meas. 78−13780
gradient index profile measurement by Babinet fringe analysis 79−49277
guided optics techniques for meas. of film props. 79−99958
heterogeneous media, local refr. index meas. *(Russian)* 78−32858
high-temperature determination method 77−85680
holographic interferometer, for optical glass homogeneity determ. 78−90401
holographic interferometry with wide field angle of view, ref. index field reconstruction 79−76637
holographic measurements of refr. index changes 78−74865
homogenoeus media, local refr. index meas. *(Russian)* 78−32858
HPLC, refr. index meas. detectors 78−45675
HPLC detection systems, review 78−48733
image-moire method 80−22420
interference microscopy for refr. index radial distrib. meas. in light focusing rods 77−57381
interference pattern, spectrally resolved, refr. index determ. 77−49763
interferometric field reconstruction, discontinuity effect 77−79138
interferometric technique for liq. CO 79−65816
IR, monochromatic line isolation methods 77−74489
IR complex refr. index spectra, FT interferometry, errors in liquid-cell expts. 77−87814
IR refractometer measurements of optical cements 79−6164
isotropic and anisotropic media, meas. at 35 GHz 80−256
Langmuir film, refractive indices and mol. lengths meas. by optical waveguide probe 77−40294
laser active mdeium, refr. index change meas. by delay method 77−58336
laser coupling, new technique for refr. index and thickness meas. 77−88965
laser material nonlinear refractive index meas. by time-resolved interferometry 77−18088
lenslike medium, method for refr. index profile determ. 78−37046
lightguide fibre testing 80−64230
liquid, determ. with cell differential refractometer, prism wedge angle effect on meas. error 80−62715
liquid, extinction coefficient meas. using coaxial dual channel laser system 80−73425
liquid, wedge-film interference method 77−22352
liquid crystal, refr. index anisotropy, meas. using different methods *(French)* 77−16274

refractive index measurement continued
liquid crystal critical angle meas. 78−60413
liquid crystals refractive index meas. by cylindrical cell method 80−11358
liquid group refractive index meas. using synchronously pumped stimulated Raman oscillator 80−55059
liquid refractive index variation with temp. meas., interferometric technique 78−74050
liquids, as function of temp., using laser beam interferometer 79−58780
liquids, depend. on concentration at different wavelengths 80−88346
liquids, effect of light obs. on meas. 77−87808
liquids, high-press. optical interferometry to 14 kilobars 77−49764
liquids, refr. index meas. method., sensitivity, geom. optics 78−12480
liquids, refr. index meas. method, sensitivity 78−12479
liquids, use of electro-optical probes *(German)* 77−5889
macromolecules in soln., refractive index increments using holographic refractometer 79−27205
microscopic specimens, heterodox methods 79−30530
monodisperse nonabsorbing particles, refractive index determ. by light scatt. *(Russian)* 77−5891
monomode fibre selective excitation for differential group delay meas. 80−99876
multilayered structure, refr. index difference between adjacent layers, meas. technique 80−101829
multimode fibre bandwidth computation from measured index profiles 80−58740
multimode fibre waveguides, optical characts. meas. by backscatt. 80−23801
multimode optical fibre bandwidth computation from refractive index profiles 79−76815
multimode optical fibres, refr. index profile meas. 77−11034
nonabsorbing film with randomly rough boundaries, refr. index and thickness meas. 77−82589
noncircular optical fibre preforms, nondestructive index profile meas. 79−14105
optical fibre, γ-irrad., differential interferometric meas. of refr. index changes 80−78952
optical fibre, elliptical, unclad 77−14797
optical fibre, index profile meas., nondestructive 78−13796
optical fibre, index profile meas. from transaxial topography, optical method *(French)* 78−66778
optical fibre, index profiles using refracted near-field technique 79−37014
optical fibre, mech. deform. meas. by light scatt. method 80−14452
optical fibre, nondestructive determ. of refr.-index profile using forward light scatt. method 79−23060
optical fibre, profile measurement 77−27340
optical fibre, refr. index profile determ. from diffr. pattern 78−25953
optical fibre, refr. index profile meas., scatt. pattern method 77−7178
optical fibre, single layer, dimensions and refractive index meas. 77−79952
optical fibre, single mode, refr. index profile meas. by refl. method 78−46756
optical fibre, single mode, refractive index profile meas., focusing method 80−33144
optical fibre attenuation, bandwidth, and refractive index meas. methods compared 80−64190
optical fibre index profiles, focusing method, nondestructive meas. 79−27375
optical fibre index profiling by video analysis of interference fringes 78−55460
optical fibre preform, nondestructive profile determ. 80−1312
optical fibre preform, refractive index profile and cross-sectional geometry meas. method 80−91893
optical fibre preform index profiling, automatic nondestructive focusing method 79−50448
optical fibre preform refractive-index profile 79−59815
optical fibre preform rod, refractive index profile meas. by transverse differential interferogram 80−64141
optical fibre preforms, axially nonsymmetric refr. index distrib., nondestructive meas. 80−106601
optical fibre preforms, index profile determ. using focusing technique 79−50464
optical fibre preforms, using X-ray absorption measurements *(Japanese)* 80−87506
optical fibre profiling using scanning optical microscope 80−87535
optical fibre radial refractive index profile determ. 78−59137
optical fibre refracted near-field scanning, calibration technique 80−99823
optical fibre refractive index profile, automatic measuring technique *(Japanese)* 78−37982
optical fibre refractive index profile meas., near-field technique 80−91931
optical fibre refractive index profile meas., nondestructive transverse interference method 78−38024
optical fibre refractive index profile meas., Q-fibre method 78−66939
optical fibre refractive index profile microdensitometry 80−106632
optical fibres, automatic nondestructive index profiling of whole fibre samples 79−81527
optical fibres, index profile meas. 80−87538
optical fibres, index profile meas. using thick samples, interf. pattern 77−61111
optical fibres, measurement techniques for transmission loss and refractive index distribution *(Japanese)* 80−87498
optical fibres, new interferometric method 79−76816
optical fibres, preformed rods, automatic optical techniques 79−18541
optical fibres, refr. index profile determ. via spatial filtering method 78−33829
optical fibres *(Japanese)* 80−10020
optical fibres 80−43458
optical material continuous heterogeneities, interf. meas. 78−93756
optical materials, refr. index, nonlinearity, optical susceptibility meas. methods *(Russian)* 77−61112
optical thin film, thickness monitoring 79−97358
optical waveguides, methods and results 77−83965
particle medium, refr. index determ. from angular, polarisation characts. *(Russian)* 77−34827
perspex prism, crit. angle method, student expt. 80−12873
phase changes in optical recording media, interferometric meas. 77−49769

refractive index measurement continued
phase error cancellation in dispersive Fourier transform spectrometry 77−45902
phase inhomogeneities, 3-dimens., shadow method obs. 77−10094
phase velocity matching method *(Russian)* 78−30406
photoelastic material, holographic method for matching and measuring refractive index 79−17466
photoelastic specimen by immersion technique 77−41671
planar diffused waveguide, WKB approx. for refr. index profile determ. 78−30086
planar waveguide, index profiles determ. from angular depend. of refl. 78−71210
plant cell wall and cytoplasm refr. index determ. by interference microscopy 78−57151
plasma, high density, refractive index measurements using laser differential interferometer 77−55170
poly(p-phenylene terephthalamide) fibres, optical anisotropy determ. 79−4786
polymeric thin film, by integrated topical techniques 78−27342
powdered material, specimen prep. 77−156
prism, using critical angle method 78−30071
prism method, for teachers 79−21
profile of single-mode fibres by scattering pattern method 78−66935
radial distribution, optical method meas. 79−80669
radiowave propag. in lower troposphere over S.England, 6-year study of RRI and PRI 79−39823
real thin films, optical consts. determ. 78−35213
reflectance extrema for film refr. index determ. 78−70178
reflectivity and interf. methods for GaSe refr. index meas., 0.45 to 330 μm 77−63387
refractive index automatic profiling 78−46836
refractodensimetric analysis, liquor samples with low total solids 78−36972
refractometric standards, Comecon, selection criteria 79−30531
roughness evaluation from interference extremum amplitudes 79−78766
schlieren probe method for measurement of refractive index profile of shock wave in fluid 80−23785
scintillometer, saturation-resistant, for refr. index struct. parameter meas. 78−65411
semiconductor heterogeneity refractive index meas., interferometric method 79−6172
simple method for liquid 79−54174
single mode fibre transmission characts. and refr. index profile meas. from exit radiation pattern 80−9986
solid dielectrics, refractive index meas. in sub-mm. wavelength 77−18074
solid object, 3-dimens. of refr. index distrib. from multidirectional interferogram 77−71363
solid transparent samples, refr. index meas. by interferometry 79−95722
solids, Fabry-Perot interferometer 80−52297
solids, Fabry-Perot interferometric technique *(Russian)* 78−82023
spectrograph, continuously recording, for transparent/opaque insulators and semiconds. 79−17467
sugars, detect. in HPLC systems using polarimetry, refractometry and optical rot. 78−48734
surface layer of material, refr. index meas. using diffr. method 79−30532
tetrafluoroethane, specific refractivity, interferometric meas. 80−95124
tetrafluoromethane, specific refractivity, interferometric meas. 80−95124
thick planar films, transmission method for index meas., modal effects 80−102862
thin films, micromethod for refr. index determ. using liq. standards 79−67378
thin films, optical transmittance and reflectance, bulk optical props. determ. 80−88954
thin films for integrated optics, modified Abeles method *(Italian)* 78−1427
time-resolved interferometry, nonlinear refr. index meas. of glasses and crystals 79−3737
transferrin, human anal. density gradient equilib. centrifugation for determ. of mol. wt., sp. vol., preferential hydration 77−64160
transmission technique for planar film index-profile measurements 80−33230
transparent film, from zero refl.-induced ellipticity angles of incidence 78−41345
transparent film thickness and refr. index meas., polarisation-independ. reflectance matching 77−65052
transparent films, independent determ. of thickness and refractive index by MIS-11 microscope 77−49770
transparent films, on absorbing substrate, refr. index, thickness, ellipsometric meas. 77−52194
transparent layer refr. index and thickness determ., optical interf. method 78−89528
transparent solids, multiple-beam interferometers 80−52299
troposphere, radio refr. index and potential refr. index, S.England 79−34928
two dimensional distribution of refr. index changes in $LiNbO_3$:Ti strip waveguides 79−86254
vacuum automatic ellipsometer for condensing film homogeneity determ 80−101825
variable wavelength method for epitaxial garnet film 77−77309
very-small-angle light scatt. apparatus design and performance 77−10082
water vapour, from 0.3 to 1.5 THz 77−82596
weakly absorbing layers, interferometric determ. of optical parameters 79−17471
wedged film technique for As_2S_3 film 79−14066
$CdInGaS_4$, layered structure crystals, refractive index meas. method 80−98966
CdS, nonlinear refr. index meas. by nonlinear lens method *(Russian)* 79−26111
Cl_2, quadrupole moment determ. by refr. index anisotropy meas. method 80−78722
Ge single cryst. prism, refr. index meas., interlaboratory comparison 78−54443
Ge_xSe_{1-x} glasses, optical props. and local struct. *(French)* 77−77162
HF in absorption, anomalous dispersion meas. 80−95881
He-Ne 3.39 μm laser interferometer, length and refr. index meas. 80−68172
$LiNbO_3$:Ti, planar and channel optical waveguides, anisotropic diffusion expts. 80−64200
refractive index measurement continued
light-focusing rod refr. index profile determ., Interphako interf. microscopy method 80−101832
Si wafers layers, multilayer ellipsometry, layer thickness and refr. index determination of layers 80−95121
SiC, nonlinear refr. index meas. by nonlinear lens method *(Russian)* 79−26111
SiNH films, thickness and refractive index meas., comparison of techniques 80−8957
SiO amorphous film, optical transmittance and reflectance, bulk optical props. determ. 80−88954
SiO_2 films, thickness and refractive index meas., comparison of techniques 80−8957
SiO_2 HF plasma sputtered dielectric layer thickness and refractive index obs. 79−56931
Ta_2O_5 sputtered film for integrated optics, refr. index meas. *(Italian)* 79−32088
$TlInS_2$, layered structure crystals, refractive index meas. method 80−98966
refractivity *see refractive index*
refractometers
Abbe refractometer, self-calibration of polystyrene reference prism 77−55764
Abbe-type, IRF-454, specification, testing method and facilities 80−73424
automatic dioptometer with projection readout system 79−50455
automatic vee block refractometer design for glass refr. index meas. 80−68243
biomedical, IRF-454 and IRF-456 models 80−104715
cell differential, for liqs., prism wedge angle effect on meas. error 80−62715
differential, effect of light scattering in double-prism cuvette on error 79−75573
differential, for size exclusion chromatography of polyethylene glycols, response correction 79−34375
differential deviation, for liquid chromotography, high sensitivity and time response conditions *(Czech)* 78−80810
differential refractometer for continuous liq. phase residence time distrib. studies 80−17999
digital, for atmospheric radiowave refractive index meas. 78−86321
digital laser, interference band counter, automatic measurement appl. 77−67492
eye refractor, automatic, optical system 78−61274
Fabry-Perot interferometer as refractometer 80−264
fibre optics refractometers for liquid chromatographic use 77−2683
Fresnel cell redesign for REMAT 20 refractometer 78−21207
frustrated total internal reflection refractometer, optical consts. of absorbing media 80−9021
frustrated total internal reflection refractometry, for refractive index meas., foreign and Soviet refractometers 79−6165
holographic, for refractive index increments for macromolecules in soln. 79−27205
interference, for use with automatic interference comparator, length measurement appl. *(German)* 78−77966
interference fringes in wedge-shaped film, for teaching 78−61994
interference type, obs. of phosphatidylcholine dispersion phase transitions 78−44459
IR goniometric refractometer, construction and test results 79−71513
laser detector for anal. of liquids 80−101830
laser microrefractometer, temperature gradients in liquid, meas. 80−57362
low temperature refractometer for inert gas refr. index meas. 77−57382
microwave radio refractometer, expendable, lightweight, construction and performance 79−8708
microwave refractometer using Fabry-Perot interferometer, appl. to degree of moisture of air 77−18073
objective detection of light contrast limit, errors 77−74490
opticophysical and physicochemical meas. instrum. 80−13121
optoelectronic refractometers, design, construction and quantitative characteristics *(Russian)* 80−62716
photoelectric, semiconductor scanistor and operational amplifier design 77−53971
prism developments for PR2 Pulfrich refractometer 78−24848
Rayleigh interferometer, two-freq., performance as refractometer and anemometer 79−75579
recording refractometer for optical glasses, 300 to 2600 nm range 80−57363
REMAT 20 process-control refractometer, of photoelec. differential flow-through type 77−45885
spectrograph, continuously recording, for transparent/opaque insulators and semiconds. 79−17467
UV region SP-129 refractometer 80−31846
variable-focal-length, with wide meas. range *(Czech)* 77−18076
refractometry *see refractive index measurement*
refractories
see also ceramics; cermets; clay
abrasion test machine for use at high temp. 79−52505
actinide compounds, synthesis from oxides and single cryst. growth 80−16229
actinide oxide/rare earth oxide system, high temp. vaporization, valence effects 79−99309
actinide oxides, thermodynamic props. and high temp. chem. behaviour, comparison with lanthanide oxides 79−100127
Al_2O_3-SiO_2 refractories, using neutron-2 equipment 80−45612
alkali metal borides, prep., cryst. struct., thermal stability, phys. and chem. props., book contrib. 78−47304
alkaline earth oxide based compounds, thermodynamic study using CaF_2 electrolyte 78−53241
alloy, heat resistance and cold brittleness, achievements and trends 78−95718
alloy composites, refractory fibre reinforced, diffusional reaction, effect of alloying calc. 80−20851
alloys, creep mechanism and struct. changes *(Russian)* 79−52299
alloys, spectrochem. anal. using high-voltage unipolar spark discharge *(Russian)* 78−15750
aluminosilicate, high density prod. with spodumene additives 77−90310
aluminosilicate refractories, X-ray struct. determ. of quantitative phase contents 77−52707
aluminosilicate refractory, wetting by molten steel 79−82415

refractories continued
amorphous-crystalline substances, high temp. plastic deform. interpret. 77−35627
and UO_2-Gd_2O_3 solid soln., high temp. thermal expansion, 298-1700K 78−83979
apparent density determination, using surface γ densimeter 80−35464
badde-leyite-corundum refractories, qualitative X-ray phase anal. 78−7112
baddeleyite-corundum refractories, creep and annealing 78−84907
baddeleyite-corundum refractories, fused, elec. resist., 1300-2300°C 79−28345
baddeleyite-corundum refractories, thermophysical props. 79−82398
Bakor 33, refractory, stress relaxation capacity determ. 80−60910
blast furnace blocks, carbon-containing, apparatus for thermal conductance determ. 77−57329
bonding material of basic refractories, effect of SO_3, Na_2SO_4 and V_2O_5 79−83343
boride RF sputtered wear-resistant coatings, XPS study of adherence 79−34191
borides, book 78−48292
borides, manufacture and appl. in electronic and electrotechnic field *(French)* 80−40311
borides, metallic, sintering, review, book contrib. 78−48359
borides, proposed classification 80−19741
borides, refractory compounds, classification 79−94985
borides, transition metal, rare earth, and actinide, mag. props., book contrib. 78−47978
borosilicate glass, powder, sintering, foaming by chemical reactions 80−81017
carbide additions to sintered high-speed steel, effect on hardness and cutting performance 77−66608
carbide coating, oxidation protection 77−32704
carbide RF sputtered wear-resistant coatings, XPS study of adherence 79−34191
carbides, manufacture and appl. in electronic and electrotechnic field *(French)* 80−40311
carbides, thermodynamic evap. charcts., cluster-component calcs. 78−51704
castable, stability in steam-N_2 and steam-CO atmos. at 199°C 78−20063
casting-pit, quality control, specific non-standardized test development *(French)* 77−90297
cement, hardened paste, fracture meas. 77−4837
cemented carbides, fracture roughness testing 80−104410
ceramic, creep meas. in tension and compression 78−31486
ceramic, creep testing, equipment combination 78−11477
ceramic, deform. test apparatus and method *(Russian)* 78−35613
ceramic, heterogeneous, significance of non-elastic deform. in fracture 79−47765
ceramic coatings, for high temp. use, current status *(Japanese)* 80−71619
ceramics, synthetic raw materials, sintered and fused, use in refractories industry, slagging, creep, thermal thick resistance *(German)* 79−4937
chamotte concretes, phosphate binder based, strength props. 80−89305
chrome-forsterite-periclase refractory constitution and props., phase reactions during firing *(German)* 78−11175
classification according to brittleness and thermal shock resistance determ. 79−83321
coatings, deposited by electron evaporation, struct. and props. 79−23871
commercial, soln. in soda-lime glass, 1200-1350°C 78−95821
composite materials, creation of matrices with operating temp. of 1100°C *(Russian)* 77−55913
composites, fibre reinforced, directionally solidified tensile tests, in HVEM, deform. and fracture *(French)* 78−68785
compressive strength, hot 77−12677
concrete, refractory, high temp. mech. props. *(French)* 77−56019
concretes, review of new developments *(French)* 79−15636
corrosion rate in glass melt 79−70196
corundum, corrosion resist. in fused Li rel. to phase and microstruct. changes 77−44378
corundum, spinel formation during reducing heating 77−36427
corundum, thermal strength, effect of additives 78−19770
corundum refractories, dense production and performance 80−20866
corundum refractory ceramic deformation curve analysis *(Russian)* 79−90716
corundum-based refractory lining, wear resistance in combustion gas flow *(Russian)* 79−8370
corundum-based refractory lining specimen, thermal softening assessment *(Russian)* 79−83237
creep measurement, high temp., vacuum and rarefied gas flow installation 79−91864
creep testing, high-temperature, at different loadings, laboratory equipment *(Russian)* 78−19970
creep-rupture strength of EP199 in NH_3 and decomp. products *(Russian)* 77−52534
critical consts., review 78−59931
crystal growth, high temp., appl. of Stober technique 77−28709
crystal growth, use of Xe-lamp imaging furnace *(Japanese)* 80−50547
crystal high temp. properties *(Japanese)* 78−48418
curvilinear lining, thermal stresses 78−5649
dense, sintered, role of isostatic pressing 79−28995
dense products, high-temp. rheology *(French)* 77−32629
development from organosilicon polymers by heat treatment 80−81014
dielectric coatings appl. using electrodeless capacitor HF plasmotron 77−69984
dolomite, powders sintering, decarbonisation cycle effect 80−104102
double oxides, thermodynamic obs. using galvanic cells with CaF_2 solid electrolyte *(French)* 80−85190
elastic moduli measurement, US method for up to 2000K *(French)* 80−104373
elastic properties, test unit for up to 1500°C 79−57167
electrodeposition on liq. cathode, duty ratio 77−24975
electron structure, and phys. props. of infusible compounds 80−54585
electronic structure and chem. bonding 79−27948
electrosparking and surface hardening of steel *(Russian)* 78−95849
emission and adsorption props., rel. to electronic struct., review 77−76899
erosion resistance during action of highly concentrated energy fluxes 80−55562
exam. of brittle fracture props., using Hertzian indentation 79−11686
fatigue, effect of texture/crack relationship *(German)* 80−25829
refractories continued
fatigue behavior, effect of texture and crack kinetics, AE anal. *(German)* 80−21061
fibre, effect on high-temp. strength of refractory coatings *(Russian)* 77−52536
fibre, inorganic, refractory behaviour testing 77−25204
fibre, metallisation by continuous casting in Al and Al alloys *(Russian)* 78−35538
fibrous refractory, exam. of deform. behaviour and thermal cond. *(French)* 79−15719
filament, temp. control method and its appl. to W 79−9215
film evaporator with axially symmetric electron source 79−83125
film laser detector 78−41350
films, stability, high temp. and electron irrad. effects 77−39747
firing temperature effect for MgO containing refractories *(French)* 79−38770
fissure fixing for struct. anal. with television microscope 77−63846
flexural creep 79−29155
fracture toughness role in spalling resistance *(German)* 77−73316
fracture under thermal shock, AE study 80−25865
fusion reactor materials, neutron irrad., microstruct., voids, nucleation TEM study 80−29065
gas cooled reactors, internal insulation 80−47537
GCFR core-catcher crucible, material compatibility for UO_2-316 stainless steel graphite system 79−59171
glass fabric, effect of phosphate binders on properties 78−44075
glass making refractories, progress, review 78−3089
glass-making, progress, review 80−40303
graphite, CVD of TiB_2 coating 80−21131
graphite materials, wetting by pyroceramic melt, lining material 77−1831
graphite-based, survey 78−56609
graphite-SiC-FeSi crucible mat., oxidation loss and wettability of inorganic fluxing materials *(Japanese)* 78−84755
graphitised 79−82362
hard coating prep., electron beam evaporation in reactive atm. 77−44396
hardness, methods of increasing by prod. method 80−25643
heat conduction, contrib. of segregation and diffusion 80−20001
heat of formation determ. using self-propagating high-temp. synthesis 80−3392
heat resistance criteria on surface during convective heat exchange 77−15642
heat treatment of transformer steel, resistance of refractories in contact 80−66554
heat-resisting alloys, VM-1 and VX-4, thermal fatigue rel. to struct. changes *(Russian)* 78−11302
high temp.-high flux material testing, solar power station appls. 80−40668
high temperature materials problems, review 77−65329
high temperature metallic species, absorpt. and fluoresc., high temp. fast flow reactor technique 80−42231
high-temperature materials, technological requirements, R and D, report 80−45222
high-temperature materials for space power systems, mech. props. 79−57045
hot-wire test, critical review and comparison with BS 1902 panel test 80−104409
hydrogen embrittling effects from acoustic emission meas. 80−11742
integral degrees of blackness 77−35725
internal friction meas. from 20 to 2000°C in superhigh vac. 77−86249
ion bombarded surfaces, spectral refl. 77−55308
kyanite-sillimanite concentrate, sintering and mullitisation of basic minerals 77−59726
kyanite-sillimanite concentration, mullitisation and sintering, props. of refractory products 80−20867
laser heating system, for meas. of high-temp. props. of materials over wide press. range 77−77699
laser vaporised surface, free jet expsn. of vapour 78−1703
leucosapphire single cryst., W grid reinforced, growth 77−16530
lift-off process, appl. to high T_c supercond. circuits 79−47626
lubricating coating, solid, elemental anal. by proton-stimulated X-rays 78−88687
luminescence characteristics of pure surface acted on by flux of field emission electron 80−100695
magnesial refractory concretes, cast. props. 80−89306
magnesian-spinel materials form. using heat treatment 79−38773
magnesite, powders sintering, decarbonisation cycle effect 80−104102
magnesite artifacts, roasted, props., filler porosity effect 80−104099
magnesite refractories, spinel bindal, with reduced thermal cond. 79−83162
magnesite refractories, unfired, by resin phosphate binding 80−104101
magnesite-chromite powder, exam. of rheological charcts., compaction 78−60628
magnesite-dolomite refractories, tar bound, fracture and wear 80−104287
magnesite-phosphate mortar, rheological props. 77−23927
masonry with gunite coating adhesion strength determ. apparatus, breakaway tests 78−35618
metal, adhesional reactions with Ti 79−29280
metal, body centred, thermodynamic study of interstitial solid solns. *(Ukrainian)* 79−37845
metal, disturbed layer depth on abrasive lapping with TiC, NbC, WC micropowders 77−44391
metal, evaporation in inert gas atmosphere *(German)* 79−55879
metal, generalised model for prediction of periodic trends in sintering activation 78−64498
metal, group VI, activated sintering mechanism 79−91605
metal, refractory, BCC, free migration of self-interstitials 78−47574
metal, refractory, water vapour attack, immersion heater appl. in vacuum radiation furnace *(German)* 80−21184
metal, strength charact., effect of thermal test conditions 78−39994
metal, strength charact., error evaluation 77−16771
metal, surface geometry and emission parameters, changes during directional mass transport 78−2344
metal, vapour-phase epitaxial-growth *(Russian)* 77−59227
metal borides and carbides, thermal stability 79−8286
metal compounds, diffusive creep, theory *(Russian)* 80−40437
metal dichalcogenides and Ga alloys, mixing powders using US treatment 79−24454
metal powder adhesion forces on metallic substrates, electrostatic eval. method 77−52564

refractories continued
metal refractory single crystal growth by plasma heating *(Russian)* 78−35292
metal-Al_2O_3, systems, vaporis. at elevated temp., mass spectrometric obs. 79−29388
metal-H alloy prep. technique for TEM studies 77−90544
metal-Ni(Pd)(Pt)/Si interactions, phase separation 80−65303
metallic compounds, equilib. pressure of gaseous components, determ. by Knudsen method 79−52529
metals, and alloys, boride coatings, technology, props., book contrib. 78−48574
metals, Cl detect., spectrosc. method *(Russian)* 79−16095
metals, enhanced diffusion model for activated sintering 80−25612
metals, group V, diffusion of O and N, statistical calcs. on Arrhenius lines 80−59722
metals, mech. props. and diffusion figures *(Russian)* 80−40436
metals, nitriding reactions and processing conditions, thermodynamic approach *(Russian)* 80−21169
metals, oxidation, high-temp., mechanism, review *(Polish)* 79−34184
metals, technique for investigation of nonmetallic inclusions 77−52587
metals, work function, ionising radiation effects meas. method 80−6951
metals and alloys, processing by powder and vacuum melting techniques 79−33966
metals and alloys, refractory, surface investigation by FIM and atom probe *(German)* 79−55623
metals and alloys, safe-life testing *(Russian)* 79−52476
MgO:Cr^{3+}, single cryst., ESR linewidth 80−29605
MHD generator channel materials, thermophysical props. 77−28054
MHD generator duct wall, semi-hot, thermal stress design study *(Japanese)* 78−13890
MHD refractory materials, arc spot heat impact degradation *(Japanese)* 78−39819
microsamples, high-temp. mech. testing, unit 78−60904
mineral wool fibre composites, mech. props., effects of thermally induced phys. and chem. changes 77−59884
molybdenum ternary sulphides, Chevrel phase, synthesis and superconductivity *(German)* 80−25038
monocarbides, group IVa and Va, slip, microhardness, comments 78−84967
mullite, refractory ceramic creep, struct. effects 77−66679
mullite porcelain substrates, CVD growth of TiC whiskers, catalytic effect of refractory oxide 79−33211
mullite single crystal reinforced refractory with phosphate binder, compressive strength *(Russian)* 77−44293
mullite-based dispersed refractory system, rheological props. at high temp. 77−16629
mullite-corundum, reactions with FeO in different media 77−24994
multichamotte, sintering additives effect on props. 80−35147
multichannel ceramic blanks, produced from a refractory material 79−83163
multiphase systems, some novel effects, rel. to practical appls. 80−55460
Nb carbides, nonstoichiometric, elastic props., 20-2000°C 77−12661
neutron activation analysis using low energy accelerator 77−73499
nitrides, manufacture and appl. in electronic and electrotechnic field *(French)* 80−40311
nonmetallic materials, method of investigating in linear thermal loading 79−42327
nuclear fusion reactor materials development trends 77−46401
optical glass making appl., review 77−14818
oxide, coating on metal mould for Fe alloy casting, flame spraying technique *(Japanese)* 77−48586
oxide, high temp. props. conf., Odeillo, France (June/July 1977) 79−100125
oxide, solar furnace for high temp. studies *(French)* 79−70268
oxide, solid electrolytes, thermal and mech. props. at steelmaking temps., review *(German)* 78−15418
oxide, thermal shock resist. mechanisms 80−25860
oxide coating, prep. by plasma arc spraying and characterisation 79−23873
oxide development for fusion reactor first walls, chem. environment effects 80−83221
oxide electrolytes, elec. props. at steelmaking temps. *(German)* 77−90605
oxide layer growth by high-temp. electrochemical vapour deposition 78−23627
oxide-metal eutectic system 77−36483
oxides surface mass transport mechanisms obs. *(Japanese)* 80−54479
periclase refractories, props. after testing at over 2000°C 80−104317
periclase-spinel refractories, phase conversions up to 1720°C 80−25670
phosphate bonded refractory plastics, hot modulus of rupture, 1500 to 2500°F 78−19855
phosphate containing materials, technological prod. processes, review 80−97452
plasmochemical synthesis, powder dispersion control 80−55332
plasmochemical synthesis, powdered infusible compounds, props. 80−55330
powders, brittle, shock wave disintegration test method 80−66744
powders, wet decompaction and compaction 80−35150
process quality control, thermal analysis appl. *(German)* 78−35337
production by gas flame deposition from high melting oxides and compounds 77−21076
production by induction heated fusion crystallisation devices 77−63606
quartz sand, high-conc. suspension, prod. principles 80−66463
quartzite, vitrified, and quartzite based refractory concretes, prep. and props. 80−89188
radiant capacity, calorimetric meas. method 80−65259
rare earth chromite based electrode material development for MHD generators 80−84893
rare earth hexaborides, thermoelectronic props. rel. to surface state *(French)* 79−69950
rare earth monobismuthides, thermal expansion, thermal cond., 300-900K 78−91453
rare earth orthophosphates, high-temp. treatment and formation of oxyphosphates *(French)* 77−44199
rare earth oxide containing systems, highly refractive, phase equilib. and metastable phases 80−97467
rare earth oxides thermodynamic props. and high temp. chem. behaviour, comparison with actinide oxides 79−100127
rare earth oxymolybdates, growth from soln., struct., props. 77−28705
refinement during prep. by self propagating high temp. synthesis 78−60634

refractories continued
refining, at. absorpt. spectroscopy for continuous process control *(Russian)* 77−56302
refining in DC transferred arc, initiation and performance characts. 78−9866
resonant frequency meas. apparatus, elastic props. investigations 77−19576
RF sputtered, comp. by XPS 78−51839
rheological behaviour at high temp. *(French)* 77−56016
Sialon, prep. and charact. of ultrafine powders 80−11604
SiC fibre-reinforced Ti-alloy, component interaction kinetics *(Russian)* 80−55364
silicide coating, oxidation protection 77−32704
silicide coatings by local heating 77−81335
silicide RF sputtered wear-resistant coatings, XPS study of adherence 79−34191
silicides, oxidation and hot corrosion resistance kinetics 80−25896
single crystal growth, techniques 80−108341
sintered, X-ray diffraction method for assessing local stress levels 79−96265
sintered composite-liq. metal interaction, mass transfer eqn. approx. soln. 78−67262
slabs, radio wave phase method for quality control 80−40667
solid-phase reacts., effect of nonstoichiometry, thermodynamic evaluation 78−60632
solid/liquid reaction zones, electron probe microanalysis applic. *(French)* 77−32848
spectral emittance, meas. system at temp. up to 3000°C 77−22550
splat-quenching device, metals, alloys, in magnetic levitation furnace *(Croatian)* 79−11639
Spreading of liquid TiO_2 over refractory metals under the influence of surface forces 78−26749
sputtered carbides, adhesion to metal substrates, improved 80−76481
star dust, interstellar and circumstellar 77−41404
strength and thermal properties, automated test system 80−100986
strength determ., taking account of stress/deform. relations 77−28965
stress relaxation, high-temp., during alternating torsional loading 77−16636
subsidence, high temp., without load exam. using deform. during continuous heating *(French)* 79−15721
surfaces, heat of desorption of alkali metals 80−75430
swelling on proton, deuteron and He ion bombardment 78−67750
synthesis and cryst. growth by RF melting 79−70032
testing for casting bay appl. 77−25239
thermal conductivity, determ. standardisation 79−82397
thermal conductivity, hot wire meas. techniques 80−37038
thermal conductivity, hot-wire meas. method, 20-900°C 80−31759
thermal conductivity, microcracks contrib. 80−19999
thermal conductivity, rel. to gas phase mass transfer in pores and microcracks 79−73352
thermal conductivity, temp. and press. depend. 78−43188
thermal conductivity meas. at temps. above 1000°C 79−202
thermal expansion, and strain, filler content and temp. influence *(Russian)* 80−19964
thermal insulation, effective thermal cond., fibre diameter effects 80−104105
thermal shock, role of fracture toughness *(French)* 78−80618
thermal shock behaviour *(French)* 80−81084
thermal shock resist. criteria calc., rel. to deformability 79−29212
thermal shock resistance by resonant frequency expt. *(German)* 77−9009
thermal shock resistance charact. by permeability variation meas. *(French)* 79−96108
thermal strength under program controlled thermal loads 78−11325
thermal stress cracking resistance estimation 80−104288
thermal stresses produced by temp. gradient, finite element anal. *(Japanese)* 80−33538
thermomechanical testing, high-temp. installation 79−83425
thermophysical meas. above 2500K, apparatus 77−45845
thermophysical properties at high temp., conference, Moscow, USSR (May 1976) 77−28012
thermophysical props. in rarefied gaseous medium 78−34664
toughness measurement, expt. problems *(French)* 80−104368
transition metal, abrasive polishing mechanism 77−12745
transition metal borides, cryst. struct., prep. methods, chem., elec., mag. props., appls., book contrib. 78−47307
transition metal borides, refractory, single cryst. prep. methods and characterisation, book contrib. 78−48296
transition metal borides, refractory carbides, borides and nitrides, wetting by and interactions with liq. metals 80−54473
transition metal borides, silicides and germanides, binding energies from X-ray photoelectron spectra 80−49170
transition metal carbide, behaviour in Cs or K plasma 77−20979
transition metal carbides, abrasive props. of micropowders for lapping 77−63821
transition metal carbides, Group IV-VI metals, thermal expansion coeff., rel. to bond energy 78−2266
transition metal carbides, refractory carbides, borides and nitrides, wetting by and interactions with liq. metals 80−54473
transition metal carbides, solid-phase reacts., effect of nonstoichiometry, thermodynamic evaluation 78−60632
transition metal carbides, X-ray investig. of abrasive action 77−52497
transition metal carbonitrides, physicochem. props., comp. depend. 80−55370
transition metal compounds, electron and phonon behaviour 80−54624
transition metal nitrides, refractory carbides, borides and nitrides, wetting by and interactions with liq. metals 80−54473
transition metal nitrides of group IV-V, laser irrad. action, erosion strength *(Russian)* 77−56112
transition metal refractory materials, slip and microhardness 78−3211
transition metal silicides, group IV, thermal expansion, microhardness, Debye temp. meas. 77−35717
transition metal silicides, self-propag. high-temp. synthesis 80−2988
transition metal silicides for integrated circuits, review 80−100820
transition metal silicides of groups IV-VI, thermal cond., 20-1000°C 79−10992
transition metals and oxides, reactions of liq. alkali metals, relevance to reactor technology 80−85173
transitional metal sulphides, enthalpy and specific heat, temp. depend. 80−54406
tridymite, thermal expansion meas. 80−59682

refractories continued
ultra-lightweight, thermophys. characts., moisture effects *(Russian)* 77−55921
vacuum technology and wear resistant coatings, conf. Reutte, Austria, May 1977 79−57124
viscous-sheath filaments production 78−3077
wear-resistant coatings, composite struct. develop., props. 77−63618
X-ray powder diffr. meas. of phase composition, and flexural strength 80−3449
Zircon, fine ground, mechanised method of cleaning with acid 79−83357
ZrO_2 powders, stabilised, for plasma spray-coatings 80−20869
ALN, O_2 effects on sintering 77−77451
Al alloy, AK4-1, dispersion-hardening, US effects on ductility and thermal resist. *(Russian)* 77−32582
α-AlB_{12}, prep. and electrothermal props. 80−20863
AlC_xN_y, refractory deposit, prep. by thermal decomp. of Al dialkylamides and characterisation 80−11572
$AlMgB_{14}$, prep. and electrothermal props. 80−20863
AlN, cpd. form. reaction in reactive evaporation, quadrupole mass analysis *(Japanese)* 78−23628
AlN film, epitaxial growth by reactive evaporation *(Japanese)* 78−23629
AlN films, RF reactive ion-plating, struct. and morphology 80−104074
AlN, hot pressed, effect of O_2 content on flexural strength and compact density 79−11668
AlN, plasmochemical synthesis, powder dispersion control 80−55332
AlN powder, effect of O impurity on sintering and thermal cond. *(Japanese)* 79−20017
AlN powder, plasma synthesized, sintering behaviour, props. and struct. 79−100097
AlN powder, production using Al powder in N plasma with electric discharge 79−33990
AlN powder, synthesis, in low-temp. plasma 80−16257
AlN, powder shock wave compression prior to sintering 77−66615
AlN powders, synthesis and impurities 80−55329
AlN, precipitation from gas phase 78−6025
AlN, prep. and charact. of ultrafine powders 80−2983
AlN, ultradispersed powder, IR spectra 80−50312
AlN whiskers, strength rel. to growth conditions using vapour-liquid-solid method 79−11052
AlN-Si_3N_4-Be_3N_2 system, phase equilibria 80−60844
Al_2O_3, arc spot heat impact degradation *(Japanese)* 78−39819
Al_2O_3, ceramic Sinoksal, strength variation dependence on type of loading and temperature 79−57080
Al_2O_3, chemical reduction by atomic hydrogen 79−93830
Al_2O_3, composite base ceramic coating, hot pressed, H_2 permeability 77−56164
Al_2O_3 compounds, shrink free, prod. method using slips made from clay, orthophospheric acid 80−66460
Al_2O_3, crack detection caused by thermal shock, AE technique *(Japanese)* 80−21248
Al_2O_3, elastic moduli meas., US method for up to 2000K *(French)* 80−104373
Al_2O_3 electrical conductivity near melting point 77−28176
γ-Al_2O_3, film, enhanced activated reactive evaporation process, ion effect 79−66013
Al_2O_3 films, amorphous, self-supporting, vac.-tight, from electrochem. oxidation of Al in $(NH_4)_2CO_3$ solns. 80−16177
Al_2O_3, fracture, J-integral meas. 80−108537
α-Al_2O_3, fusion cast refractory, effects of glassy phase on thermal cycling resist. 78−84956
Al_2O_3, molten, specific elec. cond. up to 3000K 78−2273
Al_2O_3 porous refractories, production 80−35149
Al_2O_3, reactions with Ti-Al-Cr-Mo alloy VT3-1 80−16585
Al_2O_3 refractories, stability of refractory bond phases in steam-CO atmosphere 79−24634
Al_2O_3, sintering as function of phase comp. 80−66464
Al_2O_3, vacuum condensate, struct. and mech. props., second phase effect *(Russian)* 80−71705
Al_2O_3, vaporisation process, mass spectrometric exam. 77−1220
Al_2O_3, wettability of single crysts. by liq. metals *(Russian)* 77−43408
α-Al_2O_3/graphite mixtures, high corrosion resistance refractory materials, fracture anal. *(French)* 79−70137
Al_2O_3-Cr(Re)(Nb)(Ta)(Ti)(V) heterophase films, elec. props. rel. to Al_2O_3 content 77−15969
Al_2O_3-Na_2O, β and β'' phases, formation by solid state reaction between $NaAlO_2$ and γ-Al_2O_3 80−29912
Al_2O_3-SiO_2, SiO_2-rich glassy phase, deconvolution of microprobe conc. profiles 77−52606
Al_2O_3-SiO_2, thermomech. props., dependence on struct. and composition 78−84748
Al_2O_3-SiO_2 heat insulating refractories, prep., physical, thermal, structural props. 78−68662
Al_2O_3-SiO_2 refractory, creep, viscosity, resist. to inelastic deform. 80−89309
Al_2O_3-SiO_2 refractory concrete, elastic props. 80−89280
Al_2O_3-SiO_2-Fe_2O_3-CaO-MgO-TiO_2, refractory, corrosion and mech. behaviour correlations 80−40563
Al_2O_3-SiO_2-ZrO_2 refractories, corrosion behaviour in glassmelting furnaces *(Polish)* 80−71783
Al_2O_3-TiO_2 (1 wt.%), with and without α-Al_2O_3 laminar crystals, bend tests 77−16531
Al_2O_3-TiO_2 (1 wt.%), with and without α-Al_2O_3 laminar crystals, heat resistance 77−16532
Al_2O_3-ZrO_2 cast refractories, nucleation processes reconstruction by SEM, TEM and STEM 78−35380
Al_2O_3-ZrO_2-SiO_2, fusion cast refractory, effects of glassy phase on thermal cycling resist. 78−84956
Al_2O_3-$ZrSiO_4$, granular corundum-zircon refractory, development 80−66462
B C powders, effect of C on sintering 80−40312
B, fibre, metallisation by continuous casting in Al and Al alloys *(Russian)* 78−35538
B-B_4C materials, hot-pressed, elastic modulus and flexural strength rel. to grain size and porosity 79−79018
B_4 C, mech. and thermal props. 80−21083
BC, fine powder prod. *(German)* 77−32549
BC, sintered and hot pressed, friction and wear, 20 to 1500°C 78−60844
$B_{12}C_3$, sintering and subsequent high temp. annealing, struct. and props. 80−20858
refractories continued
B_4C, densification kinetics during hot pressing, 1800-2200°C 80−60817
B_4C, effect of fast neutron irradiation on struct. 78−26597
B_4C, FBR control rod elements, neutron damage and post-irrad. annealing 80−13581
B_4C, synthesis in HF EM field 80−20864
B_4C-Ti(V)(Cr), contact reaction with liq. Ni 80−55707
BN, contact reactions with Ti and WC-Co at high pressures 80−61029
BN, cubic, high pressure synthesis, solvent effects 80−40310
BN, cubic struct. form. from hexagonal struct. at high press., catalytic effects *(Japanese)* 77−90308
BN, degree of conversion from cubic to hexagonal, determ. method 79−15887
BN fibres, prep., struct., thermal, mech. and elec. props., appls., book contrib. 78−48360
BN, hexagonal, prod., props., uses *(German)* 79−74120
BN, hexagonal, prod. from CaB_6 *(German)* 79−74121
BN, high pressure synthesis, exam. of relationship between synthesis condition, and crystal shape, size *(Japanese)* 79−20018
BN, high temp. compatibility with insulating oxides 77−24995
BN, high-temp. plasmochem. synthesis, control of props. 80−55333
BN in contact with W, barrier layers for good high-temp. stability 79−70194
BN, low-Z material, outgassing expts. 79−209
BN, polycryst. cubic, props. 80−21013
BN powder, shock wave compression prior to sintering 77−66615
BN powder, wurtzite sphalerite struct. phase transition, effect on substruct. 80−25690
BN, shock synthesis *(Japanese)* 80−29918
BN, shock-compressed pyrolytic and hot-pressed, phase transitions to 120 GPa 77−70048
BN, sphalerite to graphite-like transform. in the 1100-1700°C range *(Russian)* 77−16572
BN, sphalerite transform., simple direct mechanism *(Russian)* 77−21135
BN, wurtzite, chem. comp. and processing props. in prep. of Geksanit-R sinterings 80−25632
BN, wurtzite-type, lattice distortions 77−11636
BN_x refractories, thermal cond. determ. using IR laser heating 79−94479
B_6O, mech. and thermal props. 80−21083
$B_{14}Si$, β rhombohedral, conduction mechanism, thermoelectric props. 80−24932
$B_{14}Si$ refractory thermoelectric material CVD and application 77−77411
$BaAl_2O_4$-Ba_2SiO_4-$BaZrO_3$, fusibility diagram 79−83184
$BaHfO_3$, $BaSnO_3$ and $BaZrO_3$, high-density ceramics prep. and elec. props. 80−60812
BaO-Al_2O_3-SiO_2-Ta_2O_5-Mo glass ceramic metal composites, cermet prep. 80−11618
$BaSc_2O_4$, synthesis, thermal stability, emissivity, reduction processes 77−8791
$Ba_3Sc_4O_9$, synthesis, thermal stability, emissivity, reduction processes 77−8791
BeO, arc spot heat impact degradation *(Japanese)* 78−39819
$Be_9Si_3N_{10}$, TEM, direct obs. of cryst. struct. 79−60339
C fibre reinforced C, appl. as refractories, toughness props. 79−38782
C impregnated oxide refractory melt, C oxidation 79−91828
C materials, thermal insulating props., furnace appls. *(French)* 78−44345
C refractories, alkali attack as catalyst for oxidation 80−40562
C, vitreous, disintegration by fluorophosphate optical glass melt 78−30101
C-refractories, thermal expansion 79−82362
$CaAl_2O_4$ compounds and cements, quantitative thermogravimetry after hydrothermal treatment 80−16737
CaO based refractory from industrial lime, with 5% added electrocorundum 80−89184
CaO, corrosion by K_2O melt, SEM obs. 77−44383
CaO-Al_2O_3-H_2O system, chemical degradation under high gaseous pressure and temp. 79−20464
CaO-MgO refractory, wettability by Fe melt *(Russian)* 78−10257
CaO-MgO-Al_2O_3-Cr_2O_3-Fe-O_2-SiO_2 system, exptl. determ. of periclase and spinel comps. 78−6906
CaO-MgO-Cr_2O_3-Al_2O_3-ZrO_2-SiO_2 system, subsolidus region characts. 80−97466
CaO-MgO-ZrO_2-SiO_2 refractories, phase diagram 80−11634
$Ca_x(PO_4)_y(OH)_z$, nonstoichiometric, wet-process formation from α-$Ca_3(PO_4)_2$ *(Japanese)* 78−84752
CaS, oxidation kinetics 79−52407
$CaSnO_3$ and $CaZrO_3$, high-density ceramics prep. and elec. props. 80−60812
$CaTiO_3$, perovskite, raw material activity and firing conditions as factors in sintering and grain growth 79−83161
$CaYAl_3O_7$, type of melting, crystallisation from melt 77−12515
CeO_2, plasma deposition of crysts. and their characterisation 80−20800
Co-Cr-WC, corrosion and corrosive wear in sea water 78−92408
Co-W-C system, η-carbide linear expansion coeff., X-ray diffr., 30-1500°C 77−25021
Co-WC, corrosion and corrosive wear in sea water 78−92408
$(Cr,Al)_2O_3$-$ZrSiO_4$, glass resist. and corrosion mechanism 79−61757
Cr-Mo-N system, at high-pressure, temp., X-ray anal., phase diagram 80−50607
Cr-Ni, high temp. strength, interatomic bonds ionic component correlation *(Russian)* 79−15761
Cr_2C_3 reactions with Ti-Al-Cr-Mo alloy VT3-1 80−16585
CrB_2, reactions with Ti-Al-Cr-Mo alloy VT3-1 80−16585
CrC electrophoretic coating, electric field strength effect on deposition rate 78−19677
Cr_3C_2 (Cr_7C_3) based coatings, detonation deposited, wear resist., 20-1000°C 80−11843
Cr_3C_2 electrophoretic alloy coatings on C steel, sintered, struct. form., Ni-P undercoat effect 80−61027
Cr_3C_2, form. from Cr_2O_3/graphite mixture in H_2 atmos. *(Japanese)* 78−92225
Cr_3C_2, reactions with Ti-Al-Cr-Mo alloy VT3-1 80−16585
Cr_xC, cathodic needle growth, at lower electric fields from $Cr(CO)_6$ vapour 80−76161
Cr_xC_y-(Ni-Cr) sprayed coatings, for gas cooled reactor heat exchangers, factors affecting performance 80−40609
CrN, deposition by hollow cathode discharge process, and hardness 79−24452

refractories continued
CrO_2 semidry refractory, struct. and mech. props., surface-active agents effect 80−89304
Cr_2O_3, RF sputtered coating for wear appls., on Inconel X-750.foil, prep. and props. 80−40605
Cr_2O_3, sintering behaviour, effect of TiO_2, C additions 80−66461
Cr_2O_3, sintering in air and reducing atmos., effects of oxide additions 77−59729
Cr_2O_3, slips and castings, rheological and technological props. 77−16779
Cr_2O_3-Al_2O_3-$ZrSiO_4$ system, electrosmelted refractories, phase comp., corrosion and glass resist. Cr^{3+} conc. depend. 79−33982
Cr_2O_3-ZrO_2 granules, from spray drying of suspensions 80−104100
Cu-Al_2O_3 dispersed composite, electron beam deposition, struct. characterisation 77−44197
Cu-Al_2O_3 dispersed system, electron beam evaporated thick film, struct./prop. relations 77−44198
Cu-BN composite electromachining tools, dynamic hot pressing 80−84889
Dy_xB_y, prep. and props., DTA study 80−20859
$3Er_2O_3$-Ta_2O_5 refractories, prep. and anal. 77−48384
Fe oxides, phase equilibrium and microstructure interpretation 80−60847
Fe-Cr-Si, heat resistive films prepared by sputtering, lifetime meas. 80−80132
Fe-Cr-SiC-B_4C powder mixture, compressibility and elec. cond. in cold pressing under low press. 78−60609
Fe-TiC pseudofused composite magnetoabrasive powders, props. 80−100926
Fe_3O_4, single cryst. growth by melt transport in DC arc 77−8745
Hf-Ta alloy, prep. by carbide-oxide reaction 77−12554
HfC, single crystal growth by plasma heating 78−60569
HfC-HfB_2 alloys, wear in vacuum, role of boride phase 80−21113
HfN_n, effect of equilib. N_2 press., 10^{-2} to 100 atm, on MP 77−36465
HfO_2, plasma deposition of crysts. and their characterisation 80−20800
HfO_2, stabilised comps., elastic props. rel. to porosity and temp. 80−81096
HfO_2-CeO_2, solid solutions 77−16549
K triple orthoarsenates, $KM^{II}Cr_2(AsO_4)_3$, prep. by high temp. synthesis, and cryst. struct. 79−66028
La compounds, plasma light reflection by free charge carriers 80−11403
La-N-C system, metallographic investigation *(German, English)* 77−52600
LaB_6 (001) surface, struct., initial oxidation, XPS, UPS, LEED, AES, work function meas. 79−99403
LaB_6 (100), (110), and (111), surface structs. and work functions 80−70512
LaB_6 surfaces, (100), (110) and (111), electron states, UPS study 80−100752
LaB_6 synthesis by heating BN with lanthanum citrate hydrate 80−100819
LaB_6 thermal and electrical conductivities, 1000-2100°C 77−69293
LaB_6, US comminution of refractory compound powders 78−23656
La_2O_3-Y_2O_3, phase diagram at high temps. *(Japanese)* 77−70038
La_2S_3-LaS_2, p-T-x phase diagram of La-S system 77−21112
La_2Se_3, La_2Te_3, mutual solubility 77−21113
La_2Te_4, thermal cond., thermoelec. power abd elec. cond. meas., 80 to 750K 78−18853
$La_{10}W_2O_{21}$, enthalpy and heat capacity at high temp. 80−70424
α-La_2WO_6, enthalpy and heat capacity at high temp. 80−70424
$La_6W_2O_{15}$, enthalpy and heat capacity at high temp. 80−70424
Li_2S-Al_2S_3, prep., phase props. and elec. cond. 79−96010
$Mg(Al,Cr,Fe)_2O_4$, spinel, elastic moduli calc. 78−6960
$MgAl_2O_4$, corrosion resist. in fused Li rel. to phase and microstruct. changes 77−44378
$MgAl_2O_4$, polycrystn., strength-grain size relations 79−79081
$MgAl_2O_4$ spinel refractory, enthalpy and specific heat determs. 80−88334
$MgCaH_{3.72}$, synthesis and struct. *(Japanese)* 78−84751
$MgCr_2O_4$, spinel refractory, enthalpy and specific heat determs. 80−88334
MgO and MgO-dolomite, crack detection caused by thermal shock, AE technique *(Japanese)* 80−21248
MgO, arc spot heat impact degradation *(Japanese)* 78−39819
MgO ceramic, erosion resistance in reaction products flow *(Russian)* 77−25173
MgO, corrosion resist. in fused Li rel. to phase and microstruct. changes 77−44378
MgO, Cr bearing basic refractory, prod. from brine MgO 79−83158
MgO, fused periclase, sintering and struct. characts. 78−23652
MgO, granular, first-order stresses due to thermal shock 77−40409
MgO, precipitation from gas phase 78−6025
MgO, rate of reduction by C 77−28743
MgO, single cryst. growth using modified plasma torch furnace, doping *(Japanese)* 79−95923
MgO single crystals, crack formation process, micro-deformation and fracture *(Japanese)* 80−24530
MgO, sintered, refractories, props. after testing at over 2000°C 80−104317
MgO, sintering, effect of Ca compound additions *(Japanese)* 80−55340
MgO, sintering by activating $3MgCo_3.Mg(OH)_2.3H_2O$ 80−89183
MgO, substructure, X-ray diffraction study, rel. to preparation by thermal decomposition 77−12581
MgO, thermal expansion, 500-1800°C, X-ray diffr. 77−35723
MgO, wettability of single crysts. by liquid metals *(Russian)* 77−43408
MgO-$(Cr_2O_3)(AP_2O_3)(Fe_2O_3)(SiO_2)$, vaporization 79−99308
MgO-Al_2O_3-Cr_2O_3 refractory system, phase conversion and props., X-ray anal. 77−90336
MgO-Al_2O_3-ZrO_2, wetting with liquid Fe and Al 78−22936
MgO-C in melts, corrosion resist., rel to oxidation, porosity, content 80−40578
MgO-$CaMgSiO_4$-$(Al_{0.5}Cr_{0.5})_2O_3(Al_2O_3)(Cr_2O_3)$, spinel phase, phase equilibrium relations and spinel bonding 80−55376
MgO-CaO refractory ceramics, thermal expansion coeffs. 79−99336
MgO-CaO-Fe_2O_3-Al_2O_3-SiO_2, clinker production from dolomite and magnesite 80−55339
MgO-CaO-FeO-Fe_2O_3-SiO_2-Cr_2O_3-Al_2O_3 spinel refractories, physicochem. prod. conditions 80−89185
MgO-CaO-SiO_2-Al_2O_3-$Na_2O.P_2O_5$, effect of $NaPO_3$ on phase composition rel. to basic refractories 78−80528
MgO-CaO-SiO_2-C, equilibrium partial press. of Mg, SiO, Ca and CO 77−36482
MgO-Cr_2O_3, vacuum vaporisation 78−91434
refractories continued
MgO-$MgAl_2O_4(FeCr_2O_4)$, thermoplastic and thermophys. props. for steel vacuuming installations 80−35281
MgO-NaCl refractory clinkers, Cr containing, densification, thermal treatment and phase composition effect *(French)* 80−76219
MgO-spinel concrete, cast, hardening by elec. heating 80−21258
Mn_xN_y, prep., rate of formation, chem. stability 78−11185
Mo, CVD films of high IR reflectance 79−52119
Mo, candidate refractory for Tokamak, thermal fatigue failure testing 80−32454
Mo, electrical resistance data in the region 300 to 2800K 77−43555
Mo, ionic siliciding, diffusion layer prod. 78−23855
Mo, liquid, spectral emissivity and brightness-temp. meas. at MP 77−43356
Mo, powder, defective structure and activated sintering, exam. 80−16240
Mo, single crystal growth by plasma heating 78−60569
Mo, specific heat near melting point, rapid pulsed heating method 77−35704
Mo, thermal conductivity and electrical resistivity, 300 to 2600K 77−35913
Mo, thermal expansion, 100-2546°C 77−66032
Mo wetting by Cu-Ag-P alloy 79−82417
Mo-Cr, powder mixture, activating effect of Group VIII metals on alloy form. during sintering 77−59728
Mo-Y(La)(Ce)-B, X-ray diffr., reciprocal lattice, crystal struct., phase equilibria 77−21122
Mo-ZrC, internal oxidation, struct. formation law, microstruct. examination 78−84836
MoB_2, hexagonal, form. by plasma heating and props. 79−28996
Mo_2B_5, monocryst., grain size, abrasive and strength props. 80−11787
Mo_2B_5-based alloys, mech. props., rel. to appl. as electrodes in electrospark machining 80−21174
Mo_2C, free energy of form. and thermodynamic props. of C in solid Mo 80−15266
Mo_2C powder form. by CVD 77−12590
Mo_2C, synthesis by ion bombard. of Mo film 78−48357
Mo_xC, cathodic needle growth, at lower electric fields from $Mo(CO)_6$ vapour 80−76161
Mo_3N, synthesis by ion bombard. of Mo film 78−48357
$MoSi_2$ film, elastic stiffness and thermal expansion coeffs. 80−107451
$MoSi_2$, oxidation in CO_2, 1200-1700°C 77−40454
$MoSi_2$, reaction VT3-1 80−16585
$MoSi_2$ refractory formation by As^+ ion beam bombardment 80−107286
$MoSi_2$, self-propag. high-temp. synthesised, sintering and props. 80−11616
$MoSi_2/TiGe_2$ mixed crystals, direct obs. of surface oxide form. *(German)* 77−12721
Na triple orthoarsenates, $NaM^{II}Cr_2(AsO_4)_3$, prep. by high temp. synthesis, and cryst. struct. 79−66028
$NaCaPO_4$-Ca_2SiO_4 partial system, phase diagram 78−35364
$NaCaPO_4$-Ca_3SiO_5 partial system, phase diagram 78−35365
NaF, sintering, relation between densification and grain growth 77−12585
Na_2S-Al_2S_3, prep., phase props. and elec. cond. 79−96010
Nb coated Mo, Ti, evaporation, carburisation and diffusion behaviour 77−44410
Nb, fusion reactor first wall material, cyclic deform. tests 80−30074
Nb, H_2 isotope release 80−37580
Nb, liq., spectral emissivity and brightness-temp. meas. at MP 77−43356
Nb, single crystal growth by plasma heating 78−60569
Nb wetting by Cu-Ag-P alloy 79−82417
Nb-Ir(Rh) system glasses, form., crystn. and microhardness, resist. obs. 80−89178
δ-Nb-N, plates and powder, oxidation *(French)* 79−66184
Nb-Nb_2C, directional crystn. using plasma heating 78−60569
Nb-W-X-C, X=Ti, Zr, Hf, quenched from liquid state, formation of nonmetallic inclusions *(Russian)* 79−57007
NbB_2, hot pressing 80−25635
$NbBe_{12}$, by diffusion saturation in vacuum, resistance to heat 78−44259
NbC, and NbC-ZrC solid soln., prep. by impregnation, strength, surface submicrocracks 77−16661
NbC crystals, electron energy spectra 80−49568
NbC, deformation behaviour during rubbing in wide temp. range 80−16486
NbC, deposition with vapour-gas phase circulation in closed circuit 77−55927
NbC, elastic modulus, porosity factor 77−21207
NbC, exam. of temp., and composition effects, on diffusion coeff. in its homogeneity range 79−33115
NbC fibre reinforced Ni-Cr, eutectic, unidirectional solidification, thermal cycling, temp. range effect on microstruct. 80−89272
NbC, high-temp. plastic deform. effects on elec. props. 77−44370
NbC micropowder surface finishing of metals, surface struct. 80−11842
NbC, recrystallisation 78−11251
NbC, refractory micropowder, geometric parameters of grains 77−16529
NbC single cryst., Vickers microhardness, slip mechanism 80−71732
NbC single crystals, synthesis and impurities 80−55329
NbC, supercond. transition temp. and lattice dynamics 79−56361
NbC, vacuum condensate, struct. and mech. props., second phase effect *(Russian)* 80−71705
$NbC_{0.98}$, single crysts., creep, 1800-2700°C *(Russian)* 79−5005
NbC_x, creep-comp. curves for homogeneous region 78−52911
NbC_x, monocrystal, work function anisotropy of electrons *(Russian)* 79−73568
NbC_x, stoichiometric and defective phases, electronic energy spectrum and physical props. *(Russian)* 77−35868
NbC_x, thermophysical props. at high temp., thermal vacancies form. 78−43141
Nb_xC powders, plastic deform. characts. on vibratory milling 78−11183
NbN preparation, by precip. from gaseous NgF_5-N_2-H_2 mixture 80−20857
NbN, supercond. transition temp. and lattice dynamics 79−56361
$Nb_{40}Ni_{60}$, 3 MeV Ni^+ ion implantation, electron microscope exam. of ion damage 78−91365
Nd_2O_3-HfO_2 system, phase relationships 80−35169
$Nd_2Zr_3O_7$-$Nd_2Hf_2O_7$, struct., elec. cond. and melting point 80−54197
Ni-(W,Cr)C, corrosion and corrosive wear in sea water 78−92408
Ni-Cr-NbC eutectic composite, unidirectional solidification, thermal cycling, temp. range effect on microstructural degradation 80−89272

refractories continued
Ni-ZrO_2, dispersion-strengthened condensate, density and mech. props. 77−44196
NiO single crysts., creep along ⟨100⟩, stresses 50 MPa-120 MPa, 950-1200°C, O diffusion *(French)* 79−20121
NiTaC, eutectic alloys, chem. incompatibility of ceramic nitrides for directionally solidifying 80−81046
Pb-Cr-O system, equil. relationships, stability limits 77−59765
Pr compounds, plasma light reflection by free charge carriers 80−11403
PuO_2 refractory, dissolution in HNO_3-HF-H_2O at 100°C 77−18683
ReS_2, prep., struct. 79−38774
Rh, single crystal growth by plasma heating 78−60569
Ru, liq., spectral emissivity and brightness-temp. meas. at MP 77−43356
Sc_2O_3, fission and phase transition enthalpies 79−99299
Sc_2O_3, liq. and solid phase elec. cond., high temp. meas. 80−84468
Si-Al-B-O-N, calc. of phase diagrams from data set 80−55362
Si-Al-Zr-O-N, calc. of phase diagrams from data set 80−55362
Si-based, survey 78−56609
SiB_{12-x}, thermam cond., temp. depend., up to 2000K *(French)* 80−70484
SiB_4, mech. and thermal props. 80−21083
SiC, abrasive, evaluation of brittleness, contact endurance by cyclic microhardness 79−15890
SiC, abrasive, wear in simulated hot grinding 78−56784
SiC, appl. of replica electron fractography 79−60237
SiC base material, electrical props., heat treatment effect 77−12645
SiC, $\beta \rightarrow \alpha$ transformation, microstructural aspects 79−8295
SiC, $\beta \rightarrow \alpha$ transformation, interfacial energetics 79−8296
SiC, CVD, microstruct. obs., optical and TEM 79−7560
SiC, chem. stability, mech. and thermal props. rel. to appls. 80−21103
SiC coated fuel particles, failure during thermal excursion above 2000°C 79−36317
SiC containing material, deform. props. investigation by pure bending 78−19823
SiC, continuous fibre synthesis with high tensile strength and Young's modulus 79−15633
SiC, controlled nucleation thermochemical deposition, charact. and props. 80−108355
SiC, dense, joining by hot pressing, and bond strength 80−66458
SiC, dissociation in silicate bonded refractories, X-ray obs. *(German)* 79−47893
SiC, dissolution rate in molten Si, Fick's law calc. 79−99319
α-SiC, effect of cryst. shape and size on plastic deform. to rupture and strength 77−56043
SiC, electron microscopical fractography *(Russian)* 77−25146
SiC, fibre, metallisation by continuous casting in Al and Al alloys *(Russian)* 78−35538
SiC fibre development using organosilicon polymer precursor 78−60627
SiC fibres obtained from polycarbosilane fibre 80−50582
SiC, form. from SiO_2 flour and coke breeze, kinetic and mechanistic study 79−15979
SiC, fracture toughness and high-temp. slow crack growth 80−81153
SiC, fusion reactor first wall appl., radiation damage 79−86822
SiC, grinding, effect of grinding wheel material, particle size, temp. *(German)* 79−43173
SiC, grinding material, grain shape optimization *(Polish)* 80−29916
β-SiC, growth kinetics by Van Arkel method 77−16479
SiC, HVEM obs. of various polytypes 80−76248
SiC heating element, resistance meas. instrument 77−71349
SiC heating elements for elec. furnaces, elec. cond. 79−69510
SiC, high density, development for heating elements using planning method 77−12584
SiC, hot pressed, bending strength *(German)* 79−24571
SiC, hot pressed, K_{Ic} and delayed fracture meas. 79−61701
SiC, hot pressed, oxidation *(German)* 79−96161
SiC, low blow Charpy impact 79−34122
SiC microtubes, formation by carburisation of Si whiskers 80−81011
SiC, one dimensional disorder 78−51492
SiC, oxidation and corrosion behaviour, formation of protective SiO_2 coatings *(German)* 80−25885
SiC, oxidation and hot corrosion resistance kinetics 80−25896
β-SiC, oxidation in CO-CO_2 mixture *(German)* 78−23844
SiC, oxide scale microstruct. of oxidised single cryst. 80−108613
α-SiC, plastic deform. 77−12673
β-SiC, polycryst., ^{30}Si self-diffusion 80−100350
SiC, polycrystalline, quantitative phase analysis, statistical estimation and mathematical splines *(Bulgarian)* 78−39753
SiC polytypes, lattice imaging studies on intergrowth structs. 80−107025
SiC, polytypic transform. during hot pressing 78−52739
SiC, polytypism, effect of furnace temp. and contamination *(Polish)* 79−27969
β-SiC, powder, synthesis by chemical vapour phase reaction from methylsilane, exam. of props. *(German)* 79−4938
β-SiC powder compact, microstruct. changes and β to α transform., Si vapour influence 78−19738
SiC, powder mixtures, composition vs. apparent density diagrams construction, model 78−60633
SiC powders, form. by vapour phase method 80−25623
β-SiC, prep. by siliconisation of C black, sinterability *(Japanese)* 79−78921
SiC, pressureless-sintered, high temp. strength *(Japanese)* 80−104299
SiC protective coatings, on graphite for HTR, corrosion *(German)* 78−3248
SiC, REFEL, strength parameters 77−1830
SiC, reaction bonded, microstruct. characterisation 78−48353
SiC, reaction bonded, microstructural characterization 79−100093
SiC, reaction sintered transform. interface morphology 78−31364
SiC, reaction-bonded , 'REFEL', microstruct. characterization 80−97490
SiC, reactions with oxidising atms. 80−11812
SiC, resist. to oxidation and corrosion at high temps. *(German)* 80−35357
SiC, self bonded, exam. of fracture 79−20149
SiC, self bonded, wetting by Si, effect of phase composition 79−33161
SiC, self-bonded, fracture characts. and rupture strength, temp. effects 79−96136
SiC, self-bonded, statistical distrib. of values of apparent density 78−68657
A-SiC, self-bonded polycryst., wetting by Si, base plate surface roughness effect 79−23809
SiC, self-bonded polycryst., electrophys. props. 80−10980
SiC single crystal, fracture toughness 78−7019
SiC single crystal, hot hardness and creep behaviour 79−100247
α-SiC, single crysts. phase struct. rel. to heat treatment, nucleation 80−38991
SiC, sintered with three dimensional crosslinked polycarbosilane 78−56601
β-SiC, sintering, B transport and lattice parameter change 80−108370
SiC, solubility, partition coeff. of Be 79−10951
SiC, specimen preparation for TEM by ion beam thinning *(German, English)* 80−11861
SiC, spray dried agglomerates, compaction response, fracture, deform. 79−43172
SiC, strength assessment by Young's modulus meas. up to 1400°C *(German)* 78−11253
SiC, subcrit. crack growth, in corrosive environment, 600-850°C 77−56080
SiC, subjected to thermal shock, study of substruct. and surface morpholoy, X-ray diffr. and TEM study 79−43292
β-SiC, submicron powder, prep. by siliconization of C black, props. *(Japanese)* 79−66192
SiC, thermal oxide layers, AES depth-profiling anal. 79−43454
β-SiC, twinned crystals, fracture characts. 80−3193
SiC, US comminution of refractory compound powders 78−23656
β- SiC, undoped compact, microstruct. development during heating 80−25746
α-SiC, uniaxial compressive damage at low homologous temps., AE and SEM obs. 79−91736
SiC, wetting by Cu-Ti and Cu-Sn-Ti melts 78−68664
B-SiC, X-ray diffr. study of anisotropic layers in twinned seams 80−107274
β-SiC/Si abrasive resistant material, prep. and props. 80−20878
SiC-AlB_2 (0.61 to 1.2 wt.%), hot pressed, microstruct. 80−93563
SiC-B_4C (B+1 wt.% C), sintering 77−36432
SiC-Si, wear resist., props. under abrasion and corrosion 80−100927
$SiCl_4$, oxidation kinetics 78−92380
SiN film, elastic stiffness and thermal expansion coeffs. 80−107451
SiN powder formation, in high-temp. N flow *(Russian)* 80−100818
Si_2N_4 powders, synthesis, charact. 79−33977
Si_3N_0 reaction bonded, strength parameters 77−1830
Si_3N_4 amorphous, crystallisation and sintering under pressure 79−87596
Si_3N_4, α to β transform., TEM and electron diffr. obs. 78−27507
Si_3N_4, α/β phase transform. 78−56632
Si_3N_4 based abrasive material for grinding unhardened steel 78−35529
Si_3N_4, bending strength, deformability, elastic moduli and brittleness 80−81191
Si_3N_4, containing MgO and Y_2O_3 additives, impurity effect on sintering 79−61543
Si_3N_4, densification, role of $Ce_{4.67}(SiO_4)_3O$ 79−61549
Si_3N_4, evidence for cavitation crack growth, SEM study 79−79086
α-Si_3N_4, exam. of chemical vapour deposition, and IR transmission and reflectance 79−19993
Si_3N_4, factors affecting α, β phase formation, during nitridation of Si powders 78−52738
Si_3N_4 film, elastic stiffness and thermal expansion coeffs. 80−107451
Si_3N_4 films, plasma etching, MOS processing appl. 80−40577
Si_3N_4, finely dispersed, high-temp. synthesis 80−55331
Si_3N_4 first pressed, mixed mode fracture from controlled surface flaws 78−27603
α/β-Si_3N_4, formation during nitridation of Si 80−50609
Si_3N_4, fracture toughness meas. using Knoop indentation method *(German)* 80−25830
Si_3N_4, grain-boundary-crystallized, thermal shock resistance 78−11308
Si_3N_4, high-speed rolling bearings, fatigue strength 80−93655
Si_3N_4, hot pressed, crack healing *(German)* 79−24599
Si_3N_4, hot pressed, effect of powder composition and sintering temp., on phase transformation kinetics, microstructure and mech. strength *(German)* 79−4939
Si_3N_4, hot pressed, rate controlling process in oxidation 78−27659
Si_3N_4, hot pressed, small surface cracks, size estimation using SAW 78−76793
Si_3N_4, hot pressed, strength and life prediction 80−3173
Si_3N_4, hot pressed, surface wave scatt. from elliptical cracks for failure prediction 80−55608
Si_3N_4, hot pressed, Y_2O_3 fluxed, microstruct. 78−64512
Si_3N_4, hot pressed with different grain struct., mech. props. 79−61700
Si_3N_4, hot pressing, effect of ZrO_2 *(Japanese)* 77−55929
Si_3N_4, hot pressing, starting powder requirements, review 79−33987
Si_3N_4, hot pressing with Mg-Si-N-O system additives *(Japanese)* 77−36437
Si_3N_4, hot pressing with Y_2O_3 and Li_2O additives 78−92220
Si_3N_4, hot-pressed, creep and strain recovery 80−100874
Si_3N_4, hot-pressed, fracture in bending *(Japanese)* 79−79113
Si_3N_4, hot-pressed, fracture mech. parameters, indentation-precracking and double-torsion methods 80−104364
Si_3N_4, hot-pressed, fracture toughness determ. using specimens with chevron and straight through notches 80−108538
Si_3N_4, hot-pressed, impurity phases, TEM obs. 79−8260
Si_3N_4, hot-pressed, proof-testing 78−80693
Si_3N_4, hot-pressed, strength anisotropy origins 80−89330
Si_3N_4, hot-pressed, viscoelastic strain recovery obs. 79−79042
Si_3N_4, intermediates in CVD, mass spectrometric detect. 78−27411
Si_3N_4, low-Z material, outgassing expts. 79−209
Si_3N_4, mechanism of α-β transition under annealing 79−87629
Si_3N_4, nitriding *(German)* 79−74414
Si_3N_4, oxidation and hot corrosion resistance kinetics 80−25896
Si_3N_4, oxidised, with Y_2O_3 densification aid, temp. and compositional stability of $Y_6Si_6O_{21}$ 78−27664
α/β-Si_3N_4, phase yields during form., influencing factors 80−108408
Si_3N_4, porous, reaction sintered, organosilicon infiltrated, decomposition, strength, density 79−29000
Si_3N_4 powder, high press. hot pressing 79−38772
Si_3N_4 powders, laser synthesis using NH_3-SiH_4 gas mixtures 79−74119
Si_3N_4, prep. and charact. of ultrafine powders 80−2983
Si_3N_4, pyrolytic, amorphous and crystalline, chemical vapour deposited fracture surfaces rel. to struct. features 79−5038
Si_3N_4, pyrolytically-deposited, engng. significance 79−38746
Si_3N_4, rapid CVD, and struct. characts. 77−28767
Si_3N_4, reaction bonded, bending strength meas., influence of loading conditions, proof testing and anal. methods *(German)* 78−31451
Si_3N_4, reaction bonded, creep, internal oxidation effects 78−56701

refractories continued
Si_3N_4, reaction bonded, effect of Si powder grain size on microstructure, and mech. props. *(German)* 79−4998
Si_3N_4, reaction bonded, exam. of Na_2SO_4 induced heat corrosion 79−20224
Si_3N_4, reaction bonded, fracture mech. pararucters, microstmet. amd temp. effect 79−24598
Si_3N_4, reaction bonded, pore size and distrib. effect on strength 79−29165
Si_3N_4, reaction bonded, post-sintering, injection moulding applications 80−60807
Si_3N_4, reaction sintered, α- and β-phase form., effect on strength 77−21075
Si_3N_4, reaction sintered, H_2 in nitriding gas, effect on strength, struct., and composition 79−24478
Si_3N_4, reaction sintered, time depend. strength degradation 79−29235
Si_3N_4, reaction sintered, microstruct. charact. 80−35145
Si_3N_4, reaction-bonded, added oxides effect on strength after oxidation 79−39012
Si_3N_4, reaction-bonded, biaxial fracture strength 79−38969
βSi_3N_4, reaction-bonded, Fe-contaminant effects on Si nitridation 78−80496
Si_3N_4, reaction-bonded, gaseous boundary layer influence on oxidation at 1400°C 79−24638
Si_3N_4, reaction-bonded, internal oxidation processes role in high-temp. mech. props. 79−38915
Si_3N_4, reaction-bonded, pore struct. variations 79−24480
Si_3N_4, reaction-bonded, quantitative microstructural analysis 79−100092
Si_3N_4, reaction-bonded, strength, effect of Si purity in production 80−100902
Si_3N_4, reaction-bonded, theoretical model of manufacture, effect of ambient reaction temp. and compact size 80−108379
Si_3N_4, reaction-bonded and hot pressed, deform. and fracture during creep 79−38916
Si_3N_4, reaction-sintered, non-axial dislocs. 77−19956
Si_3N_4, reaction-sintered, elastic moduli, fracture mechanics parameters, and strength 77−28889
Si_3N_4, reaction-sintered, strength/nitrided density relationship 77−28891
Si_3N_4, reaction-sintered, effect of oxidation on thermal diffusivity 79−86933
Si_3N_4, recrystallisation during hot pressing 77−12587
β-Si_3N_4, single cryst., growth from Si melt in N_2 atmosphere, growth mechanism 79−24429
Si_3N_4, sintering in powder bed with addition of MgO sintering aid 80−29910
Si_3N_4, sintering with Al_2O_3 and Y_2O_3 *(Japanese)* 78−19703
Si_3N_4, solid-solid reactions with Fe, Ni and Mo alloys 79−28151
Si_3N_4, struct. of slow crack interface, light and electron microscope obs. 78−68770
Si_3N_4, synthesis and props. of shapes 79−47650
Si_3N_4, Wiener filtering appl. to nondestructive evaluation, defect charact. 79−11732
Si_3N_4 with MgO, Al_2O_3 and/or spinel, pressureless sintering 77−25003
Si_3N_4 with Y_2O_3 and Al_2O_3 additions, hot pressed, exam. of mech. props., grain boundary crystallization 79−20009
Si_3N_4, Y_2O_3 doped, hot pressed, improved high temp. strength 79−61613
Si_3N_4:$(MgO+Al_2O_3)(Y_2O_3)$, hot-pressed and sintered, microstruct. and impurity distrib. 80−49261
Si_3N_4:MgO, hot-pressed, linear thermal expansion rel. to MgO content 80−70430
Si_3N_4/ZrO_2, hot-pressed, compressive surface stresses developed by oxidation induced phase change 80−60992
β-Si_3N_4-AlN-Al_2O_3-MgO, insolubility of Mg in β-Si_3N_4 79−10953
Si_3N_4-based refractories, strength and microstruct. rel. to sintering 77−63610
Si_3N_4-CeO_2 additive, hot-pressing and oxidation behaviour 80−71618
Si_3N_4-MgO, (5 wt.%), hot pressed, fracture toughness as function of initial α-phase content, SEM 80−3174
α-Si_3N_4-MgO (5 wt.%), hot-pressed, mech. strength development 78−44195
Si_3N_4-MgO (5 wt.%), microstructural changes during gas pressure sintering *(Japanese)* 77−12589
Si_3N_4-Si_2N_2O-Mg_2SiO_4, melting and eutectic studies 80−45285
Si_3N_4-SiO_2-Y_2O_2, subsolidus phase relations 80−60845
Si_3N_4-Y_2O_3, hot-pressed, oxidation kinetics 80−16520
Si_3N_4-ZrO_2, sintered and hot pressed, exam. of mech. props. 78−48509
Si_3N_4AlN-Al_2O_3 system, reaction sintering forming β-Si_3N_4 solid solns. 80−50585
Si_2N_2O, elastic props. 79−29122
Si_3Ni_4, hot pressed, subcritical crack growth boundaries at internal fracture origins 80−11748
Si_3Ni_4, hot pressed MgO fluxed grain boundary impurity phases, lattice fringe imaging obs. 79−11540
SiO_2 concrete, elastic moduli meas. during heating and cooling 80−55451
SiO_2 fused powder, difference between white and black silica, devitrification rates 80−28918
SiO_2 surface, Ar plasma-treated, O_2 adsorption reactivity, EPR obs. 79−51418
SiO_2, wettability of single crysts. by liq. metals *(Russian)* 77−43408
SiO_2-Al_2O_3, refractory fibrous heat insulating material 78−6990
SiO_2-Al_2O_3 refractories, thermal shock props., fracture mech. appl. *(French)* 79−96109
SiO_2-Al_2O_3-Cr_2O_3 system, KT-11 type, chromia-containing material production based on high-silica glass fabric 80−45266
SiO_2-base cores, for superalloys, high temp. characterisation 80−10640
SrN, impurity activated whisker growth by CVD 79−66010
SrO.HfO_2(ZrO_2), US comminution of refractory compound powders 78−23656
$SrSnO_3$ and $SrZrO_3$, high-density ceramics prep. and elec. props. 80−60812
$SrZrO_3$ coatings, plasma-sprayed, spectral emittance *(French)* 78−26709
$Sr_3Zr_2O_7.2H_2O$, cryst. struct. and thermal stability, X-ray characterisation 78−83796
$TABe_{12}$, by diffusion saturation in vacuum, resistance to heat 78−44259
(Ta,Ti)B_2 on graphite, CVD coating, hardness meas., SEM study 80−24760
Ta carbides, changes in phase structure during prolonged heating in vacuum 78−44095

refractories continued
Ta wetting by Cu-Ag-P alloy 79−82417
Ta-C-B system, mech. and physical props. 77−59731
Ta-Cr-Si-Al, heat resistive films, prepared by sputtering, lifetime meas. 80−80132
Ta-Ir(Rh) system glasses, form., crystn. and microhardness, resist. obs. 80−89178
Ta-Ta_2O_5-InP thin refractory MIS struct. deposition 80−75647
Ta-W-Hf (8,2 wt.%), T-111, O_2 absorption, effect on lattice parameter and specimen dilation 78−83958
TaB_2-Cr-Si-Al, heat resistive films prepared by sputtering, lifetime meas. 80−80132
TaB_2-ZnS:Ag(Ag,Ni)-glass binder, thermally stable, comp. 77−63617
TaC and Ta_2C, self-propag. high-temp. synthesis 80−60815
TaC, diffusion of W, correl. with self-diffusion 77−24437
TaC, reactions with Ti-Al-Cr-Mo alloy CT3-1 80−16585
TaC, single crystal growth by plasma heating 78−60569
TaC, solid-phase reacts., effect of nonstoichiometry, thermodynamic evaluation 78−60632
TaC, thermal and electrical conductivity, 1500-3000K 78−43385
TaC, ultrafine grain, high pressure hot pressing 79−70024
TaC, ultrafine powder prep. in HF plasma 77−12562
TaC-TaB_2, exam. of high temp. friction and wear, and deformation behaviour 79−34152
TaN film, growth by CVD, microhardness and corrosion resist. 77−36404
β-Ta_2N, growth by annealing Ta in N_2, cryst. struct. 77−35533
β-Ta_2N-εTaN, prep. by exothermic reaction and by zone melting, cryst. struct. 77−35533
$TaSi_2$ film, elastic stiffness and thermal expansion coeffs. 80−107451
$TaSi_2$ films, on polycrystalline Si, oxidation charact. 80−97602
$TaSi_2$ refractory formation by As^+ ion beam bombardment 80−107286
ThO_2, plasma deposition of crysts. and their characterisation 80−20800
ThO_2, thermal expansion, 500-1800°C, X-ray diffr. 77−35723
(Ti,V)C, activated reactive evaporation deposited films, annealing study, microstructure 80−24762
(Ti,V)C carbides, prep. and mech. props. 78−64518
(Ti,Zr)B_2 on graphite, CVD coatings, hardness meas., SEM study 80−24760
Ti, band struct. correlation with TiC, APW calc. *(Japanese)* 78−23017
Ti, cladding, thermal stress analysis *(Russian)* 77−59952
Ti, H_2 isotope release 80−37580
Ti, liq., spectral emissivity and brightness-temp. meas. at MP 77−43356
Ti, surface struct., HCP to BCC type struct. transition, FEM obs. *(Japanese)* 78−22938
Ti-B-C system, complex carbide phase synthesis by crystallisation from gas phase 77−16526
Ti-B-Mo system, phase equilibria at 1400°C 78−35354
Ti-Cr-B system, self-propagating high temp. synthesis, crystallochemical and mech. props. 80−20861
Ti-Nb-Na (4 to 31, 8 to 38 at.%), with uniform distribution of refractory metal, prep. *(Russian)* 77−28747
Ti-Si-C system, complex carbide phase synthesis by crystallisation from gas phase 77−16526
Ti-Zr-B system, CVD 78−60581
TiB_2 coating, on WC-Co alloy cutting plates, hardness and struct. 80−21175
TiB_2 coatings, prep. by CVD and interaction with substrate 79−24680
TiB_2, electric arc melting prep. and oxidation props. 80−20860
TiB_2, electrode, hot pressed, erosion resistance, struct. and porosity effects 78−3228
TiB_2, preparation method rel. to compressive strength 80−55327
TiB_2, reactions with Ti-Al-Cr-Mo alloy VT3-1 80−16585
TiB_2, TiB_2-ZrB_2, direct evaporation deposition, struct. and props. 77−44392
TiB_2, TiC, vacuum condensate, struct. and mech. props., second phase effect *(Russian)* 80−71705
TiB_2-TiC (BN), crucibles for vacuum evap. of Al 79−74094
TiB_2-TiC powder mixtures, hydrostatic pressing 79−100098
TiB_2-TiC(20 wt.%), sintered, US machining 77−21325
TiB_2-$TiSi_2$ composites, high-temp. oxidation, scale comp. 78−15561
TiC, activated reactive evaporation deposited films, annealing study, microstructure 80−24762
TiC, band struct. correlation with Ti, APW calc. *(Japanese)* 78−23017
TiC, CVD and activated reactive evaporation on WC-TiC-Ta(Nb)C-Co, substrate-layer interactions, AES obs. 79−24679
TiC, CVD coating on Co-bonded multicarbide substrate, SEM, RHEED, AES interface study 79−77927
TiC, CVD layers on Fe substrate *(Japanese)* 78−27415
TiC coated WC-Co cemented carbides, fracture toughness 80−85046
TiC coating, activated reactive evaporation and sputter deposition, wear charact. 77−44394
TiC coating, activated reactive evaporation and sputter deposition, ancillary props. 77−44395
TiC coating on WC-NbC-Co, ion plating, and cutting tests 79−24678
TiC coatings, on cemented carbides, struct. and hardness 80−59771
TiC coatings on steels and hard alloys 80−76414
TiC, cpd. form. reaction in reactive evaporation, quadrupole mass analysis *(Japanese)* 78−23628
TiC, deform. at high temps. 80−104239
TiC, deformation behaviour during rubbing in wide temp. range 80−16486
TiC, deposited by activated reactive evaporation, TEM and hardness 79−23872
TiC, electronic struct. and XPS, cluster method and band struct. 79−60710
TiC, fine powder form. by vapour phase reaction *(Japanese)* 79−70030
TiC, frictional charact. and contact-zone deform. in homogeneity range 80−66673
TiC, mech. props., 1073 to 2273K *(Japanese)* 79−15732
TiC, micro-Vickers hardness, up to 1500°C 77−28890
TiC micropowder surface finishing of metals, surface struct. 80−11842
TiC, oxidation at various O_2 pressures 79−96172
TiC, polycrystalline, elastic props. 78−27547
TiC powder, plastic strain of particles under vibratory milling 77−90423
TiC, production from tetrachloride and hydrocarbon, thermodynamic analysis *(Russian)* 80−7523
TiC, reactions with Ti-Al-Cr-Mo alloy VT3-1 80−16585
TiC reactively sputtered coatings on Ni-Cr-Mo-Ti (19,11,3 wt.%), adherence, XPES and wear study 80−25565
TiC, refractory micropowder, geometric parameters of grains 77−16529

refractories continued
TiC single crystal, micro-Vickers hardness meas. up to 1500°C *(Japanese)* 78−23804
TiC single crystal, prep. by floating zone technique *(Japanese)* 78−23607
TiC single crystal, work function, field emission charact. *(Japanese)* 78−19641
TiC single crystals, growth from vapour by modified hot wire method, temp. effect on habit 79−61509
TiC single crystals, synthesis and impurities 80−55329
TiC, sintering and grain growth, metallographic anal. 80−25642
TiC, solid-phase reacts., effect of nonstoichiometry, thermodynamic evaluation 78−60632
TiC sputtered coatings on Ti-Al-V (6,4 wt.%), adherence, XPES and wear study 80−25565
TiC, tool carbide, thermal shock resistance and fracture strength 77−21257
TiC, wear resistant film, activated reactive evaporation form. 77−44411
TiC, wetting by Cr-Ni-Mo-Mn alloy steel, expt. planning investigation 80−60822
TiC-(Mo-Cr-Ni-Mn) steel alloy, optimum comp. and manufacture conditions, Mn effect 80−84896
TiC-B, struct. and mech. props. 80−55461
TiC-Ni, reaction kinetics under simulated liq.-phase sintering 78−52746
TiC-Ni composite coating, activated reactive evaporation prep., structure 77−44393
TiC-Ni-Cr(Mo) hard alloy mixtures, pressing 77−63596
TiC-steel compact prod. by sintering in vacuum and in Ar or H_2 atmos. 77−63616
TiC-TiB_2, friction charact., comp. depend., 20-1000°C 80−3203
TiC-TiB_2, strength and antifriction props. over wider range of concs. 80−50673
TiC-TiB_2 alloys, wear in vacuum, role of boride phase 80−21113
TiC-TiN, hardness var. charact. in homogeneity field 80−3192
TiC-TiN system, electro- and thermo-phys. props. 80−34210
TiC-VC, mag. susceptibility, elec. cond. and thermoelec. props. 80−50033
TiC-VC(NbC)(TaC), prod. and props. 77−28772
TiC-WC-TaC carbide mixture in plasma reactor *(German)* 77−1819
TiC-ZrC, mag. susceptibility, elec. cond. and thermoelec. props. 80−50033
$TiC_{0.93}$-$TiN_{0.818}$, structural parameters, and X-ray and pycnometric densities in homogeneity range 77−90311
TiC_x film, form. by hollow cathode discharge reactive deposition process, on mild steel sheet 79−24451
TiC_x, fused material, microstruct. 78−44115
TiC_x, nonstoichiometric, densification during sintering 80−84895
TiC_x refractory layers on steel surfaces, ESCA obs. 80−39471
$TiC_{1-x}N_x$ formation in high temp. N flow, ultra disperse powder, thermodynamic anal. *(Russian)* 80−55325
TiC_xN_y, fused material, microstruct. 78−44115
TiC_xN_y, powder preparation, physical, chemical props. *(Russian)* 80−76212
TiC_xN_y, thermal cond., elec. cond., and thermal expansion 80−10714
TiC_xNy, elastic props., 290K 77−52379
TiC_xO_y, thermal cond., elec. cond., and thermal expansion 80−10714
TiN, CVD layers on Fe substrate *(Japanese)* 78−27415
TiN, cladding, thermal stress analysis *(Russian)* 77−59952
TiN coating on WC-NbC-Co, ion plating, and cutting tests 79−24678
TiN film as protective coating for vacuum deposition chamber, Auger electron spectroscopy study 80−25922
TiN formation, from TiO_2/Si_3N_4 reaction in N_2 atmosphere 80−71617
TiN, from high-temp. reaction of NH_3 and $TiCl_4$, physicochem. props. 80−55334
TiN, high dispersed superconductivity 78−43505
TiN, highly dispersed, metallic thermo-EMF 78−43363
TiN, low-energy ion-stimulated deposited, supercond. props. 80−88664
TiN, powder defect struct., thermal and elec. props. 77−59286
TiN, reactive ion plating with auxiliary discharge deposition conditions influence on film props. 80−20801
TiN, self-propag. high-temp. synthesis under high N_2 pressures 80−25630
TiN, wear resistant film, activated reactive evaporation form. 77−44411
TiN-Al_2O_3, exam. of sintering and densification kinetics, and physical props. 79−95986
TiN-AlN, composite, erosion resist. in electron stream 78−11365
TiN-Nb(Ta)N, microcomposite film prod. for radio resistors 78−3052
TiN-VN refractory powder composite, resistors, produced in low temp. 78−11182
TiN_n, effect of equilib. N_2 press, 10^{-2} to 100 atm, on MP 77−36465
TiN_x, deposition by hollow cathode discharge process, and hardness 79−24452
TiN_x, oxidation in oxygen, of plates 79−61766
TiN_xO_y, phase and structural features 77−48411
TiO_2, wettability of single crysts. by liquid metals *(Russian)* 77−43408
TiO_2-SiO_2 multilayer vacuum coatings, optical props. 80−97361
TiO_x, reactive sputtering, film prep. conditions rel. to stoichiometry 77−40370
TiS_3 synthesis 80−35141
$TiSi_2$, film, elastic stiffness and thermal expansion coeffs. 80−107451
TiW-TiO_2-InP thin refractory MIS struct. deposition 80−75647
Ti(Zr,Hf)-Gd-B system, phase equilib. 80−11629
TIBS, synthesis, struct., optical, spectral props. 79−15631
(U,Pu)C, sintering, role of Ni as sintering additive 80−84892
UC, polycrystalline, creep mechanism interpretation 78−8898
UC, sintering, role of Ni as sintering additive 80−84892
UC-based nuclear fuel materials, influence of parameters on sintering behaviour and properties 79−100100
UC_2, high temp. thermal diffusivity, thermal conductivity, spectral emissivity 77−28052
UO_2 and UO_2-Gd_2O_3 solid soln., high temp. thermal expansion, 298-1700K 78−83979
UO_2, chemical reduction by atomic hydrogen 79−93830
V, and V-H, fusion reactor first wall material, cyclic deform. tests 80−30074
V, BCC, thermal shock resistance, original struct. effects 77−63803
V, integral normal emissivity in 1300-2000K range 77−35728
V, liq., spectral emissivity and brightness-temp. meas. at MP 77−43356
V-Cr, effect of alloying additive on thermoelectric props. 77−35927
V-Mo, effect of alloying additive on thermoelectric props. 77−35927
V-W, effect of alloying additive on thermoelectric props. 77−35927

refractories continued
VC single cryst., Vickers microhardness, slip mechanism 80−71732
VC-TiC, deposited by activated reactive evaporation, TEM and hardness 79−23872
VN powder, defect struct., thermal and elec. props. 77−59286
W, BCC, thermal shock resistance, original struct. effects 77−63803
W, candidate refractory for Tokamak, thermal fatigue failure testing 80−32454
W, chemically activated sintering 77−1826
W, high-temp. specific heat, 2300-3600K, meas. of wire cooling in vacuum 77−35703
W, polycryst. surface, heat of desorption of Cs 80−75430
W, powders, defective structure and activated sintering, exam. 80−16240
W, reaction with SO_2, 1600-2100K, kinetics 79−20266
W, single crystal growth by plasma heating 78−60569
W, specific heat near melting point, rapid pulsed heating method 77−35704
W, strength, temp. depend. 77−1871
W-Co, dil., excess resistivity, temp. depend., Kondo effect 78−68011
W-Fe, dil., excess resistivity, temp. depend. 78−68011
W-Mo-Re heat resisting alloy MVR-27-VP2, high-temp. emissivity and resistivity 77−35727
W-Re, dil., excess resistivity, temp. depend. 78−68011
W-Re alloy, elec. resistivity meas. near conc. anomaly, 300 to 1200K 77−35911
W-Re fibre-reinforced Ni-base refractory alloy, struct. and props. *(Russian)* 77−59721
W-Re(Mo)(Cr), powder mixture, activating effect of Group VIII metals on alloy form. during sintering 77−59728
W-ThO_2, candidate refractory for Tokamak, thermal fatigue failure testing 80−32454
W-Ti, Ti addition effect on heat resistance and radiative props. *(Russian)* 80−25515
W-W_2C, directional crystn. using plasma heating 78−60569
W-Y(La)(Ce)-B, phase equilib., struct. of crysts. 77−21122
W-Zr, Zr addition effect on heat resistance and radiative props. *(Russian)* 80−25515
W-Zr-C, Zr and C addition effect on heat resistance and radiative props. *(Russian)* 80−25515
W_2B_5, monocryst., grain size, abrasive and strength props. 80−11787
W_2B_5, reactions with Ti-Al-Cr-Mo alloy VT3-1 80−16585
W_2B_5, sintering rel. to prod. by boron carbide process 78−11184
W_2B_5-based alloys, mech. props., rel. to appl. as electrodes in electrospark machining 80−21174
WC, deformation behaviour during rubbing in wide temp. range 80−16486
WC, electrochemical grinding, effect of mag. field 77−86214
WC, fine powder prod. from $WO_3+C+Co_3O_4$ *(Japanese)* 78−92226
WC grain, with grown-in stacking fault, contrast effects in electron micrographs 77−19959
WC, liquid phase sintering 77−4751
WC, MP depend. on press. up to 80 kbar, optical meas. *(Russian)* 77−80604
WC micropowder surface finishing of metals, surface struct. 80−11842
WC powder, sintering processing conditions 80−11614
WC, powder form. from WO_3-Co_3O_4-C powder mixture *(Japanese)* 78−92227
WC, powder prod. by vapour phase reaction in WCl_6-CH_4-H_2 system 78−60626
WC powder production from vapour phase 77−21077
WC, reactions with Ti-Al-Cr-Mo alloy VT3-1 80−16585
WC, refractory micropowder, geometric parameters of grains 77−16529
WC, sputter deposited coatings, elec. resist., mag. susceptibility and adhesion meas. 77−44395
WC, tool carbide, thermal shock resistance, fracture strength 77−21257
WC-Co, contact reaction with BN at high pressures 80−61029
WC-Co, STEM anal. of grain boundaries 80−79644
WC-Co cemented carbides, irreversible deformation, yield stress, SEM study 79−70110
WC-Co coating, sputter deposition, friction and wear charact. 77−44394
WC-Co hardmetals, β-SiC to turbostratic graphite transformation 79−74150
WC-Co hardmetals, heat-treated, single domain obs. 79−73771
WC-Co molten Zn reaction, lamellar struct. form. 79−33964
WC-Ni hard alloy composite, sintered, void healing 80−60821
$W_{50}Fe_{50}$ glassy alloy, refractory, triode sputtered 80−75185
WSi_2 film, elastic stiffness and thermal expansion coeffs. 80−107451
WSi_2, oxidation in CO_2, 1200-1700°C 77−40454
WSi_2 refractory formation by As^+ ion beam bombardment 80−107286
Y_2MoO_6, growth from soln., struct., props. 77−28705
Y_2O_3, calorimetric meas. of enthalpy, heat of fusion, heat of high temp. phase transition 77−28020
Y_2O_3, corrosion resist. in fused Li rel. to phase and microstruct. changes 77−44378
Y_2O_3, digital pyrometry in solar furnace *(Japanese)* 78−32821
Y_2O_3, fission and phase transition enthalpies 79−99299
Y_2O_3 fused single crystals, struct. 80−19804
Y_2O_3, liq. and solid phase elec. cond., high temp. meas. 80−84468
Y_2O_3, thermal expansion, 500-1800°C, X-ray diffr. 77−35723
Y_2O_3, US comminution of refractory compound powders 78−23656
Y_2O_3-$2Y_2O_3.Al_2O_3$ two-phase refractory, fracture 80−21080
YS, supercond. transition temp. and lattice dynamics 79−56361
Y_6WO_{12}:ZrO_2(MgO)(CeO)(SrO)(BaO), polycryst., elec. cond., 800-7400°C 80−15517
Z+C, band struct. correlation with Zr, APW calc. *(Japanese)* 78−23017
$ZiSiO_4$, natural and synthetic, X-ray dilatometry 77−51522
ZnO, precipitation from gas phase 78−6025
Zr, band struct. correlation with ZrC, APW calc. *(Japanese)* 78−23017
Zr, interaction kinetics with graphite, reactive diffusion 79−42318
Zr-based thermal barrier coating evaluation 80−40619
Zr-Cr-B system, self-propagating high temp. synthesis, crystallochemical and mech. props. 80−20861
Zr-O, high temp. phase diagram 78−11211
ZrB_2, direct evaporation deposition, struct. and props. 77−44392
ZrB_2, electric arc melting prep. and oxidation props. 80−20860
ZrB_2, etching method using H_3PO_4 and H_2SO_4, effect of Pt 78−44339
ZrB_2, hot pressing, applied press. effect *(Japanese)* 79−38780
ZrB_2 powders, synthesis and impurities 80−55329
ZrB_2, prod., oxidation rate, corrosion resistance 77−52274

refractories continued
ZrB_2, pure, vacuum hot-press sintering and microstruct. *(Japanese)* 78−23649
ZrB_2, reactions with Ti-Al-Cr-Mo alloy VT3-1 80−16585
ZrB_2-SiC-C(-V)(-Nb), refractory cermet, hot pressing and oxidation resist. 80−3231
ZrB_2-Ta composite, vacuum hot-press sintering and microstruct. *(Japanese)* 78−23649
ZrB_2-TiB_2 solid solns., prod., oxidation rate corrosion resist. 77−52274
ZrB_2-ZnS:Ag(Ag,Ni)-glass binder, thermally stable, comp. 77−63617
Zr(C,N), coating on Zr substrate, oxidation by water vap., kinetics, 0.2-20 torr, 500-600°C *(French)* 78−44266
ZrC, and ZrC-NbC solid soln., prep. by impregnation, strength, surface submicrocracks 77−16661
ZrC crystals, electron energy spectra 80−49568
ZrC, deposition with vapor-gas phase circulation in closed circuit 77−55927
ZrC, destruction delay time under laser impact 79−38976
ZrC, diffusion of W, correl. with self-diffusion 77−24437
ZrC, elastic modulus, porosity factor 77−21207
ZrC, electronic struct. and XPS, cluster method and band struct. 79−60710
ZrC high-temp. plastic deform. effects on elec. props. 77−44370
ZrC, high-temp. strength, affecting factors 77−63794
ZrC, isothermal sintering kinetics 79−66032
ZrC powder, plastic strain of particles under vibratory milling 77−90423
ZrC powder, struct. after vibratory milling 77−28840
ZrC powders, synthesis and impurities 80−55329
ZrC powders produced by various methods, impurities 80−11615
ZrC, prep. from $ZrCl_4$+C *(Russian)* 78−19682
ZrC, pure and with Y additions, thermionic emission, hot pressed or CVD 77−12484
ZrC, reactions with Ti-Al-Cr-Mo alloy VT3-1 80−16585
ZrC, recrystallisation 78−11251
ZrC, rupture mechanism due to internal heat evolution 77−8922
ZrC single crystals, synthesis and impurities 80−55329
ZrC, sintering 78−19700
ZrC, sintering shrinkage, effect of struct. vacancies in interstitial phases 78−60630
ZrC, solid-phase reacts., effect of nonstoichiometry, thermodynamic evaluation 78−60632
ZrC, stoichiometric, emissibility, integral hemispherical and monochromatic, N_2 content effect 78−91457
ZrC, supercond. transition temp. and lattice dynamics 79−56361
ZrC, US comminution of refractory compound powders 78−23656
ZrC, ZrC-ZrB_2, direct evaporation deposition, struct. and props. 77−44392
ZrC-C mixtures, gas composition effect on CVD, bromide process 79−24448
ZrC-NbC-MoC_{1-x} system, thermal expansion coeff. up to 2500°C 79−69267
ZrC-NbN, mag. susceptibility, zone struct., conc. and temp. depends. 77−8788
ZrC-Re, spectral emissivity, 1400 to 2500K, surface relief and composition 77−24420
ZrC-TaC solid solns., high-temp. creep 79−11661
ZrC-W (75 wt.%) eutectic refractory alloys, smelting in suspended states, components distrib. *(Russian)* 80−19913
ZrC-ZrB_2, friction characts., comp. depend., 20-1400°C 80−3203
ZrC-ZrB_2, strength and antifriction props. over wider range of concs. 80−50673
ZrC-ZrB_2 alloys, wear in vacuum, role of boride phase 80−21113
$ZrC_{0.91}$, sintered, strength charact. effect of struct. and substruct. 80−16260
$ZrC_{0.97}$-$NbN_{0.93}$, $Zr_{0.5}Nb_{0.8}C_xN_{0.98-x}$, solid solns., elastic props. expansion and hardness 77−52380
ZrC_x, change in lattice const. in region of homogeneity 77−25029
ZrC_x, creep-comp. curves for homogeneous region 78−52911
ZrC_x, micro X-ray spectral anal. of boundary zones 79−8301
ZrC_x, monocrystal, work function anisotropy of electrons *(Russian)* 79−73568
ZrC_x, thermophysical props. at high temp., thermal vacancies form. 78−43141
ZrC_xN_{1-x} coating, on Zr, oxidation kinetics, 450-600°C 50-400 Torr O_2 press. *(French)* 77−25171
ZrC_xO_y, C-stabilised low temp. cubic phase 77−36478
ZrN coating, on Zr, oxidation kinetics, 550-700°C, 50-500 Torr O_2 press. *(French)* 77−25170
ZrN, coating on Zr substrate, oxidation by water vap., kinetics, 0.2-20 torr, 550-700°C *(French)* 78−44266
ZrN high-temp. plastic deform. effects on elec. props. 77−44370
ZrN, in homogeneity range, high-temp. thermodynamic characts. 77−77464
ZrN, microhardness and resist. to brittle fracture 79−87715
ZrN, plasma-formed, ESCA and supercond. transition temp. 78−19697
ZrN, sintering in vacuum and in N_2 77−12586
ZrN-Al_2O_3, exam. of sintering and densification kinetics, and physical props. 79−95986
ZrN-Al_2O_3, sintering reaction thermodynamics 80−2989
ZrN-AlN, composite, erosion resist. in electron stream 78−11365
ZrN+W reaction, high-temp. compatibility 79−39132
ZrN_x, $0.71 \leq x \leq 0.79$, ^{15}N tracer diffusion, short cct. mechanism 77−24429
ZrN_x, MP N press. depend. 77−35669
ZrN_x, thermal diffusivity in region of homogeneity, 1000-1800°C 78−71892
Zr_3N_4, powder, form. by vapour phase reaction of $ZrCl_4$-NH_3-H_2-N_2 system *(Japanese)* 77−73247
$Zr_{0.5}Nb_{0.5}C_xN_{1-x}$, mag. susceptibility, zone struct., conc. and temp. depends. 77−8788
ZrO_2, arc spot heat impact degradation *(Japanese)* 78−39819
ZrO_2, CaO stabilised, preferred slip system 80−66585
ZrO_2 coatings, prod. by low-temp. oxidation, props. 78−23856
ZrO_2, digital pyrometry in solar furnace, freezing point *(Japanese)* 78−32821
ZrO_2, elec. cond. variation, gas flow effect 80−39581
ZrO_2, high-temp. induced porosity increase 80−35146
ZrO_2, optimum sintering characts., density, X-ray diffr., IR spectrum, UV spectrum obs. 78−76617
ZrO_2, partially stabilized, props. and appl. to extrusion dies 80−97507
ZrO_2, plasma deposition of crysts. and their characterisation 80−20800

refractories continued
ZrO_2 refractories, wettability with Fe and Al melts 77−89619
ZrO_2 stabilised with Nd_2O_3, refractories prod. and long-term high-temp. behaviour 77−59725
ZrO_2, stabilized porous refractory, mech. strength 80−35322
ZrO_2, substoichiometric, thermodynamic props. at lower phase boundary 80−29185
ZrO_2, wet vibro-grinding with surfactants, superhigh density sintering suitability 79−33989
ZrO_2, Y_2O_3 stabilized, thermal diffusivity meas. 77−28021
ZrO_2, Y_2O_3 stabilized, heat-resistant granular artifacts, procedure for making 80−35148
ZrO_2, ZrB_2, vacuum condensate, struct. and mech. props., second phase effect *(Russian)* 80−71705
ZrO_2:Nd_2O_3, in contact with $NdCrO_3$, electrical cond. meas. 78−76071
ZrO_2:Y_2O_3, in contact with $YCrO_3$, electrical cond. meas. 78−76071
ZrO_2-HfO_2(Y_2O_3) solid soln. complex refractories, sublimation *(Russian)* 78−47513
ZrO_2-Nd_2O_3(Sm_2O_3)(Dy_2O_3) eutectic, unidirectional solidification, microstruct. and crystallographic characterization 80−35176
ZrO_2-TiO_2 refractories, TiO_2 effect on props. and phase composition 79−38809
ZrO_2-Y_2O_3-CaO(MgO), long term firing effect at 2100 to 2200°C on solid soln. conc. and microstruct. 77−90309
ZrO_2-Y_2O_3-Nd_2O_3, high-temp. thermophys. props. 78−26663
ZrO_2-Y_2O_3-Nd_2O_3(CeO_2), solid solns., form. by coprecipitation, struct., X-ray, electron diffr. anal. 77−12583
ZrS_3 synthesis 80−35142
$ZrSiO_4$, plasma dissociated, improved thermal shock resistant refractories 79−52350
$ZrSiO_4$, sintering, effect of grinding and additives 78−48356
$ZrSiO_4$, synthesis, influence of rare-earth additives on props. 80−20868
$ZrSiO_4$-Al_2O_3 (SiO_2) suspensions for slip casting, prep. and props. 80−104103

refractory materials *see refractories*

refrigeration
see also cryogenics; freezing; low-temperature production
^{3}He-^{4}He dilution refrigerator process anal. 79−93150
^{3}He-^{4}He superfluid injection dilution refrigerator, process anal. 79−97394
absorption chillers, solar-fired, capacity modulation 80−66952
absorption refrigeration machine driven by solar heat for air conditioning, math. modelling 80−76651
adiabatic demagnetisation of nucl. spins, refrigeration 78−49844
Baghdad insolation and meteorological data for flate plate collector design 79−62092
circulating cooling system, exptl., with rotary pump, for supercond. mags. 77−82528
circulating systems, liquid He jet pump 79−205
closed-cycle refrigerator, 4.5K, mag. and vibration characts. 78−93706
closed-cycle refrigerator at 4.5K, features, improvement 78−93704
cold-bath, precision, laboratory appl. construction 79−26048
compressor manifold, fluid induced damping 78−83164
counterflow gas-liquid helium heat exchanger with copper grid 80−17947
cryo-tip, heat transport via metal filled epoxy glue 78−37013
cryocooler, microminiature size, scaling laws 78−93701
cryocooler for supercond. instruments, requirements 78−93710
cryocoolers, closed-cycle, design problems 78−93705
cryogenic, low power closed-cycle, split Stirling principle, SQUID's appl. 78−77921
cryogenic cycle using phase separation phenomena 79−58721
cryogenic for fusion reactor research appls. 79−49840
cryogenic molecular adsorption refrigeration systems, design theory and performance 79−58722
cryogenic refrigeration system, computer design and optimisation 79−71457
cryopreservation of cells and biological samples using electronically programmed freezer 79−62420
cryopump, refrigerator cooled 20K, with adsorption panels 77−30172
cryorefrigerator, cryopump and its appl. *(Japanese)* 78−37021
cryostat for particle separator, closed cycle operation with 300 W refrigerator 77−30742
crystal cooling device with heat exchanger 78−42850
dewar, liq. He, for space expts., long-term cooling feasibility 77−33323
dilution, history from 1951 79−41
dilution refrigeration with continuous countercurrent heat exchanger, theory 77−30152
dilution refrigerator, ^{3}He circulating, with more than one mixing chamber 77−30153
dilution refrigerator, anomalous cooling power, heat transport of ^{3}He-^{4}He solutions 80−37045
dilution refrigerator, entropy of transfer for ^{3}He-^{4}He soln. 79−56013
dilution refrigerator for neutron expts. 77−30151
dilution refrigerator with sintered Ag powder heat exchangers, millikelvin range 77−30154
electrocaloric, for 4 to 15K 79−80624
electrocaloric refrigeration for 4-20K range 78−93703
energy Doubler refrigeration system for particle accelerators 79−72013
expansion turbines, review 77−5847
fast loading dilution refrigerator 79−58702
Fermilab Central He liquefier, characts. of main components 79−67991
heat transfer by natural convection with simultaneous frosting on horizontal cylinders in a vertical array *(Japanese)* 80−58890
helium refrigeration system and cryogenic system for superconducting Switchyard magnets at Fermilab 79−67990
high vacuum cryopumps optimisation using thermal design criteria 80−22377
ice-maker heat pumps, two plate-type, Remcor and 'no-penalty' harvest schemes comparison 79−48165
Josephson process computer using superconductive logic and memory devices 79−58726
Leiden dilution refrigerator, lowest temp. and temp. gradient in counterflow capillary calc. 77−2660
liquefied gas usability *(Japanese)* 78−45638
liquid He cryopump for 1 MV accelerator, cryogenic supply and boil-off removal 79−72011
liquid He cycle using two circuits, comparison with Claude cycle 77−17993
magnetic refrigerator for operation near 2K 78−37012

refrigeration continued
magnetic refrigerators, small, to pump heat from He temp. to above 10K 78−93702
magnetic refrigerators for use at room temp. and below 79−67314
metallic thermal connectors for use in nuclear refrigeration, elec. resist. meas. 78−224
mixing chambers for dilution refrigerators 79−58703
nuclear demagnetisation refrigerator, double range, microkelvin range 80−31769
nuclear irradiation facility, refrigeration system design 77−42009
open refrigeration tube, adjustable cooling using He cryostat 79−35759
Peltier effect appl. *(French)* 77−62908
phonon-drag low temperature thermoelectric refrigeration, use of Bi 80−22366
polarised target in high energy physics, horizontal dilution refrigerator with high cooling power 80−73372
polarized target, horizontal dilution refrigerator construction 78−86708
portable self-contained refrigerants transfer system, for use with supercond. magnet dewars 80−8993
red blood cell freezing, cryopreservation and refrigeration 80−67262
refrigerator, closed-cycle, 4.5K, for supercond. susceptometer 78−93707
regenerative, generalised ideal reference cycle, isothermal systems 80−38228
saltwater drop falling in organic phase, ice growth 80−15218
semiconductor refrigerating thermojunctions with radial flow of current 79−2766
silica gel for low temp. regenerator of cryogenic refrigerator 77−17994
solar, exam. of dry absorption using $CaCl_2$-NH_3 80−61310
solar, isothermal dissociation and regeneration of $CaCl_2$-NH_3 *(French)* 80−61300
solar energy appl., H_2O-LiBr and NH_3-H_2O absorption cycles, design and optimisation 79−87974
solar energy cooling, operating systems and current developments, review 80−85265
solar energy driven absorption refrigeration system, theoretical model 80−30413
solar energy transition and materials problems 80−26115
solar flate plate evacuated collector design 79−62099
solar installation for refrigeration and water heating, energy characts. 80−101124
solar powered, single-loop conjugate cycle realisation 77−75644
solar powered refrigeration units, absorption systems with intermittent or continuous cycles 80−45729
solar refrigeration in tropical zones using flat plate collector and two-component coolant *(French)* 79−24911
solar zeolite collector for solid-gas absorpt. refrigeration system 80−35754
Stirling cryocooler, milliwatt refrigeration at temps. 3 to 4K 79−67307
storage of thermal energy, annual cycle, ice storage and three-coil heat pump 80−55917
superconducting AC machine, He rotating cryostat as thermal pump 79−58717
superconducting magnet energy doubler central liquefier 77−82530
superconducting magnet Large Coil Program, He liquefier-refrigerator and distrib. system 78−50398
superconducting RF particle separator, 300 W 1.8K refrigerator for 77−18770
superconductive energy related appls., refrigeration requirements 79−58711
superconductors, refrigeration technology 77−82529
supercritical He refrigerator, recovery time after thermal upset 77−17992
sustained thermodynamic equilib. used to control temp. of expt. chamber 77−33983
Tevatron Central Helium Liquefier, Fermilab, process control system 79−72012
thermodynamic fundamentals, system development 78−93697
thermoelectric coolers with high current pulse and finite cold junction, fast transient behaviour 80−27290
thermoelectric refrigeration at low temp. 79−93147
thermoelectric refrigerators, performance optimisation using asymptotic temp. distrib. 80−230
two-stage refrigeration and power producing arrangement, with cooling tube and thermoelectric stage 78−21142
valveless low temp. heat pump, performance 77−17991
vapour absorption refrigeration flat plate solar collector tube pitch optimisation 79−62084
zero mechanical work thermal compressor or pump, in high speed rotating frame 78−57962
He, automatic multirange liquefaction plant 80−57306
He cryorefrigerator, exergy method of anal. 80−4723
He liquefiers and refrigerators, cryogenics of Sulzer, Switzerland 80−82769
He refrigerated and liquefiers, optimisation for larger superconducting systems 80−8994
He refrigeration cycle used in H_2 liquefier 79−58740
He refrigerator, gas bearing turbine with dynamic gas bearings 79−35754
He refrigerator for temp. varying Mossbauer meas., 20-300K 80−4726
He refrigerator systems, trace impurity analyzer 79−70388
^{3}He cryostats for different refrigerating capacities 79−58749
^{3}He dilution refrigerator for neutron diffr. exam. of nucl. antiferromag. order 79−58701
^{3}He nuclear refrigeration by Cu adiabatic demagnetisation 79−67315
^{3}He refrigerator for studying Ge below 1K 80−8997
^{3}He/^{4}He dilution refrigerator, temp. inhomogeneity in glass mixing chamber 79−17429
^{3}He/^{4}He dilution refrigeration operating principles and heat exchangers, review 79−67310
^{3}He-^{4}He, dilution refrigerator, design, for Mossbauer expts. on Tm and its cpds. 78−27127
^{3}He-^{4}He dilution refrigerator, condensation stage 77−45852
^{3}He-^{4}He dilution refrigerator without pumped ^{4}He bath 77−45853
^{3}He-^{4}He refrigerator, construction and appl. to Mossbauer expts. 78−24909
N, liquid, use as cooling agent in industry 79−58709
N_2, liquid, computer design and optimization of cryogenic refrigeration cycle 79−58750
$SrTiO_3$ ceramic, electrocaloric effects for refrigeration at cryogenic temp. 80−77789

refrigerators
cryo-tip, heat transport via metal filled epoxy glue 78−37013
cryogenerators, thermally activated closed-cycle regenerative 79−58742
cryogenic refrigerators for fusion research 79−679
cryopumps, refrigerator cooled, design and performance 79−58754
dilution refrigerator using centering device, performance characts. 80−77791
dilution refrigerators, molar flow rates determ. method 77−10032
electronically programmed, for cryopreservation of cells and biological samples 79−62420
energy conservation estimates by second law anal. 80−45723
Ettingshausen refrigerator, longit., isothermal, nonstationary regimes, theory 78−18157
fast-cooling microrefrigerator 78−24801
finned tube heat transfer characts., expts. *(Japanese)* 77−23861
free piston Stirling refrigerator performance characts. determ. 80−35722
liquefier-cryogenic vessel, energy and economical aspects of vapour-cooled shield theory 79−58739
low temperature He compressor *(Japanese)* 77−53918
magnetic Stirling cycle wheel, refrigerator and heat engine modes of operation 78−57964
mechanical laser/component cooling appl. 78−22136
noise, subjective annoyance by low level sound, sound character as a physical attribute 80−35902
nuclear demagnetisation refrigerator, microprocessor controller 80−37043
nuclear demagnetization refrigerator, sintered Cu heat exchangers 79−58696
photovoltaic/thermoelectric refrigerator for medicine storage for developing countries 80−35712
reciprocating magnetic refrigerator for 2-4K operation 80−2577
rotating Carnot-cycle magnetic refrigerators for use near 2K 78−57965
solar cooling, Rankine-cycle systems, selection of working fluids 80−104515
solar evaporation and refrigeration units, assurance of specified energy parameter values, statistical analysis 80−93848
solar heating and cooling system for domestic use *(Japanese)* 80−108787
solar open cycle absorption refrigeration system, anal. and simulation 80−16788
solar-powered solid-state heat transfer device based on photovolt. and Peltier effects 80−217
spaceborne cryogenic refrigerator, ultra-reliable 79−54139
SQUID appls. portable refrigerator 80−27313
Stirling, magnetically-driven MC 80 79−58724
Stirling refrigerators, magnetically driven 79−58697
superconducting instruments in metrology, adaptation of measuring systems to small refrigerators 79−26020
temperature controller, AEG-Telefunken IC *(German)* 79−26051
thermochemical heat pump/refrigerator thermodynamic analysis 80−35716
thermoelectric cooling devices, maximum refrigerating capacity determ. 80−86318
thermoelectric microrefrigerator, single stage and two-stage, limited heat transfer anal. *(Russian)* 78−70129
H_2 target, liquid, microprocessor-based cryogenic refrigerator controller 79−45491
He, closed-cycle, containing laser diode, measurement of wave-number stability 80−31906
He, liquid, multipurpose refrigerator/liquefier for CERN 400 GeV Super Proton Synchrotron 79−58737
He, liquid, performance for different operational modes and flow impedances, 4.4 to 16K 79−58736
He, optimisation for superconducting power transmission lines, w.r.t. cost and reliability 78−24802
He refrigerators and liquefiers for large superconducting systems, optimization 79−63233
He turbo-refrigerator with regenerators 79−58723
He, use of warm ejectors 79−58725
^{3}He circulating dilution refrigerator with two mixing chambers 77−61073
NH_3-H_2O, solar absorption refrigeration system, Seoul, Korea *(Korean)* 78−51052
N_2O, thermodynamics and thermoelectric condenser design 80−108809

regenerative braking
flywheel energy storage system, composite, electric vehicle appl. 79−48185

regenerative receivers *see radio receivers*

Regge poles and trajectories
3j coeff., symmetries 79−305
$\pi^{3,4}$ theories, Regge-pole behaviour 80−18081
$\pi N \rightarrow \rho X$, trajectory data, reson. and scatt. regions, compatibility *(Russian)* 78−8703
ρ trajectory energy depend. 77−18250
ϕ_6^3 theory, anomalous dimension, Regge cut effect on structure function 80−62847
Φ^3 field theory, Regge pole behaviour 78−66053
ϕ^3 theory scatt. amplitude extrapolation between Regge region and fixed angle region 77−74596
ϕ^3 weak coupling model, s-channel cutting rules for 4-pomeron amplitude 77−38101
ω-trajectory, dual unitarisation scheme, SU(3)-breaking and baryon exchange effects 79−26316
absorption model approx. for particles with spin, Regge cuts, crossing symmetry violation *(Russian)* 80−42435
Adler zero and dual peripheral model 78−78153
analytic foundations of Regge theory 77−10202
atomic collisions, determ. of Regge poles from nonlinear Schrodinger eqn. 78−49702
atomic collisions, rainbow scattering, Regge pole anal. 78−58774
atomic collisions, scattering amplitudes, Regge representation calcs. 78−58770
bare Pomeron in four-dimensional quantum chromodynamics 79−336
barrier-top resonance and heavy ion reactions 77−38291
baryon dynamics description in dual and gauge theories 77−65138
baryon exchanges in renormalisation 77−34133
baryonium and nonexotic hadron trajectories from a color-dependent potential 80−13286
baryonium Regge trajectories exchange in medium and high energy scatt., expt. evidence 78−50022

Regge poles and trajectories continued
baryonium spectroscopy based on duality and unitarity 79−58947
baryons and baryonium, SU_6 symmetry, duality and unitarity 78−8622
Bethe-Salpeter wave function divergence at origin 78−74147
bi-local field interaction with external field 78−66030
bootstrap, planar pole, and existence of good finite mass sum rules 78−16948
boson Regge trajectories, asymptotic behaviour *(Russian)* 77−38103
bottomium, potential models, non-relativistic description 80−68426
bounds for Regge slopes and intercepts for ordinary and new hadrons 78−8627
broken global symmetries, nondegeneracy of vector meson mass, non-trivial mixing 80−13236
causality, Regge behaviour, proton electroprod. struct. function, Bjorken limit of sum rule 77−67662
charge and baryon transfers in dual unitary model 77−30337
charmed baryon mass formulae via SU(4) Regge trajectory anal. 77−79257
charmed baryon spectra in dual resonance amplitudes 79−13088
charmed baryons, Regge spectroscopy 77−38148
charmed meson masses, duality predictions 78−8619
charmed mesons, Regge spectroscopy 77−34138
charmed mesons, spectral function sum rule and onium 79−26329
charmed particles, duality constraints on spectroscopy 78−21398
charmonium, potential models, non-relativistic description 80−68426
chemically reactive system, large angle elastic scatt., interference effects, Regge pole anal. 77−58123
closed Regge eikonal formula, inclusive 6-point function, multiple Reggeon/Pomeron exchange contribs. 79−362
cluster formulation in the dual topological unitarization scheme 80−13293
compilation of coupling constants and low-energy parameters 79−22159
complex energy spectra in Reggeon quantum mechanics with quartic interactions 80−102031
complex optical potentials, Regge pole positions and residues, quantum and semiclassical calc. 79−89084
Compton scattering of protons, simple Regge pole model 78−93884
confining pot., Regge poles, coupled Schrodinger eqns. 77−61219
constituent particle scattering in the Regge region 80−37244
cosmic ray muons, scaling and charge ratio, Muller-Regge phenomenology 79−12371
cross section rise in high energy strong interactions, multipomeron exchange, Mandelstam diagrams 78−41516
crossing symmetric, unitary Regge theory for meson-meson scatt. 79−63458
crossing symmetric amplitude with Regge poles 78−54621
crossing symmetric and unitary scatt. amplitudes 78−21356
crossing symmetric unitary Regge representation 77−10201
crossover phenomenon, interactions of Reggeons and Pomerons, Reggeon field theory 79−93317
cryptoexotic states of the four-quark system 79−40762
cutting rules, simple interpretation *(Russian)* 77−46033
cutting rules, unified approach to Regge cuts models 77−6097
cylinder term structure in the topological expansion 79−13093
cylindrical mixing phenomena in dual topological unitarisation, pomerons, reggeons and gluonic states 80−86696
Deck model, rescattering effects for diffr. dissociation of hadrons 78−4844
Deck model phase for $\pi^-p \rightarrow \pi^+\pi^-\pi^-p$ 77−22709
deep inelastic electroproduction struct. funct., Abelian gauge field effects 79−71754
diffractive bumps, gluonic excitation Regge trajectories from bag and dual models 79−2978
diffractive dissociation, duality and mass-slope correl. 77−82725
diffractive reactions, pomerons and reggeons *(Swedish)* 77−65146
Dirac's large-number hypothesis, angular momentum for Regge trajectory with n=2 80−18091
disconnected quark diags., forbidden coupling and inhibited decay 77−22686
dispersion sum rules and exotic baryon resonances, reggeon scatt., E_{55} resonance *(Russian)* 80−101955
dispersion sum rules for Reggeon-particle scatt. 78−54583
double Reggeon representation of energy depend. of inclusive cross sections *(Russian)* 77−74737
double-phase representation, fixed-angle and fixed-momentum-transfer scatt. 78−8628
dual bootstrap models, solns. satisfying Lee-Veneziano relation 79−71729
dual bootstrapping and Reggeon phases 77−34132
dual models, spin in spectrum of states, helicity partition functions 77−38137
dual models, unitarised, conventional, renormalisation of new trajectory 79−85281
dual multiperipheral model, Pomeron and Reggeon slopes 78−62379
dual multiperipheral model planar bootstrap 78−4837
dual Pomeranchuk amplitude contrib. to multi-Regge limit and pomeron sister absence 80−13237
dual pomeron contrib. to inclusive distrib., triple-Regge, fragmentation, pionisation, regions 78−41509
dual resonance amplitudes, Regge spectra, symm. breaking effects, decay rates of mesons 77−82715
dual resonance amplitudes, satisfactory invariant measure 78−66093
dual topological expansion, Reggeon and Pomeron slopes 80−102032
dual topological unitarisation, higher rank cylinder kernel 80−27492
dual topological unitarisation, singular cylinder kernel 80−27493
dual topological unitarization, glueball exchange effects, pomerons and reggeons 80−52482
dual unified model and Pomeron-Reggeon amplitudes 77−57504
dual unitarisation, Reggeon, Pomeron and annihilation prod. processes 77−65143
dual unitarisation, renormalisation of trajectories with zero quantum numbers 78−21400
dual unitarisation scheme, planar amplitudes, Regge cut cancellation 77−87954
dual unitarisation scheme, Pomeron and f Regge pole prod. 78−41512
dual unitarity scheme, non-planar corrections to pomeron and reggeons 77−230
dual unitarization scheme with several trajectories, diffractive scatt. predictions 79−89133
duality, phenomenological, strong interactions description using finite energy sum rules 77−82716

Regge poles and trajectories continued
duality and four reggeon amplitudes 77−233
duality and high-energy behaviour of Regge-Regge amplitude in dual reson. model 77−10222
dynamical symmetry breaking in dual resonance model, Regge meason trajectories total renormalisation *(Russian)* 77−82717
eikonal description of nucleon-nucleon elastic polarisation data 77−13948
eikonal model, particle prod. on heavy nuclei and hadrons 77−71495
eikonal model multiplicity distrib. and Koba-Nielsen-Olesen scaling *(Russian)* 79−9355
eikonal Regge model, opacity and diffr.-dissociation cross section of grey disks 78−4845
eikonal theory, interacting Pomeron production by retaining Feynman graphs 78−8633
elastic scattering amplitude asymptotics in a supersymmetric theory *(Russian)* 79−75748
electroproduction structure functions in asymptotically free theories, Regge behaviour 78−25025
equality of radii characterising ρ and ψ Regge trajectories 79−63457
exchange degeneracy breaking, charge conjugation, in s-channel, unitarity, quark diagrams 77−22713
exchange degeneracy of Reggeon contribs. and quark model 77−13944
exchange of two different nonlinear Reggeons, struct. and props. of branchings *(Russian)* 77−74620
extended Regge trajectories, modified Chew-Frautschi plot for meson and baryon resonances 78−82176
f-trajectory, dual unitarisation scheme, SU(3)-breaking and baryon exchange effects 79−26316
factorisation of Regge slopes, ordinary and new hadron, spectroscopy, four flavour model 77−82722
factorisation of Regge slopes for ordinary and new hadrons 77−26503
fermion Reggeization without parity doubling, Reggeized absorpt. 78−54622
field theory, divergence of perturbation series 77−2754
field theory, Pomeron intercept anal. 77−6003
field theory, quantum spin model 77−45974
finite confinement potential and relativistic field theories 77−79249
finite energy sum rules, high-energy Regge expansion 77−45988
form factors of composite states, relation to Regge trajectories 77−82742
four-reggeon couplings, analogue quantum-spin model 78−45813
free-spinor field on Regge trajectory as representation of strongly interacting quark field 80−32067
gauge vector mesons and unified theories, Reggeization 79−97562
geometrical pomeron 78−37188
giant multipole resonances, Regge poles and collective model 80−13436
giant multipole resonances, spin-isospin vibrs., spin waves, Regge poles in collective model 78−89777
Glauber screening eqns. in fast backward particle prod. in high energy processes, role of short range nucleus struct. 79−63670
gluon bremsstrahlung and multiperipheral cluster models 79−22082
hadron+deuteron elastic scatt., inelastic shadow correction, complex cut integral 78−70347
hadron constituent models review, fixed angle and Regge behaviour, hard scatt., fragment X-distrib. 78−78154
hadron distributions in quark jets, pion and proton form factors 79−54317
hadron dynamics, multiparticle prod., intermol. pot. in Feynman-Wilson gas 78−477
hadron elastic scatt., high energy, review 77−257
hadron low |t| elastic scatt., polarisation effects and forward amp. in quark model *(Russian)* 77−258
hadron reactions, large, small momentum transfer regions, transition point for s-depend. 77−30339
hadron spectrum, planar amplitudes without Regge cuts 80−27464
hadron states, quark sea and non-Abelian gauge field contrib. 79−327
hadron-hadron collisions, parton model of hard and soft processes in small p_T inclusive reactions 78−41599
hadron-hadron elastic scatt. systematics at high and intermediate energies 77−22717
hadron-hadron high energy scatt., Jost-Lehmann-Dyson representation, light cone singularities 78−17049
hadron-hadron total cross-sections to 300 GeV/c, phenomenological anal. 77−38206
hadron-nucleon forward amplitudes, Reggeon exchange absorptive corrections 79−40765
hadron-nucleon total cross section 78−45888
hadron-nucleon total cross-section, regularities and systematics 77−38205
hadron-nucleus high-energy scatt., Regge theory 77−10383
hadron-nucleus total and inelastic cross-sections 77−34193
hadronic physics, Regge trajectories families, S-matrix theory, nonrelativistic linear pot. quark binding model, comparison 78−33048
hadronic reactions, trajectory slopes in gauge-dual-topological approach 80−18142
hadrons, parton distribs. calc. 78−421
hard processes, large rapidity separation of baryonic number, partons, and dual topology 80−95255
harmonic oscill. model, trajectories for old and new particles 78−12886
heavy ion+nucleus, orbiting quasimolecular system, nuclear-surface-wave interpretation 80−86914
heavy ion+nucleus scattering, Regge pole contrib., forward- and backward-angle, Coulomb and nuclear scatt. functions 80−57788
heavy ion optical potential elastic scatt., energy depend., Regge pole and Coulomb amplitudes 78−25228
heavy vector meson photoprod., vector meson dominance model anal., Regge trajectories 78−78195
heavy vector mesons associated with $\Upsilon(9.4)$ and the nature of $\Upsilon'(10)$ 78−82187
heavy-ion transfer reactions, Regge parametrisation of ang. distribs. 78−21592
high energy behaviour of a double discontinuity and the bare Pomeron 78−82179
high-energy behaviour of a double discontinuity and the bare Pomeron 79−17696
Hypercharge-exchange reactions, exchange degeneracy breaking and Regge cuts 77−71494
hypercharge-exchange reactions, K^-p and π^+p, exchange-degenerate Regge pole prediction 80−13335

Regge poles and trajectories continued
I=1 bosonic reggeon-particle scatt., dispersion sum rules *(Russian)* 80−32089
I=1 reggeon-baryon scatt., superconvergent dispersion sum rules and vertices struct. *(Russian)* 80−27494
inclusive electroproduction, final state hadrons, Regge-Mueller anal. 77−38176
inclusive interactions in triple Regge region, polarisation 77−10294
inclusive reactions, Regge Mueller approach to $\pi p \to \pi X(\rho^0 X)$, $Kp \to \pi X$, $pn \to \pi X$, $\bar{p}p \to \pi X(\rho^0 X)$ *(Russian)* 78−58218
inclusive vector and tensor meson prod. in beam fragmentation region, Mueller-Regge formalism 78−17057
inclusive vector meson production in fragmentation regions of meson at small P_T 80−105931
inclusive vector meson production in triple Regge region, absorpt. corrections 78−93867
inelastic diffraction cross section, quark model and three reggeon limit 80−102035
interatomic potentials, Regge poles positions and residues, inverse power pots. 80−83439
intercept of pomeron and inelastic binary collisions 77−67635
interference terms, phases, 1/N expansion, Lee-Veneziano model 77−18247
internal symmetry, unitarity constraints 77−41825
Jost-Lehmann-Dyson representation, high-energy scatt. 77−82660
KNO scaling and scaling in the mean for semi-inclusive processes *(Chinese)* 80−22538
large coupling expansions for eigenenergies and Regge trajectories of the general even-power potential with applications 80−86020
lattice gauge theory, string model, hadron spectrum, Regge trajectories 77−57452
leading zone distrib. and spectrum height 77−82719
lepton-hadron deep inelastic scatt., Regge behaviour, Bjorken scaling 77−244
Lie group framework for soliton eqns., Lund-Regge model generalisations 79−17605
light vector mesons, mass spectra and Regge trajectories in relativistic quark model *(Russian)* 78−93864
magnetic resonances between massive and massless spin-$^1/_2$ particles with magnetic moments 80−62895
many-hadron production at low $P_\perp$, basic concepts and models, review 79−6331
many-particle dispersion relations 77−10200
many-particle Regge poles in supersymmetric theory *(Russian)* 77−46034
meson mass spectra based on bilocal model 79−67521
meson mass spectrum, planar bootstrap, and Regge approach 80−22581
meson production by charge exchange reactions, Regge-pole model explanation 78−58200
meson Regge trajectories in the quark-gluon model 79−13042
meson resonances, high spin, natural parity, dual reson. model with non-degenerate Regge trajectories 79−359
meson resonances, narrow asymptotic Regge trajectory results 78−82178
meson spectra interrelations, heavy quarks 77−18231
meson spectroscopy, quark mixing and quantum chromodynamics *(Russian)* 79−54329
meson spectrum in simple planar bootstrap model 78−8618
meson trajectories in quark-gluon theories 78−25005
meson trajectory slope parameters on basis of two-body model 77−67634
meson-meson Regge theory with crossing symmetry and unitarity, strong coupling 77−65177
meson-meson Regge theory with crossing symmetry and unitarity, weak coupling 77−67676
meson-meson scatt., Regge theory, crossing-symmetric representation of dynamical eqns. 78−4841
mesons, mass spectrum and Regge trajectories from relativistic quasipot. eqn. *(Russian)* 80−73690
mesons, sign of unnatural-parity cylinder, Reggeon loop model 77−57506
mesons, unnatural parity, in dual unitarization scheme 77−87951
molecular elastic scattering, Regge pole anal. of differential cross sections 79−3523
moving poles in the scale-dimension plane and scaling violation 79−12983
multi-particle and inclusive reaction, at high energies, review 79−17777
multi-Regge amplitude construction by van Hove-Durand method 79−12984
multi-Regge limit of Veneziano model, exchange of new trajectories 78−33043
multi-Regge limit of Veneziano model, unconventional trajectories props. 78−33044
multi-Regge model, charge exchange and pomerons 77−65144
multi-Regge model with threshold factor for cluster prod., multiplicity distribs. in pp collisions, 50-400 GeV/c 77−18256
multi-Regge self-consistent model, overlap function and Regge cut 77−49932
multicolour QCD as dual resonance theory, mesons on rising Regge trajectories 78−16987
multiparticle Regge poles, t-channel particle repulsion *(Russian)* 78−45814
multiparticle Regge poles in ϕ^3 quantum field theory *(Russian)* 77−6057
multiparticle reggeon with $\alpha(0)>1$, quantal struct. *(Russian)* 78−445
multiparticle trajectories t-dependence, Mandelstam theory *(Russian)* 77−235
multiperipheral parton model, Reggeisation and dual unitarisation 80−37249
multiperipheral theory, unitarity condition and Reggeon theory *(Russian)* 77−30348
multiquark hadrons, Regge slope factorisation 79−22021
multiquark hadrons in two dimens. QCD, asymptotic solns. with Regge trajectory spectra 78−66085
multiquark systems in Feynman's bremsstrahlung analogy, Regge intercepts 79−97590
multireggeon processes, Yang-Mills theory *(Russian)* 77−2808
n+p→p+n, charge exchange, energy depend., possible explanation, Regge exchange 78−21465
Nambu string model, reggeon and pomeron interactions *(Russian)* 80−13294
Neveu-Schwarz dual pion model, two new Regge trajectories 77−38138
Regge poles and trajectories continued
non-Abelian gauge theory with many flavours, high energy processes, asymptotical behaviour *(Russian)* 80−101935
non-planar effects in Regge trajectories at large $t>0$ 77−234
non-Regge terms in presence of cuts in j-plane *(Russian)* 79−26261
nonlinear reggeon multiple exchanges 77−71496
nuclear elastic scatt. with optical potential, complex angular momentum methods, poles and zeros of S-matrix, REGGE 80−47445
nucleon chiral substructure, parton model 77−41787
nucleonic form factor, pion exchange, model 80−22608
optical anal. of resonances in velocity depend. square well pot. 78−62098
P+f diffraction model, two component duality and flavouring, Regge fits and pomerons 80−95261
partial wave amplitudes asymptotic behaviour, Regge models and dispersion relations 77−10204
particle correlations in multiperipheral resonance prod. model, broken SU_3 symmetry 78−45891
particle production, inclusive spectra in three Reggeon limit range *(Russian)* 79−54369
partons in Regge theory and pomerons 77−79250
perturbation expansion of multichannel Regge poles 80−86623
perturbative field theory effects and Regge pole representation, QCD, dual topological unitarisation 80−42434
perturbative Reggeon calculus, building Reggeon cuts from Reggeon tree graphs 77−13893
perturbative reggeon calculus, topological cross sections 78−8632
perturbative reggeon calculus, transverse correls., multiparticle prod. 77−2879
phenomenological consequences of new Regge trajectories on pion trajectories, dual models 78−33045
pion exchange at high energies, review 80−95259
pion multiplicity distribs. in impact parameter space, multi-Regge model 77−14001
planar bootstrap, Regge cuts cancellation, asymptotic terms 78−54619
pomeron building mechanism, in fragmentation region 78−89687
potential model, Dirac eqn. with linear confining pot., symmetric model, Regge trajectories 79−364
potential model based on Dirac eqn. with linear confining pot., asymmetric model 79−363
production at large transverse momentum 77−26502
proton-emulsion nuclei interactions, 70 GeV/c, reggeon-pomeron exchange 78−54750
proton-neutron multiplets, odd-odd nuclei, parabolic Regge trajectories, exchange of quadrupole phonon 80−52590
QCD, hadron interaction effective string lagrangian, Regge slope, charmonium pot. model 80−4939
QCD, hadronic and supersymm. string states 79−75724
QCD, in 2-dimens., bound states and asymptotic limits 79−71716
QCD, slope of leading Regge trajectory 80−42391
QCD, string constant, Regge slope and Λ parameter, empirical quarkonium approach 80−91053
QCD, two dimens., hadron scatt., leading order calcs., meson-meson scatt. 78−4831
QCD, two dimens., hadron scatt., multi-Regge and inclusive reactions 78−4884
QCD, two dimens., soln. of Bars-Durgut model for baryons 79−75741
QCD spectrum, infinite number of colours at fixed coupling, interacting string model 79−2993
quantum field scatt. theory of hadrons on Regge trajectory, bootstrap and quark interpretation 77−54046
quantum relativistic strings and the multiplicative dual model *(Russian)* 80−82958
quark conservation at meson vertices, Zweig rule model for couplings, multiRegge phenomenology 77−82709
quark fragmentation functions for inclusive hadron production, Regge formalism 80−68462
quark model, determ. of Regge pole exchange amplitudes 80−404
quark string model, hadron spectrum, semiclassical approach, baryons and exotic hadrons 79−40747
quarks, dynamic models with confinement and linear trajectories without parity doubling 77−2797
quarks, fermion field, nonlinear, origin of four quark flavours, quantum numbers, isosymmetry breaking 80−62920
Regge amplitude construction through soln. of S-matrix equations 79−49413
Regge cut contribs. in triple-Regge region 77−38146
Regge cut discontinuity formulae soln. 77−10203
Regge parametrization of NN differential cross sections and polarizations 79−17746
Regge phenomenology, review 78−24979
Regge pole calc. by formal series 77−6056
Regge pole theory, reasons for survival, review 78−24977
Regge-cut cancellations in dual unitarisation scheme planar amplitudes 77−10228
Regge-Mueller diagrams, Froissart saturation case, struct. and props. *(Russian)* 78−4808
Regge-pole approach to charmonium and bottonium 80−86697
Reggeised absorption model for reaction $NN \to \Delta(1236)\Delta(1236)$ 77−6170
Reggeised quark model, valence-core exchange 77−26485
Reggeized absorpt. with clothed, physical Pomeron 77−57469
reggeized one pion exchange model of nucleon charge exchange in inclusive reactions *(Russian)* 77−2888
reggeon amplitude from analyticity and planar unitarity 77−41828
Reggeon amplitudes satisfying good finite mass sum rules 78−16953
Reggeon calculus, physical basis and implications 77−6101
reggeon F/D ratios in SU(4), crossing invariant soln. of baryon exchange degeneracy 77−2766
Reggeon parton structure, from lepton-Reggeon scatt. data 77−6095
Reggeon quantum mechanics with quartic couplings, energy spectrum struct. 80−62889
Reggeon-Pomeranchukon cuts, Mandelstam diagram model 77−30341
Reggeons with isospin, nonplanar corrections 77−30338
relativistic mechanics of two or three point particle systems 78−4481
relativistic two-particle system and spin-mass relations of meson 79−67505
renormalisation of Regge trajectory in dual models 79−30721
review of Regge poles and multiparticle systems, book contrib. 79−21890
rising total cross sections, Regge complex-pole model 77−41871
s-channel discontinuities of Reggeon diagrams with planar vertices 77−41827

Regge poles and trajectories continued
s-channel discontinuities of torus insertion, dual unitarisation scheme, ρ-A_2 exchange degeneracy breaking 78−93866
s-dependence of proton fragmentation by hadrons, 30-250 GeV/c 78−74291
s-dependence of proton fragmentation by hadrons 4-24 GeV/c 78−74290
S-matrix, planar, building of cylinder correction in topological expansion or dual unitarisation 78−62321
sequential particle order, fundamental concept for hadron physics 79−80762
sequential particle order, fundamental concept for hadron physics, S-matrix theory 79−80763
Shapiro-Virasoro model, multi-Regge limit, pomeron sister trajectory 77−82720
short distance Regge singularities, potential models 77−38147
short distance singularities, renormalised gluon ladder in quantum chromodynamics 77−49909
singularities in multiparticle processes, limit of Veneziano model 78−29274
slope of trajectories based on vortex line models 77−18249
soft hadron-nucleus reactions at high energies, theoretical model 79−17870
soliton trajectories from nonlinear field eqns. of Dirac field, Lorentz and gauge invariant 78−4791
space-time structure of the two-Reggeon exchange process 79−9311
spin-mass trajectories and QED in null plane, free field theories 78−29259
spontaneously broken non-Abelian gauge theory 78−70287
spontaneously broken Yang Mills theories, high-energy gauge meson exchange reactions, factorisation, Reggeisation 77−18172
stochastic-field multieikonal theory, high-energy hadron dynamics 78−8634
strange quarks, Regge exchange building, K^-p data anal. 79−2995
string model, geometrical interpretation of reggeon and pomeron intercepts 77−26499
string-like configurations in Weinberg-Salam theory, Regge trajectories of excitations 78−16966
strong interaction field theory, role of tachyons and virtual fields, book contrib. 79−58889
strong interaction symmetry, calc. of fine struct. const. α 77−41788
strong interactions, introductory book using potential theory 77−223
SU(4)×SU(4) anal. of high energy cross-sections and photoprod. 77−26469
SU(4) broken symm., duality, baryon+baryon and baryon+antibaryon exotic mesons prod. 78−89629
$SU(6)\times O(3)_L$ multiplets, semilocal duality, quark-orbital Regge trajectories 80−27490
supercritical pomeron propagator, representation 77−74619
supergravity, unitarity in general covariant gauge 79−75428
superoperator generalisation of dual model with coloured quarks, three reggeon vertex *(Russian)* 78−74234
supersymmetry, field theory, fermion (meson)-meson scatt., high energy behaviour 79−295
surface acoustic waves scatt. from elastic cylinders 78−50967
symmetries of 3j and 6j coeffs. 80−86621
t-channel diffractive scatt., elastic peak and hadron size 79−45083
tachyon-reggeon scatt., string interaction, physical picture 77−18241
tachyons, role in strong interaction field theory 79−9353
tensor gauge theory with steeply-rising pot., rising Regge trajectories 77−49858
three gluon integral equation and odd C singlet Regge singularities in QCD 80−101991
threshold behaviour of simple and double Regge pole trajectories 78−16950
threshold branch pt. struct. in ladder approx. *(Russian)* 79−89136
topological dual bootstrap model and hadron collisions 77−22708
topological expansion, Pomeron and f-trajectory 77−82721
torsion gravitational theories, spinning particle motion, Lagrangian theory 79−12692
total and triple-Regge inclusive cross sections 78−400
trajectories rel. to degenerate classical solns. of eqns. of motion 79−2955
trajectories with nonplanar cylinder corrections in broken SU(4) 77−45992
trajectory intercepts and mass formulae relation *(Russian)* 79−85283
trajectory slopes based on multilocal model 77−87944
triple-Pomeron couplings in dual models 79−358
two particle system, interaction through action-at-a-distance force, relativistic mechs. 78−66055
two-Reggeon cut in the ordered phase of Reggeon field theory 80−52422
two-Reggeon cut s-channel components 77−18251
unitarised multiperipheral model and Regge cut exchange 77−57510
unitary corrections to short-range order, long range rapidity correlations 79−26315
unitary model for elast. scatt. and inclusive interactions 77−30343
universal Regge slope α' from the QCD gluon propagator 80−78026
valance quark distribs. in π, K, D, Regge trajectories, SU(3), SU(4) breaking 79−30703
van der Corput neutralisers, use in modifying pole residues 77−6093
vector meson reggeization for non-Abelian theories with arbitrary symmetry 77−2740
velocity-dependent pot., Regge trajectories, S-matrix singularities 77−57468
Veneziano model, 6-point function and new trajectories 78−16998
Veneziano-Regge trajectory, class of string models 77−2802
vertex bootstrap conditions in dual unitarisation scheme 77−38135
Z(N) strings and hadron structure 80−86572
Zweig-superconvergence relations in meson collisions 78−21397
$\Delta(1236)$ inclusive prod., absorpt. corrections in triple-Regge region 77−87956
Δ inclusive production 79−17767
ep, deep inelastic scattering on π-pole Regge *(Russian)* 78−12918
ep→epX, photon fragmentation region, Regge pole expansion 77−54108
$\gamma\gamma$ scatt., fixed and moving Regge poles 78−21406
$\gamma N\rightarrow\pi N$, fixed Regge singularities 77−74694
$\gamma p\rightarrow cX$, c=hadron, photon fragmentation region, Regge pole expansion 77−54108
$\gamma p\rightarrow N\pi$, position and residue of the pole in the $M_{1+}{}^{(3/2)}$ amplitude *(Russian)* 79−22112
$\gamma p\rightarrow\pi^0 p$, high energies, semiempirical amplitude anal. dispersion relations and Regge poles 80−86726
Regge poles and trajectories continued
$\gamma p\rightarrow$vector meson+p, elastic and total cross section using Reggeon-photon coupling analogy 78−78193
$\gamma\rho$-Pomeron-Regge vertex function, spin depend. calc., multiperipheral model 78−82223
$K(\bar{K})N\rightarrow K(\bar{K})N$, 1.5-280 GeV/c, Regge pole residues and trajectories, review 78−45886
K^0 regeneration in nuclei, effect of inelastic intermediate states, Glauber-Regge model anal. 79−54458
K_s coherent regeneration on C and Regge pole exchange theory 77−49957
K*(890) prod. at 13 GeV/c, Regge models 78−45961
KN finite energy sum rules, Regge pole models, exchange amplitudes 78−470
$K^-N\rightarrow\bar{K}^{*0}X$, inclusive cross sections and spin density matrices, 3-Reggeon model anal. *(Russian)* 79−80858
$K^\pm N$, high-energy, reaction differences and annihilations 78−74279
$Kp\rightarrow K^*p(K^{**}p)$, diffractive prod. and Reggeon-photon coupling analogy 78−45890
Kp reactions, 13 GeV/c, differential cross-sections, Regge exchange, SU_3 sum rule interpretations 77−41862
K^-p, 8.25 GeV/c, study of inclusive Λ, Σ^0 and $\Sigma(1385)$ prod. 79−30749
K^-p, inclusive Ξ^- production at 4.2 GeV/c, triple Regge formalism 78−4875
$K^-p\rightarrow\bar{K}^0X$, pseudoscalar meson prod. in triple Regge region, absorpt. corrections 78−78228
$K^-p\rightarrow\bar{K}^0n$, 25 and 40 GeV, differential cross section meas. *(Russian)* 78−25083
$K^-p\rightarrow\Lambda X$, 4.2 GeV/c, polarisation and triple Regge framework 78−45948
$K^-p\rightarrow\Lambda\eta$, 6 GeV/c, baryon exchange reactions, ηNN coupling constant, Λ polarisation, nucleon-Regge exchange 80−78098
$K^-p\rightarrow\Lambda\pi^0$, 6 GeV/c, baryon exchange reactions, ηNN coupling constant, Λ polarisation, nucleon-Regge exchange 80−78098
$K^-p\rightarrow\Lambda\pi^0$, baryon Regge exchange, FESR anal. 80−63022
$K^-p\rightarrow\Lambda\pi^0$, polarisation and differential cross-section calc. in Regge-pole model 77−54122
$K^-p\rightarrow\pi^-\Sigma^+$ and line reversed reaction $\pi^+p\rightarrow K^+\Sigma^+$, simple Regge pole model 80−78093
$K^-p\rightarrow\Sigma^-\pi^+\pi^-\pi^+$, 4.15 GeV/c, nondiffractive A_1 production, double-Regge model 80−78097
$K^+p\rightarrow K^0X$, pseudoscalar meson prod. in triple Regge region, absorpt. corrections 78−78228
$K^+p\rightarrow p+$anything, 16 GeV/c, triple Regge features 77−65184
$K^+p\rightarrow\bar{X}\Delta^{++}$, absorption corrections to three Reggeon formulas *(Russian)* 79−9423
$K^\pm p$, elastic scatt. and diffractive dissociation, Regge model with $\alpha_P(0)>1$ *(Russian)* 80−57630
$K^\pm p$ elastic scatt., dominant exchanges using Reggeon-photon coupling analogy 78−78204
$K^\pm p\rightarrow\bar{K}^0\pi^\pm p$, double Regge exchange phenomenology 79−3008
$K^\pm p\rightarrow K^\pm X$, triple Pomeron coupling, Reggeon treatment 80−68488
$K_L p\rightarrow K_S p$, 5 to 10 GeV, differential cross-section, ω Regge trajectory 80−22637
Λ inclusive prod., Regge cuts and spin depend. 78−21402
N-N Regge trajectory scheme and di-baryon resonances 77−67633
$N\bar{N}$, relativistic interacting system, eqn. of state using Regge-type interaction amplitude *(Russian)* 77−79032
$NN\rightarrow(N\pi)N$, mass-slope correl. in Reggeised Deck model 77−22712
NN elastic scattering, polarisation anal., eikonal framework 77−30405
NN low-energy pot., Regge-pole theory 78−45889
$NN\rightarrow N(N\pi)$ diffractive dissociation process, one pion Regge-pole exchange amplitude *(Russian)* 80−42491
NN potential from Regge pole theory in momentum space, S-matrix theory formalism 79−67525
NN potential from Regge pole theory, pseudoscalar meson potentials, M/E factor 79−67526
NN potentials from Regge pole model, one boson exchange, coupling consts., masses 78−70346
NN spin-polarisation meas. 78−74272
np charge exchange amplitudes, Regge behaviour of imaginary parts, polarisation 77−38145
np charge exchange cross sections, Regge pole and cut behaviour at Fermilab. energies 78−441
np elastic scatt., 70-400 GeV/c, cross sections, simple Regge pole model 80−63032
np high-energy scattering, review 77−79283
np→pn, 8 GeV/c, Regge anal. of charge exchange scatt. 77−22756
np→pn charge exchange amplitudes, energy dependence, up to 60 GeV/c 77−6171
np→px, baryonium exchange, triple-Regge couplings 80−86763
$\nu\bar{N}\rightarrow\pi^\pm\Delta$, dynamical model 79−401
νp interactions, charmed meson prod., Regge pole model, cross sections 78−33052
$\nu p\rightarrow\mu^-D^+X$ or $\mu^-D^{*+}p$, cross sections estimation using V+A form of charm current 77−41839
p electroprod. struct. function and constituent-particle scatt. 78−45931
p+nucleus, inclusive production of neutral strange and charged particles, collective tube model 80−52538
pd scatt., intermediate inelastic states and triple-Regge couplings, Pomeron 80−4972
$pK^-\rightarrow\Sigma^++$anything, beam and target fragmentation processes, triple Regge anal. 77−82786
$pN\rightarrow\Lambda^0,\bar{\Lambda}^0$, 300 GeV, inclusive prod., triple-Regge behaviour 77−61328
$pN\rightarrow NN\pi$, 6 to 1480 GeV, double Regge pole model 78−45964
$pN\rightarrow N(N\pi)_{I=1/2}$, 5.7 GeV.c ρ exchange contrib., cross channel isospin amplitude anal. 78−45938
pn→np, charge exchange processes, baryonium trajectories, Regge pole description 80−9180
$pn\rightarrow p_{slow}+x$, 195 GeV/c, triple Regge model anal., dominant π exchange 78−54657
pn→pX, 100 to 400 GeV/c, slow-proton prod., Regge trajectory 80−22646
pn→pX, 19 GeV/c pion exchange model of neutron fragmentation 79−63549
$p^\pm N$, high-energy, reaction differences and annihilations 78−74279
pp, dual model, vacuum exchanges, double pomeron poles with exotic Regge poles 78−89686
pp, elastic scatt., 12 to 24 GeV, leading effective trajectories, residues, anal. 79−421

Regge poles and trajectories continued
$\bar{p}p$, pp, elastic scatt. and diffractive dissociation, Regge model with $\alpha_P(0)>1$ *(Russian)* 80−57630
$\bar{p}p$, pp high energy elastic scatt., cross section rise and polarisation, Regge model *(Russian)* 80−37301
pp, smooth interpolation between Orear- and fixed angle scaling behaviour of the scattering amplitude 80−105873
pp and pn polarisation expts. description 77−57564
pp and $\bar{p}p$ elastic scatt., dominant exchanges using Reggeon-photon coupling analogy 78−78204
pp→cX, $p\bar{c}$ exotic, triple-Regge formalism, Pomeron exchanges 80−63041
pp→charged particle+X, small-angle production from nuclear and nucleon targets, collective tube model and triple-Regge picture 80−52538
pp→Δ^{++}X, triple Regge anal., role of absorptive corrections 77−18340
$p\bar{p}$→Δ^{++}+anything, 9.1 GeV/c, Mueller-Regge theory test, fragmentation process expt. 77−61312
pp elastic, inelastic, and inclusive interactions, spin effects, polarisation 77−30434
pp elastic scattering, up to 27.4 GeV, simple Regge model for ang. distribs. 79−75799
pp large |t| scatt. and Regge cuts 78−41587
pp→Λ, 10 to 300 GeV, triple Regge framework 78−21472
pp→Λ^0X, small-angle production from nuclear and nucleon targets, collective tube model and triple-Regge picture 80−52538
pp→Λ^0X^{++}, 69 GeV/c, triple Regge anal. 77−74730
pp→ΛX, Λ polarisation and Regge cuts 77−2876
pp→$\Lambda\bar{\Lambda}$X, natural and unnatural parity exchange in triple-Regge region 77−65182
pp→nX, baryonium exchange, triple-Regge couplings 80−86763
pp→n+X, triple-Regge region, absorpt. corrections to inclusive spectrum 78−78230
$\bar{p}p$→$\bar{n}n$, 8 GeV/c, Regge anal. of charge exchange scatt. 77−22756
$\bar{p}p$→$\bar{n}n$, charge exchange processes, baryonium trajectories, Regge pole description 80−9180
pp→pX, associated multiplicity, and pomeron-pomeron cross section 79−17770
pp→pX, triple-Regge fits, duality struct. of inclusive diffr. dissoc. 78−8715
pp→pp, polarisation structure and Pomeron flip, Regge pole model 80−102073
pp→pp$\pi^+\pi^-$, 4 GeV/c, Reggeised one pion exchange model anal. *(Russian)* 79−30746
$\bar{p}p$→π^-X($\Lambda\bar{X}$), 22.4 GeV/c, test of factorisation hypothesis for leading Regge trajectories *(Russian)* 79−49561
$\bar{p}p$→$\pi^+\pi^-$X, 100 GeV/c, tests of factorisation in Pomeron and Reggeon exchange 77−74731
$\bar{p}p$→$\pi^+\rho^-$, 6 GeV/c, line reversed reaction, Δ exchange, ρ^- decay 78−12926
pp→π(K)X, 50-175 GeV, Regge parametrisation 77−14002
pp scatt., exchange degeneracy violating A_1-Z Regge amplitude and dibaryon resonances 80−4971
pp scattering, multipole Regge model, up to 5.10^3 GeV *(Russian)* 77−61324
pp-pX, Regge cut contribs. in triple-Regge region 77−38146
ϕ(1019) photoproduction on proton, 2.8-4.8 GeV 79−9381
π electroprod., light cone dispersion sum rules, Regge subtractions 78−41556
π^0 photoproduction, Regge poles and cuts 78−66127
π^-d→Δ^-p, high energy, backward Δ^- prod. mech., Δ^{++}-Reggeon exchange *(Russian)* 79−97637
πN→(ρ,Ω)N, Regge model with derivative relations between S-channel helicity amplitudes 77−74713
πN→A_2N, ρ and f Regge exchanges, an interpretation 79−63531
πN charge exchange scatt., Regge pole, model calcs. 80−102071
πN charge exchange scatt. saturation, trajectory props. *(Russian)* 79−89186
πN elastic backward scattering at 3.5 GeV/c, data anal. by Regge type models 77−61314
πN invariant scattering amplitudes, zero trajectories 80−102067
πN→πN, finite-energy sum rules, three component duality 80−82996
π^-n→pX$^-$, 21, 205 and 360 GeV/c, reggeised one-pion-exchange 80−57649
π^+n→p_{slow}+x, 195 GeV/c, triple Regge model anal., dominant π exchange 78−54657
π^+n→pX, 100 to 400 GeV/c, slow-proton prod., Regge trajectory 80−22646
$\pi^\pm$N, high-energy, reaction differences and annihilations 78−74279
$\pi^\pm$n backward elastic scatt. 20-40 GeV, Regge theory description, angular distrib., radiative corrections 78−62461
$\pi^\pm$N→ρ^0X, inclusive cross sections and spin density matrices, 3-Reggeon model anal. *(Russian)* 79−80858
πp, 16 GeV/c, diffr. dissoc. into $\bar{K}K^*$, $\bar{K}^*K$ 78−41594
πp→A_2p, diffractive prod. and Reggeon-photon coupling analogy 78−45890
πp charge exchange reactions, model of ρ Regge trajectory 78−37226
πp→K(p)X, 50-175 GeV, Regge parametrisation 77−14002
π^-p, 100 GeV/c, π^0 and η inclusive prod. in all neutral mode 79−13165
π^-p, elastic scatt., 12 to 24 GeV, leading effective trajectories, residues, anal. 79−421
π^-p→($\pi^+\pi^-$)n, 17.2 GeV/c, role of A_1 exchange, Regge pole exchange 77−61325
π^-p→Δ^{++}(1232), 15 GeV/c, multiplicity distrib. determ. 78−45982
π^-p→ηX, pseudoscalar meson prod. in triple Regge region, absorpt. corrections 78−78228
π^-p→η'n, Regge pole model with phenomenological residue functions 80−102077
π^-p→ηn, Reggeon field theory, behaviour of A_2 trajectory 80−22594
π^-p→$\eta\eta$, tensor-exchange amplitude and polarisation determ. 78−45962
π^-p→f^{0}X, tensor meson prod. in triple Regge region, cut corrections 77−46087
π^-p interaction, 15 GeV/c, ρ^0 prod. analysis within triple Regge model 78−37251
π^-p interactions, 15 GeV/c, K^0_s, Λ, $\bar{\Lambda}$ prod., Regge anal. 78−45981
π^-p→$K_1{}^0K_1{}^0$n, 40 GeV/c *(Russian)* 77−261
π^-p→K^-K^0p, double Regge exchange phenomenology 79−3008
π^-p→$\Lambda K^0(K^{*0})$, 3-6 GeV/c, Regge theory of baryon exchange 78−25074
π^-p→ωn, 20-200 GeV/c, prod. cross section, Regge formalism test 77−26546
Regge poles and trajectories continued
π^-p→ωn, 6 GeV/s, abnormal polarisation effect in Ar, two-Reggeon exchange model *(Russian)* 77−10282
π^-p→ωn, Reggeon cuts and reaction description *(Russian)* 78−45947
π^-p→p_{slow}+X^-, 147 GeV/c, differential cross sections, triple Regge anal. 79−40811
π^-p→pX, 12 GeV/c, absorbed Mueller-Regge model for backward inclusive p prod. 80−73752
π^-p→pρ^-, 6 GeV/c, line reversed reaction, Δ exchange, ρ^- decay 78−12926
π^-p→ϕn, quark line rule, violations 80−52530
π^-p→π^-_{fast}+X^+, 147 GeV/c, differential cross sections, triple Regge anal. 79−40811
π^-p→π^-X, triple Pomeron coupling, Reggeon treatment 80−68488
π^-p→π^-(π^0)X, 40 GeV, three reggeon approach, multiperipheral model evidence *(Russian)* 79−30761
π^-p→π^0X, pseudoscalar meson prod. in triple Regge region, absorpt. corrections 78−78228
π^-p→π^0(η)+anything, absorptive corrections using Regge pole amplitude 77−38204
π^-p→π^0n, 20-200 GeV, pure ρ-Regge-pole exchange model in forward direction 77−38203
π^-p→π^0n, charge exchange polarisation, Gribov Reggeon calculus, derivative rule, absorpt. model alternative 77−46076
π^-p→π^0n, helicity nonflip amplitude in Reggeon calculus 77−22765
π^-p→π^0n, pure ρ+ρ' Regge-pole anal. for 20-200 GeV/c forward scatt. 78−8702
π^-p→π^0n, π^-p→ηn, 6-200 GeV, charge exchange amplitude energy behaviour 77−22800
π^-p→π^0n, secondary trajectories propagators in Reggeon field theory, interacting Reggeons and Pomerons 79−40764
πp^-→ψ+X, ψ(3.1) inclusive prod. in fragmentation region 79−13150
π^-p→ψn, generalised Veneziano models 80−22638
π^-p→ρ^0_Ln, Reggeon cuts and reaction description *(Russian)* 78−45947
π^-p→$\rho^0\pi^-$X, diffractive contrib. in multi-Regge factorisation 80−73753
π^+p→(ρ^0,ω)Δ^{++}(1238), q_L=7.1 GeV/c, role of new exchanges *(Russian)* 79−54355
π^+p→f+X^{++} 8 GeV/c, reaction anal. 79−93457
π^+p→$K^+\Sigma^+$ and line reversed reaction K^-p→$\pi^-\Sigma^+$, simple Regge pole model 80−78093
π^+p polarisation near backward direction, partial waves anal., comparison with model predictions 77−30421
π^+p→p$\pi^+\pi^+\pi^-$, 3.1 GeV.c^{-1}, contrib. of reson. states of cross section, Regge pole exchange model anal. *(Russian)* 79−9403
π^+p→ρ^0X^{++}, 8 GeV/c, reaction anal. 79−93457
π^+p→Σ^+(1385)K^+(K^{*+}(890)) 10.3 GeV.c, Y*K and Y*K* prod. 79−49544
$\pi^\pm$p, 100 GeV/c, π^0 and η inclusive prod. in triple Regge region 79−13164
$\pi^\pm$p, 40-45 GeV, Regge anal. differential cross sections *(Russian)* 78−25081
$\pi^\pm$p, A meson prod., Regge model, polarisation anal. 78−41577
$\pi^\pm$p, elastic scatt. and diffractive dissociation, Regge model with $\alpha_P(0)>1$ *(Russian)* 80−57630
$\pi^\pm$p 100 GeV/c, π^0 and η inclusive prod., triple Regge theory test 79−6349
π^+p elastic scatt., dominant exchanges using Reggeon-photon coupling analogy 78−78204
π^+p elastic scattering, amplitude anal., σ trajectory 78−33081
$\pi\pi$ scatt., crossing symmetry and unitarity, spectral functions 77−6165
QQ mass, approx. scheme is QCD 80−42398
QQ relativistic bound states, mass formula, unification of linear Regge trajectories 79−89141
ρ recurrences in ψ→3π 77−79266
C, K^0 regeneration, Regge behaviour and nuclear effects, ω-pomeron cut 79−13347
H+Hg, differential cross sections, orbiting contribution 79−41221
H_2+Kr, elastic total cross section, orbiting effects, Regge theory 78−82814
^{4}He(γ,π^0), P-odd effects, Regge and boson pole interference *(Russian)* 79−6564
^{4}He(p,nπ^+), 18.6 GeV, invariant mass distrib., double Regge pole model comp. 79−3144
^{4}He(p,p) 18.6 GeV 79−3144
^{4}He(p,pπ^0), 18.6 GeV, invariant mass distrib., double Regge pole model comp. 79−3144
K$^\pm$p, 40-45 GeV, Regge anal. differential cross sections *(Russian)* 78−25081
Ne(α,α), A=20,22, large angle elastic scatt., 24.6-31.7 MeV, single Regge pole anal. 78−70547
$\bar{p}p$, 40-45 GeV, Regge anal. differential cross sections *(Russian)* 78−25081
$\bar{p}p$→Λ, 10 to 300 GeV, triple Regge framework 78−21472
π^-p→$\eta\eta$, Fermilab energy, Regge pole model 79−17762
^{28}Si+^{16}O, pot. for back-angle enhanced elastic scatt. 79−40953
^{28}Si(^{16}O,^{16}O), 55 MeV, Regge pole anal. using optical pots. 79−3174
^{28}Si(^{16}O,^{16}O), anomalous large angle scatt., Regge pole contrib. 79−63687

Reggeon field theory
3j coeff., symmetries 79−305
Φ^3 field theory, Regge pole behaviour 78−66053
asymptotic behaviour, quantum corrections in Reggeon calculus above critical intercept 77−45990
boson propagator in Reggeon field theory 78−74138
boson trajectories 78−89634
bound and rebound states, relativistic eikonal approximations 80−27491
broken global symmetries, nondegeneracy of vector meson mass, nontrivial mixing 80−13236
central rapidity region, asymptotic and nonasymptotic energies, nonleading terms 77−10185
critical exponents calc. by convergent numerical method 77−45991
critical exponents for Reggeon quantum spin model 78−62338
critical Pomeron intercept with block-spin methods 79−71615
crossover phenomenon, interactions of Reggeons and Pomerons 79−93317
cut Reggeon field theory on transverse lattice, inclusive distribs. determ. 78−21334
cut theory, 4-pomeron couplings 80−42366
dual models, unitarised, conventional, renormalisation of new trajectory 79−85281

Reggeon field theory continued
dual unitarisation, renormalisation of trajectories with zero quantum numbers 78−21400
exotic baryon resonance with isospins ≥5/2, existence, sum rule in Reggeon field theory *(Russian)* 78−93824
expanding disc as dynamical vac. instability 77−2774
fermion-fermion scattering in supersymm. field theory, high energy behaviour 77−13887
Feynman integral models of Regge behaviour in asymptotically free theory 77−214
finite mass sum rule and Reggeon vertices, unitarity constraint equations 80−13292
four-reggeon couplings, analogue quantum-spin model 78−45813
gauge vector mesons with unified theories, Reggeization 79−97562
hadron-nucleus high energy reactions, triple pomeron in coherent processes 77−18534
hadron-nucleus inelastic inclusive cross-sections in Reggeon field theory *(Russian)* 77−82791
hermicity properties, Schwarz trajectories 78−29274
high energy collisions of heavy nuclei, Glauber rescatt., Reggeon field theory 78−37369
high-mass diffraction in the supercritical region 79−22081
inclusive interactions of fast hadrons with nuclei, Reggeon chain *(Russian)* 78−45985
instabilities in strong coupling theory of vacuum Reggeons *(Russian)* 77−34139
instanton contributions in Reggeon quantum mechanics 79−21971
lattice approx., total cross-section anal. *(Russian)* 78−29273
lattice model, critical behaviour, Monte Carlo calc. 80−18126
Lund-Regge system, prolongation structures and connection forms 78−93805
Markov processes 78−77774
massless non-abelian gluon confinement and rising total cross sections 80−13264
meson trajectories, Markoffian approach 79−45037
multi-Pomeron couplings to external particles in Reggeon field theory, renormalisable field theory 78−78111
non-Abelian gauge theories, high energy behaviour, reggeon field theory, QCD 80−62822
non-Abelian gauge theory, nonplanar skeleton graph, vanishing graphs, planarity and Reggeisation 79−97504
non-Abelian massive gauge theory high energy behaviour via Regge field theory 77−61197
nonperturbative formulation of Reggeon field theory on lattice 77−49880
$O(\varepsilon^2)$ scaling law for $d\sigma/dt$ in the Reggeon field theory 80−101936
one-component formulation of Reggeon field theory 78−8630
ordered phase in Reggeon field theory, Hamiltonian formulation, scatt. amplitude calc. 78−4807
OZI rule violation, analyticity and duality 78−24978
particle correlations in multiperipheral resonance prod. model, broken SU_3 symmetry 78−45891
parton model of the pomeron with $\alpha(0)>1$ *(Russian)* 78−74235
path integral for Reggeon quantum mechanics 79−26259
path integral formulation of Reggeon quantum mechanics with cubic/quartic interactions 79−54283
perturbation series divergence 77−2754
perturbation theory at large orders 78−8510
pole search problem of scatt. amplitudes in L^2 norm 77−41756
pomeron flavouring in reggeon field theory with thresholds 78−41437
pomeron flavouring Reggeon field theory with thresholds 78−29275
Pomeron intercept anal. 77−6003
pomeron intercept in Reggeon field theory on transverse lattice, neg. renormalisation 78−93823
Pomeron nondiffractive renormalisation, flavour and baryon quantum nos. 78−82177
quantum chromodynamics, unified approach to gauge, dual, Gribov theories 77−18223
quantum mechanics, Reggeon, Hamiltonian formulation, S-matrix, pomeron Green functions 78−16951
quark masses and structure functions 80−22585
Regge-Mueller diagrams, rel. to dual analytical model for pomeron *(Russian)* 77−13946
Reggeization of elementary fermions in arbitrary renormalizable gauge theories 80−68367
Reggeon quantum mechanics with quartic couplings, energy spectrum struct. 80−62889
Reggeon-Gribov field theory, nonlinear Schrodinger eqn. as model 77−38100
relativistic hadron, parton distrib. and Regge field theory parameters *(Russian)* 80−62931
renormalisation group calculations for Reggeon field theory on transverse lattice 77−18203
review of recent developments 78−41439
scalar field Reggeisation in scalar QED 79−26272
secondary Reggeons, threshold approach 79−12985
semiquantum approximation for the Reggeon field theory on a lattice 79−35968
SL(3,R), unitary analytic representations, hadronic Regge sequences 78−37155
space-time structure of the two-Reggeon exchange process 79−9311
spontaneously broken non-Abelian gauge theory 78−70287
spontaneously broken nonAbelian gauge theory, Regge behaviour 78−41438
SU(2) symmetry Reggeon field theory, negative mass Reggeon multiplet 78−78110
supercritical reggeon field theory, classical kink state quantisation 78−16952
total and elastic cross sections, Pomeranchuk-type theorems, asymptotic props. 79−21972
total and triple-Regge inclusive cross sections 78−400
triple Regge region, higher order ε terms 78−16954
triple-Regge limit, cut Reggeon field theory 78−8629
tunnelling at zero transverse dimens., path integral formulation 79−12986
two-Reggeon cut in the ordered phase of Reggeon field theory 80−52422
vector meson scatt., two to three body, high energy, in Yang-Mills theory 78−17051
Yang-Mills theory, Regeisation of scalars and dual model struct. 78−16927
Reggeon field theory continued
Yang-Mills theory, spontaneously broken, reggeon field theory appl. 78−8512
zero transverse dimens., anal. using moment recursion relations 79−71661
KN scattering, reggeised particle exchanges used in Blankenbecler-Sugar eqn. 78−37230
pp total cross section rise, critical character of pomeron 77−50029
ϕ^3 theory, multiparticle Regge poles *(Russian)* 77−6057
π electroprod., light cone dispersion sum rules, Regge subtractions 78−41556
$\pi^- p \rightarrow \eta n$, Reggeon field theory, behaviour of A_2 trajectory 80−22594
$\pi^- p \rightarrow \pi^0 n$, secondary trajectories propagators in Reggeon field theory, interacting Reggeons and Pomerons 79−40764
region of escape *see exosphere*
regulation
see also load regulation
boiling water reactor optimal control, regulator problem, feedback control laws 77−54315
four-arm bridge measuring circuits with linearised characteristics *(Russian)* 79−12820
Ca^{2+} concentration in extracellular fluids in body, digital simulation of short term regulation 79−83725
regulators *see controllers*
Rehbinder effect *see mechanical properties of substances; surface phenomena*
relative density *see density*
relative humidity *see humidity*
relativistic band structure calculations
actinide dioxides, electronic struct. and ionicity 80−10872
actinide metals, Coulomb ten U and 5f electron excitation energies calc. 77−11867
actinides, electronic excitation energies calcs. 80−54592
actinides, self-consistent relativistic muffin-tin calc., atomic vol. and bulk modulus Ac-Am 78−72065
APW method, linearised relativistic using approx. pure spin basis functions 80−70581
crystal slab, 3-D, surface states, relativistic Green matrix method, muffin-tin potential 80−80345
crystal surface states, calc. by relativistic Green matrix method 79−47139
density functional formalism 80−10848
heavy elements, relativistic model pot. 78−75978
KKRZ theory of energy bands of heavy solids 79−82512
linear APW method and augmented spherical wave method extensions 79−60679
one-dimensional monatomic cryst., relativistic electronic state 80−54590
pseudopotential, norm-conserving, relativistic corrections 80−70584
rare earths, electronic excitation energies calcs. 80−54592
semiconductor with relativistic electron spectrum, bound and reson. states 77−51701
spin polarised, calc. technique and its appl. to Gd 77−85128
transition metals, relativistic electron-phonon interaction 79−82532
Au, energy band structure, X-ray N-emission spectra, relativistic APW calcs. 80−70596
Au, photoelectron spectra, bulk and surface, rel. to band struct. 80−20770
Au, self-consistent relativistic band struct. 80−75501
β'-Au-Mg, de Haas-van Alphen effect, relativistic LMTO bandstructure, Fermi surface 79−37959
$AuCu_3$, ordered, band struct. and optical props. at 30K 79−60696
Ce, density functional theory 80−15442
CuBr(Cl)(I), energy bands, relativistic KKR method, UV absorpt. spectra 80−39501
Eu, relativistic band struct. calcs., unoccupied 4f level calc., Fermi level, atomic configuration 80−49584
Gd, band structure and Fermi surface using KKR formalism 79−77993
Gd, self consistent relativistic ferromag. band struct. 78−91609
Hf, electron structure and soft X-ray emission spectrum, RAPW calcs. 79−91536
HfC, quasi-self-consistent energy band structures using relativistic KKR calcs. chemical bonding 79−51484
HfC_xN_{1-x}, X-ray valence photoelectron spectrum, 4f signal calc. 80−66391
HfN, electronic struct., relativistic energy band struct. calc. 80−34354
In, relativistic energy bands, density of states, and optical spectra, KKRZ calc. 79−51478
InSe, reflectivity and low energy absorption 80−34944
La, density functional theory 80−15442
Lu, band structure, influence of relativistic effects 78−75991
Nb, electronic struct. with non-muffin-tin pot., self-consistent relativistic APW calc. 77−66108
Os, correlation effect of crystal pot., RAPW calcs. 78−6265
PbPo, electronic struct., relativistic band struct. calc. 79−4510
PbS, energy gap anomaly, relativistic band struct. calc. 79−4510
PbSe, energy gap anomaly, relativistic band struct. calc. 79−4510
PbTe, energy gap anomaly, relativistic band struct. calc. 79−4510
Pd, electronic structre, Compton scatt., soft X-ray emission and X-ray photoelectron spectra 79−77999
SnTe, self-consistent relativistic energy bands 80−10870
TaC, quasi-self-consistent energy band structures using relativistic KKR calcs. chemical bonding 79−51484
TaN, electronic struct., relativistic energy band struct. calc. 80−34354
Th, correlation effect of crystal pot., RAPW calcs. 78−6265
Th, density functional theory 80−15442
TlCl, ground-state props., Wannier functions, and electronic struct., ab initio self-consistent calc. 80−80178
TlCl, self-consistent electronic struct. and ground state props. 80−15451
U compounds, NaCl struct. type, relativistic energy bands, LMTO calcs. 80−65442
UC, partially filled f bands, configurational and relativistic effect sensitivity 79−78002
UC, quasi-self-consistent energy band structures using relativistic KKR calcs. chemical bonding 79−51484
UF_5, electronic struct. calc. 80−6716
UGe_3, de Haas-van Alphen effect, band struct. calc. 78−72068
UN, electronic struct., relativistic energy band struct. calc. 80−34354
$U_xTh_{1-x}As$ (Sb), electronic struct., relativistic KKR-averaged T-matrix approx. method 80−107702
W, Fermi velocity calc., linear muffin-tin orbital method 79−28272

relativistic corrections
see also Lamb shift
1S Lamb shift and 1S-2S isotope shift 80−91464
6d metal superheavy hexafluorides, relativistic mol. calcs. 80−5484
ab initio effective core potential studies, relativistic effects, appl. to $HgCl_2$, AuCl, and PtH 79−93933
actinide configurations, isotope shifts rel. to $|\psi(0)|^2$ 78−17580
alkali halides, binding energy, relativistic effects 77−14370
alkali metal, high ang. momentum Rydberg states, quantum defect core polaris. depend. 77−18808
approximate relativistic Hartree-Fock eqns., soln. using Slater-type functions 80−58168
atom, bound state quantum fluctuations and variational method, relativistic HF calc. with radiative effects 80−42918
atom, contact interactions, parity-violating and parity-conserving, new evaluation techniques 79−26872
atom, electron impact excitation and ionis., relativistic effect, $Z\alpha$ and v/c depends. 79−860
atom, estimation method, relativistic corrections 80−14091
atom, HFS, many-body and relativistic effects 78−37565
atom, KLL Auger spectrum, new developments, line energies, intensities 77−18868
atom, L-subshell Auger and Coster-Kronig rates and fluorescence yields, relativistic calcs. 79−81180
atom, many-electron, in external mag. field, Hamiltonian and classical electrodynamics 77−79576
atom, nucl. quadrupole coupling const., relativistic many-body perturbation theory 78−37566
atom, orbit-orbit interaction, core and open-shell electrons 77−67989
atom, photoionisation, relativistic RPA calcs. 77−61719
atom, photoionisation cross-section, intershell interactions 79−26948
atom, quasiclassical approximation, Thomas-Fermi method, for Z>137 nuclei *(Russian)* 78−17547
atom, relativistic, level shifts, transition probabilities, perturbation theory 79−10067
atom, relativistic calcs., perturbation theory approach 79−31422
atom, screened Coulomb pots., anal. perturb. theory for relativistic case 78−21861
atom+H^+, K-shell ionis., plane wave Born approx. model 77−34748
atom+ion collisions, L-shell Coulomb ionisation, electronic relativistic effects 77−42391
atom+ion slow collisions, K-shell excitation of relativistic atoms 80−48073
atom with partially-filled shell, relativistic theory, secular operator renormalisation *(Russian)* 80−52896
atom with two electrons in open shell, level shifts *(Russian)* 80−14092
atomic data handbook 77−23398
atomic electron binding energies, determ. from relaxed-orbital relativistic Hartree-Fock-Slater calcs. 77−42255
atomic form factors, relativistic Hartree-Fock, tables for Z=1-100 79−59381
atomic ground state energy, relativistic and radiative corrections *(Russian)* 77−67991
atomic inner shell electron props., relativistic effects 77−18803
atomic photoionisation anal. using relativistic random phase approximation and multichannel quantum defect theory 80−63602
atomic radial wave functions, approx. relativistic corrections 77−421
atomic structure, ang. momentum coeffs., Fortran program MCP75 77−10605
atomic structure, review of calc. programs which take account of relativity effects 79−59379
atomic structure theory, relativistic corrections 77−57891
atomic systems, many-electron autoionisation states, transition probability and autoionisation rate, perturbation theory Z-expansion 80−52863
atomic wave functions, relativistic, Hartree-Fock calcs. 79−10009
atoms, $70 \leq Z \leq 82$, Kα X-ray linewidths and relative intensities, energy dispersive meas. 80−99483
atoms, analytical relativistic SCF calcs. 80−83248
atoms, electrostatic electron interactions, relativistic calcs. 77−57894
atoms, Hiller-Sucher-Feinberg identity, generalisation, accuracy for approx. wavefunctions 80−63512
atoms, photoionisation, multichannel relativistic RPA calcs. 80−9570
atoms, relativistic electron impact, K-shell ionisation, Z and E depend., scaling behaviour 78−42227
atoms, relativistic energies, perturbation calcs. 80−102453
atoms, review of relativistic corrections 80−47914
atoms, Thomas-Fermi model, Dirac exchange and relativistic corrections, effective EM potential 79−89614
Auger electron transition energies calcs., contributions from beyond relativistic HF limit 77−18874
beta decay, K-shell internal ionisation, many electron effect, relativistic theory 77−18890
Bethe-Salpeter equation, reduction to equiv. Schrodinger eqn., appl. to muonium and positronium 79−2933
Bose-Einstein condensation in Einstein universe 80−46959
central field approximation, RELAC method and use 80−9520
channelled relativistic particles emission spectrum, rel. to interplanar pot. 80−65115
charge transfer, resonant, spin depend. *(Russian)* 78−29850
charmonium, spectra, interaction with external quantised EM field, H-like atom 79−68332
chemistry and relativity, anomalous chemical properties of elements due to high speeds of inner electrons *(French)* 80−93839
clock synchronisation, India-W.Germany, relativistic corrections 80−95077
closed-shell atoms, approximate relativistic Hartree-Fock eqns., soln. using Slater-type functions 80−58168
closed-shell linear molecules, relativistic Dirac-Fock multiconfig. SCF calcs. 80−99455
closed-shell polyatomic molecules, relativistic Dirac-Fock multiconfig. SCF calcs. 80−99456
diatomic molecules, nucleus-nucleus interaction, Einstein relativistic correction, Born-Oppenheimer approx. 80−91463
Dirac operator, essential self adjointness anal. 80−18794
Dirac relativistic wavefunctions, momentum representation 79−13650
Dirac-Fock theory, multiconfig., relativistic SCF method, appl. to open shell ats. 77−3282
double groups, relativistic symmetry orbitals for LCAO calculations 79−10018
EHT theory, relativistically parameterised, appls. 79−49924

relativistic corrections continued
electron rest energy, using X-ray photoelectron spectrometer, student expt. 79−25802
external interaction of two charged particles with quantised field, relativistic invariance 78−74189
Feynman diagrammatic calc. 77−26981
fifth row elements, perturbation theory approach 79−31422
form factors for large momentum transfers, relativistic SCF calc. 77−83504
C_{2v}-formaldehyde, Tamm-Dancoff approx., relativistic correction, vertical excitation energy, radiative lifetimes 78−9090
four subshells of equivalent electrons, matrix elements of relativistic energy operator 78−33407
group IIB elements, interatomic potentials, relativistic effects 79−3516
H_2^+, relativistic corrections, estimation operators 79−54985
halogens, solid, intermolecular bonding influence on nucl. quadrupole interaction tensor 77−62882
heavy atom, L-shell Auger and Coster-Kronig intensities from relativistic theory 79−93962
heavy elements, covalent bonding relativistic corrections, kappa valence method 80−91461
heavy ion+atom collisions, mol. M-X-rays, self-consistent relativistic HF-Slater many electron correl. diagrams 77−14567
heavy ion collisions, radiative electron capture, line profiles 77−14565
heavy-ion collision, quasimolecular L X-rays, relativistic self-consistent correlation diagram 78−5247
high-Z atom+H(He)(O)(F)(Cl) ions, 1sσ vacancy prod., relativistic and Coulomb deflection effects 78−58801
high-Z elements subshells, photoelectron angular distribution 80−99487
highly ionised atoms, relativistic effects, book contrib. 78−74588
highly-charged ions, spectral characts., relativistic effects, theory 79−10061
hydride of Z=104, tetravalent, Dirac-Fock one-centre calcs. 77−88380
hydrides, MH^+, MH_2, M=alkaline earths: Zn, Cd, Hg, Yb, No, relativistic (non-relativistic) HF one-centre expansion calcs. 80−52908
hydrocarbons, normal, mass-spectrometric fragmentation processes, quantum field theory 80−40782
hydrogenic ions, electron capture by charge particles at relativistic energies 80−102565
inert gases, interatomic potentials, relativistic effects 79−3516
inert gases, outer shell photoionisation, relativistic RPA calcs. 80−9571
inert gases, photoelectron spin polarisation, ab initio calcs. 80−18833
ion, highly-stripped, quantum defects 79−41147
ion-atom collisions, relativistic effects in variable-screening model 77−14516
ionisation potential, periodic regularities, relativistic corrections calcs. 79−49950
ions, highly stripped, photoionisation, relativistic calcs. 79−26953
ions in $1s^{2}2s^{n}2p^{4-n}$ configurations, term-energy calcs. using perturbation theory 77−42229
ions with partly filled L-shells, relativistic Hartree-Fock energy calcs. 78−82656
jj-coupling, submatrix elements of operators derived from unit tensors 77−422
K-LL Auger spectra in intermediate-coupling scheme with CI, relativistic Dirac Hartree Slater calc. 80−52958
K-LL Auger spectrum, relativistic calc. 77−18872
K-shell atomic ionisation by heavy particle, electronic relativistic effects, Dirac wavefunctions, semiclassical effects 78−78792
K-shell Auger rates, level widths and fluoresc. yields, relativistic Dirac Hartree Slater calc. 80−52957
K-shell Coulomb ionisation, scaling parameter, relativistic correction 79−72407
K-shell ionis. by charged particle impact, electronic relativistic effects 80−28099
K-shell vacancy production, by charged particles, relativistic effects calc. 78−58600
Klein-Gordon equation, time-independent, relativistic Stark effect, resonances 80−62890
KLL Auger transition energies, relativistic multiconfig. calcs. 77−18873
l-shell Coulomb ionization by heavy charged particles, relativistic effects 79−94073
Lamb shift, anomalous mag. moment, relativistic Dirac eqn. 80−42954
lanthanoid ions, 4f photoelectron spectral intensity, relativistic calc. 79−54816
light muonic atoms, nuclear size effects, energy levels, Lamb shift 80−14254
M-shell radiationless transitions, subshell fluoresc., Coster Kronig yields and X-ray linewidths, relativistic Dirac Hartree Slater calcs. 80−52959
many electron atoms, tensor operator matrix element description 79−13649
many-electron atoms, foundations of relativistic theory, Hamiltonian H_+ and h_+ and related relativistic HF eqn. derivation 80−99458
many-electron atoms, hyperfine struct., relativistic matrix element determ. ^{209}Bi appl. 77−42251
matrix elements of relativistic energy operator, complex electronic configs. 77−30792
matrix elements of relativistic transition operators 77−30822
mesic atom, spectra, interaction with external quantised EM field, H-like atom 79−68332
metal hexafluorides, MF_6(M=W,Re,Os,Ir,Pt), ionisation energies and optical spectra in Dirac-Slater model 77−83488
methylene, singlet-triplet excitation energy, relativistic correction 80−69059
methylene, singlet-triplet separation, relativistic corrections 80−32618
molecular, relativistic orbitals for double group D_{3h} 78−41968
molecular nuclear spin-spin coupling, relativistic theory 77−61769
molecular orbital theory, relativistic, in Dirac Slater model *(Japanese)* 78−66480
molecular spinors from the quasi-relativistic pseudopotential approach 79−97963
molecule, diatomic, Zeeman effect, relativistic corrections 77−83646
molecule, estimation method, relativistic corrections 80−14091
molecule, multiple scattering relativistic Green's function method 77−20214
molecules, relations between matrix elements in relativistic Hartree-Fock-Roothaan theory 79−36521
molecules, relativistic Dirac-Fock multiconfig. SCF calcs. 80−99455
molecules, review of relativistic corrections 80−47914
molecules containing heavy atoms, program for calc. electronic struct. by quasirelativistic method 80−69088

relativistic corrections continued
Mossbauer atoms, electron densities at nuclear centre and surface, calcs. using Dirac-Fock eqn. 80−74100
muffin-tin potential, relativistic scattered-wave theory, elimination method calcs. 77−10607
multicharged ions, transitions between energy levels in strong external field, relativistic calcs. *(Russian)* 80−63547
multicharged Li-like ions, decay of metastable autoionised state *(Russian)* 78−25455
multiconfiguration Dirak-Fock program, appl. to Ba X-ray levels and 5p excited spectra 80−47865
multielectron atom, relativistic Hamiltonian calc. 77−42250
multiply charged ions, $2p_{1/2}3p_{3/2}$ config., level widths, relativistic calc., S-matrix method 80−63546
multiply charged ions, relativistic perturbation theory appls. 80−23323
multiply charged ions, superposition of quasidegenerate configurations 80−42956
multipole transitions in complex config., matrix elements for operators inc. relativistic corrections 78−5150
muonic atom energy levels, $\alpha^4(Z\alpha)^2$-vacuum polarisation contrib. 79−22867
muonic He, hyperfine struct., relativistic, radiative and recoil corrections, QED test 80−14256
muonium, bound-state solutions in relativistic two-body formalism 78−13443
n-electron atom, transition probabilities, relativistic calcs. 77−14391
nucleus+hydrogenic atom electron capture, ultrarelativistic limit relativistic corrections 80−14230
one electron atom, relativistic corrections to nonrelativistic hamiltonian 80−42955
one pion exchange currents in momentum space 77−18400
one-electron polynuclear systems, Dirac eqn., variational soln. 80−83242
open-shell molecules, relativistic self-consistent field theory 80−95518
orbit-orbit interaction, new tensor expansion, matrix and graphical forms 80−14064
oscillator strength calculations, ab initio methods for relativistic effects introduction 80−9519
oscillator strengths, isoelectronic sequences, regularities in f-value distribs. 77−38642
photoelectron ang. distrib. and spin polarisation, theory 80−91618
photoelectron angular distributions, relativistic higher multipole corrections 77−18864
pionic Ti, Klein-Gordon eqn., relativistic fine struct. term, verification 79−22868
polyatomic molecules, relativistic symmetry spinors, LCAO-SCF theory 77−420
polyatomic molecules, relativistic symmetry spinors, LCAS-SCF calcs. 77−419
ponderomotive force, relativistic corrections, plasma heating by lasers 77−65897
positronium, bound-state solutions in relativistic two-body formalism 78−13443
positronium decay, theory and relativistic wave function corrections 77−10791
pseudo pot. model Hamiltonian, spin-orbit splitting, intercombination and relativistic orbital reorganisation 78−25424
pseudopotential theories and corrections to Hartree-Fock method 80−63523
quantum defect phase shift relationship 79−771
rare earth metal atoms and ions, relativistic effects on core-polarisation contrib. to HFS 77−67990
rare earth metals, electron affinities 77−6955
RPA, relativistic, development from linearised time-depend. HF theory 80−47925
RPA appls. to He-like ions energy levels and $Mo^{30+,\ 12+}$ photoionis. 80−47913
Schwarz-Hora effect, long beating length 77−36315
screened photoeffect cross-sections, anal. calcs. 77−10643
Sommerfeld screening parameters for the K level in X-ray spectra 79−68208
spherical Gaussian basis sets, for relativistic Hartree-Fock calcs. 80−32595
spherical system, relativistic pseudopotential 78−82653
spin-flip dipole transition matrix, corrections 79−63936
superheavy molecules, Z=110, Dirac-Slater SCF relativistic mol. calcs. 78−41970
tetrahedral model systems, Dirac-Fock one-centre calcs. 79−6837
three-electron system, Breit-type three-electron eqn., Pauli approx. 79−10044
three-electron systems, autoionis. state widths *(Russian)* 79−49993
transition metal atoms and ions, relativistic effects on core-polarisation contrib. to HFS 77−67990
two-electron atom, relativistic corrections to nonrelativistic hamiltonian 80−42955
two-electron atomic system, relativistic calc. of level widths 79−3376
two-electron Hamiltonian, radiation field, relativistic corrections 78−74586
two-electron system, QED, Foldy-Wouthuysen transform. and transition operator relativistic corrections 77−74624
two-photon resonant absorpt. line profile, quadratic Doppler effect 77−34590
weak exchange currents and μ-p capture 79−75756
X-ray, lineshifts in nonrelativistic and relativistic approxs. 78−951
XPS binding energy determ. without retarding pot., relativistic mass increase 78−41377
Z=100 to 173, Dirac-Fock-Slater calcs. of energy eigenvalues and total eigenvalues 77−71739
Z=114, Dirac-Fock one-centre calcs., tetravlent hydride prediction 77−34551
Z=11 to 103, theoretical, L-shell Coster-Kronig energies 77−83524
Zeeman effect, linear, in Coulomb field 80−102484
d charge form factor accompanying high imparted momentums *(Russian)* 78−58189
Ψ family, EM decays, relativistic corrections in potential model 79−49522
ϒ, EM decays, relativistic corrections in potential model 79−49522
Ag, ionisation energies and oscill. strengths calcs. 80−5488
Ag, semiempirical, relativistic oscillator strengths including core polarisation for p-, s-, d-series 78−74609
Ag, valence-core electron exchange interactions, local approx. 80−91416
AgBr, vapour, photoelectron spectrosc., interpretation 80−95679
relativistic corrections continued
AgCl, vapour, photoelectron spectrosc., interpretation 80−95679
AgI isoelectronic series, oscill. strengths, relativistic HF calcs. 79−98034
AgI, vapour, photoelectron spectrosc., interpretation 80−95679
Al I, relativistic and cancellation effects in line strength ratios 78−82689
Ar, $1s2s3p^4P_{5/2}^{o}$-state, relativistic effects and config. mixing 79−45640
Ar 3s, photoelectron ang. distrib., relativistic Dirac-Fock calc. 79−59411
Ar, 40 keV electron scatt. 7-200 mrad, relativistic and electron correlation effects 77−34760
Ar, and isoelectronic sequence, E1 transitions, relativistic oscill. strengths 78−949
Ar, inner electron energy characteristics, validity of Hartree-Fock-Pauli approx. 80−42957
Au, ab initio effective core pot., Dirac-Hartree-Fock and Hartree-Fock calcs. 78−33426
Au, ground and excited states, pot. energy curves, relativistic effects calcs. 79−31416
Au I, relativistic oscill. strengths 77−14388
Au, relativistic 1s wavefunctions test, using exptl. Compton profiles 80−32600
Au, semiempirical, relativistic oscillator strengths including core polarisation for p-, s-, d-series 78−74609
Au, valence orbitals, Dirac-Fock scheme, direct and indirect relativistic effects 78−41969
Au_2, ground state, ab initio effective core pots., relativistic effects calcs. 79−31377
Au_2^+, ab initio SCF calcs. using relativistic effective core pot. 80−95524
AuH, AuCl, relativistic effective core potentials, ab initio calcs. 78−86767
AuI isoelectronic series, oscill. strengths, relativistic HF calcs. 79−98034
B-like ions, autoionisation states calcs. 80−43006
Ba I, low-lying, even-parity levels, ab initio relativistic SCF MCDF calcs. 78−37568
Be, and isoelectronic sequence, oscillator strengths, relativistic RPA calcs. 77−57929
Be, atom, ground state, accurate CI wavefunction 77−42245
Be, isoelectronic sequence, transition probabilities, relativistic effects calcs. 77−27028
Be, isoelectronic sequence, relativistic transition probability calcs. 77−54533
Be sequence, (Z=4 to 10, 14), $^3P_1 \rightarrow {}^1S_0$ intercombination line, CI calc., Breit interaction 78−78641
Be-like ions, oscill. strengths and transition probabilities, Breit-Pauli approx. calcs. 79−36570
Be-like ions, photoionisation, 2-channel relativistic random phase approx. calcs. 79−59407
Bi, electron config. mixing and parity nonconservation 78−13439
Bi II ion, relativistic effects in hyperfine splitting of second spectrum 80−23344
Bi V, relativistic oscill. strengths 77−14388
BiI, multiconfiguration Dirac-Fock calc. of $6p^3$, $6p^27s$, and $6s6p^4$ configurations 79−3374
Br^+, ionisation pot., periodic regularities, relativistic corrections calcs. 79−49950
Ca XV, transition probabilities, energy spectra calcs. 78−70791
Cd, Breit-Margenau correction, relativistic calcs. 77−3281
Cd, electron binding energy and shift, core level XPS 80−87088
Cd, photoionisation cross section, many-body perturbation theory, dipole length and vel. calc. 78−78674
$CdCl_2$, deformation densities, relativistic effect 80−42928
$Cd(^1S)$, dipole polarisability, relativistic effective core pot. calc. 79−76362
Ce II, isotope shift and screening, pseudo-relativistic HF calc. 78−90096
^{35}Cl XVI, beam-foil excitation, Lamb shift and fine struct., QED test 80−9549
Cr II to VI, struct. and transition probabilities, ab initio calc. using Thomas-Fermi central pot. 79−3360
Cr XVIII, XIX, spectral energy levels, relativistic corrections, config. superposition method 80−32616
Cs, isostructural transition and lattice vibrs., relativistic LMTO calc. 80−20074
CsI, isoelectronic series, oscill. strengths, relativistic HF calcs. 79−98035
CsX,(X=F,Cl,Br,I), ionis. energy, relativistic Dirac-Slater and nonrelativistic HF-Slater calcs. 77−26983
Cu isoelectronic series, Hartree-Fock line strengths 78−9122
Cu, semiempirical, relativistic oscillator strengths including core polarisation for p-, s-, d-series 78−74609
Cu-like ions, E1 transitions, wavelengths, oscillator strengths and transition probabilities, data tables 80−37780
D, 1S Lamb shift and 1S-2S isotope shift 80−91464
D_2, $_{\nu'}^{\nu}(DT^+)$, IR transition freqs. calcs. 77−88452
DT^+, adiabatic relativistic rot.-vibr. energy levels 77−57964
Eu, hyperfine interaction calc., relativistic many-body approach 77−46504
F I, and isoelectronic series, Z=10-100, L-shell energy struct. and level classification 78−55129
Fe III to VI, struct. and transition probabilities, ab initio calc. using Thomas-Fermi central pot. 79−3360
Fe XIX, XXI, spectral energy levels, relativistic corrections, config. superposition method 80−32616
Fe XXI, relativistic energy levels, Dirac-Fock multiconfig. calc., triplet state fine struct. and Lamb shift 80−23315
Fe XXI, transition probabilities, energy spectra calcs. 78−70791
$FeBr_2$, transient species, He(I) photoelectron spectrosc. calcs., relativistic corrections 80−95677
Ga I, relativistic and cancellation effects in line strength ratios 78−82689
Gd^{3+}, hyperfine interactions, relativistic CI using many-body calcs. 78−78638
H atom, energy level calcs. in superstrong mag. field 80−37737
H atom, relativistic, in superstrong mag. fields 78−90095
H atom, relativistic model of spin 1/2 particles interacting with external EM field 78−70756
H, atom in strong mag. field, relativistic corrections to binding energies using perturbation calc. 79−68186
H atom in superstrong magnetic field 80−23320
H, atomic struct., relativistic Dirac eqn., for teachers 78−62019
H, elastic electron (positron) scatt., relativistic Glauber amplitudes 79−31681
H, infinitely magnetised, ground state relativistic corrections 80−77282

relativistic corrections continued
H, line spectrum, relativistic red shift phenomenon 80−32675
H, parity mixing, relativistic neutral current interactions and nonrelativistic pots. 79−26908
H, photon emission, Bohr theory covariant eqns., teaching 80−105482
H, relativistic, in strong mag. field 80−9518
H, relativistic energy levels in strong mag. fields 80−102454
H-like atom, fine struct. and HFS levels, Zeeman effect, relativistic corrections 80−37776
H-like atoms, bound states, so(2,1) algebra 79−10016
H-like atoms, spectra, interaction with external quantised EM field, H-like atom 79−68332
H-like ion, elec. multipole polarisability, relativistic corrections, shielding factors, Dirac eqn. 78−13441
H-like ions, elastic electron (positron) scatt., relativistic Glauber amplitudes 79−31681
H-like ions, ground-state, elastic electron (positron) scatt., relativistic Glauber amplitudes 80−23550
H-like ions (Mg XII to S XVI), satellites to X-ray reson. lines, relativistic calcs. 77−88421
H^++atom, inner shell ionisation, electronic relativistic effects 77−23552
H^++Au(Bi) (U), L X-ray production cross sections, 0.3-1.8 MeV, expt. rel. to PWBA prediction 80−53115
H^++H(1s)→H(1s)+H^+, electron capture at relativistic energies, scatt. amplitude 80−1061
H_2, energy levels accurate determ. 77−46503
H_2, relativistic Dirac-Fock multiconfig. SCF calcs. 80−99455
HD^+, HT^+, adiabatic relativistic rot.-vibr. energy levels 77−57964
$H_2^+(HD^+)$, $1s\sigma_g$ state, pot. energy curves, relativistic corrections 77−57892
$H_2^+(HD^+)(HT^+)$, IR transition freqs. calcs. 77−88452
^3H, relativistic bound state calcs., off shell depend., binding energy 78−82295
^3H, relativistic correction to binding energy 77−79302
^3H, relativistic corrections to two-body pot., binding energy 78−74301
H^*, radiative magnetic energy shift, H in 2p state 78−58601
He, A=3,4, relativistic corrections to two-body pot., binding energy 78−74301
He, electron impact excitation of high Rydberg state, impact parameter method 78−62922
He excited states, relativistic corrections 78−62734
He, photoionisation, frozen-core HF perturbation theory, oscillator strength, dipole length and vel. calc. 78−78672
He-like atoms, n=2 states radiative transition rates, oscill. strengths, RRPA extension 77−34584
He-like ions, $2^3P_1^0$-1^1S_0 and $2^1P_1^0$-1^1S_0 freqs. and transition rates, relativistic calc. 79−68210
He-like ions, oscillator strengths of transitions between low-lying S and P states 78−13470
He-like ions, photoionisation, 2-channel relativistic random phase approx. calcs. 79−59407
He-like ions, radiative 2^3S_1-1^1S_0 transition, correlation effects 79−97989
$He^{2+}(H^+)$+X, (X=Nb to Gd), K-shell X-ray prod. cross-sections 77−71865
Hf III, multiconfig. Dirac-Fock theory, relativistic SCF method 77−3282
Hf IV, 6s $^2S_{1/2}$-6p $^2P°_{1/2,3/2}$ transition, relativistic oscillator strengths, influence of core polarisation 80−58132
HfH_4, Dirac-Fock one-centre calcs. 77−88380
Hg atoms, elastic electron scatt., relativistic effects 80−102568
Hg, Breit-Margenau correction, relativistic calcs. 77−3281
Hg, electron binding energy and shift, core level XPS 80−87088
Hg II, relativistic oscill. strengths 77−14388
Hg, positron scatt. at low energy 80−91670
Hg-Hg potential, relativistic effects on interactions 77−75252
Hg_2^+, electronic struct. and photoabsorpt. calcs. 80−27932
Hg_2-Pt, ^{199}Hg Mossbauer meas., isomer shift and quadrupole splitting calcs. 80−28039
$HgCl_2$, deformation densities, relativistic effect 80−42928
Hg_2F_2, ^{199}Hg Mossbauer meas., isomer shift and quadrupole splitting calcs. 80−28039
HgH, $HgCl_2$, relativistic effective core potentials, ab initio calcs. 78−86767
HgI_2, relativistic effects, photoelectron spectra, Hartree-Fock-Slater method, perturbation theory approach 80−27962
Hg(^1S), dipole polarisability, relativistic effective core pot. calc. 79−76362
I_2, relativistic effects, photoelectron spectra, Hartree-Fock-Slater method, perturbation theory approach 80−27962
In I, relativistic and cancellation effects in line strength ratios 78−82689
K, ^2P fine struct. splittings, Hartree-Fock calcs. 77−10606
Kr 4s, photoelectron ang. distrib., relativistic Dirac-Fock calc. 79−59411
Kr, inner electron energy characteristics, validity of Hartree-Fock-Pauli approx. 80−42957
Kr^{n+}+Ta(W)(Pt)(Au)(Pb)(Bi)(Th)(U), K-L level matching, X-ray obs. 79−63948
Li, ^2S ground state calc. using Hylleraas-type wavefunctions 78−33418
Li I, and isoelectronic series, Z=10-100, L-shell energy struct. and level classification 78−55129
Li isoelectronic sequence, oscill. strengths 77−3309
Li, isoelectronic sequence, transition probabilities, relativistic effects calcs. 77−27028
Li isoelectronic sequence, self-consistent relativistic density-functional theory 80−91441
Li, isoelectronic series, Hartree-Fock line strengths 78−9122
Li isoelectronic series, ionisation pot. relativistic corrections calcs. 77−46484
Li isoelectronic series, relativistic pseudopot. appl. in HF calcs. 80−27960
Li-like ions, fine struct. in $1s2p^2$ ^4P and $1s2s2p$ $^4P^0$ states 78−66471
LiH, relativistic Dirac-Fock multiconfig. SCF calcs. 80−99455
Lu III, 6s $^2S_{1/2}$-6p $^2P°_{1/2,3/2}$ transition, relativistic oscillator strengths, influence of core polarisation 80−58132
Lu, valence orbitals, Dirac-Fock scheme, direct and indirect relativistic effects 78−41969
Lw, ground state config., relativistic prediction, multiconfig. Dirac-Fock calcs. 80−106277
Mg, and isoelectronic sequence, relativistic effects on transition probabilities 77−54532
Mg, intercombination line oscill. strength, including core-polaris. and relativistic effects 78−25475

relativistic corrections continued
Mn, HFS, many-body and relativistic effects 78−37565
Mn III to VI, struct. and transition probabilities, ab initio calc. using Thomas-Fermi central pot. 79−3360
Mo XIII and XVII, spectra, perturbation theory with model pot. 78−58579
Mo XV, electronic struct. of complex ion, relativistic perturbation theory 79−22610
N, nucl. quadrupole coupling const., relativistic many-body perturbation theory 78−37566
^{14}N, spherical ground state nuclear quadrupole interaction, Breit interaction, relativistic perturbation theory 80−42939
Na, ^2P fine struct. splittings, Hartree-Fock calcs. 77−10606
Na high ang. momentum Rydberg states, quantum defect core polaris. depend. 77−18808
Na isoelectronic sequence, Bethe excitation cross-sections 78−82657
Na isoelectronic series, Hartree-Fock line strengths 78−9122
Na isoelectronic series, oscill. strengths, effective orbital quantum no. method 80−9521
Na-like ions, transition probabilities for reson. transitions 78−66494
Ne 2s, photoelectron ang. distrib., relativistic Dirac-Fock calc. 79−59411
Ne, 40 keV electron scatt., 7-200 mrad, relativistic and electron correlation effects 77−34760
Ne isoelectronic sequence, level energies and lifetimes 79−89644
Ne, isoelectronic sequence, excitation energy and oscillator strength, level crossing anomaly, relativistic RPA calc. 80−14077
Ne, isoelectronic series, ionisation pots., Ritz law and Edlen formula 80−32854
Ni cluster-H, electronic struct. calc., H-metal bonding 77−89823
Ni III to VI, struct. and transition probabilities, ab initio calc. using Thomas-Fermi central pot. 79−3360
Ni XXI, XXIII, spectral energy levels, relativistic corrections, config. superposition method 80−32616
NpF_6, energy levels and bonding, relativistic SCF Dirac-Slater calcs. 77−6691
O, isoelectronic sequences, energy spectra inc. relativistic corrections 78−924
O_2, Zeeman effect, relativistic corrects. to g_s using LCAO wavefns. 79−3492
P^+, ionisation pot., periodic regularities, relativistic corrections calcs. 79−49950
Pb IV, relativistic oscill. strengths 77−14388
Pb, K-shell ionis. probability, 25- 40-and 74-MeV α particles 77−528
Pb, muonic high-lying states transitions, electron screening effects 77−34786
Pb, relativistic 1s wavefunctions test, using exptl. Compton profiles 80−32600
$Pb+Pb^+$, δ-electrons from K- and L-shell ionisation in adiabatic collisions 80−23541
PbI, np^2→$np(n+1)s$ transition array, relativistic oscill. strengths 79−31465
PbS, relativistic electronic mol. struct., calcs. 79−761
PbS(PbSe), ab initio SCF calcs. using relativistic effective core pot. 80−95524
PbSe, relativistic electronic mol. struct., calcs. 79−761
Pd cluster-H, electronic struct. calc., H-metal bonding 77−89823
Pd_2, ab initio relativistic core pot. studies of metal-metal bonding 80−106257
PdH, ab initio relativistic core pot. studies of metal-H bonding 80−106257
Pt cluster-H, electronic struct. calc., H-metal bonding 77−89823
Pt, L-shell Auger and Coster-Kronig intensities from relativistic theory 79−93962
Pt_2, ab initio relativistic core pot. studies of metal-metal bonding 80−106257
PtH, ab initio relativistic core pot. studies of metal-H bonding 80−106257
Rb, electron scatt. differential spin exchange, differential cross section 77−535
Rb, ground state, hyperfine struct., relativistic many-body calcs. 80−23322
Rb, HFS, many-body and relativistic effects 78−37565
Rb, ionisation energies and oscill. strengths calcs. 80−5488
Rb, oscillator strength ratios for principal series, relativistic and correlation effects 79−784
Rb, valence-core electron exchange interactions, local approx. 80−91416
RbI isoelectronic series, oscill. strengths, relativistic HF calcs. 79−98035
$Re_2Cl_8^{2-}$, spectral assignment, metal-metal bonds, SCF Xα SW calcs., relativistic corrections 80−53006
S compounds, one-electron binding and Auger energies 80−52872
S, one-electron binding and Auger energies 80−52872
S^+, ionisation pot., periodic regularities, relativistic corrections calcs. 79−49950
SO, Zeeman effect, relativistic corrects. to g_s using LCAO wavefns. 79−3492
^ASb, A=121, 123, elec. and mag. hfs. 79−10224
Se^+, ionisation pot., periodic regularities, relativistic corrections calcs. 79−49950
Si IV radial wave functions of discrete spectrum calcs., dipole and quadrupole polarisation 80−5476
Si isoelectronic sequence, CI calcs. of oscillator strengths, L-S framework 80−14089
Sn, internal conversion coeffs. for inner shells of atomic ions and relativistic ionic potentials 80−68600
SnI, np^2→$np(n+1)s$ transition array, relativistic oscill. strengths 79−31465
$TeCl_2$, transient species, He(I) photoelectron spectrosc. calcs., relativistic corrections 80−95677
ThH_4, Dirac-Fock one-centre expsn. calc. 80−5485
ThO_2, electronic struct. and bonding, molecular cluster approx. 77−51657
Ti, pionic, relativistic fine struct. splitting obs. 79−10237
TiH_4, Dirac-Fock one-centre calcs. 77−88380
Tl I, relativistic and cancellation effects in line strength ratios 78−82689
Tl, oscill. strengths, semiempirical relativistic one-electron central field, model pot. calcs. 80−78575
Tl, valence orbitals, Dirac-Fock scheme, direct and indirect relativistic effects 78−41969
TlF, electric dipole hyperfine struct. calc. 80−53162
TlH, ab initio SCF calcs. using relativistic effective core pot. 80−95524
U, ab initio effective core pots., relativistic corrections 78−50483

relativistic corrections continued
U I, electronic configs., HF relativistic calc., spin-orbit const.-Slater integral relation 77−18793
U, L-shell Auger and Coster-Kronig intensities from relativistic theory 79−93962
U, relativistic Dirac-Slater calcs. *(Japanese)* 77−42252
U, valence energy levels, SCF relativistic Xalpha calc. 79−85912
^{92}U, self-consistent relativistic density-functional theory 80−91441
$U^{+}+U^{+}$, critical two-centre distance, HFS relativistic calc. 79−22801
UF_5, electronic struct., Hartree-Fock-Slater and Dirac-Slater calcs. 79−31370
UF_5, electronic struct. and geometry, ab initio calcs. using relativistic ECP 80−32606
UF_6, electronic struct., relativistic MS Xα calc. 79−85911
UF_6, energy levels and bonding, relativistic SCF Dirac-Slater calcs. 77−6691
UF_6, relativistic scattered wave calculations 80−63538
UF_6, UF_6^{+}, and UF_6^{-}, electronic struct., ab initio calcs. using relativistic core pots. 79−97987
UF_6, valence energy levels, SCF relativistic Xalpha calc. 79−85912
UH_6, Dirac-Fock one-centre expsn. calc. 80−5485
UO_{24}, electronic struct. and bonding, molecular cluster approx. 77−51657
UO_2^{+}, valence energy levels, SCF relativistic Xalpha calc. 79−85912
UO_2^{2+}, electronic struct., secondary ligands effects, Dirac-Slater model 77−411
UO_2^{2+}, relativistic X_α scatt. wave calcs. 78−46268
V, atom and ions, shell energy struct., SCF calc. by Dirac-Fock-Slater method 80−52877
Xe, 5p subshell photoelectron branching ratio, Dirac-Fock calcs. 78−42021
Xe, 5s, 5p ESCA spectrum, photoionisation many electron description 78−50516
Xe 5s, photoelectron ang. distrib., relativistic Dirac-Fock calc. 79−59411
Xe, ab initio effective core pot., Dirac-Hartree-Fock and Hartree-Fock calcs. 78−33426
Xe, atom and ions, relativistic Dirac-Fock-Slater calc., fluoresc. yield, X-ray energies shift 78−25450
Xe II, influence of relativistic effects, excited states 79−72274
Xe II $5s5p^6\ ^2S_{1/2}$ state, lifetime meas. 79−13670
Xe, inner electron energy characteristics, validity of Hartree-Fock-Pauli approx. 80−42957
Xe, low-energy 5s-ep photoionization, relativistic effects 78−50515
Xe, photoelectron branching ratio in 4d subshell 79−18164
Xe, relativistic Hartree-Fock calcs. using spherical Gaussian basis sets 80−32595
Xe_2, effective core pot., Hartree-Fock calc., relativistic and nonrelativistic effects 78−46281
Xe_2^{+}, effective core pot., Hartree-Fock calc., relativistic and nonrelativistic effects 78−46281
XeF, effective core pot., Hartree-Fock calc., relativistic and nonrelativistic effects 78−46281
Xe_2^{*}, Xe_2^{+}, Xe_2, pot. energy curves, relativistic ab initio effective core pots. 78−86800
Yb II, 6s $^2S_{1/2}$-6p $^2P^{\circ}_{1/2,3/2}$ transition, relativistic oscillator strengths, influence of core polarisation 80−58132
Yb III compounds, 4f photoelectron spectral intensity, relativistic calc. 79−54816
Zn, electron binding energy and shift, core level XPS 80−87088
Zn XX, energy levels and one electron transitions, relativistic calculations 80−87051
$ZnCl_2$, deformation densities, relativistic effect 80−42928
Zn(^{1}S), dipole polarisability, relativistic effective core pot. calc. 79−76362
Zr XI and XV, spectra, perturbation theory with model pot. 78−58579
Zr XIII, electronic struct. of complex ion, relativistic perturbation theory 79−22610
ZrH_4, Dirac-Fock one-centre calcs. 77−88380

relativistic electron beam tubes
beam surface envelope and angular vel., propag. through gas 78−46499
carcinotron, relativistic millimetre, electron beam in high current accelerator 79−68359
circular waveguide, microwave generation by relativistic electron beam 80−48128
collective ion acceleration in vacuum by linear electron beam 79−85833
critical vacuum current, virtual cathode effect 78−25790
cyclotron and space-charge wave excitation 79−86118
cyclotron resonance maser with high current relativistic electron beam 79−13942
cylindrical relativistic diode, space charge limited, voltage distrib. and current calc. 80−63437
diode, low-impedance, anode scatt. effects on electron pinch radius 77−68877
diode, pinched, particle simulation code and ion current reduction 77−68878
diode with annular cathode immersed in axial mag. field, pinching rot. and reflexing 78−9860
diode with converging mag. gradient, electron beam oscills. and ion production 78−9861
electrically pumped relativistic free-electron wave generators 80−91742
EM waves generation and amplification based on Doppler effect 80−63902
foil-less diodes, relativistic electron beam generation 78−89593
guiding props. improvement using thin insulated wire 80−74291
gyrotron efficiency, CW and pulsed power achievements 79−31849
gyrotrons and gyrokylstrons, small signal theory, fusion reactor appl. 78−70633
high-power microwave generation by relativistic electron beams 78−5444
injection into drift cavity, pot. profile finite size particle calc. 80−18987
intense microwave radiation, generation by relativistic electron beam introde 80−14887
intense relativistic electron beam generation by foilless diodes, simulation 80−63438
intense slow space charge generation appl. to collective ion accel., plasma diode 78−9863
low atomic number foil target, anomalous energy dissipation of tightly pinched relativistic electron beam 80−29833
magnetic insulation wave, propag. in vacuum coaxial line 79−27144
magnetron, intense microwave emission 79−12822
magnetron with diffracted output of EM radiation, construction and operation *(Russian)* 78−24823

relativistic electron beam tubes continued
microwave generation, planar, annular relativistic electron beams 77−83804
microwave radiation from electron beam in strong mag. field 77−79735
microwave source 78−46556
millimetre radiation, high-power, generated by intense relativistic electron beam device 77−83795
nonisochronic reflecting electron system, high power microwave emission 78−1140
O-type relativistic electron devices, linear theory 80−43242
O-type relativistic electron devices, nonlinear theory 80−43243
plasma diode, intense neutralised ion beam ballistic focusing 78−9859
polyhelical electron beam in open waveguide, diffraction radiation *(Russian)* 77−75398
ring train behaviour under longitudinal compression 79−7065
space charge wave propagation along rotating relativistic electron beam 79−55047
space-charge-limited planar relativistic diode, Poisson eqn. 79−10700
waveguide containing relativistic electron beam, slow cyclotron wave 80−106983
X band gigawatt microwave pulse, produced by relativistic electron beam injection into waveguide *(French)* 78−25781

relativistic fluid dynamics
accretion discs, fluid, orbiting Kerr black hole, analytic theory 78−36631
adiabatic blast wave, gas and cosmic ray acceleration 80−67534
anisotropic relativistic and dissipative fluid model *(French)* 77−67357
anisotropic spheres, adiabatic contraction in general relativity 80−36489
AO 0235+164, BL Lacertae object, relativistic blast-wave model for rapid flux vars. 79−9017
astrophysical media, relativistic and nonrelativistic gas flows, low press. limit 77−9655
axially symmetric flow of perfect fluid, spherical vortex 77−47116
Barotropic fluid in semi-Riemannian manifold, classical and relativistic vorticity 78−65842
basic results and shock waves 77−42933
Bianchi universes, magnetic fields and fluids with conductivity 80−83864
black holes, relativistic accreting discs hydrodynamic struct. 78−36632
Cauchy problem for general relativistic perfect magnetofluid 78−70024
channel flow rel. to beam models of extragalactic double radiosources 78−69668
charged elastic fluid sphere, interior soln. in general relativity 77−9929
charged fluid, general relativistic pulsation eqn. 77−5711
combustion fronts in relativistic MHD *(French)* 77−47115
compact extragalactic radio sources, relativistic jets model 80−4448
conducting ferrofluid, wave propagation, velocities *(French)* 77−15138
constitutive theory of general relativistic EM fluids 78−57843
constrained minimum energy problem in relativistic MHD 80−92238
cylindrically symmetric self-gravitating fluids with pressure equal to energy density 79−21612
D type perfect-fluid solutions of Einstein's equations, classification 78−21019
Eckart's relativistic temp. gradient 80−103080
Einstein's field equations, solns. for static fluid spheres, relativistic polytrope anal. 79−12669
Einstein field eqns. for rotating isentropic perfect fluid, cylindrically symmetric solns. 79−40427
elastic media, dissipative, relativistic electrodynamics 80−73219
electromagnetic fluid flows, geometrical aspects 79−72950
EM fluid flow geometry 79−4091
EM fluid flow with geometrical symmetry 79−4092
EM fluid flows, geometry 79−58601
EM fluid flows 80−52094
EM fluids and Ricci collineations 79−35605
energy momentum tensor for relativistic inviscid heat cond. fluid, evolution system 77−80233
equilibrium of slowly rotating relativistic fluids 80−46898
extragalactic radio sources, relativistic Kelvin-Helmholtz instabilities 78−45419
extragalactic rapidly varying radio sources, relativistic plasmoids dynamics theory 78−93438
ferromagnetohydrodynamics, mag. field effects on struct., waves *(French)* 79−27716
flat space-time describing perfect fluid distrib. of matter, embedding class one 78−54272
gas, arbitrarily moving, discontinuities propagation 78−73842
gas, dissociating, relativistic flows, growth and decay of weak waves, shock wave formation 80−69949
gas conducting heat, shock relns., and conservative form of hyperbolic eqns. 79−14498
gas dynamics in two dimens. 80−83863
gas with $\gamma>5/3$, accretion by Schwarschild black hole 79−17011
gas-dynamic eqns., soln. with singularities for initial value problem *(Russian)* 77−58809
general relativistic anal. of self-gravitating perfect magnetofluid 78−36905
general relativistic fluid spheres, physical solns. 79−21169
general relativistic MHD, asymptotic waves and critical time 79−41771
geodesic flows and Kepler problem, in spaces of const. curvature 78−40807
gravitational collapse, anisotropic, mag. field strength var., MHD approx. calcs. 77−11283
gravitational collapse in perfect fluid, vorticity, general relativity theory 77−11282
gravitational compression of a body within the approximation of the special theory of relativity 80−4611
Hamiltonian formalism for self gravitating relativistic perfect fluid, Lagrangian variational principle 78−16289
heat conducting fluid, dispersion relation *(French)* 79−7419
heat conducting fluid, existence and unity of Cauchy problem solns. *(French)* 78−47070
heat conducting fluid, laws of relativistic thermodynamics *(French)* 79−32713
heat conducting inviscid fluid, exceptional waves *(French)* 77−53824
heat conduction in relativistic extended thermodynamics 80−43803
heavy ion collisions at high energy, review of four theoretical methods based on classical approx. 79−89326
hydrodynamic expansion of relativistic gas, Euler eqns. 77−33331
ideal liquid, general theory of relativity, introduction of canonical variables in hydrodynamic eqns. 78−63510

relativistic fluid dynamics continued
incompressible heat-conducting relativistic fluid, four-vector form 80−33707
inhomogeneous cosmological model solns. of Einstein eqns. for perfect fluid 78−24585
irrotational shearfree motion of perfect fluid in general relativity 79−27715
isentropic perfect fluids, integration of relativistic equations of motion 78−7872
Lagrangian dynamics of polarised media with internal spin in general relativity 79−72962
magnetised relativistic continuum, shock invariants *(French)* 79−25944
magnetofluid, relativistic, and space-like conformal mappings 80−75001
magnetofluid, self-gravitating, local behaviour of congruences 78−89384
magnetofluid dynamics, eqns. of motion for charged particle and charged fluid 80−87821
magnetofluid flows, geometry 80−46895
magnetofluids, self-gravitating, collineations and motions 77−51135
magnetofluids and symmetry mappings 79−27701
magnetofluids and symmetry mappings 79−27700
magnetofluids and symmetry mappings 79−23379
magnetofluids in general relativity 77−49655
Maxwell equations, in Minkowski space-time and Poincare group 79−30301
MHD, definite material scheme 79−25943
MHD, evolution system study of generalised scheme *(French)* 77−65799
MHD eqns. with radiative reaction and relativistic Boltzmann eqn. 80−36956
MHD of heat conducting, charged relativistic fluid, Cauchy problem solutions, existence and uniqueness *(Italian)* 80−48821
MHD shock waves, plasma and condensed medium 77−24035
monatomic gas, propagation eigenmodes, Marle's 14-moment description 77−27626
neutron hot perfect fluid relativistic stars, asymptotic eigenfrequency distrib. for even parity perturbations 78−49668
Newtonian stars with stratified flows, mirror planes 78−32444
one-dimensional fluids, partial differential eqns., hodograph transformations 77−955
part-Newtonian hydrodynamics, centre-of-mass theorem 77−75
perfect fluid distrib. in general relativity, plane symmetric models 79−77295
perfect fluids flow through channels, self similar solns. and stability rel. to radio galaxies 80−62006
perfect magnetofluid, matter tensor, convective deformations 80−36922
plane wave growth eqn. in polytropic heat cond. relativistic fluid *(French)* 80−28580
projection tensor hydrodynamics: generalized perfect fluids 79−85029
projective relativity and MHD, MHD tensor struct. 79−85030
propagation of the general relativistic blast wave 80−105549
quantum relativistic hydrodynamics, nonlinear generalised equations 80−68380
quasars, two-dimensional relativistic blast waves, solns. for adiabatic case 80−22108
radio sources, formation of knots in relativistic flows as model for compact synchrotron sources variability 80−105369
radio sources, relativistic corrections in expanding synchrotron sources theory 80−12821
radiogalaxy models, relativistic channel flow, soliton soln. stability 80−56962
rapidly rotating fluid bodies, struct. and stability in general relativity beyond ang. vel. peak 79−101139
relativistic conductive additional terms 77−45746
relativistic thermodynamics of chemically reacting fluids 79−64801
review, book contrib. 78−59507
rotating fluid cylinder, field eqns. 79−50815
rotating fluids, central behaviour, tetrad formalism 80−53888
rotating fluids, Killing inequalities 77−64981
rotating shell model of relativistic star 79−88650
Schwarzschild black hole stationary spherical accretion, stability 80−51800
self inductive fluids, stress energy tensor and entropy generation 79−18975
self-gravitating charged relativistic fluid, space-time permeation 79−2689
shear-free perfect fluids, symmetry mappings leading to conservation laws 77−954
shock wave propagation in general relativity, stationary approx. 80−86172
shock wave propagation in homogeneous medium, similarity soln. 79−98826
shock waves, anal. approaches *(French)* 80−96317
shock waves, cylindrical relativistic propag. in presence of mag. field 79−53708
shock waves, plane, relativistic, propag. 79−53707
shock waves, plane, relativistic, propag. in slowly moving medium 80−62005
shock waves, relativistic, damping 77−75994
simple waves, shock damping and entropy prod. 77−17725
singular hypersurfaces, asymptotic regularisation as alternative to distrib. 80−36923
space time permeated by compressible, thermally conducting self-gravitating field, props. 79−71315
spherical charged fluid ball solns. 79−64803
spherical multicomponent fluid, hydrostatic equilib., thermodynamic interpretation, 3-component neutron star 79−49135
spherically symmetric relativistic flows, comoving-frame radiative transfer eqn. soln. 80−82181
spherically symmetric relativistic spheres, noncomoving coords. 77−87673
spherically symmetric space, isotropy conditions for relativistic perfect fluid spheres 79−14497
star, spherical, emitting neutrinos, relativistic model 78−73705
stellar relativistic centrifugal winds, appl. to pulsars 78−96473
strong shock waves in relativistic infinite electrically conducting fluids 77−39365
superluminal flow, EM wave refl. 79−27138
suspensions, nonstationary motion in grav. field, volume conc. effect *(Russian)* 80−75002
Synge's equations of motion applied to a perfect fluid 79−40433
thermal waves and growth eqn. *(French)* 80−28579

relativistic fluid dynamics continued
thermo-viscous fluid dynamics, heat conduction and wave propag. 80−24107
thermodynamics, collineation and motion, Cattneo's theory 78−51259
time conventions, effect on fundamental eqns. 77−67275
trans-relativistic shock relations, numerical solns. 80−31202
transonic flow on axially symmetric torus 80−28527
variational aspects of relativistic field theories 77−82417
variational principle for perfect and imperfect fluids in general relativity 80−90733
vector-potential Hamiltonian formulation of the general relativistic perfect fluid 79−64802
vibrationally relaxing fluid, growth and decay of weak discontinuities 80−69948
virial theorem in general relativity, consequences for spherical symmetry stability 79−21593
viscous fluids, nonstationary relativistic thermodynamics, hidden variable approach 80−68097
vorticity streets stability on curved surfaces with reflection symmetry 80−46810
wave propag. in relativistic self-inductive radiative fluid 79−41772
weak discontinuities in high temp. phenomena, relativistic theory 80−53889

relativistic mechanics
see also relativistic fluid dynamics
action at a distance, relativistic model using singular Lagrangian with multiplicative pot., rel. to nonrelativistic two-body problem 78−93531
action at a distance and relativistic wave equations for spinless quarks 79−36030
Alfven wave accelerated particles, distrib. function self-similar soln. 80−56702
angular scattering of spinor charged particles by a Kerr-Newman field 80−94996
approximately relativistic Lagrangians for classical interacting point particles 78−54179
arithmetic models formulation 78−86130
axisymmetrical body, translational-rotational motion in gravitational field of sphere, averaging methods applic. *(Russian)* 78−21049
Bhabha first order relativistic wave eqns., historical development 78−14
bilocal theory, constraints, centre of mass and quantisation 78−89619
binary pulsar, secular relativistic change in pulsar period 77−5542
Bogoliubov transforms., rigorous treatment 79−17211
book, relativistic theories of materials 78−81907
bounded system of extended bodies, relativistic eqns. of motion 78−73898
Brownian motion, space-time approach to quantum mechanics 80−31567
bubble dynamics, motion of relativistic membrane, relevance to quark confinement 79−2989
canonical systems, geometric approach to space-time struct. and symm. 77−17885
celestial mechanics, periodic solns. in Hill's relativistic problem 78−40804
charge particle free fall acceleration, relation with observed velocity 80−73170
charged particle dynamics, symmetries 77−45742
charged particle motion in HF fields with strong mag. field, averaged eqns. *(Russian)* 78−62996
charged particles, motion in relativistic fields 80−57146
charges in EM field, generalised covariant Hamiltonian formulation 80−46794
circular motion for a time-asymmetric relativistic two-body problem 79−75336
classical and prequantised mechanics without Lagrangians or Hamiltonians for relativistic particles 78−74126
classical and quantum dynamics 80−22192
classical electrodynamics, Boltzmann distrib. for relativistic free particles and Rayleigh-Jeans thermal radiation law, inconsistency 79−49036
classical quasi-relativistic two particle system, motion integrals, transform. props. *(Russian)* 77−49594
classical relativistic dynamics fundamentals revisited *(French)* 78−62074
classical relativistic Gibbs ensembles 79−63126
classical spin and the Lorentz group, a correlation 79−5979
clock problem explained by nonrelativistic premises 78−24664
composite particle scatt., quasipotl. approach 78−404
composite system of three relativistic particles with half-integer total angular momentum 79−49032
composite systems, relativistic centre of mass variable and Lie algebra of Poincare group 79−71245
conservation law derivation using digital computers 78−12552
conservation laws for particle collisions 77−33856
conservation laws for particle collisions 77−33857
constitutive equations, principle of objectivity, proper rigid frame 77−37757
continuum in generic motion, action of volume and surface forces, second cardinal equation of dynamics 80−31501
contraction of metric standards 80−82638
contrinuous media, natural theory *(Russian)* 78−41157
conventionality of simultaneity without one-way velocity assumptions 79−12594
counter-orbiting polar satellites, Earth tide information 77−2083
coupled spherical wave equation system for relativistic 2 particle interaction *(French)* 79−35549
covariant formalism for a relativistic string in a constant homogeneous electromagnetic field 79−21546
covariant wave equations of two spinning particles harmonically bound 79−71692
de Sitter space, dynamics of free particle systems 78−20958
de Sitter universe and mechanics 78−21034
deformable media, electrodynamics, relativistic field equations 78−49678
dense matter, relativistic, statistical mechs. using phenomenological quantum field model 78−89814
Dirac brackets for dynamical systems with redundant constraints 79−63078
Dirac Lorentz's equations, relativistic and nonrelativistic, maximally extensive local group of invariance 80−77946
Dirac monopole, relativistic theory, canonical quantisation 78−45517
dynamical equations of general relativity, new Hamiltonian structure 77−45745
dynamics of right angled lever 80−12900

relativistic mechanics continued
Earth artificial satellites motion, relativistic effects 79−2465
education, relativistic statics, covariant formulation 78−49593
education, relativistic torque, comment on 'right-angle lever paradox' 78−36750
eikonal function for two classical relativistic particles 78−81828
Einstein correlations, S-matrix, ψ collapse *(French)* 78−77742
elastic rotating cylinder, general relativistic formulation 80−82642
elastomechanics, compatibility relations *(German)* 78−81902
electrodynamics, moving bodies, equivalence of proposed formulations 79−35574
electrodynamics, two electron half retarded half advanced interactions, existence and uniqueness theorem 79−49035
electrodynamics of mag. monopoles and electric charges 78−28967
electron beams, collective relativistic interactions in faster than light media *(Russian)* 80−46803
electron beams, electrodynamic principles of rotating relativistic types 78−71019
electron currents in vac. relativistic generalisation of Child/Langmuirs laws *(German)* 78−36843
electron spin magnetic moment relativistic mass correction, classical reinterpretation 77−57213
electron trajectories, in homogeneous elec. fields, relativistic and classical 77−41436
elementary bodies, relativistic dynamics in seven-dimens. space 80−32015
elementary particle theory, relativistic centre of mass of extended particle with interacting constituents 79−17701
EM two-body interaction theory 78−49739
energy and momentum triangles, modified versions applicable to accelerated motions 79−88803
energy-momentum tensor of extended relativistic systems 80−46798
equivalence principle test for spin-$^1/_2$ particles 79−12707
Euclidean space, Galileo transformation 80−62467
Euler-Lagrange hyperbolic systems of second order, relativistic strings 78−54209
extended body dynamics, centre of mass description and quasirigidity 77−67359
extragalactic radio sources, model for superlight vels. 77−29944
fermions, charged relativistic, semi-classical, two-body problem, new approach 78−29284
field eqns., geometric and algebraic foundation of spinor formalism 78−37128
field theory, interpretation of advanced solns., relativistic eqns. 77−22410
Fokker type relativistic mechanics, single time form with Lagrangian 80−90665
Fokker type relativistic mechanics, single time Lagrangian form, symmetries, conservation laws 80−90666
Foldy Wouthuysen transform. group content, nonrelativistic limit for arbitrary spin 79−75387
foundations of mechanics, book 79−25837
free fall acceleration 80−90672
free particle, relativistic, in thermal radiation within classical electrodynamics, equilib. distrib. 80−8935
free relativistic spin-1/2 particle energy-momentum invariants and kinetic moment *(French)* 78−62287
general relativistic statistical mechanics, BBGKY hierarchy and Boltzmann eqn. 79−63127
generalised, spacetime quantisation and Mach's principle 78−73867
graphical evaluation of relativistic matrix elements 79−58586
gravitating particles with cylindrical symmetry, calc. of averages in equilib. system *(Russian)* 78−73904
gravitational field effects on motion and radiation of relativistic particles *(Russian)* 79−97269
gravitational wave effects as relativistic particles 79−75424
gravity mass invariance 78−57778
gyratron, coherent microwave mag. bremsstrahlung, general theory of masers *(Russian)* 78−1141
gyroscope weight reduction in left turning due to spontaneous symmetry breaking *(Japanese)* 80−98798
hadronic matter, thermodynamic props. of class of solvable statistical models 79−63452
Hamilton-Jacobi generalised theories 79−2681
Hamiltonian dynamics, constraints origin 80−17797
Hamiltonian dynamics, for closed system of N particles in mutual interaction 78−62070
Hamiltonian dynamics formulated in Lagrangian submanifolds *(French)* 77−5657
Hamiltonian formulation for an extended particle with interacting constituents 79−63022
Hamiltonian n-particle systems, advanced retarded polarisation 78−29017
hard sphere relativistic gas transport coeffs. 78−30401
harmonic anal. on Lorentz group as dynamical relativistic Fourier anal. 77−82406
heat flow in relativistic equilibrium thermodynamics 80−52017
Helmholtz flat space eqn., non orthogonal separable coordinate systems 79−75416
DI Herculis, eclipsing binary, relativistic motion of periastron 80−94830
inertial mass and potential energy 77−26225
inertial navigation equations based on relativistic effects 77−67276
infinite relativistic string with a point-like mass 79−13036
infinitesimal symplectic relations and generalized Hamiltonian dynamics 79−25878
interacting particles, two, Galilei-compatible nonconstrained Hamiltonians 80−73169
internal Galilei group for a two-particle system 79−75406
interstellar ramjet probe, relativistic flight dynamics 77−25909
interstellar rocket, laser powered, mass ratio and instantaneous efficiency 79−21134
invariantive analytical mechanics of point-like bodies 79−5978
Kepler problem and geodesic flows, in spaces of const. curvature 78−40807
kinematics of relativistic ejection *(French)* 77−73943
kinematics via principle of equivalence 79−17285
kinetic equation for weakly relativistic system with gravitational interaction 77−49671
kinetic theory, continuity of summational invariants for massless particles 79−25968
kinetic theory, continuity of summational invariants for non-zero rest mass 79−25967
Lagrangian form of relativistic mechanics for bilocal and trilocal structures, relativistic quark model 77−41809
lagrangian multipliers in frozen core Dirac-Fock calculations 78−73881
Lagrangians for classical interacting point particles 78−70048
Lorentz invariant multiparticle amplitudes, massive particle relativistic kinematics, spinor amplitudes 78−41156
magnetic monopole, relativistic classical eqns. of motion, electric dipole moment case 80−37195
magnetisable media, relativistic models, and energy-momentum tensor of EM field *(Russian)* 80−86180
magnetised relativistic continuum, shock invariants *(French)* 79−25944
magnetoelasticity, infinitesimal discontinuities *(French)* 79−25853
many-threshold amplitudes, conformal mapping, algebraic parameterisation and two-variable expansion 77−54059
mass variations obs., periodic, using electromechanical vibrating system 80−47020
Maxwell-Boltzmann statistical distrib. function, Hsu's space-light transformations, agreement with Lorentz results 80−17858
mechanical oscillator, relativistic spin quadrupole gravitational effect *(Russian)* 80−68103
Minkowski force from Frenet-Serret eqns. for curve in Riemann space 80−22208
motion in a plane, teaching 80−101686
multilocal fields in relativisitic quantum field theory 78−37125
multilocal models and string theory 79−2986
multilocal theory, relativistic mechanics of interacting particles 78−16638
multilocal theory and relativistic string 78−93845
N-body problem, direct interaction, Lagrangian formulation *(Russian)* 77−45696
N-body relativistic systems, interaction *(French)* 79−84948
N-particle systems, predictive relativistic mechanics *(French)* 77−45707
Nambu mechanics, reln. to Lagrange, and Hamilton-Dirac mechanics 78−54180
negative acceleration components on relativistic particles 78−86058
Newton-Wigner position operator, non existence for quanta with zero mass and nonzero helicity 78−62099
Newtonian gravitational theory, continua and particle dynamics 79−6038
Newtonian mechanics, four vectors 78−4477
no interaction theorem, origin from relativistic dynamics instant form 78−93530
non-inertial reference frames *(German)* 77−45720
non-interation theorem of Curie et al., expansions in c^{-1} 78−49730
nonequilibrium relativistic strain tensor, rigid disc relativistic rotation *(Russian)* 80−22195
nonlinear wave propagation in relativistic continuum mechanics 80−22203
nonspreading wave packets in quantum mechs. 78−65795
orbital equations in the relativistic two-body problem 79−44805
paramagnetism, statistical mechanics in strong mag. field 80−17865
parity-covariant relativistic two-particle forces 78−73847
particle cloud surrounding massive rotating nucleus, relativistic dynamics 79−114
particle dynamics in special relativity 78−93529
particle motion in EM field at relativistic speeds *(German)* 78−90350
particles, interacting, relativistic mechanics and bilocal theory 77−87921
path integrals for a particle in curved space 79−35598
path integrals on curved spaces, method of determination 80−31589
Poincare group, phase space representation, relativistic particle mechanics appl. 80−8784
Poincare group representations for relativistic extended hadrons 79−89099
Poincare group representations on phase space 79−88827
Poincare-Cartan integral invariant and canonical transformations for singular lagrangians 80−94956
poincare-Cartan integral invariant for constrained systems 79−63025
point charge free fall motion under weak gravitational field 80−42057
point charge moving in arbitrary way, superposition of two fields *(Russian)* 80−22251
point particle description 79−63026
Poisson sphere, global dynamics eqns. *(French)* 79−30324
polarisable media, relativistic models, and energy-momentum tensor of EM field *(Russian)* 80−86180
position operators, systems exhibiting special relativistic relation between momentum and vel. 78−89335
position operators for relativistic non-interacting n-particle system 78−41182
position variables in classical Hamiltonian mechanics 80−27123
post-Newtonian n-body problem in gravitation with PPN parameters γ and β, centre of inertia 79−17325
predictive mechanics, partial differential eqns. on accel., integration 79−44716
predictive relativistic mechanics, equivalence of two formalisms 78−69982
predictive relativistic mechanics, noninteraction theorem for interactions derived from classical field theory 79−40358
predictive relativistic mechanics, slow motion approx. 78−86152
predictive relativistic mechanics for gravitational interaction, approx. solns. 77−2541
prestressed isotropic elastic bodies, exact relativistic theory of principal wave fronts propagation *(French)* 77−67356
presymmetry in relativistic quantum mechanics, absence of kinematics 80−8843
Proca's eqn. stochastic derivation, Weyssenhoff top fluid considerations, velocity of light random fluctuations 79−97247
quantum, conserved four-vector currents for free particle 77−37778
quantum, localisation and causality 78−4514
quantum, phase space formulation 78−36878
quantum, relativistic localisation and operator density current 78−32709
quantum Hamiltonian for directly interacting particles 78−16729
quantum kinematics on stochastic phase spaces for massive particles 79−2648
quantum kinetic theory, $e\nu_e$ and $e\bar{e}\nu_e\bar{\nu}_e$ mixture 79−63140
quantum mechanics, elimination of phase angle uncertainty, charged Dirac particle+mag. monopole scatt. *(Chinese)* 78−78100
quantum mechanics, Levinson theorem generalisation *(Chinese)* 79−80461

relativistic mechanics continued
quantum mechanics, localisation problem 77−49616
quantum mechanics, role of wave fronts and torsion *(French)* 77−53795
quantum statistical appl. to spin 1/2 baryons through scalar meson field 79−67225
quantum theory, successive observations 79−88830
quantum theory of composite systems, nonlocal field theory of quark model 78−70253
radio sources, compact, relativistic particles injection in strong mag. dipole 79−17115
radio sources variable at low freqs., evidence for relativistic expansion 79−9018
ray theory in relativistic anisotropic elasticity *(French)* 80−36846
relativistic Boltzmann equation 79−17367
relativistic elasticity, one dimensional nonlinear motion 79−84953
relativistic Hamiltonian dynamics, closed system of spinless point particles, classical mechanics 79−49031
relativistic harmonic oscillator imbedded in random stochastic thermostat, stable states 79−49033
relativistic hypoelasticity, characteristic manifolds, wave propagation *(French)* 79−30227
relativistic Markov processes in quantum mechanics, Feynman path integrals 79−21576
relativistic nuclear physics, collisions of relativistic ions *(Rumanian)* 78−46104
relativistic particle sytems with confining interactions 79−63029
relativistic string dynamics, geometrical approach 80−9100
relativistic string in a constant homogeneous electromagnetic field 79−22073
relativistic string with massive ends, dynamical eqns. 78−4826
relativistic wave mechanics, stochastic model *(French)* 78−86404
restricted three body problem, appl. of Gauss method to periodic solns. form. 77−13215
rheometric structure theory, convective differentiation and continuum electrodynamics 80−86087
rotating cylinder gravitational field, equations of motion of material particles and photons 79−9157
rotating frames and continuum mechanics, relativistic appraisal 80−17795
rotating plane-fronted waves and their Poincare-invariant differential geometry 80−332
rotating stratified ellipsoids of revolution, effects on inertial frame dragging 79−2573
rotating systems, Einstein equations 80−68101
Sakata-Taketani spin 0 theory with external field interactions 77−41748
scalar particle 77−57151
Schwartz's method and Goldstein's eigenvalue problem 78−4814
second quantisation, extension of Hamiltonian formalism 79−244
separable quasipotential formulation of the relativistic dynamics for three point particles 79−12989
shock formation in elastic solids in relativity *(French)* 80−31496
short time propagators in Riemann geometries 79−63129
solar system, relativistic effects verification, comparison of obs. results with theoretical data *(Russian)* 79−80209
solitons, nontopological, and appls. to hadrons 78−32968
space-time operators, quantum mechanics incompatibility in special relativity 79−12592
space-time orbits for interacting relativistic particles, syntactic versus semantic observables 79−21976
special relativity, principle of covariance and basic inertial frame, non-invariance of rest mass 80−22194
special relativity space-time test theory, dynamical aspects 80−17798
spherical counter rotating dust bodies, relativistic dynamics 77−67358
spherical rigid body, pole-dipole singularity idealised description 79−2683
spin 1/2 particle dynamics 78−70001
spin precession in the relativistic two-body problem 79−49118
spinless particle, point form of quantum dynamics and 4-vector coord. operator 79−17213
spinning particle total reflection shifts, relativistic anal. 77−22409
spinning test particle in the manifold of the reference frames 80−62548
star clusters, isotropic relativistic, multi-term trial function stability anal. 78−73742
statistical mechanics, state indicator or negative probabilities 79−63128
stochastic particles 80−82639
string, action integral, scalar Born-Infeld eqn. 79−49038
string, longitudinal vibr. 79−13061
string dynamics, Lorentz invariant quantum theory, review *(Russian)* 79−22020
string in static field, conservation laws 79−21969
string moving in uniform static external field, 2-D space-time surface 80−57087
string theory in external field 79−97574
string with massive ends, classical and quantum theory 78−62073
strings in the embedding space 78−89654
supernova shock-accelerated cosmic rays, early radiation spectrum, cooling and escape 79−48626
surfaces, relativistic, classical theory *(Russian)* 78−69984
symplectic formulation of relativistic particle dynamics 77−57237
synchronous formulation of relativistic statics 78−24663
three point particle system, spin-mass relation 80−36845
transitive mechanical systems, param. determ. from co-adjoint action 78−12554
transport equations for one-component relativistic gas 77−966
transverse momentum in relativistic statics 78−81833
trilocal theory, constituent mass, free limit condition and quantisation 79−2984
twistor theory and particles, book 79−97485
two body problem, appl. of dynamic confinement from vel. depend. interactions 80−46800
two interacting massive particles, derivation from Lagrangian 77−54062
two interacting relativistic particles, singular Lagrangian 79−17641
two isolated particles, momentum, ang. momentum 77−2540
two or three point particle systems 78−4481
two-body gravidynamics 79−71683
two-body relativistic systems 78−69977
ultrarelativistic particle in homogeneous mag. field, trajectory, radiation damping 80−18104
unitary space of particle internal states 79−30712
vector constants and their algebras for classical Hamiltonians 79−56
wave equation of bilocal field, and mechanical model 78−29241

relativistic mechanics continued
wave mechanics, hypothesis on origin of quantum potential *(French)* 78−86405
wave mechanics, stochastic model, Newton's second law *(French)* 79−30226
wave mechanics optimal control 79−40660
weak plane gravitational wave action on two connected masses 80−17851
weakly relativistic gas, equilib. distrib. and eqn. of state 79−21649
Wigner representation, gauge invariant, electrodynamics of scalar particles 78−29251
WKBJ approx. for classical particles with spin in external field 78−32692
world line conditions for spinning particles, spin orbit forces 80−36844
world-line invariance in predictive mechanics 80−31498

relativistic plasmas
acceleration of plasma formed by relativistic electron beam 77−27657
adiabatic switch-on shock wave, in collisionless plasma, relativistic distrib. function *(Russian)* 79−55505
Alfvenic particle streaming in astrophysical plasmas 80−31206
anisotropic plasma, relativistic MHD 80−92380
AO 0235+164, BL Lacertae object, relativistic blast-wave model for rapid flux vars. 79−9017
astrophysical relativistic gas, Doppler shift distribs. 78−65492
astrophysical sources, radiation distrib. functions calc. 77−70990
astrophysical transrelativistic plasmas, photon pair prod. 78−20632
Bogolyubov equation hierarchy, plasma wave radiation damping 79−77377
Boltzmann, theory, entropy production, reference frame 78−22547
Boltzmann theory, reciprocal relations, transport props. 78−30477
Boltzmann theory, reduction of collision integrals 80−79560
bremsstrahlung, by relativistic electrons in strong mag. field *(Russian)* 77−62393
Centaurus A, nuclear gamma-ray lines, origin in relativistic plasma 80−41890
centrifugal relativistic electron beam, equilibria and stability 79−90451
charged particle drift motion under resonance conditions 80−38611
Cherenkov radiation of charged particle moving in mag. cold plasma, pulsars appl. 79−62736
closed magnetic field line plasma system form. using intense relativistic electron beams 77−24122
cold plasma, commensurable and incommensurable nonlinear waves parametric instabilities 79−66915
cold plasma, props. in general relativity theory, spherical approx. *(French)* 77−45786
collective ion acceleration by relativistic electron cloud *(Russian)* 80−48961
collective ion acceleration in vacuum by linear electron beam 79−85833
colliding relativistic plasma instabilities with relativistic temps. *(Russian)* 80−83913
collisionless plasma, EM perturbation of relativistic Vlasov-Maxwell eqns. 79−90449
Compton effect and pair production *(Russian)* 77−24052
Compton scattering of transverse waves by relativistic electrons 80−51644
conductivity tensors in collisionless plasma 79−72990
confinement of relativistic charged particles by EM wave 78−38524
cool regions in relativistic plasmas: thermal instabilities 80−17486
covariant theory of short waves in gas in gravitational field *(Russian)* 77−62370
Crab pulsar, momentum distrib. of high energy particles 78−73727
cyclotron harmonic damping in stimulated Raman scattering from an intense relativistic electron beam 79−68946
degenerate electron plasma, dielec. response function 78−71529
degenerate electron plasma, dielectric response in mag. field, plasma oscillations 80−54022
degenerate electron plasma, oscillations, dielectric response function 78−87486
dense relativistic electron gas, EM response in strong mag. fields, particle polarisation, mode struct. 80−43963
diode compression of relativistic electron beam 77−24197
diodes, relativistic, time depend. ion and pinched electron flow, computer simulation 77−89330
dispersion in warm and hot plasmas 80−48960
dispersion of small amplitude waves in relativistic magnetohydrodynamics 79−4176
dissipation phenomena formalism diffusion and heating applications 79−4111
dissipative Cherenkov instability in relativistic electron beam, theory *(Russian)* 77−47251
disturbance propag. in relativistic Vlasov plasma 77−72426
E-layer nonneutral, negative mass instability, axial energy spread effect 78−42745
echo oscillations *(Russian)* 80−53990
electron beam, inhomogeneous, space charge oscills. 80−78759
electron beam, relativistic, rotating, filamentary instabilities 77−76187
electron beam, relativistic, unmagnetised, stimulated scatt. anal. of HF incident pump wave 79−77345
electron beam, Vlasov equilib. 77−51225
electron beam, with inhomogeneous ion density, self-consistent model 80−43247
electron beam diode, low impedance, pinch profile, X-ray diagnostics 77−24207
electron beam diode, pinched relativistic, large ion current meas. 77−31428
electron beam injected into drift tube, limiting currents 79−10699
electron beam injection, higher energy density electron cloud form. *(Russian)* 77−3979
electron beam injection into drift cavity, pot. profile finite size particle calc. 80−18987
electron beam landing on equilib. orbit in toroid 77−68850
electron beam toroidal ring, equilib. config. 77−65906
electron beam transport in cusp field of Angara-Koltso system 79−68945
electron beams, laminar flow equilib., limiting currents 77−51224
electron beams, mag. focusing, equilib. surface ripples 79−3618
electron beams, relativistic intense solid, cyclotron maser instability 79−55494
electron beams in conical diodes, flow meas. 79−77416
electron cyclotron waves in plasma, relativistic nonlinear 80−10377

relativistic plasmas continued
electron energy distrib. of relativistic plasma in mag. mirror, synchrotron radn. meas. 79−10717
electron interaction, trace evaluation in strong mag. fields, REDUCE based program 79−7480
electron magnetised plasma, stability in circularly polarised EM wave field 80−87897
electron oscillations, dispersion relations in mag. field 78−34364
electron plasma, parametric instability excitation by high-freq. EM waves 79−19031
electron plasma, war, isotropic, drifting, waveguide modes, relativistic electrodynamical study 79−77393
electron power law spectra in random mag. field 80−24240
electron waves, relativistic effects 78−34310
electron-cyclotron heating, computer numerical anal. by averaging methods 77−27716
electron-positron counterstreaming beams plasma, relativistic, radiative collapse to ultrahigh densities 79−60188
electron-positron plasma, EM waves, nonlinear generation *(Russian)* 80−106973
electron-positron plasma, produced by relativistic electron beam, waves, microinstabilities, collective positron accel. 79−19053
electronic oscillations, hydrohydrodynamic model *(Russian)* 78−79434
electrons acceleration by weak MHD turbulence, energy spectrum, radio-sources appl. 79−88582
electrosound waves in strong HF field *(Russian)* 77−31466
electrostatic trapping of intense relativistic electron beam in magnetic mirror 77−24172
ELMO bumpy torus, macroscopic MHD stability and beta limit 79−31186
EM absorption around electron cyclotron freq., in finite density weakly relativistic plasma 79−64874
EM cyclotron instability 80−21912
EM ion waves in cold relativistic plasmas, astrophys. appl. 80−21910
EM radiation propag. in strong gravit. field *(Russian)* 77−3945
EM wave dispersion relations from hydrodynamical eqns. 80−79559
EM wave interaction, Doppler shift, reflected pulse duration 78−34328
EM wave propagation in cold inhomogeneous electron plasma, relativistic effects 78−26295
EM wave reflection from front of relativistic electron beam 78−34329
EM wave resonance absorpt., mode conversion, relativistic effects 77−11391
EM wave self-focusing due to relativistic electron mass variation 78−1838
EM waves propagating along mag. field in strongly anisotropic relativistic plasma, dispersion props. 80−67542
energy loss due to binary collisions in a relativistic plasma 80−24127
excitation spectrum of relativistic quantum plasma, covariant Wigner function approach 80−87938
extragalactic rapidly varying radio sources, relativistic plasmoids dynamics theory 78−93438
field-reversing electron ring generation in RECE Christa, millisec. lifetime, mag. probe meas. 77−24173
finite Larmor radius effects in absorpt. of EM waves near electron cyclotron freq. 79−94800
flux conservation, MHD and force-free approxs. 79−19081
general relativistic plasma sphere with central gravitating mass, MHD eqns. 80−6276
generalised flux theorem for relativistic plasma, covariant forms 77−55165
generalised relativistic Brillouin theory, appl. to infinite vacuum transmission line 78−87004
gyrosynchrotron emissivity peak freq. of weakly relativistic electrons in isotropic plasma 77−64633
Hamiltonian to order v^2/c^2 of slightly relativistic plasma 80−54024
hydrodynamic free expansion into vacuum 77−3980
induced Compton scatt., nonlinear classical theory 77−68857
intense relativistic electron beam focusing with large aspect ratio diodes 77−23610
kinetic equation, fully convergent, for homogeneous isotropic slightly relativistic plasma 80−54025
Langmuir turbulence, relativistic electron increase with heating *(Russian)* 79−27799
Langmuir turbulence of relativistic plasma in strong mag. field *(Russian)* 80−28678
Langmuir wave phase vel. in relativistic particle beam 79−23408
Langmuir waves, head-on approximation in second harmonic plasma emission 79−41803
laser-irradiated solid target, nonlinear dynamics 80−28767
LF wave propag. in relativistic electron gas, rel. to Crab Nebula *(Chinese)* 78−67356
linear wave props., using two fluid approx. 79−1337
longitudinal waves *(Russian)* 80−54023
longitudinal waves and beam instability *(Russian)* 79−60158
magnetic-insulation wave front struct., in waveguide 79−55517
magnetised plasma, negative absorpt. and energy distrib. function of hot electrons 79−4143
magnetised Vlasov-Maxwell plasma, current responses 79−90450
magnetoactive plasma, low frequency waves excitation, relativistic effects *(Russian)* 80−103184
Maxwellian, interaction with cyclotron radiation, absorpt. coeff., computer model 78−30478
Maxwellian synchrotron sources, spectral characts., model for 3C 273 radio and X-ray spectra 79−35107
MHD growth and decay discontinuities 80−92280
MHD shock waves 77−24035
MHD symmetric flow, eqn. of motion *(Russian)* 80−83992
microwave generation by negative-mass instability in ultrarelativistic plasma 78−51289
modulational instability of nonlinear wave propagation in relativistic plasmas 80−106911
modulational instability of nonlinear waves with nonlinear Landau damping *(Russian, English)* 80−53955
modulational instability of two transverse waves, cold plasma 79−32765
motion of relativistic charged particle in axisymmetric toroidal system 80−83991
moving magnetoplasma slab, space charge waves propag. 80−38700
moving plasma, covariant dispersion eqns. 79−37538
moving plasma, four-dimens. constitutive relations 79−37537
Navier-Stokes and mass balanace eqns., conductive additional force density term 78−75411
relativistic plasmas continued
non-linear propagation effects of relativistically strong plasma waves 79−10698
noncooperative radiation scattering, from finite vol. of relativistic plasma *(Russian)* 79−37497
nonlinear dispersion relation for transverse wave 80−87939
nonlinear EM waves, in relativistic plasma, Vlasov eqn. calcs. 77−47209
nonlinear propag. of EM wave, modulational instability 79−19047
nonlinear space charge waves, rel. to pulsars coherent radio emission 77−41386
oscillation centres and mode coupling in non-uniform Vlasov plasma 79−90448
oscillations, dispersion relations, electron fluid model approx. calcs. 78−1882
oscillations, EM and electrostatic, in isotropic relativistic plasma 80−54026
overdense plasma, nonlinear linearly polarized standing waves 78−87447
parametric resonance in a weakly turbulent relativistic electron plasma 79−55539
parametric scatt. of intense EM wave, ultrarelativistic plasma 77−84489
plasma code instability due to Lorentz force 79−7482
plasma waves relativistic self-focusing in cold plasma 79−73009
power flow in relativistically moving anisotropic warm plasma filled waveguide 78−55725
Poynting's theorem for moving media, Lerche's relativistic theory 79−48660
pulsar atmospheres, beam-plasma interaction mechanism for radio emission 78−20847
pulsar coherent radiation, relativistic soliton model *(Russian)* 78−77568
pulsar magnetosphere, generalised Ohm law 77−37610
pulsar magnetosphere, nonaxisymm., relativistic plasma streaming, particle inertia 79−21320
pulsar magnetospheres, plasma relativistic co-rotation 78−12258
pulsar magnetospheres, relativistic MHD wind or plasma wave 80−31317
pulsar neighbourhood, modulation instability rel. to pulsar radio radiation *(Russian)* 77−22258
pulsar rotating magnetosphere, charge bunching mechanism for coherent curvature radiation 77−33538
quantum electrodynamical plasmas, covariant Wigner function calcs. 79−4175
quantum scalar plasma, thermodynamic props. 78−75410
radiation scattering by high-temp. relativistic plasma, polarising props. calcs. *(Russian)* 80−53937
radiative collapse of a relativistic electron-positron plasma to ultrahigh densities 80−14929
radiative processes in relativistic plasmas, appl. to kinetic theory of free-electron lasers 78−42316
radio sources, compact, extragalactic, synchrotron and relativistic Maxwellian source models rel. to spectra 80−62299
radiosources, extended, particle accel. and radiative losses effects on source dynamics 80−46687
RECE-Berta device with external Ioffe fields, fast electron anomalous losses 77−84483
RECE-Christa device, axial translation of field-reversing E layers 79−19065
RECE-Christa device, field-reversing electron ring production, by ring stacking 77−84482
relativistic conductive additional terms 77−45746
relativistic nonneutral E layer, negative-mass instability 77−68856
resistive hose instability in relativistic electron beam 80−67947
runaway electron beams in Tokamak 77−51223
runaway electron motion in momentum space, multicomponent plasma 79−37449
runaway relativistic electron scatt. on oscills. in Tokamak *(Russian)* 80−48849
second helicon branch, relativistic electron motion, circularily polarised EM wave propag. *(Russian)* 77−47205
self-pinched beam, radial expansion with distrib. energy, anal. 80−19609
shearing field-free plasma, EM wave propag. effects rel. to pulsar microstruct. 80−17483
shock waves, in relativistic MHD 78−9770
space-charge-limited planar relativistic diode, Poisson eqn. 79−10700
space-time curvature, neutron stars and black holes 79−84873
static plasma polarisation in Schwartzschild gravitation field *(Russian)* 79−16825
statistical mechanics of relativistic dense matter, QED plasma appl. 78−89814
stellar relativistic centrifugal winds, appl. to pulsars 78−96473
stochastic heating, relativistic electron generation *(Russian)* 80−83952
streaming plasma, generalised Ohm's Law, pulsar magnetosphere relevance 78−9823
sychrotron-like X-radiation produced by intense laser beam heating 78−67322
synchrotron emissivity near electron cyclotron and upper hybrid freqs. 78−14140
synchrotron radiation from relativistic electron circ. orbits in magnetoplasma 79−55474
synchrotron radiation spectrum, canonical ang. momentum spread effect 77−47252
synchrotron radiation spontaneous emission from relativistic electrons, kinetic theory 77−72489
synchrotron turbulent reactor, relativistic electrons spectrum in nonsteady radiosources 79−40071
tearing instability in background plasma, relativistic modes 80−62012
test particle energy loss, unified theory 78−71530
thermonuclear reactions, quantum theory of electron screening effect *(Russian)* 77−17350
Thomson scatt. by fusion plasma 79−77420
toroidal plasma, equil. and circular rotation *(French)* 77−15222
trans-relativistic shock relations, numerical solns. 80−31202
transport coeffs., relativistic Boltzmann theory, variational method 78−47096
transport coeffs. of relativistic degenerate electron gas in strong mag. field 77−80346
transverse Cherenkov mode nonlinear stabilisation by external mag. field 80−38642
turbulent reactor, relativistic electron spectra, Compton effect *(Russian)* 77−19760
turbulent reactor power distrib., energy and particle flux directions *(Ukrainian)* 78−93104

relativistic plasmas continued
turbulent reactors, relativistic electrons accel. and cosmic radiosources nonlinear spectra 79−8824
two component plasma, conductivity sum rules 77−19761
ultrarelativistic beam quasilinear relativistic plasma relax. in strong mag. field, magnetobremsstrahlung *(Russian)* 80−38669
ultrarelativistic electron-positron plasma, wave prod., rel. to pulsar radiation 78−20629
ultrarelativistic particle beam in relativistic plasma, emission due to mag. bremsstrahlung 80−46390
variational principal in relativistic magnetic fluid dynamics, Lagrangian density 79−73031
virial theorem 77−89299
viscous phenomena, for relativistic plasma in EM field 78−34365
waveguide, rectangular, filled with uniaxial anisotropic relativistic warm plasma, EM wave propag. and attenuation 80−59246
X-ray emission spectrum, multiple Compton scatts. effect, Monte Carlo calcs. 78−96389
B-H, possibility of thermonuclear fuel in relativistic plasma *(Russian)* 80−37573
N_2, plasmochemical action of relativistic electron beam, calc. by degradation spectrum method *(Russian)* 79−37536

relativistic quantum field theory
4-atomism, theory 80−94967
$\lambda\phi^4_{(4,6)}$ field theory in curved spacetime 80−86556
$\lambda\phi^4$, momentum space renormalisation in curved space time 80−37158
$\lambda\phi^4$ field theory, renormalisation in curved space-time 80−42320
$\lambda\phi^4$ field theory at finite temp., Casimir effect and topological mass 80−57479
$\lambda\phi^4$ field theory renormalisation in curved space-time 80−42319
$\lambda\phi^4$ self interaction theory, symmetry breaking and mass generation by space-time topology 80−82892
$\lambda\phi^4$ theory, conformal symmetry breaking, cosmological particle creation 80−90998
$\lambda\phi^4$ theory, renormalisation in nonsimply connected spacetime 80−90999
σ-model, nonlinear, curved space, spontaneous compactification, Grassmann manifold 80−57467
ϕ_2 model, S-matrix asymptotic perturbation expansion 77−10161
ϕ^4 theory, quark confinement model 77−41811
$\bar{\psi}\psi^2/N$ interaction in four dimensions nonlocal Thirring model 79−21940
$(\bar{\psi}\psi)^2$ model in two dimens. 79−2917
•algebra, classical moment problem appl 77−54039
acceleration through random classical radiation, thermal effects 80−73191
action at a distance and wave eqns. for spinless quarks 79−36030
additive conservation laws for local relativistic quantum field theory 80−22507
algebraic structure of relativistic wave eqns. 79−67460
algebras for external EM interaction with relativistic fields 77−2722
algebras of unbounded operators *(Russian)* 79−17602
angular momentum and magnetic charge 78−41428
automorphic fields on flat space-times, vacuum stress tensor 80−22510
automorphic theory, mathematical issues 80−22509
Backlund transformation in the classical massive Thirring model 80−57456
Backlund transformations as nonlinear Dirac equations 78−49965
bags with spontaneously broken symmetry 79−264
Bargmann-Wigner equations, SO(4,2)-covariant formulation 78−37126
Bargmann-Wigner wavefunction, component minimisation 78−58105
barnacle equivalence structure in wave eqns. 79−30657
baryon interactions through scalar meson field viar Yukawa-like interaction 79−67225
baryon model on Dirac eqn. with confining potentials 78−425
Bertotti-Robinson space-time, quantum effects 79−35930
Bethe-Salpeter eqn., Lorentz deformation 79−54246
Bethe-Salpeter equation, eigenvalues 79−2925
Bethe-Salpeter equation, exact three-dimens. reduction 78−70247
Bethe-Salpeter equation, reduction to an equivalent Schrodinger equation, with appl. 79−2933
Bethe-Salpeter equation for positronium, solns. 78−93831
Bethe-Salpeter equations, two-fermion electromagnetic bound state systems, gauge props. 78−78058
Bethe-Salpeter formulation of the baryon matriz elements in hadronic weak decays 79−386
Bethe-Salpeter wave function, asymptotic behaviour as relative time approached infinity *(Chinese)* 78−82113
Bhabha first-order wave eqns. exact, closed-form, Foldy-Wouthuysen transformations and solns. 77−30254
Bhabha first-order wave eqns. summary and conclusions 77−30255
bi-local field, interaction with the external field 78−66030
bi-local field on space-like surface 80−27403
Bianchi type-I cosmologies and spinor fields 80−62347
bilinear spinor representation of space-time 77−22647
bilocal operators, spectral props., product expansion on light cone 77−41778
black hole evaporation, inevitability of associated naked singularity 80−36924
black holes, Hawking's effect, theory in curved space time 78−12268
Bose condensation in supercritical external fields charged condensates 78−8766
Bose particles in an external EM field as a one-particle problem 78−12462
Bose system with a condensate, IR divergence *(Russian)* 79−2944
Boson transformation and the extended objects 78−37140
Bosonisation in (1+1) dimens., elementary anal. 79−85208
bound state problems, dimensional continuation 77−18159
bound states with gauge monopole 79−268
bound-state equation, relativistic single-particle, numerical solutions 80−52389
Breit equation, discontinuous solns. for spin $^1/_2$ particle 80−4834
Breit equation, Klein paradox 80−57506
C*-algebras of two body interactions, existence of scatt. theory of time automorphism groups 80−31972
canonical formalism on a lightlike hyperplane 77−79214
canonical momenta, transformation props. 80−105765
canonical scalar field quantisation, scatt. operater Lorentz invariance 78−4526
Casimir effect for a self-interacting scalar field 79−97497
Casimir effect in quantum field theory 80−42330
causal A-statistics 80−22504

relativistic quantum field theory continued
causal independence of free quantum fields 79−21894
causality in homogeneous spaces 79−2699
causality of a wave equation and invariance of its hyperbolicity conditions 80−91000
characterisation by vacuum expectation valves 78−29001
characterisation by vacuum expectation valves 78−32731
charge conservations as concomitant of conformal motions coupled to gauge transforms 80−62835
charge operator anal. 77−45975
charged particles in external fields 77−49829
charged relativistic boson field, coherent state representation 79−71708
chiral symmetry, the 1/N expansion and the SU(N) Thirring model 79−12977
classical limits 77−65080
classically solvable field theory model 79−9272
Clifford-Klein space-times effective lagrangian and vacuum stress-energy tensor 79−2674
cohomology of nets over Minkowski space 78−93561
completely integrable, Hamiltonian system 77−57450
composite field theory, conjugate field quantity are relativistic wave function *(Chinese)* 79−80756
composite system, relativistic, light-front wave functions 80−73592
composite systems, field theory 78−70253
conformal anomalies in curved space-time 77−26210
conformal conservation laws in action-at-a-distance theory 80−42335
conformal invariance in field theory 78−21316
conformal invariance of relativistic eqns. for arbitrary spin particles 79−30649
conformal phase group and electromagnetism 77−67360
conformal relativity, bare mass theory 80−27417
conformal relativity, classification of particle species 78−93815
conformal relativity, classification of the metric bosons 78−93803
conformal symmetry breaking, quantisation in curved space time 78−41434
conformally, related space times, field theories, global considerations 79−67473
conformally flat spaces and solutions to Yang-Mills equations 80−57481
conservation laws in sine-Gordon and the massive Thirring models 78−29226
conserved currents in the perturbative sine-Gordon and massive Thirring models 79−9273
constrained system, compensating functional and quantisation, S-matrix 79−97527
coordinate measurements and operators 80−57458
cosmological particle pair creation as above barrier reflection, WKB approx. 79−80377
cosmology, effective Lagrangian and pair prod. 80−22123
Coulomb potential with respect to the Dirac operator 79−21988
countable systems of first-order partial differential equations, invariance groups 78−49635
coupled Einstein-SO(3) gauge field eqns. 79−274
coupled Klein-Gordon-Schrodinger equations 79−35955
covariant σ models, first order system of differential eqns. 80−31978
covariant approach for the one-soliton sector 79−17640
covariant derivatives without gauge fields 80−73584
covariant field equations for an EM string with mass points at the ends, covariant field eqns. 79−309
covariant loops and strings in a positive definite Hilbert space 77−30233
covariant quantum mechanics on a null plane 77−74581
critical mass in a two-body problem 77−26457
critical potentials, leptons, and weak currents 78−54597
crossed diagram effects in Bethe-Salpeter eqns. 77−2725
curved space anomalous currents 78−62336
curved space-time, regularisation and renormalisation 77−87890
curved space-time of a rotating star, field instability, particle creation 78−69790
curved space-time quantum stochastic processes, covariant Kolmogorov-Klein-Fock eqn. 80−18083
de Sitter gauge theory, general relativistic limit 79−58598
de Sitter groups, complex quaternious, spinor representations 78−36887
de Sitter invariant Lagrangian 80−82868
de Sitter space, quantised fields 78−92
de Sitter space-time, particle detection 77−30040
de Sitter space-time, wave eqns. for arbitary spin 77−30234
deep-inelastic structure functions for bound states in ladder approximation 79−35952
deuteron formfactor calculations with the Bethe-Salpeter eqn. 79−67554
diagonal forms of the Dirac Hamiltonian *(English)* 77−22650
diffusion theory for the sine-Gordon eqn. in three dimens. *(French)* 77−61174
dipole ghost taming 79−22019
Dirac's extended electron model 79−26269
Dirac and Klein-Gordon fields, interactions 77−30226
Dirac electrons in a gravitational field, mean motion 77−22478
Dirac eqn., exact solns. 78−45775
Dirac eqn. in Kerr-Nauman space, soln. class 77−49828
Dirac equation, 2-component form *(Russian)* 77−45934
Dirac equation, γ^5 invariant for massive particle 78−29262
Dirac equation, accurate solns. *(Russian)* 77−30289
Dirac equation, asymptotic soln. and inertial mass of electron 79−2961
Dirac equation, conformally dovariant struct. 78−41417
Dirac equation, de Sitter gauge transformations 77−67563
Dirac equation, exact solns. *(Russian)* 77−71468
Dirac equation, exact solns. 77−79205
Dirac equation, exact solns. *(Russian)* 78−49954
Dirac equation, exact solns. 79−63398
Dirac equation, formulation 78−74185
Dirac equation, general instation solns. 78−82100
Dirac equation, in N-pseydoparticle field, zero energy solns. 77−49845
Dirac equation, reduction to Pauli type eqn. *(German)* 77−9894
Dirac equation, soln. in type D vacuum space-times 77−74578
Dirac equation in a curved space of constant curvature 77−87898
Dirac equation on a lattice 78−24924
Dirac equation soln., electrons in logarithmic potentials 78−41448
Dirac equation with anomalous magnetic moment 78−82133
Dirac equation with oscill. pot., scatt. prob. *(Russian)* 77−79225
Dirac field, canonical formalism 78−49989
Dirac field, scatt. automorphisms 78−58112
Dirac field in curved spacetime, geometrical super hamiltonian and super momentum 78−45518

relativistic quantum field theory continued
Dirac field in Kerr metric, absence of superradiance 77−67578
Dirac fields in a curved space-time 80−18070
Dirac fields in Riemannian space time, geom. props. 79−75430
Dirac fields in Riemannian space-time, geom. props. 79−75431
Dirac hydrogen atom, simple form 78−37124
Dirac Lagrangians, invariance 78−4763
Dirac Lorentz's equations, relativistic and nonrelativistic, maximally extensive local group of invariance 80−77946
Dirac magnetic poles *(Russian)* 77−74606
Dirac massless field theory, potentials 77−82663
Dirac model of extended particles, physical aspect of interactions 80−9142
Dirac monopole strength 77−33764
Dirac operator, classification of terms involved 77−82672
Dirac operator, self-adjoint extension 77−18156
Dirac operator with highly singular potentials 78−21359
Dirac particle, polarisation in external EM field 78−58116
Dirac particle+two Klein-Gordon particles, relativistic three-body wave equation, preon model 80−73574
Dirac particle + fixed magnetic monopole, elec. and mag. dipole moments 78−24966
Dirac particle propagator, supersymmetric methods 80−342
Dirac propagator from path integral quantization of the pseudoclassical spinning particle 80−86577
Dirac quantisation of massive spin-3/2 field 78−58113
Dirac S-matrix in the K-plane 78−54577
Dirac singletons, equivalence with massless particles 79−21903
Dirac spinor solitons or bags 78−12817
Dirac string Lagrangian in A^0-0 gauge, path integral quantisation 80−32007
Dirac system, nongrassmann quantisation, path integral approach in phase space 79−97496
Dirac-EM field interaction, localised soln. radius 77−79212
directly interacting relativistic particles, positive energy dynamics and scatt. theory 80−82921
discrete space structure dynamics 80−52392
discrete symmetries for scalar and spinor fields in curved space-time 80−68387
dual charged solution in curved space-time 78−12827
dual string wave functional in Yang-Mills theories 79−21921
dynamical groups for the motion of relativistic composite systems 80−9115
dynamical impact parameter 79−21982
dynamics of fields of higher spin 77−74607
dyon-dyon interaction in predictive relativistic mechanics 79−26265
Dyson-Salam scheme subtractions, counterterm equivalence 80−13241
effective one-body Dirac eqn. from the Bethe-Salpeter eqn. 77−54040
Einstein vacuum and Einstein-Maxwell space-times, infinitesimal holonomy group structure and geometrization 80−73252
Einstein-Dirac field Hamiltonian 77−71428
elastic scattering between binary quark-antiquark system and local field 80−47244
elastic scattering of electrons by spatially bounded mag fields 77−13834
electron field theory 77−2779
electron pair photoproduction in field of bichromatic EM wave *(Russian)* 77−30291
electron wave equation *(Hungarian)* 79−12928
electron-monopole system, dynamics 79−54247
elementary bodies, relativistic dynamics in seven-dimens. space 80−32015
elementary domain theory 80−42318
elementary particle modeling in axiomatic relativistic field theories *(German)* 80−91009
elementary-particle symmetries in many-body theory at finite temp. and density 79−49403
EM field without indefinite metric 78−8565
energy-momentum quantised field tensor vacuum means 80−73227
energy-momentum tensor in general relativity 78−54263
energy-momentum tensor vac. expectation values, depend. on manifold geom. and topology 80−355
equations determined by the operators of the exterior derivative and generalized divergence 79−21962
equations for bound states of quarks 78−70333
Euclidean approach in curved spacetime, functional anal. 80−27181
Euclidean Dirac field, local structure, Green's function method 80−68347
Euclidean field theory, embedding the relativistic Hilbert space 77−2724
Euclidean field theory and Hawking effect 78−73732
Euclidean light cone gauge, 1/N expansions with non-isoscalar gluons 80−47169
exact diagonalization of relativistic Hamiltonians 77−34081
exact Thirring model S-matrix,perturbation theory 77−54049
excited vacuum states associated with nonabsolute minima of its effective pot., lifetime 77−26464
expanding universes, positive frequency and Hamiltonians 80−4624
extended hadrons in geometrically formulated gauge dynamics with fibre bundles 80−9141
extended model of the Dirac electron 77−22436
extended objects created by goldstone bosons 79−285
extended particles, field theory 77−22646
extended particles in two space dimensions 77−5995
extended phase space, classical fields 80−86550
extended phase space, unified meson fields 80−86551
extended phase space, unified spin 1/2 fields 80−86552
factorised S-matrices in 2-dimens., relativistic QFT model exact solns. 79−93274
factorised S-matrix in two-dimens., 0(N) isotopic symmetry 78−41432
Faddeev-Popov ghost fields, vanishing norm 78−8523
Fermi-Bose and internal symmetries with universal Clifford algebras 78−24970
Fermifield bosonisation in 1+1 dimensions 80−47172
fermion interactions, convergence difficulties, soln. 80−4836
fermion spectra in monopole fields, exactly soluble models 78−24965
fermion thermal radiation from an accelerated wall 79−54265
fermion-meron interactions in Minkowski space-time 79−2913
fermionic coordinates and quark variables 79−22018
fermions in a pseydoparticle field 77−67569
Feyman theory extension *(French)* 79−53994
Feymann propagator in curved space-time 77−45961
Feynman diagrams, appls. in advanced quantum theory, book 80−22157
relativistic quantum field theory continued
Feynman integrals with zero mass particles, asymptotic behaviour 77−57444
Feynman propagator in curved spacetime, momentum space representation 80−32004
fiber bundles, sheaf theory, and generalization of differentiable manifolds in physics 80−57459
field and particle equations for gauge theory based on (4,1) de Sitter group 79−58868
field equation of the $\lambda\phi_3^4$ QFT 77−87893
field equations, two soliton solns. 78−74124
field equations equivalence 78−74132
field equations for half odd integer spin and unique mass, graph theory 78−62290
field intensity and relativistic considerations in gauge choice in electrodynamics 79−54287
field theory for a rotating observer 79−12941
fields with complex spin, symmetry eqns. 79−21961
Fierz-Pauli field theory, smooth massless limit 80−62843
finite confinement potential and relativistic field theories 77−79249
finite Lorentz transformations in field theory 77−45976
finite regularisation algorithm for relativistic field theories 79−93283
finite temp. field theory with boundaries, extensions to curved space, stress tensor and surface action renormalisation, review 80−57455
finite temperature vacuum excitations 77−5994
finite-band solutions to the duality equation on S^4 and two-dimensional relativistically invariant systems 80−42349
finite-spectrum relativistic wave eqn. models of the quark and lepton masses 78−74130
first quantised theories, geometrical aspects 78−24697
Fisk-Tait equation for spin-3/2 particles 79−17623
five dimensional QFT, generalised free fields conformal group 80−4837
flux lines collapse, the invisible string 77−57451
Fokker-type action integrals and relativistic instantaneous interaction lagrangians of two particles 78−66046
Foldy-Wouthuysen transformations in an indefinite-metric space, relation to Lorentz transformations 77−30252
Foldy-Wouthuysen transformations in an indefinite-metric space 77−30253
free Dirac field, algebraic struct. of set of local observables 79−58883
free field quantisation, geometric approach 78−81885
free fields in stationary space-times, quantisation 77−67335
free fields on the Poincare group 78−70016
free massive spin-3 field 78−369
free massless scalar field in space-time 77−41754
free massless scalar field in two-dimensional space-time: revisited 80−105798
free relativistic particle, Lagrangian approach to quantum theory 79−58867
free scalar massless field in 2-dimens. space time 80−52426
frequency decompositions in curved space-time 80−31973
Friedmann model, spontaneous symmetry breakdown 80−51929
Galilei to Lorentz group in a general light-cone frame 77−61187
gauge field construction, lattice approx. convergence 80−37156
gauge field theory, space-time symmetry, Higgs model 80−52385
gauge invariance, time-dependent Foldy-Wouthuysen transformations, and the Pauli Hamiltonian *(English)* 77−41762
gauge invariant fermion theories, path-integral measure 79−54267
gauge symmetry spontaneous breaking in a nonstationary isotropic metric 79−21643
gauge theories, statistical mechanics of field theories with broken, global, and local SU(3) gauge symmetries 79−58881
gauge theories of interaction in conformal relativity 79−9281
Gaussian fluctuations: 't Hooft's method and an approximate method 79−85236
Gelfand-Naimark z-basis, infinite component model 77−82661
general relativistic Dirac-Pauli particle 77−45743
general relativistic nonlinear spinor equations *(Russian)* 77−45751
geometric quantization and internal symmetry 80−42089
$GL_{4,R}$, nonlinear two valued realizations, Dirac eqn. nonlinear form 79−80748
Goldstone theorem generalisation, scalar fields, conserved current and mass spectra struct. 80−68339
gravitation and universal fermi coupling in general 77−79
gravitational field and arbitrary gauge field, equations of motion, Heisenberg and classical, force term, spin-curvature coupling 80−57158
gravitational law and spinning electron eqn in de Sitter symmetric space 78−103
gravity, boson field, equal-time commutator, general relativity, indefinite-metric 80−68119
gravity coupled to non-abelian plane waves 79−35602
Green's function discontinuities across characteristic surfaces of field eqns. 79−93279
Green's function method for many-body problem for relativistic meson field theory, book contrib. 80−357
Green's functions for spin half field theory in Rindler space 78−12826
Gribov ambiguity observation in general relativity, in Coulomb gauge 79−54023
Haag's theorem and dimensional regularization 80−52409
hadronic atoms in momentum space 79−872
hadronic potentials, field theoretic interpretation 79−26266
hadrons, extended, Lorentz deformation props., O(4) and light-cone coordinate systems 80−68354
Hamiltonian dynamics 78−62070
Hamiltonian form for massless higher-spin fermions 80−52412
Hamiltonian theory, covariant formulation, on light cone, fields with spin *(Russian)* 80−9087
Hamiltonian theory, high energy representation 78−24980
Hamiltonian theory of the light cone, convariant formulation 79−2942
harmonic oscillators and hadronic structures in the quantum-mechanics curriculum 78−61971
Heisenberg equations of motion in a nonabelian gauge theory *(German)* 80−27387
Heisenberg Klein Gordon eqn., soln. in space time of const. curvature 80−62829
Higgs fields, curved space, and hadron structure 79−9275
high energy electron scattering from a two center potential 77−18187
high temperature expansion without lattice 78−58124
high-energy scattering of particles with anomalous magnetic moments 78−465

relativistic quantum field theory continued
Hilbert space sectors for solutions of non-linear field equations 77−38080
Hurley's field equation for arbitrary spin 77−6034
identical motion in relativistic quantum and classical mechanics 77−61177
impact parameter expansion of fields 77−26471
infinite component wave eqns., space-like solns. 77−61183
inhomogeneous local gauge transformations in spacetimes with torsion 79−71330
instabilities of a boson field in an external pot. 77−6017
instanton solutions on arbitrary four-dimensional compact manifolds, parameters 78−41406
interaction between particles, strings and membranes, unified theory 78−86433
interaction potentials derivation from field theory 79−12954
invariance algebras of relativistic eqns. for massless particles 79−58909
invariance groups of the Dirac and Kemmer-Duffin-Petiau eqns. 77−67320
invariant two-dimensional models in field theory integrable by the inverse problem technique 78−70291
inverse scatt. problem and 5th Painleve transcendent 79−54260
Ising field theory for $T<T_c$ Green's-Functions strings 79−271
Ising field theory for $T<T_c$ string structure 79−270
Ising field theory in a magnetic field 79−272
Ising model, two-dimsion, field theory 78−21081
isotopic spin origin from extended conformal symmetry 79−40684
Jost functions and Levinson's theorem in (1+1)-Dimensional relativistic field-theoretic model 78−54552
Kadyshevsky equation, deep bound states 77−54044
Kaluza-Klein bundle, unified theory 80−37153
Kerr metric, bound states 79−35600
Kerr-Schild geometry, spinors, and instantons 79−35601
killing field vectors and the Einstein-Klein-Gordon eqns. *(French)* 79−30340
Killing tensor, quantum no. and conserved currents in curved space 78−29249
kinematical interpretation of subsidiary conditions 77−2737
kinks and cobordism in field theories, general relativity fermions 80−98835
Klein paradox as a many particle problem 77−2717
Klein-Gordon and Dirac particles, high energy scatt. 79−40697
Klein-Gordon charged particles, perturbation theory for non-equilibrium stat. Green's functions 80−31994
Klein-Gordon charged particles, quantum distrib. function 80−31993
Klein-Gordon equation, (1+4) dimens., invariant expansion *(Russian)* 77−13875
Klein-Gordon equation, essential spectrum, self adjointness and invariance 77−18157
Klein-Gordon equation with light-cone data 78−93789
Klein-Gordon equation with optical pot. of the strong interaction 77−5990
Klein-Gordon equations, particle like piecewise analytic soln. *(Russian)* 77−30228
Klein-Gordon field in static manifolds, canonical theory 77−5718
Klein-Gordon nonlinear problems, existence of standing waves *(French)* 79−63339
Klein-Gordon particles+Dirac particle, relativistic three-body wave equation, preon model 80−73574
Klein-Gordon theory in the coherent-state representation, classical limit 79−49372
Klein-Gordon-Fock eqn., invariance with respect to Poincare group 77−57456
Klem-Gordon and Dirac eqns., phase sh.fts and quantum effects *(Russian)* 77−79207
Koornwinder's polynomials and representations of the conformal group 79−63343
ladder approximation with effective propag. and vacuum stability, Bethe-Salpeter bound state 80−47168
Lagrangian field theory, vector bundles, rth order Noether invariants 78−86409
Lagrangian formulation, conservation laws, relativistic gravitation *(Russian)* 80−68337
lagrangian formulation of spinning particles dynamics 77−18173
Lagrangian theory of relativistic rotator 77−41757
Laplace transform. inversion, non-unitary representations of MH(2) and group ax+b 80−4866
large Numbers, explanation via classical unified theory 80−57166
lattice theory for fermions, Adler anomaly nonexistence 79−71667
Lee model in EM field, mag. moment calc. using Schwinger source theory 80−42350
Lee model in S(1,1) sector 79−71590
left-flat space-times, null tetrad and restrictive conditions 80−62545
Lie algebra representations and coherent states, Trotter limits 80−22238
Lie group framework for soliton eqns' generalizations of the Lund-Regge model 79−17605
Lie group Sp(8,R), Lorentz subgroup anal., nul plane boson realisation 78−62116
Lie theory and the wave eqn in space-time 79−12968
Lie theory and the wave equation in space-time, Klein-Gordon eqn. and Poincare group 78−62292
Lie theory and the wave equation in space-time, r-separable solutions 78−62293
Lie-admissible local powers of field with the Wightman axioms 78−93793
light cone, finite normal products 78−86408
light front field theory treatment of the 2N problem 79−67579
light velocity in vacuum, quantised space, special relativity and relativistic field theories 80−82869
light-cone field theory and parton model 78−82220
light-cone quantisation of scalar field, current nonconservation 80−47220
linear field equations on self-dual spaces 80−42328
linear zero-spin fields in external gravit. and scalar fields, perturbation theory 80−31969
linearization of relativistic nonlinear wave equations 80−62837
linearly rising potential, generalisation 78−4768
local observable algebras, reconstruction from Euclidean Green's functions 78−54522
Lorentz basis of quantum fields 80−86565
Lorentz covariance and kinetic charge 79−93302
relativistic quantum field theory continued
lorentz gauge invariant vacuum functionals for quantized spinor fields in non-simply connected space-times 79−89061
Lorentz group irreducible representations, generalised function expansion with light cone support 78−70018
Lorentz space relativistic path integrals, Dirac electron perturbation expansion 79−85000
Lorentz transformation properties in the Thirring and Schwinger models 78−12837
Lorentz transformations as space-time reflections 77−57187
lorentz-invariant spin-1/2 equation for the representation (1,1/2) ⊕ (1/2,0) ⊕ (0,1/2) ⊕ (1/2,1) 80−42334
Lorentz-invariant system with exact many-soliton solutions 77−30275
low-frequency solutions of the wave equations in Schwarzschild space 80−90743
Luttinger model, thermodynamic correlation functions, bosonisation of fermion field 80−68356
M_4 factorisation, spinor algebra, Dirac equation geometrical, interpretation 80−62838
magnetic monopole and dipole soln. of SU(N) theory in curved space *(Chinese)* 78−82112
magnetic monopoles, gauge independ. formulation 78−41427
magnetic monopoles with no strings, action principle and canonical quantisation 80−31990
main equation to the Klein-Gordon eqn. 79−40660
many-body bound systems, EN props. 77−74765
many-body theory, QCD and neutron stars/supernova 79−40752
mass splitting 77−18166
massive particle production in anisotropic space-times 80−90583
massive scalar particles, coherent state representation 77−57441
massive spin-1 particles in external symmetrical tensor field, quantisation and noncausality 80−105790
massive spin-zero particles in external fields, dynamics 79−21977
massive SU(N) Thirring model, factorisation 79−12951
massive Thirring mode, static localised soln. 78−16930
massive Thirring model, bound state solns. 77−22641
Massive Thirring model, conservation law renormalisation 77−30020
massive Thirring model, conservation laws in quantum (cos 0-1) theory *(Russian)* 77−200
massive Thirring model, conserved charges 77−199
massive Thirring model, conserved currents 77−198
massive Thirring model, conserved currents 77−38087
massive Thirring model, dynamical charges 77−18171
massive Thirring model, dynamical supersymmetry 77−67586
massive Thirring model, field eqn. solns 78−41418
massive Thirring model, inverse scatt. transform method, relativistic invariant formulation 79−71598
massive Thirring model, localised solns. 77−13864
massive Thirring model, multisoliton solns. in Pohlmeyer-Lund-Regge system 80−47195
massive thirring model, particle scattering in perturbation theory 77−82674
massive Thirring model, repulsive case, new effects 80−27415
massive Thirring model, soln. method 79−21918
massive Thirring model, solns 78−8509
massive Thirring model, two-dimens., inverse scatt. method 80−4840
massive Thirring model 77−57433
massive Thirring model bound state and the sine-Gordon theory 78−74141
massive Thirring model potential, soln. reflectivity 77−74597
massive Thirring model with anticommuting variables, inverse scatt. theory 79−12626
massive Thirring model with bosons, asymptotic scale invariance 78−93799
massive Thirring-Schwinger model convergence of perturbation theory and particle structure 77−10173
massive vector boson field theory with spontaneous symmetry breaking 80−52443
massless antisymmetric tensor gauge fields of second rank, quantisation 79−257
massless boson fields, group theory 77−34098
massless bosons, collision theory 77−18155
massless Euclidean Thirring field, four point Schwinger function, Lorentz group invariant forms *(German)* 80−90980
massless field theory conformally invariant struct. 79−30656
massless fields as unitary representations of the Poincare group *(German)* 79−89056
massless fields in asymptotically flat space-time, null surface quantisation and quantum theory 80−4625
massless particle fields, arbitrary spin, Lorentz transformation laws *(French)* 80−62823
massless particles in the Dirac equation 78−4765
massless scalar field, conformal symmetry breaking and quantisation in curved spacetime 79−97523
massless scalar field in two-space time dimens. 79−12929
massless scalar free field in space-time via Lorentz expansion, IR regularisation 78−12818
massless scalar particle prod. by cosmological torsion field 80−51936
massless Thirring model, saturating field configurations 79−35923
massless Thirring-Wess model, saturating field configurations 79−35953
matrix equations for two-fermion systems with magnetic interactions 79−21904
matrix relativistic wave equations 78−372
Maxwell field quantisation in linear lorentz conformal invariant gauges 79−71666
Maxwell-Klein-Gordon fields in (2+1) dimens. Minkowski space-time 80−99038
Melosh transformation, group-theorect. anal. 77−2749
meson structure wave functions in straton model *(Chinese)* 78−50011
meson theory with internal coordinates 77−13937
mesonic test fields and spacetime cohomology 78−78065
mesons, deformations and spectral props. 80−13203
microscopic causality and quantized solitary waves 78−82095
Minkowski-space formulation of two-pseudoparticle processes 80−95220
multispinor basis of Fermi-Bose transformations 79−75676
Nelson's stochastic field, tensor field quantisation 80−105574
Nelsons stochastic mechanics, spinning particles and relativistic particles 80−31587
neutrino, Weyl, nonlocal position and momentum operators 80−73586
neutrino stress tensor regularization in two-dimens. 77−67561
non-Abelian gauge theory nucleon-nucleon scatt. 79−67573

relativistic quantum field theory continued
non-covariance in interacting spin-1 field theories 77−2720
non-linear coupling of quantum theory and classical gravity 80−27389
non-linear equations and covariance 78−49715
non-linear Klein-Gordon equations, localised solns. 78−12819
non-linear Klein-Gordon equations, Three-dimens. soliton like solns. 78−49955
non-linear spinor equations with localized solutions 78−49964
non-linear strings 77−87901
non-static nuclear forces in a Kerr-Newman background space 78−61880
noncausal effects in relativistic wave eqns. 77−45939
noncausal effects in relativistic wave equations 77−41750
noncausal propagation in spin-o theories with external field interactions 77−41770
noncompletely reducible representations of Poincare group associated with generalised Lorentz gauge 78−70249
noninstantaneous O(ν/c) relativistic effects in bound states and a covariant Schrodinger equation 80−73607
nonlinear de Sitter symmetry and restricted propagation universes 78−58140
nonlinear Dirac equations, soliton solns. 79−71591
nonlinear fermion system, excitations 78−16909
nonlinear fields, king solution in generalized geometry 79−21922
nonlinear functional theory, energy-momentum invariants, kinetic moment *(French)* 78−62287
nonlinear Klein-Gordon equation, stringlike solns. 78−82114
nonlinear Klein-Gordon equation related to Riemannian geometry, localised solns. 79−26223
nonlinear Klein-Gordon equations, solns., non-dissipative 78−62361
nonlinear quantum mechanics, model 79−12927
nonlinear scalar field theory in isotropic homogeneous 79−2676
nonlinear spinor field theory 79−45021
nonlinear super-Poincare fermion, quantisation in bag like formulation 80−4923
nonlinear wave equations and the differential geometry *(Russian)* 78−74162
nonlocal charges, new concept in quantum field theory 79−71596
nonlocal light cone expansion of current products, renormalisation group anal. 79−97526
nonlocal spinor field theory of matter 79−49141
nonpolynomial scalar interactions in four dimens., bounded interactions 80−82895
nonpolynomial scalar interactions in four dimens., quartic interaction 80−82894
nuclear many body problem as field theory 77−10336
nuclear matter, thermal conductivity calc. based on relativistic quantum field theory 79−75886
nuclear matter equation of state, relativistic quantum field theory of neutron stars 80−5088
nuclei, description in relativistic field theory, book contrib. 80−358
null infinity and Killing fields, local isometries, space-times, asymptotic conditions 80−62832
null plane fields and automodel random processes 80−32018
O(3) symmetric merons in a SU(3) Yang-Mills theory 79−30651
O(n) σ model, nonlocal charges in two dimensions 80−18075
O(n) nonlinear σ-model, field eqn. reduction 80−31979
octonions and exceptional groups *(Russian)* 79−67491
one-dimensional step potentials scatt. theory 77−49642
operator density current and localization problem 78−32709
order, disorder and generalized statistics 80−99055
oscillator formalism for hadron struct. and props. 80−9144
particle creation by time depend. elec. and gravitational fields 80−4623
particle creation in curved space, covarient description 77−13857
particle in an external EM field, coherent states 77−2721
particle model based on stringlike solitons 78−62294
particle production by white holes 80−82891
particle spin dynamics as the Grassman variant 77−41495
particles, currents and fields 78−82117
particles in standing wave fields, motion 79−58910
path integrals and Klein-Gordon eqn. 78−58144
path integrals and relativistic quantum mechanics 79−53995
path integrals and the Klein-Gordon equation 77−67553
path integrals in curved spacetime, zeta function regularisation 77−74302
Penrose graphs 78−49983
Penrose theory in particle physics, perspectives 78−29321
perturbation theory for infinite-component wave eqns. 77−61184
phase angle uncertainty, elimination in relativistic quantum mechanics *(Chinese)* 78−78100
phonon splitting in the magnetised vacuum 80−4897
photon exchange potential in configuration space 79−67527
physical states and observables, relativistic microcausality constraints 80−86589
poincare covariance of the two-dimensional string 77−6048
Poincare covariant particle model with mass and spin mixing 80−32016
Poincare generators corresponding to lightlike irreducible unitary representations 77−18193
Poincare group, mass zero representation extensions 80−57500
Poincare group and extended particle model wave eqn. 78−41414
Poincare group representations, momentum and position variables, complete decomposition theory 80−62511
pole-dipole relativistic string model 80−386
polynomial field theories, exact multiple solns. 78−45773
positronium, relativistic two-fermion equations with instantaneous potential 80−101918
potential interaction using a metric space 80−82879
Prasad-Sommerfield monopole, time depend. 79−273
Prasad-Sommerfield solution, small deformations 79−71633
pre-Schwinger model, Lorentz transforms. if operator solns. 80−47171
projective invariance in general metrical or nonmetrical space-times with torsion, spinor and Yang-Mills fields 78−57832
prolongation structure and the Backlund transformation of the anticommuting massive massive Thirring model 78−32972
prolongation structures and connection forms for Lund-Regge system 78−93805
propagators for a quantized scalar field in a static closed universe 79−35597
propositional systems in local field theories 80−105799
QCD, two-dimens. with massless fermions in 1-1 dimensions 80−62926
relativistic quantum field theory continued
QED, massless, energy-momentum tensor anomalies in spherical space-time 80−73628
quadratic lagrangians in a space with torsion and the theory of the spinor gauge field 80−91006
quadratic symmetry breaking theory, asymptotic behaviour 79−1488
quantification of free relativistic fields on curved space *(French)* 79−30639
quantised Dirac and Klein-Gordon theories 77−26472
quantization of systems with boson and fermion first- and second-class constraints 78−21337
quantum effects in systems with accelerated mirrors 80−22508
quantum microsystem evolution, nonconservation effects 80−22515
quantum stress energy in nearly conformally flat spacetimes 80−57170
quark confinement models and linear trajectories without parity doubling 77−2797
quark observation, speculations 78−24933
quark theory with internal coordinates 77−18224
quasi-light-cone frame and approximate Galilean symmetries 77−13844
quasipotential equation for scalar interactions 77−13871
quaternion formulation in curved space 78−366
quaternion quantum mechanics as the drescription of tachyons and quarks 79−30273
radial equations following from the Salpeter eqn. 79−63333
radiation from moving mirrors and black holes 77−67372
reducible wave equations 79−45003
Regge poles, approx. calc. by formal series 77−6056
regularity constraints and quantised actions 80−73601
relativistic nuclear field theory with π and ρ, cold nuclear matter calcs. 79−93527
relativistic quantum theory with correct conservation laws 80−82677
relativistic radial equations for two spin-1/2 particles consistent with the hole theory 79−93272
relativistic string dynamics, geometrical approach 80−9100
relativistic two fermion equations, Lorentz, parity and charge conjugation invariance 80−90976
relativistic two-particle system and spin-mass relations of meson 79−67505
relativistic wave equation and mass spectrum of gluonium 80−73596
relativistic wavefunctions, approx. near turning point, WKB calcs. for Z>137 80−86598
renormalisation of quantum stress tensor in curved space-time by dimensional regularisation 79−40423
renormalizable interactions in two dimens. and sharp-time fields 78−81882
renormalon singularities, contribution to Borel transform. 80−4848
resonances within nonperturbative methods in field theories 77−2750
Robertson-Walker universe, adiabatic regularisation, arbitrary coupling of scalar field to scalar curvature 80−57461
Robertson-Walker Universe, stress tensor and conformal anomalies for massless fields 77−78903
rotating system, finite temp. QFT 80−73599
S-matrix of the chiral invariant SU(N) Thirring model 79−21911
S-matrix of the massive Thirring model 78−16936
S-matrix perturbation expansion, time ordered functions definitions 77−6039
Sakata-Taketani spin-o theory with external field interaction 77−41748
Salpeter equations, integral transform and relativistic radial eqns. 80−4835
scalar field in curved space-time, particle detection and creation 77−67597
scalar field vacuum fluctuations in curved space-time localised region 80−42116
scalar meson field and many-body forces, book contrib. 80−359
scalar quantum field in an external gravitational field 80−31974
scattering amplitude zeros 79−21983
scattering in external EM field, collective excitation influence *(Russian)* 79−93318
Schwarzschild-Kruskal space-time, role in developing Maxwell field non-zero vacuum expectation value 80−62828
Schwinger model, local and Lorentz-covariant soln. 79−40668
Schwinger model, pseydoparticle configurations, role 78−32982
self dual SU(2) fields in multicentre spaces 80−73600
self-adjoint Dirac type operators 78−49992
self-dual gauge fields and space-times 80−9108
self-dual SU(2) fields in Eguchi-Hanson space 80−57483
self-dual SU(2) gauge fields in Euclidean four-dimensional space, axially symmetric solns. 79−35603
self-dual Yang Mills fields in Minkowski space 80−18078
self-generating discrete-space structure, lattice model in QFT 79−93276
short time propagators in Riemann geometries 79−63129
sine-Gordon and Thirring models, equivalence and cumulative mass effects 77−45969
sine-Gordon eqns., Lax pairs for certain generalisations 80−31997
sine-Gordon equation, intrinsic geometry 80−86553
sine-Gordon equation, separable solns. 78−89614
sine-Gordon equation, supersymmetric, prolongation struct. inverse scatt. formalism 80−99032
sine-Gordon equation in 2+1 dimensions, solns. 79−12932
sine-Gordon field theory lattice model, second order phase transition 78−78095
singular state problems, monopole pair energy levels, charged monopole-electron system *(Chinese)* 80−101733
singularities of Feynman diagrams in the coordinate space 79−58884
Sl(2,R) non-compact group for Dirac eqn. 80−22503
SO(4,2) infinite component fields, model of composite relativistic defects 80−18071
SO(N) groups representation 78−96407
soliton's and the Bethe-Salpeter equation 78−32984
soliton dynamics in non-integrable systems 78−28996
soliton mass in the sine-Gordon problem 79−40678
soliton operators for vortices and superselection rules 79−49386
soliton solutions in three-space dimensions 77−26453
soliton solutions of infinite component wave eqns. 77−26180
solitons, charged, stability, relativistic complex scalar field, direct Lyapunov method 80−62827
solitons, four-dimens. relation to two-dimens. 77−6016
solitons and supertranslations 78−45783
solitons in some geometrical field theories 80−27390
solvable scalar potentials for the non-relativistic and relativistic wave eqns. 78−58110

relativistic quantum field theory continued
space-like fields for quark confinement 80−42426
space-time, foam-like structure, Bjorken scaling violation due to gravitational field 80−77939
space-time geometry and symmetry breaking 78−54533
space-time states, book contrib. 79−58886
space-time symmetries of the lattice Dirac equation 78−4799
spectral function sum rules in relativistic quark model 79−63428
spectrum condition and Lorentz invariance of Yukawa$_2$ field theory 78−21317
spherical diffuse Yukawa sources 77−87931
spin 1 field in flat Clifford Klein space times 80−27391
spin 1 wave eqns., EM interaction in elastic scatt. 77−50104
spin 1/2, gauge invariant antisymmetric tensor spinor field 80−47184
spin 1/2 fields, tensor description 80−86597
spin 2 wave equation, minimally coupled, tenth constraint 79−54264
spin $^1/_2$ 20 component wave eqn., props. 77−45962
spin $^1/_2$ fields, wave egns. 78−21332
spin $^1/_2$ tachyons, nonecistance of conserved probability 77−67554
spin $^3/_2$ wave eqn. 77−71231
spin particles, relativistic and Galilean wave eqns. 80−82672
spin-1 particles, multispinor eqn. 80−4865
spin-1 theories in external electromagnetic fields 79−45043
spin-1/2 particles, discontinuous solns. 79−35969
spin-$^1/_2$ quantised Dirac theory, field representation 80−4845
spinning and charged particles, conformally covariant description in O(2,4) symmetry 80−22524
spinning electron 78−70250
spinning particles interacting with external fields, invariance groups 78−49962
spinning solutions of classical Yang-Mills theory 80−101937
spinor covariant derivative, geometric significance 77−26450
spinor electrodynamics, quasiclassical approx. *(Russian)* 78−49996
spinor equation admitting an infinite group 79−71645
spinor field, indefinite charge 77−71221
spinor fields, conformal, dimensions, scale invariance 80−27394
spinor formalism, geometric and algebraic foundation 78−37128
spinor models, integrability in two-dimens. space-time 80−77935
spinor operators of Weiss-Zumino type and their irreducible components 79−71602
spontaneous emission, line widths and energy shifts *(Chinese)* 79−89874
spontaneous symmetry violations 80−52411
stochastic model in wave mechnics *(French)* 78−86404
stress-tensor conformal anomaly for scalar, spinor, and vector fields 78−29023
string dynamics, lorentz invarient theory *(Russian)* 79−22039
string model, field theory in 2+E dimens. 77−57503
string theory in external field 79−97574
strings and vortices with soliton solns, unified approach 77−5674
strings in the embedding space 78−89654
strong Backlund transofrmations in four or more dimensions 79−30316
strong coupling in theory with nonlocal nonpolynomial interaction 78−21319
strong interaction field theory, role of tachyons and virtual fields, book contrib. 79−58889
strong interaction theory based on a fiber EM bundle geometry 77−79204
structured systems, the bilocal case 78−89619
SU(2|1) electroweak interactions, implications for 6 extra time dimensions 80−77998
SU(2), Yang-Mills field eqn. configurations in curved spacetimes 80−18076
SU(2) dual charges, 4-D space of constant curvature *(Chinese)* 80−68392
SU(2) gauge field configuration in curved spacetimes 80−18077
SU(3) theory of fermion-monopole systems 77−13888
superspace and local supersymmetry geometry 78−77782
supersymmetric Dirac particles in external fields 80−82918
supersymmetric relativistic oscillator, a model 77−38086
supersymmetries and the pseudoclassical electron 77−13845
supersymmetry as means to unified field theory 80−91040
supersymmetry transformations and fermion solns. in presence of instantons 78−74177
symmetrical formulation of electron-photon scattering 77−67599
symmetry breakdown and bundle representations of relativity groups 80−86610
symmetry generators, structure 79−71587
symmetry group of spin and particle number 77−64871
symmetry groups of scalar fields with self-interaction 79−30664
symplectic formulation of relativistic particle dynamics 77−57237
symplectic relations and generalized hamiltonian dynamics 79−25878
tachyons, monopoles and related topics 79−44718
tachyons, quantum field theoretical viewpoint, book contrib. 79−58887
tachyons, spinless, propagator determ. 77−74263
tachyons and quantum field theory 80−18069
Teitler's higher-spin field eqns. 77−22637
theory in de Sitter space *(German)* 77−82666
Thirring and Schwinger models, asymptotic field operator solns. 77−49847
Thirring and Schwinger models, asymptotic fields, operator solns. 77−57449
Thirring model, chiral, CP^{n-1} and SU_n, exact S-matrix 80−90985
Thirring model, massive, mass independent renormalisation, dimensional regularisation 80−57463
Thirring model, phase transitions 80−18067
Thirring model, reality symmetry 77−2731
Thirring model, renormalization and sine-Gordonization 78−37135
Thirring model, supersymmetric form 79−40682
Thirring model, two-dimens., complete integrability 78−49685
Thirring model, two-dimens., stability *(Russian)* 78−45800
Thirring model, variational anal., Thirring model 78−41426
Thirring model coupled to a Schwinger field, confined solns. 77−67572
Thirring model coupled to gravity, classical solns. in generally covariant model with fermions 80−9091
Thirring model massive phase, dynamic mass generation 80−4851
Thirring model of massless scalar field, conformal transformations 80−52428
Thirring model with SU(N) symmetry, scale invariance 79−9288
Thirring type model in 2+E dimens., fixed points and anomalous dimens. 77−54052
topology of vortices 79−40653
transformation laws in nonzero mass field theory 78−37123
twisted scalar and spinor strings in Minkowski spacetime 80−57480
two body eqn. for Dirac and Klein-Gordon Coulombic bound state 79−93275
two electron system, level shifts, transition probebilities, perturbation theory 79−22001
two-body bound state 78−82151
two-body interacting Lagrangians invariant under world line independ. reparametrization, nonexistence 79−97491
two-body relativistic systems 78−69977
two-body relativistic wave eqns. 79−63358
two-body wave equation and meson spectrum 77−30328
two-compoentn first-order equations for the quantum-relativistic electron 79−17649
two-dimensional relativistic model, spectrum 79−21955
two-fermion equations with form factors and anomalous-magnetic-moment interactions 78−372
two-particle system, relativistic mechanics 78−66055
two-photon synchrotron radiation *(Russian)* 77−2719
two-space-dimensional classical Q solitons 79−45015
U(N) symmetric thirring model, anomalous dimens., Schwinger team 77−87900
U(N)-symmetric Thirring model in indefinite metric space, boson representation 79−12942
unconventional field theories 79−21893
unified field theories, relativistic, computer field interaction simulation system 80−68412
unitarity restrictions on semi-classical approximations to certain functional integrals 80−32026
unitary quantum mechanics, nonlinear and relativistic invariant fields 80−4567
unitary relativistic wave equation exhibiting extended particle structure 80−9102
unitary transformations and reductions of relativistic Hamiltonians 77−30262
uniticity conditions for the delta/sup 1/(x,y) propagator of a scalar field in the de Sitter universe *(French)* 77−5704
universal singular fun functions in local field theory 78−32969
vacuum definition in curved space-time 80−73613
vacuum energy in a closed universe *(English)* 77−22479
vacuum polarization in a nonsimply connected spacetime 80−57531
vacuum solutions for twisted scalar field 78−93804
vacuum spacetimes, stationary and axially symmetric, homogeneous Hilbert problem, Kinnersley-Chitre transformations 80−68349
vector boson elastic and Compton scatt 77−2776
vector field, general type, group of internal symm. of quantum theory 80−47198
virial theorem and localized solns. stability 78−21342
wave eqns., second-order, causal propagation 80−90986
wave equation, reducibility criterion 77−57439
wave equation in curved space-time, compact and noncompact sources 80−73571
wave equation of bi-local field and its mechanical model 78−29241
wave equations for extended hadrons 77−18189
wave equations from space-time 77−30234
wave equations in conformal space 78−21364
wave equations without the Velo-Zwanziger pathology 78−24927
wave functions and diffraction 77−10207
wave mechanics, quantum pot., origin *(French)* 78−86405
wave mechanics of electrons in Kerr geometry 78−12622
wave packets in three dimensions 77−61186
waves and shocks on non-linear strings 78−89618
Wightman functions for interacting spinor fields on a lightlike plane 79−93284
Yang-Mills configuration constraint 80−82903
Yang-Mills equations, absence of classical lumps 78−21318
Yang-Mills theory, spinor analysis 78−8532
zero energy fermions in U(1) pointwise monopole field *(Chinese)* 80−42345
zero mass limit of massive U(N) Thirring model 77−57466
e^+e^- pair creation in strong EM fields, gravitational effects 80−42376
pp elastic scattering, 14 to 2000 GeV/c, improved impact picture 79−89178
π form factor, expt. behaviour, influence of left-hand cut on second Riemann sheet 80−13304
$q\bar{q}$ binary confined systems, elastic scatt. amplitudes 79−97576
$q\bar{q}$ spectra, heavy systems, equaltime relativistic wave eqn. with confining potential 80−77977
^{40}Ca, finite nuclear props. in relativistic quantum field theory, mass and p densities 80−9219
H atom, Dirac and Klein-Gordon relativistic eqns., energy level splitting 80−77938
^{208}Pb, finite nuclear props. in relativistic quantum field theory, mass and p densities 80−9219

relativistic scattering theory
see also elementary particle scattering; quantum field theory of elastic scattering
(0+1/2)→(0+1/2) spin reactions, differential cross-section zero 77−82693
3π dynamics, two-body unitarity and analyticity 77−18205
a covariant approach for the one-soliton sector 79−17640
absorptive scattering amplitude positivity constraints 77−71464
AKNS-ZS inverse method, canonical struct. and generalised Marchenko eqn. calcs. 80−47192
analytic extrapolations towards interior points from a cut, applic. to elementary particle scatt. theory 80−12952
asymptotic behaviour of quasipot. scatt. amplitude in plane of a complex orbital momentum *(Russian)* 79−75701
asymptotic evaluation of high energy cross sections, functional integration method 78−54551
asymptotic props. of scatt. amplitudes, where effective number of partial waves is $L=CS^{1/2}(\ln S)^M$ 77−57470
atomic electron l-shell Coulomb ionization by heavy charged particles 79−94073
average multiplicity, transverse momentum and total cross section, new upper bound 79−35970
backward scattering, Chen-Hoock formula, modulating operator formalism 79−35971
baryon resonances and electromagnetic couplings 79−9384

relativistic scattering theory continued
Bethe-Salpeter, eqn. exact three dimens. reduction, off mass shell amplitudes 78−70247
bi-local field in external source, scatt. amplitude 78−74182
book, scatt. theory in quantum mechanics 78−49573
Breit equation, Klein paradox 80−57506
bulk viscosity of relativistic matter, hydrodynamic energy-stress tensor 79−17642
canonical formulation for Lagrangian of two interacting relativistic particles 79−21973
canonical theory of relativistic interactions, N+1 interacting particles 78−33003
centre of mass covanant separation for relativistic interacting particles *(Russian)* 80−62891
charge particle-magnetic monopole scattering, zeroth order eikonal approx. 79−12990
classical and prequantised mechanics without Lagrangians or Hamiltonians for relativistic particles 78−74126
collision processes, information theoretic maximal entropy theory, rel. to scatt. theory 78−81888
complex momenta eikonal approx., hadron-nucleus collisions at asymptotically high energies *(Russian)* 78−74294
composite particles, form factors in terms of inelastic Jost functions 77−2831
Compton scattering, high intensity appl. of relativistic invariace as gauge invariance 78−41201
Compton scattering of laser photons on relativistic electrons, energy spectrum *(Japanese)* 77−13908
convergent polynomial expansion, lines of zeros, slopes of diffr. scatt. 78−45892
coordinate asymptotic behavior of (3→3) wave functions for a system of three charged particles 79−21980
covariant two-body dynamics and the Weinberg equation 79−21978
Crichton ambiguities with infinitely many particle waves 78−70311
cross-section transformation, between two moving frames 78−89369
crossing relations derivation using substitution rule 79−67483
crossing symmetric amplitude with Regge poles 78−54621
crossing symmetry of many-particle amplitudes 79−40694
deuteron electromagnetic form factors, D-wave admixture in the dispersion approach *(Russian)* 79−30737
differential scatt. cross section, influence of amplitude singularities 78−49984
Dirac particles, phase eqns. soln., method of formal series 77−45993
direct interaction scatt. theory, cluster decomposition 78−33002
direct interactions, relativistic addition in point form of dynamics 79−58907
directly interacting relativistic particles, positive energy dynamics and scatt. theory 80−82921
discontinuous solns. to relativistic eqns. for two spin 1/2 particles 79−35969
discrete two-variable expansions of scattering amplitudes for particles with spin 80−68397
divergent perturbation and partial wave expansions in scatt. theory, summation methods 79−67485
dynamical impact parameter in quantum theory 79−21982
dyon-dyon interaction in predictive relativistic mechanics 79−26265
eigenphase sum behaviour near a resonance 79−54285
eikonal and sudden approx., Moller operators and superoperators 80−86624
eikonal approx., backward and transverse effects 77−10205
eikonal approx., interaction representation *(Russian)* 78−33005
eikonal approximation, analytic props. 80−32038
eikonal approximation, Drell Hiida Deck mechanism for particle dissociation on a composite target 79−93465
eikonal approximation, some inequalities 79−44800
eikonal expansion, scalar meson exchange 78−29278
eikonal formula in QED, spin corrections using functional methods 77−13900
eikonal function for two classical relativistic particles 78−81828
eikonal multiple scattering expansion, rel. to Born series 79−30681
eikonal Regge model, opacity and diffr.-dissociation cross section of grey disks 78−4845
eikonal two-body amplitude, spin corrections 77−18204
eikonal type approximations for potential scattering 78−89635
elastic absorptive amplitudes, unitarity bounds involving total cross section, forward slope and curvature 79−75750
elastic heavy ion scatt., partial-wave expansion of amplitude 77−6423
elastic scatt., impact parameter representation *(Russian)* 80−5019
elastic scatt. with arbitrary spins, positivity props. 77−13896
elastic scattering amplitude, singularities in cos θ plane 80−37186
elastic unitarity constraints on scatt. amplitude phase 77−37787
electron+monopole, scatt. through small angles, Dirac-Schwinger monopole 80−68398
electron beam, submillimetric pulse production by stimulated magnetoresonant Raman scatt. 77−38846
electron theory 77−2779
electron-photon collision, relativistic variance of cross section *(French)* 78−45924
electronuclear sum rules, generalised, from EM structure functions 78−89806
EM wave scatt. by relativistic uniformly accel. interface 80−4891
extended unitarity in hadronic multichannel scatt. with attractive Coulomb interactions *(German)* 77−82692
factorization properties and spurious solutions in N-body scattering theories 79−12987
Faddeev approach to neutron scatt. from protons in heavy hydrocarbons in eV range 78−54728
Faddeev eqn. soln. in adiabatic approx. with separable pots. *(Russian)* 80−52437
Faddeev eqn. soln. using vel. depend. Paris pot., trinucleon bound state 78−89803
Faddeev eqns., pole approx. *(Russian)* 78−49986
Faddeev equation, product integration, choice of point, convergence 80−68396
Faddeev equations, generalised, for many-cluster problems 77−88058
Faddeev equations, two-potential formula, three-body scattering 80−4893
Fadeev's eqns., close coupling method for three-particle scatt. *(Russian)* 77−61222
fast particle scattering on exponential type singular potential 78−37157
fermion scatt. in arbitrary central force field *(Russian)* 77−22668
fermion-fermion scatt. in the eikonal limit, spin depend. 79−71662

relativistic scattering theory continued
Feynman integral evaluation in physical region using multivalue approximants 79−26262
Feynman integrals with zero mass particles, asymptotic behaviour 77−57444
field theory model of NNπ system, three-body problem, disconnectedness problem 78−29276
finite-energy bounds on the total cross section of strongly inelastic interaction between spinless particles 79−40695
forward differential cross section, t-channel singularities 77−67595
four-body final states, relativistic anal., unitarity and analyticity constraints 77−87920
four-body problem, appl. of hyperspherical functions 79−21981
four-body scatt., transition amplitudes determ. 78−24983
four-hadron isobar model 79−26263
Fresnel corrections to relativistic scatt. of particles with spin 0 and 1/2 *(Russian)* 77−13894
Friedrichs model unitary regularisation for many particle system 80−32039
froissarton coupling constant, s-channel unitarity *(Russian)* 78−45799
gas of interacting particles, phase vol. approx. 78−41225
gauge invariance, Lorentz covariance and EM props. of elementary systems 80−32037
Gegenbauer functions, expansion formulas and addition theorems 77−5634
generalised Pade approximation, explicit solns. 80−73623
Glauber high-energy approx. extension to composite particles 78−82328
Glauber model and time reversal invariance 80−91020
Glauber multiple scatt. theory, nuclear multiparticle reactions, eikonal model 79−505
Glauber theory, relativistic correction, high-energy behaviour of scatt. amplitude *(Chinese)* 78−86427
gravitational scattering, post-linear approx. 80−27190
group theoretical approach to relativistic eikonal phys. 77−82694
hadron+nucleus interaction, Glauber theory and unitarity 77−22979
hadron-Coulomb interference problem at SPS and ISR energies, operator formulation 77−54107
hadron-nucleus scatt., corrections to Glauber amplitude *(Russian)* 78−41683
hadronic diffraction mechanism, geometrical space-time formulation 78−443
hadronic potentials, field theoretical interpretation, Poincare invariance, causal solns. 79−26266
half off-shell phase eqns. for non-local interactions 78−70019
half-phase shell shift in terms of on-shell phase function 78−29279
Hamiltonian dynamics, for closed system of N particles in mutual interaction 78−62070
Hamiltonian formulation of N-body theories, effective interactions and many-body corrections 79−75938
Hamiltonian theory, physical equivalence, front and instant form interaction addition 79−97540
harmonic oscillators, relativistic two-body interaction, exactly soluble system 78−16955
heavy ion reactions, multiple collision model anal., at high and relativistic energies 78−86542
heavy-ion relativistic scatt., meson and light nucl. prod. 77−71622
helicity amplitude two particle unitarity for arbitrary spin 77−54058
high energy nucleon-nucleus scatt., spin effects, Glauber theory multiple scatt. amplitudes *(Chinese)* 79−21979
high-energy scattering amplitude, quantum field theory representation 78−24980
impact parameter amplitudes and geometrical s-channel models 77−2778
impact parameter analysis of exclusive $\bar{p}d$ and $\bar{p}p$ reactions 77−46073
impact parameter expansion of scalar and Dirac fields 77−26471
impact-parameter group, realisation on cone functions *(Russian)* 78−45817
inclusive multi-Pomeron corrections in the Regge-eikonal model, appl. to πp, Kp interactions 79−63557
inelastic, high energy, non-eikonal effects 80−42608
inelastic diffraction, compatibility of D peripherality with nondiffractive two component struct. 79−13092
inelastic eikonal phenomenology in stationary-phase approx. 78−45816
infinite momentum limit of relativistic elementary systems 80−32036
internal Lorentz basis for two-particle states 80−31499
inverse problem for general first order differential eqn. systems 78−74181
inverse problem for pot. scatt. at fixed energy, Newton Sabatier numerical method appl. 77−67593
inverse problem in abstract relativistic scatt. theory 80−4894
inverse problems in quantum scatt. theory 78−54587
inverse scattering problem in the eikonal approximation *(Russian)* 80−57522
isobar model, unitarity constraints 77−34108
isospin decomposition of three pion scatt. amplitude, partial-wave anal. 77−6061
Jin-Martin lower bound rederived 77−57473
Jost functions, S-matrix of massive Thirring model, relativistic field theoretic model 78−54552
Klein-Gordon and Dirac particles, relativistic phase shifts 79−40697
Klein-Gordon equation, time-independent, relativistic Stark effect, resonances 80−62890
ladder equations for imaginary part of scatt. amplitude, diagonalization 78−37156
large angle scattering amplitude corrections 80−37187
Lie group framework for soliton eqns., Lund-Regge model generalisations 79−17605
light-cone field-theory and the parton model, book contrib. 78−82220
Lippmann-Schwinger equation, uniqueness of solns. 79−17643
long range potentials, EM polarisabilities, interacting systems, neutral, spinless, with mag. moment 77−6058
many-body problem, on-shell integral eqns. for scatt. amplitude 77−67594
many-channel scattering, variable phase approach 79−40693
many-threshold amplitudes, conformal mapping, algebraic parameterisation and two-variable expansion 77−54059
massive spin-zero particles, consistent formulation of relativistic dynamics in external fields 79−21977
Maxwellian electrons, moment generated radiative transfer functions 78−24747
mean multiplicity of secondary particles in hadron-nuclear interactions, multiple scatt. theory *(Russian)* 80−68502

relativistic scattering theory continued
meson+proton→3 mesons+proton, partial wave anal., Ascoli anal., fireball dimens. 78−17054
meson-meson inelastic collisions, Glauber multiple-quark scatt. model, quark-quark scatt. amplitudes 78−21459
meson-meson Regge theory with crossing symmetry and unitarity, strong coupling 77−65177
meson-meson Regge theory with crossing symmetry and unitarity, weak coupling 77−67676
meson-meson scatt., Regge theory, crossing-symmetric representation of dynamical eqns. 78−4841
microwave backscatter from intense relativistic electron beam 77−38794
microwave coherent scatt. from relativistic electron beams 77−42477
minimal K-matrix model, three pion enhancements 77−6060
minimal relativistic dynamics of the 3π and $\pi\pi$N systems 79−75702
model particles, Weyl Lie algebra 79−40690
modified K-matrix formalism for meson-meson scatt. amplitudes crossing symm., unitarity 77−82774
multi-instanton solutions of the duality equation and the inverse-scattering problem *(Russian)* 79−21591
multi-particle and inclusive reaction at high energies, review 79−17777
multichannel Lippmann-Schwinger type eqns. for three particles *(Russian)* 77−79234
multichannel T-matrix, separable form 77−57471
multiparticle dynamics, cluster models, Faddeev-Yakubovskii coupling 80−105816
multiparticle prod., unitarity bounds on angular distrib. 77−38105
multiparticle scattering operators, cluster decomp. 80−22592
multiple interaction mechanism, relativistic particle prod. on nuclei at large angles *(Russian)* 77−74822
multiple scatt. from non-overlapping pots. using differential operators technique 78−82128
multiple scatt. series, eikonal approx. 78−21358
multiple scatt. theory, coherent and incoherent particle prod. in nuclei *(Russian)* 77−216
multiple scattering in the distorted-wave impulse approximation 79−45041
multiple-scattering theory of Nigam, Sundaresan and Wu, test on basis of relativistic-electron expts. 77−41793
Muskhelishvili-Omnes equation and final state interactions 79−67196
N-body scatt., filter operators in linked-cluster formalism 79−45040
n-particle relativistic phase space integral, invariant variables, Monte Carlo calc. algorithm 79−9312
N-particle system, many body correl. and scatt. amplitudes 79−30683
neutrino+antineutrino system, relativistic kinetic theory, Wigner functions 77−26239
nonlinear field equations 80−4882
nonunitary multichannel S-matrix on basis of completeness condition for wave functions *(Russian)* 77−61207
nucleus-nucleus and nucleon-nucleus collision model, Glauber's theory, classical transport eqn. 79−6522
null plane, relativistic dynamics 78−54584
off-energy-shell T matrix, frame depend., relativistic pot. theory 78−25159
Pade approximant of T-matrix elements, convergence in few-nucleon systems 79−21975
partial wave amplitudes asymptotic behaviour, Regge models and dispersion relations 77−10204
partial wave analysis, energy-dependent, for particles with spin 79−93319
partial wave analysis for supersymm. scatt. amplitudes 77−49872
partial wave construction, analytic crossing symmetric 77−87919
partial wave expansions for arbitrary spin, non-central forces 78−21535
partial wave expansions of relativistic many particle amplitudes 78−70312
partial-wave $\pi\pi$ amplitudes, Roy eqns., proof of soln. existence 78−70310
partial-wave amplitudes, crossing sum rules 78−21355
phase shift ambiguities, elastic spin-0−spin 1/2 scatt., partial waves 77−22669
phase shift anal. above inelastic threshold 79−45038
phase shift behaviour in Bakamjian-Thomas theory, relation nuclear force at high energy *(Chinese)* 79−80878
phase shift in Dirac scatt. 77−67596
phase space integral, n-particle, relativistic, Monte Carlo integration program 78−33001
phase-modulus correlations for forward scatt. amplitude without Froissart bound 78−401
plasma medium, relativistic electron beam, Vlasov eqn. 80−14910
Poincare group contraction and high energy effects 77−65119
Poincare group P(1,3), translation operator matrix elements for relativistic particles *(Russian)* 79−40696
position variables in classical Hamiltonian mechanics 80−27123
potential scatt. in 3-D, backscatt. and Fresnel diffraction 77−13895
potential scattering, matrix Pade approximants, variational bounds 77−65120
pseudoclassical Lagrangian for 2 interacting spinning particles 78−86426
QCD, gauge independence of IR cancellation, fermion-fermion scatt. 78−50006
QED, high-energy scatt., new formalism 78−66063
quantum Dirac field, scatt. automorphisms, external field perturbations 78−58112
quantum scattering in external EM field, collective excitation influence *(Russian)* 79−93318
quantum theory of composite systems, nonlocal field theory of quark model 78−70253
quark confinement, Dirac equation with relativistic linear potential, baryon properties, SU_6 representations 80−47261
quasieikonal series, exact summation, matrix method *(Russian)* 79−9313
quasipotential eqns., Levinson theorem violation, S-matrix 78−54576
quasipotential scattering amplitude, analytic props. in complex planes of rapidity and angular momentum 80−68399
radial integrals with finite energy loss for Dirac-Coulomb functions 77−23000
recoil effect, light particle scatt. by two heavy particles *(Russian)* 78−82129
recoil effects in microscopic description of inelastic scatt. 77−71465
reduced mass for relativistic quantum-mechanical problems 78−4809
Regge multiparticle poles, t-channel particle repulsion *(Russian)* 78−45814
relativistic scattering theory continued
relativistic amplitudes as wave functions, invariant diagram technique *(Russian)* 79−2957
relativistic barriers for two spin-1/2 particles, from Breit eqn. 78−62339
relativistic elastic scatt., crossed channel struct. effects *(German)* 79−58906
relativistic electron Coulomb scatt., approx. to cos γ 78−28962
relativistic particle EM interaction using universal laboratory time 79−71672
renormalised off energy shell Coulomb scatt. 77−57474
representation by Penrose graphs 78−49983
rotating dielectric column, EM scatt., relativistic soln. 78−50681
Roy eqns., regularisation with smooth cut off 78−29271
s-channel helicity conservation at γV,$\gamma\gamma$ and NN vertices, vanishing of spin-zero covariant coupling 79−40691
S-matrix theory, graduate level textbook 78−54575
s-wave pion-nucleon phase shifts in Pade approximation using ε, ρ, f, N, Δ 79−67603
scalar particle in gravitational field, high energy dispersion *(Russian)* 77−45994
scaling property of shrinking diffraction peaks, elastic unpolarised differential cross section 77−18206
scattering amplitude, punctual Pade approx. as regularisation procedure for partial wave expansions 79−17639
scattering amplitude at high energies, corrections to geom. optics in quasi-classical limit *(Russian)* 77−2760
scattering amplitude determ. from differential cross section, contraction mapping 77−10206
scattering amplitude determ. from differential cross-section, compactness theorems 77−10235
scattering amplitude zeros 79−21983
scattering amplitudes with positive imaginary parts, theory 77−71466
self-consistent field theory of electrodynamics, many-body scatt. 78−49683
semi-inclusive single particle cross-sections, upper bounds determ. 78−41442
separable nucleon-nucleon potentials and minimal relativity 80−27495
single scattering optical model, three body approach, appl. to nucleon+nucleus scatt. 78−25162
singularities in four-body final-state amplitudes 79−26264
slope parameter B(s), axiomatic lower bound determ. 78−54585
soft hadron-nucleus reactions at high energies, theoretical model 79−17870
space-time formalism for spin-zero particles 79−21974
space-time orbits for interacting relativistic particles, syntactic versus semantic observables 79−21976
spin 1/2 particles, relativistic scatt., continuous cut-off method 80−4892
spin rotation, relativistic, in elementary particle reactions *(Russian)* 78−54586
square well potential, separable representation 80−82922
stimulated collective EM scatt. from magnetised relativistic electron beam 77−38791
stimulated EM shock radiation for far IR and submillimetric wave generation 77−38997
stimulated EM shock radiation with frequency up-conversion 77−38996
Stueckelberg phases, 3-parameter exponential model 78−41440
submillimetric magnetoresonant scatt. from relativistic electron beams 77−38792
t-channel exchange model with s-channel absorptive effects, high energy polarisation data interpretation 77−30435
three body unitary formalism 78−41443
three hadron systems, resonance peaks, Brayshaw mechanism validity 80−73732
three partical expt. data, kinematically independ. representation for particle wave anal. *(Russian)* 78−89636
three particle bound states and contribution of three particle unitarity, dispersion method *(Russian)* 78−8336
three particle systems, diffractive prod. and relativistic rescatt. 79−12988
three particle systems with Coulomb interaction, modified Faddeev eqns. 79−54284
three-body Faddeev eqns., analytical soln. 77−38104
three-body problem, decoupled integral eqns. 78−24982
three-body problem, partial wave amplitude singularities for multiple scatt. series diagrams 79−71664
three-body scatt. in coordinate space, perturbative approach to Faddeev eqns. 79−30682
three-body scattering equations, nonsingular representation, partial-wave anal. 80−91021
three-nucleon bound state, perturbation approach to Faddeev eqn. 78−54691
three-nucleon bound state, soln., perturbational approach to Faddeev eqn. 79−30793
three-particle bound states, wave function calcs. 78−8558
three-particle system (two charged particles), scatt. theory *(Russian)* 79−12991
Todorov equation, Coulomb interaction between two spinless particles, infinite-multiplet spectrum 79−45039
total cross sections, asymptotic upper bound 80−105938
total cross sections, upper bound 78−12839
total scatt. amplitude eqn. in variable phase approach 79−26267
translationally invariant relativistic centre of mass observables, orbital ang. momentum, spin 77−6062
triton D-state asymptotic normalisation const., Faddeev eqn. with Reid soft core pot. 79−59017
two body correlations through tachyon exchange 80−42367
two body interactions, three particle final states, kinematics in relative coordinate system 79−67484
two body reactions, spin system constraints, quark additivity, geometrical hypothesis 78−29309
two fermion interaction, three dimens. relativistic formalism, quasipot. approach *(Russian)* 78−58143
two interacting relativistic particles, singular Lagrangian 79−17641
two particle scatt. amplitude from a relativistic Hamiltonian theory, light like case 78−78112
two particle system, interaction through action-at-a-distance force, relativistic mechs. 78−66055
two point particles, relativistic interaction, singular Lagrangian approach 80−73622
two spinless particles, scatt. amplitude and cross-section, relativistic correction *(Russian)* 78−36889

relativistic scattering theory continued
two- and three-body scatt. operators using light front dynamics 80−13238
two- and three-particle scatt. for relativistic systems in light front dynamics *(Russian)* 80−62892
two-body problem, 3-D formulation in terms of rapidities 78−49985
two-body problem, covariant canonical formulation 77−57472
two-body problem due to Kodyshevsky, Bateman method soln. *(Russian)* 77−30286
two-body t matrix, separable expansions to local potentials in a quasi-potential approach 79−63641
two-fermion relativistic eqns with form factors, anomaloys mag. moment interactions 78−372
two-particle resonance+particle interactions, scatt. amplitude, arbitrary spins *(Russian)* 77−74621
ultrarelativistic charge in absorbing plate, radiation taking into account multiple scattering *(Russian)* 77−41792
unitarity, large-angle elastic scatt., pp ang. distrib. *(Russian)* 77−61221
unitarity and analyticity bounds on multiplicity and transverse momentum 78−45815
unitary analytic isobar model, N-meson to N-meson-meson process 78−78114
unitary bounds on elastic absorptive amplitudes involving total cross section, forward slope, curvature 77−49881
unstable particle+nucleon, total cross section, from diffractive prod. on nuclei, multiple scatt. approach 78−41441
variable phase method for quasipotential equation in terms of rapidities 79−71663
Weinberg equation ladder approx., relativistic repulsive effects in nonrelativistic systems 79−35972
$^1D_2$ diproton, resonance criteria 77−18312
dd, elastic scatt. $\sqrt{s}$=53 GeV, narrow min, and inelastic shadow effects, Glauber theory 78−89740
dd collisions, 4.3, 6.3, 8.9 GeV/c, d spectra high momentum struct., multiple NN scatt. model 78−89727
dd elastic scatt., 53, 63 GeV, inelastic intermediate state effects, Glauber multiple scatt. theory 79−36104
Δ(1232), mass calc. by inverse scatt. procedure 78−403
ed elastic scatt. at high momentum transfer 80−82977
$e\bar{\nu}_e\bar{\nu}_e$, reactive mixture, bulk viscosity 78−45565
$e\bar{e}\nu_e\bar{\nu}_e$ mixture, covariant transport eqns., collision terms from Weinberg Salam theory 77−74315
eN high-energy scattering, eikonal approx. corrections, bremsstrahlung 77−215
γd→pn, 400 to 650 MeV, ang. depend. of proton polarisation and partial wave anal. of possible dibaryon resonances 79−58967
γd→π^0d, meson-exchange currents in photomesic reactions, relativistic many-body theory 80−422
^{2}H(n,n), 2.48 and 3.28 MeV, elastic differential cross section and related phase shift analyses 79−75992
K^-d, low-energy interaction, generalised final state interaction model 77−65175
$K^-d\to\Lambda p\pi^-$, Λp invariant mass distrib., ΣN bound state 77−30428
$K^-d\to\pi^-$ Λp, three body Faddeev formalism, unstable dibaryon bound state search 80−32130
$K^-d\to\pi^-$ Λp breakup process, appl. of Faddeev eqns. 79−75797
$K^-{}^4He\to\pi^-\Delta^3He$, final state interaction model, Muskhelishvili Omnes eqn. soln., πmomentum distrib. 77−30285
$\bar{K}N\to\bar{K}^*N$ energy depend. partial wave anal. 1830 to 2170 MeV 79−3046
$\bar{K}N\to\bar{K}^*N$ energy depend. partial wave anal. 1830 to 2170 MeV 79−22138
$\bar{K}N$ reaction below 1.9 GeV, dispersion theoretic discrepancy anal., SU(3), hadron coupling 78−21457
$\bar{K}N$ two-body reactions, 1480 to 2170 MeV, partial wave anals. 77−34177
K^-p, backward elastic scattering, backward differential cross section 80−63024
$K^-p\to(\bar{K}\pi\pi)^-p$, 4.2 GeV/c, partial wave anal. in Q region 80−13330
$K^-p\to K^-(\pi^+\pi^-p)$, 4.2 GeV/c, partial wave anal. of low mass $\pi^+\pi^-$p system 77−61318
$K^-p\to K^-p\pi^+\pi^-$, partial wave anal. of low-mass $p\pi^+\pi^-$ system 78−25070
$K^-p\to K^-\pi^-\pi^+p$, 10, 14.3 and 16 GeV/c, partial wave anal. of $p\pi^+\pi^-$ system 78−82251
$K^-p\to K^-\pi^+\pi^-p$, 10, 14.3, 16 GeV/c, partial wave anal. of $(K\pi\pi)^-$ system in the L-region 79−17764
$K^-p\to K^0\pi^-p$, 4.2 GeV/c, multichannel anal. 80−73736
$k^-p\to\Lambda\pi^+\pi^-$, partial wave anal. in Λ(1520) region, Λ partial decay widths *(Russian)* 80−32131
$K^-p\to\omega\Lambda$, 1.934-2.516 GeV/c expt. data, threshold to 2.436 GeV partial wave anal. 77−82767
$K^-p\to\pi^0\Lambda(1520)$, 1710 to 2170 MeV CM energy, partial wave anal. 78−33085
K^-p reactions, 1.934-2.516 GeV/c, partial wave anal., SU_3 classification of Y* states 78−25077
$K^-p\to\Sigma^-\pi^+$, backward differential cross section 80−63024
$K^\pm p\to K^\pm\pi^-n$ or $K^\pm\pi^-\Delta^{++}$, 13 GeV/c, elastic Kπ partial wave anal. 78−41593
Λ nucleus→Σ^0 nucleus, cross section, Glauber approx. *(Russian)* 78−46114
N scattering from two fixed potentials, exact multiple scatt. calc., Fresnel approx. comparison 78−66054
nd, local soft core NN pots., quasiparticle formalism 79−6529
nd backward elastic scatt., 200 to 800 MeV, ang. distribs. and relativistic momentum transfer variable 79−75783
nd elastic scattering, perturbation calcs., Faddeev eqns., Reid soft core pot. 78−33177
NN, total cross sections, medium energy dynamics, OPE three-body theory 78−25064
NN interaction, field theoretical approach with stress on OBE pot. *(German)* 78−78203
$NN\to l^+l^-X$, A depend. of lepton pair prod. on atomic nuclei *(Russian)* 79−49562
NN one boson exchange pots. with asymptotic power law energy depend. 78−82293
NN phase shifts, calc. using Blankenbecler-Sugar eqn. 79−67580
NN phase shifts and resonances, coupled channel effects 79−67574
NN scatt., 325 MeV, unique isospin-zero phase shift solution 78−50044
NN scatt., high-energy, effect of anomalous mag. moments in quantum field theory 78−465
relativistic scattering theory continued
NN scatt., impact parameter representation, taking into account spin, isospin and Pauli principle 78−58198
NN scatt., small angle, appl. of eikonal vector meson exchange theory 78−17052
NN scattering, role of non-iterative diagrams 79−67576
NN scattering in nonAbelian gauge theory, π-, ρ-, and ω-exchange, scalar Pade approx. 79−67573
np $^3S_1$-$^3D_1$, $^3D_2$ phase parameters and deuteron quadrupole moment, pot. reconciliation 79−67575
np elastic scatt., 50 GeV, amplitude parameter determ. with Glauber model 79−75798
np observables, ^{3}P-waves effects, phase shift anal. of pp expts. 78−33077
$N\pi\to N\pi$ and $N\pi\pi$, resonance region $s^{1/2}$=1380-1740 MeV, partial wave anal. 77−61315
Nπ scatt., high-energy, effect of anomalous mag. moments in quantum field theory 78−465
$N\pi\pi$ dynamics, medium energy, dispersion relations, isobar expansion for πN 80−4917
$N\pi\pi$ medium energy dynamics from πN, isobar model rescatt. corrections 80−4918
p-nucleus, high energy reaction temp., kinematic props. of nuclear fragments 78−54761
p-nucleus high energy collisions, impaet parameter anal. of multiplicity distrib. 77−79369
$pd\to d\pi^+n$, 585 MeV, Glauber theory, NN and NΔ amplitudes 78−62525
pd elastic scatt., 53, 63 GeV, inelastic intermediate state effects, Glauber multiple scatt. theory 79−36104
pd scatt., relativistic corrections to two-body pot. 78−74301
pd spin dependent total cross sections, rescattering corrections, Glauber theory 79−49536
pp elastic cross section from dressed quark model, Glauber multiple scatt. expansion 79−2977
pp helicity amplitudes at t=0, dispersion theoretic anal. 78−62340
$\bar{p}p$ high energy annihilation in nuclei, multiple scattering models 80−102079
pp high energy elastic scattering and constituent multiple scatt. model 79−67607
pp→pX, deep inelastic scatt. in nuclei, bare particles, multiple scatt. theory *(Russian)* 80−52549
$\bar{p}p\to\rho^0\rho^0,\omega\rho^0,\rho^0$f, or ωf, T(2200) region, partial wave anal. 77−34171
pp scatt. spin-dependent eikonal model for 5.5 GeV/c-2000 GeV/c calcs. 77−26545
pp small angle scattering, 398-572 MeV, polarisation, amplitude anal. 77−30407
$pp\rightleftarrows d\pi^+$, 3.2 GeV, forward scatt. relativistic study, reaction cross section 79−97633
π multiple scattering, higher order effects, NN correls., self-consistency 78−89799
π multiple scattering theories, in nuclear matter, NN correls., self consistency 78−89800
π^0-π^0 partial wave amplitudes, crossing symmetric dispersion relations 78−50048
π+nucleus interaction multiple-scattering theory 77−82967
π^-+nucleus→$\pi^+\pi^-\pi^-$+nucleus, 8.9, 12.9, 15.1 GeV/c, partial wave anal. of coherently prod. A_1, A_3 mesons 78−50047
πA, multiple scatt. theory *(Russian)* 79−49640
πd, bound states, scatt. in light front field theory dynamics 80−68477
πd, comparison of Faddeev eqn. approach with optical potential 79−76030
πd, elastic differential cross section, Faddeev calc. and π-absorption 79−75793
πd, relativistic Faddeev calc. 80−102066
πd elastic scatt., 142 MeV, elastic cross section and polarisation observables 79−75791
πd elastic scatt., 142-256 MeV, dibaryon resonance interference with Faddeev amplitudes 80−32123
πd elastic scatt., dibaryon resonance effects on differential cross section, Glauber model 79−97634
πd field theoretical model, effective semi-relativistic three-body problem 78−86454
πd scatt., relativistic kinematic effects 78−8685
πd scatt. in (3,3) reson. region, relativistic description 77−57558
πd semi relativistic field theroretical model, extended Fadde'ev and Amado-Lovelace eqns. 78−89729
πd-scattering length calc., on basis of Faddeev's equations *(Russian)* 78−33082
π^-d, 552 MeV/c, elastic differential cross section Glauber theory anal. *(Russian)* 80−52700
πK partial waves, resonance parameter determination for scatt. amplitude 79−40692
πN, partial wave analysis, S- and P-wave scatt. lengths 80−63019
πN channels, relativistic parametrization of separable pots. 79−63518
πN coupling constant from simultaneous anal. of all invariant amplitudes using rational series 78−58199
πN interactions, corrections to πN off energy shell T-matrix elements 77−6154
πN low energy partial wave anal., cross sections, Δ^0 and Δ^{++} 80−52531
$\pi N\to N\pi\pi$, 1.65-1.97 GeV, partial wave anal. including π-exchange 78−66148
$\pi N\to N\pi\pi$, 1.65-1.97 GeV/c^2, πN resonance coupling to Δπ and ρN channels 78−66149
πN partial wave anal. 1.6 to 10 GeV, possible high spin resonances in Argand plots 78−70403
$\pi N\to\pi\pi N$, 1.3 to 1.8 GeV, interference of isobars, partial wave anal. 79−63519
πN scatt., isospin violation from π^0-η mixing, partial wave anal., N*(1540) struct. 80−27426
πN scattering, partial wave analysis, high energy behaviour large momentum transfer region 79−22130
π^-N, in ^{12}C, 40 GeV/c, one- and multi-nucleon interactions, secondary charged particle multiplicity *(Russian)* 80−83013
π^-N in Ne, 25, 50 GeV/c, secondary particle multiplicity and multiple scatt. model anal. *(Russian)* 80−83014
πNN dynamics, Faddeev approach, 0-1200 MeV pp scatt. 80−57625
πp, quasi-potential reconstruction, scatt. theory inverse problem *(Russian)* 80−5016
$\pi^-p\to(\pi^+\pi^-\pi^0)n$, 12, 15 GeV/c, partial wave anal. of neutral 3π system, A-meson prod. 78−58207

relativistic scattering theory continued
π^-p backward scattering, $S_{\parallel}$ partial wave amplitude near ηn prod. threshold 77−34176
$\pi^-p \rightarrow K^0\Lambda$, threshold to 2350 MeV/c, partial wave anal. of world data 77−87997
$\pi^-p \rightarrow K^0\Lambda^0$ up to 2.375 GeV/c, resonance parameters, partial wave anal. 80−32133
$\pi^-p \rightarrow \omega\pi^-p$, 11.2 GeV/c, partial wave anal. of g-meson prod. 78−78220
$\pi^-p \rightarrow p\bar{p}n$, 18 GeV, $p\bar{p}$ resonant state partial wave anal. 80−32134
$\pi^-p \rightarrow \pi^-\pi^-\pi^+p$, 63, 94 GeV/c, A_2 meson prod. from partial wave anal. 80−37303
$\pi^-p \rightarrow \pi^-\pi^-\pi^+p$, 63, 94 GeV/c, A_1 meson existence from partial wave anal. 80−37304
$\pi^-p \rightarrow \pi^-\pi^-\pi^+p$, 63, 94 MeV/c, A_3 meson, 3π resonances in 2^- partial waves 80−37305
$\pi^-p \rightarrow \pi^+\pi^-n$, 1.33-1.38 GeV, isobar prod. near threshold, isobar model partial wave anal., bag model 79−93456
$\pi^-p \rightarrow \pi^+\pi^-n$, amplitude anal. of $\pi\pi$ scatt. 1.0 to 2.08 GeV, f, g, h mesons 79−3042
$\pi^-p \rightarrow \pi^+\pi^-n$, $\pi\pi$ scatt. partial wave anal. f, g and h mesons 80−5015
π^+p polarisation near backward direction, partial waves anal., comparison with model predictions 77−30421
$\pi^\pm p$, elastic and charge-exchange scatt., partial wave anal., Δ resonances 80−63018
$\pi^\pm p \rightarrow \pi^\pm p\pi^+\pi^-$, partial wave anal. of low-mass $p\pi^+\pi^-$ system 78−25070
$\pi\pi$, Roy eqns., S- and P-wave scatt., constraints and correl. 78−21460
$\pi\pi$ interactions, dominant resonances, pole positions, partial waves 80−63020
$\pi\pi$ low energy scatt., manifold of solutions of Roy's S- and P-wave eqns. 78−66154
$\pi\pi$ P-wave scatt. length, absolute bound 77−57563
$\pi\pi$ partial waves, resonance parameter determination for scatt. amplitude 79−40692
$\pi\pi$ S-wave phase shift, lower bounds, ε° and ρ poles 78−45953
$\pi\pi$ scatt. length, interior dispersion relations 78−45952
$\pi\pi$ scatt. sum rules on crossing-symmetry basis 77−57467
$\pi\pi$ scattering amplitudes, partial wave equations, analyticity domain 79−2956
$\pi\pi$ scattering in 1 GeV region, partial wave dispersion relation with inelastic cut 78−4877
$\pi^0\pi^0$ scatt. amplitude, new method for deriving absolute bounds 77−6059
$\pi\pi N\bar{N}$ partial-wave amplitudes, interior dispersion relations 77−82758
$\pi\pi\pi$ system, relativistic dynamics in ω channel 78−21360
CC $^{12}C(\alpha,\alpha)$, 1.37 GeV, elastic and inelastic, Glauber multiple scatt. theory 79−3161
$^{12}C(\alpha,\alpha)$, 1.37 GeV, modified eikonal multiple scattering theory 78−21576
H-like ions, ground-state, elastic electron (positron) scatt., relativistic Glauber amplitudes 80−23550
$H+H^+$, relativistic classical theory of electron capture 80−18920
$^1H(n,\gamma)^2H$, relativistic invariant approach, parity violation 79−3147
$^2H(p_0,p_1p_2)n$, 156 MeV, test on p_1-n-p_2 colliniarity reson. 79−75996
$^2H(\pi,\pi_s)$ low energy scatt., Afnan-Thomas anal. with exclusion principle 79−75792
$^2H(\pi,\pi)$, (3,3) resonance region, three body relativistic eqns., cross section calcs. 78−74405
$^4He(d,d)$, Faddeev Lovelace eqn. soln. 78−54767
$^4He(d,d)$, Glauber theory at high energy *(Russian)* 78−41732
$^4He(d,pn)^4He$, Faddeev eqns., separable pots., total cross sections 78−21571
^6Li, $\alpha+p+n$ model, numerical soln. of coupled Faddeev eqns. 79−17831
Ne^+, electron scatt., relativistic R-matrix calc., fine-struct. level transition cross sections 78−13604
pp bremsstrahlung, intermediate nucleon isobars contrib., relativistic model, nuclear force significance 78−93899
$pp \rightarrow pp\pi^+\pi^-$, 12, 24 GeV/c, p dissociation into $(p\pi^+\pi^-)$, partial wave anal. 79−22148
π^+p elastic scatt., charge exchange, partial wave anal., Δ mass splitting, P_{33} resonance 78−29348
U+U, K-shell ionis., classical relativistic trajectory method appl., 1, 10 GeV/n 80−43129

relativity
see also general relativity; light cones; relativistic mechanics; relativistic quantum field theory; relativistic scattering theory; special relativity
absolute space-time theory 78−36921
anisotropic relativistic and dissipative fluid model *(French)* 77−67357
axiomatic formulation of six dimens. phys., 3+3 dimens. spacetime 78−81834
barnacle equivalence structure in relativistic wave equations 79−30657
conformal relativity, kinematic theory of mass 78−77706
conformal relativity, special, theory of mass 78−77707
covariant representation of microscopic charge and current densities in terms of polarisation and magnetisation fields 79−71
dielectrics, relativistic effects, ponderomotive laws of electrodynamics 77−41519
education, relativistic line of charge over ideal conductor, net force 78−36762
Einstein's contribution to twentieth century physics *(Chinese)* 80−17
electrons, rest mass, continuous increase hypothesis *(Chinese)* 77−71209
equivalence principle, or formal mathematical statement, for teachers 79−71200
evolutive mechanics, relativistic analytic mechanics 77−17800
flux line collapse, invisible string 77−57451
fundamentals in quantum theory and relativity, conf. 78−54233
Galilei relativity in Newtonian mechanics, possible Lie admissible covering 78−73838
gas in closed container, relativistic thermodynamics 77−45812
gyroscopic precession machine design, calc., cost estimation *(German)* 78−21048
Hamiltonian, completely integrable relativistic system 77−57450
Klein-Gordon-Schrodinger coupled eqns. 79−35955
light velocity and gravitational potential, Laplace's deduction of differential aberration *(German)* 78−57838
linear field theories, conservation of source strength, superpotentials 77−5726
linear wave eqn., kinematical interpretation of subsidiary conditions 77−2737
Mach's philosophy, genesis of relativity theory 78−8211

relativity continued
mass spectrum in relativistic extended models of elementary particles 77−34116
metric relativity, appl. to EM dipole fields 77−64988
Newton mechanics and Kaufmann experiments *(Bulgarian)* 78−54283
non-Euclidean geometry and physical basis, Galilean geometry and relativity, book 79−62989
nonisotropic medium near critical point, space-time correlation functions of hydrodynamic fluctuations 77−30123
overturn and continuity of the hypotheses in the framing of the theory of relativity 80−90674
Planck, Max Karl Ernst Ludwig (1858-1947), quantum and relativity theories 80−68008
Poincare and Galilei groups in arbitrary dimensional spaces 78−77672
primal cosmic energy field, Birkhoff hypothesis consistent with relativity 77−30072
QED, four dimensional symmetry framework, additional concepts and universal time 78−74184
quantisation of free fields in stationary space times 77−67335
quantisation of relativistic free field, geometrical approach 78−81885
quantum field theory, relativistic, algebras of unbounded operators *(Russian)* 79−17602
quantum mechanics and relativity 78−54242
quantum theory, classical and relativistic limits 77−33901
quantum theory, unbroken wholeness extension to relativistic contexts 78−54241
quantum theory comparison 80−27175
relativistic Boltzmann eqn., series convergence 78−36949
relativistic electron model from the introduction of the chronon 78−93827
scalar particle 77−57151
scalar relativistic fields, symmetry groups, with self-interaction 79−30664
strings and vortices with soliton solns. 77−5674
strong interaction theory based on fibre bundle geom., currents 77−79204
thermodynamic quantities, relativistic transformations 77−45813
unified theory of reality 77−45722
universal metaplectic structures and geometric quantization 79−25881
vector laws of physics, reformulation 80−68036
2 NN system, bound state energies, Faddeev method *(Russian)* 79−49407

relaxation
for dislocation relaxation see dislocation damping
see also anelastic relaxation; chemical relaxation; dielectric relaxation; magnetic relaxation; stress relaxation; ultrasonic relaxation; viscoelasticity
aerosol single particle, aerodynamic relaxation time analyser 77−80205
amorphous alloy, struct. relax., compositional SRO 78−79538
amorphous metals, low-temp. annealing, geometrical relaxation model on struct. charge and kinetics *(Japanese)* 79−94908
binary gas mixtures epochal relax. 79−41783
butadiene acrylonitrile copolymer, relaxation processes *(German)* 78−31439
capture processes involving real probability depletion, relax. time approx. 79−58656
cellulose blotter/torsion pendulum technique, for relax. determ. 80−54357
critical fluctuations, cluster dynamics 77−13725
cubic crystal, relaxation effect around point defects 77−84740
elastomer, relaxation processes, statistical description *(Russian)* 79−23229
first-order phase transition, nonlinear relaxation, Ginzburg-Landau theory including fluctuations 79−35658
Fokker-Planck eqn., information theoretical derivation, drift and diffusion characterised relax. 77−49699
glass, of props. during isothermal swell period, method of calc. 78−67654
glass, refractive index during annealing, nonlinear structural relaxation model 78−44234
glass, relax. kinetics, Prigogine-Defay ratio 77−20042
glass, relaxation memory effects, exactly soluble one-dimensional model 79−1398
globular clusters, relaxation and evolution towards sphericity 77−13406
globular clusters, test computations on dynamical evolution 77−49445
inhomogeneous gravitational systems relaxation, delocalisation effect 79−62877
ionic crystals, elastic relax. associated with formation and motion of Schottky defects 80−49216
ionosphere E and F-regions, relaxation time of large-scale horizontal winds 77−78561
linear isotropic viscoelastic material, exptl. determ. of relaxation modulus 79−61810
linear relaxation theories, equations of motion, Green's functions, and thermodynamics relations 79−30352
liquid structural relaxation times, smoothed cell potential model 77−27796
liquids, relaxation, binary collision theory 78−6000
master equation, instability point, relax., fluctuation 77−13681
metallic glass, load relaxation studies 78−48441
metallic glasses, atomic transport behaviour, review *(Japanese)* 79−94907
metallic glasses, mats. props. review 77−4043
metals and alloys, relaxation, rel. to defect struct. *(Russian)* 78−19801
metastable states, relax. and fluctuation theory 78−49769
METGLAS™2826, load relaxation studies 78−48441
minerals release-adiabat measurements, effect of viscosity 80−51388
Monte Carlo studies on relaxation phenomena, book contrib., review 79−80531
noise, 1/f, superposition of relaxation spectra 80−105575
nonlinear relaxation and fluctuation 79−30373
nonlinear relaxation process, nucleation in early stage, Markov process framework 78−70060
optically oriented atoms, surface thermal relax. adsorption thermodynamics 77−24480
organic compounds, complex, nuclear relaxation influence on stimulated emission 80−48019
plastic elasticity, hardness, creep, and relaxation meas. with Vickers indenter by electroacoustic method *(German)* 78−48584

relaxation continued
polybiphenylacrylate, atactic, crystalline character effect on dynamic mech. response 78−56686
polycyclohexylphenyl acrylate, crystalline character effect on dynamic mech. response 78−56686
polyethylene, relax. phenomena, −30 to 200°C, premelting and glass transition 78−51440
polyethylene oxide, relax. phenomena, −30 to 200°C, premelting and glass transition 78−51440
polyethylene oxide, solid state relaxation, DSC study 78−9962
polyethylene oxide, solid-state relaxation, spin labelling technique 78−9963
polymer, thermolum. rel. to mol. relax. 78−11003
polymers, amorphous, segmental distrib., crystallisation and viscoelastic relax. meas. 78−51443
polymers, glassy, structural acoustic relaxation 79−95088
polymers in dilute solutions, diffusion and relaxation time 78−55964
polyoxymethylene, relax. phenomena, −30 to 200°C, premelting and glass transition 78−51440
polypyromellitimide, low temperature relax., NMR, dielec. and mech. losses 78−71686
polystyrene, glassy state, relax., free vol. fluctuations effect 80−19722
polystyrene, $T_{||}$ relax. above glass transition 79−4259
polyvinyl fluoride, relax. phenomena, −30 to 200°C, premelting and glass transitions 78−51439
polyvinylidene fluoride, relax. phenomena, −30 to 200°C, premelting and glass transitions 78−51439
QSOs black tide model, stars relaxation in isothermal sphere 77−78884
quantum dynamical semigroups and spin multipole relaxation in isotropic surroundings 78−86813
rate processes in condensed media, master eqns. 80−77687
Rayleigh waves, magnetothermoelastic, with thermal relaxation, theory 79−62
rivers, relaxation model of local scour 77−21809
rubber, loaded, effect of polyfunctional nitro-oligomers on relaxation props. *(German)* 78−48436
simple glass forming materials, universal nature of two relax. processes in region of glass transition 77−84907
solar photosphere, wave propag. and local relaxation time 77−22162
stellar systems, relaxation with close encounters 79−48862
styrene crosslinked polyester networks, low temp. γ' relaxation 78−44156
styrene crosslinked polyester networks, low temp. γ relaxation, water and chem. struct. effects 78−44157
temperature dependence of relax. rate between widely spaced levels due to gas (liq.) fluctuations 79−30366
third-order elastic const. in crystal with point defects 77−8873
thunderstorms air relaxation time, influence of cloud and precip. particles contrib. to elec. cond. 80−17332
transport-relaxation equations, time-depend. variational principle and reciprocity theorem 78−12655
two-level system, kinetics at diffusion modulated local interactions *(Russian)* 79−2716
unstable states, relax. and fluctuation theory 78−49769
unstable systems, anomalous fluctuation and relax., multimacrovariables 77−79033
viscoelastic materials with fading memory, thermodynamics of relaxation and creep processes 78−71282
viscoelasticity 77−58631
Z discharge relaxation between electrodes 80−75089
Al strips, supercond., order-parameter relaxation meas. 79−47207
As_2Se_3 glass, heat capacity and struct. relaxation of enthalpy 77−55360
B_2O_3 glass, nonlinear structural relaxation model for glassy state 78−26448
CaF:Eu(Gd)(Dy)(Tb), dimer reorientation activation volume 80−107285
Fe-Ni-P-B, metallic glasses, struct. relax., annealing effects on mag. props. 80−89261
^{4}He, superfluid, flows, healing and relaxation comparison with Khalatnikov-Lebedev theory 80−107587
^{4}He, superfluid, superflow, healing and relax. in He II flows 79−14976
Pb-Si-Sb amorphous alloys, electrical resistometric detection of relaxation 79−60278

relaxation oscillators
autogenerator displaying stochastic behaviour 79−17198
coupled Van der Pol oscillators, perturbations nonequilib. system 79−10459
forced van der Pol oscillator, frequency entrainment 78−57794
forced van der Pol oscillator, variational eqn. bifurcations 78−77681
four-level laser power and relaxation oscillation, excited-state diffusion effect 77−79834
human respiratory system, role of the Van der Pol oscillator 78−65073
polymer melt relaxation oscillators *(French)* 80−79361
respiratory rhythm generator, neural network model 77−86485
semiconductor laser direct PCM improvement by optical feedback 78−1287
symbolic dynamics and relaxation oscillations 80−90719
thermal relaxation oscillator using thermistor, temp. meas. appls. 78−73992
van de Pol eqn., transformation into S-wave Schrodinger eqn., solvable potential 78−57790
Van der Pol oscillator, renormalised perturbation theory 80−27225
van der Pol oscillator, RPA for linewidth 80−68138
Van der Pol oscillators, diffusion-coupled active medium, nonlinear waves 80−4546
Al-Pb:Bi, tunnel-junction relax. oscillator, appl. to thermometry 79−85138

relaxation time, carrier *see carrier relaxation time*

relay control
see also on-off control
radiation counting rate meter output at threshold, fluctuation and arrival shift by computer simulation 80−106240
X-ray diagnostic sets with automatic exposure relays, switching delays 77−48903

relay protection
see also circuit breakers
TFTR pulsed loads, AC electrical distribution system protective relaying 80−63387

relay systems (radio) *see radio links*

relay systems (satellite) *see satellite relay systems*

relays
see also reed relays; switches
bistable optical fibre switch, construction and performance 80−95994
broadband time relay for physical instruments 79−88940
coaxial relay current pulse generator for laser pumping 78−59014
contact erosion due to arcs, atmosphere effects *(French)* 77−72518
contacts, measurement of thermoelectric voltage for different metals *(German)* 79−26040
dry-friction periodic relay system analysis *(Russian)* 79−10455
fibre optic relay with metallic pads heated by light 78−18038
gamma spectrometer supply, simple attachment 80−57447
inductance measurement to TGL 24961 specification methods for Fe-cored coils *(German)* 80−4736
optical coupler appl. *(Swedish)* 77−774
piezoelectric, multilayer plates bending, anal. 80−40064
Pockels effect relay applications to optical data processing 79−72513
radioisotope, operation, construction and appl. *(Polish)* 80−106129
seismic testing for class 1E equipment 78−78475
X-ray quality control, automatic exposure relay 78−95893
Cu-Ni (20 wt.%) alloy appl., contour plate for spring, creep characts. obs., use of Larson-Miller method *(Japanese)* 80−55454

relays (repeaters) *see repeaters*

reliability
see also circuit reliability; quality control; standards; testing
1 Gb/s laser space communication system 77−7213
10 kbar hydrothermal installation with internal heater 79−67333
14th Annual Reliability Physics Symposium, Las Vegas (1976) 77−40514
accident at Three Mile Island, lessons learned 80−57929
advanced reactor Centralised Reliability Data Organisation 79−13463
aerospace systems and electronics, IEEE conference, Washington D.C., USA, 26-29 Sept (1976) 77−5420
$Al_xGa_{1-x}As/Al_yGa_{1-y}As$ heterostructure lasers, prep. characts., and CW reliability 80−58586
amorphous chalcogenide switching devices, reliability 79−11238
artificial blood pump fabrication for durability 79−84026
astronomical X-ray telescope, HEAO-2 Observatory, protective design considerations, system reliability 80−61983
automated NDT, vehicle reliability improvement on structural and motor parts 79−91859
automatic reverberation time meas. 79−68518
biological model parameter reliability range determ. using hybrid computer 77−44581
biological models, reliability range of model parameters 79−96500
biomedical equipment, reliability and safety aspects 80−36172
Brunswick plant post-startup optimization 80−23048
BWR, emergency core cooling system, unreliability estimates, comp. programs 77−54280
BWR, individual-tank fast shut down system, anal. *(German)* 77−54311
BWR availability improvement 77−38379
BWR power plant availability improvement by acoustic emission monitoring 79−9809
cardiac pacemaker, reliability technology conf., Gaithersburg, USA, (Jul. '76) 78−57129
cardiac pacemaker long-life battery test results 77−81735
cardiac pacemaker reliability technology workshop, Gaithersburg, USA (Oct. 1977) 80−27038
ceramic components, design criteria and structural testing 79−39083
ceramic multilayer capacitors, fracture mechanics approach to structural reliability assessment 80−89328
CERN PS booster, reliability and maintenance anal. 77−83281
Clinch River Breeder Reactor Plant reliability and safety methodology 78−29617
clinical ECG real-time telephone transmission usefulness and reliability 78−57108
CMOS microcircuit, scanning electron microscope and mass spectrometry appl. 78−21264
component, thermal neutron environment 78−21787
computer program for availability and reliability evaluation, Karlsruhe nuclear centre, complex repairable systems 77−88249
computerised nuclear reactor protection systems, reliability anal. using Markov methods 80−91229
control systems for nuclear power plants, program reliability *(Spanish)* 78−58369
coronary care unit interactive ECG monitoring 78−7481
cosmic ray variation spectrograph, data reliability ensurance 79−84610
CRO, double-beam, design 77−37910
CW injection lasers and LEDs for optical communications 77−7210
deep submergence vehicle development and reliability 77−5376
demand pacemaker, with variable-pulse-width, clinical experience 77−81696
design elements, reliability rating during fatigue failure 78−79275
dial gauges quality obs., manufactured in Rumania *(Rumanian)* 80−47049
dial pressure gauges, reliability tests and failure mechanisms *(Rumanian)* 79−40557
dissolved O_2 in rivers, reliability parameter in probabilistic programming models 80−26179
Dutch reactor safety studies, Rasmussen report eval. *(Dutch)* 79−81016
EEG, power spectral density estimates of subcortical spiking frequency 79−24972
electric insulating oils, composition, physical and chemical props. and determ. of free radicals *(Rumanian)* 80−97745
electromedical equipment, safety *(Croatian)* 78−48901
electronic devices, failure analysis of metal parts using fractography 79−61811
electronic piece parts, evaluation by neutron radiography 78−31610
equipment reliability under vibration, testing by simulated vibrations, expt. problems 80−58855
examination marks, electronic engineering educational courses 79−75305
exponential distribution MTBF confidence limits determ. using Epstein and Harters methods 80−98790
fatigue-critical structure, optimal periodic proof test based on cost-effective and reliability criteria 77−63838
fault tree anal. code SUPKIT, reactor safety appl. *(Japanese)* 78−54847
FBR, Clinch River, computer anal. and models 78−13260

reliability continued
fibre splicing, arc fusion, protection methods 80−69565
fission materials nondestructive analysis development, for EURATOM (CEC) Safeguards Directorate 79−85693
fission reactor auxiliary feedwater systems, fault tree anal. 80−63332
fission reactor component improved reliability, design consideration 79−22383
fission reactor component reliability, non-destructive testing and flaw evaluation *(French)* 79−24711
fission reactor core flooding system, reliability analysis *(German, English)* 77−38346
fission reactor fuel element sheathing, reliability, including hydration process, probabilistic model *(Russian)* 80−52742
fission reactor materials theft, fault tree and reliability relationships for analyzing noncoherent two-state systems 80−47600
fission reactor pressure component steel, fracture charact., implications for reliability 79−20199
fission reactor pressure vessel, failure risk due to manufacturing defect 79−22432
fission reactor pressure vessel reliability and sfaety, in-service inspection, surveillance specimens 79−18020
fission reactor pressure vessel safety and reliability evaluation, two-criteria approach 79−18016
fission reactor pressure vessel walls, ultrasonic inspection reliability 79−24713
fission reactor system reliability prediction, appl. of Bayes eqn. 77−67797
fission reactors, BWR decay heat removal systems, probabilistic risk assessment, fault and event tree anal. 80−63333
fission reactors, CRBR shutdown system, Markovian reliability anal. 80−27761
fission reactors, failure probability distrib. from observed failure data, beta distrib. 80−63335
fission reactors, operator reliability, Weibull distrib. model 80−63336
fission reactors, shutdown heat removal systems, reliability fault tree anal. and β-factor method 80−63331
flame photometers with automatic dilutor 78−49878
flow meas. methods and appls. for optimum reliability 79−81998
fossil fuel utilisation, reliability engineering appls. 80−61234
fracture sensitive structures, materials related aspects 78−42570
fusion reactor, BBC CQK 200-4 modulator tube for sustaining neutral beam power supply 80−99290
GCFR, 1000 MW(e), reliability anal. of decay heat removal system 77−14223
geostationary satellite, station-keeping activator subsystem reliability 78−4074
glass fibres, fatigue failure probability 79−32045
graphics plotter using linear step motors 79−93127
heterojunction laser and LED reliability rel. to facet damage and nonradiative centre formation 78−5472
hip joint prosthesis 78−11777
hydro-photovoltaic plants, peak power generation economics and reliability 80−45706
inertial navigation vibrating sensitive elements, improvement *(Russian)* 77−57302
information processing system parameters rel. to optical element characteristics 79−72510
instrument reliability assessment using mathematical models 80−22348
irradiated fuels reprocessing, French and European policies *(French)* 80−809
laminate cylindrical shells, prepared by continuous filament winding calc. of strength and reliability 80−10194
laser diode and transmitter unit lifetime tests *(German)* 78−37883
laser reliability calcs. rel. to system's operating life 77−10932
lasers for fibre-optic transmission systems 77−19342
leads, solderability of external coatings after storage at 25-400°C 78−184
LEED crystallography and reliability indices 80−54081
light-duty electrical contact, reliability assessment methods 78−29219
lightguide fibre, ensuring mechanical reliability 80−79001
liquid crystal display elements, principles and applications *(German)* 80−86277
LMFBR cooling systems 80−57838
LMFBR core components, Na test facility 77−50196
LMFBR design, risk-based approach 77−88198
LMFBR steam generators, reliability considerations 79−22437
LMFBR test facility, exptl. determ. of reliability data of sodium components 79−18015
log-normal device optimal burn-in time 80−58743
LWR, commercial, evaluation of human errors and operator reliability 78−17373
LWR, deterministic criteria vs. probabilistic analyses 80−32377
LWR, reliability demonstration test *(Japanese)* 79−26552
LWR, reliability of piping 79−18017
magnetic flowmeter construction and reliability 79−23386
and maintainability symposium, Los Angeles (1978) 78−50250
marine reactor systems, Monte Carlo reliability anal. of power and heat removal systems *(Japanese)* 78−58396
measurement reliability, statistical approach *(Russian)* 80−22317
measuring instruments, test reliability 79−75514
medical equipment reliability requirement determ. and assessment method 77−5091
metallic structures initial fatigue quality characterisation using equivalent-initial-flaw-size distribution 80−58978
metrological aspects, activities at National Institute for Metrology (INMB), Bucharest *(Rumanian)* 79−40522
microcantilever electrostatic deflection system for transmission optical modulator array 80−87512
microelectronic device bonds, glass-metal seals and weld metal, assessment using Auger spectroscopy 78−24900
micrometer, assessment method *(Rumanian)* 80−68175
microtron, operating reliability rel. to high-freq. path 77−65367
MIS solar cells, stability and degradation mechanisms 80−16806
MNOS P-channel switch, accelerated reliability testing *(German)* 80−6988
myocardial infarction diagnosis in endocardially paced patients 77−81625
NDT, methods of increasing indices 78−40010
NMR analysis system, LAOCOON3-type, reliability efficiency and error estimates 78−258
reliability continued
nondestructive evaluation and reliability in materials and structs. 77−9004
nonferromagnetic coating thickness monitoring stability and general serviceability of applied sensors 78−44326
nuclear electric power plants, failure anal. and failure prevention 77−79450
nuclear engineering risk estimates, communication techniques 80−18514
nuclear fuel drum storage capacity computation via inventory model 79−9776
nuclear industry value of reliability analysis 78−29619
nuclear installations safety, report on 1977 IAEA conference *(Dutch)* 77−83047
nuclear plant pressurized systems reliability, influence of codes, standards and practices 79−22433
nuclear plant reliability data system, quality control program in design planning 79−97774
nuclear power engineering materials certification testing for reliability 80−78360
nuclear power plant, contrib. of quality assurance to safety and reliability 79−22438
nuclear power plant, fault tree analysis, development of DICOMICS-TWIN self-adaptive algorithm for minimal cut sets determ. 78−17380
nuclear power plant, fault tree and reliability analysis, modular decomp., PL/1 program 78−17381
nuclear power plant, quality assurance requirements for reliability in developing countries 79−22452
nuclear power plant, safety-related induction motor appls. 77−3144
nuclear power plant availability improvement by acoustic emission surveillance 79−3213
nuclear power plant availability improvement by surveillance techniques 79−9812
nuclear power plant reliability technology, role of ASTM in providing standards 79−22435
nuclear power plant safety systems, reliability criteria 79−18014
nuclear power plant steam generator reliability, Canadian practice 79−22451
nuclear power plants secondary system radioactivity monitoring 80−18445
nuclear power station, probabilistic methods for risk assessment and safety standard 78−21693
nuclear power station outages, turbine-generator reliability assurance through large scale test facilities 77−3151
nuclear power station safety estimation 77−10471
nuclear power stations, aseismic design and testing of equipment and components, Japan 80−52763
nuclear power stations, aspects *(Russian)* 79−97885
nuclear power stations, availability of redundant safety systems with common-mode and undetected failures 80−91230
nuclear power stations, electrical supply system performance, reliability of protection and control systems 80−52761
nuclear power stations, probabilistic methods, safety assessment, Fed. Rep. Germany 80−106124
nuclear power stations, probabilistic methods in safety analysis and regulations in France 80−106123
nuclear power stations, structural reliability, conference, Berlin, Germany (Aug. 1979) 80−105422
nuclear power stations, turbogenerator overspeed protection, design *(French)* 77−3156
nuclear power stations, unavailability of systems under periodic test and maintenance 80−95368
nuclear power stations *(Portuguese)* 80−68844
nuclear reactor, class 1E electronic instruments, ageing 78−8945
nuclear reactor design, reliability, risk assessment, power plant safety anal. 77−71665
nuclear reactor emergency core cooling system motor operated valves, failure criteria 78−70592
nuclear reactor instrumentation, reliability improvements 80−32416
nuclear reactor redundancy systems, common mode failures 80−13641
nuclear reactor safety, fault tree anal., modular representation 78−78480
nuclear reactor shutdown system reliability, effect of operator performance 78−29611
nuclear reactor structural reliability, time-depend. nature modelling 79−18013
nuclear reactor structure, probabilistic failure mechanics anal. 77−81317
nuclear reactor technology, structural reliability *(Japanese)* 78−17315
nuclear stations, maintenance optimization through trend monitoring 80−18552
nucleonic and other meas. methods compared 77−38594
offshore operations, LEO I submersible reliability and safety 77−5373
optical couplers, test results *(Swedish)* 77−776
optical fibre cable reliability, deterioration factors, splice point reliability, coating materials, static fatigue life *(Japanese)* 80−99848
optical fibre characterisation techniques compared 80−64202
optical fibre communication systems, Soviet studies *(German)* 78−25972
optical fibre splicing, connecting and sheath jointing *(Japanese)* 80−87497
optical fibre transmission system planning *(French)* 80−87551
optical fibres, coated, research on reliability of mechanical and transmission charcts. 79−55234
optical fibres, coated *(Japanese)* 79−59822
optical fibres, compound glass, nylon-covered, reliability and verification tests and results *(Japanese)* 80−99866
optical fibres, mechanical strength reinforcing and reliability improvement methods of fabrication *(Japanese)* 80−87568
optical fibres, plastic coated fused silica, dynamic fatigue data reliability 78−87166
optical tracking system properties and advantages 79−14080
p-n junctions microplasma formation, influence of imperfections in Si crystals 77−8177
pacemaker, battery longevity estimation using statistical methods 78−57131
pacemaker base rate follow-up reliability for long-term pacing 77−81694
pacemaker implantable lead performance evaluation, status report 78−57135
pacemaker lead failure type discrimination 78−53570
pacemaker pulse generator design, manufacture and performance documentation 77−81715
pacemaker pulse generator replacement and other problems 77−81705
pacemaker reliability prediction, appls. and pitfalls 78−57132

reliability continued
particle size distributions, statistical reliability 77−53858
photovoltaic modules testing, reliability and performance 80−94063
photovoltaic power system reliability assurance methods 80−61315
plastic encapsulated and hermetic modules corrosion model 80−100937
plastics, for transmission media, thermomech. reliability 80−40666
polyethylene pipes, lifetime determ., crack growth in thermoplastics under various conditions 78−39981
polyurethane foam solar concentrator, thermal and thermohydrolytic ageing 78−92281
posterodiaphragmatic myocardial infarction diagnosis, Frank lead Y reliability 79−44038
precipitator, electrostatic, particle separation prediction reliability analysis *(German)* 79−4072
pressure vessels, prestressed concrete, safety and reliability 79−22412
pressure vessels, sensitivity to material and other factors 79−18018
pulsed laser spectroscopic instrumentation 77−18105
PWR, 900 MW, probabilistic determ. of operating rules 77−46345
PWR, reliability assessment of containment 78−78481
PWR emergency core cooling system, design, fault-tree anal. and probabilistic evaluation methods 77−74976
PWR neutron flux detectors, reliability tests *(French)* 80−32403
PWR pressure components reliability and residual life evaluation and precipitation 79−20191
PWR pressure vessel reliability, failure anal. 77−74962
PWR reliability prediction in design, empirical and Monte Carlo techniques 78−54827
PWR vessel and primary circuits estimation of reliability, probabilities and adaptive models 80−106125
PWRs, auxiliary feedwater system, fault tree anal. 78−54867
quantum dynamics of fields of higher spin 77−74607
radiochemical and chemical trace analysis, in environmental materials 78−40106
reactor loose parts monitoring, USA technology status and recommendations 79−623
reactor protection computer systems, statistical verification of reliability 80−32417
reactor safety equipment, reliability in design 80−37555
reactor Shutdown System Reliability Duty Cycle generation method 78−29620
reactor systems reliability, computer programs *(Slovak)* 78−82416
reliability physics, conference, Las Vegas (1977) 77−79086
science and technology, importance of safety and reliability, in materials testing 78−39982
seismic sensors, mechanical, improvement study *(Japanese)* 78−85722
seismographs working in standby regime 78−61585
semiconductor device degradation, recombination enhanced defect reactions 79−38094
semiconductor junction lasers *(German)* 80−19034
semiconductor light source degradation, review of recent expts. 78−82970
sintered metal parts and powders standardisation of quality control methods 79−96266
solar, hotwater and heating systems, availability aspects 80−61314
solar cell arrays, flat plate PV modules, elec. and environmental testing requirements for terrestrial appls. 80−61368
solar cell device reliability estimation using noise spectral density meas. 80−93896
solar energy concentrators, optical coatings, accelerated tests, using reliability principle 79−96419
solar photovoltaic power systems for rural areas of developing countries, technology, reliability, economics and appls. 80−61286
solar power systems availability and reliability analysis 80−35687
solar radiation and wind power measuring instrument design 79−57404
solid body motion parameters, determination reliability improvement using redundancy methods 79−30431
solid state trip system 79−6753
Space Telescope solar array requirements and design 79−96885
statistical safety factor and Bayesian analysis in reliability engineering *(Japanese)* 79−61837
steel, fission reactor pressure vessel, reliability 79−22430
steel, stainless, annealed type 304, LMFBR, creep rupture mode of failure, reliability anal. 77−3113
structural fatigue life rel. to element uncertainty 79−27593
structural reliability and safety, probabilistic methods 78−39978
structural reliability of mech. components and subassemblies of nuclear power plants, conf. 79−594
superconducting dipole magnets for CERN beam line 79−31294
superconducting magnet failure experience rel. to fusion reactors 77−26870
superconducting power transmission lines, He refrigerators optimisation 78−24802
system reliability in face of human (operator) errors, bibliography 80−94940
systems, NATO Advanced Study Institute, Liverpool, England (Jul. 1973) 77−38396
systems reliability analysis, cost effective quality control program 79−97775
telephone exchange contact reliability, effect of H_2S and organic vapours *(Polish)* 79−74573
temperature spikes stochastic analysis, contribution towards component damage exposed to nuclear radiation environment 79−7627
terrestrial solar cell reliability, accelerated stress testing 79−74528
terrestrial solar cells, accelerated stress testing 79−92083
thermal reactor safety and reliability technology 78−701
thermistor bolometers, anal. methods 78−24795
thermoelectric batteries, low-temp., stable life calculations 79−87998
TLD readers, safety of decentralised reading in Sweden 77−40780
transmission system, semiconductor device reliability tests 80−58573
tribology and technical systems reliability 78−39918
trigger circuits, QRS, reliability and precision tests using synthetic ECG *(German)* 78−92716
turbogenerators, high capacity, heating reduction measures for enhanced reliability and interval between maintenance *(Russian)* 80−96175
underground nuclear waste repositories, risk assessment using reliability models 80−57898
US multichannel shadow flaw detectors, accuracy and reliability of inspection 78−44306
US phased array diagnostic instrument with microcomputer *(Japanese)* 79−88146
vacuum beam diodes, repetitively pulsed 80−63386
reliability continued
vacuum valves, and valve traps, for production appl. 78−70140
water-moderated-water-cooled reactor VVER-1000, power plant technology 78−82501
wave power generation system, United Kingdom development 79−43739
weighing machines, reliability and performance testing 79−80579
welded structure reliability estimation, acoustic emission signal appls. 80−93702
Westinghouse plant availability anal. with operating data base 80−23050
wind power plant development, low cost approach 80−61268
wire fatigue properties, fast testing method using 23 kHz US frequency 80−89460
X-ray diffraction powder patterns, indexing reliability 80−87990
X-ray gaseous discharge proportional counters, ageing mechanism 78−78574
(Al,Ga)As long-lived DH injection lasers for fibre optic communication, degradation exam. 78−50778
(AlGa)As, CW laser diodes, long-term lifetests at room temp. 79−22963
(AlGa)As CW oxide-defined stripe laser, reliability statistical study 79−76687
$Al_xGa_{1-x}As$ buried heterostruct. laser, fabrication, optical props. and reliability 80−53322
$Al_xGa_{1-x}As$ laser diode, reliability 80−53320
$Al_xGa_{1-x}As$-GaAs LED design and characterisation for fibre-optic communications 78−46796
β-Al_2O_3-Na_2O tube life determ. for Na-S battery 79−29462
Cu electrodeposition on Su, failure anal. methods 78−24901
GaAS-$Al_xGa_{1-x}As$, DH laser and modulation developments *(German)* 78−37903
GaAlAs LED, high efficiency, long-lived, for fibre optical communication 77−79940
$Ga_{1-x}Al_xAs$ DH laser hybrid device, reliability 79−27281
$Ga_{1-x}Al_xAs$ junction-up TJS laser electron injection efficiency improvement 80−48300
$Ga_{1-x}Al_xAs$ visible diode lasers, degradation due to macroscopic defects (<730 nm) and facet oxidation (>740 nm), life tests 80−99729
GaAs FET, assessment by SEM electron beam 78−29216
GaAs-(GaAl)As DH lasers, automated LPE growth, CW reliability tests 80−20804
GaAs-(GaAl)As DH stripe lasers, CW life tests 79−98383
GaAs-$Al_xGa_{1-x}As$ DH laser, high-temp. degradation *(German)* 78−37884
GaInAsP-InP Zn diffused stripe geometry DH diode laser fabrication 79−98386
H_2 evacuation, magnetic discharge pump durability improvement 79−67326
He-Cd low-power low-cost blue lasers 77−19333
He-Ne gas lasers, 2 mW and 5 mW, reliability 80−95913
InGaAs-InGaP vapour-grown ternary heterojunction laser struct., reliability 79−98385
InGaAsP/InP injection lasers for long wavelength (1.1 to 1.6 μm) optical communication 80−58582
InGaAsP-InP vapour-grown quaternary heterojunction laser struct., reliability 79−98385
Li-I_2 battery, construction, performance and reliability 80−97771
LiI hybrid IC pacemaker, reliability, experience 77−81736
N_2 high-power pulsed laser manufacture and reliability 77−19331
Na valves for advanced reactors, reliability data collection at CREDO 80−22897
Nd:glass laser performance and reliability developments 80−78869
Ni-Cd 6.0 Ah cells, accelerated testing of cell failure for life prediction 80−35670
Ni-Cd and maintenance-free Pb accumulator characteristics *(German)* 80−97782
Ni-Cd rechargeable cells, construction, reliability and appl. 79−100509
NiCd rechargeable cardiac pacemaker system clinical experience 77−81727
Rb frequency standard, Rb lamp stability and reliability factors, expt. 77−17955
Re-Os nuclear chronometer, reliability, rel. to element rel. abundance 78−85919
U isotope separation processes *(French)* 80−806
W-Re, immersion thermocouples for ferrous metal temp. meas. 77−87767

reliability theory
see also statistical analysis
artificial satellites, future applications, reliability and cost considerations *(Italian)* 80−109334
digital m-of-n system with error indicating components, Boolean model appl. *(German)* 78−41133
downtime distrib. in reliability theory for single repairable component, time structs. 78−89959
electrical components, mathematical simulation of life *(Spanish)* 79−21532
failure rate statistical anal. 77−60918
Fourier anal. in Hilbert space of indication errors *(Rumanian)* 79−40523
importance sampling and Monte Carlo advantages 79−606
laser fusion process heat systems, reliability and maintainability anal. 79−18042
living systems, thermodynamic aspects *(Russian)* 79−20511
measurements of reaction rate consts., reliability criterion 79−8423
nuclear engineering, probabilistic systems reliability analysis for students 77−37698
nuclear reactor fuel handling system availability, minimum requirements 78−41820
nuclear reactor safety appl. 77−30653
nuclear safety system, time dependent unavailability anal., FRANTIC computer code 78−29588
optical instrument control life test design 80−87572
phased mission analysis, calc. of expected number of failures 80−68851
radioactive solid waste, storage facility, radiological safety assessment 79−17995
reactor safeguard system common-mode failure analysis 78−29618
spacecraft attitude control and navigation systems, instruments reliability enhancement 77−29623
structural reliability, using chance-constrained programming, appl. to reinforced silo 78−63338

reliability theory continued
structural system, simulation anal. of reliability and maintenance *(Japanese)* 80−62453
Weibull distribs., appl. to reliability aspects in metrology *(Rumanian)* 79−40524

remanence
see also coercive force
achondrite meteorites, brecciation and shock effects on mag. susceptibility and NRM 80−8603
acquisition in Finnish lake sediments 79−66682
Alnico 5, thermal treatment in mag. field, mag. props. 78−91905
Alnico type YuNDK25DA alloy permanent magnets, thermal mag. hysteresis 80−75818
anhysteretic remanent magnetisation for palaeomag. field intensity determ. 77−37430
anhysteretic remanent magnetisation for palaeomag. field intensity meas. 77−37431
ARM, of basalts, study with var. of AC and DC fields 79−48465
artificial rock samples, inhomogeneous remanent mag. meas. 77−45174
basaltic dyke with concentric cooling zones, remanence vars. 77−49062
basalts, mag. grains effect on remanent magnetisation 77−37191
basalts, O_2 partial press. influence on TRM 77−37190
basalts, of oceanic layer 2, occurrence of TRM questioned 78−65279
basalts from deep drill holes in Iceland, remanence rel. to mag. layer concept 77−60365
basalts from Nazca Plate, mag. props. and opaque mineralogy 78−20396
Beaufort Sea sediment cores, NRM, geomag. excursion record 78−20349
biological materials, remanent magnetization as evidence for room temp. superconduction 80−35926
chondritic meteorite, remanent magnetisation rel. to shock and metamorphic history 80−36598
chondritic meteorite magnetisation 80−36599
clay thermoremanent magnetisation, cooling-rate depend. 80−46174
Cretaceous pelagic limestone, Sicily, dual mag. polarity meas. in single bed 79−53306
detrital remanent magnetisation in five slowly redeposited long cores of sediment 79−70786
Devonian lacustrine sediments, from Caithness, Scotland, palaeomag. and mineralogy 78−28170
diabase dykes, Late Mesozoic, from S.Spitsbergen, thermomag. props. 79−92528
diamond-Co, sintered together, remanent magnetism 79−99731
DSDP abyssal igneous cores, remanent mag. inclinations, postemplacement tectonic effects 78−28161
DSDP Leg 37 basalts, oxide microstructs. and mag. props. 77−91108
DSDP Leg 37 samples, magnetisation and palaeomag. field intensity meas. 77−90996
Early Permian Ingelside Formation, N.Colorado, palaeopole position 79−29704
γ-Fe_2O_3 acicular particles, remanent coercive force 80−44872
ferrimagnetic magnetisation theoretical models, for uniparametric materials 80−65960
ferrite core, strength improvement method, SiO_2 and Bi_2O_3 additions, mag. characts. 79−24484
ferrite F-600, suspension in caster oil, residual magnetisation *(Russian)* 79−1689
ferromagnet, random anisotropy amorphous, initial magnetisation, remanence and coercivity 77−80964
ferromagnet, remanent magnetisation during thermal demagnetisation near a phase transition 78−88142
ferromagnet with random anisotropy, spin correlation 79−73722
ferromagnetic, uniaxial, remanent magnetisation from X-ray pole figure data 79−91252
ferromagnetic amorphous alloys, temp. depend. of mag. hystersis props. 79−61186
ferromagnetic materials, anomalous temp. depend. of remanent magnetisation 77−33060
ferromagnetic plate, magnetic hysteresis theory, singularities of magnetic reversals on industrial freq. *(Russian)* 78−39373
ferromagnetics, remanence rel. to palaeomagnetic studies 77−33062
ferrosuspension, residual magnetisation effect in nonuniform mag. field 79−78443
fine particle system, coercivity and remanence, particle size distrib. effect 77−73053
gyroremanent magnetisation in anisotropic mag. material 80−50142
haematite, grain size and coercive force from high temp. AF demag. 77−37189
Harp Lake Complex and associated rocks, Labrador, remanence and palaeomagnetism 77−90997
igneous rock, rot. remanent magnetisation 80−85645
igneous rock bodies, in situ mag. meas. 79−84521
igneous rocks, single domain oxide particles as source of TRM 78−65271
igneous rocks, thermoremanent magnetization 77−91113
igneous rocks, TRM and var. with grain size 78−65270
interacting single-domain grains, thermoremanence and ideal magnetization calc. 79−25232
ionic compounds, amorphous, exhibiting Mossbauer spectra, magnetic props. *(French)* 80−80490
IRM of Yellowstone Group comparison with DRM of Pearlette ash beds 80−21624
Ising chain with random bonds, remanence and non-exponential relax. 79−73751
Ising model, spin glass, mean field theory 79−4680
Ising spin glass, remanent magnetisation, Monte Carlo exam. 79−61166
kimberlites, Precambrian and Cretaceous, in S.Africa, remanent magnetisation 78−96134
kimberlites, South Africa, palaeomag. determ. of emplacement temp. 77−78180
Kirin chondrite, remanent magnetisation, early interplanetary space mag. field *(Chinese)* 78−89136
Korostenian pluton gabbro-anorthosite rocks (Ukrainian Shield), natural residual magnetisation origin *(Russian)* 79−8599
Lake Tahoe, California-Nevada, remanence, props. and palaeomagnetism 80−41371
Late Cretaceous polarity sequence, Scaglia Rossa limestone, Italy, rock and palaeomag. studies 78−11803
limestones, Upper Jurassic, from Southern Germany, mag. props. 79−25197

remanence continued
lunar palaeomagnetism, origin 78−93132
lunar rock fragments and fines from Luna 16 and 20 77−22123
lunar rocks NRM meas., ancient mag. field intensity determ. 77−37530
lunar soil, shock effects on magnetism 77−60675
magnetic fields in early solar system, recorded in lunar rocks, meteorites and planets 79−5765
magnetic particle crack detection, remanent magnetism 77−63841
magnetic tapes, static and antihysteretic mag. props. 80−44868
magnetically soft cylinders, micromagnetics of curling configurations 79−82826
magnetically-soft materials, mag. characts. determ. methods, review 79−40593
magnetite, partial thermal remanent magnetisation additivity 80−26498
magnetite monocrystals and rocks under high uniaxial press., mag. props. 78−73361
magnetite particle size effect on palaeointensity determ. 77−37186
metamorphic rocks, thermal overprinting of NMR and K/Ar ages 78−65278
meteorite impact site, Slate Islands, Canada, shock remanent magnetisation 80−30986
meteorites, evidence for primordial mag. field in parent body era 78−45293
meteorites, palaeomag. field intensity determ. from remanent magnetisation 77−37583
minerals, single-domain grains ensemble near anisotropy const. transition through zero 77−78164
Miocene rocks, Borzsony Mountains, Hungary, palaeomag. 78−32011
mountain rocks, primary remanence orientation var. rel. to palaeomag. prehistory *(Russian)* 77−44917
Mull lava succession palaeomag. study rel. to Eurasian Plate motion 77−48995
multicomponent NRM separation using difference and resultant magnetization vectors 79−66826
non-uniform magnetisation and vibrating-sample magnetometer 78−54414
NRM, multicomponent, separation method, rocks appl. 79−34805
NRM in deep sea sediments, time series anal. 79−29757
oceanic and recent lavas, NRM/ARM ratios 77−37133
oceanic crust mag. props., DSDP Leg 34 results from Nazca plate 77−17024
oceanic crustal layer 2, remanence of DSDP Leg 37 samples 77−91071
one-dimensional random Glauber model, magnetisation relax. 80−80523
ophiolite complexes, effects of alteration on NRM and implications for oceanic crust 78−65280
palaeointensity methods using AF demagnetisation and anhysteretic remanence, reliability 78−77352
Permalloy film, stripe domain struct., distrib. of magnetisation *(Russian)* 77−66396
Permalloy I bars, hysteretic props., Bitter soln. obs. and Kerr effect meas. 79−78439
permanent magnet, magnetic texture form. in double pole gap of electromagnet 77−89985
Pliensbachian limestone sequence at Bakonycsernye (Hungary), remanent magnetisation 80−90074
post-depositional magnetization in Recent tidal-flat sediments 80−101320
Precambrian schist belt, Karnataka, India, remanent magnetisation direction from aeromag. anomaly inversion 79−44094
pseudo-single domain grains, stable remanence origin 78−65275
pyrrhotite, pseudosingle-domain effects and single-domain multidomain transition 77−64274
rare earth alloys, amorphous, study of hysteresis effects using Monte Carlo technique 79−1686
rare earth alloys, R-3d alloys (3d=Mn,Fe,Co,Ni), magnetic properties 78−52231
Rayleigh hysteresis, reexam. 78−48002
red beds, secondary magnetizations significance and utilization 78−28165
ring specimens, computer controlled mag. meas. system 80−86346
rock, reversible effect of small uniaxial stress on remanent mag., single-domain theory 78−20393
rock, rotational remanent magnetisation, origin 80−61794
rock magnetism, post-depositional realignment of sediments, expts. and theory 80−109137
rock magnetism, rotational remanent magnetisation, explanation 80−51390
rock magnetism, self-reversal of remanent magnetisation of lava 80−56462
rock samples, removal of rot. remanent mag. acquired during alternating field demag. 77−60474
rocks, ARM correction method for mag. palaeointensity determ. 79−34968
rocks, characts. of psark induced TRM 78−65274
rocks, comparative anal. of chemical and thermoremanent magnetisation 77−81870
rocks, magnetic-diffusion aftereffect, Preisach-Neel diagram appl. 78−61403
rocks, multiphase magnetizations, recognition and separation techniques 78−28349
rocks, NRM stress sensitivity meas. using cryogenic magnetometer 80−26506
rocks, remanence direction from converging remag. circles 77−45182
rocks, Zijderfeld vector diagrams use in multicomponent, palaeomag. studies 80−17420
rocks and roof tiles, palaeointensity determ. by single heating method 77−37427
rocks magnetic components, separation from alternating field step demagnetisation data 79−16444
rocks remanent magnetisation, effect of stress cycling and inelastic volumetric strain 78−88820
rocks remanent magnetisation, uniaxial stress effects, stress cycling and domain state depend. 80−26505
rocks TRM, multidomain grains demagnetisation field 78−65273
rotational remanent magnetisation 77−2150
sand, specularite-bearing, experimentally deposited, mag. declination and inclination errors 80−90075
sedimentary and igneous very old rocks, palaeointensity determ. problems 77−37428
sedimentary rocks viscous remanent magnetisation, stability to AF demagnetisation, expt. results 79−79826

remanence continued
sediments, drying remanent magnetization 79−66681
sediments, fine-grained, compaction effect on acquisition of detrital remanent magnetization 78−20395
sediments, oblique anhysteretic remanent magnetisation 80−21717
sediments, upper Keweenawan, virtual geomag. pole position determ. 77−78089
sediments magnetization, depositional and postdepositional processes 77−86869
shock-diminished remanence at Charlevoix impact structure, Quebec 80−26441
silicic volcanics, Jurassic, from Nevada, USA, thermochemical remanent magnetisation 80−98310
single particle material for tape and disc manufacture, prep., props., and appls. 78−52308
Skye lavas, NW.Scotland, remanent mag. struct. 78−28167
spin glass, EPR frequency and mag. transverse susceptibility with remanent magnetisation *(French)* 80−7145
spin glass, metastability, Onsager theory 79−82796
spin glass, model, relax. of remanent magnetisation 78−91873
spin glass, remanent magnetisation using Monte Carlo methods 79−78421
spin glass, slow decay of remanence magnetisation, theory 80−11211
spin glass, theory 77−66371
spin glass, time dependent Ginzburg-Landau equation 79−61161
spin glass model, simple, magnetisation decay 80−71073
spin glasses, annealing and mag. remanence 80−60308
spin glasses, mag., transport props. *(Czech)* 78−80149
spin glasses, review 77−69578
spin-glass, two-dimensional Ising model, low temp. dynamic props. 80−20425
St. George pluton, New Brunswick, dual polarity remanences anal. rel. to palaeomagnetism 79−100809
steel, high-speed, 30Kh2N2SMKt, deform. effects on physicomech. props. 78−23741
stony meteorites, mag. props. and remanent magnetisation 79−16899
submarine basalts, remanence rel. to changes in mag. signal of oceanic crust 77−90995
terrestrial planets, remanence model for mag. fields 78−12125
terrestrial rocks, effects of shock on remanence 78−85538
Tertiary basalts with low Curie temps., palaeomag. data reliability 78−28166
Tertiary rocks, Faeroe Islands, remagnetization 78−28168
Tertiary volcanic rocks, N. Bavaria, palaeomag. and rock mag. meas. 77−64203
Thanet gabbro complex, Ontario, mag. overprinting 79−25187
Thellier-Neel's laws, distinction between juxtaposed and superimposed magnetisation *(French)* 79−84229
Thetford Mines ophiolites, Quebec, NRM props. and palaeomagnetism 80−61757
Thunder Bay Late Quaternary sediments, palaeomagnetic record from remanent mag. meas. 80−17230
Ticonal, effect of rare earth metals on mag. props., struct., and phase transformations 79−99732
Ticonal with Sm, magnetic props., phase transform. after thermomagnetic treatment 78−3155
titanomagnetite, NRM stable component in multiphase oxidised titanomagnetite 77−60366
titanomagnetite, TRM acquired by multi-domain single cryst. 80−36293
titanomagnetites, temp. depend. cation distrib., mag. prop. obs. 80−85647
titanomagnetites, TRM rel. to domain struct. temp. var. 78−65272
transition metal ferromagnetic amorphous alloys, mag. props. 77−55690
transition metal-noble metal spin glass films, mag. props. 80−60306
TRM direction, mag. shape anisotropy effect, appl. to basalts 79−29758
TRM integral characts. for palaeomagnetic field intensity determ. 78−73310
TRM origin, symposium (San Francisco, CA, 1976, December 9) 78−65269
twin crystals, magnetic reversals, role of magnetostatic interaction *(Russian)* 78−39361
twisted uniaxial polycrystals, magnetisation process, model 79−91254
Upper Cretaceous rocks at Moria (Umbrian Apennines), palaeomag. stratigraphy and remanent mag. intensity 78−96132
Upper Pliocene deposits, W Turkmenia, NRM origin and palaeomag. 79−25192
V-Fe (29-35 at%), ferromag., mag. props. near crit. conc. for ferromagnetism 78−19225
volcanic rocks, palaeointensity determ. by modified Thellier method 77−37426
weak, accurate meas. 80−68225
Wilberns Formation, Texas, palaeomag. and Lake Cambrian field for North America 77−17025
Yellowstone and Jackson Lakes, mag. props. and secular var. in sediment cores 78−48968
$Al_2Mn_3Si_3O_{12}$, amorphous insulating spin glass, susceptibility and magnetisation meas. 80−88765
Au-Fe, spin glass in low DC field, mag. viscosity, time decays of remanences 78−64209
Au-Fe (4 at.%), spin glass energy relaxation of remanent magnetisation at low temp. 79−87271
Au-Fe (4 at.%), spin glass, magnetisation and energy relax. below T_g 80−65921
Au-Fe alloy, spin glass behaviour in low DC field 77−66373
Au-Fe spin glass, energy flux associated with remanent magnetization relaxation *(French)* 80−7110
Au-Fe spin glasses in low DC fields, susceptibility and thermoremanence 77−77063
Ba-ferrite, hard magnetic, Hall effect 79−38109
$BaFe_{12}O_{19}$, Hall effect, magnetisation and elec. resist., 30 to 80°C 77−51766
$CaO-Al_2O_3-SiO_2$ glass, remanent magnetisation, log t low 78−68300
Ce-Co-Cu-Fe-Ti, sintered magnet, prep. and mag. props. 77−73043
Ce_3Al_{11}, mag. ordering at low temps. under press., relation to $CeAl_3$ props. 79−19745
$Ce_x(La_{0.76}Y_{0.24})_{1-x}Bi$, mag. phase diagrams 79−56535
$(Co,Cu,Fe)_5Ce$, sintered, mag. props. 78−68302
Co, electrodeposited coating, struct. and magnetic props. 79−46985
Co, FCC, mag. props. of single-domain powders after plastic deform. *(Russian)* 78−6554

remanence continued
Co, ferromagnetic micropowder, cryst. struct., coercivity, remanence, saturation 80−65967
Co films layered over Cr by DC sputtering for digital mag. recording 79−83118
Co vacuum condensates, Cr alloying addition effect on texture characts. *(Russian)* 80−108471
Co-Cr films, mag. props. in range of transition from thin-film to hypercritical state *(Russian)* 79−51824
Co-Cu-Fe-Ce, mag. characteristics of sintered permanent magnets 78−60312
Co-Fe-Nb-Mo, semihard magnetic alloy, magnetic props. 78−95469
Co-Ni fine particles, anhysteretic growth of exchange fixed remanent states 77−16116
Co-Ni-P, film, props. independent of mag. hysteretic and anhysteretic remanences *(French)* 80−2604
Co-Ni-P electrolytic layers, partial anhysteretic remanent magnetisation, additivity prop. *(French)* 80−44882
Co-Si-B-Fe alloy magnet, Al_2O_3 particle embedded surface, amorphous mag. anal. using electron diffr. 79−56568
Co-Si-B-Fe amorphous alloy, electron diffr., mag. anal. *(German)* 79−61182
Co-W(Mo) magnetic alloys for high temp. appl. 77−85503
$Co_{74}Fe_6B_{20}$, metallic glass, zero magnetostriction, magnetisation characts. 77−12158
$Co_{57}Fe_5Ni_{10}(Si,B)_{28}$, amorphous, soft mag. props., switched-mode power supply appls. 80−88850
$CoO-Al_2O_3-SiO_2$, amorphous, remanent magnetisation short time depend. 80−65919
$CoO-Al_2O_3-SiO_2$, spin glass, magnetic aftereffects 79−61176
CrO_2 powder, thermal-magnetic props. 79−51821
CrO_2, single mag. particle, remanent coercive force and remanent loop meas. 78−95480
Cu-Fe, dil., internally oxidised mag. and electrical prop. 77−12100
Cu-Mn, mag. irreversibility and metastability 78−19279
Cu-Mn, mictomag., massive short-range antiferromagnetism 77−12139
Cu-Mn alloy spin glass, macroscopic mag. anisotropy, transverse susceptibility and zero field NMR enhancement 80−80525
Cu-Mn spin glass, hysteresis loops, temp. and field depend. 80−15742
Cu-Mn spin glass, saturated thermoremanent magnetisation, time and temp. evolution 79−61167
Cu-Mn(1%) spin glass, remanent mag., zero-field NMR obs. 79−33492
Cu-Ni-Fe, permanent magnet, temp. effect 80−34701
CuMn, spin glass, remanence, new approach from zero field NMR 80−34785
$Dy(Fe,Al)_2$, saturation and remanent magnetostriction meas. 77−63256
$(ErEu)_3(FeGa)_5O_{12}$ film, for mag. writing and magneto-optical displays 78−6549
$Eu_xSr_{1-x}S$, insulating spin glass, mag. props. 80−2589
Fe, ferromagnetic micropowder, cryst. struct., coercivity, remanence, saturation 80−65967
Fe, fine particle dispersions, shock induced mag. effects 79−82832
Fe, first order shock induced mag. transitions characts. and discrimination from TRM 78−64205
Fe meteorites, thermoremanence hypothesis rel. to origin of magnetisation 78−65564
Fe powder, BH_4 reduced, coercive force and remanence ang. variation 80−44879
Fe powders, prep. by BH_4 process, comp. and stability 80−44878
Fe-Al-Ni-Co-Cu alloys, Ti alloying and deoxidising addition *(Russian)* 78−80181
Fe-B-Si amorphous ribbon, strain induced anisotropy, and toroid diam. effect on mag. props. 80−34623
Fe-Co, ferromagnetic micropowder, cryst. struct., coercivity, remanence, saturation 80−65967
Fe-Co-Ni-Al-Zr magnetically hard alloys, reduction *(Russian)* 78−43614
Fe-Cr-Co, permanent magnet, temp. effect 80−34701
Fe-Cr-Co hard-mag. alloys, fine cryst. struct. *(Russian)* 77−66706
Fe-Cr-Co(-Mo), mag. props. after isothermal thermomag. treatment *(Russian)* 80−25159
Fe-Mo(W), semihard magnetic alloys, magnetic, elec. mech. props. *(Japanese)* 79−70078
Fe-Ni-Al-Cu (25, 14, 4 wt.%), alloy YuND4, effect of Ti addition on structure, mag. props. 80−15714
Fe-Pd-Pt alloy powders, coercive force and specific remanence *(Russian)* 79−47302
$Fe_{80}B_{20}$ amorphous alloy, low field magnetic props. 77−55690
$Fe_{80}B_{20}$ glass, low-field mag. props. 77−8380
$Fe_{80}B_{20}$, sputter deposited amorphous, low field mag. props. 78−68335
$Fe_{80}B_{20-x}M_x$ (X=Al, Si, Ge, C, P) and $(FeCo)_{80}B_{20}$ glass, magnetisation, Curie and crystn. temps. 79−87289
FeF_3, amorphous, noncryst. magnet with antiferromag. interactions 79−91228
$Fe_{40}Ni_{40}B_{20}$, amorphous, processing conditions effect on mag. props. 79−73775
$Fe_{40}Ni_{40}B_{20}$, amorphous, casting conditions effect on mag. props. *(Japanese)* 80−34698
$Fe_{65}(Ni_{1-x}Cr_x)_{35}$, remanent magnetisation, temp. depend., anomalies near Curie temp. *(Russian)* 78−60310
$Fe_{40}Ni_{40}(Mo,Si,B)_{20}$, amorphous, soft mag. props., switched-mode power supply appls. 80−88850
$Fe_{40}Ni_{38}Mo_4B_{18}$ glassy alloy, high permeability, low field mag. characts. 78−68301
$Fe_{40}Ni_{40}P_{14}B_6$, amorhpous ribbon, influence of torsion on mag. props. 80−7138
$Fe_{40}Ni_{40}P_{14}B_6$, amorphous, mag. props. 78−10728
γ-Fe_2O_3, clean and SiO_2 coated, reduction temp. influence on coercivities, coercivity factors and rheological props. 79−69698
γ-Fe_2O_3, densified, rheological and mag. props. 80−44873
Fe_2O_3, haematite, fine-grained, hard viscous remanent magnetisation 77−56623
γ-Fe_2O_3, particle interactions, in inhomogeneous anisotropic magnetic materials, average field effect 77−32217
γ-Fe_2O_3 powders, influence of densification on mag. props. 78−95481
γ-Fe_2O_3, prep. from thermal decomp. of $[Fe_3(HCOO)_6(OH)_2]HCOO.4H_2O$ and characterisation 78−80741
γ-Fe_2O_3, single mag. particle, remanent coercive force and remanent loop meas. 78−95480
γ-Fe_2O_3:Co, impact-induced demagnetisation, magnetostriction and coercive force, appl. in mag. recording 77−16111

remanence continued
γ- Fe_2O_3-Fe_3O_4, lodestone, microstructure and mag. props., source of mag. hardening 79−82828
Fe_3O_4 ferrofluids, spin glass behaviour 80−71120
Fe_3O_4, magnetite, ARM, TRM and magnetic interactions: concentration dependence 79−44177
Fe_3O_4, magnetite, coercive force spectrum at high temps. rel. to thermal activation below blocking temp. 77−91111
Fe_3O_4, magnetite, comparison of anhysteretic remanence and thermoremanence 77−5191
Fe_3O_4, magnetite, grain size limits for pseudosingle domain behaviour, rel. to palaeomagnetism 80−11215
Fe_3O_4, magnetite, TRM props. of single-domain, pseudo-single-domain and multidomain particles 78−40544
Fe_3O_4, magnetite particles, interaction fields effect on hysteretic props. 80−54921
Fe_3O_4:Co, impact-induced demagnetisation, magnetostriction and coercive force, appl. in mag. recording 77−16111
$Fe_{75}Si_{15}B_{10}$, duplex ferromag. alloy, thermoremanent magnetization 79−73778
$Fe_{2.6-x}Ti_{0.4}Al_x O_4$, $Fe_{2.4-x}Ti_{0.6}Al_xO_4$, titanomagnetite, monodomain, mag. props. 78−56346
Fe_2TiO_4, ulvospinel, containing magnetized inclusions, mag. behaviour, cooling through Curie point 78−56314
Fe_2TiO_4, ulvospinel, mag. props. weak ferromag. in 4-200K temp. range 78−56351
$Fe_{2.4}Ti_{0.6}O_4$, titanomagnetite, single-crystal, mag. props. of multidomain TRM 78−56345
Gd alloys, amorphous, mag. props. and ferromag. reson. 80−54952
Gd-Al(C)(Cu)(Ga)(Ni)(Pd)(Rh) alloys, amorphous, mag. and elec. props. 80−80499
Gd-Co alloy, sputtered film, mag. props. determ. *(Chinese)* 78−2714
$(Ho_2O_3)_{0.194}(Al_2O_3)_{0.227}(SiO_2)_{0.579}$, amorphous, low temp. spin glass behaviour 80−60297
$(La,Gd)Al_2$ spin glasses, time depend. mag. props. 80−65909
La-Gd-Au, amorphous spin glasses, mag.-cluster description 79−42776
La-Gd-Au alloys, amorphous, high Gd content, bulk mag. props. 77−59426
$La_{1-x}Gd_xAl_2$, spin glass, thermoremanent and isothermal remanent magnetisation 79−87276
La_2MnFeS_5, antiferromag., mag. props. and mag. struct., neutron diffr. and magnetisation meas. 80−65801
$Li_{0.5}Fe_{2.5}O_4$, microwave material, mag. props., review 79−33504
$(MgFe_2O_4)_x$-$_1(Mn_3O_4)_x$, soft ferrite, squareness ratio and max. induction 79−99730
MgMn ferrite CVD epitaxial layers, bubble domains in remanence and demagnetised states 77−85516
Mn-Al-C, fine-grained cast struct., remanence and coercive force 80−60365
$Mn_{55}Al_{45}$ alloy, permanent mag. props., depend. on particle size 78−91899
MnBi particles, demagnetised, coercivity, remanence and magnetisation reversal 78−19281
$Mn_{1.88}Cr_{0.12}Sb$, thermomagnetic props., antiferromag. to ferrimag. transition 77−63194
$Mn_{2-x}Cr_xSb$ film, prep. and mag. props. 78−48009
$MnO-Al_2O_3-SiO_2$, amorphous, spin glass like behaviour at low temp. 79−61177
$MnO-Al_2O_3-SiO_2$, amorphous, remanent magnetisation short time depend. 80−65919
β-$Na_xV_2O_5$, antiferromag. props. and weak ferromagnetism 79−78337
Ni, deformed, coercivity and remanence anisotropy 78−31093
Ni, mag. props. of single-domain powders after plastic deform. *(Russian)* 78−6554
Ni-Co, mag. props. of single-domain powders after plastic deform. *(Russian)* 78−6554
Ni-Fe, new soft magnetic material for pulse transfer and choking in power electronics *(German)* 79−28555
Ni-Fe (40%), Mn coating, mag. interface effects 77−69638
Ni-Fe overlay, influence on bubble device performance 79−78466
Ni-Mn alloys, remanent magnetisation reversal, local environment model 79−33507
Ni-P, amorphous alloys, low temp. mag. props., comp. depend. 77−66387
$NiFe_2O_4$, soft ferrite, squareness ratio and max. induction 79−99730
$(Ni_{1-x}Fe_x)_{1-\delta}S$, anisotropic spin glass, mag. props. 80−39793
Ni_3Mn, partially ordered, remanence reversal 77−69619
Ni_3Mn, thermoremanent magnetisation and blocking temp. 80−34601
NiO fine particles, mag. props. rel. to physicochem. props. 78−52315
NiS film, electrolytically deposited, S content influence 80−44884
Pt-Co system, low temp. susceptibility 80−65920
Pt-Fe ordered alloy, multiply mag. phase transitions 80−60264
Pt-Mn alloy, dil., low temp. susceptibility, spin glass and Kondo behaviour 77−66372
Sm-Co, alloy powders and sintered magnets, effect of chem. treatment on mag. props. 78−60311
Sm-Co base ternary alloy, mag. props. and cryst. struct. 77−8352
Sm-Co-Cu-Fe-Zr magnet, production and mag. props. 77−40085
$SmCo_5$ based ternary and quaternary permanent mag. materials with low reversible temp. coeffs. 79−82822
$SmCo_5$, remanence and energy product, X-ray method of planar orientation 77−8342
$SmCo_5$, sintered, hard mag. material, magnetisation behaviour 80−75805
$SmCo_5$, sintered, mag. props. *(German)* 77−43852
$SmCo_5$, sintered, orientation of particle easy axes, statistical model 77−8305
$Sm(Co_{0.86-x}Cu_{0.14}Fe_x)_7$, permanent magnet, sintering and heat treatment effects 80−39817
Sm_2M_{17}, sintered magnet, hard mag. props. optimisation 77−8340
$Sr_{1-x}Eu_xS$, dilute spin glass, mag. props. 79−78386
$SrFe_{12}O_{19}$ micropowder, high coercivity, obtained by extended wet milling, prep. and mag. props. 77−8776
$TbFe_2$, amorphous, temp. depend. of mag. hystersis props. 79−61186
$(Ti_{1-x}V_x)_2O_3$ spin glass, mag. props., metallic antiferromagnetism 79−82791
$(Ti_{1-x}V_x)_2O_3$, spin glass props. and anisotropy, comp. depend. 77−66368
US, low field mag. props. 77−73047
W-Fe alloys, spin glass props., DC susceptibility and remanence meas., 1.6 to 295K 80−29560
$Y_{2.01}Gd_{0.99}Fe_{4.925-x}Mn_xO_{12}$, comp. depend. of mag. props., and stress sensitivity control 78−27057

remanent magnetism *see remanence*

remote consoles
CERN 400 GeV proton synchrotron control consoles 77−38518
disabled persons employment using traffic operator position system 80−36197

remote control *see telecontrol*

remote control equipment *see telecontrol equipment*

remote metering *see telemetering*

remote sensing
see also infrared imaging; remote sensing by laser beam
3 mm wavelength scattering and emission characteristics of natural media 78−3770
acoustic, remote measuring techniques, three-channel correlation *(German)* 79−50512
acoustic, using modified microwave dish-antenna 79−72770
acoustic Doppler and angle of arrival wind detect., comparison with direct meas. 79−39884
active, with radar, radiative transfer theory, half-space random media appl. 79−8721
active and passive remote sensing of Earth terrain, effects of scattering 80−101435
active faults, aerial photographs interpretation *(Japanese)* 78−96124
active microwave systems 77−56776
adjacency effects on imaging by surface reflection and atmospheric scattering 79−100939
Aegean Sea and surrounding regions, Landsat photographs rel. to active tectonics 78−96181
aerial data processing, automatic, for agricultural resources inventory and survey expt. 77−78505
aerial electroprospecting, transducer interference analysis *(Russian)* 77−56766
aerial landscape photography, haziness factor in image contrast *(Russian)* 77−37449
aerial multispectral-photographic lenses, Pinatar 4/125, manufacture *(German)* 78−4717
aerial photographic equipment developments, aerial survey camera and navigation telescope 77−66997
aerial photography, high altitude, aspects and results 78−36309
aerial photography, multispectral, soil survey in New Zealand 78−85728
aerial photography, stereo viewing, interpretoskop optics, modifications 80−105081
aerial photography for densification of urban geodetic nets 77−78462
aerial reconnaissance, performance evaluation of electro-optical focal planes 79−31833
aerial reconnaissance film interrogation by optical matched filtering 77−78484
aerial reconnaissance film screening using optical matched-filter image-correlator technology 78−94371
aerial survey image interactive hybrid optical/video processing system 77−53254
aerochrome IR film var. and high-altitude photographic appls. 79−2180
aerological and satellite meas. system, objective anal. accuracy determ. 79−39832
aerosol, middle atmospheric, remote sensing techniques 80−109269
aerosol atmosphere, MTF and PSF calcs. rel. to space-meteorological photography, multiple scatt. effect 79−66792
aerosol in atmos., mass concentration from Lidar-solar radiometer expt. 80−90171
aerosol layer, solar occultation technique using Skylab coronagraph 77−9540
aerosol solid particles, diffusive evaporation, laser spectrochemical analysis 79−92040
aerospace photographic image information, atmospheric effect evaluation 80−4101
aerotriangulation by Skylab Earth terrain camera photography 77−33209
Africa CITHARE project, soil thermal inertia and humidity cartography by geostationary satellite 80−76980
agricultural cover type separability in visible and IR 77−29473
agricultural cover types, separability in spectral channels and wavelength regions 80−98468
agricultural water demand information, remote sensing 79−2315
agriculture, max. likelihood estimation of signature transformation algorithm 77−78497
agriculture acreage estimates using LANDSAT data, interactive software systems 77−78504
agriculture applications 80−56329
Agulhas Current, satellite IR images, circulation modes 79−5484
air pollutants, by correl. spectroscopy, instrumental response characts. 79−5623
air pollution, pollutant gases monitoring from space using passive microwave techniques 80−76690
air pollution, population exposure in USA, evaluated by satallite 80−40936
air pollution, remote sensing via computer assisted correl. spectrometer 78−4002
air pollution detection, appl. of $LiNbO_3$ tunable parametric oscillator 78−59089
air pollution meas. expts., estimation of surface temp. 79−70854
air pollution monitoring, active and passive systems 77−70889
air pollution monitoring by satellite, correl. spectroscopy techniques 77−64456
air pollution remote sensing from space 78−61621
air pollution sensing using rotational Raman spectroscopy with Fabry-Perot interferometer 77−71384
air pollution single ended monitoring system, 1.4 to 4 μm range 78−3974
air sampling system, radio-controlled, for diffusion expts. 79−79440
air-sea search and rescue appl. of line scanner imagery 79−21519
airborne, microwave radiometer appl., stepped-frequency, 4.5 to 7.2 GHz 79−80062
airborne and spaceborne appl. *(Japanese)* 77−5338
airborne IR line-scan, tangent sweep time base for recording of data, cct. 77−9525
airborne wave tilt meas. for reconnaissance mapping at poorly cond. areas 77−78473
albedo of ground and index of absorption of atmospheric particulates, theory 79−88438
Alboran Sea, mesoscale oceanic vortex, drifting buoy and satellite meas. *(French)* 79−16473

remote sensing continued
altimetric data file acquisition automatic digital correlation method 78−61633
American Society of Photogrammetry, use of International System of Units 79−21692
American Society of Photogrammetry Annual Convention, Washington, USA (March 1978) 80−4149
angular reflectance variations of rough surfaces, near IR, correction method 77−75424
anisotropic reflection properties of vegetated surfaces 77−82010
Antarctic glaciers, radio emission spectra in 0.8-8.5 cm band *(Russian)* 77−29333
Antarctic glaciers thermal radio emission, theory for random layered media *(Russian)* 77−33106
Arctic lakes, L-band imaging radar obs. 77−21816
Arctic sea ice, layered struct. study by radar sounding *(Russian)* 78−16023
array antennas radiometric earth and atmospheric sensing systems for large structures 77−41281
artificial satellite observations *(Japanese)* 79−74977
artificial satellites, and resource sensing *(Japanese)* 78−16211
artificial satellites, Space Shuttle and European Spacelab appls. for 1980s 78−69494
artificial satellites future role in meteorological obs. 79−79965
central Asia, active faulting and Cenozoic tectonics of Tien Shan, Mongolia and Baykal 80−8278
Askja Caldera, Iceland, imaging radar obs. rel. to surface roughness 79−16426
atmosphere, above warm water surface, thermal exchange, optical meas. methods 77−49184
atmosphere, active microwave sensing *(Japanese)* 78−16213
atmosphere, aerosol properties rel. to solar aureole, photogrammetry 78−57315
atmosphere, conf. (Innsbruck, 1978 May 29-June 10) 80−31415
atmosphere, dichlorodifluoromethane spectral parameters for atm. sensing 79−84481
atmosphere, echo carrier freqs. and antenna dimensions rel. to echosonde antennas performance 78−1474
atmosphere, H_2O vapour and cloud liquid determ. by dual freq. ground-based microwave radiometry 78−93007
atmosphere, H_2O vapour and liquid, Nimbus 5 microwave spectrometer meas. 77−49129
atmosphere, humidity field objective anal. using remote sounding data 78−61524
atmosphere, ice and water content from Nimbus 6 IR sounder data 78−92925
atmosphere, mesoscale temp. and moisture fields from satellite IR radiance meas. 78−7717
atmosphere, meteorological satellites obs. appls. to weather modification programmes 78−96259
atmosphere, moisture profile estimation from satellite IR radiance meas. 78−45021
atmosphere, moisture profile meas. from brightness temps. in H_2O 1.35 cm reson. region *(Russian)* 78−81403
atmosphere, O_3 meas. in IR absorpt. bands, information content estimation *(Russian)* 78−88883
atmosphere, O_3 total content determ. using remote spectroscopy 78−65437
atmosphere, obs. from orbiting satellite, using laser 77−9571
atmosphere, operational vertical sounder on TIROS-N polar-orbiting meteorological satellite 80−77132
atmosphere, optical meas. of minor gases 79−84480
atmosphere, quantitative bistatic acoustic sounding of boundary layer 78−49176
atmosphere, radioacoustical sounding by continuous radiation method *(Russian)* 78−88927
atmosphere, satellite picture anal. 79−8713
atmosphere, satellite-derived radiance gradient rel. to upper tropospheric/lower stratospheric winds 80−98447
atmosphere, temp. and emittance effects on sensed data 77−78393
atmosphere, temp. and gaseous composition profiles by spectroradiometry 77−9568
atmosphere, temp. and press. profiles meas. via solar occultation sounding using narrowband radiometers 80−98452
atmosphere, temp. profile retrieval with passive microwave sounder using Kalman-Bucy filters 79−21053
atmosphere, temperature profile retrieval from IR satellite data 79−48586
atmosphere, turbulent, optical props. determ., He-Ne laser transmitter-receiver appl. 80−98450
atmosphere, vertical temp. profiles using ground based IR spectroradiometer *(Japanese)* 77−29499
atmosphere, VHF radar expts. 78−88938
atmosphere acoustic and radio acoustic exploration, effects of sound nonlinear absorpt. *(Russian)* 80−94567
atmosphere acoustic sounding technique, appls. to siting studies 78−81467
atmosphere boundary layer, acoustic sounder obs. from top of steep mountain 80−98409
atmosphere contaminant tele-detection apparatus using combination light scatt. spectra *(Russian)* 77−49193
atmosphere ground-based radiometry, atmospheric variables spectra deduction 79−92567
atmosphere IR mosaic background obs. from balloon altitude expt. 80−90222
atmosphere O_3 profile, determ. from outgoing thermal radiation 78−92945
atmosphere O_3 total content, determ. using satellite meas. 80−77027
atmosphere parameters, retrieval from scanning multichannel microwave radiometer obs. 80−90261
atmosphere remote sensing by satellite, thermal radiation obs. 80−85660
atmosphere sounding by interferogram measurement technique, temp. profile 80−17413
atmosphere spatial temp. and geopot. fields, thermal sensing from Earth orbit 80−36429
atmosphere temp. profiling using IR heterodyne radiometer 77−49200
atmosphere temperature, by microwave radiometry 80−46293
atmosphere temperature, impact of satellite sounding data on weather forecasts 80−77028
atmosphere temperature determination by remote sounding, aerosol attenuation effects on accuracy *(Russian)* 78−81430
remote sensing continued
atmosphere temperature field, spatial anal. from weather satellite meas. 78−20488
atmosphere temperature profile, IR remote sounding, error anal. and data acquisition *(Chinese)* 80−109273
atmosphere temperature profile, microwave radiometry charcts. *(Chinese)* 79−80188
atmosphere temperature profiles, satellite retrieved, error due to aerosol particles effects 80−98449
atmosphere temperature sounding from TIROS-N, early operational soundings evaluation 80−77133
atmosphere thermal struct., radiative eqn. 77−9498
atmosphere turbidity monitored by satellite, obs. of reflected sunlight 80−51471
atmosphere vacuum UV background, meas. 80−90221
atmosphere water vap. and liq., and wind vel. at ocean surface, satellite microwave technique 80−41573
atmospheric, four band mm-wave radiometer design 78−96324
atmospheric and Earth surface characteristics affecting tropospheric propagation of microwaves, satellite techniques 78−24353
atmospheric and oceanographic information processing system 77−78519
atmospheric boundary layer, clear air wind perturbs., dual Doppler radar obs. 79−53462
atmospheric boundary layer, vertical temp. profile determ. by ground-based microwave radiometry 79−79915
atmospheric constituents, spectral radiometric meas. 77−70883
atmospheric data, geopotential field numerical analysis 78−7814
atmospheric effects 77−56732
atmospheric H_2S, distance source sensing by statistical treatment of air quality data 77−70808
atmospheric layer thickness determ. from Nimbus E microwave spectrometry and radiosonde obs. 77−29384
atmospheric monitoring, natural sites, expt. philosophy, equipment performance *(Italian)* 77−82065
atmospheric O_3 monitoring with IR heterodyne radiometer 78−16216
atmospheric particulates, solar occultation technique, horizon radiance inversion 77−9539
atmospheric phenomena, obs. from space 79−96850
atmospheric pressure sensing by solar occultation using wideband CO_2 absorption 79−80037
atmospheric propagation, remote sensing progress and implications for local weather services 77−81990
atmospheric radiance obs., interpretation using eigenvectors of covariance matrices 77−5341
atmospheric radiation monitoring, satellite-borne polarization scanner 79−58222
atmospheric radiometry methods (Soc. Photo-Optical Instrum. Engrs., Proc. vol.91, San Diego, 26-27 Aug. 1976) 77−70880
atmospheric regional precipitation meas. by ground-based radiometer *(Chinese)* 79−84547
atmospheric remote sensing by aerosol lidar backscatter *(Dutch)* 80−4110
atmospheric temp. and humidity anomalous profiles, errors *(Russian)* 77−17266
atmospheric temp. height profile determ. by aircraft meas. of outgoing radio emission *(Russian)* 79−16574
atmospheric temp. sounding, filter for CO_2 ν_2 band 77−10998
atmospheric temp. sounding by high precision satellite, spectral band passes 77−41175
atmospheric temp. sounding with partially scanned interferograms 77−41176
atmospheric temperature, vertical profile, from satellite data, information retrieval 78−3959
atmospheric temperature and composition from satellite meas. of thermal radiation 77−45202
atmospheric temperature meas. by IR method from Earth satellite *(French)* 77−9550
atmospheric temperature sounding by IR radiometer 77−41174
atmospheric temperature sounding from CO_2 4.3 μm absorption spectrum 78−16166
atmospheric temperature turbulence and optical propag. parameters 77−45125
atmospheric temperature-pressure profile meas. by microwave remote sensing *(Chinese)* 80−4116
atmospheric total O_3 content, backscatter UV and ground-based meas. comparison 79−84430
atmospheric turbidity, skylight at South Pole station, Antarctica, polarising radiometer meas. 78−57320
atmospheric turbulence, optical method and comparison with simultaneous thermal meas. 79−34965
atmospheric UV radiation detection, space appls. 77−70881
atmospheric water vapour, passive microwave profiling technique 80−21856
atmospheric water vapour and aerosol optical depth determ. 78−65389
atmospheric water vapour and liquid monitoring using radiometry at 21 and 32 GHz 80−26628
auroral data from DMSP, calibration 80−8443
automated Earth resources surveys using satellite and aircraft scanner data for Finland 79−100988
automatic image processing 77−21931
avalanche victim detection using microwave radiometry 77−2652
backscattered pulse shape, small-angle multiple scatt. in random media 80−77079
Balloon Altitude Mosaic Measurements Program 78−81455
beach sand, spectral reflectance/grain size relationship 78−16005
Bermuda, satellite imagery and geomorphology 79−5470
bidirectional reflectance and transmission for space appl. 77−56809
black and white picture grey-differentiation displayed, using computer generated arbitrary colours *(French)* 79−81370
Brazil Patanal, drainage network mapping from Landsat-2 imagery 80−81944
brightness temps. estimates from scanning radiometer data 78−85716
C-CD space-borne Earth imager, high resolution, features 79−35097
calibration of remote sensors by time averaging *(Russian)* 77−78452
California Current, nutrient upwelling, satellite thermal imagery and chem. anal. 80−101379
California Current eddy formation 77−53072
camera, film and solid-state-array types comparison w.r.t. imagery 78−4723
canopy temp. thermal scanner meas. to estimate evapotranspiration 77−5324

remote sensing continued
Carpathian Mountains, disjunctive dislocations revealed by interpretation of space television photographs *(Russian)* 80−104958
cartography, point transfer error determ. 80−17227
cartography by Mapsat (Automated Mapping Satellite System), proposed parameters 80−17468
cartography radar image interpretation, line detection technique 78−61630
chimney plume particulate and gaseous pollutant conc. and mass flow, IR radiometry 77−37393
China, Landsat satellite imagery rel. to active faulting and tectonics 77−86848
chlorophyll, gradient map from high-altitude ocean colour scanner data 80−26551
cirrus clouds, radiative props. in NOAA 4 VTPR channels rel. to satellite exploration 79−39853
cirrus clouds, remote sensing of thickness and composition from satellites 77−64461
cirrus outflow divergence determ. using ATS 1 pictures 77−53239
citrus orchards, diseased, automatic interpretation of IR aerial colour photographs 77−56749
city lights obs. by Defense Meteorological Satellite Program 80−104494
classifier model for multi-observational anal. 77−78533
clay soil sand content, determ. from percent reflectance 80−56475
climatic change, long-term, prod. by fossil fuel usage, proposed space obs. 79−29844
climatology, hydrology, atmospheric research and meteorology from space, conference, Ajaccio, Corsica (1979 November 12 to 16) 80−62397
cloud analysis via space-derived pictures, appl. of photographic equidensity curve method *(Russian)* 77−53155
cloud bands, polar and equatorial, interaction GOES-1 imagery 79−39786
cloud classification techniques, comparative study 78−7809
cloud determination, SMS IR data appl. during GATE 80−31113
cloud diffuse reflectance, semiempirical model 79−80014
cloud microwave radiation emission meas. 80−17351
cloud motion winds from ATS 6 images comparison with coinciding SMS 1 winds 79−79954
cloud top height derivation using High Resolution IR sensor data 79−48539
cloud top heights determ. from satellite remote temp. sounding instruments 77−17256
cloud winds over oceans, satellite technique verified by aircraft obs. 80−85764
clouds, 0.35-3 μm range detection with aircraft-borne photometer 80−77085
clouds, classification from visible and IR SMS-1 data 78−77309
clouds, particle size distrib. from spaceborne line spectrum imagery, theory 79−5613
clouds, radar and satellite meas., comparison of simultaneous studies 79−58077
clouds, satellite IR nephanalyses 77−41122
clouds over NE. Pacific Ocean, Nimbus 6 liq. water data rel. to United States west coast rainfall 80−82005
cloudy atmosphere, integral humidity, integral moisture, temperature and height of drop cloud phase determ. *(Russian)* 79−5635
cloudy atmospheres, ground based microwave radiometry *(Chinese)* 80−51549
cloudy atmospheric parameter determination using microwave radiometric method 80−67435
coal gasification, in situ, diagnostic and remote monitoring instrumentation development 79−48055
coal seam thickness meas. using resonant loop as EM sensor 78−57366
coastal circulation, sewage outfall siting with dye-buoy remote sensing 78−65438
coastal currents and pollution, satellite, aircraft and drogue studies 77−37206
coastal photogrammetric mapping 80−104960
coastal zone development pressure monitoring 78−78013
coastal zones, chlorophyll a distrib. mapping 79−2294
coercive force, automatic meas. by remote means, for ferromag. metals and alloys 79−24690
coherent polarization-diversity radar techniques in meteorology 79−58111
colour compensating filters with IR film 77−33210
colour densitometry on multi-emulsion imagery 79−53555
colour image interpretation, RADC's research 77−74534
combined synthetic aperture radar/LANDSAT imagery 79−5650
composite thermal/visual display superposition technique 78−77992
computer elaboration and image processing of sensing data 78−40690
computer-based technology 77−53249
contextual classification of multispectral data, multiprocessor system 80−77149
continental ice sheet, thickness changes from Geos 3 altimetry 80−4051
continuous inhomogeneous media, extended Rytov approximation 77−19145
contour map aeromagnetic data computer processing 78−7819
convective storm, triple-Doppler radar obs. 79−39886
correlation spectrometry meas. of air pollution, 2nd CEC remote sensing campaign, report 78−88908
cosmic ray air shower remote sensing using light emission and optical detection 78−4050
crop and soil bidirectional reflectance factor calibration, remote sensing field research 80−86382
crop and vegetation studies, X-band scatterometer 79−25370
crop canopy complex aerial photographic images, analysis and electronic area meas. 79−26159
crop identification and area estimation by computer aided LANDSAT data anal. 77−78503
crop rows, effect on thermal radiation from terrestrial surface 78−16016
crop spectra, discrete absorpts. and emissions at Fraunhofer lines 78−44994
crop types monitored by side-looking radar 80−46280
crops, Landsat data, pattern recognition, temporal trend analysis 78−65440
crustal fractures and photogeology 77−44954
crustal horizontal stresses from satellite pictures *(Russian)* 79−20791
cultivated and natural vegetation mapping 77−56781
cultural and landscape interpretation from remotely sensed data 77−56782

remote sensing continued
cumulonimbus cloud top heights over Deccan Plateau and adjoining plains, radar obs. 79−48542
cumulus cloud statistics, satellite-derived, for W.Kansas 79−79955
Dakota landforms and drainage patterns, mapping by IR imagery 80−81892
data analysis of multivariate data set, canonical anal. 80−73333
data interpretation, computer-assisted analysis techniques 78−7776
data inversion from diffraction-limited multiwavelength remote sensing 79−39976
data processing, conf., West Lafayette, Ind., USA, June 1977 77−78488
data processing developments, review *(Japanese)* 78−7801
data transmission, from sensing satellite, CO_2 laser communication system 77−19427
decision tree classifier, design and pot. for remote sensing 77−56745
desert colour, Apollo-Soyuz photographs 78−65315
desert environment mapping and monitoring, worldwide 77−78489
developing countries, internationalization of remote sensing technology 79−2375
diffuse reflectance models for aquatic suspended solids measurement, test 80−8453
difluorodichloromethane, spectral data evaluation for atm. sensing 79−62582
digital crop identification, high-altitude versus Landsat imagery 79−25357
digital data processing, system performance and cost estimation 77−78517
digital image anal. for natural resources inventories 78−96326
digital image change detection 80−102637
digital image processing developments 80−14287
digital image processing for resources monitoring 78−96328
digital image processing techniques for planetary program and Earth resources information 78−96408
digital picture analysis, book 77−17962
digital sensor simulation 77−33213
digital thermal inertia image construction and interpetation 78−4001
digital thermal IR scanner data temporal correlatibility 77−78525
digitising, accuracy improvement via aided-track cursor 79−29899
directional gravity wave spectra and surface currents, with dual freq. radar 78−96323
directional sea spectrum determ. using HF Doppler radar techniques 77−17229
directional sea spectrum using HF Doppler radar techniques 77−29476
dispersion correlation spectroscopy, mask optimisation procedures 77−73857
DMSP visible imagery, causes of anomalous grey shades 80−77111
dual wavelength thermal IR scanner as potential airborne geophysical exploration tool 77−41183
dynamic, under-surface temp. pattern estimation method *(Japanese)* 78−36315
Earth, visual observations of environment from space *(Russian)* 78−40796
Earth's atmosphere, optical parameters determ. by aerial photography at sunset 80−90219
Earth's natural resource data, computerised management system, equipment 77−82058
Earth's natural resource obs. from space, present and future 79−5653
Earth's resources and environment obs., satellite meas. capabilities 79−5654
Earth's surface, air survey methods *(Dutch)* 78−3972
Earth's surface, radar techniques, review 79−12294
Earth's surface in presence of vegetation cover, microwave radiation spectra 80−68239
Earth's surface obs. contrast attenuation factors calc., using atmospheric models 80−4135
Earth albedo monitoring technique from LANDSAT data 77−78516
Earth conductivities, mapping via multifreq. airborne EM system 79−5446
Earth exploration from satellite Soyuz 22, Raduga expt. *(German)* 77−56765
Earth imagery, atmospheric blurring removal 79−88517
Earth images, atmospheric effects on classification 79−58091
Earth obs. from space and planetary resource management, conf. (Toulouse, France, 6-11 March 1978) 79−35015
Earth obs. systems, planning, design and control 79−58220
Earth observation, periodic coverage pattern quantisation and symmetry 77−78444
Earth observation from space, review 79−34983
Earth observation programme of ESA 80−109250
Earth observations by astronauts, potential appls. and results *(Russian)* 78−40795
Earth radiance obs. from Miranda (X4) satellite, IR expt. design and performance 80−72745
earth radiation budget: simulation of fluxes and accelerometric measurements *(French)* 79−84482
Earth remote sensing from space, role of 'smart sensors', book 80−62402
Earth resource imagery data processing techniques *(Italian)* 77−82063
Earth resource satellite attitude meas. and control requirements 78−65482
Earth resource thermal imaging by airborne system, possible LED use 78−93010
Earth resources, factor analysis approach to spectral interval selection 79−88503
Earth resources, remote sensing by Skylab microwave radiometer 78−16273
Earth resources exploration using satellites, review of techniques 79−16714
Earth resources sensing, LANDSAT system features 78−96330
Earth resources survey sensor, calibration linear photodiode array in push-broom scan mode, satellite appl. 80−56693
Earth resources surveying, multispectral photography from space *(Russian)* 78−16197
Earth resources surveying by satellite remote sensing 77−25788
Earth scene dynamics, satellite-borne mosaic sensor performance 80−90321
Earth surface, 0.8 cm radiation emission mapping by satellite *(Russian)* 80−77145
Earth surface, active microwave sensing *(Japanese)* 78−16214
earth surface, electron system for image transformation and coding in conventional colours 80−4117
Earth surface, Heat Capacity Mapping Mission 79−5640

remote sensing continued
Earth surface, photomontage of Europe and Asia *(Russian)* 78−16199
Earth surface albedo, atmospheric transfer function influence on aircraft and satellite meas. *(Russian)* 77−60464
Earth surface albedo, satellite meas. over NW.Africa 79−2368
Earth surface features classification atm. turbidity effects 78−16204
Earth surface multispectral photography from space *(Russian)* 78−16198
Earth surface obs. satellite remote sensor/attitude control system interface 78−65481
Earth surface obs. satellites and remote sensor/attitude control interface 78−45182
Earth surface UV reflectance, meas. from airborne platform 80−98453
Earth-atmosphere radiative heating effects on climate, NOAA radiometer meas. 80−8425
Earthnet, monitoring Earth's environment 78−88921
East African swidden farming, computer processed LANDSAT data interpretation 77−78494
ecosystem succession detection by aerial IR photography 78−81459
electric and magnetic sensing system appls. 78−69538
EM modelling of transmissions through in situ gasified coal seam 79−12298
EM remote sensing, reconstruction algorithms for geophysical applications in noisy environments 80−77168
EM remote sensing of inhomogeneities in ground, numerical modelling 80−77165
EM response of Earth surface, aircraft remote sensing *(Chinese)* 80−104859
EMF properties of air 77−17182
energy balance maps from remotely sensed imagery 77−37433
energy conservation for reflectivity and transmissivity at a very rough surface 80−53188
environment, conf., Detroit, Michigan, USA (Nov. 1977) 78−96300
environment, from space, automated digital data handling 78−3960
environment, survey of methods and appls. 78−77364
environment remote sensing, book 77−56771
environmental obs. from space based systems, present and future 79−5657
environmental pollution monitoring, most promising trends 80−35811
environmental potential survey in Japan 78−57374
environmental remote sensing achievements and prospects 78−45028
error anal. of ill-conditioned data, inversion technique 77−66992
error probability estimation without ground truth and known a priori probabilities 77−56746
estuarine fronts behaviour study, effects on pollutants 77−78470
estuary mapping, classification algorithms for Landsat data 78−40567
European potential climatological satellite missions 79−70886
European remote sensing satellite programme benefit identification and quantification methodology 78−32231
European Space Agency remote sensing programme activities and plans 79−70885
evapotranspiration using Nimbus 5 satellite IR radiometer, evaluation *(French)* 77−17156
fault motion meas. by satellite laser ranging, San Andreas appl. 79−79786
feature identification and location experiment FILE, sensors 80−56657
feature space mapping, linear transformation for improved colour image interpretability 77−78499
feature subset selection 79−25337
field averaging spectrograph camera 77−45161
field double-beam differential spectrophotometer *(Russian)* 79−49269
flame, temp. meas. spectral remote sensing 78−32818
floating ice layer thickness meas. using nanosecond impulse X-band radar 78−62178
flood inundation of agricultural land, LANDSAT digital image anal. 80−61913
flood water movement identification 77−70710
flood-plain delineation by multispectral data analysis 77−73885
floods, Queensland, Australia, LANDSAT imagery interpretation 79−25283
fluorotrichloromethane, spectral data evaluation for atm. sensing 79−62582
fog in Cheddar Gorge, England, oblique false-colour photograph 78−57290
forest fire sources, microwave radiation spectra 80−52314
forest productivity study using LANDSAT data, computer training, USA 77−78527
forestland location in western Massachusetts, direct LANDSAT resource anal. 77−78529
forestry data analysis, digital signal proprocessing and postprocessing aspects, book contrib. 79−92634
forests, two-camera intervalometer appl. 78−77367
Fourier transform IR absorpt. spectroscopy, airborne, for atm. comp. meas. 78−61604
Fourier transform IR spectrometer, for satellite, optical design problems *(German)* 78−86360
Friuli area, LANDSAT-2 imagery of linear features 78−24284
frost prone areas, Niagara fruit belt, defined by thermal imagery 79−25314
gaseous atmospheric pollutants, teledetect. *(French)* 80−7988
gaseous pollutants, mobile Fourier transform interferometer 80−12043
gear noise, real-time bispectral anal. appl. to contactless diagnosis 77−84066
generalised method for environmental surveillance 78−57363
geologic exploration surveys 77−56631
geological faults and other linear features, detect. from LANDSAT images 80−77177
geological interpretation, from composited radar and Landsat imagery 80−56647
geological IR multispectral aircraft scanner data, image processing 80−98454
geological lineament interpretation, multi-attribute method 79−2399
geological lineaments, human perception from remote imagery, model 79−2400
geological lineaments computer-assisted photointerpretation, perception method 78−7639
geological problems application 80−109279
geological structure research, LANDSAT data anal. *(Italian)* 80−109281
geology, discrimination using dual freq. and polarization imaging radar 79−12293
remote sensing continued
geology, Washington, DC, Landsat reconnaissance 80−41444
geomagnetic depth sounding by means of oceanographic and aeromagnetic surveys 80−77166
geomagnetic field variations, at mesospheric heights 80−77124
geometric correction for LANDSAT MSS data 79−58120
geophysical applications of remote sensing by artificial satellites *(Swedish)* 77−67001
geophysical applications remote sensing technology 77−5349
geophysical environment by radiophysical methods *(Russian)* 77−78435
geophysical mapping and remote sensing by optical filtering 80−101458
geophysics, empirical study of scanner system parameters 77−56743
geophysics anal. using ERIPS and LARSYS programs *(Japanese)* 77−5340
Georgian Bay, chlorophyll conc. from airborne spectral refl. meas. 78−16202
GEOSAT, geological industry reommendations on remote sensing from space 78−69495
Geostationary Operational Environmental Satellite data acquisition analysis and display 80−17382
geothermal energy prospecting by geophys. methods, review 78−7803
geothermal research by IR scanning, image processing 77−64458
German Bight, airborne and ground data, Geoscientific Airborne Remote Sensing Programme *(German)* 80−67412
Gironde inlet and Pertuis of Maumusson, estuarine waters seaward dispersion, remote sensing study *(French)* 80−8324
glacier thickness and water content, radar measurement technique 80−98369
global phenomena monitoring by automatic satellites 77−64457
grass canopy spectral reflectance, 500-1000 nm, asymptotic value 77−64442
grass canopy spectral reflectance, soil spectra contributions 77−87126
Greak Lakes water quality, remote sensing data interpretation 80−98364
Great Lakes, LANDSAT obs. of whitings and chlorophyll distribs. 78−77283
Greenland ice sheet topography from satellite radar altimetry 78−81233
ground conditions classification of LANDSAT data by anal. of variance procedures 77−78532
ground cover remotely sensed by radar, backscatter cross-section 80−46279
ground data acquisition and processing, in developing countries, computer appl. 79−34963
ground exploration and geological evaluation using remote sensing from space platforms 78−40682
ground mapping resolution accuracy of scanning radiometer from geostationary satellite 77−73858
ground receiving system, Earth survey data, facsimile features 77−82012
ground reflectances, atmospheric effects in space meas. 80−17373
ground resistivity, airborne survey using VLF plane waves, resolution studies 80−12333
ground subsurface, EM transient response 78−57166
ground trugh index, evaluation of prediction success 79−88505
ground-truth and mission operations 77−56780
groundwater flow pathways determ. from satellite altitudes, apparent radiance data appl. 79−16522
groundwater in deserts and glaciers using radar subsurface sounding 80−67437
Gulf stream, surface boundaries measured by Geos 3 radar altimiting and IR data 80−4021
Gulf Stream cold core ring, observed formation 78−44862
Gulf Stream meanders, GOES IR meas., time series anal. 79−34842
Gulf Stream rings distrib. and number, 1975 spring period 79−39725
Gulf Stream rings obs. by satellite tracked drifter buoys 80−90242
hail, radar detection technique, quasilinear discriminant function 80−21861
hailstorm damage to vegetation, LANDSAT remote sensing epxt. *(Italian)* 77−81986
hard copy imagery from remote sensing systems, laser beam recorder appl. 79−80715
harvest prediction, man computer optimal system *(Italian)* 77−82059
height meas. from satellite images using zoom height finder 78−36308
heterodyne correlation radiometry 78−77980
heterodyne optical correlation, photogrammetric appls. 77−42497
HF radio acoustic sounder, atm. wind and temp. remote meas. 78−32235
HF sky wave radar remote sensing of sea state, minimisation of ionospheric disturbance 80−21857
high altitude low contrast imaging, sensor requirements 80−4152
high detective quantum efficiency image detectors, review 77−71010
High Energy Astronomy Observatory Program, mission 79−5730
high temperature gas diagnostics by spectral remote sensing 78−74002
Himalayas, tectonic lineaments from ERTS imageries 78−3739
Hurricane Camille, evolution, Nimbus 3/ATS 3 obs. 78−92921
hurricane sea surface wind speed, L-band radar backscatt. obs. 80−56561
hydrographic charting by multispectral and ocean colour scanners 77−5368
hydrographic charts preparation, appl. of LANDSAT MSS imagery 79−29894
hydrologic information needs and remote sensing 77−56665
hydrological features, microwave remote sensor development and appl. 80−105082
hydrothermal alteration mapping, airborne spectroradiometric data anal. and LANDSAT data appl. 79−34973
hydrothermally altered and unaltered rocks, discrimination in visible and near IR 78−7641
IBIS, geographic information system based on digital processing and image raster data type 77−56747
ice-cover thickness on rivers and lakes, pulsed radar meas. method 78−92862
iceberg volume meas. using photogrammetric techniques 77−82048
IEEE International Microwave Symposium, Orlando (1979) 79−68356
image analysis system for Earth resources surveys 79−5644
image data processing/acquisition techniques 78−61627
image interpretation and remote sensing, book 79−100985
image processing, spatial filtering 78−90385
image processing and information extraction 77−64438
image processing applications at IBM Madrid Scientific Center 80−102657
image processing techniques 78−87022

remote sensing continued
image registration, similarity measures and preprocessing techniques 78−32240
image scanner technology for digital mapping systems 80−85773
imagery interpretation and geological lineament reproducibility 77−53250
imagery multiple analysis at JPL's Image Processing Laboratory 80−82219
inaccessible target, position meas. by noninterferometric optical probe 77−74362
individualised short course 77−74182
inland wetland photointerpretation evaluation, cell analytical method 79−29898
inspection of ground sites, cost/effectiveness model 77−91319
inspection systems for nuclear power stations 79−45386
intensity fluctuations meas. using scanning laser velocimeter 77−791
interactive minicomputer array processing system for Earth science 77−78518
International Orthophoto Expt. 1972-76 results 77−44903
introductory review 77−2286
invisible information imaging techniques 77−5819
ion beam position meas. from random beam modulation 79−30606
ionosphere, props. meas. at Arecibo Observatory 78−81488
ionosphere, topside sounding and determination of electron profiles, review 80−56669
i.r., meas. techniques and devices, Earth surface imaging *(German)* 77−9567
IR atmospheric remote sensing, theoretical problems 79−80052
IR emitter/receiver device which detects objects by beam interruption or reflection *(Spanish)* 79−67389
IR film for mapping and multispectral photointerpretation 79−25356
IR Fourier spectrometer for space appl., thermal behaviour *(German)* 79−35091
IR line scanner, Reconofax XIII A, improved recording system using LED 79−25335
IR multidetector spectrometer for atm. temp. sounding 79−25365
IR optical system input diffr. effects and use of spatial apodisation 78−79113
IR parametric oscillator source for remote air pollution monitoring 77−21936
IR photography, principles and appls., book 78−82068
IR pyrometer for remote temp. meas. of high-power radiation-generating equipment 78−24799
IR radiometry, satellite radiometer calibration 80−101440
IR remote sensing, relative importance of reflected and emitted flux density in 3 to 14 μm range 79−92542
IR remote sensing measurements, conceptual considerations and surface temp. estimation, review 79−34984
IR remote sounding of atmosphere with multiple cloud formations 77−78319
IR remote sounding of cloudy atmosphere, CO_2 radiance data 77−78320
IR source classification system, non image forming, exp., simulation results 79−49296
IR spectral band transmittance, modelling, Prony's method 78−70202
IR staring mosaic sensor performance, effect of spacecraft-induced line-of-sight jitter 80−86416
IR streak camera, high speed, appls. 77−79093
IR surveillance, continuous-time signal processors 80−78781
IR technology, conf. II (San Diego, California, 1976, August 26-7) 77−45891
IR technology utilisation, symposium, San Diego, CA, USA (Aug. 79) 80−86037
isotropic reconstruction of track-type airborne geophysical surveys, 2D filler design 79−66844
Japanese weather satellite, purpose and instrumentation 78−49290
JROE II LIDAR, atmospheric gas components/aerosol meas. *(Italian)* 78−3957
Jupiter, atmosphere, $^{12}CH_4(^{13}CH_4)$ ν_4 band, line parameters, 7.7 micron transmission 78−85894
Kelvin waves in mesosphere and stratosphere, struct. and behaviour from Nimbus 5 IR meas. 80−8394
Lake, Superior, LANDSAT-1 obs. of internal standing wave pattern 78−96244
lake ice, microwave radar and radiometric remote sensing meas. 80−85691
lake identification by closed planar curve analysis using LANDSAT *(Japanese)* 80−26635
Lake Kainji, W.Africa, water columns movement, LANDSAT data 79−25284
Lake Ontario water masses, nonzero subsurface irrad. refl. at 670 nm 80−101387
lake quality monitoring, multidate Landsat data extraction progrm 80−17299
Lake Superior, remote determ. of chem. loading due to spring runoff 78−96243
lakes, ice-covered (North Slope, Alaska), radar return differences 79−2298
lakes, particulate concs. in water 80−105056
lakes, suspended solids, anal. using Landsat multispectral data 79−16523
land and sea surface temp. fields, seasonal vars., NOAA 5 satellite IR obs. 78−85676
land monitoring, techniques and equipment, Conf. on Earth resources electronics Rome, Italy (Mar.77) *(Italian)* 77−82056
land use, airphoto interpretation, teaching using computer 79−48999
land use change monitoring system based on LANDSAT 77−78542
land use classification by thermal IR scanning imagery 77−26422
land use mapping by radar imagery, techniques 80−8449
land-use map accuracy test, statistical sampling method 78−7805
land-use map accuracy testing, sampling designs 80−17226
land-use mapping by machine processing of LANDSAT-1 data 77−78467
land-use photo classification using optical spectrum anal. 78−12023
land-use/soil survey data processing for resource planning 78−7804
landform photograph three-dimensional projection system 77−74181
Landsat, digital image rectification system 77−56734
LANDSAT, proposed parameters 78−7858
LANDSAT 1 MSS imagery, plumes visible over NE.England and Midlands 78−45035
LANDSAT agricultural monitoring program to monitor corn in Iowa 77−78495
LANDSAT agriculture landuse survey, Texas 77−82050
remote sensing continued
LANDSAT and weather satellite data monitoring at new Canadian receiving station, Newfoundland 77−78600
LANDSAT colour image digital data display using matrix printer 78−12024
LANDSAT computerised data anal. rel. to global development 78−36286
Landsat data, line detection algorithm 80−77150
LANDSAT data applications 77−82060
LANDSAT data clustering, four-dimensional histogram approach 77−78524
LANDSAT Data Collection Platform for surface hydrography 77−49174
LANDSAT data correction for haze, Sun angle and background reflectance effects 77−78491
LANDSAT data digital chromaticity mapping for water quality anal. 79−29872
LANDSAT data for determining unharvested winter wheat acreage 77−78508
LANDSAT data for geological studies in India, digital anal. 77−78511
LANDSAT data for metropolitan land cover inventory 77−78536
LANDSAT data high-level computer processing 78−69546
LANDSAT data multivariate distribution relative normality measure 77−78506
LANDSAT data per-field, classification, unsupervised clustering techniques 77−64437
LANDSAT digital data for classifying vegetative cover 77−78543
LANDSAT digital data for detect. of moisture stress by Green Index Number method 80−17423
LANDSAT digital data for forest vegetation and land classification, in Minnesota 77−78528
LANDSAT digital thematic maps, radiometric interpretive legend 77−78468
LANDSAT digital thematic maps, smoothing method 77−67000
LANDSAT evaluation for land cover data in metropolitan areas 77−78538
LANDSAT image, digital anal. and appls. 78−65404
LANDSAT image anal. for terrain investigations in Florida 77−78530
LANDSAT image and digital terrain elevation data processing with parallax 77−29501
LANDSAT image classification, least square error approach 77−78523
LANDSAT image data, evaluation for land-use mapping 80−101443
LANDSAT image photointerpretation/classification using negative spectral bands 77−78498
LANDSAT image principal component technique for studying structural basin, Spain 77−78521
LANDSAT image processing, pipelined systems, design 78−96329
LANDSAT image registration performance, spatial distortion effects 77−78492
LANDSAT imagery, anal. via additive colour viewer 79−29897
LANDSAT imagery, computer aided and air-photo interpretation techniques 79−74976
LANDSAT imagery, geologic appls. 77−91321
LANDSAT imagery, operator variation in lineament anal. 77−64467
LANDSAT imagery, photographic contrast enhancement 79−29896
LANDSAT imagery, photographic data extraction 77−33212
Landsat imagery, planimetric restitution using Zeiss Stereotop 80−56648
LANDSAT imagery, spatial filter analysis 78−69490
Landsat imagery, use in land system classification of Jordan 79−2388
LANDSAT imagery for position evaluation of islands, banks and reefs in Indian Ocean 77−87123
LANDSAT imagery for surface-coal-mine inventory 77−91320
Landsat imagery for terrain analysis 78−40691
LANDSAT imagery geologic processing software 78−20521
Landsat imagery geometrical correction *(French)* 80−81889
Landsat imagery laser film recorder and processor 80−105084
LANDSAT imagery processing and enhancement 78−69545
LANDSAT imagery survey of Melaleuca problems 77−82049
Landsat images, digital differential rectification 80−41570
LANDSAT images of S.Brazil and mineral deposits rel. to tectonics 77−81855
LANDSAT images segmentation, spectral, spatial and semantic constraints exploitation 79−25336
LANDSAT information, territory administration, data aquisition *(Italian)* 77−82057
LANDSAT large area classifier MAXL4X 77−78534
LANDSAT MSS data, surface reflectivities in arid regions 77−53189
LANDSAT multispectral data, training sample size effect on classification accuracy 77−78544
LANDSAT multispectral data classification algorithms 78−61629
LANDSAT multispectral images clustering scheme 78−32241
LANDSAT multispectral sensor image adaptive coding techniques 78−45060
LANDSAT obs. of estuarine density fronts and effects on coastal pollutants 78−7659
LANDSAT pictures, interactive digital image processing system, DIBIAS 77−82062
LANDSAT ratio image dynamic range reduction technique 78−69547
LANDSAT sample selection training algorithm SEARCH 77−78535
LANDSAT satellite images; low-cost enhancement of multispectral data 78−20559
LANDSAT satellite multispectral scanner imagery of pulp mill stack plume 78−88905
Landsat satellite observations of Earth 79−84280
Landsat satellite programme for remote sensing of the Earth *(French)* 79−40058
LANDSAT scene- and map-corrected images using mini computer 78−7806
LANDSAT snow mapping data 77−82061
LANDSAT spectral data classifications, atmospheric correction 78−69548
Landsat views of Earth, book 78−7643
LANDSAT winter wheat acreage estimation in Kansas, cloud cover effect 77−78509
LANDSAT-1 digital image registration and cloud effect rectification 77−78490
LANDSAT-1 imagery for geological evaluation 77−33211
LANDSAT-based two phase sampling wheat acreage estimation 77−78502
landscape multispectral data, Karhunen-Loove analysis 80−48164

remote sensing continued
landuse anal. using BASIC interactive image processing for teaching 77−74176
landuse imagery, computer anal., change detection metrics and MIXELS 77−82070
Large Area Crop Inventory Experiment, LANDSAT image registration accuracy meas. 77−26421
large format camera for Space Shuttle, cartography appl. 80−4232
Large Format Camera for Space Shuttle 79−101043
laser stereometry using range-dependent time delay in reflected light 77−10127
lava flow terrain, radar imaged by satellite 80−98285
layered media, radiative transfer theory for scatt. 79−76553
layered random media, radiative-transfer theory 80−36413
leak detection for Tokamak Fusion Test Reactor 78−50403
lee waves generated by isolated islands, three-dimens. patterns, satellite obs. 79−44230
level and velocity measurement by random signal anal. from surface waves 79−72976
light diffusion in atmosphere, estimation using const. transmission function 80−4100
light rangefinder and profilometer, high-resolution gas laser 80−102754
lightning detection by satellite monitoring 79−92559
lightning flash detection, DMSP data 79−16593
Limb Infrared Monitor of Stratosphere (LIMS) radiometer, design and performance, expt. goals 78−61601
low orbiting satellite, microwave radar technique, CCD data handling system 77−91328
low Sun-angle photography, flight planning, interpretive techniques 77−78465
low-light sensor, DMSP nighttime images 78−88942
lower atmosphere remotely sensed by two satellites, radio illumination method 80−51550
lower atmosphere using radiowaves, ground-based measurements 80−56628
lunar regional basalt types from remote spectral refl. meas. 77−22118
lunar soil, surface refl. characts. for radar, obs. from Luna spacecraft 80−72798
lunar surface chemical composition from albedo and colour index 77−87296
lunar surface rock comp. remote sensing, regolithic radioactivity in Mare Crisium 80−62045
lunar surface unit definition and characterization using remote sensing 78−28551
machine processing of remotely sensed data, conference, West Lafayette, Indiana (1980 June 3 to 6) 80−82586
machine processing of remotely sensed data, symposium, West Lafayette, IN (1979 June 27 to 29) 79−88473
magnetosphere, elec. fields parallel to mag. field, remote sensing expt. 78−40776
mapping, remote sensing system for nationwide data bank 77−78512
marine boundary layer aerosol, optical thickness 80−17326
marine boundary layer microwave sensing, estimation techniques 79−74993
marine chlorophyll a analysis, using aircraft multispectral scanners 80−77164
marine environment characts. obtainment *(Japanese)* 77−5339
marine oil pollution surveillance, microwave remote sensing technology *(Japanese)* 80−76685
marine research from outer space, take-off of first ocean observation satellite *(German)* 79−74979
marine wind velocity, remote sensing using oceanic whitecaps 80−72554
Mentese region, SW Turkey, LANDSAT imagery appls. 78−77236
mesosphere, structures diurnal vars. in different seasons, VHF radar meas. 79−84370
mesosphere and stratosphere, O_3 and temp., satellite IR limb scanning method 80−105086
meteorological parameters *(Japanese)* 78−16205
meteorological satellite images, interpolation methods, analysis 79−58136
meteorological satellite system, LEOS and GEOS, operational, global/regional remote imaging 79−5727
meteorological satellite visible and IR image data, computer processing 79−29864
meteorological satellites, operation and appls. 79−29967
meteorology, digital satellite imagery, industrial appls. 77−91282
meteorology, satellite data uses, ESA conf. (Lannion, France, 17-21 September 1979) 80−36783
meteorology, satellite imagery appl. appl. to numerical forecasting model initial conditions assessment 80−31084
meteorology inverse problems, estimation theory appls. 79−35018
Meteosat image processing 78−36297
Meteosat imaging payload, functional aspects 78−36424
METEOSAT project, interactive image system 80−109330
METEOSAT project overview *(Italian)* 80−109331
metrological, review *(Japanese)* 77−2273
microwave, from space, synthetic-aperture radar systems and Spacelab expts. 80−36409
microwave, theory for thermal microwave emission from bounded medium containing spherical scatterers 77−87071
microwave brightness spectra of layered media 77−81898
microwave brightness temp. distrib. over Bay of Bengal using SAMIR Satellite Microwave Radiometer data at 19 and 22 GHz 80−104980
microwave ground truth data, sampling technique for soil moisture 78−65439
microwave holography appl. 78−37830
microwave monitoring Earth, from satellite, advantages 80−17409
microwave obs. of atm. vertical temp. profiles *(Chinese)* 79−84452
microwave radiation from clouds meas. by Nimbus 6 for rainfall distrib. determ. 78−3981
microwave radiometer, gain stability improvement 79−25367
microwave radiometric determ. of ocean surface wind speed during BESEX 77−29479
microwave radiometry, advances generated by progress in mm-wave region 79−25366
microwave radiometry and devices *(Japanese)* 78−16212
microwave radiometry from satellites 77−70882
microwave remote sensing expt., operation in Spacelab 80−109332
microwave remote sensing of Earth, radiative transfer eqns. 80−21855
microwave respiration monitor 79−96646
microwave scanning radiometry, appls. 78−73551
remote sensing continued
microwave scanning radiometry for ocean surveillance 78−73550
microwave scattering signature of ocean surface, aircraft AAFE RADSCAT scatterometer 77−25790
microwave scatterometer, backscatter optimisation using complex charact. polarisation concept 79−100966
microwave sensing from satellites, appl. to meteorological meas. over W.Australia 80−98485
microwave sensors in satellites, passive and active, Earth physical parameters obs. 79−80060
microwave spectroscopic imagery of Earth from Nimbus 6 satellite 78−12026
microwave thermal emission, terrain brightness temp., theory 80−77151
mineral exploration, remote-sensing appls., book 77−37450
mineral prospecting by airborne EM method *(Japanese)* 78−24392
minerals, near IR spectra for remote sensing of hydrothermally altered areas 80−81871
Mississippi embayment, remote sensing appls. to tectonics and seismicity 77−81856
MM wave radar system for remotely sensing atmospheric pressure from satellite 80−67443
MM wave radiometry conducted at Appleton Laboratory 80−67442
MM wave radiometry for atmospheric sounding 79−84551
mm-wave imaging system 77−2271
Mobile Bay, Alabama, sea truth and environmental charact. study using ERTS-1 data collection platform 77−70687
monochromatic and colour images by aero- and space methods 79−44252
Moon, orbital gamma-ray data rel. to large-scale lunar problems 78−12123
mountain aerial photography, colour film types compared 77−29500
Multi-detector Electro-optical Imaging Scanner for aircraft remote sensing 80−82085
multiband photography for geomorphology, soils and land use study, feasibility 78−12025
multiband radiometer for field research 80−90250
multichannel data sets, integrated optical comparator 80−64213
multichannel radiometer, programmable, for Earth remote sensing 80−77253
multidimensional Gaussian max. likelihood classifiers error probability estimation 77−78540
multiple-Doppler system 80−31140
multispectral aerial photography, Khomas Trough region gossaniferous outcrop identification 77−5346
multispectral aerial photography, rock type identification in NW Cape Province, S.Africa 77−5345
multispectral analysis by NOAA and METEOR satellites 77−82009
multispectral camera, use on Soyuz 22 spacecraft 78−40794
multispectral data anal., ISURSL levels classification 77−78539
multispectral data clustering, interactive approach 77−78526
multispectral data interpretation algorithms 79−88481
multispectral digital images, intensity variations and false colour display correlation 77−78514
multispectral images, region extraction and classification by entropy index 79−58130
multispectral images, vectoral representations, arithmetic processing *(Japanese)* 79−35532
multispectral imaging, geology appl. 79−34823
multispectral information vol. optimisation of natural formations 80−4118
multispectral linear arrays, alternative to LANDSAT D thematic mapper 80−4153
multispectral projector, colour synthesis instrument for evaluating multispectral photographs 78−40688
multispectral remote sensing ratio image digital processing and interpretation 78−81461
multispectral scanner, for remote sensing, parametric model 80−77261
multispectral scanner, high resolution, for Earth obs., optical design 80−82174
multispectral scanner data principal-axis transformation to colour composite picture 79−29879
multispectral scanner data processing mechanisation 77−56778
multispectral scanner image rectification, practical experience 78−88940
multispectral scanner imagery, two-dimensional digital filters appl. 80−31152
multispectral scanner imagery rectification 78−88939
multispectral sensor for satellite, analytical design 80−77262
NASA, technology transfer to State of Georgia, cost anal. 78−73519
natural resource determ. from weather satellite TV images 77−70876
natural resources, LANDSAT data handling, problems of resource management 77−82011
natural resources, satellite remote sensing, issues 78−12022
natural surface polarisation imagery 78−61625
neutral atmosphere, monitoring techniques *(Japanese)* 78−16126
Nimbus 6 high-resolution IR sounder channels, upwelling radiance sensitivity to clouds 78−32227
Nimbus-7 satellite remote sensing equipment 79−25437
NOAA spacecraft high resolution imagery data 77−78389
nonimaging airborne geophysical and miscellaneous systems 77−56777
nonphotographic optical sensors 77−56774
nonuniform dielectric regions, remote probing wave impedances 77−13781
North Sea pollution detection, appl. *(Dutch)* 78−36202
nuclear fuel plant, remote solution meas., during cold checkout runs 79−85748
nuclear power plant, siting, appl. of remote sensor data 78−21744
numerical photogrammetry, orientation, triangulation and digitisation 78−36312
ocean, atmospheric effects on refl. solar radiation field *(Russian)* 77−33086
ocean, continuously stratified, remote sensing of optical props. 78−77331
ocean, microwave scattering signature, aircraft measurements 77−17112
ocean, optical properties, one parameter characterisation for remote sensing 78−7644
ocean, radio obs. of polar regions, appls. 78−81419
ocean, remote sensing via Seasat-A experimental oceanographic satellite 78−77455
ocean, satellite imagery, atm. effects removal 78−73521
ocean, satellite IR photography rel. to low temp. skin-layer *(Russian)* 78−36180
ocean, sea level transients obs. by Geos 3 coincident orbits 80−72535

remote sensing continued
ocean, synoptic eddies *(Russian)* 80−12420
ocean acid waste dump, particulate Fe mapping 80−56497
ocean buoys, environmental data acquisition 78−36287
ocean chlorophyll content airborne meas. under cloudy sky, Gulf of Guinea appl. 79−25359
ocean colour 77−78460
ocean colour 80−8460
ocean colour and sea surface temp., remote meas. over Straits of Dover *(French)* 78−96238
ocean currents off E. coast of Argentina, SKYLAB MSS data analysis 78−65339
ocean density profile remote sensing by acoustic pulses, numerical algorithm 77−70893
ocean density profile remote sensing pulses, numerical algorithm 78−20429
ocean internal wave obs. with airborne synthetic aperture imaging radar 77−17110
ocean internal waves, acoustic reverberation data 80−41562
ocean passive radiometry, radio meteorology colloquium, Victoria, British Columbia, Canada (1978 June 14 to 21) 80−46724
ocean remote sounding instruments, quasi-optimum operating functions *(Russian)* 78−77362
ocean surface, active microwave sensing *(Japanese)* 78−16215
ocean surface, microwave radiometry remote sensing 80−36428
ocean surface, radar backscatter, friction vel. depend. 78−77246
ocean surface, roughness probability density function determination, from Geos-3 altimeter data 79−100852
ocean surface chlorophyll concentration obs. from high altitude 77−4976
ocean surface circulation, remote sensing with radar altimetry 80−46189
ocean surface currents, recent progress 77−87114
ocean surface currents and gravity waves, directional spectra, remote sensing by microwave radar 78−57364
ocean surface features interpretation on hand-held photographs from Apollo-Soyuz Test Project 79−25360
ocean surface imaging, spaceborne SAR, phase and Doppler errors 77−2323
ocean surface layer temp. sounding *(Russian)* 80−4138
ocean surface measurement using elevations from GEOS-3 altimeter 79−39882
ocean surface microwave emissivity, model of wind roughening 80−46184
ocean surface microwave radiation spectrum from multichannel meas. *(Russian)* 78−65420
ocean surface parameters, retrieval from scanning multichannel microwave radiometer obs. 80−90261
ocean surface pollutants, microwave detect. of adsorpt. and spreading films 79−5690
ocean surface radar imaging, synthetic aperture technique 78−77334
ocean surface sensing equipment, instrument characts. in presence of basic noise *(Russian)* 80−109267
ocean surface temperature measurements, derivation from Meteosat image data 80−76985
ocean surface temperature structure, subsurface mesoscale features 80−98347
ocean surface UV reflectance, meas. from airborne platform 80−98453
ocean surface wave imaging, synthetic aperture radar mechanism 79−5651
ocean surface waves, acoustic meas., theory 80−12564
ocean surface waves, radar imaging method using SAR 80−77173
ocean surface waves imaging, models 77−17237
ocean surface wind field mapping, high-resolution, skywave radar 77−17159
ocean surface wind speed meas. from HF sea scatter by skywave radar 77−17160
ocean surveillance, AGARD lecture series, Oslo (3-4 October 1977) 78−69534
ocean surveillance by US Coast Guard 78−45004
ocean surveillance techniques used by US coastguard 79−34991
ocean temperature determination by remote sounding, aerosol attenuation effects on accuracy *(Russian)* 78−81430
ocean tides mapping with satellites, computer simulation 79−39880
ocean upper mixed layer heat storage, inference from Landsat data 79−100869
upper ocean velocity field, nonlinear motion obs. using range-gated Doppler sonar 80−51422
ocean wave EM scattering theories, review 78−77243
ocean wave height meas. with satellite radar altimeter 79−44253
ocean wave height statistics, dual freq. correl. radar meas. 77−29478
ocean wave height statistics, dual frequency correlation radar measurements 77−17236
ocean wave heights, GEOS 3 radar altimeter data anal. 80−8452
ocean wave imaging and wavelength meas. by aerial photography 80−46323
ocean wave model, summary of verification results using wave height study 80−4027
ocean wave parameters using pulse compression radar scatterometer system, expt. 77−29483
ocean wave patterns under Hurricane Gloria, obs. with airborne synthetic-aperture radar 78−44873
ocean wave radar monitoring, ground wave and sky wave sensing techniques 80−109256
ocean wave spectra, remote meas., two-freq. microwave technique 78−77336
ocean waveheight nondirectional spectrum from inversion of HF sea-echo Doppler spectrum 78−16203
ocean waves, comparison between synthetic aperture radar imageries and surface truth 79−5497
ocean waves, detect. and direction meas. via microwave radars 79−5685
ocean waves, height and dominant wavelength obtained from Geos-3 altimeter study 80−4024
ocean waves, high sea state, wave height measurements from Geos-3 radar altimeter data, aircraft and shipdata−a comparison 80−4025
ocean waves off Marineland, Florida, X-band and L-band radar imagery 78−77248
ocean-disposed waste drift, satellite and current drogue studies 78−3824
ocean-dumping studies, strategies and tools 79−12138
oceanic chlorophyll gradient maps from U-2 aircraft platform over Pacific and Atlantic 80−101385
oceanic internal struct. exploration using sonar methods *(French)* 79−44274
remote sensing continued
oceanic photosynthesis, in situ quantum efficiency determ. using photoelec. sensor chlorophyll simulator 79−39760
oceanic thermal fronts off Korea, DMSP IR detection 77−21796
oceanic thermocline, depth determ. via sonar *(Russian)* 77−13132
oceanic wind fields, high resolution mapping using skywave radar 77−29480
oceanic wind speed meas. using HF skywave radar sea scatter 77−29481
oceanographic, using computer-controlled surface contour radar 79−80063
oceanographic data acquisition, CMOS CPU, low power consumption *(Italian)* 77−82068
oceanographic microwave remote sensing 80−56612
oceanographic remote sensing applications 77−56655
oceanography, LANDSAT and SEASAT data acquisition 79−12309
oceanography, large scale, radio techniques contribs. 78−77337
oceanography, Naval Coastal Systems Center (NCSC) environmental measuring system 80−12570
oceanography, nearshore bathymetry using remote multispectral imaging 78−45053
oceanography, remote acoustic monitoring of natural suspensates and slope/shelf water intrusions 79−2241
oceanography, remote sensing appls. to sea ice 80−77176
oceanography, SEASAT-A satellite scatterometer data regional integration, validation and appl. 79−5680
oceanography, spacecraft-supplied information 77−5335
oceanography, utility of polarised visible radiation 79−5498
oceanography satellite, USA proposal for 1986 launch 80−105088
oceans, Space Shuttle prospects 79−58225
Oceans 1976 conference, Washington (Sept 1976) 77−5241
Oceans '77, conf., Los Angeles, USA (Oct. 77) 78−36193
oil film on sea surface, microwave radiation characts., expt. *(Japanese)* 78−92854
oil films thickness meas. on polluted water from oil fluoresc. props. 79−79437
oil polluted sea surface, atmosphere-ocean system apparent contrast 79−25265
optical and electronic image enhancement techniques compared 77−53253
optical imaging of surface contrast reduction due to haze with nonuniform albedo 80−101431
optical preprocessor, use in Earth-resources satellites 80−67430
optical-mechanical scanners for Earth observation *(Russian)* 78−96321
optics and optical systems, book 80−101675
orthophoto accuracy and terrain height data errors 79−2176
orthophoto mapping, accuracy prediction 77−40970
orthophotography, history, advantages and uses 77−66995
orthophotography, system errors of differential rectifiers with optical projection 77−40971
orthophotoquad processing using photodensity control system 78−7807
N.Pacific, sea surface temp. meas., 1976-77, from Nimbus 6 satellite 79−20841
Pacific Ocean, E.equatorial, long waves obs. in geostationary satellite IR images 78−24308
Pacific Ocean, satellite obs. of mesoscale eddy dynamics in E tropical regions 78−24295
particle size distrib., analytical inversions, angular (spectral) scatt. in diffr. approx. 78−73509
particle size distrib., analytical inversions, multispectral extinctions in anomalous diffr. approx. 78−73508
particle size distribs., anomalous diffraction approx. solns. 80−17386
particle size distribs. remote sensing, Rayleigh-Gans-Born approx. 79−27174
passive microwave radiometers 77−56775
passive remote crosswind sensor 78−7773
PCM telemetry systems, air pollution detection/control appl. *(German)* 78−93003
Peru Current, advection obs. by satellite 78−16029
photogrammetric camera, distortion calibration using star images 79−35881
photogrammetric image quality specification and anal. 77−87125
photogrammetric online processing, general sequential algorithm 77−78463
photogrammetric system 'Zenit', automatic image processing *(Russian)* 78−24466
photogrammetry, automatic reseau meas. with simple optical correlator 78−69496
photogrammetry, high intensity dot grids appl. to accurate area determ. 80−17225
photogrammetry, least squares prediction by multiquadric and covariance functions 77−78464
photogrammetry, modern aerial lens systems 79−35868
photogrammetry, OTF/MTF standards 77−78471
photogrammetry/remote sensing courses in USA and Canada 77−74174
photographic imagery in natural resources studies, pattern classification techniques 77−64454
photographs, analytical rectification using artificial points 79−2177
photolineaments semi-quantitative geological interpretation 78−3766
photometric interpretation process for colour film 80−42251
physical principles 77−56731
phytoplankton passive remote sensing via chlorophyll α fluoresc. 77−86938
phytoplankton remote sensing from satellite, atm. optical props. 80−77105
Pioneer Venus spacecraft programme 78−61707
planetary atmosphere, remote sensor, high resolution Fourier transform spectropolarimetry 78−57469
planetary atmospheres, new inversion method 80−12677
planetary surface elemental anal. via orbital gamma-ray spectroscopy 79−12412
plant canopies reflectance meas. using spectroradiometer 80−56658
plant canopy reflectance models, theory and expt. tests for wheat and cotton 77−34822
polarimetry of particulate surfaces 78−58011
pollutant plumes, remote sensing from Landsat 78−40689
pollution detection, of coastal waters, Italian methods *(Italian)* 78−3828
population exposure to air pollution, satellite-aided evaluation 79−92116
power plant stack emission vel. and SO_2 conc., IR TV appl. 77−49197
precipitation mapping with airborne synthetic aperture imaging radar 77−87106

remote sensing continued
pressure modulator radiometer for atm. gas emission meas. 78−81457
principles, concepts and philosophical problems 77−56772
principles and interpretation, book 79−12319
qualitative and quantitative image analyses compared 77−56779
radar, 5-4 GHz region, microwave active spectrometer capability 79−25368
radar cross section, ground meas. for land and vegetation, influence of soil roughness *(French)* 77−49065
radar for mm wave propag. expt. *(Japanese)* 78−16208
radar image simulation, point scatt. model 79−12296
radar imaging of ocean surface waves, models 77−25689
radar meas. of surface roughness, soil moisture and texture with vegetation cover 79−62534
radar mosaicing, side-looking mapping errors and their reduction 77−13135
radar reflection factor data, cartesian interpolation and display 80−31136
radar scatterometer discrimination of sea ice types 77−41198
radiation exposure near nuclear power plants, remote monitoring system 79−18055
radiation from inhomogeneous and nonisothermal layers, scattering 79−37139
radiative transfer, atmospheric effects, conference, San Diego, California (1979 August 29 to 30) 80−62376
radio, acoustic and radio-acoustic sounders *(Japanese)* 78−16209
radio brightness temp. of Earth from Kosmos 243 and Nimbus 5, SHF obs. 80−72521
radio echo sounding of ice sheets, internal props. var. with depth 80−26633
radio oceanography using aircraft, inherent problems 77−25792
radiometer, polarisation effects meas. using partially polarized light 79−49266
radiometer measurements, microwave brightness temperature *(Danish)* 80−26625
radiometric imaging from space, atmosphere effects problems 80−98323
radiometric measurements, passive, influence of atmosphere in 10 to 1000 GHz range 79−88465
radiometric sounding data and operational numerical weather prediction 78−53696
radiometry, multispectral , by tethered balloon, of plants and soils 78−3958
radiometry of flat finite wave tank, three-dimensional vector modelling and restoration of meas. 77−22599
radiooceanography, using aircraft inherent problems 77−17241
radiowave backscatter from vegetation, water cloud model 78−57274
rain estimation, using geostationary satellite data from extratropical region 80−90244
rainfall estimation by satellite borne microwave radiometry 80−105085
rainfall measurement, combined usage of radar and radiometry techniques *(Chinese)* 80−109272
rainfall over land, microwave radiometry by Nimbus 6 ESMR 80−56635
rainfall rate detect over ocean and land by spaceborne microwave radiometry 80−101423
random media, active remote sensing, depolarisation effects 80−82090
random media, active remote sensing, theory 80−51571
reflected EM wave appl. for studying atmosphere, land and sea props. 78−93015
reflected sunlight polarisation, meas. from high-altitude balloon 78−61561
reflecting sea surroundings, IR contrasts 77−5211
refractive index of liquid, use of electro-optical probes *(German)* 77−5889
remote sensing and ranging systems from space, conf., Rome, Italy (March 1980) 80−105432
reservoir surface area from LANDSAT imagery 79−66834
residential building heat loss estimation by aerial IR imaging 79−74586
resource management, conf., Alamogordo, NM, USA, 1978 78−69541
review of recent developments 77−23752
river ice break-up, satellite monitoring 78−65350
river ice jams, physical meas. 79−53398
river pollution distribution determination by remote sensing, study 80−81512
River Tiber, physical processes related to discharge into sea, aerospatial obs. 80−108831
riverine and coastal effluents, remote sensing of thermal alterations and circulation patterns 79−57524
rivers and lakes, spectral response field meas. 77−78469
rivers and open channels, level and velocity meas., surface wave random signal anal. 77−45205
rivers/open channels level and vel. meas. by surface wave signal anal. 78−57328
rock type discrimination, Landsat filters assessment using laboratory spectra information 79−16791
rock type discrimination using enhanced Landsat imagery 80−41568
rocks and minerals spectral refl. data, lab. and remote obs. comparison 77−17251
rough surface average impulse response, appl. to satellite radar altimetry 77−17235
RPV, high-altitude, for environmental appls. 80−17470
Sahel region, Africa, surface albedo vars. investigation during recent drought (1967 to 1974) 80−76981
saline seep detection and mapping, IR remote sensing techniques 80−4154
salt domes, N.Louisiana, imaging radar mission 79−66833
SAMIR microwave radiometric system, Bhaskara satellite, geophysical data acquisition 80−56638
SAR/LANDSAT data set assembly and anal. 77−78493
Sargasso Sea, surface height vars. from Geos-3 altimetry obs. 80−104969
satellite acquired image geometric distortion correction 79−74588
satellite altimetry measurements for oceanic geoid determination, short arc adjustment model technique 80−21830
satellite auroral photometry, spectral albedo corrections 77−49208
satellite cloud picture recorder for reception of APT pictures 78−81434
satellite data collection with Geostationary Operational Environmental Satellite 79−29977
satellite derived cloud imagery, optical Fourier transform anal. 78−85749
satellite design for optimal continuous coverage 78−73603

remote sensing continued
satellite digital data, radiometric correction and equalisation 79−74587
satellite image data acquisition system design 79−58098
satellite image plane scanner for earth observations 79−97436
satellite image sensing and multiplexing system tradeoffs 77−60498
satellite imagery, anal., distortion free map projection 79−34986
satellite imagery, filtering to remove cloud cover 77−56744
satellite imagery, linear features enhancement by rotational exposure 79−35874
satellite imagery for Himalaya geological structure study *(German)* 77−66907
satellite imagery stereographic pairs for cloud top height meas. 78−45017
satellite images macrophotography, technique 79−29895
satellite IR pictures, automatic digital techniques for oceanic features enhancement and extraction 79−5682
satellite mapping, by synthetic aperture radar 80−12572
satellite multispectral data digital anal. for land use inventory/mapping 77−78541
satellite ocean-related imagery, appls. programme 79−5681
satellite on-board processing for Earth resources data 78−61626
satellite onboard feature classification by CCD analogue signal processing 77−70980
satellite photograph production using laser beam recorder *(German)* 80−5777
satellite picture of Ancona area, Italy, seismotectonics 78−65246
satellite radioaltimeter, rough surface average impulse response, anal. 77−25791
satellite thermal imager for Defense Meteorological Satellite Program 79−97435
satellite-borne IR scanning radiometer obs. of stratosphere, optimum field view and spacing 78−16201
satellite-generated radar images of the Earth 80−90249
SATICON return beam system 2-inch high resolution camera tube 79−5724
scatter model for leafy vegetation 79−12193
scatterometer, pulse compression system, experimental study 77−17240
scene content measurement from aerial images, appl. to building complex scene 80−78788
sea, HF radio scatter 77−17230
sea foam produced by storms, microwave remote sensing of storm intensity 80−41528
sea ice, anisotropic props. in 50-150 MHz range 80−17274
sea ice, Danish studies using Landsat and airborne sensor data 80−94527
sea ice, EM wave scattering from slightly rough boundary 78−77266
sea ice, low-salinity, radiometer studies 78−81175
sea ice, microwave remote sensing in AIDJEX main expt. 78−81173
sea ice, ocean waves SAR imaging 79−5496
sea ice, remote sensing, appls. 80−77176
sea ice age category differentiation through location and temp. observations using microwaves 80−67380
sea ice and surface temp. meas., enhanced IR satellite imagery 77−37422
sea ice in Arctic Basin, time depend. of ice conc. and multiyear ice fraction 78−81174
sea ice mapping and drift meas. using aircraft synthetic aperture radar images 79−70809
sea ice/lake SAR L-band imagery computer processing 78−36311
sea roughness investigations, radiophysical, Ukrainian Academy of Sciences 77−17233
sea state, HF sea-echo Doppler spectra statistical props. 77−29312
sea state, significant wave height extracted by algorithms 80−4023
sea state, surface roughness slope density calcs. from Geos-3 data 80−4022
sea state and wind sensing by HF skywave radar 78−24396
sea surface, radar detect. of oil contaminations *(Russian)* 77−49089
sea surface and atmosphere radio brightness temp. meas. from satellite *(Russian)* 77−60407
sea surface characts. rel. to radar returns at near-vertical sighting angles 79−57969
sea surface contour airborne radar as remote sensing instrument 80−51562
sea surface emission temps. from DMSP 77−70682
sea surface inhomogeneities sensing via sound scatt., phase function shape in shadowing conditions *(Russian)* 80−94530
sea surface radiobrightness temp. from satellite sounding *(Russian)* 77−60412
sea surface slope distrib. function determ. from Sun glitter, accuracy *(Russian)* 80−94611
sea surface temp., atmospheric effects elimination *(Russian)* 78−96311
sea surface temp. fronts, environmental satellite survey 79−2247
sea surface temp. meas. from meteorological satellite images 79−100990
sea surface temperature, 8-13 μm satellite meas. interpretation 77−17145
sea surface temperature, Noaa 4 satellite and Aries airborne radiometer meas. comparison 79−62517
sea surface temperature, radiometric observations at 2.65 GHz, atmospheric and surface corrections, Chesapeake Bay 77−17114
sea surface temperature (SST), NOAA-4 data time series anal. 79−53364
sea surface waves, remote sensing using one and two freq. microwave techniques 80−94622
sea surface wind speed and significant wave height meas. using short pulse radar 77−17234
sea surface wind speed and significant wave height using pulsed radar 77−29477
sea temp., salinity and winds, SKYLAB 1.4 GHz radiometric meas. 78−65338
sea temp. microwave radiometry, obs. at 2.65 GHz at Chesapeake Bay 77−29314
sea wave space and time structure measurement from Doppler frequency shift 77−29482
sea waves using HF radio scatter 77−25789
sea-state and surface winds in Irish and Celtic seas using MF radar 79−16725
sea-surface temperatures in tropical Pacific, satellite determ. and climatological usefulness 80−31044
sea-surface wind, meas. by radar backscatter at 13.9 GHz from Skylab 77−91304

remote sensing continued
sea-surface wind stress determination using SEASAT-A microwave scatterometer, algorithm 79−39883
Seasat, altimeter sensor file algorithms 80−94680
SEASAT, ocean wave and wind obs., appls. to offshore oil, gas and mining industries 79−80044
Seasat, radar altimeter, initial performance assessment 80−94679
Seasat, scanning multichannel microwave radiometer, antenna pattern corrections 80−94683
Seasat, scanning multichannel microwave radiometer, calibration algorithm development 80−94682
Seasat, scanning multichannel microwave radiometer, description and performance 80−94681
Seasat, scatterometer evaluation 80−94684
Seasat, scatterometer scattering coeff. algorithm 80−94685
Seasat, synthetic aperture radar system 80−94686
Seasat, visible and IR radiometer 80−94687
Seasat artificial oceanographic satellite, microwave instrums. 80−94678
Seasat Gulf of Alaska experiment, comparison data set winds 80−94570
Seasat oceanographic satellite, performance evaluation 80−94677
SEASAT program, Canadian participation 78−20535
SEASAT radar altimeter, resolution capability preliminary estimates 80−72645
SEASAT-A satellite ocean surface truth expts. 77−5419
SEASAT-A satellite project, for oceanographic research 79−84496
Seasat-A satellite synthetic-aperture-radar processor, England (Oakhanger) sited 79−21128
sedimentary sea bottoms, machine classification 79−92626
sediments below turbid water 80−8331
seismic sounding, synthetic sonic logs as process for stratigraphic interpretation 79−88483
selective modulation radiometer for gaseous pollutant remote sensing *(French)* 78−20550
selective radiant temperature mapping using layered classifier 77−56750
sensors and detectors in NASA's future mission 79−5656
sequential scene matching using edge features 78−32239
shallow aquifers detection using thermal infrared imagery 79−84326
shelf seas satellite IR imagery, fronts adjustments obs. 79−92545
shorefast sea ice melting study using multispectral LANDSAT data 77−78522
shoreline erosion, Croatan and Pamlico Sounds, N.Carolina, LANDSAT imagery appl. 79−39701
shoreline information in artificial satellites autonomous navigation problems 78−53732
short pulse radar ocean wave sensing, preliminary results 80−46315
side-looking airborne radar appl. 78−20561
signal correction optimisation considering internal noises *(Russian)* 78−16191
significant wave height, comments on airborne profilometer problems 80−4026
six channel radiometer for spectral investigations of terrestrial and planetary atmospheres *(Russian)* 77−29468
Skylab conical multispectral scanner IR data statistics 80−90223
Skylab data, inflight performance evaluation by ground-based meas. 77−64455
Skylab imagery, method to differentiate saline from non-saline rangelands 77−91322
Skylab S-192 conical scanner data digital processing 77−82046
Skylab S-192 conical scanner imagery geometric evaluation 77−82047
Skylab scatterometer meas. of hurricane Ava, anomalous data correction 79−29881
Skylab spectral channel evaluation for classification and thematic mapping 77−78500
SLAR imagery correction for flight path curvature distortion 79−53553
smoke cloud plumes from forest fires in Canada, satellite obs. 78−24367
smoke from lightning-caused fires in Alaska, NOAA-5 images 78−49079
smoke particle size and conc. meas., three-wavelength light transmission technique 79−79438
SMS images during GATE, wind field determ. accuracy 77−53147
snow, ice and rain, passive microwave obs. from Nimbus satellites 80−101422
snow, microwave signatures rel. to state and wetness 78−57235
snow albedo following dustfall, satellite remote sensing 80−17385
snow areal extent and water content estimate using LANDSAT imagery 77−78520
snow cover parameters, microwave radiometry determination 80−56652
snow cover water storage determ. using aircraft-borne gamma-ray surveys 78−16218
snow parameters, investigation by radiometry in 3 to 60 mm wavelength region 80−72561
snow parameters remote sensing, two-stream theory of reflectance 79−88376
snowfield assessment from Landsat 78−88941
snowpacks, microwave passive remote sensing, theory and expt. 80−26632
sodar meas., improved quantitative display techniques 78−77332
soil, moist, emissivity in microwave range, temp. effect 79−29797
soil, surface roughness effect on microwave emission 80−17264
soil, water content estimation via multispectral scanning 77−60479
soil and winter wheat yield on Great Plains, Landsat data 78−65351
soil automatic identification from digital terrain data 77−73884
soil moisture, by visible and IR false colour photography 80−56653
soil moisture, near-surface, theory for passive microwave remote sensing 77−87105
soil moisture, remote sensing with air temp. compensation 77−17247
soil moisture and component estimation from spectral polarisation 79−16678
soil moisture and geology mapping, thermal inertia method 80−8344
soil moisture content, determ. by meas. of reflectance in ultrashort radio wave band 78−16075
soil moisture content, microwave radiometer meas. over bare and vegetated surfaces, comparison 78−88851
soil moisture content measurement by microwave radiometry, review 80−17425
soil moisture IR thermography remote sensing through agricultural crop 80−109147
soil moisture meas. by remote microwave radiometry 79−48526
soil moisture meas. with airborne imaging passive microwave radiometer 78−36310
soil moisture measurement, microwave and radar techniques 79−70896
remote sensing continued
soil moisture measurement, microwave backscatt., surface roughness and texture effects 79−12295
soil moisture measurement, remote sensing simulator 78−49143
soil moisture sensitivity of cross-polarized radar backscatt. 79−25282
soil pattern data from aircraft/LANDSAT scanners delineation by digital anal., Indiana 77−78496
soil stored productive moisture, remote determ. technique 79−29795
soil surface moisture determination, photographic method for polarised visible light recording 79−53557
soil survey, lowland England, moisture content and soil discrimination from air photos 79−88504
solar Mesosphere Explorer mission description (1981-2), O_3 and related chemistry 80−105096
solar radiation incident at Earth surface, estimation from geostationary satellite data 80−82006
solid state imaging devices, comparison with TV camera tubes 77−83986
solid-state linear array appls., user-oriented data processing 80−4151
solid-state linear array technology appls. 80−4150
Soviet Meteor satellite imagery, reception and processing in USA 79−39872
Soyuz 22, geophysical reconnaissance *(Russian)* 77−60574
space appl. and research, WARC 1979 impact 80−105147
space data, atmospheric effects 79−58092
space information systems, real time data management 79−92600
space instrumentation for atmospheric obs. IEEE Region V annual conf. (El Paso, 3-5 April 1979) 79−58221
space observations of long-term climatic change, conf., Prague, Czechoslovakia (Sep. 1977) 79−29843
space-borne remote sensing *(Italian)* 80−109333
spacecraft remote sensors 77−56813
Spacelab and artificial satellites appls., conf., Rome, Italy (Mar. 1978) 78−96384
Spacelab incoherent scatter radar for atm. field-aligned currents meas. 77−21946
Spacelab passive atmospheric sounders 77−82113
Spacelab passive sounder packages for atm. research 77−21945
spectral bidirection refl. props. meas., at 0.52 μm, for savannah, bog, pasture, and coniferous forest vegetation 78−40649
spectral feature enhancement of Landsat data, entropy minimisation *(Italian)* 80−98473
spectral reflectance, scene composition, instrument for simultaneous recording 78−81443
spectral reflectance curves estimation from multispectral image data 78−32886
spectral reflection characts. transformation of natural formations 79−48640
spectral signatures of particulate minerals in visible and near IR 78−7620
spectral/spatial classifier development for Earth observational data 78−73555
spectroradiometer, lone wavelength Exotech model 20C, Earth resource remote sensing appl. 79−88474
spectroradiometer for airborne remote sensing 78−88943
spin scan camera system, on geostationary satellite, for global weather monitoring 78−61600
SPOT, experimental Earth observation system, features *(French)* 77−82097
staring IR sensor, acoustooptic tunable filter performance 80−36407
staring IR sensors, space and reconnaissance appln. 80−86406
step-stare spaceborne optical system image motion compensation 80−90322
step-stare spaceborne optical system smear compensation by focal plane manipulation 80−82172
stereo side-looking radar, accuracy anal. 80−56646
stereo-orthophotography, method and accuracy 77−44904
stereo-orthophotography in cadastral and general mapping 77−40972
STEREOMETROGRAPH model G with fast motor drive 77−66996
stereophotogrammetric measurements of clouds in tropics, TROPEX data 79−29833
stereophotogrammetry, automatic, using structural pattern recognition techniques 78−61632
storm zone location methods using radiothermal remote meas. of ocean *(Russian)* 78−16189
stratified acreage estimates in Illinois crop-acreage expt. using LANDSAT data 77−78501
stratified layer microwave radiation, radiometer shape effect 77−18069
stratified media, pulse-spectrum technique, permittivity determ. 79−8722
stratified media, spectral domain method 77−19138
stratosphere, aerosol and gaseous constituents from spacecraft solar extinction data, inversion retrieval 79−74961
stratosphere, artificial satellite instrums. description 80−26713
stratosphere, ClO remote meas. from IT solar spectrum obs. 79−58005
stratosphere, emission spectrum, balloon-borne far IR Michelson interferometer meas. 79−39870
stratosphere, halogen compounds global monitoring by satellite borne spectrometer 77−45162
stratosphere, laser spectroscopy relevant to photochem. 78−88951
stratosphere, O_3 vertical profile determ. by lidar sounding from ground 78−11972
stratosphere, temp. and press. determ. from OH fluoresc. lidar instrument 79−80033
stratosphere, temperatures and geostrophic winds during 1973-74, Nimbus 5 radiance meas. 79−79976
stratosphere, trace constituents correlated seasonal and climatic vars. 79−84433
stratosphere, ultralong temp. waves during 1973 austral winter 78−92901
stratosphere aerosol, satellite monitoring systems, SAM II and SAGE 80−82082
stratosphere O_3 content, Nimbus 4 UV and IR remote sensing 80−77154
stratosphere trace molecule Fourier transform spectrometer optical design 80−82099
stratospheric composition, IR meas. radiometer, H_2O vapour profile 79−8718
stratospheric composition, simultaneous IR meas., of NO and NO_2 through dawn 79−8671
subsurface radar for Earth's surface remote probing 79−8724
subsurface radar using video pulse for deep probing in Earth, pulse propag. in lossy media using LF window 80−74282

remote sensing continued
subsurface water temperature and salinity remote sensing by Raman scatt. 79−80036
S.Sulaiman Range, Pakistan, struct. and seismicity from satellite imagery 79−39715
SE Sumatra coastal environment, remote sensing appls. 79−53556
surface albedo change, monitoring by LANDSAT 78−32104
surface based remote sensors, coding technique for boundary layer echoes 80−17400
surface temperature meas. by reflection technique 77−2653
surface texture analysis with thermal and near IR scanners 79−53554
surface water pollutants, airborne monitoring by fluorescence spectroscopy 79−2397
surface wind, algorithm for wind speeds using Geos 3 measurements 80−4078
suspended sediment monitoring, universal multispectral algorithms 79−53558
suspended sediments in surface waters of Mississippi reservoirs 77−45041
Sydney Metropolitan area, Landsat data ground control points, stepwise polynomial transformation 80−104961
synthetic aperture radar appl., technology trends 79−5655
synthetic aperture radar imagery formation, effects of random phase changes 77−17242
synthetic aperture radar imaging in geosynchronous orbit 78−65442
synthetic-aperture radar on satellites, digital processing techniques 80−61914
system specification using computer image simulation 80−48439
tactical reconnaissance system, real-time, KA-102A EO LOROP camera 79−30599
target discrimination methodology in remote sensing 80−58470
technology, Canadian advances 78−16170
technology developments and appl. *(Japanese)* 79−8701
technology transfer to operational data system 77−78513
telecommunication and remote sensing, book 80−36431
teledetection of gaseous atmos. pollutants, data acquisition and anal., pollution mapping *(French)* 80−7989
telemetry, automation of information input and processing 77−78429
temperature fields meas. by IR radn. detection 77−41606
temperature meas. by IR camera, plastic processing industry appls. *(German)* 79−58685
temperature-measuring circuit uses diodes as sensor 77−53901
terrain characterisation, radar scattering 80−101464
terrain classification using colour imagery, algorithms 77−78466
terrestrial luminance field spatial structure 78−49140
terrestrial natural surfaces, reflected solar irradiance indicatrices and albedo effects 79−62514
terrestrial surface temperature sensing, emissivity correction for thermal radiation interpretation 80−82092
tethersonde system for remote meas. of wind and temp. 79−80038
S.E.Texas counties, Landsat forest and range inventory by administrative boundaries 77−56748
texture anal. in computerised picture processing 78−61628
texture analysis by hybrid optical/digital system 80−78787
thematic classified LANDSAT imagery of Portland, Oregon, tabular data base 77−78537
thematic map accuracy, statistical testing 78−77372
thematic mapper, time-delay and integration CCD imager appl. 79−35098
thermal and hydrological surveys by satellite *(Italian)* 77−81988
thermal imaging using pyroelectric vidicon *(Japanese)* 77−27359
thermal inertia imagery of Earth surface, model for calibration of survey 80−105083
thermal inertia mapping by IR imagery, mathematical model 80−109280
thermal inertia mapping rel. to surface composition and soil moisture 77−73740
thermal IR, ground truth meas. 77−91318
thermal IR scanner analogue data digital processing 77−82045
thermal IR scanning appls. to geology and hydrology 79−8723
thermal microwave emission from two-layer medium, theory 77−49170
thermal model of Earth's surface for geological mapping by remote sensing 77−53056
thermal radiation polarisation, of permanent snow fields, from meas. obtained from the 'Meteor' satellite 78−88870
thermal sounding, temp. effect on 15 μm region transmission function 78−77327
thermal spectrozonal aerial photography, capabilities and future prospects 80−18036
thermistor bolometers in Earth horizon sensor telescope 78−24795
thermosphere, middle, incoherent scatter radar studies 80−72654
thunderstorm and lightning observations from Space Shuttle 79−58078
thunderstorm growth and decay during premonsoon season, radar study, Bombay 79−48541
thunderstorm intensity from satellite data 80−41518
Tibet, active tectonics, LANDSAT imagery 79−20794
Tibetan Plateau, late Cenozoic tectonics, LANDSAT imagery 79−20795
Tien Shan region, LANDSAT imagery rel. to contemporary tectonics 79−29733
TIROS-N microwave sounder unit for global temp. distribution meas. 80−90265
TOPOCART-ORTHOPHOT C system for prod. of stereo orthophotos 77−66994
TOPOMAT all-automatic photogrammetric system for aerial photography 77−66993
trace-gas remote analysis, optoacoustic radiometry limitations 80−108759
track-type surveys, sampling requirement estimation 77−78507
transient EM wave prospecting 80−76905
transverse displacement of distant body, interferometric meas. 77−82488
tri-Doppler radar, tetrahedral scan appls. 78−16184
trichlorofluoromethane, 8-12 μm bands intensities, temp. depend. 80−43048
trophic state index for inland lakes using remote sensing data 77−5256
tropical cyclones, photometric method for estimating cloud cover from satellite data 78−4007
tropopause, detect. by partial specular refl. with VHF radar 80−8411
troposphere, O_3 distribs. meas. with airborne laser absorpt. spectrometer 79−2344
troposphere, transhorizon radiowave propag. appl. 78−44921
troposphere and stratosphere temp., O_2 absorpt. spectra at 60 GHz 80−77172
troposphere humidity, new insight with Meteosat water vapour channel 79−25292
troposphere moisture, temp., IR soundings anal. by statistical struct. and correl. functions 80−8398
tropospheric pollution from aircraft 77−49195
turbid waters, penetration depth at green wavelengths 79−66832
turbulent dispersion concentration valves, system for wind tunnel meas. 79−5191
two-layer media, microwave radiative transfer models 77−21908
ultramafic rocks from Cr-rich areas, visible and near IR spectra, remote sensing appls. 80−4000
uncontrolled thermographic mosaic compilation and videotape processing 77−29502
underground quarries, EM transmission meas. 78−57365
underwater chlorophyll *a* fluorescence sensing, sunlight penetration depth estimation 79−79874
underwater TV viewing system, lens design 77−78459
ungauged urban watershed flood frequency model parameter estimation 77−37269
upper atmosphere, constituents detection, using submillimetre wave heterodyne radiometry 78−49183
urban areas, land use, satellite temp. meas. appls. 78−65393
US applications, conference, Brighton (1977) 78−59223
USA coastal zone water quality monitoring, aircraft vs. spacecraft 77−78233
vegetation and crop development mapping, table look-up procedure 77−78531
vegetation canopy modelling for signature correction/anal. 77−78515
vegetation changes with maturity, solar elevation effects on sequential LANDSAT imagery 77−45159
vegetation layer, scatt. model 79−29880
vegetation resources interpretability for various space acquired image types 79−26160
Venus atmosphere and surface, investigation by radiosounding from Venera 9 and 10 satellites 80−101543
Venus atmospheric precipitation detect., remote sensing radar and radio techniques 80−56741
Venus surface, bistatic radiolocation by Venera-9 and Venera-10 satellites 79−48698
Venus upper atmosphere, remote temp. soundings rel. to mean circulation diagnostic model 79−58287
vertical magnetic dipole on two-layer Earth 80−76906
virgin land resources, appl. of aerial and satellite photography *(Chinese)* 79−53551
visible and infrared imaging radiometers for ocean observations 78−69536
Visible and Infrared Radiometer evaluation from SeaSat-A surface temp. obs. 80−46325
visible IR spectrometer, on Skylab, for Earth surface remote sensing 77−60567
visible range spectrometric investigation from Salyut 4, radiation characteristics of environment 80−51638
visible spectrum, photographic aspects 77−56773
volcanic rock spectral refl., 400-800 nm, obs. to compile reference data 80−90073
water covered with foam, thermal radio emission from foam structures 79−29497
water depth and bottom features mapping, from passive multispectral scans 78−40673
water penetration imagery, surface/depth data separation by multispectral scanning 78−69539
water pollution problems appl. *(Japanese)* 80−94122
water potential evaporation from soil, water and crop surfaces, eqn. for remote sensing 77−64334
water quality from Landsat imagery of Wisconsin lakes 80−41469
water suspended solid analysis by single-particle scatt. 79−79435
water vapour images from Meteosat, comparison to tropical streamline analyses 80−8384
wave heights and wind speeds from Geos 3 data 80−4079
weather forecasting processing of radar and satellite imagery data 80−109252
wheat canopy reflectance, Suits' spectral model appls. 78−7811
wind, off-shore meas. by HF Doppler ground-wave radar 78−77295
wind, strong shear obs. using pulse compression radar 78−32193
wind determination by acoustic radar *(Chinese)* 80−46290
wind fields, mesoscale, satellite-derived, covariance anals. 80−82013
wind measurements, using OMEGA radiosonde, error estimation 79−29916
wind velocity, remote meas. using video equipment for pollution monitoring *(French)* 80−7990
wind velocity estimation via optical signal processing 77−41107
wind vertical velocity, acoustic Doppler power spectra comparison with direct meas. 79−57999
wing and struct. const., MM wave and optical line-of-sight probing 80−36426
X-ray and gamma-ray remote sensing spectrometers, data analysis system for planetary mission appl. 79−12411
X-ray aurorae prod. by energetic electrons precip., imaging from Spacelab 78−61608
Zendan Fault region, Iran, struct. lineaments, interpretation of Landsat 1 obs. 80−104941
Cu deposits, exploration using LANDSAT-1 imagery 79−2398
H_2O vapour absorpt. in 10-12 μm atm. window 78−20513
NO_2 and SO_2 pollution near industrial area, meas. and remote sensing equipment *(French)* 79−74928
NO_2, remote sensing of air pollution using optical multichannel analyser 79−79439
O_3, IR heterodyne spectroscopy 77−45160
O_3, nighttime concentration (15-68 km), Nimbus 6 obs. comparison with OAO-3 obs. 80−105016
SO_2 air pollution detect. by correl. spectrometry 78−96298
SO_2, air pollution emissions in Mediterranean region, remote meas. 79−20987
SO_2, conc. determ. for coal-burning power plant stack, Fourier spectrometry appl. 77−49196
SO_2 optical depth meas., mask correlation spectrophotometry 77−82066
SO_2 remote meas. at 4 μm with continuously tunable source 78−77365

remote sensing continued
SO_3 emissions remote meas. from Asama Volcano, Japan *(Japanese)* 79−70772
SO_4^{2-} atm. aerosol hazes and long-range pollution transport, satellite detect. 79−20975
U exploration, LANDSAT data merged with geol. and geophysics data 80−56651
U, National Uranium Resource Evaluation (NURE) aerial radiometric survey data interpretation via principal components anal. 80−101438

remote sensing by laser beam
acoustic microscope, scanning laser, biomedical research and materials science appls. 78−46878
aerosol concentration deduction from 1.06 μm lidar meas. 79−25323
aerosol layer depth remote meas. by microwave-modulated laser *(Russian)* 78−57338
aerosol mass conc. meas. by Nd:glass lidar, ASSESS II Spacelab mission simulation *(German)* 78−69649
aerosol measurements with calibrated two- and three-freq. lidars 78−36334
aerosol pattern recognition *(Japanese)* 80−51028
aerosols, atmsopheric, lidar obs. 79−66841
aerosols, stratospheric, anal. by differential scatter lidar system 78−69524
air pollutant emission and emission meas. by laser *(German)* 78−40665
air pollutant sensing 77−37458
air pollutants, laser spectroscopic detection 80−17366
air pollution, CO_2 laser velocimetry techniques 78−61623
air pollution, detection by analytical spectroscopy using dye laser 78−81362
air pollution, laser spectroscopic detect. 79−57557
air pollution, long-path monitoring, using tunable lasers 78−69522
air pollution, monitoring techniques for trace gases 78−69521
air pollution, NH_3 conc. determ. on long path from CO_2 laser radiation reson. absorpt. 79−29904
air pollution detection, optical methods *(Czech)* 78−69444
air pollution detection using resonant fluorescence, Raman scattering and LIDAR *(Czech)* 78−81359
air pollution meas. using laser radar data processing system 79−57559
air pollution meas. using tunable lasers 77−60499
air pollution monitoring, electrical techniques, solid laser appls. *(Italian)* 77−82069
air pollution monitoring of ethylene and vinyl chloride, computer-controlled CO_2 laser system 78−49182
air pollution monitoring with YAG:Nd laser pumped $LiNbO_3$ parametric oscillator 77−46767
air pollution photoacoustic detector characts. at CO_2 laser freqs. 79−100554
air pollution remote meas. using chem. laser lidar system 77−21910
air pollution remote monitoring, two-dimens., via computerised tomography 79−39330
air pollution remote sensing from space 78−61621
air-truth lidar polarisation studies of orographic clouds 78−73454
airborne, particle sizing, 0.05 to 5.0 μm, using laser instrument 78−61624
airborne fluorescence system for OH and trace gas meas. 80−36425
airborne laser sensor system, using large size lightweight plastic mirror 78−66891
airborne lidar, continuous long-distance system, flight tests *(German)* 78−36338
airborne lidar, multidisciplinary, planned operation 78−36335
airborne lidar aerosol measurements during the ASSESS II mission 78−73489
airborne lidar system for geophysical and atmospheric expts. *(Italian)* 80−109277
airport environs, air pollution, remote monitoring by laser systems 80−17368
atmosphere, aerosol flow, transit-time lidar velocimeter detect. 77−13127
atmosphere, H_2O vapour conc. meas. by laser absorpt. techniques 78−61595
atmosphere, O_3 vertical distrib., shortened version of Umkehr ob. method 80−8430
atmosphere, point monitoring of gases ambient concs. using tunable lasers 78−61607
atmosphere, using discretely-tunable IR gas lasers and heterodyne detect. techniques 78−61605
atmosphere plume structure and trajectories, lidar meas. 79−58016
atmosphere remote sensing *(Chinese)* 80−46292
atmosphere temp. measurement using CO_2 laser radar 80−90225
atmospheric ^{238}U decay product detection 77−87104
atmospheric aerosol conc. meas. by lidar 78−85693
atmospheric aerosols, flash holography investigation 78−16217
atmospheric characteristics, laser beam wave case, book contrib. 79−34959
atmospheric composition meas., lidar theory and meas. *(Japanese)* 78−16206
atmospheric contaminant detection using absorption method 79−21004
atmospheric environmental research, appl. of lasers *(German)* 80−97849
atmospheric gas high sensitivity point monitoring by diode laser 78−73523
atmospheric gaseous pollutants meas., mobile lidar system 80−35814
atmospheric gases meas. using discretely tunable IR gas laser 77−49199
atmospheric measurements, laser radar system at University of West Indies 77−13134
atmospheric monitoring, book 77−25799
atmospheric monitoring, laser systems appl. 78−69520
atmospheric parameters monitoring by laser radar, water droplet remote meas. 77−91299
atmospheric pollutant gases, at CO_2 laser wavelengths 78−40647
atmospheric pollutants, real time monitoring using laser two photon ionisation spectroscopy 80−7996
atmospheric pollution, laser incoherent heterodyne detection 77−87130
atmospheric pollution *(Italian)* 79−70889
atmospheric pollution detection, high sensitivity, using tunable diode laser 78−57373
atmospheric pollution monitoring by lidar systems 78−53765
atmospheric pollution monitoring by PROBE, density profile meas. of specific constituent 78−28320
atmospheric propagation of optical signals, statistical characts. analysis 80−36412

remote sensing by laser beam continued
atmospheric properties meas., laser expts. on Spacelab missions 78−53793
atmospheric sounding, lidar characts., optical system parameters effect 80−33065
atmospheric techniques *(Japanese)* 78−45019
atmospheric temperature profiles, lidar meas. of rot. Raman and elastic scatt. 77−9515
atmospheric trace constituents, differential absorpt. lidar from Space Shuttle 78−45179
atmospheric visibility using lidar 80−31141
atmospheric water vapour, laser sounding by reson. method *(Russian)* 77−33185
bathymetry for near-shore charting appl., preliminary field test results 79−5679
Chesapeake Bay, water surface laser radar refl. as function of wind speed 77−41034
cigarette smoke, diode laser meas. of methane, ethane and H_2O vapour concs. 80−97847
cloud, vertical laser beam heating causing convection *(Russian)* 80−56529
cloud extinction coefficient, estimation from multiwavelength lidar backscatter meas. 80−98446
cloud seeding studies application of lidar remote sensing 80−109203
coherence implications for laser appls. 77−75599
coherent anti-Stokes Raman spectroscopy, appls. 77−87844
conference, laser and electro-optical systems, San Diego, CA, USA (Feb. 1980) 80−62392
cross-wind velocity meas., interference fringe visibility and spacing, atmospheric turbulence effects 80−51572
crosswind profiles, remote sensing using correlation slope method 80−31131
crystalline cloud meas., light scatt. matrices *(Russian)* 77−5317
dense particulate system, particle size meas. device based on scatt. light 78−45006
depth sounding using airborne laser land profiler 78−49173
differential absorption lidar systems for atm. gases remote meas. 78−69525
differential absorption lidars, reference range 80−89700
differential-absorption lidar technique for remote meas. of atm. gases 78−61603
dusty IR Test-1 lidar obs., transmission meas. 80−99625
dye laser, efficient forced oscillator, to meas. upper atmospheric Na layer 80−41563
dye laser, high energy pulsed, for atm. sounding 79−39868
Earth's crust, tidal displacement, Geos-3 laser ranging obs. 80−3913
Earth crustal motions detect. using spaceborne laser ranging systems 78−92995
Earth observation by airborne CW CO_2 lasers, heterodyne reception 78−40676
Earth surface intersite distances, using spaceborne laser ranging system, SPEAR 78−3978
environmental, determ. molecular chem. and biological planet surface composition 80−72651
environmental measurement, conf., Gaithersburg, Maryland, USA (Sept. 76) 78−69504
ethylene, air pollution monitoring, computer controlled CO_2 laser absorpt. system 80−89699
ethylene, high resolution spectroscopy with diode laser heterodyne system 77−91300
ethylene remote meas. using CO_2 differential absorpt. lidar 78−49122
fluorosensor performance, sea-state effect 78−92990
fluorosensor systems using N_2 and KrF lasers 80−21428
gas analysers, freq. modulation appls. 80−85246
gas measurement using discretely tunable IR lasers 77−87118
gas remote meas. using discretely tunable IR lasers 77−91298
high clouds, cirrostratus emissivity meas. 80−82061
high ice clouds, visible and LR optical props. from lidar and radiometer meas. 80−82060
high-sensitivity multipurpose remote sensor 78−40684
industrial atmospheric pollutant remote analysis by Raman lidar 80−12047
IR Doppler wind-sensing system, spaceborne, atmospheric effects 79−96828
IR laser heterodyne spectroscopy for trace gases remote detect. in planetary atms. 78−61606
IR system performance in airborne environment 78−82039
lidar, laser rangefinder, characteristics of atmospheric aerosols 80−51580
lidar and anemometer meas. of wind vel., comparison 79−39885
lidar equation for inhomogeneous atmos. *(Russian)* 80−82054
lidar measurement of Na conc. and neutral temp. at mesopause level 78−61613
lidar method for half width and intensity of gas absorption lines *(Russian)* 80−21844
lidar observation of ice clouds, microphys. props. 79−39811
lidar observations of high plains thunderstorm precipitation 78−32167
lidar probing of fogs and clouds, double scatt. approx. 78−73512
lidar Raman spectroscopy of atmosphere *(Russian)* 78−24387
lidar return signal geometrical compression, atm. remote sensing appl. 78−57329
lidar returns depolarization, scatt. from virga and source cloud 77−49169
lidar system, heavy, for environmental protection control, containerisation 78−36336
lidar system, two-freq. downward looking, for atm. monitoring 78−69523
lidar techniques for atm. struct. and comp. obs., proposed Spacelab program 78−61602
LIDAR teledetection and measurement of minority atmospheric constituents for pollution control *(French)* 80−7992
lidar temperature profiling of planetary atmsopheres 77−33352
line scan sensor, spatial and temporal coding of GaAs laser 78−83022
line scanning sensor, spatial filtering design 79−53527
line scanning sensor, spatial filtering design considerations 78−85752
long path monitoring of ambient gases, CO_2 versus semiconductor diode lasers 79−16682
lunar ranging, scientific progress, 1969-77 period 78−36476
Magnox reactors, remote corrosion monitoring, laser based instrument 78−41822
meteorological phenomena observation, mobile computerised laser radar system 80−56644
methane remote meas. by continuously tunable IR lidar 79−21025

remote sensing by laser beam continued
methanol trace detection using phase fluctuation optical heterodyne spectroscopy 80−68266
microprocessor-controlled 64-cell pulsed optical receiver for crosswind sensing 77−18096
mirror, large size lightweight scanning, for airborne laser sensor system 79−23045
multiple atmospheric parameter meas. laser radar system 78−4009
multiple gaseous air pollutants, point monitoring method by tunable laser *(Japanese)* 80−81515
ocean capillary waves, laser probe for 2D wave slope spectra meas. 77−60472
ocean subsurface temp. remote sensing using laser Raman backscatter 77−78434
ocean surface phenomena measurement *(Japanese)* 79−16716
oceanographic laser bathymetry, airborne, environmental subtraction technique 78−57372
oceanographic lidar system,; airborne, near-shore charting laser bathymetry 78−57371
oceanographic lidar system, airborne, bathymetric and fluorescing modes 78−57370
oil, remote characterisation by time-resolved laser fluorosensors, lab. expt. 78−73097
oil pollution indicator, ocean wave effects on remote sensing ability, model study 77−17255
oil pollution on sea using laser radar 78−77373
oil slicks, use of FFT in evaluation of laser Raman and Fluoresc. decay times 78−81444
oil spill detection by airborne laser fluorosensor 80−67024
oil spill remote detection by laser radar 79−25332
oil spills remote detection using laser-excited Raman backscatt. and backscatt. fluoresc. 78−32242
oil spills remote monitoring, computer controlled laser radar system *(Japanese)* 78−92994
optical fibre, use in remote inelastic light scatt. probe 80−58769
optical heterodyne line-scan imagery, speckle noise model 79−50337
optical pulse receivers for distance meas., basic params. determ. 78−33843
optical radar, logarithmic fast-response photodetector for atm. sounding, photometric properties 80−51585
passive and active environmental remote sensing techniques 77−21935
petroleum oil pollution at sea, detection by CO_2 laser radar 77−91324
photosynthesising organisms, remote laser probing by fluoresc. technique 79−66434
polar position, motion due to Earth's rot. Gen-3 laser ranging study 80−3912
radiation effect on laser system performance 80−38054
radiometer, airborne dual-channel IR heterodyne, for atm. meas. 78−57369
rain gauge, simplified optical path-averaged, based on scintillation detect. 78−40674
Raman lidar humidity sounding of atmospheric boundary layer 79−66809
Raman spectroscopy, remote spontaneous, new trends in recording of signals 80−73485
range measurements to moon, subnanosecond laser 77−82126
range resolved Brillouin scattering using pulsed laser 80−38055
real-time moving object tracking by optical correlation, using liq. cryst. image transducer 79−32035
receiving optical antenna, sensitivity to scatt. aerosol particle, laser location of atm. aerosols 77−70847
remote sensing, sensors and detectors in NASA's future mission 79−5656
saturated optical nonreson. emission spectroscopy (SONRES), appl. to air pollution elemental anal. 78−81465
sea ice, airborne laser profiles, interactive correction and anal. system 79−25338
seawater pollution studies, laser appls. *(Polish)* 78−20528
smoke and dust clouds, lidar observation at 0.7 μm, 10.6 μm 78−49181
SO_2 molecules in air, remote sensing methods assessment *(Japanese)* 78−96288
solid flaw remote sensing, laser system prod. acoustic waves, interferometric detect. 78−60975
sounding method and equipment for water absorpt. and attenuation coeffs. meas. *(Russian)* 79−34998
steel, mild, laser microspectral anal. 80−108769
stratosphere aerosol size distrib., lidar obs. at 0.6943 μm and 1.06 μm 77−41120
stratosphere aerosols, airborne lidar meas. during winter (1973) 77−33159
stratospheric dust from St. Augustine Volcano, ruby lidar meas. 77−29431
stratospheric post-volcanic aerosol decay, lidar meas. 79−53444
submillimetric wavelength bad-weather vehicle recognition system 77−19450
surface pressure, remote meas. by multicolour laser ranging system 80−8429
target classification, depolarised multispectral laser scatt. 78−50846
technology developments and appl. *(Japanese)* 79−8701
Teflon spheres-nigrosin black dye-water dispersion, turbid laser backscatt. 80−1129
teledetection of atmospheric pollutants by differential absorption of a CO_2 laser at two frequencies *(French)* 80−7991
terrain profiler, pulsed GaAs laser system 77−91297
terrain profiler, pulsed GaAs laser system 78−49145
time digitiser for laser ranging, ps. resolution, built in CAMAC minicrate 78−36301
toxic gas monitor based on laser photoacoustic spectrometer *(German)* 80−12046
trace gas monitoring system, with tunable diode laser, improvements 80−16882
troposphere, photochemical and physical transformations, obs. by tunable lasers 77−60460
tunable diode laser instruments, appl. advanced meas. and anal. 77−75600
turbulent jet, dye-dilution laser induced fluoresc. meas. 78−30397
velocimeter based on CO_2 laser for long-range anemometry 78−36333
vinyl chloride, air pollution monitoring, computer controlled CO_2 laser absorpt. system 80−89699
water depth measurement using airborne pulsed Ne laser system 80−61908
remote sensing by laser beam continued
water droplets in mists, clouds, size, density distrib. meas., laser remote sensing technique *(Japanese)* 78−49175
water in multiphase flow systems, diagnostics, laser induced Raman scatt. 77−31373
water media, remote determ. of impurity conc. by laser spectroscopy, calibration by Raman scatt. 79−16090
water pollution detection by laser-induced luminesc. techniques 78−81442
wave height profiling, depth sounding, laser beam reflection method, sea surface wavenumber effects 80−31121
weather identification by laser forward scatt., feasibility study 79−70893
wind measurements, individual particle scatt. and single-burst digital correl. 79−100980
wind speed, meas. from orbit using lidar system 80−4114
wind speed remote meas., single particle correlation by laser backscatt. 77−91302
wind speed remote meas., single-particle correl. techniques, aerosol condition, meas. rate 79−62609
wind transverse vel., remote meas. using laser Doppler velocimeter 80−4115
wind velocity and direction meas. by laser sounding, correl. method *(Russian)* 77−29474
wind velocity lidar meas. by spatial filtering 79−29901
CO absorption meas. using long-path laser, system improvements 80−3563
CO, remote sensing using freq. doubled CO_2 laser radiation 80−67025
CO_2 IR laser velocimetry, processing techniques and applications 80−87831
CO_2 laser long-path absorption system, computer automation, air pollution monitoring 78−92971
HF, CW chemical laser for remote pollution monitoring and process control, HF conc. in Al plant 79−48200
HNO_3, high resolution spectral meas. of 5.9 μm band using tunable diode laser 80−32707
HNO_3 vapour line parameters meas. by CO laser transmittance 79−26976
H_2SO_4, vapour, foreign gas broadening diode laser spectroscopy in IR 78−36261
NH_3, photoacoustic spectroscopy at 9 μm, 10 μm $^{12}C^{16}O_2$ laser wavelengths 79−21014
NH_3 remote atmospheric sensing by multiphoton sequential photodissociative excitation 79−48199
NO, reson. absorpt. meas. with CO laser, spectroscopic data for pollution monitoring 77−37350
NO_2 spatial distribution, detectivity estimation of DAS lidar 78−92991
Na enhancement and nightglow, spaced lidar obs. 80−101466
Nd:glass laser/parabolic mirror lidar for airborne aerosol mass conc. meas. 77−21937
Nd:YAG laser as source for airborne lidar system for atmospheric expts. *(Italian)* 80−109278
O remote sensing in mesosphere and lower thermosphere, two-photon lidar technique 79−39869
O_2 A band differential absorpt. lidar meas., using ruby lidar and stimulated Raman scatt. 79−39904
O_3, atm., IR heterodyne absorpt. spectrum 77−91267
O_3, atmospheric profile, airborne dual-channel IR heterodyne radiometer meas. 78−57369
O_3, high resolution spectroscopy of ν_3 band, rel. to atm. O_3 monitoring 79−63993
O_3 in troposphere, differential absorption lidar appl. 80−12554
O_3 monitoring with airborne laser absorpt. spectrometer 77−91303
O_3, stratospheric, spectroscopy with CO_2 waveguide laser 77−13117
O_3 stratospheric layer, laser-radar obs. using excimer lasers 80−17410
OH, laser absorption spectrum, scanning technique, appl. to atmospheric monitoring 78−17664
$Pb_{1-x}Sn_xSe$ diode laser absorption spectrometer, pollution detection equipment 78−40672
SF_6, trace detection using phase fluctuation optical heterodyne spectroscopy 80−68266
SO_2, absorption spectrum, meas. using frequency doubled pulsed dye laser 80−87144
SO_2, absorption spectrum, meas. using frequency doubled CW dye laser 80−87145
SO_2 air pollution detect. by differential lidar 78−96298
SO_2, atmospheric, $^{12}C^{18}O_2$ laser line absorption cross-sections 79−16661
SO_2, atmospheric concentrations, meas. using laser absorption spectrometer 79−96497
SO_2 detection, appl. of dye laser differential absorpt. lidar 77−88784
SO_2 in power station plumes, differential lidar meas. 79−57556
SO_2, long-path automatic monitoring using diode laser system 79−29892
SO_2, low conc. meas. using diode laser correlation spectrometer 77−91301
SO_2 plume in atmosphere, remote sensing mask correl. spectrosc. method 80−55966
SO_2 remote meas. by continuously tunable IR lidar 79−21025

renormalisation
(1+1) dimensional field theoretic models with soliton behaviour, exact S-matrices and form factors 79−26240
$(\theta^4)_4$ field, Borel summability, renormalization group, perturbation theory 78−16922
$\lambda_0\Phi^4$ field theory, 3 space-time dimensions, renormalisation, analytical continuation to imaginary time 80−86563
$\lambda\phi_6^3$ field theory, renormalisation group and ladder approx. 79−97524
$\lambda\phi^4$, momentum space renormalisation in curved space time 80−37158
$\lambda\phi^4$ field theory, renormalisation in curved space-time 80−42320
$\lambda\phi^4$ field theory at finite temp., Casimir effect and topological mass 80−57479
$\lambda\phi^4$ field theory renormalisation in curved space-time 80−42319
$\lambda\phi^4$ theory, renormalisation in nonsimply connected spacetime 80−90999
$\lambda\phi^4$ theory, renormalised perturbation theory, skeleton eqns. and R operation 78−54570
$\lambda\phi^4$ theory, trial wave function renormalisation using effective pot. 80−105791
σ model, explicit renormalisation in Goldstone mode 77−79218
σ model, linear in SU(n), n≥4, renormalisation in one loop approx. 79−97516
σ model, SU(3) linear, renormalisation in one loop approx. 80−68368
σ model, two dimens., nonlinear, three loop calc., minimal subtraction method 78−62289

renormalisation continued
σ model relativistic, finite temp., renormalisation, many body problem, interacting nucleons 77−18178
σ models, nonlinear, perturbative approach to symmetry restoration 80−37163
σ models, nonlinear, soft mass renormalisation of 1/N expansion 80−47164
σ SU(N) model, spontaneous symmetry breaking, renormalisation 80−42340
σ-model, nonlinear, order-parameter relaxation from renormalisation group 80−57504
σ-models, non-linear, and universality in 3-D, scaling limit, and critical behaviour, chirality 80−62824
σ-models, supersymmetric, Kahler geometry and renormalisation 80−105789
σ-models with dynamical charges, two-dimensional, renormalisation 79−85223
$\phi^{3,4}$ theory, conformal anomalies for interacting scalar fields in curved spacetime 79−49396
$(\phi^3)_6$ on mass shell parametric space renormalisation 78−24920
$(\phi^3)_6$ field theory, deep inelastic lepton-headron scatt., cut vertex theory and reciprocity relation 80−57466
ϕ^3 4-D model, existence 79−97261
ϕ^3 6-ε dimens. strong interaction theory, renormalisation group calcs. 77−82726
ϕ^3 field theory, vacuum instability in scalar field theories 79−58872
$\phi^{4,6}$ self-interacting theory, three well potential, block spin renormalization 80−57490
ϕ^4 field theory, manifestly finite, renormalisable, scatt. amplitudes 78−41407
ϕ^4 field theory, scatt. amplitude asymptotic behaviour, renormalisation group and slope parameter 79−49389
ϕ^5 field theory dual transforms., extension to 4-dimens. using renormalisation group eqns. 79−49393
ϕ^4 model, strong coupling and infrared struct., renormalisation 80−101921
ϕ^4 renormalisable field theory, virtual heavy particle effects 80−22513
ϕ^4 theory, asymptotically free, finite local field equation 79−35944
ϕ^4 theory, Euclidean, local existence of Borel transform of Schwinger functions 80−77932
ϕ^4 theory, renormalisation anal. 77−10168
ϕ^4 theory, renormalisation anal. and methods of calc. many loop diagrams 79−58885
ϕ^4 theory, renormalisation groups transformation explicit construction 80−4832
ϕ^4 theory, renormalisation of energy momentum tensor 77−6019
ϕ^4-model in two and three dimensions, real-space renormalisation for arbitrary single-site pot. 80−22307
ϕ^4-theory, soliton soln., fluctuation renormalisation and extended particles 77−5996
ϕ^6 operators in scalar systems near four dimensions, tricritical scaling and renormalisation 79−58863
ϕ^6 three-dimens. theory, consistency of 1/N expansion anal. 77−26456
$(\bar{\psi}\psi)^2$ model, spontaneous symmetry breaking, renormalisation 80−42340
't Hooft transformation, explicit solns. 80−345
A^4-coupling in abstract approach of quantum field theory, renormalisation group 80−99033
A-15 compounds, structured phase transition, renormalisation group theory 78−79743
A-15 space group struct., phase transitions, renormalisation group theory comparison with Landau theory 80−6489
Abelian and non-Abelian gauge theories, mass generation, renormalisation, chiral and unified theories 80−4871
Abelian gauge theories, renormalization using BRS symmetry 79−54257
Abelian spontaneously broken gauge model, perturbation expansions *(Chinese)* 78−8500
adiabatic regularisation, quantum field in Robert-Walker metric 78−73916
adsorbed monolayer of orientable molecules, lattice fluid model, real-space renormalisation group method 80−17882
algebraic anal. of renormalisation group eqn. 77−74575
alloy, dilute, sp. ht., electronic, mass renormalisation and band density of states influences 78−43137
alloy, quenched random, phase diagrams, multicritical points, mixed anisotropies 79−38343
alloys, binary, BCC, order-disorder transform., three-body interaction effects 80−39257
alloys with competing interactions, phase diagrams and crit. props. 79−40514
amorphous magnetism, random-axis model, low temp. renormalisation group anal. 79−61137
analytic regularization in an arbitrary number of dimensions 79−26215
Anderson localisation, real-space renormalisation approach 80−2364
Anderson localisation, real-space renormalisation group theory, decimation method 80−88461
Anderson localisation, scaling theory 80−70646
Anderson localisation in random system, renormalisation group study 80−39530
Anderson model, asymmetric, t-matrix approx., ground state 80−20061
anharmonic crystal, lattice dynamics and stability, self-consistent phonon theory 79−51209
anisotropic critical freq. depend. of spin correlation functions 78−56321
anisotropy, cubic, three-dimens., scaling-field study 79−73731
anomalies of quantum conserved currents in exactly solvable models 78−387
antiferroelectrics, multicritical points in structural phase transitions, renormalisation 80−75982
antiferromagnet, Ising model, crit. props., calc. 80−65946
antiferromagnet, phase transformations in strong mag. fields, mag. moments collapse, strengthened magnetoelastic links *(German)* 78−68227
antiferromagnet, phase transition crossover from first- to second-order in symmetry-breaking field 79−82805
antiferromagnet, quantum critical dynamics with mode coupling 80−108024
antiferromagnet chain, renormalisation group nearest neighbour interactions 80−60357
antiferromagnetic chain, Peierls distortion energy, exact limit, renormalisation calc. 79−4643
antiferromagnetic lattice, ground state energy, renormalisation procedure 79−40486
renormalisation continued
antiferromagnets, n=4 type II, phase transitions, Landau Ginzburg Wilson Hamiltonian 80−15735
antisymmetric tensor fields coupled to gravity, renormalisability 80−90765
Ashkin-Teller model, dual and star-triangle transforms. 79−30380
Ashkin-Teller-Potts model, dil., crit. behaviour 80−65897
Ashkin-Teller-Potts model, magnetic indices for percolation problem 79−63163
Ashkin-Teller-Potts model, renormalisation group anal. 79−154
asymptotic behaviour in quantum field theory, renormalisation group analysis 80−68378
asymptotic freedom in the infinite-momentum frame, SU(N) Yang-Mills theory renormalisation 80−22519
asymptotically free massless field theory, self-consistent β functions 78−16911
asymptotically free SU(5) grand unification, proton stability, renormalisation group 80−82929
atom with partially-filled shell, relativistic theory, secular operator renormalisation *(Russian)* 80−52896
axial gauge for unified gauge models, renormalisation constants 79−12930
axial vector anomalies, weak-EM interactions nonrenormalisability 80−62859
axial vector matrix elements, chiral limit, renormalisation effects 79−17190
axial vector meson model, quasi-renormalisation using BPHZl approach 80−13208
background functional, in non-abelian gauge theories 79−30663
bare Pomeron in four-dimensional quantum chromodynamics 79−336
baryon decay effective lagrangian flavour struct. and renormalisation, grand unification 80−27447
baryon-quark phase transition, asymptotic freedom studied using renormalised coupling constant 78−4830
BCC Ising model with competing interactions, fluction-induced first-order transition 80−20424
beam-plasma, renormalization procedure of EM instabilities 79−41813
Bell-Lavis 2-D bonded lattice model, critical behaviour 79−17356
Bethe-Salpeter amplitude, short distance behaviour, renormalisation constant relation, bound states 79−49387
Bethe-Salpeter model, scaling reconstruction using renormalisation group, Callan-Symanzik eqn., ϕ_6^3 theory *(Russian)* 80−42351
bicritical point crossover, asymptotic behaviour of a field theory with quadratic symmetry breaking 79−1488
binary mixtures an and liquid-gas transitions, model for coupling between molecule polarisation and order parameter 78−22823
block-cluster approach to percolation 80−161
Blume-Capel model for plane-triangular and FCC lattices 78−80114
Blume-Emery-Griffiths model, renormalisation group centred, tricriticality 80−42165
Blume-Emery-Griffiths model in 2-D, renormalisation group studies 78−54311
bond and site percolation, renormalisation group results 79−149
bond percolation in anisotropic square lattice 80−46989
bond percolation in square, cubic, hypercubic lattice, probability renormalisation group method 80−31680
bond-disordered conductance lattices, real-space renormalisation 79−7812
Borel singularities, effective one-loop Lagrangian in constant elec. field 78−16917
Borel transform, contribution of renormalons 80−4848
Borel transform and the renormalization group, review 79−26238
Bose fluid, interacting, renormalisation group approach 78−45562
Bose system condensed, crit. behaviour, renormalisation group approach 78−41231
Bose system functional formulation, renormalisation group approach 78−66026
boson system, λ-transition, renormalisation-group theory 80−143
boson system, scaling equation of state, renormalisation group transformation 78−12643
bound state formalism, modified functional formalism, self-energy and renormalisation effects 77−26463
boundary effects in quantum field theory 80−42331
Callan-Symanzik and Weinberg equations: frame dependence of fixed points 80−4838
canonical Yang-Mills field theory with invariant gauge families 79−12944
Casimir effect in quantum field theory 80−42330
causality and fixed points in the renormalization group 79−71597
changed field, electromagnetic self-energy, in non-minkowskian spacetime, gauge depend. of mass renormalisation 79−85214
charge invariance, QCD, renormalisation group, confining and asymptotically free soln. 80−62881
charged current Fermi four field point interaction, weak interaction theory, rescatt. graphs consequences 77−67555
chemical instabilities, renormalisation group approach 78−15657
chiral field, BPHZL renormalisation and 1/N expansion and critical behaviour 80−52383
chiral theory, nonlinear, superpropagator method for renormalisation consts. 77−65112
circuit based graphs for renormalized perturbation theory 79−71266
classical 2-D Heisenberg model, low temp. recursion relations, high temp. series expansion 78−10639
classical Yang-Mills theory, local harmonicity of Wilson loop integral 79−75684
collective states, improper initial or final states in nonlinear field theory 79−439
colour spin and path ordered phase factor, path integrals 80−4932
colour-flavour symm., renormalisation effects in guage theories 78−33018
complex integration method, renormalisation in QFT 77−74599
composite fields, improved effective-pot. formalism, symm. breaking renormalisation group 77−6033
composite fields, renormalisation group eqn. using Green's functions generating functional *(Russian)* 78−16934
composite fields, renormalised, in QFT *(German)* 77−82667
composite operator insertions, Wilson expansions 78−54535
composite particles, quantised theory, UV and IR divergences, renormalisation *(Chinese)* 78−24997
compressible magnet with exchange anisotropy, crit. behaviour 78−39354

renormalisation continued
Compton scattering of massless electrons; renormalisation and mass singularities 77−30237
condensed matter physics, dynamic correlations, book 80−86046
conference, critical phenomena, Sitges, Spain (June 1976) 77−22510
conference on dynamical critical phenomena, Geneva (Apr. 1979) 80−27040
configuration space renormalisation to phase space, gauge coupling 80−18074
conformal anomalies using dimens. regularisation in general metric 77−57454
conformal invariance and asymptotic freedom in quantum gravity, renormalisation group anal. 78−86213
conformal relativity, bare mass theory 80−27417
conformal spinor current anomalies 78−8520
conformal trace anomalies of stress-tensor 78−29023
conformally flat Robertson Walker space-time, explicit dimensional renormalisation of QFT 78−54539
conformally flat space-time, space tensors, trace anomalies 78−12623
conformally invariant amplitudes and field theory in a spacetime of constant curvature 79−49395
conservation laws, infinite set for Thirring model, massive and quantum sine Gordon model 78−29226
continuous spin systems, position-space renormalisation group study 79−38350
convolution regularisation and gauge invariance 77−57446
Cottingham formula renormalisation, hadron mass EM contrib., np mass difference in QCD 79−36053
Coulomb gas in d-dimensions, roughening transition 77−89718
Coulomb gauge QED, dimensional regularization and renormalization 79−89087
Coulomb scatt., perturbation theory, renormalised half-off-shell T-matrix 78−32996
counterterms in normal product formalism, Zimmermann identities 77−30268
coupled fields in one dimension: cross-over from a continuous symmetry to a discrete one 78−87758
coupled order system in 1/n expansion, fixed points critical exponent ϕ^4 theory 78−4578
coupled oscillator problem, crit. dynamics, renormalisation group approach 77−76522
coupling coefficients for cubic groups, 3j$\Gamma\gamma$ symbols for double octahedral SU(2) group 79−21571
coupling constant nonanalyticity, UV anal., logarithmic QFT models 77−49831
coupling constant relationships 80−353
coupling constant renormalisation anal. in unified theories, generalised gauge hierarchies 79−97556
coupling strengths and renormalization scale parameter in QCD by dimensional transmutation 79−6316
CP_{n-1} models and non-Abelian HP_{n-1}, quantum props., σ relation, renormalisation 80−13210
CP^{N-1} σ-model, N-component scalar QED model, renormalisation group functions 79−97500
CP^{N-1} model (D=2,3), UV renormalisation and phase transition 80−31989
CP violation in weak interaction, renormalization of QCD vacuum parameter θ 79−40683
critical dynamics, closed-form differential renormalisation group generator 78−86413
critical dynamics, dynamical scaling, mode coupling, and dynamic renormalization group, book contrib. 79−60480
critical dynamics, field theoretic method 80−27255
critical dynamics, Monte Carlo anal. of renormalisation group, scale transform. 77−22513
critical dynamics, real-space renormalisation group approach, Migdal approx. 79−63088
critical dynamics, real-space renormalisation group approach, Migdal approx., review 80−27257
critical dynamics, real-space renormalisation group approach 80−31699
critical dynamics, real-space renormalisation group study 78−49785
critical dynamics, renormalisation group eqns., scaling far from equilib. 77−28395
critical dynamics in Fokker-Planck formalism 77−22514
critical dynamics of disordered spin systems 79−40516
critical exponents by quantum field theory methods *(Russian)* 80−4869
critical interface structure, in gravit. field, renormalisation calc. in three-dimens. 78−83911
critical localisation of particle moving in given pot., renormalisation group theory 77−66135
critical phenomena, renormalisation group approach, ferromagnetic example 78−8497
critical phenomena, renormalisation group theory, critical props. of generalised 2D Ising model 80−4665
critical phenomena, renormalisation group theory, numerical method for calc. of free energy and correl. length of generalised Ising model 80−4664
critical phenomena and renormalisation group transformations *(Chinese)* 78−95128
critical phenomena and scale invariance 77−22511
critical-exponent renormalization and first-order transitions 78−70085
crossover scaling functions for two-point correlations near tricritical points 79−40510
cubic antiferromagnetic, first to second order transition crossover 78−10709
current conservation in perturbative sine-Gordon and massive Thirring models 79−9273
curved space-time, regularisation and renormaliastion of QFT 77−87890
cut vertices and dimensional renormalization in non-Abelian gauge theories 80−57484
cut vertices and their renormalisation, generalisation of Wilson expt. 79−21929
cutoff and lattice models, construction of renormalised field theories 78−4787
decimation transformations in lattice systems of continuous spins 79−25997
deep inelastic leptoproduction, normalising the renormalisation group anal., QCD twist effects 80−86690
defect states in solids, renormalisation group calc. 79−7802
derivatives of the renormalisation consts., as renormalised Green's functions 77−65111
renormalisation continued
diamond lattice, Anderson localisation, real-space renormalisation study 79−28324
diamond lattice, Gaussian model in three dimensions, differential real-space renormalisation 80−17896
dil. classical, crit. props. Heisenberg ferromagnet, position-space renormalisation group method 79−28536
dilute magnetic alloys, asymmetric Anderson model, renormalisation-group approach, static props. 80−44802
dilute magnetic alloys, symm. Anderson model, renormalisation-group approach, static props. 80−44801
dimensional anal. in renormalised perturbation theory 78−24950
dimensional regularization of composite operators in scalar field theory 80−73573
dimensional renormalisation, action principle 77−13838
dimensional renormalisation, contraction anomalies 78−45784
dimensional renormalisation, trace and axial anomalies, Zimmermann like identities, massive QED 80−101959
dimensionally renormalised Green's functions, massless particles theories 77−13839
dimensionally renormalised Green's functions, massless particles theories 77−13840
dipolar uniaxial ferromagnet, equation of motion, nonlinear response near critical point 79−99717
discrete hydrodynamics, dynamic renormalisation prescription 79−86395
disordered, two-dimens. Ising models, real space renormalisation group 79−42788
disordered spin systems, tricrit. behaviour 80−60319
disordered system, critical phenomena 78−52269
distorted gauge invariant theory, renormalisation props. 77−45967
dual models, unitarised, conventional, renormalisation of new trajectory 79−85281
dual tree and loop amplitudes *(German)* 77−65142
dual unitarisation, renormalisation of pomeron trajectory 77−2806
dual unitarisation, renormalisation of trajectories with zero quantum numbers 78−21400
dual-resonance model, M-loop amplitudes for excited states 78−50019
dynamic crit. phenomena and renormalisation group, appl. to lattice dynamic model 77−22515
dynamic critical phenomena, real-space renormalisation group methods, appl. two-dimens. kinetic Ising model 78−77810
dynamic critical phenomena 77−82477
dynamic renormalisation group in the large-n limit 80−4842
dynamic renormalization group, phenomenological fitting 79−75471
dynamical renormalisation group method, mode coupling theory 80−27254
dynamical symmetry breakdown at the two-dressed-loop level and beyond 79−294
dynamical symmetry breaking and mass generation massless field theory, renormalisation group 77−6027
dynamical symmetry breakings in quantum chromodynamics *(Chinese)* 79−22050
dynamical systems, critical transition to stochasticity 80−73265
Dyson's hierarchical model, critical props. 79−40481
Dyson's hierarchical model, essential singularities of borderline Ising case 78−31077
Dyson's hierarchical model, Heisenberg models and n-vector 78−31078
Dyson's hierarchical model, one-dimens., crit. props. 77−79038
Dyson-Salam renormalisation scheme 77−2748
Dyson-Salam scheme, generalised and improved, convergence 77−30259
Dyson-Salam scheme subtractions, counterterm equivalence 80−13241
E(6) grand unified theories, one loop renormalisation effects, stepwise symmetry breaking 80−32058
education, Lorentz-Dirac eqn. for classical charged particle, mass renormalisation 78−62007
education, renormalisation group theory, second order phase transitions, undergraduate statistical physics 78−62012
effective coupling parameters with stationary points for massless models, renormalisation group consistency 79−9292
effective critical exponents in spherical limit 79−12749
effective field theories, functional integration, renormalisations 80−86648
effective medium approach to real space renormalization 79−80539
effective potential for non-Abelian gauge theories and spontaneous symmetry breaking 80−4863
elastic constants crit. behaviour near non-elastic phase transitions 80−100298
elastic phase transitions, crit. behaviour 78−79722
elastic phase transitions, crit. dynamics 80−2146
elastic scattering total cross sections, renormalisation group method, upper bound 77−18177
elastic transitions of second order, dynamical renormalisation group method 79−40512
elastically coupled systems at marginal dimensionalities, crit. dynamics and stability 80−101769
electron ferromagnet, longit. US attenuation due to spin fluctuations 79−56588
electron gas, relativistic, ground-state energy 78−8536
energy-momentum tensor of quantum field theory in two-dimens. curved space-times 77−30239
equation of state calcs. with Wilson-Kogut renormalisation group 79−97249
equations of motion in asymptotically free theories 79−26247
equations of state, differential renormalisation-group generators, exact and approx. 78−77825
equivalence of field theories with/without boson kinetic energy terms 79−9148
Euclidean quantum field theory, n-point functions, renormalised G-convolution 80−68341
extended defect system, phase transform., critical props. 80−103455
extended objects in quantum field theory 80−86557
extended supergravity, three loop counterterms, nonrenormalisability 78−65854
FCC lattice, Gaussian model in three dimensions, differential real-space renormalisation 80−17896
Fermi gas, one dimensional with backward scatt., gap renormalisation 80−24818
Fermi one dimensional gas with long range potential, renormalisation group, exchange, Umklapp interactions 80−2351
Fermi weak interaction theory, consistent renormalisation scheme, Yang-Mills theory parallel 78−66071

renormalisation continued
fermion system, one-dimens., three-loop scaling eqns. using renormalisation group method 79−80508
fermion systems, quasipartic renormalisation of memory function approach for response functions 78−8345
ferrodistortive spin-phonon systems, crit. props. 80−88315
ferroelectric, uniaxial, crit. behaviour, electrostrictive coupling role 80−71329
ferroelectric antiferromagnetics, spin wave fluctuations in strong mag. fields *(Russian)* 79−82773
ferroelectric antiferromagnets, phase transformations *(Russian)* 80−93114
ferroelectrics, uniaxial, critical behaviour studied via renormalisation group theory 78−8367
ferromagnet, anisotropic, in external mag. field, continuous phase transition existence 80−108011
ferromagnet, disordered, low temp. renormalisation group 78−10688
ferromagnet, harmonic rotator, Coulomb plasma and related models, renormalisation group treatment 78−88135
ferromagnet, harmonic rotator, Coulomb plasma and related models, case of dimensions $D<2$ and $D>2$ 78−88136
ferromagnet, harmonic rotator, Coulomb plasma and related model, two dimens. case 78−88137
ferromagnet, random quenched, crit. behaviour, effective exponents, renormalisation 80−60326
ferromagnet, random uniaxial, dipolar interactions, crossover behaviour, renormalisation group equations numerical soln. 80−50136
ferromagnet, unaxial, random with dipolar interactions, crit. amplitude ratio change 78−31083
ferromagnet, with long-range interactions, low temp. renormalisation group 77−63206
ferromagnetic, anisotropic, in random longitudinal field, multicrit. point, theory 80−54903
ferromagnetic metal, anomalous magnetooptic effects near Curie temp., s-f exchange model 80−2736
ferromagnetic metals, s-d exchange interactions, effect on attenuation of spin waves *(Russian)* 79−19730
ferromagnetic spin system, mag. susceptibility and correl. length crossover relationship 79−78395
ferromagnetic spin system, variable distrib., convergence to normal Gaussian fixed point 79−69681
ferromagnets, easy plane, containing dislocations, static props. 79−95626
ferromagnets, exchange and dipolar coupled, spin wave renormalisation, Damon-Eshbach surface spin waves 80−2564
ferromagnets, Heisenberg and planar, exact results for spin-wave renormalisation 79−69660
ferromagnets, phase transformation theory, easy axis anisotropy, quadrupole interaction, renormalisation method calcs. *(Russian)* 79−65671
ferromagnets, quantum critical dynamics with mode coupling 80−108023
ferromagnets, translationally invariant, renormalisation group struct., crit. phenomena 77−51907
Feynman amplitudes, points splitting and dimensional renormalisation 78−86402
Feynman amplitudes, zero-mass behaviour 80−68353
field operator for unstable particle and complex mass description in local QFT *(German)* 80−90981
field-theory renormalization and critical dynamics above T_c: helium, antiferromagnets, and liquid-gas systems 78−87767
finite Fermi systems, symmetrized correl. functions, renormalisation procedure 78−4555
finite formulation of renormalisable field theory, improved operator products 78−32981
finite nonpolynomial field theories, renormalisation group, scatt. amplitudes 78−16901
finite one-dimens. Ising systems, renormalisation group transform. 79−40485
finite sine-Gordon wave function renormalisation constant determ. for field theoretic models 78−82211
finite size scaling theory, static, dynamic, based on renormalisation group approach, critical phenomena exam. 78−16745
finite system, order parameter and sp. ht. for epitaxial ordering renormalisation-group calc. 80−17862
finite temp. field theory with boundaries, extensions to curved space, stress tensor and surface action renormalisation, review 80−57455
first order phase transitions, droplet models, renormalisation, singularities 80−95050
first-order transition induced by cubic anisotropy, group fixed point removal 79−4688
flat superspace with supertorsion, supergravity, quantisation, renormalisable theory 79−2705
flavour changing self energies, contrib. to $\Delta S=1$ hadronic weak decays 79−71713
forward scattering amplitude high energy behaviour, renormalisation group eqns., ϕ^3 model 77−57448
four dimensional operators 78−16929
four fermion field theory, renormalisation in mean field expansion, Yukawa coupling 79−21939
fragmentation functions beyond leading order in QCD 80−13282
free energy derivatives, bounds, upper and lower, renormalisation group methods 80−68162
$g\phi^3$ model, supersymmetric, massive and massless, renormalised supercurrent and anomalies 79−6267
$g\phi^4$ renormalised field theory in limit $g\to\infty$, effective potential 80−99058
$g\bar{\psi}\psi\phi$ theory, trial wave function renormalisation using effective pot. 80−105791
G-convolution of n-point functions in quantum field theory 80−18065
gapless semiconductor valence band in mag. field 80−49600
gauge field models, hard anomalies, cancellation by regularisation independent renormalisation scheme 80−77931
gauge field phase diagrams, dynamic mass generation and renormalisations 80−68365
gauge field theories, $n\neq4$ axial vector anomaly, noncontribution 80−62858
gauge field theory, lecture series 77−57460
gauge field theory formulation in quantum field theory framework 79−21908
gauge field theory with multiple coupling consts., renormalisation group eqns. 78−360
gauge fields, chiral fields on loop space, colour-electric flux rings 80−42327
renormalisation continued
gauge fields, quantisation, renormalisation, and fluctuations 79−30670
gauge invariant operators, renormalisation, S-matrix elements 79−256
gauge models of weak and EM interactions, quantisation and renormalisation of gauge theories, book contrib. 79−30669
gauge theories, high temperature behaviour, symmetry restoration, renormalisation group methods 80−31996
gauge theories, renormalisation anal. 77−13851
gauge theories, renormalisation group techniques and infrared behaviour 77−45965
gauge theories, U-gauge Green's functions construction, with spontaneous symmetry breaking and Slavnov identities 79−235
gauge theories of massive vector fields without scalar fields 78−8528
gauge theory, anomalies, unitarity and renormalization, book contrib. 80−42352
gauge theory, energy-momentum tensor 77−205
gauge theory, renormalisation of ghost and Goldstone fields and ghost symmetries 80−90987
gauge theory, supersymmetric, charge renormalisation vanishing 78−24930
gauge theory, Z(2), renormalisation group calc. 80−22514
gauge theory on lattice, gauge-fixing and mass renormalisation 78−24949
gauge theory renormalisation *(Chinese)* 79−63337
gauged $N>4$ supergravity, vanishing one loop β-function, infinite renormalisation 80−86186
gaussian model, two-dimensional, differential real-space renormalization 79−54067
Gaussian random field, ferromagnets in $4+\epsilon$ space dimens. 78−73954
Gaussian stochastic processes, renormalisation group limits for Wick polynomials 78−54565
Gaussian-to-Heisenberg crossover, specific heat, renormalised perturbation theory 80−60356
Gell-Mann and Low renormalisation group and ψ^6 theory 77−71439
Gell-Mann-Low function and Borel summations in renormalizable theories 79−40670
generalised collision integral *(Russian)* 79−48
generalised Wilson expansions in dimensional renormalisation 78−86403
Ginzburg-Landau model, dynamic renormalisation group anal. in large n limit 79−9193
Glauber-Ising model, 2-dimens., crit. dynamics, real-space renormalisation group theory 78−70070
Glauber-Ising model, crit. showing-down of energylike perturbation, renormalisation group anal. 79−61133
Glauber-Ising model, real space-time depend. renormalisation group 78−49774
grand unification E_8 theory, Weinberg-Salam model reproduction *(Russian)* 80−4909
grand unified field theories, mass relations and renormalisation effects 79−49436
graphical solutions of renormalization group equations 80−4560
gravitation, covariant quantisation 78−8327
gravitational constant, and fermion pair creation in nonstationary gravit. field *(Russian)* 79−17323
gravitational field with torsion, renormalisation *(Chinese)* 79−93026
gravitational gauge field theory, renormalisable, cosmological implications 79−44839
graviton propagator calc. renormalisation and $1/N$ expansion 78−8320
gravity, dynamical affine symmetry and renormalisation 79−85048
Green's function in nonrenormalisable massless $\phi^6{}_{3+\epsilon}$ theory, removal of cutoff, vertex functions expansion 78−45772
Green's functions in nonrenormalisable massless $\phi^6{}_{3+\epsilon}$ theory, renormalisation of regularised theory 78−45771
Green functions, two-point, quantum field theory 80−9089
Gross-Neveu model, irrelevant operators and equivalent field theories 79−21912
Gross-Neveu model, renormalisation, mass generation 80−27393
Gross-Neveu model and self-consistent β-function method, fermion mass generation 79−49466
hadron polarization operator insuperrenormalizable model, rainbow approx. of $(\lambda/2)\Phi^2\phi$ model 80−105821
hadronic structure using parton anal. of deep inelastic scattering and rel. processes 79−80803
Hamiltonian formalism, construction of 2-D QED 79−21987
Hamiltonian model with scalar displacive transition, crit. dynamics, renormalisation 78−87766
Hamiltonian QFT, renormalisation group anal. 77−82662
hard-soft renormalization of massless fields 80−13214
heavy Higgs scalars and the renormalization of spontaneously broken gauge theories 79−71607
heavy particle effects through factorisation and renormalisation group, QED appl. 80−13243
heavy quark effective potential, non-perturbative semi-classical calc. 79−13053
heavy quarkonium decays, renormalisation group approach, exclusive two meson and inclusive decays 80−82972
Heisenberg, ferromagnet, classical, with dipole-dipole interaction, renormalisation group and crit. exponents 80−60351
Heisenberg antiferromagnet, magnon renormalisation, two-magnon Raman scatt., kinematic interaction 78−23228
Heisenberg antiferromagnet, one-dimens. spin 1/2 dimerised, renormalisation group and other calcs. 79−78393
Heisenberg antiferromagnetic chain, random, low temp. thermodynamic props. in zero mag. field 80−34657
Heisenberg chain, one-dimens. spin 1/2 dimerised, spectral excitations, renormalised group calc. 79−78295
Heisenberg diluted classical ferromagnet, position space treatment 79−87268
Heisenberg ferromagnet, anharmonic, renormalised magnons and phonons 78−91837
Heisenberg ferromagnet, consistent linearised Green's function theory for $s=1/2$ 79−4685
Heisenberg ferromagnet, dil. spin $^1/_2$, renormalisation group treatment 79−69679
Heisenberg ferromagnet, low-dimens., crit. temp. *(Russian)* 78−23274
Heisenberg ferromagnet, magnon renormalisation, higher approx. 78−14945
Heisenberg ferromagnet, magnon renormalisation 80−65849
Heisenberg ferromagnet, spin-wave renormalisation, $S\geq1$ 80−71070
Heisenberg ferromagnet, two-dimens., spin dynamics, renormalisation group calc. 78−47966

renormalisation continued
Heisenberg magnet, classical, with layer structure, mag. phase transitions, anisotropic lattice, theory 80−29557
Heisenberg magnet, dil., renormalisation group calcs. 79−56550
Heisenberg magnet, quasi-two-dimensional phase transition at marginal dimensionality 79−38332
Heisenberg metamagnet, collinear, mag. phase diagram 80−71035
Heisenberg model, antiferromag., phase diagram and multicrit. behaviour 78−56337
Heisenberg model, ground state energy, renormalisation calc. 79−61150
Heisenberg model, layered magnet, phase transitions 78−76252
Heisenberg model, randomly dilute, renormalisation group calcs. 80−60321
Heisenberg n-component classical model, low temp. renormalisation group and symm. breaking perturbation 79−15315
Heisenberg planar model, two dimens., renormalisation vortices, and symmetry breaking perturbations 78−10638
Heisenberg spin glass, crit. dynamics, renormalisation group approach 79−91237
Heisenberg spin systems, two-dimensional, phase diag. 80−4847
hierarchical model, ε-expansion anal. 77−71284
hierarchical model, critical and tricritical behaviour 78−10712
hierarchical model, renormalisation group anal., book 78−81921
hierarchical model, renormalisation group approach 80−34580
Higgs mechanism, implementation 78−24921
Higgs-Kibble mechanism, superfield theoretical treatment 78−89616
High energy behaviour of weak interactions and renormalisable theories, book contrib. 78−78164
high energy physics as infrared phenomenon, strong interactions in 6-ε dimens. 77−10182
high energy stability and renormalisability of gravitation, Einstein Lagrangian supplement 79−25935
high temperature series renormalization group method 80−4660
high-energy behaviour of renormalised Feynman amplitudes 78−58114
homogeneous renormalisation group equations, dispersion approach 77−41753
homogeneous renormalisation groups eqns. 77−49851
honeycomb bond lattice, renormalisation group approach 79−85089
Hubbard model, computer renormalisation-group technique 79−19716
Hubbard model, equivalent spin Hamiltonian, for phase transition studies 80−80474
Hubbard model, Green's function, functional-derivative study 80−75483
Hubbard model, magnetic instabilities, influence of short-range correlation effects 79−7963
Hubbard model, one-dimens., extended, $2k_F$ and $4k_F$ correl. functions, computer renormalisation group calcs., appl. to one-dimens. conductors 80−54625
Hubbard model, one-dimensional $2k_F$ and $4k_F$ correl. functions, computer renormalisation-group calcs. 79−78029
hydrodynamic singularities and the renormalization group 79−54063
incompressible viscous fluid, (2-ε) dimens., long-wavelength non-equilibrium props. 77−61008
indefinite-metric fields and renormalisation group 78−8529
independent value models, renormalisation of nonperturbative functional integral 78−12810
infrared behaviour of electron Green's function, renormalisation group use 79−35977
instanton correction to vac. energy densities and bag const. 80−37211
instantons and renormalisation for Yang-Mills effective Lagrangians with trace anomaly 79−85221
instantons as link between weak and strong coupling in QCD 80−42403
integral formulation divergence elimination, connecting const. renormalisation *(Russian)* 80−68369
intense field QED in continuous medium, appl. to Thomson scatt. and Cherenkov radiation 80−27435
interfacial profile, ε-expansion 78−51641
intermediate valence system, local polaron model 80−107717
introduction to renormalisation theory methods and results 77−57459
invariance props. of renormalisation group 77−22512
invariant renormalisation method for non-linear realisations of dynamical symmetries 79−108
invariant renormalization for theories with nonlinear symmetry 78−70290
inverse problem method, quantum, sine-Gordon model 80−68377
IR singularities in gauge theories, renormalisation group method, coupled massless field theories 78−54538
Ising, 2- and 3-dimens. antiferromag. lattices, appl. of Kadanoff's variational approx. 80−2583
Ising antiferromag. phase boundaries, hard-core lattice gas calcs. 80−80542
Ising antiferromagnet, FCC, nearest neighbour interactions, Monte Carlo method 80−80544
Ising chain, disordered, linear renormalisation transformations, appl. to dil. soln. model 78−34941
Ising chain, soln. of renormalisation group recursion relations 79−97310
Ising chain in transverse magnetic field, SLAC renormalisation group approach 79−67476
Ising ferromagnet, renormalised crit. behaviour 78−52272
Ising ferromagnet, site diluted, crit. props. 78−72351
Ising ferromagnet, surface tension using real-space renormalisation group methods 79−73760
Ising ferromagnet and spin glass systems, random, crit. dynamics 80−34666
Ising ferromagnet crit. props. of site and bond diluted model 79−42766
Ising lattice model with directional bonding, renormalisation group study 80−28894
Ising lattices, position-space renormalisation-group transformations, problems and proofs 78−93619
Ising lattices, triangular renormalisation group transformation, var. approximation 78−49776
Ising magnet coupled to isotropic elastic medium, first order transition, renormalisation method 80−68151
Ising model, 1-D, energy conserving relax. 80−20420
Ising model, antiferromag. case, modified Kadanoff variational renormalisation method 80−88710
Ising model, antiferromagnet, phase boundary determ. by real space renormalisation group methods 78−88134
Ising model, arbitrary spin, space renormalisation group calc. 78−27046
Ising model, bond-diluted, percolation-thermal crossover index calc. 80−11145
renormalisation continued
Ising model, compressible, crit. behaviour, applic. of renormalisation group methods 77−82464
Ising model, compressible, position space renormalisation group approach 79−56552
Ising model, continuous-variable, real-space renormalisation group method 80−100589
Ising model, correlation length, renormalisation group calc. *(Russian)* 78−77811
Ising model, crit. props. appl. of real space renormalisation techniques 79−78420
Ising model, critical dynamics, time-dependent real-space renormalisation group 80−60282
Ising model, critical exponents for high temperature series expansion 79−99701
Ising model, exact differential renormalisation at criticality 79−73755
Ising model, exact renormalisation group equations 79−73749
Ising model, ferromag. coupled, semi-infinite, with free surface, renormalisation group approach 78−14975
Ising model, ferromagnetic, band-mixed square-lattice, approx. crit. surface 80−70921
Ising model, fixed points, determ. by lower bound renormalisation transformation 80−62586
Ising model, free energy, variational calc. for 3 dimens. system 80−42167
Ising model, kinetic, Migdal type renormalisation group calcs. 79−93069
Ising model, kinetic, reliability of real space renormalisation approach 80−90793
Ising model, mixed, renormalisation group calc. 79−56547
Ising model, Monte-Carlo method appl. to evaluation of Niemeijer-van Leeuwen cumulant expansion 78−16751
Ising model, $n \geq 2$, Monte Carlo renormalisation group 79−75470
Ising model, one-dimens., real-space renormalization group 79−15317
Ising model, one-dimensional, with finite range interaction, exact renormalisation transformation 77−72963
Ising model, one-dimensional transverse-field, in complex longitudinal field, real-space renormalization group method, T=0 80−103806
Ising model, quantum renormalisation group approach 79−61126
Ising model, renormalisation group calc. for cells with inequivalent spins 79−73658
Ising model, renormalisation group calcs. on critical phenomena 80−42171
Ising model, renormalisation group transformations, cumulant expansion 78−70064
Ising model, renormalisation group treatment, stochastic weight function 79−51734
Ising model, renormalisation of the interaction amplitude 79−30384
Ising model, renormalization-group transformation for quantum lattice systems at zero temperature 79−71379
Ising model, spin-glass, renormalisation group calc. for two dimens. models 78−14968
Ising model, square lattice bond dilute, renormalisation group attempts to obtain transition line 80−44836
Ising model, surface tension, using real-space renormalisation group methods 78−47985
Ising model, three dimens., renormalisation-group transformation 77−87704
Ising model, three dimensional, crit. exponents, scaled eqn. of state 77−8262
Ising model, three dimensional, free energy, lower bound approx. 78−10707
Ising model, three-dimens., crit. index. for correl. length 78−84444
Ising model, two point correlation, renormalisation group methods 78−8353
Ising model, two-dimens., in transverse mag. field, renormalisation group studies 80−71042
Ising model, two-dimens., with transverse field, phase diagram and crit. props., from real space renormalisation group 78−52295
Ising model, two-dimensional kinetic, dynamic correlation functions, real space renormalisation group approach 80−62589
Ising model, two-dimensional renormalisation group approach 78−52261
Ising model, variational approx. for renormalization group transforms. 79−61139
Ising model, Yang-Lee edge singularity, real-space renormalisation group method 80−34643
Ising model free energy upper bound by renormalisation group methods 77−61026
Ising model in 1-D with random transverse field at T=0, real space renormalisation group method 80−4656
Ising model in transverse field in one-dimens., zero-temp. renormalisation 79−38347
Ising model of bond mixtures, spin glass transition, renormalisation group approach 78−43601
Ising model on square and triangular lattice, variational renormalisation group method 78−16740
Ising models, three-dimens., renormalisation group transform. 78−62163
Ising models, two- and three-dimens., renormalised mean-field approach 79−38339
Ising spin $^1/_2$ model, renormalisation group approach 80−2582
Ising system, with lattice anisotropy, two dimens., crit. props. 78−73932
Ising system on triangular lattice, critical dynamics, time dependent real-space renormalisation group 78−60289
Ising system with quenched impurities, high temp. expansion methods 79−78422
Ising systems, compressible, elastic anomalies inducing first order transitions 79−47288
Ising systems, finite thickness, renormalization-group transformation, real-space 80−15749
Ising type model, elastically coupled, effects of dipolar forces on crit. sound attenuation in uniaxial systems 80−50158
Ising universality class, structural phase transform., real-space renormalisation calc. 80−39255
isotropic antiferromagnets, crit. dynamics using renormalisation group methods 79−8006
itinerant electron antiferromagnetism, effect of mag. field 78−27013
itinerant electron ferro- and antiferromagnetism, spin fluctuations 79−7961
itinerant electron system, helical spin structure appl. to MnSi 78−23234
jet processes in QCD 78−82104
Jost-Lehmann-Dyson representation, high-energy scatt. 77−82660

renormalisation continued
Kadanoff lowerbound renormalization transformation for the q-state Potts model 79−44876
Kadanoff renormalisation for s-state Potts model in 3-d 78−21074
Kagome lattice, renormalisation group approach 79−85089
Kellen-Simanzik eqn., correlation function scaling behaviour in phase transitions *(Russian)* 80−57502
Kerr-Schild's gravitational fields, quantisation 80−31653
kinetic Ising chain, renormalisation group transform. for master eqn. 80−11214
kinetic Ising model, real space renormalisation group for arbitrary dimension 80−4666
Kondo Hamiltonians, rotationally invariant, universality and renormalisability 79−95573
Kondo Hamiltonians, s-d exchange, ground states, renormalisation group calcs. 80−50046
Kondo Hamiltonians with non-zero ground-state spin 79−51746
Kondo lattice Hamiltonian, ground state props., real-space renormalisation study 80−34590
Kondo-lattice model Hamiltonian, zero-temp. real-space renormalisation group method 78−34960
ladder model of QCD, hadron struct. 80−37213
Landau critical point, low temp. renormalisation group and 1/N expansion 79−35656
Landau-Ginzberg ferromagnet, static and dynamic correl. functions near magnetization curve 79−15318
large scale steady state 3-D turbulence, helicity 78−75122
large-cell Monte Carlo renormalization group for percolation 80−46994
lattice gauge theories, extrapolation to continuum limit 80−349
lattice gauge theories with fermions, phase transitions and renormalised struct. 78−82105
lattice gauge theory continuum limit, renormalised perturbation theory, lattice Lagrangian 79−6283
lattice gauge theory with fermions, renormalised phases, vacuum polarization 80−13198
lattice massive Schwinger model, renormalisation group approach 77−30246
lattice regularised field theory, renormalised and bare coupling constants 80−77960
lattice renormalisation group and thermodynamic limit 78−8359
lattice spin systems, matching conditions for crit. props., group struct. of block transforms 80−22305
lattice theory, percolation, block cluster approach, scaling laws and renormalisation groups 80−62592
Lifshitz point, critical behaviour, universal amplitude ratio calc. 79−33496
Lifshitz point, critical exponents, ε-expansion 78−65899
Lifshitz point, ferromag., renormalisation-group anal. of crit. modes in cryst. systems 79−82806
Lifshitz point, low-temp. renormalisation group 78−65898
light cone expansion in renormalised perturbation theory 80−99045
light metal, soft X-ray emission spectra, renormalisation theory 78−52595
linear conductor, interchain coupling role 78−6294
linear Ising chain, differential real space renormalisation 79−85092
lines of fixed points and physically irreducible representations 79−5964
liquid-gas system near critical point, sound attenuation and dispersion, renormalisation group calcs. 79−42149
liquid-vapour transition, non-Ising-like effects, eqn. of state, renormalisation group calc. 80−84286
local operator products, gauge invariance and renormalisation 78−358
long polymers in solution, props., direct renormalisation method for study 80−59370
Luttinger-Thirring model on lattice, real space-time renormalisation 80−62590
macromolecular solns., critical ratio in the excluded volume problem 79−64136
magnetic bicritical and tetracritical points, dynamic scaling and corrections to scaling, renormalisation group anal. 78−68247
magnetic critical phenomena, use of renormalisation group, review 77−20625
magnetic critical phenomena, Wilson renormalisation group equation, soln. by scaling field eqn. 78−68252
magnetic phase transitions, renormalisation group anal. 77−2633
magnetic system, Lifshitz point, phase diagrams and crit. behaviour 80−65928
magnetic transition at T=0, impurity effects 78−76259
magnetically ordered cryst., dislocation drag, magnetoelastic waves 80−103332
magnetism, spin-S Heisenberg model mapped onto interacting Bose field 79−47291
magnets, mixed, competing spin glass and mag. order, phase diagrams, crit. points 80−39802
magnets, randomly distributed point defects, critical exponents, renormalisation theory 80−60346
mass, physical, in ϕ^4-model, renormalisation group and mass generation 80−77948
mass generation in a normal product formulation 78−25027
mass shell applications of renormalisation group with arbitrary interpolating fields 77−13879
massive QED, renormalisation in Veltman gauge, supersymmetric transformation 77−46000
massive Thirring model, renormalisation of higher conservation law 77−30020
massive Yang-Mills Lagrangian, separation of non-renormalisable divergences 77−49854
massless $(\phi^3)_6$ theory, exponentiation of IR logarithms 80−31965
massless fields with hard-soft IR decomposition 77−54037
massless QED, dimensional regularisation in spherical spacetime 79−40698
massless quantum field theory in curved space-time 77−49834
master eqn., dynamical renormalisation group transform., Ginzburg-Landau model, kinetic Ising model 80−42170
matter-photon interaction renormalisation, coherent states in matter-photon systems 77−68199
melting model, two-dimens., renormalisation group anal. 79−42218
membrane models and generalized Z_2 gauge theories, renormalisation props. 80−86587
metamagnet, compressible, renormalisation group theory of pseudocritical point 80−60337
metastability, spinodal fixed point, renormalisation group anal. 79−40509
methane adsorbed submonolayer on graphite, structural transitions between epitaxially ordered phases 80−96740
Migdal transformation, renormalisation group, recursion relations 80−34647
Migdal-Kadanoff renormalisation scheme, surprising effectiveness 79−35652
Migdals recursion relation, harmonic rotator model in two dimens. 78−89413
mixed valence model, spinless, coherent-hybridisation states and virtual-bound states 80−107749
mixed valence model, spinless, isolated f-level problem 80−107750
monodisperse polymer solution, 2nd virial coeff., renormalisation group calc. 79−10777
Monte Carlo renormalisation group analysis, Ising model and three state Potts model calcs. 79−44880
Mott transition, spin glass description 79−65386
moving bond approach for renormalisation group transform 78−21078
multi-Pomeron couplings to external particles in Reggeon field theory, renormalisable field theory 78−78111
multicritical (order O) magnetisation eqn. of state, renormalisation group calc. 78−31085
multicritical point and problem of coexistence of two ordered phases 79−77717
multilocal struct. of spinor theories, renormalisation 77−74587
multiplicative renormalisation group, relation to critical phenomena in phase changes *(Hungarian)* 77−54042
muonic atom, heavy, $1s_{1/2}$ levels, self-energy corrections 78−55262
n-component compressible model with cubic anisotropy, critical behaviour RG calc. 78−145
n-component spin system, energy-energy correl. function calc. 80−31697
Nambu Jona Lasinio model renormalisation in mean field expansion 79−26219
nematic liquid crystal, two-dimensional, Kosterlitz-Thouless phase transitions 79−7680
nematic to smectic C phase transition, renormalisation group anal. 80−34173
nematic-isotropic transition, renormalisation group calc. 78−59937
nematic-smectic A phase transition, renormalisation group approach to crit. dynamics 80−10646
neutrino anomalies, renormalisation effects on $\sigma\bar{\nu}/\sigma\nu$ and $\langle y\rangle\bar{\nu}$ in four quark model 77−18230
neutron star matter, superfluid phase transition 79−59025
nitrobenzene-n-hexane, shear viscosity, critical conc. fluctuation rate, verification of renormalisation prediction 78−47514
non Abelian gauge theories in external electromagnetic fields *(Russian)* 80−57533
non-Abelian asymptotically free theories, composite operator renormalisation 77−65105
non-Abelian gauge fields, quantisation and renormalisation, Fadeev-Popov ghosts 77−5979
non-Abelian gauge theories, canonical methods, renormalisation 77−41764
non-Abelian gauge theories, triangle anomalies and renormalisation 77−49837
non-Abelian gauge theory, Yang-Mills phase factor renormalisability 80−95211
non-Abelian gauge theory of strong interactions, EM current renormalisation 79−63350
non-analytic mass behaviour, renormalisation group 77−67558
non-equilib. instability, k=0 hard mode transition, appl. of dynamic renormalisation group 79−21686
non-Gaussian fixed point 78−54564
non-perturbative quantum field theory, lattice renormalisation construction 80−9098
non-semisimple gauge modes, renormalization 79−6254
non-universality, polarisation and magnetisation exponents 79−40480
nonequilibrium phase transitions in chemical systems 78−54325
nonequilibrium statistical field theory, renormalisation of closed time path Green's functions *(Chinese)* 79−80758
nonlinear 3-dimens. chiral field, phase transition, 1/N renormalised expansion 79−49365
nonlinear σ model in $2+\varepsilon$ dimens. 77−13866
nonlinear scalar interactions, 1/N expansion 78−16903
nonlinear solns. of renormalisation group eqns. in large-n limit 77−61039
nonlinear spinor theories, collective phenomena and renormalisation 77−71441
nonlocal light cone expansion of current products, renormalisation group anal. 79−97526
nonperturbative renormalizability for a class of gradient-free models 79−49392
nonrandom Ising system, random-field singularities in position-space renormalization-group transformations 80−13000
nonrelativistic persistent model, Schrodinger and Klein Gordon interacting fields with Chew-Low coupling, renormalisation props. 79−54250
nonrenormalisable theories with UV stable fixed point, possible renormalisation, eigenvalue condition 78−41429
nuclear dynamics and renormalisation group relations, bulk props. 79−6469
nuclear field theory, phonon renormalisation, eigeneqns. and sum rules *(Chinese)* 80−102127
nuclear field theory, renormalisation of single particle states 78−24926
nuclei, exchange and renormalisation phenomena due to pion-nucleon couplings 77−41893
nucleon self-energy in finite nuclei; renormalisation, nucleon-meson interaction, ^{16}O calcs. 78−17110
$O(N)\psi^4$ interaction, strong coupling limit, rel. to renormalizability of chiral field 78−386
O(N) σ-model, two-dimens., mag. susceptibility, phase transitions and high temp. expansion 80−47177
O(n)-symmetric systems dynamic crit. exponents, renormalized field theory 79−12754
one dimensional conductors, Fermi gas model, reviews 79−78083
one loop equivalent gauges, one loop infinities and renormalisation constants 80−62842
one-dimensional ϕ^4 and double quadratic systems, kinks, quantum statistical mechanics 80−47197

renormalisation continued
one-dimensional electron-phonon system, renormalisation *(Russian)* 78−43314
one-dimensional Fermi gas model with two charact. energies, scaling theory 78−6287
one-dimensional superconductivity, response functions, from renormalisation group theory 80−54829
one-loop counter terms, system with derivative couplings to fermions 79−249
one-particle-irreducible renormalisation group generator for crit. phenomena 77−82475
operator-product expansion in dimensional renormalization 80−42100
optical percolation in 3-D, renormalisation group approach 80−22299
optimal truncation procedures in renormalization-group calculations 79−63075
order-disorder transitions in gauge and spin systems 78−70072
ordering alloys, nonlinear critical relaxation of the Ginzburg Landau field coupled to a conserved density 80−90803
oscillating irregular field, effective potential 79−75457
Pade approximation method as renormalisation group method 80−17909
paramagnetic-helical crit. line, near Lifshitz point 78−23278
parameter dependent renormalisation group transformations 78−87768
particles with spin J=1 described by antisymmetric tensor, renormalised theories *(Russian)* 77−13876
path integral representation for U- and S-matrix, scalar meson model renormalised S-matrix elements 78−78103
percolating two-dimens. square lattice, normal-state cond. and crit. current density, crit. exponents 80−84541
percolation at surface, appl. of real-space renormalisation group 79−93057
percolation backbone problem, large cell renormalisation group 79−69481
percolation by position-space renormalisation group with large cells 78−77805
percolation cluster numbers by real-space renormalization 79−75474
percolation conduction crit. exponent, large cell renormalisation group calc. 80−12998
percolation models, low density expansion of pair connectedness 79−67234
percolation problem, equivalence between Reynold's one-parameter renormalisation group transform. and Kirkpatrick's transform. 79−12731
percolation problem, high order behaviour in 0^3 field theories 78−65883
percolation problem, real-space renormalisation group approach 79−93059
perturbation theory, operator-product light-cone expansion 77−82680
perturbation theory, renormalisation group eqns. and analytic renormalisation 80−82865
perturbation theory, renormalisation group eqns. and analytic renormalisation 80−82866
perturbation theory, renormalised, model of 3-D nonlinear field, free of UV divergences 78−54567
perturbative QCD, chiral symmetry using dimensionless regularisation 80−27476
perturbative QCD, renormalisation improvement, charmonium decay and scaling violations 80−101993
perturbative renormalisation theory, general features, quantum action principles, pure Yang-Mills theory 80−105794
phase separation dynamics, renormalised time-depend. Ginzburg-Landau model 80−29175
phase transition in 2D Coulomb gas, sine-Gordon theory and XY model, renormalisation group anal. 80−36950
phase transition theory, renormalization group method 77−80601
phase transition with valency change, sound vel. renormalisation *(Russian)* 78−79963
phase transitions, Schlogl's chemical model, critical fluctuations near non-equilib. critical point 80−85150
phase transitions and critical phenomena, recent developments 77−87713
phase transitions with several order parameters, catastrophe and renormalisation theories 78−32782
phenomenological renormalisation group theory, general principles 80−4663
physical systems, renormalisation group anal. 80−17838
planar rotator model, one-hypercube renormalisation group transform. 78−72353
plasma, ion-acoustic solitary wave, third-order corrections, reductive perturbation method 80−43898
plasma, Langmuir turbulence, large-scale, renormalisation group method 80−38650
plasma, renormalised Vlasov turbulence 80−19579
plasma resonance absorption, mag. field generation, renormalized theory 78−47126
plasma simulation of turbulence, phase space granulation due to mode-mode coupling 80−38651
Pm3n space group struct., phase transitions, renormalisation group theory comparison with Landau theory 80−6489
polar fluid, pressure, entropy and internal energy expressions using renormalisation 79−41919
polar semiconductor, theory of excitons bound to neutral impurities 79−73441
polycrystalline material, scatt., lattice representation 78−65774
polymer, flexible chain collapse 78−87628
polymer, long, short range correlations in solution 80−59367
polymer chain, direct renormalisation group procedure 80−91712
polymer chain, phenomenological theory, renormalisation group approach 78−26418
polymer chain, renormalisation along chem. sequence 78−50669
polymer chain dynamic critical index calcs. by renormalisation method 80−87256
polymer dilute soln., critical ratio limiting values using renormalisation group methods 78−83715
polymer single chain in soln., dynamical scaling exponent, renormalisation along the chain 79−10786
polymer solution, semidilute, chain size 78−87607
polymer solutions, renormalised field theory, polydispersity 80−74270
Pomeron and critical temp. 79−12982
Pomeron flavouring and cylinder renormalisation 79−67524
pomeron intercept in Reggeon field theory on transverse lattice, neg. renormalisation 78−93823
Pomeron nondiffractive renormalisation, flavour and baryon quantum nos. 78−82177
renormalisation continued
position space renormalisation group transformation peculiarities in thermodynamic limit 79−97245
position space renormalisation of spin systems with long-range forces, hyperscaling breakdown 78−24755
position space renormalisation transformations, parameters determ. criterion 79−17357
position space renormalizations and the breakdown of hyperscaling 79−40482
position-space renormalization approach 79−30404
position-space renormalization group transformations, mathematical props. 79−75466
Potts lattice gas, crit. and tricrit. exponents using Kadanoff transform. 80−101768
Potts lattice gas, renormalisation-group treatment, Kr adsorbed on graphite 78−67908
Potts model, 1st and 2nd order transitions, renormalisation group soln. 79−99706
Potts model, appl. of Legendre transformation 78−80156
Potts model, crit. behaviour, renormalisation group calcs. *(Russian)* 79−6059
Potts model, first order phase transitions, Monte Carlo renormalisation group method 80−34645
Potts model, first-order phase transform., three-state model, Monte Carlo renormalisation group method 79−99709
Potts model, Kadanoff renormalisation 79−40483
Potts model, three-state, antiferromag. ordering 78−23279
Potts model, three-state, effects of symmetry-breaking perturbations 80−105579
Potts model, three-state, first order phase transitions 80−60333
Potts models, q-state, two-dimens., Monte Carlo renormalisation-group studies 80−77727
Potts q-state model, variational renormalisation group approach 80−31679
proton deep structure, renormalisation group approach, review 79−85302
pseudocritical phenomena near the spinodal point 78−65894
pure leptonic weak interaction with induced shadow states, renormalisable theory 78−37136
pure Yang-Mills perturbation theory, instanton sector renormalisation, zeroth sector comparison 80−105775
Q^2 dependent parton distribution function on QCD 78−93857
q-state Potts model multicritical point, singularities and scaling functions 80−57215
QCD, axial gauge, mass shell behaviour 78−49966
QCD, e^+e^- annihilation energy, asymptotically free perturbation theory 78−66045
QCD, field theoretical aspects, perturbative effects 79−26286
QCD, infrared, near-mass-shell, behaviour of non-Abelian gauge theories 78−24947
QCD, infrared behaviour of effective coupling 80−42393
QCD, jets, deep inelastic scatt., renormalisation group 79−26287
QCD, long-range correl. in forward quark-quark scatt. 78−4779
QCD, Migdal approx. and 1/N expansion, string tension 80−101992
QCD, parton transverse mass distrib. 78−8587
QCD, perturbative contributions to quark masses 80−47249
QCD, quark liberation and finite temp. renormalisation group, hadron-quark phase transition *(Russian)* 79−67515
QCD, renormalisation group and infrared behaviour 79−58931
QCD, renormalisation group calcs., cancellation of ambiguities *(Russian)* 80−62930
QCD, renormalisation group invariant charge and confinement 78−45791
QCD, review 78−37146
QCD, six-quark model, $\Delta S=1$ weak nonleptonic decays 80−22582
QCD, slope of leading Regge trajectory 80−42391
QCD, two dimens., renormalisation group functions 78−29242
QCD, two-dimens., bare pomeron graph 78−4824
QCD calc. of structure function moments, renormalisation prescription depend. 80−4948
QCD corrections at Z_0 for hadron initiated lepton pair prod., renormalisation appl. 80−86678
QCD coupling const., renormalisation prescription depend. 80−4954
QCD observables in higher order calcs. 79−9334
QCD on mass shell, Ward identities 78−16913
QCD perturbation expansions in coupling const. renormalisation by momentum space subtraction 79−63416
QCD renormalisation in two loop approx. in arbitrary gauge 80−102002
QED, conformal-invariant, Ward identity of dilation current 80−68401
QED, covariant, renormalised transition amplitudes, gauge independence, Green functions 80−57530
QED, dimensional regularisation and current commutators 78−12843
QED, dimensional renormalisation, coupling constants and masses 80−57523
QED, heavy particle effects, factorised local operators, renormalisation group 80−62898
QED, heavy particle effects, factorised local operators, renormalisation group 80−62899
QED, IR behaviour with Weinberg and 't Hooft renormalisation group eqns. 79−89085
QED, polarisation operator in ladder approx., renormalisation group 80−73629
QED, renormalisation constants, small mass behaviour 77−2780
QED, renormalisation group equations, invariant charge function 80−57529
QED, renormalisation group formulation 78−93830
QED, renormalisation group invariant charge and confinement 78−45791
QED, renorminvariant charges 77−10208
QED in external field, renormalisation and R-operation 79−26273
quadratic lattice, correlated percolation 80−68149
quantised field, renormalizable interactions in two dimensions and sharp-time fields 78−81882
quantised SU(2) gauge theory, Monte Carlo study 80−77973
quantum contour field equations, renormalisation and string like eqn. 80−86581
quantum field theory, n-point functions, renormalised G-convolution, convergence in Euclidean case 80−77930
quantum field theory in de Sitter space, renormalisation by point-splitting 78−29035
quantum flavour dynamics, renormalisability conditions 80−42404
quantum gas, renormalised collision integral *(Russian)* 79−1575

renormalisation continued
quantum gravitation without matter, renormalisation 77−37798
quantum gravity, dynamics, trapping of physical gravitons 80−31652
quantum gravity, higher-derivative, renormalisation 78−8326
quantum gravity, nonrenormalisability, one-loop divergences 80−4626
quantum gravity near two dimens., charge renormalisation const. 78−41222
quantum Ising chain, in real or complex field, real space renormalisation group method 80−71050
quantum renormalisable theories from nonrenormalisable interactions 78−383
quantum renormalisation group, zero temp., appl. to Heisenberg and Ising models 80−80526
quantum spin model, appl. of projective renormalisation group 80−84607
quantum spin system, two-dimens., frustration, renormalisation group study 80−80535
quantum spin systems, ground state energies, renormalisation techniques appls. 80−93132
quantum spin systems, Migdal renormalisation group approach 79−38333
quantum spin systems, renormalisation group transformation 78−47984
quantum stress tensor calc. by adiabatic regularisation in Robertson-Walker space times 78−32747
quantum stress tensor in curved space-time, renormalisation by dimensional regularisation 79−40423
quantum systems, one-dimens. isotropic X-Y model, zero temp. renormalisation group method 79−82800
quantum systems, two-dimens. Ising model, zero temp. renormalisation group method 79−82801
quantum-chromodynamic β function at intermediate and strong coupling 79−89108
quark confinement, bag models, field theoretic, renormalisation and translation invariance 80−62932
quark exclusive form factor, leading IR behaviour in QCD 77−54074
quark form factor and jet cross sections, high energy asymptotics 80−32112
quark form factors in quantum chromodynamics, renormalisation method *(Russian)* 78−45882
quark gas, relativistic, ground-state energy 78−8537
quark mass, current, induced isospin violations 80−32069
quark mass dependence ambiguities in gauge theory renormalisation 79−21913
quark masses from Weinberg-Salam model renormalisation group eqns. 80−42377
quark-gluon coupling constant, unified gauge theories containing Pati-Salam model 77−6072
quarkonia from charmonium and renormalization group equations 79−22055
quarks and strings on lattice, appl. of renormalisation group techniques 77−22654
quasi-two-dimensional planar spin system, mag. transition 80−65951
quenched random magnetic fields, $\epsilon=6-d$ expansion of dynamic crit. exponent 79−38335
quenched random magnets, thermodynamic behaviour from position-space renormalisation group 78−68244
radiative mass generation in perturbation theory and the renormalization group 80−86611
radiative mass generation model renormalisation, spontaneously broken symmetry, IR breakdown 79−71650
radiative transfer, noncoherent renormalisation group approach 78−65495
random and spatially inhomogeneous magnetic materials, exact model results 78−52271
random conductance lattices, conduct., renormalisation group approach 78−60100
random conductors, position-space renormalisation and exponent theory 80−153
random hierarchical model, crit. props. 80−71072
random Ising system, critical index and temp. 79−56543
random Ising system, mag. critical index 79−56544
random resistor network, $6-\epsilon$ dimensions, renormalisation group treatment 78−51956
random resistor network, elec. cond., renormalisation group approach 78−34815
random system, crit. behaviour near 2nd order phase transition lines intersection 78−68276
random walk, self-avoiding, direct renormalisation group approach 78−73933
random-spin systems, with short range interaction, static crit. behaviour 78−39328
rare earth compounds, mixed valent, renormalisation of transversal phonons 79−90749
rare earth zircons, Jahn-Teller cooperative phase transition, crossover effects 80−88316
rare gas clusters, small, structure, thermodynamic properties 80−88341
real fluids, static and dynamic crit. phenomena, theory, summer school lecture series 80−6344
real space renormalization and the honeycomb lattice, ferromag. (antiferromag.) appls. 80−11200
real-space renormalisation giving differential renormalisation-group eqns., two-dimens. triangular Ising lattice 78−65881
real-space renormalisation group, dimensionality effect 80−77716
real-space renormalisation group transformation based on cumulant expansion 79−12730
real-space renormalisation of self-avoiding walk by linear transformation 78−8360
real-space renormalization-group scheme for spin and gauge systems 80−32008
recursion eqns. for renormalisation group transforms. in lattice gauge theories including fermion variables 78−62298
Regge trajectory renormalisation in dual models 79−30721
Reggeization of elementary fermions in arbitrary renormalizable gauge theories 80−68367
Reggeon field theory on transverse lattice, renormalisation group calcs. 77−18203
regular QFT, minimal wave-packet representations 78−81883
relativistic local renormalizable field theories, basis for quark confinement and QED 79−21893
relativistic two-electron atom, level shifts, transition probabilities, perturbation theory 79−22001
renormalisation continued
relaxational dynamics in systems with many-component order parameter, renormalisation group anal. 80−42181
relaxational dynamics in systems with many-component order-parameter, scaling fields and variables 80−101772
renormalisation group and scale invariance, asymptotic fields 77−2741
renormalisation group transforms, optimal variational approx. 77−87699
renormalised Feynman amplitudes for fields with fixed masses 77−49860
renormalizable field theories with multiple fermionic excitations 79−49428
renormalized operator form of quantum action principle 80−42314
renormalons and non-renormalizability for asymptotically and nonasymptotically free theories 80−68366
resistor lattice conductivity exponent, position space renormalisation, decimation, dimensionality depend. 78−60099
Rindler, de Sitter and Schwarzschild spaces, Greens function thermal props., renormalisation 79−2686
Robertson-Walker space-times, nonconformal renormalised stress tensors 78−65852
Robertson-Walker universe, adiabatic regularisation, arbitrary coupling of scalar field to scalar curvature 80−57461
roughening transition dynamics, renormalisation group method 78−45574
scalar electrodynamics, IR divergences, rearranged perturbation expansion 77−67601
scalar field theories, finite amplitudes in perturbation theory, ϕ^n models, pass. renormalisation 78−93794
scalar field theory with $g\Pi^4$ interactions 77−2736
scale and renormalisation group transformations for renormalised field operators 77−30245
scale-breaking model of renormalisation group 78−49972
scaling, renormalisation group approach, phys. appls. 78−49634
scaling and multiplicative renormalising in solid state physics, review *(Hungarian)* 79−11289
scaling factor in renormalisation group, 2-D Ising model 78−41237
scaling properties of models of nonequilibrium phenomena, 't Hooft renorm. group method 79−26015
scattering amplitude in Regge region and fixed angle region, renormalisation group anal. 77−74596
Schwinger-Dyson eqns., particles with identical equation numbers 78−82115
second order transformations in ideal and disordered systems *(German)* 79−40508
self avoiding walk attached to a surface, tests of scaling theory 78−81927
self-avoiding lattice walks, renormalisation by non-linear transforms. 79−75468
self-avoiding random walk, real-space renormalisation group approach 79−63167
selfavoiding random walk problem, direct renormalisation method 80−77703
semi-inclusive distribs., renormalisation group anal. of scaling behaviour 79−30660
semiclassical field theory of gravitation, renormalisation scheme 80−68117
semiclassical QCD, regularisation and renormalisation 80−4925
semiconductors with direct band gaps, exciton-polariton interactions, Green's function approach 80−92831
sine-Gordon and Thirring models equivalence, cumulative mass effects 77−45969
Sine-Gordon field theory, ferromag. model, existence and renormalisation in all dimensions 79−26248
sine-Gordon problem, soliton mass, renormalisation 79−40678
sine-Gordon soliton mass, thermal renormalisation 79−54036
sine-Gordon supersymmetric model, quantisation of conservation laws and superrenormalisation 79−89058
single-loop divergences in six dimens., Ricci-flat Riemannian spaces 77−38081
single-particle properties of systems undergoing struct. phase transitions 78−26654
singular potentials, divergence problem in quantum field theory, pot. theory analogy 77−67556
singular solutions of renormalisation group eqns. 80−17840
singularities of Borel transform in renormalisable theories, massive $g\phi^4$ theory 78−62304
site percolation, infinitesimal renormalisation group transform. 80−88525
site percolation problem, finite lattice renormalisation-group approach 78−12648
site-bond percolation by position space renormalization group 79−63159
site-diluted resistor networks, renormalisation group approach 79−15128
SO(10) grand unified theories, one loop renormalisation effects, stepwise symmetry breaking 80−32058
soft pion theorem, appl. to currents in nuclear forces and matter. 79−26377
soft X-ray thresholds, exchange effects, renormalisation group theory 78−31280
solid solution, crit. phenomena of random spin systems 78−52263
soliton solutions, renormalisation and quantum corrections 80−82884
solitonlike fields, gauge phase factor operators, extended Higgs models and 't Hooft algebra 80−42324
solitons, static form factor, quantum correction in 2-D field theory with classical lump, asymptotic behaviour 80−52395
spacetime structure theory at very short distances, nonlinear sigma model 80−12979
specific heat, confluent singular term for systems with continuous symmetry, crit. amplitude ratio, calc. to order ϵ^2 80−57235
spectral forms and renormalization group equations of the Schwinger model 79−63357
spherical nuclei, absolute α-decay widths, renormalised effective interaction contrib. in shell model 79−75925
spherical shell model, renormalisation for collective model within truncated space 78−54697
spin glass, low temp. renormalisation group 78−10688
spin glass, rel. between isotropic X-Y model and mobility edge problem 78−88138
spin glass transition in random bond Ising model in 2-D, and 3-D, renormalisation group approach 78−68275
spin glasses, Ising type random bond, scaling, eqn. of state and instability 79−73753
spin glasses, localised degrees of freedom *(Russian)* 79−4691
spin glasses, long-range Gaussian-random Ising model 79−15319

renormalisation continued
spin glasses, quartic operators in Ising, X-Y, and Heisenberg systems 79−33498
spin Hamiltonian, constant-coupling, higher-order, statics and dynamics 80−60262
spin system, isotropic, N-component, with long- and short-range interactions, crit. behaviour 78−76256
spin systems, model, Monte Carlo simulation appl. 80−20421
spin systems, one-dimensional, free energy series expansion, renormalisation group series 78−31081
spin systems, operator renormalisation transform. 79−40511
spin systems, tricritical phase transition, eqn. of state, critical exponents, logarithmic corrections 78−27048
spin-1/2 models, on square lattice, sublattice renormalisation transformations 78−65878
spin-flop multicritical points in systems with random fields and in spin glasses 79−33495
spin-s Ising model, renormalisation group transformation 78−14916
spin-spin correlation function near the critical point 79−11319
spinless particle scatt. by medium, elimination of divergences, wave function renormalised 78−62320
spinor electrodynamics, anomaly free and axially coupled, bilinear gauge renormalisation 79−307
spontaneous generation of renormalisation invariant mass in IR stable theories 78−86411
spontaneously broken gauge theories, 3- and 4-point functions and renormalisation consts. 79−17600
spontaneously broken gauge theories, general struct. and renormalisation 79−17598
Spontaneously broken gauge theories, Slavnov-Taylor identities 79−12945
spontaneously broken symmetry and heavy scalar particle decoupling, renormalisation group eqn. 80−47189
spontaneously generated mass self-consistant computation anal., renormalisation group method, mass invariance 78−86412
square lattice, appl. of real-space renormalisation group to site percolation 79−30377
square lattice, critical dynamics and potential moving approx., renormalisation group approach 80−57209
square lattice Ising system, crit. relax. of temp. 79−82793
square site percolating system, renormalisation group approach 78−41241
stability and supersymmetry, general formalism, explicit two-loop appls. 77−79228
stability and supersymmetry, models with local gauge symmetry, renormalisation group anal. 78−70296
stability of critical behaviour, critical-exponent renormalization and first-order transitions 79−44895
statistical equality connecting zero Fourier harmonics with average quantities 80−133
stochastic-field multieikonal theory, high-energy hadron dynamics 78−8634
stress tensor of conformally invariant field in conformally flat spacetime, axiomatic renormalisation 78−29034
stress tensor vacuum expectation value, renormalisation, curved spacetime, covariant geodesic point separation 78−54246
stress-energy tensor of scalar field in curved spacetime 79−12697
string and quark systems, statistical mech. treatment renormalisation group meth. 77−54075
strong-coupling limit of renormalisable interacting quantum fields 78−49968
structural phase transformations, static critical behaviour 80−92640
structural stability in statistical mechanics 80−8932
structurally incommensurate systems, disordered-incommensurate phase transitions 78−91417
structure functions, deep inelastic renormalisation group sum rules 80−22611
$SU(2)_L \times U(1)$ theory, radiative corrections, simple renormalisation framework 80−101973
SU(2)×U1 unified theory, symmetry and renormalisation 80−22551
SU(2)×U(1) hybrid models, divergence cancellations and renormalisaion 77−38083
$SU(3)_{colour} \times SU(2) \times U(1)$ gauge, full operator structure of the non-leptonic $|\Delta S| = 1$ weak Hamiltonian 80−99089
SU(3)×SU(3) chiral renormalisable gauge model, nonleptonic decays 78−24938
SU(5), unification of weak, EM and strong interactions, review 80−105814
SU(6) grand unified theories, one loop renormalisation effects, stepwise symmetry breaking 80−32058
$SU(N)_L \times SU(N)_R$ nonlinear σ-model, renormalisability and struct. 79−6279
SU(N) σ model, 2 dimens., Gross Neveu model as a $Z_3 = 0$ limit 79−35949
subtraction procedure, algorithmic features 78−375
superconducting dilute alloys, eqn. for crit. temp. 78−72300
superconductivity models, nonlinear spinor models, fermions, collective bosonic states 77−18179
superconductor, renormalisation group recursion relations involving dynamics, in mag. field 80−60137
superconductors, ferromagnetic, phase transitions, renormalisation group treatment 80−29505
superconformal renormalisation anomaly determ. 77−87907
superdiagram technique for gauge theories, renormalisation 77−30267
supergravity, 2-loop divergence, with external gravitons on-shell cancellation 77−49659
supergravity, one-loop renormalisability 77−5730
supergravity, OSp(1,4) renormalisable theory with higher derivatives 80−36930
supergravity, renormalisability props., superinvariant local counterterms 77−34087
supergravity, superspace-time local symmetry, Ferru torsion preservation, renormalisability 79−12689
superheavy Higgs particles, proportional renormalisation corrections to W and Z mass, Weinberg-Salam model 79−276
superrenormalizable theories with higher derivatives 79−63344
superspace, auxiliary mass BPHZ renormalisation procedure 78−16902
supersymmetric nonlinear σ model, spontaneous breakdown of chiral symmetry 78−54549
supersymmetry, review of principles and historical development 77−18197
renormalisation continued
supersymmetry spontaneous breakdown inducing IR anomaly 77−38095
surface magnetisation profile, in crit. region by ϵ-expansion, Wilson perturbation theory calc. 80−50100
surface percolation processes, scaling theory and real space renormalisation group 80−86223
susceptibility relationship to correlation length, renormalisation group calc., anomalous-dimension crossover function 79−42780
Symanzik's approach to nonrenormalizable theories for massless models 79−26212
symmetric and mass-independent renormalisation 77−49848
symmetry breaking fields, destruction of first order transitions 79−40517
symmetry broken scalar theory, renormalisation 79−93291
symmetry mappings, renormalisation group transformations, local Lagrangian density *(German)* 78−49953
symmetry properties of renormalisation-group transformations 79−5963
thermodynamic anomalies near tricritical point, renormalisation group anal. *(Russian)* 80−13027
thermodynamic pot. at finite temp. and density, QED and QCD 78−8535
Thirring model, massive, mass independent renormalisation, dimensional regularisation 80−57463
Thirring model, renormalisation and sine-Gordonisation 78−37135
Thirring model of massless scalar field, conformal transformations 80−52428
Thirring renormalised model, construction form two massless scalar superfields 79−40682
three photon vertex in QED, renormalisation group anal., Callan-Symanzik eqn. 80−105822
three-dimensional Ising model, crit. behaviour 80−4672
three-loop charge renormalization effects due to quartic scalar self-interactions 80−57489
trace and dilatation anomalies in gauge theories 78−4790
transfer coefficients of ultrarelativistic gas of elementary particles *(Russian)* 78−8635
transiton metals, lattice dynamics calculations, superconductivity parameters 79−7655
triangular and honeycomb lattice gases, order-disorder transitions to 2×2 struct. 80−4674
triangular antiferroamgnetic lattice, ground state energy, upper bound determ. using renormalisation 78−76212
triangular Ising lattice, anal. of Kadanoff lower-bound renormalisation-group, approx. 80−8930
triangular Ising model, phase diagram 78−10631
triangular Ising model percolation props., renormalisation group anal. 78−93620
triangular spin lattice, renormalisation theory anal. of triplet interactions 77−5771
tricritical behavior in a two-dimensional field theory 80−77726
tricritical points in systems with random fields 79−33494
TTF-TCNQ, two-chain inverted band model 78−6313
turbulence, fully-developed, renormalisation group 80−28495
turbulence spectrum, fluctuation corrections by renormalisation group methods 77−42806
turbulence transition, renormalisation group with periodic behaviour 79−45013
two-dimens. U(1)-Goldstone model, QFT on lattice 78−74158
two-dimens. XY and Heisenberg spin 1/2 models 79−42727
two-dimensional anisotropic N-vector models 79−85095
two-dimensional Ising model, Monte Carlo renormalisation-group method 80−4673
two-dimensional Ising model, real space renormalisation transform. 78−2687
two-dimensional massive QED in unitary gauge as renormalisable theory 77−57478
two-dimensional spin system on square lattice, exact duality-decimation transform. 80−17890
two-dimensional SU(2) Yang-Mills theory 78−24942
two-dimensional systems, crit. percolation behaviour, renormalisation-group approach 79−4396
two-dimensional systems, phase transitions 78−68241
two-point correl. function near coexistence surface 80−44847
two-spin correlation function, dipolar crossover 80−80516
unified gauge theories, electroweak mixing angle, renormalisation 80−86651
unified gauge theories and gravitational cut-off, renormalisation group method 77−18213
unified theories of weak and electromagnetic interactions 78−81908
unified theory of strong, weak, EM interactions 78−54598
unitarity and renormalized 't Hooft identities 80−13205
unitarity of S-matrix in Yang-Mills theory 77−82681
unitary and renormalisation gauge, point transformations 77−41763
Universe, isotropic models, regularisation of fermion stress-energy tensor 78−81725
UV asymptotics and the renormalisation group, review 80−101933
UV infinity suppression in gravity modified field theories 80−105787
vacuum instability 78−41419
vacuum polarisation in intense EM fields, perturbation theory, renormalisation group calcs. *(Russian)* 80−52444
vacuum structure for a quantum field theory in curved space-time 79−21638
Van der Pol oscillator, renormalised perturbation theory 80−27225
variational approximations to renormalization groups 79−63169
variational principles in renormalisation theory 78−73951
vertex functions of chronological exponential, renormalised system of equations 79−30661
Ward identities, anomalous axial vector, renormalisation group in QED 77−61231
wave function renormalisation constants, gauge independ. in gauge field theories 80−82883
weak hypercharge embedding in strong gauge groups 79−30692
weak-coupling superconductor, effect of electron-phonon renormalisation on thermodynamics 79−99655
weakly disordered uniaxial ferromagnet, phase transition *(Russian)* 78−23291
Weinberg angle, renormalisation effects 78−62344
Weinberg-Salam theory, extension to left-right symmetry and quark-lepton unification 80−78002
Wentzel pair model in 3 space-time dimens., renormalisation, asymptotic freedom 77−49853

renormalisation continued
Wess-Zumino model, massive, dimensional regularisation, supersymmetry 80−27398
Weyl and conformal covariant field theories 79−80749
Wightman function, two-point, asymptotic behaviour 80−73614
Wilson's renormalisation group recursion eqns., critical phenomena in spin systems 78−4581
Wilson renormalisation group theory appl. to two-dimensional ferromagnetic spin model *(Norwegian)* 78−56275
Wroblewski relationship, scaling phenomena, renormalisation group eqns. *(Chinese)* 79−92986
X-Y magnets, two-dimens., with annealed non-mag. impurities 79−78391
X-Y model, ground state energy, renormalisation calc. 79−61150
X-Y model, percolation in three-dimens. model 78−80113
X-Y model, S=1/2, phase transitions at T=0, z-field renormalisation group method 80−71051
X-Y model, two-dimens., real space renormalisation group and crit. phenomena 78−56338
X-Y model, two-dimens. spin 1/2, temp. marginality by linear renormalisation transform. 79−38341
Yang-Lee edge singularity and ϕ^3 field theory 78−65882
Yang-Lee edge singularity from a real-space renormalization-group method, Ising model 79−97317
Yang-Mills fields, supersymmetric, Ward identity, one-loop level, renormalisation 80−73597
Yang-Mills massive two-dimensional theory 77−45945
Yang-Mills massless theory, exponentiation of leading IR divergences 77−13847
Yang-Mills quark prod. processes, mass singularites 77−26459
Yang-Mills theory, nonleading IR divergences in QCD, renormalisation group function 77−71422
Yang-Mills theory, renormalised eqns. and renormalisation constants, Abelian gauge invariance 77−65093
Yang-Mills theory, SU(4) supersymmetric, charge renormalisation 78−24929
Yang-Mills theory developed around an instanton, renormalisation 79−45009
Yang-Mills theory developed around instanton, renormalisation 80−32027
Yang-Mills theory renormalisation in two-loop approx. for arbitrary gauge *(Russian)* 77−49865
Yukawa field renormalisation group eqns., asymptotic freedom 77−30314
Yukawa weakly coupled model, cluster expansion convergence 77−13837
Yukawa-type interactions of strongly coupled fields 78−49969
zero mass renormalisation and triangular anomalies 78−16915
zeta function regularisation of one-loop effective pot. 78−70252
Zimmermann identities and renormalization group equation in dimensional renormalization 80−73591
β-decay, Gamow Teller matrix elements empirical renormalisation 78−66248
$e\mu$ system in QED with internal fermion excitations 80−9130
ep deep inelastic scatt., renormalisation group anal., parton model connections 79−40784
$\Gamma_{pol}N\rightarrow\pi^{\pm}N$, weak neutral interactions, QCD renormalisation 79−93433
μ, anomalous mag. moment, eighth-order contribution calc. 78−29261
μe universality violation in renormalisation theory, neutral leptonic currents *(Russian)* 78−45837
N elastic form factor, exclusive and almost exclusive process asymptotic behaviour, renormalisation group 80−42464
N renormalisation const., bounds on form factors and propagators 77−34092
ϕ^3 field theory in $6+\varepsilon$ dimensions, anomalous dimens. calc. 78−134
ϕ^4 3-D field theory, IR behaviour and connection with critical phenomena 79−71601
ϕ^6 theory, Gell-Mann and Low renormalisation group appls. 78−29224
π, wave function renormalisation const., upper bounds 78−74215
π compositeness from wave function renormalisation constant 80−101997
π longitudinal struct. function, exclusive and almost exclusive process asymptotic behaviour, renormalisation group 80−42464
$\pi^- p\rightarrow\eta n$, Reggeon field theory, behaviour of A_2 trajectory 80−22594
$\pi\pi$ elastic scatt., exclusive and almost exclusive process asymptotic behaviour, renormalisation group 80−42464
$\pi\pi\rightarrow\pi\pi$, self-interactions, nonperturbative, scatt. amplitudes containing only convergent integrals 80−68480
$\Sigma^+\rightarrow p\gamma$, $1/2^-$ resonance poles to parity-violating amplitude, two-quark weak transitions 80−78062
Ag film-Pb sandwich, supercond., effective renormalisation interactions 79−56397
^{39}Ca β-decay Gamow-Teller interaction renormalisation constant from ^{39}K(p,n) 7480-7530 keV 79−6601
$CeAl_2$, magnetic ordering, 24 component Ginzburg-Landau model 80−97095
CrN, mag. struct. and first-order antiferromag. transition 79−61132
$H+H^+$, nuclear repulsion, contrib. to charge transfer 80−18922
H_2, quantum cryst., short-range corre. and motional renormalisation of anisotropic interactions as function of density 80−34272
H_2, solid, orientational level structure of o-H_2 pairs, phonon renormalisation 79−47554
He film, jump in superfluid density, real-space renormalisation group anal. 80−44387
He, liq., critical and tricritical dynamics, renormalisation group calc. 80−29239
He monolayer, phase diagram, order-disorder transition 80−107604
^{3}He, superfluid, transport parameters, Kubo formulae and BCS-Green's functions 80−88382
^{3}He-^{4}He mixture, critical and tricritical dynamics, renormalisation group calc. 80−29239
^{4}He, superfluid, near transition, second sound damping, rel. to renormalisation gp. predictions 80−10725
K_2CuF_4, layered spin system, planar rotator symmetry, phase transition 80−65951
Li_xTiS_2, Li ordering in intercalation battery, theory 79−77580
MnS, crit. behaviour, neutron diffr. exam. 78−80169
Nb, high frequency cyclotron resonance study 79−11057
Nb-Zr, effect of band structure on elastic constants and superconductivity 79−8313
Nd, two-dimensionally modulated mag. struct. 79−78317

renormalisation continued
Ni-Pd(Pt), renormalisation of spin wave stiffness 79−51764
$Pb_{1-x}Sn_xTe$, narrow gap, many-body interaction effects, Bloch electron scatt. lifetimes, energy renormalisation 80−49637
ϕ^4 scaling limit, crit. exponents and renormalisation 77−10166
Rb_2CrCl_4, 2D-ferromag., renormalisation of long wavelength spin waves, neutron scatt. 80−60229
Si surface, (111), energy states, computer renormalisation-group calc. 80−75617
TbG_3, uniaxial ferromagnet, logarthmic corrections to crit. behaviour 78−60294
^{48}Ti, (A+2)particles-2 holes excitations, interaction renormalisation 78−29375
TmSe, Kondo lattice model 80−97063
U_2N_2Te, and related cpds., crit. behaviour 78−43605
UPTe, and UAsTe, crit. behaviour 78−43605

repackaging *see packaging*

repeaters
32 Mb/s step-index optical fibre repeater equaliser *(German)* 78−33881
32Mb/s optical fibre transmission system planning and expt. 78−1418
44.7 Mb/s fibre optic transmission system expts. 78−1420
140 Mb/s optical fibre transmission system 78−42436
400 Mb/s optical transmsion expts. 77−88954
400Mb/s SELFOC fibre transmission system expt. 78−1419
fibre optic, low-power (0.5 W) design 78−22195
fibre optic communication repeater design, high impedance input, equalisation cct. *(Italian)* 77−50758
fibre-optic repeater bypass DPDT switch 79−98484
fibre-optic system repeater error rate calc. approaches compared 77−54672
hybrid digital optical fibre transmsion system, terminal equipment and reshaping/regenerative repeaters *(German)* 78−33880
medium and long distance digital optical fibre communication systems 78−50941
monolithically integrated optical repeater, fabrication and characts. 80−28353
optical, injection laser, pump signal by Gunn diode *(Russian)* 77−83974
optical communication conference, Munich (1977) *(German)* 78−33854
optical communication systems, problems arising in development 79−3806
optical fibre communication advances, materials and techniques 80−102853
optical fibre communication for military appls., review and assessment 78−42438
optical fibre digital transmission system expt. 78−66943
optical fibre PCM repeaters with low power requirements, design and operation *(German)* 80−28315
optical fibre PWM multilevel pulse transmission, theory and expt. 79−55078
optical fibre system, optimum repeater parameter calcs. of 1.12 Gbit/sec system *(German)* 78−37989
optical fibre systems, equalising and nonequalising, comparison 77−3655
optical fibre transmission capability expansion 78−66914
optical fibres, 0.95 Gbit/s PRS signals regeneration after transmission over 0.91 km of fibre, regeneration cct. 79−59807
optical films communication systems, low noise regeneration using optical repeaters 78−66920
optical multistage repeater, consisting of nonlinear amplifiers and saturable absorbers 79−59772
optical repeater section lengths rel. to transmitter power and fibre dispersion *(German)* 78−38012
optimisation in fibre optic union for repeater spacing *(Italian)* 78−79117
photovoltaic solar cells applied to communications repeater stations 79−29450
single-mode fibre cabling for low-loss communication 80−53467
star repeaters for fibre optic links 77−34934
step-index fibre transmission system variable equaliser 79−55243
systems aspects of optical-fibre communications 77−7016
underwater housings, corrosion resistance, of Be-Cu alloy 78−15583

replica techniques
asbestos aerosol electron microscopy and analysis *(French)* 77−37461
biological material cryofixation, fast freezing device 78−28138
biological specimen replication at −150°C with improved freeze-fracture apparatus 80−85560
blood cells, red, human, frozen section prep. for electron probe anal., fracturing or cutting 79−39625
ceramic nuclear fuel, porosity characterization, optical and electron microscope exam. 78−44302
ceramic sherds, macroporosity determ. 77−34065
cord-rubber laminates, two-ply balanced, interlaminar-shear strain study 80−97526
detaching single-stage C replicas, glue films appl. 80−61038
electron microscope appl. to steel separations estimation, use of X-ray microanalysis *(Bulgarian)* 78−40012
electron microscopy, sample preparation effects on decoration patterns 79−86658
embossable surface relief structures for black and white, colour reproduction, ZOD images 78−65990
epidermal imprinting by celloidine 79−25170
epitaxial replicas for surface relief obs. on single crysts. 77−51577
extraction replica evaluation, Ashby-Ebeling model analysis *(Czech)* 80−49062
fibrous cracking, COD and initiation, replication technique 77−56069
freeze etching and related techniques, resist. monitor for automatic film thickness regulation 78−49810
freeze fracture replicas, removal of lipid contamination using chloroform 79−5426
freeze-etch device, for electron microscope laboratories 78−8474
freeze-etch unit for rotary shadowing and low temp. freeze-fracturing 79−5423
freeze-etching improvement using evaporated film 80−85558
freeze-etching results interpretation 78−28141
freeze-fracture replication, in biological research, review 78−40444
freeze-fracturing effects on membrane struct. 78−28140
freeze-fracturing preparation technique, methods and results, review 78−24776
grid-transferring technique for strain anal. of curved surfaces 79−18845
hard overcoats in replicated optics 78−66968

replica techniques continued
hard tissue matrix internal space study by SEM, dentine appl. 78−77169
laser scanner, replication process 77−58496
macromolecules, high-resolution metal replication for electron microscopy 77−25621
magnetic domain structure determ. high resolution colloid-SEM method 77−43846
metal surface replica production, nondestructive mech. and electrolytic grinding and polishing *(German, English)* 77−48607
mirrors, large scale lightweight, replication 78−66963
moire contourography, computer-aided replication of human anatomy 80−67189
MOS inverted-channel carrier scatt., effect of oxidation in Cl media 78−76156
NDT anal. and inspection technique 78−11467
off-axis beam pattern analysis using replica pulse representation 77−54821
optical component manufacture 78−66962
optical component replication, light-weight 78−66965
optical component replication 79−55253
optical image quality evaluation from aspheric replica master data, using ACCOS V SPLINE program 78−66964
optical multilayer film cross sections 77−19387
optical replication, conf., San Diego, USA (Aug. 1977) 78−66961
optical replication 78−66889
orthopaedic implants, replication techniques eval. for SEM 79−34707
preparation for SEM *(German)* 77−10140
PVC, rigid, internal struct. of diamond shaped cavities 80−66628
rapid aimed preparation, using Pt-C replicas 80−61037
refracting optics replication 78−50963
refractory metals, technique for investigation of nonmetallic inclusions 77−52587
Schmidt corrector plate replication, testing and performance calc. 78−66967
Schmidt corrector plate replication 78−66966
self-shadowed replicas, controlled sputtering 77−26434
SEM appl. 79−74334
sighting preparation method in electron microscopy 77−49810
silicate glass, low voltage electron microscopy of heated surfaces using C replica technique 80−25974
silicone rubber, crack tip replica, for determ. of J-integral values 79−52475
sputter deposition technique for fine object replication in EM 77−55219
steel, Cr-Ni-C (3, 1, 0.6 wt.%), grain boundary sulphide precip. and hot ductility *(Japanese)* 80−71654
steel, ferritic and austenitic, microstruct. study by means of replicas taken from components at 100°C 80−81256
steel nitride phase hardening, precipitation and solution kinetics after heat treatment 78−95756
surface measurement replicas, comparative study 80−36987
surface profile, reference line analysis 77−15672
TEM, dislocation struct. of slip lines in single crystals 79−27990
TGS, cleavage surface, electron microscopy using shadow decoration technique 77−7955
transmission replica system for strain measurement 79−74323
US inspection of fracture surface by replicas, determ. of reflector size by scanning 78−27689
wear measurement by surface replication 77−12771
Wolter lens component replication 80−95972
C, for TEM investigation of hard nonmetallic materials 80−61034
CaF_2, surface struct., Au decoration and C replica techniques 77−1286
CdS film, polycrystalline, photosensitive, struct., pseudoreplica method, using electron microscopy and microdiffr. 79−15030
Cu, bright galvanic coatings, crystallite size determ. 79−66221
$Gd_3Ga_5O_{12}$, garnet substrate surfaces, working damage, electron microscope investig. 77−77605
Ni base superalloy, γ' precipitate size determ. technique 79−34221
Ni-base superalloys, technique for replication of γ' 80−79648
Pt shadowing of freeze-fractured or freeze-etched specimens using electron beam gun 78−20329
SiC, appl. of replica electron fractography 79−60237
SiO_2-TiO_2 antireflection coating, 1.064 μm laser damage, barrier 80−33059
SnTe, expitaxial film, early stages of growth, replication and TEM obs. 79−65348
UO_{2+x}, sintering mechanism 77−21071

replicas
abraded surfaces, topography rel. to contact area and abrasion mechanism 80−58986
bronze bearings, TEM exam. of wear debris 77−77595
collodian, for electron microscopy, geometric stability *(Ukrainian)* 77−67536
epoxy replication of optics 77−27401
epoxy resin, plastic deform. effect on crack propag. 80−97563
extraction, for spatial struct. parameters estimation *(Czech)* 79−35668
film type, surface reproduction characteristics 80−36988
membrane fracture faces obtained by freeze fracturing, complementary struct., digital image processing 79−62205
polyethylene, high-density oriented, lamellar struct. obs. 77−55244
polythene replicas of small diameter channels, surface roughness inspection 77−30136
protein, surfaces, invertible, wetting angle 79−37900
steel, type 304, faceted fracture surfaces, selected area channelling patterns 77−77565
surface measurement replicas, comparative study 80−36987
surface topography, high-resolution polymer replication 78−10264
Zircaloys, fractographic distinction between hydride cracking and stress corrosion cracking 78−92363
$Bi_{1-x}Sb_x$ film, evaporated, cross-sectional struct., electron microscopy and replica technique study *(German)* 78−22977
C, electron microscopy, geometric stability *(Ukrainian)* 77−67536
C, stripped from pure and doped NaCl single crysts., elec. memory, Au and Ag deposition expts. 77−76691
GeS, film on Ge, evaporation, thermogravimetric, electron microscopy investigs. 77−15715
KCl, additively coloured, colloid size distrib., replica microscopy, absorpt. spectra 77−47449

replicas continued
$NH_4H_2PO_4$, dislocation obs. using electron microscopy and replica method 77−59013
S replicas of C, alloy steels, effect of methodic factors on quality 79−24691

reproduction (copying)
see also photocopying; printing
additive film copying machine, modulator mechanodigital design *(German)* 78−65987
cine film, sound film production, film sizes, tutorial series *(German)* 79−49310
cine film colour duplication, Laboratory Aim Density control method 77−5953
colour film material sensitivity, copier technology appl. *(German)* 79−26156
colour transparency projector/scanner and printer 80−52343
control, appl. of microdensitometry *(Czech)* 79−30524
diazotype radiographic duplicating system as diagnostic aid 80−8137
electron micrographs and transparencies for publication and display 77−49817
electronic imaging hard copy methods and printing systems 80−47134
embossable surface relief structures for black and white, colour reproduction, ZOD images 78−65990
film copying for TV projection *(German)* 79−49311
halftone noise characterisation, meas. technique using scanning microdensitometer 79−26151
hologram copying methods, review 79−45915
hologram copying using amorphous film as master 78−29912
image classification and tone reproduction determination, statistical method 77−74535
intaglio imaging with nuclear particles 78−65993
laser engraving unit, direct dry preparation of offset printing plates 79−18434
lenslet-array optical device for paginal information reproduction 79−27194
motion picture film, automatic system for estimation of exposure conditions *(Russian)* 79−35877
optical fibre array, gradient-index, appl. in copying machine 80−69500
photographic contact copying process, film material gap meas. 79−26166
photography, copying process for colour reversal films *(German)* 80−30254
portal film duplication using instant photography 79−30591
reflection hologram preparation by interf. copying of transmission holograms 79−45916
scintigrams recorded on X-ray films, simple method for copying and photographic data processing 79−16283
structured image reproduction, quality, information rating 77−10851
three dimensional hologram copying method 77−71957
tonal reproduction via unscreened positive printing plates 79−17517
xerographic copy line profile meas. using microcomputer/microdensitometer system 78−74088
xerographic toner, charge optimisation 77−182
xerography, amorphous Se electronic props., defects 79−97454

research and development management
allocation problem in USA, the federal role 77−9848
American Society of Heating, Refrigerating, and Air-Conditioning Engineers, thermal energy storage activities overview 80−16844
analytical instrument use and planned acquisitions 78−88684
Apollo tradition, object lesson for management of large-scale technological endeavours 78−93071
Austrian solar energy R&D activities and international cooperation 79−57374
Bell Laboratories, origin of solid-state research 77−41449
British 1977 solar energy programme 79−57369
Canadian power reactor programme, role of Chalk River research reactors 79−81073
controlled fusion research and the Joint European Torus project 80−18593
electro-optical system manufacture, test and process control changes 80−96044
energy modelling and forecasting at US ERDA 78−49629
energy resource development role of Sandia Laboratories' photometrics division 78−58077
energy resources in Britain, general survey *(German)* 80−72000
European Communities' solar energy R&D programme 79−57360
European remote sensing satellite programme benefit identification and quantification methodology 78−32231
fission and fusion reactors in Japan 80−47701
French energy research projects *(French)* 79−74497
French solar energy development 79−57368
fusion commercialisation, generalised requirements and R&D 77−34462
fusion power development program plan 77−34461
India, need for and consequences of technological assessment 80−68017
Indian national solar energy R&D programme 79−57365
information exchange, novel teleprocessing methods (NSF program) 77−2504
International Energy Agency and NATO solar energy programme status 79−57362
international team research, information networks, CAITR, CAPS examples, cost-benefit analysis 79−35441
Iranian solar energy R&D approach and philosophy 79−57377
Irish solar energy developments 79−57378
Italian national solar energy programme 79−57367
Kuwaiti solar energy research, development and demonstration programme 79−57371
Latin American solar energy prospects and programmes 79−57363
lightning strokes, artificial, experimental station in France *(French)* 80−61841
lignite deposit exploitation in W.Germany *(French)* 79−92054
LMFBR secondary cct. components 79−97793
LMFBRs, national development programmes, status assessment 80−106104
Malawi solar energy utilisation prospects 79−57379
medical ultrasonics, USA National Science Foundation incentive programme 77−66831
Mexican Solar Energy Experimental Center optimum site determ. 79−57380
modular solar collector development for large solar generators 79−96467
Monju heat transport system design and related R & D work 79−97791
Netherlands national solar energy programme 79−57372

research and development management continued
nuclear facilities in West Germany, physical protection program review 79−89450
nuclear fuel cycle length flexibility in C-E reactors 77−42116
nuclear fuel cycle sensitivity anal. system for LWR 77−42119
nuclear nonequilibrium fuel management policies at San Onofre unit 1 77−42117
nuclear optimal cycle coastdown at San Onofre unit-1, reduced enrichment requirements 77−42118
nuclear power plants, safety research in Europe, role of Joint Research Centre 77−65299
nuclear symbiotic reactor strategies, U demand 77−42120
nuclear technology transfer, collaboration of R&D centre in Sweden with small countries 77−57766
nuclear waste disposal R & D programmes by OECD countries 78−41823
nuclear waste management problem, R&D efforts 78−4991
nuclear waste management research, UKAEA programme for Iran 78−4992
ocean thermal energy conversion (OTEC), emerging programme of significance to marine community 78−44875
ocean thermal energy conversion plant design, oceanographic data interpretation, ERDA program 78−44874
OTEC ocean thermal energy conversion, commercialisation in USA 79−61957
phase equilibria data and research prog., user survey implications 78−15380
Philippine national solar energy development programme 79−57376
power supply selection for R&D instrumentation 78−246
radioactive waste disposal options, modelling studies 78−41830
radioactive waste management, regional cooperation in India 77−57730
SAW devices, US military investment and usage 77−39189
scientific Siberia *(German)* 78−24634
signal processing research programme of United States Air Force 80−48171
small-state solar energy programme structuring methodology 79−57385
solar, geothermal, hydrogen energy, and coal gasification and liquefaction, Japan's energy programme 80−3478
solar cells, power supply appls., technology and research 79−92076
solar energy R&D importance for university education and development in Sweden 79−57382
Spacelab, communications R and D project management 77−17321
submicron structures, National Research and Resource Facility at Cornell 78−38101
technological innovation, autobiological notes R.N. Noyce 80−51997
Thai rural solar energy utilisation programmes 79−57375
Third World, approaches to physics research and education 79−48987
UNIDO solar energy programme for developing countries 79−57359
United Nations System solar energy programmes 79−57361
USA Energy R&D Administration effluent date collection and reporting system 79−13545
USA Energy R&D Administration role in low-level waste management 78−94114
USA Federal solar energy programme achievements and prospects 79−57370
USA photovoltaic industry development programme 79−61976
USA solar heating and cooling R&D programme 79−57373
West German solar energy technology development status 79−57386
West German solar energy utilisation programme technologies 79−57366
Western Canadian provincial and university solar energy activities 79−57381
wind power R&D in United Kingdom 79−79370
H_2 energy economy, R&D programmes 80−26171

residual stresses *see internal stresses*

resins *see polymers*

resistance, electric *see electric resistance*

resistance coupled amplifiers *see d.c. amplifiers*

resistance furnaces
heat treatment processes, present trends 79−49233
high-temperature, for drawing out filament light guides 80−74491
industrial, transfer function determ. for DDC *(German)* 77−3709
neutron diffraction on vertical axis goniometer, high temp. diffr. furnace 77−58926
nuclear fuel element, post irradation testing *(German)* 78−29632
optical fibres drawing method for high tensile strength 78−68666
power supply control to allow interruption of analytical cycle 77−21432
programmed temperature regulator 78−86256
sintering uranium oxide appl., characteristics *(Italian)* 77−81239
temperature control 80−27307
Si_3N_4 layers deposition, high-temperature, temperature gradient and nitrogen flow influence obs. *(Bulgarian)* 80−80981

resistance noise *see thermal noise*

resistance thermometers
AC thermometry and DC heating circuitry in thermal props. meas. 78−74000
adaptive amplifier convertor using sensitivity stabilisation *(Russian)* 77−41593
Allen-Bradley resistor thermometers, one-point calibration, 2-20K 77−53922
atmosphere temperature measurement in range, 253-318K 80−46291
automatic calibration oven 80−98914
automatic contact, for liquid streams temperature meas. 80−47055
automatic resistance thermometer bridge 80−98913
automatic temperature measurement with thermojunctions, temperature sensitive ICs and resistance thermometers *(German)* 80−77778
automatic testing, transformer bridge cct., quality control, servicing appl. 77−53906
automatic testing of industrial resistance thermometers using incomplete bridge balancing technique 78−73998
bridge ccts. for differential resist. meas. 77−79126
bridge circuit errors due to changes in conductor resistance 79−30473
bridge type, with digital readout, accuracy *(Polish)* 78−49834
calibrating apparatus, automatic, 4.2-300K range 78−45624
characteristic curve linearisation method, thermistors, Si, Ni resistance thermometers appl. *(German)* 78−77913
cold wire thermometers, cct. for instantaneous temp. meas. in heated turbulent flows 78−21137
cold-wire, dynamic calibration in still air 77−5834
compensating for thermal inertia in meas. nonelectric quantities *(Russian)* 77−53885
compound carbon thermometer using Speer and Allen-Bradley resistors 80−225
computerised, TI calculator program *(Czech)* 80−13078
conductor resistance effect compensation using hexagonal bridge *(German)* 78−77910
cryogenic appl., calibration 77−26311
data logger for precision meas. of resistance temperature detectors 79−88925
DC comparator apparatus 79−75529
digital temp. measurement, novel circuit *(German)* 77−74394
digital thermometer, using a thermistor bead 79−21741
distributed temperature sensor of optical path fluctuations, calibration 77−2688
drift, correction cct. 80−98912
electrical noise thermometer, novel circuit 78−54364
electrical temp. meas. methods and trends *(German)* 78−93681
electronic digital thermometer *(German)* 78−54368
electronic sensors for clinical replacement of metethmor 78−7473
electronic thermometer, microprocessor based linearisation of thermocouple temp. charact. 80−221
electronic thermometer, using an IC LM 3911 *(Spanish)* 79−6126
environment protection when siting power station, temp. and humidity meas. methods *(French)* 79−12318
film, remote electronic testing of sensitivity 79−67298
frequency response of cold-wire thermometers used for atmospheric turbulence meas. in marine environment 80−56650
glass enclosed Pt resistance thermometer for high pressure vessels 78−70125
hermetically sealed, device for measurement of static characteristics 80−77784
high-pressure temperature meas. in liquid He region 80−31748
industrial appl., advantages 80−42221
industrial platinum: models, resistance/temp. relationship, thick film construction 78−37008
International Practical Temp. Scale, instrument interpolation, from 630.74 to 1064.43°C 79−40564
International Practical Temperature Scale 1968, fixed point determination 78−41270
linear ohmmeter for resistors having negative temperature coefficient 79−21743
linearisation of bridge measuring circuit for multi-spot temp. check *(Russian)* 80−90847
low temperature measurement in high mag. fields, instrumentation and methods, review 78−37003
low temperature resistive pickup based on Ge-Si solid soln. layer on ceramic 79−88953
low temperature thermometry, use of C black loaded field plotting paper 77−74404
low-temperature resistance thermometers 78−223
magnetic-field-induced temperature error of some low-temperature thermometers 79−12802
Matsushita C resistance thermometers, heat capacity below 1K 78−65934
measurement error due to cond. along sensor leads, correction 77−13752
measurement uncertainty estimation *(German)* 77−53909
meteorological thermometers according to Baumbach and Frankenberger, comparison *(German)* 78−65433
microprocessor-controlled, development trends 79−85135
multichannel precision temperature measuring device, minicomputer appl. *(German)* 78−77914
noise thermometry system, features, design aspects *(German)* 79−30478
operational amplifier cct. used for 1/100°C measurement *(French)* 79−63210
pH meas. instruments and appls. *(Dutch)* 79−29435
platinum resistance thermometers, state of the art review *(Spanish)* 80−52212
precision bridge using single inductive current divider 77−82517
Pt thermometers for low temp. meas., AC circuits *(Polish)* 79−97389
PWR, Pt-resistance thermometers, in-pile response time testing 79−59219
radiation temp. scales 630-1064°C relationship 78−37004
review of resistance thermometry, error sources 80−52206
semiconductor, for the interval 300K to 0.3K, thermoelectric charact. 80−73359
sensitive temperature measurement theory *(German)* 77−71323
sensor overheating, influence of meas. current *(Russian)* 79−26053
sensors, Cu and Pt types, calibration method *(Polish)* 79−26055
Speer C resistance thermometer, magnetoresist. effect 78−4624
stagnation temp. meas. in hypersonic flow using fine W wire probe 77−79095
standardisation of measuring current, meas. accuracy increase 77−74399
standards, GDR, testing *(German)* 80−90842
statistical, with temperature regimes evaluation *(Czech)* 79−63208
temperature charact. unification method *(Russian)* 78−70122
temperature meas. devices developments *(German)* 80−8986
test equipment, laboratory, using zero-setting and steam thermostats 77−74400
thermal exchange between sensor and supports, temp. fluctuation meas. in turbulent airflow 78−21135
thermal inertia compensation *(Russian)* 80−62667
thermal noise thermometer, features *(Russian)* 78−29113
thermocouples and resistance thermometers properties 78−199
thermoelectric, design and operation *(Japanese)* 79−35747
thermoelectric resistance thermometer *(Japanese)* 78−32816
thermoresistive convertor error compensation methods *(Russian)* 80−73363
thin film, Ti and GE, for surface temperature meas., design, fabrication and appl. 78−24792
thin-wire, velocity-induced harmonics 79−49226
thin-wire resistance thermometer, dynamic error correction 79−12801
time constant, influence on temperature control circuits obs. *(Czech)* 78−29114
transient hot-wire, liquids and gases thermal props. meas. 79−200
transmission function approximation by Laplace transforms and Taylor series *(Russian)* 78−62197
Wien bridge oscillator, low-power, for low-temps ~25 mK 78−93680
C, charact. in field modulation studies 77−37882
C film, for low temp. meas., manufacture and performance 77−37883
C glass, comparison of charact., stability and construction with Ge resistance sensor 77−22558

resistance thermometers continued
C resistors, 1/8 W, for thermometry around 10 mK 77−135
C resistors as low temp. sensors in low temp. reactors, gamma, neutron irrad. investig. 77−45848
C resistors for low temp. thermometry 80−86308
C, Speer grade, low-temp. magnetoresistance props. 78−49835
C thermometers with stability over wide range 78−24789
C-glass, stability characts. 80−31751
CdSb, thermometric characts. at cryogenic temps. 79−21760
Cu, heat shock influence on elec. cond. and thermophysical props. *(Russian)* 80−52210
Cu resistance temperature sensors *(Polish)* 79−97388
determination of magnetoresistance in liquid He temp. range 80−31752
p-GaAs, 4.2 to 100K range, thermometric characts. approx. 80−31746
GaAs p-type, for low temp. meas. under strong mag. fields *(Russian)* 78−89477
GaAs semiconducting, 0.3 to 350K range 79−58687
GaAs:Cu, Fe, Cr resistance thermometer expts., 0° to 200°C *(Russian)* 78−45627
Ge, characts. from 1 to 35K, ISU mag. temp. scale 78−81970
Ge, comparison of characts. stability and construction with C glass resistance sensor 77−22558
Ge, for measurements between 0.5 and 30K 80−42225
Ge, interpolation method 80−22357
Ge, resistance thermometer, low temp., approx. of calibration curve 78−45620
Ge resistance thermometer appls. below 0.1K 78−73999
n-Ge resistance thermometer material for 14 to 300K *(Russian)* 80−49731
Ge resistance thermometry, applic. of improved interpolation method for very high-precision data 77−45838
Ge resistive sensing devices, temp. calibration and reproducibility, high mag. field effect *(Czech)* 80−37029
n-Ge sensor, resist.-temp. characts., 50-125K 77−41602
Ge stability at 20K 78−41307
Ge, stability data at 3 temperatures 80−86307
Ge, stability test at 20K 78−81971
Ge thermometers, stability testing via thermal cycling apparatus 77−61066
Pt, 0-850°C meas. *(Dutch)* 77−127
Pt, 0-850°C range, principles and practice *(German)* 77−82512
Pt, calibration characts. linearisation methods *(Russian)* 78−70123
Pt, Callendar coeffs. determ. 77−26287
Pt, determination of dynamic behaviour *(German)* 80−17940
Pt, effect of oxidation on electrical resistance 80−101794
Pt, effect of pressure on readings, 294 to 1095K, up to 100 MPa 79−6124
Pt, fast response meas., features 79−195
Pt film resistance temperature detection 78−49830
Pt film resistance thermometer, fabrication, appls. 77−37890
Pt, heat leaks effect anal. 80−57296
Pt, heat shock influence on elec. cond. and thermophysical props. *(Russian)* 80−52210
Pt, in-reactor temp. meas. accuracy, thermometer construction effects 79−17969
Pt, in-situ response-time testing for nuclear power station safety systems 79−93743
Pt, linearisation characts. *(Russian)* 80−82764
Pt, linearisation circuit *(German)* 78−200
Pt, linearisation technique *(German)* 80−42224
Pt long stem resistance thermometers, Ar triple point realisation cryostat 77−26307
Pt, medium precision, A/D convertor appl. 80−86297
Pt resistance elements, temperature detectors 80−27296
Pt resistance standard capsule thermometer, for 13.81 to 273.15K, two-point calibration 79−206
Pt resistance standard low-temp. thermometer checking methods 78−37006
Pt resistance temperature probes, constructional types and state of technique *(German)* 80−52213
Pt resistance thermometer, oxidation problems 80−52206
Pt resistance thermometer response time testing in situ 79−13484
Pt, resistance thermometers for high temperatures *(Russian)* 78−57958
Pt, resistance thermometers and I_{68} calibrations, intercomparison 79−40565
Pt, response time estimation by noise anal. technique 79−93742
Pt, simple Cu holder for calibration 80−98911
Pt, TSPN-3 and a carbon thermometer (USSR), stability tests 80−62666
Pt, temp. meas. errors, 0 to 600°C 77−41605
Pt, temp. meas. in high pressure vessels 79−21744
Pt, temp. meas. in nuclear reactor appl. 79−89399
Pt, temp. range influence on error due to non-linearity *(Russian)* 80−90841
Pt thin wire resistance thermometer dynamic response 77−22549
Pt thin-film temp. sensor *(Japanese)* 80−105645
Pt type, development and cost control 77−37891
Pt type, errors due to measuring-current heating in still air 79−30472
Pt-alloy thermocouples, reference-standard testing apparatus 80−13077
Pt-Co, for low temp. appl. 78−73994
Pt-Rh, temp. convertor for nonlinearity error correction *(Russian)* 78−70124
Rh-Fe for measurements between 0.5 and 30K 80−42225
Si diode, thermometric props. in temp. range 4.2-300K 77−17998
Si, linear, superconducting transition temp. meas. 77−57330
Ti-Be-Zr base alloy, glassy, props. rel. to resist. thermometer appl. 77−82532
W resistance temp. scale for field emission electron microscopy 77−45841

resistance welding
fusion reactor superconducting magnet joints, resistance welding 80−91259
metals with high elec. and thermal cond. using C rod electrodes 77−79077
Monel, Ni-Cu-Fe-Mn, resistance spot weld quality evaluation, using stress wave emission technique 78−53066
Cu-Ni-Sn (4,4 wt.%) resistance spot weld quality evaluation, using stress wave emission technique 78−53066

resistivity *see electrical conductivity*

resistors
see also photoresistors; posistors; thermistors; thick film resistors; thin film resistors; varistors
1/f fluctuations *(Japanese)* 78−43448
absolute ohm of ETL, determ. using calculable capacitance standard *(Japanese)* 79−6137
alloy selection for cryogenic resistors with low temp. coeff. 80−98922
artificial cold resistors, electronic feedback cct. 78−32750
capacitive loss-angle resistor meas. bridge, 1 mHz to 100 Hz *(German)* 77−79125
coaxial current shunt and resistor stack, current waveform recording in μsec region 78−21178
electrolytic, 1/f noise theory 79−47940
electrolytic, regulating, for TEXT fusion reactors 78−55038
electrometer measuring unit and component requirements 77−74445
film strain resistor for temp. up to 1000°C 77−37920
fluctuations in resistance and enthalpy, response to current changes 78−34871
humidity sensitive ceramic resistor device, characts. and appls. *(Japanese)* 77−71332
liquid variable resistance, high-voltage technology appl. 77−37918
low temperature, search for standard resist. Al alloys 77−17997
manufacture, Cr-Si coatings deposition, by flash evaporation, residual gas atmosphere analysis *(German)* 80−6681
metallic, nonlinear current fluctuations, microscopic calc., heating, perturbation theory 79−69484
Noise thermometry in the range 630-962°C, thermal noise in resistors appl. 78−73995
photomultiplier arrays, efficient alignment procedure using standard dynode resistor chain 77−3229
precision variable, rotation-angle pickup appl., for goniometer 80−47047
reactive props., measurement using precision dielectric cell 79−49255
resistive ratio standard, for DC voltage meas. to 10 kV 77−18028
semiconductor strain gauge resistors, exam. of characts. in elastic waves 78−85097
semiconductor tensoresistor use for extending operating temp. range of press. transducers 78−4608
shunt, made from composition resistor, for current pulse measurement 78−4640
Speer C resistance thermometer, magnetoresist. effect 78−4624
Speer C resistors, low-temp. magnetoresist. meas. by NaF:OH and KCl:OH capacitance thermometers 78−4623
Speer carbon resistors as pressure gauges 80−95108
spiralling resistors with laser beam *(Polish)* 80−28242
strain-dependent resistors, in force meas., noise limitations 78−16771
temp. meas. by thermal noise, appl. *(German)* 78−4615
vacuum deposited resistive foils, manufacture and props. of multicomponent alloys *(Polish)* 80−35131
$Al_xGa_{1-x}As$, resistor pressure sensors 79−2756
$Al_xGa_{1-x}As$, temp. coeff. of resistance of pressure sensors 79−6108
C black-graft polymers crosslinked with epoxy resin, electrical props. *(Japanese)* 80−24920
C, high-resistance, He level gauge appl. 80−57277
C, improved thermal contacts 78−37015
C resistors, 1/8 W, for thermometry around 10 mK 77−135
C resistors as low temp. sensors in low temp. reactors, gamma, neutron irrad. investig. 77−45848
C resistors for low temp. thermometry 80−86308
$Cd_xHg_{1-x}Te$ magnetoresistor prep. and props. 79−7844
Cu, Johnson noise, rel. to absolute temp. 77−47872
Pd-Pt-Au alloys for low-temp. precision resistors 79−69490
Pt-Rh alloys, low temp. resistivity 79−60787
Si filamentary piezoresistor for pulsed wave process meas. 78−57980
Si, p-type and n-type, temp. coeff. of resist. calc. 78−91698
Si whiskers as basis for strain resistors 79−5094
Si:Sb, low energy ion implantation Schottky barrier diodes and resistors 80−88177
TiN-VN refractory powder composite, resistors, produced in low temp. 78−11182
ZnO:$^{31}P^+$ implanted nonlinear resistor production and characteristics *(Russian)* 80−49252
ZnO-based ceramic microstructure and nonlinear props., B diffusion effects *(Russian)* 80−49423

resolving power (optical) *see optical resolving power*

resonance
see also atomic beam electric resonance; circuit resonance; cyclotron resonance; dielectric resonance; Fermi resonance; magnetic resonance; magnetoacoustic resonance; molecular beam electric resonance; optical double resonance; vibrations
abyssal sediments, effect of particle size var. on DRM/ARM ratio 78−32067
acoustic, resonance frequencies in T-tube 79−14136
acoustic, unsymmetrical enclosures, LF resonances 79−18605
acoustic resonance, in control hollow cylinder in water, effect on sonar cross section 77−46844
acoustic resonance in vaneless radial diffusers with swirling flows 79−18882
acoustic resonance of planar gratings of compliant cylindrical shells, scatt. anal. 77−31157
acoustic resonant frequencies in an eccentric spherical cavity 78−90548
air column resonance spectra, meas. using basic lab. apparatus 80−41998
analytic continuation in decay-scattering systems, singularities as model basis 80−8850
annular plates under periodic radial loads, dynamic stability 79−1129
annular plates under pulsating loads, parametric resonance 79−14325
artifical Earth satellites, gravit. harmonics from shallow reson. orbits 78−40805
artificial Earth satellite, resonance due to solar radiation pressure 79−25456
artificial satellite motion, reson. eqns. in nonsingular variables 77−60581
artificial satellite orbital inclination changes due to resonance 77−17334
artificial satellites, orbital perturbations by solar radiation press., reson. effects 77−78605
asteroid, equation of motion for elliptic Jupiter orbit 79−25455
asteroid 1685 Toro, orbital resonances with Earth and Venus 79−2513
asteroid orbits in vicinity of 1:3 commensurability with Jupiter, reson. motion and orbital evolution *(Russian)* 80−36486

resonance continued
asteroids, Hilda group, resonant orbital motion of Palomar-Leiden Survey objects 77−9690
atmosphere, linear reson. of flow equilib. rel. to blocking weather systems 80−56536
atmosphere acoustic-gravity waves, behaviour at reson. 77−33270
axiomatic quantum theory and resonances 79−2907
bifurcation into invariant tori at points of reson., use of Poincare maps 79−44707
black holes, rotating, reson. freqs. of free oscills. rel. to gravit. waves 80−105271
bone, effects of geometrical parameters, shear and rot. inertia, finite element model 77−29165
box approach to resonance 80−98824
bubble resonances, effects on standing waves in gas-liq. medium 78−9474
bubbles, gas and vapour, dynamics, review 79−98788
bubbles in standing wave acoustic field, behaviour of stable arrays 77−79988
cantilever plates connected by rods, natural vibration form and frequency calc. 77−62203
cantilever sandwich beams, natural freqs. of vibr. 78−18212
cantilevered fibre-optic scanner 80−53428
cardan-suspended, gyroscopes under small vibrations, anal. *(Russian)* 77−53889
celestial mechanics; 1:1 reson. soln. appl. to Trojan asteroids theory 79−12419
celestial mechanics, asymptotic soln. to problem involving two simultaneous small divisors 77−49272
celestial mechanics, extended ideal resonance problem, comment 77−22055
celestial mechanics, props. of Delaunay-Zeipel transformation in reson. problems 80−46378
circular disk resonators in vicinity of thickness resonance, vibration mode anal. 80−48634
circular plates, asymmetric responses at nonlinear resonances 79−3951
combination, parametrically excited oscill. of coupled second order systems with nonlinear damping 80−86078
composite material, plate, natural vibration investigation using finite element anal. 77−68495
conservative, nonlinear oscillators, connection between dissipative and resonant types 79−58619
continental shelf wave side band instability and long wave resonance 78−16030
cooling towers with column supports, free vibration analysis 78−83292
crystal free vibration, resons. rel. to orthorhombic crysts. elastic consts. determ. 77−84849
cylinders and plates, dynamic deform. at high frequencies *(Russian)* 78−18223
cylindrical shell, liquid filled under nonlinear resonance conditions, vibration stability 80−99954
cylindrical shell with liquid, resonance frequencies determ. 80−43661
damped oscillators, internal reson. 77−46905
damped system, resonant peak amplitudes estimation 77−53771
decay-scattering systems, resonances and their eigenfunctionals in Friedrich's model 80−8847
depth-mode cavity resonance in turbulent flow 79−1017
diesel engines, open chamber, knock-induced cavity resonances 79−81624
disorienting collisions, nonlinear resonance induction 80−37900
Earth satellite orbits with resonance lunisolar perturbations, dependent on inclination 80−90326
Earth strain-tides, spectroscopy and reson. behaviour 78−73301
edge resonance in semi-infinite plate, variational anal. 77−78987
elastic curved body, reson. mode eigenfrequencies of creeping vibrs. 77−50817
elastic cylinder, end resonance under axisymmetric vibr. *(Ukrainian)* 80−23932
electrical activity of the brain, resonance phenomena 79−74627
electrically connected bearing, motion equation *(Russian)* 80−73164
electron relativistic ring with discrete and continuous eigenvalue spectrum, resonance crossing 78−58507
electron resonance in plasma, effects on trapped electron instabilities 77−7528
EM dominant reson. freqs. of human body 78−31857
EM power deposition in prolate spheroid models of man and animals at resonance 78−31905
external friction reduction by forced piezoelec. oscillation 80−92096
extremal properties of reson. motion, celestial body rot. anal. 77−87246
flowmeter, float-area-type, jumping instabilities of float 80−14855
fluid-loaded cylindrical shell, resonant component isolation in acoustic scatt. 80−5864
forced damped harmonic oscillators, meas. separation and half-width of components of doublets, high-Q systems 80−74590
galaxies, spiral density wave and inner Lindblad reson. caused by orbiting retrograde companion 78−96533
galaxies inner Lindblad resonance, response density in nonlinear theory 79−35366
galaxy particle resonance, nearby stellar orbits theoretical study 80−26914
gas, photon echo in a magnetic field at small areas of the exciting pulses 80−95961
gas, resonance four-photon shift, optimal focusing of high-power pumping 80−95574
gas bubbles, oscillating, appl. of subharmonic threshold to damping meas. 77−31374
giant monopole resonances in the scattering of waves from gas-filled spherical cavities and bubbles 79−50476
guitar, vibr. modes at Helmholtz and first top-plate resonances 77−35003
guitar resonance board, effect of radial ribs on reson. acoustic response, holographic study *(French)* 77−80031
gyro with damping system on vibrating base, conditions for nonlinear resonant vibrations excitation *(Russian)* 77−71312
gyroscope contactless suspension on vibr. support *(Russian)* 78−51054
gyroscope on elastic suspension, principle resonance *(Russian)* 79−30461
gyroscope resonance motion in free suspension *(Russian)* 79−10460
Hamiltonian autonomous system with 2 degrees of freedom, stability in 1st order reson. *(Russian)* 77−53776
harbours, reson. oscills. in closed L-shaped channel 77−78190
resonance continued
hemispherical monopole surrounded by plasma layer, Tonks-Dattner reson. and input admittance 80−87887
homoclinic points and resonance in dynamical systems 80−4240
hydrodynamics, generalised, extension to molecular dimensions 79−25864
impact vibrations, steady, of body having hysteresis collision characteristics 80−14602
ionosphere, satellite gyroharmonic reson. obs. interpretation 79−48614
ionosphere, spatial resonance mechanism for equatorial spread-F irregularities drifting patches 79−21095
Josephson junction current-voltage charact., resonance detection cct. 78−54406
laboratory equipment for resonance meas. in solids *(Spanish)* 80−86285
lamellar grating resonance anomalies, properties 79−50393
laser-irradiated target, electron accel. by reson. 80−75076
linearised spring pendulum system, stability anal. 77−64945
liquid surface, ripples, generation by parametric subharmonic reson. with sound waves 77−46849
liquid-filled vibr. beaker, spatial reson., energy transfer mechanism 77−39255
magnetic coated small dipole antenna, lowering of reson. freq. and improvement of radiative resist. *(Chinese)* 79−50193
magnetosphere, effect of bounce resons. on Alfven waves generation outside plasmasphere 79−12344
magnetosphere plasma resonances, on-line tracking for electron density small-scale struct. 79−35073
mechanical oscillator, effect of spin on non-linear reson. motions 77−75839
mechanical vibration, amplitude-frequency charact. recording, resonating systems 77−45829
mechanical vibrators miniaturisation 78−18229
mode finding, experimentally, when several contribute to a reson. 78−83310
model and full-scale cooling tower resonance tests 78−83291
molecular dynamics, fluctuation driven reson., hydrodynamic and kinetic theory simulation 77−55124
molecular free induction decay and optical nutation, short-term behaviour *(French)* 77−75117
Moller cross section in strong laser field, resonances and intensity depend. shifts 79−45918
multi-degree of freedom mechanical systems, antiresonances *(Chinese)* 80−42049
multi-degree of freedom systems, effects of geometrical nonlinearities 79−98648
natural VLF antenna, Deception Island, impedance meas. 79−48399
NGC 4736, spiral galaxy, ring-like structs. as Lindblad resonance tracers 77−2469
non-conservative systems, nature of resonance, comments 79−80426
nonconservative elastic systems, induced oscillations, transition through resonance *(Ukrainian)* 79−98654
nonconservative system resonance, modal analysis 78−42557
nonhamiltonian systems with one degree of freedom, forced periodic motion *(Russian)* 78−20959
nonlinear oscillations with parametric excitation, system with one degree of freedom *(Russian)* 77−89018
nonlinear resonant oscillations of body containing liquid *(Russian)* 78−18222
nonlinear systems, parametric resonance phenomenon *(Russian)* 77−57182
nonlinear systems, resonant vibrations, modified single mode method 79−86371
nonlinear two-degree-of-freedom system, internally resonanced, forced vibrs. 80−36838
nonlinear two-degrees-of-freedom system, internal resonance, forced vibrations 78−12551
nonlinear vibr. systems, secondary resonances generated by harmonic forces *(Polish)* 79−64563
nonlinear vibrating system, combination reson. response amplitude calcs. *(German)* 79−10527
nonlinear vibrating system, fourth order parametric resonance, influence of frictions 77−58620
ocean barotropic and baroclinic Rossby waves, reson. interactions and instabilities 79−57955
ocean internal waves, reson. interaction 77−45010
ocean long waves scatt. at mouth of estuaries bordered by continental shelf 77−9442
ocean shelf-wave island resonance, radial barriers effect 79−57948
oceanic long waves scatt. at river estuaries, effects of bay and shelf resons. 77−78191
oceanography, edge wave modes reson. growth rel. to surf beat 78−73380
open tubes, resonant oscillations of gas 77−68628
optical anal. of resonances in velocity depend. square well pot. 78−62098
optical anomalous resonances in anisotropic multilayer structures 79−45902
optical triple resonance, semiclassical anal. 79−93963
organic liquids, US resonance absorption 78−95110
orthotropic cylindrical panel with glued circular ribs, natural vibrations 78−22299
oscillators, weakly nonlinear, system with slowly varying parameters, resonance 80−62463
parametric complex objects, multichannel installation for stabilising vibration 80−58990
parametric dynamic systems, combination reson. determ., generalised harmonic balance method 78−90753
parametric resonance, student expts. 79−58464
Pc micropulsations, reson. theory examination by anal. of mag. fluctuations in magnetosheath and magnetosphere 79−80092
periodic motion and linear oscillation theory, stability *(Russian)* 78−86147
piezoelectric transducer, composite, of low freq. acoustic flaw detector, natural freq. calc. 80−89450
piezoelectric unbounded plate with circular electrodes, resonances 77−84175
plasma resonances in magnetosphere, JIKIKEN (EXOS-B) satellite stimulated plasma wave expts. *(Japanese)* 80−94649
plate, rectangular, dynamic stability, periodic compressive forces 77−23910
plates, nonlinear vibrs., reson. phenomena under Duffing's eqn. 79−14305

resonance continued
polyvinylidene fluoride piezoelectric film, acoustic wave reson. meas. 77−81058
pulsating stars, reson. effects on modal selection 80−82372
quantum field theory, nonperturbative, resonance states, solitons 78−380
quantum mechanical over phase space, group theory aspects 80−8852
radial-mode disc concentrators, reson. dimens. and gain 77−68301
random excitation of harmonic oscillations of single degree of freedom systems 78−54175
rectangular cylinders in heaving mode, aeroelastic instability 79−3954
resonance-bar damping, automated meas. system 77−2649
resonators, concentric tube, with unpartitioned cavities, anal. 78−90587
RF-generated magnetoplasma, wire antenna resonance near lower hybrid freq. 79−55516
rigid body resonance translational-rotational motion in sphere gravit. field, intermediate theory 79−96899
room resonance, computer-aided anal. 78−87205
rotating fluid, trapped oscillations, viscous effects, num. simulation 77−55015
satellite-satellite resonances, origin 79−16867
scattered wave focusing in periodically inhomogeneous layers *(Russian)* 78−1158
Schumann resonance problem, convergence of zonal harmonic series 79−2348
Schumann resonances, atmospheric, elec. vertical component obs. by stratosphere balloon 79−44221
Schumann resonances in Earth-ionosphere cavity, book 80−86050
self-gravitating disk, resonant interaction of three density waves 77−67130
shaft transverse vibrations resulting from longit. and transverse quasiharmonic forces *(Russian)* 77−58591
shell of revolution, resonant oscillation obs. by holographic interferometry *(Russian)* 78−22297
solar chromosphere, magnetoacoustic wave propag., resonance phenomena 77−13306
solar coronal loops, heating by Alfvenic surface waves reson. absorpt. 79−16905
solar system orbit-orbit resonances, varieties and similarities 78−4093
solid systems, errors associated with resonance curves 79−7255
solid-liquid system, connectedness of liquid and solid movements *(Ukrainian)* 79−50623
sound scattering from gas bubbles in liquid, multipole resonances 79−81606
sound scattering from water droplets in air 80−33306
sound waves, resonance interaction with plane parallel flow 77−814
spatial oscills. of gravit. oriented elastic satellite, nonlinear resonances 78−69644
spin-orbit resonance in astronomical bodies, mathematical aspects 79−12389
spring-loaded mass system vibration analysis *(German)* 80−96224
standing wave systems, errors in wave velocity meas. 79−10436
Stark effect in 1-D, resonances and continued fractions 79−59395
stellar dynamics, procedure for constructing formal third integral of motion 77−53647
stellar dynamics, reson. orbits comparison 80−56889
stellar surface large-scale pulsations, nonlinear coupling to small-scale deep-seated instabilities 80−62115
stretched wires as standards of straightness *(German)* 80−36976
strip and plate, end resonance for materials of varying Poisson ratio 77−51438
subharmonic nonlinear acoustic reson. in open tubes, open-end boundary conditions 79−14137
subharmonic nonlinear acoustic resonances in open tubes 77−72404
systems described by integro-differential eqns. with divergent arguments *(Russian)* 78−73832
systems with hysteresis, linear, and quasilinear self-oscill. *(Russian)* 77−58590
teaching demonstration, shattering glass with sound 77−57129
tensioned bar with initial curvature, parametric excitation 80−43654
tensioned sheet, with central opening, buckling behaviour and parametric reson. investigation 78−90759
p-terphenyl:pentacene, optical coherence and resonance decay 77−24859
thickness meas., US resonance method 78−48590
thin cylindrical shell, effect of cavity resonances on sound transmission 79−3850
three oscillators coupled by weak nonlinearity, response 77−68513
Trojan asteroids, long-period effects in motion and problems of 1/1 resonance 80−41755
Trojan asteroids and fictitious objects at 1/1 resonance, long-period effects 78−85830
turbine disc transverse vibration initiation 79−68633
two-particle resonances and singularities of 2→3 particle scatt. amplitude 77−49643
U-type vibrator, resonant freq. and vibration mode *(Japanese)* 77−42656
Uranus rings, reson. orbit theory and prediction of undiscovered satellite 78−81585
US backscattered wave minima for solid metal cylinder immersed in water *(French)* 80−53510
US resonance method, appl. in inspection of symmetrical products 80−89449
US rod systems, excitation and stabilisation of reson. modes 77−14839
US tool, radial mode, with statically loaded inner surface, reson. condition nomogram 78−183
US transducer design rel. to vibration geometrical effects 79−83871
US transducers array, transducer elements tuning 80−87684
vibrating orthotropic cylindrical shells 77−84182
vibration decrement determ. of nonlinear hysteresis type system from resonance peak width 77−84191
vibrational, math. modelling of built-up structures, using meas. data 80−69718
violin G-string, resonant response and excitation of wolf-note 80−53540
viscoelastic cylindrical shell, short, resonance vibrations 80−58962
waves in rotating gravitating gas cloud, resonant wave wave interaction 80−105154
waves in stratified fluid, nonlinear reson. interactions 78−83418
weakly coupled oscillatory systems 79−40357
$Co_{54}Ga_{46}$, superparamag. response to low DC fields 80−44860
Fe-Co (5 to 25 wt.%), exam. of damping capacity of Gentalloy 78−72800
resonance continued
Fe-Co-Ni-Al-Nb (15-20, 14, 9, 0.1-5.5 at.%), Nb effect on magnetic props., lattice parameter *(Russian)* 77−55689
Fe-Ni(Cr), Invar, exchange interactions between ferromag. and antiferromag. components 80−29545
$Fe_{40}Ni_{38}Mo_4B_{18}$ metallic glass, reorientation kinetics of magnetization 79−24155
He-Ne lasers, discharge reson. props. effect on radiation fluctuations, expt. 78−74883
resonance reactions and scattering, nuclear *see nuclear resonance reactions and scattering*
resonances, baryon *see baryon resonances*
resonances, meson *see meson resonances*
resonant absorption of gamma-rays *see Mossbauer effect*
resonant cavities *see cavity resonators*
resonant cavity wavemeters *see wavemeters*
resonant gamma-ray interactions in crystals *see Mossbauer effect*
resonators
see also cavity resonators; crystal resonators; resonance
30th Annual Frequency Control Symposium, Atlantic City (1976) 77−37852
accelerating resonators, for proton synchrotrons with short accel. time 77−46429
aerial ultrasonic generators using metal resonators *(French)* 80−79074
capacitive transducer with superconducting resonator for mechanical vibration meas. 78−21127
circular disk resonators in vicinity of thickness resonance, vibration mode anal. 80−48634
composite electrostrictive resonators, finite element simulation 78−59237
concentric EM resonator, gravitational wave radiation *(Russian)* 77−45772
coupled resonator chain, transverse beam instability, multimode approx. 80−52803
coupled resonators, normal mode anal. 79−14327
cylindrical, E_{010}, dielectric parameter meas., perturbation theory, error estimation *(Russian)* 77−18051
E_{112} mode, rectangular sensitivity analysis, nondestruct. control of epitaxial layers sim. structure appl. *(Russian)* 77−18052
electromechanical filter resonators, props. of materials used *(Czech)* 80−76318
Fabry-Perot resonator for precise dielec. meas. in 100 GHz range 78−70163
ferrite accelerating, for ion synchrotron, with tunable freq. from 2.5 to 30.8 MHz 79−97914
fibre optic relay with metallic pads heated by light 78−18038
flexural mode resonators, mechanical susceptance slope parameter 77−80000
fluid density meas., freq. vibration method, characts. calc. *(Russian)* 77−9985
Helmholtz, acoustic absorption properties improvement, with fibrous materials *(Spanish)* 78−14405
inductance meas. circuit, 10 mH or less, using self-excited oscillator and frequency meter 77−5867
long thin wire scattering widths, meas. using open resonator 78−46489
low-temperature rectangular resonator for observation of double electron-nuclear resonance in 3 cm range 80−98956
materials testing using frequency convertors with mechanical resonators 77−73400
mechanical, cylindrical resonator with coaxial ring flange, inherent oscillations *(Russian)* 78−34051
microwave, trapped-mode dielectric resonators coupling and tuning, for laser beam modulation 78−55389
microwave absorption by water in heterogeneous organic materials 80−15998
mode distribution, diffractals 80−8782
one-port SAW resonators, config. and cct. anal. 78−63258
open resonator methods for microwave permittivity meas. 80−15942
open transmission line, for microwave meas. of dielectric complex permittivity 77−26333
optical, tunable open resonator with cylindrical mirrors 79−90024
optical fibre, steady-state losses 77−27338
optical fibre mode coupling coeffs. determ. using fibre resonator 78−5560
plasma radial carrier density profiles, determ. using microwave resonators *(German)* 78−47160
quasidipole radiation of two circular cylinders with longitudinal slits 79−72468
radiospectrometer resonator uniaxial crystal deformation unit 80−31822
receiver design principles 78−45714
relativistic electron ring azimuthal oscillations in resonator with stabilising medium *(Russian)* 78−29889
saturable optical resonator with distributed Bragg refl. 77−3684
SAW grating resonators, mode pattern verification 78−1532
SAW metallic gratings, equivalent circuit of step discontinuity, rel. to SAW devices 80−33389
SAW resonators and resonator filters, design and performance 79−32178
SAW resonators using interdigital transducers, narrow band filters appl. *(Japanese)* 79−27478
SAW transmitting hydrophone development and performance 79−53586
slotted tube, pulsed ESR and ODMR expts. 80−86360
slotted tube resonator, use as NMR probe head at high freqs. 77−30192
spiral independently, phased, in heavy ion postaccelerator section 77−83148
split ring resonator for superconducting heavy ion booster 77−83126
stabilizing resonator of high-power klystron self-oscillator for microwave supply system of linear accelerator 80−42878
superconducting, for H^+ collective accelerator, Q-values and field profiles 78−46188
superconducting for H^+ collective accelerator 78−46187
superconducting split ring resonator as accel. struct. for ^{16}O and ^{32}S beams 77−6577
thermoquartz resonators, in geothermal field station, (GS-1) *(Russian)* 78−93000
three arm plate tuning fork, anal., mechanical filter appl. 78−22300
toroidal, for EM waves, Maxwell eqns. for toroidal geometry 80−102598
toroidal resonator excitation by uniformly moving charge 80−18726
torsion, liq. viscoelastic props. meas., 20-1200 KHz *(Russian)* 80−52196

resonators continued
travelling resonator interactions, electromech. model 77−583
two-mode hybrid resonator for nonlinear magnetisation expts. 78−58001
VHF resonator radiant energy meas., using electron beam *(Russian)* 78−77944
waveguide, RF breakdown, rel. to lower hybrid reson. in Tokamak plasma 78−26364
H_2 generator, tuning methods 77−88294

retrieval, information *see information retrieval*

revaporisation *see vaporisation*

reverberation
see also anechoic chambers; architectural acoustics; echo
acoustic absorption, classroom experiment 80−42016
acoustic chamber reverberation time, holographic meas. 79−68519
acoustic enclosure, three dimensional computer simulation 77−75747
acoustic panels, modular, for studios, computer calcs. *(Spanish)* 79−32141
acoustic systems with long reverberation, meas. transfer characts. by narrowband digital signal processing *(Japanese)* 80−64304
acoustically coupled rooms, reverberation time extension, directional microphone appl. *(German)* 79−41518
anisotropic sound energy flow effects in reverberation room plane absorber meas. precision 78−55482
appliance acoustic emission determ. facility development 77−58507
artificial, electroacoustic equipment for concert halls *(Czech)* 78−1514
assisted reverberation, in outdoor environment 78−13825
Atlantic shallow water off Argentinian coast, bottom reverberation-derived scattering strengths 78−65321
auditoria and studios, reverberation time meas. using digital instrum. *(Japanese)* 80−64321
automatic reverberation time meas. 79−68518
bat's sonar system simulation in anechoic chamber *(French)* 80−56072
Boston Symphony Hall, reverberation times in notebooks of Wallace C. Sabine 77−49545
buildings, history of meas. in America (1920-1940) 77−45663
chamber LF sound power injection analysis and response averaging 78−42496
Christchurch (New Zealand) Town Hall acoustical design aims and results 79−68490
city streets and tunnels, expressions for stationary sound pressure level 80−19159
concert hall, acoustical conditions preferred for ensemble 79−14161
critical distance measurement of rooms from acoustic energy spectral response 79−72750
cross-spectral density meas. in partially reverberant fields 78−30140
decay in room design, cinema appl. 78−33961
decay time meas. using digital freq. analyser 77−80033
decaying sound fields and spatial variation 78−79165
Demey metro station, noise level increase due to echoes from passing vehicles *(French)* 80−69600
dereverberation process evaluation by normal and impaired listeners 80−91974
diffuse sound field around objects in a reverberant room *(Japanese)* 79−1030
diffuse-field, shock excitation to determine US absorption in liquids 80−88267
diffusion in reverberation chambers 77−50842
digital reverberation and echo apparatus *(German)* 79−50554
effect on transfer function estimation, digital signal processing appl. 79−18616
Exhibition Hall of Yamaha Sportland TSUMAGOI, auditorium delay/reverberation system 78−13858
Fourier transform method for reverberation time measurement 80−74601
hall, mathematical model, rel. to speech intelligibility *(French)* 77−31175
hearing, phase change audibility in reverberant room 77−2006
hi-fi demonstration studio design *(German)* 79−94405
Hong Kong, reverberation time in high-rise areas 78−59197
house construction, acoustic power measurement appl. *(German)* 78−51024
impulse response testing of acoustic spaces 78−66987
insulating material losses and performance factors *(Spanich)* 78−55516
integrated impulse response method 78−59175
interior spaces, impulse response and lack of reverberance in certain freq. bands 80−28383
iterative calc. of reverberation time for two-dimens. enclosures 80−102934
Japanese speech intelligibility, effects of reverberation, model and articulation tests *(Japanese)* 79−90092
Joseph Haydn concert halls, room acoustics and orchestral sound *(German)* 79−18631
laboratory and domestic environments, relationship between sound power level and sound pressure level, use of noise data 80−74599
lake surface reverberation, statistical props. 79−1020
large industrial hall reverberation time 78−38145
listening room, reverberation time and reproduced sound definition *(Japanese)* 78−9499
listening room, reverberation time and reproduced sound definition 79−18606
living room loudspeaker performance problems *(German)* 79−90081
low frequency, reverberation process 79−46110
low frequency, sound power meas. 79−41514
meter for meas. reverberation time *(Japanese)* 79−37100
multipurpose hall acoustical design and construction 79−68486
music reproduction in small rooms, theory *(Spanish)* 78−38155
musical acoustics, room reverberation time meas. 80−42000
noise source investigation, industrial acoustic problems appl. 77−75742
nonrectangular reverberation chamber design and construction 78−83196
ocean reverberation spectra rel. to remote detect. of turbulence 78−38124
ocean surface reverberation model 77−34984
open plan offices, reverberation reduction via sound absorbing partial partitions 78−18116
pitch change during reverberant decay 77−14854
Poisson reverberation envelope, statistical props. 78−66984
power series for the reverberation time 80−43546
Rand-condition form generalisation in theory of chaotic movements, appl. reverberation 77−26147

reverberation continued
rectangular reverberant room, correlation coeffs. of sound pressure 79−76914
rectangular reverberant room, sound press. correl. coeffs. 78−18115
rectangular reverberant room, sound pressure correl. coeff. *(Japanese)* 78−38146
rectangular room, reverberation times determ. on basis of image methods *(Japanese)* 78−30129
rectangular rooms, prediction of reverberation using geometrical acoustics 80−23837
rectangular rooms, reverberation time dependence on wall diffusion and room shape *(German)* 80−102932
resonator appls. to hall reverberation time modification *(Dutch)* 78−22227
reverberant sound, transmission through orthotropic viscoelastic multi-layered plates 80−102884
reverberant sound absorpt. coeff. of plane porous material, theory *(Japanese)* 78−79168
room, acoustic wave diffraction at edges of absorbent wall panels, modal analysis *(French)* 80−79060
room, equivalent absorpt. area *(German)* 80−102931
room acoustics and subjective sound perception, computer simulation *(Polish)* 79−7258
room decay curve meas.; FFT methods and errors *(Japanese)* 79−27468
room resonance measurement techniques *(German)* 80−53586
room reverberation, removal from speech signals using multimicrophone signal-processing technique 78−9501
room with absorbing walls, reverberation time, absorption and impedance 78−90601
rooms sound absorpt. meas. 77−39161
Schroeder's impulse method and decay-curve averaging method comparison 78−66986
seismic reverberation periodicities, appl. to Earth crust structure investigation 79−66820
small room, image method for simulating impulse response between two points using digital computer 79−68487
sonar, incoherent and coherent processing against echo fading in shallow water 80−19142
sonar, vertical processing, concept 79−3830
sound absorption coefficient, estimation, plane porous material *(Japanese)* 78−83145
sound absorption factor influence on reverberation time 79−81631
sound absorption factors in enclosed space *(Spanish)* 79−3856
sound coverage techniques, loudspeaker placement problems *(German)* 78−87204
sound field spatial cross-correlation 79−68496
space absorber composed of porous materials, reverberant sound absorption coeff. 78−55519
spatial cross-correl. of acoustic pressures in steady and decaying reverberant sound fields 77−7232
spatial varaition of decaying fields, commnets on investigations 79−90073
speech intelligibility, reverberation effects in cases of presbyacusis 80−96139
spherical enclosure, reverberant sound decay 78−30128
spherical enclosure, uniformly absorbing, effect of surface roughness on reverberation time 79−14160
sports areas, reverberation and noise levels 78−9497
telephone speech quality, deterioration with loud speaker system 78−94488
tone sound power, reverberant room appl. 77−19502
traffic noise, reverberant meas. rel. to noise level prediction 78−75013
underwater, 4 kHz and 20 kHz tone bursts in water filled tank 80−83695
underwater sound, ocean bottom reverberation meas. at low grazing angles 79−14143
underwater sound, simulation of reverberation from surface of sea *(French)* 77−14836
urban built-up areas, external reverberation times 77−14846
urban built-up environments, room acoustical model of external reverberation 80−53563
US absorpt. in liquids at 500 kHz, determination using reverberation technique 80−38197
vol. reverberation from scatt. layers and biological meas. 78−81194
work rooms, acoustic characts. 79−81636

reverberation chambers
acoustic noise insulation, testing of Al tripole-layer wall between two reverberation rooms, road traffic noise 80−69593
appl. standing-wave tube, general acoustic instrument 79−81674
box loudspeaker study appls. *(Italian)* 78−26013
calibration, for sound power meas. in tones 77−19502
decay rate of sound in a reverberation chamber versus humidity and temperature 79−50473
decay rates of interrupted noise bands, variance determ. 79−94403
decay records, curvature meas. 79−90080
decaying sound fields, spatial variation 78−79165
diffusion in reverberation chambers provided with special devices 77−50842
eigenmode analysis of the interference patterns in reverberant sound fields 80−96112
electronic echo and reverberation generation, ccts. *(German)* 79−32138
investigation of sound transmission through pipe walls, presence of flow 80−102883
loudspeaker acoustic efficiency meas. 78−51028
monopole source, estimation of radiated power 79−10426
multitone decay variance 80−87653
noise environment study in operational aircraft voice communications 79−81662
noise source investigation, use of anechoic and reverberant rooms 77−75742
non-rectangular, resonance freq. and eigenfunctions, calculation by finite element analysis 80−64324
non-rectangular chamber design and construction 78−83196
normal mode anal. of sound power injection and effects of response averaging methods 78−42496
point-to-point correlation coefficient of sound pressure in rectangular reverberant room *(Japanese)* 78−38146
radiation impedance meas., effect of rotating diffuser 79−50510
rectangular reverberant room, correlation coeffs. 78−18115

reverberation chambers continued
reverberant absorption coeff. of plane absorber due to anisotropy of sound energy flow 78−55482
reverberation house construction in Eindhoven 78−51024
small-scale multi-purpose reverberation room 77−7259
sound absorption coefficient measurement 79−18653
sound absorption meas., method for assessing precision 78−59210
sound field ground sphere and cylinder in reverberant field *(Japanese)* 79−1030
space variance for rectangular modes 77−75746
spatial cross-correlation of acoustic pressures in steady and decaying reverberant sound fields 77−7232
velocity monopole sound power radiated under reverberant and free field conditions 79−46107

reversible shape memory effect *see shape memory effects*

reviews
see also Bibliography Index (special index bound with Author index)
(1+1) dimensional field theoretic models with soliton behaviour, exact S-matrices and form factors 79−26240
1/f noise 79−24038
1/f noise in electrical conductors, survey 80−107878
1/f noise mechanism, review of experimental investigations 78−64076
ψ(J) particle, discovery, props., experimental apparatus develop. *(Czech)* 78−78232
ψ production and decay, book contrib. 78−82208
A15 type compound, props. and one-dimensionality 80−2530
A=21-44, energy levels, excitation energies, branching and mixing ratios, lifetimes, J^{π}, resonances 79−13208
A>228 odd mass nuclei, single particle states, nuclear deform. 78−12952
A(p,d)X, A(p,t)X, inclusive reaction clustering phenomena, scaling behaviour, knockout mechanism, review 79−6441
AB-type compounds, high press. and high temp. behaviour 78−22850
abdominal abscesses detection, role of ^{67}Ga-scintigraphy, ultrasonography and computerised tomography 80−17096
abdominal disease, ^{67}Ga imaging 79−57772
abrasion and erosion, superficial plastic deformations by particles *(French)* 80−40540
abrasion resist. materials, review 80−108586
absorption coefficients meas. by transmission emittance and calorimetry 78−24839
accelerometers, performance characteristics and selection 79−177
accretion disks, theoretical review *(Polish)* 80−26739
acetylene photoelectron spectroscopy 78−50578
acid precipitation 77−37323
acoustic applications, research over past 50 years 80−96151
acoustic emission, and its appls. *(Japanese)* 80−93726
acoustic emission detection for small components production testing, review 80−16632
acoustic emission in brittle materials, book contrib. 78−11484
acoustic emission leak detection, attenuation of elastic waves in pipelines 78−27711
acoustic imaging and holography 77−58511
acoustic impedance meter, principle aspects of development 79−24999
acoustic materials for environmental noise control 77−42664
acoustic methods of materials testing 79−43504
acoustic microscopy, recent developments *(Japanese)* 78−79177
acoustic microscopy 78−46877
acoustic microscopy techniques and appls. (1979) 79−64461
acoustic noise, biological effects other than hearing, review of animal expts. 79−5314
acoustic noise, effect of LF on people 78−92673
acoustic noise measurement 80−33381
acoustic radiating parametric antenna 80−102898
acoustic streaming, nature and modern developments 79−37079
acoustic testing methods for materials exam. review 78−72987
acoustic underwater antenna arrays, adaptive 79−64467
acoustical holography and imaging 80−23841
acoustical holography in the UK *(German)* 80−53567
acoustical measurements and instrumentation, historical review 77−45666
acoustical measuring instrums. over past years 80−96152
acoustical research into life sciences 80−97925
acoustical research into superconductivity and superfluidity 80−96090
acoustical research over past 50 years on relation between acoustical behaviour and props. of solids, gases and liquids 80−96089
acoustico-optical and electro-optical modulators-areas of appl. 79−94359
acoustics, notebooks of Wallace C. Sabine 77−49545
acoustics in human communication, evolving ideas about nature of speech 80−96135
acoustics in perspective *(Chinese)* 79−37068
acoustics of auditoria, eighth annual Fairey lecture 78−13859
acousto-optic correlators, spatial or time integrating 78−9341
acousto-optic modulator applications and device technology 77−58468
acousto-optical devices, state of the art and potential 77−58464
acousto-optical signal correlators 77−58473
acousto-optics, guided-wave, with appls. to wideband communications and signal processing, progress review 80−58801
actinide compounds, magnetic and structural props. 77−63132
actinide compounds, specific heat meas., review 80−6524
actinide compounds, structure, mag. and related props., review 80−6389
actinide elements and compounds, mag. props., book contrib. 80−75727
actinide elements and compounds, mag. props. 79−4649
actinide metallic systems, magnetism 80−7076
actinide systems, mag. props. 78−84383
actinides, electronic struct. and props. 77−62813
actinides, expt. and theoret. binding and transition energies 78−50497
actinoid element alpha-decay, current state of results 78−17159
active nuclei of galaxies and quasars, role of UV obs. *(Italian)* 78−32577
active optical systems, real-time control over optical wave fronts 78−71187
active permanent magnet suspensions, scientific instruments appls. 78−24829
active Raman and Rayleigh scatt. spectroscopy, nonlinear optical methods, review 79−991
active thermal NDT, review 79−70282
adaptive optics 78−42296
adaptive optics technology, historical review and prospects 79−59793
adaptive optics technology overview, book contrib. 79−32030

reviews continued
adaptive optics technology status and prospects 80−33132
additional heating in Tokamaks, specific diagnostics review 80−28753
adenocarcinoma of colon and rectum, current place of radiation therapy *(French)* 80−17075
adenylate cyclase regulation, depend. on sugar transport system 78−69031
adenylyl cyclases, stimulation by hormones and regulation by nucleotides, review 78−15760
adhesion, surface and interfacial aspects 80−108690
adhesion, surface chemistry studies, anal. appls. 80−88440
adhesion measurement, problems and prospects 80−50817
adhesion measurement 80−50819
adhesive, pressure sensitive, radiation curing, literature review 77−86283
adhesive failure, and thin film adhesion, a prospective 80−50820
adhesive fracture mechanics 78−60773
adiabatic perturbation theory, mol. fixed moving coord. system 78−62687
adiabatic plastic deformation, shearing phenomena 80−50692
adsorbate layer, phase transition theory 80−44433
adsorbed layer, commensurate-incommensurate transition and domain walls 80−107654
adsorbed layers, photoelectron spectra, review 79−52072
adsorbed layers, two-dimensional phase transitions 80−39419
adsorbed monolayers, neutron scatt. meas. 79−65306
adsorbed surface structure and dynamics, neutron scatt. studies 79−60639
adsorption, computer simulation 79−65308
adsorption at metal surface *(Russian)* 79−46963
adsorption calorimetry for studying surface phenomena 79−40574
advanced electric power utilisation technology 79−24884
advanced lasers for fusion 79−18435
advances in basic magnetism during past twenty-five years 80−36791
advances in nuclear physics, clustering and self-consistent field theory, book 79−75879
aeroacoustic interaction, turbulent jet noise 80−87765
aeroacoustics, book contrib. 77−50807
aerodynamic heating problems with 1st order shape change, reentry vehicle 78−94735
aerosol, size meas. by optical methods, review 80−40746
aerosol fine particle charging by unipolar ions, review and expt. 78−88658
aerosol S compounds, techniques for chem. comp. determ. 78−95976
AES, qualitative and quantitative surface analysis appls. 77−90704
AES, surface composition, quantitative anal., review 79−24854
AES backscattering effects 80−81398
Afar region, geological evolution and geophysics 79−5468
ageing process, role of cell membranes, review 78−15809
agglomerate characterisation methods *(German)* 79−100443
agglomeration techniques in powder technology 78−39713
aggregate, polycrystalline, deform. 77−4816
agricultural and food products, moisture meas. methods *(Polish)* 79−2776
agricultural pollutants in runoff water 80−97831
air flow and sound generation in musical wind instruments, book contrib. 80−19174
air monitoring techniques, esp. long path optical meas. *(Italian)* 77−91329
air pollution, 1974-6 literature review 77−78405
air pollution, gaseous, aerosol and particulate methods of chemical anal. 80−7876
air pollution, long-range transport modelling 80−108823
air pollution, on site automatic analysers *(French)* 78−81451
air pollution climatic effects 78−28291
air pollution detection using lasers 77−9569
air pollution monitoring instruments 78−61590
air pollution regional scale numerical models 77−25770
air pollution remote sensing from space 78−61621
air transport noise reduction measures 78−1505
airborne dust, respirable fraction, performance characts. of samplers matched to them 78−53438
airborne IR astronomy 78−69688
aircraft dynamics, unsteady airloads prediction, aeroelastic anal. 78−71346
aircraft noise propag., report 80−64258
albedo neutron dosimetry 77−90914
Algotl, orbit, lightcurve and struct. 80−109460
alicyclic ring cpds., vibr. spectra, conformational props., book contrib. 78−78702
alkali atoms, review of exptl. methods of hyperfine struct. determ. 77−31019
alkali earth uranates, struct., phys. and chem. props., preparation methods *(Japanese)* 79−14764
alkali feldspars, TEM study of exsolutions *(French)* 78−28224
alkali halide crystals, radiation damage products, impurities and colour centres *(German)* 78−10086
alkali halide pelleting technique for solid sampling in IR spectroscopy 78−87171
alkali halide solutions, ionic hydration 78−92501
alkali halides, sputtering, thermal effects 80−35033
alkali halides and alkaline earth halides, rare earth doped, optical props, review 79−15492
alkali halides F-centre luminescence and lifetime 79−11442
alkali metal, vapour states, laser spectroscopy and applic. 80−68260
alkali metals, liquid, O_2 pot. and O_2 distrib. coeffs. between alkali and struct. metals 80−65231
alkali metals, optical spectra *(French)* 78−72558
alkaline earth monoxides, dissociation energy 77−550
alkaline earth uranates, struct., phys. and chem. props., preparation methods *(Japanese)* 79−14764
n-alkanes, vibr. data and force field consts., review 79−31750
alloy, binary, short range order calc. using equilib. diagram *(Russian)* 79−87610
alloy, cryogenic, creep, review 80−104222
alloy, $L1_2$ ordered, yield stress 77−52392
alloy, struct. transform. during ageing, book contrib. 78−11199
alloy, structural, time-depend. fatigue, nuclear reactor materials 79−1909
alloy, two phase, deform. 77−8893
alloy, two-phase, deform. struct. and recrystallisation, review 79−34061
alloy electrodeposition theories 80−11581

reviews continued
alloy film, vacuum deposition, monitoring and controlling techniques 78−11113
alloy phase diagrams, exam. of compilation activity 79−8274
alloys, amorphous, mag. props. *(Japanese)* 78−52259
alloys, austenitic, neutron irradiation effect on tensile, creep-rupture, deform., fracture props. 79−65120
alloys, crystalline and amorphous mag. props. from Rhodes-Wohlfarth plot 78−52190
alloys, ferrous and nonferrous, failure mechanisms overview 78−11322
alloys, high resoln. diffr. and imaging characterisation 80−104050
alloys, microstructural instabilities, review 78−35348
alloys, radiation effects on ageing and precipitation 80−29956
alloys, short-range order, electronic theory using pseudopot. approx. 79−47004
alloys, temper embrittlement, impurities and alloying elements role, review 80−66649
Alma Ata isochronous cyclotron, beam diagnostics, mag. field stabilising and resonator freq. control 79−54633
alpha decay theory *(Russian)* 79−49612
alternating current electrode processes 80−61107
alternative energy strategies, development of solar-based renewable resources 80−30417
ambient temperature solid state battery developments, review 80−61328
American architectural acoustics, (history to 1930) 77−45662
N.American Cordillera near Fortieth Parallel, tectonics and chronology 78−81138
amgnetic thin films, amorphous, struct. and mag. props., review 80−93148
amide group in soln., interactions, IR, Raman spectral investigs., peptide, protein struct., review 78−90330
amino acid racemization, appl. to geochronology and geothermometry 78−20341
p-aminophenol, oxidation in aq. soln., chem. equilib. of free radicals, review 79−43573
amorphous alloys, struct. and plastic flow 80−84090
amorphous alloys and metastable phases, crystallisation *(Japanese)* 80−38912
amorphous ferromagnetic alloys, domain struct. and mag. microstruct. 80−15751
amorphous ferromagnets, book contrib. 80−75743
amorphous ferromagnets, itinerant electron model, Invar anomalies 78−95413
amorphous film formation by vacuum deposition *(Japanese)* 77−66590
amorphous magnetic materials *(Chinese)* 79−33521
amorphous magnetic thin films for magnetic bubble memories, materials *(Polish)* 80−34715
amorphous magnetism *(Chinese)* 79−56508
amorphous metals, mech. props. *(Japanese)* 77−86109
amorphous metals and alloys, electronic transport props. 79−4546
amorphous metals and alloys, geometric struct. models and diffraction exam. techniques 80−79700
amorphous metals and alloys, struct. modelling 77−31596
amorphous metals and ion implantation 79−14686
amorphous semiconductors, DC and AC cond., high field effects, magnetoresist., EPR, carrier transport, review *(Japanese)* 77−35943
amorphous semiconductor, investigation into charcts. *(Croatian)* 77−39771
amorphous semiconductors, covalent, localised electronic states, Hubbard model calcs. 77−89732
amorphous semiconductors, doped, electronic props. 78−19030
amorphous semiconductors, doping effect and nature of localised states 78−14696
amorphous semiconductors, elec. and opt. props. 78−23094
amorphous semiconductors, elec. cond. mech. 79−56214
amorphous semiconductors, electronic props. and localised states 77−62871
amorphous semiconductors, photoluminesc. props. 79−56862
amorphous semiconductors, props., principles, appls. 77−4287
amorphous semiconductors, structural and electronic props. 80−64901
amorphous semiconductors, tetrahedrally bonded, electronic struct., far infrared absorption 80−45051
amorphous solids, atomic scale struct. determ., direct methods 79−37623
amorphous solids, inorganic, struct. 80−15004
amorphous solids, stochastic geometry, review, book contrib. 80−73269
amorphous state, structure determination by diffraction methods, philosophical aspects 78−50665
amphiphilic molecules and liquid crystals 79−99062
analytic signal in oscillation theory, review 79−5988
analytical atomic spectrometry *(Japanese)* 80−11990
analytical chemistry, kinetic aspects, review 1975-1977 78−85216
analytical electrophoresis, book contrib. 80−12322
analyticity in nuclear physics 78−89835
ancient geomagnetic field intensity, early research 77−37131
Anderson transition, electron localisation in disordered systems 80−29361
anelasticity due to long-range diffusion 80−60904
Anger scintillation camera, development since 1958 80−12234
angle-resolved photoemission 80−45214
Anglo-Australian Telescope, survey 77−91434
angular correlation developments at KURRI 77−42219
animal biotelemetry studies, historical perspectives and recent applications 78−69266
animal joints, mechanics, book contrib. 80−21488
animal plasma membranes, study using freeze-fracture technique 80−104842
anisotropic intermolecular potentials, mol. beam investig. 79−72376
anisotropic size effects in semiconductors and semimetals 77−32032
annular film thickness measurement 80−31439
anodic activation of passive metals, theory 80−25918
anomalous photovoltaic effect of ferroelectrics 80−65628
anomalous X-ray scattering 80−54075
W.Antarctic ice streams rel. to global climatic stability 77−64321
anthropogenic influences on climate 79−48565
antibody binding and complement interactions at the cell surface, dynamics, book contrib. 80−30689
antiferromagnetic, light absorption in freq. region of exciton and exciton-magnon transitions 77−48149
antiferromagnetic domains, indirect evidence, direct obs. methods, wall motion 79−51799
antiferromagnetic garnets, experimental data 77−80952
reviews continued
antiferromagnets, low anisotropy, nuclear spin waves spectra, relaxation, parametric excitation, NMR dynamic shift *(Russian)* 80−11180
antiferromagnets, spin waves, microwave and optical expts., review 80−50081
antigenic nature of mammalian cell surfaces, review 78−15805
antimatter cosmologies, observational tests 77−26095
antiparticle+particle reactions, high-energy, reaction differences and annihilations 78−74279
Ap stars, review of obs. and possible nucl. reactions *(Russian)* 78−20843
apatite crystal growth in skeletal tissues 80−94181
Apollo programme 77−64679
Apollo tradition, object lesson for management of large-scale technological endeavours 78−93071
appearance potential spectroscopy, recent developments *(Japanese)* 78−78052
aquatic ecosystems, acid precipitation effects 77−37257
aquatic sediment lipids, Recent and ancient 80−51583
arc, vac., anode spot and ion form. 77−80382
archaeological dating, scientific techniques, book 77−61172
archaeology, involvements of physics 78−58104
Arctic and Antarctic, Soviet meteorological research 79−34933
Arctic and Antarctic, Soviet oceanological research 79−39756
Arctic geophysical review, introduction *(French, English)* 79−48452
Arctic geophysical review, summary 79−48456
Aristotle's theory of time, Renaissance critiques 77−82355
arterial stenoses, fluid mechanics 80−35948
artificial membranes, excitable and ion-selective, review of axon and bilayer membrane props. 77−86451
artificial membranes, excitable and ion-selective, review of non-bilayer lipidic membrane props. 77−86452
artificial organs, terminology, phyiscal form 77−78042
artificial satellites future role in meteorological obs. 79−79965
Ashkin Teller model, exact results 79−58651
aspherical surface production 77−7224
aspherical surfaces, holographic methods of testing, review 80−33257
assessments of nuclear systems and use of nuclear power 79−45334
asteroid and comet dynamics and evolution 80−82260
asteroid belt structure 78−69737
asteroids, observations and theories 78−20720
asteroids, polarimetric, radiometric and spectrophotometric obs. *(Polish)* 78−36490
asteroids, sizes and albedos 77−60708
asteroids and meteorites, orbits, chem. comp. and origin *(Swedish)* 77−71048
asteroids in 1974, review of Institute of Theoretical Astronomy (USSR) activities *(Russian)* 78−49368
astigmatism, etiology of 79−16199
astroblems on Earth's surface 80−98324
astronomical gamma-ray burst origin, models review 80−82494
astronomical IR instrumentation on NASA airborne observatories 78−45224
astronomical IR interferometry, high spatial resolution methods, speckle and aperture synthesis *(French)* 80−46405
astronomical large mirror telescopes of world 77−33349
astronomical magnetic fields modification by plasma mechs. 77−73946
astronomical multiple mirror telescope 78−69687
astronomical observations of faint objects, television detection techniques 80−82208
astronomical photography, hypersensitisation, state of the art review 77−2344
astronomical photography, hypersensitisation, testing of emulsions for threshold imagery 78−32351
astronomical radio spectroscopy *(Japanese)* 80−62031
astronomical spectroscopy 79−12408
astronomical telescopes 77−33348
astronomical transient X-ray sources 77−33695
astronomy, far IR, detectors and sources 80−56726
astronomy, in vac. UV region 79−2488
astronomy, low light ground based techniques development 77−29657
astronomy, recent developments 78−16307
astronomy and astrophysics, annual review, 14th volume 77−25956
astronomy and astrophysics, annual review, 17th volume 80−12646
astronomy and astrophysics, annual review, 18th volume 79−5733
astronomy and astrophysics, annual review (volume 15) 78−24473
astrophotography, hypersensitisation 78−32348
asymptotic methods use in fluid mechanics, book contrib. *(French)* 77−87653
atherosclerosis, rheological aspects *(Japanese)* 80−94268
Atlantic continental margins, obs. and ideas 77−21691
N.Atlantic general circulation west of 50°W, determ. by inverse method 79−74901
atmosphere, mol. complexes presence and role in residual absorpt., light scatt. obs. 80−56607
atmosphere, optical phenomena, review including airglow and aurora 77−70831
atmosphere aerosols of Antarctica, origin and props. 80−90197
atmosphere natural organic aerosols of terrestrial origin, review 80−36381
atmosphere O_3 layer, transport rel. to chemistry and depletion 80−104534
atmosphere optical propagation, problems and trends 79−100947
atmosphere radar technique, for dynamic struct. of middle atmos. 80−105078
atmosphere S compounds, homogeneous chemistry 78−49119
atmosphere tides, theoretical work since 1970, review 80−94589
atmospheres of outer planets 77−5470
atmospheric ^{14}C fluctuations 79−5591
atmospheric acoustics 78−73493
atmospheric aerosol, laser beam propag., UV, visible and IR regions *(Russian)* 78−28313
atmospheric boundary layer simulation 80−51469
atmospheric chemistry: response to human influence 79−12206
atmospheric chemistry, recent advances 79−12204
atmospheric chemistry 78−81317
atmospheric dynamics on outer planets and their satellites 79−75125
atmospheric electricity, or static electrification hazard 78−28283
atmospheric gravity wave sources 80−26572
atmospheric noise propagation, review 77−84065

reviews continued
atmospheric O_3 obs. at Belsk, Poland and atm. physics research *(Polish)* 77−21825
atmospheric pollutants, gaseous, analytical control, review 80−101140
atmospheric pollution, nature and extent of unplanned releases from nuclear power stations 79−57530
atmospheric remote sensing 77−45202
atmospheric science experiments for Atmospheric, Magnetospheric and Plasmas in Space (AMPS) study 77−25802
atmospheric submillimetre wave spectroscopy 78−7796
atmospheric tides 77−86957
atmospheric trace constituents transfer past air-sea interface 79−62544
atom, KLL Auger spectrum, new developments, line energies, intensities 77−18868
atom+atom collisions at high energies 77−27150
atom+diatom, prior statistical distribs., collinear reactions 78−35670
atom+electron (positron), eikonal theory 78−25707
atom+molecule reaction dynamics, translational energy effect 80−76489
atom photoionisation, polarisation of photoelectrons 80−78584
atomic absorpt. spectrophotometry of noble metal bearing materials 78−85264
atomic absorption, bibliography, July-Dec. 1977 78−3403
atomic absorption bibliography, (July-Dec. 1977) 78−53276
atomic absorption bibliography (Jan.-June 1979) 80−31441
atomic absorption bibliography (July-Dec. 1978) 79−87888
atomic absorption spectroscopy, development in USSR, 1965-1975, science metrics investig. 78−61104
atomic absorption-chromatography analysis 77−60138
atomic and molecular fluoresc. as stratospheric species monitor 77−9472
atomic and molecular spectra, absorpt., emission, linebreadths 78−13448
atomic and molecular structure and collision data rel. to Tokamak impurity problem 80−43959
atomic beam and mol. beam scatt. from cryst. surfaces in quamtum regime 78−35244
atomic collision theory 78−1043
atomic collisions, experiments 79−81256
atomic collisions, in solids, rel. to vacuum system 80−54290
atomic double vacancy states, correl. photon and electron transition, perturbation theory 80−27968
atomic electron (positron) elastic (inelastic) scatt., 5-500 eV, perturbation treatments 77−30997
atomic electron affinity calculations 79−31439
atomic electron scattering, light atoms, intermediate energy 79−856
atomic electron scattering, matrix variational calc. 79−59577
atomic electron scattering, theoretical models 77−58166
atomic excited state collisional relax., line broadening, interat. interactions 80−43149
atomic fluorescence spectrophotometry 77−66780
atomic fluorescences spectroscopy, review of principles, instrumentation, methodologies, appls., teacher education appl. 78−69927
atomic inelastic collisions at low energies 77−30958
atomic inner shell ionisation by electron, positron and proton impact 77−19090
atomic inner shell ionisation by relativistic electrons and positrons 77−19091
atomic inner shell ionisation of electron capture decay 77−18882
atomic ionisation, inner-shell, heavy charged particles 78−42181
atomic non-Rydberg spectroscopy 78−90127
atomic photoionisation, selective, use in laser isotope separation and spectros. 80−83332
atomic processes for mag. fusion research 80−42851
atomic resonances, S-wave pot. scatt., coord. rot. method 80−28104
atomic RF spectroscopy, nonlinear and parametric effects 80−18816
atomic scattering, variational methods appls. 78−86951
atomic spectroscopy for chemical analysis 79−34381
atomic spectrum nonresonance perturbation in strong light field 77−46543
atomic structure and oscillator strengths 77−26959
atomic structure determination, experimental methods, review 79−68970
atomic transition probabilities (1914-1977) 78−74598
atomization 78−23642
atoms, AC Stark effect, multiphoton processes 77−71775
atoms, collective dynamics, hydrodynamic approach and many body approach based on RPA calcs. 80−47855
atoms, electron scattering, optical pot. methods 80−102569
atoms and molecules, autoionisation processes, and expt. methods 78−29763
atoms and molecules, scattering resonances 79−72384
atoms in high magnetic fields 77−50383
audiometers produced by Medicor Works 79−62384
audiometric thresholds, pure-time, relation to age, comparative anal. of data 79−5299
auditory evoked response, primary inhibited elements 80−94235
auditory mechanisms, lower brainstem, book contrib. 79−2084
auditory primary neurons, comparative physiology 80−94224
auditory-evoked response methodology in animals 80−46103
Auger electron spectroscopy, quantitative, problems and prospects 79−24395
Auger electron spectroscopy 79−92043
Auger microanalysis, high resolution 80−40792
Auger spectroscopy, directional effects *(French)* 80−47153
aural nonlinearity, two-tone 80−89768
aurora, results from DMSP photographs 77−13146
aurora, review of current knowledge 79−84564
aurora 78−77386
aurora of dayside cleft, and ionosphere effects 80−94633
aurora-generated gravity waves dynamic effects on midlatit. ionosphere 80−17438
auroral arcs and currents 80−77190
auroral electrons acceleration mechanisms 80−77210
auroral forms relationship with high latit. particle precip. 80−77189
auroral luminosity rel. to geomag. field changes 80−77187
auroral zone microburst precipitation phenomena 80−77208
austenitic weld testing *(German)* 78−53068
N.Australia Precambrian shields and platforms, struct. and tectonic style 80−3982
Auto-Resonant acceleration of ions, theoretical research program 80−5411
Auto-Resonant accelerator experimental program 80−5412
autocompression of plasma column, influence of external mag. axial field *(Rumanian)* 80−24148

reviews continued
autoguiders and acquisition systems for optical telescopes 80−82206
automated Earth resources surveys, Finland 79−100988
automated pattern recognition with hybrid optical/digital systems 78−63037
automatic speech recognition, advances in 1976-7 period 79−50536
automobile exhaust emission meas. and testing procedures, error statistics, survey *(German)* 77−73839
automobile propulsion using H_2 and electric power, comparative evaluation 80−16769
autoradiography, double radionuclide methods for tissue sections or cell smears, using light microscopy 77−5113
autowave processes in distributed kinetic systems 80−101721
axions 78−66183
axisymmetric elastic problems, stress function solns. *(Japanese)* 80−64371
axon, squid, Ca buffering, book contrib. 79−5267
axonal transport, components, mechanisms and specificity, book contrib. 79−96551
axoplasmic transport of proteins 80−21464
backscattered electron image in SEM 78−21304
backscattered electron imaging, SEM 80−86513
bag model of hadrons 79−75736
ball lightning, observations and theories 79−92577
ball lightning 78−88900
balsa wood, cryogenic insulation, exam. of strength specifications, props. 80−25819
Barnard's star, astrometric obs. 1916-1976, sexagintennial report 77−45432
baroclinic finite amplitude instabilities, book contrib. 80−19328
baryon-antibaryon nuclei 80−22709
baryonium, broad resonance states, S(1963), T(2190), U(2350), expt. evidence review 78−89764
baryonium, empirical evidence and theoretical interpretation review 80−42394
baryonium, review of QCD, duality, string models and bag models 78−78135
baryonium states in QCD, review 80−102001
batteries with gaseous electrodes, research and development, state of the art *(Czech)* 79−39292
Bauschinger effect, in metals, review 80−21025
BCC metals and alloys, glide and work hardening *(German)* 79−29089
BCC metals and alloys, glide and work hardening *(German)* 79−34067
BCC metals and alloys, review of plastic deformation and work hardening *(German)* 78−84946
Be stars, review 79−84809
Be stars, review of early history of studies 77−56965
Be stars, spectra and photometry 77−56966
beam diagnostic techniques for cyclotrons and beam lines 79−54731
beam-foil spectroscopy, characteristic features and comparison with other light sources, book contrib. 77−38746
beam-foil spectroscopy, lifetime meas. from decay curves, book contrib. 77−38747
beam-foil spectroscopy advances 80−9756
beam-foil spectroscopy experimental methods, book contrib. 77−38745
beam-foil spectroscopy of heavy ions 77−38643
beam-foil spectroscopy techniques 77−50563
beam-foil spectroscopy uses in atomic lifetime meas. 80−14248
bearing and frictional material, current state of prod. and development trends review 78−19902
benign thyroid disease treatment, ^{131}I appl. 80−36107
Benjamin Franklin, expts., theories and background 77−9845
benzenes, di- and mono-substituted, NMR spectral data, aromatic proton chemical shifts 77−79632
BESSY, a 800 MeV storage ring dedicated to synchrotron radiation 79−68021
beta-decay in labelled molecule, chem. and biological consequences 78−11541
beta-delayed particle emission A>70 77−22972
Bianchi cosmologies, singularities, Einstein eqn. solns. 80−12837
bibliography at. energy levels and spectra, (July 1971-June 1975) 77−71764
biliary tract disorders, evaluation by cholescintigraphy, ultrasonography and computerised tomography 80−17093
binary alloy, surface composition determ., review 79−90849
binary alloys, computer experiments on phase separation 79−43198
binary alloys, electrodeposition, recent developments 77−81233
binary stars, close, in globular clusters, preliminary report 80−109505
binary stars, freqs. on main sequence 80−26901
binary stars, main sequence, absolute dimens. determ., errors requirement review 80−109473
binary stars and cosmology 77−41393
binary X-ray sources, properties and models 77−41419
binary X-ray sources 77−17631
binocular models, characts. and design features, review 80−74468
bio-electromagnetic research 80−85444
biochemical systems stability anal., practical guide 78−73135
biochemistry and biophysics horizons, book 78−7315
biochemistry and biophysics horizons, book 78−68977
bioelectrochemistry and bioenergetics (book) 80−8749
bioenergetics and proton-electron systems of membranes, review 78−96030
biofuel large-scale prod. of ethanol and methanol from biomass 79−52864
biogeochemical cycles, role of atmosphere 79−79427
biological action of ion beams *(German)* 79−43968
biological applications of fluoresc. and fluoresc. probes 78−15932
biological effects and dosimetric data useful for RF safety standards development 80−67154
biological effects of EM radiation expt. techniques 80−8239
biological effects of EM waves, interdisciplinary and international contribs. 79−48288
biological effects of ionising radiation, current research in Canada 80−104683
biological fluid mechanics 78−35874
biological imaging by NMR *(Japanese)* 80−94312
biological macromolecules, 3D struct., electron microscopical anal. 80−35836
biological macromolecules, conformation studied by calorimetry 80−97870
biological materials, ion beam anal. in few MeV range 77−81768

reviews continued
biological molecules, X-ray absorption spectra, book contrib. 79−5436
biological rhythms and performance rhythms in animals, bibliography 77−48986
biological rhythms and performance rhythms in humans, role of light, bibliography 77−48985
biological sensors of Medicor Works 79−100769
biological specimen preparation for X-ray microanalysis 78−24214
biological specimen-conductivity problem in electron microscopy 78−24206
biological specimens, low-temp. TEM, radiation damage, review 78−57147
biological structures, X-ray and neutron small-angle scattering 79−11889
biological systems, network anal., review 80−30635
biological X-ray microanalysis 80−41349
biomagnetism, expt. investigations *(Croatian)* 79−53164
biomagnetism *(Slovak)* 78−88722
biomass system studies *(Japanese)* 80−26436
biomechanics, living tissue mechanical props., boundary value problems 77−70491
biomechanics, scope and recent trends *(Japanese)* 80−16984
biomechanics of human major articulating joints 80−56105
biomechanics of the human body, book contrib. 80−12176
biomedical applications of microprocessors 78−57095
biomedical electronic instrums. *(Japanese)* 77−56494
biomedical electronic thermometers 78−69235
biomedical electronics developments 77−13017
biomedical engineering, emerging field 80−36167
biomedical engineering, Nigeria, 3 years' practical experience 79−2147
biomedical engineering and materials for orthopaedic implants 80−76862
biomedical engineering education in Sweden and other Nordic countries 77−71169
biomedical engineering research, inc. physiology, NIGMS evaluation workshop recommendations 79−12018
biomedical engineering textbook for undergraduates 80−8750
biomedical equipment in Canadian hospitals, questionnaire answers 79−53263
biomedical equipment in some 50 years ago *(German)* 77−77994
biomedical image processing, state of art *(Japanese)* 80−56251
biomedical instrumentation elements, electrophysiology appl., book contrib. 80−12293
biomedical measurements and transducers *(Japanese)* 80−94393
biomedical tomography, equipment and reconstructive methods 80−30849
biomedical US for diagnostic medicine 79−79615
biomedical X-ray equipment, state of the art 80−81688
biomembrane, active transport, review 78−15814
biomembrane active transport of ions, elec. events 80−12068
biomembrane asymmetry 77−48768
biomembrane conductance fluctuations and ionic pores 77−90752
biomembrane excitability 78−15786
biomembrane mechanics and thermodynamics 80−45863
biomembrane mechanics and thermodynamics 80−51052
biomembrane phospholipid topological asymm. 77−90736
biomembrane properties, influence of solute environment 78−15789
biomembrane structure 77−32878
biomembrane ultrastructure rel. to function. 78−15785
biomembranes, bioenergetics and proton-electron systems 79−57596
biomembranes, dynamic aspects 78−69005
biomembranes and energy control 78−15807
biomolecules, Fe-containing, appl. of spectroscopy 79−24956
biomolecules asymmetry correl. with parity violating weak interaction 78−69000
biophysics, bioengineering, annual review, book 79−5246
biophysics and bioengineering, book 80−17723
biophysics and bioengineering, book 80−105437
biophysics and bioengineering review, book 77−86433
biophysics of photosynthesis 78−92605
biopolymer chains, intramol. reacts., enzyme catalysis appl., review 80−40953
biopolymers, assoc.-dissoc. phenomena, review 79−11884
biopolymers, circular dichroism, optical rotatory dispersion, conformational anal., review 77−3497
biopolymers, studied by circular dichroism and optical rot. 78−44457
biotelemetry, literature survey 78−80996
bipolar spatial filtering, incoherent, review 80−102822
bistable optical devices: an overview 80−58625
BL Lacertae objects, characts. and relation to QSOs and normal galaxies 78−89259
black foam films stability 80−104463
black hole quantum processes 77−17614
black holes, thermodynamics 78−93301
black holes and work of Hawking 78−8042
blast furnace reactions 78−85116
blind persons' aids 77−29227
Bloch electrons in mag. field, energy spectrum, struct. of Landau levels 80−54623
blood flow measurement, future appls. and prospects 77−78010
blood gas analysers, review 78−69238
blood pressure, indirect meas. method 80−94383
blood pressure instruments, direct systolic/diastolic meas., review 78−69234
blood pressure instruments, noninvasive arterial meas. using US Doppler effect 78−69167
blood synthetic substitutes 79−62405
blood vessel rheological props. and haemodynamic parameters meas. *(French)* 79−66587
blood volume regulation, effects of space flight, review 80−3826
BNL National Synchrotron Light Source, 2.5 GeV X-ray ring, design status 79−68023
bodies with initial stresses, elastic wave propag., review 80−38323
boiling, under increased gravitation, heat exchange mechanism, bubble form. 77−46895
boiling crisis, nuclear reactor safety and performance, state of the art review 80−63312
bone imaging in infants and children 78−77107
bone morphology and fracture, exam. 78−57036
book, axiomatic QFT, PCT, spin and statistics 78−78102
Bordoni relaxation models, internal friction and microdeformation rel. to dislocations *(French)* 79−37758

reviews continued
Borel transform and the renormalization group 79−26238
boride coatings, technology, props., book contrib. 78−48574
borides, electronic struct., review, book contrib. 78−47700
borides, hexa- and di-, electronic structs., elec. props., book contrib. 78−47701
borides, hexa- and tetra-, prep., struct., elec., mag. props., book contrib. 78−47303
borides, nature of chem. bond, book contrib. 78−47276
borides, ternary, struct. classification, props., book contrib. 78−47309
borides, transition metal, rare earth, and actinide, mag. props., book contrib. 78−47978
Borrmann-like anomalous effects in volume holography 80−102664
Bose system, Jastrow wavefunction, hypernetted chain method 80−17866
Bose-Einstein ideal gas, review 77−87692
bound excitons in semiconductors, book contrib. 80−44519
boundary layer theory, history, book contrib. 77−46992
boundary layers, unsteady, separated and attached 78−71313
boundary value problems, numerical soln. through integral eqns., review 78−81808
bow shock ion acceleration, upstream region obs. 80−31168
brain, anatomic and pathologic correls. in computerised tomography 79−34636
brain, computerised tomography, neurodiagnostic studies and head injury management 79−39470
brain tissue, microwave fixation, neurochemical technique 78−20323
breakdown phenomena in short-point-plane electrode systems, critical survey 79−4206
breast cancer induction in humans by ionising radiation 78−61217
breast cancer screening by thermography, progress and prospects 77−48915
breast carcinoma, radiation therapy as primary treatment *(Dutch)* 80−17078
breast examination methods including radiography, thermography and cytology 78−3656
Bremmer, H., scientific work 79−62984
bright plating, from zincate electrolytes, progress 80−66442
British Isles, systematic rainfall recording since 1677, tercentenary 78−44950
British optical astronomy, advances 78−69844
brittle fracture 80−29116
brittle fracture mech., review *(Russian)* 79−34139
brittle solids, shock deform., theory 80−72493
bromides and mixtures, molten, elec. cond., density, viscosity, surface tension 77−80638
bronchogenic cancer, small cell, undifferentiated, role of radiation therapy in treatment 80−67226
brontides, natural atmospheric explosive noise 80−12523
brush border of renal proximal tubule and intestinal mucosa, review 78−15815
brush plating, for wear resist. appls. 80−66443
bubble chambers, limitations and recent developments in design 77−14313
bubble counting, acoustic techniques 77−42673
bubble dynamics and cavitation, book contrib. 77−47050
bubble nucleation, theoretical experimental 79−41734
bubbles, gas and vapour, dynamics 79−98788
buckling of plate and shell structures 77−72200
building acoustics in America (1920-1940) 77−45663
buildings, service systems noise 77−34997
BWR power stations, operating record and reliability 79−22403
CAMAC system and microprocessors in physical instrum. 79−26041
camera automatic focusing mechanism principles and designs 79−30595
Canada contemporary crustal movements 80−8273
Canadian biomedical engineering research for handicapped persons 79−29662
Canadian continental margins, evolution and geophys. features 80−8274
cancer, appls. of EPR and NMR 78−69173
cancer treatment by hyperthermia *(French)* 80−17024
cancers, genetic defects, resulting from use of various energy sources 79−16259
CANDU-PHW reactors, primary and secondary water chemistry 79−22382
capacitance transient spectroscopy, book contrib. 78−10548
capillary gas chromatography 78−44412
capillary phenomena for fluid/fluid interfaces 80−70506
carbide fuels, vibro-compacted, initial stages of sintering and hot-pressing 80−16254
carbonaceous chondrite origin and classification 80−56781
carbonaceous chondritic matrix material planet forming unit, occurrence, formation review 78−53892
carciac nuclear medicine, left ventricular edges detect. methods 80−98132
cardiac arrhythmia monitors, review 78−69233
cardiac arrhythmias in ambulatory persons, review of 1000 ECG recordings 80−36184
cardiac event sequence following mental loading, spectral anal. 79−29516
cardiac fibrillation thresholds for 60 Hz currents and voltages directly applied to heart 80−101301
cardiac function and anatomy evaluation, complementary role of echocardiography and radionuclide imaging, book contrib. 80−101241
cardiac muscle, excitation-contraction coupling 79−96547
cardiac nuclear medicine instrumentation, book contrib. 80−101260
cardiac output analysers, equipment, maintenance and ccts., review 78−69239
cardiac pacemaker principles, specifications and testing, review 78−69258
cardiac shunt detection with the short-lived radioactive gases 80−94357
cardiac US and nuclear medicine, complementary roles 80−98051
cardiac valves, role in artificial heart performance 80−21575
cardiology, development progress 78−3646
cardiovascular dynamics instrumentation evolution (1940-80) 79−83983
cardiovascular nuclear medicine, an overview 80−85480
cardiovascular shunts, detection and quantitation with commonly available radioisotopes 80−94356
CARS, review 79−16051
cast iron development 78−48347
cataclysmic variables, structure 77−26018
catalysis, heterogeneous, role of surface science expts. 78−15710
catalysis and surface science 80−40740

reviews continued
catalysis research, heterogeneous IR spectroscopy appl. *(German)* 78−53256
catalyst, mag. characterisation 78−64881
catalyst surface characterisation by cyclic voltammetry 78−40092
catastrophe theory and its application *(Chinese)* 79−35534
catastrophic earthquakes in Iceland 79−84175
catastrophic earthquakes occurrence and distrib. in Europe 79−88262
cathode spot of a vacuum arc 80−24290
cavitation, acoustic field generated 80−74934
cavitation, entrainment and thermodynamic effect, viscous effects 79−10598
cavitation inception in liquids 80−38465
cavity nucleation, by plastic deform. 79−29127
CDW, impurity effects, saddle-point model 77−51678
CDW instabilities, incommensurate struct. phase transitions, neutron scatt. study 79−51231
celestial masers physics, review 79−21455
cell, membrane permeability, review 78−15813
cell adhesion 78−15803
cell binding, role of surface carbohydrates 78−15804
cell growth in vitro, rel. to cell surface 78−15808
cell membrane organisation dynamics, book contrib. 80−30687
cell membranes, effects of hydrostatic pressure, review 78−15790
cell membranes, ionising and UV radiation effects, review 78−15875
cell sorting, automated, with flow systems, book contrib. 79−5435
cell surface immunoglobulins, characts., mobility and role in immune phenomena 78−15806
cell voltage measurement using voltage sensitive dyes 79−57833
cellular precipitation features in supersaturated solid solns. *(Russian)* 80−84937
cellular receptor-mediated endocytosis and coated pits, coated vesicles 79−74611
cemented carbides, fracture toughness testing 80−104410
cemented carbides, physical and chem. nature 80−76265
cements and concretes, physics and chemistry 78−73013
Central Aerological Observatory, USSR, historical review 77−70798
central catecholamine neuron systems, anatomy, physiology of dopamine systems, book contrib. 79−2042
central nervous system, magnetic phenomena, book contrib. 79−5304
ceramic and glass prep. from metal-containing organic cpds. 77−55922
ceramic crystalline materials, IR transmission, review 78−55417
ceramic fission reactor fuels, fabrication and performance, review 78−58392
ceramic fuels, vibro-compacted, initial stages of sintering and hot-pressing 80−16254
ceramic material fracture mechanics 80−45373
ceramic nuclear fuels, high temperature chemistry 77−14238
ceramic phase diagrams, exam. of compilation activities 79−8287
ceramic powder pressing review 79−47652
ceramic utilization in fission reactors 79−93718
ceramic-metal seal technology, history and trends 78−81992
ceramics, applications in fusion system, neutron effects 80−32473
ceramics, crack extension micromechanisms 80−108567
ceramics, high performance 77−8785
ceramics, high resoln. diffr. and imaging characterisation 80−104050
ceramics, microstructure dependence of mechanical behaviour 78−88533
ceramics, oxide, TEM study of deform. 79−87686
ceramics, slip moulding method development 78−68661
ceramics, structural, state-of-art review and survey of R&D techniques 77−63605
ceramics, TEM study of radiation damage 79−86816
ceramics, thermal stress and thermal shock, review of test methods, thermal stress theory industrial problems 77−63805
ceramics, thermal stress resistance, figures of merit, review 79−83290
ceramics, transformation toughening, martensitic transforms. in crack-tip stress fields 80−104154
ceramics, utilization in nuclear industry, current status and future trends 79−45349
ceramics utilization in nuclear industry 80−32350
cerebral regional blood flow meas. with ^{133}Xe, functional landscapes in brain 78−85356
cerebrovascular disorders, computerised tomographic diagnosis 79−34638
CERN, 25 years of physics, review 80−82626
CERN's 400 GeV super proton synchrotron, design and construction 79−68064
CERN 400 GeV super proton synchrotron *(Dutch)* 77−46432
CERN ISR, facility and hadron physics program 80−873
CERN SPS, review of performance and operation reliability 79−72048
CERN-Columbia-Rockefeller-Saclay expt., electron prod. in pp collisions 77−263
cervical carcinoma, para-aortic irrad. 80−72307
cervix carcinoma, extended field technique complications, correl. of radiation and surgical parameters 80−67225
UV Ceti flare stars *(Russian)* 78−28685
chalcogenide amorphous semiconductors, ESR studies of doped Mn, review *(Japanese)* 77−90019
chalcogenide film, threshold switching mechanism, review 78−76122
chalcogenide glass, optical transitions and electronic struct. 77−76741
chalcogenide semiconductors and SiO_2, similarities and differences 78−6721
chalcogenide vitreous semiconductors, reversible photoinduced changes in optical, physicochem. and contact props. 79−24378
chalcopyrite compounds, ternary, review 79−70048
Chamberlin-Moulton cosmogony, rise and fall 78−32641
channelling 78−2184
channelling backscattering use for radiation damage studies *(Japanese)* 77−72640
channeltrons and channel plates, influence of radiations 77−26933
chaotic motion theories with appl. to controlled fusion research 78−93605
chaotic phenomena and statistical physics, review of the contributions made by J. Schwinger 79−63135
charge exchange lifetimes for ring current ions 79−25409
charge transfer ionisation reactions 77−60053
charged cosmic ray particles, fiftieth anniversary of discovery, review 79−2448
charged magnetic domains, formation, existence, dynamics, collective props. 78−23310
charged particle beams, hyperfine interactions, experimental methods *(Russian)* 79−13884
reviews continued
charged particle counters in the pre-modern period, historical perspective 79−72190
charm and heavy lepton production by e^+-e^- interactions, recent results 79−26337
charmed particle, lifetime estimates, free quark model anal. 79−67544
charmonium and QCD 78−82157
chart recorders, technology improvements 79−88933
chemical analysis by activation methods, medical appls., book contrib. 80−11995
chemical bonding in crystals, modern theories 78−2064
chemical etching of Si, Ge, GaAs, GaP 78−95832
chemical fast kinetics studied by NMR 80−55662
chemical formulae, historical development, review 78−73822
chemical ionisation mass spectrometry, survey of instrumental techniques 79−57313
chemical laser, classical dynamics of bimol. reactions, book contrib. 77−10909
chemical laser kinetics of HF, HCl and DF systems, book contrib. 77−10903
chemical laser numerical modelling, book contrib. 77−10908
chemical laser systems, ion-molecule reactions, thermal energy, book contrib. 77−50668
chemical lasers, CW H halide system, book contrib. 77−10904
chemical lasers, introduction, book contrib. 77−10902
chemical lasers, recent progress *(Japanese)* 77−38876
chemical lasers oscillating on rot., vibr. and electronic transitions 80−102716
chemical microscopy, review of literature 1976-1977 78−85221
chemical physics of solids and their surfaces, book 80−82587
chemical reactions, IR laser-induced *(Japanese)* 79−39176
chemical releases in the ionosphere 79−101049
chemical research, appl. of physical instrumentation and computers 79−70295
chemical tracer expts. on atm. precip. systems 78−24324
chemical transfer lasers, DF-CO_2 system, book contrib. 77−10907
chemisorbed atoms, indirect interaction, theory 79−46923
chemisorbed gases, replacement phenomena on metal surfaces *(Japanese)* 77−72779
chemisorption, island form., adatom interactions 79−46922
chemisorption, on metals, theoretical models *(Russian)* 78−84071
chemisorption on d-band metals, book contrib. 80−107649
chemisorption on metal films, use of external mag. field 78−72003
chemisorption on metals, historical review 79−46920
chemisorption on semiconductor surfaces, book contrib. 80−107648
chemistry, computers, and microelectronics: present and future prospects 80−55627
chemistry, status and trends 78−76864
chemistry CAI, at Syracuse Univ. 77−23
chemistry teaching, courses, laboratories, for nonscientists, bibliography, 1968-1977 79−84881
chest radiology, introduction to physiological aspects 79−25071
Chevrel phase compounds, bonding and phys. props. rel. to struct., book contrib. 80−49209
children who wear individual hearing aids in British Columbia, Canada 80−41326
chiral symmetry and pion condensation, review book contrib. 80−437
cholesteric liquid crystals, optical properties, diffraction nature 80−70123
chromatic adaptation 78−53403
chromatin, DNA-protein complexes, electron microscope visualisation, book contrib. 79−5434
chromatin research 79−79464
chromatography, aqueous gel permeation 77−36824
chromatography, reversed liq. phase, biochem. application, review 79−34371
chromatostereopsis, 28 annotated references covering 166 years 79−5290
chromosome identification, mammals, banding technique developments 77−56561
cine camera supply, control and synchronisation systems *(Russian)* 78−49936
cinematography, colour film processes and cameras, review, 1894 to date *(German)* 78−93773
cinematography review of technical progress in 1977 in USSR *(Russian)* 78−89579
circadian clocks, mathematical models 79−34470
CIRENE reactor power channel, fuel string dynamics and pressure tube fretting corrosion 79−30950
classical and dwarf novae, energy sources and systematics 79−67041
classical crystal optics, lattice dynamical background 80−97221
classical eqns. exact cylindrically symmetric solns. from compact Lie groups *(Russian)* 80−42317
classical fluid structure, Monte Carlo simulations, review, book contrib. 79−82140
classical fluids, graph theoretic techniques 78−71662
classical mechanics, invariants, stability, KAM theorem 78−41
clean metal surface physics 77−15659
climate change, anthropogenic effects 78−28293
climate modelling using radiative-convective models 79−74954
climate predictability 79−16645
climate variability, effects of volcanoes, pollution and CO_2 78−28292
climate variation throughout Earth's history, causal mechanisms 80−82048
climatic change and global air pollution 77−13120
climatic change on terrestrial planets 79−53742
climatic evolution *(German)* 78−20503
climatic variability, space and time scales 77−64413
climatic variability and causal mechanisms 77−64414
climatology, forecasting, review of major causative factors, economic and ecological effects *(French)* 79−48564
clinical decision support systems, automated medical signal anal. 79−34685
clinical engineering, USA nationwide survey of present use in hospitals 80−36177
close binary systems, starlight scatt. on gaseous extrastellar material 80−109471
closed duplex DNA, struct., reactions, book contrib. 79−5248
closed-line magnetic field approach to plasma confinement, in toroidal systems 78−42792
cloud and bubble tube detectors *(Chinese)* 80−52830
cloud electric fields measuring instruments 77−41226

reviews continued
cloud seeding with AgI *(French)* 77−78343
clouds, electrical charges fate in evaporating droplets 79−48559
cluster expansion in statistical mechanics, S-matrix formulation *(German)* 78−41256
cluster ions, formation and reactions, SIFT study 80−58435
cluster ions in gases 77−81401
cluster model, concepts and appls. 79−357
cluster model, vibronically coupled systems 79−19540
clustering aspects of nuclear struct. and nuclear forces, review 79−80887
clustering aspects of nuclear structure and nuclear reactions 79−3100
clusters of galaxies 77−64862
coal, polished section prep., structural anal. 79−15924
coal conversion plant material, corrosion and wear 78−53012
coal fired power stations, review of conventional and advanced systems 80−35625
coal hydrogasification by nuclear steam reforming of methane 80−30325
coastal circulation and wind-induced currents, review, book contrib. 80−98357
coastal current observations 79−100868
coating techniques, for SEM and X-ray microanalysis 79−12783
coatings, methods and instruments for measuring thickness 78−73000
coatings for fusion reactor environment 80−18618
coatings for wear and lubrication 79−19494
cochlear micromechanics and anatomy, review 80−76750
cochlear models−1978 80−94221
coded aperture imaging, review 80−101914
coherence and radiation laws 77−23612
coherence effects in neutron diffraction and gravity experiments 79−58616
coherence implications for laser appls. 77−75599
coherent anti-Stokes Raman spectroscopy, book contrib. 78−22177
coherent anti-Stokes Raman spectroscopy 77−71378
coherent anti-Stokes Raman spectroscopy of gases 79−27322
coherent antiStokes Raman spectroscopy 80−22443
coherent optical correlation techniques 80−43277
coherent optical spectroscopy 78−1112
coherent radio emission from pulsars 80−46596
coherent radio emission in nature, theory, solar system and pulsars appl. 80−46393
coherent Raman spectroscopy techniques 80−22440
collagen molecular organisation and connective tissues props. 80−97858
collective acceleration of heavy ions, problems and prospects 80−14013
collective accelerators, current status 79−76161
collective accelerators, review of current status 80−5394
collective coordinates with non trivial dynamics 79−26232
collective excitations, brief review of expt. and theory 77−1381
collective modes in classical monoatomic liqs., coherent neutron scatt., book contrib. 77−89371
collective props. of nuclei deduced from electron scatt., deformed nuclei, review 78−50064
collective radio-emission from plasmas 80−46392
collinear and random mag. structures, review 78−68173
collision processes, at. and mol., angular correlations, summary of review papers 80−63757
collision processes, classical theory 78−33563
collisional activation mass spectra 80−48106
collisions, at. and mol. in presence of strong radiation fields 80−63801
colloidal dispersion dynamics 80−71956
colloidal plasmas in space: some aspects of condensation and growth of solids 79−41795
color geometrodynamics, eightfold way 80−95243
colour centre physics, last fifty years 80−105487
colour degrees of freedom in hadron physics *(Russian)* 78−16979
colour filter, electrically controlled liquid crystal, state of the art 78−83113
colour matching, review of basic laws and progress during the last 15 years 78−65955
colour measuring instruments 78−93747
colour model of hadrons, SU(6), review 77−82702
colour reproduction by photography 78−309
colour vision opponent processes, psychophysical and electrophysiological studies 78−53402
colour vision recent studies *(Japanese)* 80−12127
combined heat transfer, state of the art review 80−79119
comets, physical processes 77−25985
comets, theories and observations 78−69753
comets in 1974, observations, discoveries and recoveries 78−73682
comets in 1975, observations, discoveries and recoveries 78−73683
community shelters for protection from radioactive fallout 80−5338
compact galaxy, review 80−17668
compact groups of compact galaxies 77−37656
compact H II regions, review of radio obs. 78−16507
compaction, of metal powders 80−40279
compartmental system analysis: state of the art 80−35815
complex molecules, reson. Raman spectra, vibr. scatt. 78−37644
compliance, review and extension of information for common crack growth specimens 79−3974
component containing cracks, critical review of creep 78−63321
component development, mag. systems and plasma engineering, programs status 80−99299
components for optical communication systems, review 80−87539
composite friction and bearing materials, development, friction and wear theory, review 80−60979
composite growth by eutectoid or solid-state decomposition 78−44056
composite material, fracture and fatigue, review 78−68781
composite material strength *(Japanese)* 78−39850
composite materials, mech. props., theory, review 80−64392
composite materials, optical props. 78−56496
composite materials, phys. props. 77−4720
composite materials, reliability, exam. of mech. strengths and fatigue charcts., review 80−11762
composite materials, unidirectional, three-dimens. fracture 80−64471
composite materials elastic props. 77−42746
composites, dynamic anal., review and computer programmes 77−50946
compositional depth profiling by Auger electron spectroscopy 79−52053
compound nucleus theory, recent developments, review, book contrib. 80−68636
compound semiconductor, heteroepitaxial growth and characterisation, book contrib. 79−83133
compressibility of liquids, temp. depend., eqn. 79−90710
reviews continued
compressible turbulent shear layers, book contrib. 77−47034
computation nets, significance in increasing efficiency of geologo-geophysical research 79−96835
computer applications in biomedical engineering *(Japanese)* 80−12289
computer applications in organic struct. chem. and mol. spectroscopy in USSR 78−88624
computer coupling of phase diagrams and thermochemistry 77−77460
computer development 80−4503
computer films for research 79−21512
computer generated holography 80−9827
computer industry, review of wear problems 79−20210
computer models of magnetically confined plasmas, review 77−11388
computer optics, optical system design 79−94322
computer simulation on molten ionic salts 79−19130
computer-generated holograms, techniques and appls., book contrib. 79−76645
computerised axial tomography, transmission and emission techniques 77−77973
computerised clinical EEG in perspective 79−70655
computerised tomographic scanning, engineering status 77−73571
computerised tomography, brain and body imaging 79−34659
computerised tomography, definition and scientific basis, health care needs, appls. and costs 80−36115
computerised tomography, display requirements 77−81571
computerised tomography, image documentation 79−62338
computerised tomography, introduction and review of state of the art *(German)* 80−101251
computerised tomography, quantitative, progress toward 80−81696
computerised tomography, review and comparison with classical X-ray diagnostic technique *(German)* 80−67239
computerised tomography, scanners, status in 1979 79−66536
computerised tomography, single photon emission, current status 79−66526
computerised tomography, single photon emission 80−81698
computerised tomography scanning, review of technical aspects 79−34635
computerised tomography scanning evaluation, cost containment 80−36117
computerized tomography in radiation therapy 79−20660
computing methods for recirculating flows 79−10565
comsat revolution, historical review 77−87239
concave diffr. grating, astigmatism compensation, comparative charcts. 79−32067
conceptual foundations of the unified theory of weak and electromagnetic interactions 80−95237
concrete, unbonded, prestressed, review *(Japanese)* 78−6884
condensed media, vibrational relaxation studied by picosecond or Raman spectros. 80−80797
conformal invariance in elementary particle physics *(Russian)* 79−21964
conformal invariant quantum field theory 78−86420
constituent quarks in SU(3) and SU(6), current algebra., hadron decays, book contrib. 80−47259
constituent rearrangement model and hadron reactions 79−26294
constructional materials, brittle failure resistance, calc. charcts., expt. methods 77−77662
constructional materials, use of J-integral method for assessing fracture toughness *(Russian)* 79−24602
contact electrification of dielectric solids 78−26934
contactless resistivity measurements 80−37054
contemporary acoustics, brief review *(Chinese)* 79−37069
contemporary climate changes, natural and anthropogenic factors 79−34938
contemporary frontiers in physics 79−40310
continental drift debate, historical aspects 77−29277
continental drift mechanisms 78−92813
continental tectonics and seismicity, review 79−44160
continuity eqn. numerical soln. 77−26153
continuous drawing of liquids to form fibers, review, book contrib. 80−97444
continuous flow cryostats, design and application 79−21759
continuum mechanics and field theory, role of Thomson and Maxwell 79−17179
controlled nuclear fusion, progress and problems 79−36415
controlled nuclear fusion 77−42182
convection in stars 78−69785
convective heat transfer enhancement 79−1196
convective instability, review 77−84226
convective mass transfer measurement methods *(German)* 78−46959
cool stars, mass loss *(German)* 79−16957
cooling tower meteorological effects *(German)* 77−73800
copolymer micelles in solution, review 77−21424
corona discharge applications 80−33849
corona discharge industrial applications, qualitative analysis *(Rumanian)* 80−70061
corona in atmosphere 78−26363
coronary arteriography, current techniques and equipment 78−35940
corpuscular diagnostic method of metastable atoms in glow discharge plasma *(Czech)* 80−24241
corrosion, materials science and technology problems, present situation in Japan *(Japanese)* 77−28918
corrosion and control, (1978) *(Japanese)* 79−34174
corrosion fatigue 77−4151
corrosion monitoring review 78−68849
corrosion monitoring survey 79−24684
corrosion science, surface analytic techniques 80−31929
corrosion science, use of XPS 78−15586
corrosion science and control *(Japanese)* 80−45408
corrosion studies, electrochemical methods, appl. and limitations *(Japanese)* 80−45465
cortical visual evoked potential, normal humans, bibliography of research 79−5278
corundum, grinding material, review *(Polish)* 80−29917
cosmic dust 78−16516
cosmic dust grains, observed IR props. 80−26943
cosmic dust in planetary nebulae, observational data 80−109535
cosmic dust in planetary nebulae 80−109536
cosmic gamma radiation, detection and sources 78−12059
cosmic gamma ray spectroscopy 80−67582
cosmic ray 11-year solar modulation cycle 77−13196

reviews continued
cosmic ray deuterons and antiprotons production mechanisms 79−29955
cosmic ray isotopic composition 78−20599
cosmic ray kinetics in space 77−91382
cosmic ray muon charge ratio, sea level, phenomenological model 80−67487
cosmic ray origin, recent experimental work 77−56799
cosmic ray research programme at Blackett Lab., Imperial College 79−66890
cosmic rays, high energy, obs. during August (1972) 77−25894
cosmic rays, low energy, Skylab meas. review 80−56689
cosmic rays nature and origin *(Russian)* 78−73590
cosmic rays propagation and distribution in Galaxy 78−69621
cosmic X-ray sources, review of current knowledge in 0.5 to 10 keV range 78−69915
cosmogony, origin of planetesimal theory 77−87623
Cosmology, astrophysics and elementary particle physics 80−51935
cosmology, big bang model and cosmic black body radiation 77−9830
cosmology, general relativity, big bang model, nucleosynthesis, scale covariant theory 78−73789
cosmology, rivals to big bang model 78−57705
cosmology 77−53715
cosmology and elementary particle physics 79−101061
Cosmos artificial satellites, appls. 78−69650
Couette flow, spherical, in thick layer, with revolving inner sphere, stability 79−81969
Coulomb displacement energies of analogue states in mirror nuclei, review 78−78242
Coulomb systems, statistical mechanics 80−52119
Coulomb two-centre problem in quantum mechanics *(Russian)* 77−30056
coulometric analysers with controlled potential, review 79−39244
coulostatic impulse technique 78−73048
coupling methods in single mode fibre integrated optics systems 78−59162
covalent semiconductors, electronic struct. of localised defects 80−44535
CP violation and K^0 decays 77−57532
Crab Nebula radio struct. 79−75257
crack arrest, concepts, appl., review 79−41621
crack depth measurement, ultrasonic techniques 78−95903
crack growth, anal., crack tip deform. modelling 79−41626
crack growth at high-temp., fracture mech. appl., review 79−41628
crack propagation, fracture of practical materials, anal., recent developments, review 79−43428
crack resistance in materials under long term static loading, evaluation methods 80−45461
cranial CT, valve and limitations in spreading process diagnosis *(German)* 80−36105
craniocerebral computer tomography in the neonate 79−34640
creep, irradiation induced, correlation of theory with expt. evidence 80−88255
creep damage and rupture, metallurgical and phenomenological approaches 79−20127
creep fracture 77−8944
creep of metals and plastics under combined stresses. A review 80−59567
creep rupture data analysis, development of correlation and extrapolation methods 80−58975
Cretaceous pelagic carbonate rocks, mag. stratigraphy obs. review 80−104876
critical consts. of elements and refractories with high crit. temp. 78−59931
critical dynamics, real-space renormalisation group approach, Migdal approx. 80−27257
critical magnetic behaviour and crossover phenomena, renormalisation group arguments 77−66324
critical mineral resources 79−5482
critical phenomena 77−24699
critical phenomena at low temperature 80−73297
critical point drying theory, practice and artifacts 78−24211
critical two-phase flow, bubble nuclei 80−64615
CRO design using modular system 78−93671
CROs with GHz bandpass for general purpose use 79−88936
CRT oscilloscopes, types and props. *(Swedish)* 78−62189
CRT photography, self developing film utilisation, applications 79−58811
crustacean taste analyzers, direction of bionic research *(Russian)* 79−43937
crustal stress state 79−5465
cryo-ultramicrotomy and myofibrillar fine struct. 78−53592
cryobiology, freezing and cryofixation 78−28136
cryobiology, struct. and functional aspects of freezing techniques 78−28137
cryogenic calorimetry 79−40573
cryogenic structural materials 77−17989
cryogenic targets for streamer chambers and cryofluid target supply *(Russian)* 78−13381
cryogenics, a critical review 78−89485
cryogenics, and applications *(French)* 77−53920
cryogenics 79−208
crystal, structural defects, effect on dynamical scatt. of X-rays *(Russian)* 79−64960
crystal assessment by X-ray topography using synchrotron radiation 77−84586
crystal defects *(Chinese)* 79−69100
crystal defects in integrated circuits, review 78−88547
crystal growth, conference, New Hampshire, USA (July 1977) 80−57008
crystal growth, Czochralski and related methods, diameter control 78−31328
crystal growth, from liquids at high temps. 79−15602
crystal growth, from soln., implication for industrial crystn. 80−49147
crystal growth, in pure and impure systems 80−49145
crystal growth, instabilities and pattern formation 80−35064
crystal growth, Monte Carlo simulation, book contrib. 79−80532
crystal growth, of sparingly soluble single crysts. from soluble complexes 80−29868
crystal growth and graphitization 80−89165
crystal growth and phase diagrams 80−66407
crystal growth by solid state techniques 77−85935
crystal growth from melt, history *(Japanese)* 79−4915

reviews continued
crystal growth from soln., hydrodynamic environment effects *(French)* 80−29872
crystal growth from vapour, kinetics, impurity capture 78−26468
crystal growth mechanism for glass forming systems 78−30555
crystal habit, modifications control in growth 80−49150
crystal morphology, controlling factors *(Japanese)* 77−55256
crystal nucleation and growth at surfaces, kinetic studies 78−72046
crystal optics, review of Ewald's papers from 1912 to 1968 79−23479
crystal plasticity, analytical development review *(Japanese)* 79−60424
crystal plasticity, surface effects 77−47505
crystal structure, diffr. methods 79−94932
crystal tuning fork development and biography of Jurgen Staudte *(German)* 79−30182
crystal-size distribution, population models, review 80−49153
crystalline materials, struct. of grain boundaries using diffr. techniques 80−59478
crystalline solids, electronic industry, chem. anal. instrumental methods progress 80−66903
crystallisation, technical, modern trends, computer modelling 80−66406
crystallisation kinetics, book contrib. 77−39550
crystallization and decomposition of amorphous semiconductors 79−41959
crystals of magnetic flux 79−99664
cubic metals, impurity-host force-constant changes, from Mossbauer data 78−48097
cubic semiconductors, bulk hot-electron props., review 79−99553
current algebra and electromagnetic hadron interactions, book contrib. 80−47240
current GaAs laser research 80−83613
CVD 77−63561
CVD films for interlayer dielectrics 80−45235
CVD technology, appl. to semiconductor industry 80−66431
cyclic strain diagrams recording under nonisothermal conditions, review 80−71830
cyclonic storms, mesoscale and microscale organization and struct. of clouds and precip. 79−74946
cyclotron radiation from magnetically confined plasmas 80−38722
cyclotron resonance in solids and plasmas and interband spectroscopy of semiconductors and semimetals 79−61224
V1500 Cygni (Nova 1975), review of development *(French)* 80−17598
Cygnus X-1, black hole candidate, review 78−16577
cytoplasmic membranes in somatic cell interaction and hybridisation, review 78−15792
cytoplasmic streaming, in green plants, book contrib. 79−5265
cytoplasmic streaming in amoeboid movement, book contrib. 79−5264
D-region, equatorial, ionisation processes and ion comps. review 78−36362
D-region, obs. and chem., recent advances 79−8751
D-region of ionosphere 78−77392
D-region winter anomaly, recent advances 80−17437
D-region winter anomaly, review of Western European study campaign (1975/76) 78−45122
damage analysis under nonproportional cycling 80−97556
damage parameter in continual fracture mechanics review *(Polish)* 79−32382
damped-heavy-ion collisions, book contrib. 78−82388
Danjon astrolabe planetary obs. *(French)* 80−94715
dark nebulae and globules, star form. regions 78−12347
data acquisition system assembly for pulsed fusion experiments 80−49011
data extraction from film using optical and/or digital and/or electronic devices 78−63024
data processing developments in remote sensing *(Japanese)* 78−7801
DC plasma arc, for elemental anal. 77−73478
decorated lattice gas model of critical phenomena in fluids and fluid mixtures 78−36944
deep centres in III-V compounds 79−11086
deep impurities in semiconductor, book contrib. 78−10403
deep inelastic scatt., field theoretical description, QCD, quark-parton, and light cone algebra *(Russian)* 80−42388
deep inelastic transfer reactions, between complex nuclei 78−74400
deep water waves, instabilities, review, book contrib. 80−96274
defect characterisation by mag. leakage fields 78−3296
defect clusters, in particle-irradiated crysts., TEM identification 79−69108
defect state microscopy 79−94856
defect surface structures, LEED studies 77−80685
defect theory and processes, review 80−2009
defects in mats., direct observation and characterisation 78−88617
defects in solids, influence on props. 77−7709
defibrillators, review of instruments and maintenance 78−69251
deformation of A15 compounds 78−39864
degenerate electron gas in Na_xWO_3 and heavily-doped Si:P 77−20242
denatured fuel cycles for international safeguards 79−41011
dense optically transparent media, third-order optical susceptibilities 77−38981
densitometry, review of new approaches 78−307
density functional theory of metallic surfaces 80−44698
density wave theory 80−67873
dental materials, uses and props. 78−53548
dental radiological safety, pilot survey 79−43993
dentistry, adhesion 79−20715
dentistry, problems with polymers 79−83434
depolarised Rayleigh scattering from liquids 77−40256
derivative spectrophotometry, theory and appls. *(Japanese)* 80−86451
detection of flaws in metal of atomic power plants, testing whilst in operation 78−17343
deuterons, D-state probability, review of spin, binding energy, magnetic and quadrupole moment 78−62488
development and appl. of pseudopotential theories in solid state and condensed matter physics 79−90933
diagnostic imaging systems, non-silver halide, recent developments and pot. 80−41223
diagnostic medicine, US mapping and signal processing 77−60282
diagnostic radiology, introduction to computer systems 79−34663
diagnostic techniques in nuclear medicine, review, book contrib. 80−72322
diagnostic US 79−92307
diagnostic US Doppler systems, development in Brazil 79−39455
diagnostic uses of US in medicine and biology 80−4481

reviews continued
diamond, ESR studies 78−95521
diamond, ion implantation 78−87698
diamond, optical absorption and luminesc. spectra 80−2848
diamond, semicond., band struct., elec. and optical props. 77−35862
diamond, synthesis *(Japanese)* 80−80994
diamond, synthetic, history and present status 79−33906
diamond turning, state of the art update 78−46853
diamond turning of optics, past, present and future 79−23100
diatomic molecules, excited states, electronic transition probabilities and lifetimes 80−78658
dichalcogenides, CDWs and phys. props. *(Japanese)* 80−49635
dichromated gelatin as holographic material, book contrib. 78−25833
die wear during wire drawing 80−30113
dielectric, dipolar point defects, studied by ITC 80−6405
dielectric crystal, APR and phonon spectroscopy to study paramagnetic ions 80−84634
dielectric films on semiconductor devices, deposition techniques 78−23611
dielectric permittivity in X- and γ-ray regions 80−44998
dielectric relaxational polarisation, theory development and applicability 80−11334
dielectric response of molecular interactions in liquids 80−25298
dielectric response of solids, frequency and time responses, universality, review 77−63352
dielectric wedge, review of thery of EM field behaviour 78−66712
dielectrics, transfer processes, theoretical model review 80−15529
dielectronic recombination, appls. in astronomy 80−46391
dielectronic recombination 77−36751
difference equations, linear n-term recurrences, appl. in applied math. and theoretic physics *(French)* 79−97183
difference polarography, review of method, instrumentation 80−26078
differential pressure 78−38423
diffraction gratings, review of Japanese research 80−10018
diffraction gratings produced by lasers *(Rumanian)* 80−87542
diffraction of light by sound in solids 79−18577
diffraction of partially coherent light 78−29894
diffuse reflectance spectra, model interprets. 78−32859
diffuse reflectance spectroscopy, applics., standards and calibration 78−32848
diffuse reflectance spectroscopy, calibration of reflectance standards 78−32860
diffuse soft X-ray sky, astrophysics rel. to 0.1-2.0 keV cosmic X-rays 78−16581
diffusely reflecting object, deformation meas. by lasers *(Japanese)* 80−9832
diffusion battery anal. for ultrafine aerosol particle size determ. 79−92010
diffusion in glasses and melts 78−2017
diffusion in macromolecular solutions 80−15273
diffusion in molecular crystals, and point defect struct. 79−82373
diffusion pump back-streaming 78−21155
diffusion pumps 80−57321
diffusional crystal growth mechanisms 80−3059
diffusive plasma transport across mag. field, expt. methods *(Russian)* 79−1294
digital computer control of mech. tests 79−43508
digital device noise immunity control and meas. methods *(Russian)* 77−42663
digital filtering for foetal heart rate variability 79−48353
digital image processing research, Osaka University 80−9820
digital picture processing 80−83562
digital terrain models 79−84084
digital voltmeters, microprocessor-controlled, types 79−35787
digital voltmeters, used for true effective voltage meas. *(French)* 80−42213
dilepton production in hadronic collisions, review 79−49547
dilute alloys, solute diffusion 78−47589
dimethyl ether, review of microwave spectrum, tabulated data 80−51965
diode design review, intense mag. insulated ion diodes 78−9857
diode lasers coupled to external resonators, tutorial review 79−94231
diogenesis, plate tectonic controls 80−12387
dipole oscillator strengths of atoms and molecules 78−21975
direct reactions, semiclassical theory, complex paths and uniform approximations 77−71244
discontinuous metal films, elec. cond. 78−19167
discontinuous metallic film, review of research in USSR 77−76698
discontinuous precipitation in binary metallic systems 80−3060
discovery of fission 79−26418
discrete lattice gauge fields, duality transformation 79−26236
dislocation motion, theory, book contrib. 80−107240
dislocation theory, nonlinear elastic problems, book contrib. 80−39093
dislocations, elasticity theory, book contrib. 80−39090
dislocations, state of art review, book contrib. 80−39089
dislocations, thermodynamics and thermal activation, book contrib. 80−107241
disordered quasi-one-dimensional materials 78−6361
dispersion hardened alloys, strengthening theories 80−97498
dispersion hardening, of metallic materials *(German)* 80−45316
dispersion hardening, of metallic materials *(German)* 80−50646
displacement transducers, for use below 50 mm 79−63200
DNA, conformation of native molecule, influence of solvent struct. 80−30655
DNA hybrid molecule construction and cloning 77−56559
DNA in conc. solns. of neutral salts, conformational transitions 80−81531
Doppler free multiphoton spectroscopy, review 77−79707
Doppler-free laser spectroscopy seminar 78−302
Doppler-free spectroscopy feats and fancies 80−43001
dosimeters, environmental, international intercomparison 79−63817
dosimetric primary and secondary standardization within the European Communities 80−9415
dosimetry, calibration and meas. standards at Austrian Dosimetry Laboratory 80−5362
dosimetry, secondary standard laboratory organisation in India 80−5366
dosimetry, secondary standards laboratory, role in a nuclear power utility 80−5365
dosimetry of electrons and photons, standardisation in Germany 80−5353
dosimetry standardisation in Japan 80−5359
dosimetry standardisation in UK 80−5358

reviews continued
double acoustic magnetic resonance in crystals 77−32291
Doublet Tokamak devices. TNS to demo 79−71968
drag reduction with compliant coatings, review 78−26115
Dragon HTR project 79−45326
Drell-Hiida-Deck model and diffractive dissociation *(Russian)* 79−3007
dressing effect on grinding performance 80−16502
drop formation in a circular liquid jet, book contrib. 80−19467
drop size measurement methods 80−17916
drought and weather modification in India 77−56715
drought in California and western Europe, 1976, atm. and oceanographic factors 79−48560
droughts at Kew, review and classification 77−41121
drug radioreceptor analysis applications 80−94315
dual topological unitarisation, review of S-matrix developments for hadron bootstrap theory 78−62381
dual tree and loop amplitudes *(German)* 77−65142
duality in field theory and statistical systems 80−73610
ductile fracture 77−7788
duodenum, fluid mechanics, review, book contrib. 80−97994
dust storms, Great Plains, USA, lessons 79−29486
dye indicators of membrane pot. 80−21594
dye laser technology 77−54708
dye lasers, book contrib. 80−106517
dye lasers, pulsed narrow-band 77−10915
dye lasers 77−38884
dynamic ^{13}C NMR spectroscopy 77−51971
dynamic critical phenomena 77−82477
dynamic loading of structures and plastic response 80−83756
dynamic nuclear polarisation, review of principles 78−64297
dynamic nuclear polarisation in solid dielectrics 80−29649
dynamic plasticity experiments 80−35288
dynamic self-diffraction of coherent light beams 80−102777
dynamics of mol. crysts., polymers and adsorbed species, book contrib. 77−89505
dynein biochemistry, role in enkaryotic cell motility, book contrib. 79−16178
E2, M1 multipole mixing ratios in odd-mass nuclei, A>150 77−30503
E-region, equatorial, dynamics 78−36369
Early Archaean rocks comp. rel. to crust and mantle chem. evolution 78−65222
Earth's dynamo, MHD, book contrib. 78−61331
Earth albedo, anthropogenic changes and effects on climate 80−81893
Earth and planetary sciences, 1978 annual review 79−5437
Earth anelasticity, surface waves and free oscills. 77−64231
Earth bow shock, DC mag. field obs. 80−90306
Earth bow shock, first evidence and early studies, historical introduction 80−85816
Earth core, Ramsey phase-change hypothesis 79−66662
Earth core chemistry 77−13070
Earth crust, problems of struct. and evolution 79−96749
Earth deep EM sounding and profiling 77−9326
Earth early history, review 79−20739
Earth figure and gravit. field determ., least-squares collocation method 79−48392
Earth global dynamics, Canadian contribs., 1971-79 period 80−8262
Earth heat loss through crust 80−98286
Earth observation from space, remote sensing 79−34983
Earth origin and composition models 77−25663
Earth resources surveying, multispectral photography from space *(Russian)* 78−16197
Earth resources surveying by satellite remote sensing 77−25788
Earth sciences, use of electron microscopy 80−105091
Earth seismic anisotropy, investigations in USSR 77−49038
Earth structure from seismic surface wave obs. 78−73323
Earth surface multispectral photography from space *(Russian)* 78−16198
earthquake precursors, classification 79−88264
earthquakes, Japanese prediction studies, building design and location 78−32014
EAS, 10^{15}-10^{18} eV, experimental data, implications for particle accelerators 79−8786
ECG, computer assisted interpretation, critical appraisal 80−17151
ECG, computerised systems, current status and future trends *(Japanese)* 79−44013
ECG amplifiers, instruments and maintenance 78−69232
echelle spectroscopy, astronomical applications 77−25951
echo-Doppler, range-gated, pulsed, review and evaluation 79−96642
echocardiograms, 1D and 2D, computer processing *(German)* 80−81665
echocardiology, book 77−64103
echography, real time, contrib. to diagnosis and management of palpable breast lumps 80−17027
echomammography: indications and limitations in tumours with or without calcification *(French)* 80−36039
eclipsing binary stars, period variations 80−109474
ecology and systematics (book) 80−67945
economics of energy and materials 77−77350
eddy thermoelectric currents and eddy thermoelements 77−8126
education in astronomy, review of Canadian activities 77−45626
EEG and electrooculograms, sleep research anal. 79−62377
EEG and head trauma 80−46076
EEG common clinically used montages 77−81599
EEG technique, for ABRET oral exam. candidates 78−20298
effusion and related surface processes 77−51151
EHD ionisation mass spectrometry, instrumentation, mechanisms and appls. 78−86378
Einstein's part in the development of quantum concepts 80−98781
Einstein's relativity paper (1905) and the electromagnetic world picture 78−16616
Einstein's theory of gravitation 80−90745
Einstein and the quantum theory, review 80−22237
Einstein centenary 80−46782
elastic constants, third-order, of uniaxial crystals 80−65119
elastic deflections of bars, literature review and bibliography 77−84140
elastic electron scattering at large momentum transfer, review 80−22820
elastic wave diffraction *(Russian)* 79−18795
elasto-plastic fracture mechanics, critical assessment 79−38943
elastomer, role of particulate fillers, review 80−29921
elastomers, vacuum compatible, chem. character correl. with physical characts., review 78−24804

reviews continued
elastometric glasses and porous network polymers, review of future developments 78−22657
ELDOR 78−39449
electric currents in cosmic plasmas 78−12094
electric power generation technology 79−24883
electric quadrupole interactions measured by nuclear orientation and NMR on oriented nuclei 80−92868
electric vehicle battery systems available and under review *(Dutch)* 80−72025
electric vehicle secondary cell development program of US Dept. of Energy, review 80−30442
electrical breakdown of gases, prebreakdown stage 80−106868
electrical conduction mechanism in noncryst. solids, review of developments 78−26854
electrical conductivity in inhomogeneous media 78−56115
electrical conductivity of disordered systems, Matsubara, Toyozawa, Ishida, Yonezawa theories 79−60778
electrical control of development 77−86467
electrical phenomena in polymers, nature and appl. 80−50254
electrical stimulation of stroke patients 79−48377
electro-optic and holographic meas. techniques for atmospheric sciences 78−49184
electro-optical and nonlinear-optical materials 80−74450
electroacoustics (history to 1940) 77−45665
electroanalytical chemistry, 1952-1977 78−92567
electroanalytical chemistry, recent appl. of digital computers 77−81451
electrocatalysis surfaces modified by metal adatoms 80−61110
electrochemical analysis, developments over last 25 years 77−70368
electrochemical analysis, instrumentation and dynamic techniques over past 4 years 78−85215
electrochemical analysis methods 79−43661
electrochemical electrodes in modern laboratory 77−4964
electrochemical electron transfer at electrodes in solution, in book, for teachers 78−8203
electrochemical fused salt systems, solid films and interfaces 77−77783
electrochemical healing similarities between animals and plants 79−92316
electrochemical methods for determ. of kinetic props. of solids, book contrib. 79−65251
electrode materials, for photoelectrolysis of water 79−29478
electrode process research, instruments and appls. review 78−21174
electrode-electrolyte interface, solid film props., review of expt. techniques 77−77780
electrodeposited and associated coatings 79−91596
electrodeposition 79−43162
electrodeposition and related processes, progress, (1952-1977) 78−27420
electrodialysis and its applications 80−55702
electrodynamics, Born-Infeld theory *(Polish)* 79−35576
electrodynamics, classical, field, conservation principle, history *(Russian)* 78−36849
electrodynamics, Ritz's theory based on particle interactions, review of original paper of 1908 80−47
electrofocusing, current major appls. 80−101306
electroinitiated polymerisation on electrodes 80−50854
electrokinetic phenomena in biology, book contrib. 80−12326
electroluminescence, principles and appls. 77−40288
electrolyte solution structure, (1952-1977) 78−26417
electromagnetic inspection review 80−35468
electromagnets, high field, historical review of development, mech. strength, performance limits 77−10073
electromechanical phenomena assoc. with earthquakes 78−36108
electromechanical transducers in hostile environments 80−37019
electromyography, clinical, computer anal. 78−80985
electron and ion beam generation at high power 80−13988
electron and ion emitters *(Japanese)* 77−63492
electron and positron scatt. by atoms, cross sections, review and expt. conditions 78−58828
electron beam therapy of lateralised lesions of oral cavity and oropharynx 80−12215
electron beam therapy with medium energy electrons 80−36069
electron beams as virtual electrodes 80−6861
electron bombardment ion thruster efflux, interaction with spacecraft 80−31440
electron capture processes in ion-atom collisions 78−70930
electron charge densities, coherent X-ray and neutron diffr., review 77−76260
electron cooling and new possibilities in elementary particle physics 79−68118
electron cyclotron heating in Elmo bumpy torus 80−28750
electron cyclotron maser, historical review 77−38843
electron cyclotron maser, mm-wave source appls. 77−88683
electron diffraction instrumentation 78−83683
electron distribution function, in low-temp. low press. plasma, meas. methods, review *(Czech)* 78−71534
electron emission, appl. of unified theory 78−35256
electron emission and surface physics *(Japanese)* 77−63493
electron energy loss spectrometry, local characterisation of solids 80−31948
electron energy loss spectrometry, of thin specimen sections, electron microscope chem. anal. *(French)* 79−8469
electron energy loss spectroscopy, in electron microscope, review 80−104025
electron energy loss spectroscopy and microanalysis, instrumentation developments 78−35783
electron energy-loss spectroscopy in context of TEM 80−31945
electron flow, photosynthetic and respiratory, in dual functional bacterial membrane 80−16914
electron gas, dielectric constant 80−107731
electron holography progress *(Japanese)* 80−52369
electron image processing 79−30613
electron inelastic scatt. on nuclei 77−34289
electron linacs 77−38473
electron linear accelerator, development and present status *(Chinese)* 79−54625
electron microdiffraction, book contrib. 80−10464
electron microprobe, appls. in mineralogy *(French)* 79−5628
electron microprobe instrument evolution, SEM and STEM 78−70233
electron microscope, construction, operation and special types 80−86529
electron microscope, scanning-transmission, design, operation, capabilities and limitations 80−68300

reviews continued
electron microscope image analysis 80−31947
electron microscope image contrast and localized signal selection techniques 80−37126
electron microscope resolution, prospects for extending limit 80−37128
electron microscopes, new develop. and image processing 77−41732
electron microscopy, appl. in modern science 79−26182
electron microscopy, developments of last 25 years 77−67540
electron microscopy, diffr. and imaging techniques [book] 79−67439
electron microscopy, high resolution, mol. struct. determ. 80−21595
electron microscopy, high resolution, solids fine struct. appls., advances 79−50965
electron microscopy, high voltage 77−41737
electron microscopy, HV, in situ obs., techniques and applics. *(Japanese)* 80−59351
electron microscopy, phase problem, review 80−33862
electron microscopy, possibilities and limits *(German)* 77−82652
electron microscopy, recent applications to biology 80−41347
electron microscopy, review, 1976-77 78−82077
electron microscopy, semiconductor appls., advances 80−101911
electron microscopy determ. of film thickness, electron backscatt. method 77−47703
electron microscopy in metallurgy 80−76458
electron microscopy of ferroelectric substances *(Japanese)* 80−71366
electron mobility, effect of mol. struct. and elec. field 78−2535
electron momentum densities, expt. determ., review 77−76776
electron momentum densities, theory 77−75039
electron optics, coherence, review 80−32900
electron ordered systems, orbital distrib. NQR spectra studies 79−78560
electron precipitations and polar auroras 79−29932
electron probe microanal. in SEM by means of X-ray spectrometers, review 80−95194
electron probe microanalysis of biological samples 77−86730
electron probe X-ray microanalysis, instrumentation and techniques *(Chinese)* 79−34415
electron scattering, atoms and mols., expt. and theory 78−25699
electron scattering, resonances in atoms and molecules 80−9734
electron scattering by atoms 77−34762
electron scattering by crystals 80−14969
electron spectroscopy, deconvolution methods 79−26188
electron spectroscopy, inner-shell, for microanal. 80−68303
Electron spectroscopy and molecular structure 78−1026
electron spectroscopy appls. *(Japanese)* 79−40645
electron spectroscopy for surface analysis, introductory survey, book contrib. 77−63502
electron spectroscopy of surfaces 78−92169
electron spectroscopy techniques for semicond. investig. *(Japanese)* 80−49061
electron spin echo modulation phenomena, paramagnetic species immediate environment struct., review 78−88164
electron spin-lattice relaxation, paramagnetic ions in solids 77−69672
Electron stimulated desorption: a critical review 78−22958
electron theory of metals and geometry 80−103611
electron transfer between multicharged ions and neutral targets 77−72407
electron tunnelling spectroscopy, review of principles and techniques, superconductivity 78−90253
electron-excited core level spectroscopies for surface analysis, book contrib. 77−63503
electron-hole liquid, in semiconductors, equilib. props. *(Russian)* 78−34773
electron-molecule collision theory 80−32847
electron-molecule low energy rot. and vibr. excitation 77−6943
electron-nucleus reaction mechanism at asymptotically high impact vel. 79−97700
electron-phonon interactions in alkali and Ag halides 78−63991
electronic and cohesive properties of disordered simple metals 80−44475
electronic charge distribs., theory 77−75040
electronic communication methods in geology 77−17252
electronic distance meas. technology, surveying appl. 77−67410
electronic emission spectroscopy, instrumentation 78−29166
electronic energy transfer, in excited atom collisions, book contrib. 77−40543
electronic materials rel. to cryst. growth, device appl. 80−66405
electronic measuring instruments, recent developments *(Japanese)* 78−77895
electronic properties of actinide oxides 77−28115
electronic to vibrational energy transfer, vibr. state anal. 78−37725
electronic transition laser development 79−946
electronic transport in insulators *(Spanish)* 80−84464
electronics influence on laboratory technology and instrumentation over last 25 years 77−67422
electrons and positrons in dense gases 80−103106
electrons in glass 77−66106
electrophotography, electrostatic aspects 78−25768
electrophotography, history, present status and future potential 79−2854
electrophotography, physical processes 79−17536
electrophotography, process configuration, architectures 78−29188
electrophotography developments in Western Europe (1974-77) 79−71556
electroretinography, human, psychophysical appl., review 78−35859
electrostatic double layers 78−67368
electrostatic electron energy analysers, cylindrical mirror appls. 78−21265
electrostatic image development 79−17539
electrostatic X-ray imaging, book contrib. 80−36112
electrostatics, quest for charging mechanism to end of 19th century 78−12525
electrosurgical instrumentation review 78−44680
elemental layered material prep. and growth, book contrib. 78−19647
elementary particle classification and quark model, symmetry breaking gauge theories, unified theories 79−346
elementary particle interactions, diffractive production mechanisms 79−36052
elementary particle physics, coherent production, book 79−21889
elementary particle physics, cosmological approach, review, book contrib. 80−68440
elementary particle physics, current status 79−40651
elementary particle physics 78−8493
elementary particle polarisation studies at Brookhaven AGS, past, present and future 77−30737

reviews continued
elementary particle properties review, leptons, mesons, baryons 78−66179
elementary particle strong interactions at very high energies 80−440
elementary particle subnuclear structure concept via dilepton prod. in hadronic collisions, historical review 79−93365
elementary particle weak interaction theory 78−4822
elementary particle weak interactions, resource letter, WI-1 78−16601
elementary particles, quarks and the concept of particle, Richtmyer memorial lecture 78−62286
elementary particles since J/ψ 80−57018
elementary particles strong interactions, analytic extrapolations, statistical approach *(Russian)* 79−3000
elementary processes and chemical reactions in plasma *(Czech)* 80−24126
elements origin and evolution 78−32619
ellipsometric instrumentation, review 80−101819
ellipsometry of clean surfaces, submonolayer and monolayer films 80−103546
ellipsometry work at Gakashuin University from 1955, review 80−9019
EM energy-momentum tensor and the properties of material media 79−55020
EM frequency sounding, crustal struct. determ. 78−49167
EM irradiance distribution function in turbulent media, theoretical review 79−64155
EM methods for determining dielec. const. and resistivity of ground 80−22382
EM periodic SAW transducers 78−13880
EM pump and plant with liq.-metal working fluid, review *(Russian)* 77−19639
EM scattering and radiation problems soln. by spectral domain approach 80−5663
EM waves in sea water review 77−49082
embryo, human, radiation effects on pre-natal development 79−29566
EMF production by shock compression of solids 77−31719
emission and adsorption props., rel. to electronic struct. 77−76899
emission computed tomography 80−56213
emission line galaxies 77−64855
emission spectrometry, current developments *(Japanese)* 78−86356
empirical $(1f_{7/2})^n$ model 79−17826
endocytosis 78−15816
energetic ions of ionospheric origin in magnetosphere 79−66874
energy conservation and storage, materials needs 80−66958
energy conservation through recycling 80−21388
energy conversion, intuitive thermodynamics *(German)* 79−14225
energy dispersive X-ray diffraction method, annotated bibliography (1968-78) 80−36794
energy loss of charged particles 79−95060
energy loss spectroscopy, spectrometer design, electron optical props. 79−12903
energy loss spectroscopy, tutorial 79−21872
energy resources, long-term energy systems and the role of nuclear and solar energy 80−66918
energy resources, review of alternatives to fossil fuel *(Italian)* 80−66917
energy resources and future energy concepts 79−61936
energy resources and their utilisation 79−66396
energy sources for long-term implantable devices 80−98175
energy storage and conversion, Canadian R and D program 79−29457
energy storage in power systems 79−24913
energy strategy, soft vs. hard energy technologies 79−24885
energy supply and demand, United States government analyses 80−30320
energy transport in crystalline solids, molecular dynamical calc. 78−95117
engineering education, perspective and some current problems 79−10
engineering structures, welded exam. of fracture processes, review 78−60777
enhanced diffusion mechanisms 78−67847
enteric bacteria, transport functions of the outer membrane, book contrib. 79−16179
environmental actinides, pot. carcinogenic effects 80−30780
environmental conditions at 18000 yr BP, continental record initial evaluation 80−51529
environmental noise, health effects of noise exposure 79−5313
environmental noise, review of biological effects on humans 79−5315
environmental noise exposure, medical effects, review of basic considerations 79−5312
environmental radioactivity meas. in the EEC, 1977, for air, deposition, water and milk 79−62162
environmental radioassay, Italy, appl. of quality control procedures 79−25117
environmental research, bibliography of AECL publications 79−34444
enzyme dynamics, statistical phys. 80−21439
enzymes, membrane bound, influence of membrane fluidity on activity, book contrib. 80−30688
epitaxial film growth of nonmetallic materials by sputtering 77−32521
epitaxial growth, struct. and topological aspects *(French)* 79−4483
epitaxial growth, surface reconstruction effects 77−89669
epitaxial layers, transition regions 78−14630
epitaxy, growth modes, exp. techniques, book contrib. 80−49558
epitaxy, role of lattice misfit 79−46970
epithelial mucus, rheology and mol. organisation 80−97959
epoxy replication of optics 77−27401
epoxy resin systems, synthesis review, phys. and mech. props. at low temps. 80−25650
EPR, literature July 1975 to July 1977, applications to chemical systems 78−82753
EPR, low symmetry effects 80−71159
EPR in solution 78−88165
EPR of nonsilicate minerals 78−39384
EPR of transition metal, lanthanide and actinide ions, 1974 literature 80−11253
EPR of transition metal, lanthanide and actinide ions in solids 77−69675
EPR spectra of stable radicals, slow molecular motion study, review 80−25212
equatorial counter-electrojet, geomag. aspects review 78−36367
equatorial electrojet theory 78−69607
equipment for the measurement of ions in solution 80−71983
equivalence principle, evolution to general relativity 80−98779

reviews continued
erosion, book contrib. 78−11350
ESCA, chem., technical and industrial appls., lecture 78−27875
ESCA, principles and appls. 78−27375
ESCA-ion scatt. spectroscopy-SIMS, review, chem. appls. 79−43701
ESR, appl. in photosynthesis 79−92450
ethylene-methyl acrylate, random copolymer 80−108330
Euclidean Yang Mills eqns., self-dual solns. 79−26230
European nuclear industry situation, review *(Dutch)* 77−3073
European Physical Society, growth and struct. 77−5608
European Space Agency programmes, developmental or operational status 80−72742
European Space Agency satellite, programmes and projects 79−12377
eutectic alloy, dendrite growth−the coupled zone 80−97489
evoked potential and early studies of bioelectricity 80−101158
evolution of massive stars 80−82343
EXAFS, new horizon in struct. determs. 79−19949
exceptional European weather in (1975) 77−25756
exchange effects in nuclei, introduction 79−26375
excimer laser application to laser-radar obs. of stratospheric O_3 80−17410
excimer laser systems appls., book contrib. 79−81441
excimer lasers, and applications *(Japanese)* 78−33723
excimer lasers, book contrib. 77−50665
excimer lasers, excitation mechanisms, review 80−9865
excimer lasers, optically pumped CW 80−14322
excimer lasers, theory and appl. 79−59684
excimer lasers 77−34877
excimer lasers 78−33728
excimer lasers 79−937
excimer systems, electronic structure and radiative transitions, book contrib. 79−81416
excited atomic and molecular states in strong electromagnetic fields 79−49955
excited cosmic plasmas 78−69671
excited nuclear states, 10^{-18} to 10^{-6} s, lifetimes, direct meas. 79−30804
excited semiconductor, extended phase diagram 80−44521
exciton physics, book contrib. 80−44517
excitons, condensation effects 78−2427
excitons, internal struct., book contrib. 80−44518
excitons and exciton-phonon interactions, resonant Raman and Brillouin spectroscopy, book contrib. 80−49624
excitons in crystals *(Russian)* 79−47026
excitons in magnetically ordered dielectric *(Russian)* 77−80943
exoelectronic emission, crystal defects effects *(Russian)* 77−55872
exoelectronic emission of semiconds. 77−52228
exotic atoms: a new method in nuclear and elementary particle physics *(German)* 79−76536
exotic atoms, E2 and E4 nucl. moments from HFS 78−37265
exotic atoms, props., EM and strong interaction effects within the atoms 78−9281
exotic atoms, significance of exotic atoms to particle physics 78−9282
exotic atoms, utilisation in chem. struct. studies 79−79277
expansion bellows, elastic flexibility of axially loaded omega and toroidal bellows 79−32266
experimental data on nuclear reactions and nuclear struct. Sept. to Dec. 1977 79−9430
experimental methods of heavy ion physics for radiation detection and meas. *(Russian)* 79−49900
experimental nuclear astrophysics 79−25471
experimental verification of the general theory of relativity 80−98850
exploding galaxies and supermassive black holes, review 79−80355
exponential law, concepts prior to 1900 78−86052
exposure meters for colour positive process 78−12781
extended extragalactic radiosources, models 77−26079
extended growth defect characterisation 78−30649
extensional rheometers for molten polymers 78−71302
external flows, book contrib. 77−58653
extracorporeal blood circulation apparatus, tabulated data 77−78045
extracorporeal blood oxygenator safety and efficacy 78−77153
extracorporeal processing devices, book contrib. 80−12308
extractive metallurgy, developments in basic principles and phys. chem., review 80−20819
extractive metallurgy of Pb, Zn, and Sn, developments 80−20820
extragalactic distance scale, review of distance indicators 78−93396
extragalactic radio sources (>1 arcsecond), large-scale struct. 78−57668
Extragalactic X-ray astronomy 78−73776
extragalactic X-ray sources, luminosity function and variability time scale 78−57701
extragalactic X-ray sources *(Polish)* 79−101223
extraterrestrial intelligent life 79−48692
eye, effects of UV, 300 to 400 nm, literature review 78−57042
eye movements while reading, annotated bibliography 78−53394
F-centre form. in halides, photochem. 78−63763
F-region, electron temperatures, theory and obs. 79−48618
F-region, equatorial, topside and bottomside, review of struct. 78−36373
Fabry-Perot tandem and multipass interferometers 77−34038
failure mechanisms and metallography, review 79−61833
far IR CW lasers, optically pumped 78−46588
far IR generation, difference frequency mixing of CO_2 lasers, book contrib. 77−46763
far IR IC, antennas and waveguides for integration, review 80−69553
far IR interferometry, (1950-76) 78−4456
far IR research, grating era (1925-60) 78−4455
far IR research, Rubens era (1892-1925) 78−4454
fast brittle fracture, theoretical and expt. results 77−14958
fast ion conduction materials 77−7891
fast metal assemblies, prompt alpha and reactivity meas. 78−21685
fast neutron capture, 5 to 15 MeV 77−26694
fast neutron detectors and instrumentation 77−23378
fast neutron induced nonelastic reaction cross section data, $E_n \geq 14$ MeV 77−23058
fast neutron scatt. from medium mass nuclei, i-spin depend. 77−26695
fast processes, measurement, present methods in USSR future prospects 80−57271
fast reactor plant, future design and construction plans, review of national papers SM 225/81-87 79−97797
fast transient phenomena in astrophysics, physical mechanisms affecting observations *(Italian)* 78−93105
fatigue, current aspects 77−86156

reviews continued
fatigue, fracture, statistical treatment, maintenance procedures 79−43538
fatigue, high temp. 78−56773
fatigue, multi-stage nature, review 77−21269
fatigue, static, in glass 77−40441
fatigue crack growth prediction methods 77−50983
fatigue cracks, growth rate rel. to loading cycle parameters, review *(Russian)* 79−28038
fatigue detection and rating by acoustic emission, review 80−104380
fatigue life prediction in initiation and propag. stages 79−68596
fatigue of high strength materials, strengthening *(Japanese)* 78−15513
fatigue resistance, in metals 80−94907
fatigue testing techniques and life prediction 80−21251
fault motion and earthquake occurrence, numerical and lab. simulation 79−100815
FBR, appl. in Spanish electricity supply system *(Spanish)* 79−59115
FBR, development, fuel cycle, hazards and alternatives 79−63715
FBR, safety strategies of the different phases of a hypothetical accident *(Italian)* 79−63754
Fermi gas model in 1-D 79−58636
Fermi National Accelerator Laboratory, description 77−57782
Fermi surface studies of pure cryst. materials 78−10334
Fermi surface study of disordered alloys, positron annihilation experiments 80−44480
Fermi system, Jastrow wavefunction, hypernetted chain method 80−17866
ferrite, microstruct. depend. of props. and applics., review 78−88548
ferrite, transform. kinetics, grain size, alloying element effect, carbide precip. 80−93560
ferrites, electronic cond. mechanisms, review 77−20314
ferrites, soft, production and props. 80−88801
ferrites, soft and microwave, grain-size effects on mag. props. 78−64222
ferroelectric, H-bonded, soft and central modes, mag. reson. 78−15108
ferroelectric and antiferroelectric crystals, perovskite type structure, semiconductor props. *(Polish)* 78−56437
ferroelectric and ferroelastic phase transition, dynamics, Brillouin spectra 80−55115
ferroelectric ceramics, materials and dielec. props. 80−75957
ferroelectric crystal., optically induced refr. index changes, holography appls. 77−50742
ferroelectric crystals for hologram storage, book contrib. 78−25834
ferroelectric liquid cryst., review of props. 77−85667
ferroelectric liquid cryst., chiral smectic C phase, phys. props. 80−75150
ferroelectric solid solns., perovskite struct., physical props. *(Russian)* 77−48134
ferroelectric theory and dynamics, optical, acoustic electro-optical props., Brillouin zone struct. 80−11347
ferroelectrics, bibliography, May-Sept. 1976 77−59529
ferroelectrics 77−12326
ferroelectrics bibliography, Jan-April 1976 77−48132
ferrofluids, agglomeration 80−61162
ferromagnet, 3d metal, electron spin polarisation in field emission, state-of-the-art 77−69972
ferromagnetic and antiferromagnetic domains, neutron techniques for obs. 78−64213
ferromagnetic film, phenomenology of domain walls *(Rumanian)* 78−60324
ferromagnetic film developments *(Japanese)* 77−69635
ferromagnetic ordered structures, domain structure, effect of defects, electron microscopy 78−64214
ferromagnetic particle suspensions in non-conducting and metallic liqs. 80−60372
ferromagnetic semiconductor, theory review 80−20369
ferromagnetic semiconductors, cryst. growth 77−85923
ferromagnetic surface, spin fluctuations and light scatt. 80−84727
ferromagnetic transition metal alloys, mag. props. 80−44823
ferromagnetic transition metals, electron spin polarisation 78−76591
ferromagnetic transition metals, electron spin polarisation 78−76592
ferromagnetism, itinerant electron theory, local moment approach *(Japanese)* 80−25071
ferromagnetism of disordered systems 80−29513
ferromagnets, domain struct. effects on dynamic props. 80−34678
ferrous metallurgy, nondestructive inspection and quality control review 80−21201
fertility in man, influence of radiation 80−56137
few nucleon correlations from high energy scatt. *(Russian)* 80−68549
few nucleon systems, 3N and 4N calcs., reviews 78−50094
few nucleon systems, realistic nucleon-nucleon interactions 78−62526
few-nucleon reactions for A>3, coincidence expts. 77−18518
few-nucleon system investigation using polarised deuterons 77−18578
Feynman rules for lattice gauge theory of quark confinement, Green's functions, review 78−93850
FFT in computational physics, review *(Russian)* 77−5650
fibre optic communication cable development 80−1331
fibre optic communication system components, USA military developments, review 79−46060
fibre optic communication systems, analytical review including survey of commercial systems 80−74489
fibre optic communication systems, world-wide, survey 79−46059
fibre optic communications, prospects for 1 to 1.6 μm spectral range use 80−102848
fibre optic communications 79−41455
fibre optic connection systems standardisation 79−68440
fibre optic connectors, precision and stability developments 80−69523
fibre optic connectors 79−46075
fibre optic market trends, worldwide 80−58699
fibre optic systems and field trials, review 80−58700
fibre optic transmission technology, single mode systems in 1.0 to 1.8 μm region 80−38105
fibre optic wideband transmission systems, appls. *(German)* 79−64325
fibre optical communication, research status in France 77−46814
fibre optical communication, research status in USA 77−46813
fibre optical communication devices 77−58446
fibre optics, demand explosion 77−46812
fibre optics, developments in theory 80−43457
fibre optics, diverse applications 79−27414
fibre optics, economic advantages of using optical links, compared with wire cable 79−10385
fibre optics, in medicine 77−48901
reviews continued
fibre optics, state-of-the-art and available equipment *(German)* 80−87484
fibre optics and optical links in France, industrial dossier *(French)* 78−71201
fibre optics for military appls., review and assessment 78−42438
fibre optics history of development 77−7194
fibre optics in telephone carrier systems 79−81528
fibre optics research in USA 77−27363
fibre optics sensors for measurement and control appls. 80−58780
fibre optics tasks of NASA 78−42441
fibre optics technology and connector systems, marketing 80−69522
fibre reinforced composites, AE monitoring review 79−11735
fibre reinforced composites, cracking and fracture, review 78−60772
fibre reinforced composites, fracture mechanics, review 79−27597
fibre reinforced concrete *(Japanese)* 78−31372
fibre reinforced metals and alloys 77−21060
fibre-optic interconnection techniques 79−23059
fibres, hard-elastic, morphology, mech. props., mechanisms, review 77−32612
fibres, reinforcing for plastics, review 79−61506
field desorption mass spectrometry, appl. to biochemistry, medicine, and environmental science 80−35592
field emission microscopy appls. 79−65982
field emission spectroscopy of transition metals 78−35257
field ion microscopy, developments 79−67445
field ionisation and field desorption mass spectrometry *(Japanese)* 79−66384
field ionisation mass spectrometry of inorganic cpds. 78−35764
field ionisation mass spectrometry of organic cpds. 78−35763
fifth international conference on reactor shielding, review 78−29599
filled polymer mechanical properties, particle shape effect, review 80−100864
film cleaning solvents 77−10130
film deposition and characterisation, book contrib. 79−1563
film growth, high rate, book contrib. 78−11117
film nucleation and initial stages of growth 78−75961
film- and transition-boiling heat transfer to cryogenic fluids 80−92026
films, amorphous, prep., struct., props., review, book contrib. 78−48321
films, polymorphic transforms. and phys. props. 77−43450
films and foils, mechanical testing methods, review 80−40637
FIM techniques, appl. to metallurgical problems 78−35620
final evolution of stars *(Italian)* 79−53805
fine particle magnetic materials, physical basis and applications 78−84457
finite element analysis, natural mode approach, solid mechanics appl. 79−44728
finite temp. field theory with boundaries, extensions to curved space, stress tensor and surface action renormalisation 80−57455
Finslerian relativity, development and basic theoretical principles 79−35596
fish, problem of sound perception *(Russian)* 80−41043
fissile material supervision, safety measures *(German)* 78−684
fission barrier props., expt. studies and statistical anals. review 80−102216
fission material reprocessing plant, United Reprocessors in Europe *(Dutch)* 77−14254
fission reactor design, development and commercialisation of 17 types *(Japanese)* 79−80974
fission reactor fuel preparation by spallation reactions *(Russian)* 79−22441
fission reactor LOFT program, recent results *(Japanese)* 80−673
fission reactor multiphase systems, expt. and theoretical review of density-wave oscillations 80−18369
fission reactor oxide fuel, irradiated, physical processes *(Japanese)* 80−27742
fission reactor physics 80−63245
fission reactor safety, aspects of the historical, philosophical and mathematical background to the statutory management of nuclear plant risks in the United Kingdom 80−5293
fission reactors, critical heat flux 77−57708
fission reactors, design and development of fast and high temp. reactors *(Italian)* 79−63721
fission research reactors, US National Bureau of Standards reactor, review of activities July 1977 to June 1978 79−85761
fission-fusion pellet design 79−13519
fixed charge membrane modules, pot. controlled transient gating mechanism, book contrib. 80−12067
flame, ionis. and Massey's adiabatic criterion 78−33563
flame emission, atomic absorption, and atomic fluorescence spectrometry, review of literature 1975-1977 78−85224
flare stars physical characts. 77−41383
flash lamp pumping of lasers, optimal lamp filling *(Russian)* 78−63123
flash photolysis, appl. to biological systems 78−11530
flaw sizing of real defects, review 78−53041
floating zone, under reduced gravity, Marangoni convection 80−66425
flow boiling, critical heat flux 79−4074
flow cytometric data, computerised display and anal., book contrib. 80−109082
flow interference between two circ. cylinders 78−46985
flow meas. systems 77−84361
flow measurement, international standards organisations, review 78−34246
flow measurement, review of thermal and optical methods 78−34233
flow measurement techniques for closed conduits 80−64654
flow of dense suspensions 78−67255
flow of nematic liquid crystals, book contrib. 78−59531
flow through screens, book contrib. 78−59483
flowmeter design types for gas throughput meas. in vacuum gauge calibration apparatus 77−26319
flowmeters, EM, for fast reactors 78−21686
flows with heat addition, aerospace appls. 77−916
fluctuation phenomena, mathematical formulation, review, book contrib. 80−73267
fluid dynamics, turbulence, statistical mechanics, progress in last thirty years 78−89290
fluid interfaces, isothermal and deformable, mass transfer and surface tension 80−33564
fluid mechanics, annual review, book 77−46981
fluid mechanics, annual review, book 80−17722

reviews continued
fluid mechanics, coherent structures in fluids, appl. to plasma physics 79−10621
fluid mechanics, finite element methods, book contrib. 79−32446
fluidisation research 77−24022
fluidised fine particles, turbulent ascending gas flow in cylindrical channel 78−42643
fluorescence immunoassays 79−79693
fluorescence spectrometry, anal. appls., historical review 78−93507
fluorescence spectroscopic investigations of the dynamic properties of proteins, membranes and nucleic acids 80−101148
fluorescence spectroscopy in study of biochem. processes 78−11784
fluorescently labelled molecules as probes of living cells struct. and function 80−67321
fluorometric and phosphorometric analysis, review of literature 1975-1977 78−85220
fluxgate magnetometry 79−35800
focused electron beam as probe of solid state *(Czech)* 77−24915
folding description of elastic and inelastic scattering 79−93582
for extragalactic radioastronomy, recent advances 77−17706
forced convection in channel flows, turbulence 79−1195
forced convection with rheological systems 79−1222
forced convective transition boiling, prediction methods 77−3825
Forced oceanic waves 78−73401
forced Rayleigh scattering, principle techniques and expts. 80−34938
forced Rayleigh scattering, principles and techniques 80−20646
Fort St. Vrain HTGR power station, review of design and operation 79−45353
fouling in heat exchangers 79−3902
four-wave mixing spectroscopy, recent developments 80−53383
Fourier spectroscopy and multichannel long integration time techniques 80−91751
Fourier transform IR spectrometers, history, current status and commercial future 78−58072
Fourier transform NMR spectroscopy, review 80−104486
Fourier transform spectrometry, dispersive, bibliography 79−58806
fractography, quantitative 79−39072
fracture, biaxial load effects, review 79−43433
fracture, J-integral appl. *(Japanese)* 79−81817
fracture, metals, physicomechanical characts., review 79−52368
fracture, use in engineering, industry and crafts 80−50702
fracture and plasticity, lattice-statics approach 80−39212
fracture mech. techniques, review 79−41635
fracture mechanics, plasticity, finite element anal. 79−41612
fracture mechanics, recent theoretical and experimental developments 78−60776
fracture mechanics 80−64458
fracture mechanics of yielding materials, review 78−31521
fracture mechanisms review 80−35296
fracture sustained load, ambient temperature 79−43424
fracture toughness *(Japanese)* 80−90595
fragmented analogue states produced in proton-nucleus reactions, fine struct. anal. 77−6391
free convection in rectangular enclosures filled with fluid and with porous media 80−79115
free electron laser 78−90406
free electron laser-electron storage ring system, basic characteristics and possible developments 79−68019
free neutrons, conceivable props. and expt. determ. 79−58994
free radical spectroscopy, book contrib. 77−38653
freeze-fracture replication, in biological research 78−40444
freeze-fracture techniques and appls. in struct. anal. of mammalian plasma membranes, book contrib. 80−30960
freeze-fracturing effects on membrane struct. 78−28140
freeze-fracturing preparation technique, methods and results 78−24776
French space programme 79−101045
French Tokamak research *(Russian)* 80−38690
frequency and time measurement techniques, book 79−176
fretting fatigue 77−4152
friction, lubrication and wear, review of papers published 1974 to 1976 79−15806
Frohlich brain wave model, limit cycle stability, enzyme-substrate reaction 78−44490
frontiers of time 80−12886
fuel cycles, bibliography of AECL publications 80−5
fundamental constants, summary of obs. evidence of variation 79−12759
fundamental physical and astrophys. consts., review, dimensional and dimensionless combinations *(Russian)* 77−49706
fundamental physics research in India in last three decades 79−17178
furnace combustion chamber and radiative transfer, fuel substitution effects 79−3903
fusion, ETF, engineering challenges 80−95422
fusion, international fusion technology program 80−95423
fusion, US magnetic fusion program, survey 80−91249
fusion and fast breeder reactors, a comparison, book 78−78430
fusion development status *(German, English)* 77−67874
fusion energy commercialisation, research review 79−76146
fusion hybrid blanket data and development, review, simulation test facilities 80−106170
fusion inertial confinement, advanced engineering requirements 80−95421
fusion plasma in mag. confinement, review of required diagnostic techniques 79−71951
fusion plasma reaction rates, velocity-space methods 77−79475
fusion possibilities and plasma confinement and interactions in mag. config. Tokamak, review *(French)* 80−54017
fusion power. plasma and the controlled thermonuclear reaction, review of practical problems of energy prod. 79−93826
fusion power, radiological protection review 80−9411
fusion pulsed accelerators, development, problems 78−5046
fusion reactor, ASDEX, assembly and commissioning, review 80−102334
fusion reactor, Doublet III beamline, review, component relation and config., design constraints 80−99382
fusion reactor, large superconducting toroidal field coil program, progress report 80−99335
fusion reactor, MFTF, electrical systems, overview 80−91278
fusion reactor, Nova, mechanical design, overview 80−91279
fusion reactor, PDX, 6 MW Neutral Beam Project, overview 80−106223
fusion reactor design, engineering and technology developments since 1974 79−71958
fusion reactor development, pure and hybrid reactor options 80−63389
reviews continued
fusion reactor materials, material requirements exam., review 78−50257
fusion reactor materials, neutron experiments for data testing 78−5023
fusion reactor materials, surface erosion 77−57741
fusion reactor materials technology since 1974 79−76134
fusion reactor pellet re-fuelling feasibility 80−91246
fusion reactor plasma heating and confinement 80−63388
fusion reactor pulse power supplies development 78−8990
fusion reactors, electron beam driven Tokamaks, review 80−99317
fusion reactors, high power laser appl. *(German)* 77−54361
fusion reactors, JET, state of development *(Dutch)* 77−61604
fusion reactors, Large Coil Program, superconducting mag. coil struct. design status 80−106189
fusion reactors, laser produced nuclear fusion 80−63381
fusion reactors, TEXT overview and status report 80−91273
fusion reactors, theoretical status of mirror machine confinement 77−38398
fusion reactors conceptual design 77−57749
fusion research, internat. cooperation *(Japanese)* 80−63371
fusion research, international 77−46402
fusion research, neutral beam appl. 79−45406
fusion research laser, 30 TW Omega system 79−55146
fusion technology progress 78−62607
fusion-fission hybrid reactors 80−74019
fusion-fission hybrids, mag. mirror blankets and drivers 79−13517
fusion/fission reactors, inertial confinement systems 79−13519
g-2 technique, evolution and future prospects 77−34154
gait analysis of bipedal locomotion 80−56104
galactic and intergalactic astronomy, pulsars, X-ray sources and γ-ray bursts *(Russian)* 77−57061
galactic centre region, eruptive phenomena 78−57647
galactic globular clusters, basic morphological data 79−92815
galactic magnetic field review of obs. 80−73042
galactic morphology of H and trace gases 77−26070
galactic spiral structure, density wave theory *(German)* 79−17103
galactic structure, models and theories based on gamma astronomy *(French)* 77−60829
galactic structure from gamma ray obs. 80−98743
galactic X-ray sources 77−29962
galaxies, chemical evolution 77−26068
galaxies, evolution of stars and gas 80−77486
galaxies, nearby, radio continuum obs. *(German)* 80−109544
galaxies, origin, structure and evolution *(Chinese)* 77−87551
galaxies, origin and early evolution 80−17669
galaxies, outstanding problems and future instrumental prospects 77−91626
galaxies, spatial distrib. of different types 79−84862
galaxies active and normal nuclei, radio emission 78−57646
galaxies active nuclei, continuous optical spectra 78−57644
galaxies active nuclei, emission line spectra rel. to ionised gas and dust 79−88730
galaxies formation and evolution, review 79−17100
galaxies of Magellanic type, review *(German)* 80−105348
galaxies with radio tails, review *(French)* 78−41054
galaxy classification, structure and origin 78−49541
galaxy distribution correl., appl. to Universe structure and evolution theory 79−62912
galaxy formation, props. of young galaxies 77−33645
Galilean satellites of Jupiter 79−5777
gamma camera, line spread function meas., practical considerations 79−17585
gamma ray astronomy *(Korean)* 79−12368
gamma ray spectral penetration through radiation shields 80−5343
gamma-ray astronomy, present status 79−25763
gamma-ray astronomy *(German)* 77−60853
gamma-ray astronomy 77−64888
gamma-ray astronomy *(Polish)* 78−96394
gamma-ray astrophysics, new look at universe 79−80373
gamma-ray backscattering, survey of principal research 77−65340
gamma-ray line astronomy, review 79−44641
gamma-ray picture of sky, review *(Russian)* 78−41097
gamma-resonance solid-state spectroscopy under HF excitation conditions 77−48113
garnet film, LPE growth, for bubble memory appl., book contrib. 79−70009
garnet film, physics of domain walls 79−99727
garnets, magnetic anisotropy and magnetostriction 79−99748
garnets, magnetic relaxation phenomena 79−99776
garnets, magneto-optical properties 79−99859
garnets, photoinduced phenomena 79−99718
garnets magnetic excitations 79−99695
gas analysis, isotope technique appl., ionisation detectors 79−20481
gas chromatography detectors, appl., development, sensitivity, response, operating conditions 77−1955
gas chromatography ionisation detectors 77−44564
gas chromatography techniques, mistakes made by non-specialists 80−55730
gas chromatography-mass spectrometry, integrated analytical systems, applics. in biomed. and related sciences, review 80−36200
gas chromatography-mass spectrometry integrated anal. systems, review 79−1972
gas chromatography/Fourier transform IR spectroscopy, review 80−55729
gas chromatography/mass spectroscopy integrated systems 80−68289
gas cooled reactor experience and programs in France 79−45332
gas cooled reactors, background and status in UK 79−45333
gas dynamic measurements using optical interferometry 77−35286
gas dynamics with relaxation effects, acoustic waves, nonequilibrium atmosphere effects 78−79390
gas flow, Monte Carlo simulation, book contrib. 78−59365
gas laers, frequency stabilised by saturated absorpt., synthesis and measurement of optical frequencies *(French)* 79−31966
gas laser, reson. vibr. excitation by electron impact, low energy, book contrib. 77−50662
gas laser beam-plasma interactions, in mag. field, book contrib. 77−51196
gas laser discharge oscillations 78−55339
gas laser plasmas, spectroscopic diagnostics, book contrib. 77−51242
gas laser recombination processes, book contrib. 77−50663
gas laser systems and appls., book contrib. 77−50680
gas laser with wide-band optical pumping, review 79−31885

reviews continued
gas lasers, at. and mol. vibr. and electronic metastable states, book contrib. 77−50653
gas lasers, atomic and ionic, excitation mechanisms and characts., book contrib. 80−106512
gas lasers, CO_2 high-power lasers, book contrib. 77−50651
gas lasers, electron beam ionised, book contrib. 77−50664
gas lasers, glow discharge, high-power mol. laser stability, book contrib. 77−50650
gas lasers, optically pumped IR, book contrib. 77−46718
gas lasers 77−7099
gas lasers 77−38866
gas mixtures, adsorpt. by solids 79−28211
gas phase reaction consts. for electronically excited species, relax. processes, data tables 80−16644
gas proportional scintillation counter 77−57826
gas sorption and transport in glassy polymers 80−15360
gas transport, in synthetic polymer membranes, history 78−76912
gas-cooled reactors, current development status 79−22375
gas-particle mixture flows, aerodynamic problems, French contribs. 77−42909
gas-particle mixture flows, fundamentals and applics. 77−42913
gas-particle mixture flows, German R&D 77−42910
gas-particle mixture flows, report of European developments 77−42908
gas-particle mixture flows, research at Von Karman Inst., Belgium 77−42912
gas-particle mixture flows, UK research survey 77−42911
gas-phase reactions, spectral-kinetic investig. rel. to chemical laser development *(Russian)* 77−90604
gas-solid mixture, flow in standpipes, review 79−18935
gas-solid packed bed systems, heat transfer 79−68704
gasdynamics and homogeneous nucleation 77−62292
gaseous criteria pollutant methodology and standards for USA Clean Air Act 80−94133
gaseous ion thermochemistry, metastable ion kinetic energy spectrometry 77−44537
gaseous nebulae, riddle of spectra, history 80−8676
gases, high resolution rotational Raman spectra, review 80−23425
gases, low energy positron interactions, review 78−50651
gases, rot.-vibr. Raman spectrosc., high resolution 80−22442
gases, structure determination by diffraction methods, philosophical aspects 78−50665
gases, weakly ionised, electron motion, stochastic theory of homogeneous systems, review, stochastic theory of homogeneous systems 80−77735
gases in metals, trends in modern anal. *(Russian)* 80−15123
gauge scheme of weak and electromagnetic interactions *(Russian)* 79−26278
gauge theories applied to weak interactions 77−26479
gauge theory of gravity and supergravity on a group manifold 79−21635
gauge unification of fundamental forces 80−95238
Gaussian stochastic processes in physics 79−25982
GCFR cores, heat transfer with He and Na coolants 79−45331
GCFR design studies 79−45330
gemstones, synthetic, cryst. growth *(German)* 79−33926
generalised coherent states, irreducible representations of Lie groups, anal. and applications 78−62114
generalized calculus and its applications 79−35527
generalized conductivity coefficients of heterogeneous system with chaotic structure 77−87708
generalized vector dominance, photon-hadron interaction anal. book contrib. 80−47265
geodesy, an ordering factor in society *(German)* 77−60344
geodesy, development and form. of calc. of trigonometric networks *(German)* 78−15947
geodesy, Doppler satellite positioning in Canada 77−44883
geodesy and geophysics appls. of artificial satellites 77−64183
geodetic research, objectives, meas. techniques and data processing methods *(German)* 80−101317
geoelectric phenomena assoc. with earthquakes 78−36095
geologic evolution of terrestrial planets 77−53442
geologic nuclear waste disposal, pathway anal. review 79−22424
geological data automatic contouring techniques 78−7820
geological structures, structural fracture and stress fields *(Chinese)* 79−53343
geomagnetic coast effect, review 80−94458
geomagnetic depth sounding below magnetometer arrays for atmos. research 80−98486
geomagnetic excursions and palaeomag. record 77−86779
geomagnetic influences on man-made systems 80−12887
geomagnetic Pc 3 pulsations, obs. in congugate areas around L=4 77−45260
geomagnetic variations and substorms 77−91381
geomagnetism, secular variations on historical time scale 80−36236
geophysical environment, monitoring techniques for neutral atmosphere *(Japanese)* 78−16126
geophysical environment sensing by radiophysical methods *(Russian)* 77−78435
geophysical interpretation problems, soln., correl. theory of homogeneous random fields appl. 79−100986
geophysical prediction, overview and recommendations 79−8703
geophysical turbulence, buoyant flow, book contrib. 77−60459
geophysical turbulence and air-sea interactions 78−92953
geophysics, global problems of fluid dynamics 78−96173
Geos 3 project, review 80−4224
geoscience information services, review, conf., April 1978, London 80−46183
geostationary meteorological satellites, role played in Global Weather Expt. 80−77256
geostrophic turbulence, book contrib. 80−19336
geothermal energy, environmental problems, air and water pollution, subsidence, induced seismicity, blowouts, noise 80−55797
geothermal energy 79−29447
geothermal energy prospecting by geophys. methods 78−7803
geothermal resources for elect. generation or direct heat utilisation, review 80−35636
German Standards Institute, 50 years of standardisation in surveying *(German)* 78−45591
German standards on image assessment 78−58926
giant intrinsic magnetic hardness 78−48004
giant multipole resonance in nuclei 78−13044
giant multipole resonances and inelastic pion scattering 79−85426
reviews continued
giant planet atmospheres, IR radiation 80−8568
giant pulse lasers, passive mode-locking 79−72608
giant Raman scattering by mols. adsorbed on metals 80−93343
Gilbert, Grove Karl, 1843-1918, life and contribs. to geomorphology 78−45451
glacial inception and disintegration during the last Glaciation 79−5534
glacier ice secondary and tertiary creep 77−64339
gland cells, stimulus-response coupling, book contrib. 80−108864
glass, mechanical properties 78−3162
glass, new appls. 78−3306
glass, phase separation 78−2015
glass, refractive index, freq. depend., use of dispersion formulae 79−65825
glass, refractive index gradients, form. using ion exchange diffusion 80−64227
glass, relaxation phenomena 78−2014
glass, relaxation phenomena and Raman spectroscopy, review of developments 78−22665
glass, single-component, structure, crystallite and disordered-network hypotheses 79−41964
glass, surface treatment, improvement in mech. and optical props. recent progress *(Japanese)* 79−79141
glass, ultrapure, prep. for optical waveguides 78−3086
glass capillary gas chromatography 79−57319
glass ceramics, phase transformations 80−3025
glass fibre for optical waveguide communication, state-of-the-art review 77−62052
glass fibre long wavelength optical communication, materials and devices 80−99854
glass fibre production methods for optical communications *(German)* 80−23813
glass fibre reinforced cement, review of reinforcing theory, ageing, stress/strain relations 78−44165
glass fibre reinforced plastic, fatigue processes, review 80−81176
glass fibre reinforced plastic pipe, on-line US inspection 77−86263
glass for construction purposes 78−3307
glass formation, models 78−2012
glass forming melts, crystn. kinetics processes 80−64905
glass forming processes 78−3090
glass industry, air pollution 78−3936
glass industry forming machines 78−3091
glass making process, math. and phys. models 78−3083
glass making refractories, progress 78−3089
glass making refractories, progress 80−40303
glass melting, heat transfer 78−3084
glass melting, new aspects 78−3087
glass melting furnaces, development and prospectives 78−3088
glass optical fibre, vapour phase materials and processes, review 80−58825
glass raw materials and batch prep. 78−3085
glass structure, X-ray, neutron and electron diffraction studies 77−65954
glass structure 78−2013
glass technology and applications, review of advances 77−66618
glass track detectors 77−23370
glass-metal bonding *(German)* 79−83167
glasses, acoustic and dielec. props. at low temps. 78−6128
glasses, ESR studies 80−108049
glasses, US props. 77−69048
glasses and amorphous semiconductors, band struct. and forbidden gap, review 78−75987
glasses as bioactive materials, review 78−3698
glassy metals, structure, transport props., magnetic behaviour 80−70138
glassy state and highly viscous liq., rheology 80−70130
global nuclear power is alternate source of energy, prospects and issues 80−7897
global reactor calcs., homogeneous and heterogeneous methods 78−58341
globular star clusters, age and chemical comp. determ. *(Polish)* 78−61751
globular star clusters, dynamic evolution, review of obs. and numerical theories 78−77585
glottic cancer, early, radiotherapy 80−12217
glottic cancer, early, radiotherapy 80−12218
glow discharge as welding heat source, appls. 79−73051
gradient-index optics: a review 80−69478
grain boundaries, cubic materials, intergranular structures, geometrical approach *(French)* 80−59482
grain boundary segregation, critical assessment 80−75362
grain boundary struct. 77−4110
grain boundary struct. and energetics 78−14359
graphite, electron-phonon interactions, rel. to elec. transport 80−34156
graphite, pyrolytic, galvanomag. effects, effect of fast neutron irradiation 80−34465
graphite, synthetic materials, radiation defects, review 77−47494
graphite compound, metallic electronic props. and correl. with chemistry 80−44567
graphite intercalation compounds, electronic props. review 78−30860
graphite intercalation cpds., electronic props. 78−34744
graphite intercalation cpds., Raman scatt. and IR refl. 80−45066
graphite-based composite mats. and refractories 78−56609
gravitating fermions, thermodynamic functions 79−80552
gravitating fermions, thermodynamic potentials 79−80551
gravitation, gauge group deformations, generalised Gupta program 80−12957
gravitational experiments in space 79−6042
gravitational field gauge theories 80−98848
gravitational field influence on turbulent flow and heat exchange, review 79−86427
gravitational interaction, spin, rotation and quantum effects 80−37203
gravitational radiation, multipole expansions 80−73240
gravitational radiation detection *(Japanese)* 78−77792
gravitational wave research, current status and future prospects 80−73254
gravitational waves and radiation detectors 79−126
gravitons in Minkoswki space-time, review 77−87683
gravity waves nature and role in tropospheric processes 79−92575
guided acoustic waves in the ocean 79−39753
guided optics techniques for meas. of film props. 79−99958
guided wave devices, use of ferroelectric materials, review 78−38048
guided wave optics, appls. 79−37054

reviews continued
gyrotron, stimulated emission of cyclotron radiation 77−34865
H II regions in Cygnus X region 77−9783
hadron+hadron elastic scatt., >100 GeV, asymptotic theorems *(Czech)* 78−29357
hadron+hadron high energy collisions, variables and optical concepts 80−444
hadron collisions, lepton and photon production 79−405
hadron constituent models review, fixed angle and Regge behaviour, hard scatt., fragment X-distrib. 78−78154
hadron elastic scatt., high energies 77−257
hadron EM interactions 80−412
hadron induced lepton production, state of art 79−26340
hadron interactions, inclusive processes, multiplicity and scaling, resonance production, additive quark model, SU(6) theory 80−63043
hadron interactions, multi-particle production processes, interaction models 78−33024
hadron photoproduction, high energy diffractive processes, book contrib. 80−47309
hadron photoproduction nondiffractive processes, review, book contrib. 80−47313
hadron physics at high p_T 80−73743
hadron resonance, EM decay and excitation, review, book contrib. 80−47300
hadron-hadron collisions at high energy, large transverse momentum processes *(Russian)* 79−26351
hadron-hadron diffractive phenomena 77−57552
hadron-hadron multiparticle prod. *(Russian)* 77−2875
hadron-lepton deep inelastic scatt., book contrib. 80−47260
hadron-nucleus collisions at high energy, expt. data 77−50120
hadron-nucleus interactions at high energies, phenomenological models 78−8859
hadron-nucleus reactions, multiple production, expt. results *(Russian)* 79−3118
hadronic high momentum transfer scatt., spin meas. and polarisation review 79−63498
hadronic massive lepton pair prod., theory review, Drell-Yan model 78−89752
hadronic structure using parton anal. of deep inelastic scattering and rel. processes 79−80803
hadrons and quarks in high energy collisions, review 79−49482
haematologic disorders, radionuclide therapy 80−36109
haemoglobins and chlorocruorins, extracellular respiratory, physico-chemical and functional props. 80−3581
hail-meas. instruments 77−33196
Hall effect, discovery and applications 80−31477
Hall effect in disordered and ordered systems, theoretical view 79−51605
halogen and inert gas cpds., chem. bond, MO LCAO SCF calcs. 79−41104
Hamiltonian dynamics, integrable and nearly integrable systems historical review 78−93521
hand prostheses, ideas on sensory feedback 80−51295
handicapped persons technical aids, R&D in Sweden *(Japanese)* 78−48934
hard superconductors, mag. instabilities 77−89908
hardfacing 78−72937
harmonic generation, state of art 80−33090
Hartree Fock Bologiubov theory, appl. to light/heavy nuclei, book contrib. 79−75881
^{4}He thin film, superfluidity 80−107594
hearing mechanism, phys. 77−90808
heart rate and blood pressure biofeedback, literature review 80−21484
heart rate and blood pressure biofeedback theoretical models review 80−16974
heart valve prostheses development 77−56523
heat and mass transfer, bibliography, Soviet works 78−22343
heat and mass transfer, book contrib. 77−58693
heat and mass transfer, Polish works, (1975-1976) 78−38320
heat and mass transfer, Soviet bibliography 79−68701
heat and mass transfer bibliography, Soviet work 77−39288
heat and mass transfer bibliography−Polish works (1977-1978) 80−57020
heat and mass transfer bibliography−Soviet works 79−23318
heat and mass transfer bibliography−Soviet works 80−90618
heat and mass transfer development in USSR 79−14201
heat conduction in region with moving boundaries, analytical soln. methods for boundary-value problems 77−75768
heat exchangers, R and D in Japan 80−35737
heat of adsorption determ., expt. methods 79−42370
heat pipes and their instrument applications 77−10010
heat transfer, 1976 literature 78−5740
heat transfer, 1977 literature 79−14392
heat transfer, bibliography, 1975-76 77−27526
heat transfer, bibliography, Japanese works 78−22344
heat transfer, bibliography, Japanese works 1974-76 77−15012
heat transfer, Japanese literature (1975-1976) 78−79314
heat transfer, review of 1978 literature 80−23860
heat transfer bibliography, Japanese works 79−23317
heat transfer bibliography, Japanese works 80−31442
heat transfer bibliography 78−75141
heat transfer bibliography 79−68700
heat transfer bibliography 80−51978
heavily doped semiconductors and devices 79−47039
heavy current electron beams prod., survey 78−33337
heavy element nucleosynthesis, current astrophysical theory review 77−29644
heavy element origin, supernova model, r- and s-processes 77−56825
heavy ion, deep inelastic reactions, as probes of nuclear matter 78−46083
heavy ion accelerator facilities in Europe 80−42880
heavy ion collisions, perturbed stationary state method, low energy collision and mol. resons. 80−78320
heavy ion collisions at high energy, review of four theoretical methods based on classical approx. 79−89326
heavy ion direct transfer reactions, DWBA approach review 79−49614
heavy ion dissipative collisions, ang. momentum transfer 80−13501
heavy ion elastic and inelastic scatt., book contrib. 80−27668
heavy ion fusion, expt. data comparison with classical trajectory models 80−9324
heavy ion reactions, dynamical properties, field overview 80−18327
reviews continued
heavy ion reactions, energy depend. struct., book contrib. 80−27671
heavy ion reactions, reaction types, reaction theories 78−74401
heavy ion reactions at relativistic energies, nuclear matter 77−26781
heavy ion science research in Japan *(Japanese)* 79−25813
heavy ion transfer reactions, book contrib. 80−27669
heavy ion-nucleus collisions, friction model 78−86546
heavy lepton, τ, discovery, props., prod. in $e^+e^- \rightarrow \tau^+\tau^-$ 78−89694
heavy lepton τ, experimental evidence for production in e^+e^- annihilation 79−75758
heavy lepton properties, experimental evidence, theoretical predictions 77−57582
heavy leptons in e^+e^- interactions, short review 77−30473
heavy nuclei, photoproton reaction, isospin effect 79−80926
heavy particle elastic collisions, quantum effects *(Japanese)* 78−21015
heavy quarks, elementary particle physics developments 79−22053
heavy quarks and new particles 80−73661
heavy-ion accelerators, book contrib. 78−90003
heavy-ion beam inertial-confinement fusion, commercial power generation 79−6762
heavy-ion charge exchange reactions 77−57690
heavy-ion collisions, supercritical fields, charged vac. and pion condensate effects 78−21600
heavy-ion elastic and inelastic scatt. 78−37375
heavy-ion stripping, semi empirical expressions 78−13395
Heisenberg ferromagnet surface, spin behaviour, review 77−20527
hepatic mass evaluation, relationship of ultrasonography, nuclear medicine and computerised tomography 80−17092
hepatobiliary functional scintillation recording *(German)* 80−30874
AM Herculis (4U 1814+50), X-ray emitting mag. white dwarf binary, review of props. 80−105403
hereditary damage [review] after low-level radiation exposure 80−67165
heritable lesions, radiation induced, in proliferating mammalian cells 79−20602
heteroatomic cpds., paramag. reagents for ligand mol. struct. determ. from NMR 79−13741
heterodyne holographic interferometry 79−86141
heteroepitaxial structures based on III-V compounds, appl. in optical electronics, defect form. 78−23160
heterogeneous flows of multi-component mixtures in porous media−review 78−59471
heterojunction lasers, for fibre optic data systems 79−55149
heterojunction solar cell, relation between efficiency and heterojunction parameters, review 79−74523
heterostructures for integrated optics 77−39112
HF current surgery, instruments and problems *(Hungarian)* 80−98172
HF heating in Tokamaks and stellarators 80−28736
HF radio oceanography 78−77241
high detective quantum efficiency image detectors 77−71010
high dynamic pressure measurements in solids 80−47070
high electrical resistance measurement 80−57331
high energy collisions, theoretical overview 80−42682
high energy electron diffraction, theory 79−68985
high energy interactions of nuclei 79−22326
high energy neutrino experiments, state of art 79−26322
high energy particle interactions on nuclei, review 80−42658
high energy photon absorption cross section for matter *(Japanese)* 78−74506
high energy physics, quest for charm, D and F particle discovery, superheavy leptons *(German)* 78−66184
high energy physics and applied superconductivity 77−26949
high energy physics CAMAC hardware 79−13617
high energy physics in USSR, book contrib. 79−21890
high energy resolution X-ray spectroscopy 80−14959
high impact strength materials, laser beam effects 80−21073
high intensity Raman interactions 79−76759
high level radwaste management, storage, transportation, disposal, review 79−54522
high magnetic field generation in Grenoble and appls. 80−13110
high power laser propag., thermal blooming 78−30035
high power lasers and their applications 78−87092
high power neutral injectors 80−18656
high Prandtl number convection, geophs. appl. 79−81875
high pressure molecular beam mass spectrometric sampling 80−52355
high pressure phases of materials 79−8289
high pressure physics 77−43278
high pressure production at low temps. 78−12709
high resolution NMR of solids 78−6582
high resolution tunable laser spectroscopy 77−74515
high resolution UV solar spectroscopy, review 78−45313
high strain rate processes 80−84864
high strength structural mats., microstruct. influences on fatigue and fracture resist. 78−56728
high temperature corrosion *(Japanese)* 78−72911
high temperature materials problems in fusion reactors 77−65329
high temperature mechanical behaviour of crystalline solids 80−59568
high temperature vapours, phase transitions, equations of state, appl. of laser pulse heating 80−52230
high-energy physics, progress and prospects 78−45989
high-energy two-body and inclusive reaction data 78−29370
high-power lasers 80−32950
high-resolution electron microscopy, present state of instrumentation 79−2887
high-temperature alloys, hot corrosion, book contrib. 78−11444
high-temperature chemistry, book contrib. 77−40545
high-temperature electron diffraction, by gases 80−52237
high-temperature materials, technological requirements, R and D, report 80−45222
high-temperature plasma, X-ray spectroscopy 77−31434
high-temperature power-technological industrial processes use of nuclear power, reviews 79−26729
high-temperature superconductivity non-specialist review 77−12070
highly excited atoms, collision processes 77−58146
highly excited atoms, review of recent expts. 80−23325
highway traffic noise prediction, state of the art review 77−65651
Hinkley Point B AGR station computer control system, performance review 79−89457
hip joint diseases from radiological and pathological-anatomical view points *(German)* 79−83920
historical climatology 79−16641
historical introduction, weak interactions, book 78−78133

reviews continued
historical supernovae and possible remnants *(Italian)* 79−53837
history of science, continuity of scientific ideas, problems rel. to evaluation and assessment 79−44694
History of Sciences Collections, Royal Swedish Academy of Sciences, catalogue 78−81789
hollow cathode discharges for gas lasers 80−83599
hollow cathode discharges for gas lasers 80−99717
hologram copying methods 79−45915
hologram recording in white light 77−7033
holographic interferometry in mechanical testing 79−87788
holographic memories, used for data recording 80−58478
holographic method of small particle analysis 79−13924
holographic microscopy, theory and appls. 78−45690
holographic recording materials and devices, book contrib. 78−25838
holographic vibration measurement *(German)* 78−33709
holography, 1948-78 development *(Czech)* 79−98315
holography, applications and theory review, background and current status 78−74866
holography, industrial applications, review *(Japanese)* 78−78958
holography, principles, materials, applications *(Italian)* 77−42507
holography, research and development of Soviet State Optical Institute 79−94199
holography in dentistry 78−48859
holography today and tomorrow *(Japanese)* 78−78957
hopping conductivity in ordered and disordered solids, review 77−1420
hopping conductivity in ordered and disordered solids 77−15851
host cell membranes in animal virus reproduction, review 78−15791
hot carrier noise, exptl. and theoretical aspect, survey 79−28389
hot electron phenomena, calc. 78−26870
hot electron physics *(Japanese)* 80−49754
hot electron quantum magnetotransport 78−30940
hot pressing 79−74113
hot stars, mass loss *(German)* 79−16958
hot-wire test, critical review and comparison with BS 1902 panel test 80−104409
HTGR, nonelec. appl., prod. of H_2 and synthetic hydrocarbons 79−45329
HTGR, US R and D programs for steam supply plant, fuel and materials 79−97757
HTGR development and its process heat, steam-cycle and gas turbine appls. 80−63250
HTGR utilisation in technological processes and electric power generation 79−97886
HTR, reactor types, design, uses *(French)* 77−67857
HTR LEU oxide fuels, performance data review 80−42780
HTR material developments, Dragon Project 77−65273
HTR power station, design development, operation and appl. *(German)* 79−76088
human factors in nuclear power plants 79−89463
Hume-Rothery Phases, electronic struct., main features 79−23883
hurricanes and tropical meteorology 79−39785
HV electron microscopy, recent progress, book contrib. 79−67442
HV lines to 800 kV, elec. and mag. field effects on human beings *(French, English)* 80−72209
hybrid image processing, potential of optical methods 79−27185
hybrid reactors, fusion driven fissile fuel breeder systems 80−57954
hydrocarbon crystal, calc. of internal friction resulting from molecular defects 78−31448
hydrocarbon fuels combustion prod. plasma with alkali impurity, elec. cond. 79−55466
hydrocarbons, volatile, detection and meas. in atm. 77−64492
hydrocarbons emissions inventory in United Kingdom 79−62158
hydrodynamic instability in isotropic fluids, book contrib. 77−89098
hydrodynamic interfacial instability, mechanical, chem. and elec. constraints, review 80−34278
hydrodynamic models in star formation *(Polish)* 80−67709
hydrodynamic stability problems with time-depend. boundary conditions, numerical simulation methods 80−19411
hydrodynamics 77−14973
hydroelectric power generation in Pakistan 79−34423
hydrology instrumentation *(French)* 79−39979
hydrometallurgy, developments 80−45252
hydrometeorological information in USSR, economic effectiveness 79−29909
hydrometeorology, new directions review 78−96240
hydrophobic interactions, lipid-protein binding, thermodynamics, book contrib. 79−16129
hydrothermal alteration in active geothermal fields 79−5535
hyperfine fields on fast ions in ferromagnetic media 78−37283
hypernuclear physics, beginnings 80−47418
hypernuclei, ground state prod. and props., present status of experimental research 79−30799
hypernuclei general props. with experimental methods 79−22224
hyperon beam physics, book contrib. 80−68503
hyperthermia, deep local, induction by US and EM fields, problems and choices 80−94283
hyperthermic tumour-cell devitalisation in vivo 77−70424
hyperthyroidism, childhood, role of radioiodine treatment 80−41182
hysterosalpingography, appraisal of current indications 80−56169
ice Ih, dislocations, effect on physical and mechanical props. *(French)* 77−55287
ice nucleation, study of different modes 79−48530
ice nucleation in atmosphere, natural nuclei origin 79−48531
iconics and image processing 79−94173
identification of materials, review of available methods 78−95876
igneous rocks, thermoremanent magnetization 77−91113
II-VI compounds, electron energy radiation damage thresholds, EPR and luminescence 77−84799
II-VI cpds. in solar energy conversion 77−77377
II-VI semiconductor Franz-Keldysh effect modulators for laser radiation *(Russian)* 77−88813
II-VI semiconductors, impurity and defect centre energy states, luminesc. meas. 80−55150
II-VI semiconductors, injection electrolum., book contrib. 77−73174
II-VI semiconductors, radiation effects, optoelectric props. control 80−25458
III-V compound MIS structs. 78−95372
III-V compound semiconductors, electronic uses 79−65538
III-V compounds and alloys, MBE process and problem areas 80−10815
reviews continued
III-V quaternary alloys, melt and soln. growth of bulk single crysts. 80−35079
III-V semiconductor, point defects and dislocation climb 79−82209
III-V semiconductor properties and optoelectronic device appls. 79−74088
III-V semiconductors, deep level defects, review 80−24841
III-V semiconductors, electrolum. and related props., book contrib. 77−73173
III-V semiconductors, p-n heterostructures, epitaxial growth techniques, appl. to optoelectronics 80−54770
III-V semiconductors, radiation induced defects 77−80544
III-V semiconductors, radiative recomb., optical evaluation review 80−60647
III-V semiconductors, transport phenomena, review 79−19587
III-V semiconductors for optoelectronic appls. 78−30975
III-VI compound layered materials, prep. and growth, book contrib. 78−19661
Illinois climate centre, review 80−77118
image assessment; review of German standards 78−50724
image deconvolution, complex spatial filters 77−10860
image intensification in medical and industrial radiology *(French)* 77−30223
image processing in nuclear medicine 80−81694
image reconstruction by projection *(Italian)* 79−53207
image reconstruction formulae, computer implementation 80−52179
imaging and optical communication through atmospheric turbulence, book contrib. 79−34960
imaging process efficiency and quality, electrophotographic process, electronographic cameras and image intensifiers 78−78932
immunological effects of irrad. 80−81660
impact, abrasion, wear, review *(German)* 78−88536
impact noise, review and bibliography 79−3848
impinging free shear layers, self sustained oscillations, book contrib. 80−19466
implantable prostheses 80−101292
implanted atoms, Mossbauer studies 80−39913
implanted cardiac pacemaker experience and trends 77−81701
implanted ion lateral spread *(Japanese)* 79−4322
implanted semiconductors, laser annealing 80−107301
impulse/impact noise, current knowledge 80−79056
impurity centre conc. meas., junction capacitance technique *(Japanese)* 78−79958
impurity centres, electron-phonon coupling from structured optical spectra 80−89038
impurity conduction phenomena, review of exptl. work *(Japanese)* 80−49737
impurity defect interaction influence on radiation hardening and embrittlement 80−35199
impurity depth profiling of H and He isotopes within near surface region of solids using ion beams 79−7622
impurity scattering theory in crystals 77−85172
Inca people (Peru), evidence of astronomical knowledge *(Swedish)* 78−32640
inclusive high energy particle-nucleus interactions, A depend. of multiplicity, cross section, rapidity, momenta distrib. 77−79291
incoherent scatter radar technique appl. to lower thermospheric dynamics 79−8734
Incoloy 800, chem. behaviour and mech. performance in HTR He at high temps. 79−47842
Incoloy 800, corrosion resist. props. in high temp. steam, review 79−47839
Incoloy 800, design codes and lifetime prediction aspects for nuclear and non nuclear appls. 79−47778
Incoloy 800, high temp. corrosion and mech. props. in Na environment 79−47840
Incoloy 800, high temp. gaseous corrosion in sulphidising environments 79−47838
Incoloy 800, review of mech. props. up to 600°C 79−43368
Incoloy 800, review of structural charact., heat treatment and comp. effects 79−43297
Incoloy 800, review on high temp. gaseous corrosion in carburising and oxidising environments 79−47837
incommensurably distorted structures, rel. to structural phase transition 80−10665
incommensurate structural phase transformations, recent neutron scatt. studies, review 79−42205
incommensurate structural phase transitions and phason interpret. *(Japanese)* 78−22827
incompressible boundary layer separation; book contrib. 77−51033
indeterminate−mass particles 79−26319
Indian nuclear medicine 80−36082
inductive storage technology, new applications 78−55019
inductively coupled plasma-AES, present and future position in analytical chem. 80−7887
industrial gases, density meas. at melting, boiling points, survey of methods, apparatus *(German)* 79−30421
industrial lasers, multikilowatt CO_2 lasers, survey 77−46731
industrial metallurgical processes, alteration due to political considerations, and raw material availability 79−4901
industrial meteorology and American Meteorological Society, history 77−49543
industrial radiography and radioscopy, basic physical principles 77−38067
inelastic electron scattering as analytical tool 78−24010
inelastic electron tunnelling spectroscopy, past and future 78−90255
inelastic electron tunnelling spectroscopy, vibr. spectra 77−54632
inelastic electron-matter interactions 80−104024
inert gas crystals with imbedded impurities, struct. and diffusion props. 80−10563
inert gas excimer lasers, book contrib. 79−81417
inert gas fluoride lasers 78−71083
inert gas halide excimer lasers, book contrib. 79−81418
inert gas halide high-efficiency UV lasers 77−54706
inert gas halide high-power lasers, efficiency and energy scaling 79−36887
inert gas halide lasers, kinetic processes 78−63098
inert gas solid, long range forces, book contrib. 77−51347
inert gas solids, band struct. and excitons, book contrib. 77−47731
inert gas solids, cryst. struct., book contrib. 77−51348
inert gas solids, lattice dynamics, book contrib. 77−47522

reviews continued
inert gas solids, research history, book contrib. 77−49547
inert gas solids, self-consistent phonon theory, book contrib. 77−51460
inert gases, interatomic pots., book contrib. 77−46615
inert gases, short and intermediate range forces, book contrib. 77−50494
information transmission by laser *(German)* 77−54810
information transmission with laser beams 77−38821
infrared astronomy 79−35153
infrared heterodyne spectroscopy in astronomy 78−85859
infrared multiphoton dissociation of molecules *(Japanese)* 80−11885
infrasound waves, in the Earth's atmosphere *(Russian)* 78−32143
inhaled heavy elements deposited in vivo, external counting, review 80−36152
inhomogeneous materials, electronic props., metal-nonmetal transitions 78−56073
injection lasers, mode comp., control with selective cavities 80−19037
injection lasers, state of research *(German)* 79−7146
inner shell (e, 2e) symmetric reacts., for ats. and mols. 77−19092
inner shell excitation, impact parameter dependence 77−19047
inner shell excitation in molecules by electron impact 80−37899
inner shell excitation processes in heavy ion-atom collisions 80−37874
inner solar system, mag. fields, plasmas and coronal holes 79−58212
inorganic crystals, vibr. spectroscopy 80−55093
inorganic glasses, IR transmitting materials, appl. in 1 to 6 μm range, mech. props., review 79−4250
inorganic ion exchanges, appl. in U, Pu separation from fission product solns. 79−85625
inorganic oxide glasses, internal friction *(Polish)* 79−95078
inorganic photochemistry, review 80−3382
inspection of part quality, coarse struct. materials, LF US methods 80−81264
instantons in field theory 79−71642
instrument science, introductory article 77−53847
instrumented impact testing, critical review 77−36725
insulating crystals, growth mechs., practical techniques, review 77−69975
insulating thin films on Si, instability phenonema 77−12037
integrated electro-optic modulators 79−37058
integrated optical devices fabricated by MBE 79−95943
integrated optics, device principles 78−1429
integrated optics, film appls. 78−71234
integrated optics, for communications, present status 77−46822
integrated optics, GaAs technology and device develop. 77−46823
integrated optics, new wave phenomena, thin films, review 77−54817
integrated optics (1977) 78−33916
integrated optics and guided wave devices 78−42468
integrated optics and optical waveguide devices 78−66948
integrated optics and thin-film technology 77−54815
integrated optics bibliography 78−66959
integrated optics for wavelength division multiplexing, review of recent developments 78−38079
integrated optics using periodic structures 77−39109
integrated-optics elements with distributed coupling, surface waves 79−64361
intense particle beams, production and handling 79−76117
intense pulsed ion beam accelerators 77−71707
intense sources of fast neutrons 79−22522
intensity fluctuation spectroscopy studies of Brownian motion 80−52129
intensive care unit/coronary care unit safety 78−69252
interactions between two light nuclear systems, two-body pots. 77−18501
intercalation *(Japanese)* 77−68930
intercalation compounds, metal guests in chalcogenide hosts, struct., review 79−46627
intercalation compounds, synthesis *(French)* 78−27429
intercalation properties *(Japanese)* 80−49838
interface of two phases or liquids, selective processes induced by resonance laser radiation 78−64867
interferometry, including holographic interferometry 78−37050
intergalactic matter and evolution of galaxies 80−109543
Interkosmos program and Magion satellite project 80−98535
intermediate energy nuclear physics, review of recent expts. 78−50061
intermediate valence, review of theoretical situation 79−4536
intermediate valency compounds, properties and appearance conditions 80−103649
intermetallic compounds 78−15333
intermetallic compounds of rare-earth and 3d transition metals, struct., props. 78−10668
intermolecular forces, Raman scatt. obs. 80−23427
intermolecular interaction potential, adsorption, Henry const. 78−22948
intermolecular interaction theory, modern state, rel. to large mols. 80−14186
intermolecular interactions and biomol. organisation 77−64006
intermolecular interactions and potential energy wave calcs. 80−43140
internal flow, book contrib. 77−58654
internal ocean waves, book contrib. 80−21781
international architectural acoustics standards *(Japanese)* 80−64294
International Astronomical Union 1976 system of constants *(Russian)* 78−73611
International Magnetosphere Research programme, review *(Russian)* 80−17467
International Magnetospheric Study, progress report 78−20587
international radiation standards, role of ICRU 80−9414
International Reference Ionosphere, goals and status 79−5714
international standard reference radiations and their application to the type testing of dosimetric apparatus 80−9416
International Sun-Earth Explorer (ISEE) mission, review 80−90320
International Sun-Earth Explorer spacecraft, expts. and instruments 78−85785
interpenetrating polymer networks, and related materials 78−42923
interplanetary dust, origin and composition 79−75154
interplanetary H, review 78−49272
interplanetary magnetic field heliocentric distance dependence 78−73675
interplanetary magnetic field polarity effects on equatorial geomagnetic field and ionosphere 78−36416
interplanetary scintillation, appl. for solar wind probing 78−45178
interstellar CH and CH^+ molecules 77−33625
interstellar communication, theory 80−4271
interstellar gas, dust and molecules in Galaxy 78−54006
interstellar magnetic field 77−26048
interstellar matter 79−53900
interstellar matter distrib. and dynamics in spiral galaxies 78−16540

reviews continued
interstellar molecule reactions 77−9790
interstellar molecules, identified and unidentified, R&D progress *(German)* 77−67122
interstellar molecules, pioneering investigations 1935-42 period 78−69855
interstellar molecules 77−78856
interstellar molecules radio obs. 77−33616
interstellar radiating dust clouds 77−78863
interstellar radio recombination line obs., review *(Russian)* 77−57080
interstellar radio spectrum lines 77−71138
interstellar wind effect on interplanetary environment 79−5721
interstitial alloys, interstitial atomic arrangement and mobility at high degrees of interstice filling *(Russian)* 80−107223
intracranial cystic abnormalities, children, computerised tomography diagnosis 79−34641
intracranial pressure measurement, some considerations 80−17155
intraocular lenses, literature review 1976-1977 79−96707
intraocular pressure survey, pediatric patient emphasis 80−30712
intraplate seismicity, zones of weakness, alkaline magmatism and tectonism 79−74882
Invar-type alloys, review of magnetomechanical effects and state of art of materials 78−52330
inverse problem for scalar planar sources radiometry and coherence, book contrib. 79−31797
inverse problem uniqueness, scatt. object reconstruction, book contrib. 79−31824
inverse scattering problem and instanton construction by algebraic geometry 80−47203
inverse scattering transform eqns., survey of developments 78−57795
iodides and mixtures, molten, elec. cond., density, viscosity, surface tension 77−80638
ion+molecule reaction rate coeffs., ions containing C and H, review 77−25260
ion+molecule reactions, upper atmospheres of Earth and planets, interstellar clouds 78−33563
ion accelerators and their use for controlled thermonuclear reactions *(German)* 79−67933
ion accelerators pulsed power, for inertially confined fusion *(Russian)* 77−67915
ion assisted deposition *(Japanese)* 77−73227
ion beam, plasma and reactive ion etching 80−108621
ion beam appl. to corrosion 77−8963
ion beam deposition, thin film formation technique *(Japanese)* 80−35107
ion beam induced light emission 79−95850
ion beam sources, for sputtering technology 78−72719
ion beam sputtering, review of technique, appl. 78−68587
ion beam utilisation for etching and film deposition 77−32522
ion beams, compensated, handling and expts. *(Russian)* 79−46461
ion bombardment, electron microscopical anal. of surface effects and volume defects *(Rumanian)* 80−29093
ion channels in development, book contrib. 79−96549
ion implantation, appls. to colour centre research 79−19272
ion implantation, chemical and electrochem. aspects 80−100271
ion implantation, dosimetry techniques 80−32527
ion implantation, limits of comp. achievable 79−14827
ion implantation, metastable phases in metals 80−49254
ion implantation, problems and perspectives 78−75687
ion implantation and integrated optics 77−23781
ion implantation and superconductivity 78−52134
ion implantation appl. to electronic device fabrication 78−87692
ion implantation formation of amorphous layer *(Japanese)* 78−22746
ion implantation studies in tribology, corrosion, catalysis, chem. synthesis and amorphous metals 77−43236
ion implanted films, props. and appls. 78−71752
ion implanted metal layers, book contrib. 79−1835
ion microanalyser, appls. in mineralogy *(French)* 79−5628
ion microanalysis 79−96404
ion optics and mass spectrometers *(Japanese)* 77−58247
ion recombination 77−30947
ion scattering, low energy, struct. and comp. analysis of single cryst. surfaces 79−87547
ion scattering spectra, fine features 78−15267
ion selective electrodes 78−85165
ion sources, negative 78−33345
ion sources for low energy accelerators 78−58521
ion sources for low-energy accelerators 78−66445
ion transport in simple ionic crystals 78−63878
ion trapping and gas release effects in cryst. lattices, thermal desorption spectrometry 77−43262
ion-beam plasma and compensated ion beam propagation 77−80317
ion-bombardment induced photon emission, spectral features, mechanisms, band struct. depend. 77−44072
ion-implanted materials, SIMS characterisation 79−49331
ion-induced kinetic electron ejection, pot. emission, semiconductors and insulators 77−44109
ion-induced X-rays 79−96405
ion-molecule reactions, gas phase, and high-press. mass spectrometer *(Japanese)* 78−64830
ion-selective electrodes for blood serum anal. 78−3645
ion-sensitive solid-state-membrane electrodes−properties and applications *(German)* 79−1954
ion-surface scattering, low-energy elastic case 80−40211
ion-surface scattering, low-energy inelastic case 80−40212
ionic and mixed conductors for energy storage and conversion systems 77−76596
ionic channels and gating currents in excitable membranes 77−90764
ionic conduction in solid electrolytes *(Czech)* 77−59142
ionic crystal, intrinsic electronic excitations and defects *(Russian)* 80−10881
ionic crystal, surface vibrational properties 78−71928
ionic crystal surfaces, defect struct. 79−19439
ionic crystals, defects, computer modelling, review 80−107205
ionic crystals, dielectric loss and relaxation theory and kinetics 80−11335
ionic crystals, dislocations 80−107236
ionic crystals, model potentials 77−27845
ionic crystals, spectroscopy, lattice localised modes 80−50375
ionic crystals, thermocurrents 78−60381
ionic liquids, structural props. 80−96430

reviews continued
ionic mechanisms of excitation in Paramecium 80−21458
ionic melts, unusual elec. props., review 79−99338
ionic nitriding thermochemical process, equipment, process details and advantages and prospects *(French)* 80−108641
ionic reactions rate coeffs. in thermosphere, AE satellite meas. 79−48594
ionic solute hydration, thermodynamic and transport props. 78−27815
ionising radiation, primary standards and transfer methods in France *(French)* 80−5352
ionising radiation, review of sources 79−88149
ionising radiation calibration, meas. standards, CNEN, Italy 80−12273
ionization phenomena, appls. in medical diagnosis and treatment 80−67240
ionizing liquids, non-aqueous, review *(French)* 79−69255
ionosphere, anomalous resistivity 77−64528
ionosphere, atomic processes, book contrib. 77−37482
ionosphere, D-region electron loss *(Russian)* 78−85756
ionosphere, electron density models 79−48617
ionosphere, equatorial scintillation rel. to irregularities 78−36380
ionosphere, high-latit., ion velocity distribs. 79−101018
ionosphere, research in Netherlands *(Dutch)* 78−4029
ionosphere, time dispersion of EM pulses 80−94645
ionosphere and plasmasphere studies using ATS-6 satellite 80−56677
ionosphere radiowave scintillation, nighttime equatorial F-region 80−26681
ionosphere-magnetosphere system, induced elec. fields 80−94647
ionospheric drifts, review 78−36364
ionospheric EM wave propag., ducting at high-freq. 80−21872
ionospheric modification and parametric instabilities 79−101019
ionospheric scintillation 77−21995
ionospheric scintillation theory, mini-review 77−5393
ionospheric topside sounding and determination of electron profiles 80−56669
ions, spectra at high ionisation 78−62755
IR and sub-MM astronomy with balloon-borne telescopes 80−8547
IR and submillimetre astronomy, book *(Russian)* 80−72773
IR astronomical current instrumental developments 78−61737
IR astronomy and galactic dust *(French)* 78−12352
IR astronomy on Tenerife 78−69684
IR detectors, survey of different detector charact. 77−10106
IR detectors in 10 μm region *(Japanese)* 78−24862
IR ellipsometric spectroscopy, appl. to study of adsorbed species 80−39434
IR generation, difference freq. mixing, parametric oscill. and stimulated Raman scatt., book contrib. 77−46762
IR generation, optical mixing, SHG and parametric oscills., book contrib. 77−46764
IR instrumentation in ambient air monitoring, overview 77−49194
IR laser systems, for 16 μm range *(Rumanian)* 80−87408
IR lasers, and laser techniques in mol. spectroscopy 78−8455
IR materials, high transparency 77−27326
IR materials, laser residual absorpt. 2 to 10 μm 78−25906
IR non-destructive testing of bonded materials, theory and practice 80−93708
IR observations of cosmic dust at Jena University Observatory *(German)* 77−26047
IR photovoltaic detectors for 8-14 μm range *(Italian)* 78−54451
IR radiation, parametric up-conversion to visible range 80−64104
IR remote sensing measurements, conceptual considerations and surface temp. estimation 79−34984
IR spectrometry, review of literature 1976-1977 78−85223
IR spectroscopy, reflection-absorption, of adsorbed layer systems, review, book contrib. 80−84747
IR spectroscopy, ultra-high resolution *(Japanese)* 80−31912
IR spectroscopy observations of solid/liquid interface interactions 80−40733
IR spectroscopy of metal surfaces *(Japanese)* 78−19470
IR stars, review of observational data *(Russian)* 77−49377
IR stimulation and quenching of luminescence *(Russian)* 80−11455
IR technology evolution 77−5934
IR technology fundamentals 77−61120
IR window materials, optical phenomena, book contrib. 78−9420
IR-ATR spectroscopy, appl. to struct. investigation of biological material in aq. environment 80−61735
irreversible thermodynamics, basic formulations of nonequilib. thermodynamics 79−35657
irreversible thermodynamics, review of foundations postulates and implications 78−12658
island films, diffusive mass transfer 80−20054
isobar components of nuclei, experimental tests, review, book contrib. 79−97668
isostatic hot compaction 79−33960
isothermal and non-isothermal stress relaxation following steady state shear flow *(German)* 79−77044
isotope separation, new methods 78−1111
isotopic anomalies in the early solar system 79−25522
ISR projects situation (1979) *(Czech)* 80−870
IV-VI material production and physical props. for microelectronics *(Russian)* 78−11108
IV-VI narrow gap semiconductors, fabrication, IR laser and detector appls. 77−77415
IV-VI optoelectronic devices, MBE techniques 79−95942
IV-VI semiconductor film technology, review 78−3034
Jahn-Teller effect in ionic crystals 78−64015
Japanese medical technology, development and future problems *(Japanese)* 80−12287
jet, of gas, axisymmetric, free, steady-state, sound emitted *(French)* 78−67244
jet noise, current research 79−32602
jet studies and large transverse momentum collisions 79−22143
jets, turbulent, structure 80−48760
joint replacement development 77−90960
Josephson effect applications 77−20503
Josephson effects applications 77−8243
Jovian planet interior heat production 80−98606
Jupiter, IR and visible spectrum, C/H ratio 79−48729
Jupiter magnetosphere-satellite interactions, aspects of energetic charged particle loss 80−36566
Jupiter radiation belts 79−58296
Jupiter upper atmosphere, photochemical models 80−36567

reviews continued
K(K)N—K(K)N, 1.5-280 GeV/c, Regge pole residues and trajectories 78−45886
kaons 78−78173
KEK proton synchrotron, status of beam lines 77−10499
kimberlite and kimberlitic intrusives of SE-Australia 80−51392
kimberlite pipes and mantle rocks, review 79−2205
knee biomechanics, review of some basic assumptions 80−94265
Knudsen effusion cell, interactions with systems, high-temp. mass spectrometry 80−52354
Kondo alloy, low temp. props. 80−2569
L^2 discretisation of atomic and mol. electronic continua 79−59425
laboratory modelling of global geophysical flows *(Russian)* 77−81958
laboratory plasma devices 80−79589
BL Lacertae objects 77−26069
laer Doppler anemometry meas. in water flows 77−58818
lake modelling, temperate ecosystem 80−81949
Lamb shift in high-Z hydrogenic ions, expt. and calc. 77−54534
Lambert, J.H., self-taught scientist, life and work on cosmology 77−82354
lamellar intercalation compounds, NMR studies 80−39882
laminar flame propagation, asymptotic anal., review and extension 79−47926
Langmuir probes for high pressure plasma study 77−3982
Langmuir turbulence 78−51302
Langmuir turbulence and modulational instability in unmagnetised, completely ionised plasma 79−37496
large angle hadron-hadron scattering, power automated asymptotic behaviour *(Russian)* 78−17050
Large Coil Program, research and development activity 80−99336
large transverse momentum and large mass production in hadronic interactions review of theoretical models 79−89115
large transverse momentum physics review, diagnosis and prognosis 78−78215
large-scale elec. energy storage 80−89676
larynx carcinoma, primary radiotherapy 80−12216
laser anemometry, fringe-type, review of high-speed wind tunnel appl. in France and Germany 77−35272
laser anemometry, high Reynolds number flow, review, data anal. for photon correl. method, simulation 79−60082
laser annealing, review and anal. 80−25741
laser application in Raman spectroscopy 78−65979
laser applications in biomedical meas. *(Japanese)* 80−94311
laser applications in medicine and biology, bibliography, 1963-74 77−25539
laser applications in medicine in USSR 77−73555
laser applications in metrology *(German)* 77−698
laser applications in nucleas physics, review, book contrib. 80−68504
laser applications in otology 78−48860
laser applications to chemistry, overview 79−58800
laser atmospheric studies 79−66789
laser beam, spectral analysis, photomixing method 78−46698
laser beam applications in medicine and surgery *(French)* 79−34626
laser beam detection of atmos. constituents *(French)* 79−34952
laser beam materials processing, thermophys. and hydrodynamic effects 78−19957
laser beam propagation in atmosphere, book 79−34955
laser beam propagation through atmospheric turbulence 80−41550
laser beam wave case and remote sensing, book contrib. 79−34959
laser biomedical research in USSR 78−48858
laser clocks for psec. meas. 78−12676
laser Doppler spectroscopy, biology appls. 79−66598
laser Doppler techniques for flow measurement 79−68883
laser frequency measurements: a review, limitations, extension to 197 THz (1.5 μm) 78−81952
laser fusion research, present (1977) status *(Japanese)* 78−37439
laser glass charact. 79−27262
laser gyro, tutorial review 80−1266
laser induced fluorescence 78−37678
laser induced photochem. of vibr. excited mols. 80−71925
laser interaction with matter, nature of light, nonlinear spectroscopy 77−50712
laser ion source, appl. in mass spectrometry 80−89564
laser isotope separation, book contrib. 78−9280
laser isotope separation, mol. photodissociation processes, overview 78−55257
laser isotope separation 77−34784
laser isotope separation *(Japanese)* 78−5048
laser isotope separation 78−37758
laser isotope separation 79−18304
laser isotope separation 79−36789
laser isotope separation 80−32851
laser light polarisation *(Japanese)* 78−5516
laser material processing, overview 78−56826
laser plasma, strong mag. field effects *(Russian)* 78−38462
laser processing of thin films 77−23684
laser purification of rare earths, photochem. separation methods 79−61883
laser radiation, selective action on matter 80−7832
laser radiation induced elec. breakdown of gases, book contrib. 77−51256
laser radiation interaction with plasma 80−43953
laser Raman spectroscopy, biological appls. 77−52940
laser selective photophysics and photochemistry, book contrib. 79−79273
laser speckle photography *(Chinese)* 79−35880
laser spectroscopy, high resolution *(German)* 79−26138
laser spectroscopy, multiphoton and multistep methods, review 79−35842
laser spectroscopy, picosecond processes, review 79−54194
laser spectroscopy, present problems and tunable laser status 78−24867
laser spectroscopy, problems 77−5927
laser spectroscopy, review of new techniques 78−32893
laser spectroscopy, review of progress 78−82867
laser spectroscopy, theoretical foundations 79−35846
laser spectroscopy in mol. beams 80−22446
laser spectroscopy of atoms and molecules 79−55002
laser spectroscopy of diatomic mols. 77−46602
laser spectroscopy of primary energy conversion in photosynthesis 79−66461
laser surgery, state of the art 77−40729
laser techniques for biophys. studies 77−90975
laser technology, overview, past, present and future 77−75537

reviews continued
laser thermonuclear fusion 77−34449
laser thermonuclear synthesis for future energy production *(Russian)* 78−89978
laser wavelength measurement 78−50841
laser wavelength measurements, why? how? and how accurate? 78−89446
laser wavelength measurements 80−48320
laser-Doppler velocimetry in ionized gases 80−48975
laser-excited luminescence spectrometry in chem. analysis 80−40800
laser-induced grating phenomena 77−46752
laser-induced radiative collisions 79−10196
lasers, far IR, present and future problems 78−5466
lasers, high-efficiency, high-power, fusion appls. *(Japanese)* 78−5486
lasers, influence in biological and medical research, review 80−26318
lasers, organic cpds. as active media *(Russian)* 80−38015
lasers, research in International Business Machines Corp., USA 80−23696
lasers, tunable, principles, charact. and appl. *(Japanese)* 80−74330
lasers and masers, fluctuating intensity regimes 80−19015
lasers in metrology 77−694
lasers in metrology *(German)* 77−14734
lasers in metrology and testing 77−5817
latent image formation in Ag halides, nucleation, growth and developability 79−20395
latent-image formation: the contribution of the Research Division, Kodak Limited, Harrow 80−22458
lathe during metal removing automatic vibration control systems *(Russian)* 78−70118
lattice defects, review of resistomatic studies in metal *(Japanese)* 78−59799
lattice defects and irrad. effects in actinide oxides 77−27873
lattice defects in actinide carbides 77−27874
lattice dynamics, microscopic theories, developments 78−59870
lattice dynamics of trigonal Se and Te 80−54327
lattice energy, calcs., problems and solns. *(French)* 80−19746
lattice gauge fields, review 78−45797
lattice gauge theory, extreme environments and duality transform. 79−13024
lattice gauge theory and spin systems 80−22528
lattice imaging by electron microscopy 79−77467
layer perovskites, $(C_nH_{2n+1}NH_3)_2MX_4$ and $NH_3(CH_2)_mNH_3MX_4$, cryst. growth, solubility and props. 78−43999
layered compounds, modulation spectroscopy, book contrib. 77−40267
layered compounds, optical props., book contrib. 77−44023
layered compounds, photoemission, book contrib. 77−44133
layered semiconductors, transport props., book contrib. 77−43587
layered structures, single-crystal growth methods, review 77−59680
layered structures, superconductivity, book contrib. 77−39994
layered superconductors, Josephson coupling effects, review 80−84554
LEED, surface characterization, tutorial 79−68986
LEED crystallography 79−14656
LEED surface crystallography, past and present 78−14253
LEED surface studies 79−10764
left ventricular function, radioisotope evaluation with nonimaging probes 80−85484
left ventricular function assessment using radionuclide techniques, technical considerations, book contrib. 80−101261
Lemaitre's cosmology *(Polish)* 77−17737
lenses for projection photolithography 77−58423
lepton direct production in hadron-hadron collisions, interaction models 77−236
lepton measurements, QED and CPT, CP and T invariance tests 80−77996
lepton mixing and neutrino oscillations, cosmic neutrinos, heavy leptons, μ decay 78−82193
lepton mixing and neutrino oscills, review, 'solar neutrino puzzle' 78−66192
lepton-hadron scatt., polarised beam and target, review and survey of expts. and theoretical implications 79−67560
lepton-nucleon deep inelastic scatt., quark-parton model 77−57545
level crossing and high resolution laser spectroscopy 77−30835
Lie transform, approach to classical perturbation theory, plasma physics appl. 78−93510
lifetime meas. in atoms, mols., ions 77−30832
Lifshitz point, occurrence in mag. alloys 78−52265
light, fundamentals summary *(German)* 79−94145
light beam choppers, electromechanical 77−27346
light elements, Z>10, K-LL Auger process, review 78−50523
light guide data transmission, review *(German)* 80−95996
light hadronic spectroscopy, expt. and quark model interpretations, review, book contrib 80−68438
light ion direct reactions, polarisation expts., tensor polarised deuteron beams 78−54732
light nuclei, alpha transfer reactions, review, book contrib. 80−68699
light nuclei, cluster struct., review 78−50107
light nuclei, n-particle n-hole struct. from few nucleon transfer reactions, review 78−50062
light nuclei structure, multicluster model 79−3102
light quark spectroscopy 80−42424
light reflection by rough surface 80−18996
light scattering by liquid He 80−54454
light scattering near phase transition pts. in pure and defect containing crysts. 80−93361
light sources, LEDs and laser diodes, 1.06 to 1.6 μm range 79−45969
light sources for simulating sunlight 80−87454
light wave transmission technology, survey 79−55213
lightning charact. 80−51470
lightning discharge, HF effects, report 79−88456
lightning energy estimates, survey 79−100925
lightning main discharge theories 78−32132
lightning stepped leader theories 79−25320
limnological theses and dissertations concerning Texas waters, 1897 to 1976 period 78−7680
linear analogue ohmmeter circuits design 78−37031
linear elastic beams, shells and plates, elementary theories review 80−69677
linear electron accelerators, development for industry and medicine 79−45480
linear isotropic elasticity, boundary problems, book contrib. 80−39092
reviews continued
linear laser spectroscopy, absorption, opto-acoustic and fluorescence techniques 78−29170
linear molecule liquids, computer simulation and theory 78−38604
linear response theory and area preserving mappings 78−62174
linear-chain conductors 80−24887
lipid films, at fluid interfaces, phys. chem., book contrib. 77−39725
lipid requirement of membrane-bound enzymes 79−20521
liquation cracking during welding, comp. influence 80−66645
liquid, diatomic mol., spontaneous Raman scatt., vibr. dephasing 77−28568
liquid, simple, equilib. theories 80−38887
liquid alloys, magnetic properties, review 79−51741
liquid alloys, thermodynamic properties *(German)* 78−18794
liquid column chromatography, scintillation counters *(Czech)* 80−27885
liquid crystal appl. *(Polish)* 78−30537
liquid crystal electro-optical appls. 77−43136
liquid crystal materials and display devices 79−99056
liquid crystal phases and phase transitions 78−2006
liquid crystals, acousto-optical effect, instabilities generated by US field 78−91235
liquid crystals, book contrib. 77−39544
liquid crystals, defects, struct., optical, electron microscopy *(French)* 79−46567
liquid crystals, mol. conformation and orientational order, NMR studies 80−75151
liquid crystals, struct. and props. 77−43134
liquid crystals, symmetry and thermodynamic states 80−10493
liquid crystals, textures, deform. and struct. order 77−43135
liquid crystals, thermotropic, struct., two-dimens. order, and symm. props. 79−86698
liquid crystals, X-ray diffr. studies 80−100166
liquid crystals *(Chinese)* 79−32905
liquid crystals in living and dying systems 77−44602
liquid dielectrics, electrical conductivity and breakdown, liquid impurity effects 80−11340
liquid electron diffraction 78−83686
liquid intermolecular relaxation spectroscopy 79−95844
liquid metal, electron states, esp. opt. and mag. props. 78−2882
liquid metal embrittlement 79−15798
liquid metal embrittlement 79−29272
liquid metal embrittlement micromechanisms 80−108637
liquid metal embrittlement of metals 80−3257
liquid metal MHD, review of flow problems and cellular motion 78−83498
liquid metals, review of research, phys. aspects, Knight shift, elec. resist. *(Dutch)* 77−7657
liquid metals, thermoelectricity, expt. methods review 79−65451
liquid mixing, volume changes 79−90782
liquid props. review, viscoelasticity and lubrication 79−7356
liquid solutions, reaction rates, mol. mobility effects, book contrib. 77−40526
liquid spreading on solid surfaces, static and dynamic contact lines, book contrib. 80−20015
liquid surfaces, theory and appl. *(German)* 77−62710
liquid theory 77−7653
liquid-liquid interfaces in isolation and in interaction, review 77−47651
liquid-solid equilib., expt. methods of determ. *(Rumanian)* 79−28078
liquid-vapour interface nature, non uniform classical fluids statistical mechanics 79−77468
liquids, transparent isotropic, electro-optical and magneto-optical effects 78−84553
living cells, laser Raman spectra 80−56113
living system biophysical interaction mechanism with RF and microwave radiation 79−79602
LMFBR, commercial plants, French development program 79−97762
LMFBR, post accident heat removal technology review 78−41839
LMFBR, response to abnormal events, applied mechanics in design and safety review 78−70611
LMFBR, safety research and development 79−36362
LMFBR materials, exam. of material requirement 78−50256
LMFBR plant system design *(Japanese)* 79−80973
LMFBR safety 78−13257
LMFBR steam generators, flow induced vibr. 77−23240
LMFBR thermal explosion hazards, review of present understanding and simulation expts. 78−82464
LOCA, extreme loads and associated safety aspects 79−22405
local atomic arrangements, associated with ordering 80−50632
local moments and localised states, review of early work on Anderson model 78−72327
local moments and localized states, theory 79−23935
long-range order in two dimensions 79−65307
long-range weather forecasting, art and science 80−109184
long-wavelength IR spectroscopy, obs. of intermol. interactions in condensed medium 80−34927
Loran-C signal, ground wave propag. theory 80−94580
Lorentz microscopy, thin film and bulk specimen, recent advances 78−35002
Lorentz transformations derivation by Ives (1945) 80−4523
loudspeaker technology *(German)* 79−50559
low cycle fatigue, design of structural elements 77−3788
low energy atomic collisions, ionisation processes, chemi-ionisation, review 78−22024
low temp. dense plasma electrode phenomena 80−33743
low temperature measurement in high mag. fields, instrumentation and methods 78−37003
low temperature research activities and facilities in Italy 79−93146
low-dimensional mag. systems, neutron scatt., review 80−50103
low-energy recoil meas. in high-energy physics 77−38593
low-frequency acoustic nondestructive test methods 79−79204
low-temperature chemical reactions, book contrib. 77−40542
low-temperature physics, early investigation to present day discoveries 78−69958
low-temperature spectroscopy techniques *(Japanese)* 78−291
lower hybrid heating in toroids, US experimental program 80−28748
lubrication, boundary conds. and cavity-fluid interface, review 77−55058
luminescence, conduction band behaviour, defects and impurity centres *(Chinese)* 79−33535
luminescence, worldwide research survey 78−10986
luminescence and luminescent devices, lecture 78−27323
luminescence research, new trends 79−47503

reviews continued
Lunar and Planetary exploration programs, United States 78−77461
lunar dynamics studies before laser ranging 77−64183
lunar gravity determinations and their implications 77−60653
lunar highlands crust, origin and comp. and effects of meteorite bombardment 80−109381
lunar igneous rocks supercooling, review of analogue information 77−60652
lunar laser-ranging 77−5459
lunar magnetism origin, theories 80−36522
lunar mare basalts, crystal chemistry, mineralogy and petrology 77−45334
lunar materials, KREEP origin 80−4279
lunar radar mapping 80−12694
lunar samples, assessment of results from Mossbauer spectra 77−60655
lung ^{239}Pu burden, assessment of tissue substitutes for calibration purposes 79−16307
lung cancer, interstitial brachytherapy, 20 year experience 80−72302
lung lavage for removal of inhaled radioactive particles 78−3618
lung ventilator, development, engineering appraisal 78−3673
LWR, review of alternative fuel schemes *(Italian)* 79−63784
LWR, structural integrity of pressure boundary 78−66334
LWR accidents, in-reactor expts. on fuel behaviour *(Japanese)* 79−63760
LWR in-core fuel management techniques *(Italian)* 80−18447
LWR LOCA safety analysis, thermohydraulic phenomena *(German)* 79−13430
LWR local corrosion causes and preventive methods *(French)* 78−8963
LWR safety research programs by US NRC 80−42796
lymphocyte plasma membrane components, distrib. and mobility, book contrib. 80−30690
lymphocyte surface morphology, human, SEM obs. 78−53599
B Lyrae, eclipsing binary system, current knowledge 80−105289
RR Lyrae stars, observational review of multiperiodic behaviour 77−87430
macromolecular adsorption, onto inorganic substrate, surface struct. 79−69342
macromolecular chain configuration-dependent props., review 77−38758
macromolecular random chains, spatial configurations, review 77−38757
macromolecular solutions, Rayleigh scatt., elec. induced variations, spectral width and intensity meas. 78−48187
macromolecule functional groups, reaction kinetics and statistics *(Russian)* 79−87825
macromolecules, epitaxial crystallisation 79−42409
macroscopic metal catalysts, morphology and etching processes 80−7856
Magellanic Clouds, evolution struct., and intensity *(French)* 79−71131
magnetic alloys, dil., transition metal hosts, props. 78−84417
magnetic anisotropy, book contrib. 80−11191
magnetic bubble materials, props. and preparation models *(Rumanian)* 80−93149
magnetic bubble materials 80−50153
magnetic bubble wall dynamics 80−75823
magnetic bubbles, electron microscope obs. 77−28417
magnetic chains in solids 80−15737
magnetic circular dichroism of biological molecules, book contrib. 80−109080
magnetic confinement of plasmas 78−94928
magnetic critical phenomena, hyperfine expts., selective review 78−43722
magnetic critical phenomena, use of renormalisation group 77−20625
magnetic densities and magnetic excitations, neutron studies, book contrib. 80−11170
magnetic disordered systems, Monte Carlo anal., review, book contrib. 79−82809
magnetic domain walls and bubble dynamics 77−69599
magnetic domain walls and bubbles, dynamic props. 80−88784
magnetic domains, cylindrical, static and dynamic props. of isolated domain *(Russian)* 77−51915
magnetic electron spectrometers and their in-beam use 79−68128
magnetic excitations, submillimetre spectroscopy applic. 77−37955
magnetic field meas., 1980 status *(French)* 80−95114
magnetic field measurement in toroidal plasma systems 80−49004
magnetic fluids, mag., optical, and hydrodynamic props.,, expt. study 80−60376
magnetic flux quanta in superconductors, electron-optical obs. 77−47945
magnetic fusion program in US, recent exptl. results 79−85781
magnetic inelastic neutron scatt., book contrib. 77−89944
magnetic levitation methods for tracked high-speed traffic 79−49011
magnetic materials, elastic props. 80−7142
magnetic materials, spin polarised electron emission 77−73215
magnetic monopoles in quantum field theory 79−26234
magnetic ordering in actinide intermetallics 77−20598
magnetic oxides, hydrothermal crystallisation, for mag. appl., book contrib. 79−69974
magnetic props. meas. in high mag. fields, review *(Japanese)* 78−52303
magnetic resonance, book contrib. 80−11242
magnetic separation, review of current activity 77−63961
magnetic soft and hard materials, garnets, magnetic properties and applications, structural props. 80−65760
magnetic spectrographs, use in nucl. reaction studies *(Rumanian)* 80−87012
magnetic surface states, in spin wave resonance, theory 80−84654
magnetic susceptibility, review of literature 1975-1977, instrumentation, chem. anal. applications, and bioscience 78−82006
magnetic system, Lifshitz point, phase diagrams and crit. behaviour 80−65928
magnetic systems, exptl. studies of multicritical points 77−66325
magnetic systems and mixtures, phase diagrams, Monte Carlo studies, book contrib. 79−82313
magnetically-soft materials, mag. characts. determ. methods 79−40593
magnetics research, materials development and appl. during past 25 years 80−36792
magnetism, one dimensional model systems, theoretical survey 78−68129
magnetism investig. by neutron scatt., review *(Japanese)* 78−52227
magneto-microwave effects, rel. to ESR 77−69667
magneto-optic imaging, domain struct. obs. 77−48151
magneto-optic memories, state of the art 77−42494
magneto-optical spectra, appls. to inorganic materials 77−52050
magnetocardiography overview 79−92246
magnetocrystalline anisotropy *(Rumanian)* 80−25125
magnetoelastic effects in metallic glasses 78−68352
reviews continued
magnetoelastic waves *(Japanese)* 78−23317
magnetoelectrets 80−25289
magnetoelectric dipole gas as explanation of biocosmic phenomena, summary of phenomena 80−8241
magnetoelectric effects in magnetic materials, review *(Japanese)* 80−50159
magnetosphere, double layers and electrostatic shocks review 80−36460
magnetosphere, elec. and mag. fields at high latits. 78−12057
magnetosphere, large-scale elec. fields 77−87208
magnetosphere, macroscopic elec. fields 78−49238
magnetosphere, magnetic field models 77−9629
magnetosphere, open model plasma populations 80−90295
magnetosphere, plasma waves and instabilities in polar cusp 78−12058
magnetosphere, quantitative models of 0 to 100 keV near Earth plasma 80−36459
magnetosphere, response to August 1972 solar flares 77−25888
magnetosphere 77−45253
magnetosphere and ionosphere, elec. and mag. fields, rel. to coupling 79−66870
magnetosphere and ionosphere, mag. field aligned elec. fields 77−9618
magnetosphere physics 79−12356
magnetosphere plasma, hot ion component rel. to electron component, obs. and implications 79−80106
magnetospheric convection driving force 79−8782
magnetospheric energetic ions expected charge states 79−80105
magnetospheric heavy ions 79−80104
magnetospheric physics, review of selected topics 78−65466
magnetospheric plasma physics, global problems and soln. 78−20588
magnetospheric simulation expts. 80−46347
magnetospheric studies 78−65496
magnetostriction, book contrib. 80−11241
magnetostriction, temperature dependence, origin, elastic and magnetoelastic energies *(Rumanian)* 80−34747
magnetostrictive materials and devices *(Japanese)* 78−23316
magnetotail dynamics 79−80100
magnetotelluric sounding, inverse problems soln. 78−49162
magnetotelluric sounding method development in USSR 78−49169
magnetotelluric studies in USSR 78−49168
magnetron sputtering, appl. to sputtered thin compound films *(Japanese)* 80−25561
magnons, general lecture 78−27026
major solar energy research programs 80−40843
malignant thyroid disease treatment, ^{131}I appl. 80−36108
mammal gonads, radiation induced morphological and endocrinological changes *(Russian)* 78−77090
mammalian cell membranes, plasma membrane responses, book 78−15787
mammalian cell membranes and cellular functions, book 78−15784
mammalian surface membrane turnover, review 78−15788
mammary carcinoma, primary radiotherapy *(German)* 80−61693
mammography, experience with 153 breast carcinoma cases *(German)* 80−12244
mamography, risks, radiation dosage and picture quality *(German)* 80−36103
Mandel'shtam and nonlinear oscillations and wave theory 80−105515
mantle convection models 79−5464
many body theory, appls. review of development 80−46968
many-body forces in nuclear physics, review, book contrib. 79−97670
many-dimensional oscillator problems, 'Arnold diffusion' instability 79−75334
many-hadron production at low $P_{\perp}$, basic concepts and models 79−6331
marine atmosphere diurnal kinetic photochemistry 79−48549
marine geology and geophysics, 1967-77 77−64260
marine geophysical exploration 77−41196
marine pollution by oil *(French)* 79−48193
marine research in China 77−64312
Mars, as seen at end of Viking mission 80−72839
Mars, props. of surface and atmosphere *(Russian)* 78−20667
Mars, solar wind interaction, satellite meas. with charged particle traps 77−13200
Mars, surface morphology review 80−56748
Mars, tectonics and volcanism review *(Russian)* 79−48726
Mars, upper atmosphere structure and dynamics 77−33382
Mars, Viking biological investigations review and status 79−80263
Mars 77−74002
Mars atmosphere 77−13273
Mars Viking mission, biological implications 79−8872
martensite formation, and lattice props. rel. to elastic constants 80−50630
martensitic transformations, electron microscope study of cryst. geometry *(Russian)* 80−108441
martensitic transformations 80−3037
Martian satellites, 100 years since discovery, review of studies 78−73670
mass loss from late-type stars 80−67755
mass spectrometer sources, field ionisation and desorption, experimental techniques, review 79−26176
mass spectrometric ion anal. based on periodic motion along closed trajectories 78−78029
mass spectrometry, laser-probe, analytical capabilities 78−64902
mass spectrometry, review of literature, 1975-1977 78−85226
mass spectrometry applications in study of porphyrins and related tetrapyrroles 80−51306
mass spectrometry by Wien-Thompson method 80−45613
mass spectrometry instrumentation for chemists and biologists 80−42297
mass spectroscopy, developments over last 25 years 77−67528
mass transfer between solid spheres and oscill. fluids 77−42902
massive stars evolution, observational review 80−90416
matched filtering improvements for coherent optical pattern recognition 80−78786
material phase diagram determination techniques, review of more sophisticated technique 79−7673
material processing by high power lasers, comparison of available systems 78−30003
material properties associated with dynamic deformation of matter, acoustics and the props. of materials 80−64234
material science, current topics, book 80−46747
materials, dimensional stability for precision machine parts *(Japanese)* 79−39116
materials for human implantation 79−96709
materials for noise and vibr. control, review 78−13854

reviews continued
materials in history and society 79−38725
materials involving fluorine *(Japanese)* 79−96282
materials problems and basic research needs rel. to energy resources and storage 78−86703
materials research for advanced energy technology, appl. of crystallography, review 79−96429
materials review of mech., corrosion, thermal, elec. props., appl., economics, design considerations 79−1818
materials science, book 78−11089
materials science, high resolution microanal., using electron energy loss measurements 77−56190
materials science, life prediction and design, review 77−16475
materials science and design *(Japanese)* 77−69974
materials science and engineering as a multidiscipline 79−38726
materials sciences in space, first Skylab mission 77−36377
materials technology 77−8733
mathematical modelling, vibrational resonances of built-up structures, use of meas. data 80−69718
matrix isolation spectra of high-temp. and interstellar molecules 78−46340
matrix isolation studies of high temp. species 80−57399
matter-antimatter asymmetry of Universe, review of speculations and data *(French)* 79−35439
Max Born, biography, review of contributions to physics 78−86100
Mayer waves, history and methodology 79−29537
MBE crystal growth 78−39707
MBE of injection lasers, integrated optics device fabrication 79−90042
MBE of semiconductor films 77−73239
MBE study of semiconductor surface and crystal physics 79−95289
measurement, the measures of man 77−9981
measurement microphones, comparison of performance and environmental charact., and applications 79−1038
mechanical properties of soft animal tissue, in vitro testing, apparatus 78−31985
mechanical props. of vapour deposited coatings 78−6247
mechanical stability in creep conditions *(Russian)* 79−18758
mechanical test methods and strength of structures 79−43507
mechanics of biological tissues 78−69131
mechanochemical reactions, phase transformation and synthesis, review 80−3024
medical appls. of low-temp. biology *(Japanese)* 77−44870
medical B-scan US, technical factors influencing the imaging of small anechoic cysts 80−98049
medical CRT displays, review 78−69240
medical diagnosis, EM techniques 80−36063
medical diagnostic, X-rays, effects, risks and protection 78−3591
medical diagnostic imaging techniques and instruments 79−96635
medical dosimetry standards programme of the National Bureau of Standards, USA 80−8187
medical elec. equipment international standardisation, current problems 77−73603
medical engineering, review of developments and facilities 80−12292
medical engineering, review of present state 80−17023
medical image processing in diagnostic radiology 80−81690
medical imaging by NMR, book contrib. 80−36064
medical imaging overview 80−98082
medical imaging techniques, developments 80−26324
medical physicists, training, survey of program directors 79−17159
medical research, laser applications, biophysical aspects 80−51201
medical US and its biological effects 79−96614
medical US applications and new developments 78−11712
medicine, diagnostic radiology, radiation therapy, nuclear medicine, sensitometry, review 78−20260
melting, dislocation theory 80−65198
membrane bilayers, quasitwo dimens., theoretical models 80−76713
membrane energy transduction probes 77−21666
membrane excitability mechanisms, book contrib. 80−12062
membrane filters in air anal., review 79−79316
membrane separation processes, principles, practice and prospects 78−92505
membranes, biological and synthetic, 1/f noise 79−24969
membranes, synthetic, use in biophys. research 77−70418
8-mercaptoquinoline, synthesis, physiochem. props., review *(Russian)* 79−39140
Mercury: magnetic field and interior 78−65524
Mercury, Mariner 10 2nd and 3rd encounters 77−73989
Mercury, post-Mariner 10 assessment 80−12697
Mercury, tectonic and volcanic history inferred-from scarps, ridges, troughs and other lineaments 79−16855
Mercury surface history from Mariner 10 77−37537
mesic atomic and molecular processes in H_3 isotope mixtures 80−23580
mesomorphic monolayers, quasitwo dimens., theoretical models 80−76713
meson exchange currents, configuration mixing, role in nucl. mag. moment, beta decay, review, book contrib. 80−478
meson spectroscopy, review of SU_3 quark model, quark confinement and bound states 78−74228
meson theory of nuclear vector and axial vecotr exchange currents, review, book contrib. 80−474
mesonic processes and quarks in nuclei 80−42564
mesophase, and high modulus C fibres from pitch 79−94867
mesosphere, major charact., processes and dynamics 77−25734
mesosphere winds at equatorial latits., observational aspects review 78−36229
metabolic regulation and math. models 77−90714
metal, BCC, deform. 77−4815
metal, cond. electron relax. time *(Japanese)* 78−30910
metal, deformed struct. role in recrystallisation nucleation, review 79−34060
metal, diffusion of H(D), slow neutron scatt. obs. 80−34248
metal, FCC polycrystalline, work hardening, plastic deform *(Hungarian)* 77−77504
metal, He migration and defect interactions, role in radiation damage processes 77−28041
metal, ion implanted H(D), interstitial positions and vibr. amplitudes, fast ion channelling study 80−79848
metal, irrad., containing self-interstitials and vacancies, electronic transport props. 78−60105
metal, light element implantation, radiation damage review 80−88219
metal, plastic deform. *(Russian)* 78−19825

reviews continued
metal, point defect clusters, TEM obs., review 78−26564
metal, radiation induced damage, review 78−51580
metal, recovered dislocation substructure, prod. and utility, review 77−84749
metal, review of chemisorption 79−42377
metal, self-diffusion, atomic jump processes 78−47562
metal, self-diffusion 78−47561
metal, self-interstitial atoms, review 78−47332
metal, thermodynamic props. of grain and phase boundaries, review *(German)* 79−34012
metal, vacancies and interstitials, electronic struct. 78−47320
metal, vacancy concentration 78−47319
metal, vacancy defect mobilities and binding energies obtained from annealing studies 78−47325
metal, vacancy-solute interaction 78−47409
metal atom oxidation lasers, book contrib. 77−10913
metal colloids in ionic cryst., preparation, optical, mag. resonance, elec. props. 80−59459
metal corrosion in ionising solvents 77−8973
metal crystallites, polyhedral, growth in inactive gas 79−27934
metal crystl, anisotropy of electron radiation damage 77−84796
metal film thickness meas. methods and instruments *(German)* 78−32787
metal films, on alkali halide substrates, nucleation and growth, surface study techniques 80−10809
metal forming, limit anal. appl., book contrib. 78−11140
metal halide layered materials, prep. and growth, book contrib. 78−19648
metal hydrides use as energy conversion media *(Japanese)* 80−55934
metal hydroxide layered materials, prep. and growth, book contrib. 78−19649
metal ion lasers, hollow cathode 80−99708
metal matrix composite, state-of-the-art review, book 78−72706
metal mirrors for CO_2 laser fusion systems, material constraints and fabrication 78−5476
metal monolayers, on metal cryst. surfaces, surface struct., review 80−80067
metal silicides, fabrication technique and characterisation *(Japanese)* 80−60779
metal structures, thin walled, crack growth problems 80−55527
metal surface, atomic and mol. beam scatt. 80−40203
metal surface, He implantation lateral stress, role in bluster form. mech. 78−95068
metal surface, kinetics of adsorpt., desorpt. and migration, review 79−46921
metal surface, reactivity, review of electron spectra 77−62748
metal surface struct. and initial stages of reactivity, review 78−68837
metal surfaces, clean polycrystalline, ion-induced electron emission 80−35032
metal surfaces, laser heat treatment, wear resist., corrosion protection, hardening 78−72939
metal vaporisation, optical spectral methods of vapour press. meas., review 79−66381
metal vapour excimers, book contrib. 79−81419
metal vapour lasers, hollow cathode *(Rumanian)* 80−87409
metal-electrolyte interfaces, optical reflectance specta, interpretation 80−93263
metal-gas interactions, kinetics and mechanisms, book contrib. 78−11558
metal-H, phase transitions 80−50631
metal-H alloys, phonon dispersion relation, neutron scatt. studies 79−60451
metal-H system, electro- and thermotransport of H, book contrib. 80−24644
metal-H system, hydride formation in high press. range 80−65235
metal-H system study by neutron scattering, review *(French)* 80−34226
metal-H systems, anelastic and plastic props., review 80−49298
metal-insulator transitions 79−15082
metal-ligand bonds, frequencies, predominantly stretching vibrations 79−41154
metal-metal metal-polymer sliding, wear mechanisms, review 79−70174
metal-nonmetal transitions in fluids 78−2529
metal-rich compounds, pnictides, chalcides and halides, struct. and bonding, review 79−46626
metal-semiconductor contacts 78−2566
metal-semiconductor rectifier, theory, technology and appl. 78−52089
metal/air batteries, status and potential, review 80−55828
metallic alloy, random, first principles band theory, review 80−44473
metallic components, damage investigation 79−74330
metallic film, struct. of small particles 77−89671
metallic films, vapour deposited on polymer, ageing, adhesion, elec. cond., electrochem. pot. *(Russian)* 79−33362
metallic glass, bulk and surface properties, review 80−44147
metallic glass, corrosion behaviour 80−89421
metallic glass, current exptl. data on struct. 80−88058
metallic glasses, annealing behaviour, thermal stability and crystn. 80−75167
metallic glasses, atomic transport behaviour *(Japanese)* 79−94907
metallic glasses, electronic structure rel. to elec. cond., supercond. and mag. props. 80−65429
metallic glasses, formation, stabilities, and props. 80−64912
metallic glasses, formation, structure and thermal stability, review *(German)* 78−83747
metallic glasses, mats. props. review 77−4043
metallic glasses, prep., characterization, struct., formation, electronic, mag. and mechanical props. 78−3074
metallic glasses, review 80−88051
metallic glasses, struct., stability and prod., elec., mag. and mech. props. 80−44134
metallic glasses, struct. and props. 78−47245
metallic glasses *(German)* 79−41962
metallic glasses and amorphous magnetism 79−82818
metallic glasses formation 77−66606
metallic surface, self-consistent electron theory 80−88616
metallic thin film, electrical resistance, effect of gas adsorption *(Rumanian)* 79−82691
metallic thin films, optical props.; effect of quench condensation 79−78773
metallography, quantitative methodology *(French)* 80−30205
metallurgical coatings, fabrication, struct., and appls. 80−80121
metallurgical industry, mathematical modelling appl. 77−73429

reviews continued
metallurgical industry, mathematical models appl. 77−70276
metals, 3d and 4f, electron impact excited soft X-ray spectra, resonances and many body effects 80−50468
metals, adsorption of gases *(Japanese)* 79−46930
metals, aspects of impact testing 79−79111
metals, BCC, low temp. softening 79−34113
metals, BCC, plastic deform., review 80−104213
metals, charge perturbations around impurities 77−85582
metals, compression, effect of press. on lattice defects *(Japanese)* 77−72654
metals, dynamical props. of point defects, book contrib. 80−103317
metals, electronic struct. and magnetism 80−70573
metals, FCC, hardened, plasticity 79−11683
metals, ferromag. elec. cond. 77−31993
metals, friction and wear rel. to comp., struct. and props., review 80−25872
metals, grain boundaries, struct. and props. recent developments 79−99217
metals, H_2 embrittlement, kinetics, review *(Russian)* 79−15762
metals, H effect on mech. props., review 80−50718
metals, H trapping, book contrib. 80−24491
metals, high press. expts., review *(Japanese)* 78−71790
metals, hydrogen brittleness measurement 80−104291
metals, ion-implanted, friction and wear, review 80−40555
metals, lattice defects, positron annihilation study, book contrib. 79−99977
metals, liq., structure and dynamical properties 79−55648
metals, point defect diffusion controlled reaction theory, book contrib. 80−103318
metals, positron annihilation, localised probe of lattice defects 80−55224
metals, positron annihilation expts., electronic struct. and Fermi surface studies 80−54594
metals, radiation damage, FIM and atom probe FIM expts. 78−35623
metals, slow positron studies 80−55223
metals, solid and liq., optical props. by spectroscopic ellipsometry, review 80−103929
metals, stacking fault energy meas. by electron microscopy *(French)* 79−42079
metals, storage of H_2 79−10956
metals, surface effects in hydrodynamic model 79−78148
metals, use of ion beams to study radiation effects 79−10883
metals and alloys, close-packed, temp. depend. of stacking fault energy 79−19266
metals and alloys, electron momentum density, positron annihilation meas., book contrib. 79−99976
metals and alloys, fatigue behaviour, vacuum effect 80−35309
metals and alloys, FCC, tensile fracture mechanism, review of pressure effects 77−70155
metals and alloys, NMR results, brief survey 79−73830
metals and alloys, shock wave effect on martensitic transform. *(Russian)* 80−96595
metals and alloys, sulphidation mechanism, review *(Polish)* 80−45413
metals and alloys, thermodynamic props., evaporation, optical spectral method appls., review *(Russian)* 78−75822
metals and semimetals in strong mag. fields, EM excitations 77−8130
metals for mirror substrates, manufacturing processes 78−5542
metals hardness testing 79−87773
metals in road transportation, review 78−88622
metamagnetism, materials, theories and phys. props. 78−19248
metastability, rigorous molecular theory, review, book contrib. 80−73271
metastable alloy formation by ion implantation 79−14828
metastable microcrystalline alloys, appls. 80−84887
metastatic thyroid cancer, use of ^{131}I 80−36084
meteoric nightglow, review of historical obs. 80−94761
meteorites collisions with planets, review 79−8884
meteoritics, early chemical and mineralogical work 77−71175
meteorological observations in urban environment 79−25312
meteorological physics, recent developments 79−25313
meteorological satellite observations 77−22041
meteorology, numerical modelling of the atmosphere 79−44234
meteors, observation methods in Poland *(Polish)* 78−61750
methane-ethane liq. mixture, phase equilib., heat of mixing, vol. change, data evaluation 80−15233
methanol, and $-d_{1,3,4}$, thermodynamic props. struct. and spectroscopic data 77−39396
methyl formate, microwave spectra, rot. consts., moments and struct., radio astronomy appl. 80−17637
methylfluoride laser, CW, 496 microns, rate equation model 78−55343
methylhydropolysiloxanes, equilibration by catalysts *(German)* 78−35722
MHD channel and boundary layer flow, rel. to energy sources 79−37403
MHD dynamo theory of planetary and stellar magnetic fields *(French)* 79−35161
MHD materials 80−40240
mica, crystal chemistry 79−46612
micelles, reversed, solubilisation and catalysis 80−45545
micro-organism propulsion, cilia and flagella, fluid mechanics, book contrib. 77−48833
microanalysis by direct obs. of nucl. reactions 79−96409
microchannel plate technology and applications 79−23075
microcomputer applications in physics teaching 79−30171
microdosimetry, role in radiobiology 80−61705
microelectronics and thin film components frontiers 80−73123
microelectronics revolution, appl. in telecommunications, medicine, education 80−31446
microfabrication techniques for integrated optics 78−38091
microhydrodynamics, characteristic effects, developments 77−68681
microinstability theory in Tokamaks 78−75292
microkymography, and related techniques 80−36215
micrometallurgy and microelectronics *(Russian)* 77−55874
micron scaled cathodoluminescence of semicond. with SEM 78−23537
microneutronographic and neutron-induced autoradiographic techniques, review of appl. in metallurgy 78−60892
microoptic signal processing research, review 78−38073
microorganisms, photobehaviour, book contrib. 79−5329
microparacrystals in physics *(German)* 79−27933
microparticles, quantitative anal. with electron beam instruments 79−21866
microphones, development and calibration accuracy 80−96167
microphysics to macrochemistry, discrete simulations 80−54102

reviews continued
micropinch in a high-current diode 80−103183
microprocessor, in industry *(French)* 80−17729
microprocessors in bioscience 80−21557
microscopic calcs. of nuclear optical model potls. 77−26648
microscopic cluster model, light nuclei as proving ground 79−3101
microscopic equipment, methods and appls., bibliography 80−62406
microscopic optical pots., summary 79−97691
microscopic theory of collisions in atomic phys. survey of recent developments 78−46410
microscopy, quantitative, appl. of statistical methods, review 79−17484
microscopy bibliography 80−90619
microstructure fabrication, using STEM and X-ray lithography and reactive ion etching, appl. 79−15844
microvoids as pigments in polymeric materials, review 79−52617
microwave biological effects, research in Soviet Union and Eastern Europe since 1976 80−35971
microwave effects on blood-brain barrier 80−56121
microwave holographic imaging 80−23645
microwave instrumentation 79−212
microwave meas. advances reviewed 78−57984
microwave potentially hazardous radiation sources 78−73173
microwave power for fusion machines 80−23151
microwave spectroscopy of short-lived molecules, review 79−50010
microwaves in cancer therapy, review of 4 years 80−56162
mictomagnet props. review 79−24183
mid-ocean ridges, obs. and implications of ridge crest hot springs 80−98304
middle atmosphere dynamics 80−17338
middle atmosphere processes revealed by satellite observations 80−21803
MIGMA, colliding beam fusion power source 79−18031
Mikhail Lomonosov, research vessel, 20 years of scientific results *(Russian)* 78−69485
MIM, thin film, use as non-heated source of electrons 80−84516
MIM sandwich structures with anomalous props. 77−59337
MIM tunnelling junction for inelastic electron tunnelling spectroscopy, zero bias anomalies 79−4603
mineral insulated cables in nuclear reactor instrumentation *(German)* 77−6573
minerals, preferred orientation, review and outlook 79−83220
mining and prospecting research, examples of mineraology contrib. *(French)* 79−5475
minor planets 79−88619
mirror electron microscopy, theory and appl. 79−67443
mirror machine, fusion reactors, survey 80−47721
mirror machine end-loss processes, review 77−55164
mirror plasma confinement, recent developments *(Japanese)* 79−7475
MIS solar cells 79−39300
MIS structures, review of applications, ion sensitive techniques 79−33353
mitochondrial cytochrome b, evidence for two or more components 79−24944
mitochondrial permeability, transport and energy-coupling processes, effect of fatty acids and acyl-CoA 77−21498
mixed gas adsorption, review of theories 78−75942
mixtures, high-press. vap.-liq. equilib., phenomenological description 78−30737
mixtures, physical-chemical separation and thermodynamics *(German)* 78−18774
mm wave atmospheric slant path propag., 15 to 40 GHz 79−84465
MNOS structure, trap parameters determ., review of expt. techniques 77−55612
modern electrometer techniques 80−37052
modulation meters, history of development, selection, special features, calibration *(French)* 77−53948
modulation spectroscopy in vacuum UV, with synchrotron radiation 78−4710
modulators, photoelastic radiation polarisation 80−102846
moire topography, historical review 80−9024
molecular, rotational energy levels, quartic and sextic centrifugal effects, book contrib. 78−21910
molecular beam epitaxy, review of recent progress *(Japanese)* 77−63566
molecular biology, electron microscopy, detection and resolution of atom images *(French)* 79−66595
molecular biology, origins, autobiographical review 80−57052
molecular charge transfer complexes, mol. and cryst. struct. 78−62942
molecular chemical tunnelling, facts and hypotheses 79−59520
molecular clouds, summary of obs. 78−16512
molecular collisions, vibr. and rot. excitation cross-sections, meas. and calcs., book contrib. 77−38720
molecular crystal, dynamics, neutron spectroscopy appl. 79−42166
molecular crystal spectroscopy, 1975 bibliography 77−77159
molecular crystals, electronic energy transfer, book contrib. 77−39789
molecular crystals, rot. excitations and tunnelling 79−46579
molecular crystals, simple, lattice vibrations, Raman and IR obs. 78−43079
molecular dynamics method in statistical physics 80−18895
molecular electronic spectra, vibrational struct., determ. by Franck-Condon method, book contrib. 78−21911
molecular electronic structure theory, 1972-75, book contrib. 77−38595
molecular emission cavity anal., vapour generating systems, cool flame spectroscopy 80−81396
molecular forbidden rot. transitions, expt. and theory 77−34612
molecular gas, thermalisation under reson. excitation by laser radiation *(Russian)* 78−26231
molecular gases, non-self sustaining discharge for CW laser excitation, review 78−42849
molecular graphs, matrix descriptions 77−38737
molecular ion beams, mass spectrometry absorpt. spectra 79−89808
molecular ions, gas phase, spectrosc. props. 78−33501
molecular kinetic spectroscopy 79−94110
molecular laser, optically pumped 80−58519
molecular photoelectron spectroscopy 78−94283
molecular radiation biology, time effects 80−72269
molecular relaxation, statistical treatment, review 77−51284
molecular reorientation in fluids, extended rotational diffusion models, unified treatment 77−27797
molecular reorientation of symmetric top molecules, in liquid state, book contrib. 78−22623

reviews continued
molecular self-assoc. and complex form. in soln., IR and Raman spectra, book contrib. 78−21931
molecular spectroscopy with coherent radiation sources, review 77−3343
molecular substances, positron annihilation and phase transitions 78−95614
molecular tunnelling in chemical reactions *(Russian)* 77−52615
molecular vibr. freq. tables, up to 13 atom mols., and Raman and IR values 77−79614
molecular vibration, spectra, summaries and reviews of recent work, book 78−21894
molecule-surface scattering, appls. 78−39653
molecules adsorption on oxide surfaces, UPS studies 80−84374
molecules in molecule (MIM) model, appl. to π-electron systems *(German)* 79−36506
molten salt, thermal cond., heat storage *(Japanese)* 80−6573
molten salts, IR, Raman, EPR and NMR spectroscopy, review *(French)* 79−69832
molten salts, pure, theories of the modynamic props. 79−19380
molybdates of trivalent metals, solid-state chem. 77−24288
monocarbides of subgroups IVa and Va, kinetic props., review 78−47613
monocrystals, EM radiation of relativistic positrons and electrons during axial and planar channelling 80−79845
monodisperse Ag halide photographic emulsion production methods, review of patents 1955-75 *(Russian)* 78−58084
monolayer on graphite, neutron scatt. studies 80−107655
Monte Carlo computer simulations, of cryst. surfaces and cryst. growth 79−14710
Monte Carlo methods, struct. of liq. water and dil. aq. solns. 80−54101
Monte Carlo studies on relaxation phenomena, book contrib. 79−80531
Moon, chemical history rel. to Earth and achondrite parent body 77−60639
moon, mare basalt petrogenesis, expt. studies 77−13258
Moon, mascon basins: lava filling, tectonics and origin 80−98583
Moon after Apollo era 77−33373
Moon ancient magnetic field, intensity and origin 77−60656
Moon and satellite distance meas. by laser 77−9673
MOS processing for III-V semiconductors 78−10570
MOS structures, hot electron transport, expt. review 78−30994
MOS structures, quasi-2-dimens. system 79−33352
Moscow State University, synchrotron radiation research review 78−66730
Mossbauer effect in solid-state physics, overview *(French)* 78−2782
Mossbauer spectroscopy, high field, recent developments 79−73863
Mossbauer spectroscopy, matrix isolation techniques appls. 78−46376
Mossbauer spectroscopy, review of literature 1976-1977 78−84501
Mossbauer spectroscopy development in Soviet Union 77−32311
motion in depth, binocular and monocular stimuli 80−61570
motor systems, neurological control of locomotion, book contrib. 79−5272
Mott insulator electronic struct. 78−18963
multi-nucleon transfer and direct reactions, nuclear struct., review 78−50060
multi-particle and inclusive reaction, at high energies 79−17777
multibarrier kinetics, subcritical crack velocity stress depend., review 80−23958
multicritical phase transitions 79−30385
multielectron target+multiply charged ion, electron capture 80−63812
multihadron production in nuclear matter and hadron struct., space-time description *(Russian)* 80−68571
multimegawatt neutral beams for Tokamaks 79−76234
multiphoton molecular photofragmentation, high order 78−82797
multiphoton scattering spectra of laser light 79−6979
multiphoton transitions, perturbation theory, atomic ionisation and intermediate reson., dissoc. 79−41145
multiple ion scattering at solid surfaces 77−63517
multiple scattering of waves by particle ensembles, radiation transport 77−95
multiply charged ion+one-electron target, electron capture 80−63811
multiply ionised atoms, spectroscopy 79−10060
muon capture progress, weak interaction form factors 80−42643
muon g-factor anomaly, review of theoretical contribs. 77−30384
muon physics 78−82260
muon spin rot., appl. to mag. investigs., review *(Japanese)* 78−52417
muon spin rotation, review of recent advances 79−24252
muon spin rotation method, review *(Polish)* 80−88901
muon two-frequency precession in muonium atoms, probe for study of matter. 77−28505
muonic X-rays, formation and expts. 80−43215
muonium and μ^+ physics and chemistry *(Russian)* 77−50566
muonium formation and charged particle tracks 79−57259
muscle, excitation and contraction processes, book contrib. 79−5262
muscle cell cultures biology, book contrib. 79−2031
muscle contraction cross-bridge model 78−44475
musical acoustics, review of recent work 79−76920
musical acoustics 80−10096
MWPC, appl. to radiation localisation problems in medicine and biology 79−5432
MWPC, review of operating principles and functions 79−3293
MWPC and drift chambers, operation principles 77−83465
myocardial blood flow, ^{133}Xe studies, theoretical, technical and practical aspects 80−94355
myocardial perfusion imaging, quantitative aspects 80−94358
myopia, Prentice Memorial Lecture [optometry] 80−27089
myosin and actomyosin kinetic anal. 80−21441
narrow band gap semiconductors, physics 77−28112
narrow band gap semiconductors effects 79−95437
narrow gap semiconductors, recombination mechanisms 80−96905
narrow-gap semiconductors, microwave effects, review 79−82618
natural convection in enclosures 79−1193
natural convection in porous media and geothermal systems 79−1194
natural mineral crystal growth characts. 78−32072
natural sciences school curriculum *(Hungarian)* 79−71167
natural water chem. anal., modulated polarographic, voltammetric techniques 77−37253
nature, unity of, as an incentive to research *(German)* 80−77533
Navier-Stokes eqns., finite difference methods, recent advances 77−80136
Navier-Stokes equations, theory and numerical analysis, book 78−77721
NBS National Measurement System 79−21688
NDT, equipment for production line inspection 79−29320
reviews continued
NDT, use of accelerated electrons 80−35480
NDT 77−36700
NDT of wire ropes using EM methods 79−83423
near-Earth radiation environment 79−12359
near-space radio noise environment characteristics and sources 78−89034
nearly closed shell atoms, binding energy and isotope shift correl. 80−27980
negative ion lifetimes, book contrib. 80−9529
negative ion sources, generation by sputtering in Cs plasma, recent developments 79−49884
negative ions, at. and mol. collisions electron detachment for energies near threshold 80−63797
negative ions, form. processes and props. *(Japanese)* 80−53127
negative ions 77−27194
negative molecular ions, theoretical calcs. 78−37552
nematic liquid crystal, total internal reflection 80−96445
nematic liquid crystals, coherent neutron scatt. studies 79−41956
neoplasm localisation with radionuclides 80−67215
nerve cell cultures biology, book contrib. 79−2031
nerve cells and circuits, insights into construct. by genes 79−39411
nerve impulse, physical mechs., ion transport through membranes 78−85306
nerve impulse conduction, modulation along the axonal tree, book contrib. 80−108872
nerves, electrochem. theory, steady and transient pots., in book, for teaching 78−8202
nervous system, circadian pacemakers, literature review, book contrib. 79−2028
nervous system, clinical disorders, sensory evoked potentials, book contrib. 79−2029
nervous tissues, Ca dependent K activation, book contrib. 79−5266
neural nets, rhythmic movement generation, lobster, leach, book contrib. 79−5273
neural prostheses 80−21576
neuromuscular disorders, biofeedback therapy, conscious control of motor neurons 79−34702
neuronal membranes, organisation book contrib. 79−2032
neuronal spike-train statistical anal. methods 78−73149
neurons, transport of substances 80−89745
neuroscience, annual review, vol.I, book 79−2027
neurosurgery, laser appls. 80−26317
neurotransmitter modulatory actions, book contrib. 79−96550
neutral+high Rydberg atom, thermal collisions 80−63756
neutral atoms, electron interaction, free-free radiative transitions, review 78−90295
neutral beam injection heating in Tokamaks, review 80−28729
neutral current effects in nuclei 79−40859
neutral currents, expt. verification of theoretical predictions 79−89097
neutral currents and gauge theories 79−13011
neutral particles, detect. and energy anal. 78−82590
neutral upper atmosphere, density, temp. and winds 79−75006
neutrino astrophysics, review, book contrib. 80−72769
neutrino experiments at high energies, total cross sections by currents, review 79−49511
neutrino expts. at CERN, neutral current results 77−34145
neutrino interactions, appl. to weak interaction and nucleon struct. investigations 79−80823
neutrino interactions, expt. bibliography to 1976 77−22730
neutrino interactions involving weak neutral currents, expt., theory, gauge models 77−49901
neutrino physics, high-energy (>10 GeV), development, book contrib. 78−82201
neutrino-hadron interactions 78−78171
neutrinos, historical review 78−89288
neutrinos, review of discovery, production, meas. and appls. *(Russian)* 80−13344
neutrinos as ultimate astrophysical probe, review 78−77486
neutron absorption radiometric testing of materials, review 80−71860
neutron activation anal., appl. using ^{252}Cf neutrons 80−18728
neutron activation analysis, $1/E^{1+\alpha}$ epithermal neutron spectrum, α-determ. methods, accuracy 80−71977
neutron activation analysis 79−66378
neutron cross-sections for reactor dosimetry, status 77−23304
neutron D-T sources, accelerator prod. neutrons of high flux rate 77−23342
neutron damage simulation, using HVEM, state-of-the-art 77−51417
neutron data importance in fission reactor appl. 77−23192
neutron diffraction, struct. investigations of melts and amorphous substances *(German)* 80−44108
neutron diffraction by macroscopic bodies, dynamical theory 79−4211
neutron diffraction investigation of liq. struct. book contrib. 79−60230
neutron diffraction magnetisation density distrib. expt. determ. 77−77034
neutron diffraction of disordered structs., book contrib. 79−60228
neutron diffraction studies of mag. materials, book contrib. 80−11169
neutron diffractometry, automatic, development 79−27879
neutron diffractometry, profile analysis of powder data 77−68900
neutron distribution in nuclei, elastic and inelastic proton scattering 80−22649
neutron dosimeters, personnel, recent developments 79−63818
neutron dosimetry with solid state nuclear track detectors, brief review 78−33299
neutron induced fission, role of double humped barrier 77−26659
neutron induced fission resonances, spin determ. using polarised beam and target 77−26796
neutron inelastic scatt. expts., book contrib. 78−1959
neutron intense high-energy sources for fusion reactors and radiotherapy 77−83419
neutron physics, recent advances 77−26640
neutron polarisation expts. 77−26700
neutron radiative capture cross section meas. techniques 77−26932
neutron radiative capture data, nucl. struct. anal. 77−26701
neutron radiography, application in industrial analysis 79−52609
neutron radiography, equipment and methods review, beam production, sources and image recording 78−60889
neutron radiography, H and water transport studies review 78−59961
neutron radiography, industrial applications in USA, review of data and neutron effects 78−60891
neutron radiography, technological development review, neutron props. and history 78−60887

reviews continued
neutron radiography, trends *(German)* 77−32745
neutron scatt. anal. of biological structs. 77−29238
neutron scattering by molecules, polymers and absorbed species 79−41911
neutron scattering from adsorbed mols., surfaces, and intercalates, review, book contrib. 80−84394
neutron scattering of high-energies, review 77−79283
neutron scattering studies of one- and two-dimens. mag. systems 77−66254
neutron small angle scattering, expt. techniques, and appl. 79−46515
neutron star, thermal X-ray emission 80−41849
neutron star X-ray emission models 80−62175
neutron stars, nonequilibrium shells, role in X-ray emission and nucleosynthesis 80−67774
neutron stars, review of nuclear physics 79−92797
neutron stars thermal properties and detectability, cooling and heating processes 80−31323
neutron therapy radiobiology 77−5076
neutron time of flight correlation spectrometers, operation and circuitry 77−6605
neutron time-of-flight spectrometers, historical review of developments 79−72179
neutron transport theory, collision probability method 80−27706
neutron-nucleus reactions 77−26702
neutrons, review of props., their expt. determ. and degree of precision 79−58961
Nevis synchrocyclotron facility, status and exptl. program 77−14279
'new particle' searches and discoveries, 'Review of Particle Properties' 1976 supplement 77−57515
Newman-Penrose formalism and its application in general relativity *(Russian)* 79−21595
Newman-Penrose method in general relativity, book contrib. 80−46905
Newtonian cosmology for unbounded Universe *(Italian)* 80−12836
nitrides, structs. and cryst. growth 80−29865
NMR, ESR, NQR and theoretical chemistry 77−18943
NMR, high-resolution studies of double helical polynucleotides 77−86450
NMR, of liq. metals and alloys 78−2755
NMR, ring current theories 80−53020
NMR and molecular biology research *(Chinese)* 79−39459
NMR applications to phosphoryl transfer enzymes, and metal nuclei of metalloproteins, book contrib. 80−109081
NMR chemical applications, literature review July 1975-July 1977 78−85217
NMR chemical shift, nucl. other than protons, semi-empirical calcs. 77−75188
NMR in coupled spin systems 78−48072
NMR of proteins, ^{13}C 77−86449
NMR of solid electrolytes and solid soln. electrodes 80−60432
NMR spectroscopy, appl. to organic compounds anal. 80−16756
NMR studies of nucleoside and nucleotide conforms. 78−76990
NMR studies of water in biological systems 80−3886
NMR study of molecular conform. in soln., use of La ion probe 77−60324
NMR system, multi-level, coherent phenomena *(Japanese)* 79−73831
NMR-NQR double resonance, two-freq. methods, resonance spectrometers 80−20512
nMTCB task analysis of nuclear medicine technology 80−8753
Nobel prizes, scientometric papers and data sources 79−97123
noble metal complexes, hexafluoro, review of struct. obs., pseudorot., press. effects 78−6045
noble metals and their dil. alloys, electronic struct., de Haas-van Alphen studies, book contrib. 79−37967
noctilucent clouds, advances in space era 80−105095
noise and vibration control systems 77−11090
noise and vibration control systems 78−30127
noise measurement, engineering aspects, techniques of noise evaluation 77−39178
noise signals, pitch, evidence for central spectrum 77−36942
noise standard, OSHA regulation at 29 CFR 1910.95 (b) (1), review 79−14157
noise-induced sleep disturbances and their effects on health 79−5317
non-classical effects in the statistical properties of light 80−99686
non-ionising radiation, hazards in the laboratory 79−57708
non-linear optics, recent advances 80−33075
non-linear properties of thermal convection, review 79−18893
non-Newtonian fluid mechanics 79−60010
non-Newtonian fluids, literature review 77−23999
non-Newtonian fluids, scale-up problems 79−23342
non-Newtonian fluids 80−33637
non-oxide ceramics, hot pressing 80−25641
non-reactive heavy particle collision calculations 79−59541
non-solar X-ray astronomy 77−33698
noncrystalline materials, personal review by Sir Nevill Mott 78−55811
noncrystalline materials, properties, current and potential applications 78−30539
noncrystalline solids, struct. models and exptl. methods 78−22655
noncubic metals, elec. field gradients, nuclear electric quadrupole interaction 79−65420
nondestructive assay of irradiated nuclear fuel for safeguards, review 78−82495
nondestructive evaluation 80−71855
nondestructive inspection methods, review 79−43535
nondestructive materials testing, review of radiographic principles and methods 78−53065
nondestructive testing methods *(German)* 77−77724
nonelectrolyte solutions, liq. theory, book contrib. 77−39523
nonequilibrium electron gas, fluctuation theory 79−54043
nonequilibrium phenomena in superconductors 80−49982
nonequilibrium statistical mechanics, exactly solvable models 79−30365
nonfilm TV method of high-speed process coords. meas., review 78−5093
nonionising electromagnetic radiation bioeffects research and related occupational health aspects 78−73172
nonlinear σ model, 2-D, topology and higher symmetries 79−26241
nonlinear acoustics, model eqns., book contrib. 80−19126
nonlinear crystals for frequency conversion of optical radiation *(Russian)* 80−38068
nonlinear finite element analysis, review of soln. techniques 79−3914

reviews continued
nonlinear high resolution laser spectroscopy, review of techniques 78−29171
nonlinear laser spectroscopy, density matrix methods 78−74071
nonlinear materials for tunable coherent light sources in middle infrared 77−38991
nonlinear optical resonators, radiation excitation, review 80−69462
nonlinear optical uniaxial crystals, review and summary of data 77−75615
nonlinear optics, three-wave interaction 79−86209
nonlinear optics 77−50716
nonlinear photoelectric emission from metals by high power layer radiation review 78−48288
nonlinear relaxation and fluctuation 79−30373
nonlinear spectroscopy, at. and mol. techniques 77−50564
nonlinear three wave interactions, space-time evolution in homogeneous medium 79−84966
nonlinear wave theory 80−36874
nonmathematical review of gravitational capture 80−26734
nonuniform fluid state, Van der Waals theory, thermodynamics, struct. and phase stability 79−77475
nonverbal thought in technology 78−8210
norepinephrine and epinephrine neuron systems, anatomy and physiology, book contrib. 79−96548
North Sea oil production platforms, use of steel and concrete in construction 79−78985
notch testing, short term tension tests 79−61829
nova outburst, thermonuclear runaway model 77−82262
novae, 50 years research 78−4239
novae explosions 79−67042
NQR, NMR and EPR, spectral parameters, influence of mol. motion dynamics, review 80−20486
NRC Reactor Safety Study (the Rasmussen Report) 79−63750
nuclear, vertex constants *(Russian)* 78−33155
nuclear and atomic research review 80−43216
nuclear and particle science, book 80−67940
nuclear applications for low-temperature heat 80−7903
nuclear astrophysics, recent developments 78−4100
nuclear beta-decay, extended Siegert theorem 77−41924
nuclear cluster correlation in heavy ion-nucleus collisions, book contrib. 80−27670
nuclear clustering, microscopic description 80−487
nuclear collective props., rotation effects *(Russian)* 78−37299
nuclear data sheet for A=58 to June 1976 77−18372
nuclear data sheet for A=58 to June 1976 77−18373
nuclear data sheets for A=237 to November 1977 78−82267
nuclear data sheets for A=241 to November 1977 78−82268
nuclear data sheets for A=48 to September 1977 78−82266
nuclear decay rate variations produced by physical or chem. means 77−41931
nuclear decays as test of elementary particle theory, review 78−21361
nuclear detector data acquisition and processing equipment, evolution 79−72219
nuclear detectors and systems 79−72188
nuclear dipolar magnetic ordering, dipole-dipole interactions 77−85475
nuclear energy, future integrated reactor systems fuel strategy 79−49696
nuclear energy levels and structure in A=16, 17 nuclei 77−46116
nuclear field theory, appl. to ^{209}Bi struct. 77−67692
nuclear forces and isobar configs. in nuclei, review 78−50093
nuclear frictional effects in reacts. 78−78336
nuclear fuel, inspection by neutron radiography, review 78−60890
nuclear fuel, U and Pu decontamination, sorption and distillation methods, review *(Czech)* 78−82496
nuclear fuel cycle, uncertainties rel. to reprocessing and waste management 80−5315
nuclear fuel cycle materials, neutron and photon assay techniques and instrumentation 80−18426
nuclear fuel cycles and waste management 78−54863
nuclear fuel nondestructive assay techniques and instruments *(Japanese)* 77−57716
nuclear fuel reprocessing plants, general characteristics 79−85717
nuclear fuel reprocessing technology, development up to current status 78−58393
nuclear fuel structure characterisation methods, review 79−49802
nuclear fusion engineering developments 79−3240
nuclear fusion potential 77−75000
nuclear fusion power, state-of-the-art and problems to be overcome *(Dutch)* 80−37574
nuclear fusion research, review of T chemistry *(Japanese)* 79−63806
nuclear fusion technology development in France and UK 77−18695
nuclear giant E1 resonances 77−79350
nuclear giant multipole resonance excitation through inelastic scatt. 77−57593
nuclear giant multipole resonances 77−14087
nuclear giant multipole resonances 77−79351
nuclear heat for urban district heating, costs and technology 80−26118
nuclear imaging, apparatus, techniques and performance 80−51237
nuclear industry safety criteria 77−65302
nuclear instrumentation, historical perspective of early detectors and counters 79−72189
nuclear ion microprobe at MeV energies production and use 80−7883
nuclear isobar configurations in few nucleon systems 78−37294
nuclear isomers, 10^{-4} to 10^{-1} sec lifetime, decay spectra, meas. procedure 79−36167
nuclear isotopes far off stability line, production, props. *(Hungarian)* 79−9927
nuclear K-harmonics and shell model methods *(Russian)* 77−82836
nuclear magnetic double resonance, in solids, nuclear spin systems dynamics *(Rumanian)* 78−55189
nuclear magnetic double resonance spectroscopy *(Rumanian)* 79−15380
nuclear magnetism and ultralow temperature *(Japanese)* 80−86806
nuclear magnetism of liquid systems in the Earth field range 80−50206
nuclear mass estimation, Garvey-Kelson generalised mass relations *(Rumanian)* 79−75827
nuclear materials, actinide determ. review of procedures at Rockwell Hanford Operations 79−81050
nuclear matter, variational and Brueckner-Bethe calcs., review 78−93959
nuclear matter, variational techniques 80−22748
nuclear medical instrumentation, mobile 80−101262
nuclear medicine, appl. of computers *(German)* 80−41214

reviews continued
nuclear medicine, computer appls. in image and data processing 79−16294
nuclear medicine, computers and quality control 79−16295
nuclear medicine, trends *(French)* 80−26327
nuclear medicine, tumour-localising radionuclides in retrospect and prospect 80−42036
nuclear medicine, understanding and using statistics 80−12233
nuclear medicine and emission computed tomography *(Japanese)* 79−70610
nuclear medicine and metrology of ionising radiations *(French)* 80−17057
nuclear medicine display systems 79−16298
nuclear medicine in Europe, present status and future trends 80−94331
nuclear medicine instrumentation, recent developments 80−81692
nuclear medicine instruments and radiopharmaceutical production *(French)* 80−17056
nuclear methods of NDT 77−32756
nuclear microprobe as analytical tool 79−87913
nuclear molecular resonances in heavy ion collisions 79−22313
nuclear moments, elec. and mag., review of data 78−37266
nuclear moments and moment ratios determ. by Mossbauer spectroscopy 77−22885
nuclear muon capture, developments in theory and expts. 80−42642
nuclear muon capture, present knowledge 77−50090
nuclear optical model potl., theory 77−30538
nuclear orbital electron capture, theoretical status and exptl. methods 77−26629
nuclear orbital electron capture probabilities, experimental techniques, review 77−18893
nuclear orientation, brute force, review of accomplishments and problems 77−59466
nuclear orientation, induced by laser, at. and nucl. applications 78−37310
nuclear orientation and NMR of oriented nuclei, appl. to solid state magnetism 80−44928
nuclear particle detectors 79−54740
nuclear physics, current trends *(Hungarian)* 80−57786
Nuclear Physics Dept., Saclay, research programs *(French)* 79−437
nuclear physics in Australia 77−88021
nuclear physics with synchrotron radiation 80−106216
nuclear polarisation, recent advances in technique 79−30822
nuclear power, comparability study of fission and fusion reactors w.r.t. safety, costs and development time 79−59114
nuclear power, environmental impact 80−101143
nuclear power, future prospects, technical, economic and political review *(Spanish)* 79−59116
nuclear power development in Germany 79−63716
nuclear power generation, safety, proliferation and theft 77−74953
nuclear power in Czechoslovakia *(Czech)* 79−31157
nuclear power nonelectrical energy production 79−26728
nuclear power plants, seismic safety 77−374
nuclear power station corrosion research, review of problems *(Czech)* 78−62598
nuclear power station response to aircraft impact 78−41875
nuclear power station with desalination plant, steam-cycle and optimisation calc. 79−26724
nuclear pumped lasers, review of developments at Illinois University 80−63996
nuclear quadrupole double resonance techniques 77−36153
nuclear radiation as a probe of chemical bonding, review of theory and expt. techniques 79−79339
nuclear reaction backward angle peaks, exchange processes, review *(Russian)* 77−79392
nuclear reaction polarisation phenomena *(Russian)* 78−33162
nuclear reaction theory for nuclear engineers *(Japanese)* 80−99155
Nuclear Reactions Lab., Dubna, USSR, review of 30 years work 79−36204
nuclear reactor accident, human exposure to radiation, biological consequences 78−7407
nuclear reactor computational benchmark problems 77−79413
nuclear reactor control and safety, development of a reliable single-channel direct-digital reactor-control system 79−89458
nuclear reactor fuel element codes, structural anal. 80−78362
nuclear reactor fuel elements, struct. anal. 78−41814
nuclear reactor materials, radiation damage, fast breeder and fusion reactors *(Japanese)* 79−81011
nuclear reactor materials development for LMFBR primary and secondary circuits 77−46295
nuclear reactor pressure vessels, pre-stressed concrete, historical review 79−601
nuclear reactor reactivity determinations for performance of reactor safety, economics, operability *(Japanese)* 78−17332
nuclear reactor safety, probabilistic analysis, review of ANS symposium 79−45354
nuclear reactor system, joints, review of design and anal. techniques 77−3098
nuclear science 78−82263
nuclear shadowing of electromagnetic processes, vector dominance model anal., book contrib. 80−47266
nuclear shape, review 77−79308
nuclear shell model continuum calcs., status and prospects 78−54698
nuclear spectroscopy techniques in at. and mol. physics 78−22055
nuclear spin and moment data tables 77−22881
nuclear spin relaxation spin relaxation spectroscopy, appls. 77−83619
nuclear spin-spin coupling consts. calcs. 77−30889
nuclear spontaneous fission, of transuranium isomers, exptl. work 77−79405
nuclear structure at high angular momenta *(German)* 79−40832
nuclear structures, probabilistic design, state of art, research needs 78−94055
nuclear symbiosis, development of FBR and thermal spectrum near breeder reactors 79−45335
nuclear techniques for bulk, surface anal. 78−85238
nuclear testing 1975-1978 79−67958
nuclear track etching, review of appl. in other scientific fields 79−97934
nuclear variable moment of inertia model, theories of collective motion 77−57611
nuclear vibrations 79−89219
nucleation, theory for high and low supersaturations, review 80−49142
nucleation 80−49143
reviews continued
nucleation theories (1930 to 1960) 79−86897
nucleation theory, fundamentals *(Spanish)* 78−43101
nucleation thoery, role of replacement free energy 77−62611
nuclei, exchange and renormalisation phenomena due to pion-nucleon couplings 77−41893
nuclei and particles, introductory text book 78−78234
nuclei far from line of beta stability, mass spectroscopic anal. techniques, book contrib. 80−69014
nuclei with A=194, review of struct. information to July (1977) 78−89769
nuclei with A=207, review of struct. information to August (1977) 78−89770
nuclei with A=209, review of struct. information to September (1977) 78−89771
nucleic acid-water interactions 78−44448
nucleic acids, H_2 exchange kinetics and internal motions 80−21440
nucleic acids and their aggregates, optical activity, book contrib. 80−108847
nucleic acids functions, interactions with metal ions 80−3577
nucleon form factors, dispersion theory 77−34155
nucleon resonances in nuclei 77−26563
nucleon-antinucleon systems, nonrelativistic scatt., quasinucl. systems 78−25065
nucleon-nucleon bremsstrahlung expts. review, comparison of results with theory 78−62447
nucleon-nucleon high energy elastic and inelastic scatt., review of phenomenology 77−30441
nucleonics, review Nov. 1975 to Nov. 1977 78−82262
nucleus shapes and motions in even-even and odd A nuclei 80−5054
numerical modelling of fatigue, crack, creep and corrosion test results, review 78−30243
numerical weather prediction, appl. of telescoping method *(Polish)* 79−16557
O_3, atmospheric, near surface meas. at Hohenpeissenberg, historical review *(German)* 78−65369
objective lens manufacturing, present status and future prospects 79−94323
observational cosmology since 1958, progress and problems 78−28873
obstetric practice, the place of real-time and static B-mode scanning, educational syllabus 80−86057
occupational radiation exposure, evaluation and control, US research program 80−5370
ocean biological instrumentation requirements 79−12049
ocean current meas. near surface, general problems, review 78−45048
ocean current meas. with moored meters, intercomparisons 78−45050
ocean eddies and the general circulation of model gyres 80−56490
ocean optics, blue-green laser technology 77−78458
ocean sediment geotechnical prop. determ. instrumentation problems 79−12304
ocean surface, microwave radiometry remote sensing 80−36428
ocean synoptic eddies 79−5491
ocean thermal energy, renewable power source 79−5503
ocean thermal energy conversion, review of engng. problems for technical and economic development 80−3486
ocean tides 80−98349
ocean wave EM scattering theories 78−77243
ocean waves and wind meas., radar techniques 78−81418
ocean waves of continental shelves, recent advances 80−98348
ocean-atmosphere interface, coupled energy transfer, turbulent and radiative 79−2290
ocean-atmosphere momentum, heat and H_2O vapour fluxes, meas. methods 78−32213
oceanic and atmospheric fields, linear prediction models 80−56590
oceanic crust, seismic vel. evolution 79−5457
oceanic tides 77−73762
oceanography, microwave radiometry appls. review 78−81415
ocular physiology review 80−56023
odd mass nuclei, 59≤A≤149, E2, M1 multipole mixing ratios 78−4911
Ohio Sky Survey and other radio surveys, review 77−45325
oil demand projections to 1985 80−3482
oil shale, in situ technological developments 80−30354
oil shales, review of thermophysical properties 79−100479
Oklo fossil reactor 77−60377
Oklo natural fission reactors, formation, propagation and control *(French)* 80−21774
Oklo natural fission reactors, geophysical eval. of U distrib., topography, sedimentology and structure *(French)* 80−21755
Oklo natural fission reactors, review of French geological research *(French)* 80−21744
Oklo natural reactors, data on stability and remobilisation, summary *(French)* 80−21771
Oklo natural reactors, review of mineralogical and petrographic studies at Strasbourg *(French)* 80−21745
oligomers, polymer-derived, mass spectral charact. 80−37916
oncology, role of radionuclides 77−9248
ondulatory radiation sources, theory and appl. 80−37947
one dimensional conductors, electron-electron interactions and Kohn anomaly 80−24895
one dimensional conductors, Fermi gas model 79−78083
one dimensional Fermi gas model in relation to spin and field theoretical models 80−24816
one-dimensional charge transfer conductors, press. effects on mag. props. 78−6505
one-dimensional conductors, Fermi gas model, review 79−47090
one-dimensional conductors, struct. aspects, book contrib. 78−10429
one-dimensional inverse scattering problem for stratified inhomogeneous media 80−46346
one-dimensional metals and charge density wave effects in these materials 79−78085
operational and reliability experience with ractor instrumentation for AGR and magnox reactors 79−89453
ophthalmic literature, optic nerve, tracts and visual cortex diseases 79−83762
ophthalmology and physics 79−53084
ophthalmolscopic and vision function meas. instruments 79−96689
optical astronomy, high-resolution techniques, book contrib. 77−33357
optical attenuators *(Japanese)* 79−98475
optical cements, commercial, trials and meas. *(French)* 79−50452
optical centering devices, vertical collimators, for geodetic appl. 78−13807

reviews continued
optical coatings, basic developments 78−74964
optical coatings 77−83946
optical coherence, review 80−48140
optical communication, present and future developments 80−69521
optical communication status and prospects *(German)* 78−33855
optical communications research and technology, fibre optics 78−87151
optical computing and applications 77−10852
optical constants of metals and alloys, expt. methods 79−33655
optical data processing extension to space-variant and nonlinear operations 78−78940
optical design, contemporary, aspects 80−23766
optical device performance assessment, British standards 78−50729
optical elements, diamond turning 77−27400
optical estimation of surface roughness statistics from light scatt. 77−61916
optical fibre applications outside data transmission and communication 80−74482
optical fibre as a transmission medium 80−14456
optical fibre cable, design, performance and development projections, review 79−46069
optical fibre communication, cabling, light source and receiver technology 78−59125
optical fibre communication, progress review of fibre design, low-loss and low-dispersion *(German)* 80−28325
optical fibre communication systems, optoelectronics devices 79−76858
optical fibre communication systems 77−65629
optical fibre connector technology 79−68439
optical fibre data buses, single distribution system and crosstalk isolation 79−3802
optical fibre light sources for 1.0 to 1.2 μm emission, review 77−38894
optical fibre manufacturing, cabling and splicing, developments in Japan 78−59124
optical fibre manufacturing processes, status report 77−46815
optical fibre preparation methods and performance factors 80−69557
optical fibre processing techniques 79−50460
optical fibre system connectors 78−42414
optical fibre systems for civil telecommunications, state-of-the-art review 78−25979
optical fibre technology for military aeronautic appl. *(French)* 78−46813
optical fibre theory 78−1351
optical fibre transmission coming of age 79−98487
optical fibre transmission systems comparsion, 0.8 to 1.4 μm 78−46824
optical fibre waveguide, low loss, radiation induced transmission loss behaviour 80−38111
optical fibre waveguides, book contrib. 77−31141
optical fibres, bandwidth and backscatter measurements 79−64356
optical fibres, development since 1966 in information transmission *(German)* 77−50760
optical fibres, measurements of characts. 80−43458
optical fibres, progress and components *(French)* 80−69524
optical fibres in Italy, short distance appl. 79−50369
optical fibres in medicine *(Italian)* 78−53540
optical glass and single crystal production 79−94308
optical IC developments *(Japanese)* 77−62077
optical image processing, analogue and digital, feedback, review 80−102639
optical inhomogeneities of ferroelec. oxide crysts. for electrooptics and nonlinear optics *(Japanese)* 77−65613
optical instrument design, partial coherence effects 80−78767
optical isotope shifts, (1918 to October 1976) 77−57932
optical lenses, technological development trends *(German)* 78−33805
optical magnetometry optically pumped, design, characts. and development 79−93177
optical materials rain erosion mechanisms 78−83049
optical measurement techniques of thermodynamic props. in flow fields 77−35279
optical microscopes, scanning, imaging props. and appls. 80−82811
optical mixing in metal vapours, book contrib. 77−46766
optical parametric oscillators 77−75620
optical pattern recognition, deformation invariant, space variant, book contrib. 79−76619
optical power spectrum meas., error sources in diffr. pattern sampling 78−63030
optical precision expts. using lasers 78−42246
optical production and orientation of ground state diatomic mols. *(Russian)* 79−27046
optical properties of films 78−76540
optical properties of rough surfaces, discontinuous films, heterogeneous materials, review 80−103935
optical properties of small inorganic and organic metal particles 80−45106
optical pumping appl. of atomic density matrix irreducible components 77−46546
optical pumping of gaseous atoms *(Japanese)* 78−25489
optical reading and recording instruments using lasers *(Japanese)* 77−72023
optical recording media 78−71172
optical rectification effect and meas. appls. 80−91835
optical resonator design for chemical lasers, book contrib. 77−10964
optical software survey for digital image processing 77−75431
optical storage medium specification and performance trends 80−43415
optical stress analysis using moire fringe and laser speckles 80−10217
optical studies from space, Soviet 78−85815
optical system, evaluation criteria and problems *(German)* 80−43268
optical thin-film waveguides fabrication *(Polish)* 79−3775
optical tolerance, glass and plastics comparison 79−59780
optical wave propagation in turbulent medium, modern theories, book contrib. 79−34957
optical waveguide fibre coating technology, overview 80−58828
optical waveguide image transmission in coherent light 79−59831
optical waveguide lenses *(Japanese)* 80−10019
optical waveguide process and materials, review of progress 80−23768
optical waveguide processes and materials 79−50459
optical waveguide resonant tunnelling 77−780
optical wavelength division multiplexing transmission technology 80−58727
optically pumped far IR laser design and performance 79−31917
optically pumped mid-IR lasers 79−22961
optically pumped waveguide gas lasers 78−5490

reviews continued
optics, recent advances 80−28155
optics of condensed matter, linear and nonlinear lecture 78−25918
opto-acoustic spectroscopy *(Japanese)* 78−89554
optoelectronic devices, digital data processing, review 80−19106
optometric education in Nigeria, three year programme 79−25781
orbital disease, appl. obs. computerised tomography scanning 80−56174
ore minerals, recent developments in microscopic meas. of spectral reflectance *(French)* 79−5627
ore-deposition through geological time 78−77235
organ doses from isotropic γ-ray fields 80−109026
organic compounds, high-press. thermodynamics 79−24500
organic electrochemistry, progress, 1952-77 77−60078
organic molecular crystals, intermolecular interactions, spectroscopic studies, review 80−103958
organic molecular crystals, photoemission, book contrib. 80−16158
organic molecules, UV photoelectron spectroscopy, systematic review 80−28057
organic reaction mechanisms, generalised mol. orbital theories 78−44366
organic scintillators, review of development 79−72198
organic solids, vibr. relax. and dephasing, Raman spectra 80−88987
organometallics, photochemistry with applications to imaging systems 77−4914
origin of elements, review 80−62359
origin of life 80−4111
origin of the elements 79−97118
ORNL fusion power demonstration study 79−71969
orographic effects on SW.monsoon 78−44962
oropharyngeal epithelioma treatment, role of radiation therapy *(French)* 80−41190
oropharynx, squamous cell carcinomas 80−67925
Orsay MP tandem 78−13352
orthopaedic engineering in Oxford 80−17187
orthopaedic load meas. using strain gauges 80−56262
oscillator strengths for atoms, calc. methods 78−17616
osteogenic sarcoma treatment, role of radiation therapy *(French)* 80−17077
OTEC, technology development, US DOE program 80−94098
OTEC ocean engineering 80−66989
OTEC power system development and environmental impacts 80−66990
OTF of radiographic imaging systems 80−17085
outer solar system, fields and plasmas 79−58213
oxide, solid electrolytes, thermal and mech. props. at steelmaking temps., review *(German)* 78−15418
oxide and related single crystals, melt growth 78−31322
oxide ceramics, dependence of props. on raw materials, exam. using ceramic magnets as model *(German)* 79−4936
oxide semiconducting glasses, electronic cond. mechanism 80−65562
oxides, excited states of F-centres 78−64006
oxides, impurity diffusion and self-diffusion, review and bibliography 80−59719
oxides, sputtering, thermal effects 80−35033
oxides, thermally stimulated exoelectron emission *(German)* 80−66404
oxiphenol developers, free radicals *(Russian)* 79−39138
(p,2p) reactions, intermediate energies, distorted wave impulse approx. anal. review, $^{40}Ca(p,2p)^{39}K$ illustration 78−62541
pacemaker, electrode leads, transvenous, anchoring measures 79−84008
Pacific island and seamount ages rel. to volcanic chains origin 77−64242
palaeoclimatic research, status and opportunities 80−51527
palaeoclimatology, overview, and European air temp. trends *(German)* 79−16639
paleomagnetism of the peri-Atlantic Precambrian 79−5451
pallasites, metal comp., classification, relationship with Fe meteorites 77−64709
palliative treatments for fretting fatigue, review 80−21126
Palomar Hale telescope, first 30 years 80−72774
pancreas disorders, integrated nucleus medical diagnosis *(German)* 79−16293
pancreatic disease, study by multiple imaging modalities 80−17094
pancreatic scanning 77−9237
Papua New Guinea, Late Cainozoic geotectonics and volcanism 80−51372
paracrystals, review, appl. to cryst. struct. investigs. *(German)* 77−39552
paralysed, treatment by elec. stimulation *(Slovenian)* 80−81771
paralysis of extremities, electrical stimulation treatment, basis, technology and role 79−34620
paramagnetic impurity ions in crystals, Jahn-Teller effects, review 78−34809
parametric processes in CTR plasmas, review 78−30430
paraplegic patient muscles, provision of functional use by elec. stimulation 80−101289
parity non-conservation in nuclei 80−32207
parity non-conserving processes, weak interaction theory, review 78−50002
parity nonconserving nuclear interactions and weak neutral currents 77−41936
parity nonconserving weak interaction between nuclear particles 77−6295
parity-non-conserving nuclear forces, theoretical and phenomenological approach review 80−42556
partial coherence studies, bibliographic review 77−27244
particle accelerator developments *(Czech)* 77−42196
particle accelerators, historical review, impact on scientific culture 80−868
particle accelerators, operating principles and construction *(French)* 79−45486
particle beam excited state populations, preparation, measurement and control 79−30607
particle capture from laminar flows, review, book contrib. 77−47078
particle coherent and incoherent prod. in nuclei, multiple scatt. theory *(Russian)* 77−216
particle detectors, methods of detection and appl. of electronics and computer technology 80−106235
particle identification systems including magnetic analysis 79−72181
particle motions in a viscous fluid, review, book contrib. 80−96289
particle physics overview, role of CERN and FERMILAB *(Dutch)* 77−45928
particle properties, leptons, mesons, baryons 80−67944
particle scattering, solid and liq. struct. determ., Fourier transforms 77−27772

reviews continued
particle size distribs., determ. methods for particles <10μm, review *(German)* 78−60894
particles, massive, with any spin. consistent eqns., Klein-Gordon divisor 80−73577
parton model, QCD and hard processes 80−47258
parton model 77−57498
parton model appl. to large momentum transfer interactions 79−17686
passive ground-based electro-optical detection of artificial Earth satellites 79−62717
passive optical rotation sensors using guided waves, developments 80−58781
passivity, in metals and alloys 80−50750
path integrals in quantum theory, basic concepts 80−52066
patient exposure to diagnostic X-rays, anal. of 1972-1975 NEXT data 79−39505
PBHTR, design operation and applications 79−45328
Peach Bottom 1, HTGR nuclear power station, review of design and operation 79−45327
Pecs University Biophsyics Unit, Hungary, 25 years of radioisotope appls. *(Hungarian)* 80−90647
Penning collision processes *(Japanese)* 79−64092
PEP, polarisation expts., review 77−34487
peptide linkages, H bonding effects 77−10783
percolation clusters, scaling theory of lattice 79−80542
percolation theory, review, appl. and polychromatic percolation 79−58626
percolation theory 80−98868
percussion instrument acoustics, multidimens. vibrs. 77−57128
perimetry, automated, history, theory and practical application 79−92402
peripheral circulation evaluation, noninvasive techniques 80−56163
peripheral nervous system, trophic mechanisms, book contrib. 79−2043
peristalsis, review of functions and waveforms, book contrib. 79−16245
permanent magnets, theory, materials, fabrication and applications 79−42801
personnel dosimetry performance, testing standard 80−9421
personnel monitoring for radiological protection, current status and developments 79−22490
perturbation theory, large order estimates 79−26237
perturbation theory developments in reactor physics 77−14227
perturbative QCD and hard scattering processes 79−45075
petroleum industry materials, plant, service failure modes gen. review 78−95904
phase diagrams, thermodynamic calc. 79−91620
phase microscopy techniques 78−45684
phase ordering *(Japanese)* 80−2352
phase profiles generation, recent advances, book contrib. 79−76644
phase reconstruction problem for wave amplitudes and coherence functions, book contrib. 79−31823
phase relationships and equilibria for U-Pu monocarbonitrides 77−21126
phase screen statistical features from scatt. data, book contrib. 79−36851
phase separation and glass structure concept changes 77−65955
phase stability under irradiation, review 79−77722
phase transformations, Ising and other models, book contrib. 77−37825
phase transformations in metals and alloys, thermodynamic and mechanistic classification 80−2995
phase transformations of minerals and Earth's deep interior materials *(Japanese)* 78−28225
phase transition theory, renormalization group method 77−80601
phase transitions and critical phenomena, recent developments 77−87713
phase transitions in strongly random systems 79−58647
phase transitions under shock-wave loading 77−84888
Philippines, high wind study 78−36257
philosophy of science, contemporary competing positions *(German)* 79−71217
phoniatric diagnostics of speech organ disorders, objective acoustic methods 80−104598
phonon perturbation by complex defects, expt. studies review 79−42190
phonon-phonon interactions in liquid He-4 77−55410
phonons, high-frequency, spectroscopy, transport phenomena 80−49325
phonons and neutron scattering, book contrib. 77−89504
phosphate containing materials, technological prod. processes review 80−97452
phosphate laser glasses 80−9888
phosphates, condensed, crystal chemistry 79−86745
phospholipids, exchange between membranes, book contrib. 80−30695
photicon, 2D array imaging detector for visible light, review of imaging characts. 79−45554
photoacoustic effect and appls., review 79−41786
photoacoustic spectroscopy, biological and medical appls., book contrib. 80−109078
photoacoustic spectroscopy, of solids *(Japanese)* 80−31887
photoacoustic spectroscopy, operation of instruments and test results 78−4705
photoacoustic spectroscopy, theory, techniques and appls., book contrib. 80−9050
photoacoustic spectroscopy 79−89013
photoactive catalyst used in light induced photocuring of coating systems 80−7820
photocells and photomultipliers, USSR 80−57371
photochemical formation of self-sustaining coacervates, rel. to origin of life 78−11611
photochemistry and dynamics of the ozone layer of atmosphere 79−5590
photochromic glass, with Ag halides:Cu, formation and theoretical models 80−43418
photochromic inorganic materials for hologram storage, book contrib. 78−25835
photodesorption 79−51424
photodetectors, thermal detectors and photondetectors, operating conditions and applications 80−47110
photodissociative ionisation, 16-41 eV 77−18995
photoelectric setting microscopes, recent developments 77−41681
photoelectrochemical solar energy conversion principles, review 80−35695
photoelectrochemical systems, energy conversion 79−52941
photoelectrolysis of water with semicond. surface *(Japanese)* 78−6440
photoelectromagnetic effect, current research status, review 79−69559
photoelectron counting statistics, theory, fully quantum 80−52312
photoelectron spectroscopy, biological appls. 77−56558
reviews continued
photoelectron spectroscopy, charact. of vapours oven heated inorganic solids 80−52239
photoelectron spectroscopy, solid-state, with synchrotron radiation, review 80−71570
photoelectron spectroscopy, synchrotron radiation appls., book contrib. 80−14035
photoelectron spectroscopy and catalysis *(French)* 77−29045
photoelectron spectroscopy of adsorbed atoms and molecules 78−27372
photoelectron spectroscopy of valence bands in solids 78−39668
photoelectronic streak-tube technology 77−79184
photoemission, book contrib. 77−32506
photoemission, theoretical aspects 80−45213
photoemission spectroscopy, book contrib. 77−63546
photogrammetry, OTF/MTF standards 77−78471
photographic information recording, new techniques *(German)* 77−26411
photographic information recording and retrieval techniques *(German)* 77−26410
photographic method optimisation in astronomical obs. *(Russian)* 79−35144
photographic process, simultaneous developing and fixing *(Russian)* 78−86372
photographic process physics, silver halide phys. props. and sensitivity *(Japanese)* 77−54007
photographic reactions, quantum chemistry *(German)* 78−53229
photographic reactions, quantum mechanical interpretations *(German)* 78−61034
photographic sensitometry, black and white, photographic testing procedures, film evaluation 78−29191
photographic speed determ., methods used to relate sensitometry and exposure 79−89020
photographic zoom lens systems for 8 mm and super-8 cameras *(German)* 78−93771
photography semiconductors and ICs used in cameras *(German)* 79−58813
Photoinduced heterogeneous catalysis 78−40080
photoionisation, atoms and molecules review, expt. techniques, processes, theory 77−14402
photoionisation of atomic systems 77−27125
photolytic generation of transient radicals for EPR spectroscopy 80−11271
photometric analysis methods 79−43660
photomultipliers for photon counting, one-electron characts. 78−58038
photon antibunching in reson. fluoresc. from two-level atom, quantum nature of light 79−85251
photon correl. spectroscopy, macromolecular soln. dynamics, review 79−59603
photon dosimetry, practical problems 77−60261
photon echo spectroscopy of crysts. 80−83648
photon-nucleus reactions, medium energy, above giant dipole resonance 77−79358
photonuclear research at Lund and future accelerator plans 77−82907
photoplastic effects *(Japanese)* 78−6121
photopolymer industry in Japan 80−4800
photoproduction at high energies, total cross section for p and nuclei 78−78186
photoreceptor membranes, dynamic aspects of molecular texture 79−79519
photoreceptor rod cells, vertebrate, visual transduction, book contrib. 79−96561
photorefractive materials for optical storage and display, phase hologram form. 77−75445
photorefractive materials for optical storage and display 77−71961
photoresists for relief phase hologram recording, book contrib. 78−25837
photoselective bimetallic aggregation, new route to bimetallic clusters 80−53182
photostimulated processes in inorganic materials and optical information storage 78−82926
photosynthesis, delayed light 77−86466
photosynthesis, electronic structural props. of relevant mols. 80−16902
photosynthetic productivity engineering 79−62209
photosynthetic reaction centre, chlorophyll function, book contrib. 79−5251
phototropism of coprophilous Zygomycetes 77−90851
photovoltaic materials and devices for terrestrial solar energy applications, R and D status review 80−101112
photovoltaic power systems, US DOE R and D program 80−55874
physical acoustics, history and future 77−49548
physical acoustics *(Polish)* 79−55258
physical chemistry, annual review, vol.28 (book) 78−40019
physical measurements under ultrahigh press. *(Japanese)* 77−67457
physical mechanisms of adhesion of solids *(French)* 78−6231
physics, quantum mech. appls., history 77−18773
physics and its methods in medicine *(Polish)* 80−12048
physics syllabuses in schools 79−62952
physiologic tomography, noninvasive meas. of myocardial metabolism, blood flow and function 80−104730
Pi3, long-period irregular mag. pulsations, reviews 78−45164
piano acoustics *(Japanese)* 80−33375
picosecond chemistry 77−5933
picosecond flash photolysis in biology and biophysics, book contrib. 79−5328
picosecond interactions in liquids and solids, book contrib. 77−65057
picosecond light pulse techniques, historical overview of rapid phenomena meas., book contrib. 77−65026
picosecond nonlinear optics, book contrib. 77−65609
picosecond photochronoscopy, generation and meas. of pulses from mode-locked lasers 79−76734
picosecond pulse generation methods, book contrib. 77−61138
picosecond pulse measurement techniques, book contrib. 77−61139
picosecond pulses generation and meas. 79−41401
picosecond Raman techniques, vibr. dynamics in liqs. 80−52325
picosecond relaxation measurements in biology, book contrib. 77−64166
picosecond relaxation processes in chemistry, book contrib. 77−61788
picosecond spectroscopy, appl. to chem. and biological reactions 79−80697
picosecond spectroscopy 78−37081
pictorial electrophotography, image quality and development 79−17538
picture taking parameters display in amateur cameras 78−89578

reviews continued
piezoelectric ceramic materials, reviews appl. and recent developments 79−78628
piezoelectric materials, piezoelec. props. review *(Japanese)* 77−73115
piezoelectrics, absolute config., bibliography 77−48129
pigmented biomembranes, photoelec. and magneto-orientation effects 77−48766
pinch effect in solid-state plasma 77−1441
pion absorption and production expts. 77−10435
pion exchange at high energies 80−95259
pion excitations and phase transitions in nuclear matter, review, book contrib. 80−483
pion low energy scattering 79−85529
pion production from proton-proton collisions at medium energies 78−62441
pion radiotherapy, review *(Japanese)* 78−40321
pion-nucleus absorption and scattering, pion condensation 78−8858
pion-nucleus elastic low energy scatt., corrections to multiple scatt. series 77−6439
Pioneer Venus mission, expts. descriptions 77−73928
pionic atoms, nuclear and atomic research review 80−43216
pipe, US testing 79−100316
planar Feynman diag. enumeration 79−26239
planar optics, goals, methods, potential appl., principles and trends 80−33231
planet interior differentiation processes, trace elements as probes 80−98584
planetary and solar system origin, model comparisons 80−17508
planetary atmospheres, research developments 78−69720
planetary atmospheres, review 78−32377
planetary atmospheres 78−69719
planetary dynamo theories *(German)* 78−40852
planetary magnetic fields, survey of expt. data 78−73664
planetary magnetism 80−98585
planetary nebulae, advances in optical studies 80−109522
planetary nebulae, gas dynamics and evolution 80−109533
planetary nebulae, review of UV obs. 80−109523
planetary nebulae, spatial and vel. distrib. statistics 80−109518
planetary nebulae, UV spectra 79−92843
planetary nebulae 77−17665
planetary nebulae 78−16510
planetary nebulae central stars, spectra, temps., binaries and peculiar stars 80−109435
planetary nebulae chemical abundances 80−109530
planetary nebulae role in heating stirring and ionisation of interstellar medium 80−109540
planetary ring systems, review of physical studies 80−72874
planetary rings 79−101096
planetary theory developments in 1973-6 period 78−77505
planets, major, pre-Voyager understanding of ionospheres 80−90351
plant biophysics, book 77−60180
plant condition monitoring in nuclear power generating industry 80−47612
plant growth and development regulation, role of light 78−11695
plant lipids and their role in membrane function 79−83716
plasma, drift-dissipative instability in mag. field 77−7536
plasma, H line Stark broadening, role of ion dynamics simulation 80−24144
plasma, high-temp. anomalous transport, solenoidal fusion system appls. 78−22460
plasma, laser-produced, electron density determ. by multicharged ion K-spectra obs. 79−64908
plasma, low-temp., with nonequilibrium ionisation 80−96343
plasma, nonideal, excitations and macroscopic props. 80−43842
plasma, nonlinear wave effects, comparison of theory and experiment 79−7460
plasma, reflection coeffs. for light ion-surface interaction *(Russian)* 80−38663
plasma, reversed field pinches, theory and experimental results 77−24126
plasma, strongly coupled classical plasmas in laser fusion and astrophysics 79−10634
plasma, supplementary heating in toroidal plasmas in France 77−24101
plasma, toroidal theta-pinch theory, Scyllac config. 77−24125
plasma chemistry, history, diagnostics, production, organic cmpd. synthesis 80−61099
plasma chemistry, principles and problems 77−48644
plasma collisionless shocks, simulation and laboratory expts. 80−87893
plasma confinement in cusp-shaped mag. fields 77−76178
plasma confinement in fusion reactors, alternative approaches 78−87477
plasma deposition, of inorganic thin films 80−50564
plasma diagnostics, high press. 77−47268
plasma diagnostics by laser interferometry *(Russian)* 77−11409
plasma diagnostics for controlled thermonuclear fusion experiments *(Spanish)* 79−63805
plasma diagnostics in Tokamak, far IR lasers development for Thomson scatt. 80−24242
plasma diagnostics using laser submillimeter methods 77−72498
plasma etching, mech. 79−83348
plasma etching techniques in semiconductor manufacture 79−20238
plasma generation and diagnostics by lasers 77−35371
plasma heating, neutral beam US development program and review 80−92348
plasma heating by laser beams 77−19735
plasma heating expts. in Japan 77−65889
plasma heating using negative ion based neutral beams 80−42852
plasma indicator, moving-coil type, construction, charact. *(German)* 78−8393
plasma industrial utilisation, synthesis, powder, metallurgical and surface treatments *(French)* 80−96398
plasma instability, suppression by feedback method automatic control, stabilisation methods 78−63564
plasma ionic-covalent nonadiabatic coupling 80−38535
plasma MHD ideal equilibria, computer codes 77−27712
plasma microinstabilities nonlinear effects 78−14150
plasma parametric instabilities *(German)* 77−31440
plasma RF heating, state of art in France and European community 77−47232
plasma shock waves, transverse mag. field effects 80−103153
plasma spectroscopy techniques development 80−43991
plasma turbulence, strong, Langmuir, simulations 80−59237

reviews continued
plasma wave propag. linear effects 78−14149
plasma waves, fundamental radn. theory 79−23409
plasma waves, radn. from point sources 79−23411
plasma waves, radn. from point sources 79−23410
plasma waves in magnetosphere 78−28451
plasma waves stimulated in ionosphere by RF topside sounders 78−45128
plasma-surface interactions in Tokamaks 79−73017
plasma-wall interaction; impurity introduction mechanism, fusion temps. 77−42990
plasma-wall interactions in Tokamaks 78−94123
plasmas, optical scattering of light by atoms, techniques theory 80−54044
plasmasphere, large scale elec. fields and currents, related geomag. vars., review 80−105121
plasmasphere of Earth, review 79−12329
plasmons, general theory 78−26826
plastic, metal electroplated, durability and struct. 78−3242
plastic deformation during freeze-cleavage 78−14400
plastic scintillation detectors, timing props. 79−22540
plastic surgery, biomechanical aspects 80−56103
plasticity, theory and constitutive equations *(Japanese)* 78−83267
plastics coatings 79−96163
plate tectonics, driving force models for plate stress 80−56450
plate tectonics 77−44959
plates and shells, fabrication from polymers, composite materials, physical props. 78−67056
Pluto, long term orbital motion, librational character 80−94753
Pluto (book) 80−82591
Pluto and its satellite, physical parameters and current research *(French)* 79−70994
PNP project, prototype HTR and coal gasification plant 80−5393
Pockels readout optical modulator, current status and appls. 77−72085
point defect chemistry, book contrib. 78−10044
point defects and interactions, book contrib. 78−10043
point defects in Si and Ge *(Japanese)* 77−89428
polar, magnetotail lobe and interplanetary low energy electrons, satellite obs. 78−73587
polar D-region aeronomy 77−53311
polar materials, appl. to SAW and other devices 80−66114
polar molecules, elastic and inelastic electron scatt. 78−94322
polar polymer, piezoelectricity and pyroelectricity 80−7267
polarimetric methods for polarisation state complete determ. 77−45882
polarisation model, appl. to hydrated Li^+ 80−54115
polarised beam experiments, low energy, in nuclear physics, book contrib. 80−68642
polarised H and D ion sources, recent advances 79−45498
polarised light in materials research, birefr., electro-, magneto-, elasto- and acousto-optics 77−48143
polarised neutron production and appls., book contrib. 79−58843
polarised photoelectrons from ferromagnets 77−32505
polariton modes at interface between two conducting or dielec. media 78−87922
polaritons in semi-infinite crystals 78−72087
polarization phenomena in hadronic reactions 80−52527
polarized-ion sources production methods 79−63841
polarographic methods of analysis 78−35769
polarography, amalgam, film, with accumulation, appl. to micro-, macro-object anal., review 78−61098
polarons, dielec. and molecular, comparison and new props. 79−28298
pole figures, automatic determ. 79−87819
poly-N-vinylcarbazole, polymerisation, struct., props., elec. charact. 79−41972
poly-phase microstructures, quantitative metallography, review 79−15925
polyacetylene, doped, p-n junction, elec. props. *(Japanese)* 80−29410
polyatomic mol. gas phase spectra, struct., review and tabulation 80−14136
polyatomic molecule, continuous and diffuse spectra, freqs. of 0,0 transitions 79−93965
polyatomic molecule, electronic relax. process, energy depend., book contrib. 77−34688
polyatomic molecules, photodissociation dynamics, review 78−37697
polyatomic mols., multiple photon IR processes 80−43125
polycrystalline surface texture analysis, modern methods 78−75914
polyelectrolyte 'catalysis' of chem. reactions 79−57217
polyelectrolytes in soln., conform., small-angle neutron scatt. investigs., review 79−873
polyester thermoplastic, for electrical insulators 80−103685
polyethylene, hexagonal, high press. crystn. 79−23529
polyethylene, lightly crosslinked, processed under mol. orient., struct., props., review 80−38957
polyethylene, vibr. data and force field consts., review 79−31750
polymer, amorphous, bulk, structure models and exptl. methods 78−22671
polymer, amorphous, segmental distrib., light-, neutron- and X-ray scatt., piezooptical and dielec. meas. 78−51444
polymer, crack extension micromechanisms 80−108561
polymer, crystalline, crystallisation, morphology rel. to props. 77−39546
polymer, long-term durability prediction methods 79−20320
polymer, neutron scatt. studies of chain conform. and dynamics 78−83753
polymer, piezoelectricity and pyroelectricity 77−8514
polymer, synthetic, solns., assoc., quantitative evaluation, review 79−10773
polymer chain dynamics, review 77−38759
polymer chains, with volume interaction, statistical physics problems, coils and globules, review 78−94347
polymer crystallisation, review 80−64925
polymer crystallisation 78−51430
polymer dry insulation, for power cables *(Spanish)* 80−81024
polymer fibres, ultra high modulus, prep. by soln. and melt spinning, review 79−11544
polymer films, between contacting surfaces, effect of contact pressure and temp. 78−60842
polymer films, electronic cond., electro-, photoresponsive effects, review 79−56261
polymer gels, thermodynamic props. *(German)* 78−20073
polymer macromolecules, volume interactions, coil-globule transition, statistical physics 80−78737
polymer mechanics, use of statistical methods, review 78−67031

reviews continued
polymer membranes transport from liq. phase 80−16720
polymer microstructure morphogenesis, book contrib. 78−83757
polymer mixtures, thermodynamics, review 79−1506
polymer molecule, flexible chain shape measures 78−17832
polymer orientation measurement methods, review 78−48589
polymer reactants in organic reactions 78−95923
polymer science, contribution of neutron scatt. 78−14245
polymer self-diffusion 80−29193
polymer solns., cooperative phase transitions 80−45850
polymer solns. and gels dynamic behaviour by light scatt. 80−55727
polymer solution, rigid, exciton transport 79−69431
polymer solutions, diffusion coefficients estimation methods, review 79−90807
polymer solutions, microgel-containing, physico-chem. and rheological props., light scatt. obs. *(Polish)* 78−50704
polymer solutions, mol. dynamics, book contrib. 77−39268
polymer solutions, thermodynamics, Flory-Huggins lattice theory appls. 77−40574
polymer solutions, thermodynamics *(German)* 78−18530
polymer surface, struct., bonding and reactivity, ESCA meas. 79−52073
polymer systems, binary, high mol. wt., phase transform. assoc. with spinodal decomposition 79−70062
polymer systems, crystallisation from solution 80−84105
polymer systems, crystallisation kinetic data, status of anal. 80−84104
polymer testing by dynamic mech. anal. 80−16626
polymer transformation reactions, kinetics, statistics and mechanisms 79−43584
polymer-cement composite, review 79−70039
polymer-polymer and metal-polymer sliding wear mechanisms, review 79−70174
polymeric alloys, props. and struct. 78−44076
polymeric compositions containing elec. cond. filler, struct. effect on elec. props. *(Russian)* 79−33317
polymeric dielectric materials exposed to partial discharges, degradation product anal. 79−4765
polymeric liquids, rheology and kinetic theory 78−38611
polymeric materials, prop. struct. concepts 77−7301
polymeric materials, stress meas., X-ray diffr. technique, review 78−5713
polymeric systems, fluid, rheology, characterised by mol. int. distrib., review 80−1504
polymeric systems, rheology 78−87317
polymeric systems, supported on inert substrates, dynamic thermomech. study 80−55623
polymerisation chemistry, mol. wt., chain-unit struct. control, review 77−40544
polymers, adhesional strength *(Russian)* 79−52619
polymers, amorphous, semicryst., mech. motions, review 77−32616
polymers, anal., literature review 1974-76 77−77815
polymers, and molecular solids, surface props. 78−34886
polymers, as engineering materials 79−56918
polymers, broadline NMR 80−11277
polymers, crystalline, homophase and heterophase, small-angle neutron, X-ray and light scattering, recent developments 79−10751
polymers, crystn., texture studies, review 79−83221
polymers, deformation of materials 78−68749
polymers, dielec. breakdown *(Japanese)* 80−60501
polymers, diffusion coeffs. of gases, sorption, permeation investigs., review 78−67868
polymers, elec. props. and morphology, correl. 78−43786
polymers, electronic structure 80−59860
polymers, fatigue, fracture 79−43425
polymers, fracture and fatigue, review 78−68781
polymers, long-term strength prediction, review 80−104226
polymers, multiple dielectric relax. processes, mol. aspects, book contrib. 80−50264
polymers, nonisothermal rheology, significance in polymer processing 79−90206
polymers, pyrolysis-mol. wt. chromatography−vapour phase IR spectrophotometry, on-line system, reviews 80−55768
polymers, specific fracture surface energy, meas., review *(French)* 80−104275
polymers, struct., bonding, reactivity by ESCA 78−53299
polymers, synthetic, chiral, with aromatic side chains, conform. from circ. dichroism 79−55014
polymers, synthetic, dil. solns., NMR relax. 79−89693
polymers, synthetic, radiative degradation, chem., phys., environmental, technological effects, review 80−40948
polymers, thermal cond., temp., crystallinity and orientation depends. 78−10234
polymers, torsion pendulum dynamic mechanical testing 80−55620
polymers and composites, fracture and fatigue 78−68781
polymers containing main chain heteroatoms, struct., ^{13}C NMR investigs., review 79−55013
polymers in medicine, book contrib. 80−12307
polymorphic phase transitions induced by shock waves 80−15188
polynucleotide electron energy band studies 80−72132
polyolefins, elec. cond., 78−26867
polyquinones, ladder, partially-ladder, synthesis, struct., props., review *(Russian)* 80−7529
polystyrene-polyisoprene two-block copolymer soln., conformation, small angle neutron scattering, X-ray diffraction *(Rumanian)* 80−6348
polytypism in crystals 78−83764
polyvinylidene fluoride, structure, and its electret *(Japanese)* 80−10510
POPOP dye vapour lasers, optical and electron beam pumping 80−48237
population inversion models for chem. lasers, book contrib. 77−10910
position sensitive detectors for thermal neutrons *(Japanese)* 78−78589
positive muon probes, metal studies 80−103909
positron annihilation, positron basic props., annihilation line shape, positronium formation, book contrib. 80−2893
positron annihilation exam. of crystal defect recovery kinetics *(German)* 77−44082
positron annihilation investigation apparatus 80−23240
positron annihilation study of neutron damage in metals 78−71769
positron camera system, ring detector, brain research, computed transaxial tomography 80−61739
positron circular ring cameras for computerised tomography, trends and prospects 79−66524
positron emission computer-assisted tomographic scanner 80−36116
reviews continued
positron emission tomography and its applications 79−11996
positron scattering by atoms, computer simulations, review 77−79692
positron studies of annealing in cold worked state 79−100163
post-dryout heat transfer 79−1094
potential energy surfaces of chemical reactions, nonempirical calcs. 80−35505
Potts model, exact results 79−58651
powder, dynamic compaction, review 78−3071
powder and particle charact., review of current instruments 77−66735
powder coatings, in metal finishing, review 80−104330
powder forging, review 79−43166
powder metallurgical parts, development, and manufacture of semifinished products 80−50578
powder metallurgy, particle shape analysis 77−1820
powder metallurgy, review of instruments for particle and powder charact. 77−66735
powder science *(Japanese)* 78−15326
powders, phonon electroacoustic echoes, storage mechanisms 80−75606
power reactors worldwide, review 77−67856
power sources for biomedical appl., progress survey 78−15917
powerful VLF waves, nonlinear effects on magnetosphere/ionosphere plasma *(Russian)* 78−32287
prealbumin-DNA-hormone interactions, X-ray studies, review 78−53322
precision measurements using stabilized lasers 79−55151
premartensitic phenomena, nucleation, shape memory effect, review 80−3041
pressure meas. and control instruments 79−2781
pressure transducers in clinical use 79−96692
pressure vessels, multicavity PCRV, design and anal: for ultimate strength calc. 78−44182
prestressed secondary containments, explosive charact. near ultimate load, 79−30968
primary dosimetric standards at the Memorial Sloan-Kettering Cancer Center, NY, USA 80−8190
principle of maximum entropy and irreversible processes 80−86198
probabilistic ideas in field theory and statistical mechanics 78−8230
probing solids and liqs. with photons and neutrons 77−43102
propagation in glass optical waveguides 79−90015
proportional and drift chambers in applied research 79−26824
proportional counters, RC-line encoded position-sensitive, recent improvements 79−9963
prosthetic circulatory device fluid mechanics and haemolysis 80−46101
prosthetic joint replacements, mech. factors 80−56286
prosthetic material mech. props., effects of physiological environment, cardiovascular appls. 80−8212
protective coatings for metals, chemically vapour deposited 78−44261
protein network formation dynamics, review, book contrib. 80−97995
protein sequencing, solid-phase techniques 77−56557
protein structure, areas, vols. and packing 77−86441
protein structure prediction from amino acid sequence 78−24026
protein X-ray crystallography, book contrib. 77−40958
protein-lipid interactions 77−90719
proteins, H_2 exchange kinetics and internal motions 80−21440
proteins, stress-induced struct. and activity changes 79−43812
proteins involved in active membrane transport, struct., book contrib. 80−108844
proteins of membranes, props. rel. to function 77−44601
proton decay, β-delayed proton radioactivity, book contrib. 78−82322
proton deep structure, renormalisation group approach 79−85302
proton radiography 79−91896
proton relaxation enhancement, biochem. appls. 79−89692
proton scattering at 1 GeV 79−26428
proton spin imaging by NMR 77−5877
proton-nucleus scattering, 1 GeV, review 78−70536
pseudorandom noise method *(Japanese)* 78−77688
psychological and physiological acoustics, history (1920 to 1942) 77−45664
pulmonary fluid dynamics, book contrib. 77−52829
pulmonary physiology, pathology, and ventilation-perfusion studies 79−29613
pulmonary radiograph interpretation, review of models used 80−36089
pulsar magnetosphere radio emission, plasma supply and elec. forces 80−46595
pulsars, book 78−8035
pulsars, obs. parameters and dispersion measures 77−9763
pulsating aurora, review 78−73562
pulse discharges in gases under conditions of strong ionization by electrons 80−44064
pulse propagation, narrow-band high-freq. in homogeneous medium 77−6982
pulse radiolysis appl. to biomolecule reactions and struct. 78−61145
pulse-power particle beam sources as fusion drivers, review 79−18066
pulsed and CW optically pumped lasers for novel applications in spectroscopy and kinetics 78−90413
pulsed H halide chem. and chem. transfer lasers 77−10906
pulsed ICR, with one-region trapped ion analyser cell, review 79−2876
pulsed laser fluorescence for atomic and mol. excited states obs., book contrib. 80−9760
pulsed laser spectroscopy 79−26140
pulsed neutron sources for epithermal neutrons 79−45516
purple membrane of Halobacterium holobium 77−86457
PVC plastisol pastes, dispersion and characteristic functions, review *(German)* 79−55015
PWR power stations, operating record and reliability 79−22404
PWR steam generator blowdown review of international handling procedures 80−690
pyrocarbon coatings, deposition in fluidized bed, TEM, changes by irradiation 80−34084
pyroelectric detector technology 79−2827
pyroelectric detectors and materials 78−49901
pyroelectric radiation detectors 77−45889
pyroelectricity, 1976-7, literature guide 78−43797
pyroelectricity, literature guide, 1974-1975 77−12323
pyroelectricity, literature guide, 1975-6 77−59515
pyroelectricity literature guide (1977) 78−95552
pyrometallurgy, industrial methods and research, book contrib. 77−40407
pyrometallurgy, process developments 80−25596
pyrophosphate myocardial imaging 80−94359
QCD, inclusive deep-inelastic scatt., asymptotic freedom 80−32084

reviews continued
QCD anal. of the low energy behaviour of hadrons 79−80813
QCD and hadron dynamics 79−97593
QCD and superdense matter, quark and gluon plasma, hadronic structure, neutron stars, hadron collisions 80−73683
QCD perturbation theory, predictions and applications 79−13026
QCD perturbation theory test for various processes, review 79−326
QCD perturbative appl. 79−97571
QCD phenomenology, quarks and gluons in medium energy nuclear physics 80−42563
QCD vacuum props., strong interaction theory 79−26233
QED, review of classical limit 78−8563
QED, review of experimental status 79−63399
QED, strong and supercritical fields, book contrib. 78−74193
QED and general relativity, physics of strong fields 78−8561
QED of small distances *(Russian)* 77−217
QSO line spectra 77−26081
QSO/galaxy associations, redshifts and distances 80−31369
QSOs, emission-line spectra and redshift distrib. 78−57677
quadrupole mass spectrometric applics. in at. and mol. physics 77−23581
quantisation of nonlinear systems, semiclassical methods 77−71238
quantitative analysis of multicompnent mixtures from absorpt. spectra 79−52811
quantitative electron microscopy, recent developments, review 77−70250
quantum amplifiers and their application in space research 80−36503
quantum beats 80−22444
quantum chemical methods appls. 80−93752
quantum chromodynamics, review 78−37146
quantum chromodynamics, strong interaction theory *(Dutch)* 77−46016
quantum chromodynamics 79−67498
quantum electronics, nonlinear optics and holography *(Russian)* 79−45950
quantum field theory, classical soliton solns. and semi-classical quantisation techniques 78−8255
quantum field theory, notes for history 78−28904
quantum field theory, solitons and instantons 78−8495
quantum field theory methods and models review using Schwinger source theory *(German)* 78−86406
quantum field theory methods for many-body isotropic Fermi systems 78−8338
quantum field theory of crystals and extended objects 79−42164
quantum fluids and crystals, Monte Carlo methods and results, book contrib. 79−82405
quantum interference effects in psychology, Schrodinger's cat 80−73158
quantum interference effects in two photon spectroscopy, improved techniques review 78−94224
quantum liquids, neutron scatt. 78−59990
quantum mechanical perturbation theory, convergence props., energy series 78−80
quantum mechanical theories of magnetism, review of properties and explanations 78−76215
quantum mechanics, Bell's theorem. Experimental tests and implications 79−17280
quantum mechanics, development and Heisenberg's role *(Polish)* 78−89291
quantum mechanics, key to understanding magnetism 79−24125
quantum mechanics, logical and mathematical structures 77−33904
quantum mechanics based on position 80−52048
quantum mechanics in secondary schools, review of Dutch program *(Hungarian)* 79−44657
quantum optics, transition phenomena 80−32944
quantum theory, boson expansion method, appls. 78−36884
quantum theory, review of attempts at experimental verification 78−54245
quantum theory of solitons 78−70288
quantum transport effects in DC elec. resistance of solids, review 79−40500
quantum-chemical π-electron system, molecules-in-molecule model *(German)* 80−5490
quark bag model, spectroscopic appls., baryonium, gluonium, quark phase of matter 78−50008
quark confinement, dynamical and topological considerations, review 79−26296
quark confinement 77−34121
quark distributions and quark jets from the CERN bubble chamber neutrino experiments 79−45085
quark model, implications of magnetic field topology in particle physics 78−8583
quark model and hadron spectroscopy 79−80808
quark model of resonances, $SU_6 \times O_3$, form factors 77−67624
quark model with SU(n) symmetry, 3 colours and 5 flavours 79−9343
quark models and unified field theories 79−80805
quark parton model 79−93368
quark-line rule for hadron nonets, review 79−26304
quarks, monopoles, tachyons etc., review of expts. 78−12872
quarks 79−22052
quarks and leptons, fermion physics in terms of SU(2)×SU(1) gauge theory 78−74197
quarks with colour and flavour *(Czech)* 77−41807
quasars, discovery and theories 77−60847
quasars and young galaxies 78−32582
quasi-one-dimenional organic conductor, chem. trends and stabilisation of nearly one-dimens. state 78−10328
quasi-one-dimensional conductors 78−60070
quasi-stellar objects, absorpt. line spectra review 78−57679
quasielastic cluster knockout theory, review, book contrib. 79−75874
quasifree cluster knockout reactions, cluster spectroscopic factors, medium and high energies, review 79−6440
quasiresonant atomic collisions, asymptotic calcs. 80−23512
Quaternary buried palaeosols 77−2151
Quaternary of Chile, state of research 78−44980
QUISTOR, ion kinetic energy calc., survey 80−78468
radar appls. in meteorology and atmospheric behaviour research, review 78−77371
radar observation of lower atmos., VHF pulsed Doppler method 80−46277
radar remote sensing of Earth's surface, techniques 79−12294
radiation, low-level, current estimates of hazards to human populations, review 78−57043
radiation, public health aspects 78−35895
radiation blistering 80−44239

reviews continued
radiation chemistry, present status, future trends and applic. *(Japanese)* 78−31659
radiation chemistry and applications *(Japanese)* 77−73456
radiation damage, defects and surfaces in bulk metallic, covalent and ionic systems 80−34049
radiation damage, mechanisms in semiconductors and insulators 80−107315
radiation damage by electrons, cryst. and organic materials 80−79840
radiation damage effects, in metals, neutrons and heavy ions, rel. to reactor technology 77−43255
radiation damage in crystals, computer modelling methods 77−7760
radiation damage in high-resolution electron microscopy of biological materials 79−5331
radiation damage physics, current status in USSR 79−95049
radiation detectors, methods of pulses positions meas. 77−65410
radiation effects on optical components 78−83054
radiation exposure and other hazards, comparison of relative risks 79−2111
radiation exposure in daily life 77−49535
radiation exposure of UK population 79−62373
radiation induced creep, fundamental mechamisms *(Italian)* 80−55457
radiation induced defects, X-ray diffraction study *(Japanese)* 80−15152
radiation induced exchange reaction kinetics of H_2, D_2 and T_2, review 78−61005
radiation injury, repair and sensitisation of micro-organisms 78−11700
Radiation Oncology Research Program, recommended research proposals 80−3787
radiation physics, interaction with matter *(Japanese)* 80−39149
radiation protection standards, quantitative risk 80−61708
radiation safety, X-ray diffraction and fluorescence anal. equipment 79−12017
radiation science, role of models 80−67144
radiation therapy, calibration and meas. standards in USA 80−8188
radiation therapy, chamber factor reliability, United States institutions 79−20685
radiation therapy, current usage of fast neutrons 79−16270
radiation therapy, history of the use of radioactive iodine 80−42032
radiation therapy, intracavitary uses of colloids 80−36110
radiation therapy, total body techniques for bone marrow transplanation 80−104738
radiation thermometry, applied precision, current status 80−52224
radiation-induced segregation in binary and ternary alloys 79−78970
radiative, (-conductive) heat transfer, direct differential methods, review 80−64352
radiative and combination heat transfer 79−81703
radiative and nonradiative recomb. at metal ions, core struct. effects 79−4834
radiative corrections in gauge theories, QCD current algebra formulation, weak interaction universality 78−93883
radiative polarisation in particle accelerators 78−33335
radiative transfer, irreversible processes *(French)* 80−13002
radio astrometry 77−25952
radio propagation in natural waveguides, survey 77−78328
radio signal transmission, long-delay echoes generation, models 80−26670
radio telescopes, tiltable, design and improvement 77−45313
radio transmission in Earth-ionosphere waveguide, concise theory 79−48616
radioactive atoms, hyperfine spectrosc., nucleus-electron interactions 79−72259
radioactive decay lifetimes, influence of chemical environment 79−75911
radioactive ions beams, for nucl. expts. 79−97922
radioactive tracer appls. to ventilation and air pollution studies 78−28306
radioactive waste, decay heat estimation, summation calcs. and Standard eqns. 80−63317
radioactive waste, final disposal possibilities, waste conditioning, storage and safety 79−26554
radioactive waste, low and intermediate level, current development program 80−13733
radioactive waste, reprocessing, solidification vitrification of liquid waste, review 79−9762
radioactive waste disposal criteria proposals by EPA and NRDC 80−18484
radioactive waste management in Canada, bibliography 79−6755
radioactive waste processing, consequences of separation of long-lived α-emitters *(Czech)* 80−5251
radioactivity incidents, national arrangements 80−102355
radioassays, automated data processing 79−16299
radioastronomical equipment, techniques and observations *(German)* 77−56827
radioastronomy, interferometry theory and appl. 80−12676
radioastronomy, pioneering work by Jansky, and Penzias and Wilson 79−44655
radioastronomy image reconstruction 80−56718
radiochemical quality control of short-lived radiopharmaceuticals 77−52876
radiocommunication, propag. problems connected with infinitesimal point source 80−90194
radiocommunication, propag. problems connected with special source structs. 80−87272
radiography, computerised tomographic scanning 77−16973
radiography, computerised tomography, present state and technical perspective *(French)* 77−16974
radiography, physical processes and math. methods review, neutron-nucleus interaction effects 78−60888
radiography of breast, recent techniques *(French)* 77−81564
radioimmunoassay, probe for fine struct. of biological systems, review 78−73217
radioimmunoassay as aid to diagnosis *(French)* 80−21522
radiointerferometry, Mandel'shtam's research 80−105488
radioisotope counting techniques for analytical appls. in biology and medicine 80−81794
radioisotope emission computed tomography 78−44599
radioisotope imaging, computer application to rapid dynamic studies 79−16297
radioisotope scanning in thromboembolic disease diagnosis 78−7434
radioisotope scanning of bone, historical survey 80−42029
radioisotope therapy in bone and joint disease 80−36111
radioisotope tomographic imaging, historical review 80−42038

reviews continued
radioisotopes, artificial, 25 years of use and production in Hungary *(Hungarian)* 80−94340
radioisotopes, development in use *(Hungarian)* 80−90645
radiological anatomy of the ear round window 79−62332
radiological fine puncture and biopsy, efficiency and technique in tumour diagnosis *(German)* 80−41212
radiology, past and future techniques 77−12984
radiology instrumentation, new industrial contributions 78−31924
radiolysis of DNA and other bipolymers 80−67163
radiolysis of heterogeneous inanimate systems, radiobiology appl. 80−66824
radiometry and applied radiation *(Japanese)* 77−33984
radiommunoassay, book contrib. 80−109021
radionuclide evaluation of cadiac trauma 80−94361
radionuclide imaging, merits rel. to US imaging and computerised tomography 79−48324
radionuclide imaging techniques, book contrib. 80−36113
radionuclide therapy, pot. future appl. 80−36031
radionuclide venography for investigation of thromboembolic phenomena 78−7439
radiopharmaceuticals for tumour detection 79−48318
radiosources, astronomical, with superluminal rels. 77−78882
radiotherapeutic agents, props., dosimetry and radiobiologic considerations 80−36106
radiotherapy *(French)* 80−21523
radiotherapy accelerator neutron leakage survey 80−51269
radiotherapy electron accelerator photoneutron prod., survey of European meas. 80−51241
radiotherapy of malignant disease, changing patterns 77−56446
radiowave scatter communications 79−34935
radiowave studies of ionosphere, incoherent scatter technique development 78−81503
rail/wheel noise research 80−48496
railway tunnels, structure-borne sound levels 80−48499
rainbow, physics, historical review 77−73854
rainfall event, S.England, 1968, September 14-16, hourly rainfall maps and mesoscale motions 77−45122
rainfall measurement by radar, methods and interpretation of data 80−81969
Raman and Brillouin spectra of transparent solids *(Chinese)* 79−33714
Raman effect, interacting elementary excitations in solids 78−43846
Raman high-resolution molecular spectroscopy, rot. and rot.-vibr. spectra 78−42064
Raman laser, IR, high-power tunable 79−7140
Raman laser, IR source, physical processes, theory 78−17943
Raman laser uses in molecular spectroscopy and atmospheric constituents detection 80−55762
Raman lasers, high-power, liquid, N_2 and O_2 as possible active media 80−19028
Raman scattering cross-sections in gases and liquids 80−23426
Raman scattering of light by polaritons 80−34928
Raman spectroscopy, in high temp. chem. 80−52234
Raman spectroscopy, literature review, 1975-1977, chem. anal. applications 78−85218
Raman spectroscopy, recent advances 78−41359
Raman spectroscopy, remote spontaneous, new trends in recording of signals 80−73485
Raman spectroscopy, vap., medium resolution, appls. 78−42065
random motion and Brownian rotation 80−73266
rapid automated nuclear chemistry, short lived fission products, reactor safety 80−81353
rare earth alloys, amorphous, mag. props. rel. to struct. 79−15298
rare earth alloys, RFe_2, magnetostriction studies, book contrib. 80−39846
rare earth alloys, RM_2, (M=Fe, Co, Ni), magnetism, review 80−20365
rare earth alloys and compounds, Kondo effect 79−69506
rare earth complexes, formation and props., book contrib. 80−43204
rare earth compounds, intermediate valency 79−91001
rare earth compounds, Raman light scatt., phonons and valence fluctuations, review 77−63415
rare earth compounds, valence changes, book contrib. 80−39533
rare earth hydrides, props., book contrib. 80−45291
rare earth intermediate valence systems, neutron scatt. 80−49674
rare earth intermetallic compounds, ferromag. props., book contrib. 80−75726
rare earth intermetallic cpds., cryst. chemistry, book contrib. 80−39010
rare earth intermetallic cpds., mag. props., book contrib. 80−39759
rare earth ions in soln., absorpt. and fluoresc. spectra, book contrib. 80−45112
rare earth iron garnet single crystal films, synthesis and props., review 78−48013
rare earth iron intermetallics, RFe_2, magnetostrictive, book contrib. 80−75838
rare earth luminescence, relaxation phenomena, book contrib. 77−32439
rare earth metal, alloy and cpd., static and dynamical aspects of hyperfine interaction, NMR investigation 79−91299
rare earth metal atomic spectra analysis, present state and trends 78−62749
rare earth metal-B systems, phase equilibria, phase diagrams, book contrib. 78−48389
rare earth metals, diffusion 79−69281
rare earth metals, elastic and mechanical properties 79−70132
rare earth metals, hydrides and oxides, film prep., struct. and props., general review 80−54556
rare earth metals, low temp. heat capacity 79−69263
rare earth metals, mag. and transport props. 79−69658
rare earth metals, mag. excitations, neutron inelastic scatt. 79−47265
rare earth metals, optical props. 77−40259
rare earth metals, preparation methods and properties 79−69969
rare earth metals and alloys, ferromag. props., book contrib. 80−75725
rare earth metals magnetism 77−63123
rare earth molybdates, cryst. growth, cryst. chem., and phys. props., book contrib. 80−44194
rare earth orthochromites, mag. interactions and weak ferromagnetism 78−52220
rare earth oxides, binary, struct. and props., book contrib. 80−45292
rare earth oxides, mixed, phase relations and struct., book contrib. 80−45293
rare earth perovskites and garnets, prep. and props. book contrib. 80−44193

reviews continued
rare earth semiconductors, studies in Soviet Union 80−96875
rare earth systems, cryst. field interactions, book contrib. 80−39540
rare earth systems, high pressure studies 79−69193
rare earth systems, magnetic structures and inelastic neutron scattering 79−69654
rare earth systems, NMR, EPR, and Mossbauer effect, book contribs. 80−39883
rare earth systems, superconductivity 79−69621
rare earth-Co permanent magnets, processing and props., review *(Japanese)* 77−73049
rare earth-nonmagnetic metal intermetallic cpds., struct. and props. 79−95377
rare earth-transition metal alloys, amorphous, struct. and mag. props., book contrib. 80−39818
rare earths, and their alloys and cpds., photoemission, rel. to electronic struct., book contrib. 80−16157
rare earths, atomic props. and electronic struct. 79−68204
rare earths, electronic structure, calc. methods 79−69405
rare earths in metallic environment, mag. moments 78−6515
rare earths industry 80−25537
rare gas liquids, ionisation and scintillation, appl. to radiation detectors *(Japanese)* 78−35206
rare-earth magnetically hard materials 77−73051
ray optics, theory of light field, statistical optics, light meas., photometry, polarimetry 77−79748
reaction rate theory in bioluminesc. and other life phenomena 77−90716
reactive DC sputtering, magnetron-plasmatron processing and instrumentation 80−35090
reactive molecular collision calculations 79−61851
reactive sputtering of low-Z materials by H_n^+, expts. rel. to plasma-wall interactions 77−48297
reactivity of surfaces, exptl. techniques and appls. *(French)* 79−92000
reactor cooling and heat recovery methods *(Italian)* 78−4978
reactor coupled-core kinetics, research review *(Japanese)* 79−63733
reactor safety 77−61510
real-time optical Fourier spectrum analysis using acousto-optic diffr. 78−5430
receiver design for optical fibre communication systems 78−30077
rechargeable sealed battery systems 79−43753
reciprocal effects and other quark theories, charm quarks, J/ψ discovery, gauge theories *(Danish)* 79−30698
recorders, direct-writing analogue type, biomedical appls., techniques and maintenance, review 78−69241
recording of fast processes, photographic and cine methods 80−57413
recrystallisation 77−4790
red dwarf stars 79−16954
refractories, role of fracture toughness in thermal shock resistance *(French)* 78−80618
refractory borides, carbides, nitrides, manufacture and appl. in electronic and electrotechnic field *(French)* 80−40311
refractory ceramic coatings, for high temp. use, current status *(Japanese)* 80−71619
refractory concretes, review of new developments *(French)* 79−15636
refractory materials for optical glass making 77−14818
refractory metals, oxidation, high-temp., mechanism, review *(Polish)* 79−34184
refrigeration with expansion turbines 77−5847
Regge phenomenology 78−24979
Regge pole theory, reasons for survival, review 78−24977
Regge poles and multiparticle systems, book contrib. 79−21890
Reggeon calculus, physical basis and implications 77−6101
Reggeon field theory, recent developments 78−41439
relativistic atomic structure calculations 79−59379
relativistic electron beam induced turbulence and heating 80−38672
relativistic experiments in gravitational fields 80−42135
relativistic hadron couplings, unified framework, symms., quark models *(German)* 78−50012
relativistic heavily ionising particles, energy loss 80−32583
relativistic heavy ion collisions, reaction mechanism and recent topics, review 80−42683
relativistic heavy ion reactions, central collisions, review 78−50195
relativistic heavy ion reactions, review of recent expt. and theoretical evidence 79−67765
relativistic heavy ion-nucleus reactions, book contrib. 80−27672
relativistic string dynamics, Lorentz invariant quantum theory *(Russian)* 79−22020
relativistic strings and dual models of strong interactions 78−439
relativistic theory of the classical electron 80−12923
remaining creep life for components under stress at elevated temperatures 80−59566
remote sensing, appls. of technology 77−5349
remote sensing, introductory review 77−2286
remote sensing, recent developments 77−23752
remote sensing of Earth's resources using satellites, review of techniques 79−16714
renal imaging with radionuclides, US and computerised tomography 80−17095
renewable energy sources in West Germany *(German)* 79−87958
renormalization group and ultraviolet asymptotics 80−101933
reprocessing of nuclear fuels 79−26662
reproductive epitaxy, exam. 80−55303
research uses of early data, from Meteosat-1 80−77257
residual latency techniques and related physiological procedures 79−44001
residual stress, X-ray evaluation, treatments for nonlinear distribs. 80−25966
residual stresses, methods of detecting, review *(German)* 78−44291
residual stresses, review 80−44245
residual waste treatment technology 80−40932
resin, highly crosslinked, fracture, review 77−4846
resistance thermometry 80−52206
resolution methods in free surface problems 77−54954
resonance interaction of intense light with atoms 79−68216
resonance ionization spectroscopy and one-atom detection 80−22441
resonance light pressure, anal. of forces and applications 79−18156
resonance Raman scattering, polariton theory, book contrib. 79−38551
resonance Raman scattering with tunable lasers, review, appls. 78−94247
resonance Raman spectra of biomols. 77−90976
resonance Raman spectroscopy, uses in analytical chem. 79−92014

reviews continued
resonance scattering methods in atomic spectroscopy 80−53167
resonant light scattering from magnetic excitations 80−97290
resonant Raman effect, appls. and theories, book contrib. 77−38676
resonating group method, recent investigation results 79−3098
resonating-group method for nuclear many-body problems 79−9497
resource letter on environmental noise control 78−61949
respiratory mass-spectrometer, medical fields of appl. 79−62383
respiratory monitors, instrumentation and maintenance, review 78−69236
retina, current research and study, selected review 80−30710
retina, excitation and interaction, book contrib. 79−5282
retina physiology, single cell studies on lower vertebrates, book contrib. 79−96558
retinal diseases, literature review (1975-76) 78−35836
retinal ganglion cell functional pathways, book contrib. 79−96559
retinal research and study, selected review 80−108874
retinal stimulation by Ra 79−71213
retinol-binding proteins in retinal pigment epithelium 79−20525
reversed field pinches, bibliography, 1958-75 77−24171
reversible temper embrittlement, book contrib. 78−11334
review of literature, 1975-1977 78−85225
review of reactions involving few-nucelon systems at intermediate energies 78−13054
review of three years e^+e^- research at SPEAR 79−63490
RF accurate voltage measurement 77−18043
RF heating of toroidal plasma 79−98939
RF separators 77−13821
RF telemetry exposure effects on biosystems 77−86533
rheological equations for polymer solutions and melts 79−86391
rheology of concentrated dispersions, review 77−19578
rhodopsin visual pigment, photochemical transformations 79−66472
rigid body, vector anal. of finite rotations, literature review 78−36819
ring compounds, three-membered, vibr. spectra and struct., book control 78−78701
ring galaxies 80−62281
ring laser, resonance phenomena with saturated absorpt. *(Russian)* 78−59048
river ice, book contrib. 78−61476
river meandering, book contrib. 78−61475
river water quality, modelling and control problems 79−57519
road traffic, noise control procedures 79−34464
rock mechanics rel. to earthquake prediction 79−16449
rock volume changes during fracture and frictional sliding 79−16450
rocks, steady state flow 77−9412
room temperature phosphorimetry, anal. technique, review, methodology, instrumentation, appls. 78−95972
Rosenstiel School of Marine and Atmospheric Science, University of Miami, review 80−8755
Rossby waves in ocean and atmosphere, book contrib. 78−61435
rotating fluid dynamics *(French)* 78−30300
rough surface contact, review of expt. work 80−76377
rough surface light scatt., vector theory, surface plasmon effects 79−59638
rubber, analysis and characterisation, 1974-6 literature review 77−77814
rubber, dynamic mechanical properties models *(Polish)* 79−43349
rubber, natural, crosslinked by dicumyl peroxide, modulus, swelling relations 80−59551
rubber elasticity, molecular aspects book contrib. 78−84886
rubber-like networks, thermoelasticity, rel. to rubber elasticity theory 77−31219
runaway electrons in toroidal discharges 79−64892
Rutherford backscattering, review of technique and applications 79−43082
Rydberg atom+molecule, reaction channels, expt. vs. theory 80−63755
S-matrix theory, quark as redundant concept, order concept, review 79−25786
Salyut, international spaceport, review 80−31196
Salyut space stations, review 80−31195
San Andreas fault, California, Palmdale Bulge as precursor event 78−36114
satellite geodesy *(German)* 77−44905
satellite solar power stations 79−8984
satellite time transfer technology 80−47029
Saturn's satellites, surfaces and interiors present knowledge 80−4297
SAW design and appls., review 77−50853
SAW device materials development 78−6636
SAW devices, signal processing appls., review 80−38204
SAW devices and signal processing appls., book contrib. 79−50519
SAW filter appls. in consumer electronics 80−74675
scaling and multiplicative renormalising in solid state physics *(Hungarian)* 79−11289
scanning Auger microanalysis, review 79−43699
scanning Auger microscopy, developments 80−101909
scanning electron micrographs, optical techniques for anal. 79−21864
scanning electron microscopes, operation and appl. 79−49348
scanning electron microscopy, recent developments of microscopes and techniques *(Chinese)* 79−30627
scanning electron probe microanalyser, development of x-ray microanalysis 80−37139
Schrodinger equation, current research 77−41509
science and society in London, 1796-1807 77−41450
scientific career migration, bibliography 79−71220
scientific growth, review of measurement indicators 79−58519
scientific instrum. in India 77−79087
scintigram improvement by computer processing 79−16296
scintigraphy, computerised image processing and display methods, multicentre comparison 79−53233
scintigraphy in paediatrics *(French)* 78−44590
scintillation cameras, deadtime meas., scatter conditions simulating nuclear cardiography 79−16276
scintillation counting anal. for radioactive dating 78−82586
scintillation detectors for neutron physics research 79−72199
scintillation pickups with plateau in counting characteristic 80−47811
scission of deformed nucleus, review of fission process 77−14096
Scorpius X-1 review 78−16576
Scripps Institution of Oceanography, research projects and education review 78−69464
δ Scuti and related stars, review 79−62847
search for interplanetary quantity controlling development of magnetospheric storms 80−17447

reviews continued
Second European Conference on Optical Fibre Communication, September 1976 *(Italian)* 78−5552
secondary cells, membrane appls. *(French)* 78−3374
secondary complex ion emission *(Russian)* 80−108305
secondary electron emission, angular and energy distrib. 80−100718
secondary electron emission spectroscopy of solid surfaces 77−36326
secondary ion mass spectroscopy, nuclear engineering appl. 79−30602
secondary ion-ion emission, primary ion beam optimum current density review 77−52211
secondary ion-ion emission ionisation of solids during sputtering, exam. of mech. *(Russian)* 79−33878
Secondary Standards Dosimetry Laboratory, review of role 80−5361
secondary-ion emission, ionisation process 80−35040
sedimentary basins subsidence mechanisms 77−21746
sedimentation, concentration and pressure effects 77−32835
sedimentation of flocculent suspensions 80−35577
sediments magnetization, depositional and postdepositional processes 77−86869
seismic anisotropy in lithosphere 77−49011
seismic data deconvolution 78−53736
seismic data processing hardware developments 77−60355
seismic design of power plants 77−3179
seismic instrumentation for nuclear power plants in Germany 79−620
seismic surface waves, theory and obs. *(German)* 77−64227
seismicity of western Canada, 1899-1975 period 79−5452
seismological observatories and seismic instrument construction in Poland *(Polish)* 77−21911
seismology, use of dislocation theory, book contrib. 80−109119
selective surfaces for high temp. photothermal conversion 78−1364
selenodetic investigations in USSR, bibliography (1928 to 1975) 79−88609
self-consistent calculations of nuclear properties with phenomenological effective forces 79−22218
self-consistent field calcs., NN interactions, and results of appl., book contrib. 79−75880
self-gravitating rotating masses, book contrib. 80−21915
self-powered neutron and gamma-ray detectors 79−45558
self-sustaining oscills. of flow past cavities 78−94645
SEM, low-temp. 78−54510
SEM, magnetic contrast, techniques and appls. 79−6236
SEM, recent trends and developments 79−2897
SEM, state-of-the-art review and future trends 78−21282
SEM, wet, live and frozen objects 79−26183
SEM channelling patterns 77−55217
SEM contrast mechanisms 78−21296
SEM field emission sources 78−21299
SEM image processing systems, summary of useful techniques and anal. 79−12901
SEM microanalysis techniques 80−71995
SEM specimen chamber use for dynamic expts., state-of-the-art review 78−23918
semi-insulating substrates, monolithic integration of optical and electronic devices 80−58543
semi-leptonic interactions 78−78162
semiclassical radiation theory within quantum mechanical framework, book contrib. 79−75705
semiconducting biopolymers and their part in biochemical phenomena 80−12053
semiconducting solid solutions, optical transitions 78−2908
semiconductive conjugated polymers, synthesis and elec. props. 80−15513
semiconductor, cubic, tetrahedral and layered cpds., surface struct. 77−85032
semiconductor, deep levels, review 80−103640
semiconductor, impact ionization 80−65577
semiconductor, magneto-impurity effect 79−91081
semiconductor, nonpolar, empty surface states and surface order effects on sorption 77−85281
semiconductor, optical props. under intense laser field 79−43040
semiconductor, optical props. under intense laser fields 78−72513
semiconductor, phonon-assisted cyclotron reson., single and two-phonon pinning, review 79−15356
semiconductor, phonon-assisted nonradiative recomb. phenomena, review *(Polish)* 77−69339
semiconductor, recomb. at deep traps 79−38100
semiconductor, resonant Raman scatt., book contrib. 77−36251
semiconductor, spin orientation by optical pumping 79−38410
semiconductor, strong electron-lattice interaction *(Japanese)* 80−49664
semiconductor, surface electronic props., optical spectroscopic techniques 80−11070
semiconductor, Wannier-Mott polaritons in mag. fields 78−2437
semiconductor, waveguide method of measuring electric parameters at microwave frequencies 79−93170
semiconductor, zero-gap props. correlated to Γ_8 symmetry, review 80−6717
semiconductor cyclotron resonance 78−6575
semiconductor detectors for charged particles and γ-rays, principles of operation and appl. 79−68154
semiconductor device characterisation using electron beam induced current technique 78−21302
semiconductor diode lasers, book contrib. 80−106525
semiconductor epitaxial structures, atomic diffusion 77−85110
semiconductor film, heteroepitaxial, on insulating substrates, characterisation, book contrib. 79−82497
semiconductor film growth, multilayer systems, spectroscopic ellipsometry 80−103603
semiconductor gamma radiation detectors, operation, energy resolution, efficient and appl. 79−68156
semiconductor gas sensors *(German)* 80−55974
semiconductor heterostructures, elec. and optical phenomena, discrete devices 78−72250
semiconductor homojunction lasers, gradual degradation process expt. *(Polish)* 77−68213
semiconductor impurity anal. by photoelectric spectroscopy 77−24584
semiconductor interface and overlayer electronic struct. 80−49841
semiconductor inversion layers, spectroscopy in high mag. fields 79−60889
semiconductor laser diodes, present status and technology *(German)* 80−58561

reviews continued
semiconductor laser material requirements, multicomponent solid solns. 77−14718
semiconductor lasers, recent progress, review 78−17938
semiconductor lasers 77−38892
semiconductor LEDs, high-radiance lamps and lasers, degradation 77−28630
semiconductor material phase diagrams, exam. of compilation activity 79−8288
semiconductor materials for junction lasers *(Polish)* 80−19029
semiconductor monocrystal-amorphous radiation-induced transitions 77−80554
semiconductor oxide crystals, forbidden energy gap, spectroscopic props. 78−2876
semiconductor physics in high mag. fields *(Japanese)* 80−50192
semiconductor radiation detector, development 79−68153
semiconductor step l-h junction, elec. struct. analytical methods 80−100507
semiconductor superlattices, optical and transport props. *(Slovak)* 80−20288
semiconductor surface, atomic geometry, ELEED meas. 79−51399
semiconductor surface, electron-electron interaction and electronic props. of space charge layers 78−60210
semiconductor surface electron states, optical methods of detection 77−66191
semiconductor surface structure and properties *(Japanese)* 80−49483
semiconductor waveguide switches, and modulators, review of development progress 78−38045
semiconductor with anisotropic conductivity, elec. and photoelec. props., review 78−10447
semiconductor-ferrite layered structs., SHF spin wave interaction with electrons 79−95507
semiconductors, atomic diffusion 79−4423
semiconductors, capture of carriers by attractive centres 79−7836
semiconductors, chemical thermodynamics 80−55692
semiconductors, current instabilities, theory and expts. *(Hungarian)* 77−39857
semiconductors, cyclotron-phonon reson., review 79−56615
semiconductors, deep centres, ODMR *(French)* 80−60461
semiconductors, electrical characterisation 78−60120
semiconductors, elemental amorphous, vibr. props. 77−84873
semiconductors, exciton condensation and electron hole liquids, state-of-the-art 80−49625
semiconductors, impurities and other point defects, electronic struct. 79−7803
semiconductors, interface and surface physics 80−49872
semiconductors, intervalley electron transfer, drift velocity and diffusion coefficient 80−39594
semiconductors, ion implantation, recent progress 79−14831
semiconductors, ion implanted, laser annealing 80−65023
semiconductors, p-type, spin-flip Raman scattering 80−108209
semiconductors, photoelectron spectra and band struct., book contrib. 80−16155
semiconductors, properties and use for making devices, review 78−60131
semiconductors, temp. depend. electronic cond. 80−59975
semiconductors, tetrahedrally coordinated, electron states associated wtih dislocations 79−82544
semiconductors, thermoelectric and thermomagnetic effects, heat transfer due to quasi-particle subsystems *(Russian)* 80−24959
semiconductors and insulators, role of electron-hole interaction in optical spectra, review 80−45113
semiconductors in noncrystalline states, diffr. investigations of struct. 77−72559
semimagnetic semiconductors 80−49702
semimetals, group V, low temp. transport props. 80−49708
sensory substitution systems−current status and future trends *(Japanese)* 80−36195
Seyfert galaxies and quasars, spectra and relationships 79−2571
shape isomers, spontaneous fission, static and decay props. and excitations, review, book contrib. 78−82402
shape memory effect 77−4144
sheet metal forming, material behaviour 78−95787
shell and isotope effects in neutron-nucleus interactions, review of Soviet research 79−36168
shell structure in nuclei 78−86493
SHG in laser plasma 80−53993
ship boundary layers, book contrib. 80−19346
shock acceleration of particles in astrophysical plasma 80−82192
shock compression of solids 80−24534
shock tube measurements of elem. gas reaction rate coeffs. 80−3299
shock wave interactions with boundary layers, review, book contrib. 80−96283
shock waves, terrestrial and cosmic 78−15967
shock waves on Earth and in space 78−3897
short-life radionuclides and regional lung function 79−53211
Si epitaxy, vapour phase deposition technology 80−75472
SI units in Journal of Physics E: Scientific Instruments 77−13733
Sigma cameras, development since 1960 79−63328
signal transmission in the nervous system, review of axonal and synaptic transmission 79−100593
silicate planets, crustal evolution 78−61774
silicates, ESR 78−88166
simple ionic liquids, struct. and dynamics 79−60243
simple metals, photoemission theory, book contrib. 80−16159
SIMS, appl. to surface anal. 80−40204
SIMS, in-depth profiling *(Japanese)* 78−85246
SIMS, quantitative 80−61195
SIMS anal. appl. to biological specimens 79−44074
simulative wear study critically reviewed 77−28968
single crystals under large loads, theoretical elastic behaviour, review and appl. 80−71681
singular potentials in non-relativistic quantum theory *(Russian)* 80−68345
sintered permanent magnets, development history, magnetic and physical props., appl. 80−29901
sintering, rel. to definition powder metallurgy 80−20841
sintering by diffusion mechanisms, kinetics of contact form. 77−85956
sintering science 79−15621
skeletal demineralisation osteopathy, quantitative diagnosis *(German)* 80−30872
skin friction in turbulent boundary layers, meas. techniques 78−1770

reviews continued
skull, frontal diagnostics of injuries *(German)* 80−36104
Skylab obs. of quiet and active solar events 77−56891
sliding anvil device for high press. and large volumes *(French)* 80−47067
small angle diffraction in electron microscopes, review 79−50966
small molecules, spectroscopic techniques 77−54554
small particle identification 78−48739
small superconductor in magnetic field, first and second order phase transitions 80−2519
soft connective tissues, biomechanical behaviour 80−56102
soft magnetic materials, meas. methods 80−86345
soft X-ray microscopy and lithography using synchrotron radiation 78−66018
soft X-ray sources 77−26094
softwoods, flow paths *(Japanese)* 80−3288
soil moisture content measurement by microwave radiometry 80−17425
solar, air heating/cooling systems for buildings 80−45754
solar activity, cosmic-ray variations, and neutrino fluxes 79−84599
solar activity, general problems 77−53544
solar activity effects on weather and climate 79−16644
solar and stellar flares 78−7973
solar astrophysics, extension to stellar and galactic astrophysics 77−9736
solar atmosphere, bound-free and free-free electron transitions 78−33563
solar atmosphere models, survey of last 30 years' research 78−69764
solar cell, photovoltaic effects in p-n junctions, Schottky barriers *(Czech)* 77−24583
solar cell, thin film polycryst. Si, research and develop. overview 80−93921
solar cell array fabrication, review of present status and future prospects 80−61343
solar cell developments and appls. for large scale electricity prod. 80−40861
solar cell manufacture, alternative technology for cost reduction 79−74514
solar cells, developments, appls., and economics of solar photovoltaic conversion *(German)* 80−26132
solar cells, heterojunction thin films, survey or semi-conductor combinations 80−50974
solar cells, manufacture of Si photopiles *(French)* 79−24895
solar cells, materials aspect, review 80−50971
solar cells, power supply appls., technology and research 79−92076
solar chromosphere, present knowledge 79−66976
solar collectors, design, thermal performance and economic anal. 80−51001
solar constant, Smithsonian Astrophysical Observatory program, (1902 to 1962) 80−36606
solar cooling 80−85265
solar cooling systems for buildings 80−45756
solar corona, struct. and activity 79−71014
solar coronal heating 79−75180
solar coronal holes, modulation effect on cosmic ray intensity 80−77370
solar coronal holes and high-speed wind streams 78−12187
solar coronal magnetic fields 78−77533
solar cosmic rays, origin, nature and effects *(Russian)* 79−66893
solar cosmic rays, relativistic 80−56798
solar cosmic rays during August (1972) 77−25895
solar electricity production by direct and indirect conversion schemes, review 80−50981
solar energy, review using rational units 80−30389
solar energy collector developments *(Japanese)* 77−62031
solar energy conversion, materials science aspect 80−66957
solar energy conversion, solid state physics aspects 79−74518
solar energy conversion technology, assessment and contemporary criteria, 1978-79 80−76650
solar energy exploitation 77−46903
solar energy R and D in Thailand 80−26113
solar energy storage 80−55916
solar energy utilisation, chemical aspects 77−83977
solar EUV output, present knowledge and accurate meas. techniques for aeronomy 78−57535
solar fine structure radio bursts at meter wavelengths *(Russian)* 78−16386
solar flare mechanisms *(Italian)* 78−96463
solar flare plasma instability and turbulence 80−62100
solar flares, current sheet models 77−17475
solar flares, observational and theoretical status 80−51728
solar flares, particle and EM emissions *(Italian)* 78−93192
solar flares, studies using optical, X-ray and radio data 78−89156
solar flares ground based obs. 77−17489
solar flares of August 1972, anal. of dynamics 77−25992
solar flares of August 1972, ground-based radio obs. 77−25993
solar hard X-ray flare events 78−89144
solar heat storage using chemical reactions 77−86333
solar heating and cooling systems design, operation, feasibility 80−45755
solar hectometric and kilometric emission in August 1972 77−25994
solar IR continuous spectrum, review *(Italian)* 79−88638
solar magnetic field meas. review 78−81607
solar magnetic fields, primordial field theory 77−56902
solar material, primitive chemistry 77−25959
Solar Maximum Year project and related space experiments, review 80−90404
solar neutrino astrophysics, review 79−16917
solar neutrino problem, theory versus obs. 80−17566
solar oscillations 78−69777
solar passive space heating, review and development of direct, mass wall and attached sun space systems for residential appls. 80−76619
solar photoelectrochemical cells, review of cell types and electrode props. 80−61385
solar photoelectrolysis with semiconductor electrodes photodecomposition of electrodes 79−74533
solar photosphere magnetic flux, appearance 79−40161
solar photovoltaic energy conversion 79−100530
solar photovoltaic research and development in Japan, review 80−12012
solar photovoltaic systems, design for intermediate-sized appls. 80−30490
solar ponds, nonconvecting 80−61407
solar ponds for thermal conversion/storage 80−30550
solar power, direct conversion and storage, review of developments 79−43741
solar power in Great Britain, availability, collection methods, and some research projects 79−100482

reviews continued
solar power systems 77−73798
solar power utilisation 80−16790
solar radio burst emission mechanisms 80−72917
solar rotation, obs. methods 79−75179
solar selective surfaces for thermal absorbers, review of basic physics and requirements 80−45752
solar system orbital resonances 77−25998
solar system origin, relation to supernova explosions 80−17509
solar system origin theories, critical review *(Chinese)* 77−22117
Solar System stability and evolution 80−82235
solar temperature control system, modern control theory appl. 80−66949
solar thermal conversion, collectors, storage systems, energy transport and economics 80−51003
solar thermal technology 80−30555
solar UV irradiation flux meas. between 120 and 400 nm, current position and future needs 78−57536
solar wind, effect on terrestrial weather *(Swedish)* 79−79910
solar wind, plasma fluid aspects 80−90313
solar wind, plasmadynamical processes review *(German)* 80−109323
solar wind characts. rel. to solar activity, review 80−94777
solar wind data measured on lunar surface 80−77556
solar wind holes and solar mag. fields 79−58312
solar wind physical processes 79−75071
solar wind plasma kinetics 77−91512
solar wind plasma microinstabilities, review of theory 80−98530
solar wind plasma obs. during August 1972 solar-terrestrial events 77−25902
solar wind properties 77−41372
solar wind theoretical research (since 1958) 78−49281
solar-cometary relations and events of June to August (1972) 77−25983
solar-H_2 energy systems 80−61447
solar-terrestrial events of August 1972, interplanetary mag. field obs. 77−25903
solar-wind exposure effects in the lunar soil 79−75070
solar/interplanetary events during August 1972, interdisciplinary summary 77−25991
solid, near phase transition, light scatt. 80−29752
solid dielectrics, electric breakdown mechanism, discharge development, electron impact ionisation 80−15961
solid electrolytes and their applications *(Japanese)* 77−70308
solid film, electrolyte systems, materials characts. and appls., review 77−77781
solid ionic conductors *(German)* 78−79795
solid lasers, nanosecond and microsecond pulse generation 78−71130
solid polymers, NMR 80−88888
solid soln. spectroscopy, investigs. by F. Klement *(Russian)* 80−8767
solid solution hardening in metals, review of theories *(Czech)* 80−3084
solid solutions, polycrystn., rheological study of crystallographic order on creep *(French)* 80−97548
solid state CW lasers 77−38901
solid state dosimetry, tissue-equivalent systems *(Hungarian)* 80−91291
solid state lasers, book contrib. 80−106529
solid state materials, struct. and props., appl of μ^+SR 79−65781
solid state nuclear track detectors, past and future uses 78−17484
solid state nuclear track detectors, visualization of latent damage trails etching, decoration and observation techniques 80−91382
solid state nuclear track detectors 80−37696
solid state phase transformation, detection techniques 80−2996
solid state physics, review of experimentation, undergraduate level *(Spanish)* 80−82624
solid state physics rel. to solar cells 80−49601
solid surface, microgravimetric-IR study 80−76577
solid surface, physics *(Japanese)* 78−79870
solid surface, structure and gas interactions 79−37912
solid surface and thin film anal. methods, review 79−34410
solid surface characterisation techniques 78−22945
solid surface monolayers, anal. by mass and energy spectrometry methods 77−56248
solid surfaces, scattering of atoms and mols. 78−31291
solid-Earth geophysics, bibliography 77−2078
solid-gas and solid-liquid interfaces, struct. rel. to reactivity 77−72775
solid-solid interface chemistry, characterisation, theory 80−75448
solid-solid reactions, analysis and reaction development 80−16648
solid-state convection in planetary interiors, numerical methods 79−84693
solids, acoustic wave emission, absorpt. and propag. in THz range 80−65164
solids, reactivity control 80−50853
solitary waves, review, book contrib. 80−94962
soliton theory 80−47204
solitons, lecture 78−24690
solitons, review of concepts and methods in theory *(Polish)* 80−68057
solitons in condensed matter: a paradigm 80−77632
solitons in dispersive media, nonlinear evolution eqns. soln. 78−60
solution X-ray scattering, review of recent developments, book contrib. 80−109077
solvated electron electrochemistry 77−16829
solvent structure, at polarisable interfaces, mol. models 80−59359
somatosensory evoked potentials, in man, cerebral, subcortical, spinal and peripheral nerve pots. 80−16961
somatosensory evoked potentials, review of acquisition and anal. 80−101281
sonar, technology development, review 78−55500
sonic and ultrasonic applications 77−27404
sonic bangs 77−42858
sonography, diagnosis of tumours, comparison with other methods *(German)* 79−34614
Sorb-ac wafer pumps, behaviour in plasma machines 78−70627
Soret coefficients, meas. methods 77−39685
SOS single crystal films, struct. and elec. props. *(Japanese)* 77−63009
sound analysis by the ear 80−104593
sound and TV recording appls., general principles 77−34844
sound and vibration instrumentation for dynamic meas. 77−72124
sound propagation, HF, in metals and semiconductors, nonlinear effects 80−88279
sound propagation in atmosphere, historical review 78−15
Soviet 6 metre reflecting telescope, review *(Norwegian)* 78−36456
Soviet acoustics, progress in ninth five-year plan (1971-1975) 77−14824
Soviet meteorological satellite development 78−16266
Soviet physics, review articles, book 80−46742
reviews continued
Soviet seismology evolution during 1917-77 period 79−84142
Soviet Tokamaks *(Russian)* 79−4192
space environment, fluid behaviour, review 79−46410
space exploration, 1946 to 1978 period 79−80195
space exploration and astronomical research, first 20 years *(Russian)* 78−16267
space instrumentation for charged particles meas. *(Russian)* 77−17368
space research, 1976-77 period 79−25449
space science, status and development, reviews 79−80190
Space Shuttle, history, principle features and uses 78−36427
Space Shuttle, operational features 78−36428
space stations for the international future 78−32322
Space Telescope 77−17363
space telescopes, optical systems *(Russian)* 77−17367
space vehicle nuclear propulsion, historical review of advanced consent 80−36475
space-variant coherent optical processing 80−102638
spacecraft solar arrays, in-orbit performance 80−94054
spaceflight factors combined effects on man 78−53537
Spacelab project, zero gravity physics review 77−29619
spatial resolution of subwavelength sources from optical far-zone data, book contrib. 79−31825
special relativity, ether drift, historical review 80−49
special relativity, neo-Lorentzian relativity of G. Builder 80−46
special relativity and time dilation 79−25840
specific heats of magnetically-ordered materials 79−42763
speckle, optical information processing, photography and interferometry appls. 77−83820
speckle, properties and applications *(Japanese)* 78−22085
speckle interferometer construction 77−71369
speckle interferometry, book contrib. 79−75584
speckle pattern statistics, book contrib. 77−31070
speckle propagation through turbulent atmosphere research progress 79−66803
spectral analysis, review of methods biomedical appls. 80−21560
spectral data sampling and smoothing 77−34031
spectral selectivity of composite materials, optical props. and fabrication of composite solar absorbers 79−74520
spectral sensitisation, theory *(German)* 79−39172
spectral sensitisation of Ag halide emulsions 78−4719
spectral sensitization theory, review *(German)* 79−39174
spectrally selective solar absorber coatings 80−61404
spectrally selective surfaces and their impact on photothermal solar energy conversion 79−74519
spectrally selective surfaces for photothermal conversion of solar energy 80−101125
spectrochemical analysis, derivative and wavelength modulation 79−79317
spectrochemical analysis, noise and signal-to-noise ratios 79−43671
spectrochemical analysis, noise and signal-to-noise ratios 79−43672
spectrochemical emission spectroscopy, literature review 1976-1977 78−80797
Spectrochemical properties of certain light emitting sources *(French)* 78−3426
spectrofluorometer components, state of the art *(Slovak)* 78−56940
spectrophotometer, prism instruments, Beckman Instrument Inc., historical review 77−61125
spectrophotometric methods of determination of Pd, Pt, Rh, Ir 78−61115
spectroscopic and molecular consts., extremal props., book contrib. 78−78678
spectroscopic effects in dense and ultradense plasmas 80−43990
spectroscopic factors for single-nucleon transfer in A=21-44 region 77−71563
spectroscopic information in visible and UV for diatomic astrophysical molecules 77−88459
spectroscopic instrument developments, overview *(French)* 78−293
spectroscopic techniques, anal. with STEM for electronic anal. and obs. of defects in semiconductors 79−14812
spectroscopy, RF, of positive ions, using optical pumping 78−1107
spectroscopy of small molecules, recent developments 79−3426
spectroscopy using lasers, coherent optical transients, atom, mol. and solid 77−53986
speech maturation, anatomical and neuromuscular, evidence from acoustic studies 77−5014
speech recognition and anal. *(French)* 79−68509
speech synthesis, current topics *(Japanese)* 80−91973
speech synthesis, digital electronics technology 79−90095
speech waveform coding technique developments in Japan 80−33353
spent fuel storage in water pools, technology assessment 79−36357
spent nuclear fuel reprocessing, separation technologies 78−89965
spherical shell model, collective features, review 78−50098
spin and charge density theoretical determ., review 77−75045
spin echo spectroscopy, two-freq. 80−20506
spin glasses, random ordered phases, review *(Japanese)* 78−47993
spin glasses, review of recent expt. and systems 78−52274
spin glasses, theory 78−2696
spin glasses and mictomagnets 77−69578
spin glasses and other glasses, symmetry and topology concepts 79−28541
spin labels and biomembranes, review 78−69265
spin-flip Raman laser spectrometer as source for high resolution mol. spectroscopy and photochem. 78−32894
spin-reorientation transitions in rare-earth magnets 77−36073
spinodal alloys characterisation techniques, props. and appls. 80−50588
spinodal decomposition, phase transitions via unstable states 80−96657
spiral galaxies radio continuum morphology 77−26071
splat-cooling devices, quenching efficiency 79−29106
splint making materials, comparative study 79−39606
spontaneous fission of heavy nuclei 79−36289
spontaneous symmetry breaking and symmetry defects 80−95231
spray in atmospheric surface layer, lab. and oceanic results 79−70844
sputtered neutral particle flux props., ion bombardment of polycryst. targets 77−44110
sputtered particles, energy and mass distribs. 80−84822
sputtering and ion trapping, technological appls. 77−44107
sputtering and SIMS *(French)* 78−80450
sputtering mechanisms 80−40213
sputtering of single cryst., differential yield, surface struct. 77−44112
sputtering process and sputtered ion emission 80−35044

reviews continued
sputtering use in depth profiling 80−40214
SQUID, review of development and future 79−33398
SQUIDS, weak magnetic field meas. 80−86267
SS 433, review of obs. and theories 80−72987
stability and nuclear props., review of research 79−89218
stability of matter, nonrelativistic quantum mechanics 77−5696
stacking fault, antiphase boundary energies, investig. methods, review, appls. to FCC metals *(French)* 79−42080
standard specimens for spectral analysis of metallurgical substances 78−7273
standard volt by BIPM since 1932 77−82566
standards in meteorology 79−21032
Stanford Synchrotron Radiation Laboratory, operation and development 79−68020
star charts for amateur astronomers 79−62762
star formation, IR obs. 78−7988
star formation, observational studies 78−93215
star formation and protostellar clouds, review 80−101589
STARFIRE project, an overview 80−106183
stars, nonradial oscillations, theories and obs. 77−26003
stars with anomalous mass, examples 80−72929
statistical geodesy, engineering perspective 78−81099
statistical mechanical theory of the kinetics of phase transitions, review, book contrib. 80−73270
statistical mechanics, Monte Carlo and mol. dynamics calcs. 77−37807
statistical methods appl. to planetary surfaces 80−101540
statistical shell model, spectrum fluctuations 77−26599
statistical tests, less well known 77−67239
statistical theory of turbulence, book book contrib. 77−84234
statistical thermodynamics appl. to fluid phase 78−83703
statistical treatment of experimental data, book 78−77834
steady state evoked potentials, recording and appls. review 78−35823
steam generators of water cooled nuclear power plants, corrosion phenomena 80−558
steel, alloy, Fe-Ni-Cr-Mo-V-C, HY130, effect of H_2 and impurities on brittle fracture, review 78−60765
steel, atom probe microanalytical expts. 78−35622
steel, austenitic stainless, fast neutron irrad., effect on mech. props. 78−92309
steel, austenitic stainless in liq. Na, mechanical props. 79−20150
steel, austenitic type EI-69, carbide transformations on precipitation of C from austenite *(Russian)* 80−97487
steel, C and HSLA, grain size and substruct. control by alloying and thermomech. treatment 80−3082
steel, C and low alloy, size effect in bending fatigue strength and its prediction 79−43411
steel, cast, mech. props., fatigue behaviour, influence of microdiscontinuities, review 78−35512
steel, clean, review 80−84839
steel, continuous casting machine design, based on heat flow analysis, review 77−21048
steel, corrosion resistant, review of heat treatment, mech. and corrosion resist. characts. *(Korean)* 79−24653
steel, Cr-C, structural, struct.-prop. resl., high strength and toughness design criteria 80−97491
steel, cryogenic, creep, review 80−104222
steel, deep-drawing, texture problem after processing through continuous annealing 79−87659
steel, effect of H_2 on phys. and mech. props. 80−101657
steel, environmental fracture, metallurgical variables effects, review 77−28887
steel, fatigue crack growth eqn., correlation of threshold stress intensity factor, review 79−34127
steel, fatigue crack propag. near to threshold stress intensity 80−100898
steel, ferritic, crack extension, cleavage micromechanisms 80−108562
steel, H effect on weldability 80−50720
steel, intergranular failure, role of grain boundary composition 79−20155
steel, low alloy, creep crack growth, microstruct., fatigue effects 80−7672
steel, low alloy, temper embrittlement, review 79−20154
steel, low C, deep-drawing, mechanism of recrystn. texture formation 79−87658
steel, low C, endurance limit, effect of coatings *(Russian)* 77−25145
steel, microalloyed, review of development 79−47699
steel, plasticity of two-phase, coarse microstruct.-material *(German)* 77−59882
steel, pressure vessel for light water reactors, corrosion fatigue, data review 79−79169
steel, proeutectoid reaction 77−4777
steel, rare earth addition effects and behaviour, review *(Chinese)* 79−43257
steel, rare earth additions review 78−72786
steel, solidification of castings in mould *(Russian)* 78−27502
steel, stainless, 316, 304, LMFBR primary piping materials, mech. props., review 77−25151
steel, stainless, sintered, prod. methods and props. for machine components, review 79−100082
steel, stainless ferritic, Cr-Mo, corrosion behaviour, review 79−39018
steel, toughness, review of joint tests *(German)* 80−65142
steel, type 4340, effect of H_2 and impurities on brittle fracture, review 78−60765
steel, ultra high strength, historical 80−7609
steel, wear resistant, abrasive adhesive and rolling wear *(Korean)* 79−24624
steel A533A, review of data in reln. to fracture toughness at upper shelf temp. 79−15797
steel casting, meas. and significance of residual stresses 80−21253
steels, austenitic and type 316, neutron irradiation effect on tensile, creep-rupture, deform., fracture props. 79−65120
steels, brittle transition temp. determs. from impact ductility tests, comparative evaluation 79−15888
steels, ferritic and martensitic, C and N migration at low temps., monograph 80−22149
steels, nuclear pressure vessel, small specimen predictions of fracture toughness 80−81172
steels, secondary hardened, microstruct. rel. to mech. props. 80−25851
steels, solute segregation and intergranular fracture 80−60957
steels, stainless, effect of metallic second phases 78−31503
stellar, ouflowing atmospheres across HR diagram, review 79−66996
reviews continued
stellar chromospheres, observational indicators, empirical models 80−12755
stellar chromospheres, review *(German)* 80−109421
stellar clusters, use as cosmic calibrators 78−57599
stellar coronae, evidence for existence from X-ray and UV obs. 80−12756
stellar evolution, final phases rel. to supernova phenomenon *(Italian)* 79−88646
stellar interferometry, high ang. resolution obs. 77−33355
stellar opacity 77−26002
stellarator fields 78−30467
stellarators 77−47239
STEM, metallurgical appl. 77−44422
STEM optical system, practical considerations 78−21301
stereoscopic microscopes, domestic, review 80−27342
steroid research using mass spectrometry 80−51308
stethophonendoscopes, design and production 80−104686
stimulated Brillouin scatt. in laser plasma expts. 79−10706
stimulated Raman scattering, appls. 77−735
stimulated resonance Raman scattering 77−79897
stimulated resonance Raman scattering in excited and ground state mols., theory *(German)* 77−58013
Stirling cycle machine anal. using nodal anal. techniques 80−30532
stochastic cooling of particle beams 80−37675
stochastic gravitational fluctuations in a self-consistent mean field theory 80−90734
stochastic instability theory applics. to nonlinear plasma systems, review *(Czech)* 80−38580
stochastic interpretation of quantum mechanics 78−70056
stochastic processes, review, book contrib. 80−73268
stochastic quantisation processes, review, Markov processes, Martingales, quantum dynamics 80−94969
stochastic self-oscillations and turbulence 80−4537
Stokeslets and eddies in creeping flow, review, book contrib. 80−96265
stopped-flow systems, automated, for fast react. rate anal. methods, review 78−95971
storage batteries, vehicle and storage appl. 80−72031
storage cell impedance theory and experimental data review 80−55667
strain measurement methods, state of art *(German)* 77−11152
stratified and rotating fluids, review of selected aspects 77−68660
stratified water, turbulence and mixing, book contrib. 78−59444
stratosphere, H_2O vapour distrib. 77−45112
stratosphere, photochemistry interpretations 79−74943
stratosphere, trace constituents, in situ meas. 79−8676
stratosphere and mesosphere, general circulation, radiative transfer, transport processes 78−49105
stratosphere and mesosphere radar studies, UHF and VHF, review 80−90180
stratosphere turbulence near tropopause, review of radar obs. 80−90179
stratospheric aerosol layer and climatic effects 78−81331
stratospheric Aitken particles 77−87050
stratospheric atomic processes 77−37339
stratospheric H_2O, maintenance of extreme aridity 80−105028
stratospheric warmings, obs. and theory 79−74944
stress analysis of isotropic thick plates, review of problems of plates with geometric, and load discontinuities 79−46218
stress corrosion cracking, crack propagation, exam. of kinetic control processes 78−60884
stress corrosion cracking, role of H_2, state of art review 80−61017
stress corrosion cracking control measures 77−90509
stress corrosion cracking failure, predictive approaches 80−97611
stress corrosion cracking theory, geophys. appls. 77−62212
stress relaxation in crystals 79−73248
string and quark systems, statistical mech. treatment renormalisation group meth. 77−54075
stringed musical instruments, acoustics 79−7261
stripe-geometry heterojunction lasers 80−53288
strong external fields, fermion and boson interactions 78−49987
strong spin-two interaction and general relativity 79−45046
structural defects, interaction effects *(Russian)* 79−42098
structural materials, radiation effects 80−49267
structural morphology, of crystals *(French)* 79−4266
structural phase transformations, static critical behaviour 80−92640
structural phase transforms. and phonons, book contrib. 77−89518
structural phase transition, intrinsic and extrinsic central peak properties 80−34168
structural phase transition induced refractive index changes in crysts. 80−16000
structural phase transitions, crit. dynamics and quasi-elastic scatt. 80−92641
structural phase transitions, Landau theory 80−92639
structural wall test results, applicability to seismic design 79−592
structure and crystallisation, review 78−2008
Struves of Pulkovo, family of astronomers 78−24632
styrene-butadiene block polymers, multiphase systems, struct., props. 77−31600
SU(2) gauge group, magnetic monopole as finite energy smooth soliton soln., review 78−89625
SU(2) Yang-Mills theories, classical solns., historical development and general introduction 79−93295
SU(2) Yang-Mills theory, Coulomb gauge fixing 79−26235
SU(5), unification of weak, EM and strong interactions 80−105814
sub-Doppler line shapes, saturation and two-photon spectra, elastic collisions, review 78−82697
sub-picosecond optical pulses, generation and meas. 80−23731
subjective effects of the sound fields and acoustic design of rooms *(Japanese)* 80−64293
submersibles, 1977 review 78−69499
submillimetre wave laser waveguides 78−5505
submillimetre wave mixers 78−45712
submillimetric wave atmospheric spectroscopy 77−41240
submonolayer films on metallic surface, struct. and props. review 78−38972
subnuclear physics 77−67623
subsoil liquifaction during earthquakes in Japan 78−36118
substrate prep. for film deposition using glow discharge techniques 79−24438
sulphide minerals, superstructure and modulated struct. 79−99146
Sun, active and quiet, atm. and interior struct, solar energy 78−40895
Sun, active regions, open mag. field lines struct., review 80−85924

reviews continued
Sun, angular momentum flow 77−45396
Sun, differential rot. and global-scale vel. fields 77−53545
Sun, prominence-corona interface 80−4333
Sun, quiescent prominence formation, support and stability 80−4334
Sun, rotation theories 77−53563
Sun-weather long-term relationships, critical review 79−48558
sunspot research, past and present, review *(Norwegian)* 79−75312
super-dense matter, phase transitions in gauge theories and cosmology 79−44654
superalloy, hot consolidation of rapidly solidified powders, review 79−33965
superconducting A15 compounds, martensitic and supercond. transition models, anisotropy of vortices and US anomaly *(Japanese)* 78−23216
superconducting band gap anisotropy, Eliashberg eqns. *(Spanish)* 80−84544
superconducting critical temps. theory *(Chinese)* 79−38241
superconducting film, geometrical reson. effect, electron tunnelling density of states meas. *(French)* 78−2626
superconducting film, metastability and T_c 78−64161
superconducting magnet conductors, props. and fabrication techniques *(Japanese)* 80−25042
superconducting magnet stability problem at accelerators under high-energy particle irradiation *(Russian)* 80−68972
superconducting materials, large scale appls. 79−69640
superconducting materials, table of props. 77−4460
superconducting metastable alloys, review of current work 80−81002
superconducting order parameter fluctuations, pair tunnelling 79−1642
superconducting properties of $(SN)_x$ 78−6474
superconducting thin films, vortices, phase transitons 80−88698
superconducting transition critical temperature, BCS theory, phonon spectra *(Spanish)* 80−84535
superconducting weak links, review of physical processes 79−60983
superconductivity, inhomogeneous, Ginzburg-Landau theory 80−88672
superconductivity, nonequilibrium 78−52146
superconductivity, technological survey *(German)* 79−65573
superconductivity and elementary particle theory 80−4911
superconductivity and magnetism *(Hungarian)* 79−47226
superconductivity and phonons 80−84543
superconductivity and superconductors *(French)* 79−7931
superconductivity applications in electron microscopy 77−38059
superconductivity at Intermagnetics General Corp. 79−58699
superconductivity coexistence with mag. order 78−19177
superconductivity in thin films *(Russian)* 78−19172
superconductor flux-flow noise theory 79−24115
superconductor metal interface proximity effect *(French)* 78−2625
superconductor preparation, multifilamentary Nb_3Sn by 'in situ' and cold powder methods 80−93522
superconductors, A15-type, structure and props. 80−70909
superconductors, electric field penetration and collective oscillations 80−88678
superconductors, nonequilib. distribs. *(Russian)* 79−19688
superconductors, search for new materials 77−59350
superconductors, thermoelectric effects 80−11133
superconductors, tilted vortices, mixed state features in surface layers *(Russian)* 80−29512
superconductors, type II, review of mechanical behaviour and stress effects 77−86083
superfluid state of matter 79−42328
superfluidity and the two dimensional XY model 79−28498
supergravity review, phenomenological appls., and lower spin fields unification 78−77788
superheavy element research 80−37411
superheavy elements, search and synthesis, review 78−50117
superheavy elements, searches in nature and accelerators 77−57616
superheavy elements in nature, recent searches 79−79845
superionic conducting oxides 80−49414
superionic conductors, dynamics *(Japanese)* 78−30791
superionic conductors, light scatt. and IR absorpt. book contrib. 80−25382
superionic conductors, mag. reson., book contrib. 80−25240
superionic conductors, some experimental facts and fallacies 79−23774
superionic conductors, sublattice disorder and dynamics, exptl. techniques 78−91476
superionic conductors, theoretical models, review 80−107465
superionic conductors, transitions, structures, dynamics and spectra 79−60549
superionic conductors, transport props. 77−62671
superluminal frames and tachyons, introductory review, generalised Lorentz transform. derivation 78−69983
superluminal motion in compact extra-galactic radio souces 80−77504
supernova remnants in Magellanic Clouds, optical obs. review 79−75259
supernova remnants X-ray emission 77−87521
supernovae, historical and theoretical review *(Norwegian)* 79−80329
supernovae, review of props. 77−87455
superplastic materials, flow and failure 80−50690
superplasticity, deformation mechanisms 80−50691
supersaturated vapour, critical clusters, theory and Monte Carlo simulation 80−82734
supersonic flow, self-induced oscills. 78−67215
supersonic mixing chem. lasers, gas dynamics, book contrib. 77−10905
supersymmetry, algebraic props., applic. to particle physics 77−87918
supersymmetry and supergravity, review of present status 79−63112
supersymmetry and supergravity *(Czech)* 80−86183
supraventricular tachycardia, diagnosis and management, instrumentation and therapeutic techniques 79−39598
surface, characterisation, literature review 1970-76 77−77816
surface acoustic waves 79−95254
surface anal. tools 80−103540
surface analysis, appl. to lubrication problems *(French)* 80−45616
surface analysis, by secondary ion mass spectrometry, review 78−68949
surface analysis, probing and imaging techniques 80−54487
surface analysis, review of AES technique and applications 78−68946
surface analysis, review of ESCA technique, instrumentation, and appl. 78−68947
surface analysis, review of ion scattering spectroscopy 78−68948
surface analysis, spectroscopic methods *(Chinese)* 79−34414
surface analysis techniques appl., electrification phenomena 80−80354
surface analytical instruments, present status *(Japanese)* 78−80823
surface analytical techniques, quantification 80−65342
surface anisotropy, review of characterisation processes 79−12770
reviews continued
surface blistering by ion bombardment, energy, dose and target temp. depends. 77−43261
surface charact., combined ion scattering spectrocopy, SIMS, SEM, energy dispersive X-ray techniques 79−43702
surface characterisation, physical methods *(French)* 80−7889
surface characterisation, state-of-the art and need for standards 78−38916
surface chemical bonding, electron spectroscopy, book contrib. 80−24992
surface crystallography by LEED 78−83691
surface damage, plastic deformation cause in fatigue, wear, fretting and rolling fatigue 80−40537
surface defects 78−14551
surface electron state characterisation by X-ray techniques 77−55868
surface exciton polaritons, book contrib. 80−49623
surface Green's function matching, physical and physicochem. appls. 77−78954
surface labelling techniques for eukaryotic cells 77−56560
surface lattice vibrations, interaction with low-energy electrons 78−30820
surface layer anal. by small-angle Rutherford backscatt. 77−44108
surface phonon-polaritons on semi-infinite crystals, attenuated total reflection spectroscopy 77−89827
surface physics research development *(Chinese)* 79−37898
surface rheology 77−42792
surface science, survey of recent research 80−39384
surface science 79−19427
surface science in metallurgy 79−42388
surface segregation, influence in metallurgical props. *(French)* 80−80045
surface spark discharges high current, light emission props. and appls., book contrib. 79−77449
surface structure determination, ion scatt. methods 78−71907
surface structure studies by LEED *(Russian)* 79−14994
surface treatment processes in France *(French)* 80−16528
surface vibrational spectroscopy using stimulated Raman scatt. 80−38062
surface-active agents, determ. in waste waters 79−53007
surfaces, optical examination and monitoring 79−67375
surfactant-water liquid crystal phases 80−28913
surgical diathermy units, selection guidelines 77−73613
surveying, literature survey for the year 1976, with appendices *(German)* 77−90993
suspension concentrates, physical stability criteria 80−45562
suspensions, rheology, colloidal forces role, review 80−103063
suspensions, statistical theory, review, book contrib. 80−96288
Swedish underground nuclear reactor containment studies 79−600
swirl defects in single crysts. 80−44200
swirl flows in combustion 78−1755
swirling or asymmetric flow meas., review 77−84360
switches, high press. surface discharge 80−103208
symbolic algebraic computation, appl. 79−58535
symmetries and nuclei 79−80883
symmetry groups in QFT, supersymm., space-time symm., internal symm. groups *(Russian)* 77−49871
symmetry principles, historical review *(Hungarian)* 78−73818
synaptic slow responses, props. and possible underlying mechs., book contrib. 80−108873
synchrotron radiation, appls. 78−9010
synchrotron radiation, appls. 78−74825
synchrotron radiation, origin, charact. and appls., review 77−58243
synchrotron radiation, props. and appls., review 79−36830
synchrotron radiation, review of props., facilities, and source parameters and optimisation 79−68018
synchrotron radiation, sources, properties, and research appl. 77−75403
synchrotron radiation, spectroscopic appls. 77−58239
synchrotron radiation and its appl. *(Danish)* 79−81345
synchrotron radiation and its applications 79−44997
synchrotron radiation applications 79−67448
synchrotron radiation for VUV and X-ray spectroscopy, lecture 78−24870
synchrotron radiation research 79−22505
synchrotron radiation source, Daresbury 2 GeV storage ring with 600 MeV booster synchrotron 79−68022
synchrotron radiation sources and utilisation 78−41390
synoptic windfinding technique, Loran and VLF navaids used with radiosondes 80−17392
synovial fluid, rheological eqns. 79−62285
synovial joints, immobility effects, pathomechs. of joint contracture 80−97954
synthesis, structure and electrical properties of doped polyacetylene 80−15623
synthetic ceramic raw materials, exam. of chemical preparation methods *(German)* 79−4930
synthetic-aperture radar 78−81445
Ta-You Wu festschrift: science and matter, book 79−44688
tandem accelerators 78−13351
TCNQ salt, $(TSeF)_x(TTF)_{1-x}$-TCNQ, struct., elec. and mag. props., review 80−20158
technical, cooperation among developing countries, evaluating potential of technology transfer 80−82628
tectonics and mineral resources of USSR *(Russian)* 78−40536
tektite origin 77−67078
TEM, advances, catalytic chem. appls. 80−85214
TEM, appl. to organic solid-sate chemistry 79−60235
TEM, experience at Univ. of California (Berkeley) 80−37130
TEM, principles and practice of in situ experimentation 79−71574
TEM, specimen prep. methods for image processing, review 79−17405
TEM, STEM, and SEM: microscopy to microfabrication 78−32936
TEM 77−56189
TEM observation of cavities 80−14974
temperature and thermal sensing devices *(Japanese)* 77−71318
temperature measurement, high-speed pyrometry in laser-pulse heating expts. 80−52225
temporal visual resolution, annotated bibliography 77−60199
ternary semiconductor crystals for nonlinear optical applics. 78−33782
ternary semiconductor device applications 78−39207
ternary semiconductors, pot. practical appl. 79−10344
ternary semiconductors, review of developments 78−34737
terrestrial planets, gravity anomalies and tectonics, review 80−98593
terrestrial planets, solid-state convection, obs. evidence 79−84692

reviews continued
testing materials and structures 78−3298
tetrahedrally coordinated semiconductors, surface structure, chem. and spectroscopy 80−59764
texture meas., expt. methods 79−87815
texture study, use of crystallographic orientation distrib. function 79−52228
theoretical physics at Kharkov Inst., Ukrainian SSR *(Russian)* 79−12558
theory of defectsin solids 80−6400
therapeutic radiologists, training in USA, 1978 survey 79−84878
thermal analysis, developments over last 25 years 77−70369
thermal analysis, multiple methods, instrums. and appls. 77−70363
thermal analysis applications 80−26083
thermal blooming in atmosphere, book contrib. 79−34961
thermal imaging systems, pyroelectric technology, review 77−14794
thermal insulation of animal coats and human clothing 78−73139
thermal methods of NDT, review of theoretical and experimental problems 78−44325
thermal neutron scatt. of condensed matter under high press. 79−37592
thermal plume modelling 79−4056
thermalization of neutrons, review of Soviet research 79−36300
thermionic emission of transition metal nitrides *(Japanese)* 77−63522
thermo-gasdynamic control in laser beam guidance, review of developments 78−74942
thermoconvective instabilities of confined fluids 80−38399
thermocouple thermometry 80−52207
thermocouples, development, pitfalls in their use 80−62664
thermocouples, types and selection guidelines 79−194
thermodynamic energy conversion efficiencies 80−101081
thermodynamic parameter changes in solids and resultant processes 78−22868
thermodynamic temperature, meas. techniques and concept. 80−52204
thermodynamics, non-equilib. systems 77−26255
thermodynamics appl. to fundamental Earth physics 78−36125
thermodynamics for calculating chem. equilibria, review for teachers 77−26108
thermodynamics of irreversible processes 80−13020
thermoelectric power generation, isotopic and nonisotopic, 1978 state and development trends 79−43780
thermography, cm and mm wave, tumour detect. survey 79−100690
thermogravimetric methods 78−3408
thermogravimetry, development in United States 77−90668
thermomechanical treatment 77−4796
thermometry 80−86305
thermometry considerations in localised hyperthermia 78−53561
thermonuclear fusion and the Tokamak *(Italian)* 79−31177
thermonuclear fusion by lasers, state-of-the-art review *(Japanese)* 78−21768
thermonuclear fusion research, economic factors 80−73991
thermonuclear reactor development *(German)* 77−34425
thermophysical properties, standardisation of meas. methods 80−52197
thermophysical properties, temp. measurement methods at high temp. 80−52208
thermophysical properties dynamic meas. techniques 80−52219
thermophysical property research, metallurgical applications 80−97457
thermoplastic hologram recording, book contrib. 78−25836
thermoplastic media for hologram recording *(Russian)* 78−58948
thermoplastic optical phase recorder for data processing 77−72081
thermoplastic photoconductor media *(Japanese)* 78−78956
thermoregulatory system, human, engineering models 77−81471
thermoset and coating technology, torsional braid and thermal anal. 80−55622
thermosphere, dynamics at high latits., magnetospheric convection effects 79−8733
thermosphere, tidal and planetary wave propag. 77−87147
thermosphere and ionosphere, chemical processes 80−17431
thermosphere global comp. and temp. 79−8732
thermosphere waves 77−45211
thermospheric dynamics 80−21866
thermotropic liquid crystals, NMR relax. 78−39436
thick film conductor, adhesion meas. 80−50808
thin film, and surface anal., modern methods 80−54486
thin film and integrated optics review, theory, expt. techniques, waveguides 78−22220
thin film growth due to crystallite surface migration 80−10810
thin film technology, appls. in energy, optics, and electronics 80−78932
thin films, chem. anal. by energy loss spectroscopy 80−104493
thin films, deposition techniques 80−80964
thin films and interfaces, analytical techniques 80−80120
thin-film solar cells, recent developments 78−80016
thixotropy 79−59959
Thomas-Fermi statistical model of atoms, solids, plasmas 77−84
three and four nucleon low energy scatt. expts., review 79−80945
three body systems, review of recent theoretical anal. 79−80842
three body systems in nuclear physics 78−517
three point bending tests, calc. of yield stress 78−92310
thrombosis, rheological aspects *(Japanese)* 80−94268
thrombus detection radiopharmaceuticals, selection, prep. and evaluation 78−11731
thyroid, radionuclide in vivo studies, technical considerations, developments 78−85372
timbre perception, review 78−77068
time differential perturbed angular correlations, appl. to chemistry and solid state physics 79−75665
time domain spectroscopy of dielectrics, survey 80−68212
time meas. *(French)* 78−49802
time of flight detectors for heavy ions 79−72178
time-domain reflectometry 78−37038
timing devices selection and appl. 77−82492
tissue, mammalian, survey of US vel. and attenuation data 80−46744
tissue quantitative characterisation by US 80−81670
tissue substitutes in experimental radiation physics 79−20680
Titan, atmosphere organic chemistry, review 80−90364
titration calorimetry, research developments 79−40575
TLD characteristics and recent trends *(Korean)* 80−41253
TLD utilisation in field of atomic energy *(Japanese)* 79−26764
TNS fusion reactors, review of plasma engineering, design and program planning for future developments 79−71959
Tokamak, recycling and surface erosion processes 80−33805
reviews continued
Tokamak and tandem mirror reactors, neutral beam injection and superconducting magnets 80−63391
Tokamak demonstration power reactors, engineering problems rel. to system components 80−32511
Tokamak experimental results 79−98968
Tokamak experiments and apparatus 79−98967
Tokamak fusion reactors, neutral beam driven, physical basis and engineering parameters 77−54360
Tokamak hydromagnetic stability, ideal and resistive, review 78−34358
Tokamak magnetic confinement, recent progress in Tokamak expts. for fusion energy prod. 79−71948
Tokamak plasma diagnostics 78−47163
Tokamak reactors, role of α-particles 80−86971
Tokamaks, ion beam anal. of surface modifications 79−46457
Tokamaks, small-scale 78−42831
Tokamaks, transport computations, heating, treatment of neutral gas, and impurities 79−98966
tomography, transaxial scanners for reconstructing objects from their X-ray projections, review 80−102632
topographically trapped waves, review, book contrib. 80−96273
topology and physics, historical review *(Russian)* 80−8770
torsional method for metal plastic props. investig. at elevated temps. 79−43509
total α and β counting of thick samples 79−36488
total current spectroscopy 80−45185
total pressure meas., ultrahigh vacuum 80−31782
toughness-porosity phenomena 78−72874
tracking microscope, design and operation 80−36214
transactinide elements, atomic and chemical props. by gas chromatography and aqueous chemistry, book contrib. 78−85121
transequatorial radiowave propag. over 21 year period, VHF/UHF signals, theories 80−109311
transfer standard flowmeters, critical appraisal 77−84370
transformation of nonlinear variables in construction of statistical models 80−57081
transient lunar phenomena 77−60683
transient X-ray sources, review 78−12425
transition metal, magnetic ground state props., simple one-electron theory 77−63063
transition metal alloys, dilute, spin glasses, mag. ordering, book contrib. 80−75787
5d-transition metal antifluorite crystal, struct. props. and lattice dynamics, mag. struct. 80−44268
transition metal borides, cryst. struct., prep. methods, chem., elec., mag. props., appls., book contrib. 78−47307
transition metal carbide emitters *(Japanese)* 77−63521
transition metal chalcogenides, quasi-one-dimens., elec. mag., and supercond. props. *(Russian)* 80−93022
transition metal chalcogenides, struct. and mag. props., book contrib. 77−43808
transition metal complex, CNDO method for study of electronic struct. and props. 77−88392
transition metal compound surfaces 80−84349
transition metal compounds, band struct. calc. 78−18956
transition metal compounds, localisation of electrons 80−49650
transition metal diborides, C32-type, phys., chem. props., appls., review, book contrib. 78−47308
transition metal dichalcogenides, phys. props. *(Japanese)* 77−69225
transition metal dichalcogenides, physical props., *(Japanese)* 80−33969
transition metal dichalcogenides prep. and growth, book contrib. 78−19650
transition metal ferromagnetic amorphous alloys, mag. props. 77−55690
transition metal hydrides, H ordering 80−60850
transition metal hydrides (binary ternary systems with metallic cond.) review of research on catalytic props. 80−30273
transition metal itinerant magnets, neutron scatt. expts. 77−73002
transition metal layered dichalcogenides and their intercalation compounds, physical props., review 78−27443
transition metal magnetic alloys, dilute, props., review of theory 79−15282
transition metal magnetic clusters, neutron inelastic scatt. 80−50083
transition metal oxides, defect struct. review 79−42052
transition metal oxides, extended defects, review 78−63753
transition metal pyrites, mag. and elec. props., review *(Japanese)* 78−47941
transition metal silicides, growth and characterisation 80−66408
transition metal silicides, refractory for ICs 80−100820
transition metal-H systems under high H pressure, phase diagrams., electrical cond., mag. props. 80−29923
transition metal-metalloid amorphous alloys, mag. props. review 78−52300
transition metals, 3d, ferromag. props., book contrib. 80−75724
transition metals, and their alloys and cpds., photoelectron energy distrib. curves, rel. to band struct., book contrib. 80−16156
transition metals, chemisorption of H, O and CO 78−2378
transition metals, H diffusion 80−29219
transition metals, reaction with gases, exam. of mech. and kinetics *(Russian)* 79−57289
transition metals, surface magnetism 77−73071
transition metals and their alloys, struct. 77−51304
transition oscillator strengths of alkali metal atoms 80−52937
transition radiation and transition scatt. 79−27143
transition state theory generalisations 80−26002
transition state theory generalisations 80−26003
transmission and emission computed tomography *(Japanese)* 78−81042
transonic flow numerical calculation methods and problems 77−58723
transonic plane flows past oscillating airfoils, review, book contrib. 80−96278
transonic steady potential flow 77−72324
transparent conducting coatings, book contrib. 78−10587
transparent dielectric destruction by laser radiation 77−50702
transuranic nuclear waste management, evaluation of alternatives 80−18490
transuranium elements, resuspension from contaminated surfaces 79−62376
treeing in solid extruded electrical insulation, bibliography 77−24788
tribology, material aspects in manufacturing processes 80−81210
tribology, review of current understanding 77−59066
triboluminescence 78−19581
triboluminescence 79−11478

reviews continued
triple star dynamics 79−44559
triple stars and close approaches dynamics, review 79−44560
TRIUMF meson factory, basic and applied research 78−21792
tRNA in soln., selected topics, book contrib. 80−108839
tropical meteorology, review 77−64365
tropical waves in atmosphere, ionosphere and oceans 79−74945
troposphere, composition, natural and effects of pollution 78−28262
troposphere, radar obs. during clear air conditions, review 80−90178
troposphere, refr. theories of radio wave propag., review 78−69425
tropospheric studies, microbarograph, sodar, FM-CW radar 77−91332
TTF-TCNO, optical evidence for Coulomb interactions 78−6704
TTF-TCNQ, physical properties *(Japanese)* 80−24883
TTF-TCNQ and $(SN)_x$ polymer, electronic props. 78−6306
tube inspection, magnetic leakage flux method 78−95891
tumour localisation, animal tumour models for evaluation of radioactive agents 77−9249
tunable acousto-optic filters 78−5570
tunable diode laser instruments, appl. advanced meas. and anal. 77−75600
tunable diode laser IR spectroscopy 78−82061
tunable IR lasers, principles and operating charact. 79−98376
tunable IR lasers with $F_A(II)$ and $F_B(II)$ colour centres 78−90420
tunable laser progress 80−43344
tunable laser spectroscopy, of semiconductors 79−93231
tunable lasers *(Japanese)* 79−27270
tunable lasers appl. to spectroscopy 79−64270
tunnelling MIS structures photovoltaic energy conversion, band struct. 80−92995
tunnelling spectroscopy *(German)* 78−91776
tunnelling spectroscopy appls. 78−92588
turbine flowmeter, for gaseous hydrocarbon, construction and performance, review 78−34244
turbomolecular pumps, advances 80−62676
turbulence, 2-D, hydrodynamic and plasma applications, dynamical eqns., diffusion, MHD, superfluidity 80−69769
turbulence, current theory and practical examples *(French)* 80−64523
turbulence, fully developed, statistical mechanics 78−51150
turbulence, fully-developed, renormalisation group 80−28495
turbulence, progress and problems 77−39278
turbulence, universality and scaling 79−58548
turbulence creation *(Hungarian)* 79−23312
turbulence in stellar atmospheres 79−30056
turbulence measurement by laser Doppler anemometers, book contrib. 80−19538
turbulence models for heat transfer 79−4017
turbulence review of present research 79−98687
turbulence theory 80−4536
turbulence-generated noise in pipe flow, book contrib. 78−59385
turbulent flow separation 80−1543
turbulent shear flow structure problems, new developments 77−31286
turbulent wall flows, constant press. and press. gradient flows, book contrib. 80−19347
TV-rate stereo SEM systems, design and performance 79−12906
twin composition plane as extended defect, structure-building entity 80−44218
twistor programme, self dual solns. to reduced equations 79−26231
two dimensional system, ordering 80−107407
two dimensional systems, phase transition, review 80−52149
two photon transitions in solids 77−69240
two-dimensional system, phase transitions and metal-insulator transitions 80−2143
two-nucleon pot. and meson physics, nucleon-nucleon interactions, review 78−89802
two-phase flow, mixing and condensation in high-speed flow 78−47014
two-phase flow, transient and statistical meas. techniques 77−11287
two-phase flow characterisation using neutron techniques *(Italian)* 80−19479
two-phase gas-liquid mass transfer in packed beds 77−31381
two-phase two-component heat transfer 79−1239
two-photon spectroscopy, dipole-forbidden transitions, double excited configurations, CNDO-CI methods 80−58332
two-photon spectroscopy 77−67510
type II superconductors, mag. hysteresis and flux profiles 79−1651
ultra high vacuum technology developments *(Japanese)* 78−49845
ultra-cold neutrons, review of prod., transport and appl. 79−40982
ultra-high vacuum systems for surface anal. 79−67323
ultra-sensitive particle identification systems based upon electrostatic accelerators 79−72182
ultra-short light pulse generation *(Japanese)* 79−45973
ultracold neutrons, extraction, transportation and storage 77−26826
ultracold neutrons, review of Soviet expt. research on prod. and storage 79−97923
ultramafic bodies in S.Appalachians 78−65288
ultranarrow resonance, use in spectroscopy and for gas laser freq. stabilisation 79−59775
ultrapure water, trace metal determ. 80−81394
ultrasonic flaw detection, of welded joints, in USSR 79−87768
ultrasonic materials testing reference blocks and transducers, survey 78−68858
ultrasonic testing techniques 77−74899
ultrasonic velocity measurement methods 77−84094
ultrasonics, trends in research work *(Japanese)* 78−33946
ultrasonography of the kidney in 1979 *(French)* 80−56149
ultrasonography rel. to computerised tomography in upper abdomen and retroperitoneum exam. 80−21506
undersea acoustics, review of history (to 1950) 77−45667
underwater explosions, book contrib. 77−47035
underwater explosions, surface effects 80−14745
underwater sound, deep ocean LF attenuation data 80−33318
underwater sound scattering by marine organisms, report 80−64269
undulators and 'free-electron lasers' 80−9794
unidirectional wave motions, book 78−77730
unification of fundamental forces in nature, elementary particle constituents, SU(3), gauge symmetry 80−27448
unified gauge theories, grand, asymptotic freedom constraints 80−62914
United States, available energy resources, 1985-2000 period 79−43711
United States fusion power, overview 80−95395
Universe long-term future, review 80−41927
university physics curricula 79−62953

reviews continued
unnamed space probes, recent achievements, financial restrictions and their effect on future programmes 80−72743
unstable quantum systems, decay theory review 78−65871
unsteady aerodynamics of lifting surfaces using computer, book contrib. 77−51076
unsteady boundary layers, separated and attached, review 79−77086
unsteady subsonic and supersonic inviscid flow 78−71350
upper atmosphere, dynamical properties 79−75005
upper atmosphere, responses to August 1972 mag. storms 77−25858
upper atmosphere, structure, composition, temperature and motion, general review 79−39997
upper atmosphere perturbations assoc. with mag. storms 80−98495
upper atmosphere research applics., of quadrupole mass spectrometer, book contrib. 77−25911
upper limb joint replacement 78−3674
uracil, RNA component, review of props. 79−53035
urea-formaldehyde resins, book 80−73114
urodynamic parameter meas. systems 79−96690
SU Ursae Majoris stars, important sub-group of dwarf novae, photometric props. 80−101596
US applications in obstetrics and gynecology, safety and pot. hazards 80−67170
US B-scanning in medicine, book 78−73180
US defectoscopy, development of and problems in theory of normal waves 80−81265
US diagnosis in medicine and biology, bibliography 78−69166
US diagnostic uses, bibliography 79−62322
US equipment safety standards, BRH, FCC, CPSC, FDA and OSHA regulations 77−57311
US evaluation, computer-assisted, review 79−43536
US flaw detection, progress in theory and principles 80−81262
US imaging, single-transducer technology, state of art review 77−843
US imaging and holography, devices, medical uses *(French)* 77−827
US imaging modalities for medical appls. 80−81669
US imaging of abdomen, book contrib. 80−36046
US imaging of carotid arteries, book contrib. 80−36047
US imaging over view, appls. and future trends 80−48536
US in medical diagnosis, appls., principles and equipment 78−11709
US in medicine and biology 77−66830
US in ophthalmic diagnosis 80−81673
US inspection, of seamless drill casting and linepipe, review 78−95879
US inspection of coarse grained metals, struct. reverberation interference 80−45456
US materials testing, future development 79−79196
US National Shoreline Erosion Control Demonstation Program 78−16163
US nuclear fuel cycle 79−54585
US phased array sector scanning, medical diagnosis 80−36038
US propag. props. of nematic liquid crystals 78−63668
US props of mammalian tissues 78−88727
US testing 80−104360
US therapy device surveys, performance standard drafting 79−79613
US tomography 78−31876
US tomography techniques survey 80−30823
US transducer 2-D array technology, state of art review 77−844
US transducer arrays 79−59898
US wave damping in solid material, instruments for determ., review 78−92429
US wavefront visualisation and meas. methods 79−64459
uterine venography, value in diagnosis of pelvic pain in women *(French)* 80−17079
UV and IR instrument material mech. and thermal props. 80−106584
UV and light absorption spectrometry, review of literature 1975-1977 78−85222
UV effects on eye 78−80917
UV high-power laser material, refractive props. and optical constants 80−106555
UV molecular lasers with transverse electronic pumping *(French)* 79−31880
UV radiation physics and the skin 80−81661
UV radiometric standards, gas discharges, plasma diagnostics appls. 80−47088
UV sky surveys 78−93111
UV solar radiation effects on upper atmosphere, review of Saha's work 79−53599
UV/visible gas lasers, appls. in commercial photochemical processes, review 79−55123
vacuum arc cathode, cathode spot phenomena, classification 77−24223
vacuum gauge calibration, review 77−22563
vacuum gauge calibration techniques *(German)* 77−87778
vacuum gauges, types and charact. 79−26064
vacuum physics progress *(Chinese)* 79−35768
vacuum systems for optical coating prod. 77−58493
vacuum technology *(German)* 77−79100
vacuum UV optics, reflecting coatings and transmitting filters, review 79−46029
vacuum UV special application coatings, reflectance, transmission, technology 79−59788
vacuum UV tunable coherent radiation generation by lasers 77−54705
van der Waals interactions between surfaces of biological interest 77−44609
van der Waals molecules, book contrib. 77−38709
vapour deposition of wear-resistant surfaces 78−72938
vapour growth, element incorporation 78−30556
vapour pressure isotope effects, bibliography 80−77558
vapour pressure measurement, effusion method, review 80−51995
vapour quenching techniques 80−80977
variable stars, physical and eclipsing, surveys and obs. 80−12772
variational principles, complementary 78−41135
variational theory of nuclear matter 79−89262
vegetation canopy modelling for signature correction/anal. 77−78515
velocity meas., analogue electrical methods *(German)* 79−178
venous occlusion plethysmography for the detection of venous thrombosis 80−56268
ventricular arrhythmia detector, arrhythmia data base of American Heart Association 79−62391
ventricular fibrillation and defibrillation 80−81769
ventricular performance, 1st pass radioisotope assess. 80−85482
Venus, atmosphere thermal balance 77−73994
Venus, current knowledge 77−73991

reviews continued
Venus, review of surface and interior 77−73996
Venus, review of Venera data 80−72804
Venus, upper atmosphere structure and dynamics 77−33382
Venus atmosphere, dynamics, winds, circulation and turbulence 77−78706
Venus ionosphere, characts. and interaction with solar wind 77−73995
Venus solar wind interaction, review of present understanding 79−58288
vesicular film sensitometry, review 78−16878
vestibular control of oculomotor and postural mechanisms 80−72151
vestibular mechanisms, rel. to eye movement control, book contrib. 79−96588
vibration damping materials, testing and development 77−84059
vibration isolation, survey of use and characterization 80−19144
vibrational dynamics of liquids and solids, Raman scatt. of picosecond light pulses 78−94414
vibrational nonequilib. in gases 79−18270
video microscopy 79−58784
Viking mission, review of surface sampling and landing of second vehicle 77−17403
Viking mission to Mars 77−73933
Viking orbiters, scientific missions 78−20612
Viking project, summary 78−20611
vinyl alcohol-vinyl acetate copolymers, mol. architecture and physicochem. props. 80−44103
viral infections diagnosis, contrib. of electron microscopy *(Italian)* 80−109024
viruses envelopes, plasma membranes, book contrib. 79−5257
viscoelasiticity linear, Boltzmann and Maxwell theories, review 77−71216
viscoelastic bodies, adhesion and fracture mechanics 78−83336
viscoelastic fluids, secondary flows 77−68644
viscoelastic liquids, steady non-viscometric flow, review, book contrib. 77−47049
viscous compressible flows at high Reynolds number, book contrib. 80−19424
viscous transonic flow, book contrib. 78−59416
visibility of isolated alphabetic letters and numerals, annotated bibliography 78−53411
vision, human, pattern detection and recognition, review 77−73527
vision, light deprivation and maturation, bibliography 78−15843
vision, parallel pathways 80−89751
vision, pattern recognition functional mechanisms in humans 80−81609
vision, photopigment and receptor props. in Drosophila compound eye and ocellar receptors 80−8063
vision, photostable pigments, function in fly photoreceptors 80−8058
visual acuity in human infants, comparison of studies 79−53112
visual acuity threshold variation, study of research literature *(French)* 79−5283
visual areas of mammalian cerebral cortex, book contrib. 79−96560
visual development, environmental effects 79−11926
visual evoked cortical potentials, transient response, techniques review 78−35844
visual evoked potentials in neurological disorders 79−24981
visual information processing *(German)* 77−64034
visual perception, failure of classical optics, to account for observed phenomena 79−5289
visual pigment chromophores, models, spectroscopic and photochemical studies 80−30723
Visual pigment systems, implications of bistability 80−8059
visual pigments, reson. Raman studies 77−90729
visual stress, functional consequences, annotated bibliography 80−26222
visual system variability and periodicity, bibliography 78−27936
visually evoked potentials, speed methods for vision assessment, normal and amblyopic eyes 80−61661
VLF heating methods, thermonuclear prospects 80−28738
VLSI processing by low-pressure CVD 79−87581
voice synthesis and voice recognition *(German)* 79−50530
void swelling simulation in reactor materials 78−8906
voids, review of diffusional growth of creep voids 78−71720
volcanic evolution of the Cascade Range 79−5466
voltage clamp of multicellular preps. 77−40955
voltage contrast, a review 79−21863
voltammetry, phase selective anodic stripping type 80−40788
volume phase holographic storage in ferroelec. crysts. 78−82929
vortex breakdown structure, book contrib. 78−59407
vortex flow aerodynamics, review of developments rel. to design 79−77140
vortex interactions, book contrib. 80−19410
vortex methods for flow simulation 80−106801
vortex shedding research 78−14021
wakes in stratified flow, book contrib. 80−19473
Wannier excitons, fine structure, lineshape and dispersion 80−44520
water, chemical analysis 80−7877
water, density, effects of isotopic comp., temp., press., and dissolved gases 78−26616
water, liquid structure *(French)* 78−26424
water, struct. and liq. theory, book contrib. 77−39525
water, viscosity, international formulation 78−26714
water at biological interfaces, struct. and functional aspects 78−40121
water resources management, systems anal. and modelling techniques appl. 79−5518
water resources policy, scientific and technological considerations 79−8642
water solution calorimeter, determination of energy equivalent, with standard substance 78−23961
water supply in United States, effects of climate and climatic changes 78−49044
water transport in soils, review, book contrib. 80−96308
water wave diffr. and radn., numerical methods, book contrib. 78−59412
waterdrop interaction experiments 78−11974
wave energy convertors, materials aspects 80−85262
wave propagation and scattering in random media 77−75376
wave propagation in active and passive periodic structures 77−3504
wave propagation in random media, oceanic appls. 79−5987
wave propagation in turbulent medium, classical theory, book contrib. 79−34956
wave-formed bars, sedimentation and equilib. 79−92521
wavelength stabilisation for light interferometry *(German)* 80−57250
wavepower 77−81919
weak, non-leptonic interactions 78−78163

reviews continued
weak current interactions 80−73654
weak currents of hadrons, unified gauge theories 79−80786
weak electron-nucleon interactions, testing Laporte's rule, review 78−37564
weak interaction effects in atoms 77−13890
weak interaction studies with the DUMAND detector 79−63463
weak interaction theory review, Higgs bosons 78−78131
weak interactions, high-energy behaviour 78−78164
weak neutral current, effects in stellar collapse, review, book contrib. 78−85964
weak neutral currents, parity non-conservation in e-N, μ-N forces 77−57484
weak shock propagation in liquid-filled tubes 78−26004
weak-EM decays of π and K *(Russian)* 77−2818
wear, debris anal. and condition monitoring review 78−68854
wear, delamination theory, review 78−3229
wear mechanisms 78−72891
wear resistance, surface treatments, selection procedure, review 78−72892
wear study, analytical surface tool, review 78−64718
weather, numerical prediction review 78−69393
weather and climate numerical prediction 78−96276
weather forecasting, overview and future work 77−91196
weather modification economics, review, future anal. 79−20927
weather modification technology, statistical approach 78−53706
weather prediction, development and status 77−82358
weather prediction, objective methods, book contrib. 78−61535
Weissenberg effect, review of expts. 79−60025
welding, appl. of high energy density heat source *(Japanese)* 79−29329
Western Australian Shield, struct. and tectonic style 80−3983
whistler propagation at low latits. 78−73586
whistler propagation theory 77−45261
whistlers, nature, types and observations 80−36458
whistlers, present state of research and history 80−46348
white dwarfs, physics of structure and evolution 79−25606
white dwarfs, review 80−82356
wideband integrated optic signal processors 79−89864
wildlife biotelemetry 80−30966
wind characteristics in Japan 78−36253
wind energy conversion, fluid dynamic aspects 80−7909
wind energy conversion, review of the US Wind Energy Programme 80−50929
wind-driven currents on the continential shelf, review, book contrib. 80−98358
wing section theory of Kutta and Zhukovski, book contrib. 80−1514
worldwide energy prospects, synthesis of studies published in 1976 and 1977 *(French)* 79−29443
wustite solid solns., props. connected with localised electron state 80−107734
X-ray, and neutron small-angle scattering, appl. to materials science 79−10752
X-ray analysis in the TEM/STEM 78−24014
X-ray and extreme UV lasers, basic physical concepts 79−31850
X-ray and neutron diffraction techniques, advances, book contrib. 79−67453
X-ray and neutron diffuse scattering, direct methods of anal. 79−94845
X-ray and neutron small angle scattering, recent developments in instrumentation and data anal. 79−10750
X-ray and synchrotron orbit radiation spectroscopy *(Japanese)* 79−26142
X-ray and synchrotron radiation inelastic scattering in crystals 78−39625
X-ray astronomy, 1960-1980 period 78−49567
X-ray astronomy, techniques, electronic image processing *(Italian)* 79−16826
X-ray astronomy 77−78892
X-ray astronomy 78−32604
X-ray astronomy satellites and missions 79−8793
X-ray binary stars, optical photometry and spectra 78−12429
X-ray binary stars, review of types and props. 80−109564
X-ray binary stars *(Italian)* 78−32516
X-ray burst sources, review 78−12427
X-ray burst sources, review 78−49566
X-ray burst sources 78−12416
X-ray computed tomography, annotated bibliography 80−30876
X-ray diagnostics appl. to laser induced fusion, review 77−55176
X-ray diffraction, review of literature, 1976-1977 78−83646
X-ray diffraction chem. anal., historical review 77−70383
x-ray diffraction studies of the heart, book contrib. 80−109079
X-ray diffractometry, diffraction pattern parallel meas. 79−94848
X-ray diffractometry handling problems, survey 80−1898
X-ray edges theory 77−66556
X-ray emission induced by heavy charged particles, analytical appl. 77−4967
X-ray energy spectrum analysis *(Chinese)* 79−30635
X-ray flash techniques 79−49356
X-ray fluoresc. anal., energy dispersive, least squares, Monte Carlo methods, mathematical anal. techniques 78−85243
X-ray fluorescence analysis, equations of bond, review 80−66898
X-ray fluorescence analysis, overview 78−3425
X-ray fluorescence matrix correction methods using scattered radiation 80−3456
X-ray galaxies 79−58422
X-ray imaging, image intensification systems and techniques 80−51236
X-ray lasers, plasma, production, optical transitions of multiply charged ions, population inversion, review 77−19227
X-ray optics in 1 to 300 Å wavelength range 78−29221
X-ray phosphors and screens based on compounds activated with rare-earth elements 79−8169
X-ray photoelectron spectra of solids, satellite lines *(French)* 77−36363
X-ray photoelectron spectroscopy, development (1900-1960) 79−12560
X-ray photoelectron spectroscopy 1900 to 1960, review 77−82359
X-ray planigraphic examination of the abdomen 80−21529
X-ray science, survey of former students of Oregon State University 79−9
X-ray sources, periods 78−12424
X-ray sources in globular clusters, review 78−12428
X-ray spectra excited by high-energy ions 79−49976
X-ray spectral analysis, energy dispersive, using semicond. detectors 80−85237

reviews continued
X-ray spectral analysis 78−23981
X-ray spectrometry, empirical influence coefficient methods 80−3455
X-ray spectroscopic anal., mathematical correction procedures, review 77−56308
X-ray spectroscopy, chemical aspects, review of literature 1975-1977 78−85219
X-ray spectroscopy in ferrous metallurgy 79−39242
X-ray spectroscopy of metals and alloys 77−55849
X-ray stress anal., recent German activities 77−81359
X-ray synchrotron source, design status 79−68024
X-ray tensometry *(Czechoslovakian)* 77−28958
X-ray topographic images, direct display systems, review 77−68899
X-ray topography, techniques and interpretations 79−67454
X-ray topography assessment of crystals, developments, review 80−64836
X-ray transient sources, galactic distrib. and physical nature 79−84867
X-ray transient sources *(Polish)* 77−17720
X-ray transmission computerised tomography 77−48860
X-ray tube technological and philosophical changes over a decade 80−37136
X-Y model critical properties 77−66326
X-Y recorders, commercially available *(Norwegian)* 77−37869
xerography, amorphous Se electronic props., defects 79−97454
xerography and mammary microcalcifications *(French)* 80−51224
XUV astronomy, review *(German)* 80−109372
Yang-Mills 2-D theory in leading 1/N expansion 79−26242
Yang-Mills type gauge fields, geometrical setting 80−32014
yeast, sensitivity to ionising radiations and damage repair 80−81659
YIG, optical absorption and magneto-optic spectra 79−99860
yrast spectroscopy, nuclei with high angular momentum, review 78−50063
zeolite surface, bonding of Cu^{2+}, Cr^{3+}, Co^{2+} ions EPR, optical spectroscopy investig. *(German)* 79−95266
zero differential overlap approximation, theory, parametrisation, methods 78−82622
zero-gap semiconductors, electronic energy spectrum 77−66118
zero-gap semiconductors, reson. states 79−82558
zeros of classical polynomials and Bessel functions, diophantine props. 79−35530
zeugmatography, state of the art 78−74043
ZGS, polarised beam results 80−99361
ZGS polarised ion source development activity 77−34493
Zircaloy 2 and 4, oxidation kinetics appl. to loss of coolant accidents, data review 78−19958
Zwicky's compact galaxies, properties 78−49542
α-clustering and spectroscopic factors, shell effects and deformation correlations in (^{6}Li,d), (d,^{6}Li) 79−6436
β-decay, time reversal invariance and second class weak currents 78−37309
(e,e′) in giant resonance region, review 79−93585
ed→ed, nucleon forces, meson exchange current effects, impulse approx. 80−57603
e^-e^+ annihilation, >2 GeV, production of charmed particles and charged τ lepton, review 78−17006
e^-e^+ colliding beam physics 77−74700
e^+e^- annihilation, radiative corrections, review, book contrib. 80−47320
e^+e^- annihilation by one-photon processes, book contrib. 80−47272
e^+e^- annihilation experiment review, ψ spectroscopy and charmed particles D and F 79−49533
e^+e^- collisions, hadron prod., tests of QED 77−57551
e^+e^-→hadron jet, 3 to 17 GeV, including charm threshold and upsilon resonances 80−47321
e^+e^-→hadrons, jet behaviour 80−52524
e^+e^- interactions 79−80833
e^+e^- storage rings, expt. review of beam polarisation 79−63837
eγ cascade widths, review of expt. evidence and calcs. 78−85779
eN→eX, form factors and structure functions, book contrib. 80−47294
eN→e+hadrons, E<2 GeV, formalism, book contrib. 80−47312
γ high energy experimental physics at Fermilab, review 78−50028
γ sources, properties, produced by neutron capture 80−14029
γN, many body processes, book contrib. 80−47303
γp→X, strong interaction model anal., review, book contrib. 80−47310
K→2π and 3π, transition amplitude determ. using least-squares anal. 79−58956
KN anal. in resonance region below 3 GeV/c 77−6163
Λ- and Σ-hypernuclei, γ-transitions, spin-orbit components of single particle pots. 80−42574
Λ- and Σ-hypernuclei and hyperon-nucleus interactions, review 80−42575
ΛN, reaction-matrix calc. of Λ binding energy in nuclear matter 79−36185
μ g-factor, (g−2) expts., review, book contrib. 80−68403
μ^- spin rotation, μ relaxation and repolarisation, muonic X-rays 80−42644
N-N potential 79−71795
NN charge exchange models at high energies 77−30444
NN elastic scatt. at large transverse momentum, spin-spin forces 78−78216
NN interaction in pion exchange, nuclear matter and pion condensation, review 80−42557
NN resonances and total cross sections, expt. evidence review 80−42558
NN scattering E<1 GeV, TRIUMF and SIN expt. programs 79−63501
NNN bound state problems, hyperspherical harmonic expansion 80−91136
(p,α), polarised p, anal. power, direct 3-nucleon transfer reactions, microscopic approach review 79−6545
(p,d), intermediate energy study review 80−42653
(p,γ), exclusive single nucleon transfer, theoretical status 80−42652
(p,p), elastic, inelastic, polarised and unpolarised, intermediate energy study review 80−42653
(p,p), elastic scattering theory, multiple scatt. test review 80−42654
(p,π), exclusive single nucleon transfer, theoretical status 80−42652
(p,π), hopes and realities, review, book contrib. 80−73849
(p,X), experimental information review, polarisation phenomena 80−42655
p+nucleus, intermediate and high energies, research review 78−94010
pn→$\mu^+\mu^-$+anything, review of data, explanation using quark models, new quarks 78−74202
pp, neutral particle production in 4 to 2100 GeV interactions *(Russian)* 80−68489
$\bar{p}$p atoms, quasiatomic and very energetic γ-rays 80−42574

reviews continued
pp elastic scatt. at high energies and large momentum transfer, review *(Russian)* 80−105926
pp→pp, medium energies, inelasticity and struct., pure spin total cross section data 78−62439
(π^-, γ), high spin isomer state excitation, review 79−49569
(π,π), 80-300 MeV, nuclear struct. studies around (3,3) resonance region 79−85528
(π,π) elastic scattering, microscopic theory 80−47511
(π,X), reaction mechanisms, at low energy and near 3.3 reson. region 79−80958
(π,X), reaction mechanisms, nuclear environment and models 80−42700
π, photoproduction in E<450 MeV region, dispersion relations, CT invariance, book contrib. 80−47311
π factories, multidisciplinary role 78−21791
π photo and electroproduction in first πN-reson. region *(Russian)* 78−54636
πd elastic scattering, microscopic theory 80−47511
πN elastic amplitude, off-shell behaviour, and separable potential model 79−85327
πN scattering, low-energy, nonlinear chiral dynamics description *(Russian)* 78−17043
πp, neutral particle production in 4 to 2100 GeV interactions *(Russian)* 80−68489
π^+p, elastic and charge-exchange scatt., partial wave anal., Δ resonances 80−63018
$\pi\pi$ scattering amplitude and single π prod. results 78−62455
ψ/J discovery and charm prod., quark models 77−54113
ψ/J particle discovery, experimental details, personal recollection 77−54112
ψ/J particles, expt. results and interpretation *(Russian)* 77−269
τ particle, discovery and props. *(Polish)* 79−89216
$\tau^\pm$ heavy lepton in e^+e^- annihilation, review 79−49505
^{227}Ac fission expt. data, review *(Russian)* 79−49641
Ag halide, photographic material, sensitivity and struct. characts. *(Russian)* 79−2868
Ag halide crysts., dislocations, survey of post-war research 80−62449
Ag halide monocrystal detectors, reference listing 79−72196
Ag halide photographic materials for holography, book contrib. 78−25832
Ag halide photographic materials, theory of supersensitisation *(Russian)* 80−62786
AgBr, determ. of ionic transport processes 77−89578
AgBr, photoexcited electrons and holes in latest image form., review 80−73496
AgCl, determ. of ionic transport processes 77−89578
AgI, interfacial electrochem., review 78−80748
AgI type solid electrolytes, expt. props. 78−63877
Al alloy, engineering problem solution 77−66605
Al and alloys, critical pitting potential meas., review 79−43501
Al bronze, plasticity of two-phase, coarse microstruct. material *(German)* 77−59882
Al I to XIII, energy levels and ionisation energies, data compilation 80−14100
Al-In emulsion, solidification mechanisms at zero gravity, review 78−88458
Al-Mg-Si, Guinier-Preston zones, inception and effect on ageing *(Hungarian)* 79−11627
AlGaAs heterostructures in integrated optics 77−75713
Al_2O_3-Ni cermets, prep. and props. *(French)* 80−20877
and associated metals recovery, from secondary sources, recent developments 80−100800
As, amorphous, optical, vibr., transport and defect-related props., review 79−51935
As_2S_3, amorphous semicond., photo-induced optical and structural changes *(Japanese)* 78−47244
As_2S_3, As_2Se_3, optical props., electronic struct., photocond., book contrib. 77−44024
B, and borides, cryst. chem., struct., B cryst. growth, review, book contrib. 78−47278
B, and refractory borides, book 78−48292
B, chem. props., reacts., review, book contrib. 78−48653
B compounds, ^{13}C NMR spectroscopy 79−89691
B fibre prep. 79−28983
B, filament CVD technology, book contrib. 78−48352
β-B, rhombohedral, EPR, book contrib. 78−48041
α-B, rhombohedral, prep. methods, book contrib. 78−48295
B-O(S)(Se)(Te)(Po) compounds, prep. and struct., book contrib. 78−47306
BC, EPR, book contrib. intensity correl. with elec. cond., Hall coeff., book contrib. 78−48041
BN, EPR, book contrib. 78−48041
BN fibres, prep., struct., thermal, mech. and elec. props., appls., book contrib. 78−48360
B_2O_3-PbO(ZnO) glass-ceramic-cement composites, review 79−38783
$BaMnF_4$ phase transitions 79−78378
Bi electron properties, carrier spectrum 78−84137
Bi, electronic props. 77−15742
Bi_2O_3-based solid electrolytes, ion cond. and oxide ion vacancy 79−28139
C and graphite, mechanical props., high temp., review 79−38897
C cardiovascular prosthetic devices and dental implants, review 77−44835
C fibre, vapour-grown, growth mechanism and props. *(Japanese)* 77−66598
C fibre and glass fibre hybrid reinforced plastics, review of physical properties 80−55496
C fibre reinforced composites for spacecraft use, prep., props. and struct. 80−71625
C fibre reinforced plastic aircraft structural appl., non destructive testing 78−35599
C fibre structure, recent advances 80−81069
C glass fibre hybrid plastics, review of mech. props 79−20107
C, soft and hard, sp. ht. anomalies and spin-spin interactions, review 79−69261
C stars, spectroscopic problems 80−56832
C-fibre reinforced cement 77−21082
CO, chem. laser, book contrib. 77−10911
CO laser, theoretical and experimental developments *(Japanese)* 78−25857

reviews continued
CO_2 laser, non-self sustaining discharge for CW laser excitation, review 78−42849
C_2S mineral, chem. and polymorphism 79−69051
^{12}C, 3-α struct. in boson model 78−17124
^{13}C, NMR of peptides and proteins, review 78−24023
^{13}C-^{13}C spin-spin coupling consts., data compilation, meas. and appls. review 80−17725
^{14}C analysis of soil, dating 78−36299
^{14}C radioactive dating, determ. of $^{14}C/^{12}C$ ratio, review of methods *(Hungarian)* 79−48578
Ca I to XX, energy levels and ionisation energies, data compilation 80−14101
Ca^{2+}, passive and active fluxes across membranes 80−97886
CaCl, aq., mean activity and osmotic coeffs., free energy, 298.15K 77−81411
Ca_2SiO_4-$CaMgSiO_4$, T phase, review 80−50612
CdI_2, polytypism, review 77−11498
CdS solar cells 80−76638
CdTe, applications review 77−72894
CdTe, charge carrier transport prop. meas. by time of flight technique 77−39850
CdTe, defect struct. 77−39581
CdTe, donor impurity compensation models, impurity-vacancy complexes 77−39601
CdTe, melt-growth review, including liquid encapsulation method, defect charact. 77−40350
CdTe optical applications 77−42580
CdTe, physical props. 77−39833
CdTe sensors, review of medical appl. 77−64147
^{252}Cf, status, application and prospects 77−26914
ClO_x, reaction rate consts., atmospheric gas phase reactions, review 77−81390
Co, impurity hyperfine fields 79−99518
Co, physical, mech. and chem. props. 79−95909
^{60}Co teletherapy dosimetry survey of facilities 79−62367
Cr, antiferromagnetic structure, mag. field effect, spin density wave model *(Russian)* 80−70953
Cr I to XXIV, energy levels, ionis. pots., g-factors, from spectral data 77−79556
CrO_2 and tetravalent Cr oxide derivatives, chem. and phys. props. 78−31069
Cs arc, low-voltage hot-cathode, plasma production and props. 77−27766
Cu and Cu alloys, diffusion in systems involving group VA elements 77−39697
Cu, production and extractive metallurgy, developments 80−20821
Cu-Ag-X, X=metals, P, S, Se, phase diagrams and thermodynamic props., iso-activity coeff. curves 77−81249
Cu-Fe system, ageing and reversion phenomena study 80−89274
Cu-Ni-Al, memory alloy wire and ribbon reversible martensitic transformation, ageing effect 80−7564
Cu-Zn-Al, memory alloy wire and ribbon reversible martensitic transformation, ageing effect 80−7564
CuCl, biexcitons existence 77−69239
Cu_2S-CdS solar cells, thin film fabrication processes and conduction mechanism 79−74522
D-T, solid, estimated heat capacity, enthalpy, thermal cond. and diffusivity 77−4228
D-T fusion, energy deposition, damage and neutronics data 77−26880
DT fusion reactors, environmental aspects *(German)* 79−54599
EuO(S)(Se)(Te), cryst. and electronic struct., mag., elec., and optical props., book contrib. 80−39760
EuO(S)(Se)(Te), spin order and fluctuations, Raman scatt. study 80−97273
EuO(Se), complex elec. cond. anomalies 80−107812
F, spin-spin coupling constants, review 77−23511
Fe abundance in solar system rel. to nucleosynthesis 77−53435
Fe alloys, hydrogen embrittlement mechanisms 78−72853
Fe, brittle fracture mech., review *(Russian)* 79−34139
Fe, effect of H_2 on phys. and mech. props. 80−101657
Fe electrodes, semicond. model of passive layer 80−26022
Fe, impurity hyperfine fields 79−99518
Fe making industry, evolution, review 77−73431
Fe meteorites, mineralogy 77−87348
Fe, neutron magnetic critical phenomena, review of new effects 79−56534
Fe^+, isoionic study, excited config. position and level struct., review 80−32621
Fe-C, martensitic transformation, thermodynamical study *(Chinese)* 80−55395
Fe-C solid solution, martensite, carbide decomposition, electron microscopy and X-ray diffr. obs., review *(Russian)* 79−33998
Fe-Cr-Mo alloy castings, thick-section, factors affecting 80−108374
Fe-Cr-Ni austenitic alloys, environment sensitive cracking, metallurgical variables effect 80−35391
Fe-group, atoms and singly ionised, f-value meas., review 78−17617
Fe-Ni alloys, thermal props., let. review *(Russian)* 78−18805
Fe-Si, grain-oriented sheets, high permeability, low losses, review 80−88790
Fe-Si, non-oriented sheets, production and props. 80−88797
Fe-Si (3 wt.%), transformer steel, grain-oriented, magneto-optical domain obs., magnetisation mechanism 77−12364
Fe-Si-B-N-S, B, S, N effects on grain boundary segregation and grain growth inhibition, review 80−3047
Fe-Zn, galvanised coating appl., metallurgy review 79−96199
$Fe_{1-x}O$, thermodynamic props. of wustite phase of iron-oxygen system 78−79780
Fe_3O_4, magnetite, electronic cond. mechanisms, review 77−20314
Fe_xO_y crystal dissolution, electrical potential effect, review 79−46809
FeS_2, cryst. growth, literature review 78−31318
Ga chalcogenides, cryst. struct. types 77−15392
GaAs, and its alloys, as integrated optics materials, book contrib. 79−64362
GaAs, elec. props. of dislocations *(Japanese)* 78−6325
GaAs, ion implantation 78−6080
GaAs, ion implantation review 80−88184
GaAs ohmic contacts fabrication, review 80−49901
GaAs-GaAlAs DFB and distributed Bragg reflector lasers, historical review 77−31102
GaInAs-InP injection lasers with longer wavelengths for optical fibre communications *(Japanese)* 78−25892

reviews continued
$Ga_{0.47}In_{0.53}As$, photodetector applications 80−95140
$Ga_yIn_{1-y}As_xP_{1-x}$, LPE growth 80−66440
GaP, green luminesc. efficiency 77−28636
^{67}Ga imaging of peritoneum and retroperitoneum, anatomic correls. 80−17097
^{67}Ga, status in tumour detection 80−98074
^{67}Ga tumour scanning 77−9250
^{67}Ga, use in diagnosis of pulmonary disorders 79−57771
Gd, impurity hyperfine fields 79−99518
$Gd_3Ga_5O_{12}$, single cryst. growth for mag. appls., book contrib. 79−69968
Ge, electron-hole-liquid in mag. fields, expt. and theoretical investigations 79−60720
Ge, self-interstitials, vacancies and their clusters 77−80500
H assisted cracking, mechanisms, review 80−50721
H biological photoprod. using sunlight 80−45777
H diffusion, and solubility in solid metals 80−49422
H energy, industrial appls. of liquid and gaseous H 80−45801
H energy, R and D programs 80−45802
H II regions, dust content 78−16508
H lines, Stark broadening in plasma 78−42001
H photoelectrolytic production by H_2O decomposition using sunlight 80−45774
H production, EPRI R and D program for electric utility industry 80−30610
H production and utilisation, EEC R and D program review 80−45821
H production by H_2O electrolytic dissociation 80−30429
H, storage, transmission and distribution 80−30596
H storage electrolysis-based technology R and D at BNL 80−40920
H storage in metals, book contrib. 80−26175
H thermochemical prod. by H_2O decomposition 80−45800
H^- form. by surface and vol. processes, neg. ion source appl. 80−58375
H_2 and isotopes, vap. press., 4 to 30K 77−72674
H_2 electrolytic production, design and operation of advanced H_2O electrolysers 80−61449
H_2 energy bibliography 80−12863
H_2 energy research programs in Japan 80−61435
H_2 high press. afterglows 80−64823
H_2 photobiological prod., key enzymes and biochem. systems, tech. problems of H_2 prod. 80−61446
H_2 photochemical production by H_2 dissociation utilising solar energy 80−61452
H_2 photoelectrochem. prod., semiconductor-liquid junction systems 80−61453
H_2 production and utilisation, EEC R&D program progress and results 80−16767
H_2 production by biological and biochemical solar energy conversion 80−61454
H_2 production by direct solar energy conversion at sea 80−61456
H_2 production by direct thermal decomposition of H_2O utilising solar energy, thermodynamics 80−61450
H_2 production by H_2O decomposition using solar energy conversion 80−97813
H_2 solid, fundamentals, static props., review 80−75403
H_2 storage, transmission and distrib. 80−61439
H_2 thermochemical prod. by H_2O decomposition utilising solar heat 80−61451
H_3, form. and dissoc., kinetics, historical review, book contrib. 77−40527
$H_2(D_2)(T_2)$, ortho-para transition, catalytic-, radiation-, and self-induced conversion 77−90633
H_2O pyrolysis by solar-H_2 energy systems, thermodynamics 80−61448
H_3PO_4, technology development for commercial systems 80−30464
$^2H(\pi,\pi)$, expt. and theoretical work, present status, model testing, πN interaction 80−42699
He, condensed phases, neutron scatt. techniques and results, book contrib. 80−2230
He cooling systems, large, review of hydrodynamics and heat transfer 79−204
He film, adsorbed, NMR measurements 80−107605
He film, from two to three dimens. 78−47633
He, liq., two-dimensional electron system *(Japanese)* 78−51771
He, liq. films 78−60002
He mass spectrometer leak detection 77−67447
He, quantum solid behaviour, defect and impurity diffusion 77−7945
He, solid, theory and thermodynamic props., book contrib. 77−47646
He-Ne laser discharge tubes, design and technology *(Czech)* 79−72586
^3He and ^4He monolayer systems, book contrib. 79−99390
^3He, dynamic props., neutron scatt. studies 79−50972
^3He, liq., normal phase, Landau Fermi liquid theory and low temp. props., book contrib. 79−99386
^3He, liquid, low-temp. props. 79−37896
^3He, solid, mag., theory 78−38906
^3He, superfluid, expt. props. 78−59998
^3He superfluid, hydrodynamics and inhomogeneous states 80−49453
^3He, superfluid, order parameter, sp. ht., mag. props., sound propag., hydrodynamic props., book contrib. 79−99388
^3He, superfluid phases, theoretical and expt. work 77−76639
$^3He/^4He$ dilution refrigeration operating principles and heat exchangers 79−67310
^3He-^4He, superfluid, osmotic and mag. props. *(French)* 80−10733
^3He-^4He mixtures, review 78−60000
^4He, crit. phenomena and superfluid transition 78−59989
^4He, liq., dynamical behaviour close to λ-line, light scatt. 79−7717
^4He, liquid comprehensive theory 79−73361
^4He, superfluid, thermodynamic props. 77−39708
^4He superfluid film, dissipation by pinned vortex lines 77−80662
Hg determ. in environmental samples, neutron activation anal. methods, review 77−56284
$Hg_{1-x}Cd_xTe$, props. and appls., book contrib. 77−39834
HgI_2 detectors, state-of-art crystal growth and nucl. spectroscopic evaluation 78−41895
HgTe, zero gap semiconductor 77−31944
I photochemical laser, book contrib. 77−10912
I_2, use as test mol. in modern spectroscopy 78−90317
^{125}I-fibrinogen uptake test for detect. of deep vein thrombosis, review of current practice 78−7436
^{131}I, milk transfer coeff., review of meas. values 79−2141
^{131}I therapy, review of contamination and exposure hazards 80−41257
^{131}I-ortho-iodohippurate absorbed kidney dose calc., literature review 80−76841

reviews continued
(In,GA)(As,P) binary, ternary and quaternary, hydride vapour phase epitaxy, cryst. growth and props. 80−66434
In chalcogenides, cryst. struct. types 77−15392
In electrodeposition 79−83144
p-InP, prep. of single and bicrysts., epitaxial layers and polycryst. films for photovoltaic applic. 77−81211
InSb, charact. and phys. props. *(Japanese)* 80−39576
^{192}Ir, specific γ-ray constant and exposure rate constant 79−36187
K_2CuF_4, ferromag., orbital ordering *(Japanese)* 78−76224
KD_2PO_4, electron beam addressed light valve, optical processing appl. 78−83099
KD_2PO_4, optically addressed light valve, optical processing appl. 78−83101
$K_2Pt(CN)_4Br_{0.3}.3H_2O$, one-dimensional cond., phys. props. *(Japanese)* 78−30916
KrF, excimer lasers, state of art 80−95879
LaB_6, synthesis and props. *(Japanese)* 80−40255
Li, Auger and autoionisation spectra, collisional excitation mechanisms 77−19042
Li ion conductors 77−84979
Li powered pacemaker status and performance 77−81740
Li solid electrolytes 77−84980
Li solid electrolytes for electrochem. batteries 80−107524
Li-$SOCl_2$ battery, nonaqueous 79−100505
$Li_{0.5}Fe_{2.5}O_4$, microwave material, mag. props. 79−33504
LiF thermoluminescent detectors 80−68964
LiH (D), single crystals, electronic excitations *(Russian)* 78−72574
α-$LiIO_3$ single crystals, research work, review *(Chinese)* 79−69782
$LiNbO_3$:Fe, phase hologram storage and fixing, review 77−19210
Mg ternary alloys, constitution, review 77−90319
MgO, electronic excitations and luminescence *(Russian)* 78−72575
Mn chalcogenides-II-VI compound solid solutions, cryst. growth and physicochem. props. 79−14711
Mn, energy levels, Mn I to Mn XXV 78−21841
Mo-Mo bonds, review 77−76352
$MoSi_3$, high temp. material, coatings, powder metallurgy, review *(German)* 79−74295
N_2, N_3, spectroscopic data review 77−38680
NH, heat of formation, review and new value 79−70362
NH_3-metal, soln., thermophysical props. 79−77758
NH_4IO_4, high order phase transition, quadrupole coupling temp. depend. 80−54371
NH_4ReO_4, high order phase transition, quadrupole coupling temp. depend. 80−54371
N_2O, in atm., sources and sinks 77−37374
Na, Auger and autoionisation spectra, collisional excitation mechanisms 77−19042
Na fires, origination and mechanism form. and sedimentation of Na aerosols *(Czech)* 79−30956
Na permeability inactivation in squid giant nerve fibres, review of exptl. work 78−73154
Na/S traction batteries, development progress and problems 80−61326
Na_3AlF_6-LiF-CaF_2-AlF_3-Al_2O_3, electrolyte, exam. of phase equilibria, review 79−11590
NaI(Tl) scintillation counters, review of techniques and appl. 79−72197
Nb, RF superconductivity, appl. to particle acceleration, overview 79−31244
NbH(D), structs. phase diagrams, morphologies, prep. methods, book contrib. 80−25675
Nb_3Sn, supercond. props. and appls., state-of-the-art 79−33413
Nd:YAG pumped tunable sources, appl. to spectroscopy 80−58576
Ne, nonlinear laser spectroscopy, inside Doppler line *(Russian)* 78−21231
negative ion detachment cross sections for neutral gas targets 80−63796
Ni base alloys, production methods, review of powder metallurgy methods, mathematical-physical considerations 79−95970
Ni, impurity hyperfine fields 79−99518
Ni-H, in high press. H conditions, published results anal., atomic ratio calcs. 79−69254
O I and N I forbidden lines emission in nightglow, historical review 79−5699
O_2 analyser instrumentation and operation 78−69237
O_2, singlet state, form., quenching and reactions 77−29002
O_3, atmospheric, review of concs. over Australia 80−109223
O_3, global distribution, effects of pollutants, book contrib. 77−29429
^{17}O, NQR at natural isotope abundance, double reson. new techniques 80−53013
^{31}P NMR analysis of intact tissue 80−26432
Pb chalcogenide diode lasers, recent advances 80−5732
^{208}Pb region, finite Fermi systems 78−537
Pd-H, in high press. H conditions, published results anal., atomic ratio calcs. 79−69254
Pd-H and Pd alloy-H systems, review of props., book contrib. 80−24605
Pd-H and Pd alloy-H systems, α-β phase transform., compositional relationships, hysteresis of press. 80−60859
PdH, supercond., book contrib. 80−25037
$Pr(OH)_3$, low temp. heat capacity, thermophys. props. optical spectra, anal. of Schottky contributions, review 80−24611
Pu environmental contamination 80−101136
Pu recycle programme fuel cycles with reduced proliferation characteristics, review 79−18024
(π,π), elastic and inelastic, use in nuclear struct. determ. studies, review 79−85527
^{226}Ra fission expt. data, review *(Russian)* 79−49641
Rb atomic frequency standard, optical pumping phenomenon and techniques, review 77−65022
$RbMnF_3$, nuclear spin waves spectra, relaxation, parametric excitation, NMR dynamic shift *(Russian)* 80−11180
Ru, hazards and control in nuclear fuel cycle 79−36392
S air pollutants, large scale study in Canada 79−20979
S containing aerosols, physical charact. 78−96284
S cycle of NE United States, role of man-made S sources 80−26178
S-S bond chirality, biomolecule struct. and activity depend., review 78−27889
SF_6 electric breakdown mechanisms 78−59699
$(SN)_x$, preparation and properties 78−27389
SO_4^{2-} atmospheric aerosols, dynamics 78−96286
Sc compounds with O_2 donor ligands, literature review 79−99122
Si, (001) and (111), geometrical and electronic struct., review 80−80039
Si, charge transport properties 77−39851
reviews continued
Si concentrator solar cells, high efficiency, state-of-the-art design and processing 80−93958
Si crystal growth, for electronic devices 80−66419
Si devices, ion implantation damage 77−27899
Si epitaxial detectors 77−54406
Si epitaxial layer regrowth due to laser annealing mechanism, liquid and solid phase regimes 80−100712
Si, heteroepitaxial, prep. and props., book contrib. 79−83128
Si high efficiency solar cells, laser annealing, reviews 80−93976
Si, interstitials and lattice vacancies 78−10038
Si inversion layers 77−80842
Si, ion-implanted, disorders, nature and annealing behaviour 78−83836
Si oxidation, effect of chlorinated ambients 79−100278
Si oxidation, high press. techniques 79−100279
Si, oxidation, oxidation-induced lattice defects, review *(Japanese)* 78−39931
Si, oxidation in presence of Cl and Cl cpds. 78−53009
Si, reconstructed surface physics, review 80−10766
Si, ribbon growth via RTR technique, process update and material characterisation 78−76597
Si ribbons, edge-defined film-fed growth technique for solar cells 80−89138
Si, self-interstitials, vacancies and their clusters 77−80500
Si solar cells, current developments 80−108801
Si solar cells, perform. parameters of amorphous and polycryst. thin film cells 80−93882
Si solar cells, review of physics underlying recent improvements 80−93974
Si, status of defect studies 77−84742
Si substrate, defects 77−39597
Si, technology and physics 80−34353
Si, thermal oxidation, Cl effects 80−108622
Si, vertical etching, at very high aspect ratios 80−50744
Si/metal system, silicide form. by thin film interactions 80−49429
Si-based composite mats. and refractories 78−56609
Si-H amorphous film, reactively sputtered, prep. and props. 79−78889
Si-SiO_2 interface, electronic states 78−30992
Si-SiO_2 interface, inversion layer transport, radiation hardness effects 79−19673
Si-SiO_2 interface, props. 78−23170
SiC, radiation damage 77−80553
SiC, resist. to oxidation and corrosion at high temps. *(German)* 80−35357
SiN_x film reactive plasma deposition enhancement 77−77405
Si_3N_4, hot pressing, starting powder requirements, review 79−33987
Si_3N_4 reaction bonded, microstructure, formation, properties, phase composition 79−56947
SiO_1, vitreous, viscosity meas. 80−103513
SiO_2, electronic struct., review of spectroscopic and theoretical data 77−76749
SiO_2 films, on Si, role of H_2 79−69376
SiO_2, ion mobility and trapping 80−92985
SiO_2 on Si, thermally grown, breakdown 78−23172
SiO_2 surface, bonding of Cu^{2+}, Cr^{3+}, Co^{2+} ions, EPR, optical spectroscopy investig. *(German)* 79−95266
SiS, and isotopes, microwave spectra and consts., review 77−23493
Sm monochalcogenides, semicond.-metal phase transition 79−47017
Sm monochalcogenides, valence related optical and other studies, review 78−31215
SmB_6, mixed valent semicond., transport props. and electonic struct. 80−96877
$Sm_{1-x}R_x^{3+}S$, (R is rare earth metal), semicond.-metal phase transition 79−47017
^{151}Sm, gamma spectra, energy levels *(Dutch)* 80−47430
Sn polymorphic transformations (β→α), effect of impurities, exam. 80−7557
Sn reactions in aqueous electrolytic solutions 77−86337
SnO_2, optical props. 77−1673
$Sn_xPb_{1-x}Te$ mixed cryst., cryst. growth and assessment 78−80463
TaH(D), structs. phase diagrams, morphologies, prep. methods, book contrib. 80−25675
TaS_2(1T) pure and doped, Mott and Anderson localisation, commensurate phase transition 80−39641
Tc, radiochemical charact. and role in nuclear fuel reprocessing, review *(Czech)* 78−82496
^{99m}Tc-fibrinogen, usefulness of phlebography for pulmonary embolism patients 80−36093
Th-H system, supercond., book contrib. 80−25037
$ThBr_4$, new inorganic scintillators for nuclear particle detection, review of props. 79−45549
$ThCl_4$, new inorganic scintillators for nuclear particle detection, review of props. 79−45549
^{232}Th cycle, review of low cost fuel cycles using two separate fuels 79−45389
^{232}Th cycle for prod. of ^{233}U for thermal neutron reactors 79−45388
^{232}Th utilisation in reactor fuel cycles 79−45390
Ti, mechanical props. and appls. 79−66104
Ti powder metallurgy, developments 80−100801
Ti, production methods, review of powder metallurgy methods, mathematical-physical considerations 79−95970
Ti-Al-V (6,4 wt.%), corrosion fatigue behaviour, surgical implant material 79−39027
$TiS_2(Se_2)$, modelling contrasting semimetallic characters 78−43393
Tl chalcogenides, cryst. struct, types 77−15392
Tm monochalcogenides, valence related optical and other studies, review 78−31215
$(U,Pu)O_2$ FBR fuel cycle 80−47682
U, exploration and assessment technology survey 79−53564
U ore processing plant development in Spain *(Spanish)* 79−59231
U, review of Australian resources 79−87941
UF_6 conversion to UO_2 80−23099
UO_2, 5f-magnetic semiconductor, spectroscopic data, review 80−97299
UO_2, point defects and electronic props., theoretical survey 77−31657
UO_2, review of diffusion coeff. of fission product rare gases 78−33248
UO_2, vapour press. meas. up to 500K, critical point data prediction, present state of art 79−45347
^{235}U decay heat meas. and calcs. 80−13732
^{238}U, proton-induced fission, asymm. region, nucl. charge distrib. 78−4967
V-H(D), phase diagrams, struct. studies 80−66491

reviews continued
V_3Ga multifilamentary supercond. wire, fabrication and props., crit. review 79−38271
VH(D), structs. phase diagrams, morphologies, prep. methods, book contrib. 80−25675
VO^{2+} EPR in solids, review 80−11254
V_2O_5 and lower oxides, defect structures and related props. 80−59454
W, LEED and electron microscopic investigs. *(Hungarian)* 77−47654
Xe_2 coaxial-diode tunable vacuum UV excimer laser systems 77−54738
XeCl, excimers and excimer lasers 80−48217
YIG crystals, bulk growth from high temp. solns., props. 80−66413
YIG, elec. props. 79−99552
YIG, single cryst. growth from high temp. soln. 78−31315
Zn, elastic properties, compilation and review 78−27551
$ZnO-B_2O_3-SiO_2$ glass-ceramic-cement composites, review 79−38783
ZnS, epitaxial growth, appl. to electronic devices *(Japanese)* 80−55281
Zn_2SiO_4 ore, processing review 77−48365
Zr alloys, crystallographic texture, quantitative charact., review 78−21647
Zr, and its alloys, TEM obs. of irradiation damage, critical review 79−10879
Zr-Nb (2.5 wt.%), oxidation kinetics appl. to loss of coolant accidents, data review 78−19958
ZrO_2 films on Zr alloys, X-ray stress meas. 79−49694
revolution *see rotation*
revolving *see rotation*
rewinding *see winding (process)*
Reynolds number *see flow*
r.f. amplifiers *see radiofrequency amplifiers*
r.f. filters *see radiofrequency filters*
r.f. heating *see radiofrequency heating*
r.f. oscillators *see radiofrequency oscillators*
r.f. sputtering *see radiofrequency sputtering*
r.f.i. *see radiofrequency interference*
RHEED *see reflection high energy electron diffraction*
rhenium
see also nuclei with .....
activated sintering 77−52262
adatom, on W (110), dipole moment, field emission meas. 77−47674
adsorbed atoms and dimers, surface diffusion on W(211) 77−20183
adsorbed on W (110), long range interatomic interactions with coadsorbed Pd 80−59789
adsorption, of k, an (10$\bar{1}$0) surface, electron-adsorption props. 79−33192
adsorption of Au on low index planes, FEM 78−14597
adsorption of C, CO, H_2 and C_2H_4, work function changes *(French)* 77−28075
adsorption of CO, effects of surface steps on CO β state *(French)* 78−43250
adsorption of CO and electronic struct., XPS, UPS, and thermal desorption study 80−71571
adsorption of CO on basal (0001) and stepped |14(0001)×(10$\bar{1}$1)| planes 78−14594
adsorption of ethylene and acetylene on polycryst. and (0001) single cryst. Re surfaces 78−38947
adsorption of H within wide temp. range 80−10778
adsorption of Hg, work function change 77−7966
adsorption of K, work function changes, FEM obs. 77−72772
adsorption of O_2, CO, NO, and H_2O on (0001), XPS, UPS and temp. programmed desorption 80−71574
adsorption of O_2, effect of struct. defects, steps and kinks 80−29269
adsorption of O_2 on vicinal faces, mirror electron microscopy, LEED and AES obs. 79−65323
adsorption of Zr, low-temp. mobility, surface struct. 77−20197
Anderson-Gruneisen parameter, bulk modulus and compression curves 78−30690
atom, even config., parametric calcs. 78−82631
atom, nuclear K-X-ray satellites, Z=50-83, by α-bombard., 17.5-22.5 MeV 80−42984
atom, reson. Raman X-ray scatt., K-vacancy excited state widths 79−45661
atomic vibr. and fermion behaviour of HCP metals 80−6474
carburised, spectral emissivity at 0.65 μm 80−75374
catalyst, supported, chem. anal. method 77−25332
catalytic activity during adsorption of HD 79−69358
cermets with rare earth oxides, prep. and props. 78−27466
chemisorption of alkali metal ats., bond, adatom valence energy level broadening *(French)* 79−33176
chemisorption of CO on (0001) surface, role of d-orbitals, angular resolved UPS and thermal desorption meas. 80−40232
coadsorption of ethylene and O_2 *(French)* 78−85194
coating on cemented carbides, CVD, hardness *(German)* 78−64777
desorption of Na, neutral and ionic rates meas. via surface ionisation detector with field reversal 77−2710
desorption of O_2, electron-induced *(French)* 77−85853
determination in Mo-Re, W-Re alloys electrochem. method 79−16073
determination in W-Re alloy, polarography 79−16071
electrical resistance and Hall effect at low temp. *(Russian)* 78−47760
electrical resistance anisotropy, temp. depend. *(Russian)* 78−76041
electrical resistivity, quadratic contrib., 2 to 40K *(Russian)* 80−92874
electrical resistivity temp. depend., plastic deform. effects *(Russian)* 77−35909
electrodeposited from fused salts, (10$\bar{1}$1) texture *(Russian)* 80−92791
emissivity, integral hemispherical degree of blackness, 1200-3000K 78−43154
epitaxial film growth on sapphire *(Russian)* 78−35311
epitaxial growth *(Russian)* 77−43443
ESCA on in situ cleaned surface 79−83101
EXAFS, and L_α and L_β satellites 79−33861
Fermi surface, determ. from RF size effect 79−23889
Fermi surface, Landau quantum oscill. meas. in magnetostriction, stress and strain derivatives 80−107691
Fermi surface, RF size effect, temp. depend. 80−65424
Fermi surface, strain depend., from US vel. oscills. 78−84133
Fermi surface, stress depend., quantum oscills. obs. 78−91599
Fermi surface hydrostatic press. depend., de Haas-van Alphen phase shift meas. 80−54593
field emitter tip, condensation remoulding, field emission microscopy 78−2995
field evaporation, search for high ionic charges 78−35269
rhenium continued
filament, NH_3 decomposition at low press. above 500K 79−61906
filament adsorpt. of CO, H_2, temp. controller for filament heating appl. *(Japanese)* 77−51603
film, electrodeposition on Cu, packing defects, X-ray diffr. 77−1333
film, phase comp. depend. on thickness, deposition rate and substrate temp. 77−31915
film, prep. by laser melting 80−84859
flow stress temp. depend., effect of interstitial atom clustering and embrittlement *(Russian)* 78−34538
Hall effect, for single cryst., at 4.2K, under 12 kbar press. *(Russian)* 77−80762
HCP, elec. field gradient 78−14698
hydrosols, coagulation under action of US irradiation 80−58853
ion prod. in hollow cathode source 78−74525
isotope exchange reactions for O_2 and CO 77−70338
lattice dynamics, third order elastic consts. and thermal expansion 77−76505
metal losses during annealing in O_2, air, water vapour, high temp., low press. *(German)* 77−8856
metal oxides, high temperature interactions with Re 80−16665
metallo-ceramic, deform. and cold working by cold rolling *(Russian)* 78−56655
Mossbauer meas., elec. field gradients at ^{186}Os nuclei 79−47373
nuclear quadrupole alignment of $^{183,184,186,188}Re$ in single cryst. at low temps. 78−48091
oxide formation of clean surface, struct. rearrangement, field ion microscope obs. 77−28936
photodesorption of CO forming CO_2 79−52777
photoemission, from (0001) surface, effect of CO chemisorption 79−74060
plastic deform. rel. to low temp. sp. ht., supercond. *(Russian)* 78−31005
Raman scattering spectrum at room temp. 80−25373
resistive film, electron diffr., structure obs., heat treatment effects 77−51620
RF size effect, electron-electron scatt. 78−68025
RF size effect, Fermi surface dimensions determ. 78−91598
sedimentary rocks, epithermal neutron activation anal. 77−9153
single crystal growth by plasma heating 78−60569
sintered, preparation, thermal cond., linear expansion up to 1000K 79−61533
size effect in electrical resistivity *(Russian)* 78−87961
specific heat, elec. cond., emissivity, 1600-2400K 78−67835
sulphiding with H_2S 78−3078
superconducting film, T_c and residual resist., variation with coating thickness 78−47900
surface, adsorption of NO and water vapour *(French)* 79−69344
surface, field depend. of spectral line energy of He-H_2 adsorbate 79−78853
surface, He ion irrad., blistering, SEM obs. 78−87722
surface, interaction with F_2 and fluorides at low temp. and high press. 78−39700
surface, interaction with N_2^+ beam, reaction dynamics studied by XPS and thermal desorpt. spectrometry 80−93797
surface, interactions between adsorbed HD or D_2 and CO 79−86987
surface, long range and temp.-depend. interaction with alkali metal atom, theory 80−59802
surface, supported, CO chemisorption, activated surface processes, IR spectra 80−16724
surface, with adsorbed O_2, Na ionisation, field reversal and surface ionisation expts. 77−90232
surface (10$\bar{1}$0), struct., LEED anal. 80−75414
surface dopant in Mo, effect on fatigue *(Russian)* 80−7660
surface electron density crimping, Ashcroft potential, density functional calcs. *(Russian)* 79−82653
surface ionisation by laser-excited Li beam, quantum yield 79−87540
TF electron emitters props. obs. 80−66403
thermal desorption of CO and NO from Re single crystal surface *(French)* 78−22959
thermal expansion, 1200 to 2300K 80−103500
thermal expansion, X-ray determ., 113-1700K 78−67838
thermal expansion of single crysts., 2-300K *(Russian)* 79−55904
thermionic emission, work function in atmospheric pressure gases 78−76575
thermionic work function of low index planes 80−55255
thin film preparation, by laser melting *(Japanese)* 79−78909
vapour deposited tubes, hot burst strength, thrust motor appl. 78−44021
vapour-phase epitaxial growth *(Russian)* 77−59227
wear coefficients determ. using pin-on-disc apparatus 80−76366
Cs_2NaYCl_6:Re,Tm, fluorescence, two-step blue up-convertors 78−95603
$Cs_2TeCl_6:Re^{4+}$, vibronic transitions progressions, intensity distrib. 79−78735
$Cs_2ZrCl_6:Re^{4+}$, cryst., mag. circularly polarised emission 77−28613
films, plasma deposited, from $Re_2(CO)_{10}$ vapour decomp. 80−20799
Mo alloy:Re, effect of Re on mechanical props. 80−35196
MoO_2:Re, current carrier sign, Fermi surface cross section variations *(Russian)* 80−84420
MoO_3:Re, ESR and optical absorption obs. 77−36127
$MoSe_2$:Nb(Re), layered, elec. props., semicond.-metal transition 77−11922
$NaReO_4$, EPR spectra of paramag. centres and free radicals 80−108072
Pt-Re bimetal sheet specimens, interdiffusion, 1500°C *(Russian)* 77−62683
$Rb_2TeCl_6:Re^{4+}$, vibronic transitions progressions, intensity distrib. 79−78735
Re, atomic masses and mass differences, mass spectrometric obs. 77−42433
Re I, isotope shift meas. by HFS, methods, $5d^46s^26p$ level classification 79−49988
Re, pionic 4f→3d transition, pionic 3d state strong interaction level shift and width 79−98251
Re XLVIII X-ray spectra from laser produced plasmas 80−42981
Re:C, work function, graphitic layer formation 80−96966
Re:Ir, electric quadrupole orientation of $^{186,188-190}Ir$ 80−78140
Re/Al_2O_3, catalyst, Re-O_2 surface interactions; 77 to 773K 79−79286
Re/Os cosmochronology, nuclear correction factor 80−17485
Re-Al_2O_3 heterophase film, elec. props. rel. to Al_2O_3 content 77−15969
Re-Mo bimetal sheet specimens, interdiffusion, 1500°C *(Russian)* 77−62683
Re-O_2, surface interactions and catalysis, 77 to 773K 79−79286

rhenium continued
Re-O-Cl system, gas-transition metal interaction, kinetic model *(French)* 80−108740
Re_2, adsorbed on W (211) surface, dissoc., thermodynamics 78−87861
^{186}Re labelled EHDP preparation and possible use in osseous neoplasms treatment 80−56215
$^{187}Re/^{186}Os$ in Earth mantle, rel. to use of Os isotopes as petrogenetic and geological tracers 80−89989
^{187}Re-^{187}Os systematics in meteorites, rel. to solar system early chronology and Galaxy age 80−41778
n-Si, Re-compensated, deep levels, electron traps, photocond. 77−15902
Si:Re, diode, barrier capacitance and photocapacitance, uniaxial press. effect 77−20416
n-Si:Re, photon-capture cross sections of Re levels, spectral depend. 77−89726
Si:Re diode, photocapacitance and induced photocapacitance spectra 77−4404
n-Si:Re diode photocapacitance spectra, Re centre dissociation 79−90997
n-Si-Re Schottky contact barrier height meas. 80−65675
$SnO_2:Re^{4+}$, direct mechanism in supertransferred hyperfine interaction 79−23936
W:Re, polygonisation in diffusion process, glide dislocation interactions 80−38998
W-C-Re, vacuum melted, phase composition, struct. and props. 78−31403
W-Re immersion thermocouples for ferrous metal temp. meas., reliability/accuracy improvement 77−87767

rhenium alloys
see also rhenium compounds
Cr-Re binary system, isomorphous transition region, phase diag. *(Russian)* 77−55945
HCP-BCC binary systems, electronic struct. and supercond. *(Russian)* 79−33375
rare earth alloys, $R(Fe_xRh_{1-x})_2$, mag. props., Mossbauer spectra 80−25108
Ar-Re, phase diagram between 1866 to 1913K 79−100115
Co-Re, sputtered film, high coercivity and high hysteresis loop squareness 79−91259
Co-Re sputtered films, mag. props. and microstructures 79−82837
Cr-Re, dil. alloy, mag. susceptibility temp. depend., thermal expansion coeff. *(Russian)* 78−76225
Cr-Re, Invar alloys, thermal expansion, plasticity *(Russian)* 79−55907
Cr-Re, mag. excitation, neutron spectrometry 79−4654
Cr-Re, mag. excitations in commensurate antiferromag. phase 80−50079
Cr-Re, phase transformations and magnetostriction *(Russian)* 80−103869
Cr-Re, surface spin-density wave near T_N 79−91238
Cr-Re (0.18 wt.%), mag. excitations in longitudinal and transverse SDW phases 80−70946
Fe-Rh, mag. phase transitions, triple point 79−1672
La-Re-B, annealed and quenched, X-ray structural and phase anal. 78−11207
Mo-Re, cold worked, strength 78−31426
Mo-Re, integral hemispherical degree of blackness, 1200-3000K 78−43154
Mo-Re, prep. from reduction in Mo-Re-O system *(Russian)* 80−16225
Mo-Re, recovery after deform. and annealing, destrengthening mechanism *(Russian)* 80−97546
Mo-Re, solid soln., dislocation internal friction *(Russian)* 78−23748
Mo-Re, supercond. energy gap and transition temp., tunnelling meas. 79−56405
Mo-Re, σ phase alloy, critical mag. field, elec. resistance 80−54850
Mo-Re, thermoelec. power, 4.2 to 300K 80−70683
Mo-Re (5 at.%), enhanced lattice sp. ht. due to LF reson. modes 78−14882
Mo-Re alloy MR47-VP, dislocation struct. and fatigue damage during room temp. deform. *(Russian)* 79−20111
Mo-Re alloys, fractography of deformed samples *(Russian)* 78−19889
Mo-Re alloys, Re determ., electrochem. method 79−16073
Mo-Re film, electron beam deposited, supercond. transition temp. conc. depend. 77−28279
Mo-Re wire, high-strength, fracture mechanism *(Russian)* 77−25126
Mo-Re-C (0.3, 0.2 at.%) time-of-flight atom-probe expts. 80−55741
Mo_xRe_{1-x}, (x=0.4 and 0.6), search for strong coupling superconductivity 79−28441
$Mo_{1-x}Re_xCo$, mag. state of Co impurity, NMR exam. 78−27100
Nb-Re, dil., impurities effect on elec. resist. at 0.4 and 77.3K *(Russian)* 79−91196
Nb-Re, kinetics and thermodynamics of reaction with N_2 *(German)* 79−74415
Nb-Re and Nb-V-Re, supercond. crit. temp. and crit. field, Re alloying effect 77−85375
Nb-Re-N system, N_2 solubility and solubility limit *(German)* 77−4205
Nb-Re-N system, spectral emissivity, lattice parameter, initial rate of N_2 absorption *(German)* 77−4204
Nb-Re(Ru)-N, α-solid soln., thermodynamics *(German)* 77−12600
Ni-Re, dil. alloys, two-band Mott conductivity *(Russian)* 78−60118
Ni-Re, sintering, limited solid solubility, peritectic diagrams 77−28754
$NpRe_2$, mag. susceptibility 78−68182
Os-Re alloy, mag. suscept. of HCP transition metal alloys *(Russian)* 78−80138
Pt-Re dil. alloy, 0.5 at.%, ^{195}Pt NMR for local mag. susceptibility 78−84484
Pt-Rh thermocouple, Ta-sheathed, Al_2O_3-insulated, large decalibrations above 1330°C 78−24790
Pu-Pt-Rh, exam. of phases and crystal structure 78−80518
Pu-Rh, exam. of phases and crystal structure 78−80518
$PuRe_2$, mag. susceptibility 78−68182
Re-Al-Si , X-ray determ.of system *(Russian)* 78−19763
Re-Al-Si system, phase equilibria, $ReAl_{1.2}Si_{0.8}$, $ReAl_{1.25}Si_{0.75}$ prod., struct. 78−35357
Re-Cu-Al phase diagram, X-ray structural and microscopic anal. *(Russian)* 80−20895
Re-Fe-Al, physical-chemical investigation *(Russian)* 78−15362
Re-Hg, dil., anomalously high elec. field gradients below 0.05K 78−72442
Re-Ir (1 wt.%), positron annihilation, photon ang. distrib. meas. effect of deformation, annealing temp. *(Russian)* 78−35220
Re-Mo (up to 4.4 wt.%), X-ray diffr. study of conc. and temp. depend. of lattice parameters 79−94965

rhenium alloys continued
Re-Os nuclear chronometer, reliability, rel. to element rel. abundance 78−85919
Re-Ta-Mo, phase diag. *(Russian)* 77−59747
Re-W (up to 6.1 wt.%), X-ray diffr. study of conc. and temp. depend. of lattice parameters 79−94965
Re-W alloy, mag. suscept. of HCP transition metal alloys *(Russian)* 78−80138
Re-W/C multilayer films for X-ray mirrors 79−44992
Re-Zr-V, constitutional diagram *(Russian)* 79−56956
(Re-Mo)-Pt bimetal sheet specimens, interdiffusion, 1500°C *(Russian)* 77−62683
Re_5Ge_3, RF sputtered, supercond. crit. temp. 78−14853
$ReSi_2$, atomic volume deviations and supercond. T_c and elec. cond. 80−75203
Re_5Si_3, X-ray cryst. struct. determ., microhardness rel. to Re content 80−84142
Rh-W disc bonded to graphite, for X-ray tube rotary anodes *(German)* 80−105760
$Sc_{(3)}Re_2Si_3$, X-ray cryst. struct. determ. 80−39009
Ta-Re, kinetics and thermodynamics of reaction with N_2 *(German)* 79−74415
Ta-Re (20 at.%), with N_2, spectral emissivity, N_2 absorption rate, N_2 solubility, thermodynamic data *(German)* 77−25026
Ta-Re film, amorphous, temp. stability 78−63948
Ta-Re-Y-La alloy, Y, La determ., spectrochem. method 79−16076
Ta-Re-(N), deformed at 77K, dislocation substruct. 77−32647
$ThRe_2$, mag. susceptibility 78−68182
U-Re, high temp. phase diagram, thermodynamic props. of refractory metal solutes in liquid U 77−25022
U-Re system, γ-solid solns., thermo-EMF, temp. depend. *(Russian)* 79−73496
U-Re-C, crystalline struct. of a compound 77−25023
URe, mag. susceptibility 78−68182
$U_4(Re_{0.17}Si_{0.83})_{13}$, X-ray diffraction anal. of crystal struct. *(Ukrainian)* 78−83773
$U_4Re_7Si_6$, X-ray diffraction anal. of crystal struct. *(Ukrainian)* 78−83773
URh_3, magnetisation density 78−52203
V-Re, and V-Nb-Re, supercond. crit. temp. and crit. field, Re alloying effect 77−85375
V-Re, X-ray K-emission spectra *(Russian)* 77−55851
V-Re alloy, thermo-EMF and resistivity at 0 to 1500°C 77−43571
V-Re system, discovery of supercond. A-15 phase 78−88060
V-Rh alloys, short range atomic order exam. *(Russian)* 78−63696
V_3Si-SiO_x-Mo_3Re_2, supercond. tunnel junctions 80−107961
W-Mo-Re heat resisting alloy MVR-27-VP2, high-temp. emissivity and resistivity 77−35727
W-Re, amorphous wire, elec. resist., 2-20K, dimens. and mag. field depend., quantum localisation 80−39547
W-Re, dil., excess resistivity, temp. depend. 78−68011
W-Re, integral hemispherical degree of blackness, 1200-3000K 78−43154
W-Re, ion irradiated, recovery behaviour studied by field ion microscope 80−29074
W-Re, neutron irrad. effects on phase stability free energy changes 79−11566
W-Re, optical props., temp. depend., 4.2-300K 78−2874
W-Re, phase form. and diffusion interaction with liquid Al, under weightlessness *(Russian)* 78−22876
W-Re, sigma phase stability and irrad. effect 78−11200
W-Re, substruct. stability of single crysts. on high temp. annealing *(Russian)* 77−66666
W-Re, surface diffusion 79−56048
W-Re, thin wires, fatigue limit and tensile strength 80−25834
W-Re, wire, elec. resistance, low-temp. continuous and cyclic heating effects, compared with W 78−92370
W-Re (3%), W adatom-substitutional Re atom interaction, FIM obs. 77−89626
W-Re alloy, effect of thermal prehistory on resistivity meas. 78−3241
W-Re alloy, elec. resistivity meas. near conc. anomaly, 300 to 1200K 77−35911
W-Re alloy, prep. by powder metallurgy technique, appl. in lighting industry 80−29904
W-Re alloy thermocouples, calibration, 77 to 290K 77−57324
W-Re alloys, anomalous conc. depend. of elec. resistivity 77−35917
W-Re alloys, polarographic determ. of Re 79−16071
W-Re alloys, Re determ., electrochem. method 79−16073
W-Re alloys, sintered, preparation, thermal cond., linear expansion up to 1000K 79−61533
W-Re alloys, thermal EMF instability, heat treatment effects 80−75553
W-Re amorphous alloys, phase-slip and localisation diffusion lengths 80−107747
W-Re fibre-reinforced Ni-base refractory alloy, struct. and props. *(Russian)* 77−59721
W-Re film, amorphous, temp. stability 78−63948
W-Re film, obtained by electron beam volatilisation and vac. condensation, props. *(Russian)* 77−24490
W-Re films, amorphous, one-dimensional quantum localisation 80−80413
W-Re thermocouple, thermal EMF var., stability 77−41604
W-Re wire, CVD coatings of SiO_2 and Mo, for neurological electrode, elec. cond. and bending props. 78−11752
W-Re/C multilayer, periodic and near-periodic, small-angle interferences of reflected X-rays 79−94846
W-Re(Mo)(Cr), powder mixture, activating effect of Group VIII metals on alloy form. during sintering 77−59728
$W_{0.65}Re_{0.35}$, search for strong coupling superconductivity 79−28441
Y-Re-B, annealed, and quenched X-ray structural and phase anal. 78−11207
Zr-Nb-Mo-Re, alloying effect on dislocation core struct., determ. by discrete lattice modelling 78−30618
ZrC-Re, adsorption of H 79−19467
ZrC-Re, in H_2, thermionic emission residual gas effects 78−48269
ZrC-Re, spectral emissivity, 1400 to 2500K, surface relief and composition 77−24420

rhenium compounds
see also rhenium alloys
alkali halide:ReO_4^{2-}, frozen solns., absorpt. spectra, 4.2 to 300K 79−87467

rhenium compounds continued
alkali hexahalogeno compounds: $ReCl_6^{2-}$($ReBr_6^{2-}$), low symm. splittings in vibronic spectrum due to phase transitions 80−55161
alkali metal hexahalogenostannate: $ReBr_6^{2-}$, vibronic transition $\Gamma_7(^2T_{2g})\rightarrow\Gamma_8(^4A_{2g})$, intensity distrib. 80−45142
alkaline earth-ReO_6, ordered or perovskite type struct., magnetic and elec. props. 79−65053
hexaoxy ions, octahedral, mol. consts. calcs. 80−106317
mass spectrometer gas-chromatography chemical analysis Re cpds. formed from Re filament 79−74465
$AgReO_4$, NQR 77−20745
Co_2RhS_4, mag. semicond., mag. and elec. props. 80−93121
Cs_2ReF_6(-Cs_2GeF_6) cryst., ReF^{-2}_6 ion electronic absorpt. spectra, Raman, visible, IR and UV, liq. H and room temps. 77−77193
Cs_2SnCl_6:$ReCl_6^{2-}$, luminesc. and absorpt. spectra, relax. processes 77−85779
$ErRh_4B_4$, ternary superconductor, paramagnetic relax. effects 78−68112
$FeRh_2S_4$, mag. semicond., mag. and elec. props. 80−93121
KCl:ReO_4^- nonlinear absorption for CO_2 laser pulse compression and mode locking 80−74443
KCl(Br):ReO_4^-, vibronic absorption spectra 78−10924
K_2ReCl_6, displacive phase transition, thermal expansion meas. 78−10188
K_2ReCl_6, struct. props. and lattice dynamics, mag. struct. 80−44268
K_2ReCl_6-K_2ReBr_2 solid soln., mixed ligand complexes 77−72585
$KReO_4$, NQR and thermal expansion 77−20745
K_2SnCl_6:$ReCl_6^{2-}$, (K_2PtCl_6:$ReCl_6^{2-}$), luminesc. and absorpt. spectra, relax. processes 77−85779
$La_6Re_4O_{18}$, X-ray cryst. struct. determ. Patterson and Fourier methods *(French)* 79−14745
$(Mn_xRe_{1-x})_2(CO)_{10}$, Raman spectra, intramol. vibr. coupling, ^{13}C substitution 79−47431
$Mn_xRe_{1-x}(CO)_5X$(X=Cl, Br), $0<x<5$, vibr. spectra in the 2000 cm^{-1} region of mixed and isotopic crystals 78−84585
NH_4ReO_4, NQR and thermal expansion 77−20745
$NaReO_4$, NQR 77−20745
$NdReSi_2$, cryst. struct. determ. 78−95037
PbO-Re_2O_7 system, gas phase components obs. using mass spectrometry *(Russian)* 79−96354
Pu-Re-C systems, phase relationships 77−21127
RbI:ReO_4^-, IR absorpt., half width, temp. depend. *(Russian)* 79−78722
Rb_2SnCl_6:$ReCl_6^{2-}$, luminesc. and absorpt. spectra, relax. processes 77−85779
Re complex, $((C_2H_5)_4N)_2$ [ReI_6], electronic resonance Raman spectrum, 80K *(German)* 79−82982
Re complex, $AsPh_4ReOCl_4$, cryst. and mol. struct. determ. 77−47390
Re-Hg-O system, solid state synthesis of 5 crystn. compounds, thermal and X-ray anal. *(French)* 79−66281
ReB_2, electron struct., Fermi energy and surface, bonding 80−20076
ReB_2 possibility of semicond. props., rel. to atomic volume 77−69317
$ReBr_6^{2-}$ doped K_2PtCl_6 type crystals, vibronic side band intensity distrib., $\Gamma_7(^2T_{2g})\rightarrow\Gamma_8(^4A_{2g})$ transition 80−10609
$ReBr_6^{2-}$, IR luminesc. spectra 79−45745
$ReBr_6^{2-}$, in cubic crysts., luminesc. spectra and relax. processes 78−68552
Re_3Br_9, atomic clusters, electronic struct. and photoelectron spectra 80−69287
$Re_2(CO)_{10}$ vapour decomposition, for plasma deposited Re films 80−20799
$Re(^{12}CO)_{5-y}(^{13}CO)_yX$(X=Cl, Br), $0<y<5$, vibr. spectra in the 2000 cm^{-1} region of mixed and isotopic crystals 78−84585
$Re(CO)_5Cl$(Br)(I), thermodynamic props. tabulation 79−24808
$Re(C0)_5Br$-$Mn(C0)_5Br$, polycryst., ν(C0) vibr. intermol. Raman intensity transfer 80−60564
$ReCl_5$, photoelectron spectra 79−821
$ReCl_6^{2-}$ doped in various host lattices, luminesc. spectra and vibr. struct. 79−43024
$ReCl_6^{2-}$ doped K_2PtCl_6 type crystals, vibronic side band intensity distrib., $\Gamma_7(^2T_{2g})\rightarrow\Gamma_8(^4A_{2g})$ transition 80−10609
$Re_2Cl_8^{2-}$, in acetonitrile and dichloromethane solns., 300K, emission spectra and lifetimes 79−59447
$Re_2Cl_8^{2-}$, $Re_2Cl_8^{3-}$, ab initio calcs. of metal-metal bond 78−82633
$Re_2Cl_8^{2-}$, spectral assignment, metal-metal bonds, SCF Xα SW calcs., relativistic corrections 80−53006
$(Re_3Cl_{12})^{3-}$, atomic clusters, electronic struct. and photoelectron spectra 80−69287
$Re_3Cl_{12}^{3-}$, cluster ground state electronic struct. SCF Xα SW calc. 79−3607
Re_3Cl_9, atomic cluster, electronic struct. and photoelectron spectra 80−69287
Re_3Cl_9, cluster ground state electronic struct. SCF Xα SW calc. 79−3607
Re_3Cl_9 metal cluster complexes, He(I) photoelectron spectrum, SCC DV Xα calcs., $Re_2Cl_8^{2-}$ comparison 80−28063
$Re_3Cl_9^-$, electronic struct. and metal-metal bonding, HMO calcs. *(Russian)* 78−1118
ReF_6, cryst., Raman and absorpt. spectra, Jahn-Teller effect 78−6675
ReF_6, electron affinities from collisional ionisation with alkali atoms 78−55226
ReF_6, ionis. energies, optical spectra, Dirac-Slater model 77−83488
ReF_6^+, force consts. and vibr. props., GVFF calcs. 77−14417
ReF_7, generalised quadratic valence pot. calcs., Wilson's F-G matrix 79−93966
ReF_7, molecular vibr. calc. 79−18169
$ReNCl_4^-$, EPR in Ph_4As[$RuNCl_4$], hyperfine splitting and spin Hamiltonians 78−64272
ReO_3, absorpt. of H_2, electron diffr. obs. of H_xReO_3 phase 79−60513
ReO_3, coeff. of linear thermal expansion, 100-500K 79−10972
ReO_3, compressibility collapse phase transition, NQR study 80−39282
ReO_3, cubic lattice stability, screening effect on vibrs. 80−75356
ReO_3, de Haas van Alphen signal anal. by linearly recursive approx. 78−91603
ReO_3, elastic consts. determ. 77−11617
ReO_3, elastic stiffness const. determ. by Brillouin scatt. 78−19494
ReO_3, electronic density of states calc. for perovskite struct. cryst. 77−76720
ReO_3, Fermi surface, pressure induced anomaly 79−19505
ReO_3, hardness anisotropy, comp. depend. 79−29181
ReO_3, intra- and interband plasmons, inelastic electron scatt. exam. 78−72098
rhenium compounds continued
ReO_3, lattice parameters, thermal expansion 291 to 464K, Bond technique meas. 78−75617
ReO_3, mag. breakdown above compressibility collapse transition 80−103617
ReO_3, open orbits in cryst., EM induction meas. 79−73421
ReO_3, phase transition at high press., Fermi surface and X-ray studies 79−65188
ReO_3, positron annihilation, Fermi surface shape 79−46997
ReO_3 related oxides, elastic strain energy of matrix between shear planes, array microstruct. 78−43033
ReO_3 related oxides, formation energy of isolated crystallographic shear planes 78−43032
ReO_3 type lattice, group-theoretical symmetry anal. of vibr. *(Russian)* 80−10610
ReO_4^- doped alkali halide, saturable absorber at 10.6 μm 80−53384
ReO_4^-, in halide salt aqueous solution, absorpt. spectra, 4.2 to 290K *(Russian)* 78−60499
ReO_4^- ions in $R(ReO_4)_3.4H_2O$, R=Nd, Eu, Gd, Dy, vibrs. rel. to static field *(Russian)* 78−76470
ReO_4^- molecules in alkali halide matrices, CO_2 laser saturation of internal vibr. modes 78−86922
ReO_4^-, valence level electron struct. by XPS 77−4712
ReO_3Cl, near UV absorpt. spectra, dynamical Jahn-Teller effect 78−86881
$(Re_2OCl_{10})^{3-}$, reson. Raman, IR and electronic spectral studies 79−10118
ReP_4, synthesis and cryst. struct. 79−99124
$Re_{12}P_{26}$, binary crystals containing plane Re_4 clusters *(French)* 80−19774
ReS_2, layer cryst., dislocations and domain struct. 80−39102
ReS_2, prep., struct. 79−38774
$ReSe_2$, layer cryst., dislocations and domain struct. 80−39102
$ReSe_2(Te_2)$, high-press. modifications 77−51354
$ReSi_2$, atomic volume deviations and supercond. T_c and elec. cond. 80−75203
Rh_2ReO_6, preparation, X-ray powder diffractograms 78−76615
Sm_3ReO_8, cryst. struct. determ. *(French)* 77−4073
U-Re-C systems, phase relationships 77−21127
$V_{1-x}Re_xO_2$ ($0\leq x\leq 0.15$), insulator-metal transition, DTA, X-ray, mag. and elec. meas. 78−10353
Xe-MF_6, M=W, Mo, U, Re, Ir, charge transfer interactions, VUV and IR obs. 78−50664
$(Y,Re)_{3-x}Ca_xGe_{5-x}Ge_xO_{12}$, garnet films, LPE growth for bubble memory appls. 77−11813
Y-Re-Si system, phase diagram at 800°C 79−38806

rheology
see also biorheology; plasticity; viscoelasticity
acrylic dispersions, conc., shear thinning and thickening rheology 77−48691
acrylic dispersions, shear thinning and thickening rheology 77−52676
acrylonitrile-styrene copolymer melts, rheological behaviour *(German)* 77−51012
amorphous plastic injection moulding, frozen-in orientation, pressure loss during filling 79−77047
anisotropic micropolar fluid theory 80−31515
aqueous polymer solns., shear stress and normal stress meas. using cone-and-plate rheogoniometer 80−1496
basaltic lava flows, degassing effects on rheology 79−12115
Bingham plastic flow through annuli 80−64521
biomacromolecules, rigid, modelling approaches of hydrodynamic props. 80−61613
bitumen, rheological model of Maxwell-Norton type *(French)* 79−64614
bitumen constitution, struct., and rheological props. *(French)* 79−18853
bitumen-silica composites, dynamical mechanical props. 80−58996
bituminous pitch oils, flow curves, mag. field effect 80−33553
BKZ fluid, shear, integral rheological relations 77−11159
butadiene-styrene block copolymer, star shaped, rheological props. 77−68542
butadiene-styrene block copolymer, viscoelastic props. 79−8336
butadiene-styrene three-block copolymer, rheological props., 60-110°C *(Russian)* 79−23292
cement paste, mathematical model relating flow curve to water/cement ratio 78−34100
ceramic composition rheological meas. device for 20° to 90°C and constant moisture content 78−85079
ceramic suspensions, effect of grainy filler 80−43685
chromorheology, exptl. verification of numerical solns. of elastic-plastic problems 80−48659
chromorheology, new exptl. method 80−48658
circular plates, thermoviscoelastic anal. of a thermorheologically simple material 80−10161
clays, heat treatment, effect on rheological props. of enamel slips 80−60809
coating, rheological characterisation with regard to appl. and film formation 79−77970
cohesionless granular materials, flow at high deformation rates and low stress levels 78−90810
colloidal dispersion dynamics, review 80−71956
colloidal dispersions, microrheology, Brownian diffusion of doublets of spheres 77−4942
colloidal dispersions, microrheology, chains of spheres in shear flow 77−7354
colloidal dispersions, microrheology, pairs of interacting spheres in shear flow 77−7352
colloidal dispersions, primary and secondary doublets of spheres in shear flow 77−7353
colloids, nonlinear rheological behaviour and shear dependent struct. 79−7358
colloids, rheological props., terminology and symbols 80−26065
composite material viscoelastic properties modelling 78−75082
concentrated disperse systems, min. energy dissipation principle 77−72339
concentrated disperse systems, non-Newtonian shear viscosity in steady flows 79−81957
concentrated disperse systems, non-Newtonian viscosity model 79−77231
concentrated dispersions, review 77−19578
concentrated suspensions, self consistent field theory *(German)* 77−14972

rheology continued
concrete, workability, predictions from viscosity-elasticity analogy, effect of aggregate volume conc. 77−25087
condensed systems *(French)* 78−22310
cone and plate oscillatory motion, secondary flow effects, perturbation anal. 78−1618
cone and plate rheometer, press. distrib. in gap for viscoelastic fluid with high shear rate *(German)* 77−51143
continuous models of suspensions, nonequilib. thermodynamic approach 80−28479
convective heat transfer in coaxial horizontal channel, influence of electro-viscous effects 79−77100
cooperative diffusion in temporary network 78−77820
Coulomb contributions to rheology *(French)* 79−18730
creep theory in nonuniform hereditary-ageing media 77−35059
crosslinked polymer systems, probabilistic theory 80−19314
crude oils, heavy, and solvents, flow of mixtures through porous medium *(Spanish)* 79−98800
cumene, films, thin, wetting, rheological characts. determ., capillary method 78−51788
cyclic loading, elementary and classical rheological models, global behaviour *(French)* 80−22197
n-decane, films, thin, wetting, rheological characts. determ., capillary method 78−51788
dense suspensions, rheological behaviour 79−32431
dielectric suspension, convective heat transfer, rheodynamics, in horizontal coaxial cylindrical channel 78−59494
dilute polymer solns., rheology, role of rigidity constraints 79−81928
dipolar dumbbells in a viscoelastic Oldroyd liquid, dilute soln., electric field effect on rheological behaviour 80−6009
disc rotating in non-Newtonian liquid, rheodynamics 77−15067
disperse hydrocarbon system electrokinetic and polarisation phenomena *(Russian)* 79−83514
disperse system, plastoviscous, cone plastometer for strength props. determ. 80−76426
disperse systems, plastic, laminar flow in circular tubes 80−87798
dispersed system, concentrated, rheology and principle of minimum dispersed energy *(French)* 78−22313
dispersion systems, concentrated, shear thickening effect 77−7351
drag reducing polymer solns., dynamical behaviour, mol. conformation and optical props., expt. and rheological model 79−60034
dumbbell kinetic problem, rheology, Langevin approach 78−42633
dumbbells, nearly-Hookean, dilute soln., rheological equation of state 80−100321
Earth lithosphere bending at trench, elastic-perfectly plastic anal. 78−81135
Earth upper mantle, micromechanisms of flow and fracture 78−69331
elastic fluid, homogeneous and inhomogeneous stretching 79−86392
elastic viscoplastic body, differential rheological eqn. *(Ukrainian)* 78−55617
elastohydrodynamic contact, rheological model 80−33544
elastohydrodynamics, solns. to steady-state problems 77−35107
elastomer-oligomer system, flow props. *(German)* 77−28868
electrochemical solutions, diffusion coeff. determ. using pipe wall electrode 79−14947
electrolyte solutions in glycerol, investigation by US shear strains 80−88266
electrorheological suspension, effect of contamination *(Russian)* 77−44519
electrorheological suspension flow, vibr. effect *(Russian)* 80−53877
electrorheological suspensions, spontaneous rotation of dielectric rotor 77−15130
electrorheological suspensions, struct. form in electric fields *(Russian)* 77−86390
electrorheological suspensions, struct. form. in electric fields *(Russian)* 77−86391
elongational flow in non-Newtonian fluids, effects 77−23998
emulsions, concentrated, rheological props. 80−99981
emulsions, unstable water-oil type, rheological props. obs. non-Newtonian obs. 77−75866
enamel slips, control of rheological props. 79−29136
ethylene methacrylic acid polymer and Na salt, ionic aggregation and melt rheology, H_2 bonding effect 78−67159
extensional flow capillary rheometer for extensional viscosity meas. 78−55704
extensional rheometer, elongation props. meas. of polymer melts 80−6004
ferromagnetic suspension, magnetorheological characts. meas., errors 80−33550
ferrosuspension, magnetorheologic characts. *(Russian)* 77−65786
ferrosuspensions, mag. field effects on mech. props. 78−87321
fibre suspension, rheology, rel. to turbulent drag reduction 78−22315
fibrous structures, mech. relax. theory 78−13916
filled polymer melts, appl. of parallel-plate plastometer 79−77036
flexible macromolecule solutions, mol. models for mech. props. 79−59957
flow curve model, drilling muds, cement slurry appl. *(French)* 79−64615
flow curves determ. by method of representative viscosity *(German)* 77−68642
flow regulating system operating with Newtonian and non-Newtonian fluids *(German)* 80−1535
flowing viscoelastic fluid, bubble and solid particle separation through apertures *(German)* 79−37389
fluid, effects of normal stresses, interference meas. method 78−94624
forced convection with rheological systems, review 79−1222
forsterite, ^{18}O self-diffusion expts., high-temp. creep implications 80−81870
gas-solid fluidisation, solid pot. flow around rising bubbles 79−86501
gels, props. by Weiler-Rhebinder method, polymer conc. *(Russian)* 78−53274
glass fibre reinforced polyethylene melt, rheological props. 79−37273
glass fibre reinforced polypropylene, effect of injection speed on fibre orientation 79−4944
glass workability rel. to melting history, microstruct., apparent liquidus temp., mechanical props. 80−11633
glassy state and highly viscous liq., rheology 80−70130
graphite-epoxy resin, hydrothermal ageing 77−52367
heart muscle preparations, isolated, viscoelastic props., math. model *(German)* 79−53167
rheology continued
heating of viscous and non-Newtonian fluids on a rotating disk 79−77095
heterocyclic polymer, rheological props. conc. soln. 79−68671
hydrodynamic stability of structurally viscous medium, effect of elastic factor 80−19303
hydrodynamic thermal breakdown in viscous fluid, Couette flow between cylinders 78−83391
hydroxylpropylmethyl cellulose, aq. solns., turbulent flow characts., friction-reducing props. 78−94649
ice, columnar grained, rheology 79−57044
inertial effects in rheometrical flow systems, orthogonal rheometer theory 77−51016
isothermal melt spinning, Lagrangian and Eulerian viewpoint 79−7357
journal bearing rheometer, experimental investigations *(German)* 80−6014
kaolin, aq. suspension, flocculated and dispersed, rheological behaviour in pipe flow 79−37361
kaolin suspensions, aq., flocculated and dispersed, rheological behaviour in pipe flow 80−64510
lamellar liquid cryst. phases, form. at liquid-liquid interface, rheological props. 79−99063
laminar viscoelastic boundary layers, role of fluid relaxation time 79−81829
landslides, hydrogeological conditions rel. to stability, rheology *(Russian)* 77−25683
Langevin analysis of dumbbells with hydrodynamic interaction 79−77042
lava, field meas. 79−12114
LDPE melt, nonlinear shear creep and constrained elastic recovery 78−87318
liquid lamellar liquid crystalline system, rheological props. 79−23289
liquid on surface of vibrating acoustic radiator 79−94573
longitudinal instabilities in exit flow from a slit, surface tension origin 79−98684
LPDE melt, tensile stress overshoot in uniaxial extension, single integral constitutive eqn. 80−1507
lubricant, shear rheological behaviour at high press. 80−35342
lubrication of cylindrical surfaces with Rivlin-Ericksen fluid *(French)* 77−80126
lunar lavas, effusion rates and rheology 77−60654
lyotropic liquid crystals formed by phosphated polyoxyethylene surfactants, n-hexane, water, rheological props. meas. 77−54947
macromolecular solutions, kinetic theory and rheology 77−7424
macromolecules, coiled linear, effective diffusion tensor of chain mol. in shear flow 77−50579
magnesial refractory concretes, cast. props. 80−89306
magnesite-chromite powder, exam. of rheological characts., compaction 78−60628
magnesite-phosphate mortar, rheological props. 77−23927
magnetic micro-rheometer evolution and theory 80−92099
magnetic suspensions, magnetic and rheological props. *(Russian)* 79−55350
maleate-acrylate polyester resin, with phenol and glass microspheres, rheological behaviour 78−53267
mantle return flow and non-linear rheology 80−46152
material functions for steady circ. shear in orthogonal rheometer 79−23385
Maxwell models, uniaxial elongation 77−42751
measurement of rheological properties of fluids with rotary viscosimeters under nonisothermal conditions 79−68664
metals, rheological interpretation of planar deformed state in extremal friction regime *(Russian)* 80−64385
metals and alloys, yield criterion, rheological interpretation *(Russian)* 80−21014
motion with constant stretch history, algorithms 77−62175
mullite-based dispersed refractory system, rheological props. at high temp. 77−16629
multiphase non-Newtonian systems, rheological props. variation in barotreatment 80−19304
nearly viscometric glide bearing fluid *(German)* 79−81830
non-Newtonian fluid, kinematical tensors, rheological eqns. of state 78−30326
non-Newtonian fluid, stretching jet profiles, simple rheological models 77−75955
non-Newtonian fluid rheometry, flow curve evaluation 78−83352
non-Newtonian fluids, capillary and slit methods of normal stress measurements 80−43807
non-Newtonian fluids, mass transfer from cylinders to power law fluids 80−83826
non-Newtonian fluids, mass transfer from spheres to power law fluids 80−83825
non-Newtonian fluids, rheological props., pressure induced change of yield stress 80−53736
non-Newtonian liquid, hydraulic behaviour *(Italian)* 78−38376
non-Newtonian solid-filled systems, transfer phenomena, interface-adjoining phase struct. effects 79−77099
nonisothermal flow of anomalous systems in pipes, rheological aspects *(Russian)* 80−43775
nonisothermal flow of anomalously viscous liquids in channels of screw extruders 80−19305
nonlinear behaviour 77−39267
nonlinear rheological media, variational criterion of material stability 80−28480
nonlinear viscoelastic materials, stress formulation relations *(German)* 79−76987
nonlinear viscoplastic media, dispersion in circular tubes for laminar motion case 77−58626
nonlinearly viscoplastic liquids, rheodynamics 78−83265
nonviscometric flow, drop suspension model, deformation and vorticity 79−60022
nylon 6.6 in 100% H_2SO_4, primary normal-stress difference coeff., dependence on molecular wt. 80−87752
4-n-octyl-4′-cyanobiphenyl, smectic A liq. cryst., shear-induced textures and rheology 78−91228
olivine, rheology rel. to thermal stability or instability of asthenospheric shear flow 78−20370
olivine in mantle, local nonsimilarity boundary layers rel. to shear flow beneath oceanic plates 78−40521
orthogonal stagnation flow, a framework for steady extensional flow experiments 80−1653

rheology continued
paraffin oil, aq. emulsion, polyelectrolyte stabilised, mech. props. 79−39223
phenolic novolac resin-rubber mixture, glass transition, mixing ratio effect *(German)* 79−77732
physical constants of a flowing continuum, theory 79−60012
pigment dispersion rheology, kinetic model, expt. results 79−7361
pitch and coke-pitch disperse system, viscoelastic props. 80−1500
plastic, fluid, charact. by torque rheometer 77−32751
plastic disperse systems, generalised flow theory with account of wall effect 78−87320
plastic powder compact rheological characteristics *(Japanese)* 78−95770
plastics, extrusion props. prediction using capillary rheometer 79−90204
Poiseuille flow of viscoelastic fluid between eccentric cylinders 80−1652
Poiseuille flow viscosity of a couple stress fluid 79−25011
poly-1-olefin melts, steady-state and dynamic rheology 79−59956
poly-α-methylstyrene, shear flow, transient stress effects, network rupture constitutive eqn. 77−11157
poly-γ-benzyl-glutamate, conc. soln., rheology, liq. cryst. transition 79−94574
poly-N-vinylcarbazole, polymerisation, struct., props., elec. charact., review 79−41972
poly-p-aminobenzhydride terephthalamide in dimethyl sulphoxide soln., rheological study 80−43683
poly-p-phenyleneterephthalamide solns., rheological props. comparison with nylon 6,6 soln. 80−6007
polyacrylamide, very dil. drag reducing soln., nonlinear viscoelastic props. 79−7355
polyacrylamide in glycerine-water dilute soln., rheological props. in extensional and shearing expts. 77−58630
polyacrylamide Separan MG200, aq. soln., rheological props. 80−64507
polyacrylamide solution, drag reducing, rheological props. meas. 79−37271
polyacrylamide solution, tube flow, friction and convective heat transfer, rheological changes effect 79−1220
polyamide coating on steel roller, experimental exam. of contact parameters 78−68842
polyamide in isoamyl alcohol solutuibs, spin coating process modelling and appl. 78−27655
polyamide-hydrazide solns., rheology 79−64978
polyanide, thermorheological and mech. props. 79−96067
polyaryloxyphosphazene copolymers, thermal, morphological and rheological props. 80−103265
polybutadiene, high cis-1,4, orientation effects induced by shear rate in capillary rheometer 77−51014
polybutadiene, hydrogenated, linear and star branched, melt rheology 80−23978
polybutadiene, linear and star branched, rheology 80−23977
high cis-,1,4-polybutadiene, orientation effects induced by shear rate in capillary extrusion 77−48389
polybutadiene soln., rheological behaviour of flow patterns around agitators 77−31269
polyethylene, high density, filled with pearlite, melt rheology *(Japanese)* 77−54942
polyethylene, high-density, polymer melt, shear stress at wall 80−19450
polyethylene, linear, melt rheology 80−23976
polyethylene, low density, melt elongation, stress and recovery maxima 79−90209
polyethylene, low density, melt flow, mech. degradation *(Russian)* 79−50691
polyethylene, low density, rheology and molecular struct. effect on viscoelasticity 77−62227
polyethylene, low density melts, temp. depend. of the elongational behaviour 80−6012
polyethylene, low-density, melt, critical deform. in rotary rheometer with active cone-plate pair 77−89080
polyethylene, rheological behaviour at high shear strain rates *(French)* 80−66574
polyethylene, ultradrawing, effects of temp. and drawing rate *(Japanese)* 79−91760
polyethylene extruded melt, elongational viscosity, tensile props. 78−67163
polyethylene film, minimum running thickness, biaxial extensional flow study 80−100993
polyethylene film-resin melts, rheological props., prep. method depend. 78−34099
polyethylene melt, nonlinear shear behaviour, strain-dependent memory function 78−67161
polyethylene melt, rheology and molecular struct., melt identification from mech. props. 77−11490
polyethylene melt, rheology and molecular struct., relaxation spectra, charact. relaxation time 77−72255
polyethylene melt, rheology in shearing and extensional flow 77−72256
polyethylene terephthalate, preoriented sheet, plastic deform., anisotropic behaviour 79−8335
polyethylene terephthalate, solid, rheology, deform. 77−11140
polyethyleneoxide dilute solns., flow birefringence at high rates 79−81834
polyethyleneterephthalate-polycaproamide melts, two-phase blend, rheological props. *(Russian)* 80−58997
polyisobutylene, soln., stress deform., integral rheological relations 77−11159
polyisobutylene soln., start-up tests, relaxation meas. of shear and normal stress *(German)* 78−67166
polyisobutylene solution in cetane, hyperelasticity, filler effect 80−10223
polyisobutylenes, shear behaviour of Vistanex LMMH and L 100 80−1443
polyisoprene, rheological props., accelerator and temp. effects *(German)* 78−34101
polymer, filled, rheology, steady state shear flow and periodic deform., relaxation time, spectra, viscosity 79−96066
polymer, filled, solution, normal stresses and hyperelasticity under simple shear flow 80−1506
polymer, plastoelasticity theory 78−75712
polymer, viscofluid, extensional vibrorheometer 77−70257
polymer extrusion dynamics, visual study 78−94625
polymer extrusion flow and heat transfer relationships, numerical anal. 79−77188
polymer flow, birefringence meas. of normal and tangential stresses 77−58625

rheology continued
polymer liquids, elastic and Newtonian, vel. distrib. determ. in channel terminals 79−77046
polymer melt, deformation, loss of fluidity 77−89078
polymer melt, exit press. meas. from capillary or slit rheometer 77−72260
polymer melt, flow birefringence meas., influence of parasitic birefringences 80−88963
polymer melt, network models, loss of junctions due to stretching of material planes 79−77043
polymer melt, particulate mixing, fluid dynamics, rheological and energetic considerations 80−43686
polymer melt, polydispersity, estimation from rheological data 80−6535
polymer melt, rheology and mol. struct. 78−63405
polymer melt, shear stress over wide shear rate range, in falling coaxial cylinder, rheometer 79−7363
polymer melt, viscoelastic, 2-dimens. nonisothermal processing between calender rolls, mathematical model 79−68670
polymer melt in intermittent shear flow, transient birefringence 78−63457
polymer melt mixtures, thermodynamically incompatible, specific fibre formation mechanism 77−23926
polymer melt suspension, plastic-viscoelastic constitutive eqn. 79−60014
polymer melt viscosity meas., Brabender torque rheometer calibration and reading's interpretation 79−10620
polymer melts, annular flow, secondary normal stress difference 80−106816
polymer melts, elastic, uniform extension by const. force, rheology 80−43682
polymer melts, elongational behaviour in const. elongation rate, tensile stress and tensile force expts. 80−38372
polymer melts, elongational properties, microscopic stretch history 80−23981
polymer melts, extensional rheometers, review 78−71302
polymer melts, flow in cooled channels, dimensional anal. *(German)* 79−81833
polymer melts, isothermal and non-isothermal stress relaxation following steady state shear flow *(German)* 79−77044
polymer melts, meas. of elongation props. with universal extensional rheometer 80−6004
polymer melts, rheological props., effects of hydrostatic press. 80−48663
polymer melts and solns., rheological constitutive eqn. 79−41647
polymer melts and solutions, rheological equations, review 79−86391
polymer model adhesives, peeling, morphology and rheology obs. 78−92439
polymer molecular weight correlation with physical and rheological props. 77−51011
polymer processing, applications of 77−23925
polymer rheology nonlinear singularly perturbed Volterra integrodifferential eqn. 79−23290
polymer soln., diffusion in boundary layer 78−87368
polymer soln., dil., rheological constitutive eqn. eval. 79−90208
polymer soln., dil., rheological constitutive eqn. eval. 79−94577
polymer soln., viscoelasticity, rheological props., prep., transport and processing effects, tensile and shear flow *(German)* 78−13982
polymer solns., not infinitely dilute, second-order fluid coeffs., conc. depend. 80−106771
polymer solns., rheological props. in flow through porous media 80−53819
polymer solns., shear and normal stress behaviour, flow hardening *(German)* 78−67165
polymer solns., turbulent boundary layer in pipe flow 78−67256
polymer solution, conc., constitutive eqn. applic. to shear and elongational flow 79−90292
polymer solution, conc., rheological props. rod-like mol. model 78−75114
polymer solution, highly elastic, vel. meas. in die entry region of capillary rheometer 80−99988
polymer solution, laminar capillary tube, critical shear rate 78−34170
polymer solution, mechanical model for flow, extensional viscosity 78−22378
polymer solution, rheological eqns. of state, macromol. elasticity and internal viscosity effects 77−80127
polymer solution, rheology, rel. to turbulent drag reduction 78−22315
polymer solution, stress deform., integral rheological relations 77−11159
polymer solution rheology based on a finitely extensible bead-spring chain model 80−83775
polymer solutions, concentrated, rheological relationships 77−75867
polymer solutions, concentrated, viscous function, hyperelasticity and viscoelasticity 80−48662
polymer solutions, drag-reducing, in U-tube 79−1217
polymer solutions, intrinsic stress, birefringence tensor, bead/spring model, freq. depend. 78−42574
polymer solutions, liquid cryst., rheo-optics of shear and elongational flow, quiescent and flow birefringent charcts. 80−83773
polymer solutions, microgel-containing, physico-chem. and rheological props., light scatt. obs., review *(Polish)* 78−50704
polymer solutions, normal stress meas. using flight velocity 79−77039
polymer solutions, rheology, finitely extensible nonlinear elastic dumbbell theory 78−9617
polymer solutions, shear flow, transient stress effects, network rupture constitutive eqn. 77−11157
polymer solutions, single-relaxation-time constitutive model 77−11156
polymer substrates, amorphous Se vac. deposited, with dynamic coating device 80−100792
polymeric liquid, entropic elasticity and time temp. superposition principle, thermodynamic eqn. of state 78−63406
polymeric liquids, dynamics, kinetic theory, book 77−42795
polymeric liquids, rheology, fluid mechanics, book 77−65772
polymeric liquids, rheology and kinetic theory, review 78−38611
polymeric systems, fluid, rheology, characterised by mol. int. distrib., review 80−1504
polymeric systems, rheology, review 78−87317
polymerisable mass, unsteady viscosity meas. method *(Russian)* 79−23293
polymers, conc. solns. in volatile solvents, high temps., method for viscosity meas. 80−19535
polymers, nonisothermal rheology, significance in polymer processing 79−90206
polymethylmethacrylate, rheological meas. with new rotational rheometer *(German)* 77−51006

rheology continued
polyolefins, molten, basic rheological characts., industrial appl. *(Polish)* 79−50689
polyoxymethylene-copolyamide mixture melt, plasticiser effect on props. and fibre form. during flow 77−27500
polyoxymethylene-copolyamide mixtures, melt rheological props., extrudate microstruct. *(Russian)* 80−7530
polypeptides, helical, conc. solns., rheological behaviour and liq. cryst. order 80−83771
polyphenylquinoxaline, synthesised in different media, mass-mol. distrib. *(Russian)* 79−61862
polypropylene, stretching flow for film prod., bubble blowing in solid phase 78−71303
polypropylene, stretching flow for film prod., stretching over canonical mandrel 78−71304
polypropylene melt, particle filled, blow moldability eval. by melt rheology *(Japanese)* 79−94578
polypropylene-polyethylene blends, capillary flow, rheology and morphology 80−59088
polypropylene-polyethylene blends, flow behaviour in capillaries 80−59087
polystyrene, non-isothermal rheological response during elongational flow 78−38262
polystyrene, nonisothermal rheology 77−32619
polystyrene conc. sols. in toluene, rheological behaviour *(German)* 78−55618
polystyrene in chlorinated biphenyl, flow birefringence on appl. of step-shear strain 80−25335
polystyrene melt, molecular weight effects in die swell and in shear rheology 79−94575
polystyrene melt, rheological props. 79−37273
polystyrene melts, flame-retardant high-impact, shear viscosity-temp.-shear rate relationships 80−59691
polystyrene monomer, high purity, soln., rheological behaviour of flow patterns around agitators 77−31269
polystyrene soln., rheological behaviour of flow patterns around agitators 77−31269
polystyrene solns., correlations of network model parameters 80−106772
polystyrene solution, constitutive models, exptl. tests based on birefringence data 80−100015
polythene melts of high density, viscosity meas., entropy and compressibility *(German)* 78−67162
polytrifluorochloroethylene, rheological props. *(Russian)* 80−6015
pore geometry effects on pressure loss, model channels with varying diameter *(German)* 80−1677
porous solids, hot rolling, rheology, stressed state determ. 79−100194
powder-water-oil system, cohesion of powder particles with water, rheological prop. *(Japanese)* 80−14647
power law fluid, data treatment from cylindrical viscometer 77−3893
power-law liquid, dil. suspensions of dipole dumbbells, rheological eqns. of state and shear flow in elec. field 79−86473
PPT in 100% H_2SO_4, primary normal-stress difference coeff., dependence on molecular wt. 80−87752
primary macromolecules, mol. wt. distrib. influence on crosslinked polymer systems 80−19313
primary normal stress function from shear viscosity data 77−68548
propergol, during polymerisation *(French)* 78−23762
prosthetics, haemodynamic design considerations 78−40428
PTFE, rheological props. below m.p. with certain low molecular smectic states 79−87675
pump with fixed and moving wall, steady shear flow *(German)* 78−87367
PVC, flow behaviour, particulate and melting flow, rheology 79−3981
PVC, plasticised, processing-morphology-mech. props. relation 79−8264
PVC, rheology, viscoelasticity, panel discussion 79−3984
PVC, rheology, viscoelasticity 79−3982
PVC, suspensions, melts, rheological props. rel. to struct. 79−3983
PVC composite, MBS type multifunctional impact modifier effect on mech. and rheological props. *(Polish)* 78−52751
PVC compositions, influence of formulation on the compounding and rheological props. 80−40321
PVC dispersion, rheology, particle size effects 79−92007
PVC pastes, rheological, surface props. rel. to density of prep. foams *(Polish)* 78−85212
PVC plastisol, steady shear rheological behaviour 79−37274
PVC plastisol films, thermally hardened, struct. and props. *(German)* 79−70097
PVC plastisols, thermally hardened, rheological props. *(German)* 79−29154
PVC plastisols, viscosity props. 79−86724
PVC suspension rheological props. *(German)* 79−94579
rate-dependent materials, integral formulation of constitutive eqn. *(French)* 79−90150
Rayleigh-Taylor instability of two viscoelastic superposed fluids 79−72869
rectilinear flow, pressure error upper and lower bounds with pressure gradient 80−6010
refractory, rheological behaviour at high temp. *(French)* 77−56016
refractory products, dense, high-temp. rheology *(French)* 77−32629
Reiner-Rivlin fluids, rheological props. 80−14646
reinforced fluid, supporting strain in flow direction 77−51017
resin impregnated glass tape, friction and rheological props. 77−63806
resin slab, stress response, fluctuating external moisture (temp.) effects 78−55620
rheocasting, review 77−4757
rheogoniometer, Weissenberg, modification to normal stress meas. unit 80−69750
rheogoniometry, viscous heating and heat transfer 79−82013
rheological equations, for thixotropic-dilatant structs. 79−64616
rheometer, high freq., operation, calibration, appls. 78−83345
rheometer for the investigation of disperse systems 79−82012
rigid ellipsoidal particles in external field, dil. suspension, rheological eqns. *(Ukrainian)* 80−48661
Rivlin-Ericksen fluid, dispersion medium on rheological behaviour of dilute suspension of dipolar dumbbells, viscoelastic props. 80−99983
rocks, growth of banded perturbation structures 78−36152
rocks, partially melted, critical phenomena 78−32080
rotational rheometry, edge effects and related error sources 80−19536
rotational viscometer use in calc. of rheological props., programme *(German)* 77−60026
rubber, vulcanized, rheological props., stress-strain rels. 77−32608
rheology continued
rubber and crumb mixtures from scrap pneumatic tyres, rheological behaviour 78−55619
rubber creep processes associated with uniaxial compression, rheological props. 78−68734
Rzhanitsyn-Koltunov nucleus, anal. determ., relax. function for shear and stretching 80−58932
shear elasticity in liqs., oscillat cup expt. 77−72190
shear viscosity of settling suspensions meas. 79−82011
sheared coagulated sols, energy dissipation during sheared flow 78−63461
shearing motion, unidirectional simple, analysis of automorphous model 78−5718
sickle blood cell rheology, pressure-flow curves 77−25503
silicone oil, Newtonian, vel. meas. in die entry region of capillary rheometer 80−99988
simple fluid shear depend. viscosity, central force interactions 80−79970
simple fluids, small strain oscillatory squeeze film flow, polymeric liquids 80−92765
sintering, rheological and microscopical models, relationship 79−95963
sodium carboxymethyl cellulose solns., rheodynamics of immersed rotating disc 77−15067
soil mechanics, classical numerical models *(French)* 77−72261
soil-structure coupling. Nonlinear rheological relationships and boundary conditions in soil mechanics 79−7354
solid-liquid mixtures, rheological characts., shear stress/strain rate relationships 80−10287
spectrophasemeter, for polymer systems meas. 80−33547
spherical particle, free-fall rate in immobile liq. 80−19302
stress relation to deformation, theory 79−59958
stress transient meas. in cone and plate flow, geometry effects 77−31407
structured hydrocarbon systems, flow, rheological behaviour 78−59429
styrene butadiene rubber, peroxide cured, strain independent nonlinearity 78−59353
styrene-butadiene block copolymers, in 1-chlorohexadecane, rheological props., viscoelasticity 79−23288
styrene-butadiene copolymer, soln., rheological behaviour of flow patterns around agitators 77−31269
styrene-butadiene-styrene block copolymer, melt rheology 80−87751
styrene-butadiene-styrene block copolymer, nature of melt rheological transition 78−75113
styrene-butadiene-styrene block copolymer, stress relax. following steady-state flow, residual shear stress development 80−83772
styrene/acrylic terpolymers, viscoelastic props. 80−64509
styrene/MMA copolymers, struct. and rheology 80−1444
surface chemistry, rheological props., terminology and symbols 80−26065
surface rheology, review 77−42792
surfactant solns., rheological props., hydraulic loss reduction in tube flow 77−65768
suspension, fibre, conc., rheology of tube flow, uniform fibre length distrib. 77−58628
suspension, fibre, conc., rheology of tube flow 77−58627
suspension, finely dispersed, rheological props., steady flow 79−18930
suspension, rheological thixotropy analogue simulation study with plane-cone Ferranti-Shirley viscometer *(French)* 77−65725
suspension, rigid ellipsoids, rheological props. *(Russian)* 78−75187
suspension, viscoelastic properties 79−92006
suspension, wave motion in flow down inclined plane *(Ukrainian)* 79−77220
suspension concentrates, physical stability criteria, review 80−45562
suspension in nonstationary flow, rheological behaviour 80−6130
suspension of charged rigid spheres, suspension mechs. 78−40086
suspension of deformable particles, elastohydrodynamic theory 77−35104
suspension of spherical particles, Brownian motion effect on bulk stress 78−7246
suspensions, rheology, colloidal forces role, review 80−103063
technical fabrics, viscoelastic compliance, appl. of stress-time analogy method 80−1497
thermomechanical theory of viscoelasticity for incompressible material *(Russian)* 78−63327
thermoplastic sheet, extruded, thickness adjustment and cooling between calender rolls 79−68597
thermorheological behaviour and coupling problem of struct. materials 77−3718
thermorheological problems, numerical soln. 78−13910
thermotropic liquid crystals, anomalous rheological responses, spectrometer study 80−6358
thick film circuit pastes to determine their suitability for serigraphy *(French)* 77−11154
thixotropic materials, characterisation via extrusion rheometer 77−63876
time constants from shear viscosity data 79−37275
transient natural convection in curly viscous fluids 79−77096
triblock copolymer, model for rheology 80−23979
turbulent flow with polymeric additives, convective heat transfer 79−77098
turbulent heat transfer in dilute surfactant or polymer solutions 79−77101
turbulent shear flow without solid boundaries, effect of polymeric additives 79−77084
upsetting tests developments for better stress/strain curve results *(German)* 80−38368
urethane elastomers, rheo-optical const., Young's modulus *(Polish)* 79−70108
variational Lagrangian irreversible thermodynamics of nonlinear thermorheology 77−27467
viscida, buckling and stretching, surface tension effects 79−10512
viscoelastic converging pipe flow, vel. vectors and radial stresses, rheological model and laser anemometry 79−60028
viscoelastic droplet break-up, in nonuniform shear flow 80−64588
viscoelastic fluid, deformed sphere motion 79−81831
viscoelastic fluid, free surface problems, domain perturbations of rest state 77−68549
viscoelastic fluid, reduction of turbulent friction, rheological model 79−86408
viscoelastic fluid, rot.-oscill. flow, rheological consts. determ. 78−30251
viscoelastic fluid, suspension of two identical spheres, interaction anal., general homogeneous flow 78−63455
viscoelastic fluid flow, heat transfer at low Deborah numbers, rheological effects 80−19445

rheology continued
viscoelastic fluid flow between rotating coaxial disks, numerical anal. 79−77041
viscoelastic fluids, Weissenberg rheogoniometer, R-17, axial compliance reduction 80−106859
viscoelastic material, rheological relations invariance with rel. to orthogonal time depend. transform. of coords. 78−1623
viscoelastic material, stress-strain behaviour, mathematical simulation *(German)* 80−1442
viscoelastic materials, under prolonged loading, failure hypothesis 80−3180
viscoelastic system, fracture mechanics 78−67145
viscoplastic material, mixing process, Bingham model, two-dimens. flow *(German)* 80−92076
viscous fluid, squeezing between elliptic plates 80−28478
viscous incompressible two dimensional slow flow, finite deform. of ellipsoidal inhomogeneity 77−51013
water, films, thin, wetting, rheological charcts. determ., capillary method 78−51788
water in single capillary, electrokinetic and rheological parameters 80−10220
water-fluidised bed, viscosity meas. by oscills. damping 78−59475
wavy rod rotated, induced secondary flow, method of domain perturbations 78−63456
Weissenberg Rheogoniometer, addition of polarizing microscope 79−68838
Weissenberg rheogoniometer, computerised calib. and meas. of Newtonian fluids 78−87323
xanthan gum, rheology 79−37272
Ag-Mg (18.5 wt.%), rheological study of crystallographic order on creep *(French)* 80−97548
Al-Si alloy, eutectic, quasiisotropic 80−79165
Al_2O_3 suspensions, grinding method influence on rheology and suitability for high-density sintering 79−29001
$Ba(PO_3)_2$-MgF_2=0.4AlF_3.0.6CaF_2 glass system, vsicosity and energy parameters of rheological props. *(Polish)* 79−73331
C black conc. suspensions in low mol. wt. vehicles, rheology anal. 80−19312
C mixes, rheological props. at very low shear rates using capillary rheometer 77−65691
C mixes, rheological props. using capillary rheometer, binder content depend. 77−65692
Cr_2O_3, slips and castings, rheological and technological props. 77−16779
Cu-Zn, rheological study of crystallographic order on creep *(French)* 80−97548
Fe_3-Al, solid soln., rheological study of crystallographic order on creep *(French)* 80−97548
γ-Fe_2O_3, densified, rheological and mag. props. 80−44873
Fe_2O_3, flocculated suspension in ethylene glycol, intrinsic viscosity rel. to shear rate 80−1502
Li-Na ferrite powders, props. rel. to Fe_2O_3 chem., thermal, mech. historical 79−11539
Mg_2SiO_4, ^{18}O self-diffusion expts., high-temp. creep implications 80−81870
MnZn ferrite powders, reactive, mag. materials obtained by compaction 80−89182
Ni-Al, rheological study of crystallographic order on creep *(French)* 80−97548
$PbCrO_4$, paste, anomalous viscous flow 79−64617
Si_3N_4, aqueous suspension rheological and processing props. 77−23928
TiO_2, aq. suspension, flocculation effect on dilatant flow 79−61916
TiO_2 suspension in glycerine, Bingham plastic flow through annuli 80−64521

rho mesons
$\pi N \rightarrow \rho X$, trajectory data, reson. and scatt. regions, compatibility *(Russian)* 78−8703
ρ-exchange isovector parity-violating potential 79−93525
chiral $SU_2 \times SU_2$ mixing and decay widths of ρ and A_1 77−30369
chiral SU(3)×SU(3), ρ-meson as dormant Goldstone boson 80−368
chiral SU(3)×SU(3) representation, spontaneous symm. breaking, VDM, PCAC 77−57512
DCI vector meson resonances, $q\bar{q}$ excitation explanation using quark pair creation model 78−70342
decay of ρ'(1275) vector meson nonet 77−79267
Deck model, rescattering effects for diffr. dissociation of hadrons 78−4844
diffractive muoproduction in μp reactions at 147 GeV 77−30391
duality and dual models rho mesons diffraction model [Neveu-Schwarz dual model for ρπ system] 78−82175
dynamic ππ resonance, failure of inelastic N/D eqns. to produce, criticism of method 77−10198
$e^+e^- \rightarrow \pi^+\pi^-(\pi^0\omega)$, ρ'(1250) description, EM form factors, bound states, N/D method *(Russian)* 80−42465
electroproduction, parity-violating effects 80−9178
EM form factor, elec. quadrupole and mag. dipole moments 78−12913
EM mass difference using ρ-ω mixing and quark model 77−2834
equality of radii characterising ρ and ψ Regge trajectories 79−63457
exchange, lepton-hadron relation and the nucleon-nucleon potential 79−22207
exchange in $^2H(\pi,\pi)$ and $^4He(\pi,\pi)$ 78−21610
inclusive distribs. of ρ^0 mesons from cascade decays of τ heavy leptons *(Russian)* 79−9390
inclusive prod. in pp interactions in 9.1 GeV/c 79−6355
inclusive production of ρ^+, ρ^-, ρ^0 in πp^+, pp interactions, cross sections, quark model 78−93912
interaction cross sections in QCD *(Russian)* 80−4968
intermediate states in πN scatt. Chew-Low theory modifications 79−479
lepton pair width regularity of vector mesons, ρ, ω, φ, ψ and γ 79−63472
lifetime and proton mass relationship, quantum of time 77−22716
magnetic moments of light nuclei, ρ-meson exchange 78−17100
mass of radial excitation, quark confinement potential calcs. 78−93860
masses in QCD lattice gauge theory 80−4928
meson strong decay, 2 quark-antiquark pair model 80−52496
meson-baryon interactions, comparative study of ρ^0, ω, $K^{*0}(890)$ and $\bar{K}^{*0}(890)$ production 78−58200
model independent partial wave anal. of $\pi^+\pi^-$ prod. in $\pi^- p \rightarrow \pi^+\pi^- n$ at 17.2 GeV/c 79−54363
N/D calc. of ρ reson. prod. 77−71461
N/D calculation in Veneziano model, ππ scatt. anal. 77−67627

rho mesons continued
nuclear reactions, ρ meson exchange anal. 78−82397
pion-nucleus reactions, intermediate state of ρ-propagation in static model 79−67781
potential model, Dirac eqn. with linear confining pot., symmetric model, π^0 and ρ^0 79−364
production in high energy pp interactions 79−17760
production in $K^- p \rightarrow p^- Y^+$, $Y^+ = \Sigma^+$ or $Y^{*+}(1385)$ 80−82997
progenitor sum rules, π-nucleon coupled fields, ρ-mesonic effects 78−17111
QCD, lattice-gauge theory calc. of π and ρ-meson decay consts. 78−74154
QCD and resonance physics, appl. of sum rules to ρ-ω mixing 79−22060
QCD and resonance physics, appl. of sum rules to reson. props. of mesons 79−22059
QCD exclusive processes, π, K, ρ form factors, hadronic wavefunction evolution eqns. 80−18135
QCD spectrum calcs. in lattice gauge theory using Wilson's fermion method, ρ mass 79−367
quantised particle lifetimes, reln. to hypothesis of quantised time 77−38106
quark effective-bare mass distinction 78−12866
radiative decays anal., ω' meson at 1.2 GeV 77−46045
resonance pole position in ππ system 77−6096
resonance vertex functions and scatt. amplitudes resonance-nucleon scatt. ρ rescatt. *(Russian)* 80−105918
size in quark multiple scatt. model 79−54349
spontaneously broken gauge theory model, ρ' vector meson, e^+e^- colliding beam data 77−2845
strong-gravity contributions to the electromagnetic field of an elementary particle 79−36076
structure function from deep-inelastic scatt. on virtual particles 77−18292
SU(8) symm. mag. moments of charmed vector bosons 78−4794
time quantisation, relation between proton mass and ρ-meson lifetime 78−76
vector meson radiative decay evaluation in spectrum generating SU_4 scheme 79−54342
$D^0 \rightarrow K^- \rho^+$ strong signal, $(\bar{c}s)_R$ current implications 79−36070
$\delta(980) \rightarrow \rho\gamma$, radiative decay width using a vector dominance model 78−82205
e^+e^- annihilations, radial excitations of ρ, ω, φ mesons 78−4866
$e^+e^- \rightarrow e^+e^-\rho$, bremsstrahlung production of neutral vector mesons 80−5006
$e^+e^- \rightarrow$hadrons, QCD perturbation theory sum rule, ρ, ω and φ mesons 79−85268
$e^+e^- \rightarrow \pi^+\pi^-$, 4π, dispersion anal., ρ°(1250), ρ''(1600) prod. 78−8677
$e^+e^- \rightarrow \rho^0$X, 1.45 to 1.61 GeV 79−63489
$e^+e^- \rightarrow \rho \rightarrow \pi^+\pi^-\pi^+\pi^-$, 1.55 GeV 80−82984
$e^+e^- \rightarrow \rho\pi\pi$, radiative corrections, model estimates 77−10271
$e^+e^- \rightarrow \tau^+\tau^- \rightarrow$cascade π and ρ, parity violation from weak and EM interaction interference *(Chinese)* 79−49504
$e^+e^- \rightarrow$VX, polarisation states and differential cross sections for πA_1 and $\rho^+\rho^-$ *(Russian)* 80−102059
$e^+e^- \rightarrow$xπ, even G parity hadronic cross section, ρ'(1600) 2π branching ratio 78−12921
$ep \rightarrow ep\omega_{1,}$ prod. by virtual photons, ω prod. to ρ^0 prod. ratio 79−6344
$ep \rightarrow ep\pi^+\pi^-$, exclusive ρ^0 prod. by virtual photons 79−22113
$ep \rightarrow ep\rho^0$ or eX, polarised beam and target, cross section asymm., vector-meson dominance model 77−6135
η'→ργ, radiative widths, δ and S* background, SU(3) and VDM anal. 80−419
ηγ decays of ρ^0, ω and φ, widths 77−22736
(γ,ρ^-), forward photoprod. on Al, Be, C, Cu up to 4.5 GeV *(Russian)* 77−50113
γ→πω, transition and π form factors, p'(1200) resonance *(Russian)* 79−22098
γd→pd, double scatt. at high energy, unstable particle scatt. amplitude 78−45929
γN, 7.5-10.5 GeV, inelastic ω and $\rho^\pm$ prod. 78−45930
$\gamma n \rightarrow \rho^0(p\pi^-)$, 7.5 GeV, cross channel isospin amplitude meas. and anal. 77−18299
γp, 30-180 GeV, ρ and φ elastic photoprod. cross sections 80−95278
$\gamma p \rightarrow pe^+e^-$, prod. of ρ, ω, φ anal. 78−50037
$\gamma p \rightarrow \pi^+\pi^- p$, Lagrangian model, ε(700), ρ(770), f(1260), Δ(1236) resons. 78−17028
$\gamma p \rightarrow \pi^+\pi^-\pi^0\pi^0 p$, 20-70 GeV, $\omega\pi^0$ state enhancement at 1.25 GeV 80−78078
$\gamma p \rightarrow \pi^+\pi^-\pi^0\pi^0 p$, ρ'(1.6) production 80−102056
$\gamma p \rightarrow \rho^- \Delta^{++}$, 2.8 to 4.8 GeV, cross-sections, ρ spin density matrices 80−62999
$\gamma p \rightarrow \rho^- \Delta^{++}$, 9.7 GeV, pion exchange mechanism anal. 77−82750
$\gamma p \rightarrow \rho^+ n$, 2.8 to 4.8 GeV, cross-sections, ρ spin density matrices 80−62999
$\gamma p \rightarrow \rho^+ n$, 9.7 GeV, pion exchange mechanism anal. 77−82750
$\gamma p \rightarrow \rho'(1500)p$, $\rho'(1500) \rightarrow \pi^+\pi^-\pi^+\pi^-$, photoprod. at CERN SPS and search for charmed mesons 79−26336
γp→ρ+anything, 2.8, 4.7, 9.3 GeV, cross section, multiplicity, energy depend. 77−61303
$\gamma p \rightarrow \pi^+\pi^- p$, 20-70 GeV, dipion enhancemment, ρ'(1600) observation 80−78079
K_L^0-K_2^0 transmission regeneration on deuterons and neutrons, 10 to 50 GeV/c 80−4985
$K^0 N$ interaction, 10 to 50 GeV/c, residue of partial ρ amplitudes *(Russian)* 78−41590
$K^- p$, 32 GeV/c, vector and tensor meson prod., with quark model anal. 79−80854
$K^- p \rightarrow \Lambda\rho(760)$, transversity amplitude analysis 79−80847
$K^- p \rightarrow \rho^- \Sigma^+(1385)$, φΣ°(1385), ωΛ(1520) or 0(1520), cross sections, momentum transfer 77−71531
$K^- p \rightarrow \rho^-(760) + \Sigma^+(1385)$, amplitude anal. 79−97635
$K^- p \rightarrow \rho^0$+anything, 10, 16 GeV/c, central and fragmentation contribs., quark model predictions 78−62467
$K^- p \rightarrow \Sigma^- \pi^+\pi^+\pi^-$, spin-parity $1^+ \rho\pi$ enhancement at 1.04 GeV 77−71532
$K^\pm p$, 32 GeV/c, ρ, K*, φ inclusive prod., quark fusion model 80−32135
$\mu^+\mu^-$ pair system, meson reson., leptonic decay *(Russian)* 77−67646
μN deep inelast. scatt., inclusive ρ^0 prod. 78−37216
$\bar{N}N \rightarrow (\pi, \rho, \omega, f)$, statistical model 80−102028
NN scattering in nonAbelian gauge theory, π-, ρ-, and ω-exchange, scalar Pade approx. 79−67573

rho mesons continued
$\bar{p}p$ charged current interaction, inclusive ρ^0 prod. 80−62963
ω−ρ^0, effects of EM mixing on pn mass difference *(Russian)* 78−74255
$\bar{p}d \rightarrow p_s\pi^+\pi^-\pi^-\pi^0$, 0.4 to 0.9 GeV/c, meson resonance production 79−93447
$\bar{p}n$ annihilation, 5.55 GeV/c, meson resonance prod. and transverse spectra 79−93450
$pN \rightarrow NN\rho^0$, 7-24 GeV, isospin anal. 77−46083
$\bar{p}N \rightarrow \bar{N}(N\pi)_{I=1/2}$, 5.7 GeV/c ρ exchange contrib., cross channel isospin amplitude anal. 78−45938
$\bar{p}p$, 100 GeV/c, inclusive ρ^0 and f^0 prod. 78−41605
pp, 405 GeV/c, ρ^0, f, g^0, h meson prod., cross sections 80−105930
$\bar{p}p$, azimuthal correlations at 22.4 GeV, ρ^0, Δ^{++} reson. prod. 79−67611
$\bar{p}p \rightarrow 2\pi^+2\pi^-$, 5.7 GeV/c, pion ang. distribs., ρ^0, f^0, prod. rates 77−2857
$p\bar{p} \rightarrow e^+e^-$, magnetic nucleon form factor, p-meson type contribs. 80−57596
$pp \rightarrow e^+e^-X$, 53 and 63 GeV, prod. of high transverse momentum low mass e^-e^+ pairs 79−54365
$\bar{p}p$ inclusive prod. of π^-,η,ρ^0,ω,f, mesons at 0.7 GeV/c 77−65170
pp inelastic collisions, ρ-dominance in collision model 78−37238
$pp \rightarrow n\Delta^{++}$, 6-1500 GeV/c, differential cross-section 78−8700
$pp \rightarrow ppX$, cross sections at ISR energies, ρ, ω, A_2 and f meson prod. 79−40815
$\bar{p}p \rightarrow \bar{p}p2\pi^+2\pi^-$, 100 GeV/c, diffraction and ρ^0 prod. in exclusive interactions 78−93909
$pp \rightarrow \pi^+\pi^-X$, 405 GeV/c, indictive ρ^0 and f meson prod. 79−45111
$\bar{p}p \rightarrow \pi^+\rho$, 6 GeV/c, differential cross sections, line reversal symmetry test for baryon exchange 78−78202
$\bar{p}p \rightarrow \pi^+\rho^-$, 6 GeV/c, line reversed reaction, Δ exchange, ρ^- decay 78−12926
$pp \rightarrow \rho^0X$, OZI rule violation 79−58929
$pp \rightarrow \rho^0X$, study of ρ^0 prod. using Heisenberg uncertainty relation *(Russian)* 79−49560
$\bar{p}p \rightarrow \rho^0+X$, 22.4 GeV/c, cross section, average transverse momentum 78−62468
$pp \rightarrow \rho^0+X$, $S^{1/2}$=23.6 to 63.0 GeV, inclusive cross section meas. 79−75805
$\bar{p}p \rightarrow V^0\pi^0 \rightarrow e^+e^-\pi^0$, annihilation at rest, heavy vector meason prod., ρ' (1250), ρ'' (1600) existence 77−13971
$\phi\pi \rightarrow \rho\pi$, analytic quasi-unitary isobar model anal. 79−36099
π, form factor, resonant space and time like, radiative correction, ρ resonance interference 79−54341
π form factor, analytic representation at all Q^2 accommodating higher vector meson states 78−58188
π^0-meson condensation, alternating layer-spin struct. of nucleon system 79−13236
π^-+C(Al)(Cu)(Pb)(H), 3.7 Gev/c, incoherent prod. of ρ^0 mesons *(Russian)* 78−33084
π^+d, 6 to 100 GeV/c, $P_\perp$ distribs. of K^0, π^-, ρ^0, f, equilibrium temp. 79−49540
πN data, energy depend. of ρ trajectory intercept 78−45959
$\pi N \rightarrow \pi^+\pi^-N$, 4-17 GeV/c, ρ^0 and f prod. mech. 80−436
$\pi^-n \rightarrow p\pi^-\pi^0$ or $\rho^-\pi^-p$, 5, 9 GeV/c, model independ. anal. of final states 78−25071
$\pi^-N \rightarrow \rho^0(\omega)X$ at 40 GeV/c, cross sections 77−18359
$\pi^+n \rightarrow \pi^+\pi^-p$, 15 GeV/c, longit. phase space anal., ρ^0, f^0, Δ^0, N^* 77−74727
$\pi^+N \rightarrow \rho^+\gamma N$, bremsstrahlung in vector meson prod. at high energy *(Russian)* 79−80851
$\pi\omega \rightarrow \pi\omega$, $\rho'(1250)$ meson and two channel $\pi\pi$, $\pi\omega$ problem, N/D method *(Russian)* 80−37297
πp charge exchange reactions, model of ρ Regge trajectory 78−37226
$\pi p \rightarrow \rho p$, 6 GeV/c, differential cross sections, line reversal symmetry test for baryon exchange 78−78202
$\pi^-p \rightarrow$ meson pair + X, 11.2 GeV, longit. and azimuthal correlations 77−6180
π^-p interactions, 15 GeV/c, vector meson prod., polarisation props. 78−37251
$\pi^-p \rightarrow n\pi^-\pi^+$, 12 GeV/c, ρ and f prod., differential cross section, baryon exchange 79−423
$\pi^-p \rightarrow n\pi^+\pi^-$, 8 GeV/c, backward meson and baryon reson. prod. 79−415
$\pi^-p \rightarrow p\pi^-\pi^0$, 9 and 12 GeV/c, backward e^- prod. 78−8704
$\pi^-p \rightarrow p\rho^-$, 6 GeV/c, line reversed reaction, Δ exchange, ρ^- decay 78−12926
$\pi^-p \rightarrow \pi^-\pi^+n$, narrow epsilon resonance under rho 80−5021
$\pi^-p \rightarrow \rho^0+X$, 100-360 GeV, cross sections 79−40816
$\pi^-p \rightarrow \rho^0n$, Reggeon cuts and reaction description *(Russian)* 78−45947
$\pi^-p \rightarrow \rho^0\pi^-X$, diffractive contrib. in multi-Regge factorisation 80−73753
π^+p, 32 GeV/c, π and ρ^0 inclusive prod., f and η cross section estimates *(Russian)* 80−68499
π^+p, 6 to 100 GeV/c, $P_\parallel$ distribs. of k^0, π^-, ρ^0, f, equilibrium temp. 79−49540
$\pi^+p \rightarrow (\rho^0,\omega)\Delta^{++}(1238)$, q_L=7.1 GeV/c, role of new exchanges *(Russian)* 79−54355
$\pi^+p \rightarrow \pi^+p\pi^0$, 1 GeV, N^{*+}, N^{*+} and ρ^+ prod., single π distribs. 77−74716
$\pi^+p \rightarrow \pi^+p\pi^0$, p diffractive dissociation, ρ^+ prod., one-pion-exchange model 78−21451
$\pi^+p \rightarrow \pi^+\pi^-\Delta^{++}$, narrow epsilon resonance under rho 80−5021
$\pi^+p \rightarrow \rho^0\Delta^{++}$, positivity conditions in joint vector-meson Δ prod. 77−13975
$\pi^+p \rightarrow \rho^0\Delta^{++}$, quasi eikonal model anal., πP cut contribution, enhancement coefficients *(Russian)* 79−40798
$\pi^+p \rightarrow \rho^0X^{++}$, 8 GeV/c, reaction anal. 79−93457
$\pi\pi$, ρ-meson contrib. in broken chiral symmetry model, phase shifts and lengths *(Russian)* 80−86756
$\pi\pi$ interactions, dominant resonances, pole positions, partial waves 80−63020
$\pi\pi$ P-wave anal., ρ pole parameters 77−46079
$\pi\pi \rightarrow \pi\omega$, $\rho'(1250)$ meson and two channel $\pi\pi$, $\pi\omega$ problem, N/D method *(Russian)* 80−37297
$\pi\pi \rightarrow \pi\pi$, p-resonance production, quasipotential approach, linear σ-model 80−86755
$\pi\pi \rightarrow \pi\pi$, $\rho'(1250)$ meson and two channel $\pi\pi$, $\pi\omega$ problem, N/D method *(Russian)* 80−37297
$\pi\pi$ resonance, N/D calc., rebuttal of criticism N/D calc., rebuttal of criticism 77−71462
$\pi\pi$ S-wave phase shift, lower bounds, ε° and ρ poles 78−45953
$\psi \rightarrow 3\pi$, ρ recurrences, quantitative study 77−79266

rho mesons continued
ρ, photoproduction at high energy, parton model, γ hadronic props. 78−74266
$\rho(767)$, $p\pi$ scatt., separable interactions for three-body problems 78−78113
$\rho \rightarrow e^+e^-$, decay widths from QCD *(Russian)* 78−45812
$\rho \rightarrow \eta\gamma$ radiative decay width determ. 78−467
$\rho \rightarrow \eta\pi\gamma$, three body decay width 79−36083
$\rho \rightarrow \pi+\gamma$, radiative decay in the MIT bag model 78−66110
$\rho \rightarrow \pi\gamma$, EM decay rates, spectrum generating SU(4) approach 79−26334
$\rho \rightarrow \pi\gamma$, quark anomalous mag. moments 79−17693
$\rho \rightarrow \pi\gamma$, radiative decays, final state interaction, π rescatt. *(Russian)* 78−89710
$\rho \rightarrow \pi\gamma$, SU_3 symm. breaking schemes, radiative widths 77−6114
$\rho \rightarrow \pi\gamma$ decay width, explanation using SU(3)-scalar term in the EM current operator 78−82206
$\rho(\rho') \rightarrow \pi\gamma$, obs. in $A(\pi^\pm,\pi^2\pi^0)A$ *(Russian)* 79−9639
ρ/ω amplitude ratio for radiative decay, sea quark γ emission 79−63440
ρ-A_1-π system, radial excitations, and EM mass difference of pions 79−40775
ρ-A_2 exchange degeneracy breaking, estimate from Fermilab π^-p ($d\sigma/dt$) data 79−13162
ρ-ω interference in $K^-p \rightarrow \pi^+\pi^-(\Lambda,\Sigma^0)$ at 4.2 GeV/c 77−30429
ρ-ω mixing, quark mass differences 80−37243
ρ-ω mixing charge symmetry breaking force, nonlocal contribs., ^{3}He-^{3}H mass difference 78−70458
ρ-π puzzle, possible soln. in neutrino-nucleon inelastic scatt. and weak neutral currents 79−17714
$\rho^- \rightarrow \pi^-+\gamma$ decay width, comments 77−13959
$\rho^- \rightarrow \pi^-\gamma$, nonet symmetry scheme 79−63480
$\rho^- \rightarrow \pi^-\gamma$, radiative decay width from pion excitation anal. 80−57599
ρ^0, high multiplicity pp prod. at 300 GeV/c 77−22807
ρ^0, Klein paradox and the mass spectra of the neutral vector mesons 79−26299
ρ^0, multiparticle production in multiperipheral resonance model complemented by duality 79−36050
ρ^0, production cross section in π^-p inclusive interactions *(Russian)* 78−33098
$\rho^0(770)$, polarisation meas. in $\psi \rightarrow \rho^0\pi$ 78−74251
ρ^0 and ρ^- photoprod. at 3 GeV 77−30390
$\rho^0 \rightarrow e^+e^-$, obs. in 4.0 GeV/c π^+p interactions 77−38199
$\rho^0 \rightarrow \eta\gamma$, decay rates calc. SU(3) theory 78−58181
$\rho^0 \rightarrow \pi^0\gamma$, decay rates calc. SU(3) theory 78−58181
ρ^0-ω mixing, sign of single particle exchange nucleon force, charge asymm. pot. 77−88048
ρ^+ diffr. prod. in high energy νp collisions 78−54625
$\rho^+ \rightarrow \pi^+\pi^0$, decay widths calc. in MIT bag model 77−74681
$\rho^\pm \rightarrow \pi^\pm\gamma$, parity nonconservation effects in $np \rightarrow d\gamma$, short dist. contrib. to γ circular polarisation 77−41855
ρ', suppressed hadronic decay and particle degeneracies 77−74684
$\rho'(1250)$ leptonic decay, observations in $\gamma p \rightarrow pe^+e^-$ 900 to 1500 MeV expts. 79−30738
$\rho'(1260)$ existence, vector meson leptonic width, duality between vector mesons and perturbative QCD 80−57589
$\rho'(1600)$, Veneziano model, two pion decay mode suppression 77−46031
$\rho'(1600)$ diffractive photoprod. in two pion final state 80−22624
$\rho'(1600)$ meson resonance from 2- and 4-pion distribs. in photoproduction data 80−95279
$\rho' \rightarrow \rho\pi\pi$, current algebra techniques, pole plus remainder model, chiral symmetry breaking and QCD 80−62972
$\rho\pi$ scatt. in Bardakci-Halpern model 1^+ channel, N/D anal., A_1 status 79−40688
$\rho\pi$ system, resonance-particle prod. amplitude phase shift, S-channel unitary relations *(Russian)* 78−74278
$\rho\pi$ system effective Lagrangian *(Russian)* 77−6036
$\tau \rightarrow \nu\rho\pi$ decay parameters from PCAC and current algebra, A_1 characts. 80−37314
$\tau \rightarrow \rho\nu\tau$, halflife and mass determination from e^+e^- interactions 78−89765
$\tau^- \rightarrow \rho^-\nu$, branching fraction meas. 80−13296
Be(K^-,$\rho\omega$X), *(Russian)* 79−9637
$^4He+\pi^+ \rightarrow \pi^+\pi^-$ ppd, 1.7 GeV/c, cross section, $\Delta(1232)$ and $\rho(770)$ resonance prod. 78−89911
$\mu^+\rho$ scattering, exclusive vector meson prod. ρ, ρ^0 and ω cross sections 79−49528
$\rho K \rightarrow \rho K$, analytic quasi-unitary isobar model anal. 79−36099

rhodium
see also nuclei with .....
adsorbed S on (110), surface struct. anal. using hybridisation model 80−44423
adsorption, of CO and H_2, on (111) surface, 2-dimens. phase separation 80−107634
adsorption of $C^{16}O$ and $C^{18}O$, inelastic electron tunnelling spectra obs. 79−65331
adsorption of CO, AES obs. 77−35818
adsorption of CO, dispersed on Al_2O_3, ^{13}C NMR obs. of adsorbed states 80−96733
adsorption of CO, inelastic electron tunnelling spectra obs. 79−46962
adsorption of CO+H_2 mixtures, reflection-absorption IR and thermal desorpt. obs. 78−6226
adsorption of H_2, mass spectra 78−38970
adsorption of H_2S on (100) surface, (2×2) surface struct., LEED anal. 79−99426
atom, Kβ/Kα rel. intensity obs. 80−32665
atom, Lα X-ray spectra, $_{40}$Zr to $_{48}$Cd, linewidths 79−41131
atoms, $N_2N_3N_{45}$ super Coster Kronig processes 80−106303
band structure and photoemission from low index surfaces 80−24790
band structure and X-ray emission spectra calcs. 77−28105
band structure calc., ground state and effects of change of volume 79−77994
catalyst, interaction of CO, NO and H_2, NH_4OCN formation 78−73082
catalytic oxidation of CO on polycrystalline sample 79−79294
chemisorbed CO on (111), dissociation probability, isotopic exchange and AES meas. 80−40743
chemisorption, of CO, ^{13}C NMR obs. 80−1000
chemisorption, of N_2 and H_2, on perfect surfaces 79−86979
chemisorption, of NO, flash desorption spectra, titration, reaction kinetic calcs. 78−61045
chemisorption of CO, IR spectra, species identification 79−39198

rhodium continued
chemisorption of CO and CO_2 on (111), high resolution EELS, thermal desorption, and LEED study 80−44419
chemisorption of CO on (110) face 78−6225
chemisorption of ethane, sticking coefficient per landing site 79−46941
chemisorption of ethylene and acetylene on (111) surface; EELS, LEED and thermal desorption mass spectrometry 80−80057
chemisorption of formaldehyde, catalytic decomposition, transmission IR spectra 79−39199
chemisorption of H_2 on (111) surface, thermal desorption spectra and LEED obs. 79−86989
chemisorption of methane, vibr. excitation and surface reactivity 79−73393
chemisorption of water on (111) surface, effect of adsorbed O, H, or CO, LEED and thermal desorption meas. 80−75435
coadsorbed CO and O, desorption spectra, Langmuir-Hinshelwood reaction between O and CO 79−47965
coadsorption of CO and H_2, thermal desorption mass spectroscopy meas. 79−46948
coadsorption of O_2 and H_2 below 140K on (111) surface 80−29276
core level binding energies 80−71564
de Haas-van Alphen effect 77−35851
dissociative chemisorption of CO_2 on (111) surface, EELS and thermal desorption spectra meas. 80−6656
double beam photoemission study of electronic struct. 79−83098
electrode, evaporation rate from cathode spot in vac. arcs. 80−49024
electronic struct. determ. from optical refl. meas. 77−62812
epitaxial growth on (001)W and (001)Mo 79−99450
field evaporation patterns, multilayer 77−59675
field ion emitter, calibration using energy distrib. of free space field ionisation 77−69971
film, annealing effect on struct., TEM, electron diffr. study 78−76682
film, deposited by cylindrical magnetron sputtering, internal stresses 80−24773
film, evaporation onto single crystal Ag films and mica cleavages 77−40375
film, optical absorption meas. using synchrotron radiation, 20-250 eK 77−12457
film, work function rel. to degree of coverage of Th film *(Czech)* 78−80039
foil, work function determ. rel. to heat treatment temp., extrinsic photoeffect meas. 77−39918
gamma-laser launching, quadrupole spin echo technique using ^{103}Rh 77−79794
lattice parameters, densities and atomic vols., tabulation for Pt metals 79−65033
LEED, (100) surface struct. determ. 77−69152
LEED, (111) surface struct. study 79−14987
magnetic ground state props., simple one-electron theory 77−63063
melting point determ. 79−1491
multilayer thin film system, scaling law for interdiffusion 79−65262
neutron detectors, self-powered, reliability anal. 79−41078
planar interface, first phase to nucleate 77−62764
proton-induced L-shell ionisation cross-sections 80−100707
recovery and use of noble metals from radioactive waste 80−99242
self powered neutron detectors, influence of Rh burnup on sensitivity 80−63462
spectrophotometric methods of determination, review 78−61115
stopping power for 28 MeV α-particles, re-evaluation 78−79651
stopping powers for 28.8 MeV α-particles 77−80556
superconductivity, search for, at very low temps. 78−91799
supported catalyst particles, adsorption of CO, inelastic electron tunnelling spectra 79−3509
surface, (100), structural determ. using reliability factor proposed for LEED 78−43224
surface, (110), chemisorption of CO and NO, LEED, AES, XPS, UPS, and desorption obs. 79−77899
surface, (110), S-adsorbed, LEED crystallographic determ. of struct. 80−44422
surface, (111), AES, LEED, and thermal desorption mass spectra meas. 79−77900
surface, (111), catalytic reaction between adsorbed O_2 and gaseous H_2 79−83503
surface, (111), chemisorbed and condensed CO, energy level shifts 78−87865
surface, (111), dissoc. chemisorption of methane, vibr. activation 79−57292
surface, (111), UPS meas. of chemisorbed and condensed CO using synchrotron radiation 79−33902
surface, (111) and (100), chemisorption of H_2, O_2, CO, CO_2, NO, C_2, ethylene, acetylene, LEED, AES and thermal desorption meas. 78−38951
surface, chemisorption of CO, thermal desorption mass spectrometry and LEED meas. 79−77917
surface, pulsed laser atom-probe FIM, expts. 80−66402
surface(111), geometry, vibrational props., Debye temp., LEED study 78−87852
surface (111), catalytic reaction between adsorbed O_2 and H_2, LEED obs. 79−52773
surface (111), co-adsorption of H_2 and CO segregation of co-adsorbed species 80−65361
surface (111), interaction with O_2, thermal desorption spectra, AES and LEED obs. 79−51428
surface (111), LEED crystallography and reliability indices 80−54081
surface atoms, Debye temps. determ. during field evaporation and LEED 80−39406
surface catalyst for CO hydrogenation to methane and higher mol. wt. compounds 78−73034
surface structure, LEED exam. 78−87853
surfaces (755), (331), chemisorption of H_2, O_2, CO, NO, CO_2, C_2H_4, C_2H_2, and C, desorpt. temp. and decomp. characts. 79−65318
thin films, polycryst., resistivity and temp. coeff. of resistivity 80−88648
wear coefficients determ. using pin-on-cisc apparatus 80−76366
X-ray emission L-spectra, influence of temp., liq. N_2 temps. *(Russian)* 80−80907
X-ray reflection intensities, charact. temps. 78−18731
X-ray tube for silicate rock X-ray fluorescence analysis 78−88945
Fe:^{103m}Rh, γ-detected NMR of 40 keV metastable state, 0.5 to 14 kG external fields 77−59499
LiD:Rh, EPR spectra of Rh centres, UV-irrad. cryst. 79−65724
LiH:Rh, EPR spectra of Rh centres, UV-irrad. cryst. 79−65724
rhodium continued
LiH(D):Rh, EPR of axial impurity complex 77−40123
$LiNbO_3$:Rh, Czochralski-grown oxide crystals, fluid-flow effect on gas-bubble entrapment 80−84121
MgO:Rh^{2+}, EPR of Jahn-Teller ions, ^{17}O superhyperfine structure 77−32253
Pt/Rh thermocouple, Type B, HI BX extension wire, EMF characteristics 78−49832
Rh^+, Rh^{2+}, field evaporation, field ion mass spectra and field ion appearance spectra study 80−7479
Rh:H, energy and electron density of states 78−51929
Rh/Al_2O_3 catalysts, surface interaction between NO and CO, IR study 79−70369
Rh/γ-Al_2O_3 disperse δ-phase, chemisorpt. of CO, IR spectra, site distrib., mol. mobility 78−72496
Rh-H system, energy and electron density of states, improvements to theory 80−70636
Rh-Si thin film interaction, interdiffusion, temp. depend. 80−54443
Rh-TiO_2 catalyst, adsorpt. of H_2, surface states, NMR spectrosc. investig. 80−103891
^{106}Rh, radioactive decontamination methods, effectiveness for different terrains 78−96104
^{103m}Rh, separation from ^{103}Ru by solvent extraction 78−58857
^{106}Ru-^{106}Rh, accumulation by marine organisms, sediment and sea water influences 78−80981
Si:Rh, p^+-n-n^+, n^+-n-n^+, p^+-n-p^+, structs., S- and N-type I-V characts. 77−43706
Si:Rh, Schottky diode, capacitance characts., donor and acceptor levels 77−43697
Si-Rh interface, RhSi form. by lattice diffusion 78−71891
Si-Rh Schottky diode, X-ray effects on elec. props., irrad. induced diffusion 77−4439
Si-Rh Schottky diode, X-ray irradiated, radiation-accelerated diffusion of Rh in Si 78−26952

rhodium alloys
see also rhodium compounds
ferromagnetic Heusler alloys, peaks in low field AC susceptibility 80−50071
neutron activation determ. of microcomponents Pt, Pd, Ir, Rh, in noble metal alloys *(Russian)* 77−32858
Permalloy-Rh, film, influence of Rh on corrosion resist. and mag. props. 80−3235
rare earth alloys, RRh_2X_2 (X=Si,Ge), cryst. struct. 80−1964
rare earth intermetallics, $R Rh_2$, (R=Y, La, Ce, Lu) 77−85564
rare earth rhodium tin intermetallic cpds., synthesis, supercond. and mag. props. 80−100547
rare earth-Sn-X, X=Rh, Ir, Ru, Co, cryst. growth and cryst.-chem. invest, supercond./mag. ternary cpds. 80−100777
Ag-Rh film, valence band spectra, XPS meas. 78−52618
Al-Rh, composite, paramagnetic resonance and electron-positron annihilation *(Russian)* 79−87314
$AmRh_2$, crystal structure and mag. props. of Laves phases 77−27851
Au-Rh, dil., Friedel d-reson. scatt. and elec. resists. 80−44566
BaRh, gaseous, dissoc. energies, obs. and calc. values 78−58864
$CePd_{3-x}Rh_x$, resistance behaviour and intermediate valence effects 79−78068
$CeRh_2$:Nd^{3+}, ESR investigation 79−78514
Ce_3Rh_2, structure determ., rhombohedral Er_3Ni_2 type 77−80443
$CeRh_{3-x}Pd_x$, electronic and cryst. struct. comparison, catalytic behaviour 78−84398
$CeRh_{3-x}Pd_x$, lattice spacing and mag. suscept., effect of prep. and hydrogenation 77−58976
$CeRh_{3-x}Pd_x$, powdered alloys, catalytic behaviour correlation with electronic struct., lattice struct. and surface comp. 79−82181
Cr-Rh, dil., hyperfine fields meas. 79−47056
Cr-Rh, magnetic transformations, triple point *(Russian)* 80−88747
Cu-Rh (0.5 at.%), nucl. quad. relax. 79−82898
Cu-Rh (4 at.%), anneal hardening mechanism 80−60879
DyRh, direct Coulomb contrib. of cond. electrons to crystalline elec. field 77−76784
DyRh, direct coulombic contrib. of cond. electrons to cryst. elec. field 79−91005
DyRh, exchange coulombic contrib. of cond. electrons to cryst. elec. field 79−95376
$DyRh_{1.1}Sn_{3.6}$, new supercond./mag. cpds., X-ray powder diffr. data 80−100215
$Er_{1-x}Ho_xRh_4B_4$, mag. and supercond. transitions, cryst. field effects 80−107950
$ErRh_4B_4$, reentrant supercond., mag ordering, neutron diffr. obs. 78−14879
$ErRh_4B_4$, supercond., electronic props. of Er^{3+} using Mossbauer effect in ^{166}Sr 79−56651
$ErRh_4B_4$, supercond. and mag. props. 79−4631
$ErRh_4B_4$, supercond. and mag. props., influence of mag. fields 79−56374
$ErRh_{1.1}Sn_{3.6}$, new supercond./mag. cpds., X-ray powder diffr. data 80−100215
$ErRh_{1.1}Sn_{3.6}$, synthesis, supercond. and mag. props. 80−100547
$Er_{1-x}Tm_xRh_4B_4$, mag. and supercond. transitions, cryst. field effects 80−107950
$Eu_{0.25}La_{0.75}Rh_2$, high press. Mossbauer spectra, interconfig. charge fluctuations 77−63341
$EuRh_2$, H_2 absorbing, degradation by cycling 78−34628
$EuRh_2$, mech. of H absorption, Mossbauer, mag. and X-ray diffr. meas. 78−38846
$EuRh_{2-x}Pt_x$, intermediate-valance state, XPS obs. 77−28687
Fe-Rh, ferromag., spin wave stiffness constant calc. 79−38307
Fe-Rh, hyperfine field distrib., spin echo NMR meas. 78−76351
Fe-Rh, mag. hyperfine interactions, Mossbauer effect meas. 77−66442
Fe-Rh, spin wave spectrum in antiferromag. and ferromag. phases, inelastic neutron spectrometry 77−63158
Fe-Rh alloy, nonmag. and mag., band theory 79−37973
FeRh, antiferromag., band structure and effect of Fe impurity on mag. props. 77−28377
FeRh, antiferromag., band struc., off-stoichiometry effects 78−10341
FeRh, antiferromag.-ferromag. transition, appl. of interacting virtual bound state picture 77−69464
FeRh, transition mechanism, interacting virtual state approach 77−72987
$Fe_{1-x}Rh_x$, press. effects on mag. phase transition, resist. meas. 77−4516

rhodium alloys continued
$Fe_{48}Rh_{52}$, hyperfine mag. field at ^{57}Fe and ^{119}Sn nuclei, press. depend. *(Russian)* 78−80266
Gd-Rh, amorphous, mag. and elec. props. 80−80499
Gd-Rh, amorphous, mag. props. and ferromag. reson. 80−75862
Gd-Rh, amorphous alloy, mag. coupling 78−88108
$Gd_xEr_{1-x}Rh_4B_4$, effects of Gd ion on supercond. transition temp., mag. transition temp. and upper crit. field 79−56392
$Gd_xEr_{1-x}Rh_4B_4$, ferromag. and structural transitions, low temp. calorimetric meas. 79−55888
$Gd_{0.99}Ho_{0.01}(Rh_{1-x}Fe_x)_2$, spin echo meas. on ^{165}Ho, quenching effect of Fe substitution 78−48079
$Gd_{1-x}La_xRh_2$, NMR, contribution of Gd neighbours to Gd hyperfine field 77−8423
$GdRh_2$, H_2 sorption props. 79−86980
$Gd(Rh_{1-x}Fe_x)_2$, $x \leq 0.15$, magnetisation and EPR studies 80−34767
$GdRh_2H_x$, struct. and mag. props., Mossbauer and magnetisation meas. 80−71271
Ir-Rh/Ir alloy, thermocouple, appl. to temp. meas. in atm. press. flame 77−86314
$LaRh_2$, ESR of Yb^{3+} 79−87315
$LaRh_2$, H_2 sorption props. 79−86980
$LaRh_2$:Nd^{3+}, ESR investigation 79−78514
$LaRh_2$:Nd^{3+} cubic metallic host, spin-lattice relaxation, ESR obs. 79−1710
Li-Rh-H system, intermetallic cpds. and phase relationships, cryst. struct. 78−44084
$LiRh_3$, cryst. struct. 77−11506
$LuRh_2$-Nd^{3+}, dil., ESR, hyperfine crysts. of $^{143,145}Nd$, g-factor, crystalline field splitting 78−52349
Mh-Rh-Cr, mag. transition, effect of press. 77−16077
Mo-Rh, secondary electron emission and inelastic refl. coeffs. 78−15264
Mo-Rh film, amorphous, temp. stability 78−63948
Nb-Rh, dil., neutron irradiation at 4.6K, influence of impurities on defect prod. 79−55790
Nb-Rh, radiation disorder model of phase stability 80−16297
Nb-Rh, σ-phase alloy, superconductivity and resistance behaviour 80−70882
Nb-Rh system glasses, form., crystn. and microhardness, resist. obs. 80−89178
Nd_3Rh_2, structure determ., rhombohedral Er_3Ni_2 type 77−80443
$NdRh_{1.2}Sn_{4.1}$, new supercond./mag. cpds., X-ray powder diffr. data 80−100215
Ni-Fe-Rh films, mag. and corrosion props. 80−34702
Ni-Rh, disordered, local environment effects, neutron scatt. expts. 78−68172
Ni-Rh, disordered, vol. paramagnetostriction calc. 77−80985
Ni-Rh, ferromag., local-environment effects, mag. diffuse neutron scatt. cross-section meas. 77−55664
Ni-Rh, ferromag., press. effect on Curie temp. 79−51781
Ni-Rh, local environment and mag. props. effect of disorders 77−63085
Ni-Rh, mag. moment distrib., one-mag.-species model calc. 80−65788
Ni-Rh, thermal EMF, elec. resist., mag. susceptibility, mag. moment and Curie temps., 18-500°C *(Russian)* 77−20288
Ni-Rh ferromagnetic alloy, mag. moment spatial distrib. 77−66275
$(Ni_{1-x}Rh_x)_{99}Mn$, ferromagnetic, NMR study of local environment effect 80−7192
$(Ni_{1-x}Rh_x)_{99}Mn$, ferromagnetic, NMR study of local environment effect, relaxation mechanism 80−7193
$NpPd_{3-x}Rh_x$, Mossbauer spectra, hyperfine interactions and mag. ordering 77−20783
Pd-Rh, and Pd-Rh-Ag, effects of press. and alloying on Pd electronic struct., susceptibility meas. 78−91581
Pd-Rh, dil., hyperfine anomaly between bound negative muon and Rh nucleus 79−56707
Pd-Rh, dilute, low temp. sp. ht. and mag. susceptibility 77−62650
Pd-Rh, disordered, Hubbard model for electron correl. and spin susceptibility 77−76762
Pd-Rh, disordered, vol. paramagnetostriction calc. 77−80985
Pd-Rh alloys, soln. of H_2, partial thermodynamic parameters determ. 77−66027
Pd-Rh-Ag, mag. susceptibility, pressure effect up to 4000 atms. 77−16142
Pd-Rh-Ag, magnetic susceptibility press. depend., d-band deform. and exchange var. 77−47967
Pd-Rh-H, band struct. and supercond. props., APW calc. 79−56354
Pd-Rh-H, hydride formation in high press. range 80−65235
$Pd_{0.91}Ag_{0.045}Rh_{0.045}H_x$, supercond. transition temp. rel. to optical phonon spectrum 79−56355
PdFeRh, ferromag., Curie temp. depend. on susceptibility, non-mean field theory 80−44829
PdHg-Rh, dil., quadrupole interaction of ^{100}Rh 79−99520
$PdPb_2$-Rh, dil., quadrupole interaction of ^{100}Rh 79−99520
$Pd_{0.9}Rh_{0.1}$, lattice dynamics, inelastic neutron scatt. meas. at 296K 80−29135
$Pd_{0.95}Rh_{0.05}$, exchange-enhanced, phonon dispersion relations exam. 77−84868
$Pd_{95}Rh_5$, low-temp. spin-fluctuation resist., effect of pot. scatt., effect of Ni addition 77−15840
$(Pd_{95}Rh_5)Co$, exchange enhanced system, AC susceptibility meas. 77−16096
$(Pd_{1-y}Rh_y)_{100-x}Fe_x$, exchange-enhanced alloys, mag. ordering 79−61050
$Pd_{1-y}Rh_yH_x$, electronic struct. and supercond., APW calc. 79−95318
$(Pd_{95}Rh_5)_1H_x$, elec. resistivity studies 80−59957
PdSb-Rh, dil., quadrupole interaction of ^{100}Rh 79−99520
PdTe-Rh, dil, quadrupole interaction of ^{100}Rh 79−99520
$PrRh_2$, hyperfine sp. ht. and magnetisation meas. at 4.2K 80−75775
$PrRh_2$, sp. ht., differential susceptibility and elec. resist. meas., 1.4-40K 80−71063
$PrRh_xSn_y$, crystallography X-ray powder diffr. study 80−100217
Pr_3Rh_2, structure determ., rhombohedral Er_3Ni_2 type 77−80443
Pt-Rh, elec. cond., temp. influence *(Russian)* 80−39549
Pt-Rh, surface comp. determ. by ion scatt. spectroscopy 80−6602
Pt-Rh, surface composition using ion scatt. spectroscopy 79−82422
Pt-Rh alloy, on rock salt, epitaxial growth and struct. 77−20211
Pt-Rh alloys, low temp. resistivity 79−60787
Pt-Rh alloys, surface behaviour on heating in air, XPS and SIMS *(French)* 77−40327
Pt-Rh dil. alloy, 0.5 at.%, ^{195}Pt NMR for local mag. susceptibility 78−84484

rhodium alloys continued
Pt-Rh-W (30, 8 wt.%), intergranular embrittlement by Se vapour 80−3185
Pt-Rh-W alloy corrosion by radioisotopic power system insulating and thermoelec. materials 78−7094
$Pt_{90}Rh_{10}$/Pt thermocouple, Inconel sheathed, MgO-insulated, decalibrations during 1200°C use, ion microprobe obs. 78−57957
$Pt_{86}Rh_9Au_5$, $Pt_{74}Rh_{17}Au_9$, low temp. sp. ht. 79−73320
PtRh5 alloy, phosphate glass addition effect on high temp. strength *(German)* 80−25807
$Pu_{31}Rh_{20}$, crystal struct. determ. 77−80445
Pu_5Rh_4, cryst. struct. 77−19909
Pu_5Rh_4, cryst. struct. 77−58974
Pu_5Rh_4, cryst. struct. determ. 77−55267
Rh-Al, transition metal group VIII aluminide, NMR near equiatomic composition *(Russian)* 80−20479
Rh-C (graphite), adhesion and wettability of graphite *(Russian)* 80−20008
Rh-Co (20 at.%), mag. virtual bound state alloys, XPS of core states 79−47588
Rh-Cu catalyst, Al_2O_3 supported, chemisorbed CO, IR spectra *(French)* 80−60559
Rh-Cu(Si), melts, surface props. *(Russian)* 78−26750
Rh-Fe, competing interactions in FCC alloys 78−95453
Rh-Fe, dil., anti-Kondo effect, de Haas-van Alphen obs. 79−73427
Rh-Fe (25, 20 at.%), mag. virtual bound state alloys, XPS of core states 79−47588
Rh-H system, energy and electron density of states, improvements to theory 80−70636
Rh-Ir, local environment and mag. props. effect of disorders 77−63085
Rh-Ni alloy, onset of ferromag. 79−56533
Rh-Pd, mag. moment of Ni, Co, Fe, Mn and Cr impurities 78−95416
Rh-Pd-Co, dil., local moment formation 78−43562
Rh-Pd-Co(Fe), dil., local environment and mag. props. 78−64187
Rh-Pt, local environment and mag. props. effect of disorders 77−63085
Rh-Si thin film interaction, interdiffusion, temp. depend. 80−54443
Rh-Sn-M M=Mg, Ca, Sr, Sc, Y, Zn, Cd, In or Th 80−100777
RhCo, disordered itinerant-electron system, spin-glass condensation 79−78424
Rh_2CoSn, ferromag., crit. exponent of ^{119}Sn hyperfine field, Mossbauer obs. 78−92008
Rh_2CoSn, ferromag., mag. hyperfine fields of ^{119}Sn, Mossbauer meas. 78−10816
Rh_2CoSn, ferromag. Heusler alloys, hyperfine fields, spin echo meas. 77−63314
Rh_2CoSn, hyperfine mag. fields at ^{119}Sn, under press., Mossbauer expts. 79−99812
Rh_2CoSn, metallic ferromagnet, hyperfine mag. field temp. depend. *(Russian)* 78−80265
Rh_2FeSn, ferromag., mag. hyperfine fields of ^{119}Sn, Mossbauer meas. 78−10816
Rh_2FeSn, ferromag. Heusler alloy, hyperfine fields, spin echo meas. 77−63314
Rh_2FeSn, Heusler alloy, Sn and Fe hyperfine field, Mossbauer exam. 77−43920
Rh_2FeSn, hyperfine mag. fields at ^{119}Sn and ^{57}Fe, under press., Mossbauer expts. 79−99812
Rh_2FeSn, metallic ferromagnet, hyperfine mag. field temp. depend. *(Russian)* 78−80265
RhH, electronic struct. and supercond., APW calc. 79−95318
Rh_7Mg_{44} structure types, alternative description of cryst. struct. 79−7577
Rh_2MnGe, ferromag. Heusler alloy, hyperfine mag. field meas. by TDPAC technique 79−78580
$Rh_2MnGe(Pb)$, hyperfine mag. field at Cd impurity, TDPAC study 80−39905
Rh_2MnPb, hyperfine fields, ferromag., NMR and Mossbauer effect studies 80−71259
Rh_2MnSb, hyperfine fields, ferromag., NMR and Mossbauer effect studies 80−71259
Rh_2MnSn, and related cpds., with Heusler and Heusler-related struct., mag. props. 77−8311
Rh_2MnSn, ferromag., mag. hyperfine fields, time differential PAC meas. 77−81040
Rh_2MnSn, ferromag. Heusler alloy, hyperfine fields, spin echo meas. 77−63314
Rh_2MnSn, ferromag. Heusler alloy, hyperfine mag. field meas. by TDPAC technique 79−78580
Rh_2MnSn, Heusler alloy, Sn hyperfine field, Mossbauer exam. 77−43920
Rh_2MnSn, Heusler alloys, hyperfine mag. field at Sn 78−39482
Rh_2MnSn, mag. hyperfine fields at Rh and Sn sites, and their temp. depend. 78−43708
Rh_2MnX, (X=Al, Ga, In, Tl, Sn, Pb, Sb), Heusler and Heusler-related cpds., mag. and cryst. props. 77−20568
Rh_2NiSn, Heusler alloys, hyperfine mag. field at Sn 78−39482
RhSi-Si interfaces, chemical state, AES expts. 78−91767
Rh_xSi_y-n-Sn Schottky diodes, rectifying barrier height meas. 80−49896
RhTh, mol. vapour above Th-U-Rh-graphite, dissoc. energy, mass spectra 78−78832
RhU, mol. vapour above Th-U-Rh-graphite, dissoc. energy, mass spectra 78−78832
Sc-Rh, electronic struct., susceptibility, sp. ht. and Knight shift meas. 77−43485
Sc-Rh-Si system, partial phase diagram, X-ray diffr. and microprobe anal. 80−25659
ScRh, electronic struct., NMR relax. times meas. 79−51871
ScRh:Gd, influence of cryst. field on EPR 78−52346
$ScRhC_{1-x}(B_{1-x})$, stabilising effect of C and B on alloying behaviour of Sc 77−36454
Sm_3Rh_2, structure determ., rhombohedral Er_3Ni_2 type 77−80443
Ta-Rh, σ-phase alloy, superconductivity and resistance behaviour 80−70882
Ta-Rh system glasses, form., crystn. and microhardness, resist. obs. 80−89178
$Tb(Fe_{1-x}Rh_x)_2$, Fe sublattice spin reorientation possibility, Mossbauer spectra *(Russian)* 79−78335
$TbRh_xSn_y$, crystallography X-ray powder diffr. study 80−100217
$TmRh_4B_4$, mag. and supercond. props., mag. susceptibility and sp. ht. meas. 79−78344
URh_3, de Haas-van Alphen effect, Fermi surface obs. 77−28099

rhodium alloys continued
V-Rh, constitution diagram 77−44216
V_3Rh, nuclear spin-lattice relax. time, electronic density of states 77−59354
YRh, electronic struct., susceptibility, sp. ht. and Knight shift meas. 77−43485
YRh_2:Nd^{3+}, ESR investigation 79−78514
Zr-Rh, absorbed interstitial H_2 energy 79−82198
Zr-Rh, $\alpha \rightleftarrows \beta$ transform. *(Russian)* 78−80540
Zr-Rh, high temp. modification, X-ray diffr. obs. *(Ukrainian)* 79−32947
Zr-Rh alloys, amorphous, thermal relax. effects on electronic and supercond. props. 79−65575
Zr-Rh-H(D), superconducting transition temp., effect of H(D) conc. 80−84532
$(Zr_{1-x}Er_x)_3Rh$, amorphous, influence of mag. ordering on supercond. props. 80−29511
$Zr_{75}Rh_{25}$, amorphous, evidence for short wavelength cutoff in fluctuation spectrum 78−68113
$Zr_{75}Rh_{25}$, amorphous superconductor, high-κ, upper and lower crit. fields 79−4629
$ZrRh_{3-x}Pd_x$, electronic and cryst. struct. comparison 78−84398
$ZrRh_{3-x}Pd_x$, powdered alloys, catalytic behaviour correlation with electronic struct., lattice struct. and surface comp. 79−82181

rhodium compounds
see also rhodium alloys
anodic oxide film, two-colour electrochromic system 80−66150
borides, RRh_3B_2 (R=rare earth), supercond. and mag. props. 80−97028
double oxides, elec. cond. 80−34438
oxidised surface, bonding of cadmium arachidate monolayers XPS 79−15011
rare earth borides, RRh_4B_4, coexistence of superconductivity and long-range magnetic order 79−11264
rare earth borides, ternary, superconducting, phase diagrams and upper crit. fields 80−2531
rare earth compounds, RRh_4B_4, coexistence of supercond. and ferromag. order 79−65579
rare earth compounds, RRh_4B_4, supercond. and long range mag. order coexistence 80−15642
rare earth cpds., RRh_4B_4, coexistence of supercond. and mag. ordering *(Russian)* 80−84542
rare earth rhodium borides, RRh_4B_4, NMR and sp. ht. in supercond. and mag. ordered phases 80−7037
rare earth ternary borides, RRh_4B_4, supercond., re-entrant magnetism, energy band calcs. 78−52140
$(Co,Rh,Fe)_3O_4$ film magnetooptical switch for synchronization of CO_2 and red laser beams 80−58615
$Cr_{1-x}Rh_xO_2$, oxidative prep. method, mag. props. 80−44863
$Er_{1-x}Gd_xRh_4B_4$, supercond. and mag. transitions at press. up to 19 kbar 79−38236
$Er_{1-x}Gd_xRh_4B_4$, ternary superconductor, mag. interactions 79−73613
$(Er_{0.6}Ho_{0.4})Rh_4B_4$, reentrant supercond., magnetisation meas. near lower crit. temp. 80−25043
$(Er_{1-x}Ho_x)Rh_4B_4$, superconductive and mag. interactions, hydrostatic press. effect 80−49973
$Er_{1-x}Ho_xRh_4B_4$, ternary superconductor, mag. interactions 79−73613
$ErRh_4B_4$, ferromag. superconductor, vortex phase 80−80441
$ErRh_4B_4$, mag. supercond., NMR study of ^{11}B 80−107957
$ErRh_4B_4$, supercond., electronic struct. and reentrant magnetism 78−10340
$ErRh_4B_4$, superconducting and mag. transitions, alpha particle irradiation damage effects 79−60954
$ErRh_4B_4$, superconducting and normal state props. 79−73632
$ErRh_4B_4$, superconducting, magnetic dilemma 80−75680
$ErRh_4B_4$, superconducting thin films, critical mag. field 80−75693
$ErRh_4B_4$, superconductor, neutron scatt. exam. of mag. phase 79−73680
$ErRh_4B_4$, ternary superconductor, mag. interactions 79−73613
$Er_xY_{1-x}Rh_4B_4$, supercond. phase transitions, recentering temp. to normal ferromag. state 80−7024
$Gd_xEr_{1-x}Rh_4B_4$, mag. ordering near supercond. region 79−73696
$GdRh_4B_4$, magnetic and electrostatic props., NMR study 80−93195
Hf-Rh-B systems, phase equilib. and cryst. structs. 80−15072
$Ho(Ir_xRh_{1-x})_4B_4$ pseudoternary system, supercond. and mag. ordering 80−70876
$HoRh_4B_4$, electronic struct. and reentrant magnetism 78−10340
$HoRh_4B_4$, ferromag., mag. struct., neutron diffr. obs. 79−78323
Li-Rh-H system, intermetallic cpds. and phase relationships, cryst. struct. 78−44084
$(Lu_{1-x}Ho_x)Rh_4B_4$, interaction between superconductivity and magnetism 79−38248
$LuRh_4B_4$, magnetic and electrostatic props., NMR study 80−93195
$LuRh_4B_4$, superconducting and normal state props. 79−73632
MRh_4B_4 (M=trivalent transition metal, usually rare earth) supercond. and ferromagnetism, role of Sc 78−95438
$MoRh_2O_6$, crystn. and cryst. struct., paramag. and elec. cond. props. *(French)* 77−80480
$Mo_{6-x}Rh_xTe_8$, synthesis, struct., and elec. props. 80−92877
NaRhY zeolite, Rh complexes with CO and methyl iodide ligands, spectrosc. obs. 80−85159
$Ni_{1-x}Rh_xS$, nonvolume effect of Rh substitution on paramag. metal-antiferromag. nonmetal transition 79−28277
$Pd_{1-x}Rh_xTe_2$, high-press. phase transform. obs. 77−15584
Rh complex, di-μ-chlorobis[(1,5-cyclooctadiene)rhodium (I)], IR and Raman spectra 79−19877
Rh complex, h^5-indenylbis(ethylene)rhodium(I), ethylene displacement reactions 79−15975
Rh complex, trans-dibromotetrakis(pyridine)rhodium III bromide, excited state geometry calcs. 77−27047
Rh complex, trans-dichlorotetrakis(pyridine)rhodium III chloride, excited state geometry calcs. 77−27047
Rh complexes, Rh(III) halopentaammines, solns., luminesc. and excited state lifetimes, photoaquation 79−8175.
Rh complexes with adenosine, xanthosine, prep., elec. cond., IR spectra, characterisation 78−92065
$RhBr_3$, bond distances exam. by EXAFS 78−26525
$Rh_4(CO)_{12}$, bond energy terms from thermochem. data 78−62967
$Rh_6(CO)_{16}$, bond energy terms from thermochem. data 78−62967
$Rh_6(CO)_{16}$, UPS investig., comparison with metal/adsorbate system 77−51598

rhodium compounds continued
$RhGe_{1.5}S_{1.5}$, new skutterudite relation compounds, prep. and charact. 78−52700
RhH, electronic struct. and supercond., APW calc. 79−95318
Rh(III) complexes, luminesc. rise time meas. by wavelength shifter 80−50390
Rh_xSi_y-n-Sn Schottky diodes, rectifying barrier height meas. 80−49896
$(Rh_xV_{1-x})O_3$, impurity doping effects, elec. props. obs. 80−75609
Sc-Rh-B system, phase equilib. and cryst. structs. 80−15072
$SmRh_4B_4$, coexistence of supercond. and antiferromag. order 80−11140
$SmRh_4B_4$, mag. ordered, persistence of supercond. 80−54834
Th-Rh-C, phase diagram *(German)* 77−48413
YRh_4B_4, supercond., anomalous cond.-electron polaris. 80−25047
YRh_4B_4, supercond., electronic struct. and reentrant magnetism 78−10340
Zr-Rh-B system, phase equilib. and cryst. structs. 80−15072
Richardson effect *see thermionic emission*
ridge waveguides *see rectangular waveguides*
Riemann-Cristoffel tensors *see general relativity; tensors*
Righi-Leduc effect *see thermomagnetic effects*
rigidity *see shear modulus*
ring lasers
accelerated, Sagnac effect and four-vector pot., classical EM theory 77−68232
active medium dispersion effects on radiation intensity in mag. field *(Russian)* 77−83900
angle meas. appl., principle 78−16777
anisotropic cavity single isotope type, oppositely travelling waves competition 78−50825
anisotropic resonator, polarisation and freq. splitting of opposite waves 80−33037
anisotropic resonator with natural optical rotator and Faraday cell, lasing characts. *(Russian)* 77−19351
annular optical cavity, integral eqn., amplifying medium of limited dimens. 78−82996
backscattering influence on ring laser operation with methane cell 79−10329
backward wave interaction phenomenon study *(Russian)* 77−34899
beam divergence, mode competition effect 80−48303
beat frequency stability, slowly varying parameter effects calcs. *(Russian)* 77−61981
beat regime, with resonator freq., existence and stability *(Russian)* 78−71125
beat regime with nonlinear absorber, appl. to ang. vel. sensor *(Russian)* 78−1273
beat regime with resonator freq., existence, stability 79−50326
beat signal, luminesc. effects *(Russian)* 77−54742
beat signal, spectral characts., broad-band noise effects calcs. *(Russian)* 77−19352
bistability of ring cavity system, multiple-valued stationary state 79−94301
bistable absorber system, in ring cavity, photon statistics 79−31847
bistable absorption in Fabry Perot ring cavity 78−50821
body dither laser gyro, scale factor nonlinearity 78−79062
Brillouin optical fibre ring oscillator 78−1275
Brillouin ring laser, fibre-optic, use for inertial sensing 80−87411
capture zone minimum, in dynamic beat regime *(Russian)* 78−29987
cavity, dispersive bistability in homogeneously broadened systems 80−14306
cavity dumping using antiresonant ring and electrooptic phase modulator 77−88792
cavity dumping using antiresonant ring and electrooptic phase modulator 78−17980
coherence theory, counter-rotating laser modes 78−55387
collision model, averaged, in active medium polarizability theory 80−95924
conference, laser and electro-optical systems, San Diego, CA, USA (Feb. 1980) 80−62392
CW lasers, homogeneously broadened, with uniform distribution loss, exam. of output power 78−55332
CW oscillation in presence of passive medium, stability 78−37913
cylindrical mirror and quadratic amplifying medium *(Russian)* 78−74929
de-adjusted medium, optical axis and stability 78−82999
detuning, generation of high-frequency pulsations 80−48304
differential four frequency laser, precision angle meas. appl. *(Chinese)* 80−64083
diffraction biased unstable ring resonators, appl. in laser gyroscopes 80−1238
diffraction splitting of oppositely travelling waves, gain transverse distrib. effect 77−58353
diffraction theory, Gaussian approx. 80−53338
diffraction theory, perturbation method 80−95919
dispersive optical bistability in ring cavity 79−18386
drift splitting of opposite wave frequencies, effect of elastic collisions 80−14370
dual mode, capture zone constriction, interference effect *(Russian)* 77−88796
dual polarised ring laser, simultaneous four state oscill. 77−88787
dye, operation principles and tuning methods 77−10914
dye, optical bistability and first order phase transition 80−95918
dye CW laser, high efficiency, tunable single-freq. radiation over visible spectrum 79−72589
dye CW laser, ring resonator, mode selection 80−14371
dye laser, continuously pumped, pulse compression with slow saturable absorber 79−31959
dye laser, CW, feedback controlled pulse self-excitation 78−22152
dye laser, CW, optical diode to enforce one-direction travelling wave operation 80−69427
dye laser, CW, second-harmonic, single, freq. UV type 79−41392
dye laser, CW, technology developments and appl. 80−43383
dye laser, CW, travelling wave oscills. 77−23699
dye laser, injection-locked pumped by Xe ion laser, 4-mirror ring-cavity 80−48280
dye laser, new high efficiency system *(German)* 79−10325
dye laser, tunable, flashlamp pumped, ultra-narrow bandwidth 80−9897
dye laser, unstable ring resonator, N_2 laser pumped 80−53326
dye laser resonator, CW, astigmatism compensation using lenses 78−29978
dye laser spectral props., hole-burning effects 80−102718

ring lasers continued
dye ring laser, flashlamp pumped, injection of N_2 laser excited oscillator beam 80−5754
dye ring laser, performance and appl., internal freq. doubling possibility *(German)* 79−36927
dye ring laser charact. *(German)* 80−14365
dye solution, amplitude-spectral asymmetry of stimulated emission 79−10299
dye travelling-wave CW laser, mode locking 80−43354
emission spectrum control by mag. field induced phase anisotropy of active medium 79−94264
far IR ring laser 79−7153
Faraday element fabrication for intracavity laser appls. 78−66852
fibre laser gyroscopes 77−46728
fibre Raman ring laser 79−22981
free generation modes of travelling wave ring lasers with uniform spread *(Russian)* 77−46736
frequency characteristic distortion, by two sinusoidal signals *(Russian)* 78−22155
frequency noninteraction of oppositely travelling waves in gas ring laser 80−38043
frequency nonreciprocity of oppositely travelling waves 79−64255
frequency response of ring laser with reversible pedestal 80−48308
frequency stabilisation for two and three-mode operating regimes 77−75578
gas, limiting charact. of power resonances 80−19058
gas, nonlinear interaction of opposing beam waves with arbitrary polarisation, anal. *(Russian)* 78−82993
gas annular laser, with anisotropic resonator, longit. mag. field effects 79−27293
gas laser, mode self-locking 78−1283
gas laser, nonlinear Zeeman effect 78−71123
gas laser, opposite wave freq. difference, mag. field 79−7156
gas laser, reson. radiation trapping and nonlinear interaction of waves 79−18452
gas laser, scale factor for saturating oppositely travelling waves 80−9910
gas laser discharge oscillations, review 78−55339
gas laser freq. synchronisation region of colliding waves 80−83620
gas laser interaction of elliptically polarised opposing waves 80−38044
gas laser under gain modulation conditions 77−72011
gas laser with automatic freq. control, long-term instability and irreproducibility of freq. 79−45962
gas ring laser, synchronous four-wave regimes boundary 77−721
gas two-mode laser with two-isotope active medium, freq. charact. 77−79864
general relativity test, precision ring laser interferometry technique 80−52117
grating coupled ring laser investigation 77−31102
gyro, anomalous dispersion and gas flow effects 79−98430
gyro, dispersion and gas flow effects 80−1267
gyro, integrated 3 axis design 80−1268
gyro, low-scatter low-loss mirror prod. 80−1272
gyro, positive scale factor correction 77−34894
gyro, Rockwell programme 80−1271
gyro, tutorial review 80−1266
gyro, two-mode, four-mode soln. to locking problem 80−1270
gyro, two-mode ring laser, multioscillator approach to locking problem 79−59742
gyro, Zeeman laser, beat-note sensitivity 80−53340
gyro evaluation plan and test results 80−9934
gyro performance analysis using fast Fourier transforms 80−9933
gyro progress 78−46704
gyros system, military appl. 78−42370
gyroscope, accuracy limit, model calc. 80−1241
gyroscope, empirical model for drift estimation 79−72605
gyroscope, multioscillator approach to locking problem 78−79042
gyroscope, nuclear radiation vulnerability 80−9935
gyroscope, operation principle 79−23007
gyroscope, passive ring resonator, for inertial rot. meas. 77−58352
gyroscope, Raytheon four freq., mag. mirror, Faraday and Zeeman biassing 80−1269
gyroscope, structure and basic charact. 79−23006
gyroscope, using passive ring resonator 77−88828
gyroscope, vibratory laser, steepness charact. and S/N ratio anal. *(Russian)* 78−59070
gyroscope application *(German)* 80−53337
gyroscope applications 79−23008
gyroscope for missile guidance using magneto-optic bias mirror 78−79061
gyroscope with induced mode locking, limiting sensitivity 79−59744
high-power, single-mode, CW dye ring laser 78−13731
homogeneously broadened, mode competition, intensity fluctuations 80−43375
homogeneously broadened laser, two mode operation, analytical string signal analysis 78−55331
inertial rotation sensors, conf., San Diego USA (Aug. 1978) 80−1265
instabilities for coherently driven absorber in ring cavity 78−50822
intensity fluctuations taking spatial population-inversion grating into account 80−14364
laser gyroscope, accuracy limit *(Russian)* 79−10343
light drag coefficient determination 77−83810
lock-in width calc. 79−55156
longitudinal mode analysis 77−14766
longitudinal modes in resonators filled with inhomogeneous material 79−81463
magnetic angle convertor accuracy test method 78−77948
mean field model for absorptive and dispersive optical bistability with inhomogeneous broadening 78−50823
methane absorber narrow nonlinear resonances at low press. *(Russian)* 79−76722
mirrors, high precision reflectivity meas. technique 77−23698
misalignment sensitivity analysis for non-planar resonator 78−29985
misalignment sensitivity of ring resonator with focusing elements 80−1242
mode competition and anticorrelation calc. and expt. 80−102740
mode competition at line centre 78−25898
mode locked ring-laser with two isotope medium, two-mode emission 78−1278
mode selection, CW, laser with homogeneously broadened gain 77−61978
modes in system of two coupled ring resonators 79−10328

ring lasers continued
modes of resonator with additional return mirror 78−46677
multilayer light scattering and laser gyro 78−33764
multimode, containing saturable absorbers, bistable operation 80−91862
multimode, high-Q power resonances, expt. investigation 78−82997
negative branch unstable resonator, with self imaging aperture 79−977
nonlinear nonreciprocity effects, laser placed in longit. mag. field 80−43377
nonlinear phenomena in laser with inhomogeneous nonreciprocal element 78−50824
nonlinear polarisability of two-isotope active medium 80−14369
nonlinear resonance appl. for frequency stabilisation and spectrometry *(Russian)* 79−94261
nonreciprocal effects, longit. mag. field effect 78−17986
nonreciprocal effects on appl. of transverse mag. field to active medium 80−53341
open cavity matrix eqns. in diffraction theory 80−69429
optical cavity, nearly confocal, with spatially inhomogeneous medium, threshold gain 80−43373
optical elements with mag. circular dichroism, laser props. 79−31951
optical resonator with diaphragmed spherical mirror and spatially inhomogeneous amplifying medium *(Russian)* 80−64082
output characteristic coefficient determ. 77−7123
passive resonant ring laser gyroscope design 80−99768
perturbed cavity calculations 80−102739
plane-mirror ring cavity with diaphragm and with spatially inhomogeneous amplifying medium 79−55162
plasma, laser gas discharge, Faraday rot. diagnostics 80−43981
Polarisation-frequency characteristics of compound ring anisotropic resonators with one and two mirrors *(Russian)* 77−83901
power resonances shape 77−58355
PT asymmetry and four-fold EM degeneracy lifting, appl. to ring laser mode splitting 80−23606
pulse train generation in dye laser with saturable absorber *(German)* 77−38936
quasiclassical equation of motion, spontaneous emission in lasing channel *(Russian)* 78−90434
Raytheon laser gyroscope using MnBi magnetic mirror 78−79064
Raytheon multioscillator gyroscope 78−79063
relativistic Doppler effect, two-wave mode instability and optimum tuning 77−38940
resonance phenomena with saturated absorpt. *(Russian)* 78−59048
resonator loaded with periodically inhomogeneous active medium, spatial struct. of field 79−81462
resonator with arbitrarily situated medium, axial contour and stability *(Russian)* 79−89939
resonator with diaphragmed spherical mirror and inhomogeneous amplifying media *(Russian)* 80−28256
rhodamine 6G, ring struct. laser emission, resonator exit mirror effect 77−38941
rhodamine 6G dye in ethylene glycol, broadband optical diode, one directional traveling wave operation of ring laser 80−58606
rhodamine 6G in ethanol, injection locked ring amplifier 77−88788
rhodamine 6G thin film ring laser, emission features 79−64221
rotating, eigenfrequency splitting, effect of medium refr. index 79−98414
rotating for plane angle meas., error anal. *(Russian)* 77−38942
rotating ring laser, freq. charact., mode composition effects 77−54741
rotation rate sensors, Air Force appls. 80−9932
ruby ring laser with forced mode locking 80−95915
Sagnac fibre-ring interferometer gyro with electronic phase sensing 79−17472
saturating opposite waves interaction 77−50695
self pulsing in dispersive optical bistability in ring cavity 80−78890
self-locking type II mode, freq. depend. effects 78−5506
self-mode locking phenomena *(Japanese)* 77−58307
semiclassical equations of motion for system with spontaneous emission in generation channel 80−1240
semiconductor-waveguide lasers in bent-guide structs., charact. *(Japanese)* 78−87062
SHG, computer controlled intracavity, in CW ring dye laser 80−91841
soft apertures, method of controlling inversion profile in amplifier 79−98427
solid, synchronisation regimes of opposite waves and beats *(Russian)* 79−3717
solid ring laser with additional mirrors, stabilisation by external signal 78−82998
solid state, with intracavity bleachable filter, conditions for CW stimulated emission 80−14368
solid-state, interactions between opposite waves, self-modulation and beats 78−17983
solid-state, synchronisation modes of colliding waves and beats 79−72602
solid-state, with weak external signals 77−23702
solid-state laser, mode locking theory 79−41399
solid-state laser, travelling-wave, linear stage of field development 80−23724
solid-state ring laser, generation of microsecond pulses 80−9913
solid-state ring laser, single-freq., spontaneous antiphase fluctuations, theory 80−91821
spatial field structure in resonator filled by periodically inhomogeneous active medium *(Russian)* 79−976
stability of oppositely travelling waves 79−98415
synchronisation region width calc. *(Russian)* 78−46681
transient processes, influence of radiation interaction with reflector material 79−13993
travelling wave, mode self-synchronisation 80−83605
travelling wave, operation with periodically varying resonator parameters 78−46678
travelling wave amplifier, spontaneous radiation channelling 79−27294
travelling wave cross-saturation asymmetry 80−43371
travelling wave generation, beat freq. dispersion *(Russian)* 77−38946
travelling wave laser, harmonic var. in cavity freq. difference, beat signal phase 77−75571
travelling wave lasers with periodically varying cavity parameters, operation anal. 78−37917
travelling-wave Zeeman gas laser operating at high radiation intensities, theory 80−9912
tunable laser progress 80−43344
tuning, freq. shift and splitting for opposite waves, spatially inhomogeneous media 79−7155

ring lasers continued
two-mode, intensity fluctuations 80−33038
two-mode, intensity fluctuations meas. near threshold 78−55388
two-mode ring laser, correl. functions 79−76720
two-photon absorbent, pulse evolution 79−10326
ultrashort laser pulses, interaction with condensed matter *(German)* 79−27335
ultrashort-pulse generation by lasers with saturable absorbers 78−46687
unbalanced antiresonant ring cavity, perturbed Gaussian modes 77−718
unidirectional, modes 80−91818
unidirectional system efficiency comparison *(French)* 79−76717
unstable optical resonators with tilted spherical mirrors, design eqns. 78−74930
Zeeman, four-mode operation 80−19053
Zeeman laser, interaction of modes characterized by orthogonal circular polarizations 80−48306
Zeeman multioscillator ring laser gyro, props. 79−72604
AlGaAs-GaAs ring laser, injection type, laser oscill. 77−75570
CO_2 laser compact wideband ring modulator 77−88803
CO_2, optical coupling modulation in travelling-wave cavities 77−42553
GaAlAs DH injection laser, half-ring, room temp. operation 80−58558
GaAs-(GaAl)As injection lasers with circular resonator 80−74377
GaAs-$Ga_{1-x}Al_xAs$, optically pumped ring laser fabricated by LPE over chemically etched channels 77−10958
GaAs-$Ga_{1-x}Al_xAs$ half-ring laser, fabrication by LPE over chemically etched channels 77−684
He-Ne, 0.63 μm emission, difference freq. depend. on active medium gain 77−722
He-Ne, angular meas., experimental appl. *(Japanese)* 79−71408
He-Ne, anisotropic ring laser cavity, polarisation characts. 79−59726
He-Ne, freq. shift of 3.39 μm methane transition 79−27298
He-Ne, nonlinear polarisation interaction of opposite waves 78−50828
He-Ne, nonlinear Zeeman effect 78−71123
He-Ne, operating well above lasing threshold Zeeman effect 80−33039
He-Ne, opposite waves competition dynamics 77−72008
He-Ne, rapidly pumped, competition between opposite waves 78−17985
He-Ne, rotating, output characts. 78−29982
He-Ne, two-mode, stimulated emission regimes 77−657
He-Ne, with nonlinear absorber, competition of orthogonally polarised modes 78−17984
He-Ne, Zeeman effect, influence of reson. radiation trapping 77−75574
He-Ne gas ring laser, unidirectional two-mode lasing, stability region width 79−76721
He-Ne laser, Ne $3s_2$-$2p_4$ transition relax. consts. using cross saturation of travelling waves 79−76374
He-Ne laser, two-mode ring laser power resons. 78−1211
He-Ne laser placed in longit. mag. field, nonlinear nonreciprocity effects 80−43377
He-Ne ring laser, 0.6328 μm, self-pulsing conditions 80−87414
He-Ne ring laser, absorbing medium press. influence on power resonance characts. *(Russian)* 80−23725
He-Ne ring laser, influence of pressure on Zeeman effect 80−19056
He-Ne ring laser, methane stabilised, nonlinear resonance freq. shift due to back scatt. *(Russian)* 80−78874
He-Ne ring laser, Ne isotopic composition changes during prolonged discharge *(Russian)* 78−22110
He-Ne ring laser, nonlinear spectroscopic technique 80−91819
He-Ne ring laser, nonreciprocal effects with transverse mag. field applied to active medium 80−91820
He-Ne ring laser beat frequency deviation rel. to dispersion and modulation 79−68410
He-Ne ring laser with methane absorpt. cell, power reson. characts. 80−28255
He-Ne two mode ring laser for interferometry 78−1260
He-Ne two-mode travelling-wave laser, Zeeman beats 78−50827
He-Ne-methane ring laser, frequency stabilized, operating charact. 80−14366
He-Ne-methane ring laser, power resonances 80−99761
He-Ne-methane ring laser, freq. synchronisation interval for oppositely directed waves 80−99762
He-Ne-methane stabilised ring laser, freq. stability calcs. *(Russian)* 78−9401
I photodissoc. ring laser, lasing regimes, emission and polarization characts. 80−48236
Na_2 optically-pumped three-level dimer lasers, amplification profiles and dynamic Stark effect 79−41367
Nd garnet ring laser, with return mirror, mode locking 80−99764
Nd laser, continuously tunable, pulsed, operation and output, characts. 79−18448
Nd:glass, continuous dynamic freq. tuning of pulse radiation 78−29986
Nd:glass, mode-locking, unidirectional travelling wave operation 77−61976
Nd:glass, pulsed ring laser, quasistationary single-freq. generation *(Russian)* 77−83897
Nd:glass laser, short pulse mode-locked, using prisms 80−83617
Nd:glass laser, with nonlinear absorber, pulsed Q switching 78−9400
Nd:glass mode locked ring laser, unidirectional travelling wave operation 77−88812
Nd:glass ring laser, actively mode-locked and Q-controlled, props. 79−18445
Nd:glass ring laser, holographic dispersion element *(Russian)* 78−59051
Nd:glass ring laser, single synchronizable ps pulse generation 77−14739
Nd:glass synchronised ultrashort laser pulse, appl. to diagnosis of CO_2-produced plasmas 78−42825
Nd:glass travelling-wave sweep laser, emission spectrum dynamics 78−50829
Nd^{3+}:YAG CW ring laser, axial mode locking by electrooptic $LiNbO_3$ phase modulator 78−50835
Nd^{3+}:YAG CW ring laser, fluctuation spectrum 80−9914
Nd^{3+}:YAG stabilised single-freq. travelling wave laser 79−18449
Ne ring laser, two-mode, oppositely travelling waves, beat freq. obs. 77−10963

ringers *see bells*

riometers *see ionospheric measuring apparatus*

ripplons
conference, Moscow, USSR (Apr. 1978) 80−62378
L-α-dipalmitoyl phosphatidyl choline, monolayers, laser-ripplon scatt. at air-water interface 79−99894
He, liq., adiabatic approach in theory of electron-ripplon scatt. at surface *(Russian)* 77−80660

ripplons continued
He, liq., dynamic struct. factor function, surface contrib. 77−47634
He, liq., electron-charged surface, nonlinear wave propag., theory 78−67879
He, liq., hot electrons on surface *(Russian)* 78−87832
He, liq., phonon coupling of two-dimens. Wigner cryst. with second surface sound *(Russian)* 80−92756
He, liq., surface, high freq. cond. of electrons 78−10238
He, liq., surface, two-dimensional electron gas, ripplon scatt. effect on cyclotron 79−60566
He, liq., surface, two-dimens. Wigner cryst., electron-ripplon reson. anomalies *(Russian)* 80−92754
He, liq., Wigner 2-dimens. lattice, on surface, reson. linewidths 79−86949
He liq. surface, cyclotron reson. of two-dimens. electrons *(Russian)* 80−88374
He, liq. surface, electron solid, phonon-ripplon coupling 79−42337
He, liquid, charged surface, current instability theory *(Russian)* 80−29243
He, liquid, effect of short-wave surface excitations on damping in two-dimens. electron gas *(Russian)* 79−10995
He, liquid, short-wave surface excitation study using electron gas nonlinear I-V characts. *(Russian)* 80−10717
He, liquid surface, electron-ripplon spectrum in mag. field normal to surface *(Russian)* 80−49444
He liquid surface, localised electron states 78−60007
^{3}He-^{4}He, charged interface, ripplon softening 80−34269
^{3}He-^{4}He interface, charge induced ripplon softening and dimple crystallisation 79−28170
^{4}He film, heat cond. by ripplons 79−51375
^{4}He, liq., atomic scattering at free surface 78−56003
^{4}He, liq., excitations produced by ^{4}He atomic beam 78−10241
^{4}He, liquid, surface electron interaction with EM radiation *(Russian)* 80−54449
^{4}He liquid surface, hot carrier mobility 78−59988
^{4}He, superfluid, ^{4}He atom scatt., quantum interference 79−99382
^{4}He, superfluid, free surface, book contrib. 80−2231
^{4}He, superfluid, microscopic theory 78−14525
^{4}He, superfluid, ripplon canonical conjugate momenta 79−55951
^{4}He, superfluid, ripplon damping at low temp., calc. 79−7720
^{4}He, superfluid, surface, ripplons, adsorbed ^{3}He and heat conduction meas. 80−49459
^{4}He, superfluid film, long wavelength excitations, ripplon dispersion 79−73356
^{4}He surface, hot electrons theory 79−42329

rivers
see also lakes
acid mine drainage problems treatment for Monongahela river basin, QUAL II simulation 79−29806
acid rain, neutralization in Hubbard Brook ecosystem 79−74922
acidification of headwater stream, New Jersey Pinelands 80−81945
acoustic noise from breaking ice 78−53671
aeration system subject to random disturbances, optimal control 78−16078
agricultural land urbanisation hydrologic impact, distributed watershed model 77−37277
Aisne, France, N contamination assessment by use of differential temp. calcs. 79−66730
Alberta bankfull discharge, effects of channel enlargement by river ice 80−8369
alluvial bed load transport estimation 78−20444
alluvial channels in Kansas, gradient, discharge and particle-size data rel. to braiding 79−20869
alluvial soils and flooding relationship in Piedmont Lowland, SE.Pennsylvania 79−88385
Almond, Scotland, sediment discharge measurements 79−88386
Amazon, ^{18}O concs. and rel. discharges in Negro and Solimoes rivers 77−5268
Amazon, bed sediment size distrib. 80−101392
Amazon, organic C oxidation and transport 80−105007
Amazon discharge effect on surface salinity and dissolved silicate, in Caribbean 79−39722
Amazon River, fine sediment non-uniform vertical distrib. 79−84313
Amazon River, sediment loads meas. 79−44206
Amazon suspended sediment reaction with seawater, cation exchange characts. 80−8337
Amur basin rivers, anal. and forecasting of dates of ice breakup *(Russian)* 77−53088
ancient big river systems significance and origin 78−77281
annual average discharge processes, long-range intraseries couplings 77−78260
annual discharge variations, long-range intraseries couplings for ultralong range forecasting 77−78261
annual floods of E.Australia catchments, freq. distribs. 80−105012
annual river flows, Box-Jenkins modelling appl. 77−87633
annual streamflow record extension by correl. methods 80−81950
aqueous heavy metals, adsorption on inorganic minerals 78−49006
Arno flood study 79−88373
arroyo cutting near Santa Fe, New Mexico 77−70698
artificial aeration optimal control methods 78−36203
asbestos mining area river pollution meas. by proton-induced X-ray emission 79−100556
atmosphere contribution to stream water chem., North Cascade Range, USA 80−61824
Australian streams, preliminary estimation of reservoir storage 77−86947
average slopes of watersheds and rivers, improved formulae 78−61448
Baltic Sea sedimentation, role of river suspensions *(Russian)* 78−7616
bank erosion rate, obs. in Devon, England 80−105002
bank-full discharge of rivers 79−88381
basin hydrology, tests of random network model 77−45029
basin recharge, Dupuit-Forchheimer and potential theories 77−25722
basin study simulation model 80−31079
basin water resource, Pareto region, stochastic multicriterial problem in control 80−4055
beach sediments, lower St. Lawrence Estuary, Quebec, frost effects 78−7609
Beatton River, British Columbia, regional trend to meander migration 80−101391
bed evolution rel. to river flow and sediments *(Russian)* 77−29330

rivers continued
bed forms and unsteady flow, classification 77−45036
bed forms and unsteady processes 77−29352
bed load transport, Bagnold's granular fluid model 80−51442
bed load transport by natural rivers 77−73778
bed load transport by submerged jets, laboratory expts. 80−81942
bed material mobility, probabilistic model and obs. *(Italian)* 78−53665
bed scallops and ripples formed by flowing water, size and origin 79−27628
bed shear stress and vel. profiles over various bed configs. in river bend 78−20439
Bedford Ouse River, systems model of stream flow and water quality 80−81956
bedload dynamics, grain-grain interactions in water flows 80−31069
bedload stresses and Bagnold's bedform theory 77−70695
bedload transport measurement, calibration of acoustic device 80−56620
bedload transport oscillations, circuit for acoustic detect. 77−45168
Belgium, pluviometric system normals 79−66723
Belorussia, annual runoff, land reclamation effects 78−16076
bend, fluid flow behaviour, simulation 79−100885
Bhagirathi River, West Bengal, unidirectional alluvial channels, metamorphosis philosophy 80−31075
big river sands, modern, petrology and chemistry 79−25274
Biya and Katun rivers, evolution of river bed in confluence node 78−3839
Black River, Ontario, streamflow record synthesis, feature prediction model appl. 80−98372
Blue Ridge and Piedmont provinces, stream patterns rel. to Recent vertical crustal movements 79−79794
bore propagation theory based on classical hydraulic theory 79−84312
Brahmaputra river, flood of Aug. 1962, synoptic aspects 80−81939
braided features rel. to braided Martian channels 79−2507
Breg in W.Germany, uranine tracer for karstified aquifer 80−26564
Britain, runoff and water balance, 50000 yr BP to present day 80−72566
Bulgarian river flow prediction, methods 80−26562
Burhi Gandak, severe floods in 1974 and 1975 79−20891
canal, converging, unsteady 2-D compressible boundary layer flow 79−20885
Caniapiscau River, Canada, shaping by ice during the last 6000 years *(French)* 80−12439
canyon rivers, rapids charact. 80−72564
Caspian Sea feeders, continental runoff contrib. to biogenous elements balance 80−31073
catchment model parameters sensitivity anal. 78−77288
channel bottom, kinematic charact. of nonuniform flow, limiting stability, erosion 80−94547
channel charact. and discharge, conceptual model 79−74907
channel development, dynamic process-response model 79−74909
channel factors simulation in numerical computations of flow *(Polish)* 79−25280
channel flow resistance due to large obstructing boulders 80−81947
channel geometry, adaptive adjustment 77−45027
channel network development and stream link length freq. distrib. 77−91164
channel network evolution in mature drainage basins, relief factor 77−66932
channel networks, link slope distrib. 77−5258
channel turbulence charact. and deform. in inshore zone 77−78258
chemical composition, of river water, in northern Okinawa Honto, Japan *(Japanese)* 79−96782
chemical composition rel. to atmospheric humidity, temperature data 1971-75 period *(Japanese)* 79−70874
Chesapeake Bay and Potomac River, nontidal variability, nonlocal atm. forcing 78−92829
N.Chesapeake Bay estuary, agglomerated suspended sediments microstruct. 79−53336
coarse riverbed material, probability density function of biased samples 80−12445
Cochin backwater, India, estuarine water, particulate heavy metal content 80−7964
Cochin Harbour mouth, India, hydrographic charact. and tidal prism 80−41452
cohesionless bottom sediments, limiting stability in turbulent channel flow, erosion 80−94546
cohesionless soils on channel bottom and sloping sides, onset of motion 80−94548
Colorado River and Quaternary climatic change in central Texas 77−91251
Colorado River in Grand Canyon, control of rapids and pools 79−62537
Columbia Icefield, shrinkage or growth on river systems 78−61445
Columbia River discharge effect on radioactivity field in NE.Pacific *(Russian)* 79−39761
composite beds, continuous free-surface flow *(French)* 79−100877
SW Connecticut, detect. of nonpoint pollution of small streams 77−33099
Connecticut River offshore plume, motion field obs. 77−33111
contaminant, buoyant, in shallow channel, longitudinal dispersion 77−21805
Corsica (France), Quaternary fluvial deposits props. and chronology 78−57234
Cumbarjua Canal, Goa, India, hydrographic conditions and flow pattern 77−91146
currents in fjord-type lake 78−49051
daily flow, non parametric Markov model, appl. to Cheyenne river 80−81948
Dakota drainage pattern mapping IR thermal imagery remote sensing 80−81892
Danube, distrib. of artificial radionuclides at mile 34, 1976 79−39323
Danube, radioactive pollution meas. 1972 to 1975 by γ-spectrometric anal. *(Bulgarian)* 79−88019
Danube hydroenergetic potential, utilisation in Austria and other European countries *(Czech)* 79−66401
Danube water and sediments, radionuclides detec. during 1977 79−12158
data base system for river basin management 79−25288
Dauguvos, plume influence on Baltic Sea *(Russian)* 80−98345
Delaware River, evidence for former extension to Wilmington Submarine Canyon 77−37255
delta evolution, sediment transport modelling 78−15993
deltas, variability of types 77−73769

rivers continued
denudation, fallacy of stream equilib. assumption 77−78236
Devitsa River, 1975 spring flooding charact. 77−78256
discharge effects on oceanic residence times of trace metals 77−78228
discharge forecasting using hydrologic model of Mahanadi basin 80−31130
discharge gauging using weirs and flumes, Soviet rules 80−26561
discharge volume after marsh reclamation, theory including gorundwater 80−36349
discharge volume estimation, correction for channel and floodplain morphology 80−85695
dissolved Fe, Mn organic matter, estuarine mixing implications 80−17296
dissolved O_2 reliability parameter in probabilistic programming models 80−26179
dissolved oxygen and biochemical oxygen demand, random signal anal. applic. 77−45047
diversion, effect on Mediterranean circulation 80−77014
Diyala catchment, Iraq, water balance between Derbendikhan and Himrin dams 80−12462
Dnieper navigable lock, V.I. Lenin hydroelectric power station, geological problems *(Russian)* 77−86883
downstream pollution short-term prediction, one-dimensional transient model 80−81496
drainage basin characteristics, network power model 80−61823
drainage basin composition, random model appl. 77−45030
drainage basin peakedness var. with area 77−45022
drainage basins, computer, analysis *(French)* 78−7786
drainage basins, snow estimated water equivalents and melting charact. determ. 78−96249
drainage density and channel network geometry, post-Hortonian studies 79−20874
drainage density estimation from topological variables 80−61831
drainage density prediction techniques, evaluation of surrogate methods 80−8365
drainage headwater development, modelling 79−20875
drainage history of karstic limestone terrain, Texas 80−56501
drainage network change in Britain 80−81934
drainage network composition analysis 78−81226
drainage network mapping of Pantanal Brazil, Landsat-2 imagery 80−81944
drainage networks, topological classifications, evaluation 78−81254
drainage patterns, link magnitude var. with map scale 77−25723
drainage water from spruce trees, acid content determ. method 77−37448
drought definitions 80−105010
drought flow hydrographs, regionalised, from mature glaciated plateau 77−91180
drought in streamflow series, statistical charact. 80−105009
dynamic features of deficit forms in translational flows 79−39775
East Fork River, Wyoming, 1976 bedload meas. 78−49055
East River tidal strait, New York, hydrodynamic charact. 77−37222
Ebro river hydrological study *(French)* 77−78239
Elbe estuary on North Sea nested model 77−37212
Elta reservoir, rock slide stability, geological survey *(German)* 78−7636
energy extraction possibilities, developing countries appl. 79−43729
England and Wales, 1975-6, water balance investigations 78−88865
entropy concepts reevaluation in fluvial geomorphology 80−12453
ephemeral streams in arid regions, aquifer recharge 79−5521
erodable riverbed, channel deformations, hydraulic modelling 80−77024
erodible sandy channel, rate and time of deform. due to artificially compressed flow 77−78259
erosion and sedimentation, problems rel. to water supply, research needs 78−61444
estaurine sediments, methyl mercury growth and decay during storage 77−66937
estuaries, chemical speciation of Cd, Cu, Pb and Zn in mixed freshwater-seawater solns. 78−20409
estuaries, contaminants, long-term dispersion 77−78229
estuaries, control of stratification in almost-enclosed regions 79−46358
estuaries, hydrodynamic model using smooth elements, accuracy 80−98356
estuaries, nontidal, hydrographic network changes under influence of natural factors and water management measures 79−29792
estuaries, stratified, water circulation forecasting for water quality management planning 79−5543
estuaries, stratified turbulent flow, finite element method appl. 78−90964
estuaries, transport, erosion and deposition of cohesive sediments, modelling 78−15994
estuaries, two dimensional, approx. solution to obtain the streamfunction 78−81187
estuaries, two-layer transport capacity of a constriction, barotropic current fluctuations 77−60396
estuaries, very low salinity regions, chemical and biological reaction sites 78−81199
estuaries bordering continental shelf, scatt. of oceanic long waves 77−78191
estuaries of variable breadth and depth tidally induced residual currents 80−72544
estuarine and coastal waters, suspended particles surface charge 80−36331
estuarine dynamics, mass balance eqn., longitudinal dispersion function estimation 77−37262
estuarine environment, natural suspended matter flocculation and electro-kinetic pot. *(French)* 80−61817
estuarine environments, Cu inorganic speciation 78−69371
estuarine flow, nonlinear partial differential eqn., finite element anal. *(Japanese)* 78−8233
estuarine fronts remote sensing, behaviour study, pollutant effects 77−78470
estuarine hydrography and sedimentation, measurement techniques, book 80−36788
estuarine mixing, dissolved humic acids and Fe removal 79−34830
estuarine mixing, flocculation of dissolved Fe, Mn, Al, Cu, Ni, Co and Cd 79−29774
estuarine sediments, heavy metal pollution detection 78−73546
estuarine surface microlayer and trace metal cycling in salt marsh 79−57984
estuarine tidal front, trace metal enhancements in biotic and abiotic components 79−2265

rivers continued
estuarine water in Solent area, dissolved Se meas. 78−57230
estuarine water-quality model in an oscillating constant-volume reference frame 79−34871
estuarine waters, behaviour of trace chem. constituents 79−16512
estuary, flow onto continental shelf, simple theoretical model 78−49030
estuary, Jamaica Bay, New York, dissolved O modelling 77−17146
estuary, mass and salt transfers and halocline depths 77−29322
estuary, nonlinear response to tidal action for potential hydroelectric power generation 77−70692
estuary, spread of river jet, models 80−98353
estuary, tidal two-dimensional hydrodynamic digital simulation by finite element method 78−92846
estuary, volatile petroleum hydrocarbons contrib. to organic C budget 79−70473
estuary, well mixed, buoyancy effects on longitudinal dispersion 80−85681
estuary and river sited power plants, water discharge and chlorination, simulation 78−96250
estuary circulation (partially mixed), two-dimens. model 80−109161
estuary halocline, expt. simulation, salt diffusion in tap water, educational aspects 78−61980
estuary mapping, classification algorithms for Landsat data 78−40567
estuary models of Tampa Bay, Florida, comparison 78−77269
estuary pollution model development, wind and freshwater flow influence 78−81207
estuary proportioning with sinusoidal tidal wave *(Italian)* 79−20839
estuary unsteady-state two-dimensional salinity intrusion model 78−77271
estuary water quality management for P treatment 77−21823
estuary water quality models, finite difference and finite element methods 78−77375
estuary with uniform reversing tidal flow, suspended sediment model 78−7648
Euphrates watershed, free water surface evaporation losses 80−81957
evaporation from water surfaces in Armenian SSR 78−7673
extreme floods, rainfall rel. to runoff, nonlinear analysis 78−81247
fall height rel. to water vel. 78−7678
Finnish river water pollution monitoring network 80−89686
fjords, river fronts in surface waters 79−57953
flash floods, American National Weather Service (NWS) warning and disaster preparedness program 79−25289
floating ice layer thickness meas. using nanosecond impulse X-band radar 78−62178
flood and tidal flows, network hydraulic model 79−12162
flood calculations, analogue rivers selection 78−16073
flood control planning 78−81245
flood estimation, critical duration of rainfall 77−41084
flood event real-time predictors, stochastic model 80−67383
flood flows routeing in rivers, parameter optimisation 77−37263
flood forecasting in river, by unit hydrograph method 77−5254
flood forecasting model from rainfall catchment and evaporation data, retention hysteresis 80−81951
flood freq. estimates, reliability 77−86944
flood freq. model for snowmelt in northern subarctic basin 77−9454
flood frequency, regional analysis 77−60431
flood frequency analysis, log Pearson type 3 distrib., max. likelihood theory 78−61470
flood frequency analysis, Pearson type 3 and log Pearson type 3 distribs. 77−78285
flood frequency analysis with a generalized skew coefficient 79−5531
flood inundation of agricultural land, LANDSAT digital image anal. 80−61913
flood levee reliability, anal. 77−91182
flood levels in Brest and Gomel' region *(Russian)* 77−29332
flood prediction computer-operated telemetered gauge network 77−21818
flood sequences, apparent regional skew 77−64355
flood storage distribution and travel time isochrones from tracer study on small watershed 77−91174
flood warning system, on-line, based on adaptive model, desk-top computer appl. 79−34977
flood water movement identification 77−70710
flood wave propagation in channels with storage areas, diffusion eqn. 79−25277
flood-plain delineation by multispectral data analysis 77−73885
floodplain planning 78−81246
floods, 1975 August, in Orissa, India 79−20886
floods, partial duration series models, Poisson assumption anal. 80−8374
floods and morphometry in small drainage basins 77−29340
floods in Plynlimon expt. catchments, Wales, geomorphological effectiveness 80−81932
flow, bed topography, grain size and sedimentary struct. in open channel bends 78−20443
flow, effects of drought in England and Wales, 1975-6 period 78−88867
flow prediction, nonlinear feedback system model 80−98375
flow prediction by multiplicative model 79−53399
flow-routing techniques, linear system vs. finite difference models 77−29512
FLUCOMP numerical river flow model 80−26653
fluid dynamics conference, Aug. 1978, Strasbourg, France 80−36764
fluvial geomorphology, rate law for relaxation times 77−33098
fluvial streams, sedimentology, Rayleigh-Ritz method appl. 78−92878
fluviatile environment, artifacts as sedimentary particles 78−70239
forested watershed streamflow during storm, dominance of flow through soil 80−61825
Fraser River, B.C., Streamflow record synthesis, feature prediction model appl. 80−98372
Fraser River estuary, British Columbia, surface currents obs. using airborne inertial sighting system 78−73384
frazil ice conc. meas. system using laser Doppler velocimeter 77−25796
free-surface sediment conveying river bed flow, flowrate and momentum correction factors 80−36339
frictionless tidal channel behaviour, finite element and finite difference methods appl. 78−92876
fuzzy equations, water pollution control appls. 79−57523
Ganges Basin water supply, groundwater recharge by pumping along rivers 80−81952
Garonne-Gironde river estuary system, radioactive tracing of physio-chemical behaviour of Zn $(OH)_2$ *(French)* 80−7994
Georges River, Sydney, changes in urban water resource 77−70697

rivers continued
geostrophic adjustment in wide estuaries, theory and laboratory expts. for two-layer system 79−48503
geothermal steam samples from Lanzarote (Canary Islands) isotopic comp. 77−49048
geothermal waste water, environmental effects on river system 79−29487
Ghaggar River, India, hydrometeorological study of rainfall trend in catchment area 77−56660
Gironde estuary, turbidity max., numerical simulation *(French)* 79−79869
Gironde estuary vertical circulation, real time two-dimensional model *(French)* 79−62519
Gironde inlet and Pertuis of Maumusson, estuarine waters seaward dispersion, remote sensing study *(French)* 80−8324
Goulais, overbank alluvium rel. to Nipissing Great Lakes events 79−84251
Grand, Ontario, geomorphic effects of catastrophic flood 78−28248
granular bed material, erosional capacity of smoothly varying streams, particle size 80−94545
gravel river, grain size var. statistics 79−5513
gravity waves propag. over permeable bed *(Polish)* 78−38353
Great Lakes, runoff rel. to W. Lake Michigan shoreline erosion 79−5542
Great Miami River, Ohio, behaviour and transport of industrially derived Pu 78−16061
Grote Nete basin, Belgium, geomorphology *(Flemish)* 78−61452
groundwater recharge mechanism, Los Naranjos area, Mexico, using environmental isotope methods 80−12458
N.Gulf of Alaska, river runoff rel. to coastal flow meas. by drogued drift buoys 80−51431
gulf of St. Lawrence, buoyancy driven current system, mixing and circulation 80−90095
Gulf of St. Lawrence and estuary, geochem. of Zn, Cu and Pb in sediments 78−92855
Gulf of Taganrog salinity, after restriction of exchange with Sea of Azov 80−36335
gully erosion, gravel pad appls. *(French)* 79−62533
headwater streams, Vermont and New Hampshire, chemical charact. 77−78290
headwaters, wear of unsound pebbles 79−92557
heat and mass transfer data to atmosphere 78−96253
heavy metals, distrib. and speciation in aquatic systems, analytical techniques 78−69390
heavy metals and organic C conc. in surface microlayer, physical processes effects 79−57978
high-water peaks, annual recurrence *(French)* 80−77020
hodograph method, use of reference function 79−84323
Hope, Jamaica, shear stress and competence determ. 78−61474
Hudson, ^{226}Ra flux from estuarine and continental shelf sediments 78−32061
Hudson Bay rivers, historical freeze-up dates as climatological data, content anal. 77−2224
Hudson estuary, Ba and ^{226}Ra desorption from river-borne sediments 79−79877
Hudson Estuary, salinity and temp. distrib. 77−17136
Hudson River estuary, ^{222}Rn distrib. and transport across sediment-water interface 78−16064
Hudson River estuary, man-made radionuclides and sedimentation 77−2183
Hunter, sand supply at New South Wales coast 78−16066
Hurricane Agnes storm and flood, geomorphic effects, SE.Pennsylvania 78−77280
hybrid river models software support 80−56499
hydrobiological studies at nuclear sites, conception and main data *(French)* 80−76665
hydrograph calc. problems for mountain river 78−7676
hydrologic data set distribution functions, extremes and confidence intervals 78−24313
hydrological forecasts, automatic processing of operational information 78−3842
hydrological system, state space modelling and identification 79−79908
hydrometeorological series stationary properties study, Oise river basin appl. *(French)* 78−36210
hydrophobic pollutants, sorption on natural sediments 79−83651
hydrophysical apparatus, channels with automatic transfer function correction *(Russian)* 78−16193
ice, book contrib. 78−61476
ice, influence on behaviour and use of rivers 79−62525
ice break-up, satellite monitoring 78−65350
ice jams, form. conditions and forecasts 78−92863
ice jams, physical meas. 79−53398
ice processes, radiohydroacoustic monitoring method 80−26649
ice-cover thickness, pulsed radar meas. method 78−92862
ice-covered streams, water discharge meas. 79−12160
ice-jam backwater levels cutoff period 79−39778
impurities dispersion, model *(Dutch)* 79−88011
in-stream settling basin sediment routeing, convective dispersion model 77−37272
Indian rivers, chemical and sediment load input into world oceans 79−34870
inorganic pollutant meas. by nuclear techniques 77−41102
interfluvial area of Minija and Sventoji, marginal formations structures *(Russian)* 77−25708
Iowa, wind-aligned drainage in loess 80−41467
Ireland west coast, runoff effects from seawater colour, UV absorbance and salinity meas. 78−85603
Isar River, Bavaria, trace elements distrib. in sediment, suspension and water samples by neutron activation analysis 78−3834
isotopic distribution in waters from high altitude region north of Jolma Longma mountain, geochem. charact. *(Chinese)* 79−2304
Jamaica Bay, NY, estuarine P model parameter estimation 77−21777
Jordan River, Utah, steady state quality modelling 78−81248
Kakogawa River basin, multiobjective optimisation of water resources problems 79−57993
Kama Reservoir, USSR, forecasting spring inflow 80−105008
Kicking Horse River, bar evolution and stratification in gravelly braided stream 77−64332
kinetic energy distributions in small watersheds, urbanisation effects 79−25275
Krishnapatnam coastal inlet, stability rel. to wave conditions and longshore currents 80−41449

rivers continued
Kumbel River, 1975, Aug. 19 mudslide 77−78257
Kuskokwim River drainage, Alaska, Hg dispersal from lode sources 78−40600
Lake Ontario feeders, sediment and nutrient loadings, methodological arguments 78−77278
Lake Ontario tributary waters, N and P conc. determ. 79−79418
Late Wisconsin flood into Gulf of Mexico 79−29775
level and velocity measurement by random signal anal. from surface waves 79−72976
Liard River, SE Yukon, exposed late Tertiary-Quaternary stratigraphic sequence 79−62499
lichenometry rel. to river channel capacity 77−45033
Lithuania, lake vegetation influence on river runoff *(Russian)* 79−12154
Lithuania, river flood durations rel. to rainfall (1946-72) *(Russian)* 79−5516
Lithuanian inter-river relief, kames structure *(Russian)* 79−48486
Lithuanian lake overflow influence on river runoff *(Russian)* 78−16070
Lithuanian river groundwater discharge long-term fluctuations *(Russian)* 79−92554
local scour, stable numerical model 77−21809
Loch Lomond Stadial in British Isles 79−79887
longitudinal slope determ. 80−82108
Louisiana canals hydrologic simulation model 80−31080
Macdonald Valley, NSW, catastrophic channel changes in 1949-1955 period 78−16065
Mackenzie, Canada, asymm. transverse valley profiles 78−20446
Mackenzie, Canada, ice-push features stability 78−28247
Mahanadi basin, India, climatic study of river regime 80−81941
Main River, County Antrim, N and P loads meas. by discrete and intensive sampling 79−44213
management operational system development using weather radar 78−40718
Mandovi estuary, circulation and sedimentation rel. to Aguada bar 77−73756
old Mangalore Port, India, sediment transport and siltation of navigational channel 80−56488
old Mangalore port, seasonal vars. in estuarine and oceanic waters hydrographic conditions 80−41451
Manning's roughness coeffs. for open estuarial river system 79−79897
maximum rain runoff calc. for USSR far eastern rivers 78−81238
meander of small stream with sand bed, flow and sediment transport 80−41466
meandering, review, book contrib. 78−61475
meandering and braiding of alluvial rivers, stability theory 78−36212
meandering River South Esk, Scotland, flow and sedimentary processes 77−29350
meanders, disturbed periodic model 77−29351
meanders, disturbed periodic model 77−45034
Meghadri river effects on temp. and salinity of Visakhapatnam coastal waters 77−73757
meltwater channels near Calgary, episodic Holocene alluviation 77−81921
meltwater from glacier, elec. resist. obs. showing water origin 80−85689
Merrimack River Basin, water pollution abatement benefits, survey results 78−61456
Merrimack River spring runoff rel. to LF currents in Massachusetts Bay 77−37228
Mersey estuary, H_2S effect on methyl Hg in sediments 79−2295
Meuse, run-off rel. to transit time distrib. for Netherlands coastal waters 78−65336
Michigan surface waters, N_2O concs. 78−57223
Mississippi, Ba non-conservative behaviour during mixing of river and Gulf of Mexico waters 78−32120
Mississippi basin, magnitude and freq. of transport of solids by streams 77−78235
Mississippi Pascagoula Estuary water quality planning using Gauss-Seidel iterative technique 78−73402
Mississippi River computerized data bank 78−73520
Mississippi River delta, inner shelf temp. and salinity structure 77−37229
Missouri River, mean motion of dispersing fluid particles 77−9453
Moisie River, Quebec, gully flow development after heavy rainfall 77−5249
monsoon floods, diluting of industrial pollution in Cochin backwaters 80−76668
montane arroyos and gully development 79−74905
monthly streamflow, hydrologic persistence modelling 77−25713
morphology of river beds 80−77017
morphometric and hydraulic channel characteristics, in integration of St. Venant eqns. 78−3838
Moscow River basin, automated surface water quality monitoring system 77−78266
Moscow river water pollution modelling *(Russian)* 77−29328
mountain basin morphology, river branches and sides, models *(Italian)* 78−3829
mountain rivers, evaluation of max. discharges distrib. parameters 78−3840
mountain stream, mean motion of dispersing fluid particles 77−9453
mountain streams, channel roughness coeffs., Chezy-Manning relation 78−49045
mountain watershed with ski basin, heavy metals concs. in snowpack and streams 79−20903
mudflow formation in Akzhar and Kokcheka river basins *(Russian)* 77−29331
multi-inflow reservoirs, flow dynamics 78−20452
Murray, Australia, air-sea-river interactions 77−45032
Murray-Darling river system, Australia, symposium (Melbourne, 13 October 1977) 79−92556
Nadym River, bottom sediments and sandwaves 77−78254
natural channel flow simulation by computer-controlled RC network 77−45046
natural streamflow control coeff., analytical calc. method 79−39777
near-field model for dissolved O_2 and other water quality parameters 78−81261
nested tributary basin classification, drainage basin shape anal. 77−41079
network design for runoff prediction 77−41083
neutron activation analysis of Cr after preconc. on activated C 78−3993

rivers continued
Nevezis and Jura, Lithuania, river basin hydrographical characteristics *(Russian)* 79−84311
central New England, denudation rate determined from estuarine sedimentation 79−92550
New England, USA, heavy metal content in non-industrial area 80−61477
New York State, regional runoff errors rel. precipitation meas. 77−45095
Niger delta, sedimentation rel. to struct. of continental margin 77−21693
Nile, climate variation affecting discharge 80−81946
Nile, evolution from heavy mineral analysis 77−17151
Nile, Kalman forecasting model 80−31081
Nile, water budget and potential reserves of East Africa source region 79−100880
Nile Cone, Lake Quaternary stratigraphy and sediment dispersal, climatic response 77−45040
Nile Delta, inner shelf sediment types and deposition 79−79868
nonuniform suspended load, non-equilibrium transportation *(Chinese)* 80−8339
nuclear power plant siting, ecological and environmental constraints *(Croatian)* 79−92092
numerical modelling appls., conf.; Southampton, England (July 1977) 78−77285
Ohio, power curve regression eqns., statistical computer program 78−61472
Oise, at Sempigny, low water level, forecasting *(French)* 77−37250
old Mangalore port, India, channel siltation study 80−77005
open channel, two-dimensional tidal propagation model, difficulties 78−77272
open streams, hydraulic-hydrometric method for water flow determ. 78−7672
Ord River, W.Australia, sedimentation in arid macrotidal alluvial system 79−44205
Ottawa, methylmercury equilib. concs. in sediments 78−11923
Otway region, palaeocurrent directions in S.E.Australia 78−20449
outflow to sea, 3D model, Herault river example *(French)* 78−36209
overland flow model, infiltration and rainfall effects 77−25720
overland flow model, natural watershed appls. 77−25721
overland flow model, soins. for converging geometry 77−25719
palaeocurrents and sediments in Tertiary deltaic succession 77−17147
Par River estuary, India, pollution transport and abatement methods 80−104521
Parana river, water balance rel. to inflow and outflow of moisture through atmosphere *(Russian)* 77−53090
Pascagoula River basin estuary, model for water quality planning 77−64343
Passaic River, New Jersey, nitrification, historical and expt. investigation 80−7968
Pee Dee River−Winyah Bay estuary, S.Carolina, ^{226}Ra behaviour 80−98360
Periyar, S.India, pollution profile 79−57510
pesticides in USSR rivers, 1973-1976 period 80−81495
Po, bed sediments, trace metal anal., sampling programme 78−69389
Po delta, coastal current flows, mathematical model *(Italian)* 77−70667
pollutant dispersion, boundary conditions effect 78−85611
pollutant dispersion in channels with non-uniform vel. distrib. 79−16556
pollutants, radioactive tracers appl. *(French)* 80−7995
pollution, dynamic behaviour of distributed systems *(Dutch)* 80−3542
pollution, thermal, due to power plants water effluents *(Czech)* 79−57505
pollution by Pb smelter, trace metal deposition in sediment 80−61475
pollution control, appl. of decision theory, Rhine river study 77−66946
pollution dilute capacity at tributary confluence, mathematical model *(French)* 79−8646
pollution distribution determination by remote sensing, study 80−81512
pollution from chlorinated drinking water, effect on organic content 80−97824
Polomet River, stream kinematic struct., sandwaves 77−78255
Pomme de Terre River, Missouri, USA, Holocene erosion and climate 80−51446
porous elastic bed response to water waves 78−67208
Port River estuary, S.Australia, tidal and thermal propag., numerical model 79−12133
Providence River, Narragansett Bay, nontidal flow, stochastic approach to estuarine circulation 77−17132
Puget Sound, Fe geochemistry 78−69370
QUAL II river model soln. algorithm characts. 78−65348
quality modelling by sequential extended Kalman filters 78−81248
radioactive tracer detection techniques, flow problems appl. *(Japanese)* 78−96320
radioisotope applications in agriculture, hydrology, medicine industry etc., booklet 78−35947
radiotracer methods for speciation study in natural waters 79−88490
rainfall intensity effect on storm flow and peak discharge from forest land 77−78271
rainfall-runoff process identification, Semois river appl. 79−5537
rainfall-runoff relation, deterministic nonlinear model 78−85615
Red River Valley, June-July 1975 record storms and flood 77−91193
remote velocity and level meas. using cross correlation techniques 78−57328
Rhine, run-off rel. to transit time distrib. for Netherlands coastal waters 78−65336
riffle-pool stream, flow geometry simulation 79−48521
River Po low water flow characteristics *(Italian)* 79−84306
riverine lake inflow and lake temperatures, effect on spring circulation 80−26555
Rother catchment, W.Sussex, fine sediment mineralogy of source rocks and suspended sediment 79−20827
runoff dependence on climatic factors in Lithuania and Kaliningrad region *(Russian)* 78−16067
runoff generative process and yield from arid talus mantled slopes 77−45031
runoff in Lithuania rel. to lake level oscills. *(Russian)* 78−16068
runoff kernel for basin, mathematical derivation 80−61832
runoff response to suburban development, seasonal vars. 77−78289
runoff time series models, evaluation of practicality and complexity 77−29341
runoff travel time curve, approximation using statistical distribs. *(Russian)* 77−53089

rivers continued
Saguenay fjord, trace metals rel. to runoff inputs 77−5251
lower Saint Lawrence estuary, sediments of Rimouski shelf region 79−62530
salinity calc. in estuary, semiempirical turbulence theory appl. 79−57967
saltation and suspension trajectories in water stream 77−44517
sand-wave motion of sediment along nonerodible bottom in open channel flow 78−16074
sandwave bottom river, turbulent flow expts. 80−36350
sandy bed streams, sand discharge, leveed rivers, coastal flood plains 77−53086
Saruhashi River, Japan, heavy metal pollution *(Japanese)* 78−40599
S.Saskatchewan River, streamflow record synthesis, feature prediction model appl. 80−98372
Sava River and Lake, possible interconnection with Ranney wells determ. by environmental T meas. 78−20447
Sava water pollution influence on ranney wells in Belgrade 78−40602
Sawmill Creek, near Argonne National Laboratory ^{239}Pu and ^{240}Pu concs. 77−45037
seasonal streamflow in Himalayas from satellite snow cover obs. 77−64349
secondary currents direct meas. at inflexion point 79−79888
secondary currents direct meas. in river bends 77−91166
sediment evolution 79−100876
sediment leachates, trace element anal., multielement-direct reading method 78−69514
sediment source identification, mag. meas. techniques 80−8348
sediment supply to Atlantic 79−12157
sediment transport 77−86943
sediment transport in steady unidirectional flow, scale modelling test 80−81933
sediment transport modes in channelised water flows, appl. to Martian outflow channels erosion 80−98363
sediment yields of Western Southern Alp rivers, New Zealand 80−21787
sedimentation in open-channel bends, mathematical model and FORTRAN program 77−37245
sediments, average Hg content in European Economic Community 79−8687
sediments, of Tigris and Euphrates, comparison with old red sandstone 78−81160
sediments, P content, bonding form., in Elbe, Trave, Eider, Schwentine *(German)* 79−34868
sediments, polymodal, of river-lake system, interpretation 79−25273
sediments, suspended, in translational flow, vertical distrib. 78−3841
sediments from granitic rocks area, petrographical investigation, Yakuwa River, Japan *(Japanese)* 77−70694
self-formed straight river, gravel, equilib. banks and mobile bed, model 79−34863
self-formed straight river, sand-silt equilib. banks and mobile bed, model 79−34862
Sepik River coast, Papua New Guinea, trace gases and breezes 78−85642
Severn estuary, seasonal and spring neap tidal depend. of axial dispersion coeffs. 80−94534
shallow channels with running water, upstream long waves 77−25726
shallow floods, finite element method appl. 78−92847
shallow flows, turbulence in depth-limited boundary layer 80−12406
E. Siberia, hydromorphometric relationships for rivers 79−39776
Siberia, river diversions to south, effect on Arctic ice cover, climate 80−41541
Silica Springs, New Zealand, spring water and alumino-silicate deposit anal. 78−32124
Skagit, Washington, annual runoff rel. to cloud seeding project 79−79949
solute loading and chem. denudation rate mapping in Devon, England 78−69375
South and East Lithuania rivers, hydrochemical regime peculiarities *(Russian)* 77−25709
South Esk, Glen Clova, Scotland, flow and sedimentation in meander bend 77−49093
South Saskatchewan River, streamflow data, pattern recognition 79−5527
spring break-up of estuaries on Hudson Bay 78−11930
spring-flood forecasting, loss of runoff due to soil water absorpt. 80−109178
Squamish, British Columbia, mean flow struct. in meanders 79−62532
Squamish River, B.C., concave bank benches 79−84305
St. Lawrence, E.Canada temp. and salinity changes rel. to magnetotelluric fields time depend. 80−26451
St. Lawrence, estuarine front, tide-induced 77−37209
St. Lawrence Estuary, inorganic B content determ. *(French)* 78−77274
St. Lawrence Estuary turbidity maximum, sediment, salinity, suspended matter study 80−4015
St. Lawrence River valley, Canadian quickclays and landslide process 77−44970
St. Venant equation modelling *(German)* 80−90103
stages digital simulation model 80−31078
steppe-zone river, spring-runoff norm, estimation method 80−85694
stochastic models of floods 79−5528
storm runoff, flow component separation, solute conc. and contact time study 80−8358
storm runoff effected by rainfall spatial distribution in small catchment 80−8357
storm water and sediment hydrographs simulation from small watersheds 77−37264
stormwater runoff from various land cover types, characterisation and impact 78−88852
straight alluvial streams, unsteady flow, dune modification 79−62535
stratified flow, finite element analysis, book contrib. 79−34875
stream bed, movement of cohesionless grain, relative protrusion effect, shear stress 77−13094
stream channels, natural high-gradient, width and discharge var. 77−78270
stream draining agricultural watershed P input, sampling 77−33116
stream flows, effects of wind 77−21808
stream gradient correl. with valley side slope angle 77−70699
stream hydrograph, major base flow components identification and separation 79−79898
stream link length organisation and network scale dependencies in network diameter model 77−41085
rivers continued
stream network changes due to suburbanization 77−78288
stream networks, distances determ. 77−91183
stream piracy near Balcones fault zone, central Texas 77−91165
stream pollution controller design via pole assignment 77−60434
stream pollution dissolved O concentration optimisation using instream aeration 77−17153
stream sediment, heavy metal ion removal in clay suspensions 77−86955
stream sediment sources, use of metals as tracers, field expt. 78−81227
stream sediments, Cd content determ., geochem. 78−36170
stream temp. modelling, 'dishonest' method 78−81454
stream temps. during snow melt period *(Japanese)* 78−88860
stream water, dissolved forms of trace elements, dialysis cell meas. 80−97851
stream water solute conc. rel. to throughflow 80−31070
stream-connected aquifer system, lumped parameter stochastic model 78−81241
stream-pollution model with random deoxygenation and reaeration coefficients 79−70472
stream-well-aquifer system groundwater flow anal., linear system models 78−77289
streambank erosion, stereometric meas. 80−17421
streambed particles, erosive forces *(French)* 78−36211
streamflow, empirical data, multivariate gamma distrib. fitting 78−81240
streamflow, Hurst phenomenon in turbulent flows 78−59377
streamflow, low flow estimates using watershed and climatic parameters 78−61471
streamflow, max. expectation levels, standards improvement 78−7674
streamflow, multiple monthly series, reconstruction and prediction 78−24373
streamflow, shot noise models for synthetic data generation 77−64348
streamflow, skewed annual flows generation using fast fractional Gaussian noise generator 79−53395
streamflow, small sample estimation of Hurst coeff. 78−61467
streamflow calc. from discharge vols. for winter periods 79−25285
streamflow changes after reclamation, errors of estimates 79−29794
streamflow data, empirical, fitting of multivariate gamma distribution 79−34878
streamflow data, Pearson type 3 distrib. fitting 78−49061
streamflow data network design, economics of resource information systems 77−73893
streamflow fluctuations in no precipitation periods 77−64406
streamflow generation rel. to fog drip 77−64405
streamflow in cedar-hemlock catchment, silicone antitranspirant effects 77−78272
streamflow meas. in remote catchments, natural pollution loads estimation 77−70714
streamflow of large Soviet rivers, agricultural afforestation effects 78−7675
streamflow record synthesis, feature prediction model appl. 80−98372
streamflow synthesis, two- and three-parameter log normal distribs. 78−81255
streamflow turbulence effect on bottom topography 79−39780
streams, chem., hydrological, thermal characts., Haney, British Columbia 80−8350
streams, surface films and foams, source and metal transport 79−16549
streams draining granite terrain, S.Carolina, dissolved Fe as groundwater component indicator 80−12444
subsurface water chemistry study, coring and squeezing technique 78−57332
summer droughtand autumn rainfall, England, 1976, effects on stream solute levels 79−48523
surface water chemistry and weathering processes, Absaroka Mts., Wyoming 78−32125
Susquehanna River basin, $^{87}Sr/^{86}Sr$ ratio in streams 77−29349
Susquehanna River system, use of ^{210}Pb as heavy metal tracer 78−49046
Suwannee River sill, effect on Okefenokee Swamp water level 80−8356
synthetic streamflow, Bayesian generation of multivariate model 77−78274
Tagus Estuary, water quality study *(French)* 79−66706
Tarmanskii Marsh, influence of human activity on hydrological and thermal regimes 78−92864
telescopic alluvial fan complex, intersection points 79−20877
telluric field increase near water streams 78−65176
temperature forecasting, Fourier series and communication theory techniques 77−25718
Thailand, water pollution problems 78−88853
Thambraparani river, Tamil Nadu, India, large floods 77−53081
Thames, extreme ebbs, historical record 78−73417
Thames Estuary, Flandrian sea level changes rel. to land subsidence in England and Wales 78−24304
Thames estuary, surge and tide interaction 78−96219
thermal convection downstream from thermal power plant warm water disposal constructions 79−83647
thermal discharges, unsteady temp. distrib. in rivers, modelling 77−5264
thermal pollution by discharges into waterways, mixing problems 79−8645
thermal regime, influence of industrial effluents and sewage 79−29793
Thompson River effects on Kamloops Lake, B.C. 78−49051
Tiber, physical processes related to discharge into sea, aerospatial obs. 80−108831
tidal, discharge model, acoustic flowmeter meas. 79−68878
tidal computations, explicit-implicit water level model 78−44886
tidal currents calc. in homogeneous estuaries 78−7654
tidal flow, interlacing channels, nonlinear computer model 79−34828
tidal propagation in shallow rivers, diffusive model 79−2303
tidal stream diffusion and transport phenomena, two step difference method *(German)* 78−57877
tidal wave profile distortion on entering river *(Russian)* 77−17115
tidal wave propag., nonlinear model 79−5512
tidal waves in channel, energy dissipation due to bottom friction and eddy losses 80−31058
tidal waves in rivers and estuaries, finite element models 79−53370
tidally-generated residual motion in St. Lawrence estuary, numerical model 80−94541
tide waves in channel, bottom friction in perturbation method 80−98354
Tigris watershed, evaporative losses from free water surface 80−81957
Tokyo Bay, central Japan, buried river valley system 78−44818

rivers continued
Tolaga Bay Flats basin, recent alluvial infilling estimation using tephra marker beds 78−11925
Tomaki River, New Zealand, bed material transport 80−40547
Tornio River (Finland), hydroelectric power suitability 78−57236
total sediment transport model for sandy river *(Chinese)* 79−96779
trace elements determination using routine neutron activation analysis 78−3992
transport props. and particle shape characts., Fourier analysis *(Japanese)* 79−88506
transverse mixing in meandering nonuniform natural channels 77−5263
triangular channel, free surface seepage, variational inequality method 78−81251
tributary diameter, topologically random channel networks anal. 80−8372
tributary junctions, channel geometry changes 80−98376
tributary spatial arrangements 80−81929
turbid estuarine waters, optics, approxs. and appls. 79−66712
turbid waters, remote sensing penetration depth at green wavelengths 79−66832
turbid waters, spectral scatt. props. 80−72560
turbulent channel flow, energy aspects 78−7677
turbulent flow over sand wave field 80−51441
turbulent open channel flow, dissipation and fine-scale structure 79−16546
ungauged rivers, distributed numerical model development for estimating runoff and sediment discharge 77−91178
ungauged rivers, distributed numerical model for estimating runoff and sediment discharge 77−91177
ungauged rivers runoff and sediment discharge estimation, distributed numerical model 77−91179
ungauged urban watershed flood frequency model parameter estimation 77−37269
unit hydrographs for Barakar and Yamuna catchments, flood forecasting 79−20887
urban bulk precipitation and streamflow quality relationships 79−88382
urban flood control programs, ecological and social aspects 79−2316
US east coast, runoff isotopic composition 79−100879
USSR rivers, streamflow variation (1961-1976) 80−101394
valley basin in Hertfordshire, lateral translocation of soil plasma 77−45026
Vellar estuary, Fe precipitation, conc. determ. 80−77015
Ventos, plume influence on Baltic Sea *(Russian)* 80−98345
Victoria Falls, erosion rate and Batoka Gorge archaeological dates 77−2184
Volga, spring floods long-range forecasts, study of effectiveness 78−3837
volumetric flow gauging, electronic methods 77−73891
Walker Branch Watershed, atmospheric input and origin of elements 77−86956
water, chemical composition, correl. with water-rock partition coeffs. 79−44200
water balance of lower Sutlej catchment, estimation by Thornthwaite's method 79−48525
water erosion characteristics in Siberia, Russian plains and central Asia 78−61449
water exam., L65 turbidity meter description *(Dutch)* 77−27332
water pollutants, airborne monitoring by fluorescence spectroscopy 79−2397
water pollution control mathematical modelling, book 78−73418
water pollution detection, multielement anal. 78−69511
water quality, math. deterministic model, Blackwater catchment appl. 79−66732
water quality, math. deterministic model, formulation and description 79−66731
water quality, modelling and control problems, review 79−57519
water quality and stream networks in S.England during and after 1976 drought 78−73409
water quality assessment, Willamette River basin, Oregon, implications of a prototype project 79−20896
water quality control, robust decentralised control 79−57522
water quality controller, observer-based, polluted river stream appl. 77−81938
water quality management stochastic programming model 79−57507
water quality modelling and operational control 79−16555
water quality modelling of high mountain stream of Bishop Creek, California 78−53666
water quality models, Monte-Carlo anal. 80−8367
water quality models near effluent outfalls 79−62157
water quality monitoring, sampling freq. 79−53380
water quality sampling program 78−69388
water quality surveillance, optimal sampling frequency selection, autocorrel. techniques 79−53001
water quality system, recursive estimation techniques appls. 79−5538
water quality variations operational forecasting from streamflow vars. 77−78265
water resource problem with multiple objectives, interactive optimisation, Yodo River basin, Japan appl. 79−57516
water resources planning, use of multiattribute utility theory 78−11932
water-data bank compilation, Adour-Goronne river basin *(French)* 79−66720
watercourse/atmosphere single-dimensional time-depend. heat exchange, anal. *(Bulgarian)* 78−57221
watershed geochemistry, aqueous solns. control by soil materials 78−20445
watershed geomorphology, relative scales of time and effectiveness of climate 78−81229
watershed models, sensitivity of optimised parameters 79−5523
watershed stream network, model of rainfall-runoff process 77−29347
watershed stream network run-off anal. model, appl. to Nagara River *(Japanese)* 79−16529
well-mixed rivers cooling, simple non-linear models 79−20902
Westend basin, S.Pennines, England, slope form and basal stream relationships 77−45025
wide rivers, acoustic flow meas. 79−72975
wind stress coefficient over water surfaces, new evaluation 80−72603
Yamuna and Damodar, India, raingauge station network for flood forecasting 78−32126
Yangtze delta, Holocene formation and development *(Chinese)* 79−16528
Yangtze River middle reaches, channel development after completion of aritficial cutoffs 79−44210
rivers continued
Yarra estuary, metals in water profile 79−16552
Yarra River estuary, dissolved I 79−34855
Yellow River, flow with heavy sediment concentrations *(Chinese)* 79−79886
Zuari estuary, Goa, India, environmental parameters monitoring 78−81214
As conc. meas., column chromatography versus flameless atomic absorption spectrophotometry 80−55969
B abundance determ. 78−85559
Cd sorption and accumulation in sediment of Tama River 79−52972
Cd sorption and accumulation in sediment of Tama River 79−74924
Cl^- ion concentrations in river, spring waters in Okinawa Honto, origin *(Japanese)* 79−39324
^{137}Cs, runoff coeff. from surfaces of river basin soils 79−44212
Fe, determ. in waters, colorimetric-acid digestion method 78−61088
Fe removal in estuaries, mechanism 78−20437
^3H, conc. in atmospheric precip., rivers, and seas, USSR 79−74560
^3H, environmental transport from atm. release of mol. ^3H 78−11987
Mg mass balance in continental runoff 79−34859
Mn, dissolved, in river water, rapid precip. rel. to estuarine Mn distribs. 79−62516
NO_3^--N export from drainage basins, Toronto, Ontario 79−66729
Na determ. by flame emission meas. 77−36850
O_2 and pH fluctuations, math. model 78−92866
P concentration, in streams draining from agricultural watershed 80−61474
P control in estuaries, parallel shooting models, Corpus Christi Bay (Texas) and Jamaica Bay (New York) appls. 79−57521
Se (−II,0), -(IV) and -(VI) composition of water, by gas chromatography method 80−81928
^{90}Sr concentration in freshwaters of USSR 79−39770
^{90}Sr, runoff coeff. from surfaces of river basin soils 79−44212
U in natural waters, field meas. technique 78−85705
U in world rivers, evidence for higher natural content 79−44208

RKKY interaction
alloy, binary random Heisenberg ferromagnet transition temp., crit. conc. RKKY model 78−52266
amorphous ferromagnet, effective-field distrib. and resistivity minima 79−73501
amorphous magnet, range of indirect exchange interaction 79−15295
anisotropic metal, with impurities, long-range interactions of spins 79−47092
conduction electron polarisation and RKKY interaction 78−91859
CuCr, dil., specific heat, impurity contrib. Kondo temp. 80−65903
dilute alloys, mag. impurity ordering 77−28370
dilute local moment local magnetisation, Kondo-like deviations from free spin behaviour 80−44800
dilute RKKY spin glass, Bethe-Peierls theory 78−39351
ferromagnetic metal, RKKY oscills. in surface spin density, density functional formalism 77−20512
finite ionic spin distribution, effect on RKKY interaction 77−69526
finite magnetic core size, effect on RKKY interaction 77−69525
heavy rare earth metals, RKKY theory of magnetism, electron-electron interactions 79−73667
Heusler alloys, ionic spin distribution and RKKY interactions 78−27028
Heusler alloys, preasymptotic form of RKKY interaction 77−32184
indirect exchange calc., omission of self energy terms 78−56113
Ising model, spin glass in Bethe-Peierls-Weiss and other mean-field approximations 79−65682
Ising spin glass, with RKKY interaction, props. 79−24177
itinerant electron antiferromagnet, localised spin coupling 78−68142
itinerant ferromagnetism, local-band theory, equivalent Heisenberg model 79−82745
Kondon lattice, impurity interactions, ground state calc., impurity conc. effect 80−65782
magnetic electron gas induced by van Vleck ion, spin polarisation, ion mag. moment 79−56176
magnetic semiconductor, doping effects on exchange interaction mechanism 78−31064
metal, amorphous ferromagnetic, paramagnetic Curie temp. determ. 78−76242
metallic very small particles, mag. ordering temps., ferro- and antiferromag. spin structures 77−73027
metals, indirect exchange interaction, partial wave expansion 80−88523
metals, indirect mag. coupling between local moments 78−52207
mixed-valence systems; short-range-order model 79−78049
nearly free electron system, RKKY interaction 79−51771
paramagnetic impurities in conductors, relaxation and indirect exchange interaction 78−2728
particles, quantum size effect obs. by CESR and NMR 77−20700
random Heisenberg model for mag. alloys, RKKY type interaction 80−44788
random magnetic alloys, mean field effective medium theory, Ising model appl., phases 78−84438
rare earth dodecaborides, mag. susceptibility temp. depend., 90-1200K 80−20374
rare earth hydrides, magnetic props., book contrib. 79−82754
rare earth intermetallics, mag. props. 78−84380
rare earth intermetallics, RGa_2, ordering and exchange interactions 80−39779
rare earth metal, RKKY interactions, anisotropic effects from spin-split bands 80−15712
rare earth metallic compounds, indirect multipole interactions 77−4308
rare earth metals, mag. structs., nonspherical Fermi surface in RKKY theory 77−63227
rare earth systems, metallic, with unstable valence, model for thermodynamic props. 77−69487
Ruderman-Kittel interaction at finite temp. *(Russian)* 80−96835
scalar interactions, microscopic, histogram collection by FORTRAN program 78−34958
semiconductor, doped, indirect interactions between localised mag. moments 77−66296
semiconductors, magnetic, static magnetic properties, mean field approach 80−7090
spin glass, conc. depend. of low temp. sp. ht. 77−12135
spin glass, FCC lattice with RKKY interaction, numerical calc. 78−52275
spin glass, generalised mean field theory with spin correls. 78−2691

RKKY interaction continued
spin glass, low temp. susceptibility, spin-depend. curvature, Ising model MRF approx. 77−66366
spin glass, metallic, computer simulation 77−32203
spin glass, resist. max. rel. to Kondo temp. and RKKY interaction 77−20307
spin glass, RKKY, dil., approach to fully magnetised state 80−60302
spin glass freezing temperature, fluctuations in nearest neighbour distance and damping effects 77−51913
spin glass system, RKKY interaction exam. 78−52290
spin glasses, Ising, sp. ht. 1/T behaviour 80−11210
spin glasses, phase transition, fluctuations of local spins, mean-field theory 80−34661
spin glasses, recent progress in numerical simulation 79−69689
spin glasses, resist. maximum, press. and conc. depend. 77−69300
spin glasses, resist. maximum, s-d exchange interaction 77−69586
spin glasses, RKKY free energy, pair approx. 79−56557
spin glasses, second virial coeff., magnetic field depend. 79−65690
spin glasses, transition temperature, conc. depend. 77−85463
spin system, random thermodynamic props. using Bethe-Peierls-Weiss approx. 79−78387
superconducting amorphous metals, mag. impurity interactions 80−44777
superconducting dilute mag. alloys, effects of indirect coupling upon nucl. spin-lattice relax. 77−80874
superconductivity-ferromagnetism coexistence in two-band model *(Russian)* 80−84539
superconductor, ferromag., spin correls., effect on nonlocality 79−82708
system with electron hole pairing, interaction between localised moments *(Russian)* 78−88111
Van Vleck compounds, LF dynamics, NMR linewidth, RKKY exchange mechanism role 80−103812
Ag-Mn, spin glass, mag. susceptibility hydrostatic press depend., RKKY interaction 80−44845
$Ag_{0.6}Au_{0.4}Mn$, dil., effect of mean free path on strength of RKKY interaction 78−39291
AgCr, dil., specific heat, impurity contrib. Kondo temp. 80−65903
Au-Cu-Fe spin glass alloys, impurity mag. resist. meas. 80−59972
Au-Fe, dil., approach to saturation of magnetisation 78−56293
Au-Fe, spin glass, transition temp., freq. depend. 80−97113
Au-Fe, spin-glass, characteristic temps. 79−38348
Au-Fe alloys, spin correlations, neutron diffr. meas. 80−80482
Au-Fe film spin glass, low temp. resistivity, mean free path effects 78−80163
Au-V, dil., ^{51}V CW NMR line width anal., RKKY broadening 78−15033
Bi-Mn, dil. liq. alloy, static and dynamic props. of localised Mn moments 79−82755
$Cd_{1-x}Mn_xTe$, spin-orbit coupled bands, indirect exchange interaction via electrons 80−34407
$CeAl_3$, singlet ground state at T=0, mag. ordering 2.5-6K 78−84388
$Ce_xEu_{1-x}B_6$, mag. susceptibility, 80-1000K 79−73674
$Ce_{0.72}Ho_{0.27}Ru_2$, superconductors, mag. correlations and crystal-field levels 80−34547
$Ce_xLa_{1-x}B_6$ solid solutions, Weiss const. antiferromagnetic ordering calcs., mag. props. *(Russian)* 79−91212
Cu, nuclei, antiferromag. ordering, mean field theory 79−78333
Cu-Al-Fe, dil. liq. alloy, localised mag. state interactions *(German)* 77−1539
Cu-Mn, classical RKKY model, thermodynamic props. 78−39333
Cu-Mn, spin glass, transition temp., freq. depend. 80−97113
Cu-Mn alloy, classical RKKY model, zero temp. dynamic struct. factor 78−68271
Cu-Mn-Au(Pt) spin glasses, anisotropic exchange interactions, effect of nonmag. impurities 80−80534
Cu_2MnAl Heusler alloy, inelastic magnon scatt. of neutrons 77−4509
Eu chalcogenides, heavily doped mag. semiconductors, effect of carriers statistics on indirect exchange 77−69280
EuB_6, exchange interaction, EPR obs. in $Sr_xEu_{1-x}B_6$ and $La_xEu_{1-x}B_6$ 80−20457
EuSe:Gd, mag. props. explained by band struct. 78−43324
EuX_5, X=Cu, Zn, Ag, Au, cond. electron spin polarisation effects 77−63136
$Fe_xPd_{82-x}Si_{18}$ metallic glass, long range interaction and spin wave interactions 80−65949
Gd, RKKY interactions, anisotropic effects from spin-split bands 80−15712
Gd-Al, amorphous film, microwave mag. reson. 78−91948
Gd-Al(C)(Cu)(Ga)(Ni)(Pd)(Rh) alloys, amorphous, mag. and elec. props. 80−80499
Gd-Al(Cu)(Ga)(Rh)(Pd), amorphous alloys, mag. coupling of rare earth moments 78−88108
$Gd(Al_{1-x}Cu_x)_2$, thermoelec. power, exchange interactions 80−24881
$Gd_xDy_{1-x}C_2$, solid soln., mag. susceptibility, temp. depend. 79−87239
$Gd_{1-x}M_x$, M=Co, Ni, Fe, temp. depend. of magnetisation 77−77043
GdN, mag. interaction and carrier conc. 80−71005
$GdN_{1-x}O_x$, magnetic interaction and carrier conc. 80−71005
GdP-GdS systems, mag. exchange interactions, free carrier conc. 78−60278
$(Gd_xY_{1-x})Al_2$, ferromag. and spin glass like behaviour, magnetisation meas. 80−75734
$(Ge,Pb)_{1-x}Mn_xTe$, mag. and elec. props. meas. 80−29534
$HgCr_2Se_4$, n-type ferromag. semicond., galvanomagnetic props. 80−70727
$Hg_{1-x}Mn_xSe$, spin-orbit coupled bands, indirect exchange interaction via electrons 80−34407
$Hg_{1-x}Mn_xTe$, spin-orbit coupled bands, indirect exchange interaction via electrons 80−34407
$(La,Ce)B_6$ dil. alloy, Kondo effect, impurity-impurity interaction, mag. susceptibility, mag. to non mag. transition 78−47948
$(La,Gd)Al_2$, mag. props. 78−52299
$(La, Gd)Al_2$ spin glass, suscept. and sp. ht., mag. field depend. 79−61173
$(La,Gd)B_6$, dil. alloy, spin glass behaviour, 4.2 to 200K AC mag. susceptibility, RKKY calcs. 78−47994
La-Gd-Au, amorphous, mag. field depend. of resist. minima 77−59275
La-Gd-Au, amorphous spin glasses, mag.-cluster description 79−42776
$La_xEu_{1-x}B_6$, EPR linewidth conc. depend., $Sr_xEu_{1-x}B_6$ comparison, exchange interaction in EuB_6 80−20457
$La_{80-x}Gd_xAu_{20}$, amorphous dil. alloy, RKKY interaction, magnetisation meas. 77−32207

RKKY interaction continued
$La_{3-x}V_xS_4$:Gd^{3+} localised moment-conduction electron interact., ESR obs. 78−88183
Mo-Fe, dil., Kondo effect of RKKY interaction 78−31052
$(Ni_{100-x}Fe_x)_{79}P_{13}B_8$, amorphous dil. alloys, spin glasses, magnetisation meas. 79−61178
Ni_2MnSn alloy, ionic spin distribution and RKKY interactions 78−27028
Pd-Fe alloy, dil., cond. electron polarisation studied by positive muons 77−28397
Pd-Fe and Pd, muon$^+$ Knight shift, cond. electron polarisation, RKKY oscill. 77−66450
Pd-H-Gd, dil., ESR exam. of low temp. region of phase diagram, and electronic props. 80−29930
PdGdH, diagram of state elec. props., indirect exchange interaction, EPR study *(Russian)* 80−50179
PdH_x (α')$Fe_{0.003}$ 79−61054
PdH_x-Fe, dil., Kondo system, local moment hyperfine studies, Mossbauer expt. 80−39908
$PdH_xFe_{0.003}$, Kondo system, local moments, hyperfine fields, Mossbauer study 80−80478
Pd_2MnSn alloy, ionic spin distribution and RKKY interactions 78−27028
$PrNi_5$, LF dynamics and ^{141}Pr thermal relax., coupling parameter and RKKY exchange mechanism 80−103812
Pt-Mn-Sn alloy, mag. hyperfine fields 79−1737
Sc-Gd, spin glasses, low temp. sp. ht. and magnetisation 80−65913
$Sr_xEu_{1-x}B_6$, EPR linewidth conc. depend., $La_xEu_{1-x}B_6$ comparison, exchange interaction in EuB_6 80−20457
$(Ti_{1-x}V_x)_2O_3$ spin glass, mag. props., metallic antiferromagnetism 79−82791
Y-Gd, spin glasses, low temp. sp. ht. and magnetisation 80−65913
$Y_{1-x}Co_x$, temp. depend. of magnetisation 77−77043
YIG-rare earth garnet solid solutions, magnetisation temp. depend. calcs. 80−20388

road traffic
acoustic behaviour near traffice lights, computer simulation 78−90597
acoustic noise, effect of intermittent truck noise on deep sleep 79−5310
advection-diffusion model for pollutant dispersion near roadways 79−21003
air pollution, statistical models with reference to Los Angeles Catalyst Study (LACS) data 80−30620
air pollution ejections control model 77−21900
air pollution in Geneva, evaluation by daily profiles meas. *(French)* 78−92969
air pollution reduction via bus lane network simulation 79−52991
air pollution source inventory for Tehran, methodology and approach 79−52996
background noise effects on assessment of aircraft noise 79−86288
contamination of roadside soils and plants in Alexandria district, Egypt, with Cd, Ni, Pb and Zn 78−81171
control and surveillance system for anti-pollution programme *(Japanese)* 77−56726
cumulative noise measure for general annoyance prediction of traffic and aircraft noise 77−80010
energy and air pollution consequences of traffic systems management 79−52990
exhaust gases, as atmospheric N_2O source 78−85631
formaldehyde in New Jersey air, statistical anal. 77−73833
freeway noise barrier, expt. eval. 79−34463
ground vibration by traffic, effects on LaCoste and Romberg gravimeter meas. *(Japanese)* 78−65400
highway noise shielding methods 78−9492
Hong Kong, roadside noise meas. 78−30125
microtremor measurement, by He-Ne laser interferometer *(Japanese)* 80−9025
motorway free-flow traffic noise obs. 78−90591
motorways, fog meas. and traffic control 79−16608
mountain watershed with ski basin, automobile exhaust heavy metals pollution 79−20903
noise, a socioeconomic approach to subjective responses 80−67022
noise, acoustical correlates of aversiveness 79−41511
noise, analysis of sequence of sound level readings *(Japanese)* 80−35806
noise, annoyance and activity interference patterns 80−48504
noise, attenuation around buildings 78−1498
noise, bus noise levels in the New York City and Albany metropolitan areas 80−76684
noise, close proximity vehicle noise survey method 80−102926
noise, close to light motor vehicles 80−83701
noise, community reactions from social survey in Manchester 77−84073
noise, community response prediction 77−80012
noise, computer simulation of traffic flows, road intersections having traffic lights 80−72109
noise, control of noise level of moving vehicles 80−99894
noise, echoes from vehicles, Demey metro station *(French)* 80−69600
noise, effect of skewness and standard deviation on sampling errors 80−35803
noise, effect of structure-borne tunnel vibrations on buildings 80−48492
noise, effect on hearing levels, academic achievement of children, exp. study 79−20553
noise, effect on sleeping subjects 80−48509
noise, effects of tyre tread and road surface 77−14850
noise, environmental impact in Britain 80−48508
noise, equally spaced line sources model *(Japanese)* 78−33954
noise, exponentially distrib. vehicles model *(Japanese)* 77−88983
noise, highway noise barrier perceived benefit 80−102920
noise, highway noise barriers, optimum weight with respect to effectiveness and cost 80−67021
noise, human response in residential areas 80−55962
noise, importance in France 80−48510
noise, improvements to the equally-spaced vehicles model, grouping effect *(Japanese)* 80−55963
noise, individual diffs. in sensitivity from public surveys 78−33953
noise, kerbside study of vehicles 80−79050
noise, meas. accuracy using digital instrums. 80−79075
noise, meas. radiating height of cars and lorries, effectiveness of sound barriers 80−64325
noise, microsampling technique 79−55264

road traffic continued
noise, model investigation on acoustical performance of courtyard houses 80−10077
noise, Monte Carlo simulation methods, effect of vehicle spacing on results 80−72110
noise, multivariate joint probability expression of general random processes, finite expansion terms 80−69592
noise, prediction of time pattern of fluctuating sound levels *(Japanese)* 80−55965
noise, prediction problem for various types of vehicles and multilanes *(Japanese)* 77−3699
noise, prediction using a scale model 80−45838
noise, presentation of statistical results 80−67019
noise, reduction by correct building placement, noise emitted by single source in open space 80−87647
noise, reduction by multiple acoustic screens *(French)* 78−13844
noise, relationship to air pollution levels 80−69594
noise, relationships between multidimens. correlation props. of intensity and higher order information, Stratonovich's stochastic theory for random points system 80−87645
noise, responses of Chinese firemen 77−39157
noise, reverberant meas. rel. to noise level prediction 78−75013
noise, sampling errors with gamma headway distributions 77−84072
noise, sound immission mapping in urban areas 80−48533
noise, sound pressure prediction 77−84071
noise, statistical theory based on component response waves composition 77−84070
noise, statistical treatment in arbitrary sound propag. environment *(Japanese)* 78−59199
noise, subjective annoyance, lab. expt. on students 80−102921
noise, test procedures *(Japanese)* 78−38141
noise, time sampling, uncertainty in sound level eval. 77−42658
noise, traffic control effect on evaluation index 80−51024
noise, traffic passing through road intersections controlled by roundabouts, model 80−64280
noise, traffic-induced building vibration 80−96098
noise, use of sloped barriers for noise abatement 80−102925
noise, use of theoretical and empirical models in prediction *(French)* 80−67020
noise, wall insulation, prediction of output probability distribution of noise level 80−69593
noise abatement, noise propag. characts. identification under different conditions, Kalman filter theory appl. *(German)* 80−99896
noise above ideal reverberant city, aerial meas. 77−50827
noise and sleep disturbance 77−42659
noise annoyance, lab. study 77−80013
noise annoyance measurement, simulated 80−28379
noise at signalized intersection, influence of traffic structure *(Japanese)* 79−37082
noise attenuation by masonry subdivision perimeter fence 79−74578
noise control, systematic trial and eval. diagrams *(Japanese)* 79−23132
noise control procedures 79−34464
noise data, appl. of multivariate joint probability function of state variables with quantized levels 80−36836
noise generated by single vehicles in freely flowing traffic 78−38139
noise in a high-rise city 78−94482
noise level definitions and building design criteria 78−83174
noise levels, relationship with traffic volume *(Japanese)* 80−33335
noise levels on high rise building balconies 79−50504
noise levels prediction 77−14842
noise measurements in Antwerp and Brussels and their relation with annoyance 80−33332
noise monitoring, errors between sampled data and continuous data 79−81618
noise nuisance in residential areas, individual responses 77−31167
noise pollution, new road traffic noise model *(Japanese)* 80−35804
noise poly-freq. spectral anal. based on filtered Poisson process model 79−52998
noise prediction, state of the art review 77−65651
noise prediction *(Japanese)* 78−13853
noise prediction calc. on straight road in suburbs *(Japanese)* 80−19147
noise prediction method for traffic noise in urban Sydney 77−34994
noise propag., scale model anal. 78−59196
noise propag. in city area, investigation using scale models and field measurements *(Japanese)* 80−19152
noise propag. in streets, multiple-reflection diffuse-scatt. model 78−87190
noise propagation by motor vehicles, prediction technique 77−75744
noise propagation characts. estimation trial 79−53000
noise protection of buildings 77−68324
noise reduction by closed balcony shielding on buildings 78−33951
noise reduction by multiple finite barriers, prediction method 80−38171
noise screening effect by buildings *(German)* 80−10076
noise spectra, simulation model 77−46865
noise studies based on traffic flow models 79−52999
noise survey, comment on method 79−37083
noise survey, Turin, Italy 77−84063
noise vertical distrib. in Hong Kong 77−19475
noise with interrupted traffic flow, meas. 77−62106
pollutant dispersion over highways, wind and temp. study of turbulence 80−12038
practical air pollution model at signalised intersections in Tokyo metropolitan area 79−52987
quiet tyres use, cost and safety aspects 77−65652
road vehicle tyre/road noise mechanism study 77−19485
Rome road traffic noise, 24-hour obs. and statistical analysis *(Italian)* 80−87651
site selected variables effect on human responses to traffic noise 80−61491
site selected variables effect on human responses to traffic noise 80−61492
statistically stationary traffic noise shielding by simple obstacles 78−90590
Teheran, gasoline consumption contrib. to atmosphere Pb concs. 79−21011
total noise exposure and time average statistics *(Japanese)* 79−70499
tyre noise, meas. and anal. technique 78−33969
urban centres, CO emissions 77−21895
urban noise level variation and attenuation with height 80−10078
urban traffic noise, contrib. of heavy vehicles 78−38136
vehicle generated air pollutants, correl. study 79−21012

road traffic continued
vehicle noise attenuation over short grass 80−19146
CO, pollution from road traffic, street level conc. 80−81500
NO_x emissions from European cars, control 79−48198
Pb pollution in Egypt 79−12255

road vehicles
audible warning devices, effectiveness on emergency vehicles 78−87200
automobile exhaust pollutants diffusion 79−52985
buses, noise levels in New York City and Albany metropolitan areas 80−76684
car and motorcycle speed and cross-country races, noise inconvenience to local residents 77−84064
diesel engine noise radiation mechanisms 79−32135
diesel engine noise research at Perkins Engines 79−32136
electric vehicles, energy economy aspects *(German)* 80−30427
heavy commercial vehicle cab noise reduction techniques 79−37087
infrasound, effect on people, exptl. study of levels 78−88726
linear one degree of freedom system with random excitation 78−34057
microphone windscreens, acoustic sensitivity 78−38133
motorcycle carrier stress anal. 79−43545
noise emission from point sources on road, analysis *(Japanese)* 77−23804
noise from single vehicle, stationary test method 77−34998
noise measurement, large anechoic chamber, instrum. room and services room *(German)* 77−72121
noise measurements, single vehicles at roundabouts 78−90594
noise radiating height measurement, roadside sound barrier effectiveness calculations 80−64325
optimized speed-controlled suspension of a 2-DOF vehicle travelling on a randomly profiled road 79−72847
response to profile-imposed excitation 77−72219
solar powered automative transport utilising stirling heat engine 80−55824
sound meas. standards 80−14531
stopping distance, weight transfer effect, for teaching 79−25800
thermal energy storage system for a Stirling engine powered highway vehicle 80−30584
tyre/road noise mechanism study 77−19485
Pb contamination of soils, air exchange in cities *(German)* 79−70470
Pb from motor exhausts on motorways 79−12248

robots
see also artificial intelligence
adaptive industrial, orientation angle calc. method *(Russian)* 80−42192
aerospace systems and electronics, IEEE conference, Washington D.C., USA, 26-29 Sept (1976) 77−5420
appendages, manipulators and robotics prospects 78−53582
bipedal walking, linear stabilisation *(Russian)* 78−51055
compact servo master-slave manipulator 79−9214
manipulator, computer controlled, for use as remotely controlled arm 78−81083
manipulator compliance, kinetostatic error distrib. 79−18697
and manipulators, symposium, Warsaw (Sept., 1976) 78−53574
master-slave manipulators and remote maintenance in nuclear research 77−71682
medical engineering, appl. of automatic meas. and automata 79−62381
micromanipulator for biological experiments, versatile remote control, economic construction 79−25163
oceanographic robot submarine with computer control 77−5375
remote manipulation systems for fuel recycling, design and performance 77−67854
retinal hue signal generation, optoelectronic robot model 80−3647
two-phase servo master-slave manipulators, triac output control system 79−9213
underwater robot/manipulator, development 78−77356
voice command of a six-degree-of-freedom manipulator, robotic arm appl. 80−12313

Rochelle salt
ammonia Rochelle salt, temp. depend. of optical axis angle, phase transitions *(Russian)* 80−97216
ammonium Rochelle salt, incommensurate ferroelectricity 79−61311
ammonium Rochelle salt, incommensurate phases and ferroelectricity 78−52455
ammonium Rochelle salt, thermodynamics of ferroelec. transition 80−84702
ammonium Rochelle salt-Rochelle salt mixed cryst., elastic props., piezoelec. reson. method 78−76390
chemical reactions in plasma generated near ferroelectric surface, obs. 78−68931
crystal, oriented, intrinsic absorpt. edge shape 77−66505
dehydration kinetics in ferroelec. and paraelec. phases, surface acoustic waves influence 80−97204
deuterated, complex dielec. const., 5 MHz-24GHz, −45 to +45°, relax. mechanism 80−15983
dielectric props. near upper Curie pt. under hydrostatic press. 79−82935
dielectric relaxation, freq. and temp. depend., 10 kHz-1 MHz, 16-28°C 79−82930
dipole interaction symm. aspect 77−20805
electrogyration during phase transitions 79−19859
electromechanical behaviour, influence of ferroelec. phase transitions 77−8510
ferroelectric, Raman and IR study 80−71406
ferroelectric phase, ^2H NMR spectrum, correl. effects 78−76324
ferroelectric phase transition, external field induced 80−29700
ferroelectric phase transitions in pseudo-spin lattice coupled mode model 80−108161
ferroelectric props., student expt. 79−97162
ferroelectric surface creep discharge plasma channel and domain interactions 80−15996
ferroelectric thin crysts., struct. investig. 79−27962
ferroelectrics, external field effect on phase transitions 79−73888
gas-liquid inclusions, in crysts., movement in temp. field gradient 79−55942
heat capacity, meas. by adiabatic low temp. calorimeter *(Japanese)* 80−52218
irradiated crystal, and deuterated form, primary reactions, EPR obs. 80−3370
layered domain struct. form., theory and expt. 77−52029
mechanoluminescence and crack mobility, charge prod. during fracture 78−88370
optical characteristics in UV region *(Russian)* 78−84550

Rochelle salt continued
paraelectric-ferroelectric phase transition, relaxing defects effects 79−61320
phase transition at low temp., dilatometric exam. 77−11691
phase transition mechanisms by optical spectroscopy 79−15411
phase transitions, free energy in symm. group representation of parent phase 79−69790
phase transitions, high-resolution sp. ht. meas. 78−48128
phonon echos in SiO_2, ADP, KDP, and Rochelle salt *(Japanese)* 79−51213
polarisation echo, near ferroelec. transition 78−88266
polarisation echo in ferroelec. phase transition region 79−42920
polarisation relaxation, US vel. and attenuation meas. 77−28512
positron lifetime meas. during phase transitions 78−6644
rectilinear system of transition parameters 78−48126
refractive index, dispersion and temp. depend. 77−16275
refractive index, X-ray radn. effect on dispersion and temp. depend. 78−72480
Rochelle salt, crystal, X-ray topographic obs. of localised vibr. 79−24264
(Rochelle salt)$_{1-x}$(ammonium Rochelle salt)$_x$, phase transitions, hydrostatic press. effects 80−93246
spectra of absorption edge, low-temp. 79−4819
structural phase transitions 78−83938
thermal expansion and spontaneous strain meas., −40 to 40°C, electrostrictive consts. 77−16262
unified phenomenological theory, spherical system of transition parameters for phase transitions 77−31751
X-irradiated, radical II struct. and location, ENDOR 77−51991
Ag electrodeposits, dendritic growth inhibition by tartaric acid and tartrates *(French)* 78−87894
$NaND_4C_4H_2D_2O_6.4D_2O$, ferroelec. phase, incommensurate satellite refls. 78−84531
VO^{2+} doped Rochelle salt, EPR study 80−34762

rock magnetism
see also palaeomagnetism
abyssal sediments, effect of particle size var. on DRM/ARM ratio 78−32067
alkaline rocks and magnetic anomalies *(Rumanian)* 80−12338
ancient metamorphic rocks, mag. characts. correl. with superimposed metamorphism *(Russian)* 79−8630
ancient oceanic lithosphere, mag. props. as alteration indicators, Othris ophiolite example 80−8297
anisotropy of magnetic susceptibility variations in Icelandic columnar basalts 79−44175
anomalies and magnetizations in Coast Mountains, British Columbia, rel. to subduction 78−11796
ARM correction method for mag. palaeointensity determ. 79−34968
artificial rock samples, inhomogeneous remanent mag. meas. 77−45174
ash-flow tuffs, microanalytical recognition of TRM components 80−72497
automatic AF demagnetiser for igneous rock specimens 79−25347
basalt, anhysteretic remanent mag. study with var. of AC and DC fields 79−48465
basalt, hypervelocity cratering and impact magnetization, lunar surface simulation 77−91115
basalt, mag. mineral identification by rot. hysteresis loss 80−67428
basalt, mag. props. rel. to crust and upper mantle struct. and development 79−79816
basalt, monodomain behaviour in multiphase oxidised titanomagnetite 77−60366
basalt, titanomagnetites domain struct. temp. var. 78−65272
basalt flows from Absaroka Mountains, Wyoming, mag. stability rel. to palaeomag. study 77−86765
basalt thermomagnetic study for S.E.Sicily samples 77−33056
basaltic bodies, mag. susceptibility anisotropy meas. rel. to flow and emplacement direction 79−29766
basaltic dyke with concentric cooling zones, var. of mag. props. 77−49062
basalts, from deep drill holes in Iceland, mag. studies rel. to mag. layer concept 77−60365
basalts, from N Pacific, mag. props. rel. to Pacific plate tectonics 78−40543
basalts, mag. coupling in partial self-reversal assoc. with increased mag. viscosity 77−73717
basalts, mag. grains effect on remanent magnetisation 77−37191
basalts, mag. props. rel. to form. conditions 78−73360
basalts, mag. susceptibility anisotropy meas., torque and spinner magnetometer comparison 78−21185
basalts, O_2 partial press. influence on TRM 77−37190
basalts, oceanic, viscous remanent mag. characts. 78−85540
basalts, of oceanic layer 2, occurrence of TRM questioned 78−65279
basalts from Nazca Plate, mag. props. and opaque mineralogy 78−20396
basement rock type determ. using magnetic anomalies 77−45166
biotite, thermal decomposition, stability of ferromag. products 78−57195
Bishop tuff, in Long Valley caldera, mag. model rel. to hydrothermal alteration 77−86846
Butte mining district, Montana, palaeomagnetism, rock magnetism and aspects of structural deform. 80−101326
Caerfai Bay Shales, S.Wales, diagenetic magnetisation of Lower Cambrian rocks 80−36227
Cambrian rocks of Morocco, magnetisation rel. to African palaeomag. poles *(French)* 77−37125
Cambrian slate belt of N Wales, mag. susceptibility anisotropy and correl. with strain 79−79832
E.Canada ophiolites, thermomagnetic evidence for native Fe 78−3760
chemical and thermoremanent magnetisation, comparative anal. 77−81870
clay thermoremanent magnetisation, cooling-rate depend. 80−46174
Upper Cretaceous limestones from Munster Basin, NW.Germany, magnetisation age 80−89949
critical field calc. of single domain particle with two types of anisotropic energy 78−61404
crustal rocks, magnetisation rel. to long-wavelength mag. anomalies over Canada 80−85594
Curie isotherms in deep crustal mag. anomalies, mineralogical constraints 78−44805
deep sea drilling project Glomar Challenger, international phase *(German)* 77−70837
deep-sea sediments, magnetisation, particle flocculation effects 79−70781

rock magnetism continued
demagnetising factors in nonellipsoidal samples 77−17083
depositional detrital remanent magnetisation of organic mud 80−61795
detrital remanent magnetisation in five slowly redeposited long cores of sediment 79−70786
Devonian John O'Groats Sandstone, N. Scotland, superimposed magnetisations resolution 79−92481
Devonian Onondaga limestone (New York), palaeomagnetism re-examination 80−3928
diabase dykes, Late Mesozoic, from S.Spitsbergen, thermomag. props. 79−92528
dolerite dykes, India, density, mag. susceptibility and lithologic comp. 78−85542
domain structure obs. by Lorentz electron microscopy 80−72502
drilling induced remanence, origin and stability 77−33059
DSDP Leg 37 basalts, oxide microstructs. and mag. props. 77−91108
DSDP Leg 37 samples, magnetisation and palaeomag. field intensity meas. 77−90996
dyke rocks of Permian S.W. Sweden 80−36228
Exeter pluton, New Hampshire, mag. fabric 79−70791
ferromagnetic component indication by magnetic hysteresis 77−64271
ferromagnetic components comp. and struct. from coercive spectra of rock samples 79−62490
ferromagnetics, remanence rel. to palaeomagnetic studies 77−33062
ferromanganese freshwater nodules, antiferro- to speromag. order 77−70649
ferruginous quartzites of Ukrainian shield, magnetic props. at high press. and temp. *(Russian)* 78−15999
in folds, magnetic fabric 78−85481
fracture zones mag. features 77−78092
Galapagos hot spot, bathymetry, magnetic anomalies and basalt magnetization 77−5132
Guil valley Permian volcanics (French Alps), relations between tectonic stresses and mag. props. *(French)* 77−25679
gyroremanent magnetisation in anisotropic mag. material 80−50142
haematite, fine-grained, hard viscous remanent magnetisation 77−56623
haematite, grain size and coercive force from high temp. AF demag. 77−37189
haematite, natural and synthetic samples, thermomag. anal. 77−56622
haematite, single domain, defect moment origin and props. 79−16438
haematite-bearing rocks, effects of haematite reduction to magnetite 78−65277
haematite-bearing rocks and concentrates, peaked thermomag. curves 79−79824
Haliburton intrusions, remanences $^{40}Ar/^{39}Ar$ dating for Grenvillian palaeopoles calibration 79−20778
hemoilmenites, mag. anisotropy, torque balance obs. 80−98309
Iceland, reversely mag. rocks, evidence for geomag. reversal during Wisconsinan Ice Age 78−61327
NE Iceland, rock magnetic investigations rel. to ΔZ mag. anomalies 80−89951
Icelandic columnar basalt, anisotropy of mag. susceptibility vars. 77−86859
igneous rock, mag. props. rel.to composition and Fe-oxide grains 80−36294
igneous rocks, thermoremanent magnetization 77−91113
inductive magnetisation sounding, inverse mag. problem numerical soln. *(Russian)* 79−34747
initial susceptibility, uniaxial stress effect on reversal, theory 77−9401
interacting single-domain grains, thermoremanence and ideal magnetization calc. 79−25232
intrusive granitoids chem. comp. influence on mag. props. *(Russian)* 78−85535
kimberlites, Precambrian and Cretaceous, in S.Africa, remanent magnetisation 78−96134
Korostenian pluton gabbro-anorthosite rocks (Ukrainian Shield), natural residual magnetisation origin *(Russian)* 79−8599
Lake Tahoe, California-Nevada, remanence, props. and palaeomagnetism 80−41371
Late Cretaceous polarity sequence, Scaglia Rossa limestone, Italy, rock and palaeomag. studies 78−11803
lava flows of Mt. Etna, partial self-reversal and NRM 80−46126
lodestone, microstructure and mag. props., source of mag. hardening 79−82828
lodestones, magnetic and microstructural props. 78−16004
long grains method for palaeomagnetic field strength and direction 80−77148
magmatic rocks, magnetic anisotropy, depth var. 77−9407
magnetic anisotropy, principles of quantitative interpretation 77−44973
magnetic anisotropy and ductile deformation of rocks in zones of progressive regional metamorphism 78−81149
magnetic components, separation from alternating field step demagnetisation data 79−16444
magnetic susceptibility anisotropy var. in deep-sea sediments, controls 79−66680
magnetic vector determination of rock specimen, statistical method 80−51556
magnetic-diffusion aftereffect, Preisach-Neel diagram appl. 78−61403
magnetite, coercive force spectrum at high temps. rel. to thermal activation below blocking temp. 77−91111
magnetite, depth calc. of piezomagnetic effect rel. to earthquake prediction 78−11816
magnetite, grain size limits for pseudosingle domain behaviour, rel. to palaeomagnetism 80−11215
magnetite, magnetisation of immobilised particles, shape factors 80−72499
magnetite, partial thermal remanent magnetisation additivity 80−26498
magnetite, TRM props. of single-domain, pseudo-single-domain and multi-domain particles 78−40544
magnetite, weak field TRM is single domain grain, cooling rate effect 80−109139
magnetite (Fe_3O_4), mag. susceptibility under hydrostatic press. and implications for tectonomagnetism 80−26504
magnetite (Fe_3O_4), piezomag. response depth depend. rel. to tectonomagnetism as earthquake precursor 80−26465
magnetite and Fe, grain-size thresholds, palaeointensity determ. appl. 77−37188
magnetite grains, ARM, TRM and magnetic interactions: concentration dependence 79−44177
magnetite monocrystals and rocks under high uniaxial press., mag. props. 78−73361

rock magnetism continued
magnetometers, RF-driven SQUID, rock magnetism and palaeomag. appls. 77−45201
marble, mag. susceptibility anisotropy development through cryst. preferred orientation of calcite 78−56286
marine ophiolite complexes, evidence for past magnetism 80−109092
measurement of magnetisation of laboratory sample, combination of individual vectors 80−46271
metalliferous sediments and Fe-Mn concretions, magnetomineralogical study, East Pacific Rise 79−62481
metalliferous sediments of E.Pacific Rise, three-dimensional distrib. and mag. props. 80−21705
metamorphic rocks, thermal overprinting of NMR and K/Ar ages 78−65278
Mid-Atlantic Ridge at 37°N, anomalies rel. to mag. source layer thickness 77−91070
mineral identification in rocks, mag. rot. hysteresis loss meas. 80−67428
minerals, Curie temp., HF meas. method *(Russian)* 79−39992
Mississippian Madison limestone from N-central Wyoming 79−8626
Mount Shasta, magnetisation implications for virtual geomag. poles determ. from seamounts 79−39637
multicomponent NRM separation using difference and resultant magnetization vectors 79−66826
multiphase magnetizations, recognition and separation techniques 78−28349
New Brunswick, density and magnetic susceptibility meas. 77−44968
Nizky Jesenik Mts., Czechoslovakia, mag. anisotropy meas. rel. to rock cleavage origin 77−9410
NRM, multicomponent, separation method 79−34805
NRM, stress sensitivity meas. using cryogenic magnetometer 80−26506
NRM in deep sea sediments, time series anal. 79−29757
oblique anhysteretic remanent magnetisation 80−21717
ocean floor rocks, metamorphism rel. to magnetism and seismic layering 77−13068
oceanic basalts, titanomagnetites low-temp. oxidation rel. to mag. anomalies statistical anal. 80−36233
oceanic crust magnetisation 77−2088
oceanic crust random magnetisation, effect on coherence of short-wavelength marine mag. anomalies 80−36225
oceanic crustal layer 2 magnetisation, results from DSDP (Leg 37) 77−91071
oceanic gabbro, dredged, mag. props. and marine mag. anomalies source 79−16437
olivine, Fe-rich superparamagnetic clusters, Mossbauer study, appl. to thermal histories of rocks 79−82831
ophiolite complexes, effects of alteration on NRM and implications for oceanic crust 78−65280
ophiolite complexes limitations as models for mag. layer of oceanic lithosphere 78−81145
ophiolitic and continental margin pillow lavas from Quebec Appalachians, magnetic signatures *(French)* 79−79813
E.Pacific Rise−Gapalagos Rise system, magd mag. anomalies and rock magnetism 78−73331
palaeointensity determination of laboratory rock sample 80−61917
palaeomagnetic record carriers synthetic analogues, preparation, characterisation and mag. props. 78−65276
Pearson Formation (Great Slave Supergroup, NWT), multicomponent magnetisation and Coronation loop 78−77179
Permian volcanics in western Southern Alps, palaoemag. and rock magnetic props. 80−89948
Pliensbachian limestone sequence at Bakonycsernye (Hungary), remanent magnetisation 80−90074
Pliocene rhyolite from San Vincenzo, Tuscany 80−56357
post-depositional realignment of sediments, expts. and theory 80−109137
primary magnetisation direction, rock folds slope angle effects 77−53041
psarks, nature and existence rel. to pseudo-single-domain phenomena 78−65274
pseudo-single domain grains, stable remanence origin 78−65275
pyrrhotite, pseudosingle-domain effects and single-domain multidomain transition 77−64274
pyrrhotites and kholodninskoye ore deposit 77−60367
recent remagnetisation, occurrence rel. to deficiency of high-latit. palaeomag. poles 78−65181
red beds, Moenkopi Formation, Arizona, detrital mag. 79−79820
red sandstone from N.Calcareous Alps, Permo-Triassic palaeomagnetism 80−56358
redbeds of Great Slave Supergroup, Canada, mag. susceptibility anisotropy 77−78160
remanence acquisition in Finnish lake sediments 79−66682
remanent magnetisation, effect of stress cycling and inelastic volumetric strain 78−88820
remanent magnetisation, uniaxial stress effects, stress cycling and domain state depend. 80−26505
remanent magnetization, reversible effect of small uniaxial stress, single-domain theory 78−20393
remanent magnetization of single-domain grains ensemble near anisotropy const. transition through zero 77−78164
Reydarfjordur area, E.Iceland, dyke magnetisation and upper crustal struct. 77−78139
Rossville-type diabase, Pennsylvania, probably pseudo single domain behaviour 77−56621
rotational remanent magnetisation, explanation 80−51390
rotational remanent magnetisation, origin 80−61794
rotational remanent magnetisation 77−2150
rotational remanent magnetisation acquired during alternating field demagnetisation 80−36295
rotational remanent magnetisation of igneous rock, expt. and theory 80−85645
RRM and anhysteretic remanent magnetisation, expts. on laboratory samples 80−90076
sand, specularite-bearing, experimentally deposited, mag. declination and inclination errors 80−90075
sandstone (Dunnet Head), scattered magnetisation direction, down to small scale 80−90077
sediment, artificial, const. vol. deform. effects on magnetisation 78−65265
sediment magnetisation, surface tension effects 80−85644
sediment magnetisation, water content effects 79−70785
sediment magnetisation studies, high-press. cell for chem. demagnetisation 80−31126
rock magnetism continued
sedimentary rocks, magnetisation rel. to palaeomagnetism and Cretaceous-Tertiary extinctions 78−32013
sediments, drying remanent magnetization 79−66681
sediments, fine-grained, compaction effect on acquisition of detrital remanent magnetization 78−20395
sediments anomalous magnetic fabric which records apparent geomag. field excursion 78−81152
sediments from Lake Zurich, magnetisation of detrital and chemical samples 79−70787
sediments magnetization, depositional and postdepositional processes 77−86869
self-reversal of remanent magnetisation of lava 80−56462
serpentinite protrusions, in oceanic crust, contrib. to mag. anomalies 77−5149
serpentinites from Burro Mountain, California, magnetic study 79−79814
shock, effect on terrestrial rocks magnetism 78−85538
shock effects and remanence in hypervel. impact expt. 79−29755
silicic volcanics, Jurassic, from Nevada, USA, thermochemical remanent magnetisation 80−98310
single domain grains, mag. blocking temps. during slow cooling 80−90082
slate, ferromagnetic mineral grain orientation model 77−5192
spin glass, rock magnetism type behaviour 77−66361
St. Bees Sandstone, N.England, diagenetic development of unstable and stable magnetisation 77−29287
stratified anisotropy diagnosis possibilities 77−33061
stress wave attenuation, linear magnetic hysteresis model *(Chinese)* 79−39702
stressed rocks, mag. behaviour rel. to earthquake prediction 78−32068
submarine basalts, mag. props. rel. to changes in oceanic crust mag. signal 77−90995
submarine pillow basalts, seafloor weathering effects on geomag. palaeointensities determ. 80−3927
Sudbury Basin, Ontario, mag. susceptibility anisotropy as rock strain indicator 77−78170
sulphide mineralisation zones of NW Ukrainian Shield, rocks mag. props. *(Russian)* 79−96758
susceptibility anisotropy meas. using inductive magnetometers 78−85541
Swedish Ordovician limestones, mag. directions 78−28169
tectonomagnetic experiments, noise reduction by multivariate linear regression 79−84515
tectonomagnetics and small scale secular variation, symposium, Seattle, Washington (1977 August 22) 80−22133
Tertiary volcanic rocks, N. Bavaria, palaeomag. and rock mag. meas. 77−64203
Tertiary volcanics from Sardinia 80−56343
Thetford Mines ophiolites, Quebec, NRM props. and palaeomagnetism 80−61757
titanomagnetite, Al-substituted, monodomain, mag. props. 78−56346
titanomagnetite, prepared at different oxidation conditions, hysteresis props. 78−56352
titanomagnetite, single-crystal, mag. props. of multidomain TRM 78−56345
titanomagnetite, single-domain particles identification by TEM 79−88342
titanomagnetite, TRM acquired by multi-domain single cryst. 80−36293
titanomagnetite from African rift zones, spinodal decomposition and partial self-reversal of magnetisation 77−81869
titanomagnetites, hysteresis props., grain size and comp. depend. 77−37187
titanomagnetites, temp. depend. cation distrib., mag. prop. obs. 80−85647
TRM, multidomain grains demagnetisation field 78−65273
TRM, prod. by single domain oxide particles 78−65271
TRM, var. with grain size 78−65270
TRM direction, mag. shape anisotropy effect, appl. to basalts 79−29758
TRM origin, symposium (San Francisco, CA, 1976, December 9) 78−65269
ulvospinel, containing magnetized inclusions, mag. behaviour, cooling through Curie point 78−56314
ulvospinel, mag. props. weak ferromag. in 4-200K temp. range 78−56351
Upper Pliocene deposits, W Turkmenia, NRM origin and palaeomag. 79−25192
viscous magnetisation, use of distrib. functions for time consts. in Preisach-Neel diagram 77−9408
viscous remanent magnetisation in sedimentary rocks, stability to AF demagnetisation, expt. results 79−79826
volcanic rocks from Mt. Etna, stress effects on magnetic props. 77−37192
Yellowstone and Jackson Lakes, mag. props. and secular var. in sediment cores 78−48968
Yerington mine, Nevada, in situ induced polarisation and mag. susceptibility meas. 80−51323
Au deposit location in Canton Bousquet, Quebec *(French)* 77−53051
Fe ore deposits, magnetic prospecting, 3-D anisotropic body mag. field calcs. and algorithm 80−4141
Fe ore formation, Addatigala, India, mag. profiles 79−34808
FeOOH minerals, magneto-mineralogical props. 77−81872
$Na_2(Fe,Mg)_5Si_8O_{22}(OH)_2$, riebeckite, low temp. Mossbauer obs. of oriented single cryst. behaviour and mag. props. 80−84674

rocket vehicles *see rockets*

rockets
see also missiles; space vehicles; weapons
aerospace acoustic emission instrumentation and applications 77−33322
Ariane launch vehicle, acoustic environment *(French)* 79−81620
Ariane launch vehicle, model firing tests, acoustic field, heat flux, press. distrib. 78−4062
astronomy and atmosphere programs, conf. Bournemouth, England (1980, Aug.) 80−105433
attitude control, solar sensor system pointing accuracy *(Japanese)* 78−24420
attitude measurement using laser system 79−12763
attitude measurement with Hall-effect magnetometers 79−21148
attitude sensing using albedo sensor sounding rocket appls. 79−101044
ballistic, intercontinental, Keplerian paths, pencil with two common points, nongravitational foci 80−52005

rockets continued
base flow at supersonic vel., rockets and re-entry vehicles appl. 78−67243
charge neutralisation of rocket payload during electron beam emission, laboratory studies 80−77258
China 2 rocket (1971-18B), orbit determ. and geophysical interpretations 80−4231
conducting tubes in polarized plane wave fields, surface currents and charges 78−42256
Cosmos 408 rocket orbit rel. to upper atmosphere winds 78−73559
debris and jettisoned boosters as UFO phenomena 77−64607
Echo IV electron beam-emitting rocket, neutral N_2 cloud effect on elec. charging in ionosphere 79−75017
eddy current torques, air torques, and spin decay of orbiting cylindrical rocket bodies 78−93074
electric field structure in disturbed zone behind cylinder streamlined by rarefied plasma 79−53623
electric potential of rocket, and electron beam injection expts. *(Russian)* 78−93069
electrical potential determ. device 79−21146
electron accelerator expt. on POLAR-5 sounding rocket, for use within aurora 80−77170
electronic units development, within INTERCOSMOS programme *(Spanish)* 77−91401
European space technology developments, Swiss role *(German)* 80−4234
exhaust anemometry, Doppler difference and two focus methods, correlator and photon counting 79−60084
exhaust plumes, short-duration, rapid-scan instrumentation for spectrally and spatially resolved radiance measurements 80−13164
exhaust turbulence parameter meas., laser crossed beam correl. technique 79−86541
gaseous-fuelled nuclear engine, reactivity effects 77−54354
geomagnetic aspect horizontal component sensor *(Japanese)* 78−24421
hydrazine fuel in ambient air CO_2 laser absorption spectra and photoacoustic detection 80−104540
impulse recorder for small rocket engines 80−77595
intermediate thrust arcs in rotating potential force fields 80−52007
interstellar appls. of electrostatic/EM ion collection techniques 77−70974
interstellar ramjet acceleration runway 79−101047
interstellar ramjet probe, relativistic flight dynamics 77−25909
interstellar rocket, laser powered, mass ratio and instantaneous efficiency 79−21134
interstellar rocket relativistic navigation problem, three-dimensional eqn. of motion 79−21136
ionosphere satellite wake, assessment ion current distrib. 80−101527
ionosphere sounding, ion temperature probes system design *(Japanese)* 80−85838
ionosphere sounding rocket, POLAR-5, elec. charge accumulation due to electron expt. 80−77213
ionospheric rocket expt. high-power electron gun *(Japanese)* 78−61566
IR emission meas. using versatile sensitive radiometer 77−70887
jet engine reactive thrust using lasers 77−38905
laser evaporation of target, nozzle for impulse augmentation 79−23439
laser-powered interstellar ramjet 77−70975
launching of large payloads into Earth orbit by intense relativistic electron beams 79−21135
M-3C, meteorological obs. for launching *(Japanese)* 79−25304
meteorological rocket systems in 1960s in America *(Russian)* 77−21927
meteorological rocket telemetry system *(German)* 77−64606
monoaxial controlled solar pointer for atmospheric occultation meas. *(Japanese)* 78−32312
multiple propulsion concept, theory and performance 80−4229
Nike-Apache, ion plasma oscills. prod. in ionosphere 79−40012
Nimbus 1 rocket (1964-52B), 15th-order resonance effects 78−65168
nuclear gas-phase rocket motor, MHD rot. of conducting fluid in crossed field *(Russian)* 78−47059
nuclear reactors, laminar flow, temp.-viscosity induced instabilities in gaseous heated channel 77−18689
orbit transfer of rocket between elliptic orbits, globally optimal solns. 78−8236
payloads for Project ARAKS 79−21140
plasma spraying utilisation in research work 79−83117
potential and charge neutralisation, electron beam injection in Araks expt. *(Russian)* 80−17472
propulsion and dynamics theory, early stages 78−16
propulsion project for engineering students 77−9839
ram-augmented interstellar rocket performance 77−25908
rocket and satellite space obs. (1966-76) *(Japanese)* 78−28481
rocketborne IR spectrometer 78−81460
S-310-5 rocket, ionospheric current obs. *(Japanese)* 80−94635
satellite, orbit injection autonomous system 78−65485
Skylab 1 rocket, 1973-27B, orbit determ. and anal., geopotential resonance 80−67515
Skylark, vertical, weightlessness expts., metallurgy and electrolysis *(German)* 79−19980
Skylark rocket attitude control using magnetometers and Moon sensor 79−25436
solar sensor data processing cct. *(Japanese)* 78−24423
solid propellant effluent, effect on ice nucleation 79−88446
solid propellant stress transducer evaluation 80−81245
sounding rocket attitude estimation using star sensor data 79−25435
sounding rocket attitude stabilisation H_2O_2 jet system *(Japanese)* 78−28482
sounding rocket three-axis attitude control system *(Japanese)* 78−24422
Space Shuttle, environmental effects during launch and reentry 78−85681
space shuttle model, exhaust effluents meas. using electrets 79−53548
static electricity form. during ionised gas discharge from nozzle 79−40060
thrust limited relativistic, interstellar drag effects on minimum time trajectory 78−49286
Vanguard orbits, geopot. resonances 77−32978
Vertical'-6 flight results rel. to 1978 International Reference Ionosphere 80−90285
Vertical-6 rocket flight results on upper atmosphere parameters 80−90268
wind meas. by meteorological rocket sounding methods, since World War II 80−17398

rockets continued
Zarnitsa.2 electron injection expt., circumrocket glow spectral obs. *(Russian)* 80−12596
Al particles produced by rocket launch 80−81503
H_2, laser-heated, analysis of nozzle flow 80−10283
HCl sources (solid fuel rockets), detection using DF laser absorption 77−27059

rocks
see also geology; minerals; rock magnetism
acoustic anisotropy of sedimentary rocks, due to overburden press. 80−56455
acoustic emission and creep at high confining press. and differential stress 77−73716
acoustic emission techniques appl. to rock mechanics, rel. to earthquake prediction *(Chinese)* 78−24279
acoustic emissions, meas. at high temp. and press. by wide-band optical-mechanical system 78−1525
acoustic microscope images of sedimentary rock samples 79−12292
actinide abundance determ. for rocks using NaI detectors 79−80043
active hydrothermal systems, intrinsic fluid and rock resistivity anal. 78−40480
Adirondack anorthosite, deform. characts. 78−61399
AE appl. to mechanics *(Japanese)* 78−56845
S.African kimberlites, $^{40}Ar/^{39}Ar$ anals. of phlogopite nodules and phlogopite-bearing peridotites 79−34769
alabaster, US waves in crack preparation region rel. to seismic waves 77−9405
Alcaparrosa Formation (Upper Ordovician), Argentina, palaeomagnetism and K-Ar age 78−96135
aleurolite, buried explosions model studies 77−52999
alkaline, neutron activation analysis, destructive and nondestructive methods 78−92573
alkaline basaltoid and pyroxenite inclusions, Tien-Shan, elec. cond. under high temp. and press. 77−53039
alkaline lava flows from El Salto-Almafuerte Argentina, palaeomagnetism 78−85471
alkaline lavas from Antarctica, rare earth geochemistry 77−41030
alpha activity of natural samples, appl. of Kodak LR 115 dielectric track detector *(Czech)* 79−8711
alpha and beta radioactivity meas. *(Rumanian)* 77−49067
alpine peridotite near Pinchi Lake, BC, tectonic fabric 77−44987
Alpine tectonite lherzolites, Sr isotope comp., evidence for mantle origin 78−65302
Amadeus Basin, Central Australia, Precambrian-Cambrian boundary sediments palaeomag. direction 79−29697
Amitsoq gneiss, W.Greenland, initial Pb isotopic comp. and implications for Earth age 78−20371
amphibole from upper mantle, planetary-type rare gases 78−96167
amphibolite facies, Chenaillet Massif, Hautes Alpes, France, example 78−65304
analysis, for C_2-C_9 hydrocarbons, gas chromatographic method 79−39226
analysis, quantitative, spectral appl. of microdensitometry *(Czech)* 79−30524
analysis by instrumental neutron activation, automated method 78−3769
ancient deep-sea fan in Cantabrian Mountains, growth 78−44813
ancient metamorphic formations, appl. of geophysical and geological data combined anal. *(Russian)* 79−8630
andesite, amphibole stability 79−66678
andesite, neutron activation analysis, destructive and nondestructive methods 78−92573
andesite melt, viscosity at high press. 77−29291
andesites, Andean region, petrogenetic composition variations 80−8313
andesites, high $^{87}Sr/^{86}Sr$, O isotope comp. rel. to origin 79−34817
andesites from S.America, Nd and Sr isotope data 79−29726
anelastic strain rel. to virgin stresses, possible meas. method 77−9416
anisotropic elastic const. meas. by uniaxial compression test *(Japanese)* 79−79822
anisotropic elastic deformation, effective stress law, appl. to saturated porous rocks 80−51385
anisotropic rock, chip form. 78−61407
anisotropy evolution under isotropic cyclic compression *(French)* 77−41021
anorthosite and associated plutons, S Nain complex, Labrador 79−20825
anorthosite complexes, Marcy (New York) and Morin (Quebec), rare earth element abundances 77−78177
anorthosite gneisses, trace element comp. rel. to petrogenesis 78−65224
anorthosite in Kalka Intrusion, central Australia, genesis by plagioclase flotation and remelting 77−60371
anorthositic dikes, southern Nain complex, Labrador 79−84246
Antarctic Peninsula igneous rocks, transverse geochemical vars. rel. to calc-alkaline magmas genesis 80−56466
Antarctic plate boundary near Bouvet triple junction, petrology 78−53639
Antarctic rocks, seawater dissolution rate rel. to silica budget of Antarctic waters 78−20436
Aphebian alkaline plutonic and hypabyssal rocks, Great Slave Lake 79−84255
apparent resistivity changes under uniaxial compression *(Chinese)* 80−3995
Archaean basalts and peridotites, rel. to mantle heterogeneity and Earth comp. 78−11844
Archaean clastic metasedimentary rocks, $^{18}O/^{16}O$ as petrogenetic indicator for Archaean gneisses 78−20410
Archaean Dalembert tuff, Rouyn-Noranda, Quebec, Canada, petrography, and eruption mechanism 79−62472
Archaean granite in Yellowknife, Northwest Territories, Canada, rare earth and trace element data 80−4007
Archaean granite-greenstone terrains rel. to mafic dikes 79−57881
Archaean granites from NE.Minnesota, Th, U and K distribs. 78−61356
Archaean granulites model for lower continental crust, evidence from mantle Nd-Sr isotope correl. 80−94498
Archaean layered greenstone from Pilbara Block, age of volcanics 78−53627
Archaean metamorphic rocks, Zijderfeld vector diagrams use in multicomponent palaeomag. studies 80−17420
Archaean metasedimentary rocks from Kambalda, Western Australia, rare earth element geochemistry 80−109143
Archaean migmatites in Lofoten-Vesteralen, Norway, Nd, Sr and Pb isotope data interpretation 79−34773

rocks continued
Archaean peridotitic komatiites in La Motte Township, Quebec, emplacement 78-77234
Archaean plutonic rocks, Pb isotope comp. 78-65223
Archaean rocks, press.-temp. data rel. to continental geotherms 79-34780
Archaean ultramafics of Bulong Complex, W.Australia, fractionation rel. to igneous layering 77-56626
Archaean volcanic rocks S content rel. to ocean floor basalts 78-88824
Archean greenstone belts, Nyanzian System, W.Kenya, trace element model study 77-60375
Archean sedimentary rocks, Kalgoorlie, Australia, rare earth elements and crustal evolution 77-60374
Archean supracrustal Rb-Sr ages, Rocks and Amitsoq gneisses, Isua, Greenland 78-16013
Archean ultramafic rocks, discrimination between extrusive and intrusive on chemical basis 79-84256
Archean variolites, quenched immiscible liquids, discussion 78-20394
Arendal orthogneiss, geologically meaningless Rb-Sr total rock isochron 80-31014
Armenian basic and ultrabasic rocks, elastic wave vels. at high pressures 77-44972
artificially disturbed strata, temp. distrib. during air filtration *(Russian)* 77-25667
artificially fractured rock, heat transfer agents flow patterns 80-17239
artificially fractured rock beds, heat extraction with water 77-44949
Arunta Block, Australia, sapphirine-bearing rocks with sedimentary and volcanogenic protoliths 79-44185
ash-flow tuffs, Lake Precambrian in E. Newfoundland 79-84258
assay-activation analysis, use of Au and Ag standards based on phenol formaldehyde resin 78-3419
asymmetric folding, finite-element simulation 78-77222
Mid-Atlantic Ridge, geophysical and petrological constraints 78-85508
Mid Atlantic Ridge crest, geological and geophys. investigations 80-8284
attenuation and mechanical hysteresis loops of anelastic solid 79-100826
Australia and Timor Trough, facies rel. to topographic wave migration during past 3 million years 78-49018
Australian post-Archaean sedimentary rocks, rare earth patterns and crustal evolution 77-41015
avalanches and landslides, mechanism based on law of dry friction 80-8314
axial-plane slaty cleavage and schistosity development, expt. 78-7625
Azorean lavas, REE and LIL element compositions 77-25669
Baikal rift zone, petrochem. of Cenozoic basalts and assoc. rocks 78-36171
Baja California, ancient lithospheric lherzolite xenolith in alkali basalt 77-81888
Baltic Shield, petrological model *(Russian)* 77-33020
banded deformation structures description and origin, regional strain, local perturbs. 78-7629
banded perturbation structures, growth, rheology 78-36152
banding phenomena, calcs., nonlinear partial differential eqns. appls. 80-4510
Barberton region, South Africa, Archaean granitic rocks, trace element geochemistry 78-11895
Barre granite, crack growth and development during creep 79-84237
Barre Granite, microfracture opening and strain relaxation mechanism 77-91116
Barre granite, prop. determ. and wave propag. 77-56617
Barre granite, static and dynamic fracture strength 77-44976
basalt, $^{238}U/^{235}U$ ratio and comparison with chondritic meteorites 80-85903
basalt, amphibole stability 79-66678
basalt, chemical comp. rel. to Earth bulk comp. and lunar basalt 77-60636
basalt, deep-sea, Mossbauer study of core-to-rim alteration 79-66688
basalt, elasticity freq. depend. and seismic vel. dispersion 77-73727
basalt, erupted at Reykjanes Ridge crest, vesicularity 78-73351
basalt, feasibility of geologic repository for nuclear waste 80-18479
basalt, hydrothermal alteration by seawater, chemical exchange exptl. results 79-20828
basalt, internal friction Q-factor meas. 77-27499
basalt, mag. mineral identification by rot. hysteresis loss 80-67428
basalt, measurement of magnetic torque acting on rotating sample using air sample 80-31811
basalt, naturally occurring, high-temperature quantitative DTA analysis 80-77144
basalt, oceanic, Pb isotope comp., rel. to mantle evolution 78-65217
basalt, optical props. compared with Mars disc IR spectra 78-85879
basalt, S.Atlantic, glass inclusions as samples of early magmatic liquid 77-37202
basalt, shock effects and remanence in hypervel. impact expt. 79-29755
basalt and gabbro, elec. resistivity meas., oceanic crust model 79-29703
basalt dykes, Newfoundland, occurrence of sodic amphibole, arfvedsonite 78-65287
basalt flows from Absaroke Mountains, Wyoming, palaeomag. study 77-86765
basalt from DSDP Leg 34, cooling effects on texture and mineralogy 79-44148
basalt geochemistry rel. to mantle heterogeneity in N.Atlantic 79-29745
basalt glasses from FAMOUS area, Mid-Atlantic Ridge, regional var. and petrogenesis 80-31041
basalt glasses from Mid-Cayman Rise spreading centre, geochemical var. and petrogenesis 80-101364
basalt melt, viscosity at high press. 77-29291
basalt thermomagnetic study for S.E.Sicily samples 77-33056
basalt xenoliths in Massif central France, deform. rel. to mantle struct. and geodynamics *(French)* 79-48424
basalt-andesite, phase comp. at 30 kbar crystallization intervals 79-20816
basalt-seawater alteration reactions, studies via dynamic hydrothermal experimental system 79-5686
basalt-seawater interaction, trace element and Sr isotopic vars. in glassy basalt 80-8286
basaltic and gabbroic rocks from W. Mariana basin and Mariana trench 78-65254
basaltic andesite dykes, Iritono, central Abukuma plateau, plagioclase grain size 78-7618
basaltic bodies, destruction by high-vel. impact 77-64704
basaltic lava flows, degassing effects on rheology 79-12115
rocks continued
basaltic magmas, O_2 fugacity, role of gas forming elements 78-77218
basaltic magmas classification, use of Ti, Zr, Y, Sr, K, P and Nb distribs. 77-5150
basaltic pillars, in collapsed lava pools on deep ocean floor 80-3991
basaltic rocks from DSDP Leg 37, geochemistry 77-91127
basalts, altered mid-oceanic, radioactive disequilibrium 78-96186
basalts, crystallisation temp. determ. 79-88343
basalts, deep sea, statistical anal. of clinopyroxenes 78-88828
basalts, deep sea, trace element distrib. pattern, neutron activation anal., rel. to genesis 78-11879
basalts, DSDP Leg 37, U concs. 77-91075
basalts, from Central North Atlantic, Sr isotope geochemistry and Azores mantle plume 77-5179
basalts, from Juan de Fuca-Gorda Ridge area, comp. rel. to mag. anomalies 77-29242
basalts, from Pacific Ocean Basin, Sr isotope comp. rel. to mantle comp. 78-65218
basalts, Indian, elec. cond. meas., 475-1100K 78-69336
basalts, mag. grains nature and implications for palaeomag. 79-84243
basalts, oceanic, elec. resistivity meas. 80-21713
basalts, oceanic, noble gas abundance patterns controlling factors 78-65220
basalts, open system cryst. fractionation and incompatible element var. 77-66916
basalts, Palaeocene, of Mull and Skye, immobile trace elements rel. to palaeotectonic affinities 79-34816
basalts, redox state 78-77217
basalts, stability region of ferromagnetic minerals 78-16000
basalts and mantle derived materials, K and Rb relations rel. to phlogopite source 77-5165
basalts from DSDP Leg 37, S isotope comp. of sulphides 77-91101
basalts from DSDP Leg 37 and FAMOUS area, compositional and petrogenetic comparisons 77-91077
basalts from DSDP Leg 37 cores, Pb and U isotopes 77-91123
basalts from DSDP site 332, geochemical characts. and evolution 77-91126
basalts from Faeroe Islands, compressional and shear wave vels. at high temp. and press. 79-84244
basalts from Great Meteor and Josephine seamounts, K-Ar ages 77-9399
basalts from Mid-Atlantic Ridge in central N.Atlantic, geochemical var. 79-39675
basalts from mid-ocean ridge, major and trace element data 79-88316
basalts from Nauru Basin, trace element abundances 80-94499
basalts from Project FAMOUS area, petrogenesis from 0 to 15 kbars exptl. study 79-29768
basalts from Reykjanes Ridge and Iceland, Cl and Br contents rel. to degassing 78-36136
basalts from Sao Miguel, $^{143}Nd/^{144}Nd$ and $^{87}Sr/^{86}Sr$ ratios 79-74873
basalts from Tyrrhenian Sea, geochemistry 79-53329
basalts geochemistry from back-arc spreading centre, East Scotia Sea 80-3989
basalts with xenoliths from S.E. Arizona, petrogenesis 80-8303
beach rock erosional features morphological zonation 79-48447
beam, laterally-constrained ultimate strength investigation with constrained beam test apparatus 79-29299
bedded formations tectonics, struct.-forming props. from modelling data *(Russian)* 79-8627
bedrock freeze-thaw weathering in Colorado front range alpine zone 80-31039
Belingwe Greenstone Belt, Rhodesia, petrogenesis of peridotitic komatiites 78-32087
bentonite, examples of devitrification and early diagenesis 80-81860
Berea sandstone, effects of pore fluids on bulk and shear attenuation 80-51386
N.Black Hills, S.Dakota, evidence for late Tertiary volcanic activity 77-78142
Black Sea continental slope, Cretaceous rock outcrops 79-44173
black shales rel. to geologic-oceanographic model of Lower Palaeozoic 78-61436
Blair dolomite, shock wave expts. 80-67362
blueschists, from Ile de Groix, France, isotopic ages, metamorphic episodes determ. 77-66896
blueschists at Shangla Pass, N.Pakistan, early Tertiary, evidence for subduction 79-2229
Bohus granite, relation between uniaxial tensile strength and sample size 78-81153
Bohus granite area, SW Sweden, geothermal investigations 80-85631
boninites, komatiites and ophiolitic basalts 79-92539
borehole activation analysis, neutron energy distrib. in low-porosity rock 77-64286
Borrowdale Volcanic Group, English Lake District, palaeomag. results 77-32984
Boston Bay Group, Massachusetts, origin and significance of cylindrical sandstone structs. 78-69343
Bouvet triple junction, S.Atlantic Ocean, geochem. and petrology of dredged basalts 78-11877
boxed sets of rock and minerals from Geological Survey of Canada 77-37203
Brantford-Woodstock area, S.Ontario, bedrock rel. to late Wisconsinan till sheets trend surfaces 78-92858
Brezovica peridotite base, Jurassic metamorphism 78-96169
British Trias, hydrogeophysical props. 77-41074
brittle material under compressive load, crack extension from flaws 78-95812
Bucegi Conglomerate, Romanian Carpathian submarine slope deposit 79-8632
bulk chemical anal. calc. from mineral phases obs. in thin section, BULK computer program 79-2378
calc-alkaline igneous rocks, Sr isotope data and crustal contamination model 79-79762
calc-alkaline volcanic rocks of Cerro Galan, NW.Argentina, Sr isotope evidence for crustal contamination 80-98318
calcareous rocks, seismic transverse waves propag. expts. 77-21682
calcite, crack propagation obs. 77-73725
calcite rock, compression wave studies 78-81151
calcite rocks, experimentally deformed, texture development 79-83230
calcite rocks, plastically deformed, texture transitions 79-83227
Caledonian granites of Scotland and N.England, isotopic evidence for provenance 80-109146

rocks continued
California rock P-wave velocity, high press. and temp. expts. 80−61783
Cambrian greenstone belts, Australia, marginal sea crust slices in Lachlan Fold Belt 79−29765
Canada Maritime Provinces, rocks radioactive heat prod. rel. to heat flow meas. 79−100819
Canadian Precambrian Shield, N.W.Ontario, $^{18}O/^{16}O$ ratios 77−78130
Canadian Shield surface crystalline rocks, O isotope comp. 79−62496
Cantal continental volcanic system (France), ^{87}Rb-^{87}Sr constraints on genesis and evolution 79−88327
carbonate, trace element anal. using computerised automatic X-ray fluoresc. spectrograph 77−56320
carbonate bearing rocks, fluorite mineralisation dynamic model 80−81876
carbonate breccia beds, submarine, depositional model 79−84259
carbonate rock, interrelation of flow or fracture and phase transition during deform. 80−51389
carbonates, dissolution kinetics, lithology effects 77−78172
carbonates, Texas, high-temp. metamorphism in shallow crustal environment 77−2128
carbonatites, origin by liq. immiscibility 79−57928
carbonatitic igneous rocks, apatite comp. vars. 79−57929
Carboniferous Andacollo series (Argentina), palaeomagnetism, K-Ar dating and hydrothermal overprinting age 79−29698
Carboniferous Limestone, in-situ seismic methods for crack anisotropy in NW.England 80−17240
carboniferous rock, cyclically layered, seismic response from synthetic seismograms 78−69293
E.Carpathian volcanic rocks, rare earth elements and Y, Rb, Sr, Cs, Ba, Pb, Th, U, Zr, Hf and Sn concs. 77−5151
caved faces of Appin Colliery, rock pressure distrib. 77−9420
cenotypal volcanogenic rocks under hydrostatic press., longitudinal wave vel. *(Russian)* 77−73722
Central American andesites petrogenesis, Sr isotope evidence 79−20833
chabazitic tuff, a zeolitic rock for thermal storage of solar energy 80−94117
chalk of S.E. England, soils and geomorphology 77−44993
Chamita Formation stratotype (Mio-Pliocene) of northcentral New Mexico, mag. polarity stratigraphy 77−78087
characteristics examination by US method *(German)* 77−91314
Charlevoix structure, Quebec, shock produced mosaicism in plagioclase 77−44988
charnockite formation in S.India and ancient crustal metamorphism 79−44154
charnockite series, form. temp. and press., evidence for geothermal gradients 78−40553
charnockites from Sao Paulo State, Brazil, geochemistry 79−44145
charnockites from Visakhapatnam, India, allanite occurrence 78−65285
chert, Ce as indication of form. in marine environment 77−37200
chert, prehistoric Hertzian fracture 77−29292
cherts, deep sea, stable isotope geochem. 77−5182
cherts, from South Africa, O isotope geochem. 79−34820
N.Chilean ignimbrites, REE data and Sr isotopes rel. to petrogenesis 79−44146
Clarno Formation, central Oregon, volcanism on thin continental margin 77−29296
clastic rock softening characteristic tests *(Japanese)* 78−49013
clay layer, non-homogeneous, consolidation estimation method 79−58110
clays, seismic transverse waves propag. expts. 77−21682
cleavage, morphological classification 80−21736
coal, anisotropic elec. props. meas. 80−98312
coal formations seismic tracing, interference waves appl. *(Russian)* 79−74858
coal seams, approx. seismic wave diffrac. theory for transparent half-planes 80−89974
coal-bearing rocks of Bonnet Plume Basin, Yukon Territory, Canada, evaluation from gravity profile 80−76898
colour values from diffuse reflectance spectra *(French)* 78−11881
complex resistivity meas. by freq. domain method *(German)* 80−4001
composite dike, geochemistry of co-existing acidic and basic melts 79−2233
composite dike geochemistry, magmas commingling model for coexisting acidic and basic melts 80−12391
composition, porosity and depth rel. to density-vel. relation *(Russian)* 79−48461
compressibility, nonelliptical crack effects 79−2227
compressional and shear wave velocities, temp. depend. 78−7579
compressional and shear wave velocities under high press., effect of high-low quartz transition 80−12380
compressional and shear waves in saturated rock during water-steam transition 80−30995
compressional wave vel. meas. in lab., transient effects 79−16447
compressional wave velocities at high temps. and press., rel. to crustal low-vel. zones 80−41435
compressional wave velocity and damping, minerals and rocks at high-press. *(German)* 80−31031
concretions in Otway sediments, S.E.Australia 78−20417
conglomerates of flat pebbles, stone rosettes, as indicators of ancient shorelines 80−26489
continental and oceanic basalts, $^{143}Nd/^{144}Nd$ ratio vars., rel. to magma sources and mantle struct. 77−21708
continental crust, metamorphic rocks model for lower crust 77−81840
continental volcanics, $^{143}Nd/^{144}Nd$ and $^{87}Sr/^{86}Sr$ ratios 78−53635
Conway granite, reinvestigation of 4.4 MeV alpha-activity 78−57210
cooling orogen, magnetic and isotopic blocking temps. 78−65226
cooling orogen, magnetic blocking temp. 78−65227
cooling plutons, transport phenomena in assoc. hydrothermal systems 78−36206
cordierite-bearing rock, $^{40}Ar/^{39}Ar$ age spectrum, effects of excess radiogenic ^{40}Ar 77−29456
cordierite-garnet bearing assemblages in granulite facies terrains 78−44810
Cordilleran granites, mantle origin 77−21710
Corsican granite, deformation effects on ^{39}Ar-^{40}Ar systematics 79−53347
crack growth and thermoelastic behaviour 80−26502
crack propag. in diametrically-compressed rock discs 79−48463
crack propagation, branching model 77−23918
cracked, slip surface development 78−15480
cratering explosion, pulsed hydrodynamic model 78−51180
creep, stable sliding, and premonitory slip 79−16410
rocks continued
creep laws for mantle 78−69305
crenulation cleavage, mechanical significance investigations 80−21737
crenulation cleavage, morphologic classification 77−70646
crenulation cleavages microstructure, cleavage origin indicator 79−70784
Cretaceous black shale, thermal alteration by basaltic intrusions in E.Atlantic 78−61396
Cretaceous deep-sea basalts, $^{40}Ar/^{36}Ar$ for trapped mantle gases 79−16423
Cretaceous kimberlites and mantle xenoliths from Southern Africa, Pb and Sr isotopes 77−60372
Upper Cretaceous limestones from Munster Basin, NW.Germany, palaeomagntism 80−89949
Cretaceous mid-ocean ridge basalt (MORB), Nd and Sr isotopic comps. and rare earth element abundances 80−94520
Cretaceous Pirgua Subgroup (Argentina), palaeomag. rel. to age of opening of S Atlantic 77−90998
critical dilatant volume at tertiary creep onset 78−28220
crustal, deep structure to NW of Cape Verde Islands 79−2201
crustal rocks, exponential relationship between seismic vel. and radioactive heat prod. 79−70793
crystalline, thermal cond., rel. to energy extraction from hot dry rock geothermal systems 79−70790
crystalline basement rocks deformation, mechanical processes rel. to ductile deform zones and mylonites form. 79−53344
crystalline physiology, model for non-chemical form of life 77−90978
crystalline rocks, transient creep and semibrittle behaviour 79−16460
crystalline rocks from 5.3 km depth in Michigan Basin, microcracks obs. 79−39705
cylindrical shell, thin, instability rel. to mechanical anal. of geologic structs. *(Chinese)* 78−73364
cylindrical stress waves generated by moving axisymm. super-seismic pressure pulse 77−44979
Dalradian metabasaltic rocks, petrochemical affinities 77−5202
Dalradian metabasaltic rocks, petrochemical affinities 77−5203
Dalradian sediments, Scotland, evidence for Cambrian opening of Iapetus Ocean 80−98299
debris flows on vegetated screes in Black Mountain, Carmarthenshire 77−44992
Dedham granodiorite, E.Massachusetts, Rb-Sr whole rock age determs. 77−81835
Deep Sea Drilling Project Leg 37-1974, conference Edmonton, Canada, (May, 9176) 77−91069
deep-sea basalts, clinopyroxenes chemistry statistical anal. 80−41437
deep-sea basalts, He and Xe as measure of magmatic differentiation 80−31040
deep-sea cherts and porcelanites, mineralogy of silica phases 77−86856
deformability, determ., in situ tests 79−53341
deformability, determ. by in situ methods 80−17411
deformation, fault slips, processes 80−8263
deformation, non-coaxial, of elliptical particles 79−79829
deformation, time dependent, meas. via triaxial loading apparatus 77−9538
deformation, time-dependent, not purely elastic specimens 78−32075
deformation, transition between regimes dominated by intercrystalline diffusion and creep 77−53047
deformation and failure of rock masses, time-dependent multilaminate model 78−16002
deformation and fracture under general triaxial stress states, anisotropic dilatancy *(Japanese)* 78−56750
deformation data rel. to elastic-plastic lithosphere flexure model 79−20785
deformation experiment on granular material in transmitted light 77−86860
deformation in brittle rock masses preceding earthquake rupture, failure models 80−8255
deformation mechanisms, international colloquium (Perros-Guirec, France, 1-5 October 1978) 79−96757
deformation of foliated medium due to plane strain, theory 80−21720
deformation under pressure, failure precursors, laboratory study 80−8298
deformation under uniaxial compression 77−53043
deformational history of the Delhi rocks around Biliawas, Central Rajasthan 79−25246
deformed flysch sequence, S.W.England, vein arrays, hydraulic fractures and press. soln. structs. 77−78169
deformed rocks, solid-body rot. natural indicators 79−79842
Denchai Basalt, N.Thailand, paleomagnetism, age and geochemistry 80−41421
density determ. by pulsed gamma-ray method, theory *(Russian)* 79−39956
density logging, influence of standard material comp. on readings *(Russian)* 79−74989
description, LSD02 computer-based system 77−33071
desert varnish, cyclic Mn deposition 79−16469
desert varnish, importance of clay minerals 77−86893
desert varnish of Sonoran Desert, comp. from optical and electron probe microanal. 79−79834
destruction by meteorite impact 77−66910
destruction by water jet, theory based on drag force on grains in permeable medium 78−55691
Devonian carbonate rocks, NE British Columbia, barite origin hypothesis 79−25240
Devonian metamorphism, in the Bas-Limousin areas (Massif Central, France) 78−96204
Devonian old red sandstone, comparison with Euphrates and Tigris river sediments 78−81160
diabase, dilatancy anisotropy and response to large cyclic loads 80−21715
diabase, seismic attenuation rel. to crack and grain boundaries 80−72495
diabase, thermal expansion at high-press. 80−21719
diabase pebbles of val d'Illiez conglomerates (Haute-Savoie), geochronology *(French)* 78−92810
dielectric relaxation measurement using blocking layer method 80−103914
differential thermal expansion of pore fluids, fracture propag. and microearthquakes 77−70641
dilatancy and fracture induced vel. changes rel. to frictional sliding 79−16458
dilatancy anisotropy and response to large cyclic loads 80−21715

rocks continued
dilatancy in dry rock, quantitative model and appl. to Westerly granite 79−16445
dilatancy induced fluid migration and vel. anomaly 77−33065
dilatancy rel. to earthquake prediction *(Chinese)* 79−88254
dilatancy-magnetic effect, local mag. vars. assoc. with earthquakes *(Chinese)* 78−61333
dilatancy-magnetic effect to explain earthquake assoc. mag. variation *(Chinese)* 80−56374
discontinuities, suggested methods for quantitative description 79−84513
discontinuous, photoelastic anal. *(German)* 79−34811
displacement meas. in rock masses, two-dimens. coordimeter 79−35016
dolerite, in Tasmania, terrestrial heat flow meas. 77−33018
dolerite dykes, India, density, mag. susceptibility and lithologic comp. 78−85542
dolerite sills, 'Twin Sisters', Baluchistan, Pakistan, petrology 79−44188
dolomite, form. in Floridan Aquifer 79−53346
dolomite, modulated struct. 79−100832
dolomite, ramp wave compression studies 77−78161
dolomite, strain rate depend. inferred from impact and static compression studies 77−44977
dolomites, low temp., microstruct. 79−62487
drill cores, joint systems description *(German)* 79−66690
dry hot rock hydraulic fracture characterisation acoustic instrumentation 77−33221
DSDP Leg 34 basalt, clay mineral form. 79−29767
DSDP Leg 37 basalts, oxide microstructs. and mag. props. 77−91108
DSDP Leg 37 basalts, trace elements and petrogenesis 77−91076
DSDP Leg 37 cores, Pb concs. and isotropic comp. 77−91074
DSDP Leg 37 rocks, O isotope geochemistry 77−91072
ductile deformation in zones of progressive regional metamorphism 78−81149
dunite, anisotropic, compress. wave vel. temp. depend. 78−77224
dunite, elec. cond during shock compression from 12.5 to 45 GPa 78−85536
dunite, thermal expansion at high-press. 80−21719
dyke strain relief meas. near mine working in Boksburg, S.Africa 80−17263
dynamic deformation, at nonuniform triaxial loading *(Russian)* 77−56619
dynamic fracture strength 79−62486
dynamic strength determ., reflected shear wave technique 78−57344
dynamic testing, hydraulic press 79−87789
Early Archaean rocks comp. rel. to crust and mantle chem. evolution 78−65222
Early Precambrian rocks of W.Greenland and Minnesota River Valley, U-Pb ages on single zircons 78−11845
Earth interior, influence of press.-induced phase transitions on Gruneisen parameter 79−1497
Earth mantle materials, Nd-Sr isotopic correl. and geodynamic consequences 79−92512
eclogite, garnet content *(Chinese)* 78−20413
eclogite production in overthrust orogenic zones, metamorphism 79−44142
ecologite, C-type, existence in Xingyang metamorphic belt, tectonic significance *(Chinese)* 79−84264
edge-fracture anal. method 77−21765
elastic anisotropy, investigations in USSR 77−49038
elastic dykes, pre-cleavage, at New Paltz, New York, redistrib. by folding 79−100837
elastic longitudinal wave vels. during nonelastic deform. 78−61402
elastic potential and eqn. of state in geophysical compression range *(Russian)* 77−91112
elastic properties, experimental studies rel. to Earth crust press.-temp. conditions modelling *(Russian)* 78−96207
elastic properties determination, modified borehole jack method 78−81448
elastic props. of rocks rel. to deep crustal composition *(Russian)* 79−48460
elastic wave absorption meas. and recording instrument *(Russian)* 79−29891
elastic wave vel. before earthquakes 80−8256
elastic wave velocity, brittle rocks undergoing deformation at high-press. *(German)* 80−36296
elastic wave vels. of metamorphic rock mass, seismoacoustic methods 77−81871
elastic-plastic deformation 79−92531
elasticity and density simultaneous meas. using high-press. apparatus *(Russian)* 77−70851
elasticity theory, self-consistent imbedding approx. 77−33066
elastoplastic coupled boundary-value problems, rock mech. appl. 77−14918
electrical conductivity meas. in lab., transient effects 79−16447
electrical conductivity of cracked solid 79−91117
electrical conductivity of sandstone, limestone and granite, comments 79−34806
electrical conductivity rel. to random networks and mixing laws 77−44971
electrical parameters of rock forms. determ., probes number and type *(Russian)* 79−39969
electrical properties, of water-bearing and frozen geological conductors *(German)* 79−5472
electrical resistivity changes in rocks during frictional sliding and fracture 79−16457
element analysis of geological and extraterrestrial samples, laser mass spectra 79−16717
element determ. in National Institute for Metallurgy (S.Africa) reference samples 79−88356
Elsonian magmatism in Labrador, age, characts. and tectonic setting 78−73365
Eltanin fault zone, Pacific Ocean, crustal struct. from petrographic data 80−12376
EM wave transmission along drill rod in conducting rock 79−59618
energy dispersive X-ray fluorescence anal. of trace elements in rocks 77−44565
Eocene limestones, on Mid-Atlantic Ridge, tectonic significance 79−12106
epidote-banded greenstones, origin rel. to deformed pillow lavas from Tauern, Austria 79−79833
epithermal-neutron field in medium with inhomogeneous water distribution 79−17957
rocks continued
epizonal granitic intrusions, geothermometry and geobarometry from Fe-Ti oxides and feldspars 77−5140
evaporites, of giant late Jurassic sabkhas of Arabian Tethys 77−66918
explosion in brittle rock, props. gas cavity expansion, soil dilatation 79−8608
explosions, spalling, tensile stresses 79−7324
extension veins of deformed rock, crack-seal mechanism 80−61798
external environmental radiation levels of naturally of occurring radioactive sources 78−9001
facies differentiation caused by wrench deformation along a deep-seated fault system (Leon line, Cantabrian Mountains, North Spain) 78−88831
failure, role of acoustic fluidisation 80−85653
failure, scale invariant properties 78−3758
failure precursors during anelastic deformation 78−61405
failure processes and AE under compression *(Japanese)* 78−56749
fault gouge, possible existence at depth in San Andreas fault zone 79−12097
fault gouge, structural changes during stable sliding and stick-slip 78−32079
fault gouge composition effect on frictional sliding stability 78−3759
fault surfaces, stiffnesses and stick-slip phenomena 79−16463
faulting inception in rock mass with weakened zone 77−33064
faults and shear zones, assoc. deep focus earthquakes 80−61786
fenitisation and fracture granite replacement in mesocratic dike 77−64276
fibrous dissemination, elect. characts. and models 80−4002
finite strain anal. using lines with initial random orientation 78−20568
finite-strain lineations, theory of dispersion 78−88832
fissured media, transient flow tests *(French)* 79−48459
flow heterogeneities 79−57934
fluid distrib. in partial melt, mech. and thermodynamic constraints 80−21685
fluid-infiltrated elastic materials, deformation of cavities and inclusions 78−51073
fluid-saturated rocks, elastic dilatancy and earthquake dynamics 77−21683
Fohnsdorf tertiary basin, Styria, in situ tension measurements *(German)* 80−21665
fold propagation, finite element anal. 77−53049
fold propagation in viscous layer, finite element model 78−32083
folding, experimental, under confining press., drape folds partially scaled models 79−58127
folding, three-dimens. strains in hinge zones 77−81863
folding in simple shear, expt. anal. 78−32077
folding of sedimentary rocks, Malaguide Complex, Spain 80−8312
folding of single viscous layer, exact infinitesimal-amplitude soln. 77−73729
folding of single viscous layer, role of initial perturbs., finite element anal. 78−49003
folding stress outside buckled layers, theory 80−4003
folding under confining pressure, anal. of faulted drape-folds 78−7626
folds, symmetrical, simple derivation of straight limbs shortening/rot. relation 79−79841
folds and gravity tectonics in ice and rocks 77−70658
forested watershed Oesling, Luxembourg, chemical erosion 77−81930
fracture, assoc. microacoustic signals anal. 78−32070
fracture, role of crack inertia 80−109138
fracture and frictional sliding of samples with saw cut, earthquake prediction appl. *(Chinese)* 79−100825
fracture granite replacement in mesocratic dike 77−64276
fracture intensity, expressed as fracture surface area per vol. 80−8301
fracture measurement in laboratory, under geological conditions 80−46171
fracture prediction problem 79−25230
fracture processes, adsorption-sensitive, control and appl. 77−52468
fracture propagation by transient cooling 79−84236
fracture regularities with internal friction and dilatancy 78−85537
fracture toughness meas. technique for downhole stress condition 79−43543
fracture under uniaxial compression *(Chinese)* 77−37183
Franciscan complex, California, compressional vel. 78−40548
Franciscan rocks, dry, compressional wave vels. to 8 kbar and 300C 77−64273
French Western Alps, internal mineralogical and petrological investigations of Alpine metamorphism 78−36157
friction 79−16451
friction and earthquake prediction, conf. (Stanford, 28-30 April 1977) 79−16448
friction and stick-slip mechanics 79−16459
friction effect of confining pressure, temp. and pore pressure 79−16455
friction modelling, expt. results and constitutive eqns. 79−84240
friction modelling, preseismic slip simulation 79−84241
frictional sliding, asperity-surface interaction and surface damage 79−16456
frozen sand-argillaceous rocks, elastic moduli 77−9406
frozen sandstones and shales, US vels. and elec. props. 77−78157
fused, X-ray fluoresc. anal., fundamental parameter method 77−77820
gabbro, compression expts., microcrack development and seismic vel. anal. 80−17250
gabbro, long-term creep, large and small specimen results obtained over 20 and 3 years respectively *(Japanese)* 78−56705
gabbro, long-term creep tests, rel. to crustal rheology 79−79828
gabbro-anorthosite, reduction of Fe, Ti, Si when heated in H atm., X-ray photoelectron spectra 79−25527
gabbros of Gettysburg Bank, N.Atlantic Ocean, K-Ar data for age and evolution 79−88322
Galapagos spreading centre, hydrothermal deposits and assoc. basement rocks 79−29750
Galesville sandstone, for compressed air energy storage appls. 80−30576
gamma-rays from extended sources, energy distrib. calc., rel. to remote spectroscopy 78−61586
garnet lherzolite, high-press. phase equilibria and Mg^{2+}-Fe^{2+} partitioning among constituent minerals 79−66687
garnet lherzolite, in upper mantle, melting from expts. on fluorites and fluoroberyllates 77−51475
garnet lherzolite xenoliths, disequilibrium, rel. to palaeogeotherms 78−57179
garnet-cordierite gneisses, geothermometry of granulite facies rocks from Rogaland, Norway 78−96193

rocks continued
gas-oil-source rock masses, lithogenesis *(Russian)* 80−4006
Gassetts schist, Vermont, prograde reaction histories from compositional zonation and inclusions in garnet 78−36159
geochemical classification of radiolarian cherts and siliceous sediments *(French)* 78−96319
geochemical haloes analysis using X-ray radiometric methods 77−53231
geological anal., nuclear track technique, B, Li, U, Th mapping 78−20553
geothermal energy, review 79−29447
geothermal energy extraction by two-loop systems 77−78134
geothermal energy extraction problem, thermal convection in shattered rock zones 77−78162
geothermal heat, extraction by water circulation through crack in dry hot rock mass 79−57355
geothermal saturated strata maintained by linear, ring batteries of wells, heat exchange 80−45630
Giant Mascot ultramafic body, near Hope, British Columbia, K-Ar ages 77−5147
gneiss, pre-carboniferous basement near Trail, British Columbia 79−84253
gneiss domes structural analysis, Saint Malo massif example *(French)* 78−7627
gneisses, radioactive dating, igneous and metamorphic events, Fiskenaesset region, Greenland 79−84250
Godthaabsfjord area, W.Greenland, U-Pb dates on zircons from early Precambrian rocks 77−29256
Gondwanaland Mesozoic tholeiites, Rb-Sr mantle isochrons and lithosphere chemistry vars. 78−28201
grain orientation in sheared dispersion, appl. to sedimentary and igneous rocks 80−3420
Grande Kabylie (Algeria), epimetamorphic pre-alpine rocks, pressure characts. *(French)* 79−48458
granite, b-value changes during movement on cut surfaces, lab. expt., rel. to earthquake prediction 79−12109
granite, critical dilatant vol. at tertiary creep onset 78−28220
granite, deformation and permeability of crushed samples 77−21763
granite, dilatancy anisotropy and response to large cyclic loads 80−21715
granite, dissolved elements in leaching surface water *(French)* 77−41029
granite, elasticity freq. depend. and seismic vel. dispersion 77−73727
granite, exam. of fracture mech. under dynamic loading 79−29218
granite, extraction of fission Xe, anomalous fission yields 78−96216
granite, failure expts., pore press. stabilisation 80−90079
granite, feasibility for radioactive waste repository 80−18481
granite, inert gas abundance patterns, Sudbury phenomenon *(Japanese)* 77−73735
granite, long-term creep, large and small specimen results obtained over 20 and 3 years respectively *(Japanese)* 78−56705
granite, long-term creep tests, rel. to crustal rheology 79−79828
granite, methods for determining electrical conductivity of core samples 79−67345
granite, seismic attenuation rel. to crack and grain boundaries 80−72495
granite, shear and tension hydraulic fracture 77−91119
granite, slow crack growth anal., appl. to rad waste disposal 79−89452
granite, static fatigue, effect of confining press. and stress difference 80−81872
granite, stressed, crack-crack and crack-pore interactions 79−84238
granite, thermal expansion at high-press. 80−21719
granite, vol. changes before stick-slip failure 79−12110
granite, weathered, bearing capacity determined by graphical soln. of pole trail method *(Japanese)* 78−56706
granite cylinders, failure under impact loading, brittle fracture process 77−86864
granite emplacement in Outer Zone of S.W.Japan 78−3767
granite in W. Great Kabylia (Algeria), deform. by ductile shear *(French)* 79−39716
granite intrusions, Rb-Sr ages and tectonics, coastal Labrador 77−81836
granite magmatism initiation and thermal diversity 78−65240
granite microfracture, source process rel. to earthquake prediction 80−104919
granite of N.Central New Brunswick, Rb-Sr age 77−81837
granite plate, crack propagation by projectile impact load 78−60741
granites, Caledonian, in Britain, geochemical and geophysical evidence on geothermal pot. 79−74486
granites, from cliff deep in N.Atlantic 77−5180
granites, Nanling region, southern China, K-Ar and U-Pb dating 77−2132
granites from British Late Caledonian, O and Sr isotope ratios 80−36276
granites from Hyderabad, US profiling 78−44786
granites from Mt. Rokko, electron probe X-ray microanalysis 80−31038
granites microcracking and heating, new evidence from cathodoluminescence 80−51391
granites of Great Britain, Caledonian suture zone, geophys. correl. 80−17259
granitic and migmatic rocks of Argentera Massif garnet mineralogy 78−85554
granitic basement, $^{87}Sr/^{86}Sr$ for fracture-filling calcite 77−29267
granitic clasts selective weathering 79−92532
granitic magma of Bushveld Complex, crystallisation history as revealed by trace element abundances 80−109145
granitic magmas, sources, water content and crystallization sequence 77−5187
granitic plutonic rocks, origin and stability of drilling induced remanence 77−33059
granitic rocks, formation and destruction during continental crust evolution rel. to U deposits 79−84201
granitic rocks of Bear-Slave provinces boundary, NW Canadian Shield, geochronology 77−91080
granitic rocks rel. to country rocks in Japan 78−81119
granitic tafoni in S.Australia, role of salts in fracture development 79−44183
granitoid plutons in Hackett River greenstone belt, Slave Province, NWT, emplacement rel. to regional deforms. 79−100834
granitoid rocks, Nd-Sr isotopic relationship and continental crust development, chemical approach to orogenesis 80−94522
granitoid rocks between Hindu Raj and Gilgit River (W.Karakorum), absolute age 79−100818
rocks continued
granitoids from Bulgarian Staro-Planina mountain range, metasomatic displays, geology, struct., form. *(Russian)* 79−5476
granodiorite, fracture under uniaxial compression, mech. and AE meas. *(Japanese)* 78−56748
granodiorite, late Precambrian, strain anal. of shear zone 78−77223
granodiorite, naturally deformed stress corrosion cracking of mica and feldspar 80−36299
granodiorite intrusions in Shuswap Metamorphic Complex, B.C., Rb-Sr dates 77−81838
granodiorite weathering, REE mobility and fractionation 79−62512
granulite xenoliths from Lesotho kimberlites, chemistry rel. to lower continental crust comp. 78−24268
granulites of central Australia, Rb-Sr chronology 79−53326
granulitic outcropping, trace elements determination by thermal and epithermal neutron activation *(Portuguese)* 80−7874
graphite, occurrence of carbyne forms of C 79−77450
Green River oil shales, anal. of depend. of thermal transport parameters on organic content 79−79817
Green River oil shales, thermal diffusivity depend. on organic content 80−76965
SW Greenland, Fiskenaesset, Archaean aluminous ultrabasic rocks 78−11892
groundwater flow through rock, radioactive waste storage study 80−82111
Guil valley Permian volcanics (French Alps), relations between tectonic stresses and mag. props. *(French)* 77−25679
half-space, impact of steel cylinder and effects 80−85649
hardness and abrasiveness determination, suggested methods 78−96313
Harp Lake Complex and associated rocks, Labrador, palaeomagnetism 77−90997
harzburgite xenolith, evidence for upper mantle multiple spinel-garnet peridotite transitions 78−65309
Hawaii xenolithic dunites, excess ^{129}Xe and high $^{3}He/^{4}He$ ratios 79−34814
Hawaiian alkalic basalts, thermoluminescence dating 77−86832
Hawaiian basalt, petrologic data from silicate melt and other inclusions in olivine 77−2146
Hawaiian lavas, contamination evidence from ^{230}Th-^{238}U data 77−5166
Hawaiian lavas, palaeomag. directional data sets shape 79−39881
Hawkesbury sandstone, mechanical props. 78−65263
heat conduction, nonstationary, by rock massif near horizontal size *(Russian)* 77−56620
heat transfer with liquid filtration into shattered rocks 79−81962
high pressure props. of Earth interior, dynamic compression expts. 80−98315
high-pressure metamorphic rocks ('knockers') in subduction zones, material transport within accretionary prisms 80−101353
high-pressure metamorphism in New Caledonia, phase equilib. in Ouegoa district 78−44811
Himalayan, Rb-Sr age and initial Sr isotopic ratio *(Japanese)* 77−17060
Himalayan granites, origin 78−44809
Hinterland Belt, Canadian Cordillera, deformation episodes 78−88825
Hispaniola, Cretaceous and Tertiary rocks palaeomag. study 79−44103
hot, dry, hydraulically fractured linearly expanding cracks, eqns. *(Japanese)* 79−34809
hot dry rock, heat extraction siting criteria and appl. to Switzerland 79−39275
Huronian sedimentary rock outlier, Goulais River area, Ontario 79−25243
hydraulic fracturing, growth rate of penny-shaped crack 77−29289
hydraulic fracturing, penny-shaped crack growth rate 77−17084
hydraulic fracturing for stress meas. in hard and soft earthen material 77−9577
hydraulically fractured cracks in hot dry rocks 79−62491
hydraulically induced crack, mapping by point source signals diffr. meas. 79−48572
hydrofracturing stress meas. technique, American field results 77−9576
hydrogen embrittling effects from acoustic emission meas. 80−11742
hydrostatic loading and unloading relation for porous materials with various fluid contents 78−28222
hydrothermally altered and unaltered rocks, discrimination in visible and near IR 78−7641
hypersthenic magmas, water contents 80−72507
hysteresis effects under loading 80−21712
Iceland, Hg natural conc. 77−64244
Iceland, Skagi and Langjokull volcanic zones, petrology and structure 79−2195
Iceland, Skagi and western neovolcanic zones, geochemical vars. 78−96171
Iceland-Faeroe Rise, magmatic rocks 77−78155
Icelandic basalts, general mixing eqn. appl. 78−53625
Icelandic igneous rocks, Mossbauer anal. 80−17253
Icelandic rhyolites, generation by melting of plagiogranites in oceanic layer 77−86885
Icelandic subglacial volcanic rocks, thermal and physical studies 80−101350
igneous, actinide sorption from radioactive waste 80−95367
igneous, granitic comp., trace elements appl. to petrogenesis 78−65215
igneous, major element analyses, PETROS data bank 77−2249
igneous and metamorphic, ^{18}O distrib. among mineral triplets 78−32071
igneous and metamorphic rocks, O isotope partitioning among minerals 77−86870
igneous intrusions, convective cooling of infinite sill 79−20787
igneous layered rocks, magma double-diffusive crystallization 80−90081
igneous rocks, average comp. rel. to Earth crust chemical balance 77−86831
igneous rocks, microscopic tubes 77−29286
igneous rocks, thermal cycling cracks props. 79−29759
igneous rocks, type rel. to lanthanides relative concs. in titanite 79−62492
igneous rocks from Michigan Basin borehole, palaeomag. results 79−39636
ignimbrites with low aspect ratio, charact. 80−41423
ijolitic igneous rocks, apatite comp. vars. 79−57929
Ile de Groix blueschists, progressive shear rel. to subduction or obduction 78−53652
immiscible picritic liquids, Ni partitioning 78−32069
impact and comminution processes in soft and hard rock 78−3763

rocks continued
impermeable rock hydrofailure, plane circular crack propagation *(Russian)* 79−70788
impulse response estimation, numerical method and appl. to laboratory data 79−80049
impulsive fracture, criteria 80−85646
impure dolomitic limestone, progressive metamorphism 77−33053
in situ strength from triaxial testing 77−44975
in situ stresses relationship with depth, trends 79−29729
inclined asymmetric upward-moving gravity structs. 78−7637
indentation fracture in brittle rocks and glasses 77−41023
Indian limestone, electrical conductivity of cylindrical cores 78−61401
Indian Ocean, magmatic rocks, petrographic study 79−20807
W.Indian Ocean, mantle uplifted block 79−25228
Indian Shield basement rocks, heat prod. meas. from geothermal study of Jharia Gondwana basin 80−98276
Indiana limestone fracture toughness, confining pressure effect 78−57197
induced (galvanic) polarisation, theory *(German)* 79−88344
induced polarisation theory, stochastic rock model appl. *(Russian)* 79−88250
inorganic gas chromatography for determ. of H_2O and CO_2 in rocks and minerals 80−85767
insular phosphorite from Ebon atoll, Micronesia, U series dating 78−81121
internal cracks, nondestructive obs. in stressed state 77−73726
internal friction and resonant freqs. 78−65268
IR multispectral aircraft scanner data, image processing 80−98454
IR spectra exam. 78−84567
irreversible deformation of anisotropic rock under hydrostatic pressure 77−73724
Isla Tortuga volcanics, trace element and $^{87}Sr/^{86}Sr$ characts. 79−66657
Isle of Skye granites, rare earth elements and origin 78−11890
Isua supracrustals, Greenland, Sm-Nd isotopic investigations and implications for mantle evolution 78−36129
Iwanai-dake peridotite mass, chromian spinel lamellae in olivine 78−96205
Jacupiranga carbonatite, Sao Paulo, Brazil, manganoan magnesian, ilmenite and titanian clinohumite 78−85552
Jamaican blueschists, coaxial pure shear rel. to deform. assoc. with subduction 79−2236
Japanese island arc volcanic rocks, relation between chemical comp. and gravimetric data 78−32102
Japanese islands, lateral var. of phenocryst assemblages in volcanic rocks 77−86886
joint orientation meas. evaluation in terms of regional stress 77−64487
joint orientations, tectonic interpretation, Muskoka region, Canada 77−70653
joint surface roughness, statistical representation 79−48464
jointed, strength and deformation characteristics in true triaxial compression 79−84235
jointed blocks of peridotite xenoliths in basalts and mantle dynamics 80−61796
jointed granite in situ, elastic and transport props. 77−66909
jointing, Griffith crack concept appl. 77−53048
joints, mapping via photogrammetry and EDP appl. 80−56470
joints filled with wet clay, shearing at high-press. 80−41438
joints roughness determination, new laboratory method 78−96315
Josephine Peridotite, anomalous noble gases 79−79761
Josephine Peridotite, effect of partial melting on mineral comp. rel. to geothermometry and geobarometry 77−81880
josephinite, excess ^3He and ^{21}Ne 78−65313
josephinite, Widmanstaetten patterns in metal-bearing rock 80−81887
Jura Mountains, incompetent beds rel. to geometrical adjustments during rot. of fold limbs 77−21747
Jura type platform folds, centrifuge expt. 78−49001
Jurassic evaporites of Gulf of Mexico-Caribbean area, distrib. rel. to Permian-Triassic continental reconstruction 80−56431
Jurassic rock in N.Armenia, palaeomagnetic directions rel. to remanent magnetisation 80−104870
K-rich ultramafic magmas from peridotitic mantle source 79−2200
kaersutite, amphibole from upper mantle, planetary-type rare gases 78−96167
Kapuho lava, Hawaii, olivine phenocrysts excess ^{129}Xe and high $^3He/^4He$ ratio 79−34814
Karmutsen volcanics, burial metamorphism, N.E.Vancouver Island 77−17063
karst depressions in Jamaica, morphology and hydrology 77−44991
karstic rocks and karst waters tidal movements 77−86940
Kayenta Sandstone, deform. in triaxial stress tests 80−81880
Kayenta sandstone, influence of pore press. on mechanical props. 78−81150
Kerguelen igneous rocks, petrology and isotopic geochemistry rel. to continental or oceanic character 79−57924
Kerguelen Islands igneous rocks, Nd isotopic study rel. to enriched oceanic mantle sources 80−98319
Ketilidian metamorphic rocks, SW Greenland, palaeomagnetism and apparent polar movements, 1850 to 1600 Myr 77−13059
Keweenawan rhyolites, anomalous Li content 79−84252
khondalites from E.Ghat belt, India, physical and elastic props. 77−5188
Kiglapait intrusion, Labrador, influence of augite on plagioclase fractionation 80−12390
Kilauea 1977 lava flow, heat transfer meas. 80−85632
kimberlite, from India, U and Th abundances 77−60376
kimberlite and kimberlitic intrusives of SE.Australia, review 80−51392
kimberlite nodule data on palaeogravity since late Precambrian 78−24217
kimberlites, micaceous, chemistry of micas 79−16465
kimberlites, Precambrian and Cretaceous, in S.Africa, remanent magnetisation 78−96134
kimberlites, South Africa, palaeomag. determ. of emplacement temp. 77−78180
kimberlites, Sr isotopic studies in Indian samples 79−92536
kimberlites and plate tectonics in W. Africa 78−11868
kink bands, theoretical analysis of geometry 77−64269
kinking, ultimate locking angles for conjugate and monoclinal kink bands 78−88821
Klamath Mountains, Oregon, Rogue and Galice formations petrology, Jurassic island arc sequence identification 79−100836
komatiites and high-MgO lavas, origin, crystallisation 78−65312
rocks continued
komatiitic lavas, Ni partitioning between magma and cryst. phases 77−49061
L-S fabric scheme appl. to structural mapping and palaeostrain anal. 77−78176
laboratory hydraulic fracturing in intact and pre-fractured rock 77−73723
laboratory spectra, intrinsic information appl. to Landsat filters assessment for rock type discrimination 79−16791
laminar rock, stress distrib. during sliding failure 79−2225
landslide mechanisms 79−96762
landslides, hydrogeological conditions rel. to stability, rheology *(Russian)* 77−25683
landslides following 1946 June 23 central Vancouver Island earthquake 80−21637
landslides on Ryuohzan Mountain, Japan, geology, model *(Japanese)* 78−96217
Late Cretaceous granodiorites, Jamaica and Haiti, Greater Antilles, Sr isotope geochemistry 79−57927
Late Palaeozoic slate belt, structural succession and tectonic significance 78−81140
lattice thermal conductivity at mantle press. and temp. 78−69338
lava, flowing of South Novo-Tolbachinsky volcano eruption, elec. cond. 80−72498
lava, rheological props., field meas. 79−12114
lavas from Archaean volcanism in Malartic Group, Abitibi, petrography and geochemistry 80−17258
Laxfordian deformation in Carloway area, Isle of Lewis, Scotland 78−7638
leucite, under water vapour pressures up to 25 kb, expt. investigation 77−70648
Lewisian gneisses, Sm-Nd systematics and implications for granulites origin 79−20777
Lewisian gneisses of NW.Scotland, ages from Pb isotope meas. 77−70625
Lewisian rocks of NW.Scotland, effective seismic vels. var. with press. 79−44179
lherzolites, comp. rel. to comp. of Earth mantle 80−76940
lignite deposit, mapping via multifreq. airborne EM system 79−5446
limestone, complete refr. index meas. in visible and IR 78−40541
limestone, crystalline, variation of elastic wave velocity *(Japanese)* 78−11887
limestone, dry and saturated, P and S wave attenuation, US obs. 80−72494
limestone, erosion under soil due to acid waters 77−45023
limestone, estimation of short-term vars. in erosion processes 77−81935
limestone, finegrained, superplastic flow 78−20398
limestone, fracture toughness meas., influence of microstruct. and environment *(French)* 77−81874
limestone, high press. effects on plastic state 79−74889
limestone, seismic attenuation rel. to crack and grain boundaries 80−72495
limestone, thermal expansion at high-press. 80−21719
limestone diagenesis simulation, computer model based on Sr depletion 78−73358
limestone plate, crack propagation by projectile impact load 78−60741
limestone tubes, dynamic torsional failure obs. 80−85648
limestone-granite contact zone, props. of peculiar carbonate mineral *(French)* 78−69339
limestones, geological aspects of calcite microstruct. 79−57933
linear and planar structure, rot. and strain in three-dimens. progressive deform. 77−78171
lithosphere petrology and plate tectonics, comparison with Venus tectonics and comp. 80−72805
lithosphere rocks, elec. conds. rel. to EM waves lateral-wave propag. 79−92482
Lithuanian upland and plateau palaeoperiglacial blanket deposit formation *(Russian)* 80−81882
Lochseiten limestone, differential stress in Glarus overthrust 78−88822
Lonar Crater, India, chem. study of impact glasses and basalts 79−20836
long-term solar energy storage in native rock 79−57474
longitudinal wave vel. and absorpt. in rocks and minerals at high press. and temp. 79−39704
Los Pinos pluton, S.California, petrology and emplacement 77−5200
lower mantle rocks Gruneisen parameter, evidence for approximation $\gamma\rho$=const. 80−3970
Lower Triassic sediments, Skrino anticline strain var. determ. from deformed reduction spots 77−37184
mafic belts along margins of Japanese Islands, origin, geophys. survey 78−32100
magma, solubility and saturation of apatite, laboratory expts. 80−72504
magma genesis, mineral phases and parental rocks, $^{87}Sr/^{86}Sr$ ratios 77−25671
magma mixing, petrological process and volcanological tool 77−37201
magma/water solutions, appl. of Gibbs-Duhem eqn. 78−57205
magmas, genesis 79−12103
magmas, influence of volatile components 80−41418
magmas, mineral trends on alkali-Fe-Mg diagrams 78−85551
magmatic, anchieutectic comp. 80−12381
magmatic differentiation models, computer program for interactive testing 79−2377
magnetic-diffusive after-effect 77−70640
Magnitskiy-Birch additivity hypothesis, shock adiabat testing 77−9379
major element whole rock anal. using sample fusion technique with electron microprobe 77−64494
Makapansgat Formation (South Africa), palaeomag. results and age 77−25637
Malaguide complex, structural facing and Palaeozoic rocks 77−49046
Malaysia offshore areas, rocks thermal cond. rel. to heat flow estimation in wells 80−67349
Manicouagan impact melt, Quebec, chemical interrelationships with basement rel. to form. processes 78−81165
Manicouagan impact melt, Quebec, stratigraphy, petrology and chemistry 78−81164
Manicouagan impact structure, Quebec, melt rocks petrogenesis 78−81166
Manicouagan melt sheet, Rb-Sr isochron age 78−81168
Mantaro landslide, Peru, seismological and geological aspects 78−96248
mantle hydrous nodules 80−56420

rocks continued
mantle material, shear heating as explanation for lithosphere-mantle decoupling 79−20790
mantle peridotite, high-temp. anelasticity and elasticity 80−17256
mantle peridotite, petrogenetic grid and conditions for magma generation 77−5137
mantle peridotites, origin of olivine subgrain boundaries 78−85544
mantle peridotites, stress estimates from structural studies 78−69330
mantle rocks, thermally activated point defects interpretation of low vel. zone 78−88806
mantle rocks in kimberlite pipes, nature and origin 79−2205
mantle xenoliths, equilibrated Nd and unequilibrated Sr isotopic comp. meas. 80−98321
mantle xenoliths, olivine grain sizes rel. to recrystallised grains geopiezometer applicability 78−85715
marble, diametral compressive testing method 80−35495
marble, layer, absolute thickness meas. of dielectric material 79−67253
marble in Pikikiruna Range karst, solution processes 79−74906
marble thermal expansion at high-press. 80−21719
Marda calc-alkaline suite, rare earth elements, Archean geochem. analogue of Andean-type volcanism 78−11898
Marianas trench, Pacific Ocean, basic and ultrabasic rocks 77−21757
marine, U content distrib. and meas. by neutron induced fission track method 79−79809
marine basalts, U conc. and distrib., implications 77−81886
marine sediments and rocks, sound vel.-density relations 78−50982
Massif Central, peridote xenoliths deform. rel. to upper mantle struct. and geodynamics 78−81120
mathematical models for stress relaxation and deformation 77−14923
mechanical behaviour of rocks from radical jack test *(German)* 79−66689
mechanical properties rel. to cooling *(Japanese)* 80−31036
mechanical strength parameters, drillability *(German)* 79−74888
mechanics, American studies rel. to earthquake prediction 79−16449
mechanics testing, lateral deform. gauge 79−57163
megascopic textures of constituent rock types of epidote amphibolite masses, Mt. Higashi-akaishi region, Japan 77−70663
melting drills, thermal analysis 77−17258
Mesozoic igneous rocks from N.Brazil and S.Atlantic opening time 79−44089
Mesozoic pillow lavas from French Alps, clinopyroxenes comp. trends, cooling rate effects 77−5154
Mesozoic tholeiites from Antarctica, interpretation of discordant $^{40}Ar/^{39}Ar$ age spectra 77−49047
metabasalt block from Mid Atlantic Ridge, metamorphic mineral data 77−64279
metabasalts from Point Sal ophiolite, California, rare earth and trace element geochemistry 78−32092
metabasites, geothermometry of granulite facies rocks from Rogaland, Norway 78−96193
lower metadiabase from Michigan Basin basement, preliminary petrological study 80−4009
metagabbro at bottom of Michigan Basin deep drill hole, Rb-Sr geochronologic anal. 79−39680
metagabbronorite from DSDP hole 334, high-temp. deform. and recrysts. near Mid-Atlantic Ridge 77−91125
metamorphic, margarite stability and compatibility relations as press.-temp. indicators 77−5183
metamorphic, tabular grain shapes prod., shear displacement 78−96199
metamorphic, visible and near IR spectra rel. to comp. 77−17087
metamorphic bathozones and bathograds, meas. of regional scale post-metamorphic uplift and erosion 78−81113
metamorphic rocks, quartz c-axis fabrics anal. via photometric method 80−101456
metamorphic rocks, thermomechanical expts. using shear machine *(French)* 79−5474
metamorphic rocks of Yap arc-trench system, petrology and geochemistry 78−32093
metamorphism, rate laws 79−16467
metamorphosed chert from W.Greenland ^{18}O composition 78−81155
metasedimentary sequence of N.Hill End Trough, NSW, metamorphism and deform. time relations 80−26510
metastable phase transition models and their bearing on the development of Atlantic-type geosynclines 79−20822
metavolcanic rocks, Montauban-Les-Mines, Quebec, geochem., mineralization 78−36161
meteorite impact, craters, internal struct. model 78−44825
meteoritic Earth model validity *(Italian)* 77−44982
Mexican andesites, Sr isotope evidence for petrogenesis 78−28203
N.Mexico Mesozoic formations, palaeomag. pole positions 77−2099
Michigan Basin deep borehole, Phanerozoic and Precambrian rocks density from gravimeter survey 79−39634
Michigan Basin deep hole metagabbro, mineralogy and geochemistry compared to seawater hydrothermal alteration 79−39710
microfracture *(Japanese)* 78−7020
microwave brightness spectra of layered media 77−81898
Mid Atlantic Ridge, FAMOUS area, petrogenesis of basalts 78−11891
Mid Atlantic Rift Valley, basaltic rocks from FAMOUS area, petrological diversity and structural setting 77−78150
Mid-Atlantic Ridge, geology of submarine hydrothermal field at 26°N latit. 80−85641
Mid-Atlantic Ridge, rock densities and fracture zones struct. in equatorial Atlantic *(Russian)* 80−104932
Mid-Atlantic Ridge, sulphides in DSDP Leg 37 drill core 77−91122
Mid-Atlantic Ridge basalts from DSDP sites 332 and 335, petrology and alteration 77−91124
Mid-Atlantic Ridge mafic and ultramafic rocks, Pd, Ir and Au contents 77−91073
mid-ocean ridge basalts, comparison with lunar mare basalts 79−16424
mid-ocean ridge basalts, density var. rel. to magma mixing and primitive lavas scarcity 80−56460
mid-ocean ridge basalts, rel. to Earth comp. and mantle evolution 78−11844
mid-ocean ridges, estimators for heat flow and deep rock props. 77−86843
Middle Ordovician volcanic rocks from Quebec, palaeomagnetism 78−15965
Mieville granite deformation, feldspars superplastic flow and cryst. chemistry changes 79−79831
migmatite rise, numerical expts. based on continuum dynamics 80−51381
migmatite tectonics, Hidaka metamorphic belt, Japan 80−8310
mineral composition of rocks at great depths, prediction from longit. elastic wave vels. *(Russian)* 80−104956
mineralized zones, probability and uncertain number theory appls. *(Rumanian)* 77−29509
minettes, REE and trace element contents and origin 79−74864
late Miocene shallow marine sediments, New Zealand, C isotope stratigraphy appl. 80−26479
Mohr-Coulomb material, axisymmetric compression around circular hole 79−57914
Moine Thrust Zone, Eriboll, Scotland, palaeostress estimates 79−79835
monolithic materials for creating high pressures, anvil device with lune toroid 80−73377
Montagne de Saint-Anselme Formation, Quebec, deposition rel. to Appalachian orogen margin tectonics 79−20824
Monterey Shale, O isotopes rel. to diagenetic silica minerals 77−64267
mountain rocks, problems of mag. prehistory *(Russian)* 77−44917
movement, suggested methods for monitoring using borehole extensometers 79−84512
movement monitoring using inclinometers and tiltmeters 78−28318
Mt. Burnet Dunite, high-temp. creep meas. 78−7624
Mt. Givens granodionite solidification 79−44151
mudstone, in Tasmania, terrestrial heat flow meas. 77−33018
multielement anal. by sequential instrumental and radiochem. neutron activation 78−7798
multielement analysis by photon or neutron activation 78−12018
multielement analysis with DFS-36 quantometer and ES-1020 computer 79−70392
multielement determination, instrumental neutron activation anal. 79−53550
multiple surface waves on viscoelastic half-space 78−79254
Munchberg Gneiss Massif, NW.Bavaria eclogitic rock dating 79−34774
Murnaghan constants evaluation as function of pressure 80−31037
Murrumbidgee granite batholith, Rb-Sr isochrons and Sr isotopic equilibration 77−41026
mylonites, grainsize reduction and grain boundary sliding rel. to flow strength 80−21721
mylonites from Grenville Front Tectonic Zone, Ontario, distortional strain estimation 78−7628
Nain anorthosite (Labrador), palaeomagnetic results and tectonic implications 78−77178
Nain anorthositic complex, Labrador, examples of contrasted magmas commingling in plutonic environment 80−104959
Nanling mesozoic granites, geochronology *(Chinese)* 79−62468
Naxos island, Greece regional metamorphism, petrology and geothermal gradients 77−44985
Neogene trench-slope deposits, Nias Island, Indonesia, sedimentology and palaeobathymetry 80−104950
nepheline syenite, dating, Rb-Sr internal isochron, ^{39}Ar-^{40}Ar plateau age methods *(French)* 78−32031
neutron activation anal., gamma-ray spectra processing with computer graphics 79−2228
neutron activation analysis, accuracy 78−11589
neutron borehole measurements, rock density effects *(Russian)* 79−88500
neutron slowing props. in water bearing containers *(Russian)* 77−73720
SW New Brunswick and SE Maine, stratigraphy and tectonic setting of Palaeozoic sedimentary rocks 78−57199
New Brunswick rock units, palaeomagnetism rel. to N.America Lower Palaeozoic tectonics 79−100809
Newfoundland Basin seamounts, rocks rel. to Mesozoic evolution 78−32045
NW.Nigeria, calc-alkaline volcanics and possible Pan-African suture zone 78−32086
NIMROC reference materials, for neutron activation anal. 78−7288
Nizky Jesenik Mts., Czechoslovakia, cleavage origin from mag. anisotropy meas. 77−9410
noncylindrical flexural slip folds, in nature and expt. 77−53024
nondestructive neutron activation analysis of environmental samples using low-energy photon spectrometry 78−3995
North Mountain Basalt, Nova Scotia, K-Ar isochron method for age determ. 80−3960
Norwegian eclogites, Caledonian Sm-Nd ages and crustal origin 80−76978
Norwegian gneiss eclogites, giving evidence for Precambrian continent-continent collision 77−49057
Norwegian monzonitic rocks, heat generation versus crystallisation depth 78−65228
Nova Scotia southern plutons, geochemistry of tonalitic and granitic rocks 77−49064
nuclear power plant design for underground rock cavity location, safety aspects 79−13398
obsidian, from Koyukuk River, Alaska, elemental anal. by at. absorpt. spectrophotometry 77−34062
obsidian, hydration 79−8629
obsidian, hydration profiles meas. by sputter-induced optical emission, rel. to dating technique 79−24871
obsidian, Japanese, ^{57}Fe Mossbauer spectra of naturally occurring glasses 80−67364
obsidian from northern New Zealand, U, Th determ., archaeological sourcing method appl. 79−2239
obsidian source identification by thermoluminescence 79−26195
ocean basalt, seawater reactions, chemical exchange, Fe, Mn, and S species results 80−17294
ocean floor basalts, parental magma, MgO content 79−44155
ocean floor spilites, seawater/basalt ratio effects on chem. and mineralogy 78−92819
ocean ridge basalts, trace elements, rel. to mantle comp. 78−65219
ocean-floor hydrothermal metamorphism of ophiolitic metabasic rocks in Italy 78−7613
ocean-floor hydrothermal metamorphism of ophiolitic rocks of Troodos Massif 78−7614
oceanic basalt, U exchange during low-temp. alteration, isotopic evidence 79−29744
oceanic basalt glass, noble gas comp. of neutron activated samples 79−74866
oceanic basalts, differential Sm/Nd evolution 78−61391
oceanic basalts, hydrothermal alteration by seawater at high temp. 78−69327

rocks continued
oceanic basalts, trace element mobility during hydrothermal alteration 78−69328
oceanic basalts, variations in $^{143}Nd/^{144}Nd$ and $^{87}Sr/^{86}Sr$ ratios 77−29295
oceanic basalts melting, press. depend. of solidus temps. and elec. cond. 77−91109
oceanic crust basalt, U abundance, heat flow implications, fission track anal. 80−8287
oceanic igneous rocks, $^{40}Ar/^{39}Ar$ studies 79−53325
oceanic layer 2 basalts, DSDP Leg 37, low-temp. fluid lateration 77−91102
oceanic tholeiites siderophile contents compared with lunar highland rocks 80−8562
oceanic upper mantle seismic anisotropy, evidence from ophiolite complex 80−21677
oil and gas-bearing structures, seismic exploration *(Russian)* 77−45195
oil shale, dry and saturated, P and S wave attenuation, US obs. 80−72494
oil shale, dynamic fracture strength, expt. determ. method 79−48584
oil shale, shear and tension hydraulic fracture 77−91119
oil shale, transient temp. distrib. due to combustion flame in retort 79−37110
oil shale from Piceance Creek Basin, Colorado, permittivity by microwave radiation method 80−12378
oil shale from Rock Springs, Wyoming, dynamic modelling Maxwell model 78−57196
oil shales, review of thermophysical properties 79−100479
oil shales of Green River, USA, thermal decomposition rel. to elec. cond. obs. 80−104495
Oklo natural fission reactors, temp. of mineral phase assemblages and rock textures 80−21722
Oklo natural reacors, fluid phases contemporaneous with sandstone diagenesis, and tectonic movements *(French)* 80−21746
Olby lava flow, $^{230}Th/^{238}U$ dating rel. to Olby-Laschamp geomag. polarity event age 79−12067
olivine, steady state flow creep eqns., implications for mantle rheology 80−104924
olivine fractionation equations for basaltic and ultrabasic liquids 79−20818
olivine-rich rocks, activation vol. for creep, rel. to upper mantle 79−44184
olivine-sulphide assemblages, metamorphosed, from W. Australia, Fe/Ni partition 77−5185
olivine/liquid distrib. coeffs. and test for crystal-liquid equilib. 77−81889
Onverwacht Group, Transvaal, sedimentology rel. to early Earth characts. and evolution 78−44812
oolitic calcarenites, Ste. Genevieve Limestone (Mississippian), permeability est. techniques *(French)* 79−34801
oolitic limestone, fold strain analysis using elliptical particles 80−61787
ophiolite complex, early Caledonain age, on Karmoy island, Norway 79−2235
ophiolite complex of Point Sal, California, seismic vel. struct. 80−109110
ophiolite complexes, evidence for ocean-floor metamorphism, appl. to seismic layering and magnetism 77−13068
ophiolite emplacement on continental margins, similarity to thrust faulting 77−2136
ophiolite fractionation trends, Bay of Islands, Newfoundland, polycyclic cumulate sequences 77−78179
ophiolite genesis, tectonic regimes 79−57898
ophiolite nappes emplacement, Mesozoic-Cenozoic examples 77−41012
ophiolite peridotite, seismic anisotropy rel. to oceanic upper mantle 78−53645
ophiolite rocks of Samail, Oman, study of petrogenesis and hydrothermal alteration 80−46177
ophiolite suite, dynamothermal aureole of Bay of Islands 80−51355
ophiolites, Chilean, hydrothermal metamorphism vars., ocean floor metamorphism implications 79−88354
ophiolites, identification in oceanic crust 78−81117
ophiolites, seismic vels. and oceanic crustal struct. 78−77226
ophiolites of Pan-African province of Anti-Atlas (Morocco), geodynamic interpretation *(French)* 80−76952
ophiolites of S Quebec, oceanic crust of Betts Cove type *(French)* 79−57923
ophiolites of S.Quebec, Betts Cove type oceanic crust 77−81885
ophiolitic melange, significance in Fleur de Lys Supergroup, N.Appalachians 77−78175
ophiolitic metabasalts in Mediterranean area, clinopyroxene comp. 79−57925
ophiolitic peridotites structures, role of young lithosphere thrusting in subduction zones 80−56446
ophiolitic rocks tectonic emplacement in Precambrian Mona Complex, Anglesey 79−8631
Ordovician conglomerates and Midland Valley evolution in Scotland 79−92540
Ordovician sandstones from Tourelle Formation, Quebec rel. to Taconic orogeny 79−57919
Ordovician volcanic rocks, N.Maine, magmatic affinity and tectonic significance 77−44984
Upper Ordovician volcanics, geochemistry and tectonics in E. and SE.Ireland 79−44144
oriented cracks, differential strain analysis 78−53647
orthorhombic olivine layer, seismic body waves propag. 77−49020
P- and S-wave velocities in dry and saturated rocks, influence of cracks, model 78−20366
P-V meas., 5 to 45 kb *(Chinese)* 79−23676
P/S-wave velocity ratio for rocks, statistical study *(Japanese)* 77−17036
Central Pacific Basin, $^{40}Ar/^{39}Ar$ ages of diabase sill and basalt, rel. to ocean floor history 77−66897
E.Pacific Rise, igneous rocks of young cratered volcanoes pair 80−12374
Palaeogene komatiites from Gorgona Island 79−44168
palaeogeotherms from xenolith suites in basalts and kimberlites 77−2127
palaeostrain analysis, distortion and dilatation 77−78167
Pantelleria peralkaline lavas, glass inclusions in quartz and anorthoclase *(French)* 77−9389
paratectonic porphyroblasts, inclusion trails spiral direction reversal 79−39717
Parece Vela Basin, E.Philippine Sea, petrology rel. to evolution 80−41431
partially melted rocks, struct.-sensitive physical props. 79−12116
passive rock bed storage system for domestic solar air heating 79−57490
pavement surface aggregates, exam. of polishing characts. 78−53057
pebble abrasion studies 80−4004
pegmatites, U^{235} estimation by homogenised fission track anal. using solid state track detector 80−97719
pegmatites in Enderby Land, Antarctic U-Pb ages 80−76946
peralkaline rhyolites, assoc. with andesitic arcs of SW.Pacific 78−32043
peridotite, elastic modulus and internal friction 78−85550
peridotite, equilibration conditions in upper mantle, exptl. determ. of geochemical parameters 77−2130
peridotite, from upper mantle, rare earth fractionation patterns in partial melts 77−37198
peridotite hornfelses, Washington, limits to forsterite-anorthite assemblage 77−5184
peridotite xenoliths, Nevada, Cr-rich pyroxenes comp. rel. to formation press. and temps. 77−5139
peridotite xenoliths from Assab, element partitioning in clinopyroxene-orthopyroxene pairs 79−62488
peridotite xenoliths of SW.Japan island arc, appl. to uppermost mantle differential stress lateral var. determ. 80−98275
peridotite-H_2O-CO_2 system, phase relationships, rel. to planetary mantles 78−77506
perlite, water content obs. by electron microscopy *(Russian)* 77−66908
permeability and penetrating water zone propag. 78−7671
permeability changes due to stress 79−16452
permeability from resistivity and pore shape 77−86866
permeability of whole and fractured porous rock with confining pressure 79−53342
Permian sediments, Skrino anticline, strain var. determ. from deformed reduction spots 77−37184
Permian volcanics in western Southern Alps, palaeomag. and rock magnetic props. 80−89948
Peru-Chile Trench basalts, fractionation and mantle heterogeneity 78−53626
S.Peruvian coast, two-billion-year granulites in Late Precambrian metamorphic basement 78−28204
petrology, error assoc. with point-counting 78−32232
petrology rel. to extreme metamorphism, symposium (Sydney, August 1976) 78−44821
phanerozoic peridotitic and pyroxenitic komatiites from Newfoundland 79−79772
phosphate fertilizer, specific activity of U and Th rel. to particle size 80−106244
phosphate materials, U assay 78−82589
phosphate rocks, processing for fertiliser prod. and byproduct U recovery 78−17398
Phosphoria Formation shale, subaerial weathering of sedimentary organic matter 78−57206
phosphorites from Spanish continental margin, geochemistry and mineralogy *(French)* 78−65258
phosphorites from Spanish continental margin, geology and petrology *(French)* 79−79837
photon attenuation coeffs. for determ. secondary radiation intensities 79−39708
physical parameters from 4000-6000 m deep cores *(Rumanian)* 79−57892
physical properties, investigation using high-press. apparatus *(Russian)* 77−70850
physical properties and struct. geol., conf. (1978), Toronto, Canada 80−101666
physical properties under mantle conditions, conf., Durham, England (Aug. 77) 78−69333
physics and chemistry, conf., Newcastle, England (April 1974) 77−37194
pianlintic clay, a new sedimentary rock *(Chinese)* 79−96759
picrite calculation of Gruneisen parameter and specific heat from measurements of US vel. 80−41436
picrites from E.Pacific Rise 79−79810
Pierre clay shale, longit. modulus meas. at varying strain rates 77−53038
piezo-magnetic effect to explain earthquake assoc. mag. variation *(Chinese)* 80−56374
piezomagnetic effect, lake ground loading, during filling 80−8346
pillar monitoring during ore extraction at Mount Isa Mine 77−9418
pillow lava, spreading cracks props. 79−79780
pillow lavas, deformed, rel. to origin of epidote-banded greenstones from Tauern, Austria 79−79833
pink westerly granite, wave propag. study by holographic interferometry 78−20536
plastic deformation, fabric development simulation, appl. to quartzite 78−49015
plastic limit analysis with anisotropic parabolic yield function 77−91114
plastic-brittle behaviour, hardening and softening constitutive eqns. 77−21270
plate, loaded by projectile impact, crack propag. 79−83296
plateau lavas from S.America, Nd and Sr isotope data 79−29726
Pleistocene carbonates, in E.Africa, isotopic evidence for dramatic climatic changes 77−56723
Late Pleistocene tephra in South Island, New Zealand, identification and significance 80−8306
Pliensbachian limestone sequence at Bakonycsernye (Hungary), remanent magnetisation 80−90074
Pliny Range, New Hampshire, intrusive complex, mineralogy and petrology 78−36158
Pliocene Centerville Beach section (N.California) age and palaeomag. stratigraphy 77−60346
plutonic granitic rocks, O and H isotope comps. 78−65221
plutonic rock, discrimination and spectral reflectance, visible and IR obs. 80−90083
plutonic rocks from Whitehorse map area, Yukon, ages 80−31005
Poisson number determ., discrepancies *(German)* 78−69324
polycrystals of anisotropic substances under hydrostatic press., microstresses 79−25231
polygonal strain markers adaption 78−20567
pore aspect ratio spectrum determ., seismic velocities inversion 80−51387
pore fluids and seismic attenuation in Massilon sandstone 79−44120
porosity and permeability, rel. to transport phenomena in hydrothermal systems 78−36205

rocks continued
porosity of upper igneous crust in N.Atlantic, seismic refraction studies 78−53629
porous, dry and water-saturated, plane shock wave studies 80−21714
porous, saturated with low cond. fluid, thermal cond. meas. systematic errors 77−86871
porous, seismic wave vels. rel. to saturation 77−2114
porous, self-consistent imbedding and ellipsoidal model 80−26503
porous, shear stress enhancement of void compaction 79−69182
porous rocks, US absorpt. from wave attenuation and scattering on random inhomogeneities *(Hungarian)* 77−86791
potassic igneous rocks from Roccamonfina volcano, Roman comagmatic region, Italy,, O isotope geochemistry 80−41420
Potsdam Sandstone, outcrop fractures and in situ strain relaxation 77−91117
Prairie Evaporite, S.Saskatchewan, influence on local seismotectonics 79−20757
Precambrian, seismic reflection sounding 79−79743
Precambrian basement rocks of N Saskatchewan, var. in lithology and tectonometamorphic relationships 77−91132
Precambrian Gardar lavas, S.Greenland, mag. stratigraphy and mag.-petrologic props. 77−40973
Precambrian igneous rocks, Pb isotope inhomogeneity in K-feldspars 78−32095
Precambrian metamorphic, folding *(Chinese)* 79−96761
Precambrian metamorphic rocks, from SW.Montana, mineral-pair geothermometers 80−81846
Precambrian metamorphic rocks of Neumayerskarvet area, W Dronning Maud Land, Antarctica 77−86894
Precambrian metavolcanics in Orange River region, S.Africa, isotopic study 79−44147
Late Precambrian rocks of Adelaide Geosyncline, Australia, palaeomagnetism 80−101325
Precambrian surface rocks, rel. to earthquake hazards in East-Central USA 78−11834
pressure wave, two dimens. cylindrical, excited by moving load, propag. in acoustic medium 77−68300
primary stresses, meas. at Eisenhower Memorial Tunnel, Colorado 79−29727
Proterozoic low-potash, high Fe charnockitic Tromoy gneisses, chemistry and origin 77−86882
proton activiation analysis of B and Li local levels in minerals, rocks and ores 79−74477
N Pyrenean metamorphism, age and tectonic implications 79−34819
pyroclastic flow deposits, utilisation 80−12365
pyroxenes from planetary basalt, silicate mineralogy study 80−72802
pyroxenite, spheroidal aggregates in Bushveld Complex as special case of silicate liq. immiscibility 79−88351
quartz bearing rocks, RF EM emission with fracture 77−86863
quartz cryst. axes orientation, in metamorphosed volcanic sediment 80−85655
quartz preferred orientation and quartz content interdependence in deformed rocks 78−88818
quartz-bearing, search for piezoelec. effect 77−73728
quartz-bearing and quartz-free, high temp. and press. effects on compress. wave vel. 78−32081
quartz-feldspar mylonite, microstruct. and fabric development 78−96201
quartz-rich rocks folding, implications of c-axis fabrics of experimentally folded ice 79−57983
quartzite, critical dilatant vol. at tertiary creep onset 78−28220
quartzite, deformation in Earth crust, dislocation climb mechanism 79−60425
quartzite, grain boundary and struct., analogue expts. using ice 80−21718
quartzite, Gruneisen parameter at high press. 80−8299
quartzite, naturally deformed, textural and microstructural development, metallurgical approach 79−83228
quartzite, thermal expansion at high-press. 80−21719
quartzite breccia, Onaping Formation, Sudbury Basin, quartz orientations 77−9402
quartzite cleavage, pressure soln. mechanism *(Portuguese)* 78−65260
quartzites, intracrystalline deform. comparison in natural and exptl. deform. 79−79830
quartzites, microscopic deform. and flow laws, South Mountain Anticline 78−77220
Quaternary lavas, Snake River Plain, Idaho, mineralogy and petrology 78−20402
Quaternary magmas of NE Japan, H_2O contents lateral vars. 79−57899
Quaternary volcanic rocks across NE.Japan, trace element contents, lateral variation 80−104926
Quaternary volcanic rocks of New Hebrides geochemistry and origin 78−20375
radioactive high-level waste disposal in deep geologic formation, environmental aspects 79−49712
radioactive waste, geologic isolation repositories, long-term safety assessment 79−49714
radioactive waste disposal, retention of Am and Pu by rock 77−71679
radioactive waste geologic disposal, migratory props. of waste elements 79−67893
radioactive waste interactions with surrounding rock at disposal sites 78−54853
radioactive waste repository in geologic primation 79−49713
radioactive waste storage, Am sorption on major rock-forming minerals 80−13716
radioactive waste storage in crystalline rock, temp. distrib. calc. *(German)* 78−86631
radioactivity, determ. of bulk α and β radioactivity *(Rumanian)* 79−88346
radioactivity of large volume geological samples, absolute activity determs. 80−56643
radiochemical neutron activation anal. of environmental matrices for Hg and noble metals 80−16889
Raft River Valley, Idaho, surveys of geothermal system 79−84307
rapakivi granite, anorthosite and charnockitic plutonism 78−28234
rare earth element, abundances in layered Komatiite lava flow, Ontario, Canada 79−29764
rare earth elements, determ. by neutron activation anal. 78−27870
rare earth elements, determ. in geological materials, using thermal and epithermal neutron activation 78−7797
rare earth elements determination, neutron activation analysis, optimum method 79−88491

rocks continued
rare earth elements determination by neutron activation analysis 79−88492
rare gas fractionation rel. to Earth-atmosphere evolution model 77−13077
reconnaissance using enhanced Landsat imagery 80−41568
resedimented conglomerates of Huronian age, Lake Huron north shore, deposition from sediment gravity flow 78−36164
residual gravity anomalies interpretation *(Russian)* 79−88232
residual stress development in cooling rock bodies, elastic models 78−88819
residual stress meas., microcracking effects 77−91118
rheology of partially melted rocks, critical phenomena 78−32080
Rhynie chert, isotopic ratio of palaeoatmospheric Ar 77−66917
rhyodacitic pillow lava and isolated-pillow breccia from Fishguard Volcanic Group, SW.Wales 80−12389
Rio Grande rise volcanic rocks, petrology 77−81866
Rn emanation rate measurement from specimens and powders 80−63494
Roccamonfina volcano caldera wall, petrochem. of pumiceous layers *(Italian)* 77−49051
rock, failure process under compression, fracture mechanics *(Japanese)* 79−57915
rock beam, laterally-constrained, ultimate strength investigation with constrained beam test apparatus 79−29299
rock salt from New Mexico Salado formation, mech. props. at high-press. 80−72492
rock samples, dry and water-saturated, at high press., elastic wave vels. and v_P/v_S ratio 79−92529
rockburst fault gouge microscopic features, SEM obs. 79−74891
rockfalls, Surprise Valley, Jasper National Park, Canada 77−44998
Rother catchment, W.Sussex, fine sediment mineralogy of source rocks and suspended sediment 79−20827
rupture and particle velocity during frictional sliding 79−20820
rupture by elastic shock wave superposition in multiple detonations *(Russian)* 77−35082
rupture rel. to Rn content var. before earthquakes, model expt. *(Chinese)* 78−24225
S-tectonites, finite and incremental deforms. recorded by planar subfabrics 77−21767
S-wave vel. meas. in soil and bedrock using down-hole method 80−98458
Sabaloka Igneous Complex, Sudan, petrography and chem. analyses 78−32097
salt deposits, Upper Triassic, of western N.Atlantic, obs. from Newfoundland Grand Banks 80−94516
salts, dissolving and outwashing from soil and rock, hydromechanical treatment *(Russian)* 78−77279
Sambagawa schist, Central Shikoku, Japan, relationship between albite porphyroblasts growth and deform. 80−26509
sample f/α particle track anal. for U, Th and isotopic disequilibria 78−7799
sandstone, determination of Biot parameters using static tests 79−20299
sandstone, fault development, deformation bands and slip surfaces 79−20819
sandstone, fluid injection effects on fracture 78−7622
sandstone, fracture toughness and acoustic emission characts. *(Japanese)* 79−34810
sandstone, mech. props. rel. to water content *(Japanese)* 77−44980
sandstone, porosity destruction through press. soln. 77−91110
sandstone, seismic attenuation rel. to crack and grain boundaries 80−72495
sandstone, seismic compressional wave absorpt. 80−72433
sandstone, small faults as deformation bands 79−25235
sandstone, stress and size-depend. sonic vel. 77−9417
sandstone, stress relaxation, water effects 79−16453
sandstone, U ores assessment by charged particle track analysis 80−91405
sandstone (Dunnet Head), scattered magnetisation direction, down to small scale 80−90077
sandstone elastic wave velocity, function of moisture content 80−56459
sandstone litho-stratigraphy in Hungary, petroleum exploration aspects 77−86884
sandstones, electrical conductivity of cylindrical cores 78−61401
sandstones, Indian east coast, post-Pleistocene age 79−48485
sandstones, stress conditions and rupture characts. var. from triaxial tests *(Chinese)* 79−74962
sandstones, tectonic and climatic significance from modern big river sands anal. 79−25274
sandstones of Southland syncline, New Zealand, zeolite facies alteration 78−32084
S.Saskatchewan, composition study of sands 79−84254
Saxony Granulites, petrofabric anal. by optical and X-ray diffr. studies 80−21740
Scandinavian rocks, giant and dwarf haloes rel. to unknown radioactivity 78−81157
Scotia Sea Island arc and back arc tholeiites, geochemical study 78−11872
NW Scotland Tertiary continental volcanics, Nd and Sr isotope evidence for crustal contamination 79−66693
scree slope rockfall model 77−44990
sea-floor basalt, rare earth elements behavior during weathering 79−57910
Seal Group, Quebec, magnetisation study of igneous rocks 80−3918
seawater-saturated ocean crust and oceanic island basalts, elec. props. freq. spectrum 79−25229
sedimentary, Cd content determ., geochem. 78−36170
sedimentary, element distrib. rel. to O_2 in Precambrian atmosphere 77−5272
sedimentary, fluid saturation effects on dynamic elastic properties 77−17082
sedimentary, measurement of thermal conductivity using semi-automatic apparatus 79−100970
sedimentary, rare earth elements, Huronian sequence 79−92511
sedimentary, sieve size statistics from grain meas. 77−70645
sedimentary, visible and near IR spectra rel. to comp. 77−17086
sedimentary rocks, epithermal neutron activation anal. of Re 77−9153
sedimentary rocks, Th and U abundances rel. to crustal evolution and sedimentary recycling 80−85654
sedimentary rocks as precursors of tektites and microtektites, chemical evidence 77−82179

rocks continued
sedimentary rocks containing water and oil, dielectric constant and losses *(Russian)* 79−20747
sedimentary rocks from Michigan Basin borehole palaeomag. results 79−39636
sediments, average rock comp. rel. to Earth crust chemical balance 77−86831
seismic anisotropy of crustal and mantle rocks under high-press., high-temp. conditions 77−49059
seismic attenuation, role of grain boundary friction 79−34755
seismic classification of rock mass qualities, vel. data 80−17248
seismic flow of rock mass, vel. of vertical crustal motions 77−33035
seismic flows of rock masses, deform. vels. calc. 79−74850
seismic velocity of rocks, expts. on two-phase aggregates 80−56463
seismic wave attenuation in dry and saturated rocks, lab. meas. 80−3998
seismic wave attenuation in partially saturated rocks 80−3997
seismic wave attenuation mechanisms in dry and saturated rocks 80−3999
seismoelectric effect in rocks, nature 77−44974
SELLO, FORTRAN IV program for skewed distributions for normality transform 77−9502
serpentinised pyroxenitic and saxonitic rocks, petrophysical props., factor anal. 80−90087
serpentinite, protrusions in oceanic crust 77−5149
serpentinite, quarried, rel. to environmental asbestos pollution 77−91261
serpentinite diapir W. of Galicia Bank, rel. to Iberian margin ocean-continent boundary 80−94489
serpentinite intrusions, origin rel. to deep magmatic diapir folds evolution *(Russian)* 80−104957
serpentinites, Glenrock, New South Wales, foliation development 80−21738
Setul Limestone (Ordovician-Silurian), NW Peninsular Malaysia, palaeomag. evidence 80−89936
shackanite and related analcite-bearing lavas in British Columbia 79−57921
shale-sandstone (-limestone), P-, SH- and SV-wave vels. computation 80−98249
shatter cone surface spherules from Vredefort structure, S.Africa 77−53046
shatter cones, geometry and description procedure 80−51398
shear microcrack propag. in triaxially-compressed brittle rocks 80−90080
shear resistance, effect of normal stiffness 77−17089
shear strength, empirical laws of friction and fracture 77−21762
shear strength of joints 78−28226
shock deformation of brittle solid, review of theory 80−72493
shocked rocks in Goat Paddock cryptoexplosion crater W.Australia, petrology 80−98322
Sibley Group, Thunder Bay district, Ontario, Canada, stratigraphy and depositional setting 80−94517
E. Sicily, genetic implications of isotope and trace element variations 78−11893
Sierra Leone Rise, equatorial Atlantic, alkali-rich volcanics 79−2215
silicate, chem. denudation rates in tropical catchments 78−73414
silicate, multielement anal. by epithermal neutron activation, detector systems 78−20123
silicate, trace element anal. using computerised automatic X-ray fluoresc. spectrograph 77−56320
silicate, X-ray spectral fluoresc. anal. 78−3762
silicate anal. on small samples using X-ray quantometer 78−61112
silicate magmas, liquid immiscibility in K_2O-FeO-Al_2O_3-SiO_2 system 77−13076
silicate rock X-ray fluorescence analysis 78−88945
silicate rocks, Br determ. by epithermal neutron activation anal. 78−35741
silicate rocks, quartz-stishovite transitions, shock wave processes 79−88347
silicate rocks and minerals, instrumental neutron activation anal. 78−20548
silicates, Ru determ., preseparation procedure for neutron activation anal. 77−44547
silicates, Zr/Hf determ. by neutron activation 78−20547
siliceous dolomites, petrogenetic grid extension to mantle peridotite and magma generation 77−5137
silicic igneous rocks, Burlington Peninsula, Newfoundland, Rb-Sr ages, deform. 78−65212
siltstone, fracture toughness testing, plane strain, simple meas. method 77−73381
single layer folds arc lengths, comparison between theory and obs. 79−53345
single-layer folds, shape at small but finite amplitude 80−56473
Siwalik Group, Dhok Pathan, Potwar Plateau, Pakistan, mag. polarity stratigraphy and age 79−29725
Skaergard intrusion, E.Greenland, Sr, Pb, O isotopic anal. 79−29763
S.Kivu, Zaire, basaltic flows on Idjwi Island *(French)* 77−64246
slates age studies, $^{40}Ar/^{39}Ar$ stepwise outgassing method applicability 79−29721
slaty cleavage development across Nackara Arc, Adelaide Geosyncline 79−66694
slaty cleavage development in French Alps 77−73736
slip propag. along frictional surfaces 79−25236
soft, vibrating wire stress gauge 77−84199
Sokoman Iron Formation near Ardua Lake, Quebec, mineralogy and petrology 78−77228
Solenhofen limestone, US propag. at high press. 79−29756
solute partitioning, diffusive isothermal, in layered material 77−16896
solvsbergite and fracture granite replacement in mesocratic dike 77−64276
sound velocity determination, suggested methods 78−81433
South Africa, kimberlites, rare gases in phlogopite and phlogopite bearing nodules 78−11894
South Fork Mountain Schist (N Coast Ranges, California), early Cretaceous metamorphic age 78−81114
S.Spain, high-temp. peridotites contact relations in Serrania de Ronda 77−73737
specific resistivity in high Tatra, Poland *(Polish)* 79−96735
spectral reflectance data, lab. and remote obs. comparison 77−17251
spectral reflectance of volcanic rocks, 400-800 nm, for remote sensing studies 80−90073
spectrographic description, suggested method 78−81431
speleothem fluid inclusions, D/H ratio rel. to meteoric precipitation 79−44201

rocks continued
speleothems, stable isotope geochemistry rel. to climatic change, 230000 to 100000 BP 79−2234
spilite and keratophyre from Permo-Triassic volcanic arc terrane, Oregon-Idaho, petrogenesis 79−20826
spilitic rocks, rare earth element mobility and geochem. charact. 77−86887
spilitic rocks from Michigan Basin deep drill hole, petrology 79−39711
spinel lherzolite nodules from Pleistocene cinder cone, upper mantle origin 78−65299
spinel lherzolite xenoliths, implications of texture composition depend. 79−25244
spinel lherzolites from S.Rio Grande Rift, evidence for underlying oceanic mantle 79−29724
stability of elastoplastic half-space around spherical cavity, rock deformation appl. *(Russian)* 79−27551
stability of solid freezing front 78−63844
stalagmite, New Zealand, $^{18}O/^{16}O$ ratios rel. to temps. and climate change during last millennium 79−62574
steady state flow, review 77−9412
steady state flow rel. to lithospheric stress 77−91120
stick-slip sliding dynamic props. appl. to earthquakes 78−48983
Stone Canyon well, California, rock fracturing rel. to P-waves in situ vel. study 79−57865
strain and rotation in a multilayered fold 78−88823
strain determination using randomly oriented strain markers 78−3765
strain distribution across experimental single-layer fold 78−32076
strain ellipsoid estimation for large clasts in deformed rocks, down-plunge viewing method 79−92610
strain estimation from deformed ellipsoidal objects, algebraic method 77−21766
strain field at intermediate distance from ellipsoidal inhomogeneity 78−85534
strain patterns in crestal region of immature diapirs 79−29752
strain-softening of brittle geologic materials 79−16442
strained units, stratigraphic thickness determ. 79−21034
strata layer interface, eigenstresses of sphere embedded in bonded dissimilar half-spaces 77−23886
strength determination in triaxial compression, suggested methods 78−81432
strength tests, irregular specimen versions 78−7791
stress, in situ, in N. America, compilation 79−29728
stress changes, in situ monitoring 79−29884
stress corrosion theory of crack propag. as earthquake mechanism 78−24235
stress evolution rel. to compressive strengths and plate tectonics 77−9421
stress meas., conference (Sydney 11-13 August 1976) 77−9573
stress meas. in bored raise at Mount Isa Mine 77−9414
stress meas. methods in Norway 77−9422
stress meas. using CSIR triaxial strain cell 77−9574
stress measurement, borehole jack fracturing technique 77−64488
stress measurement, hydrofracturing method and recent field results 79−29885
stress measurement by overcoring, diagnostic stress-relief curves 79−29886
stress measurements in north China *(Chinese)* 79−88312
stress memory of crystalline rocks in acoustic emission 79−44180
stress relief boring, monitoring programme at Akabira coal mine 77−9423
stress state determ. in transversely isotropic rock mass 77−56752
stress wave attenuation, linear magnetic hysteresis model *(Chinese)* 79−39702
stressed rocks, crack induced anisotropy, effective elastic moduli and attenuation 80−56461
stresses and displacement distrib. in body with system of parallel shear cracks 78−49012
structural and vibr. bedrock props. in Sweden, seismic events 79−16402
structure analysis, acoustic method *(Russian)* 80−85760
structure fracture and the stress fields of geological structures, review *(Chinese)* 79−53343
structure monitoring instrumentation 78−7790
submarine basalts, sea water weathering effect on K-Ar age 77−86830
submarine lithosphere, geophys., geochem. and petrological model 80−3994
submarine pillow basalts, abundance and distrib. of H_2O, C and S in glassy rims 79−12111
subsolidus attenuation at simultaneous high temp. and press. 78−3764
supracrustal rocks, Isua area, W.Greenland, least radiogenic Pb occurrence 78−44816
surface rock stress meas. using new cylindrical jack 77−9575
surface waves, direction-sensitive displacement analysis by multiple freq. holographic interferometry 78−54338
Surkhob fault zone, rock compression 78−15979
Swedish dolerites, Rb-Sr and palaeomagnetic evidence rel. to Grenville Belt magnetisation age 77−81839
Swedish rapakivi suite, palaeomag. study rel. to Proterozoic tectonics of Baltic Shield 80−56346
symmetrically extending plane crack, self-similar pressure profiles 78−69340
Tauern eclogites, role of buoyancy in exotic eclogite blocks preservation 79−88350
tectonites, quartz ⟨a⟩ axes preferred orientation 78−96200
Tehilla igneous complex, Sudan, petrology and evolution 77−81891
tektite-like material in archaelogical remains, Indonesia 80−101365
tektites and natural glasses, N concs. 80−41446
tektites-irgizites, Fe ions state rel. to form. conditions 78−61420
Tennessee sandstone, Carrara marble, fracture toughness, double torsion testing method 79−84239
Tennessee sandstone, frictional sliding, displacement rate effects 79−16461
Tennessee sandstone, mechanical behaviour studies by stress relaxation testing method 78−96309
tensile strength determination, suggested methods 78−96314
tensile strength indirect measurements, new theoretical aspects 79−29883
tensile strength of discs or rings under diametral compression, calcs. *(French)* 77−70638
tephra attributed to Glacier Peak, Washington, electron microprobe data 78−24273

rocks continued
tephra set W, Mount St. Helens, Washington, electron microprobe anal. of glass shards 78−24274
Tertiary igneous complex of Skye, $^{18}O/^{16}O$, D/H, and $^{13}C/^{12}C$ ratios 77−33012
Tertiary submarine gabbros and peridotites, Zijderfeld vector diagrams use in multicomponent palaeomag. studies 80−17420
texture goniometer for analysis of rocks 80−26630
texture heterogeneity, study via dielectric const. and elec. resistance *(Russian)* 78−96195
thermal conductivity and diffusivity using modified Angstroem or impulse method 80−90085
thermal conductivity and thermal expansion, conference, Chicago, USA (Nov. 79) 80−31425
thermal conductivity determ. from fragment meas. *(Rumanian)* 78−20563
thermal conductivity meas., steady-state plate method *(Chinese)* 80−56615
thermal conductivity measurements on saturated rocks at permafrost temperatures 79−84232
thermal conductivity of granular media, results for greisen and granite *(French)* 78−11880
thermal diffusivity and elastic anisotropy meas. at high press. in cubic press. 78−69337
thermal expansion, effects of cracks 78−28218
thermal properties of dry, water-saturated and petroleum-saturated specimens *(Russian)* 78−92817
thermal props. of near-surface rocks in Ukraine *(Russian)* 77−91084
tholeiitic basalts, rare earth elements behaviour during submarine weathering 78−73369
tholeiitic basalts from Japan, geochemical types 78−96206
tholeiitic rocks and Ni and MgO content of magmas 79−88318
tholeiitic submarine basalts, volatile abundances 79−34795
till on Lake Huron E coast, mag., physical and lithologic props. and age 77−33057
Tilting Harbour igneous complex, Fogo Island, Newfoundland, petrology 78−77230
Tirumalai hill range AP, porphyritic granite fracture pattern interpretation 79−44156
Toba Tuff from late Pleistocene eruption, K-Ar age 79−16427
Tokyo, base rock, seismic explosion obs. *(Japanese)* 80−41403
trace element behaviour in magmatic processes, quantitative models 78−65214
trace element determ., neutron activation anal., coaxial, planar detection comparison appl. 77−81443
trace element separations in igneous rocks, possible diffusional effects 77−41008
transient effect in sample under simulated upper crustal conditions 77−29293
transient thermal conductivity meas., thermal contact resistance 78−53744
transitional basalts and tholeiites from E.Pacific Rise at 9°N 79−84218
transversal bent fold, stress and strain rate, stress relax. effect 79−66651
transverse wave vels. in dry and water-saturated samples, up to 2 kbar press. *(Russian)* 78−28219
transversely layered isotropic media, seismic wave vel. calcs. 80−12344
Triassic sandstone, porosity determ. using electrical resistivity meas. 77−9528
trondhjemitic basement enclave, near Favourable Lake volcanic complex, NW.Ontario, Canada, age 80−94518
Troodos Massif, Cyprus, preliminary tectonic results 77−17072
Troodos ophiolite metamorphism, implications for marine mag. anomalies 80−81812
Troodos ophiolitic complex, major oxide geochemistry and origin 80−98317
tuff, deform. charact., expt. study *(Japanese)* 78−56704
two phase convection driven by phase change instability mechanism 77−86834
Tyrrhenian Sea floor, tholeiitic basalts 78−11873
Uivak II gneiss from Saglek area, Labrador, zircon age meas. 80−3958
Ukrainian shield, effect of high hydrostatic pressure on elec. props. *(Russian)* 77−73721
Ukrainian Shield, rock mag. props. map rel. to composition and metamorphism 80−17229
Ukrainian shield rocks, correls. of electrical parameters at high temps. *(Russian)* 79−8628
ultrabasic, diffusion and diffusion creep, rel. to upper mantle deform. 77−9409
ultrabasic xenoliths, elastic anisotropy up to 10 kb pressures 77−56624
ultramafic, appl. to mantle thermal gradients estimation 77−5138
ultramafic, elastic props. 77−9413
ultramafic, elec. cond. meas., 670-1820K 78−69335
ultramafic, from Cr-rich areas, visible and near IR spectra, remote sensing appls. 80−4000
ultramafic nodules, crystalline phases, Co and Sc fractionation 78−65306
ultramafic nodules, from Kimberley pipes, South Africa 79−34821
ultramafic partial melt fluid distrib. under hydrostatic stress, expts. 80−21716
ultramafic xenolith suite from Tahiti, petrology and genetic significance 80−90086
ultramafic xenoliths, Baja California, textures, microstructs., deform. 78−20420
ultramafic xenoliths from Elwin Bay kimberlite, first Canadian palaeogeotherm 77−91078
ultramafic xenoliths rel. to tectonites *(French)* 79−44141
ultramafics from Owen fracture zone, NW Indian Ocean, petrology rel. to nature of oceanic upper mantle 80−94519
ultrametamorphism and granitoid genesis 78−44808
Umfraville gabbro, Ontario, 1180 Ma Grenvillian stock palaeomagnetism 78−92777
underground destruction, seismic meas. method 77−9419
underground mine openings design rel. to stress meas. 77−9425
underground openings, stress release, improved method 77−9424
uniaxially compressed rock cylinders, longitudinal splitting anal. 80−17249
Upper Cretaceous Plutonian, in Maritsa neointrusive zone, palaeomag. stability 77−37124
Upper Jurassic pyroclastic rocks in Skye, W.Scotland 77−29297
upper mantle, rare earths partitioning between silicate melt, amphibole and garnet peridotite 79−20775
rocks continued
upper Mesorzoic subduction complexes along N.America west coast, distrib. and character 78−81136
upper Palaeozoic rocks of W.Canadian Cordillera rel. to Cordilleran evolution 78−7632
uraniferous materials, disequilib. variability and ^{222}Rn emanation factor 79−62498
US pulse transit times, simultaneous stress and strain monitoring 77−91046
W.USA Cenozoic geodynamics rel. to Columbia-Snake River-Yellowstone region magmatism 77−73738
Vajont rock slide (Italy, 1963) analysis, new approach 79−8633
vaporisation to elements, meteorite impact study 80−36583
velocity anomalies in dilatant rock 79−20821
velocity anomalies prior to failure and violent slip 79−16409
Vempalle dolomite, Andhra Pradesh, India, petrography and thermoluminesc. characts. 77−17088
vertical orogenetic profile, relation between rocks mechanical characts. and terrestrial heat flux *(German)* 78−81123
viscoelastic properties of fluid-saturated cracked solids 78−36154
viscoelasticity equations, methods for numerical soln. 77−89042
volcanic, evolution in island arc, batch fractionation model, example from Japan 79−34818
volcanic, from W.Pacific island arcs, $^{87}Sr/^{86}Sr$ ratio 77−33031
volcanic, glass inclusions as samples of early magmatic liquid 77−37202
volcanic, in Eifel fields, pliocene and quaternary volcanic phases, K/Ar age determ. 80−46160
volcanic, isotopic comp. rel. to mantle local and regional isotopic equilib. 78−65216
volcanic, Lesser Antilles island arc, palaeomagnetic and geochronological survey 80−8265
volcanic, Mariana Island arc and trough, volatiles content 79−92535
volcanic, Sr isotopic comp., role of ancient lithosphere in young continental volcanism 77−2133
volcanic, Tetagouche Group, Canada, geochem. rel. to origin 78−65298
volcanic ash, examples of devitrification and early diagenesis 80−81860
volcanic belt, Kisseynew, Canada, Pb isotope studies of ore deposits, ages 79−5479
volcanic material alteration in marine sediments, SE.Pacific Ocean 80−3990
volcanic material from Klyuchevskaya Sopka volcano (1974), chem. anal. 80−101351
volcanic rocks, mass fractionation of rare gas isotopes as indicator of gas transport to or from magma 80−98292
volcanic rocks, nucleoside phosophates adsorpt. rel. to origin of life 77−91273
volcanic rocks, relation between major element chemistry and tectonic environment 78−16006
volcanic rocks, W abundances 79−16468
volcanic rocks classification using Irvine and Baragar classification scheme, FORTRAN IV program 78−57203
volcanic rocks from Hess Rise, W.Pacific 80−90026
volcanic rocks of Marcus-Necker Ridge, comp. and stages of development 80−36282
volcanics, Rb/Sr whole-rock systems and chemical control 78−61366
volcanics from Archaean Prince Albert Group, Melville Peninsula, N.W.T., geochemistry and origin 79−53324
volcanics from Capraia, Italy, geochronology and palaeomagnetism 79−16418
volcanics from Nasu zone, NE.Japan, trace element vars. 79−88317
volcanics of E.Avoca-Ballard mineralised belt, U content 78−69346
volcanogenic formations, uranium redistrib. and mobility during metamorphism 77−64283
volume changes during fracture and frictional sliding, review 79−16450
Wairakei thermal region, thermal water transport of major rock constituents 77−81844
water flow, shear thinning and shear thickening polymer additives 80−72100
water flow through rock specimen, average pore vel. meas. 79−5473
water-saturated, dynamic props. of seismoelec. effect 79−25233
water-saturated rock, electrically charged, effect on seismic wave propag. and damping coeff. 80−76921
wave dielectric log curves in formations of limited thickness, interpretation *(Russian)* 79−74990
wave propagation, frictional attenuation, amplitude depend. 80−31034
weathered Athenian schist, basic geotechnical and mineralogical props. 78−61408
weathering, correction method in seismic sounding 79−44255
weathering by chemical decomposition, rate meas. by now U isotope method 80−77142
Weber sandstone, hydrofracture at high confining pressure and differential stress 77−64272
Westerley Granite, changes in seismic vel. and attenuation during deformation 78−28221
Westerly granite, dry, deform. behaviour 78−36153
Westerly granite, electrical conductivity of cylindrical cores 78−61401
Westerly granite, failure under triaxial compression 78−11884
Westerly granite, high temp. frictional sliding mechanisms 78−73357
Westerly granite, permeability changes during water flow at 100-400°C 78−40546
Westerly granite, stress effects on cracks 77−25676
Westerly granite, stress-strain hysteresis loops shapes 80−26499
Westerly granite, stress-volumetric strain behaviour statistical var. 78−96196
Westerly granite, vel. anisotropy, dilatancy effect 79−2226
Westerly granite fracture propagation, crack interaction effects on critical stress 79−25234
Woodroffe thrust, deform. and fold axes reorientation in ductile mylonite zone 78−32101
X-ray fluorescence, major-element data processing, SORT, REORD and MW programs on FORTRAN 77−86398
X-ray fluorescence spectrometry of geological samples, element analysis *(Rumanian)* 77−33217
xenoliths, mantle-derived, from S.Africa 79−34775
zeolite-bearing rocks, multicomponent, quantitative thermogravimetry 79−16082
$^{40}Ar/^{39}Ar$, shock press. effects 77−60360
$^{40}Ar/^{39}Ar$ dating, appl. of isochron diagrams 79−29873
^{40}Ar-^{39}Ar geochronological studies on submarine rocks from W.Pacific 77−17075
^{40}Ar-^{39}Ar systematics, temp. and pressure effects 79−44178

rocks continued
As determination in rocks and soils by at. absorpt. 79−88475.
Au, determ. in rocks, minerals by at. absorpt. spectrometry 77−29067
B abundance determ. 78−85559
$^{13}C/^{12}C$ ratio in magmatic gases of Afar ridge volcanism 80−21732
^{14}C dating of geological and archaeological samples 78−92993
$CaCO_3$ production of mare incognitum, upper windward reef slope, Enewetak Atoll 78−7662
Cd isotopic abundances, survey of diabase, sulphide ore and tonalite 78−53891
Fe formation in Early Precambrian Isua supracrustal belt, W. Greenland, cosmic grains discovery 80−72508
Ge-Si and Ga-Al fractionation in Hawaiian volcanic rocks 79−12112
Li rich pegmatites, petrogenesis 79−57918
Na determ. in rock, mineral samples, X-ray fluoresc. quantometer modification 78−61589
Nd-Sr isotopic patterns rel. to petrogenetic mixing models 80−3965
$^{187}Os/^{186}Os$ in terrestrial samples, rel. to use of Os isotopes as petrogenetic and geological tracers 80−89989
Pb determ. by atomic absorption 79−88035
Rb/Sr chronology, Rainy Lake Archean granitoid batholith 79−84188
Rb-Sr ages, Hopei, China *(Chinese)* 79−20776
Rb-Sr dating, deformation in Hellroaring Plateau area, Beartooth Mountains, Montana 80−17238
Rb-Sr whole rock isochron, Newry Granodiorite, N.E.Ireland 77−5162
Rb-Sr whole rock isochron age from Kangamiut dykes rel. to Hudsonian orogeny in W.Greenland 79−5459
Rb-Sr whole-rock isochron age, 2390 Myr, for Scourie dykes, NW.Scotland 79−39690
Rn diffusion through inactive rock sections 77−5194
$^{34}S/^{32}S$ ratio in magmatic gases of Afar ridge volcanism 80−21732
Sc determination by neutron activation analysis using ^{46m}Sc 79−79356
Sn determ. by thermal neutron activation anal. 77−44552
Sn determ. in rock samples by neutron activation method 78−85258
SnO_2, from rocks, quantitative determination by Mossbauer effect *(Rumanian)* 78−49178
$^{87}Sr/^{86}Sr$ ratio reduction during hydrothermal alteration of basalts 79−16446
U analysis in geological samples, delayed neutrons method *(Rumanian)* 79−88507
U containing conglomerates, Witwatersrand type, significance of diagenesis for origin 79−84265
U deposits, distribution and mode of occurrence 79−84266
U deposits in South Africa and South West Africa 79−84268
U determination in whole rock samples by fission track method 77−73880
U distribution and evolution in oceanic lithosphere 79−84226
U in rock samples, meas. by track registration in plastic detectors 78−73533
U isotope disequilibrium due to α-recoil and soln. effects 80−98314
U mineralisation rel. granite magmatism, British Isles 79−84273
U movement during higher grade metamorphism 79−84274
U, Th contents, rel. to ^{14}C prod. in groundwater and implications for dating 80−85690
U-bearing rocks, radioactive disequilib. determ., isotopes relative abundance meas. 78−57330
$^{234}U/^{238}U$ ratio disequilibrium in natural samples, mechanisms involving recoiling alpha-emitting nuclei 79−16466
Yb isotopic and elemental abundances 78−32419
Zr, isotopic composition, at. wt., rock standards, chondrite composition 79−3591

Roentgen ray *see X-rays*

rolling
see also cold rolling
alloy, vacuum rolling at high temp. *(Russian)* 79−15708
austenitic stainless steel, recrystallisation transformation energies, α' to γ, effect of Si content and deformation by rolling *(French)* 77−48433
austenitic steel, 17G1S struct. and austenite transformation kinetics variation on deform. *(Russian)* 79−70060
austenitic steel, 45G17Yu3, structure and loss of strength after hot deform. by rolling *(Russian)* 78−39794
bimetal rolling, calc. of strains by variational method *(Polish)* 80−45323
α-brass, (211)[$\bar{1}$11] single crystal, rolling deform. 77−21174
α-brass, deformation mode during rolling *(Japanese)* 79−79001
α-brass, dislocation structure around crack tips in early stage of fatigue 78−60830
brass, FCC, rolling texture development 79−87657
brass, FCC rolling texture origin with rolling plane parallel to {111} 79−91674
brass, orientation change in (211) [$\bar{1}$11] single crystals during rolling *(Japanese)* 78−60712
brass, orientation distribution, texturised materials, Ghost effect demonstration 80−70080
α-brass, polycrysts., deformed in tension or rolling, anneal hardening *(Japanese)* 80−93564
α-brass, recrystallisation texture, rel. to rolling temp. 80−11664
brass, rolling texture development and deform. struct., shear bands effect *(Japanese)* 80−84952
brass, shear band development during rolling, twinning, metallographic obs. *(Japanese)* 78−39849
brass, simulation of rolling and shear texture, using an adapted Taylor theory 78−52835
brass, tensile curve and specific value of anisotropy coeff. *(French)* 77−28867
α-brass, texture, recrystallised orientation distrib. function comparison with 40°(111) rolling texture 80−25723
α-brass, thin sheet, plastic anisotropy 77−63683
brittle fibre reinforced composite, sheet manufacture without fracturing *(Russian)* 77−55914
bronze, Al, electrode strip, short-time sintering 77−1824
circular blank, stress-strain state during forging *(Russian)* 79−52231
contact fatigue failure, of rolls of hot strip mills 80−60950
contact fatigue life, traction and microgeometry effects 79−20205
critical line nature in multiple-roll passes *(Russian)* 80−38347
critical reduction effect on chemicothermal treatment processes 77−70073
cross-rolling and compression textures, numerical prediction 80−40382
crystallite deformation in rolling, computer simulation *(French)* 78−31421

rolling continued
deformation by lamination, hydrodynamic analogy, utilisation of current function *(French)* 80−19292
elastohydrodynamic film thickness, meas. of artificially produced dents and grooves 80−36975
elastoplastically deformed strengthened material, stress deformed state during rolling *(Russian)* 80−54299
elastostatics element method to determine elastic behaviour of 4 high stands, appl. to strip rolling *(German)* 77−36541
extrusion and forming of solids, plastic deform., nonNewtonian flow, numerical solns. 78−19824
fatigue life dispersion in rolling contact, new model 78−59349
f.c.c. alloy, rolling texture *(Russian)* 77−1843
FCC and CC metals, behaviour during rolling, numerical simulation study *(French)* 78−84891
FCC metal, polycrystalline, computer simulation of rolling texture *(Japanese)* 77−63686
Fe, cast, high Cr, hardfacing of roll, wear resistance and thermal durability 80−7686
ferrite, transform. kinetics, grain size, alloying element effect, carbide precip. 80−93560
flat, with spread, cross-section warping *(German)* 80−92064
Gauss principle, in rolling theory, deformed and kinematic eqns. *(Russian)* 80−65124
glass ball rolling on adhesive viscoelastic material, contact area 79−52394
glass on rubber rolling friction, humidity effect 79−79118
granular materials, rolling, granule kinematics 80−84875
granule rolling process, energy and force parameters determ. 77−63577
heat transfer, total coeff. determ. tests for industrial cooling system of continuous hot rolling mills *(German)* 77−89005
hot longitudinal, periodically charging sections with flash, pressures calc. *(Polish)* 80−89257
hot rolling, simplified load calcs. incorporating material strain rates 77−52359
hot rolling, torque calc., mechanical model 79−20078
hot rolling exam. of empirical relations for plastic flow strength 79−61630
Inconel 617, microstruct., mech. props., thermal ageing effect 77−36557
inhomogeneous deformation model 80−48650
Invar, deformed, magnetism and temp. depend. of effective field on ^{57}Fe *(Russian)* 79−24234
large sized tube milling by planetary skew rolling, theoretical anal. *(Chinese)* 79−74180
metal, BCC, rolling texture, effect of critical shear stress ratio of {112} and {110} 79−91673
metal, ductile fracture criterion 78−60817
metal, FCC, polycrystalline, quantitative anal. of cross-slip and twinning 79−90677
metal, flow during rolling *(Russian)* 78−27561
metal, internal stresses during rolling friction and their evaluation 77−28912
metal, pack rolling, bonding, deform. struct., small reduction before seizing 77−90503
metal, plastic flow rate during rolling under two dimensional strain *(Russian)* 79−52264
metal, vacuum rolling at high temp. *(Russian)* 79−15708
metal electroplastic deformation meas. pulse generator *(Russian)* 80−25931
metal powder, mean normal contact stress in rolling 77−12571
metal powder, rolling, overall strain co-eff. 77−24984
metal powders, contact stresses distrib. 79−66083
metal powders, strip densification in forward slip zone in rolling 79−95972
metal ribbon, amorphous, fluid-flow-temp. model for casting by melt extraction 79−56942
metal ribbons, amorphous Newtonian-quenched, formed by melt spinning and melt extraction, dimens. variations 79−56943
metal sheet, recovery strain during unloading in tensile test, roll-forming appl. *(Japanese)* 79−100182
metals, complex sections, unified anal. function of surface of strain focus *(Russian)*. 80−21017
metals, cubic struct., numerical simulation of cross-rolling textures *(French)* 79−20061
metals, longitudinal flow velocity distribution in rolling *(Russian)* 80−93575
metals, wave movement, resonance phenomena in deformation zone during rolling *(Russian)* 80−65123
metals porous, mean principal stress in rolling without lateral expansion 80−25803
multilayer materials, vacuum rolling at high temp. *(Russian)* 79−15708
Ni-Cr alloy Kh20N80, sintered sheet material, stopping power and pore size relationship 78−19693
Ni-Cr-Mo and Ni-Cr, impact strength, effect of modified ausforming *(Japanese)* 79−11692
nylon 66, doubly oriented, annealing of drawn and rolled samples, struct. 78−52859
plasticity problem soln. by symbolic computer processing of formulae 80−17803
β-poly(vinylidene fluoride) films, single cryst. orientation, piezoelec. 80−20591
polycarbonate, effect of rolling on mech. props. 78−52837
polyether sulphone, effect of rolling on mech. props. 78−52837
polyethylene, lightly crosslinked, processed under mol. orient., transparent film prep. 80−38957
polyethylene, struct. changes on hot-rolling 77−86051
polyethylene, structural changes on hot-rolling 77−86052
polymer, ultrahigh modulus, production 77−52277
polymer melt, viscoelastic, 2-dimens. nonisothermal processing between calender rolls, mathematical model 79−68670
polymer solutions, high mol. wt., birefringence lines in elongational flow *(French)* 80−25337
polysulphone, effect of rolling on mech. props. 78−52837
porous materials, contact stresses in hot rolling 77−77515
porous metal gauze materials, struct. and hydraulic characts. 80−11729
porous solids, hot rolling, rheology, stressed state determ. 79−100194
powder, particle size effect on conditions of strip shaping process 77−12565
powder strip, rolled, effect of densification zone shape on density distrib. 79−95960

rolling continued
powder strip shaping device, deform. zone configuration effects 77−24979
powders, agglomerate structure parameters of powders in the incoherent zone in rolling 80−84876
powders, critical speeds 79−70011
pressure calculations, mathematic treatment *(Chinese)* 79−100171
profile measurement of hot rolled strip during hot rolling *(German)* 80−25929
PVC, reaction with maleic anhydride in heated roll mill *(Japanese)* 79−38856
PVC, rolled, anisotropic, creep fracture *(Japanese)* 79−34132
rolled stock, stat. quality control w.r.t. mech. props. 79−43510
rolling discs, coeff. of friction 79−14360
rubber, loaded, effect of polyfunctional nitro-oligomers on relaxation props. *(German)* 78−48436
shaped strip, tension during rolling 78−84890
shear band formation models, in rolling and extrusion 80−3152
sheet metal, texture heterogeneity, numerical simulation *(French)* 78−92274
square blank, rolling process, math. model based on plasticity theory *(Russian)* 80−16335
steel, 0.2 to 0.8% C, ferrite-pearlite transformation, tensile strength, cooling rate effect 80−7549
steel, 0.45% C, annealed, roller, macroscopic and microscopic changes in surface layer due to rolling contact 77−77518
steel, 0.45% C, annealed, roller, rolling contact fatigue life, effect of changing rolling direction 77−77519
steel, 3Kh2V8F, brittleness depend. on high temp. deform. at high stress. temp. *(Russian)* 80−50698
steel, 45G17Yu3, deformed, influence of hot rolling on struct. *(Russian)* 77−25073
steel, AISI 4340, sulphide inclusion behaviour during thermomechanical treatment 78−3151
steel, Al-Cr-Mo, nitride hardened roller, surface fatigue failure under pure rolling and sliding rolling contacts 79−79183
steel, Al-Cr-Mo, nitride hardened rollers, surface fatigue resistance under pure rolling and sliding-rolling contacts 79−79184
steel, alloy, high speed, type R18, hot deformation and recrystn. 80−16391
steel, alloy, sheet, crack-propag. resist. in heat-affected zone in presence of H, rolling direction and preliminary plastic tensile strain effects 80−60971
steel, alloy, uphill diffusion during homogenization 77−90381
steel, anisotropic rolled plate, fatigue crack growth, rel. to laminated struct. and inclusions 78−92313
steel, anisotropic rolled plate, torsional fatigue in middle and high cycle fatigue ranges *(Japanese)* 77−12691
steel, austenite decomposition, controlled rolling rel. to substruct., props. 79−29014
steel, austenitic, 16H2NMB, struct., texture and mech. props. of product of transform. 78−92273
steel, austenitic, 30KhGSA, heat treatment, preliminary, cold deform., elec. heating rel. to mech. props. 79−24554
steel, austenitic, dislocation structural changes on hot rolling *(Russian)* 77−59805
steel, austenitic, low-C, transform. kinetics rel. to temp., deform., struct., mech. props. 79−24519
steel, austenitic, metastable, 0Kh14AG12M, Cr-Mn and Cr-Mn-Ni, phase transform. kinetic effect on mech. props. *(Russian)* 79−34024
steel, austenitic, microalloyed with V and N, hot rolling 77−52364
steel, austenitic stainless, 08Kh18N10T, hot-worked precipitation kinetics and struct. of dispersed phases, Ti effect 80−29964
steel, austenitic stainless, 12Kh18N10T, intercrystalline corrosion, hot rolling effect 79−79010
steel, austenitic stainless, grain growth kinetics, effects of C content and rolling *(French)* 77−81269
steel, austenitic stainless, recrystallization after hot rolling 79−47734
steel, austenitic stainless, structural inhomogeneity, electron and optical microscope exam. 78−72827
steel, bainitic, low C and alloy, quenched microstruct. effect on mech. props. *(French)* 79−79003
steel, ball bearing, martensitic decay during rolling contact fatigue 77−32682
steel, ball bearing with modified chem. comp., improved rolling contact fatigue 78−64732
steel, bearing, corrosion resistant, rolling element fatigue life 79−20090
steel, C, contact fatigue strength, effect of austenite grain size 79−100254
steel, C, fatigue failure in type 45, strength charact. 79−52373
steel, C, isoforming and warm rolling, effect of mech. props. 80−11673
steel, C, naval, corrosion in harbour anaerobic sediments, rolling direction and tensile stress effects 80−30135
steel, C, naval, corrosion in natural seawater, rolling direction and tensile stress effects 80−30134
steel, C, pearlite grade ShKh15, struct. transformations, hot plastic strain influence *(Russian)* 80−20927
steel, C, rolling contact fatigue, tufftriding effect on 0.2% C cylindrical specimen 80−100954
steel, C, structural strength, increase by high temp. mech. treatment with austenite isothermal decomp. 79−24555
steel, C and Ni-Cr surface hardened, rolling contact fatigue failure 80−16608
steel, C-Mn, corrosion in acidic soln., metallurgical factor effects 79−70206
steel, C-Mn and C-Mn-Nb, weldable, high temp. thermomechanical treatment 79−15709
steel, C-Mn-Nb, Nb microalloying, weldable, structural, recrystallization and precipitation induced by high temp. deform. *(French)* 79−61632
steel, C-Mn-V-Cb-N, high strength low alloy, controlled-rolled 80−100803
steel, case-carburized, low alloy, rolling contact fatigue 78−35518
steel, comp. and processing effects on microstruct. and props. rel. to low temp. applic. 77−52365
steel, constructional, struct., props., isothermal thermomechanical working *(Russian)* 77−25076
steel, correlation links between mech. props. 80−35234
steel, Cr (17 wt.%), stainless, hot-rolled texture, effect on cold-rolled and annealed textures 80−55425
steel, Cr-Mn type, martensite struct. after quenching and HTMT, X-ray diffr. obs. 80−84975
rolling continued
steel, Cr-Ni, case hardened rollers, surface fatigue failure under pure rolling and sliding rolling contacts 79−52472
steel, Cr-Ni, rolled and sintered, to produce capillary structured filter material, exam. of mech. props., and production 80−16235
steel, Cr-Ni(-Mo) austenitic, strengthening by modified ausforming 78−76665
steel, Cr-Ni (16,14 wt.%), Si effect on texture, grain growth after rolling or recrystallisation *(French)* 77−55986
steel, die, thermal fatigue resistance, high temp. thermomech. treatment effect 80−50715
steel, electric sheet, hot-rolled, recrystallization and texture formation during ht. treatment 77−44271
steel, high C, plate, rolling residual stress meas. by X-ray diffr. *(Japanese)* 79−66081
steel, high C, tensile strength, working and heat treatment effects *(Japanese)* 80−104209
steel, high C, thermomech. treated, strengthening factors 77−8862
steel, high Mn, austenite grain size, effect of rolling and V, Ti and Zr additions *(Korean)* 77−12632
steel, high Mn alloy G22, phase transform. during plastic deform. 77−16576
steel, high speed, R18 and R6M5, rolled and annealed carbide phase investigation 77−90374
steel, high strength, low C, with N_2, yield strength, Mo effects 77−90410
steel, high strength, Nb(C, N) precipitation in austenite, effect on mech. props. *(Japanese)* 77−21186
steel, high strength, thermally strengthened by rolling heat, H_2 embrittlement *(Russian)* 77−77562
steel, high-speed, 30Kh2N2SMKt, deform. effects on physicomech. props. 78−23741
steel, high-speed, cast, mech. props. at high temps. 79−20135
steel, hollow cylinder, thick walled, effect of thermomech. treatment 80−11674
steel, hot rolled, low C, low alloy, bainitic alloying addition effects on microstruct. and props. 77−36546
steel, hot rolled, M1 tool type, microparticle distributions and mech. response 77−44279
steel, hot rolled Al killed sheet, strain ageing control 79−61628
steel, hot rolled strip and plate shape meas. device 80−35498
steel, hot rolled strip formability, mech. testing and mech. props. *(German)* 79−66089
steel, hot rolling, simulation while preserving criteria of similarity *(Russian)* 79−52266
steel, hot-rolled high quality sheet use of stat. maths. for NDT determ. of mech. props. 79−11749
steel, impact and tensile props., Si effects 79−24614
steel, ion nitrided, rolling wear props. *(Japanese)* 77−48554
steel, Kh15N5AM3, combined heat treatment and mech. working *(Russian)* 77−55997
steel, laser erosion value depend. on metallic props. anisotropy during plastic deform. *(Russian)* 78−31452
steel, lightly alloyed, S effect on failure following controlled rolling *(Russian)* 79−57086
steel, low alloy, naval, stretch zone width meas., COD for ductile crack initiation 78−68813
steel, low alloy, strengthening by strain tempering, deform. effects 78−15424
steel, low alloy, type 3sp, effect of temp. at end of rolling on mech. props., and coercive force 78−72799
steel, low alloy composite, ferrite-carbide struct., cold plastic deform. 77−90408
steel, low C, bainitic, optimal struct., heat treatment effects 77−16624
steel, low C, crack propagation energy rel. to temp., time factors 79−29179
steel, low C, deform. form effect on texture *(Russian)* 78−3141
steel, low C, deformed, comp. of precipitated carbonitrides, X-ray diffr. anal. *(Russian)* 79−20051
steel, low C, effect of heat treatment on resistance to fatigue crack propag. 80−11675
steel, low C, hot rolled and cold deep drawn, nonmetallic inclusion distrib. in microcavities *(Russian)* 79−52265
steel, low C, hot rolling effects on struct. *(Russian)* 78−19793
steel, low C, low alloy, ferritic-pearlitic, high temp. mech. treatment, cooling effect 80−104193
steel, low C, Mb-Nb, reheated, quenched, tempered, microstruct. 77−36550
steel, low C, microalloyed, heat treatment, mech. props. 79−24551
steel, low C, Mn, recrystallisation and grain growth in hot rolling 79−47714
steel, low C, Mn, strain hardening parameters, electron microscope obs. 77−63690
steel, low C, Mn effect on recrystallisation and texture *(French)* 80−3110
steel, low C, Mn-Nb, quenched and tempered, microstruct. and props. 77−36549
steel, low C hot rolled sheet, drawability improvement by Al addition *(Ukrainian)* 79−78996
steel, machining, 12L14, effect of Pb and Te on hot-shortness mechanism 80−104190
steel, maraging, effect of deformation on props. 80−21032
steel, martensitic, low C wire, strain tempering by rapid heating *(Japanese)* 78−31428
steel, medium C, internal cracks in continuous casting billet and rolling products *(Chinese)* 79−43375
steel, medium C 80−11752
steel, microalloyed, hot-rolled, Nb(C,N) precip. and austenite recrystn. 80−97513
steel, microalloyed, precipitation effect on microstruct. and mech. props. *(French)* 80−25708
steel, microalloyed, types V1599, V1600, V1286, NbCN precipitation in undeformed austenite 80−89230
steel, mild, implantation of Cu(Cr), annealing and rolling behaviour of conc. profiles 78−75684
steel, mild, rolled, critical angle US reflectometry of stressed bar, book contrib. 79−100324
steel, mild, rolled, texture, analysis, vector method 79−83218
steel, mild, solderability, annealing effect *(Japanese)* 80−89244
steel, Mn, as rolled bainitic, tensile, impact and machinability props., transport appl. 78−88503

rolling continued
steel, Mn-Mo-Ni-Cr, bainitic, microstructures and mechanical properties *(French)* 80−16362
steel, Mn-Ni-Cr-Mo, high tensile strength, control-rolled, transformation textures 79−83225
steel, Mn-Ni-Mo, PWR pressure vessel, irrad. induced embrittlement, chemical composition effect *(French)* 79−20195
steel, Mn-Si-Cr-Mo, dual phase, as-rolled, continuous cooling transformation diagram to optimize composition 80−100829
steel, N_2 effect on grain boundary migration rate during secondary recrystallisation *(Czech)* 77−59812
steel, Nb,(V),(Al), hot-rolling, laboratory simulation, recrystn. of austenite 80−97512
steel, Nb, controlled-rolled into ferrite temp. range, soln. temp. and rolling effects 80−11678
steel, Ni-Cr, case hardened rollers, macroscopic and microscopic changes in surface layer due to rolling contact 77−77518
steel, Ni-Cr, case-hardened, surface durability in rolling contact fatigue testing 77−63684
steel, Ni-Cr, case-hardened roller, rolling contact fatigue life, effect of changing rolling direction 77−77519
steel, Ni-G rollers, case hardened, surface durability in pure rolling and sliding-rolling contacts 79−61739
steel, nonmetallic inclusion, effect on hot ductility 80−29999
steel, plastic, thermally strengthened, not prone to H_2 embrittlement, prod. *(Russian)* 79−52267
steel, plastic deform. resist. during continuous hot rolling *(Russian)* 80−55462
steel, plastically deformed, force and speed criteria interactions during hot rolling *(Russian)* 80−55463
steel, plate, alloying, normalising, controlled rolling 77−48459
steel, plate, thickness and rolling ratio influence on inclusion behaviour 80−16340
steel, rare earth additions, effect on physicomechanical props. 77−12639
steel, rolled, anisotropic, fatigue fracture surface obs. *(Japanese)* 80−108546
steel, rolled, fisheyes produced by exposure to H_2 at room temp. 77−90455
steel, rolled, low-cycle torsional and push-pull fatigue anisotropy 78−27589
steel, rolled, used of statistically justified methods in determining heterogeneity and mech. props. 79−52516
steel, rolled 15 MND 6, nuclear reactor cell material, determination of non-cracking threshold *(French)* 79−52367
steel, rolled sections, continuous rolling process considerations *(Rumanian)* 79−29097
steel, Si(3 wt.%) grain oriented, high permeability obs. 77−1881
steel, Si (3 wt.%), hot rolled, effect of initial texture on secondary recrystallisation *(Czech)* 79−91711
steel, Si-Mn, 27SG, heat treated sheets, underwater explosive forming *(Polish)* 79−34052
steel, sintered, mech. props., effect of small cold reduction 79−39048
steel, stainless, Cr-Cu (17, 0.6 to 1.1 wt.%), texture 80−84957
steel, stainless, deformation temp. determ. for high yield strength 78−44177
steel, stainless, duplex, hot ductility and fracture mechanism 78−60731
steel, stainless, ferritic, tensile strain direction and roping phenomena 77−36533
steel, stainless, Frank-Read dislocation source obs. in grain boundary 77−84756
steel, stainless, gas liberation in vac., effect of different methods of surface treatment *(Russian)* 80−45429
steel, stainless, grain growth after deform. by rolling, C effects on kinetics *(French)* 77−28866
steel, stainless, hot rolled texture, effect on cold rolled and annealed textures *(Japanese)* 78−48425
steel, stainless, hot rolling resist., multistage mode of deform. effects *(Russian)* 78−80583
steel, stainless, Kh18N10T, struct. and mechanical props., effect of previous deform. in rolling *(Russian)* 79−29099
steel, stainless, maraging, grain growth, temp. effect 79−57019
steel, stainless, sintered sheet material, stopping power and pore size relationship 78−19693
steel, stainless, tempering after air hardening from rolling heat *(German)* 80−93571
steel, stainless Cr (17 wt.%), hot rolled sheets, martensite distrib. effect on ridging phenomena 79−1887
steel, stainless/Al laminate, sandwich sheet material, plane strain compression and rolling 79−57062
steel, strain-hardened subsurface layer, residual stress change in fatigue 80−81185
steel, tensile prestrained strength of anisotropic rolled steel, rot.-bending fatigue tests, slip bands 78−27590
steel, thermomechanical treatment effect on mech. props. and microstruct. *(French, German)* 79−66090
steel, transformations, influence of type of cold plastic strain *(Russian)* 79−52232
steel, transformer, EM losses, influence of charact. of substruct. distrib. *(Russian)* 78−7058
steel, transformer, formation of perfect cubic texture in thin sheets *(Russian)* 78−80557
steel, transformer, texture formation tendency *(Russian)* 77−59803
steel, two-phase austenitic-ferritic, plastic deformation under hot working conditions 77−48466
steel, types 15Kh2NMFA and 45, fatigue tests, low cycle, material variance distrib. law 79−91799
steel, V, high C, faceted Mn sulphide formation on crystn., thermomech. treatment effect on dendritic struct. *(Russian)* 80−50621
steel, V and V-N , high strength, mech. props. and strain ageing, processing variables effects 77−59819
steel, very low C, delamination study by impact testing 78−3218
steel, W-Mo, high speed, hot deform. and heat treatment effect on props. 77−90372
steel, wear resist., effect of rolling friction strengthening, oil abrasive environment *(Russian)* 79−15799
steel alloy, austenite transformation in hot rolled strips 80−55407
steel austenite, recrystallisation diagrams, heating, plastic deform. rel. to struct. 79−20067
steel M16C, low C, natural discrete microlamellar composite *(Russian)* 78−39810
rolling continued
steel plate, rolling direction determ. with notched bend test specimen *(German)* 77−60003
steel plates, hot rolled, anisotropic texture, exam. of elastic deformation behaviour *(Japanese)* 78−64586
steel rolled, low-cycle torsional and push-pull fatigue anisotropy 78−27589
steel sheet, hot and cold rolled, cold formability, notched tensile test and stretch bend test *(German)* 80−61031
steel ShKh15, fatigue strength and residual stress distrib., machining method effects 78−31528
steel spheroidised type AISI 1090, hot rolled H_2 promotion of plastic instability 78−60725
steel St 52, textured, rolled, REK and lattice strain distrib. *(German)* 79−29095
steel-Al bimetallic wire for overhead lines, manufacturing methods 80−16247
steel-bronze bimetal mech. props., diffusional interlayer effects 79−29169
steels, die, mech. props. high temp. thermomech. treatment 79−20086
steels, induction hardened bearing, rolling contact strength *(Japanese)* 80−93568
steels 45, 17G2AF, 55S2, 60S2, faceted Mn sulphide formation on crystn., dendrites *(Russian)* 80−50621
stress analysis of plastic zone during rolling under plane strain conditioner, Fourier calcs. *(Russian)* 78−80555
stress distrib. during asymmetrical processes, two dimensional strain, conditions *(Russian)* 78−94601
stress distrib. in rolled material 80−48651
strip rolling, kinetostatics *(Russian)* 80−38348
strip rolling, rigid-plastic anal. *(Russian)* 79−29085
surface damage, plastic deformation cause in fatigue, wear, fretting and rolling fatigue 80−40537
surface damage eval. by X-ray diffr. technique *(Japanese)* 80−25892
sylvite powder, compression in smooth faced rolling presses, preferred orientation *(German)* 79−33959
temperature field in hot rolled T-section finite element anal. *(Russian)* 79−29101
tension in tandem rolling, mathematical treatment for computer contol *(Chinese)* 79−43278
texture control, theoretical and practical study 79−87656
texture development, shear band effect 79−91675
theory, applic. of similarity theory *(Russian)* 78−80556
thermoplastic sheet, extruded, thickness adjustment and cooling between calender rolls 79−68597
transverse deformation theory, development to fourth stage *(Russian)* 77−56027
tube with hexagonal bore, crack formation during rolling *(Russian)* 78−80622
tubes in round passes, evaluation of moments *(Russian)* 80−97442
unhealed porosities and crystalline steps in flakes *(Chinese)* 79−74179
unidirectionally reinforced composite, plane strain deform. processing limits 77−55918
vibratory, contact strains *(Russian)* 77−65722
Zircaloy-4, plain strain ductility dependent of struct. and texture 77−8885
Ag, recrystallisation texture, rel. to rolling temp. 80−11664
Ag, rolled, dislocation struct. and recovery during annealing *(Russian)* 79−29084
Ag-Ga (27 at.%), cooling rate depend. of thermal arrest, transform. temp. 79−29053
Al alloy, dil., recrystallisation during hot rolling 79−47732
Al alloy 2219-T851, fatigue crack initiation, effect of intermetallic comp. and microstruct. 79−5054
Al alloy 6061, thermomechanically treated elev. temp. mech. props. 79−8310
Al alloy 7050, fatigue, effect of intermediate thermomech. treatments 79−8352
Al alloy AK5M2 granules, rolling speed effects 78−60604
Al alloy granules, lubricants for rolling 80−60980
Al alloy granules, rolling, temp. and speed effects 79−70015
Al alloys, thermomech. treatments, effects on microstruct. 80−100858
Al, alloys, thermomechanical working effect on mech. props. *(Russian)* 77−21181
Al and Al alloy granules, hot rolling, angle parameters and forward slip 80−25601
Al, atomized powder, metallic contact for hot rolling in air 77−73294
Al, high purity, development of rolling and recrystallisation textures 77−25070
Al, powder, nonuniformity of stress and strain distrib. over width of rolled powder strip 77−12577
Al, recovery and recrystallisation during temperature strain *(Czech)* 77−73287
Al, recrystallisation and recovery during temperature strain *(Czech)* 77−70071
Al, rolled single crystal, annealing texture 79−91678
Al, rolled strip from granules, coeff. of deform. 77−90422
Al sheet, texture evolution, effect of rolling or tensile deform., rel. to strain ratio 79−91672
Al, tensile curve and specific value of anisotropy coefficient *(French)* 77−28867
Al, tensile deformed single crystal, form. of recrystallisation textures 77−12647
Al, wire, appl. of subgrain control 77−86060
Al-Ag (5 wt.%), diffuse effects accompanying rolling, in terms of Guinier-Preston zones *(Russian)* 77−12627
Al-Al_3Ni eutectic composite, substructural matrix hardening *(Russian)* 77−21162
Al-Al_6Fe, fibre reinforced eutectic, deformation behaviour by rolling, TEM and SEM study 79−29129
Al-Cu-Mg, rolled plate fatigue charact. *(Russian)* 80−16437
Al-Cu-Mn (6.3, 0.3 wt.%), Al 2219-T851, fatigue crack initiation and early propag. 77−32684
Al-Fe (0.02 wt.%), Mossbauer spectrum of ^{57}Fe associated with vacancies 77−85636
Al-Mg-Bi -Na, Bi additions to prevent Na embrittlement 77−86153
Al-Mg-Si, deformed, orientation of recrystallisation nuclei 79−91681
Al-Mg-Si, heavily rolled, electron microscope obs. of cube oriented region, rolling texture 79−29093
Al-rare earth alloys, granules, rolling to form foil, exam. 80−20825
Al-Si-Cu, granules, energy conditions of rolling 77−12578

rolling continued
Al-Zn-Mg granules and bands rolled from them, heat treatment 80−100862
AlZnMgCuO.5, static crack growth, stress state effect, elec. pot. meas. 78−7007
B fibre reinforced Al-Zn-Mg, packet rolling, thermodeform. process parameters *(Russian)* 80−55433
Be foil, nucl. target fabrication 80−23225
Be, ultra fine-grained, recrystn. after deform. 79−52239
Co-Ni (32 wt.%), FCC, rolling texture development 79−87657
Cr bronze Sn, recrystn. props., hot rolling, annealing, polygonisation *(Russian)* 80−55419
Cr-Al_2O_3 powder targets for plasma-ion spray deposition of resistance films 80−84897
Cu and Cu alloys, deformed, texture development 79−87653
Cu and Cu-Cr (0.6 wt.%), electron microscope obs. of shear bands *(German)* 77−48454
Cu, deformed by rolling and torsion, stored energy *(German)* 79−29160
Cu, foil recrystallisation during annealing in high voltage electron microscope, grain growth *(Russian)* 79−100159
Cu, heavily rolled, electron microscope obs. of cube oriented region, rolling texture 79−29093
Cu, plane strain deformed, electron microscope obs. of morphology 78−31424
Cu, recrystallisation and recovery during temperature strain *(Czech)* 77−70071
Cu, recrystallisation and recovery during temperature strain *(Czech)* 77−73287
Cu, recrystallisation texture, rel. to rolling temp. 80−11664
Cu, rolled, dislocation struct. and recovery during annealing *(Russian)* 79−29084
Cu, rolled at room temp. and 200°C, variation in props., hardness and X-ray meas. *(Russian)* 77−73285
Cu, rolled sheet, texture transform. during primary recrystallisation as function of annealing time 79−91683
Cu, rolling textures and texture inhomogeneities, exam. of development in single- and poly-crystals 79−11637
Cu single crystals, influence of friction and geometry of deformation, on texture inhomogeneities during rolling 78−72792
Cu, sintered strip, external friction of rolling 77−1845
Cu, solderability, annealing effect *(Japanese)* 80−89244
Cu, strip, formed by high deform., mech. props. charact. *(Russian)* 78−27534
Cu, tensile curve and specific value of anisotropy coefficient *(French)* 77−28867
Cu, texture after rolling of single crystal at room temp. 77−25067
Cu wire rod, rolling temp. effects 77−70084
Cu, wires, effect of heat treatment during drawing 78−56659
Cu-AL(Zn), effect of original grain size on struct. and props., after deformation and annealing 78−44178
Cu-Ag, solid soln., nonhomogeneity of deform. 78−84889
Cu-Al (15 at.%), rolled single crysts., metallographic study of deformation struct., orientational change, shear bonds *(Japanese)* 79−24582
Cu-Al (4.5 at.%), alloy, dislocation recovery anomalies *(Russian)* 77−21163
Cu-Al (6.4 wt.%), rolled low stacking fault energy alloy, struct. and texture 78−52844
Cu-Sn-Al, deform at high temps. *(Polish)* 80−89284
Cu-Zn (30 wt.%), rolled, electron microscope exam. of recrystallisation 78−76663
Cu+Fe+Cd, nucl. target preparation by evaporation and rolling 80−23224
Cu+Fe+Sn, nuclear target proparation by evaparation and rolling 80−23224
Fe based amorphous alloys, Invar effects, mag. and elastic props. *(Japanese)* 79−20100
Fe, cast, wear resist., effect of rolling friction strengthening, oil abrasive environment *(Russian)* 79−15799
Fe, magnetic powder, particle deformation effects on mag. props. 77−63236
Fe powder, density distrib. in rolling deformation region 80−40288
Fe, pure, rolling texture *(German)* 77−86054
Fe/Fe-Cr composite powder, X-ray diffr. exam. of densification during rolling 80−40289
Fe-C (0.64 wt.%), quasicleavage during fatigue crack propag., pearlitic microstruct. effect 79−11702
Fe-Co heterogeneous alloys, fabrication by powder metallurgy, tensile strength 77−63600
Fe-Mn-Ni, fracture toughness, thermomechanical treatment effects 78−60794
Fe-Mo (15.5 and 19.5 at.%), modulated struct., heat treatment effects, TEM obs. 79−100192
Fe-Ni, crystallization texture, rolling, effect of impurities 78−15425
Fe-Ni, reactive metal alloy, effects of thermomechanical processing on strength and toughness 79−70112
Fe-Ni (31%) alloy, deformed by slip, misaligned zones in $\{259\}_A$-martensite crysts. *(Russian)* 77−59850
Fe-Ni-C (19.5, 0.73 wt.%), banded struct. formed by deform., TEM and optical obs. 78−39869
Fe-Ni-C (24, 0.5 wt.%), recovery and recrystallisation of stable austenite after hot rolling *(German)* 77−32591
Fe-Ni-C alloy, austenitic, pre-deform. effects on TRIP *(Japanese)* 77−8890
Fe-Si, internal friction, domain boundary area *(Russian)* 79−24562
Fe-Si (3 wt.%), (110)[001] oriented single crystal, form. of rolling and annealing texture 77−16608
Fe-Si (3 wt.%), chemical comp. and hot rolling effect on brittleness *(Czech)* 80−50712
Fe-Si (3 wt.%), mag. anisotropy induced by rolling in (110) plane *(Russian)* 78−34978
Fe-Si (3 wt.%), texture form., plastic strain effect, hot rolled 79−79002
Fe-Si (6.5%) alloy, struct. and rolling texture 79−79006
Fe-Si-B, high induction, hot rolling treatment 80−89266
Fe-Si-B, melt C content effect on grain growth and induction 80−35351
Fe-Si-MnS-Al, Al effect on hot rolling struct., recrystallization, texture magnetic props. *(Chinese)* 78−11237
$LiNbO_3:Cr^{3+}$ glass, roller quenched, crystn. kinetics 80−44143
MO-B, B effects, rolled, segregation of implanted elements, Auger spectroscopy exam. *(Russian)* 78−35389
MgO single crystal, absorbed fluid effect on rolling contact deform. 78−64719
rolling continued
Mn-Cu structural alloys, physicomechanical props. 77−12652
Mo alloy TZM bonding to Fe by vacuum rolling, corrosion protection appl. 79−29283
Mo, cellular structure, initial stages of formation in rolled single crystals 79−23611
Mo, electron beam melted with C additions, mech. props. *(Japanese)* 77−48449
Mo, foil dislocation struct. of rolling texture *(Russian)* 78−59810
Mo, fracture surface, effect of plastic deform. by rolling at 950°C *(Russian)* 77−59893
Mo, macroscopic heterogeneity of plastic deform., metallographic examination *(Russian)* 79−100210
Mo, plastic deform. by rolling at 293K, dislocation struct. *(Russian)* 77−48481
Mo, plastic deformation during rolling at 293K, crystallography of slip *(Russian)* 77−32588
Mo, proton irradiated, annealed and rolled, void form. 78−22774
Mo, rolled and annealed, zone-refining effect on recryst. grain orient. 77−36532
Mo, rolled single cryst., polygonisation and recrystn., strain depend. *(Russian)* 77−81270
Mo sheet, conc. of interstitial elements on lamination surface 77−86038
Mo, single crystal, subjected to plastic deform., substruct. using X-ray diffr. 79−70083
Mo, single crystals, recrystn. textures, effect of fine precipitates 78−88480
Mo, stress-to-rupture strength at high temps., struct. effect 77−70175
Mo-Zr-C (0.08, 0.02 wt.%), struct. and banding tendency, thermomechanical treatment effects 77−86063
Mo-ZrO_2 dispersion hardened, rolled, grain struct. and props. 77−77492
Nb_3(Al, Ge), effect of thermal treatment on superconducting props. 79−61016
Nb_3Al tape, effect of thermal treatment on superconducting props. 79−61016
Ni alloy, rolled, annealing texture *(Russian)* 77−21159
Ni, alloying effect of magnetostriction and rolling texture *(Russian)* 77−32229
Ni, and Ni alloys, rolling and oxidation, effect on magnetostriction and texture 77−36671
Ni, electrolytic and carbonyl grades, sintered sheet material, stopping power and pore size relationship 78−19693
Ni, FCC, rolling texture development 79−87657
Ni, high-purity, softening of strained single crystals *(Russian)* 80−40499
Ni, rolled, dislocation struct. and recovery during annealing *(Russian)* 79−29084
Ni, texture nonhomogeneity during rolling 79−91670
Ni-containing alloys, hot workability after reheating using S-containing fuel 80−108483
Ni-Cr-Al_2O_3 powder targets for plasma-ion spray deposition of resistance films 80−84897
Ni-Ti (48 at.%), annealed and rolled electron microscope and probe analysis of structure 79−100189
Pb, sample length effect on plasticity 78−44179
Pb, stress-strain state of central part during rolling of tall narrow strips *(Russian)* 79−52262
Pb-Sn, directionally solidified lamellar eutectic, deform. induced microstruct. instability 77−32623
Pb-Sn, superplastic eutectic, roll load and torque necessary for rolling *(French)* 78−95761
Pb-Sn (62 wt.%), superplastic eutectic, exceptional ductility 78−27579
$Pd_{82-x}Ag_xSi_{18}$, amorphous, roller-quenching conditions determ. 77−21051
Π, electrolytic powder, rolling of porous sheets 77−63578
Ta, rolled and annealed, zone-refining effect on recryst. grain orient. 77−36532
Tc, temp. depend. of hardness and hot plastic strain *(Russian)* 79−74202
α-Ti alloy, rolled, elastic stiffness and Bauschinger effect accompanying anisotropic hardening *(Russian)* 80−40435
Ti alloy, VT22, thermomechanical treatment, effects on struct. and props. *(Russian)* 78−19785
Ti alloy sheet, plastic microstrain study during rolling under industrial conditions *(Russian)* 79−52263
Ti alloy VT22, hardening during thermomechanical treatment, precipitate particle internal struct. *(Russian)* 79−91657
Ti alloys, texture strengthening 78−23724
Ti alloys, wear under conditions of rolling stress 79−20211
Ti bonding to Fe by vacuum rolling, corrosion protection appl. 79−29283
Ti lamellar single cryst. formation by heat treatment *(Russian)* 77−59800
Ti, rolling texture, determ. by three-dimens. anal. 77−86049
Ti, sintered sheet material, stopping power and pore size relationship 78−19693
Ti, strip prod. by powder rolling 78−80493
Ti, wear under conditions of rolling stress 79−20211
Ti-Al (6.1 wt.%), hot rolled sheet, ductile fracture nuclei, SEM obs. 78−64654
Ti-Al-V, rolled, elastic stiffness and Bauschinger effect accompanying anisotropic hardening *(Russian)* 80−40435
Ti-Al-V (6, 4 wt.%), annealed and rolled plate, elevated temp. plastic anisotropy 79−61663
Ti-Al-V (6,4 wt.%), heat treated and rolled, texture instability 77−63689
Ti-Al-V-(Sn), surface finishing effect on internal stresses, X-ray study *(German)* 79−34210
β-Ti-Mo-Cr-Al (8, 4.5, 2.5 wt.%), metastable, tensile ductility, α-phase morphology and distrib. effect 77−86098
Ti-Nb-Zr (35, 3 wt.%), martensitic τ phase, X-ray diffr. obs. 80−16300
Ti-Ni-Mo (1.5, 2 wt.%), Mo effect on microstructure 77−36536
V foil, nucl. target fabrication 80−23225
W [310] tip, prep. from rolled sheet 80−97447
W and alloys, wire, increasing plasticity, by electroplastic rolling *(Russian)* 79−29103
W brittle alloy rolling, contact stresses *(Russian)* 80−93576
W, foil, nucl. target fabrication 80−23225
W sintered rods, hot rolling with four roll passes, effect on struct. and mech. props. 79−100195
W wire from rolled rods, mech. props. and struct. 80−25743

rolling continued
Y, plastic deformation props., deformation ageing, plastic flow, dislocation-impurity interactions *(Russian)* 80−66582
Zn, hot rolled, grain boundary fine structures, TEM exam. 78−76680
Zn-Al alloys, comp. effects on intergranular slip during superplastic deform. *(Russian)* 77−32633
Zr, deformation texture during rolling in sequential passes 79−11674
Zr-Mo(-Al) (3, 1 wt.%), β-phase stability 78−39742
$Zr_{50}Co_{50-x}Ni_x$, transform. and deform. studies 79−1864

rolling mills
cold, work roll spalling, prevention measures 77−55981
cold rolling, Sn plate, roll-force model 77−4788
cold rolling mills, roll service life, rehardening by heat treatment 80−16347
cold sheet rolling, thermoviscoelastic problem, numerical soln. 77−39236
force meas., using semiconductor strain gauge based extensometer 78−41296
non-Newtonian or Newtonian liqs., two-roll mill problem 78−42616
performance monitoring, extensometer appl. 77−41590
plane symmetric rolling mill, vector field system soln. *(German)* 78−63333
product speed and length meas. by laser velocimeter *(German)* 79−72614
steel, hot rolled strip and plate shape meas. device 80−35498
steel high-temperature ultrasonic testing *(Italian)* 79−96242
strip production, employing US and electroplastic effect 78−84941

roots of polynomials *see polynomials*

rotamers *see rotational isomerism*

rotating bodies
see also angular velocity measurement; centrifuges; gyroscopes; rotation
76-115-B, tumbling cylindrical Earth satellite, rot. axis location using visual obs. 79−80201
1978 CA and DA, photoelectric obs. of asteroid rotation periods 79−101106
1979 VA, precise posns., and rotation period from UBV photometry 80−17534
A-type stars, quest for differential rot. 77−45409
A-type stars, rot., mixing and variability 77−87397
absorbed dose of cylindrical rotating object in collimated electron beam 77−25558
accretion disc in soft potential well, excess surface density ring form. 80−8532
acoustic field effects on spinning velocities and first order torques 77−23798
acoustic half-space, transient response to rotating point load 79−3844
acoustic sources, radiation characts. in circular motion 77−23803
adiabatic pulsations of uniformly rot. compressible Maclaurin spheroids 77−73941
aircraft structures, ang. vibr. prediction 77−39253
887 Alinda, light curves and rotation period for Amor object 79−44401
angular acceleration and velocity meas. by miniature linear accelerometers 78−12679
anisotropic explosion of rotating, self-gravitating uniform spheroids, astrophysical appls. 79−8822
Ap stars, mag. fields struct., and precession in oblique rotator model 77−2432
Ap stars, orientation of mag. and rot. axes; decentred mag. dipole theory 78−4241
Ap stars, rapidly rotating, discovery of mag. fields 77−33511
Ap stars in open clusters, rot. vels. and mag. braking 77−33500
Ap-type stars, rot. rel. to atmospheric mag. fields *(Russian)* 77−17594
387 Aquitania, slow spinning asteroid with rot. period of nearly one day, photometric evidence 80−17529
β Arietis, rapidly rotating, Am star, spectroscopic obs. and curve of growth anal. 77−22237
artificial satellite, spinning, symmetric, in planar periodic orbit, attitude stability 80−4220
artificial satellite, unstabilized weakly perturbed, orientation determ. 79−8809
artificial satellites, dual-spin, nutational motion damping *(Russian)* 77−60570
asteroid, 1980 AA, rot. period observed photometrically 80−36558
asteroid 129 Antigone, photoelectric photometry and synodic rot. period 77−45343
asteroid 1580 Betulia, Amor object, photographic lightcurve and rot. period 77−91465
asteroid 186 Celuta, slowly spinning asteroid, photometry rel. to rot. period and comp. type 78−61782
asteroid 194 Prokne, photoelectric photometry and rot. period 79−84727
asteroid 1978 CA, rotation period from UBV photometry 78−36486
asteroid 22 Kalliope, light curves, phase function, pole and dimensions 78−53857
asteroid 26 Proserpina, photoelectric photometry and rot. period 79−84727
asteroid 287 Nephthys, photoelectric photometry and rot. period 79−84727
asteroid 32 Pomona, photoelectric photometry, composite light curve and synodic period of rot. 77−9691
asteroid 337 Devosa, unusual object with triple extrema in photoelectric light curve, rot. period 79−40116
asteroid 349 Dembowska, rot. period and phase curve 79−35174
asteroid 354 Eleonora, rot. period and phase curve 79−35174
asteroid 41 Daphne, photoelectric photometric and synodic rot. period 77−45343
asteroid 52 Europa, photometry and rot. period 78−12133
asteroid 554 Peraga, photoelectric photometry and rot. period 79−84727
asteroid 624 Hektor, light curve indicating elongated shape 80−98600
asteroid 7 Iris, photometry rel. to rot. and pole orientation 77−74004
asteroids, light curves and rot. periods from photographic photometry during 1977 and 1978 80−72844
asteroids, photoelectric photometry and rot. periods of seven objects 79−35175
asteroids, photoelectric photometry and rotation period for three large and dark objects 79−44402
asteroids, rotation period near 24 hours, problems 79−21220
asteroids, rotation rates, collisional evolution theory 80−17532
asteroids, rotation rates, pole positions and shapes 80−17531
asteroids, synodic rotation periods from photoelectric lightcurve 78−45259

rotating bodies continued
asteroids 1978 CA and DA, UBV photometry, rotation periods, albedos and diameters 78−36489
astronomical bodies, spin-orbit reson. mathematical aspects 79−12389
asymmetric rigid body problem, arbitrarily torqued, variation of parameters approach 78−93528
asymmetric rotators, singular motions, demonstration 77−13533
asymmetric top, rotational Brownian motion 78−8349
asymmetric top rotational Brownian motion and electric polarisation calc. 80−15949
asymptotically uniform rotation of rigid body about fixed point *(Ukrainian)* 78−65761
asynchronous cardan mounted gyroscope, stability of stationary motion *(Russian)* 77−62147
attitude control in inertial space *(Russian)* 79−9101
axially symmetric body rot. in Ostwald fluid, rate distrib. near wall *(French)* 77−42847
axisymmetric top filled with liquid, regions of stability of uniform rotation *(Russian)* 77−62148
axisymmetric top filled with liquid, sufficient conditions for stability *(Russian)* 77−62149
axisymmetrical body, translational-rotational motion in gravitational field of sphere, averaging methods applic. *(Russian)* 78−21049
B2 0055+26 (NGC 326), radio galaxy with precessing beam model 79−17118
B-type stars, UV obs. of six rapidly rotating objects 77−56938
bacterial cells, tethered, rot. rate and direction detect. apparatus 77−73620
ball, radius of gyration determ., using air track, undergrad. demonstration 78−49606
ballistic axisymmetric space vehicle, spin during atmospheric entry 77−64591
bar, gravitational field, and forced oscill. of resonant antenna 80−52090
bar, radially rotating, of variable cross-section, deflection and lateral vibr. *(Japanese)* 80−94954
bars, extensional vibrations 78−30213
Be stars, rot. vels. rel. to Paschen line emission and IR excess 77−22234
Be-stars, rotation rel. to Hα and Hβ meas. 77−56983
Be-stars, spectra rel. to rotational hypothesis 77−56981
beam, rotating, nonlinear flap-lag-axial eqns. derivation 77−84134
beam with tip mass, vibration 80−58960
776 Berbericia, slow spinning asteroid with rot. period of nearly one day, photometric evidence 80−17529
Bernoulli's principle, spin of balls and coins 80−77592
binary galaxies, angular measures, rotation and morphological type 79−53914
binary stars, ang. momentum loss and mass exchange instability 77−49433
black hole, exponential amplification in gravitational field of ultrarelativistic rotating body 78−93594
black hole, in mag. field, particle creation 77−2452
black hole, interaction with weak mag. field, ang. momentum changes 77−74080
black hole, Kerr metric effect on EM wave plane of polarization 80−94827
black hole, light propag. and sky appearance from accretion disc 80−17605
black hole, spin entropy 79−75246
black hole and accretion disc seen by non rotating observers, light propag. 80−17606
black hole ang. momentum reduction in dense stellar system 77−29874
black hole in Cygnus X-1, obs. test 77−33699
black holes, geometrical optics appls. to Kerr metric, analytical results 77−29637
black holes, Kerr naked singularities, accretion disks 79−30084
black holes, nonsymmetric disc accretion *(Russian)* 80−36661
black holes, rot. rel. to free oscills. reson. freqs. and gravit. waves 80−105271
blade, vibr. analysis using holographic interferometry 78−32807
bladed disc, finite element anal. of vibr. modes 77−39250
blades on rotary lawn mower, noise control method 77−34995
brittle disk, probability theory appl. to rupture strength 80−43662
Brownian motion of rot. body, graphical method 77−13702
3C 33, 98, 184.1 and 218, rotation axes 80−26997
3C 33, rot. axis. of assoc. optical galaxy 78−4355
952 Caia, rot. period and light curve from photoelectric obs. 80−46454
α Canis Majoris, Fourier transform method to determine projected rotational vels. 77−29655
cantilever, stability and instability conditions, Lyapunov function method *(Russian)* 80−36840
cantilever (Timoshenko), elastically restrained, with attached masses, follower force stability 78−63347
celestial body, rotating electrically conducting sphere behaviour in time-independ. homogeneous external mag. field 78−49309
centre of mass rel. to centre of rotation, demonstration 80−77579
centrifugal fans, geometrical parameter influence on sound power level 79−37084
β Cephei stars, rot. rel. to pulsation excitation 77−87425
chair, quantitative ang. momentum expt. 77−75789
charged dust, Newtonian and general relativistic treatments 78−73908
circular cylindrical elastic membranes bifurcation 80−33494
circular disc with time depend. shearing stress on outer edge, anal. 77−68415
circular plate on floating central collar, moving load stability theory 77−46863
circular saws, aerodynamic noise source, point dipole model 79−50503
close binary stars, tidal friction effects on rot. 77−57013
Comet Donati (1858 VI), rot. period of nucleus 78−57506
comets, long-period, rot. direction rel. to nongravit. orbital perturbations 79−70998
comets with fan-shaped comae, rotating nucleus model 79−44414
composite devices, fibre-reinforced, rotating strength, stress distrib., failure criterion rel. to mould process 78−76701
composite rotating plasma, gravitational instability, including Larmor radius, Hall currents, collisions 77−60591
compound pendulums, teaching appls. 78−12474
concave hamburger equilibrium of rotating bodies 80−109422
condensation for mixed dynamic FE analysis of rotational shells 79−32231
conducting mag. top, fast rot. in inhomogeneous alternating mag. field 79−41264

rotating bodies continued
conducting sphere, gyrating in mag. field 79−10241
cone, flow and heat transfer obs., disc theories applicability 77−58673
contact binary stars of low mass, ang. momentum loss and evolutionary fate 77−2453
contactless gyroscope, influence of nonconservative moments on precession *(Russian)* 79−80421
continuous bodies under gravity load, centrifugal force, optimum strength shape 79−98665
convective heat transfer coefficient measurement using heat-flux sensor, error anal. 79−94463
corotational stretch theories, higher order, nonlinear finite element anal. appls. 79−32245
cosmic bodies, ang. momentum-mass relation 80−77528
creep analysis of rotating orthotropic disks 80−33476
Cygnus A, rot. axis of assoc. optical galaxy 78−4355
cylinder, fatigue fracture 78−30238
cylinder, partially full of mag. liquid rolling on mag. field 77−19515
cylinder, permeable, in viscous fluid, friction coeff. 79−46385
cylinder, rotating, non-steady temp. distrib. *(Polish)* 78−13885
cylinders, stagnation flow-based profiles for boundary layers 77−89096
cylindrical annulus, model for Earth mantle-core interface 78−28194
cylindrical gas system, rotating and self gravitating, thermodynamic instability 80−82191
deflection analysis of cylindrical shell, with end plate subjected to centrifugal force, finite element method appl. *(Japanese)* 79−1104
deformable gyroscope in non-Euclidean space, classical non-relativistic theory 77−30004
dense stars, ang. momentum loss by neutrino emission 77−49371
dielectric rotor in electrorheological suspensions 77−15130
differential geometry, appl. to mechanical systems, gyroscopic forces *(Russian)* 79−63016
differential rotation and dynamo presence 77−53582
disc, centrally clamped rotating, nonlinear vibration 79−59938
disc, drag reduction in polymer soln., laminar to turbulent transition 78−75173
disc galaxies, rot. vels. effect on superdense gaseous cores form. 80−90526
disc rotating in non-Newtonian liquid, rheodynamics 77−15067
disc system, mass transfer 77−15041
discs, burst strength and necking 78−79226
discs, irregularly rotating elastoplastic, tangent tension optimisation *(Russian)* 79−50609
discs, stability under edge load 78−38219
discs, with radial cracks, appl. of linear-elastic fracture mechanics 77−54929
driven member rotation uniformity test installation 80−92094
dual spinning spacecraft, extension of dual magnetometer method 78−77459
dust sphere, slowly rotating, maximal slicing condition, initial value equations 80−73246
200 Dynamene, photoelec. light curve, rot. period, low spin rate object 78−32383
dynamic balancing, electrical measuring methods *(German)* 78−86261
dynamic balancing, influence coefficient method, balancing of rigid rotors 80−53724
dynamics of shells of revolution under axisymmetric load involving shear deformation 78−79210
early B-type stars in local spiral arm, var. of axial rot. vels. with galactocentric distance 77−56929
Earth, liquid core convection model 78−28193
Earth satellite, tumbling, cylindrical, rot. axis location using visual obs., theory 79−80200
education, infinitesimal rotations, invalidities in usage 80−57036
education, moments of inertia and Mohr's circle 77−45643
education, relativistic rot. disc circumference 77−87603
education, rigid rotator, account suitable for basic quantum mechanics course 77−33773
education, rotating water sprinkler anal. 79−9064
eigenvalue problem, stationarity principle 77−35027
Einstein vacuum field eqns. solns. using local symm., rotating body neutrics 78−54257
elastic, in supersonic flow, stability of 77−39257
elastic disc, stress intensity factors for two collinear edge cracks 77−65717
elastic disc with transverse load system, stability anal. 77−19562
elastic rotating cylinder, general relativistic formulation 80−82642
elastic stress analysis of an anisotropic compound rotating disc under thermal loading 78−67036
elastic viscoplastic disk, uniformly rotating, axially symmetric stress state *(Russian)* 79−50611
electrically conducting sphere behaviour in time-independ. homogeneous external mag. field, lab. approx. *(German)* 78−37785
electrooptical meter for rotation angle meas. 79−88908
elliptical galaxies, rot. meas. rel. to oblate models 78−16529
elliptical galaxies, scale free axisymmetric models with little ang. momentum 80−82493
elliptical galaxies, three-dimens. shapes 80−51868
elliptical galaxies 78−54052
elliptical galaxy rotation curve determ. 80−46675
59 Elpis, photoelectric lightcurves and rotation period of asteroid 78−69729
182 Elsa, photoelec. light curve and rot. period of asteroid 80−56750
EM field of rotating perfectly conducting sphere, boundary value soln. 77−23597
433 Eros, rotation axis motion *(Chinese)* 77−67058
45 Eugenia, rot. period and photoelec. light curve determ. 80−72846
247 Eukrate, UBV photometry, light curve and rot. period 80−21942
exponential Fourier and densities on SO(3) and optimal estimation and detection for rotational processes 79−49030
fan blade, vibration frequency of a curved beam with tip mass 79−37223
finite rigid-body rotations, kinematics 78−12482
flexible rod, effect of small tip mass on vibr. 79−41608
flexible rods, unstable vibration and buckling 78−79242
flexible rotors, basis for a unified balancing method 80−74732
flexible structures, modal anal. 77−31235
fluid mass, axisymmetric, asymptotic estimates 80−98542
flutter-unstable dynamical system with gyroscopic (circulatory) forces, nonlinear behaviour 78−63276
flywheel, buckling and vibr. of rotating spoke, anal. 78−71288

rotating bodies continued
Fourcade-Figueroa galaxy near NGC 5128, spectrum and vel. gradient 78−73758
free asymmetric rotors, vectorial correl. functions for classical system 78−20960
free gyroscopes, reorientation, kinetic moment control under influence of orthogonal moments *(Russian)* 79−80423
galactic bar, isolating integrals of motion for stellar orbits 80−4404
galaxies, angular momenta and magnetic fields 78−93405
galaxies, corrugation waves in differentially rotating gas layer 77−5571
galaxies, dissipation and merging rel. to rotation 80−4444
galaxies, distrib. of ang. momenta 78−20886
galaxies, dynamical development and struct. of six rotating collapsing models 79−25710
galaxies, early-type, rot. curves meas. 78−54034
galaxies, elliptical, large radio sources preferred orientation rel. to oblate rotator model 79−92880
galaxies, extended optical-rotation curves for spirals 79−97083
galaxies, extent of bars rel. to inner Lindblad Resonance and corotation radius 80−46666
galaxies, flat, with double-peaked rot. curves, spiral struct. generation 80−46679
galaxies, high-luminosity spirals, rotation curves for Sa→Sc types 79−17092
galaxies, instability of gravitating rot. viscous gaseous systems rel. to ring struct. form. 77−17690
galaxies, kinetic theory of differentially rotating interstellar medium *(Russian)* 77−91617
galaxies, late-type, max. rot. vels. from H I obs. 78−86015
galaxies, mass and ang. momentum, statistical relations 80−8689
galaxies, N-body simulation 80−17670
galaxies, nonlinear stability theory for rotating gravitating disc 80−17488
galaxies, rot. curve and stochastic star form. rel. to spiral struct. 78−93395
galaxies, rot. curves rel. to stellar disc central density min. 80−17663
galaxies, rot. rel. to elliptical galaxies form. by tidal interactions 77−78865
galaxies, rotation curves, rel. to nearby galaxy presence *(Russian)* 80−77496
galaxies, spheroidal interstellar medium equilib. forms *(Russian)* 77−91616
galaxies, spiral arm development, sufficiency conditions 80−77483
galaxies, stability anal. of finite uniformly rotating disc 79−88732
galaxies, tidal torque theory, numerical simulations 79−25730
galaxies in turbulent layers with proto-galactic eddies 78−54040
Galaxy, dynamical friction in galactic disc 79−35367
Galaxy, N-S asymmetry and fluctuations of rotation 79−17085
Galaxy, pattern speed of one-dimensional spiral shocks 77−64849
Galaxy, rot. curve accounting for interstellar gas expansion *(Russian)* 79−48938
Galaxy, rot. curve to R=16 kiloparsecs 79−97081
Galaxy, rot. effect on mag. field leading to corona prod. 80−82492
Galaxy, rotation parameters from O-type star radial vels. 79−12523
galaxy, two-component, polytropic model 79−25712
galaxy central bar, spiral density waves response near corotation radius 77−17689
galaxy M31, rotation of nuclear region 78−45395
galaxy NGC 5907, rotation and mass of edge-on object *(French)* 78−77595
148 Gallia, UBV photoelectric lightcurves and rotation period of asteroid 79−101105
gas cloud, accretion onto point gravit. source, rel. to Jupiter formation 78−20630
gas cloud, self-gravitating rotation and Kelvin-Helmholtz instability 79−46287
gas clouds, gravit. collapse, fluid-in-cell method 77−5523
gas-dust clouds, mass transport processes rel. to solar system origin 80−8556
gaseous rotating masses with mag. fields, stability and existence of bifurcation point 78−53924
general relativity of rotating sources, eqns. of motion in linearised gravity 79−93004
geodesics in rotating systems 79−6028
Goryachev-Chaplygin case, qualitative anal. *(Russian)* 77−65671
gyro, free tuned, expt. method for finding tuning speed 78−90701
gyroscope, Earth orbiting, rot. motion according to general relativity 79−84651
gyroscope, stability of Staude's permanent rot. with damping 78−21126
gyroscope, strong field precession from d'Alembert's principle appl. in general relativity 78−40812
gyroscope drift, elastic deform effect on rot. gimbals with base vibr. *(Russian)* 77−14894
gyroscope with contactless suspension under ang. vibr., stability conditions *(Russian)* 79−80420
gyroscope with tuned elastic suspension, dynamical charact. 80−79133
gyroscopic eigenvalue problems in elasticity, nonconservative 80−101708
gyroscopic motions of body with fixed point, rot., precession *(Italian)* 77−13601
gyroscopic system, linear, damped, modal anal., appl. to satellite 78−63275
gyroscopic systems, appl. of theory of singularly perturbed eqns. 77−57183
gyrostat, almost axial, almost symmetric, torque free spin near osculation condition 79−49029
gyrostat, nonregular precessions in a Newtonian central field *(Italian)* 78−81825
gyrostat, reorientation 80−8780
gyrostat inertial motion, ang. velocity hodographs *(Russian)* 78−86137
gyrostat inertial motions, hodograph eqns., dividing motion *(Russian)* 78−86138
gyrostat motion, analytic props. of soln. *(Russian)* 78−86132
gyrostat precessions in a pot. force field *(Russian)* 79−63017
gyrostat with elastic shaft: a contribution to the theory of centrifuges *(German)* 79−67149
gyrostatic bodies, control of motion by means of gyroscopes *(Italian)* 78−12549
gyrostatic satellite in Kepler orbit, rot. motions 80−86080
gyrostats, kinetic energy bounds 80−46793
HD 116458, binary Ap star, period, 5200 Å depression index and light vars. 77−64767

rotating bodies continued
HD 128220, peculiar spectroscopic binary, photometric separation rel. to cool star rot. *(French)* 77−57014
heat pipe, centrifugal, cylindrical, heat transfer, heat flux density and vap. press. effects 78−79188
heavy chain rotating, duality principle for non-convex optimisation, calculus of variations 79−71237
heavy gyrostat, steady motion stability for free and restrained dynamical systems 80−46791
heavy particle on rotating surface, stability of equilibrium, including damping 77−13604
helical motion of rigid body, meas. by double exposure speckle method 78−16775
high-speed rotating anode disc, spot motion and erosion calc. 78−71498
high-speed rotation instrum. for production of centrifugal fields of 10^8 times gravity 79−75524
homogeneous ellipsoidal figures evolution 77−33333
hot-wire sensor, effect of centrifugal and Coriolis forces on rotating probe 78−94862
HR 3089, He-rich star, rot. vel. and comp. 77−9751
HR 5153, Ap star, rot. vel. and light vars. period 77−17593
human body in weightlessness, biomechanical model 78−96106
IC 5152, low-luminosity barred galaxy, struct., rot. curve and redshift 80−56950
ice, floating sheet, viscoelastic response under prolonged loading 78−51093
indenters, rigid, rough, rotating, plane strain collapse theory 80−79172
inertially spinning rotor, for dynamic meas. of matter creation 78−28868
instantaneous axis of rotation, theory and demonstration apparatus 79−84903
intermediate-axis theorem, undergraduate demonstration expt. 78−61990
interplanetary dust, effect of spin and solar radiation on motion *(Japanese)* 78−20732
interstellar clouds, axially symmetric collapse and protostellar form. 80−77380
interstellar clouds, multiple star system formation 78−93366
interstellar clouds, rotating, nonaxisymmetric collapse theory rel. to protostar form. 80−85927
interstellar clouds, stability against fragmentation from three-dimensional hydrodynamical calcs. 80−62236
interstellar clouds, structure and evolution under external pressure 78−61898
interstellar gas, differential rot. ahd helical turbulence rel. to galactic dynamo 78−81685
interstellar grains, disorientation in suprathermal rotation 79−92824
interstellar grains, spin-related magnetism 79−5883
interstellar grains, suprathermal rotation 79−92823
interstellar gravitating gas cloud, wave-wave interactions 80−105154
ionized medium, technique for rot. freq. meas. 80−41730
isothermal disc, heat transfer meas. using Mach Zehnder interferometer 80−38223
Jovian planets, polar moment of inertia determ. 80−94694
Jupiter, effect of rot. on inflated magnetosphere, similarity model 78−57492
Jupiter, linear polarisation obs. at 6, 11 and 21 cm, vars. with rot. 77−87313
Jupiter, magnetosphere, planetary spin period accel. of particles 77−9701
Jupiter, natural vibration spectrum, rot. effects, calc. 80−8583
Jupiter, radio emission maps at 2.7 GHz at different rotational phases 80−82272
Jupiter, rot. as magnetosphere energy source, comparison with Earth 79−58201
Jupiter, rot. changes rel. to particle accel. in magnetosphere 79−12428
22 Kalliope, pole coordinates from photoelectric photometry 80−31230
Kelvin, background, teaching motivation, demonstrations 80−42025
keplerian motion and gyration 78−77472
Kerr black hole, electrodynamics and Carter tetrad 77−49426
Kerr black hole, EM extraction of energy and ang. momentum 77−53621
Kerr black hole with tilted accretion disc, mag. alignment 77−60789
Kerr black holes, stable circular orbits of test particles moving in equatorial plane 80−85970
Kerr naked singularity, classical instability 78−57834
Kerr naked singularity evolution surrounded by accreting disc of matter 79−75245
kinetic energy of rotating wheel, expt. using rocket accel., for teachers 79−17168
Kovalevskaya gyroscope, new class of motions 80−68037
kovalevski hodographs of gyroscope angular velocity in the Delone case *(Russian)* 79−63013
L134, interstellar dust cloud, formaldehyde absorpt. vels. rel. to rot. 77−5558
Lagrange gyroscope, stationary out-of-balance, stabilisation *(Russian)* 79−63019
Lagrange gyroscope motion, geometrical investigation, hodograph curves *(Russian)* 79−63015
Lagrange gyroscopes, system of n, stability of uniform rotation *(Russian)* 78−86136
Lagrange gyroscopes, system of two, stability of regular precessions *(Russian)* 77−62145
Lagrangian gyroscope, hodographs of ang. velocity *(Russian)* 78−86133
Lagrangian gyroscopes, moving ang. velocity hodograph *(Russian)* 78−86134
Lake Kinneret (Sea of Galilee), mean flow in rotating basin 80−81937
393 Lampetia, long rotation period from photoelectric lightcurve 79−40120
68 Leto, rot. period and photoelec. lightcurves determ. for asteroid 80−98594
lubrication, elastohydrodynamic, between two rot. cylinders, with non-Newtonian fluids 78−83435
α Lyrae, Fourier transform method to determine projected rotational vels. 77−29655
M82, Ne II 12.8 micron emission obs. and rot. curve 79−17082
M87, rot. and dynamical evidence for central mass concentration 78−49529
M 31, spiral struct. morphology rel. to rot. 78−65690
machinery, measurement of torsional vibr. 79−23287
machinery subharmonic vibration diagnosis 79−3971
magnet, rot. near Cu disc, field lines, lecture room demonstration 78−54131
rotating bodies continued
magnetic field effects, exponential damping 78−69645
magnetic field meas., effects and properties 78−17837
magnetic oblique rotator, EM field prod., exact vacuum soln. 80−58442
magnetic oblique rotator production of EM field, lowest order solns. 79−21176
magnetic stars, equatorially symmetric rotator model 78−8020
magnetic stars, kinematic mechanism for oblique rotator model 77−45407
magnetic stars, models with toroidal fields and circulation 77−45406
magnetic stars, steady-state models 77−45405
magnetic variable Ap stars, light vars., rot. and evolution 77−87426
magneto-gravitational effect *(Russian)* 77−9935
main-sequence stars, appl. of strained coordinate methods to struct. 77−56910
Mars, dynamics obs. from Viking lander tracking data anal. 80−77314
Mars, longit. var. of thermal inertia and 2.8 cm brightness temp. 80−105191
Mars, rot. axis orientation and rot. period from Viking landers tracking data 78−20685
Mars, rot. model, including precession and nutation 80−21938
Mars, rot. period determ. from transits of albedo stations across central meridian (1659 to 1971) 80−98588
Mars, rotation theory in Euler angles 80−51684
Mars, spin axis orientation and Viking 1 lander posn. from radio tracking data 77−13269
mechanical oscillator, effect of spin on non-linear reson. motions 77−75839
mechanical oscillator, relativistic spin quadrupole gravitational effect *(Russian)* 80−68103
mechanical resonance, $J_0(x)$ obs. on reson. rot. vertical chain 80−42006
18 Melpomene, rot. period from photoelec. obs. 80−82258
Mercury, reson. rot. rel. to internal convection 78−12127
Mercury, rotation and solar tidal torques 79−66940
Mercury, slow rot. rel. to escape of natural satellite 78−16323
Mercury, tidal despinning rel. to global tectonics 78−85874
meteoroids, meteor train initial radius, rotation effect 79−16893
9 Metis, pole coordinates from photoelectric photometry 80−31230
9 Metis, UBV photometry, light curve and rot. period 80−21942
metric torsion field effect on spinning particle, equ. of motion 80−62543
microconvective heat, mass transfer processes 79−86435
moment of inertia in quantum mechanics, Harris cranking model, for teachers 79−35475
Moon, free librations determined from laser range meas. 77−37521
Moon, rotation around centre of mass, historical development of understanding 80−57064
Moon, tidal effect in rot. theory 77−13259
motion, in linearised gravity 79−85020
motion equations for rot. finite bodies in extended parametrised post-Newtonian formalism 77−64628
moving atmosphere simulation by rotating phase plate 80−79021
moving rigid body, axoid nondevelopable character 80−62460
nebula Barnard 213 NW, rotation and vel. structure rel. to parent cloud 78−41007
128 Nemesis, long rotation period from photoelectric lightcurve 79−40120
Neptune, rotation period from IR photometric light curves 78−40869
Neptune rotation period, correction, photometric and spectroscopic results comparison 80−82301
neutron stars in X-ray binaries, rotational spin-up 77−71154
NGC 1052, elliptical galaxy, H I system rot. 78−69873
NGC 1084, NGC 7331, spiral galaxies, surface photometry and rot. curves rel. to mass distribs. 79−40265
NGC 128, S0 galaxy, rot. curve 77−33631
NGC 1313, barred spiral galaxy interferometric study 77−49474
NGC 1313 barred spiral galaxy, asymmetric rot. *(French)* 79−97082
NGC 157, spiral galaxy, surface photometry and rot. curve rel. to mass distrib. 79−40264
NGC 2742, spiral galaxy, rot. and mass. *(French)* 78−89255
NGC 2997, late-type galaxy, rot. and mass 79−21409
NGC 3115, S0 galaxy, rotation and mass of inner 5 kiloparsecs 80−105326
NGC 3256, peculiar galaxy, kinematics 78−96537
NGC 3379, elliptical galaxy, spectroscopic obs. rel. to rot. and vel. dispersion 78−49529
NGC 4378, anaemic Sa galaxy, extended rot. curve 79−8990
NGC 4594 (Sombrero Galaxy), rot. vels. and mass 78−36685
NGC 4736, spiral galaxy, rot. model from H I model 77−57090
NGC 4762, S0 galaxy, rot. curve and dynamics 78−28774
NGC 488, Sb galaxy, rotation curve from emission line spectra 80−62266
NGC 5195, M51 companion galaxy, rot. and relative mass 77−22306
NGC 5236 (M83), Sc galaxy, CO vels. rel. to rot. curve 78−65689
NGC 5383, barred spiral galaxy, vel. field 78−24549
NGC 5728, barred spiral, vels. and mass distrib. of galaxy 80−94863
NGC 612, rotation of lenticular radio galaxy 80−51874
NGC 935-IC 1801, close pair of spiral galaxies, rot. curves and mass distribs. 77−45556
nonholonomic system, motion eqns. derivation *(Russian)* 78−20956
nonholonomic systems under external influences, sledge on incline, gyroscope in cup *(Russian)* 80−52011
nonlinear vector products calc. methods 77−71201
nonspherical body, rot. Brownian motion, ang. vel. 77−33860
nose surface, press. distrib. of bodies of revolution, α=0 to 10° 77−27549
44 Nysa, pole coordinates from photoelectric photometry 80−31230
O-type stars, rotational vels., V sin i and macroturbulence 77−45411
open cylinder, internal flow, wave-transition spectra and vacillation 78−14020
orientation stability of double spin satellite 77−53398
Orion OB 1 association stars, rot. vel. effects on uvbyβ photometry 77−82288
orthogonal base functions and consistent diagonal mass matrices for two-dimensional elements 79−90125
orthotropic rotating discs, flexure, stresses and deflection 80−5927
ovalling oscillations of cylindrical shells in cross flow, comments 80−59045
overhung shaft-disc system with disc effect, critical speed determ. 79−46172
parameter and combination resonances of rotor systems having asymmetric elements *(German)* 79−50578

rotating bodies continued
118 Peitho, rot. period and light curve from photoelectric obs. 80−46454
pendulums, example of arbitrarily slow irreversibility 78−70083
Periodic Comet d'Arrest (1976 XI), nucleus light curve and rotation 78−53877
Periodic Comet Encke, changes in orbital period due to rotation of nucleus 80−62078
Periodic Comet Encke, spin axis precession, nongravitational motion and sublimation 80−46483
Periodic Comet Halley, rotation period from halo diameter meas. 80−51694
Periodic Comet Schwassmann-Wachmann 1, rotation and outbursts 80−67655
plane periodic motion of two rigid bodies *(Russian)* 78−73840
planet form., behaviour of system of particles at high press. 77−87261
planetary satellites rotation, secular effects of tidal friction 79−8860
planets, atm. circulation estimated characts. 77−17393
planets, Coriolis phenomenon and rotational alignment 80−90636
planets, differential rotation, gravitational effects 79−8862
planets, differentially rotating, gravit. field and figure 78−7893
planets, global tectonics following tidal despinning 77−60698
planets, gravitational quadrupoles *(Russian)* 79−58285
planets, kinetic energy of atm. circulation 77−13261
planets, rotation resulting from accumulation process, numerical expts. *(Russian)* 80−8557
planets, spin motion and axial inclination *(Italian)* 79−21210
planets, tidal hypothesis for origin of rot. 79−8859
planets and Sun, shape due to rot. 77−13541
planets capture into resonance rotation, tidal friction 77−78620
planets rotation and figure of giants 79−96934
plastic rotating discs, anisotropic, finite deform. 79−41586
plate, spinning nutating, resonant excitation 79−64504
platforms, rotational and turning, kinematics 79−30220
polytropes, uniformly rotating, equilib. struct. investig. using iterative method 78−32441
308 Polyxo, photoelectric lightcurves and rotation period 80−46455
precession rel. to vertical of heavy rigid body with fixed point *(Russian)* 77−62142
pressure gauge, gas-operated, effect of piston-cylinder relative rot. on meas. 77−41631
790 Pretoria, C-type asteroid, light vars. obs. and rot. period 80−21941
projectile, axisymmetrically rotating, stability of nonstationary motions *(Russian)* 78−24659
projectile in impact expts., axial rot. elimination via rectangular-bore gas gun 77−41588
protoplanetary cloud, ang. momentum transfer by meridional currents 77−53436
protostellar cloud, rotating, collapse and stability, turbulent viscosity effect 80−109510
protostellar cloud ang. momentum problem, mag. breaking 80−82342
protostellar cloud rotation, mag. braking of aligned rotator during star form., exact time-depend. soln. 80−90493
protostellar clouds, ring form. during dynamic collapse 80−56820
protostellar gas clouds, fragmentation 80−51827
pseudowork-energy principle nonrigid or rot. bodies, for teaching 78−49602
pulsar, dynamics of differential rotating sphere 77−37609
pulsar, hollow-cone beam models rel. to pulse wave forms 77−2449
pulsar relativistic beaming process rel. to pulses 77−29870
pulsar-type superfluid system, rotating, dynamics of Onsager-Feynman vortices *(Russian)* 77−82270
pulsars, angular momentum and energy loss, physical processes 77−91557
pulsars, hollow-cone model of radiation geometry 77−9761
pulsars, mag. dipole moments secular var. 77−9764
pulsars, space vel. vector orientation rel. to spin axis 77−53619
pulsars in massive X-ray binary systems, rot. history 77−49412
pulsars magnetic alignment, classification system 77−45476
pulse phenomena produced by a flat mass on one of its supports *(Italian)* 80−4514
quantum mech. nonaxial top, coherent states *(Russian)* 77−45739
rectangular prismatic bodies, free motion, translatory and auto-rotating modes 80−43605
red giants, rotational enhancement of mass loss 77−56928
reference manometer free-piston rotation with changes in tilt angle 77−57316
relativistic rotating body, initial value eqns. 78−95
relativistic rotating systems, Einstein equations 80−68101
relativistic spherical mass, effects of rot. on gravit. focusing of light 80−105155
ridig body rotation in 3D space from body fixed linear acceleration meas. 80−68040
rigid, computation of functionals over sample paths 77−74212
rigid body, heavy with fixed point, necessary conds. for existence of precessions rel. to vertical *(Russian)* 78−86139
rigid body, motion in Newtonian force field, phase coords. determ. *(Russian)* 78−89049
rigid body, regular motions stability in Newtonian gravit. field 77−26165
rigid body, translational-rotational motion of gravit. field of sphere 80−62000
rigid body, vector anal. of finite rotations, literature review 78−36819
rigid body containing liquid, uniform rotation, stationary solns. *(Russian)* 78−86140
rigid body in central Newtonian field, stability of rotation *(Russian)* 77−33328
rigid body motion about fixed pt., order reduction of differential eqns. *(Russian)* 77−49590
rigid body motion about fixed pt., perturbed Euler-Poinsot problem, splitting of separatrices *(Russian)* 77−49591
rigid body near Earth's surface, stability of flight *(Russian)* 78−89048
rigid body orientation, rot. gradient operator and torque calcs. 77−67266
rigid body with fixed point, angular velocity hodographs *(Russian)* 77−62144
rigid body with fixed point, effect of viscous damping on spin stability 77−78974
rigid body with fixed point, motion, variants of soln. *(Russian)* 77−62143
rigid body with fixed point, Riemannian struct. of continuum of configs. *(Italian)* 78−12548
rotating bodies continued
rigid elastic body system, turning round fixed point, linear viscoelasticity theory *(French)* 80−69646
rigid rotor in elastic ball bearings, free oscillations *(Russian)* 79−18773
rigid shaft in short journal bearings, aperiodic behaviour 78−46905
rigid shaft rotating in antifriction bearings, motion stability 80−68038
ring, oscillatory behaviour, influence of Coriolis forces on power transmission belts *(German)* 78−87255
rod buckling, critical rotation speed, extended Galerkin method 77−35064
rolling contact with dry friction, Duvorol computer code 79−90194
rolling disc motion, new generalised Hamilton-Jacobi method 77−5663
rolling missile, apsidal limits 79−3909
rotational-oscillatory system with many degrees of freedom, resonant motions *(Russian)* 77−33859
rotor, flexible, on flexible bearing, viscous-damping, vibr. and balancing 78−63352
rotor, partially filled with viscous incompressible fluid, stability anal. 80−64359
rotor, passing through crit. speed, with gyroscopic effect, asymptotic calc. 78−63354
rotor blades, dynamic characts. 77−39251
rotor blades in low-pressure axial flow fan, chord length and camber effects on noise 77−42661
rotor blades in low-pressure axial flow fans, turbulent noise modelling 77−42660
rotor dyanamics analysis using tapered beam finite element 80−38316
rotors, elastic wave stability 78−87297
sample holder with voltage readout, for low-temp. CW US expts. 78−13873
satellite, spinning notion, optimal nutation damping by flywheel 77−53396
satellite in elliptic orbit, stability of cylindrical precession *(Russian)* 77−42729
satellites, magnetic damping of rotation, shielding effects 78−69646
satellites, spin-stabilised, effect of orbital eccentricity and nodal regression on gyroscopic motion 78−45206
Saturn, natural vibration spectrum, rot. effects, calc. 80−8583
Sc galaxies, rot. props. from major axis visible spectra obs. 80−90517
separatrix motions of a Lagrange gyroscope *(Russian)* 79−63014
shaft, whirling motion, stability analysis 78−13894
shaft, with nonlinear spring characteristics, vibrs. 77−75836
shaft, with single disc nonlinear inner damping forces, stability *(German)* 78−1562
shafts, noncircular cross section, effect of external forces and internal friction on rotary motion *(French)* 78−63274
shafts, torsional vibration meas., laser Doppler system 79−50685
shell, rotating, conducting, in mag. field, forces and moments 78−37786
shell, thin cylindrical, dynamic behaviour under high-speed rotation 77−75834
shell subjected to centrifugal force, stress anal. *(German)* 80−23900
shells of revolution, computer program for linear and geometrically nonlinear static analysis *(Japanese)* 80−64500
140 Siwa, C-type asteroid, light vars. obs. 80−21941
slowly rotating nonhomogeneous bodies, quasistationary gravit. collapse in general relativity 77−49289
SMC X-1, X-ray pulsar, spin-up rate meas. 77−29956
solid body dynamics with one fixed point, inverse problems *(Russian)* 80−52010
solid body orientation control by an excess number of power gyroscopes *(Russian)* 79−80419
solid body rotation in Newtonian force field *(Russian)* 79−35546
solid body steady rotation about nonprinciple axes, stability conditions *(Russian)* 79−63018
solid elastic bodies, ultimate motion of a system gravitating to a fixed point *(Russian)* 80−90664
solids, uniqueness and stability under config. depend. loading 78−30194
spacecraft, eigenvalue problems solution, with real symmetric matrix of same dimension 80−12895
spacecraft, flexible, in gravitational field, stability 77−25906
spacecraft, orientation control by solar radiation pressure 77−53397
spacecraft, rotation control by mass ejection 77−41278
spacecraft, spin-stabilised, optimal aerodynamic attitude control 80−77250
spacecraft detumbling, using movable telescoping appendages 77−54868
sphere, internal gravit. field in weak-field approx., appl. to astrophysical objects *(Russian)* 79−25939
spin 1/2 plane waves interacting with rot. body, gravitational scatt. helicity depend. *(German)* 80−52088
spin axisymmetric high speed rotor, approx. anal. soln., coord. system linked to precession and nutation 77−17802
spindle unit on test stand, wheel failure 80−19277
spinning cable with tip mass, free vibr. anal. 78−94609
spinning masses, gravitational fields, exact solns. with arbitrary integer deltas 77−67351
spinning particle total reflection shifts, relativistic anal. 77−22409
spinning shell, Magnus instability 79−18693
spinning top, on surface with friction, behaviour 79−58467
spinning tops, mechanics *(German)* 78−87253
spiral galaxies, max. rot. vel. rel. to morphological type in stochastic star form. model 80−12818
spiral galaxy NGC 1961, rotation curve 79−62898
spiral vibration of rotating shaft rubbing against interference element *(German)* 78−87252
stabilisation by passive dampers, asymptotic methods use *(Russian)* 78−20957
stability according to Cassini laws and Poincare periodic solns. *(Russian)* 79−40066
star, neutrino ang. momentum losses during collapse 77−56916
star, rotating 2 $M_\odot$ Fe-O object, gravitational collapse *(Russian)* 78−4199
star, thermal props. of self-gravit. plane-symm. gas 77−13323
stars, adiabatic stability of rotating gaseous masses 77−91516
stars, differential rot. effects on struct. of novae shells and planetary nebulae 77−64746
stars, effects of rot. and mag. fields on models calc. *(German)* 77−17592
stars, equilib. problem in rotating convection zone 77−56917
stars, equilib. struct. and oscill. of uniformly rotating mag. polytrope 77−87366

rotating bodies continued
stars, equilib. struct. of uniformly rot. mag. polytrope with large toroidal field 77−87367
stars, evidence for discrete rot. vel. states 77−22307
stars, exact solns. for Emden-Chandrasekhar axisymmetric solid-body rotating polytropes with (n=0, 1 and 5) 80−109419
stars, F- and G-type, mag. accel. of winds and ang. momentum loss 77−13334
stars, in close binary systems, rot. rel. to precession and nutation 77−13392
stars, internal struct. of rot. relativistic polytropes *(Russian)* 77−91513
stars, massive, in slow rot., vibr. instability and oscill. props. 77−5536
stars, meridional flow calc. method for slowly rotating bodies 77−56880
stars, models with circulation-free rot. laws 77−67088
stars, rot. distortion of polytropes by analytic approx. 77−74039
stars, rot. rel. to evolution, exploratory calcs. 77−13316
stars, rotational darkening or brightening 77−60750
stars, rotational vels. determ. via appl. of Bessel transform 77−49369
stars, uniformly rot. polytropes, boundary eqn. 77−74040
stars, upper main sequence, rotational effects in spectra 77−71104
stars in close binaries, rotational angular momenta 77−57057
stars spherical rotating system, free collapse 78−93325
steel shells, spinning, aerodynamic ablation, side force 79−37347
stellar models, rapidly rot. spheroids of n=1 polytropic index 77−17539
stellar models, secular instability of Maclaurin spheroids due to gravit. radiation and viscosity 77−17538
stellar rotation, thermomagnetic torque 77−53574
stellar systems, two-dimensional, nonlinear nonradial oscills. stability 78−53992
stochastic mechanics of Bopp-Haag spin model, higher spin states 77−30039
strain gauge for recording deformation of rotating parts, exam. of design 78−76820
stratified ellipsoids of revolution, inertial frame dragging effects 79−2573
strings, elastic, heavy, whirling, nonlinear eigenvalue problems, bifurcating branches of solns. 80−73174
563 Suleika, rot. period and photoelec. lightcurves determ. for asteroid 80−98594
Sun, ang. momentum outward transport by gas convection rel. to equatorial accel. 77−53531
Sun, angular momentum flow 77−45396
Sun, angular vel. distrib. 77−56904
Sun, chromospheric rotation during 1972-73, years of declining activity 78−4186
Sun, convection in deep rotating spherical shell 77−53562
Sun, convection zone and angular vel., Boussinesq model 77−56898
Sun, coronal EUV holes, rot. charact. from Fe XV 284 Å spectroheliograms 77−53547
Sun, coronal rotation investigation by spectroscopic method 77−53551
Sun, differential rot. and giant cell circulation of Ca II network 77−53546
Sun, differential rot. and global-scale vel. fields 77−53545
Sun, differential rot. differences 77−53548
Sun, differential rot. from mm wave obs. 77−2378
Sun, differential rot. maintenance rel. to surface Reynolds stresses 77−2379
Sun, differential rotation for unrestricted rot. rates, 2-dimens. stochastic motions 77−56899
Sun, equatorial rot. rel. to climatic changes 78−7960
Sun, evidence for distortion rotating with period of 12.2 days 77−17502
Sun, fact var. in sunspot rotation during 19th and 20th cycles 77−53552
Sun, large scale circulation in convection zone rel. to differential rot. 77−22164
Sun, large scale magnetic dipole and multipole progressive waves in photosphere 77−17505
Sun, limb effect of redshift rel. to solar activity 77−53553
Sun, oblateness, rot. period and faculae 77−9735
Sun, rot. mag. core model, rel. to neutrino flux 77−2381
Sun, rot. period rel. to pulsation and sunspot cycle periods 77−53519
Sun, rotation from obs. of sunspot umbrae 77−45374
Sun, rotation theories, review 77−53563
Sun, surface rot. during Maunder minimum 77−2377
Sun, two-dimensional stochastic motions rel. to differential rot. problem 77−53518
superlinear Hammerstein operators and nonoccurrence of secondary bifurcation 78−16641
surface temperature contactless meas. instrument 78−57946
87 Sylvia, UBV photometry, light curve and rot. period 80−21942
symmetric gyroscope motion, differential eqns. stabilisation procedure including perturbing torques 80−4244
synchronization mode of rotating solid celestial body 78−7869
ζ Tauri, high-resolution spectra of λ1920 and λ1720 features rel. to rapid rot. 78−4236
BU Tauri (Pleione), polarisation rel. to rot. axis orientation 77−45500
temperature meas., minimisation of contact drop error 78−73991
thick flexible ring rotating at high speed, vibration anal. 79−37227
88 Thisbe, photoelectric light curves and rotation 80−17528
three rigid bodies problem, translational motion solns. with uniform rot. *(Russian)* 80−61999
tippe top, spinning motion 77−33735
top, properties and complex motion, expt. study 78−55557
translatory-rotary motion of gravitating spheroids *(Russian)* 78−73841
translatory-rotary motion of three rigid bodies, Euler solns. *(Russian)* 78−53802
triaxial planetary satellites, Cassini's laws 79−8812
turbine disc transverse vibration initiation 79−68633
turntable accessories, for rotational motion phenomena demonstrations 80−77571
two spinning bars with Coulomb friction bearing, differential equation of motion 79−64601
Uranus, rot. period meas. 78−7920
Uranus, rotation period from geometric oblateness and J_2 harmonic of gravity field 80−67649
Uranus, rotation periods rel. to methane band strength var. 78−49376
Uranus, rotation rate from ellipticity derived from SAO 158687 occultation 80−67648
Uranus, rotation velocity determ. 78−36508
AN Ursae Majoris, nova-like variable, white dwarf rot. rel. to circular polarisation vars. 78−8018
W Ursae Majoris stars, rot.-convection interaction rel. to light curves 77−57008
vacuum black holes, gravit. radiation scatt. 78−65648
variational principle for spinning liquid-filled solid bodies 80−43609
Venus, Earth-synchronous rot. theory 79−25531
Venus, free wobble damping time 80−17516
Venus, nonresonance rotation 79−66944
Venus, resonance rotation 80−109387
Venus, rot. period and atmospheric circulation problems 79−70977
Venus, rotation and atmospheric tides 78−85877
Venus, rotation pole 79−66943
Venus, slow rot. rel. to escape of natural satellite 78−16323
Venus, spin and atmospheric tides 77−87301
Venus, spin evolution 80−46423
Venus, spin vector determ. by radar obs. 80−105185
Venus, tidal theory and torque balance 80−46422
Venus, upper atm., rot., photographs 1927-1975 in UV *(French)* 79−2504
vestibular research, rotating room acceleration and damping 79−84048
viscous liquid filled cavity in solid, free rotational motion 80−38420
volcanic ash particles, influence of shape and rot. on atmospheric settling vel. 79−84364
vortex noise from rotating blades 78−38143
VV 8, galaxy, rot., mass and surface brightness obs. *(Russian)* 79−48937
white dwarf stars, rot. and gravit. redshift 77−29816
white dwarfs, rigidly rotating, critical ang. vel. 77−5525
wind turbines, rotational dynamics, eval. of turbine response to wind speed changes 80−55785
He, cryostat, rotating, centrifugal field rel. to residual press. in vac. cavity 80−42232

rotation
see also angular velocity measurement; Earth rotation; molecular rotation; optical rotation; rotating bodies; rotational flow; stellar rotation
about arbitrary axis, matrix formalism 77−60922
angular momentum, operator props. through three-dimens. rot., teaching 80−105469
asteroids, initial rotation periods and relative formation times *(Chinese)* 80−105182
asteroids shape and spin axis orientation determination, photometric method *(Russian)* 80−8581
astrometry, rot. of fundamental coordinate system 79−62727
astronomical systems, ang. momenta mass depend. rel. to self-similarity 80−36490
bicycle dynamics, nongyroscopic aspects, lab. demonstration, for teaching 78−36769
brachistochrones, tautochrones, evolutes, and tesselations, for teaching 79−25798
Brillouin ring laser, fibre-optic, use for inertial sensing 80−87411
centrifugal barrier, radial Schrodinger eqn., use of phase integral formulae 78−54222
chemically induced dynamic spin polarisation, orientation depend. 80−63656
Coma I galaxy cloud, redshifts rel. to rot. 77−45575
Dedekind ellipsoids, deformed figures in post-Newtonian approximation to general relativity 78−32734
double group theory, half-shell and two-level system, optical polarisation 78−49594
double group theory, half-shell and two-level systems, rot. and half integral spin states 78−45447
education, Coriolis machine, inertial motion viewed from rot. reference frame, coordinate transformation 78−69934
education, eigenvector of general rot., geometrical construction 80−57025
education, holographic double exposure interferometry for small rot. meas. 78−36758
education, rotation matrix formalism for rots. 77−82349
elbow three-dimensional rotation 78−69129
fibre optic rotation sensor, signal detection and processing, inertial reference device 79−54111
finite rotations, associated displacement vectors 77−49589
fluid, binary mixture, in centrifugal field, crit. dynamics 80−44310
galactic halo, rot. from subdwarf kinematics 80−22003
galaxies, bright, elliptical, effect of form. by merging on rot. 80−56922
galaxies, elliptical, rot. vels. and vel. dispersions rel. to equilib. models 80−94865
galaxies, role of vortex generation in protogalactic medium 80−62360
galaxies, spiral, rot. direction determ. by means of edge-on systems *(Russian)* 80−36722
galaxies rotation, contrib. from galaxy merging 80−4439
Galaxy, determ. from proper motions of AGK3 stars 77−45402
Galaxy, rot. consts. and solar motion, from stellar proper motions 78−32440
Galaxy, rot. curve to R=16 kiloparsecs 79−97081
Galaxy, rot. model rel. to Cepheids kinematics between l∼294° and 331° 79−48910
Galaxy, rot. models rel. to low-latit. pulsars H I absorpt. meas. and distances 80−101606
Galaxy, rot. rel. to H I clouds kinematics in solar vicinity 79−8971
galaxy clusters, rotation as opposed to transverse vel. 80−94876
Galaxy H I subsystem, rot. curve *(Russian)* 80−36724
Galaxy rotational spiral struct. parameters, derivation from stellar kinematics 80−17665
Galilean satellites volcanism and rotation, influence of Jupiter mag. field 80−31247
gases, rot.-vibr. Raman spectrosc., high resolution, review 80−22442
granular medium, grains rot. rel. to wave propag. 77−23909
hadrons, uncharmed, rotational states 80−22596
Hill's case of ave. three-body, problem, stability of plane orbits *(Russian)* 77−67271
IC 342, Scd galaxy, H I rot. curve obs. 80−67857
infinitesimal operators of translation and rot., dynamic eqns. lineage 80−17788
interplanetary magnetic field, imperfect corotation as source of cosmic ray semidiurnal var. 80−8497
joint instantaneous centre of rotation, least square analysis 79−29555
Jupiter, fast moving bright spot obs. in North Temperate Current C 80−67640
Jupiter atmosphere, origin of differential rot. 80−46467

rotation continued
Jupiter corotating magnetosphere, self-consistent model 78−89109
kinetic analysis of rotation with air-cushion apparatus *(Hungarian)* 79−25811
knee joint, human, torsional load-displacement charact. in vitro 78−40235
large cosmical masses, expansion and rot. momenta *(Russian)* 77−17351
Liapunov's periodic motions at heavy rigid body with fixed point *(Russian)* 80−22190
M31 nuclear bulge, rotational vels. meas. 80−41888
M33 rotation curve, influence of warped optical phase 80−56944
Moon, peculiarities of translatory-rotatory motion caused by force function third and higher harmonics *(Russian)* 80−90349
Neptune, equatorial flow model rel. to rot. 80−67653
Neptune rotation period, effects of seeing on reflected spectrum 80−46479
NGC 1023, SB0 galaxy, H I obs. rel. to rot. and mass/luminosity ratio 80−67886
NGC 1055, 681, 4594, galaxies, rot. curves and mass distribs. *(Russian)* 80−90541
NGC 3115, S0 galaxy, rotation and mass of inner 5 kiloparsecs 80−105326
NGC 3686 galaxy quartet, spectra and rot. curves rel. to mass distribs. and group stability 80−62297
NGC 4945, late-type spiral galaxy, mean rot. curve and excited gas kinematics 80−109547
NGC 5128 (Centaurus A), disc rot. curve rel. to galaxy struct. and evolution 80−4429
NGC 520, Irr II galaxy, new photographic and spectroscopic obs. 80−41889
NGC 741, 1316, 7626, radio galaxies, rot. axes and dynamics 80−94871
ocean closed basin with topography, planetary vorticity gradient rel. to normal Rossby modes 78−73385
Orion Molecular Cloud, rotational explanation of high-vel. mol. emission 80−36688
periodic system induced oscillation and rotation analysis 77−37753
photosphere magnetic fields assoc. with coronal holes, differential rot. 77−22167
planets, initial rotation periods and relative formation times *(Chinese)* 80−105182
quantisation in spherical coords. *(Russian)* 78−21012
relativity of inertial forces, modified Thirring shell model 79−12667
rigid body resonance translational-rotational motion in sphere gravit. field, intermediate theory 79−96899
rigid body translational-rotational motion in gravit. field of sphere, Poincare periodic solns. of third kind 80−46377
rocks rotational deformation, reversal of inclusion trails spiral direction in paratectonic porphyroblasts 79−39717
rotation matrix for rot. around arbitrary axis, Euler vector representation 78−62011
rotor, linear (triaxial) (asymmetric), action-angle variables in quantum mechanics 80−31543
sample rotation, biaxial, in supercond. solenoid *(Czech)* 80−37010
Saturn atmosphere, origin of differential rot. 80−46467
sea ice field of Okhotsk Sea coast of Hokkaido, divergence and rot. meas. *(Japanese)* 78−96223
solar coronal holes, June 1973-January 1974, EUV obs. rel. to differential rot. 77−56893
solar prominences, evidence for rot. mass motions from inclined spectral features 80−62098
space vehicle, disordered rotation damping by elastically suspended ballast *(Russian)* 77−45287
spontaneous symmetry breaking and bifurcations from the Maclaurin and Jacobi ellipsoids 79−35616
steady motions of complex rotating systems, computational anal. 80−53618
Sumatra, late Cenozoic clockwise rot. 77−60363
swift rotation, appl. in beam choppers, turbine drives, etc., history 78−32643
teaching, torque and Newton's third law 78−12517
ultraprecision spindle unit construction on aerostatic supports 78−77880
Uranus, equatorial flow model rel. to rot. 80−67653
Uranus, rot. period spectroscopic determ. 80−51691
Uranus rotation period, effects of seeing on reflected spectrum 80−46479
vacuum chamber target, two-axes sample positioning mechanism 77−61076
Venus rotation, possible dynamical evolution since formation 80−56742
Venus stratosphere, retrograde rotation meas. with Fabry-Perot radial vel. spectrometer 79−44389
vestibulo-ocular reflex gain in monkey at high rot. freqs. 78−56973
vorticity vector, rot. theory 80−82604
wave functions of 1/2-integral spin particles, 720° rot. effect, teaching models 79−62958
H I, extended, in M51 system, vel. field and rot. 78−89253
He, liq., ht. transfer in centrifugal acceleration fields, free convection and boiling regimes 77−89604
$KCN:HCN^-$, structural props. using ESR 80−25205

rotation by magnetisation *see Einstein-de Haas effect*

rotational flow
see also vortices
abruptly rotated cylinder, turbulent boundary layers, numerical anal. 80−43716
acoustic resonance in vaneless radial diffusers with swirling flows 79−18882
aerated systems, oblong, flow and mixing, transverse circulating flow of liquid, longitudinal dispersion 80−69900
aerodynamics, rotating cylinder for circulation control on airfoil 77−7401
aerosol vortex jet streams, impingement zone, particle motion soln. and expt. 77−65773
air, partially filled rot. cylinder, horizontal, steady flow soln. 77−84260
air flow, turbulent, in infinite medium spatial speed distrib. *(Rumanian)* 80−53826
air flow in vertical annular channel with rot. inner cylinder, heat transfer 77−58679
air-water surfaces, turbulence charact., mass transfer and eddies 80−14665
analytic solutions to nonlinear eqns. 78−1670

rotational flow continued
angular velocity determ. for rotating liquid figures in equilib. *(Russian)* 79−10572
annual review of fluid dynamic, book 80−94927
annular axial compressor nonaxisymmetric flow anal. 79−32679
annular diffuses with conical walls, swirling flow and separation 80−43715
annular flow, vel. distrib., expt. determ. 80−38510
annular gap with axial flow and rot. inner cylinder, heat transfer coeffs. 79−27489
annular jets, velocity distrib. and profile meas. 79−50829
annular turbulent flow with rot. core tube, numerical predictions 77−55010
annuli, spherical rot., stratified convection of viscous Boussinesq fluid 79−27635
annulus, rot. inner cylinder, outer cylinder heat transfer to enclosed flowing liq. 78−83478
annulus, spherical, rot., forced thermal convection of viscous fluid 79−27634
annulus experiment, Rossby regime, ocean circulation appl. *(Japanese)* 79−66709
annulus with inner rot. tube, heat transfer 79−1204
annulus with rotating inner cylinder, momentum integral soln. of developing flow 77−35149
asymmetric Stokes flow from closed torus in quiescent viscous flow 80−43719
asymptotic drag formulas for rapidly rotating radial channels of rectangular cross section 80−6065
atmosphere, effects of Earth rot. rate vars. rel. to climate 80−4097
atmosphere and oceans, wave disturbances 78−32209
autooscillations, azimuthal wave type, rot. Couette flow stability loss 77−75882
autorotating flat plate wings, moment of inertia, geometry and Reynolds number effects 79−68719
axial flow in annuli, instability 78−55631
axial flow under pressure gradient, turbulent boundary layer on rot. cylinder 77−62256
axial-flow fan, quadrant duct bend effect on noise emission *(German)* 77−27539
axisymmetric body in viscous conducting rotating fluid in mag. field, slow motion 79−50805
axisymmetric cavity flow, viscous, numerical calcs. 79−98737
axisymmetric convection in rotating sphere, non-slip surface effects 79−64657
axisymmetric convection in shallow rotating cylinder, centrifugal acceleration effects 80−96260
axisymmetric disturbances, evolution in fluid *(Russian)* 79−34848
axisymmetric equilibrium figures for rotating incompressible fluid 78−18307
axisymmetric flow boundary with temp. gradient in rotating annulus 78−90911
axisymmetric flow stability 79−23300
axisymmetric inertial fluid oscillations in cylindrical cavity during spin-up from rest 78−5750
axisymmetric potential flow for two spheres, exact soln. 79−32536
axisymmetric rotating round nosed bodies, flow and heat transfer, buoyancy effects 80−79306
axisymmetric streaming flow past torus, Stokes eqn. soln. method 78−14026
backflow appearance conditions for rot. fluid in channel, stability *(Russian)* 79−86439
backswept centrifugal impeller, laser-Doppler investigation of flow 79−77304
baroclinic fluid, rapidly rotating, sine-Gordon eqn. model 80−46820
baroclinic fluid, soliton behaviour 79−72898
baroclinic instability in rot. eccentric annulus 77−11197
baroclinic two-layer flow in channel, instability, geophys. appl. 79−55420
baroclinic unstable wave field modulation 77−33144
Benard convection, asymptotic sidewall effects 78−14014
between rot. and static discs, with radial flow, numerical method 78−59403
between two counter rotating infinite plane discs, numerical soln. by multiple shooting 78−42621
binary homogeneous mixtures, motion in infinite rot. cylinder, generalised diffusion theory 80−79328
binary mixture over infinite rotating disk, species distrib., existence and uniqueness of solns. 77−15044
bispectral analysis, turbulent rot. vel.-derivative data computations 77−920
blade to blade flow, anal. with Thomas algorithm 78−24669
blades, vibr. due to rotating stall, aerodynamic force meas. 80−92172
blocking phenomenon in rot. liq. 79−64668
Bodewadt flow, spin-up, angular momentum adjustment 80−28511
body force effect on turbulent transport near surface 78−26116
body of revolution with heating and cooling, boundary layer transition and separation 80−64518
body-propeller combination, numerical soln. including swirl and data comparisons 80−19407
boiling crisis in swirled flow of water in pipes 79−90241
bottom waves in rotating stratified fluid 79−2274
boundary layer, three-dimens., along enclosed rot. disc, roughness effects 79−94628
boundary layer close to rotating disc, numerical soln. *(Russian)* 77−54969
boundary layer growth on spinning sphere, screw motion 77−31315
boundary layer modification by axial vel. imposition in rotating fluid 79−77133
boundary layer on rot. cylinder, stability, transition and growth 77−31309
boundary layer on rot. disc, drop interaction 78−47020
boundary layer turbulence, streamline curvature effects 78−13998
boundary layers, vertical, in rapidly rot. gas 77−19609
bounded coaxial jets, convective heat transfer in turbulent mixing, swirling 80−64541
Boussinesq convection in deep rotating spherical shell, temp. boundary effects 79−64655
Boussinesq convection in deep rotating spherical shell, vel. boundary effects 79−64656
Boussinesq differentially heated fluid, struct. 80−109190
Boussinesq fluid, helicity effects 77−42924

rotational flow continued
Boussinesq viscous fluid, inertial instability, appl. to atm. 80−90131
bubble, single rising, internal mass transfer coeffs. 79−86487
bubble motion in rotating liquid, computer study, Runge Kutta Nystrom method 77−47063
bubble motion in rotating liquid under residual gravity 78−55679
bubble motion under gravity in rotating fluid, differential equations of motion *(German)* 78−90918
buoyant cylinder within rapidly rotating horizontal cylindrical container, steady flow 79−86441
burner with diffusive control, intermixing of gas streams with transverse swirled air flow 78−87418
capillary fluids rot. in cylindrical vessel, free oscill. *(Russian)* 77−27542
cascade flow, varying flow rate, finite element anal. 78−90910
cascade flow in large distorted periodic flow, finite element soln. 78−87348
cascades, annular, secondary flow, shear flow turning or departure of exit flow 80−69842
with cavitation, around circular cylinder, pressure distrib. *(French)* 78−67234
cellular convection in rot. fluid annulus steady linear theory 78−38339
centrifugal buoyancy forces from energy considerations 80−82609
centrifugal injectors, submerged flow charcts. 77−58701
centrifugal instabilities of circumferential flow in finite cylinders, nonlinear theory 80−99989
centrifugal nozzle, similarity criterion and flow swirl ratio 77−24010
centrifugally driven thermal convection in rot. cylinder 78−51172
centrifugally stratified helical Couette flow, stability 77−89183
centrifuge, two-fluid spin-up 78−30301
centrifuged flow with recirculation, book contrib. 80−1604
channel with arbitrary end wall, Kelvin wave reflection 78−5751
chaotic circular Couette flow, reemergent order 79−27651
circle theorems for inviscid steady flows 80−59043
circular channel with centrifugal forces, laser Doppler meas. of vel. field 78−34225
circularly polarised inertial wave vectors in rot. fluid 77−3829
circulation flows near wall, ideal liq., two-dimens. anal. in Cartesian coords. 78−51173
closed torus, virtual mass in axisymmetric motion 79−32437
closed torus in Stokes flow, eddy-type motion and vortices 77−42850
coaxial circular discs, hydrodynamical problem 80−24032
coaxial cyclone flow, heat transfer from a cylinder 80−48698
coaxial discs, multiple solutions of flow equations 77−55002
coaxial rotating cylinders, concentric flow in gap, stationary lower bound 79−68714
combined laminar and turbulent flow, over a rotating disc 77−3809
combined Taylor vortex and axial flows, heat transfer characts., Reynolds analogy soln. 79−59974
combustion and non-combustion flow fields with swirl, numerical anal. 79−98821
compressible atmosphere, vertically rotating, critical levels 80−6073
compressible finitely conducting rotating fluid in mag. field, Rayleigh-Taylor instability 80−10228
compressible flow, in rot. cylinder, linearsed anal., appl. to gas centrifuges 78−71345
compressible flow, variational principle and finite element method 79−46336
compressible fluids, thermal instability in presence of mag. field and rotation 77−89204
compressible inviscid fluid, profile of isogradient vaneless diffusor with swirl flow 79−86445
compressible Newtonian fluid, laminar flow between rotating discs 77−31320
compressible swirl flow with closed streamlines, high Reynolds no. 77−84269
concentric spheres, unstable motion of viscous fluid *(Russian)* 78−55649
condensation of laminar film on helical elliptical cylinders, governing eqns. soln. 78−9689
conducting fluid, flow and heat transfer in channel in mag. field *(Russian)* 78−75218
conducting fluid, laminar rot. in cylindrical vessel, elec. and mag. field effects *(Russian)* 78−75222
conducting fluid in horizontal mag. field, Rayleigh instability 77−15126
conducting fluids, dynamics under rotational mag. forces 80−48820
cone-cylinder body, boundary-layer flow in uniform stream 77−23965
conical diffuser, with suction, compressible boundary layer swirling flow 78−38360
conical diffuser performance change by swirl addition 79−14403
conical flow, Pohlhausen method appl. to 3-D boundary layers 77−65746
conical tube, heat transfer with internal cooling by swirling air jet 77−55063
constriction meter orifice, swirling flow component effect on discharge coeffs. 78−63514
convection in rotating annulus with negative radial temp. gradient 78−90912
convective flows in spherical shell, bifurcation and stability 80−28507
convective heat transfer from a confined jet in a centrifugal force field 79−98720
convective modes and convective stability, of rotating fluids 79−16818
Couette flow, amplitude steady secondary flow past marginal state, Landau's conjecture 79−77128
Couette flow, spherical, in thick layer, with revolving inner sphere, stability, review 79−81969
Couette flow and heat transfer in rot. system 77−75878
Couette flow stability, transformation of perturbation eqns. 77−7474
Couette modulated circular flow, energy stability 77−31313
critical heat flux in swirl flow *(Russian)* 79−10558
cryostat, rot. vap. column flow anal. 80−4722
curly-viscous fluids, three-dimens. free convection about slender bodies of revolution 77−75943
cyclone, reverse flow, efficiency anal., using monodisperse methylene blue-uranine 78−34142
cyclone flow, boundary layer on cylindrical insert surface 80−10251
cylinder, rot., with inner cylinder eccentric torque-free rot., viscous flow 78−34144
cylinder, rotating, 3D boundary layer eqn. expansion 77−84259
cylinder, rotating, visual observation of flow past 78−90915
cylinder, source-sink flows, numerical anal. 79−4018

rotational flow continued
cylinder in conducting fluid, radial mag. field effects *(Russian)* 77−3874
cylinder in rotating system, flow separation 79−68720
cylinder on β-plane, prograde and retrograde rot. flows, boundary layer separation 80−92189
cylinder oscillating in viscoelastic fluid, secondary flow 79−60037
cylinder rotation in stream of viscous fluid, numerical soln. *(Russian)* 77−58704
cylindrical pipe turbulent nonisothermal flow, temp. fluctuation and pulsatile heat flux calc. 78−83475
Czochralski bulk flow in the growth of garnet crystals 80−38979
deformable medium, rotational dynamics 78−20631
detached shear layers and boundary currents in rot. liq. 80−81984
developed flows in rotating channels having rectangular cross section *(German)* 79−86516
diatomic gas, transient flow, temp. and conc. profiles, by rot. Raman scatt. 77−75995
diffuser, conical, swirl effect on press. recovery coeffs. 78−63474
diffusive instabilities in rotating elec. conducting compressible layers 80−38379
disc, inviscid cell chain with viscous interlayers 80−53794
disc, rot., laminar to turbulent boundary layer shear flow, three dimens. 78−38284
disc, rotating, convective mass transfer 80−43707
disc, spin up, fluid motion analytical-numerical anal., shear wave trains 77−15040
disc in viscous fluid, decleration 80−28515
disc pair, air flow between, exptl. obs. and theory *(Russian)* 77−55009
disc pair, flow between rotating and stationary porous discs 78−90914
disc rotating in fluid with surfactant surface layer 80−10284
disc rotating in jacket in presence of transitional boundary layer, local heat transfer 79−94608
disc rotating in stagnant surroundings, local heat transfer, two-eqn. model 77−58690
disk, fluctuating flow induced by periodic suction 77−68592
dissociating fluid layer, heated, effect of rot. on Benard convection 79−4020
double boundary layers on an electrically conducting plane surface in a rotating environment 79−46397
drag on a sphere moving axially in a long rotating container 79−50734
drag reduction polymer additive in helicoidal flow, screw pump press. head 78−26166
driven polar cross section cavity, laminar incompressible recirc. flow 78−46988
droplet dispersion produced by rotating perforated drum 77−11244
drops, rotating, captive between co-rotating parallel faces, shapes and stability, capillarity eqns. 80−64592
duct, plane, with sudden expansion, aerodynamics 79−94722
duct rotating around perpendicular axis, flow and heat transfer, finite difference method 78−94752
ducts, eddy motions induced by water waves and periodic flows 80−33679
ducts, rapidly rot., variable area, rectangular, steady flow, inertial perturbations for small divergences 80−59112
dusty Maxwell flow between concentric spheres, torsional transient motion 79−90258
dusty viscous fluid flow through rotating circular cylinder 77−68675
dynamo action associated with random waves in a rotating stratified fluid 80−33687
eccentric rot. cylinders, Newtonian flow inertial effects 77−919
eccentric rotating cylinders, flow where clearance is relatively large 78−1667
eccentric rotating discs, torque and energy balances for flow 77−68641
eccentricity of rotating cylinder, error calc. in viscosity meas. *(German)* 78−67291
Einstein field eqns. for rotating isentropic perfect fluid, cylindrically symmetric solns. 79−40427
Ekman and Hartman layers on plate with variable suction or blowing 78−38416
Ekman layer, mechanically induced unsteady compressible, theory 80−24033
elastic-viscous fluid, steady flow through annulus of porous rotating coaxial cylinders 77−72349
elastico-viscous fluid rot. in mag. field, unsteady flow induced by oscill. plate 78−67273
elasticoviscous flow between rotating disc and stationary porous disc 77−54964
electrically conducting medium, rotation at exit of coaxial MHD channel 80−83853
electrolyser, rotating, flow field 79−52682
ellipsoid of revolution rot. around equatorial axis *(French)* 77−68593
elliptically rotating liquid, generation of vortical perturbations as atm. model *(Russian)* 77−49146
energy stability for the flow between rotating, coaxial disks 80−14712
energy stability theory of decelerating swirl flows 80−59054
equation of state and Euler's turbine eqn. *(Rumanian)* 78−79400
exit region central source flow, between finite close parallel rot. discs 77−42849
falling particles, in rot. fluid 78−55675
fan jets with swirling, self-similar soln. 78−90950
ferrofluid, helical flow with heat cond. between coaxial porous tubes 79−23371
ferrofluid constitution examination by rotating test tube method 80−33693
ferrofluid devices, magnetostatic and centrifugal, nonmagnetic body motion 80−33700
ferromagnetic colloids, helical flow in mag. field *(Russian)* 78−75213
ferromagnetic fluid rotating about vertical axis, convective instability of layer 79−27698
ferrosuspensions, internal rotations and the other transport phenomena 80−28573
fibre bundle, centrifugal flow, fluid vel. and press. distribs. *(Polish)* 78−51236
film cooling efficiency, axisymmetric air flow rot. cylinder, main flow swirl effect 78−75132
film cooling of rotating surface, efficiency 79−98718
finite amplitude two dimensional Benard convection, in finite rot. system, weakly nonlinear theory 78−83394
finite difference and finite element anal., review 79−10565

rotational flow continued
finite shrouded disc, laminar boundary layer in rot. compressible isothermal flow 80−43727
finite-amplitude thermal convection and geostrophic flow in a rotating magnetic system 80−87813
fire whirl phenomenon, model 79−72958
flat surface, jet impingement, rotational flow model calcs. 80−64596
flow around rotating cones and discs, momentum, heat and mass transfer 79−1203
flow between coaxial rotating cones, frictional moment coeff. determ. *(Japanese)* 77−39299
flow between rot. disc and fixed wall, friction coeffs. 78−63439
flow between rot. discs, multiple solns. 78−79324
flow between rot. discs, three kinds of solns. 78−79323
flow between rotating discs, finite element anal. using exponentially weighted basis functions 78−16655
flow past a rotating cylinder energy-dissipation model of turbulence 77−58696
flow past porous plate, rotation effects 80−10256
flow profile measurements of gas in a rotating cylinder [^{235}U enrichment] ^{235}U enrichment processes 79−49793
fluctuating boundary layer in a rotating fluid with variable suction 79−50718
fluctuating flow due to rot. disk 79−18898
fluctuating flow of viscous cond. fluid on porous plate in rot. medium with transverse mag. field 79−90340
fluid, convective heat transfer with alternating circulation, mathematical model *(Rumanian)* 79−14208
fluid, perfect, 3-dimens. rot. flow, Lagrangian invariants appl. 80−43720
fluid containing particles, laminar throughflow between corotating disks 79−77136
fluid dynamics expts. and problems *(French)* 78−9645
fluid dynamics on rotating plane, averaged equations 78−42617
fluid layer heated, turbulent convection 80−100003
fluid motion between two parallel rot. plates, Navier-Stokes eqn. soln. 79−68713
fluid motion within ellipsoidal cavity, influence of Coriolis force field *(Russian)* 78−81296
fluid of spherical configuration, wave propagation 80−106804
fluid-fluid interface, rotlet or sphere rot., torque values 79−86494
fluidised bed, two-dimensional, with transverse gas supply, fluid dynamics obs. *(German)* 78−34192
forced oscillations in rotating stratified liquid 78−63478
forced oscillations of an enclosed rotating fluid under a uniform magnetic field 79−32688
free and forced convection flow in rot. channel bounded by permeable bed 79−23366
free atmospheric convection, rigorous formulation using matched asymptotic expansions *(French)* 77−65740
free convection in laminar boundary layer along rot. plate, nonsimilarity solns. 77−31307
free oscillation in a rotating spherical shell 80−19409
free shear layer behavior in rotating systems 80−1545
freesurface breakdown in rot. liq., wavelets 78−59402
frictional force and torque in anisotropic spatially inhomogeneous viscosity fluid, variational principle 79−37367
frictional torque nonstationary brake flow in liquid filled cylinder *(German)* 77−72304
fully developed turbulent channel flow, perturbation propag. in viscous sublayer and wall region 80−19513
gas, perfectly conducting compressible in mag field under gravity, wave dispersion relations *(Chinese)* 80−77276
gas, rapidly rotating, spin-up problem, perturbation calcs. 78−75147
gas, rot. in mass-transfer equipment, eddy contact element radial press. distrib. 78−26126
gas, rotating, convective instability in gravitational field 79−27642
gas, Stewartson 1/3 layer in countercurrent centrifuge *(French)* 77−928
gas, strong diverging cylindrical shock propagation 80−79350
gas centrifuge, fluid flow anal., computer calcs., appl. to UF_6 77−75924
gas centrifuge, numerical anal. of weakly compressible rotating flows 80−47726
gas centrifuge with insulated end walls, Stewartson layer struct., temp. distrib. 78−46973
gas centrifuge with insulated side wall, Stewartson layer struct., linearised eqns. 78−46974
gas centrifuges, axisymmetric flow driving mechanisms 77−15039
gas cloud, self-gravitating rotation and Kelvin-Helmholtz instability 79−46287
gas ejector, energy separation 79−68774
gas flow, plane and helical, restrictions on instabilities 79−98745
gas in rot. cylinder, velocity profile meas. 79−50737
gas turbine asymmetric swirling flow anal. 79−27694
gas turbine combustion chamber flow three-dimens. calc. 80−79405
generalised Benard problem for stratified fluid, rotation effects 80−24031
geophysical fluid dynamics theory, book 80−105443
geophysical fluid motion, Rossby and Kelvin waves, open boundary conditions 80−61810
geostrophic adjustment in rot. fluid 77−66952
geostrophic flows in rapidly rot. gases, thermally insulating boundaries, Ekman and Stewartson layers 80−14711
gravitational forces in rotating channel 77−11194
gravitational instability in presence of suspended particles and rot. 79−64633
gyrotropic turbulence spectra, Wilde diagram anal. *(Russian)* 79−4000
Hall effect on MHD flow induced by oscill. disc in rot. fluid 79−18968
Hamels spiral flow, temp. and vel. distribs. *(German)* 80−87779
Hartmann boundary layer control of spin-up of stratified, conducting fluid 77−42923
heat and mass transfer from rotating disk with sink flow 80−19402
heat conducting simple fluid with memory, nonsteady helical flow 79−81900
heat exchange from rotating disc. into unbounded rotating fluid, thermal and hydrodynamic boundary layers 80−59050
heat transfer, cylinder in stabilised swirl flow having aerodynamic axis parallel to flow, calc. 80−79321
heat transfer, cylindrical shrouded cavities, with rot. and coolant through flow 77−72294
heat transfer, liq. in rot. cavity 79−81899
heat transfer from rot. disc with axisymmetric heat source distrib. in laminar flow 79−46314
rotational flow continued
heat transfer from rot. disc with liq. jet impingement 79−4055
heat transfer from rotating short radial blade, laminar and turbulent flow 78−18294
heat transfer in laminar cyclone 78−55548
heat transfer through rotating channel in porous medium 79−72932
heat transfer to circular cylinder in stabilised twisted flow 77−72309
heated fluid annulus with semicond. walls, temp. gradients, lab. expt. 77−65744
heating of viscous and non-Newtonian fluids on a rotating disk 79−77095
heavy viscous rotating fluid system, normal oscillations *(Russian)* 79−14417
helical flow in simple fluid, uniqueness 78−14017
helical flows, static press. distrib., analytic deriv. 78−94748
helical flows in a sphere 80−59052
hemisphere in MHD rotating stratified fluid 80−100039
homogeneous rotating fluid, topography/shear flow interaction 79−55354
homogeneous turbulence, rotation effect on double vel. correlations *(French)* 78−63435
homogeneous turbulence, with internal rotations, theory 80−69772
homogeneous turbulence under rigid rotation and uniform mean vel. gradient *(French)* 79−23306
horizontal rotating fluid layer, heated from below, convection rolls nonlinear props. 80−6066
horizontally heated rotating fluid, spatial oscillations 77−55004
hydraulic resistance of channel during rot. about axis perp. to channel axis 77−58698
hydrodynamic, sticking and slipping boundary conditions, friction of rot. bumpy cylinder 78−63410
hydrodynamic resistance and heat exchange from flow past rotating cylinder *(Russian)* 80−1586
hydrodynamic thermal breakdown in viscous fluid, Couette flow between cylinders 78−83391
hydromagnetic convection, thermally driven, in rapidly rotating sphere 80−14548
hydromagnetic free convection past infinite porous flat plate in rot. system, slip effects 79−81989
hydromagnetic free shear layers in rotating flows 79−14493
hydromagnetic penetration in a rotating fluid, fluid fluctuations 80−14839
hydromagnetic Stokes flow past rotating sphere 79−32694
hydromagnetic thermal instability of rotating fluid layer, Hall current effects 79−27699
hydromagnetic viscous fluid between rotating surfaces of revolution *(Polish)* 77−55096
hydroplaning of a rotating cylinder on water 78−63522
impeller, centrifugal, impeller width effect on flow 78−63513
imploding rotating liquid cylinder, viscous boundary layer formation on free surface 79−81894
inclinable pipe, suspension in turbulent flow, Markovian model, eddies 80−48790
incompressible cholesteric liquid crystal static magnetic field effect 78−6010
incompressible isotropic simple fluids, universal motions 79−68758
incompressible rotating simple fluids, velocity fields and strain histories of motions 78−59401
incompressible turbulence, statistical investigation of eddy viscosity 80−14675
inertial and frictional effects on flow over topography 77−45106
inertial oscillations of rotating fluid in rigid axisymm. container 78−1673
inertial oscills. in rot. fluid, DuFort-Frankel difference scheme 77−51035
inertial wave and flow struct. for disturbances at low Rossby number 78−22360
inertial waves, produced by obstacle in deep rotating container 79−59993
inertial waves and an initial-value problem for a thin spherical rotating fluid shell 78−55656
inertial waves frequency in rotating sectored cylinder 77−47031
infinite viscoelastic liquid, unsteady slow flow due to rot. sphere 78−75112
internal currents, struct., kineticity effects 77−68570
internal flows with initial swirl, generated heat and mass transfer law 80−24025
internal wave diffraction by vertical half plane in rotating basin *(French)* 77−68603
internally heated rotating annulus, axisymmetric states 77−45157
inviscid, rotating, compressible fluid, linear stability 80−92161
inviscid rotational flow through sprays 79−46328
isothermal spinning, network theory 77−68601
jet, axisymmetric, vel. distrib. and swirl effects, low speed results 79−46351
jet, axisymmetric free shear flow with Reynolds stress closure 80−19469
jet, coaxial, initial swirl of inner and outer flows effect on aerodynamics 77−68652
jet, viscous laminar flow, tangential twist eddy flow form., numerical soln. 77−89179
jet mixing in transverse subsonic crossflow, vortex strength 79−14447
jets, swirling, radial, in free space, velocity components 78−55669
jets and plumes, swirling, integral method model 79−60040
journal bearing in rotating MHD flow, system characts. *(French)* 79−1263
Karman equations for rot. fluid motion in presence of infinite rot. disc 77−54999
Kelvin wave diffraction from rotating channel with infinite and semi-infinite barrier 79−46331
Lagrangian dynamics of polarised media with internal spin in general relativity 79−72962
laminar and turbulent boundary layers on some rotating bodies in axial flows *(Japanese)* 79−77127
laminar boundary flow over spinning blunt body of revolution, Magnus forces 78−94745
laminar boundary layer, on finite disc, vel. profile *(Russian)* 77−84219
laminar boundary layer heat transfer over rot. bodies 79−32517
laminar boundary layer on rot. cylinder 77−89130
laminar boundary layer on rot. disc in counter-rot. fluid 77−35113
laminar boundary layer on rot. sphere 79−27648
laminar boundary layer on rotating sphere in still fluid *(Japanese)* 77−35112

rotational flow continued
laminar boundary layer swirling flow with heat and mass transfer in conical nozzles and diffusers 79−81842
laminar compressible boundary layer swirling flow in nozzle, flow and heat tranfer 78−94795
laminar Couette flow in rot. fluid between coaxial cylinders, Taylor instability 77−51066
laminar flow in rot. annulus, stable stratification effect 78−94797
laminar flow in rotating porous annuli, Navier-Stokes eqns. 77−68687
laminar incompressible flow past rot. elliptic cylinders 77−27538
laminar motion in rot. channel 79−68717
laminar non-Newtonian fluid jet, swirling, impinging on normal plane 77−42889
laminar swirled flow in annular channel 79−90260
laminar swirling flow, integral method of anal. *(Japanese)* 80−28512
laminar swirling impinging jet, heat transfer, numerical calc. 79−1228
laminar throughflow between closely spaced rot. discs 78−51170
laminar to turbulent boundary layer stability, rotating disc 78−38283
laminar to turbulent transition, laser Doppler velocimetry expt. 79−77073
large eddies in wake and turbulent boundary layer, vel. fluctuations 80−24036
laser heated nozzle flow with swirl, axisymmetric comp. boundary layer 80−14775
liquid, motion instability in vessels of elliptical cross-section *(Russian)* 77−51062
liquid filled spinning spheroids, stability via Liapunov's second method 80−48677
liquid film, instability on surface of rot. sphere 80−59006
liquid film flow regimes, on rot. disc 78−1671
liquid film flowing over rot. disc 78−38342
liquid film on rot. cylinder in gravitational field, steady soln. 78−83411
liquid films, thin, effect of Coriolis force on film dynamics 78−94747
liquid flow in-rotating spherical layers, stability and nonuniqueness 79−77135
liquid He, pool heat transfer, in high centrifugal accel. field 77−15034
liquid in closed rot. annular cavity, heat exchange, flow regimes 78−5753
liquid in rotating cylindrical cavity, dynamics *(Russian)* 77−68594
liquid layer heated from below, form. and interaction of three-dimens. convective cells 79−14397
liquid layer on rot. Archimedes spiral, heat transfer 79−14410
liquid layer on rot. Archimedes spiral, mass transfer 79−14413
liquid metal rotor energy storage device, secondary flow due to Alfven waves 77−39353
liquid metals, MHD rot., vel. meas. by vane type sensor *(Russian)* 77−47123
liquid spiral flow, self-oscills., loss of stability 77−80171
liquid-gas flow without mass transfer, centrifugal scaling 77−35209
local heat transfer at rotating disc, Prandtl's mixing length hypothesis 77−27540
longitudinal counterrotating vortices, wall boundary layer of flow with ang. momentum *(German)* 77−75922
magnetic field growth in helical turbulence 79−18967
magnetic flow of viscous gas between rotating surfaces of revolution 79−46395
magnetic fluid, cylindrical column, motion in rot. mag. field *(Russian)* 78−75212
magnetic fluid, in homogeneous rot. mag. field, torques, hydrodynamics 79−94632
magnetic fluid, spherical drop, motion in rot. mag. field *(Russian)* 78−75212
magnetic fluid in rotating vessel, flow in homogeneous mag. field 80−33691
magnetic fluids, response to mech., mag. and thermal forces 80−59122
magnetic gyrotropy in a medium with inhomogeneous density 79−94730
magnetic instabilities of rot. gas in presence of radial gravit. force and azimuthal mag. field 78−47046
magnetic-velocity shear, hydromag.-intertial-gravity waves propag. 79−55422
magnetisable fluid, motion in rotating homogeneous mag. field 80−28572
magnetohydrodynamic flow between rotating and stationary porous coaxial discs 80−43799
mass force field boiling crisis, critical heat flux for swirling tube flow 79−90248
mass transfer from rotating cylinders 78−42613
mass transfer from rotating wedge-shaped bodies 78−30305
mass transfer in rotating disc system 77−15041
mass transfer near rotating disc at high swirl rates 79−14405
material lines in viscous and elastic flow between eccentric co-rot. cylinders 77−23966
MBBA, homeotropic nematic layer, torsional shear flow in normal elec. field 79−82155
mean flows driven by weak eddies in rotating systems 80−103032
measurements of rotating flow around circular cylinder, azimuthal velocity in gas centrifuge 80−74890
meridional flow of compressible fluid in a rapidly rotating short cylinder 80−106812
MHD, gas boundary layer swirling nozzle and diffuser flows with mag. field 80−1693
MHD, Hall effect on unsteady flow due to rotating infinite disc 78−18354
MHD, heat transfer between porous discs, one rotating one at rest 80−28561
MHD, stability in axial and toroidal mag. fields 77−31394
MHD, steady, diffusive instability, rel. to geomagnetism 79−50807
MHD, viscous flow between two rotating porous cylinders, in axial mag. field 77−72364
MHD between coaxial cylinders, difference eqn. soln., Dean's problem 79−94731
MHD boundary layers, unsteady on porous plate in rot. system 77−24027
MHD convection in rapidly rot. fluid layer, stability, rel. to geomagnetism 79−50808
MHD convective instability in rot. viscoelastic fluid layer heated from below 77−58800
MHD Couette flow, Hall effect in rot. system 80−74991
MHD Couette flow and heat transfer in rotating system 77−35246
MHD Ekman layer on free convection past infinite porous flat plate 80−14830
rotational flow continued
MHD flow between a rotating and a stationary disc 78−63502
MHD flow in cylinder, inviscid, axial field and point force 78−18349
MHD flow in rot. channel, wall conductances effect on heat transfer 78−51245
MHD flow over oscillating porous plate, Hall current and rot. effects 78−5803
MHD fluid layer, stability in rot. frame of reference with temp. and conc. gradients 77−27600
MHD helical flow, linear and nonlinear stability 79−37408
MHD of fluid with stratification, Boussinesq. approx. of linearised eqns. 78−79387
MHD rotational flow, homogeneous fluid in cylindrical tube past circular disc 79−46398
MHD rotational stability sufficiency conditions 79−10616
MHD shift flow, in strong field, of viscous fluid 80−28576
MHD stratified flow between oscillating disks, boundary layers 80−28570
MHD turbulent boundary layers in rot. circ. vessel, drag 80−33697
micropolar fluid, steady flow due to rotating disc 79−72897
micropolar fluid flow due to an oscillating plane subject to rotation 79−98763
micropolar liquid between two infinite slowly rotating discs 80−53796
micropolar liquid flow between two infinitely slowly rotating discs 77−35150
natural convection, in slightly inclined rectangular box heated from above 79−59976
Navier-Stokes eqns. for rotating flow above rotating disc, non-unique solns. 77−47020
Navier-Stokes eqns. numerical solns. *(German)* 80−59057
Navier-Stokes equations, finite element anal., upwind scheme 79−1201
nematic liquid crystal, cylindrical Couette flow, stability 79−32526
Newtonian flow between rotating cylinders 77−80186
Newtonian fluid flow between eccentric rot. cylinders and related problems 79−10570
Newtonian liquid, coating on to rotating roll 79−41692
Newtonian liquid, Weissenberg effect 79−59990
non Newtonian fluid, mass transfer due to rot. disc 79−41717
non-axisymmetric small particles, rot. in simple shear flow 79−68722
non-isothermal disc rot. in quiescent compressible gas, heat transfer 80−14704
non-Newtonian creeping flow around rotating spheroidal spindle, torque calcs. 77−15073
non-Newtonian flow between rotating cylinders 77−80186
non-Newtonian flow between symmetric rotating bodies of revolution, natural coord. system 77−15081
non-Newtonian flow classification criteria for rigid motions, viscometric flow and elongational flow 80−69881
non-Newtonian fluid, free convection, heat and mass transfer 79−68765
non-Newtonian fluid, rot. liq. film, free surface instability 79−37294
non-Newtonian fluid, rot.-oscill. flow, rheological consts. determ. 78−30251
non-Newtonian fluid, unsteady laminar incompressible boundary layer eqns., flow, heat and mass transfer, similarity solns. 79−32590
non-Newtonian fluids in jacketed agitated vessel, heat transfer, viscosity correl. 78−75143
non-Newtonian nonisothermal flow, in slowly converging channel 77−89168
non-Newtonian or Newtonian liqs., two-roll mill problem 78−42616
non-Newtonian rot. symmetric flow *(German)* 78−55667
nonequilibrium free jet expansion, rotational temp. meas for N_2 80−69890
noninertial particle transfer to rotating in laminar flow under external force field 80−10250
nonisotropic turbulence model of swirling flow 77−55001
nonlinear axisymmetric flow between concentric rot. spheres, numerical anal. 80−19412
nonlinear convection in rot. fluid 77−68597
nonlinear split-disc problem for free shear layers in rot. fluid 77−42851
nonlinear stability of motion of viscous liquid between concentric rotating cylinders 79−14409
nonspherical particle, friction coeffs. in incompressible fluid with spin 78−87350
nonstationary convection in a rotating system, book contrib. 80−1593
nonstationary eqns. soln., appl. to flow between discs 80−28516
nonstationary flow between rotating coaxial porous discs, porosity effects 79−32657
nonstationary rotating disc flow, Navier-Stokes eqns., analytic and num. results 79−41694
nonuniform grids in finite difference approximations, application to fluid flow problems 80−105507
nose separation for laminar boundary layers on body of revolution 80−59091
nozzle, axisymmetric choked, transonic swirling flow analysis 77−58761
nucleate boiling of liq. Ar, N_2, in centrifugal accel. field, heat transfer and flux 78−94538
ocean, exptl. study of nonlinear baroclinic instability and mode selection in large basin 80−85669
ocean, potential vorticity distrib. rel. to equatorial undercurrent dynamics 80−72558
ocean, spread of mixing in stratified fluid and analogue in rot. fluids 79−57949
ocean, stability of solitary Rossby waves over variable relief, analytical theory 80−101371
ocean, stability of solitary Rossby waves over variable relief, numerical expts. 80−101372
ocean, wind driven, new class of steady solns. to wind-driven ocean problem 80−85667
ocean, wind-driven flow in zonal channel on rotating Earth 80−51402
ocean circulation, modelling expts. 79−57952
ocean deep-water channel flow, rotating hydraulics theory 80−94539
ocean internal waves, wind-generated exptl. study *(French)* 79−62518
ocean residual circulation, topographic generation by oscillatory tidal currents 79−57954
oceanic warm front propag., rotating stratified fluid theory 80−94538
oscillating radial flow between two parallel rotating disks 79−55393
oscillatory free stream flow past rotating disk, Navier-Stokes solns. 79−14416
overstable convection in horizontally treated rotating fluid 78−67202
paramagnetic fluid, non-conducting sphere steady rotation 79−72900

rotational flow continued
partially filled container rot. about horiz. axis, stable laminar secondary flow 77−51026
particle migration, in turbulent boundary layer of rot. disc 78−22333
particles, falling under gravity, in rot. drying drum, turbulent gas flow 78−1728
penetrative convection in rotating fluid, finite difference method 79−81902
perforated flat plate over porous medium, turbulence penetration, eddies, mass transfer 80−64528
permeable spheres in incompressible fluid, hydrodynamic interaction, mobility tensors 78−71395
permeable spheres in incompressible fluid, hydrodynamic interaction vel. fluid, friction consts. 78−75202
photon correlation technique, appl. to sinusoidally perturbed flow characts. meas. 77−42945
pipe, containing anomalously viscous liq., convection intensification by spiral swirlers 79−94461
pipe, rotating, curved, convection heat transfer, appl. to spacecraft spin system 78−94737
pipe, swirled flow, friction law and form parameters 79−37329
pipe, swirled flow, integral calc. method 79−37402
pipe flow, rotating pipe of elliptic cross-section 80−92220
pipe inlets, turbulent local mass and heat transfer, swirling effects 80−64542
pipe rotating perpendicular to axis, liq. fully developed heat transfer 77−58689
planetary boundary layer model with variable eddy viscosity coeff. 77−9482
plasma, rotation speed measurement, in external magnetic field *(German)* 78−42821
plate, rotating, 3-D boundary layer turbulence, effects of rotating radial end-plates 80−69843
plates, eddy motions induced by water waves and periodic flows 80−33679
point source in rotating fluid in cylindrical tube in mag. field 79−14490
Poiseuille flow, plane, horiz., rot., stability, effect of Coriolis force 78−67203
Poiseuille pipe flow of incompressible second order fluid *(German)* 78−87395
Poiseuille-like flow of rot. gas 77−15043
polymer solns., mass transfer and drag reduction near wall, electrochemical methods 79−77138
polymer solution, flow visualization near rot. disc 79−72914
polymer solution, semidilute, hydrodynamic interaction of two permeable spheres, method of reflections 78−71394
polymer solutions, mol. diffusion coeff. meas. using impedance meas. technique 79−23328
polymers, unsteady flow in rotary devices 80−24061
porous cylinder, rot., lift, torque, appl. to wind power generation 78−46987
porous disc and fluid at infinity, noncoaxial rotations, Navier-Stokes eqns. soln. 77−68600
porous disc and rot. disc, fluid flow 80−64569
porous tube array, flowfield struct., turbulence and vorticity distribs. 77−27589
porous tube entrance segment, heat transfer anal. with initial flow swirl and transverse injection 77−24025
potential flow about body of revolution, axial singularity distribs. 80−64570
power law liquid, flow between eccentric rotating cylinders 77−65766
pressure distribution in elastic hydrodynamic contact of cylinders 77−84208
propeller wake, stalling conditions, 3-dimens. flow field obs. 78−46972
pulsating flow in rotating straight pipe 77−62258
pump, centrifugal, impeller flow, quasi two-dimens. method of singularities 78−46986
quasi-geostrophic two-layer turbulence, simple special case 78−81186
quasi-viscometric flow around rot. sphere 79−60023
quasiperiodic flow between rot. cylinders, second charact. mode visualisation 80−28519
radial convergent duct, air flow heat transfer boundary conditions, turbulent and transition flow 78−83476
radial pipe with liq. film, Coriolis effect, film width and vaporisation 79−18955
radial turbomachine, meridian plane characts. for subsonic and transonic flow, finite element calcs. *(French)* 80−38418
radially progressive surface waves from rot. circular cylinder 80−14722
radially rotating pipe, heat transfer coeffs. in various flow regimes 78−1668
rapidly rot. gas, free jet expansion, Newtonian thin shock layer approx. 80−74888
rapidly rotating flows in geophysical fluid dynamics 77−45102
rapidly rotating gases, thermally-driven axially antisymm. geostrophic flows, flow field calc. 79−90259
rarefied gas, laminar boundary layers with swirl in slip regime 77−31336
Rayleigh-Taylor instability in presence of rot. 77−19591
Rayleigh-Taylor instability in presence of rotation 80−53749
rayleigh-Taylor stability of a rotating liquid shell 79−14381
recirculating flow behind backward-facing step, mean vel. and Reynolds stresses meas. 80−19355
recirculating laminar flow between shrouded rotating disks, num. soln. 79−64667
rectangular channels, heat transfer, press. drop calcs. *(German)* 80−1594
recycling flow over bottom topography in a rotating annulus 78−90916
Reiner centripetal effect in liquids, interferometric meas. for H_2O and alcohol-glycerine 78−51174
Reiner-Rivlin fluid, slow and steady rotation of solid formed by revolution of limacon 77−72306
relativistic case, centre of stationary rotating star, tetrad formalism 80−51222
relativistic rotating fluid cylinder, field eqns. 79−50815
resolving spheroid, instantaneous motion of surrounding liquid, viscous flow *(French)* 77−42845
retarding torque on rot. concentric spheres in viscous fluid 77−15042
rheometer, rot., inertial normal force correction 78−63520
rimming flow, numerical simulation of free-surface flow with surface tension 78−22353
Rivlin-Ericksen flow, between 2 parallel plates 78−30320
Rivlin-Ericksen fluids, steady universal motion 79−68757
roll-cell instability, rot. laminar and turbulent channel flows 77−946
Rossby wave interactions and stability in rot. two-layer fluid on β-plane 80−10257
Rossby waves, topographically induced, laboratory expts. and theory 77−64289
Rossby waves in rot. two-layer fluid on β-plane, reson. interactions 79−77145
Rossby waves in rotating annulus, laboratory and theoretical study *(Russian)* 80−19509
rotating channel flow, hydraulic control theory 77−56642
rotating channel with porous walls, heat transfer and temp. distrib. 78−30355
rotating coaxial disks, Newton-Raphson method 77−72308
rotating disc, laminar boundary layer heat transfer, Prandtl no. effects calcs. 77−31306
rotating disc in polymer solutions under a turbulent regime 80−33634
rotating disc problem, Taylor coefficients, computational methods 80−106802
rotating disc with suction and stationary disc, flow between 78−46975
rotating disk, in Ostwald fluid, nonstationary mass transfer 79−23328
rotating fluid dynamics, review *(French)* 78−30300
rotating gaseous masses, secular stability and points of bifurcation 77−42843
rotating liquid figures in equilibrium, angular velocity determ. *(Russian)* 78−51176
rotating rods and plates, mass transfer and flow regimes 80−79326
rotating sphere, small yaw ang., laminar boundary layer *(Japanese)* 78−38272
rotating spheres, heat transfer coeffs. for gas-solid two-phase flow 80−19369
rotating square cavity, laminar flow, flow problems with body forces soln. 79−68715
rotating stratified fluid, appl. of radiation condition for a source 79−64676
rotational transonic flow and inviscid potential computation by quasi-natural numerical methods 79−64666
salt fingers, rot. effects 79−50767
sea straits and wide estuaries, geostrophic adjustment, theory and lab. expt. 79−20847
sea straits geostrophic adjustment, theory and laboratory expts. for two-layer system 79−48503
second-order fluid between infinite rot. discs with injection 77−11223
second-order fluid forced flow against rot. disc with uniform high suction 77−27564
secondary flow in cascades, theory *(Japanese)* 78−83412
secondary flows and stability study of rotating spherical layers at arbitrary Rossby numbers 79−18899
secondary polyvortex currents in rotating elliptical cylinders *(Russian)* 78−38338
selfgravitating liquid ring with inner flow *(Russian)* 78−65783
separated flow, free shear layer behaviour in rotating systems 79−77137
separator intertray space, development of liq. laminar flow 79−81893
shock and detonation wave anal. 80−53792
slightly rarefied gas, unsteady motion about rotating cylinder, slip effects 77−39312
slow viscous flow due to motion of sphere on axis of circular cone 80−14654
slow viscous rotation of a sphere on the axis of a circular cone 80−87777
slowly rotating sphere submerged in fluid with surfactant surface layer 80−48717
small sphere in slow viscous flow, shear and rot. flow, forces calc. 79−37282
small sphere motion in rot. vel. field, rel. to particles suspension in turbulence 77−58771
sound generation by vorticity waves in swirling duct flows 77−62261
sound propagation, as example of flow-acoustics 77−75903
sound wave, effect of rotation on flow past flat plate due to standing sound field 80−24028
spatial oscillations of horizontally heated rotating fluid 79−10569
sphere, nonconducting, slowly rotating in steady MHD flow, exact soln. 80−33695
sphere rotating in viscous fluid, induced flow 77−15036
sphere slow rotation in confined vol. of dilute gas 79−77187
spherical annulus flow, torque characts., secondary flow effects 80−43718
spherical Couette flows, loss of stability between two rotating spheres 80−1527
spherical mass. MHD stationary equilibrium in uniform rotation *(Italian)* 77−55093
spherical movements of viscous incompressible fluids, meteorological model 79−16598
spherical permeable shell motion at axis of rotating viscous incompressible fluid 79−18944
spherical rot. fluid shell with non-uniform heating, thermal stability 77−31314
spherically symmetric polymer, time depend. compressible flow, Faxen theorems 79−23345
spheroid, slow motion in rotating fluid 80−14710
spin up, in cylindrical container, numerical solns. and laser-Doppler meas. 78−46977
spin up of rapidly rot. gas 78−55652
spin-up and spin-down, vel. meas., stability 77−11196
spin-up and spin-down, Wedemeyer model extension 77−11195
spin-up from rest of fluid in cylinder 78−14023
spinning disc causing laminar and turbulent flow, mass transfer 79−41691
spinning yawed axisymmetric body, three-dimens. flow 80−38422
spiral flow between coaxial cylinders, branching and stability loss 80−19406
squeeze-films, elastico viscous, torsional balance rheometer meas. 77−3851
squeeze-films, elastico-viscous, superimposed rotation 77−3850
stability of flow between two rotating cylinders, effect of thermal diffusion 78−18308
stability of viscous flow between rotating concentric cylinders with an axial flow 79−59989
stability problems with time-depend. boundary conditions, numerical simulation methods, review 80−19411

rotational flow continued
stationary cellular convection, rotation effects *(German)* 79−81904
stationary disc in rotating cylinder, laminar compressible flow 80−43728
stationary Ekman flow, bifurcation into stable periodic flow 79−32449
stationary flow between porous rotating cylinders in a radial magnetic field 80−83857
stationary motion of finite mass of fluid 79−23331
stationary nonlinear waves in stratified rot. fluid, periodic solns., solitary waves *(Russian)* 79−7378
steady and unsteady, fluid in finite cylindrical container 80−14708
steady flow between a rotating and a porous stationary disc in the presence of transverse magnetic field 78−79382
steady flow between a rotating circular cylinder and fixed square cylinder 80−24035
steady flow between rotating disc and stationary naturally permeable disc 79−72934
steady flow in porous region between two rot. spheres 79−46382
steady flow in rapidly rot. variable area rectangular ducts, small divergences 77−62260
steady rotating flow over topography, steady β-plane channel, quasi-linear theory 80−92159
steady screw motion, impossibility in Navier-Stokes fluid 79−94627
steady streaming induced between oscillating circular cylinders 80−1602
steady viscous incompress. flow between rotating spheres, improved solns. 79−81892
steam condensation on external entrance length of cooled rot. tube 77−75906
steel shells, spinning, aerodynamic ablation, side force 79−37347
Stewartson layer, stability in a rapidly rot. compressible fluid 78−46979
Stokes, non-stationary, rotational historic term 79−41654
Stokes flow, separation, appl. of bipolar coordinates to two-dimensional creeping motion of liquid 79−14375
Stokes flow, slender body theory for viscous incompressible fluid 80−92160
Stokes flow, three-dimensional Moffatt-type eddies due to Stokeslet in corner 80−74891
Stokes flow due to body rot. in micropolar fluid 78−38372
stokes flow due to circular scraping 79−46329
Stokes flow in conical trenches 78−83413
Stokes series, computed extension, circular boundary flow 78−42583
stratified and rotating fluids, review of selected aspects 77−68660
stratified Boussinesq fluid, in rotating spherical annuli, small Reynolds number convection 80−6047
stratified flow, in horizontal mag. field, stability 78−67246
stratified flow in rot. annulus, expt. 77−31357
stratified fluid, internal and inertial waves 78−67245
stratified fluid, parallel shear flow, baroclinic and barotropic instability 80−98328
stratified fluid, rot., MHD stability 78−55692
stratified medium, rotating, small oscillations, internal waves 77−68664
stratified rotating fluid, mass transfer between layers causing vortex 80−12401
stratified rotating liquid, waves energy relations *(Russian)* 77−27575
streamline patterns and eddies in low-Reynolds-number flow 80−33612
subcritical steady plane flow past profile with sharp trailing edge, smoothness and circulation *(French)* 78−18312
subsonic rotational and transonic mixed flows, numerical simulation using fast super-dashpot time-dependent technique 80−83813
subsonic turbulent jet, entry zone flow wave struct., eddies 80−14773
supercritical He, pool heat transfer, in high centrifugal accel. field 77−15034
superfluid, gauge wheel of superfluid ^{4}He, two fluid model 80−44379
superposed fluids, MHD instability, flow through porous medium 78−14089
surface waves, comparative theorem 79−50745
surface waves, finite depth rotating fluid, Green's function anal. 79−37324
surface waves in a rotating fluid due to sources and internal boundaries 79−37323
surface waves of rotating cylindrical layer of fluid *(Russian)* 77−925
surge and rot. stall, flow instabilities 80−106803
suspension, centrifugal sedimentation of large particles 78−59462
swirl flows in circular pipes *(Japanese)* 77−47022
swirl flows in combustion, review 78−1755
swirl nozzle with annular exit section, anal. of outlet flow rate *(Chinese)* 79−32624
swirled flow, sprayed liquid hydrodynamics 80−79325
swirled flow characts. in swirl-nozzle type injector 79−86444
swirled flow in pipe entrance, heat transfer law 78−5754
swirled jet, stream parameters at exit cross section of annular nozzle 77−15090
swirled jet propag. in channel 77−58755
swirled turbulent flow in cylindrical channels, heat and momentum transport, local props. 80−14819
swirling film cooling in initial tube section 79−1256
swirling flow, fluid between rotating discs, nonmonotonicity of solns. 78−59404
swirling flow, non-unique solns. to Navier-Stokes eqns. 79−46321
swirling flow hydrodynamic parameters in flow transducer input, expt. 77−72390
swirling flow in composite pipe bends 79−32667
swirling flow managment, appl. to wind tunnel and duct flows 79−41754
swirling isothermal flow in long tube, local and integral parameters 78−83489
swirling jets, confined, axisymmetric viscous incompressible flow, numerical prediction 77−84286
swirling one- and two-phase liq.-gas flow in tube, heat and mass transfer 78−30339
swirling or axisymmetric flow, meas. using press. difference meter 80−10330
swirling particle fluids, computer studies, evolution of planetary-type bodies 79−35121
swirling recirculating reacting turbulent jets passing through diffusers 79−50764
swirling turbulent radiative arc heater flowfield, model 79−41764
swirling water bells 79−50733
symmetric Couette and Taylor flow between rotating coaxial cylinders, Navier-Stokes eqn. solns. *(German)* 78−94750
symmetric flow between concentric spheres *(German)* 80−1609
Taylor column for hemisphere, nonlinear effects 77−11199
rotational flow continued
Taylor column irregularity in rapidly rotating MHD fluid, mag. field effects 80−43786
Taylor instability, transition to turbulence 80−28491
Taylor vortex flow, heat and mass transfer with const. axial flow rates 77−15035
Taylor vortices near instability point, amplitude, mode-coupling theory 77−68598
temperature boundary layer on rotating curved surface, constant wall temp. case 79−81903
thermal boundary layer, axisymmetric rot. body, arbitrary surface temp. distrib., exact solns. 78−75133
thermal convection in rotating fluid subject to horizontal temp. gradient, baroclinic waves 77−84251
thermal diffusion and convective stability, role of rotating container 79−68725
thermal instability in horizontal rotating fluid layer, surface viscosity and deformation 78−63438
thermally driven rotating annulus, cyclic vars. of imposed temp. const. 79−7377
thermally forced stratified rot. fluids, axisymmetric steady motion 80−69844
thermally stratified rot. fluid, secular spin-up, expt. and numerical study 79−77217
thermoelectric MHD, pipe end problem, boundary layers and rotation 80−69942
three dimensional parallel shear flows, stability and transition for rot. disc 80−74887
three-dimensional flow in highly-loaded axial turbomachine, vorticity effects 78−26130
throughflow between rotating and stationary disk calc., laminar, finite difference method appl. *(Japanese)* 80−6064
topographic effects in rapidly rot. flow over transverse ridge 78−28245
torque suppression in mech. stirred liqs. and multiphase systems, additives 77−3864
torsionally oscillating impermeable disc and stationary naturally permeable disc, flow streamlines 80−24030
transitional flow conditions on rot. disc 78−46980
translational-rotational flow stability, Rayleigh method generalisation 77−58702
transonic, nozzle, relaxation solution 78−30312
transverse force on a spinning porous sphere at small Reynolds number 79−77243
trapped oscillations in rotating fluid, viscous effects, num. simulation 77−55015
trapped vortices in rotating flow 78−55650
tube array, whirling instability, phase relationships 78−51175
tube flow, with spiral blades, heat transfer, drag resistance 78−1672
tube inlet zone, flow and heat transfer with injection into swirled flow 79−98717
turbomachine annuli with swirl, small shear disturbance propag. 77−84258
turbulence, non isotropic homogeneous, pure rotation influence *(French)* 80−33568
turbulence characteristics *(Russian)* 79−59991
turbulence in rot. layer, convective wave motion *(Russian)* 77−58670
turbulence in rotational Couette flow, power spectra of nonlinearly coupled waves 78−30261
turbulence onset *(Russian)* 79−46327
turbulent, velocity vector and stress tensor component measurement *(Russian)* 80−83867
turbulent convection within rapidly rotating superadiabatic fluids with horizontal temperature gradients 78−90913
turbulent flow, annular, with inner cylinder rot., computation 80−1544
turbulent flow, curved and rot., press. gradient-vel. correls. 78−26128
turbulent infinitely long axisymm. theoretical anal. 77−68599
turbulent recirculating jet flow, initial mixing region meas. 77−27570
turbulent shear flow, fully developed, local closure condition *(German)* 77−11179
turbulent swirling flow 78−71337
turbulent thermal convection in presence of rot. and mag. field, stellar and planetary dynamos appl. 80−6042
turbulent transport coefficient, rot. fluid, rel. to stellar interiors 78−36452
turbulent transport to rot. cylinder 77−7402
turbulent two-dimens. recirculating flow, numerical model calcs. 80−19358
turbulent wake of axial flow turbomachinery rotor blades, numerical anal. 80−1596
twisted gas flow in pipe, numerical soln. 77−84261
two coaxial cylinders, fluctuating flow and heat transfer for incompressible fluid 80−24013
two coaxial rotating discs, viscous fluid unsteady motion and heat transfer 79−94633
two dimensional recirculating flow, finite difference grid for non-rectangular flow fields 79−14374
two moderately rotating porous discs, heat transfer 80−103028
two parallel corotating discs, laminar flow and heat transfer, shear pump appl. *(German)* 80−69840
two rotating discs, air flow in gap between 80−92156
two spheres rotating perpendicular to an interface 79−90313
two-dimensional rotational flow, large Reynolds no., numerical calc., discrete vortices with random walk 77−31312
two-layer fluid, barotropic and baroclinic Rossby waves interactions and instabilities 79−57955
two-phase flow, annular, crit. heat flux, swirl effect 80−10113
two-phase flow between parallel corotating discs, laminar or turbulent throughflow, bulk-parameter anal. 77−39336
two-phase mixture flow in rotary mixer, optimal dimensions 78−63485
two-phase recirculating flow, num. calc. procedure 77−55081
two-phase swirling flow in short vortex chamber 79−72924
ultracentrifuge, flow, isotope conc. field, numerical model 79−1199
unsteady axisymmetric 1-dimens. motions of ideal incompressible liquid, small perturbations 80−59004
unsteady flow arising from rotating fluid above a fixed plane 80−24029
unsteady forced convection heat transfer from impulsively started circ. cylinder 79−27633
unsteady heat transfer from rotating disc or cone with large suction 77−47025
unsteady laminar boundary layers, collision at equator of rotating sphere 79−72896

rotational flow continued
unsteady long wave reflection from walls of rotating channel 77−3832
unsteady MHD flow in rotating system, Hall current effects 80−33704
unsteady rotating boundary layer flows between porous plates 77−47112
unsteady similarity equations for the flow above a rotating disc in a rotating fluid 79−41697
velocity distrib., wall friction in rotational turbulent laminar boundary flow *(German)* 80−1526
velocity measurements inside a rotating cylindrical cavity with a radial outflow of fluid 80−96275
viscoelastic flow past stationary and rotating cylinders 80−43744
viscoelastic fluid, free surface between cylinders rotating at different speeds 80−59082
viscoelastic fluid, steady flow and heat transfer between two coaxial rot. discs 80−14755
viscoelastic fluid film, flow along conical rotor 78−1697
viscoelastic fluid flow between rotating coaxial disks, numerical anal. 79−77041
viscoelastic liq. film in rot. mixer 79−90291
viscoelastic liquid, heat transfer in rot. flow, suction and injection effects 80−33596
viscoelastic liquid steady flow about porous rotating disc 79−32586
viscoelastic Maxwell liquid, torsional transient motion between concentric spheres 77−62283
viscoelastic non-Newtonian fluid flow between eccentric rotating cylinders 77−84282
viscometric flow around rotating sphere *(German)* 77−80187
viscous axial flow in annulus entry region with rotating inner cylinder, stability 77−23967
viscous axial flow in annulus with rot. cylinder, instability 77−7404
viscous axial motion, gas between rotating plate and container wall *(German)* 78−90919
viscous boundary layers in rot. fluid driven by periodic flows 77−3804
viscous flow, between concentric rot. spheres, visualisation and meas. 77−15038
viscous flow between rot. coaxial cylinders, hydrodynamic instability 77−72307
viscous flow between rotating discs with injection on the porous disc 80−14713
viscous flow between two concentric rotational spherical surfaces *(German)* 78−94751
viscous flow between two revolving spheres, unstable motion *(Russian)* 79−32530
viscous flow in a partially filled rotating horizontal cylinder, effect of speed of rotation on bubble position 79−77125
viscous flow in a rotating channel bounded below by a permeable bed 78−91013
viscous flow in cylinder with circular barrier on the bottom 79−41693
viscous fluid, flow and heat transfer due to disc small torsional oscills. 79−68691
viscous fluid, steady rot. screw motion 79−50736
viscous fluid flow due to rotating torus 80−43713
viscous fluid flow through slot between fixed and rotating surfaces of revolution *(Polish)* 78−79300
viscous fluid in rotating channel pulsatile flow 80−10311
viscous fluids in spherical motion, asymptotic behaviour *(French)* 77−65743
viscous incompressible flow between rotating spheres, numerical anal. 79−4019
viscous incompressible liquid flow, momentum eqn. anal. *(Russian)* 79−59992
viscous liquid filled cavity in solid, free rotational motion 80−38420
viscous liquid flow through annular clearance over rotating inner cylinder 80−64626
viscous rotation of sphere on axis of circular cone 78−79326
viscous toroidal eddy generation in cylinder, Stokeslet streamlines 80−19404
von Karman swirling flows 80−74894
vortex breakdown regimes, in rot. cylindrical cavity, identification 79−50731
vortices formation near reson. for elastoid-inertia waves 80−12473
vortices in rotating stratified fluids, theory and atmospheric appls. 79−39814
water, apparent Weissenberg effect 80−83787
wave linear propagation in rotating fluid, critical level absorption and valve effects 80−106805
wave propagation, gravit. instability, rot. and streaming effects 79−37293
wave transport in stratified, rotating fluids 78−89192
wave-transition spectra and vacillation in open rotating cylinder 78−14020
wave/mean flow interaction, mean motion induced by transient inertio-gravity waves 80−105029
waves, low-freq., in rot. stratified channel 77−47030
wavy rod rotated, induced secondary flow, method of domain perturbations 78−63456
weak polymer solutions, flow props. in narrow channel between rotating and stationary discs *(Russian)* 80−59089
Wedemeyer spin up model, Ekman compatibility conditions, Navier-Stokes eqns. 80−83802
Weissenberg effect, review of expts. 79−60025
Fe_2O_4, suspension in oil, motion in rotating mag. field *(German)* 77−75983
He, superfluid, thermal counterflow in rot. flow, vortices and turbulence 79−86946
^{3}He, rotating superfluid, equilibrium order parameters, chemical potentials 80−96713
^{3}He, superfluid A-phase, internal struct. of de Gennes disgyration 79−60584
^{4}He, rotating, second sound attenuation in presence of const. supercritical heat flow *(Russian)* 77−55409
^{4}He, rotating superfluid, equilibrium order parameters, chemical potentials 80−96713
^{4}He, superflow in thin rotating annulus 77−55407
^{4}He, superfluid, nonstationary rot. regime ref. to superfluidity of pulsars 80−98683
^{4}He, superfluid, rotating Couette flow, hydrodynamic instabilities, attenuation of second sound resonances 79−55964
^{4}He, superfluid film, thinning in persistent flow 77−35792
^{4}He, superfluid rot. film, melting of two-dimensional vortex lattices 80−2539

rotational flow continued
Hg layer with rot. and mag. field, cell sizes at thermal convection onset 77−54991
MHD flow and heat transfer, porous disc eccentric rotations at infinity 79−18965
Na current surge tank, flow meas., LMFBR cooling system *(Czech)* 77−67792
Sn, molten rotating stream, vortical filament generation during solidification *(Russian)* 78−88460
U fuel enrichment, flow profile meas. of gas in rotating cylinder 77−46382

rotational isomerism
1,3-butadiene-1-one, spectroscopic consts., IR and microwave spectra, prep. 80−18859
S,S′-dimethyldithiocarbonate, pot. for rot. about C(sp^2)-S bonds, electron diffr. obs. 80−23572
AB_5, non-transition element complexes, shapes and other props. 78−86790
acetaldehyde, first triplet state geometry, fragmentation into free radicals 80−47915
acetaldehyde, internal rotation barriers, exchange energy and orbital orthogonality effects 77−75049
acetic, acid, ideal gas thermodynamic props. 78−51275
acetic acid, methyl group dynamics, NMR 78−29802
acetophenone, liquid, far IR absorpt., mol. vibrs., internal rot., dipoles *(French)* 77−24827
acetyl cyanide, (^{15}N), microwave spectrum, rot. consts., internal rot. barrier 77−75141
adamantane, derivatives in solution, mol. motion and methyl group rot. barriers from ^{13}C NMR relax. times 80−74179
L-alanine, solid, H bonding, wide line NMR obs. 78−52362
alcohol, dielec. const., hindered mol. rot. influence 78−43767
aliphatic alcohols, conform., rot. isomerism calcs. *(German)* 78−50541
alkane chain internal rot. correlation times, from ^{13}C T_1 data 78−17688
alkanes, ab initio calcs. using FSGO, internal rot. 78−82639
n-alkanes, liq., Raman spectra, longit. acoustic modes and gauche-trans energy difference 80−93295
alkyl chains, ^{13}C longitudinal relax. times and nuclear Overhauser enhancement anal. 80−83390
N-alkyl free radicals, ESR study, conformational anal. of N-alkyl group 78−62831
alkyl trichloroacetates, solns., intramol. rot., permittivity and dielectric loss, microwave meas. 78−31145
allene, C-C double bond rot. barrier, ab initio open-shell restricted SCF calc. 78−1099
allene, internal rot. in ground electronic state 77−67975
allene, transition state for internal rot., HF/STO-3G calcs. with correlation energy corrections 78−25430
allylamine, N-cis lone-pair gauche rotamer ground state microwave spectrum anal. 78−82720
amide C-N bond character, metal ion bonding effects 77−6801
amide group molecules empirical pot. model EPEN/2, development, parameter testing 79−54935
amino acid side chains, NMR relax. due to multiple internal rots. 78−94340
aminoborylpolyynes, intermolecular interaction through triple bonds, internal rot. 80−106370
aminopolyynes, intermolecular interaction through triple bonds, internal rot. 80−106370
aniline, amino group inversion and torsion, far IR spectra 77−10670
aniline-ND_2(-NHD), far-IR vap. phase spectra, assignments pot. function calcs. 77−75144
anilines, substituted, in benzene soln., dielectric relax. time, dipole moment 80−50259
anilines, substituted, in nonpolar solvent, dielec. relax. obs. 80−55022
anisole and -d_3, Raman spectra, low freq. vibrs., torsional barrier 78−25543
anthronyl radicals, ESR, temp. depend. phenyl twist angles 79−18210
p-(9-anthryl)-N,N-dimethylaniline derivatives, excited emitting states in polar solvents, fluoresc. 78−5263
antimony ethyl derivative, Et_3Sb, IR and Raman spectra, rot. isomerism 79−41167
apomyoglobin reconstituted with ^{111}In(III)mesoprotoporphyrin IX, rot. correl. time determ. 80−76698
aromatic polyesters, with S atoms, configurational props. 80−74269
arsenic ethyl derivative, Et_3As, IR and Raman spectra, rot. isomerism 79−41167
2-aryl-3-benzylidenamino-4-thiazolidones, IR and NMR spectra, solvent effects and isomer conform. *(Italian)* 79−3596
aziridine, anhydrous and hydrated, inversion calc. 78−9272
azomethane, steric strain relief accompanying isomerisation 79−10230
benzaldehyde, and isomeric phthalaldehydes, dipole moments meas., config., ab initio MO calc. 80−58410
benzaldehydes, o- and m-substituted fluoro- and chloro- forms, rot. isomerism, $n\pi^*$ spectra obs. 80−5631
benzaldehydes in EBBA liq. cryst., NMR, mol. struct., reorientation and order matrix 78−5251
benzene, torsion, one-electron props. variation, electronic and nuclear components partitioning 77−83491
benzenes, substituted, cryst., reorientation motion, site models with non-equivalent sites, dielec. relax. 79−11382
benzenesenol, CCl_4 soln., PMR, barrier to internal rot. 78−1006
benzil, in PMMA glass, luminesc. temp. depend. matrix controlled photorotamerism 79−22743
benzotrifluoride, and mono-substituted derivatives, vibr. spectra, internal rot. 77−83598
benzyl carbonium ion, internal rot. barrier, MINDO/2(3) forces method 78−9078
benzyl fluoride, mol. struct., NMR and gas electron diffraction obs., ab initio and mol. mechanics calcs. 80−23574
benzyl-phosphonium radical, EPR spectra temp. depend., H-P coupling consts., conformation and rot. *(German)* 77−18950
Δ^6-bicyclo(3,2,0)heptane, conformational mobility 80−99587
bicyclopropyl, Raman study of rotational isomers 79−18194
1,1′-binaphthyl, conformational changes, picosec. dynamics 78−25625
1,1′-binaphthyl, $T_n \leftarrow T_1$ absorption spectrum in rigid and fluid media, CNDO/A study 79−76355
bis(fluoroxy)difluoromethane, ab initio MO calcs. of geometry, torsional barriers 78−90313

rotational isomerism continued
bis(trifluoromethyl)peroxide, gas and solid, Raman, IR spectra, internal rot. barrier of CF_3 78−29789
bond order rel. to internal rot. 79−36498
4-bromo-m-thiocresol, liq., dielectric relax. mechanisms 79−42891
bromoethane, mol. parameters, vibr., pot. barrier height etc., data tables 79−76409
2-bromopropene, barriers to internal rotation 78−9273
bromtrinitromethane, electron diffr. study of gas phase mol. struct., rot. isomerism 78−1080
1,3-butadiene, FSGO calcs. of orbital energies, locations, dipole moments, charge distribs. 77−67976
n-butane, conformational hypersurface, anal. 79−41252
n-butane, LF vibr. spectrum, methyl torsional pot. function, internal rot. 79−89670
butane, liq., enthalpy difference between rot. isomers, IR spectrosc. obs. 80−106404
n-butane, skeletal alkane fluid simulation, vibr., rot., torsional gauche/trans relax., diffusion const. 79−1378
n-butane, vibr. shrinkages, mol. struct., electron diffr. obs. 77−50535
n-butane in tetrachloromethane, gauch-trans equilib. const., mol. dynamics and Monte Carlo anal. 79−70308
tert-butanol, mol. dynamics, liq. and cryst. states, neutron inelastic scatt. obs. 78−75599
trans-2-butene, Raman and IR spectra, torsional mode pot. function 79−89676
1-butene oxide, gas, microwave spectrum 79−13703
t-butyl acetate, rot. isomerism, dielect. and Raman spectra 80−106328
t-butyl formate, deuteration effects, IR and Raman spectra 79−50016
t-butyl formate, rot. isomerism, dielect. and Raman spectra 80−106328
butylsilane-d_0,($-d_n$), vibr. spectra, normal vibrs. and rot. isomerism 79−31523
3-butyn-1-ol, vibr. spectra, assignments, rot. isomerism 80−58257
carbenes, bond angles, inversion barriers, singlet-triplet energy differences, struct. fragments method 77−10782
chloral, liq., permittivity, dielec. loss, up to 60 GHz 78−60384
chloro(ethyl)silanes and its C derivatives, Raman spectra, mol. vibr. and rot. isomerism 80−87134
3-chloro-1-butene, rot. isomerism, vibr. spectra assignments 78−58702
1-chloro-2,2-dimethylpropane, IR and Raman spectra, vibr. assignment 80−74169
3-chloro-2-methylpentane, IR spectra of film, rot. isomerism 79−59595
1-chloro-2-methylpropane, IR and Raman spectra, vibr. assignment 80−74169
2-chloro-4-methylpentane, IR spectra of film, rot. isomerism 79−59595
4-chloro-α-toluothiol, liq., dielectric relax. mechanisms 79−42891
chloroacetaldehyde, s-trans conformation barrier height 77−61872
o-chlorobenzoic acid, solid, H bonding, wide line NMR obs. 78−52362
p-(N-chlorobenzylidene)-p-chloraniline, cryst., polymorphism, cryst. struct. rel. to mol. conform. 78−75611
2-chlorobuta-1,3-diene, far IR and Raman spectra, internal rot. 79−89668
4-chlorobutyrylchloride, Raman and vibr. IR spectra of solid and liq., rot. isomerism 78−62810
3-chlorodiphenyl, in dipolar aprotic solvent, internal rot. barrier, ^{13}C T_1, obs. 78−29860
2-chloroethanol, IR and Raman spectra, normal coord. anal., isomerism 78−74661
2-chloroethyl radical, struct., ab initio calcs. 80−83252
chloromethyl cyclopropane, microwave spectra, rot. and distortion consts. 79−36625
chloromethyl formate($-d_1$,d_2,d_3), gas, solid. and liq., IR spectra assignments and struct. 80−32715
chlorotrinitromethane, electron diffr. study of gas phase mol. struct., rot. isomerism 78−1080
cinnamyldehyde, rotational isomerism study by US absorpt. and vel. meas. 77−27196
compounds with hindered internal rot., microwave spectra, free rotor states obs. 79−18179
condensed phase mol. reorientation, correlation times, librational model 78−1968
conformational dynamics and the rotational isomeric state model 78−90315
conformations of rotational isomers, interactive access data program 78−62786
coupled molecular rotational diffusion and conform. change 78−22613
crotonaldehyde, rotational isomerism study by US absorpt. and vel. meas. 77−27196
cyclobutadiene, π face bonding with CO, HCN, benzene 79−98180
cyclobutanol-d_0,-d_1, conformation, microwave spectrum 78−86852
cyclobutylmethylether, IR and Raman spectra, config. 79−31525
cyclododecane, force field, PMR of deuterated isotopomers 79−45695
cycloheptane, conformation maps 77−57900
cycloheptane, cyclooctane, high resoln. rot. Raman spectra 77−75163
cyclohexane, conformation maps 77−57900
cyclohexanol, polymorphism, Raman spectroscopy 77−73138
cyclopentadienyl platinum (IV) complexes, mech. spectroscopy to meas. ring rotation 80−74259
cyclopentane, pseudorot., effect of 10 fold barrier 78−74792
cyclopopane, conformations, rot. consts., microwave spectrum 79−98075
cyclopropyl carbinyl cation, internal rot. barrier, MINDO/2(3) forces method 78−9078
decylammonium chloride micelles, ^{13}C longitudinal relax. times and nuclear Overhauser enhancement anal. 80−83390
di thioformic acid, cis and trans isomers, rot. microwave spectra and config. 79−63989
trans-1,2-di-(1-napthyl)-ethylene, conformeric fluoresc., chromophoric fragments rot. 77−485
1,4-di-(2-naphthyl)-benzene, conformic fluoresc., chromophoric fragments rot. 77−485
2,4-di-p-bromophenyl pentane, polystyrene model mol., US relax., mol. dynamics 79−73258
dialkyl carbonates, liq., US, microwave dielect. relaxation 79−56717
diamond clusters and corresponding saturated hydrocarbon ab-initio HF and PCILO calcs. 78−42951
diarylethylene, luminesc. spectra and rot. isomerism 79−85991
meso-2,3-dibromo-1,4-dichlorobutane, rot. isomerism, IR and Raman spectra 80−981
dibutyl-phenyl-benzoyloxy-benzoate, nematic liq. cryst., rot. barrier, PCILO and CNDO/2 calcs. 80−33874
rotational isomerism continued
dicarbonyl compounds in soln., internal motion, dielectric relax., ^{13}C NMR relax., far IR spectra 77−28517
3,5-dichlorobenzyl mercaptan, PMR, barrier to rot. about C-C bond 78−17696
1,2-dichloroethane, conformer equilibrium by effusive beam-matrix IR spectroscopy 80−48100
1,2-dichloroethane, enclathrated, conform., reorientation, PMR line shape anal. 79−91300
trans-1,2-dichloroethane, solid, NQR at high press., hindered rot. 79−95672
dicyanoalkanes, in benzene soln., microwave absorption, internal rot. 78−60385
N,N-diethyl formamide, dipole moment, dielectric relax., internal rot., microwave absorpt. 79−56716
diethylcarbonate, liq., alkoxy group internal torsion, extended microwave/far IR anal. 78−19457
diethylsilane-d_0($-d_n$), vibr. spectra, normal vibrs. and rot. isomerism 79−31524
1,2-difluoroethane, gauche-trans conformers, IR and Raman spectra, vibr. 78−17667
1,2-difluoroethane, internal rotation temp. frozen in supersonic jet, matrix IR spectroscopy 80−9594
diformamide, torsional pot. barriers, ab initio and partition of energy methods 77−88588
dihydroxycarbene, singlet and triplet state rot. pot. surfaces 80−32627
1,4-dimethoxy-2,6-dimethylbenzene, methyl reorientations, NMR relax. and inelastic neutron scatt. obs. 79−61253
4-4′-dimethoxyazoxybenzene-d_{14}, orientational order and internal rot., D NMR obs. 79−50987
dimethoxymethane, vibr. spectra and rot. isomerism 80−106325
dimethyl ether, internal rot., struct. relax., ab initio SCF calcs. 78−90077
dimethyl ether -d_0, -d_3, -d_6, internal rot., far IR and Raman spectra 77−79612
dimethyl phosphate, potentials of internal rot. 77−16901
dimethyl selenide-d_6, microwave spectrum in ground and excited torsional states *(German)* 77−57992
dimethyl tin difluoride, solid, methyl reorient., low temp. phase transition, neutron scatt. obs. 79−27932
dimethylallene, excited states, microwave spectrum and strong Coriolis coupling 78−9141
dimethylboric anhydride, IR and Raman spectra, vibr. and struct. 78−25531
2,3-dimethylbuta-1,3-diene, IR, Raman spectra, torsional pot. function, thermodynamic function 80−43046
dimethylcarbonate, liq., alkoxy group internal torsion, extended microwave/far IR anal. 78−19457
1,1-dimethylcyclopropane-d_0,-d_6, internal rot., Raman spectra 78−985
1,2-dimethyldiborane, IR and Raman spectra of cis and trans isomers 78−86868
dimethylformamide, intramolecular exchange rate determ. from ^{13}C spin-lattice relax. times 80−69169
3,3-dimethyloxetan, far IR spectra, ring puckering vibration 78−42058
dimethylphosphine, microwave spectra, internal rot. barrier 78−5205
dimethylsulphate, cryst., liq., and oriented film, vibr. spectra, internal rot. 79−91444
p-,(m-)dioxane, conformation maps 77−57900
2,4-diphenyl pentane, polystyrene model molecule, US relax. 77−6965
dipyridylethylenes, photoelectron spectra, conformation, SCF LCAO calcs. 77−79651
1,4-disilabutane, rot. isomerism, Raman and IR spectra 80−74168
disilylmethane, microwave spectrum, struct., dipole moment and internal rot. 79−13699
dithioformic acid, pot. for rot. about $C(sp^2)$-S bonds, ab initio calc. 80−23572
divinyl ether, microwave spectrum, doublet splitting, vinyl group internal rot. 78−86849
effective hamiltonians, pseudopotentials and applics. 77−30754
electric polarisation in strong field for mol. with two hindered rot. groups 79−76361
electronic and nuclear energy balance in conformational change 77−54623
epichlorohydrin, microwave spectra, rot. and centrifugal distortion consts. 79−36626
ethane, barrier and one electron charge transfer states in strong orthogonal group function theory 78−13421
ethane, d_2, microwave spectra for internal rot. barrier 79−93986
ethane, internal rot. barrier, energy decomposition anal. 77−75327
ethane, internal rot. splittings, vibr.-rot.-torsion energy levels perturbations 80−91531
ethane, internal rotation barriers, exchange energy and orbital orthogonality effects 77−75049
ethane, rot. anal., perturbational MO analysis of ab initio SCF-MO wave functions 77−57867
ethane, rot. barriers, MS-SCF-X_α calcs. 80−106267
ethane, valence electronic struct., model pot. in floating spherical GO formalism 78−74563
ethanes, substituted, dielec. relax. by intramol. motion 78−23391
ethaneselenol, IR, Raman and microwave spectra, barriers to internal rot. 77−38666
ethanoic, acid, ideal gas thermodynamic props. 78−51275
ethenediol, σ conjugative interactions role in rot. isomerism 79−31443
ethenethiol, σ conjugative interactions role in rot. isomerism 79−31443
ethenol, σ conjugative interactions role in rot. isomerism 79−31443
ethyl alcohol-d_0(-d_1)(-d_1)(-d_2), internal rot. and microwave rot. spectra 80−69128
ethyl cyanoformate, conformers, dipole moments, rel. energies, microwave spectra 78−55164
ethyl fluoroformate, microwave spectra of rot. isomers 79−10097
ethyl formate, relax. processes rel. to US absorpt. intervals 77−1183
ethyl iodide, microwave spectra and internal rot. anal. 80−69130
ethyl methyl sulphide, low freq. vibr. spectra, methyl torsional pot. functions and internal rot. 80−5543
ethyl nitrite, microwave spectra, rot. isomerism and dipole moments 79−93990
ethyl radical, C-C bond barrier rot., IR spectra 80−76536
ethyl-3-chloropropionate, liq., microwave absorption and relax. 78−60386
ethyldifluoroborane, microwave, Raman, IR spectra, conform., dipole moments, vibr. assignment 78−90155

rotational isomerism continued
ethylene, C atom pyramidalisation rel. to bonding, ab initio SCF calcs. 79−93936
ethylene, C-C double bond rot. barrier, ab initio open-shell restricted SCF calc. 78−1099
ethylene, rot. around double bond, four orbital-four-electron model 80−95592
ethylene, S_0,S_1-states, twisting vibrs., pot. curve calcs., absorpt. spectra 77−83576
ethylene(−d_4), Rydberg states assignments, electron energy loss specta 80−53153
ethylene-d_0, -d_4, hindered internal rotation, vibronic luminesc. and absorption spectra 79−54883
ethylgermane, microwave, IR and Raman spectra, struct., internal rot., dipole moments 77−79605
ethylidenimine, pyrolysis product, microwave spectra, rot. distortion and electric quadrupole const. and rot. barriers determ. 80−78608
ethylmethylamine, low freq., vibr. spectra, methyl torsional pot. functions, mol. struct. 80−43045
ethylmethylether(-d_3), low freq. vibr. spectra, methyl torsional pot. functions, internal rot. 79−26978
ethyltrichloroacetate, liq., permittivity, dielec. loss, up to 60 GHz 78−60384
fluoro sulphuric acid methyl ester, rot. isomerism 78−86964
4-fluoroaniline, amino group inversion and torsion, far IR spectra 77−10670
o-fluoroaniline, conformation by microwave spectroscopy, rot. consts. 78−9144
pfluorobenzaldehyde(-d_1), in smectic mesophase, mol. struct. and reorientation, NMR 77−27093
fluorophores, limited rot. motion, differential phase fluorometric obs. 79−22741
fluoroxyperoxytrifluoromethane, ab initio MO calcs. of geometry, torsional barriers 78−90313
formaldehyde-d_0(-d_1)(-d_2), matrix isolated, IR spectra, monomer absorpt. 80−99503
formamide, mol. geom., self-consistent MINDO calcs., torsion and relax. effects 77−42243
formic acid, ideal gas thermodynamic props. 78−51275
furfuraldehyde liquid, US relaxation meas. 77−20016
guanidinium ion, rot. barriers, ab initio calcs. 78−41923
1-halo-1-n-propylcyclohexanes, conform. equilib., and pot. barriers, IR spectra *(Russian)* 78−21928
haloacetaldehydes, rot. isomerism, semi-empirical model calcs. 78−50659
haloacylhalides, rot. isomerism, semi-empirical model calcs. 78−50659
haloalkanes, rot. isomerism, semi-empirical model calcs. 78−50659
2-haloethanols, Raman spectra, rot. isomerism and conform. energies 79−10117
halomethylsilanes, internal torsion modes, inelastic neutron scatt. 77−19105
halomethylstannanes, internal torsion modes, inelastic neutron scatt. 77−19105
Hamiltonian of a molecular type system with internal rotation 80−18842
HCl-inert gas mixtures, van der Waals molecules, far IR spectra 80−95610
helical wormlike chains, angular correls. 79−45871
hexa-deutero dimethyl selenide, microwave spectrum, first excited torsional states, top-top interaction 77−10668
hexafluoroethane, rot. barriers, MS-SCF-X_α calcs. 80−106267
hexafluoropropene, mol. struct. by electron diffr. of gas phase 79−59572
4-n-hexyloxybenzylidene-4′-n-propylanilene, smectic S_H and S_m phase structs. 79−14673
holomethylgermanes, internal torsion modes, inelastic neutron scatt. 77−19105
hydrazonium tartrate enantiomers, and deuterates, struct. and opt. props. 77−68954
hydrocarbon chain, gauche-trans isomerisation, ^{13}C relax. times and nucl. Overhauser enhancement model 78−33520
hydrocarbons, conformational anal., modified Urey-Bradley force field, gauche-H_2 interactions 77−6749
hydrocarbons, unsaturated, empirical potential model EPEN/2 parameterisation, testing 79−50103
2- and 4- hydroxypyridine tautomers, ab initio SCF LCAO MO calcs. 79−81154
internal rotation barriers, exchange energy and orbital orthogonality effects 77−75049
inversion geometry, ab initio SCF calcs., basis set effects 80−78532
1-iodo-2-methylpropane, IR spectra, vibrational anal., stretching bands 78−90168
1-iodo-3-methylbutane, IR spectra, vibrational anal., stretching bands 78−90168
iodoethane, mol. parameters, vibr., pot. barrier height etc., data tables 79−76409
2-iodopropene, barriers to internal rotation 78−9273
2-iodopropene, microwave spectrum, quadrupole coupling consts., internal rot. barrier 79−45710
IR molecular absorption spectra, effect of rotational coupling on torsional bands 78−13497
isobutene-d_0, -d_6, torsional pot. functions, spectra anal. 78−25528
isopropyl fluoroformate, microwave spectrum and conformation 79−10098
lithium acetate, methyl group dynamics, NMR 78−29802
macromolecular chain configuration-dependent props., review 77−38758
macromolecular helical wormlike chain statistical mechanics, persistence vectors, comparison rot. isomeric state model 77−50573
membrane-active complexon fragments, nonrigidity effects calcs. 80−91704
methanediol, bond length distortions and torsion pots., ab initio calcs. 79−6836
methanes, substituted, internal torsion modes, inelastic neutron scatt. 77−19104
methanoic, acid, ideal gas thermodynamic props. 78−51275
methanol, and −$d_{1,3,4}$, thermodynamic props. struct. and spectroscopic data 77−39396
methanol, and -d_1, -d_4, photoelectron spectra, internal rot. in ground ionic state 77−65509
methanol, internal rotation barriers, exchange energy and orbital orthogonality effects 77−75049
methanol molecle enclosed in β-quinol clathrate, O-H group rot., dielectric meas. 78−2026
methanol-d_1(-d_4), far-IR internal rotation spectrum 80−47989
rotational isomerism continued
methanol-water, assoc. mixture, rot. barrier solvent effect, CNDO/2 calc. 78−29861
2-methoxyethanol, methyl torsional barriers to internal rotation calc. 80−95603
2-methoxyethylomine, microwave spectra, H-bond, torsional motion and mol. vibr. obs., rot. isomerism, mol. moments determ. 80−95603
3-methoxypropionitrile, microwave spectrum, rot. conformer, rot. consts., vibr. state 77−14419
methoxytrifluorosilane and -d_3, IR and Raman spectra, vibr. anal., barrier to internal rot. 79−18185
methyl 2-bromopropionate, IR and Raman liq. phase spectra, rot. isomerism 78−58680
methyl 2-chloropropionate, IR and Raman liq. phase spectra, rot. isomerism 78−58680
methyl acetate, microwave spectra and internal rot. 80−87100
methyl alcohol, and -d_3, far IR spectra of internal rot. 78−5222
methyl alcohol, internal rot. barrier, energy decomposition anal. 77−75327
methyl azidoformate, microwave rot. spectrum, satellite transitions 80−69127
methyl compounds with hindered rot. ^{13}C spin-rot. relax. times 79−50049
methyl fluoroformate, isomer conformation, CNDO and ab initio STO calcs. 80−58151
methyl group, conform. problems, correlation effects 79−97999
methyl group, proton spin relax. due to intermol. proton coupling, reorientation 78−25564
methyl group hinderance barrier, spin-rot. relax. times 80−53011
methyl group internal rot., pot. barrier and activation energy, absolute rate theory 79−79220
methyl groups, barriers to internal rot., orbital calcs. 77−68138
methyl groups in solids, tunnelling freq. for internal rotation in pot. function 80−49134
5-methyl isoxazole, microwave spectrum internal rot. barrier 78−58665
3-methyl l-butanethiol, Raman and vibr. IR spectra of solid and liq., rot. isomerism 78−62810
N-methyl m-fluoroaniline, conformational anal., microwave spectra obs. 80−58247
methyl mercapto acetate, Raman and vibr. IR spectra of solid and liq., rot. isomerism 78−62810
methyl nitrate, internal rotation temp. frozen in supersonic jet, matrix IR spectroscopy 80−9594
s-methyl nitrite, methyl group rot. barriers in cis and trans forms, ab initio calcs. 80−74111
methyl selenocyanate, and isotopic forms, microwave spectrum 79−13705
methyl top barrier to internal rot. in five membered heterocyclic mols. 78−78833
methyl vinyl ether, and -d_3, IR and Raman spectra, vibr., torsion and internal rot. 78−94250
methyl vinyl sulphide, rotational isomerism, variable temp. photoelectron spectroscopy appl. 77−6846
methyl vinyl sulphide, syn-gauche equilib., force field and ab initio calcs., microwave and Raman spectra 80−23573
methyl-3-bromopropionate, liq., microwave absorption and relax. 78−60386
methyl-4-chlorobutyrate, liq., microwave absorption and relax. 78−60386
2-methyl-pyrimidine, microwave spectrum, V_6 barrier, dipole moment, rot. consts. 77−3345
N-methylacetamide, and isotopic forms, low-freq. Raman spectra, internal torsional mode 79−26992
methylamine, internal rot. barrier, energy decomposition anal. 77−75327
methylamine, membrane-active complexion fragments, nonrigidity effects calcs. 80−91704
methylamine, vibr.-inversion-internal rot.-rot. Hamiltonian 78−86840
methyldiborane, microwave spectra, bond lengths, dipole moments, rot. consts. 77−83579
methyldisilylamine, and -d_2, vibr. assignment and barriers to internal rot., IR and Raman spectra 78−13496
N-methylformamide, cis-isomer rot. struct., IR absorpt. spectrosc. obs. 80−14138
methylphosphorous pentafluoride, CH_3PF_4, pseudorotation, quantum dynamics 77−34570
methylpropylether, trans-trans isomer, microwave spectra, struct., dipole moment and rot. barriers calcs. 80−83348
methylpropylsilane, vibr. spectra, normal vibrs. and rot. isomerism 79−31524
N-methylpyrazole, microwave spectrum, internal rot. barrier 78−58666
methylpyridines, rot. tunnelling, NMR relax. and inelastic neutron scatt. 79−4733
micellar interface, reaction kinetics, rotamer population, fast proton transfer 80−26050
molecular conformational props., internal rot. barriers, PCILO-CNDO calcs. 77−75056
molecular multiple internal rot., ^{13}C-{^1H} nuclear Overhauser enhancement, ^{13}C spin lattice relax. 77−479
molecular rotational spectra, doublet splittings caused by tunnelling, perturbation treatment 80−91541
molecular structures, topological code, modified Morgan algorithm 80−58122
molecule, nonrigid, sum of states, isometric group, symmetry no., thermodynamic functions 80−58186
molecules with hindered internal rotation, vibronic luminesc. and absorption spectra 79−54883
molecules with internal rot., forced diffusion, correlation function 77−80402
monochloroacetic acid, isolated molecules, internal rotation, CNDO/2 calcs., IR spectra 80−69254
monothioformic acid, cis-, trans-rotamers, rot. spectrum, force consts. and isotopically substituted struct. 78−9145
monothioformic acid, pot. for rot. about C(sp^2)-S bonds, ab initio calc. 80−23572
muonic radicals, μSR spectra obs. 80−69279
N-methylhydroxylamine, microwave spectra, struct., moments, internal rot., HFS and rot. consts. 79−45708
1- and 2-naphthol, ideal gas thermodynamic props., vibr. fundamentals, rot. isomerism 79−24813
1-β-naphthyl-2-N-piperidinoethane, intramol. exciplex form., ground state conform. control 80−102547
nitrocyclopropane, vibr. spectra struct. and bonding 80−102520

rotational isomerism continued
nitromethane, torsional barriers, electronic spectrum 79−59424
nitrosomethane, mol., spectra 600-720 nm, and geom. change on excitation 79−72329
nitrosomethane-d_3, electronic excitation, conformational changes obs. 79−98233
3-nitrothiophene, rot. transitions, torsion, microwave spectra 77−42313
NMR and dielectric relaxation, defect diffusion models 79−15375
NMR spectral lineshape analysis of two-site exchange kinetics, student expt. 77−26118
nonbonded interactions, density response theory, appl. to rot. barriers 78−41913
nonbonded ligand interactions, mols. with hindered internal rot., symmetry determined investigation 78−70960
noncyclic molecules, bent bonds, electron density maps 79−49960
norbornane, derivatives in solution, mol. motion and methyl group rot. barriers from ^{13}C NMR relax. times 80−74179
normal vibrations classification in mols. with internal rot. according to microwave spectra data 77−18909
n-octane fluid, gauche-trans. relax. 79−69002
one-top molecule, barrier height determ. from self-consistent harmonic approx. 77−57977
optical torsion transitions, barrier heights from vibr. optical freqs. 77−42308
organic carbonyl compounds, empirical pot. model EPEN/2, development, parameter testing 79−54934
organic compounds, structural energy characteristics, rotational isomerism, mol. motion *(Russian)* 79−56602
organic molecules, saturated, empirical potential model EPEN/2, parameterisation testing 79−54933
organic ortho compounds, solid, H bonding, wide line NMR obs. 78−52362
organic polycyclic compounds, ^{13}C NMR, spin-lattice relaxation meas., rot. barriers in hindered methyl groups 77−10689
organo tin dichlorides, tetrahedral, dilute soln., dielec. and thermodynamic behaviour, microwave region 77−36170
oxalyl chloride, rot. isomerism, CNDO and EHT-type methods 78−58591
oxide semiconducting glass, structural energy characteristics, rotational isomerism, mol. motion *(Russian)* 79−56602
oxirane, triplet state, torsional motion relax. 79−49959
oxirane cation, struct. rearrangement following vertical ionisation, ab initio CI calc. 80−58191
oxiranecarboxaldehyde, microwave spectrum, torsional excitation energy, partial struct., dipole moment 77−38655
PAA, nematic liq. cryst., rot. barrier, PCILO and CNDO/2 calcs. 80−33874
PCILO-INDO method, theory and appls. 80−58153
pentane, liq., enthalpy difference between rot. isomers, IR spectrosc. obs. 80−106404
peptide, NMR spectroscopy study 78−88694
perfluoro-1,3-butadiene, vibr. spectra, struct. and barrier to planarity 78−9147
perfluorocyclobutane, matrix isolation Raman and IR spectra, pot. function 77−3352
periodic potential functions, with sine and cosine terms, matrix elements for level calcs. 77−57904
phenols, halogenated, internal rot. barriers, torsional vibr. freqs. 77−68041
9-phenylanthronyl radical, ESR, temp. depend. phenyl twist angle 79−18210
phospholipids, ^{31}p NMR, slow-motional lineshapes for very anisotropic rot. diffusion 80−5644
phosphonatomethylene radical, EPR spectra and rot. barrier height, comparison CNDO calcs. 79−74409
pivalic acid(-d_1; d_9), liq. and soln., Raman assignments, CH_3 rot. barrier, dimerisation 79−26991
pivalic anhydride, liq. and soln., Raman assignments, CH_3 rot. barrier, dimerisation 79−26991
poly-1,3-pentadiene, microstruct., IR, NMR, X-ray determs. 79−37637
poly-4-methyl-1-hexene, optically active, ^{13}C NMR obs. of conform. 77−10801
polybut-1-ene and but-1-ene-polypropylene copolymers in solution, ^{13}C spin-lattice relax. and mol. motions 79−95670
polydimethysiloxane, conc. soln. in benzene, polarised Raman scattering 78−9286
polyene derivatives, horizontal radiationless transitions, singlet-pot. and rot. angle, semi-empirical model 78−42109
polyethylene, γ-irrad., alkyl radicals ESR and hindered oscill. 78−85182
polyethylene, elongation, conform. set change IR obs. *(Russian)* 78−37778
polyethylene, perdeuterated, skeletal vibr. spectrum 78−23445
polyethylene terephthalate, conform. statistics *(Russian)* 78−70993
polyethylene terephthalate, elongation, conform. set change IR obs. *(Russian)* 78−37778
polymer, conformational transitions, Brownian dynamics, simulation 79−45873
polymer, molecular mechanism of orientation 77−69033
polymer, rot. isomeric state model, approx. anal. soln. 77−58214
polymer, rot. isomeric state model, monomer-monomer distrib. function 77−71897
polymer, structural energy characteristics, rotational isomerism, mol. motion *(Russian)* 79−56602
polymer chain dynamics, ang. correl. function decay by multiple rot. pot. diffusion 80−3569
polymer dynamics simulation, relax. rates and dynamic viscosity 78−91211
polymers containing main chain heteroatoms, struct., ^{13}C NMR investigs., review 79−55013
polymethylene, intramol. scatt. function calc. 77−38761
polymethylene, short chains, rot. isomeric representation 80−87254
polymethylene flexible biradicals CIDNP and chain dynamics, field depend. 77−88473
polynucleotides, potentials of internal rot. 77−16901
polyoxide chains, config. partition functions, entropy, (CH_2)y-o- repeat unit 78−17829
polypeptides, helix-random coil transition rates, mean relaxation rate, internal friction 77−38763
polyynes, intermolecular interaction through triple bonds, internal rot. 80−106370
propane-d_0 and -d_3, Raman spectra, torsional pot. function 77−58015
rotational isomerism continued
propanes, substituted, rot. isomerism, semi-empirical model calcs. 78−50659
propargyl mercaptan (−d_1), microwave spectra, struct., rot. anal. 77−18916
2-propene-1-imine, rot. isomers, microwave spectra 78−58670
propenoyl chloride, far IR and Raman spectra, internal rot. 79−89668
propenoyl fluoride, far IR and Raman spectra, internal rot. 79−89668
propionitriles (-O, NH, S), conformational investig., NMR, IR and semiempirical MO methods 80−95650
propyl formate, relax. processes rel. to US absorpt. intervals 77−1183
propylene, rot. anal., perturbational MO analysis of ab initio SCF-MO wave functions 77−57867
propylsilane-d_0(−d_n), vibr. spectra, normal vibrs. and rot. isomerism 79−31523
protein, NMR spectroscopy study 78−88694
proteins, amide unit electron organisation, mol. orbital theory 79−2000
protocatechualdehyde, PMR, 77-427K, OH group rot., struct. 77−30886
pseudopotential calcs. of barriers to internal rotation 77−14352
pyridine-3-aldehyde, partially oriented in nematic solvent, rot. isomerism and conformation, NMR obs. 77−71820
Raman spectroscopy, vap., medium resolution, appls., review 78−42065
revolution manifold isometric stereohedra 79−82170
saturated ring cpds., six- and seven-membered, conformation mapping 77−57900
scalar properties of mols. with internal rot., symmetry aspects, appl. to ethane skeleton 78−70959
second-row molecular orbital calcs., INDO calc. for Na to Cl 78−82643
selenoacetaldehyde, microwave spectrum, struct. internal rot. barrier 78−74645
selenocyclopentane, interconversion barrier, spectra and struct. 79−10115
semirigid molecules, Stark effect, isometric groups, elec. dipole moments theory 78−29815
L-serines-d_0 and -d_4, IR and Raman spectra, rot. isomers *(French)* 79−45714
short chain molecule, dielectric relax. 79−95706
silacyclopentane, Raman spectra, pot. energy surface, barrier to interconversion 78−25541
silanes, ab initio calcs. using FSGO, internal rot. 78−82639
Δ^5-steroids, methyl group rot. barriers from ^{13}C relax. data, geometry effect 78−13626
stilbene, diphenylpolyenes, photoisomerisation, 'phantom' photochem. singlet state, PPP SCF CI calcs. 78−73058
stilbene, horizontal radiationless transitions, singlet-pot. and rot. angle, semi-empirical model 78−42109
stilbene, trans-, cis-forms, singlet excited state, picosecond dynamics 78−17677
succinonitrile, plastic phase, molecular reorientation, rotational isomerism, incoherent neutron scatt. study 79−51021
N-sulphinylaniline, microwave rot. spectra, torsional freq., dipole moment and internal rot. barrier 78−973
symmetric rotor, internal rot. splitting 78−94232
symmetric top, rigid, rot. partition function 78−46260
symmetric top mol. with internal rot., extended diffusion and reorientation in fluids 77−20101
tangential isotropic polarisable atomic unit model, optical rotation calc. *(French)* 79−54989
TCNE-substituted benzene complexes, isomers, stability, rel. to charge transfer band intensity 77−68051
TCNQ, and anions, PRDDO method using Slater orbital basis 79−764
teaching, mol. models based on Petri dishes 78−73817
terpenes, methyl groups internal rotation, ^{13}C spin lattice relaxation times and force field calcs. 80−74255
2,2,3,3-tetrachlorobutane, vibr. spectra, liq. and solid-state, conform. struct. 79−73936
1,1,1,3-tetrachloropropane, Raman and IR obs. of rot. isomerism, entropy difference between vapour and liq. phase isomer *(Russian)* 79−31529
1,1,2,2-tetrafluoroethane, anti- and gauche-rotamers, struct., spectra, electron diffr. 77−50439
tetramethyldiphosphine, UV photoelectron spectra trans/gauche isomer equilib. 79−31600
thioacetaldehyde (-d_1), microwave spectrum, substitution struct. internal rot. barrier, dipole moment 77−6762
thioacetamides, CNDO calcs., internal rot., ionisation pots., photoelectron spectra 78−5143
thioacetic acid, −d_1, principle axis method anal. of microwave spectra 78−9139
thioformic acid, g-values, mag. susceptibility, quadrupole moments, rot. Zeeman effect, isomer effects 78−25520
thiophosgene, vibronic anal. of electronic transition, inversion doubling splittings obs. 80−83388
thiourea, ground and first excited triplet state configs., ab initio SCF calcs. 79−89597
toluenes, substituted, methyl torsion, internal rot., neutron inelastic scatt. 77−43160
torsional potential analysis, from spectrosc. data 78−62787
torsional vibrs., effect on gas electron diffr. determ. of molecular configuration 78−25743
total dipole moment orientation calcs. 80−91705
transformation of operators of coordinates and momenta 79−63982
transition metal complexes, mol. dissymmetry, book 80−27057
tri-i-propygermylamine, and isotopomers, IR and Raman spectra, normal coord. anal. *(German)* 80−32716
tri-t-butylstannylamine, and isotopomers, IR and Raman spectra, normal coord. anal., Mossbauer spectrum *(German)* 80−32716
bis-triazolopyridazines, conformation calcs. by mol. mechanics and CNDO/2 method 80−69079
bis-triazolyls, conformation calcs. by mol mechanics and CNDO/2 method 80−69079
triethylsilylamine, and isotopomers, IR and Raman spectra, normal coord. anal. *(German)* 80−32716
1,1,1-trifluorethyl halides, internal rot. barriers and LF Raman spectra 77−65478
1,1,1-trifluoro-3-chloropropane, Raman and IR obs. of rot. isomerism, entropy difference between vapour and liq. phase isomer *(Russian)* 79−31529
trifluoroacetates, methyl and ethyl, intramol. relax. at microwave freqs. 80−55020
trifluoroacetic acid, ab initio MO calcs. of geometry, torsional barriers 78−90313

rotational isomerism continued
1,1,2-trifluoroethane, mol. struct., gas phase electron diffraction, rotamer abundance 79−76514
trifluoromethane, rot. isomerism, internal rot. splitting 78−94232
2,2,5-trimethyl-1,3-dioxane-4,6-dione, cryst., X-irradiated, methyl group hindered rot. tunnelling, EPR, ENDOR, and ELDOR 79−68328
trimethyl-d_9-vinylsilane, IR and Raman spectra, struct., vibr. assignment, barriers to internal rot. calc. 80−87102
trimethylaminegallane, microwave, IR and Raman spectra, struct., vibr. assignment 80−95600
trimethylene, singlet state, rot. barrier origin, MINDO/2 calc. 79−81170
trimethylene biradical, rot. barrier of mol., INDO calc. 79−68192
trimethylene diradical, generalised Hartree-Fock natural orbital config. interaction approach 77−75062
trimethylvinylsilane, IR and Raman spectra, struct., vibr. assignment, barriers to internal rot. calc. 80−87102
trinitromehtane, electron diffr. study of gas phase mol. struct., rot. isomerism 78−1080
trioxolane, methyl substituted, stability, pseudorotation, electronic effects in final ozonide 79−45654
trioxolanes, methyl substituted, stability, pseudorotation, electronic effects in primary ozonide 79−49961
trioxolanes, pseudorotation surface, mol. struct. and conform. 79−45653
trithiane, Raman spectrum, press. effect on internal rot. angle 78−37642
vibrational level classification by Longuet-Higgins group 80−43030
vibrational spectra, linewidth, temp. depend. calcs. 77−83594
vinyl azide, microwave spectrum 77−57985
vinyl isocyanate, and vinylcyano ether, geometry and conform., ab initio minimal STO-3G MO calcs. 80−23337
vinyl mercaptan -d_0, -d_1, anti rotamer, conform., microwave spectrum 80−9592
vinyl mercaptan -d_0, -d_1, synrotamer, conform., microwave spectrum 80−5535
vinyl polymers with flexible side chains, configurational statistics, dipole moments 77−38760
2-vinylanthracene, conform. conversion kinetics, fluoresc. 80−9631
vinylcyano ether, and vinyl isocyanate, geometry and conform., ab initio minimal STO-3G MO calcs. 80−23337
vinylcyclopropane, Raman study of rotational isomers 79−18194
n-vinylformamide, torsional pot. barriers, ab initio and partition of energy methods 77−88588
aminoarsines containing As-NH group, IR spectrometry, configuration isomers and hybridization state of N *(French)* 77−23495
AsH_3, inversion barrier calc. 78−9271
BCl_2SH, BCl_2SD, Raman and IR spectra, barrier to internal rot. 78−5223
$(CH_3)_2X$ molecules, perturbational MO anal., methyl rot. barriers, fragmentation mode 77−88386
$ClNO_3$, far IR rot. and torsional spectra 77−79609
$Co(NH_3)_4Cl_2Cl$, cis and trans isomers, XPS, shake-up satellites 78−82783
Cu complex, $Cu(NH_3)_2(NCX)_2$, X=O, S, electronic struct., stereochem. 80−58156
Cu complex, L-alanyl-L-serine, PMR, EPR and absorpt. spectra 78−46367
N,N-dimethyloxamide, conform. anal., CNDO/2 energy optimisation, mol. props. 77−75328
Ge_2H_6, rot. barriers, MS-SCF-X_α calcs. 80−106267
Ge_2H_6, valence electronic struct., model pot. in floating spherical GO formalism 78−74563
H_2O-HF heterodimer, H bonding, microwave rot. spectrum, mol. geometry and moment 80−99501
H_2O_2, geometry, internal rot. barriers, electron correl. calcs. 78−70751
H_2O_2, hindered rot. pot., strongly orthogonal geminal calcs. 77−71751
H_2O_2, hindered rot. pot. recreation, electron pair wavefunction transferability 77−71752
H_2O_2, internal rot., pot. energy calcs. 79−3521
H_2O_2, internal rotation barriers, exchange energy and orbital orthogonality effects 77−75049
H_2O_2, struct. and barrier to internal rot., HF and Rayleigh-Schrodinger perturbation calcs. 79−13636
H_2O_3, struct., barrier to int. rot., HF and RS-MP perturb. calcs. 79−13637
H_2PNH_2, inversion-rot. mechanism, basis set and geometry optimisation effects 80−83273
HS_2, rotamers, electronic and geometrical structs., ab initio floating GO basis calcs. 78−74572
H_2S_2, rot. barriers, internal rot. and electronic struct., valence electron study 80−83344
H_2Se_2, rot. barriers, internal rot. and electronic struct., valence electron study 80−83344
H_2Te_2, rot. barriers, internal rot. and electronic struct., valence electron study 80−83344
Mo complexes, organic derivs. of heteropolymolybdates 77−79701
$(N_2)_2$, Van der Waals molecule, struct. and internal rot. barriers determ., interaction pot. from ab initio calcs. 80−91626
NCl_3, ab initio LCAO SCF calc. for ground state, inversion barrier 78−25426
N_2D_4, ^{14}N quadrupole coupling consts., inversion barrier, microwave spectrum 77−54556
N_2D_4, microwave spectrum, barrier to inversion determ. 78−62793
NH_3, and -d_n IR matrix isolation spectra, rotation and inversion 78−5218
NH_3 dimer, inversion, influence of H-bond, SCF calc. 77−50556
NH_3, geometry changes during inversion, ab initio calcs. 78−5154
NH_3, inversion, one-electron props. variation, electronic and nuclear components partitioning 77−83491
NH_3, inversion splitting calc., variable pot. barrier 79−18177
$^{14}NH_3$, $^{15}NH_3$, submm-wave rot.-inversion transition, ν_2 state 77−75138
$^{14}NH_3$, inversion spectrum 79−3438
$^{15}NH_3$, inversion doublets, T_1 and T_2 M depend. 78−13489
N_3H_3 radical, lowest two electronic states 80−925
NH_xF_{3-x}, geometry changes during inversion, ab initio calcs. 78−5154
$(NH_4)_2S_5$, Raman spectra, vibrs. and rot. isomers of Sn^{2-} (n=4-8) *(German)* 78−13504
NO_2^- hydrate clusters, ground-state HF pot., Monte Carlo simulation, energy surfaces and rot. barriers 80−106412
$NbCl_5$, mol. struct., vibr. assignments, barries to pseudorotation 78−29858
rotational isomerism continued
$(Ni[NH_3]_6)(ClO_4)_2$, reorient. correlation times of NH_3 and ClO_4 groups, Raman obs. 79−28748
PF_3, microwave l-type reson. transitions in v_4=1 state 77−57988
PH_5, rearrangements, CI calcs. in large at. orbital basis 79−94106
P_2H_4, conformation, ab initio, HF, PNO-CI and CEPA calcs. 77−46495
PH_xF_{3-x}, geometry changes during inversion, ab initio calcs. 78−5154
Pd complex, L-alanyl-L-serine, PMR, EPR and absorpt. spectra 78−46367
$PtCl_2(NH_3)_2$, cis- and trans-isomers, electronic struct., SCF-Xα study 80−18795
S_4Cl_2, Raman spectra, vibrs. and rot. isomers of S_n^{2-} (n=4-8) *(German)* 78−13504
SH_3^+, geometry and inversion barrier, basis set depend. 80−921
ScH_3^+, inversion barrier calc. 78−9271
o-semiquinone, radicals, intra- and intermolecular H^+ transfer, ESR 77−16840
SiH_3 radical, in Ar(Kr)(N_2) matrix, anisotropic ESR spectroscopic parameters 80−63687
Si_2H_6, barrier to internal rotation 78−66680
Si_2H_6, rot. barriers, MS-SCF-X_α calcs. 80−106267
Si_2H_6, valence electronic struct., model pot. in floating spherical GO formalism 78−74563
$(SiH_3)_2S$, rot. consts., internal rot. parameters, anal. of microwave spectra 78−46316
$(SiH_3)_2S$, microwave spectrum, r_0-struct., elec. dipole moment, internal rot. barrier 79−3439
$TaBr_5$, gaseous, electron diffr. obs. of vibr. assignment, mol. struct. and barrier to pseudorot. 79−81293
$TaCl_5$, mol. struct., vibr. assignments, barries to pseudorotation 78−29858
$TcCl_8^{3-}$, metal-cluster, EHT calcs. of electronic struct., metal-metal bonding *(Russian)* 77−61687
XeF_6, energy levels, nonrigid mol. effects 78−41931

rotator phase in solids *see nuclear magnetic resonance; plastic crystals*

rotatory dispersion power *see optical rotation*

rotons
^{4}He, superfluid, one phonon excitation spectrum and interaction pot. 80−54455
Bose fluid, structure factor determ. 78−34667
Boson system, hard spheres, condensed phase, Jastrow wave function 78−84018
boson system, strongly interacting, excitation spectrum 78−71897
condensed Bose system, roton spectrum 79−63133
ferromagnet, amorphous, spin-wave excitations, roton minimum 78−80139
ferromagnetic, amorphous, magnetic and phonon rotons 79−61087
second sound and roton-roton interaction pot. 79−51328
second sound in relax. time approx. 77−66050
second sound velocity, roton-roton interaction pot. 78−75898
superfluidity, model Hamiltonian 80−44377
Yukawa Bose fluids, Jastrow wave function, Monte Carlo computation 79−73375
p-D_2, solid, roton dragging librons 78−67886
o-D_2, solid, up to 150 kbar, 5K, Raman spectrum 80−50332
H_2 solid, localised excitations due to p-H_2 impurity 79−65288
H_2, solid, rotational excitations, higher order effects 80−6591
o-H_2, solid, roton dragging librons 78−67886
He, film, superfluid props. 80−34270
He II, superfluid, single atom neutron scatt. and two roton connected state branches *(Russian)* 80−44381
He II-^{3}He, roton lifetime from neutron inelastic scatt. meas., 1.27-2.15K 79−56011
He, liquid, short-wave surface excitation study using electron gas nonlinear I-V characts. *(Russian)* 80−10717
He, superfluid, inelastic neutron scatt. spectra, roton-roton interactions 78−95194
He, superfluid film, bulklike rotons, neutron scatt. 77−7942
^{4}He superfluid, phonon-roton excitation 80−107586
^{3}He, fluctuations, rotons and solidons 79−95228
^{3}He-^{4}He, liq., excitation spectrum and quasiparticle interactions, perturbation theory 78−10250
^{3}He-^{4}He, liquid mixture, second sound, quantised vortex creation at constrictions, excitation model 80−44383
^{3}He-^{4}He, superfluid soln., dil., low temp. props., book contrib. 80−15330
^{3}He-^{4}He mixture, dil., ^{3}He excitations, calc. 79−7730
^{3}He-^{4}He mixture, dil. solns., dielec. model of roton interactions 78−55998
^{3}He-^{4}He mixture, roton spectrum *(Russian)* 77−4240
^{3}He-^{4}He mixtures, excitation spectrum, exptl. studies using neutron inelastic scatt. 77−59170
^{3}He-^{4}He mixtures, excitation spectrum, neutron inelastic scatt. study 79−46877
^{3}He-superfluid ^{4}He mixture, dispersion law of ^{3}He quasi-particles under press. *(Russian)* 79−42336
^{4}He, bound roton pairs 78−59993
^{4}He, elementary excitations, Brillouin-Wigner perturbation theory with correlated basis functions 78−2319
^{4}He film, adsorbed, few atomic layers, excitations, two-dimensional roton. 80−39381
^{4}He film, third sound, two-dimens. hydrodynamics and elementary excitations 79−7721
^{4}He, liq., excitations produced by impinging ^{4}He atomic beam 78−10241
^{4}He, liq., excited states, variational calcs. 80−80017
^{4}He, liq., hard-sphere roton interaction, transition temp. calculated 78−51767
^{4}He, liq., negative ion motion at supercritical drift velocities 77−80667
^{4}He, liq., neutron scatt., book contrib. 80−2230
^{4}He, liq., sp.ht., 65-850 mK, and phonon dispersion 79−4442
^{4}He, liq., two-dimens., excitation spectrum and thermodynamic props. 79−86959
^{4}He, superfluid, bound 2-roton state by neutron scatt. meas. *(Russian)* 79−86951
^{4}He, superfluid, bound roton-ion states, energy spectrum *(Russian)* 79−4445
^{4}He, superfluid, bound states of rotons to impurities 78−55999
^{4}He, superfluid, density regions, λ transition and roton physical picture 79−82402
^{4}He, superfluid, dispersion of roton second sound 77−31819

rotons continued
^{4}He, superfluid, elementary excitation line shapes, energies and linewidths, neutron scatt. obs. 79−60572
^{4}He, superfluid, elementary excitations, μeV resolution study by neutron spin echo 80−65327
^{4}He, superfluid, evaporation by rotons and phonons, heat-pulse technique 79−33135
^{4}He, superfluid, excitation spectrum, Bogoliubov theory 79−7722
^{4}He, superfluid, excitation energy spectrum, roton contrib. 80−24699
^{4}He, superfluid, excitation spectrum, RPA calc. involving simple pseudo-pot. 80−92738
^{4}He, superfluid, isotopically pure, roton-driven mech. for nucleation of negatively charged vortex rings 80−59746
^{4}He, superfluid, Landau critical velocity meas., excitations 80−103528
^{4}He superfluid, maximum roton vel. obs. 77−31818
^{4}He, superfluid, negative ion vortex nucleation rate for ions whose drift vels. are limited by roton emission 79−55969
^{4}He, superfluid, neutron scattering, role of two-roton bound state 78−55993
^{4}He, superfluid, neutron scattering, role of two roton bound state 79−4446
^{4}He, superfluid, neutron spin-echo study of excitations 80−80014
^{4}He, superfluid, polarisation pots. and elementary excitations at low temps. 77−15643
^{4}He, superfluid, pressurised, vortex nucleation by neg. ions, thermal roton influence 80−10721
^{4}He, superfluid, Raman expts., interpretation 79−73362
^{4}He, superfluid, roton energy determ. from neutron diffr. exam. 77−24458
^{4}He, superfluid, roton interactions 77−7926
^{4}He superfluid, roton lifetime, inelastic neutron scatt. meas. *(Russian)* 79−7723
^{4}He, superfluid, roton lifetime effects on thermodynamic props. 79−55957
^{4}He, superfluid, roton-roton interactions and excitations at large wavevectors 77−28058
^{4}He, superfluid, roton-roton interactions, neutron scatt. meas. 79−46860
^{4}He, superfluid, roton-roton interactions and thermodynamic props. 79−60571
^{4}He, superfluid, roton-roton interaction for large and zero momentum 80−84336
^{4}He, superfluid, rotons and solidons 79−95228
^{4}He, superfluid, two- and three-dimens., energy spectrum and phase vel. 80−70489
^{4}He, superfluid, two-dimensional, roton spectrum 77−11751
^{4}He, superfluid, two-dimens., microscopic theory, excitation spectrum and thermodynamics props. 80−24709
^{4}He, superfluid, velocity-field characts. of negative ions, effect of one-roton emission process 78−47622
^{4}He, superfluid, viscosity and thermal conductivity *(Russian)* 80−10720
^{4}He, temp. depend. of spatial correls. 78−71896

rotors
automatic balancing using CO_2 laser *(Russian)* 78−70115
bicycle rotors for vertical axis wind turbines, design and performance 80−30367
coil planetary motion, angular velocity control method 80−42202
Coriolis ocean turbine energy system status 80−45628
cryogenic, for 50 MVA superconducting generator 79−58710
cryogenic gyroscope suspension conditions *(Russian)* 79−30459
cryoturbogenerator transition process simulation, cryostat damping casings electrical characteristics determination *(Russian)* 80−8996
dynamics analysis using tapered beam finite element 80−38316
elastic hydrostatic sliding bearing, forced vibrs. of vertical rotor 79−18798
elastic wave stability 78−87297
elastically supported, automatic balancing *(Polish)* 79−10458
flexible asymmetric, convergence factor for residual unbalances 79−81785
flexible unbalanced rotor, bending vibration behaviour and accel. through critical speeds 79−81783
flywheel energy storage interface unit for photovoltaic applications 80−30571
flywheel energy storage system, rotating flywheel in an evacuated casing 80−30570
flywheel energy storage system 80−30569
flywheel rotor design utilising natural cellulosic materials for energy storage appls. 80−30568
flywheel rotor with high energy density for energy storage 80−30565
flywheels, development of low loss magnetic bearings, for energy storage appls. 80−30566
flywheels, performance of retainerless bearings for vehicular energy storage appls. 80−30567
forgings, crack detection, US holography method 77−66730
fusion reactor, inductive and rotating machinery energy storage and transfer 79−85782
gas turbine, vibration contactless meas. system *(Russian)* 80−8982
gyroscope, scanning laser based vibration detector *(Russian)* 80−22351
high speed unequally spaced fan, acoustics and performance anal. 80−96163
high temperature metallurgical problems 79−52089
large rotor forgings, metallurgical opportunities to improve reliability 79−52089
lathe off-balance during metal removing, automatic vibration control systems reviews *(Russian)* 78−70118
linear rotary convertor angle meas. *(Russian)* 79−63192
low pressure turbine blades, metallurgical opportunities to improve reliability 79−52089
noise generation by transonic open rotors 80−69599
noncrystalline solid, dispersion relation of phonon-like excitations 78−18727
phase wound rotor, in AC contactless machine of double supply *(Russian)* 77−17375
refrigerant circuit for superconducting AC machines, used as thermal pump, He rotating cryostat 79−58717
Savonious, two-dimensional vortex sheet model 79−83552
sine cosine rotating transformer, angular displacement meas. apparatus *(Russian)* 79−97344
spinning tops, mechanics *(German)* 78−87253
steam power plants, metallurgical problems and opportunities to improve reliability 79−52089

rotors continued
steam turbine, rotor steel type EI-415, low-cycle fatigue and short term creep investigation 77−25238
steel, Ni (3.5 wt.%), heavy rotor forgings, temper embrittlement, metallurgical investigations *(German)* 80−16471
three phase induction motor heat flow model, locked rotor and running-up temp. rise calcs. *(German)* 79−90115
titanium low pressure turbine blades and large rotor forgings, reliability improvements 79−52089
transonic compressor, single-stage, flow measurement using 2-probe synchronized sampling technique, calibration 80−14865
turbine blade vibration meas., optical methods *(French)* 78−71300
turbomolecular pump, development and use 79−63251
two-phase AC servomotor, vibration reduction method *(Japanese)* 77−45704
ultracentrifugation, rotor matching, laboratory use 79−40556
vibration control using feedback control system *(Russian)* 78−70116
wind power generation, large-scale, 10 MW windmill design 79−43713
wind turbine aerodynamics, machine performance and rotor aerodynamics 80−74904
wind-operated, reciprocating water pump, stroke adjusting mechanism for rotor speed control 80−50930
He, liquid, effect of short-wave surface excitations on damping in two-dimens. electron gas *(Russian)* 79−10995

roughness measurement *see surface topography measurement*

roundoff errors
long geodesics computation on ellipsoid through Gaussian quadrature, computational, roundoff and truncation errors 79−100806
molecular integrals' errors, influence on RHF energy values 77−50354
Numerov algorithm, note 79−2643
penalty functions techniques error anal., constraint definition in linear algebraic systems appl. 77−41467
plasma simulation, anal. of time integration 79−50886

rovibronic levels *see molecular rotation-vibration*

RPA calculations
π-electron systems, screened potential, excitation energies determ. in RPA 79−22597
actinides, electronic struct., Hubbard's alloy approx. 79−73665
alcohols, chiral, circular dichroism, RPA calc. 79−36672
allyl-radical, pi-electron system, appl. of UHF Green's function method 77−61684
amorphous semiconductor, non-polar, mobility gap temp. variation calcs. 78−10339
Anderson model coupled to boson field, HF approx. and RPA 77−40033
anisotropic magnet, low-temperature properties 79−65633
anisotropic paramagnet, statistical mechanics using second order Green's function theory 80−25074
antiferromagnet, itinerant electron, mag. excitations 78−56305
antiferromagnet, spin-1, with biquadratic exchange, sublattice magnetisation and Neel temp. 77−47953
antiferromagnetism itinerant electron theory, spin susceptibilities 78−6504
atom, inner shell, generalised oscill. strengths, with outer shell effects 78−50507
atom, open-shell, 1st order transition matrices calc., graphical method in RPA 80−47846
atom, photoionisation, relativistic RPA calcs. 77−61719
atomic electron scattering, many-electron correlations 77−42409
atomic oscill. strength, gauge props. of HF and RPA approx. 78−950
atomic photoionisation anal. using relativistic random phase approximation and multichannel quantum defect theory 80−63602
atoms, collective dynamics, hydrodynamic approach and many body approach based on RPA calcs. 80−47855
atoms, mag. hypersusceptibility *(Russian)* 77−14598
atoms, photoionisation, multichannel relativistic RPA calcs. 80−9570
benzene, mol. semiempirical RPA calc. using PPP Hamiltonian, triplet instability 79−26893
Bethe lattice, random ordered phase, statistical theory 77−85457
borazine, triplet instability, RPA calculations 80−27938
Bose fluids, normal, conserving evaluation of dynamic struct. factor, Fermi liq. generalised RPA 79−14975
Bose gas, two-dimens., charged, in zero mag. field, dielec. response 80−142
trans-butadiene, mol. semiempirical RPA calc. using PPP Hamiltonian, triplet instability 79−26893
butadiene, oscillator and rotatory strengths, RPA in ab initio calc. 78−25617
trans-2-butene, twisted, oscillator and rotary strengths, ab initio calculations 77−65510
(X)-D-camphor, circularly dichroic band at 3000 Å, RPA calc. 78−94267
CDW distorted solid, quasi-one-dimens., charge density fluctuations and dielec. matrix 80−107726
CDW dynamics in presence of free carriers 80−6760
chemical bond energy, ground state correlation energy 80−47847
chemisorption, spin-fluctuation description 77−76666
closed shell nuclei, elementary excitations unified model 77−67712
closed-shell systems, interactions, correl. energy, RPA calcs. 78−25646
collective excitations from high-q electron scatt., RPA AND ATDMF calcs. 80−22673
collective excitations in nuclei, microscopic model of giant dipole resonance 77−54135
collective states and crossing symmetry 79−93497
consistent ground state characteristics 79−59346
cooperative Jahn-Teller systems of T nature, electron-phonon excitation branches 78−63823
cooperative Jahn-Teller T-systems dynamics vibronic excitation branches 80−10934
coordinate space formalism derivation, interaction strength and transform. coeffs. for Skyrme interactions 78−70473
Coulomb isospin mixing, self consistent theory, isobaric states in RPA, isovector forces *(Russian)* 79−22181
coupled bands in even-even nuclei in RPA approach 80−32143
coupled spin $^1/_2$ phonon system, existence of sharp transition 79−69204
coupling with pairing vibration approximation, Green's function calcs. 77−5754
current conserving random phase approximation 79−75878
deformed nuclei, coupled rot. bands, RPA type approach 78−89775
deformed nuclei, first monopole excitation energies in systems with pairing forces 77−61364

RPA calculations continued
deformed nuclei, giant quadrupole resonance description *(Russian)* 77−50045
deformed nuclei, low and high energy collective states and giant resonances, RPA calc. 79−17779
deformed nuclei, yrast level ground state correlations, RPA anal. 80−86777
deformed nuclei with isoscalar and isovector interactions, one-phonon states 79−3071
degenerate electron liquid, compression modulus, perturbative calc. 80−36942
degenerate electron system, low-freq. polarisability, RPA calc. with temp. correction 79−95354
dense electron gas response at any degeneracy, RPA calcs., plasma modes, screening 78−36930
derivation of RPA using generalised Schwinger representation of fermion pairs 77−38233
dielectric function, inverse RPA calcs. at metal-vacuum interface 78−14789
dielectric function, time-dependent Hartree-Fock formalism 79−69448
disordered Heisenberg spin model, magnetisation calc. 80−60167
dynamic polarisability, TDHF theory and RPA sum rules 78−78292
elecronic excitation properties, RPA-CI calcs. using hypervirial relations as constraints 79−76413
electrical conductivity of bond-type disordered system, random phase model 78−51952
electron correlations in solids, local approach 80−29344
electron dielectric function, second-order RPA 78−49753
electron gas, collective modes, ground state energy 77−66134
electron gas, coupled-cluster expansion, inclusion of ring and exchange effects 77−76764
electron gas, degenerate, in metal or semicond. slabs, surface plasmon damping 80−88501
electron gas, dense, response at any degeneracy 77−71269
electron gas, exchange and correlation effects, self consistent theory 77−85161
electron gas, generator coordinate method 78−60077
electron gas, interacting, local-field correction to dielectric constant, review 80−107731
electron gas, interacting, quadratic electronic polarizability 78−6310
electron gas, paramag. susceptibility, RPA calc. 78−43559
electron gas, partially degenerate, thermal cond. 77−71266
electron gas, semi-infinite, nonlocal cond. tensor calc., effective optical surface region 80−20283
electron gas, spin polarised, correlation energies for local spin density calcs. 80−107725
electron gas, spin polarised, model for conduction electrons of simple metal in mag. field and ferromag. Gd 77−8034
electron gas with surface, Green function theory, exchange and correlation effects 77−8164
electron liquid, dynamic structure factor 79−78023
electron liquid, spin-dependent, correlation energies for local spin density calcs. 80−107725
electron-hole pair condensation and liquefaction in strong mag. field, RPA and variational calcs. 78−63984
electron-hole plasma, two particle state influence on dielectric function 79−56154
electron-phonon quasi-one-dimensional system, fluctuations anal. 77−89703
energy weighted sum rules for spin-dependent excitations of nuclei 80−86833
energy-weighted moments, relations between nucl. collective theories 78−33130
ethylene, π-electron system, self-consistent many-body theory 78−25432
ethylene, mol. semiempirical RPA calc. using PPP Hamiltonian, triplet instability 79−26893
ethylene, RPA hypervirial relation, ab initio minimal basis calcs. 77−18779
ethylene, twisted, oscillator and rotary strengths, ab initio calculations 77−65510
exact removal of spurious states in RPA calculations 79−22217
excitation operators and extended RPA 78−13412
excited nuclei, self-consistent theory of giant dipole resonance, thermodynamic RPA *(Russian)* 80−5106
excitonic insulator, quasi-one-dimens. 79−90966
fast charged particle traversing ferromag., dynamic mag. field 79−73230
fast ion in solid, oscillatory wake, trapped electron binding energy, RPA calc. 80−96575
fermion system, two-body operators with dynamic effective interactions, t-channel 77−41898
fermion system, two-body propagators with dynamic effective interactions, s-channel 77−41897
ferromagnet, anisotropic exchange interaction, random phase and Callen approximations *(Japanese)* 79−95560
ferromagnet, inter-atomic interaction effect on dynamic susceptibility, RPA calcs. 79−65662
ferromagnet, itinerant, spin waves, surface effects, RPA calc. 80−60226
ferromagnet, uniaxial with single-ion and exchange anisotropies, magnetisation in transverse mag. field 78−56277
ferromagnet with single ion anisotropy, collective modes 77−28354
ferromagnetic partially ordered alloy, spin wave stiffness const. 79−24150
fluids, critical-point universality 78−22826
formaldehyde, triplet instability, RPA calculations triplet instability, RPA calculations 80−27938
four-body correl., mode-mode coupling model, light nuclei 77−10322
Frenkel exciton system, phase transition and exciton-photon coupling 78−23024
gauge invariance in second quantisation, Hartree-Fock and random phase approximations 79−75395
generalised Schwinger representation of fermion pairs to anharmonicity 78−89807
giant dipole resonance of deformed even-even nuclei, ^{152}Sm to ^{238}U, semimicroscopic calcs. 77−50096
giant electric and magnetic multipole resonances in closed shell nuclei 78−538
giant monopole vibrs., RPA and collective field description, surface compressibility 80−102100
giant resonance description, RPA, GCM, and semiclassical theories unification 78−54671
gradient approx. anal., nonuniform electronic system 80−96810
RPA calculations continued
heavy ion+nucleus, RPA theory, time dependent, quasi-boson approx. 80−57800
Heisenberg, ferromagnet, spin-one, uni- and biaxial anisotropy, RPA and mol. field approx. 78−34989
Heisenberg anisotropic ferromagnet, longit. correl. function, generating Green functions 78−6500
Heisenberg antiferromagnet, Green function theory 80−107975
Heisenberg antiferromagnet, second order Green's function 78−43545
Heisenberg antiferromagnet, uniaxial, props. by Green's function method 77−85406
Heisenberg ferromagnet, anisotropic, collective Green's function, dynamical RPA 80−70925
Heisenberg ferromagnet, consistent linearised Green's function theory for $s=1/2$ 79−4685
Heisenberg ferromagnet, correlation functions in ferromagnetic and paramagnetic regions, RPA 80−71075
Heisenberg ferromagnet, dil., CPA theory, spin-wave stiffness and Curie temp. 78−31080
Heisenberg ferromagnet, isotropic, second-order Green's function theory 80−2578
Heisenberg ferromagnet, surface magnetisation profile and localised magnons 80−70985
Heisenberg-Mattis model, long-wavelength dynamic response 80−20409
hexatriene, mol. semiempirical RPA calc. using PPP Hamiltonian, triplet instability 79−26893
high spin rot. motion, TDHF cranking model and RPA descript. 80−102091
high spin states and band coupling, theory and heavy ion expts. *(Russian)* 80−18160
hydrocarbons, conjugated, effect of semi-empirical parameters on simple RPA calcs. 79−10037
hypervirial relation, sum rules for ordinary and rotatory intensities in finite bases 77−18779
impurity screening in strong mag. fields 79−47054
inelastic positron scatt. in electron gas, plasmon excitation 80−92843
inert gas atom photoelectron ang. distribs., theoretical calcs. comparison 79−59412
inert gases, outer shell photoionisation, relativistic RPA calcs. 80−9571
inert gases, photoabsorption to bound state and photoabsorption to continuum state (ionisation), comparison, HF calcs. 80−47910
inert gases, photoelectron spin polarisation, ab initio calcs. 80−18833
inert gases, photoionisation cross-sections, multiconfig. Hartree-Fock calcs. 77−50373
infinite nuclear matter, response function, quantum field theory of fermion systems 78−70480
interacting many-level system, thermodynamics, from RPA Green's functions 78−43549
interatomic electron interactions, effect of electron correl. 79−38010
interatomic interactions between electrons 78−64017
Ising, quenched dil. random-bond model, CPA difference eqn. and crit. curves 80−2584
Ising paramagnet in transverse field 77−8260
isoscalar effective charge in large A limit Tamm-Dancoff and RPA calcs. 80−42534
isoscalar effective charges with scaling and HF wavefunctions 77−26559
isoscalar giant quadrupole resonances, RPA calcs., E2 strength fragmentation, spectroscopic factors 80−13437
isoscalar giatn resonances, sum-rule approacH 77−82898
itinerant electron ferromagnet with domain struct., spin waves 78−64182
itinerant ferromagnet, surface spin waves 77−69480
Jahn-Teller cooperative T-(e+t) system, thermal cond. 80−70479
jellium metal, bounded, linear response function in RPA 79−69444
kinoform synthesis by Fresnel transform evaluation, least squared error method *(Russian)* 79−22913
layer metal particles, surface plasmons 77−1465
linear aggregates, small, polarisability determ., CNDO method and analytical models *(French)* 80−29298
linear chain with anharmonic pot., SC phonon, RPA and transfer integral methods 77−51452
linear Hubbard model, RPA and CI test calcs. 78−25411
linear response and Hartree-Fock, coordinate space representation and gradient iteration 80−18216
liquid, simple, equilib. theories, review 80−38887
liquid structure function evaluation, using optimised cluster expansion 80−49085
magnetised semiconductor, coupled LO phonon-plasmon modes 79−73459
magnetised solid state plasma, theory of neutron scattering 79−38015
medium heavy nuclei, pairing correlations, RPA ground states 79−54401
metal, quasi one dimens., plasmon dispersion relations, RPA and HF calcs. 78−34789
metal, screening energies in photoelectron spectroscopy of localised electron levels 77−1781
metal, semi-infinite, transverse dielec. response, surface effects 77−47878
metal, surface plasmons in thin film, circular cylinder and spherical void, RPA calcs. 77−80823
metal surface, exchange-correlation hole 78−80037
metal-insulator transition, Ising model, for transition temp., Green's function calc. 79−15084
metallic sphere, very small, surface plasmon dispersion, RPA 77−47886
metals, classical plasma frequency in long-wavelength limit, quantum correction 80−107728
metals, density of states and spin susceptibility, normal and giant surface effects 78−10322
metals, simple, quasiparticle props., density functional approx., electron gas calc. 80−96808
metals, spin fluctuations, mag. field effect, electronic sp. ht. and elec. resist. 80−108026
mixed valence compounds, dynamic susceptibility, RPA study of Anderson lattice 80−97075
molecular electronic struct., UHF Green's function method, appl. to allyl-radical 77−61684
molecules, chemisorbed on metal surface, spectrosc., electron gas effects 80−54504
multicomponent electron-hole plasma correlation energy by RPA and mean component approx. calc. 80−24824
multihadron production processes, high energy, strong correls., RPA scheme 78−41506
multiple basis set calcs. 77−5755
multipole excitation of doubly-open shell spherical nuclei 78−21507

RPA calculations continued
multipole residual interaction strength, radial depend. in RPA 80−83026
n-type semiconductors, plasmon-local phonon mode interaction, RPA, CPA theory 78−87932
nematic liquid crystals, molecular statistics, random phase approx. 79−41954
non-magic nuclei laser states, self-consistent theory *(Russian)* 79−9483
nonlinear extension, appl. to even Ni isotopes 77−61366
nuclear, oblate high spin isomers, pairing Hamiltonian anal. 78−12996
nuclear collective coordinates, systematics of giant multipole resonances *(Russian)* 77−74751
nuclear collective excitations, macroscopic eqns. of motion and dynamic polarisability 77−41903
nuclear collective excitations, sum rules 79−59002
nuclear collective monopole and quadrupole oscills., decoupling anal. 77−10343
nuclear form factors of 0^+-0^- transition in A=16 system, nuclear struct. effects 80−18246
nuclear giant magnetic resonances and effective Mλg-factors, RPA anal. 77−2897
nuclear giant multipole resonances, energies, transition densities, sum rules from RPA eqns. 77−61365
nuclear giant resonances, self-consistent microscopic anal. including particle continuum 77−2896
nuclear ground state correls. and isotope effect in ^{40}Ca and ^{48}Ca 77−6238
nuclear isovector M6 excitations, open shell RPA calcs., appl. to electron scatt. form factors 78−50112
nuclear large amplitude collective motion coupling to RPA excitations 77−74787
nuclear microscopic model, wobbling motion in fast rotating nuclei 78−21505
nuclear particle-hole states, microscopic self-consistent calc., ^{16}O levels 77−67713
nuclear quadrupole excitation, microscopic description 77−41901
nuclear quasirotational bands, RPA eqns. of motion 78−54663
nuclear struct., self-consistent RPA calc., Skyrme forces 77−50072
nuclear struct. calcs. *(Rumanian)* 77−26602
nuclear structure, pairing rotation and intrinsic Hamiltonian 80−57708
nuclei, transitional, pairing rotations and quadrupole modes 80−18165
octupole low-energy resonances in deformed nuclei, RPA calc. 77−82892
one dimensional electronic systems, instability due to electron-phonon interaction 79−99536
open shell atoms, LS-coupling, RPA with exchange 77−30838
open shell nuclei by seniority and reduced isospin projections 80−47415
open shell RPA unitary group formulation, Hartree Fock stability eqns. 80−52860
oscillating dipole-metal surface interaction, jellium model and random phase approx. 80−92955
pairing vibration in closed-shell nuclei, RPA calc. 77−67710
particle-hole propagator, order analysis 77−38602
Peierls transition, interchain bandwidth effect at low temp. 78−10352
perturbative anal. of two-body effective interactions from large matrix diagonalisations 78−41644
phonon anomaly near Fermi surface topological transition 78−95120
photoionisation, one-electron excitations, local pots., many-electron effects 79−54817
plasma, complex dielectric function long wave limit, Coulomb systems with bound states, elec. cond. 80−33738
plasma, electronic, classical, dispersion relation, RPA method 79−55481
plasma, one-component, coupling of single particle and collective modes, memory function 77−68749
plasma, spectral line broadening, non-thermal effects 79−46433
plasma oscillations, higher surface modes near plane metal-vacuum interface 78−42760
plasmon dispersion, correlation correction 80−43917
polar semiconductor, electron-hole liq., phase diagram 77−89706
polyene band struct. calc., excitons in polyene chain 78−26816
polyenes, linear, π-electron system, appl. of extended RPA excitation operators 79−97993
quantum field theory, four fermion interactions 79−12653
quasi-one-dimensional solid, CDW distorted, macroscopic dielec. function 80−39515
quasi-two-dimensional electrons, electrodynamics 77−89829
radiative lifetimes, polarisation propagator approach 77−18844
random Ising bond interactions, paramag. phase, thermodynamic props. 77−20523
randomly diluted Heisenberg spin system with anisotropic exchange coupling, crit. temp. 79−99702
rare earth compounds, Kramers, temp. renormalised spectrum of mag. excitations, cryst. field level ordering 77−20516
rare earth deformed nuclei, high spin region excited rot. bands, RPA calcs. 80−78108
rare earth metals, electronic struct., Hubbard's alloy approx. 79−73665
relativistic, appls. to He-like ions energy levels and $Mo^{36+,12+}$ photoionis. 80−47913
relativistic effects in oscillator strength calculations, ab initio methods 80−9519
relativistic RPA development from linearised time-depend. HF theory 80−47925
Rochelle salt, ferroelectric phase transition, external field induced 80−29700
RPA ground state correls. and isotope effect in ^{40}Ca and ^{48}Ca 77−6238
s-d shell, two nucleon effective interaction, intruder state, RPA correlation 80−57701
self consistent cranking model, anomalies 79−26382
self consistent cranking model with RPA corrections, high spin states, conservation laws 77−14047
self consistent RPA for three body forces in Fermi systems 78−89810
self-consistent quasiparticle RPA in nuclear structure theory 80−86835
semiconductor, amorphous and liq., Hall conductivity in random-phase model 80−65599
semiconductor, crystalline, local field effects on static dielec. const. 77−59264
semiconductor, electron scattering interaction with coupled plasmon-polar-phonon modes 79−42536
semiconductor, light scatt. spectra, interference effects 79−82977
semiconductors, electron-hole liquid 80−6743
semiconductors, free electron scattering and dynamical cond. 78−2476
spectral density, time-depend. perturbation theory calcs. 77−13525

RPA calculations continued
spherical nuclei, M1 transition strength distrib. at high excitation energies 79−75895
spherical nuclei, small amplitude vibrs., giant resonances, TDHF, fluid dynamics comparison 78−66233
spin exchange and polarisation changes, RPA breakdown from HF connection 80−99142
spin glass, Heisenberg mode, RPA approx. 80−65904
spin systems, coupled itinerant localised systems, dynamic magnetic response 80−34583
spin-one system, quadrupolar to paramagnetic phase transition 77−80934
spin-systems, double-time Green functions method, thermodynamics 79−15313
star clusters, spherical, frozen in pot. waves 79−67070
strongly disturbed bands in the high spin region described by rotating bosons 78−78239
structural phase transitions and anharmonic phonons 78−14433
sum rule, cubic inverse energy-weighted and adiabatic inertial parameters in HF calcs. 77−79316
superconductor, dynamical electrical conductivity below transition temp. 78−2623
superlattice, plasma oscillations 77−72878
surface, positron-electron correlations, RPA calc. 80−40181
surface correlation energy, plasmon contrib. 77−69397
surface dielectric response in local representation, microscopic theory 77−85289
time dependent HF polarisability and RPA sum rules, collective model restoring force 79−6461
time dependent HF polarisability and RPA sum rules, isovector giant resonances 79−6462
transition metal alloys, dilute ferromagnetic, itinerant d-electron(hole) degenerate, spin stiffness constant 80−70930
transition metal magnetic alloys, dilute, props., review of theory 79−15282
transition metals, role of electron correlation 77−72974
s-triazine, triplet instability, RPA calculations 80−27938
TTF-TCNQ electronic props., PMR 78−2763
TTF.CuBDt, spin 1/2 Heisenberg chain, spin-Peierls transition 79−61135
TTFCuBDT, spin-Peierls transition in spin 1/2 Heisenberg chains, RPA calcs. 80−25150
two nucleon transfer, RPA theory, pairing vibrs., and extended basis shell model 79−481
two-dimensional classical plasma, on dielectric film, collective excitations *(Russian)* 78−34788
two-dimensional electron-hole metallic liquid, RPA calc. 77−47743
two-dimensional quantum plasma de Haas-van Alphen oscill. in correlation energy 79−60738
two-electron systems, RPA eigenvalue eqns., excitation frequencies and oscillator strengths 78−17570
unpolarised atoms, spin polarisation of ejected photoelectrons 79−45682
van der Pol oscillator, RPA for linewidth 80−68138
vibrational nuclei, quasiparticle RPA nonlinear generalisation for anharmonic effects 79−63579
weak ferromagnet, with easy plane anisotropy correl. functions and magnetisation, temp. depend. *(Russian)* 80−84581
X-Y ferromagnet, S=1, with uniaxial anisotropy, Curie temp. 79−78425
X-Y model, biquadratic, spin one, variation of Curie temp. 80−97102
zero gap semiconductor, thin layer, dielec. response 80−103635
zero-gap semiconductor, ferroelec. phase transitions, effect of Coulomb interaction on RPA calc. 79−28691
(π,π) scatt. in 3,3 resonance region, Δ-isobar dynamics, optical potential and RPA calcs. 77−34347
π-electron systems, self-consistent many-body theory 78−25432
Al, plasmon dispersion, effect of band struct., dielec. function calc. 78−26825
Al, polycryst., anisotropy of plasmon dispersion, RPA dielectric function 78−23039
Ar, isoelectronic sequence, many-body photoionization calcs. 78−17631
Ar, ns→εp photoelectrons, spin polarisation 80−37792
Ar, outer $p_{1/2}$ subshell photoionisation, polarised electrons, relativistic RPA calcs. 80−83331
Ar, polarisation effects in photoionisation *(Russian)* 79−3420
Ar, Raman scatt., single particle HF approx. and RPA many-electron correlations calcs. 80−23374
^{36}Ar, mode-mode coupling model for four-body correls. 77−10322
Be, and isoelectronic sequence, oscillator strengths, relativistic RPA calcs. 77−57929
Be, oscillator strengths, generalised RPA with exchange calcs. 79−98030
Be-like ions, photoionisation, 2-channel relativistic random phase approx. calcs. 79−59407
Bi, gas-liquid type transform. and sound attenuation in strong mag. fields, electron-hole correl. effects 80−88598
Bi hole pocket, far-IR magnetospectroscopy, electron-electron interaction effects 77−77211
^{12}C, electroexcitation of collective M1 resonances 77−46104
^{12}C, residual interactions, current conserving RPA calculations 80−57710
^{12}C, spreading widths of giant reson. calc., core-coupling RPA approx. 77−74827
^{A}Ca, A=40,48, static and transition densities, self consistent RPA theory test in fast particle (p,p), (e,e) scatt. *(Russian)* 79−49604
^{A}Ca, A=40 to 48, giant multipole resonances, mass dependence of energy weighted sums 80−63144
^{40}Ca, coupling of 4p and 4h modes 78−93926
^{40}Ca, giant monopole resonance widths, RPA calcs. based on Skyrme interaction 78−93984
^{40}Ca, residual interactions, current conserving RPA calculations 80−57710
^{40}Ca, vibrating nucleus, eigenvalues of Baranger-Veneroni operator, RPA solns. 79−40863
^{44}Ca, mode-mode coupling model for four-body correls. 77−10322
Cd(p,p)Cd, A=110, 112, 5-9 MeV, isobaric analogue reson., QRPA calc. 78−576
Ce compounds with group V elements, antiferromag., temp.-renormalised longit. mag. excitations 77−51862
Cl, photoionis. cross sections, RPA with exchange method generalisation 79−10077
$Co(C_5H_5NO)_6(ClO_4)_2$ $[(BF_4)_2]$, X-Y antiferromagnet, Neel temp., spin correlation functions 80−60345

RPA calculations continued
^{124}Cs, β-decay props. of collective 1^+ states 78−13028
^{126}Cs, β-decay props. of collective 1^+ states 78−13028
$Cu_{0.98}Mn_{0.02}$, spin glass, Heisenberg mode, RPA approx. 80−65904
$ErCo_2(Fe_2)$, mag. excitations, RPA theory 80−65830
$Eu_xSr_{1-x}S$, Heisenberg spin glass system, excitations 80−84610
EuTe, field depend. correl. function theory of Raman scatt. near antiferromag.-paramag. transition 78−68490
F^-, photodetachment cross section, Stieltjes imaging method 78−55149
F_2, eqns. of motion method, transition energies, oscill. strengths, electron impact Born cross section 77−18983
Fe-Ni, fcc alloys, spin wave energy calc. 79−87247
GE, microscopic inverse dielec. matrix, local field correction and acoustic sum rule 77−84863
n-GaAs, temp. depend. density of states, impurity densities, activation energy, screening, chem. pot. calcs. 79−56109
Ge, electron-hole droplets, luminesc. and absorpt. lineshapes, RPA theory 80−49613
HF, linear response function, diagonal ARPA calcs. 78−74594
H_2O, linear response function, diagonal ARPA calcs. 78−74594
He, oscill. strength and first derivative, optical limit 77−3305
He, photoabsorption, modified RPA calcs. with exchange 78−13477
He, RPA eigenvalue eqns., excitation frequencies and oscillator strengths 78−17570
He, slow positron elastic scatt. phase shifts, simplified RPA calcs. 77−10759
He-like atoms, n=2 states radiative transition rates, oscill. strengths, RRPA extension 77−34584
He-like ions, oscillator strengths of transitions between low-lying S and P states 78−13470
He-like ions, photoionisation, 2-channel relativistic random phase approx. calcs. 79−59407
^{3}He, liq., dynamic form factor, particle density, spin density correlation, RPA calcs. 79−46873
^{3}He, liq., elementary excitations, RPA model using extended Landau theory 78−14527
^{3}He, liq., neutron scattering, dynamical form factor, RPA calc. 77−7938
^{3}He, normal liquid, elementary excitations, density and spin density, zero sound mode, press. depend. RPA model calcs. 80−59749
^{4}He, liq., HF cond. of electrons trapped at surface 78−10238
^{4}He, superfluid, excitation spectrum, RPA calc. involving simple pseudopot. 80−92738
$He(2^{1,3}S)$, inelastic scatt., RPA and 1st Born approx. calcs. 80−53148
$HoCo_2$, ground state spin excitations, inelastic nneutron scatt. study 80−50077
In, photoionisation cross section calc. for $4d^{10}$ subshell in RPA with exchange 77−23479
InSb inversion layer, electromagnetic mode 78−60080
K, Pauli susceptibility and Knight shift meas., electron wave functions 80−44937
Kr, ns→εp photoelectrons, spin polarisation 80−37792
Kr, outer $p_{1/2}$ subshell photoionisation, polarised electrons, relativistic RPA calcs. 80−83331
La, intense 4d-f resons., cross-sections, spectra, calcs. 79−31426
La, soft phonons, f-band induced instability 78−83907
Li, autoionisation spectrum, theory *(Spanish)* 79−89647
LiH, linear response function, diagonal ARPA calcs. 78−74594
Mg, isoelectronic series, oscill. strengths and excitation energy, RRPA calcs. 78−13471
Mg, photoabsorpt. and photoionisation, RPA with exchange calcs. 77−54543
Mn, FCC, itinerant antiferromag., spin susceptibilities and co'llective excitations, many band effects 77−63140
^{A}Mo(d,d) A=92-100, 21.5 MeV, elastic and inelastic cross sections, RPA and folding model 79−553
N_2, Raman intensity, ab initio calc. 80−1028
α-N_2, solid, librational motion, theory 77−43303
NH_3, linear response function, diagonal ARPA calcs. 78−74594
^{15}N(n′,n)^{15}N, continuum random phase approx. 80−27635
^{16}N, random phase approx. including continuum treatment 79−59024
Na, photoabsorpt. and photoionisation, RPA with exchange calcs. 77−54543
Nb-Mo system, electron-phonon coupling const. and supercond. transition temp., average T-matrix approx. 80−39707
^{A}Nb, A=90,92,94, Gamow-Teller strength distrib., RPA calcs. 80−78218
Ne, autoionising resons. near 575 Å, ab initio relativistic RPA calc. 80−32681
Ne, isoelectronic sequence, many-body photoionization calcs. 78−17631
Ne, isoelectronic sequence, excitation energy and oscillator strength, level crossing anomaly, relativistic RPA calc. 80−14077
Ni even isotopes, quasiparticle RPA nonlinear generalisation for anharmonic vibr. spectra 79−63580
Ni-Cr(V)(Co)(Mn)(Mo)(Ru)(Fe), spin wave stiffness consts., RPA CPA band model 79−61088
Ni-V(Mo)(Ru)(Cr), weak ferromag., stiffness const., low-temp. meas., rel. to RPA-CPA theories 78−31063
^{A}Ni, A=58,60,62,64, tensor open-shell RPA calcs., M2, M8 excitations 79−22216
^{16}O collective and giant multipole states, Brueckner RPA particle-hole state description 80−32169
^{16}O, giant monopole resonance widths, RPA calcs. based on Skyrme interaction 78−93984
^{16}O, pion condensation effects, RPA calcs. *(Chinese)* 80−47407
^{16}O, random phase approx. including continuum treatment 79−59024
^{16}O, residual interactions, current conserving RPA calculations 80−57710
^{16}O, spreading widths of giant reson. calc., core-coupling RPA approx. 77−74827
^{16}O, vibrating nucleus, eigenvalues of Baranger-Veneroni operator, RPA solns. 79−40863
Pb muonic isotopes, A=204, 206, 207, 208, nuclear polarisation energy shifts, RPA calcs. 78−94334
Pb pairing vibr. band, microscopic struct. and wave functions from (p,t), (t,p) 80−91126
^{208}Pb, core-coupling RPA calcs. of NGR, electric multipole strength fragmentation 78−50142
^{208}Pb, excitations, EM transitions in renormalised RPA 77−82857
^{208}Pb, isobaric analogue states, effects of Coulomb isospin coupling, random-phase method *(Russian)* 80−86808
RPA calculations continued
^{208}Pb, isoscalar electric giant dipole resonance, from RPA calc., nuclear compressibility 78−86520
^{208}Pb, M1 reson. states fine struct., 2p-2h states in RPA 77−22831
^{208}Pb region, finite Fermi systems, review 78−537
^{208}Pb, static and transition densities, self consistent RPA theory test in fast (p,p), (e,e) scatt. *(Russian)* 79−49604
^{208}Pb(α,α′), RPA calcs., existence of breathing mode 78−25163
^{208}Pb(d,d′), RPA calcs., existence of breathing mode 78−25163
^{208}Pb(e,e′), RPA calcs., existence of breathing mode 78−25163
$(SN)_2$, theory of plasmon excitations 77−69266
^{36}S, mode-mode coupling model for four-body correls. 77−10322
Se, trigonal, dielec. matrix calcs. 80−54630
Si, continuum-exciton effect in optical spectrum 80−25416
Si inversion layers, stress effects on electronic props. 78−43476
Si, microscopic inverse dielec. matrix, local field correction and acoustic sum rule 77−84863
Si, optical spectrum, many particle effects, band struct. 80−89024
Si, screening of donor ions by delocalised electrons 79−69466
Si(100)-SiO_2 interface, mobility in Si inversion layers, screening and neutral impurity effects 79−28412
^{148}Sm(^{18}O,^{16}O), interference effects, coupled channels calc. with BCS+RPA wavefunctions 77−26787
^{150}Sm(^{16}O,^{18}O), interference effects, coupled channels calc. with BCS+RPA wavefunctions 77−26787
α-Sn, gapless semicond., sound propag., RPA calc. 77−31721
^{132}Sn, doubly magic, RPA calc. of level scheme 78−50087
TbP, singlet-groundstate magnetism, static mag. props. 80−7109
$Tb_cY_{1-c}Sb$, elec. resist., cryst. field and exchange interaction contribs. 80−39556
Te, trigonal, dielec. matrix calcs. 80−54630
^{44}Ti, mode-mode coupling model for four-body correls. 77−10322
Tl, photoionis. cross section, spin polaris. and ang. distrib. of photoelectrons, RPA calc. 78−13478
Tm, intense 4d-f resons., cross-sections, spectra, calcs. 79−31426
UAl_2, spin fluctuations, mag. field effect, electronic sp. ht. and elec. resist. 80−108026
Xe, $5s^2$ subshell, discrete excitations, generalised oscill. strength calcs. 77−65441
Xe, atom, photoionis., collective level existence RPA with exchange calc. 78−42025
Xe, ns→εp photoelectrons, spin polarisation 80−37792
Xe, outer $p_{1/2}$ subshell photoionisation, polarised electrons, relativistic RPA calcs. 80−83331
Xe, photoelectron branching ratio in 4d subshell 79−18164
Xe, photoelectron studies of 5p branching ratio 80−37793
Xe, polarisation effects in photoionisation *(Russian)* 79−3420
Zn isoelectronic sequence, RRPA calcs. of resonance transitions from $4s^2$ $^1S_0$ 78−17612
Zn, XPS and Auger spectra, many-body calcs. 79−49995
^{90}Zr, static and transition densities, self consistent RPA theory test in fast (p,p), (e,e) scatt. *(Russian)* 79−49604

rubber
see also rubber industry
abrasion pattern analysis and obs., rel. to growth of cracks 79−38988
ABS polymer, fracture behaviour, rubber content effects 77−32676
ABS-rubber modified, two-phase struct. influence on fracture toughness *(German)* 80−66666
acoustic, dry entry of ultrasound appl., for glass-reinforced plastics testing 77−90563
acoustic scatt. from silicone rubber cylinders and spheres 78−79149
acoustic transducer-receiver configuration, flexible, activated by laser 80−83724
adhesion and friction, surface charge contribution 77−80826
adhesion on Perspex, surface topography effects 78−15644
adhesion with glass, propag. of cracks, effect of humidity 77−86133
adhesive bonds, physical modelling, US attenuation effects 78−7141
ageing, natural and accelerated, comparison 79−24625
alteration of mechanical properties of epoxy resins using reactive elastomers *(German)* 79−100106
amorphous polymers, intrinsic time to fracture criterion 78−92320
amorphous solids, time-temperature-pressure superposition phenomena, free volume theory 78−26059
analysis and characterisation, literature review, 1974-76 77−77814
angle tearing testing appliance 78−7140
balloon, internal press. eqn., for teachers 79−14
balloon bursting under biaxial strain, tear behaviour 80−19287
belt, cord reinforced, finite cylindrical deformation, stresses 78−38203
biaxial deformation of rubber-like solids 80−1431
binary polymeric mixtures, soln. viscosities meas. 80−54423
blooming by waxes 80−104109
bonding to metal, XPS appl. 78−15648
bronze scrapers, wear by rubber 79−66173
butadiene, stressed, microcrack generation under const. elongation, struct. depend. 77−90459
butadiene methylstyrol, exam. of low temp. relaxation processes *(German)* 78−92291
butadiene nitrile, exam. of low temp. relaxation processes *(German)* 78−92291
butadiene nitrile rubber, air permeability, subject to high press. 78−27823
butadiene rubber, polymer melt, extrusion at constant deformation rate 78−68744
butadiene styrol base elastomer, relaxation mech. *(German)* 77−36565
butadiene styrol rubber, effect of polyfunctional nitro-oligomers on relaxation *(German)* 78−31441
butadiene-nitrile, stressed, crack generation under const. elongation, struct. depend. 77−90459
butadiene-styrene gum elastomers, compounds, viscoelastic props., stress relaxation meas. 77−7321
butadienepstyrene, surface phenomena in struct. rearrangement after deform. *(German)* 78−19913
butyl rubber, resin cured, filled, relaxation study *(German)* 80−35243
butyl rubber dispersion, electron-microscopic investigation 78−53268
butyl rubber ethylene propylene ternary copolymer mixture, permeability, diffusion of gases and solvents 79−95217
butyl rubber solution, shear flow, rel. to rheologic theory 77−55051
butyl rubber vulcanisation with resins, use of organic accelerator *(Polish)* 79−74129

rubber continued
C black filled, friction behaviour sliding against Al, applied voltage effects 79−74266
carbon black-loaded styrene-butadiene rubber, elec. cond., effect of milling and thermal-oxidative ageing 77−55529
carboxyl terminated butadiene nitride-diglycidyl ether of bisphenol A epoxy resin, struct. and mech. props. 78−52901
composites with asbestos, classification 80−7484
compressibility anisotropy of rubber-like solids 79−43302
contact charge density, true meas. using soft rubber 78−43462
contact interaction between spherical surfaces under press. in various media *(Russian)* 77−7958
cord-rubber laminates, two-ply balanced, interlaminar-shear strain study 80−97526
crack growth, at rubber springs bonds, energy calc. and meas. 79−83316
creep processes associated with uniaxial compression 78−68734
cross linked, thermodynamic approach to stress induced crystallisation 79−41984
crystallising, tensile test specimen prep. 80−71838
cutting resistance measurement in absence of friction 79−5035
cyclic compression, heat generation and thermal conduction 79−52283
cyclorubber with bisazides, effect of photoresist layer thickness on photosensitivity *(Russian)* 80−73510
cylinder, circular, uniformly heated, combined extension and torsion 80−92057
cylinder, effect of stretch on wave speed 80−1467
cylinder against glass plate, elastohydrodynamic lubricant film form., expt. and theory 77−28910
deformation, associated volume changes 77−68447
denture base polymers, fatigue test machine 80−66712
dielectric properties of natural rubber-channel black, natural ageing effects 77−24777
dimethylpolysiloxane rubber reinforced film in membrane oxygenator 79−48373
dispersion with liquid crystals, prep. and props. 77−27821
dynamic material constants measurement using automatic progressive wave apparatus 79−91866
dynamic mechanical properties models *(Polish)* 79−43349
education, Brownian motion, melting, surface tension and rubber networks, thermodynamic anal. 80−73132
elastic deformation, nearly isochoric, anal. of volume changes 79−10471
elasticity, Gaussian statistical and Mooney-Rivlin theories 77−46935
elasticity, molecular aspects, book contrib. 78−84886
elasticity, network entanglement contrib. 80−39203
elasticity, new statistical theory 77−35623
elasticity, props. prediction on basis of microscopic structure, small angle neutron scattering appl. 80−3113
elasticity theories, statistical, applicability to polymer melts 78−42579
elasticity theory for highly entangled regime 77−90385
elasticity theory for rubber-like materials 78−67049
entrapped liquid lenses at elastomer-glass interface, formation and geometry 77−85021
epoxy rubber photoelastic coating combined with moire method for strain meas. *(Japanese)* 79−32400
epoxy-rubber glass transition rel. to filler, cooling rate 79−4403
epoxy-rubber particulate composite, toughness and fracture mech. 80−71727
ethylene, propylene rubber, effect of electrode profile on dielec. breakdown voltage, epoxy resin insulation system 80−60502
ethylene-propylene, fracture energy determ. 77−62208
ethylene-propylene, synthetic rubber, mathematical simulation of kinetics of thermal expansion *(Russian)* 78−55958
ethylene-propylene rubber, for dry insulation in power cables *(Spanish)* 80−81024
ethylene-propylene rubber, highly deformable, fracture surface roughness 78−44197
facings, rubber-metal, vulcanisation degree determ., γ-ray method 80−61043
filled, birefringence 78−68472
filled, light scatt. by strains, theory and expt. 80−28162
filled, viscosity, anomalous conc. depend. at low filler concs. *(Russian)* 77−44287
filled epoxy polymers, dense-woven, fracture characts. 80−11757
filled low-mol. wt. diene rubbers, IR spectroscopic study of mol. struct. *(Russian)* 78−76627
filled rubber, stress/strain behaviour at moderate strains 80−38293
film, on glass surface, interfacial dislocations spontaneously created by peeling 78−73011
fluorosiloxane, use in orthotopic artificial heart 77−78048
fracture in viscoelastic systems under cyclic loading 80−81195
friction against paper and polymer film surfaces, microroughness effect 80−71763
friction coefficient, role of adhesion *(French)* 77−52495
friction of rubber containing $CuSO_4$ paired with steel, selective transfer mechanism 80−55544
gamma irradiated, effect on dielec. props. *(Hungarian)* 78−59836
gas permselective membranes, irrad. effects on permeation and separation performances 78−29591
gasket inspection, US system, gas pipe appl. 80−30178
graphite filled, performance assessed against steel structures under water lubrication conditions 80−21123
gum and C black filled vulcanisates, rubber, natural and styrene/butadiene, unixial and equibiaxial fatigue 79−8363
Hysol 8705, mathematical model of impact loading behaviour 77−54890
hysteresis under uniaxial extension, test of Fitzgerald's concept *(Russian)* 77−86065
hysteretic behaviour, thermomech. study 78−76692
impact force vs. displacement curves, expt. determ. 78−83344
insulating material, temp. depend. of elec. resist. determ., expt. *(Croatian)* 77−74426
isoprene, stressed, microcrack generation under const. elongation, struct. depend. 77−90459
laser processing capacity using CO_2 laser 77−5820
latex+free polymer, dispersion flocculation, equilib. anal. 80−45574
latex films, surface struct., vulcanisation, radiothermoluminesc. obs., 100-230K 78−75575
latex particles in ionic solution, in aq. soln., hindered diffusion through small pores 79−43622
latex solids, agglomerating and dewatering 80−104470
latex sphere aggregates, dynamic shape factors determ. by sedimentation vel. meas. in capacitor 80−26063
rubber continued
liquid, viscosity meas. using manual viscosimeter *(German)* 79−27729
loaded, effect of polyfunctional nitro-oligomers on relaxation props. *(German)* 78−48436
lung tissue simulation, O_2 exchange in silicon rubber capillaries 79−44060
materials testing *(German)* 77−73399
mechanical and electrical strength, effect of Se, after mechanical and electrical ageing *(Russian)* 79−52396
mechanical model for rubbers containing entanglements 79−81315
methylstyrene type, relaxation time spectra calc. from stress relax. data *(Russian)* 77−44288
mixture, wear determ. device 80−21226
mixtures in range of reversion, vulcametry, cross-linking model *(German)* 80−104113
modified epoxy system, sub-T_g annealing expts. 79−11643
modified glassy polymers, thermal stresses 77−77567
Mooney-Rivlin constants correl. with polymer chain cross-section 77−11624
natural, crosslinked by dicumyl peroxide, modulus, swelling relations 80−59551
natural, oriented, crystallisation kinetics and melting 78−75554
natural, stretching effects on glass transition, sp. ht. obs. *(German)* 78−79753
natural, thermal properties depend. on temp. and press. 79−95223
natural, transverse nuclear magnetisation decay rel. to slow mol. motions *(Russian)* 78−72423
natural, viscosity meas. when various accelerators were added *(German)* 78−30688
natural, with furnace soot or acetylene black, natural ageing and dielectric props. *(German)* 78−19795
natural rubber latex, mechanical and chemical stability enhancement, by potassium fatty-acid soaps 79−96034
natural rubber latex ^{13}C NMR spectra 80−15816
natural rubber vulcanisate, network changes during physical testing 80−60936
natural rubber vulcanizates, vulcanization temp. and systems effect on struct. 78−19705
network, crosslinks and trapped entanglements, two-network model 80−38962
network, elasticity, mol. theory 80−38290
network, finite linear viscoelastic theory, time-depend. deform. behaviour 80−38292
network, highly swollen, long time dynamics 80−38291
nitrite, heat ageing, light scatt. method study *(Russian)* 80−40407
nonGaussian theory, under biaxial strain, mech. props. 80−16366
nonGaussian theory, under biaxial strain, optical props. 80−16367
NR, glass-rubber transition, time-temp. superposition, shear creep compliance meas. 80−88309
orientation averages for drawn networks 79−10819
oxidation, for prep. of diene oligomers with hydroxyl groups *(German)* 80−85175
partially hydrogenated, ^{13}C NMR 80−20472
peeling initiation and propag. 78−76824
penetrant diffusion, statistical mech. model 80−44352
photoelastic analysis, material and optical props. 77−42734
poly(butadiene-co-styrene), rubber, radiation cured, dynamic phys. props. 77−69003
poly(cis 1,4-isoprene), cryst. phase, elastic modulus 79−57037
poly(dimethylsiloxane) rubber, filled with modified silica, cross-linking 79−95990
poly-α-methylstyrene-polybutadiene, light beam and Curie point pyrolysis investigation *(German)* 79−57223
polybutadiene, carbon black-filled, ESR 77−90036
polybutadiene, cross linked, deform. below T_g, radical form. and crazing 79−52307
polybutadiene, dihydroxy-terminated, with unattached styrene-butadiene copolymer, stress relax. 80−104202
polybutadiene, exam. of wear in steel due to rubber 79−15810
cis-1,4-polybutadiene, vulcanised composite system, viscoelasticity 77−75823
polybutadiene rubber, modified with oligoester acrylate, plastic-elastic and rheological props. *(German)* 80−19871
polybutadiene rubber, rheological props., 60-110°C *(Russian)* 79−23292
polybutadienes, use of high modulus inclusion gauge, in stress analysis 80−21254
polybutediene rubber-styrene copolymers, control of morphology and props. *(Bulgarian)* 80−35153
polychloroprene and polychloroprene vulcanizates, γ-radiation effects on struct., physicomech. props. 77−1840
polydimethylsiloxane, rubber elasticity in uniaxial tension, compression 79−15714
polyisoprene, from guayule rubber, TEM exam. of crystallisation 80−10508
polyisoprene exam. of wear of steel 79−15810
polymer-elastomer mixtures, temp.-time analogy 79−19317
polystyrene, polarised Rayleigh scatt. near glass-rubber relax., photon correl. spectroscopy 80−40124
polystyrene, rubber modified, two-phase struct. influence on fracture toughness *(German)* 80−66666
polystyrene, rubber-filled, mech. props. *(German)* 80−35320
polystyrene, rubber-modified, fracture mechanics anal. of effect of rubber content, craze formation 79−29190
polystyrene latexes, monodisperse, model colloid systems 80−89545
polystyrene modification, impact-strength analysis 79−38972
polystyrene modification, rubber particle morphology influence 79−94925
polystyrene-polybutadiene systems, phase separation obs. 79−94926
polyurethane, photoelastic, behaviour at elevated temps. 77−25094
powdered, prod. and processing, powder preblend mixes 79−52149
powders, finely dispersed, sedimentometric anal. 80−66883
prestrain effect on dynamic modulus of elasticity and attenuation coeff. in nonconducting materials 80−29110
prosthetic heart valves, materials eval. 77−56533
protective coating for optical fibres, pressure sensitivity meas. and limitation 80−106605
PV, glass-rubber transition, time-temp. superposition, shear creep compliance meas. 80−88309
PVC, rubber-modified, stress whitening and yield mechanism 79−8324

rubber continued
PVC-g-butyl rubber grafted copolymer, tensile strength increased by S_2Cl_2 curing 79−95993
radiation heating effect on creep 80−35285
radiation processing, conf., Miami, FL, USA (Oct. 1978) 80−36772
radiation resistance of cable insulating materials for nuclear power stations, expt. 78−59835
radical and unsaturated polymer interactions, MO calcs. 77−44481
replication of fibrous cracks in steel 77−56069
resin vulcanisation, effect of Sn halides, IR spectra *(Bulgarian)* 79−33994
resin vulcanisation, effect of Zn halides, IR spectra *(Bulgarian)* 79−33993
rigidity and loss factor, meas. under steady vibr. 80−55602
rolling friction of glass on rubber, humidity influence 79−79118
rubber, natural, materials eval. 77−56533
rubber, nondestructive testing during production, portable instrument 78−23892
rubber blend, computer controlled pyrolysis gas chromatography 79−20493
rubber mixtures, synthetic, natural ageing effects on dielec. props. 77−24778
rubber-brass interface, adhesion failure, XPS study 80−40671
rubber-epoxy resins, heterogeneity analysis, light scatt. and statistical methods 78−2024
rubber-metal interface, adhesion mechanism, XPS study 80−65382
rubber-resin mixtures, viscoelasticity 79−43303
rupture life calc. 77−59933
SBR, fracture energy determ. 77−62208
Schallamach waves, rel. to friction of elastomers 79−29225
seal technology, advances 80−93730
sheets, circular, elastic deformation profiles 79−66481
shell, spherical, mode of loading effect on stability 80−24528
silastic, magneto-electret of tubular shape, surface charge 78−56419
silastic strain gauge as in vivo muscle force transducer 79−29680
silicon rubber model for design and stress analysis of large parts 77−7350
silicon-Pb(Zr,Ri)O_3:Nb flexible composite pyroelectric, dielectric props. 80−80704
silicone, biomed. eval. for passive prosthetic devices 79−29666
silicone, dimensional stability, surface roughness testing by interferometric gauge 79−21807
silicone, ring membranes appl., *(Slovak)* 80−61141
silicone, RTV 560, diffusion of outgassing species, kinetics data 79−15010
silicone rubber, arc resistance tests in various gas insulators *(Japanese)* 80−81250
silicone rubber, crack tip replica, for determ. of J-integral values 79−52475
silicone rubber, prosthetic heart valves materials eval. 77−56533
silicone rubber, room temp. vulcanising, as optical element coupler 77−39002
silicone rubber, room temp. vulcanising, as variable focal length lens 78−66888
silicone rubber, vulcanizing, possible substitute for damaged/diseased parts of eye 79−74788
silicone rubber biomaterial, filler free, radiation chemical and physical evaluation 79−39608
silicone rubber membrane, inert gas separation appl. 77−36791
silicone rubber mixtures evaluated for selective vascular occlusion 77−37104
silicone rubber substrata, appl. to study of cell locomotion 80−104835
silicone rubber vulcanisates, as alloprosthetic material 77−25596
silicone rubber with radiation-grafted methacrylate, for burn wound dressing 79−29657
siloxane rubber, energy investigation of softening during deform. 77−4819
sliding of hard ellipsoid, orientation effects, theory and expt. 77−86188
sliding wear mechanism 77−63810
steel scrapers, wear by rubber 79−66173
steric hindrance, rubber-elastic networks, stress-deformation behaviour *(German)* 80−35277
strain-energy density function for rubber-like materials 80−25773
stress relaxation in N_2 of irradiation cured samples 78−84884
stress/strain relations, uniaxial extension and compression 78−80578
stretching strength, long-term, testing apparatus 79−15907
styrene butadiene, dielectric const. and loss, lignin content depend. 80−29670
styrene butadiene rubber, dicumyl peroxide cured, behaviour in moderately large deform. 78−60692
styrene butadiene rubber, peroxide cured, strain independent nonlinearity 78−59353
styrene butadiene rubber, strain energy function, temp. effects 78−56684
styrene butadiene rubber-glass bead composites, network density determ. from stress/strain meas. 79−34112
styrene-butadiene rubber, fracture time variability, endochronic prediction 78−76734
styrene-butadiene rubber, highly deformable, fracture surface roughness 78−44197
styrene-butadiene rubber, reinforcing effect of fillers, strain energy meas. *(Japanese)* 78−31468
styrene-butadiene uncrosslinked gum rubber, viscoelastic behaviour in moderately large deform. 77−89079
styrenebutadiene, intrinsic time to fracture criterion 78−92320
surface strain field meas. on rubber structures, optical method 77−34017
surface texture effect on hysteretic friction 79−61741
swollen, low-freq. dynamics, optical and mech. props. 80−43626
swollen, stretch testing, attachment to strength testing machine 79−15905
swollen rubber network, stress-optical coeff. and amorphous order 77−77169
synthetic, advances review 77−55938
synthetic, network fracture mechanism, particle reinforcement 80−41928
synthetic, nonlinear anelastic behaviour at finite strains 79−3923
teacher resource paper on entropy an rubbery elasticity 80−17777
tear resistance testing, instrument for controlled notching 79−70258
testing, statistical anal., method variance *(Polish)* 77−28962
thermoluminescence data numerical anal., glass-rubber transition temp. spread 77−52189
thermoplastic elastomers, crosslinked by secondary valence interactions, elasticity and processing, crosslinking behaviour 80−40320
rubber continued
thermoplastic rubber morphologies and applications 78−26457
thick tube, large elastic deform. theory and unstable deformations 77−73298
toughened plastics, ABS- and AAS-resin, flow props., effect of heating and shearing hysteresis *(Japanese)* 79−94685
toughened polystyrene, polystyrene-Kraton G blend, charact. by SEM 79−14697
tube, inflation and extension, biaxial strain studies 78−83251
tube pressure-radius relationships, exptl. and theoretical artery model comparison 77−64078
tyre rubber blends, analysis using computer-controlled pyrolysis gas chromatography 79−96396
tyre treads, scrap, rheological behaviour of rubber and crumb mixtures 78−55619
urethane rubber, viscoelastic disc, contact problem, photoviscoelasticity obs. *(Japanese)* 78−30202
US vel. in 25-150 kHz range 77−31726
viscoelastic response to small deformations superposed on large stretch 77−72187
vulcanisates, creep under tension, O_3 effects 78−92302
vulcanisation, by S addition and γ-irradiation *(German)* 78−64599
vulcanised, biaxial deformation study *(German)* 79−70129
vulcanised, cryogenic grinding technique 77−32555
vulcanised, device for dynamic modulus of elasticity determ. *(Polish)* 77−28963
vulcanized, biaxial finite deformation props. *(Japanese)* 78−84939
vulcanized, longevity computation, fracture 79−96131
vulcanized, rheological props., stress-strain rels. 77−32608
vulcanized-rubber protection and waterproofing in seawater environment for strain gauge 78−16787
wear mechanisms, optical microscope obs. *(French)* 77−21285
X-ray scatt., differential radial distrib. function 79−14703
S vulcanisation, sulphenamide-accelerated, use of *N*-(cyclohexylthio) phtalimide as retarder 79−83169
Si rubber as electro-optic material for optical hydrophones 80−43412

rubber industry
computer controlled pyrolysis gas chromatography 79−20493
computerised automatic tensile tester, ISO and ASTM standards 77−26284
elastomer reinforcement, carbon black-polymer interaction 79−83171
instrumentation and control automation, conf., Brussels, Belgium (1976) 77−27638
microwave appl., w.r.t. economics and safety 80−3754
polyester fibres, thiuram and dithiocarbamate rubber accelerator degradation 79−78986

rubbing (abrasion) *see abrasion*

rubidium
see also nuclei with .....
absolute zero isotherms and polymorphic transition 79−73310
accommodation coefficients, of Na, Rb and Cs on Ni, 658-1095K 77−47666
adion-surface interaction energy, density formalism calcs. for Al and W surfaces 78−68069
adsorbed film on Ni (100), plasmon losses in electron energy loss spectra 79−61480
adsorption on GaAs (InSb), LEED, AES, EELS study 78−68068
anions, THF soln., photolysis, appl. to photogalvanic cell 80−85294
Ashcroft pseudopotential, unified study of props. 80−39239
atom, 1st reson. level, effective electron-ionis. cross sections, plasma discharge method 78−13603
atom, 4^2D-state, hyperfine struct. calcs. 77−67970
atom, 4p level He II photoelectron spectra, energies and intensities 80−5511
atom, 4p subshell excitation spectra, 15 to 19 eV, a new interpretation 79−777
atom, $5^2P_{3/2}$ state, Hanle effect intensities 78−66521
atom, 5^2S-n^{2}S transitions, Rydberg levels, high resolution two photon spectra obs. 80−52923
atom, 6^2D excited levels, assoc. ionisation efficiency 77−10747
atom, ^{2}D states, fine struct. 78−90098
atom, ^{2}P photodissoc. product, fine struct. anal. 80−78665
atom, π-photoionisation spectra in DC field, Fano profile 79−59410
atom, anomalous emission in blue wings 77−46517
atom, circ. polarised reson. fluoresc. excited with π polarised D_2 line, 0-170 G 79−41133
atom, Doppler-free superradiance, polarisation characts. 79−782
atom, Doppler-free two-photon absorpt. spectrum 80−42975
atom, ejected electron spectrum of autoionis. levels excited by electron impact 77−58174
atom, electron excitation cross sections for six autoion. config., Born approx. calc. 78−25713
atom, electron impact excitation, combined classical theory and free fall model 79−98229
atom, electron impact excitation velocity consts. for reson. levels, meas. *(Russian)* 78−1086
atom, electron scatt. differential spin exchange, differential cross section 77−535
atom, excited np states, fine struct., core electrons effect 77−18807
atom, F states, highly excited, natural radiative lifetime meas. 79−3404
atom, fine struct. intervals in 6^2F and 7^2F states, RF spectroscopic meas. 77−71766
atom, fine-struct. splittings in visible region, ^{2}D states 78−50656
atom, first reson. line oscillator strength, phase matching condition determ. 77−10638
atom, fluoresc., far wings profile of self-broadened reson. lines 79−76388
atom, forbidden quadrupole lines, oscill. strengths meas. 77−50390
atom, ground state, hyperfine struct., relativistic many-body calcs. 80−23322
atom, HFS, many-body and relativistic effects 78−37565
atom, high lying Rydberg states, atomic beam laser spectra 79−94101
atom, highly excited P-states natural radiative lifetimes 77−6727
atom, hyperfine struct. density and temp. shift coeffs., at high buffer gas densities 79−18138
atom, in Rb_2SO_4, study of 4d excited states 77−26989
atom, induced mag. moment by laser excitaion *(Russian)* 79−68327
atom, inner core neutral binding energies, relaxed orbital relativistic Hartree-Fock-Slater calc. 78−13433
atom, ionisation energies and oscill. strengths calcs. 80−5488
atom, isotopically selective ionisation through Rydberg states 78−5186

rubidium continued
atom, $K\beta/K\alpha$ rel. intensity obs. 80−32665
atom, L-shell soft X-ray emission spectra, oscillator strengths 80−32651
atom, laser saturation spectra, collision broadened line struct. *(Russian)* 79−45678
atom, lowest metastable autoionising level identification by RF spectroscopy 77−426
atom, multiphoton ionis. processes, fine struct., hybrid reson. 77−18877
atom, n^2D states, fine struct. near ionisation limit, two-photon spectra 77−30843
atom, observation of superradiance in the vapour 79−45691
atom, optical reson. line electron impact excitation cross sections, polaris. 78−55244
atom, oscillator strength ratios for principal series, relativistic and correlation effects 79−784
atom, oscillator strengths of 5s-4d first forbidden lines 78−86824
atom, outer-shell photoelectron ang. distrib. 80−37797
atom, photoionis. cross section, elec. field depend. 80−37796
atom, photoionisation from ground state in DC elec. field, narrow resonances *(French)* 77−61718
atom, photoionization cross-section, reson. induced by elec. field 79−13689
atom, polarisability constant, Stark interaction for excited states, laser spectroscopy 77−50404
atom, polarisation transfer collisions with inert gases, NMR of inert gases 78−33453
atom, principal series doublets, oscillator strengths 79−22656
atom, radiative lifetime, time resolved laser induced fluorescence 80−37781
atom, radiative lifetimes up to n=12 excited states, pulsed dye laser and superradiance excitation 80−83322
atom, radiatively excited states, ionis. rate coeffs. in two atom collisions 80−43160
atom, radioisotopes, hyperfine spectroscopy, nucl. props. 80−57677
atom, resonance spectral lines, Stark broadening and shift 77−75097
atom, resonantly excited in cylindrical discharge plasma, effective lifetimes 78−79413
atom, Rydberg levels, Stark patterns, expt. and central pot. calc., positions and intensities 79−93953
atom, Rydberg S and P states, hyperfine struct., RF spectroscopic meas. 77−57911
atom, Rydberg states, detection using freq. doubled CW dye laser 78−17592
atom, self-broadened first reson. lines, near-wing asymmetries 80−9535
atom, situated in external elec. field, near zero energy reson. anal. 80−63563
atom, spectral broadening and shift, inert gas collision 79−22663
atom, Stark const., β_{jj} of $6^2P_{3/2}$ state, level-crossing method 77−88424
atom, two-photon excitation, stimulated IR emission, simultaneous parametric radiation 77−10651
atom, two-photon transitions to Rydberg levels, dye laser reference wavelengths 78−94221
atom, valence p-shell HeIIα photoelectron spectra, final state CI effects 80−14121
atom, XPS, free atom core binding energy 78−74699
atom, Zeeman resonance lineshapes, motional narrowing, expt. 77−46525
atom+atom, radiatively excited states, chemi-ionisation, ionisation rate consts. determ. 80−58363
atom+bromomethane (iodomethane), product translational energy calcs., energy depend. 79−70314
atom+inert gas, D_2 line collisional broadening and shift, and HFS 79−22664
atom+inert gas, quenching cross sections of alkali n^2P states, 5-100 eV 79−76505
atom in Xe, collision-induced dipole transitions, absorpt. meas. 80−95718
atom-atom collisions with He, Kr, Xe, disorientation cross-section temp. depend. 77−23546
atomic and ionic spectra 79−59388
atomic beam, optical pumping 79−26941
atomic energy level ordering, in excited states 79−81162
atomic frequency standard, optical pumping phenomenon and techniques 77−65022
atomic HFS of optically inaccesible excited states 78−37582
atomic spectra, superradiant cascading effects, Rydberg levels 79−31491
atomic vapour, Doppler-free two-photon dispersion and optical bistability 80−95940
atoms, valence-core electron exchange interactions, local approx. 80−91416
BCC crystal, elastic constants, thermal expansion and bulk modulus 80−6452
calc-alkaline rocks from the East Carpathians, K, Rb and Sr distrib. 78−85555
CESR linewidth and g-shift in presence of spin-orbit perturbation, spin-phonon scatt. 77−63285
chemisorbed on Ag (111), struct., and reactivity towards NO 79−28207
conduction-electron spin flip by phonons, expt. data anal. 79−61219
crystal nucleation and symmetry, interaction pots. effect 80−34169
crystal struct., van der Waals and repulsive interaction 80−84137
crystal structure, effect of Van der Waals forces 79−99111
determination, by X-ray fluoresc., for radiometric age meas. 77−70356
diffusion in Bi, mechanism 79−77819
discharge lamp, spherical, electrodeless, spectral profile of D_1 line 77−50744
elastic constants, cryst. equilib. and electronic contrib. 79−73243
elastic scattering amplitudes, for high energy electron scattering, by ionised atoms, numerical calcs. 80−49057
electrical resistance meas., search for supercond. at high press. 79−56359
electrical resistivity, data tables, 1-2000K 79−78072
electrical resistivity, phase transforms. under high press. *(German)* 80−107763
electrical resistivity, temp. depend., anharmonic effects 78−76045
electrical resistivity, temp. depend., free energy approx., anisotropic continuum dispersive model 77−43557
electrical resistivity, thermal cond. and thermoelec. power, 40-300K 79−73490
emission, anomalously intense, Rb atomic lines in shock heated salt vapour 78−63089
equation of state meas. 80−19905
rubidium continued
equations of state determ. 80−24564
erythrocytes, rabbit, increased passive efflux of ^{22}Na and ^{86}Rb on microwave irrad. 80−108957
expanded fluid, struct., Monte Carlo study 78−83720
Faraday effect for reversible depolarisation, optical communication scrambling appl. 77−42596
Fermi surface, de Haas-van Alphen meas. 78−2411
Fermi surface and quasiparticle props., density functional approx. 80−96771
Fermi-surface press. dependence 80−96772
film, elec. props. *(Russian)* 77−47906
film, inert gas impurities, optical excitation spectra obs. 77−24876
fluid, simulated, atom pairs, dynamic behaviour 80−44098
fluorescent excitation anal. of stable Rb, erythrocyte survival determ., rabbits 80−81788
frequency standard, Rb lamp stability and reliability factors, expt. 77−17955
frozen solution in HMPA, Wannier-Mott impurity ground state, EPR 77−8054
graphite, Rb-intercalated, theory of order-disorder phase transitions 80−19908
ground state alkali molecules, mag. shielding and spin-rot. interaction 80−87186
ground state of solids, spin density functional method, binding energy, compressibility 80−65477
Gruneisen parameter temp. var. for BCC struct. 78−6137
hexamethylphosphoramide-K(Cs)(Rb), low temp. glass, EPR of solvated ats. 78−91927
high pressure effect on supercond. and high temp. resist. 77−47917
interatomic function from phonon-dispersion curves and Heine-Abarenkov-Shaw optimised model pot. 79−19185
interatomic pair potential, phonon spectra 80−33927
interatomic potentials from experimental phonon spectra 78−75621
intercalation compound with graphite, superlattice struct., electron diffr. study 80−75214
intercalation compounds with graphite, Raman scatt. from in-plane lattice modes 78−15168
ion mobility in He, Ne, Ar, H_2, N_2, O_2, CO_2 77−11305
isotope, neutron deficient, supermultiplet mass predictions 79−85359
isotope shifts and high resolution laser fluoresc. spectroscopy in deep blue spectral region 77−82622
Landau Fermi-liquid-theory parameters, conduction-electron spin wave meas. 79−42472
lattice dynamics, OPW calc. in Lindgren approx. of conduction-core exchange 79−1481
lattice dynamics, phenomenological model 77−20017
lattice sp. ht. and thermal vibrs. 78−30768
lattice vibrations, modified tensor force model 79−86853
lattice vibrations, seven parameter non-central force model 80−44270
liquid, backflow of quasiparticles in classical system 79−27614
liquid, classical, long-time anomalies suppression 80−24339
liquid, coherent scatt. function anal. by self consistent field method 79−55651
liquid, coherent scatt. function calc. 78−22635
liquid, coherent scatt. function calc. 78−42875
liquid, computer-simulated, search for atomic vacancies 77−84620
liquid, cryst. nucleation and growth, mol. dynamics calcs. 79−74144
liquid, current-fluctuation spectra, mode-coupling theory 79−4231
liquid, density fluctuations, coherent scatt. function, SCF method 78−18527
liquid, density fluctuations from mol. dynamics simulations 80−100161
liquid, dynamic struct. factor, two-relax. time model 77−1068
liquid, dynamic struct. factor 78−30533
liquid, dynamical struct. factor 78−38612
liquid, effective interionic pots. determ. from expt. data 77−47338
liquid, electrical resist. temp. depend. calc. 77−55507
liquid, equation of state, press. and entropy along melting curve 77−47540
liquid, equilib. props., self consistent field methods calcs. 79−10767
liquid, expanded, eqn. of state, transport up to 1700°C, 400 bar 80−2136
liquid, expanded, struct. factor up to 1400K, 200 bar 77−47335
liquid, freq. moment and viscosities calc. 80−88348
liquid, higher order struct. functions in long wavelength limit, improved perturbation approx. 79−37606
liquid, isothermal compressibility, harmonic pot. model calc. 79−14870
liquid, kinetic model, dynamic struct. factor 79−10768
liquid, kinetic theory of self motion, memory function of vel. autocorrel. function calc. 80−14986
liquid, long wavelength collective motion 78−38601
liquid, long wavelength limit, triplet and higher correls., Percus-Yevick eqn., perturbative anal. 79−37613
liquid, longitudinal modes, transverse modes and velocity correlations 78−94954
liquid, mode coupling theory of simple classical liquids 79−55630
liquid, mol. dynamics data, test of Born-Green eqn., pair pots. determ. 77−1057
liquid, non-Markovian system, Fokker-Planck eqn. 77−47313
liquid, nuclear spin relax. of 13.9 msec ^{88m}Y 77−12270
liquid, phonons, collective modes calcs. 78−2218
liquid, resist. and thermo-electric power using corrected parameters of Shaw model 79−19566
liquid, resistivity calc. 77−85190
liquid, self-consistent calc. of coherent scatt. function 77−51308
liquid, shear viscosity coeffs., model calcs. 78−47549
liquid, shear viscosity correlation function 78−47460
liquid, shear wave modes and velocity correl. spectra 78−63654
liquid, short-wavelength density fluctuations 79−46550
liquid, simultaneous meas. of density, elec. cond., absolute thermopower up to 1400°C and 400 bar 77−1402
liquid, static struct. and electronic transport props., pseudopotential calc. 79−7543
liquid, struct. factor, improved perturbation anal. of Percus-Yevick eqn. 77−58942
liquid, struct. factor and compressible rel. to metal-nonmetal transition 78−2529
liquid, struct. factor determ. by neutron diffr. up to 1400K and 200 bar 77−1064
liquid, structure and dynamics, SCF calcs. 77−51303
liquid, structure factors, higher order distrib. functions 77−51299

rubidium continued
liquid, T_c, P_c V_c, from eqn. of state 78−2228
liquid, transverse correlations in simple liqs., effective field approach 79−82135
liquid, van Hove's dynamical structure factor for classical liquids 79−55631
liquid, vel. correl. function, memory function calcs. 80−49081
liquid model, derivation of vel. autocorrelation function from incoherent scatt. function 79−77491
liquids, pair interaction pot., thermodynamic, neutron diffr. calcs. 77−11463
maser oscillator freq. domain meas. of freq. stability 80−83574
maser response to coherent Zeeman perturbations 78−58972
melting at high pressures, thermodynamics 78−91426
melting thermodynamics *(Russian)* 78−71840
metal impurity effect on residual elec. resistance *(Russian)* 80−84457
metallic compressibilities, general pseudopotential approach 80−54631
methyl iodide+K(Rb), reaction cross sections 78−40043
MHD generation appl., owing to low ionisation potentials *(Hungarian)* 80−3526
microwave transmission modes at cryogenic temps. 79−42473
molecular beam, I_2 surface chemi-ionis. 78−7231
molten, enthalpy and specific heat meas. in 320 to 1220K range 77−35711
muscle single fibres, Rb^+, Cs^+ and Na^+ localisation, autoradiographic demonstration at 77K 79−96726
nepheline syenite, dating, Rb-Sr internal isochron, ^{39}Ar-^{40}Ar plateau age methods *(French)* 78−32031
optical filter, ultrahigh-Q isotropically sensitive, using at. reson. transitions 79−55216
optical pumped magnetometer *(Japanese)* 79−21790
optical pumping light source 79−46023
optical pumping of vapour, in mag. field, alignment due to π-polarised light 79−31476
optically pumped at. beam clock, theory 77−34866
oxidation, adsorbate-induced structs., UPS obs. 79−47828
phonon dispersion, calc. using electron fluid model 78−75738
phonon dispersion, modified de Launay model 78−34573
phonon frequencies and Gruneisen parameter, model pseudopotential calc. 77−35643
phonon spectral density, pseudopotential calcs. 80−39234
photoionisation, 3d subshell absorption spectra 77−10648
PIXE anal. method 77−63973
plasma impurity conc. determ., HFS intensity redistrib. method 77−84498
plasma temp.and density, HFS brightness ratios 77−89310
portable clock for transcontinental and intercontinental time comparison 78−57908
positronium, formation in positron+alkali metal atom collisions, first Born approx. 80−83525
positronium formation in positron+alkali metal atom collisions, pseudopot. calcs. 80−83524
pseudopotential, energy-depend., for Fermi surface distortion and phonon dispersion calc. 77−15737
pulsed polarised electron source with high repetition rate 77−10517
quasiparticle dynamics, density-functional approx. 79−60682
quenching cross sections, highly excited states 79−89761
resonance cell frequency standard XSRM 78−41281
resonance lines 7800.23 and 7947.6 Å, Stark broadening obs. 78−66508
Righi-Leduc and Hall coeffs. meas., 2 to 120K 77−66156
Rydberg levels in intense mag. field, diamag. struct. 79−26958
separation from potash salts, ion exchange methods *(German)* 78−23940
soft X-ray outer-shell absorption and emission, one-electron calc. 79−69904
specific heat at high temp., Monte Carlo calc. 80−29182
Stark shift of $6^2P_{1/2}$ to $5^2S_{1/2}$ line, mag. scanning meas. 80−27977
structural energies, pseudopotential formalism 80−39519
Sub-microsecond intercontinental time comparisons by satellite 77−82494
superradiance between degenerate levels, polaris. characts., coupled transitions 80−58493
surface energy, barrier height and work function, jellium model calc. rel. to fracture model 77−72907
surface energy, self-consistent calc. including ion pot. perturbation effect 77−8166
surface wave, momentum exchange with moving atom 79−64359
thermal resistivity, ideal, free-electron approx. 77−51724
time standards study review *(French)* 79−174
two photon spectrum, Doppler free, self-broadening and shift meas. 80−5506
UV absorpt. spectra 80−2780
UV absorption spectra, threshold singularities of p-shell absorpt. in XUV region 77−36261
vacancy formation energy calcs., electron density functional method 80−19801
vapour, 1.06 micron conversion to 420 nm range 79−14040
vapour, dynamic Stark tuned for IR laser 78−63126
vapour, Gaussian pulse propag. under two-photon near reson. conditions 80−87441
vapour, inelastic light scatt., mol. form. and fluoresc. *(Russian)* 77−61787
vapour, IR stimulated Raman scatt. 79−27325
vapour, mag. props. changes under laser irrad., induced EMF obs. 80−100059
vapour, reson. four-photon difference freq. mixing of Nd:YAG and dye lasers 78−50854
vapour, spectral profiles of D-lines, spherical lamp case *(French)* 78−18032
vapour, stimulated electronic Raman scatt. for tunable IR output 79−76754
vapour, thermal cond. meas. 80−14870
vapour, time-reversed optical wave front generation by degenerate four-wave mixing 79−14028
vapour, viscosity rel. to thermal cond. 79−72982
wire, low temp. elec. resist., size and temp. depend. 77−76958
wires, size effect and temp. depend. of resist. 79−51691
wires, size effect and temp. depend. of resist. 79−51692
X-ray K absorption edge, fine struct. 77−77319
X-ray production, K-shell, on N^+ impact 77−75090
AgCl:Rb^+, impurity effect on plasticity, brittleness 78−14398
rubidium continued
CsBr:Rb^+, impurity induced IR absorpt. spectrum, breathing-shell model 77−77256
CsBr(Cl)(I):Rb, optical absorpt. investig. of F_A-centres 77−44029
H^++Cs(Rb)(K)(Na), charge exchange, H(2s) form. 79−64101
He+Cs(Rb), interatomic pots., hyperfine shifts, diffusion coeffs., perturbation exchange theory 79−41220
Hg+Ne(Na)(K)(Rb), elastic scatt., interatomic pots. 77−58122
K-Rb arc lamp development for space laser communications 78−46646
KBr:Rb, H-centre interaction with Rb^+ ion 78−75662
KBr:Rb, microcrystalline powders, isothermal decay of colour centres 80−2804
KBr:Rb, U-centre modes, Green's function method calc. 77−24372
KBr:Rb^+, elastic interaction of H-centre with impurity, dynamic effects 77−76396
KCl:Rb^+, entropy changes associated with point defect form. calc. 77−7741
KI:Rb^+, lattice relaxation around tetragonal and rhombic defects 79−95110
$KMnF_3$:Rb, phase transition and atomic motions, NMR study 80−75872
$(NH_4)_2SO_4$:Rb, ferroelec. transition, light scatt. meas. 78−43822
$^{81,82m}Rb$ production for positron emission tomography 80−98068
Rb, $5^2P_{1/2}\rightarrow5^2S_{1/2}$ resonance line perturbed by inert gases, depolaris., broadening and shift 78−21880
Rb $6^2P_{1/2}$ state, fluoresc. electric scanning method, polarisability 79−76381
Rb I, D_2 resonance line ^{85}Rb-^{87}Rb shift, mean square charge distrib. values inversion *(French)* 77−57931
Rb I, lifetime meas. of lowest ^2D-states, elec. quadrupole excitation 78−42004
Rb I isoelectronic series, transition probabilities, oscill. strengths, lifetimes, branching ratios 78−33470
Rb II, lifetimes in $4p^55p$ config., precision meas. and calc. 80−102488
Rb induced radiation in multiphoton excitation above ionisation limit *(Russian)* 79−3425
Rb^-, in tetrahydrofuran soln., transient photoelectron nutation 79−3418
Rb^-, photodetachment, electron affinity 78−90132
Rb^+ diffusion in molten (Li-K)NO_3, wave-front-shearing interferometry study 79−60535
Rb^+, electron impact excitation, absolute cross-sections 78−82849
Rb^+, free-ion polarisabilities, empirical values 77−20792
Rb^+ in Kr(Xe) gas, longit. diffusion and generalised Einstein relation 79−10625
Rb^+, ionic mobility in Ar, Kr and Xe, interaction pot. determ. 79−18991
Rb^+, levels direct excitation, cross sections and transition probabilities determ. 80−52899
Rb^+, longit. diffusion coeffs. in elec. field, mass spectrometric determ. 77−7502
Rb^+ mass spectrometer quadrupole mass filter transmission 79−21851
Rb^{2+}, crossed beam electron impact excitation, cross sections 80−43190
Rb^{2+}, dissoc. energy from ionisation rate coeffs. of Rb+Rb 80−58363
Rb^{2+} formation during electron-ion collisions, ultrasoft X-ray spectroscopic study *(Russian)* 80−43193
Rb^{33+}, ^1P and ^3P energy levels relativistic RPA calc. 80−47913
$^{85,87}Rb$, high Rydberg levels, press. broadening and shifts 80−52902
^{85}Rb, $5^2P_{3/2}$ state, Hanle effect *(French)* 78−42018
Rb:Kr film, metal-insulator transition, cond. and optical absorption meas. 77−24598
Rb-Ar, oscill. strength, for induced dipole transitions, pot. energy curve 77−75100
Rb-Cs plasma, electron collision induced charge exchange *(Russian)* 77−68740
Rb-Sr dating of Brazilian rocks, appl. of solid-source mass spectrometer 77−70840
Rb-tetrahydrofuran soln., photolysis, photoelectron emissive EPR signal, scavenger electron affinity reactivity 78−53224
Rb-Xe mixture, nonreson. third harmonic generation of I laser radiation 79−3746
Rb-Xe mixture, third harmonic generation with Nd:glass mode-locked laser 77−27318
Rb+$_5{}^{10}B^{n+}$, 4-38 MeV, K-shell ionis., X-ray obs. 79−59549
Rb+^{131}Xer, spin-exchange cross section, ^{131}Xe nucl. spin relax. obs. 80−37868
Rb+Ar(Kr)(Xe), spectral line breadth and shift, Van der Waals pot. calc. 78−90126
Rb+atom, Rb Rydberg states, collisional ionisation, rate consts. 80−32817
Rb+H^+, atomic K-shell ionis., X-ray emission 79−18280
Rb+H^+, single photon emission following double K-shell ionisation, contrib. to superheavy element search data 78−50625
Rb+H^+(H), single-electron capture total cross sections 80−91656
Rb+He, quasielastic and inelastic collisions in S and D Rydberg states 80−83462
Rb+He(2^3S_1), Penning ionis. in stationary afterglow 78−42184
Rb+Hg, 15-1400 eV, electronic excitation, integral cross sections 80−43159
Rb+inert gas, hyperfine struct., broadening and shift calcs. 77−58153
Rb+inert gas atom, ground-state pots. from elastic cross sections 77−75258
Rb+iodomethane, reaction cross section, translational energy depend: min. 77−66753
Rb+Kr, STS components shift and broadening 77−68014
Rb+methane (and deuterates), $5^2P_{1/2}\rightleftarrows5^2P_{3/2}$ excitation transfer, isotope effects, temp. depend. 80−91630
Rb+methyl bromide$\rightarrow$RbBr+CH_3, yields, crossed mol. beam study 79−34293
Rb+Mg^+, charge exchange and excitation processes 78−17772
Rb+N_2, spin relax. rate 77−19027
Rb+Na, spin exchange cross section 78−33637
Rb+Ne(Ar), spin relax., van der Waals mols. form. 77−19027
Rb+Rb, ^2P states, near IR spectra, collision induced features 77−10637
Rb+Rb^+, total resonant charge transfer cross section determ. using model pot. simulation 79−64073
Rb+Rb**, freq. shift, line broadening, phase interference effects, Doppler free two photon spectra 80−58200
Rb+Rb(Cs), continuum- and bound-state pair absorption, 2300-3100 Å, 410-540°C 80−42970
Rb+Xe, interatomic spectrum, theoret. and exptl. obs. 78−9112
Rb+Xe system, reson. fluoresc., quasimol. states *(Russian)* 79−85935
Rb^++Ar(Kr)(Xe), elastic beam scatt., repulsive pots. 79−98184

rubidium continued
Rb^++Cu crystal, elastic scatt., ang. and energy relationships, 1-3 keV *(Russian)* 79−78802
Rb_2, absorpt. spectrum in visible and near visible 78−46356
Rb_2, B-X system vibr. consts. from mag. rot. spectra 79−76530
Rb_2, laser-induced photodisintegration *(Russian)* 79−89719
Rb_2, mol. spectra, population inversion, high-power laser appls. 77−3406
Rb_2, photodissoc., ^2P products, at. fine struct. anal. 80−78665
Rb_2, vapour, laser radiation absorpt. superradiance 78−46553
Rb_2, $X^1\Sigma_g^+$ state, Raman spectra, fluoresc., vibr. energy 78−46345
Rb_2^+, $^2\Sigma$ and $^2\Pi$ state pot. energy curves, two-centre model 79−26906
Rb_2^+, adiabatic pot. curves, ground and excited state, Hellmann-type model pots. 78−78647
Rb_2^+, core-core interaction potential calc. 78−25645
Rb_2^+, form. by electron impact in elec. discharge, low-press. vap. 79−10738
Rb_2^+, pot. energy curve, pseudopot. calc. 77−6703
Rb_2+Br→RbBr+Rb*, product electronic state distrib., chemiluminesc. 77−40529
RbI isoelectronic series, oscill. strengths, relativistic HF calcs. 79−98035
^{79}Rb, low energy ions systematic range meas. in Ar and N_2 gases 79−1472
^{81}Rb, excitation functions of proton induced nuclear reactions on ^{85}Rb, medical appls. 80−78286
^{81}Rb, prod. and characts. for myocardial imaging studies 79−29628
^{81}Rb/^{81m}Kr ratio as radioactive tracer study of organic bleeding *(Dutch)* 80−3807
^{82}Rb generator with alumina column, radioactive Sr adsorption 80−12257
^{82}Rb generators, alumina-based, medical evaluation and appl. 80−41237
^{84}Rb, preparation by on-line isotope separation 77−23328
^{85}Rb cell filtering action, press. shift and broadening by foreign gases 79−3403
^{85}Rb, ground state dipole HFS diamagnetic shift, high field optical pumping expt. 78−90129
^{85}Rb, HFS affected by strong mag. fields 78−37759
^{85}Rb, hyperfine struct., diamag. shift obs. 77−61717
^{85}Rb unperturbed hyperfine transition frequency determ. 77−7047
^{85}Rb, unperturbed hyperfine transition freq. meas. 77−17954
$^{85}Rb^+$($^{87}Rb^+$), hyperfine struct., in-flight saturated absorption laser spectrosc. 78−78650
^{86}Rb, countercurrent fluxes through bilayer lipid membranes 79−70528
^{86}Rb, in molten alkali nitrates, diffusion coeffs. meas. 80−70437
^{87}Rb, decay consts. for use in geochronology and cosmochronology 78−28189
^{87}Rb dose-rate contrib. in thermolum. dating of pottery 78−70242
^{87}Rb double resonance, signal intensity characts. due to pumping light 77−34603
^{87}Rb, freq. displacement meas. by passing pumping light through ^{85}Rb filter cell 77−41702
^{87}Rb, ground state g-factor, rel. to ^{39}K, spin-exchange optical pumping meas. 77−34596
^{87}Rb, hyperfine transition, light shifts, buffer gas shifts, rel. to maser freq. stability 79−98029
^{87}Rb maser and related oscillators, time- and frequency-domain stability 78−58968
^{87}Rb optically pumped freq. standard, buffer mixtures for gas cell 78−82938
^{87}Rb passive frequency standards, line inhomogeneity effects 79−54106
^{87}Rb resonant frequency change, due to spectral profile of pumping light 78−45590
^{87}Rb, Stark effect on $5^2P_{3/2}$ state 79−3399
^{87}Rb, surface wave polarisation in hyperfine dipolar mag. transitions *(French)* 78−50504
^{87}Rb+^{129}Xe, spin-exchange cross-section meas. 80−78686
^{87}Rb+Kr, D_1 line broadening and shift 77−38640
^{87}Rb+inert gas, D_1-line hyperfine components perturbation, interferometer obs. 80−32635
^{88}Rb fractional uptake, meas. of myocardial blood flow, compared to microspheres 79−34656
Rb*+He(Xe), thermal, 5p $^2P_{1/2}$ state depolarisation cross-sections 77−71852
Rb*+Xe+Xe, mol. form., eikonal approx. calcs. 77−14531
Rb_2*, optically excited, cascade predissoc. *(Russian)* 79−10159
^{85,87}Rb, first excited D-level, hyperfine struct. meas. by cascade, fluoresc. spectrosc. 80−69101
Rb(6^2P)+He(Ar)(Xe), fine-struct. transition cross sections, semiclassical calcs. 77−30972
Rb(nP)+Rb(inert gas), collisional depopulation Rydberg P state 77−75281
Rb(nS, $nD_{3/2}$)+Rb(ground state), collisional quenching cross sections 80−43146
Ru^{3+} isoelectronic series, radial charge distrib. calc. 80−9507
$SrCl_2$:Rb^+, X-irradiated, recomb. luminesc. between trapped electrons and self trapped holes 77−73162
SrF_2:Gd^{3+}, Rb^+, EPR of orthorhombic Gd^{3+}-univalent metal ion complexes 80−11262
^{82}Sr-^{82}Rb biomedical generator, performance obs. 79−53247
^{82}Sr-^{82}Rb generator improvement using inorganic exchangers 80−17135

rubidium alloys
Au-Rb, charge transfer, Mossbauer effect ^{197}Au isomer shifts, XPS valence-band spectra 80−2676
K-Rb, dil., anisotropic scatt. of conduction electrons by impurities 78−18944
K-Rb, dil., anisotropy of electron-impurity scatt., de Haas-van Alphen effect meas. 78−18943
K-Rb, dil., calc. of press. depend. of low-temp. transport props. 78−30905
K-Rb, extreme UV absorpt. spectra 80−97294
K-Rb, internal energy, heat of mixing, entropy, dielectric function 80−88340
K-Rb, liq., elec. resistivity, temp. depend. 78−39084
K-Rb, liq., form factors and transport coeffs., pseudopot. perturb. theory 80−44561
K-Rb, liquid, resistivity calc. using general method pseudopot. 77−55506
K_cRb_{1-c}-alloys, lattice dynamics of substitutional alloys, force constant disorder 78−75786
Na-Rb, liq. alloys, electromigration driving force expression 78−51714
Na-Rb, liq. calc. of electromigration forces and resist. 79−82572
Na-Rb, liquid, resistivity calc. using general model pseudopot. 77−55506

rubidium alloys continued
Pb-Rb, phase diagram *(Russian)* 78−19720
Rb-Au, electron diffusion thermoelectric power calc. 77−28161
Rb-Cs, liq., elec. resistivity, temp. depend. 78−39084
Rb-Cs, liquid, electron theory of chemical potential and activity *(Japanese)* 77−72702
Rb-Hg liquid amalgams, thermodynamic props. determ. from conc. cell EMFs 77−1246
Rb-K, dil., dynamical props. of quasiparticle excitations, de Haas-van Alphen effect meas. 78−84128
Rb-K, lattice vibrs. in CPA, comparison to neutron scatt. meas. 79−42165
Rb-K alloys, localised phonon modes, classical mol. dynamics compuer simulation 78−10147
Rb-K(Cs)(Na), solute atom-grain boundary interaction energy, electron-statistical calcs. *(Russian)* 79−73175
Rb-Se system, phase equilibria 78−44079
RbAu, NMR line shape, Knight shift, X-ray diffr. study, struct. props. 78−68402
RbAu, photoelectron spectroscopy and energy bands calc. 78−76581
$Rb_{1-c}K_c$, local mode exam. by neutron diffr. 79−37781
$Rb_{1-x}K_x$, phonon spectra, single site CPA 78−10142
$Rb_{1-x}K_x$, influence of many electrons exchange and correlation effects on vibr. props. 79−69443
$Rb_{71}K_{29}$, lattice dynamics, molecular dynamics study 79−37782
Ru-Nb alloy, mag. suscept. of HCP transition metal alloys *(Russian)* 78−80138

rubidium compounds
see also rubidium alloys
acetate, molten mixtures, elec. cond., density 77−15613
n. alkanoates, long-chain, phase transformations, in melt, DTA obs. 77−76536
graphite, intercalation compound, C_8Rb, elastic and inelastic neutron scatt. 78−30597
graphite intercalation compound, RbC_8, first stage intercalation cpd., X-ray crystallographic obs. *(French)* 79−32966
graphite intercalation compounds with Rb Raman scattering 78−35130
graphite-Rb compounds, intercalates IR active lattice mode obs. 80−45072
graphite-Rb lamellar cpd., reversible intercalation of tetrahydrofuran 80−16211
halide crysts., phonon dispersion curves, shell model calc. 77−55331
halide-CuI(Cl) systems, AC cond. rel. to phase diagrams 77−72712
halides, absorpt., emission and lifetime data, temp. depend. 77−4671
halides, cohesive energies, effect of three body interactions 77−76516
halides, elastic constants, temp. derivatives at constant volume 80−59549
halides, He II photoelectron spectra, ionisation energy 77−18977
halides, moments of phonon spectrum from sp. ht. data 77−35649
halides, photoelectric yield spectra, 10 to 40 eV photon energy 79−28887
halides, polymorphic transitions, temp. depend. of transition press., thermodynamical data *(French)* 78−38843
halides, spin lattice relaxation meas. of O_2^- centres 80−88863
halides, vibrational surface modes of (001) unrelaxed face, shell model 77−43420
intercalation compound with graphite, resistivity anomalies and phase transform. 78−26839
intercalation compounds with graphite, phase transitions, resistive anomalies, electronic props. 79−95405
low-temp. cryst. modification, gyrotropy *(Russian)* 77−85684
mixed oxides, cryst. struct., electron microscopy study 78−91310
platino-oxalate, one-dimens. conductors, prep., struct. and elec. cond. 80−24900
$RbBiF_4$, anionic conductivity exam. *(French)* 77−35952
RbBr, structural phase transition, Born-model and effects of hydrostatic and non-hydrostatic stresses 79−23721
RbCl:Ag^+ IR absorpt. spectrum and vibr. of substitutional impurity 77−81135
RbH_2PO_4, attenuation const. meas. by SHF dielec. resonance 79−47406
rubidium propanoate, solid state transitions and melting process, diffr. and conductometric meas. 80−10670
rubidium tetramethylborate, vibr. spectra and force constants *(German)* 79−26981
rubidium uranyl propionate, low temp. absorpt., luminesc. spectra, intermol. interactions 80−2830
tartrate, optical rot. dispersion, dichroism and spectra, in soln. and cryst. *(Russian)* 77−90124
TCNQ salt, Rb^+TCNQ^-, cryst. struct. of new form 77−24311
TCNQ salt, Rb-TCNQ, ^{14}N NQR, Zeeman perturbation study, charge transfer 78−39438
TCNQ-Rb, X-ray exam. of phase transitions 78−55933
ternary chlorides, $ABCl_3$ type, optical props. 78−35111
tetracyanoplatinate conductors, IR and Raman spectra, cyanide stretching vibrs. 79−11415
trisoxalatoferrate complexes, Mossbauer studies of electronic relax. phenomena 80−44973
X-ray K absorption edge, fine struct. 77−77319
$Ag/RbAg_4I_5/I_2$ solid state battery, low temp. degradation 80−61331
$Ag/RbAg_4I_5/Ta$, solid electrolyte timing cell and coulometer 80−68216
AgI/RbI quasibinary system, solid state reactions and transport props. 80−96700
AgI-RbI films, vacuum deposited, cond. determ. 77−39689
Ag_4RbI_5, interfacial polarisation effects 79−60538
$Ag_5Rb(PO_4)_2$, struct., density and elec. cond. 80−33952
β-Al_2O_3-Na_2O-Rb_2O, cation interstitial pair modes in vibr. spectra 79−37788
β-Al_2O_3-Rb_2O, far IR absorption and ionic cond. 78−72512
β''-Al_2O_3-Rb_2O, single cryst. Raman scatt., cond. mechanism and cryst. struct. 80−66209
β-Al_2O_3-Rb_2O, X-ray diffuse scatt. 78−71725
β-Al_2O_3.Rb_2O, low temp. sp. ht., tunnelling states and diffusion theory 77−43345
As_2O_5-$Rb_2O(Rb_2CO_3)$ system, phase diagram, polymorphic transform. 79−83181
B_2O_3-K_2O-Na_2O-Rb_2O-Cs_2O glass, small angle X-ray scatt. exam. of struct. 80−38922
$C_{24}Rb$, graphite intercalated, de Haas-van Alphen effect, cyclotron reson., and transport props. 80−44479
C_8Rb, graphite intercalated, phonon dispersion relations and Raman spectra 80−44272

rubidium compounds continued
$CdRbI_3H_2O$, cryst. struct., X-ray diffr. 77−19918
$Cs_{1-x}Rb_xMF_3$ (M=Mg, Co, Ni, Zn), hexagonal fluoride perovskite structural evolution by cationic substitution *(French)* 80−24430
$Cs_2RbMO_3F_3$, (M=Mo, W), low temp. phase transitions *(French)* 78−92036
Cs_2RbTmF_6, mag. behaviour 2.9 to 251.3K, cryst. field levels, ang. overlap model *(German)* 80−29520
Cs_2RbYbF_6, mag. behaviour, 3.5-251.3K *(German)* 80−50041
$Cs_{10}Ta_{29.2}O_{78}$, cationic exchanger with crossed tunnel struct., cryst. struct. *(French)* 78−83797
DyF_3-RbF, phase diagrams and ternary fluorides *(French)* 80−81040
K-Rb silicate glass, thermal expansion 77−4186
KCl:RbCl, $SrCl_2$, IR window material, cryst. growth and props. 78−31333
KCl:RbCl, $SrCl_2$, laser window material, prep., grain boundary stability 77−46774
KCl-RbCl fused binary mixtures, electrocapillary phenomena on liq. Bi 77−40553
$K_{1-x}Rb_xBr$, lattice dynamics on pseudo-crystal model 78−75762
$K_{1-c}Rb_cCl$, impurity centre local vibrs., comp. depend. of spectral parameters 80−79898
$K_{1-x}Rb_xCl:HF_2^-$, dynamic inhomogeneous broadening of bands of local vibr. 78−92102
$K_xRb_{1-x}Cl:HF_2^-,SO_4^{2-}$, nonuniform broadening of IR vibr. absorpt. bands of impurities *(Russian)* 77−16357
$K_xRb_{1-x}Cl_yBr_{1-y}$, far IR absorption spectra 79−33695
$K_xRb_{1-x}Cl_yBr_{1-y}$, IR reflection spectra 78−76474
$K_xRb_{1-x}HF_2$, nuclear spin-lattice relax. and internal motion mechanism 79−99787
$K_{0.5}Rb_{0.5}I$, mixed cryst., phonons, neutron scatt. 77−1192
$K_xRb_{1-x}I$, Debye temp. conc. depend. 79−90746
$K_xRb_{1-x}TiOPO_4$, new nonlinear optical material 77−14784
(Li-Rb)NO_3, molten, internal cation mobility meas. 79−60534
LiCl-RbCl, molten, Chemla effect, mol. dynamics simulation, self exchange vel. 80−79967
$Li_{1-x}Rb_xI$, intrinsic optical absorpt. spectra 78−23500
$MgCl_2$-RbCl, binary melts, surface tensions *(Japanese)* 78−10260
$MgRb_2(SeO_4)_2.6H_2O:Mn^{2+}$, EPR spectra 80−100608
$(NH_4,Rb)Cl$, negative isotope effect on II-III phase transition *(German)* 78−95155
$(NH_4)_xRb_{1-x}Al(SO_4)_2.12H_2O:Cr^{3+}$ EPR study, effect of monovalent ions on trigonal distortion 80−11255
$(NH_4)_{1-x}Rb_xCl(Br)$, and $(ND_4)_{1-x}Rb_xCl(Br)$, phase diagrams, DTA and birefr. obs. *(German)* 79−83185
$((NH_4)_{1-x}Rb_x)_2SO_4$, isomorphic impurity effect on dielec. and nonlinear optical props. 80−88911
$((NH_4)_{1-x}Rb_x)_2SO_4$ mixed cryst., EPR of NH_3^+ and SeO_3^- radicals 80−50190
$(NH_4)_{2(1-x)}Rb_{2x}SO_4$, mixed crystal, dielectric and US meas. of ferroelec. phase transition *(Japanese)* 80−7305
$(NH_4)_{2(1-x)}Rb_{2x}SO_4$, stoichiometry defects, electron probe microanal. 80−39143
Na-Rb silicate glass thermal expansion 77−4186
NaCl-RbCl fused binary mixturs, electrocapillary phenomena on liq. Bi 77−40553
$NaNO_3$-$RbNO_3$-$Pb(NO_3)_2$, crystn. heat of eutectic, thermodynamic anal. *(Russian)* 77−63644
Na_2WO_4-Pb_2WO_4-WO_3 system investigation, crystn. from melt, coordination compounds form. 79−52189
$NbSe_2Rb_x$ intercalation cpd., EXAFS study 80−2897
Rb halides, high-resolution spectroscopy in far UV 77−66484
Rb halides, role of quantum effects in lattice dynamics, Debye temp., shell model calcs. 80−70336
Rb-inert gas molecule, excimer transitions, absorpt. spectra 77−475
Rb-TCNQ-II, two-carrier cond. 80−44625
Rb-tetrahydrofuran solution, polarised photoelectron and loose ion pair (Rb^+, e) obs., optical-ESR study 80−85196
Rb-U-O system, cryst. chem. 77−39568
$Rb_2(CU(CO_3)_2)H_2O$, crystal struct., X-ray determ. *(French)* 79−99164
Rb_2AgCl_3 luminesc., absorpt. and excitation spectra 77−12424
$RbAg_{4-x}Cu_xI_5$, solid electrolyte, elec. cond. 77−15624
$RbAg_4I_5$, 208K phase transition, Jahn-Teller-like model 77−35694
$RbAg_4I_5$, Ag^+ ion pot. energy calcs. 79−10828
$RbAg_4I_5$, contact in solid state cells, electrochem. study 80−76527
$RbAg_4I_5$, critical dynamics, role of acoustic phonons, and Z-branch 77−84887
$RbAg_4I_5$, cryst. growth from soln. 79−33916
$RbAg_4I_5$, crystal nonequilibrium thermodynamics, quasielastic light scatt., systematic anal. 79−61391
$RbAg_4I_5$, depolarisation of light by crit. fluctuations 79−61333
α-$RbAg_4I_5$, dynamic cage effect 80−107541
$RbAg_4I_5$, EXAFS, RDF studies 79−87526
$RbAg_4I_5$ film, thermopower meas. temp. depend., correl. effects role 80−107539
$RbAg_4I_5$, I_2 diffusion obs. using ^{131}I radiotracers 78−18830
$RbAg_4I_5$, ionic cond., effect of press. 78−51733
$RbAg_4I_5$, ionic cond. near order-disorder transition 77−11728
$RbAg_4I_5$, ionic conductivity and heat capacity near T_c 78−47584
$RbAg_4I_5$, low temp. phases, $\alpha\rightarrow\beta\rightarrow\gamma$ transitions 77−15586
$RbAg_4I_5$, phase transitions and dynamics 78−59924
$RbAg_4I_5$, phase transition, statics and local dynamics, mean field and Mori theory 80−39347
$RbAg_4I_5$, single cryst., dielectric relax. *(German)* 79−4764
$RbAg_4I_5$, single particle excitations, inelastic neutron scatt. obs. 80−59599
$RbAg_4I_5$, solid electrolyte, polarised Raman scatt. meas. 77−12376
$RbAg_4I_5$, solid electrolyte, compatibility with polyiodide cathodic materials of I_2-Ag current source 77−40555
$RbAg_4I_5$, solid electrolyte, cond., phase transitions 77−84972
$RbAg_4I_5$, solid electrolyte, electronic cond. meas. 78−2483
$RbAg_4I_5$, solid electrolytes, co-ionic cond. 78−26721
$RbAg_4I_5$, solid electrolyte, neutron scattering study 78−79696
$RbAg_4I_5$, solid electrolytes with glass-like struct., thermodynamic and electrochem props. 79−10978
$RbAg_4I_5$, solid electrolyte, Rayleigh-Brillouin and low-frequency Raman spectra 79−33720
$RbAg_4I_5$, solid electrolyte, thermodynamics and electrochem. behaviour of I_2 electrode 79−70348
$RbAg_4I_5$, solid electrolyte, Raman spectra 79−73934
rubidium compounds continued
$RbAg_4I_5$ solid electrolyte, interface with metal, photocurrent obs. on illumination 80−34513
$RbAg_4I_5$, solid electrolyte, contrib. of non-Brownian motion to transport props. 80−70453
$RbAg_4I_5$, solid electrolyte development, Ag^+ cond. 80−107532
$RbAg_4I_5$, static and dynamic NMR effects at 208K and 122K phase transitions 80−108105
$RbAg_4I_5$, struct. transition at 209K, Ising like behaviour 78−14460
$RbAg_4I_5$, superionic conductor, absence of Hall effect for Ag ions 77−31805
$RbAg_4I_5$, superionic cond., US absorpt., ionic cond., relaxing sp. ht. 78−14505
$RbAg_4I_5$, superionic conductor, evidence for first-order phase transition 78−83949
$RbAg_4I_5$, superionic conductor, phase transition detection by thermoelectric power method 80−92669
$RbAg_4I_5$ superionic films, elec. cond. and optical absorpt. studies 79−99355
$RbAg_4I_5$, superionic phase transition, dynamical and crit. pt. props. 80−107535
$RbAg_4I_5$, third order elastic consts. at room temp. using 110 cut 78−59848
$RbAg_4I_5$, US attenuation near 208K phase transition 79−33085
$RbAg_4I_5$:AgI,Rb_2AgI_3, polycryst., ionic cond., impurity conc. effects 78−51734
$RbAg_4I_5$-metal interface, photocurrents, photoelectrochem. effects 78−34897
Rb_2AgI_3, cryst. struct. and polarised Raman spectrum 77−69813
$RbAg_3Se_2$, crystal struct., X-ray study *(German)* 78−83795
$RbAlCl_4$, solid state Raman spectra, 298-80K, vibr., struct. 79−28745
$RbAlF_4$, single cryst., prep. and struct. *(French)* 80−79762
$RbAlF_4$, dissoc. enthalpies, mass spectrometric determ., heat of form. 80−97720
$RbAlF_4$, hydrothermal growth method in presence of hydrofluorhydric acid *(French)* 80−25543
β-$RbAlF_4$, struct. and irreversible and topotactic phase transition $\beta\rightarrow\alpha$ mechanism 80−107132
α-$Rb_5Al(MoO_4)_4$, cryst. struct. 79−19219
$RbAl(SO_4)_2.12H_2O$, ENDOR of $^{57}Fe^{3+}$ in trigonally distorted octahedral sites 79−38405
$RbAl(SO_4)_2.12H_2O$, spin-Hamiltonian with trigonal S^3I terms for describing $^{57}Fe^{3+}$ ENDOR spectra 80−75885
$RbAl(SO_4)_2.12H_2O:Cr^{3+}$, high order EPR transitions 79−22736
$RbAlSi_2O_6$, elec. cond. meas. 78−47787
$RbAsO_3$, new compound, prep. and crystallographic characterisation *(French)* 79−66280
Rb_3AsO_4, new compound, prep. and crystallographic characterisation *(French)* 79−66280
$Rb_4As_4O_7$, solid-state synthesis, X-ray powder data *(French)* 80−15079
$Rb_2B_{12}H_{12}$, cryst. growth from soln. and morphology 77−44145
$Rb_2B_{12}H_{12}.RbBr$, cryst. growth from soln. and morphology 77−44145
$Rb_2B_{12}H_{12}.RbCl$, cryst. growth from soln. and morphology 77−44145
$RbBO_2$, mean geometrical config., vapour phase electron diffr. 77−46651
$RbBO_2$, mol. struct. determ. by gas phase electron diffr. 79−10227
$RbBO_2$, vapour over heated solid, XPS, obs. 80−87171
Rb_2BRCl_6, B=Li,Ag,Na, systematic structs., X-ray Guinier-Simon method *(German)* 80−44186
$Rb(B_xW_{3-x})O_9$ (B=Na, Ca, Co, Ni, Cd, Ga, Bi, Nb, Ta) cryst. struct., temp. dielec. anomalies 80−1998
$Rb_{2-2x}Ba_{3x}Ti_{6-x}O_{13}$, $0<x<0.2$, struct. evolution, tunnel struct. 79−65049
$Rb_2Be_2Si_2O_7$, cryst. struct., X-ray obs. 77−24293
Rb_3Bi, cubic and hexagonal structs., transition 78−26480
Rb_3BiBr_6, cryst. struct. determ. 78−75638
RbBiF, new solid electrolytes, conductivities and activation energies 79−28137
$RbBiF_4$, fast ionic conduction of F^- ions 79−99360
RbBr, cation defects creation mechanism 80−75224
RbBr crystals, positron annihilation, Doppler broadening 80−40180
RbBr, evaluation of photoelastic consts. 80−50297
RbBr, exciton mechanisms of electron sputtering 77−55857
RbBr, F-centre emission, mag. circular polarisation 80−108251
RbBr, far IR complex refr. indices, dispersive Fourier transform 78−80322
RbBr, harmonic and anharmonic props. from phonon dispersion at three temps. 80−39235
RbBr, hyperfine struct., qudrupole coupling consts., vibr. depend. *(German)* 77−34565
RbBr, liq., dynamic density fluctuations, diagonalized relax. theory 78−47230
RbBr, mode anharmonic self energies, freq. depend. 78−59908
RbBr, molten, density and charge fluctuations 79−55645
RbBr, molten, dynamical struct. factor calc. 78−22627
RbBr, optical absorpt. centre formation time meas. 80−40081
RbBr, parallel and perpendicular Stark effect of F-centre 77−1703
RbBr, phonon freqs. at 80, 290, 370K, neutron inelastic scatt. study, comparison to Gruneisen parameters 78−51631
RbBr, photo-elastic constants and pressure derivatives of shear moduli 80−75284
RbBr, self trapped exciton, optical detection of spin relax. processes 78−60358
RbBr, self trapped exciton form. time at $^1\Sigma_u^+$ state under pulsed electron beam in ps range 80−97347
RbBr, self-trapped exciton and F-centre form. by picosecond laser pulses 80−10546
RbBr, sign of thermal expansion coeff. at low temps. 77−84954
RbBr, sputtering of atoms by 540 eV electrons, delay times 80−35025
RbBr, suprapure, thermolum. glow and emission studies at room temp. 80−7423
RbBr, thermal cond., press. depend., up to 10 kbar, jump at phase transition 77−62694
RbBr, thermal cond. under press. meas. 78−30802
RbBr, two photon absorpt., 2p excitons relax., F-centre 79−91462
RbBr, UPS exam., band struct. determ. 77−40330
RbBr, UV two-photon absorpt. relative to known Raman cross section 79−81487
RbBr, Xe^+ ion bombard., sputtering processes, time of flight meas. 78−88392

rubidium compounds continued
RbBr:Ag^+, press. tuning of motional behaviour in shallow off-centre pots. 79−78718
RbBr:Ba^{2+},Sn^{2+}, thermal depolarisation meas., relax. processes 78−23389
RbBr:Cu^+, off-centre ion position, ionic thermocurrent study 80−7271
RbBr:Eu^{2+}, single cryst. optical absorpt. spectra 80−45117
RbBr:I^-, OH^-, luminesc. of interstitial atomic H 80−89062
RbBr:O_2^- centres, luminesc. polarisation temp. depend. 78−87943
RbBr:V, covalency effects, EPR meas. 77−85557
RbBr-Ag, mag. field effect on luminesc. of paired Ag^- ions 78−27313
RbBr-$CdBr_2$-H_2O, Gibbs free energy, H_2O activity, 25°C *(Russian)* 78−31678
RbBr-$MgBr_2$ system, thermochem. and struct. investigation *(German)* 79−1423
RbBr+Ag^+, IR absorpt. spectrum and vibr. of substitutional impurity 77−81135
RbBr(Cl) F centre, EPR in relaxed excited state, via mag. circular polarisation of emission 79−24232
RbBr(Cl):Ag^+, off to on centre defect transitions under hydrostatic press. 78−15199
RbBr(I), sputtering, depend. on beam energy and target temp. 79−1804
$RbBrO_3$, ^{17}O NQR, spin echo double reson. method, electronegativity 80−54970
$RbBrO_3$, hexagonal modification, temp. depend. of NQR freq., interpretation of long-wave spectra 80−25243
RbC_8, intercalated graphite, band struct. determ. by angle-resolved photoemission 80−45203
RbC_x, lamellar cpds. with graphite, EPR studies 80−44902
RbC_x, lamellar cpds. with graphite, ^{13}C NMR studies 80−44936
RbCN, acoustic and optical phonon dispersion at 300K 80−84266
RbCN, crystal props., log potential model calc. 78−63829
RbCN, cubic, temp. and press. derivatives of elastic consts. 80−6456
RbCN, cubic phase, temp. depend. of elastic consts., Brillouin spectra obs. 79−56805
RbCN, ferroelasticity and F- and M-centres absorpt. 79−87475
RbCN, molecular motion and ordering from dielec. and Raman techniques 79−73932
RbCNS, single cryst. factor group anal. of IR and Raman multiphonon bands 77−4644
Rb_2CO_3, high press. phase relations, DTA 77−43329
Rb_2CO_3, molten, IR emission spectra *(Japanese)* 78−19469
$Rb_2C_2O_4(SbF_3)_2$, growth from soln. and X-ray diffr. study *(French)* 77−80481
$RbCaCl_3$, phase transitions, optical and dilatometric meas. 79−61394
$RbCaCl_3$, Raman scatt. study of phase transitions 80−71411
$RbCaF_3$, ^{87}Rb NMR at cubic to tetragonal phase transition 79−82885
$RbCaF_3$, 193K phase transition, lattice dynamics 78−10160
$RbCaF_3$, 193K phase transition, crit. neutron scatt. obs. 78−10161
$RbCaF_3$, crit. scatt. at phase transition, Mossbauer diffraction 79−1733
$RbCaF_3$, critical scatt. at struct. phase transition, Mossbauer diffr. 80−20546
$RbCaF_3$, cubic to tetragonal phase transition, neutron diffr. obs. 79−23730
$RbCaF_3$, cubic to tetragonal phase transition, ^{87}NMR meas. 80−7187
$RbCaF_3$, cubic to tetragonal phase transform., X-ray, neutron, Mossbauer diffr. study 80−49360
$RbCaF_3$, cubic to tetragonal phase transition, ^{87}Rb NMR study 80−70392
$RbCaF_3$, elastic consts. near phase transition by Brillouin scatt. 78−38844
$RbCaF_3$, first order improper ferroelastic phase transition at 194K, phenomenological description 80−70397
$RbCaF_3$, influence of domains on struct. phase transition 79−28097
$RbCaF_3$, lattice consts. temp. depend., X-ray examination, 194K transition *(French)* 78−10184
$RbCaF_3$, NQR obs. of struct. transition at 198K 79−65191
$RbCaF_3$, neutron scatt. central peak rel. to soft mode 78−75794
$RbCaF_3$, nonlinear elastic behaviour, US velocity, 1 bar-3 kbar 78−59851
$RbCaF_3$, optical absorpt. of radiation produced defects 77−28604
$RbCaF_3$, phase transitions due to octahedra rots. in perovskite struct., order-disorder model 80−70151
$RbCaF_3$, phonon scatt., thermal cond. meas. 77−7916
$RbCaF_3$, precursor order and Raman scatt. near displacive phase transitions 80−45061
$RbCaF_3$, shift of first order transition under hydrostatic press. 80−59649
$RbCaF_3$, sp. ht. anomaly at struct. transform. 78−14426
$RbCaF_3$, struct., phase transitions, neutron diffr. study 80−33918
$RbCaF_3$, structural phase transition, superlattice points, neutron diffr. obs. 80−19944
$RbCaF_3$, thermal props. near phase transition 78−75850
$RbCaF_3$, V_K centres, lattice distortion in tetragonal phase, EPR meas. 77−20699
$RbCaF_3$:Gd_2O_3, Gd^{3+}-O^{2-} pair, EPR study of displacive transform. *(French)* 78−27088
$RbCaF_3$:Gd^{3+}, O_h-D_{4h} struct. transition, ESR obs. 80−50178
$RbCaF_3$:Gd^{3+}, struct. phase transition, EPR study 80−71171
$RbCaF_3$:Gd^{3+}, uniaxially stressed, transcrit. behaviour, EPR obs. 79−33086
$RbCaF_3$:Mn^{2+}, overlap and covalency contrib. to zero field splitting, LCAO-MO calc. 80−24850
$RbCa_{0.95-x}Mg_xEu_{0.05}F_3$, green luminesc. obs. 77−32428
$Rb_2Ca(SO_4)_3$, phase transitions, dielec. props. obs. 78−6643
$RbCdBr_3$, cryst. struct., X-ray diffr. 77−19917
$RbCdBr_3$, polarised Raman spectra 78−76443
$RbCdCl_3$, birefringence, twinning and structural phase transitions 79−38480
$RbCdCl_3$, crystal struct., polarised Raman spectra and X-ray diffraction obs. 78−76443
$RbCdCl_3$, n.q.r. spin-lattice relax. near cubic-tetragonal transition, soft modes 77−1616
$RbCdCl_3$, struct. phase transitions, NMR obs. 78−83943
$RbCdF_3$, cubic crystal, phase transitions with three-component order parameter, elastic anomalies *(Russian)* 79−37837
$RbCdF_3$, Fe^{3+}-O^{2-} pair EPR probe for struct. phase changes 77−36113
$RbCdF_3$, nonlinear elastic behaviour, US velocity, 1 bar-3 kbar 78−59851
$RbCdF_3$:Cr^{3+}, EPR meas. of phase transition 79−61206
$RbCdF_3$:Gd^{3+}, EPR 79−91289
$RbCdF_3$:Gd^{3+}, O_h-D_{4h} struct. transition, ESR obs. 80−50178

rubidium compounds continued
$RbCdF_3$:Gd^{3+}, struct. phase transition, EPR study 80−71171
$Rb_2Cd_2(SO_4)_3$, ferroelec., X-ray study on phase transition 77−85665
$Rb_2Cd_2(SO_4)_3$, pyroelectric and dielectric props., ferroelectric transitions 79−38458
$Rb_2Cd_2(SO_4)_3$ single cryst., growth and phase transitions 79−33918
$Rb_2Cd_2(SO_4)_3$, structural phase transition, phenomenological theory 79−7693
RbCl, aqueous soln., high precision viscosity meas. 80−10695
RbCl aqueous solutions, IR absorpt. ν_1 (CN) band parameter temp., conc. study *(Russian)* 80−80801
RbCl, cation defects creation mechanism 80−75224
RbCl containing K additive impurity, local modes due to U-centres 78−22805
RbCl, defect modes due to substitutional anion-pair and cation-pair impurities in ionic crystals 80−92540
RbCl, diffusion by $^{20}Ne(^{22}Ne)$, isotope effect 78−18841
RbCl, diffusion of ^3He (^4He), isotope effect 78−18841
RbCl, electron beam excited, luminesc. and cond. of nonideal degenerate electron-hole plasma 78−10488
RbCl, electron bombard., colour centre photoemission, surface contamination and escape depth 80−66392
RbCl, enthalpies of solution and formation 79−61892
RbCl, evaluation of photoelastic consts. 80−50297
RbCl, F-centre ESR in relaxed excited state, isotropic superhyperfine interaction consts. 79−65733
RbCl, F-centre emission, mag. circular polarisation 80−108251
RbCl, F-centre optical absorpt., estimate using symmetry-adapted wave functions 80−11448
RbCl, F-centre trapping of conduction electrons, photocond. study 78−56179
RbCl, far IR complex refr. indices, dispersive Fourier transform 78−80322
RbCl films, breakdown on appl. of electric voltage pulses 80−66109
RbCl, fundamental luminescence at high ionisation levels *(Russian)* 80−103985
RbCl, Gruneisen parameter, high press. phase transitions 79−60467
RbCl, lattice localised modes due to U-centre pairs 79−77709
RbCl, M-centre, lifetime data for excited state 78−35193
RbCl, molten, struct., mol. dynamics study 77−47328
RbCl, nearest-neighbour atom displacements derived from EXAFS spectra, temp. depend. 79−87524
RbCl, Pb colloid effect on particularities in vac. evaporated Cr film growth 79−82496
RbCl, permittivity and polarisation behind shock wave front 77−52013
RbCl, photo-elastic constants and pressure derivatives of shear moduli 80−75284
RbCl, photofragment spectra, bond energies and excited state symmetries 80−87190
RbCl, positron-trapping colour centre dynamics, positron annihilation study 80−108294
RbCl, Raman spectra and vibrational modes of V_K centre meas. 78−80338
RbCl, self trapped exciton, optical detection of spin relax. processes 78−60358
RbCl, sp. ht., thermal cond. and thermal diffusivity, meas. by pulse method, influence of press. 79−7701
RbCl, sp. ht. at low temps., Debye temp. determ. 80−2177
RbCl, structural phase transition, Born-model and effects of hydrostatic and non-hydrostatic stresses 79−23721
RbCl, thermodynamic props., lattice-dynamical calc. 77−35715
RbCl, thin film, crystal-vacuum (100) surface, mol. dynamics computer simulation 80−34288
RbCl, third order elastic constants 78−6117
RbCl, U-centre local modes calcs. 77−62603
RbCl, UPS exam., band struct. determ. 77−40330
RbCl, undoped and Sn doped, γ-irrad. crysts., thermolum. and emission, 300 to 560K 79−15539
RbCl, vacuum UV absorption spectra, exciton splitting rel. to exchange interaction 78−23494
RbCl, vibrational contribution to surface thermodynamic functions 77−47659
RbCl, with divalent impurity, reorientation of impurity-vacancy complexes, thermally stimulated depolarisation 77−65977
RbCl, Xe^+ ion bombard., sputtering processes, time of flight meas. 78−88392
RbCl:Ag, dynamic behaviour of off-centre Ag^+ defects, NMR study 79−28634
RbCl:Ag_n phosphor, luminesc., absorpt. and excitation spectra 77−12424
RbCl:Ag_n^+, first-order impurity-induced Raman scatt. 77−77216
RbCl:Ag^+, off-centre system, quadratic-coupling phonon-assisted defect-tunnelling theory 79−55849
RbCl:Ag^+, press. tuning of motional behaviour in shallow off-centre pots. 79−78718
RbCl:Ag(Cu), strong IR luminesc. obs. of Ag_F^0 centres 78−6736
RbCl:Au, EPR and optical absorpt. 78−39397
RbCl:Au^-, optical absorpt. bands and MCD, electron-lattice interaction 80−108236
RbCl:Br^-(I^-), interstitial atomic H centres, formation kinetics and struct. MO calc. and EPR studies 80−75854
RbCl:Ca,H, ENDOR studies of localised vibrations of substitutional atomic H 78−80248
RbCl:Ca^{2+}, thermolum. and optical absorption studies 80−104002
RbCl:Co^{2+}, dielectric loss, impurity sites 79−91348
RbCl:$CoCl_2$ system, precipitate form., ionic cond. meas. 80−96653
RbCl:Cu, X-irrad., ESR of noncentral Cu^0 atoms, 20-180K 77−24739
RbCl:Cu^+, off-centre ion position, ionic thermocurrent study 80−7271
RbCl:Eu, electron-irrad., photostimulated luminesc., ionic processes 78−52561
RbCl:Eu, γ-irrad., thermoluminesc., EPR meas. 78−84670
RbCl:Eu, luminescence and absorption of color centres in RbCl:Cu and KCl:Eu crystals 78−92118
RbCl:Eu^{2+}, EPR of $^{153}Eu^{2+}$ and $^{151}Eu^{2+}$ 80−11259
RbCl:Eu^{2+}, optical absorpt. meas. for Eu^{2+} conc. determ. 79−51137
RbCl:Eu^{2+}, single cryst. optical absorpt. spectra 80−45117
RbCl:Eu^{2+}, tetragonal sites, spin Hamiltonian parameters, EPR and UV absorpt. spectra obs. 80−50177
RbCl:F (Br^-)(I^-), anion impurities substitution, energies of soln., association and migration 78−83831
RbCl:H, dynamical superhyperfine interaction 80−2663

rubidium compounds continued
RbCl:H^-, defect pairs of F-centres and U-centres, Raman meas. 79−7599
RbCl:I, H, fluorescence of interstitial H-centres 79−73987
RbCl:Li, tunable CW IR lasers using F-centres 77−88725
RbCl:Li F_A(II) centre laser, pumped by flashlamp-pumped dye laser 80−102737
RbCl:Li^+, new off-centre defect system, studied with dielec. techniques under hydrostatic press. 79−19834
RbCl:Li^+,Na^+, F_A(II) to F_B(II) centre crystals, CW laser oscill. with extended tuning range 80−32997
RbCl:Li(Na), tunable IR lasers with F_A(II) and F_B(II) colour centres 78−90420
RbCl:Mg_2 γ-irrad., thermoluminesc. 79−47528
RbCl:Mn^{2+}, spin-Hamiltonian parameters anal., superposition model applicability 79−28592
RbCl:NH_4Cl, PMR, NH_4^+ ion proton spin-lattice relax. time temp. depend. 78−27104
RbCl:NO_2^-, first-order Raman scatt. meas. 77−52085
RbCl:Na, F_A-centre optical absorpt., estimate using symmetry-adapted wave functions 80−11448
RbCl:Na, U-centres, HFS consts., g-factors, EPR spectra 80−39869
RbCl:Na^+, F_B(II) colour centres, tunable CW laser operation obs. 77−83877
RbCl:Sn, Sn-centres study, X-ray and coloration effects 78−76500
RbCl:Tl, absorpt. spectra, 210-300 nm 79−87473
RbCl:Tl_2 origin of 3.55 eV emission band 80−7401
RbCl:V^{2+}, EPR spectrum temp. depend., crystal field theory 77−16163
RbCl:V^{2+}, phonon induced zero field splitting 78−39073
RbCl:V^{2+}, spin-lattice relaxation 78−91941
RbCl/KCl interface, diffr. studies of conc. variations 79−42322
RbCl-$CdCl_2$-H_2O, Gibbs free energy, H_2O activity, 25°C *(Russian)* 78−31678
RbCl-CuCl, solid electrolyte, AC cond. and phase relations meas. 77−72713
RbCl-KCl powder blends, diffusional homogenisation, X-ray diffr. exam. 78−18847
RbCl-KCl(H_2SO_4)-H_2O, water activity, 0 and 50°C, conc. depend. *(Russian)* 78−31679
RbCl-UCl_3 melts, density, surface tension and viscosity 78−67764
$RbCl_3$-$NiCl_2$, impurity ion and vacancy aggregation, thermally stimulated depolarisation exam. 78−18678
RbCl(Br):Eu, Eu^{2+} ESR meas. 78−80209
$RbCl_xBr_{1-x}$, IR refl. spectra, temp. depend. 77−28573
RbCl(Br)(I), acoustic non-linearity parameter in cubic crysts. 77−51444
RbCl(Br)(I), cubic crysts., third-order elastic consts. from US vels. 77−80566
RbCl(Br)(I), emission band of F-centre 80−76071
RbCl(Br)(I), thermal shifts in energy level separations, ESCA 77−8723
$RbClO_3$/$RbBrO_3$ mixed crystals, internal optic modes obs., Raman and IR reflectance spectra 80−76024
$RbClO_4$, AC elec. cond. temp. and freq. depend., obs. and unified defect struct. model 80−88554
$RbClO_4$, electrical conductivity, frequency dependence 80−65288
$RbClO_4$-$LiClO_4$, binary melt, Raman spectra, polarised line width, temp. depend. 78−84578
2RbCl.CuCl, and 2RbCl.3CuCl, phase transform. heats, DTA obs. *(Russian)* 80−55698
Rb_2CoBr_4, ferroelec., Curie temp. determ. 79−38485
Rb_2CoCl_4, ferroelec., Curie temp. determ. 79−38485
$RbCoCl_3.2D_2O$, metamagnetic phase transition, crystallographic and mag. struct., neutron diffr. meas. 80−44174
$RbCoCl.2H_2O$, Dzyaloshinsky-Moriya linear chain magnet, spin counting 79−38304
$RbCoCr_2(VO_4)_3$, synthesis and cryst. struct. 80−88114
$RbCoF_3$, antiferromag., anisotropic exchange, dispersion relations of mag. excitations 77−69532
$RbCoF_3$, mag. space group and Raman tensors in antiferromag. phase 79−82760
$RbCoF_3$, single oriented antiferromag. domain, polarised Raman scatt. under uniaxial stress 78−23463
$RbCoF_4$, 2-dimens. Ising antiferromag., mag. excitons, Raman scatt. obs. 80−66181
Rb_2CoF_4, critical fluctuations near Neel temp., US attenuation study 80−108013
Rb_2CoF_4, pseudo Ising antiferromag., inelastic light scatt. by mag. excitons 80−11377
Rb_2CoF_4, two dimens. Ising like antiferromag., spin wave excitations 78−72342
Rb_2CoF_4:^{57}Fe, Ising antiferromag., Mossbauer spectra, critical dynamics 80−15884
Rb_2CoF_4:^{57}Fe, Mossbauer spectra, critical region anal. 80−15888
$Rb_2Co_{0.95}Mg_{0.05}F_4$:^{57}Fe, Mossbauer spectra, critical region anal. 80−15888
$Rb_2Co_cMg_{1-c}F_4$ mag.-nonmag. two-dimens. antiferromag. Ising system, spin fluctuations 80−80545
$Rb_2Co_cMg_{1-c}F_4$, magnetic specific heat, dilution on a two-dimensional Ising-like antiferromagnet 78−91871
$Rb_2Co_cMg_{1-c}F_4$, random 2D antiferromag., neutron inelastic scatt. 79−28505
$Rb_2Co_cMg_{1-c}F_4$, random two-dimens. Ising antiferromag., unstable mag. long-range order, neutron scatt. obs. 80−44839
$Rb_2Co_pMg_{1-p}F_4$, dilute antiferromag. two dimens. Ising system, phase boundary effective medium theory 80−50130
$Rb_2Co_xMg_{1-x}F_4$, antiferromag., static critical phenomena, neutron diffr. obs. 79−56528
$Rb_2Co_xMg_{1-x}F_4$, neutron scatt. exam., obs. of two dimens. mag. long range order 78−56295
$Rb_2Co_xMg_{1-x}F_4$, two-dimens. Ising antiferromag., fluctuations near percolation threshold 79−78390
$Rb_2Co_{0.5}Mn_{0.5}F_4$, two dimens. random antiferromag., excitations 80−107997
$RbCrCl_3$, α-β phase transition, dynamical aspects and thermodynamic theory 80−70404
β-$RbCrCl_3$, co-operative Jahn-Teller distorted struct. determ. 78−63713
γ-$RbCrCl_3$, cooperative Jahn-Teller distorted structure 79−90604
$RbCrCl_3$, Jahn-Teller induced phase transitions 80−70391
Rb_2CrCl_4, 2D-ferromag., renormalisation of long wavelength spin waves, neutron scatt. 80−60229
Rb_2CrCl_4, cryst. growth by Czochralski technique 77−28710
Rb_2CrCl_4, NMR of ^{53}Cr 78−10798

rubidium compounds continued
Rb_2CrCl_4, optical absorption intensity, short-range spin correlation 80−108185
Rb_2CrCl_4, planar ferromag., spin waves 80−65835
Rb_2CrCl_4, spin wave temp. depend. 79−4662
Rb_2CrCl_4, two-dimens. easy-plane ferromag., cryst. and mag. struct., temp. variation of moment 77−66255
Rb_2CrCl_4, zone centre magnon gap determ., exciton-magnon combination band meas. 79−61082
$RbCrI_3$, radiocrystallographic and mag. study *(French)* 79−46632
Rb_2CrO_4, diffuse reflectance spectra 78−88326
Rb_2CrO_4, domain struct., ferroelastic 78−18702
$Rb_2Cr_3O_{10}$, hexagonal form, cryst. data *(French)* 80−28979
$Rb_2Cr_8O_{16}$, Hollandite type compound, synthesis, struct. and magnetic props. 79−11543
$RbCs^+$, adiabatic pot. curves, ground and excited state, Hellmann-type model pots. 78−78647
Rb_2CsSb, evaluation as photocathode material 78−11072
$Rb_2CuBr_4.2H_2O$, dynamic props. in paramag. state, spin-lattice relax. time meas. 80−71214
$Rb_2CuBr_4.2H_2O$, ferromag., static and dynamic mag. props. 80−50074
$Rb_2CuBr_4.2H_2O$, ferromag., hyperfine and exchange interactions, NMR study 80−50208
$(Rb)_2CuBr_4.2H_2O$, hyperfine and super-exchange interactions 80−103654
$RbCuCl_3$, quasi-1-dimens., NQR obs. 80−54987
Rb_2CuCl_4, layered, mag. sp. ht., two-dimens. $S^1/_2$ Heisenberg ferromag. behaviour 77−32206
$RbCu_4Cl_3I_2$, development of Cu^+ ion cond. 80−107532
α-$RbCu_4Cl_3I_2$, solid electrolyte, cryst. struct. and anal. 79−82382
$Rb_2CuCl_4.2H_2O$ and $Rb_2CuBr_4.2H_2O$, exchange anisotropy by NMR 77−55714
$Rb_2CuCl_4.2H_2O$, and isomorphs fine struct. on NMR lines due to indirect nuclear spin-spin coupling 79−61244
$Rb_2CuCl_4.2H_2O$, BCC Heisenberg ferromag., transferred hyperfine interactions of ^1H, ^1D and ^{17}O 77−69725
$Rb_2CuCl_4.2H_2O$, Bloch-wall NMR, anisotropic hyperfine interaction 79−51864
$Rb_2CuCl_4.2H_2O$, ferromag., hyperfine and exchange interactions, NMR study 80−50208
$Rb_2CuCl_4.2H_2O$, hyperfine and super-exchange interactions 80−103654
$Rb_2CuCl_4.2H_2O$, NMR spectra, second-order effects of mag. hyperfine interaction, pseudoquadrupole interaction 79−78540
$RbCuCr_2(VO_4)_3$, synthesis and cryst. struct. 80−88114
$RbCuF_3$, ^{63}Cu NQR meas. 80−50219
$Rb_4Cu_{16}I_7Cl_{13}$ in CuCl-CuI-RbCl system, high Cu ion cond. solid electrolyte, elec. props. and powder X-ray diffr. anal. 80−15295
$Rb_2Cu(SO_4)_2.6H_2O$, single cryst., fine struct., mag. dipole coupling, EPR obs. 78−68360
$Rb_2CuX_4.2D_2O$, X=Cl, Br, quadrupolar interaction, 4-300K, reorientation 79−73848
$Rb_2CuX_4.2H_2O$, (X=Cl, Br), fine struct. due to indirect coupling of nuclear spins 79−78541
RbD_2AsO_4, ferroelectrics, Raman spectra, coupled tunnel-phonon modes and isotope effect 79−69205
$RbD_{2x}H_{2(1-x)}PO_4$, deuteration effect on refr. index 77−59550
$Rb(D_xH_{1-x})_2PO_4$, D distrib. during crystallisation from aq. soln. 77−11496
$Rb(D_xH_{1-x})_2PO_4$, isotope exchange during crystallisation from aqueous solns. 78−18569
RbD_2PO_4, ferroelectrics, Raman spectra, coupled tunnel-phonon modes and isotope effect 79−69205
RbD_2PO_4, struct. at room temp., diffractometer study 80−1994
$Rb_3D(SO_4)_2$, djelec. props. and phase transitions 80−60482
$RbD_3(SeO_3)_2$, ^2D NMR struct. anal. 80−2661
$RbD_3(SeO_3)_2$, DMR, electric quadrupole coupling, ferroelec. transition 79−91312
$RbD_3(SeO_3)_2$, incommensurate nature of intermediate phase, neutron diffr. obs. 80−50276
$RbD_3(SeO_3)_2$, phase transform., inelastic neutron scatt. study 78−39514
$RbD_3(SeO_3)_2$, spontaneous polarisation meas. below T_c 77−24801
$RbDy_3F_{10}$, $RbDy_2F_7$ and Rb_3DyF_6, cryst. symm. and cell parameters *(French)* 80−81040
$RbDy(MoO_4)_2$, Dy^{3+} doublets, temp. anomaly in splitting separation due to structural phase transformation *(Russian)* 80−39274
$RbDy(MoO_4)_2$, low temp. phase transitions *(Russian)* 78−87787
$RbDy(WO_4)_2$, cryst. struct. and refinement 77−65969
$Rb_5Er(MoO_4)_4$, cryst. struct. 77−62510
$RbEu_3F_{10}$, crystal struct., X-ray studies *(French)* 80−33955
Rb_3EuF_6, Rb_2EuF_5, $RbEu_2F_7$, $RbEu_3F_{10}$, cryst. struct., X-ray diffr., equilib. in RbF-EuF_3 *(French)* 78−44107
$RbEu(PO_3)_4$, vibr. spectra 80−34905
$Rb_3Eu(PO_4)_2$, synthesis and IR spectra 80−16019
RbF, dil. aq. soln., elec. cond., 25°C 77−69105
RbF, ESR study of interstitial atomic H centres 79−56609
RbF, high press. B1 to B2 phase transition, X-ray diffr. obs. 79−23722
RbF, one electron props., SCF-Xalpha scattered wave method 80−83279
RbF, quadrupole coupling, vibr. and rot. effects, Morse oscill. calcs. 77−6805
RbF, RbCl and RbI, monomers and dimers, Ar matrix-isolated, IR spectra, vibr. assignments and calcs. 79−45718
RbF, UPS exam., band struct. determ. 77−40330
RbF, vibrational contribution to surface thermodynamic functions 77−47659
RbF:Li(Na), F-centres, saddle-point configuration, molecular model parameter 80−107234
RbF-AlF_3, ion-molecule equilibria studied by mass spectrometric method, heats of dissoc. and form. calc. 80−104479
RbF-CsF, solid solution, fundamental absorption 79−11433
RbF-EuF_3 system, thermal anal. and X-ray diffr., phase equilibria *(French)* 78−44107
RbF-HoF_3, cpd. formation 77−44226
RbF+Eu^{2+}, cryst., hyperfine splitting, EPR 78−2733
RbF+K, complex form., decay, branching fraction and cross-sections, translational energy depend. 77−21374
RbF+K collision complex, rot. energy effect on branching fraction for reactive decay 78−73023
$(RbF)_n$-FeF_3, antiferromagnetic systems, dimensionality and spin reduction effects, Mossbauer study 80−39947
RbF(Cl)(Br), shock adiabatic, nonparametric equation of state 78−10121

rubidium compounds continued
$RbF(Cl)(Br)(I)$, chem. shift in X-ray absorpt. spectra, correl. with ion contrib. to bond 78−76559
$RbF.H_2O_2$, X-ray and neutron diffr. struct. determ. 78−67698
$RbFeCl_3.2H_2O$, pseudo one-dimens. Ising-like system, mag. heat capacity and metamag. transitions 77−66351
$RbFeCl_3$, linear chain ferromag., optical absorpt. and dichroism in mag. field 77−77237
$RbFeCl_3$, linear chain cryst., quadrupole and mag. reson., rel. to $CsFeCl_3$ 79−38403
$RbFeCl_3$, one-dimens. ferromagnet, lowest excitation, far IR study 80−66186
$RbFeCl_3$, pseudo-one-dimens. singlet ground state ferromag., mag. excitations, neutron scatt. study 80−97064
$RbFeCl_3$, singlet ground state 1-D ferromag., far IR Zeeman spectra 77−52098
$RbFeCl_3$, singlet ground state one-dimens. ferromag., 2-magnon excitation, far IR spectra obs. 77−69831
$Rb_2FeCl_5(Br_5).H_2O$, antiferromag. props. and struct. 78−31056
$Rb_2FeCl_5.H_2O$, cryst. struct., superconducting susceptometer mag. meas. 79−73717
$RbFeCl_3.2D_2O$, cryst. and mag. struct., neutron scatt. and NMR expts. 79−7969
$RbFeCl_3.2H_2O$, 2D Ising system, crit. fluctuations, Mossbauer spectra study 80−44842
$RbFeCl_3.2H_2O$, pseudo one-dimens. Ising cpd., multiple magnon bound states 79−42723
$RbFeCl_3.2H_2O$, pseudo-one-dimens. canted Ising antiferromag., spin-cluster reson. 79−61233
$RbFeCl_3.2H_2O$, pseudo-one-dimens. canted Ising antiferromag., spin cluster reson. 79−61235
$RbFeCl_3.2H_2O$, pseudo-one-dimensional canted Ising antiferromag., spin-cluster excitations 80−70989
$RbFeCl_3.2H_2O$, rectangular Ising cpd., Mossbauer meas. 80−71252
$RbFeCl_3.2H_2O$, spin cluster excitation expts. 80−66039
$RbFeF_3$, antiferromag., Mossbauer study of mag. axis 79−4752
$RbFeF_3$, magnetisation density of Fe^{2+} 79−78313
$RbFeF_3$, Mossbauer spectra, mag. phases 80−15878
$RbFeF_4$, Mossbauer and optical evidence for crystallographic transition 79−14931
$RbFeF_4$, Mossbauer spectra, struct. and hyperfine field 77−12266
$RbFeF_4$, two dimensional structural phase transitions, sp. ht., optical, dielec., X-ray diffr. meas. 79−69240
$RbFeF_5$, one dimensional antiferromagnets, field depend. spin reduction temp. variation, spin flopping 79−78586
Rb_2FeF_4, antiferromagnet, two-dimensional, mag. excitations 80−80492
Rb_2FeF_4, two dimensional planar antiferromag., mag. excitations, Raman and far IR spectra obs. 78−72343
Rb_2FeF_4, two-dimensional antiferromag., with easy plane anisotropy, mag. excitations and two-magnon Raman scatt. 80−65839
Rb_2FeF_5, 1D antiferromagnetic system, Mossbauer investigation 78−95533
Rb_2FeF_5, mag. struct. and one-dimens. antiferromagnetism 80−60209
Rb_2FeF_5, Mossbauer spectra, 1D antiferromag. 80−15886
Rb_2FeF_5, one-dimensional antiferromag. systems, Mossbauer studies 80−71266
α-Rb_xFeF_3, mixed valence compound, Mossbauer effect appl. to charact. 79−51883
Rb_2FeI_4, X-ray cryst. struct. determ. and refinement 79−69070
$Rb_5Fe_3O(SO_4)_6.5H_2O$, cryst. struct. determ. 80−92482
$RbFeS_2$, crystal ligand field theory, band assignment, absorpt. spectra study 80−20657
$RbFeS_2^{+}$, ^{57}Fe Mossbauer hyperfine interaction, covalency effects, point charge model 78−39484
$RbFeSi_2O_6$, elec. cond. meas. 78−47787
$RbGa_3Br_{10}$, cryst., vibr. spectrosc. *(French)* 78−6667
$Rb_{5-x}Ga_{11+x/5}O_{30}$, synthesis, non-stoichiometry, density and ionic cond. meas. *(French)* 78−52741
$RbGa(SO_4)_2.12H_2O$, ENDOR of $^{57}Fe^{3+}$ in trigonally distorted octahedral sites 79−38405
$RbGa(SO_4)_2.12H_2O$, spin-Hamiltonian with trigonal S^3I terms for describing $^{57}Fe^{3+}$ ENDOR spectra 80−75885
Rb_2GeF_6, A=Si, Ge, Sn, IR absorpt. spectra, integrated intensity 79−73944
Rb_2GeF_6, IR absorpt. spectra, integrated intensity, 100-300K 79−73945
$Rb(H,D)_3(SeO_3)_2$, improper ferroelec. phase transition, anomalous elastic props. 79−33634
RbH, structural transition from NaCl to CsCl type under high press. 80−96458
RbH^{+}, Σ state pot. energy, Hellman pseudopot. calcs. 78−70764
RbH_2AsO_4, acoustooptical and photoelastic props. 78−27181
RbH_2AsO_4, and deuterated isomorph, E-mode splitting in ferroelec. phase, Raman scatt. meas. 77−16296
RbH_2AsO_4, and deuterated isomorph, ferroelectric mode and molecular vibr. press. depend. 78−19424
RbH_2AsO_4, and RbD_2AsO_4, IC spectra and phase transitions, under pressure 78−31180
RbH_2AsO_4, attenuation const. meas. by SHF dielec. resonance 79−47406
RbH_2AsO_4, ferroelec., attenuation of LF elastic oscills. 77−7791
RbH_2AsO_4 ferroelec. cryst., internal friction, torsion pendulum obs. 78−72474
RbH_2AsO_4, ferroelectrics, Raman spectra, coupled tunnel-phonon modes and isotope effect 79−69205
RbH_2AsO_4, microhardness, expt. determ. 79−24603
RbH_2AsO_4, phase transition, dielec. pyroelec. and internal friction meas. 77−16261
RbH_2AsO_4, pres. depend., LF dielec. response, ferroelec. props. 78−15120
RbH_2AsO_4, pyroelectric investig. in ferroelec. phase 77−12321
RbH_2AsO_4, Raman scatt. near T_c, search for soft modes 78−15114
RbH_2AsO_4, ruby SHG, comparison with other KH_2PO_4 isomorphs 78−50856
$RbHF_2$, heat capacities, transitions and melting 79−10967
RbH_2PO_4, acoustic longit. mode coupling to order parameter and effect on ferroelec. phase transition 79−51914
RbH_2PO_4, acoustooptical and photoelastic props. 78−27181
RbH_2PO_4, and RbD_2PO_4, IC spectra and phase transitions, under pressure 78−31180
RbH_2PO_4, critical and tricritical phenomena, susceptibility, exponents 80−75976

rubidium compounds continued
RbH_2PO_4 crystals, plastic deform. and mech. props. 79−79035
RbH_2PO_4, electro-optic props. near ferroelec. transition 78−19445
RbH_2PO_4, electrostrictive effects, US rel. 80−75941
RbH_2PO_4, ferroelec., attenuation of LF elastic oscills. 77−7791
RbH_2PO_4 ferroelec. cryst., internal friction, torsion pendulum obs. 78−72474
RbH_2PO_4, ferroelec., dielec. props., four-cluster approx. 80−97202
RbH_2PO_4, ferroelec. phase transition, birefringence studies 80−108162
RbH_2PO_4, ferroelectric, US propag. near ferroelectric phase transition temp. 78−23417
RbH_2PO_4, ferroelectric-ferroelastic phase transition, γ-ray diffr. 78−43819
RbH_2PO_4, ferroelectrics, Raman spectra, coupled tunnel-phonon modes and isotope effect 79−69205
RbH_2PO_4, for tunable frequency-doubled CW dye laser 80−53372
RbH_2PO_4, harmonic and sum freq. generation, tunable CW UV radiation prod. 78−46712
RbH_2PO_4, high press. phase diagram 78−52457
RbH_2PO_4, high temp. phase transition, dielec. const., elec. cond. and IR refl. meas. 78−43118
RbH_2PO_4, IR overtone spectra and temp. depend. 79−47456
RbH_2PO_4, longit. US wave propag. near ferroelectric phase transition temp. 78−84536
RbH_2PO_4, microhardness, expt. determ. 79−24603
RbH_2PO_4, phase transitions study, role of cryst. struct. determ. 80−75197
RbH_2PO_4, polarisation and dielec. const. 77−59527
RbH_2PO_4 powder, phase transition in paraelectric (upper) phase by measuring damping const. and amplitude of phonon echoes 79−19855
RbH_2PO_4, proton modes, dielec. spectroscopy 80−75915
RbH_2PO_4, pyroelectric investig. in ferroelec. phase 77−12321
RbH_2PO_4, Raman scatt. near T_c, search for soft modes 78−15114
RbH_2PO_4, static dielec. props., and Curie temp., press. depend. 79−87405
RbH_2PO_4, tetragonal phase disordered struct. 78−42980
RbH_2PO_4, transverse elec. susceptibilities 80−50273
RbH_2PO_4, X-irradiated, hysteresis effects obs. by ESR 80−103928
RbH_2PO_4, X-ray cryst. struct. refinement 79−14787
$Rb_2HPO_4.RbH_2PO_4.Te(OH)_6$, monoclinic, cryst. struct. *(French)* 80−33964
$RbHSO_4$, acoustic and dielectric props. near phase transition 80−55053
$RbHSO_4$, anisotropy of US anomaly near ferroelec. phase transition 78−72473
$RbHSO_4$, compressed powder, dielectric const. and particle size, 77-335K 78−76371
$RbHSO_4$, dielec. dispersion near ferroelec. phase transition 80−2684
$RbHSO_4$, ferroelec., Curie-Weiss behaviour, dielec. const. meas. *(Japanese)* 77−43940
$RbHSO_4$, ferroelec., dielec. crit. phenomena, spontaneous polarisation meas. 77−85641
$RbHSO_4$, ferroelec. with small Curie-Weiss const., dielec. props. 78−39496
$RbHSO_4$, ferroelec. phase transition, US attenuation and velocity 78−39511
$RbHSO_4$, ferroelec., dielec. dispersion 80−97179
$RbHSO_4$, ferroelectric phase transform. model, SO_4 group ordering 77−77156
$RbHSO_4$, isotope effect, dielec. const. and spin polarisation investigation 80−20574
$RbHSO_4$, phase transition, sp. ht. and dielec. permittivity meas. 77−85672
$RbHSO_4$, volume expansion, spontaneous strain, second order phase transitions 79−65224
$Rb_3H(SO_4)_2$, dielec. props. and phase transitions 80−60482
$Rb_3H(SO_4)_2$, phase transitions at 56°C and 126°C, dielec. const. meas. 78−76405
$RbHSeO_4$, ferroelec. props. and domain struct. 79−78637
$RbHSeO_4$, ferroelec. phase transition, X-ray study 80−7309
$RbHSeO_4$, ferroelec. props. rel. to struct. 80−71345
$RbHSeO_4$, ferroelec., far IR spectra 80−71404
$RbHSeO_4$, successive phase transitions 80−15985
$RbHSeO_4$, X-ray cryst. struct. anal. 79−4292
$RbH_2(SeO_3)_2$, improper ferroelectric phase transformation, neutron scattering study 78−80302
$RbH_3(SeO_3)$, ferroelectric phase transition, Raman spectra meas. 79−19871
$RbH_3(SeO_3)_2$, ^{87}Rb NMR, elec. field grad. temp. depend. 79−78536
$RbH_3(SeO_3)_2$ crystal, incommensurable phase, quadrupole moment study 80−97213
$RbH_3(SeO_3)_2$, crystal lattice monoclinic distortion determ. by phase transition from elec. meas. results 79−73887
$RbH_3(SeO_3)_2$, dielec. relax. near ferroelec. Curie temp. 80−97207
$RbH_3(SeO_3)_2$, ferroelec., thermodynamic theory of phase transitions 77−90112
$RbH_3(SeO_3)_2$, ferroelec., location of H atoms in cryst. struct., neutron diffr. meas. 78−2093
$RbH_3(SeO_3)_2$, ferroelec. phase transition, X-ray study 79−38479
$RbH_3(SeO_3)_2$, ferroelec. domain struct., obs. using dew method 80−50283
$RbH_3(SeO_3)_2$, low temp. struct., neutron diffr. 78−38669
$RbH_3(SeO_3)_2$, order parameter 77−66460
$RbH_3(SeO_3)_2$, paraelec. phase, H bonding, neutron diffr. 77−47420
$RbH_3(SeO_3)_2$, phase transitions, elastic compliance temp. depend. 77−90116
$RbH_3(SeO_3)_2$, phase transitions *(Japanese)* 79−65812
$RbH_3(SeO_3)_2$, piezoelectric effect, near nonintrinsic ferroelectric phase transition 78−2815
$RbH_3(SeO_3)_2$, Raman spectra meas. 78−10899
$RbH_3(SeO_3)_2$, repolarisation in region of improper ferroelec. phase transition 77−8497
$RbH_3(SeO_3)_2$, US vel. and absorpt. near ferroelec. Curie temp. 80−97206
$RbH_3(SeO_3)_2$: VO^{2+}, EPR spectra, spin Hamiltonian parameters 80−100609
$RbH_3(SeO_3)_2$:Mn^{2+}, single crystal, EPR 78−72396
$Rb_3H(SeO_4)_2$, phase transitions, dielec. behaviour 79−90777
RbHe(Ne), spin relax., Rb hyperfine interaction in Van der Waals mol. 78−94201
$Rb_4Hf(C_2O_4)_4.nH_2O$, electric field gradient at metal site, γ-ray perturbed ang. correlation meas. 78−52380

rubidium compounds continued
$RbHgC_4$, and $RbHgC_8$, intercalation cpds., synthesis and struct. 80−44183
$Rb_2Hg(CN)_4$, spinel, ferroelasticity and phase transformation 79−7646
RbI aqueous solution, US study of apparent molar compressibility 78−10125
RbI, edge emission of excitons 77−59606
RbI, edge luminesc. under UV excitation 77−77273
RbI, elastic constants determ. by inelastic neutron scatt. 78−79659
RbI, electron irrad., polariton effects in reson. emission 79−33843
RbI, evaluation of photoelastic consts. 80−50297
RbI, exciton mechanisms of electron sputtering 77−55857
RbI, F-centre trapping of conduction electrons, photocond. study 78−56179
RbI, far IR complex refr. indices, dispersive Fourier transform 78−80322
RbI, free exciton reson. luminesc. lines 77−77272
RbI, ground vibr. state rot. transition, quadrupole HFS and coupling consts. *(German)* 77−57990
RbI, hyper-Raman spectra by single channel method 78−84591
RbI, IR active and silent modes, hyper-Raman scatt. obs. 79−61376
RbI, intra impurity local oscill. composition tone absorpt. band anharmonic temp. broadening *(Russian)* 80−60642
RbI, intrinsic luminesc. quenching, by X-ray induced coloration 78−19539
RbI, luminesc. spectra induced by pulsed Ne^+ and electron beams and X-rays 80−80851
RbI, mosaic struct. in metastable press. region, gamma-ray diffr. meas. 77−20065
RbI, NaCl to CsCl phase transition by elastic diffuse and inelastic neutron scatt. 80−2162
RbI, non-linear press. depend. of phonon freq. 77−35650
RbI, optical absorpt. centre formation time meas. 80−40081
RbI, parallel and perpendicular Stark effect of F-centre 77−1703
RbI, phase transition, diffuse neutron scatt. in metastable press. region 78−67825
RbI, phase transition NaCl→CsCl type, preferred orientation of CsCl type 80−49160
RbI, photo-elastic constants and pressure derivatives of shear moduli 80−75284
RbI, photostimulated recomb., electron spin polarisation 80−60673
RbI, press. depend. of I nucl. relax. press. induced polymorophic transform. study 79−1720
RbI, self-trapped exciton and F-centre form. by picosecond laser pulses 80−10546
RbI, sign of thermal expansion coeff. at low temps. 77−84954
RbI, single cryst., press.-induced B1-B2 phase transition, X-ray diffr. meas. 78−63852
RbI, single crysts., mosaic struct. changes, press. induced 77−51507
RbI, solutions, preferential solvation, NMR obs. 78−95919
RbI, sputtering of atoms by 540 eV electrons, delay times 80−35025
RbI, Stark effect in F-centre emission 77−63434
RbI, structural phase transition, Born-model and effects of hydrostatic and non-hydrostatic stresses 79−23721
RbI, temp. depend. of second order Raman spectra 78−68512
RbI, two photon absorpt., 2p excitons relax., F-centre 79−91462
RbI, UPS exam., band struct. determ. 77−40330
RbI, vaporisation thermodynamics, mass-loss Knudsen effusion, mass spectrometry 79−28093
RbI, Xe^+ ion bombard., sputtering processes, time of flight meas. 78−88392
RbI, zero phonon and LO phonon assisted luminesc. of free excitons 79−28799
RbI:AgI, thermal reorientation kinetics of I_2^-, decay of optical anisotropy 77−52138
RbI:H^-, U-centres, force consts. using Green's functions 79−46775
RbI:HF_2^-, anharmonic interaction of impurity intramol. vibrs. with cryst. phonons 77−77217
RbI:Pb_2 absorpt. spectra of Pb^{++} centres 80−76058
RbI:Pb^{2+}, luminescence under B-band excitation 78−35192
RbI:Pb^{2+}, optical and elec. props. 79−15493
RbI:ReO_4^-, IR absorpt., half width, temp. depend. *(Russian)* 79−78722
RbI:TeO_3^{2-}, IR absorpt. of impurity complexes *(Russian)* 79−33746
RbI:Tl, emission and excitation spectra, press. effects 79−83028
RbI:Tl, emission bands, press. effect 79−33789
RbI-CdI_2-H_2O, Gibbs free energy, H_2O activity, 25°C *(Russian)* 78−31678
RbI-NaI_3 binary molten mixture, surface tension meas. 79−65294
$RbICl_4$, ^{35}Cl NQR spectra, press. cond. temp. depend 80−20501
$RbICl_4$, NQR of ^{35}Cl, press. and temp. depend., phase transform. obs. 80−15820
$RbICl_4$, NQR press. depend. 77−12225
$Rb_5I(I_3)(BiI_6)(H_2O)_2$, cryst. struct. 77−58989
$RbIO_3$, hexagonal modification, temp. depend. of NQR freq., interpretation of long-wave spectra 80−25243
$RbIO_3.2LiIO_3$, crystal struct. refinement, Li atom localisation in I atom presence, cell parameters 79−77585
$RbIn_3F_{10}$, crystn. struct., unit cell parameters, coordination *(French)* 77−80485
$Rb_2In_3F_{11}$, crust. struct. *(French)* 78−42966
$RbIn(MoO_4)_2$:Fe^{3+} monocrystals, EPR spectrum in the phase transition neighbourhood 80−2624
$Rb_2InOH(SeO_4)_2.H_2O$:Eu^{3+}, synthesis and luminesc. 79−91488
$RbIn(SO_4)_2.4H_2O$, refinement of cryst. struct., interatomic distances, bonds 80−59448
$RbIn(WO_4)$:Gd^{3+} hyperfine struct. in ESR spectrum 77−8399
Rb_2IrCl_6, hyperfine spectra of mag. ordered state at very low temp., Mossbauer meas. 77−69744
$Rb_xK_{1-x}MnF_3$, struct. transitions, NMR and birefr. expts., 60-300K 77−47577
$(Rb_xK_{1-x})AgI_3$, cryst. struct. 77−51360
$(Rb_xK_{1-x})Ag_4I_5$, cryst. struct. 77−51360
$Rb_xK_{1-x}H_2PO_4$, 90° phase matching in freq. doubling, appl. to lasers 80−33088
$Rb_3KMO_3F_3$, (M=MO, W), low temp. phase transitions *(French)* 78−92036
$Rb_2KMoO_3F_3$, ferroelec., transition obs. 80−75989
Rb_2KTiF_6, bonding, struct., ligand field splitting, electron gas calcs. 78−17557
$Rb_2KWO_3F_3$, ferroelec., transition obs. 80−75989
rubidium compounds continued
$Rb_xK_{1-x}[GaSi_2O_6]$, partially ordered leucite-type struct. *(German)* 79−51088
RbKr, magnetic resonance meas. of spin-rotational interaction 78−33528
$Rb_2LiMO_xF_{6-x}$, M=Nb or Mo, high press. transforms. *(German)* 77−89400
$RbLiSO_4$, field induced ferroelec. phase 79−78633
$RbLiSO_4$, new ferroelectric materials *(Japanese)* 77−28529
$RbLiSO_4$, successive struct. transitions, X-ray diffr. 80−10521
$RbLiSO_4$, thermal and dielectric props., ferrielectricity 79−28688
$RbMF_3$ (M=V, Mn), flux growth of crystal 79−78861
$RbMF_3$:Mn^{2+}, (M=Mn,Cd,Ca), zero-field splitting of Mn^{2+}, superposition model *(French)* 79−15267
$RbMF_4$ (M=Ti, V), flux growth of crystal 79−78861
$Rb_{12}M_{33}O_{90}.(12H_2O)$, cation exchanger with intersecting tunnel struct. *(French)* 78−20014
$Rb^+M^{III}(SO_4)_2$, M=Al^{3+}, Cr^{3+}, Fe^{3+}, Raman and IR spectrum study *(French)* 79−47453
$RbMgCr_2(VO_4)_3$, synthesis and cryst. struct. 80−88114
$RbMgF_3$, irradiated, thermal conductivity 78−22909
$RbMgF_3$:Mn, low-temp. radiation damage, optical absorption meas. 78−22761
$RbMgF_3$:Mn^{2+}, EPR obs. and struct. interpret. *(French)* 80−50167
$RbMg_xMn_{1-x}F_3$, impurity induced fluorescence, thermal depend. 77−85776
$Rb_2Mg_2(SO_4)_3$, langbeinite type cryst., search for ferroelec. phase transition 77−59535
$RbMnBr_3$, EPR linewidth anisotropies 80−103878
$RbMnBr_3$, X-ray cryst. struct. determ. 80−54187
$RbMnCl_3$, antiferromag. static mag. props. *(Russian)* 78−60270
$RbMnCl_3$, birefringence, twinning and structural phase transitions 79−38480
$RbMnCl_3$, cryst. struct., X-ray diffr., Weissenberg photograph 77−19922
$RbMnCl_3$ crystal, structural phase transition 80−15243
$RbMnCl_3$, high-pressure cubic phase, mag. props. 79−47260
$RbMnCl_3$, specific heat near Neel temp. *(Russian)* 80−100340
$RbMnCl_3$, structural phase transition 78−91442
$RbMnCl_3$, twinning struct., cryst. domains, orientation mag. transition *(Russian)* 80−107275
$RbMnCl_4$, changes in birefr. due to spin flopping 79−73910
$RbMnCl_4$, quadratic layer antiferromag., intrinsic emission obs. 77−20906
Rb_2MnCl, layer antiferromag., optical absorpt., temp. and mag. field depend. 80−20661
Rb_2MnCl_4, 2D Heisenberg antiferromag. spin wave analysis 80−54879
Rb_2MnCl_4 antiferromagnet, spin flopping of sublattice mag. moments in mag. fields 79−69687
Rb_2MnCl_4, cryst. struct. determ. 77−80473
Rb_2MnCl_4, Heisenberg antiferromag., spin wave anal. 79−61237
Rb_2MnCl_4, IR active modes, interlayer and intralayer forces 77−59575
Rb_2MnCl_4, perovskite type layer struct., far IR reflectivity and Raman spectra 77−15511
Rb_2MnCl_4, perovskite type layer struct., lattice dynamics, rigid-ion model calc. 77−15512
Rb_2MnCl_4, rare earth doped, energy transfer, emission spectra obs. 80−20684
Rb_3MnCl_4, quasi-2D-antiferromag., linear birefr. and optical absorpt. spectra 80−71385
$Rb_3Mn_2Cl_7$, cryst. struct. 78−79578
$Rb_3Mn_2Cl_7$, two dimens. double layer antiferromag., neutron diffr. exam. 77−8277
α-$RbMnCl_3.2H_2O$, pseudo-one-dimensional mag. system, low-temp. sp. ht. 77−85471
$RbMn_{1-x}Co_xF_3$, Raman scatt. by mag. excitations 77−55775
$RbMnF_3$, ^{19}F spin-lattice relax., 0.1-3K 77−20743
$RbMnF_3$, acoustic nucl. spin echo *(Russian)* 77−48088
$RbMnF_3$, antiferromag., temp. depend. of NMR linewidth 77−63292
$RbMnF_3$, antiferromag., multi-magnon luminesc. sidebands 78−76525
$RbMnF_3$, antiferromag., mag. props. 79−8032
$RbMnF_3$, antiferromag., spin-wave lifetimes calc. 79−7980
$RbMnF_3$, antiferromag. domain struct. in fields exceeding spin-flop value 79−69693
$RbMnF_3$, antiferromagnetic resonance, optical detection, luminescence 80−7174
$RbMnF_3$, EPR and NMR, solid and liq. states, 300-1450K 77−73077
$RbMnF_3$, exciton and exciton-magnon emission 79−33779
$RbMnF_3$, Faraday effect mechanism in paramag. phase 80−60552
$RbMnF_3$, Heisenberg antiferromagnet, paramag. region, NMR, spin pair correl. 78−15032
$RbMnF_3$, Heisenberg antiferromagnet, spin diffusion below T_N 78−34968
$RbMnF_3$, isotropic antiferromagnetic, T-H phase diagram as test of theory 77−32192
$RbMnF_3$, isotropic antiferromag., phase diagrams, US meas. 78−68350
$RbMnF_3$, isotropic antiferromag., crossover behaviour of mag. phase boundary, US meas. 78−80145
$RbMnF_3$, isotropic antiferromag., crossover behaviour of mag. phase boundaries 79−78370
$RbMnF_3$, Jahn-Teller coupling consts., LCAO calc. 80−59940
$RbMnF_3$, NMR, modes interaction *(Russian)* 77−59468
$RbMnF_3$, nucl. spin waves *(Russian)* 78−34973
$RbMnF_3$, nuclear spin echo of ^{55}Mn, freq. pulling 77−69727
$RbMnF_3$, nuclear spin waves spectra, relaxation, parametric excitation, NMR dynamic shift *(Russian)* 80−11180
$RbMnF_3$, pure and Fe, Co or Ni doped, thermal cond., spin wave and mag. impurity contribs. 77−40046
$RbMnF_3$, radiation damage, energy transfer, radiolysis, effect of defect centres 78−2161
$RbMnF_3$, reflectivity, 8-60 eV, excitonic struct. 77−20871
$RbMnF_3$, solid and molten paramag., high-temp. EPR linewidth meas. 77−4548
$RbMnF_3$, spin wave lifetime, theory compared with expt. 80−60228
$RbMnF_3$, spin wave widths 80−97081
$RbMnF_3$, spin waves, light scatt. lineshape 78−23476
$RbMnF_3$, triplet states, piezospectroscopy 79−38562
$RbMnF_3$, two-spin Raman scatt. at high temp. 77−40225
$RbMnF_3$ universal relations among crit. amplitude, calc. up to order ϵ^2 for systems with continuous symm. 77−17936
$RbMnF_3$, zone-boundary magnon energy and damping, Raman scatt. meas. 78−31202

rubidium compounds continued
$RbMnF_3$:^{111}Cd, antiferromag., spin deviations and hyperfine fields, PAC meas. 77−48104
$RbMnF_3$:Er^{3+}, absorption, emission, excitation and lifetime meas. 80−71460
$RbMnF_3$:Fe^{2+}(Co^{2+}), high-temperature EPR linewidth, impurity fast relax. effects 77−85556
$RbMnF_3$:Fr, pure and doped, unirradiated and electron irrad., energy transfer 80−108254
Rb_2MnF_4, antiferromag. reson. relax., multimagnon processes 77−4564
Rb_2MnF_4:^{111}Cd, antiferromag., spin deviations and hyperfine fields, PAC meas. 77−48104
$Rb_3Mn_2F_7$, double-layer antiferromag., mag. prop. meas. and calc. 77−55666
$Rb_2MnF_5.H_2O$, X-ray cryst. struct. anal. 79−4290
$RbMn_{1-x}Mg_xCl_3$, dilute pair antiferromag., mag. susceptibility and ESR meas. 79−78338
$Rb_2Mn_{0.5}Mg_{0.5}F_4$ and $Rb_2Mn_{0.5}Ni_{0.5}F_4$, neutron scatt. obs. of mag. behaviour 77−66254
$Rb_2Mn_cMg_{1-c}F_4$, dil. antiferromag., mag. correlations, neutron scatt. meas. 77−66356
$Rb_2Mn_cMg_{1-c}F_4$, two-dimens. antiferromag., spin fluctuations, neutron diffr. study 80−44846
$Rb_2Mn_xMg_{1-x}F_4$, random magnetic-nonmagnetic 2-dimens. antiferromag., spin fluctuation dynamics 77−63147
$Rb_2Mn_xMg_{1-x}F_4$, spin dynamics near percolation threshold, EPR study 80−39859
$Rb_2Mn_xMg_{1-x}F_4$, two-dimens. Heisenberg-Ising antiferromag., fluctuations near percolation threshold 79−78390
$Rb_2Mn_{0.5}Ni_{0.5}F_4$, site-random two-dimensional antiferromag., crit. behaviour, quasielastic neutron scatt. 77−85468
$RbMnP_3O_9$, form. in $RbPO_3$-$Mn(PO_3)_2$ system 79−78943
$Rb_2Mn(PO_3)_4$, form. in $RbPO_3$-$Mn(PO_3)_2$ system 79−78943
$RbMnP_2O_7.3H_2O$, physicochem. characts. 77−39562
$Rb_3MoO_3F_3$, ferroelec., phase transitions, crystallographic, DTA, dielec. and pyroelec. meas. *(French)* 77−85671
$Rb_3MoO_3F_3$, ferroelec. and order-disorder phase transitions 78−92037
$Rb_3MoO_3F_3$, ferroelec., transition obs. 80−75989
RbN_3, heat capacity from 5 to 350K 79−55901
RbN_3, lattice vibration Raman study, tetragonal-cubic phase transitions 79−77743
RbN_3, polycryst., IR-active lattice vibr., optical consts. 77−77185
RbN_3, Raman spectra, weaker features obs. 77−68045
RbNCO, polycryst., IR and Raman spectra, lattice and internal modes 77−32369
$Rb^+(NH_3)_n$, gas phase clusters, relative bond strengths, thermodynamic props. 78−35649
$RbNH_4SO_4$, ferroelec., ion group reorientation temp. and press. depend., PMR obs. 78−72470
$RbNO_2$, Raman spectra temp. depend., NO_3^- ion external librational modes, IV→III transition, Raman spectra temp. depend., NO_3^- ion external librational modes 79−78662
$RbNO_3$, anhydrous, kinetics of crystallisation 77−43164
$RbNO_3$, cubic to rhombohedral transition, X-ray diffr. obs. 78−22681
$RbNO_3$, cubic to rhombohedral transition induced by orientation-shear strain coupling 78−22682
$RbNO_3$, high pressure phase V, X-ray struct. determ. 80−28953
$RbNO_3$, melt, NO_3^- ion struct., pulsed neutron diffr. obs. 78−22631
$RbNO_3$, melt, Tl^+ high dilution diffusion, interferometry 78−47546
$RbNO_3$, molten, X-ray diffr. structural anal. 78−42887
$RbNO_3$, permittivity and dielec. cond. press. up to 5 kbar, antiferroelec. transition obs. 77−36183
$RbNO_3$, phase transition, IR spectra 80−7350
$RbNO_3$, single cryst., DC cond., dielec. and thermophys. props., temp. depend., transitions interpret. 78−26682
$RbNO_3$, struct., high temp. phases, neutron diffr. study 80−79756
$RbNO_3$-KNO_3, liq., electromigration cation and mobility and isotope effect 80−10691
$RbNO_3$-$LiClO_4$, binary melt, Raman spectra, polarised line width, temp. depend. 78−84578
$3RbNO_3-2Ca(NO_3)_2$, glass form. from liq., struct. transform., Raman spectrum obs. 80−64916
Rb_2NaHoF_6, NMR spectra of ^{165}Ho, 1.6 to 13K 80−80620
$RbNaMg_2M_2Si_{12}O_{30}$ (M=Cu, Fe, Mg), cryst. struct., X-ray diffr. and IR spectra *(French)* 80−107158
Rb_2NaTbF_6, NMR spectra of ^{159}Tb, 1.6 to 13K 80−80620
Rb_2NaTiF_6, bonding, struct., ligand field splitting, electron gas calcs. 78−17557
$Rb_{10}Nb_{29.2}O_{78}$, cationic exchanger with crossed tunnel struct., cryst. struct. *(French)* 78−83797
$Rb_{12.20}Nb_{33.56}O_{90}$, tunnel cryst. struct., X-ray diffr. 78−18611
$Rb_8Nb_{22}O_{59}$, cryst. growth from melt, and instability 78−35294
$Rb_4Nb_6O_{17}.3H_2O$, cryst. struct. by X-ray diffr. *(French)* 80−92503
$Rb_{0.5}NbS_2$, supercond. props., alkali cation and topotactic solvation influences 79−87180
$RbNbTeO_6$, pyrochlore struct. and its relatives 79−14773
$Rb_2Nb_6TiO_{18}$, cryst. struct. *(French)* 78−6040
$RbNbWO_6$, pyrochlore related structures, phases of type AM_2X_6, acentricity and phase transitions, X-ray diffr., DSC and NMR study 79−27943
$RbNbWO_6$, pyrochlore struct., tetragonal to cubic phase transition 80−75355
$RbNbW_2O_9$ crysts., growth and props. 80−104054
$RbNdP_4O_{12}$, crystal struct. determ. 77−80459
$Rb_3Nd(PO_4)_2$, synthesis and IR spectra 80−16019
$RbNgF_3$, radiation defect F,M,R-centre absorpt., emission, excitation spectra 79−43000
$RbNiCl_3$, cryst., ^{35}Cl and ^{87}Rb NMR down to 1.3K 79−42848
$RbNiCl_3$, mag. props. 79−73736
$RbNiCl_3$, nearly one-dimensional antiferromag., spin-flop transition 78−6527
$RbNiCl_3$, noncollinear magnetic order and spin wave spectrum in presence of competing exchange interactions 80−65834
$RbNiCr_2(VO_4)_3$, synthesis and cryst. struct. 80−88114
$RbNiF_3$ and Rb_2NiF_4, MCD and stress linear dichroism on double excitonic transitions 77−52051
$RbNiF_3$, high-temperature mag. sp. ht. *(Russian)* 80−88757
$RbNiF_3$, neutron scatt., automatic data processing *(Russian)* 80−54079
$RbNiF_3$ spin lattice, susceptibility, Heisenberg model *(Russian)* 80−65893
Rb_2NiF_4, obs. of short range order by optical birefringence 79−11318
rubidium compounds continued
Rb_2NiF_4, planar antiferromagnet, cluster-Bethe-lattice method 80−22306
Rb_2NiF_4, quadratic layer antiferromag., optical spectra obs. 77−16326
Rb_2NiF_4, specific heat capacity, critical amplitude, cross-over from 2-D Ising to Heisenberg behaviour 80−39791
$RbNiFeF_6$, pyrochlore, Mossbauer spectra in paramag. and mag. ordered states 77−52003
$RbNi_xMn_{1-x}F_3$, powder, mag. props. 80−2560
$Rb_2Ni_3(P_2O_7)_2.nH_2O$, thermal dehydration 80−35513
RbO_2, low temp. phases, mag. order, EPR and antiferromag. reson. 79−95630
RbO_2, X-ray low temp. phase study, crystallographic domains and unit cell dimens. 78−63728
RbO_2-Na_2O-P_2O_5 glasses, Raman and far IR spectra, vib. at cation site, struct. 78−60435
$Rb_{1-x}O_x$, metallic glass, prep., elec. props. and struct. 78−67652
Rb_2O, high temp. X-ray anal. using special cell for reactive substances *(French)* 79−68978
Rb_2O-GeO_2 glass, He permeability, diffusivity and solubility 79−51308
Rb_2O-Li_2O-P_2O_5 glasses, Raman and far IR spectra, vib. at cation site, struct. 78−60435
Rb_2O-Nb_2O_5 mixed oxides, cryst. struct., electron microscopy study 78−91309
Rb_2O-Nb_2O_5(Ta_2O_5), phase equilib. relns. and crystal chemistry, structs. useful as ionic conductors 79−20033
Rb_2O-Ta_2O_5 mixed oxides, cryst. struct., electron microscopy study 78−91309
Rb_2O-Ta_2O_5 mixed oxides, cryst. struct., electron microscopy study 78−91310
Rb_2O-TeO_2 glass, struct. and props. *(Japanese)* 79−32917
Rb_9O_2, ionic clusters in alkali metal suboxide cryst., struct., vibr. freqs., Raman spectra 79−37772
RbOH, quadrupole hyperfine struct., Δ-level splitting, microwave spectra 77−88446
$Rb_2O.SrO.4B_2O_3.12H_2O$, real Patterson function determ., method of rhombs. 78−5986
$RbPO_3$, form. from dihydroorthophosphate dehydration, reaction thermodynamics 79−52643
$RbPO_3$, He(I) photoelectron spectra, UTARC calc., assignments 79−72357
$RbPO_3$, vitreous, microhardness 80−25864
$RbPO_3$-$AgPO_3$ system, phase diagram 77−25033
$RbPO_3$-$Mn(PO_3)_2$ system, $Rb_2Mn(PO_3)_4$ and $RbMnP_3O_9$ form. 79−78943
$RbPbCl_6(Br_6)$:$ReCl_6^{2-}$($ReBr_6^{2-}$), vibronic side bands 80−10609
$Rb_2PbCu(NO_2)_6$, incommensurate Jahn-Teller phase transitions 79−65185
$Rb_2PbCu(NO_2)_6$, incommensurate Jahn Teller phase transitions 79−95156
$Rb_2PbCu(NO_2)_6$, incommensurate Jahn-Teller transition, Huang scatt. 80−70401
$Rb_2PbCu(NO_2)_6$, uniaxial stress, EPR meas. 80−20455
$RbPbI_3.2H_2O$, X-ray cryst. struct. determ. 80−64958
$Rb_2Pb(MoO_4)_2$, and $Rb_2Pb(WO_4)_2$, domain struct. and phase transition *(Russian)* 78−6159
$Rb_2Pb[Co(NO_2)_6]$, struct. study 80−88106
Rb_2PdCl_4, single cryst. growth from gel and soln., morphology 77−77360
$Rb_{1.75}Pt(CN)_4$. $1.5H_2O$, quasi 1D metals, electric conductivity meas., semiconductor-metal transition 79−99538
$Rb_{1.75}(Pt(CN)_4).1.5H_2O$, 1-D cond., IR spectra 77−85703
Rb_2PtCl_4, single cryst. growth from gel and soln., morphology 77−77360
Rb_2PtCl_6, physical properties, application as lens or laser window materials 79−98450
Rb_2PtI_5, synthesis and cryst. struct. *(German)* 78−79588
Rb_2PtI_6, cryst., role of ordinary and harmonic Raman processes, ^{127}I nucl., spin-lattice relax., obs. 79−8063
Rb_2PtI_6, cubic to tetragonal phase transition 79−1500
$RbRF_4$, R=La, Ce, Pr, Nd, Sm, phase equilib. and cryst. struct. *(French)* 78−44107
$RbReO_4$, external lattice vibr. modes and elastic wave vels., dispersion relations 79−33050
$RbReO_4$, IR matrix-isolation spectra 80−87108
$RbReO_4$, quadrupole coupling, cation electric field gradients 78−35060
Rb_2SO_4 molecules isolated in inert gas matrices, low freq. IR spectra 78−50547
Rb_2SO_4, solid-to-solid transition temperature under hydrostatic pressures to 0.6 GPa 80−24586
Rb_2SO_4-$(NH_4)_2SO_4$ mixed cryst., ferroelec. transition, structural and dielec. props., proton spin-lattice relax. 78−39512
$Rb_2SO_4.3MoO_3$-In_2O_3, phase diags., chem. reactions 77−86008
$Rb_2Sb_{0.5}M_{0.5}^{IV}O_6$, ($M^{IV}$=Se, Te, Sn), ^{121}Sb Mossbauer effect 78−84506
$Rb_4Sb_2O_7$, solid state synthesis *(French)* 80−104438
$RbSbO_3$.1/6RbF, dielec. spectroscopy study, 100 Hz to 10 MHz, 238 to 417K *(German)* 80−108144
$RbSbS_2$, cryst. struct., space groups 79−7592
$Rb_6Sb_4(SO_4)_3F_{12}$, dielec. props. and phase transitions 79−69765
$RbSc(MoO_4)_2$:Gd^{3+}, hyperfine struct. in ESR spectrum 77−8399
$RbSc(WO_4)_2$:Gd^{3+}, hyperfine struct. of ESR spectrum 77−8399
Rb_2SeO_4, single cryst., orthorhombic, Raman spectra 77−73140
Rb_2SiF_6, A=Si, Ge, Sn, IR absorpt. spectra, integrated intensity 79−73944
Rb_2SnBr_6:$ReBr_6^{2-}$, luminesc. spectra and relax. processes 78−68552
$RbSnCl_6$:$ReBr_6^{2-}$, vibronic transition $\Gamma_7(^2T_{2g})\rightarrow\Gamma_8(^4A_{2g})$, intensity distrib. 80−45142
Rb_2SnCl_6:$ReCl_6^{2-}$, luminesc. and absorpt. spectra, relax. processes 77−85779
$RbSnCl_6(Br_6)$:$ReCl_6^{2-}$($ReBr_6^{2-}$), vibronic side bands 80−10609
Rb_2SnF_6, A=Si, Ge, Sn, IR absorpt. spectra, integrated intensity 79−73944
Rb_2SnF_6, thermal stability and thermolysis *(French)* 78−10011
$Rb_2Sn(NH_2)_6$, cryst. struct. determ. *(French)* 77−47384
$RbSnX_{3(5)(6)}$ (X=Cl, Br, I), single cryst. gel growth, X-ray diffr. study 80−29870
Rb^+TCNQ^-, optical absorpt. spectra of small particles 78−19505
Rb^+TCNQ^-, triplet exciton dipolar splitting tensors rel. to mag. susceptibility 77−62839
Rb_2TCNQ_3, X-ray cryst. struct. determ. at 113K 79−99169
$Rb_{10}Ta_{29.20}O_{78}$, layered cryst. struct. 80−107166
$Rb_{10}Ta_{29.2}O_{78}$, cationic exchanger with crossed tunnel struct., cryst. struct. *(French)* 78−83797

rubidium compounds continued
$Rb_{0.33}TaS_2$, supercond. props., alkali cation and topotactic solvation influences 79−87180
$Rb_2Ta_6TiO_{18}$, cryst. struct. *(French)* 78−6040
Rb_2Te film electron affinity and photoelectron work function obs. 79−69959
Rb_2Te_3, synthesis and cryst. struct. 80−88115
$Rb_2(TeBr_6)$, far IR and Raman spectra and phase transitions 80−11376
$Rb_2(TeCl_6)$, IR and Raman spectra, lattice and internal modes, phase transition 78−6659
$Rb_2TeCl_6:Re^{4+}$, vibronic transitions progressions, intensity distrib. 79−78735
$RbTeCl_6(Br_6):ReCl_6^{2-}(ReBr_6^{2-})$, vibronic side bands 80→10609
$RbTiMO_5$ (M=Ta, Nb), ion exchange props., synthesis and crystallographic props. *(French)* 80−28997
$Rb_{1-x}(Ti_{1-x}M_{1+x})O_5$, M=Nb, Ta, layer compound, cryst. struct., nonstoichiometry 80−64972
$Rb_2Ti_4O_9$, preparation, cryst. struct. determ. 78−75646
$RbTl(SeO_4)_2$, $Rb_3Tl(SeO_4)_3$, and $Rb_5Tl(SeO_4)_4$, cryst. struct. *(French)* 80−84148
$RbUO_3$, EPR and mag. susceptibility, temp. depend. 79−33451
$Rb_2UO_2Cl_4$, fluoresc. decay rate of pure and impure cryst. 79−47487
$Rb_3UO_2F_5$, normal coordinate anal. 79−22596
$Rb_4(UO_2)_2F_8{\cdot}2H_2O$, IR absorpt. and Raman spectra, normal coordinate anal. *(French)* 78−52509
$RbUO_2(NO_3)_3$, fluoresc. decay rates, temp. depend. 80−25429
$Rb_4(UO_2)_4O_2Cl_8(H_2O)_4$, cryst. data 77−76367
$Rb_2(UO_2)_4O_2(OH)_2Br_4(H_2O)_6$, cryst. data 77−76366
$Rb_2(UO_2)_4O_2(OH)_2Cl_4(H_2O)_6$, cryst. data 77−76366
$RbVCl_3$, mag. props. *(French)* 77−16059
$RbVF_3$, antiferromag. ordering points, thermal anal. and X-ray diffr. meas. *(French)* 78−84421
RbV_2F_6, flux growth of crystal 79−78861
$Rb_{0.25}VF_3$, cryst. struct. examination by electron diffr. using TEM 79−23583
α-Rb_xVF_3, mag. props. *(French)* 77−80933
Rb_xVF_3, non-stoichiometric, struct. depend. on composition 79−99152
$RbVO_3$, cryst. struct. 78−6043
$RbVO_3:Cr^{3+}$, study of ESR spectra 80−80601
$Rb_{0.30}WO_3$, struct. anal. *(French)* 78−59786
$Rb_{0.33}WO_3$, supercond. and special phonons, neutron scatt. obs. 80−15643
$Rb_{22}W_{32}O_{107}$, crystal atomic struct. 78−14313
Rb_xWO_3, anomalous supercond. transition temp., electron pairing by acoustic plasmon exchange 79−56358
Rb_xWO_3 bronze, elec. resist. meas., anisotropy 80−75569
Rb_xWO_3, low lying phonon dispersion curves, neutron scatt. study 80−92622
Rb_xWO_3, phase transitions, supercond. transition temp. and elec. props. 79−28431
Rb_xWO_3, resistivity, Hall effect and Seebeck coeff. from 1.5 to 300K 80−6879
$Rb_3WO_3F_3$, ferroelec. and order-disorder phase transitions 78−92037
$Rb_3WO_3F_3$, ferroelec., transition obs. 80−75989
$Rb_{20+x}(W_4O_6)_{1/3-x/12}W_{32}O_{108}$, struct. *(French)* 79−60321
$Rb_9(XeO_3Cl_2)_4Cl$, neutron and X-ray diffr. struct. determ., Xe-Cl bonding 78−30591
RbXe*, far-wing line spectra undulations, semiclassical methods 77−61808
Rb_2ZnBr_4, average struct. determ. from neutron diffr. diagrams 79−32955
Rb_2ZnBr_4, dielectric const. and ferroelectric hysteresis 78−84535
Rb_2ZnBr_4, ferrielectricity, triple 60 Hz D-E hysteresis loops 80−71365
Rb_2ZnBr_4, ferroelec., Curie temp. determ. 79−38485
Rb_2ZnBr_4, ferroelec., photovoltaic and photorefractive phenomena 80−75598
Rb_2ZnBr_4, ferroelectricity, hysteresis loops and dielec. const. meas. 78−23416
Rb_2ZnBr_4, incommensurate phase transition, neutron-scatt. obs. 79−4390
Rb_2ZnBr_4, incommensurate phases, neutron scattering study 79−15417
Rb_2ZnBr_4, incommensurate and commensurate phases, neutron scatt. meas. 79−82936
Rb_2ZnBr_4, modulated struct., far IR transmission, temp. depend. 80−71408
Rb_2ZnBr_4, modulation phase transitions, neutron scatt. 79−95712
Rb_2ZnBr_4, quasicrystalline state, incommensurate phase transformation 79−99310
Rb_2ZnBr_4, Raman scatt., normal-incommensurate-commensurate phase transitions, soft modes 80−40071
Rb_2ZnBr_4, soft modes at phase transforms., far IR spectrum study 80−107398
Rb_2ZnBr_4, soft modes obs. by Raman scatt. 80−97283
$Rb_2ZnBr_4(Cl_4)$, Raman spectra near incommensurate phase transitions 80−76013
Rb_2ZnCl_4, ^{35}Cl NQR, incommensurate struct. phase transition 79−47401
Rb_2ZnCl_4, commensurate-incommensurate phase transition, crit. behaviour, sp. ht. meas. 80−71342
Rb_2ZnCl_4, commensurate-incommensurate phase transition, ^{35}Cl NQR study 80−75966
Rb_2ZnCl_4, dielec. dispersion, 5-900 MHz, near incommensurate-commensurate transition 80−60522
Rb_2ZnCl_4, ferrielectricity, triple 60 Hz D-E hysteresis loops 80−71365
Rb_2ZnCl_4, ferroelec., Curie temp. determ. 79−38485
Rb_2ZnCl_4, ferroelectricity, hysteresis loops and dielec. const. meas. 78−23415
Rb_2ZnCl_4, incommensurate phase form., domain struct. near phase transition, NQR obs. 79−33643
Rb_2ZnCl_4, incommensurate phases, neutron scatt. 79−38501
Rb_2ZnCl_4, incommensurate phase transition, ^{87}Rb NMR study 80−75967
Rb_2ZnCl_4, incommensurate phase transitions, ^{35}Cl NQR study 80−75968
Rb_2ZnCl_4, NQR exam. of noncommensurate superstructures produced by phase transitions 79−69791
Rb_2ZnCl_4, phase transitions, soft mode, Raman scatt. meas. 79−4389
Rb_2ZnCl_4, phase transition, Raman scatt. evidence 80−40116
Rb_2ZnCl_4, phase transitions, thermal expansion coeff. 80−100638
Rb_2ZnCl_4 single crystals, Raman scatt. spectra, temp. range covering two phase transitions 80−7340
rubidium compounds continued
Rb_2ZnCl_4, spin-lattice relax. in incommensurable phase, phason and amplitudon excitations 80−50213
Rb_2ZnCl_4 type ferroelectrics, phase transitions and physical props. *(Japanese)* 79−78636
Rb_2ZnCl_4, US vel. and attenuation at normal-incommensurate phase transition pt. 79−55833
Rb_2ZnCl_4, US velocity and attenuation, around normal-incommensurate phase transition 80−40072
$Rb_2ZnCl_4(Br_4)$, cryst. with modulated struct., neutron scatt. obs. 79−95713
Rb_2ZrS_2, intercalation cpd., X-ray K absorption edges 78−39627
$^{85,87}RbCl$ isotope enriched cryst., optical registration of EPR F-centres *(Russian)* 80−103886
$Rb_2[C_2O_4].D_2O_2$, neutron profile refinement at 5K 80−88103
$Rb_2[Cu(H_2O)_6](SO_4)_2$, Tutton's salts, stereochem., neutron struct. determ. 78−18609
$Rb_2[M^{II}(H_2O)_6][(UO_2)_2F_8]$, M^{II}=Mn, Co, Ni, Cu, Zn or Cd, structural type, IR spectra 77−35525
$Rb_2[MnBr_4]$, X-ray cryst. struct. determ. 79−32961
$Rb_2[Pt(CN)_4Br_2]$, neutron diffr., cryst. struct. 77−35522
$Rb_2[Pt(CN)_4].1.5H_2O$, energy band calcs. 77−39780
$Rb_2[Pt(CN)_4].3H_2O$, DC elec. cond. props. 77−51582
$Rb_{1.75}[Pt(CN)_4].xH_2O$, one-dimensional, X-ray diffuse scatt. meas. 77−19937
Ru_7B_3, stella quadrangula as struct. building unit 80−15055
α-$RuCl_3$, reflectivity and absorpt. spectra, thermo-reflectance 79−47438
$Te(OH)_6.Rb_2HAsO_4.Rb_2H_2AsO_4$, synthesis and cryst. data *(French)* 80−33948
$TlNO_3$-$RbNO_3$, melt, cationic self-diffusion coeffs., temp. and conc. depends. 78−22879
$ZnRb_2(SeO_4)_2.6H_2O:Mn^{2+}$, EPR spectra 80−100608

ruby
abrasive grains, single, wear on steel, exam. *(Japanese)* 78−44230
acoustic phonon focusing, direct obs. *(Russian)* 77−59075
acoustic phonons, 10^{12} Hz, optical detect. 77−36272
brown colouring due to specific growth, annealing and irrad., exam. of visible, infrared and UV spectra 79−11440
chamber calibration using ruby R_1 luminescence line shift, 80 to 550K 78−86284
coherent transients obs. by Stark switching with narrow optical hole burning 78−37947
concentrational inhomogeneities, appl. of vacuum decoration method 79−14835
connectors, plug and socket, for single optical fibres *(German)* 79−46039
Cr^{3+} ion doped, R-line region, absorpt. spectrum, dispersion rel. to mag. field 80−2732
cross-relaxation studies of $3d^4$ impurity ions 79−99755
cross-relaxation to $(3d)^1$ ions 80−71163
crystal, photon echo generation, control method 80−87440
crystal, radiation amplification, spatial coherence 80−99737
crystal orientation determ. by Laue method, computer calc. *(Chinese)* 79−32853
crystal structure and compression up to 46 kbar 79−37682
CW backward wave generation by degenerate four-wave mixing 78−71147
distant nuclei ESR and ENDOR experiments, dipole-dipole reservoir importance 80−71241
double electron-nuclear resonance at Cr^{3+} B1, B2 absorpt. lines, optical detection *(Russian)* 80−7194
dynamic nuclear polarisation, correlated ESR and NMR c-axis variation effect 78−72436
electric field induced double quantum transitions 80−80595
electron-nuclear spin system, equilib. establishment *(Russian)* 77−43904
ENDOR of Cr^{3+} ions, elec. field effect *(Russian)* 79−8071
energy diffusion distance, upper limit within fluoresc. lifetime 80−29789
energy migration and transfer to N-line traps 79−83006
energy transfer between different emitters and spatial diffusion 80−103978
EPR, effect of relax. processes on microwave signal detection 77−66413
EPR, thermally detected of Cr^{2+}, Cr^{3+} and Cr^{4+} ions 77−63273
EPR intensity standard, description and use 79−54164
EPR method of predicting cryst. characts., laser appl. 79−11345
EPR spectrum, temp. depend. 78−15016
EPR study, comparison of Verneuil and Czochralski grown crystals 78−91945
ESR and NMR correl. line broadening effect assoc. with external mag. field inhomogeneities 80−50227
ESR line saturation of Cr^{3+}, dynamical mag. susceptibility increase in zero mag. field 77−40122
ESR of Cr^{3+} excited state as function of delay time, Zeeman levels explained 78−43695
excited state spin-phonon interaction, time resolved spectroscopic exam. 78−19549
far IR to visible conversion for tunable quantum counter 77−5909
fibre, sapphire-clad, single-crystal, growth by floating-zone technique 77−90268
fibre laser, room temp. continuous operation without cooling, crystal growth, heating effects 78−66833
fluorescence decay of red R lines used in biological thermometer 80−86306
fluorescence line narrowing, energy transfer studies 78−84642
fluorescence line shift, appl. to press. distrib. meas. in diamond anvil press 78−12710
fluorescence press. gauge, calibration, 0.06-1 Mbar, specific vol. meas. for Cu, Mo, Pd, Ag 78−70150
fluorescence spectrum, appl. to glass transition, fluid press. determs. 77−26321
fluorescent R-lines, appl. in press. calibration at ambient and low temps. 77−18106
forced Rayleigh scattering, 50 to 300K 77−42564
gain probing by intracavity dye laser spectroscopy 77−7092
heat transfer at very low temp., ^{27}Al NQR relax. times 79−65757
heat-pulse induced energy transfer, time-resolved optical spectroscopy 77−24456
high energy phonons, generation and detect. spectroscopy 78−83893
high pressure single cryst. struct. determ. for press. up to 90 kbar 78−83875
implantation temperature meas. using impurity luminesc. 79−52012

ruby continued
irradiated, low temp. UV bleaching 79−23646
laser, μs pulse laser with negative feedback 77−714
laser, and Nd:glass laser placed parallel in cavity, for efficiency increase *(Russian)* 77−10954
laser, application to high-speed photography of fast processes 77−68236
laser, battery powered, pulsed, based on electronic flash, for portable holo-camera 79−3711
laser, continuously pumped, repetitive self-Q-switching 78−50781
laser, crystal defects influence on energetic effectiveness obs. *(Czech)* 78−79022
laser, CW, pumping by Ar ion laser 78−1253
laser, CW operation 77−38901
laser, double mode locking using dye saturable absorber 80−99763
laser, effect of unexcited part of rod on generation 79−18422
laser, focusing effects during laser emission in relaxed state *(French)* 77−34896
laser, frequency-stabilised using Fabry-Perot interferometer 80−58566
laser, generation, amplification of high power picosecond pulses depend. on superluminescence 80−53305
laser, giant pulse self-modulation at 90K 77−38961
laser, graphical method for pumping coeff. estimation 80−14343
laser, low-temp. ruby, with optical delay line inside resonator, cooling system 79−36922
laser, microsecond pulse production, with quadratic loss in laser cavity 77−7147
laser, mode synchronisation during loss modulation on freq. difference *(Russian)* 77−61989
laser, modulation by US surface waves on resonator mirror 77−50699
laser, negative feedback, cavity Q insertion effect on parameters of modulated pulses 80−43376
laser, negative feedback, external perturbations, effect, spectral depend. 77−83908
laser, negative feedback, ultrashort pulse generation 78−13714
laser, nonuniform amplification effects *(Russian)* 77−14722
laser, one-freq. tunable one-pulse, selector parameter optimisation 78−74935
laser, operating principles 79−27265
laser, output spatial characts. using FTIROS material 79−68414
laser, passive Q-switched oscillator, damage limited pulsewidth 78−83004
laser, passive Q-switching by I_2 vapour bleaching 77−79872
laser, passive Q-switching using colour centres in SrF_2 78−71157
laser, passively mode-locked, subnanosecond pulse generation using saturable absorber 79−86197
laser, peak generation for active mode phasing *(Russian)* 79−14000
laser, picosecond pulse generation by electrooptic shutter passive switching 79−36942
laser, polarised radiation freq. mixing with Nd laser radiation in $LiIO_3$ cryst. 79−55181
laser, power enhancement by intracavity plasma 80−53330
laser, pulsed with active spectrum phasing, dynamics and energy characts. *(Russian)* 78−9387
laser, Q-factor passive modulator unloading, in resonator with prism *(Russian)* 77−68234
laser, Q-switched, laser induced damage, influence of pores 77−83918
laser, Q-switched, parameter depend. on ruby quality 78−46608
laser, Q-switched, photographic film calibration for energy meas. 78−5517
laser, Q-switched, power dependent freq. sweep 77−19256
laser, Q-switched, spectroscopic props., operation modes, pulse amplification *(Rumanian)* 80−48265
laser, radiation automodulation with passive switching of electro-optical shutter *(Russian)* 78−74936
laser, radiation characts. rel. to pumping intensity in long-time operation *(Russian)* 77−68214
laser, radiation effects on Xe plasma *(Russian)* 78−22514
laser, radiation self-modulation with passive closing of electro-optic shutter 79−64258
laser, refraction effects and gain meas. 79−31905
laser, rotating beam generation 80−1258
laser, self-synchronisation of modes *(Russian)* 78−74937
laser, single-pulse, controllable phototropic shutter design 80−23699
laser, slot method for radiation extraction 77−50694
laser, spark control cavity dumping 78−59053
laser, spiked regime, dynamic theory 79−27260
laser, total mode self-synchronisation 79−64259
laser, two single-phase generation *(Russian)* 77−46725
laser, ultrashort pulse generation by internal phase and amplitude modulation 80−106551
laser, unstable Q-switched resonator in negative branch confocal config. 79−13980
laser, variable radiation loss 77−50685
laser, weak passive Q-switching in spherical resonator 78−50834
laser, with active phasing of spectrum, double Pockels shutter performance *(Russian)* 79−98419
laser, with electrooptical shutter, emission spectrum narrowing and single freq. giant pulse lasing 80−78877
laser, with small active volume, mode-locked ultrashort pulse generation 79−89932
laser, with stimulated Brillouin scatt. complex conjugate mirror 80−87438
laser and $LiNbO_3$ cryst. in difference freq. laser, tunable MM range emission 80−5764
laser beam spatial coherence interferometry 79−14003
laser crystal, excited state absorpt. and energy output 77−65595
laser elements, laser backscatt. by bulk damage zones 79−23000
laser generating ultrashort light pulses, saturating absorber efficiency increase 80−23700
laser induced damage, influence of pores 77−83918
laser material, threshold pumping energy depend. on loss coeff. *(Russian)* 77−46723
laser resonator, lasing spectrum singularities and Q-factor, for z-dimens. beam path *(Russian)* 77−88795
laser rod, absorption coeff., loss coeff. and population inversion *(Japanese)* 78−37888
laser rod, exoemission parameter rel. to optical strength 77−732
laser satellite ranging, compact ruby oscillator-amplifier system 79−966
laser single pulse formation kinetics with self-modulation of quality factor *(Russian)* 77−27312
ruby continued
laser sweep generator, spectral-kinetic characts., singularities *(Russian)* 77−83894
laser with special resonator Q-switching 77−38958
lasers, freq. synchronisation and locking by passive modulator 80−1249
lasing action, spectrum, luminesc. spectrum effects *(Russian)* 78−13716
lasing feasibility in far IR, pumping via ruby laser 79−81435
leucosapphire-ruby boundary, laser backscatt. at inhomogeneities 79−23000
light echo signal correlation with exciting pulse shape *(Russian)* 80−106576
light echo signals, advance and retardation effects *(Russian)* 78−71158
luminescence, absorption of R and N lines, effect of mag. field 80−60550
luminescence, energy transfer time const. between single Cr^{3+} and Cr^{3+} pairs 79−38627
luminescence, ground state of Cr(III) pair 79−33782
luminescence, nonequilibrium, of hot electrons, nonradiative transition probability 77−32436
luminescence, red emission intensity at various temps., mag. field depend. 77−32423
magnetic dipole moment, phase meas. 78−72394
magnetic double resonance, nonstationary, consideration of dipole-dipole reservoir 77−4580
magnetisation precessing, optically induced, near level anticrossing points in $^4A_2$ 77−36111
maser, K-band, 500 MHz bandwidth 80−63966
maser, reflected-wave, with K-band tuning range and large instantaneous bandwidth 79−50275
maser, research and development 80−27094
maser with wide tuning band 80−53247
NMR laser, ^{27}Al nucl. spin system, collective ordering phenomena, instabilities 80−11278
NMR laser, dynamic props. from point of view of synergetics 80−43341
NMR line width of ^{27}Al, charact. features of behaviour 79−69734
nonradiative spectral and spatial energy transfer 77−44037
nuclear quadrupole transitions of ^{27}Al, acoustic and elec. saturation 77−90071
nuclear spin-flip maser pumped by dynamic nuclear polarisation 77−31084
optical absorption and dispersion in R-line region, mag. field effects *(Russian)* 78−92056
optical echo intensity depend on mag. field, Cr^{3+} and ^{27}Al nuclei superhyperfine interaction 79−68419
optical energy storage and retrieval 77−73165
optical free induction decay modulation and absorpt. line struct. due to superhyperfine interaction 80−33091
optical hole burning, Stark and pump-probe studies 80−48356
optical hole burning obs. using Stark field sweeping 77−46768
optical nutation echoes, Stark switching obs. 80−69467
optical pair spectrum, Stark effect with AC elec. field modulation 78−10911
optical properties, effect of annealing near melting point 78−90419
optical pumping, bottlenecked 29 cm^{-1} phonon spectral width 77−12425
optical spectra of Cr^{3+} ions, freq. shifts press. depend., nonperturbative theory 78−23499
optical strength rel. to surface defectiveness 77−28665
optically excited, diffusion of bottlenecked 29 cm^{-1} phonons 80−6472
optically induced magnetisation 78−76292
optically induced two-phonon processes connecting ^2E states 80−25443
optically pumped ruby far IR quantum counter 77−38001
optically-pumped, excited-state Raman processes 79−4798
optics fabrication 79−23099
phase modulated conjugate wave generation, hologram model 80−83643
phonon bottleneck effect, 29 cm^{-1} phonons 78−68562
phonon bottleneck of direct decay within $\bar{E}(^2E)$ state, optical detection 80−10608
phonon heat conduction of single crysts. by quantum acoustic method 77−11748
phonon propag., 29 cm^{-1}, reson. scatt. and lifetime *(Russian)* 78−34581
phonon scattering time, inelastic, appl. of time resolved phonon spectroscopy technique 77−31733
phonon spectrum, thermal pulses under diffuse phonon propagation conditions 80−103434
phonon spectrum of high energy heat pulses generated in thin metal films 77−20140
phonons, at 29 cm^{-1}, stimulated emission 80−45114
phosphorescence, decay obs., impurity effects *(Russian)* 79−15530
photoacoustic spectroscopy, nonradiative processes obs. 77−90185
photon echo, modulation in μs pulse separation regime 78−30029
photon echo generation, depend. on pulse parameters and temp. 79−10364
photon echoes, optical free induction decay, Stark switching technique 79−7182
piezo-spectroscopy of exchange coupled Cr^{3+} pairs 79−33783
pink, electronic excitation spatial diffusion meas. by degenerate four-wave mixing 79−64274
polishing features of hard crystals 80−64225
pressure calibration system improvement using ruby R_1 fluorescence 80−98928
pulsed diode simulators of solid lasers $Al_xGa_{1-x}As$ and $Ga_xIn_{1-x}P_{1-y}As_y$ solid solns. 80−91816
quantum counter for far IR radiation 77−53977
quantum efficiency, photoacoustic meas. 80−73472
R_1 zero phonon line, resonance fluoresc. meas. 80−89055
radiation-induced optical processes, impurity effects 80−66310
radiative spectral transfer, time resolved fluoresc. 78−2900
Raman ^2E and phosphorescence transitions, line widths, time correl. study 80−20621
Raman effect to probe dynamical processes of Cr^{3+} photoexcited states 80−2740
Raman transition from optically pumped excited state 78−39531
raser, instabilities and first order phase changes *(German)* 80−48263
resonance interaction of electronic two-level states and short-wave phonon radiation 80−24551
resonance radiation transfer and nonequilibrium phonon *(Russian)* 78−80418
resonance trapping of 0.87×10^{12}Hz acoustic phonons in mag. field 78−91400
resonant cross-relaxation to Jahn-Teller Cr^{4+} ion 79−65723

ruby continued
resonant scattering and trapping of 29 cm^{-1} acoustic phonons in $Al_2O_3:Cr^{3+}$ 80−93403
resonantly trapped 29 cm^{-1} phonons, spectral diffusion 78−92113
reversed light echo due to two pulse laser resonance excitation *(Russian)* 80−87439
ring laser with forced mode locking 80−95915
rod TW amplifier with variable Cr^{3+} conc. *(Russian)* 79−94202
rods, quality control, EPR method 79−14047
ruby:Cr^{3+}, diffusion of localised optical excitations and trap emission 77−24887
ruby:Cr^{3+}, high mag. field spin-lattice relax. rates in ground state of ion 79−61407
ruby:Cr, lifetimes of laser-induced population density gratings, comparison with fluoresc. lifetimes 79−64276
ruby:Ni, cross relaxation 78−39389
ruby, anisotropic 29 cm^{-1} phonon capture *(Russian)* 80−6471
ruby, induced absorpt., radioluminesc., thermoluminesc., Cr^{3+} conc. depend. *(Russian)* 77−90206
ruby, spectral absorption coeff., 0.25-1.25 micron, up to 1800K, and 3.5-5.2, up to 1200K 78−27204
ruby NMR laser, spontaneous nucl. spin system self organisation 79−916
saturation effects by double-quantum transitions 78−80197
spatial diffusion of weakly bottlenecked 29 cm^{-1} phonons, quasi-stationary techniques 79−73996
spatial gratings, transient light-induced, by successive optical coherent pulses 80−64115
spectral absorpt. coeff., 1800K 78−27252
spin dependency of optical feeding into $\bar{E}(^2E)$ metastable doublet 79−28812
spin lattice relaxation rate of Cr^{3+} 78−52340
spin level population inversion, coherent phonon amplification and generation *(Russian)* 77−24364
spin-lattice relaxation time meas. inhomogeneously broadened ESR lines 79−15343
spin-strain coupling tensor meas. US modulated EPR obs. 80−50170
Stark induced optical transients, photon echo 78−33785
stimulated photon echo modulation 80−38074
structural defects due to laser irrad. *(Russian)* 80−100303
surface disruption after polishing investigation by chemical etching in single crystal *(Russian)* 79−38995
synthetic, cryst. growth, review *(German)* 79−33926
thermal stress, effect of, by thermal shock on substruct. and surface morphology 79−43292
thermochemical etching, Cr impurity influence 80−88190
thermoluminescence, red, and thermal bleaching *(Russian)* 79−56868
two level spin system, second harmonic generation, time depend. 79−65719
two-photon spectroscopy of reson. three-level spin system, reson. shift 79−82864
ultrashort pulse attenuation in active medium, calc. *(Russian)* 78−1295
yield point, under compression and extension, temp.-time depend. 78−6988
yield stress, compression tests, temp.-time depend. 78−48484
Zeeman effect in $^4A_2{}^2E$ pair states in first nearest neighbour Cr (III) pair 79−15440
Zeeman effect of R-absorpt. lines 79−47416
Zeeman spectra of laser excited E and 2A levels 78−43908
Zeeman splitting, MG field production and appls. 79−71491
$Al_2O_3:Cr^{3+}$, inhomogeneous spin system, time evolution towards saturated state 80−88869
$Al_2O_3:Cr^{3+}$, shock compression, absorpt. spectra 80−20675
^{27}Al, distant ENDOR and dynamic nucl. polarisation 80−2664
^{27}Al NMR line acoustic saturation, appl. in quantum acoustic strain detector 77−51009
Ar pumped CW ruby laser 77−68227
Cr content determ. *(Russian)* 77−48745
Cr^{3+} doped, exchange integral, pressure depend., test of theory 78−87741
Cr^{3+}, electronic states interactions with crystal odd vibrs., R-lines vibr. recurrences 78−84639
Cr-doped, relaxation behaviour, EPR study, environmental effects 80−66021

Rudermann-Kittel-Kasiya-Yosida interaction *see RKKY interaction*

Runge-Kutta methods
black liquid solar collector analysis and expt. 79−62097
bubble motion in rotating liquid, computer study, Runge Kutta Nystrom method 77−47063
buoyancy induced flow adjacent to vertical uniform flux surface in cold water 80−69834
celestial mechanics, satellite motion prediction by extrapolation methods *(Russian)* 78−49299
Curtis' (11,8) explicit Runge-Kutta method 77−17796
differential equations soln. using imbedding techniques 79−21536
dynamical astronomy numerical simulation, new Runge-Kutta algorithms 79−12387
electron mass, truncated, gauge dependence 80−22542
electron propagator singularities, using Runge-Kutta method 79−49427
EPR and saturation transfer EPR, fast computation, master supermatrix eqn. soln. 78−62213
Fehlberg treatment for numerical integration of stellar orbits 79−21361
finitely conducting cross grating theory 80−106635
heat conduction, inverse problem, Fourier eqn. Runge-Kutta integration 78−89417
inclined surfaces, wave instability of laminar mixed convection flow 80−69837
integration of ordinary and partial differential equations, appl. of semi-implicit Runge-Kutta methods 78−12542
integration technique for dynamic behaviour of stiffened strings 77−75837
linear inhomogeneous differential eqn. systems with variable coeff., integration *(German)* 78−8235
material particles movement, differential equation, numerical solution *(Croatian)* 79−25983
meteorology, prognostic models, automatic timestep control 77−86975
muonic atom energy levels, computer calc. codes 79−31743
Navier Stokes eqns. in fixed bed reactor radial flow 79−10546
neutron spectrum in heavy gas moderator, series methods, Runge Kutta integration 77−34365

Runge-Kutta methods continued
nonlinear elastic continuum, comparison of Runge-Kutta-Nystrom method and Newmark method *(German)* 78−87273
nonlinear partial differential eqns. solution, fluid flow problem appl. 77−42796
optimal m-fold Runge-Kutta algorithm for celestial mechanics 77−25930
particle track fitting in mag. field 79−31782
partitioned parallel method for weakly coupled ordinary differential eqns. 78−36806
pipe, curved, in creep, flexibility 78−34039
ray tracing in general index distributions 80−14279
Runge-Kutta-Nystrom condition equations, resolution through eighth order 77−22398
second order hyperbolic differential equations, initial value problems *(German)* 78−20952
solar regenerator buoyancy effects, analysis 79−68709
thin hyperelastic spherical shell, finite amplitude oscillations 78−93533
viscous liquid emerging from slot, nonlinear differential equation, Runge-Kutta numerical integration 80−52030
$H+H^+$, classical 3 body collision, cross section, energy transfer, computer calcs. 78−17783
Na vapour bubble growth in superheated liquid, numerical anal. 78−29576
O silent discharge, numerical simulation 78−63629

Russell-Saunders coupling
atom, inner-shell multiplet, Auger transition rate calc. 77−6743
atomic electron scatt., intermediate coupling strengths from LS coupled R-matrix elements 79−18292
atoms, P-state collisions, quantum mechanical treatment, angular momentum coupling 80−99541
Auger transition probability for config. with incomplete shell, LS and JJ coupling cases 77−42302
complex spectra; Gel'fand states for pure and mixed configs. 77−75079
equivalent electrons, J allowed values in jj coupling, teaching 80−90624
inert gas, atomic photoionisation, Dirac-Fock calcs., branching ratios and angular distrib. in p shells 80−63601
ion, three-electron, 2s2p1s config., intermediate coupling state, energy level calcs. 79−3353
$l_1^{n1}l_2^{n2}l_3^{n3}$ configuration, hyperfine struct. theory 77−67964
lanthanides, doubly ionised, f-d interaction 78−90102
LS coupling, fractional parentage coeffs. and submatrix elements of transposition operators for spin and quasispin quantum numbers 77−71736
many-electron atoms, determination of matrix elements of operators describing hyperfine structure 77−46505
many-electron atoms with different coupling types, transform. of wave functions 77−67956
matrix elements, algebraic expressions for operators for atomic quantities 77−6664
multiplet ratios for photoionisation and electron attachment, shell model, LS coupling and correl. 78−17636
multipole transitions in complex config., matrix elements for operators inc. relativistic corrections 78−5150
plasma electron density, determ. by spectral line width, at. oscill. strength effects 77−51230
reactance matrices, fine struct. cross sections, JAJOMPRE program 78−90312
second Born approx., small angle elastic electron scatt. from atoms, high energy limit 78−78811
spin factoring for spectroscopic term determ. 77−61695
three-electron systems, transition probabilities calcs. 80−99479
transformation matrices, jj-LS, for p^n and d^n configurations 80−47862
transition metal complexes, vibronic coupling and spin relax. NMR decay rate study 80−18870
two electron systems, coupling schemes, transition energies and probabilities of autoionising states 80−18828
Ar, optical oscillator strengths, 3p-ns and 3p-nd transitions, independ. particle model 78−86816
C, optical oscillator strengths, independent particle model, excited state wave functions, LS coupling and Born approx. 80−32674
Cd^+, polarised emission of light following photoionis, Cooper-Zare model 79−81179
^{57}Fe, configuration interaction, SL-dependent, effect on hyperfine structure 80−37749
Ga, J_1J_2 transition from LS, revised assignments for $d^9s^2p^2$, $d^9s^2p^3$ 79−45630
Ge, J_1J_2 transition from LS, revised assignments for $d^9s^2p^2$, $d^9s^2p^3$ 79−45630
He, jK and LS coupling between states, transition probs., depend. on elec. field 80−37782
He-like ions, highly charged, electron impact, intermediate-coupling strengths for fine struct. transitions 80−32837
HoF_3, single cryst., Ho^{3+} energy level spectrum calc. 79−1586
In, J_1J_2 transition from LS, revised assignments for $d^9s^2p^2$, $d^9s^2p^3$ 79−45630
Li I, $2s^2sp$ and $1s2s^2$ decay rates many-body perturbation theory calc. 79−59376
Li, optical oscill. strengths calcs. 80−91495
Na like ions, dielectronic recombination rate, scaling props. 80−32668
Ne, $2p^6(^1S_0)$ ground state electron impact excitation cross sections 80−23558
O III, electron impact excitation cross sections, independent particle model calcs. 80−63823
O, isoelectronic sequences, energy spectra inc. relativistic corrections 78−924
Pb, J_1J_2 transition from LS, revised assignments for $d^9s^2p^2$, $d^9s^2p^3$ 79−45630
Si isoelectronic sequence, CI calcs. of oscillator strengths, L-S framework 80−14089
Sn, J_1J_2 transition from LS, revised assignments for $d^9s^2p^2$, $d^9s^2p^3$ 79−45630
Tl, J_1J_2 transition from LS, revised assignments for $d^9s^2p^2$, $d^9s^2p^3$ 79−45630
TmTe, f^{12} and f^{13} config. photoemission fractional parentage coeffs., intermediate and LS coupling calc. 80−84829
Xe_2^*, Xe_2^+, Xe_2, pot. energy curves, relativistic ab initio effective core pots. 78−86800

rust prevention *see corrosion protection*

ruthenium
see also nuclei with .....
adsorbed layer of CO on (001) surface, electron induced dissociation 77−59215
adsorption, CO on Ru(001), IR spectra and LEED 79−37914
adsorption and desorption kinetics of CO from clean and S covered Ru 80−6643
adsorption and desorption kinetics of H_2 from clean and S covered Ru 80−6644
adsorption of CO on (001), temp. depend. ordering processes 80−80773
adsorption of CO on (001) surface, IR spectra, LEED, and thermal desorption meas. 80−70533
adsorption of H_2S, H_2, and S on (110) surface, UPS and work function change meas. 79−78834
adsorption of H_2S, H_2, and S on (110) surface, UPS and work function meas. 79−99424
adsorption of H_2S and S on (001) surface, LEED, UPS, AES, and thermal desorption meas. 79−99420
adsorption of NO, inelastic electron scatt. dissoc. energies adsorbed state depend. 78−95956
adsorption of NO and CO, coadsorbed on Ru(001), adsite symmetry by electron energy loss 79−99412
adsorption of NO on (001) surface, EELS obs. 80−20741
adsorption of NO on (001) surface, KPS, UPS, and X-ray AES meas. 80−6655
adsorption of O_2, H_2, and CO on (11$\bar{2}$0) surface, ellipsometry-LEED study 80−103570
adsorption of SF_6 on surface (001), XPS expts. 77−69178
adsorption of SF_6 XPS exam. 77−55866
Anderson-Gruneisen parameter, temp. depend., third-order elastic consts. calc. 79−46776
atom, hyperfine interaction parameters, effect of local exchange, Xα and HF calcs. 78−78622
atom, Lα X-ray spectra, $_{40}$Zr to $_{48}$Cd, linewidths 79−41131
atomic vibr. and fermion behaviour of HCP metals 80−6474
atoms, $N_2N_3N_{45}$ super Coster Kronig processes 80−106303
catalyst, interaction of CO, NO and H_2, NH_4OCN formation 78−73082
chemisorbed CO and O_2, CO+O_2 surface reaction, electron energy loss spectra 79−46924
chemisorption, dissociative, of CO, isotope exchange 79−34354
chemisorption, of acetylene, substrate effects on bonding, electronic spectrum 78−63933
chemisorption and decomp. on Ru decomp. of NO 78−18903
chemisorption by GaAs, surface recombination rate reduction 80−49866
chemisorption effects on grain boundaries in n-GaAs solar cells 80−55879
chemisorption of CO, surface structural chemistry and electron impact props. 77−1312
chemisorption of H_2O, conformation, electron stimulated desorption ion ang. distribs. 77−89637
chemisorption of NO and CO on (10$\bar{1}$0) surface 77−72783
chemisorption of NO via mobile precursor state 78−43247
chemisorption of O_2, on (001) surface, high resolution electron scatt. spectra 79−11013
chemisorption of O_2 on (001) surface, uptake meas., thermal desorpt. spectroscopy and AES 80−108739
coadsorption of O_2 and CO on (001), uptake and flash desorption meas. 80−39450
comparator for epithermal neutron activation anal. appl. 77−81441
core level binding energies 80−71564
Debye-Waller factor and Lindemann parameter, temp. depend., lattice dynamical model calcs. 80−59610
desorption, associative from mixed adlayers of O and N 80−54512
determination, in automobile exhaust-emission, by chem. ionisation mass spectrometry 78−61079
determination in silicate rocks, preseparation procedure for neutron activation anal. 77−44547
diffusion in liquid Cu *(Japanese)* 78−10204
electrical contact material, environmental interactions and prep. 80−29463
electrical resistance anisotropy, temp. depend. *(Russian)* 78−76041
electrical resistivity, quadratic contrib., 2 to 40K *(Russian)* 80−92874
electrodes, adsorption and surface reactions, cyclic voltammetry and X-ray emission spectrometry 78−61018
electrodes, reversibility and growth behaviour of surface oxide films 79−20263
electronic structure and mag. breakdown, galvanomag. props. obs., 1.3-20.4K 78−91600
Fermi surface, influence of press. *(Russian)* 79−4501
Fermi surface energy spectrum, de Haas-van Alphen effect *(Russian)* 79−37964
field emitter, adsorption of H_2, field-induced redistrib. processes 79−78854
fission product, isotope anal., U and Pu fission investig. *(German)* 77−63996
hazards and control in nuclear fuel cycle, review 79−36392
HCP, elec. field gradient 78−14698
impurity in Cu-Ni sulphidised alloys, behaviour during carbonylation *(Russian)* 80−40584
ion plating, crack-free layers, 2-3 μm thick 78−11131
isotopes, cumulative yields from U and Pu neutron induced fission 79−576
isotopic analysis of U ore 80−21764
isotopic composition of Oklo reactor and other samples *(French)* 80−21765
kinetic and thermal props. at high temp., anisotropy 77−43563
kinetics of C deposition from adsorbed CO on (110) surface 80−76553
lattice dynamics, sp. ht., thermal expansion 79−82363
lattice dynamics, thermal expansion and bulk modulus 77−59079
lattice parameters, densities and atomic vols., tabulation for Pt metals 79−65033
lattice sp. ht. calc. 79−69262
liquid, spectral emissivity and brightness-temp. meas. at MP 77−43356
magnetic breakdown trajectories, quantum oscillations of thermo EMF and Nernst effect *(Russian)* 78−95290
magnetoresistance and Hall effect under mag. breakdown conditions *(Russian)* 79−95389
metallography 78−3289

ruthenium continued
neutron deficient isotopes, gas thermochromotographic separation from AgCl 79−865
nuclear fuel reprocessing by fluoride volatility process, distrib. of Ru contaminants 80−13743
optical constants of (11$\bar{2}$0) Ru, meas. in visible region 77−1650
optical properties 79−24282
oxidation resistance in Ar and air 77−25201
physisorption of SF_6, XPS interpretation 77−89830
radioactive, processing from nuclear fuel by aluminosilicate gels *(Japanese)* 80−22973
radioactive waste, chem. treatment prior to evaporation 77−54327
recovery and use of noble metals from radioactive waste 80−99242
selective on-line gas phase separation from fission products 79−97907
size effect in electrical resistivity *(Russian)* 78−87961
stopping power nucl., in ferromag. Gd, transient mag. field 78−34555
surface, (0001), adsorbed Xe layer, 5p photoemission, local surface struct. influence 80−2920
surface, (0001), adsorption of H_2, N_2 and NH_3, AES, LEED and thermal flash desorption meas. 78−38954
surface, (000$\bar{1}$), growth, struct. and electronic props. of Cu films 79−77958
surface, (001), adsorbed CO, electron stimulated desorption, correl. with other meas. 78−47658
surface, (001), adsorpt. of cycloparaffins, LEED, ESD study 78−87872
surface, (001), clean and CO(O_2) adsorbate covered, characteristic slow electron energy loss meas. 79−47562
surface, (001), CO desorpt. 79−15001
surface, (001), dissociation of adsorbed H_2S, chemisorption and electronic struct. of S layer 79−79292
surface, (10$\bar{1}$0), interactions with N_2O 80−55713
surface, (10$\bar{1}$0), oxide form., thermal desorption and ESCA obs. 79−82442
surface, (101), O_2 chemisorption, CO+O_2 interaction 77−73471
surface, (110), methanol reaction, thermal desorpt. meas. 78−31685
surface, clean, oxidation, atom probe anal. of oxide films 79−47797
surface, clean, oxidation, FIM study 79−47796
surface, decomp. of formic acid into H_2, CO_2, H_2O and CO 79−79245
surface, stepped (~001) cryst., O_2 chemisorption, LEED and AES obs. 80−11947
surface (0001), adsorption and desorption of NH_3, effects of electron beam 78−38955
surface (001), adsorbed hydrocarbons, characterisation by electron-stimulated desorpt. 78−71958
surface (001), chemisorption of CO, electron stimulated desorption ion ang. distribs. bonding geometry and bending vibrs. 79−33189
surface (001), geometric struct. of chemisorbed CO, LEED obs. 79−51429
surface (10$\bar{1}$0), dissociative adsorpt. of NO, LEED and AES expts. 77−90642
surface (110), formaldehyde adsorption, UPS study, 80K 78−73080
surface CO adsorbed particle interactions, lattice gas quasi-chem. approx. 80−49529
thermo-EMF and Nernst effect under mag. breakdown conditions *(Russian)* 80−24878
thermopower and magnetoresistance meas., mag. breakdown 78−47766
thermopower oscillations due to magnetic breakdown trajectories 79−60688
thin film, electrographic investigation of interaction with atmospheric O_2 *(Russian)* 77−25196
transport props., anisotropy, high temp. obs. 78−26843
wear coefficients determ. using pin-on-cisc apparatus 80−76366
X-ray emission spectra and electronic structure 77−20960
X-ray reflection intensities, charact. temps. 78−18731
AgBr(Cl):$Ru^{3+,2+}$, dopant vacancy config., EPR 79−91288
Cd:^{99}Ru, quadrupole interaction temp. depend., PAC method, electric field gradients 77−73105
KCl:Ru, optical absorption bands, complex form. 77−1705
NaCl:Ru, optical absorption bands, complex form. 77−1705
Pt/Ru electrocatalysts for methanol oxidisation in acid electrolyte with improved steady state activity for fuel cell appls. 80−76629
Ru (III) chemisorption on photoanode of n-GaAs/K_2Se-K_2Se_2-KOH/C solar cell, effect on performance 80−3516
Ru^{4+}, Sternheimer valence shielding antishielding factor including exchange 77−85182
^{97}Ru preparation investigation 80−30891
^{97}Ru radioisotope preparation at variable energy cyclotron of Frederic Joliot Hospital Service *(French)* 77−65361
^{103}Ru, ^{106}Ru, radioactive decontamination methods, effectiveness for different terrains 78−96104
^{103}Ru, diffusion behaviour in SiC, 1650 to 1850°C 78−79814
^{103}Ru in determination of rate of passage of food through gut of captive wild birds 80−26425
^{103}Ru, separation of ^{103m}Rh by solvent extraction 78−58857
^{106}Ru, errors in activity ratio determ. in reactor RA used fuel element 79−41061
^{106}Ru sorption on natural sorbents clinoptilolite and vermiculite *(Russian)* 77−38370
^{106}Ru-^{106}Rh, accumulation by marine organisms, sediment and sea water influences 78−80981
Si:Ru, photon- and carrier-capture cross sections of Ru levels 79−90995
Sn:^{99}Ru, quadrupole interaction temp. depend., PAC method, electric field gradients 77−73105
TiO_2:Ru^{4+}, rutile, EPR and cryst. field const. 80−60415
U ore dating from meas. of ^{238}U and Ru conc. 80−21863
YIG:Ru, optical absorpt. and MCD obs. of Ru^{4+} site occupancy 80−71456
YIG:Ru(Ru,Zn), mag. anisotropy 77−69544
Zn:^{99}Ru, quadrupole interaction temp. depend., PAC method, electric field gradients 77−73105

ruthenium alloys
see also ruthenium compounds
ferromagnetic Heusler alloys, peaks in low field AC susceptibility 80−50071
rare earth alloys, R_3Ru and R_5Ru_2, cryst. struct. 80−1965
Ag-Ru film, valence band spectra, XPS meas. 78−52618
Al-Ru, composite, paramagnetic resonance and electron-positron annihilation *(Russian)* 79−87314
$AmRu_2$, crystal structure and mag. props. of Laves phases 77−27851
Be-Ru, dil., quadrupole interactions at ^{99}Ru, TDPAC meas. 78−91996

ruthenium alloys continued
$Ce_{1-x}Gd_xRu_2$, superconductivity and ferromagnetism coexistence, 60 mK-4.2K, spin echo NMR 78−84349
$Ce_{0.73}Ho_{0.27}Ru_2$, spontaneous mag. order below superconducting transition temp., Mossbauer study 80−39701
$Ce_{0.73}Ho_{0.27}Ru_2$, superconductors, mag. correlations and crystal-field levels 80−34547
$(Ce_{1-c}Ho_c)Ru_2$, superconducting, mag. props., neutron scatt. study 80−44808
$CeRu_2$ and $Ce_{1-x}Gd_xRu_2Zr_3Co$, spin-pairing state investig. via Josephson effect 77−47942
$CeRu_2$, change of valence of Ce ions, induced by H absorption, supercond. disappearance 79−47185
$CeRu_2$, H absorption induced Ce valence change, mag. and supercond. props. 80−50042
$CeRu_2$, type II supercond., ESR of Nd^{3+} meas. 79−28444
$CeRu_2$:Nd^{3+}, ESR investigation 79−78514
Co-Ru, dil., mag. hyperfine fields, TDPAC meas. 78−43702
Cr-Ru, dil. absence of mag. hyperfine field, TDPAC meas. 80−50237
Cr-Ru, Invar alloys, thermal expansion, plasticity *(Russian)* 79−55907
Cr-Ru, magnetic transformations, triple point *(Russian)* 80−88747
Cr_2Ru, σ phases, ordering, X-ray cryst. struct. determ. 80−107107
$Dy_xCe_{1-x}Ru$, supercond., mag. order 79−87189
$Dy_xCe_{1-x}Ru_2$, supercond., mag. props. 79−11267
Fe-Ru, antiferromag. ordering, hyperfine fields 80−15867
Fe-Ru, CC hexagonal phase, ^{57}Fe Mossbauer study 79−91321
Fe-Ru (30-60 at.%) mag. ordering, Mossbauer obs. 77−4585
Fe-Ru-SiO_2 supported catalysts, Mossbauer spectra 80−11296
Gd-Ru, amorphous, mag. props. and ferromag. reson. 80−75862
$Gd_xCe_{1-x}Ru_2$, magnetic ordering by ^{155}Gd Mossbauer spectroscopy 78−27139
$Gd_xCe_{1-x}Ru_z$, coexistence of supercond. and spin glass mag. freezing 77−28283
$GdRu_2$, H_2 sorption props. 79−86980
$GdRu_2H_x$, struct. and mag. props., Mossbauer and magnetisation meas. 80−71271
$Gd_xTh_{1-x}Ru_z$, coexistence of supercond. and spin glass mag. freezing 77−28283
$(La,Ce)Ru_2$, supercond. transition temp., its press. depend., and structural phase transform. 78−6473
$(La_{.993}Lu_{.007})_{1-x}Gd_xRu_2$, exchange enhanced supercond., compensation effect on H_{c2} 77−4474
$LaRu_2$, H absorption induced Ce valence change, mag. and supercond. props. 80−50042
$LaRu_2$, H_2 sorption props. 79−86980
$LaRu_2$, supercond. disappearance on H absorption 79−47185
$LaRu_2$, type II supercond., ESR of Nd^{3+} meas. 79−28444
$LaRu_2$:Nd^{3+}, ESR investigation 79−78514
Mo-Ru, electron beam melted, alloying addition effects on brittleness and ductility 79−61728
Mo-Ru, recovery after deform. and annealing, destrengthening mechanism *(Russian)* 80−97546
Mo-Ru film, amorphous, temp. stability 78−63948
Mo-Ru-C, deformed, singularities of fragmented structs. *(Russian)* 77−44289
Mo-Ru-V alloys, phase equilib. and corrosion resist. *(Russian)* 79−52165
Mo-Ru(-Si), amorphous superconductors, prep. by electron beam evaporation and liq. quenching, crit. temp. 80−103776
$(Mo_{0.6}Ru_{0.4})_{82}B_{18}$, supercond. metallic glass, neutron irrad. effects 80−29060
$Mo_{48}Ru_{32}B_{20}$, amorphous, local symmetry around glass-former sites, elec. quadrupole effects, NMR 80−80618
$(Mo_{0.6}Ru_{0.4})_{0.8}G_{0.2}$-Fe (G=P,B), amorphous supercond., upper crit. field as function of temp. 79−73646
$(Mo_{0.5}Ru_{0.5})_{80}P_{20}$, amorphous normal and mixed supercond. state, ^{31}P NMR 79−87193
$(Mo_{1-x}Ru_x)_{80}P_{20}$, amorphous, liq. quenched, mag. susceptibility, supercond. and electronic props. 79−56376
$(Mo_xRu_{1-x})_{80}P_{20}$, amorphous supercond., high-κ, upper and lower crit. fields 79−4629
$(Mo_{0.6}Ru_{0.4})_{80}Si_{10}B_{10}$, amorphous supercond. matrix, flux pinning by MoRu precips. 80−65756
Nb-Re(Ru)-N, α-solid soln., thermodynamics *(German)* 77−12600
Nb-Ru, dil., impurities effect on elec. resist. at 0.4 and 77.3K *(Russian)* 79−91196
Nb-Ru, impurity diffusion and vacancy-impurity binding energy 80−15307
Nb-Ru, kinetics and thermodynamics of reaction with N_2 *(German)* 79−74415
Nb-Ru-N system, N_2 solubility and solubility limit *(German)* 77−4205
Nb-Ru-N system, spectral emissivity, lattice parameter, initial rate of N_2 absorption *(German)* 77−4204
Ni-Ru, environmental effects and mag. moment distrib., magnetisation and neutron scatt. meas. 79−91211
Ni-Ru, spin wave stiffness consts., RPA CPA band model 79−61088
Ni-Ru, weak ferromag., stiffness const., low-temp. meas., rel. to RPA-CPA theories 78−31063
Ni-Ru (3.3 at%), magnetisation, magnetocrystalline anisotropy, magnetostriction and elastic consts., thermal variations 79−28563
Ni-Ru (≤4 at.%), influence of alloying on mag. anisotropy 80−71010
Ni-Ru peritectic alloys, rapidly cooled, crystn. peculiarities *(Russian)* 80−20922
$Ni_{0.97}Ru_{0.03}$, mag. form factor and moment distrib., obs. using polarised neutrons 78−68171
$Ni_{0.97}Ru_{0.03}$, mag. moment distrib. polarised neutron study 79−42738
$(Ni_{1-x}Ru_x)_{99}Mn$, ferromagnetic, NMR study of local environment effect 80−7192
$NpRu_2$, spin fluctuation cpd., sp. ht., 3-25K 77−63212
Pd-Ru, dilute, low temp. sp. ht. and mag. susceptibility 77−62650
Pd-Ru, effects of press. and alloying on Pd electronic struct., susceptibility meas. 78−91581
Pd-Ru, electron transport props., 50 mK-4.2K 78−14707
Pd-Ru-W(V)(Ti), elec. resist. and thermal cond. *(Russian)* 78−19017
PdRu (4.7 at.%), effect of alloying on activation energy of H_2 diffusion 80−107571
$PrRu_2$, hyperfine sp. ht. and magnetisation meas. at 4.2K 80−75775
$PrRu_2$, sp. ht., differential susceptibility and elec. resist. meas., 1.4-40K 80−71063
Pt-Ru, surface segregation, appl. of quantification of atom-probe FIM data 78−62263

ruthenium alloys continued
$PuRu_2$, intermetallic cpd., sublimation thermodynamics 80−96639
$PuRu_2$ Laves phase cpds., thermodynamic props. 77−20092
Ru-Al, transition metal group VIII aluminide, NMR near equiatomic composition *(Russian)* 80−20479
Ru-Cu catalyst, electron spectroscopy exam. 78−44405
Ru-Cu clusters, EXAFS study 80−84804
Ru-Fe, dil., local magnetisation, Mossbauer meas. 80−66091
Ru-Fe, dil., localised spin fluctuation system, supercond. transition temp., conc. depend. 78−56253
Ru-Hf, dil., ^{178}Hf Mossbauer transition, electric quadrupole interaction 80−39928
Ru-Sn compounds, type of binding *(German)* 77−35503
Ru-Sn-M, m=Mg, Ca, Sr, Sc, Y, Zn, Cd, In or Th 80−100777
Ru_2FeSn, ferromag. Heusler alloys, hyperfine fields at nonmagnetic atoms in various sites, Mossbauer effect and NMR meas. 80−66089
Ru_2FeSn, hyperfine mag. field, Mossbauer spectra 80−15865
Sc-Ru, dil., elec. field gradient, Mossbauer meas. 80−80665
Sc-Ru, elec. field gradient and temp. depend. TDPAC meas. 80−60477
Sc-Ru, electronic struct., susceptibility, sp. ht. and Knight shift meas. 77−43485
ScRu, electronic struct., NMR relax. times meas. 79−51871
ScRu, UPS exam. 78−48276
$ScRu_3C_{1-x}$, stabilising effect of C on alloying behaviour of Sc 77−36454
$ThRu_2$, type II supercond., ESR of Nd^{3+} meas. 79−28444
$ThRu_2$:Nd^{3+}, supercond. state, ESR investigation 79−78514
Ti-Ru, radiation disorder model of phase stability 80−16297
Ti-Ru (0.05 to 90 wt.%) hardness, thermal EMF, electrical conductivity, in annealed or quenched state *(Russian)* 77−55998
Ti-V-Ru system, metastable phases form. *(Russian)* 77−21098
URu_3, sublimation thermodynamics 80−97722
V-Ru, electronic states calculation 78−95255
VRu, soft X-ray emission, photoelectron spectra and electron structure 79−37978
W-Ru based refractory transition metal-metalloid glass, struct. 80−1938
Y-Ru, elec. field gradient and temp. depend. TDPAC meas. 80−60477
Y_3Ru, cryst. struct. 80−96474
Zr-Ru, alloy Zr rich, Ru solubility, eutectic decay, $\alpha \rightleftarrows \beta$ transform., struct. *(Russian)* 80−65227
Zr-Ru, heat treated, mech. props. and struct. 78−80571
Zr-Ru film, amorphous, temp. stability 78−63948
$Zr_3Co_{1-x}Ru_x$, phase stability and supercond. T_c 78−80519

ruthenium compounds
see also ruthenium alloys
acetylacetonate, nucl. spin-lattice relax., electron spin density matrix theory 78−13521
tris(2,2′-bipyridine) ruthenium(II) cation, IR-optical double reson. and thermal modulation spectra 78−25576
borides, RRu_3B_2 (R=rare earth, Y, Th, or U), supercond. and mag. props. 80−97028
charge transfer transitions, mixed valence and outer sphere complexes, solvent effect 77−75127
chemisorption, of O_2, by catalysts, EXAFS obs. 78−15708
complex, HF calc., electron densities and Mossbauer isomer shift, chemical binding 78−50470
complexes, luminescent, non-radiative pathways in solvents 77−3393
double oxides, elec. cond. 80−34438
reactor fuel reprocessing, separation of Ru from PuF_4 79−31091
reactor fuel reprocessing fluorination of Ru 79−31090
ruthenium tris-bipyridyl, excited state electron transfer quenching, H_2O photoreduction mediators effects 80−102536
ruthenocene, cryst. and soln., dynamic struct., NMR expts. 77−15328
ternary and quaternary oxides, prep., cryst. struct., and mag. props. 79−14771
trisbipyridyl ions in surfactant solns., excited state decay kinetics 80−83407
$Ba_2Bi(Y)RuO_6$, perovskites, prep., struct., emission control catalysts 77−68957
$Ba_4NbRu_3O_{12}$ and $Ba_4TaRu_3O_{12}$, $(Ru_3O_{12})^{13-}$ cluster obs. in presence of orbital degeneracy and spin-orbit coupling *(French)* 80−70655
$Ba_3Ru_2MO_9$, (M=Mg, Ca, Sr, Co, Ni, Cu, Zn, Ca), Mossbauer spectra 80−108136
$Ba_4Ru_3MO_{12}$, (M=Ta, Nb), Ru oxidation state, Mossbauer study 80−44965
$H_4Ru_4(CO)_{12}$, polycryst., PMR chem. shift 79−95655
$LaRu_4B_4$, X-ray cryst. struct. determ. 79−32959
$La_8Ru_4O_{21}$, mixed valence oxide of new hexagonal struct. type 78−51503
$Li_{0.5}Fe_{2.5}O_4$ Ru substitution effect on struct. and mag. props., and max. solubility determ. 80−75364
$RRuB_4$, R=Y, Cd, Tb, Dy, Ho, Er, Tm, struct. and mag. props. 78−79584
$Rh_2Cl_2(CO)_4$, non-empirical pseudopot., PSIBMOL algorithm 79−76335
Ru bipyridine ion, electron transfer limiting efficiency and rate constant meas., step excitation method expt. 79−91929
Ru complex, (2,2′-bipyridyl)$_3$ruthenium^{2+}, excited-state redox processes, electron transfer theory 79−39126
Ru complex, [Ru(bipy)$_3^{2+}$], decay times and bimolecular quenching, ultrafast kinetics expt. for students 77−26116
Ru complex, [Ru(bpy)$_3$]$^{2+}$-Ti (III), photochem. H_2 prod. from aq. soln. 80−85192
Ru complex, acetylacetonate, relaxation studies in magnetic resonance spectroscopy 79−73841
Ru complex, Creutz-Taube ion, ground state, single crystal EPR obs. of mixed valence Ru dimer ion 80−34766
Ru complex, electrogenerated chemiluminesc., production of excited states by direct heterogeneous electron transfer 79−20371
Ru complex, photooxygenation, actinometric laser intensity meas. appls. 77−30193
Ru complex, Ru(II)-polypyridine, excited charge transfer states, multiple emissions 79−3468
Ru complex, Ru(2,2′-bipyridine)$_3$Cl$_2$-6H$_2$O, photocond., optical absorpt. and fluoresc. 77−80807
Ru complex, Ru(bpy)$_3^{2+}$, excited, in aq. soln., optical absorption spectrum 79−50032
Ru complex, ruthenium(II) tris(2,2′-bipyridine), absorption spectrum and quantum yield of formation *(French)* 80−5554
Ru complex, tris-1,1,1-trifluoro-2,4-pentanedionate, struct., chem. ionisation mass spectra 78−61079

ruthenium compounds continued
Ru complex, tris-(2.2′-bipyridyl)-Ru(II) complex, photoelectrochemical systems, solar energy utilisation *(German)* 80−45713
Ru complex in PMMA matrix, mag. induced circular polarisation of emission meas. 78−58058
Ru complexes, $[Ru(bipy)_n(pq)_{3-n}]^{2+}$ mixed-ligand, electronic absorpt. and emission spectra meas. 80−71441
Ru complexes, carbonyl hydrides, pre-reson. Raman spectra, Ru-Ru and Ru-C modes 78−43854
Ru complexes, $K_{\alpha 1}$ lines chem. shift, donor-acceptor capacity of ligands 79−33867
Ru complexes, $Ru(NH_3)_6^{2+}$ and $Ru(en)_3^{2+}$ in soln., UV spectra, solvent effects 79−94010
Ru complexes, $Ru(bipy)_3Cl_2.6H_2O$ and $Ru(bipy\text{-}d_8)_3\ Cl_2.6H_2O$, soln. electronic excitation energy, deactivation determ. 80−55173
Ru complexes with adenosine, xanthosine, prep., elec. cond., IR spectra, characterisation 78−92065
Ru dimers, mixed-valence, electron transfer rate consts. calc. from intervalence transfer absorpt. bands 79−81164
RuB_2, possibility of semicond. props., rel. to atomic volume 77−69317
$Ru(CO)_{5(g)}$, chem. thermodynamics 78−18799
$RuCl_5NO^{2-}$, polarised Raman and IR spectra, vibr. anal. 77−69819
RuF_5, mag. props. 80−15707
$Ru_2Ge_{3-x}Sn_x$, and $Ru_2Ge_{3-y}Si_y$, diffusionless phase transitions, elec. and mag. props. 80−96871
Ru(II) complex, carbonyl(pyridine)-phthalocyaninatoruthenium(II), optical hole burning, matrix effects 80−102522
Ru(II) complex, tri-biphenyl, electrochem. electron transfer reactions at $SnO\text{-}H_2O$ interface 79−52675
$Ru(NH_3)_6^{3+}$, isotropic chem. shift, pseudocontact contrib. 80−91577
RuO_2 anodic coating on Ti, struct., electrochem. props. *(French)* 79−83385
RuO_2, as elec. contact material, environmental interactions and prep. 80−29463
RuO_2, catalyst on isopropanol surface active sites during dehydrogenation 79−43621
RuO_2, electronic struct., XPES obs., rel. to TiO_2, IrO_2 78−52632
RuO_2, photoelectron spectra, X-ray and UV polycrystalline 79−28889
RuO_2 porous powder electrodes, proton diffusion meas. 80−54436
RuO_2, thermal conductivity meas., rel. to elec. cond. 80−65317
$^{99,101}RuO_2$, NQR spectroscopy 80−63664
RuO_2-based anodes, electrochem. props 79−96332
RuO_2-TiO_2 anode, wear-resistant, use in applied electrochem. 80−40701
RuO_2-TiO_2 coatings for Ti anodes, microstructural investigations 79−43469
RuO_4, catalytic reduction in radioactive liquid waste processing 79−76092
RuO_4, mol. vibrs. and reaction pathways, min. energy coords. and compliance consts. 77−57966
RuO_4, $\nu_3(F_2)$ IR band contour, isotopically pure cpds., mol. consts. 77−61746
RuO_4, SCF Xα SW calcs. of ground state 78−90081
RuO_4^{2-}, antireson. Raman effect, excitation profile 79−50019
$^{106}RuO_4$ in lung, in vivo meas. and dosimetry 78−53515
RuO_x, catalyst at anode of solid polymer electrolyte cell, corrosion 79−20376
RuO_x, confinement of oxides volatilised during nucl. fuel reprocessing 80−47680
RuO_x working electrodes in nonaqueous solvents, props. 79−91960
$Ru_4O_{16}^{12-}$ clusters, thermodynamic props., exchange interactions effects 79−24180
$(Ru_2OCl_{10})^{4-}$, reson. Raman, IR and electronic spectral studies 79−10118
RuP_2, oxidation resistance in Ar and air 77−25201
RuP_2, prep. and characterisation 78−39679
RuS_2 amorphous, preparation at ambient temp., magnetic susceptibility meas. 80−35119
$RuTe_2$, decomposition press. and thermodynamic props. 78−3366
$Ru_{1-x}Ti_xO_2$ solid solns., metal-nonmetal transition 78−91735
$Ru_xTi_{1-x}O_2$ films, elec. props. and IR spectra 79−38207
$Ru_xTi_{1-x}O_2$ films, percolation elec. cond. in strong electric fields *(Russian)* 80−84471
$Sr_2Bi(Y)RuO_6$, perovskites, prep., struct., emission control catalysts 77−68957
Th-Ru-C, phase diagram *(German)* 77−48413
$Ti/RuO_2/MnO_2$ electrode, anode characts. 78−68897
Ti-RuO_2 anode, electrochem. stability 79−70346
TiO_2-RuO_2 surface, photocatalytic decomp. of H_2O 80−85194

rutile *see titanium compounds*

S-matrix theory
see also dispersion relations; network parameters
(1+1) dimens. Todd chain and $e^{\phi}+e^{-2\phi}$ model, exact factorised S-matrices 80−18094
(1+1) dimensional field theoretic models with soliton behaviour, exact S-matrices and form factors 79−26240
1+1 dimensional field theories, bound state problem, S-matrices 79−71609
$\lambda\phi^4$, momentum space renormalisation in curved space time 80−37158
σ model, two-dimens., nonlinear, anal., nonlocal charges determ. 78−54532
ϕ_2^4 theory, mass and S-matrix Borel summability 79−89054
Φ_3^4 weakly coupled model, nontriviality of scatt. matrix 77−87891
$P(\phi)_2$ field theory, non-relativistic limit for two particle phenomena 78−16906
A^4-coupling in abstract approach of quantum field theory, renormalisation group 80−99033
A^4-phonon theory, model S-matrix negative in Brillouin zone 78−41257
abstract scattering systems, S-matrix energy bound 79−54274
adiabatic S-matrix and perturbation theory for systems in a periodically-varying external field 79−9133
adjoint SU(N) representation, exact factorised S-matrices 79−71647
Adler zeros, as group theoretical consequence of mass zero asymptotic free fields 77−22655
algebras of observables in the S-matrix approach 79−71648
amplitude props. in supersymm. theories 77−67582
analytic struct., of distribs. and essential support theory 77−10191
analytic struct. for some classes of potls., Jost functions appl. 78−70294
analytical continuation of bound state, scatt. wave function construction 77−74258

S-matrix theory continued
anomalies of quantum conserved currents in exactly solvable models 78−387
applied inverse problems, book 79−49017
asymptotic perturbation expansion, time ordered functions in relativistic quantum field theory 77−6039
asymptotic relations, cross sections of inclusive processes 77−65187
atom+atom, inelastic scattering data inversion, interaction function recovery 79−89741
atom+diatom, CS approximation, total angular momentum labeled, inadequacies 79−22777
atom+diatom, inelastic cross-sections, rot. quantum number, energy scaling 77−83692
atom+diatom, sudden approx. of Cross, computational tests, cross section factorisation, scatt. phenomena 80−58352
atom+diatomic molecule, coupled states, P-helicity, and effective pot. methods comparison 77−30944
atom+molecule rot. inelastic scatt., coupled eqns. for single initial state, variation-iteration method 79−68301
atom surface scatt., reflection and sticking coeffs., short range forces, low energy limit 80−40208
atomic collisions, by molecular theory, electron translational effect 77−88528
atomic collisions, determ. of Regge poles from nonlinear Schrodinger eqn. 78−49702
atomic electron scattering, free-free transition of electron, multichannel theory 78−1078
atomic excited state collisional relax., line broadening, interat. interactions, review 80−43149
atomic ion, electron scatt., S-matrix calc. 79−45847
atoms, photon exchange between neutral neighbours and cooperative radiation 77−27141
baryonium, S-matrix representation 80−399
baryonium dual S-matrix approach 80−52526
bilocal fields, ϕ^3 vertex, unitary S-matrix 78−62323
black hole evaporation, predictability, CPT invariant superscatt. operator and S-matrix 80−46600
block diagrams, divergence cancellation in energy level perturbation theory 79−80751
book, graduate level 78−54575
book, scatt. theory in quantum mechanics 78−49573
bootstrap topological colour and disc mating unitarity as the source of zero triality 79−49492
boson resonant state S-matrix pole residue relationship with wave function asymptote 79−9499
boson theory, probability struct. in Euclidean domain 79−89071
boson-soliton scatt., sine-Gordon model 80−9109
bound proton-neutron system, basis functions and collective states 79−67688
bound proton-neutron system, operator averaging technique, recurrent construction of collective variables 79−67689
near bound states in the continuum 77−87663
bound states near limit of lower continuum 77−49885
bubble diagram functions, u=0 structure theorem 79−2946
causality, generalized integral condition for S-matrix, reln. to algebraic approach 78−37150
causality condition in field theory with momentum space of const. curvature 78−395
charged particle scatt. in laser radiation field, S-matrix formulation, low freq. approx. 79−93299
charged particle scatt. in laser radiation field 79−12996
charged particle scatt. in quantising mag. field 80−46853
chemically reactive system, elastic scatt., parametrised S-matrix models 79−79225
chemically reactive system, large angle elastic scatt., interference effects, Regge pole anal. 77−58123
chiral fields, two-dimens., hidden symm. 78−29243
chiral invariant SU(N) Thirring model, exact S-matrix 79−21911
chiral O(N)×O(N) and SU(N)×SU(N) 2-dimens. models, conservation laws and S-matrices 80−68389
chiral SU(N) Thirring model, S-matrix bound state poles fixing 80−360
classical limit S-matrix for nuclear Coulomb excitation reactions 77−3036
classical sources, conditions for quantum scalar field with higher order derivatives 79−63365
cluster expansion in statistical mechanics, S-matrix formulation *(German)* 78−41256
collision amplitudes, structural anal. 77−10188
conservation laws, infinite set for Thirring model, massive and quantum sine Gordon model 78−29226
conserved currents and symmetries of the S-matrix 80−9110
consistent S-matrix with nonlocal Yukawa interaction and relativistic form factor 79−93300
in constructive quantum field theory of self-interacting bosons *(Russian)* 77−209
continuum S state wavefunctions for the Debye potential by Ecker-Weizel approximations 78−78104
Coulomb electron atom scatt. in laser field, asymptotic dynamics 79−94084
Coulomb matrix elements, semiclassical approx. including distorting nuclear potentials 77−57640
Coulomb scatt., perturbation theory, renormalised half-off-shell T-matrix 78−32996
coupled channel R-matrix propagation equations, Green's function method 79−54273
coupling strength of particle production, Ball-Zachariasen model of diffractive scattering 80−9158
cross section of deep inelastic collisions, general form using S-matrix theory 78−566
crossing properties of scattering operators 80−32028
crossing-symmetric four-body unitarity condition 79−67480
curve-crossing collisions, scatt. matrx. 78−70891
cut extrapolation method for data anal., crossed channel Mandelstam cuts, symm. $\pi\pi$ scatt. 77−49867
cut-off potential, asymptotic energy behaviour of Green function 80−27165
Debye expansion convergence 79−40679
deflection functions for curve-crossing collisions 79−94051
degenerate perturbation theory, energy shifts and S-matrix 79−75693
determinant of S-matrix, relation to number of eigenvalues due to perturbation 78−58132

S-matrix theory continued
diatom+atom (electron) scatt., vibr.-rot. excitation, generalised field theory method 77−23537
diffraction peak width, upper bound derivation 78−12831
diffusing layers, characteristic matrices for inhomogeneous layers 78−87015
diffusing layers, characteristic matrix and general props. 78−87014
Dirac S-matrix in k-plane 78−54577
dispersion relations with two substractions in frames of field localisable theories *(Russian)* 78−41433
dual chiral pion model, partially conserved axial-vector current, S-matrix theory 78−58175
dual topological unitarisation, review of S-matrix developments for hadron bootstrap theory 78−62381
dual unitarisation and baryons 78−16999
dynamical equation for scattering operator 79−12936
education, S-matrix theory, quark as redundant concept, order concept, review 79−25786
effective radius outside energy surface, approx. *(Russian)* 77−14039
eigenphase sum behaviour near a resonance 79−54285
eikonal approximation, some inequalities 79−44800
Einstein correlation, S-matrix and Feynman zigzag 78−77761
elastic scatt., new semi-classical approach 78−32706
elastic scatt. amplitudes, asymptotic bounds on derivatives 78−12892
elastic scattering, semiclassical time-independ. formulation in three-dimens with complex trajectories 80−27605
elastic scattering, Sommerfeld poles and backward peaks 78−21357
elastic wave scatt. from cylindrical cavity, nuclear resonance theory 78−87290
electron scattering from ats.(mols.), partial resonance widths, Siegert eigenvalues, basis-set calc. 80−37880
electron-molecule scatt., adiabatic nuclei theory 79−45846
energy averaged reaction cross sections, S-matrix pole expansion examination 78−58259
ergodic behavior in the statistical theory of nuclear reactions 79−17888
exact from factors in field theoretic models with soliton behaviour 78−82211
exponential model, two-state, comment on Stueckelberg phase calcs. 79−3514
extended baryon fields and meson-baryon interaction, S-matrix construction 77−41751
extended particle relativistic field theory, S-matrix to 4th order 77−22646
extended supergravity, SO_2 model, minimal set of auxiliary fields 79−58608
extrapolation method for perturbative expansion of S-matrix, high energy hadron collisions, ϕ^4 model calcs. 78−394
factorisation, analogy of 2-dimens. perturbation theory structural props. in higher dimens. 78−70293
factorisation in the 2 dimens. linear σ model in $1/N$ expansion 79−35936
factorisation of classical and quantum S-matrix, rel. to conservation laws 77−30277
factorised completely X symmetric S-matrix characterisation, multicomponent field theories 80−105800
factorised S-matrices in 2-dimens., relativistic QFT model exact solns. 79−93274
factorised S-matrix framework, antiparticles as bound states of particles 79−49411
factorizable S-matrix with Z(N) symmetry 79−93301
factorized U(n) symmetric S-matrices, two dimens., scatt. of solitons 78−45802
few nucleon systems, 3N and 4N calcs., reviews 78−50094
Feynman integrals, holonomic character and local monodromy struct. 77−54038
fine-structure transition probability, semiclassical multichannel scatt. matrix 80−37854
formal manipulations relating the S-matrix and density matrix formalisms 80−99064
functional integral construction of S-matrix 77−57458
G-parity and exchange degeneracy breaking 77−71449
gas linear molecules, symmetrised Liouville basis vectors, appl. to spectral linewidths 80−83457
gas phase nucl. mag. relax., DWBA cross sections from S-matrix formalism 77−27151
gauge dependence in the Yang-Mills S matrix 80−351
gauge invariance, Lorentz covariance and EM props. of elementary systems 80−32037
gauge invariant operators, renormalisation, S-matrix elements 79−256
gauge invariant QED construction in stochastic space 79−21998
gauge invariant S-matrix elements with Yang-Mills SU(2) instantons and antiinstanton 80−22511
gauge singlet operators instead of bound states 80−99063
Gell-Mann-Goldberger formula for long-range pot. scatt. 77−6040
Glauber approx. for particle-atom collisions 77−10716
glueball singularity, flavour loops and the Harari-Freund picture 80−42433
gluon bremsstrahlung and multiperipheral cluster models 79−22082
gravitation, covariant quantisation 78−8327
gravitational and Yang-Mills fields interaction 80−42315
Gross-Neveu and nonlinear σ-model, scatt. amplitudes in $1/N^2$ perturbation theory 78−70261
Gross-Neveu chiral model, scatt. theory, $1/N$ expansion 80−348
Gross-Neveu model, chiral invariant, S-matrix direct calc. 80−68362
Gross-Neveu model, exact S-matrix theory 78−24937
hadron+hadron, cluster model, field theoretic, multiperipheral production, Feynman scaling violation 80−57576
hadron nonlinear string model 77−87901
hadron S-matrix topological expansion, dual unitarisation 77−74662
hadronic targets, spin-$^1/_2$, Compton scatt., optimal sum-rule inequalities 80−105815
half off-shell t-matrix elements for class of equivalent pots., ΛN scatt. 77−2562
Hamilton-Jacobi equation solns. in Coulomb pot. and quasiclassical approx. 80−46765
heavy ion inelastic scatt., closed form quantal description, DWBA anal. 77−14147
heavy ion large-angle scatt., elastic cross-section, excitation functions 80−52689
heavy ion large-angle scatt., inelastic cross-section and collective state excitation 80−52690
S-matrix theory continued
heavy ion potential scatt., multiple reflection expansion 78−41753
heavy ion scatt., optical potential resonances, semiclassical method, S-matrix amplitude 79−3120
heavy ion transfer reactions, recoil effect, kinematics of mol. states approach 78−62557
heavy particles, reson. scatt., pseudocrossing problem 79−49412
heavy-ion deep inelastic collisions, general form of cross-section 78−13131
Higgs-Kibble mechanism, superfield theoretical treatment 78−89616
high energy collisions of heavy nuclei, Glauber rescatt., Reggeon field theory 78−37369
hyperquantisation of multi-mass vector spinor field in EM interaction, S-matrix unitarity 77−61232
identical particle effect and symmetrization in Mueller amplitude 79−30672
inclusive coherent interference phenomena between pions in S-matrix theory 77−61206
indefinite metric quantum field theory of general relativity 78−65853
indefinite metric quantum gravitation theory, subsidiary conditions and physical S-matrix unitarity 79−9171
integrable system, finite dimens., scatt. behaviour investigated via associated matrices 77−82415
intense field QED in continuous medium, appl. to Thomson scatt. and Cherenkov radiation 80−27435
interacting extended boson fields, scatt. amplitude, self energy 78−66047
interacting spin-1 field theories, anomalies, expansion of S-matrix into Feynman graphs 78−45798
inverse scatt. problem, fixed point theorem 79−280
inverse scatt. problem 77−45981
inverse scattering problem, quantum field theory 78−363
ion, three-electron, 2s2p1s config., intermediate coupling state, energy level calcs. 79−3353
ions, multiply charged, level lifetimes relativistic calc., S-matrix approach 80−47942
IR dynamics, classical current models 77−60947
IR interaction with mols., classical/semiclassical theory 78−90164
J-dependence of statistical bootstrap mass spectrum, S-matrix and semiclassical formalism comparison 78−86448
Jost function and S-matrix for pot. of general form., Schrodinger eqn. soln. in hypergeometrical functions *(Russian)* 78−81870
Jost functions, S-matrix of massive Thirring model, relativistic field theoretic model 78−54552
Korteweg de Vries eqn., self similar solns. and pots. with trivial S-matrix 79−30266
Kugo-Ojima formalism for gauge theories, unitary proof validity 80−37164
large-scale lossy groove array finite difference analysis 77−27420
Lehmann-Symanzik-Zimmermann formulas in a gauge-independent path-dependent formalism 79−21942
level dneisty distribution effect on energy average of scatt. function 77−82686
Levinson's theorem for nonlocal interactions, phase shifts, continuum bound states 77−26195
linear Boltzmann equation, scattering matrix 77−18643
Lippman-Schwinger equation, soln. for n delta-shell pots. 78−41112
long range forces in quantum theory, book contrib. 78−82811
low-frequency photons in processes involving particles with spin 80−9131
lower bounds on total cross sections and slope parameter 78−32997
macrocausality of S-matrix, LSZ asymptotic condition 77−26452
many channel scattering model, exactly soluble 80−43127
many-photon ionization, resonance scattering on a nonstationary potential, and complex poles of the S-matrix 79−22677
mass generation for fermion field in absence of chiral symmetry breaking 80−347
massive Thirring model, complete S-matrix, sine-Gordon solitons 78−16936
massive Thirring model, conservation laws in quantum (cos $\phi-1$) theory *(Russian)* 77−200
massive Thirring model, particle scatt. in perturbation theory 77−82674
massive Thirring model, S-matrix calcs., required number of conserved currents 80−42329
massive U(1) Thirring model, S-matrix and dynamical supersymm. 77−67586
massless fields in asymptotically flat space-time, null surface quantisation and quantum theory 80−4625
meson interactions, LSZ reduction formulae, soliton asymptotic theory 78−4774
meson-meson Regge theory with crossing symmetry and unitarity, strong coupling 77−65177
meson-meson Regge theory with crossing symmetry and unitarity, weak coupling 77−67676
micro-analyticity of the S-matrix and related functions 79−54272
mode-coupled multimode W-fibre, analytical anal., scattering matrix method 80−99872
model factorized S matrix and an integrable Heisenberg chain with spin 1 *(Russian)* 80−101767
modified Bethe-Salpeter equation from the matrix Pade approximants 79−93286
molecular collinear scattering, information content, dynamical approach 80−23500
molecular collisions, factorisation of matrix 79−72380
molecular electron impact excitation, threshold structures, non-adiabatic theory 79−72431
molecular electron scatt., vibr. struct. of resonances 78−17813
molecular scattering, semiclassical S-matrix, by generalised phase shift approach 79−89725
Moller wave operators for pot. scatt. 78−45495
monotone dependence in scattering theory, proof from S-matrix explicit formula 78−74163
Morse function off-shell K-matrix, computation method 78−74164
multichannel partial-wave dispersion relations, coincident thresholds, pole approx. 79−9293
multichannel resonances, combined Hamiltonian and S-matrix methods *(Russian)* 79−63645
multichannel T-matrix, separable form 77−57471
multimass field hyperquantisation, S-matrix unitarity 77−22645
multiparticle amplitudes, discontinuity formulas 77−13881
multiparticle collision amplitudes, physical-region props. 77−13880
multiparticle S-matrix factorisation in two dimens. space-time models 79−281

S-matrix theory continued
multiparticle S-matrix in field theory two dimens. space-time models, factorisation 78−62324
multiparticle scatt. operators representation satisfying unitarity and crossing props. 80−32029
multiparticle scattering operators, cluster decomp. 80−22592
multiple Coulomb excitation of heavy ions, semiclassical S-matrix integral representation 78−630
multiple normal threshold discontinuities for 2 to 4 processes 77−60982
multiply charged ions, $2p_{1/2}3p_{3/2}$ config., level widths, relativistic calc., S-matrix method 80−63546
Muskhelishvili-Omnes equation and final state interactions 79−67196
Muskhelishvili-Omnes integral eqn. with inelastic unitarity 78−8546
n-body potentials in QED and quantum gravity 78−24969
n-body quantum system, time depend. scatt. theory for infinite delta function pots. 78−49704
n-electron atom, transition probabilities, relativistic calcs. 77−14391
N-particle scatt. ionisation T matrix 79−44777
N-quantum approximation in Bronzan-Lee extended-source static model 78−8507
NDO in terms of power series expansion in S-matrix 80−69080
non local theory, canonical quantization, with form factor in interaction Lagrangian 79−75691
non-Abelian theories, struct. of leading IR divergences 78−4785
nonadiabatic collision processes, electronic degrees of freedom, classical analogue, appl. to mol. system 79−64063
nonlinear Bose systems, Dyson-Wick expansions 78−73921
nonlocal continuous potentials, theory of integral operators and eigenvalue anal. 78−8274
nonrelativistic multichannel potential scattering model, confined channels, Hamiltonians 77−5684
nonunitary multichannel S-matrix on basis of completeness condition for wave functions *(Russian)* 77−61207
nuclear and chemical reactions, variational techniques 77−60966
nuclear collision, K-matrix theory, method for compensating for neglected open channels 78−13039
nuclear deep inelastic collisions, parametrised S-matrix approach 80−32249
nuclear elastic scatt. with optical potential, complex angular momentum methods, poles and zeros of S-matrix, REGGE 80−47445
nuclear optical model S-matrix, energy depend. anal. using WKB 77−34275
nuclear reaction threshold phenomena, K-matrix description 79−30809
nuclear reactions, energy ave. and ensemble ave. equality 78−17170
nuclear resonance reactions, strong absorption and the distribution of zeros of the S-matrix 79−36214
nucleus-alpha back-angle anomalies, S-matrix continuation to complex l-plane 77−30613
null surface quantization and quantum field theory in asymptotically flat space-time *(German)* 79−25959
O(N) nonlinear σ-model, particle prod. and factorising S-matrix 79−71613
off shell scattering amplitude, S-matrix, pot. scatt., Mittag-Leffler expansions of Green's function, convergence 78−73874
off-energy-shell T matrix, frame depend., relativistic pot. theory 78−25159
on shell S-matrix relations for pot. scatt. variable phase method eqns. 79−9149
on-shell counterterms and nonlinear invariances 80−22522
one-dimensional scatt. theory, stability of direct and inverse problems 78−4523
one-electron atom, rearrangement collisions in laser radiation field 80−74225
one-soliton sector, covariant functional approach 78−78092
open systems, S-matrix and density matrix formalism 79−88872
optical fibres, mode-coupled multimode, baseband transmission theory based on scattering matrix 80−14468
optical potential, imaginary part, effect on total reaction cross sections 79−9534
ordered hadron S-matrix, quark interpretation, selection rules 78−62322
ordered hadronic amplitude graphs, mathematical props. 80−42354
ordered S-matrix theory, quark struct. and charge conjugation connections, hadron zero triality 79−12973
oscillating potentials, scatt. matrix 80−57126
overlapping resonances, constraints imposed by analyticity and unitarity 77−22656
$P(\phi)_2$ field theory, time ordered operator products and S-matrix 77−10162
$P(\phi)_2$ quantum field theory, asymptotic perturbation expansion 77−10161
Pade approximants and πN scattering 80−22634
partial wave amplitudes asymptotic behaviour, Regge models and dispersion relations 77−10204
path integral formulation, central scattering potentials 80−82906
path integral representation for U- and S-matrix, scalar meson model renormalised S-matrix elements 78−78103
path integral representation of QFT for S-matrix, meson field-nucleon field interaction 79−2947
perturbation expansion of multichannel Regge poles 80−86623
perturbation theory, in 1/Z expansion, S-matrix theory appl. *(Russian)* 79−1565
photoionisation, relativistic R-matrix theory 78−5184
photonuclear reactions, S-matrix element transformation, particle polarisation 79−89293
pion-nucleon low energy scatt., local and nonlocal pots., inverse scatt. reaction matrix anal. 78−8684
planar, building of cylinder correction in topological expansion or dual unitarisation 78−62321
Poincare-like groups, Kronecker product decomposition, appl. to Weyl group 78−49632
point transformations and non-linear system quantisation, S-matrix from perturbation theory 79−109
pole factorization theorem in S-matrix theory 78−12830
pole trajectory in three neutron model 78−82296
poles, connection with resonances, local distortion technique 77−74609
potential scatt., amplitude, quasiclassical asymptotic behaviour, quantum correction 78−62325
potential scattering , perturbation methods for local and nonlocal pots. 78−16696
principal value collision integrals, reduction scheme 77−57234

S-matrix theory continued
QED, S-matrix anal. as three-body interaction Klauder phenomenon interpretation 79−80777
QED in an external gravitational field, S-matrix evaluation, pair prod. 78−82131
QED in external gravitational field, S-matrix construction 78−78116
quantal Coulomb excitation scattering matrix, asymptotic approxs., error estimates, using nonlinear Riccati matrix differential eqn. 77−49866
quantisation of relativistic systems with first-and second-class constraints 78−21337
quantum action method in quantum field theory 79−40659
quantum collision theory, generalised sensitivity anal. 80−31542
quantum Dirac field, scatt. automorphisms, external field perturbations 78−58112
quantum field theory, operator ordering, interaction Hamiltonian noncommuting operators, S-matrix expansion, Feynman rules 80−57472
quantum field theory in curved space-time, S-matrix existence 79−63120
quantum field theory of electrostatic potential in gravitational field 78−54270
quantum gravitation without matter, renormalisation 77−37798
quantum mechanics, decaying states in rigged Hilbert space formulation 80−62521
quantum theory of solitons, review 78−70288
quark-parton model from dual topological unitarization 79−93361
quasi-particle scattering, kinetic eqns. in statistical T-matrix approx. 77−65011
quasipotential eqns., Levinson theorem violation, S-matrix 78−54576
R-matrix theory, atomic continuum processes 77−83478
ray representation of scattering amplitude in the presence of resonances 79−21587
reaction matrix theory, phase equivalent pots., general case 78−58131
reduction formulae for matrix elements, Yang-Feldman relations 77−30276
Regge amplitude construction through soln. of S-matrix equations 79−49413
Regge pole calc. by formal series 77−6056
Regge trajectories families, S-matrix theory, nonrelativistic linear pot. quark binding model, comparison 78−33048
Regge trajectories for vel.-depend. pots., S-matrix singularities 77−57468
Reggeon quantum mechanics, Hamiltonian formulation, S-matrix, pomeron Green functions 78−16951
relativistic constrained system, compensating functional and quantisation, S-matrix 79−97527
relativistic elastic scatt., crossed channel struct. effects *(German)* 79−58906
relativistic factorised S-matrix in two-dimens., O(N) isotopic symm. 78−41432
relativistic factorised S-matrix in two-dimens. space-time with isotropic symmetry *(Russian)* 78−8547
relativistic Fermi-Bose system quantisation, by compensated functional method *(Russian)* 80−42142
relativistic gas of interacting particles, phase vol. approx. 78−41225
relativistic harmonic oscillators and hadronic struct., 1st year graduate quantum mechs. 78−61971
relativistic quantum fields, particles and currents, book 78−82117
relativistic S-matrix of dynamical system with boson and fermion constraints 77−74610
renormalisation group transformations as symm. mappings, local Lagrangian density *(German)* 78−49953
renormalisation group with arbitrary interpolating fields, mass shell appls. 77−13879
Riemann boundary value problems, partial wave mixing in S-matrix, Jost matrix evaluation 79−89072
S-matrix for analytical continuation over complex k-plane 78−49978
Sato's conjecture, validity using concrete expressions for Feynman amplitudes 78−74123
SAW two-port, terminal characts., S-matrix approach 77−23848
scaling of energy and quantum no. for nonreactive collisions 80−9695
scattering amplitude at high energies, corrections to geom. optics in quasi-classical limit *(Russian)* 77−2760
scattering function energy average, differential equation approach 77−18514
Schrodinger eqn., radial, general pot. props. for soln. by hypergeometric functions 80−4581
Schrodinger eqn. with Hardy pot. 80−96
Schrodinger equation, Laplace transform 78−57806
second virial coefficient, low temp., S-matrix pole representation 77−37834
second virial coefficient from the scattering operator 78−24730
self-interacting boson field, interaction with classical current, S-matrix elements 79−21963
semiclassical collision theory, non-integer Bessel uniform approx. 79−36730
semiclassical Coulomb excitation theory, classical-limit S-matrix, orbital dynamics 78−33205
semiclassical perturbation expansion of the multichannel scattering matrix 79−49410
semiclassical propagator, focal points, phase 79−76
semiclassical wave propagation matrix method, S-matrix calc. 79−101
sequential particle order, fundamental concept for hadron physics 79−80762
sequential particle order, fundamental concept for hadron physics, S-matrix theory 79−80763
sine-Gordon model, quantum solitons, exact two-particle S-matrix *(Russian)* 77−57463
sine-Gordon S-matrix, origin of double poles 78−70292
sine-Gordon soliton form factors, massive Thirring model S-matrix 77−45952
sine-Gordon solitons, exact two-particle S-matrix 77−74608
sine-Gordon supersymmetric theory, exact S-matrix 78−62313
Slavnov-'t Hooft identities in Mandelstam's formalism 78−45776
SO(3) gauge invariant theory, quantisation, spontaneous broken gauge theory, S-matrix gauge independ. 79−269
soft spin 3/2 massless fermions, gravity, supersymm. 77−49869
soliton conservation laws, construction of form factors and correl. functions *(German)* 79−9274
soliton field theory, construction of Green's functions from an exact S matrix 79−71629
spectral and scattering inverse problems 79−17282
spherically symmetrical coherency strain contrasts, S-matrix theory calcs. 80−100133

S-matrix theory continued
spin dependence, composite hadrons, S-matrix theory, TeV energy range 78−58164
spin-1/2 tachyons, scatt. from EM field 77−5693
Stiefel manifolds, 2-dimens. nonlinear σ-model, S-matrix regularities 80−86576
stimulated and Cherenkov radiations, differential eqns. with respect to coupling constants, S-matrix 79−50278
stimulated electron radiation due to wiggled magnetic field 80−58451
strong coupling in quantum field theory with nonlocal nonpolynomial interactions 78−21319
Stueckelberg close-curve-crossing phases 78−22
Stueckelberg phases, 3-parameter exponential model 78−41440
SU(2)×SU(2), dynamical rearrangement of symmetry 78−49979
SU(5) without symmetry constraints, unified model of quarks and leptons, conservation laws 80−101968
supergraph anal., gauge supersymmetry, S-matrix 80−27422
supergravity, auxiliary fields for closed algebra using S-matrix 78−81911
supergravity, covariant canonical formulation, subsidiary conditions and physical S-matrix unitarity 80−12974
supergravity, four particle S-matrix one-loop renormalisability 77−5730
supergravity, Hamiltonian formalism, quantisation and S-matrix 78−16972
supergravity, S-matrix difficulties, graviton elastic scatt. amplitude 79−135
supergravity 77−46010
supersymmetric nonlinear σ model, S-matrix determ. 78−66052
tachyons and quantum field theory 80−18069
tensor test functions in the scattering matrix theory 79−30671
Thirring massive SU(N) model, factorisation 79−12951
Thirring model, chiral, CP^{n-1} and SU_n, exact S-matrix 80−90985
Thirring model S-matrix, exact soln., agreement with perturbation theory 77−54049
three particle reactions, multichannel scatt. theory, kinematic props. 78−54578
three-body scatt. in coordinate space, perturbative approach to Faddeev eqns. 79−30682
threshold cusp 79−58893
time delay in N-body scattering 79−75389
time delay in N-body scattering 79−75695
time-delay operator from scale-invariance 77−79227
time-ordered products and Schwinger functions 79−26216
transition operators, CCA class, under particle interchange, unexpected behaviour 79−75694
two-body spin 1/2 reactions at fixed s and t 78−37149
two-body transition matrix and UPA model, convergence props. of generalised separable expansion 78−16939
two-particle scatt., elasticity, factorisation and S-matrices in (1+1) dimens. 78−16937
unidirectional wave motions, book 78−77730
uniqueness of purely elastic S-matrix in (1+1) dimens. 77−49868
unitarity, causality of functional S-matrix in renormalized QFT 78−4793
unitarity and crossing in high energy scatt., differential cross section in diffraction region *(Russian)* 79−80764
unitarity and renormalized 't Hooft identities 80−13205
unitarity of S-matrix in Yang-Mills theory 77−82681
unstable particles description in quantum field theory, S-matrix poles 77−6024
unstable quantum states and rigged Hilbert spaces in nonrelativistic scatt. theory 80−8849
van de Pol eqn., transformation into S-wave Schrodinger eqn., solvable potential 78−57790
variational principle for calculating poles 78−74165
wave packet dynamics, classical S-matrix limit 77−17836
wave-spreading effects in nuclear scattering at intermediate energies 80−18252
weakly interacting systems, S-matrix, density matrix, Pauli and Boltzmann eqns. 79−88871
Wightman formulation, nontranslationally covariant currents and symm. of S-matrix 78−58133
Yang-Mills field, canonical quantisation, interaction Lagrangian *(Chinese)* 79−21950
Yang-Mills massive theory, S-matrix unitarity in zero-mass limit 77−2732
Yang-Mills theory, covariant canonical formulation, phys. S-matrix unitarity, phys. state subsidiary conditions 78−37141
Yang-Mills theory, massive, appl. of path integrals to non-perturbative study 80−32020
Yang-Mills theory, non-Abelian structure, IR finite asymptotic states 79−265
Yukawa pot. problem, S-matrix exact evaluation from transformed Schrodinger eqn. 78−82120
Yukawa potentials, finite sum S-matrix 80−101940
Z_4-symmetric factorized S-matrix in two space-time dimensions 80−4883
α-nucleus large-angle pot. scatt. 77−71614
$\Delta(1232)$ pole position, stabilized bias free method 78−24968
$f' \rightarrow \pi\pi$ analytic S-matrix theory, Zweig Iisuka rule compatibility with unitarity 77−41782
$K\bar{K} \rightarrow \pi\pi$, analytic S-matrix theory, Zweig Iisuka rule compatibility with unitarity 77−41782
KN scatt. length and forward cross sections for S-wave I=0 78−37231
^{3}n system, S-matrix pole trajectories 79−67679
nd quartet scatt., many-body theory *(Russian)* 77−38190
NN, relativistic interacting system, eqn. of state using Regge-type interaction amplitude *(Russian)* 77−79032
NN interactions, phase shift anal. *(Rumanian)* 78−45942
NN potential from Regge pole theory in momentum space, S-matrix theory formalism 79−67525
NN scatt., high-energy, effect of anomalous mag. moments in quantum field theory 78−465
NN scatt. formalism 78−21463
np scatt., two-channel Jost matrix construction on second-order S-matrix *(Russian)* 79−9294
Nπ scatt., high-energy, effect of anomalous mag. moments in quantum field theory 78−465
(p,p), isobaric analogue resonances, microscopic and phenomenological parameters, S-matrix eval. methods 78−13045
pp scattering matrix determ. from scatt. meas., exptl. technique 78−25063
S-matrix theory continued
π-π interaction, lectures, theory and expt. results, analyticity, unitarity, phase-shifts, current algebra 77−50008
πN coupling constant determ. using forward dispersion relations 79−45098
πN interaction, Coulomb corrections, phase shift anal., S-matrix theory, below 300 MeV 79−85325
$\pi N \rightarrow N\pi\pi$, 1.65-1.97 GeV, partial wave anal. including π-exchange 78−66148
πN off-shell t-matrix, P-wave states calc. 77−61205
πN S-matrix, inelastic effects in sidewise dispersion relations for nucleon EM form factors 78−82212
πN scatt., low energy, determ. of low eqn. 78−8688
πNN form factor, $\Delta(1236)$ contrib., calc. 80−22609
πNN vertex function and off-mass-shell πN scatt. 80−73739
$\pi\pi$ S-wave phase shift, lower bounds, ε° and ρ poles 78−45953
$(\bar{\psi}\psi)^2$ model, kinks, S-matrix elements 78−93809
$^{10}B(t,\alpha)^9Be^*(2s_{1/2})$, resonant spectra 80−22691
$^{11}B(d,\alpha)^9Be$, non-relativistic, analytic S-matrix theory *(Spanish)* 77−67754
Br_2+H, classically forbidden vibr. excitation, S-matrix 77−516
CO+H_2, rot. excitation, rel. between tensorial cross sections 80−83454
CO_2, 3.8 eV resonance, vibr. struct. in electron-molecule scatt. 78−17813
$^{12}C(d,p)^{12}C^*$, reaction mech., relation to $^{12}C(d,d)$, S-matrix theory, 1.63 to 2.05 MeV *(Chinese)* 78−78393
H+H^+, nuclear repulsion, contrib. to charge transfer 80−18922
H+HR→H_2+R, (HR=hydrocarbon), tunnelling reaction, classical S-matrix calc. 77−29007
H+Hg, differential cross sections, orbiting contribution 79−41221
H+highly stripped ions, S-matrix construction 79−3527
HBr+He, classically forbidden vibr. excitation, S-matrix 77−516
$H(1s)+O^{8+}(He^{2+})(H^+)$, charge transfer, 0.025-200 keV/amu 79−22823
He I plasma lines, Stark broadening, quantum mechanical calcs. 80−43880
He neutron rich isotopes, reaction matrix calcs., stability 78−66225
^{5}He+n, pole positions of ^{5}He resonances, models calcs. 78−70530
Li+He, $P_{1/2\text{-}3/2}$, fine-structure transition probability, semiclassical multichannel scatt. matrix 80−37854
$^6Li(n,\alpha)^3H$, low energy, deuteron exchange mechanism, S-matrix theory 79−30840
^{7}Li, energy of first 3/2$^-$ excited state from S-matrix anal. from $^6Li(n,t)^4He$, 0-3.9 MeV, ^{7}Li, energy of first 3/2$^-$ excited state from S-matrix anal. 79−473
N_2, 2.4 eV shape resonance, vibr. struct. in electron-molecule scatt. 78−17813
N_2, elastic electron scatt., low-energy, static exchange in R-matrix 78−13601
$^{15}N(n',n)^{15}N$, continuum random phase approx. 80−27635
^{238}U deformed even-even nucleus, rot. vibr. band excitation, classical limit S-matrix 79−3067

S-parameters
amplifier, fast DC coupled linear pulse, gain and phase response design 80−58088
asymmetric three-transducer configuration analysis 77−39165
complex dielec. and mag. props., modified von Hippel least square fit determ. 78−21179
lossy volume holograms, representation 79−36858
nondestructive evaluation transducer figure of merit 77−27457

safety
see also accidents; alarm systems; fission reactor safety; health hazards; protection
accidents during work, mapping of reasons using error beams by function sensed computations of admission probabilities *(German)* 80−68027
ACS Tenth Biennial Education Conference on Safety and Health in Academic Lab., recommendations 79−80387
actinide partitioning from high-level radioactive wastes, arguments against 77−61570
actinide separation in nuclear fuel and wastes, hazard assessment 79−85806
active noise reduction system for ear defenders 78−92748
air filters, portable electrostatic devices 80−36158
air traffic, solar power station hazards, photometric photography of dazzling heliostat mirrors *(French)* 80−61295
antennas, 10MHz to 1GHz, ANSI and EPA recommendations 80−30765
atmospheric electricity, or static electrification hazard, review 78−28283
atrioventricular sequential demand pacemaker, R-wave sensing methods *(Japanese)* 79−5406
aviation, meteorological conditions forecasting procedures development and improvement 78−92950
balloon pump counterpulsation, increasing operational safety 80−3869
barracks heating using solar energy *(German)* 79−87970
biological effects of radiation, methods of safety estimation and problems encountered *(French)* 80−98003
biological fluid mixing and bottling unit improvement 78−61291
biomedical electronics, recommendations for Spanish hospitals *(Spanish)* 80−72350
biomedical equipment, reliability and safety aspects 80−36172
biomedical equipment, safe voltage differences, practical equipot. limits 78−44649
biomedical instruments, problems and prospects 77−40812
blood pressure instruments, direct systolic/diastolic meas., review 78−69234
breeder reactor security and environmental impact *(French)* 80−47614
BWR power plant, routine checks and radiation protection 78−74462
BWR power plant turbine building, radiation protection, calc. and obs. 78−74461
CANDU irrad. fuel bundles, sheathed in Zircaloy-4, long term stability investig. 80−13774
capacitance meter operation with 10 kV Bias Isolation Unit 77−57364
cardiac electrodes, safe voltage limits 79−16344
cardiac fibrillation, reduced risk using conductive catheter 78−35972
cell drying, critical point drying alternatives for specimen prep. 78−24210
chemical laboratory, airborne contaminants monitoring, USA regulations 80−12869
choke-earthed surgical diathermy circuit analysis 79−20705
clean air cabinets, standards 79−67273

safety continued
clinical engineering safety and technical service centres *(German)* 80−98151
coal mining, deep-level seams, bed rocks instability obs., by monitoring acoustic emission activity *(Japanese)* 80−10071
collective dose commitment for estimate of radioactive pollution, concept and calcs. *(German)* 78−74504
combustion process hazard modelling and logic theory 79−91953
computer-assisted monitoring of vinyl chloride monomer exposure, gas chromatograph system 79−21727
computer-controlled stimulator for ventricular myocardial function analysis 77−60267
concrete slab, reinforcement optimisation by linear programming 77−89022
Conference, nuclear materials, safeguards and accountability meas., Williamsburg, USA (May 1978) 79−81045
containment and surveillance techniques for the IAEA 79−85645
Creys-Malville station, safety arrangements *(French)* 79−30946
critical point drying theory, practice and artifacts, review 78−24211
criticality of U-Pu aqueous solns., oxides and nitrates, effect of Gd, Gd-B neutron absorbers 77−34393
current nuclear power plant safety issues, 1980 conf. preview 80−95360
cutting edges, response of living pig skin 77−36980
data acquisition shelf monitor system for special nuclear material real-time inventory 79−45426
decommissioned nuclear facilities, radiation exposure pathways 80−13957
decommissioning, activation and dose rate calcs. 80−13958
decommissioning of commercial power reactors, environmental, economic and sociological effects 79−67901
decommissioning of commercial power reactors, technical feasibility, cost, environmental effects 79−67902
defect evaluation rel. to fracture mech. *(German)* 80−100908
defibrillation, myocardial damage rel. to high-energy elec. current 78−57051
defibrillation, transchest damped sine wave shocks producing cardiac damage 78−57052
defibrillator ground-loop current elec. skin burn computer simulation 77−78039
demand pacemaker, with variable-pulse-width, clinical experience 77−81696
dense plasma focus, capacitor bank system design and safety 78−54889
density of fluid meas., using gamma radiation, theory, practices and appl. 80−73325
dental radiological safety, pilot survey 79−43993
design safety principles and safety assessment techniques for nuclear chemical plants 80−820
diagnostic ultrasonics, electronic techniques, present applications and future developments *(German)* 79−100683
dialysis equipment elec. hazards and safety 79−84010
ear protectors, performance estimation 78−40192
earplugs, real-ear noise attenuation and effectiveness 78−87199
earthquake prediction and warning, theoretical review 79−5455
electric shock, protection of people, safety curves as function of ambient conditions *(French)* 77−17012
electrical measuring instruments, new CEI standards *(Italian)* 80−31789
electrical operated equipment, safety standard 77−65046
electrical safety, one-day seminar for nurses 77−37701
electrical stimulation parameters, cortical response to callosal stimulation 80−3614
electro-medical apparatus, guideline for provisional safety standard *(Japanese)* 78−73274
electro-medical equipment, leakage current due to mains transformers *(German)* 78−3625
electro-medical measuring equipment, leakage current protective measures *(German)* 78−3629
electro-medical servicing, quality maintenance 78−77126
electroconvulsive therapy, servo-controlled volt. machine 78−77148
electrode safety models, evoked pots. recorded from cat cerebral cortex 78−31797
electrode stimulating and sensing characteristics 77−81743
electrode stimulation of nervous system, electrochem. safety aspects 77−21659
electromedical equipment, reliability *(Croatian)* 78−48901
electromedical equipment, safety by monitoring leakage currents *(German)* 80−81749
electromedical equipment and installations, safety standards *(Croatian)* 80−104795
electromedical equipment and radiological apparatus, standardisation *(French)* 77−73602
electron accelerator, linear highfrequency, hazard factors and conditions for safe operation *(Czech)* 80−52794
electronic diagnostic apparatus, input earth isolation 77−48905
electrosurgery system using HF surgery unit Radiotom 704 78−73292
electrosurgical return electrode capable of steam sterilisation and reuse 77−40911
electrosurgical safety precautions 79−92317
EM absorption in multilayer cylindrical models of man 80−30767
EM fields, range 3-30 MHz, exposure, maximum permissible intensity and duration, physiological effects *(German)* 80−12179
EM non-ionising radiation, influence of quality on bioeffects, exposure standards 78−44558
EM radiation protection, in transmission stations, Polish and international regulations *(Polish)* 78−61263
energy generation, human health risk, comparison of conventional and nonconventional technologies 79−87956
energy sources, role of health physicist in development of safe sources 78−36088
energy systems, comparative risk anal. 80−30423
energy technologies risk assessment, conventional vs. non-conventional (renewable) resources 79−52862
environmental pollution by nuclear fission products 78−85607
equipment safety in diagnostic X-ray departments 79−48346
explosion causing mixtures, Li/SO_2 cells, differential scanning calorimetry studies 79−52919
explosion hazard, electrostatic volt., capacitance and energy storage charcts. of human body 77−40954
explosive device detection using NMR techniques 79−6158
explosive materials detectors evaluation, for use in nuclear facilities 79−89451
safety continued
extracorporeal blood oxygenator safety and efficacy, review 78−77153
Exxon nuclear fuel recovery and recycling center, safety analysis 79−36389
exxon nuclear fuel recovery and recycling center facility description 79−36388
eye injury potential of propelled objects, assessment system 80−21591
fast reactor fuel cycle, safety considerations 79−36396
fatigue, failure interrelation between stress and magnitude of safety and fatigue crack *(German)* 79−32385
fatigue crack growth prediction, aircraft structures, under flight-by-flight loading 79−50651
fibrillation threshold for intracardiac catheter, vs. current flow duration and electrode area 77−37101
fibrillation threshold for intracardiac catheter as function of 60 Hz current duration and electrode area 77−86675
fire extinguishing, experience in laboratory safety course 79−48995
fissile material supervision, aspects *(German)* 78−684
fission materials nondestructive analysis development, for EURATOM (CEC) Safeguards Directorate 79−85693
fission product decay heat removal with fusion-fission hybrid mobile blanket 80−99282
fission reactor materials management, using dynamic materials accounting methods 79−85738
fission reactor processing facility, safeguards instrumentation 80−63362
fission reactors, fast breeder, using uranium-plutonium cycle, Na-cooled, technical and economic viewpoints of application *(German)* 80−99202
flash point meas. of liquid wastes for safe disposal 80−47051
flowmeters, turbine-type, made in Bulgaria, survey *(Bulgarian)* 80−6173
fracture mechanics, fundamental aspects and new developments, evaluation aspects *(Italian)* 78−34086
fuel cycle and material international safeguards, current technical issues 79−26714
fuel cycle optimization with nonproliferation objectives 80−730
fuel elements recycling and thermal re-irradiation, technical, economic and safety problems *(German)* 80−99269
fuel fabrication and reprocessing plants, Pu neutron emission checks *(French)* 79−26720
fusion power plant, vacuum outer containment, safety, T control and monitoring 78−74498
fusion power plant safety and environmental impact 77−67876
fusion reactor, JT-60, grounding system design 80−102313
fusion reactor, JT-60, grounding system pot. rise during lightning strike, anal. 80−102314
fusion reactor, mirror hybrid type, T handling systems 78−62617
fusion reactor, safety and environmental aspects 77−34454
fusion reactor, safety of superconducting fusion magnets: twelve problem areas 80−102348
fusion reactor electrotechnical component practicalities, operational safety and economics *(German)* 78−94140
fusion reactor factors *(German)* 79−13527
fusion reactor large magnet systems safety 78−770
fusion reactor LOCA accidents in Li cooled fusion blankets 78−777
fusion reactor magnetic fields, biological implications 78−768
fusion reactor second generation designs, safety anal. 78−771
fusion reactor vacuum system (Princeton TFTR), description, operation, safety 78−74497
fusion reactors, air detritiation operation, computer model and scale expt. 78−66413
fusion reactors, liquid Li, safety anal. and support facilities 80−63380
fusion reactors, missile ejection from confining magnets, kinetic energy release 78−779
fusion reactors, reliability requirements for admissible radiological hazards 78−58447
fusion reactors hazards assessment *(Czech)* 78−86681
fusion-fission hybrid blanket designs, accidental criticality 78−778
fusion-fission hybrid power reactor, blanket cooling under LOCA conditions 78−775
fusion-fission hybrid reactor blanket design accidental criticality 80−32497
Gammacell self-contained irradiators, safety programme 77−29211
GCFR with N_2O_4 coolant, power plant nuclear and chemical safety 79−30969
geologic nuclear waste disposal, pathway anal. review 79−22424
guarded double insulation, reduction of shock hazard of grounded elec. systems in hospitals 77−56497
hazardous atmospheres, max. explosion press. affected by low ambient temp. 78−44380
health physics in the Novazza (Bergamo, Italy) uranium mine *(Italian)* 79−74764
hearing protectors, attenuation-frequency charcts. meas. using cadaver ears 79−11947
hearing protectors, determination of effectiveness 79−14156
HFEF/N, equipment repair room modifications 79−45439
high intensity radiation equipment, radiation safety during operation, personnel dose 77−73601
high level radioactive waste management, safety and protection aspects *(French)* 79−26656
highly enriched U plates, assay in random driver, absorption modified multiplication effects 80−32399
HLLW, safety analysis of tank storage 80−740
hospital, radioactive, substances, Health and Safety at Work Act 80−98906
hospital critical care unit instrumentation care and servicing; book 78−69231
hospital laboratories, general aspects 80−95089
hospital radiation protection staff, Delhi, behavioural aspects 79−39527
hospital safety design, probabilistic approach, use of basic n-element configurations for safety education 77−57137
human factor studies, conf., San Francisco, USA (Oct. 1977) 78−48742
HV photovoltaic arrays, safety from high reverse voltages 80−93953
HV transmission line, electrostatic field effects on human body *(French)* 77−21562
hydrogen fuels, safety aspects of a future hydrogen technology 79−74551
IAEA safeguards, instruments and techniques for nondestructive assay 78−33302
ice, detection using surface acoustic waves 78−18129
implantable stimulation electrode, standardisation problems 77−64151

safety continued
in-situ transuranium element measurement technique for wastes associated with power reactor fuels 79−85715
incendiary sparks of minimum ignition energy, spark formation 79−10729
industrial centrifuges, vibration monitoring, safety and economic aspects 79−49218
industrial radiation safety programme for accelerators 77−83115
industrial radiography, accidental over-exposure to ^{192}Ir source 77−56472
industrial radiography radiation exposures, causes, safety training program 80−17141
intensive care instrumentation, book 77−17006
intensive care unit/coronary care unit safety 78−69252
iontophoresis device for safe elec. administration of ionised drugs 78−31965
irradiated fuel elements recycling plant design modifications and safety of used nuclear fuel during storage and disposal *(German)* 80−99219
irradiated LWR fuel, European transport experience 80−63309
irradiated nuclear fuels, passive neutron assay, burnup determination 80−32398
isotopic correlations in irradiated nuclear fuel, fissile material accounting 79−40994
laboratory instruments, survey of sources of information 79−80596
laboratory safety standards realisation 78−77879
laparoscopic surgery, bipolar sterilising forceps and uterine manipulator 77−48926
large scale nuclear facilities and reprocessing plants, international safeguards 79−26715
laser, beam diameter meas. methods survey 80−53348
laser applications for discotheque light effects, safety considerations with respect to output power and exposure time, regulations and recommendations *(German)* 80−101224
laser beam operation in surgery and treatment 78−35903
laser controlled fusion reactor, safety considerations 79−89497
laser fusion generating stations, safety, environmental effects 78−50337
laser fusion reactor, environment and safety features 78−50333
laser fusion research, safety aspects, control measures and protective eye-wear 77−40711
laser light dosimeter, health physics evaluation of operating conditions at laser installations 80−76835
laser medicine development trends 80−51198
laser radiation, calc. of max. permissible exposure levels 79−96666
laser safe operation control measures 80−9928
laser safety considerations 77−77940
laser safety eyewear, filter glasses 79−39525
lasers, basic classification concepts 79−39524
Lawrence Livermore Laboratory accelerator safety program 77−83118
line isolation monitor with adjustable alarm level for hospital elec. systems 77−56496
liquefied natural gas, safe handling, measurement system, prediction of roll-over 80−27269
LMFBR fuel preirradiation for improved proliferation resistance 79−49826
LNG, transport and storage hazards 80−45620
Loviisa-1 Nuclear Power Station, in Finland, safety during design, building, and operating stages *(Russian)* 80−106128
low inductance circuit apparatus, raised frequency current inflammability *(Russian)* 79−86626
low-level solid radwaste, regulations and guides 80−5263
LWR, radwaste solidification processes, safety aspects 80−13673
LWR and coal power stations, effects on ambient media from mining to waste disposal *(Spanish)* 77−75005
LWR fuel cycle effluent model for ENFORM system 78−94111
LWR fuel fabrication plant, Japanese national safeguards system 79−26717
LWR fuel reprocessing and mixed oxide fuel fabrication plant safety 79−26710
LWR spent fuel reprocessing plant, integrated safeguards assessment 79−89418
LWR stowaway fuel cycle effluent projections 78−94110
LWRs at Harrisburg and Mulheim-Karlich, safety systems comparison *(German)* 80−22966
magnetic safety valve 80−8966
magneto-inductive flowmeters, installation, earthing, isolation, protection against explosion *(German)* 80−64662
materials flammability testing, problems, language and scientific basis 79−5092
medical devices, safety and efficacy, legislation 77−2062
medical elec. equipment international standardisation, current problems 77−73603
medical electrical equipment, safety problems 80−56228
medical electrical safety programme on low budget, with offline inventory control 77−40821
medical electro-optics, 1980 development trends 80−85464
medical equipment, leakage currents meas. and minimising 78−11748
medical instrumentation and elec. safety, for nurses, book 78−57100
medical use of radioisotopes, regulatory controls 79−96660
metal casting workplace lighting, vision problems, Swedish report *(Swedish)* 77−77896
methane, stored energy needed to ignite by discharger from charged person 80−54063
methane gas interferometer for coal mine safety 78−44423
MHD test facility safety analysis methodology and documentation system 80−61388
microwave and RF radiation protection, American and European standards 78−80973
microwave appl., in industry, science and medicine 80−3754
microwave biological effects, book 77−90850
microwave power symposium, Monaco (1979) 80−3758
microwave radiation, emission and exposure standards 78−44619
microwave radiation safety, meas. and instrumentation 78−44618
microwave radiometric methods and the problem of forest and peat fires 80−31877
mirror fusion-fission reactor, safety 79−22461
MM-wave interaction with biologically active compounds and polar liquids 80−16707
molten fuel-coolant interaction studies, simulated reactor accident, wind-scale shock tube rig 78−58363
MOX fuel fabrication, safeguards systems alternatives 79−89474

safety continued
MPD reduction suggestion fo meet requirements of higher safety 80−85499
Na loop safety facility expts., disassembly at HFEF/N 79−45444
neutral beam accelerator electrodes, spark discharge protection, for fusion reactor 78−62609
nonionising RF and microwave radiation hazards *(French)* 80−3824
nonproliferation treaty safeguards implementation, nuclear facilities in USA 78−820
nuclear, criticality accidents at facilities processing fissile material, characts., detect. and action procedures *(French)* 78−55054
nuclear, gamma spectrometric mobile computerised analysis and data processing system 79−9959
nuclear, Integrated Safeguards Information Systems requirements 79−85681
nuclear accident phenomena, human elements *(French)* 78−57084
nuclear energy industry, impact on human health and safety 77−25508
nuclear energy systems, proliferation risk assessment 79−89384
nuclear facilities, tamper-indicating seal program development and implementation 79−85689
nuclear facilities, vital area identification, fault tree analysis appl. 79−85691
nuclear facilities in West Germany, physical protection program review 79−89450
nuclear facility, enriched uranium, diversion path analysis 79−85739
nuclear facility, large, neutron interaction anal. 79−63822
nuclear facility, Pu reactor, continuous controllable containment, West German safeguards system 79−85683
nuclear facility safeguard effectiveness computing, based on SAFE methodology 79−85674
nuclear facility safeguards meas. systems analysis controllable unit approach appl., multiple closure equations effectiveness determ. 79−85746
nuclear facility safety assessment, material control and accounting system 79−85673
nuclear fast critical facilities 79−85611
nuclear fuel, irradiated, highly radioactive, safe transportation 77−74956
nuclear fuel accountability and control, use of novel data collection and processing techniques 79−85749
nuclear fuel centre, fuel and waste facilities, safety, protection and socioeconomic aspects 78−58395
nuclear fuel cycle, safeguards implementation technology 78−86660
nuclear fuel cycle, USA policy in fuel reprocessing analysis 79−85737
nuclear fuel cycle environmental assessment methodology 78−94112
nuclear fuel cycle facility, Guard Tactics Simulation exercise 79−85742
nuclear fuel cycle facility, physical security assessment results synthesis, using decision analysis 79−85740
nuclear fuel cycle material, computerised transportation model shipment 79−85743
nuclear fuel cycle plants, accident anal., special completeness proof for licensing 80−817
nuclear fuel cycle safeguards techniques development and appl. in European Community 79−26719
nuclear fuel cycles, U enrichment and nonproliferation safeguards *(French)* 79−26698
nuclear fuel processing plant operation, critical safety criteria *(German)* 78−74440
nuclear fuel reprocessing, on-line control *(Russian)* 78−74460
nuclear fuel reprocessing plant instrumentation for internat. safeguards 78−721
nuclear fuel reprocessing plant safety aspects 79−26708
nuclear fuel storage options compared, dry, shallow pool and deep pool 79−9843
nuclear fuel transport by air, feasibility and economics 78−94154
nuclear fusion, environmental and safety aspects 78−766
nuclear fusion reactor materials, social aspects *(Dutch)* 80−106153
nuclear installations, radioactivity release, air monitoring, emergency procedures 78−70610
nuclear installations, seismotectonic map of France for antiseismic design 80−860
nuclear irradiated fuel, safe transport 77−79445
nuclear material accountability, analytical methods and laboratories, present and future 79−81047
nuclear material accounting, decision anal. 79−81049
nuclear material control and accountability system (DYMCAS), prototype terminal 79−89485
nuclear material control for safeguard purposes in Czechoslovakia, anal. methods 79−26546
nuclear material inventories, management information system, at BWR fuel fabrication plant 79−85750
nuclear material inventory differences interpretation, game theory appl. 79−85744
nuclear material safeguarding, tamper and radiation resistant instrumentation 77−61584
nuclear materials, IAEA safeguards appl., technical criteria survey 79−85678
nuclear materials, mechanisms for assuring accurate meas. 79−81048
nuclear materials, safeguards against theft or diversion 77−23213
nuclear materials, supervision in West Germany, by Euratom and IAEO *(German)* 80−18415
nuclear materials, use of US identified seals 79−85677
nuclear materials accounting, perimeter monitors 79−89509
nuclear materials accounting data analysis, dynamic 79−85684
nuclear materials dynamic control, DOE development and demonstration program 79−85745
nuclear materials management, Conf., Cincinnati, OH., USA, (June 1978) 79−85672
nuclear materials management, in U enrichment facility, based separation nozzle process 79−85747
nuclear materials security, advanced safeguards system as proliferation deterrent 79−89383
nuclear medicine department, radiation safety 80−89868
nuclear medicine laboratory, radiation safety 80−104772
nuclear plant, aircraft crash probabilities for selected plant parts 80−859
nuclear plant design, seismic response spectrum normalisation 78−50415
nuclear plant equipment response to aircraft impact 78−50416
nuclear plant fuel cycle closing, ecological problems solution *(German)* 77−54344
nuclear power, reprocessing and enrichment plants, IAEA safeguards 78−33282

safety continued
nuclear power engineering materials certification testing for safety 80−78360
nuclear power plant, fire hazard 78−50269
nuclear power plant, intrusion detection system 80−47787
nuclear power plant, occupational radiation exposure minimisation at Yankee Atomic, USA 77−18712
nuclear power plant, radiation monitoring systems, review 78−33292
nuclear power plant containment buildings, integrated leak rate testing *(Spanish)* 79−54518
nuclear power plant decommissioning problem solutions and costs *(German)* 79−89487
nuclear power plant safety systems, common mode failures, investigation *(German)* 78−694
nuclear power plant security system, American experience 80−47786
nuclear power plants, environment protection problems during construction *(French)* 80−76663
nuclear power plants, environmental studies organisation *(French)* 80−76664
nuclear power plants, hydrobiological studies, conception and data obtained *(French)* 80−76665
nuclear power plants, safeguards network anal. procedure, SNAP, appl. 80−47672
nuclear power plants, security in America 80−47785
nuclear power project, 480 V and 125/250 V auxiliary elec. unit design 77−3143
nuclear power projects, public opposition, international experience review 77−18642
nuclear power station, full scale tornado-missile impact tests 78−41876
nuclear power station, seismic anal., slab modelling 78−50414
nuclear power station accident prevention, 1300 MW nuclear reactor steam isolating valve blowdown tests *(German)* 80−22967
nuclear power station earthquake simulator 78−5681
nuclear power station protection against seism-aseismic bearings 80−857
nuclear power station response to aircraft impact 78−41875
nuclear power stations, aspects *(Russian)* 79−97885
nuclear power stations, Czechoslovak Research Institute activities *(Slovak)* 80−83188
nuclear power stations, earthquake response spectra determ. 79−97910
nuclear power stations, leakage tests, Spanish policies *(Spanish)* 80−5247
nuclear power stations, nuclear materials, safeguarding experiences *(German)* 80−611
nuclear power stations, radiation dosage determination, monitoring and control for personnel safety *(German)* 80−842
nuclear power stations, radiation safety prediction 79−45435
nuclear power stations, risk due to seismic activity in New York and New Jersey 79−8611
nuclear power stations, seismic category I building design, structural anal. 80−858
nuclear power stations, the need for evacuation to protect public safety at TMI 80−99352
nuclear power stations *(Portuguese)* 80−68844
nuclear reactor, assessment by reliability technique 77−30653
nuclear reactor, multigoal fuel cycle optimization including nonproliferation objectives 80−52764
nuclear reactor fuel reprocessing plant, technical safety rules, catalogue and classification 78−58384
nuclear reactor protective system, optimum supervision intervals and order of supervision 78−37419
nuclear reactor redundancy systems, common mode failures 80−13641
nuclear reactor spent fuel bundle absence from position in storage basket, monitor for detection 77−61511
nuclear reactor spent fuel storage vault, criticality safety determ. *(Korean)* 80−37478
nuclear research facilities, inventory verification 79−85600
nuclear safeguards, anal. chem. in nucl. fuel reprocessing 79−13505
nuclear safeguards technology, present status *(Japanese)* 79−26783
nuclear safety, national programmes, aspects 78−697
nuclear safety aspects at power and fuel cycle plants in USSR *(Russian)* 79−26709
nuclear safety exercises carried out in French industrial facilities *(French)* 78−55051
nuclear sites, workers' protection against radiation hazards 79−59267
nuclear technology, West German practice *(German)* 77−75004
nuclear waste disposal problems and safety 78−86636
nuclear waste management safety assessment, use of safety indices 79−89413
nuclear wastes as heat source 78−41838
ocean wave forecasting service, pot. benefits case study anal. 78−77357
ocular contusion injury from propelled objects, evaluation model 79−43955
offshore operations, LEO I submersible reliability and safety 77−5373
operating theatre safety fundamentals *(Japanese)* 79−2149
optical cables, LED- and laser-fed, safety aspects 78−74968
optical cables, LED- and laser-fed, safety aspects 78−74969
optical cables, minimum obs. distance 77−83955
orthopaedic implants and biomaterials, mech. testing 78−36057
pacemaker interference, 60 Hz field and current effects 78−88769
pacemaker interference, body potentials and currents from ELF elec. fields and household appliances 78−88770
pacemakers, fixed-rate type, safety of competition with intrinsic ventricular beats 77−81706
particle accelerator decommissioning, radioactive waste management 80−18720
particle accelerators, radiological safety in design and operation, American National Standard 79−89511
patient electrical safety in crit. care areas using isolated patient environment 77−40914
patient safety design, probabilistic approach by appl. of Markov chains to n-element environments 77−37106
permit-to-work certification scheme, for use in health building laboratories 80−22338
personal radiation monitor checker 79−16312
PGFR seismic risk anal. 80−99298
Philips PW 1360 X-ray diffraction tube shield, mechanical safety interlock device 78−36989
plutonium, biologically important physicochemical props. and methods of human contamination *(French)* 80−98004
PMMA, critical stress-intensity factor, determ. under mixed mode loading conditions by shadow optics 78−68868
safety continued
PNC Pu fuel and reprocessing facilities, safety aspects 79−26711
political and social decision making rel. to fracture, failure, risk anal. and safe design 78−77661
portable glove box system, HFEF/N 79−45440
powder handling, electrostatic spark hazard identification and control 80−69291
power leakage from microwave-excited light sources 78−36988
power line elec. field effect on communication line maintenance personnel 78−40353
power plants, operational danger levels, mathematical model determ. *(German)* 80−13633
pressure catheters, resist rel. to applied volt., elec. shock risk 77−40818
pressure vessel, stress concentrations around multiple windows photoelastic anal., strain gauge tests 77−72254
pressure vessels, prestressed concrete, safety and reliability 79−22412
principles underlying IAEA nuclear safety programme 80−95361
proliferation-resistant reprocessing methods 80−27792
PWR assemblies, pool-site fuel inspection and exam. techniques 80−18567
PWR fuel production, quality study *(French)* 77−3110
PWR power plant, safeguard system, diagnosis of fault conditions using fault trees 77−6549
radiation, in high-altitude air traffic 78−44620
radiation, low-level, current estimates of hazards to human populations, review 78−57043
radiation, public health aspects 78−35895
radiation, risk to health assessment 80−41124
radiation monitoring, microprocessor based systems 77−67897
radiation protection, environmental modelling 77−48878
radiation protection, safety standards for X-rays and ionising radiation 80−98146
radiation protection, US Nuclear Regulatory Commission practices for assuring worker protection 80−5367
radiation protection European regulation in EEC countries *(French)* 79−48347
radiation safety, X-ray diffraction and fluorescence anal. equipment 79−12017
radiation safety glasses, physical factors determining the utility 80−46067
radiation safety in laboratories 80−73154
radiation safety system, computerised 77−25562
radiative waste, low- and medium-level surface and concrete-lined trench storage, seven years' experience report *(French)* 77−61579
radio transmitters, VHF and UHF energy deposition in human tissue 77−73541
radioactive, high-level vitrified waste, risk anal. of repository in geologic salt formation 78−17362
radioactive fuel, nonproliferation charcts. 80−5304
radioactive I adsorption on charcoal filter, safety evaluation *(Japanese)* 78−33267
radioactive materials, IAEA regulations for safe transportation 80−63410
radioactive materials, IAEA transport information collection system, influence on improved safety measures 80−63413
radioactive materials, IAEA transport regulations, underlying radiation protection principles 80−63414
radioactive materials, international regulatory control for safe transportation 80−63411
radioactive materials, package design, construction and testing for safe transportation 80−63412
radioactive materials, risk anal. of transport using Monte Carlo and probability methods *(Norwegian)* 79−13437
radioactive materials, safe transportation, using type A, exempt and LSA packages 80−63401
radioactive materials, transportation, safety aspects 79−67968
radioactive materials transportation, safety anal. 79−63814
radioactive reprocessing, comprehensive system of major hazard control 80−818
radioactive solid waste, storage facility, radiological safety assessment 79−17995
radioactive waste, disposal by bituminisation, fire safety and explosion prevention 79−71920
radioactive waste, disposal methods in German Democratic Republic, use of abandoned salt mine 77−61574
radioactive waste, geologic isolation repositories, long-term safety assessment 79−49714
radioactive waste, high level and α-bearing, international co-operative research programmes 79−36363
radioactive waste, high-level, repository site selection, concerns of Michigan State 79−49716
radioactive waste, high-level, ultimate disposal in salt domes, waterproof geometry on safety aspect 77−61576
radioactive waste, land disposal, repository, packaging and cost estimate *(Japanese)* 78−66351
radioactive waste, long-term risk assessment of waste disposed in geologic formation 78−17361
radioactive waste, off-shore discharge *(French)* 77−18678
radioactive waste disposal *(German)* 78−54836
radioactive waste disposal into salt deposits, fault tree anal. appl. to safety assessment 78−55046
radioactive waste final disposal in asphalt products, safety evaluation *(Japanese)* 77−50254
radioactive waste geologic disposal, safety anal., functional relations of risk to input data uncertainties 80−83189
radioactive waste management, storage, disposal, safety 77−65291
radioactive waste surveillance, using real-time unfolding algorithm 79−85679
radioactivity warning symbol, design history 79−67135
radiographers, safety training 78−81961
radiography equipment safety and preventative maintenance in rural community hospitals 77−40758
radioisotope thermoelectric generator, safety programme for LES 8/9 mission 77−46412
radiological safety rules at CEGB 80−5369
radionuclide movement from hypothetical nuclear waste repository, Waste Isolation Safety Analysis Program 80−16853
radionuclide users in Israel, surveillance and accident prevention 78−57077
radiotherapy Cathetron linkages, safer coupling collar 77−73612
reactor blowdown anal., two-phase crit. flow models 77−6531

safety continued
reactor buildings safety, solid-structure interaction behaviour 79−97912
reactor fuel, inventory checks, accounting data optimal linear combinations for nonconstant loss detection 79−81057
reactor used fuel shipment, risk assessment 79−81013
reactor waste disposal in geological form., long term risk assessment 78−58387
reflection holographic portraits, diffraction efficiency and safety 80−37968
reliability and maintainability symposium, Los Angeles (1978) 78−50250
remote decontamination facility and repair station for hot-cell manipulators, Whiteshell, Canada 79−45453
reprocessing plant safety and protection anal. *(French)* 79−26713
research reactor Caramel UO_2 fuel, proliferation resistant fuel service 80−27746
research reactors, safeguards requirements for highly enriched uranium and reduced enrichments 80−22952
reverse-buckling safety discs, release pressure 78−89489
review, worldwide variation of energy production, future Hungarian energy requirements *(Hungarian)* 78−70580
RF and microwave exposure, USA occupational safety and health standards 80−3727
RF EM fields, review of effects and dosimetric data, safety standards development 80−67154
RF EM fields (300 KHz-100 GHz), human exposure safety level 80−89869
RF industrial heaters, elec. and mag. field strengths meas. 80−52175
risk anal. for Austrian nuclear power plant site *(German)* 77−65321
risk analysis methods, practical applications 80−12894
risk assessment of energy production *(Japanese)* 79−83543
road, visual perception test using liquid crystal device *(French)* 77−36930
road traffic, cost and safety aspects of quiet tyres use 77−65652
roller pumps, clinical, automatic safety shutdown 78−44720
safeguard application to Italian nuclear power plants and fuel cycle 79−26716
safety and environmental pollution *(German)* 80−63370
science and technology, importance of safety and reliability, in materials testing 78−39982
scientific apparatus, in-house design and construction 79−80595
seal, electronic, self-monitoring 79−85690
SEM laboratory, health and safety hazards 78−21295
SLAC, beam containment electronics operational experience 77−83466
sodium reactor experiment decommissioning, radiation protection 80−9432
solar concentration system health hazards 80−3492
space considerations, conf., Lisbon, Portugal (Oct. 1975) 77−25913
space frame transient analysis in large displacement 77−14955
space vehicle radioisotope power system, using Rankine conversion cycle, emergency cooling by multifoil insulation melting 79−48168
spacecraft external surfaces, conductive materials for grounding 78−45187
spent fuel assembly storage racks, dynamic anal. 80−13639
spent fuel measurements using high resolution gamma systems 80−32400
spent fuel transportation, commercial experience in US 80−63310
static electricity generation, dangers and safety precautions *(Italian)* 80−28131
statistical safety factor and Bayesian analysis in reliability engineering *(Japanese)* 79−61837
steel components, safety anal. for loading conditions 78−39979
sterilisers, ethylene oxide, evaluation of effectiveness and hazards 77−60269
structural reliability and safety, probabilistic methods 78−39978
superconducting magnet failure experience rel. to fusion reactors 77−26870
superconducting magnets for fusion reactor, safety and structural aspects 77−26874
superconducting Tokamak TF coil system, protective control features 78−62625
suppression of industrial explosions 80−31725
sweat test equipment safety improvement 79−29649
Swiss emergency organisation for nucl. and chem. accidents 78−57078
Tokamak central station fusion power reactors, potential safety 77−6562
tokamak fusion reactor, generic PSAR for TF coil system 78−58407
transthoracic intramyocardial pacing wire for emergencies 78−69254
tritium, permeation test facility at Julich, safety measures and monitoring 79−36428
tsunami, warning system based on sub-oceanic Rayleigh wave amplitudes 77−81806
tsunami risk, estimation via stochastic model 77−21685
underground nuclear waste repositories, risk assessment using reliability models 80−57898
underground solidified high-level radioactive waste retrieval system development 79−9818
US applications in obstetrics and gynecology, safety and pot. hazards, review 80−67170
US diagnostic equipment, US power and intensities produced 78−69162
US diagnostic instrument performance evaluation, work of USA AAPM and AIUM 78−69170
US equipment, review of BRH, FCC, CPSC, FDA and OSHA regulations 77−57311
UV and IR radiation effects on eyes, safety measures *(Japanese)* 78−35881
UV and IR rays, effect on skin, safety measures *(Japanese)* 78−35882
vacuum technique problems, with modern semiconductor processes *(German)* 80−86330
Venice, defences against high water and subsidence, implications of altimetry *(Italian)* 77−86740
VHF radiowave induction heating of biological tissue from portable transmitter, expt. 78−57039
volatile fission product atmospheric release from nuclear reactors and fuel reprocessing plants 79−34461
water pool spent fuel storage units, neutron anal., criticality state *(Spanish)* 80−32517
wood, load bearing capacity, and deformability, evaluation of timber structure safety *(German)* 78−39983
X-ray crystallography, absorpt. attachment for powder diffr. camera 77−41744

safety continued
X-ray locking window shutter and collimator coupling to comply with Health and Safety at Work Act 77−39505
X-ray production equipment, USA safety standard 78−29223
X-ray tubes, rotating anode, upper limitation of output, radiographical appls. 79−30631
Cs sputter source, T beam prod. 78−29684
DT fusion reactors, environmental aspects, review *(German)* 79−54599
H production and distrib., US safety regulations and standards, bibliography 80−41976
H_2 fuel, safety anal. 79−74552
He liquid, safety aspects for cryostats and storage containers 79−58730
^{125}I, procedures for safe working in labs. 79−35698
$Li/SOCl_2$ D cells, optimisation with respect to energy density, storability and safety 80−97775
LiAl/FeS batteries, principles and construction, load levelling of nuclear stations 80−21392
Pu fuel facility damage from high winds, risk anal. 80−63356
Pu inventory verification of ANL, IAEA safeguards 78−821
Pu, isotopically denatured, diversion resistance 79−89385
Pu nondestructive assay, gamma-spectrometric method 79−81068
Pu nondestructive rapid isotopic anal. gamma-ray spectrometric method 79−81069
Pu recycle and nuclear proliferation, economic analysis 80−5302
Pu, safe working, safety measures 79−41040
Pu-containing reactor fuel, safety training program 79−18053
Pu-contaminated solid waste, operational techniques for minimisation, segregation and accounting 77−61567
Pu-contaminated waste management techniques 77−61568
^{238}Pu, sources for cardiac pacemakers, manufacture and safety tests *(French)* 77−44751
^{239}Pu, use in weapons and energy prod., radiological hazards, security 77−10492
Ra storagé safe, design, safety, ease of use 78−92736
^{99m}Tc generators, comparison of weekly and biweekly systems rel. to radiation safety 77−2049
U and UF_6, mining, manufacture and purification processes, safety and waste disposal *(Spanish)* 79−63785
U enrichment plant criticality analysis *(Japanese)* 78−46156
U fuel fabrication facility, integrated US/IAEA safeguards exercise 79−85736
U isotope separation processes *(French)* 80−806
U water flooded rod lattices, effect of soluble neutron absorbers in criticality prevention 79−85725

safety systems
see also alarm systems
analogue safety data link, for Princeton Large Torus control room 78−54938
anti-collision, for cars, microwaves and non-conventional appl. survey *(Italian)* 80−13093
BWR passive containment system, LOCA safety features 79−13466
device for gamma ray source containers 78−5051
electron storage ring, SRS, press. meas. 79−63264
fission reactor safety channel system with on-line testing capability 77−65278
flame sensor-trigger device for explosion barrier in underground mines 80−52313
flood warning system, on-line, based on adaptive model, desk-top computer appl. 79−34977
hermetically sealed valve for the safety systems of a nuclear power station *(Russian)* 78−89952
Maine Yankee reactor protection system setpoint calc. 79−13479
modular instrumentation system for nuclear industry 77−67780
nuclear, time dependent unavailability anal., FRANTIC computer code 78−29588
nuclear facilities, material control and accounting systems assessment 79−85675
nuclear facilities entry-control system, computerised 79−85688
nuclear facility physical protection system, role of barriers 79−85686
nuclear fuel reprocessing plant, material diversion, probability of detection, optimisation of safeguards 77−14258
nuclear material control system simulator 79−85685
nuclear material diversion safeguards IAEA, containment and surveillance systems 79−85676
nuclear material monitoring, VACOSS electronic sealing system appl. 79−85687
nuclear material safeguards, human performance characts. 79−85741
nuclear power, human factors, safety system problems and risk assessment 80−22968
nuclear power plant safety systems, common mode failures, investigation *(German)* 78−694
nuclear power station, pressurized water, Gosgen *(German)* 79−63763
nuclear power stations, electricity supplies for safety system, German Regulation KTA 3701.1 *(German)* 80−37466
nuclear reactor safety-channel trip comparator, fail-safe logic elements 77−65277
reactor safeguard system common-mode failure analysis 78−29618
remote maintenance to comply with new legislation limiting occupational radiation exposure, in United States 80−106210
safety closure with deflector 80−53425
Shiva laser beam diagnostics 78−59037
thermal imaging with pyroelectric vidicon camera 80−86288
valves, for high and ultrahigh vacuum 79−63246
wind power plant development, low cost approach 80−61268
^4He pumping lines, low press. safety value 78−32822
T facility at Lawrence Livermore Laboratory, quality assurance of systems 77−50297

salt water conversion *see desalination*

samarium
see also nuclei with .....
abundance in HD 18474 giant star *(Spanish)* 79−25605
adsorbed on W, conc. depend. of lifetime and heat of adsorption of Sm atoms 79−69364
adsorption and absorption of $H_2(D_2)$ 77−4257
adsorption and condensation on Ir, thermal desorption mass spectra and thermionic emission meas. 79−69362
adsorption and initial stages of condensation of Sm on Ir covered with graphite monolayer 79−69366
adsorption on W foils, kinetics meas. by flux modulation method 79−69363

samarium continued
atom, coherent ground state transients, beat meas. 80−948
atom, excited state lifetimes, oscillator strengths 77−83531
atom, excited states hyperfine struct., isotope shifts, laser-RF double reson. obs. 79−41140
atom, hyperfine struct. second order effects, on isotope shifts 78−25476
atom, in inert gas matrix, pseudolocalised vibr. modes, UV/vis. spectra 78−46289
atom, keV electron impact, L X-ray prod. cross section 79−18293
atom, laser isotope separation by two step photoionisation 77−61720
atom, multiphoton ionisation by laser beam, Sm^{+} and Sm^{2+} form. 77−58093
atom, optical isotope shifts, optical heterodyne method 79−22630
atom, photoabsorpt. spectra 77−88417
atom, UV photoelectron spectra, config. interaction effects 77−50413
atom, VUV emission spectra, 5p electron excitation by electron impact 77−68007
atomic lifetime meas. by dye laser excitation 78−25465
atomic spectra, spectra, 2900 to 7100 Å relative oscill. strengths, Rozhdestvenskii hooks 77−75084
atoms, Hanle effect expt. on $4f^6 6s 6p\ ^7F_1$ level 80−43004
charged particle stopping power meas. by 100 keV proton induced X-ray emission 79−45593
crystal structure, P-T phase diagram 78−84776
decay chain expansion significance 79−9712
determination by X-ray fluorescence 78−61127
divalent surface states, photoemission meas. 78−47841
electrical resistivity, Neel temp., 15 to 300K 80−54672
electron radiation damage, elec. resistivity change rates 80−59954
film, elec. props. 80−107929
film, elec. resist. results 78−84326
film, electrical resistivity in 77 to 300K range 77−59339
film, ion plating deposition system using electron beam evaporation *(French)* 80−20802
film, XPS, 50-250 eV, 4d→4f transition and surface mixed valence 79−15588
fluoride, MF_2:Sm^{3+}, (M=Ba,Ca,Cd), far IR Stark and Zeeman splitting 77−48190
gamma-ray scattering, incoherent, total at. cross section 79−13679
inert gas:Sm, absorpt. and emission spectra, phonon sidebands 79−43021
ion recoiling into gas and vac., hyperfine field and correl. time meas. 78−66240
ions, hyperfine interactions, decoupling meas. 78−37761
isotope anomalies in Allende meteorite 78−89134
isotope separation, laser two-step photoionisation 78−46461
isotope separation by two step photoionisation method 77−58205
isotopic anomalies in Allende meteorite inclusion 79−35208
Isua supracrustal rocks, Sm-Nd isotopic investigations and implications for mantle evolution 78−36129
magnetic and structural transitions, X-ray K-line shift, 77-1000K *(Russian)* 77−4518
magnetic properties, of polycrystalline Sm with ferromag. impurities, 1.5 to 300K 77−69547
magnetoresistance, longit., at low temps. and up to 80 kG 77−55515
magnetoresistivity and elec. resist., 4.2 to 300K *(Russian)* 80−88539
metal, XPS evidence for weak s ..face divalent component 77−39808
metastable phase modification formation during quenching from molten state *(Russian)* 79−91636
Oklo natural fission reactors, migration in core sample, appl. to dating of reactions *(French)* 80−21760
oxide glasses:Sm^{3+}, optical transitions 79−61430
phase transition, low temp. *(Russian)* 79−32937
phosphate glass: UO_2^{+}, Sm^{3+}, energy transfer from UO_2^{+} to Sm^{3+} 79−78732
phosphor:Sm^{3+}, rel. band intensities in luminesc. spectra *(Russian)* 77−48238
poisoning transient anal. in fission reactors using XESAMO code *(Spanish)* 80−52749
praseodymium ethylsulphate:Sm, one-dimens. X-Y system, spin dynamics, electron spin echo meas. 80−66031
praseodymium ethylsulphate:Sm, XY system, mag. relax. and spin dynamics 79−61211
resistivity and thermopower anomalies at high temp. 78−64027
spectral emittance above 1000K 77−4211
sputtering, thermal and collisional effects influence on energy spectra 80−66370
surface, electron spectroscopy of 4f energy shift 80−2925
surface, valence change 79−56280
surface, valence transition in first atomic layer 80−70652
surface, X-ray prod. by 5 MeV/amu deuterons (oxygen ions), projectile Z depend. 80−42982
surface electronic structure, XPS study 80−55259
surface mixed valence, XPS study 80−60753
surface valence state from surface tension props. 79−95462
thermal conductivity at low temps. *(Russian)* 79−11100
transport properties, low temp., effect of mag. field 80−70679
vacuum sublimation method of prod. *(Russian)* 79−70012
valence state, mag. susceptibility expts. 78−95270
water assemblies, poisoned, thermal neutron diffusion calc., absorption discontinuity effect 78−13191
X-ray production by 9.5 to 41.8 MeV Fl ions, total L-shell cross-sections 77−85847
XPS, electronic struct. determ. for surface 80−20765
$BaBr_2$:Sm^{2+}, radiationless coupling, $4f^5 5d$ band effects, spectra 77−8627
$BaBr_2$:Sm^{2+}, spectra, ^5D states, Lauer-Fong formula and SCC model 79−15513
$BaCl_2$:Sm^{2+}, radiationless coupling, $4f^5 5d$ band effects, spectra 77−8627
$BaCl_2$:Sm^{2+}, spectra, ^5D states, Lauer-Fong formula and SCC model 79−15513
BaClF:Sm^{2+}, energy levels, optical props. 78−84631
BaClF:Sm^{2+}, radiative and radiationless transition rate meas. using tunable pulsed dye laser 77−24891
BaClF:Sm^{2+}, radiationless processes 79−33792
BaF_2:Sm^{2+}, vibronic spectra and dynamics of impurity-contaiing lattice 79−1787
$BaTiO_3$:Eu(Sm), absorption spectra, Ti^{3+} ion and Z-centre formation 77−24871
CaF_2:Eu^{2+}, Sm^{2+}, relaxed resonance acoustic phonons in vibronic anti-Stokes luminescence *(Russian)* 80−93404
CaF_2:Sm, capture of thermalised positrons by activator impurities 77−40299
samarium continued
CaF_2:Sm, charge transitions, positron annihilation exam. 78−92143
CaF_2:Sm, positron annihilation polarisation effects, electron momentum distribution 80−55225
CaF_2:Sm^{2+}, coherent population oscills. and hole burning observed using polarization spectroscopy 80−71457
CaF_2:Sm^{2+}, luminesc. spectra, vibronic wing, 2K 79−8182
CaF_2:Sm^{2+}, optical absorption and magneto-optic. props. 77−59595
CaF_2:Sm^{2+}, phonon spectrum of thermal pulses by fluorescence 79−95860
CaF_2:Sm^{2+}, pseudo-Jahn-Teller effect 79−69476
CaF_2:Sm^{2+}(Eu^{2+}), cubic crysts., vibronic spectra, induced dichroism method 77−81131
CaF_2:Sm^{3+}, VUV absorpt. spectra 80−108230
$CaSO_4$:Sm phosphors, mag. susceptibility temp. depend. 300-453K 78−52196
$CaSO_4$:Sm phosphors, X-ray induced fluorescence and phosphorescence 80−55179
$CaSO_4$:Sm phosphors, X-irrad., thermoluminesc., charge compensation effects 80−97351
$CaWO_4$:Sm^{3+}, energy transfer after red edge excitation 78−52552
CdF_2:Sm^{3+}, photoconverted, thermally stimulated relax. 80−84476
Dy-Sm, magnetic moment growth due to Sm addition *(Russian)* 80−34608
EuO:Sm, electron transition and valence state of impurities, X-ray spectroscopy and structural anal. 78−39064
EuO:Sm^{3+}, hyperfine field at Sm, TDPAC meas. 80−93215
EuS:Sm, electron transition and valence state of impurities, X-ray spectroscopy and structural anal. 78−39064
GaSb:Sm struct., thermo EMF, galvanomag. props. rel. to dopants, eutectic $Mn_{0.6}Ga_{0.4}Sb$ form. 77−15869
KCl:Sm^{2+}, spectra, ^5D states, Lauer-Fong formula and SCC model 79−15513
$KMgF_3$:Sm^{2+}, absorpt. spectra and Zeeman effect, 3000-12000 Å, 4.2-295K 79−24341
$KMgF_3$:Sm^{2+}, luminesc. spectra 4.2, 77 and 295K and Zeeman spectra, 4.2K 77−81146
LaCl:Sm, mech. for X-ray luminesc. and thermolum. 79−8170
LaF_3:Sm, cryst. field anal. of triply ionised ion spectra 80−2796
La_2O_3-Al_2O_3-SiO_2:Sm^{3+}, luminesc. selective laser excitation line narrowing 80−25434
LaOCl:Sm^{3+}, conc. quenching of X-ray and UV-excited luminescence *(Russian)* 77−55829
LiCl-KCl:Ln^{n+}, fused eutectic, electrolytic behaviour *(Japanese)* 79−16009
Na borate glass:Sm, Nd, nonradiative energy transfer from Sm^{3+}→Nd^{3+} 78−80394
$NaMgF_3$:Sm^{2+}, absorpt. spectra and Zeeman effect, 3000-12000 Å, 4.2-295K 79−24341
$NaMgF_3$:Sm^{2+}, luminesc. spectra 4.2, 77 and 295K and Zeeman spectra, 4.2K 77−81146
$POCl_3$-MCl_4:Sm^{3+} (M=Sn,Zr,Ti), splitting of Sm^{3+} near IR absorpt. bands 80−2750
$POCl_3$-$SnCl_4$, Sm^{3+} fluoresc. quenching temp. depend., near reson. interaction 79−65915
$POCl_3$-$SnCl_4$: Tb^{3+}, Sm^{3+}, lifetime and quantum yield of fluoresc. emission 77−20909
Si:Sm, implanted impurity location, Mossbauer and channelling expts. 80−39128
n-Si:Sm,P, carrier conc. and mobility, electron irrad. effects *(Russian)* 77−66168
Sm, and isotopes, hfs, laser-RF double reson. spectroscopy 80−58170
Sm I $^{144}Sm^{152}Sm$ isotope shift J depend., in ground term. 77−75101
Sm I spectrum from laser-atomic-beam spectroscopy 78−37578
Sm II, lifetimes of $^8G^0_{5/2\text{-}15/2}$ excited levels 79−3407
Sm II, spectral transition probability, 3000-7000 Å, solar abundance 79−31453
Sm II isotope shifts for $4f^6 6s$ and $4f^6 5d$ 79−67647
Sm XVI, UV spectra, 60-600 Å reson. lines 78−33455
Sm^{3+} in cubic environment, importance of T^{-5} and T^{-7} terms in spin-lattice relax. time 80−25192
Sm^{3+} in magnetically ordered Sm compounds, crystal-field effects on crossover temp. of magnetisation 79−69656
Sm^{3+} in molten $LiNO_3$-KNO_3, transition probabilities in absorpt. and fluoresc. spectra 79−50085
Sm^{3+}:NaCl(KCl), absorption spectra at 4.2 K, anal. 80−7378
Sm+$F_2(N_2O)$, chemiluminesc., absolute photon yields determ. 77−86317
Sm+H^{+}($^3He^{+}$), X-ray intensity ratios, projectile energy depend. 80−23535
Sm+N_2O, mol. beam chemiluminescence, cross section energy depend. 77−32792
SmI, laser atomic beam spectroscopy, isotope shifts, hyperfine struct., transitions 80−102468
^{A}Sm, A=144-154, charge distrib. and hyperfine splitting from muonic X-rays 79−40838
^{149}Sm polarising filter for thermal neutrons 78−54502
^{150}Sm, stopping power in Ni, (Au) 80−70284
^{152}Sm, KLM- and KLN- Auger transitions 77−18884
SrF_2:Sm^{2+}, interconfig. luminesc., spectral and kinetic characts., appls. 77−4677
SrF_2:Sm^{2+}, interconfig. luminesc. spectra, vibronic wing 79−24358
SrF_2:Sm^{2+}, pseudo-Jahn-Teller effect 79−69476
SrF_2:Sm^{2+}, spectra, ^5D states, Lauer-Fong formula and SCC model 79−15513
SrF_2:Sm^{2+}, vibronic spectra and dynamics of impurity-contaiing lattice 79−1787
$SrTiO_3$:Eu(Sm), absorption spectra, Ti^{3+} ion and Z-centre formation 77−24871
TbF_3:Sm^{3+}, induced visible emission of Sm^{3+} 80−97330
YIG:Sm^{3+}, mag. anisotropy, effect of Sm^{3+} ferromag. reson. study 80−80615
$Zn_3(BO_3)_2$:Sm^{3+}, photoluminescence obs. *(Spanish)* 79−73986
ZnO:Sm, electro- and photoluminesc. 79−83024
ZnO:Sm, electrolum. brightness, field strength and freq. depend. 80−100696
ZnO:Sm, phosphor, electrolum. and photolum. spectra 78−80421
ZnO:Sm phosphors, electrolum. 79−99946
ZnS:Ag,Sm, recomb. centre interaction, luminesc. quenching 78−10946

samarium alloys
exchange and crystal field effects on temp. depend. of Sm^{3+} magnetisation 77−8302
magnetisation of Sm^{3+} in ordered compounds, exchange and cryst. field effects 77−51890
misch metal, improvement of Al alloy 51S, for space appl. 80−55466
mischmetal-based magnets, $MM_{1-x}Sm_xCo_5$, demagnetisation, temp. depend., 175 to 425K 79−78440
Ticonal with Sm, magnetic props., phase transform. after thermomagnetic treatment 78−3155
Ag-Sm system, phase diagram, eutectic temps., microstruct. *(German)* 80−104119
Ce-Sm-Co-Fe-Cu, permanent magnet props. 79−8013
$CeMM_{0.8}Sm_{0.2}Co_5$, (MM=mischmetal), thermal props. *(German)* 77−8359
Co-Cu-Fe-Sm magnet, microstruct. exam. after ageing, TEM meas. 77−48555
Co-Mn, permanent magnetic materials 78−8426
Co-Sm, dilute, magnetic annealing effect, induced anisotropy 77−73054
Co-Sm film, magneto-optic coeff. and refr. index, ellipsometric determ. 80−71501
Co-Sm magnets, H_2 atm. sintering effect on mag. props. 77−85504
Co-Sm permanent magnet, grain alignment determ., metallographic method using eutectoid transform. of Co_5Sm 77−9003
Co-Sm-Cu, phase diagram 79−91632
Co-Sm-Gd(Ho) magnets, prep. and characterisation 77−8351
Co-Sm-Sn-$Co_{17}Sm_2$ eutectic fibre composite, coercive force 77−40084
Co_5Sm, coercive field of hard mag. materials, planar defect influence 77−24710
Co_5Sm, coercive field temp. depend. 77−8358
Co_5Sm, coercive force variation as function of annealing temp. *(Japanese)* 79−47787
Co_5Sm crystals, microstruct., homogeneous precip. and nucleation 80−104160
Co_5Sm, magnetic domains, nucleation and pinning, magneto-optical Kerr effect 80−39811
Co_5Sm sintered magnet, effect of surface conditions on mag. props. 79−28556
Cr-Sm-Pr, Sm and Pr additions and plastic deform. effects on texture *(Russian)* 77−55983
Dy-Sm, elec. resist. singularities and mag. transitions *(Russian)* 79−47075
Dy-Sm, mag. props. at low temp. in high mag. fields 79−56570
$Dy_{1-x}Sm_x$, magnetoresist. of polycryst. specimens in fields up to 44 kOe *(Russian)* 80−92880
Gd-Sm, mag. props. at low temp. in high mag. fields 79−56570
Ho-Dy-Sm, magnetic moment growth due to Sm addition *(Russian)* 80−34608
Ho-Sm, Hall effect, field and temp. depend., 4.2-150K, singularities *(Russian)* 80−29387
Ho-Sm, mag. props. at low temp. in high mag. fields 79−56570
Ho-Sm, magnetic moment growth due to Sm addition *(Russian)* 80−34608
Ho-Sm, magnetic phase diagrams, helicoid-ferromag. transform. *(Russian)* 80−50089
HoSm elec. props. in temp. range near zero to 150K *(Russian)* 79−11098
La-Sm-Au, amorphous, surface effects on Sm valence, XPS and X-ray absorption meas. 80−108325
La-Sm-Sn, dil. alloy, Kondo effect obs., supercond. transition temp. meas. 77−51837
$La_{1-x}Sm_xSn_3$, Kondo scatt. from Sm ions 77−51734
Mg-Sm, phase diagram and mech. props. *(Russian)* 80−20892
Mg-Sm, solid soln., phase diagram *(Russian)* 77−25015
$Nd_xPr_ySm_zCo_5$ permanent magnets, coercive force, low-temp. annealing influence *(Russian)* 80−39812
$(Nd_xSm_{(1-x)})_2(Co_{0.7}Fe_{0.3})_{17}$, mag. anisotropy 80−34622
Ni-Cr-Si (10, 1.8 wt.%), Zr, Hf, La or Sm alloying additions effect on oxidation resist. 77−63831
Pb-Sm, vacuum deposited supercond. films, T_c chem. comp. depend. *(Russian)* 78−19174
$Pd_{0.97}Sm_{0.03}$ dil. alloy, assist. meas. 79−19583
$Pr_{0.75}Sm_{0.25}Co_5$ magnets, struct. and props. sintering temp. depend. *(Russian)* 79−82819
$Pr_xSm_{1-x}Co_5$, magnetisation and magnetocryst. anisotropy 78−68215
$Sc_xY_{0.95-x}Sm_{0.05}$, ^{119}Eu isomer shift, at. vol. depend. 77−43915
$Sm_x(Co,M)_{17}$, (M=Fe, Mn, Cr), exchange and crystal field parameters, anisotropy meas. 77−69535
Sm-Al(Fe)(Co)(Pt), hyperfine field exam. by NMR spin echo 78−23365
Sm-Au, amorphous, surface effects on Sm valence, XPS and X-ray absorption meas. 80−108325
Sm-Co, alloy powders and sintered magnets, effect of chem. treatment on mag. props. 78−60311
Sm-Co, amorphous, plasma-sprayed, role of Ar or H_2 atm. in mag. props. and crystn., rel. to H_2 storage 80−64898
Sm-Co, decomp. kinetics when aged, X-ray mag. props. and metallography study *(Russian)* 78−56644
Sm-Co, permanent mag., O ion impact, 5.5 keV, secondary Co ion emission, magnetisation depend. *(Russian)* 78−2967
Sm-Co alloy, mag. anisotropy origin 79−38319
Sm-Co alloy magnets, operational control of residual induction, maximum mag. energy 79−15324
Sm-Co base ternary alloy, mag. props. and cryst. struct. 77−8352
Sm-Co deposit, arc plasma sprayed, crystal and micro struct. exam. 79−28248
Sm-Co ring magnets for BWO, 110 to 170 GHz, design and appl. *(German)* 80−105684
Sm-Co-Cu, with Sm_2Co_{17} struct., aged, TEM high coercivity material, TEM obs. of microstruct. 77−77073
Sm-Co-Cu permanent magnets, phase diagram 77−21106
Sm-Co-Cu-Fe, single phase 2-17 sample, hard mag. props. 77−8349
Sm-Co-Cu-Fe-Ti magnets, comp. and sintering effects on coercivity 79−15326
Sm-Co-Cu-Fe-Zr, reversible changes in coercive force and struct. state during heat treatment 400-800°C *(Russian)* 80−29574
Sm-Co-Cu-Fe-Zr magnet, production and mag. props. 77−40085
Sm-Cu phase diagram *(Russian)* 78−27477
Sm-Cu system, phase struct. investigation by X-ray diffr. *(Russian)* 80−49185
Sm-Dy (3 wt.%), electrical resistivity, Neel temp., 15 to 300K 80−54672

samarium alloys continued
Sm-Eu, dil., mag. and elec. hyperfine interac., TDPAD obs., paramag. behaviour, exchange integral 80−103908
Sm-Fe, dil., valence impurity state, inference from mag. susceptibility 78−95270
Sm-Fe-B ternary systems, phase equilibria and cryst. struct. *(Ukrainian)* 80−11626
Sm-Ga, phase diagram *(Russian)* 78−27478
Sm-Hf-Co alloy, rare-earth electron transfer 77−40028
Sm-Pr-Co, added Fe_2Sn, permanent magnets, demagnetisation curves, X-ray obs. 78−91900
Sm-Pr-Co, mag. props. and struct., comp. depend. *(Russian)* 80−20430
Sm(-Pr)-Co, sintered, cryst. phases *(Russian)* 80−39004
$Sm_{21}Ag_{79}$, amorphous, sp. ht. at low temp. 80−75780
$SmAl_2$, exchange and cryst. field effects 80−24857
$SmAl_2$, hyperfine fields, ferromagnetic coupling between rare earth spins, NMR study 80−39880
$SmAl_2$, orbital and spin polarisations of cond. electrons 80−65791
SmAu, diode sputtering, negative ion MFP 78−95641
SmAu, significance of negative ion formation in sputtering and SIMS anal. 78−72663
$SmAu_{3.6}$, ordering temps. and effective moments 78−60283
$SmAu_6$, mag. props. temp. depend. *(French)* 77−51879
$SmCO_5$ based permanent magnets, props. and cryst. orientation *(Russian)* 80−20431
$SmCO_5$, etched microparticles, Barkhausen discontinuity, nucleation, and domain wall pinning 79−87288
$SmCO_5$ magnets, sintering time effect on props. 79−95977
$Sm_{11}Cd_{45}$, cryst. struct. similarity with γ-brass and α-Mn clusters 78−75625
$Sm_{1-u}Ce_u(Co_{1-x-y-w}Fe_xCu_yCr_w)_z$, permanent mag., improved mech. props. 79−87593
$Sm_2(Co, Cu, Fe, M)_{17}$, M=Nb, V, Ta, Zr, effect of M on mag. props. 77−89978
Sm(Co, Cu) alloys, coercivity mech. 80−44862
$Sm(Co,Cu)_5$, eutectoid transform. 77−8799
$Sm(Co,Cu)_z$, precip.-hardened, mag. and metallographic props. 77−8339
$SmCo_2$, hyperfine interactions and exchange fields acting on Eu^{3+}, Mossbauer obs. 77−63338
$SmCo_5$, adsorption and desorption charact. of H_2 *(Japanese)* 77−47667
$SmCo_5$, amorphous, supermag.-ferromag. transition and directional crystallisation 80−65891
$SmCo_5$, and related alloys, nucleation and pinning at 360° domain walls 77−73042
$SmCo_5$, and $SmCo_{3.5}Cu_{1.5}$, anisotropy and coercivity, Kerr effect, magnetisation and aftereffect expts. 77−8300
$SmCo_5$ based alloys, dissociation process *(Russian)* 78−27542
$SmCo_5$ based permanent magnets with low reversible temp. coeff. 79−51814
$SmCo_5$ based solid soln., X-ray diffr. obs. of decomp. *(Russian)* 77−81264
$SmCo_5$ based ternary and quaternary permanent mag. materials with low reversible temp. coeffs. 79−82822
$SmCo_5$, Bloch wall energy determ. *(German)* 78−19271
$SmCo_5$, coercivity, random substitution of Sm by Co *(Chinese)* 77−8343
$SmCo_5$, Cu-modified, magnetisation reversal mechanism 77−8350
$SmCo_5$, domain wall nucleation sites and magnetization reversal 79−56563
$SmCo_5$, domain wall pinning rel. to coercive force 77−1561
$SmCo_5$, EXAFS and shape of K absorption discontinuity of Co 77−20955
$SmCo_5$, electronic struct., X-ray photoelectron spectra 77−20992
$SmCo_5$, exchange and cryst. field effects 80−24857
$SmCo_5$ films, struct. transformations effect on coercive force and mag. reversal *(Russian)* 80−20436
$SmCo_5$, H_2 absorption in thin film hydriding alloys 80−65238
$SmCo_5$, hard mag. props., book contrib. 80−39759
$SmCo_5$, high coercivity isotropic plasma-sprayed magnet, eutectoid decomp. 80−80568
$SmCo_5$ hydride films, mag. props. 78−68306
$SmCo_5$ hydriding kinetics, inverse over pressure effect 80−55944
$SmCo_5$, improvement of mag. domain contrast in SE-mode of SEM *(German)* 77−51920
$SmCo_5$, intrinsic coercivity losses, temp. depend. 78−95468
$SmCo_5$, intrinsic magnetic props. 79−82779
$SmCo_5$ isotropic plasma sprayed magnet, high coercivity 78−68295
$SmCo_5$, isotropic plasma-sprayed high coercivity magnet, eutectoid decomp. 80−75810
$SmCo_5$, mag. properties in low temp. range, obs. *(Russian)* 77−73050
$SmCo_5$, mag. props., effect of phase and struct. transforms. during liq.-phase sintering 79−100086
$SmCo_5$, magnetic aftereffect of H and D 79−56573
$SmCo_5$ magnetic alloys, pressed, sintering rel. to mag. props., cryst. struct. 78−60600
$SmCo_5$, magnetic anisotropy, Co contrib., ^{59}Co NMR Obs. 78−43583
$SmCo_5$, magnetic fastening for piezoelectric accelerometer 79−77035
$SmCo_5$ magnets, ageing at high temp. 80−7129
$SmCo_5$ magnets, effect of heat treatment on coercive force *(Russian)* 79−1684
$SmCo_5$ magnets, magnetisation and demagnetisation, heating effects 79−38357
$SmCo_5$, nucleation of reversed domains at Co_7Sm_2 precips. 80−75791
$SmCo_5$ permanent magnet, liq. phase sintered, hysteresis loops, ageing, temp. depend. *(Chinese)* 77−51921
$SmCo_5$, permanent magnet stability, during long-term ageing *(Chinese)* 80−55428
$SmCo_5$ permanent magnets, crystal texture effects on props. 80−100600
$SmCo_5$, polished, domain wall grooving, optical microscopy and SEM obs. 77−8334
$SmCo_5$, powder, comminution temp. effect on mag. props. 80−39819
$SmCo_5$, powder, exam. of protective preps. of organic media against oxidation 79−96220
$SmCo_5$ powder alloy, densification by cold working 77−4753
$SmCo_5$, powder prod. by electroerosion mag. props. 77−59718
$SmCo_5$ powders, orientability and texture, milling time effect 79−100168
$SmCo_5$, radial pulse magnetisation, magnetising and testing fixtures 77−8354
$SmCo_5$, remanence and energy product, X-ray method of planar orientation 77−8342

samarium alloys continued
$SmCo_5$, single cryst., grown-in dislocations and stacking faults, TEM investigation 79−19253
$SmCo_5$, single cryst. and liq. phase sintered, magnetostriction, field depend. 77−63245
$SmCo_5$ single crystals subjected to shock waves, magnetisation, creation of high-coercivity state *(Russian)* 77−66384
$SmCo_5$, single crysts., mag. props. study and role of anisotropy *(French)* 79−38356
$SmCo_5$, single-cryst. and liq. phase sintered, elastic stiffness consts., US velocity obs. 77−73066
$SmCo_5$, sintered, anisotropic thermal expansion and fracture of radially oriented toroids *(Chinese)* 80−10686
$SmCo_5$, sintered, hard mag. material, magnetisation behaviour 80−75805
$SmCo_5$, sintered, high coercivity, microstruct. and mag. props. 77−69629
$SmCo_5$, sintered, mag. after-effect, expt. and model 80−75816
$SmCo_5$, sintered, mag. props. *(German)* 77−43852
$SmCo_5$, sintered, magnetic reversal processes *(German)* 77−32216
$SmCo_5$, sintered, orientation of particle easy axes, statistical model 77−8305
$SmCo_5$ sintered alloy magnetic properties *(Russian)* 78−72369
$SmCo_5$, sintered alloy permanent magnets, temp. depend. of domain struct. *(Russian)* 77−66380
$SmCo_5$ sintered magnets, periodic struct. and coercive force *(Russian)* 79−28554
$SmCo_5$ sintered magnets, struct. and magnetic charact., sintering temp. influence *(Russian)* 79−52397
$SmCo_5$ sintered magnets, eutectoid decomp. 80−89219
$SmCo_5$, sintered permanent magnet, mag. props., 4.2-300K, fields up to 100 kOe 77−8341
$SmCo_5$, sintered permanent magnet manufacture 80−20838
$SmCo_5$, Sm_2Co_{17}, magnetisation temp. depend., exchange and cryst. field effects 77−51890
$SmCo_5$, specific heat and kinetic props. at elevated temp. *(Russian)* 79−28530
$SmCo_5$ spheres, exam. of sintering in vacuum and Ar atmospheres 78−84738
$SmCo_5$, spin polarised energy band struct., APW calc. 78−10342
$SmCo_5$, sprayed magnet, microstruct. and mag. props. between 650°c and 800°C 79−82829
$SmCo_5$, substituted alloy, low reversible temp. coeff. 78−68178
$SmCo_5$, temp. depend. of Sm^{3+} magnetisation, exchange and cryst. field effects 77−8302
$SmCo_5$, temp. depend. of Sm mag. form factor, polarized neutron expts. 79−78329
$SmCo_5$ thin film, hydride form., kinetics, mag. monitoring 80−35571
$SmCo_5$, vacuum-deposited, eutectoid decomp. *(Russian)* 77−66621
$SmCo_5$, X-ray K absorpt., chem. shift 79−91531
$SmCo_{5+x}$, Cu and Fe modified, coercive force, demagnetization curves *(Czech)* 79−42805
$SmCo_x$-Fe composite permanent magnet material, mag. props. 77−40089
Sm_2Co_{17}, coercive force depend. on annealing temp. 80−65964
Sm_2Co_7 sintered magnets, coercive force and constitution, annealing temp. depend. *(Russian)* 80−88786
Sm_xCo_y, mag. and struct. investigations of intermetallic systems 78−95440
Sm_xCo_y, mag. props. 78−43568
$Sm_2(Co_{1-x}Al_x)_{17}$ *(Russian)* 78−64202
$Sm_2Co_{17-x}Al_x$, magnetisation, Curie temp., anisotropy 77−89947
$SmCo_3B_2$, high coercive forces, ferromag. ordering and saturation moments 77−24711
$Sm(Co_{0.65}Cu_{0.35})_{5.6}$, cryst. struct. and coercive force, heat treatment effects *(Russian)* 80−44170
$Sm(Co_{0.84}Cu_{0.16})_{6.9}$, microstruct. and domain struct., mag. reversal *(Russian)* 80−20429
$Sm(Co_{0.87}Cu_{0.13})_{7.8}$, coercivity and microstruct. 79−56569
$Sm(Co_{1-x}Cu_x)_{7.8}$ alloys, coercive fields, domain wall energies, mag. and metallographic exam. 78−91897
$SmCo_{3.5}Cu_{1.5}$, mag. aftereffects, coercive mechanism, magnetisation reversal 77−69634
$SmCo_{3.5}Cu_{1.5}$, single cryst., domain wall motion and domain form. 78−39359
$SmCo_{3.5}Cu_{1.5}$, single crysts., mag. props. study and role of anisotropy *(French)* 79−38356
$SmCo_{3.5}Cu_{1.5}$, time dependent magnetisation 78−80176
$SmCo_4Cu$, domain boundaries shift, mag. reversal processes 79−87286
$SmCo_4Cu$, nonuniform comp., domain struct. and mag. reversals process *(Russian)* 79−1681
$SmCo_{4.3}Cu_{0.7}$, highly anisotropic ferromag., mag. state after large Barkhausen jump *(Russian)* 79−4699
$SmCo_{5-x}Cu_x$, giant intrinsic mag. hardness obs. 77−59432
$SmCo_{5-x}Cu_x$, giant intrinsic mag. hardness 79−91255
$SmCo_{5-x}Cu_x$ magnet alloy, metallurgical study *(Korean)* 77−8853
$SmCo_{5-x}Cu_y$, giant intrinsic magnetic hardness, high field meas. 78−68289
$Sm(Co_{0.81}Cu_{0.15}Fe_{0.04})_{6.9}$ and $Sm(Co_{0.84}Cu_{0.16})_{6.9}$ powders, mag. props. *(Russian)* 80−20434
$Sm(Co_{0.86-x}Cu_{0.14}Fe_x)_7$, permanent magnet, sintering and heat treatment effects 80−39817
$Sm_2(Co_{1-x}Fe_x)_{17}$, anisotropy consts., conc. and temp. depend. *(Russian)* 78−64202
$Sm_2(Co_{1-x}Fe_x)_{17}$, magnetocryst. anisotropy, Tb, Mn or Cr substituent effects 77−8297
$Sm(Co_{0.85}Fe_{0.05}Cu_{0.10})_z$, coercive force meas. 77−4530
$Sm(CoFeCuMn)_7$, coercive force and anisotropy temp. depend. 78−68297
$Sm_2(Co_{0.8}Fe_{0.14}Mn_{0.04}Cr_{0.02})_{17}$, sintered, hard mag. props. 77−8340
Sm_3Co_3Ga, crystal struct., X-ray determ. *(Russian)* 79−27951
$Sm_2(Co_{1-x}M_x)_{17}$, bulk magnetisation and magnetocryst. anisotropy, interpretation 77−40055
$Sm_2(Co_{1-x}M_x)_{17}$, magnetocryst. anisotropy 77−40054
$Sm_2Co_{17-x}M_x$, M=Cr, Ni, effect of substitution on mag. props. 79−78363
$SmCo_2Ni_3$-Y(Pr)(Gd)(Tb)(Er), giant intrinsic magnetic hardness 78−56347
$SmCo_{2.5}Ni_{2.5}$, mag. after effect *(Russian)* 78−6544
$SmCo_{5-x}Ni_x$, giant intrinsic mag. hardness, temp. and time depend. 77−69627
$SmCo_{5-x}Ni_x$, giant intrinsic magnetic hardness, high field meas. 78−68289
$SmCo_{5-x}Ni_x$, giant intrinsic magnetic hardness analysis 78−88146

samarium alloys continued
$SmCo_{5c}Ni_{5-5C}$, exchange fluctuations and giant intrinsic mag. hardness 78−56310
$Sm_2Co_{17-x}Ni_x$, effect of Ni on mag. props. 78−68296
$SmCu_5$, X-ray K absorpt., chem. shift 79−91531
$SmCu_4Ag$, mag. props. and cryst. struct. 77−20562
$Sm_2Cu_{1.6}Zr_{0.16}Fe_{3.3}Co_{12}$, enhancement of mag. props. 79−82825
$Sm_xDy_{1-x}Co_5$, temp. compensated magnetic material, mag. and struct. characterisation 78−68177
$Sm_xEr_{1-x}Co_5$, temp. compensated magnetic material, mag. and struct. characterisation 78−68177
$SmFe_2$, ferromagnetic-ferrimag. cpds., mean field exchange consts., Stoner itinerant model calcs. 80−50084
$SmFe_2$, highly magnetostrictive props. 77−12180
$SmFe_2$, hyperfine interactions and exchange fields acting on Eu^{3+}, Mossbauer obs. 77−63338
$SmFe_2$ powder, mag. and hysteresis props. rel. to high anisotropy *(Russian)* 79−42800
$SmFe_2$, spontaneous magnetoelastic distortion, X-ray diffr. expts. 77−63253
$SmFe_3$ and Sm_6Fe_{23}, magnetostriction, room temp. to 80K 80−65993
$SmFe_4Al_8$, mag. props. 78−52250
SmGa, ferromag., mag. props., 4.2 to 350K 77−63230
$Sm_{1-x}Gd_xAl_2$, hyperfine fields, ferromagnetic coupling between rare earth spins, NMR study 80−39880
$Sm_{2-x}Gd_xCo_{17-y}Mn_y$, saturation magnetisation and anisotropy field temp. depend., suitability for microwave/millimetre wave TWT 79−82824
$Sm_{11}Hg_{45}$, cryst. struct. determ. 79−77555
Sm_2In, mag. props., 4.2 to 270K 79−56512
Sm_3Ir, X-ray cryst. struct. determ., isotypic compound types 79−69057
Sm_5Ir_2, cryst. struct. 80−96473
$Sm_{1-x}La_xS$, electron struct., lattice consts., X-ray spectral study *(Russian)* 80−100432
Sm_2M_{17}, sintered magnet, hard mag. props. optimisation 77−8340
$Sm_{1-w}MM_w(Co_{1-x-y}Cu_xFe)_z$, (MM-mischmetal), mag. meas. and metallographic exam. 77−56119
$Sm_6Mn_{23-x}Fe_x$, magnetic behaviour, temp. and comp. depend. 80−93090
$Sm_{1-x}Nd_xCo_5$ alloys, magnetisation, magnetocrystalline anisotropy, 4.2 to 280K 78−91863
$Sm_xNd_{1-x}Co_5$ powders, mag. props. *(Russian)* 79−51812
$SmNi_2$, hyperfine interactions and exchange fields acting on Eu^{3+}, Mossbauer obs. 77−63338
$SmNi_{5-x}Cu_x$, giant intrinsic mag. hardness due to randomised cryst. field interactions 78−68208
$SmNi_4M$, M=Fe, Cu, Al, intrinsic mag. hardness 77−85506
$Sm_{10}Pd_{21}$, X-ray cryst. struct. anal. 79−99118
$Sm_{0.5}Pr_{0.5}Co_5$, sintered alloy permanent magnets, temp. depend. of domain struct. *(Russian)* 77−66380
$Sm_{0.5}Pr_{0.5}Co_5$ sintered magnets, periodic struct. and coercive force *(Russian)* 79−28554
$Sm_{1-x}Pr_xCo_5$ single crystals, magnetocryst. anisotropy and stepwise mag. reversals *(Russian)* 77−66291
$Sm_{1-x}R_xCo_5$ (R=Y, La, Ce, Nd), mag. props., domain boundary pinning on statistical conc. heterogeneities *(Russian)* 79−99728
$Sm_{0.6}R_{0.4-x}M_xCo_5$ (R=Gd, Dy, M=Pr, Nd), temp. coeff. of magnetisation 80−34688
Sm_3Rh_2, structure determ., rhombohedral Er_3Ni_2 type 77−80443
$SmSn_3$, NMR Knight shift, extension to low temp. 77−20735
$Sm_xTb_{1-x}Co_5$, temp. compensated magnetic material, mag. and struct. characterisation 78−68177
SmZn, ferromag., cond. band antiparallel polarisation exceeding 4f moment 80−60207
SmZn, unusual form factor, polarised neutron scatt. 79−99684
$Sm_{0.91}Zr_{0.09}(Co_{0.68}Cu_{0.10}Fe_{0.22})_{6.7}$, alloy permanent magnet, coercive force *(Russian)* 80−65966
$SnCo_5$, magnetisation and cohesive strength 77−55688
Tb-Sm *(Russian)* 80−34608
V-Sm, vacuum deposited supercond. films, T_c chem. comp. depend. *(Russian)* 78−19174
$Y_2Co_{17-x}Ni_x$, effect of Ni or mag. props. 78−68296

samarium compounds
see also samarium alloys
chalcogenide, valence fluctuations 78−67985
chalcogenides, metal-dielectric phase transitions involving valence changes *(Russian)* 79−51489
complex, mono-, di-, tri-glycolate, IR absorpt. spectra, vibr. freq. and co-ordination number 78−58684
LPE growth, saturation magnetisation, collapse field, bubble diameter 78−95703
magnetisation of Sm^{3+} in ordered compounds, exchange and cryst. field effects 77−51890
mixed valence, metals or small gap insulators, two-band Hubbard Hamiltonian 80−34399
monochalcogenides, local effects and valence transitions 79−51533
monochalcogenides, semicond.-metal phase transition 79−47017
monochalcogenides, valence related optical and other studies, review 78−31215
monochalcogenides doped with Nd, Gd, Eu, electronic phase transition, semicond.-metal transition, X-ray shifts 77−28116
oxalate, IR and Raman spectra exam. *(French)* 78−48159
phthalocyanine solutions, bleaching by ruby laser beam 78−30030
SmS film, metallic, interpretation of optical absorption spectrum 78−27344
$(YSmEuCa)_3(FeGe)_5O_{12}$, garnet film, ion implanted, bubble domain props. 78−88152
Al_2O_3-Sm_2O_3, phase diagram at high temps. *(Japanese)* 78−19732
Al_2O_3-Sm_2O_3, phase diagram at high temp. *(Japanese)* 78−92253
$Ba_{1-x}Sm_xB_6$, prep., elec. cond. and thermoelec. props. 80−49697
$Ba_{1-x}Sm_xS$, electron config. of Sm ions, X-ray L-absorpt. spectroscopy 80−60715
Bi_2O_3-Sm_2O_3 eutectoid system, isothermal deformation 77−63625
CaB_6-SmB_6, mag. props., comp. depend. 80−50034
CaB_6-SmB_6 system complex borides, prep. and props. 78−52703
$Ca_2Nb_2O_7$-Sm_3NbO_7 system, phase equilib. 80−20907
$Ca_{1-x}Sm_xF_{2+x}$, luminesc. expt. suggesting Sm^{3+} ion pairing 80−76065
$Ca_{1-x}Sm_xS$, electron config. of Sm ions, X-ray L-absorpt. spectroscopy 80−60715
CdF_3:SmF_2 films, electroluminesc. meas. *(French)* 79−11471
$(ErSm)FeO_3$, spin reorientation, Faraday rot. meas. 77−8547
$EuCl_3$, coord. in aq. Cl^- soln., X-ray diffr. obs. 80−92445

samarium compounds continued
$Eu_{0.98}Sm_{0.02}O$, ferromag. semicond., elec. cond. meas. 80 to 370K, press. effect to 20 kbar 77−51751
$Eu_{1-x}Sm_xO$, ferromag. semiconductor with elevated Curie temp. 77−51903
$Eu_{1-x}Sm_xO$, mag. semicond., thermodynamics of mag. quasimols. 78−19266
$EuSm_2S_4$, mag. props. 78−68237
$Eu_{1-x}Sm_xS$, ESR, exchange interaction, susceptibility, elec. cond., thermoelectric power 80−93174
$Eu_{1-x}Sm_xS$, electron config. of Sm ions, X-ray L-absorpt. spectroscopy 80−60715
$Eu_{1-x}Sm_xS$, electronic transition in Sm impurity ions, rel. to exchange interactions, L absorpt. spectra 77−59644
GaS-SmS system, phase diagram 79−78939
HfO_2-Sm_2O_3, X-ray diffr. obs. of phase relations 79−61566
HfO_2-Sm_2O_3 solid solns., prep., crystn. 78−42909
$KSm(PO_3)_4$, cryst. struct. 77−43188
La-Sm-Lu iron garnet film grown as NdGaG substrates, mag. props. 80−44888
LaB_6, surface (100), atomic struct., angle-resolved XPS, LEED and ISS investigation 80−10765
LaB_6-SmB_6 exam. of secondary ion-ion emission, due to bombardment by 8 keV Ar ions 79−33882
$(LaLuSm)_3(GaFe)_5O_{12}$ bubble garnet film, coercivity 79−78459
$La_{0.58}Sm_{0.42}B_6$, FIM study 80−71578
$La_xSm_{1-x}B_6$ solid solns., mag. susceptibility meas. *(Russian)* 79−28501
$NaY_{1-x}Sm_xF_4$, luminesc. expt. suggesting Sm^{3+} ion pairing 80−76065
$Pb_{1-\alpha x}Sm_xTiO_{3+x(1.5-\alpha)}$, permittivity as function of temp. 79−33586
SMS, band struct. and semicond. metal phase transition 80−80180
$(Sm,Er)(Ga,Fe)_5O_{12}$, LPE, non-grooved film, thermomag. writing 78−76278
$(Sm,Lu)_3Fe_5O_{12}$, submicron bubble films on rare earth-Ga garnet substrates, prep. and mag. props. 78−91909
$(Sm,Y)_3(Fe,Ga)_5O_{12}$, epitaxial mag. layer, LPE, growth rotation rate, effect on props. 78−56053
Sm chalcogenides, semiconductor-metal transition, extended Felicov-Kimball model calcs. 80−70616
Sm complex, with ortho-phenanthroline and $\alpha\alpha'$-dipyridyl tris-trifluoroacetate, absorption spectra 79−98113
Sm-Cr-B system, phase equil. at 800°C, boride lattice parameters *(Russian)* 78−31388
Sm-H, phase equilibria 80−66492
Sm-S system, L-X-rays absorpt. spectroscopy, conc. of ions with various numbers of f electrons 77−28646
Sm-YIG garnets, implanted and Permalloy coated, comparison between planar domain walls in bubbles 77−85520
Sm_2ASe_5, A=Ge, Sn, diffuse refl. spectra and band gaps 79−51963
$SmAl_3[BO_3]_4$, thermal stability, X-ray struct. anal., refractive indices 79−4297
SmAs, low temp. props. 79−28528
SmB_2, high press. synthesis 78−18608
SmB_4, antiferromag. props. *(French)* 77−20566
SmB_4, mag. and elec. props., metallic character 80−20386
SmB_6, ^{11}B nucl. quadrupole interaction, NMR meas. 80−2660
SmB_6 (001) surface, azimuthal anisotropy in low-energy ion scatt. 79−28875
SmB_6, crystal preparation, elec. resistance, phase transitions 80−97427
SmB_6, f-d hybridisation, optic phonon anomalies 78−92080
SmB_6, FIM study 80−71578
SmB_6, field emission patterns and emission characts. *(Japanese)* 77−85900
SmB_6 film, prep. by electron beam evaporation, and optical and elec. props. 80−20793
SmB_6 films, crystn., struct. and elec. resist. 77−63559
SmB_6, intermediate valence, ^{11}B NMR study 80−93193
SmB_6, metal insulator transition, cond. processes 80−96787
SmB_6, mixed valence cpd., EPR and heat capacity obs., metal-semicond. behaviour 80−20456
SmB_6, mixed valence state, conduction band struct. 80−103624
SmB_6, mixed valent, DC transport props., metallic or insulating props. 78−68029
SmB_6, mixed valent, large low-temp. Hall effect and resist. 80−39611
SmB_6, mixed valent semicond., transport props. and electonic struct., review 80−96877
SmB_6, resistivity press. variation, lattice consts. 80−100456
SmB_6, specific heat anomalies 80−34199
SmB_6, surface mixed valence, XPS study 80−60753
SmB_6, thermophys. props., 700 to 1200K 79−37850
SmB_6, valence fluctuating state, sp. ht. 80−20127
SmB_6, valence fluctuation system, ground state and elementary excitations, Anderson lattice model Hamiltonian, dense Kondo problem 80−54656
SmB_6, valence mixed state, Kondo lattice, Anderson localisation models *(Japanese)* 78−51945
SmB_6, valence mixing, XPS 77−21000
SmB_6, work function, thermionic and field emission retarding pot. meas. 77−90233
SmB_6, work functions from thermionic and field emission retarding pot. methods 79−65537
SmB_6, XPS of 4f-levels, Sm^{2+}/Sm^{3+} valence ratio 77−63537
SmB_6:$Gd^{3+}(Eu^{2+})$, mixed valence compound, ESR g-shifts and linewidths 78−48035
$SmB_4(B_6)$, growth by soln. method, struct. and mech. props. 80−16168
$Sm(BH_4)_3$, synthesis from chloride salts and $NaBH_4$ in tetrahydrofuran 80−30222
$Sm(BO_2)_3$, single cryst., IR absorpt. spectra 80−34903
$Sm_{1-x}B_xS$, valence transition induced by alloying 80−96829
SmBi, low temp. props. 79−28528
SmBi, thermal expansion, 20-800°C 79−14942
Sm_4Bi_3, mixed valence system, X-ray absorption spectroscopic study 80−80906
Sm_4Bi_3, press. induced valence instability, elec. resist. transition 78−95317
Sm_4Bi_3, press.-induced valence instability 80−20261
$SmBiTe_3$, prep., elec. props., and crystallographic date 80−59981
SmCaGe garnet LPE bubble film, coercivity, thickness depend. 78−68324
$Sm_{1-x}Ca_xS$, XPS, electronic struct. excitonic effects, insulator to metal transition 78−43988
$SmCl_2$, mag. props., 77-292K 78−52197
$SmCl_3$, coord. in aq. Cl^- soln., X-ray diffr. obs. 80−92445
samarium compounds continued
$SmCl_3$, heat capacity and Schottky anomaly, 5 to 350K, entropy 77−47588
$SmCl_3$, photoacoustic spectra, spectrometer sample cell design investig. 77−74520
$Sm(ClO_4)_3$, osmotic coeffs. 80−45556
$SmCl_3.6H_2O$:Gd^{3+}, X-ray band EPR lines, exact anal. using intensity operator 80−20448
$SmCo_5$, heat treated, coercive force exam. 78−68298
$SmCo_5$, mag. domains structure rel. to crystal defects, electron microscopy 80−103856
$SmCo_5$ magnets for mini-orange spectrom. 78−58531
$SmCo_5$ permanent magnets for accelerators 79−31273
$SmCo_5$ permanent magnets, free suspension in const. mag. field with aid of pyrolytic graphite 80−101807
$SmCrO_3$, spin reorientation phase transition, second order nature 77−80950
$SmCrOS_2$, single cryst. X-ray diffr. struct. determ. *(French)* 79−23581
$Sm_8Cr_2Si_6N_2O_{24}$, apatite-like struct. study *(French)* 77−27854
Sm_2CuO_4, catalytic props., mag. and elec. props. 79−66350
Sm_2CuO_4, magnetic properties obs. 80−70937
$Sm_{0.7}Er_{0.3}FeO_3$ spin reorientation photomagnetic motor 78−2695
SmF, vaporisation, sublimation, Knudsen effusion method 80−6508
SmF_2, thermal props. *(German)* 80−81355
SmF_2-SmF_3 system, four new compounds Sm_mF_{2m+5}, X-ray powder patterns, lattice parameters *(German)* 78−42999
SmF_3, ^{19}F spin-lattice relax. and mag. couplings 79−65753
SmFX mixed halides, synthesis and lattice parameters 78−30594
$SmFeO_3$, HF susceptibility, crit. divergence in spin reorientation temp. region *(Japanese)* 77−43836
$SmFeO_3$, magnetisation direction angle meas. in spin reorientation region 77−26366
$SmFeO_3$, magnetostriction meas. in spin reorientation region 78−2721
$SmFeO_3$, orthoferrite, anisotropy of Faraday rotation 79−61341
$SmFeO_3$, Raman scatt. from magnons, anisotropy consts. determ. 80−66178
$Sm_3Fe_5O_{12}$, spin reorientational phase transitions *(Russian)* 78−39349
$Sm_3Fe_5O_{12}$, spin-reorientation phase transition, NMR spectra and anisotropy consts. meas. 77−28458
SmGa garnet film, scratch-modified mag. domain patterns 78−48007
$Sm_2Ga_2BeO_7$, melilite struct., synthesis 77−81236
$Sm_3Ga_5O_{12}$, elastic and thermoelastic consts., US meas. *(German)* 77−59061
$Sm_3Ga_5O_{12}$, garnet-perovskite transform 80−15239
$Sm_{0.8}Gd_{0.2}S$, low temp. phase transition, X-ray diffr. expts., 110-293K 77−59115
$Sm_{0.8}Gd_{0.2}S$, single cryst., fracture stresses meas. 77−31718
$Sm_{0.8}Gd_{0.2}S$, valence transition, positron annihilation study 80−15454
$Sm_{0.85}Gd_{0.15}S$, metal-semicond. transition, X-ray diffr. obs. 90-473K 79−95333
$Sm_{1-x}Gd_xS$ (x=0.15 to 0.18), magnetic susceptibility meas., phase transition 77−63071
$Sm_{1-x}Gd_xS$, calorimetric exam. of metal-semiconductor transition 78−18967
$Sm_{1-x}Gd_xS$, electron mechanism of high temp. phase transform., X-ray K-line shift obs. *(Russian)* 77−89704
$Sm_{1-x}Gd_xS$, metal-insulator transition, induced by temp. and press. *(Japanese)* 79−51488
$Sm_{1-x}Gd_xS$, metal-semicond. isomorphous transition curve, low temp. crit. point, lattice parameter changes 79−95334
$Sm_{1-x}Gd_xS$, phase transition temp. depression by mag. field, hybridisation 77−62828
$Sm_{1-x}Gd_xS$, press. induced electronic transitions 78−68058
$Sm_{1-x}Gd_xS$, resistivity investig. of metal-semicond. transition, press. effects 77−62829
$Sm_{1-x}Gd_xS$ system, equilib. of isomorphous phases and crit. point 78−34772
$Sm_{1-x}Gd_xS$ system, semicond. to metallic isomorphous phase transition mechanism 80−2338
$Sm_{1-x}Gd_xS$, XPS, electronic struct. excitonic effects, insulator to metal transition 78−43988
$(Sm_{1-x}Gd_x)_3S_4$, mixed valence compound, elec. cond. transition 80−70777
$Sm_4Ge_3O_9(OH_6)$, cryst. struct. 78−14330
Sm_2GeSe_5, elec. props., 300 to 1100K 79−51585
$SmH_{2.2.84}$, low-temp. sp. ht., mag., elec., and cryst. field splitting effects 80−49379
SmH_2, low temp. sp.ht., antiferromag. ordering and cryst. field splitting effects 78−84439
$SmH_{2.84}$, sp. ht., second-order phase and cryst. field splitting effects 79−87279
SmH_x [x=2.78, 2.85, 2.91], electrical resistance anomalies at high pressures 80−29381
SmI, Zeeman coherence, transient and stationary, polarisation spectroscopy 80−58212
SmIG, hysteresis in spin-orientation phase transitions 79−73761
SmIG, mag. phase transitions, Mossbauer spectroscopy obs. 80−80509
Sm_3InS_6, X-ray struct. determ. *(French)* 77−80453
$Sm_{0.8}La_{0.2}AlO_3$, high temp. Raman spectra, phase transition 79−61367
$Sm_{1-x}La_xB_6$, valence transition, lattice parameter and mag. susceptibility meas. 80−59929
$Sm_xLa_{1-x}B_6$, solid solns., exam. of structure, elec. props. 80−39290
$Sm_{1-x}La_xS$, mag. suscept., moment, impurity effects, indirect exchange interaction 78−68147
$Sm_{1-x}La_xS$, magnetoresist. in semicond. and metallic phases 80−96914
$Sm_{1-x}La_xS$, press.-induced semicond.-metal transition, refl. and lattice compression meas. 77−62826
$Sm_{1-x}La_xS$, valence transitions, theoretical model 79−69474
$(SmLu)_3(FeAl)_5O_{12}$, film epitaxial growth on $Gd_3Ga_5O_{12}$ substrate, mag. props. lattice mismatch 80−65402
$Sm_{0.3}Lu_{0.2}Tm_{0.2}Y_{1.45}Ca_{0.85}Fe_{4.15}Ge_{0.85}O_{12}$, LPE growth, saturation magnetisation, collapse field, bubble diameter 78−95703
$(SmLuYCa)_3(FeGe)_5O_{12}$ film, ion implant profile 79−78477
$Sm_{0.5}M_{0.5}CoO_3$, (M=Ca, Sr, Ba), catalytic props. 80−66875
$Sm_{1-x}M_xS$, M=Eu,Ca,Yb, valence transition under high press. 79−73551
$Sm_{1-x}M_xS$, M=transition metal, valence charges, band struct. 80−20131
$Sm_2Mg_3(NO_3)_{12}.24H_2O$:$Mn^{2+}$, EPR spectra, 77-298K 79−15342
Sm_2MoO_5, cryst. struct., IR spectra, elec. and mag. props. 80−33954
SmN, form. conditions 80−101019

samarium compounds continued
SmN, magnetic props., neutron diffr. and mag. susceptibility meas. 80−50036
SmN, miscibility with UC *(German)* 80−96654
SmN, vaporization enthalpy, Knudsen cell vaporization of rare earth nitrides 79−10936
$Sm(NO_3)_3$, osmotic coeffs. 80−45556
$SmNbO_4$-$CaWO_4$, phase transitions of fergusonite-scheelite *(French)* 80−19942
Sm_3NbO_7, grain growth kinetics 77−85969
$Sm_{1-x}Nd_xSe$, Nd substitution effect on lattice const., resist., and colour 79−56763
$Sm_3Ni_6Ga_2$, X-ray struct. determ. *(Russian)* 79−27959
SmO, cryst. field parameters due to $4f^{N-1}5D$ configs. 80−80230
SmO, dissoc. energy, mass spectrometric determ., rel. to EuO 77−58199
SmO film, new reduced variant due to annealing 77−89660
SmO, intermediate valence state *(French)* 80−20132
SmO, mag. props., lattice consts., and X-ray absorpt. spectra 80−44798
Sm_2O_3, 'monoxide' film reidentified as sesquioxide formed by oxidation by hydride 79−19474
Sm_2O_3, B-type monoclinic, DC(AC) elec. cond., thermoelectric power, dielectric const., temp. depends. 80−59980
C-Sm_2O_3, cryst. struct., electron diffr. 77−31650
Sm_2O_3, elec. cond., thermoelec. power, dielectric const. 79−69763
Sm_2O_3, from reactive evaporation, struct. and polymorphic transform. 79−51441
Sm_2O_3, isotopically enriched target preparation using electron gun 80−23226
Sm_2O_3, microhardness anisotropy of single cryst. *(French)* 77−52489
Sm_2O_3, polymorphic transitions rel. to $Sm_2Ti_2O_7$ form. 79−11606
Sm_2O_3, reaction with liq. Li and liq. Li-N 79−66276
Sm_2O_3, surface step thickness measurement 80−103555
Sm_2O_3-Ga_2O_3 system, garnet-perovskite transform., phase diagram relationships 80−97460
Sm_2O_3-HfO_2, kinetics of initial stages of formation of cpds. 77−48617
Sm_xO_y film, struct. electron microscope and diffr. obs. 79−11028
$Sm(OH)_3$, mol., XPES, satellite phenomena 79−27035
$SmOs_4Sb_{12}$, prep. and cryst. struct. 80−100211
SmP, low temp. props. 79−28528
Sm_3PO_7, IR and Raman spectra, vibr. assignments, cryst. struct. characts. 80−97258
$Sm_{1-x}R_x^{3+}S$, (R is rare earth metal), semicond.-metal phase transition 79−47017
Sm_3ReO_8, cryst. struct. determ. *(French)* 77−4073
$SmRh_4B_4$, coexistence of supercond. and antiferromag. order 80−11140
$SmRh_4B_4$, cryst. struct., X-ray diffr. 77−89423
$SmRh_4B_4$, high supercond. transition temp. 77−89893
$SmRh_4B_4$, mag. ordered, persistence of supercond. 80−54834
SmS (001) surface, mixed valency and phase transitions 80−39658
SmS (100), resonant photoemission 79−28895
SmS, and $Sm_{0.8}Tb_{0.2}S$, resistivity and thermopower 80−20260
SmS, crit. point for isostructural black to metallic phase transition, thermoelec. power meas. 78−60174
SmS, cryst. struct. in homogeneity region 78−91334
SmS, Debye temps., vibr. amplitudes, X-ray diffr. determ. 78−2222
SmS, Debye-Waller factor, X-ray diffr. meas. 77−11659
SmS, defect struct., precipitate colonies, dislocation loops, TEM obs. 80−44214
SmS, divalent and trivalent ion doped, electronic struct., Mossbauer spectroscopy 78−39022
SmS, electron mechanism of high temp. phase transform., X-ray K-line shift obs. *(Russian)* 77−89704
SmS, electron-phonon interaction, lattice dynamical model 80−96610
SmS, electronic config., Mossbauer spectra meas. 77−16228
SmS, electronic phase transition, mechanism, trivalent metal impurity effects 80−49604
SmS, energy of metal-semicond. transition, optical and DSC expts. 77−62830
SmS, energy of metal-semicond. phase transition and threshold recording energy density 79−28386
SmS, f-d hybridisation, valence fluctuation and phonon spectrum, Raman scatt. expts. 78−60464
SmS, f-d hybridisation, optic phonon anomalies 78−92080
SmS film, laser beam threshold recording energy density meas. method 78−5520
SmS, film, laser generation of US using metal-insulator transition 79−90734
SmS film, semicond. and metallic modifications, elec. props. 77−32098
SmS film amplitude-phase hologram recording *(Russian)* 79−94192
SmS film for holographic storage, laser-induced semicond.-metal transition 77−88676
SmS, first-order transition from semiconducting to metallic state 78−52040
SmS, Hall effect near semicond.-metal transition 77−62968
SmS, high-pressure mixed-valence phase, diagram and electronic entropy, neutron diffr. obs. 79−33267
SmS, induced magnetic form factor, polarised neutron studies 80−25078
SmS, intermediate valence compound, pressure-temperature phase diagram 79−28283
SmS, intermediate valency, three-site model 79−78047
SmS intermediate valence, low lying states 80−96826
SmS, LO phonon freq. softening in semicond. and metallic phases 80−96619
SmS, mag. susceptibility in semicond. phase, in homogeneity region 79−28502
SmS, mechanical polishing, stabilisation mechanism for metallic phase on surface 78−60015
SmS, metal insulator transition, cond. processes 80−96787
SmS, metallic, optical refl. investig. of valence fluctuations 77−63428
SmS, metallic, thermal modulation of reflectivity, 1.2-3.8 eV 79−99909
SmS, metallic, transmission, refl. and absorpt. spectra 78−19587
SmS, metallic phase, compressibility anomalous behaviour 80−29114
SmS, mixed valence, induced mag. form factor 78−68163
SmS, mixed valence states at surface 77−20398
SmS, mixed valent, DC transport props., metallic or insulating props. 78−68029
SmS, nonorthogonal orbitals in intermediate valence 78−43323
SmS, optical props. and electronic struct., Kramers-Kronig model anal. 79−69859
SmS, phase diagram in p-T plane, theory 79−28278
SmS, phonon anomalies and electron-lattice coupling 80−39490

samarium compounds continued
SmS, physical and physicochem. props., review 80−96875
SmS, press. effect on lattice parameter, mag. susceptibility, and reflectivity 79−56272
SmS, relative intensity of optical bands calc. 77−8603
SmS, semicond., anomalously high magnetoresist., Hall coeff. and elec. resist. meas. 78−10479
SmS, semicond., photocond. meas. 78−60164
SmS, semicond. and metallic phases, electronic struct., optical props. 0.03 to 12 eV 77−28594
SmS, semicond. phase, cond. band model, elec. and thermal cond. meas. 77−39854
SmS, semicond. thin film, absorpt. and refl. spectra, fine struct., cond. band extremum 79−69897
SmS, semicond.-metal transition, phase struct. determ. 78−91618
SmS, semicond.-metal transition, cond. band type, deform. pot. determ. 79−69417
SmS, semiconducting, piezoresistance at 80K 80−59990
SmS, single cryst., fracture stresses meas. 77−31718
SmS, single crystals, crystallographic slip 78−18659
SmS, thermal expansion meas. using galvanomagnetic dilatometer 78−87797
SmS, trivalent rare earth substituted, stability of Sm^{2+} 80−65508
SmS type cpd., fd mixing effect on impurity levels, local valence transition 80−24831
SmS type semiconductors, electronic struct., influence of point defects 80−70650
SmS, valence fluctuation phenomena 80−24800
SmS, valence fluctuation system, ground state and elementary excitations, Anderson lattice model Hamiltonian, dense Kondo problem 80−54656
SmS, valence transition, positron annihilation study 80−15454
SmS, valence transition, entropy and phase diagram 80−59877
SmS, valence transition, two band model 80−65507
SmS, vol. changes at press. up to 20 kbar 78−71791
SmS:Eu, excited-state exchange interactions, EPR meas. 78−68374
SmS:P, neutron irrad., semiconductor-metal transition 80−24975
Sm-S-based alloy, preparation and properties 78−44034
Sm-CdS system, T-p-X diagram, semicond.-metal transition 79−69421
SmS-GdS system, crit. effects and phase equilibria 79−7692
Sm_2S_3 films, refl. and transmission spectra at 300K 80−80889
Sm_2S_3, mixed valence compound, mag. and thermal props. 79−78400
Sm_2S_3-Sm_3S_4, valence related optical and other studies, review 78−31215
Sm_3S_4, cryst. struct. and valence state of Sm *(German)* 78−75636
Sm_3S_4, inelastic light scatt. 77−55788
Sm_3S_4, mag. susceptibility meas., valence state of Sm 80−15684
Sm_3S_4, magnetic susceptibility and valence fluctuations 77−8266
Sm_3S_4, mixed valence compound, mag. and thermal props. 79−78400
Sm_3S_4, mixed valence system, inelastic light scatt., photoluminesc. 77−90145
Sm_3S_4, sp. ht. anomaly 77−89550
Sm_3S_4:Eu, excited-state exchange interactions, EPR meas. 78−68374
$SmS_{1-x}As_x$, magnetoresist. in semicond. and metallic phases 80−96914
$SmS_{1-x}As_x$, optical investig. of substitution effects on metal-semicond. transition 77−63427
$SmS_{1-x}As_x$ solid solns., intermediate valence phase, lattice const. and mag. susceptibility meas. 79−87245
$Sm_2(SO_4)_3.8H_2O$, cryst. struct. refinement 77−89418
$Sm_2(SO_4)_3.8H_2O:Gd^{3+}$, cryst., EPR 77−59455
$Sm_2(SO_4)_3.8H_2O:Gd^{3+}$, EPR, zero field splittings, spin-Hamiltonian parameters 78−91949
$SmS_{1-x}P_x$, intermediate valence cpd., lattice parameter and mag. susceptibility 80−7091
$SmS_{1-x}P_x$, valence changes, XPS and UPS study 80−97402
SmSb, crystal field effect in thermal expansion 78−19305
SmSb, forbidden band gap and electrotransfer parameters 80−39497
SmSb, low temp. props. 79−28528
$SmSb_{1-x}S_x$, magnetic ordering and configuration mixing 78−68179
$SmSb_xS_{1-x}$, intermediate valence, susceptibility and lattice parameter meas. 78−51943
SmSe, Debye temps., vibr. amplitudes, X-ray diffr. determ. 78−2222
SmSe, electronic struct., optical props. 0.03 to 12 eV 77−28594
SmSe, formation and crystallographic charact. of thin film phase 78−91574
SmSe, pressure-induced reflectivity changes and semiconductor-metal transition 79−56763
SmSe:Eu, excited-state exchange interactions, EPR meas. 78−68374
Sm_3Se_4, mixed valence compound, mag. and thermal props. 79−78400
Sm_3Se_4, valence fluctuation, mag. susceptibility meas. 80−97056
$SmSi_2$, valence band struct. *(Russian)* 79−15076
Sm_2SnS_5, X-ray cryst. struct. determ. *(French)* 80−19760
$Sm_{1-x}Sr_xCoO_3$, electronic and mag. props., itinerant ferromagnetism obs. 78−10660
$SmTaO_4$, heat of form. 79−83494
$Sm_{0.05}Tb_{0.45}FeO_3$, singularities of domain struct. in spin-flip region 78−19272
$Sm_{0.55}Tb_{0.45}FeO_3$, orthoferrite cryst., domain memory effect *(Russian)* 77−55693
$Sm_{0.55}Tb_{0.45}FeO_3$ orthoferrite, optical and magneto-optical props. 79−61396
$Sm_xTb_{1-x}FeO_3$, gyrotropic props. and birefringence, in spin reorientation range 80−7324
$Sm_xTb_{1-x}FeO_3$, mag. reorientation, temp. *(Russian)* 79−87263
$Sm_xTb_{1-x}FeO_3$ orthoferrites, crystallo-optical props. 79−42027
$Sm_xTb_{1-x}FeO_3$, rotation of polarisation plane, ang. depend. 77−43961
SmTe, Debye temps., vibr. amplitudes, X-ray diffr. determ. 78−2222
SmTe, electronic struct., optical props. 0.03 to 12 eV 77−28594
$Sm_{1-x}Th_xS$, XPS, electronic struct. excitonic effects, insulator to metal transition 78−43988
$Sm_2Ti_2O_7$, ferroelec., layer type struct., cryst. growth 80−108348
$Sm_2Ti_2O_7$, ferroelec., temp. depend. of SHG intensity 79−24267
$SmTi_{1.5}W_{0.5}O_6$, Stark sublevels in mag. suscept. and luminesc. 77−51876
$(SmTm)_3(FeGa)_5O_{12}$, small-bubble appl. 79−82845
SmTmIG, epitaxial layer with submicron bubbles, mag. props. 77−12172
$Sm_{1-x}Tm_xS$, optical investig. of substitution effects on metal-semicond. transition 77−63427
$Sm_2(WO_4)_3$, mag. susceptibility, paramag. Curie temp., 300-900K 79−82753

samarium compounds continued
$Sm_2(WO_4)_3$, molar mag. susceptibility, DC elec. cond., thermopower meas. 79−15172
Sm_2WO_6 and $Sm_{14}W_4O_{33}$, high-temp. enthalpy and specific heat 80−34205
Sm_2WO_6, growth from soln. in melt 77−1806
$(SmYCa)_3(FeGe)_5O_{12}$ epitaxial layer, growth kinetics and struct. as functions of cryst. lattice parameter mismatch 80−6677
$(SmY)_3(FeGa)_5O_{12}$, LPE on $Gd_3Ga_5O_{12}$, growth kinetics, 920-980°C 78−3064
$Sm_{0.4}Y_{2.6}Fe_{3.8}Ga_{1.2}O_{12}$, LPE. improved method of stirring 78−68641
$Sm_{0.4}Y_{2.6}Fe_{3.8}Ga_{1.2}O_{12}$ epitaxial films, uniaxial mag. anisotropy, ferrimag. reson. study 80−80577
$Sm_xY_{3-x}Fe_5O_{12}$, magnetostriction comp. depend., 78 to 300K 77−77082
$Sm_xY_{3-x}Fe_5O_{12}$, spin reorientation transitons 78−2686
SmYGa garnet, bubble motion depend. on wall pinning 79−78455
$Sm_{0.4}Y_{2.6}Ga_{1.1}Fe_{3.9}O_{12}$, LPE, growth rate anisotropy and kinetic coeffs. of vicinal faces 78−51846
$Sm_{0.4}Y_{2.6}Ga_{1.2}Fe_{2.8}O_{12}$, H^+ implanted film, epitaxial, mag. bubbles, walls and fine struct. 77−63241
$Sm_{0.25}Y_{0.75}S$, phonon anomalies and electron-lattice coupling 80−39490
$Sm_{0.7}Y_{0.3}S$, Debye-Waller factor, X-ray diffr. meas., evidence of optic phonon softening 77−11659
$Sm_{0.75}Y_{0.25}S$, intermediate-valence-state system, phonon dispersion meas. 79−19342
$Sm_{0.75}Y_{0.25}S$, intermediate valence system, mag. excitations 79−60771
$Sm_{0.75}Y_{0.25}S$, intermediate valence compound, phonon investigation by neutron scatt. 80−6476
$Sm_{0.75}Y_{0.25}S$, mixed valence, phonon dispersion theory 80−34153
$Sm_{0.75}Y_{0.25}S$, mixed-valence, electron-lattice correlations, EXAFS studies 80−76103
$Sm_{0.76}Y_{0.24}S$, induced magnetic form factor, polarised neutron studies 80−25078
$Sm_{0.76}Y_{0.24}S$, mixed valence, induced mag. form factor 78−68163
$Sm_{1-x}Y_xS$, anomalies in phonon dispersion 79−73268
$Sm_{1-x}Y_xS$, CPA calc. of rare-earth impurity, valence change 77−63096
$Sm_{1-x}Y_xS$, effect of valence fluctuations on lattice dynamics 78−47493
$Sm_{1-x}Y_xS$, electronic config., Mossbauer spectra meas. 77−16228
$Sm_{1-x}Y_xS$, magnetoresist. in semicond. and metallic phases 80−96914
$Sm_{1-x}Y_xS$, metal-semicond. isomorphous transition curve, low temp. crit. point, lattice parameter changes 79−95334
$Sm_{1-x}Y_xS$, mixed valence system, electron-phonon coupling, theory 80−70343
$Sm_{1-x}Y_xS$, mixed valence, phonon softening and linewidths, calc. 80−75319
$Sm_{1-x}Y_xS$, press.-induced semicond.-metal transition, refl. and lattice compression meas. 77−62826
$Sm_{1-x}Y_xS$, valence transitions, theoretical model 79−69474
$Sm_{1-x}Y_xS$, XPS, electronic struct. excitonic effects, insulator to metal transition 78−43988
$Sm_{1-y}Yb_yB_6$, valence transition, lattice parameter and mag. susceptibility meas. 80−59929
$Sm_{1-x}Yb_xS$, optical investig. of substitution effects on metal-semicond. transition 77−63427
$Sm_{1-x}Yb_xS$, simultaneous Sm^{2+}-Sm^{3+} and Yb^{2+}-Yb^{3+} electron transitions *(Russian)* 79−60711
$Sm_2Zn_3(NO_3)_{12}.24H_2O$:$Gd^{3+}$, EPR X-band, fine struct., low field lines 79−15351
$Sm_2Zr_2O_7$ pyrochlore phase, O ion conduction 80−24654
Sm_2ZrS_5, mag. and sp. ht. meas. on polycrystalline samples 78−23253
$(SrCaSm)_2(Cr_xGa_{1-x})O_4$, mag. 2-D oxide, phys. props. 78−47974
$SrSm_2S_4$, mag. props. 78−68237
$Sr_{1-x}Sm_xS$, electron config. of Sm ions, X-ray L-absorpt. spectroscopy 80−60715
$(Y,Sm,Ca)_3(Fe,Ge,Si)_5O_{12}$ single-crystal films, props. 78−64247
$(Y,Sm,Ca)_3(Fe,Ge)_4O_{12}$, garnet thin film, mag. anisotropy, Faraday effect meas. 79−42812
$(Y,Sm,Ca)_3(Fe,Ge)_5O_{12}$, domain wall, radial motion, method of dynamic collapse of mag. bubbles 79−8026
$(Y,Sm,Ca)_3(Fe,Ge)_5O_{12}$ epitaxial films, mag. props., growth condition effects 80−97124
$(Y,Sm,Ca)_3(Ge,Fe)_5O_{12}$ film, bubble wall state stability obs. 77−20651
$(Y,Sm,Ga)_3(Fe,Ge,Si)_5O_{12}$ film, static and dynamic mag. props., 20-160°C 77−24725
$(Y, Sm, Lu, Ca)_3(Fe, Ge)_5O_{12}$:$Ne^+$, film, S=1 bubbles dynamic props., temp. depend. 77−20658
$(Y,Sm,Lu,Ca)_3(Fe,Ge)_5O_{12}$, bubble memory chip, dynamic conversion comparison with $(Y,Eu,Lu,Ca)_3(Fe,Ge)_5O_{12}$ 78−68319
$(Y,Sm,Lu,Ca)_3(Fe,Ge)_5O_{12}$ garnet film coercivity, new annealing method 78−84459
$(Y,Sm,Lu,Ca)_3(Fe,Ge)_5O_{12}$ bubble magnetic garnet film, LPE grown, props., $CaCO_3/GeO_2$ molar ratio influence 80−50152
$(Y, Sm, Lu, Ca)_3(FeGe)_5O_{12}$ LPE films, factors affecting coercivity 79−91267
$(Y,Sm,Lu,Ca)_3(Ga,Ge,Fe)_5O_{12}$, film growth and mag. props. for bubble-memory appl. 79−87297
$(Y,Sm,Lu,Cu)_3(Fe,Ge)_5O_{12}$, ion implanted, hard bubble suppression 80−11238
$(Y,Sm,Lu,Tm,Ca)_3(Fe,Ge)_5O_{12}$, epitaxial garnet film, temp. depend. mag. props. 80−39825
$(Y,Sm,Lu)_3(Fe,Ga)_5O_{12}$, LPE mag. film, suitability for 1 to 3 micron bubble devices 78−68323
$(Y, Sm, Tm)_3(FeGa)_5O_{12}$ LPE films, factors affecting coercivity 79−91267
$(Y,Sm)_3(Fe,Ga)_5O_{12}$ film, static and dynamic mag. props., 20-160°C 77−24725
$(Y,Sm)_3(Fe,Ga)_5O_{12}$, garnet LPE films, growth rate anisotropy 80−54558
$(Y,Sm)_3(Fe,Ge)_5O_{12}$, Ca, Ge substituted garnet LPE films, elec. props., charge imbalance, Seebeck effect 78−68101
$(Y,Sm)_3(Ga,Fe)_5O_{12}$ epitaxial layers, annealing effect on mag. props. 79−61191
$(Y,Sm)_3(Ga,Fe)_5O_{12}$ film, domain boundary mobility, effect of easy magnetization axis inclination 78−19293
$(Y,Sm)_3(Ga,Fe)_5O_{12}$ films, growth from melt, growth property control 78−27395
$(Y,Sm)_3(Ga,Fe)_5O_{12}/(Eu,Er)_3(Ga,Fe)_5O_{12}$ double-layer self-biasing garnet films, dynamic behaviour of domain walls 80−34722
Y-Sm ferrogarnet *(Russian)* 80−71140
$(YBiSmCa)_3(FeGe)_5O_{12}$ epitaxial layer, growth kinetics and struct. as functions of cryst. lattice parameter mismatch 80−6677

samarium compounds continued
$(YLuSmCa)_3(FeGe)_5O_{12}$ garnet film, bubble domain expansion, fuzzy wall struct. 80−71128
$(YLuSmCa)_3(GeFe)_5O_{12}$ bubble garnet film, coercivity 79−78459
$(YLuSmCa)_3(GeFe)_5O_{12}$ garnet films, bubble expansion saturation vel., sampling optical photography 80−75820
$Y_{1.62}Sm_{0.21}Lu_{0.27}Cu_{0.9}Ge_{0.9}Fe_{4.1}O_{12}$, implanted bubble garnet, anisotropy profile, FMR study 80−7103
$(YSmCa)_3$ $(FeGe)_5O_{12}$ mag. bubble garnets, ion implantation induced stress influence on props. 79−91274
$(YSmCa)_3(FeGe)_5O_{12}$ LPE films, optimum growth conditions for low coercivity 78−95499
$(YSmCa)_3(FeGe)_5O_{12}$ LPE film, growth and coercivity 79−4707
$(YSmCa)_3(FeGe)_5O_{12}$ films, cc $(YSmLuCa)_3(FeGe)_5O_{12}$ films, mag. bubble props. mag. bubble props. and LPE conditions 79−74107
$(YSmCaLu)_3(FeGe)_5O_{12}$, bubble film inhomogeneity, spin wave reson. meas. 80−44439
$Y_{2.2}Sm_{0.4}(Fe,Ga)_5O_{12}$, garnet film, strip domain struct. behaviour in applied field 78−68341
$(YSm)_3(FeGa)_5O_{12}$ film, LPE on $Gd_3Ga_5O_{12}$, interface processes, horizontal dipping obs. 80−49552
$(YSm)_3(FeGa)_5O_{12}$, growth rate anisotropy and kinetic coefficients of vicinal faces 78−63954
$Y_{2.6}Sm_{0.4}Fe_{3.8}Ga_{1.2}O_{12}$, garnet films, LPE growth, mag. anisotropy field control 77−69642
$Y_{3-y}Sm_yFe_{5-x}Ga_xO_{12}$ film, LPE process exam. by induced striation 77−69643
$Y_{3-y}Sm_yFe_{5-x}Ga_xO_{12}$ film, LPE growth induced mag. anisotropy 78−2709
$Y_{2.6}Sm_{0.4}Fe_{5-x}Ga_xO1_2$, epitaxial, domain wall crit. vel., effect of material parameters 79−99740
$Y_{3-x}Sm_xFe_5O_{12}$, cubic and induced anisotropy, temp. depend., 100-300K, ferromag. reson. obs. *(Russian)* 78−39313
$Y_{3-x}Sm_xFe_5O_{12}$:^{57}Fe film, ion implanted, Mossbauer conversion spectra study 80−80663
$Y_{2.6}Sm_{0.4}Ga_{1.2}Fe_{3.8}O_{12}$ film, ion-implanted, bubble domain behaviour 77−12177
$(YSmLuCa)_3(FeGaGe)_5O_{12}$, reproductibility in bubble garnet LPE growth 78−92204
$(YSmLuCa)_3(FeGe)_5O_{12}$, mag. props. and growth of 2 μm bubbles 78−91910
$(YSmLuCa)_3(FeGe)_5O_{12}$, LPE growth, growth reproducibility of bubble props. 78−92208
$(YSmLuCa)_3(FeGe)_5O_{12}$ films, mag. bubble props. and LPE conditions 79−74107
$(YSmLuCa)_3(FeGe)_5O_{12}$ film, bubble propagation direction effects on high frequency bias margin 79−78480
$(YSmLuCa)_3(FeGe)_5O_{12}$, double layer struct., LPE growth from molybdate and Pb borate fluxes 80−39827
$(YSmLuCa)_3(FeGe)_5O_{12}$, bubble material, dynamic characterisation, comparison between transport and FMR methods 80−39833
$(YSmLuCa)_3(FeGe)_5O_{12}$, mag. loss and domain wall mobility 80−65980
YSmLuCaGe garnets, 7 μm-period bubble devices 80−44887
$(YSmLuCa)_3(GeFe)_5O_{12}$, garnet film, refractive index dispersion 78−88273
$(YSmLuCa)_3(GeFe)_5O_{12}$, LPE low defect density films, prep. for mag. bubble device fabrication 79−87590
$(YSmLuCa)_3(GeFe)_5O_{12}$, stripe domain wall, form. and punch-through of horizontal Bloch line 79−99723
$YSm_{0.5}Lu_{0.7}Ca_{0.8}Ge_{0.8}Fe_{4.2}O_{12}$ film, magnetic bubble propagation with 8 μm period ion implanted propagation patterns 79−78475
YSmLuCaGeIG, mag. props. and defects, depend. on B_2O_3 conc. on growth in PbO-B_2O_3 solvents 78−68321
YSmLuCaGeIG films, epitaxial growth with 3 μm magnetic bubbles 79−61518
$(YSmLu)_3(FeGaSc)_5O_{12}$, submicron mag. bubble garnet 80−54929
YSmTmCaGe garnets, 7 μm-period bubble devices 80−44887
$(YSmTmCa)_3(GeFe)_5O_{12}$ film, YY pattern racetrack discrimination and state stability of S=1 and 0 bubbles 78−91908
$(YSmTm)_3(FeGa)_5O_{12}$, small-bubble appl. 79−82845
$Yb_{1-x}Sm_xS$, electron config. of Sm ions, X-ray L-absorpt. spectroscopy 80−60715
ZrO_2/SmF_3 mirror coatings, light scatt. and optical strength in UV range 80−106595
ZrO_2-Sm_2O_3 eutectic, unidirectional solidification, microstruct. and crystallographic characterization 80−35176
ZrO_2-Sm_2O_3 solid solns., prep., crystn. 78−42909

sample and hold circuits
amplifier for stimulus artifact suppression in bioelectric recordings 78−77163
boxcar integrator/US recording unit using sample-and-hold circ., for student lab. 80−27083
luminous flux meas., automatic null method *(French)* 80−27331
magnetoresistive head Barkhausen noise voltage meas. 79−82821

sampled data systems
see also discrete time systems; Z transforms
aphasia treatment session recording, momentary and interval sampling 79−96704
biological temperature telemetry, domestic fowl appl. 78−57152
conditional sampling, detection and data signal phase relation, turbulent boundary layer appl. 78−24772
electronic delay, dynamically variable, for real-time US imaging 79−46142
eye movement hierarchical control model 77−25429
imaging systems, linear gradient model for suppression of aliasing 78−33686
online real-time data acquisition system design 78−35994
plasma probe, digitised random signal analysis method, power spectrum, phase vel. 77−84509
radioactive tracer kinetics, compartmental system identification by optimum sampling 77−86615
saccadic ocular dysmetria simulation using sampled-data model 77−56373
space variant systems, holography using phase coded reference beams 78−33698

sand
aeolian sedimentation on Earth and Mars, comparisons 80−31042
ancient big river systems significance and origin 78−77281
aqueoglacial deposit lithology of E.Lithuanian upland *(Russian)* 78−16011

sand continued
arenaceous aquifers, matrix conduction props. of argillaceous sand 77−64347
Athabasca oil sand behaviour under cyclic and uniaxial loading and hydrostatic press. 79−48468
Athabasca oil sands, electrical props. 80−31030
Baltic beach scouring and detritus accumulation in short-term disturbance *(Russian)* 80−36288
SE.Baltic mainland shore moderately accumulative section morphodynamics *(Russian)* 80−67359
SE.Baltic shore development due to hydrotechnical constructions *(Russian)* 78−36145
Baltic underwater coastal slope sand grain size and mineral composition *(Russian)* 80−76963
Banks Island, Canada, deposits and aeolian processes *(French)* 78−36163
barrier beach shoreline accumulative section, protective dune ridge morphodynamics *(Russian)* 80−36287
barrier beach shoreline transit section, protective dune ridge morphodynamics *(Russian)* 80−36286
beach and dune sands on Goa coast, mineralogy 77−41028
beach dynamic profile equilib. in frontal wave action *(Russian)* 79−88331
beach sedimentology of Mustang and Padre Islands, time series approach 78−77211
beach sediments, lower St. Lawrence Estuary, Quebec, frost effects 78−7609
beach slope sand granulometric composition variations during wave cycle *(Russian)* 78−15991
beaches, rhomboidal lattice struct. 77−37178
beaches, SE Rio de Janeiro state, sediment textural charact., grain size *(Portuguese)* 78−81144
bedload dynamics, grain-grain interactions in water flows 80−31069
capillary mass transfer 77−7443
clay soil/sand mixtures, reflectance 80−56475
clock, historical development 80−22185
Cuba, north coast, morphologic and lithodynamic study using luminescent tagged sands 77−64264
cyclic liquefaction strength 80−3996
desert, containing TiO_2, photoreduction of N_2 to NH_3 79−83483
desert colour, Apollo-Soyuz photographs 78−65315
dissolution, during glass melting, kinetic equation for interaction between grain material and liq. 80−84901
dune fields and sand sheets rel. to Late Quaternary aridity in W. Australia 77−13113
dune formations in Canada 80−12386
dune ridge morphodynamic characteristics on spit of Kurshyu Nyariya, abrasional section *(Russian)* 78−36149
dynamic features of deficit forms in translational flows 79−39775
dynamic properties w.r.t. seismic risk prediction, stress condition effect *(Japanese)* 80−17235
Dzukija massif ancient inland dunes, geomorphology, lithological charcts. *(Russian)* 77−21709
enriched heavy minerals in sand grains, enhanced natural radiation exposure *(German)* 80−51018
erosion of windblown quartz and basaltic sand on Mars 80−17525
evaporation rate from porous surfaces, wind tunnel *(French)* 77−80684
excess pure pressure measurement with liq. manometers 77−52566
fixed dunes, Sahel, central Niger, erosion 78−81225
flow law of sand, limiting condition 77−54948
fluidised, determ. of flow parameters by simple model and new distributor design 78−83493
Fraser River (British Columbia) deltaic sediments and heavy metals content 77−33048
frozen sand-argillaceous rocks, elastic moduli 77−9406
fulgurite formation, elec. discharge into sand layer expts. 78−81322
Gippsland, Victoria, Pliocene eustasy and sand barrier form. onset 79−74886
glacial till landforms, fabric anal. 77−44989
grain size distrib. functions 77−29999
granular media, nonuniform, nonlinear flow analysis 77−58779
Green and Ampt infiltration eqn. parameters depend. on initial water content 79−79899
W Greenland continental margin, Mesozoic and Cenozoic sediments provenance 79−62479
Grote Nete basin, Belgium, geomorphology *(Flemish)* 78−61452
groundwater flow, unconfined, tunnel opening, 2-D finite element anal. 78−11922
heated, thermoluminescence, appl. to radiation dosimetry 77−61613
Hellespontus dunes, terrestrial analogues 77−29697
Holocane aeolian landforms in Belarabon area, NSW, dunefield 77−53054
Hunter River, sand supply to New South Wales coast 78−16066
impact craters in ice and ice-saturated sand, Martian implications 80−67614
interfluvial area of Minija and Sventoji, marginal formations structures *(Russian)* 77−25708
Labrador continental margin, Mesozoic and Cenozoic sediments provenance 79−62479
laser sand detector to discriminate between bubbles and sand, oceanography appl. 79−58109
Late Quaternary sedimentation on W.African continental margin 77−21753
liquefaction during Friuli 1976 earthquakes 78−24280
longshore sediment transport and sediment budget for Malpeque barrier system, Gulf of St. Lawrence 78−36140
Mars, sand sea (erg) in north polar region, wind patterns 80−67624
S.Mediterranean Ridge sand, petrographic analysis 79−70782
microwave propagation, path attenuation during sandstorms 79−70834
Miramichi estuary, New Brunswick, tidal current control of submarine morphology 78−36174
Moisie River, Quebec, gully flow development after heavy rainfall 77−5249
moisture content, microwave optics determ. 77−37684
monazite sand, determ. of Th, U, and K from spectrometry of natural γ-activity 78−20408
Newcastle-Port Stephens area of Australia late Quarternary deposits 79−88352
ocean bottom profile form. mechanism under translational flow 79−29751
particles in air, effect on breakdown voltage 78−81363
sand continued
pore water pressure changes in sand deposits during earthquakes 79−88308
quartz beach samples, spectral reflectance/grain size relationship 78−16005
quartz sand, pilot tests of acoustic device for dressing 78−7271
quartz sand, press. soln. expt. 77−60370
quartz sand, thermal conductivity rel. to moisture content *(Russian)* 77−54864
resin-coated, curing effects on physicomech. props. *(Korean)* 78−60855
resistivity-porosity-particle shape relationships for marine sands 79−53339
riffle formation model 78−63482
river, sand-silt equilib. banks and mobile bed, model 79−34862
river sediment, sand-wave motion along nonerodible bottom in open channel flow 78−16074
Rudnaya Bay, Sea of Japan, layer of storm network of sediments 79−2224
lower Saint Lawrence estuary sediments, clay-sand sequence chronology in Rimouski shelf region 79−62530
Sakhalin Island, grain size distrib. along underwater slope 77−64265
S.Saskatchewan, composition study of sands 79−84254
sea floor, mobile sand grains underwater detect. 78−96192
sediment movement behaviour, current, wave and wind effects *(French)* 77−78151
sedimentary deposit, porous, NaCl mass transfer to stationary water region *(Japanese)* 77−25700
sediments of old coast formations of E.Lithuanian upland *(Russian)* 78−16012
shear bands formation, bifurcation problem 78−73362
shear strength at const. vol. 77−63865
shoreline changes due to dredged holes, math. and lab. models *(Japanese)* 78−11878
shoreline evolution, beach sand transport modelling 78−15993
shoreline forms and dynamics of USA Atlantic coast 77−91106
slope stability and valley form. in glacial outwash deposits, Norfolk, England 79−20880
slopewash and wind action, Quaternary morphogenesis in Belgium 77−81924
soil, experimental and simulated P transport 77−66940
soil, sandy, mech. charcts. under static loadings 79−88345
soils, sandy and clay, microwave absorption *(Russian)* 78−81162
specularite-bearing sand 80−90075
Spit of Kursiu Nerija, morphodynamical characteristics of protectional dune ridge *(Russian)* 78−20389
surface texture rel. to wind vel. conditions 80−41443
suspended clastic material, in ocean, movement over shore slope under storm conditions 79−2223
terrigenous and volcanogenic deep sea bottom sediments chem. comp., Sea of Japan 77−21758
thermal diffusivity measurement, constant rate heating method *(Japanese)* 80−6572
tidal sand waves study in White Sea 79−2218
titanomagnetite sand from New Zealand, density, elec. and mag. prop 80−98311
tracer dispersion under progressive water waves, laboratory and field obs. 80−46170
triaxial test, bifurcation anal. 79−70783
Tunisian sand, N_2O decomposition 79−16014
unconsolidated porous sand reservoirs, elastic props. 78−61400
under-surface temp. pattern estimation by dynamic remote sensing *(Japanese)* 78−36315
underwater cusps, rare form of shallow water bottom relief 77−86855
unsaturated Plainfield sand, longit. and transverse dispersion coeffs. 79−53382
US attenuation in fluid-saturated sand 80−33307
Waipipi ironsands in New Zealand, mag. assessment technique for titanomagnetite 80−17254
water content, hysteretic steady state profiles 77−91172
water infiltration into horizontal sand column, flow charcts. 77−78280
water-saturated, broadband meas. of acoustic attenuation 80−83719
wave-formed bars, sedimentation and equilib., review 79−92521
waves on shelf of tidal sea 79−12313
White Sea, periodic forms of bottom relief on shelf 78−44804
Al-C-silaceous sand mixture in N_2 atmos., weight loss during heating, compaction *(Japanese)* 80−35151
Co radioactive release from reactor cooling water, fixation by sandy soil *(Japanese)* 78−74443
Hg pollution of Mediterranean sediments around Alexandria, Egypt 80−3538
U in sea foams and adhered to sea sands *(Japanese)* 79−29785
$ZrSiO_4$, zircon, thermoluminesc. glow curve and spectrum 79−33847

sapphire
acoustic phonon geometric propag., anisotropic continuum 77−4169
chemical analysis, O conc. determ. using non Coulomb H ion backscatt. 80−55753
clad ruby fibres, single-crystal, growth by floating-zone technique 77−90268
complex dielec. const. at audio freqs., 5.5 to 380K 80−25272
composite leucosapphire single cryst., W grid reinforced, growth 77−16530
concentrational inhomogeneities, appl. of vacuum decoration method 79−14835
contact electrification 78−88018
creep deform. of 0°, fracture anal. 77−56035
crystal defects from X-ray irradiation, F-centres, X-ray luminesc. obs. 80−55176
crystal growth, rel. between growth angle and shape of lateral surface 79−94936
crystal growth and slicing developments 77−77371
crystal growth by edge-defined film-fed growth process 80−104057
crystal growth from melt, capillary shaping, expt. results 77−47364
crystal growth from melt by Stepanov's method, axial temp. distrib. 80−103280
crystallisation from melt, capillary conditions 78−3020
Czochralski crystals, formation of low angle grain boundary macrostruct. 78−47392
damage by UV laser radiation, self-focusing mechanisms 80−76110
dielectric losses, HF, loss angle upper limit *(Russian)* 77−24785
dislocation detection by divergent polychromatic beam method 77−35568

sapphire continued
dislocation obs. by weak-beam TEM 77−47461
dynamic deformation by projectile impact back reference holography obs. *(French)* 78−42307
dynamic nuclear polarisation, correl. ESR and NMR strain-broadening effects 77−48090
edge dislocation loop obs. by high resolution lattice imaging 80−103346
epitaxy of Si, cryst. perfection rel. to MOS transistor mobility 78−75956
ESR pressure cell for meas. at hydrostatic pressures to 60 kilobars 78−54418
etching, HF ion-plasma, cryst. surface layers treatment and study *(Russian)* 80−16517
etching of arrays of orifices using Pt-Cr composite layer mask 80−3216
excess charge carriers, generation, transport and trapping 79−82646
F-centre, fluorescence decay below 75K 80−60664
F-type centre induction, 6.1 eV optical absorpt. band 78−88332
fibre reinforced Mo, strength at rupture 80−104286
fibres, meas. of bending strength 80−25964
fibres, strength at rupture 80−104286
filament, cryst. growth by laser-heated floating zone technique 77−32518
flat films growth from melt for SOS LSI/VLSI technology *(German)* 79−95918
float zone growth, laser heated, of const. diameter crysts., meniscus angle meas. 80−108347
float zone growth, maximum stable zone length 79−91582
fracture anisotropy of ⟨1$\bar{2}$10⟩ zone 79−61726
gas-solid interface, EPR centres induced by microwave gas plasma 78−80215
growth angle determ. from cryst. lateral face shape and solidified separation drops 80−103282
heat transfer at low temps., lattice thermal cond. 78−34665
interface with dilute ^{3}He, heat transfer at very low temp. 79−56003
interface with Pb, heat transfer coeff. meas., 2-80K 80−88419
interface with superfluid ^{4}He, 0.25K, ballistic phonon pulse transmission 79−19415
interface with superfluid ^{4}He, ballistic-phonon-pulse transmission at 0.25K 79−95229
interface with vac., phonon refl. 80−15358
internal friction, low temp. peak 80−2033
ion bombardment, 15-keV, chem. implantation, isotopic trapping effects and induced hygroscopicity 77−59030
lamellar crystal, growth twinning 77−4113
lamellar crystal, growth twinning investig. 77−4113
leucosapphire, crystal growth by Kyropoulous method, temp. effect on structural and optical quality 80−20784
leucosapphire, electronic band struct., optical props. 79−95329
leucosapphire, large cryst., UV transmittance 77−88876
leucosapphire, phosphorescence, decay obs., impurity effects *(Russian)* 79−15530
leucosapphire, spectral absorpt. coeff., 1800K 78−27252
leucosapphire, spectral absorption coeff., 0.25-1.25 micron, up to 1800K, and 3.5-5.2, up to 1200K 78−27204
leucosapphire, supercooling and crystn. temp. determ. 79−51237
leucosapphire, unique polishing features of hard crystals 80−64225
leucosapphire 80−88190
leucosapphire crystal, kinetics of radioluminescence flare-up *(Russian)* 77−12439
leucosapphire crystals, block boundary energies 78−55877
leucosapphire crystals, gaseous inclusions 78−2151
leucosapphire fibres, multicapillary growth 80−44459
leucosapphire large crystals, anomalies in block struct. formation 80−9972
leucosapphire-ruby boundary, laser backscatt. at inhomogeneities 79−23000
liquid metal container for neutron scattering expts. up to 1900K 79−63215
luminescence centres of pure and doped samples 79−33791
luminescence of F centre 79−73990
metal-sapphire interface, effect on shear strength of adsorbed species 80−49485
natural, origin of colour 79−70794
neutron bombarded, F-centre fluorescence, photoluminescence 80−100676
neutron damaged 14.8 MeV, optical vibronic absorption spectra 80−50384
nondestructive testing, using IR and UV specular reflectance meas. 80−108684
optical detection of acoustic phonons at THz freqs. 80−75320
optical strength anisotropy, absorbing microdefects effect 78−2952
optics fabrication 79−23099
phonon conductivity, calc., 0.4-4K 78−18852
phonon energy contours, in bc-plane, inelastic neutron scatt. obs. 77−59083
phonon transmission from incoherent radiator into cryst., anisotropic continuum acoustics 77−47521
phosphorescence, decay obs., impurity effects *(Russian)* 79−15530
polishing with colloidal SiO_2 78−39925
profiled growth, struct. perfection 78−68621
pulsed laser induced damage at DF laser wavelengths 77−46751
ribbon crystal, interface growth feature rel. to voids 78−34456
ribbon crystal growth by edge-defined film-fed growth technique *(Japanese)* 78−27396
ribbon crystals, EFG growth and charact., voids, grain boundaries and dislocations 80−103283
ribbon crysts., grown by edge-defined film-fed growth technique, X-ray topography study of dislocations 79−4305
ribbon edge-defined film-fed growth, substrate for heteroepitaxial Si 80−108342
ribbon microvoid distribution control in edge-defined film-fed SOS growth 77−77370
rod, torsional waves at low freqs. 77−84053
sapphire :Ti^{4+}, deformation history effects on precipitation hardening 79−83209
sapphire filaments in Al_2O_3:MgO matrix, single cryst. boundary migration 80−44369
sapphire-^{4}He interface, transmission of ballistic longitudinal and transverse phonon pulses at 0.25K 79−51416
sapphire-Al interface barrier, transport and trapping obs. 77−76921
sapphire-H_2O interface, SiO_2 sputtered film performance as acoustic antireflection coating 80−106686
sapphire continued
sapphire-LiF film system, ATR, substrate surface polaritons reson. effect *(Russian)* 77−32384
second sound observation by heat pulses method, phonon scatt. processes *(Russian)* 79−99273
shaped single crystals, porosity, microstruct. 78−2125
shock compressed, refractive index, density, and polarisability behaviour 80−50295
single-crystal clocks and frequency standards 78−57915
solid phase Si regrowth in Si-Al-Al_2O_3 system, Hall effect 80−100413
solid-state oscillator with superconducting sapphire resonator, freq. stabilisation 79−12823
SOS early growth, island coalescence model 77−76704
SOS early growth, transmission electron microscope obs. 77−76703
SOS films, cryst. quality improvement by Si ion channelling, annealing 80−44222
SOS structure, radiation dose at interface due to electron beam aluminisation 78−68089
SOS structures, high-field electron transport, drift vel. meas. 80−80387
SOS substrate quality evaluation by X-ray rocking curve technique 77−76262
SOS wafer for beam profile monitoring in high-current ion implantation systems 80−13182
substrate, anthracene ultrathin film deposition 80−59812
substrate, Czochralski grown, etch pits and dislocations 79−37708
substrate, influence on adherence fracture energy of glass bonded Pt-Au thick film conductor 77−56075
substrate, RF sputtering of Hf high stress in graded interfacial layers, AES meas. 77−43446
substrate, single crystalline AlN film, low temp. growth by RF reactive planar magnetron sputtering method 80−76175
substrate, surface quality determ. by optical reflectance methods 78−43862
substrate, VPE of GaN, crystallographic aspects 78−2387
substrate, with epitaxial Si layer, characterisation, X-ray rocking curves 80−75458
substrate crystallisation of amorphous Si layers, RF-sputtered, CW ion laser annealing 80−80109
substrate film for Si, laser annealing non-thermal theory expt. test 80−89273
substrate for crystallisation of Ni, Ni-B films, struct. evolution *(Russian)* 80−75455
substrate for directed crystallisation of GaSb thin layers 80−35111
substrate for directed crystallisation of InSb thin layers 80−35112
substrate for epitaxial Si, misfit, strain and dislocations, book contrib. 79−82499
substrate for $K_3Li_2Nb_5O_{15}$ film for optical waveguide, cryst. struct., dielectric props. 80−79016
substrate for Mo epitaxial layer production by electron beam deposition in vacuum *(Russian)* 77−59228
substrate for Nb and V highly-oriented films, surface chem. treatment 77−66097
substrate for Si epitaxial film growth by MBE 80−76186
substrate for Si film, laser annealing dynamics epitaxial regrowth, optical reflectivity 80−29285
substrate for V, Ta, Mo, W, Nb epitaxial films, growth texture, nucleation texture *(Russian)* 80−75454
substrate for vacuum deposited heteroepitaxial Si films, struct. and elec. props. 80−15390
substrate for vapour phase epitaxial growth of GaN 79−4919
substrate surface evaluation for SOS 77−76653
substrate with Si layer in SOS technology, gettering effect by O implantation, Hall and Rutherford backscattering meas. 79−65103
substrates, prep. for GaN epitaxy 78−39929
synthetic, heat capacity, 300 to 550K 79−21754
synthetic, pure, enthalpy determ., 900-1900K 79−42275
synthetic and natural, optical spectra comparison and identification 80−40138
synthetic arc lamp envelope, basal plane cleavage 79−66146
TFTR diagnostic windows, radiation damage 80−34063
thermal stress, effect of, by thermal shock on substruct. and surface morphology 79−43292
thermophysical props., temp. wave methods 80−24624
time dependent phonon irrad. of detector area from pulsed incoherent phonon radiator 78−38790
torsional vibrations of sapphire rod, numerical description 77−51435
unintentionally doped, defect struct. 79−60755
vacuum UV spectra, Cr^{3+} impurity and anion vacancy conc. 78−84605
wave propagation along sapphire rod, theory 77−51434
wetting by AuSi and Si 77−85022
white, brittle fracture, microstruct. depend. 80−16469
white, three-point bending test, dislocation climb *(Japanese)* 79−96104
work hardening 77−16604
Al-sapphire-Si capacitor, effect of electron-beam aluminisation on Si-sapphire interface 77−89856
α-Al_2O_3:Co,H, Co and proton ENDOR, IR and optical spectra charge compensator nature and defect struct. 80−44956
α-Al_2O_3:Cr^{3+}(Ti^{3+})(Ti^{4+}), solid soln. hardening, yield stress conc. depend. 77−28823
Si-Al_2O_3, inversion layer subbands, magnetocond. oscills. 78−64124
Si-saphhire, Si ion implanted wafer, laser annealing 79−99989
Si-sapphire, interface radiation induced charge trapping, rapid anneal phenomena 79−19666
Si-sapphire interface charge trapping, effects of sapphire type and epi growth conditions 77−20447
Si-sapphire interface in SOS ICs, elec. investigation 80−11097
Si-sapphire interface states exam. by transient current anal. 77−43736
Si-sapphire interface structure, SIMS obs. 77−76675
Ti^{4+} doped, plastically deformed, precipitation hardening, TEM study 80−7592
Ti-sapphire interface, solid-state reaction 78−72008
W/α-Al_2O_3, heteroepitaxial structs., refined formulation of relative orientation criterias 80−44448
W/α-Al_2O_3 heteroepitaxy, orientation relationships, X-ray diffr. study 79−60661
ZrO_2, wear chart, exam. *(German)* 78−35521

satellite atmospheres *see extraterrestrial atmospheres; planetary satellites*

satellite computers
Navy navigation satellite system TRANSIT, on-board computer 79−29978

satellite links
see also artificial satellites
20 and 30 GHz, crosspolar phase variations on satellite-Earth path, meas. 77−81957
20 and 30 GHz radiometer calibration using ATS-6 satellite beacons 77−74500
22.75 GHz microwave attenuation characts. at high elevation *(Japanese)* 80−27346
aerospace systems and electronics, IEEE conference, Washington D.C., USA, 26-29 Sept (1976) 77−5420
aircraft satellite data link, for meteorological reconnaissance data transmission 78−96299
atmospheric attenuation meas. using radiometer *(Czech)* 78−36351
ATS 6/Geos 3, satellite to satellite range-rate obs. for 5° mean gravity anomalies recovery 80−41366
ATS-6, near horizon meas. over water at 30 GHz 78−24345
attenuation and cross polarisation meas. at 20 GHz, ATS-6 satellite and radar system caused by hydrometeors 79−20912
attenuation meas., satellite Earth path, in the freq., bands 20 and 30 GHz 78−7822
beacon signals from ATS-6 satellite, ground refl. effects on polarization 78−40612
Canadian government research, role and development in communications 80−43481
Canadian satellite receiving station, Newfoundland, LANDSAT and weather satellite data monitoring 77−78600
causing fading, investigation ionospheric radio lenses 78−7833
communications satellite system measurements 78−61712
Communications Technology Satellite beacon, 12 GHz meas. of Earth-space propag. 78−73422
comsat revolution, historical review 77−87239
Comstar beacon cumulative slant path rain attenuation statistics, 28.56 GHz 80−26582
COMSTAR beacon propag. expts. in 19 and 28 GHz range by Bell Laboratories, overview 78−73420
COMSTAR beacon receiver diversity experiment 78−73421
crosspolarization of microwaves due to rain on satellite to Earth path 80−21789
data communication, real-time system to increase information output 79−92600
Earth-satellite paths, 11.5 GHz, annual and annual-worst-month statistics of fading 78−57238
educational broadcasting for developing countries, case for use of satellites 80−4485
European Space Agency activities *(German)* 80−8516
exact time signal transmission using artificial satellites 77−79069
forward scatter and cross-polarisation from spheroidal ice particles 77−25733
frequency scaling of attenuation above 10 GHz due to rain 79−5595
geomagnetic monitoring system for International Magnetospheric Study 79−29882
GEOS, IUE and METEORSAT Earth Station antennas, design, charcts. *(German)* 77−56764
GEOS, IUF, and METEOSAT ground stations, weather obs., Earth exploration *(German)* 77−56763
GEOS-3/ATS-6 satellite-to-satellite tracking data for ionospheric refr. index determ. 78−93039
geosynchronous satellite orbit determination using VLBI and computer program *(Japanese)* 80−21925
Global Weather Expt., roles played by METEOSAT and TIROS-N 80−26714
ground receiving system, Earth survey data, facsimile features 77−82012
INTASAT, ionospheric plasma obs., data analysis *(Spanish)* 78−16270
integrated optical devices and applications 79−14117
intercontinental clock synchronisation, ramp method 80−47034
intercontinental time comparison by spread-spectrum random-access geostationary satellite system 77−5815
international time synchronisation, precision tracking package TEMPUS, NAVSTAR satellite network appl. 80−22332
ionosphere, UHF and VHF scintillation, signals from geostationary satellite 80−56674
ionosphere scintillations at 4 and 6 GHz using INTELSAT programs 79−5715
Ionosphere sounding satellite control, automated system 77−60572
ISEE-1 and -2, results of meas. on magnetosphere 79−29935
Kiku-2 satellite-to-Earth link, MM wave propag. expts. 79−79909
lake identification by closed planar curve analysis using LANDSAT *(Japanese)* 80−26635
Landsat D wideband communications system 80−101529
lightning crosspolarisation model 78−11961
low angle transmission effects, VHF and UHF 78−7747
low elevation-angle space-diversity expt. for 12 GHz radio path 77−70914
lunar noise effect obs. *(Japanese)* 80−82239
medium scale broadcasting satellite for experimental purposes, rain-scatter interference 79−8668
meteorological, SMS-1, SMS-2, GMS-1, METEOSAT systems *(Polish)* 79−58219
meteorological information provision for weather sensitive economic activities 80−46244
Meteosat for weather data collection, single cabinet telecommunication equipment 78−36419
Meteosat ground facilities, European/W.Indian network *(French)* 78−45183
Meteosat image processing 78−36297
METEOSAT synchronisation and image channel system *(Italian)* 77−82110
microwave, crosspolarisation phase due to ice crysts. 78−7684
microwave and satellite terminal fibre-optic links 77−27377
microwave attenuation statistics influenced by rain cell orientation 77−5278
microwave attenuation through rain, correl. with predicted values using radar 77−5279
microwave depolarisation, rain and imperfect antennas combined effects 78−92936
microwave Earth-space link, rain cell attenuation 80−94586
microwave rain attenuation, 11.6 GHz, diversity meas. at Etam and Lenox, West Virginia 79−79922
microwave rain attenuation distributions on Earth-satellite paths, empirical calc. 79−5592

satellite links continued
National Bureau of Standards time code relay to western hemisphere by satellite 80−47039
navigation using radio interferometric systems 79−25375
Northern Ontario interhospital telemedicine satellite link 77−56495
offshore oceanographic buoy with new mooring design, antenna for satellite telemetry systems 79−5660
optical, CO_2 laser intracavity electro-optical modulator 77−19443
optical, CO_2 laser system for Earth sensing satellite 77−19427
optical CO_2 laser 400 Mb/s communications terminal 77−19441
optical Nd:YAG laser 1 Gb/s satellite communication system 77−19440
orbital antenna farm, concept 80−8514
OTS payload performance, in-orbit RF meas. 80−82167
path diversity and baseline orientation [rain cell effects], geometrical approach for circular cylindrical rain cells 79−20913
polarisation fading freq., ionospheric wave disturbances, effect, simulation 78−69572
precise time recovery from Transit satellites 80−47037
PSK modems, high rate data communication 77−49268
radar reflectivity profile classified by rain types 80−101420
rain attenuation, Earth/satellite radio links, site diversity, statistical study *(Japanese)* 79−5555
rain attenuation, seasonal var. of statistics due to bright-band height 79−100889
rain attenuation above 10 GHz, regression curves for tropical areas, telecommunication, broadcasting systems appl. 80−90111
rain attenuation and depolarization of Earth-satellite transmissions at freq. greater than 10 GHz *(French)* 78−53689
rain attenuation and site diversity effect, statistical studies 78−88892
rain attenuation at 11, 14 GHz, Darwin, Australia 79−62541
rain attenuation distribution estimation, formulae, worst-month, worst-year distribution, Japan *(Japanese)* 79−100890
rain attenuation effects on multiple access transmission of data via satellite 78−77313
rain attenuation for Earth-space links, comparison between radar- and radiometer-derived data 78−24343
rain attenuation in microwave and MM wavebands, estimation of duration time distribution *(Japanese)* 80−21788
rain attenuation meas. at 35 GHz along slant paths over two sites at different altitudes 79−8667
rain attenuation of 19 GHz COMSTAR satellite beacon signals 79−5593
rain attenuation on microwave link slant path 79−66737
rain effects above 10 GHz 80−8410
rain effects on propag., prediction 77−41126
rain rate distrib. study, Japan, attenuation in telecommun. systems 78−92934
rain rate distribution study, Japan, attenuation above 10 GHz appl. 78−92934
rain slant path attenuation statistics prediction at various locations 78−24344
rain-scatter interference between satellite, terrestrial communications systems *(Japanese)* 79−16612
remote sensing by artificial satellite *(Japanese)* 79−74977
satellite VHF/UHF communications, effect of ionospheric scintillation 77−41264
satellite-to-satellite tracking, ionospheric range-rate effects 79−58174
shadow mapping to study rain attenuation on satellite microwave links 77−29505
SHF signal attenuation by rain, monitored by radar 80−51567
SHF waves for satellite broadcasting, rainfall attenuation characts. *(Japanese)* 80−12501
signal depolarisation, thunderstorms 78−3854
SIRIO, 11.6 and 17.8 GHz attenuations relationship 79−84340
SIRIO, atomic clocks synchronisation at ground stations experiment *(Italian)* 79−2751
SIRIO, microwave attenuation, fade statistics for 11.6 and 17.8 GHz *(Italian)* 80−4095
SIRIO 1 experimental satellite, propag. meas. in circular polarisation on satellite-Earth path 79−84334
SIRIO radiowave propag. data for earth-space rain-cell modelling 80−36352
SIRIO satellite, 11.6 and 17.8 GHz cumulative attenuation statistics 79−84339
SIRIO satellite down link propagation expts. in Finland 79−84338
SIRIO satellite link, 11.6 GHz, propag. meas. in Munich 79−84337
SIRIO satellite link, propag. meas. in Eastern USA 79−84343
SIRIO satellite link 11.6 GHz attenuation, meas. and estimated from sky noise temp. 79−84341
SIRIO satellite reception, atten. meas. during first year at Deutsche Bundespost Earth station at Leeheim 79−84335
SIRIO satellite signal propag. meas. by Netherlands PTT ground station, and equipment 79−84344
SIRIO satellite to Earth propagation path, precipitation scatter meas. 79−84336
SIRIO satellite transmissions near 11.6 GHz at Slough UK, meas. 79−84333
SIRIO VHF telemetry emission, use for ionospheric meas. 78−69553
SIRIO-1, analysis of oblique propag. measurements made at Gometz-la-Ville Earth station *(French)* 80−56504
slant path rain attenuation 77−86988
slant path rain attenuation characteristics in 20 and 30 GHz bands 79−8678
solar activity and effects on satellite performance 80−56812
Solar Maximum Mission GSTDN/TDRSS compatible RF system 78−45198
solar power, microwave power beaming, for long range energy transfer 79−34427
SOLRAD satellite measurements of solar radiation for ionospheric disturbance forecasting 79−58134
sound, graphical picture transmission, distrib. via domestic satellite, education appl. 80−31463
space diversity improvement, squall line direction effects 77−91205
space technology and scientific satellites, conf., Rome, Italy (Mar. 1977) 77−82107
sputnik Meteor series, TV link *(Russian)* 77−64612
standard transmissions stability on transionospheric paths 79−84577
stationkeeping, orbital perturbations of communication satellites, literature survey 78−89039
stochastic dynamic model of rain attenuation 79−53506

satellite links continued
Sub-microsecond intercontinental time comparisons by satellite 77−82494
Symphonie geostationary satellite, time transfer link for atomic clock synchronisation 80−47038
synthetic aperture radar, satellite borne, terrestrial surface mapping appl. 80−12572
time and frequency, conf., Helsinki, Finland (Aug. 1978) 80−46728
time of signal passage determination method, time scale synchronisation appl. 78−89444
time transfer experiment using Nova satellite time signals 80−47036
time transfer technology, review 80−47029
TIROS-N weather satellite, detection circuits and sync pulses for picture facsimile machine 79−53577
transionospheric propagation from a satellite, observations on the beyond-the-horizon statistics 77−25825
tropospheric fading at low elevation angles, meas. of satellite signals *(French)* 78−49069
TV broadcasting, tropospheric EM wave propag. meas. in 1978, eval. of long-term meas. *(German)* 79−84441
TV broadcasting satellite, use for precise real-time signal dissemination 80−47033
universal telemetering system *(German)* 77−73924
VHF, weather radar data transmission appl., expt. 78−20569
VHF signals, ionospheric radio fluctuation obs. from geostationary satellite 79−21091
VHF signals from satellite radio beacons, ionospheric scintillations 79−53634
VLBI, general considerations of international systems *(Japanese)* 80−17501
VLBI, Japanese domestic system, general aspects *(Japanese)* 80−17502
VLBI, Japanese domestic system, receiver and local oscillator *(Japanese)* 80−21923
VLBI, Japanese domestic system, recording signal generator *(Japanese)* 80−21924
VLBI, Japanese domestic system, selection of radio sources and experimental procedure *(Japanese)* 80−21922
VLBI, principles of measurement *(Japanese)* 80−21921
VLBI between geostationary satellites for hectometric observations of radio stars *(Japanese)* 80−21928
WARC 1979 regulations, impact on space appl. and research 80−105147
weather forecasting satellite Meteosat 78−45196
weather picture transmission, NOAA satellites 77−60458
weather-satellite picture facsimile machine, sample-and-hold detector and line dividers 77−17260
zero cross-polarisation mode for orthogonally polarised signals in rain 77−81991

satellite relay systems
aerospace systems and electronics, IEEE conference, Washington D.C., USA, 26-29 Sept (1976) 77−5420
Air Droppable Random Access Measurement System buoy sea ice tracking 77−5363
Appalachian Education Satellite Project activities and outcomes 78−12450
atmospheric noise measurement ATS-6 satellite link, 30 GHz *(Dutch)* 78−7742
ATS-6, 30 GHz signal attenuation measurement, effect of weather appl. *(Dutch)* 78−7741
automated meteorological data transmission from commercial aircraft via satellite 78−57327
biomedical broadband communication network combining satellite link and TV broadcast techniques 77−64145
BWO appl., 110 to 170 GHz, using Sm-Co ring magnets *(German)* 80−105684
CETI from Earth satellite orbit 80−4275
communication satellites, history 77−64602
CTS biomedical communications expt., selection of Earth terminal parameters 77−48898
data collection, developmental program for environmental data using Anik 1 satellite 79−39867
developing countries, economic problems 77−64604
direct broadcasting in Europe and associated European Space Agency programme 80−12638
diversity reception results, geostationary satellite ATS-6 *(Italian)* 78−49072
environmental telemetering service, geostationary, polar orbiting satellites 80−56592
geostationary, effect of solar eclipses by the Moon on broadcast satellites, prediction of occurrence 80−31199
geosynchronous orbiting, interference from solar power satellites 80−45634
Global Positioning System, computationally efficient modelling for long-term prediction of orbits 79−80198
high precision time comparison, via satellite, synchronisation discrepancy obs. 77−17953
integrated optical devices and applications 79−14117
INTELSAT V solar array design and test results 79−96471
Interkosmos program and Magion satellite project, reviews 80−98535
International Microwave Symposium, San Diego, Calif., USA (June 1977) 78−5478
large deployable solar array development for communications spacecraft 79−96469
meteorological data relay, aircraft-to-satellite 80−17380
Meteosat, weather and communications satellite 79−16790
Meteosat data-collection system, description and appl. 80−77122
MM wave space applications and technology in 100-1000 GHz range 79−92650
NTS-1, propagation effects near mag. equator 78−7839
Ogo 4, VLF signals reception, numerical study using waveguide concepts 80−90282
Orbital Test Satellite, system design rel. to communications 77−64603
PALAPA, Indonesian domestic telecommunications satellite 77−64601
radionavigation, plasmaspheric time delay effects 78−7831
rain attenuation, year and worst-month rain rate distrib. estimation method 79−5648
rigid foldout solar array development for geostationary satellites 79−96468
SARSAT, search and rescue satellite, ionospheric effects on Doppler frequency 79−58183

satellite relay systems continued
single carrier per channel system, Japanese, using medium-capacity communication satellite 77−60573
SIRIO 2, meteorological data communication from Africa appl. 79−96806
Spacelab, high rate data handling in space and on ground, multiplexing system 79−21138
Spacelab, payload data path from user input (on-board) to user ouput (laboratory) 79−21137
Spacelab data communication and acquisition system 79−84643
synchronous telecommunication and research satellites *(German)* 78−20610
TDRSS, Ni-Cd secondary batterys system design 80−30460
time dissemination using TV signals from broadcasting satellite 77−60334
time system for utility companies 79−12774
tracking, data relay satellite system, NASA, exp. data transmission appl. 79−21131
Transit, precise time dissemination system 80−57263
TRANSIT Navigation satellite, phase fluctuation and ionospheric irregularities observations 78−7832
TRANSIT satellite-referenced ionospheric propagation correction for USAF SPACETRACK radar systems 79−58131
TV instruction system, India, reception systems, overall appraisal 78−8185
V_d ratio specification atmospheric noise models 77−81992
waverider buoy GOES satellite relay system reporting 79−5663
wideband polarisation separation network with adaptive control 77−78394
worldwide maritime satellite system 77−64600

satellite vehicles *see artificial satellites*

satellites, artificial *see artificial satellites*

satellites, planetary *see planetary satellites*

saturable absorption, optical *see optical saturable absorption*

saturable core reactors
three-phase frequency meas. transducers with saturating transformers 78−77893

saturable reactors *see saturable core reactors*

saturation control *see chemical variables control*

saturation effects, optical *see optical saturation*

saturation measurement *see chemical variables measurement*

Saturn
1966 S 2, positional obs., 1980 March 15 80−85893
1979 S 3, discovery of possible satellite 80−26802
1979 S 3 to 6, 1980 S 1, possible new satellites, discovery 80−46472
1980 S 10, precise positions, 1980 March 15 to 16, and relation to Dione 80−85893
1980 S 1, 3, 6, 25, new Saturnian satellites, positional obs., (1980 March 9 to 14) 80−94749
1980 S 2, new Saturnian satellite, discovery and possible orbital periods 80−46473
1980 S 3, 13, positional obs. (1980 March 15 and 16) 80−85893
1980 S 7 to 14, Saturnian satellites, obs. (1980 March 13 to April 8) 80−62068
A and B rings, surface brightness obs. *(Russian)* 80−72872
A-ring, azimuthal brightness var. and particles size 78−32391
acetylene, detect. in Saturn atmosphere using IUE satellite 79−48731
ammonia and N mixing ratio in troposphere 80−94748
aperture synthesis study of Saturn and rings at 3.71 cm wavelength 79−96963
astrolabe obs., 1977 Jan.-April *(French)* 78−32390
astrolabe obs. at Paris (1971-6) *(French)* 78−85896
astrometry, obs. with Paris astrolabe (1975-1976) *(French)* 78−89115
astrometry, positions determ. with Odessa meridian circle, (1974 to 1975) *(Russian)* 79−44394
atmosphere, far IR spectrum, PH_3 and NH_3 absorpt. lines 78−12147
atmosphere, H_2 2-O quadrupole spectrum obs. 77−45351
atmosphere, H_2 content from spectral line equivalent width *(Russian)* 78−12143
atmosphere, inhomogeneous models 78−12149
atmosphere, ionisational nonequilib. shock layer effects on entry heating 77−25979
atmosphere, IR radiation, review 80−8568
atmosphere, latit. differences in cloud layer struct. 78−20725
atmosphere, PH_3 photochemistry 77−16807
atmosphere, Pioneer 11, IR radiometry data 80−82290
atmosphere, probe flight characts., scale model expts. 78−7854
atmosphere, Raman scatt. 78−28571
atmosphere, review 77−5470
atmosphere, seasonal phenomena from $3\nu_3$ methane band obs. 80−26803
atmosphere, struct. and comp. models, aerosols occurrence *(Russian)* 77−53465
atmosphere, thermal profile from IR meas. inversion 78−4144
atmosphere, thermal struct. 79−84735
atmosphere, upper clouds, NH_3 frost near IR refl. spectra 79−8135
atmosphere, UV photometry from Pioneer 11 probe 80−82288
atmosphere constituents, comparison with Jupiter, visible spectra obs. *(French)* 80−101550
atmosphere differential rotation, origin 80−46467
atmosphere upper layers, physical props. *(Russian)* 78−40867
atmospheric VHF refraction 80−98608
Axel dust props., Mie theory 77−37565
B-ring, optical reflectance polarimetry (1958-76 obs.) 79−44408
B-ring, optical reflectance polarimetry interpretation 80−31248
Bode's law and the 'missing moons' of Saturn 79−58480
brightness coefficient of disc centre, phase effect 80−98602
brightness temps. of Saturn and its rings at 39 μ 77−41351
C-ring structure and dynamics 78−81574
colour photographs from space probe *(German)* 77−53445
cosmic ray cutoff rigidities, theory 80−72873
D-ring, methane 890 nm band obs. 79−44407
D-ring, visual obs. (1973 September) 79−96966
decimetric radio obs., brightness temp. 80−46474
differentially rotating models, gravit. field and figure 78−7893
dynamics and He distribution, in He-He fluid planet 78−28555
E-ring, obs. during (March 1980) 80−67647
E-ring radial structure, 1980 March CCD obs. 80−105201
E-ring rel. to Enceladus orbit, max. density from CCD obs. 80−94750
echelle spectrogram 78−96426

Saturn continued
eclipse of Iapetus by shadow of planet and rings (19-20 October 1977) 78−16342
eclipses of Iapetus by Saturn and its rings, 1977, Oct. 77−91471
Enceladus, IR photometry rel. to presence of water frost 78−12146
Enceladus, near IR spectra and JHK photometry 80−56761
equatorial atmosphere, radiative portion model 77−37566
equatorial limb scans at 20 microns 79−2517
equatorial satellites motion, appl. of problem of four fixed centres 78−28493
external gravit. field, tidal perturbs. due to rings, mass of rings calc. 79−35189
F-ring, discussion based on Pioneer 11 obs. 80−105202
F-ring and new satellite, Pioneer II discoveries 80−8585
faint satellites existence, reexamination of evidence 79−16877
far IR obs., temp. determ. 79−12431
far IR photometry, atm. thermal models 79−75151
far IR spectral obs. of planetary disc and rings 78−16341
far UV spectrum, rocket obs. 78−53867
figure, hydrostatic equilib. eqn. numerical soln. 79−62773
figure parameters and gravit. moments, fifth approximation calc. 78−65547
formation of planet and satellites *(Chinese)* 78−69712
gravitational contraction history 77−33405
gravitational potential of Saturnian system 79−75152
H_2 quadrupole lines in spectrum 79−70990
Hyperion, IR photometry rel. to membership of new class of satellites 78−12146
Hyperion, near IR spectra and JHK photometry 80−56761
Hyperion, radius and albedo from 20 μ obs. 79−40136
Iapetus, brightness and B−V colour index 77−60719
Iapetus, eclipses by Saturn and rings, 1977 Oct. 19-20 and 1978 Jan. 7-8 predictions 77−53467
Iapetus, near IR reflectivity of dark and light faces 80−26800
Iapetus, radius from 1974 March 30 lunar occultation 78−36505
Iapetus, relative reflectance meas. at 1.6 and 2.2 μm 80−98607
Iapetus, theory of motion, perturbations 78−28577
imaging, photometry and polarimetry obs. from Pioneer 11 probe 80−82289
innermost satellites, separations and times of elongation, (1980 February 29 to March 18) 80−56762
insolation, latitudinal, seasonal and atmospheric effects 77−60704
interferometric obs. of Saturn and rings, at 3.71 cm wavelength 79−96962
interior model for luminosity and mag. determ. 80−109393
interior models, phase separation 78−36507
interior Vashchenko Zubarev formula for Gruneisen parameter 80−90030
ionosphere, chem. and phys. props., model calcs. 80−26801
ionosphere, model, ionization by galactic cosmic rays and solar EUV radiation 78−4142
ionosphere, spectral broadening meas. by Pioneer (11) 80−109391
IR photometry, 5-8 μm obs. 77−29711
IR scans at 7.8 to 25 μm, (1977 to 1978) 80−90363
IR spectrum 17-25 μ, comparison with thermal struct. models 77−45348
limb darkening and brightness temp., 1.30 cm interferometry obs. 80−82279
long term variation of H_2 and methane absorpt. 77−71058
Love numbers 78−16338
lunar occultation, normal reflectances of Rhea, Titan and Iapetus 78−85897
Lyman α emission from disc and ring system 78−12150
magnetic dipole axisymmetry 80−56361
magnetic field, dynamo precession model *(Russian)* 80−94752
magnetic field meas., Pioneer 11 obs. 80−82292
magnetic field origin 80−36564
magnetic moment, prediction from scaling law test 80−21934
magnetopause, affected by Jupiter's mag. tail 80−12706
magnetosphere, bowshock and magnetopause detect. by Pioneer 11, mag. field determ. 80−82283
magnetosphere, energetic ions and electrons, Pioneer 11 obs. 80−82286
magnetosphere, interactions with satellites and rings 80−82285
magnetosphere, review 78−12145
magnetosphere, trapped radiation, absorpt. by satellites and ring, Pioneer 11 obs. 80−82284
magnetosphere, trapped radiation belts, particle absorpt., Pioneer 11 obs. 80−82287
magnetosphere interaction with solar wind, Pioneer 11 obs. 80−82282
Mariner Jupiter/Saturn 1977 mission 77−73932
Mariner-Jupiter-Saturn low energy charged particle expt. 77−70971
mass, determ. from Phoebe (Saturn IX) orbital motion (1904 to 1969) 79−88621
mass determ. from Pioneer 11 trajectory var. carrier freq. Doppler shift 80−82294
methane, deuterated, obs. in 5 μm spectrum 79−25543
methane and NH_3 in outer atmosphere, obs. and model *(Russian)* 77−33406
millimetre radiation, short wave, obs. with wide-band radiometer based on superconducting point contact 79−96916
Mimas and Tethys, orbital theory including perturbs. 80−36568
natural vibration spectrum, rot. effects, calc. 80−8583
near IR polarisation, obs. 78−85899
near IR spectral albedo, obs 80−31242
NH_3 abundance from visible obs. 80−82269
oblateness parameters and satellite masses 77−56872
occultations by eclipsed Moon, 100 BC to 3000 AD period 77−49319
orbit, stability of Jupiter-Saturn-Sun system 77−9679
orbit second-order perturbations, semi-major axis secular vars. *(French)* 79−2474
orbital elements of satellites rel. to Saturn's position and mass 77−74007
orbital resonance in dissipative medium rel. to asteroids and Saturn's rings 78−28491
origin and evolution, arguments against Kumar's theory 78−45266
original evolution, evidence for accretion hypothesis 77−87311
outer ring, discovery and extent 80−46472
outer ring search, 1979 November obs. 80−17543
particle flux, Pioneer 11 meteoroid detector obs. 80−82291
perturbation of Jupiter, first order theory, critical term elimination 79−35183
Phoebe, near IR spectra and JHK photometry 80−56761
Pioneer 11 investig. 80−46476

Saturn continued
Pioneer 11 post-Jupiter trajectory midcourse manoeuvre sequence for Saturn targeting options 78−7857
planetary model using fourth order theory and molecular eqn. of state 77−82155
polar moment of inertia determ. 80−94694
position determ. in 1978 using Double Zeiss Astrograph, Belgian obs. *(French)* 80−72809
positional photographic obs. of Saturn and satellites at Pulkovo, (1971 to 1974) *(Russian)* 79−96965
positions, obs. with Algiers Observatory Danjon astrolabe (1969 to 1974) *(French)* 78−61794
positions, obs. with CERGA Observatory Danjon astrolabe, (1974 to 1976) *(French)* 78−61793
protoplanetary core formation by rain-out of Fe drops 79−66932
radio emission flux density at 102.5 MHz, upper limit meas. *(Russian)* 78−4146
radio emission in H_2O 1.35 cm line 78−20664
regular satellite system, form. model rel. to masses 78−69714
Rhea, icy satellite, mass-radius relationship 80−31222
Rhea, planetary, 1976 to 1979, rel. to possible solar variability detect. 80−98623
ring A, Encke division, photometric confirmation from Iapetus eclipses 78−45273
ring A, spiral struct. explanation for asymm. brightness 77−9705
ring A profile from stellar occultations 79−35187
ring brightness, model for azimuthal brightness variation 80−31251
ring brightness temp. meas. at 8 mm wavelength 78−36502
ring detection by focal coronograph *(French)* 80−72772
ring disappearances (1600 to 2100) 80−72876
ring E, inferences from obs. of radiation belt particles 80−41762
ring formation, particle size distribs. 77−41338
ring particle composition and size distrib. from radar obs. 78−36501
ring shadow eclipses of Iapetus, predictions 77−91472
ring system, brightness enhancements rel. to existence of supposed satellites (1980 S 7 and 23) 80−94749
ring system, ephemeris for Earth ring plane crossing (1979 October 27) 79−101115
ring system, numerical simulation of systems of colliding bodies in gravit. field 77−29634
ring system, origin and location of narrow rings 80−56764
ring system, polarimetry of light scatt. during 1979 opposition 80−36570
ring system, radii rel. to break-up and accretion limits and origin 79−84737
ring system, review of physical studies 80−72874
ring system, statistical mechanics of Keplerian orbits 78−20625
ring system, summary of recent research 80−72875
ring system, thickness from low tilt angle photometry 79−35186
ring system origin, Roche problem for polytropes in central orbits 80−82179
ring system vicinity, origin of Lyman-alpha emission 79−12430
ring system-ionosphere interaction 80−94751
rings, 22.7 μ brightness versus solar declination 78−20724
rings, 2-4 μ spectrum 77−82159
rings, 3 mm obs. and props. 80−46470
rings, amorphous ice, formation, stability and observability 79−35188
rings, anisotropic optical scatt. 77−41352
rings, apparent and true thickness 79−21225
rings, azimuthal brightness var. 78−36503
rings, azimuthal brightness vars., obs. at intermediate tilt angle 78−4145
rings, Cassini division formation, reson. with Mimas 78−61796
rings, effect on direct solar radiation reaching top of atm. 79−70992
rings, five-colour photometry 78−36504
rings, four colour phase curves, analysis 80−4295
rings, gravitational field 77−87320
rings, history and perturbation anal. *(French)* 80−82281
rings, ice sputtering by radiation belt protons 78−89116
rings, influence on gravitational field *(Russian)* 77−74008
rings, International Planetary Patrol obs. and data reduction 80−4294
rings, IR brightness and eclipse cooling obs. 80−56763
rings, maintenance by planet gravit. quadrupole moment 78−53869
rings, mass estimate from gravitational model of Saturnian system 77−60722
rings, model constraints from radar obs. of polarisation and albedo 80−82277
rings, optical thickness of Cassini division 77−71059
rings, structure and origin 78−73674
rings, structure from refl. sunlight polarization obs., disc of rock bodies 79−53767
rings, thickness caused by satellite and solar perturbs. and planetary precession 80−36569
rings, tilt effect, multiple scatt. 77−60721
rings, two-freq. radar obs. 77−33404
rings, unilluminated side, 20 μm brightness temp. 80−109392
rings, vel. dispersion calc. 78−61795
rings, vertical struct. and thickness 79−53769
rings, vertical struct. and thickness 80−4296
rings, wavy deformations caused by gravitational perturbations 78−57496
rings and regular satellite system formation 80−41746
rings azimuthal brightness vars., obs. at tilt angle (B~11.°5) 79−48732
rings composition, frost-coated semiconductor 77−29716
rings diffuse reflection, mutual shadowing effect classical calc. extensions 79−84666
rings mechanics, transversal viscosity effects on colliding bodies systems in gravit. field 77−67026
rings optical thickness, nearby faint satellites obs., possible new satellite 79−16876
rings thickness, photometric determ. 79−66959
satellite, obs. of possible new satellite 78−7921
satellite, orbits near Jupiter and Saturn, post-Newtonian effects 79−101054
satellite I-IX, astrometry obs. from McDonald Observatory (1975-1976) 80−105199
satellite system, orbit-orbit resons. 78−4093
satellites, 1966 December and 1980 March positions for five objects 80−94750
satellites, 1978 opposition astrometric obs. 79−75149
satellites, 1980 March Pic du Midi obs. 80−67646
satellites, analyses and electronographic obs. (1980 March) 80−77346

Saturn continued
satellites, astrometric obs. from McCormick Observatory (1977) 80−105200
satellites, astrometric results from 1974 lunar occultations 78−36506
satellites, light curve, surface meteoroid bombardment effects 80−26786
satellites, mutual eclipses and occultations, diameter calcs. *(Swedish)* 79−92695
satellites, precise positions during 1973 77−17421
satellites, surfaces and interiors, review 80−4297
satellites 1966 S 2 and 1980 S 15-18, separations 80−67645
satellites 1980 S 24 and 1966 S 2, 1980 April obs. 80−82280
satellites and exterior ring obs. (1980 Feb.-March) 80−51690
satellites icy interiors and surfaces evolution 78−61771
satellites mutual phenomena in 1979-1980, ephemerides 78−53868
satellites position meas. 78−81573
Saturn/Titan system, satellite aided capture of external body 79−75087
South Pole temp. enhancement, spatially resolved IR obs. 79−25541
spatially resolved IR obs., 10 and 20 μm disc scans at (B′=−11°.8) 79−84741
spectrophotometry in far IR 78−85890
stratospheric seasonal climate model 79−75150
structure and evolution, effect of dense cores 80−98603
surface temperature excess, attributed to EM phenomena *(French)* 77−60714
temperature inversion in atmosphere, model 78−12148
Titan, 16-30 μm spectroscopy 80−56760
Titan, atmosphere, review 77−5470
Titan, atmosphere organic chemistry, review 80−90364
Titan, Axel dust props., Mie theory 77−37565
Titan, brightness changes, solar activity effects 79−75177
Titan, brightness temp. at 6 cm wavelength 79−101114
Titan, contaminant terrestrial microorganisms, limitations to growth 77−41355
Titan, dynamo mag. fields possible strengths 79−16873
Titan, icy satellite, mass-radius relationship 80−31222
Titan, inhomogeneous scattering model of atmosphere 79−44406
Titan, IR spectrum from 0.8 to 2.5 microns 80−21946
Titan, Kuiper bands detect. in spectrum 78−85898
Titan, long term light vars. *(Italian)* 78−93147
Titan, N_2 atmosphere evolution 79−30005
Titan, optical props. and vertical distrib. of aerosols in atmosphere 80−46471
Titan, photochemistry of hydrocarbons in atm. 79−53766
Titan, search for H_2 (3,0) S1 line in spectrum 78−4143
Titan, secular brightness increase, 1972-76 period 78−16346
Titan, sources of UV absorpt. in spectrum 77−41353
Titan, spectral reflectivity in 0.32-0.86 μ range 79−35181
Titan, suspected near IR variability 80−46469
Titan, upper ionosphere photoionisation 77−60720
Titan (Saturn VI) eclipse, 1979 December 20, photometric obs. 80−31250
Titan atmosphere, non-Maxwellian effects assoc. with H_2 thermal escape 79−80264
Titan atmosphere, photochemical aerosols identification 80−31249
Titan atmosphere, photochemical models 80−36567
Titan atmospheric aerosol distribution, constraint 79−96964
Titan-Hyperion orbit-orbit resonance, appl. of spin-orbit theory 78−24451
Titan-Hyperion orbital resonance origin, observational test 79−25542
Titan-Hyperion resonances and close approaches, restricted three-body problem anal. 80−77347
UBV photoelectric pinhole scans of disk 79−40135
upper atmosphere, struct. from Titan eclipse light curve 80−90362
upper neutral atm. and ionosphere, vertical struct., Pioneer 11 radio occultation obs. 80−82293
UV observations by TD1A and OAO-2 satellites 77−91459
visual mapping and photometering, 1973-4 period 77−87321
Voyager imaging experiment 78−24427
Voyager IR spectroscopy and radiometry experiments 78−24428
Voyager low energy charged particle experiment 78−20618
Voyager magnetic field experiment 78−24431
Voyager mission objectives 78−24426
Voyager photopolarimeter experiment 78−20616
Voyager planetary radioastronomy experiment 78−24433
Voyager plasma experiment 78−20617
Voyager plasma wave system 78−24432
Voyager project, purpose and experiments *(Norwegian)* 79−92646
Voyager radio science experiment 78−24430
Voyager reconnaissance missions *(German)* 78−20619
Voyager spacecraft, receiver for measuring LF planetary radio emissions 78−4075
Voyager UV spectrometer experiment 78−24429
C/H, $^{12}CH_4/^{13}CH_4$ ratios, from 0.1 cm^{-1} resolution near-IR spectra 77−9698
$^{12}C/^{13}C$, evidence for telluric ratio in atmospheres of Jupiter and Saturn 78−20723
H atom cloud, generated by photo-sputtering of ice in rings 80−46475
H-He immiscibility, chemical differentiation rel. to excess luminosity 78−69798
H_2, metallic, solubility of He, Gibbs energy, fluid state model, He conc. in giant planets 79−60602
HD detect. at 6063.88 Å, D/H abundance ratio calc. 78−57495
HD search at 6045 Å, D/H ratio upper limits 78−85892
NH_3 1.56 μ band study 77−17422
NH_3 atmospheric abundance 78−12142
NH_3 vertical density profiles from IR and radioelectric emissivity data 80−82267
PH_3 abundance, IR obs. 80−82278
SAW *see surface acoustic waves*
SC (sudden commencement) *see magnetic storms*
scale invariance *see scaling phenomena*
scalers (circuits) *see scaling circuits*
scales *see balances*
scaling circuits
add-substract digital correlator, using multichannel scaler 77−61053
CMOS ICM 7216B multifunction counter used for time, frequency or period measurement *(German)* 80−74092
dead time correction of measurements using scaledown units 79−93892
decade, 133 series integrated microcircuits, vacuum luminescent display tube 77−18754
scaling circuits continued
Digitron fast multichannel time recorder 77−67949
eight-channel 64 bit scalar with static CMOS memory 78−17531
flexible multi-scaler system with micro-processor control 78−90037
four-terminal high capacitance standard 77−5869
multichannel scaling using 8-bit microcomputer 78−82595
nonlinear scaling, via programmable power supply for use with multichannel analyser 77−42218
RAMs used for multiple counters, nuclear medicine appl. 79−85870
strain gauge transducer, digital output obtained from counter and logic ccts. 79−67281
surface contamination meter 79−22494
X-ray diffractometer scanning block modernisation by scaler adjustment 80−31958

scaling phenomena
see also elementary particle theory; renormalisation
0.7-8 GeV, scaling and nonscaling of inclusive π prod. 79−22296
$(\theta^4)_4$ field, Borel summability, renormalization group, perturbation theory 78−16922
ξ scaling in lepton-hadron inclusive interactions 77−61298
σ-models, non-linear, and universality in 3-D, scaling limit, and critical behaviour, chirality 80−62824
ϕ^2 field, scaling limit in anharmonic oscillator 79−63341
ϕ^4 Euclidean field theory, scale limit of ϕ^2 80−333
ϕ^4 Grinzberg Landau Wilson model, dispersion theory and ϵ expansion for $T>T_c$ 79−12753
ϕ^6 operators in scalar systems near four dimensions, tricritical scaling and renormalisation 79−58863
A^4-coupling in abstract approach of quantum field theory, renormalisation group 80−99033
A(p,d)X, A(p,t)X, inclusive reaction clustering phenomena, scaling behaviour, knockout mechanism, review 79−6441
A(p,p)X, quasi-two-body scaling appl., single scatt. model validity 79−3151
Abelian gauge theories with dynamical symmetry breaking, effective pot., scale and chiral invariance *(Russian)* 80−57503
anharmonic oscillator, perturbed, applics. of scaling transformations 77−82384
anisotropic bond percolation in d-dimens. hypercubic lattice 79−75464
arbitrary N critical phenomena in three dimens., critical exponents 79−80746
asymptotic energy scale factors for pseudoscalar meson scatt. and charmed meson couplings 78−8620
asymptotic free field anal. of μ-p deep inelastic scaling violations 78−4863
asymptotic freedom infrared instability 80−73678
asymptotic scale factors for pseudoscalar scatt. and charmed meson couplings 77−38202
asymptotic validity of scaling in the mean, 78−479
asymptotically free colour gauge theory, electroprod. local duality and precocious scaling 77−22630
asymptotically free field theories, operator mixing and scaling deviations 77−18181
asymptotically free gauge theories, scaling violations in leptoproduction 78−4769
asymptotically free gauge theory, higher-order effects for coupling const. 77−34095
asymptotically free theories of deep inelastic muon, and electron scatt. 78−21430
atom+diatom, inelastic cross-sections, rot. quantum number, energy scaling 77−83692
automodelling validity disturbance and problem of scaled variables *(Russian)* 79−2943
baryon-baryon scatt., ang. depend. of differential cross-section 77−255
BBGKY hierarchy, scaling method of kinetic eqn. derivation 78−54286
Bethe-Salpeter model, scaling reconstruction using renormalisation group, Callan-Symanzik eqn., ϕ_6^3 theory *(Russian)* 80−42351
Bjorken and Feynman scaling violation, connection, wee parton region 77−18229
Bjorken asymptotic behavior of deep inelastic scattering form factors and the general principles of field theory 79−21958
Bjorken scaling, deep inelastic struct. function for rest frame, quark-parton model 77−87942
Bjorken scaling, review of parton model 77−57498
Bjorken scaling in neutrino expts., quark charged current tests 77−22726
Bjorken scaling law violation, mass dependent, quark-quark interactions 80−9160
Bjorken scaling violation, dynamical approach, N struct. functions 77−49976
Bjorken scaling violation, model of quarks with size and excited states 78−74208
Bjorken scaling violation, QCD and models of quarks with substructure 80−105851
Bjorken scaling violation models of quarks with substructure 79−26305
Bjorken scaling violations in large angle electroprod. 77−87980
Bloom-Gilman duality, scaling violations 78−21399
bond percolation, Monte Carlo anal. of scaling 78−77804
Bose gas, impenetrable, one particle reduced density matrix, Painleve-type eqn. 80−62576
Bounds on slope of diffraction peak and zeros of absorptive differential cross sections 78−74282
Callan-Gross relation, instanton violation, nonperturbation correction asymptotic behaviour 80−27409
canonical scaling in hadronic high-p_T processes, parton Fermi motion 78−45977
cascade models, transverse momentum depend. of quark fragmentation functions 79−45068
causality, Regge behaviour, proton electroprod. struct. function, Bjorken limit of sum rule 77−67662
central rapidity region, asymptotic and nonasymptotic energies, Reggeon field theory, nonleading terms 77−10185
charged particle multiplicity distrib., high energy p-emulsion and π^--emulsion collisions, KNO scaling 78−70568
charm production, mass scales, in deep inelastic processes, parton model, generalised VDM 77−13930
charm quark prod., scaling violation as threshold effect 78−66088
charm quark prod. in deep inelastic lepton scatt. 78−21436
charmed particles, inclusive semileptonic decay, struct. functions, scaling limits 78−82165

scaling phenomena continued
charmonium potential models, testing Q^2 duality 79−45082
chiral models in three space dimens., finite energy static solns. 77−203
classical, cross-section generating solutions of field equations 79−97488
classical and quantum scaling 79−35626
colour gauge theory, quark elastic scatt. and large transverse mom. hadron prod. 78−8610
complex scaling transformations in stationary and scattering problems 79−18124
compound quarks, gluons and parton confinement 79−22017
conference, lepton-hadron physics, Karlsruhe, Germany (Sep. 1978) 80−73098
continuous mass spectrum, scale and conformal invariance, scalar currents 78−62335
cosmic gamma ray high energy families, f' spectrum 78−28466
cosmic ray EAS, conflict with scaling, 10^{15} to 10^{17} eV 77−61336
cosmic ray muons, scaling and charge ratio, Muller-Regge phenomenology 79−12371
cosmic ray muons, sea-level spectrum, Dao scaling model for $pp \rightarrow \pi^- X$ 78−61694
cosmic rays at 1-10 TeV, γ-ray, electron, muon spectra 77−64576
cosmic rays ultrahigh energy interactions, scaling deviations and modified models 79−80172
covariant derivatives without gauge fields 80−73584
covariant parton model, pattern of scaling violation, openings of new channels 77−41815
critical dynamics, Monte Carlo anal. of renormalisation group, scale transform. 77−22513
critical exponents, three dimensional system with short-range interaction, calc. 80−42348
critical phenomena and scale invariance 77−22511
critical scattering theory, book 79−25913
cumulative π, electroproduction from d, effect of rescatt., scaling effects *(Russian)* 78−74265
current-induced reactions, dual unitarisation 78−74233
cyclical meas. ambiguity elimination, alphabetic soln. rule selection *(Russian)* 79−21689
deep inelastic $F_2^n(x)/F_2^p(x)$ near $x=1$, chirality 77−10258
deep inelastic lepton-hadron interactions, scaling deviations 78−32991
deep inelastic lepton-hadron scatt. in massive vector gauge models 78−74262
deep inelastic leptroproduction, meson bound state contrib. to σ_L/σ_T 80−78029
deep inelastic scatt. and lepton pair prod., covariant parton model approach to scaling 78−21431
deep inelastic scatt. and rising $\sigma(\bar{\nu})/\sigma(\nu)$ ratio, neutron-proton structure function difference 77−49978
deep inelastic scattering, struct. functions, 2nd order corrections, theoretical calcs. in QCD 79−71688
deep inelastic struct. functions, direct method for QCD predictions of scaling violations 79−80800
deep-inelastic leptoproduction off nucleons, struct. function model in asymptotically free gauge models 79−40786
diffractals (wave interaction with fractals) 79−58549
diffraction peak scaling, collisions of arbitrary spin particles 77−18252
diffusion in bistable potential, systematic WKB treatment 80−46975
dilepton production and scaling in hadron interactions 77−50031
dimensional anal. in renormalised perturbation theory 78−24950
dimensional symmetry rearrangement in renormalised quantum field theory 77−5982
dimuon continuum production in hadron collisions, nonscaling behaviour 79−22156
diquark contribs. to scaling violation and deep inelastic σ_L/σ_T, structure functions, QCD 80−22573
discrete symmetry scaling and the virial theorem 79−58894
discriminative deep inelastic tests of strong interaction field theories, QCD scaling violations 79−89105
disordered systems, mode softened unified theory 79−55637
double-phase representation, fixed-angle and fixed-momentum-transfer scatt. 78−8628
Dreel-Yan processes, gluon corrections 78−8597
Drell-Yan conjecture in asymptotically free theories 79−17689
Drell-Yan process, heavy lepton pair prod., non-scaling parton model 77−13928
Drell-Yan scaling, absorptive corrections, for initial and final hadronic state interaction 80−4950
dual two-loop graph double Pomeron region, particle prod. 79−75751
duality model, scaling violation in ν and μ interactions 78−8623
dynamical scaling violations, evidence from neutral current anomalies 79−17664
dynamical scaling violations, slow rescaling discrimination using neutral current anomalies 77−49896
dynamical symmetry and asymptotic scale invariance in ladder models 79−21959
EAS, validity of Feynman scaling 78−28469
eight quark model, modified left-handed currents, ν reactions and e^+e^- annihilations 78−16982
eikonal model, multiplicity distribs., KNO scaling 78−41514
eikonal model multiplicity distrib. and Koba-Nielsen-Olesen scaling *(Russian)* 79−9355
elastic differential cross sections, model independ. aspects 77−256
elastic form factors, asymptotic behaviour, Callan-Symanzik eqns. *(Portuguese)* 80−18137
elastic hadron-hadron diffraction scatt. processes, scaling, conformal mapping without spurious cut 80−82992
elastic phase transitions, crit. dynamics 80−2146
elastic scattering of elementary particles, relativistically invariant scaling law 77−13986
electromagnetic and neutrino scattering, scaling violations 79−17713
electroproduction data, model-independ. anal. of precocious scaling 77−5999
electroproduction struct. functions scaling props. and Gross-Nevau model anomalous dimens. 77−67660
elementary particle phenomena, rel. to undergraduate physics 78−54118
EM form factors in Bjorken limit and their Fourier transforms on light cone 79−26246
emulsion nuclei, 28 GeV proton interactions *(Korean)* 80−18299
energy inclusive meas., parton model and scaling laws 77−74733
equation of state scaling function in $1/n$ and ε expansions 77−87718
Euclidean fields, low momentum behaviour scale limit 80−62834

scaling phenomena continued
exclusive meson electroprod. on nucleon, cross section asymptotics, scaling functions *(Russian)* 79−22111
Fermi-motion, canonical scaling of partons in hadronic high p_T processes 78−29314
fermion system, one-dimens., three-loop scaling eqns. using renormalisation group method 79−80508
fermion-fermion high energy scatt., transverse momentum cut-off hypothesis, Yang-Mills theory 80−86575
Feynman scaling, interaction model for 10^6 GeV cosmic rays in atm. 77−45271
Feynman scaling, multihadron prod. through intermediate reson. 78−78152
Feynman-Wilson fluid, density fluctuations, multiparticle event asymptotic struct. 79−36040
Feynman-Wilson gas, KNO scaling, phase transitions 77−30094
Feynman-Wilson gas, statistical model for multiparticle physics 79−22071
fine structure of inclusive and semi-inclusive spectra, fragmentation, cluster, Chew-Pignotti models *(Chinese)* 79−58984
fine structure of inclusive spectra, sum rules and Feynman-Yang scaling generalisation *(Chinese)* 79−49557
finite Bose system, condensate fraction growth, boundary condition effects 77−74318
finite size scaling theory, static, dynamic, based on renormalisation group approach, critical phenomena exam. 78−16745
form factors of deep inelastic scattering, Tauberian theorems in quantum field theory 80−68375
G_1, spin depend. struct. function, scaling violations 78−93880
gauge theory and neutrino physics, book 79−30726
geometrical aspects of statistical physics, scaling and fractals 79−58625
geometrical pomeron, shielding cut mechanism 77−2807
geometrical scaling at inelastic threshold, appl. to K^+p, $\pi\pi$, $K\pi$ 77−22797
Ginzburg-Landau model, scaling at low temp. 77−30121
gluon fragmentation functions from quark jets 79−49453
hadron+hadron, cluster model, field theoretic, multiperipheral production, Feynman scaling violation 80−57576
hadron+hadron, high-energy, inclusive spectra of secondary pions, Feynman scaling and statistical model 80−42502
hadron+hadron$\rightarrow\gamma\gamma$X, scaling and quark mass dependence, quark parton model 80−73749
hadron+hadron interactions, Drell-Yan dynamics, lepton pair from $q\bar{q}$ collision, energy scaling breakdown 78−54610
hadron+nucleus cross-section, energy depend., multiplicity, scaling violation model *(Russian)* 79−22350
hadron dynamics, multiparticle prod., intermol. pot. in Feynman-Wilson gas 78−477
hadron interactions, local thermodynamic equilibrium *(Russian)* 80−9155
hadron interactions, violation of scaling model *(Russian)* 78−78231
hadron reactions, large, small momentum transfer regions, transition point for s-depend. 77−30339
hadron-hadron diffraction scatt., convergent polynomial expansion, scaling 79−45096
hadron-hadron hard collisions, calorimeter trigger, Ochs-Stodolsky scaling law derivation, parton model 79−17775
hadron-hadron interactions, scale invariant variable *(Russian)* 78−82227
hadron-hadron interactions, scaling law 78−41606
hadron-nucleus reactions, 20-400 GeV, multiplicity of relativistic charged particles *(Russian)* 80−5191
hadron-proton amplitudes, real parts from 3-universality 77−49926
hadronic amplitudes in scaling region for e^+e^- and e^-+hadron 78−41484
hadronic collisions violation of Feynman scaling, central region, fragmentation, mixed two component model 77−26551
hadronic constituents with size and excited states and scaling violation 78−29299
hadronic EM current, short distance scaling, R(s) behaviour as $s\rightarrow\infty$ 79−22095
hadronic interactions, 10^{12} to 10^{15}eV, and cosmic ray components in atmosphere 79−62708
hadronic large p_T reactions, K^+ and K^- prod. as model test, hard quark scatt. 79−40735
hadronic massive lepton pair prod., theory review, Drell-Yan model, scaling violation 78−89752
hadronic muon pair prod. QCD radiation and mean scaling, longitudinal and transverse momentum 80−42405
hadronic phase transitions, evidence from present data phenomenology 79−45006
hadronic reactions, universal scaling law 80−18082
hadronic structure using parton anal. of deep inelastic scattering and rel. processes 79−80803
hard QCD processes, relations through mass singularity universality 79−22054
heavy black and grey prongs in nuclear emulsions, scaling in multiplicity distribs. 79−49555
heavy meson hadroproduction, QCD effect on scale breaking 80−37239
helical curve motion and soliton eqns., scaling invariance 78−49667
high energy cosmic rays, EAS and energy deposition 79−66898
high energy inelastic hadron reactions, π prod., scaling law, fireball model 78−74287
high energy interactions, above 100 TeV, scaling violation, momentum transfer increase, and exotic phenomena 79−63563
high energy interactions, scaling, limited fragmentation, cosmic ray models 77−10211
high energy interactions and cosmic ray components in the atmosphere 79−62707
high energy two-particle interactions, scaling 78−4878
high mass dilepton prod., comparison with Drell-Yan formula in asymptotically free theories 80−4942
high-energy cosmic-ray components in atmosphere 78−93062
hydrodynamic model, scaling and logarithmic multiplicity of secondary hadrons *(Russian)* 77−10221
hydrodynamic theory of multiple hadron production, new approach *(Russian)* 79−6332
hydrodynamical model of multiparticle prod., scaling solns. 78−8616
hyperon-nucleon high energy reactions, differential cross sections, inclusive hyperon resonance prod. 77−18331
hyperscaling and the critical exponent ν 79−80747

scaling phenomena continued
inclusive and semi-inclusive reactions, relation of Feynman scaling 79−35962
inclusive and semi-inclusive scaling-in-the-mean functions 78−4880
inclusive charged current scatt., new quark flavours and scaling 77−82731
inclusive cross section density matrix and scaling props. 77−41872
inclusive electroproduction, local duality and precocious scaling, quantum chromodynamics 77−2842
inclusive form factor scaling w.r.t. generalised scaled variable 80−417
inclusive hadron production in high energy particle+nucleus collisions, sum rules, scaling law 77−57673
inclusive leptoproductions, scaling violation, colour-octet model effect 79−13077
inclusive process, quark confinement in nonlocal quantum field theory 77−13915
inclusive processes, scaling hypothesis for the rapidity distributions and information theory 80−73747
inclusive production of hadrons in high energy nucleus+nucleus collisions, scaling laws 78−33204
inclusive production of hadrons in particle-particle collisions at high energies, scaling law 78−54656
inclusive single-particle distribution function structure, urbaryon model 77−18343
indefinite-metric fields and renormalisation group 78−8529
Ising field theory, Z_2 duality algebra in D=2 quantum field theory 79−75685
Ising model, scaling limit 78−45573
Ising model, surface tension, using real-space renormalisation group methods 78−47985
Ising model amplitudes and extended lattice-lattice scaling 78−6495
Ising model with free surface, series anal. 80−25062
Ising rectangular ferromagnet, pair correlation function using spinor technique 78−70063
Ising spin 1/2 model, confluent singularities and hyperscaling 79−73655
Ising spin $^1/_2$ model, renormalisation group approach 80−2582
jet and lepton-pair production in high-energy lepton-hadron and hadron-hadron scattering 79−17729
jet model, uncorrelated, implications of Bose-Einstein statistics 79−22070
jet model with quantum statistics, Touschek invariant meas. 79−22068
Jost-Lehmann-Dyson representation, scale invariance breaking and spectral function 80−13316
Kellen-Simanzik eqn., correlation function scaling behaviour in phase transitions *(Russian)* 80−57502
kinematical scale breaking in high p_T interactions, parton fragmentation function 80−367
kinematical scale breaking in high P_T interactions 79−13064
KNO deviation at high energies in multiperipheral n-particle prod. *(Russian)* 77−34141
KNO scaling, automodel behaviour of multiplicity distrib. as function of inelasticity factor *(Russian)* 79−89213
KNO scaling, possible struct. in correlations *(Russian)* 77−2887
KNO scaling and multicomponent cluster models 77−49918
KNO scaling and scaling in the mean for semi-inclusive processes *(Chinese)* 80−22538
KNO scaling for high-energy multiplicity distribs., distrib. functions 77−18237
Koba-Nielsen-Olesen scaling, asymptotic behaviour of multiplicities 78−78083
Landau crit. point, mean-field theory, scaling theory and crit. exponents to second order in ϵ^2 79−4395
Landau hydrodynamical model of multiparticle prod. due to viscosity 78−4836
large $p_\perp$ photoproduction, gluon fragmentation function extraction, scaling 80−105853
large p_t inclusive interactions, scaling behaviour of γ/π prod. cross section ratio, models testing 77−50032
large transverse momentum hadronic reactions, hard scatt. model of urbaryons with two-jet struct. 77−41813
lattice field theory, Ising model and scaling 77−5991
lattice gauge theories, extrapolation to continuum limit 80−349
lattice Hamiltonian field theory, finite-size scaling 80−73580
lattice-lattice scaling, reln. to scaled eqn. of state, appl. to Ising model 78−70067
lepton+hadron, deep inelastic scatt., quark-parton model with logarithmic scaling violation 80−78071
lepton pair production in hadronic collisions, parton model and scaling approach 78−82150
lepton scatt. off protons and deuterons nonscaling behaviour 78−8642
lepton-hadron deep inelastic scatt., massive vector gauge model, Bjorken scaling violation *(Russian)* 78−89720
lepton-hadron deep inelastic scatt., Regge behaviour, Bjorken scaling 77−244
lepton-hadron generalised scaling variable in parton model 77−10259
lepton-hadron hard reactions, scaling features, correlating quark rearrangement model 79−58939
lepton-hadron inclusive cross sections, kinematical scaling isolation 78−8671
lepton-hadron inclusive interactions, quark and target mass effects, colour SU_3 theory 77−6090
lepton-hadron relation and a new KNO-type of scaling 79−9414
Lie groups, compact, simple, rank 2, irreducible representations *(Chinese)* 80−68391
Lifshitz point, critical wavevector 78−36954
Lorentz invariant hypothesis, appl. to single particle distrib. functions 77−38214
magnetic critical phenomena, use of renormalisation group, review 77−20625
many-body systems, resons., extended virial theorem, complex scaling, Schrodinger operators 79−21575
many-electron systems, time depend., complex scaling and resons. calcs. 79−22612
many-hadron production at low $P_\perp$, basic concepts and models, review 79−6331
mass corrections to scaling in deep inelastic processes 77−13929
mass scale effects in parton model 78−25017
mass scaling for molecular systems, quantum mech. theory 77−83475
massive lepton pair production in meson-nucleon collisions 79−63532
massive particle decoupling in field theory, scaled mass, Feynman amplitudes 79−71585

scaling phenomena continued
massive Thirring model with bosons, asymptotic scale invariance 78−93799
Mellin transform hologram scale invariance obs. *(Russian)* 79−94183
meson-baryon scatt., ang. depend. of differential cross-section 77−255
metrical connection in space-time, Newton's and Hubble's laws 78−57435
minimal metallic cond., localisation scaling theory *(Russian)* 80−103671
MIT bag, one-dimens., Bjorken scaling, mass corrections 78−62356
MIT bag model cavity approx., parton distribs., Bjorken scaling 78−89664
moving poles in the scale-dimension plane and scaling violation 79−12983
multi-particle and inclusive reaction, at high energies, review 79−17777
multiparticle inclusive prod., cluster sequential decays, scaling violations 77−49934
multiparticle prod. in hadron-hadron collisions, scaling and multiperipheral model, review *(Russian)* 77−2875
multiparticle reactions on deuterons, multiperipheral parton model anal. to rescatt. 79−22154
multiple hadron generating models, transition to KNO scaling *(Russian)* 79−22051
multiple production, scale invariant solution in hydrodynamic theory *(Russian)* 78−45896
multiplicative renormalisation group, relation to critical phenomena in phase changes *(Hungarian)* 77−54042
multiplicity, average, energy depend. and scaling-in-the-mean 78−29369
multiplicity distrib. scaling law at high energies 77−54083
multiplicity distribs. for nonasymptotic energies, concept of similarity *(Russian)* 78−41522
muon scattering at Fermilab, inclusive scatt., quark models, scaling violation 80−5001
n-component spin system, anisotropic Brillouin zone, Wilson-Feynman graph technique, universality 77−5764
neutral currents and scaling violation 78−41529
neutrino scattering scale breaking models 79−13107
non-Abelian gauge theories, canonical methods, renormalisation 77−41764
non-equilibrium systems near instability, systematic scaling expansion 77−49669
non-linear transport equations: Properties deduced through transformation groups 80−4680
nonequilibrium statistical mechanics, scaling for space-time coarse graining 79−40521
nonequilibrium statistical mechanics, space-time coarse graining scaling, kinetic eqns. 79−75445
nonrenormalisable field theories, scale-invariant solns. *(Russian)* 77−34097
nonscaling parton model, large p_T processes in hadron collisions 79−352
nuclear backward π^+ prod., momentum depend., scaling, Monte Carlo calcs. 79−13305
nuclear coherent recoil dominance, basis for quasi two-body scaling 78−50140
nuclear interactions around 20 TeV, characts., comparison with Monte Carlo simulation 79−58991
nuclear reactions, quasi-two-body scaling 78−8791
nucleon, constituent quarks and deviations from Bjorken scaling 77−6089
nucleon form factors, asymptotic relations from quark-gluon model, scaling violation 80−42463
nucleon structure function, empirical formula, scaling violation 77−38171
nucleon structure functions from quark distrib. functions anal. of μp and μd interactions 78−50035
$O(\epsilon^2)$ scaling law for $d\sigma/dt$ in the Reggeon field theory 80−101936
one particle reduced density matrix of impenetrable bosons in one dimension at zero temperature 80−17863
one-dimensional cascade model of interacting nuclei, scaling law 78−17233
one-dimensional electron-phonon system, renormalisation *(Russian)* 78−43314
one-dimensional Fermi gas model with two charact. energies, scaling theory 78−6287
operator products near light cone, expansion in terms of regular bilocal operators 77−87899
particle and antiparticle prod. by 200 GeV/c p is CERN SPS charged hyperon beam 79−71768
parton model, mass scale effects 78−21389
parton model in renormalisable field theory, anomalous dimension 77−22682
parton model of large transverse momentum processes, logarithmic corrections to Bjorken scaling 77−71483
parton model scaling violation mechanisms, electroprod. as quark sea effects *(Russian)* 79−9344
parton transverse momenta, scaling violation effect 78−41483
parton transverse momentum distrib., scaling violation mechanism 78−89661
percolation backbone problem, large cell renormalisation group 79−69481
percolation in 1-D, ghost fields, pair correctedness and scaling 78−4560
percolation theory, scaling assumption for lattice animals 78−54313
percolation theory at the critical dimension 79−152
perturbative QCD, jets, inelastic distribs., colourless clusters, scaling, multiplicity and tree evolution 80−52459
perturbative QCD, renormalisation improvement, charmonium decay and scaling violations 80−101993
phase cyclic meas. ambiguity elimination *(Russian)* 79−6072
photoemulsion nuclei, π^+ absorption, up to 114 MeV, nuclear scaling *(Russian)* 78−25247
photon structure functions, anomalous components, using Altarelli-Parisi eqns. for QCD scale breaking 79−63479
planar-rotator model with short range interaction 79−80540
point like spin-3/2 quarks, contrib. to deep inelastic struct. functions 80−47250
position space renormalizations and the breakdown of hyperscaling 79−40482
precocious scaling, asymptotically-free field theory 77−18182
precocious scaling in field theories 78−8525
proton and neutron struct. functions, parton model 78−16988

scaling phenomena continued
proton electroproduction struct. function, elastic form factor, scaling function, causal representation 79−13138
pseudospherical surfaces in soliton eqns., conservation laws, Backlund and scale transformations 79−75688
QCD, Bjorken scaling violations 79−22033
QCD, hadronic semi-inclusive processes, calc. of scaling props. 79−13027
QCD, high transverse momentum meson prod., scale breaking 78−45861
QCD, impulse approx. and scaling phenomena 79−22043
QCD, inclusive distributions in extended leading logarithms 79−13066
QCD, leptoprod. and Drell-Yan processes beyond leading approx., Bjorken scaling 79−6323
QCD, quark and gluon propagators 80−52469
QCD, scale breaking for quark and gluon distribs., diagrammatic anal. 79−71706
QCD, scaling violation pattern, higher order terms 80−27468
QCD, Schrodinger equation scaling props. 79−67496
QCD, slope of leading Regge trajectory 80−42391
QCD effects, parton transverse momenta, large-p_T hadron prod. 78−66083
QCD extended leading logarithm approx. for inclusive distribs. and lepton pair prod. 80−379
QCD hadron jets, branching processes, multiplicity distrib., KNO scaling *(Russian)* 80−101998
QCD observables in higher order calcs. 79−9334
QCD opposite two hadron correl., scale violations in quark/gluon fragmentation functions 79−54299
QCD perturbation theory, quark decay functions, heavy hadron prod. 78−62364
QCD predictions, subtraction scheme depend., struct. function scaling 79−49450
QCD predictions of deep inelastic scaling violations, non-perturbative effects 79−40732
QCD scale parameter from quark matter phase transition 79−89112
QCD vacuum, effects on hadronic currents, instantons, e^+e^- annihilation and precocious scaling 79−332
QED, conformal-invariant, Ward identity of dilation current 80−68401
QED, heavy particle effects, factorised local operators, renormalisation group 80−62898
QED, scale and conformal covariance 77−6067
QFT, scaling variable 78−70269
quantum chromodynamics, scale violation in presence of instantons 77−61196
quantum chromodynamics, two dimens., confinement form factors, deep inelastic scatt. 77−30322
quantum-chromodynamic predictions for inclusive spin-spin asymmetries at large transverse momentum 79−49472
quark fragmentation functions in Monte Carlo quark parton model of e^+e^- annihilation 79−80791
quark model, relativistic, with linear scaling pot. 77−38125
quark-parton distributions model, large transverse momentum hadrons, logarithmic scale breaking 78−16989
quark-parton model, Large-p_T correlations in scale-breaking model 77−82704
quark-parton model, with scaling violations, large p_T processes anal. 78−45927
quarkonium, quantum mechanical applications, masses and leptonic widths of ψ and Υ 80−27484
quarkonium, scaling and prescaling 79−40726
quarkonium level splittings, scaling behaviour, semiclassical methods 79−75742
quarks with substructure and new Bjorken scaling 79−17674
radial scaling analysis in single particle inclusive reactions 77−18351
radiointerferometric phase meas. ambiguity detection, recurrence relationship *(Russian)* 79−25513
rapidity in distrib. in inclusive reacts. *(Russian)* 78−41518
Reggeon field theory on a lattice, critical behaviour, Monte Carlo calc. 80−18126
relativistic form factors for clusters with nonrelativistic wave functions 77−30382
renormalisation group, scale breaking model 78−49972
renormalisation group, scaling factor, 2-D model 78−41237
renormalisation group and scale invariance, asymptotic fields 77−2741
renormalisation group and scale transformations for renormalised field operators 77−30245
renormalisation group approach to scaling, phys. appl. 78−49634
renormalisation group equations in critical dynamics, scaling far from equilib. 77−28395
renormalisation group model with non-Gaussian fixed point 78−54564
renormalisation group transformations as symm. mappings, Kadanoff global scaling laws *(German)* 78−49953
resonance-saturation picture, scaling violation patterns 80−82940
resonances and complex scaling: a rigorous overview 79−17258
resonant pole trajectories in complex scaling, stationarity, appl. to H atoms 79−18126
s-dependence of proton fragmentation by hadrons, 30-250 GeV/c 78−74291
s-dependence of proton fragmentation by hadrons 4-24 GeV/c 78−74290
S-matrix time-delay operator from scale-invariance 77−79227
scalar field theories, finite amplitudes in perturbation theory, ϕ^n models, pass. renormalisation 78−93794
scale breaking parton model for electron and neutrino deep inelastic scatt. 78−66122
scale dependent quark mass in colour gauge theory, $e^+e^-\rightarrow$hadrons anal. 77−30320
scaling and multiplicative renormalising in solid state physics, review *(Hungarian)* 79−11289
scaling in the mean, connection with Feynman scaling, semiinclusive reactions at asymptotic energies 78−29363
scaling laws with account of positivity props. 77−6013
scattering amplitudes and complex scaling 79−17257
scattering amplitudes satisfying geometrical scaling, low and high-energy props. 78−86447
Schrodinger eqn., charmonium 78−54613
second order transformations in ideal and disordered systems *(German)* 79−40508
self avoiding walk attached to a surface, tests of scaling theory 78−81927
semi-inclusive distribs., renormalisation group anal. of scaling behaviour 79−30660
scaling phenomena continued
semi-inclusive processes of multiparticle productions, scaling laws 79−30684
semi-inclusive rapidity distrib., scaling in the mean 79−93309
semi-inclusive reactions, many particle, new types, rapidity gap, scaling and exptl. results *(Chinese)* 77−74729
semi-inclusive single particle cross-sections, upper bounds determ. 78−41442
semi-infinite systems, critical behaviour 78−4563
short distance and the maximal degree of a field theory 79−54279
shrinking diffraction peaks, scaling property, elastic unpolarised differential cross section 77−18206
single particle semiinclusive distributions, scaling in the mean at asymptotic energies 77−57576
solitons, scale invariance 79−58866
space-time, foam-like structure, Bjorken scaling violation due to gravitational field 80−77939
spacetime structure theory at very short distances, nonlinear sigma model 80−12979
spinor fields, conformal, dimensions, scale invariance 80−27394
superconformal unified field theory 78−12848
t-flavoured meson production in photonuclear and pp collision, parton distribution functions with scale breaking 80−22623
thermodynamic stability and ctit. points, ferromagnets and simple fluids 78−16766
Thirring model, massive, with internal U(n) symmetry, zero mass limit 77−57466
Thirring model with SU_n symmetry, scale invariance 79−9288
Thomas-Fermi type picture of EM structure of π and N 80−9170
three resonantly interacting particles, scatt. processes and bound states *(Russian)* 79−54017
Tokamaks with shear, scaling law for trapped ion anomalous diffusion 80−32492
totally inclusive leptoprod., scaling anal., target mass corrections in QCD parton model 80−102052
transient nonlinear fluctuations, scaling theory, macroscopic order formation 79−80520
transverse mass scaling 78−25018
tricritical behaviour, nonuniversality 78−93640
turbulence universality and scaling, review 79−58548
two gluon jets in e^+e^- annihilation, scaling limit ang. distrib. 79−54314
two-current two-particle amplitude, narrow-reson. model, gauge invariance and scaling 77−74576
two-dimensional systems, crit. percolation behaviour, renormalisation-group approach 79−4396
two-hadrons inclusive reactions and correl., large p_T, scale-violating quark model 78−74292
two-well oscillator, eigenvalues, scaling properties, WKB approx. 79−25897
uncorrelated jet model at high energy, quantum statistics, soft pion prod. 78−16995
unified scalar-free theory, order-R vacuum functional, with spontaneous scale breaking 80−78003
unitarity and crossing in high energy scatt., differential cross section in diffraction region *(Russian)* 79−80764
vector meson-nucleon scatt., scaling 78−45810
violation in infinite-momentum frame 78−70286
violation in QFT 78−66037
violation of scaling anal. 78−62406
virtual Compton amplitude, high-energy deep-inelastic scatt. 78−41550
weak charmed-baryon resonance prod., neutrino inclusive interactions, scaling behaviour 78−8645
weakly random system, limit $n\rightarrow\infty$, scaling function for eqn. of state 78−73953
WKB approx. and scaling behaviour for Hellmann-Feynman and virial theorems 78−86193
Wroblewski relationship, scaling phenomena, renormalisation group eqns. *(Chinese)* 79−92986
(e,e), A=2, 3, 4, scaling laws in relativistic impulse approx. model, spin effects 80−52662
e(μ)(ν) deep inelastic scattering, minimal mass corrections 79−30740
e(μ)p, polarised deep inelastic scatt., scaling props. of struct. functions 78−45926
e-p deep inelastic scaling at SLAC, possible valence gluon evidence 77−30310
ed, deep inelastic scatt., nucleon struct. function moments anal., asymptotic freedom critical tests 79−54344
ed, elastic and inelastic scatt., quarks and dimensional scaling 77−6132
ed deep inelastic scatt. cross sections, quark-parton model with broken scaling *(Russian)* 80−32109
ed deep inelastic scattering, phenomenological determ. of electroprod. struct. functions 79−63478
ed inelastic scatt. at high momentum transfer, scaling anal. 77−26531
eē scattering, energy depend. scale dimens. in QED 77−79239
$e^+e^-\rightarrow$ hadrons, scaling and quark struct. 80−425
$e^+e^-\rightarrow$ hadrons, two-fireball model, jet problem 77−65165
e^+e^- annihilation and deep inelastic scatt., VDM approach 77−46068
e^+e^- annihilation and quark fragmentation functions, Monte Carlo quark-parton model 79−22119
e^+e^- annihilation channel, differential dispersive theory of ψ/J 78−45933
e^+e^- collisions, jet prod. and two-photon annihilation, hadron spectra 80−91121
$e^+e^-\rightarrow\Delta X$, polarisation effects in nonperturbative parton model, scaling 80−105912
e^+e^- final states, $q\bar{q}$ decay, semiclassical model, vacuum polarisation by colour field 80−63011
$e^+e^-\rightarrow h^{\pm}X$, 13 and 25 GeV^2, cross sections, scaling 77−49989
$e^+e^-\rightarrow h^{\pm}X$, dynamical scaling 77−6137
$e^+e^-\rightarrow h^{\pm}X$, violation Bjorken scaling, momentum fluctuation, range of timelike photon 79−3033
$e^+e^-\rightarrow$hadrons, 53 GeV^2, $\pi^{\pm}$ and $K^{\pm}$ cross sections, scaling 78−78201
$e^+e^-\rightarrow$hadrons, asymptotically free quark model predictions in complex plane 77−71522
$e^+e^-\rightarrow$hadrons, deviation from Bjorken scaling, differential dispersive anal. 77−74698
$e^+e^-\rightarrow$hadrons, multiplicity, scaling, inclusive spectrum, simple hadron cascade model 78−66135
$e^+e^-\rightarrow$hadrons, scaling and quark binding anal., generalised vector dominance 77−249

scaling phenomena continued
e^+e^- inclusive annihilation, scaling and cluster decay phenomena 77−2854
e^+e^- inclusive annihilation, scaling function in multiperipheral fireball model 77−87985
$e^+e^-\rightarrow q\bar{q}g$, (3g), jet-mass spectra, perturbative QCD 80−63006
e^+e^- scaling in bound state models 77−38181
eN, scaling violation, Callan-Gross relation, colour excitation 77−65159
eN deep inelastic scattering, scaling prediction and prod. struct. functions 79−17738
eN→hadrons+anything, scale invariant limit on average transverse momentum 77−67659
eN scattering, scaling violation patterns, p-n mass difference 77−57536
ep, deep inelastic scatt., nucleon struct. function moments anal., asymptotic freedom critical tests 79−54344
ep, deep inelastic scatt. cross sections, quark-parton model with broken scaling *(Russian)* 80−32109
ep, deep inelastic scattering, scaling deviations, parton model anal. 79−58966
ep deep inelast. scatt., QCD perturbative corrections 78−74263
ep deep inelastic scatt., asymptotically free field theory anal., scaling breaking *(Russian)* 78−78190
ep deep inelastic scatt., density matrix appl. to scaling props. 78−8673
ep deep inelastic scatt., scaling violations and QCD parametrisations, struct. functions *(Russian)* 80−37277
ep deep inelastic scattering, scaling property *(Chinese)* 77−10257
ep deep inelastic scattering, rest frame quark-parton model of proton, scaling 78−70374
ep deep inelastic scattering, phenomenological determ. of electroprod. struct. functions 79−63478
ep→e+hadron+x, parton picture from QFT, structure function scaling behaviour 79−402
ep inclusive cross-sections meas. at 50° and 60°, 6.5-19.5 GeV 77−2843
γ-ray families, multiparticle prod. above 10^{14} eV, Monte Carlo anal. 78−49257
K*(890) and K*(1420) prod. in 405 GeV/c pp interactions 79−30757
K^+n, inelastic charge exchange scatt., diffraction approach, convergent polynomial expansion, scaling 80−78095
$K^-p\rightarrow\Lambda X$, 8.25 GeV/c, off shell KK and pp interactions, KNO scaling 80−52534
K^+p, 100 GeV, topological cross-sections and multiplicity distribs. meas. 77−30464
K^+p, geometrical scaling at inelastic threshold 77−18323
K^+p, K_S^0 and Λ inclusive production at 147 GeV/c 80−52539
$K^\pm p$, 130, 200 GeV, jet prod. cross sections, QCD anal. and scale breaking 80−99111
$K^\pm p$, fireball model, universal scaling function 80−57646
$K^\pm p$, inelastic charge exchange scatt., diffraction approach, convergent polynomial expansion, scaling 80−78095
Kπ, geometrical scaling at inelastic threshold 77−18323
Kπ asymptotic scattering amplitudes, positivity anal. 79−45102
lp→lX, scaling violation due to charm prod., conventional ideas 77−74691
μ+nucleus deep inelastic processes, nucleon struct. function, scale breaking 78−78185
μd, deep inelastic scatt., nucleon struct. function moments anal., asymptotic freedom critical tests 79−54344
μN deep inelastic scatt., dimuon prod. and scale violation 78−62407
μN→μX, nucleon struct. function meas., scaling violation obs. 79−45091
μN→μX, scale breaking, modified quark distrib. function for description 77−57543
μp, 219 GeV, proton struct. function determ. 78−82216
μp, deep inelastic scatt., nucleon struct. function moments anal., asymptotic freedom critical tests 79−54344
μp, deep inelastic scattering, scaling deviations, parton model anal. 79−58966
μp high energy data, QCD energy momentum sum rule, gluon fraction of proton 77−49971
μp inelastic scatt., p struct. function determ. 77−61290
μp→μX, deep inelastic processes, nucleon struct. function, scale breaking 78−78185
N, EM form factors, dipole fit and scaling law, electroproduction in Δ_{33} energy region 80−22625
N structure function model from hard consistent quark interactions, scaling violations 80−86719
N-N low multiplicity events, scaling and multiperipheral testing at cosmic ray energies 77−18342
n+nucleus, high momentum study, quasi-two-body scaling, differential cross sections 77−57665
NN multiplicity distributions at very high energy, universality hypothesis 77−26550
NN semi-inclusive reactions, secondary pion production, 1000 GeV, scaling phenomena 79−22157
$\nu,\bar{\nu}$ cross-sections and scaling violations 77−87970
ν and $\bar{\nu}$ charged-current reactions, Bjorken scaling violations 78−74246
ν deep inelastic scatt., scale-breaking effects from asymptotic freedom 78−45905
$\nu(\bar{\nu})$ deep inelastic scattering, scaling violations of struct. function moments and perturbative QCD 79−40736
$\nu(\bar{\nu})$ inclusive scattering, weak neutral currents with longitudinal cross sections, scaling 78−17007
$\nu(\bar{\nu})$N 2-200 GeV, differential cross section, struct. functions, Bjorken scaling, Callan-Gross ratio 79−392
$\nu(\bar{\nu})$N 50-200 GeV, deep inelastic scatt., charged current cross section, Bjorken scaling 78−89699
$\nu(\bar{\nu})$N deep inelastic scatt., 45 to 205 GeV, scaling and struct. functions 78−62386
$\nu(\bar{\nu})$N high energy scatt., scaling violation and generalised vector meson dominance 77−67644
$\nu(\bar{\nu})$N inclusive scatt., scaling violation evidence, QCD test 78−89701
$\nu(\bar{\nu})$N scattering, modified GIM model, scaling violations, naive parton model 78−21414
$\nu(\bar{\nu})N\rightarrow l^-(l^+)X$, differential cross section in scaling limit, sea quark contribution 78−37196
$\nu_\mu(\bar{\nu}_\mu)$N charged current total cross sections, (V-A) interactions, nucleon struct. function scaling 78−25033
ν_τ, charged current interactions, scaling variable distributions 79−378
νN, charged and neutral current interactions, cross sections and scaling variable distribs. 80−57581
$\bar{\nu}$N, charged current high energy reactions, μ^+ events scaling-variable distribs. 77−74672
scaling phenomena continued
νN, charged current inclusive interactions in Fe at 30-200 GeV, struct. functions, scaling phenomena 79−75764
νN, deep inelastic scatt., structure functions, form factors, negative scaling violation 78−74241
νN, eN, μN inelastic scattering, comparison of scaling deviations, energy depend. 77−49948
νN, heavy-quark production, t and b-quarks, SU(2)×SU(2)×U(1) gauge group mixing angles 80−68445
νN, $\bar{\nu}$N, y-distributions, nonscaling and longitudinal struct. function effects 78−33053
νN, scaling violation, quarks with size and excited states 78−74242
νN charged current reacts., appl. of new scaling rule 78−89703
νN deep inelastic charm particle prod., breaking of scaling *(Russian)* 77−46043
νN inclusive interactions, nondiagonal neutral currents, six quark model with slow rescaling 77−49949
νN interactions, book contrib. 78−78171
$\bar{\nu}N\rightarrow\mu^+e^-X$, relative prod. rate, Vee yield and scaling variable distrib. 79−40768
$\nu N\rightarrow\nu\pi X$, scale breaking effects 79−40770
νN total cross-sections, scaling violations, Wilson operator product expansion 77−87967
$\bar{\nu}\bar{\nu}$, y-distrib. energy and x-depend., quark right handed coupling 79−26325
$\bar{\nu}$p, deep inelastic interactions, scaling variable distribs. 79−13101
νp inelastic interactions, scaling deviations in secondary hadron energy distrib. 80−9161
$\bar{\nu}_\mu$p(n), charged current interactions in Ne, cross section ratio, scaling variables 79−75763
p-n mass difference, anal. of expt. data, scaling violation and renormalised struct. functions 79−97628
p-nucleus collisions, $\bar{p}$ and K subthreshold prod., struct. function 78−21564
p-nucleus multiparticle production data anal. using charged particles created as variable 79−3155
p-nucleus shower particle multiplicity distribs. at 6.2-300 GeV. scaling hypothesis 77−50019
p+nucleus, inclusive production of neutral strange and charged particles, collective tube model 80−52538
$Pn\rightarrow l^+l^-X$, scaling predictions, Drell-Yan model 80−73756
pp, 100 GeV, topological cross-sections and multiplicity distribs. meas. 77−30464
$\bar{p}p$, 22.4 GeV/c, inclusive γ, K_S^0, Λ $\bar{\Lambda}$ production, KNO scaling test *(Russian)* 79−30759
pp, 53, 63 GeV, massive electron pair prod., Υ ang. decay, scaling function 80−68495
pp, 53, 63 GeV, Υ and ψ prod., dielectron decay angles 80−68496
pp, K_S^0 and Λ inclusive production at 147 GeV/c 80−52539
$\bar{p}p$, pp, 130, 200 GeV, jet prod. cross sections, QCD anal. and scale breaking 80−99111
$\bar{p}p$, pp, Drell-Yan processes, scaling violation effects 80−382
pp, smooth interpolation between Orear- and fixed angle scaling behaviour of the scattering amplitude 80−105873
pp ($p\bar{p}$) μ-pair, W and Z prod., asymptotic freedom and scaling violations 77−26554
$p\bar{p}$ annihilation, 100 GeV/c, general features of charged particle prod. 79−75803
pp→cX, scaling parameters at ISR energies, cosmic ray muon charge ratio 78−58212
pp→CX, $C=\pi^\pm, K^\pm, \bar{p}$, scaling-in-the-mean hypothesis 80−68497
pp→charged particle+X, small-angle production from nuclear and nucleon targets, collective tube model and triple-Regge picture 80−52538
pp collision inclusive spectra, fast pionisation at high energies, z-scaling *(Russian)* 80−47339
pp collisions, real photon prod. at large p_T, cross section calc. 79−13149
pp diffraction scattering, convergent polynomial expansion and scaling 79−40797
pp Drell-Yan lepton pair prod. processes, π structure function and scaling phenomena 80−405
pp elastic amplitude, geometrical scaling real part effects 78−37232
pp→γX, large p_T direct photon prod., QCD scale violation effects 79−71772
pp→hadrons, phase transition in Feynman-Wilson analogue fluid, multiplicities, plateaux, cross-sections 80−73744
pp→hadrons, scaling violation in fragmentation region in quark model, 10^6 GeV *(Russian)* 79−3051
pp inclusive interactions, multiplicity distribs. of negative particles, energy depend. of KNO scaling parameter *(Russian)* 79−80860
$\bar{p}p$ inclusive $\pi^\pm$ prod., 100 GeV/c, R-distrib. 77−50028
pp inclusive reacts., 100-400 GeV, $\pi^\pm$, $K^\pm$, p and $\bar{p}$ spectra 78−17059
pp interactions, multiplicity of particle production, correl. with increasing primary energy 79−58979
$pp\rightarrow l^+l^-X$, massive lepton pair prod., quark-gluon-parton model, scaling 79−428
$pp\rightarrow l^+l^-X$, parton density scale violations and quark-gluon correction to Drell Yan formalism 79−63560
pp→lX, p_T behaviour and scaling violations with conventional ideas 77−74691
$pp\rightarrow\Lambda^0X$, small-angle production from nuclear and nucleon targets, collective tube model and triple-Regge picture 80−52538
$pp\rightarrow\mu^+\mu^-X$, 62 GeV, ψ and γ cross sections, scaling function 80−105932
pp→NX, ISR energies, low p_T secondary prod. and lepton-hadron relation 79−45112
pp→pX, 28.5 GeV/c, π charge multiplicity, scaling and Hagedorn temp. 77−26553
$\bar{p}p\rightarrow p(slow)+X$, 22.4 GeV/c, associative multiplicity *(Russian)* 80−5031
$pp\rightarrow\Pi^-+X$, ISR energies, scaling variable, derived sea level muon spectrum 77−13995
$pp\rightarrow\pi^0X$, one-gluon-exchange quark scatt. 78−8714
$pp\rightarrow\pi^0X$, scaling in the mean hypothesis and Feynman variable energy depend. 80−42501
$pp\rightarrow\pi^+X$, non-plateau behaviour in central region 77−6182
$pp\rightarrow\pi^++X$, inclusive reactions, ISR energies, scaling variable 77−50021
$pp\rightarrow\pi^+\pi^-X$, 405 GeV/c, indictive ρ^0 and f meson prod. 79−45111
$pp\rightarrow\pi^\pm X$, charge ratio for cosmic pion spectrum in atmosphere 78−28463

scaling phenomena continued
pp→πX, Pomeron struct., effects on one particle inclusive cross sections 79−89210
pp scatt. at higher energies, differential cross section ratio scaling 80−73741
pp scatt. cross section at high momentum transfer, geometrical scaling, energy depend. *(Russian)* 80−102064
pp semiinclusive collisions, hypergeometric distrib., KNO scaling 77−2883
pp single-lepton spectra at high p_T, parton p_T and gauge invariance 77−18352
pp→xπX, QCD radiation and mean scaling, longitudinal and transverse momentum 80−42405
ϕ^3 field theory in 6+ε dimensions, anomalous dimens. calc. 78−134
ϕ^4 3-D field theory, IR behaviour and connection with critical phenomena 79−71601
π compositeness from wave function renormalisation constant 80−101997
π EM form factor, asymptotic behaviour in scale-invariant quark model 78−37211
π electroprod., bare mass of nonstrange quarks, scaling functions 78−41556
π production spectrum derivation from primary cosmic ray spectrum and scaling consts. 77−25897
π-nucleus, barionic cumulative effect in nuclei collective nature *(Russian)* 79−22339
π^0 high p_T prod. ang. depend., inclusive cross sections, scaling 80−91119
π^-+nucleus, inclusive at 3.9 GeV/c, Λ Feynman scaling obs. *(Russian)* 79−9635
π^-+p→Λ+X, relative scale invariance *(Russian)* 77−88003
π^-d, 360 GeV/c, multiplicity distribs. and double scatt. effects 78−66165
π^+d, 6 to 100 GeV/c, $P_\perp$ distribs. of K^0, π^-, ρ^0, f, equilibrium temp. 79−49540
πN exotic channels in fragmentation region, early scaling 77−18361
$\pi^\pm$N, 16 GeV, dimuon prod., qq̄ annihilation contrib., exact scaling deviations 79−89196
πp, direct photon prod., Compton and annihilation process contrib. 80−105925
πp, inelastic charge exchange scatt., diffraction approach, convergent polynomial expansion, scaling 80−78095
πp→ηn, pion-nucleon charge exchange scatt. and scaling of differential cross section 79−26348
π^-p, 147 GeV/c, neutral particle prod., K_S, Λ, Λ̄, γ, multiplicity scaling form 80−22645
π^-p, 200 GeV/c, inelastic diffractive-dissociation cross section 79−22151
π^-p, 5-40 GeV/c, distribs. of total multiplicity of secondary particles *(Russian)* 77−22820
π^-p Drell-Yan lepton pair prod. processes, π structure function and scaling phenomena 80−405
π^-p→η′n, Regge pole model with phenomenological residue functions 80−102077
π^-p→γX, 5 GeV/c, invariant struct. function *(Russian)* 77−74717
π^-p→γ+X, 5 GeV/c, scaling obs. *(Russian)* 78−45986
π^-p inclusive interactions, 40 GeV/c, associative multiplicity of charged particles, automodel behaviour of spectra *(Russian)* 77−10295
π^-p→π^0+X, 5 GeV/c, scaling obs. *(Russian)* 78−45986
π^-p→π^0n, pion-nucleon charge exchange scatt. and scaling of differential cross section 79−26348
π^-p→π^0n or ηn, nondiffractive reactions, scaling of differential cross sections 78−62462
π^+p, 6 to 100 GeV/c, $P_\perp$ distribs. of k^0, π^-, ρ^0, f, equilibrium temp. 79−49540
π^+p, K_S^0 and Λ inclusive production at 147 GeV/c 80−52539
π^+p, 130, 200 GeV, jet prod. cross sections, QCD anal. and scale breaking 80−99111
$\pi^\pm$p, fireball model, universal scaling function 80−57646
ππ, geometrical scaling at inelastic threshold 77−18323
τ decay dynamics, scaling prop. and Michel parameter 78−37195
υ prod. from duality and new quark charge 78−74224
Be+p, 400 GeV/c, two hadron correlation, x_e scaling 78−46060
Be+p, high mass symmetric hadron and pion pair prod., scaling props. 79−22291
^{9}Be(p,p)X, 0.8 GeV, inclusive cross sections, quasi-two-body scaling 79−3150
^{40}Ca(e,e′), quasi-elastic scatt., scaling law test, knockout process contribution 79−22274
Cu+π^-→$\mu^+\mu^-$X, 16, 22 GeV, quark annihilation model interpretation, scaling 79−36277
Cu(α,π), 0.7-8 GeV, scaling and nonscaling of inclusive π prod. 79−22296
Cu(p,π), 0.7-8 GeV, scaling and nonscaling of inclusive π prod. 79−22296
H, positron scatt., analytic model, complex scaling 79−18257
^{A}H(p,π), A=1,2, 0.7-8 GeV, scaling and nonscaling of inclusive π prod. 79−22296
^{3}He-^{4}He mixtures, tri-critical phenomena, Callan Symanzik study of $\lambda\phi_3{}^4+g\phi_3{}^6$ theory 77−35788
^{3}He(e,e), form factors and dimensional scaling quark model 78−93991
^{4}He(e,e), form factors and dimensional scaling quark model 78−93991
^{6}Li(p,p)X, 0.8 GeV, inclusive cross sections, quasi-two-body scaling 79−3150
pp→μ pairs, 200, 300, 400 GeV, test of scaling hypothesis 78−4888
$\bar{p}p$→$\mu^+\mu^-$X, scale violating effects in large q_T interactions 79−22125
π^-p, 100 GeV, topological cross-sections and multiplicity distribs. meas. 77−30464
^{181}Ta(p,p)X, 0.8 GeV, inclusive cross sections, quasi-two-body scaling 79−3150

scaling tubes *see counting tubes*

scandium
see also nuclei with .....
adsorbed on 4d or 5d metal, work function, O_2 coadsorpt. effects, thermionic emission obs. 78−11064
adsorption and absorption of $H_2(D_2)$ 77−4257
atom, arc spectra, energy levels assignment *(French)* 77−83522
atom, arc spectra, Zeeman effect *(French)* 77−83521
atom, HFS and g_j-values, calc. 78−21860
atom, ionisation potential, term value, correlation energy by vertical anal. 78−41964
scandium continued
atom, rel. at. transition probabilities, by flame at absorption spectroscopy 79−89642
atom, X-ray production by protons by 0.5 to 2.0 MeV energy 78−66646
band structure, density of states, absorpt. spectra, KKRZ calc. 80−70593
Compton profile, electron momentum distrib., renormalised free atom model 77−1756
crystal field potential calc. 77−59366
crystal surface, N and O adsorption, refl. electron energy loss spectra obs. 80−20742
CVD, open-tube technique 80−89128
Debye-Waller factor and Lindemann parameter, temp. depend., lattice dynamical model calcs. 80−59610
electric field gradient, of ^{181}Ta substitutional atoms, press. depend. 78−52385
electron and positron multiple scatt. 80−15171
electronic excitations, charact. energy loss meas. up to 50 eV 80−60723
electrotransport behaviour of C, N_2 and O_2 77−11738
filter for 2 keV neutron beam facility 77−23346
fractionation of Co and Sc versus Fe content for crystalline phases of ultramafic nodules 78−65306
HCP, elec. field gradient 78−14698
HCP, lattice heat capacity, third order elastic consts., thermal expansion 79−82352
HCP, LCAO description of (0001) surface electron states 78−72232
HCP, nonlocal effects in lattice dynamics 78−91397
HCP, optical examination of electronic struct. 77−89694
interband, collective and atomic (p,d) excitations, Z-160 eV, fast EELS 80−93443
Kohn anomalies and phonon dispersion, model including exchange-correl. corrections 78−59886
lattice dynamics, sp.ht. and bulk modulus 78−71814
magnetic form factors, neutron diffr. study 79−47234
magnetic susceptibility, temp. depend., theoretical explanation 78−47944
oxidation by O_2 and H_2O, XPS obs. 79−47827
phonon dispersion, phenomenological model 79−7660
phonon dispersion relations and dielectric screening 77−35646
photoabsorption spectra, at. ionisation, band struct. mechanisms, electron energy loss investig. 77−24909
proton stopping power meas. at 100 keV, using ion induced X-ray emission 78−48725
rocks, Sc determination by neutron activation analysis using ^{46m}Sc 79−79356
secondary ion emission, energy spectra, 0-55 eV, contamination levels 79−15573
specific heat data rel. to electronic props. 78−83971
spin susceptibility, exchange correlation enhancement 77−85167
sputtered excited states, secondary photon emission, role of transition probability 80−102483
strength and plasticity 77−90429
superconducting high-pressure phase 79−33378
surface, (0001), H adsorption, geometric vs. electronic factor in surface electronic structure 80−70788
surface, single cryst., segregation of impurities 79−65299
surface (0001), surface states 79−91120
thermal expansion anisotropy, 78-783K, X-ray determ. 78−83983
thin films, obtained in vac. of 10^{-5}-10^{-6} torr, struct. and elec. resist. 80−107931
X-ray emission spectra and electronic structure 77−20960
XPS, core level binding energies, plasmon peaks 78−6828
XPS, valence bands 78−35249
$BaNi_2M_xFe_{16-x}O_{27}$, effect of $M=Sc^{3+}$ or In^{3+} on props. 77−47978
Cl^{5+}+Ca(Sc)(Ti) thick targets, 30 MeV, near symmetry collisions, double-K-vacancy sharing 79−3391
GeO_2:Sc^{3+}, trapped-hole centres, ESR meas. 79−77597
LaB_6:Y, Sc effects of impurities thermionic emission 78−60542
$LuPO_4$:Sc, Gd^{3+} EPR spectrum, satellite resonances 78−2734
O_2+La(Y)(Sc), crossed beam chemiluminescence reaction, spectral simulation, hyperthermal energy meas. 78−80732
S II in ζ Ophiuchi interstellar spectrum, abundance upper limit 80−82445
Sc I, hyperfine struct., far-config.-mixing effects 77−42240
Sc I, oscill. strength calc. 80−78571
Sc I to Sc XXI, energy level tables derived from atomic spectra anal. 80−101672
Sc II, 3d4p ^{1}P and ^{3}F levels, beam-foil mean-life meas. 77−3306
Sc II, visible spectra and ionisation limit 80−74143
Sc IV, atomic structure determ. by model pot. method 78−86777
Sc IV, autoionising transitions ns^2np^6−$nsnp^6mp$ 77−88419
Sc XI, wavelengths and energy levels, spectral obs. 77−428
Sc^+, excited config. position and level struct., review 80−32621
Sc-F_2(ClF)$(Cl_2)(SF_6)(Br_2)$, visible chem. laser development from reactions yielding visible chemilum. 78−63111
Sc+$^{28}Si^{n+}$, K-shell ionisation, projectile charge state depend., theory 78−17786
Sc+Ar^+, charge exchange obs. through spectral line enhancement 79−7005
Sc+$H_2O(D_2O)$(alcohols), O atom abstraction, product internal state distrib., fluoresc. study 78−48643
Sc+H^+, K X-ray production, 0.2-0.5 MeV, ionis. cross-section 79−31459
Sc+NO_2, chemiluminesc., nonequilib. product distrib. 80−101014
Sc+$O_2(NO_2)(N_2O)(O_3)$, oxidation, single collision chemiluminesc. 77−25267
Sc+O_2(NO)(SO_2), nascent product state distribs., laser fluoresc. detect. 78−7187
Sc+O_2→ScO+O, chemiluminescence, $A^2\Delta X^2\Sigma^+$ transition 77−1927
ScIV, photoionisation, multichannel CI calcs. 79−93931
^{47}Sc carrier-free radiopharmaceutical prep. with epithermal neutrons in ^{47}Ti(n,p) reaction 79−79652
Si:Sc, photocapacitance and photoconductivity 80−107859
α-SiC:Sc, quasiline luminesc. spectrum 77−4686
SiC:Sc, various polytypes, photolum. meas., identification of 4H and 6H polytypes 77−63459
SiC:Sc energy distrib. in photolum. spectra, influence of synthesis conditions 79−52009
YIG:Sc, diamagnetically substituted, annealing effects on cation distrib. 79−1455
YIG:Sc, magneto-optical Kerr effect, reflectivity spectra 80−66157

scandium alloys
see also scandium compounds
rare earth alloys, mag. phase diagram 78−10684
Al-Sc, dil., thermomigration of Sc 79−69280
Al-Sc, elec. resist. determ. 80−92876
Al-Sc, solid solubility and residual resist. 79−51265
Al-Sc foil, alloying effect on strength characts. and weldability 80−55475
AlSc, lattice parameter changes in Al 3d alloys 77−62504
$Ce_{1-x}Sc_xAl_2$, fluctuating valence system, quadrupole interaction temp. depend. 80−54972
$Ce_2Sc_3Si_4$, X-ray cryst. struct. determ. 80−92480
Cu-Sc, dil., impurity effects on annealing and resist., vacancy-Sc interaction 79−51142
Dy-Sc, magnetic relax. phenomena 79−33579
$Dy_{0.9}Sc_{0.1}Al_2$, hyperfine field, NMR spectra 80−15811
Gd-Sc, Curie temp. and saturated mag. moment, nonmag. solute effects 78−39301
Gd-Sc, dil. alloy, ferromag. hyperfine field determ. 77−43919
$Gd_{1-x}Sc_x$, Mossbauer spectra, hyperfine interactions 80−15923
$Gd_{1-x}Sc_xPt$ Laves phase alloy, NMR, nonstoichiometry 77−63298
Nb-Ga-Sc, superconducting transition temp., X-ray, microscopic and microprobe anal. *(Ukrainian)* 80−75667
$(Ni_{1-y}Y_y)_3Al_{1-x}Sc_x$, quarternary γ' ($L1_2$) pseudobinary props., revealed by ionicity modified pair model 78−19725
δ-PuSc (5, 12, 18 at.%), f.c.c., contraction by self irradiation at 4.2K *(French)* 77−4129
Sc, In, itinerant electron ferromagnet, magnetovolume effects 80−60397
Sc-[Co,Ni,Cu]-Ga, phase equilibria, diagrams of state, X-ray, microstructural study *(Russian)* 80−55356
Sc-Ag(Cu)(Pd)(Rh)(Ir)(Ru), electronic struct., susceptibility, sp. ht. and Knight shift meas. 77−43485
Sc-Au, dil., elec. field gradient, Mossbauer meas. 80−80665
Sc-Co-Si, phase equil. and atomic struct. *(Russian)* 77−77462
Sc-Co(Ni)(Cu), phase diagram determination, using X-ray diffr., metallography and DTA techniques *(Russian)* 79−34004
Sc-Dy, dil., high field magnetisation 78−56292
Sc-Er, dil., high field magnetisation 78−56292
Sc-Fe, dil., elec. field gradient, Mossbauer meas. 80−80665
Sc-Fe, electrotransported, low temp. sp. ht. meas. 77−7872
Sc-Fe system phase diag. *(Ukrainian)* 78−84773
Sc-Fe-Ga system, isothermal sections of phase diagram *(Ukrainian)* 78−92235
Sc-Fe-Si system, phase obs. at 800°C *(Russian)* 78−23661
Sc-Ga system, phase diagram from 20-75 at.% Ga, intermetallic compound identification *(Russian)* 77−55944
Sc-Gd, dil., reverse resist. anomaly and negative magnetoresist. 80−84459
Sc-Gd, spin glasses, low temp. sp. ht. and magnetisation 80−65913
Sc-Gd spin glass, sp. ht., 0.3-10K 80−25145
Sc-Gd(Tb), spin glasses, low-field susceptibility, role of single-ion anisotropy 77−48000
Sc-H, conc.-temp. depend. at room temp. of elec. resist. thermo-EMF, mag. susceptibility, and Hall coeff. 80−29382
Sc-Hf, binary continuous solid solution, elec. resist. and thermoelec. power behaviour 79−69492
Sc-Ir, dil., elec. field gradient at ^{193}Ir, Mossbauer meas. 80−66090
Sc-Mg, low-temp. heat capacity 80−75370
Sc-Mn-Ga, system, isothermal sections of phase diagram *(Ukrainian)* 78−92235
Sc-rare earth, dil. alloy, cryst. field parameter determ. 78−10650
Sc-rare earth, dil. alloy, cryst. field determ. 78−10651
Sc-Rh-Si system, partial phase diagram, X-ray diffr. and microprobe anal. 80−25659
Sc-Ru, dil., elec. field gradient, Mossbauer meas. 80−80665
Sc-Ru, elec. field gradient and temp. depend. TDPAC meas. 80−60477
Sc-Tb, dil., high field magnetisation 78−56292
Sc-Tb, induced-moment spin glass, simple mean-field theory 80−29553
Sc-Zr, binary continuous solid solution, elec. resist. and thermoelec. power behaviour 79−69492
Sc-Zr, low-temp. heat capacity 80−75370
Sc-Zr(Hf), thermopower composition depend. 79−65445
ScAg, electronic struct., NMR relax. times meas. 79−51871
ScAg(Pd)(Ir)(Ru), UPS exam. 78−48276
$ScAl_2$, density of states, ^{45}Sc NMR 77−63276
$ScAl_2$-Eu, intermediate valence on Eu ions, Mossbauer isomer shift 80−84587
$ScAl_2$-Gd, dil., EPR, comparison with YAl_2, $La Al_2$, $LuAl_2$ 77−63276
$ScAl_2Er(Dy)(Nd)$, dil., EPR and mag. susceptibility 80−15797
Sc_3Co, new struct. type related to Fe_3C and Re_3B by periodic unit-cell twinning 79−4268
$ScCoC_{1-x}$, stabilising effect of C on alloying behaviour of Sc 77−36454
Sc_2Co_3Si, struct. determ. by X-ray powder method *(Russian)* 77−55261
ScCu, electronic struct., NMR relax. times meas. 79−51871
$ScFe_2$, mag. props., 80-1300K *(Russian)* 80−75750
$ScFe_2$, Mossbauer effect of ^{57}Fe 80−75903
$ScFe_{2-2x}Al_{2x}$, mag. props., composition depend. 77−20593
$Sc(Fe_{1-x}Co_x)_2$, magnetic saturation moment, Co conc. depend., NMR exam. 78−15037
$ScFe_2H_2$, Mossbauer effect of ^{57}Fe 80−75903
Sc_2Fe_3Si, struct. determ. by X-ray powder method *(Russian)* 77−55261
ScGa and Sc_5Ga_3, exam. of X-ray K spectra of pure Sc, Ga in alloys *(Russian)* 79−15562
$ScGa_2$ atomic structure determ. using single crystal method *(Ukrainian)* 80−70165
ScH_2, electron diffr. investigation 80−107112
ScH_x thin films, struct. and elec. props. 80−107931
Sc_3In, itinerant electron ferromagnet, spin fluctuations 77−73096
Sc_3In, itinerant electron ferromag., NMR and relax. 78−6586
Sc_3In, itinerant electron ferromag., low temp. sp. ht., mag. field depend. 79−42765
$Sc_3InC_{1-x}(B_{1-x})$, stabilising effect of C and B on alloying behaviour of Sc 77−36454
ScIr, electronic struct., NMR relax. times meas. 79−51871
ScIr:Gd, influence of cryst. field on EPR 78−52346
$ScIr_3C_{1-x}(B_{1-x})$, stabilising effect of C and B on alloying behaviour of Sc 77−36454
Sc_2Ni_3Si, struct. determ. by X-ray powder method *(Russian)* 77−55261
$Sc_3PbC_{1-x}(B_{1-x})$, stabilising effect of C and B on alloying behaviour 77−36454
ScPd, electronic struct., NMR relax. times meas. 79−51871

scandium alloys continued
Sc_2Pt, X-ray powder struct. anal., Debye-Waller factors 79−77553
$Sc_{(3)}Re_2Si_3$, X-ray cryst. struct. determ. 80−39009
ScRh, electronic struct., NMR relax. times meas. 79−51871
ScRh:Gd, influence of cryst. field on EPR 78−52346
$ScRhC_{1-x}(B_{1-x})$, stabilising effect of C and B on alloying behaviour of Sc 77−36454
ScRu, electronic struct., NMR relax. times meas. 79−51871
$ScRu_3C_{1-x}$, stabilising effect of C on alloying behaviour of Sc 77−36454
$Sc_3SnC_{1-x}(B_{1-x})$, stabilising effect of C and B on alloying behaviour 77−36454
$Sc_3TlC_{1-x}(B_{1-x})$, stabilising effect of C and B on alloying behaviour of Sc 77−36454
$Sc_xY_{0.95-x}Sm_{0.05}$, ^{153}Eu isomer shift, at. vol. depend. 77−43915
Tb-Sc, mag. ordering temps., susceptibility meas. 80−25136
TbSc, basal plane magnetocrystalline anisotropy and ferromag. ordering 79−1667
$Th_{65}Sc_{35}Ce$, supercond., magnetisation of Ce impurities, sp. ht. meas. 78−47904
V-Ga-Sc, phase diagram, metallographic and X-ray meas., solubility boundaries *(Russian)* 78−56618
$Yb_xSc_{1-x}Al_3$, valence fluctuation system, suscept. meas. 78−68149
Zr-Sc-Ga, phase equilibria 800°C *(Ukrainian)* 80−35157

scandium compounds
see also scandium alloys
compounds with O_2 donor ligands, literautre review 79−99122
dihydirdes, structs. and stabilities 80−107146
germanates, cryst. struct. and cryst. chemistry 77−39571
germanates, crystallisation in high temp. aq. solns. 77−24942
hydrides, mag. susceptibility, mag. props. in single-phase region explained by proton model *(Russian)* 78−47961
oxalate, IR and Raman spectra exam. *(French)* 78−48159
rare earth garnets, mag. props. 77−47979
scandium octaethylporphyrin, μ-oxo bridged dimer, triplet states and geometrys, ODMR obs. 80−9625
scandium octaethylporphyrin, triplet states and geometrys, ODMR obs. 80−9625
silicates, cryst. struct. and cryst. chemistry 77−39571
silicides, $ScM_{0.25}Si_{1.75}$, (M=Mn,Fe,Co,Ni), X-ray determ. of struct., new representative of struct. type $ZrSi_2$ 78−79595
silicides, ScMSi, (M=Co,Ni), X-ray determ. of struct., new representative of struct. type TiNiSi 78−79595
silicides, valence band struct. *(Russian)* 79−15076
sulphides, RR'_3S_6, where R,R'=rare earth, Sc or Y, struct. organisation *(French)* 77−11519
zeolites, type Y, catalytic activity, NMR, mechanism 79−29405
ArO_2-ScO_3 solid electrolytes, thermoEMF 78−95184
$Ba_3Sc_4O_9$, $Ba_3Sc_2WO_9$ and Ba_2ScTaO_6, elec. cond. nature, depend. on comp. and medium thermodynamic parameters 80−70773
$Ca_3Sc_2Si_3(Ge_3)O_{12}$, garnets, refined cryst. struct. 78−87654
$Cd_3Sc_2Ge_3O_{12}$, garnet, refined cryst. struct. 78−87654
$Ce_{1-x}Sc_xPd_3$, intermediate valence of Ce, susceptibility, lattice const., ESR meas. 80−103648
CrN-ScN, rhombic distortion of cryst. lattice at low temp. 78−2253
Eu_2O_3-Sc_2O_3-Ta_2O_5 system, orthotantalate section, X-ray diffr. and luminesc. obs., conc. depend. 80−54205
$KSc(MoO_4)_2$, soft modes and Raman spectrum at ferroelastic phase transitions 79−47450
$K_4Sc_2(OH)_2Si_4O_{12}$, crystal struct., X-ray diffr. study 80−79763
(La, Y, Sc)B_6 solid solns. electron work function, thermal emission technique 80−20755
LaB_6-YB_6-ScB_6, thermionic emission 78−11068
$(NH_4)_3Sc(SeO_4)_3$, cryst. struct. 79−99122
NaF-ScF_3 system, ionic equilib., mass spectra 78−7222
$Na_3Sc_2(PO_4)_3$, ferroelectric props., X-ray diffr. study 79−69789
$Na_3Sc_2(PO_4)_3$, X-ray cryst. struct. determ. 79−60341
$Na_3Sc_2P_3O_{12}$, superionic cond. synthesis, cryst. struct. and ionic cond. 80−107519
$Na_6YSc[SiO_7]_2$, crystal struct., atom coordinates, X-ray study 80−59446
Pb(Zr,Ti)O_3:ScO elec. cond. study 79−11120
(Sc,M)Rh_4B_4, M=Ca, Th or rare earth, supercond. and ferromagnetism 78−95438
Sc complex, $Sc(BH_4)_3$ with THF, synthesis and struct. 79−51068
Sc-H, conc.-temp. depend. at room temp. of elec. resist. thermo-EMF, mag. susceptibility, and Hall coeff. 80−29382
Sc-H, p-T phase diagram and influence of H pressure, on decomposition temp., DTA exam. 80−29929
Sc-H system, phase transforms. at high H_2 press. 78−63853
Sc-M-B systems (M=Rh,Ir), phase equilib. and cryst. structs. 80−15072
$ScAlO_3$ perovskite, elasticity meas. to 6 kbar 77−51428
$ScB_{\sim 28}$, β_2-rhombohedral cryst. struct. by X-ray diffr. 78−34464
$ScBO_3$:Fe^{3+}, ESR spectra, lattice parameters 80−93170
$ScBO_3$:Tb^{3+}, vacuum UV excitation spectra and quantum efficiencies 79−28811
Sc_4C_3, superconducting phase synthesis at high press. and temp., critical field *(Russian)* 80−65732
ScCl, electronic struct., self-consistent and non-self-consistent band calcs. 80−44499
$ScCl_3$, phonon dispersion curves 80−2130
$ScCl_3$-NaCl-CsCl ternary system, cpd. form., thermographic investig. *(Russian)* 80−66490
Sc_2CoSi_3, X-ray cryst. struct. determ. and refinement 79−60343
$Sc_3Co_2Si_3$, X-ray cryst. struct. determ. and refinement 79−60343
ScD, emission bands in 5580 and 8603 Å regions 78−990
ScD_2, surface, interactions with reactive gases 78−23964
ScF, Franck-Condon factors and R-centroids, rot.-vibr. effects 78−50596
ScF supersonic mixing flame, spontaneous emission, electronic transition chem. laser pot. 78−66817
ScF_2, ESR spectra of radical in Ar matrix, 12K, hyperfine splitting 79−98122
ScF_3, metastable high press. phases, X-ray diffr. and IR absorpt. expts. 77−11499
ScF_3, pyramidal struct. and force field coeffs., electron diffr. obs. 78−9250
ScF_3-CaF_2, phase relationships at 100 kbar and 1200°C 77−43335
$Sc_2Fe_3Si_5$, cryst. struct. determ. 78−18620
$Sc_{0.995}Gd_{0.005}H_{1.9}$, low temp. anomaly, Gd^{3+} EPR linewidth and X-ray meas. 77−69687
ScH, $^1\Sigma$ state, Dirac-Fock one-centre calcs. 80−23301

scandium compounds continued
ScH, emission bands in 5580 and 8603 Å regions 78−990
$ScH_{1.9}$:Pt, Gd, effect of Pt on Gd^{3+} ESR lineshape 78−68371
ScH_2, CVD 79−24420
ScH_2, electronic struct., optical studies, 0.2-5 eV, 4.2-340K 79−78005
ScH_2, electronic struct., band theory 79−78006
ScH_2, electronic struct., photoelectron spectra study 80−50527
ScH_2, optical interband struct. and low energy plasmons 78−31200
ScH_2, self-consistent bond struct., charge transfer 80−49590
ScH_2, self-consistent energy bands, KKR method with Hedin-Lundqvist approx. 80−49593
ScH_2, synchrotron XPS obs., rel. to theory for metal dihydrides 80−55275
ScH_2, XPS, core level binding energies, plasmon peaks 78−6828
ScH_3, valence mol. orbital energy, nonempirical pseudopot. 79−22592
ScH_x:Er, ESP determ, of proton locations 80−34768
ScH_x:Er, ESR evidence of octahedral site occupation 79−78512
ScH_x:Er, proton distrib. and site energies, ESR meas. 80−59509
$Sc(H_2PO_4)_3$, synthesis, struct. and stability 77−47423
$Sc(HSeO_3)_3$, cryst. struct. 78−51485
$ScH(SeO_4)_2.2H_2O$, single crysts., X-ray diffr. struct. anal. 78−95020
$ScH(SeO_4)_2.2H_2O$, $Sc(HSeO_3)_3$, cryst. struct. 79−99122
ScI_3, mass spectra and vapour press., and thermochemistry for dimerisation 78−27809
ScI_3, vaporisation thermodynamics, sublimation and formation 80−54366
$Sc_{11}Ir_4(Os_4)(Ru_4)$, cubic struct. type described by cluster concept, X-ray determ. 80−33933
$(Sc_xLu_{1-x})_2V_2O_7$ 80−29547
ScM, (M=Ru,Rh,Pd,Ag), electronic struct., self-consistent local density functional calcs., LMTO method 79−11059
$Sc_{(x+2)/3}Mg_{(x-2)/3}O_x$, 145 Å superstructure 79−99143
$ScMo_6X_8$ (X=S, Se), supercond., sp. ht., 1 to 14K 79−51720
$Sc(NO_3)_3.4CO(NH_2)_2$, cryst. struct. determ. 79−23588
$ScNiSi_3$, cryst. struct., X-ray diffr. meas. 78−10027
$ScNi_2Si_3$, cryst. struct., X-ray structural anal. 78−95044
ScO, absorption spectra, in flame, optogalvanic spectrosc. obs. 79−18202
ScO, chemuluminesc. from Sc+O_2 reaction 77−1927
ScO emission spectrum, intensity distribution, spin decoupling, theory, expt. 77−23504
ScO, fluoresc. spectra, atom+ROH O atom abstraction reactions, fluoresc. study 78−48643
ScO molecule, $B^2\Sigma$-$X^4\Sigma$ system, Franck-Condon factors and r-centroids 80−1025
ScO, optical emission spectrum, wave functions and intensity factors, using effective Hamiltonian *(French)* 78−5114
ScO, pot. energy curves and dissoc. energy of $X^2\Sigma$ state 80−69203
ScO, r-centroids and Franck-Condon factors for $A^2\Pi$-$X^2\Sigma$ and $B^2\Sigma$-$X^2\Sigma$ systems 77−61809
Sc_2O, atomisation energies and stand. ht. of formation 77−54622
Sc_2O_3 and double oxides, photon multiplication and secondary electron-hole pairs generation *(Russian)* 80−66262
Sc_2O_3 catalyst for CO+N_2O reaction, kinetic obs. 79−29389
Sc_2O_3, elec. cond. at 1300°C 77−80813
Sc_2O_3, elec. cond. rel. to defect struct. 77−80814
Sc_2O_3, electronic excitations, charact. energy loss meas. up to 50 eV 80−60723
Sc_2O_3, fission and phase transition enthalpies 79−99299
Sc_2O_3, heat treated, elec. cond. rel. to O_2 partial press. 77−15845
Sc_2O_3, hot pressing charact. 78−27456
Sc_2O_3, interband, collective and atomic (p,d) excitations, Z-160 eV, fast EELS 80−93443
Sc_2O_3, liq. and solid phase elec. cond., high temp. meas. 80−84468
Sc_2O_3, Mandelshtam-Brillouin spectra, transverse phonon contrib., elastic and photoelastic consts. 77−81115
Sc_2O_3, photoabsorption spectra, at. ionisation, band struct. mechanisms, electron energy loss investig. 77−24909
Sc_2O_3, polycrystalline, elastic props., porosity and temp. depend. 77−52384
Sc_2O_3, reduction in Li vapour, 1800-2500K, thermodynamics 77−90595
Sc_2O_3, solid, enthalpy investig. at high temp. 80−103498
Sc_2O_3, solid and liq. phases, thermophysical and electrophysical props. 80−103495
Sc_2O_3, solid solubility in MgO 80−15247
Sc_2O_3, XPS, core level binding energies, plasmon peaks 78−6828
Sc_2O_3:MgO, defect struct., X-ray diffr. and pyrometric density 78−34524
Sc_2O_3-Bi_2O_3-SiO_2, three-layer antirefl. coatings, form. and props. 77−58420
Sc_2O_3-Ho_2O_3 (Dy_2O_3), solid solution, use of segregation phenomena to exam. solidification phase diagrams *(French)* 79−8293
Sc_2O_3-R_2O_3, regular soln. approx. of solidification diagram *(French)* 79−24505
Sc_2O_3-R_2O_3 (R = rare earth or Y), phases and phase transitions at high temp. *(French)* 79−100126
Sc_2O_3-ScF_3 system, phase ratios at 100 kbar press. 78−19729
Sc_2O_3-ZrO_2 (HfO_2), cubic solid soln., lattice parameters 79−82186
Sc_2O_3+Sb(V) reaction, phase formation, structs. 77−84712
Sc_2O_4, polycryst., form. conditions of anion vacancies, phase comp. 80−54220
ScOF, metastable high press. phases, X-ray diffr. and IR absorpt. expts. 77−11499
ScOF, ordering and structure, NMR and crystallographic determ. *(French)* 79−90618
$Sc(OH)_3$, metastable high press. phases, X-ray diffr. and IR absorpt. expts. 77−11499
ScO(OH), metastable high press. phases, X-ray diffr. and IR absorpt. expts. 77−11499
Sc_2O_2S, cryst. atomic struct. determ. *(French)* 79−10837
ScP, electronic struct., self-consistent Hedin-Lundqvist and Xα APW calcs. 80−29322
ScP, energy band struct., exchange-correl. pot. effects, APW calcs. 80−29321
ScP, thermodynamics and high temp. vaporisation 80−88310
ScP(As)(Sb)(Bi), coupling between Gd 4f electrons and conduction electrons, EPR linewidth 78−52347
$Sc(PO_3)_3$, cryst. struct. determ. from X-ray intensity data 78−95043
$ScPO_4$, enthalpy and heat capacity, 298.15-1600K 77−12559
$ScPO_4$, $Sc(PO_3)_3$, mass spectra 77−47567
$ScPO_4$:Gd^{3+}, zircon struct. EPR investig., rel. to radiation resistance 80−97138
$Sc_4(P_4O_{12})_3$, cryst. struct. determ. *(French)* 78−55842
$Sc_2Re_3Si_4$, X-ray struct. determ. *(Russian)* 79−27958
ScRh, gaseous, dissociation energies, high temp. mass spectrometric determ. 80−93790
$ScRu_4B_4$, superconducting and crystallographic data 80−33968
ScS, $B^2\Sigma$-$X^2\Sigma$ system, rot. struct. and hyperfine effects near IR spectrum 80−5544
ScS, IR spectrum, vibr. consts. 77−10669
ScS, supercond. props. at press. up to 20 kbar 79−24111
$Sc_{0.8}S$, order-disorder transition, ionic model appl. 80−107096
Sc_xS, high temp. vaporisation, enthalpy, atomisation, dissoc. energies 77−1223
$Sc_2(SO_4)_3$ aq. soln., dielec. relaxation spectroscopy in microwave region, double-beam interferometry *(German)* 80−71309
$Sc_2(SO_4)_3$+$Al_2(SO_4)_3$ aq. solns., complex form. reacts., kinetics, US relax. investig. 79−1942
$ScSbO_4$, polymorphism at high pressure, X-ray phase anal. 79−46804
Sc_2Se_3, elec. resist., thermoelectromotive force, temp. depend., 300 to 1400K *(Russian)* 78−84243
$Sc_2(SeO_4)_3$, cryst. struct. determ. 78−63708
$Sc_2(SeO_4)_3(.5H_2O)$ cryst. struct. 79−99122
ScSi, effects of non-sphericity on intensity variations and their minimization, a priori estimates of errors in intensity 79−23489
ScSi, paramag. susceptibility 80−50035
$Sc_2(SiO_3)_3$, mag. susceptibility, temp. depend., 77-800K 80−20372
$Sc_2Si_2O_7$, high press. pyrochlore struct. 77−47426
$Sc_2Si_2O_7$, IR and Raman spectra, internal and external modes 79−61365
$Sc_2Si_2O_7$, polymorphism at high press. and temp., thortveitite struct. stability *(French)* 80−10657
$Sc_{(x+2)/3}Si_{(x-2)/3}O_x$, 145 Å superstructure 79−99143
$Sc_{0.65}Th_{0.35}Rh_4B_4$ and $Sc_{0.5}Th_{0.5}Rh_4B_4$, cryst. struct., X-ray diffr. 77−89423
$Sc_{0.75}Th_{0.25}Rh_4B_4$, high supercond. transition temp. 77−89893
$(Sc_xTi_{1-x})_2O_3$, semicond.-metal transition, sp. ht. meas., 300-600K 77−43347
$ScVO_4$, ^{51}V NMR, nucl. quadrupole coupling const., chem. shift 77−90055
$ScVO_4$, electron energy loss spectra 79−11490
$ScVO_4$:R^{3+}, R=Nd, No, Tm, Sm, Dy, Er, Eu, Tb, electronic struct. and spectra of VO_4, RO_8 clusters 78−10953
$Sc_2(WO_4)_3$:Cr(Eu), and undoped crystals, luminesc. obs. 80−89047
$Sc_2(WO_4)_3$:Er^{3+}, growth, solubility, absorption spectrum and thermal expansion meas. 77−36391
$Sc_{2/3}\square_{1/3-y}Sc_yS$, elec. props. variation at high temps. *(French)* 79−82649
Si_2O_3-TiO_2 system, phase transform. at high temp. 77−84926
Si_3Si_5, X-ray spectra, valence band struct. *(Russian)* 79−1798
TiO_2-Sc_2O_3 system, dislocation mechanism of diffusion processes 79−77837
Ti_2O_3, Sc_2O_3 doping effects on struct. changes 77−55276
$(Ti_{1-x}Sc_x)_2O_3$, crystal struct. determ., metal-metal distance, effect on electronic struct. 77−47431
Tl_2WO_4-$Sc_2(WO_4)_3$, cpd. formation and single cryst. growth 77−86010
U_3O_8-Sc_2O_3, solid soln. electrode, high temp. electrochem. appl. 80−6828
$UScS_3$, cryst. struct. determ. *(French)* 78−79576
Y_2O_3-Sc_2O_3 fused powders, production of ceramics of good thermal strength 77−63607
YScIG, expitaxial film, magneto-spatial interaction, conversion coeffs. 77−55774
ZrO_2-Sc_2O_3, phase system, X-ray and thermal anal. 78−27494
ZrO_2-Sc_2O_3 system, high-temp. phase transitions, elec. cond., thermal props. 77−16573

scanning antennas
plasma antenna system, multilayered, electronically scannable, for space communication 79−4151
UHF/SHF tropospheric scatter radio links, scanning beams 78−81276

scanning electron microscope applications
adhesion measurement, locus of failure, bond failure in adhesive joints 80−50801
adhesive energy, meas. techniques for metal/ceramic system 80−50803
AES in SEM, high resolution, electron sources comparison 77−25330
Aspergillus niger dying spores, electron refl. and transmission SEM expts. after irrad. 80−56111
autoradiography for location and study of microscopic β-active particles 77−57425
biological specimens, macromolecular resolution 80−72401
biomedical studies, cathodoluminescence method 80−72400
bipolar transistors, emitter/collector pipes obs., use of electron-beam-induced current mode of SEM 79−82665
bulk mode analysis using energy-dispersive X-ray fluoresc. spectrometer 77−60140
cathodoluminescence analysis 78−32949
chemical vapour deposition conditions, quick survey method 78−44019
conference, Chicago, USA (Mar.-Apr. 1977) 78−21281
conference, Lannion, France (June 1977) 78−41378
cultured cell obs., SEM STEM comparison 79−74801
dentistry, in situ ion etching 79−30629
diffraction grating writing for integrated optics, charact. 79−68450
dynamic SEM with video tape recording 78−32952
dynamic techniques developments 78−32953
EBIC characterization of HgCdTe crystals and photodiodes 79−67385
EBIC SEM, stroboscopic principle and resolution enhancement 80−100515
electon energy loss spectrometry, with electrostatic mirror 77−61168
electrical conductivity meas., appl. to TTF-TCNQ 80−86507
electron beam for GaAs FET failure anal. 78−29216
electron beam particulate analysis of air samples 80−40785
energy despersive analysis, simplex spectral deconvolution method 79−80722
energy-dispersive X-ray microanalysis, background reduction due to back-scatt. electrons 78−20121
equipotential and mag. intensity contour line visualisation 79−6149
forensic science, backscattered electron detector 80−68319
glass micropipettes, comparative calibration by optical microscopy and SEM *(German)* 80−98201
IC local voltage measurement 79−54156
IC reliability assessment 78−24902
IC template fabrication, SEM and electron lithography optics 79−75662

scanning electron microscope applications continued
leukocytes in motion, surface struct. obs. 77−29116
light duty electrical contact reliability assessment 78−29219
Lorentz microscopy, mag. domain images resolution, computer calcs. 78−35004
Lorentz microscopy, thin film and bulk specimen, recent advances 78−35002
LSI circuits, appl. of electron beam meas. techniques for verification of computer simulations 79−21875
LSI circuits, wafer defect classification using modified scanning electron microscope 79−21876
metallurgical applications, of Kossel diffr. in scanning electron microscope 79−20335
microbeam analysis developments, mag. contrast obs. with HV SEM, quantitative analysis by ion microprobe with quadrupole mass filter *(Japanese)* 78−3432
microcircuits, radiation hardness design, SEM as diagnostic tool 79−21869
microfilm, reproduction and scale changes of recorded information 78−93775
mineralogy, backscattered-electron/low vacuum mode appl. 80−82077
minority carrier diffusion length determ. near p-n junction, SEM appl. *(French)* 78−43466
minority carrier lifetime-meas. technique using SEM-electron beam induced current 80−59999
MIS structures investigation 78−95377
monolithic ICs, measurement of SiO_2 thickness 79−30619
MOS, capacitors, SEM investigs. using electron beam induced current technique 78−23177
MOS struct., minority carrier nonuniform generation obs. 78−72273
operation and appl. of SEM, review 79−49348
optical grating direct writing using SEM 78−83121
optical integrated circuits, SEM written gratings in chalcogenide films 79−32087
p-n junction, planar, nondestructive determ. of depth by SEM 78−19132
particle track detectors, electron microscopy of etch pits 80−99424
particulate materials, quantitative three-dimens. characters. using polished sections and computer-controlled SEM system 77−2714
photography, positive print, of CRT image 78−82082
picosecond pulse stroboscopic SEM for semicond. device voltage contrast images 79−71565
planar diode, heavily doped, collection efficiency and surface recomb. vel. modulation 80−20291
planar diode characterisation using SEM with movable Faraday cup, illuminator and backscatt. diode detectors 78−21292
quartz crystal US vibrations, SEM obs. 79−56733
research, quality control and education ISI Model 7, parameters 79−89044
SAW device diagnosis, voltage contrast obs. 80−69618
SAW resonator transverse modes, phase effects 79−68452
scanning laser microscope, electron beam excited 80−52303
Schottky barriers use in SEM electron beam induced conductivity obs. of semicond. 78−34898
semiconductor, elec. parameters determ. by electron probe method 79−9259
semiconductor, induced conductivity mode expts., apparatus requirements 79−9260
semiconductor, micron scaled cathodoluminescence with SEM, review 78−23537
semiconductor, TEM/SEM observations comparing diffr., elec. and luminesc. contrast from dislocations 78−38714
semiconductor, with high quantum yield and recomb.-radiation reabsorpt., induced-current, in SEM 79−11140
semiconductor device characterisation using electron beam induced current technique, review 78−21302
semiconductor induced current obs., stroboscopy appl. 77−19855
semiconductor lasers, SEM evaluation *(Japanese)* 77−71992
semiconductor material research *(German)* 79−94854
semiconductor materials and devices, SEM characterisation methods 80−49064
semiconductor resistivity meas., two dimensional plotting by SEM 77−39852
semiconductor structures, defect obs. using stroboscopic SEM 79−9261
semiconductor substrate surface, low loss electron and Auger images correl. 78−22944
shift register reliability assessment 78−29215
Si, single cryst. characteris. by SEM using Schottky barrier charge collection microscopy 77−4444
sintering studies, high temp. SEM, development and appl. 79−21873
solar cells, defects, rel. to elec. parameters, SEM electron beam induced current investig. 79−43772
stereoscopic observation and three-dimens. meas. instrument 78−21287
stroboscopic, microcomputer controlled, for measuring signal waveform at arbitrary positions on MHz IC 79−21871
surface analysis, corrosion research 80−99004
surface roughness measurement methods using SEM techniques, research and development *(German)* 80−105612
surface topographical measurements at grazing incidence, alignment problem 80−99014
thermistor bolometer failure anal. appl. 78−24795
thickness meas. 78−29218
two-dimensional magnetic stray field imaging 80−86514
visualization method for concanavalin A receptors on lymphoid cells 79−74800
X-ray image processing, quantitative, with SEM, surface meas. appls. *(French)* 78−41379
X-ray microanal. of frozen-hydrated biological specimens 77−56552
X-ray microtomography in SEM 80−101308
X-ray projection microscopy, using energy dispersive spectrometer 79−17593
Fe dust particles, respirable, meas. of mass and thickness by SEM backscattered electron imaging 79−21707
n-GaAs Schottky barrier junction, SEM meas. of hole diffusion length, surface effects 79−87110
Si p-n junction local temp. meas. using pulsed SEM, induced-current mode 80−54775
Si photodiodes, linear arrays, use for high-energy electrons detection, SEM assessment 78−32951
Si, RTR ribbon, defect obs. rel. to photovoltaic potential 79−11186
Ti, 300 keV He^+ irrad., exfoliation, flaking, blistering, in-situ SEM obs. 77−35598

scanning electron microscope examination of materials
see also scanning electron microscopy
ABS polymer, fracture behaviour, rubber content effects 77−32676
ABS polymers, deposited in internal magnet magnetron sputtering system, adhesion of Cu films 79−83121
acrylonitrile-butadiene-styrene copolymers, micromechanism of deform. and rupture *(German)* 80−35276
adhesion, surface anal. techniques appl. 80−65381
AES, ionisation enhanced diffusion effect obs. 80−71497
air pollution, particulate matter, analysis 77−41150
aircraft parts, microfractographic fracture analysis exam., SEM exam. *(Japanese)* 78−52950
alite paste, mature, microstructure study by SEM, TG and X-ray diffr., corrosion 78−92381
alkali borosilicate glasses, observation of phase separation using SEM-EDX technique 80−76224
p-alkoxy-phenyl-p-acryloyloxy benzoate polymers, mesomorphic struct. 80−38905
Allende meteorite, occurrence of Fe-Ni-Cr-S-O compounds *(French)* 78−32411
alloy, two phase microstrct. revealed by selective sublimation 79−24698
alloys, absorbed current image, contrast, noneffect of sample resistivity 77−45922
alloys, embrittling residuals categorisation by Auger electron spectroscopy 80−66739
alumina, polycryst., compressive strength, microplasticity 77−36620
alumina deposition by activated reactive evaporation, struct. obs. 77−44176
alveolar brush cells of rats 79−34517
amino acid-quinone complexes, surface bubble form. during SEM obs. 77−15450
amino acids, surface bubble form. during SEM obs. 77−15450
aortic elastin, freeze-dried, SEM 78−65160
aramid fibre reinforced acrylic bone cement, tensile strength and fracture toughness, SEM study 79−29667
arcing and surface damage in DITE Tokamak, SEM obs. 78−59611
automobile materials, appl. of microfractography 77−56199
bagasse fibre reinforced phenol formaldehyde, tensile strength and Young's modulus, SEM study 80−60952
Barre granite, crack growth and development during creep 79−84237
basalt, cement reinforcing fibre, alkali resist. 80−89377
biological implant, ion beam sputter of surface morphology SEM exam. 77−44836
biological material freeze-fracture preparation 78−61290
biological materials, low-temp. SEM, X-ray microanal. 79−39627
biological specimen freeze-drying process obs. by SEM 78−28142
bituminous coal, identification of constituents for petrographic anal. 80−81888
blood cell exam. technique 79−74812
bone, compact, fatigue damage, residual strength and stiffness 77−90834
bone china body, MgO effect on vitrification mech. props. *(Japanese)* 79−78922
borosilicate microporous glasses, structural anisotropy and birefringence 79−8114
α-brass, Al bearing, high temp. relief cavitation, SEM, STEM, TEM, SIMS and EDX anal. 79−5039
brass, corrosion pretreatment effect on corrosion inhibition 79−100280
α-brass, fractographic obs. of cracks in early stages of fatigue *(Japanese)* 78−7023
α-brass, stress corrosion cracking in 15N ammonia solns., fractographic aspects 80−16547
α-brass, with few inclusions, shear mode of ductile fracture 77−36652
α-brass stress corrosion cracking in nontarnishing ammoniacal environment, fractography, chemical anal. 77−40466
calcium oxalate trihydrate and monohydrate, dissolution kinetics charact. by SEM 79−42250
CANDU irrad. fuel bundles, sheathed in Zircaloy-4, long term stability investig. 80−13774
cartilage, articular, meas. of surface microgeometry 80−3880
case hardened and structural steel fracture obs. *(German)* 77−60032
cast iron, white, high Cr-Mo, fracture toughness 80−50726
cavitation erosion, observation of eroded surface by SEM 78−15536
[CC] Ag−(100)InP, metal-semicond.cathode contact, metallurgical, physical, chemical processes 80−107911
cell membranes, at mol. resoln., introduction 80−104841
cellulose diacetate membrane, diffusive permeability 80−104460
cement, hot pressed, type III, role of admixtures on pastes and H_2O cured cement, exam. 78−44073
cement, Portland, static and fatigue cracking morphology 77−52493
cement hydration, SEM, new technique 77−40503
cementite, in white pig Fe, deform. and fracture 77−4827
ceramic, brittle, specimen prep. for optical and SEM obs. *(German, English)* 80−35457
ceramic nuclear fuel, porosity characterization, optical and electron microscope exam. 78−44302
ceramics, crack propagation, microstructural aspects 79−15771
charcoal, active, heat-treated, spiral growth structs. *(German)* 78−44141
cholesteric liquid crystal, pitch observation, SEM freeze etching method 77−15316
clay, isotropically consolidated sample prep. with random fibres 77−90531
clay soft, increase in shear strength and rigidity due to Fe^{3+} addition *(Japanese)* 78−31463
CMOS ICs electrically active stacking faults, anomalous leakage currents 79−78191
coal chemical analysis, computer evaluation of SEM images 80−71994
coated arc electrodes, identification of types and brands using SEM with energy-dispersive X-ray detector 80−81400
cold stage thick specimen heating model 78−61289
collagen fibres, mech. props., role of struct. organisation 80−72207
colloid-SEM method, fine magnetic domain observation *(Japanese)* 78−37105
coloured coatings on Al, prod. in AC electrolysis, thick coatings case 80−25908
coloured coatings on Al, prod. in AC electrolysis, thin coatings case 80−21176
Columbia Resin, CR-39, fracture mirrors, static and impact tests 78−27601
compound eye of Cicindela tranquebarica herbst, fine struct. 80−85382
conference, Chicago, USA (Mar.-Apr. 1977) 78−21281

scanning electron microscope examination of materials continued
conference, Lannion, France (June 1977) 78−41378
α′ copper phthalocyanine and chlorinated derivative mol. crysts., radiation damage in electron microscope 80−107328
corundum single crystal, premetallizing with Mo-Mn-SiO_2 79−47792
Cr_2O_3, pure, hydrothermal reactive sintering 77−36431
crack and fracture behaviour, simultaneous acoustic emission and SEM techniques *(German)* 79−96240
crystal, accelerator irradiation, heavy ion irradiation damage 80−100291
crystal morphology, interfacial angles meas. by SEM, sample holder 77−27792
crystalline contrasts from defects in thin and thick specimens 78−22611
crystalline materials, observation of single defects using electron channel imaging 80−64848
crystalline materials observation using diffr. effects, bibliography 78−22612
cyano-biphenyl LC alignment on obliquely evaporated SiO_2 films 80−79677
deformed crystal, optical method for quantitative evaluation of electron channelling patterns *(German, English)* 77−7777
desert varnish, importance of clay minerals 77−86893
diamond, accelerator irradiation, heavy ion irradiation damage 80−100291
diamond, cracking and fatigue under repeated indentations 77−59905
diamond, industrial, anal. cathodoluminesc. studies in SEM 80−81410
diamond, metastable overgrowths in dissoln. medium in Ni presence at atm. pressure, SEM surface study 79−51030
diamond, polycryst., growth at high temp. and press., morphology 77−11495
diamond, polycrystalline film growth from gas phase 78−48332
diamond, sintered compact, fracture and fatigue 79−52352
diamond, synthetic, external crystal morphology, SEM obs. 79−73078
diamond, synthetic, oxidized in fused salts, etch features 80−97604
diamond, synthetic grits, crystal morphology of cyclic twins 80−2037
diamond cathodoluminesc. at dislocations 79−47524
diamond coatings, for increased wear resist. 80−76371
diamond subsurface damage exam. using cathodoluminescent mode of SEM 77−80398
diamond tool, metallic binder, microstruct. charact. by electron probe anal., SEM obs. *(Rumanian)* 79−74114
dielectric, thermal mechanism of plastic deformation and fracture by laser beam 77−11553
diffusion welded joints, creep deformation effect on characts. 80−25806
discharge breakdown, mechanism determ. in solid dielectrics using scanning electron microscope 77−85649
disilicate, piezoelectric glass ceramic, recrystallisation, pyroelectric response, permittivity 80−80703
dispersion hardened metallic matrix composite, powder metallurgically produced effective interparticle distance effects *(German)* 78−52727
ductile erosion, prediction, mechanistic model 77−12709
elastin ultrastruct., freeze-fracture electron microscopy 80−8036
electrochemical displacement reactions, electron microscope obs. of nucleation and growth, comparison of Cu/Fe and Cu/Al cementation systems 79−47939
electrode-electrolyte interface, solid film props., review of expt. techniques 77−77780
electron contrast effects from oscillating quartz crystals 78−88255
electronics microstructure analysis 79−80723
enstatite-type glass-ceramic, crystn. kinetics and mechanism 77−55241
epoxy, mica filled, polishing by abrasive papers and lapping cpds. 80−108620
epoxy resin, filled, wear props., SEM obs. 80−16500
epoxy resin, thermosetting, crosslinking kinetics and structure *(German)* 78−76624
epoxy resins, struct. changes under mag. field action 80−40516
erythrocytes, technique for observing 3D dim. struct. with a cryo-SEM 78−92765
etched thin foils, comparative SEM, STEM and TEM analysis 80−100144
ethylene-vinyl acetate-vinyl chloride graft copolymers, rel. between morphology and toughness *(German)* 80−66665
euglenoid flagellates, sputter and vacuum evap. coating, comparative effects on delicate features 78−24205
failure anal. 78−27710
failure characts. of steel 15G2AFDps, effect of loading freq. and temp., SEM exam. of failure surface 78−84995
ferrite, transform. kinetics, grain size, alloying element effect, carbide precip. 80−93560
ferroelectric materials, repolarisation in SEM 79−15424
ferromagnets, domain structure image obtained by SEM *(Polish)* 80−34682
fibre reinforced composite, hybrid C and glass fibre, fracture energy 78−95801
fibre reinforced ionomer composites, fracture surface *(Japanese)* 78−92339
fibreglass laminates, investigation of fracture processes using hydraulic tensile straining stage 79−54227
finely grooved solid surface, apparent contact angle of liquids, SEM study 77−51573
fission reactor mixed oxide fuels, SEM obs. of gas bubble morphology 80−57843
fluorocarbon polymer film, prep. by RF sputtering and plasma polymerisation, props. 77−55890
fluoropolymer adhesive joints, fracture and surface anal. by SEM and ESCA 77−55434
fly ash particles, effect of chem. variability on cell exposure 79−16172
fractographic study of early stage fatigue cracks in vacuum *(Japanese)* 79−61781
fracture, surfaces *(Chinese)* 80−11849
fracture anal. appl. 79−61834
fracture surface SEM analysis, microtopography 80−68312
fracture topography-microstruct. correlations in SEM 77−32687
fused silicon substrate, directional reactive ion etching at oblique angles 80−66428
garnet film, domain obs. by SEM 77−69646
glass, float, low-Fe, weathered, surface, characterisation 80−93666
glass, impact damage, localised 77−44306
glass, laser irrad. effects, SEM meas. *(German)* 80−24492
glass, surface flaws, decoration technique 78−14547
glass fibre reinforced epoxy, short aligned fibres, mech. charact., SEM and optical obs. 78−72761

scanning electron microscope examination of materials continued
glass fibre reinforced epoxy laminate, failure, fractographic study 79−96111
glass fibre reinforced polyester, fatigue behaviour 80−25856
glass fibre reinforced polypropylene, effect of injection speed on fibre orientation 79−4944
glass fibres and spheres, microscopic, production and charact. for microanal. 79−24487
glass fragments, classification into window and non-window types 80−81401
glass rods, compressively clad, residual stresses, comparison of optical and fractographic meas. 80−108539
glass spheres, small, technique for full surface exam. in SEM 79−21874
glass-plumbite-treated cotton, form. of coating at interface 79−15058
glasses, high vol. low cost, as solar reflectors, compositions and weathering effects 80−106589
glazed surface, abrasion resistance testing *(German)* 77−32728
glioma cells, cultured, influence of microwave irradiation 79−100661
glow discharge and ion-microprobe sputtering, SEM and ion-microprobe mass anal. 78−43977
goniometry, from photographs or angle-true sketches 79−55619
grain boundary sliding model 80−75237
granite, stressed, crack-crack and crack-pore interactions 79−84238
graphite, D^+ bombardment, surface damage, sputtering, SEM study 80−32459
graphite, H^+, D^+, He^+ ion bombardment, Raman scatt. and SEM anal. 77−35609
graphite, pyrolytic crystals, surface topography, bombarded with Ar^+, N^+, He^+ ions 78−6820
graphite, surface morphology changes after irrad. with energetic He ions 78−21767
graphite fibre electrodes, coating by electropolymerisation, adhesion to epoxy matrix 79−15644
graphite intercalation cpds., struct. and order-disorder transforms. 78−71710
graphite/epoxy laminate with third phase reinforcement, static and impact behaviour 77−40447
graphitic Ceylon and California, occurrence carbyne forms of C, X-ray and SEM anal. 79−77450
graphitic materials deformation, crack and fracture behaviour, SEM exam 80−11706
grinding, fracture and deform. mech., SEM obs. *(Japanese)* 79−15620
guanidine aluminium sulphate hexahydrate, SEM obs. of ferroelec. domain struct. in single crysts. 80−97219
guanidinium aluminium sulphate hexahydrate, surface obs., SEM and AES expts. 80−71362
Gunn domain dynamics, two-dimensional, study using strobosocopic SEM 79−23978
Gunn domains, obs. at 1 GHz by picosecond pulse stroboscopic SEM 77−85228
gypsum, strength changes on setting *(Japanese)* 77−36619
Hastelloy X, grain size effect. creep and creep-rupture *(Japanese)* 80−16382
Hastelloy X, high temp. low cycle fatigue tests, ductility, fracture 77−90523
Hastelloy-X, fatigue crack propag. at elevated temps. in solid solution strengthened superalloys 78−39895
Hasteloy B, equilibrium surface bombarded with high dose He^+ ions 78−95091
Haynes alloy 188, fatigue crack propag. at elevated temps. in solid solution strengthened superalloys 78−39895
Haynes alloy 188, SEM exam. of fracture surface, due to low cycle fatigue at 700°C *(Japanese)* 78−52963
Haynes Stellite 6B, Al_2O_3 particle erosion of surface, SEM obs. 78−88545
height meas. of surface features 77−60019
high-resolution AES in diffusion-pumped SEM 77−40515
hot-pressed with crystn. grain boundary phases 78−95716
hydrogel coatings, and impregnations in silastic, dacron and polyethylene 79−20719
III-V multilayer structure, as-grown, assessment of defects by differentiated cathodolum. topography 80−59819
III-V semiconductor ternary alloys, VPE growth lattice mismatch effects 79−28220
impact, abrasion, wear, review *(German)* 78−88536
Incoloy 800, contamination and decontamination of samples from KFA experimental duct of DRAGON reactor 79−45600
Incoloy 800, exam. of caustic stress corrosion cracking, comparison with type 304 stainless steel 79−29261
Incoloy 800, fatigue crack behaviour in bending and pull-push modes 77−81315
Incoloy 800, high temp. oxidation in low O_2 pressures, SEM obs. of oxide morphologies 79−47844
Inconel 600, cold sintering under high pressures, correlation to plastic props. and diffusion 79−38757
Inconel 600, equilibrium surface bombarded with high dose He^+ ions 78−95091
Inconel 600, exam. of caustic stress corrosion cracking, comparison with type 304 stainless steel 79−29261
Inconel 600, PWR primary corrosion products 80−13578
Inconel 617, creep, morphological changes of carbides, affect on creep props. 80−108509
Inconel 625, nitriding in N_2-H_2 glow discharge 80−16590
Inconel 625, plasma nitriding, surface topography obs. by SEM 80−45442
Inconel 718, superalloy, wear of superhard tool during cutting, SEM and metallographic obs. 78−64720
Inconel 738, SEM and electron beam analyser study *(German)* 79−20056
insulating films, on Si, struct. stability 80−54564
ion bombarded faceted cone symm. rel. to ejection patterns 78−64439
ion etching device for SEM samples 80−82847
jute, cement reinforcing fibre, alkali resist. 80−89377
kaolin bodies, effect of mineralizers on firing shrinkage, microstruct. and strength 80−97488
Kapton, pyrolysed, cond. polymer, transport and mag. props. 80−96887
laser mirror, SEM obs. of laser induced damage *(German)* 78−37929
LED, diffusion lengths and near-junction luminescence-efficiency profiles from SEM scans 77−77301
liquid crystal carbonaceous mesophase, disclinations 77−43147
liquid phase sintering, role of grain and phase boundaries 78−72747

scanning electron microscope examination of materials continued
macroscopic metal catalysts, morphology and etching processes, review 80−7856
magnesium stearate-containing powder mixtures, bonding 78−84731
magnetic contrast in SEM with reference to bubble domain struct. 78−18511
magnetic domain, SEM obs., method of removing fine magnetite particles from surface *(Japanese)* 80−108655
magnetic domain imaging by SEM, computer simulation 80−71091
magnetic domain obs. 77−69606
magnetic domains, image formation in reflection mode of SEM *(Japanese)* 77−32212
magnetic domains and domain walls, image contrast 77−4528
material analysis by electron beam bombardment *(Japanese)* 77−86416
material characterisation, in a scanning electron microscope environmental cell 79−17577
material surface texture analysis 80−73548
materials failure and corrosion, microstructural aspects, obs. 79−52610
materials science experiments, use of closed circuit TV as teaching aid 79−71209
Mersilene mesh, herniorrhaphic reinforcing prosthetic, mech. and struct. props., SEM study 79−74789
metal, ion beam texturing 77−44402
metal, magnetic, and SEM exam. of fatigue, dynamic strength problems *(German)* 77−86272
metal, microanalysis of migration processes 77−36706
metal cutting, direct SEM obs. of adhesion and frictional sliding 80−104412
metal film and foil, surface IR wave propag. distance, imperfection and oxidation effects 77−28641
metal fracture surface 79−34220
metal layered contacts, low temp. diffusion *(German)* 80−6538
metal oxide metaphosphate glasses, vibr. study of metal cation reduction at surface 78−56797
metal oxide smoke particles, prep. by burning metal in Ar-O_2 gas, electron microscope obs. 77−52238
metal oxide smoke particles prepared by gas evap., morphology and coalescence growth 80−97738
metal tip profile change meas. for evaporation rate determ. 77−24403
metal-C system, spheroidal graphite formation, role of high angle boundaries *(Russian)* 80−81065
metal-semiconductor contacts, new phases struct. 78−34899
metallic surfaces, adsorption of inorganic and organic molecules, mechanism and effects, exam. *(German)* 78−51828
metallography, failure analysis appl., conf., Houston, USA (July 1977) 79−61832
metallurgical and mineralogical specimens, electron beam microanalysis 77−60152
metallurgical problems, struct.-props. relation use of TEM and SEM and optical microscopy 77−56186
metals, cryogenic fracturing, appl. to surface layer struct. investig. 77−30219
metals, extending SEM capabilities using SIMS attachment for chem. charact. 79−17555
metals, mechanical props., testing and modelling 80−25811
meteorite, Kirin, fusion crust microstruct. from SEM study *(Chinese)* 79−2525
Metglas 2826 ribbons, ferromagnetic resonance and SEM obs. 80−15804
microbeam anal., conf., Ann Arbor, MI, USA (June 1978) 79−39258
microcrystals, method for indexing *(German)* 78−22608
micrographs, calc. of cell surface area and vol. for human erythrocytes 79−5259
microsection assessment for machine failure prevention *(German)* 79−8412
mild, anodic polarisation behaviour in hot alkaline sulphide solns. 80−100949
mineralogy, appl. of cathodolum. microscopy and spectrometry 77−69919
minority carrier lifetime mapping 80−96903
mischmetal-cobalt alloy, $MMCo_5$, polished, domain wall grooving, optical microscopy and SEM obs. 77−8334
mitochondria in rat liver and monkey cardiac muscle 79−34516
MOS devices, SEM, electron beam induced currents, Si stacking fault investig. appl. 79−42665
Multimet, fatigue crack propag. at elevated temps. in solid solution strengthened superalloys 78−39895
Murchison carbonaceous chondrite meteorites, Si in metal grain, electron probe anal. 80−77363
myocardial cells, cats, improved techniques for studying surface topography by SEM 79−34712
myoepithelial cells, SEM examination 79−34713
near surface region of solid, H_2 effect on deform. and fracture, Rebinder-Westwood effect 79−39001
Ni powder 2JJ, porous, effect of sintering conditions in struct. and strength 80−20823
Nimomic PE-16, equilibrium surface bombarded with high dose He^+ ions 78−95091
nosean identification, in sodalite and conversion of nosean sodalite 80−84907
nuclear ceramics, quantitative image anal. using light and SEM obs. 79−12912
nylon, stress cracking induced by $ZnCl_2$ solns. 78−27594
nylon 66, fatigue crack propagation, effect of moisture 80−3166
nylon 66 films, superstructural ordering 80−15344
Nylon 6, unidirectionally reinforced, mech. props. and fracture 77−21252
nylon-6, pressure-crystallised, morphology and structure 77−84669
optical fibre, mechanical strength, fractographical analysis, review *(Japanese)* 80−35319
optical fibres, fractographic anal. of fracture surface, after proof stressing, SEM exam. 78−38093
optical glass diamond grinding kinetics 80−64224
optical multilayer film cross sections 77−19387
orthodontic adhesive joints, adherend topography effects 77−52916
orthopaedic implants, SEM study of wear 78−15926
orthotropic laminates, torsion strength and shear modulus determ. 80−92587
oxide phase equilibria, high temp. appl. 79−8416
p-n junction, short circuit, SEM investigation 80−6957
p-n junctions, minority carrier surface recombination velocity, lifetime, AM electron beam determ. 79−87145

scanning electron microscope examination of materials continued
paper sheets and single fibres, fracture behaviour, SEM investigation 79−34149
particulates, quantitatives charact. by computerised high voltage, SEM 79−48036
pearlite, SEM obs. of tensile deform. and fracture 78−84897
pearlite spheroidization, quantitative meas. 77−44275
Permalloy film, corrosion induced defects, scanning Auger microscopy 77−40464
Permalloy thin-film head pole struct., domain configurations, SEM obs. 80−65975
phenolic resin, linen impregnated, abrasion, SEM obs. 78−64742
Phosphate conversion coatings on steel 78−3251
phosphosilicate glass coatings, measurement of P content using SEM and energy-dispersive X-ray analyser 80−76588
phosphosilicate glass passivation layer P content, SEM analysis and interpretation 78−35759
planar Gunn diode, high-field domain dynamics anal. using stroboscopic SEM 79−56232
plant material, cryofracturing and low temp. SEM 78−24207
PMMA, abrasion, SEM obs. 78−64742
PMMA, quartz- and glass-particle reinforced, abrasive wear 80−97594
PMMA-mortar composite, thermocatalytically polymerised, fracture morphology and mech. props. 78−27595
poly(ethylene terephthalate), surface props. rel. to UV irrad. *(Japanese)* 78−79859
poly-1,6-dip-toluenesulphonyloxy-2,4-hexadiyne single cryst., twinning 80−33906
poly-(p-alkoxy-phenyl-p-acryloylbenzoates), nematic polymer, struct. determ. 79−99064
poly-(phenyl-p-acryloyloxybenzoate), nematic polymer, struct. determ. 79−99064
polyacetylene, nascent morphology obs. 80−24379
polycarbonate, deform. and failure modes, surface craze characts. 79−91753
polycarbonate blends, yield and deform. behaviour, impact modification 77−36572
polydiacetylene single crysts., twinning 78−23777
polyethylend, high molecular weight film, fibril structure induced by oriented crystallisation *(Japanese)* 79−90575
polyethylene, fibrillar, high mol. wt., oriented crystallisation, heat treatment effect *(Japanese)* 80−25738
polyethylene, filled, linear, struct., strength 79−29149
polyethylene, high density, crystallisation struct. revealed by solvent extraction 78−42922
polyethylene, high density, wear mechanism at steel surface, SEM, TEM and DTA 78−64727
polyethylene, linear, injection moulded at high press. struct. 79−11640
polyethylene, low density, SEM exam. of environmental stress cracking 78−53011
polyethylene, obtained from heterogeneous Ziegler-Natta catalysts, cryst. morphology and growth 80−38941
polyethylene, SEM meas. of fine lamellar struct. 79−51007
polyethylene, ultra-high modulus, micromorphology 77−63621
polyethylene, ultra-high-strength filaments, soln. spun/drawn, mech. and thermal props. 80−40440
polyethylene, ultradrawn linear, kink bands by compression, interfibrillar motion 79−24581
polyethylene electrets, charge trapping mechanism, TSC, DTA and optical meas. 80−11322
polyethylene films, internal lamellar struct. obs. by ion etching and SEM 79−73076
polyethylene flow crystallisation, in extensional flow developed by convergent capillaries, props. 80−84111
polyethylene melt spinning, extensional flow induced crystallisation 78−55818
polyethylene total joint replacement, props. improvement by C fibre reinforcement 78−24183
polymer blend morphology, methods for study and specimen prep. 78−75580
polymer blends, interdiffusion, meas. method 79−69271
polymer model adhesives, peeling, morphology and rheology obs. 78−92439
polyoxymethylene, wear mechanism at steel surface, SEM, TEM and DTA 78−64727
polypropylene, drawn fibres, SEM and US study 78−47249
polypropylene, impurities redistribution during crystn. 78−75577
polypropylene fibre, with helical internal texture, SEM obs. of surface morphology 80−39394
polypropylene fibres, helically twisted, small-angle light scatt. 79−1765
polypropylene film, effect of crystallinity on deformation mechanism of biaxial stretching 77−80426
polypropylene film and fibre, plasma etching 78−95871
polypropylene-nylon 11 fibres, bimodal cryst. texture, X-ray diffr. and electron microscopy 78−75567
polypropylene/peanut-hull flour composite, strength 79−8365
polystyrene, (-Kraton G blend), rubber toughened, charact. by SEM 79−14697
polystyrene, coarse shear bands and fracture, SEM study, craze fracture surfaces 79−29191
polystyrene, glassy, fracture surface, formation and struct. of striations 77−28892
polystyrene filament, melt spun, struct. and mech. props., effect of drawing, twisting, annealing, untwisting 80−45331
polystyrene-polymethylmethacrylate system, phase relationships and fracture surface morphology 79−61571
polyvinylidene fluoride, chem. etching of fission tracks, growth of fine holes, TEM, SEM study 79−76297
porcelain, crack propag. data applicability to failure prediction 80−81154
porcine skin, herniorrhaphic reinforcing prosthetic, mech. and struct. props., SEM study 79−74789
Portland cement mortar, micromorphology and interfacial zone around aggregates, SEM obs. 79−61598
portland cement paste, microstructure study by SEM, TG and X-ray diffr., corrosion 78−92381
Portland cement-fly ash, physico-mech. props., SEM and X-ray diffr. anal. 79−74239
powder and sintered material particles, dimension and shape evaluation by SEM 80−40278
PTFE, abrasion, SEM obs. 78−64742

scanning electron microscope examination of materials continued
PTFE, wear mechanism at steel surface, SEM, TEM and DTA 78−64727
pulmonary fibrosing disease diagnosis, histological section SEM and energy-dispersive X-ray microanalysis 80−72314
PVC, ductile fracture, SEM investig. 77−44343
PVC, high temp. creep 78−48453
PVC, oriented mouldings, struct. order 80−60896
PVC, rigid, craze and yield zones in fracture 80−50701
PVC rigid plate specimens, Charpy impacted, SEM exam. of fracture surface *(Japanese)* 78−52953
PVC-chlorinated polyethylene blend, optical characterisation methods 79−8408
PVC-poly-ε-caprolactone, interdiffusion, meas. method 79−69271
PZT/polymer composites, simplified fabrication 80−40323
quantitative electron microscopy, recent developments, review 77−70250
quartz, grains, fission track dating, Oklo uranium ore deposit 78−20555
quartz, grinding and surface treatment by ball mill in cetyl alcohol *(Japanese)* 80−25890
quartz, ion-etching of grooves for SAW devices 78−95822
quartz, surface damage by X-rays, γ-rays, neutrons, SEM study 80−79837
quartz, synthetic, as-grown and etched cobbled Z-surfaces *(French)* 80−24719
quartz crystals, oscillating, surface patterns obs., energy trapping appl. 80−71323
quartz glass, ^{252}Cf fission fragment tracks 78−17526
quartz grains, from sub-glacial and assoc. environments, characterisation using SEM 79−25238
quartz grains of podzols, surface texture, SEM study 78−36151
quartz high-transmittance antirefl. film, vacuum-etched 80−74449
quartz overgrowths, in quartz, cathodoluminescence and microstruct. 79−25239
quasi-cleavage fracture, characteristic length parameter, correlation with fracture toughness *(Chinese)* 80−104246
radiative samples, appl. of SEM with X-ray spectrometer, shielding design 77−189
reflection electron diffraction method, electron channelling and microdiffraction from surfaces 80−59355
refractory coatings, deposited by electron evaporation, struct. and props. 79−23871
Rene 95, as hot isostatically pressed (HIP) and HIP+forged, low cycle fatigue 80−25854
replica technique for increased information from SEM 79−74334
replication, NDT anal. and inspection technique 78−11467
rockburst fault gouge microscopic features 79−74891
rubber, silicone, biomed. eval. for passive prosthetic devices 79−29666
sapphire, synthetic arc lamp envelope, basal plane cleavage 79−66146
semiconductor diffusion length and surface recombination velocity determ. by intensity modulated SEM 78−10472
semiconductor, defect state microscopy, review 79−94856
semiconductor, localised defects, theory of SEM charge-collection imaging 79−1374
semiconductor, SEM electron beam induced current images of dislocations and stacking faults, computer simulation 80−70198
semiconductor defects, charge-collection images, contrast formation 80−70087
semiconductor defects, SEM in EBIC mode vs. HVEM images 78−9923
semiconductor devices and materials, characterisation by electron beam induced current, charge collection process 79−17580
semiconductor diffusion length and lifetime meas. and assessment 80−96902
semiconductor dislocations, SEM charge-collection image contrast and resolution 79−46662
semiconductor impurity distrib. and defect structure analysis by charge collection SEM 78−9924
semiconductor materials, high resolution charact. 78−64794
semiconductor substrate surface, low loss electron and Auger images correl. 78−22944
semiconductor viewing in a stroboscopic SEM, spatial resolution of luminescence and spectra 77−20936
semiconductors, extending SEM capabilities using SIMS attachment for chem. charact. 79−17555
semiconductors, II-VI cpds., dislocation motion obs. by SEM in cathodolum. *(Japanese)* 79−46666
semiconductors, minority carrier diffusion lengths meas. 79−60848
semiconductors, surface potentials using electron energy anal., SEM study 80−15582
semiconductors depth profiling, using carrier collection models 80−70723
sensitised photolysis and latent image structure 79−24768
SiC, attritious wear in grinding 77−32696
silica optical fibres, surface flaws obs., fracture strength 77−14793
single electron field emission non-destructive SEM method 78−88410
sintered pellets, oxidation mechanism and kinetics, optical and SEM study 79−79137
sodalite, crystallisation process, effect of solid and liq. boundary layers, SEM 79−23544
sodalite single crystals, exam. of growth mech. in hydrothermal method, using SEM 79−52105
spacecraft materials failure, metallurgical exam. 80−71868
sputtered coatings, metallurgical characterisation 79−15056
stainless steel:C, surface, obs. at very low accel. voltage (200 V-1 kV) by SEM 80−10764
stainless steel, coated with C, surface damage by D^+ and He^+ ions irrad. 80−23146
stainless steel rod adaptor, failure anal. in Fast Burst Reactor 77−54307
steel, 12% W, eutectic carbides struct. and comp. during heating 80−76283
steel, 12Kh18N9T-TiB_2, eutectic alloy, high temp. props. 78−84931
steel, 18% Ni maraging, fracture surface investigation by SEM 78−23805
steel, (0.36 wt.% C) Ni-Cr-Mo, electroslag refined, fracture toughness and fatigue behaviour 80−81171
steel, alloy, Si-Mn(Mn-Cr), heat treated, exam. of microfractographic aspects of fatigue cracks *(Japanese)* 78−52959
steel, alloy, wear particles, spheroid form. by cavitation erosion 79−52382
steel, ATSI 9310, fretting, selected fretting resistant surface treatments 79−29223
steel, austenitic and duplex 308 stainless, mech. of intergranular corrosion and pitting corrosion 79−91846

scanning electron microscope examination of materials continued
steel, austenitic stainless, 18-8, effect of H on martensitic transformation *(Chinese)* 80−55394
steel, austenitic stainless, ageing at high temp., effect on creep props. SEM 80−97516
steel, austenitic stainless, Cl^- stress corrosion cracking 79−20287
steel, austenitic stainless, DIN 1.4970, influence of He on high temp. mech. props. 79−7636
steel, austenitic stainless, exam. of fatigue crack fracture surface 78−64688
steel, austenitic stainless, fretting corrosion of orthopaedic implant materials by bone cement 80−104813
steel, austenitic stainless, He implanted 1.4970, high temp. fracture 77−86186
steel, austenitic stainless, in boiling $MgCl_2$ solns., alloying elements effect on stress corrosion cracking and K_{ISCC} *(Japanese)* 80−93692
steel, austenitic stainless, intergranular corrosion evaluation 77−16741
steel, austenitic stainless, of type 55 23 33, slow strain rate testing under electrochem. control in high temp. water 80−97650
steel, austenitic stainless, precipitates and grain orientation by non aqueous electrolyte potentiostatic etching method *(Japanese)* 80−15102
steel, austenitic stainless, rel. between polarisation behaviour and susceptibility to stress corrosion cracking *(Japanese)* 80−93693
steel, austenitic stainless, unlubricated, friction, wear and microstruct. of types 304, 316 and Nitronic 60 80−108589
steel, austenitic stainless type 304, time-depend. fatigue, mechanistic model 80−100925
steel, ball bearing, fatigue damage, influence of dispersed phases in martensitic matrix 80−108549
steel, C1020, dual phase, mech. behaviours and structs. *(Korean)* 80−25779
steel, C, corrosion and self protection in hot saline soln. 79−1925
steel, C, failure mechanisms in impact fatigue 80−40493
steel, C, fatigue subsurface crack initiation, result of residual stresses 80−25833
steel, C, fretting fatigue damage, SEM exam. 78−88541
steel, C, heat treated, exam. of microfractographic aspects of fatigue cracks *(Japanese)* 78−52959
steel, C, transition from initiation to propagation of fatigue cracks 78−68802
steel, C (0.18 wt.%), fatigue strength, atmospheric press. effect *(Japanese)* 77−77573
steel, C and stainless, ductile fracture, in situ obs. of microprocess of failure *(Chinese)* 80−55492
steel, C-Ni-Cr (0.6, 1, 1 wt.%), grain boundary segregation of S, N, P, As, Sb and Bi *(Japanese)* 78−15405
steel, carbide cracking as source of acoustic emission 78−19872
steel, carburised, microstruct. and fracture 79−24658
steel, carburised, with non martensitic microstruct. at surface, fatigue *(Japanese)* 77−48535
steel, carburized, fractography of fatigue fractures 77−86137
steel, cast, thermal fatigue crack propag. *(Japanese)* 79−83305
steel, cast structural, heat treatment and mech. working influence on mech. props. *(Russian)* 80−40392
steel, cavitation during superplastic flow, affecting factors 78−60728
steel, cementite coarsening in type 1080 in a temp. gradient 78−88486
steel, Ck 45, alternating bending, fracture surface appearance *(German)* 78−52995
steel, cold-rolled, good and bad paintability, AES, SEM and X-ray diffr. characterisation of surfaces 79−42344
steel, composition effect on carburizing 80−35432
steel, continuously cast, ductility near melting pt., hot tearing 79−83314
steel, continuously cast slabs, formation of longitudinal midface cracks 79−83315
steel, Cr-Mo:P (2.25, 1 wt.%), stress relief cracking, effect of P segregation 80−89324
steel, Cr-Mo, oxidised, mechanism of crack decoration of oxides by electrodeposition 80−97560
steel, Cr-Mo, toughness of heat treated steels of equal tensile strength *(German)* 80−25727
steel, Cr-Mo (10-14, 2-6 wt.%), heat-resist., creep-rupture strengths 80−104271
steel, Cr-Mo (1, 0.5 wt.%), heat treated creep failure, role of stress state 79−5047
steel, Cr-Mo (2.25, 1 wt.%), damage accumulation and microstruct. changes during creep 80−3129
steel, Cr-Mo (2.25, 1 wt.%), small changes effect in impurity elements, creep life 80−25790
steel, Cr-Mo-V, rupture ductility rel. to cavitation, density and SEM obs. 79−34142
steel, Cr-Ni-Mo, 'light spots', fractographic anal. 79−29204
steel, Cr-V (1.5, 0.5 wt.%), ferritic, effect of temp. and microstruct. on creep damage 79−5023
steel, creep resistant, fine grained, structural, welded-joints, cause of cracking during stress relieving *(German)* 77−70141
steel, ductile fracture in presence of elongated sulphides *(French)* 80−45394
steel, ductile fracture under cold metal forming conditions, metallurgical struct. influence 79−34125
steel, ductile structural, fatigue crack propag. rate and striation spacing 80−93635
steel, eutectoid, high strength, unnotched specimens, fatigue crack init. and propag. 77−56098
steel, ferritic stainless, type 444 welds, ductility loss mechanism 80−85002
steel, gas nitrosulphurized, in temp. range 813-903K, wear props., surface and cross-sectional hardness, X-ray diffr. and SEM study *(Japanese)* 79−29224
steel, hard, high speed and tool, linear elastic fracture mech. appl. 78−48518
steel, heat-exchanger alloys for use in nuclear steam coal gasification plant 78−15589
steel, high C, tensile strength, working and heat treatment effects *(Japanese)* 80−104209
steel, high speed type M-50 and 18-4-1, fracture and fatigue 80−16457
steel, high strength, fatigue crack initiation and early growth 78−7009
steel, high strength, H_2 embrittlement due to cathodic charging during specimen prep. for SEM *(German, English)* 80−11760
steel, high-speed, eutectic carbide structure, determ. by SEM 78−85075

scanning electron microscope examination of materials continued
steel, high-speed, fracture toughness of powder metallurgy vs. conventionally produced steels 78−64647
steel, homogenisation of sulphide inclusions 77−32605
steel, hot forging die type, fractography *(Japanese)* 80−108547
steel, hydrogen embrittlement *(German)* 78−19858
steel, inclusion, grain boundaries and H_2 attack, fracture analysis 77−32695
steel, inclusion behaviour investigations using SEM 78−23916
steel, industrial, surface chem. characterisation by SIMS, glow discharge spectrometry and other techniques 80−66907
steel, Kossel patterns, small area 79−1375
steel, low alloy, crack form. during stress relief in heated zones *(German)* 79−74242
steel, low alloy, medium strength, SEM obs. of fracture surfaces, cleavage fracture model 77−36649
steel, low alloy, SMCM 8, tempered, fractographic study of stress corrosion cracking *(Japanese)* 79−66214
steel, low alloy ferritic, sub-micron cavity nucleation, SEM obs. 78−95753
steel, low C, built-up edge form., direct SEM obs. 80−104303
steel, low C, corrosion, heat treatment and plastic deform. effects 77−63825
steel, low C, effect of water vapour, on fatigue crack plasticity 78−64678
steel, low C, fatigue and creep observation using imaging of subgrains 80−66609
steel, low C, rimmed, structural damage in sheet metal forming 78−64614
steel, low S, overheating 77−21185
steel, low-alloy, study of deformation and fracture processes by acoustic emission transient anal., SEM and optical microscopy study 79−43311
steel, marageing 300 grade, serrated flow in austenitic state 80−30041
steel, maraging, 18 wt.% Ni, solution heated and aged, surrface damage during machining, unlubricated 78−15599
steel, maraging and low-alloy, electron fractographic analysis of fatigue fractures 79−38965
steel, martensitic, age hardening with Cu, Nb additions, exam. of hardness 80−7681
steel, martensitic stainless, in SO_4 solns., activation pH and susceptibility to H_2 assisted stress corrosion cracking 80−97619
steel, medium C, Mn, type 42Mn2 cylinders, flake immunisation by hot working *(Chinese)* 80−66540
steel, medium C, Ni-Cr-Mo, overheated, fractographic study *(Chinese)* 80−66616
steel, medium C, shell-shaped fracture due to B embrittlement *(Chinese)* 80−55493
steel, mild, AISI 1009 and 1018, corrosion incipient processes in hypersaline geothermal brine at 90°C 80−50753
steel, mild, Al-Zn alloy coated, interface struct. 79−52466
steel, mild, conical rider on Cu surface, SEM exam. of plastic deformation and wear at friction junction 78−88542
steel, mild, hot shortness mechanism, surface enrichment of residual elements and oxidation *(Chinese)* 79−74230
steel, mild, origin of spherical particles on fatigue fracture surfaces and ferrograms 79−79112
steel, mild, programmed fatigue crack propag., crack tip residual stresses 77−36644
steel, mild, shear mode of ductile fracture 79−91785
steel, mild and type EN31, eval. of cold rolling oils and boundary lubrication characts. by SEM 80−85068
steel, Ni-Cr, exam. of caustic stress corrosion cracking, comparison with type 304 stainless steel 79−29261
steel, Ni-Cr, temper embrittlement by Sn 77−86149
steel, Ni-Cr temper embrittlement by P 77−40448
steel, Pb and MnS inclusions 77−77685
steel, pearlite, deform. and fracture mechanisms, HV SEM obs. 80−104243
steel, rail, toughness, effect of Sn, SEM exam. 80−97569
steel, rolled, anisotropic, fatigue fracture surface obs. *(Japanese)* 80−108546
steel, rusted, exam. of tannin treatment action mode 78−88564
steel, Si, nonoriented elec. sheet, solute oxidation effect on mag. props. 79−83335
steel, Si-Mn-Cr-C (1.1, 0.9, 1.0, 0.29 wt.%) 30KhGSA, heat treatment effect on strength and toughness 78−15437
steel, spheroidised, H_2 embrittlement, fracture surface study by SEM and optical microscopy 79−57109
steel, spheroidized, shear mode of ductile fracture 79−61714
steel, stainless, 18Cr-2Mo-Ti, atmospheric corrosion 80−85078
steel, stainless, 316, crack propag. in low cycle fatigue below 600°C, SEM obs. 78−64631
steel, stainless, 316, surface analysis by SIMS, SEM AND ESCA 79−52825
steel, stainless, 316 and 304, equilibrium surface bombarded with high dose He^+ ions 78−95091
steel, stainless, AISI 304, dislocation substruct. around fatigue cracks, SEM obs. 78−15516
steel, stainless, annealed 310, deform. at erosion sites, TEM and SEM studies 78−64725
steel, stainless, blistering owing to He^+ bombard., 2 MeV 80−49279
steel, stainless, corrosion fatigue cracking in NaCl aqueous solution, fractographic anal. *(Japanese)* 78−53023
steel, stainless, emittance meas. rel. to surface roughness parameters 80−100342
steel, stainless, Fecralloy, creep-rupture props., 650-800°C 80−97535
steel, stainless, He ion irrad., fracture behaviour, in-situ HV electron microscopy 80−29089
steel, stainless, PWR primary corrosion products 80−13578
steel, stainless, spatial distribution of limiter material and impurities on the first wall of TFR 400 79−651
steel, stainless, stress corrosion cracking, due to boiling $MgCl_2$ solution, SEM exam. *(Japanese)* 78−53025
steel, stainless, stress corrosion testing, slow strain rate, elevated temp. and high press. study 80−97615
steel, stainless, type 304 welded, low temp. sensitisation, nucleation of CR carbide nuclei along grain boundaries TEM, SEM study 79−38851
steel, stainless, type 309, low-cycle fatigue, effects of notches on crack initiation 79−74249
steel, stainless, type 316, blistering by 2 MeV He^+ ions, optical microscopy and SEM obs. 79−42119
scanning electron microscope examination of materials continued
steel, stainless, type 316, low cycle fatigue props. in vac., fracture mode 80−85021
steel, stainless, type 316, microstruct. changes in creep ductility, SEM, TEM, optical microscopy and X-ray diffr. study 79−38927
steel, stainless 304, elevated temp. low cycle fatigue, heat treatment effect 78−27626
steel, stainless 304, stress corrosion cracking 78−31565
steel, stainless 304, stress corrosion cracking in boiling $MgCl_2$, crack growth rate study by SERT method *(Japanese)* 79−100290
steel, stainless 310, erosion at 975°C in combustion gas atoms. 77−66704
steel, stainless 316, ion sputtered, surface anal. by Auguer effect and SEM 78−95632
steel, stainless 316, low cycle fatigue life, relation with striation spacing, and macroscopic crack growth at 625°C 78−11317
steel, stainless casts, creep ductility, Auger spectroscopy study 80−60917
steel, stainless sheet, texture effect on sputtering erosion by Ar^+, SEM-electron channelling study 79−91856
steel, stainless type 304, effects of waveshape on crack initiation in low-cycle fatigue 79−79108
steel, stainless type 316, thermally aged, accelerated creep-fatigue crack propag. 80−89326
steel, stainless unpolished, electron field emission sites 77−21008
steel, struct. type 05KhGM, crack initiation and propagation during H_2 embrittlement 80−35313
steel, structural, impurity effect on crack initiation, dynamical loading *(Czech)* 80−60955
steel, structural, naturally and artificially weathered, SEM characteris. 78−23882
steel, structural, second phase particle effects on impact strength 80−108581
steel, tool and high speed samples, emission spectral and X-ray fluorescence anal., SEM microstruct. obs. *(Japanese)* 79−43232
steel, type 27KhGSNL, castings, exam. of cracks due to treatment 78−44205
steel, ultra high strength, P induced 350°C embrittlement 79−57099
steel, V-Nb and Cr-Mo-V-Nb, supercooled austenite isothermal decomp., struct., strength and fracture characts. 80−60966
steel C60, machined, surface morphology, struct., SEM, topographic investigs. *(German)* 77−73372
steel gas nitrosulphurising, S25C, wear property 80−50729
steel hardness and ductility variations and micrographs rel. to heat treatment and phase diagram obs. 79−87609
steel mesh, herniorrhaphic reinforcing prosthetic, mech. and struct. props., SEM study 79−74789
steel-polymer wear mechanism during fretting corrosion 78−35522
steels, austenitic stainless, crack propag. rates under high-temp. low cycle fatigue conditions 80−21088
steels, free-machining, fractography and X-ray photoelectron spectroscopy 80−7673
steels, obs. and anal. of sulphides, using non-aqueous electrolyte-potentiostatic etching method *(Japanese)* 80−89433
steels, stainless, surface characterisation rel. to adhesive bonding chem. etching, SEM, AES, XPS and electron probe microanal. 80−88416
steels, structural St 37-2, cleavage fracture, report 80−25868
steels, welded, types D36, D50, secondary ion anal. of segregation 80−7580
stretched zone anal. by means of stereo matching method *(Japanese)* 80−108544
superconductor, magnetic flux quanta, TEM, SEM and STEM obs. 77−47945
superconductors, low temp. SEM appl. 80−80443
superconductors, multifilamentary, voids growth obs., via hot stage SEM 80−70089
surface charact., combined ion scattering spectrocopy, SIMS, SEM, energy dispersive X-ray techniques 79−43702
surface microstructure determ. and microanalysis by ultrahigh vacuum field emission gun SEM 80−96423
surface potentials visualisation and meas., electron energy analysis 80−68307
surface topography, high-resolution polymer replication 78−10264
Teflon foils, cryst. struct. and texture changes due to polarisation process *(Polish)* 80−35209
textile fibres, polymer treated, sectioning technique 79−2891
thermoelectric materials, B_4C_x and $(B,Si)_4C_x$ P-type LaS_x N-type alloys, fabrication and thermoelectric props. 80−107771
thermoplastic, partially crystalline, microscopic methods of struct. anal. *(German, English)* 80−30198
thermoplastics, internal stresses revealed by artefacts produced in SEM 78−35634
thin films, thickness determination, using backscattered electrons as tool 79−21704
thin films cryst. defects obs. in SEM *(French)* 77−31662
thinned semiconductor device, SEM, electron beam induced cond. of defects, rel. to TEM 80−107027
tooth enamel organic phase, sample prep. technique 77−52952
tribopolymerised lubricants, mechanism of action, SEM expts. 79−29226
TTF-TCNQ, elec. cond., SEM technique 80−86507
turquoise, crystalline, Nogales Mexico, SEM and TEM study 79−29760
Udimet 500, microstructural instability in industrial gas turbine engine vane 77−28833
unhealed porosities and crystalline steps in flakes *(Chinese)* 79−74179
untreated insulating materials, direct viewing without charging, modification to Cambridge SEM 80−47150
vacuum, ultra-high, secondary electron emission dependence on electron beam density dose, surface interactions from AES and ELS 80−61209
vacuum vessel wall surface conditions, long term changes, PLT appl. 79−653
4-vinylpyridine acrylonitrile copolymer membrane, reverse osmosis charact. *(Japanese)* 78−31694
volcanic ash, examples of devitrification and early diagenesis 80−81860
volcano eruption cloud particles, St. Augustine, Alaska 78−57186
wear measurement by surface replication 77−12771
wear study, analytical surface tool, review 78−64718
wet, live and frozen objects, review 79−26183
white Fe castings, morphology of eutectic M_3C and M_7C_3 80−108427
wood, clean cut surface preparation for SEM studies 78−15935
X-ray dispersive crystal spectrometers, geometric accuracy *(Chinese)* 80−22495
Zircaloy, breakaway mechanism, corrosion kinetics in steam 80−61030

scanning electron microscope examination of materials continued
Zircaloy, deposits on inside surface in LWR cladding, SEM obs. 79−6741
Zircaloy, PWR primary corrosion products 80−13578
Zircaloy-2, effect of simulated fission products on elongation fractography and metallography 80−649
Zircaloy-2, mech. props. after exposure to I_2-methanol solutions, SEM study 80−93689
Zircaloy-2, TEM and SEM of anodically formed oxides 77−21313
Zircaloy-2 cladding, bonding to UO_2 fuel, mechanisms determ. by SEM and EPMA 78−17317
Zircaloy-4, resistance-welded, microstruct. of weld region 80−66549
Zircaloy-4, strain rate dependent mech. response 77−21254
Zircaloy-4 cladding rubes, burst strain and stress corrosion cracking, I influence 80−3248
Zircaloys, fractographic distinction between hydride cracking and stress corrosion cracking 78−92363
Zircaloys, I_2 induced stress corrosion cracking 79−8381
ZnO, film, reactively RF sputtered, anal. of texture 78−67921
β-2CaO-SiO_2, hydration mechanism and rate, SEM and chem. anal. 79−79218
Ag, cluster growth and nucleation on Mo (100), UHV-SEM, AES/(RHEED or LEED) obs. comparison 78−63956
Ag electrode, prepared by sintering and by chemical method 79−87851
Ag electrodeposits, dendritic growth inhibition by tartaric acid and tartrates *(French)* 78−87894
Ag, film, chem. deposited, agglomeration, SEM and TEM obs. 80−59828
Ag film, sputtered, hillock growth and agglomeration by annealing, SEM obs. 80−2309
Ag, film, sputtering mechanism, SEM 80−29839
Ag film growth on Si (111), nucleation and growth modes, SEM study 80−100423
Ag films, hillock form. hole growth and agglomeration 80−44455
Ag halide photographic emulsions, SEM investig. of grain props., specimen prep. technique 77−41715
Ag, implanted grain boundary cavities effect on cavity growth kinetics and creep fracture 78−52935
Ag, in 0.1 M Na_2SO_4, passive (Ag_2O, AgO and Ag_2SO_4) films properties obs. *(Japanese)* 79−8399
Ag ion plated film on permalloy, Cu and Vicalloy substrate, AES, SEM and X-ray study *(Japanese)* 78−11128
Ag layers, on W, scanning Auger microscopy, effect of backscatt. electrons on resolution 79−2898
Ag, loosely packed powder, sintering SEM and dilatometry obs. 80−20843
Ag on Si and W substrates, UHV-SEM studies of Stranski-Krastanov growth 80−79722
Ag, ultrafine powder, role of evap. during sintering 78−64505
Ag-(100)InP contacts, interface struct. 79−60922
Ag-Al polycryst. thin-film couples, interaction process 79−51443
β'-Ag-Cd (45 at.%), growth kinetics of bainite plates and Widmanstatten needles 77−36551
Ag-Cd (approx. 50 at.%), disordered hcp to ordered bcc transition, meas. of activation energy 78−72773
Ag-Cu, directionally solidified, obs. of cutting deform. zone *(Japanese)* 78−15422
Ag-Cu (6.2 at.%), with discontinuous precipitates, quantitative struct. anal. using SEM 79−43527
Ag-Ni (10 wt.%) wire, plastically deformed, fracture struct. *(German)* 80−71744
AgCl, epitaxial growth on TGS, model system for orientation mechanism determ. during epitaxy 79−11022
α-Ag_2S whiskers, growth in VLS system, SEM and X-ray diffr. anal. 79−46989
Ag_2Te, Ag movements, X-ray microanal. by SEM *(French)* 79−42304
Al alloy, anodic finish exam. by SEM and electron probe micro anal. obs. 79−96278
Al alloy 7075-T7351, fretting fatigue crack form. 80−35344
Al alloy surfaces anodized in phosphoric acid 80−81241
Al alloys, fatigue crack arrest, corrosive environment, at low stress intensities 78−92415
Al alloys aged, local plastic strain distrib. by selected areas channelling patterns 77−44349
Al and Al alloy anodised oxide films, for adhesive bonding appls., AES and SEM study 80−66689
Al, annealed, and sintered powder, sputtering under D^+ and He^{4+} bombardment, microstruct. effects study 80−84821
Al, atomized powder, metallic contact for hot rolling in air 77−73294
Al, Auger electron microscopy, edge effect, Monte Carlo simulation 79−1801
Al, cavitation erosion in water flow, initial stage 78−27648
Al coating, plasma sprayed on steel substrate, microstructural investigation and oxidation effects 78−11426
Al, coating on steel by thermal decomposition of alkyls 78−15590
Al, contrast of electron channelling patterns, estimation from low index refl. 78−9921
Al, erosion by solid particle impingement at normal incidence, SEM obs. 80−104304
Al FCC single crystal, crystal rotation accompanying scratch deform. *(Japanese)* 79−15733
Al, fatigue crack initiation, pre-existing subgrain effect 80−97565
Al film, deform. under He ion bombardment 80−65073
Al film, ion plated, morphology exam. by SEM 79−28251
Al film, MBE and field emission deposition on III-V semiconductors, comparative study 79−87016
Al film, meas. of stress gradients generated by electromigration, X-ray topography and SEM 77−51541
Al film, vacuum deposited, 7 to 65 μ thick, morphology and purity determ. 77−76699
Al, fracture mechanism 80−100903
Al, high temp. creep, grain boundary dislocations 78−43065
Al, high temp. fracture, SEM obs. 77−59918
Al lithographic sheet, AC etching, surface study 80−35547
Al, oxidation, in water, oxide growth rate and struct. 78−76783
Al, plasma-sprayed, effect of Si substrate surface conditions and impact velocity of sprayed particles 80−21145
Al, polishing, electrolytic and chemical, SEM exam. of gassing defects 79−34206
Al, polycrystalline, fatigue damage detection by exoelectron emission meas. *(Japanese)* 77−55871

scanning electron microscope examination of materials continued
Al, sacrificial anode dissolution, Hg effect study using ion implantation 79−39016
Al, scanning Auger electron microscopy, Monte Carlo calc. 78−19610
Al sheet surfaces, chem. characterisation by SIMS, glow discharge spectrometry and other techniques 80−66907
Al, sliding wear in NaCl of varying pH 78−3240
Al, step coverage optimisation by computer simulation and SEM 78−51838
Al, surface deformation and wear track obs. using analytical electron microscope 80−108687
Al, surface exfoliation and blistering induced by He ion bombard. in energy range 10-80 keV 80−39173
Al, tribological investigation using two-cylinder tribometer *(German)* 77−25164
Al, wear particles, spheroid form. by cavitation erosion 79−52382
Al-Ag (15 wt.%), precipitation hardenend cyclic stress-strain response 78−35412
Al-Al_3Ni, electrolytic prep. of Al_3Ni fibres, SEM and anodic polarisation 80−100817
Al-Al_3Ni eutectic composite, structural response to shape variations 79−83190
Al-Al_6Fe, fibre reinforced eutectic, deformation behaviour by rolling, TEM and SEM study 79−29129
Al-alloy type 7075-T6, effect of shot peening on fatigue behaviour 79−79102
Al-Bi(Cd)(Pb)-Ti, containing low-melting pt. inclusions, mech. props. 80−93632
Al-Cu, type 2219-T851, fracture mechanics and surface chemistry of fatigue crack growth 80−81168
Al-Cu (Mg)(Zn), corrosion of chill zone, solidification microstruct. effect 77−36687
Al-Cu (4 wt.%), aged to contain Guinier Preston zones, crystallographic fatigue crack growth 78−60832
Al-Cu (4 wt.%), supersaturated and aged conditions, high strain deform. 80−60907
Al-Cu (4.5 wt.%) alloy, controlled electropotential corrosion in NaCl soln., microstruct. exam 78−39948
Al-Cu-Mg, tpye RR55, high strength, creep behaviour, effect rel. to anodic coatings, SEM study 80−97542
Al-Cu-Mg (4,1 wt.%), behaviour during ductile fracture, SEM *(Rumanian)* 80−21062
Al-Cu-Mg/mica particulate composite mech. props. 80−100919
Al-Cu-Mn (6.3, 0.3 wt.%), alloy Al 2219-T851, crack closure load meas. during fatigue 77−63870
Al-GaAs interface, thermal ageing of Al film, optical microscopy and SEM obs. 77−20203
Al-Li-Mn (2.8, 0.3 wt.%), recrystallised sheet, fracture behaviour, SEM and TEM study 80−97566
Al-Mg, homogenisation process, effect of solidification rate and alloying *(Polish)* 79−78949
Al-Mg (1 wt.%), behaviour during ductile fracture, SEM *(Rumanian)* 80−21062
Al-Mg_2Si (0.95 wt.%), excess Si effect on ductility 78−27580
Al-Mg_2Si(1.42 wt.%), aged, dislocation structs. caused by plastic deformation 80−25786
Al-Mg-Si alloys, dendritic non-homogeneity 78−56641
Al-Mg-Si alloys, effects of dispersoids upon micromechanism of crack propagation 79−83286
Al-Pd eutectic, microstruct. morphology 80−3018
Al-Si, eutectic colonies morphology by stereometric microanal. *(Russian)* 77−81247
Al-Si eutectic alloy, banded struct., SEM and optical microscopy 80−104144
Al-Si hypereutectic alloy, dissolution and primary crystallization of Si *(French)* 77−59832
Al-Si-Cu-Mg-Ni cast alloy, fractography *(German, English)* 79−87809
Al-Si-N-O system, comps. corresponding to β'-sialon phase reaction hot-pressing 80−84891
Al-silicide-Si systems with $CoSi_2$, $Pt_xNi_{1-x}Si$, and $MoSi_2$ as silicide, diffusion, compound form., and microstructure 80−34253
Al-Zn-Mg, stress conversion cracking based on micromech. surface reactions 80−7716
Al-Zn-Mg alloy AA-7039, stress corrosion cracking, SEM obs. 80−104323
Al-Zn-Mg type 7017 and 7018 alloy plate, fractographic study of stress-corrosion crack propag. 79−57158
Al-Zn-Mg-Cu, age hardened, effect of strain rate, temp. and environment on ductility 80−45368
Al-Zn-Mg-Cu alloy 7075-T651, adiabatic shear localisation and erosion 79−96157
(AlGa)As DH lasers, comparison of 'normal' lasers and lasers exhibiting light jumps 80−106519
AlGaAs-GaAs proton irradiated solar cells, deep-level defects, recombination mechanisms, performance characts. 80−81459
$Al_xGa_{1-x}As$ epitaxial diode, neutron and γ-irrad. effects on cathodolum. in SEM 79−11473
$Al_xGa_{1-x}As$, point defects, recomb. enhanced interactions with dislocation networks 79−60398
AlN film, oriented c-axis, low temp. deposition by reactive magnetron sputtering 80−76180
AlN films, RF reactive ion-plating, struct. and morphology 80−104074
Al_3Ni dendrite facets, determ. cryst. direction by SEM *(French)* 78−87893
$Al_{2+x}O_3$, sintered, elec. cond. temp. and comp. depend., thermoelec. power 80−2438
Al_2O_3 (96 wt.%), fractographic criteria for subcritical crack growth boundaries 80−81155
Al_2O_3, abrasive, wear in simulated hot grinding 78−56784
Al_2O_3, calcined, exam. of morphological changes during calcination by SEM, exam. of sintering behaviour *(German)* 79−4931
Al_2O_3, defect microstructure due to ion bombardment, TEM study 80−34100
Al_2O_3, dense, steam-enhanced Ca segregation, AES and SEM obs. 79−83352
Al_2O_3, fibrous, thermal diffusivity and conductivity 78−10232
Al_2O_3, grinding and polishing, quantitative control and optimization *(German, English)* 80−35460
Al_2O_3, hot pressing, microstruct., texture 80−40299
Al_2O_3 plasma-sprayed, struct. and thermal diffusivity 79−86932
Al_2O_3 sintered surfaces, premetallizing with Mo-Mn-SiO_2 79−47792

scanning electron microscope examination of materials continued
Al_2O_3 sintering in liq. phase presence, particle rearrangement 79−29004
Al_2O_3, sintering response with const. rate of heating, depend. on processing related pore distrib. 79−28992
Al_2O_3, sintering with $SrTiO_3$ admixture *(Polish)* 78−19699
Al_2O_3, spray dried agglomerates, compaction response, fracture, deform. 79−43172
Al_2O_3, subject to elastic/plastic indentation, crack initiation threshold 79−70157
Al_2O_3 substrate, notched, grain struct., SEM study *(German)* 80−33860
Al_2O_3 substrates, grain growth during sintering 80−40302
Al_2O_3 substrates, tape-casted, fracture strength analysis 80−60948
Al_2O_3, twinning and microcrack nucleation during indentation 77−63793
Al_2O_3, unflawed polycryst., tensile failure, SEM and acoustic emission expts. 78−27598
Al_2O_3:Ni anodised films, electrolytically coloured, spectrally selective surface 80−11490
Al_2O_3-Al, disordered, energy diagram model 79−56110
Al_2O_3-Cu composite, vapour deposition, microstruct., texture and surface topography 77−70001
Al_2O_3-glass mixture, microstructural changes and shrinkage during sintering 80−25640
Al_2O_3-SiO_2 particles, new method for X-ray micro-anal., based on peak to background meas. 79−24881
Al_2O_3-ZrO_2 cast refractories, nucleation processes reconstruction by SEM, TEM and STEM 78−35380
$3.5Al_2O_3.2SiO_2$, mullite, decomposition by SiO_2 volatisation 80−61082
Al_2TiO_5, eutectoid decomposition, kinetic study *(Japanese)* 77−55941
Au black solar absorbing film, particulate nature 77−39003
Au, contrast of electron channelling patterns, estimation from low index refl. 78−9921
Au, electrodeposition in 2 μm layers 79−74104
Au, film, grain boundary electromigration, tracer meas. 77−31802
Au film, interface reaction with n-type $Ga_{0.7}Al_{0.3}As$ and GaAs 80−39482
Au film, ion plated, defect growth structs., SEM obs. 80−24768
Au film, MBE and field emission deposition on III-V semiconductors, comparative study 79−87016
Au film, whisker growth due to high current densities 77−69191
Au film on Cr adhesion layer, etching, SEM anal. of abnormal undercutting 79−5075
Au, hardening mechanisms, grain size effect 80−35302
Au, vapour deposited on Au with Cr interlayer 77−20202
Au wire, microparticle trigger discharges and impact damage in HV vacuum insulated gap 77−24227
Au/Ti thin film, temp. and humidity effect on interdiffusion 79−51317
Au-Co electrodeposits, heating effect on microstruct. and surface topography 77−43456
Au-Ge contacts on GaAs, SEM and TEM obs. of struct. 80−100522
Au-refractory film interdiffusion obs., by combination of scattering techniques 80−65308
Au-Sn evaporated films, comp. and annealing behaviour, 20-400°C 77−76695
Au-$Ti_{0.3}W_{0.7}$, thermal annealing study of metallisation on Si 80−80134
Au_3Si, room temp. dissociation 78−35672
Au_3Zn, R_2-phase, long period domains, transmission, scanning and optical microscopy obs. 79−38801
B fibre, fracture, Griffith criterion appl. 77−12684
B fibre reinforced Al, thermal degradation of tensile strength, due to fibre strength degradation 78−39861
B fibre reinforced Al alloy, influence of band strength on failure *(Russian)* 79−43387
B-B_4C materials, hot-pressed, elastic modulus and flexural strength rel. to grain size and porosity 79−79018
B_4C, effect of fast neutron irradiation on struct. 78−26597
B_4C, morphology and struct. of vap. grown crysts. 79−7562
B_4C rings, Al bonded, exam. of fabrication techniques 78−72748
BN, cubic, growth pressure-temp. region in system BN-Mg 79−66053
BN, cubic struct. form. from hexagonal struct. at high press., catalytic effects *(Japanese)* 77−90308
BN external crystal morphology, SEM obs. 79−73078
B_2O_3-SiO_2, optical waveguide glass, sintering kinetics 80−84898
B_2O_3-SiO_2-Na_2O phase-separated glass, creep fracture morphology 80−81151
Ba hexaferrites, mech. and mag. props., fractography study 79−70151
$BaCO_3$, grown in silica gel medium in test tube 77−36379
$BaFe_{12}O_{19}$ particles, magnetic domain study by colloid-SEM method 80−97120
$BaFe_{12}O_{19}$ powders, fast reaction presintering 80−97445
$BaMoO_4$ crystals, growth in SiO_2 gel under influence of elec. field 80−93469
$BaMoO_4$, grown in silica gel media in test tube 77−36379
BaT:O_3, surface microrelief revealed by ion irradiation 80−54485
$BaTiO_3$ ceramic, PTC-type, voltage contrast imaging for low and high Ti excess 77−28183
$BaTiO_3$ ceramics, calcination effects, TiO_2 powder eval. *(Japanese)* 78−64516
$BaTiO_3$, domain structure obs. using SEM 77−1647
$BaTiO_3$, epitaxial vacuum condensates struct. 79−95290
$BaTiO_3$ powder, US dispersed, SEM study *(German)* 80−33860
$BaTiO_3$, powder compacts, sintered, physical and chem. inhomogeneities 79−87594
$BaTiO_3$, pure and doped crysts., surface and domain struct., AES and SEM expts. 80−71363
Be, implanted D and He, interaction and radiation enhanced oxidation 80−39120
Be, machining damage, SEM exam. 78−39990
Be, neutron irradiated, annealed, tensile props. and swelling, effect of He bubbles 78−22765
Be, thick film, amorphous, RF magnetron sputtering 80−80971
Be-Cu strip surface quality and preparation 80−50779
Bi film, structure and electronic props. 80−70562
BiOCl, exam. of crystal structure and morphology, as function of growth conditions, using electron microscopy 79−52103
n-$Bi_2(Te,Se)_3$ semiconducting solid solns., plastic deform. during hot extrusion 79−20143
p-Bi_2Te_3-Sb_2Te_3 semiconducting solid solns., plastic deform. during hot extrusion 79−20143
C CVD coating, surface damage and erosion under energetic D^+ and $^4He^+$ irrad. 80−39174

scanning electron microscope examination of materials continued
C, colloidal layers, sputtering, chem. etching in DC glow discharge 78−27667
C fibre, metal-coated with Cu, Co or Ni, coating struct., SEM study 80−97605
C fibre, morphological charact. rel. to fracture, SEM obs. 77−63791
C fibre layers on arc anodes props. and cooling behaviour 79−52245
C fibre reinforced epoxy and C fibre, elastic moduli 77−86069
C fibre reinforced plastic, SEM obs. of fatigue 80−11737
C fibre reinforced plastic, fractography of fracture surface under three-point bending *(Japanese)* 80−55506
C fibres, from mesophase pitch, tensile strengths, Weibull parameters, SEM study 79−79031
C fibres struct. and physical props. effects of B additions and heat treatment temp. 78−68715
C, microscopic features of carbons obtained from aromatic hydrocarbons using carbonisation catalysts 77−66597
C, morphology and growth mechanism of carbons formed by Ni-catalysed decomp. of hydrocarbons 78−35679
C, nongraphitizable, catalytic graphitization by Cr_2O_3, MnO_2 80−97440
C vacuum deposited coatings for prosthetic devices 77−40374
C-C composite, oxidised, SEM study 77−52522
C-fibres, fracture surfaces, SEM study 79−69649
CC Nb single cryst., He ion implantation, depend. of blister deckeldicke and depth profiles on incidence angle, SEM study 79−73226
$CaAl_2O_5$, form by interdiffusion of CaO and Al_2O_3 79−28998
CaF_2, cathoduluminescence 80−100700
CaF_2:Eu, CaF_2:Eu,Mn(Gd), single crystal predisintegration phenomena, SEM cathodolum. obs. 80−59502
CaF_2:Eu, Mn, stroboscopic cathodoluminescence meas. appl. 80−70088
CaF_2:Mn, CaF_2:Eu,Mn, single crystal predisintegration phenomena, SEM cathodolum. obs. 80−59502
CaO, corrosion by K_2O melt 77−44383
CaO, produced from $CaCO_3$ powder decomp. in vac. and in CO_2 80−45255
β-(CaO_2)-SiO_2-H_2O, SEM and X-ray diffr. exam. of structure, crystallisation props. 78−73012
$3CaO.Al_2O_3$-$CaSO_4.2H_2O$-CaO-H_2O, citric acid effect on reactions 78−27725
$Ca_x(PO_4)_y$, soln., coagulation effects on light scatt. obs., TEM, SEM 80−45090
$Ca_{10}(PO_4)_6(OH)_2$, hydroxyapatite, prep. by hydrotherm. recrystn., composition and props. study 79−33913
$Ca_5(PO_4)_3OH$ bioceramic, material props. 80−93523
Ca_3ScO_5, fracture surfaces, quantitative anal., energy dispersive X-ray spectrometry with Si(Li) diodes *(French)* 80−89571
β-Ca_2SiO_4, very reactive powder, prep. 77−55924
Ca_3SiO_5, P containing, hydrated, microstruct. and IR struct. 79−29074
Cd film on C steel, tribological behaviour 80−89364
Cd films, nucleation and growth, props. 80−29878
Cd-Zn alloys, splat-quenched, X-ray diffr., SEM and TEM study of struct. 79−66077
$CdCr_2Se_4$, spinel film, struct. SEM study, props. 78−79905
$Cd_xHg_{1-x}Te$, correlation between structural and chemical inhomogeneity *(Russian)* 80−49484
$Cd_xHg_{1-x}Te$ film, vacuum deposited, struct. and elec. props. 77−59344
$Cd_xHg_{1-x}Te$, vac. evap. film struct. rel. to carrier scatt. 77−85116
$CdI_{2-x}Br_x$, vapour grown mixed cryst., growth and polytypism 79−69044
$CdIn_2S_4$ film, vac. deposited, growth, struct., optical and photoelectronic props. 80−10831
CdS, Au deposition; Schottky diodes and MIS devices, surface treatment effects, SEM obs. 80−54794
CdS, diffusion length determ., resolution limit of EBIC technique 79−21865
CdS film, prep. by hot wall technique, morphology and semicond. props. 79−95292
CdS film growth, with smooth surfaces through boundary layers 79−28244
CdS films, spray pyrolysis deposition, SEM study, aerodynamics of nozzles 79−68782
CdS, ion irrad. damage, obs. using SEM in cathodolumin. mode 79−7633
CdS, local cathodolum. of single crysts. under colour contrast conditions in SEM 79−8191
CdS, reversible hardening induced by electron-beam irrad. 77−62580
CdS solar photovoltaic panels, deposited by spray pyrolysis, film and junction structure studies 80−45689
CdS, vacuum epitaxial growth on $CuInSe_2$ 78−92193
CdS:Ga crystal cathodoluminescence, SEM analysis 80−97349
CdS/Cu_2S heterojunction solar cells diffusion length determ. using minority carrier SEM 80−61359
CdS(Se), small-angle boundaries, SEM obs. 80−24456
CdSe film, vac. deposited, elec. resist. and surface changes by laser annealing 80−2491
Cd_2SnO_4 and Cd_2SnO_4:CdO, thin film electrodes in H_2SO_4 electrolytes, reduction, AES and SEM 80−65674
n-CdTe, cathodoluminescence microscopy obs. of dislocations, compared with etch pit pattern 79−69105
CdTe film, growth by photostimulated VPE, electrophys. props. 77−40390
CdTe, laser window material, vap. deposition, mech. props. 77−46776
CdTe sputtered films, struct., photocond., and trap distrib. 80−29489
$CePd_3$ single crystal Czochralski growth and characterisation 80−60767
Co ferrite film prep. by vac. evaporation and annealing 77−85939
Co film, electromigration exam. from structural changes and resistance increases 77−20213
Co, superalloy, attritious wear in grinding 77−32696
Co-B-Si ternary system, partial phase diagram, Co rich region 77−52293
Co-Cr superalloy, type MAR M509, high temp. fatigue behaviour 80−40485
Co-Cr-Ni-Ta-Al-Y (25, 10, 5, 3, 0.5 wt%), exam. of hot corrosion 79−20251
Cr coatings, ion-plated, deposition parameter influence on struct. and hardness 79−82485
Cr, deposited by high rate sputtering, mech. props. 77−36630
Cr film, evaporated, on die-cast Zn, microstruct. and intrinsic stresses, substrate temp. effects 78−10304
Cr films, photoresist film on reverse gas plasma etching 80−97634

scanning electron microscope examination of materials continued
Cr whisker cryst., growth incorporated with field electron emission 80−44458
Cr/Au layered films, microstruct. and interdiffusion during ageing, 423 to 573K 79−46965
Cr-Cr_2O_3, black chrome films, surface microstruct. rel. to optical props. in solar absorbers 79−52036
Cr-Cr_2O_3, black chrome solar selective absorber, microstruct. 79−56875
Cr-Cr_2O_3 black, electroplated solar collector coatings, high temp. optical and struct. degradation 80−66995
Cr-Cr_2O_3 black solar absorber surfaces, microstruct. rel. to electroplating parameters 80−61418
Cr-rare earth, dil., oxidation of Cr, effect of rare earth impurities 79−79160
Cr-SiO, thin film, laser beam-treated, emission mode of SEM 79−28226
Cr-V-B-Y system, fatigue strength and fatigue fracture at 20 and 1100°C, SEM study 80−3194
Cr_3C_2-(WC)-Ni, sintered, cavitation erosion resistance *(Japanese)* 77−52500
CrO_2, ferromag., new prep. method by high-pressure oxidation, SEM characterisation 79−43164
CrO_2, ferromag. films, epitaxial growth in air, electron diffr. and SEM obs. 79−42410
Cr_2O_3 films, black, microstruct. depend. of optical props., SEM, XPS, and sputter depth-profiling 79−43049
Cr_2O_3, grain growth during sintering *(Japanese)* 80−16261
Cr_2O_3, monocrysts. formed on heat treatment of Ni-Cr based alloy in air, struct. obs. 79−52455
Cr_2O_3, reduction by H_2, reaction kinetics 80−11950
Cr_2O_3/Cr solar-absorber surfaces, chemical and struct. anal. 79−95283
Cr_2O_3-Cr black, solar collector coating, microstruct., FIM and SEM obs. 80−26166
Cr_2O_3-Cr film, electrodeposited, optical degradation rel. to surface morphology, SEM and AES obs. 79−79401
$Cr_{1-x}RH_xO_2$, ferromag., new prep. method by high-pressure oxidation, SEM characterisation 79−43164
$Cr_3Si_2(C_2)$, sputtered films, microstruct. and wear props. 78−64733
Cs/W, work function measurement in SEM 80−80918
Cu adhesion to Au, surface treatments and surface impurities 77−15701
Cu alloys, appl. of SEM to brittleness study 78−3214
Cu alloys, cavitation during superplastic flow, affecting factors 78−60728
Cu, appl. of SEM to brittleness study 78−3214
Cu, bright galvanic coatings, crystallite size determ. 79−66221
Cu cathode, oxide-coated, arc erosion rates, SEM expts. 77−55185
Cu, cementation, characterisation of nucleation and growth from aq. soln., TEM and SEM study 79−28972
Cu, cementation, on Fe, deposit struct., reaction rates, SEM 80−104421
Cu, commercial pure, creep-rupture props., vacuum,, SEM and X-ray diffr. meas. *(Japanese)* 78−72843
Cu, contrast of electron channelling patterns, estimation from low index refl. 78−9921
Cu, corrosion protection by benzotriazole pretreatment 80−16555
Cu, crack propag. and fracutre kinetics in creep, optical microscopy and SEM obs. *(Russian)* 79−52342
Cu, cracks in earlier stages of fatigue, fractography *(Japanese)* 77−8924
Cu, deformation band, role in fatigue crack nucleation and propag. 79−24585
Cu, ductile fatigue crack growth mechanism in single crystals, in situ SEM obs. 79−61695
Cu electrodeposits, collagen and chloride additions effects obs., on morphology and crystal orientation 78−51852
Cu, erosive wear mechanisms, combined TEM and SEM obs. 80−108601
Cu, FCC single crystal, crystal rotation accompanying scratch deform. *(Japanese)* 79−15733
Cu, fatigue behaviour effect of Zn, Au diffused coatings 78−72850
Cu, fatigued specimens, 'etch pit slip', SEM obs. 79−100258
Cu film, on W substrate, cementation, vac. deposition, and electroplating, growth characts. 79−95291
Cu, film, sputtering mechanism, SEM 80−29839
Cu, friction and prow form. in scratch process by diamond cone 78−11349
Cu, ion bombarded, cone form. and associated surface features 77−59054
Cu, ion plated, defect growth structs., SEM obs. 80−24768
Cu, irradiated with 20 keV He^+, surface damage and gas trapping profile meas. *(French)* 80−84219
Cu, loosely packed powder, sintering SEM and dilatometry obs. 80−20843
Cu mirror, surface defect layer form. on mech. polishing 80−33122
Cu, oxidation, electron scattering study 79−83377
Cu, oxidation kinetics, influence of intermediate annealing treatment 80−89412
Cu, plastic strain meas. due to sliding wear 78−64731
Cu plastically deformed crystals, SEM exam. of light and dark etch pits, dislocation arrangements 78−87679
Cu, point emitter, surface microrelief under explosive electron emission 78−2973
Cu, polycryst., creep and fracture behaviour, effects of prestrain and O 80−97544
Cu rich dental amalgams, SEM and energy dispersive X-ray analysis 78−24184
Cu single crystal spheres, dissolution, formation of etch pits, surface structure study using SEM 79−23735
Cu, single crystals, effect of stacking fault energy on extrusion and intrusion development 78−72826
Cu spheres, rotation and translation during sintering onto a substrate, grain boundary energy SEM study 79−38759
Cu, thin film, oxidation, RMEED/SEM studies 80−100968
Cu, tough pitch wire, cupping fracture surface, SEM study *(Japanese)* 79−79087
Cu, tribological investigation using two-cylinder tribometer *(German)* 77−25164
Cu whisker, H_2 reduction of CuI, growth mechanism 78−30853
Cu, whiskers, Ar^+ ion implanted, X-ray study on lattice defects *(Japanese)* 79−99230
Cu, with Al_2O_3 inclusions, breakdown and emission props., effect of inclusions 79−87389

scanning electron microscope examination of materials continued
Cu:Au:C, surface, obs. at very low accel. voltage (200 V-1 kV) by SEM 80−10764
Cu/Au planar interface, formation of ordered phases CuAu and Cu_3Au 79−82392
Cu/Sn-Ni/Au tricouples, electrodeposited, interdiffusion obs. 80−84331
Cu-Al (14.3 wt.%), ^{110}Ag diffusion in β/γ_2 interphase boundary 80−79989
Cu-Al thin film multistructure, Xe^+ ion beam cratering 80−66708
Cu-Al-Ni-Fe system, corrosion behaviour in sea water 80−45421
Cu-Al-Sn system, coexistence of different and brass like phases 80−89206
Cu-Au film, aged, strength failure due to Kirkendall porosity 79−77969
Cu-Au thin films after accelerated ageing, failure by Kirkendall porosity, SEM study 80−6675
Cu-based metallisation systems, in 85°C 78% RH SO_2 contaminated environment, performance 79−74304
Cu-Be, dynode surface, SEM and Auger microanalysis 80−100384
Cu-Bi, grain boundary struct. intergranular fracture, segregation role 80−66648
Cu-Bi (0.02 wt.%) alloy, intergranular fracture, Kossel X-ray diffr. in SEM obs. 80−108579
Cu-Ga, binary alloy constituent EDS anal., secondary fluorescence, SEM study *(Chinese)* 80−85231
Cu-Ge, primary coplanar slip, role in deform. of FCC crystals *(Japanese)* 77−52412
Cu-mild steel explosively welded interface, SEM examination *(German, English)* 80−96746
Cu-Nb (7 wt.%), solidification microstruct., SEM 77−12611
Cu-Nb multifilamentary composites, in situ formed, anomalous strength increase 79−43323
Cu-Nb multifilamentary composite, in situ formed, high temp. tensile strength, SEM microstruct. study 79−61602
Cu-Nb_2Sr, multifilamentary supercond. composites, in situ formed, critical currents 79−65625
Cu-Ni alloys 706 and 715, corrosion in flowing sea water, dissolved sulfide effect 80−35379
Cu-Ni crystals, growth, H_2 reduction of CuI-$NiBr_2$ mixture, habit study by X-ray difr., optical and SEM 79−60665
Cu-Ni diffusion couple, diffusion bonding process, fracture surface exam. *(German)* 77−35762
Cu-Ni:polyethylene, surface, obs. at very low accel. voltage (200 V-1 kV) by SEM 80−10764
Cu-Ni-Cr (28, 2.8 wt.%), spinodal alloy, microstruct. and tensile props. 78−39858
Cu-Ni-Zn alloy, surface comp., outdoor exposure influence 80−59770
Cu-Sn alloy, surface comp., outdoor exposure influence 80−59770
Cu-Sn-P (5, 1-5 wt.%), effect of P on friction and wear characts. 80−16494
Cu-W, powder, prod. by controlled reduction in H_2O/H_2 mixture of $CuWO_4$ 79−24458
Cu-water interface, natural boiling site cavities, SEM obs. 77−31763
α-Cu-Zn (5.3 to 21.8 wt.%), single crystals, effect of stacking fault energy on extrusion and intrusion development 78−72826
Cu-Zn alloys, surface comp., outdoor exposure influence 80−59770
α-Cu-Zn-Al (18, 7 at.%), deform. and mech. props. 79−29159
Cu-Zn-Al alloys, dendritic struct. obs. 77−8810
Cu-Zn-Sn-Pb (5, 5, 5 wt.%) alloy, analysis in glow discharge lamp and in ion microprobe, sputtering processes 77−52730
CuCl, photosensitive film formation on Cu 77−9105
CuCoNi ferrite magnetoacoustic oscills. rel. to microstruct. 77−85536
CuO-Ag film solar absorbers, mechanism of high-temp. instability 78−22971
Cu_2O, anodic form. on Cu electrodes immersed in NaOH, chronopotentiometry, SEM and TEM obs. 77−48573
Cu_2S, epitaxial overgrowths on Cu(111), struct. and morphology 79−82494
Cu_2S-CdS thin film solar cells, Cu_2S layer separation, struct. 79−95282
Cu_xS, diffusion length determ., resolution limit of EBIC technique 79−21865
Cu_xS-CdS, SEM meas. of diffusion lengths, recombination vel. and junction collection efficiency 80−16808
Cu_xS-CdS solar cell, minority carrier diffusion length, SEM determ. 77−72911
Cu_xS-CdS solar cell, p-n junction shape and struct. 77−55599
$Cu_{46}Zr_{54}$, devitrification effect on mech. props. 80−30082
Dy, single crystal, plastic and magnetoplastic deform. 77−63713
$ErRh_4B_4$, film, sputter deposition and low temp. props. 80−2948
EuS, defect struct., etch pitting and electron microscopic obs. 79−27989
$Eu_{0.14}Si_{0.31}O_{0.55}$ glass, optical, magnetic, and magneto-optical props., chemical clustering 79−42951
$Eu_{0.14}Si_{0.31}O_{0.55}$, insulating amorphous mag., optical, mag., and magneto-optical props. 79−61344
EuTe, high-temperature evaporation and reactivity 80−103469
α-Fe, 0.14 wt.% P addition effect on creep 77−90420
Fe and alloys, brittle fracture, quantitative determ. of transcryst. and intercryst. portions by opt. and SEM fractography 77−52464
Fe, Armco, borided surface layers, Mossbauer and metallographic anal. 80−50769
Fe, atomically clean, N_2 treatment, corrosion inhibition 78−19954
Fe, cast, abrasive wear rel. to lamellar or spheroidal graphite content *(German)* 78−85000
Fe, cast, fracture mech. and fractography *(Japanese)* 78−7031
Fe, cast, grey, solidified in oscillatory and rotating moulds, metallographic study 80−89213
Fe, cast, heated in CO atm., obs. cracks around graphite flakes *(Japanese)* 78−84974
Fe, cast, nodular graphite, annealed, fracture behaviour at low temps. 78−72875
Fe, cast, nodular graphite form. by Bi and Pb additions *(Japanese)* 77−63693
α-Fe, cold rolled, hydrostatic press. effect on microstructural changes during creep 78−39871
α-Fe, crack initiation study at low-cycle fatigue using slip bands *(Slovak)* 79−38949
α-Fe, creep life, meas. by microstruct. changes 78−35443
Fe, ductile, with different secondary struct., abrasive wear *(German)* 80−25871
Fe, ductile fracture, fractographic characts. SEM exam. of fracture surface necking obs. 78−35506

scanning electron microscope examination of materials continued
Fe, effect of atm. corrosion on fatigue crack nucleation and fracture surface morphology, in air and vacuum *(Japanese)* 79−8387
Fe, free surface and grain boundary O_2 and S chemistry 80−75410
Fe, high purity, boriding with cryst. B powder 80−84951
Fe, microcracks formed by H_2 precipitation, SEM and TEM obs. *(Japanese)* 79−70071
Fe, nitriding by ion beam 80−2095
Fe, oxidation, under low O_2 partial press., wustite whisker form. obs. 79−77972
α-Fe, plastic deform. in neck leading to fracture 78−64655
Fe, polycryst. whisker, microstruct. SEM and TEM 77−39755
Fe, pure, cathodic charging effect on creep and tensile deformation 80−76320
Fe, pure, fatigue crack direct obs. by SEM, propag. mechanism *(Japanese)* 79−20164
Fe, pure, hydrogen-charged, initial cracking obs. 80−108580
Fe, pure, splat-quenched, martensite morphology, SEM study 80−7547
Fe, pure ductile fracture analysis, allowance for discontinuity *(Russian)* 77−25133
α-Fe single crystal whiskers, controlled growth by H reduction of ferrous halides, X-ray and SEM exam. of crystals 78−60554
Fe, sintered, fatigue, metallographic obs. 78−64646
Fe surface, form. and decomp. of nitrides 79−24831
Fe, whisker, H_2 effect on deform. 78−68755
Fe whisker growth, on wustite, Wagner's mechanism 80−10847
Fe whiskers, cryst. morphology and dislocation struct. study using optical and SEM, X-ray diffr. topography 79−23876
α-Fe whiskers, pure, ductile fracture initiation, macroscopic obs. of deform. history and failure 80−85043
Fe/ZrB_2, metal-like cpd. form. in diffusion layer during solid phase saturation 80−19994
Fe-Al-Cr (10, 5 to 10, wt.%), corrosion by coal char, SEM and X-ray diffr. exam. 78−88573
Fe-Al-(Nb), fatigue deform. 77−44350
Fe-C (0.64 wt.%), quasicleavage during fatigue crack propag., pearlitic microstruct. effect 79−11702
Fe-C system, effect of microstruct. on fatigue crack propagation 79−79097
Fe-C-Si, high purity, vacuum melted, nodular graphite form. 80−108452
Fe-Cr, from ore reduction, metallographic investigation, optical miroscopy and SEM *(French)* 78−68648
Fe-Cr (13 wt.%)+polycarbosilane, powder metallurgy, charact. 77−85962
Fe-Cr (20 wt.%), role of rare earths and reactive elements in high-temp. oxidation 79−79178
Fe-Cr (20 wt.%) high temp. oxidation behaviour with small La additions (0 to 1.3 wt.%) *(Japanese)* 78−85039
Fe-Cr-Al, electrical heating material, SEM obs. and surface analysis of oxide films formed at high temps. 77−16738
Fe-Cr-Al, HOS 875, oxidation, cyclic, role of thermal shock 80−97640
Fe-Cr-Al, scales, α-Al_2O_3, early stages development at high temp. 80−89413
Fe-Cr-Al (0.3 wt.%), oxidation behaviour at high temps. *(Japanese)* 80−35404
Fe-Cr-Al (7, 5 wt.%), expt. stainless alloys, phys. and mech. props. 80−97637
Fe-Cr-Al-Ce, Ce effect on high temp. oxidation 79−100301
Fe-Cr-Al-Ce, high temp. oxidation *(Japanese)* 78−11413
Fe-Cr-Al-Y, oxidation resistance, heat treatment and Al^+ ion implantation 80−71785
Fe-Cr-Al-Y, scales, α-Al_2O_3, early stages development at high temp. 80−89413
Fe-Cr-Al(-Y), isothermal oxidation behaviour at 1200°C, SEM 80−50755
Fe-Cr-Al(-Y), thermal cycling influence on oxidation behaviour at 1200°C, SEM 80−50756
Fe-Cr-Ni alloys, oxidation-sulphidation in gas mixture, kinetics, SEM exam. 78−72932
Fe-Cr-Ti (18, 0.1-0.9 wt.%), high temp. oxidation *(Japanese)* 80−71806
Fe-Cr-Y, Y addition effect on high temp. oxidation resistance *(Japanese)* 79−70223
Fe-Mn alloy, splat-quenched, martensite formation obs. 77−44247
Fe-Mn-Ni, fracture toughness, thermomechanical treatment effects 78−60794
Fe-Mn-Ti alloys, austenitic, precipitation strengthened 80−25714
Fe-Ni, oxidation, Mossbauer spectroscopy, metallography, SEM and X-ray diffr. anal. 78−15577
Fe-Ni, secondary recrystn. and mag. props. 80−89247
Fe-Ni alloys, graim growth texture 79−91687
Fe-Ni superstructure in metal particles in chondrites 80−12713
Fe-Ni-Al (10, 0.1 wt.%), clustering of Al_2O_3 inclusions 79−83205
Fe-Ni-Al system, multiphase diffusion at 1000°C, diffusion structs. and props. 80−19995
Fe-Ni-Al(2.5, 7.5 at.%), fracture surface morphology, ageing temp. effects 77−16600
Fe-Ni-C, lenticular martensitic alloy, fractured at liquid N_2 temps., crack propag. mode *(Japanese)* 77−48524
Fe-Ni-C, model alloy, intercrystalline brittleness caused by segregation and precipitation in austenite *(Slovak)* 79−70073
Fe-Ni-C (23, 0.39 wt.%), austenitic or martensitic structs., corrosion faces anal. *(French)* 80−21181
Fe-Ni-C (26.4, 0.24 wt.%) martensite, partially twinned, slip lines obs. 78−84913
Fe-Ni-C (26.4, 0.24 wt.%), austenitic single crysts., effect of prior deformation on martensite burst transformation, SEM obs. 79−38823
Fe-Ni-C alloy, splat-quenched, martensite formation obs. 77−44247
Fe-Ni-C alloys, obs. of banded struct. formed by deformation 79−79050
Fe-Ni-C austenitic single crysts., deform. props., martensitic transformation, SEM study 79−29143
Fe-Ni-C martensite, autoradiographic evidence of C clustering 79−83203
Fe-Ni-Cr, high Ni content, intergranular corrosion, effect of Cr *(French)* 80−7708
Fe-Ni-Cr (30.6, 21.3 wt.%), Alloy 800, high temp. oxidation at low O_2 press., SEM, AES and electron probe microanal. study 80−93688
Fe-Ni-Cr-Al-Y, oxidation mechanism, Y addition effect on kinetics and oxide adherence 80−97623
Fe-Ni-Cr-Mn-Al-Ti Incoloy 800, exam. of scale morphology, alloying element distrib. after oxidation 78−80677

scanning electron microscope examination of materials continued
Fe-Si, grain oriented, fatigue crack direct obs. by SEM, propag. mechanism *(Japanese)* 79−20164
Fe-Si (2.4 wt.%), ductile fatigue crack growth mechanism in single crystals, in situ SEM obs. 79−61695
Fe-Si (3 wt.%), grain-oriented, effect of forsterite coatings in domain struct. 78−23293
Fe-Si (3 wt.%), total losses under tensile stress, rel. to orientation near (110)[001] 78−76272
Fe-Si (3 wt.%) cores with insulative coatings, morphological and struct. SEM characteris. 78−23881
Fe-Si (3 wt.%) sheet, obs. through surface coating of domain struct., SEM 77−85482
Fe-Si (3.22 wt.%), topographic and type-2 magnetic contrast, effect of collector position in SEM 79−12909
Fe-Ti-C, rapidly quenched by splat-cooling 80−84923
Fe-TiB_2, eutectic alloy, high temp. props. 78−84931
$Fe_{80}B_{20}$, metallic glass, ferromag. props. 77−16107
$(Fe_xCr_{1-x})_2O_3$ corundum-type solid solution single crystal growth, chem. vapour transport 80−93465
Fe_4N, hard coating preparation by ion beam methods 80−25579
$Fe_{72}Ni_8P_{13}C_7$ glass, erosion craters produced by spark machining, scanning microscopy obs. 78−44268
$Fe_{0.925}O$, wustite, kinetics of reduction at moderate temps. 79−83154
β-Fe_2O_3 film, CVD and characterisation 77−44172
Fe_2O_3 haematite platelets, growth and cross-connection in consolidation of haematite pellet *(Chinese)* 80−104186
Fe_2O_3 sputtered films, optical transmission and reflection spectra depend. on substrate temp. 79−91517
Fe_3Pt austenites, ordering kinetics 80−104155
FeS_2, pyrite, single cryst. growth by chem. vapour transport, surface struct. and morphology using SEM 79−23550
Fe_2S_3, existence and thermal stability, Mossbauer study 78−83733
$Fe_{2-x}SiO_4$, fayalite, oxidation kinetics and growth of Fe_2O_3 whiskers 78−84113
GE, RF etch sputtering under controlled atmosphere 77−44397
GaAS, binary alloy constituent EDS anal., secondary fluorescence, SEM study *(Chinese)* 80−85231
GaAlAs 79−64964
GaAlAs DH laser, In solder deterioration, Au diffusion in In 80−33019
$GaAs_{1-x}Al_xAs$ visible diode lasers, degradation mechanisms 80−64026
GaAs, adsorpt.-desorpt. of Zn, thermal desorpt., at. beam adsorpt., AES, SEM, RHEED 78−14591
GaAs, alloying with Au and Au alloy ohmic contact metallisations, SEM and optical study 80−70820
GaAs, dislocation loops, rel. to dark defects in LEDs 77−80509
GaAs, electron-beam induced conductivity 80−10922
GaAs, epitaxial, polycryst., monocryst. layers and whiskers growth by CVD, SEM obs. electron diffr. study *(French)* 79−43150
GaAs epitaxial films on strongly doped substrate, basic parameter meas. utilising magnetoresist. and SEM techniques under cathodoluminesc. conditions 80−65728
GaAs epitaxial layers on polycryst. GaAs substrates, LPE growth charact. 80−75471
GaAs, etch pit pattern made by light irradiated electrolytic etching 79−95012
GaAs Gunn domain appearance and movement, SEM obs. 77−80785
GaAs laser diode, SEM electron beam induced current study, contamination effect 79−43773
GaAs, polycrystalline films, meas. of effective diffusion length by SEM 80−80424
GaAs, SEM defect study, transmission cathodoluminescence 79−64964
GaAs, surface recomb. velocity, determ. from SEM expts. on p-n junctions 77−55601
GaAs, VPE, fast growth at low temp. and high partial pressure 79−51446
GaAs, VPE layer growth with abrupt doping profile 80−24746
n-GaAs wafer, defect studies by ASLEEP, SEM and scanning AES 79−19256
GaAs:Au, back surface gettering 80−10758
GaAs:Se cathodoluminescence decay obs. with SEM and streak camera, 90 to 300K 80−97348
GaAs:Se(Zn) polycrystalline film, Hall effect, resistivity meas. 80−96911
GaAs:Si defect density before and after Zn diffusion, SEM and TEM obs. 80−96529
GaAs:Si(Cr), LPE, spiral growth patterns, dopants role 77−72800
GaAs:Te, microcathodoluminesc. of effect of struct. defects on radiative recomb. 79−11475
GaAs:Te, phonon-dislocation interactions, nonstoichiometry effect *(French)* 77−43298
GaAs:Te Schottky barrier solar cells, diffusion length determ. using minority carrier SEM 80−61359
GaAs:Te-implanted by laser-annealing, ohmic contacts 79−19658
GaAs:Zn, implanted, laser annealing, elect., Rutherford backscattering and SEM meas. 80−100273
$GaAs-Al_xGa_{1-x}As$ buried-heterostructure lasers, current injection confinement, MBE/LPE hybrid technique 80−74374
$GaAs-Al_xGa_{1-x}As$ current injection multi-quantum-well heterostructure lasers, MBE grown 80−19042
$GaAs-Ga_{1-x}Al_xAs$ DH lasers, electron beam induced current microscopy 80−95899
$GaAs-Ga_xAl_{1-x}As$ DH laser material crystal cathodoluminescence, SEM analysis 80−97349
GaAs-GaAlAs wafers, defects and degradation, transmission cathodolum. evaluation 80−65395
$GaAs_{1-x}P_x$, mol. beam epitaxial growth, cryst. quality, composition investig. *(Japanese)* 77−55895
$GaAs_xSb_{1-x}$-GaAs epitaxial films and multilayer heterostruct., SEM obs. under cathodolum. conditions 79−11023
GaInAsP-InP DH layers, lattice deform. and misfit dislocations 79−19473
$Ga_xIn_{1-x}P$, real struct. exam. by electron microscopy and channelling 78−2143
GaN, epitaxial layer, charact. from cathodoluminesc. 78−35208
GaN, VPE, on sapphire, crystallographic aspects 78−2387
GaN:Al, VPE grown, luminesc. and elec. props. depend. on doping conc., bound excitons 80−20688
GaP, dislocation obs., SEM EBIC vs SEM CL micrographs 77−80511
GaP, dopant dislocations, scanning electron micrographs, cathodoluminesc. 78−91340

scanning electron microscope examination of materials continued
GaP, electrical recomb. behaviour at dislocations 79−82606
GaP, epitaxial layers, dislocation recomb., SEM cathodoluminescence studies 79−42558
GaP, epitaxial struct., cathodolum. in SEM 78−10991
GaP, green cathodolum. from cryst. defects, SEM, TEM study 80−80870
GaP, LEC growth of dislocation-free crysts., microdefects and striations 78−9974
GaP LED, SEM study of charge collection and cathodoluminesc. 80−65661
GaP, light emitting diode structure, effect of neutron irradiation on cathodoluminesc. 79−28843
GaP, minority carrier lifetimes at dislocations, SEM meas. using photon counting 78−23109
GaP, mol. beam epitaxial growth, cryst. quality composition investig. *(Japanese)* 77−55895
GaP polycrystals, subgrain boundaries, cathodolum. in SEM 79−1440
GaP, SEM, cathodoluminesc., impurity and defect detect. 78−83695
GaP, VPE layer structures for LED's, SEM, and TEM obs. of dislocation density reduction expt. 80−100425
GaP:N LED structures, local dopant conc. determ. using SEM cathodolum. spectra 80−101057
GaSb, CVD using organometallics, epitaxial growth 80−29879
GaSb film, gamma-irradiated, struct., TEM and SEM obs. 79−15033
$\alpha(\beta)$-Ga_2Se_3, cryst. growth, optical, X-ray diffr. and SEM study 80−71587
$Gd_3Ga_5O_{12}$, garnet substrate surfaces, working damage, electron microscope investig. 77−77605
Gd_2O_3-Ga_2O_3 system, phase diagram relationships of garnet-perovskite transform. 80−97460
Ge, electrodeposited, X-ray, electrochem., and electrorefl. characterisation 78−14624
Ge film, evaporated amorphous, angle of deposition effects, electron microscopy 77−43451
Ge, surface electronic props. meas. by SEM, sand-blasting effect 77−62976
Ge, thin crystal, SEM, contrast features, variation of specimen thickness 79−23508
Ge-Au-Ni(Pt)(Pd) trilayered films, annealing, interdiffusion 78−22902
Ge-Si n-n heterojunction, topography study 78−14804
Ge-Te-Se/Si amorphous film-cryst. heterojunction, electron-beam-induced current 79−24060
$GeSe_2$ chalcogenide film, struct. changes due to laser induced transmittance oscill., SEM obs. 78−6240
$GeSe_2$-Te, phase diagram and vitrification region determ. by DTA, SEM, X-ray diffr. *(French)* 77−72565
Ge_xSe_{1-x}, $0<x<0.2$, crystallisation in amorphous bulk and thin films 78−55813
Hf, RF sputter deposition, ion bombardment and ion implanation 80−25564
HfN on stainless steel, activated reactive evaporated coatings, high rate deposition, microhardness 80−25580
HfN, RF sputter deposition, ion bombardment and ion implanation 80−25564
Hg lamps, RF-excited, dark film anal. 80−92789
Hg-Ag-Sn, dental amalgams, corrosion penetration in crevices 80−3238
HgCdTe, cryst. and photodiode, imperfections and surface conditions using electron induced current technique 79−67385
$HgCr_2Se_4$:Cd, precipitations during growth by chem. transport method 80−55409
α-HgS films, sputter-deposited in Hg vapour, growth and props. 80−75467
InAs epitaxial layers, on GaAs substrate, electron diffr. and SEM exam., electronic props. 79−1552
InAs, MBE growth, SEM, RHEED, optical microscopy and elec. meas. 78−18925
InBi single crystal, deform. mode under dynamic indentation 80−88163
InGaAsP, epitaxial layer, defect evaluation by cathodoluminescence 80−2866
p-InP, RF sputtering on CdS and other substrates, and grain size obs. 77−90272
InP substrate, LEC-grown, defect evaluation by cathodoluminescence 80−2866
n-InP wafer, defect studies by ASLEEP, SEM and scanning AES 79−19256
InP:Fe, precipitate mixture 77−77485
InP-Au contacts, conditions of fabrication that control interfacial microstruct. 79−42643
InSb film, gamma-irradiated, struct., TEM and SEM obs. 79−15033
InSb, RF etch sputtering under controlled atmosphere 77−44397
InSb surface, Cu deposition, ohmic contact formation obs. 77−51817
Inconel-718, blistering by 2 MeV He^+ ions, optical microscopy and SEM obs. 79−42119
Ir-W (0.3 wt.%): Al(Fe)(Th)(Ni)(Rh), effect of additions on grain boundary composition 79−83309
K-rich globules in Luna 20 soil, SEM obs. 80−67591
KCl, agglomeration of crystals from aqu. soln. 79−90580
KCl, cryst. laser irrad. effects, electron microscopic obs. 77−73192
KD_2PO_4, domain structure obs. using SEM 77−1647
$K_xWO_{(3+y)}$, direct imaging of ordering 77−11511
LaB_6, high temp. interaction with 0_2, AES and mass desorption expts. 80−7698
LaB_6 single crystal needles, thermal field emitted electron total energy distribution spread 80−45218
$LaCoO_3$, conducting oxide powder prod. by freeze drying 79−95984
$LaNi_{5-x}Fe_x(Cr_x)$, Fe and Cr electron hydride formation, X-ray and SEM obs. *(Japanese)* 79−43202
$La_{0.5}Sr_{0.5}CoO_3$, conducting oxide powder prod. by freeze drying 79−95984
Li electrode, in lithium perchlorate-propylene carbonate solution, surface anal. *(French)* 80−50859
Li electrode, passivation layer, in $LiClO_4$-propylene carbonate solution, composition *(French)* 80−11899
Li particle size distrib. meas. by SEM 80−101775
Li, surface characterization of film growth 80−81240
Li-$SOCl_2$ hermetic D cells, effect of $Li_2B_{10}Cl_{10}$ and $Li_2B_{12}Cl_{12}$ on performance 80−12000
$LiAlO_2$, fuel cell electrolyte matrix, prep. and struct. charact. 78−80488
LiF crystal, contact damage obs. by cathodoluminesc. 80−71728
scanning electron microscope examination of materials continued
LiF, single crystal, neutron and gamma irradiation, SEM and Bragg profile anal. 80−15158
$Li_{0.5}Fe_{2.5}O_4$, spinel ferrite, prep. by thermal treatment of spray-dried formates, scanning electron microscope examination 79−24482
Li_2GeO_3 piezoelectric glass ceramic, recrystallisation, pyroelectric response, permittivity 80−80703
Li_3N, ionic cond., annealing, trans- and intercryst. resist. 78−43176
$LiNbO_3$ pure and Fe doped, IR induced acousto-photorefractive memory effect 80−80746
LiO_2 pellets, sintered, exam. of microstructure 78−72749
Li_2O-Al_2O_3-SiO_2 glass, aq. corrosion 79−61753
Li_2O-SiO_2 glass, bulk crystn., SEM and optical microscope studies 80−44142
Li_2O-SiO_2 glass, crystallisation study 79−90567
Li_2SiO_4, piezoelectric glass ceramic, recrystallisation, pyroelectric response, permittivity 80−80703
Mg film, deposition using low-energy ion beam, Rutherford backscatt. and SEM anal. 77−59700
Mg film, deposition using low-energy ion beam, Rutherford backscatt. and SEM anal. 77−70004
Mg, inclusions, types and size distrib. *(German, English)* 80−97492
Mg-Mn-Ce (1.5%, 0.3%) alloy, dislocation slip during superplastic deform. *(Russian)* 77−21214
Mg-Ni-S, electroforming, mech. props. rel. to heat treatment 80−35133
Mg-Zr alloy, cavitation during diffusion creep 77−44296
$MgCr_2O_4$-TiO_2, porous ceramics, humidity-sensitive electrical conduction 80−107782
MgIn, atmospheric corrosion, SEM, electron diffraction and electron probe obs. 79−24681
MgO (:CaO) powder compacts, sintering studies, SEM obs. 79−78918
MgO, cathodoluminesc. at dislocations 79−47524
MgO crystal, contact damage obs. by cathodoluminesc. 80−71728
MgO crystal cathodoluminescence, SEM analysis 80−97349
MgO, hot pressed, microstruct. influence on microhardness 79−38971
MgO, hot-pressed, elasticity props. of polycrystals and single crystals 80−54301
MgO, lattice misorientation and displaced vol. for microhardness indentation 78−64617
MgO, precipitate morphology, strain energy effects 80−40358
MgO single crystal, grain boundaries, cathodolum. in SEM 79−1440
MgO, single crystals, compressed, SEM exam. of cathodoluminescence 78−56525
MgO, smoke particles, size distrib. 80−104471
MgO, solid solubility of Sc_2O_3, Al_2O_3, Cr_2O_3, SiO_2 and ZrO_2 80−15247
MgO, spherical particle impact damage, effect of crystallographic orientation 79−79135
MgO:Fe, cathodolum. after plastic deform. 79−95849
MgO-Al_2O_3-SiO_2, exam. of microstructure and crystallisation kinetics 78−80501
Mn micronodules from NW Atlantic, morphology and chemistry 80−81869
Mn nodules, deep-sea, diagenetic features, X-ray spectral and SEM anal. 79−16099
Mn-Zn ferrite, single crystal, surface damaged layer study *(Japanese)* 77−86260
MnAs, single cryst. whiskers, morphology and cryst. orientation, SEM and X-ray diffr. study 79−60664
MnBi, thin film, fine mag. domains, SEM obs. 79−24202
$MnCO_3$ crystals, gel. grown, Ca^{2+}, Ni^{2+} impurity influence, SEM study 80−20778
$Mn_{46}Co_{54}$, amorphous alloy prep. by high-rate sputtering, struct. and prop. characteris. 79−24462
$MnCo_2O_4$ DC sputtered films, struct. and elec. props. 80−54812
MnZn ferrite, spray dried agglomerates, compaction response, fracture, deform. 79−43172
MnZn ferrite, surface damaged layer, mag. domain obs. by taper section SEM 77−59423
Mo alloys, fractography of deformed samples *(Russian)* 78−19889
Mo, blister erosion reduction by multi-groove surface microstruct. 78−95211
Mo, C doped sheet, electron beam welded, low temp. ductility 79−87685
Mo cast alloy, shape, size, distrib. of carbides and oxides 79−24528
Mo, D^+ impact, surface blistering, SEM study 78−71774
Mo fibre reinforced Al and Al alloys, SEM study *(Slovenian)* 78−84923
Mo film, evaporated, annealing behaviour, SEM obs. 80−65397
Mo film, on SiO_2/Si substrate, effect of heat treatment after deposition on internal stress 78−22973
Mo flame sprayed coatings, comp., microstruct. and mech. props. 80−16598
Mo, fracture and crack propag. tested in tension along [001] axis *(Russian)* 80−50697
Mo, gas driven blister growth on He ion bombardment, SEM obs. 77−76473
Mo, H, H^+(H_2^+) energy refl. coeffs., surface damage obs. 78−54969
Mo, irradiated by H^+ and H_2^+ ion beams, grain ejection from surface 78−6819
Mo laser mirror, optical and metallurgical characterisation 80−33129
Mo, mech. props., influence of temp. on singularities of deform. *(Russian)* 78−6970
Mo, point emitter, surface microrelief under explosive electron emission 78−2973
Mo powder, cold sintering under high pressures, correlation to plastic props. and diffusion 79−38757
Mo, recrystallised sintered sheet, C addition effect on ductility 79−8319
Mo sheet, shock-induced intergranular cracks 79−57087
Mo, surface blistering by 75 to 350 keV He ions, SEM study 78−72657
Mo whisker cryst., growth incorporated with field electron emission 80−44458
Mo-B-Al-C system, fractography of static and fatigue fracture 79−87729
Mo-base alloy, TZM, blistering under He ion bombard. 80−92567
Mo-Mn alloy, plasticity, fracture, strength depend. on C content *(Russian)* 80−35257
Mo-Nb-TiN, dispersion hardened with strong interface, fracture mechanism 79−5058
Mo-Re alloy, type MR47VP, fractographic of static and fatigue fracture 79−87729
Mo-Ti(B)-Zr(Al)-C, stress cycling at room temp. *(Russian)* 77−25148
Mo-W (30 wt.%), wrought, fracture, characteristic features 80−104278

scanning electron microscope examination of materials continued
Mo-Zr (0.15 wt.%), wrought, fracture, characteristic features 80−104278
MoO_3 topotactic transform into MoO_2, electron microscopy, X-ray anal. 80−107417
MoS_2 film, sputtered, solid lubricant, morphological growth 77−35825
MoS_2 hydrotreating catalysts, Co, Fe and Ni effects on microstruct., TEM, SEM and EPMA obs. 79−52762
MoS_2, RF sputtered, solid lubricant on mild steel, morphology 78−6239
$MoSi_2$, sputtered films, microstruct. and wear props. 78−64733
$NH_4Fe_3(SO_4)(OH)_5$, jarosite, decomposition 80−11624
$5(NH_4)_2O.12\ WO_3$, thermal decomp., 100-500°C, thermogravimetric, evolved gas, X-ray and SEM expts. 77−56223
NaCl, {100} face, subject to elastic/plastic indentation, crack initiation threshold 79−70157
NaCl cleavage step decoration, nucleation and growth of metallic thin films 77−69200
NaCl, damage process preceding semibrittle fracture, plastic strain depend. 77−32692
NaCl, dislocation density, laser beam effect, electron microscopy of etch pits 77−11553
NaCl, single cryst., crack healing at low temp. 77−36622
$NaO-CaO-SiO_2$ glasses, fluorinating agents effect on comp. and surface struct. 80−35364
$Na_2O-Al_2O_3-SiO_2$ glass, formation from alkoxides, phys. and chem. evolution 78−80503
Na_2O-CaO glass, shear deform. under pyramidal indentations 80−84989
$Na_2O-CaO-Si_2O$ glass, mixed mode fracture 79−79083
$Na_2O-CaO-SiO_2$, plates, exam. of Hertz crack branching 78−72887
$Na_2O-CaO-SiO_2$ glass, fractographic anal. of delayed failure 80−45387
$Na_2O.Al_2O_3.10TiO_2$, crystallized bronze, chem. comp., morphology, optical and thermal props. *(Japanese)* 80−16172
Nb, 14 MeV neutron sputtering, ion microprobe, SEM, He^+ backscatt. anal. 77−36317
Nb, Ar ion surface erosion 77−36342
Nb, blister diameter and blister skin thickness correl. under He ion irrad. SEM obs. 79−82266
Nb, blister form. on single crystal under Ne^+ ion bombardment 78−71772
Nb, CVD, kinetics and microstruct., pressure and temp. depend. 80−11569
Nb CVD coatings on graphite, grain struct. depend. on temp. 80−25574
Nb fibre glass composites, new technique for producing fine metal fibres 80−108384
Nb film, sputter-deposited on stainless steel, electron microscopy and ESCA 77−52554
Nb film sputtered onto Cu substrate, microstruct. and supercond. props. 77−85370
Nb, flaking and blistering due to He and Ne ion bombardment 80−29092
Nb, H_2 embrittlement, microscopic obs. at low temps. 77−32666
Nb, local heating during abrupt strain, catastrophic slip band formation 80−7652
Nb, single crysts., plastic relaxation of internal stresses during mech. twinning at 4.2K, optical and SEM study *(Russian)* 79−66108
Nb, sputtering yield, SEM and scanning Auger microprobe obs. 79−87545
Nb, superconducting bridges by electron beam lithography and ion implantation Josephson effect 80−20355
Nb/Cu-Sn-Mg, superconductor, effect of Mg addition to Cu-Sn matrix 80−25028
Nb-Ge-Si film, CVD, struct., comp., stability and homogeneity 80−15421
Nb-NbO system, single- and two-phase, sputtering yield, SEM and scanning Auger microprobe obs. 79−87545
Nb-Si compounds, CVD, struct. and supercond. props. 79−24447
Nb-Zr (1%), He bubbles and voids with ringed images SEM and TEM exam. 78−51529
Nb-Zr sputtered films on Ta, struct. and supercond. props. *(Japanese)* 78−52138
$Nb_{40}Fe_{40}P_{14}B_6$, metallic glass, explosive compaction, mech. props. 80−89176
Nb_3Ge films, magnetron sputtered preps. and microstruct. 79−38276
Nb_3Ge sputtered film, struct. and superconducting props. 77−28337
Nb_3Ge tape, prepared continuously by CVD, props. 78−60257
NbN, Nb_4N_3-NbN, Nb_2N-Nb_4N_3, Nb_2N, cryst. growth parameters and morphology of chem. vapour deposition, X-ray diffr. and SEM study 79−23861
NbO, cryst. growth and microstructure 79−95913
NbO_2, cryst. growth and microstructure 79−95913
NbO_2 hollow needles, and continuous coatings of crystallite NbO, electrodeposition from molten fluorides, SEM study 79−24423
$Nb_{12}O_{29}$, cryst. growth and microstructure 79−95913
Nb_2O_5, cryst. growth and microstructure 79−95913
α-Nb_2O_5, reduction in H_2 discharge, AES and SEM anal. 77−59708
Nb_2O_5, single cryst. growth by chem. transport reactions involving $TeCl_4$ 77−36382
Nb_3Sn composite wires, supercond., degradation mech. under tensile strain at 4.2K 79−38284
Nb_3Sn film, electron beam codeposited, growth morphology and tensile props. 78−10301
Nb_3Sn, flux density gradient determ. by Faraday effect 80−107969
Nb_3Sn, vap. deposited supercond. film, effect of N_2 and tape heating 78−34939
Nb_3Sn-Cu multifilamentary composite wire, Nb_3Sn filament morphology and grain size 80−100855
Nd:YAG, solid-state formation 80−35121
Ni alloy 718, intermetallic second phase obs. using electrolytic extraction and SEM 79−34074
Ni base alloys, hot corrosion in coal conversion system atmos. 79−96200
Ni base alloys, IN-702, IN-601, TD-Ni-Cr-Al, B-1900+Hf, oxidation, cyclic, role of thermal shock 80−97640
Ni, blistering by $^4He^+$ bombardment, temp. depend. 78−43967
Ni, corrosion, high temp., SO_4 induced, studied at 900°C in O_2+4.2% SO_2 80−97639
Ni, corrosion in SO_2, high temp. 79−20281
Ni, erosive wear mechanisms, combined TEM and SEM obs. 80−108601
Ni, fatigue cracks, use of SEM in quantitative stereofractographic anal. 78−80645
Ni, grain boundary cavities growth under applied stress and internal pressure 80−29032

scanning electron microscope examination of materials continued
Ni, low-temp. fracture, electron fractography obs. *(Russian)* 77−90437
Ni, Medicus matrix cathode, surface charact. 80−66378
Ni monocrystals, struct., effect of stress applied during electrodeposition 78−26777
Ni, neutron irrad., slip bands, TEM and SEM obs. 78−51596
Ni, oxidation, high temp., effect of C on cavity form., SEM study 80−97638
Ni, oxidation kinetics, influence of intermediate annealing treatment 80−89412
Ni, plasma-sprayed, effect of Si substrate surface conditions and impact velocity of sprayed particles 80−21145
Ni, powder, correlation between specific surface area and technological props. 78−64503
Ni, preoxidised, reaction with SO_2 at high temp. 79−39047
Ni, single crysts., H and liq.-Hg embrittlement 80−25862
Ni, sintering kinetics, metallographic study 80−93519
Ni solar collector coating, microstruct., FIM and SEM obs. 80−26166
Ni, solar selective black coatings, electrochem. deposition on Zn surfaces 80−29885
Ni tensile-deformed single crystal glide step heights, latex sphere and SEM obs. *(German)* 77−59018
Ni-Al, (2 and 6 wt.%), oxidation, α-Al_2O_3 growth, microstruct., precip. 80−108626
Ni-Al film, co-evaporated, comp.-depend. struct. and morphological changes 79−87020
Ni-Al-Cr_3C_2, eutectic alloy, directionally solidified resistance, influence of Y 80−89409
Ni-Au, dil., orientation depend. of surface segregation, AES and SEM obs. 78−71908
Ni-Co-Al alloys, continuous precip., SEM, TEM, X-ray diffr. study 80−89220
Ni-Co-W, electrodeposition, surface morphology and cryst. struct. 80−71602
Ni-Cr, degradation after exposure to 1% H_2S/H_2 gas mixture at 1000°C 80−89408
Ni-Cr (2 wt.%), role of hydrostatic pressure on sintering of creep cavities 79−28980
Ni-Cr-Ce, Ce effect on oxidation 79−43484
Ni-Cr-Fe-Mo-Co (21.41, 19.28, 8.64, 2.16 wt.%), Hastelloy alloy X, exam. of thermal stability 78−84865
Ni-Cr-NbC eutectic composite, unidirectional solidification, thermal cycling, temp. range effect on microstructural degradation 80−89272
Ni-Cr-TaC eutectic-like composite, obs. of interfacial diffusion by high resolution TEM 79−4432
Ni-Cr-W, oxidation behaviour in air at 1000-1250°C 80−89407
Ni-Cr-Zr, degradation after exposure to 1% H_2S/H_2 gas mixture at 1000°C 80−89408
Ni-Fe-Ce superalloy, vacuum melted, Ce effects on microstruct. 77−36552
Ni-Fe-W alloy, electrodeposition, SEM and optical obs. 79−66018
Ni-ferrite powders, form. in presence of Li_2SO_4-Na_2SO_4 molten salts, prep. and charact. 80−84869
Ni-Nb (5, 10 at.%), oxidized specimen study using SEM, HEED X-ray diffr. and ion backscattering anal. *(Japanese)* 79−24651
Ni-P, electroless deposition on Al 79−90907
Ni-Pd surfaces, electrochem. passive film form. and comp. determ. by SEM, SIMS, XPS 80−39401
Ni-pigmented anodic Al_2O_3, for selective absorpt. of solar energy, optical and struct. props. 80−55892
Ni-S incongruently subliming system, SEM and TEM obs. of high temp. transitions, temp.-comp. diagrams 80−104136
Ni-Si-B powder, oxidation at 850°C, SEM, ESCA, and elec. cond. meas. 80−7717
Ni-ThO_2, oxidation, cyclic, role of thermal shock 80−97640
Ni-Ti (1.6, 7.64 wt.%), monophase high temp. scaling, metallography study 80−21159
Ni-V, dil., oxidation behaviour at 1200°C 77−77636
Ni-W surfaces in contact, deform. and adhesion at very low loads 80−39457
β-NiAl, oxidation, α-Al_2O_3 growth and microstruct. 80−108627
Ni_3(Al.Ti), single crysts., flow and fracture behaviour tested in tension 79−79075
$Ni(CO)_4$, form. on single Ni cryst., reaction kinetics and induced surface facetting 80−71948
NiF_2 film preparation and characterisation 80−59815
$Ni_{2/3}Fe_{7/3}O_4$, precipitation of α-Fe_2O_3, optical microscopy, SEM and TEM studies *(French)* 80−11650
Ni_3Ge single crystal, cleavage fracture 79−61694
NiO, stress relief and plastic flow in temp. range 1323-1473K 80−89302
NiO_2 single crystals, welding, optical and SEM study 79−65097
PLZT, ferroelectric domain struct. obs. by SEM and optical microscopy *(Japanese)* 78−15136
PLZT, thin film epitaxial growth and characteris. 79−28918
(PLZT)(PLZN) system, ferroelec. transparent, prep. and study 79−42911
Pb, electrode, potential effect on surface struct. in H_2SO_4 in anodic region 80−16592
Pb, filament production, ejection of molten metal through nozzle, jet stability *(Japanese)* 78−52719
Pb, film, hillock formation by grain boundary sliding 80−107673
Pb, film, sputtering mechanism, SEM 80−29839
Pb film, thermal strain, strain relax. mech. 79−42427
Pb films, hillock growth upon cycling to cryogenic temps. 80−88448
Pb superconducting microbridges, two-dimens. imaging of resist. voltage changes caused by electron irrad. 80−15659
Pb thin films, thermal strain, multiple cycling to 4.2K effects 79−90918
Pb:O, thin film, microstruct. and thermal stress, doping effects 80−88458
Pb-In (40 wt.%), solid soln., single phase, superplastic behaviour 80−21048
Pb-Sn (62 wt.%), intercrystalline and interface boundary sliding, tensile tests, SEM obs. 79−38886
Pb-Sn eutectic, cavitation during superplastic flow, affecting factors 78−60728
$Pb_{1-x}Cd_xS$ metastable epitaxial films, growth and physical props. 78−27417
PbO, polycrystalline layers, influence of prep. conditions on phase comp., texture and struct. 79−4495
PbO, reactively evaporated photoconductive film, phase transform. induced by water vapour 79−78233

scanning electron microscope examination of materials continued
PbO-SiO_2, glass on Si, emission mode of SEM 79−28226
PbO-SiO_2 glass, modifier release in acid soln. 79−43450
PbS, chem. deposited thin film, effect of morphological struct. on photosensitivity 80−70760
PbS, chemically deposited film, photosensitivity, effect of morphological struct. 79−82647
PbS film, soln. grown on Si, struct. and comp. of heterojunction 80−54530
PbS-$(PbSO_4)_x(PbO.PbSO_4)_y$ heterosystem, cathodoluminescence spectra 79−24370
PbS-Si heterojunction, PbS film growth and struct. 80−96762
$Pb_{1-x}Sn_xTe$ (x=0.15 to 0.20), SEM study, dislocation density, and carrier density and mobility 79−69107
PbTe, effect of pressing and sintering, study of induced defects by SEM 80−59983
PbTe thermoelectric materials, microstructure anal. using SEM X-ray microanalysis 80−107211
Pb(Zr, Ti)O_3 cast tape, densification by pressing for piezoelec. devices 79−87595
$PbZr_xTi_{1-x}O_3$ ceramics, morphotropic phase boundary 80−81035
Pd coated Si wafers, interference effects on irrad. with laser beam 80−66333
Pd, film form. on Si surface by ion beam plating 77−90284
Pd on UHV-cleaved mica substrate, obs. using scanning Auger microscopy 80−80149
Pd sponge powder, sintering shrinkage kinetics 80−29900
Pd-Ag(Au)(Cu) film on $BaTiO_3$ dielectric ceramic substrate, interaction between film and substrate during sintering 79−33958
Pd-Cu-Si glass, cold drawn, serrated plastic flow, optical and SEM study 79−79052
Pd-Si layers, form. by laser irrad. of Pd film on Si substrate 79−99438
$Pd_{781}Cu_{55}Si_{164}$ glass, erosion craters produced by spark machining, scanning microscopy obs. 78−44268
Pt catalyst surface morphology, faceting induced by NH_3 and propane oxidation 77−52669
Pt-Si layers, form. by laser irrad. of Pt film on Si substrate 79−99438
PtRh5 alloy, phosphate glass addition effect on high temp. strength *(German)* 80−25807
PtSi surface, and interface with Si, impurity effects 80−80037
Pu, $\beta \rightarrow \alpha$ and $\gamma \rightarrow \alpha$ transforms., microstructures and kinetics 77−25048
Re, activated sintering 77−52262
Re, He ion irrad., blistering, SEM obs. 78−87722
Ru layer, 2-3 μm thick, ion plating and characterisation 78−11131
RuO_2 anodic coating on Ti, struct., electrochem. props. *(French)* 79−83385
S^- ion-selective electrode, sensitivity, surface heterogeneity effects 78−92526
Sb_2S_3:Ag, sensitised photolysis and structure of latent photographic image 78−89574
Se amorphous film, threshold and memory switching 79−82651
Se film, epitaxially grown on Te substrates, crystallinity, RHEED and SEM meas. 77−40373
Se film, trigonal, sputtered and evaporated nucleation and growth processes 77−31920
Se, red amorphous film, textural change, thermal and photo effects 78−63951
Se-As film, evaporated, thickness, substrate temp. effects 79−15610
Si, amorphous, hydrogenated film, struct. determ. using electron microscopy 80−10806
Si, Ar bombarded, blistering effects, SEM obs. 78−67745
Si, CVD on SiO_2 and Si_3N_4, SEM study *(Dutch)* 80−2960
Si, contrast of electron channelling patterns, estimation from low index refl. 78−9921
Si, crucible grown, virgin and implanted, laser irradiation effects on surface structure 80−92768
Si crystal, obtained by local epitaxial accretion, facing and shape meas. 77−4270
Si, crystal defects and impurities interaction obs. by electron microscopic methods 80−65003
Si, Czochralski grown, dislocation free, swirl defect form., doping effect 80−92519
p-Si, Czochralski grown, microdistrib. of O, SEM and spreading resist. obs. 80−79830
Si, damage in electron bombardment, threshold voltage 77−27910
Si, diffusion of Ga in closed capsule, surface damage elimination 78−87691
Si, dislocation images, comparison of SEM and scanning optical obs. 79−51112
Si, dislocation study by high voltage electron microscopy and SEM 79−82217
Si, dopant striae, SEM obs. by Schottky barrier charge collection 77−31684
n-Si, edge dislocation and stacking fault defect electrical recombination efficiency 80−15106
Si, electrical recomb. behaviour at dislocations 79−82606
Si, electron channelling patterns, contrast mechanisms, lattice-defect images 79−27884
Si, electron-channelling imaging, defect obs. 80−10471
Si, energy losses on C contaminated surfaces, secondary electron spectra, AES, and SEM 79−99997
Si, epitaxial, elec. activity of stacking faults, determ. using SEM in EBIC mode 77−43445
Si, epitaxial regrowth and grain struct. of Al metallisation on ⟨100⟩Si 78−79901
Si, etching in He-F_2 plasma, etch rates, mass spectra, direct ion sampling study 80−79510
Si, fibre, growth and struct. 79−69970
Si, filamentary crystals, branching and bending obs. 77−7954
Si film, CVD or evaporated, covered with Al layer, solid-phase crystn. obs. 77−85100
Si film, electron beam evaporation, for solar cell appl., heat exchanges and columnar growth 79−15609
n-Si film, epitaxial, electrical activity of stacking faults 77−39744
Si film, MBE, cryst. defect props., substrate treatment effects 80−70551
Si films, electron-beam-deposited on W substrates, growth and struct., AES and SEM obs. 79−46972
Si films, polycryst., glow discharge deposited below 250°C, struct. and morphology 80−49535
Si, fluorocarbon ion beam etching characts. 80−35363
Si, four-point probe meas. error factors, SEM obs. 79−71484
scanning electron microscope examination of materials continued
Si, heat-treated dislocation-free, elec. props. of stacking faults and precipitates 77−39796
Si, high fluence deuteron bombard. and implantation 77−59033
Si, implanted annealed layers, amorphised structure formation mechanism and crystallographic nature 80−29091
Si, ion implantation radiation damage, electron beam absorpt. meas. 78−75696
Si, ion implanted, electron beam annealing, surface struct. study using SEM 80−70235
Si, ion implanted, laser annealed, elec. characterization 79−69137
Si, ion implanted, scanning electron beam annealing 80−6420
Si, ion-implanted, defect struct., SEM, TEM and X-ray topography expts. 77−51399
Si, ion-implanted layers, epitaxial regrowth by laser beam and flash annealing 80−100420
Si, measurements of electron channelling pattern linewidths 80−62805
Si, minority-carrier diffusion length and drift mobility determ. using a modulated SEM beam 79−19607
Si multilayer structure dopant distrib. and minority carrier diffusion length, SEM obs. *(Russian)* 78−10543
Si n^+-p junction, microplasma sites, SEM and TEM characterisation 77−43702
Si, near (111), fracture by painted indenter, SEM study 80−71734
Si on sapphire, deposition kinetics and interface characteris. 79−28234
Si oxides, grown in Cl-containing ambients, correl. between elec. and material props. 80−39479
Si p-n junction, charge carrier recomb. at dislocations, combined SEM and TEM study 80−15105
Si, p-n junction, dopant conc. diffusion length and lifetime variations, SEM obs. 79−82604
Si phototransistors, slow contamination and fast surface state effects, SEM study 80−107896
Si polycrystalline solar cells, recombination, electron-beam-induced current characterisation 80−81470
Si porous layer, struct. and heat-treatment effect 79−1557
Si, pseudo-Kikuchi patterns in refl. expts. during scanning of single cryst. by intermediate energy electrons 78−1964
Si ribbon grown by capillary action shaping technique, electron channelling analysis 77−76418
Si, single cryst., heterogeneities meas. *(Japanese)* 77−35549
Si solar cells, SEM electron beam induced current study, contamination effect 79−43773
Si, strip-type crystals, growth mechanism, morphology 79−7559
Si substrate for PMMA electron sensitive layer, 400 Å linewidth electron beam lithography 80−65392
Si surface, planar and O_2 etched, CO adsorption, SEM, AES, and desorption meas. 78−63934
Si, V-grooves formed by etching, phosphosilicate glass bridge struct. 80−104312
Si wafer, defect studies by ASLEEP, SEM and scanning AES 79−19256
Si:As(B), ion implanted, pulsed laser annealing appl. to device fabrication 79−73180
Si:B, diffusion length, SEM-EBIC/Schottky diode 79−82605
Si:B, implanted, oxidation-induced stacking faults, EBIC and TEM expts. 78−39923
Si:B, SEM obs. of dislocations using Schottky barrier EBIC technique 78−79614
Si:B film, sputter-deposited, elec. props., struct., SEM and TEM obs. 79−95298
Si:B radiation damage and minority carrier lifetime, SEM-EBIC obs. 80−96573
Si:B^+, ion implanted, lateral spread of B^+ ions through SiO_2 mask 79−51130
Si:B(BF_2), p^+-n junction form., ion implantation damage, leakage current 77−24334
p-Si:Cu, Cn precipitation effects, for solar cells appl. 79−69249
Si:H, amorphous films, plasma-deposited, defect states, IR, ESR, and refractive index meas. 79−65944
Si:H plasma deposited film, amorphous, microstruct., TEM and SEM obs. 80−10801
Si:N wafers, Si_3N_4 layer growth by high dose implantation and annealing, elec. props. 80−70227
p-Si:P p-n junctions, dislocations investig. rel. to P diffusion, SEM, X-ray topography techniques 77−76433
Si:P^+, ions implanted through SiO_2 mask window, lateral spread 79−77627
Si:Sb, in solar cell struct., heavily doped, dopant striation, SEM 79−39312
p-Si-Al, ohmic contacts, Si dissoln. and recrystn. effects, computer calc. 80−103749
Si-Al interface in semiconductors, electronic parts, electromigration aspects 80−39355
Si-Al-Al_2O_3 system, solid phase Si regrowth on sapphire 80−100413
Si-Al-O-N, high-temp. fracture and diffusional deform. mechanisms 80−40509
Si-Al-O-N, oxidation mechanisms 80−40570
Si-Al-O-N ceramics, grain boundary segregation determ. by X-ray microanal. and lattice fringe imaging 79−15681
Si-$CoSi_2$Si, double heteroepitaxy, solid phase and MBE 80−104063
Si-Pd-Ti, silicide form. in evaporated films 80−80006
Si-Pt(Ni)(Pd), laser-induced reactions of metal films with Si, surface struct. obs. by SEM 79−19471
SiAlON, prepared from siliceous sand and Al powder, hot pressing, steatite contamination effects *(Japanese)* 80−93528
SiC, abrasive, wear in simulated hot grinding 78−56784
SiC, appl. of replica electron fractography 79−60237
SiC, blistering and flaking due to light ion bombardment *(Japanese)* 80−70264
SiC coating on Mo, CVD and stability under thermal cycle conditions 80−7500
SiC, film, synthesized by RF reactive ion plating, struct. 77−40391
β-SiC, fluidised bed deposited coatings for nucl. fuel granules, microstructural obs. by SEM 77−14233
SiC, H^+, D^+, He^+ ion bombardment, Raman scatt. and SEM anal. 77−35609
SiC, hot pressed, bending strength *(German)* 79−24571
SiC, identation plasticity and microfracture 79−70158
SiC, impurity redistrib. and anomalous grain growth effects during polytypic transform. 80−15033

scanning electron microscope examination of materials continued
β-SiC, oxidation in CO-CO_2 mixture *(German)* 78−23844
SiC particles in EFG ribbon solar cells, EBIC and ion microprobe anal. 80−93838
SiC, pyrolytic particles for high temp. reactor fuel, X-ray and SEM study *(French)* 78−22734
SiC, reaction bonded, microstruct. characterisation 78−48353
SiC, reaction-bonded, impact erosion by ang. Al_2O_3 particles 80−89362
SiC, single cryst., friction and wear behaviour in sliding contact with various metals 80−21112
SiC single cryst., reaction-bonded and hot pressed, hardness and wear behaviour 79−38970
α-SiC, sintered, influence of B, C additives on microstructure, SEM exam. 79−8262
SiC, spray dried agglomerates, compaction response, fracture, deform. 79−43172
β- SiC, undoped compact, microstruct. development during heating 80−25746
α-SiC, uniaxial compressive damage at low homologous temps., AE and SEM obs. 79−91736
SiC-Ni based superalloy reaction, at elevated temps., interface obs. 80−3287
$SiCl_4$-$GeCl_4$-BCl_4 particulate layers consolidation, in fabrication of optical fibre preforms 80−60787
$Si_{12}Ge_{10}As_{30}Te_{48}$ glass surface, heat treatment and electron bombard. effects obs., rel. to switching filament form. 77−47700
SiN_x film, d.c. reactive sputtering, and characterisation 78−3047
Si_3N_4, α/β phase transform. 78−56632
Si_3N_4, bending strength, deformability, elastic moduli and brittleness 80−81191
Si_3N_4, dielectric film, on Si. crysts. from amorphous state 79−28225
Si_3N_4, evidence for cavitation crack growth, SEM study 79−79086
Si_3N_4, hard coating preparation by ion beam methods 80−25579
Si_3N_4, hot pressed, high temp. compressive cracking, optical and electron microscopy exam. 78−76733
Si_3N_4, hot-pressed, fracture mech. parameters, indentation-precracking and double-torsion methods 80−104364
Si_3N_4, hot-pressed, strength anisotropy origins 80−89330
Si_3N_4, pyrolytic, amorphous and crystalline, chemical vapour deposited fracture surfaces rel. to struct. features 79−5038
Si_3N_4, reaction bonded, effect of Si powder grain size on microstructure, and mech. props. *(German)* 79−4998
Si_3N_4, reaction bonded, pore size and distrib. effect on strength 79−29165
Si_3N_4, reaction-bonded, microstructural analyses 77−8782
Si_3N_4, reaction-bonded and hot pressed, hardness and wear behaviour 79−38970
Si_3N_4, reaction-sintered, SEM fractographs 79−86933
Si_3N_4-CeO_2, surface stress development during oxidation 80−50736
Si_3N_4-CeO_2 additive, hot-pressing and oxidation behaviour 80−71618
Si_3N_4-MgO, (5 wt.%), hot pressed, fracture toughness as function of initial α-phase content, SEM 80−3174
Si_3N_4-Y_2O_3, hot-pressed, oxidation kinetics 80−16520
SiO_2, dielectric film, on Si. crysts. from amorphous state 79−28225
SiO_2, etching in He-F_2 plasma, etch rates, mass spectra, direct ion sampling study 80−79510
SiO_2 fibres, freeze formed from polysilicic acid aq. soln. 80−71609
SiO_2 films, RF-diode-sputtered, step coverage 80−80117
SiO_2, fluorocarbon ion beam etching characts. 80−35363
SiO_2 grown on polycryst. Si, surface asperity mechanism of cond., SEM obs. 78−19153
SiO_2, reduction by Mg vapour, reaction mechanism, SEM obs. 77−1944
SiO_2 relief, plasma etching, tapered wall prod. 80−97606
SiO_2:Al_2O_3, ultrafine and ultrapure powder prep., SEM study 79−70025
SiO_2-C mixture, nitridation to form. Si_3N_4 additives effects, exam. 78−44068
SiO_2-Na_2O glass, fracture initiating flaws, depth meas., crack propag., SEM exam. 78−48494
SiO_x layers, grown in HCl/O_2 ambients, struct. and comp. 79−42404
SiO_x thin films, deposition and characterisation study 80−80133
$Si_xO_yN_z$, dielectric film, on Si. crysts. from amorphous state 79−28225
Si⟨111⟩Al/Si, growth kinetics of ⟨111⟩Si through Al layer, SEM and electron probe anal. 79−28236
$SmCo_5$, improvement of mag. domain contrast in SE-mode of SEM *(German)* 77−51920
$SmCo_5$, polished, domain wall grooving, optical microscopy and SEM obs. 77−8334
Sm_2O_3-Ga_2O_3 system, garnet-perovskite transform., phase diagram relationships 80−97460
Sn droplets, on Bi, Zn and Al, heterogeneous nucleation 80−44294
Sn film epitaxially grown on KCl substrate 79−99441
Sn-Ni electrodeposit, metastable, transform. kinetics, X-ray and SEM meas. 78−38979
Sn-Pb surfaces, contaminant growth on ageing, SEM 80−108625
SnO_2 CVD coating on glass, elec. resist. rel. to cryst. microstruct. 80−84520
SnO_2, film, effects of Sb and In additions on struct. and resist. 77−20469
$SrAl_2SiO_8$, micro-crystal, appl. of method for indexing *(German)* 78−22608
$SrTiO_3$, surface microrelief revealed by ion irradiation 80−54485
TZM, D^+ impact, surface blistering, SEM study 78−71774
$(Ta,Ti)B_2$ on graphite, CVD coating, hardness meas., SEM study 80−24760
Ta, CVD, kinetics and microstruct., pressure and temp. depend. 80−11569
Ta, evidence for slow strain-rate embrittlement due to O_2, SEM study 79−79109
Ta, film, CVD on silica, struct. and mech. props. 77−24965
Ta film sputtered onto Cu substrate, microstruct. and supercond. props. 77−85370
Ta foil, crack growth resistance, straining stage in SEM 77−25124
Ta powder, cold sintering under high pressures, correlation to plastic props. and diffusion 79−38757
Ta single crystal, H_2 embrittlement *(Japanese)* 80−66636
Ta_2O_5, anodic oxide film, adhesion, ductility and fracture, spectrophotometric thickness meas. and SEM obs. 79−99460
Ta_2O_5, e-modification, cryst. struct. and microstruct. 79−51083
Te, evaporated deposition, absorptivity and emissivity 80−25473
Te film, surface morphology depend. on vacuum deposition angle 80−103553
scanning electron microscope examination of materials continued
Te film, vacuum deposited, growth and morphology of crysts. 80−96766
Te, vacuum deposited on NaCl, crystallite growth and morphology, electron microscopy 80−65401
^{122}Te-Au interface, target fabrication for cyclotron isotope prod. 77−83406
$(Ti,Zr)B_2$ on graphite, CVD coatings, hardness meas., SEM study 80−24760
Ti, 300 keV He^+ irrad., exfoliation, flaking, blistering, in-situ SEM obs. 77−35598
Ti alloy, fracture surface and metallographic features exam. by precision sectioning 77−36638
α-βTi alloys, high strength, heat-treated weldments, intergranular fracture 80−21097
Ti anodic film, growth kinetics, determ. *(French)* 78−76788
Ti, beta III powder compact, fatigue origins 77−44351
Ti, cold rolled, transcrystalline SCC in methanol-bromine soln., crystallographic texture effect 79−15872
Ti, corrosion in H_2SO_4, estimated from weight loss meas. at 270°C and 56 bar *(French)* 80−85080
α-Ti, fatigue crack growth, influence of grain orientation, SEM study 80−108550
Ti, fatigue damage, SEM, X-ray diffr. and surface trace anal. 80−85040
Ti film, ion plated, morphology exam. by SEM 79−28251
Ti oxidation, high temp., exam. and comparative study with Ti-Cu, Ti-Ni oxidation *(French)* 79−20285
Ti, oxidation behaviour under pure O_2 atmos., temp. range 600-800°C 80−89415
Ti oxidation in air, scanning electron microscope meas. 79−61794
Ti, RF sputter deposition, ion bombardment and ion implanation 80−25564
α-Ti, recrystallised commercial purity, Fe-rich precipitates obs. *(French)* 80−50637
Ti, tribological investigation using two-cylinder tribometer *(German)* 77−25164
Ti-Al (6.1 wt.%), hot rolled sheet, ductile fracture nuclei, SEM obs. 78−64654
Ti-Al-V (6, 4 wt.%), fretting corrosion of orthopaedic implant materials by bone cement 80−104813
Ti-Al-V (6, 4 wt.%), hot isostatically pressed casting, fatigue crack initiation 79−79078
Ti-Al-V (6, 4 wt.%), solution treatment temp. effect on fracture morphology 79−61620
Ti-Al-V (6, 4 wt.%), Widmanstatten, microstructurally sensitive fatigue crack growth obs. 78−27627
Ti-Al-V (6,4 wt.%), β-annealed, subsurface fatigue crack initiation 80−108553
Ti-Al-V (6,4 wt.%), effect of air exposure on fracture characts. 80−100890
Ti-Al-V (6,4 wt.%), fretting fatigue behaviour of temps. up to 600°C 80−21104
Ti-Al-V (6,4 wt.%), phase transformation after hydrogenation 80−7560
Ti-Al-V-Sn (6,6,2 wt.%), H_2 induced crack growth, in-situ scanning Auger anal. 79−8355
Ti-Al-V-Sn (6,6,2 wt.%), depend. of K_{ISCC} on loading rate and crack orientation 80−45427
Ti-Al-Zr (6,5 wt.%), alloy IMI 685, SEM exam. of crack growth 78−72849
Ti-Al-Zr-Mo alloy 685, phase at α/β interface *(French)* 80−25661
Ti-Cu (Ni), oxidation, high temp., comparative study with Ti *(French)* 79−20285
TiB_2 CVD coating, surface damage and erosion under energetic D^+ and $^4He^+$ irrad. 80−39174
TiB_2, coating, D^+ and $^4He^+$ irrad. effects 80−20753
TiB_2 coatings, CVD, electron microprobe, SEM, X-ray diffr. characterisation *(French)* 78−43271
TiB_2 coatings, prep. by CVD and interaction with substrate 79−24680
TiB_2-(Ni) (20 wt.%), initial stage sintering under high press., lattice strain 77−55905
TiC, CVD coating on Co-bonded multicarbide substrate, SEM, RHEED, AES interface study 79−77927
TiC coatings, on cemented carbides, struct. and hardness 80−59771
TiC whiskers, CVD growth on various metals and refractory oxides, SEM examination 79−33211
TiC-Au film, prep. by activated reactive evaporation, struct. and mech. props. *(Japanese)* 78−3252
TiC_x-TiN double-layer films, on C steel, CVD in US field, X-ray and SEM characterisation 79−65338
TiC_xN_y monolayer films, on C steel, CVD in US field, X-ray and SEM characterisation 79−65338
TiN film, magnetron DC reactive sputtering, X-ray diffr. and SEM 77−44160
TiN, RF sputter deposition, ion bombardment and ion implanation 80−25564
TiN-Ti_2N, activated reactive evaporation formed deposits, microstructure, transformation depend. on depositing conditions 80−24761
(U,Pu)C, fracture and crack healing, SEM study 79−79080
α-U, strain rate effect on flow and fracture 80−100887
α-U, strain rate effect on tensile flow and fracture 80−84992
UO_2, fission gas bubble distrib. from high temp. irradiated SGHWR fuel pins 77−46284
UO_2-20CeO_2 mixed powder, X-ray and microprobe exam. of homogenisation 80−25609
^{238}U, determ. of time since arrival in matrix existing at time of discovery in Pakistan 79−34822
V and V-Mo, mechanical properties, O, N_2 and C addition effects 79−52356
V, first wall material, irrad. with 40 keV ^{4}He ions, blistering 78−55897
V, He ion bombard., blister diameter and skin thickness, SEM obs. 79−28019
V, irradiation with 2 MeV He ions, low cycle at elev. temp. 78−95086
V-Nb-Ti-N alloy, dispersion hardened, fracture characts. 79−15794
VC-TiC coating, high rate deposition by activated reactive evaporation, and characterisation 78−11372
V_3Ga superconducting tape, stress effect on critical current *(Japanese)* 80−50020
VO_2 films, chemically deposited, chemical transition layers at interface with substrate, AES and SEM obs. 79−95533
V_2O_5, (001) surface modification, during catalytic oxidation of propene *(French)* 80−45557

scanning electron microscope examination of materials continued
V_2O_5 cathode, used in Li-V_2O_5 reserve cells, microstruct. optical reflectance, elec. cond. meas., chem. anal., SEM obs. 79−43752
W alloys, deformed, vacuum technology appl., mech. props. *(German)* 79−57046
W cast alloy, shape, size, distrib. of carbides and oxides 79−24528
W, drawn wire, microstruct. effect on fracture 80−3177
W, electron channelling map *(Chinese)* 79−73229
W, electron-channelling patterns, crit. voltage effects 80−79647
W fibre reinforced Cu, interface porosity formation, on thermal cycling 80−30092
W, from $WO_{2.96}$ reduction 77−28744
W, hot emitter, surface struct. change during baking above 2000K 79−65971
W, plasma-sprayed, effect of Si substrate surface conditions and impact velocity of sprayed particles 80−21145
W, SEM expts., anomalous patterns *(Chinese)* 80−59349
W spheres, in liq. Ni, sintered, coalescing, crystallographic orientation, SEM study 80−45249
W, thin wires, electron emission into gases under strong elec. fields 79−83108
W whisker cryst., growth incorporated with field electron emission 80−44458
W wire, AKS-doped, second phase particle obs. by TEM, SEM and atom probe microanalysis 80−108457
W wire, microparticle trigger discharges and impact damage in HV vacuum insulated gap 77−24227
W wires, KSiAl doped cavity formation *(German)* 78−31524
W, with different microstructs., temp. depend. of yield strength 80−16404
W, work function measurement in SEM 80−80918
W:Os coated dispenser cathode, chemical and physical process obs. 79−28885
W/Cu powders, liq. phase sintering, particle rearrangement 80−45253
W-Al_2O_3 cermet films, oxide evaporation deposited on Mo, Ti, Al_2O_3 substrates, struct., props. 80−25581
W-Cr solid solution, precipitation behaviour, reaction front motion, lattice parameters *(German)* 80−55401
WAl_4, diffusive interaction of solid W and Al melt *(Russian)* 78−26735
WC base alloys, uncoated and TiC or Al_2O_3 coated, wear charact. 78−92365
WC, crystallite size distrib. of powder, SEM method *(German)* 78−47218
WC-Co, on-line computer anal. of SEM obs. 79−87807
WC-Co (10%) alloy, high cycle fatigue, optical microscopy and SEM obs. 77−52494
WC-Co alloys, brittle fracture, precision matching of mating fracture surfaces, by SEM fractographs 78−60807
WC-Co carbide, crack paths, SEM study *(Japanese)* 80−50710
WC-Co cemented carbides, irreversible deformation, yield stress, SEM study 79−70110
WC-Co cemented composites, abrasion by quartz 80−16495
WC-Co cermet, dynamic SEM wear obs. 77−36667
WC-Co DC and RF sputtered coatings, bias effect, struct., X-ray-Auger study 80−70565
WC-Co molten Zn reaction, lamellar struct. form. 79−33964
WC-Co sputter deposited film, struct. and comp. 78−72023
WC-Co sputter deposited film, friction and wear 78−72918
W_6Co_6C cemented carbide substrate, TiC CVD coating, structure, composition and hardness exam. 78−11425
$W_{50}Fe_{50}$ glassy alloy, refractory, triode sputtered 80−75185
W_xO_y, carburisation/reduction with CO, morphological study 79−47977
YAG, molten, complexity in solidification behaviour, SEM electron images 79−43229
YIG, film, LPE, annealing-induced relief of compressive misfit strain 78−2386
Y_2O_3 film in Y-Y_2O_3-Au junction, defect struct. and local conduction 78−26970
Y_2O_3, grain size depend. of fracture energy, SEM study 79−34130
$(YSmLuCa)_3(GeFe)_5O_{12}$, LPE low defect density films, prep. for mag. bubble device fabrication 79−87590
YbTe, high-temperature evaporation and reactivity 80−103469
Zircaloy-4, heat treated in SiO_2 capsules, Zr and Si vapour transport surface struct. anal. of deposits 80−55437
Zn alloys, anodic corrosion in seawater 77−77628
Zn, chromated, electroplate on steel, corrosion, effect of chromate content 79−20286
Zn electrodeposition, on Zn and Al single crysts., from H_2SO_4 bath, SEM obs. *(Japanese)* 80−93502
Zn, film, sputtering mechanism, SEM 80−29839
Zn on Be, zincating conditions, film characts. 77−40397
Zn-Ge, eutectic, stereomorphology using SEM, TEM and optical microscopy *(Russian)* 79−52187
$Zn_{1-x}Ni_xFe_2O_4$, heat treatment and sintering effect on porosity 80−25610
ZnO, CVD of epitaxial films on sapphire, SAW interdigital transducer fabrication 80−66430
ZnO, ceramic varistor, physical props. of elec. barriers by AES and electron microscopy 77−20326
ZnO ceramics, microstructural evaluation 79−55750
ZnO crystals, SEM study *(German)* 80−33860
ZnO films, DC reactive magnetron sputtering technique, quality study 79−78877
ZnO microcrystals, morphology, formed by Zn anodic electrocrystn. 77−80432
ZnO piezoelectric films, RF planar-magnetron sputtered, characterisation 80−96751
ZnO RF sputtered films, post deposition annealing behaviour 80−100416
ZnO, sintered, impurity ion effects on crystalline state *(Japanese)* 77−28768
ZnO, thin Zn or O rich layers, thermolysis, photolysis, SEM, XPS 77−11821
ZnO:Ba, Co, rare earth metal varistors, microstructure-prop. relations 80−100249
ZnO/Al_2O_3, microstratified mixing of suspensions, viscosity dependence 79−70023
ZnO_2, polycrystn., determ. of crystallographic orientation of grains 79−69049

scanning electron microscope examination of materials continued
ZnS, hot pressed, water drop impact damage, SEM exam., IR transmission 78−88543
ZnS striated platelets, SEM studies of local variations in cathodolum. 78−15232
$ZnSO_4$, electrolyte evaluation by cyclic voltammetry and SEM 77−29076
ZnSe, electron beam induced current study of grain boundaries by SEM 80−59479
ZnSe:In films, MBE growth, doping effect on photoluminesc. 80−10818
ZnSe-Ge(GaAs)(mica) epitaxial heterostructs., growth struct. 78−43257
Zn_2SiO_4-SiO_2 dielectric, struct. exam. by optical, photoemission electron and SEM 78−80706
ZnTe, elec., SEM and TEM studies of impurity segregation during long annealing 80−30001
ZnTe, low voltage green LED, struct. double diffusion procedure 80−100697
ZnTe, SEM and luminesc. study of Li segregation 79−38657
ZnTe:B^+ native and implant-created defects 77−76446
ZnTe:Li, diffusion investigation by SEM and TEM 80−10706
ZnTe:Li, impurity segregation during short annealing and quenching, SEM, TEM and elec. meas. 80−10676
Zr, blistering by 2 MeV He^+ ions, optical microscopy and SEM obs. 79−42119
Zr, breakaway oxidation at 573K, SEM study 79−74305
Zr, breakaway oxidation kinetics at 623K, SEM study 80−97633
Zr diffusion in Cu, microstruct. and microanal. study of coating formed *(Rumanian)* 78−19917
Zr, foil bending by in situ ion irrad., neutron damage simulation, room temp. oxide growth 80−107342
Zr, RF sputter deposition, ion bombardment and ion implanation 80−25564
Zr-Al-Fe (8.9, 0.001 to 0.006 wt.%) Fe partitioning to Zr_2Al during peritectoid transformation 78−39784
Zr-CR (1.9 wt.%), β-quenched and tempered, tensile props. rel. to tempered conditions, SEM study 79−66109
ZrN, RF sputter deposition, ion bombardment and ion implanation 80−25564
ZrO_2, porous, sintered stabilised microspheres, strength and fracture studies 80−85019
ZrO_2, sintering response with const. rate of heating, depend. on processing related pore distrib. 79−28992
ZrO_2, spray dried agglomerates, compaction response, fracture, deform. 79−43172
ZrO_2-SiO_2, liquid immiscibility, microstruct. of plasma dissociated $ZrSiO_4$ 80−107429
ZrO_2-Zr cermet composite, hot pressed, fracture toughness 78−27604

scanning electron microscopes
see also scanning electron microscopy
100 kV, with energy dispersive X-ray spectrometer 77−26441
accessory for obs. of wet objects in cathodolum. mode 78−11782
adaptation for transmission mode 79−71579
attachment for meas. of elec. microfields 79−2789
Auger, calc. of effects of backscattered electrons on spatial resolution 80−81412
Auger, with beam brightness modulation *(Hungarian)* 78−29210
Auger, with computerised image processing 80−68304
Auger digital scanning electron microscope 78−12797
Auger microprobe, backscattered electron images, tailored modulation techniques appl. 80−68305
Auger microscope using microprobe with thermal field emission source 80−68297
Auger SEM, spatial resolution *(Japanese)* 78−21278
automatic focusing and stigmating system for the SEM 79−12893
backscattered electron detector, forensic appls. 80−68319
backscattered electron detector, solid state, operating at TV scan rates in scanning electron microscope 79−18089
backscattered electron image, effects of collector take-off angle and energy filtering 80−62802
backscattered electron image, enhancement of type-2 mag. contrast by lock-in technique 80−62806
backscattered electron image, review 78−21304
backscattered electrons, contrast mechanisms and detectability limits 78−21305
beam chopping by electrostatic deflection 77−22619
beam splitting by HF square-wave deflection 79−75654
Broers type LaB_6 gun design 78−21283
Cambridge, modification for viewing untreated insulating materials 80−47150
carousel stage for multisample microanal. by SEM and energy dispersive X-ray spectrophotometry 77−40611
cathodoluminescence, detector system 80−101898
cathodoluminescence detection system for transmission optical fluorescence analysis 78−23999
cathodoluminescence in electron beam instruments, review 78−4740
chamber attachment for fracturing and coating frozen biological samples 78−69260
charged particle behaviour, obs. 77−74556
chopping systems comparison and universal system development 80−68306
collector with energy analyser for SEM 79−6226
combined deformation/heating stage, acoustic emission rate meas. 80−101892
conference, Chicago, USA (Mar.-Apr. 1977) 78−21281
contamination buildup, investigations using backscattered electron imaging technique 80−62807
converted backscattered electron detection 80−68318
cryo-unit for SEM, rapid prep. technique for highly water-swollen membranes 79−89047
cyclic loading stage 78−37106
design and operating characts. of REM-200 79−6221
development, refinements of lens correction, recording of individual electrons, holography, image quality monitoring *(German)* 80−57430
development and appls. 80−13187
digital Auger SEM incorporating concentric hemispherical energy analyser 77−79199
dynamic observations, microelectronic system *(Spanish)* 77−38065
electron beam irradiation damage and contamination 78−29217
electron beam photographic recording system 80−101903

scanning electron microscopes continued
electron gun brightness improvement by ZrC coating on W filament 79−67438
electron gun emission instability, grid aperture contamination in guns using directly heated LaB_6 sources 79−12907
electron gun evaluation unit for electron optical parameters meas. 78−21285
electron microprobe Auger spectrometer with ultra high vac. SEM capability *(Japanese)* 78−27849
electron scattering influence on detection of fine topographic detail 78−21290
electron-acoustic microscope, using US imaging 80−95192
energy dispersive spectrometer 80−27378
equipotential patterns obtaining, accuracy increase 80−57423
exposure numbering, Cambridge 600 modification 78−62266
fiducial grid for high resolution metallography 77−25230
field emission, enhanced secondary electron detection at small working distance 78−21303
field emission, high resolution image 80−86520
field emission electron gun, comparison of cold and thermal types used in the same electron microscope 80−101890
field emission electron gun for SEM *(Czech)* 79−6240
field emission gun SEM column electron-optical performance obs. and model 80−68328
field emission high resolution type HFS-2, development 77−18146
field emission micro SEM, for UHV surface anal. 80−86519
field emission sources, review 78−21299
filter for removing backscattered electrons in energy-dispersive analysis 80−13189
flying spot scanner for conversion of SEM to lithography system 80−86512
focusing and stigmating system using minicomputer 78−37113
heating stage for the Stereoscan SEM, construction 80−95190
hexapole spherical aberration corrector 79−76571
high resolution, multipurpose, REM-100-75, auxiliary devices 79−6222
high-energy electron up to 5 MeV 79−80728
high-performance, new *(German, English)* 77−74559
image analyser FAS II, interactive terminal 78−89597
image formation, phase and amplitude, simultaneous, use of circular solid state detector 78−12795
image formation in scanning microscopes with partially coherent source and detector 78−58923
in-situ gas reaction cell, for field emission SEM 80−81415
induced conductivity mode expts. on semiconds., apparatus requirements 79−9260
insulating specimen charge neutralization using very low energy ions 80−68309
ion etching facility, and its appl. 77−54020
ISI Model 7, for research, quality control and teaching *(German)* 80−57429
ISI Model 7, technical parameters and appl. 79−89044
ISI-100, high performance SEM 79−6238
lens, spherically corrected, apochromatic *(German)* 77−22620
lens system design snorkel or condenser-objective 80−57438
liquid He state 80−9073
magnetic contrast, type-2, effect of collector position in SEM 79−12909
magnification standard reissue 80−27375
metrical features of micrographs, calibration procedure 78−32922
microprobe analyser, scanning cathodolum. 80−81409
microprobe instrument evolution, SEM and STEM 78−70233
microprocessor controlled vector scan pattern generator 80−13188
microradiography stage development and applic. 78−32946
microrelief, quantitative anal., SEM method and apparatus 79−7530
minimum measurable voltage estimation 77−82646
modification for direct obs. of insulators 77−2712
movable Faraday cup, illuminator and backscatt. diode detectors for planar diode characterisation 78−21292
multisample stage for SEM 78−4738
noise in deflection channel, effect on resolution *(Russian)* 78−86391
objective lens, moving, design 78−74829
objective lens, spherical and chromatic aberration coeffs., meas. method 78−21286
on-line stereo processing technique using minicomputer 78−37114
operating parameters, identification for optimal results 79−12900
operational features and appl. *(German)* 77−5965
Philips SEM 505 with multifunction detectors 80−101880
phosphor scintillators, prep. and evaluation 79−230
picosecond pulse stroboscopic SEM for semicond. device voltage contrast images 79−71565
piezoelectric displacement device, inchworm operation in vac., SEM X-Y stage driving appl. 79−21729
precision SEM image analysis system with full-feature EDXA characterization 80−68311
principle and degrees of sophistication 80−37124
REhM-200, secondary electron collector for local electric field meas. 78−4736
REhMP-2 SEM modification to examine p-n junctions 78−58095
resolving power, improvement of REMN-2 scanning microscope 79−26185
review, TEM, STEM, and SEM: microscopy to microfabrication 78−32936
review of recent developments of microscopes and techniques *(Chinese)* 79−30627
sample preparation for X-ray microanalysis, cryogenic stage 80−42306
sampling circuitry for fast repetitive waveform exam. 78−37109
scan generator, digital, microprocessor based, interface to image processing computer 79−12902
scintillating substances, YAG *(Czech)* 78−21280
selected area channelling patterns, optimum instrumental procedures 78−34408
semiconductor detector for testing SEM quality parameters 80−22484
shielded specimen holder for X-ray microanalysis in JOEL U3 SEM 77−49816
shielding design for SEM with X-ray spectrometer, studies of radioactive samples 77−189
signal processing devices 78−78040
signal-to-noise ratio, in recorded images, by random variations in angle of incidence of electron beam 79−12910
source imaging detector 78−21284
spatial resolution enhancement for cathodlum. and electron beam induced current modes 78−21293
scanning electron microscopes continued
specimen holder, for cold tensile deform. and its appl. to Pb-Sn eutectic *(French)* 77−36704
spiral scanning attachment for electron channelling studies 79−2889
state-of-the-art review and future trends 78−21282
stereoscopic observation and three-dimens. meas. instrument 78−21287
stereoscopic viewing technique 78−37112
stereovision in SEM 80−73532
straining stage, 10 kN hydraulic tensile, for investigation of fracture processes in fibreglass laminates 79−54227
stroboscopic, GHz Gunn effect device appl. 78−89606
stroboscopic, picosecond pulse, electron optical design 79−21870
teaching methods for short courses 80−73533
three-dimensional stereo data acquisition, presentation and treatment 78−21297
TV-rate stereo SEM systems, design and performance 79−12906
ultra high resolution, with electron optical system and microprocessor control 80−99002
ultrahigh vacuum field-emission SEM 80−62812
vacuum improvement technique 80−27381
vacuum system specification and design 80−82779
view port 79−75655
voltage measurement system improvement 77−49813
voltage state prediction 79−40644
LaB_5 gun, optimum brightness problem 78−21298
MgO coated detector for SEM backscatter to secondary electron conversion 80−68332

scanning electron microscopy
see also scanning electron microscope applications; scanning electron microscope examination of materials; scanning electron microscopes
absorbed current image, contrast, noneffect of sample resistivity 77−45922
algae, Lugol preserved, rapid preparation technique for SEM 79−39620
application in modern science, review 79−26182
artifacts, obs. in energy dispersive X-ray spectrometry in SEM 79−21888
asbestos aerosol electron microscopy and analysis *(French)* 77−37461
asbestos fibre counting by automatic image analysis 80−73538
atmospheric aerosol, particle size, opt. and geom. determs. *(German)* 77−91259
Auger, instruments and appl. 80−52370
Auger, S/N aspects 80−71993
Auger, synchronous modulation technique 79−17570
Auger electron microscope, Monte Carlo calc. of spatial resolution 78−41383
Auger electron microscopy, edge effect, Monte Carlo simulation 79−1801
Auger electron spectroscopy for analysis of biological material 80−73535
Auger electron spectroscopy microanalysis 80−101058
Auger microanalysis, effect of backscatt. electrons on resolution 79−2898
Auger scanning electron microprobe, analytical techniques 79−79359
Auger scanning microscope, spatial resolution, Monte Carlo calcs., Ag edge on W profiles 79−85204
Auger scanning microscopy, backscattered electron lateral resolution effects 78−15262
Auger SEM using digital integrator 80−37131
Auger spectroscopy, resolution, quantification and sensitivity 80−81411
auto-zero electrometer for analytical electron beam instruments 78−12721
automated X-ray microanalysis with electron microprobe and SEM 78−27840
automatic quantitative anal. of images obtained in SEM 79−6229
automatic topographical surface reconstruction 80−62803
automation, quant. anal. of elementary images *(French)* 78−78045
automation of comparative morphological analysis 79−23509
backscattered, using CdS layer scintillator reflected SEM proposal 78−21291
backscattered electron conversion to secondary electrons, detector system 80−62804
backscattered electron detection mode, nondirectional, high efficiency for SEM 79−12911
backscattered electron detector, small solid angle, cryst. orientation contrast and contrast reversal 79−17579
backscattered electron image, effects of collector take-off angle and energy filtering 80−62802
backscattered electron image, enhancement of type-2 mag. contrast by lock-in technique 80−62806
backscattered electrons, energy filtering *(French)* 77−74558
backscattering theory, using Boltzmann transport equation 80−57439
bacterial growth obs., improved method 78−15933
beam brightness modulation, in Auger scanning microscopy 79−16097
beam chopper for subnanosecond pulses in scanning electron microscopy 78−58096
biological objects, image interpretation 78−53597
biological SEM, for physicists and engineers 79−17581
biological specimen-conductivity problem in electron microscopy, review 78−24206
biological specimens, efficient processing methods 77−60317
biomembrane surface charge visualisation 80−85566
blistering by ion bombardment, ion energy, dose and target temp. depends., review 77−43261
blood cell, red, Fe content anal. by electron microprobe and scanning electron microscopy 79−53065
blood cell profile direct meas. using SEM beam reference lines 78−81094
bone, technique for studying collagen fibres and ground substance 78−57150
BS 350, HV stabilised supplies for 25 kV SEM *(Czech)* 79−21858
capsular organ observation, method based on epoxy removal from embedded material 79−20728
cathodoluminesc., spatial resolution anal. *(Russian)* 77−32448
cathodoluminescence, bibliography of papers till 1977 79−21482
cathodoluminescence analysis of impurities, localisation and sensitivity 78−95985
cathodoluminescence detection of Giemsa stain and its appls. 80−67323
cathodoluminescence images, polarisation contrast 79−7529
cathodoluminescence microscopy, mirror detector system 78−24000
cathodoluminescence mode SEM, efficient spectroscopic detection system 77−5964

scanning electron microscopy continued
cathodoluminescence probing of biomol. species at 100 Å resolution or below 78−24197
cathodoluminescent microscopy of biological materials, improved resolution 77−56549
cathodoluminescent mode for subsurface damage detection 77−80398
cell cycle and topography in nonsynchronised monolayers, autoradiography and time-lapse use for rigorous SEM obs. 78−24212
cell drying, critical point drying alternatives for specimen prep. 78−24210
cell element observations in same sections by light microscopy, TEM and/or SEM 80−85556
cell organelles, ultrastructure from SEM of thick sections etched by O plasma 80−21584
cellular identification of free cells by light microscopy and SEM 78−53589
ceramic materials, techniques for exam. *(German)* 78−56832
channel plate multiplier as emissive mode detector 78−339
channelling contrast technique for material deform. obs. 78−23917
channelling patterns, contrast meas. 78−9921
channelling patterns, review 77−55217
circle mounts for elemental anal. or morphological studies 77−45921
coating techniques, for SEM and X-ray microanalysis 79−12783
cold stage microscopy, thin frozen hydrated specimens, temp. rise and sublimation of water 78−24198
cold storage specimens, electron beam heating temp. profiles 79−5422
colour images, electronic adding-up and storing 79−21879
computer-aided topographical analysis 80−70094
conductive treatment of specimen to prevent charging 80−101883
conference, Chicago, USA (Mar.-Apr. 1977) 78−21281
conference, Toledo, USA (Sep 1978) 79−100796
conference, Washington, DC, USA (Apr. 79) 80−57003
contamination buildup in microscopes, investigations using backscattered electron imaging technique 80−62807
contrast detector and area evaluator, low cost SEM 80−73531
contrast features, variation of specimen thickness 79−23508
contrast mechanism of electron channelling patterns 78−1965
contrast mechanisms, review 78−21296
contrast mechanisms in electron channelling patterns obtained with SEM 79−27884
coordinated, multidiscipline courses 80−67965
correlative light microscopy, SEM and TEM of argentaffin cells 80−85557
correlative microscopy, comparison of SEM, TEM, STEM, scanning work on TEM, transmission work on SEM 79−17576
correlative SEM-TEM of primate infundibular recess 78−20336
cover-slip and mounting-slide with graticule for light microscope and SEM exam. 78−29153
crack and fracture behaviour, in situ techniques with simultaneous acoustic emission obs. *(German)* 79−96240
creation energies for secondary electrons [SEM applications], SEM appl. 79−99994
critical point drying, semi-automatic method 79−17406
critical point drying of hydrated specimens, principles and procedures 80−76882
critical point drying theory, practice and artifacts, review 78−24211
cross-section preparation and handling, chick embryo appls. 80−21588
cryofixation of tissue specimens studied by cooling rate measurements and scanning electron microscopy 80−94430
crystal defects, obs. using SEM fitted with field emisson gun *(French)* 77−35452
crystal morphology, interfacial angles meas. by SEM, sample holder 77−27792
crystalline contrasts from defects in thin and thick specimens 78−22611
crystalline materials observation using diffr. effects, bibliography 78−22612
crystallisation process, effect of solid and liq. boundary layers 79−23544
crystallographic contrast and channelling electron patterns 79−86657
cultured cell obs., SEM STEM comparison 79−74801
cultured cell preparation for electron microscopy, ethanol and chem. dehydration methods comparison 78−24208
cultured cells preparation by air drying from org. solvents 77−48965
defect state microscopy, review 79−94856
deformation heat attachment for scanning electron microscopy *(German)* 79−20297
dehydration of specimens, bibliography (1974-8) 80−73544
detects in materials, direct observation and characterisation 78−88617
development and appls. 80−13187
diffraction unit for RHEED, THEED and dark field microscopy 78−83699
diffractogram online computation 80−70095
diffusion model for electron probe into solid target, energy depend. 78−71652
digital scanning electron diffractometer, appl. to radiation sensitive materials 78−87596
direct elemental analysis by electron energy loss spectroscopy 80−71998
direct grounding tool for uncoated specimens examination 80−4821
dislocation density determination using selected area channelling patterns 78−34407
dislocation imaging, electron channelling appl. 80−70214
dynamic experiments in specimen chamber, state-of-the-art review 78−23918
dynamic SEM with video tape recording 78−32952
dynamic techniques developments 78−32953
egg shells, electron microscope embedding medium for pore studies 80−98194
electric microfields meas. with SEM attachment 79−2789
electrocrystallisation, recent progress in electrochem. and physical methods *(French)* 80−7510
electron backscattering patterns, in field emission gun SEM 80−100142
electron beam induced conductivity, determ. defects in thinned semiconductor devices 80−107027
electron beam induced current, charge collection process 79−17580
electron channel imaging used in microscope for observation of single defects in crystals 80−64848
electron channelling band width, SEM study *(Chinese)* 78−91366
electron channelling patterns 78−83697
electron channelling patterns in SEM, contrast depth 78−18512
electron probe, compensation of aberrations, dynamical focusing with stigmator 80−87291
scanning electron microscopy continued
electron probe microanal. in SEM by means of X-ray spectrometers, review 80−95194
electron scattering, in the scanning electron microscope 79−21880
electron-channelling imaging, defect obs. 80−10471
elemental analysis, X-ray, energy dispersive vs. wavelength dispersive concepts 80−16739
elemental concentration, estimations, in small particles using X-ray anal. in SEM 79−16098
elemental mapping techniques in microscopic domain 78−24013
emission area of back scattered electrons 77−27795
energy dispersive filtration for simultaneous energy and wavelength dispersive analysis 79−12918
energy dispersive microanalysis, in SEM, artifacts *(German)* 80−73561
energy dispersive spectroscopy 80−27378
energy dispersive X-ray imaging techniques and appls. 78−48740
energy dispersive X-ray particle analysis system using beam blanking and digital scan-stop 78−24004
energy dispersive X-ray spectrometry, qualitative and quantitative analysis problems 80−85249
energy loss spectroscopy, spectrometer design, electron optical props. 79−12903
energy-dispersive X-ray analysis, false peaks and other problems 77−52731
environmental particulate exposure in humans, documentation 80−76886
etching of red blood cells by ion beam sputtering 80−85554
fatigue crack propagation, new measurement and observation techniques 80−45463
fatigue crack tip displacement visualis. and meas. using stereo viewer 79−24700
ferritin particle visibility in SEM with field emission gun 79−25174
field emission instability effects on SEM display, electronic removal device 78−21279
filter for removing backscattered electrons in energy-dispersive analysis 80−13189
fissured biological object prep. for SEM, vacuum deposition and cathode sputtering comparison 80−72390
fractographic quantitative analysis, develop. and exptl. verification 77−60023
fracture surface SEM analysis, microtopography 80−68312
freeze drying technique for SEM 80−104828
freeze etching SEM with glycerinated biological tissues 77−64157
freeze fractured chicken erythrocyte nuclei, 3D view of chromatin 80−8229
freeze substitution for preservation of ciliated surfaces for scanning electron microscopy 79−74805
freeze-drying of articular cartilage for investigation of rat femoral heads 80−26433
Freon-TF freeze drying method for SEM sample 79−74802
fringe field measurements, automation 79−12891
fundamentals for biologists, bibliography 78−24213
gas in SEM sample chamber, electron scatt., appl. to N_2 79−49342
geological samples, prep. for SEM 79−12785
gradient image processing using on-line digital computer 78−21288
haematopoietic malignancy diagnosis, significance of SEM 80−85529
hard tissue matrix internal space study by SEM, dentine appl. 78−77169
hardwired image analyser software control 78−57917
health and safety hazards in SEM laboratory 78−21295
heart muscle cells, paraffin-embedded, cryofracture, SEM and TEM obs. 78−57148
high specimen chamber pressure techniques 80−22483
high temperature SEM, development and appl. to sintering studies 79−21873
high-speed SEM voltage contrast waveform display 79−67432
hip replacements, total, causes of failure 77−81662
history of SEM and electron microprobe *(German)* 78−41381
human metaphase chromosomes, SEM examination of uncoated specimens 79−84034
human platelets, air-dried, topography and thickness measured by correlative TEM and SEM 79−84041
HV, for electron channelling pattern anal. 79−4213
image anal. attachment 77−57427
image enhancement and digital reproduction 77−38060
image processing systems, summary of useful techniques and anal. 79−12901
imaging techniques, and X-ray microanal. 80−57432
imaging with backscattered electrons 80−86513
information representation by equal signal lines 80−95196
instant imaging systems appls. 78−21300
insulating surfaces, charge neutralisation by gas ionisation 79−6235
intercellular junctions in FANFT-induced carcinomas of rat urinary bladder in tissue culture 80−8230
ion etching, in-situ, scanning electron microscopy appl. in dentistry 79−30629
ion etching, SEM dynamic study 80−50734
ion microprobe mass analyser and SEM combined depth profiling 79−74481
ion microradiography, of hydrated cells with SEM imaging 79−16360
Kossel diffraction, in scanning electron microscopes, metallurgical appls. 79−20335
Kossel diffraction application developments 78−34405
Kossel patterns, SEM attachment, parameters affecting minimum diffracting volume of back reflection lines 79−1375
Kossel technique in SEM for crystallographic orientation 80−75133
Kossel X-ray technique, for obtaining crystallographic data in the SEM 78−34391
light element detection, meas. near detectability limits with a horizontal cryst. spectrometer 79−21877
linewidth meas. artifact fabrication and calibration 78−41375
low-temperature, appls., techniques and specimen prep., review 78−54510
low-temperature biological SEM, comprehensive freezing, fracturing and coating system 80−76883
low-temperature biological SEM and X-ray microanalysis 79−74818
LSI surface analytical techniques applied to electronic components [Si LSI chip inspection] 80−81392
lymphocyte surface morphology, human, review 78−53599
magnetic contrast, techniques and appls. 79−6236
magnetic contrast, type-2, isolation by lock-in technique 80−13184
magnetic domain, image profiles and resolution in SEM 78−47996

scanning electron microscopy continued
magnetic domain structure determ. high resolution colloid-SEM method 77−43846
magnetic heads scattered fields anal. 79−89045
mass analyzer using electron-beam-guiding type ion source 80−31933
material surface texture analysis 80−73548
materials investigations uses 77−60015
measurement of backscattering coefficient and secondary electron yield 80−86515
metallic deposition in specimens presenting cavities using sputter coater 78−77171
microanalysis of solid matter in a scanning electron microscope *(Czech)* 79−8465
microanalysis techniques, reivew 80−71995
microcrystal orientation, precise determ. using electron back-scatt. patterns 77−76268
microdissection of biological tissues, techniques utilizing real-time stereo SEM 79−80724
microfield effects on spectrum of electrons emitted from surface 79−6227
micrographs, anal. by optical diffractometer and convolution square camera 79−21864
microprobe, particle analysis and identification in pharmaceutical industry 78−61125
microrelief, quantitative anal., SEM method and apparatus 79−7530
microscopic equipment, methods, appls. and related topics, bibliography 80−73124
microscopic tip regeneration and cathode polishing by explosive emission 77−16472
microspreading on rough surfaces by SEM 77−72746
mineralogical use of energy dispersive X-ray spectrometry with Si(Li) diodes *(French)* 80−85251
minicomputer controlled for image and microtopography anal. 78−29214
minority carrier diffusion lengths in semiconds. meas. interpretation 78−80002
module for continuous rotation of cylindrical specimens 80−22486
moist environment ambient temp. scanning, for untreated fresh biological specimens 79−100797
Monte Carlo calculations, use in electron probe microanalysis and SEM 77−74562
multiphase polymers, morphology using electron microscopy 78−91271
multispecimen holder for matrials processing and critical point drying 77−57429
mycoplasma contamination detect., SEM sensitivity 80−85568
myelinated axon identification, SEM technique 80−85570
non-conductive specimens, determ. of thickness and grain size of deposited films by TEM 78−77170
object microrelief analysis by SEM, metallurgy appls. 80−73319
online topographical analysis in SEM 80−68310
orthopaedic implants, replication techniques eval. for SEM 79−34707
oxide phase equilibria, high temp. appl. 79−8416
Pacific marine aerosol, continental component identification by combined neutron activation and SEM with X-ray anal. 78−3990
particles, collecting, handling and mounting for SEM characterisation 79−21867
particulate analysis, aspects of specimen prep. and a limitations of precision by SEM and TEM 79−17574
passivation, effect on obs. of voltage contrast 79−21856
peak-to-background method for quantitative anal. of single particles, with electron probe, developmental progress 80−73541
phase contrast, appl. to obs. of cryst. atomic planes *(French)* 77−35451
photogrammetry, simplfied numerical transform. for distortion correction *(German)* 79−17572
photographic densitometry, appl. to chromosomes 78−77168
photomacrography and photomicrography, oblique transmitted light techniques 78−306
photomicrograph analysis with symmetric pair scintillation detector 79−6232
Plato IV network, SEM teaching 80−68003
polycationic substance layer for preparing suspended biological materials for SEM 77−64156
polymers, multicomponent-multiphase, bulk struct. by rheo-optical techniques 78−91267
pore size measurement, comparison of methods 80−62622
potential distribution mapping technique 79−21857
powder crystallite size determ. using SEM *(German)* 78−47218
powder scintillators, type P-47 80−22487
power plant stack emissions, trace element analysis techniques 78−3938
preparation technique for emulsion particles, freeze drying 80−62799
present state and possible future development 79−12892
principles and examples of SEM photographs *(German)* 80−33860
pseudo-Kikuchi patterns in refl. expts. during scanning of single cryst. by intermediate energy electrons 78−1964
reflected, viewing specimens in air 80−82853
replica preparation for SEM *(German)* 77−10140
reproduction of electron micrographs and transparencies for publication and display 77−49817
resolution degradation, effect of collector field 80−52372
review, TEM, STEM, and SEM: microscopy to microfabrication 78−32936
review, trends in SEM 79−2897
review of recent developments of microscopes and techniques *(Chinese)* 79−30627
sample holder for critical point drying 80−22485
sample preparation, for materials microanal. with SEM 80−37129
sample preparation, IBMA equipment for ion bombardment *(Czech)* 77−61161
sample preparation apparatus for freeze drying and vacuum evaporation 78−335
SAW propag., photographs on TV images of travelling waves using strobed electron beam 80−102894
scanning AES, appl. to cathode studies 79−40643
scanning Auger electron microscopy, Monte Carlo calc. 78−19610
scanning Auger microscopy, developments 80−101909
scanning Auger microscopy, effects of backscattering on resolution 80−104021
scanning electron microscopy (conf., Los Angeles, USA (April 78)) 79−12899
scanning microprobe microscopy, conf., Paris, France (Oct. 1979) 80−82569
scanning electron microscopy continued
scanning mirror electron microscopy, quantitative evaluation of elec. microfields 78−74110
scintillation detector, electro-optical props. 80−52819
sectioning technique for exam. of polymer treated textile materials 79−2891
selected area channelling patterns, optimum instrumental procedures 78−34408
SEM, and assoc. microanal. by X-ray dispersive spectrometry applic. to mineralogy *(French)* 79−5630
SEM cathodoluminescence detection system for transmission optical fluorescence analysis 78−23999
SEM-AES-IMA combination with SIM spectrometer, Si device anal. appls. *(Japanese)* 78−85249
semiconductor, minority carrier diffusion length meas., primary electron accel. voltage effect *(Czech)* 78−34844
semiconductor, SEM meas. of diffusion const., lifetime and surface recomb. vel. 78−91701
semiconductor, spatial distrib. of traps obs. with SEM *(Russian)* 77−32449
semiconductor crystal growth and defects, appl. of analytical techniques 80−73546
semiconductor layers, thin, theory of lifetime meas. with SEM, transient anal. 80−88573
semiconductor structure defect exposure 79−23507
semiconductors, cause of appearance of potential contrast 79−27883
semiconductors, charge collection microscopy, surface barrier method, for defect investig. 79−37598
shadow scanning method for studying magnetic fringing fields 79−6233
signal treatment, backscattered electron spectral distrib. *(French)* 80−42305
SIMS, attachment for chem. charact. of semiconductors and metals 79−17555
SIMS/SEM, surface anal. appls. 79−26187
skeletal muscle preparation 80−94431
slide/tape modules use in teaching SEM 80−68005
small particle identification, review 78−48739
soft X-ray microscopy, high resolution, appl. to biological materials 77−87889
solar cell interaction with SEM electron beam anal. 80−7943
solid, backscattering coeff. meas. of 15 to 60 keV electrons at various angles of incidence, rel. to SEM 80−80919
solid surface characterisation techniques, review 78−22945
spatial resolution of SEM electron beam induced conductivity images 80−6327
specimen carrier storage disc system for SEM of cell culture substratum on stainless steel 78−20328
specimen cleaning by puncture perfusion 78−57149
specimen coating by ion sputtering deposition 80−76184
specimen mounting device for precise alignment 77−87878
specimen mounting epoxies, aerosols, and adhesive tapes 79−71580
specimen preparation, metal coating by sputtering, specimen heating *(German)* 80−73338
specimen preparation for inner surface struct. study of giant axon membrane 77−70579
specimen preparation ion beam techniques 78−24778
specimen stage for energy dispersive anal. for Stereoscan S-600 79−71564
specimen surface coatings, comparison of nature and mode of appl. 79−5421
specimen-electron interactions 80−68317
sputter coating for SEM sample prep. conversion of vacuum coating units 77−34058
sputtering coating in oil-contamination free vacuum for SEM 79−12784
square wave modulation technique appl. to scanning Auger electron microscopy 78−14257
state-of-the-art review and future trends 78−21282
steel, maraging, 18 wt.% Ni, annealed surface damage during machining, lubricated conditions 77−59948
steel, maraging 18 wt.% Ni, annealed, surface drainage during machining, unlubricated conditions 77−59947
steel, mild, cathode arc craters, oxide thickness effects meas. *(German)* 78−38558
steel, stainless cathode arc craters, oxide thickness effects meas. *(German)* 78−38558
stereoimaging displacement and strain meas. and obs. 80−68314
stereological analysis in SEM 80−22482
stereoscopic, mag. tape roughness meas. 79−67254
stereoscopic depth perception and measurement 80−68313
stereoscopic SEM micrographs, quantitative anal. 80−57433
stereoviews and morphological data on microcrystals 78−18510
sterostopic SEM pictures, method for taking by eucentric rotation in tilted specimen plane 79−12908
stray field reduction for voltage contrast meas. 79−67431
stress-strain, recording attachment 80−25961
stroboscopic, for meas. of local temp. in specimen 79−9258
stroboscopic microcomputer-controlled, function testing of bipolar IC and LSI 80−68294
stroboscopic procedure for obs. of defects in semicond. structs. 79−9261
subgrains imaged from bulk specimens in study of localized plasticity 80−66609
surface anal. tools review 80−103540
surface analysis, AES and ESCA combined with SEM *(French)* 80−47154
surface analysis, coordinated, using SEM, electron probe microanalysis and electron spectroscopy 79−96381
surface analysis techniques and appls., symposium, Dayton, USA (Jun. 1979) 80−62363
surface associated microorganisms, effects of specimen preparation on preservation 80−21582
surface physics experiments with ultrahigh vacuum SEM 78−38925
surface potential and work function meas. from secondary electron emission energy in SEM 80−66343
surfaces and interfaces, analysis by combined Auger, X-ray and SEM studies 80−81413
table top SEM for undergraduate training 80−68002
teaching methods for short courses 80−73533
teaching philosophy and methodology 80−67964
temporal event representation by colour microphotography 79−17566
thickness measurement of SiO_2 layer 80−57435
thin film, and surface anal., modern methods 80−54486

scanning electron microscopy continued
thin film coating techniques for specimen preparation 80−68308
three-dimensional stereo data acquisition, presentation and treatment 78−21297
tissue dimensional changes during SEM specimen prep. 78−24209
tissue preparation, removal of epoxy resins 79−5424
two-surface analysis, of polished sections in scanning electron microscope 80−77912
US imaging, appl. in scanning electron microscopy 80−95192
vacuum techniques, contamination management 79−17575
vacuum-sealed specimen stage for air-sensitive materials 79−17571
vascular smooth muscle cells adventitial aspect visualisation 79−20523
video tapes in SEM teaching, evaluation 80−68004
visualization of dermal elastic fibres 79−84036
voids in sintered materials, qualitative and quantititative investig. 80−16212
voltage contrast, a review 79−21863
voltage contrast in scanning electron probe, device ground level floatation 80−73527
voltage contrast in SEM, electron beam current-recording relationship 80−73528
voltage contrast mode at semiconductor surfaces *(Czech)* 79−35897
wet, live and frozen objects, review 79−26183
wet objects, use of gas microchamber 79−21855
X-ray analysis using combination of SEM and WDS 79−12917
X-ray microanalysis, pellet mould for bulk specimens 80−95191
X-ray spatial resolution, for SEM and STEM specimens, Monte Carlo methods 80−101066
ZAF corrections, quantitative X-ray anal. programs 79−21878
Al thin films spontaneous destruction by atmospheric pressure *(Croatian)* 77−76711
$Al_xGa_{1-x}As$, LPE, cathodoluminesc. obs. 78−68565
Au coins, surface anal. by X-ray fluoresc., SEM and scanning Auger spectroscopy 80−89552
Au decoration technique, TEM and SEM study of localisation of decorating crystallites *(French)* 80−10470
Cu cathode arc craters, oxide thickness effects meas. *(German)* 78−38558
Cu electrodeposition on Su, reliability anal. 78−24901
LaB_6 cathodes for Kohler illum. and brightness meas. 80−68296
Li, electrochemical behaviour, in propylene carbonate, SEM study *(French)* 78−56899
Ti/Cu/(Au) thin films thermocompression bonds degradation by thermal ageing 80−66546
YAG:Ce^{3+}, new fast scintillator for SEM 78−86394

scanning radiography
see also computerised tomography; radioisotope scanning and imaging
abdominal aortic aneurysms, comparative study of computerised tomography and ultrasonography 79−29586
abdominal examination by X-ray planigraphy 80−21529
angio-tomographic device, posterior fossa midline visualisation 79−34642
angiotomography in the diagnosis of intracranial tumours 79−48333
Arnold-Chiari malformation: diagnosis by iodo-myelo-tonsillography with tomography 80−36088
artifact-free region-of-interest reconstruction from coded-aperture recordings 79−89863
axial tomography of skull, modified technique 77−86600
bidimensional array design for B- and C-scan US imaging system 79−47877
bone mineral analyser, microcomputer based 79−53218
brain, clinical interest of coronal and sagittal sections using computerised tomography 79−29587
brain, computerised tomography, neurodiagnostic studies and head injury management 79−39470
brain, computerised tomography scanning, traumatic and emergency patients 79−34639
brain, sella and parasella lesions, sagittal and coronal reconstructs. using computerised tomography 79−39471
brain metastasis, clinical symptomatology and computerised tomography 79−29584
cerebral regional blood volume, variations meas. by computerised axial tomography 79−29583
cerebrovascular disorders, CT diagnosis, reviews 79−34638
chest tomography by gamma camera and external gamma source 78−61250
colour TV system with soft X-ray preferred display 80−56186
Compton scatter imaging of transverse sections, corrections for multiple scatt. and attenuations 77−40742
computer cardiotomography, methods and results of morphological anal. 79−34647
computerised tomography, brain and body imaging, review 79−34659
computerised tomography, correction for X-ray beam hardening 79−25082
computerised tomography, display instrumentation *(Japanese)* 79−70688
computerised tomography, functional principles and applications *(French)* 79−70691
computerised tomography, information extraction at different energies 79−39488
computerised tomography, merits rel. to radionuclide and US imaging 79−48324
computerised tomography, reconstruction method for limited field of view 79−48325
computerised tomography, role and relation compared to radionuclide imaging, brain studies 79−34637
computerised tomography, scanners, radiation beam and image slice parameter evaluation technique 79−39487
computerised tomography, X-ray, Rotate/Rotate type whole body scanner using direct magnification 80−21565
computerised tomography scanning, review of technical aspects 79−34635
convolution algorithms for arbitrary projection angles 79−66509
convolutional reconstruction from cone-beam projection data 79−66512
craniocerebral computer tomography in the neonate, review 79−34640
craniofacial anomaly assessment, computerised versus conventional tomography 78−73239
digital image-enhancement, used for human anatomy scanning 80−94408
digital tomogrpahic restoration 78−40322
dynamic radiography, automatic control system design 77−60244

scanning radiography continued
EMI brain and body scanners, patient radiation dose 79−48341
fan-beam scanners, suppression of ring artefacts by software algorithm 79−5394
fast plastic scintillators for medical applications 77−44744
flashing tomosynthesis, 1st clinical results 80−104746
flashing tomosynthesis, coded aperture X-ray imaging 77−40848
flashing tomosynthesis, pre-folded Fourier-filter reconstruction of coded-aperture images 80−53222
flexible scanning industrial X-ray/fluoroscopic inspection 80−89459
grating acoustic scanner for material defects 79−47878
grid for novel and effective Bucky movement 80−104754
grid-coded flashing tomosynthesis, heart phantom radiographs 80−51206
halftone screen techniques for photographic film response shaping, medical X-ray image processing 79−83895
image enhancement of conventional transverse-axial tomograms 79−57758
image formation by back-projection 79−83916
image intensifier tomofluorography, expt. evaluation and clinical potentialities 79−62331
image intensifier tomography in exam. of larynx 78−40312
image reconstruction from parallel projections *(French)* 80−3808
image reconstruction of non-scalar parameters 79−66510
image two-dimensional reconstruction algorithms 77−82379
imaging theory with very limited number of projections 79−53219
intracranial cystic abnormalities, children, computerised tomography diagnosis, review 79−34641
kymography, motion picture apparatus 80−30851
kymography, theoretical aspects 80−30844
laser imploded targets, three-dimens. reconstruction of X-ray emission 80−79563
linear tomography, deterioration of image-phase performance using automatic exposure control *(German)* 79−39500
longitudinal tomography and imaging with masked mirror 78−92695
microtomography in SEM 80−101308
NDT, beam-absorption system, param. selection for extended sources 77−81376
nephro-urography by rapid intravenous injection for urinary system exam. 77−86694
non-metallic materials, flaw detection by tomodensitometry *(French)* 79−20295
paediatric urography, tomography with short exposure times 79−48336
para-nasal sinus tomography with conventional and rare-earth screens, eye dose 77−37055
phased-array US scanners, coarse phase quantisation effects 79−57739
picture reconstruction, quality, accuracy 77−40849
point spread function synthesis, geometrical optics approach, transaxial tomograph processing 79−94163
positron imaging instrumentation 77−44745
pulmonary hila, 55° posterior oblique tomography 80−41189
pulmonary nodules, noninvasive diagnosis using computerised tomography 79−29582
radiotherapy, analogue tomography for tissue organ anal. 79−43984
Radon inversion formula for diverging X-rays 77−37088
Radon transform for higher dimensions 79−5969
Radon transform sampling with finite width beams 79−5968
reconstruction from projections, uniqueness and resolution, book 79−43989
rotation coronary angiography 80−104744
scanography with rotation of the rotation of the radiographic tube, new method 80−98130
SEM, microradiography stage development and applic. 78−32946
spatial multiplex tomography, coherent optical analysis 77−86684
spine, upper cervical, pathology evaluation using computerised tomography 79−29585
spiral tomography, optimum blurring 78−69181
straight-line tomography, linearising mechanisms 78−35934
Synthalyzer, three dimens. synthesis and analysis by optical dissection 78−81011
thoracic region, diagnostic capability of computerised tomography *(German)* 79−39498
three dimensional imaging MTF, optimum blurring figure determ. 77−40851
tomodensitometry, image quality 78−44589
tomograph information characteristics 77−25541
tomograph noise filtering, lung boundaries determ. using neuristic search 78−73240
tomographic image quality evaluation 77−86607
tomographical imaging using uniformly redundant arrays 79−58852
tomography, comparative survey of multi-directional units 78−61242
tomography, emission, compensation of tissue absorption 79−70686
tomography, linear, optimum spread functions 77−66846
tomosynthesis, 3-D X-ray imaging using holography or electronics 77−40847
transaxial tomograms, simplified apparatus 79−11997
transaxial tomography, analogue reconstruction methods 77−12998
transaxial tomography, possibility of an optical treatment for expt. data *(French)* 79−22898
transaxial tomography, simple pupil function for OTF synthesis 79−41349
transaxial tomography camera, photographic image reconstruction, analogue recording system 78−82085
transverse axial film tomography with a therapy simulator 80−81716
transverse section reconstruction, statistical errors, effects of projection angle number and projection sampling 77−52869
tuberculous thoracic aortic aneurysm, early diagnosis, using computerised tomography 79−34634
twin-cone beam projections, 3D reconstruction by algebraic reconstruction technique 79−2155
undersampled images, bounds on errors in reconstruction 79−89858
X-ray generators, tomographic applications 79−16288
X-ray tomography, non-computed, using coherent light reconstruction 80−17116
X-ray topography of large single crystals 80−96415
CdTe detectors, portable miniature scanner, bone mineral meas. using ^{125}I X-rays 77−44750
CdTe detectors in nuclear medicine, capabilities, limitations, X-ray transmission tomography appl. 77−44748
Mo film, constrained, 20 MHz thermoelastic wave generation 79−47880

scanning-transmission electron microscope examination of materials
see also scanning-transmission electron microscopy
acetylene, catalytic decomposition, STEM of catalyst particles 80−24328
alloy, lamellar multiphase, struct. and spatial comp. variation, analytical STEM 78−24011
aluminosilicate glass, phase separated, phase characterization by STEM and X-ray microanal. 80−50643
amorphous materials, small area struct. studies 80−44087
asbestos, elemental intensity ratio variation used to identify fibres 80−3462
biological samples, origin of contrast in images *(French)* 79−66593
biological specimens, contrast and radiation damage 79−66592
biological ultrathin section, electron probe microanalysis, local mass thickness meas. using STEM 79−62416
catalyst, metal oxide, convergent beam electron microscopy obs. 80−108689
cold stage thick specimen heating model 78−61289
composition profiles meas., statistical variation limitation 80−61208
diamond, natural type-IIb, single dislocations, cathodoluminescence obs. by STEM 80−80871
diamond cathodoluminesc. at dislocations 79−47524
dislocation core, symmetry of dynamical electron microdiffraction patterns 80−100140
dislocations and microplasma sites, STEBIC/STEM/EELS correlation 80−96528
electrolytic Fe based composite metal-powder coating structure *(Russian)* 79−83170
etched thin foils, comparative SEM, STEM and TEM analysis 80−100144
FCC metal, microdeform. at low temp. 80−47155
ferromagnetic film domain wall profile determ. by differential phase contrast electron microscopy 79−61195
ferromagnetic thin film, direct determ. of mag. domain wall profiles, using split detector STEM 80−103867
fibre, environmental, convergent beam electron microscopy obs. 80−108689
field emission gun appl., X-ray analysis of metals and ceramics inhomogeneities 80−59354
film, evaporated, metastable phases, convergent beam electron microscopy obs. 80−108689
graphite, Fe-catalysed gasification, electron, microscopy 80−104358
graphite, zone-axis pattern maps 80−100137
II-VI semiconductors, lattice defects, X-ray diffr. and electron microscopic study 80−15088
image resolution and penetration in amorphous and polycrystalline materials, comparison with conventional TEM 80−14976
lipoprotein, low density, from human serum, STEM and FE-TEM obs. 79−100566
Metglas 2826A, direct meas. of decomp. on crystn. by X-ray microanal. in STEM 79−48025
microarea analytical system 77−56188
natural type-IIb, single dislocations, cathodoluminescence obs. by STEM 80−80871
Nimonic 105, quantitative STEM chem. anal. using standard and standardless programs 79−17578
nonmetallic materials, appl. 79−87796
paraffin, single crystal, STEM versus CTEM beam damage 80−103393
phase diagrams, electron microprobe and STEM determ. exam. of techniques 79−6241
plessite structure in Carlton Fe meteorite, analytical study 78−32422
polyacetylene, nascent morphology obs. 80−24379
polyethylene, single cryst. and spherulites, microstruct., deform. micromechanisms 78−83758
polyethylene single crystals, advantages over TEM, microarea diffraction patterns specimen radiation damage 79−55620
polyethylene spherulites, high density, microstruct. and mech. props. 78−42921
polyethylene spherulites, STEM and microdiffr. obs. of micromorphology 78−34444
precipitate free zones, X-ray microanal. 80−108768
principle and advantages 79−30611
protein molecular weight and ultrastruct. determ. in STEM 80−85562
quantitative electron microscopy, recent developments, review 77−70250
rare earth oxides, segregation study by electron energy-loss spectroscopy 80−79953
semiconductor, STEM spectroscopic techniques for simultaneous electronic and defect obs. 80−100145
semiconductor defects, spectroscopic techniques to study of electronic props. 80−84446
semiconductor devices, appl. of STEM 78−23155
semiconductor-metal contact, convergent beam electron microscopy obs. 80−108689
small particles, characterisation and microanal. by STEM combined with other techniques 80−50901
spot scan TEM technique 80−82846
stainless steel, quantitative STEM chem. anal. using standard and standardless programs 79−17578
steel, carbide particles, EM400 electron microscope 80−24328
steel, commercial alloy ferritic, meas. of alloy and impurity elemental distrib. using STEM 80−35601
steel, Cr (10 wt.%), precip. free ferrite form., STEM 80−84941
steel, Cr ferritic stainless, meas. of alloy and impurity elemental distrib. using STEM 80−35601
steel, Cr-Mo, ferritic, grain boundary segregation, X-ray microanal. by STEM 80−66740
steel, Cr-Mo (2.25, 1 wt.%), small changes effect in impurity elements, creep life 80−25790
steel, Cr-Mo low alloy ferritic, meas. of alloy and impurity elemental distrib. using STEM 80−35601
steel, dual phase HSLA, compositional anal., TEM 80−85253
steel, ferritic Cr-Mo type, microanalysis of precipitates using TEM 80−108688
steel, ferritic stainless, Cr-Mo (12,1wt.%) microstructure influence on localised corrosion behaviour 80−61018
steel, stainless, duplex, STEM obs. of localized corrosion 80−104324
steel, stainless, ferrite to austenite decomp. 80−93554
steel, stainless, precip. obs using convergent beam electron microscopy 80−108689
steel, stainless, sensitized, direct evidence of Cr depletion near grain boundaries 77−90358
steel, stainless, weld metal, segregation, S-TEM obs. 77−48431

scanning-transmission electron microscope examination of materials continued
steel, stainless AISI 316, Si and Ti effect in phase stability and swelling behaviour 79−78972
stress induced martensitic transformations 80−47155
superconductor, magnetic flux quanta, TEM, SEM and STEM obs. 77−47945
thin specimen STEM antisymmetric phase function imaging 79−21861
thorium phthalocyanine, phase contrast characteristics in STEM 80−100153
transition metal chalcogenide layer compounds, convergent beam electron microscopy obs. 80−108689
vitrinite, in bituminous coal, microporosity and micromineralogy, small-angle X-ray scatt. study 79−12117
X-ray microanal. of epon sections after O plasma incineration 79−17584
Al and Al alloy anodised oxide films, for adhesive bonding appls., AES and SEM study 80−66689
Al anodising, porous films formed in chromic acid 80−100966
Al, prepared for adhesive bonding, oxide morphologies 79−70203
Al, small spheres, bulk plasmons damping 80−75561
Al surface, porous anodic films, cell walls anal. by STEM and energy dispersive X-ray anal. 79−19476
Al, surface deformation and wear track obs. using analytical electron microscope 80−108687
Al-Mg_2Si, ageing sequence study by electron microdiffr. 80−81068
Al-Mg_2Si alloy, microdiffr. obs. of precip. struct. 80−104167
Al-Mn (1.8 wt.%), cold-rolled, precipitation and recrystallisation 78−27540
Al-Ni (6 wt.%) alloy, misorientation between subgrains, second-phase particles role, STEM microdiffr. obs. 80−104415
Al-water vapour reaction, stress corrosion susceptibility STEM study, Mg addition effect 80−3247
Al-Zn-Mg-Cu alloy 7075, SCC from T6 to overaged T7X 77−90487
Al-Zn-Mg-Cu foil, STEM-microanal., specimen thickness effect on X-ray count rates 77−70374
Al_2O_3:MgO, grain boundary segregation of Ca and Mg X-ray spectrosc. and STEM study 80−107269
Al_2O_3-ZrO_2 cast refractories, nucleation processes reconstruction by SEM, TEM and STEM 78−35380
Au, thin foil, spatial resolution of X-ray microanalysis 80−101065
$BaTiO_3$:Fe ceramic, dopant distrib., STEM obs. 79−82255
C amorphous film, adsorpt., atomic imaging using the dark-field annular detector in the STEM 80−6331
Cu alloy matrix with Cr and SiO_2 particles, low resolution STEM imaging 80−108685
Cu, extinction distances and anomalous absorpt. coeffs. 78−42872
Cu-Au-Cu thin film, diffusion induced grain boundary migration 79−77833
Cu-Be-Co, discontinuous reaction, analytical TEM 80−100842
Cu-Bi alloys, embrittled grain boundary obs. using STEM, Cu-SiO_2 comparison 78−38730
Cu-Bi alloys, grain boundary segregation 79−61596
Cu-Nb_2Sr, multifilamentary supercond. composites, in situ formed, critical currents 79−65625
Cu-Ni-Nb (30, 0.9 at.%), precipitate free zones, X-ray microanal. 80−108768
Fe-Cr-C, austenite to ferrite+precipitate reaction, TEM/STEM study 80−3075
Fe-Cu-Ni, austenite to ferrite+precipitate reaction, TEM/STEM study 80−3075
Fe-Ni, grain boundary segregation, X-ray microanal. by STEM 80−66740
Fe-Ni (3 wt.%), grain boundary segregation of Sn and P embrittling additions, STEM microanal. 78−76654
Fe-Ni (3 wt.%), grain boundary segregation microanal. using X-ray (STEM) and AES 78−87685
Fe-Ni (3 wt.%) alloys, embrittled, microanalysis of grain boundary segregation using STEM 78−35633
Fe-Ni meteorite, STEM/X-ray microanalysis across α/γ interface 80−105212
Fe-Ni-(P), phase diagram determ., 700 to 300°C 80−108399
Fe-V-C, austenite to ferrite+precipitate reaction, TEM/STEM study 80−3075
$Fe_{1-x}Pd_x$ film, vac. deposited, oxidation and corrosion, AES, XPS and STEM obs. 79−100286
$Ga_{1-x}Al_xAs$, STEM techniques for simultaneous electronic anal. and obs. of defects 79−14812
$Ga_{1-x}Al_xAs$ structures, STEM and scanning deep level transient spectroscopy in defect centre anal, cathodoluminesc. techniques 80−103642
$Ga_xAl_{1-x}As$:Cu epitaxial layers, spatial distrib. of nonradiative defects, STEM imaging spectroscopic technique 77−89438
$Ga_{1-x}Al_xAs_{1-y}P_y$ epitaxial layer heterojunction, nonradiative recombination at misfit dislocations 80−96901
MgO, cathodoluminesc. at dislocations 79−47524
MgO, deformed, cathodlum. obs. by STEM 80−76088
MgO-NiO, STEM microanal., absorpt. effects 80−80902
Nb, electron energy losses due to H, obs. by scanning TEM 80−79850
Nb_3Ge, sputtered on Cu, film-substrate interface obs. by electron microscopy 80−65398
Nb_3Sn filamentary superconducting composites, mechanical properties and microstructure 79−57054
Ni alloy, STEM microanalytical techniques comparison for precip. comp. determ. 78−35790
Ni superalloy, STEM microanal. of precipitates and their nuclei 80−81067
Ni-base superalloy, STEM microanalysis of precipitates 80−104492
Ni-Si, intergranular segregation of Si, electron energy loss spectrometers, X-ray anal. *(French)* 79−8388
$NiAl_3$, quantitative STEM chem. anal. using standard and standardless programs 79−17578
Ni_4Mo alloy, high temp. oxidation, oxide layer growth, struct., mech. behaviour 78−44269
Pb, supercooled liquid thin films, liq. struct. factor determ. by STEM 80−10487
Pd, catalyst, Z-contrast, in STEM 79−46530
Pt, catalyst, Z-contrast, in STEM 79−46530
Si, amorphous, scanning TEM studies of cryst. inclusions 80−79699
Si p-n junction depletion layer, electron beam damage inhibition 80−70817
Si, single-electron excitations, image contrast from delocalised excitations 79−46529

scanning-transmission electron microscope examination of materials continued
Si:As, ion implanted, pulsed laser annealing, partial solid-state regrowth 80−103591
Si_3N_4:$(MgO+Al_2O_3)(Y_2O_3)$, hot-pressed and sintered, microstruct. and impurity distrib. 80−49261
Ti-Cr, phase transformation, appl. of Philips STEM400 system 80−25689
U atomic motion on thin C substrate, low-temp. obs., biomolecule marking appl. 79−25176
V, electron energy losses due to H, obs. by scanning TEM 80−79850
V-Ti-C, elemental anal. by EELS 80−101069
WC-Co, STEM anal. of grain boundaries 80−79644
ZnO-Bi_2O_3 varistor, grain boundary segregation, STEM study 79−78980
ZnS platelets, cathodolum. analysis using STEM 78−32950
ZnS, single electron excitation study, cathodoluminescence image contrast using STEM 80−89072

scanning-transmission electron microscopes
see also scanning-transmission electron microscopy
50 kV, 0.3 nm resolution, with scintillation crystal detector scheme 79−58848
Auger STEM, UHV, for thin foil anal. *(German)* 78−12794
biological specimens, frozen, obs. single heavy atoms 80−89921
combined CTEM and STEM, using condenser objective lens and 100 kV LaB_6 gun 80−86516
computer driven, image registration 80−104838
crystals study, two-dimens. diffr. patterns obs. and recording system 80−79650
design, operation, capabilities and limitations, review 80−68300
double focus electron probe, lens for STEM 80−9074
electron energy analysis in Vacuum Generators HB5 STEM 80−73543
field emission, microanal. by energy loss spectrometry 78−53286
field emission gun, for X-ray microanal. 80−85260
field emission STEM for single atom imaging 78−32923
field-emission gun STEM and microanalysis use 78−32948
filtered diffr. patterns and images, direct prod. 80−31950
fine microstructural details, characterisation 80−24328
foil lens, correction of spherical aberration, appl. to STEM 80−87294
future improvements and potential advantages 80−86532
hexapole spherical aberration corrector 79−76571
HV, detection efficiency and performance estimation 80−101899
image accumulation, storage and display system 80−37132
image formation 80−86399
linear imaging of strong phase objects by differential phase contrast 78−32959
microanalysis uses of high resolution STEM system 78−24012
multichannel detector system 80−68331
optical system, practical considerations, review 78−21301
partially coherent image form. 77−190
phase contrast, energy loss effect 78−32960
Philips EM400 TEM/STEM performance, with field emission gun and twin lens 80−57441
post specimen optics, corrected spectrometer 77−38062
quadrant detector, appls. 80−77914
review, TEM, STEM, and SEM: microscopy to microfabrication 78−32936
scan generator, digital, microprocessor based, interface to image processing computer 79−12902
scanning system, for 5 MeV STEM 79−12913
scintillation detector use 80−101897
shadow image processing, a posteriori focusing 79−80726
single atom microscopy, instrumental aspects 80−86522
specimen stage, low temp. in-situ deform. of metals 80−47155
spectrograph, recording of energy loss spectra 80−86525
transmitted and backscattered electrons use 78−37118
vacuum dependent scientific instruments, hydrocarbon contamination 79−63259
X-ray analysis in the TEM/STEM, review 78−24014

scanning-transmission electron microscopy
see also scanning-transmission electron microscope examination of materials; scanning-transmission electron microscopes
accelerator system, magnetic shielding and voltage divider chain 78−340
amorphous thin film, high resolution STEM 79−37597
analytical microscopy, contamination reduction 80−68316
asymmetrical dark field detectors, elastically scatt. electrons 78−8477
atom images under dark field, STEM and TEM comparison 78−83696
atomic imaging using the dark-field annular detector in the STEM 80−6331
atomic number contrast, supported catalyst particles 80−79651
atomic resolution, adsorpt. and diffusion of heavy atoms on light element substrates 77−24484
beam damage sensitivity, STEM versus CTEM 80−103393
biological, on-line data processing system 78−24202
biological, specimens, low-dose, using digital data processing system 78−24203
biological macromolecule observation using CTEM and STEM with negative staining 80−85561
biological STEM dark-field mode capabilities 79−74821
biological thin sections, energy dispersive X-ray analysis, detection limits 78−24215
bright field single atom images with half plane detectors 78−66010
bright-field image contrast and resolution 80−95200
cathodoluminescence analysis 78−32950
ceramic materials, techniques for exam. *(German)* 78−56832
chemical analysis, principles, instrumentation, resolution 79−39262
cold storage specimens, electron beam heating temp. profiles 79−5422
computer graphics analysis of images 80−73539
computerised data recording and replay 80−57440
contamination and countermeasures 79−71578
contamination rate reduction at 10^{-5} torr *(German)* 77−61167
convergent beam, materials science appls. 80−108689
correlative microscopy, comparison of SEM, TEM, STEM, scanning work on TEM, transmission work on SEM 79−17576
coupling to small computer 79−54235
Crewe's Z-contrast technique, study of the Pt and Pd catalysts 79−46530
crystal defects, extinction distances and anomalous absorpt. coeffs. 78−42872
crystal structures and cryst. defects, electron microscope imaging 80−88006
crystalline specimen imaging, image contrast *(German)* 7?−24251

scanning-transmission electron microscopy continued
cultured cell obs., SEM STEM comparison 79−74801
damage, compared with proton microscopy, ratio of elastic to inelastic cross-sections 77−22625
defocus and astigmatism, automatic correction method 80−68298
defocus fringes, exptl. obs. of contrast 77−54021
detects in materials, direct observation and characterisation 78−88617
differential phase contrast role, quadrant and first moment detectors comparison 80−95202
diffraction patterns and bent contours visibility in thick composite amorphous-crystalline specimens 80−1906
diffusion of heavy atom on thin film substrates, direct obs. by STEM 77−89644
displacement energy determ. by electron beam induced conductivity 80−70097
EELS, in STEM, multi-channel averaging 80−101061
electron beam fabrication, using STEM 80−104104
electron energy-loss spectra, progress in quantitation 80−73542
electron microdiffraction patterns, point group symmetry from dislocation cores 80−100140
energy dispersive X-ray analysis in STEM, optimum kV selection 78−24008
energy dispersive X-ray analysis in STEM, semiquantitative analysis method using ref. spectra and empirical scale factors 78−24005
energy dispersive X-ray analysis in TEM/STEM, sensitivity limits for thin specimen analysis 78−24007
energy loss spectrometry, differentiated 78−35786
energy loss spectroscopy, detect. limit improvement using coincidence techniques 77−25345
energy loss spectroscopy, spectrometer design, electron optical props. 79−12903
energy loss spectroscopy, tutorial 79−21872
field emission, Fresnel fringes 78−8476
fine microstructural details, characterisation 80−24328
grain boundary segregation, critical assessment 80−75362
high resolution, microscope design principles and practical advantages 77−49815
high resolution energy filtered images 78−24891
illumination system for thermal cathode, for round beam electron probe systems 80−57436
image analysis and beam damage, instrumental aspects 78−32954
image contrast, radiation damage, STEM and CTEM 77−49811
image formation, 2-D computer simulation of heavy atom model compounds 80−75135
image formation, partially coherent, two dimens., computer simulation 80−106434
image processing, real-time 79−25181
image processing systems, summary of useful techniques and anal. 79−12901
image resolution and penetration in amorphous and polycrystalline materials, comparison with conventional TEM 80−14976
image signals, and detector configurations for STEM 79−12904
images, matching illum. to specimen struct. 80−73551
imaging at high resolution, influence of detector geometry 80−62811
in-situ deform. of metals, room temp. to 16K 80−47155
incoherent imaging in STEM with large annular detector 77−87884
lattice imaging, diffr. patterns for periodic specimens 78−34398
limiting factors in specimen thickness in STEM and conventional TEM, expts. on Si 77−19852
linear imaging of strong phase objects using asymmetrical detectors in STEM 79−97476
lithography, new appl. for microstruct. fabrication in mat. science and biology 79−15844
Lorentz microscopy using STEM for domain wall profiles determ. 78−35003
macromolecular assemblies, struct. anal. with STEM 79−16147
magnetic contrast in STEM 79−21854
magnetic spectrometers, approx. and ideal design, appl. to STEM 78−8475
mass measurements and associated errors 80−73537
mass thickness recording 77−71300
materials science, appl. combined with energy dispersive X-ray anal. and electron energy loss spectroscopy 80−103228
materials science applications 80−76460
materials science role, progress and prospects 78−32957
metallurgical applications, review 77−44422
metallurgical specimen, low resolution imaging problems and soln. 80−108685
microanalysis, precipitates in Ni-base superalloy 80−104492
microanalysis technique, appls., review 79−39261
microanalysis uses of high resolution STEM system 78−24012
microbeam anal., conf., Ann Arbor, MI, USA (June 1978) 79−39258
microdiffraction, nonstandard imaging and microanal. 79−49344
microdiffraction methods, comparison, using STEM 79−19129
microdiffraction patterns, effect of cryst. defects 78−22610
molecular resolution, quantitative approach 77−10143
molecular weight determination by STEM 79−92451
multi-signal detection and processing 80−73552
non-optimal apertures 80−62801
object wave reconstruction, off-axis holograms 79−54230
orientation and position accuracy of electron diffr. 78−22606
particle mass determination method 78−21294
phase contrast, Lorentz object imaging 79−12898
phase contrast characteristics 80−100153
phase contrast transfer with different imaging modes 78−70232
phase determ. of multiply scattered electron beams 77−87885
phase determination, of inner dynamical reflections 79−14660
plural scattering, influence on image quality of thick amorphous objects 80−86533
post-specimen optics, lens-spectrometer system optimisation 77−22621
principle, material science appls. 79−30611
quantitative energy-loss spectroscopy, treatment of inner-shell electron energy losses 79−12905
review, TEM, STEM, and SEM: microscopy to microfabrication 78−32936
scanning electron microscopy (conf., Los Angeles, USA (April 78)) 79−12899
scanning system for HV electron microscope 77−45917
SEM adaptation for transmission mode 79−71579
semiconductor, STEM spectroscopic techniques for simultaneous electronic and defect obs. 80−100145

scanning-transmission electron microscopy continued
semiconductor device characterisation 78−34893
single-electron excitations, image contrast from delocalised excitations 79−46529
spatial resolution, improved X-ray microanalysis of thin specimens 80−104490
specimen contamination problems 79−71577
specimen orientation modes 78−34406
spectroscopic techniques, with STEM for anal. of electronic props. of defects and impurities in semiconductors 79−14812
split detector, direct determ. of mag. domain wall profiles in ferromag. thin films 80−103867
split detectors in STEM, ptychography 78−89603
structural and chemical analysis, appls. 80−88003
structure image high-speed calc. methods 79−55622
surface originating contamination and its elimination 80−68315
thick objects, influence of detector geometry on image props. 77−56554
thick objects, micrograph anal. 80−82856
thin films, chem. anal. by energy loss spectroscopy 80−104493
thin foil microanalysis using XPS and STEM, surface film effects 78−35789
thin specimens, intensity distribs. using phase object approx. 77−55218
transfer functions concept appl. to imaging of phase objects *(German)* 78−32931
transmitted and backscattered electrons use 78−37118
two-dimensional molecular assemblies construction 78−24201
unstained biological sections 78−31990
X-ray analysis in the TEM/STEM, review 78−24014
X-ray microanalysis, electron probe dispersion influence on spatial resolution 80−85257
X-ray microanalysis, spatial resolution 80−84039
X-ray microanalysis in scanning transmission electron microscope, limitations 78−20122
X-ray spatial resolution, for SEM and STEM specimens, Monte Carlo methods 80−101066
X-ray standardless thin film analysis in electron microscope 78−24006
X-rays, spurious, produced in the scanning transmission electron microscope 79−17573
zone-axis pattern formation using four sets of coils 80−70091
C film on substrates for supporting specimens, prep. and observation 80−93496
LaB_6 cathodes for Kohler illum. and brightness meas. 80−68296
V-Ti-C, elemental anal. of second phase carbides using electron loss spectroscopy 79−20500

scattering
see also acoustic wave scattering; backscatter; electromagnetic wave scattering; potential scattering
3-body problem with one infinite mass particle, Schrodinger and integral eqn. soln. equivalence 80−77636
Aharonov-Bohm scatt. by thin impenetrable solenoid 79−9058
algebraic theory, existence of wave operators *(French)* 78−24692
amplitude phase construction by iteration of bounds from unitary integral 80−57142
amplitudes, unitarity condition homogeneous linear inequalities, calc. program 79−85013
analytic continuation in decay-scattering systems, singularities as model basis 80−8850
analytic extrapolations towards interior points from a cut, applic. to elementary particle scatt. theory 80−12952
angular scattering of spinor charged particles by a Kerr-Newman field 80−94996
anisotropic random medium, scatt. in depth direction 79−2635
approximate coupled equation method 80−73215
asymmetry estimation from incomplete azimuthal ang. distribs. 79−81142
Backlund transformation in language of jet bundles *(French)* 78−28913
Bessel functions, asymptotic approx. 80−31562
binary reaction amplitudes for particles with spin 77−74273
Boltzmann equation, exactly soluble, with persistent scatt. 80−46997
Borel-type sums in scatt. theory, computation method 78−57823
classical dynamics scattering theory 79−49109
classical inverse scattering in one dimension 80−82595
classical limit for scattering in liquids 80−17842
classical predictive electrodynamics, energy and 3-momentum balance and scatt. cross sections 79−88818
completeness value for eigenfunctions of second order differential eqns. 80−31564
continental shelf waves, scattering by longshore bottom topography vars. 80−67376
continued fraction expansions and statistical nonequilib. mechanics 78−45523
cosmic rays, multiple scatt., energy balance in randomly nonuniform mag. field *(Russian)* 78−49252
Coulomb problem, symmetry and invariance, canonical transformations 80−41989
Coulombic scatt. of charged particle by random distrib. as two-body process 77−38789
critical scattering theory, book 79−25913
cross-section transformation, between two moving frames 78−89369
decay-scattering systems, resonances and their eigenfunctionals in Friedrich's model 80−8847
density matrix of scattered particles, comments on 80−22219
density matrix of scattered particles 80−22218
diffuse wave scatt. by short range order, improved mean spherical approx. 79−9127
Dirac equation, Levinson's formula, inverse problem of scattering theory *(Russian)* 79−9315
education, multiple scatt., elastic and inelastic, two particle system with fixed wall, air track expt. 80−73135
eikonal approximation, some inequalities 79−44800
elastic reflections of particle in expanding sphere, rebound function 78−86196
elastic unitarity integral, angle-dependent lower bound on soln. and new uniqueness condition 79−40414
elastic waves, diffusion approach to propag. in highly scatt. medium 77−86804
elastic waves, multiple scattering by elastic ellipsoidal inclusions, self-consistent approach 78−63372
elastic waves, reciprocity relations, forward amplitude theorems 77−49605
scattering continued
elastic waves, scattering by elastic sphere embedded in isotropic elastic medium 80−96214
elastic-scattering in several coordinate dimensions, global nature of semi-classical wavefunctions 79−63092
electron beam scatt. by plate, soln. to mixed type PDE 77−67388
Faddeev integral eqns. for three charged particles *(Russian)* 80−8830
few-body scatt. in quantum mechanics, soln. methods 79−85010
finite cross section for three-particle scattering 79−67195
fission-fragment scattering kinematics multiparametric anal. electronic meas. system, semiconducting detectors 78−78551
Fokker-Planck eqn., kinetic effects due to detailed equilibrium violation, elastic scatt. *(Russian)* 80−31687
forward or backward scatt. amp. with three constraints, variational pattern 80−94995
forward scattering contrasts in multicomponent systems 80−90728
Froissant bound saturation for two particle elastic scatt. 79−75680
general residual interactions, natural distrib. props., direct proof 79−97262
gravitational radiation, long-wave, primordial, induced scatt. by galaxies 80−17661
Haag-Ruelle scattering theory as scattering theory in different state spaces 80−4593
hard corrugated surface, wave scatt., iterative series 78−89355
hidden symmetries in dynamical systems 80−37168
high-frequency scattering by a convex soft or a rigid obstacle 80−90727
holonomic quantum fields, classical scatt. in Minkowski space time 79−80472
internal Galilei group for a two-particle system 79−75406
internal waves with finite fluid depth, inverse scatt. problem, Backlund transformation 80−31517
interplanetary recurrent proton streams, 1.3 to 2.3 MeV protons diffusion and scatt. mean free path 79−16774
inverse scattering and solitons, geometric considerations 80−4550
inverse scattering problem, class of singular integral eqns. 77−17878
inverse scattering problem in Rayleigh-Debye approx., diameter distrib. functions of helical structs. 80−27182
inverse scattering solution for three dimens. three-wave resonant interaction 80−77633
inverse scattering theory second-order difference eqn. on whole axis *(Russian)* 77−29990
3×3 inverse scattering transform, soliton perturb. scheme 80−27151
inverse scattering transform, Wronskian technique, isospectral flow eqn. 78−8275
inverse scattering transform eqns., survey of developments 78−57795
ion, comparison of time-of-flight and stripping cell low-energy ion scattering methods 80−73522
ionosphere, photoelectron thermalisation and transport, isotropic scatt. 77−70933
Langmuir solitons, prolongation struct. 79−88814
levinson's theorems in classical scattering 80−90729
linear Boltzmann equation, transport and scatt. props. and solns. 78−93628
longitudinal wave scattering by sphere-like bodies of revolution *(Ukrainian)* 80−22202
magnetic heads scattered fields anal. 79−89045
magnetic irregularities in extragalactic compact radio sources, ripple scatt. and low-freq. variability 79−21450
many body wavefunction struct. 78−62119
many boson non-relativistic systems, classical field limit of scatt. theory 79−80501
mean impact parameter for fixed scatt. angle 79−58589
microwave backscatter, ploughed soil, surface roughness meas. *(French)* 80−82072
Miura's transform. of modified Korteweg deVries eqn. 79−75356
multichannel, optimised anomaly-free and restricted anomaly-free variational methods 79−3515
multichannel, theory, in two spaces 79−88839
multiparticle scatt., time depend., arrangement-channel quantum mech. 77−41503
multiparticle scattering, weighted Hilbert space 79−75380
multiple scatt. in 1-D 79−44754
multiple scatter problems, use of physical concepts 79−21561
multiple scattering in one-dimens. of monochromatic waves 78−4528
multipoles and excitons in higher order coherence 80−82680
N-body scattering, general formalism, relationships between formulations 79−75412
N-body scattering equation approach using pole decomposition of Green's function 80−62540
N-body scattering wave functions, singularity anal. 79−71286
neutron transport integrals, quadrature sums, Gaussian, orthogonal polynomial method 80−83139
nondiffractive scattering from kaleidoscopes 80−86155
nonrelativistic models for inelasticities in N/D eqns. many channel scatt. problems 77−49879
ocean continental shelf waves, scatt. by isolated topographic irregularities 80−51423
ocean internal waves, damping by scatt. on rough bottom *(Russian)* 78−24293
ocean long waves, scattering at estuaries bordering continental shelf 77−78191
oceanic internal waves, elastic scatt. reson. interaction 77−45010
Painleve transcendents, geometric struct. and inverse scatt. problems 80−31600
paired summation eqns. with legendre associated function kernels, effective solution 79−84968
particle diffusion and scatt. length, Green's function methods 77−13629
periodic hard corrugated surface, wave scatt., formalism and numerical solns. 78−81876
periodic surface scatt., existence theorems *(Russian)* 78−73890
phase of scattering amplitude, uniqueness, variational calc. 80−86156
phase space packets, time depend., differential cross sections obtained by superoperator methods 80−105544
plane wave scatt. by lossless penetrable obstacles, low freq. expansions 77−26211
plane wave scatt. by moving obstacle 79−71254
Poisson summation formula, generalisations 80−4565
polycrystalline material, scatt., lattice representation 78−65774
principal value collision integrals, reduction scheme 77−57234
quadratic forms, Schechter's theorem 77−41512
quantum dynamics, sensitivity anal., Green's function method 79−67178

scattering continued
quantum field systems, scattering theory asymptotic conditions, field and Hamiltonian props. 80−13222
quantum inverse scattering method and Heisenberg ferromagnet 79−61029
quantum mechanical description of scatt. by dissipative and diffusive scatt. centre 79−75410
quantum scattering theory with different state spaces of perturbed and free system 79−40406
randomly varying medium, with quasistatic fluctuations, average field weakening calc. 79−71367
reaction matrix representation, no-go theorem for polarisation struct. 78−62120
real-space information, interpretation of from small angle scattering experiments 79−50925
relativistic electrons in strong mag. field, Raman scatt., pulsar radiation *(Chinese)* 77−53418
resonance transfer rate of electron excitation, model of convergent terms, effect of diffusional motion of particles 80−8936
resonances, scattering theory and rigged Hilbert spaces 80−94987
rigged Hilbert space and decaying states 80−4591
rotated hamiltonians, complex-coordinate rotation and least-squares variational method 80−68075
Rutherford scatt., electron deflection, inverse 1st, 2nd and 3rd power field, program 77−87594
scalar waves, high freq. scatt. by plane boundary stratified medium 77−67297
scattering amplitudes with positivity constraints, analytic extrapolation, integral eqns. 79−35589
scattering medium description by number of particles scattered 78−93623
Schrodinger equation, Laplace transform 78−57806
Schrodinger equation, scattering solutions decay at least logarithmically 79−25901
Schrodinger equation, time-depend., explicit integration method 78−57805
seismic Rayleigh waves, scatt. by ridge 77−78125
seismic waves, attenuation and scatt. by randomly distributed inhomogeneities *(Hungarian)* 77−86791
seismic waves, effect of multiple scatt. on wave field spectral comp. *(Russian)* 79−8607
seismic waves, energy transmission in intensively scatt. environment 77−73685
seismic waves, scattered waves in coda of P 77−73684
seismic waves, single isotropic scattering approx. for coda waves near hypocentre 78−11828
semiconductors, hot electron transverse escape galvanomagnetic effects *(Russian)* 80−80289
small angle scattering, by ellipsoid of rev. or sphere distrib., equivalence 80−99
solid layers, conversion electron scatt. processes anal. 80−45181
solids, chemical bonding studied using scattering theory concepts 80−103289
spectral and scattering inverse problems 79−17282
Spencer-Lewis eqn., orders of scatt. soln. 79−85098
spin-rotation model, for adiabatic anal. of collisions 79−40402
stationary state scatt. theory for density operators 77−26207
symmetric collision theory, T-operator matrix elements 80−73214
Szego's theorem for Hankel determinants 79−49106
temporally inhomogeneous nonlinear scatt. theory 77−37788
theory, existence and completeness of wave operators, eigenvector orthogonal complement 79−9150
theory, for orthogonal polynomials on the unit circle 79−30294
theory, propagation of singularities for the transmission problem and application to the inverse problem of scattering *(French)* 80−94994
theory for domains with non-smooth boundaries 79−30293
thermal averaging deconvolution in scatt. expts., using integral transform methods 78−92442
three body Schrodinger operators, scatt. theory, using abstract stationary theory 79−17265
three-particle scatt., finite cross section 79−85011
three-particle scattering without divergence difficulty 78−93555
translation kernel upper bound *(French)* 78−62118
transport scattering coefficients from reflection and transmission measurements 79−93078
two Hilbert space scatt. theory, recent progress 79−75411
two space scatt. theory, Cook-Kuroda theory 79−67194
two-body scattering in force field 79−85012
two-channel scattering problem variable phase method *(Russian)* 77−74269
two-particle resonances and singularities of 2→3 particle scatt. amplitude 77−49643
two-particle scattering systems, general, sum rules 80−8862
unitarity constraints on scatt. amplitude phase 77−37787
unstable quantum states and rigged Hilbert spaces in nonrelativistic scatt. theory 80−8849
variational principle for scatt. phase 80−68084
wave, multiple, theoretical analysis *(German)* 79−75362
wave equation, reduced, fixed incident field, inverse problem 80−62484
wave scattering, fluctuating inhomogeneous media, model for teachers 79−21492
wave scattering, second order approx. in planar linear sheet 80−17812
wave scattering in presence of background slab, algorithm for profile reconstruction 80−94644

scattering matrix *see S-matrix theory*

scattering parameters *see S-parameters*

SCF calculations
for MS SCF (MS Xalpha) calculations see Xalpha method
see also HF calculations; Xalpha calculations
π-electron system, self-consistent many-body theory, self-energy effect 79−63901
acetaldehyde, first triplet state geometry, fragmentation into free radicals 80−47915
acetic acid, cryst. binding, ab initio MO SCF calc. 79−37657
acetic acid, dimer, config and energy, ab initio MO SCF calc. 79−37657
acetone, ab initio CI valence and Rydberg states, spectral assignments 77−14346
acetonitrile, quadratic force fields, MOCIC pot. functions calcs. 80−5475

SCF calculations continued
acetophenones, di- and trisubstituted, π^*-π systems, UV electronic absorpt. spectra 80−74132
acetophenones, mono substituted, semi empirical Π-electron calcs. 80−74131
acetophenones, spectrosc. characts. using PPP SCF CI calcs. 80−102448
acetylene, and cation, SCF MOGO calc. of electronic struct. 77−34556
acetylene, force consts. of symmetric stretch motions, accurate ab initio calcs. 77−83567
acetylene, ground and triplet states, electronic and geom. struct. 78−94184
acetylene, mol. and cluster Auger spectrum calc., SCF core-valence-valence spectra 80−48045
acetylene, multipole moments and polarisabilties, SCF calcs. 80−5471
acrolein, excitation, ionisation and electron affinity, expts., HAM/3 calcs. 80−18790
actinides, self-consistent relativistic muffin-tin calc., atomic vol. and bulk modulus Ac-Am 78−72065
adenine, tautomeric forms protonation, ab initio HF Roothaan SCF calcs. 80−78534
adenine tautomers; relative stabilities, nonempirical MO calcs. 80−21442
adsorbate relaxation energies in XPS 78−15283
adsorbed atoms on metallic surface 77−7976
adsorption anisotropy for molecule SCF MO LCAO calcs. 77−89643
advances in nuclear physics, clustering and self-consistent field theory, book 79−75879
alkali borate glass networks, π-electron distrib. SCF INDO LCAO-MO calc., O basicity 78−79924
alkali metal atoms and anions, electron affinity, model pot. SCF and CI calcs. 77−38609
alkali metal diatomics, pot. curves, selected valence electron SCF MO calc. 79−10053
alkaline earth compounds, valence shell electronic struct., ab initio SCF calc., photoelectron spectra 79−31383
alkanes, linear, electronic struct., electronic relax. during photoemission *(French)* 78−5283
alkanes, linear, K-shell ion relax. energy chain length depend. 79−72252
n-alkanes, methane to n-tridecane, ESCA of core electron relax. and valance bands 77−18978
n-alkanes, mol. Rydberg $S_0 \leftarrow S$ and $S_0 \leftarrow T$ transitions, semi-empirical SCF MO calc. 80−91453
alkanes, saturated, ab initio LCAO MO SCF calcs., core ionis., electronic relax. 77−71745
alkyl chlorides, proton affinity correl., ab initio SCF calc., MINDO/3, STO and G basis sets 78−33421
alkyl fluorides, geometries, props. and protonation, ab initio mol. orbital study 79−22588
all-valence LCAO MO SCF INDO method, for mol. ground and excited state props. 78−37556
allene, C-C double bond rot. barrier, ab initio open-shell restricted SCF calc. 78−1099
allene, internal rot. in ground electronic state 77−67975
allyl radical, ab initio SCF solns., doublet stability 78−33423
allyl radical, restricted ab initio SCF LCAO solns., doublet stability 77−79539
allyl radical, restricted SCF and MC SCF calc. of C_{2v} and C_s structs. 80−83289
amide C-N bond character, metal ion bonding effects 77−6801
amides, geometry from ab initio calcs. 80−23338
amino acid protonation ab initio Hartree-Fock-Roothaan SCF calcs. 80−9503
α-aminoisobutyric acid, cryst., γ-irrad., cation radicals, ESR obs., SCF-MO-INDO calcs. 78−11537
anharmonic crystals, unsymmetrised SCF approx. 78−63830
anharmonically coupled oscills., time depend. Hartree theory, susceptibility, absorpt. and Raman spectrum 80−58241
anisotropy of long-range interaction 79−36734
anthracene, cryst., radiation induced radicals, optical absorpt. bands, SCF-CI MO calc. 79−91463
aromatic heterocycles, MC-SCF and CI calcs. in PPP framework 79−26892
ascorbic acid adduct model systems, SCF calc., rel. to protein internal charge transfer 80−69072
atom, bound state quantum fluctuations and variational method, relativistic HF calc. with radiative effects 80−42918
atom, orbital rel. to total SCF energies, HF SCF approx. formula 78−21837
atom, SCF electron-gas local-spin-density model including correlation, appl. to He through Ar 80−9488
atom, SCF treatment of higher excited states, method and its appl. to Si II 78−82658
atom-ion core level shifts, ΔSCF calcs. 80−87176
atom-pair interactions in molecules, semi-empirical MO calc. 80−915
atomic anions positron complexes, ground and excited states theoretical studies 80−42934
atomic collisions, mol. approach, radial couplings between approx. wavefunctions 77−38713
atomic electron binding energies, determ. from relaxed-orbital relativistic Hartree-Fock-Slater calcs. 77−42255
atomic excited states, SCF wavefunctions 78−90099
atomic form factors for large momentum transfers, relativistic SCF calc. 77−83504
atomic nonrelativistic binding energy, statistical theory, agreement with SCF calc. 78−25438
atomic quadrupole shielding factors calc. using elec. field variant orbitals 80−106276
atomic scatt. factors and momentum densities, asymptotic form 80−74105
atomic struct., numerical HF radial function during SCF iteration, convergence 78−58574
atoms, analytical relativistic SCF calcs. 80−83248
atoms, complete active space method, comparison of super C I and Newton Raphson scheme 80−47904
atoms, near threshold struct. in K-shell spectra, photoionisation or fast charged particle ionisation 80−87064
atoms, nucl. vol. isotope shift theory, many electron effects 80−47851
atoms and ions, central analytic potential with three parameters 77−71737
atoms and molecules, config. interaction calcs. for SCF basis sets 78−58593

SCF calculations continued
atoms on semi-infinite linear chain, chemisorption theory and superoperator formalism 80−93800
autonitryl, electronic struct. and geometry, open-shell SCF calcs. 79−18106
azabenzenes, multipole moments, polarisabilities and long-range interaction coeffs. calcs. 79−89599
azacyclobutadienes, conjugated mols. electronic struct. and geometry, Hartree-Fock instability 80−69055
azomethane, trans-cis isomerisation, INDO-SCF and CI calc. 78−25440
bacteriochlorophyll, π-electronic struct., ASMO-SCF-CI calc. 77−36868
bacteriopheophytin, π-electronic struct., ASMO-SCF-CI calc. 77−36868
band structure, optical cond., Compton profile, self consistent calcs. 80−65435
bases, K^+ affinities ab initio SCF calc. 78−58585
benzaldehyde, nπ* and pi pi* triplet states, props., SCF calcs. 77−6695
benzene, π electron system, excitation energy, appl. of MBPT 80−52876
benzene, ab initio model calc., variational 77−46492
benzene, dipole polarisability, finite-field SCF MO calcs. 80−83255
benzene, electronic struct. calc. using free-electron orbitals basis set 77−79537
benzene, ionised, H atom scrambling, SCF calcs. 77−9062
benzene, LCAO-MO-SCF calcs., MODPOT, VRDDO and MODPOT/VRDDO procedures 77−71742
benzene, mol., directional Compton profile, ab initio SCF LCAO MO calc. 78−62857
benzene, protonated, electronic struct., SCF MO LCAO calcs. 78−82638
benzene, SCF-EHT polarisability calc. 80−47895
benzenediazonium compounds, structure-property relationships, quantum chemical calcs. 79−22605
benzonitrile, LCAO-MO-SCF calcs., MODPOT, VRDDO and MODPOT/VRDDO procedures 77−71742
benzophenone, metastable triplet state, SCF CI calcs. 79−54776
beryllocene, gas phase struct., ab initio LCAO SCF calc. 78−41942
biacetyl, lower excited electronic states, ab initio SCF and CI calcs., absorptiop band assignment 78−74589
1,1′-binaphthyl mononegative ion conformation 77−30774
biomolecule, ab initio study of Na^+ interaction with purine and pyrimidine bases of nucleic acids 77−64005
biomolecules electrostatic model of solvation, SCF MO calc. 79−96305
bond orbital model, atomic charges calcs., fully localised SCF method 80−42923
bond orders, lengths, MO calc. methods, correl. with experimental values, teaching appl. 77−29974
boron trihalides, quadratic potential functions, Coriolis consts. calcs. 79−72239
Bose interacting gas, energy spectrum and specific heat 77−15656
boson system, one-dimens., ground-state props., SCF approx. 78−49761
bromomethane, ab initio SCF MO calcs., ionis. pots., dipole moment, config., electronic props. 78−1104
trans-butadiene, polarisability, nonlinear elec. susceptibility, SCF calcs. 80−95547
butadiene, twisted zwitterionic excited states, SCF calcs. 80−58179
trans-1,3-butadiene, valence electronic excited states, SCF ab initio GVB and CI calcs. 79−31423
butadiene-acrylonitrile copolymer, electronic struct., reactivity, SCF CNDO calc. 77−50580
n-butane, conformational hypersurface, anal. 79−41252
cis- and trans-2-butene, Compton profiles, theory and expt. 78−50597
t-butyl radicals, ab initio geometry calc., ^{13}C hyperfine coupling 77−10580
caffeine, semi-empirical excited state Morokuma's EHP calc., geometry and order of states 78−46256
carbenes, core ionised states, singlet and triplet state binding energy, struct. changes, LCAO-SCF calc. 79−97982
carbonic anhydrase, active site substrate binding, environmental effects, CNDO and SCF LCAO calcs. 80−8002
carbonyl compounds, ^{13}C chem. shifts, approximate SCF perturbation theory 77−6804
carbonyl fluoride, vertical electronic states, ab initio SCF CI calc. 79−49942
carbonyl halogen substituted cpds., geometric and electronic struct., LCAO-SCF calc. 79−89603
carbonyl to oxacarbene rearrangement, conformation, ab initio SCF MO calcs. 77−32780
carbonyls, core ionisaton phenomena, nonempirical LCAO MO SCF investig. 80−37906
β-carotene, optical absorpt., theory 79−62189
charged liquid, SCF equation, partial soln. *(Russian)* 78−74823
chemisorption, embedding problem, SCFMO formalism 78−71977
chloromethane, mol., valence and core ionis. energy, RHF-SCF and PNO-CEPA calc. 79−85890
chromium formate, mol., Hartree-Fock instability of SCF wavefunctions 80−9492
closed shell Hartree theory with orthonormal orbitals 80−69051
closed-shell configurations of isoelectronic ions and atom, SCF and STO energies 79−89598
closed-shell linear molecules, relativistic Dirac-Fock multiconfig. SCF calcs. 80−99455
closed-shell polyatomic molecules, relativistic Dirac-Fock multiconfig. SCF calcs. 80−99456
closed-shell SCF calcs., mol. symmetry 78−41930
closed-shell system, polarisability and mag. susceptibility calc. by SCF and CI method 80−99443
complex heteroorganic molecule, semi empirical SCF-CI MO method 79−63917
composite medium, elastic props. 78−51078
condensed matter, orbital and pot. functions calc., eq. of state 80−44463
configuration interaction, spectroscopic calcs., general parametrisation method 78−94228
conjugated hydrocarbons, conformational analysis and heats of form. by force field method 77−60105
convergence, effect of electron distrib. nonuniformity 77−18778
convergence by level shifters, general many shell theory 78−17548
convergence in SCF calcs., reverse level shifting technique for accel. rate 78−70735
core hole state and ground state equilibrium geometry differences 79−41186
coronene, excited state Faraday values mag. circular dichroism spectra and MO CI calcs. 80−18877

SCF calculations continued
coupled HF-perturbation theory of atomic and mol. props., correl. corrections 80−106269
coupled multiconfiguration SCF perturbation theory, analytic techniques 78−17550
coupled oscillator system, SCF-state interaction method 80−58239
coupled oscillators, approx. and exact quantum energies and eigenfunctions 79−26961
coupled vibration systems, eigenvalues, semi-classical SCF calcs. 80−27929
covalent surface, pot. and charge distribs. and dangling-bond state 78−2537
crystal, SCF theory, boson transform. 77−80430
crystals, anharmonic, with complex lattice, equations of state 80−107399
cubic crystal electronic energy band calc. by LCGO method, FORTRAN IV program 78−75977
cubic lattices, dipole moments of point polarisable atoms, uniform applied electric field, SCF equations 80−50257
cyanine dyes, all-reactive-electrons closed-shell SCF-CI MO calcs. 79−36541
cyanoacetylene, IR absorpt. bands, integrated intensities, ab initio and LMO calcs. 79−72234
cyclic 3- and 4-membered ring cpds., saturated, ab initio struct. anal. 80−58192
cyclobutadiene($-d_1$), singlet and triplet ground states, vibr. freqs., MINDO/3 and ab initio SCF calcs. 78−13429
cyclopentadiene, LCAO-MO-SCF calcs., MODPOT, VRDDO and MODPOT/VRDDO procedures 77−71742
cyclopropane, γ-ray Compton profile meas., MO calcs., rel. to propene 77−10706
cyclopropane, electron correlation, double SCF method 78−17575
cyclopropenyl radical and anion, planar, E state pot. surfaces, CI and SCF calcs. 78−5155
cyclopropyl chloride, ab initio SCF-MO calc., electronic and mol. struct. 78−25425
deoxyhaemoglobin, porphin-Fe-imidazole system, SCF-LCAO-ASMO and CI calcs. of low-lying multiplets and excited states 80−94155
diagrammatic review and implications, appl. to ferromagnetism 77−74313
diamagnetic susceptibility, Curie law, SCF calcs. *(Russian)* 78−64183
diamond, (100) surface states, SCF extended tight-binding method 77−47881
diamond, (111) surface states and relax., modelling and using mol. SCF calcs. 78−39186
diamond, cluster, electronic struct. of deep levels, LCAO, SCF method 79−82555
diamond, electron density, bulk and surface atoms, from ab initio model calcs. 79−4590
diamond, five-atom clusters, unrestricted Hartree-Fock calcs. 77−11866
diamond, tetrahedrally bonded valence crystals, SCF perturbation theory appl. 79−37658
diatomic molecules, ab initio calcs., book 78−90080
diatomic molecules, homonuclear, individual orbital contribs. to SCF virial 79−3349
diatomic mols., one electron props., SCF-Xalpha scattered wave method 80−83279
diatomic systems, Penning and assoc. ionisation, correl. diagrams calcs. 77−50521
diazines, LCAO-MO-SCF calcs., MODPOT, VRDDO and MODPOT/VRDDO procedures 77−71742
diazoles, LCAO-MO-SCF calcs. MODPOT VRDDO and MODPOT/VRDDO procedures 77−71742
1,1-dichlorocyclopropane, ab initio SCF-MO calc., electronic and mol. struct. 78−25425
difluoromethane, ionisation energies, SCF Xα calcs. 77−14360
diformamide, torsional pot. barriers, ab initio and partition of energy methods 77−88588
dihydroquinoxalinediones, conjugated mols. electronic struct. and geometry, Hartree-Fock instability 80−69055
dihydroxycarbene, singlet and triplet state rot. pot. surfaces 80−32627
diimide, trans-cis conversion in lowest excited states, SCF calcs. 78−46284
dimethyl ether, internal rot., struct. relax., ab initio SCF calcs. 78−90077
dimethylether, ab initio SCF calcs., force field, IR and Raman intensities 77−79601
dimethylether, equilib. struct., ab initio SCF calcs. 77−3265
dipyridylethylenes, photoelectron spectra, conformation, SCF LCAO calcs. 77−79651
Dirac-Fock theory, multiconfig., relativistic SCF method, appl. to open shell ats. 77−3282
direct orbital optimisation for MC SCF theory by unitary transformations 80−87049
discrete variational Xα cluster calculations, applic. to metal clusters 78−90332
dislocations, continuously distributed, kinetic eqns. in SCF approx. *(Russian)* 79−14806
DNA, proton transfers between base pairs, LCAO SCF all-electron PRDO method 78−80829
double excitation wavefunctions, multiconfigurational SCF method 77−10604
doublet and quartet states, abstraction reactions, pot. energy surfaces calcs. 78−31627
dynamical damping in ab initio MO SCF calcs., energy minimisation method 80−18777
education, one-dimens. many body model with two- and three-body forces, exact Hartree soln. 79−9065
effective convergence to complete orbital bases and at HF limit through systematic Gaussian primitive sequences 80−14065
eigenvalue independent partitioning and direct minimisation of SCF theory 77−26970
eigenvalue sum rel. to total SCF energy for ats. and mols. 79−9993
elastic scattering, reson. width, stabilisation method, variational calc. 77−19011
electron affinity, MNDO semi-empirical SCF-MO calcs. for atoms, mols., negative ions 78−74578
electron affinity, variation-perturbation approach 77−54513
electron correlation, double SCF method 78−17575
electron density at nucleus, press. depend., elements Ag to Te, Hartree SCF calcs. 78−56411

SCF calculations continued
electron exchange and correlation phenomena, effect of local electron speed 79−95356
electron gas, quasi-one-dimensional, pair correl. function and plasmon dispersion curve 77−62851
electronegativity, spin-orbital, and catalytic activity 78−73078
electronic structure calcs., self-consistent, accelerating convergence of iterative process 80−87037
electrostatic interactions in liquid state, effect on frontier orbitals and chem. reactivity 80−84046
EM wave transient scattering, time domain method 80−38655
energy functional, direct minimisation in LCAO-MO density matrix formalism 78−5118
equations of state of crystals with strong sixth-order anharmonicity 80−92637
ethane$^+$, stability and struct., CI-SCF ab initio calc., Franck Condon anal. 77−54575
ethane, multipole moments and polarisabilties, SCF calcs. 80−5471
ethane, rot. barriers, MS-SCF-X_α calcs. 80−106267
ethene, dipole polarisability, finite-field SCF MO calcs. 80−83255
ethene, general valence force field, ab initio calcs., IR and Raman intensities 77−71746
ethyl radical, geom. struct., Hartree-Fock calcs. 78−62722
ethylene, and radical ion, SCF-MO calc., bonding and electronic struct. 77−38610
ethylene, C atom pyramidalisation rel. to bonding, ab initio SCF calcs. 79−93936
ethylene, C-C double bond rot. barrier, ab initio open-shell restricted SCF calc. 78−1099
ethylene, dimer interaction, lattice energy, multipole expsn., at.-at. pots. 78−9218
ethylene, excited states, continuum embedded, SCF-stabilisation approach 78−928
ethylene, mol. and cluster Auger spectrum calc., SCF core-valence-valence spectra 80−48045
ethylene, multipole moments and polarisabilties, SCF calcs. 80−5471
ethylene, planar, V-N vertical transition, SCF and correlation energies 77−68032
ethylene, planar dissociation, electronic rearrangement, states, bonds, ab initio multiconfigurational SCF calcs. 80−27937
ethylene, polarisability, nonlinear elec. susceptibility, SCF calcs. 80−95547
ethylene, quasidegeneracy and effective Hamiltonians, canonical transformation cluster expansion formalism 80−52888
ethylene, self-consistent many-body theory, self-energy effect 79−63901
ethylene, vertical, $N(^1A_g)$, $T(^3B_{1u})$, $V(^1B_{1u})$ states, large scale CI calc. 78−70752
ethylene+cis-N_2H_2, chem. reaction, intermediate geom. calcs. 78−35655
ethylene+Cl_2(Br_2) complex, intermolecular interaction and struct. SCF-MO-LCAO CNDO/2 calc. 78−58763
ethylene+H⇌ethyl radical, pot. energy surface, analytic function 79−11779
ethylene glycol, IR spectra, ab initio calcs., vibr. anal., conformations of isotopic modifications 78−5210
ethylene molecules, long range forces in multipole expsn., ab initio calcs. 78−9219
ethylene ozonide, ab initio gradient and MC SCF calc., conformational anal. 80−83290
ethylene radical cation, electronic states assignments, ab initio SCF CI calcs. 77−10584
ethylene-LiF complex, molecular orbital calcs., Li bonding exam. 78−29745
ethynol, ab initio calc., energy levels and geom. struct. of C_2H_2O isomers 78−62716
ethynol, struct., isomerisation, ab initio SCF MO calcs. 78−41941
ethynyl radical, vertical electronic spectrum, CI calcs. 77−34656
excimer laser, electronic structure, pot. energy curves, radiative transition probabilities, quantum mech. calcs. 79−10284
excitation energy, validity of excited minus ground state calcs. using HF/pair correlation 77−38620
excited state, applic. to hole states of free atoms 77−10610
excited states, perturbation and SCF calcs. 80−102455
excited states of closed-shell systems, SCF scheme 79−6885
exponential transformation, quadratically convergent SCF procedure, appl. to closed shell ground states 80−47875
extrapolation procedure 78−82604
fermion one-dimensional many-body system 77−62699
ferroactive crystals, geometric effects 79−38493
ferrocene, metal to ring distance, ab initio MO SCF calcs. 80−47870
ferrocyanide ion, electronic struct. and related props., calc. by SCF $X\alpha$-scattered wave method 77−15809
ferroelectric semiconductor phase transitions 77−52028
first-row atoms, SCF calcs. using cusped-Gaussian basis sets, polarisation effects 80−74118
first-row transition metal ions, core ionised states, ΔSCF MO calcs. 80−78523
floating orbital geometry optimisation with floating outer-shell basis functions 80−95517
fluorene conjugate bases, chem. shift, ring-current and excess-charge effects, semi-empirical calc. 78−33523
fluoro sulphuric acid methyl ester, rot. isomerism 78−86964
fluoroethyl radical, unimol. dissoc., pot. energy characts. and energy partitioning calcs. 80−45488
fluoroform, quadratic force fields, MOCIC pot. functions calcs. 80−5475
fluoroformaldehyde, pot. energy surface characts., substitution effect 80−89505
fluoromethanes, ab initio calcs. of K-shell ionisation potentials 77−18784
fluoromethanes, GVFF from SCF ab initio energies 78−74635
fluoromethanes, ionisation pots., SCF-multiple scatt.-$X\alpha$ calcs. 78−5141
fluoromethanes, vibr. spectra, force consts. and geom., SCF ab initio calcs. 78−62785
fluoromethanes, $X\alpha$ calcs. using ΔSCF formalism 79−6861
formaldehyde, and cation, vertical proton affinity in singlet and triplet states 78−90079
formaldehyde, core ionisation, valence orbital relax. calcs. 78−5135
formaldehyde, electronic struct., dipole moments, mol. polarisability, force fields, ab initio calcs. 80−78531
formaldehyde, MC SCF method in full and pseudopot. versions 77−83487
formaldehyde, mol. Rydberg S←S and S←T transitions, semi-empirical SCF MO calc. 80−91453

SCF calculations continued
formaldehyde, orbital contribs. to relax. energies accompanying core ionis., ΔSCF HF calcs. 78−82642
formaldehyde, photodissoc., pot. energy surface features 79−79271
formaldehyde, semi-empirical excited state Morokuma's EHP calc., geometry and order of states 78−46256
formaldehyde, X^1A_1, a^3A'' and A^1A'' states, SCF and CI ab initio calcs. 79−36545
formaldehyde+formaldehyde, medium distance interaction, SCF LCAO MO, supermol., perturbation and MCF calc. 79−837
formaldehyde.H_2S(H_2O) complexes, ab initio SCF MO calcs., binding energy dispersion contrib. 80−27967
formamide, comparison of theoretical and experimentally determined electron density distrib. 78−82634
formamide, force consts. and dipole moment derivatives, ab initio MO calcs. 80−95521
formamide, hydration by H_2O mol., point charge model 77−34569
formamide+formamide, medium distance interaction, SCF LCAO MO, supermol., perturbation and MCF calc. 79−837
formamide dimer, hydrogen bond, ab initio MO calcs. 78−58588
formamide-glyoxal, charge transfer theory, Mulliken population, ab initio calc., multiconfiguration scheme 80−106392
formic acid, conform. hypersurface determ. and analysis 80−1078
formic acid, cryst. binding, ab initio MO SCF calc. 79−37657
formic acid, dimer, config. and energy, ab initio MO SCF calc. 79−37657
formic acid, dimerisation energy, non-empirical MO SCF calc. 79−37656
formic acid, lattice energy, non-empirical MO SCF calc. 79−37656
formic acid dimer, hydrogen bond, ab initio MO calcs. 78−58588
formyl-triglycyl amide-H_2O, analytical pot., ab initio calc. 79−48206
fourth row element ions, relativistic Dirac-Fock-Slater orbital binding energies, one-electron transition energies 79−25778
frozen core AO approx. in Roothaan's MO LCAO SCF method 77−3264
fully coupled SCF perturbation theory in matrix form, simultaneous perturbations 77−34548
fully symmetric nonlinear theories, Green's function methods, SCF theory 77−61180
fulvene, ground and excited states, electronic correl. and struct. 79−26898
g-shell nuclei, charge distrib., self consistent calc. *(Russian)* 77−38234
Gaussian geminal basis set optimisation, with crude SCF reference state 77−57885
Gaussian-70 MO program, LCAO-SCF eqn. soln., population anal., appl. 78−70742
general SCF coupling operators, arbitrariness 80−99439
generalised Brillouin theorem and generalised forces in SCF and MC SCF theories, and H-F limits 77−14366
generalised SCF transition operator 78−41925
geometry optimisation with explicit inclusion of electron correl. 80−37748
glyoxal-alkali (alkaline earth metal) complex, ab initio MOSCF calc., chelate effect 79−31386
guanine, tautomeric forms protonation, ab initio HF Roothaan SCF calcs. 80−78534
guanine tautomers, relative stabilities, nonempirical MO calcs. 80−21442
H-bonded and H-like bonded systems 78−9068
halogen atom, 1s hole states, ionisation, ab initio SCF calcs. 78−17568
halogen compounds, chem. bond, MO LCAO SCF calcs. 79−41104
halogen diatomic molecule, 1s hole states, ionisation, ab initio SCF calcs. 78−17568
HAM/3 formalism, semiempirical, energy expression derivation 80−903
HAM/3 semiempirical MO theory, correl. energy, self-repulsion 78−13416
HAM/3 semiempirical MO theory, SCF method 78−13413
HAM/3 semiempirical MO theory, unoccupied orbitals, excitation energies and electron affinities calcs. 78−13415
Hartree, anal. of dilute polymer solns. 80−5648
Hartree Fock calcs., NN interactions, and results of appl., book contrib. 79−75880
Hartree iterative solution of general SCF eqns., convergence criteria 77−61675
Hartree problem, 1 dimens., exactly soluble (undergraduate level) 77−23418
Hartree problem, iterative diagonalisation soln. 79−6829
Hartree-Fock theory, constraints, stability 77−57870
Hartree-Fock wave functions, convergence in Roothaan's SCF eqns., 'level-shifting' method 78−41920
heat of reaction, basis set of effect and approx. natural orbitals in SCF CI GTO calcs. 78−76904
heavy ion+atom collisions, mol. M-X-rays, self-consistent relativistic HF-Slater many electron correl. diagrams 77−14567
heavy ion-nucleus reactions, time dependent SCF theory 79−17932
Heisenberg antiferromagnet, AFMR freq. temp. depend., integral peak intensities *(Russian)* 80−54951
helical systems, energy band calcs. using Hartree-Fock SCF-LCAO formulae 78−10329
Hellmann-Feynman theorem for open-shell and multiconfiguration SCF wave functions 79−89591
heterocyclic conjugated compounds, electronic struct., spectra, ionisation pot., INDO-CI LACO-MO-SCF calcs. 79−54834
heteronuclear molecules, alternant mol. orbitals energies, generalised formula 79−6867
heteroorganic molecules, all-reactive-electrons closed-shell SCF-CI MO calcs. 79−36541
hexafluoroethane, rot. barriers, MS-SCF-X_α calcs. 80−106267
hexatriene, polarisability, nonlinear elec. susceptibility, SCF calcs. 80−95547
trans,trans-1,3,5-hexatriene, valence electronic excited states, SCF ab initio GVB and CI calcs. 79−31423
HF wavefunctions, restricted and unrestricted, convergence problem 77−418
hydrides, third row, electron binding energies, one-centre expansion method 77−6677
hydrocarbon, conjugated, nonlinear susceptibility, extended basis set calcs. 79−27107
hydrocarbons, Compton profiles, deviations from bond additivity, rel. to strain energy 79−81240
hydrocarbons, liq., Compton profiles, bond additivity 80−93423

SCF calculations continued
hydrocarbons, small, electron momentum distribs. in π orbitals from (e,2e) expts. 80−14239
hydrocarbons proximity and conform. effects, ^{13}C chem. shifts at γ position, INDO computations 77−50451
hydronaphthyl radicals embedded in naphthalene cryst., optical transition energies and ionisation energies 80−78595
β-hydroxy acrolein, lower excited states, electronic struct. and H-bonding, ab initio SCF and CI calcs., photochemical mechanism 80−83278
β-hydroxyacrolein, intramol. H bonds, orbital and transition energies, ab initio SCF and SCF CI calcs. 77−14345
para-hydroxyaniline, mol. complex., electronic struct., basis set and correlation effects 80−91436
hydroxymethyl cation, geom. and electronic struct., ab initio SCF calc. 79−76331
2- and 4- hydroxypyridine tautomers, ab initio SCF LCAO MO calcs. 79−81154
hyperpolarizability, freq. depend., time depend. HF eqn., second order LCAO SCF pertubation theory 79−31388
inert gas compounds, chem. bond, MO LCAO SCF calcs. 79−41104
inorganic binary iono-covalent compounds, cryst., inorganic static effective charge calcs. *(French)* 80−2331
interconversion pot. energy surfaces, geometries, electronic structs. 78−35660
intermolecular energies calculation from delocalised pictures, artifacts and elimination 80−18899
intermolecular forces, ab initio calcs. applicability and accuracy 80−18898
internal conversion calc., Hartree-Fock-Slater and Hartree-Fock models 80−18238
intrinsic reaction coordinate ab initio SCF calc. method 77−48626
invariance requirements in approx. SCF MO theory 79−6824
inversion geometry, ab initio SCF calcs., basis set effects 80−78532
ion clusters, 3-body pots., SCF energy partitioning calcs. 80−18953
ionic crystal, electronic struct., SCF calc. method 79−56125
ionisation potential, vertical, inner and valence shells, ab initio SCF MO CI perturbation calc. method 78−74800
isomerisation, model reaction, SCF-SI theory calcs. 80−23399
isotope exchange reactions, equilib. consts., adiabatic correction, electron correl. effects 78−88626
iterative sequences, convergence accel. 80−91435
k-particle generalisation and new generalisation of SCF type theories 80−102432
ketene, ab initio calc., energy levels and geom. struct. of C_2H_2O isomers 78−62716
ketocarbene-ketene rearrangement, reaction path, ab initio calc. 78−20008
Koopmans atomic valence electron ionisation energy, $1/Z$ expansion method, reorganisation corrections 78−78623
β-lactam antibiotics, ab initio SCF-MO-LCAO calcs., amidic bond breaking, methoxy substitution effect 80−78533
Landeu model, critical multiple correlations 79−75440
large complex systems, mixed electrostatic-quantum chemical approach 79−89605
LCAO, atomic d orbitals in basis sets, symmetry criterion 79−45622
level shift technique, unconditional convergence in SCF formalism 77−50339
light atom molecules, general quadratic force fields, semiempirical MOCIC calcs. 80−5474
light atoms, large-q form factors, calcs. for ^3Li to ^{19}K, ^{22}Ti 78−58589
limited CI with optimal generalised combination of SCF MO symmetry subsets 77−42246
limited MC SCF theory 79−36537
linear triatomic hydrides, ab initio SCF CI electric dipole moments 79−31410
lipid, monolayer, backfolding, self-consistent field theory 79−8451
liquid crystal, nematic, phase transform. *(Russian)* 77−89528
liquid crystals, mesomorphic state formation mechanism and molecular struct. correlation 80−54128
lithium acetylene, SCF MOGO calc. of electronic struct. 77−34556
lithium ethylene, SCF-MO calc., bonding and electronic struct. 77−38610
liver alcohol dehydrogenase, proton relay system, SCRF PCE theory, CNDO/2 calcs. 80−85325
LNDO/S, semiempirical SCF-CI method for calc. ionis. pot. and electronic transition energies 79−18117
localised fixed orbitals, construction, pseudopot. method using multi-config. SCF theory 77−14334
localised orbital construction for calcs. using multiconfigurational SCF methods *(Russian)* 78−922
lone pair localised MOs, energy contribs. and second moments in 10-electron hydrides 77−14341
magnetic impurities and Kondo effect, theoretical model 79−33455
magnetic ordering in superconductors, SCF model *(Russian)* 79−15253
magnetic system, spin correlation function, dynamic SCF approx. 79−7952
many-body perturbation theory, modified pots., 3- and 4-body contribs. 77−88376
many-shell SCF theory, convergence, first order perturbation anal. 79−9999
maximum overlap mol. orbitals versus ab initio HF-SCF-MO calc. dipole energy 78−9070
MC-SCF equations, restricted, open- and closed-shell, soln. algorithm 79−63891
MC-SCF theory, modified one-electron Hamiltonian, iteration convergence 79−6871
MC-SCF theory, orthonormality-constrained orbital optimisations 78−86766
MCSCF and CI wave functions, two-particle density matrix and graphical unitary group approach 80−63558
MCSCF functions optimisation, generalised Brillouin theorem appl., CI calcs. 77−67960
MCSCF method improvement 80−52857
MCSCF procedures, 2nd- and approx. 2nd-order, convergency, appl. to Be and O_2 79−93907
metal, d-band, generalized pseudopotential theory, density functional formulation 78−10389
metal, simple, vacancies and vacancy clusters, electronic struct. 79−11077
metal atom cluster compounds, bonding calc. using d-orbital overlap model, SCF-Xα-SW calc. 80−102595

SCF calculations continued
metal porphin, triplet state, spin density and zero-field splitting, PPP-SCF-CI calc. 79−68200
metal surface, mol. chemisorption, self-consistent calc. 79−95260
metal surface, narrow-band, self consistent model calcs. of electronic states 77−85295
metal surface, work function, change-in-SCF theory 78−84282
metal-diamond interface, Schottky barrier theory, ionicity depend. 78−52086
metallic ultrathin filaments, dielectric and superconducting fluctuations, Peierls transition *(Russian)* 80−65742
metals, compressiblities, general pseudopotential approach 80−54631
metals, free-electron-like, electron struct. of single and interacting H impurities 79−95365
metals separated by dielectric, electronic component of metal-metal interaction force, calc. 78−52056
metals with $Z \leq 49$, supercond. props. 77−66221
methane, ^1H and ^{13}C mag. shielding, He and methane intermol. effects 78−37571
methane, and -t_1, β-decay, ab initio SCF MO calcs. 77−71842
methane, bond dissociation, MCSCF LMO calcs. 77−57886
methane, core 1s shakeup study, XPS and Xalpha calcs. 80−69064
methane, core ionis., single orbital relax., LCAO MO SCF calcs. 78−29739
methane, elec. dipole polaris., near Hartree-Fock value, using EFV GTOs 77−88591
methane, freq. depend. polarizability, LCAO SCF perturbation theory 79−31387
methane, H-X bond position, correlation with electronegativity 78−9069
methane, localised orbital construction for calcs. using multiconfigurational SCF methods *(Russian)* 78−922
methane, mol. and cluster Auger spectrum calc., SCF core-valence-valence spectra 80−48045
methane, mol. nuclear spin-spin coupling, ab initio SCF perturbation theory 78−33525
methane, multipole moments and polarisabilities 79−85910
methane, orbital relax. energy for single and double ionis. from valence shells 80−106253
methane, pot. energy curves, Monte Carlo and SCF LCAO MO calcs. 80−63526
methane, SCF calcs. including polaris. functions 80−87034
methane $+H_2O$, pairwise interaction pot. function, ab initio SCF MO calc. 79−22786
methanol, ab initio calcs. of K-shell ionisation potentials 77−18784
methanol, equilib. struct., general valence force field, ab initio calcs. 77−3265
methanol, field ionisation, geometry changes, INDO-SCF-MO calc. 77−38614
methanol, polymers, structs., binding energies, LCAO SCF MO calcs. 77−83498
methyl chloride, ab initio SCF-MO calc., electronic and mol. struct. 78−25425
methyl group, conform. problems, correlation effects 79−97999
methyl halides, mol. force field at SCF ab initio levels, quantum-mechanical calc., LCAO-MO method 80−106319
methyl halides, mol. force fields, IR intensities, and vibr. props. 80−47879
3-methyl lumiflavin in soln., optical absorption, theory 78−74569
methyl radical and anion, electron affinity determ., ab initio SCF and CI calcs. 78−5149
N-methylacetamide, vertical excitation energies, ab initio SCF CI calcs. 79−45647
methylacetylene, quadratic force fields, MOCIC pot. functions calcs. 80−5475
methylamine, affinities for $H^+(Li^+)(K^+)(CH_3^+)$, ab initio SCF calculations 80−102443
methylamine-t_1-NH_3, β^-decay effect on H-bond, ab initio LCAO SCF MO calc. 78−76894
methylene, 2^1A_1 state, CI and multiconfiguration SCF calc. 79−10052
methylene, geometry, SCF and CI calcs., basis set effects 78−62715
methylene, photoelectron spectra, singlet and triplet state calcs. 78−42127
methylene, singlet-triplet separation, configuration interaction study 78−13438
methylene ion, pot. energy surfaces of excited states, ab initio GTO SCF CI calcs. 78−58602
methylene manganese, electronic struct., equilib. geometry, ab initio SCF calcs. 77−71747
methylene peroxide, multiconfig. SCF CI calcs. 80−18803
methylene radical anion and dimer, semiempirical CNDO/2 and nonempirical SCF calcs. 77−79535
methylenimine, $n \rightarrow \pi^*$ transition, ab initio SCF MO CI calc. 78−58584
methylnitrene, symmetry restricted multiconfiguration annihilation of single excitations calcs. 78−62695
MNDO semiempirical calcs. accuracy rel. to current MO methods 80−47893
mol. and cluster Auger spectrum calc., SCF core-valence-valence spectra 80−48045
molecular, geometry optimisation in ab initio SCF calcs., appl. of Hellmann-Feynman force 79−49927
molecular aggregates, nonvalidity of SCF vibronic spectra calcs. 77−10655
molecular consts., di and triatomic mols., mol. model pot. calcs., approx. 77−65420
molecular crystal, action of external forces on mesogenic struct. form. 80−2147
molecular diamagnetic susceptibility, interatomic charge transfer in diatoms, mol. second moments, additivity formulas 78−70961
molecular dynamical damping, ab initio calcs. 79−54762
molecular electric polarisabilities, hyperpolarisabilities, nonlinear optical coeffs., MNDO calc. 79−13641
molecular electronic structure, semiempirical CNDO method, calc. progam 78−86782
molecular electronic structure, solid state approach 80−9508
molecular electrostatic potentials influence of polarisation functions 79−839
molecular energy gradient, ab initio HF program 79−89606
molecular excited states, restricted SCF method calcs. 77−88405
molecular excited states, SCF calcs. using Binkley-Pople-Dobosh formalism 77−6694
molecular excited states, SCF wavefunctions 78−90099

SCF calculations continued
molecular force constants, SCF method with fixed orbital basis, H_2 mol. appl. *(French)* 79−94107
molecular force fields, MINDO/3 semiempirical SDF MO calc. 79−76408
molecular geometry, basis set effect and approx. natural orbitals in SCF CI GTO calcs. 78−76904
molecular ionisation potential, quark influence, ab initio SCF calcs., appl. to H_2O and SO_2 79−10058
molecular liquid, dielectric solvent effects, quantum chem. calcs. 77−14375
molecular multipole magnetisability, mag. shielding, multiple SCF perturbation theory 77−34549
molecular nuclear spin-spin couplings between ^1H, ^{13}C, or ^{19}F, LCAO-MO-SCF-MINDO/3 approx. calcs. 79−94019
molecular orbital and energy level calc., program of SCF-Xα scattered wave method 78−50453
molecular orbital methods, speed and accuracy, comparison of methods 79−41106
molecular orbital SCF and total SCF energies, approx. relation 78−5123
molecular orbital theory, sum rules for circular dichroism in spectroscopy 78−58059
molecular orbitals, counterintuitive orbital mixing, SCF perturbation methodology 78−74564
molecular polarisability finite-field calcs., SCF and Galerkin treatments 77−54497
molecular quadratic potential functions, calc. MO constraint of interaction coordinates 78−74631
molecular spinors from the quasi-relativistic pseudopotential approach 79−97963
molecular static polarisability, ab initio SCF wave functions 80−74106
molecular symmetry, electronic energy gradient rel. to nucl. coords., HONDO calcs. 78−66463
molecular systems, improved SCF method in representation of basis expansions 78−17567
molecular systems, saddle points and min. energy paths, constrained simplex optimisation procedure 80−42943
molecule, electron pair distrib. functions, SCF CI wavefunctions 78−41966
molecule, method of calc. from fragments 79−63905
molecule, numeric MCSCF method, unicentre expansion 79−45623
molecule, orbital energies rel. to total energies, approx. calc. 77−30764
molecule, orbital rel. to total SCF energies, HF SCF approx. formula 78−21837
molecule, orbtial and total SCF energies, Ruedenberg's formula evaluation 78−37537
molecule, single spin-config. singlet states, wavefunctions, energies 77−83505
molecule, total energy of molecule, local spin density functional approx., LCAO SCF calc. 79−93920
molecule, valence states and binding energies 77−30757
molecule with second-row atoms, bond functions in SCF calcs. 77−14349
molecules, complete active space method comparison of super C I and Newton Raphson scheme 80−47904
molecules, energy partitioning scheme for ab initio SCF calc. interpretation 79−93918
molecules, interacting, rigid, HF, self-consistent nonorthogonal group function approx. 79−31430
molecules, multiconfigurational wave functions, optimization scheme 77−57889
molecules, natural orbitals, Brillouin-Levy-Berthier theorem, multiconfigurational SCF optimisation 80−27936
molecules, relations between matrix elements in relativistic Hartree-Fock-Roothaan theory 79−36521
molecules, relativistic Dirac-Fock multiconfig. SCF calcs. 80−99455
molecules involving B and C atoms, self-consistent charge calcs. of core-electron binding energy shifts 80−69084
molybdenum formate, mol., Hartree-Fock instability of SCF wavefunctions 80−9492
dimolybdenum tetraformate, metal-metal bond energy, SCF-Xα-SW calcs. 80−78538
monofluoromethane, force consts. and IR intensities, ab initio SCF finite difference method 78−86783
monothioformate anion, protonation site, ab initio SCF calc. 79−47894
Mott transition in the presence of impurities, Hubbard model and SCF anal. 80−10878
muffin-tin approximation in mol. calcs. and solid state 77−409
multi-config. SCF super-CI calc., density matrix formulation 80−78547
multi-configuration Hartree-Fock program 78−50471
multiconfiguration Dirak-Fock program, appl. to Ba X-ray levels and 5p excited spectra 80−47865
multiconfiguration Hartree Fock problem, finite-difference Newton-Raphson soln., He 1s2s^{1}S state appl. 77−6663
multiconfiguration SCF theory, hierarchy eqns. for reduced transition operators 77−54516
multiconfiguration SCF theory, modified one-electron Hamiltonian 78−33412
multiconfiguration wave functions, optimisation 78−33411
multiconfigurational Hartree-Fock procedure, second-order, 2-electron integral transformations 80−87045
multiconfigurational paired excitation SCF theory 77−42224
multiconfigurational SCF method, yielding Fock-like operator 79−36540
muonic atoms, Dirac-Fock method 78−74805
naphthalene, cryst., radiation induced radicals, optical absorpt. bands, SCF-CI MO calc. 79−91463
naphthalene, dipole polarisability, finite-field SCF MO calcs. 80−83255
naphthalene, inclined dimers, transition energies and moments, excitation energy, four-electron MO-CI treatment 77−42237
naphthalene, LCAO SCF MO CI calcs., integral approx. scheme using semiorthogonalised orbitals 79−6873
naphthalene, triplet excimer conformation, σ-π interaction transitions 77−6701
1,4-naphthoquinone, and derivatives, singlet electronic transitions, SCF MO CI calcs. 79−49948
negative ions, electronic structure, stabilisation calcs. using big mol. Gaussian SCF/CI program 79−18121
neopentane, spherical Compton profile, rel. to diamond C-C bond, SCF calcs. 77−75232
neutral molecules, total energy and eigenvalue sums 78−21835
nitrofuranes, substituted, electron affinity, HAM/3 calc. 79−27109
nitroimidazoles, substituted, electron affinity, HAM/3 calc. 79−27109
nitromethane, ab initio SCF MO calcs. of geom. and bond energies 79−31381
nitromethyl anion, ab initio SCF ab initio MO calcs. of geom. and bond energies 79−31381
nitrosomethane, ground state and nonvertical n-π^* excitation energy calcs. 80−18804
NMR coupling constant, SCF INDO calc., zero overlap approx. *(French)* 79−50047
nuclear level densities 77−2909
nuclear particle-hole states, microscopic self-consistent calc., ^{16}O levels 77−67713
nuclei acid phosphate group, analytical atom-pair pot., SCF-LCAO calc. 79−70516
nucleic acid bases, Zn^{2+} binding, ab initio SCF (pseudopot.) calcs. 80−12052
octane, first-order props. of simulated ab initio molecular orbital wave functions comparison with SCF wavefunctions 79−41094
one-dimensional electron-phonon system, dynamics, Frohlich model 77−15781
one-dimensional molecular crystals, electronic struct., mol. orbital theory 80−54588
one-electron Hamiltonian method applied in SCF theory to states with open shell 80−23302
open shell orbitals, iterative process 78−90066
open shell SCF MO LCAO method in unrestricted Hartree Fock formalism 79−31389
open shell theory 78−94179
open-shell SCF calcs. with model pot. method 77−57875
open-shell SCF secular eqn., iterative algorithm soln. 80−52868
open-shell SCF theory, one-electron Hamiltonian method 78−90055
open-shell system, polarisability and mag. susceptibility calc. by SCF and CI method 80−99443
orbital equations, closed-shell, open-shell, and multiconfig., orthogonal gradient soln. method 79−36503
orbital functional theory for exchange and correl., local spin density approx., self interaction correction 79−76347
organic carbonyls, all-reactive-electrons closed-shell SCF-CI MO calcs. 79−36541
organic compound, substituent π-conjugative effects, ab initio calcs. 79−45633
organic molecules, core ionisation and electronic redrganisations, LCAO MO SCF calcs. 79−18115
organic molecules, quadrupole moments, dipole quadrupole A and C polarisabilities, perturbation theory anal. 80−27934
organic molecules, relax. phenomena, following core ionis., LCAO MO SCF calc. 79−10030
organic system, nonlinear second-order optical susceptibility 80−9947
organolithium cpds., ab initio SCF-MO calcs. of C-Li bond character 77−410
oriented molecules, inelastic low energy electron scatt. 78−72653
oxalic acid, cryst. binding, ab initio MO SCF calc. 79−37657
oxiranylidene, struct., isomerisation, ab initio SCF MO calcs. 78−41941
oxirene, ab initio calc., energy levels and geom. struct. of C_2H_2O isomers 78−62716
ozone, $^1A_1$ ground state, dipole moment function, ab initio SCF and CI calcs. 80−32628
path-integral approach to time-dependent self-consistent field theories 79−59023
Peierls one dimensional model, exact solution, electron spectra, static lattice deformation *(Russian)* 80−70609
pentofuranosyl nucleosides, isomeric, ^1H NMR coupling consts., SCF FPT INDO approx. calc. 80−14156
peptide architectural units, ab initio SCF MO calcs. 78−96004
periodic systems electronic struct., LCAO SCF ab initio HF calcs. method 80−65419
perturbation theory, variable basis sets, numerical finite perturbation vs. analytic approach 79−59330
perturbational MO analysis of ab initio SCF-MO wave functions 77−57867
perturbed energies, 2nd order, coupled HF iterative procedure, geometric approx. 79−9991
phenol-phenyl complex, electrostatic mol. pot. contour maps, MODPOT and VRDDO calcs. 80−102463
phosphate-H_2O-Na^+ system, interactions 77−30773
photochemical reaction, avoided crossings in excited states potential energy surfaces 78−76881
photoemission relaxation energies, non-relativistic ΔSCF-optimised HFS calcs. *(French)* 77−36357
photoionisation cross-section, molecules, orthogonalised-plane-wave approx. 79−41202
photon energy band, low energy photon diffr. 79−78795
photosynthetically relevant mols., electronic structural props. 80−16902
phytochrome chromophore, models, absorption wavelengths and oscillator strengths calc. 77−81469
pinacyanol dye, adsorbed on CdS substrate, aggregation effect on mol. electronic states 80−37757
PMDA, ab initio SCF MO wavefunctions for ground and excited states 79−10028
polar molecule, excited state MCSCF wave functions, BeO appl. 80−47916
polar molecule clusters, 3-body pots., SCF energy partitioning calcs. 80−18953
polarisability of conjugated hydrocarbons and aromatics, linear and dynamic polarisability 79−98242
polarization Green's function with multiconfiguration self-consistent-field reference states 80−37724
poly-ynes, struct., vibr. freqs., ionis. energies, MNDO calc. 77−88390
polyacenes, electronic transition bands, Franck-Condon factors, PPP SCF MO/CI calc. 78−33430
polyacenes, spectra, correlation effects 79−81199
polyacetylene, pure and doped, electronic props. from one-dimens., tight-binding LCAO-SCF-MO calcs. 79−56123
polyacetylenes, fluorinated, electronic struct., tight-binding LCAO-SCF-MO calcs., prep. 80−70591
polyacrylonitrile, electronic struct., reactivity, SCF CNDO calcs. 77−50580
polyatomic molecule, SCF-SI theory applic. to coupled vibr. motion 80−23399

SCF calculations continued
polyatomic molecules, relativistic symmetry spinors, LCAO-SCF theory 77−420
polyatomic molecules, relativistic symmetry spinors, LCAS-SCF calcs. 77−419
polyatomic molecules, triplet states, var. and perturbational calcs. 77−61680
polyatomic system, large, ALGOL-60 program for MO LCAO calcs. in Mulliken-Rudenberg approx. 77−88388
polyatomic systems, MC SCF computation scheme 79−10039
polybutadiene, electronic struct., reactivity, SCF CNDO calcs. 77−50580
polycrystals, single phase, stress strain relations by X-ray diffraction *(Russian)* 80−5999
polycyclic aromatic hydrocarbons, diamagnetic susceptibility NCHF (SCF-PPP) calcs. 77−6686
polydiacetylene backbone sequence, electronic structs., unrestricted HF approach 78−63975
polydiacetylenes, electronic struct., cyclic vs. linear models 80−54587
polydiacetylenes, electronic structure, bond length variations effect, Xα SCF calc. 78−5378
polyene, deformed excited state, bond length rel. to bond order 77−75071
polyene, linear, band gap calcs. 77−31969
polyenes, linear, two-photon absorptivities, SCF-PPP-CI calcs. 79−31631
polyethylene, deformation, Hartree-Fock SCF calcs. 80−18949
polyethylene, electronic band struct., tight-binding approx. with MNDO 77−89691
polyethylene(-d_4), vibr. freqs., MNDO semiempirical SCF calcs. 78−1114
polyglycine, band struct., ab initio SCF LCAO calcs. 79−22874
polyisoprene, electronic struct., reactivity, SCF CNDO calcs. 77−50580
polymer chain, irregular, lattice distortions, SCF perturbation calcs. 78−6018
polymer chains, Coulombic contributions, LCAO-SCF-CO method, Fourier representations 80−32862
polymer excluded vol., SCF theories 78−70983
polymers, adsorption of molecules, Green matrix local impurity SCF calcs. 80−92778
polymers, connection between Yvon-Born-Green and Kirkwood hierarchies in SCF approx. 78−42882
polymers, electron problems by SCF method, HF matrix 77−79718
polymers with defects, energy bands, ab initio SCF crystal orbital calcs. 78−30884
polypyridines, photoelectron spectra, SCF LCAO calcs. 78−33551
porphin, MCD, LCAO MO SCR π-electron calcs., PPP approx. 78−9178
porphyrin a, MCD, LCAO MO SCR π-electron calcs., PPP approx. 78−9178
positive atomic ions, orbital SCF energies, rel. to total SCF energies 79−3350
positron+H(He), second-order nonadiabatic polaris. pot. for elastic scatt. 79−22836
potential energy first derivative, open-shell restricted HF and MC SCF calcs. 79−98004
prop-1, 2-dienyl radical, ab initio SCF HF MO calc., electronic struct. and one electron props. 77−42231
propene, γ-ray Compton profile meas., MO calcs., rel. to cyclopropane 77−10706
propene, force constants, SCF ab initio calcs. 77−34780
n-propyl radical, and propane, struct., ab initio calc. 79−98006
propyleneimine, circular dichroism, optically active Rydberg transitions 77−18952
protein architectural units, ab initio SCF MO calcs. 78−96004
protein internal charge transfer, ascorbic acid adduct model systems, SCF calc. 80−69072
protoporphyrin, MCD, LCAO MO SCR π-electron calcs., PPP approx. 78−9178
proximity-effect sandwiches, self-consistency conditions for two pair potentials 79−1646
pseudo pot. model Hamiltonian, spin-orbit splitting, intercombination and relativistic orbital reorganisation 78−25424
pseudopotential form factor determ., exchange interaction and correlation effects 80−49639
pyrazine, dimer interaction, lattice energy, multipole expsn., at.-at. pots. 78−9218
pyrazine, excited and N_{1s} ionised states, ab initio calcs. broken orbital symm. 80−27931
pyridines, monosubst., H_2O complexes, n-π* transitions, H bonding, MO theory 80−95550
pyrrole, excited state electronic struct., ab initio SCF and CI calcs. 78−78644
pyrrole, ground state, (π-π*) state, ab initio SCF CI calcs. 78−33438
quadratically convergent SCF procedure based on Newton-Raphson iteration procedure 79−59335
quark affinity to water molecule, centre expansion SCF calcs. 80−43213
quasi-relativistic SCF-MO-LCAO methods, CNDO and MWH appls. 78−41953
radical, small, isotropic hyperfine coupling consts., MINDO/3 calcs. 80−52894
random binary alloy, self-consistent theory of localisation 78−34805
relativistic atomic wave functions, Hartree-Fock calcs. 79−10009
relativistic self-consistent field theory for open-shell molecules 80−95518
roughening transition, self-consistent calc. of statics and dynamics 79−27939
row element ions 79−25778
Ruedenberg energy relation, deviations, theory 79−93909
Ruedenberg relation, in ab initio calcs. of at. and mol. SCF energies 79−89596
SCF-LCAO-MO calculation, semi-empirical, correct orthogonalisation of basis set 80−32613
SCF-Xα-scatt. wave calcs. for photoionisation cross sections and asymmetry parameters 80−63542
second-row atoms, SCF loge localised wave functions 78−41932
second-row hydrides, nucl. spin-spin coupling consts., ab initio calcs. 80−95647
self-consistency accel. procedure 80−78529
semi-empirical SCF-LCAO calc. including energy minimisation, GEOMO program 77−23428
semiconductor, deep transition metal impurity states, SCF CNDO cluster calcs. 80−100442
SCF calculations continued
semiconductor, defect electronic struct., SCF method 80−80208
semiconductor, electronic struct. of deep levels, LCAO, SCF method 79−82555
semiconductor in quantizing mag. field, plasma surface states of electrons 79−11195
semiconductors, deep levels, self consistent LCAO MO calcs. 80−29353
separated electronic pair functions, direct minimisation of energy functional, LCAO-MO SCF, density matrix formalism 79−31392
SiH_5, SCF calcs. including polaris. functions 80−87034
silaethylene, singlet-triplet energy separation 78−58594
silaethylene, singlet-triplet energy separations 77−57866
silaethylene, triplet carbenoid isomers, thermodynamic stability 78−90076
silyl radical, conform., hyperfine struct., nonempirical calcs., vibr., effects 79−97998
single-particle density matrix, perturbation expansion 80−54635
singlet states with two open shells of equal symmetry, orthogonality constrained SCF theory 77−26962
$(Sn)_x$ chain, energy band struct., Hartree-Fock and CDW solns. 79−23885
solid insulator, effective screening function 78−10383
solid surfaces, review of electronic struct. calcs. 77−28226
sparse s and p type Gaussian basis set LCAO MO SCF calc., mol. props. 80−23306
spherical nuclei, self-consistent Thomas Fermi method 77−57607
spherical system, relativistic pseudopotential 78−82653
spin optimised SCF general spin orbitals, theoretical formulation 78−5125
stilbene, diphenylpolyenes, photoisomerisation, 'phantom' photochem. singlet state, PPP SCF CI calcs. 78−73058
strongly anharmonic crystals, improved unsymmetrised SCF approx. 78−75791
struct. and props., SCF calcs. 80−106260
structural phase transitions, de Gennes pseudospin model, lattice phonons tunnelling effects 79−73290
superconductivity, theory of collective excitations, appl. of generalized self-consistent field method 78−10598
superheavy molecules, Z=110, Dirac-Slater SCF relativistic mol. calcs. 78−41970
supermolecule calcs. with additive procedure, intermolecular interactions and binding energy 80−52880
surface lattice dynamics and density response 78−71930
surface states, three-dimens. cryst. ab initio SCF LCAO calc., impurity clustering 78−56201
symmetry adapted multiconfiguration SCF wave functions, single excitation annihilation calcs. 77−46481
symmetry restricted multiconfiguration annihilation of single excitations calcs., applic. to methylnitrene 78−62695
syndnone, semi-empirical excited state Morokuma's EHP calc., geometry and order of states 78−46256
TCNE-benzene, charge transfer theory, Mulliken population, ab initio calc., multiconfiguration scheme 80−106392
$TCNQ^x$, (x=0, −1, −2), elec. dipole polarisability, π-electronic components, SCF calcs. *(Russian)* 78−84204
TCNQ anion, one-electron Hamiltonian method in SCF theory 78−9055
TCNQ salt, NMP-TCNQ, electronic struct., SCF calc., total energy polarisation effects 80−15469
tempered orbital energies, relation to Mulliken-Walsh ordinate and extended Huckel orbital energies 79−763
tetrafluoromethane, Auger transition energies, transition state approx. SCF Xα calc. 77−65426
tetrahedrally coordinated solids, charge distrib., localised mol. orbitals 79−23560
1,3,6,8-tetraphenyl-pyrene, UV absorpt. spectra, SCF CI method 79−59479
thiocarbonates, mol. struct., S-substitution effect *(French)* 80−23335
thiocarbonyl halogen substituted cpds., geometric and electronic struct., LCAO-SCF calc. 79−89603
thioformaldehyde, electronic struct., dipole moments, mol. polarisability, force fields, ab initio calcs. 80−78531
thionitrates, mol. struct., S-substitution effect *(French)* 80−23335
thiourea, ground and first excited triplet state configs., ab initio SCF calcs. 79−89597
thiourea, struct., hydration, ab initio SCF calcs. 80−58142
third row element mols., general harmonic force field, SCF-MO-MNDO and freq. calc., MOCIC pot. 80−27948
thirene, ab initio SCF calc., thermodynamic stability 78−25420
three-body interatomic forces, electron gas model and SCF calcs. 78−33564
three-dimensional crystal, Hartree-Fock theory of surface states 80−44468
total HF SCF energy, of ats. and ions, approximation methods comparison 79−31366
total molecular energies, calcs., SCF orbital energies rel. to total SCF energies 79−59337
transition elements, higher types, electronic config. and nucl. quadrupole interaction, atomic SCF Hartree-Fock calcs. 79−60777
transition metal alloy, ground state properties, self-consistent calc. 78−91587
transition metal atom, many-config. approx. in X-ray and electronic spectra interpret. 80−32615
transition metal chlorides, 4d-series, electronic struct. and spectra, multiple scatt. calcs. 77−83486
transition metal complexes, counterintuitive orbital mixing in semiempirical, ab initio MO calcs. 78−90078
transition metal dihydrides, gas phase geometrical struct. calcs. 80−42951
transition metal hydrides, homoleptic, electronic structure, ab initio calcs. 79−89601
transition metal nitrides, liquid interactions, ab initio LCAO MO SCF calcs. 79−18256
transition metal surface clusters, Hartree-Fock-Slater model calcs. 77−72899
trimethylamine, SCF calcs. including polaris. functions 80−87034
trimethylene diradicals, geometry optimisation ab initio SCF CI calcs., energy gradient 79−85903
triphenylene, excited state Faraday values mag. circular dichroism spectra and MO CI calcs. 80−18877
twisted conjugated molecule, zwitterionic excited states investig. 80−58179

SCF calculations continued
two linear harmonic oscillators, coupled by interaction pot., SCF calc. 78−37625
two-level atoms, multiphoton cooperative radiation, SCF approx. calcs. 80−95856
ultrathin doping levels as model for 2-dimens. systems 78−60182
umbelliferone, excited states, in ethanol-water soln., absorption and emission spectra 79−13763
unimolecular reactions, pot. energy surfaces, SCF perturbation theory 79−91918
urea, single crystal Compton profiles, H-bonding and dimer config. effects, calc. and meas. 78−80431
variation-iteraction soln. of Hartree Fock eqns., Green's integral operator, SCF formalism 79−6842
vinyl alcohol, struct. from ab initio calcs. 78−29857
vinyl fluoride, geometries, props. and protonation, ab initio mol. orbital study 79−22588
n-vinylformamide, torsional pot. barriers, ab initio and partition of energy methods 77−88588
virtual orbitals modification, computational implementation 79−85880
visual chromophores, two-photon absorptivities, SCF-PPP-CI calcs. 79−31631
water, NMR shielding constants of ^{1}H and ^{17}O, paramag. contrib., triple perturbation theory 79−10127
water+glycine(serine) zwitterions, interaction pots., ab initio SCF LCAO calcs. 78−48747
water elec. dipole polaris., near Hartree-Fock value, using EFV GTOs 77−88591
water molecule, nucl. spin-spin coupling consts. geometric approx. 79−59380
X-ray transition energy data, rel. to theory 79−76378
e^+A^-, positron-containing ground-state negative ions, self-consistent Fock field 80−47888
e^+Br^-, positron-containing ground-state negative ions, self-consistent Fock field 80−47888
e^+I^-, positron-containing ground-state negative ion, self-consistent Fock field 80−47888
Ag (110), electroreflectance, surface state contrib. 80−80755
Al, SCF Xα scattered wave calc. for clusters up to 43 atoms 78−10323
Al, single vacancy formation energy calc., SCF-LCGO modified solid state scatt. theory 80−54637
Al-H_2O, mol. complex, electronic struct. calcs. 78−66465
Al_2, repulsive region ground state pot. curves, SCF with STO basis set calc. 80−14188
Al_2^{6+}, repulsive region ground state pot. curves, SCF with STO basis set calc. 80−14188
Al_5, chemisorpt. of Na, Si and Cl, core hole induced electronic relax. 79−90874
$Al_2(Al_2^-)(Al_2^+)$ configurations, ab initio study, LCAO, STO, MO-SCF and CI calcs., binding energy *(French)* 80−91447
Al_2Cl_6, ab initio LCAO SCF minimal basis set calc., struct. 79−49943
AlF_6^{3-}, octahedral complex, ionis. energy, SCF-Xα study 78−70967
Al_2F_6, ab initio LCAO SCF minimal basis set calc., struct. 79−49943
AlH, SCF pot. curves, 0.1-10 Bohr, ground and excited states 78−58610
AlH^+ radical cation, EPR matrix isolation obs., hyperfine components calcs. 80−14158
AlH^+, SCF pot. curves, 0.1-10 Bohr, ground and excited states 78−58610
α-Al_2O_3, charge distribution determ., SCF calc., Slater-type orbitals, Madelung type const. 80−107100
β-Al_2O_3-Na_2O, adsorption of Na, surface electronic struct. calcs. 80−75431
Al(111), chemisorption of O_2, SCF X_α scatt. wave MO calc. 79−42374
Ar, aqueous soln., dil., energy and struct., pair pot. energy function, Monte Carlo calc. 80−54107
Ar, electron binding energies, one-centre expansion method 77−6677
Ar, electron impact ionis., calc. for $3s^2$ subshell 79−31700
Ar, Koopmans' ionis. pot., relax. correction 79−18308
Ar, solid, self consistent field calcs. of isotherms and thermodynamic props. *(Russian)* 80−10633
Ar, solid, thermodynamic props. under press., multiparametric pairwise and Lennard Jones potential calcs. 80−39316
$Ar+HHe^+$, ab initio pot. energy data, SCF-LCAO calcs. 80−63530
Ar_2, excited state pot. curves, ab initio CI calc. 78−78643
Ar_2, interatomic potential single parameter 80−48059
Ar_2, short range interactions between two rare gas atoms 79−26888
Ar_2 van der Waals dimer, intermol. pot., SCF CI ab initio calcs. 80−106274
Ar_2^+, electronic states, pot. curves, with/without spin-orbit interaction 78−33443
Ar_2^+, electronic struct., pot. energy curves, spectroscopic consts. 79−18114
ArCl, neutral and negative ion states SCF pot. energy curves 78−62745
ArH, neutral and negative ion states SCF pot. energy curves 78−62745
$Ar_nH(H^+)$, excited and ground state struct. energies and binding energy, vibr. modes, LCAO-SCF-MO calc. 79−3608
Ar.HCl, Van der Waals mols., SCF energies and dispersion forces 80−74279
Ar.HF, Van der Waals mols., SCF energies and dispersion forces 80−74279
Ar.H_2O, Van der Waals mols., SCF energies and dispersion forces 80−74279
As_3, 3-body nonadditive interaction, nodal struct. 78−1049
AsF_3, inversion barrier, STO SCF calc. 80−63567
Au (110), electroreflectance, surface state contrib. 80−80755
Au, energy levels from ab initio effective core pot. 78−33426
Au, ground and excited states, pot. energy curves, relativistic effects calcs. 79−31416
Au_2, ground state, ab initio effective core pots., relativistic effects calcs. 79−31377
Au_2^+, ab initio SCF calcs. using relativistic effective core pot. 80−95524
B, ground state wavefunction, SCF HF calc. 78−90070
B_2, ground state, multiconfig. SCF CI calcs. 78−58590
BF_3, dissoc. pathways and mol. vibr., compliance consts. and min. energy coords. 78−35661
BH, electron density and localizability partitioning calcs. 78−21847
BH, SCF and CI wavefunctions for electronic struct. and one-electron props. 77−67978
BH_3, electronic wave function determ., genealogical technique using Clebsch-Gordan coeff. 80−95529
B_2H_6 and $B_2H_5NH_2$, electronic struct. and bonding, comparative calcs. 79−31397
B_2H_n, struct., ab initio SCF calcs. *(French)* 79−22598
B_3H_n, struct., ab initio SCF calcs. *(French)* 79−22598
$B_{n+3}H_{n+8}$, n=1-7, ab initio 6-3G and 3G/MODPOT LCAO-MO-SCF calcs. 79−10026
BH_3NH_3, complexation energies and interatomic distances, SCF and CEPA calcs. 78−25446
B(1) hydrides, ab initio calcs., proton and hydride affinities 79−10029
BN, cubic, ab initio SCF calcs., band struct., ground state props. 78−51891
BN tetrahedrally bonded valence crystals, SCF perturbation theory appl. 79−37658
B_2O_3, bipyramidal struct., stability, ab initio SCF-MO calcs. 80−99446
$(B(OH)_3)_2$, hydrogen bond, ab initio MO calcs. 78−58588
^{11}B, ground state, two-determinant numerical self-consistent at. orbitals appl. 79−93937
Ba I, low-lying, even-parity levels, ab initio relativistic SCF MCDF calcs. 78−37568
BaF_2, U-centre, electronic struct. and optical transition energies, SCF MS Xα calc. 79−4532
$BaTiO_3$ crystals, octahedral TiO_6^{8-} cluster atomic population, ionisation energy, SCF MS Xα calcs. 79−72244
Be cluster, multibody expansions, convergence 80−23594
Be, ground state energy, split valence GO basis set SCF calc. 77−34554
Be, ground state wavefunction, SCF HF calc. 78−90070
Be, SCF ion improved virtual orbitals, excited configs. calc. 77−10585
Be^{2+}, numerical Hartree-Fock calc. of $1s^2$ ground state 79−81155
Be_2, pot. curve of ground-state, many-body perturbation theory and SCF-CI method 79−36563
Be_3, 3-body nonadditive interaction, nodal struct. 78−1049
Be_3, Be_4, Be_5, atomic clusters, nonadditive interactions, SCF energy anal. 78−25765
Be_4 (Be_4^-), atomic clusters, electronic struct., LCAO-MO-SCF and HF calcs. 80−63880
BeF_2^-, electron binding, extended basis SCF calc. 79−49944
BeF_2^-, ground state, conform., electron affinity, extended basis SCF calcs. 79−72253
BeO, MCSCF and CI calcs. 80−95526
BeO, tetrahedrally bonded valence crystals, SCF perturbation theory appl. 79−37658
^{7}Be, electron capture radioactive decay probabilities in atoms and ions 79−59556
$Be(2^3P)$+methane, reaction, ab initio MO calcs. 79−8431
BiI, multiconfiguration Dirac-Fock calc. of $6p^3$, $6p^27s$, and $6s6p^4$ configurations 79−3374
Br^-+He, electron detachment, SCF calcs., $BrHe^-$ and BrHe pots. 80−23503
Br_2, model potential SCF calcs. 80−95528
BrF, He(I) photoelectron spectra, interpretation 79−13766
BrF_3, electronic struct. and ionisation pot., SCF DV Xalpha method 80−69057
BrF_5, electronic struct. and ionisation pot., SCF DV Xalpha method 80−69057
$Br^-(H_2O)_n$, hydration energies, orientation, ab initio-LCAO SCF MO calcs. 80−27944
C, first-principles pseudopotential in the local-density-functional formalism 79−59328
C, ground state wavefunction, SCF HF calc. 78−90070
C-H bond, acidity in organic mols. and anions, SCF MO calcs. 77−83497
C_2, band system transition moment ab initio SCF and CI calcs. 79−13770
C_2, transition moments of Swan band system, SCF-CI calc. 78−58746
C_2, valence states, CI calcs. 79−45642
C_2^{6+}, total SCF energy estimation from orbital energies 79−63908
C_3, ground and excited states, vibr., pot. curves, CI calcs. 77−83509
$C_2(C_2^-)$ pot. energy curves calc. using SCF, MCSCF and CI methods, dissoc. energies, bond lengths, electron affinity 80−95523
CF_3, CF_3^-, and CF_3^+, optimised struct. and bonding, ab initio SCF MO calc. 80−23334
CH, photoionis. and photodissoc. near ionis. threshold, SCF MO CI and Steltjes imaging 78−58749
CH radical, SCF theory, multiconfig., direct orbital optimisation 80−87049
$C_2H_2+OH^-\rightleftharpoons C_2H^-+H_2O$, equilib. consts., ab initio SCF and CEPA calcs. 78−3361
$C_2H_3^++HF$, interaction, struct. and stability, ab initio calcs. 80−58347
$C_2H_7^+$, ab initio SCF, CI, CEPA-PNO struct. and energy calcs. 78−94197
CH_3CO^+, ground-state, two-config. SCF wavefunction 77−46481
$C_2H_5O^+$ and $C_2H_5S^+$, stability, proton affinity, ab initio SCF, CEPA PNO, MINDO/3 and MNDO calcs. 79−59357
$(CH_3)_2X$ molecules, perturbational MO anal., methyl rot. barriers, fragmentation mode 77−88386
CN, CN^-, HF electron affinity, SCF calcs. 77−67979
CN^-, electron density distrib., SCF mol. orbitals calcs. 78−9058
CN^-, finite field method calc., moments, polarisability, field-induced shifts in mol. props. 78−74561
CN^+, ground state, identity, ab initio CI calcs. 80−5468
CN^+, ground state, SCF pot. energy curves calcs. 79−13782
CN^+, lower states, pot. energy curves, equilib. distances SCF CI calcs. 80−27957
$(CN^-;^+)$ complex, ab initio LCAO SCF calc., positron affinity and excitation energy 79−49945
CO, $^1\Sigma^+$ state, ionisation pots., dissoc. energy, atoms-in-mol. calcs. 77−88410
CO ($^1\Sigma^+$), X-ray and electron diffr. scatt. intensities, electron correlation effects 78−17577
CO, $a^3\Pi$ and $A^1\Pi$ states, dipole moment, CI calcs. 77−79548
CO and $(CO)_6$, electronic struct. and bonding, SCF-Xα-MSW calcs. 78−25431
CO, CO^+, MO correlation diagrams 77−61689
CO, core ionis., electric field depend. 78−13424
CO, core ionisation and single orbital relax. calcs. 78−5133
CO, core ionisation single orbital relax. energy, LCAO-SCF basis set depend. 79−89604
CO, dipole moment functions for $d^3\Delta$ and $a'^3\Sigma^+$ states, MCSCF calc. 78−78636

SCF calculations continued
CO, electronic struct., binding energy and interatomic distance, SCF variational cellular calc. 80−9498
CO, electrostatic interaction energies for point charge and NaCl (100) surface 78−74592
CO, finite field method calc., moments, polarisability, field-induced shifts in mol. props. 78−74561
CO, numerical coupled Hartree-Fock parallel polarisability, partial wave SCF calc. 78−9079
CO, one-election props., SCF and CI calcs. 80−27951
CO, orbital contribs. to relax. energies accompanying core ionis., ΔSCF HF calcs. 78−82642
CO, polarisability derivatives, bond length depend., SCF and CI calcs. 80−58162
CO^+, ab initio pot. energy curves, full valence CI with minimal STO 79−72361
CO_2, $^1\Delta_u$ valence state, vertical energy level MC-CI wavefunction 79−45644
CO_2, ab initio SCF calcs., force consts., vibrs., pot. energy surface 78−5209
CO_2, anomalous energy minima surfaces 78−86791
CO_2, localised mol. orbitals, ab initio PRDDO SCF calc., isoelectronic struct. 78−25441
CO_2, low energy electron (positron) collisions, ab initio adiabatic polarisation pots. 80−14240
CO_2, nonbending, vibr. motion calc. using SCF-SI theory 80−23399
CO_2, SCF vertical spectrum for valence, mixed character and Rydberg states 77−50375
CO_2, stretch-stretch interaction force const., electron correlation influence, ab initio CI study 80−58161
CO_2^+, $^1\Pi_g$, mixed charact. state, vertical energy level MC-CI wavefunction 79−45644
CO_2+$H_2(D_2)$, ab initio LCAO-MO-SCF intermolecular pot. energy surface, V→T transfer 77−50489
CO_2+He, rot. inelastic collision, ab initio SCF, electron gas and pot. energy surfaces 80−83468
CO_3^{2-}, localised mol. orbitals, ab initio PRDDO SCF calc., isoelectronic struct. 78−25441
COH^+, orbital contribs. to relax. energies accompanying core ionis., ΔSCF HF calcs. 78−82642
CO_2H^+, SCF CI equilib. struct. calc., CO_2 proton affinity 77−10599
CS, perturbation parameters between valence states 77−26975
CS_2, symmetric stretch mode, moments and polarisability derivatives, SCF calcs. 80−901
C_3S_2, electronic struct., optical and photoelectron spectra 78−70745
C_3S_2, electronic struct., optical and photoelectron spectra 78−70982
Ca, forbidden transitions, radiative lifetimes, MCSCF and CI calcs., time of flight spectra for metastable state 80−91498
Ca_2^+, pot. energies in Ca^+ and Rydberg Ca** collisions with Ca 79−27055
CaF_2, U-centre, electronic struct. and optical transition energies, SCF MS Xα calc. 79−4532
CaF_2:Dy(Tm), cryst. fields, overlap and covalency contribs. 77−1397
CaH, low lying electronic states, ab initio SCF-CI calcs. 80−52893
CaH, spin doubling, SCF calcs. 80−95649
CaO, electronic struct., SCF calcs. 78−66462
Cd_2 as 470 nm absorber, multiconfig. SCF calcs. 80−32731
Cd^*_2, 470 nm absorber, multiconfiguration SCF calcs. 80−27963
Cl^-, pair polarisability, ab initio SCF MO energies 78−70741
Cl-containing systems, core Auger and core electron binding energy shifts, ab initio LCAO SCF MO UHF calcs. 77−30777
Cl_2, model potential SCF calcs. 80−95528
Cl_2, one electron props. and polarisability, SCF and CI calcs. 80−58159
$(Cl_2)_2$, binding, dispersion energy predominance 78−25421
ClCO radical, struct. and props. calcs. 80−74112
Cl_2CS, potential energy surfaces and equilibrium geometries for ground and excited states 79−45634
ClFCS, potential energy surfaces and equilibrium geometries for ground and excited states 79−45634
$ClHCl^-$, deuteron quadrupole coupling const., nuclear mag. shielding, geometry depend. 78−58586
ClO, MCSCF-CI electronic wavefunctions, dissoc. energy, dipole and transition moment 77−75052
ClO_4^-, dummy spheres in SCF Xalpha calcs. 80−69056
ClO_4^-, ionisation energies, SCF-Xα transition state calcs. 80−74115
ClOO radical, struct. and props. calcs. 80−74112
$ClO(X^2\Pi_i)$, radical, He(I) photoelectron spectrum, ΔSCF calcs. 79−72359
Co, Auger spectrum, ab initio MO LCAO SCF CI calc. many electron contribs. 80−87169
Co complex, metal-metal bond, correl. effects, SCF calc. 77−65425
Co-porphine, ab initio LCAO SCF MO calcs. 79−6860
$Co(CN)_6^{3-}$, electronic struct., ab initio LCAO SCF MO calcs. 79−18112
$CoCl_4^{2-}$, electronic energy levels calc. by conventional and X alpha Hartree-Fock methods 78−66470
$CoCl_4^{2-}$, mol. orbital energy levels, semi-empirical calc. 77−3271
$CoCl_n$, electronic struct., INDO theory 80−42948
$Co(NH_4)_2(SO_4)_2.6H_2O$ Tutton salt, low-temp. spin orientation, mag. props. 0-0.1K 79−15286
CoO, ab initio SCF and CI calcs. on d-d transitions, CoO_6^{10-} cluster d-electron localisation 77−35897
Cr_i Koopmans' ionis. pot., relax. correction 79−18308
Cr^{3+} in octahedral fluoride lattice, optical spectrum open shell SCF MO cluster CI calc. 78−19501
$Cr(CO)_6$, electronic struct. and bonding, SCF-Xα-MSW calcs. 78−25431
$CrOCl_3$, electronic structure and valence ionisation energies, obs. by ab initio and SW-Xα methods 80−69073
$CrOCl_3$, ionisation energy, CI and ΔSCF methods 79−68194
Cs^+ and Cs, analytic SCF HF ground state wave function, ionis. pot., mag. props. 77−18785
Cs_2^{2+}, low-lying states, MC SCF+CI 80−69053
$CsH^-CsH^+(CsH)$, ab initio ground-state pot. energy curves, electron affinities 78−41946
$CsNpF_6$, optical spectrum anal. 79−26963
$CsX_i(X=F,Cl,Br,I)$, ionis. energy, relativistic Dirac-Slater and nonrelativistic HF-Slater calcs. 77−26983
Cu (001) monolayer, electronic struct., self-consistent LCAO calc. 79−4606
Cu (100) monolayer, self consistent electronic struct. 80−6926
SCF calculations continued
Cu (110), electroreflectance, surface state contrib. 80−80755
Cu, chemisorption of CO, electronic struct. of $(M)_5CO$ clusters 78−95948
Cu surface, with chemisorbed CO, cluster calc. using SCF-Xα-scatt. wave method 77−62742
Cu-Ni(Fe)(Mn)(V), dil., local mag. moments and Kondo effect, theoretical model 79−69651
Cu-Ni(Zn)(Ga)(Ge), dil. impurity electron struct., self-consistent Korringa-Kohn-Rostoker Green's function calc. 79−78040
Cu_2, bonding, ab initio pseudopot. calcs. 79−6857
CuCl, electronic struct., ab initio HF SCF MO calcs. of $CuCl_4^{3-}$ cluster 78−95262
$CuCl_4^{2-}$, ESCA satellite intensity, ab initio SCF calcs. 80−74103
$CuCl_4^{2-}$, electronic energy levels calc. by conventional and X alpha Hartree-Fock methods 78−66470
$CuCl_n$, electronic struct., INDO theory 80−42948
$CuCl_2(Cl_4^{2-})(Cl_6^{4-})$, electronic struct. studies by SCF, MSXα and INDO method 80−74119
$CuF_2(F_6^{4-})$, electronic struct. studies by SCF, MSXα and INDO method 80−74119
CuO, ab initio HF-MC-SCF with GTO basis set, dissoc. energy and bond length 80−47890
D_3 Rydberg states, spectroscopic B_0 consts. 80−74109
DCN, electronic spectra, vibr. struct., ab initio calc. 78−9166
EuO, electronic struct. and props., mol. cluster approx. 77−11852
EuS, electronic struct. and props., mol. cluster approx. 77−11852
$F(^2P_{1/2})+H_2$, quenching, classical path calcs. 79−22800
F compounds, ground states, mol. parameters, MINDO calcs. 78−41955
F^-+fluoromethane, S_N2 reaction, ab initio LCAO SCF calcs. 77−81402
F_2, Compton scatt. profile, SCF MO theory calcs. 78−58577
F_2, correlated wavefunctions, ionisation pot. 77−67986
F_2, electron impact excitation, dissoc. of lowest electronic state 80−63839
F_2, mag. shielding and susceptibility, finite perturbation mol. orbitals calcs. 77−46513
FBO, electronic struct. calcs. 77−30772
FCO, radical, struct. and props. calcs. 80−74112
F_2CS, pot. surfaces, X^1A_1, a^2A_2 and $a^3A_2(b_1)$ states, ab initio SCF calcs. 78−86795
$FClO^+$, radical cation, struct. and electronic props., ab initio RHF SCF MO calc. 80−52883
FH-OH_2(dimethyl ether), H-bonded complexes, cubic force consts. calcs. 80−47868
FH_2^+, reactive processes, ab initio MCSCF-CI and diatomics in mols. calc. 78−56881
FH_3^+, stability, ab initio calcs. 77−30775
$FHCl^-$, deuteron quadrupole coupling const., nuclear mag. shielding, geometry depend. 78−58586
FHF radical, struct. and stability, ab initio SCF and CI calcs. 77−71887
FHF^-, deuteron quadrupole coupling const., nuclear mag. shielding, geometry depend. 78−58586
$F^-(H_2O)_2$, 3-body pots., SCF energy partitioning calcs. 80−18953
FHe^+ dissociation energy calc., β decay of FT 78−56910
FNO, ground and lowest excited states, SCF ab initio calcs. 78−37544
F_2O, geometry, electron spectrum, vert. ionis. pot. ab initio calc. 80−58187
F_2O_2, geometry, SCF CI calcs. 78−55126
FOO radical, struct. and props. calcs. 80−74112
F_2S_2, electronic struct. and stability of isomers, gaussian SCF MO calc. 79−93921
$F_4S_4N_4$, SCF-Xα-CNDO/BW calcs., comparison 78−25435
FSO (FOS), struct. and props., SCF calcs. 80−106260
FSS, struct. and props., SCF calcs. 80−106260
$(F^-;e^+)$ complex, ab initio LCAO SCF calc., positron affinity and excitation energy 79−49945
Fe complex, $[Fe(CN)_6]^{3-}$, electronic struct., optical transitions, XPS, Mossbauer isomer shift, valence ionisation pot., SCF-MSX calc. 79−6864
Fe complexes, Mossbauer isomer shift and core electron binding energies of Fe 78−82620
Fe, ferromagnetic, hyperfine fields; SCF calcs. 77−8061
Fe, model potential method, in Roothaan's open-shell scheme 79−36513
$Fe(CN)_6$, Mossbauer isomer shift const., ab initio SCF calcs. 78−43751
$FeCl_n$, electronic struct., INDO theory 80−42948
FeF, electronic states, ab initio calcs., UV spectrum elucidation 78−74570
FeF_6, Mossbauer isomer shift const., ab initio SCF calcs. 78−43751
FeO_4^{2-} ion, electronic struct., hyperfine interactions, SCF Xα calcs. 79−37951
Fe_3O_{fg} SCF X_α calcs. of one-electron energy levels 78−47727
FeS_6^{4-}, electronic struct., SCF-Xα scatt. wave calcs., rel. to spectra of FeS, FeS_2 78−5138
Fr I, wavelength estimate of first and second resonance lines 78−58617
n-GaAs-$Ga_{1-x}Al_xAs$, superlattice, subband struct. and optical spectra, self-consistent calc. 80−15443
Ge, effective screening function 78−10383
GeH_3^-, electronic struct., electron affinity, inversion barrier, ab initio SCF Gaussian basis calc. 80−63552
Ge_2H_6, rot. barriers, MS-SCF-X_α calcs. 80−106267
H adsorption and desorption, self-consistent model calc. 79−46943
H atom finite chains, HF solns. stability and symmetry breaking, independent particle model calcs. 80−87035
H, bond energy, chem. substitution influence 80−37718
H, chemisorbed on Be(0001), mol. cluster theory 79−15002
H halides, ab initio SCF calc. of dipole polarisabilities 79−89600
H, He atmosphere, hyperfine press. shift, MCSCF-variational procedure 77−6735
H_i in spherical box 77−54508
H^-, electronic structure, stabilisation calcs. using big mol. Gaussian SCF/CI program 79−18121
H^-, numerical Hartree-Fock calc. of $1s^2$ ground state 79−81155
H-bonded systems, core and valence ionis., nonempirical LCAO MO SCF calcs. 77−67973
H-bonded systems, cyclic and bifurcated, ab initio MO calcs. 79−41100
$H+Br_2 \rightarrow HBr+Br$, pot. energy surface, ab initio generalised valence bond calc. 78−73026
H+He(Ne)(Ar)(Kr)(Xe), low energy elastic scatt. cross section MCSCF calc., van der Waals forces 78−70897

SCF calculations continued
$H+Li_2$, collinear reactions, SCF correl. diagram for Li_2H form. 77−70292
$H+NH_2 \rightarrow NH_3$ react., force, density anal. 78−60997
$H^+ + 2HF$, interaction pot., monopole approx., supermol. SCF and perturbation schemes 77−27139
$H^+ + CO$ ($^1\Sigma$), ground state pot. energy surface, ab initio SCF calc., protonated equilib. geometry 80−83301
$H^+ + Kr$, mol. orbit approach, spin-orbit interaction, adiabatic pot. and projected valence band treatments 77−533
H_2, adiabatic polarisation, ab initio calc., static electric dipole polarisability 79−72229
H_2 chain, infinite, lattice distortions, CNDO/2 calcs. 78−6018
H_2, electron total scatt. intensity, first Born approx. , SCF CI calc. 77−10755
H_2, electronic energies of $D'^1\Pi_u$ and $B''^1\Sigma_u^+$ states, wave functions 77−23438
H_2, limited MC SCF calculations 79−36537
H_2 molecule dimer, ab initio SCF intermolecular interaction energy calcs. 80−78537
H_2, nucl. mag. shielding, elec. field, accurate coupled Hartree-Fock 78−25434
H_2, nucl. mag. shielding and susceptibility, elec. field depend., SCF-Hartree Fock method 80−18791
H_2, octapole magnetisability, multiple SCF perturbation calc. with STO basis set 77−34550
H_2, polarisability, finite field MC SCF calcs. 80−14075
H_2, relativistic Dirac-Fock multiconfig. SCF calcs. 80−99455
H_2, repulsive intermol. pot. 80−32794
o-H_2, solid FCC, orientational ordering, SCF approx. 78−2029
H_2, total energy, HF SCF approx. formula, internucl. distance depend. 78−21837
H_2^+, Compton profile and momentum distribution, impulse approx. 78−25626
H_2^+, individual orbital contribs. to SCF virial 79−3349
H_2^+, mol. energy in strong magnetic field, MO SCF calcs. 79−6858
H_2-H_2, intermol. pot. surface, ang. depend., nonorthogonal CI calc. 77−46613
H_2-H_2 intermol. pair pot., ab initio SCF-CI surface 80−91457
$H_2+D_2 \rightleftharpoons 2HD$ catalysis, MgO surface, SCF UHF calc. 77−9120
H_2+H_2, interaction polarisability comparison with the He diatom, ab initio SCF calcs. 80−27943
H_2+H_2, van der Waals pot., electron tunnelling, charge transfer 77−54588
H_2+He potential surfaces, SCF and MRD-CI calcs. 79−10172
$(H_2)_2$, ab initio calcs., perturbation dispersion energy versus CI treatment 77−26976
H_3, Rydberg states, spectroscopic B_0 consts. 80−74109
H_3, spin-optimised SCF general spin orbitals calcs. 78−5125
H_3 , dissociating states, lowest singlet and triplet PE surfaces, HF calcs. 79−81160
H_3^+, $^3\Sigma_g^+$ excited level, GO SCF calcs. 77−46507
H_4 and H_4^+, H_4^- ions rectangular configurations, stability, SCF MO LCAO calcs. 77−42235
H_4 excimer, electronic and geom. struct., ab initio CI calc. 79−76348
H_{4u} ground and excited states, SCF MO CI calcs. 77−6693
H_4^+, ground and excited state pot. energy surfaces and geom. struct., SCF and CI calcs. 78−78769
HBr^{n+}, highly charged, repulsion energies, nucl. internal conversion, ab initio calcs. 79−76341
HC_2, ground state energy surface, ab initio SCF calc. 78−33446
HC_2 radical, electron affinity, ab initio SCF and CI calcs. 78−50468
HC_2^-, ground state energy surface, ab initio SCF calc. 78−33446
HCCN, a cyanocarbene, geom. struct., electron correl. effects 80−1077
HCN, electronic spectra, vibr. struct., ab initio calc. 78−9166
HCN, electronically excited states, SCF CI calc. using Slater type orbitals 78−78645
HCN, Fermi and Coulomb correl. holes, SCF and CI wave functions 80−69085
HCN, finite field method calc., moments, polarisability, field-induced shifts in mol. props. 78−74561
HCN, H-CN dissoc. curves, SCF CI calc. 79−100405
HCN, HNC, electronic reorganisation, with core ionisation 78−94196
HCN, orbital calculation, SCF+CI method 79−93928
HCN, SCF ab initio ground state pot. energy surface, geometry, rel. to HCN^- 78−78646
HCN, semi-empirical excited state Morokuma's EHP calc., geometry and order of states 78−46256
HCN^-, SCF ab initio ground state pot. energy surface, geometry, rel. to HCN 78−78646
HCN^+, $^2\Sigma^+$ and $^2\Pi$ states, SCF and CI calcs. for determ. optimum linear geometries, bond angles calc. 80−74114
HCN^+, A and B $^2\Sigma^+$ states, pot. surfaces, ab initio SCF calcs. 80−27959
HCN^+, photoelectron spectra of third electronic state, ab initio calc. of pot. energy surface 78−70871
HCN-CO complex, charge transfer theory, Mulliken population, ab initio calc., multiconfiguration scheme 80−106392
$H_2CN^+H_2 \rightarrow HCN^+H+H_2$, ab initio GO SCF pot. energy surface, saddle point, reaction path 77−50379
HCO^+, orbital contribs. to relax. energies accompanying core ionis., ΔSCF HF calcs. 78−82642
H_2COLi^+, geom. and electronic struct., ab initio SCF calc. 79−76331
HCS^+-CSH^+, struct. and stability, ab initio SCF calcs., CNDO calcs. 80−32608
HCS^+-CSH^+ system, pot. surface for H abstraction, internuclear bending for ground and excited states 78−29744
H_2CS, potential energy surfaces and equilibrium geometries for ground and excited states 79−45634
H_3CS^+, struct. ab initio (4-31G) SCF calc. 79−68201
HCl, one electron props. and polarizibility, SCF and CI calcs. 80−58159
HCl, one-centre-expsn. SCF calc., electric field grad., Sternheimer effect 78−37550
HCl^-, reson. states by electron impact, GO and SCF+CI methods, dissociation channels 77−71883
HD, nuclear spin coupling const. calc., using ab initio LCAO MO SCF method 78−25558
HF, Auger transition energy calcs. 77−34704
HF, core ionis., single orbital relax., LCAO MO SCF calcs. 78−29739
HF dimer, stabilisation energies, harmonic free constants, intermolecular vibration, SCF and CEPA PNO calcs. 79−98177
SCF calculations continued
HF, elec. dipole polaris., near Hartree-Fock value, using EFV GTOs 77−88591
HF, geometries, props. and protonation, ab initio mol. orbital study 79−22588
HF, H-X bond position, correlation with electronegativity 78−9069
HF, mol. hyperpolarisability, second-order SCF perturbation method, coupled Hartree-Fock calc. 78−33422
HF, mol. props. internucl. separation depend., MCSCF calc. 78−70965
HF, nucl. mag. shielding and susceptibility, elec. field depend., SCF-Hartree Fock method 80−18791
HF, nuclear spin-spin coupling, ab initio SCF perturbation theory 78−33525
HF, numerical coupled Hartree-Fock parallel polarisability, partial wave SCF calc. 78−9079
HF, orbital relax. energy for single and double ionis. from valence shells 80−106253
HF, SCF theory, multiconfig., direct orbital optimisation 80−87049
HF, $X^2\Sigma^+$ state, 3- and 4-body perturbation theory modified pots. 77−88376
HF-HCl, SCF energy hypersurface, stationary points, thermodynamics of form. 80−102436
$HF+H^-$, reaction, ab initio pot. energy surface calcs. 79−39127
HF+HF, interaction energy, MCF and perturbation calculations 77−27139
HF+HF, medium distance interaction, SCF LCAO MO, supermol., perturbation and MCF calc. 79−837
$HF+H' \rightarrow H+H'F$, transition state geometry, SCF CI calcs. 78−2000°
$HF+Li \rightarrow LiF+H$, pot. energy surface, SCF and CI calcs. 80−71904
$(HF)_2$, energy decomp. anal. of H-bonding, ab initio SCF MO calcs. 77−57868
HF_2^-, mag. shielding and susceptibility, finite perturbation mol. orbitals calcs. 77−46513
$(HF)_3$, 3-body pots., SCF energy partitioning calcs. 80−18953
HFCS, potential energy surfaces and equilibrium geometries for ground and excited states 79−45634
HFF radical, struct. and stability, ab initio SCF and CI calcs. 77−71887
H_2^+He, total energy, interat. dist., geometric configurations, LCAO MO SCF calcs., stability, binding energy 77−42236
HI, dipole moment function, multiconfiguration SCF calc. 77−75330
HN_3, ground $^1A'$ state, SCF and CI calcs., conform., geom., vibr. freqs. and dissoc. 80−18806
H_3N-HF, energy decomp. anal. of H-bonding, ab initio SCF MO calcs. 77−57868
HNC, finite field method calc., moments, polarisability, field-induced shifts in mol. props. 78−74561
HNC^+, $^2\Sigma^+$ and $^2\Pi$ states, SCF and CI calcs. for determ. optimum linear geometries, bond angles calc. 80−74114
HNCO, barrier to linearity, ab initio SCF and CI calcs. 79−3363
HNO, CI-SCF-MO basis function calc. 77−42246
HNO, ground and lowest excited states, SCF ab initio calcs. 78−37544
HNO, HON, electronic reorganisation, with core ionisation 78−94196
HNO, vibr. freqs. from anharmonic ab initio/empirical PE functions 79−76406
HNO^+, ab initio SCF and CI comparison of struct. and spectra, rel. to NOH^+ 77−26972
HNO_2, isomers, protonation mechanism, electrostatic pot. prediction limits 78−11506
HO_2 and HOCl, struct., vibr. freqs., IR intensities, ab initio calcs. 79−98007
HO_2, pot. energy surface for $H+O_2 \rightarrow HO_2^* \rightarrow OH+O$ reaction, MC SCF CI method 79−74353
HO_2, struct. and props., SCF calcs. 80−106260
HO_2^+, ab initio calc. of three lowest states 78−62711
H_2O, ab initio SCF CI calcs., ground state energy, config. and force consts. 77−18782
H_2O affinity for $Li^+(Na^+)(K^+)$, ab initio SCF calcs. 80−58125
H_2O, bond dissociation, MCSCF LMO calcs. 77−57886
H_2O, core 1s shakeup study, XPS and Xalpha calcs. 80−69064
H_2O, core ionis., single orbital relax., LCAO MO SCF calcs. 78−29739
H_2O, correlated wavefucntions 78−70755
H_2O, double SCF method for electron correl., stretching force const. 78−17575
(H_2O), electron affinity, ab initio SCF calcs. 79−76343
H_2O, electron affinity, mol. geom. effects calcs. 78−82618
H_2O, electronic ground state, SCF HF and CI calcs, pot. energy hypersurface, spectroscopic consts. 78−50473
H_2O, equilib. struct., ab initio SCF calcs., general valence force field 77−3265
H_2O, excited states, pot. energy curves w.r.t. bond ang., one-centre expansion approx. 79−6886
H_2O, geom. and electronic struct., ab initio SCF calc. 79−76331
H_2O, geometry, SCF and CI calcs., basis set effects 78−62715
H_2O, ground state ionis. pots., generalized Mo theory 80−52907
H_2O, H-X bond position, correlation with electronegativity 78−9069
H_2O, mol., Compton profile, directional, polarisation functions 79−36706
H_2O, mol. Rydberg S←S and S←T transitions, semi-empirical SCF MO calc. 80−91453
H_2O, multiplet states, SCF theory 80−69062
H_2O, nucl. mag. shielding and susceptibility, SCF calcs. 77−14351
H_2O, nuclear spin-spin coupling, ab initio SCF perturbation theory 78−33525
H_2O, one-electron props., SCF Xα SW functions 78−62719
H_2O, open-shell SCF calcs. with model pot. method 77−57875
H_2O, orbital relax. energy for single and double ionis. from valence shells 80−106253
H_2O, perfect pairing valence bond model, ab initio SCF calcs. 77−6689
H_2O, polarisability and mag. susceptibility calc. by SCF and CI method 80−99443
H_2O, SCF calcs. using cusped Gaussian basis sets, polarisation effects 80−74118
H_2O, SCF energy optimisation with regard to Slater's exponents *(French)* 79−49936
H_2O, sum rule props., SCF optimizations of MO and VB calcs. 78−5156
H_2O, vibr. freqs. from anharmonic ab initio/empirical PE functions 79−76406
H_2O^-, electron affinity, mol. geom. effects calcs. 78−82618
H_2O^+, pot. energy surface, linear approach 78−41978

SCF calculations continued
H_2O^+, X^2B_1 and B^2B_2 states, pot. surfaces, SCF and CI calcs. 77−3338
H_2O-H_2S supersystem, ab initio LCAO MO SCF calcs. of H bonding 79−89607
H_2O-lysozyme, interaction, intermol. pot. calcs. 77−75250
$H_2O+H_O(F^-)(CH_4)$, interaction energy calc. using minimal basis sets 80−9678
H_2O+H_2O, interaction energy, MCF and perturbation calculations 77−27139
H_2O+H_2O, medium distance interaction, SCF LCAO MO, supermol., perturbation and MCF calc. 79−837
$(H_2O)_2$, energy decomp. anal. of H-bonding, ab initio MO calcs. 77−57868
$(H_2O)_3$, geometric config. energies, SCF LCAO MO calcs. 80−63551
$(H_2O)_n$, n=2 to 8, correlation energies, ab initio and SCF calcs. semiempirically corrected 80−43223
H_3O^++2HF, interaction pot., monopole approx., supermol. SCF and perturbation schemes 77−27139
$H_5O_2^+$, aq. soln., IR continua with polarisable H-bonds 79−26979
HOCl, photodissoc., ab intio SCF CI calcs. 78−50604
HOCl, vibr. freqs. from anharmonic ab initio/empirical PE functions 79−76406
HOF, nucl. mag. shielding and susceptibility, SCF calcs. 77−14351
HOF, vibr. freqs. from anharmonic ab initio/empirical PE functions 79−76406
$H_2O(H_2O^+)$, ab initio SCF study of low lying electronic states 79−49946
$HO_2.H_2O(NH_3)$ complex form., ab initio calcs., min. energy configs. 77−14340
H_2O...HF complex, force field, vibr. freqs., equilib. geometry bond energy, ab initio calc. 77−65450
HPO, mol. struct. and props., ab initio, calc., Gaussian lobe orbital 78−62713
HS_2, ground and first excited states, geometry, ab initio SCF calcs. 78−50657
HS_2 radical, ab initio calcs. of geometry and spectra 77−34552
HS_2, rotamers, electronic and geometrical structs., ab initio floating GO basis calcs. 78−74572
H_2S, electronic struct., ab initio CI SCF calc., spectra assignments 77−10586
H_2S, gas-phase, states in valence photoelectron spectrum 78−94284
H_2S, ground and excited states, SCF and CI calcs. 77−414
H_2S, KLL Auger spectra of S, ab initio LCAO SCF calcs. 77−65515
H_2S, KLL Auger spectrum, obs. and ab initio SCF CI calc. 78−50654
H_2S, $L(S_2)$-MM Auger energies, MC SCF calcs. 78−21977
H_2S, mol. polarisability and derivatives, ab initio SCF CI calc. 79−59597
H_2S, SCF energy optimisation with regard to Slater's exponents *(French)* 79−49936
H_2S, valence and Rydberg excited states, SCF-Xα-SW mol. oribtal study 79−36550
H_2S_2, electronic struct. and stability of isomers, gaussian SCF MO calc. 79−93921
$(H_2S)_2$, hydrogen bond, proton transfer, pot. energy surface 77−67977
HSO, ground and first excited states, geometry, ab initio SCF calcs. 78−50657
HSO radical, ground and excited first states, ab initio SCF and CI calcs. 77−30776
HSS, struct. and props., SCF calcs. 80−106260
H_3SiCl, mol., valence and core ionis. energy, RHF-SCF and PNO-CEPA calc. 79−85890
HSiN-HNSi isomers, MRD-CI calcs. of struct. and stability 78−82635
H_2SiO, electronic struct., dipole moments, mol. polarisability, force fields, ab initio calcs. 80−78531
He, freq. depend. polarizability, LCAO SCF perturbation theory 79−31387
He, ground state wavefunction, SCF HF calc. 78−90070
He, Koopmans' ionis. pot., relax. correction 79−18308
He, numerical Hartree-Fock calc. of $1s^2$ ground state 79−81155
He, photoabsorption, modified RPA calcs. with exchange 78−13477
He, quantum-mechanical calculations 77−14350
He, SCF ion improved virtual orbitals, excited configs. calc. 77−10585
He through Ne, static polarisabilities and hyperpolarisabilities, numerical SCF method 79−36567
$He+ArH^+$, ab initio pot. energy data, SCF-LCAO calcs. 80−63530
$He+H_2$, pot. energy surface, ab initio calcs., van der Waals const. determ. 80−106372
$He+H_2$, Van der Waals pot., ab inito SCF model 78−74728
He_2, He_2^+, MO correlation diagrams 77−61689
He_2, pair polarisability correl. effects, SCF-CI-GTO-SO calc. 78−82651
He_2, short range interactions between two rare gas atoms 79−26888
He_3, 3-body nonadditive interaction, nodal struct. 78−1049
He_3 three-body interatomic forces, electron gas model and SCF calcs. 78−33564
$HeCN^+$, SCF calcs., dissoc. energies, rot. and hyperfine const. determ. 80−95531
$HeCl^+$, interaction potential, HF dissociation energies, LCAO SCF calcs. 77−6880
HeH, neutral and negative ion states SCF pot. energy curves 78−62745
HeH^+, bond energy calcs., using density matrix partitioning 78−46417
HeH^+, collisional formation, SCF calcs. 77−6893
HeH_2, collision induced dipole IR spectra, ab initio SCF LCAO calc. 79−89737
HeH_2^+, electronic struct. 79−31414
He_2H^+, quantum-mechanical calculations 78−33424
^4He, liquid, inclusive of exchange-overlap three-body SCF term in Sinanoglu solvent effect method 79−41120
Hf III, multiconfig. Dirac-Fock theory, relativistic SCF method 77−3282
HfC, quasi-self-consistent energy band structures using relativistic KKR calcs. chemical bonding 79−51484
Hg_{2_n} model calc. of electronic struct. and spectroscopy 79−3352
Hg_2^+, electronic struct. and photoabsorpt. calcs. 80−27932
H_n^+ (n=7, 9, 11, 13), geometry optimisation, ab initio SCF calcs 80−53180
I, model potential method, in Roothaan's open-shell scheme 79−36513
I_2, band system, MC SCF pseudopot. calcs. 78−78632
I_2, model potential SCF calcs. 80−95528
IF, He(I) photoelectron spectra, interpretation 79−13766
$I_2(I_2^+)(I_2^-)$, HF and SCF calcs., pot. curves, electron affinity and quadrupole moment determ. 80−95527

SCF calculations continued
K^+ in molecular complexes, K-edge absorpt. spectra, Z+1 analogy, theory-expt. comparison 80−47935
KCl, Compton profile anisotropies, charge and momentum distrib., LCAO-SCF-MO calc. 79−3500
KCl, polarisability, near-Hartree-Fock limit SCF MO calc., bond length 78−42239
KD_2PO_4, H-bonded phase transitions, SCF approach 78−92030
KF, ab initio SCF MO energy, dipole moment and polarisability 80−1085
KH_2PO_4, H-bonded phase transitions, SCF approach 78−92030
KOH, MHD plasma mol., pot. energy curves and dipole moment, bond lengths 78−71462
Kr, Koopmans' ionis. pot., relax. correction 79−18308
Kr_2^+, electronic states, pot. curves, with/without spin-orbit interaction 78−33443
Kr_2^+, electronic struct., pot. energy curves, spectroscopic consts. 79−18114
Li clusters, dissociative chemisorption of H_2, ab initio SCF-MO calcs. 79−77918
Li, doublet open-shell restricted SCF eqns. 79−59350
Li, ground state wavefunction, SCF HF calc. 78−90070
Li isoelectronic sequence, self-consistent relativistic density-functional theory 80−91441
Li, s^2S and 2^2P states, spin-optimised SCF general spin orbitals 78−82617
Li, SCF ion improved virtual orbitals, excited configs. calcs. 77−10585
Li^+, ab initio SCF binding energies, with −NCO, −CO, −COO−, O, N, and −CN 77−50352
Li^-, numerical Hartree-Fock calc. of $1s^2$ ground state 79−81155
Li^+, pair polarisability, ab initio SCF MO energies 78−70741
Li/H_2O_2 surface energy for 10 atom Li model using ab initio SCF calc. 79−69359
Li-H_2O(ethylene) 78−66465
Li-like ions, partial photoionis. cross-sections and radiative recomb. rate coeffs. 80−52951
Li^+-H_2O complex, charge transfer theory, Mulliken population, ab initio calc., multiconfiguration scheme 80−106392
$Li+H_2$, inelastic collision, ab initio pot. energy surface 79−10055
$Li+H_2O \rightleftharpoons LiOH+H$, equilib. consts., ab initio SCF and CEPA calcs. 78−3361
Li+LiH, collinear reactions, SCF correl. diagram for Li_2H 77−70292
Li^++CO, pot. energy surface, equilib. distance, SCF calcs., correl. effects 77−3430
$Li^++CO(N_2)$, differential cross-sections, classical trajectory calcs. 78−29841
Li^++ether(thioether)(amide), pair pots., ab initio LCAO SCF MO calcs. 80−58184
Li^++He collisions, K-shell vacancy sharing, ab initio LCAO-SCF, CI calcs. 77−19054
Li_2, $A^1\Sigma_u^+$ state, vibr. energy levels calcs. 77−83566
Li_2, and anion, electronic struct., spin-unrestricted, spin-restricted SCF HF calc. 78−90331
Li_2, $B^1\Pi_u$, pot. energy curve, MC SCF approx. calcs. 77−38618
Li_2, charge distrib. anal. rel. to Berlin's binding and antibonding regions 79−6875
Li_2, lowest $^1\Pi_g$, $^1\Pi_u$, $^3\Pi_g$, $^3\Pi_u$ states 77−54517
Li_2, MCSCF and CI calcs. 80−95526
Li_2, MCSF accurate pot. energy curves for $^3\Sigma_u^+$ and $b^3\Sigma_g^+$ states, level crossing 77−50369
Li_2, mol. struct. 2-electron integral evaluation by Multipole Expansion of Diatomic Overlap 78−908
Li_2 SCF polarisability, polarisation potentials, ab initio calc. 79−89602
Li_2, second virial coeffs., Konowalow MCSCF potential calcs. 80−23312
Li_2, total SCF energy estimation from orbital energies 79−63908
Li_2, $X^1\Sigma_g^+$ and $A^1\Sigma_u^+$ states, electronic struct. and spectra 79−89615
Li_2^-, electronic struct., ab initio calcs. 77−34553
Li_{2n}, (n=1, 2, 3), stable cluster configs., ionisation pots., binding energies, vibr. freqs., al initio SCF and CEPA calcs. 80−14265
Li_3, electronic struct., SCF and SCF-CI calcs. 80−87044
Li_3^-, electronic struct., SCF and SCF-CI calcs. 80−87044
Li_3^+, electronic struct., SCF and SCF-CI calcs. 80−87044
Li_4, MCSCF and CI calcs. 80−95526
Li_4, plane configs., ab initio SCF calc., rel. to condensation *(French)* 77−4062
$LiAlF_4$, struct. pot. energy surface, Li^+ migration, ab initio LCAO SCF calcs. 80−23305
LiBr, pair pot., dipole moment, polarisability tensor, bond length depend., finite field SCF calcs. 80−58127
LiCN, electron density distrib., SCF mol. orbitals calcs. 78−9058
LiCl, Compton profile anisotropies, charge and momentum distrib., LCAO-SCF-MO calc. 79−3500
$Li_nCl^{(n-1)+}$, energy cluster expansion convergence 80−91715
LiF, ab initio SCF MO energy, dipole moment and polarisability 80−1085
LiF, F centre study by mol. SCF calcs. 80−44530
LiF oligomers, struct., stability SCF and CEPA-PNO calcs. 78−78640
LiF^-, ground and excited states, ab initio calcs. single config. and multiconfig. SCF calcs. 80−52873
LiF-NH_2 adduct, mol. consts., ab initio SCF LCAO MO calcs. *(French)* 78−13423
LiH, direct optimisation of orbitals for multiconfiguration self-consistent field theory by unitary transformations 80−63544
LiH, electron correl., double SCF method, mol. dissoc. energy 78−17575
LiH, finite-field method calcs., dipole moment gradients, polarisability gradients and elec. field effects 77−88589
LiH, LiH^-, pot. energy curves, electron affinity, spectroscopic consts. 78−5129
LiH, $LiHe^+$ and $LiHe_2^+$ systems, ab initio SCF LCAO calcs. of stability and spectroscopic consts. 77−71748
LiH, limited MC SCF calcs. 79−36537
LiH, mol. struct. 2-electron integral evaluation by Multipole Expansion of Diatomic Overlap 78−908
LiH, numerical calc. of one-electron props. from SCF-Xα-SW calcs. 77−6688
LiH oligomers, struct., stability SCF and CEPA-PNO calcs. 78−78640
LiH, positron affinity, ab initio LCAO MO SCF calc. 78−82870
LiH, relativistic Dirac-Fock multiconfig. SCF calcs. 80−99455
LiH, SCF ab initio calcs. with noninteger Slater orbitals 77−26969
LiH_2 SCF calcs., undergraduate exercise 80−82597
LiH^+, spin densities, SCF and CI calcs. 79−3362

SCF calculations continued
LiH-NH_3(ethylene)(acetylene), struct. and props., SCF ab initio calcs. 80−106250
LiH+H→Li+H_2, linear LiH_2 pot. energy surface, MCSCF functions optimisation 77−67960
$(LiH)_3$ complex, SCF interaction energy nonadditivity 80−91487
LiH^-(LiH), ab initio ground-state pot. energy curves, electron affinities 78−41946
$LiNH_3^+$, $LiNH_2$, Li_2NH, localised orbital anal., bond props. 77−6676
$LiNO_3$, mol. struct. ab initio calcs. 79−26884
$Li^+NO_3^-$ ion pairs and hydrated ion pairs, MO calcs., matrix isolation data 78−46267
LiNa, and anion, electronic struct., spin-unrestricted, spin-restricted SCF HF calc. 78−90331
LiO, struct., spectra, SCF MO calcs. 78−17559
Li_2O (LiOLi, LiLiO), struct., spectra, SCF MO calcs. 78−17559
Li_2O^-, electronic struct. and config., ab initio SCF study 79−85898
LiOH, geom. and electronic struct., ab initio SCF calc. 79−76331
$LiOH^-$, electronic struct. and config., ab initio SCF study 79−85898
$Li^+(OH_2)_2$, 3-body pots., SCF energy partitioning calcs. 80−18953
LiOO, struct., spectra, SCF MO calcs. 78−17559
Mg cluster, multibody expansions, convergence 80−23594
Mg_2, Mg_2^+, electronic struct., pot. energy curves, multiconfig. SCF calcs. 78−5124
MgF_2, ground state, nonempirical LCAO SCF calcs. 78−66469
MgF_2^-, ground state, conform., electron affinity, extended basis SCF calcs. 79−72253
$Mg_4(Mg_4^-)$, atomic clusters, electronic struct., LCAO-MO-SCF and HF calcs. 80−63880
MgO, compressed, SCF electronic struct. calcs., necy. press. for conversion to metallic state 78−43300
MgO, electronic struct., approx. SCF calcs. 79−56125
$Mg^{2+}.nH_2O+PO_4H_2^-$, binding mechanisms, SCF ab initio calcs. 79−22586
Mn-C_2H_2 and Mn-C_2H_4, π-bonded, pot. energy curves, SCF calc. 78−5136
$MnCl_4^{2-}$, electronic energy levels calc. by conventional and X alpha Hartree-Fock methods 78−66470
MnO, SCF CI calcs., ground and first excited states, bonding mechanism 77−14347
Mo complex, hexadimethylamino molybdenum, electronic description of triple bonds and verification by photoelectron spectroscopy 78−41949
Mo complex, metal-metal bond, correl. effects, SCF calc. 77−65425
Mo, electron states, calc. using SCF-Xα-SW method 77−15797
Mo, localised electronic states near dislocations 79−33257
Mo, localized electronic states near ⟨100⟩ edge dislocation compared with perfect lattice 78−30888
Mo_2 metal-metal bond energy, SCF-Xα-SW calcs. 80−78538
$Mo_2Cl_8^{4-}$, metal-metal bond energy, SCF-Xα-SW calcs. 80−78538
$Mo_2Cl_9^{3-}$ complexes, cluster exchange coupling consts. SCF-Xα-SW calcs. 80−74120
$Mo_6Cl_{14}^{2-}$, cluster ground state electronic struct. SCF Xα SW calc. 79−3607
$Mo_2(NH_2)_6$, electronic description of triple bonds and verification by photoelectron spectroscopy 78−41949
$Mo_2(OH)_6$, electronic description of triple bonds and verification by photoelectron spectroscopy 78−41949
$Mo_6X_8^{4+}$ cluster cpds. (X=F, Cl, Br, I), SCF-SW-Xα calcs. 80−74276
N-containing cpds., ^{13}C chem. shift calcs. using approx. SCF perturbation theory 77−18945
N_2, $^5\Pi_u$-$^5\Sigma_g^+$ transition, MC-SCF calcs. 79−76412
N_2, 50 eV elastic electron scatt., centrifugal-dominant channel decoupling 80−32831
N_2, ab initio MO-LCAO-SCF and Gordon-Kim intermolecular pot. for seven different orientations 80−95522
N_2, core ionisation, single orbital relax. energy contrib. calcs. 78−82637
N_2, electron scattering, charge polarisation effects, SCF treatment 79−50132
N_2, electron-mol. adiabatic polarisation pots. and ab initio SCF polarisabilities 80−9499
N_2, electronic struct., binding energy and interatomic distance, SCF variational cellular calc. 80−9498
N_2, electrostatic interaction energies for point charge and NaCl (100) surface 78−74592
N_2, finite field method calc., moments, polarisability, field-induced shifts in mol. props. 78−74561
N_2, ground state ionis. pots., generalized Mo theory 80−52907
N_2, low energy electron (positron) collisions, ab initio adiabatic polarisation pots. 80−14240
N_2, mol. struct. 2-electron integral evaluation by Multipole Expansion of Diatomic Overlap 78−908
N_2, multi-config. SCF super-CI calc., density matrix formulation 80−78547
N_2, multiple moments, polarisabilities and anisotropic long range interaction coeffs. 80−43206
N_2, N_2^+, MO correlation diagrams 77−61689
N_2, one-electron props., polarisabilities and polarisability derivatives, SCF and CI calcs. 80−37746
N_2, polarisability derivatives, SCF and CI calcs. 79−59348
N_2 SCF calcs. using cusped Gaussian basis sets, polarisation effects 80−74118
N_2, static polarisabilities, ab initio SCF HF calcs., internucl. separation depend. 78−9073
N_2^+ 1s hole satellite spectrum, large-scale CI calc. 77−65428
N_2^{2+}, low-lying electronic states, pot. energy curves calcs. by SCF technique, vibr. and ionisation consts. 80−69091
N_2^{n+}, Coulomb explosion following heavy ion impact, ab initio SCF calc. 79−18277
N_3^- electronic struct., SCF Xα scatt.-wave calcs. 77−50364
N_3^-, low-lying excited states 79−31425
N_3^-, theoret. electron density distrib. cf. expt. density distribs. of NaN_3 and KN_3 77−46489
NCNCO, geometrical struct., INDO calcs. 79−22602
NCO^+, CI-SCF-MO basis function calc. 77−42246
NCO^+, partial pot. energy surfaces, ab initio SCF CI calcs. 78−37554
NCl_3, ab initio LCAO SCF calc. for ground state, inversion barrier 78−25426
NF_3, NF_3^-, and NF_3^+, optimised struct. and bonding, ab initio SCF MO calc. 80−23334
NH_2, geometry, SCF and CI calcs., basis set effects 78−62715
SCF calculations continued
NH_2 radical, (NH_2^+), ab initio SCF study of low lying electronic states 79−49946
NH_2, X^2B_1, A^2A_1 and B^2B_2 states, ab initio SCF CI calcs. 78−29746
NH_2^-, mol. geom., diffuse functions in SCF calcs. 79−10226
NH_2^+, low lying states, ab initio MRD-CI pot. surface calcs. 79−89611
NH_2^+, quintet states, pot. energy surfaces, ab initio SCF MO calc. 78−25419
NH_3, ab initio SCF calcs., force consts., vibrs., pot. energy surface 78−5209
NH_3, affinities for $H^+(Li^+)(K^+)(CH_3^+)$, ab initio SCF calculations 80−102443
NH_3, affinity for $Li^+(Na^+)(K^+)$, ab initio SCF calcs. 80−58125
NH_3 bond dissociation, MCSCF LMO calcs. 77−57886
NH_3, core 1s shakeup study, XPS and Xalpha calcs. 80−69064
NH_3, core ionis., single orbital relax., LCAO MO SCF calcs. 78−29739
NH_3 dimer, inversion, influence of H-bond 77−50556
NH_3, elec. dipole polaris., near Hartree-Fock value, using EFV GTOs 77−88591
NH_3, freq. depend. hyperpolarisability, time-depend. Hartree-Fock calcs. 79−36559
NH_3, geometry changes during inversion, ab initio calcs. 78−5154
NH_3, H-X bond position, correlation with electronegativity 78−9069
NH_3, HF geometry calcs. and SCF calcs. 80−47877
NH_3, lowest triplet state geometry, SCF and CEPA-PNO calc. 80−914
NH_3, mol. nuclear spin-spin coupling, ab initio SCF perturbation theory 78−33525
NH_3, mol. Rydberg S←S and S←T transitions, semi-empirical SCF MO calc. 80−91453
NH_3, orbital relax. energy for single and double ionis. from valence shells 80−106253
NH_3, photodissoc., ab initio SCF and CI calcs. 78−21984
NH_3-CO_2 complex, matrix isolation IR spectrum, struct., ab initio SCF calcs. 78−5209
NH_3-lithium halide complex, ab initio calcs., Li bond rel. to H bond 77−14343
NH_3+2H_2, triplet n3S Rydberg state, ab initio UHF Cl SCF calc. 80−53095
NH_3+He, interaction potentials, ghost orbital SCF and Gordon-Kim calcs. 79−94057
NH_5^+, stability, ab initio calcs. 77−23419
N_2H_2, model rearrangement system, electron correlation and basis set effects 80−3317
N_2H_2, $N_2H_2^+$, ab initio calcs., electronic struct., geometries relative energies 77−46487
N_2H_2+ethylene reaction, H transfer, ab initio SCF GO calcs. 77−44469
N_3H_3 radical, lowest two electronic states 80−925
NH_4Cl, gas $^1A_1$ ground state, pot. surface 80−32626
NH(D) radical, and isotopic species, laser mag. reson., hyperfine parameters 77−10694
NH_xF_{3-x}, geometry changes during inversion, ab initio calcs. 78−5154
$NH_2(F_2)(Cl_2)$, SCF-MO-HF calc., struct. and one-electron props., population anal. indices 79−76338
NH_2T, β-decay, ab initio SCF MO calcs. 77−71842
NH_2TNH_3, β⁻ decay effect on H-bond, ab initio LCAO SCF MO calc. 78−76894
NO_2, electronic states, pot. energy surface calcs. 77−6673
NO_2, ground state pot. surface, ab initio LCAO MO SCF calcs. 80−102461
NO_2, NO_2^+, NO_2^-, SCF and MC SCF CI calcs. 78−46280
NO_2, peroxy isomer, stability, ab initio SCF calcs., bond strength 77−14605
NO_2, vertical electronic spectrum, SCF and CI calcs. 77−30878
NO_2, vertical electronic spectra, ab initio calcs. 78−66538
NO_2^-, electron detachment energy, equations of motion method calcs. 77−50478
NO_2^+, vertical electronic spectra, ab initio calcs. 78−66538
NO_2^+, gas phase equilib. geometry, force consts., vibr. freq., dipole moment function MCSCF/CI calcs. 80−78520
NO_2^+, vertical electronic spectra, ab initio calcs. 78−66538
$(NO_2)_2$, struct. and force fields of isomers, ab initio calcs. 77−18783
N_2O, X-ray fluoresc. obs., ionis. pot., fine struct., LCAO SCF calc. 77−68055
N_2O^+, ground state potential energy surfaces 77−27175
N_2O^+, electronic ground state, INDO SCF MO calcs. 78−82644
N_2O^+, pot. energy hypersurface characts. calc. in $O^+ + N_2 \rightarrow N + NO^+$ react. 78−60996
NOF and ONF, ab initio calcs. of geometry and electronic struct. 79−76342
NOH^+, ab initio SCF and CI comparison of struct. and spectra with HNO^+ 77−26972
$N(^4S)+O_2(^3\Sigma_g^-)\rightarrow NO(^3\pi_u)+O(^3P)$ doublet surface minimum energy path calcs. 78−7194
^{14}N quadrupole coupling consts., ab initio calcs. 80−58283
^{15}N-^{13}C spin-spin coupling constants calc. using SCF and INDO method 80−32609
Na $A^1\Sigma_u^+ \rightarrow X^1\Sigma_g^+$ system, transition moments and radiative lifetimes calcs. 77−34697
Na clusters, electronic relaxation energies in $KL_{2,3}L_{2,3}$ Auger transitions, SCF-Xα-SW calcs. 78−90334
Na core polarisation effect on oscillator strengths and energy level locations 78−82688
Na, doublet open-shell restricted SCF eqns. 79−59350
Na, metallic, Auger cross relaxation energy, SCF cluster model calc. 79−46945
Na^+, interaction with purine and pyrimidine bases of nucleic acids 77−64005
Na^++ether(thioether)(amide) interaction, pair pots., ab initio SCF LCAO MO calc. 79−36721
Na_2, and anion, electronic struct., spin-unrestricted, spin-restricted SCF HF calc. 78−90331
NaCl, Compton profile anisotropies, charge and momentum distrib., LCAO-SCF-MO calc. 79−3500
NaF oligomers, struct., stability SCF and CEPA-PNO calcs. 78−78640
NaH oligomers, struct., stability SCF and CEPA-PNO calcs. 78−78640
NaH^-(NaH), ab initio ground-state pot. energy curves, electron affinities 78−41946
Na(1s), X-ray photoelectron spectrum, binding energy, at. compared with metal 78−70800

SCF calculations continued
$Na^+.nH_2O+PO_4H_2^-$, binding mechanisms, SCF ab initio calcs. 79−22586
NbC, electronic struct. of vacancies, effect on supercond. transition temp. 80−29347
Ne, atomic interaction energy, basis set effects in SCF calcs. 77−83678
Ne, core ionis., single orbital relax., LCAO MO SCF calcs. 78−29739
Ne, ground state wavefunction, SCF HF calc. 78−90070
Ne, ionisation potential, KLL Auger energies, SCF transition operator calcs. 78−41925
Ne, Koopmans' ionis. pot., relax. correction 79−18308
Ne, temp. perturbed Thomas Fermi eqn., variational principle 80−69074
$Ne+H_2$, Van der Waals pot., ab inito SCF model 78−74728
$Ne+H_2^+$, reaction pot. energy surface, LCAO-MO-SCF energies 77−1917
$Ne+HeH^+$, collinear reaction, pot. energy surface SCF-LCAO-MO and DIM calc. 78−92467
Ne_2, short range interactions between two rare gas atoms 79−26888
Ne_2, van der Waals mols., interatomic energy, SCF supermol. ab initio calcs. 77−42370
Ne_2^+, electronic struct., pot. energy curves, spectroscopic consts. 79−18114
Ne_3, 3-body nonadditive interaction, nodal struct. 78−1049
$NeCN^+$, SCF calcs., dissoc. energies, rot. and hyperfine const. determ. 80−95531
Ne_nH clusters, ab initio LCAO MO SCF calc., struct. and energy 78−66704
Ne_nH^+ clusters, ab initio LCAO MO SCF calc., struct. and energy 78−66704
Ni, (001) surface, local density of states, asphericity of pot. and charge transfer, ab initio self-consistent calcs. 79−15064
Ni (100), surface electronic struct., self-consistent local orbital calc. 80−65649
Ni, chemisorption of CO, electronic struct. of $(M)_5CO$ clusters 78−95948
Ni cluster-H, electronic struct. calc., H-metal bonding 77−89823
Ni clusters local densities of states 80−88466
Ni complex, nickel-bis-dithiolene, pseudopot. MCSCF and limited CI calcs. 80−83292
Ni, correlation effects on energy bands 79−60697
Ni, FCC, H-Ni_n self-consistent electronic screening charge density 79−33255
Ni surface, adsorbed CO, N_2, valence band photoemission, SCF MO CNDO calc. 80−100754
NiCO, and core ionised, binding and relax. energy ab initio LCAO MO SCF calc. 78−62712
NiCO, liquid interactions, ab initio LCAO MO SCF calcs. 79−18256
$Ni(CO_4)$, ionisation energies, approx. SCF Hartree-Fock-Slater calcs. 77−75334
NiF_2+CO, Ar matrix isolated, ab initio MO calcs. 78−92458
NiNO, ground and core hole states, config. depend. HF LCAO SCF calc., relax. and binding energy 80−29453
$Ni(Ni)_2$-ethylene cluster complex 78−82641
NiO, ab initio SCF and CI calcs. on d-d transitions, NiO_6^{10-} d-electron delocalisation 77−35896
NpF_6, electronic struct. and transitions, SCF-Xα-SW calcs. 78−78627
NpF_6, energy levels and bonding, relativistic SCF Dirac-Slater calcs. 77−6691
O^{n-} (n=0 to 2), core binding energy shifts, ΔSCF calcs. 80−95558
O-containing organic molecules, LCAO-SCF calc. core binding and relax. energies, rel. to polymer surface oxidation 79−76344
O_2, $a^1\Delta_g$ and $b^1\Delta_g^+$ state, MCSCF wavefunctions 78−37561
O_2, electronic struct., self-consistent pseudopot. calc. 80−9508
O_2, RH-GTO-MCSCF calc., 1s photoelectron spectra, multiplet intensity ratio 78−5134
O_2, Schumann-Runge continuum, oscill. strength and electron impact excitation 80−69121
O_2^-, $A^2\Pi_u$ state pot. energy curve, MCSCF calcs. 80−63565
O_2^-, ab initio pot. curves of $X^2\Pi_g$, $A^2\Pi_u$, $a^4\Sigma_u^-$, $^2\Sigma_u^-$ states 78−66483
O_2^+, electron impact dissoc. recomb., pot. energy curves calcs. 80−53150
$O_3 \rightarrow O_2+O$, MNDO semi-empirical SCF MO calc. 77−44465
O_3, open and closed forms, bond angle and length, MC SCF and MC CI calcs. 78−78831
O_3, open-shell SCF secular eqn., iterative algorithm soln. 80−52868
O_4 molecule, equilib. struct., vibr. freqs., SCF closed shell calcs. 80−74101
O_4 molecule, SCF-CI calcs. 80−78517
O_5^{2-}, hypothetical, mol. self-consistent study, possible prep. method *(French)* 80−91717
OCl_2^+, radical cation, struct. and electronic props., ab initio RHF SCF MO calc. 80−52883
$OH^-+CO_2 \rightarrow HCO_3^-$ react., MO-LCAO-SCF calcs., energy barrier 78−76846
OH_4^+, stability, ab initio calcs. 77−30775
OH_n, ab initio LCAO SCF calcs. of ionisation pot., electron, proton, H and hydride affinities 77−88387
OH_n, LCAO-MO-SCF with Gaussian polarisation functions, energetic effect of p-, d-, and f-functions 78−41944
OHT, β-decay, ab initio SCF MO calcs. 77−71842
ONCN, IR spectra isotope shifts and ab initio calc. for harmonic force field 79−13715
ONCl, vibr. freq., anharmonic ab initio/empirical pot. energy functions 80−99457
ONF, vertical electronic spectrum, CI and SCF calcs. 77−75123
P_4, closed-shell SCF calcs., mol. symmetry 78−41930
PF_6^-, octahedral complex, ionis. energy, SCF-Xα study 78−70967
PH_2 radial, pot. energy curves. config., ab initio SCF-MO calcs. 77−50419
PH_5, rearrangements, CI calcs. in large at. orbital basis 79−94106
PH_3F_{3-x}, geometry changes during inversion, ab initio calcs. 78−5154
$PH_2(F_2)(Cl_2)$, SCF-MO-HF calc., struct. and one-electron props., population anal. indices 79−76338
PO_4^{3-}, ionisation energies, SCF-Xα transition state calcs. 80−74115
Pb, muonic high-lying states transitions, electron screening effects 77−34786
PbS, first-principles calc. of eqn. of states 80−49649
PbS, thermomech. props., SCF Xα scatt. wave theory 78−71704
PbS(PbSe), ab initio SCF calcs. using relativistic effective core pot. 80−95524
Pd cluster-H, electronic struct. calc., H-metal bonding 77−89823
Pd_2, ab initio relativistic core pot. studies of metal-metal bonding 80−106257
$Pd(CO)_4$, ab initio LCAO MO SCF results invalidate pseudopot. calc. 77−6675
PdH, ab initio relativistic core pot. studies of metal-H bonding 80−106257
Pd(111) chemisorption of H, photoemission spectra, SCF electronic struct. 79−33320
Pt cluster-H, electronic struct. calc., H-metal bonding 77−89823
Pt_2, ab initio relativistic core pot. studies of metal-metal bonding 80−106257
$(PtCl_6)^{2-}$, quasi-relativistic SCF-MO-LCAO methods, CNDO and MWH appls. 78−41953
PtH, ab initio relativistic core pot. studies of metal-H bonding 80−106257
PuF_6, electronic struct. and transitions, SCF-Xα-SW calcs. 78−78627
PuF_6, energy levels and bonding, relativistic SCF Dirac-Slater calcs. 77−6691
Rb, density functions, SCF method, coherent scatt. function 78−18527
Rb, liquid, coherent scatt. function anal. by self consistent field method 79−55651
$Re_2Cl_8^{2-}$, spectral assignment, metal-metal bonds, SCF Xα SW calcs., relativistic corrections 80−53006
$Re_3Cl_{12}^{3-}$, cluster ground state electronic struct. SCF Xα SW calc. 79−3607
Re_3Cl_9, cluster ground state electronic struct. SCF Xα SW calc. 79−3607
Re_3Cl_9 metal cluster complexes, He(I) photoelectron spectrum, SCC DV Xα calcs., $Re_2Cl_8^{2-}$ comparison 80−28063
S_2, low lying bound molecular electronic states 79−45643
S_3, open and ring isomers, electronic struct., ab initio SCF calcs. 77−57862
S_4^x, x=2−, 0, 2+, struct. differences explained, SCF Xα scatt. wave MO calcs. 78−74784
S_8, cyclic, electron deformation density distrib., SCF-Xalpha-scatt. wave method 78−33425
S_8^{2+}, electronic struct. and localised MOs, bonding nature and geom. struct. 80−18798
SF_2, ab initio LCAO MO SCF calcs., elec. struct., mol. props. 77−14344
SF_6, ab initio electronic struct., and photoelectron spectral assignment 79−54764
SF_6 and SF_6^+, excited states investig. 77−57882
SF_6, KLL Auger spectrum, obs. and ab initio SCF CI calc. 78−50654
SF_6, KLL spectra of S, ab initio LCAO SCF calcs. 77−65515
SF_6, octahedral complex, ionis. energy, SCF-Xα study 78−70967
SH, ionis. pot. of $(X^2\Pi_i)$ radical, ab initio ΔSCF calc. with electron correl. 79−98153
SH_n, LCAO-MO-SCF with Gaussian polarisation functions, energetic effect of p-, d-, and f-functions 78−41944
SN, electronic states, ab initio, SCF, and CI calcs. 77−75053
$(SN)_x$, quantum chem. calcs. of electronic struct. 78−6257
$(SN)_x$, tight-binding SCF MO calcs., interchain interaction 78−30859
S_2N_2, $(SN)_x$, (x=2 or 3), minimal STO-3G basis HF ab initio LCAO SCF MOC, geometry 78−903
S_2N_2, electronic states, ab initio, SCF, and CI calcs. 77−75053
S_2N_2, polymerisation, mol. struct., INDO calcs. 77−70301
S_4N_4, electronic struct. calc. using free-electron orbitals basis set 77−79537
$S_4N_4H_4$, SCF-Xα-CNDO/BW calcs., comparison 78−25435
SO, low lying bound mol. electronic states, SCFCI calc. 80−23314
SO_2, analytical pot. functions, several surface minima 78−5158
SO_2, ground state, ab initio and MOD POT calcs. 78−66466
SO_2, KLL Auger spectra of S, ab initio LCAO SCF calcs. 77−65515
SO_2, KLL Auger spectrum, obs. and ab initio SCF CI calc. 78−50654
SO_2, SF_2, SO_2F_2, bond function parameter transferability 77−30770
SO_3, dissoc. pathways and mol. vibr., compliance consts. and min. energy coords. 78−35661
SO_4^{2-}, ionisation energies, SCF-Xα transition state calcs. 80−74115
SOH, ground and first excited states, geometry, ab initio SCF calcs. 78−50657
SOH radical, ab initio SCF and CI calcs., electronic states and transitions 77−46488
SbH_3, inversion barrier, ab initio SCF calcs. 78−78615
Se, amorphous, defect states, SCF pseudopot. and tight-binding calc. 79−65415
Se_8^{2+}, electronic struct. and localised MOs, bonding nature and geom. struct. 80−18798
Si (111), chemisorbed Cl layer, SCF LCAO band struct. calcs. 78−88010
Si (111), surface relax., mol. SCF calcs. 78−91522
Si (111) covalent surface, pot. and charge distribs. and dangling-bond state 78−2537
Si II, transition probabilities between excited states, SCF treatment 78−82658
Si, isolated vacancy, electronic struct., SCF method 80−80208
Si, Jahn-Teller distorted vacancy, electronic struct. 80−10869
Si, solid, electron rearrangement after inner shell ionisation by heavy charge particle impact 80−87043
Si, vacancy, self-consistent electronic states 80−29354
Si_2, charge density and pseudo charge density, pseudopot. and SCF calcs. 78−70740
Si_2, electronic struct. and bonding, atomic effective pot. appl. 80−95745
SiF_4, XUV spectra, overlapping core-valence and core-Rydberg transitions and resons. 80−32735
SiF_6^{2-}, octahedral complex, ionis. energy, SCF-Xα study 78−70967
SiH_2, electron affinity, theoretical exam. 78−29863
SiH_4, ab initio Hartree-Fock SCF-LCAO-MO method 78−94195
SiH_4, mol., valence and core ionis. energy, RHF-SCF and PNO-CEPA calc. 79−85890
SiH_4, SCF calcs. including polaris. functions 80−87034
SiH_4, SiH_3F, SiH_2F_2, CH_3SiH_3, core Auger shifts, ab initio LCAO MO SCF calcs. 78−904
Si_2H_4 ground state struct., ab initio SCF calcs., singlet silylsilylene 80−27945
Si_2H_6, barrier to internal rotation 78−66680
Si_2H_6, bond lengths, photoelectron spectrum, mol. orbitals calcs. 78−5132
Si_2H_6, rot. barriers, MS-SCF-X_α calcs. 80−106267
Si_2H_6, tetrahedral edge sharing, distortions, MO calcs. 77−14380

SCF calculations continued
SiH_2F_2, ab initio Hartree-Fock SCF-LCAO-MO method 78−94195
SiH_3F, ab initio Hartree-Fock SCF-LCAO-MO method 78−94195
$(SiH_3)_3N$, SCF calcs. including polaris. functions 80−87034
$SiH_4(SiF_4)$, electron rearrangement after inner shell ionisation by heavy charge particle impact 80−87043
$SiH_2(SiH_2^+)(SiH_2^-)$, electronic structure, ab initio LCAO MO SCF calcs. 79−10027
SiO $^3\Pi$ valence states, struct. and perturbations 79−59369
SiO, valence ionis. energy, calc. including correl. effects 79−68185
SiO, $X^1\Sigma^+$, $A^1\Pi$, $C^1\Sigma^-$ and $E^1\Sigma^+$ states, SCF CI calcs. 79−45641
SiO_2, mol., ab initio SCF calcs., ground state stability, struct., vibr. freqs. 78−86781
Si_2O_2, tetrahedral edge sharing, distortions, MO calcs. 77−14380
Si_2S_2, tetrahedral edge sharing, distortions, MO calcs. 77−14380
SiX_4 (X=Cl,H,F), chemical shifts, relax., X-ray spectra, SCF Xalpha calcs. 80−27928
SrF_2, U-centre, electronic struct. and optical transition energies, SCF MS $X\alpha$ calc. 79−4532
TCNQ, ab initio SCF LCAO band struct. calc. 80−70608
TTF, ab initio SCF LCAO band struct. calc. 80−70608
TaC, quasi-self-consistent energy band structures using relativistic KKR calcs, chemical bonding 79−51484
TaO_6^{7-}, octahedral cluster, ionisation energies and atomic populations, XPS and SCFMS $X\alpha$ calc. 79−93923
$Tc_2Cl_8^{3-}$ ion, visible spectra, electronic struct. 78−5240
Te_4^{2+}, pseudopot. SCF-MO calcs., spectrum assignments 80−83269
$ThF_4(Cl_4)$, electronic struct., MS-SCF-$X\alpha$ calcs. and VUV photoelectron spectra 80−63710
Ti complex, bis cyclopentadienyl Ti:N_2, liquid interactions, ab initio LCAO MO SCF calcs. 79−18256
Ti, Koopmans' ionis. pot., relax. correction 79−18308
Ti_2, electronic structure of five and ten atom chains SCF-Xα-SW calcs. 80−5483
$TiCl_4$, optical and Ti 2p core photoemission spectra, SCF Xα anal. 79−94032
TiF_2, TiF_4, X-ray emission, core level chem. shift calcs. 80−53010
TiH, electronic structure of five and ten atom chains SCF-Xα-SW calcs. 80−5483
TiH_4, X-ray emission, core level chem. shift calcs. 80−53010
TiH_3F, X-ray emission, core level chem. shift calcs. 80−53010
TlCl, ground-state props., Wannier functions, and electronic struct., ab initio self-consistent calc. 80−80178
TlH, ab initio SCF calcs. using relativistic effective core pot. 80−95524
U, valence energy levels, SCF relativistic Xalpha calc. 79−85912
^{92}U, self-consistent relativistic density-functional theory 80−91441
UC, quasi-self-consistent energy band structures using relativistic KKR calcs. chemical bonding 79−51484
UF_6, electronic struct. and transitions, SCF-Xα-SW calcs. 78−78627
UF_6, energy levels and bonding, relativistic SCF Dirac-Slater calcs. 77−6691
UF_6, valence energy levels, SCF relativistic Xalpha calc. 79−85912
UF_6^+, electronic struct., ab initio calcs. using relativistic core pots. 79−97987
$UF_4(Cl_4)$, electronic struct., MS-SCF-Xα calcs. and VUV photoelectron spectra 80−63710
UO_2^{+z}, valence energy levels, SCF relativistic Xalpha calc. 79−85912
UO_2^{2+}, electronic struct., secondary ligands effects, Dirac-Slater model 77−411
V, atom and ions, shell energy struct., SCF calc. by Dirac-Fock-Slater method 80−52877
V, X-ray band spectra calcs. 79−33860
VN, electronic struct. of vacancies, effect on supercond. transition temp. 80−29347
W, first-principles pseudopotential in the local-density-functional formalism 79−59328
W(001), surface states and surface resonances, self-consistent electronic struct. 80−96960
Xe, energy levels from ab initio effective core pot. 78−33426
Xe, photoabsorption, local field effects 80−74151
Xe_2^+, electronic states, pot. curves, with/without spin-orbit interaction 78−33443
Xe_2^+, electronic struct., pot. energy curves, spectroscopic consts. 79−18114
$XeCl_2$, electronic structure, MSW-SCF-Xα method 80−78539
XeF_2, pseudopotential SCF-MO studies, equilib. struct., stretch-stretch interaction force const. 80−95525
XeF_4, pseudopotential SCF-MO studies, equilib. struct., stretch-stretch interaction force const. 80−95525
XeF_5^+, pseudopot. SCF MO studies, steric aspects of struct. and force fields, Jahn-Teller effect 80−99444
XeF_6, pseudopot. SCF MO studies, steric aspects of struct. and force fields, Jahn-Teller effect 80−99444
XeF_x, x=2, 4, 6, electronic structure, MSW-SCF-Xα method 80−78539
Xe_2*, Xe_2^+, Xe_2, pot. energy curves, relativistic ab initio effective core pots. 78−86800
Yb, atom, scalar relativistic approximation 79−26899
Zn_2, ab initio SCF LCAO MO calcs., contracted basis set effects 77−83495
Zn_2, electronic states, CI calcs., rel. to Hg_2 77−10601

scheduling
antitumor drug dosage schedule, cell cycle kinetics approach 77−86700
fusion reactor, TFTR, preoperational test plan, manpower loading and scheduling 80−102340
nuclear power plant startup scheduling 80−13687
nuclear power reactors in elec. utility system, short range system analysis method 77−50252
PWR refuelling fuel shuffle scheduling 79−9866

schizons *see elementary particle weak interactions*

schlieren systems
acoustic field quantitative visualization, using closed circuit TV system 78−46867
acoustic wave fronts image profiles in schlieren obs. 77−11093
acousto-optic modulator efficiency optimisation, sound diffraction profile model and expt. 80−106615
amplitude transfer charact., Monte Carlo method 80−28336
arc, high current, rotating, hot wake investigation by streak photography and schlieren systems 80−1862
axisymmetric schlieren interferometry, quantitative appls. 77−41677
boundary layer transition, detection using holography 78−14101

schlieren systems continued
brass/water interface leaky Rayleigh wave reflectivity loss meas. 78−59187
breakdown in air gaps obs., using high-speed schlieren technique 78−87518
bubble dynamics, laser schlieren meas. 79−41773
colorisation of schlieren images, using electro-optical technique 78−33904
colour images of inhomogeneous transparent media 78−33905
composite material delamination visualisation, US pulsed schlieren method 79−70289
crossed beam correlation method, localised turbulence props. meas. 78−34223
current disruption, in Tokamak plasmas, schlieren signal meas. from millimetre waves 80−48998
diaphragm shape var. effect on charact. 78−30080
dielectric liquid, elec. stressed, motion due to Coulomb, electromech. forces, schlieren image obs. 80−100037
discharges, selfluminous, schlieren system for time and space resolved photography 80−87471
electric field distrib. in dielectrics, schlieren method for determ. 80−31720
electrical breakdown in liquid hydrocarbons, high speed laser schlieren techniques 78−15093
electron beam fusion compression targets, fuel preconditioning studies 79−81076
exploding wire cylindrical blast wave high-speed photography for material impact testing 79−79189
flow visualisation of hypersonic sphere in air, obs. with open microwave resonator 79−77301
flowing gas conc. fluctuation meas., laser schlieren technique 80−3444
gas trace anal. by laser-induced Schlieren technique 80−9929
gradient index material profiles and chromatic props. 80−14409
high speed interferometry to measure effects of neutral gas density reduction on negative pulseless glow-spark transition 80−33850
high speed photography, in aeroballistic range, track facilities of von Karman gas dynamics facility 78−37094
high-speed cine schlieren photography for meas. of V-gutter stabilised flame 77−35263
hologram production using shearing interferometers with a wide light source 80−43293
holographic interim recording 79−76641
holographic schlieren investigation of laser-induced plasma density 77−72503
holographic schlieren photography and interferometry, coloured patterns appl. *(Russian)* 77−34852
hydrophone, multimode, fibre-optic 80−102938
hypersonic ballistics experiment, application of laser light source 78−38433
injection of the He for visualisation of air flow patterns past models 77−58813
instrument large-aperture adapter for optical surface quality evaluation 79−14122
interferometer, 3-D vol., radiation transfer, probability model 77−87818
interferometer, triangular path inverting, for schlieren system appl. 77−34018
interferometry with schlieren microscopy 77−34016
irregular phase objects, dynamic interferometry, differential holography using phase conjugate refl. 80−37969
laser beam probe method for measurement of refractive index profile of shock wave in fluid 80−23785
laser irradiated solid target, picosecond microphotography 78−42828
laser thermonuclear fusion, shell target parameters meas. using X-ray schlieren method 80−14942
lens, residual wave aberration due to schlieren, diminished image quality *(German)* 77−14788
light optical imaging, of focused US field *(German)* 80−3275
light valve projection systems classification 78−33812
microscopic imaging analysis applied to phase, schlieren and interf. microscopy 78−45688
microscopy, colour schlieren technique 78−29151
multiple slit grating, optical inhomogeneity study *(Hungarian)* 80−69515
negative DC corona study in atmospheric air using Schlieren and interferometric techniques 80−49023
phase object projection, imaging charact., recording conditions 78−25977
photography, aberration and diffr. effects on resolution 77−34040
photography of exhaled air, detection of abnormal nasal escape 80−64145
projector, phase image reflection, coherent light source *(Russian)* 78−38025
projector for visualisation for information recorded on photothermoplastic material 80−87544
pulsed discharge, air, elec. wind and sonic wave (350 m/s) initial growth, Schlieren obs. 78−87587
quantitative schlieren technique, using doubly refracting crysts. 77−11040
rapid events, photographic study by picosecond techniques 78−42826
refractive index gradient, chromatic variation meas. technique 80−74471
relief recording with circular iris, luminous efficiency 78−83095
resonant optical schlieren system for plasma flow studies 78−5940
shadow Schlieren obs. of cathodic diffusion boundary layer free convective flow 78−68894
shell target monitoring by X-ray Schlieren method 80−86263
shock flow, time analysis using dual microwave and dual schlieren systems 77−15143
shock wave vel. determ. by laser schlieren method 77−39370
sound-intensity meas. by schlieren optical filtering for light diffracted from US beam 80−87672
Spacelab optical techniques for liquid flow and temp. meas. 79−82007
spatial filtering techniques represented by phase contrast function 80−9813
submerged cylindrical target, comparison of schlieren and holographic techniques 78−38157
supersonic air flow through high press. gas valves into atm., noise and flow pattern obs. 80−59067
Talbot-Schlieren interferometric method to see US waves 77−10099
temperature measurement of laser irradiated transparent materials, Moire-Schlieren technique 80−53392

schlieren systems continued
threshold sensitivity of schlieren instrums. to turbulent inhomogeneities 78−79134
trace analysis in gases by laser-induced schlieren technique 80−3436
tracking system properties and advantages 79−14080
transfer function of optical systems with small residual aberrations, schlieren effects *(German)* 80−32923
transformer oil, optical obs. of pre-breakdown and breakdown 77−80386
transient cavitation, on marine propellers, high-speed photography 78−38432
two-lens standard phase inhomogeneity 79−14111
ultrasonic wave visualization using schlieren technique 78−30118
unipolar acoustic pulses, quantitative schlieren visualization 78−38125
US pulse scattering observations, elastic cylinder appl. *(French)* 80−53500
US rel. meas. in metastable liquids 78−55535
US transducer evaluation in exptl. and theoretical domains 79−46153
US visualisation for NDT of solids 80−22424
US visualisation of defects, stroboscopic schlieren apparatus 79−87811
US wave visualisation at low freqs. 78−55501
vibration insulation of equipment for optical system performance testing 78−90543
vortex investigations, small inner diameter fluid jets, appl. schlieren photography 80−74935
water-sediment interface US reflection with bidirectional displacement 78−60017
ClF+Ar, shock wave, vibr. relax., laser schlieren meas. 78−90267
O_2, liq., stimulated Raman scatt., vibr.-translational relax. rate, schlieren technique meas. 80−9955

Schottky anomaly
methane-d_1(-d_2,-d_3), solid, struct. of phase III from thermodynamic meas. 79−82193
methane-d_2, orientational ordering and tunnelling states meas. 79−10963
pyridinium pentasilver hexaiodide, sp. ht. and cond., gradual solid electrolyte transition 77−76604
rare earth hydroxides, heat capacity from near 5 to 350K, lattice and Schottky contribs. 80−49374
rare earth sesquisulphides, $RS_{1.5}$ (R=La,Lu), sp. ht. between 2 and 20K, Schottky type contrib. 79−60518
terbium ethyl sulphate, mag. and thermal props. 79−7971
ytterbium ethyl sulphate, crystal field effects on mag. and hyperfine props. of Yb^{3+} 80−97101
Ag-Dy, dil., Schottky effect, sp. ht. meas. 78−34633
$BaCl_2(F_2)$, sp. ht. meas., Schottky-type diffuse phase transitions, defect form. energies and entropies 80−107441
CaF_2:Ce^{3+}, Kapitza limited spin-bath relax., paramag. Faraday effect meas. at liq. He temp. 79−95642
CaF_2:Dy^{3+}, cubic cryst. field effects 80−2368
CaF_2:Tm^{3+}, 8.2 keV excited state, mag. props., Schottky ht. capacity, nucl. quadrupole splitting 78−76037
$CdInGaS_4$:Er^{3+}, cryst. field parameters, thermal and mag. props. calc. 77−20540
$CdIn_2S_4$:Er^{3+}, cryst. field parameters, thermal and mag. props. calc. 77−20540
$CeAl_3$, cryst. field effects, inelastic neutron scatt. meas., Schottky sp. ht. calc. 77−51710
ErGa garnet, crystal field theory calcs. 77−8259
$EuCl_3$, heat capacity and Schottky anomaly, 5 to 350K, entropy 77−47588
$Fe_{1-x}Ni_x$, FCC, anomalies in sp. ht. and thermal expansion 79−19739
$Fe_{0.5}(Ni_xMn_{1-x})_{0.5}$, FCC, anomalies in sp. ht. and thermal expansion in paramag. temp. range 79−19739
$HfB_{2.036}$, $HfC_{0.968}$, ht. capacity, thermodyn. props., 5-350K 77−47590
$HoRh_4B_4$, low temperature magnetic properties 80−88728
$LaCl_3$, ht. capacity meas., 5-350K 77−31784
$LaPd_3$, heat capacity at low temps. 79−28547
$NdAl_3$, cryst. field effects, inelastic neutron scatt. meas., Schottky sp. ht. calc. 77−51710
$NdCl_3$, ht. capacity meas., 5-350K 77−31784
$Nd(OH)_3$, heat capacity from 10 to 350K, lattice and Schottky contribs. 80−84300
$NiZrF_6.6H_2O$, uniaxial ferromagnetism 78−80143
PbF_2, sp. ht. meas., Schottky-type diffuse phase transitions, defect form. energies and entropies 80−107441
$PrAl_3$, crystal-field effects, inelastic neutron scatt. meas., Schottky sp. ht. 77−8268
$PrCl_3$, ht. capacity meas., 5-350K 77−31784
$PrIr_2(Pt_2)(Rh_2)(Ru_2)$, hyperfine sp. ht. and magnetisation meas. at 4.2K 80−75775
$Pr_2Mg_3(NO_3)_{12}$, sp. ht. and elec. susceptibility 77−85642
$Pr(OH)_3$, low temp. heat capacity, thermophys. props. optical spectra, anal. of Schottky contributions, review 80−24611
PrP, sp. ht., 20-300K, cryst. field effects contrib. 77−16092
$PrPd_3$, heat capacity at low temps. 79−28547
PuC_{1-x} and Pu_2C_3, sp. ht., 10 to 300K, mag. ordering 77−28403
SmB_6, mixed valence cpd., EPR and heat capacity obs., metal-semicond. behaviour 80−20456
$SmCl_3$, heat capacity and Schottky anomaly, 5 to 350K, entropy 77−47588
SmH_2, low temp. sp.ht., antiferromag. ordering and cryst. field splitting effects 78−84439
$SrCl_2$, sp. ht. meas., Schottky-type diffuse phase transitions, defect form. energies and entropies 80−107441
$Tb(OH)_3$, heat capacity from 10 to 350K, lattice and Schottky contribs. 80−84300
YAG, Yb^{3+} crystalline field, Schottky specific heat, paramagnetic susceptibility temp. depend. 77−11882
YAG:Er^{3+}, crystal field theory calcs. 77−8259
YGa garnet, Yb^{3+} crystalline field, Schottky specific heat, paramagnetic susceptibility temp. depend. 77−11882
$ZnIn_2S_4$:Er^{3+}, cryst. field parameters, thermal and mag. props. calc. 77−20540
ZnS:Fe^{2+}, thermal expansion and heat capacity, effect of Fe^{2+} 77−31782

Schottky-barrier diodes
see also semiconductor-metal boundaries
ageing, influence of metal electrode 79−99620
BARITT devices, boundary conditions, RF performance 80−49955
barrier formation and shape determ. factors *(Russian)* 78−84295

Schottky-barrier diodes continued
barrier height control using knock-on effect in ion implantation 77−76919
barrier height variation techniques 80−20284
capacitance, differential, epitaxial layer carrier conc. profile obs. 77−12036
capacitance, inverse square, for p-type Schottky diodes with deep acceptor impurities 80−2468
charge carrier speed, p-n vs. Schottky diodes, for various appls. *(Dutch)* 80−65662
current transport analysis 77−1484
current voltage characts. of Schottky diodes with high series resistance 79−95491
deep impurity levels, spectroscopic determination by compensation method 80−108229
deep level properties measurement, capacitance spectrometer *(German)* 80−15471
detector for submillimetre laser Thomson scatt. system for plasma diagnostics 77−84526
diffusion length and surface recomb. vel. determ., light excitation 78−91725
drift field Schottky barrier solar cell calcs. 77−15953
edge current modelling, agreement with thermionic-field emission theories 78−56227
EM radiation probes, implantable, design factors 78−73258
far-IR heterodyne radiometric measurements with quasioptical Schottky diode mixers 78−77958
n-GaAs:O, press. depend. of deep level associated with O, transient capacitance meas. 78−64000
grid devices, preparation on Zn_3P_2, performance evaluation 80−44708
heavily doped IR diode without substrate, noise equivalent power 77−24618
high frequency rectification, transport theory 79−82660
hybrid-type integrated photodetector using partially metal-clad dielectric-slab waveguide struct. 77−11050
hydrostatic pressure effect on V-I curve and barrier height *(Russian)* 77−39934
I-V impurity profiling under Schottky barrier 78−19148
II-IV-V_2-Cu, pseudo-straight-zone semiconductor, Schottky barriers, IR photosensitivity and photocond. *(Russian)* 77−8195
III-V semiconductor based layered multielectronic systems, electronic process investig. survey *(Russian)* 80−107891
impurity space distrib. in near-contact region, meas. instrument 77−19976
interfacial layer theory, surface fixed charge, voltage drops 80−96967
IR C-CD staring sensors, operation and performance 80−10029
IR capacitive mixing and detect. at high, intermediate or modulation freqs. 80−77864
IR detector, nomographs for parameter evaluation, 77K 80−31870
laser pulse monitor, 50 psec detector 77−3600
light intensity detector integrated with GaAs-GaAlAs laser 79−89917
low noise mixing in far IR region, appl. of Schottky barrier diodes 78−68083
magnetic surface levels in presence of depletion-type band bending 80−20285
magnetodiode, integrated mag. sensor Si on sapphire 80−68223
mesa diode, axial pressure effects on surface-state density redistrib. *(Russian)* 77−89847
metal-$Cd_xHg_{1-x}Te$ contacts, schematic energy band diag., transport props. 77−47897
metal-GaAs(GaP), elec. props. under mech. stress 80−11087
metal-Ge Schottky barrier quantum detectors, optoelectronic props. 80−13146
metal-InP contacts, metal beam epitaxy, struct. and elec. props. of films on ion bombarded InP 79−28922
metal-merocyanine solar cells, photovoltaic props. in terms of exciton transport 79−43763
metal-semiconductor junctions, fabrication aspects 80−88632
minority carrier diffusion length, Schottky barriers, electron bombard. investigation 78−68037
MIS Schottky barrier and conducting diodes with interface traps, capacitance and conductance 78−10564
MM-wave and sub MM-wave receiver elements 80−11558
monolithic detector dielectric plate antenna 79−30548
non-degenerate diode, current-voltage characts., analytical approx. 79−95494
one-sided abrupt junctions, normalized representation of avalanche breakdown behaviour 80−65666
oxide layer between metal and semicond., effect on barrier height, avalanche breakdown 77−20432
p-n structures, lowly doped, effective barrier height calc. 77−39941
photochemical diode using p-n heterojunction or Schottky barrier immersed in electrolyte 77−66201
photodetectors, picosecond, for 257 nm to 1 μm laser pulses 79−67388
photodiode, quantitative meas. of body motion using laser beam 80−12207
photovoltaic IR detector, Schottky barrier 80−9040
point-contact, for detection of 10 μm radiation 77−37979
polyacetylene, pure and doped, metal; and semicond.-semicond. junctions 79−95474
pulsed radiation effects on elec. cond. and EMF relax. 77−89842
quantum noise at low temperature 80−103733
quantum photoelectric yield, theoretical anal. 77−39939
quasioptical superheterodyne radiometer for upper atmosphere 77−41241
rectification properties of CdS diodes with evaporated Au-Ti blocking contact 77−85319
rectifier, theory, technology and appl. 78−52089
rectifying metal-semiconductor contact, method for determ. of pot. barrier height 77−1486
resonant tunnelling spectroscopy, deep centre detection 80−96968
SEM by Schottky-barrier charge collection, dopant striae obs. in Si 77−31684
solar cell, back wall type, possible performance and potential advantages over front-wall cell 77−4438
solar cell, comparison of thin film and bulk single cryst. 78−80053
solar cell, doping density effect on efficiency 80−101100
solar cell, improvements due to Al-Si metallurgical reaction 77−72914
solar cell, on amorphous hydrogenated Si *(French)* 79−24897
solar cell, open cct. voltage 77−32078
solar cell, optimum thickness indicator for barrier metal 78−21120
solar cell sensitivity computation 79−62004

Schottky-barrier diodes continued
solar cells, back-illuminated, theoretical performance 80−61345
solar cells, efficiency depend. on thickness of interface layer 80−76637
solar cells appl., props. obs. by electron beam induced currents 80−3518
solar-cells, barrier height change and current transport in presence of interfacial layer 80−61353
strip-coupled varactor SAW convolvers, parametric cct. anal. 78−71245
sub-micron size, for submillimetre wave detection 77−34024
submillimetre heterodyne detection 77−37983
submillimetre heterodyne detector 77−34028
submillimetre mixing, high order, for heterodyne detect. 77−5910
submillimetre wave detector, monolithic, printed resonant antenna 77−34025
submillimetre wave mixers, review 78−45712
submillimetric low-noise Schottky-barrier coherent detector materials 77−37995
subminiature Schottky-barrier diode video detection and heterodyne mixing 77−37996
superconducting, space appl. 80−85836
superconductor-semicond. device research, future prospects 79−28467
ternary semiconductor based Schottky diodes with tunnel device characts. 78−39215
thermally degenerated Schottky diodes, resonant tunnelling 80−100503
thermionic emission-diffusion theory validity, thermodynamic conditions 77−12003
thermographic diagnosis, high resolution dynamic method, detector system 80−41167
trap refilling, depth and capture cross section determ. 78−80052
tunnel junction mixers, quantum limited detection 80−18015
tunnelling current assisted by deep traps in Schottky barrier, theoretical evaluation 77−43722
uncooled millimeter wave receiver for radioastronomical observations, appl. *(Swedish)* 78−24461
wavelength-modulated photoresponse spectra *(Russian)* 78−84300
wide-band mechanically stable quasi-optical detector for 100-300 GHz 79−67382
Al contact of p-type Si surface-barrier diode, ageing 77−32077
Al/GaAs contacts, metallization of surfaces covered with absorbed S *(French)* 80−107909
Al/metal-free phthalocyanine Schottky barrier solar cells, photovoltaic props. 79−100527
Al/NiSi/Si system, high temp. interaction study, elec. and struct. characts. by Schottky diodes 79−24075
Al-CdSe thin film diode, vac. evaporated, I-V and C-V characts. 78−10555
Al-copper phthalocyanine-Ag diode struct. with Schottky barrier 77−43740
Al-GaAs, Richardson const., recomb. at interface traps 77−20424
Al-GaAs-$Al_xGa_{1-x}As$ Schottky barrier diodes, prep., characts. 80−6948
Al-Ge photovoltaic cell, charact. 79−40612
Al-InP Schottky barrier, increase 80−15603
Al-Pd_2Si contacts on Si, elec. and structural characterisation 77−43695
Al-poly-Si Schottky-barrier solar cells, grain boundary effects on electrical behaviour 80−85279
Al-Si, with Ti contact, voltage-current characts., appl. to ignition circuits 80−11088
AlGaAs laser array on Si heat sink, optical power detection 80−74383
$Al_xGa_{1-x}As$ epitaxial film based device, microstruct., effect on elect. characts. *(Russian)* 80−107671
$Al_xGa_{1-x}Sb$-Pd contacts, struct., preparation elec. props. 80−65684
$Al_xGa_{1-x}Sb$-Pd contacts, band gap depend. of barrier height 80−65685
Au/n-TiO_2 Schottky diodes, I-V and C-V characts. 80−96988
Au-$Al_{0.5}Ga_{0.5}As$ -GaAs heterojunction Schottky-barrier solar cells, barrier height enhancement 80−85284
Au-CdF_2, degradation, thermal stability of CdF_2 79−23969
Au-CdS, piezoelec. effect due to mech. bending 77−69779
Au-CdS junction diodes, chemically etched CdS cryst. surfaces effect on barrier layer 80−44722
Au-CdTe, fabrication and characterisation *(German)* 80−89151
Au-CdTe-Au structure, current transport props. 80−80408
Au-Cr-GaAs Schottky-barrier diodes, effect of γ-radiation on current-voltage charact. *(Russian)* 80−2459
Au-$Ga_{1-x}Al_xAs$ Schottky diodes, band struct. from I-V, C-V meas. 80−96989
Au-GaAs, fabrication using LPE 77−40357
Au-GaAs, photosensitivity losses, field and spectral depend. 80−2452
Au-GaAs, Richardson const., recomb. at interface traps 77−20424
Au-GaAs LPE production methods, X-band application 77−8192
Au-Ge Schottky diode, phonon energies, barrier heights, photovoltage spectra 78−64112
Au-InP, Schottky diodes, behaviour under heat treatment 79−78172
Au-InP Schottky diodes, barrier height study 78−52088
Au-InS Schottky-barrier diode, tunnelling current due to thermionic-field emission 79−33340
Au-n-AlGaAs-n-GaAs Schottky-barrier solar cells, band readjustment effect 80−81458
Au-n-GaAs, interface state density model 77−39937
Au-p-n-Si Schottky barrier solar cell, photovoltaic characts., barrier heights, carrier mobility 79−83601
Au-Si Schottky barrier solar cell interface props. and stability 79−61984
Au-Ti/n-GaAs contacts, interdiffusion and Schottky barrier height variations 77−89849
Au-W/n-GaAs contacts, interdiffusion and Schottky barrier height variations 77−89849
Au-ZnS electrolum. Schottky barrier diode, S^+-implanted, blue emission 80−76082
Au-ZnSe:Ga(Al), Schottky diode, wavelength modulated photoresponse spectra 78−6714
CdF_2-metal, photoemission, capacitance and I-V meas. barrier heights 78−26950
CdS, Au deposition, Schottky diodes and MIS devices, surface treatment effects, SEM obs. 80−54794
CdS-Au Schottky diode, elec. props. under stress 79−15222
CdS-Cu_2S junctions, carrier trap density, deep level defects 80−107801
CdTe diode, generation-recomb. and ionisation processes, temp. depend. *(Russian)* 77−39942
CdTe, Schottky diode, AC small signal capacitance 79−7899
CdTe Schottky solar cell, barrier height, open circuit voltage 77−43721
CdTe/Langmuir film photovoltaic structures for solar cells 80−49918
CdTe-Ag diode, Schottky type, elec. and photoelec. props. 77−43719

Schottky-barrier diodes continued
CdTe-Au Schottky barriers, quantum photoelectric yield, theoretical anal. 77−39939
Cr-GaAs, metal-nn^+ Schottky diode, I-V characts., inverse branch, effect of dislocation defects *(Russian)* 79−15217
Cr-GaAs, Schottky-barrier diode, surface electron states 79−73578
Cr-Si, cleaved junction, interface states, capacitance meas. 79−91118
Cr-Si, metal-nn^+ Schottky diode, I-V characts., inverse branch, effect of dislocation defects *(Russian)* 79−15217
Cu/$CuGaSe_2$ Schottky-barrier cells, photovoltaic effect 79−96440
Cu-$CdSiP_2$, photoelec. props. 77−4442
Cu_2O solar cell, low barrier heights, Auger spectra obs. 79−15224
Cu_2O-Au(Mg)(Mn)(Yb) solar cells, surface anal. using AES 79−43759
Cu_2O-Cu diode junction, Schottky barrier, electronic structure and minority carrier diffusion length *(French)* 80−65682
GaAS, proton isolation layer, lateral spread, elec. meas. 77−80520
$Ga_{1-x}Al_xAs$ Schottky barrier, oxide free, surface composition and fabrication 78−68084
$Ga_{1-x}Al_xAs$ Schottky directional coupler switch, construction and operation 78−25960
n-GaAs, boat-grown, deep levels *(Japanese)* 79−47043
GaAs, CVD on W coated graphite, characterisation, and Schottky barrier solar cell characts. 79−28930
GaAs, deep level profile anal., double correlation technique 77−80830
GaAs, detection down to 70.5 μm, submicron size contacts 77−10103
GaAs, device quality, polycrystalline, epitaxial growth on Ge/Mo substrates 79−69988
GaAs diode, with Schottky barrier, photoluminesc. *(Russian)* 79−28410
GaAs, elec. props. 77−59331
GaAs epitaxial film based device, microstruct., effect on elect. characts. *(Russian)* 80−107671
GaAs epitaxial layer and Sn-doped bulk characterisation 79−82596
GaAs epitaxial layers, structural defect and conc. inhomogeneities influence on barrier diode I-V characts. 80−15602
GaAs epitaxial layers, surface impurity gradients, Schottky barrier capacitance meas. 80−70782
GaAs fast light detector, beat freq. generation between visible lasers 80−1253
GaAs films for solar cells appl., deposition and characterisation 80−84853
GaAs, gamma and electron irrad. defect formation depend. on interface, luminescence study 80−34057
GaAs, MIS, radiation effects 79−24078
GaAs MOS and Schottky systems, electromodulated reabsorption of luminesc. 79−15524
GaAs MOS diodes, interface states, deep-level transient spectroscopy 80−44727
GaAs, polycryst. Schottky barrier solar cells, effect of grain size on efficiency 80−50968
GaAs, radiation defect obs. using Schottky diode characts. 78−76024
GaAs, reverse-biased, current-controlled negative resist., switching investig. 77−69410
n-GaAs Schottky barrier diode, electron processes at interface *(Russian)* 78−84301
n-GaAs Schottky barrier junction, SEM meas. of hole diffusion length, surface effects 79−87110
GaAs Schottky barrier with Au and Au-Ga contacts, high temp. annealing behaviour 77−43725
n-GaAs Schottky diode, impurity photoluminesc. 80−29781
GaAs Schottky diode, influence of γ- and electron irradiated on recomb. characts. near GaAs surface 80−71478
GaAs Schottky diode, use in acoustic memory correlator 78−66989
GaAs Schottky-barrier diode submicron layer LPE reactor 77−77439
GaAs solar cell, for terrestrial photovoltaic energy conversion 79−15242
GaAs, strain sensitivity mechanism 79−38165
GaAs, submillimetre receivers, heterodyne radiometry 78−45713
GaAs, temp. depend. of intervalley gap, generalisation of thermionic emission theory 79−73586
GaAs thin layers, MBE, growth conditions and phys. props. *(German)* 80−55307
GaAs thin Schottky barrier metallisation, thermal reactions 79−78176
GaAs, trap levels, admittance spectroscopy 79−51672
GaAs, under high neutron fluence, current transport 80−65679
n-GaAs, undoped, proton radiation defect detect. by transient capacitance spectroscopy 79−11089
n-GaAs vapour phase epitaxial film electrophysical props. rel. to growth temp. *(Russian)* 80−49961
GaAs/Ni-Ge-Au cathode struct., with enhanced injection efficiency, contact resist. 77−20431
GaAs-Al, prep. by MBE on GaAs, and characts. 78−72257
n-GaAs-Au Schottky barrier diode, thermally assisted tunnelling currents 77−20412
GaAs-Au Schottky diode, electroless plating of Au, fast characterisation of epitaxial layers 79−33347
n-GaAs-Au(Al) Schottky diodes, interface state density model 77−80840
GaAs-metal contacts, use of Ga to eliminate large As loss peaks 80−80370
GaAs-metal diode, surface-barrier, excitons effect on photocurrent 79−82670
GaAs-metal Schottky barrier diodes, impedance, freq. and voltage depend. 78−64114
$GaAs_{0.6}P_{0.4}$, deep level profile anal., double correlation technique 77−80830
n-GaP, Schottky barrier height data for several contact systems 80−60080
GaP:Cu-Ni, Schottky barrier, TSC meas., trap levels 78−91709
GaP-Ag(Au), Schottky barrier, stress effects on elec. props. 80−34512
n-GaP-Au, Au overlayer potential on photoelectrodes, I-V curves 77−89848
GaP-Au, layer formation, elec. and optical props. 78−91766
GaP-Au, Schottky barrier, layer formation, elec. and optical props. 78−91766
Ge, lightly doped, IR response and extended HF model 77−80836
Ge-metal Schottky barrier photodetectors, near IR interband transitions and optical parameters 80−73449
Ge_xSe_{1-x} thin film, photovoltaic effect 77−15895
Hg-InP Schottky-barrier diode, contact times, I-V characts. 80−96971
HgCdTe Schottky barrier diode and n-p diffused junction IR detectors, comparison 80−9039
$Hg_{1-x}Cd_xTe$ photodiodes, for IR detection 80−13144

Schottky-barrier diodes continued
In-Ge:As, Schottky barrier tunnel junction, zero bias resistance, temp. depend. 78−72258
InP, barrier height control by S diffusion 77−85309
InP detector, unbiased, operation in submm. wave region 80−105707
n-InP/Au-Ti Schottky diode, elec. characts. and barrier height 77−59329
n-InP/Au-Zn Schottky barrier diodes, fabrication and elec. props. 79−33348
n-InSb, forward biased Schottky barriers on low doped surfaces, current transport 79−24074
$LiNbO_3$-gap coupled Schottky diode memory correlator, grating coupled optical imaging 80−64143
Mo-Si, sputtering damage effects on I-V and C-V characts 77−39940
Ni/Au-Ge/nGaP system, specific contact resistance calc. 78−43474
Ni-Pt silicide Schottky diodes, current-voltage characts. and comp. profiles 80−84508
NiSi, parallel contacts, Schottky barrier height meas. 80−96965
PbS_xSe_{1-x}, multispectral photovoltaic IR detectors 80−105710
PbS_xSe_{1-x}, Schottky-barrier IR detector, comp. tuning 78−12752
$Pb_xSn_{1-x}Se$, multispectral photovoltaic IR detectors 80−105710
PbSnTe(Se) Schottky barrier diode and n-p diffused junction IR detectors, comparison 80−9039
Pd-Si Schottky barrier chemical sensor, for H_2 detect. 78−44646
Pd-TiO_2 Schottky barrier, work function depend. on adsorbed species 80−54782
Pd-W, substrate temp. influence on shallow contact formation on Si 80−96963
Pd-ZnO, H_2 sensitivity 80−11085
Pd_2Si-Si, grown by solid phase epitaxy, orientation and temp. effects 77−80837
Pt-n-GaAs Schottky diode, microplasma breakdown 79−91140
Pt-Si contact, annealed in H_2 ambient, elec. props. 78−64110
Pt-Si Schottky diode/$LiNbO_3$ acoustoelectric integrating correlator 77−88990
Pt-Si thermally degenerated Schottky diodes, resonant tunnelling 80−100503
Pt-W, substrate temp. influence on shallow contact formation on Si 80−96963
PtSi diode, sputtering-induced defects, elec. characts. 78−51941
PtSi film formation by ion sputtering and annealing, form. and exam. problems 80−100782
PtSi, parallel contacts, Schottky barrier height meas. 80−96965
PtSi Schottky-barrier monolithic IRCCD focal plane 80−86427
PtSi-n-Si, photoelec. barrier height and elec. props. 79−33344
Rh_xSi_y-n-Sn Schottky diodes, rectifying barrier height meas. 80−49896
S:P, ion implanted, defect annealing 450-800°C, deep-level transient spectroscopy 79−47042
Si, amorphous, hydrogenated, electronic density of states determ. from Schottky diode meas. 80−49907
Si, amorphous, luminesc. of diode structures 77−8656
Si, amorphous, photovoltaic diodes, influence of mag. field on charge transport 80−49891
Si, amorphous, Schottky barrier solar cell, large-area RF sputtered, contact form, scaling and optimisation 80−45679
Si, clean-cleaved, Schottky barrier height meas. accuracy 78−52081
Si, dislocation electronic states, Schottky diode meas. 79−82548
Si, electron beam scan annealed, deep levels 80−65481
Si, electron irradiated, high resist. surface layer, Schottky barrier meas. 78−64093
Si, ion implanted, laser annealed, deep levels study in n-type Schottky diodes 79−69457
Si, metal contacts to O_2 contaminated surfaces, Schottky diodes 79−56309
Si, photocell, ionized cluster beam deposition and epitaxy, cell characts. 77−77416
Si, planarized solid state epitaxy for Schottky barrier diodes 78−35302
Si, radiation detector, barrier heights, electron and hole currents, Schottky contact effects 79−33293
Si Schottky barrier solar cell, V-I characts. and efficiency 78−14828
Si, Schottky diodes on sputtered amorphous Si:H, light induced ageing effects, interpretation of photovoltaic stability 80−54780
n-Si, temp. anomalies, I-V and C-V characts. 78−14823
Si:Al, P-diffused, recomb. centres, thermally stimulated capacitance meas. 77−72834
Si:B, diffusion length, SEM-EBIC/Schottky diode 79−82605
Si:B, RF glow discharge sputtering damage centres, barrier formation 79−33329
Si:B, SEM obs. of dislocations using Schottky barrier EBIC technique 78−79614
Si:F,H, amorphous, glow discharge deposited elec. props. and device aspects 80−44744
Si:H, amorphous, band tail absorpt., photocurrent meas. for Schottky barrier solar cell 80−60032
Si:H, amorphous, RF sputtered, Schottky barrier solar cells, photovoltaic props. and capacitance-voltage charact. 80−45678
Si:H, amorphous, Schottky diode, spectral response and hole drift mobility 80−39673
Si:H, amorphous, Schottky barrier solar cell, degradation mechanisms affecting stability and operation 80−45680
Si:H, amorphous, Schottky barrier solar cell, deposition parameter effects on elec. props. 80−45681
Si:H, amorphous, Schottky diodes, elec. props., light-induced effects 80−103741
Si:H, amorphous Schottky solar cells, prep. and characts. of diode RF reactive cathodic sputtered films *(French)* 80−61347
a-Si:H Schottky barrier diodes, capacitance studies 80−49908
a-Si:H/Pt, Schottky diode, influence of prep. conditions on forward bias currents 79−78171
n-Si:Pd Schottky diodes photocapacitance meas., photon and carrier capture cross sections 80−20309
Si:Rh(Pd), Schottky diode, capacitance characts., donor and acceptor levels 77−43697
Si:Sb, low energy ion implantation Schottky barrier diodes and resistors 80−88177
Si/In(-Cd), Si/Cd Schottky contacts, electrochemically deposited 80−88633
n-Si-Ag, excess current mechanism under uniaxial press. 78−91771
Si-Au Schottky barrier solar cell fabrication, doping of a-Si 80−50969
Si-Au Schottky diodes, role of O in formation mechanics 79−42639
Schottky-barrier diodes continued
Si-Au Schottky-barrier, formation process anal., V-I characts. *(French)* 78−91768
Si-Au(Rh)(In), Schottky diode, X-ray effects on elec. props., irrad. induced diffusion 77−4439
n-Si-Cu Schottky contacts, electrochem. deposition, barrier height and ideality factor 80−75641
a-Si-H sputtered solar cells, temp. depend. of Schottky barrier characts. 80−45669
p-Si-In Schottky barrier structure, optical quenching of photovoltaic effect 77−55608
Si-In(Rh)(Au) Schottky diodes, X-ray irradiated, radiation-accelerated diffusion of impurities in Si 78−26952
Si-IrSi interface microstructure and Schottky barrier height 80−34508
n-Si-$IrSi_x$, rectifying barrier height meas. 79−99619
a-Si-metal, I-V characts., barrier heights 77−8191
n-Si-Ni, Schottky-barrier, I-V characts. of elec. contact 79−19662
Si-Ni(Pt)(Al), type II localised interface states, Si surface prep. effects 78−39210
Si-$Pd_{80}Si_{20}$, amorphous, Pd_2Si layer form., shallow contact 80−103586
Si-Pt, silicide layer, struct. and elec. props., sputter etching and annealing ambient effects 77−62991
Si-Rh(Au)(In), radiation-stimulate diffusion of contact materials in surace layer of Si 77−55394
Si-SnO_2 heterojunction, barrier height meas. by HF capacitance method 77−69406
Si-TiO_x-Ni, MIS amorphous solar cell, increase in open-circuit voltage and short-circuit current on addition of TiO_x layer 79−57425
SnO_2-copper phthalocyanine-Ag systems, elec. and electroluminescent behaviour 80−80864
Zn-tetraphenylporphine/metal electrode, photocurrent generation mechanism 78−76868
$ZnAs_2$ Schottky diodes, elec. and photoelec. props., excitons 80−65653
ZnO-on-Si SAW convolver development 77−27430
ZnP_2 Schottky diodes, elec. and photoelec. props., excitons 80−65653
Zn_3P_2 photovoltaic material and Schottky diode characteristics 78−64066
Zn_3P_2, single crystal, growth, electronic and device props. 80−25551
Zn_3P_2, solar cell appl. 79−7839
Zn_3P_2-Au Schottky diodes, influence of additional laser illumination on photoresponse spectra 77−89852
ZnS Schottky-barrier diodes, blue light emission 79−38671
ZnS:Mn Schottky diodes, reverse-biased, electroluminescence, hot electron impact excitations 80−25005
ZnSe, electroluminescent MIS diodes, surface state density determ. 77−35993
ZnSe surface barrier diode, hot charge carriers, elec., photoelec., and electroluminesc. props. *(Russian)* 79−33841
ZnSe:Mn^{2+} Schottky barrier diodes, spin depend. cond. and photovoltage 79−91141
ZnSe-metal contact, elec. props. 78−14826
$ZnSiP_2$, electroluminescence under forward and reverse bias conditions 77−63466
$ZnSiP_2$-In Schottky diode, photovoltaic spectra 80−2423
ZnTe single crystal, Schottky-barrier diodes and ohmic contacts props. 80−96987
ZnTe:Cu, red centre, electric and optical props. 80−20239
ZnTe-In Schottky diodes, photocapacitance determ. of electron-hole recomb. *(French)* 79−47119

Schottky barriers *see Schottky effect*

Schottky defects
alkali halides, intrinsic point defects, generalised Mott-Littleton approach 77−51698
alkali halides, Schottky defect correl. of form. enthalpy and melting point 78−43015
alkali perchlorates, elec. transport during struct. transforms. 78−59971
enthalpy, possibility of decrease with increasing temp. 80−2012
inert gas crystals, internal energy, Monte Carlo calcs. 77−72577
ionic crystal, defect formation volume, temp. and press. depend. 78−26563
ionic crystals, elastic relax. associated with formation and motion of Schottky defects 80−49216
ionic crystals, nonstoichiometric, equilib. with gas phase in mech. vibr. field 78−43388
semiconductor, atomic displacements and enthalpy of vacancy formation 78−38690
AgBr, Br^- diffusion plot, anomalous curvature 79−60548
AlH_3, dark electrical cond., exam. 80−39624
CsBr, Debye-Waller factors, lattice dynamics, Schottky form. energy, X-ray determ. 78−75792
CsBr-TlBr, phase diagram and pt. defect parameters 79−96017
CsCl-TlCl solid soln., point defect parameters 80−54224
CsI, Debye-Waller factors, lattice dynamics, Schottky form. energy, X-ray determ. 78−75792
He, solid, ion current modulation by thermal waves 78−91506
KBr, energy of form. of Schottky defects 77−7714
KBr, quenched, absorpt. spectra, role of Schottky defects 77−59599
KCl, energy of form. of Schottky defects 77−7714
KCl, entropy changes associated with formation of defects, Schottky defects 77−62552
KCl, ionic cond., defect parameters, diffusion coeffs. 80−79978
KCl:$Sr^{2+}(SO_4^{2-})$, ionic cond., defect parameters, diffusion coeffs. 80−79978
KCl:$Sr^{2+}(SO_4^{2-})$, defect parameters, self-consistent set, ionic cond. meas. 80−107487
$KClO_4$, AC electrical conductivity meas., mechanism involving Shottky and Frenkel defects 79−99367
LaF_3, ionic transport, NMR and cond. studies 80−107555
LiH, solid, anion and neutron diffusion, NMR relax. and linewidth obs., Schottky disorder 80−15815
MgO, lattice defects., calcination temp. effect 80−15091
NH_4Br, Debye-Waller factors, lattice dynamics, Schottky form. energy, X-ray determ. 78−75792
NH_4Cl, Debye-Waller factors, lattice dynamics, Schottky form. energy, X-ray determ. 78−75792
NaCl, energy of form. of Schottky defects 77−7714
NaCl, formation enthalpy, entropy, temp. effects, correction 78−10039
NaI:Ca^{2+}, pure and doped, lattice defects, entropy and enthalpy of formation and migration 80−96687

Schottky defects continued
$PbBr_2(Cl_2)(I_2)$, ionic cond. and activation volumes, high press. effects 80−100353
PbFCl, ionic cond. mechanism, ^{19}F NMR meas. and struct. considerations 79−55927
Si inversion layers, magnetocond. in ground Landau level, defect diffusion in Wigner cryst. 77−39914
TlBr, Debye-Waller factors, lattice dynamics, Schottky form. energy, X-ray determ. 78−75792
TlCl, Debye-Waller factors, lattice dynamics, Schottky form. energy, X-ray determ. 78−75792
TmSe, nonstoichiometry, high temp. chem. and valence instability *(German)* 79−23743
ZnO, defect struct. calc., doping effects 80−107218
ZnO single crysts. with stoichiometry deviations, intrinsic defects, thermodynamic analysis 79−42485
ZnSe:Al(As), and pure single cryst., defect struct., Hall effect and Zn self-diffusion meas. 79−1427
ZnSe:Ga, defect struct., Hall effect and resist. meas. 79−1428

Schottky effect
see also work function
1/f noise, expt. and analytical dependences *(Russian)* 79−19648
1/f noise in barrier layers 79−82666
amorphous barrier, capacitance-voltage meas., localised density of states determ. 80−49900
avalanche breakdown instability mechanism, microplasma form. 78−72262
avalanche multiplication 78−84289
barrier, theory and complex band struct. 79−15220
barrier formation, chemical effects 78−91753
barrier heights, semi-empirical tight-binding calc. 79−28408
barrier T_0 anomaly, comparison of Levine and Bardeen models 77−39938
barriers, Bardeen and Schottky limits of interface index 80−49868
barriers at metal-covalent semiconductor interfaces, independence of work functions *(Japanese)* 77−69417
charge carrier conc. determ. from low-field electrorefl. spectra 77−85320
contacts, submicron, high-field pulsed electroplating technique 80−49899
deep level profile anal. by double deep level transient spectrosocpy 77−20378
degenerate semiconductor-metal Schottky barriers, low temp. capacitance 80−60075
diamond Schottky barrier, electronic struct., pseudopot. calc. 78−95364
diamond Schottky barrier, electronic struct., pseudopotential method, jellium model 79−38162
diamond Schottky barriers, photocapacity meas. 78−52057
dielectric, carrier-dominated, low-frequency dispersion 79−47380
dielectric film transient thermal emission current model *(Russian)* 77−15982
diode, interfacial layer theory, surface fixed charge, voltage drops 80−96967
doping inhomogeneity, meas. by low field electrorefl., in Schottky-barrier config. 77−11584
electrical contacts at low temps., contact resist. characts. 78−68072
electrode-insulator boundary, current injection in presence of space charge 79−1619
electronic structure of Schottky barrier, calcs. 79−1613
epitaxial film, dopant profile and Schottky barrier height determ. by second differential method *(Chinese)* 80−49257
exciton reflection band burning in Schottky barrier field *(Russian)* 79−47479
excitonic reflection of light 80−10885
GaAs, back-wall Schottky barrier solar cell with interfacial layer 77−62993
GaAs, Schottky barrier, effect of oxide composition on elec. behaviour, AES meas. 79−87141
GaSb surface, Au overlayer, adatom interactions, photoemission obs. 79−33898
grain boundary diffusion, chemical reactions, contamination, AES and SIMS 80−72066
hexatriacontane single cryst., elec. cond. and dielec. breakdown 80−6849
homogeneous random fields, modelling realisations 80−8911
II-IV-V_2-Cu, pseudo-straight-zone semiconductor, Schottky barriers, IR photosensitivity and photocond. *(Russian)* 77−8195
III-V oxide interface state and Schottky barrier form., unified mechanism 80−44724
III-V semiconductor, $(SN)_x$ and HgSe as contact materials, compared with Au 77−85312
III-V semiconductor Schottky barrier formation, Fermi-level pinning, defect mech. 78−95358
III-V semiconductors, MBE developments in device fabrication, Schottky barriers 79−78902
inert gas, liq., electron mobility, role of shallow traps 80−34440
insulator, space charge effect on time dependence 78−14735
ionicity and Schottky barriers 78−30972
jellium-semiconductor interface, role of ionicity pseudopot. method 77−47888
lead phthalocyanine:O_2(I), Schottky barrier effect on AC current response 80−75623
metal surfaces, dipole barrier and work func. calc. 79−15208
metal-CdS contact photovoltage 78−95337
metal-chalcogenide glass-metal structure, freq. response characts. 77−76951
metal-diamond interface, Schottky barrier theory, ionicity depend. 78−52086
metal-InP contacts, intermediate adsorbed layer effect on electronic props. 80−39674
metal-semiconductor barrier heights, chemical trends 78−84293
metal-semiconductor contact, elec. characts., interfacial reaction effects, book contrib. 79−1623
metal-semiconductor contacts with thin interfacial films 80−96969
metal-semiconductor interface, photoelectron injection, quantum mech. transmission and optical phonon scatt. 80−84511
metal-semiconductor interface, Schottky barrier formation, microscopic model 78−52087
metal-semiconductor junction carrier migration and equivalent cct. analysis *(Russian)* 78−84294
metal-semiconductor junctions, Schottky barrier heights for low ionicity semiconds. 79−42640

Schottky effect continued
metal-semiconductor Schottky barrier junctions, characterisation and appl. 80−92971
metal-thin oxide-semicond. structures, physical processes and microelectronics applications *(Russian)* 78−84307
minority carrier diffusion length, Schottky barriers, electron bombard. investigation 78−68037
minority carrier injection effect on Schottky barrier height approaching semicond. band gap 77−20434
minority carrier lifetime-meas. technique using SEM-electron beam induced current 80−59999
minority carrier traps, detection using transient spectroscopy 79−65402
MIS device, optically biased, tunnelling 77−85334
MIS tunnelling Schottky barrier, reverse biased, appl. to photodetection 79−7904
MIS tunnelling Schottky barrier, surface state effect on electrical characts. 78−47877
MOS structs., Schottky barrier characterisation by scanned internal photoemission 80−49915
n-p structure, Schottky-gate, depletion layer, pot. fluctuations 80−88512
ohmic contacts, recomb. beneath, and adjacent oxide covered regions 79−47164
organic semiconductor Schottky barriers, capacitance meas. 79−82659
p-n junctions, excess currents 78−56223
photocathodes, alkali metal multilayers, high field enhancement of photoemission 78−19639
photocurrent, recomb. losses in Schottky barriers *(Russian)* 80−2470
photoelectrochemical solar cells, semiconductor/redox electrolyte junctions, functions examples and problems 80−45714
photoelectron injection at metal-semicond. interface, theory and expt. 77−85314
photoemission and Auger spectroscopy for anal. of semiconductor-oxide interface and Schottky barriers 80−50536
photosensitivity losses 80−2452
polyacetylene films, AsF_5 doped, photocond. and junction props. 80−70770
polypropylene thin film conduction mechanism, expt. obs. 77−28271
polytetrahydrofuran films, electrochemically prepared between metal electrodes, DC elec. props. 80−39695
polyvinyl acetate:Cu, and undoped, thermally stimulated currents exam. 78−35083
rectifying barrier formation with metal-semiconductor junction *(Russian)* 78−84296
resonant tunnelling through traps, theory 78−10553
Schottky barrier grid devices, preparation on Zn_3P_2, performance evaluation 80−44708
Schottky barrier solar cells, interfacial layer effect 79−57429
Schottky-barrier solar cells fabrication by electroless Ni plating 79−83591
SEM electron beam induced conductivity obs. of semicond. using Schottky barriers 78−34898
semiconductor, spatial resolution of SEM electron beam induced conductivity images 80−6327
semiconductor, TEM/SEM observations comparing diffr., elec. and luminesc. contrast from dislocations 78−38714
semiconductor, with defects adsorbed mols. and metal overlayers, electronic structure 79−95466
semiconductor characterisation, by electron beam induced current, charge collection process 79−17580
semiconductor characterisation, cond. type determ. by pot. profiling 80−73387
semiconductor materials, shallow and deep level evaluation using Schottky contacts, conc. and distrib. 80−49669
semiconductor metal interface, Schottky barrier, chemical reaction and charge redistrib. 78−95365
semiconductor on insulator substrate, capacitance meas. for Schottky barrier 80−39678
semiconductor-metal boundary, Schottky barrier form., chem. mechanisms 80−49869
semiconductor-metal contact, ionised mixture effects, I-V characts. *(Russian)* 77−24622
semiconductor-metal contact, tunnel effect theory, random field contrib. 77−43727
semiconductor-metal interfaces, Schottky barriers, chemical trends 78−95363
semiconductor-metal Schottky barrier height modification by interfacial oxides 79−47163
semiconductor-metal Schottky barrier interfaces in pairing model, covalent-ionic trend 78−95367
semiconductors, charge collection microscopy, surface barrier method, for defect investig. 79−37598
semiconductors, isothermal and non-isothermal C-V deep level meas. using Schottky contacts 80−88515
shellac, electrical cond. mechanisms, Schottky and Poole-Frenkel processes and work function 80−29402
Si, single cryst. characteris. by SEM using Schottky barrier charge collection microscopy 77−4444
n-Si-electrolyte junction, Schottky barrier height and reverse current 80−6979
silicide contacts on Si, Schottky barriers, elemental description 80−60085
solar cell, photovoltaic effects in p-n junctions, Schottky barriers, review *(Czech)* 77−24583
solar cells, electrochem. liquid-junction, Schottky barrier height, photovoltage and photocurrent 80−26162
solar cells, metal-semiconductors contacts, collection vel. of excess minority carriers 77−15954
solar cells n-type Schottky barrier, theoretical anal. of band edges, Fermi levels 80−50975
squarylium and cyanine-TCNQ dye Schottky-barrier sandwich cells 79−29468
surface barrier current instability in Schottky-barrier structs., uniaxial crystal compression 80−20310
thermal emission from damage near interface, effect on TSC and transient current expts. 77−11982
thin film technology, appls. in energy, optics, and electronics, review 80−78932
transition metal oxide films, dielec. dispersion and polarization 78−2803
transition metal silicides, refractory for ICs, review 80−100820
zinc blende type ionic semiconductors, vacancies, bound state energy level calcs., tight binding approx. 80−44694

Schottky effect continued
n-Si, deep levels in p-n junctions or Schottky barriers determ., hybrid method 79−24067
Ag, adsorbed on Si (111), electronic and cryst. struct., Schottky barrier form. obs. 78−84091
Ag monolayer on (111)Si surface, Schottky barrier, interface electronic nature and epitaxy 79−77934
Al/GaAlAs, film, epitaxial growth on (100) GaAs by hot vac. deposition and characterisation 79−56085
Al-Al_2O_3-Al junctions, Dy doped at Al_2O_3-Al interface, electron transport mechanisms and barrier height 78−91778
Al-Al_2O_3-Dy junctions, steady state and nonsteady state behaviour 79−78205
Al-Al_2O_3-GaAs backwall MIS Schottky barrier solar cell, anal. model 80−85289
Al-Al_2O_3-Hg structure, I-V charact. at room temp. for different thicknesses 79−47172
Al-GaAs interface, thermal ageing of Al film, optical microscopy and SEM obs. 77−20203
Al-GaAs-Al sandwich-type sputtered film, elec. props. 78−91780
Al-n-n^+-GaAs, deep centre reson. charging, photocapacitance meas. on Schottky barrier 78−26908
Al-polyacrylonitrile-Al films, current-voltage characteristics 80−11125
Al-Si-Al(Mo), sputtered Si film, photovoltaic props. 77−24623
Al-SiO_x-(p-)Si barrier structs., minority carrier injection ratio meas., MIS solar cell model 80−93007
Al-silicide-n-Si systems with $CoSi_2$, $MoSi_2$, and $Pt_xNi_{1-x}Si$ as silicide, Schottky-barrier height 80−34520
Al-Sio-Al structure, with amorphous SiO, VLF behaviour 77−76946
Al_2O_3, MIS Schottky structures, photovoltaic response 80−101115
Al_2O_3, porous film, elec. cond. charact. 78−76179
Au films on Si substrate, solid-solid reactions 78−95369
Au Schottky barrier with III-V and II-VI semiconds., correl. of barrier height with anion electronegativity 77−20430
Au-AlGaAs-GaAs heterojunction Schottky barrier solar cells, barrier height enhancement 80−94071
Au-CdS, Schottky junction, surface defects, photovoltaic, piezoelectric and V-I characteristics *(French)* 80−49898
Au-$Ga_{1-x}Al_xSb$ Schottky barriers, barrier height 80−96986
Au-GaAs Schottky barrier, photocurrent, recomb. losses *(Russian)* 80−2470
Au-GaAs Schottky barrier solar cells, effect of interfacial oxide layer on cell charcts. 80−61365
Au-GaS, Schottky-barrier electroreflectance spectra under uniaxial stress 79−56767
Au-InP, MIS Schottky barriers, interfacial parameters determ. 79−95505
Au-InSb Schottky-barrier, photovoltage, temp. effects 77−69415
Au-n-$Al_xGa_{1-x}As$-n-GaAS Schottky barrier solar cells, prep. and props. 80−26140
Au-n-Si Schottky barrier solar cells, recombination in space charge region 80−61351
Au-Si Schottky contact elec. props. rel. to AES 77−85322
Au-SiO-Au structure AC conductivity, bulk and interface effects 80−54798
Au-W-GaAs Schottky barrier, elec. and chem. props., AES 80−96973
Bi-NbO_2-Bi system, Schottky barrier effects in transport and dielec. props. 80−29486
CdS, deep level electron trap charcts. 79−78036
CdS, electron traps, admittance spectra on hetero- and Schottky junctions 79−56159
CdS, low resist. single cryst., photodeform. mechanism 77−89806
CdS Schottky barrier solar cells, spectral distrib. and photocapacitance 80−55864
CdS-Au contacts, electronic states, vacuum UV photoelectron spectra 80−70827
CdS-metal interface, chemical reactions and local charge redistrib. 79−19661
CdS(Se)-metal Schottky barrier form., transition with chemical reactivity 78−30986
CdSe (11$\bar{2}$0), surface electronic struct. and chem. struct. 78−14788
CdSe-Au contacts, electronic states, vacuum UV photoelectron spectra 80−70827
CdSe-metal interface, chemical reactions and local charge redistrib. 79−19661
CdSe-Mo, Schottky barrier, charcts. study 79−51673
p-CdTe, barrier heights of metals on etched surface 80−80378
CdTe, Schottky diode, AC small signal capacitance 79−7899
CdTe sputtered film with In contact, electrophysical props. *(Russian)* 79−42642
CdTe-Au contacts, electronic states, vacuum UV photoelectron spectra 80−70827
CdTe-Au(Al) Schottky barriers, defect effects 79−60921
CdTe-metal contact, surface barrier exam. 78−64111
CdTe-$SnCl_2$ electrolyte heterojunction photoelec. props., feasibility as solar energy convertors 77−76918
Cu-CdS, Schottky barrier, Cu diffusion and photovolt. mechanism 80−6980
Cu-CdS, Schottky barrier, reverse differential capacitance, diffusion of Cu *(French)* 80−15424
Cu-CuGaSe Schottky barriers, electrical and photovoltaic props. 80−92940
GaAlAs, surface vacancies, bound state energy levels calc., rel. to Schottky barrier formation 80−80340
$Ga_{1-x}AlAs$ (110) oxide-free Schottky barriers, surface comp. and charcts., AES obs. 79−82661
$Ga_{1-x}Al_xAs$:Sn, layer Schottky barrier, deep level spectroscopy 80−49666
n-$Ga_{1-x}Al_xAs$-Au, Schottky barrier height as function of AlAs content 79−65535
$Ga_xAl_{1-x}As$, Schottky barrier, effect of oxide composition on elec. behaviour, AES meas. 79−87141
GaAs (001)-Ag contact, surface stoichiometry and struct., and electronic surface states 78−95361
GaAs (110)-Al(Ga)(In), Schottky barrier form., defect mechanism 80−49902
GaAs, annealed, surface cond. change, Schottky barrier meas. 78−64095
GaAs anodic oxide, states, electrochemical meas. 80−80176
GaAs conducting MIS structures and metal-semicond. structures, effects of ultrathin oxides 79−1626

Schottky effect continued
GaAs, deep level trap emission identification by indirect conduction minima technique 78−84163
GaAs electro-optic rib waveguide directional-coupler switch with stepped $\Delta\beta$ Schottky electrodes 79−98507
GaAs MIS solar cells, effects of thin oxide layers on charcts. 80−89624
n-GaAs, metal filmed photoelectrochemical cell, energy conversion charcts. 80−101118
GaAs, p-n junction, conductance oscillations in a two-dimensional impurity band 79−95477
GaAs Schottky barrier, Auger de-excitation of metastable state 79−65410
GaAs Schottky barrier charge-accumulation detector, photosensitivity spectrum 77−55582
GaAs, Schottky barrier electrorefl. under uniaxial stress, band struct. 77−48193
GaAs, Schottky barrier electrorefl. meas. by sample rotating technique 80−60544
GaAs Schottky barrier function capacitance meas., determ. of deep electron traps 77−39797
GaAs, Schottky barrier solar cells, diffusion length meas. 79−61973
GaAs Schottky barrier solar cells with grain boundary edge passivation 79−83592
GaAs Schottky barrier structure, defects from proton irradiation, thermal transients and optical capacity *(French)* 80−59534
n-GaAs, Schottky barriers, minority carrier trap meas. 78−26951
p-GaAs, Schottky barriers on polar (111) and ($\bar{1}\bar{1}\bar{1}$) surfaces 80−88631
GaAs Schottky-barrier, linear and quadratic electroreflectance, minicomputer-controlled meas. 80−97241
n-GaAs, spectra, light induced, electrolyte and Schottky barrier techniques of meas. 80−76046
GaAs, sputtered-etched surface, Schottky contact characterisation and its recovery by annealing 79−99603
GaAs structures, charge accumulation and transmission, physical modelling *(Bulgarian)* 80−6947
GaAs substrate, Pd/Ge film sintering, Auger spectra, Schottky barrier energy 79−69581
GaAs, surface, vacancies, bound state energy level calcs., tight binding approx. 80−44694
GaAs thin film polycrystalline Schottky barrier solar cells, grain boundary chemistry 80−94067
GaAs, vacuum deposited Shottky barrier metallisation 79−78153
GaAs:Ag, diffusion of Ag at 1000°C, profiles, Schottky barrier and Hall effect meas. 80−54435
GaAs:Cr, deep levels, wavelength-modulated photocapacitance spectroscopy 80−76055
GaAs:Cr, Schottky barrier, effect of trapping processes on photocapacitance 77−76866
GaAs:O, evidence for metastable state of O centre, Schottky barrier photocapacitance meas. *(French)* 78−10556
GaAs:Te Schottky barrier solar cells, diffusion length determ. using minority carrier SEM 80−61359
GaAs/anodic oxide interface, characterisation of proposed model 80−103754
GaAs/Au-Ge/Ni, Schottky barrier energy var. with interdiffusion 77−20435
n-GaAs/Pt/Cr Schottky contact, barrier height change due to heat treatment 79−47165
GaAs-$(SN)_x$ semiconductor-polymer solar cell 79−15219
GaAs-Au, Schottky barrier energy var. with interdiffusion 77−20435
GaAs-Au polycrystalline Schottky barriers, transition with grain size from electrode-limit to bulk-limited cond. 80−65676
GaAs-Au(Ag) Schottky barrier solar cells, interface problems, AES, SIMS and XPS study 80−89627
GaAs-metal contacts, excess capacitance, depend. on nonlinear dielectric susceptibility 78−43475
GaAs-metal interface, metal-induced chem. reactions and surface states 80−20311
GaAs-metal Schottky barrier, surface states and barrier height, I-V (C-V) charcts. meas. 77−85310
GaAs-metal Schottky barrier contacts, interface chemistry 79−74049
GaAs-metal Schottky barrier height rel. to chem. reactivity 80−25008
n-GaAs-metal Schottky barrier, ultrathin native oxide, thickness determ. from C-V and photoresponse meas. 80−70821
GaAs-Pb junctions, electron tunnelling under high press., transition temp., energy gap, phonon energies 79−15257
n-GaAs-W contact, Schottky barrier 78−39213
$GaAs_{1-x}P_x$ epitaxial layers, charge carrier conc. determ. from low-field electrorefl. spectra 77−85320
GaAs(Sb), Schottky barrier and semicond./insulator interface states formation 80−49906
GaInAs:Cs-O, occurrence of Schottky effect 79−8227
n-GaP, deep state controlled minority carrier lifetime 80−20211
GaP Schottky barriers, voltage fluctuations, meas. 80−15604
p-GaP, Schottky barriers on polar (111) and ($\bar{1}\bar{1}\bar{1}$) surfaces 80−88631
GaP:Cr-Au Schottky barrier, local level near valence band of semicond. 79−11080
GaP-Hg, elec. props. using Schottky barrier capacitance techniques 78−47870
GaP-metal Schottky barrier height rel. to chem. reactivity 80−25008
p-GaP-NaOH interface, Schottky barrier model of photoelectrochemical effect 80−55673
GaSb-Au structure, metal-semicond. interaction, soft XPS meas. 78−60203
p-GaSe, back wall Schottky barrier cells, diffusion length, RT spectral response meas. 80−107806
Ge, amorphous, doping, Schottky barrier and p-n junction form. by RF sputtering 77−8187
N-Ge, electrorefl. spectra, light induced, electrolyte and Schottky barrier techniques of meas. 80−76046
Ge, Schottky barrier, electronic struct., pseudopot. calc. 78−95364
Ge Schottky barrier, electronic struct., pseudopotential method, jellium model 79−38162
Ge, Schottky barrier electrorefl. under uniaxial stress, band struct. 77−48193
Ge-metal interface, internal photoemission mechanisms 80−60077
Ge-metal Schottky barrier junction, surface electron states spectrum *(Russian)* 78−84297
n-Ge-metal Schottky barrier contacts, IR optoelectronic props., quantum detector appls. 80−75640

Schottky effect continued
Ge-Si_3N_4 system, potential barriers determ. from photoinjection carriers trapping 80−103756
GeS film, between Al(Zn)(Sn) electrodes, Schottky and Poole-Frenkel cond. mechanisms 80−54799
GeS, Schottky barrier, photovoltaic props. 79−7854
GeSe amorphous films, blocking metal contacts characteris. and photo/EMF obs. 77−76924
Hg-InP Schottky-barrier diode, contact times, I-V charcts. 80−96971
HgSe/CdSe lattice-matched heterostructs. as Schottky barriers, CVD epitaxial growth and elec. props. 80−49877
II-VI semiconductor, $(SN)_x$ and HgSe as contact materials, compared with Au 77−85312
In-GaAs(Ge)(Si) Schottky barrier interface, covalent bonding of metal atoms 77−20429
In-$SrTiO_{3-x}$ contacts, differential capacitance, elec. field depend. permittivity effect 80−54779
In-ZnSe:Al-In, MSM structure, mechanism of current flow *(Russian)* 79−78208
p-InGaAsP-Au, Schottky barrier height comp. depend., photoelec. meas. 77−20433
$In_{1-x}Ga_xSb$ alloy system, interband magnetooptical study using Schottky barrier 79−8124
$In_{1-x}Ga_xSb$-Au, photovoltaic effect and Schottky barriers 80−49897
InP (001)-Ag, contact, surface stoichiometry and struct., and electronic surface states 78−95361
n-InP barriers, low leakage, near ideal 78−39212
InP, cleaved surface, metal contact props. and influence of intermediate adsorbed layers 80−49905
InP, deep level trap interaction with lowest and upper cond. minima 80−49654
InP electrode-electrolyte interface, Schottky barrier obs. 78−52079
InP, Schottky barrier and semicond./insulator interface states formation 80−49906
n-InP Schottky barriers, photocapacitance effects of deep traps 78−43325
InP surface, interaction with Cl, rel. to Schottky barriers at metal-InP interface 78−56036
InP surface preparation for Schottky barrier and ohmic contact formation 80−39671
InP, surface space charge layers and Schottky barrier form., Raman scatt. study 80−50319
InP, surface vacancies, bound state energy levels calc., rel. to Schottky barrier formation 80−80340
InP thin films for photovoltaic devices 80−93972
InP-Ag Schottky barrier, hot electron attenuation length 80−49904
n-InP-Al(Hg), Schottky barrier height and stability characterisation 80−54786
InP-Au, semiconductor-metal boundary, effect of interfacial layers on barrier height 78−14824
InP-Au Schottky contacts, interfacial oxide layers used to increase effective barrier height 79−7896
InP-Au(Ag)(In), electronic structure 78−10554
InP-$In_xGa_{1-x}As$ alloy photocathodes, semiconductor photoemitters, field-assisted, 1-2 μm range 80−97396
n-InP-metal Schottky barriers, effective lowering using thin VPE n^+ lasers 77−43717
InP-metal Schottky barriers, effects of heat treatment characterised by SIMS 78−6446
n-InP-metal surface barrier struct., props. 79−11223
InSb-Au Schottky barrier, photovoltaic spectra and magneto-optical transitions, Landau levels and excitons 77−47858
$In_{2-x}Sn_xO_{3-y}$-CdTe(InP) photovoltaic heterojunctions, surface and interface studies, efficiency 80−45691
IrSi, Schottky barrier height meas. 79−47160
$KTaO_3$, electromech. props. and electron tunnelling 78−23403
$LaAl_2$, doped with Tb, Nd, or Pr, crystal field effects, tunnelling within mK range 80−70907
$LaPb_3$, doped with Tb, Nd, or Pr, crystal field effects, tunnelling within mK range 80−70907
$LaSn_3$, doped with Tb, Nd, or Pr, crystal field effects, tunnelling within mK range 80−70907
Li plasma, electrode pot. layer charcts., surface ionisation and Schottky effects 77−15260
Mo-n-Si Schottky barrier, sputtered, freq. cond. charact. 77−20426
Nb on thin Si membranes, super-Schottky and Josephson-effect devices 79−28469
Nb-Nb_2O_5-Nb structure, Schottky barrier effects on capacitance and loss tangent 77−8203
NiSi, parallel contacts, Schottky barrier height meas. 80−96965
Pb-Si:Sb Schottky tunnel junction, variable range hopping assisted tunnelling 80−39670
PbI_2-Ag(Au)(Cu), light sensitive, internal photoelectric emission 80−107910
$Pb_{0.8}Sn_{0.2}Te$-Pb, Schottky barrier form., Auger depth profiling and I-V meas. 80−49903
PbTe-Au Schottky barrier junctions, Landau level oscills. in tunnelling data 80−49945
Pd/Si, barrier type devices, chemical and polarisation characteristics, comparative study 79−78173
Pd/Si, Schottky-barrier type devices, chemical and polarisation characteristics, comparative study 79−78173
$Pd/SiO_2/Si$, barrier type devices, chemical and polarisation characteristics, comparative study 79−78173
Pd-W, substrate temp. influence on shallow contact formation on Si 80−96963
Pt-Si Schottky barriers on Si, laser formation and charcts. 80−60079
Pt-W, substrate temp. influence on shallow contact formation on Si 80−96963
PtSi, parallel contacts, Schottky barrier height meas. 80−96965
$(SN)_x$ Schottky barrier with III-V and II-VI semiconds. prep. and evaluation 78−6442
Sb_2O_3 anodic layers on Sb, semicond. props. 79−56303
Si (111) 7×7 surface, Schottky barrier formation, photoemission, exam. of filled surface states and band bending 77−28250
Si (111) surface, Al overlayers, theoretical study 78−95366
Si (111) surface with Al overlayers, electronic struct., self-consistent pseudopotential method 79−4595
Si, amorphous, doping, Schottky barrier and p-n junction form. by RF sputtering 77−8187
Schottky effect continued
Si, amorphous, in contact with electrolyte, Schottky barriers at interface 79−78169
Si, amorphous, Schottky barrier and p-n junction props. 79−28407
Si, amorphous, Schottky barrier solar cells, deep hole traps, spectral response and TSC meas. 80−50962
Si amorphous films, RF sputtered, appl. as Schottky barrier solar cells 79−34434
Si, back-wall Schottky barrier solar cell with interfacial layer 77−62993
Si, chemically etched, metal contact, electron and hole currents correl. 78−91769
Si, cleaved surface, metal contact props. and influence of intermediate adsorbed layers 80−49905
Si, heavily doped, doping density striation effects in studies of metal-nonmetal transition 79−28383
Si MIS solar cells with Cr, Hf, Be, Sc and Y as barrier forming metals, expt. investigation 80−94077
Si polycrystalline-metal Schottky barrier solar cells, elec. and photovoltaic contact props. 80−93936
Si Schottky barrier metallisation characteristics 77−76922
Si, Schottky barrier structs., proton bombarded, defect states 80−29356
n-Si wafer, trap centres of self-interstitials 80−75516
Si:Fe(Au)(Pt)(Ag)(Ti), photoionisation cross-sections and energy levels 79−87060
Si:H, amorphous, RF sputtered, suitability as solar cell material 80−40864
Si:H, amorphous, RF sputtered, Schottky barrier solar cells, photovoltaic props. and capacitance-voltage charact. 80−45678
Si:H, amorphous, sputtered Schottky barrier solar cells, conduction mechanism 80−104506
Si:H, amorphous Schottky barrier solar cells, depletion region, capacitance study 80−50963
a-Si:H solar cells, photoexcited carrier collection efficiency 79−100526
Si:H(F), amorphous, Schottky barrier profiles, depletion region width 80−49871
Si:O, O rich polycryst. film, carrier transport 78−80076
Si:Pt, deep level, exam. by thermally stimulated current and capacitance techniques 79−1579
Si/metal system, silicide form. by thin film interactions, review 80−49429
Si/Pd-W, contact reactions, backscattering, X-ray diffr. meas. 80−20040
Si-Al(Ga)(In) interface, electron energy loss spectra of Schottky barrier states 77−48290
p-Si-Au, Schottky barrier IR detector 77−37985
n-Si-Au Schottky barrier, role of surface states in appearance of photo EMF 79−11222
Si-Au semiconductor-metal boundary, effect of interfacial layers on barrier height 78−14824
Si-Au(Ag) contacts, Schottky barrier heights and interface states 77−85317
n-Si-Cr, Schottky barrier IR detector 77−37985
Si-IrSi interface microstructure and Schottky barrier height 80−34508
Si-metal contact, transport theory of Schottky barriers 80−80372
Si-metal Schottky barriers, surface states and barrier heights 77−80838
p-Si-metal Schottky contact surface state spectra and current transport mechanism *(Russian)* 78−43472
Si-metal systems, interfacial reaction and Schottky barrier 80−39672
Si-Ni Schottky barriers, thermionic field emission at room temp. 78−6445
n-Si-Ni structure formed by elec. explosion of metal, rectifying barrier 78−72263
n-Si-Ni surface barrier junction, rectifying, struct. and elec. charcts., effect of low temp. annealing 78−14821
n-Si-Pd_2Si contact, interface struct. and Schottky barrier height, correl. obs. using TEM 80−100504
Si-Pd_2Si Schottky barrier, resistivity, elec. charcts., solar cell use 78−14825
Si-PtSi Schottky barrier, resistivity, elec. charcts., solar cell use 78−14825
n-Si-Re(Os) Schottky contact barrier height meas. 80−65675
Si-refractory metal contacts, thermally cleaned surfaces 80−100521
Si-SnO_2 heterojunctions, complementary Schottky barriers 79−78166
Si-transition metal silicide Schottky barrier, effect of glassy membrane 77−85311
SiC film, amorphous, reactively sputtered, effects of S/C ratio and H content on elec. and optical props. 79−90906
SiH_x amorphous films, internal photoemission, metal contacts 80−96964
SiH_x amorphous reactively sputtered films, in Pd Schottky barrier devices, photovoltaic props. 80−49910
$Si_{1-x}H_x$, amorphous, gap states, DLTS 80−49656
Si_3N_4 layers, cond. process kinetics 77−76991
SiO_2-Si interface, hot electron capture process, expt. method for study 79−38180
SiO_x film, in MIM sandwich, elec. props. 77−72933
SiO_x thin film dielec., in MIM struct., interfacial props. rel. to non-stoichiometry 80−80399
$Si_{12}Te_{48}As_{30}Ge_{10}$-Au, Schottky barrier props. 79−7897
SnO_2/V_2O_5-P_2O_5/Si heterojunction, static optoelectronic charcts. 79−87146
Ta-Ta_2O_5-InP thin refractory MIS struct. deposition 80−75647
Ta_xO_y on Ta, anodic film, electrochem. reactions by tunnel current 77−81340
Te-Se-Cd rectifying sandwich structs., elec. forming action, Schottky junction form. 80−80371
Ti-anodic oxide-Au(Al), electronic cond. *(French)* 79−95512
TiO_2 film, ion plated, DC cond. study 80−100457
TiW-TiO_2-InP thin refractory MIS struct. deposition 80−75647
Tm_2O_3 film, between Al electrodes, prep. and elec. props. 80−60103
Tm_2O_3 film, electron beam deposition, elec. props., and struct. 79−87580
V_2O_5-metal Schottky barrier, contact-limited conduction 79−95493
V_2O_5-P_2O_5 glass, dielec. relax. mechanism, SDRC investigation, Schottky barrier formation in metal-glass-metal systems 78−60388
WO_3 films on Si, sapphire, glass and metal substrates, colour intensity dependence obs. *(Russian)* 80−2430
ZnO ceramic, nonohmic, drift phenomena of capacitance and current 80−39587
ZnO, nonhomic ceramic, current oscillation phenomena 79−69515
ZnO, nonohmic ceramic, current creep 79−69514
ZnO:Ce(Sm) phosphors, electrolum. 79−99946

Schottky effect continued
ZnS-metal interface, metal-induced chem. reactions and surface states 80−20311
ZnS-metal Schottky barrier height rel. to chem. reactivity 80−25008
ZnSe layers, cond. type determ. by pot. profiling 80−73387
ZnSe:Mn(Al)(I), Schottky diode, direct impact excitation of luminescent centres 79−7900
ZnSe-metal Schottky barrier height rel. to chem. reactivity 80−25008
n-$ZnSiP_2$, deep impurity levels, Schottky TSC meas. 79−95419
$ZnSiP_2$-Au(Ni) Schottky contact, production and props. 79−7901

Schottky gate field effect transistors
400 Mb/s optical fibre communications, integrating and transimpedance front end performance comparison *(German)* 78−33879
carrier concentration and mobility profiles in thin semicond. layers meas. 79−87170
Josephson FET, hybrid, feasibility 80−80451
$Ga_{1-x}Al_xAs$ low threshold stripe geometry DH laser, Be implanted, on semi-insulating substrate 80−69409
GaAs, deep trapping effects at GaAs-GaAs:Cr interface 78−72245
GaAs epilayer, hot carrier noise 79−24035
GaAs, etching soln. system H_3PO_4-H_2O_2-H_2O for MESFET fabrication 78−11379
GaAs, fabrication using dual-bubbler CVD system 78−6856
GaAs, hydride VPE growth for FETs, and characterisation 78−27407
GaAs LPE buffer layers for MESFET appls. 80−29887
GaAs MBE physical characteristics and applications *(German)* 79−7618
GaAs, MBE prep., device props. 77−77417
GaAs MESFET, for fast pulse modulation of semiconductor laser 77−88797
GaAs, MESFET, low temp. VPE growth by halide process 77−90279
GaAs MESFET, optical detector appl., sensitive high-speed device 80−13143
GaAs MESFET layers, low-temp. halide epitaxial growth 77−77403
GaAs, MESFET structure, buffered, LPE growth 80−40271
GaAs MESFET struct., high-resolution deep level meas., photo-FET method 80−44531
GaAs, monocrystalline, lateral definition, prep. by MBE 80−108357
GaAs, obs. of localisation in two-dimens. systems 78−60213
GaAs, possible use of anodic Al_2O_3 for passivation, elec. props. of GaAs-Al_2O_3 interface 80−49934
GaAs Schottky-gate FET, monolithic integration with GaAlAs injection laser 80−48275
GaAs type FET with buffer, bias effects due to deep centres in struct. *(French)* 80−107917
GaAs, VPE by pyrolysis, producing power GaAs MESFETs 78−23623
GaAs:Cr, buffer layer, epitaxial, exam. of doping using $Cr(CO)_6$ 78−72737
GaAs:Fe, for FET, VPE and characterisation 78−19672
GaAs:Sn films, MBE power MESFETs 80−50563
GaAs:Sn layers, MBE growth, DC I-V characts. 77−15952
GaAs-GaAlAs, injection laser and MESFET monolithic integration on GaAs substrate 79−64242
GaAs-W-Au Schottky barrier FET, elec. and chem. props. 80−96973
InP, VPE growth for MESFET's 80−103602
SiC, growth techniques of epitaxial layers 80−108360

Schottky noise *see random noise*

Schrodinger equation
3-body problem with one infinite mass particle, integral and Schrodinger eqn. equivalence 80−18255
3-body problem with one infinite mass particle, Schrodinger and integral eqn. soln. equivalence 80−77636
σ model, nonlinear, quantum fluctuations of pseudoparticles 77−87897
abstract equipartition of energy theorems 79−71273
acoustic wave propag. in shallow water, soln. of wave eqn. based on eigenfunctions of Schrodinger eqn. *(French)* 79−41505
adiabatic oscillator and related pots., spectral and scatt. theory 79−58568
Alfven waves, circularly polarised, spiky soliton soln. to nonlinear evolution eqn. 80−38590
algebra of three-dimensional generalized functions, associative, involution and differentiation 80−68080
alternating direction method 78−21011
an inhomogeneous Schrodinger equation and its solutions in scattering theory 79−63073
analogue computer solution *(German)* 78−28903
anharmonic oscillator, moment recursions and the Schrodinger problem 79−35584
anharmonic oscillator, three-dimensional, radial Schrodinger eqn. 80−86144
anharmonic oscillator pot., eigenvalues and eigenfunctions 80−27163
anharmonic oscillator with polynomial pot., asymptotic forms of energy eigenvalues 78−45509
anharmonic oscillators, single or quartic coupled, energy levels 78−70014
approximate method of soln. *(French)* 78−81867
approximate soln. through continued fractions for eqn. with central potls. and positive energies 77−17852
approximated solutions, variation method 77−30029
asymptotic completeness of wave operators 77−74259
asymptotic distribution of eigenvalues for the multidimensional Schrodinger equation 80−94985
asymptotic expansions in motion of two electrons in nuclear field 78−66459
asymptotic soln. of radial Schrodinger eqn. for singular pot. 79−30288
atom, bound state decay in external field in semiclassical approx. 80−12941
atom, ionis. by pulse of coherent radn. 77−38647
atom, multiphoton ionisation, resonant, with intense monochromatic laser, appl. to H(Na)(Cs) 80−32689
atom, soln. using model statistical potential *(Russian)* 77−22444
atom+diatom, energy correction of infinite order sudden approx., improved phase shift approach 80−95710
atom+diatom, planar reaction, cross section calcs., vibr. and rot. convergences 77−21376
atom+diatom, planar reaction, Schrodinger eqn., expansion as partial differential eqns. 77−21375
atom+diatom, three dimens. reaction, Schrodinger eqn. soln. for Porter-Karplus pot. energy surface 77−21378
atom+diatom, three dimens. reaction, theory 77−21377

Schrodinger equation continued
atom+molecule, collinear reactive scattering, generalised hyperbolic coords. 79−74363
atom+molecule, IR induced vibr. transition, Schrodinger eqn. distorted wave calc. 77−23538
atom interacting with strong classical radiation, exact soln. *(Russian)* 78−49697
atom models, ionisation time depend. under intense EM fields 80−32683
atom near metallic surface, resonant state, Schrodinger eqn. soln., jellium model 78−80033
atomic collisions, determ. of Regge poles from nonlinear Schrodinger eqn. 78−49702
atomic collisions, rotationally induced transitions in two-state model 80−47945
atomic hyperfine interactions, modified delta-function pot. 79−3378
atomic model potentials soluble in closed form 80−23287
atomic scatt. factors and momentum densities, asymptotic form 80−74105
atomic system, two-electron, Schrodinger local energies 79−41090
atomic theory, few-charged particle problem 77−26977
atoms, many body problem, Schrodinger eqn. standard solns. 80−47863
atoms, P-state collisions, quantum mechanical treatment, angular momentum coupling 80−99541
attractive potential, $r^{-(s+2)}$ type, SL(2,R) acting on quaternions 80−57125
Backlund transform. for nonlinear partial differential-difference eqns. 78−16625
Backlund transformations as canonical transformations 78−81855
band struck. in 1-D, continued fraction approach 80−6694
band struct. of 1-D periodic system in scaling limit 79−80454
baryon spectroscopy and photoproduction couplings using new baryon wavefunctions 80−102016
baryonium four body problem, Schrodinger eqn. soln. by stochastic variational method 79−36008
binding of Schrodinger particles through conspiracy of potential wells 79−75374
bistable potential field, model for diffusion, soln. to Schrodinger eqn. 79−75458
bistable potentials, diffusion, Schrodinger and Fokker-Planck equations 80−62528
Bohr Hamiltonian, collective states of Ba and Xe isotopes 77−67695
Born series, 2 cluster→2 cluster scatt., two, three, four particle Schrodinger operators 79−49072
Born-Oppenheimer approx. for levels of diatomic molecules 77−46478
Born-Oppenheimer nuclear motion wave function determ., incl. conical intersections and identical nuclei 79−54932
Bose Hamiltonian, bilinear, nonstationary solns. 78−73864
boson, nonrelativistic, potentials, attractive discreteness of ground state 80−46957
boson quantum thermodynamical system in one space dimension, high-order perturbation expansion 80−4636
boson system, 1-D, with δ-function interactions, time-depend. Hartree approx. 79−9184
bound s-state of electron in screened Coulomb field 78−58581
bound state continuum, necessary and sufficient condition of existence 78−45496
bound state for one-dimens. operator in weak coupling limit 78−62
bound state solutions, var. calcs. 77−33747
bound state systems, kinetic energy and path curvature 78−19998
bound state wavefunctions, normalisation, semiclassical results 80−86128
bound states, bound on number, spherically symm. pot. 77−2564
bound states, impedance and zero energy wavefunction 77−74253
bound states for higher angular momenta, scatt. length 80−22209
bound states in attractive potentials, existence condition *(French)* 80−57113
bound states of bispherical and toroidal potentials *(French)* 80−75
bounds on number of eigenvalues of Schrodinger operator 78−49693
box approach to resonance 80−98824
bremsstrahlung, stimulated, high intensity, convergence of approx. 78−16687
Brownian motion interpretation challenged 80−94974
Cauchy problem, classical mechanics of diffusion and Schrodinger eqn. 78−28985
Cauchy problem, general case, class of nonlinear Schrodinger equations 79−84994
Cauchy problem, jump process in quantum theory *(French)* 80−31596
Cauchy problems average boundary conditions 77−2561
central potentials, energy levels and level ordering 79−80463
central potentials, wave function at origin for large-n S-wave levels 79−35585
charged particle scattering in homogeneous mag. field, transition amplitude 79−10218
charmonium, ψ and χ states, hyperfine struct. 78−12878
charmonium and similar two fermion systems, effective Hamiltonian 78−21381
charmonium models, energy perturbation series from Schrodinger eqn. 79−6005
charmonium spectroscopy, explicit soln. of wave eqn. for arbitrary power pots. 80−403
classical bounds for energy distribs. of Hamiltonian operators in EM fields 78−45490
classical two fluid process, relationship with Schrodinger quantum theory 79−40385
coherent states of a nonrelativistic charged particle in a constant electric field 80−18103
collective motion frictional and conservative forces, frictional Schrodinger eqn. 79−85357
collision processes, time-depend. eqn., explicit integration method 78−57805
completely integrable class of mech. systems, Korteweg-de Vries eqns., multicomponent Schrodinger eqns. particle motion 78−54218
completely integrable operator evolutionary eqns., Schrodinger Korteweg-de Vries, KdV eqns. 79−97248
completely integrable systems for Schrodinger and KdV equations *(French)* 79−25879
complex diffusion processes, transforms., and nonrelativistic quantum mechanics 80−82670
complex WKB method, asymptotic behaviour of phase integrals 77−67332
confinement pots. in Schrodinger theory, analytic continued fraction theory 79−44786

Schrodinger equation continued
confining pot., eigenvalue problem for Schrodinger operator 80−27154
confining pot., Regge poles, coupled Schrodinger eqns. 77−61219
construction of L^2 dependent potentials 80−86129
continuation property for hamiltonians 80−77642
continued fraction expansions and statistical nonequilib. mechanics, for asymptotic soln. 78−45523
continued-fraction soln. method, convergence behaviour 77−64963
continuity of generalised eigenfunctions of Schrodinger operator 78−45511
continuous singular spectrum of the Schrodinger operator 80−86138
continuum S state wavefunctions for the Debye potential by Ecker-Weizel approximations 78−78104
correlated electronic wavefunctions, Schrodinger eqn. variational form, generalised k-particle Brillouin conditions 79−81146
correspondence rules and path integrals 80−31590
cosmological particle pair creation as above barrier reflection, WKB approx. 79−80377
Coulomb energy dissipation in reactions with heavy ions 79−76014
Coulomb potential, exponential cosine, critical screening parameter 80−82673
Coulomb problem, zero-energy 78−62097
coupled, nonlinear with complex coeffs., analytical and numerical anal. of wave-wave interaction 78−54220
coupled equations, perturbative method, piecewise constant reference potential 80−86111
coupled second order differential equations, soln. 79−40398
coupled-channel Schrodinger eqn. bound states, renormalised Numerov method 79−13627
cranking model, all orders solution, system with energy gap 77−82838
critical point of infinite type, exact sol. in one dimens. 79−9199
crystals, Schrodinger eqn. calcs. variational cellular method, general formulation 78−94192
cubic, perturbed plane-wave solns. 79−58587
current research, review 77−41509
currents and continuous symmetry restoration in two dimens., perturbation theory 79−21910
damped double solitons in the nonlinear Schrodinger equation 79−64853
damped oscillator approach to nuclear structure 80−27569
Darboux theory, appl. to construction of general soln. with Poshl-Teller potential *(Russian)* 78−12607
density matrix, coherent-state basis 78−21060
derivation from scale invariance 77−41507
derivative nonlinear, under nonvanishing conditions, exact solns. 78−62093
derivative nonlinear eqn., exact soln. using inverse scatt. technique 78−49703
diagrammatic many-body perturbation expansion, computer program 78−50454
diagrammatic many-body perturbation expansion, ladder energies, computer program 78−50455
diagrammatic many-body perturbation expansion, ring energies, computer program 78−50456
diatomic mol. scatt., phase shift differences for some trigonometrical potentials 80−43132
diatomic molecular scattering, phase shift difference, trigonometric pots. 79−22787
diatomic molecule, vibr. energies and functions, cubic splines method calcs. 80−78594
diatomic molecule, wave function computation, iterative method compared with Langer's method 78−86762
diatomic molecules, vibr.-rot. coupling const. calc. 79−31503
diffraction problem, non-homogeneous media, non-stationary problem 80−22211
dilated three-body Schrodinger operators, scatt. theory 79−17256
dipole absorption oscillator strengths, simple approx. method for computing radial wave functions 78−62111
Dirac's time dependent perturbation theory, appearance of singularities 79−21984
Dirac bubble potential, moving particle problem 79−80456
discontinuous pots., variational methods with global trial functions 77−30035
discrete inverse scatt. theory and continuum limit, difference approxs. 78−32724
discrete-time Schrodinger eqn., linear harmonic oscill. 78−49717
discreteness conditions of the spectrum of Schrodinger operators 79−17260
dissipative dynamical system, stochastic quantisation 77−56
dissipative phenomena and new interpretation 77−26202
dissipative system, nonlinear von Neumann equations 79−25976
dissipative systems, calc. of propagators in the Caldirola-Karai-Schrodinger equation 79−6009
dissipative systems, Schrodinger-type eqn. 79−49085
distorted wave Glauber approximation, Pauli eqn. soln. 78−57809
divergent series summation by order depend. mappings 79−88819
double exponential pot. and large coupling consts., perturbation theory 77−87662
double well Schrodinger operators 80−90698
dynamical symmetries, rotationally invariant time-dependent potentials, degeneracy and dynamical algebras 80−62510
dynamical symmetries in spherical geom. 79−40394
education, electron spin, nonrelativistic quantum mechanics derivation from Schrodinger eqn. 78−69942
education, linear differential eqns. with polynomial appl. Schrodinger eqns. 77−49522
education, particle in box, position versus momentum representation 77−33762
education, Schrodinger eqn. for free particle, wave packet spreading in coord. representation 80−17736
education, Schrodinger eqn. solns. using approximate nucleon-nucleon and Λ-nucleon pots. 80−62429
education, two-electron atom, 1snl excited levels, ionisation energy calc., perturbation, Schrodinger eqn. methods 80−17728
effective potential calculation to order ħ using functional Schrodinger Rayleigh-Ritz approach 77−74257
eigenfunction expansion of Schrodinger operator 77−74260
eigenstates, pointwise bounds, probabilistic approach 78−93544
eigenvalue and eigenfunction computation by stepwise potential function approximation 77−17853
eigenvalue bounds, method for obtaining formulae 79−75392
eigenvalue nonexistence condition 78−24682
Schrodinger equation continued
eigenvalue problem in nonlinear field equations for meson spectroscopy 78−89689
eigenvalue problem soln. with long range pots. 80−83
eigenvalues, perturbation theory calc. without complete set of eigenfunctions 80−105519
eigenvalues for particle in monotonic pot. 79−40412
eigenvalues in singular perturbation problem 79−49088
eigenvalues of infinite multiplicity, existence theorem 80−94989
eigenvalues of Schrodinger operators, proof of nonexistence 78−81878
eigenvalues of stochastic differential operator, approx. soln. of mean problem *(German)* 78−12540
eikonal theory of high-energy pot. scatt. 78−16675
El Gendi approximation method, solution of Schrodinger integral eqn. 78−77749
electron, free, motion in uniform mag. and elec. fields, Schrodinger eqn. soln. 78−24985
electron diffraction, generalised nonlinear Schrodinger eqn. 77−14650
electron diffraction and channelling, Schrodinger eqn. separation, case of systematic refls. 79−46522
electron gas, thermodynamic properties, weak field expansions, in uniform mag. field at T=0K 79−85066
electron in multicentre Coulombic field of nuclei, integral Schrodinger eqn. soln. 79−30285
electron moving in Coulomb field of two charged nuclei 77−23403
electron moving in several Coulomb centres' field, justification of LCAO MOs 77−57854
electron nonlinear waves in strongly magnetised plasma 80−79472
electron optics, quantum phenomena in dense electron beams, soln. of Schrodinger eqn. 79−76568
electron reflection and transmission through surface potential barrier 80−87998
electron shell, types of collective motion 79−63886
electron wave function in vicinity of planar defect 'on edge' 80−88002
electron-atom collision theory, soln. of coupled integro-differential eqns. by computer program 78−86948
electron-molecule scattering, Schrodinger eqn. Fourier transform 79−64105
electron-photon interaction, gauge and hybrid transforms. 80−22544
electronic density of states, Schrodinger eqn. with random pot. 79−65414
electrons in helical mag. fields, quantum theory 79−80470
electrons in logarithmic pots. 78−41447
energy approximants and perturbation theory 80−22232
energy functional, unification with Hohenberg and Kohn functionals 77−413
energy levels, lower bounds determ. 78−16672
energy levels for linear plus Coulomb-like pot. 78−4521
energy spreading in solns. to nonlinear eqn. 80−86147
envelope wave stability 80−43410
evolution equations, completely integrable, natural generalisation *(French)* 80−27152
exact scatt. soln. of eqn. with short range pot. 79−17268
exact solution of damped nonlinear equation, for parabolic profile 79−17278
exact solutions for one-dimens. eqn. with continuous plus δ-functions 80−98827
exactly soluble Schrodinger eqn. with bistable pot. 80−67950
exciton-neutral donor complexes, dissociation energy 80−34364
explicit method stabilisation difference eqn. *(Italian)* 77−71225
exponential cosine screened Coulomb pot., s-states, Ecker-Weizel approx. calcs. 80−101732
exponential nonlinearity, soln. of Schrodinger eqn. in time independent case 78−14168
exterior domains, nonexistence of nontrivial solns. 78−65819
factorised completely X symmetric S-matrix characterisation, multicomponent field theories 80−105800
fermion many body systems, Tamm-Dancoff method based on SO(2N+1) regular representation 79−35629
fermion many-body systems, Schrodinger eqn. on (2N+1) spinor space 78−41227
few-body scatt. in quantum mechanics, soln. methods 79−85010
Feynman path integral and quantum mech. as $\hbar \to 0$ 77−2557
Feynman path integrals, generalised meas. 78−384
Feynman theory extension *(French)* 79−53994
Feynmann path integral, cylindrical approx. 79−105
field intensity relaxation, in medium with quasi-static fluctuations *(Russian)* 79−2715
finite difference approach, inverse problem in nuclear physics 77−54195
finite difference of Schrodinger eqn., math. props., appl. to free electron *(Italian)* 77−78993
finite element formulation in space-time continuum 77−67333
finite nucleus model for the Fermi contact interaction 79−36601
finite range potentials, inverse problem 79−49097
finite-difference, with time dependent operator, soln. 77−5692
fission, asymmetric, nuclear mass parameter 78−13053
fitting technique approach in pot. scatt. theory 77−79000
fluid dynamical form of the linear and nonlinear Schrodinger equations 80−90720
form factors, bound state, relation to binding potential using nonrelativistic Schrodinger eqn. 78−58187
free, invariance algebra 78−81
free particle, two space-one time dimens., symmetries 77−17781
free polaron multiphoton absorpt. spectra, electron reson. coupling via longit. optical phonons 79−95347
friction, stochastic quantisation, nonlinear Schrodinger equation 80−27164
friction, stochastic quantisation, nonlinear wave eqn. 80−98825
friction in quantised Langevin systems, Schrodinger eqn., damped harmonic oscill. solns. 79−21570
frictional quantum mechanical system, one-dimens. scatt. model for coherence in stopping power problem 80−101736
Friedrich extension for differential operators with strongly singular potentials 80−27150
Fues potential, vibr.-rot. spectra, Schrodinger eqn. soln., pot. energy curves *(Spanish)* 78−36784
functorial geometric quantization and Van Hove's theorem 80−86108
fundamental solution construction 79−75397
Galilean invariant Schrodinger eqn., relativistic wave eqn. derivation, Lie algebra 80−105555
gaseous dipolar media, semiclassical theory, appl. to gas laser 80−83586

Schrodinger equation continued
gaseous molecules, persistence of p, d, f and g orbitals, ang. functions, Schrodinger's eqn. and cardinal number anal. 80−102426
gauge invariance in second quantisation, Hartree-Fock and random phase approximations 79−75395
Gauss-Hertz principle continuum form, derivation of Schrodinger eqn. in time domain 78−73851
gausson collisions, logarithmic nonlinear Schrodinger eqn. solns., resonance energy interval 78−89357
Gel'fand-Levitan equation, non-self adjoint operators, eigenfunctions, spectral representations 80−86131
Gel'fand-Levitan equations with comparison measures and comparison potentials 80−12931
Gel'fand-Levitan kernel for 3-D Schrodinger eqn. 80−36892
Gel'fand-Levitan method as a generalized Jordan-Wigner transformation 80−77962
Gelfand-Levitan eqn. generalisation 78−28984
general light cone frame, from Galilei group to Lorentz group, appl. to Schrodinger-Pauli eqn. 77−61187
general relativity, path-integral formulation, DeWitt-Morette measures 78−123
generalisation from new reversible evolution principle approach *(French)* 79−5995
generalisations of finite element and R-matrix methods 78−24676
generalised nonlinear eqn., solns. in 2-D 79−40397
generalized solitons of the Schrodinger equation with unitary nonlinearity 79−71294
gluon exchange in short distance hadron-antihadron pot. quark motion, Schrodinger eqn. 79−328
Grassman functional Schrodinger equation appl. to perturbation theory 79−21915
Grassmann functional Schrodinger description for fermions 79−30642
gravitational gas, one-dimens., Schrodinger eqn. for N-body problem 77−33943
gravity waves, nonlinear Schrodinger eqn., Fermi-Pasta-Ulam recurrence 79−10579
gravity waves, nonlinear Schrodinger eqn. exact solns. 79−77147
Green functions for discrete-time Schrodinger equation 80−46859
group projective representations 77−37773
hadronic atoms in momentum space, Dirac, Schrodinger and Klein-Gordon eqn. eigenvalues 79−872
Hamilton's principle function for Brownian motion, Schrodinger-Langevin eqn. 78−41233
Hamiltonian expectation values for time-depend. Foldy-Wouthuysen transformations 77−49633
Hardy pt., S-matrix formalism 80−96
harmonic oscillator, damped, coherent states and reson. 79−97251
harmonic oscillator, general time depend., quantal fluctuations and invariant operators 80−36898
harmonic oscillator, numerical soln., teaching aid 78−8188
harmonic oscillator, three-dimens., Green's function 80−73211
harmonic oscillator, vibr.-rot. interaction eigenvalue estimate 79−12628
harmonic oscillator damped, transitions between pseudostationary states, quantum treatment 78−65
harmonic oscillator in box, quantum-mechanical soln. 77−13632
harmonic oscillator in random EM field radiative corrections stochastic electrodynamic treatment 77−45736
harmonic oscillator wavefunctions, asymptotic behaviour 80−67979
harmonic oscillator with λx^M perturbation 80−27161
harmonic time depend. oscillator with damping and perturbative force 80−82
Hartree equations, time-dependent, global solutions, and nonlinear Schrodinger eqn. 80−73193
heavy baryon spectroscopy in the QCD bag model 80−105866
heavy ion scattering, optical model code A-THREE 78−89837
heavy ion scattering cross-sections, WKB calcs., unphysical reflection phenomena 80−27656
heavy leptons, existence in quantum theory 78−21363
heavy-ion scatt., inelastic, with Coulomb interaction, soln. of coupled eqns. 77−65232
Heine-Abarenkov optimised potential for 27 elements, radial Schrodinger eqn. soln. 77−11833
Heisenberg algebra commutation relation, general representation, Schrodinger eqn. soln. 79−2653
Heisenberg ferromagnet eqn. equivalence to nonlinear Schrodinger eqn. 79−95563
helical curve motion and soliton eqns., scaling invariance 78−49667
higher order modified pot. for effective phase integral approx. 79−44779
Hilbert space formalism for probability theory 77−60955
hypergeometric partial solutions in the problem of two Coulomb centers 80−4582
hyperon+nucleon interactions, one boson exchange pot. approach, multichannel Schrodinger eqn. soln. 77−57556
hyperspherical 1-D Schrodinger eqn. derivation, two-body interaction 78−49721
hyperspherical coords., discrete spectrum of charged particles 77−49627
hypervirial theorem, form of intermediate operators 79−44784
ideal gas, self-trapping of electrons, nonlinear Schrodinger eqn. soln. 79−2662
instanton phenomena, real time approach, multidimens. potential with continuous symmetry 79−2922
integral inequalities and separation for Schrodinger type operators in $L_2(R^n)$ 78−77680
integral Schrodinger eqn. for atomic evolution operator, transitions to continuum, Fredholm method 79−72223
integral transform groups for differential operators from Lie algebras 80−4887
interacting particle system with Lennard-Jones pot., Schrodinger eqn. eigenvalues 79−71292
interaction of type $\lambda x^2/(1+gx^2)$ 79−91
invariance algebras of Schrodinger and Dirac eqns. *(Russian)* 80−68081
invariance group, reln. to conformal extensions of Galilei group 78−36877
invariance principle in scatt. theory, proof 79−75378
inverse problem for pot. scatt. at fixed energy, Newton Sabatier numerical method appl. 77−67593
inverse scatt. method generalisation, generalised nonlinear Schrodinger eqn. eigenfunction 79−92994
inverse scatt. problem *(Russian)* 77−22982

Schrodinger equation continued
inverse scattering, one-dimens. Schrodinger eqn. pot. from S-matrix 80−57127
inverse scattering in three dimens. 80−86130
inverse scattering method, massive Dirac system soln. using connection with matrix Schrodinger eqn. 79−2655
inverse scattering problem, incorrect nature 80−86139
inverse scattering transform for potentials of compact support 79−97
inverse scattering transform solvable nonlinear evolution eqns., existence, Lax's method extension 78−32711
inverse scattering transformation, correl. with exact quantum eigenstates 79−58873
inverse scattering transforms, Zakharov-Shabat and Schrodinger-type, connection 78−21006
inverse spectral problem for one dimens. Schrodinger eqn. with additional linear pot. 79−2656
ion+atom collisions, ionis., charge transfer, model 77−75278
ion cyclotron resonance spectrometry, collisionally damped ion motion 80−57419
ion-acoustic wave modulation instability, effect of finite ion temp. 79−1307
ionic crystals, surface F centres, electronic struct., numerical soln. of one electron Schrodinger eqn. 78−64091
Jost function and S-matrix for pot. of general form., Schrodinger eqn. soln. in hypergeometrical functions *(Russian)* 78−81870
Jost solutions and Green's functions for the three-dimensional Schrodinger equation 79−71277
Jost solutions for general Gaussian potentials 80−46854
Jost solutions for Yukawa potentials 80−86132
JWKB phase integrals, to high-order 80−5632
Kepler stationary orbits of electron with velocity-depend. oscillatory perturbations 80−52062
kink Schrodinger equation and one dimensional non-linear solitons, general method for soln. 80−46871
Klein-Gordon eqn., meson masses calc. using harmonic oscillator pot. 79−93392
Klein-Gordon Schrodinger coupled equations, global C^∞ solns. 79−35955
KMS condition for Schrodinger dynamics 80−36896
Langmuir and dispersive ion acoustic waves, coupled nonlinear Schrodinger eqn. 79−77362
Langmuir collapse, dimensionality and dissipation 80−87880
Langmuir plasma, self-magnetised collapse dynamics 80−92327
Langmuir waves, modulated, nonlinear Landau damping effect 78−81849
Laplace transform, appl. to scattering 78−57806
large radius polaron model, soliton excitations 79−42470
laser beam propagation eqn., finite difference approx. *(French)* 77−72017
laser beam self-channeling Schrodinger nonlinear eqn. exact soln. *(Ukrainian)* 79−94278
laser excitation, stepwise, coherent Schrodinger vs. incoherent rate eqn. approaches 78−74871
layered crystal, mag. quantisation investig. *(Russian)* 78−23054
layered crystal, wave functions, exciton spectrum, light absorpt. *(Russian)* 80−100436
Lee model, V-V sector 78−24967
linear confining pot., soln. with combinatorics functions 78−32719
linear dynamic mol. system, correlated radiation impulse sequence interaction 80−38058
linear physical field, propagator expansion in power series of coupling constant 79−30647
linear potential hill, incident quantum wave, for teachers 78−12492
linear potential wavefunctions, generalised hypergeometric functions 80−62512
linear recursion relns., discrete path approach 78−24678
Liouville-Green uniform asymptotic method, used to obtain eigenvalues of Schrodinger eqn. (3-d), with a radial Gaussian pot. 78−20995
local bound states, existence conditions in weak fields, stationary Schrodinger eqn. calcs. 80−36904
local decay of scatt. solns. 78−77744
local distortion technique, resonances, poles of S-matrix 77−74609
local scaled Schrodinger relations and the virial theorem, kinetic energy operator 80−78527
local symmetries, oscill. problem 77−17847
localised wave field evolution, nonlinear Schrodinger equation exact soln. 80−53191
locality principle, governed by Schrodinger eqn. 79−88834
logarithmic, nonlinear gausson solns. 80−46865
logarithmic pot., soln. for quark model particle spectroscopy 80−32065
logarithmic Schrodinger equation, soliton dynamics 80−57130
low-frequency approximation for scattering in a laser field 79−92996
lower bound Hamiltonians for atoms and mols., projection operator method 78−82602
magnetic charges, quantum strings and gauge invariance 78−33009
magnons, nonlinear, multidomain ferromagnets with 180° Bloch walls 78−34967
many body Schrodinger operators, ground state energy per particle 80−68064
many electron atomic Hamiltonians spectral props., method of configuration interaction 79−59368
many particle systems with $1/r^2$ pot., Riccatti eqn. and completely integrable systems *(French)* 79−12711
many-body, description of electromagnetic and hadronic reactions, intermediate energies 77−79363
many-body operator decomposition 77−22434
many-body systems, resons., extended virial theorem, complex acaling, Schrodinger operators 79−21575
many-electron systems, electron density, Schrodinger inequalities and asymptotic behavior 78−21845
many-particle Hamiltonian with two-particle singular pots., self-adjointness 77−67311
many-particle wave function, hyperspherical expansion, singularities at partial wave origin 77−74264
massive gauge theories, with instantons, wave functions, energies, vacuum and heavy quarks, WKB Schrodinger eqn. 79−35951
massless non-Abelian fields, study of state vectors using Schrodinger equation *(Russian)* 79−30667
matrix equations for two-fermion systems with magnetic interactions 79−21904
metallic alloy, random, first principles band theory, review 80−44473

Schrodinger equation continued
microscopic system mechanics, solitons and 1-dimens. Schrodinger eqn. 79−12934
minimal operator self adjointness 80−17836
MISIM struct. inversion layer, symmetrical, carrier conc. calc. 80−75651
mixed local-global variational approach and its application to a discontinuous potential 79−58564
modified Coulomb potentials, bounds for phase-shifts 80−57112
molecular energy levels, accurate determ., appl. to H_2 77−46503
molecular Hartree-Fock integral eqns., soln. 79−76325
molecular multicentre potential, X_α scattered waves method and Schrodinger eqn. soln. 80−37740
molecular nuclear motion, time dependent adiabatic approx., Born-Oppenheimer approx. 77−23491
molecular rot.-vibr. anal. by finite difference perturbation method 77−50420
molecular state stability, symmetry breaking for a non-linear Schrodinger equation 79−26867
molecules, composite particle, vibr. amplitude and vibr.-rot. anal. 80−74158
momentum invariance with Schrodinger prescription 79−2659
momentum space, bound-state energies and eigenfunctions 79−92972
momentum transfer cross section, ave. force and force correlation formulas 79−92
monopole theory without strings 77−49625
Monte Carlo solution for molecular systems 78−46255
moving electron in field of two Coulombic ions fixed in space, rel. to H_2^+ line spectrum 80−42083
multi-soliton solutions of a derivative nonlinear Schrodinger equation 80−105528
multichannel scatt. theory for temp. depend. Hamiltonians, charge transfer problem 80−90695
multicomponent chiral and gauge models, stationary solns. 79−85213
multicomponent nonlinear Schrodinger equation, generalisation of prolongation struct. for AKNS system 77−45730
multicomponent nonlinear Schrodinger equation, soliton solns. 77−9907
multidimensional, nonlinear evolution eqns. 77−13630
multiple well anharmonic oscillators and perturbation theory 79−49086
multistep laser excitation, pulse modulation, Schrodinger eqn. anal. 78−63046
muonic atom energy levels 79−76533
n-body Schrodinger eqn., exp(S) formalism for nucl. matter 77−22918
N-body Schrodinger operators, eigenfunctions, wave packets, pointwise bounds 79−12634
n-electron atoms, compactness proof for infinite systems of linear equations 79−72247
N-electron system, Schrodinger eqn. soln. using antisymmetrisation 80−106246
N-particle Schrodinger eqn., macroscopic behaviour, superconductor and fermion systems 78−60242
N-particle system eigenvalue problem, survey of general results 77−45713
Nelson's probabilistic derivation, discussion 77−33908
neutron star model appl. 77−49418
non-Abelian massless fields, discussion of Schrodinger equation 79−17614
non-Abelian phase factors, Yang-Mills Hamiltonian 80−73575
non-Abelian quantum gauge theory, Schrodinger representation 77−2757
non-affine path algorithm in the functional integral calculus of Schrodinger kernels 80−31593
non-Gaussian wave packet time evolution 80−57133
non-linear coupling of quantum theory and classical gravity 80−27389
non-local potentials and positive energy bound states 80−73200
non-uniqueness in writing Schrodinger kernel as a functional integral 79−54006
nonadiabatic collision processes, electronic degrees of freedom, classical analogue, appl. to mol. system 79−64063
nonadiabatic transition amplitudes, semiclassical calcs., adiabatic theorem in complex plane 78−20993
nonconservative systems, irreversible behaviour 79−81
noninstantaneous $O(\nu/c)$ relativistic effects in bound states and a covariant Schrodinger equation 80−73607
nonlinear, appl of variation of action method of one field solitons 80−331
nonlinear, as model for Regge-Gribov field theory 77−38100
nonlinear, Benjamin-Feir instability and recurrence 78−81874
nonlinear, Cauchy problem anal. using theory of monotone operators *(French)* 79−53993
nonlinear, classical systems with infinite set of conservation laws 80−86102
nonlinear, comparison of exact quantum and quasiclassical results 77−64965
nonlinear, conservation laws group theoretic aspects 77−30016
nonlinear, conservation laws soln. method 79−63066
nonlinear, constrained harmonic motion 80−77625
nonlinear, discrete version with variable coefficient 80−8819
nonlinear, envelope solitons and holes for sine-Gordon, nonlinear Klein-Gordon eqns. 77−2553
nonlinear, explicit formulae for solns. *(Ukrainian)* 77−30031
nonlinear, in cylindrical symmetry, return and collapse of solns. 80−90711
nonlinear, inverse scatt. method generalisation, Schrodinger equation 79−75381
nonlinear, inverse scatt. problem method 80−4577
nonlinear, Lie theory calc. of invariants 80−22234
nonlinear, modulation of torsional waves in elastic rod 77−62195
nonlinear, Moller operator construction, Lax pair operator quantisation 79−97250
nonlinear, perturbation expansion, nonlinear Landau damping influence 78−62110
nonlinear, perturbation expn. 78−47124
nonlinear, soliton-like soln. 79−44790
nonlinear, three dimens. stability of solns. 80−57141
nonlinear, three-dimens., helicon packet three-dimens. self-localisation *(Russian)* 79−15176
nonlinear, under nonvanishing conditions, inverse scatt. method 78−57808
nonlinear, variational approach 79−58583
nonlinear, variational principle appl. 79−63065
nonlinear differential eqns. with N-depend. coeff. 79−71275

Schrodinger equation continued
nonlinear dispersive and dissipative wave propagation 77−74231
nonlinear dispersive systems, 2-D lumps 79−92955
nonlinear dispersive wave eqns., modulational instability and envelope solns. 78−54199
nonlinear electron plasma waves in cylindrical waveguide 79−4134
nonlinear eqn., damped, soliton soln. 78−12605
nonlinear eqn., exact stationary soliton soln. 78−12604
nonlinear eqn., slowly varying solitary wave solns. 80−73
nonlinear equation, Cauchy problem soln. blowing up 78−8220
nonlinear equation, energy bands 79−58581
nonlinear equation, soliton soln. *(Chinese)* 79−92987
nonlinear evolution eqns., soln. by inverse spectral transforms 77−57228
nonlinear evolution eqns. associated with energy depend. pots. 77−17841
nonlinear evolution eqns. in one space dimens., inverse scatt. soln. 79−97222
nonlinear evolution equations, exact solns. 79−25873
nonlinear evolution equations solvable by inverse spectral transform of rank 4 matrix Schrodinger eqn. 78−41187
nonlinear field eqn. and differential Schrodinger eqn. correction *(French)* 80−77637
nonlinear field equations, quantum inverse scattering transform method, 2-D ice and ferroelectric lattices 80−68348
nonlinear field equations, scattering theory 80−4882
nonlinear field theory, scatt. of quantised solitons 77−49842
nonlinear focusing and Kelvin-Helmholtz instability 80−83785
nonlinear generalisations, exact solns. 79−35569
nonlinear mixed eqn. and soliton solns., inverse method 80−68065
nonlinear propagation of wave-packets on fluid interfaces 77−47032
nonlinear quantum mechanics, appl. of Gauss tranformation to $^1/_2$ fields 79−63082
nonlinear quantum mechanics, Gauss transform. appl., Schrodinger eqn., nonlinear integro-differential eqn. 79−6013
nonlinear Schrodinger eqn., global solns. in 1,2,3-dimens. 79−5993
nonlinear Schrodinger eqn., soliton solns. 80−27173
nonlinear Schrodinger eqn. and anomalous backward scatt. 78−17232
nonlinear Schrodinger eqn. inverse scatt. problem, prolongation structs. 77−33890
nonlinear Schrodinger equation, appl. to deep water waves, $O(\varepsilon^4)$ perturb. anal. 80−4569
nonlinear Schrodinger equation, existence, uniqueness and regularity *(French)* 77−67202
nonlinear Schrodinger equation, spectral transform soln., charact. behaviour of solitons 78−70005
nonlinear Schrodinger equation, transverse instability of soliton solns. 79−58561
nonlinear Schrodinger equation solns., recurrent motion in continuum dynamical systems 80−22235
nonlinear Schrodinger equation with nonlocal interaction *(French)* 79−63061
nonlinear Schrodinger equation with periodic pot., existence of solns. 78−57820
nonlinear Schrodinger-Hartree eqn., soln. asymptotic behaviour 77−37728
nonlinear stationary operator equations, evolution *(French)* 80−46845
nonlinear time-dependent frictional or optical pot. Schrodinger eqns., one dimens. wave packet solns., Fortran program 77−9897
nonlinear tunnelling of soliton pulse 78−57811
nonlinear variant search using neutron interferometry 80−52064
nonlinear variants, proposed neutron interferometer expt. 79−92984
nonlinear wave and soliton propagation, arbitrary density profile, adiabatic approx. 78−49676
nonlinear waves in cold plasma, classical Vlasov plasma description through quantum numerical methods 80−92288
nonlinear wind waves, theoretical model using nonlinear Schrodinger eqn. 79−77154
nonlinearity of integral type, existence, uniqueness and regularity result *(French)* 77−67316
nonrelativistic electron wave diffraction by cylindrical capacitor 79−72473
nonrelativistic Markoff field, stochastic quantisation 79−67181
nonrelativistic one-dimensional problems, perturbation theory algorithm 80−82671
nonrelativistic persistent model, Schrodinger and Klein Gordon interacting fields with Chew-Low coupling, renormalisation props. 79−54250
nonseparable, series solns. and variational principle, appl. to H_2^+ and He 79−36504
nonseparable potentials, vibr. energy level semiclassical calc. 80−8832
nonspreading wave packets 79−44672
nonspreading wave packets in quantum mechs. 78−65795
normalised form, appl. to determ. of H atom energy *(Hungarian)* 79−3339
nuclear deep lying level props. in strong electrostatic field *(Russian)* 77−2910
nuclear elastic scatt. with optical potential, complex angular momentum methods, poles and zeros of S-matrix, REGGE 80−47445
nuclear pot., short-range, central, two-nucleon problem 77−65203
nuclear potential, solitons as model 80−83081
nuclear single-particle resonances, numerical anal. 78−29436
numerical integration, using WKB approx., eigenvalue estimates 78−12486
numerical integration leading to Bohr-Sommerfeld formula, alternative to JWKB calcs. 80−86119
numerical integration of Schrodinger eqn. with double-minimum potential 78−58573
numerical soln., exponential-fitting methods 78−49694
numerical study of phase-integral connection formula 77−71230
Numerov algorithm solutions, roundoff error study 79−2643
Numerov scheme for Schrodinger eqn. soln. 80−52046
off-shell, nonrelativistic two-body amplitudes, generalisation of Jost formalism 78−49687
'On the theory of the Schrodinger equation', Leontovich and Mandel'shtam, 50th anniversary 79−49090
one dimens. WKB soln. effect of pot. function defined on finite interval 78−28978
one dimensional, Fourier transforms *(French)* 77−37766
one dimensional, gap between asymptotic degenerate eigenvalues, quantum and semiclassical methods 78−57803
one dimensional, with energy dependent potential, inverse problem, pt.I 77−26186

Schrodinger equation continued
one dimensional, with energy dependent potential, inverse problem, pt.II 77−26187
one dimensional, with gradient coupling, quantum mechs. as generalised stochastic theory in phase space 78−45505
one dimensional, WKB approx., numerological anal. to large order 78−16688
one dimensional electrical model, T network, unreal components *(German)* 77−53792
one dimensional systems with resonance interaction, collective particle like excitations, Schrodinger eqn. 80−46868
one-body approx., disordered system spectral props., Schrodinger eqn., random fields 80−90696
one-dimensional band calculations using perturbation theory 80−44460
one-dimensional crystal, electron problem in uniform elec. field 77−20280
one-dimensional eigenvalue problem, bound state solns., numerical methods 78−20992
one-dimensional model crysts., surface density of states, rel. to adsorbed molecule 80−107889
one-dimensional motion, relation between phase function and Green's function 80−105543
one-dimensional Schrodinger eqn., almost periodic soln. *(Ukrainian)* 78−89360
one-dimensional Schrodinger eqn. scatt. pot., reflection coeff. rescaling effects 79−71291
one-dimensional singular potentials 77−13522
one-dimensional systems, with reson. interaction, soliton-like solns. 80−46831
one-dimensional time-independent, stationary path integral formalism 77−67315
one-particle quantum mechanics, duality between confining pots. and $(R+L_c^\infty)$ pots. 80−31574
open system, new classical Hamiltonian-Lagrange mechanics 80−36900
operator eigenvalue calc., linear error minimisation *(German)* 77−33880
operator evolution equations, completely integrable, nonlinear Schrodinger eqn. 80−12938
operator regularisation stability with singular repulsive pot. 79−88841
operators in uniform norm 77−64954
operators with L_{loc}^{p} pots., closure 77−45718
operators with long range potentials, spectral representations, book 80−73088
operators with wildly oscillating potentials, essential adjointness, sufficient condition 79−44772
optical fibre minimal dispersion refractive index profiles, Schrodinger eqn. analogy 79−98469
oscillating Hermite-Gaussian wave functions for harmonic oscillator Schrodinger eqn. 78−70004
oscillatory integral approach, semiclassical, linear and parabolic potentials 80−57124
overlapping avoided crossings, rel. to quantum stochasticity 80−90694
partial-wave Schrodinger differential and integral eqns., comparison of numerical solns. 78−16671
particle beam, potential scatt. into cone 79−97234
particle motion in potential channel, waveguide-optical analogy 80−12942
particle motion in ring shaped potential, spin-orbit coupling 80−101723
particle-boson interactions and the weak coupling limit 79−49100
path integrals for a particle in curved space 79−35598
pendulum, representation of canonical relns. 80−42084
periodic pot., one-dimensional Schrodinger operators 77−49629
periodic potential energy levels, late terms, asymptotic expansions 79−25895
perturbation problem, two-level atom interacting with EM field 80−52056
perturbation theory applications to numerical integration methods 80−12926
perturbative methods of solution, choosing step sizes 80−86110
perturbative numerical methods, local and accumulated truncation methods 80−62536
perturbed boundary conditions, for differential equations in theory of atoms 78−33432
perturbed equation with cubic linearity, soliton-like soln. 79−7765
perturbed nonlinear eqn., soliton interactions 77−87661
perturbed nonlinear equation, inverse problem method 77−60968
perturbed oscillator energies, numerical calc. method 79−58580
phase integral formulae for level densities, normalisation factors and quantal expectation values 78−54222
phase scattering, quasiclassical approximation *(Russian)* 79−89
phase shifts of certain potentials using recurrence relations for spherical Bessel functions 78−89364
phase shifts produced by repulsive, strongly singular, inverse power pots., high-energy behaviour 79−97233
photons, quantum mech. theory 77−13519
plasma, cold, modulational instability of two transverse waves 79−32765
plasma, collisionless, nonlinear Langmuir wave modulation 77−89256
plasma, inhomogeneous, modulated nonlinear ion acoustic waves 79−86576
plasma, laser-irradiated, Langmuir soliton generation at crit. density 80−6267
plasma, modulational instability of ion acoustic waves in the presence of density gradients 79−64840
plasma, nonlinear eqn. for dispersive media, ion-acoustic and Langmuir waves 77−31463
plasma ion waves, nonlinear Schrodinger eqn., perturbation method 78−75301
plasma wave propagation, nonlinear Schrodinger equation, modified Zakharov-Shabat inverse scatt. problem 80−59200
point spectrum, non-existence of eigenvectors of compact support *(French)* 80−68063
polar semiconductor, theory of excitons bound to neutral impurities 79−73441
polyatomic mol. gas, laser-induced rate processes, collision-free dynamics 77−30934
polynomial conservation laws in (1+1) dimens. classical and quantum field theory, nonlinear Schrodinger eqn. 78−54224
polynomial factor eigenfunctions, corresponding pots. *(Chinese)* 80−22236
position evolution of wave function, new type of Schrodinger eqn. 80−27178

Schrodinger equation continued
potential barrier, axially symmetric, tunnelling calc., appl. to energy level splitting and well broadening *(Russian)* 79−58588
potential having feature, spectra of self-conjugate extensions *(Russian)* 77−22381
potential problems, non-local, Perey effect, WKB method 80−68077
potential scattering, inverse problem, radial Schrodinger eqn. solns., analytic investigation *(Russian)* 79−87
potential scattering, wave operator completeness breakdown 79−40388
potential well particle escape, time-depend. Schrodinger eqn. soln. 80−86118
potential without spherical symmetry, sufficient condition for existence of bound states 80−68070
potentials with Coulomb tails, eigenenergy calc. 79−58560
prolongation structure for a nonlinear equation with explicit space dependence 80−82664
proper functions and absence of bound states for Schrodinger operator 80−4563
QCD, Schrodinger equation scaling props. 79−67496
QED external EM fields, time-dependent, particle interpretation, Fock representations of Fermi field operators. 80−52439
quadratic Hamiltonians in phase space and their eigenstates 80−86127
quantal matrix elements between unbound states, for radial Schrodinger eqn. 79−97240
quantal problems, soluble, using solns. of Schrodinger eqn. 77−67307
quantisation of matter without quantising related fields 80−105525
quantum chemistry, simple approximation method *(Hungarian)* 79−3341
quantum collision theory, generalised sensitivity anal. 80−31542
quantum damped oscillator, master equation and pure state representations 80−8823
quantum decay models, complex energy eigenstates for pot. scatt. 79−6011
quantum dynamics, sensitivity anal., Green's function method 79−67178
quantum field theory of solids, book 77−31922
quantum friction equations from Schrodingers equation 79−49069
quantum mechanical perturbation problems, resolution using integral eqn. 80−58112
quantum system subject to random pulses, Blume's integration of Schrodinger's eqn. 79−97232
quantum theory, physical foundations, stochastic formulation, proposed expt. test 80−52049
quantum theory equations of motion, deterministic model 78−24689
quantum theory of neutrons in helical magnetic fields, Schrodinger eqn. solns. 79−35581
quantum three particle system, action-angle variables 80−95708
quantum tunnelling, reaction coord. method 80−62500
quark-quark interaction, phenomenological, from s-wave baryon spectrum 80−101984
quarkonium, quantum mechanical applications, masses and leptonic widths of ψ and Υ 80−27484
quasi-discrete states in complex pots., Schrodinger eqn. with Woods-Saxon pot. *(Russian)* 78−86194
quasi-particles with variable effective mass *(Russian)* 78−4497
quasi-recurring energy leakage in the two-space-dimensional nonlinear Schrodinger equation 80−82676
quasirelativistic equation of motion, invariance group 79−12649
quasistationary state decomposition, effect of transient excitation *(Russian)* 78−77769
quasistationary states decay in nonrelativistic quantum mechanics 79−21584
radial, conversion to recursive eqn., pocket calculator determ. of energy eigenvalues 77−57215
radial, direct and inverse problem generalisation 79−9144
radial, fourth-order numerical method of soln. 80−86107
radial, general pot. props. for soln. by hypergeometric functions 80−4581
radial, product integrals appl. 77−74251
radial, propag. method, appl. to close coupled eqns. 80−42096
radial, propagation method 80−8816
radial Coulomb eqn., soln. by double Chebyshev expansion technique 77−37768
radial one-dimens., second order perturbative numerical calcs. 80−31580
radial reduced Coulomb Green's function 80−31559
radial Schrodinger eqn. global numerical soln. by second order perturbation theory 80−68079
radial Schrodinger equation, eigenvalues, matrix elements, phase shifts 80−86133
radial Schrodinger equation, numerical anal. technique 79−67191
radial Schrodinger equation, solns., inversion formulae by expansions by squares *(Russian)* 79−12629
radial wave equation, particle in asymptotically Coulomb pot., eigenvalues and eigenfunctions calcs. 77−57214
radical eqn. for n-dimensional scatt. 78−24679
random Gaussian pot., one dimens. charge density wave *(Russian)* 79−19534
random potential, behaviour of Wiener integrals as $t\to\infty$ and density of states 79−2720
random pulses in quantum systems, Schrodinger eqn. soln. 78−86189
random walk calcs., method of successive corrections 79−68180
randomly fluctuating interaction term, uncertainty in nature 80−62499
Rayleigh-Schrodinger, appl. of Pade approximants 78−65806
rearranged perturbation theory, nonlinear transformation 80−105542
relative magnitudes of the derivatives of 1P(D,F,...) and 2P(D,F,...) wave functions at the origin 79−67182
relativistic Bethe-Salpeter harmonic oscillator 80−32006
relativistic quantum mechanics, space-time formalism for spin-zero particles 79−21974
relativistic spinless particles, one particle quantum theory 79−17255
relativistic two body Schrodinger equation, generalisations of quasipot. eqn. for scalar interactions 77−13871
repulsive quadratic potential, energy eigenvalues determ. 79−9136
rescaling Schrodinger eigenvalue problem perturbation series 79−92980
resolvent operator expansion, generalised method, Schrodinger eqn. soln. appl. 80−86126
resonance fluorescence of N two-level atoms in a weak EM field, Heitler-Ma approach 79−93950
resonance theory in indefinite metric spaces 80−101730
resonant pole trajectories in complex scaling, stationarity, appl. to H atoms 79−18126

Schrodinger equation continued
resonant states in the presence of Coulomb interactions, Schrodinger eqn. 80−91161
Riemann solution in one-dimen. inverse problem 78−28979
Ritz-Givens-Householder method, anharmonicity type λx^{2m}, Schrodinger operator energy levels 78−28970
rotating harmonic oscillator, eigenvalues of radial Schrodinger eqn. 79−67184
S-matrix for analytical continuation over complex k-plane 78−49978
S-wave for finite range pot., Stieltjes functions and approximate solutions of an inverse problem 79−49094
scalar potential inter-relation between non-relativistic and relativistic wave eqns. 78−58110
scaling, nonrelativistic Schrodinger eqn. charmonium 78−54613
scattering and local absorption for the Schrodinger operator 78−93546
scattering by hard corrugated wall potential, Schrodinger eqn. exact soln. 79−40404
scattering matrix for rapidly oscillating potentials 80−57126
scattering medium, with quasistatic fluctuations, average field weakening calc. 79−71367
scattering phase shifts and eigenvalues of eqn. with singular pots. 78−62102
scattering problem with separable potentials 80−90708
scattering solutions decay at least logarithmically 79−25901
scattering theory, general case, class of nonlinear Schrodinger equations 79−84995
scattering theory and continuous spectra for class of strongly oscillating potentials 80−77638
scattering theory with different state spaces of perturbed and free system 79−40406
scattering wave function construction using analytical continuation of bound state 77−74258
Schmidt orthogonalisation in the continuum 78−8266
Schottky barrier formation and shape determ. factors *(Russian)* 78−84295
Schrdoinger-Kepler eqn., perihelion precession rate in system of two charged masses 78−73897
Schrodinger's route to wave mechanics 80−17783
Schrodinger's variational quantisation method in stochastic framework 80−105532
Schrodinger kernel as functional integral, non-uniqueness 80−31594
Schrodinger-Langevin eqn. derivation, stochastic quantisation of open systems 77−30090
Schrodinger-Pauli wave equation without approximation 79−12648
screened Coulomb pot., Schrodinger eqn. with Hulthen pot., variational soln. 77−23427
screened Coulomb problem, group theoretic approach 77−87655
screw dislocation, scattering of tight-binding electrons, numerical solution of Schrodinger equation 79−51540
self-adjointness and spectral anal. of Schrodinger operators 77−45712
self-adjointness of Schrodinger-type operator powers 78−81877
self-focusing of waves on deep water surface *(Russian)* 80−94536
semi-classical bounds for eigenvalues of Schrodinger operators 78−70010
semiclassical perturbation expansion of the multichannel scattering matrix 79−49410
semiclassical strong coupling parabolic connection formulae 77−9903
semiclassical theory for near adiabatic photon assisted mol. collisions 79−5141
semiconductor doped surfaces, inversion layers, quantum model 78−30961
separable quasipotential formulation of the relativistic dynamics for three point particles 79−12989
short range local interactions, radial wave functions and scatt. phase shift calc. program 79−84976
short time propagators in Riemann geometries 79−63129
short-time stochastic electron, modified Brownian particle, Schrodinger eqn. 78−36853
single channel Schrodinger eqn. for e-scatt. off static pot., de Vogelaere's method 79−63062
single particle state obeying Schrodinger eqn. new bound state to continuum formulation 78−78335
singular perturbation pots. 77−60952
singular potentials, Gel'fand-Levitan theory of the inverse problem 79−49098
singular potentials in the non-relativistic quantum theory *(Russian)* 79−63063
singular Schrodinger operators, eigenfunction expansions 77−53793
SL(2,R) approach to Schrodinger spectral problem with pseudosingular potential 80−8845
smooth distribution group and Schrodinger equation in $L^p(R^n)$ 79−97227
solids, Bloch waves, Lame eqn. interpretation 80−39489
soliton equations, perturbed, variational approach 78−89366
soliton formation in warm magnetised Vlasov plasma 79−90396
soliton scattering in non-linear Schrodinger theory 78−8256
soliton solutions, stability, nonlinear term of form $\psi|\psi|^\nu$ 78−70013
soliton solutions to derivative nonlinear Schrodinger eqn 79−44773
soliton stability, 3-D nonrelativistic *(Russian)* 80−4583
solitons, lecture 78−24690
solitons as nonlinear magnons 78−6523
soluble Kisslinger pot., associated Schrodinger eqn. 79−85416
solution, hybrid method 80−94968
solution by hand-held calculator 80−52052
solution method for specjal class of potentials 80−36897
solutions for $\lambda x^2/(1+gx^2)$ interaction with g small and λ large 79−92967
solutions with time depend. pots. and associated scatt. theory 79−17263
spectral and scatt. theory, Schrodinger operator with singular attractive potential 80−86151
spectral and scatt. theory of Schrodinger operators, Stark effect 77−22435
spectral props. of many electron atomic Hamiltonians, appl. to 2-electron atoms 79−63922
spectrum of $p^2+V(x)+\varepsilon x$, periodic V, complex ε 80−22225
spectrum of Schrodinger operator with damped oscill. pots. 78−77748
spherical potential, bounds on number of states *(French)* 77−67312
spherically symmetric charged dust distrib., Brans-Dicke theory, Schrodinger eqn. soln. 79−12693
spin particles, relativistic and Galilean wave eqns. 80−82672
spin-orbit coupling origin in Schrodinger representation 80−42914

Schrodinger equation continued
spinless particle eqn., for free and external scalar field interactions 79−58575
spinless particle scattering by central pots., soln. 80−27156
spinless particles through one dimens. pot. barrier, formal series method, refl. coeff. 78−32700
spinning particle in helical mag. field, nonrelativistic quantum theory 80−77651
square well potential, bound state energies, for teachers 79−35478
square-well potential, integral eqns. and scatt. solns. 80−31451
stability of self-adjointness of Schrodinger operators under positive perturbations 80−94990
Stark effect in 1-D, resonances and continued fractions 79−59395
stationary connected multisoliton formations, Schrodinger eqn. with nonlocal nonlinearity *(Russian)* 80−57105
stationary nonlinear Hartree eqn., asymptotic soln. 78−49723
stationary theory of scattering, spectral forms 77−45714
STO basis set, removal of singularities in numerical integration 79−6847
stochastic action integral interpretation of quantum mechanical transformation function 80−77644
stochastic electrodynamics, derivation of quantum mechanics 78−36801
stochastic electrodynamics, derivation of Schrodinger eqn. 77−82411
stochastic origns, model 80−81
stochastic resolution, analyticity and integrability, existence and uniqueness of soln. *(French)* 80−73195
stochastic solution, asymptotic behaviour *(French)* 80−46844
Stormer approach and the solution of two coupled Schrodinger equations 80−62526
strong coupling QCD, variational approach, Schrodinger eqn. and effective Hamiltonian 80−95245
strong coupling theory, scatt. on nonrelativistic particle 79−40675
Sturm-Liouville equation, convergence, rel. to nucleon-nucleus pot. 79−6534
Sturm-Liouville equation, math. aspects rel. to nucleon-nucleus pot. 79−6533
SU_n Heisenberg spin chain derivation 80−37184
superposed Yukawa and inverse square potentials, eigenenergy expansion 79−30281
surface gravity wave packet development when moving over an uneven bottom 79−41700
surface potential barrier, Schrodinger eqn., anal. and numerical soln. incl. spin-orbit interaction 79−58492
symposium, 50 years of Schrodinger equation, Vienna, Austria (June 1976) 77−45711
system subject to random pulses 77−74245
term entry into continuum in presence of Coulomb field 79−21583
s-tetrazine, pot. surface of low-freq. out-of-plane modes 78−62741
thermodynamics, subquantum 78−24751
third-order constants of motion in quantum mechanics 79−6002
third-order JWKB approximation method applic. to absolute continuity criteria derivation, approx. operators construction 78−12591
third-order JWKB approximation method applic. to absolute continuity criteria derivation, approx. operators and estimates 78−12592
three body problem for general even power potential with applications 79−25900
three body systems, spectral and scatt. theory 77−45715
three fermion system with exchange potential, asymptotic soln. 77−38229
three level system, interference between one and two photon processes, occupation probabilities 80−63965
three particle nuclear molecular states, Schrodinger eqn., wave functions and energy spectrum *(Russian)* 78−86497
three-body problem, bound state eigenvalues lower bounds, upper bounds by Rayleigh-Ritz method 80−68068
three-body problem, number of discrete levels 77−49636
three-body problem with hard cores, 1-D, eigenvalue lower bounds 80−68069
three-body problem with hard cores, 1-D, reduction to 2-D Helmholtz eqn. 80−62523
three-body problems, Schrodinger perturbation theory in adiabatic rep. *(Russian)* 77−60976
three-level system, strongly-excited, statistical broadening and population loss 79−41359
tight lower bounds to eigenvalues of the Schrodinger equation 80−94984
time depend., explicit integration method, comment 79−72224
time depend., two-dimens. finite difference schemes 80−97
time depend. eqn., solutions comparison 78−12596
time dependent eqn., initial value problem, fund. soln. 79−25902
time dependent Schrodinger eqn., alternative approx. soln. for heavy ion reactions 80−32296
time dependent Schrodinger eqn. from time evolution in subquantum model 78−41189
time evolution operator in quantum mechanics 80−82610
time independent, soln. for particles inside Coulomb barrier, computation 77−2914
time recurrent behaviour in the nonlinear Schrodinger equation 80−90704
time-dependent, optimisation of approx. solns. 78−73885
time-dependent harmonic oscillator type Hamiltonians, explicit invariants, Schrodinger wavefunctions 78−8259
time-dependent variational principles, Schrodinger eqn. 77−26208
transformation, for infinite-order perturbation theory 78−12589
transformation groups for resolution of partial differential eqns., appl. to gravity, quantum mech. and heat transfer *(French)* 79−49099
transformation to accel. reference frame, equivalence principle, for teaching 78−24614
transit time measures in scattering theory, time depend. Schrodinger eqn. 80−73194
transition metal clusters, symmetric, higher-order isotropic exchange, Schrodinger model 79−7955
translation invariant harmonic matter, exact Schrodinger eqn. soln. 78−65802
translation invariant N-body harmonic oscillator problem 80−31558
translation invariant N-body problem, exact solns. to Schrodinger eqn. 78−65801
translation kernels for velocity depend. interactions 78−24680
translation-invariant harmonic atoms, exact solns. 78−32725
transmission coeff. for 1-D potential barrier, discretisation of Schrodinger eqn. 80−57123
transport theory integral eqn. soln. in Green's function formalism, scatt. amplitudes 80−4566

Schrodinger equation continued
triangular matrix Schrodinger problem, evolution eqns., inverse spectral transform 78−70007
triatomic molecule, large amplitude vibr. model, appl. to H_2O 79−41150
triatomic molecule, large-amplitude Hamiltonian for vibr.-rot. 78−25511
trotter formula for the Schrodinger operator with a complex singular potential *(French)* 79−49070
Trotter product non-standard formula 78−32710
truncated space calculation of exact bound state energies, comment 79−88837
tunnelling phenomena, electronic energy distrib., Schrodinger wave eqn. solutions 80−103743
two body problem with nonlocal separable central and tensor interaction, exact analytical soln. 78−69997
two cluster scattering amplitudes, dilation anal. reson. rel. to scatt. reson. 79−40389
two component derivative nonlinear Schrodinger equations, Alfven waves appls. 80−48883
two dimensional Schrodinger equation, finite element package MANFEP 78−36870
two-body problem, relativistic, appl. to muonium and positronium 79−2933
two-channel scattering problem variable phase method *(Russian)* 77−74269
two-photon spectroscopy, Laplace transform method 79−10084
ultracold neutrons in traps, damping of quasistationary wave functions 78−9013
vacuum polarization connection to atomic spectrum in a strong magnetic field 80−42369
van de Pol eqn., transformation into S-wave Schrodinger eqn., solvable potential 78−57790
velocity dependent nuclear potential, matrix soln. 79−25892
velocity dependent pot. uncoupled Schrodinger eqn. soln. using Green's technique 78−69998
von Neumann's measurement theory, phase relationship observation 80−105539
water, X^1A, ground state, large-amplitude Hamiltonian for vibr.-rot. 78−25511
water surface, oscillotory waves, Korteweg-de-Vries and Schrodinger eqns. solns. and expt. 78−26131
water wave, partial reflection by nonuniform adverse currents 79−64681
water wave packet evolution, Schrodinger and Korteweg-de Vries eqn. models 79−72902
wave diffraction, stationary problem in non-homogeneous media 80−68
wave function, normalisation consts., Poschl-Teller and $B_0 \tan h\ z\text{-}U_0 \cos h^{-2} z$ pots. 78−65818
wave functions, generalised wave operators for system of three charged nonrelativistic particles 79−75398
wave functions at pot. discontinuities, continuity conditions for teaching 80−27077
wave mechanics, invention, Schrodinger-Einstein correspondence 79−84898
wave modulation in multi-dimens. space, reductive perturbation method *(Japanese)* 77−41472
wave operators for oscillating pots. 78−49714
wave packet reduction in quantum mechanics: a model of a measuring apparatus 79−84977
wave-packet motion in Eckart and quadratic pots., appl. to H interstitials in transition metals 80−52067
wave-packet self-modulation, in nonlinear dispersive medium 78−41192
wavefunction mass depend. 79−92974
weakly bound particle ionisation, perturbation theory series convergence in alternating field 80−4575
weakly coupled one-dimensional Schrodinger operators, asymptotic behaviour of ground state 80−22220
with random. potl., cure. Green's functions 78−86
WKB approx. and scaling behaviour for Hellmann-Feynman and virial theorems 78−86193
WKBJ five term approx. 80−31569
Yang-Mills fields, quantisation by separation of gauge variables 79−67474
Yang-Mills theories, quantum dual string wave functional 79−21921
Yukawa pot. problem, S-matrix exact evaluation from transformed Schrodinger eqn. 78−82120
Yukawa potential, double integral representation 77−57224
Yukawa potential bound states, Sturmian group theoretical approach 80−8825
D^+-D^0, D^{*+}-D^{*0} mass differences using modified nonrelativistic Schrodinger eqn. 78−58186
K+nucleus, opt. pot., distorted waves, 100 to 200 MeV, difference between Schrodinger and Klein-Gordon wave functions 78−94033
NN potential from Regge pole theory, pseudoscalar meson potentials, M/E factor 79−67526
NNN bound state problems, hyperspherical harmonic expansion, review 80−91136
π+nucleus, opt. pot., distorted waves, 100 to 200 MeV, difference between Schrodinger and Klein-Gordon wave functions 78−94033
ψ meson, phenomenology and quark confinement 78−29308
qq interactions and nonrelativistic quark model 80−73682
Θ_2^4 quantum field theory, numerical methods, anharmonic oscillator approx. 80−52390
Ag, electronic and mag. structure calcs. of mag. impurities 80−80213
$Be, {}^1S$, Schrodinger eqn. random walk soln., electron spin effects 77−18780
CN ($A^2\Pi$-$X^2\Sigma^+$) transition, Franck-Condon factors, r-centroids, by Langer's approx. method 78−37685
$^{12}C+{}^6Li(^{16}O)$ scatt., anomalous backscatt. from nonlinear Schrodinger eqn. for nuclear matter 79−6465
Cu, electronic and mag. structure calcs. of mag. impurities 80−80213
$H, {}^2P$, random walk soln., electron spin effects 77−18780
H atom in box, 2-D Schroedinger equation, influence of constant elec. field, finite-element method 80−31544
H atom in mag. field, Schrodinger eqn., Monte Carlo soln. 80−31545
H atom lattice impurity, H atom confined to spherical box with penetrable walls 79−84987
H atom theory, Schrodinger-Dirac spaces of entire functions 77−54494
H hyperfine splitting inside paraboloidal surfaces 80−99445
H like wave functions in spherical and hyperbolic coords. *(Russian)* 77−9911
H, Schrodinger eqn. in two-dimens., for teaching 80−31457
H, Schrodinger equation, trigonometric soln. of polar function 77−67308
H, Stark effect, iteration procedure for any field strength 80−69104
H, uniform mag. field, low lying levels below 10^9 G, adiabatic approx. 79−72235
H^++H, 15-200 keV, excitation and charge transfer cross sections, Sturmian expansion 77−19024
H^++H, charge transfer cross section calc., up to 100 keV 78−55235
$H_2, {}^3\Sigma_u^+$, Schrodinger eqn. random walk soln., electron spin effects 77−18780
H_{2s}, mol. ion, Burrau approx., series solns. 77−30763
H_2^+, coupled-channel Schrodinger eqn. bound states, renormalised Numeroy method 79−13627
H_2^+ energy spectrum, variational cellular method calcs. 78−94192
H_2^+, HD^+ electron reduced mass use in electronic Schrodinger eqn. 77−10576
H_3^+, $D_{3h}{}^1A_1'$, Schrodinger eqn. random walk soln., electron spin effects 77−18780
$H_4, {}^1\Sigma_g^+$, Schrodinger eqn. random walk soln., electron spin effects 77−18780
HF, dipole moment function, Schrodinger eqn. soln. using Morse pot. 77−79703
H_2O, rot.-vibr. Schrodinger eqn. soln., bond lengths and angles, force consts. 79−41151
$^2H(n,n)$, nonlocal nonsymmetric pot., treatment of Schrodinger eqn. 78−82325
He atom, Schrodinger eqn. in symmetric coordinates 79−21589
He, isoelectronic sequence, Schrodinger eqn. finite difference soln. 79−31373
He like systems, ground state one electron density decay 79−76337
He, Schrodinger eqn. solns., existence criterion, for teachers 78−41117
He-He, energy and interaction potential of two ground-state atoms 80−63740
^{3}He, HCP, and adsorbed ^{3}He with triangular lattice, exchange and mag. order 80−107606
^{3}He, liq., binding energy and effective interactions, interactions, variational calcs. 80−107596
$He(2^3S)+H(D)$, Penning and assoc. ionis. cross sections, vel. depend. 79−22815
Hg atoms, elastic electron scatt., relativistic effects 80−102568
^{6}Li bound states, six body hyperspherical soln. to N-body Schrodinger eqn. 79−9490
N_2, Raman intensity, ab initio calc. 80−1028
NaF, quasimolecular struct. characts. of $NaL_{II,III}$ absorpt. edge 80−93436
Ne, noncoplanar symmetric (e,2e) reaction, factorised distorted-wave approx., 0.4-2.5 keV 78−55245
$Sr(^1S)+Ar$, $Sr(^1P)$ collisional excitation in nonreson. laser field, four-state model 79−10191
U (M,f), muon excitation probabilities, muonic atoms, Schrodinger eqn. 80−47515
Xe, noncoplanar symmetric (e,2e) reaction, factorised distorted-wave approx., 0.4-2.5 keV 78−55245

Schroedinger equation *see Schrodinger equation*

Schwarz-Hora effect
free electron devices for light prod., history, book contrib. 79−27147
long beating length, relativistic dielec. correction 77−36315

Schwarzschild metric
see also cosmology
adiabatic accretion onto Schwarzschild black hole 80−77445
artificial satellite orbits and general relativity, motion in Schwarzschild metric 77−64622
black hole, absorpt. and emission spectra, computational methods, cross sections 79−2558
black hole, elastic scatt. and absorption of waves 79−5857
black hole, master differential eqn. for perturbations 77−26214
black hole, point source spherical model, Schwarschild coord. frame, nature of interior universe 77−67107
black hole, prob. distrib. of incoming radiation 78−8300
black hole, scalar and electric charge at rest *(French)* 77−67108
black hole, slow rot., weakly charged, space-time and physical fields perturbs. *(Russian)* 78−36634
black hole, wave scatt. and adsorpt. cross-section 78−8283
black hole in external mag. field, radiation from moving particles *(Russian)* 78−49474
black hole in external mag. field, relativistic particle radiation 80−22035
black hole in radiation heat bath, stochastic evolution 80−85971
black hole in radiation-dominated non-relativistic gas, Bondi accretion problem 78−77575
black hole perturbatiors, transformations between governing eqns. 77−60790
black hole perturbations, zero rest mass fields in algebraically special curved space-time 77−74078
black holes, existence of gravit. field outside black hole 79−9158
black holes, massive, rotating, charged, phenomena based on Schwarzschild and Kerr-Newman metric solns. 79−71064
black holes, stable circular orbits of test particles moving in equatorial plane 80−85970
black-hole space-times, mass positivity 80−8880
Bonnor electrovac counterparts of Tomimatsu-Sato solns. of Einstein eqn. 78−57835
bundle boundary for the Schwarzschild and Friedmann solutions 80−31603
celestial mechanics, astron. meas. and coord. systems 80−36481
circular orbits, existence and stability in a Schwarzschild field with nonvanishing cosmological constant 79−92660
classical pseudoparticle solutions in general relativity 78−89390
collapsing shell, Schwarzschild-de Sitter space-time, thermodynamics and radiation 80−17607
conformal flatness and the Schwarzschild interior solution 79−30333
conformal uniqueness of Schwarzschild interior metric 77−30064
cosmic censorship, black holes, and particle orbits 79−44802
cyclotron instability, mechanism for cosmic radio emission 78−65724
Einstein-Maxwell equations, some Robinson-Trautman solns. 78−89374
electrodynamics, rel. to black holes and neutron stars 78−77480
electron self-energy 78−49681
electrostatics, electric fields and black holes *(French)* 79−40432
EM field of charge near singularity *(Russian)* 77−13652
EM radiation, partial polarisation in Schwarzschild gravitational field *(Russian)* 80−51801
EM radiation near black holes and neutron stars 78−53978

Schwarzschild metric continued
fluid sphere interior soln., const. gravitational mass density 77−79015
geodesic equation, rel. to Hawking's black hole area theorem 80−90468
gravitation, modified theory with regular solns. *(German)* 79−88844
gravitation, relativistic theory, static solutions and Poincare press. 80−31648
gravitational effects in 6-D general relativity, Schwarzschild metric, orbital precession 80−62550
gravitational field energy localisation, logic 78−49728
gravitational inertial field and critical systems, free motion 78−93484
gravitational Michelson-Morley expt., proposed, experimental and Schwarzchild metrics, black holes 79−97289
horizon stability in asymptotically flat spacetime 78−29021
index theorem, axial-vector anomalies, in Schwarzschild and Taub-NUT spaces 78−93832
irradiated Schwarzschild object, Petrov type-II electrovacuum soln. 78−106
Israel's theorem, uniqueness of Schwarzschild black hole 78−4097
Kerr-Taub-NUT soln. generalisation 78−49734
Klein-Gordon equation in Kerr Newman background space, Schwarzschild black hole 77−22262
Kruskal extension from vacuum field eqns. 80−42112
Kruskal metric, nominal source 80−12956
local relative motion in general relativity 80−42123
Lorentz-covariant model of the system of two gravitating particles 80−8865
low-frequency solutions of the wave equations in Schwarzschild space 80−90743
massive particle finite motion in Kerr and Schwarzschild fields *(Russian)* 79−8833
matter-vacuum matching 78−21032
neutrino emission from cylindrically symmetric cluster of many gravitating masses 80−94707
nonlinear scalar field dynamics 79−275
nonspherical perturbations, nonlinear behaviour gravit. field outside collapsing object 77−2581
null radiation gravitation deflection by relativistic spherical masses 79−58600
pair production by gravitational waves in field of black hole 77−22474
particle creations in the pseudoparticle gravitational fields 79−2704
particle motion in external gravitational field, Schwarzschild metric calc. *(German)* 77−9923
particle speed when approaching Schwarzschild metric 78−57776
particles in stationary spherically symmetric gravit. field 77−41293
point mass alternative space-time 80−31638
quadratic theory of gravitation *(Russian)* 77−45754
$R+R^2$ theory of gravity, with torsion, Brikhoff theorem, vacuum field eqn. solns. 79−71337
radial coord. as measure of proper distance 78−70034
radial wave functions in Schwarzschild space-time, global prop., irregular singular point 77−2567
red-shift of static config. with core and envelope 77−22058
Rindler, de Sitter and Schwarzschild spaces, Greens function thermal props., renormalisation 79−2686
scalar pot. and event horizon 78−101
scalar waves in Schwarzschild metric, approx. scheme 79−54025
Schwarzschild black hole in ext. mag. field, radiation emitted by relativistic particles 78−96501
Schwarzschild-Kruskal space-time, role in developing Maxwell field non-zero vacuum expectation value 80−62828
spherical cavity in an Einstein Universe 80−95013
spherical symmetric field, spin ang. momentum tensor calc. 80−42107
spinor representation, Kerr-Schild metrics 77−57253
stability proof 79−75420
static plasma polarisation in Schwartzschild gravitation field *(Russian)* 79−16825
static scalar field, possibility 77−45765
stellar collapse and the black hole limit from a dynamical view 79−30081
stress tensor trace anomalies, Hawking effect 77−67110
supergravity, classical solns. 78−122
superluminal particles motion in gravit. field of nonrot. black hole *(Russian)* 78−93103
supersymmetric black holes in supergravity, spin 3/2 perturbation of Schwarzschild black hole 78−93300
symmetry constraints in general relativity and the Schwarzchild interior metric 80−4605
tachyonic scalar waves in Schwarzschild space-time 78−45558
test particle motion, criticism of other result 77−67348
test particle motion, reply to critics 77−67349
test particle motion in Schwarzschild field *(Russian)* 78−12612
tetrad field of orthonormal vectors, new definition of Schwarzschild metric 78−89372
three body circular problem, periodic soln. of Schwarzschild's type 80−90730
rel. to Tolman metric *(Russian)* 78−12611
transformation to Kruskal-Novikov coordinate system 80−68098
two-body problem, nonlinear effects 79−8799
uniform electrovacuum space time, observer dependent effects, Bertotti-Robinson line element 79−122
vacuum energy-momentum tensor in Schwarzschild de Sitter space time 80−52091
variable quasars and active galactic nuclei, strong gravity effect on light curve 79−16812
white holes, nonexistence, anal. of star bursting Schwarzschild barrier 78−32506
white holes present appearance 78−61881
world function of Schwarzschild field, power series representation 80−12954
zero rest mass scalar wave eqn. solns. 79−93010

Schwarzschild space *see Schwarzschild metric*

Schwinger source theory
(1+1) dimens. Todd chain and $e^{\phi}+e^{-2\phi}$ model, exact factorised S-matrices 80−18094
(1+1) dimensional model field, fermion-boson correspondence, Klein transformation 80−42379
θ-vacua and confinement in two-dimensional models 80−77990
$\lambda:\Phi^4:/4!$ massive Euclidean field theory, perturbation expansion, cutoff bounds on n-point Schwinger function 79−71630

Schwinger source theory continued
$\lambda\phi_2^4$, Glimm-Jaffe-Spencer expansion for classical boundary conditions and phase coexistence 79−54245
ϕ^4 theory, Euclidean, local existence of Borel transform of Schwinger functions 80−77932
anomalous spectral regions in source theory 79−63354
axial anomaly and meron configurations in 2-dimens. Euclidean Schwinger model 80−86545
Bertotti-Robinson metric, pair production, semi-classical treatment 79−2702
charge confinement, Schwinger model compared with $(QED)_4$ 80−62902
chiral rotations and the fermion-boson equivalence in the Schwinger model 80−101919
chiral symmetry breaking and vacuum structure in Schwinger model 78−89615
conference on particle physics, Honolulu, Hawaii (Aug. 1977) 79−49485
consistent approx. scheme based as Laguerre polynomials 80−336
covariance problems in two-dimens. QCD 80−22575
dressed electron propagator solution without renormalisation 79−312
EM field, minimal coupling, relativistic wave equations for particles of unique mass, constraints 80−22526
equivalent boson theory, anomaly-free Ward-Takahashi identities 80−82873
Euclidean Dirac field, local structure, Green's function method 80−68347
Euclidean QED_2 on lattice, continuum limit, Schwinger functions, vacuum expectation values 80−73624
evolution operator, quark struct. of states, two dimensional massless electrodynamics *(Russian)* 80−73630
exponential interaction in R^n 79−63361
Fermifield bosonisation in 1+1 dimensions 80−47172
fermion, massless, quantum electrodynamics of Schwinger model, perturbation anal. 77−65109
$g\phi^4$ quantum field theory, clusterlike expansion based on static ultralocal approx. 80−62839
gauge field models, hard anomalies, cancellation by regularisation independent renormalisation scheme 80−77931
gauge transformations and vacuum structure 77−30260
generalised Schwinger boson realisations and oscillator-like coherent states, rot. groups and asymmetric top 79−80743
generating function in terms of non-Gaussian functional measure, soliton soln. appl. 79−21892
gravitino, axial current anomaly, Faddeev-Popov ghosts 80−68120
hypercomplex number approach 77−71416
introduction and applications to high energy elementary particle physics 79−49409
Ising field theory, 2-D, $T<T_c$, three point function string structure 79−270
Ising field theory 2-D, $T<T_c$, Green's function strings in n-point functions 79−271
Ising field theory in mag. field, cut breakup in two point function 79−272
Keldysh's perturbation formalism 80−13217
kink solutions on null plane, quantisation of 1+1 dimensional field theory 80−57505
Lagrangian formulation generalisation 80−42332
lattice Schwinger model, form factors of dipole states 78−66029
Lee model in EM field, mag. moment calc. 80−42350
lepton-hadron deep inelastic scattering, source theory anal., polarisation 77−34160
linear physical field, propagator expansion in power series of coupling constant 79−30647
Lippmann-Schwinger type integral eqn. of motion, quantum corrections 78−62318
Lorentz transformation formula correction, Thirring and Schwinger spinor field models 78−12837
massive Schwinger model, asymptotic completeness and confinement 78−66028
massive Schwinger model, saturation, fermion confinement and instantons 80−47175
massless Euclidean Thirring field, four point Schwinger function, Lorentz group invariant forms *(German)* 80−90980
multiparticle production in chromoelectric flux tube model in 1+1 dimens. field theory 80−73666
multispinor basis of Fermi-Bose transformations 79−75676
new local and Lorentz-covariant soln. of Schwinger model for arbitrary gauge 79−40668
nonperturbative gauge technique soln. for Schwinger model of 2-dimens. electrodynamics 78−78120
nonstationary theory, Schwinger variational principle *(Russian)* 79−30668
one dimensional gauge field theories, at finite temp. and densities, props. and quark confinement 79−49468
order, disorder and generalized statistics 80−99055
phase transitions, structural, first order, anharmonic oscillator model in (1+1) dimensions 80−86239
phenomenological Lagrangian construction 79−63356
photon gravitational interaction, QED corrections 77−65131
pre-Schwinger model, Lorentz transforms. if operator solns. 80−47171
QCD, two-dimens. with massless fermions in 1-1 dimensions 80−62926
QCD, weak coupling approx. Schwinger-Dyson eqn. *(Chinese)* 80−52476
QCD lattice gauge theory, matrix Pade approximants, ratio of hadron to nucleon mass 80−4928
quantised rotator, Schwinger boson representation, derivation of cannonical variables 80−18164
quantum field theory methods and models review using Schwinger source theory *(German)* 78−86406
quantum mechanics, experiments on reinterpretation, new ideas 77−26204
Reggeon field theory on a lattice, critical behaviour, Monte Carlo calc. 80−18126
Schwinger equations, compact description 80−13204
spectral forms and renormalization group equations of the Schwinger model 79−63357
spin-$^1/_2$ particle, energy in constant coloured mag. field 79−80742
spinless particle scatt. by medium, elimination of divergencies, Lippmann-Schwinger eqn. 78−62320
static ultralocal solutions, 1/N expansion of O(N) symmetric theories 80−52401
SU(N) groups, Weyl invariants generating function *(French)* 79−93304

Schwinger source theory continued
sum rules, deep inelastic, source theory approach 77−61190
supergravity and local supersymmetry, source formalism for Fermi-Bose transform. 79−63114
superradiance from vacuum persistance amplitude 80−48195
synchrontron radiation, quantum corrections 80−37193
Thirring model with SU_n symmetry, scale invariance 79−9288
Thirring-Weiss model, massless, saturating field configurations 79−35953
three body problem, Lippmann-Schwinger eqns. 79−44785
time-ordered products and Schwinger functions 79−26216
tunnelling amplitudes in Schwinger model, path integral representation 79−49364
two-dimensional gauge model perturbation theory, Schwinger and massive vector meson models 79−6269
U(1) Goldstone boson, anal. of BRS invariance in nonAbelian gauge theories 79−80798
vacuum degeneracy and quark confinement 78−78090
vacuum polarisation, influence on confinement 79−71715
vacuum struct. generators in Lowenstein-Swieca gauge for the Schwinger model 79−6259
vertex function, spectral representation, ghostless electron propagator, infra-red and ultraviolet behaviour considerations 79−58911
Ward identity, fermion axial vector current divergence, chiral invariant regulator field 80−57524
Weinberg-type fields in curved spacetime, stress tensor conformal anomaly 79−25960
Yukawa$_2$ model, analyticity and Borel type summability of Schwinger functions *(French)* 78−54523
Yukawa$_2$ model, Schwinger functions, analyticity and Borel type summability *(French)* 80−73570
D, D*, Schwinger phenomenological and dyon description 78−82109
F, F*, Schwinger phenomenological and dyon description 78−82109
ψ'', Schwinger phenomenological and dyon description 78−82109
T, Schwinger phenomenological and dyon description 78−82109

science education *see education*

scientific societies *see societies*

scintillation
see also phosphorescence; phosphors
acoustooptic FM and freq. shifted heterodyne CO_2 laser system 78−5568
anthracene, α-particle tracks, excited states, creation and evolution 78−43934
anthracene, (100) and (110), scintillation response of α-particles in planar channelling and blocking expts. *(German)* 79−14869
anthracene, dissolved in toluene and cyclohexane, scintillation from α-particles, time depend. *(Spanish)* 79−99950
anthracene, electron irrad., creation and evolution of excited states, scintillation obs. 78−92128
anthracene, scintillation response to deuteron bombardment, energy, temp., and deuteron direction depend. *(German)* 78−6779
anthracene crystals, α-particle induced scintillation, mag. field effects 80−40161
anthracene scintillator, response to low energy electrons 77−54391
AO 0235+164, BL Lacertae object, interplanetary scintillation obs. and radio halo struct. 78−4386
AO 0235+16.4, BL Lacertae object, search for interstellar scintillation rel. to expansion vel. 77−2482
aromatic scintillators radioluminesc. yield *(French)* 78−52574
astronomical bodies, determ. of stratosphere density inhomogeneity struct., Salyut obs. *(Russian)* 80−109186
atmosphere, amplitude scintillation meas. at 36 GHz rel. to refr. index struct. parameter 78−81316
atmosphere, optical and IR waves, simulation 77−82005
atmosphere, phenomenological model 77−9491
atmosphere, refr. index profiles, upper and lower atm. contribs. 77−87070
atmosphere, refractive turbulence profiles, meas. by spatial filtering of scintillation 77−5331
atmosphere, turbulence and wavelength effect on scintillation fading at mm. wavelengths 78−85623
atmosphere, turbulent, conditional fading statistics of scintillation 78−66757
atmosphere scintillation, theory for millimetre and submillimetre wavebands 80−61884
atmosphere turbulent boundary layer, scintillation intensity rel. to refr. index struct. charact. *(Russian)* 80−94597
atmospheric, in optical lunar occultation meas., statistically rigorous reduction 78−73650
atmospheric amplitude scintillation temporal spectra at 10 and 36 GHz 79−12192
atmospheric optical propagation through strong turbulence 79−66802
atmospheric scintillation effect, optical pulse detection 77−7004
atmospheric scintillation effect on capacity of polarisation and amplitude modulated links 77−75428
atmospheric vertical profile of refr. index turbulence, stellar scintillation meas. 77−45126
auroral oval, VHF amplitude scintillation 78−61660
auroral zone, nighttime scintillation localised enhancements struct. 80−98506
binary optical communication system, atm. scintillation effects 77−71943
biomedical liquid scintillation counting, apparent and actual ^{14}C retention 80−36080
4C 03.59, BL Lacertae object, interplanetary scintillation obs. and radio halo struct. 78−4386
3C 48, 3C 273, 3C 295, scintillation at 25 MHz rel. to ang. struct. 78−65711
2-carbethoxy-5-chloro-7-aminoindole, soln., liq. scintillator, UV excitation, energy transfer and quenching 78−64395
cosmic ray interplanetary scintillations at 250 GV, statistical props. 80−8496
cosmic ray transient diurnal var., scintillation model confirmation from spectrum anal. 79−25416
dioxane liquid scintillators, scintillation yield, chloroform and carbon tetrachloride quenching effects *(French)* 77−3217
9,10-diphenyl anthracene, cyclohexane soln., solute excited state form. kinetics in pulse radiolysis 79−79263
direction scintillation meas. with split image range finder *(German)* 78−83076
Earth-space-Earth retroreflector link, scintillation statistics 78−11996

scintillation continued
electron-optical convertor, multielectron scintillation statistics 79−72695
electron-optical convertor detection characteristics, multielectron scintillation effect 79−72686
EM or optical pulse arrival time statistics in turbulent media 80−48154
EM propag. through troposphere at 30 GHz, scintillation effects meas. on ATS-6 satellite *(French)* 78−49065
equatorial ionosphere, phase scintillation of 40 MHz signals rel. to ionisation irregularities 79−44303
extended source in turbulence, asymptotic parameters, scintillation scales 77−606
extragalactic decimeter sources flux variability 79−62924
F-region, equatorial, scintillation obs. rel. to irregularity patches localised origin 78−77404
F-region, scintillation rel. to aurora 77−87158
film scintillators for extended UV response Si detectors 80−86412
finite aperture optical scintillometer, for profiling wind and refr. index struct. parameter 79−25331
finite optical beam in extremely strong turbulence, variance, covariance of irradiance 78−63008
focused radiation scintillations, freq. correl. by speckle interferometry 79−94153
glycine sulphate:L-alanine, unirradiated, optical spectroscopy of scintillations 80−80863
inert gases, secondary scintillation under mag. fields, effect in gas proportional counters 80−58055
inhomogeneous media, phase fluctuations, strong scintillations *(Russian)* 77−75417
interplanetary, joint Gaussian statistics anal. 77−2316
interplanetary, m wavelength, bispectral anal. 78−12153
interplanetary, theory and appl. 79−8880
interplanetary density discontinuities rel. to radiosource scintillations 77−17314
interplanetary medium, velocity distrib. from scintillation obs. 80−105143
interplanetary plasma dynamics from temporal scintillation spectra data 77−25980
interplanetary radiowave phase scintillation rel. to search for VLF gravit. radiation 79−70995
interplanetary scintallation, appl. to solar wind recurrence determ. at high heliographic latits. 80−62106
interplanetary scintillation, appl. for solar wind probing 78−45178
interplanetary scintillation, mathematical anal. in weak scatt. approximation 77−9706
interplanetary scintillation, multi-station obs. and solar wind vel. estimation 78−73601
interplanetary scintillation, obs. for turbulent plasma radio imagery 79−92645
interplanetary scintillation, obs. rel. to solar wind plasma irregularities anisotropic struct. 80−67489
interplanetary scintillation, obs. rel. to solar wind speed latit. and longit. struct. 79−40049
interplanetary scintillation, obs. rel. to solar wind speed out of ecliptic 77−5409
interplanetary scintillation, obs. using fully automatic system 79−101064
interplanetary scintillation, prediction of geomagnetic disturbances 79−58215
interplanetary scintillation, synoptic anal., rel. to solar wind turbulence 79−2460
interplanetary scintillation activity as precursor of solar induced geomag. activity 79−58214
interplanetary scintillation in N.Polar Spur and scintars 79−44579
interplanetary scintillation meas. in conditions of strong radio interference 80−46413
interplanetary scintillation meas. of electron density power spectrum in solar wind 78−77448
interplanetary scintillation obs. and solar wind vel. meas. 78−49278
interplanetary scintillation observations, solar wind vel. determ. *(Russian)* 79−80185
interplanetary scintillation of quasars, red shift-magnitude link *(Chinese)* 80−12828
interplanetary scintillation of radio background, sources mean ang. size determ. 77−5453
interplanetary scintillation pattern, nature of temporal restructuring 78−45280
interplanetary scintillation pattern, rearrangements 79−96879
interplanetary scintillation rel. to latit. gradient in solar wind vel. 77−25900
interplanetary scintillation response to solar wind density struct. var. 79−2455
interplanetary scintillation spectra, radio spectrograph obs. 80−72741
interplanetary scintillations, dispersion anal. of solar wind vel. 78−7852
interplanetary scintillations, freq. correlation *(Russian)* 77−17427
interplanetary scintillations spectra, influence of source sizes, obs. 80−46361
interplanetary shock waves, flare-generated, scintillation obs., 1977 Sept. 79−48638
interplanetary shock waves during second STIP interval (1976, March 15-May 15), scintillation obs. 78−81514
interstellar electron density determ. from decorrel. bandwidth of pulsar scintillation 77−78850
interstellar plasma irregularities, space-freq. correl. function 77−13444
interstellar scintillation method for quasar and galaxy superfine radiostructure *(Russian)* 80−77297
interstellar scintillation of low-freq. variable radio sources, evidence for relativistic expansion 79−9018
interstellar scintillation of pulsar radio emission, decorrelation bandwidth rel. to dispersion measure 80−85964
interstellar scintillation of pulsar radio emission, scale height determ. 80−85965
interstellar scintillation of radio sources, compact source discovery in supernova remnant (G78.1+1.8) 79−101213
ionosphere, auroral zone, irregularities, simultaneous rocket probe, scintillation and incoherent scatter radar obs. 80−94640
ionosphere, daytime satellite radio scintillation rel. to sporadic-E layer near mag. equator 77−45225
ionosphere, diffr. from discrete and homogeneously structured irregularities 79−48612
ionosphere, DNA Wideband satellite expt., complex signal scintillation 78−45133

scintillation continued
ionosphere, Doppler fluctuations and angle-of-arrival var. caused by scintillation 78−77411
ionosphere, equatorial, scintillation obs. rel. to irregularity patch form., motion and decay 80−67456
ionosphere, equatorial scintillation at 40, 140, 360 and 860 MHz, simultaneous obs. 78−57393
ionosphere, equatorial scintillation rel. to irregularities 78−36380
ionosphere, F-region irregularities and scintillations in equatorial region, VHF radar maps 78−36382
ionosphere, horizontal struct. of scintillation-producing irregularities in southern mid-latits. 79−12339
ionosphere, long-term 1.5 GHz amplitude scintillation meas. at mag. equator 80−85792
ionosphere, mid-latit., geostationary satellite signals scintillation at 137 MHz 79−25388
ionosphere, morphological aspects of quasiperiodic scintillations 77−91361
ionosphere, multifreq. scintillation data from ATS-6 radio beacon expt. 77−45250
ionosphere, persistent subauroral scintillation enhancement obs. in Alaska 78−20573
ionosphere, radio signals, scintillations of phase and quadrature components 79−80077
ionosphere, radiowave scintillation calc. by thin phase screen approx. 77−53298
ionosphere, scintillation, power law phase screen model, strong scatt. 80−61962
ionosphere, scintillation, power law phase screen model, weak scatt. 80−61961
ionosphere, scintillation meas. at 1.5 and 4 GHz 77−29581
ionosphere, scintillation probability distrib. function 80−41598
ionosphere, scintillations of ISIS-1 VHF beacon signals 79−8752
ionosphere, severe disturbances of VHF and GHz waves during mag. storm 80−109302
ionosphere, spaced scintillation obs. of ionisation irregularity drift motion 80−82133
ionosphere, temporal amplitude and phase spectra from ATS-6 radio beacon expt. 77−45251
ionosphere, VHF and L-band scintillation over Huancayo 78−36381
ionosphere, VHF scintillation rel. to peculiar Faraday rotation fluctuations 78−61663
ionosphere, VHF scintillations, equatorial, nature and dynamics of irregularities 79−48601
ionosphere amplitude scintillations, multifreq. spectra 77−87161
ionosphere F-layer, large-scale artificial inhomogeneity spectrum 80−98515
ionosphere mid-latit. scintillation rel. to plasma instabilities assoc. with subtrough density gradients 78−40753
ionosphere mid-latitude trough, scintillation of extraterrestrial radio noise sources signals 78−73574
ionosphere night-time scintillations at mag. equator, obs. 79−44292
ionosphere scintillation, calcs. based on in situ irregularity spectra 78−28415
ionosphere scintillation, effect of VHF/UHF satellite communications 77−41264
ionosphere scintillations, assoc. with features of equatorial ionosphere 80−77191
ionosphere SHF scintillations, refr. scatt. explanation 79−48615
ionospheric, obs. at Lunping Observatory, geomagnetic activity influence 79−88545
ionospheric radiowave scintillation, signal-statistical and morphological model 79−58185
ionospheric scintillation, critical prop. freq. up to 1 GHz 78−7827
ionospheric scintillation, effects on received signal level 78−93047
ionospheric scintillation meas. at 1.7 GHz at midlatitude 79−2434
ionospheric scintillation of solar bursts at 30 and 60 MHz, STEREO-5 obs. 78−61822
ionospheric scintillation theory, mini-review 77−5393
ionospheric scintillations at GHz freqs. power spectra model comp. 77−45233
ionospheric turbulent layer, propagation, phase and frequency spectra, after nuclear explosion 78−24405
IR propag. over long atm. paths, instrumentation 79−39875
irradiance enhanced variance from target glint 80−5691
Jupiter ionosphere, radio spectral broadening obs. under weak scintillation conditions 80−109391
laser absorption spectrometer, long path length, effect of scintillation and multiwavelength coherence 78−40653
laser aerosol deflector for energy parameters meas., scintillation phenomenon 78−25916
laser beam, in turbulent atmosphere 79−80018
laser beam scintillation beyond turbulent atm., numerical calc. 77−7005
laser beam vertical propagation through troposphere 79−39851
light scintillations in weak turbulence, source temporal coherence effects 79−50223
liq. scintillator, UV excitation, energy transfer and quenching 78−64395
liquid scintillation counting of ^{3}H or ^{14}C amino acids, optimisation factors 80−30951
liquid scintillation vial system, new container geometry for better sensitivity 80−46021
liquid scintillators, theory of fluorescence, appl. *(Rumanian)* 79−81135
Mars atmosphere, scintillation rel. to occultation of ϵ Geminorum (1976 April 8) 77−37545
α-methylnaphthalene, scintillators activated by 1,3,5-triarylpyrazolins containing difluoromethylsulphonyl group *(Russian)* 77−52187
multipath scintillation spectra, phase and fluctuation 77−11076
naphthalene single crystal, 4.50 MeV α bombardment, scintillation response, planar channelling, blocking *(German)* 78−6780
NE 213 liquid scintillator, temp. depend. of pulse shape discrimination props. 77−79507
night vision equipment matching to human observer 77−40937
optical scintillometer, large-aperture, fine calibration, optical estimate of turbulence inner scale 79−21026
organic liquid scintillator, γ-irrad., energy transfer and quenching 77−8622
organic liquid scintillator system, energy transfer, fluoresc. intensity-max. solvent depend. 78−21966
organic scintillator, captured γ quanta yield, fast neutron irrad. 77−46457
scintillation continued
oxazole scintillator solns., two- and three-component, laser emission spectra 80−32980
partially coherent source in extremely strong turbulence, irradiance scintillations 79−64176
PBD, dissolved in toluene and cyclohexane, scintillation from α-particles, time depend. *(Spanish)* 79−99950
phase autocorrelation function, scintillation behind deep random phase screen 77−79751
photoelectron counting distributions of laser light signal through turbulent atm. *(Japanese)* 77−50711
Pilot U scintillation response to neutrons, 50 to 120 MeV 77−54453
PKS 2025−15, occultation by Comet Kohoutek (1973 XII), vars. rel. to tail plasma irregularities 77−13285
planetary atmosphere, occulting spacecraft signal, turbulence determin. 80−94734
planets, strong scintillation at Earth's night horizon, Salyut 4 obs. 77−9590
plastic scintillator detectors, fluorescent response to heavy ions, $Z<36$, $E<170$ MeV 77−3228
plastic scintillator excited by ^{60}Co γ-rays, absolute radioluminesc. yield meas. 80−2829
plastic scintillators, bistilbenes used as mixers of luminesc. spectra 77−23373
plastic scintillators, quenched, sub-nanosecond 77−54419
plastic scintillators, radioluminesc. absolute output following ^{60}Co γ-ray irrad. *(Russian)* 78−92124
plastic scintillators, study of light pulse shapes 77−54450
plastic scintillators, sub-nanosecond time response studies using laser produced X-ray pulsed excitation 77−54434
plastic ultrafast scintillators, primary energy transfer process 78−90026
polyethylene-2,6-naphthalate fluorescence, transparency decay, possible appl. as polymer scintillators *(Chinese)* 79−93870
polyvinyltoluene scintillators, energy transfer in organic systems 78−92127
POPOP, dissolved in toluene and cyclohexane, scintillation from α-particles, time depend. *(Spanish)* 79−99950
powder scintillators, type P-47, for SEM 80−22487
PPO, dissolved in toluene and cyclohexane, scintillation from α-particles, time depend. *(Spanish)* 79−99950
PSR 0531+21, interplanetary scintillations at 74 MHz 78−36625
pulsar scintillations, freq. cross-correl. and finite bandwidth effects 80−4392
pulsar signals, cosmic ray streaming or mirror instability effects 80−51845
pulsar signals, interstellar density fluctuations effect 80−46649
pulsar signals, interstellar medium mirror instability growth effects 80−46648
pulsar signals interstellar scintillation, analytic soln. of second-order moment eqn. 80−26726
pulsars, freq.-time struct., means for detecting interstellar electron density irregularities 80−101608
pulsars, interstellar scintillation rel. to vels. 77−78811
pulsars, modified Rickett diagram for charact. freq. scale versus dispersion meas. wavelength parameter 77−17609
pulsars scintillation, mathematical anal. of physically thin screen 78−28501
pulse shape meas. by single photon technique 79−35810
quasars 3C 345 and 454.3, 102 MHz obs. of interplanetary scintillations *(Russian)* 80−94889
radar propag. through turbulence, scintillation detection using monopulse techniques 78−85717
radiation-optical converter of single crystal, diameter calc. 79−68445
radio beacon signals, ATS-6, plasmaspheric electron content and scintillations *(French)* 79−58184
radio noise from discrete sources, travelling ionospheric disturbances effects 77−91353
radio source scintillation from artificial ionosphere inhomogeneities at 25, 240 and 290 MHz 80−36454
radio sources, extragalactic, interplanetary scintillation rel. to existence of compact sources at low freqs. 80−90553
radio sources, extragalactic, varying at low freqs., interstellar scintillation rel. to microsecond, struct 78−16550
radio sources, faint, interplanetary scintillation statistical study at 81.5 MHz 80−51893
radio sources, faint, interpretation of interplanetary scintillation meas. at 81.5 MHz 80−90554
radio sources, interplanetary scintillation during August (1972) 77−25901
radio sources, weak, low freq. scintillation obs. 79−53921
radio wave scintillation caused by equatorial ionospheric bubbles, model computations 80−94641
radioisotope-powered photovoltaic generator 79−22495
radiosource scintillation obs., ionospheric irregularities determ. 79−84579
radiosource structure meas., scintillation effects 79−96922
radiosources scintillation, appl. to detect. of solar wind whistler turbulence 78−45173
radiowave scattered by 1-D power law phase screen 80−77220
radiowave scintillation by ionosphere, statistical study 80−109306
radiowave scintillation in ionosphere, UHF and VHF radiocommunication 80−56674
radiowave scintillation studies using ATS-6 radio beacons at Delhi 78−69600
radiowaves, equatorial ionospheric scintillations, freq. depend. 79−35050
radiowaves, wind velocity effects on amplitude scintillations of mm waves, wind vel. effects 78−61496
rain gauge, simplified optical path-averaged, based on scintillation detect. 78−40674
rain parameters, meas. by optical scintillation, correl. method simulation 78−36290
rain parameters meas. by optical scintillation 77−82015
refractive index structure parameter meas. by optical scintillator 78−65411
ring scintillation detectors, determ. of efficiency 77−46458
satellite laser ranging, scintillation statistics 77−88900
saturated scintillations, irradiance variance 77−27252
Saturn ionosphere, radio spectral broadening obs. under weak scintillation conditions 80−109391
simultaneously-produced scintillation and Cherenkov radiation separation method 79−93893

scintillation continued
SN 1408, evidence for marked scintillation from Japanese guest star record 80−90641
sodium salicylate, vac. UV scintillators, characteristic props. at 253.7 nm 79−71525
solar wind, radial depend. of props. from Helios 1/2 and Pioneer 10/11 radio scintillation 78−28595
solar wind 74 MHz interplanetary scintillation and IMP 7 obs. during 1973 78−89033
solar wind large-scale density fluctuations, meas. using dual freq. phase scintillations 77−13198
solar wind vel. meas. from scintillation obs. of H_2O and OH maser sources *(Russian)* 78−69704
source bandwidth and receiver response time effect on scintillation index in random media 77−42473
spectral covariance, 1.6 km path, 0.488 and 10.6 μm 77−607
starlight in Earth's atmosphere, twinkling 78−53726
stars, scintillation meas. for astronomical site testing 77−29645
stellar, aperture averaging effects, photon counting meas. 77−91519
stellar, speckle patterns and plane scintillation, statistics 79−100948
subnanosecond X-ray framing camera, fibre array technique 78−41394
synchronous satellite beacons at equatorial and high latitudes, empirical models 79−58182
p-terphenyl, cyclohexane soln., solute excited state form. kinetics in pulse radiolysis 79−79263
p-terphenyl, vac. UV scintillators, characteristic props. at 253.7 nm 79−71525
p-terphenyl solns., mag. field effects on scintillation pulse shape, ion pair recomb. 77−16835
TGS:L-alanine, unirradiated, optical spectroscopy of scintillations 80−80863
thin screen theory for spherical wave 78−13645
toluene, scintillators activated by 1,3,5-triarylpyrazolins containing difluoromethylsulphonyl group *(Russian)* 77−52187
transionospheric radio wave scintillation, time struct. 80−90281
1,3,5-triarylpyrazolins containing difluoromethylsulphonyl groups, scintillation activators for toluene and α-methylnaphthalene *(Russian)* 77−52187
turbulent plasma, wave scintillations, fourth-order moment eqn., astrophys. appl. 80−46381
Venus atmosphere, turbulence from Pioneer multiprobe radio scintillations 80−46437
VHF, UHF and SHF equatorial scintillations calc. using disturbed ionosphere model 77−17289
VHF and SHF scintillations and F-region irregularities correl. meas. 77−21977
VHF multi-satellite scintillations correl. with spread-F and sporadic-E increase over Brisbane 77−53297
VHF satellite signals, 40 MHz, ionospheric characts. determ. 79−88529
VHF satellite signals, 40 MHz, scintillations obs. at Kurukshetra 79−88527
VHF scintillation at high-latitude, analytical formulas 80−77224
VHF scintillation at high-latitude near 70°W 80−77221
VHF scintillation late evening enhancements at low latits. 79−75031
VHF signal scintillation, from ETS-2 satellite, obs. of Waltair and Calcutta 80−109295
VHF signals from satellite radio beacons, ionospheric scintillations 79−53634
VHF/UHF, ionospheric irregularities 80−46345
Ar, condensed, luminescence decay under α- and β-particle excitation 79−38678
Ar, liquid, ionisation and scintillation, application to radiation detectors, review *(Japanese)* 78−35206
Ar, liquid, scintillation decay due to α-particles and electrons 78−55099
$Bi_4Ge_3O_{12}$, low-temp. scintillation props. and appl. to high-energy γ-imaging devices 80−55191
$Ce_xLn_{1-x}P_5O_{14}$, UV luminescence lifetimes obs. 78−6775
CsI:Tl, gamma-scintillation growth front, external elec. field effect 80−34984
CsI:Tl(Na), light yield under charged-particle bombardment 80−93409
Gd_2O_2S scintillation convertor screen characterisation, portable neutron radiographic system 77−40510
KCl:Ag, hole capture radius, scintillation luminesc. obs. *(Russian)* 78−39582
KCl:Pb, 420 nm A-emission band *(Russian)* 79−56852
Kr, liquid, ionisation and scintillation, application to radiation detectors, review *(Japanese)* 78−35206
^{6}Li-loaded liquid scintillators with pulse-shaped discrimination 79−59310
$MgO-Al_2O_3-SiO_2:Ce^{3+}$ glass scintillator, energy transfer, luminesc. efficiency under UV and charged-particle excitation 79−95821
NaI:Tl, and unactivated NaI, scintillation response to random and channelled ions 77−48255
NaI:Tl, scintillation excitation mechanism for γ-rays *(Russian)* 78−92126
NaI:Tl, scintillation excitation mechanism 80−2857
NaI:Tl, triple-peaked scintillation pulse height spectra for MeV channelled ions 77−48254
NaI(Tl) decay time constant temp. depend., influence on detector appls. 77−54417
Na_2ZrSiO_5, scintillation props., excited by α particles 80−29809
$Na_2ZrSiO_5:Ln^1,Ln_2$, scintillation, α-excited *(Russian)* 79−28841
Ta_2O_5 anodic film, scintillation 79−91500
$ThBr_4$, inorganic scintillator, use in nucl. and accelerated particle detection 78−58540
Xe, condensed α scintillation kinetics 79−26828
Xe gas scintillation proportional counter, UV emission spectrum, prod. mech. 77−26935
Xe, liquid, ionisation and scintillation, application to radiation detectors, review *(Japanese)* 78−35206
ZnS, rare earth activated phosphor, scintillation mechanism *(Russian)* 78−48231
ZnS scintillator with faster decay 77−42217
ZnS:Tm(Er)(Nd) phosphors, optical scintillation mechanism 79−56867
$ZnWO_4$, scintillation characts. 80−66256

scintillation chambers
see also scintillation counters
alpha-in-air monitoring system, real-time 80−23155
biomedical γ-chamber, operating model 80−30848
cosmic ray neutron detector, large underground telescope, Russia *(Russian)* 78−73589
scintillation chambers continued
high-speed single-input system for pulse indentification 80−891
plastic ball multi-detector large angle spectrometer for Belavac 80−58028
radiometric path automatic stabilisation 77−23372
screen containing Li for neutron introscopy 79−76302
Kr photo-ionization proportional scintillation chamber 80−58056
^{85}Kr monitoring system with permselective membranes 79−3260
T monitoring using scintillation chamber 79−89519

scintillation counters
see also photomultipliers; position sensitive particle detectors
α-particle, neutron yield from D-T generator meas. *(German)* 77−23336
β-spectra, nucleus identification 79−26805
acrylic industrial scintillators coupled to wavelength shifter material (BBQ) 79−81126
acrylic low cost scintillators 80−37699
acrylic pieces of small surface area, cementing technique, appl. to light guides 78−13404
acrylic scintillator and wavelength shifter material, radiation induced degradation 80−5442
activation of materials during spaceflight, data for assessment 77−23382
adjustable response detector for lung clearance studies 77−56451
aerosol particles size meas., for medical use, inhalation technique development *(Slovak)* 79−74750
AGC circuit for scintillation probe containing long plastic scintillator 77−57833
air showers for 10^4 to 10^6 particles, lateral distrib. of EM component, detection 80−17459
albedo-type neutron dosimeter, description and calibration data 77−65389
alpha scintillation counter for determ. of low natural conc. of ^{222}Rn and ^{226}Ra 80−9456
alpha-emitting soil contaminant field monitoring using ZnS and phoswich detector 78−70646
amplitude characteristics 79−26820
analog mean-timer circuit for use with large-volume scintillation counters 80−63477
Anger camera dead-time, effect of window fraction 77−86598
Anger rectilinear tomographic scanner 78−20257
Anger scintillation cameras, state-of-the-art in suitable photomultiplier tubes 78−40304
anthracene, decay time determ. using low energy spectra 79−9964
anthracene, meas. of cosmic ray neutron spectrum at sea level 77−5405
anthracene crystals, meas. of light pulse shapes 78−74534
aqueous soln. liquid scintillation counting optimisation 79−76269
aromatic scintillator prod. 79−81126
arrays, testing with computer controlled LED flashing system 77−57802
ARS-1 attachment, for radiometry of samples containing alpha-radioactive isotopes 77−75022
atmospheric electrons, MeV range registration instrument 79−5645
atmospheric radioactive gas monitoring by silicone oil absorbent scintillation counter 80−12044
beam profile monitor, determ. of intensity and polarisation profiles 79−76251
Benjamin detector unfolding, MATXUF improved on-line uncertainty calc. 79−85876
beta counting of ^{90}Y(^{90}Sr), improved method with reusable phosphors 78−9024
beta detector with ring-type conical phosphor 80−27881
beta ray plastic scintillator survey meter for directly absorbed dose meas. *(Japanese)* 80−848
beta-ray detector, equiangular spiral light guide performance 77−3212
binary encoded position-sensitive scintillation hodoscope with reduced photomultiplier, pion detection 78−17506
Bonner sphere spectrometer, least-squares technique for extracting neutron spectra 78−33366
bronchoscopic tumour localisation, small radiation detector probes, scintillation and semiconductor detectors 80−61676
calorimeters, fluorescent wave shifters and calorimeters 79−59303
CAMAC autonomous system for control of scintillation and Cerenkov counters 78−21833
camera, 3-dimens. gamma-ray imaging 78−11734
camera, 70 mm photographic camera with roll film *(Japanese)* 77−70546
camera, ^{123}I imaging, detect. performance and quality factor 77−40743
camera, ^{99m}Tc detect., effect of small amounts of ^{131}I 77−16972
camera, multidetector design with 254 channels 77−40739
camera based on image intensifier tubes for nucl.-medicine appls. 77−5069
camera collimator image form. 80−89844
camera control, Pilotix module *(French)* 77−37040
camera data, recording method for low and moderate count rates 79−8539
camera deadtime in meas. of left ventricle ejection fraction 79−62355
camera electronics capable of high processing rates, clinical significance 77−40740
camera field uniformity, global and local, statistical features 80−61677
camera for ECG-triggered scintigraphy of intracardiac space 78−28033
camera interface to scintigraphic data and computer 77−21613
camera performance monitoring equally-spaced parallel-bar phantom 77−2041
camera with 2 mm intrinsic resolution, biomedical appl. 77−70525
cameras, deadtime meas., scatter conditions simulating nuclear cardiography 79−16276
cameras, effect of photon energy on field uniformity tests 79−16278
cameras, large-field-of-view 78−44596
cameras for radioisotope imaging *(Spanish)* 78−7428
capture gamma-ray detector, neutron sensitivity 80−18767
cellulose nitrate plastics, heating and alpha track revelation characts. 79−49910
cerebral radiographic scintillation detection unit fixture 79−57749
CERN OMEGA spectrom., slow proton trigger 78−17467
characteristics linearisation method *(Russian)* 79−729
charge collection effects on time resolution, anomalies *(French)* 77−57801
Cherenkov liquid scintillator counter, ^{18}F and ^{14}C radioactivity meas. 79−26817
chromatographic scanning procedure, for ^{32}P-labelled compounds 77−9151

scintillation counters continued
composite detectors for medium energy electron beams, cathodoluminesc. props. *(Russian)* 79−41080
Compton telescope, appl. of Anger camera principle, for gamma-ray astronomy 79−80223
computer assisted ring detector positron camera system for brain reconstruction tomography 78−40306
computer controlled gain stabilizing system for scintillation spectrometer using LED, processor in feedback 78−17473
computerised tomography, positron emission, crystal size optimisation 80−61681
computerised tomography, positron emission, data acquisition and processing electronics 80−61690
conical, time resolution meas. with constant fraction discriminator 77−65408
coordinate detectors based on liquid scintillators 79−68140
coordinate sensing detector with high time resolution 77−6621
coordinate-sensitive time-of-flight scintillation system, in large area gamma-ray telescope 79−84676
cosmic gamma-ray telescope in 10-30 MeV range 78−73638
cosmic ray muon lifetime, undergraduate teaching 78−81752
cosmic ray neutron detector, efficiency determ. by Monte Carlo method 78−21809
cosmic ray spectrometer, for study of 6 to 50 MeV electrons 78−45235
cosmic ray telescope of Sydney Univ., results 78−25388
Crystal Ball data acquisition system 79−89531
crystal ball detector, MWPC compact chambers and electronics 79−45534
Daly-type ion-electron-scintillation detector *(German)* 77−88331
Darmstadt linear accelerator, detector system and performance of elec. scatt. system 78−70680
dead time of detection systems, determination method *(Slovenian)* 80−47815
decay time meas. in nanosecond range 77−46461
defectoscope, multichannel, spectrometric method of recording γ-radiation in scintillation counter 78−53099
delay curves measurement by single photon counting technique *(Japanese)* 78−78555
detector amplifier for widely varying input amplitudes 77−50335
detector array, 200 m^2 for examining central sections of EAS 77−61648
dioxane based gel, scintillation yield and mechanisms involved study *(French)* 80−52816
dioxane liquid scintillators, scintillation yield, chloroform and carbon tetrachloride quenching effects *(French)* 77−3217
direct meas. of β absorbed dose rate by discriminator and filter *(Japanese)* 78−74511
discriminator principle slow neutron counting 78−29717
dose equivalent measuring instrument for rapid use in mixed radiation fields 78−15901
dose rates in mixed beta-gamma fields, plastic scintillator system 77−60254
dosimeter for gamma radiation, design calibration and construction *(Spanish)* 80−5437
drift chamber, electroluminescent 79−22545
drift chamber, transition radiation detection 79−22546
dual-probe system for rapid bedside assessment of left ventricular function 77−2039
dye solutions, liq. scintillation counting, rel. to colour quenching ability 79−1790
EAS array at Durham 77−91391
ECG-gated scintigraphy, appl. to studies of heart 78−7440
ECG-gated scintillation probe meas. of left ventricular vol. 78−31891
efficiency meas. for fluxes of 5-100 keV photons 80−14044
electro-optical properties, in SEM 80−52819
electro-optical stabilisation of subnanosecond lifetime spectrom. 77−34508
electron gun, portable containing source, monochromator, counters, for particle detector calibration 78−78539
electron multiplier scintillator detector for positive/negative ions pulse counting, mass spectrometer appl. 78−89583
electron scattering experiments, detection system, Saclay linear accelerator facility 80−52809
electron spectrometers, pulse shape anal. in fosfich detector 77−65387
electron-photon cascades separation 78−78563
electronic techniques for high energy expts. 79−59315
elongated scintillation counter characts., optimum design for cosmic ray detection 77−61652
EM shower detection in Pb glass blocks and scintillation hodoscope 80−58034
EM shower sampling counters, characteristics of plastic scintillator and radiator layers 78−58530
emulsion scintillation counting of ^{222}Rn and ^{226}Ra in biological samples 78−81089
emulsion stack connected with ionis. calorimeter for high energy cosmic ray obs. 78−25386
energy resolution optimisation at high energies 80−37697
environmental γ flux meas. method using NaI(Tl) scintillation counter and photomultiplier 78−21786
EOSCOR: A light weight, microprocessor controlled solar neutron detector 79−101063
external standards channels ratio, time-dependent change obs. 80−69036
fast particles, separation of simultaneously produced scintillation and Cherenkov radn. 79−18076
fast plastic scintillators for medical applications 77−44744
fast-neutron detector for use as criticality monitor 77−65391
fast-pulsed electron beam energy meas. using bremsstrahlung absorption spectroscopy 78−49940
fibre-optic data transmission systems for plasma diagnostics 80−79571
fission and radiative capture cross sections ratio meas. in reson. region 77−50175
fission reactor loss of coolant studies, gamma densitometer detector comparison 80−57881
flaw detection systems based on semicond. detectors and scintillation crysts. for hard bremsstrahlung 79−11748
flight chamber, fast large area zero time detector 77−18743
flow cell type detector for continuous monitoring of tritiated water activity 78−82524
fluorescence decay times determ. in nanosec. and subnanosec. range 80−5443
focusing gas scintillation proportional counter 77−83461
fusion reactor radiation attenuation meas., sensitivity response of liquid scintillator detector 79−67951
gain stabilising scheme, gated radioactive source and broad digital window 80−63453
gain stabilized NaI(Tl) γ-ray detector, electronics, disc-based minicomputer, power shape in LWR core 78−33284
gamma, Anger-type, time resolution *(German)* 77−13000
gamma camera, anal. of basic characts. 78−57059
gamma camera, electronically collimated, for single gamma emission computed tomography 78−44603
gamma camera imaging, recent advances 80−17127
gamma camera oscilloscope display, performance meas., computer simulation 78−7425
gamma camera performance comparison 78−44595
gamma camera transfer function, statistical study 77−70541
gamma camera with brightness amplifier *(French)* 77−37036
gamma cameras, appl. of orthogonal light propag. 77−16979
gamma cameras, performances under high counting rates 79−16277
gamma detector in isotropic radiating medium, efficiency 77−30728
gamma dosimeter testing, effect of air scattered radiation 79−6774
gamma imaging, optical device 77−5056
gamma photon energy spectra estimation based on 34×34 matrix 79−41059
gamma ray appl. to fluid density meas., theory, practices and appl. 80−73325
gamma ray detection system, 3-D, fabrication and efficiency 80−63483
gamma secondary radiation, from pulsed ruby laser 79−76303
gamma-ray astronomy, direction of high energy gamma-rays, active coded aperture imaging 80−62022
gamma-ray detection, scintillator response, pulse height spectra unscrambling, computer program 78−55092
gamma-ray detector, nonhydrogenous organic liquid scintillator sensitivity function calc. 78−78572
gamma-ray spectrom. temperature characteristics of α-datum stabilizers 79−26808
gamma-ray spectrometer with various shaped scintillators, for gamma-ray spatial pattern anal. 79−16831
gamma-ray spectrometers; calc. of radioactivity induced during spaceflight 80−102382
gamma-ray telescope, spark chamber, scintillation counter time-of-flight system 80−62017
gamma-ray tomographic imaging by scintillation camera, algorithm 79−57773
gas, use of vacuum photodiode as light sensing element 79−13601
gas counter with selective level population for high-intensity neutron fluxes detection 80−23253
gas proportional, using inert gases, principle and appl. *(Czech)* 78−86727
gas proportional counter, review 77−57826
gas proportional scintillation counter, performance and applications evaluation 79−3289
gas proportional scintillation counter for use in large area detector systems without photomultipliers 79−59302
gas proportional scintillation detectors with uniform electric fields, secondary scintillation model 80−74087
gas scintillation counter, for high count rate X-ray detection 80−14052
gas scintillation counter for spectral line studies in X-ray astronomy 77−13247
gas scintillation counter X-ray spectrometer performance figures astronomy appl. 79−48673
gas scintillation drift counter for fast X-ray detection 80−888
gas scintillation proportional counter, burst length discrimination system 78−21824
gas scintillation proportional counter, gas fillings, preliminary studies 80−58054
gas scintillation proportional counter, large-area focusing, for X-ray astronomy 79−25494
gas scintillation proportional counter coupling to photoionisation detectors 78−82581
gas scintillation proportional counter for first Spacelab mission 79−25488
gas scintillation proportional counter for X-ray astronomy 77−71004
gas scintillation proportional counter of large area for X-ray astronomy 79−80222
gas scintillation proportional counter using a photomultiplier tube array 79−76294
gas scintillation proportional counters, large vacuum photodiode imaging appl. 80−58050
gas scintillation proportional counters, props. in soft X-ray detection 79−13600
gas scintillation proportional large area counter, X-ray astronomy appl. 79−45556
gas scintillation spectrometer for X-ray astronomy, performance characteristics 80−56709
gas scintillator in electric field, light signal amplification changes *(Russian)* 77−46462
gas transmission, neutron flux determ., 1-30 MeV, proton recoil method 77−23366
gas-filled electroluminescent detector for soft X-rays, constr. and characts. 80−32569
gas-scintillation proportional counters, high resolution, for X-ray astronomy, developments 77−54439
gaseous, basic properties and physical characteristics *(Czech)* 79−36467
hadron cascade energy and position, large area scintillation counters 78−37512
hard X-ray camera for study of gamma ray burst sources 79−25502
heavy ion detection, using two dimens. gas-scintillation drift chamber 78−86730
heavy ion detection in low-press. noble-gas scintillation counter 77−83446
helical cathode position sensitive proportional counter system for use in a broad range spectrograph 78−82578
high pressure gas scintillation spectrometers for X-ray astronomy 80−105166
high resolution gas scintillation proportional counter for studying low energy cosmic X-ray sources 80−58052
high-speed camera using plastic phosphors 79−93888
high-speed pulse shaper/discriminator for scintillation and Cherenkov counters 78−86748
highly efficient counters 79−31329

scintillation counters continued
hodoscope, automatic system for meas. of transmission channels 77−3219
hodoscope, high resolution, using spherical mirror 77−393
hodoscope, track correlator as fast trigger in π-μ Coulomb bound states detection 79−45574
hodoscope containing scintillation counters, and small FEU-87 photomultipliers, charged particle meas. 78−78562
hodoscope counter for beam meas. in CERN SPS 79−36472
hodoscope for low energy light ions, spatial, timing and pulse height resolution 77−38555
hodoscope for meas. of ionisation losses of relatistic particles 80−42892
hodoscope using fibre optic light guides 78−37514
hodoscope with 1 mm granularity 77−34515
hodoscopes, LED test system 78−58556
hodoscopes, with hodoscope photomultipliers 80−47817
hodoscopes for high intensity muon beam, high-rate photomultiplier-base and precise timing calibration 79−22544
hodoscopic spectrometer, gamma-quanta coordinate meas. in NITsE scintillation spectrometer 78−78549
hydrocarbon scintillators, Monte Carlo predictions of neutron detection efficiency 79−68150
hydrogenous scintillator, fast neutron sensitivity, calibration with ^{252}Cf fission neutrons 77−23376
IEEE conf., scintillation and semiconductor counters and nucl. power systems 77−54389
image intensifier scintillation cameras for nuclear medicine 77−40732
imaging gas scintillation counter for X-ray astronomy 80−98551
in-beam Ge(Li)-NaI(Tl) Compton suppression spectrom. 77−88325
inert gas and mixtures, detection gas suitability for proportional scintillation counter *(German)* 78−41901
inert gas scintillation counters for energetic heavy ion detection 79−45550
inert gases, secondary scintillation under mag. fields, effect in gas proportional counters 80−58055
inner-shell vacancy filling detector, scintillation counter 77−18749
inorganic scintillators, decay charact. determ. using two-photomultiplier method 79−13589
inorganic solid-solution single-cryst. scintillator containing U, prototype fission detector, performance 77−54445
integrating counting technique, appl. to ^{197}Au Mossbauer spectroscopy 78−25377
ion detector, Daly-type, plasma ion energy meas. 78−22570
isotope conveyor weigher, errors caused by profile variations and shift of material 77−67933
large, light collection uniformity improvement 78−78569
large area counter, geom. effects, simple model 77−57817
large area counters for cosmic ray work light collection 78−74538
large area liquid, for EAS expts., calibration 77−397
large counter light collection inhomogeneity 78−82573
large field scintillation gamma cameras, performance charact. 78−7441
large field-of-view camera, dynamic leg scintigraphy 78−73215
large time compensated scintillation counters for neutron high energy TOF meas. 78−55085
large-area gas-scintillation proportional counters for in-vivo measurement of plutonium and americium 80−58086
light collection improvement in scintillation detectors 79−45548
light distribs. within light diffusion boxes, algorithm 79−49908
light guide design for timing meas. in large counters 77−38554
light pulse propagation in pipes, model 78−30068
liquid, ^{3}H and ^{14}C determ. in whole-body sections *(German)* 77−5114
liquid, ^{3}H filled glass microsphere assay 80−63481
liquid, ^{45}Ca and ^{32}P determination in biological samples by Cherenkov and liq. scintillation counting 80−98183
liquid, α-ray meas. due to air luminescence 79−36479
liquid, American National Standards Institute quality assurance programme 77−38585
liquid, colorimetric analysis appl., use of miniature ^{14}C and ^{3}H standards 80−21346
liquid, continuous radio-scanning method for chromatograms and electrophoretograms 77−70367
liquid, determ. of 14 MeV neutron spectrum 79−45526
liquid, influence of quenching on background 79−18082
liquid, modified commercial detector and sample changer for low-background Pu assay 77−54474
liquid, quench monitoring, H Number concept 78−82576
liquid, radiometric determ. of U content *(Czech)* 78−69487
liquid, Series 8000 system with microprocessor 77−14308
liquid, simultaneous meas. of ^{59}Fe and ^{51}Cr in blood 77−29195
liquid, single solvent cocktail for counting of ^{3}H in aqueous samples 78−856
liquid, tests of counters made with extruded acrylic panels 79−49906
liquid, unified approach to counting process, optimising optical design 77−3241
liquid, unified approach to counting process, stochastic model 77−3240
liquid, use of Aquasol in plastic Mini-Vials for ^{3}H assay 77−26934
liquid, use of plastic scintillator to determine activity of solid samples 77−88333
liquid, vessels for beta ray spectrometers 77−26920
liquid (NE 224) high-efficiency time-compensated neutron spectrom. 78−17468
liquid column chromatography, scintillation counters, review *(Czech)* 80−27885
liquid counters, external standard quench correct. capability, inexpensive method for acquisition 80−47810
liquid high efficiency counter for background characteristics meas. 77−3223
liquid rare gases, ionisation and scintillation, review *(Japanese)* 78−35206
liquid scintillation, counting technique, review 78−82586
liquid scintillation alpha counting and spectrometry , appl. to bone and tissue samples 77−25617
liquid scintillation alpha particle spectroscopy, pulse-shape discrimination cct. 78−21823
liquid scintillation alpha-particle assay with energy and pulse shape discrimination 77−23350
liquid scintillation counting, ^{3}H meas. 79−22554
liquid scintillation counting, conf., San Francisco, USA (Aug. 1979) 80−58074
liquid scintillation counting, single and double labels, absolute activity analyser vs. on-line computer 77−83470
scintillation counters continued
liquid scintillation counting, single and double labels, quench correction with on-line computer 77−79520
liquid scintillation counting of ^{45}Ca in plant and soil material 77−44536
liquid scintillation counting of solns. containing ^{14}C-$NaHCO_3$, prevention of radiocarbon loss 78−21811
liquid scintillation counting sealed standard production 79−68145
liquid scintillation counting waste vol. reduction by distillation 78−78556
liquid scintillation detector module for bulk-sample and whole-body counters 77−3216
liquid scintillation high resolution alpha spectroscopy, optimisation of detector and electronics 78−13370
liquid scintillation instrumentation development 78−86728
liquid scintillation solutions for use in ^{3}H urine analysis 77−9273
liquid scintillation spectrom. meas. of internal conversion electrons 79−89520
liquid scintillation spectrometry, of low alpha activities *(Slovak)* 77−83453
liquid scintillation spectrometry sample pre-processing 78−21816
liquid scintillation spectrum, (n,γ) thermal react. cross section meas. 78−25382
liquid scintillation system ^{32}P Cherenkov effect detect. efficiency meas. using ^{60}Co external source 78−25387
liquid scintillation techniques, appl. in low level activity assessment 80−58082
liquid scintillation tube appls. 78−13383
liquid scintillation vial for radiometric assay of lymphocyte carbohydrate metabolism in response to mitogens 78−61248
liquid scintillation wastings, combustion system *(Japanese)* 80−63503
liquid scintillation wastings, vaporisation apparatus *(Japanese)* 80−63502
liquid scintillator, 1,4 dioxane based radioactive decontamination and recovery 79−22536
liquid scintillator containing O_2, selective activation detection of neutrons 78−25392
liquid scintillator determ. of dose rates from homogeneously distrib. β,γ- and EC,γ-emitters in phantom organs 78−53501
liquid scintillator solvents, solubility of Xe and Kr, meas. using radioactive tracers 77−57808
liquid scintillators, theory of fluorescence, appl. *(Rumanian)* 79−81135
liquid xenon proportional scintillation counter, detection of ^{207}Bi conversion electrons 79−45563
liquid-scintillation vial system, biphasic, for radiometry, modifications 80−101253
low radiocarbon activity, determ. by $^{14}CO_2$ absorption in liq. scintillator 78−74550
low-background detection system for neutron reaction expts. 77−54395
low-background system for neutron activation anal. 77−36843
low-efficiency counter, for meas. of average number of charged particles 80−23252
low-noise photon counting system using photosil detector 77−45890
lung monitor for assessment of low energy photon emitters 79−25067
magnetic α spectrograph performance 79−31316
magnetic large acceptance spectrom. using wire chambers 78−46207
magnetostatic shield fabrication 78−5053
MEA, magnetic detector at Adone 78−33367
medicine, nuclear, digital filtering and edge detection 80−58065
medicine, nuclear, microprocessor systems for data acquisition, image processing, RIA anal., patient data retrieval 80−61670
Metapol HC100 as non-ionic detergent in liq. scintillation counting 78−21815
microprocessor controlled digital spectrum stabiliser 77−38572
microprocessor-controlled, with programming facilities 79−26831
MISO low energy γ-ray telescope 79−25472
mixed β-γ dosimetry, ionisation and scintillation counters 80−57975
mixed n-γ field portable scintillation spectrometer with pulse shape discrimination 77−77992
mixed neutron-gamma ray field, γ contrib. to proton recoil counter spectrum 77−88337
MLS type compact scintillation counter assembly, operational principles and test results 79−36484
modular electron calorimeter, relative and absolute calibration 78−78578
Mossbauer spectroscopy, fast γ-ray detection system 78−25376
MTF calc. on programmable pocket calculator 77−66844
Muehllehner's tomographic camera, quantitative evaluation of depth effect 77−86609
multi-functional standards, use of miniature glass vials 77−70370
multicrystal camera, left ventricular ejection fraction determ. 78−73213
multidetector arrangement for on-line meas. of neutron and γ-ray multiplicities 78−50440
multiparameter gas-scintillation counter for heavy charged particles 80−58051
multiplane tomographic scintillation camera image quality improvement 79−92338
multiplicative core selector for EAS axis determ. 80−41682
multistage parallel-serial time averaging filters to reduce time jitter in scintillation counter time meas. 80−102405
muon telescope for slow muon spectra and zenith angle depend. meas. 78−49324
NE102, proton loss by nuclear inelastic interactions 77−71729
NE213, detection efficiency meas. for 130 MeV neutrons 80−27888
NE213, organic liquid, Monte Carlo calcs. of electron energy loss spectrum for incident gamma-rays 77−6613
NE213 liquid cylindrical neutron spectrom., anisotropy of response 80−5434
NE213 liquid scintallator, light output for electrons and protons, coincidence spectrometer 80−32564
NE213 neutron counter, efficiency calibration 80−27877
NE213 organic liquid, response functions to high energy neutrons 77−6634
NE213 organic scintillators, effect of light output efficiency of charged particles on unfolded neutron spectrum 78−29700
NE213 spectrom. in LiF assembly, Monte Carlo calc. of neutron flux perturbation 79−85855
NE 111 matrix doped with benzophenone, acetophenone and piperidine, emission spectra and selective filtering 79−76280
NE 111 scintillators, timing charact. exam. by single photon counting tech. 80−78494
NE 213, Munich pulse shape discrimination cct., low energy performance 78−46233
NE 213, n-γ pulse shape discrimination 77−57816

scintillation counters continued
NE 213, proton loss by nuclear inelastic interactions 77−71729
NE 213, pulse shape discrimination, appl. to neutron spectrometry 80−27862
NE 213 liquid scintillator, decay under neutron and gamma excitation *(German)* 78−55097
NE 213 liquid scintillator, deuterated, decay mode *(German)* 78−55096
NE 213 liquid scintillator, temp. depend. of pulse shape discrimination props. 77−79507
NE 213 scintillator, neutron response functions, energy range to 40 MeV *(Japanese)* 80−18756
NE 238 fast liquid scintillator, scintillation decay and n-γ discrimination *(German)* 78−55101
NE-110 scintillation counter, obs. neutron flux meas. 80 to 500 keV 79−735
NE-111 thin homogeneous scintillator foils, alpha particle energy loss and straggling 77−83472
NE-213, proton recoil data, neutron spectrum unfolding with AMTXUF 78−74553
NE-213 neutron spectrom., continuous functional representation of response surface 79−81116
NE-213 organic liquid, two-dimensional pulse height analyser for gamma-ray spectroscopy *(Japanese)* 77−46451
Ne-213 organic scintillation counters, energy calib. by γ-rays 79−45553
NE-213 spectrom. system, meas. of neutron leakage spectra from Fe, Nb, Be, polythene spheres, integral test of cross sections 77−23033
NE-213 spectrum system for 1.0-20 MeV neutrons 77−88346
NE-213 system, 1-15 MeV, Pu-Be and ^{252}Cf neutron spectra meas. 77−26930
neutral particle detector and spectrometer for plasma diagnostics 79−23455
neutron, calibration of threshold 80−23258
neutron, with electronic device for rapidly changing the multiplication of a photomultiplier 80−74074
neutron activation analysis of Sn at nanogram level by ^{121}Sn liq. scintillation counting 78−3693
neutron and γ-ray spectra meas. on radial shielding model of KS-150 reactor *(Slovak)* 78−21624
neutron counter, scintillation, photomultiplier noise characteristics 80−74077
neutron counter (60 element) calibration in energy range 8.5 to 450 MeV 79−6798
neutron detection, effective solid angle anal. 77−57819
neutron detection, test of Monte Carlo calcs. by ^{12}C(p,n) and ^{12}C(p,p′) cross section meas. 80−37713
neutron detection efficiency meas. using Monte Carlo simulation program 78−17045
neutron detection from short-lived plasma 80−23263
neutron detector efficiency calc. using Monte Carlo computer program 79−63874
neutron detector for TOF meas. with very fast burst source *(French)* 80−14040
neutron detectors, black and grey 79−9971
neutron detectors with nanosecond time resolution 80−69029
neutron flux meas., 250-1000 keV neutrons, >95% efficiency 77−26938
neutron scatt. facility in 20-40 MeV range 77−26888
neutron scintillating glasses, effects of temp. on pulse height and cond. 77−10547
neutron scintillating glasses, pulse decay time meas. at room temp. 78−46225
neutron scintillating glasses activated by Ce^{3+}, luminesc. 79−38668
neutron spectrom. meas. of ^{16}O(γ,n) and D(γ,n) spectra *(Dutch)* 79−3281
neutron spectrometer, with pulse-height discrimination against γ-ray background 78−13378
neutron spectrometers, with LED and PIN photodiode, stabilising system 80−47821
neutron spectrometry by means of the stilbene spectrometer and hydrogen-filled proportional counters 79−63860
neutron totally absorbing TOF spectrom. 78−850
neutron transit time and interaction coord. determ. 79−26807
neutron-gamma pulse shape discrimination, digital technique 77−403
neutrons with binding energy >40 MeV, search in fission reactor spectrum *(Russian)* 79−89515
nuclear geophysical borehole logging system 79−25353
opaque metal coatings on plastic scintillator 78−3049
optical fibre-scintillator system, for high bandwidth radiation diagnostics 78−46820
optical multiplexing of scintillation detector arrays 77−54438
optical system evaluation program 77−34523
optical wave propagating through turbulence, scintillations meas. detector aperture effect *(Slovak)* 80−63921
optronic converters with Cu_2S(Se)-CdS(Se) p-n heterophotoelements, props. on X-irrad. of scintillator 80−34505
organic, neutron response functions, Monte Carlo program 80−14047
organic, temporal characteristics and saturation effects for low energy X-rays 79−81125
organic, use of logarithmic pulse height and energy scales 80−37690
organic compounds, ^{35}S-labelled, liquid-scintillation counting, automatic sample prep. 78−70688
organic detectors for neutron physics research 79−72199
organic scintillator efficiency using Monte Carlo code 80−889
organic scintillators, review of development 79−72198
organic scintillators, saturation effects to nanosec. pulses of low energy X-rays 79−93880
personal monitoring, effect of environmental radiation, thermoluminescent dosimeter *(Japanese)* 80−61707
phosphor, detection efficiency and performance estimation, of HV STEM 80−101899
phosphor scintillators in scanning electron microscopes, prep. and evaluation 79−230
phoswich battery operated portable detector for field monitoring of transuranic contaminants 79−683
phoswich detector, in vivo meas. of transuranic elements at CRNL 77−77993
phoswich detector, reduction of low energy background 77−23369
phoswich detector for ^{147}Pm in-vivo meas. 78−28087
phoswich-type scintillation detector system for X-ray astronomy 78−49328
photomultiplier arrays, efficient alignment procedure using standard dynode resistor chain 77−3229

scintillation counters continued
photomultiplier gain stabilisation system for high counting rates 79−76277
photomultiplier gain stabilization, computer control software 78−13369
photomultiplier tube imbalance, field nonuniformity of scintillation camera, effects on cold lesion detectability 79−5352
photon counting, vacuum UV region, 120-200 nm, detection limit of apparatus *(German)* 78−45691
pickups with plateau in counting characteristic, gamma and neutron radiation, review 80−47811
Pilot U scintillator for 55-225 MeV neutrons 80−18762
Pioneer Venus Orbiter Gamma Burst Detector 80−67505
plasma-ion analyser for H conc. in metals using pulsed laser and thin film scintillation detector 78−15746
plastic, accurate time meas. 78−82582
plastic, beta-ray absorbed dose rate, direct meas. *(Japanese)* 77−73589
plastic, of high transparency containing Gd, props. 78−78567
plastic, unsaturated response to relativistic heavy ions 78−17502
plastic calorimeters, light guides containing fluorescent radiation converter 79−740
plastic capillary method, self-diffusion in liq., using β-active tracers 77−50333
plastic cylinder, perparation gained physical parameters *(Czech)* 80−74076
plastic detector, large-volume, for aerial gamma-ray spectroscopy 79−58126
plastic detectors, status of timing 79−22540
plastic large area fast neutron detector 78−90022
plastic neutron scintillation detector efficiency in 80-220 MeV range 78−78568
plastic scintillation counter, time resolution meas. for 16 MeV neutrons 77−83460
plastic scintillation counter NE-102A, pulse-height spectrum prod. by 14.8 MeV 78−845
plastic scintillation counter response to relativistic heavy ions 79−36473
plastic scintillation counter with air light guide 78−29713
plastic scintillation detector system for low level environmental radiation meas. 77−38567
plastic scintillation fast-slow coincidence spectrom., K-shell photoelectric cross section meas. 78−86754
plastic scintillation filament detector system for $^{14}CO_2$ breath anal. tests 78−65122
plastic scintillation granules, efficiency of α radiation recording 78−9028
plastic scintillator, neutral radiation incident spectrum determ. 77−54398
plastic scintillator, Q_β value determ. from endpoint energies of β-spectra 80−27864
plastic scintillator blocks for gamma-ray burst astronomy, comparison with NaI scintillators 77−64648
plastic scintillator detectors, fluorescent response to heavy ions, Z<36, E<170 MeV 77−3228
plastic scintillator props. meas., streak camera technique 78−66450
plastic scintillator telescope for pion beam monitor in (π^-,γ) experiments 79−49913
plastic scintillators, fluoresc. meas. 78−86747
plastic scintillators, polymerisation of blocks with large dimensions 77−65400
plastic scintillators, specific luminescence, semi-empirical expression 77−57820
plastic solid state nuclear track detectors, sensitivity and struct. variation 79−49912
plastic ultrafast scintillators, primary energy transfer process 78−90026
plexiglas 1921, linear response and energy resolution results 78−78586
polyethylene mini-vials, construction of permanent standards 77−38550
polystyrene scintillators, extrusion prod. 80−37698
portable camera, for ^{125}I contamination monitoring 78−85388
portable microprocessor controlled neutron spectrometer, NE213 organic scintillator 80−58022
portable neutron spectrometer/kerma-rate meter, design, performance 78−33361
portable spectrometer/dosimeter for low level neutron radiation meas. 79−49869
position sensitive, light signal propag. speed. for spatial resolution determ. 80−69028
position sensitive gas scintillation proportional counter for X-ray astronomy 80−58053
position sensitive target counter for photons above 50 MeV 79−76285
positron annihilation coincidence detection tomography, circular ring camera system 77−64124
positron camera, 3-dimens., for nucl. medicine 78−73225
positron camera, cylindrical, multilayer hybrid computed tomographic system, $Bi_4Ge_3O_{12}$ scintillation crysts. 78−48876
positron circular ring transverse axial camera system, efficiency optimisation 77−12994
positron computerised transaxial tomography, effect of detector response 77−12993
positron emission transaxial tomograph, PETT IV and computer system 78−80959
positron emission transverse tomograph, PETT IV 78−40299
positron imaging device resolution limit 77−60243
positron imaging instrumentation 77−44745
positron imaging system using annihilation coincidence detection, model, design, performance 78−40303
positron lifetime spectrom., improved time resolution in liquid scintillator NE 238 78−29696
positron ring, 280-crystal, design and construction for 3D imaging 78−28063
positron spectrometer, low-background, many cryst. scintillation triple βγγ coincidence 77−54446
probe detector in assessment of cardiovascular disease 80−3800
proportional, built-in K getter 78−29707
proportional large area gas counter for X-ray astronomy 78−49321
proportional large area gas counter for X-ray astronomy 78−49322
proportional response photon counter 80−87021
proportional scintillation in Ar, Kr, and Xe 79−81131
proton counter telescope, efficiency for 89-466 MeV protons 77−57843
proton detection, 2.43-19.55 MeV, response of NE-228A, NE-228, NE-224, and NE-102 scintillators 78−58542
proton spectra, high energy, emerging from 680 MeV synchrocyclotron shielding 78−17530

scintillation counters continued
pulse shape analyser, effect of pulse pile-up on discrimination between neutrons and gamma rays 80−91402
pulse shape analysers for phoswich detectors in space borne hard X-ray expts. 80−36501
pulse shape discrimination for alpha-gamma separation with trans-stilbene 78−13386
pulse-width discriminator for multilayer scintillators 80−27883
pulsed beam time pickoff system for nanoampere beams 78−13393
pulsed proton radioluminescence in binary liquid scintillators 79−52731
quenching curves, solns. by second-order polynomial regression 77−3220
quenching equation for scintillation, relationship between counting rate and quenching agent conc. 80−99411
radioactivity meas., fly-ash radioactivity meas., environmental protection *(Polish)* 77−14318
radioimmunoassay appls. of Philips gamma counter PW 4800 and scintillation counter PW 4700 80−56173
radioisotope hybrid scanner, design of detector and collimators 78−7423
rate dependent photomultiplier gain, time depend. 80−87020
recoil spectrometer for 5 GeV pion-He interactions 78−90011
rectilinear scanner, large crystal, improved focused uptake probe 78−28053
reflectors, comparison of light collection efficiency 78−70702
resolution function determ. for scintillation associated particle TOF system for d(n,n) scatt. meas. 78−58535
response function of NE-213 liquid scintillator, Monte Carlo calc. 79−97926
review of nucl. particle detectors 79−54740
sampling grid scintillator, calibrated intensity monitor for intense high energy charged particle beams 80−69034
sawtooth pulse generator cct., for monitoring scintillation counters *(German)* 78−25395
scale stabilizer based on ^{40}K photopeak for scintillation detector 79−26823
scintigraphic camera systems and their assessment by computer 78−57063
scintigraphic image adaptive restoration 80−27914
scintillating imaging proportional counter as X-ray to light image convertor 77−65063
scintillation cameras, automatic field uniformity corrections 80−17128
scintillation spectrometers based on flight time 79−26818
scintillation spectrometric path, switch shaper 77−6641
4π scintillation system for low activity beta counting 77−65405
scintillation techniques for calibration light sources 77−71720
scintillator photodiode detector, for intense pulsed ion beams diagnostics 77−61160
scintillators, liquid and plastic with improved decay time and emission characts. 78−58539
Searle Pho/Con tomographic multiplane scanner, tomographic plane separation and detector distance determ. 78−20258
self-triggered liquid xenon drift chamber by the use of proportional ionization or proportional scintillation 79−45562
short lifetime meas., β-spectrometer, plastic scintillator, effects of light guide and mag. field *(Japanese)* 78−90016
shower separation in conjunction with cathode readout MWPC 79−3273
signal shaper-discriminator 78−33387
SILYA-4 light nucleus isotope spectrometer for cosmic ray obs. above atmosphere 79−80111
slow proton detectors, 10-30 keV range 79−68137
soft X-ray sealed gas electroluminesc. detector, design and characts. 79−733
solar gamma ray emissions study, Solar maximum mission, detector assembly and electronic assembly 80−63476
solgel scintillators for liq. scintillation counting of aqueous and non-aqueous samples 77−38546
solutes in liquids, conc. determ. by (n,α) and (n,γ) reacts., scintallation counting 80−35602
spaceflight, radioactivity induced in scintillator materials 78−85822
spectrometer stabilisation using LED reference light source 80−91365
spontaneous fission low background detection system 79−36475
stability analysis 80−99406
stack gas monitor, β scintillation detector+Ge(Li) detector system, environmental γ dose *(Japanese)* 79−3246
statistical resolution meas. 79−93874
status of equipment, microprocessor appls. 79−76271
stilbene, n-γ pulse shape discrimination 77−57816
Stilbene, proton loss by nuclear inelastic interactions 77−71729
stilbene crystal, fast neutron counting efficiency 77−71719
stilbene crystal, separation of neutron and gamma-ray spectra in mixed field *(Czech)* 77−50327
stilbene crystals, meas. of light pulse shapes 78−74534
stilbene scintillation fast neutron spectrom. with pulse shape discrimination 78−55084
stilbene scintillation spectrometer, meas. of fast neutron spectrum from NA-2 generator *(Czech)* 77−71710
subnanosecond lifetime measurements, system using microchannel plate photomultiplier 78−37520
subnanosecond plastic scintillators 80−69037
superconducting mag. spectrom. for cosmic ray flux meas. 78−25383
symmetric-pair, use in photomicrograph anal. in SEM 79−6232
system for cosmic ray EAS research above 2×10^{14} eV 77−61649
tetralin based scintillator, appl. in neutron spectrometry 77−30723
thin cylindrical, spectral characteristics for fast neutron spectrom. 79−26806
thin detector for thermal neutrons, LiF and ZnS (Ag) vac. coated layers 77−54456
thin film, heavy ion detectors, book contrib. 79−31335
thin film detector for heavy ion identification 79−13596
thin film plastic scintillator for light ions 78−29711
thin film waveshifter coatings for fluorescent radiation converters 80−32574
three-dimensional scintigram processing algorithm 78−7446
time compensated, high efficiency neutron detector for TOF studies 77−23363
time of flight directional coincidence telescope for gamma ray telescopes 77−390
time of flight spectrom., for He-jet produced α-source recoil particle obs. 78−86717
time of flight spectrom., ion discrimination using thin scintillator films 78−86718
scintillation counters continued
time of flight telescope, compensated, for spaceborne cosmic ray measurements 77−67939
time-amplitude convertor for 20 to 100 ns 77−50334
time-dependent properties of proportional counters SRPO-304 used with scintillation detectors 80−42894
time-of-flight electronics system for Mark II Detector 80−58093
time-of-flight telescope for cosmic γ-ray preselection 78−82572
time-resolved coded aperture imaging system, for nuclear fuel motion HCDA conditions 78−45764
timing errors evaluation 80−5445
TOF high efficiency detectors for high energy neutrons, subnanosec. time resolution 78−37481
TOF spectrom., intrinsic time resolution of detectors 78−849
tomograph, positron emission, ring detector, attenuation, scatt. radiation and random coincidences 80−61684
tomography of positron emitters, high resolution computed 77−66837
track-finding trigger processor for mag. detector 78−46244
tritium detection in gases and liquids, state of art *(Czech)* 77−86403
ultra-cold neutron scintillation detectors, optimisation 80−74090
ultra-fast detectors for laser fusion diagnostics, quenched plastic scintillator with microchannel plate photomultiplier 80−74084
ultrafast scintillators, response 78−41393
upper atmosphere, background effects in scintillation telescopes 78−85823
variable sampling-time technique for improving count rate performance of scintillation detectors 79−22565
weak γ-ray transitions observed in coincidence with summed cascades 79−76264
well-type, improved model with enhanced resolution power and higher sensitivity 79−68143
whole body counter, portable chair type for in vivo internal contamination monitoring 78−61260
whole-body counter, 4 π, at Hamburg, performance parameters 77−16975
whole-body counter based on liq. scintillation detector modules 77−48883
whole-body counter for meas. of radionuclides in large dogs 78−11786
whole-body counter in vivo calibrations for quantitative retention estimation 78−3579
whole-body imaging methods and devices, comparison 78−44597
whole-body K content, ^{42}K calibration of whole-body counters 79−25086
windowed ang. correl. method for positron annihilation params. meas. 77−34528
X-ray crystal spectrograph with active readout 80−4826
X-ray detector calibration in 183 to 932 eV range 77−71717
X-ray detector for radioisotopes low energy radiation meas., absolute method 78−878
X-ray fluorescence gamma coating-thickness meter, performance improvement 79−35670
X-ray imaging gas scintillating proportional counters, performance in medical appl. 79−2153
X-ray imaging scintillation detectors, design 79−25511
X-ray position-sensitive scintillation detector for portable stress analyser 80−13190
X-ray telescope for Aryabhata satellite project 79−84638
X-ray-β particle coincidence technique to exam. β-decay of ^{252}Cf fission fragments 80−74094
YAG, for electron microscopy, using auto emission gun *(Czech)* 78−21280
α scintillation kinetics in condensed Xe 79−26828
β-decay surface contamination, comparison of counter efficiency 78−25398
β-γ-γ coinc. spectrom. using GM-Ge(Li)-Na(Tl) counter combination 78−46210
$e^+e^-\rightarrow2\gamma$, ang. correl. meas. device *(German)* 78−86726
γ-ray pulse-height response of NE-213 scintillation detector 78−17508
π^- discrimination and absolute counting for nucl. capture at rest expts. 80−5432
π^0 photoprod. on ^4He meas. 78−29694
Ag activation detector, determ. of neutron yield from pulsed neutron sources 79−31332
Ar gas, high press., recombination luminescence in scintillation induced by alpha particles 78−50441
Ar, liquid, scintillating target, fast neutron polarisation analyser 80−47833
Ar, liquid, scintillation decay due to α-particles and electrons 78−55099
Ar-N_2 gas scintillation MWPC for high-intensity 5-10 keV X-rays 78−82575
^{41}Ar release from TRIGA reactor, comparison of γ-ray detectors 78−57309
B, liquid scintillation slow neutron detector with n-γ separation cct. 78−862
^{10}B-loaded liquid scintillator with pulse-shape discrimination 79−59309
^{10}B, neutron cross section standards, detection techniques 79−9970
BaF_2, Ce activated counters 77−65402
$Bi_4Ge_3O_{12}$, 38 mm scintillator, γ-ray response 80−58048
$Bi_4Ge_3O_{12}$ as potential scintillation detector in positron cameras 78−3586
$Bi_4Ge_3O_{12}$, low-temp. scintillation props. and appl. to high-energy γ-imaging devices 80−55191
$Bi_4Ge_3O_{12}$ scintillators, appl. as high energy gamma detectors 80−47827
C_6D_6, n-γ pulse shape discrimination 77−57816
$C_6H_{6_1}$n-γ pulse shape discrimination 77−57816
CO_2-^{14}C animal exhalation meas. by liquid scintillation counting *(French)* 79−48384
CSF detector, positron emission tomography 80−61688
^{14}C counter system using proportional counters of plastic scintillator 77−60491
^{14}C dating, apparatus for β-counting 79−80048
^{14}C detection, $NaH^{14}CO_3$ liquid and $Ba^{14}CO_3$ gel suspension, scintillation cocktails efficiencies 79−3283
^{14}C, high accuracy meas. by gas proportional and liq., scintillation counting 78−74544
^{14}C liquid scintillation counting using thick-walled vials 78−857
^{14}C, liquid scintillation counting efficiency, volume and quenching effects 79−76270
^{14}C low level liq. scintillation counting using small vol. teflon-Cu vial 80−16887
$^{14}CO_2$ trapped in solns. of NaOH, reliable scintillation counting method 79−62410

scintillation counters continued
CaF_2, Ce activated counters 77−65402
CaF_2 scintillation counter activated with Eu, ^{85}Kr conc. determ. at high pressures using β-ray count 78−13385
CaF_2:Eu, scintillation detector, in STEM 80−101897
CaF_2(Eu) and NaI(Tl) scintillators in phoswich config., low background β counting 78−37521
CaF_2(Eu) Phoswich detector, evaluation for ^{90}Sr in situ anal. 80−58067
4π-CaF_2(Eu) spectrum for X-ray and electron meas. 77−398
CdS, layer scintillator for backscattered SEM, reflected SEM proposal 78−21291
CsF scintillator, pot. advantages for a time-of-flight positron camera 80−81706
CsI crystal, growth time of scintillation pulse activator concentration and ionisation density 80−23251
CsI crystals, in scintillation counters, nonstatistical counting rates due to phosphoresc. 78−95597
CsI, proton loss by nuclear inelastic interactions 77−71729
CsI:Tl, gamma-scintillation growth front, external elec. field effect 80−34984
CsI(Na) scintillating crystals in cosmic X-ray detectors, growth of deactivated layers 77−10554
CsI(Tl), characteristics of γ-emission scintillation detection units 78−33365
CsI(Tl) crystal light output when exposed to protons at 3-15 MeV 78−78570
CsI(Tl), params. of FEU-118 photomultiplier in operation with NaI(Tl), CsI(Tl) dets. 79−3284
CsI(Tl) thin film detectors, light output and resolution 78−9030
Fe calorimeter, hadronic cascade curves between 20 and 8000 GeV 80−36464
Fe scintillator calorimeter, segmented, structure of hadronic and EM showers 80−74078
Fe-liquid scintillator multilayer calorimeter transition effects, muon burst rates 78−90019
Gd loaded large liquid scintillator, neutron radiative capture cross-section meas. 78−25380
Ge diode detector telescope for particle spectroscopy, design and performance 78−13384
Ge gamma camera, computer controlled, nuclear cardiology appl. 80−61682
Ge(Li)-NaI(Tl) Compton suppression spectrom. for low-level activity meas. 78−9022
H scintillating gaseous drift chamber for use as positron sensitive target 80−9457
^3H calibration of photomultipliers on liquid scintillator *(Czech)* 79−31324
^3H counting efficiencies and sample time stabilities in a Triton X-100/toluene scintillant 80−52813
^3H environmental levels, problems of detection 77−9489
He high press. gas counter, neutron polarisation meas., Monte Carlo convections 80−14061
He scintillation counter use in neutron time of flight spectrometer for 0.4-4 MeV range 79−68134
He-Xe scintillators, fast neutron polarisation expts. 78−13052
^{123}I two-crystal coincidence counting 78−13394
^{125}I airborne vapour detection 80−51027
^{125}I surface contamination meas., sensitivity comparison with other detectors *(Czech)* 79−34673
^{125}I, variation of γ-counting efficiency with sample composition 80−83238
In loaded liq. scintillator for solar neutrino spectroscopy at low energies 78−73639
Li glass NE-912, neutron detection efficiency *(Russian)* 80−27901
Li-glass scintillator, pulse height distrib., neutron energy depend. 79−54751
Li(I), response functions of spherically moderated neutron detectors 80−37687
Li_2O-MgO-Al_2O_3-SiO_2 glass scintillator for pulsed neutron detection 80−87019
^6Li glass counter, determ. of $^6Li(n,\alpha)T$ 70 to 3000 keV cross section 79−85471
^6Li glass detector, threshold photoneutron spectra meas. 77−88334
^6Li glass detectors for neutron physics research 79−72199
^6Li glass scintillators, appl. as neutron detector, problems and consequences 79−9968
^6Li sandwich counter, meas. of neutron spectra in fast neutron systems 80−27884
^6Li-salicylate neutron detectors with pulse shape discrimination 79−97950
$^6Li(n,\alpha)^3H$ reaction, as standard in neutron flux meas., instruments review 79−9969
MgO scintillator prep. for viewing accelerator beam spots 79−6803
Na I (Tl) detector for gamma-ray from fast neutron radiative capture 77−26925
NaI (Tl) surrounded by thick plastic scintillator for high energy γ-rays, pp studies 78−62443
NaI absolute photopeak efficiency, relationship between point- and extended source geometries 77−26944
NaI collimated detector response matrix generation 79−22553
NaI counter telescopes, energy resolution 77−57822
NaI detector absolute photopeak efficiency calc. for water as source medium 78−78558
NaI detector calibration using large diam. sources 78−33396
NaI detector efficiency for 10 to 150 keV gammas, 4π geometry vs. well- and face-type cryst. 77−3214
NaI detector system, front end electronic, pulse height anal. 79−45587
NaI detectors, lung counter system, improvements to overcome interference from neighbouring compartments 79−2132
NaI detectors, proton react. losses determ. 78−74540
NaI detectors, synthesis of response functions to gamma-rays 78−94158
NaI dual-crystal probe, coincidence-counting assays of ^{123}I 77−14320
NaI face-type detector efficiencies for 10 to 150 keV γ-rays 77−3215
NaI gamma spectrometer with ^6LiH shielding for neutron background reduction 78−90012
NaI, γ-ray self-absorpt. in vol. shaped source, Monte Carlo calc. 77−26909
NaI, meas. of fast neutron capture cross sections 78−74530
NaI opposed detector/turntable γ counter for voluminous samples 79−100706
NaI position sensitive detector, test results 79−76288
scintillation counters continued
NaI, proton loss by nuclear inelastic interactions 77−71729
NaI pulse height spectra for >1.5 MeV gamma-rays, model modification 79−36459
NaI scintillation counter, calc. of self-shielding and detector efficiency 80−99419
NaI scintillation detectors, efficiency values, point and extended volume source geometries 78−13387
NaI scintillation spectrometer, gamma-ray energy released from fission products, response matrix *(Japanese)* 80−42888
NaI, scintillator props. in temp. range 125 to 293K 80−58047
NaI scintillators for gamma-ray burst astronomy, comparison with plastic scintillators 77−64648
NaI, sex-dependent calibration factor, ^{42}K whole-body content meas. 79−29593
NaI spectrometer, response matrix for 6 MeV γ-ray penetration meas., benchmark data 78−50432
NaI, through well, well type detectors, comparison 78−90020
NaI well-type detectors, efficiency values for 10 to 150 keV gammas, point and needle sources 77−3213
NaI well-type detectors, effect of well dimensions in photopeak efficiency 77−88332
NaI:Tl, American National Standards Institute quality assurance programme 77−38585
NaI:Tl, right-circular cylindrical detector, Monte Carlo calc. of efficiency 79−734
NaI:Tl, scintillation excitation mechanism for γ-rays *(Russian)* 78−92126
NaI:Tl scintillation crysts., analytic calc. of photofractions to monoenergetic γ-rays 79−52038
NaI:Tl scintillator response, γ-ray, (X-ray) rel. $^1/_2$-width energy depend., undergrad. expt. 78−49600
NaI:Tl spectrometer meas. of activity of radioisotope emitting two gammas in cascade, geometrical effect 77−88320
NaI(Tl), ^{237}Pu $T_{1/2}$ determ. 78−8775
NaI(Tl), anomalous intensity variation of backscattered gamma ray peaks 80−37691
NaI(Tl), appl. in NBS positron annihilation in flight facility 79−31306
NaI(Tl) array, calibration using 500 keV Van de Graaff proton accelerator 79−45524
NaI(Tl), background charact., appl. as low-level γ detectors 79−68144
NaI(Tl) crystal, 400×200 mm, energy resolution 77−6622
NaI(Tl) crystals for volume cylindrical sources, efficiency of γ-ray detection 80−63457
NaI(Tl) decay time constant temp. depend., influence on detector appls. 77−54417
NaI(Tl) detector response using X-ray monochromator 79−93876
NaI(Tl) detectors, determ. of full energy peak efficiency 79−31318
NaI(Tl) detectors, response functions to terrestrial γ-radiation, computer program 80−83233
NaI(Tl) large area multi-crystal detectors for X-ray and gamma-ray astronomy 77−22070
NaI(Tl) linear response photon counter 79−45567
NaI(Tl) long narrow rectangular polycrystalline scintillator, test and evaluation 77−54418
NaI(Tl) modularised detector, crystal ball prototype 78−37498
NaI(Tl), on International Sun-Earth Explorer C spacecraft, for solar flares and cosmic γ-ray obs. 78−85787
NaI(Tl), params. of FEU-118 photomultiplier in operation with NaI(Tl), CsI(Tl) dets. 79−3284
NaI(Tl), pile up reduction in low intensity rad. counting, fractional charge collection technique 77−88345
NaI(Tl), plume exposure monitoring system for LWR plant 80−42875
NaI(Tl), portable, natural soil radioactivity monitoring 80−31148
NaI(Tl) positron ring cameras for emission computed tomography 77−44742
NaI(Tl), pulse shape discrimination of high-energy neutrons and gamma rays 78−33395
NaI(Tl), review of techniques and appl. 79−72197
NaI(Tl) right circular cylindrical crystal detectors, simple model for γ pulse-height spectra prediction 77−6611
NaI(Tl) scintillation counter, γ-ray flux meas., appl. to environmental γ radiation anal. *(Japanese)* 77−71732
NaI(Tl) scintillation counter, bremsstrahlung meas. from β decay of ^3H 78−55042
NaI(Tl) scintillation survey meter, for ^{131}I meas. in human thyroid gland 78−80970
NaI(Tl) scintillation detectors, temp. depend. of radiation-induced coloration 79−72204
NaI(Tl) scintillation spectrometer, used simultaneously with Ge(Li) semiconductor, in neutron activation cross-section meas. 80−78485
NaI(Tl) scintillation detectors, microprocessor-based multichannel analyser 80−91378
NaI(Tl) scintillator, specific sensitivity in γ-ray recording from radioactive ores 78−81449
NaI(Tl) scintillator, electron detection efficiency for electrons and gamma-rays > few keV 79−36461
NaI(Tl) scintillator, evaluation as fast neutron monitor 79−45559
NaI(Tl), simple algorithm for Gaussian peaks best fit *(Italian)* 78−58538
NaI(Tl) single-crystal scintillation camera, image artifacts at high photon fluence rates 78−85364
NaI(Tl) total efficiency calc., algorithm for small calculators 79−9938
NaI(Tl), use in anti-Compton spectrom. 79−26804
NaI(Tl) well type detector calib. for absolute counting of ^{85}Kr and ^{133}Xe 78−9036
NaI(Tl) well type detector, efficiency determ. 78−55087
NaI(Tl), well-detector, low-background γ-spectrometry, comparison with CsI(Tl) 78−86724
NaI(Tl) well-type detector calibration 79−85858
NaI(Tl) well-type detectors, photopeak efficiency values, expts. and calcs. 80−63454
NaI(Tl)-Fe(Li), Compton suppression spectrometer for in-beam expts., design and performance 78−78553
Na(Tl), circular ring transaxial positron camera, coinc. electronics 78−31953
Na(Tl) scintillator detectors for neutron-gamma discrimination 80−102386
Pb spectrom. for fast reactor fuel pins 80−37461
Pb-acrylic shower detector, meas. of electron and pion cascades 79−81124

scintillation counters continued
Pb-foiled plastic scintillator, γ-ray meas. *(Japanese)* 77−57825
Pb-foiled toluene based scintillator, γ-ray meas. *(Japanese)* 78−90032
Pb-glass total absorption counters, photomultiplier size at high energy 80−74085
Pb-liquid large area shower detector with high spatial and energy resolution 79−742
Pb-plexipop calorimeter module viewed by wavelength shifter bars 79−81127
Pb-scintillation counter, modular EM shower detector for CERN ISR 79−76275
Pb-scintillator calorimeter, electron energy and positron measurement 79−76273
Pb-scintillator sandwich EM shower detector, perform. charact. 80−102385
Pu-Am survey instrument, β-α-γ-X-ray scintillation detect. probe 78−33376
Rn continuous monitor response to transient Rn concs. 80−32519
^{222}Rn alpha-scintillation counting, statistical counting error calc. 77−3211
^{222}Rn concentrations in water, rapid meas. with commercial liq. scintillation counter 78−28339
^{222}Rn low conc. meas. in air, α-scintillation method 78−92970
^{222}Rn scintillation counting, standard deviation estimation 77−79519
Si(Li)-NaI spectrometer, L X-rays, meas. of trace radionuclides in soil 80−58020
T in air, scintillation detection using liquid adsorbent 79−76291
T monitoring using scintillation chamber 79−89519
T_2O, injectable soln., radionuclidic purity using liquid scintillation counter *(French)* 78−73118
^{99m}Tc-EHDP accumulation in canine tibia, meas. method 78−20245
$ThBr_4$, crystal, self-induced α-spectra 77−67943
$ThBr_4$, inorganic scintillator, use in nucl. and accelerated particle detection 78−58540
$ThBr_4$, new inorganic scintillators for nuclear particle detection, review of props. 79−45549
$ThCl_4$, new inorganic scintillators for nuclear particle detection, review of props. 79−45549
U activity, liquid scintillation counting 80−27873
U analysis in phosphate fertilisers and other materials using liq. scintillation spectrometry 78−53280
U assay of phosphate materials 78−82589
U exploration, airborne phoswich detector system 79−53576
U stored in lung, meas. using NaI and solid-state detectors 78−28090
Xe filled gas scintillation proportional counter in space environment, background radiation rejection efficiency 78−21819
Xe filled proportional scintillation detector for charged particles 80−32572
Xe gas counter, meas. of ^{235}U(n,f) and ^{238}U(n,f) cross sections 77−26806
Xe gas scintillation proportional counter, UV emission spectrum, prod. mech. 77−26935
Xe high pressure proportional, scintillation camera for X-and γ-ray imaging 80−99412
Xe, liq., for imaging of positron emitters 77−2042
Xe, liq. and solid, for scintillation cameras *(French)* 77−37034
Xe proportional scintillation detector, energies and angles of emission of ^{252}Cf fission fragments 80−63488
Xe uniform field gas proportional scintillation counter, secondary scintillation output 77−54428
Xe-Kr mixtures for gas proportional scintillation counters 77−83464
YAG:Ce^{3+}, new fast scintillator for SEM 78−86394
YAG:Ce^{3+}, scintillation detector, in SEM, electro-optical props. 80−52819
ZnS scintillator with faster decay 77−42217

scintillation detectors *see scintillation counters*

scintillation spectrometers *see particle spectrometers; scintillation counters*

scintillators *see scintillation; scintillation counters*

scintillometers *see scintillation counters*

scorching *see combustion*

Scott effect
Knudsen mol. gas, thermo-mag. force on heated cylindrical body *(Russian)* 78−26235
polyatomic Knudsen gas, kinetic thermomag. phenomena 78−75246
rarefied gas, thermomagnetic force kinetic theory *(Russian)* 79−94765
trifluoromethane, polar gas thermomagnetic torque meas. 77−42960
N_2O, polar gas thermomagnetic torque meas. 77−42960
OCS, polar gas thermomagnetic torque meas. 77−42960

s.c.r. *see thyristors*

screening *see shielding*

screening, nuclear *see nuclear screening*

screens, fluorescent *see fluorescent screens*

screens, phosphorescent *see fluorescent screens*

screens (display)
see also fluorescent screens
cathodoluminophors, characteristic calcs. 78−10993
electroluminescent, laser-addressed, use of CdS:Cu,Cl photocond. film 77−51777
Faraday screen, for nuclear magnetic resonance spectrometer with crossed coils 78−4670
halosodalites, synthesis, cathodochromism, reflectivity spectra 77−40399
holographic reader-copier development and speckle suppression 79−81395
holographic screens for colour flat image projection *(Russian)* 80−9066
II-VI semiconductor laser screens, for electron-hole tubes, stimulated emission mechanism 79−94237
interactive satellite video display systems for atmospheric analysis 79−58229
laser electron-beam tubes for projection TV 79−59743
light transmitting stereo screen *(Russian)* 80−86480
liquid crystal screen, coherent optical image spotty structure reduction 79−14109
liquid crystal translucent screens, resolution 80−28335
neuronal response analyser with microprocessor *(French)* 79−20730
passive thermal screen for IR scene simulation 77−62060
phosphor film electroluminescent devices, book contrib. 77−73176
photoelectric screen convertor, accuracy, reading system ang. aperture effect 77−62066

screens continued
projection TV using electron beam pumped semiconductor laser 77−88830
radiographic intensifying screens, sensitivity to scattered radiation 77−77970
random nucleated halftone screen 78−62192
spatial image projection on to lenticular screens with hexagonal structure, raster and holographic projection appl. *(Russian)* 80−86481
speckle free rear projection screen, two close moving screens 77−19412
TV, large pictures obtained by using projection system *(German)* 79−80660
TV, use of cholesteric-nematic phase transitions of liquid crystals *(Chinese)* 80−79922
X-ray film/intensifying screen system, MTF and Wiener spectrum, film and screen quality effect *(German)* 80−73560
CdS, CdS_2Se_{1-x}, single cryst. ingot, laser screen for CRT 77−75561
CdS, CdS_xSe_{1-x}, scanning semiconductor laser with transverse electron-beam pumping 80−9904
CdS screen for laser CRT, stimulated emission with TV type operation 78−59028
CdS single crystal laser screen, photolum., determ. of layer depth disturbed by polishing 78−17977
CdS_xSe_{1-x} laser electron-beam tube, possibility of acceleration voltage lowering 79−89929
PLZT ferroelectric display electro-optical props. *(Russian)* 79−9211
ZnSe, single cryst. ingot., laser screen for CRT 77−75561

screw dislocations
absorbing crystals, dislocation contrast in the case of anomalous X-ray transmission 80−100240
alkali halide, morphology of growth and evaporation surface 78−79544
alkali halide, screw dislocations in puncture rosettes, motion-starting-stresses, surface-active media effects *(Russian)* 78−10051
alkanes, thin plate microcrystals, transmission electron diffraction intensities 78−83821
alloy, $L1_2$ ordered, yield stress 77−52392
alloy, ordered, conservative jog slip on superpartial screw dislocations, work hardening 77−7731
alloys, single cryst., work hardening phenomena and screw dislocation dipole clusters 80−100845
amorphous Lennard-Jones solid, edge and screw dislocation, stability, elasticity, simulation 80−15099
anisotropic crystals, infinite rectilinear dislocation, vibrs. 80−44210
antiferromagnet, magnetic dislocation domains, mag. moment distribution 80−2601
BCC lattice, core struct., rel. to α-Fe slip 79−82211
BCC metal, discrete-continuum hybrid method for dislocation-point defects interaction 77−89467
BCC metals, HF mech. relax. peak 78−91379
BCC metals, influence of screw dislocations on cryst. lattice rotations during deform. *(Russian)* 78−6966
BCC transition metals, screw dislocations, electronic theory, Peierls stress, core energy calc. 78−71737
Burgers vector sign determ. for nearly screw dislocations, X-ray dynamical theory applic. 80−59467
channelled ions, energy loss effect of screw dislocations 78−67761
coherent motion, lattice dynamics 78−71738
coherent precipitation near dislocations 79−95016
continuum mechanics, non-local, at atomic scale 78−12563
crack analysis, concentric circular arc cracks in anti-plane strain, screw dislocation pile-up model 77−54927
crack propagation effect of 2- or 3-dimensional macrodefect *(Japanese)* 80−104261
crack tips, yielding on inclined planes 80−33525
cracked bar under torsion and shear, elastoplastic stress and strain calc. from screw dislocations 79−68654
cross-slip processes in high temp. recovery-creep 77−19965
crystal face, growth behaviour in presence of screw dislocations 80−103276
crystal growth, generalised kinetic eqn. 77−55249
crystal growth, imperfect faces, Monte-Carlo growth rates 77−11493
crystal growth models, attachment energy at habit controlling factor 80−59420
crystallite with screw dislocation, determination of particle size and distortion 80−15098
cube growing from infinite quiescent soln., conc. field at dislocation 77−47361
cubic crystal, high vel. screw dislocations motion and interatomic force law 77−43214
cubic crystal edge and screw dislocation−point defect elastic interactions 80−15151
deformation potential operator, electron dislocation interaction *(Russian)* 80−2021
diamond, natural type-IIb, single dislocations, cathodoluminescence obs. by STEM 80−80871
diamond lattice, dynamic symmetry and plastic deform. 80−24527
diffraction, optical analogue using simulated models 78−38723
disclination dipole of infinitesimal width and straight dislocations 79−51104
dislocation, straight line, motion in conc. solid soln. computer simulation 77−81268
dislocation motion, lattice resist., effect of impurity interstitials 80−84170
dislocation-phonon interaction in cryst. with anisotropic slip system 80−29137
displacement field when moving in elastic nonlinear medium *(Russian)* 80−44206
double cross-slip mechanism 78−22720
dynamic Peierls stress in cryst. model with slip anisotropy, screw dislocation motion 78−95056
electrolytic crystal growth, role of screw dislocations 80−54540
electron scattering due to screw dislocations 78−60101
electron-microscope image of dislocations, in anticlassical scattering region, dislocation axis contrast 80−38877
etch figure rosettes, dislocation interaction in screw rays 78−47376
FCC anisotropic crystals, extended screw dislocation, ⟨110⟩ misfit defect elastic interactions 80−100232
FCC crystal, elastic interaction of 60° and screw dislocations with point defects 78−63786
FCC metal, dislocation dissociation 80−107235

screw dislocations continued
feldspar, dislocation image contrast in electron microscopy and X-ray topography 78−26573
ferromagnet, dislocation motion, mag. moments around screw dislocations, spin waves retarding dislocations 78−87670
ferromagnet, rectilinear screw dislocation, magnetisation distrib. 80−44897
ferromagnet, with screw dislocation, density of magnon states 78−84402
finite-two phase bodies, response to internal and external stresses, numerical considerations 80−24742
foils, trapezoidal splitting of partial dislocations 77−51376
friction stress and back stress from hysteresis loop anal. during fatigue 79−42076
graphite, single crystal, from Fe-C melt, morphology 78−42932
HCP crystal, dislocation-point defect interactions, anisotropic elasticity theory, appl. to Zr 77−11588
HCP crystals, dislocation-point defect interactions in slip systems 78−47417
helical electric current flowing along screw dislocation 78−51959
hexagonal elastic crystal with long range interatomic interactions, theory 78−59807
III-V crystals, piezoelectric effect due to dislocations 77−81059
III-V semiconductor, absence of effect on carrier mobility 78−60124
III-V semiconductor, dislocations, velocities and internal friction 79−82231
III-V semiconductor, local resist. near dislocations, eqns. 78−60123
image and surface dislocations models, comparison 79−23605
image stress field, attractive and repulsive forces 77−39584
inelastic neutron scattering phonon dispersion curves 78−75774
interaction with Wannier-Mott exciton 78−10361
interactions with Wannier-Mott excitons *(Russian)* 79−4513
interface, screw like dislocations behaviour with lattice frictional forces 80−64999
Invar, dislocation motion anomaly 80−10554
ionic crystal, solid soln. hardening by aliovalent cations 77−44265
isotropic and anisotropic crystals, stress fields around defects of dislocation-aggregate type 77−39591
laser optical simulation of diffr. from distorted lattices 79−23612
lattice model near surface 77−7719
lattice models of screw dislocation high velocity motion, lattice model effects 79−77600
lattice-statics approach to dislocation calculations, modified, formalism 78−75668
like dislocations near interface in presence of lattice frictional forces 77−47454
local vibration associated with rectilinear screw dislocation *(Russian)* 77−35652
long-wave quasiparticle states localized at screw dislocation *(Russian)* 78−95126
magnetically ordered cryst., dislocation drag, magnetoelastic waves 80−103332
metal, BCC, ⟨111⟩ screw dislocation−vacancy interaction energies 77−15415
metal, BCC, atomic displacement about ⟨111⟩ screw dislocations 77−15414
metal, BCC, core structure, kinks and constrictions *(German)* 77−24316
metal, BCC, energies of kinks and constrictions *(German)* 77−19950
metal, BCC, motion under shear and uniaxial stress, computer simulation 77−4102
metal, BCC, relation between elastic energies of dislocations and choice of slip system *(Japanese)* 78−18656
metal, FCC or BCC, dislocation annihilation during tensile and cyclic deform. and limits of dislocation densities 80−34007
metal, HCP, atomic struct. of defects 78−30611
metal, polycrystalline, strain hardening, dislocation link length model 80−84953
metals, atomic mobility under pulsed loading conditions *(Russian)* 80−96684
metals, BCC, dislocation processes, straining expts., electron microscope obs. 80−29025
metals, BCC, effect of screw dislocations, on mech. props. *(Russian)* 78−60704
metals, BCC, plastic deform., review 80−104213
metals, dislocation motion depend. on electrons *(Russian)* 79−65260
metals, FCC, misfit defect and extended screw dislocation anisotropic elastic interaction 80−96563
metals, Snoek-Koster relaxation, theory 80−16369
microstress field, study by X-ray dynamic focusing 79−23613
modelling of linear and surface defects 77−89450
monostearine crystals, spiral growth from organic soln. 80−93467
motion, in simple cubic lattice, anal. of displacement field 77−11551
motion, soliton like piecewise linear force model 78−2119
naphthalene-p. chloronitrobenzene system, eutectic, solidification 78−64530
nonlocal elasticity theory 77−31659
nonplanar screw dislocation cores, Peierls-Nabarro eqns. approx. solns. 79−32993
nonuniformly moving screw dislocation, transient subsonic motion 80−79790
nucleation of second phase on screw dislocation 78−51540
octacosane crystals, complex growth polytypism and periodic polysynthetic twins 77−47360
ordered alloy, noncoaxial dislocation loop behaviour 77−11549
Peierls model, dislocation core energies 79−27984
Peierls stress in simple model 77−76401
Peierls-Nabarro model, screw dislocation with nonplanar core 77−1126
phonon dispersion curves of localised modes, inelastic neutron scatt. 77−72661
pile-ups as fatigue crack growth 77−3774
plastic deformation controlled by screw dislocation's motion 78−51605
point-force array description 78−18646
polyethylene, crystal, elastic line energies and line tensions of dislocations 79−90656
polyethylene, lamellar stacks, screw dislocations 80−19728
polystyrene, lamellar stacks, screw dislocations 80−19728
pyramids of different slopes, growth on cryst. face at const. supersaturation, model interpret. 78−2050
quartz, synthetic, growth spirals on prism faces, electron and optical microscope obs. 77−7723
roughening transitions of finite order 80−38975
screw dislocations continued
scattering of tight-binding electrons, numerical solution of Schrodinger equation 79−51540
screw subboundaries as dislocation sources, creep 80−100234
semiconductor, containing screw dislocations, impurity centres 78−72111
semiconductor, free carrier scatt. due to screw dislocation strain field 77−1416
semiconductor, tetrahedrally coordinated, effect of doping on dislocation mobility 79−82550
similarity with disclinations in nematic liquid crystals 77−11477
slip band steady-state expansion, dislocation vel. theory 77−24320
solid-on-solid model, rel. to correl. in X-Y model 78−63691
stearic acid crystals grown from solution, spatial correlation between growth spirals and inclusions 80−96527
steel, 12Kh1MF, influence of preferred dislocation orientation on high-temp. strength *(Russian)* 79−4999
steel, austenitic, substructure change in hot deform. process *(Russian)* 77−16617
steel, stainless, single crystals, shear cracks, electron microscope study 80−40522
stress field, diffusing elastic fluid, mechanical interaction effects 78−63766
stress-free motion of dislocation arrays 79−65083
surface dislocation model, Z-phase interface boundary problem 80−39085
surface shear stress, strain and displacement in vertical slab with shear modulus contrast 77−56594
surface-dynamics of growing crystals 80−44160
Ta, single crystals, microyielding, high amplitude damping 77−52396
TEM, image theory, iconic approx., and its generalisation 78−79509
thermal and thermoelastic fields around moving dislocations *(Russian)* 78−22731
three-phase anisotropic medium, antiplane line force 78−67041
tight-binding electron scatt. off screw dislocations 79−91012
transition metal oxide catalysts, reduction, cryst. defects influence, in-situ electron microscopy 80−81322
transition metals, BCC, interaction energy between self-interstitial and screw dislocation, calc. 80−70248
type II superconductor, dielastic interaction of flux line lattice with internal stresses of cryst. imperfections 78−56270
Vibration modes of split screw dislocations in BCC metals 78−22804
Volterra dislocation in nonhomogeneous medium 78−14342
web dendrites, dislocations, stacking faults, X-ray topographic study *(Chinese)* 80−88148
Zircaloy-2, irradiation growth, reaction rate theory calcs. 80−88212
Ag, crystal (100) faces, polynuclear growth mechanism during electrocrystallisation *(German)* 78−18562
AgBr(Cl), vapour-deposited epitaxial film 80−59814
Al, anharmonic effects associated with ⟨110⟩ screw dislocations 78−30625
Al bicrystals, isoaxial, fatigue crack initiation in grain boundary affected regions *(Japanese)* 80−89338
Al, cold-worked, plastically deformed, internal friction spectrum, Hasiguti peaks associated with dislocations 80−7618
Al, screw dislocation core, atomic struct. calc., modified lattice-statics approach 78−75669
Al, single crysts., misfit recrystn. dislocations formation study during recrystn. by X-ray synchrotron topography 79−38849
Al-Mg (0.3 wt.%) single cryst., dislocations obs. by high voltage electron microsc. 80−79796
Al-Mg (5.5 wt.%), effect of stress changes during creep on dislocation struct., TEM study 79−74214
$Ca_5(PO_4)_3F$, dislocation struct. exam. *(Russian)* 78−63770
CdS, acoustic wave attenuation, phonon viscosity and dislocation drag 80−70319
CdS, deformed, dislocation struct., TEM obs. 80−54250
CdS, dislocation charges determ. 78−2136
CdS, plastically deformed, optical and electronic transport anisotropies 77−8611
Cr_2S_3, single crystal, exam. of unit cell structures by interference contrast microscopy 78−67670
CsCl crystal, BCC and BCC ordered, core struct. of ⟨100⟩ dislocations, atomistic calc. 78−30637
CsCl type intermetallic compounds, correlation between dislocation character and operative slip system 79−10852
CsCl-type lattice, (111) superlattice screw dislocation motion, computer simulation 80−79793
Cu alloys, FCC, climb of extended dislocations due to irradiation in HVEM 80−103343
Cu, cross-slip at low stresses 77−11564
Cu, etch pit formation on single cryst. planes by dil. H_2SO_4 78−14348
Cu, fatigued single crysts., temp. depend. of saturation stress and dislocation substruct. 80−44211
Cu, layered cell structures and slip lines in deformed cryst., TEM obs. 79−99209
Cu, neutron irrad. cryst., edge and screw dislocation groups, mean vel. 79−7607
Cu plates, thin, dislocation-dislocation interaction inducing cross-slip, X-ray topographic anal. 80−49233
Cu, single crystals, neutron irradiated, stresses and secondary slip between overlapping and dislocation arrays 80−88162
Cu-Cd (1.0 wt.%), yield stress and flow stress 80−97524
Cu-Cr-SiO_2 system, age and dispersion strengthened, dislocation struct. around SiO_2 particles 80−108468
Cu-Cr(-SiO_2), single crysts., yield and pre-yield behaviour rel. to aging time 80−81103
CuAu, calc. of elastic interaction between locally transformed regions with screw and edge dislocations 78−83844
Fe, Armco, dislocation struct. after hot and cold rolling *(Russian)* 77−8847
Fe, Armco, flat-rolled and annealed, dislocation struct. and mech. props. *(Russian)* 79−20062
Fe, Armco, screw dislocation effect on mech. props. *(Russian)* 78−60704
Fe, BCC surface ledge simulation, dislocation-like relaxation 78−30620
α-Fe, crack initiation study at low-cycle fatigue using slip bands *(Slovak)* 79−38949
α-Fe, creep and fracture between 77 and 673K 79−7649
Fe, deformation, influence of crystallographic lattice type *(Russian)* 79−34106

screw dislocations continued
Fe, deformed, dislocation structure determ. from magnetic props. 78−55874
Fe, deformed single crystal, dislocation distrib. 77−59880
Fe, effect of H_2 on phys. and mech. props. 80−101657
α-Fe film, deform. in electron microscope, dislocation mechanism 79−82227
α-Fe, internal friction for low temp. deform. 80−40420
α-Fe, internal friction peaks from dislocation relax. in plastically deformed and/or neutron irrad. sample 78−48438
Fe, pure, deformed, internal friction, dislocation relax. and dislocation-defect interactions 79−29125
Fe, quenched-in hydrogen, yield stress decrease of prestrained specimens 80−16454
α-Fe, screw dislocation motion, orientation depend., tight-binding type electronic theory 79−51109
Fe, softening and hardening by H_2 charging during tensile deformation 80−16453
Fe whiskers, struct., dislocations, mag. domains *(Polish)* 79−33210
Fe whiskers, undeformed, X-ray topographic study 77−80716
Fe-Cr-Co alloy, spinodally decomposed, micro-twinning 80−92537
Fe-N, single cryst., solid soln. softening, effect of interstitial N 80−97496
Fe-Ni (29 at.%), calc. of elastic interaction between locally transformed regions with screw and edge dislocations 78−83844
Fe-Si (3 wt.%), degeneration of slip on (211) planes *(Russian)* 78−80587
Fe-Si (3 wt.%), single crystals, cyclic deformation oriented for single glide 79−100224
FeAl single crystal, compressed, dislocation arrangement 78−14354
$FeCr_2S_4$, vapour grown, growth mechanism of multisteps on surface 78−75605
Ga whisker growth from GaN/Ga layered films 80−92800
GaAlAs-GaAs DH lasers, degradation caused by growth of dislocation networks 80−53289
$Ga_{0.7}Al_{0.3}As$ epitaxial film, inclusion-generated dislocation clusters 77−89445
GaAs cryst., creep and dislocation vel. at different doping and temps. 78−95783
GaAs, LPE layers, optical microscope obs. 77−35561
GaAs pure and Se-doped, photoluminescence at dislocations, band gap electronic levels 79−99926
GaAs:S(Te)(Zn), dislocation-free, TEM study of microdefects 79−82213
GaSb, acoustic wave attenuation, phonon viscosity and dislocation drag 80−70319
$Gd_3Ga_5O_{12}$, single cryst., helical dislocation obs. by etching 77−11558
Ge, amorphous, struct., dislocation model 78−42911
Ge chalcogenides, screw dislocations in layer crystal growth from vapour *(Russian)* 80−1953
Ge, cross-slip of single dissociated screw disclocations, double etching and X-ray topography studies 80−15104
Ge, dislocation mobility 77−76413
Ge, dislocation motion near surface 79−82219
Ge, dislocations under high stress, stacking fault energies, TEM study 80−70202
Ge, elastic moduli, drag coeffs. and Keating's parameters 79−73238
Ge mobility of screw and 60° dislocation at low stresses 77−11554
Ge monocrystal, dynamic interaction of screw dislocations with flat clusters of dislocations on other slip planes *(Russian)* 79−86800
Ge, motion of partial dislocations 79−82229
Ge, screw dislocations, effect of dislocation dissociation on localised electron and hole states 79−82546
Ge, short dislocation line movement at low stresses *(Russian)* 77−47462
GeS, gas-phase single-cryst. growth, photoelec. props. 77−36381
^{4}He solid-liquid interface mobility under 1 MHz sound wave *(French)* 80−100373
n-InP, defects in homoepitaxial layers, on p-type substrate, accurate lattice parameters 78−47675
InP, photoluminescence at dislocations, band gap electronic levels 79−99926
KCl, cryst. isolated pore healing under press., dislocation struct. evolution *(Russian)* 80−100245
KCl, melt-grown, spiral growth, screw dislocation mechanism, phase-contrast microscopy obs. 78−87637
KCl, motion of dislocation half-loops, influence of prestart loading and ensemble nature 78−71745
KCl, stepwise motion of edge and screw dislocations *(Russian)* 77−84748
KCl-KBr single crysts., yield strength and dislocation mobility, solid soln. hardening model 77−72649
KH_2PO_4, Burgers vector sign determ. for nearly screw dislocations, X-ray obs. 80−59467
Li, temp. depend. of dislocation behaviour between 90 and 300K 80−88146
LiF crystal, contact damage obs. by cathodoluminesc. 80−71728
LiF, dislocation distrib. on surface parallel to Burgers vector 79−65090
LiF, dislocation structure, influence of variable deform. temp. 80−70211
LiF, multiplication of screw dislocations during deform., yield stress depend. 77−24321
LiF, plastic strain accompanying local rise in surface temp., of natural shear *(Russian)* 80−6411
LiF, radiation induced voids, formation on dislocations 80−15159
LiF, slip band steady-state expansion, dislocation vel. theory 77−24320
LiF:Mg^{2+}, deformed in ^{3}He and ^{4}He, dislocation struct. characteristics 79−69112
$MgAl_2O_4$, dislocations, sessile dissoc. 79−46663
MgO, crack propagation during in-situ deform., plastic zone formation 80−16468
MgO crystal, contact damage obs. by cathodoluminesc. 80−71728
MgO crystal, yield strength and dislocation mobility 80−93601
MgO crysts., geometrical-statistical parameters of dislocation interactions with point obstacles 80−103341
MgO crysts., plastic deform. activation parameters, rel. between macroscopic and in-situ HVEM expts. 80−103355
MgO crysts., radiation damage influence on deform. in HVEM 80−103391
MgO, point-obstacle distance distrib. during motion of screw dislocations 77−11744
MgO, single cryst., tensile creep, stress induced dislocation structs. 80−96539
screw dislocations continued
MgO single crysts., dislocation processes, obs. by HVEM in-situ deform. 80−103340
Mg_2SiO_4, dislocations revealed by etching 79−99199
Mo dislocation a ⟨100⟩ stability, plastic deform. at high-press. 78−43030
Mo film, deform. in electron microscope, dislocation mechanism 79−82227
Mo, mechanical props. and dislocation struct., mag. field effect 80−54935
Mo, pure and He doped, at. config. of $^1/_2\langle 111\rangle$ screw dislocation 79−65081
Mo, single crysts., work hardening and softening in cyclic strain 80−20957
MoO_3, reduction at low temps., surface defects obs. in HV electron microscope 77−35564
MoO_3, reduction at low temp., role of defects, electron microscope obs. 77−77755
$Na_2Al_2Si_3O_{10}.2H_2O$, natrolite, cleavage etching in acidic and neutral media 80−6407
NaCl, atomistic calc. of core config. 79−23606
NaCl, cross slip of screw dislocations during deform. at room temp. 77−84758
NaCl crystals, config. of screw dislocation halfloops *(Russian)* 77−89436
NaCl, dislocation density in monocrystal deformed under high hydrostatic press. 80−70216
NaCl, dislocation distrib. on surface parallel to Burgers vector 79−65090
NaCl, dislocation half loop mobility 78−59817
NaCl, dislocation mobility under high press., temp. depend. 80−75235
NaCl, dislocation movement, effects of adsorpt. of octadecylamine *(Russian)* 77−51372
NaCl, dislocation ordering influence on integrated X-ray coeff. 80−103357
NaCl, electric field gradients near dislocations, resulting NMR line-shapes 80−75225
NaCl, integrated intensity of X-ray diffr. by polygonization walls 77−89447
NaCl, motion of individual surface dislocation semi loops *(Russian)* 78−51542
NaCl, plastically deformed, recovery of work hardening *(German)* 77−35626
NaCl, screw dislocation mobility under high hydrostatic press. 79−69109
NaCl single crystals, screw dislocations, influence of interionic potentials on core configs. 80−34000
NaCl, spiral dislocation mobility depend. on elec. field, relaxation time 80−39105
$NaClO_3$, dislocations rel. to growth mechanism from aq. soln., X-ray topography 80−59464
Na_2O-B_2O_3 melt, crystallisation of $Na_2B_8O_{13}$ 78−59763
Na_2SiF_6, precipitation from H_2SiF_6 soln., mechanism, kinetics, habit 77−44142
Nb, deformed, α′-peak in internal friction spectra 80−16368
Nb, effect of electron irradiation on low temp. deform., tensile stress-strain curves 79−55784
Nb film, deform. in electron microscope, dislocation mechanism 79−82227
Nb, high purity, dislocation relaxation by internal friction meas. over wide freq. range 79−38876
Nb, mechanical props. and dislocation struct., mag. field effect 80−54935
Ni, cyclically deformed, polarisation stress field, dislocation shuttling, computer calcs. 79−96095
Ni, rectilinear screw dislocation, magnetisation distrib., mag. moment anal. 80−44897
Ni-Al, solid soln. and solid soln. hardened, stead state creep 78−27578
Ni-Cr, movement and dislocations using SEM and diffr. contrast method *(Chinese)* 79−51110
Ni_3 (Al.Ti), flow stress and work hardening, exam. of temp. depend. by tensile tests 78−84839
$Ni_{0.33}Fe_{2.33}O_4$, {001} ⟨110⟩ glide system, room temp. TEM obs. 79−90660
Ni_3Ga, with $L1_2$ struct., dissociated struct. of superlattice dislocations 79−37706
$PbFe_{12}O_{19}$, dislocation etch pit morphology study *(Chinese)* 80−88150
Si, (111) surface structure phase transform, screw dislocations RHEED study 80−88153
Si, cross-slip of single dissociated screw disclocations, double etching and X-ray topography studies 80−15104
Si, dislocation generation in local oxidation 80−107245
Si, dislocation growth during laser melting and solidification 80−2022
Si, dislocation mobility 77−76413
Si, dislocation motion near surface 79−82219
Si, dislocation velocities as function of electronic doping 77−4117
Si, dislocation velocities meas. 79−82230
Si, doped, motion of partial dislocations 79−82229
Si, filamentary crystals, branching and bending obs. 77−7954
Si, HVEM struct. images of extended 60° and screw dislocations 80−59466
Si, screw and 60° dislocations velocities 79−86798
Si, screw dislocation networks, TEM study 80−70204
Si, self-implanted, ⟨100⟩ and ⟨111⟩, crystallised layers by laser annealing, struct. 78−47644
Si, stacking fault energies, intrinsic and extrinsic, by TEM 80−10562
Si:B(P), dislocations under high stress, stacking fault energies, TEM study 80−70202
Si:P, interstitial supersaturation near P-diffused emitter zones 79−65541
Si:P(B), high temp. impurity diffusion via vacancies and self-interstitials 80−24667
SiC, eccentric growth spirals 78−26470
SiC, high period polytype at interface of two interacting spirals 80−20041
SiC, polytypism, reflection electron diffr. 78−83694
SiC, spiral growth of polytype struct. from faulted matrix, 15R and 4H struct. 77−4778
Sn chalcogenides, screw dislocations in layer crystal growth from vapour *(Russian)* 80−1953
Sn, single crystal, dislocation walls consisting of double arrays 79−46664
SnS_2, cryst. growth, photoconductivity 77−85912

screw dislocations continued
Ta, flow stress at superconducting transition, temp. and strain rate depend. 78−2617
Ta, single crystal, microyielding microflow parameters 77−52395
Te, c-slip, asymmetry and orientation depend. 77−27888
Te, induced acceptor levels and free-carrier mobility due to c-screw dislocations 77−89730
Te, piezoelectrical free-carrier scatt. by screw dislocations, Hall effect and cond. meas. 80−24926
Te, screw dislocation substruct. studied by torsion expt. 79−10859
Te, screw-dislocation-induced scatt. and acceptor states, galvanomag. and optical expts. 77−28142
Te single crystals, c screw dislocation prod. by pure shear deform. 77−81367
Ti, single crysts., recrystallised, X-ray topography obs. 78−10054
TiO_2 rutile single crystals, stoichiometric, dynamic strain ageing 80−50661
$TiS_{1.7}$, hexagonal polytypes form. mechanism 78−9990
$TiS_{1.7}$, screw dislocs., X-ray topography 77−47460
$(U,Pu)O_2$, thermal creep in 40 to 100 N/mm^2 stress range 77−28881
UO_2, thermal creep in 40 to 100 N/mm^2 stress range 77−28881
V, slip geometry and dislocation struct., rel. to degree and temp. of deform. *(Russian)* 78−38717
V, strain hardening, screw dislocations and microtwinning *(Russian)* 80−29971
V-Ta (5 wt.%), strain hardening, screw dislocations and microtwinning *(Russian)* 80−29971
W, screw dislocation motion, orientation depend., tight-binding type electronic theory 79−51109
W single crystal, creep, excess edge and screw dislocation density calc. *(Russian)* 78−34519
W, twinning dislocation, math. model 77−59024
WC grain, with grown-in stacking fault, contrast effects in electron micrographs 77−19959
Y_2O_3, plastically deformed monocryst., HV electron microscopy obs. of dislocation config. *(French)* 79−55747
Zn, basal dislocation−prismatic dislocation ring interactions by method of moments *(Russian)* 80−10550
Zn, dislocation damping on $\{\bar{1}2\bar{1}2\}\langle\bar{1}2\bar{1}\bar{3}\rangle$ slip system above Debye temp. 77−62538
Zn, line energy of basal screw dislocation, exptl. determ. 80−88154
Zn polycrystals, deformation, grain sizes effect at room temp. *(Czech)* 80−45359
Zn, pyramidal edge and screw dislocation mobility, compressional stress pulse technique 77−19957
ZnS crystal, inhomogeneous, microscopic struct. investig. using synchrotron radiation 77−76424
ZnTe:Ag, doped during frowth and by diffusion, defect form. 80−15129
Zr alloys, creep and growth, irradiation induced, microstruct. depend. 80−93602
Zr, creep, optical and electron metallographic anal., 473 to 873K 78−39986
Zr, irradiation growth, reaction rate theory calcs. 80−88212

scrubbing (abrasion) *see abrasion*

scuffing *see abrasion*

SDI *see information dissemination*

sealing *see seals (stoppers)*

seals (stoppers)
see also glass-metal seals
Araldite, high vacuum sealant at liq. N_2 temp. 80−57319
bakeable seals development for large noncircular ports on Tokamak fusion test reactor 80−82777
battery, secondary, using catalyst (gas recombination) plug system *(Japanese)* 79−83586
breeder reactor cover gas seals, design approach 80−47562
ceramic-metal seal technology, history and trends 78−81992
compression for high-pressure chemical apparatus, sealing characteristics determination *(German)* 78−21160
conical plug seals, plastic flow under pressure, tightness mechanism 78−54386
cryogenic flange connection 79−71460
cryogenic flange joint design and characteristics 78−86277
cryogenic-vacuum chamber, shaft seal method for rotation transmission 77−26314
Dependex fittings, modification for sealing with Cu 77−65040
Dewars, simple valve seal for vacuum space saving 77−5851
elastomer, easily demountable, for cryogenic appl. 79−207
elastomer, valves for high and ultrahigh vacuum 79−63246
elastomer seal for large toroidal vacuum chamber 80−27315
elastomeric seals for nuclear service, selection 78−46152
elastomers, vacuum compatible, chem. character correl. with physical charact., review 78−24804
elastometer materials, selection for vacuum seals 80−77797
electric lead-ins with composite seal for high pressure chambers 80−105665
electrically-insulating high-pressure seal for use at cryogenic temps 77−41633
far IR gas cell, high press., low temp. 77−30207
ferrofluid seal against liq. 80−57270
ferrofluids, application as seals 79−95609
ferromagnetic liquid seal, dynamic loading 78−62186
flexible plate sealing incompressible liquid, removal of anomaly in perturbation anal. 78−38201
friction-activated semi-demountable hermetic feedthrough seal 77−67452
fusion reactor, Demonstration Power Tokamak Reactor, vacuum outer containment and metal seals feasibility study 80−95458
fusion reactor, TFTR, large noncircular ports, development of bakeable seals 80−95454
gasket, large diameter elastic metal gasket for ultra-high vacuum flange connections 80−95106
glass and ceramic developments for electrical industry appls. 79−78925
glass-ceramic, annealing effect on internal stresses 80−40389
high speed vacuum seal 79−93151
high-pressure low-temperature seal, simple closure 78−4626
high-temp. metal foil, formed by seam welding 79−80597
hydrocarbon contamination, of vacuum dependent scientific instruments 79−63259
hydrostatic step seal, charact. of micropolar lubricant 77−86189
inlet for elec. conductor into high-pressure chamber 78−74016

seals continued
laser technology, parallel plate, polarisation problems obs. and solution 80−1225
liquid jet vacuum seal, inflow, rel. to electron beam emergence into atmosphere 80−78469
LMFBR, 1000 MW(e), selection of reactor cover seals and bearings 80−5219
LMFBR, equipment design, Na-NaK engineering handbook 79−97815
lubrication static contact shape and kinetic behaviour 80−97598
magnet spectrometer, QQDDQ Big Karl, cryopump system 79−63257
magnetic fluid, high-speed cryogenic for high-vacuum chambers 80−57314
magnetic liquid vacuum seals 79−63244
magnetic safety valve 80−8966
magnetofluid seals appl. to rot. cryostats 80−4721
metal hollow O-ring seal, for UHV and cryogenic use *(Japanese)* 80−22374
metal-seal valve for high radiation use in high vacuum 80−233
metal-sealed all-metal gate valve, design developments 79−63243
NMR sample tube self-positioning anti-vortex plug 77−21434
noble-metal tubes, cold-weld sealing 80−41556
nuclear facilities protection, tamper-indicating seal program development and implementation 79−85689
nylon chamber sealing for use at low temp. 79−6131
O-ring compounds, resistance to heat and ionizing radiation 78−29584
polyimide thin film gasket seal fabrication for ultrahigh vac. 77−57334
pressure-mode soft-metal vacuum seal, for glass and ceramics 80−17952
PTFE seal for superfluid He 78−4625
remotely operable large vacuum seals for fusion reactors 78−50405
rubber seal technology, advances 80−93730
self-monitoring, electronic 79−85690
semiconductor packages, hermetically sealed, calibration and anal. of moisture by gas mass spectrometry 80−90928
shaft seal, high-speed mag. fluid, heat dissipation 80−59032
short tube drawing from thin metal sheets 78−86248
sliding contact seal, thermoelastic instabilities 78−18257
strain gauge protection, sealants suitability determ. 78−4610
teflon rope, vacuum sealing material 80−98925
Teflon seals, spring-loaded, ultrahigh vacuum appl. 79−6133
Teflon superleaktight gasket seals for use at low temps. 78−16806
thermocouple installation in IR spectroscopy and reaction cells 80−57398
thermovacuum chamber, criteria for choice of elastomer seals 79−71466
trident, thermal expansion differential test 79−61815
UHV bakeable vacuum chamber, use of Al alloy *(Japanese)* 80−52248
vacuum, axial-rotation, for independent rotation of objects on common axis 80−31772
vacuum feedthroughs, coaxial and multipin, cryogenic performance 80−8995
vacuum grease, for analytical electron microscopy, reduction of contamination *(Japanese)* 80−11978
vacuum pressure, with thermomechanical drive of Ti-Ni 80−31773
vacuum seal, demountable, for low temp. conditions 77−45857
vacuum seal, demountable, operating at low temps. 77−67445
vacuum seal between stainless steel and Al_2O_3 ceramic, bakeable and moveable 79−35767
vacuum seal design, construction and application 80−82780
vacuum seal for 5000 r.p.m. rotation 77−53923
vacuum seals, Cu-ceramic, metallisation process 80−37046
vacuum system, break-seal shattering, novel method 78−41322
very high vacuum appl. of field electron emission gauge 79−71476
Al windows, unbacked, for He discharge lamps directly mountable as part of Cu seal between UHV flanges 79−97397
Al wire gaskets for demountable, bakeable ultrahigh vac. seals *(Japanese)* 79−93154
Al_2O_3-glass seals, diffusion of Al, electron microprobe study 80−107577
As_2S_3 thin films, vacuum deposited on Ge and PbS, sealing props. and TEM 80−35097
BaF, CaF windows, process for vacuum tight joints prod. 77−26312
In seal fabrication by prepressing 80−101800
In solder joints, thermal conductance at low temps. 77−30150
Mo-Mn-Fe-Si/Al_2O_3 ceramic seal, interfacial phases 78−72011
PbF_2, use in vacuum sealing LiF window to Au or Cu thin-walled cylinder 77−54820

seawater
abyssal shear zone east of Newfoundland Ridge, temp., salinity and nephel meas. 78−73386
acoustic absorption, chemical relaxation studies using resonator method 80−96073
acoustic attenuation due to chem. relax.-absorpt. 79−34851
acoustic nonlinearity parameter meas., comparison with distilled water 78−75727
acoustic wave scattering by sea surface, props. *(French)* 80−53502
acoustical props. of laboratory sediments, temp. variation 80−96069
Adriatic Sea, chem. parameters, spring and winter time obs. 80−41447
N.Adriatic Sea, trace element analysis by neutron activation 77−21801
alpha and beta radioactivity meas. *(Rumanian)* 77−49067
amino acid formation in ultrasound in water masses of primordial Earth 77−37409
analysis, Schales and mercuric nitrate methods *(French)* 77−78432
Antarctic Circumpolar Current S of Australia, cyclonic eddy obs. from R/V Professor Zubov 79−48500
Antarctic Intermediate Water in SE.Pacific and S.Atlantic 80−36306
Antarctic Ocean, ^{226}Ra distrib. 77−5220
Antarctic surface water, glacial ice melting effects 79−34866
Arabian Sea, hydrochem. and hydrographic features of northern basin 77−41059
Arabian Sea, inorganic N system equilib. 77−41060
Arabian Sea, inorganic phosphate distrib. during SW monsoon season 77−41061
Arabian Sea, trace metal content obs. and marine chem. 80−56495
Arctic fjord, mixing 79−48504
N.E.Atlantic, heavy metals and petroleum products 78−3827
Atlantic, particulate I distrib. 77−5237
N.Atlantic, sea surface temp. year to year changes, (1948 to 1974) 80−67367
W. Atlantic abyssal waters, ^{14}C distrib. 77−5228
N.Atlantic deep water, production since Miocene, sediment evidence 80−46186
E.Atlantic Ocean, 23°N to 47°N, dissolved Cu concs. 77−5239

seawater continued
Atlantic Ocean, ^{226}Ra distrib. 77−5219
Central Atlantic Ocean, results of underwater irradiance meas. *(Russian)* 78−77257
S.Atlantic Ocean, sea water hydroptic struct. variability *(Russian)* 78−77262
Atlantic surface particulates, composition, settling rates and dissolution in deep sea 77−5236
N Atlantic water columns, trichlorofluoromethane (F-11) exploratory anals. 78−88847
attenuation matrix photometer *(Russian)* 77−78453
bacteria, attachment to solid surface, influence of substratum critical surface tension 79−79493
SE.Baltic coast transit section, suspended load composition in calm and storm *(Russian)* 80−67360
Baltic Sea, density meas. 77−56635
Baltic Sea, P, N and organically bound C conc. annual vars. 77−49084
Baltic Sea, salt transports determ. from conservation calculations in natural coordinates 80−51433
Baltic Sea Basin, suspended matter, quantitative distrib. and comp. 77−21783
Baltic Sea inshore waters, light scatt. matrices *(Russian)* 77−29311
E.Baltic upper shelf suspended matter distribution and structure *(Russian)* 78−36187
banded salt finger structure, form. 78−85570
basalt alteration, radioactive disequilibrium 78−96186
basalt-seawater alteration reactions, studies via dynamic hydrothermal experimental system 79−5686
basalt-seawater interaction, trace element and Sr isotopic vars. in glassy basalt 80−8286
Bay of Bengal, total N and P determ. 78−81213
Black Sea, F content 78−32118
Black Sea, H_2S and O_2 zone boundaries rel. to water mass dynamics *(Russian)* 80−12435
Black Sea upper layers, temp./salinity anal. of seasonal vars. *(Russian)* 78−77264
Bombay coast region, water pollution physicochemical studies 80−104522
bottom boundary layer of deep ocean, short-term variability 79−2269
bottom nepheloid layers and bottom mixed layers, obs. on continental shelf off Oregon 78−16027
boundary layer during evaporation, optical interferometry *(Russian)* 80−61919
brass, admiralty, dezincification conditions in fresh or seawater, thermogalvanic method 80−16548
bromide determ. using bromide ion-selective electrodes 78−3996
bubble populations in coastal waters, photographic analysis 79−100849
bulk viscosity and l.f. sound attenuation, Be and B influence 77−3696
S California coastal waters, Ba as pot. indicator of marine drilling contamination 77−2180
E.Canadian Arctic, sea ice meltwater, isotope study 80−77002
Canaries Current eastern branch, density-depth relation rel. to current tidal component *(Russian)* 78−77263
Cariaco Trench, temp. salinity and chemistry 80−98359
NW.Caribbean, methane content of deep water indicating seepage 80−81924
E.Carribean, deep water silicate content distrib. 80−76984
catastrophic chemical events, ^{34}S rises 77−56645
cathodic protection in seawater, sacrificial anode performance 79−57246
Chesapeake Bay, water surface laser radar refl. as function of wind speed 77−41034
chlorinated, sunlight-induced bromate form. 77−49088
chlorinity and salinity determ., possible use of neutron methods *(Russian)* 78−65422
chlorinity determination, appl. of gamma-radiation from neutrons radiative capture *(Russian)* 78−77360
chlorophyll *a* fluorescence sensing, sunlight penetration depth estimation 79−79874
chlorophyll concentration, estimation from outgoing radiation spectrum meas. from helicopter 80−36333
coastal submarine hydrothermal activity off northern Baja California 78−61431
coastal zone, particulate U, Pu, and Po in biogeochemistries 79−29787
Cochin backwater, India, estuarine water, particulate heavy metal content 80−7964
Cochin Harbour mouth, India, hydrographic characts. and tidal prism 80−41452
colorimetry using Technicon Autoanalyzer II, systematic absorbance errors 79−21802
complex permittivity meas. at microwave, method 77−45184
composition, correl. with water-rock partition coeffs. 79−44200
composition rel. to atmospheric CO_2 evolution through geologic time 78−73515
concrete, cracking in seawater due to embedded metal corrosion 80−30116
conductivity/temperature/pressure profiler errors 77−5377
Connecticut River offshore plume, motion field obs. 77−33111
convection of fluid cooling from surface *(Russian)* 80−1582
convective fluxes, temp. and salinity from atm. obs. 80−104986
cooling through free surface, critical value of boundary Rayleigh number *(Russian)* 78−61426
coral reef water, O isotope composition rel. to evaporation and precipitation 80−46202
corrosion of Cu, hydrostatic pressure effects 79−52420
corrosion protecting, of Be-Cu alloy, for repeater housings 78−15583
crystal unusual growth 80−26516
Cs accumulation in muscle tissue of marine fishes 80−35797
current measurement from a surface following data buoy 79−84290
Dead Sea rift valley, Sr behaviour in subsurface $CaCl_2$ brines 80−17295
deaeration procedure for conducting electrochemical expt. 79−29366
deep ocean, salinity and pot. temp. profiles rel. to boundary mixing 78−73388
deep ocean, temp. fine struct. rel. to internal gravity waves and wave breaking 78−85578
deep Sargasso Sea, organic carbon flux at 3.2 km, annual variation 80−41460
deep water density, N. Atlantic and N. Pacific 77−5208
deep water formation in N.Atlantic during last ice age 80−94535
density, dependence on temp., salinity and press., math. expressions 80−94540
seawater continued
density, vertical structure meas. using optical interferometry *(Russian)* 80−51569
density determ., active nuclear methods appl. *(Russian)* 79−39902
density determ. using gamma radiation *(Russian)* 77−82037
density large-scale anomalies, non-linear evolution *(Russian)* 79−16479
density maximum points meas. 78−57900
density meas., Mediterranean Sea samples 79−5486
density relation for pure and saline comp. 78−2185
density vertical struct. influence on dynamics of small basins, Adriatic sea appl. 78−53654
density vertical vars., review of math. models 78−49022
desalination by wind power, anal. 80−108781
desalination plants using simplified nucl. reactor 78−13315
determ. in coastal sediments and seawater, activity ratios, disequilib. 78−27851
dielectric constant at microwave freqs., improved model 77−17113
dielectric permeability calculation, algorithm *(Russian)* 78−77261
differential isothermal compressibility meas., hydration and ion-water interactions 77−73761
diffuse irradiance refl., two flow model 77−29301
dimethyl sulphide in seawater rel. to S budget 78−96237
dissolved and particulate organic material meas. using automatic sampling buoy 78−49149
dissolved free amino acids, concs. in seawater rel. to organic pollution 78−44883
dissolved gases comp. determ. using hermetically sealed sampler-degasser 77−49191
dissolved I in Yarra River estuary water 79−34855
dissolved O determ., comparison of polarographic electrode and Winkler tritration determ. 77−70848
dissolved O studies using electrochemical meter *(Russian)* 77−78227
dissolved organic Fe, determ. in seawater 78−81208
dissolved organic matter, fluoresc. spectra *(Russian)* 77−13083
dissolved trace gases in tropical Pacific 80−41509
electric conductivity meters with automatic correction of characts., seawater appl. *(Russian)* 78−65426
electrical conductivity and salinity, temp. and press. depend. 80−67368
electrical conductivity compared to KCl standard solution, salinity scales 80−72646
electrical conductivity meas., var. with temp. 78−20531
electrical energy tapping 79−5504
electrochemical potential of pure metals *(Chinese)* 80−31062
electrolysis, for H_2 and O_2 prod. 80−30435
electrolytes partial molal vol. estimation, specific interaction model 77−60429
electrolytic dissociation, utilisation of ocean hydropower systems for H prod. 80−30374
EM properties, at frequencies below 1000 GHz, various Earth surface forms 78−24310
EM waves, review 77−49082
energy-extraction, from warm surface waters 79−83577
equation of state, use for PVT props. of lake waters 77−49095
equation of state at high press. 80−101369
equation of state for bounded depths *(Russian)* 77−60424
equation of state for open ocean salinity, temp. and press. ranges 77−66922
equatorial Indian Ocean, seasonal temp. and density fields caused by monsoons *(Russian)* 78−44839
estuaries, very low salinity regions, chemical and biological reaction sites 78−81199
estuary halocline, expt. simulation, salt diffusion in tap water, educational aspects 78−61980
evaporation variation with salinity and temp. 77−53083
flow, vertical boundary layer convection, salinity and press. depends. 79−37316
fractionally charged particles conc. in large samples of matter *(Russian)* 79−88341
freezing, induced haline convection expts. *(Japanese)* 78−88843
freezing point depend. on salinity 78−3803
Galapagos Rift, submarine thermal springs 80−8295
Galapagos Rise hot spring field, water natural radionuclides ratios rel. to clam growth rate determ. 79−84300
gamma radiation field of seawater and atm. surface layer rel. to cosmic ray neutrons *(Russian)* 79−39746
Golf of Fos and Canal Caronte, seawater physical and chemical characts. 78−44877
Guaymas Basin, ^{3}He meas. rel. to mantle volatiles injections in Gulf of California 80−85640
NE Gulf of Alaska, processes affecting suspended matter distrib. and transport 80−12398
W.Gulf of Maine, current, temp. and press. obs. rel. to winter circulation 80−51430
N.Gulf of Mexico, anoxic hypersaline basin 77−86936
Gulf of Mexico, aromatic hydrocarbons concs. in seawater at proposed deepwater port sites 78−44880
Gulf of Taganrog salinity, after restriction of exchange with Sea of Azov 80−36335
Gulf Stream ^{14}C concs., determ. from annual coral rings. meas. in Florida 79−16513
hydrocarbon pollution detection, caution on use of Niskin sampling bottles 78−45039
hydrochemical structure in NE tropical Atlantic *(Russian)* 80−17284
hydrographic data, appl. to current flow vel. determ. 80−17415
hydrological and biological characteristics, statistical relationships with transparency field *(Russian)* 79−88361
hydrothermal alteration of basalt by seawater, chemical exchange exptl. results 79−20828
hydrothermal sulphide deposits in Cyprus, ^{87}Sr enrichment confirms ore form. by circulating seawater 77−81887
hydrothermal water in Galapagos, excess ^{3}He and ^{4}He 78−40593
ice melting model, appl. to Antarctic ice shelf and icebergs 80−4036
ice nuclei off Nova Scotia coast during 1975 Summer 78−16104
Iceland high-temperature geothermal systems, seawater aquifer chemistry 78−96245
ignimbrite/sea water explosions, volcanic ash generation 80−26480
N.Indian Ocean, dissolved petroleum content 80−98361
Indian Ocean, Pacific water incursion 79−16511
Indian Ocean floor, geothermal convection through oceanic crust and sediments 79−79812

seawater continued
inert gases dissolved in seawater rel. to hydrophysical studies *(Russian)* 77−60425
inherent optical props. rel. to Secchi depth 79−16472
IR relative reflectance spectra and complex refractive indices, meas. 77−45013
Ireland west coast, surface waters colour, UV absorbance and salinity 78−85603
Irish sea, Pu oxidation state 79−16516
irradiance attenuation coefficient in a stratified ocean, meas. technique 80−98325
isolation of humic substances and alcohol soluble organic matter 77−64448
isotopic cycle of oceanic phosphate 77−5232
Java, East China and South China Seas, seawater optical props. 77−21792
jet drops from bubbles bursting in seawater, ejection height rel. to organic material 79−39727
Knudsen-Ekman equation of state, possible replacement 77−33083
Kuroshio jet current system region, density field calc. 78−92843
Laccadive Sea, chemical oceanography 80−104995
Laccadive Sea, trace metals concs. 80−104997
Laccadive Sea (Lakshadweep), physical charact. 80−104966
Laccadive Sea waters, total Hg concs. 80−104996
laser sounding method and equipment for water absorpt. and attenuation coeffs. meas. *(Russian)* 79−34998
laser velocimeters appl. to ocean meas. 78−36325
layer 2, geochemistry of secondary minerals in basalts from (DSDP Leg 37) 77−91127
light attenuation index meas. errors *(Russian)* 78−16041
light field rel. to hydro-optical charact. *(Russian)* 80−17279
light scattering, Henyey-Greenstein indicatrixes *(Russian)* 77−60411
light scattering by particles of different shapes 78−40565
light scattering obs. in frontal zones 79−2266
light scattering props., statistical and physical models *(Russian)* 78−96222
light scattering rel. to size distrib. determ. of spheroids *(Russian)* 78−36279
low-temperature alteration of oceanic layer 2 basalts of (DSDP Leg 37) 77−91102
low-temperature interaction with basalt, effect on S distrib. in oceanic crust layer 2 80−41432
Mangalore coast, India, 1976-7 nearshore water conditions 80−8315
old Mangalore port, seasonal vars. in estuarine and oceanic waters hydrographic conditions 80−41451
Marianas Trench, Pacific Ocean, water charact. meas. at depths >10 km 78−61423
marine aerosol, Bermuda, alkali and alkaline earth chemistry 77−70727
marine aerosol alkali and alkaline earth metal chemistry 77−70726
marine boundary layer, optical beam propag., analytical model 80−8329
marine sediments interstitial solns. comp. and diagenesis, seawater-sediment interface fluxes 80−3988
Mediterranean Sea, heat and water budgets, dependence on climate and Atlantic waters 79−84291
E.Mediterranean Sea, later Quaternary density stratification rel. to Ionian Sea sapropels 78−73350
E.Mediterranean Sea, T and O_2 profiles 80−17298
Meditteranean water, identification in intense mesoscale eddy off Bahamas 79−74902
metal transport in hot seawater rel. to Cyprus sulphide ores 77−44997
microscale studies of vel., temp. and cond., stable platform development 79−5669
microwave attenuation by salt water droplets 78−7725
microwave meas. of reflectance, at 100, 140 and 180 GHz 79−84552
mixed salt solution approximating seawater composition, dielec. and radiation charact. 80−97184
multilayered stratified flow investigation *(Russian)* 80−1703
multiradionuclide analysis, ^{134}Cs, ^{137}Cs, ^{210}Pb, ^{226}Ra and ^{228}Ra concs. determ. 79−88370
Narragansett Bay, USA coast, natural radionuclide content 80−12399
neutron activation analysis of Cr after preconc. on activated C 78−3993
North Sea, N_2O, ^3H, chlorofluoromethanes and salinity vertical profiles meas. *(German)* 78−3814
North Sea, sea surface temp. year to year changes, (1948 to 1974) 80−67367
North Sea and Baltic pollution, natural and man-made influences *(German)* 79−5508
nutrient-rich seawater, artificial upwelling induced by ocean currents 78−81217
ocean basalt reactions, chemical exchange, Fe, Mn and S species results 80−17294
ocean floor spilites, seawater/basalt ratio effects on chem. and mineralogy 78−92819
ocean optics, conf. proceedings (San Diego, 30-31 August 1978) 80−8325
ocean thermal energy conversion systems 79−29456
ocean thermal energy conversion to electricity *(French)* 80−21389
ocean upper mixed layer, temp. and heat storage inference from Landsat data 79−100869
oceanic finestructure, wave-induced and intrusive structs. separation 79−48502
oceanic fronts, optical and particulate matter properties 80−51418
oceanic residence times of trace metals, river discharge effects 77−78228
oil conc., continuous meas. by towed fluorometer 80−45846
oil contaminations on sea surface, radar detect. *(Russian)* 77−49089
oil migration, mixed Lagrangian-Eulerian model 80−45830
oil pollution, review of effects on water and marine life *(French)* 79−48193
optical anisotropy coeff., temp. fluctuation, optical meas. method 78−69488
optical classification using solar radiation spectral attenuation meas. 79−12127
optical coherence loss meas. in Atlantic coastal waters 80−8333
optical props. in region of large variability 80−8327
optical structure in S.anticyclonic gyre *(Russian)* 79−100866
optical transfer function meas. in Sargasso Sea 80−8328
organic chemistry of particulate matter 78−65344
P-V-T props. calculated from US derived eqn. of state 79−25264
NW.Pacific, ^{226}Ra, ^{210}Pb and ^{210}Po disequilibria 77−5227
E.Pacific, Ra and Th isotopes in surface waters 78−96234
N.Pacific, size distrib. of suspended particles in surface water 80−4047

seawater continued
Pacific deep waters, mineralogical and radioisotope studies 77−5235
Pacific equatorial zone, water transparency *(Russian)* 78−16043
Pacific Ocean, computerised high-precision titrations of major constituents 77−66926
Pacific Ocean, December sea surface temps. correl. with spring rains in California 80−77064
N.E.Pacific Ocean, deep water ^{226}Ra maximum 77−5221
Pacific Ocean, Mn distrib. 80−56494
E Pacific Ocean, surface temp. annual development in Panama Gulf and coast *(French)* 77−17109
E.Pacific Ocean, tropical, N_2O meas. in sea water and marine air 80−94542
N.Pacific Ocean, west, depth, var. of temp., salinity and sound vel. meridional gradients 80−51429
equatorial Pacific Ocean, XBT sections and sea level meas. rel. to currents strength monitoring 78−73383
N Pacific Ocean waters, density 78−73391
Pacific Ocean waters, nitrate N distrib. 80−31065
E.Pacific Rise, hot springs and geophysical expts. 80−101360
E.Pacific Rise, hydrothermal vents on seabed issuing H_2 and methane 80−41422
E.Pacific Rise geothermal system, physical limits on geothermal fluid temp. and role of adiabatic expansion 80−101362
Pacific surface waters, ^{210}Pb and ^{210}Po distrib. 77−5226
paint coatings, corrosion fatigue resistance *(Russian)* 77−59979
palaeosolinity determination, implications of B loss from shells during weathering 77−78204
palaeotemperatures, determ. from larval bivalve shell morphometry 79−53510
particulate Mn over Galapagos Spreading Centre, hydrothermal source 79−39699
penetration imagery, surface/depth data separation by multispectral scanning 78−69539
permittivity at microwave freqs., modelling 77−25690
permittivity at mm wavelengths 80−66098
petrols, optical consts. in 0.25 to 25 micron region, sea pollution detection appl. *(Russian)* 78−76976
pH, effect on low-freq. sound absorpt. 77−49072
phosphate budget, P accumulation rates in metalliferous sediments on E.Pacific Rise 77−60364
photographic film, exposure while immersed in seawater, effects on props. *(Russian)* 77−79180
pollution, industrial waste dispersion meas. technique 78−44884
pollution by dinitrotoluene isomers, occurrence and determ. in seawater 80−7966
pollution studies, laser appls. *(Polish)* 78−20528
potential temp. calc. for arbitrary reference press. 77−73746
potential temperature calc. from effect of pressure on entropy 79−74897
Practical Salinity Scale 1978, for in-situ meas. of seawater 80−67419
predominance-area diags. and equilib. ratios for Co and Ni inorganic forms 78−3819
purification, method for obtaining Si-free and PO_4-free water 78−3817
quality instrumentation system test 77−41066
quarks, search for occurrence in seawater, ocean sediment deposits and volcano lava *(Russian)* 77−64288
radiative transfer in atmosphere-ocean system, matrix operator approach 80−8330
radiative transfer in turbid water 80−8331
radioactive contamination, rapid determ. of levels of ^{54}Mn, ^{59}Fe, $^{58,60}Co$ 78−85608
radioactivity of advected water masses, calc. from salinity meas. *(Russian)* 78−77275
radioactivity-salinity correlation *(Russian)* 77−78199
radiobiological protection aspects *(French)* 78−11744
radionuclide distribution among green alga, marine sediments and sea water 78−53534
radionuclide migration in seawater and marine sediments *(French)* 78−11916
rain-formed mixed layer 80−36323
reaction with Amazon suspended sediments, cation exchange charact. 80−8337
Red Sea brines, evidence for mantle He content 77−25693
Red Sea brines origin, new isotopic evidence 78−96236
REE data and Fe formations 79−66715
refractive index microstruct. from diffusive and turbulent ocean mixing 80−56486
refractive microstructure from diffusive and turbulent mixing 80−8326
relative conductivity and density of standard seawaters 77−64296
rocks hydrothermal alteration, rel. to Michigan deep hole metagabbro mineralogy and geochemistry 79−39710
Ross Ice Shelf, circulation and melting 79−88363
Ross Ice Shelf sea temperatures 79−88362
Saguenay Fjord, suspended particulate matter geochemistry 78−92852
saline water trace element analysis problems 78−45051
salinity, meas. via microwave radiometry 78−81416
salinity and density from gamma-ray attenuation *(Russian)* 79−39897
salinity and temperature meas. using bathometer sonde 77−78480
salinity calc. in estuary, semiempirical turbulence theory appl. 79−57967
salinity determ. from sound vel., measurement errors 77−70679
salinity measurement, elec. cond. obs., temp. and conc. depend. 80−67421
salinity of standard seawater, elec. cond. compared to KCl soln. 80−67420
salinity of standard seawater, elec. cond. obs. 80−72647
salinity of standard seawater, elec.cond./salinity/temp. relations 80−67422
salinity rel. to specific electrical conductivity and temp. *(Russian)* 78−16039
salinity standard, definition and calc. 78−40687
salt analysis of seawater by neutron activation *(Russian)* 79−39898
salt finger size and shape near marginal state 77−17122
salt mixing, double-diffusive intrusions into density gradient 78−85569
Santorini area, neutron activation trace element anal., role of Ge(Li) high-resolution detector 77−56324
Sargasso Sea, hydro-optical study *(Russian)* 78−85594
Sargasso Sea, narrow warm water tongue intrusion obs. using satellite and in situ data 78−73382
Sargasso Sea, optical props. of seawater *(Russian)* 80−94532
scalar quantity, conservative, undergoing advection, time-depend. 79−48507

seawater continued
sea and beach persistent oil spill identification methods 80−90101
seawater density determ., possible use of beta-emitting radioisotopes *(Russian)* 78−65423
sediment-water interface in coastal zone, chem. exchange traced by ^{222}Rn obs. 80−101386
self-diffusion coefficient for water molecules (1 to 7000 kg/cm^2, 0 to 60°C) *(Russian)* 77−64291
shelf sea fronts adjustments, results from satellite IR imagery 79−92545
side convection characteristics *(Russian)* 80−1580
silicates dissolved in deep water of Bering Sea 80−31061
sound absorption, theory 78−1481
sound absorption contour chart for Atlantic, Indian and Pacific Oceans 80−36303
sound absorption in seawater, borate-complex relaxation 80−36304
sound speed eqns. for varying salinity and temp. 78−81193
sound speed in seawater at high press., meas. 78−13837
sound vels. in sea salts at 25°C 77−84042
south-east Baltic Sea silt granulometric and mineral composition *(Russian)* 79−96755
St. Lawrence Estuary, inorganic B content determ. *(French)* 78−77274
standard seawater, preparation and chlorinity calibration 79−74898
standard seawater as elec. cond. standard, reliability 79−29779
standards, history 79−79871
stanol/stenol ratio control process in Black Sea water and sediments 79−92549
steel, notched specimens in sea water, endurance limit enhancement, specimen size, freq. effects 80−93678
steel, structural, notched, cathodic polarisation effect on fatigue in seawater 79−47805
subantarctic intermediate in S.Atlantic *(Russian)* 79−100865
sulphate concentrations, indirect anals. by atomic absorpt. 80−89556
sulphate reduction and marine sediment deposition rate 78−53642
sunlight polarisation, reflection, and biological effects 77−56648
surface charge 80−36331
surface current probes, rapid method for data recovery 79−84518
surface IR emissivity, meas. of vars. *(Russian)* 77−60384
surface microlayer, ^{210}Pb and ^{210}Po enrichment obs. 80−56496
surface microlayer chemical composition *(Russian)* 80−104998
surface particulates, Atlantic and Pacific Oceans 77−5234
surface particulates, minor metal content 78−92853
surface pollutants, microwave detect. of adsorpt. and spreading films 79−5690
surface salinity, mean annual var. in Baltic Sea *(German)* 79−62521
surface temperature, appl. in climate change predictions 80−8377
surface temperature, influence of mesoscale eddies *(Russian)* 78−81191
surface temperature, meas. 200 km from land rel. to air-sea heat transfer coeffs. 80−72552
surface temperature, response to vars. in atmospheric wind forcing 79−48505
surface temperature (SST), NOAA-4 data time series anal. 79−53364
surface temperature contouring, appls. of satellite ocean-related imagery programme 79−5681
surface temperatures in shallow seas, 18.6 year cycle due to tidal mixing vars. 78−73387
surface tension, effect on development of waves from periodic disturbances in non-uniform fluid *(Russian)* 78−77253
surface water, remotely sensed by microwave radiometry 80−36428
surface water masses, marine plankton C isotope ratios 79−29783
suspended heavy metal compounds 79−74904
suspended material concentration, estimation from outgoing radiation spectrum meas. from helicopter 80−36333
suspended matter, trace metal chemistry, atmospheric input 79−44199
suspended particle size distrib. shape stability in Baltic sea 79−79876
suspended particles, rel. to chem. processes in Atlantic and Pacific oceans 78−36201
synthetic, solubilities and activity coeffs. of $CaSO_4$ and $SrSO_4$ 79−91986
temperature, meas. via microwave radiometry 78−81416
temperature fluctuations, small-scale, in upper ocean layer, statistical regularities *(Russian)* 80−94528
temperature gradient meas., anal. of two methods 80−31149
temperature meas. by enhanced IR satellite imagery 77−37422
temperature vertical gradients, meas. via moored vector averaging current meters 80−12561
thermal energy conversion programme, review 79−92066
thermodynamics at one atmosphere pressure 77−17108
thermohaline intrusions lie across isopycnals 79−84289
trace element estimation using radioactive ^{14}C *(Dutch)* 77−29459
trace element meas. by neutron activation and atomic absorption methods *(French)* 77−41238
trace elements determination using routine neutron activation analysis 78−3992
trace metal composition of N.Pacific, Cd, Ni, Cu, Cd vertical profiles 80−67381
trace metal composition using microprocessor-assisted flow-through anodic stripping voltammeter 78−36324
transfer matrix elements of scattering medium *(Russian)* 78−36181
transition metal, determination in estuarine and sea water by at. absorpt. spectra 79−74557
transmission props. for underwater laser communication 80−33069
transparency, rel. to hydrochemical charcts. distrib. 80−31057
transparency at 30 m depth in tropical Atlantic *(Russian)* 77−64307
transparency meter, Se photocell device, for biological activity 80−8442
Tunis Strait area, carbonate system elements 77−53075
turbid, vol. scatt. function and light field charcts. *(Russian)* 79−13902
underwater irradiance in Norwegian and Barents Sea, relation to water temp. 80−31055
underwater light field, scatt. light influence anal. 77−64322
upper ocean temperature and salinity structure, obs. during POLE expt. 80−72536
US east coast isotopic composition rel. to salinity, river runoff contrib. 79−100879
Velsao and Colva beaches, Goa, India, water quality charcts. 78−81218
vertical buoyancy flux, atmospherically induced 80−4039
vertical eddy viscosity, effects on Rossby and Eady waves 80−51404
visible light refl. and scatt., utility of polarisation in oceanographic remote sensing 79−5498
warm front, oceanic, propagation, theory with appl. to Sagami Bay Kyucho phenomenon 80−94538
water, fluorometric dye meas. background variation expts. 80−45844
seawater continued
wave energy conversion, using half-plane and omni-directional convertors 79−52875
Weddell Sea, bottom water origin, chem. tracer considerations 80−76982
Weddell Sea, bottom water variability 80−67366
γ-ray field of seawater, meas. method *(Russian)* 80−109268
Al conc. from clay minerals dissolution 77−66928
Al concentration and distrib., control by biological activity 78−61437
Al content controlled by inorganic processes 80−61815
Al-air, seawater activated secondary cell 80−26128
^{26}Al in seawater rel. to oceanic residence time of dissolved Al 79−34856
Am, vertical distribution in Mediterranean Sea 79−84301
As distrib. and speciation in natural waters and marine algae 78−81210
Ba concentrations, at GEOSECS stations in Atlantic and Pacific, comparison with ^{226}Ra 77−5222
Ba, non-conservative behaviour during mixing of Mississippi River and Gulf of Mexico waters 78−32120
^{10}Be in seawater rel. to oceanic residence times of dissolved Be 79−34856
CO_2 content, gradual increase 79−29786
CO_2 equilibrium partial pressure, temp. coeff. 79−74903
CO_2 increase, direct obs. 79−34854
CO_2 solubility temp. coeff. in ^{13}C air-sea interchange calc. 80−61814
CO_2 solution in ocean surface waters, role of homogeneous buffer factor 80−21783
^{14}C distribution, Ross Ice Shelf Project ice hole 79−88371
Ca^{2+}, total activity coeff. determ. 80−31064
$CaCO_3$ and scale formation on OTEC heat exchangers 80−41461
Cd, determ. in sea and fresh waters, interlaboratory comparison 78−81209
Cl, Br content, origin by continuous mantle fluxing 78−65342
Cl disappearance meas. 79−88372
Cl, residual, in saline cooling waters, determ. via modified amperometric membrane probes 80−82112
Cr-Ni-Mo steel, low-cycle fatigue in sea water, mechanism *(Russian)* 77−59970
$^{137}Cs/^{134}Cs$ radioisotopes in seawater, Cs-selective resin determ. 80−94137
Cu, effect of addition of bromides and iodides on corrosion in seawater 78−80670
Cu, inorganic speciation in estuarine environments 78−69371
Cu-Al-Ni-Fe system, corrosion behaviour in sea water 80−45421
Cu-Ni alloys 706 and 715, corrosion in flowing seawater, O_2 effect 79−43460
Cu-Ni(10 (30) wt.%), seawater corrosion rate meas., electrochem. method validity 80−45426
F conc., potentiometric determ. 78−3820
Fe, conc. determ. by graphite furnace atomic absorpt. spectroscopy 80−40768
Fe-(ni), influence of Ni content on seawater corrosion props. *(German)* 80−35370
H isotope exchange between clay minerals and seawater 78−69329
H_2 conc. in near-surface air and dissolved in seawater, tropical N.Atlantic 79−39729
H_2 dissolved in N.Atlantic surface water, interchange with air 80−77057
H_3BO_3 evaporation from seawater, major source of atm. B 79−2293
HCO_3 apparent dissociation consts. 77−5238
H_2S, dissociation 78−3816
^3H, conc. in atmospheric precip., rivers, and seas, USSR 79−74560
^3He distrib. in deep water over Mid Atlantic Ridge 77−5242
^3He excess in Mid-Atlantic Ridge bottom waters, hydrothermal activity 80−101383
Hg determ. in sea and fresh waters, interlaboratory comparison 78−81209
Hg, determ. in sea and inland waters, differential pulse anodic stripping voltametry method 77−70361
Hg determination, error anal. 78−69519
Hg, dissolved, conc. determ., automated UV digestion-AAS method 78−44414
Hg, in fish and waters of Irish Sea and other United Kingdom fishing grounds 78−36204
Hg, neutron activation anal. for low levels in water 79−70503
^{203}Hg, tracer for Hg conc. in seawater expts., ^{75}Se tracer 80−21420
K determ. using selective membrane electrode 79−53368
KCN, determination in seawater *(Chinese)* 79−52966
Mg-noble metal, sintered, superconducting for heat and H_2 gas generation, seawater reaction 78−15607
Mn conc. and balance, surface samples 78−3815
Mn, conc. determ. by graphite furnace atomic absorpt. spectroscopy 80−40768
Mn determination in environmental waters by neutron activation anal. 79−74584
Mn diffusion-controlled fluxes, rel. to deep-sea nodules growth model 79−2212
Mn dissolved in NE.Pacific water 80−101384
Mn, hydrothermal, in deep sea, scavenging residence time and $Mn/^3He$ relationships 78−32121
NO_2^-, photolysis as source of free radicals in productive surface seawater 79−62522
N_2O composition of Pacific surface water 80−51519
NaCl, monoelectrolyte, highly mineralised salt soln., dielec. and radiation charcts. 80−97184
NaCl, solution, seawater, with trace quantities of Cs, adsorption behaviour on paper *(Russian)* 77−73766
Nd isotopic composition of sediments of different oceans 80−21704
Nd, Sr isotopic ratios, rel. to island arcs sources 78−32044
O isotope comp. of water in Sea of Azov 77−49083
O isotope fractionation in dissolved O in the deep sea 77−5231
O isotopes exchange with oceanic crust, results from (DSDP Leg 37) 77−91072
O_3 oxidation of Br, Cl and organic C 79−16518
^{231}Pa, determ. in coastal sediments and seawater, activity ratios, disequilib. 78−27851
^{210}Pb, particulate and soluble activities in the deep sea 77−5223
$^{210}Pb/^{226}Ra$ and $^{210}Po/^{210}Pb$ disequilibria in seawater and suspended particulate matter 77−5224
Pu, vertical distribution in Mediterranean Sea 79−84301
^{226}Ra concentrations, at GEOSECS stations in Atlantic and Pacific, comparison with Ba 77−5222

seawater continued
^{222}Rn in Hudson River estuary, distrib. and transport across sediment-water interface 78−16064
SO_2-seawater, thermodynamics 77−52660
SO_4/Cl ratio in Ionian Sea coastal waters *(Italian)* 79−5499
$^{33}S/^{32}S$ ratio in ocean water SO_4^{2-} 78−65340
Se (−II,0), -(IV) and -(VI) composition of water, by gas chromatography method 80−81928
^{75}Se, tracer for Se conc. in seawater expts., ^{203}Hg tracer 80−21420
SiO_2, dissolved silica content over opaline sediments 80−51419
Sr isotopic composition, comment 77−29323
$^{87}Sr/^{86}Sr$ ancient seawater composition, Jurassic to Pleistocene, Israel groundwater obs. 80−61804
$^{87}Sr/^{86}Sr$ ratios of interstitital waters from DSPD sites rel. to sediment geochem. 79−34794
T distribution, Ross Ice Shelf Project ice hole 79−88371
T in Arctic Ocean and East Greenland Current surface water 77−5230
T in deep N.Atlantic current, from weapons tests 80−101380
^{234}Th removal from Funka Bay, Japan 80−61803
U complex, binding, by brown coal, from seawater, IR spectroscopic obs. 78−82855
U conc. and $^{234}U/^{238}U$ activity ratios in open ocean 78−36197
U determination in environmental waters by epithermal neutron activation 79−53010
U determination in sea water by preconc. on Chelex 100 and neutron activation 79−53009
U exchange during low-temp. alteration of oceanic basalt 79−29744
U extraction, around British coastal power stations 78−21788
U extraction, by sorption techniques 79−29902
U extraction, tests of adsorbents 78−36198
U extraction from seawater *(Japanese)* 78−36199
U, extraction from seawater by polymer-bound macrocyclic hexaketone 79−92052
U extraction from seawater using composite absorbents 80−24730
U from sea-water by interfacial electrolysis *(Japanese)* 77−1931
U in sea foams and adhered to sea sands *(Japanese)* 79−29785
U_3O_8 recovery from seawater, R and D program 80−99217
U(VI), extraction from sea water using polyacrylamide gel containing metal hydroxides 78−54861
U(VI) extraction from sea water using hydrous metallic oxide binded with hydrophilic polymers *(Japanese)* 79−48102
V determ., preconc. on charcoal, neutron activation anal. 77−44549
Zn, conc. determ. by graphite furnace atomic absorpt. spectroscopy 80−40768

second-order optical susceptibility *see nonlinear optical susceptibility*

second sound
see also liquid helium sound propagation
BCC lattice, semi-infinite, heat transfer, mol. dynamics study 77−24453
boson system, struct. factor and sound vel. 78−34668
calorimetry, acoustic thermometry appl. to low temp. optical spectroscopy of solids *(French)* 77−87840
CBOOA, isotropic, nematic, smectic-A phases, Brillouin scatt. 80−11421
metal, electron-phonon drag and interaction of first and second sound 77−66009
molecular dynamics study 79−42207
monatomic BCC lattice under intense excitation, energy transport 78−59922
optic mode second sound in distortive phase transitions 79−73366
roton second sound and roton-roton interaction pot. 79−51328
roton second sound in relax. time approx. 77−66050
rotons, second sound velocity, interaction pot. 78−75898
sapphire, second sound observation by heat pulses method, phonon scatt. processes *(Russian)* 79−99273
smectic A LC, second sound excitation in insulating and conducting crystals 80−103244
superfluid, acoustic turbulence, first and second sound kinetic eqn. soln. *(Russian)* 78−43193
superfluid ^{3}He-^{4}He mixtures, two-phase sound 79−86958
superfluid prop. meas., review 80−96090
superfluid turbulence, penetration through porous filters 79−46855
vortices pinning in nucleopores, effect on second sound resonators 80−49439
He II-^{3}He, ^{3}He diffusion coeff., order parameter relax., second sound 78−30808
He, liq., phonon coupling of two-dimens. Wigner cryst. with second surface sound *(Russian)* 80−92756
He, liquid, first and second sound generation by immersed Ge cryst. optical pumping 80−6581
He, sound transmission at liq. solid interface, probe of melting kinetics 80−92734
He, superfluid, self-focusing of second sound *(Russian)* 79−10996
He, superfluid, transformation of first sound into second sound *(Russian)* 77−11755
^{3}He, A_1 phase, broken relative symmetry and dynamics 80−24705
^{3}He, superfluid, hydrodynamic modes interaction, sound propag. and spin waves *(Russian)* 79−37897
^{3}He, superfluid, second viscosity and attenuation of fourth and second sound near transition temp. 77−31830
^{3}He-^{4}He, dilute, second sound vel. and absorpt. 77−20154
^{3}He-^{4}He, dilute soln., second-sound damping meas. 79−73370
^{3}He-^{4}He, liquid mixture, second sound, quantised vortex creation at constrictions, excitation model 80−44383
^{3}He-^{4}He, solution, capillary waves and second sound, mag. excitation 79−60594
^{3}He-^{4}He, superfluid solns., nonlinear sound interaction 80−34267
^{3}He-^{4}He, superfluid solution, second sound velocities *(Russian)* 79−33150
^{3}He-^{4}He, superfluid solutions, second sound attenuation and dissipation processes, 1.3-2.0K *(Russian)* 79−42335
^{3}He-^{4}He dilute mixture, ballistic phonons, transition to second sound 78−10249
^{3}He-^{4}He mixture, dil., ^{3}He excitations, calc. 79−7730
^{3}He-^{4}He mixture, dil., 1.1-1.9K 78−63898
^{3}He-^{4}He mixture, dilute, second sound absorpt. and vel., phonon-^{3}He interactions 77−31835
^{3}He-^{4}He mixture, superfluid phase transition, universality and scaling laws 77−11763
^{3}He-^{4}He mixtures, propag. conditions and vels. for first, second and fourth sound, singular surfaces theory 77−47643

second sound continued
^{3}He-^{4}He solution, first and second sound interaction, hydrodynamic approx. *(Russian)* 77−69142
^{3}He-^{4}He superfluid mixture, second sound velocity, influence of spin 77−80676
^{3}He-^{4}He superfluid solution in superleak waveguide, acoustic-modes *(Russian)* 79−90842
^{3}He-superfluid ^{4}He solns., second sound vel. and absorpt. 79−56008
^{4}He, counterflowing, superfluid transition temp., second sound vel. 77−89606
^{4}He, crystalline, shape anal. of pulsed second sound 78−14537
^{4}He, liq., dynamic scaling near λ point 79−14977
^{4}He, liq., dynamic scaling near T_λ 80−34264
^{4}He, liq., dynamic structure factor near λ temp. 77−66049
^{4}He liquid, first and second sound attenuation near lambda point 79−95227
^{4}He, liquid, second sound, quantised vortex creation at constrictions, excitation model 80−44383
^{4}He, optically observed second sound resonance 78−71894
^{4}He, pulsed perturbation relaxation, intense short heat pulse passage, compression wave propagation *(Russian)* 79−82400
^{4}He, rotating, second sound attenuation in presence of const. supercritical heat flow *(Russian)* 77−55409
^{4}He, small liq. drop model for vacancy 78−51784
^{4}He, superfluid, boundary conditions 79−46857
^{4}He, superfluid, continuum theory based on classical theory of irreversible processes 80−29236
^{4}He, superfluid, dispersion of roton second sound 77−31819
^{4}He, superfluid, flows, healing and relax., first, second and fourth sound 78−47617
^{4}He, superfluid, fluctuations in turbulent counterflow, vortex line density fluctuation power spectra 80−84335
^{4}He, superfluid, Kapitza resistance, role of second sound 79−33132
^{4}He, superfluid, Kapitza resist. meas. *(Russian)* 80−88375
^{4}He, superfluid, liq.-vap. sound propag., crit. props. of sp. ht. 79−33134
^{4}He, superfluid, near transition, second sound damping, rel. to renormalisation gp. predictions 80−10725
^{4}He, superfluid, nonlinear combination interactions between first and second sounds *(Russian)* 77−69125
^{4}He, superfluid, nonlinear conversion of second sound to first sound within a waveguide 79−55974
^{4}He, superfluid, precision second sound meas. 77−15648
^{4}He, superfluid, reson. mode conversion and other second order effects 77−51559
^{4}He, superfluid, resonant nonlinear mode conversion 78−79831
^{4}He, superfluid, rot., second sound vel., mutual friction 78−51766
^{4}He, superfluid, rotating, mutual friction parameters crit. region meas. 77−15647
^{4}He, superfluid, rotating, effect of hysteresis, second sound attenuation meas. *(French)* 79−55965
^{4}He, superfluid, rotating Couette flow, hydrodynamic instabilities, attenuation of second sound resonances 79−55964
^{4}He, superfluid, second sound shock waves, pulse characts. and temp. depends. 78−67876
^{4}He, superfluid, second sounds, nonlinear profile, heat pulse method 78−75896
^{4}He, superfluid, second sound shock waves, detection by superconducting thin film probe 79−73355
^{4}He, superfluid, second sound damping, hydrodynamic regime below T_λ 80−10727
^{4}He, superfluid, second sound discharge and compression shock wave propagation *(Russian)* 80−103529
^{4}He, superfluid, sound absorption, theory *(Russian)* 77−89607
^{4}He, superfluid, sound conversion phenomena at free surface, acoustic coeffs. 80−96709
^{4}He, superfluid, sound pulse amplitude meas. method sound transform. at free surface 80−54451
^{4}He, superfluid, spatial distribution of order parameter, spectral approach of inverse problem *(Russian)* 77−80659
^{4}He, superfluid, stationary flow, 1.5K 79−73358
^{4}He, superfluid, stationary flow, combined meas. 80−49446
^{4}He, superfluid, surface deformation and surface motion due to standing second sound waves 79−55984
^{4}He, superfluid, turbulence in counterflow jet 77−72732
^{4}He, superfluid, turbulent counterflow, steady-state vortex-line density 78−95198
^{4}He, superfluid, turbulent counterflow, vortex line density by second sound burst technique 79−55963
^{4}He, superfluid, vorticity threshold and vortex-core parameter near T_λ, second sound probe meas. 77−85007
^{4}He superfluidity, macroscopic quantum waves, bound quasi-particles 80−39378
^{4}He-^{3}He, dil. soln., ^{3}He quasiparticle excitation spectrum and second sound vel. meas. 80−24708

secondary cells
advanced energy systems, future needs and developments 78−8197
alkali and alkaline earth metal electrodes, in nonaqueous secondary cells, electrochem. behaviour 80−35665
alkaline accumulators parameters improvements *(Czech)* 79−70447
ambient temperature solid state battery developments, review 80−61328
batteries for automobile propulsion, current designs and their limitations 79−66405
batteries for transport and stationary appl., advanced systems development 79−43756
batteries with gaseous electrodes, research and development, state of the art review *(Czech)* 79−39292
battery appls. and developments, conf., Brussels, Belgium (Jan. 1979) 80−72032
battery energy storage, 1979 status and prospects *(Japanese)* 80−76655
Battery Energy Storage Test facility, test programs and data processing 80−30449
bipolar, Li-Al alloy/FeS_2, using LiCl-KCl eutectic or LiF-LiCl-LiBr melt 79−48117
characteristics of Gates' cylindrical, sealed lead-acid cells for float applications 80−66964
comparison of available primary batteries and accumulators *(German)* 79−70444
criteria for electric vehicle and energy storage applications 80−72031
developments in electrochemical energy sources *(German)* 80−97770

secondary cells continued
electric vehicle power sources, battery design requirements for commercial use *(Dutch)* 80−72024
electric vehicle power sources, fuel cell/secondary battery hybrid appls. *(Dutch)* 80−72037
electric vehicle secondary cell development program of US Dept. of Energy, review 80−30442
electrode materials for solid state, high energy batteries 80−55836
energy conversion, Conf., San Diego, CA, USA (Aug 1978) 79−48038
fast ion conduction materials, props. review 77−7891
fast ion transport in solids, conf., Lake Geneva, USA (May 1979) 80−57006
fast ion transport in solids, conf., Lake Geneva, USA (May 1979) 80−105427
forced ionisation powered secondary batteries 79−43755
future energy concepts, Conf. London, England (Jan.-Feb. 1979) 79−43709
galvanic cells, high energy, with molten salt electrolytes *(German)* 80−72036
halide-aluminate media, positive electrode materials, experimental study 79−52923
high performance batteries, materials requirements 80−12002
high power batteries, possible use of honeycomb-type structs. 80−72027
intercalation compound electrodes, thermodynamic and transport props. 80−66963
membrane appl., review *(French)* 78−3374
metal-air batteries for electric vehicle propulsion, comparison of Li, Al, Zn, Fe systems 80−30444
metal/air batteries, status and potential, review 80−55828
mixed conducting electrodes, kinetic parameters determ., method and appl. to Li_3Sb 78−14772
mixed conductor applics. and characterisation 77−76596
molten salt Na/β-alumina/$SbCl_3$ cells, performance evaluation 79−52922
Na-S batteries, solid electrolyte β-Al_2O_3 formation from m-Al_2O_3 by new method 80−89606
Pb-acid batteries, testing of PVC cases *(German)* 78−85093
Pb/acid, design and performance characteristics for remote photovoltaic applications 80−55833
performance limits, technical and economic factors 80−45657
Plante cell formation using NO_3^- process 79−96437
plaster of Paris based rechargeable cell 79−96433
polyphenylquinoxaline-cellulose acetate, battery separator membrane, diffusion meas. 80−35574
redox flow battery, quantum parameters separation in continuum of ferromag. liquid insulation 80−61338
reversible solar galvanic cell 79−62016
sealed, using catalyst (gas recombination) plug system *(Japanese)* 79−83586
solar electricity battery storage Systems optimisation of solar cell/ battery 80−51007
solar energy plant electricity storage, battery appls. potential 80−72067
solar energy systems with battery storage, domestic appl. *(German)* 79−39307
solid electrolyte, layer and tunnel compounds, fast ion transport and electrochem. storage 80−61324
solid solution cathodes for electrochem. power sources, dynamic aspects 80−3508
solid solution electrodes, characterisation and performance 80−72033
solid state storage batteries, investigation 79−43754
space power systems, 1979 state of art and development trends 79−100506
standard cells combination with low temp. coeff. for Josephson voltage standard maintenance 80−101788
superionic conduction accumulator with high energy density *(French)* 80−26131
superionic conductor applics. and characterisation 77−76596
thermal management of battery systems for electric vehicles and utility load leveling 80−30458
wind energy conversion system, electricity storage using batteries 80−72008
$Ag/RbAg_4I_5/I_2$ solid state battery, low temp. degradation 80−61331
$Ag/RbAg_4I_5/Ta$, solid electrolyte timing cell and coulometer 80−68216
Ag-H_2 electrochemical cell design using rolled stack configuration 80−101084
Ag-H_2 energy storage system, long-life, light-weight, spacecraft appl. 79−48108
Ag-Zn battery, baseline characts. comparison with Ni-Zn battery 79−48110
$Al/AlCl_3$-NaCl/FeS_2 secondary cell, preliminary study 80−108793
Al-air, seawater activated cell 80−26128
β- Al_2O_3-Na_2O-CaO, microstruct. and ionic resistivity 80−44357
β-Al_2O_3-Na_2O, solid electrolyte, battery appl. *(Polish)* 80−12005
β''-Al_2O_3-Na_2O, solid electrolyte, behaviour at high current density, sodium heat engine mode 80−61330
β-Al_2O_3-Na_2O electrolyte development for Na-S battery 79−29461
β''-Al_2O_3-Na_2O solid electrolyte, strength degradation under electrolytic conditions 80−61329
β-Al_2O_3-Na_2O tube life determ. for Na-S battery 79−29462
β''- Al_2O_3-Na_2O-Li_2O (8.85, 0.75 wt.%) pressing powders, prep. by spray drying 80−40294
$Ba_{0.5}FeS_2$ cathodes for nonaqueous Li batteries 80−3506
C gas-diffusion O_2 electrode in acid, electrochem. performance 78−31652
C-air electrodes in alkaline electrolytes, ageing mechanism study 80−101087
Cu, cyclable solid-state cell based on intercalated electrodes 79−100511
Fe/Ti battery system, soluble, discharge characts. 79−92070
Fe-air, for electric vehicles 79−48118
Fe-air batteries, bifunctional air electrode 80−72028
Fe-Ni, for electric vehicles, Japanese development *(Japanese)* 79−83589
H_2-Br_2 cell for energy storage appls. 80−72029
H_2-Cl_2 cell, electrochemically regenerative, mass and heat balances 80−3503
$HUO_2PO_4.4H_2O$ proton conductor applications 79−29466
Hg-Zn, for rechargeable pacemaker free from EM interference 77−40925
$KFeS_2$, cathodes for nonaqueous Li batteries 80−3506
Li battery, use of MoS_3 as cathode 80−29892
Li battery solid electrolyte evaluation 79−29465
secondary cells continued
Li battery with dissolved S and THF electrolyte, capacity, rate and rechargeability 79−100510
Li corrosion in alkaline soln. 77−73367
Li, electrochem. props. of amorphous MoS_2 cathodes 80−40851
Li, electrochemistry of amorphous V_2S_5 80−76626
Li, high energy density, mixed electrolyte solns. of propylene carbonate and dimethoxyethane 80−76627
Li long life battery systems, standby power for data retention in volatile memory systems, selection criteria 80−61337
Li metal for battery industry, sources and preparation 80−97781
Li salt based solid electrolyte, synthesis and characterisation, secondary cell appl. *(French)* 80−72034
Li solid cathode cells, Li closoboranes as electrolytes 80−108794
Li solid electrolyte materials, review of crystal and electrochem. props. 80−107524
Li, use of V_6O_{13} cathode materials 79−92073
$Li/Li^+/M_xV_{1-x}S_2$ cells (M=Fe, Cr), effect of metal substitution of Li intercalation 79−100395
Li/MS_x, electric vehicle appl., improved design 79−48116
Li/SO_2, safety studies, DTA of constituents 80−16795
Li/SO_2 cells, safety studies, kinetics of Li-organic solvent exothermic reactions 80−72030
Li-Al alloy electrode performance, effects of metal additives 78−23953
Li-Al alloy/LiCl-KCl eutectic/FeS_2, for vehicle propulsion appl., cycle life, self-discharge rates and edge losses obs. 79−48117
Li-Al alloy/LiF-LiCl-LiBr melt/FeS_2 for vehicle propulsion appl., cycle life, self-discharge rates and edge losses obs. 79−48117
Li-Al/FeS, electric vehicle appl., improved design 79−48116
Li-Al/FeS cells for electric vehicle propulsion 80−30446
Li-Al/MS_2, electric vehicle appl., improved design 79−48116
Li-Al-FeS, high temp. battery, ceramic powder, as electrode separators 79−61966
Li-FeS battery eng. problems for elec. load levelling plant design 80−30457
Li-FeS_2, for electric vehicles and stationary energy storage devices, ANL development with industrial participation 79−48113
Li-FeS_2, Li-Si alloys eval. as negative electrodes, thermodynamic props. 77−16547
Li-FeS_x molten salt battery, anodic corrosion rate of candidate current collector metals 79−100512
Li-FeS_x molten salt battery, anodic corrosion rate of candidate current collector metals 79−100513
Li-organic electrolyte batteries, corrosion-resistant materials 79−100387
Li-S, Li exchange current in LiCl-KCl eutectic melt at 400°C 80−93867
Li-Si alloy/FeS, development for load levelling and electric vehicles appl. 79−48115
Li-Si alloy/FeS_2, performance for electric vehicle appl. 79−48114
Li-TiS_2, electrochemical pot. spectroscopy, thermodynamic props. meas. 79−100426
Li-TiS_2 cells, intercalation chemistry and electrochemical energy storage 79−100541
Li-TiS_2 nonaqueous batteries, mechanism of Li intercalation, optical and X-ray studies 79−100394
Li-TiS_2 storage batteries *(German)* 80−12001
LiAl/FeS, battery system research developments at ANL 80−61323
LiAl/FeS batteries, principles and construction, load levelling of nuclear stations 80−21392
LiAl/FeS electric vehicle battery, charging system developments 80−30447
LiAl/FeS experimental cells with molten salt electrolyte, self-discharge behaviour 80−104501
LiAl/FeS_2 cell with negative electrode prep. by powder metallurgy, performance 80−26130
LiAl/metal sulphide high temp. battery with multi-foil insulation container for electric vehicle appls. 80−30448
LiAl(Si)/FeS(S_2) battery developments for electric vehicle propulsion and load levelling appls. 80−61325
LiBr, surface characterization of film growth on Li anode 80−81240
Li_xCoO_2, cathode material for batteries of high energy density 80−101089
$LiNO_3$, power capacity assessment 79−34428
Li_3Sb, mixed conducting electrodes, kinetic parameters determ. 78−14772
$Li_xV_2O_5$ ($0.1<x<1.0$), phase relationship in ambient temperature system 80−20912
$Li_2VS_2(Se_2)$ based topochemical cells, low voltage behaviour 79−92069
Li_xWO_2/Li_yTiS_2 cyclable organic electrolyte cell, using 2 intercalation electrodes 80−76625
MgO sintered-ceramic separator plate development, Li-Al/LiCl-KCl/FeS battery applications 80−61321
Na/S, for rail traction, dimensions optimisation 79−48112
Na/S, pulse characts. for electric vehicle propulsion 79−48109
Na/S, recharging characts. in two liquid phase region 80−26127
Na/S batteries, load levelling and traction 80−21391
Na/S battery, development of β-Al_2O_3-N_2O electrolyte 80−71615
Na/S battery, high-temperature, for vehicle appl. 79−43757
Na/S battery, mass transport phenomena in molten S-Na_2S_5 system 80−72026
Na/S battery development program at GEC for utility lead levelling with beta alumina solid electrolyte 80−61327
Na/S cell, principles *(German)* 79−57421
Na/S cells, casing material selection 79−52924
Na/S cells, evaluation of sintered SiC as electrode 80−35355
Na/S cells operating with dissolved catholyte, elec. props. 80−101085
Na/S load levelling batteries, optimisation of fabrication process of beta Al_2O_3 solid electrolyte 80−72035
Na/S sintered battery material *(German)* 80−21394
Na/S traction batteries, development progress and problems, review 80−61326
Na-$Na_5ErSi_4O_{12}$-TiS_2, electrochem. characts. 80−107518
Na-S, fabrication of β''-Al_2O_3 solid electrolyte tubes from cast ceramic tape 80−60819
Na-S, processing+props. of β''-Al_2O_3 and NASICON ceramic electrolytes 80−60820
Na-S, solid electrolytes, appls. *(German)* 79−29460
Na-S, with dynamic S electrode, electrical characts. obs. 79−100515
Na-S accumulator, electrical energy storage *(French)* 80−55835
Na-S batteries, current development trends and characts. 80−55830
Na-S batteries, energy storage for peak power generation 80−30455

secondary cells continued
Na-S batteries, load levelling and motive power appls. 77−86321
Na-S batteries, reproducibility and performance of large prototype cells 80−30454
Na-S battery, appls. *(French, German)* 80−61322
Na-S battery, blocking defects in β''-alumina observed by high resolution electron microscopy 78−55879
Na-S battery, improved capacity *(French, German)* 80−30441
Na-S battery for energy storage 80−30453
Na-S cells, factors affecting S electrode operation 79−29463
Na-S cells, failure anal. of β-Al_2O_3-Na_2O-Li_2O membranes 80−12003
Na-S cells, S electrode potential distrib. model 79−96435
Na-S cells, S electrode resistance calc. 80−35667
Na-S interconnected cell performance 79−29464
β-Na_2O-Al_2O_3, single cryst. Czochralski growth 77−77367
$Na_2O.Li_2O.Al_2O_3$, comp. and props. for use in Na-S battery 79−87745
Nc-Cd accumulators, efficient charger cct. based on Fairchild, μA78S40 IC *(German)* 80−66961
Ni-Cd, hybrid system with solar cells *(Japanese)* 79−83599
Ni-Cd, lightweight, long-life, development of aerospace appl. 79−48106
Ni-Cd, Nimbus-Landsat spacecraft power subsystems, flight performance 80−30459
Ni-Cd, plastic bonded Cd electrodes, production methods 80−45659
Ni-Cd, plastic-bonded electrodes positive active layer study 80−101088
Ni-Cd, sealed aerospace cells, H_2 recombination during over discharge 80−30461
Ni-Cd, with plastic bonded Ni oxide electrodes, basic electrochemical parameters 80−50951
Ni-Cd 6.0 Ah cells, accelerated testing of cell failure for life prediction 80−35670
Ni-Cd accumulators, plastic bonded electrodes, active layer composition influence on galvanostatic and potentiostatic discharge curves 80−55834
Ni-Cd accumulators, sintered negative electrodes props. evaluation, impregnation method influence 79−57422
Ni-Cd all with MnO_2 doped positive electrodes 79−96439
Ni-Cd and maintenance-free Pb accumulator characteristics *(German)* 80−97782
Ni-Cd batteries, button and cylinder types, self discharge behaviour during storage *(German)* 80−66960
Ni-Cd batteries, prep. of plates by electrolytic precipitation *(Chinese)* 79−57237
Ni-Cd batteries, sealed, quick charge characts. *(Japanese)* 79−83587
Ni-Cd batteries for standby power systems 80−104500
Ni-Cd battery, sealed, cylindrical, 'PANANICA' H type, trickle charge characts. *(Japanese)* 79−83588
Ni-Cd battery, state-of-charge nondestructive determ., using impedance parameters 79−57423
Ni-Cd battery reconditioning and long term performance, in geosynchronous orbit spacecraft 79−52929
Ni-Cd battery system design for tracking and data relay satellite system 80−30460
Ni-Cd cell lifetime prediction, computerised pattern recognition 80−3504
Ni-Cd cells, characts. limitations, future developments 80−89607
Ni-Cd chargeable batteries, advantages and appl. 79−96434
Ni-Cd parameters improvements, use of oxalic acid and combined Cd/Zn electrodes *(Czech)* 79−70447
Ni-Cd pocket plate batteries characteristics, solar applications 80−61332
Ni-Cd rechargeable cells, construction, reliability and appl. 79−100509
Ni-Cd sealed battery electrode performance meas. 80−66962
Ni-Cd spacecraft batteries, power system perform. anal. using computer modelling 80−30497
Ni-Cd system, characteristics and new developments for telephone industry applications 80−55829
Ni-H_2, Navigation Technology Satellite-2 appl., first-year operating experiences 79−48107
Ni-H_2 50 Ahr battery for low earth orbit satellite appls. 80−30463
Ni-H_2 battery for satellite energy storage, prelaunch and orbital performance through one eclipse season 80−81430
Ni-H_2 cells for space appls., characterisation and simulated low earth orbit cycling 80−30462
Ni-Zn, traction, using high-rate tapered DC charge method 79−48111
Ni-Zn battery, baseline characts. comparison with Ag-Zn battery 79−48110
Ni-Zn cells, heat transfer anal. 80−30458
Ni-Zn electric vehicle battery, performance characts. 80−30443
Ni-Zn sealed cylindrical dry-cell batteries, high working voltage 80−40852
NiCd rechargeable cardiac pacemaker system clinical experience 77−81727
NiCd, rechargeable sealed battery systems, review 79−43753
Pb accumulators, improvements w.r.t. weight, service life and maintenance *(Czech)* 79−70446
Pb acid battery plants, current and future trends, telecommunications emergency power supply 80−61333
Pb batteries with gel-electrolyte, charging and discharging *(German)* 79−92068
Pb battery anode reverse polarisation corrosion test method *(Bulgarian)* 80−50950
Pb porous electrode oxidation in H_2SO_4, potential step expts. 79−96438
$Pb/HBF_4/PbO_2$ electrochemical system, performance, electrolyte impurity effects 79−52927
Pb-acid, cell design analysis computing for optimal electrical performance characterisitics 80−55832
Pb-acid, cylindrical, pure lead, design features and performance experiences in float service applications 80−55831
Pb-acid, electrodes, structure obs. 79−100516
Pb-acid, oxidation of porous Pb electrodes obs. 79−100514
Pb-acid, response to chopper-controlled discharge, in electric vehicle 79−48120
Pb-acid, traction, using high-rate tapered DC charge method 79−48111
Pb-acid 'G-cell', construction and design and performance charact. for UPS systems 80−61335
Pb-acid based, Cyclon, rechargeable sealed battery systems, review 79−43753
Pb-acid batteries, DSA type positive grids, characts. improvement, soln. 80−35668
Pb-acid batteries, for elec. vehicle propulsion, heat transfer, math. anal. 80−3509
Pb-acid batteries for electric vehicles 80−30445
Pb-acid batteries for electric propulsion *(Dutch)* 80−72025

secondary cells continued
Pb-acid battery, effect of H_3PO_4 on positve electrode, constant pot. corrosion studies 79−92071
Pb-acid battery, effect of H_3PO_4 on positive electrode, mechanism 80−26129
Pb-acid battery, grid corrosion, effect of addition agents 80−3505
Pb-acid battery, sealed, deterioration mechanism of overdischarge characts. obs. *(Japanese)* 79−83585
Pb-acid battery, thermopassivation of PbO_2 plate 80−3507
Pb-acid battery charge determ. from internal impedance 79−96436
Pb-acid battery charging from photovoltaic array energy source, problems and efficiency 80−61336
Pb-acid battery positive, cyclic corrosion 79−92072
Pb-acid cells, heat transfer anal. 80−30458
Pb-acid cells, PbO_2 formation on Pb and antimonial Pb alloy 80−76628
Pb-acid negative battery plate, form., physicochem. processes 77−4907
Pb-acid storage batteries for uninterrupted power supply appls. 80−61334
Pb-acid system, characteristics and new developments for telephone industry applications 80−55829
Pb-Ca batteries, float current 80−12004
Pb-Ca-Sn alloys for battery grids, proposed phase diagram, grain struct. development, corrosion phenomena 77−16546
Pb-H_2SO_4 battery negative plates, impedance, theory 78−27771
Pb-H_2SO_4 cells, Sb alloying effect on solid Pb electrochemical properties 80−55668
Pb-PbO_2 storage batteries, gas tight with recombination, advantages *(German)* 79−52921
Pb-Sb battery grids, ageing behaviour obs., effects of casting and cooling 79−100517
PbO_2 compressed powder magnetoresistance and apparent carrier mobility 80−35669
PbO_2 powder, electronic conductivity, separation of particle core and surface resistance 80−104442
$4PbO.PbSO_4$, oxidation to PbO_2 in positive plate of Pb-acid battery 79−70336
$4PbO.PbSO_4$, paste mixing and curing for Pb acid batteries, effect of CO_2 79−61968
$Sr_{0.5}FeS_2$ cathodes for nonaqueous Li batteries 80−3506
Y_2O_3 sintered-ceramic separator plate development, LiAl/LiCl-KCl/FeS battery applications 80−61321
Zn electrode development, dispersed, electric vehicles appl. *(French)* 80−72023
Zn electrodes, shape change resulting from cell cycling, quantitative study 79−43591
Zn, props. of alternate electrolytes 80−104502
Zn-Ag_2O, concentration changes in porous Zn electrodes during cycling 80−35666
Zn-Br, performance anal. in electric vehicle and utility applications 80−101086
Zn-Br_2 battery for utility energy storage appls. 80−30450
Zn-Br_2 non-circulating storage batteries 80−30451
Zn-Cl_2, 100 MWh peak-shaving battery plants development 79−48119
Zn-Cl_2 batteries for electric vehicles, battery design modelling 80−30452
Zn-Cl_2 battery, half-cell overpotential measurements 80−21393

secondary electron emission
4π proportional counters, spurious Malter pulses 77−54452
accelerated electron beam current monitor using secondary emission detection 78−78033
acceleration by protons in vacuum, ion bombardment effects 77−52210
air, weakly-ionised, secondary electron distrib., produced by electron source distrib. 80−6211
alkali halide, under bombard. by multiply charged Ar^+-Ar^{5+} and Kr^+-Kr^{5+} ions 78−11046
alkali halides, secondary electron emission statistics, photomultiplier appl. 79−47564
alkali metal halide electron elastic reflection and secondary emission, 1 to 30 eV obs. 78−11037
n-alkanes, conduction band struct., LEED, secondary electron emission and UPS study 80−70601
amorphous semiconductors, universal yield curve verification 80−45179
angular and energy distrib. 80−100718
angular dependence, model, and its appl. to Al (001) and (110) 77−73197
angular distribution, cosine law theory 78−35233
atmospheric positive streamer corona, primary wave emission, secondary electron emission 80−44008
attenuation length, escape depth and probability for excited electrons in solids 78−76593
Bendix layer, channel electron multiplier, secondary electron emission yield, energy depend. 77−54471
Boltzmann equation, appl. *(French)* 80−20740
cascade background correction, Auger peaks, Cu(110) surface appl. 79−43079
CdS thin films, slow electron mean free path 79−99998
conducting surfaces used in multistage depressed collectors 78−31288
conference on inelastic ion surface collisions, Hamilton, Ontario, Canada (Aug. 1978) 80−31402
controllable method for particle detection 77−30711
convoy electrons from solids, ion vel. and Z and target material depend. 78−84692
copper phthalocyanine, autoionisation in electron energy loss spectra 78−35232
coronene, metastable inert gas atom impact, surface electron emission energy distrib. 78−43970
creation energies for secondary electrons [SEM applications], SEM appl. 79−99994
diamond, inelastic scatt. differential cross-sections 77−76652
diamond, semiconducting, (111) surface, quantum photoyield and secondary-electron distribs., stable negative-affinity emitter 79−100023
diamond, total secondary electron emission spectrum 77−72759
diatomic molecules, N_2 and CO nuclear pumped lasers, electron impact cross section meas. 80−63985
dielectric, irrad. by electron beams, effect of bulk and surface cond. on pot. 80−2446
dielectric theory of secondary electron spectra 80−93442
discharge, RF, gamma regime, ionis. balance and plasma characts., model 80−44022
discharge in heterogeneous medium 80−38858
discharge tube, secondary electron emission at wall 77−27762

secondary electron emission continued
discharge tube wall, secondary electron emission in cathode fall region of tube wall 80−44001
elastic and inelastic contribs. to secondary electron yield struct. 78−72642
elastic reflection of electrons from solid surface, Boltzmann eqn. 79−43078
electrically stressed insulator-vacuum interface, secondary electron avalanche 77−81185
electron backscattering in Si surface-barrier detector 78−55095
in electron beam deposition, electron interactions near condensing surface *(Russian)* 77−59698
energy analysis in 6 to 150 eV range *(German)* 79−75649
energy dependence of yield, based on range-energy retardation power formula 79−47565
ethylene, conduction band struct., LEED, secondary electron emission and UPS study 80−70601
Fano plot application to secondary electron yield data 77−1770
Faraday cups for laser plasmas diagnostics, secondary emission meas. 78−5941
fast electron irradiated material, defect and secondary electron generation, model 78−11030
film, conducting or insulating, kinetic electron emission when penetrated by H^+ ions with 0.3 to 30 keV energy 79−91554
flashover of insulator surface in vacuum mag. inhibition 77−11411
gas, weakly-ionised, electron stopping model and secondary-electron distrib. 80−6263
gas-filled counters, secondary electron emission, elec. field at cathode 78−17529
glow discharge, HV, electrode surface effects 79−64955
glow discharge, secondary electron emission mechanism 77−19800
glow discharge breakdown, temporal development of electrode pot. 80−44003
graphite, sintered powder, energy losses, secondary electron spectra, AES, and EELS 79−99997
graphite film, secondary electron emission and EELS rel. to plasmons 80−50481
Inconel 625, electron yields under ion bombardment for clean and oxidised surfaces 80−66368
inert gas nuclear pumped lasers, electron impact cross section meas. 80−63985
insulator, secondary electron escape probabilities 78−72651
insulator films, porous, field-enhanced SEE coeff., nature of fine struct. 77−20970
insulators, free-electron scatt. theory and plasmon theory 79−8211
insulators, soft X-ray induced secondary-electron emission, models and meas. 79−74034
ion induced, energy and angular spectra 80−71547
ion-bombarded solid, direct and recoil-induced electron emission 80−11526
ion-bombardment Auger spectroscopy for studying surfaces of solids 79−20497
ion-electron emission energy spectra in small and large solid angles 78−2964
ion-electron emission from spherical targets 79−52066
ion-induced kinetic electron ejection, pot. emission, semiconductors and insulators, review 77−44109
ion-induced X-rays, review 79−96405
ionic crystal, ion-electron mechanoemission mechanism 78−3002
kinetic emission from electron and ion bombardment 80−66342
kinetic ion-electron emission, ion charge depend. 78−11045
kinetic ion-electron emission coeff., target at. no. depend., and role of recoil atoms 78−2966
laser channel with secondary emitter, transverse microwave discharge He-Ne laser 80−9899
laser plasma, ion emission, secondary electron emission effects on detect. efficiency 80−100096
local and integral emission meas., electron emission microscope adaptation 79−93258
low energy distrib. meas. using double-pass cylindrical mirror analyser 80−68293
lunar regolith, secondary electron emission charact. determ. method 80−12687
mechanical system for multi-specimen cleavage and rotation 78−36987
metal, creep-electron emission relation 78−6994
metal, secondary electron emission, Monte Carlo calc. 79−69932
metal oxides, Ar ion impact, comparative secondary electron emission *(Russian)* 77−8707
metal secondary electron emission coefficient recorder 78−58094
metal surface, appl. to energy anal. of energetic neutrals in plasma diagnostics 80−59278
metal surface, clean, ion impact, mol. effects in electron emission 78−80446
metal surface, electron emission induced by low energy light ions 79−61482
metal surface, heterogeneous cluster ion bombardment, secondary electron emission 80−60742
metal surface, inert gas bombard., 1.05 keV, electron yields, Fermi energy estimate 78−52611
metal surface, interaction with He metastable atoms 79−91558
metal surface, keV neutrals energy determ. method 80−89100
metal surface, linearised secondary electron cascades, surface and subsurface sources 78−11036
metal surface, linearised secondary electron cascades 78−11035
metal surface, oxide covered, primary electron beam effect on secondary emission coeff. *(French)* 79−47563
metal surface with incident microwave radiation, secondary emission discharge 77−1026
metal surfaces, clean polycrystalline, ion-induced electron emission, review 80−35032
metal surfaces, linearized secondary-electron cascades, line-shape synthesis 79−74035
metallic elements, gamma-ray irradiated, energy spectra of secondary electrons 78−84683
metals, Ar ion or electron impact, comparative secondary electron spectra *(Russian)* 77−8706
metals, electron absorpt. and transmission charact., 5 to 30 keV, film-massive block method 78−88387
metals, electron penetration and energy transfer in solid metal targets, film bulk method 78−2963
metals, influence of oxide films on photoemission *(Russian)* 77−81194
metals, nearly-free-electron, secondary electron emission, role of plasmon decay 77−81186
metals high density collision emission cascades following heavy ion bombard. 80−71531
microdosimetry, secondary electron emission and two-target theory 80−12274
minimum ionising particle detection, test of low density KCl layers 77−54475
model, absorption of electrons with energies greater than 1 MeV *(Russian)* 77−55304
MOS structures, electron beam induced charge carriers *(German)* 77−12007
multialkali photocathodes, secondary emission charact. 78−84687
multipactor microwave discharge, electron vel. distrib., homogeneous polyphase reson. anal. 77−7628
naphthacene, metastable inert gas atom impact, surface electron emission energy distrib. 78−43970
near dielectric-metal interface, and elec. fields 79−38697
due to negative corona discharges 78−67592
open microchannel multiplier secondary electron multiplication efficiency and nonlinearity 77−79513
perylene, metastable inert gas atom impact, surface electron emission energy distrib. 78−43970
photomultipliers noise figure, secondary electron emission model 78−86336
piezoelectric insulator, nonlinear interaction of SAW with electron beam 80−70517
plane electrode, space-change limitation 79−4871
polyethylene, solid liq., secondary electron emission spectroscopy 80−80916
polyethylene film, soln.-cast, low energy electron scatt. obs. of band struct. 80−16131
polymer film on Pt, energy losses, secondary electron spectra, AES, and EELS 79−99997
polystyrene latex sphere beams 77−24914
pulsed surface flashover mechanism involving electron-stimulated desorption 80−70055
pyrographite, surface struct., amorphisation, secondary electron spectra and AES 79−43077
raster electron microscope in secondary electron emission regime, interaction between probe and object material 79−93259
reflection and transmission secondary emission *(Japanese)* 80−45180
response delay using storage commutation by slow electron beam *(Russian)* 78−88386
retarding field analyser, spurious effects of electron emission from grids 77−20968
saturated liquid polydielectrics, secondary electron emission and energy loss spectra 80−55239
secondary electron emission spectroscopy of solid surfaces 77−36326
secondary electron imaging system for a nuclear microprobe 79−26799
SEM, ultra-high vacuum secondary electron emission dependence on electron beam density dose, surface interactions from AES and ELS 80−61209
SEM accuracy increase, equipotential patterns obtaining 80−57423
SEM specimen-electron interactions 80−68317
semiconducting channel ion sorce, secondary emission and ion feedback 80−31936
semiconductor glasses, scattered electrons emission angle and energy distribution 79−91545
semiconductors, electron absorpt. and transmission charact., 5 to 30 keV, film-massive block method 78−88387
semiconductors, soft X-ray induced secondary-electron emission, models and meas. 79−74034
single crystals with lowered work function, secondary and Auger electron emission anisotropy 80−100716
solid, cascade emission theory during penetration 78−11033
solid, cascade emission theory during reflection 78−11034
solid, heavy ion bombard., Mach shock electron distrib. 80−45194
solid, secondary electron emission effect of alkali and alkaline-earth ion bombardment 79−8212
spectrometer for Auger spectroscopy, secondary electron emission effects 78−23564
spectroscopy, total current, study of surface regions and bulk physics 80−31952
spectroscopy based instrument applic. to rate controlled deposition of alloy films *(German)* 80−89152
spherical crystalline target, ion-electron emission 79−28878
spherical target, ion-electron emission 79−65966
sputtering, at. excitation mechanism 78−43971
sputtering, ionised and excited particle production, validity of thermodynamic models 79−52062
stainless steel:C, surface, obs. at very low accel. voltage (200 V-1 kV) by SEM 80−10764
steel, stainless, ion and electron desorption of neutral molecules from type 304 79−83507
steel, stainless, proton and deuteron irrad. 0.5-2.5 MeV 77−63512
steel, stainless, secondary electron emission, ion-induced for cluster ions V_n^+, Nb_n^+, and $V_nNb_n^+$ 80−35035
surface AES with secondary emission imaging 78−11475
surface analysis, AES and ESCA combined with SEM *(French)* 80−47154
surface analysis techniques and appls., symposium, Dayton, USA (Jun. 1979) 80−62363
surface electron states, electron emission spectroscopy probe 77−51798
surface film, method of obs. of contact area and mech. breakdown 79−37939
surface plasma source, H^- ion form. and secondary electrons *(Russian)* 78−71503
surface potential and work function meas. from secondary electron emission energy in SEM 80−66343
surface spacings from secondary electron yield 80−66341
targets, deformation process investigation 79−99995
theory 78−76564
thin solid target, proton bombarded, secondary electron bremsstrahlung, directional anisotropy 77−69953
threshold studies from ion-surface impact 80−66360
Tokamak, time resolved heat flux to wall meas., sheath model with secondary electron emission 78−79468
Tokamak limiter, influence of secondary electron emission on energy transport 79−3236

secondary electron emission continued
trifluoroiodomethane nuclear pumped lasers, electron impact cross section meas. 80−63985
vacuum arc, secondary electron emission by multiply charged ions 77−19791
wake-bound electron contrib. to convoy electron vel. distrib., effect of ionic field 80−60729
water vapour ionised by He^+ and He^{2+}, electron yield obs. 80−102562
X-ray detection in 60-190 Å range using secondary-electron multipliers 77−21446
X-ray induced, model 77−59669
yield from ion-surface impact 80−71544
Zircaloy, breakaway mechanism, corrosion kinetics in steam 80−61030
Ag (111) surface, ionic bombardment, diffr. effects in angular distrib. of emitted secondary electrons 79−15577
Ag coating on refractory metals, energy struct. determ. at two monolayer thickness 80−100392
Ag discontinuous film on (001) MgO, low energy electron spectrum 77−48288
Ag, evaporated layer, secondary electron energy distrib. and work function *(French)* 79−99993
Ag film, on Au substrate, monolayer overgrowth, quantitative AES method 80−10813
Ag, low energy distrib. meas. using double-pass cylindrical mirror analyser 80−68293
Al (001) and (110), anisotropy of secondary emission, Monte Carlo calc. 79−99996
Al, (001) and (110) surfaces, ang. depend., model 77−73197
Al, adsorbed S(O)(N)(C), internal and external sources of electrons 77−44097
Al, appl. of Boltzmann equation *(French)* 80−20740
Al, characteristic energy losses on C contaminated surfaces, secondary electron spectra, AES, and EELS 79−99997
Al, clean and oxidised surfaces, secondary electron spectrum, EELS and AES, comparison 80−55237
Al, collective properties of degenerate electron gas, (e, 2e) technique *(Russian)* 79−56149
Al, evaporated layer, secondary electron energy distrib. and work function *(French)* 79−99993
Al film, (e, 2e) reaction, ang. correlation functions, plasmon satellites 79−19955
Al film, transparent, 10-100 keV primary electron energies 77−32477
Al, foil, secondary electron emission due to α-particle irrad. *(Russian)* 80−66344
Al, influence of oxide films on photoemission *(Russian)* 77−81194
Al, ion-induced electron emission, ion charge depend. 80−108315
Al, multiple scatt. of fast electrons and inner secondary electron generation 77−1160
Al, proton and deuteron irrad., 0.5-2.5 MeV 77−63512
Al, proton bombarded, secondary electron bremsstrahlung, directional anisotropy 77−69953
Al, proton or α-particle bombarded, secondary electron emission 77−36346
Al, rel. to high-current electron beam refl. coeffs. *(Russian)* 78−84690
Al, secondary electron emission, role of plasmon decay 77−81186
Al, secondary electron emission characts. calc. by Monte Carlo methods 79−28868
Al, secondary electron emission, Monte Carlo calc. 79−69933
Al, secondary electron emission by reflection, Boltzmann eqn. resolution method 80−45178
Al, secondary-electron energy distribution in high-energy photoemission 77−48305
Al, X-ray induced electron emission, secondary electron energy distrib. 77−59669
Al-Al_2O_3 films, coincidence energy spectra for (e, 2e) reaction 79−69936
Ar, high resoln. pulsed electron beam time-of-flight ejected electron spectra 77−3462
Ar, secondary electron energy distrib. on fast electron impact 77−34763
As_2S_3, secondary electron emission, fluctuation state effect 80−40193
Au, adsorbed layer comp. anal., by ion-forwarded electron spectra 77−31850
Au, Boltzmann eqn. appl. *(French)* 80−55238
Au, evaporated layer, secondary electron energy distrib. and work function *(French)* 79−99993
Au film, transparent, 10-100 keV primary electron energies 77−32477
Au, foil, electron spectra from α-particles and fission products 77−24918
Au, foil, X-ray induced electron emission 77−4713
Au, low energy peaks interpretation 78−39638
Au, multiple scatt. of fast electrons and inner secondary electron generation 77−1160
Au, X-ray cathode, secondary electron energy distrib. excited at 277 and 1487eV 77−8716
Au, X-ray induced electron emission, secondary electron energy distrib. 77−59669
BaO, electron energy loss and secondary emission mechanisms, plasmon losses 78−76565
$BaTiO_3$, piezoelectric ceramic, secondary electron emission yield 79−91546
Be film, on Cu substrate, monolayer overgrowth, quantitative AES method 80−10813
Be, multiple scatt. of fast electrons and inner secondary electron generation 77−1160
Be, slowly oxidised, secondary electron yield changes, and AES characterisation 80−71524
Be thick film or Au substrate secondary electron emission 80−104022
Be-Cu surface, secondary electron yield, for electron multiplier ion detector 78−74094
$Bi_{12}GeO_{20}$, piezoelectric, secondary electron emission yield 79−91546
C, film, secondary electron emission rel. to energy loss 77−16438
C films, surface struct., graphitisation, secondary electron spectra and AES 79−43077
C, foil, electron spectra from α-particles and fission products 77−24918
C, secondary electron spectroscopy 77−85854
C-foil, secondary electron yield from heavy ion beam-tilted-foil expts. 78−62889
CO, adsorbed layer, electron impact, electron impulsive ionisation spectroscopy obs. 80−60720
CaF_2 film, ionic migration study by Rutherford scatt., defects, secondary emission *(French)* 78−55982

secondary electron emission continued
CaO epitaxial layer, on Mo, secondary electron emission, struct. effects, LEED and AES expts. 78−2959
CaO, optimum composition of dielectric materials for AC-operated plasma display panels 80−14945
CdS, explanation for total current spectrum 77−8693
Cr-SiO, thin film, laser beam-treated, emission mode of SEM 79−28226
Cs halide porous layers, electron bombardment induced cond., meas. 78−56550
Cs halides, storage layers stability under electron bombardment 78−27355
Cs/W, work function measurement in SEM 80−80918
CsCl, transmission and refl. secondary emission 78−27356
CsI, depth of emission of secondary photoelectrons 79−8228
CsI film, secondary emission yield, primary electron ang. of incidence effects 78−2961
CsI, potential and limitations as dynode material for electron multiplier 78−23566
CsI, secondary electron spectra, primary electron energies up to 30 eV 77−12473
CsI, secondary electron emission statistics, photomultiplier appl. 79−47564
Cu (100), 30 keV ion impact, scatt. ion-electron emission correlation 77−52209
Cu (100), linearized secondary-electron cascades, line-shape synthesis 79−74035
Cu, Boltzmann eqn. appl. *(French)* 80−55238
Cu, evaporated layer, secondary electron energy distrib. and work function *(French)* 79−99993
Cu, low energy distrib. meas. using double-pass cylindrical mirror analyser 80−68293
Cu, low energy peaks interpretation 78−39638
Cu, multiple scatt. of fast electrons and inner secondary electron generation 77−1160
Cu, rel. to high-current electron beam refl. coeffs. *(Russian)* 78−84690
Cu, secondary electron yields from ion impacts, stopping power calcs. 78−11053
Cu, spherical and plane surface, ion-electron emission 79−65966
Cu, spurious peaks from grid of retarding field analyser 77−20968
Cu, surface, C and H ion bombardment, secondary electron coeff. experimental technique 79−78804
Cu, surface contaminant anal. by ion-electron spectroscopy 80−54490
Cu, work function meas., SLEEP and retarding pot. techniques 77−32067
Cu:Au:C, surface, obs. at very low accel. voltage (200 V-1 kV) by SEM 80−10764
Cu-Be-O surface, $O(^3S)$ impact, secondary electron yield 78−58797
Cu-Ni:polyethylene, surface, obs. at very low accel. voltage (200 V-1 kV) by SEM 80−10764
CuBe, electron emission following ion bombardment of electron multiplier dynode 78−23576
CuBe, emission coeffs. for multiply charged ion bombard. 78−11051
D_2, solid, electron and ion induced 79−1803
D_2, solid, electron emission under bombard. by keV electrons, H and D ion beams 77−73196
D_2, solid 0.5-3 keV electron penetration depth 78−56549
Fe, proton and deuteron irrad. 0.5-2.5 MeV 77−63512
Fe, secondary electron emission characts. calc. by Monte Carlo methods 79−28868
GaAs, excitation by 2-4 KeV Ar^+ ions, electron energy spectra 80−11529
GaAs-Cs-O, negative electron affinity emitter 78−11031
GaAs-Cs-O, negative electron affinity, refl. of slow electrons, 0.4-3 eV 78−11038
GaAs-Cs-O film, polycryst., secondary emission props., activating coating effects 78−2957
GaP, Cs(Cs-O) activated, with negative electron affinity, near UV photoemission and secondary emission 78−11074
GaP film, polycrystalline, with negative affinity *(Czech)* 78−52604
n-GaP films, reduced work function, energy spectra of secondary electron emission 79−28867
GaP:Cs-O simultaneous adsorption, oxidation interface chemical struct. 80−103584
GaP-Cs-O, negative electron affinity emitter 78−11031
Ge, ion irrad., accumulation and annealing of struct. defects, secondary emission obs. 78−2167
$H^+ + He$, proton energy degradation, approx. yield spectrum 79−31643
H_2, solid, 0.5-3 keV electron penetration depth 78−56549
H_2, solid, electron and ion induced 79−1803
H_2, solid, electron emission under bombard. by keV electrons, H and D ion beams 77−73196
$H^+(H_2O)_n$, secondary electron emission from charged clusters on 2.4 keV Ar bombarded surfaces 79−15580
$H^+(NH_3)_n$, secondary electron emission from charged clusters on 2.4 keV Ar bombarded surfaces 79−15580
H_2O, vapour, fast electron impact, secondary electron energy distrib. 77−58148
He, high resoln. pulsed electron beam time-of-flight ejected-electron spectra 77−3462
He I beam-foil excitation, 60-180 keV, alignment production, foil temp. depend. 79−54956
HgCdTe, crystal and photodiode, imperfections and surface conditions using electron induced current technique 79−67385
InP, excitation by 2-4 KeV Ar^+ ions, electron energy spectra 80−11529
KBr film, field enhanced, transmission mode, electron energy spectrum obs. 77−1771
KBr, porous insulator films, field enhanced emission, energy spectrum 77−20969
KCl, electron irrad., secondary electrons and radiation defects 79−55782
KCl film, field enhanced, transmission mode, electron energy spectrum obs. 77−1771
KCl film, porous, injection mechanism for transmission secondary electron emission 78−19643
KCl, porous insulator films, field enhanced emission, energy spectrum 77−20969
KI, secondary electron spectra, primary electron energies up to 30 eV 77−12473
K_2O-SiO_2, glass, influence of electric charge phenomena on AES *(French)* 80−50478
LiF, film, characteristic energy loss and secondary electron spectra *(Japanese)* 78−15266

secondary electron emission continued
LiF film, secondary emission yield, primary electron ang. of incidence effects 78−2961
LiF, transmission and refl. secondary emission 78−27356
LiF(Cl)(Br) film, electron emission under metastable He and Ne atom impact 80−20747
$LiNbO_3$, monodomain ferroelec. cryst., secondary electron emission coeff. 78−11032
$LiNbO_3$, piezoelec., SAW interaction with secondary electrons 80−80708
Mg, adsorbed S(O)(N)(C), internal and external sources of electrons 77−44097
Mg, influence of oxide films on photoemission *(Russian)* 77−81194
MgO, adsorption of Cs and Li, AES, LEED, work function, and secondary electron emission meas. 80−44407
MgO coated detector for SEM backscatter to secondary electron conversion 80−68332
MgO film, delayed secondary electron emission 78−19617
MgO film, ion induced secondary electron emission 77−44104
MgO film, with high secondary electron emission, growth on Al-Mg alloy 78−35590
MgO film with ordered structure slow electrons escape depth 77−20971
MgO secondary emitter, increasing of efficiency by coating with Cs or Li film 78−2960
MgO secondary emitter efficiency improvement for low primary electron energies 79−69931
MgO surface, secondary electron emission effects on voltage breakdown curves in Penning mixture for insulated electrode discharges 78−19616
MgO-Ag porous layer, secondary electron emission from ion impact, gas discharge device appl. 78−68586
MgO-Au cermet film, high intensity electron bombard. effect on secondary electron yield 77−81184
Mo [110], metastable He impact, secondary electron spectra 78−95642
Mo {100}, anisotropy of secondary electron emission from oblique incidence of electrons 79−99999
Mo, adsorption of CO, O_2, metastable He de-excitation spectroscopy and UPS study 80−34314
Mo, effect of ion implantation with K^+ and Ba^+ ions 79−91544
Mo, proton and deuteron irrad., 0.5-2.5 MeV 77−63512
Mo surface, metastable He atom beam contamination by fast neutral atoms, effect on secondary emission 80−55253
Mo:Ba^+, temp. depend. 77−69947
Mo-Nb alloy, secondary electron emission coefficient 77−77333
Mo-Rh, secondary electron emission and inelastic refl. coeffs. 78−15264
Mo(100) face, struct. of secondary emission characts. 77−16439
Mo(100) single crystals, anisotropic ionisation loss of electrons, orientational effects 79−69935
N_2, solid, interaction of 1-3 keV electron beam, range and secondary emission 79−15568
NO, adsorbed layer, electron impact, electron impulsive ionisation spectroscopy obs. 80−60720
Na_3AlF_6 film, evaporated, electron bombard. effect on secondary electron emission, Auger peak shifts 80−2903
NaCl, electron irrad., secondary electrons and radiation defects 79−55782
NaCl, secondary electron emission, appearance of collective and individual interactions of slow electrons 77−69948
NaF(Cl) film, electron emission under metastable He and Ne atom impact 80−20747
Nb, electron bombardment, high-energy, secondary electron emission 80−80917
Nb, for supercond. microwave cavities, secondary electron emission and AES meas. 79−56895
NbN, for supercond. microwave cavities, secondary electron emission and AES meas. 79−56895
Nb_2O_5, for supercond. microwave cavities, secondary electron emission and AES meas. 79−56895
Nb_3Sn, for supercond. microwave cavities, secondary electron emission and AES meas. 79−56895
Ne-Ar (0.1%) mixture, AC plasma panel, Paschen breakdown curves 77−11418
Ni (100), clean and chalcogen-covered, electron ejection by metastable He atom impact 79−8217
Ni (100), with absorbed O_2 monolayer, surface EXAFS, secondary electron yield meas. 79−47544
Ni, (100) surface, secondary electron spectra, adsorbed elements effects 80−50480
Ni, adsorbed S(O)(N)(C), internal and external sources of electrons 77−44097
Ni, effect of ion implantation with K^+ and Ba^+ ions 79−91544
Ni, emission coeffs. for multiply charged ion bombard. 78−11051
Ni, secondary electron emission under Ar^+ ion bombard. near Curie point 80−29838
Ni stepped surface, secondary electron emission, diffraction features 79−83068
Ni substrate, electron bombard. in residual gas containing hydrocarbons, secondary electron yield *(German)* 77−40315
NiO(100), low-energy secondary electron emission, 8 and 12 eV peaks 77−28668
Pb glass, secondary electron emission yield, reducing and heat treatment conditions *(German)* 79−56894
Pb, rel. to high-current electron beam refl. coeffs. *(Russian)* 78−84690
β-PbF_2 film, ionic migration study by Rutherford scatt., defects, secondary emission *(French)* 78−55982
PbO-SiO_2, glass on Si, emission mode of SEM 79−28226
PbS, film, total current spectrum and energy struct. 80−100719
Pb(Zr,Ti)O_3:La(Cd,W), electro-optical ferroelec. ceramic, secondary electron emission yield 79−91546
Pd (111) surface, clean and CO covered, metastable He impact, electron emission, energy and ang. distrib. 80−60744
Pd, secondary electron emission, discrete levels in energy distrib. 79−87535
Pt surface, secondary electron current, Hg(6^3P_2) impact, in Hg(6^3P_1) stepwise electron excitation function meas. 79−858
Ru (001) surface, clean and CO(O_2) adsorbate covered, characteristic slow electron energy loss meas. 79−47562
Si, 1-10 keV H^+, He^+ irrad., role of Auger processes in electron emission 79−15579
Si (111), MEED, secondary electron emission under surface state reson. 78−84688
Si (111) 7×7 surface, emission from surface state resonances 79−69930
Si (111) surface, anal. by ion-electron spectroscopy 78−72670

secondary electron emission continued
Si, (111) surface, Cu phthalocyanine dye deposition, low energy electron optically modulated transmission increase 79−78133
Si (111)-Cl(7×7), angle resolved secondary emission and electron energy loss study of electronic struct. 79−61477
Si, energy losses on C contaminated surfaces, secondary electron spectra, AES, and SEM 79−99997
Si, irrad. by 50 keV N^+ and P^+, depth distrib. of struct. defects, secondary emission obs. 78−2168
Si, low energy primary electron irrad. 79−69934
Si negative electron affinity, statistics of transmission secondary emission 77−48287
Si, secondary electron energy spectra due to He^+, Ar^+ ion impact 78−11049
Si_3N_4, N K-edge EXAFS, secondary electron yield meas. 79−47544
SiO_2, electron-beam-induced cond., appl. to obs. of voltage contrast in SEM 79−21856
SiO_2 layer, thickness measurement by secondary electron emission 80−57435
SrO epitaxial layer, on Mo (110), secondary electron emission and struct., LEED and AES expts. 78−2958
SrO, optimum composition of dielectric materials for AC-operated plasma display panels 80−14945
Ta, emission coeffs. for multiply charged ion bombard. 78−11051
Ta, energy distrib. of secondary electrons during relax. of metastable inert gas atoms *(Russian)* 77−85861
Ti, chemisorption of N_2, O_2 and CO on polycryst. surfaces, secondary electron yield obs. 78−71971
Ti, for supercond. microwave cavities, secondary electron emission and AES meas. 79−56895
Ti, polycryst., chemisorption, of N_2, O_2 and CO, secondary electron yield spectrum obs. 78−38933
TiN, for supercond. microwave cavities, secondary electron emission and AES meas. 79−56895
TiO_2, UV photon induced secondary electron emission 79−52079
TiO_2, UV photon induced secondary electron emission 79−78835
$Tl_2SeAs_2Te_3$, secondary electron emission, fluctuation state effect 80−40193
UF_6 nuclear pumped lasers, electron impact cross section meas. 80−63985
V, proton and deuteron irrad. 0.5-2.5 MeV 77−63512
V_2O_5-P_2O_5 glasses, secondary electron emission 79−87534
V_2O_5-P_2O_5-$Cs_2O(Na_2O)$ glasses, enhanced secondary electron emission yield 80−93441
W (001), surface reson. bands, dispersion relations 77−51797
W (001), surface resonance bands 78−47843
W, ion induced secondary electron emission, probe for adsorbed O 80−55251
W, LEED and electron microscopic investigs., review *(Hungarian)* 77−47654
W, O_2-covered, slow Ar ion induced electron emission 80−60740
W, secondary electron emission rel. to LEED 78−84689
W, secondary electron emission characts. calc. by Monte Carlo methods 79−28868
W, secondary electron emission spectra, angular depend. and phenomenology 79−43076
W, secondary electron yields from ion impacts, stopping power calcs. 78−11053
W, secondary emission and photoemission props., effect of one-electron density of states 80−16152
W, semi-infinite cryst., secondary electron emission, obs. of electronic struct. 79−33871
W surface, clean and CO covered, He metastable atom bombard., secondary electron emission 79−47581
W surface, impact determ. of inert gas ion beam metastable fractions, secondary electrons obs. 79−28873
W, surface cleanness control using secondary electron spectroscopy *(Russian)* 79−90858
W, surface diffusion of adsorbed O, secondary electron emission study 80−76117
W, transmission induced struct. in electron emission spectra 78−43965
W, work function measurement in SEM 80−80918
ZnS, emission coeffs. for multiply charged ion bombard. 78−11051

secondary emission
see also secondary electron emission; secondary ion emission
atomic resonance charge exchange in laser field, secondary emission 79−27081
conference on solid-vacuum interface, Amsterdam, Netherlands (June 78) 79−42342
ion implantation dose meas., secondary particle collection 78−62731
noise, in particle flux, due to reduction and multiplication processes 79−21672
solid, hot luminescence and relaxation processes in resonant secondary emission 78−52549
Be, secondary photon emission following ion bombard. 80−71493
Cu (001) surface, with adsorbed O, Ar^+ bombarded, particle ejection ang. depend. 80−50489
Cu surface, secondary charge emission coeffs., low energy H^0 flux meas. 80−25509
p-Si, defect form. due to multiple N^+ and B^+ irrad. 79−90706

secondary ion emission
see also secondary ion mass spectra; secondary ion mass spectroscopy
alloy surface, anal. by secondary ion-ion emission 77−56200
alloy surfaces, sputtering process and sputtered ion emission models 80−35044
bombarding ion dependence of secondary ion emission and sputtering yield 79−33879
caesiated surface, negative ion emission *(French)* 80−108314
channel plate, for secondary ion images obs. *(French)* 79−58840
competitive atomic and molecular ion emission from solids 78−68588
conference, Stanford, USA (Aug. 1979) 80−105419
desorption, heavy-ion induced, of organic cpds. from solid surfaces 80−100739
elements, sputtering process and sputtered ion emission models 80−35044
energy spectra of secondary ions emitted during ion bombardment 78−23573
fission fragment and alpha recoil induced secondary ion ejection 80−71533

secondary ion emission continued
flooded on noble metal surface, effect on sputtered negative ion yields 78−11056
high energy molecular beam apparatus for solid and surface anal. 77−21443
intensity changes, correction via new total ion monitoring method 78−12796
ion analysis, conference, Paris, France, (May 1977) 77−86406
ion beam analysis, conf., Paris, France (May 1978) 79−58837
ion implantation, quantitative, current practice and appls. 79−69141
ion microanalysis, review 79−96404
ion-surface impact, surface atomic struct., effect on recoil atom energy distrib. 80−35050
ionisation of solids during sputtering, exam. of mech. *(Russian)* 79−33878
ionisation process, review 80−35040
layer structures, raster scanning depth profiling 77−16441
mechanism, energy spectra 79−100013
metal, obs. of initial oxidation stages 78−11386
metal, positive secondary ion and sputtered atom energy distrib. 77−32485
metal, sputtering induced photon and ion emission similarities, O_2 adsorpt. effect 77−28674
metal, with adsorbed Cs effects on photon and secondary ion emission during sputtering 80−35038
metal interface of unlike metals, secondary ion-ion emission 78−11050
metal surface, adsorbed C^+ removal, by 20-30 keV Ar^+, in plasma 77−76103
metal surface, anal. by secondary ion-ion emission 77−56200
metal surface, ion bombarded, secondary negative ion emission 79−28879
metal surface, ion bombarded evidence for recomb. mech. of cluster emission 79−100007
metal surface, ionisation of atoms 79−68310
metals, polycrystalline, secondary ion energy spectra 79−24401
mica, surface impurity levels by static SIMS, cleaning treatment effects 77−59190
microanalysis, transfer optics *(French)* 79−58838
oxide layers on Ni-Cr and Fe-Ni-Cr alloys, compar. study using secondary ion emission and electron probe analysis *(French)* 77−56286
oxidised surfaces, sputtering process and sputtered ion emission models 80−35044
positive secondary ion emission from solid surface, meas. apparatus, spherical condenser *(German)* 77−44103
quadrupole ion microprobe for secondary ion emission investigs., ion optics 79−35892
quadrupole-type SIMS development and applications *(Japanese)* 77−86414
review, secondary complex ion emission *(Russian)* 80−108305
secondary ion-ion emission, primary ion beam optimum current density review 77−52211
semiconductor, positive secondary ion and sputtered atom energy distrib. 77−32485
semiquantitative analysis, one fitting parameter approach 80−108762
silicate glass, silicates, matrix effects in secondary ion emission 80−76125
silicates, ion bombardment, secondary positive mono-atomic ion emission, cation conc. depend and matrix effects *(French)* 80−50487
silicates, quantitative anal., linear variation of secondary ion yield *(French)* 80−108763
SIMS, secondary ion emission mechanism, autoionis. process model *(Japanese)* 79−26177
slow ion secondary emission model, rel. to Anderson model *(French)* 79−56902
solid surface, energetic particle irrad.,, collision cascade 80−45186
sputter ion source, appl. to IMA analysis *(Japanese)* 79−54734
sputtering, at. excitation mechanism 78−43971
sputtering, Saha-Langmuir eqn. appl. 77−8698
sputtering, secondary-ion emission probability 79−87548
sputtering yield meas. by integration of secondary ion energy distrib. 77−77334
steel, austenitic, non-oxidising, B and by secondary ion emission and X-ray microanal. *(French)* 80−11985
steel, stainless 304, secondary ion emission due to H ion bombardment 79−8216
surface, secondary ion emission during O_2^+ ion bombardment *(Japanese)* 78−84691
surface analysis, quantitative, using ion-induced secondary ion and photon emission 77−86423
surface plasma, influence on secondary ion and photon emission under medium-energy ion bombard. 79−33881
tissuelike medium α trajectory heavy secondary ion ejection 80−9466
Tokamak fusion devices, secondary ion emission, appl. to impurity control 80−37584
transition metal borides, secondary ion sputtering, ionisation, energy distrib. characts., atom binding energy *(Russian)* 79−69940
transition metal carbides, secondary ion sputtering, ionisation, energy distrib. characts., atom binding energy *(Russian)* 79−69940
water clusters around alkali metal ions, secondary emission obs. 77−63518
yield, linear variation, quantitative anal. of mineral silicates *(French)* 80−108763
Al, Ar^+ ion bombard., photon and secondary ion emission, single cryst. struct. effect 77−59660
Al, energy spectra, 0-55 eV, contamination levels 79−15573
Al, ion bombarded, photon and ion emission, simultaneous meas. 78−15276
Al-Li solid soln., decomposition exam. by secondary ion ion emission *(Russian)* 78−68696
Ar ion bombardment and Cs flooding of metallic surfaces, secondary negative ions *(French)* 77−85866
Au, energy spectra, 0-55 eV, contamination levels 79−15573
BC, ion bombarded, chemical effects on secondary photon and ion emission 78−95637
Be, clean and O covered, secondary-ion emission energy depend. 80−50502
Be, ion bombarded, chemical effects on secondary photon and ion emission 78−95637
Be surfaces, O and H covered, secondary ion emission, coverage dependence 80−35043
Bi_2O_3, doped, secondary ion emission, at. and mol. processes 78−68588
secondary ion emission continued
Bi_2O_3, molecular versus atomic secondary ion emission, rel. to quantitative analysis 79−61481
C, ion bombarded, chemical effects on secondary photon and ion emission 78−95637
Co-Si alloy, secondary ion mass spectrometry *(Dutch)* 79−1809
Cr, energy spectra, 0-55 eV, contamination levels 79−15573
Cr, ion bombard. induced photon and secondary ion emission in O_2 atmosphere 77−90231
Cr, secondary negative ion emission, effect of adsorbed O_2 *(Russian)* 79−28881
Cs flooding and Ar ion bombardment of metatlic surfaces, secondary negative ions *(French)* 77−85866
Cu (001), sputtering of atoms and positive ions along [011] and [101] directions, ang. depend. 77−24917
Cu (110), O adsorption, low-energy ion bombardment investigation 80−34302
Cu alloy film, multicomponent secondary ion emission meas. of composition var. laws *(Russian)* 77−80704
Cu, chain effect for fast recoils, Ar^+ ion beam impact 78−56554
Cu, Cs^+ impact, 5.5 keV, negative secondary ion emission obs., comparison with phosphor bronzes *(French)* 77−66562
Cu, energy spectra, 0-55 eV, contamination levels 79−15573
Cu matrix, small oxide precipitates, two-phase system, sputtering and secondary ion emission 78−39650
Cu, secondary negative ion emission, effect of adsorbed O_2 *(Russian)* 79−28881
Cu-Al alloy, chemical emission by Ar^+ ion bombardment *(French)* 77−86410
Cu-Ni alloy, chemical emission by Ar^+ ion bombardment *(French)* 77−86410
Fe alloys, secondary-ion emission under varying bombardment condition 77−48292
Fe, effects of initial ion bombardment and oxidation 77−1777
Fe, energy spectra, 0-55 eV, contamination levels 79−15573
Fe-Al alloy, chemical emission by Ar^+ ion bombardment *(French)* 77−86410
Fe-Cr, alloy, composition determination using secondary ion emission *(French)* 77−86409
Fe-Cr alloy, Ar ion bombard., O_2 flooded, secondary ion yield as function of original conc. *(French)* 78−39643
Fe-Cr-Ni alloy, quantitative anal. method based on ion bombardment induced secondary ion and photon emission 79−19963
Fe-N alloys, secondary ion emission, phase transforms. effect *(Russian)* 80−66347
Fe-Ni, alloy, composition determination using secondary ion emission *(French)* 77−86409
Fe-Ni alloy, Ar ion bombard., O_2 flooded, secondary ion yield as function of original conc. *(French)* 78−39643
Fe-Ni alloys, qualitative analysis of order-disorder structure by secondary ion-ion emission *(Ukrainian)* 77−69950
GaAs thin film, effect of O on thin film compositions obtained by secondary ion emission 80−26079
Hf, energy spectra, 0-55 eV, contamination levels 79−15573
LaB_6-SmB_6(YbB_6), exam. of secondary ion-ion emission, due to bombardment with 8 keV Ar ions 79−33882
Mo, secondary ion emission mechanism, under Hg^+ ion bombardment 79−100013
Mo, surface, electron-stimulated desorption of negative ions, work function 78−72654
NaCl, doped, secondary ion emission, at. and mol. processes 78−68588
NaCl, molecular versus atomic secondary ion emission, rel. to quantitative analysis 79−61481
Nb, secondary ion emission mechanism, under Hg^+ ion bombardment 79−100013
Ni, desorption of CO due to ion bombard., comparison of surface anal. methods 79−8213
Ni, energy spectra, 0-55 eV, contamination levels 79−15573
Ni, integranular precipitation after annealing, ion imaging microanalysis *(French)* 79−61594
Ni, secondary negative ion emission, effect of adsorbed O_2 *(Russian)* 79−28881
Ni-Cr, alloy, composition determination using secondary ion emission *(French)* 77−86409
Ni-Cr alloy, Ar ion bombard., O_2 flooded, secondary ion yield as function of original conc. *(French)* 78−39643
Ni-Cr(20 wt.%), oxidation in pure O_2, 800 to 1200°C, secondary ion emission exam. of oxide film *(French)* 77−59995
Ni-Fe alloy, chemical emission by Ar^+ ion bombardment *(French)* 77−86410
O_2 covered metals, secondary ion yield, quantitative determ. *(German)* 79−48003
^{18}O, concentration profile, secondary emission of negative or positive ions *(French)* 79−60395
Pb halides, doped, secondary ion emission, at. and mol. processes 78−68588
Pb halides, molecular versus atomic secondary ion emission, rel. to quantitative analysis 79−61481
Pb-In films, atom redistrib., ion-ion emission obs. *(Russian)* 78−18926
PbO, doped, secondary ion emission, at. and mol. processes 78−68588
PbO, molecular versus atomic secondary ion emission, rel. to quantitative analysis 79−61481
Pt-GaAs contacts, sintered, eval. of W, Ti, Mo and Hf barrier metals 77−8193
Re, electron-induced desorption of O_2 *(French)* 77−85853
Ru (001), chemisorption of CO, electron stimulated desorption ion ang. distribs. bonding geometry and bending vibrs. 79−33189
Sc, energy spectra, 0-55 eV, contamination levels 79−15573
Si, Auger electron emission, ion induced and secondary ion emission 80−71546
Si bombardment with atomic and molecular noble-gas ions, secondary ion emission 80−35042
Si, epitaxial film on sapphire, optical absorption and interface comp. profiles 77−12459
Si thin film, effect of O on thin film compositions obtained by secondary ion emission 80−26079
SiC, thin film, effect of O on thin film compositions obtained by secondary ion emission 80−26079
Si_3N_4 thin films, Ga and As concentration measurement by CAMECA probe *(French)* 77−86411
SiO_2 on Si, ion bombarded surface, de-excitation processes 77−16446

secondary ion emission continued
Sm-Co, permanent mag., O ion impact, 5.5 keV, secondary Co ion emission, magnetisation depend. *(Russian)* 78−2967
steel, quantitative anal. method based on ion bombardment induced secondary ion and photon emission 79−19963
Ta, secondary ion emission, normalised energy spectra from Hg^+ impact 80−45193
Ta, surface, secondary ion emission mechanism, under Hg^+ ion bombardment 79−100013
Ti, and alloys, intergranular precipitation after annealing, ion imaging microanalysis *(French)* 79−61594
Ti, energy spectra, 0-55 eV, contamination levels 79−15573
TiO_2, (100) surfaces, ionisation of sputtered-atomic particles 80−20750
TiO_x, surface film on plasma anodised Ti, comp. determ. 77−48591
V, anomalous secondary ion emission, normalised energy spectra from Hg^+ impact 80−45193
V, energy spectra, 0-55 eV, contamination levels 79−15573
V, oxidation during energetic particle irrad., influence of reactive gases on sputtering and secondary ion emission 78−72656
V, secondary ion emission mechanism, under Hg^+ ion bombardment 79−100013
V surface interaction with O_2, H_2, H_2+O_2 and H_2O, SIMS, EID 77−62753
W, electron-induced desorption of O_2 *(French)* 77−85853
W, energy spectra, 0-55 eV, contamination levels 79−15573
W, oxidation during energetic particle irrad., influence of reactive gases on sputtering and secondary ion emission 78−72656
W^+, relative ion sputtering yield, integration of secondary ion energy distribution, retarding dispersive ion energy analyser 79−33875

secondary ion mass spectra
active ion bombardment induced chemical reactions at surfaces detected by SIMS 79−16034
adhesion, surface anal. techniques appl. 80−65381
alkali halides, sputtering and cluster formation, mass spectra and SIMS 79−19959
amino acid, monolayer on solid, SIMS anal. 79−89038
amino acid overlayers, on Ag, XPS and SIMS study 79−86986
amino acid overlayers, static SIMS exam. 79−83074
amino acid valine, heavy ion induced desorption, time-of-flight mass spectra anal. 80−54509
anodic oxide film, exam. using SIMS and ellipsometry 79−61770
ceramics, local in depth anal. by neutral beam SIMS 80−89565
chromel and alumel thermocouples, decalibration, quantitative SIMS anal. 80−4705
coating chemical characterisation by surface and near-surface sensitive techniques 79−15053
conference, Stanford, USA (Aug. 1979) 80−105419
depth profiles by sputtering in SIMS and AES 79−56891
depth profiling, dynamic range of 10^6 80−107302
diamond:B, B conc. and impurity-to-band activation energy 79−56165
diamond:B epitaxial layer, SIMS obs. of impurity distrib. 78−19169
diamond:Li, ion implantation, investigation of Li^+ distrib. 79−77630
electron microprobes and scanning electron microscopy, conf., Orsay, France, Dec. (1978) 80−11979
ferrite spinel films, LPE growth and props., SIMS, X-ray diffr., and spin wave reson. obs. 80−34323
fluoride salts, static SIMS, mol. rearrangement, cluster formation 78−64440
fluoropolymers, determ. of microstruct. by secondary emission mass spectrometry *(Russian)* 77−31604
$GaP/In_xGa_{1-x}P/GaAs$:(Cs-O) high sensitivity transmission photocathodes, photosensitivity, electron diffusion length 79−78832
garnet LPE layers, SIMS in-depth conc. profiling 77−24489
glass/polymer interface exam. using ion scattering spectroscopy and scattered ion mass spectrometry 78−60641
glasses, SIMS quantitative analysis, accuracy 79−39266
graphite, energetic ion sputtering, appl. of AES-SIMS (IMA)-FDS combined systems to physical and chemical processes 78−95636
graphite fibre, Type-A, surface comp. and energetics 77−70024
graphite fibres, HM, surface comp. and energetics 80−54480
histological section, high mass resolution by ionic analyser *(French)* 80−109069
implanted ion depth distrib., secondary ion mass spectra 80−79829
impurity flux in scrape off layer of Tokamaks TFR 400 and 600 79−652
insulators, primary-ion charge compensation in SIMS anal. 79−57322
ion beam material characterisation, conf., Aleria, Corsica (Sept. 1976) 79−96403
ion etching, secondary ion monitoring 79−91551
ion yields, depend. on ionisation pot. and matrix sputtering yield 79−8214
ionic clusters, struct., thermodynamic functions, energy surfaces and SIMS 80−63881
ionisation of sputtered atoms, microscopical quantum-mech. model 79−8220
lubrication, spectroscopic methods for surface anal. *(French)* 80−26095
mass peaks identification in SIMS using computer program 80−101867
metal, H detect., SIMS method with quadrupole mass filter 77−32854
mica, surface impurity levels by static SIMS, cleaning treatment effects 77−59190
mica surface, static SIMS anal. 78−38922
MIS solar cells, interface problems, AES, SIMS and XPS study 80−89627
molecular ion cluster emission, parity rule applics. in SIMS *(French)* 80−63882
MOS structure, electrical behaviour and SIMS depth profiling 78−84308
Nimocast, diffusion of Cs, AES, SIMS depth profile study *(German)* 78−84008
oxidation and O_2 adsorption studies 78−15273
phosphor bronzes, surface Cs^+ impact, 5.5 keV negative secondary ion emission obs., rel. to Cu *(French)* 77−66562
polyfluorvinylide, determ. of microstruct. by secondary emission mass spectrometry *(Russian)* 77−31604
polysiloxane-metal oxide interfaces, bonding mechanism, surface anal. by XPS and static SIMS 78−15643
polytrifluorclorethylene, determ. of microstruct. by secondary emission mass spectrometry *(Russian)* 77−31604
quantitative, review 80−61195
recording, optimisation 79−43683

secondary ion mass spectra continued
sapphire-Si interface structure, SIMS obs. 77−76675
semiconductor materials, quantitative anal. 80−101052
semiconductor microstructure fabrication, ion channeling effects 80−70230
semiconductor thin films and heterojunctions, grain boundary and interdiffusion studies, AES and SIMS 79−77842
semiconductors, characterisation of thin epitaxial layers and bulk material *(French)* 80−50904
semiquantitative, one fitting parameter approach 80−108762
soda-lime glass, depth profiles of Na and Ca by SIMS and AES 78−51805
solid surface anal. by secondary ion mass spectrometry *(Rumanian)* 77−47655
sputtered particles, energy and mass distribs. 80−84822
sputtering, preferred, phenomenological model for SIMS and Auger profiling 80−55254
sputtering yield meas. by integration of secondary ion energy distrib. 77−77334
sputtering yield variations, substrate matrix effects under O^- and Cs^+ ion bombard. 79−15571
stainless steel, in $MgCl_2$ solutions, Cl distrib. in oxide films *(French)* 80−108765
stainless steel, neutron dose determ., from isotope abundance ratio, mass spectra obs. 80−61220
steel, C, friction faces, S, O content, secondary ion-ion emission obs. 80−55545
steel, continuously cast, segregation at halfway cracks 80−60869
steel, Ni-Cr, oxide layer form., SIMS obs. 79−52464
steel, stainless type 304, surface cleanup and sputtered ion production, AES and SIMS obs. 79−66209
steels, welded, types D36, D50, secondary ion anal. of segregation 80−7580
surface analysis, appl. of SIMS, review 80−40204
surface analysis, atomic beam scatt., SIMS, and vibr. spectra, book contrib. 79−42357
surface analysis, using SIMS, Mossbauer spectra and spectrometry 79−16050
surface charact., combined ion scattering spectrocopy, SIMS, SEM, energy dispersive X-ray techniques 79−43702
surface problems, in materials science and technology, conference, Gothenburg, Sweden, June 1979 80−51950
surface science, conf., York, England (March 1977) 78−14540
surface segregation, effect on metallurgical props, SIMS, XPS and AES *(French)* 80−80045
tetrafluorethylene-ethylene copolymer, determ. of microstruct. by secondary emission mass spectrometry *(Russian)* 77−31604
thin film, and surface anal., modern methods 80−54486
yield calculations for oxidised metal surfaces, empirical formula 78−6821
a-Si:H, effect of H conc. on photovoltaic props. 79−99577
Ag, Cu diffusion, SIMS investigations 80−59717
Ag, ion beam plating using mass analysed ions, SIMS and AES expts. 78−19673
Ag surface, CO chemisorption, SIMS, XPS study 80−84382
Ag-Au, surface layer, effect of Ar^+ bombardment, AES and SIMS 80−25504
Al, 1100, anodic barrier film characts., ISS/SIMS 78−53021
Al anodic film, H profile meas. by SIMS 78−27847
Al, film and polished bulk specimens, initial stages of oxidation obs. 80−81239
Al, oxide coated, inhibitive and aggressive ion effects, secondary ion mass spectrometry 77−8974
Al, polycryst., secondary ion emission angle, energy distrib. depend. 78−76569
Al, propane adsorption SIMS and EID obs. 77−69167
Al-base alloys, semiquantitative anal. with SIMS, AES and wet chemical anal. 77−48291
Al-Mg-Zn, O_2^+ ion bombard., SIMS and photon emission spectra, local thermodynamic equilib. model 80−20751
$Al_xGa_{1-x}As$, MBE grown film, in situ surface characterisation by RHEED, SIMS and AES 77−43410
Al_2O_3 anodic layer formation in H_3PO_4 solns., surface charact. 78−15603
Au film sandwiches, recovery kinetics and early stages of diffusion, DC resist. expts., correl. with SIMS 79−77971
Au, ion beam plating using mass analysed ions, SIMS and AES expts. 78−19673
Au-Cu-Cr, thin layer, deposited on glass or Si substrate, X-ray microanalysis *(French)* 80−50902
Au-Y_2O_3-Y junctions, migration of Au rel. to voltage-controlled negative resist., SIMS obs. 79−91157
BN, chem. bonding and electronic struct., AES and SIMS meas. 80−50512
B_2O_3, chem. bonding, electronic struct., ESCA, Auger, and SIMS spectra 80−50512
Bi surface, detection of high mass cluster ions by SIMS and XPS surface monitoring 77−16442
Bi_2O_3, molecular versus atomic secondary ion emission, rel. to quantitative analysis 79−61481
CO adsorption on polycryst. metal 78−14585
CdTe surfaces, SIMS, Rutherford scatt. and ellipsometry 79−56046
CdTe, trace anal. by heavy ion induced X-ray emission and SIMS 80−55755
Ce oxidised surface, comparative sputtered neutral mass spectrometry and SIMS studies 79−90856
Co, microanalysis for epilepsy study, use of electrostatic filter and transfer optic *(French)* 79−62414
Co, monolayer, oxidation, quasisimultaneous SIMS, AES, XPS 78−72919
Co-Si alloy, secondary ion mass spectrometry *(Dutch)* 79−1809
Cr, oxide film form., combination anal. using ESCA, AES and SIMS 79−16092
Cr-O system, initial oxidation 78−72924
Cr_3C_{2+}, bond energy and ionization efficiencies from SIMS 79−24400
$Cr_pC_n^+$, p=1 to 4, CrC_n^-, clusters, electronic props., mass spectra obs. *(French)* 79−45877
CsI, high mass secondary ion clusters detected by SIMS 78−88400
Cu (001), chemisorbed O, Ar^+ bombardment, angle resolved SIMS, surface struct. 79−77913
Cu, chemisorpt. of CO, SIMS, AES, desorpt. meas. 78−87875

secondary ion mass spectra continued
Cu, Cs^+ impact, 5.5 keV, negative secondary ion emission obs., comparison with phosphor bronzes *(French)* 77−66562
Cu, diffusion of stable Ge isotopes, isotope effect, SIMS anal. 79−60552
Cu, ion-bombarded, particle ejection, SIMS obs. 79−78810
Cu, polycryst., secondary ion energy spectra, ionisation mechanisms 79−38700
Cu, polycryst. surface, Ar^+ sputtered, ion to neutral yield ratio, SIMS anal. 78−72659
Cu polycrystals, oxidation, secondary ion energy spectra 80−71788
Cu, SIMS depth profiling, surface roughening by low energy ion irrad. 80−60727
Cu, self-sputtered, secondary ion mass spectra 79−74044
Cu surface, low energy Ar^+ ion scatt., binary collision approx., SIMS meas. 79−47582
Cu-Co-Si (0.36, 0.11 wt.%), surface layer struct. on annealing, SIMS and AES exam. 80−88415
Cu-Ni, chemisorpt. of CO, SIMS, AES, desorpt. meas. 78−87875
Cu-Ni, clean surface, surface segregation and growth process of altered layer *(Japanese)* 80−24720
Cu-Ni, surface layer, effect of Ar^+ bombardment, AES and SIMS 80−25504
CuBe, Be distrib. in vicinity of oxidation boundary *(French)* 80−11984
CuO, monolayer on Cu, SIMS anal. of oxidation 79−89038
Fe (110) surface, adsorption and decomposition of NH_3, identification of surface species using SIMS 79−90862
Fe, cast, graphite nodule form., ion microprobe mass anal. appl. 79−43295
Fe-Cr, high-temp. oxidation, borate inhibitors 80−66705
Fe-Cr-Ni alloy, quantitative anal. method based on ion bombardment induced secondary ion and photon emission 79−19963
Fe-Ni-Cr, oxide film form., combination anal. using ESCA, AES and SIMS 79−16092
Fe-O system, initial oxidation, combination anal. using ESCA, AES and SIMS 78−72924
Fe-TiB_2, phase composition, secondary ion-ion emission study *(Russian)* 80−20896
$Fe_pC_n^+$, p=1 to 4, clusters, electronic props., mass spectra obs. *(French)* 79−45877
$Fe_{40}Ni_{40}B_{20}$ glass, ^{10}B self-diffusion, meas. by SIMS 80−49406
α-Fe(111), adsorption of water under the influence of 2.5 keV electrons 79−28199
$Ga_{0.1}Al_{0.9}As$ LPE layers containing low-cond. regions, charging effects in SIMS anal. 80−66348
GaAs, annealing with Si_3N_4, Cr profiles meas. 79−90693
n-GaAs, anodic oxide film, exam. using SIMS and ellipsometry 79−61770
GaAs diffusion of ion implanted Be, SIMS and electrical profiling 78−47605
GaAs, electron trap at E_c-0.75 eV, direct evidence for nonassignment to O 79−90988
GaAs, MBE grown film, in situ surface characterisation by RHEED, SIMS and AES 77−43410
GaAs oxide, passivated layers, quantitative in-depth profile, AES-SIMS thermal, anodic and plasma oxidations 78−84087
GaAs, oxide layers prepared by anodic, thermal and plasma oxidation, in-depth profiles and annealing effects 79−61768
GaAs, polycryst., wet and dry oxides, comparative study by AES, SIMS and XPS 80−80116
GaAs, SIMS, energy distrib. of sputtered ions 79−38706
GaAs, semi-insulating, effects of heat treatment characterised by SIMS 78−6091
GaAs, single cryst., adsorbed mol. lifetimes and desorption activation energy meas. 78−20072
GaAs solar cell, polycryst., grain boundary passivation by oxidation, AES, SIMS and XPS obs. 80−81467
GaAs, solid solubility of Se, SIMS 78−67830
GaAs, surface segregation of implanted alkali metals, photoemitter prep. and characts. *(French)* 78−60544
GaAs, surface studies during MBE growth 79−90899
GaAs:^{11}B, physicochem. and resistivity meas. 80−24933
GaAs:Be, annealing effect during MBE 78−79898
GaAs:Cr, bulk and epitaxial, ion implanted, Cr conc., depth distrib. and diffusion coeff. 80−49243
GaAs:Cr, Cr distrib. and heat-treatment migration studies by SIMS 80−107305
GaAs:Cr capless annealed, under As press., Cr redistrib., SIMS obs. 80−59503
GaAs:Cr substrates and LPE layers, Au film deposition, Cr redistrib., TEM and SIMS 80−15312
GaAs:S, depth profiling using Cs^+ bombardment and negative SIMS in UH vac. 79−99232
GaAs:Se, fast diffusion of elevated temp. ion implantation, SIMS meas. 78−34527
GaAs:Se, implanted, depth profile, SIMS obs. 78−30655
GaAs:Se, ion implanted, Cr redistrib. during annealing, SIMS anal. 80−10570
GaAs:Se depth profiles, Cs^+ SIMS anal. appl. 79−39265
GaAs:Se^+, Cs^+-SIMS and negative ion spectrometry 79−12882
GaAs:Si, ion implantation, thermal annealing, Hall meas., SIMS atomic profile meas. 80−75243
GaAs:Sn thermal diffusion from spin-on SnO_2/SiO_2 source 80−96691
GaAs-Au(Ag) Schottky barrier solar cells, interface problems, AES, SIMS and XPS study 80−89627
n-$GaAs_{0.6}P_{0.4}$, anodic oxide film, exam. using SIMS and ellipsometry 79−61770
$GaAs_{0.6}P_{0.4}$:Be, implanted annealing studies, elec. resist., Hall effect meas. 78−84213
$GaAs_{1-x}P_x$, SIMS, energy distrib. of sputtered ions 79−38706
$GaAs_yP_{1-y}$ alloy, composition effects in growth by MBE 80−59816
GaN:Al, VPE grown, luminesc. and elec. props. depend. on doping conc., bound excitons 80−20688
GaP:Cr epitaxial layers, Cr conc. profile determ. 80−65029
GaSb, diffusion of In, 520 to 712°C 80−79995
Gd oxidised surface, comparative sputtered neutral mass spectrometry and SIMS studies 79−90856
$Gd_3Fe_3O_{12}$, electron irrad., primary-ion charge compensation using SIMS 79−57322
Ge amorphous film, O depth profiling by SIMS 80−39480
H_3BO_3, chem. bonding, electronic struct., ESCA, Auger, and SIMS spectra 80−50512

secondary ion mass spectra continued
$H(H_2O)_n^+$, macromol. clusters, detect. by SIMS 79−39239
H_2O, ordered monolayer adsorbed on KCL (100), secondary ion mass spectra 77−76660
HfC, bond energy and ionization efficiencies from SIMS 79−24400
In, chemisorption of O_2, XPS and static SIM spectral study 80−80055
In film, oxidized polycrystalline, spectra obtained from combined XPES and SIMS investigation of surface 80−52377
$InAs_yP_{1-y}$ alloy, composition effects in growth by MBE 80−59816
InP (100) substrates, for MBE, ion-cleared, contamination, SIMS meas. 78−11353
InP (110), low coverage adsorption, SIMS study 80−49500
InP, VPE growth for MESFET's 80−103602
InP-metal Schottky barriers, effects of heat treatment characterised by SIMS 78−6446
Li_3N thin film, vacuum evaporation on WO_3, retarded deposition 80−108351
$MgO-Al_2O_3-SiO_2$ glass/polysulphone adhesive failure, ISS and SIMS obs. 80−55626
Mo, adsorption of O_2, low energy SIMS and electron induced desorpt. exam. 77−76667
Mo, chemisorption of CO, low energy SIMS and electron impact desorption expts. 78−38941
Mo, coadsorption of CO_2 and O_2, AES and SIMS obs. 79−46928
Mo, diffusion of Cs, AES, SIMS depth profile study *(German)* 78−84008
Mo, ion bombard., ion and photon yields, CO adsorption effect 80−89098
Mo, monolayer, oxidation, quasisimultaneous SIMS, AES, XPS 78−72919
Mo-O system, initial oxidation 78−72924
Mo_2C, bond energy and ionization efficiencies from SIMS 79−24400
Mo(100), chemisorpt. of O_2, low-energy SIMS, ion yields depend. on surface chem. and primary ion energy 78−73105
N_2 adsorbed on W, effect of SIMS sputtering induced recomb. anal. 80−55243
N_2^+, active ion bombardment of pyrolytic graphite or Si (100), SIMS obs., 79−16034
NaCl, molecular versus atomic secondary ion emission, rel. to quantitative analysis 79−61481
$Na_2O-Al_2O_3-SiO_2$ glass, diffusion of Ca and Mg, SIMS study 79−82387
$Na_2O-CaO-SiO_2$, Al-coated glass, electron bombarded, SIMS analysis 79−66376
Nb (110) and (750), interaction with O_2, LEED, AES, SIMS, and EELS obs. 80−44408
Nb foils, coated with H-permeable Pd film 79−52467
Nb, interaction with O_2, AES and low-energy SIMS meas. 79−47832
NbC, bond energy and ionization efficiencies from SIMS 79−24400
Ni (001), azimuthal anisotropies of ejected dimer ions, SIMS expt. 80−60730
Ni (100), adsorption of CO, SIMS and XPS meas. 79−42378
Ni (100), adsorption of water $(O_2)(H_2)(CO)$, combined XPS/LEED/SIMS exam. 79−83075
Ni (100), chemisorption of O_2, SIMS and XPS 79−15019
Ni (100) and polycrystalline surfaces, CO chemisorption, low energy SIMS and AES 80−34309
Ni, (110), (100) and (111) surfaces, coadsorption of CO and H_2S, surface coverage meas. by SIMS 79−90876
Ni, (110) and (111) surfaces, oxidation exam. at room temp. by combined SIMS-AES/LEED method 79−20241
Ni alloys, dilute, near surface composition, effect of irradiation and sputtering 79−33168
Ni, chemisorpt. of CO, SIMS, AES, desorpt. meas. 78−87875
Ni, chemisorption of O_2 and CO, ion bombard., particle ejection, SIMS obs. 79−78810
Ni, desorption of CO due to ion bombard., comparison of surface anal. methods 79−8213
Ni, diffusion of Cs, AES, SIMS depth profile study *(German)* 78−84008
Ni, integranular precipitation after annealing, ion imaging microanalysis *(French)* 79−61594
Ni, ion bombard., ion and photon yields, CO adsorption effect 80−89098
Ni, oxidation, chemisorption and oxide nucleation stages, low-energy SIMS and AES obs. 79−43083
Ni, polycryst., O_2 interaction obs. 78−76568
Ni, reaction of H_2 and O_2 on polycryst. surface, SIMS and thermal desorption meas. 80−40742
Ni surface, adsorpt. and decomp. of formic acid, obs. using combined SIMS-FDS-AES system 78−40076
Ni surface, polycryst., interaction with O_2, SIMS and flash filament meas. 79−47829
Ni-base alloy, semiquantitative anal. with SIMS, AES and wet chemical anal. 77−48291
Ni-Cr(Fe)(Cu) alloy, matrix effect in SIMS anal. using O_2^+ primary beam 80−76576
Ni-O system, initial oxidation, combination anal. using ESCA, AES and SIMS 78−72924
Ni-Pd surfaces, electrochem. passive film form. and comp. determ. by SEM, SIMS, XPS 80−39401
O_2 covered metals, secondary ion yield, quantitative determ. *(German)* 79−48003
Pb halides, molecular versus atomic secondary ion emission, rel. to quantitative analysis 79−61481
Pb surface, oxidation, XPS and SIMS study 79−15873
Pb-Sb alloy, Sb distrib. profile as function of depth in corrosion films 80−21177
PbO, molecular versus atomic secondary ion emission, rel. to quantitative analysis 79−61481
Pd surface, CO chemisorption, SIMS, XPS study 80−84382
Pd-Ag, thin layer, deposited on glass or Si substrate, X-ray microanalysis *(French)* 80−50902
PdAg surface, CO chemisorption, SIMS, XPS study 80−84382
Pt film on Si, PtSi form. kinetics, AES, SIMS, EPMA 77−11800
Pt-Rh alloys, surface behaviour on heating in air, XPS and SIMS *(French)* 77−40327
Re, dissociative and mol. adsorption of NO and H_2O, XPS, AES and SIMS study *(French)* 79−69344
Si, amorphous, asymmetrical profile of ion implanted P 79−46693
Si, amorphous, epitaxial regrowth, structure and impurities effect 80−84401

secondary ion mass spectra continued
Si, amorphous, hydrogenated, diffusion of D_2, SIMS anal. 78−75877
Si, annealing, using laser pulses, impurity incorporation at melt-cryst. interface 80−59504
Si, dry etching induced surface contamination, SIMS, AES, and XPS obs. 80−11810
Si, high sensitivity depth profiling of As and P, SIMS 77−7742
Si layers amorphized by molecular ions, laser annealing 80−103379
Si microdot standards, ion implanted, SIMS anal., detection limits 79−39264
Si, multigrained, grain boundary elec. and compositional props., surface anal. 80−76575
Si, multigrained, impurity segregation to grain boundaries, AES and SIMS obs. 80−65027
Si, O_2 adsorption and oxidation 78−15273
Si on sapphire, deposition kinetics and interface characteris. 79−28234
Si oxidation, dopant redistrib., Cs^+ SIMS anal. appl. 79−39265
Si, oxidation induced by ion or electron bombardment, AES-SIMS study 80−108606
Si ribbon, EFG, C contaminant conc. determ. by nuclear techniques and SIMS 80−59506
Si wafer, ion etching, secondary ion monitoring 79−91551
Si wafer surface sputtering, secondary postive ion mass and kinetic energy anal. 78−88391
Si:As, depth profile detect. limit of 3×10^{15} atom cm^{-3} using Cs^+ bombardment negative SIMS 77−65988
Si:As, SIMS, energy distrib. of sputtered ions 79−38706
Si:As(P), depth profiling using Cs^+ bombardment and negative SIMS in UH vac. 79−99232
Si:B, ion implanted, laser annealed, thermal annealing effect 79−73191
Si:B(Be)(Li) ion implanted, channelling and random equivalent depth distrib. 80−100293
Si:B(P)(As)(Cu)(Fe), dopant profile changes induced by laser irrad. using SIM and backscatt. meas. 79−69148
Si:B(P)(As)(Sb), ion implanted, redistrib. of dopants by pulsed laser annealing 79−7620
Si:B(P)(As)(Sb)(Cu)(Fe), ion implanted, doping profile, pulsed laser annealing effects 80−88197
Si:Be, ion implanted, correl. of atomic distrib. and implantation induced damage profiler 80−88199
Si:Cr, ion implanted, Cr conc., depth distrib. and diffusion coeff. 80−49243
Si:D, ion implanted, D depth distribs., SIMS meas. 80−54279
Si:Ga^+, impurity distrib. profiles using SIMS and Hall effect method 79−69152
Si:H amorphous film, H quantitative depth profiling by nuclear reactions and SIMS 78−14373
Si:Na, quantitative analysis of residual impurities with SIMS 78−87688
Si:O_2^+, in-depth distrib., Cs^+ SIMS anal. appl. 79−39265
Si:O(C), implant redistribution, annealing effects, SIMS meas. 80−96561
Si:P, diffusion-doped laser irradiation effects, electrical reactivation of P 80−39124
Si:P, N implantation through Si_3N_4 film, depth distrib. of knock-on N, SIMS meas. 78−10066
Si:P(As), conc. profiles of P (or As) and recoiled O atoms after ion implantation into SiO_2-Si, SIMS obs. 79−51138
Si:Sb, low energy ion implantation, profile determ. 80−88176
Si-Al solid-phase epitaxial growth, substrate effects, SIMS and backscatt. spectra 79−42421
Si-SiO_2 interface, chem. struct. of transitional region 78−95824
Si-SiO_2 interface struct., transient region 77−85115
Si-SiO_2 interfacial region on TCE/O_2 and CCl_4/O_2 oxidised Si, struct. and comp. 80−50741
Si-SiO_2 laminar ion-implanted systems, struct. change investig. by MSSI method *(Russian)* 80−107918
Si-SiO_2 transition region width, SIMS depth profiling 80−39454
SiC, energetic H and Ar ion sputtering, AES-SIMS-FDS combined obs. 78−80444
SiC, energetic ion sputtering, appl. of AES-SIMS (IMA)-FDS combined systems to physical and chemical processes 78−95636
SiC, sputtering processes by energetic ions, combined SIMS-AES study 80−40201
SiO_2, amorphous, ^{30}Si diffusion *(French)* 80−59696
SiO_2, amorphous, diffusion of ^{30}Si *(French)* 80−107482
SiO_2, dry etching induced surface contamination, SIMS, AES, and XPS obs. 80−11810
SiO_2 film, quantitative secondary ion mass spectrometry of O isotopes and other light elements 77−9147
SiO_2 films, amorphous to cryst. transform. induced by diethyl ether vapour 79−55667
SiO_2:Na, film, depth profiling by SIMS 78−79624
SiO_2-CaO-Na_2O, glass, layers near surface, anal. using SIMS 80−88041
SiO_2-Li_2O, glass, layers near surface, anal. using SIMS 80−88041
SiO_2-Si interface, detection of SiO_2^- ions by SIMS 77−77848
Si(111), ion-bombard., O_2 adsorption, SIMS study 80−70522
SmAu, significance of negative ion formation in sputtering and SIMS anal. 78−72663
SnTe, ^{117}Sn diffusion coeff. meas., stoichiometric deviation, SIMS 80−34236
SnTe, diffusion of ^{125}Te, diffusion profiles by SIMS meas. 80−84325
steel, quantitative anal. method based on ion bombardment induced secondary ion and photon emission 79−19963
TZM, diffusion of Cs, AES, SIMS depth profile study *(German)* 78−84008
Ta, anodic barrier film characts., ISS/SIMS 78−53021
Ta foils, coated with H-permeable Pd film 79−52467
Ta, O_2 adsorption and oxidation 78−15273
β-Ta sputtered film, stabilisation by Ta-Si interlayer, SIMS depth profiling 80−54568
TaC, bond energy and ionization efficiencies from SIMS 79−24400
TaN, sputtered thin films, cross-sectional composition by SIMS, elec. resist. calcs. 79−77953
Ta_2O_5 preferential sputtering by Ar^+ ions, SIMS obs. 79−83083
Ti, adsorption of O_2, CO and CO_2, SIMS expts. using 500 eV primary Ar^+ ions 77−72785
Ti, and alloys, intergranular precipitation after annealing, ion imaging microanalysis *(French)* 79−61594
Ti, monolayer, oxidation, quasisimultaneous SIMS, AES, XPS 78−72919
Ti, oxidation in monolayer range, SIMS, AES and XPS meas. 77−86215
TiC, bond energy and ionization efficiencies from SIMS 79−24400
TiC_x film, formation by hollow cathode discharge reactive deposition process, on mild steel sheet 79−24451
TiH_x and $TiD_{0.9}$, surface characts., AES, EELS, SIMS, and XPS study 80−65343
TiN film as protective coating for vacuum deposition chamber, Auger electron spectroscopy study 80−25922
TiO_2(-Cr_2O_3), rutile, Cr_2O_3 effects on O_2 tracer diffusivity, depth profile meas. by SIMS 80−24651
U, quantitative analysis 77−73498
V foils, coated with H-permeable Pd film 79−52467
V-H, H on polycrystalline V, H detection by SIMS, flash-desorption obs. 79−24405
VC, bond energy and ionization efficiencies from SIMS 79−24400
W (100), coadsorption of Zr and O_2 at high temp. 80−6653
W dispenser cathodes, Ba-activated, surface characts., ion scatt. spectrometry and SIMS study 80−66377
W, O_2 chemisorption hysteresis effect 77−72771
WC, bond energy and ionization efficiencies from SIMS 79−24400
W(100), chemisorpt. of O_2, low-energy SIMS, ion yields depend. on surface chem. and primary ion energy 78−73105
W(100)-O chemisorption system, static mode SIMS 78−34712
ZnO, adsorption of H, space charge accumulation layers effect on secondary ion yields, H conc. meas. 79−83087
$ZnSiP_2$:Ga, doping conc. meas. 78−76077
ZrC, bond energy and ionization efficiencies from SIMS 79−24400

secondary ion mass spectroscopy
adhesion measurement, locus of failure, bond failure in adhesive joints 80−50801
alloys, surface composition after fabrication by SIMS 80−65351
apatite, secondary ion mass spectra 78−68965
axially symmetric quadrupole SIMS, using mirror type ion-electron convertor 79−5232
biological specimens, SIMS anal. appl. 79−44074
Cameca ion analyser, modifications 79−58841
channel plate, for secondary ion images obs. *(French)* 79−58840
chemical characterisation, of semiconductors and metals, extending SEM capabilities using a SIMS attachment 79−17555
chemical surface analysis, low energy ISS compared with SIMS 78−64908
computerised system for energy spectra determ. 80−3423
concentration profiles depth differential, evaluation 80−59531
conference, Stanford, USA (Aug. 1979) 80−105419
contamination levels in metals, meas. by improved sensitivity 79−15573
corrosion science, surface analytic techniques 80−31929
crystalline solids, electronic industry, chem. anal. instrumental methods progress 80−66903
data quantification, theoretical model and sensitivity factor calcs. 78−21255
depth profiles, edge effects, anal. correction 80−80925
depth profiles obtained by ion-beam sputtering, edge-effects correction 80−55757
depth profiling, automatic sequential mass analysis 80−108764
depth profiling, dynamic range of 10^6 80−107302
depth profiling by ion microprobe with high mass resolution 79−46894
depth profiling techniques for thin film interdiffusion and interfacial reactions, book contrib. 79−1564
detector discrimination, negative ions ion-to-electron converter yield factors 79−17553
detector discrimination in SIMS: ion-to-electron converter yield factors for positive ions 78−73100
detector sensitivity improvement 79−26172
dielectrics, use of Cs^+ beams in secondary ion mass spectra 80−90929
doping profiles meas. appl. *(German)* 78−95978
duoplasmatron ion source for secondary ion mass spectrometry 79−85196
electronic material and device characterisation using surface-sensitive analytical techniques 80−65341
element distributions obtained by ion microprobe, images quantification 78−73101
energy band centre, procedure for adjustment *(French)* 79−58839
energy selection effect on quantitative anal. 77−44539
ESCA-ion scatt. spectroscopy-SIMS, review, chem. appls. 79−43701
film surface analysis techniques survey, for development and production *(Hungarian)* 80−54537
flint implements, provenance determ. possible appl. of SIMS 80−61197
garnet LPE layers, SIMS in-depth conc. profiling 77−24489
gas ion probe, instrument for gas conc. profile meas. in solids 79−39238
high energy molecular beam apparatus for solid and surface anal. 77−21443
high temp. relief cavitation, SEM, STEM, TEM, SIMS and EDX anal. 79−5039
III-V semiconductors, surface and interface anal., secondary ion mass spectrometry technique 80−59763
image quantitation, by microphotodensitometry and digital processing 78−32914
imaging analysis, sensitivity, lateral and depth resolutions 78−48738
in-depth profiling by SIMS *(Japanese)* 78−85246
instrument combining XPES and SIMS for surface studies 80−52377
instrumental discrimination effects, evaluation 79−35888
intensity changes correction via new total ion monitoring method 78−12796
interface composition determ. methods 79−70396
interfacial impurities, quantitative anal. 80−84396
intermetallic compounds, significance of negative ion formation in sputtering and SIMS anal. 78−72663
ion beam analysis, conf., Paris, France (May 1978) 79−58837
ion bombarded surfaces, energy analysed SIMS with Auger and XPS meas. 79−4457
ion implantation by laser annealing, characterisation, solar cell applications 80−70247
ion microanalysis, review 79−96404
ion microprobe anal., secondary ion mass spectrometry at close to single-atom concentration using DC accelerators 79−48004
ion-implanted materials, SIMS characterisation 79−49331
ISS/SIMS, developments 78−76971
layer structures, raster scanning depth profiling 77−16441

secondary ion mass spectroscopy continued
LSI surface analytical techniques applied to electronic components [Si LSI chip inspection] 80−81392
MACS mass and charge analysis technique, principle and appl. 80−73521
mass and energy spectrometer, for secondary ion anal. 77−13814
metal, H detect., SIMS method with quadrupole mass filter 77−32854
metal and oxide surfaces, and interfaces, slow exchange processes study using SIMS 80−55653
metal oxidation, secondary ion energy spectroscopy 80−71788
metal surfaces, characterisation by SIMS and XPS 79−16054
metallurgical applications of XPS, AES, and SIMS *(French)* 80−81253
microanalysis, principles, practice 79−39259
microanalysis, transfer optics *(French)* 79−58838
microbeam anal., conf., Ann Arbor, MI, USA (June 1978) 79−39258
monolayers on solid targets, design of a SIMS apparatus 79−89038
multifeature mass analysis utilising digital image processing, Fe anal. appl. 79−43684
negative ion formation, by sputtering, work function depend. 78−39645
negative ion techniques 79−5235
NODUS, ion scatt. spectrometer for surface composition anal. 78−76968
nuclear engineering appl. 79−30602
p-n junction potential step meas. 80−34503
particle analysis, detection limits, sensitivity 79−43695
photovoltaics and absorber/reflectors, diffusion, chemical reactions, contamination, AES and SIMS 80−72066
primary ion beam profile effects on monolayer analysis 78−68589
primary ion sources, selection 79−39267
quadrupole mass filter, adaptor unit for secondary ion anal. *(German)* 79−75650
quadrupole mass spectrometer, to study secondary and sputtered ions 79−83072
quadrupole mass spectrometer, transmission of narrow ion beam *(French)* 80−105747
quadrupole-type SIMS development and applications *(Japanese)* 77−86414
quantitative, one fitting parameter method 79−39263
quantitative analysis, test on U sample 77−73498
quantitative analysis of glasses and silicates using SIMS 77−56285
quantitative evaluation using Saha-Eggert type eqns. 77−60164
quantitative investigations, results and possibilities *(Hungarian)* 80−73523
quantitative multielement anal., derivation of working curves 77−44563
quantitative techniques in SIMS 78−76942
review on sputtering and SIMS *(French)* 78−80450
second-generation ion microanalyser description and performance *(French)* 80−101055
secondary ion emission mechanism, autoionis. process model *(Japanese)* 79−26177
SEM-AES-IMA combination with SIM spectrometer, Si device anal. appls. *(Japanese)* 78−85249
SEM/SIMS, surface anal. appls. 79−26187
semiconductor crystal growth and defects, appl. of analytical techniques 80−73546
semiquantitative analysis 77−86407
sensitivity improvements, Cs^+-SIMS and negative ion spectrometry 79−12882
SIMS, AES and ESCA analysis of thin films, expt. *(Hungarian)* 77−4952
SIMS-AES-X-ray photoelectron spectral analysis system, for solids anal. 79−39268
SIMS/AES instrumentation and appls. in Japan 79−35883
single-atom concentration, using DC accelerator 79−92042
soda-lime glass to Fe-Cr seal, field-assisted bonding, SIMS anal. 79−34399
solid substance surfaces, physico-chemical props. investigations *(Czech)* 80−90927
solid surface and thin film anal. methods, review 79−34410
solid surface and thin film analysis 78−80825
solid surface characterisation, tridimensional 78−73110
solid surface investig. applications *(Rumanian)* 80−49510
solids, elemental analysis 80−97748
specimen charging control for SIMS and AES of insulators 80−101875
specimen current integration, appl. 79−43685
spectrometer, cluster formation obs. in alkali halide sputtering 79−19959
sputtering use in depth profiling, review 80−40214
steel, cold-rolled sheet, surface chemistry 80−61146
steel, industrial, surface chem. characterisation by SIMS, glow discharge spectrometry and other techniques 80−66907
surface analyser, combining secondary ion mass spectrometry and ion scattering spectrometry 79−5189
surface analysis, advantages and disadvantages of SIMS rel. to ion scattering spectrometry 79−12883
surface analysis, appl. of SIMS, review 80−40204
surface analysis, appl. to lubrication problems, review *(French)* 80−45616
surface analysis, by secondary ion mass spectrometry, review 78−68949
surface analysis, combining secondary ion mass spectrometry and ion scatt. spectrometry 77−60158
surface analysis, probing and imaging techniques 80−54487
surface analysis, spectroscopic methods, review *(Chinese)* 79−34414
surface analysis by ion scattering and secondary ion mass spectrometry 77−40621
surface analysis techniques and appls., symposium, Dayton, USA (Jun. 1979) 80−62363
surface analytical techniques, quantification, review 80−65342
surface characterisation, physical methods, review *(French)* 80−7889
surface reactions, appl. of SIMS *(French)* 80−45603
surfaces and thin film studies by combined system of SIMS, AES and XPS 80−86536
thin films, surface anal., survey of ESCA, AES, SIMS, and ISS *(Hungarian)* 80−70544
three-electrode emission lens, appl. for secondary ion microscopy 79−41324
XPS/SIMS combined apparatus, system for transferring samples between chambers in UHV 79−12809
Al sheet surfaces, chem. characterisation by SIMS, glow discharge spectrometry and other techniques 80−66907
Au-refractory film interdiffusion obs., by combination of scattering techniques 80−65308
Au-Si contacts, O depth distrib. determ. by SIMS 79−4482
AuGe/n-GaAs, SIMS study Au behaviour during annealing 78−75947
Be-Cu dynode, depth profiling anal. of surface layer 80−2253
Cs^+, ion source for secondary ion mass spectrometry 78−32913
Cs^+, semicond. doping profile anal. appls. 79−39265
Cu, sputtered, ionisation probability, energy dependence 80−35041
Fe-Ni-Cr-Al-Y, oxidation mechanism, Y addition effect on kinetics and oxide adherence 80−97623
GaAs, quantitative anal. of O impurities 79−5233
GaAs:Be, implanted, determ. of Be concentration profiles 79−4335
GaAs:Si(s), generation of high mobility n layers 80−103375
GaN, film, secondary ion mass spectrometric qualitative anal. 78−7265
H embrittlement in metals, assessment of techniques for local detection 78−3439
In_2O_3:Sn, thin films, prep. by pyrolitic method, charact. by SEM, electron diffr. and SIMS, solar energy appl. 79−43143
$LiNbO_3$:Ti, planar and channel optical waveguides, anisotropic diffusion expts. 80−64200
Ni, sputtered, ionisation probability, energy dependence 80−35041
Ni:Mn, radiation-enhanced diffusion, effect of point defect fluxes 77−89588
^{18}O, concentration profile, secondary emission of negative or positive ions *(French)* 79−60395
Pd-silicate transport in Si-Pd_2Si-Si, correl. with C contamination 79−4491
Si, EFG ribbon, characterisation by ion beam tech. 80−79833
Si, grain boundary elec. props./impurity correl. using surface anal. of multigrained samples by SIMS and AES 80−79816
Si, H^+ and H_2^+ ion implantation profiles determ. 79−4334
Si wafer surface doping profile determ. 79−77618
Si:As sputter rate meas. SIMS combination with Rutherford backscatter 80−21334
SiO_2 prepared in O_2-HCl and H_2O-HCl ambients, Cl conc. profiles using SIMS 79−65110
SnNi electroplate, anal. by SIMS, ion scatt. spectrometry, and Rutherford backscatt. 78−95979
SnO_2:F, thin films, prep. by pyrolitic method, charact. by SEM, electron diffr. and SIMS, solar energy appl. 79−43143
W (100), chemisorbed O_2 or H_2, isotope effects obs. by SIMS 79−5234

security of data
see also data handling
astronomical data base standards, management and security 77−82282
automatic speech recognition, speaker authentication and data entry 79−94419
computer trends, effects on society 80−47590
confidential data storage in sandwich holograms 79−76631
picture scrambling holographically for confidential picture taking technology 77−19208

security of information *see security of data*

sedimentation
see also disperse systems; sediments; water treatment
aeolian sedimentation on Earth and Mars, comparisons 80−31042
aerosol, diffusion and sedimentation in Poiseuille tube flow 78−59463
aerosol, in closed finite tubes in random orientation 79−24841
aerosol, simultaneous diffusion and sedimentation in rectang. tube 77−11266
aerosol cylindrical particles, overall drift angle in sedimentation 79−50777
aerosol diffusion and sedimentation in horiz. cylinder 78−3385
aerosol dry deposition, filtration model rel. to trace metal deposition from atmosphere 78−73441
aerosol flows in finite tubes in random orientation, sedimentation 79−50778
aerosol particle deposition in sampling lines, expts. 78−81472
aerosol particle settling and diffusion from stationary gas in tube or duct 77−52678
aerosol particle settling in flow in parallel plate channel, diffusion effect 79−66371
aerosol particles, gravity settling in horizontal rectangular tube with diffusion 77−84310
aerosol particles diffusion and gravitational settling in tube 78−90976
aerosol particles growing, gravitational deposition from laminar tube flow 80−59099
aerosol particles in flow type chamber, coagulation, deposition 80−69908
aerosol systems, with sub-micron fractions, in confined space, expts. *(Russian)* 79−5182
aerosols, particle deposition from laminar flow 79−47988
aerosols, submicrons, in aluminised Mylar bags, electrostatic deposition losses 79−58114
NW Africa, Late Palaeozoic-Early Mesozoic palaeogeography 77−70659
airborne sea salt sedimentation meas., effects on vegetation 78−3847
alumina powder, particle size analysis, using centrifugal sedimentation *(German)* 78−57890
ancient deep-sea fan in Cantabrian Mountains, growth 78−44813
apatite deposition in Laccadive Sea, rel. to seawater and low F^- concs. 80−104995
aqueoglacial deposit lithology of E.Lithuanian upland *(Russian)* 78−16011
aqueous metals, adsorption on inorganic minerals 78−49006
Archaean aeon, sedimentary basins development 80−89986
S.Atlantic, evolutionary history from deep sea drilling results 77−21756
NE Atlantic continental margin, sediments differential deposition and distrib. by bottom currents 80−12372
Atlantic continental margins and deep sea Late Quaternary sedimentation 77−21751
Atlantic-type continental margins, post-Permian, sedimentary histories 77−21738
axisymmetrical sedimentation by rough plates *(Russian)* 79−79300
Baltic Sea, estuary region, suspension distrib. under river drifts influence *(Russian)* 80−98345
Baltic Sea coast sedimentary material differentiation *(Russian)* 80−104951
Baltic Sea sedimentation, role of river suspensions *(Russian)* 78−7616
bed forms and unsteady flow, classification 77−45036
Benin Gulf, Africa, struct. and sedimentation of continental margin 77−21693
binary fluid mixture, in centrifugal field, crit. dynamics 80−44310
binary particle mixtures 80−40757
biological isotope separation by sedimentation process 79−44066

sedimentation continued
biphase liquid cylindrical vortex, mass force effect on dispersion phase distrib. *(Russian)* 80−79388
Biya and Katun rivers, evolution of river bed in confluence node 78−3839
Black Sea, large rockslide formations rel. to Cenozoic sedimentation 78−3751
blood, at controlled shear rates 77−66877
blood, three-component anal. by method of charact. 77−70577
blood sedimentation rate free from gravity influence, rapid determ. from density meas. *(German)* 78−81085
Brazil, coastline Quaternary formations, littoral zone evolution 77−21755
carbonate minerals precipitation in natural water systems, influence on isotope evolution 79−20882
Caspian Sea, lake bottom sedimentation contrib. to biogenous elements balance 80−31073
Cenozoic oceanic sedimentation rates for Atlantic, Indian and Pacific Oceans 77−91107
Chad basin, Africa, active intra-continental sedimentary basin 77−21726
clay minerals in DSDP Leg 34 basalt, form. 79−29767
clay minerals in estuarine and coastal waters, role of suspended particles surface charge 80−36331
coarse angular particles in water, fall velocity 79−74430
cohesive sediment entrainment in fresh water 80−90107
colloidal, suspension, electrophoretic clarification 77−60127
colloids, sedimentation hydrodynamic interaction between spherical particles, effect of repulsive interparticle forces 80−45577
concentration and pressure effects, review 77−32835
continental ice sheets, deposition 79−25276
continental margin and craton sedimentary basins, conf., Durham, England (Apr. 1976) 77−21715
continental margins, sedimentary basins rel. to oceanic fracture zones, appl. to Equatorial Atlantic 77−21695
continental shelf zones development and sedimentogenesis 77−64263
continuous sedimentation theory, effects of density gradients and velocity profile 77−60125
Cretaceous-Tertiary boundary, sedimentation, geomag. field and extinctions 78−32013
deep sea cores sedimentation rates determ. by fission/alpha track counting 78−61392
deep-sea sedimentation, time scales and dynamic models 78−15988
Deimos, loose material downslope movement obs. 80−94737
deposition, onto rot. disc, convective diffusion, external force field 78−40081
disperse suspension of solid particles in viscous fluid, Markov model 80−28551
dissaggregation effects, porous solid matrix stresses, aggregate max. size 80−16732
DNA, double-helical model, sedimentation coeff., X-ray scatt. 77−14629
DNA, high mol. wt., sedimentation data, radiation-induced single-strand breakage, additives effect 80−30667
DNA, sedimentation constants, direct meas. by analytical ultracentrifugation *(French)* 80−8004
electrokinetic phenomena within multiparticle systems, sedimentation pot. 77−9090
elutriator, inclined tubular, for spherical particles, collection efficiency 79−90354
enhanced sedimentation in settling tanks with inclined walls 79−70382
equilibrium eqns. derivation using hard spheres in Percus-Yevick approximation 80−66884
erosion and sedimentation, problems rel. to water supply, research needs 78−61444
erythrocyte distribution profiles during sedimentation as determ. by HeNe laser light 80−81563
erythrocyte sedimentation rate, for teaching 78−49610
erythrocyte sedimentation rate in inclined tubes 80−67048
estuarine particle dynamics, math. model, phys. and chem. processes 77−21793
estuarine sedimentation, measurement techniques, book 80−36788
fine grains, compaction effect on acquisition of detrital remanent magnetization 78−20395
fine particle sedimentation phenomena investigated by vibrational force field and interferometry 79−60086
floc, settling velocity, rel. to permeability 79−43636
flocculated fine sediments, depositional props. 77−21807
flocculent suspensions, review 80−35577
Floridan Aquifer, transgressive-regressive sedimentation cycles and dolomitisation 79−53346
flow, bed topography and grain size in open-channel bends, calc., mathematical model and FORTRAN program 77−37245
fluorides deposition in Laccadive Sea, rel. to seawater and low F^- concs. 80−104995
fly ash from coal-fired power plant, downwind elemental deposition 79−20838
fouling in heat exchangers, review 79−3902
gels, non-linear behaviour under strong deform. 78−7240
geophysical flow, turbulent bursting phenomenon, sedimentological implications 77−13093
Gironde estuary, sediment transport from vertical circulation real time two-dimensional model *(French)* 79−62519
glacier-fed lake with low sediment input, sedimentation processes and patterns 78−88849
Grand River, Ontario, geomorphic effects of catastrophic flood 78−28248
gravity, basic theory and experimental demonstrations 80−66885
Guacanayabo Bay, Cuba, tectonic processes rel. to Holocene sedimentation 78−3752
central Gulf of California, sedimentation rate effects on heat flow 80−3968
Gulf of Gdansk, lithodynamical processes, theoretical anal. and scale model tests *(Polish)* 78−40540
heavy metal sedimentation rate in Saanich Inlet, British Columbia, ^{210}Pb technique 78−32063
heavy metals in Susquehanna River system, use of ^{210}Pb as tracer 78−49046
Hercynian front in Ireland, Caledonoid lineaments control on sedimentation and struct. 78−32035
Hercynian Ocean northern margin, sedimentary facies and basin subsidence 77−21725
histones H_2A and H_4, mixed solns., oligomer structs. 80−30648
Hudson River estuary, man-made radionuclides and sedimentation 77−2183
Iapetus Ocean, eustatic events and pelagic sedimentation during Ordovician and Silurian 79−29776
ice wedge casts in NE county Wicklow, sedimentary environment rel. to form. 78−69379
ice-crystal fog, aerodynamic and opt. props. 77−90648
Indian intra-cratonic sedimentary basins, deep struct. features and evolution 77−21728
W.Indian Ocean, clay mineralogy and sedimentation 77−29279
Indian Ocean, deep-sea sedimentation, lithologic and palaeomag. study 79−20810
interferometrically recorded sedimentation, diffusion and thermal diffusion expts., reference marks arrangement 77−87813
Kicking Horse River, bar evolution and stratification in gravelly braided stream 77−64332
Lake Eyre North, S.Australia, bottom profile rel. to sedimentation 78−69376
Lake Ontario, Late Wisconsin sediments, aspartic acid racemisation and ^{14}C dating 78−73415
Lake Ontario, sedimentation rates determ., ^{210}Pb dating method 78−73408
Lake Van tectonic activity and sedimentation study *(German)* 78−3843
laminar aerosol flow through inclined circ. tubes, gravitational deposition of particles 77−89192
Late Quaternary sedimentation on W.African continental margin 77−21753
latex, monodisperse, phase transition pressure determ. from sedimentation equil., Alder transition model 77−70344
latex sphere aggregates, dynamic shape factors determ. by sedimentation vel. meas. in capacitor 80−26063
leukocytes of human blood, gravity sedimentation anal. 80−98197
liquid mixture, crit. soln. point, sedimentation and density gradients in high gravit. field 77−59121
liquid-liquid critical solution point, and density gradients, high gravit. field 78−47526
Long Island Sound, estuarine sedimentation rel. to central New England denudation rate 79−92550
longshore sediment transport by tidal current, outside surf zone 80−76961
lymphocytes, living and dead, mag. props. and mag. sedimentation 80−35925
macromolecular solns., associating sedimentation equilib. distrib. anal. 77−14628
macromolecular solns., expt. determ. errors due to diffusion *(Russian)* 78−76934
macromolecular solution, conc., sedimentation behaviour rel. to particle shape 77−81428
macromolecular solution, semidilute, scaling law describing conc. depend. 79−70377
magnetic fluids, barbotage and sedimentation, multivelocity model 80−61161
Mandovi estuary, circulation and sedimentation rel. to Aguada bar 77−73756
old Mangalore Port, India, sediment transport and siltation of navigational channel 80−56488
old Mangalore port siltation, meas. of seasonal vars. in seawater hydrographic conditions 80−41451
marine detritus, rel. to atm. CO_2 from burning wood 78−81368
Markov model, three-parameter 78−34183
Markov model for very slow settling of dilute suspension 78−22406
E.Mediterranean Sea, sedimentation rel. to tectonic elements and crustal struct. 78−44801
mineral particles settling in liq., X-ray photography 79−20469
molten metal binary mixtures with wide immiscibility range, gravitational layering of components *(Russian)* 80−104092
mud suspension, batch sedimentation in inclined tube 79−64743
multigranular suspensions, aqueous, sedimentation in oblique plate separator under laminar flow conditions *(German)* 77−44513
near-shore and lake sedimentation process, fallout radionuclide tracer obs. 80−81864
North American Atlantic continental margin, rapid Cretaceous subsidence and sedimentation 77−21722
W Norway, Devonian basins subsidence and sedimentation 77−21727
ocean, particulate ^{210}Pb scavenging model 77−5223
ocean, rates determ. by nondestructive gamma-gamma coincidence spectrometry 78−85709
ocean floor abyssal regions, gigantic accumulative relief forms 77−21759
oceanic phosphorites, Fe, Ti and Al behaviour during initial form. stages 80−31029
old Mangalore port, India, channel siltation study 80−77005
E.Pacific Rise, P accumulation rates in metalliferous sediments 77−60364
Pacific-Nazca plate boundary, sedimentation in fast slipping transform fault zone 79−25226
palaeoenvironmental conditions, organic geochemical indicators 78−40539
palaeohydrologic phenomena recorded by lake sediments 77−66936
particle deposition, in laminar flow in tube, thermal effects 77−58764
particle interactions in fluid suspension, effect on sedimentation velocity 78−23972
particle layer deposition from gas dispersion turbulent flow in tubes, heat exchanger appl. 79−55409
particle separation, high-resolution, by sedimentation field-flow fractionation 77−73473
particle size analysis using ^{55}Fe X-ray source and sedimentation cell 79−75491
particle size distribution measurement by laser Doppler velocimetry technique *(Japanese)* 78−24913
particle track photography, semiautomatic device for photograph analysis 77−44515
particulate, mixture theory formulation 77−21423
particulate sedimentation, stability, two-dimens. anal. 80−69768
permafrost layer thickness and temp. variations under sedimentation or denudation conditions 77−78241
Philippine Sea, clay sediments comp. and accumulation rates 79−2221
poly-4,4-diphenylphthaleinterephthalamide, mol. mass distrib., sedimentation and fractionation method meas. *(Russian)* 80−71957
poly-m-phenyleneisophthalamide, sedimentation coeff. distrib. at 25°C *(Russian)* 77−63971

sedimentation continued
polydisperse polymer, anal. of mol. mass. distrib. *(Russian)* 77−31038
polydisperse randomly branched polymer, sedimentation coeff. 77−63966
polyethylene oxide, semidilute aq. soln., sedimentation of large colloidal particles 78−95965
polymer, absolute mol. wt. and mol. heterogeneity determ. from sedimentation vel. in ultracentrifugation *(German)* 80−14261
polymer solns., ultracentrifuged, effect of pressure on sedimentation *(Russian)* 79−34369
polymer solution, Debye-Brinkman equation, macroscopic derivation 77−10799
polymer solution, sedimentation rates for low mol. wt. materials in dilute region 80−108756
polymer solutions and gels, dynamic behaviour obs. using light scatt. 80−55727
polymer systems, sedimentation field-flow fractionation in macromolecule characterization 80−66879
polymers diffusive broadening of distrib. function, from single record using model functions *(Russian)* 77−63970
polyphenylquinoxaline, soln., conform., equilib. rigidity *(Russian)* 79−55643
polystyrene, conc. solns., diffusion and sedimentation, frictional coeff., crit. soln. temp. 79−95195
polystyrene, sedimentation coeff. distrib. at 25°C *(Russian)* 77−63971
polystyrene, soln. in cyclopentane, sedimentation vel., conc. and temp. depend. 79−70385
polystyrene, solns., sedimentation behaviour, branching effects determ. 80−66887
polystyrene, suspension of monodisperse spherical colloidal particles, layered sedimentation 79−39217
polystyrene solution in benzene, thermodyn. interaction coeff. determ. 78−3367
polyvinylacetate solution, long-chain branching characterisation, molar masses 79−94122
powders, grain size determ. by sedimentation, automatic recording system 78−60897
Pyrex glass, sedimentation pot. meas. device and ζ pot. determ. *(Spanish)* 77−70236
pyrex-H_2O(aq. KCl) systems, electrokinetic coeff. determ. from sedimentation pot. 80−3365
quartz, grinding and surface treatment by ball mill in cetyl alcohol *(Japanese)* 80−25890
radioactive waste, medium-level, sedimentation method of bituminisation, thermogravimetric charcts. of products 77−61561
remanent magnetisation, acquisition by settling organic mud 80−61795
reservoir sedimentation process and detention structure model 78−44892
river deltas, variability of types 77−73769
river estuaries, Fe precip. mechanism 78−20437
River South Esk, Glen Clova, Scotland, flow and sedimentation in meander bend 77−49093
rivers, dissolved humic acids and Fe removal during estuarine mixing 79−34830
Rockall Trough, hydrographic and geological inferences from near-bottom traverse 79−62483
rubber powders, finely dispersed, sedimentometric anal. 80−66883
salt marsh sedimentation rates determ. by ^{137}Cs dating 78−96247
sandy bed streams, sand discharge, leveed rivers, coastal flood plains 77−53086
seismic signatures of sedimentation models using synthetic seismograms hydrocarbon exploration appls. 77−21913
serum albumin, diffusion and sedimentation in conc. solns. 77−48749
settling convection, obs. and continuum fluid mechs. model 78−14070
settling instability, horizontally homogeneous suspension 78−42652
settling velocity scale 80−81376
Siberian platform, main structures development history and dynamics 77−21732
W Siberian platform development history and dynamics 77−21731
E.Sivash waters, carbonate sedimentation rel. to ^{90}Sr content *(Russian)* 78−77282
smoke, natural sedimentation, photographic, visual and laser sonde obs. *(Russian)* 78−32216
smokes, atmospheric, gravitational seidmentation, velocity *(Russian)* 78−85619
solar nebula, fine dust grains clustering and sedimentation time 80−26937
solid particles in viscous incompressible fluid, action of gravity, sedimentation *(French)* 77−75964
speleothems from Britain, palaeoclimatic and geomorphic implications of ^{230}Th/^{234}U dates 78−36128
sphere, small, in viscous fluid bounded by two perpendicular walls 78−90975
sphere sedimenting in viscous fluid, lateral force 79−27685
spherical particle, in stagnant bounded fluid, lateral migration 77−48695
storm beach sedimentation mechanism 78−20386
streams, straight, alluvial, unsteady flow and individual dunes modification 79−62535
sulphide deposits of E.Pacific Rise (21°N) physics of geothermal system fluid 80−101362
supracrustal relics in Archaean of W.Africa, zonation rel. to sedimentary environments 78−44815
suspended load sedimentation in reservoirs, analysis and prediction method 78−53664
suspended sediment transport theory, elliptic boundary value problem 79−14466
suspension, centrifugal sedimentation of large particles 78−59462
suspension, conc. distrib. determ. by radioactive solids 79−32634
suspension, settling velocity 79−46360
suspension of spherical particles *(Russian)* 78−67254
suspensions, creeping flow, hindered settling, particle shape effect 80−14797
suspensions, fluid dynamical aspects of operating conditions of suspension stirrers *(German)* 80−26058
suspensions, settling, accelerated by addition of buoyant particles 79−96369
suspensions of charged particles, laminar tube flow, entrance deposition 80−59100
suspensions of equal spheres, cluster settling, appl. of distrib. of kth nearest neighbours 80−40758
suspensions of particles of two or more sizes, model and expt. 79−87881
Sverdrup Basin, Arctic Canada, evolution, subsidence and uplift 77−25673

sedimentation continued
theory and expt. comparison 77−40577
thick clay suspensions, electroenforced sedimentation in consolidation region 80−26057
thick water film in turbulent flow over impermeable slope, erosion and sedimentation *(French)* 80−43692
tracer theory, nonsteady state systems 79−5646
transport phenomena, hydraulic electronic instrumentation *(Italian)* 77−91334
urban erosion and sedimentation prediction and control 77−37282
urethane elastomer, thermoplastic, dilute soln., viscosity and sedimentation 80−103512
W. interior USA, tectonics and late Cretaceous sedimentation 78−81134
velocity-voidage relations for sedimentation and fluidisation 80−24076
vibration-frequency method of sediment analysis 79−49202
viscoelastic fluid, deformed sphere motion 79−81831
viscoelastic fluid, homogeneous shear flow, rigid particle slow motion 77−84308
water flow, bed topography, grain size and sedimentary struct. in open channel bends 78−20443
wave-formed bars, sedimentation and equilib., review 79−92521
white dwarfs external layers, metals sedimentation rel. to interpretation of spectra 79−62824
AgI hydrosols, kinetics and mechanics of colloid systems formation 80−101045
Fe particles, dispersed in Hg, mag. props., aggregate form. 80−60375
Fe_2O_3, powder, preparation conditions rel. to morphology 77−8777
Mn, deep sea sedimentation rates from hydrothermal Mn scavenging residence time 78−32121
Mn deposition and nodule growth in Jervis Inlet, British Columbia, effect of sediment-water exchange 78−96187
Mn, dissolved, in river water, rapid precip. rel. to estuarine Mn distribs. 79−62516
Pu in Irish Sea, oxidation state rel. to solubility and sedimentation 79−16516

sediments
see also rocks; sedimentation
α-spectrometric dating method, using ^{210}Po 78−28350
abrasion as source of sedimentary material in Atlantic Ocean, shore erosion 79−2217
abyssal clay containing meteoroid ablation spheres 80−46500
abyssal marine sediment, organic ^{14}C activity 79−16434
abyssal marine sediments, biological stirring, dissolved and adsorbed materials redistrib. 78−69321
abyssal sediments, effect of particle size var. on DRM/ARM ratio 78−32067
acoustical props. of laboratory sediments of seawater, temp. variation 80−96069
N.Adriatic Sea, trace element analysis by neutron activation 77−21801
aeolian sedimentation on Earth and Mars, comparisons 80−31042
aerobic pelagic sediments, denitrification 78−77214
W.Africa continental margin, subsidence and uplift, DSDP Leg 41 geological results 77−21754
age determination, ^{210}Pb radioactive dating, plastic nuclear track detector 78−20554
alluvial bed load transport estimation 78−20444
alluvial channels in Kansas, bed material particle size rel. to gradient, discharge and braiding 79−20869
alluvial ground surface dislocation due to buried fault movements *(Japanese)* 80−21723
Amazon River, bed sediment size distrib. 80−101392
Amazon River, fine sediment non-uniform vertical distrib. 79−84313
Amazon River, sediment loads meas. 79−44206
Amazon suspended sediment reaction with seawater, cation exchange characts. 80−8337
N.America, Plio-Pleistocene glacial sediments rel. to Pleistocene stages terminology 79−62470
analysis, neutron activation, using standard reference materials as multielement irrad. standards 78−80815
ancient big river systems significance and origin 78−77281
anomalous magnetic fabric which records apparent geomag. field excursion 78−81152
anoxic pore waters, silicate content and effects of oxidation during sampling 78−61394
aquatic sediment lipids, Recent and ancient 80−51583
Arabian Fan of NW.Indian Ocean floor, sediment sound vel. 80−72488
Arabian Sea, DSDP Site 220, Fe, Mn and Ti distrib. 77−73708
Arakapas fault belt, Cyprus, sedimentation and metallogenesis along fossil oceanic fracture zone 79−29769
Arctic Ocean, sediment thicknesses and upper mantle temps. from magnetotelluric soundings 79−48454
Arctic Ocean, sediment thicknesses over Alpha Ridge rel. to spreading centre hypothesis 79−48455
Arctic Ocean, sedimentary sequences rel. to geophysics 79−48456
Arctic Ocean sediments, ^{10}Be deposition rate 77−81865
artifacts as sedimentary particles in fluviatile environment 78−70239
S.Atlantic, $CaCO_3$ and radiolarian distribs. rel. to glacial and interglacial oceanographic conditions 80−72556
N.Atlantic, Mesozoic and Cainozoic, calcareous sediments depth distrib. 80−81866
N.Atlantic, palaeocirculation, benthic forminifera, and ^{18}O 79−92548
Atlantic, Vema Channel, Antarctic bottom water fluctuations effects of sediments 77−81903
Atlantic coast barrier islands, shoreline periodicities and edge waves 80−12375
mid-Atlantic continental shelf, bottom current and sediment movement 79−57964
N.Atlantic Foraminifera sediment, ocean deep water production since Miocene 80−46186
Atlantic Jurassic red sediments from DSDP leg 11, remanent magnetisation 77−81787
Atlantic nuclear waste disposal site, radionuclide redistrib. 80−85309
S.Atlantic Ocean, Cretaceous, study of clay minerals and organic matter *(French)* 79−84220
S Atlantic Ocean, depositional history during last 125 million years 78−44798
Atlantic Ocean, early Cenozoic calcareous plankton palaeobiogeography and climatic fluctuations 78−16143
Atlantic Ocean, Holocene sediments thickness in bottom deposits 79−2216

sediments continued
S.Atlantic Ocean, palaeoenvironment of anaerobic sediments in Late Mesozoic 77−17074
Atlantic Ocean, quartz distrib. relation to climate in last glaciation 80−8308
Atlantic Ocean, river sediment supply 79−12157
NW.Atlantic Ocean, sterol geochemistry 79−74885
N.Atlantic recent sediments, volcanism effects on mineral comp. 78−44802
Atlantic-type continental margin off New York, subsidence 79−29722
Australia and Timor Trough, facies rel. to topographic wave migration during past 3 million years 78−49018
Australia continental slope and shelf, sedimentary basins evolution from Mesozoic times 78−96175
authigenic silicate minerals in marine sediments and oceanic Mg budget 77−86858
Baie des Chaleurs, Gulf of St. Lawrence, sediments distrib. and depositional history 77−64257
Baltic beach sedimentary material stratification (autumn/winter 1976-7) *(Russian)* 80−76962
Baltic coastal beach scouring and accumulation by moderate sea disturbances *(Russian)* 80−81867
Baltic Sea, continuous underwater gamma-survey 80−12377
Baltic Sea coast sedimentary material differentiation *(Russian)* 80−104951
Baltic Sea Upper Quaternary sediments, physical props. 78−3753
SE.Baltic shore development due to hydrotechnical constructions *(Russian)* 78−36145
Baltimore Canyon, submarine mass-wasting of sediments 80−101354
Banks Island, Canada, deposits and aeolian processes *(French)* 78−36163
Barents Sea, morphostructural map of SE region 78−3749
Barents Sea, sediments rel. to origin of Pliocene and Pleistocene glaciations 78−57227
Barents Sea sediments, continuous seismic profiling with two receiver systems 80−31150
barite, deposits at deep-sea hydrothermal site on strike-slip fault 80−21710
barrier island breach morphology and dynamics, study in stability 80−12371
barrier island migration computer simulation 78−20384
barrier islands, global distrib. in terms of tectonic setting and sediment supply 79−2214
barrier reef and lagoon, Guadeloupe Island, geomorphology and sediments *(French)* 79−29749
bars, longitudinal axis when formed at a shore inlet within a contour *(Russian)* 79−92522
bars, shallow profile coastal, calcs., choice of wave parameters *(Russian)* 79−88330
Bay of Biscay, sedimentary sequences rel. to rifting, crustal attenuation and subsidence 79−2209
Bay of Fundy, Canada, bedforms and hydraulic stability in tidal environment 78−88814
Bay of Naples, bottom sediment contamination 79−16519
beach changes in S.California, statistical prediction 80−98305
beach deposits, elevated, near Al Jubail, Saudi Arabia, evidence for recent coastal uplift 79−79799
beach deposits sedimentary material differentiation and bedding form. dynamico 80−26496
beach ridges in S.Australia, palaeomag. chronology rel. to Milankovitch theory of ice ages 80−98307
beach sedimentology of Mustang and Padre Islands, time series approach 78−77211
beach sediments, lower St. Lawrence Estuary, Quebec, frost effects 78−7609
beaches, SE Rio de Janeiro state, sediment textural characts., grain size *(Portuguese)* 78−81144
Beaufort Sea sediment cores, NRM, geomag. excursion record 78−20349
bed material mobility, probabilistic model and obs. *(Italian)* 78−53665
bedded formations, modelling of structure-forming props., results *(Russian)* 79−48429
bedload stresses and Bagnold's bedform theory 77−70695
bedload transport oscillations, circuit for acoustic detect. 77−45168
Benguela upwelling system off N.Namibia, late Miocene origin, sediment evidence 80−104993
Benue Trough, stratigraphic evolution and implications for W.Africa Upper Cretaceous palaeogeography 79−2230
Berendon Glacier, BC, Canada, movement, ice structures and medial moraine at confluence 78−61441
Bering Sea shelf sediments, denitrification estimates 80−12433
Bermuda, sediments transport rel. to geomorphology, results from Landsat imagery 79−5470
Bhagirathi River, West Bengal, unidirectional alluvial channels, metamorphosis philosophy 80−31075
big river sands, modern, petrology and chemistry 79−25274
Black Sea, dark lamina form. in sediments, photosynthetic bacteria mass mortality mechanism 78−88815
Black Sea, first expts. with Pisces submersible vehicles 79−44267
Black Sea, primary minerals of uraniferous sediments *(German)* 78−65257
Black Sea, sediments as source of mag. anomalies *(Russian)* 78−85473
Black Sea, U anomaly in sediments, accumulation mechanism 77−91105
Black Sea, Upper Quaternary deep-sea sediments stratigraphy 79−20811
Black Sea and Bay of Biscay, grain size and mineral comp. of shelf sediments 79−20812
Black Sea Pleistocene clay sediments, physical and mechanical props. 78−3755
Black Sea sediment cores, organic geochemistry 78−49040
Black Sea water and sediments, stanol/stenol ratio control process 79−92549
Blake Plateau, Late Cenozoic sedimentary record rel. to Gulf Stream vel. fluctuations 80−12432
block folding of sedimentary strata, mechanical model 77−81841
N Bohemia, heat flow meas. in Palaeogene, Cretaceous and Permo-Carboniferous sediments 77−44946
Bolivia, evidence for glaciation 3.27 Myr BP 79−34865
Bombay Harbour sediments, elemental concs. 77−73709
Boston Bay Group, Massachusetts, origin and significance of cylindrical sandstone structs. 78−69343

sediments continued
bottom reflection loss for a class of marine sediments, effects of density gradients 78−55498
boulders of canyon rivers rapids, resistance to movement rel. to rapids stability 80−72564
N.Brazil continental margin, evolution, sediment distrib. and hydrocarbon potential 77−21697
N.Brazil continental margin, sedimentation 77−21748
S Brazil intracratonic and marginal basins tectonic evolution 77−21743
S.Brazilian continental margin, sediment thicknesses rel. to struct. 77−21694
British Columbia, S central, late Pleistocene stratigraphy 78−92804
British geomagnetic master curve 10000-0 yr B.P. for dating European sediments 79−70740
Brunhes epoch deep sea sediment core palaeomagnetic intensity variation 77−32995
Bulgarian continental shelf, morpholithodynamic study 80−26495
Calangute beach, Goa, sediment transport and rip currents 77−73755
calcareous deep sea sediments, vel. anisotropy in semi-indurated samples 79−48466
calcareous ooze and chalk, Ontong Java Plateau, W Pacific, sound vel., sonobuoy data 78−40542
calcite dissolution by fossil fuel CO_2, effect of sediment mixing 78−81212
coastal California, late Quaternary sediments rel. to climate and existence of Ice Age refugium 78−57293
California-Mexico coastal basins, sediments ^{241}Pu and ^{241}Am concs. 80−98303
Canada west coast, sediment thicknesses and crustal struct. from marine seismic survey 79−100820
Cape Basin, S. Atlantic, scour and deposition at Walvis Ridge base 77−91103
carbonate breccia beds, submarine, depositional model 79−84259
carbonate minerals precipitates in natural water systems, isotopic comp. theory 79−20882
Caribbean Sea floor, sedimentary cover struct. and thickness *(Russian)* 78−77212
Carpathian region sedimentary cover, elec. conduction 80−89940
Cenozoic explosive volcanism recorded in deep sea cores, tectonic effects, climatic implications 77−49052
Chaine des Puys, France, lava flow-baked sediments ages and palaeomag. field strengths 79−44100
chemical exchange across sediment-water interface 79−5505
Chesapeake Bay, pollution history 79−34445
N.Chesapeake Bay estuary, agglomerated suspended sediments microstruct. 79−53336
Chesapeake Bay sediment, time depend. transport, temp. and chloride obs. 80−81863
E.China Sea sediments, mineral comp. and distrib. *(Chinese)* 80−8293
chronological strategies and metal fluxes in semi-arid lake sediments 79−34860
classification by ocean subbottom acoustic Q meas. 80−46168
clay minerals, distrib. in sediments of Bay of Bengal 78−81146
clays in S.E.Baltic, physical props. *(Russian)* 78−15990
Clear Lake, California, absence of Mono Lake geomagnetic excursion in sediment palaeomagnetic record 78−11801
coarse riverbed material, probability density function of biased samples 80−12445
coastal marine, ^{134}Cs, ^{137}Cs, ^{210}Pb, ^{226}Ra and ^{228}Ra concs. determ. 79−88370
coastal marine sediments, fossil C effect on ^{14}C ages 80−98308
coastal muds, interstitial water isotopic behaviour during evaporation *(French)* 79−79811
coastal sediment U isotope ratios along Indian W. coast 77−41020
Cochin Harbour, siltation in outer channel, tidal streams and longshore currents 78−36144
cohesionless bottom sediments, limiting stability in turbulent channel flow, erosion 80−94546
Colombia basin, Caribbean Sea, crustal struct. from profiler-sonobuoy meas. 78−28198
concave-bank benches on the Squamish River, British Columbia, Canada 79−84305
conductivity of marine sediments from EM field of water currents 79−62480
contamination of marine sediments, trace metals from wastewater 79−83643
continent-derived sediments, contrib. to volcanic rocks of Aleutian and Pribilof Islands, Alaska 78−57185
continental margin basins, sediment loading and lithosphere flexure 77−21717
continental margin morphology 79−12098
continental margin sedimentation, computer simulation 78−15998
continental platform subsidence mechanisms and eustatic sea level changes 77−21718
continental shelf sediment mapping, Huntec Seabed Project 77−13130
Continental Shelf sediment sonar signal processing 78−61622
continental shelf sediment transport, turning effect in bottom boundary layers 77−37235
continental shelf sediment transport modelling 78−15995
continential shelf sediment core, anomalous declination due to slumping 80−76964
coring method for lake surface sediments 77−9520
Corsica (France), Quaternary alluvial deposits studies 78−57234
Cos θ similarity coefficient, approximate levels of significance 77−86877
Cretaceous plankton species extinction due to comet impact 80−76977
Cretaceous-Tertiary boundary, plankton extinction and geochem. indicating extraterrestrial event 80−76976
Cretaceous-Tertiary boundary sediments, Red Deer Valley, magnetostratigraphy, biostratigraphy and geochronology 79−57888
crustal, deep structure to NW of Cape Verde Islands 79−2201
cycling models, global processes 78−16162
Danakil Depression and Dead Sea Rift, comparative study of sedimentary fills 78−69347
Danube water and sediments, radionuclides detec. during 1977 79−12158
dating of marine sediment, α-scintillation counting of ^{230}Th 80−72636
Dead Sea Rift and adjoining areas, gravity rel. to sedimentary section thickness 79−57893
deep ocean, compressional wave attenuation 80−79033
deep ocean sediment thermal conductivity meas. platform rel. to nuclear waste storage 80−46175

sediments continued
deep sea, fine-grained sediment laminations, origin, model 78−77213
deep sea benthic mixing, radioactive tracer study 80−8294
deep sea carbonates, thickness and ^{14}C age of mixed layer 79−29742
deep sea cores from Project FAMOUS, radiocarbon and ^{210}Pb distrib. 77−37179
deep sea sediment cores, Au, Pd, Ir, Mn sources, neutron activation anal. 80−17247
deep sea sediments, fission/α anal. of radioactive disequilibria 77−29497
deep sea sediments, palaeomag. study using thin sections 77−78099
deep-sea, O_2 uptake and nutrient exchange meas. 80−3564
deep-sea cores, ^{231}Pa dating via ^{227}Th counting 78−32238
deep-sea micronodules, near 14 Å mineral of birnessite group 79−74892
deep-sea Mn nodules, quant. distrib. and metal content *(Japanese)* 80−8292
deep-sea sediment core, thermoluminesc. dating 79−74871
deep-sea sediments, 20000 yr SiO_2 O isotopes record in diatoms 78−32247
deep-sea sediments, magnetisation, particle flocculation effects 79−70781
deep-sea sediments, unmixing of O isotope record rel. to deglacial melt-water spike 78−3746
deep-sea sediments cores and Minoan tephra from bronze age eruption of Santorini Volcano 78−24272
deep-sea sulphide ore deposits, discovery on E. Pacific Rise 79−34799
deformed flysch sequence, S.W.England, vein arrays, hydraulic fractures and press. soln. structs. 77−78169
deluvial deposits in SE Lithuanian periglacial valleys and ravines *(Russian)* 78−16010
denitrification rate seasonal var. determ. by use of ^{15}N 79−100883
Derwent Reservoir, N.England, Zn, Cd and Pb in water, sediments and submerged plants 79−25286
descending lithosphere, effects of accretion on geometry 77−29275
determ. in coastal sediments and seawater, activity ratios, disequilib. 78−27851
detrital remanent magnetisation in five slowly redeposited long cores of sediment 79−70786
Devonian lacustrine sediments, from Caithness, Scotland, palaeomag. and mineralogy 78−28170
Devonian old red sandstone, comparison with Euphrates and Tigris river sediments 78−81160
Deweras Group sedimentary environment, Rhodesia, palaeorift system 78−53650
Dezadeash flysch sedimentology rel. to strike-slip faulting along Denali Fault 77−17098
Dnieper-Donets depression, deep struct. from magnetotelluric sounding data *(Russian)* 78−96170
Dnieper-Donets depression, sedimentary cover struct. along Jagotin-Baturin profile *(Russian)* 78−92806
dredger spoil, dumping ground obs., motion of fine particles with current 80−17287
dredging from Gulf of La Napoule in France, pollution abatement attempt results 80−16857
drying remanent magnetization 79−66681
DSDP interstitial waters, Ca and Mg profiles 77−5177
DSDP Leg 35, Bellingshausen Abyssal Plain, interstitial water profiles and diagenetic reactions 77−5178
duststorm fallout, Kuwait, summer 1978 obs. 80−81966
dynamic features of deficit forms in translational flows 79−39775
East Fork River, Wyoming, 1976 bedload meas. 78−49055
elastic waves, propag. in model sediments 77−73672
elasticity theory, self-consistent imbedding approx. 77−33066
NE Ellesmere Island, NWT, Canada, glacial and marine deposits ages 78−77233
ellipsoidal grain thin sections, Monte Carlo simulation 77−5332
eolian transport during dust storms, Slims River Valley, Yukon territory 79−5552
equatorial Pacific Ocean, deep-sea sediments rel. to southern trade winds and upwelling 78−57217
erosion and sedimentation, problems rel. to water supply, research needs 78−61444
erosion and sedimentation, society's needs and professional opportunities 77−64342
estuarine, methyl mercury growth and decay during storage 77−66937
estuarine and continental shelf sediments, ^{226}Ra flux 78−32061
estuarine environments, Cu partition between water and suspended sediments 78−69371
estuary heavy metal pollution, Mosquito Lagoon, Florida 80−76671
estuary sediment containing lead pollution, rel. to flood control measures, California 80−76670
estuary with uniform reversing tidal flow, suspended sediment model 78−7648
Eurasia continental shelf, postglacial transgressions from slope of abrasional-accumulative surfaces 79−20813
evaporites from lower Proterozoic, East Arm, Great Slave Lake 77−78181
evolution of sedimentary basin on viscoelastic lithosphere 79−8615
fan sedimentation, computer simulation of turbidity current flow 78−15997
ferromanganese concretion deposits in Shebandowan Lakes, Ontario 79−84257
ferromanganese concretions in Baltic Sea, trace metal distrib. rel. to accretion rates 77−81864
ferromanganese nodules, oriented, U-Th series nuclides rel. to growth rates and turnover times 79−29740
fine-grained, compaction effect on acquisition of detrital remanent magnetization 78−20395
flocculated fine sediments, depositional props. 77−21807
Florida Straits, seabed sediments, current-induced movements 79−79807
fluviatile evolution 79−100876
NE.France, forest borealisation rel. to last (Eemian) interglacial abrupt end 80−21818
Fraser River (British Columbia) deltaic sediments, heavy metals content 77−33048
Fraser River estuary, British Columbia, silt plume obs. using airborne inertial sighting system 78−73384
free-surface sediment conveying river bed flow, flowrate and momentum correction factors 80−36339
freshwater, microbial degradation of organic molecules 79−84331
Galapagos Rift hydrothermal mounds, obs. with DSRV Alvin and detailed heat flow studies 80−51383
Galapagos Rift mounds, deep tow hydrothermal obs. 78−11871
sediments continued
Galapagos sea floor sediments, hydrothermal mounds, stratigraphy and chem. 80−26497
Galapagos spreading centre, hydrothermal deposits and assoc. basement rocks 79−29750
gas-bearing, meas. of sound speed and attenuation, gas bubble models 80−87670
gas-bearing sediments, characterization of acoustic props. 80−87630
gas-bearing water-saturated sediment, sound vel. as function of bubble distrib. 79−39703
geochemical classification of radiolarian cherts and siliceous sediments *(French)* 78−96319
geochemistry, environments and processes involving an aqueous phase 77−86888
geoelectrical prospecting in marine areas, dipole and unipole resistivity methods 80−56641
geomagnetic excursions and palaeomag. record 77−86779
geophone and hydrophone recordings in Californian offshore sediment 80−46192
Georges Bank, NW.Atlantic, seismic vel. of sediments to 1.4 km depth 80−21644
N.German sedimentary basin, cond. distrib. from widely spaced areal magnetotelluric meas. 79−74833
Gilbert Islands region, sedimentary mantle and basement struct. 79−2219
Gippsland, Victoria, Pliocene eustasy and sand barrier form. onset 79−74886
Gironde estuary, turbidity max., numerical simulation *(French)* 79−79869
Gironde inlet and Pertuis of Maumusson, suspended sediment seaward dispersion, remote sensing study *(French)* 80−8324
glacial deposits, Holocene and latest Pleistocene, in Shuswap Highland, British Columbia, ages 78−92856
glacial deposits, wind action on sub-Antarctic Marion Island 80−31093
glacial sediments of English Lake District, pre-Devensian till 80−94523
glacial till landforms, fabric anal. 77−44989
glacier-fed lake with low sediment input, sedimentation processes and patterns 78−88849
grain shape effects on settling rates 78−81232
graph model based on instantaneous unit sediment graph 79−53394
gravel river, grain size var. statistics 79−5513
N.Great Barrier Reef, ^{14}C dating 79−84225
Great Barrier Reef, Bewick and Stapleton cays, drilling investigation 79−84223
Great Barrier Reef, general nature and environment, 1973 expedition, inter-reef sediments 79−84221
Great Barrier Reef, geological history and structure from seismic profile, sedimentary accumulations 79−84222
Great Barrier Reef, sedimentation trends in lee of ribbon reefs 79−84224
Great Lakes, inorganic sediment, spectral absorptance and backscattering coeffs. 80−98364
Great Lakes, sediment chemical composition, anthropogenic loadings 77−37256
Greatlakean Substage replacing Lake Michigan basin Valderan Substage 77−17104
E.Greenland, Jurassic sedimentation and basin evolution 78−73344
S.E.Greenland, sediments of continental margin 77−33014
W Greenland continental margin, Mesozoic and Cenozoic sediments provenance 79−62479
W.Greenland Cretaceous-Tertiary volcanic region, sediments thickness rel. to magma traps theory 79−70776
Grote Nete basin, Belgium, geomorphology *(Flemish)* 78−61452
Gulf of California, varved sediment core appl. to ^{32}Si half life determ. 80−91153
Gulf of Kutch, element distrib. in sediments 79−48450
Gulf of Kutch, geomorphology, sediment and tectonic instability origin 80−76960
Gulf of Kutch, sediment distrib. in high energy tide dominated environment 79−48448
Gulf of Maine, polycyclic aromatic hydrocarbons 79−74555
N.Gulf of Mexico, anoxic hypersaline basin 77−86936
W.Gulf of Mexico, sedimentary section, multichannel seismic refl. results 77−21749
W.Gulf of Oman, Mahran deformed sediment prism rel. to tectonics 80−8279
Gulf of Oman, sediment deform. and plate tectonics 77−5176
Gulf of Sidra (Mediterranean Sea), platform upper sediment mantle geological struct. 80−36290
Gulf of St. Lawrence and estuary, geochem. of Zn, Cu and Pb in sediments 78−92855
Gulf of Suez, sediment layers rel. to multiple seismic refls. and head waves 80−56400
Gulf of Thailand, currents and particulate matter movements 77−49090
gypsum hydration water, isotopic comp. 79−20829
heavy metal pollution detection in estuarine sediments 78−73546
heavy metal sedimentation rate in Saanich Inlet, British Columbia, ^{210}Pb technique 78−32063
Hebridean continental margin, seismic evidence for Mesozoic age sedimentary troughs 78−53643
W. Hellenic Trench, high sedimentation rates and variable dispersal patterns 78−57193
Hepworth carboniferous sediment geochemistry, Fe minerals and concretions origin 80−17262
hillslope profiles in mid-Wales, sedimentological anal. 77−70666
Holocene alluviation in meltwater channels near Calgary, Alberta 77−81921
Holocene lake sediments, N.Poland, palaeomag. 80−21616
Holocene lake sediments, N.Poland, palaeomag. records anal. rel. to short period secular geomag. vars. 80−98221
Hope River, Jamaica, shear stress and competence determ. 78−61474
Hudson Bay beach ridges, 8000 yr. palaeoclimatic record of 'Double-Hale' 45 yr. solar cycle 77−78401
Hudson estuary, Ba and ^{226}Ra desorption from river-borne sediments 79−79877
Hudson River estuary, ^{222}Rn distrib. and transport across sediment-water interface 78−16064
Hunter River, sand supply to New South Wales coast 78−16066
hydrocarbons at Argo Merchant wreck site, gas chromatography 79−83645
hydrocarbons in Antarctic marine sediments 79−92096

sediments continued,
hydrocarbons in surface sediments on Scotian Shelf 78−49008
hydrological investigations, nuclear radn. appls. 79−39981
hydrophobic pollutants, sorption on natural sediments 79−83651
hydrothermal deposits on Mid-Atlantic Ridge FAMOUS area 78−65259
hydrothermal mounds near Galapagos Rift, chemistry 79−29739
Iapetus Ocean, eustatic events and pelagic sedimentation during Ordovician and Silurian 79−29776
ice-wedge casts in NE county Wicklow, distrib. and struct. 78−69379
in-stream settling basin sediment routeing, convective dispersion model 77−37272
India, continental shelf sediments, carbonate fraction 77−73711
India, recent shelf sediments, Fe partition patterns 77−73710
India, W. continental shelf, $CaCO_3$, Mg^{2+}, and Ca^{2+} content 80−8289
India, W. continential shelf, marine sediment P_2O_5 content 80−8288
W.India continental shelf, topography and sediments 80−56454
Indian coast, Paradip port sediment movements 77−73712
Indian continental shelf, distrib. patterns of Al, Ti, Mn, Cu and Ni in sediments 79−25225
Indian Ocean, bottom sediments geochem. studies 79−20808
W.Indian Ocean, clay mineralogy and sedimentation 77−29279
E.Indian Ocean, clay minerals distrib. in sediments 79−44172
Indian Ocean, clay minerals in Cenozoic bottom sediments 79−53335
Indian Ocean, deep-sea sedimentation, lithologic and palaeomag. study 79−20810
Indian Ocean, palaeotemps. during Brunhes epoch from sediment core study 80−12429
E.Indian Ocean, volcanoclastic material in Quaternary deposits 77−78154
Indian Ocean floor, geothermal convection through oceanic crust and sediments 79−79812
mid-Indian Ocean Ridge and Marie Celeste Fracture Zone, metal accumulation rates 77−33052
Indian rivers, chemical and sediment load input into world oceans 79−34870
Indo-Australian plate, deformed oceanic sediments rel. to plate internal deform. 80−109134
Infracambrian glaciogenic sediments from Sierra Leone 78−69378
inshore submarine slope cross-profile changes and littoral drift balance *(Russian)* 78−15989
interfluvial area of Minija and Sventoji, marginal formations structures *(Russian)* 77−25708
Ionian Sea, sapropel distrib. and E.Mediterranean Sea late Quaternary palaeoceanography 78−73350
Iowa lakes, suspended material rel. to water transparency 79−2308
Isar River, Bavaria, trace elements distrib. in sediment, suspension and water samples by neutron activation analysis 78−3834
Israel coast, nearshore sediment pollution by trace metals derived from sewage effluent 78−44882
Isua sediments, W.Greenland, isotope averages and Archaean C and O cycles 79−84262
Japan Trench, Tertiary continental sediments discovery rel. to eastward extension of Honshu *(German)* 79−84200
Kambalda, W.Australia, precious metal values from komatiite sequence interflow sedimentary rocks 79−20830
Kamchatka basin, W.Bering Sea, seismic refr. meas. 77−17053
Keweenawan turbidites in Michigan, foundered basin sequence developed during protoceanic rift system evolution 79−39712
Kimmeridgian black shales, N Atlantic region, rare earth elements distrib. 79−44187
Komyoike volcanic ash horizon sediments in Osaka Group, palaeomagnetic study 79−70742
Kuskokwim River drainage, Alaska, Hg dispersal from lode sources 78−40600
Kuwait Bay, organic matter in sediments rel. to pollution 79−62154
Labrador continental margin, Mesozoic and Cenozoic sediments provenance 79−62479
Labrador Sea, sediments rel. to surface wave study of 1971 December 7 earthquake 77−91040
lacustrine, selective chem. extraction of CO_3^{2-} associated metals 78−65406
Lake Biwa (Japan), sedimentary sequence rel. to late glacial age chronology 79−34872
Lake Bonneville sediments, EM depth sounding 77−45173
Lake Constance, eutrophication effects on sedimentation 79−79889
Lake Lisan-Dead Sea aragonite, element and isotropic comp. rel. to pleistocene geochemical evolution 78−49047
Lake Magadi basin (Kenya), sediments rel. to hydrochemistry 77−49098
Lake McIlwaine, Rhodesia, distrib. of P, N and organic C in sediments 77−33114
Lake Michigan sediment cores, palaeomag. records of geomag. secular var. 77−60347
Lake Monona, Wisconsin, sediments, Cu concs. and environmental chemistry 79−44214
Lake Naini Tal, India, metal pollution in water and sediment 80−97828
Lake Ontario, Late Wisconsin sediments, aspartic acid racemisation and ^{14}C dating 78−73415
Lake Ontario, sediment and nutrient loading 77−81922
Lake Ontario, sediment and nutrient loadings, methodological arguments 78−77278
lake sediment pollution records in New York State 80−85311
Lake sediment radioactivity, mixing by benthic organisms 78−16060
lake sediment sequences, pre-Pinedale, Yellowstone National Park, geology, palynology, climatology 79−66727
lake sediment thermal diffusivity estimation from field obs. 77−2253
lake sediment-water interface sampling with gravity corer 79−88512
lake sediments, E_h meas. reliability conditions 79−48528
lake sediments, PO_4^{3-} adsorption equilibria 79−66354
lake sediments as indicators of heavy-metal pollution 77−25710
lake sediments from New Guinea Highlands, evidence for recent palaeomag. secular var. 79−12069
Lake Tahoe, California-Nevada, sediments, palaeomag. and sedimentological studies 80−41371
Lake Vanern, Sweden, wind, fetch and water depth rel. to sediment distrib. 77−66934
Lake Vuokonjarvi, Finland, palaeomagnetic secular variation 78−32004
lakes, ^{210}Pb determ. by direct gamma-ray meas. 77−5156
lakes, radionuclide geochronology and pollution history 78−61451
lakes, suspended solids, anal. using Landsat multispectral data 79−16523
lakes, vertical mixing by tubificid oligochaetes 80−101390
lakes of western USA, benzo(a)pyrene conc. 80−61476

sediments continued
Lakes Ontario and Erie, comparative ^{210}Pb, ^{137}Cs and -pollen geochronologies of sediments 79−66728
Lakes Ontario and Erie, comparison of bluffs and sediments composition 77−5248
Lakes Superior, Huron, St. Clair, Erie and Ontario, N. distrib. and C/N ratio in sediments 78−28250
Lakes Superior and Huron, sediment composition, anthropogenic inputs 79−79419
landscape periodicity, slope deposits, soil pattern and erosion in small catchment area 78−11924
Late Palaeozoic sediments of Gondwana, garnets anal. rel. to nature of glaciation 79−100874
Late Pleistocene and Holocene dry lake deposits, Mexico, palaeomag. record 80−21618
Late Quaternary climatic changes, W.Africa, from deep sea sedimentation 78−73355
Late Quaternary deposits lithobiostratigraphic characteristics, Baltic Sea *(Russian)* 79−88332
late Quaternary lakes, Arabian Desert, ^{14}C chronology 77−5161
Late Tertiary Verde Formation, Arizona, magnetostratigraphy 78−65179
lateral textural grading in overwash sediments 78−20385
leachates trace element anal., multielement-direct reading method 78−69514
littoral alterations, Messina coastline, Sicily *(Italian)* 79−5469
Llyn Goddionduon, sediment influx, magnetic susceptibility meas. 79−74915
Loch Lomond, Scotland, palynology, palaeomag. and ^{14}C dating of Flandrian marine and freshwater sediments 78−81234
Loch Lomond sediments, geomagnetic secular var. record 79−44088
loess, in Iowa, wind-aligned drainage 80−41467
loess profile near Einbeck, W.Germany, stratigraphic arrangements and material *(German)* 79−20823
loess-formed quartz silt thermoluminescence and dating *(Chinese)* 78−57226
Long Island Sound sediment core, biological mixing effects 79−66672
longshore sediment transport and sediment budget for Malpeque barrier system, Gulf of St. Lawrence 78−36140
Los Angeles Basin SW block, sedimentary record rel. to thermal subsidence and petroleum generation 80−3967
Lower Tertiary laterite on Iceland-Faeroe Ridge, rel. to Thulean land bridge 78−85514
Lower Triassic sediments, Skrino anticline strain var. determ. from deformed reduction spots 77−37184
magnetic remanance, post-depositional realignment of sediments, expts. and theory 80−109137
magnetic remanence acquisition in Finnish lake sediments 79−66682
magnetic spherules, $^{40}K/^{41}K$ ratio rel. to possible meteorite origin 78−11874
magnetic spherules in Arctic Ocean sediments 80−26488
magnetic spherules in marine sediments, K and Ca isotopic comps. 79−44423
magnetic susceptibility anisotropy var. in deep-sea sediments, controls 79−66680
magnetisation, surface tension effects 80−85644
magnetisation, water content effects 79−70785
magnetisation of artificial sediment, const. vol. deform. effects 78−65265
magnetisation of detrital and chemical sediments from Lake Zurich 79−70787
magnetisation studies, high-press. cell for chem. demagnetisation 80−31126
magnetization, depositional and postdepositional processes 77−86869
magnetostratigraphy of San Juan Basin, Cretaceous-Tertiary boundary 77−53055
Mahalanobis' D^2 distance for sediment distinction *(Portuguese)* 78−61388
Mahone Bay, Nova Scotia, Late Quaternary sediments 78−77232
Mamontova Gore silt, Siberia, radiocarbon dates and late Quaternary nonglacial stratigraphy 78−44819
marine, ^{26}Al decay meas. with cyclotron, dating technique 79−71819
marine, acoustic wave penetration as function of physico-mech. characts. *(French)* 80−33324
marine, acoustic wave vel., attenuation and refl., math. model 77−91104
marine, classification, using broadband deep towed seismic system data 79−16721
marine, containing gas hydrates, thermal cond. and acoustic wave vel. meas. 79−79819
marine, correl. between geotechnical and acoustic props. bottom refl. coeff. meas. near sea floor 79−96756
marine, from W Indian coast, geochem. of Th and daughter products 77−41019
marine, hydrostatic press. effect on Cl^- diffusion, in situ expt. 78−44878
marine, in situ gamma-ray spectroscopy, appl. to radioactive waste detect. 77−57806
marine, interstitial water extraction using pneumopress 80−26643
marine, ionic exchanges at water-sediment interface in Norwegian Sea and Intertropical Atlantic *(French)* 79−62523
marine, mag. stratigraphy using susceptibility meas. 79−84520
marine, near drilling sites, Ba content, potential pollutant indicator 79−12144
marine, occurrence of inositol isomers 77−5240
marine, piston core behaviour recording device 78−20532
marine, presence of azaarenes 77−37181
marine, quantitative investigation by neutron activation anal. *(Russian)* 78−92814
marine, radioactivity uptake, rel. to metal pollutants monitoring 79−12145
marine, radiocarbon dating by benzene variant method aboard ship 80−85770
marine, radionuclide conc. rel. to residence time near Maine Nuclear Power Reactor 78−49021
marine, rapid field method for oil pollution detect. 79−12143
marine, ratio of compressional wave vel. to shear wave vel. and Poisson's ratios 80−12404
marine, reflected and scatt. US waves, granulometric mode determ. *(French)* 78−92815
marine, sand velocity gradients 79−68465
marine, saturated, acoustic nonlinearity 80−19132
marine, sulphate reduction and methanogenesis 78−49009

sediments continued
marine, surface organic layer containing U and Th, thickness meas. 78−40592
marine, underconsolidated, adhesive resistance 79−20814
marine deposition rate and sulphate reduction 78−53642
marine environment monitoring through sedimentation 77−29319
marine environmental impact due to Cu mining activities, Chile 79−12140
marine gamma-spectrometric surveying problems 79−2390
marine laminated diatomaceous sediments of Gulf of California, climate record 80−98351
marine Mn concretion growth rates, nonradiometric considerations 78−61393
marine sample petroleum analysis by gas chromatography and mass spectrometry 77−4977
marine sands, resistivity-porosity-particle shape relationships 79−53339
marine sediment analysis and pollutant detection by X-ray fluorescence 77−5361
marine sediment heat flow, Indian Ocean equator region 80−76958
marine sediments, acoustic anisotropy due to overburden press. 80−56455
marine sediments, cosmic origin of black magnetic spherules 78−24494
marine sediments, in situ acoustic impedance meas. method 78−9519
marine sediments, interstitial methane profiles 80−12373
marine sediments, removal from interstitial waters in reducing environments 79−66673
marine sediments, response to seismic activity, seafloor meas. system development 79−5689
marine sediments, seismic vel., density and attenuation models from multibounce phases 79−57864
marine sediments, subsurface layered media parameters estimation using linearised multiple refl. model 79−5691
marine sediments, water-saturated, finite-amplitude wave propag. 78−1476
marine sediments and rocks, sound vel.-density relations 78−50982
marine sediments diffusion coefficients determ., resistivity techniques validity 79−92601
marine sediments interstitial solns. comp. and diagenesis, seawater-sediment interface fluxes 80−3988
marine sediments interstitial waters, dissolved organic matter nature and reactions 78−49039
marine seismic data for detrital sediments, petroleum exploration 78−96303
Martinique Beach, Nova Scotia, nearshore currents and beach topography 78−7646
Matanuska Glacier, Alaska, basal zone entrained debris origin from O isotope investigation 79−79884
Matanuska Glacier, Alaska, pebble orientation in ice and deposits 80−98366
meandering River South Esk, Scotland, flow and sedimentary processes 77−29350
E.Mediterranean, crustal struct., sedimentary layers 78−69311
E.Mediterranean, during glacial max., surface temp. and salinity from foraminifera in sediments 80−41456
E.Mediterranean Sea, palaeoclimatic record of long deep sea core 78−57294
Mediterranean Sea, salt diffusion in sediments 79−57909
E.Mediterranean sediments, heavy metal content, off Lebanon coast 80−97830
Melanesia Basin deep-sea sediments, palaeomag., polarity reversals 78−36102
Mesozoic-Cainozoic sedimentary basins development in W. North America 77−5169
Messinian sediments, rel. to salinity crisis and late Miocene eustatic changes in world ocean 77−91151
metal enrichment of sediments, partitioning of metals, Ranafjord N. Norway 79−83641
metal-enriched sediments from the TAG Hydrothermal Field 79−20805
metal-rich deposits at ocean ridge crests, form. 80−41430
metalliferous sediment components, microprobe study 79−34792
metalliferous sediments and Fe-Mn concretions, magnetomineralogical study, East Pacific Rise 79−62481
metalliferous sediments on E.Pacific Rise, P accumulation rates 77−60364
metasomatic garnets, low-temperature, in marine sediments, paragenesis 77−86857
meteoritic spherules in oceanic sediments, trace element concentrations 79−84755
microparticles of cryst. sediment in bubbles in glass, density determ., flotation method 79−24692
Mid Atlantic Ridge, SW of Azores, deep seismic sounding results 78−3747
Mid-Atlantic Ridge, submarine hydrothermal deposits at 26°N latit., lithology and struct. 80−85641
mid-ocean ridges sediments, role of ridge crest hot springs 80−98304
Middle Ordovician formations, E.Tennessee, tectonic significance of distal turbidites 78−65296
Middle-America Trench, visual obs. of sea-floor subduction line 77−66902
Minch waters and sediments, Windscale effluent 77−91158
minerals diogenesis, plate tectonic controls 80−12387
Miocene, Carpathian Foreland, statistical anal. of repeated borehole meas. 78−49146
Lower Miocene, O isotope anal., parallel changes in species diversity and palaeotemp. 79−39866
Mioceneglaciomarine, southern Ross Ice Shelf 80−36292
mirex in lake Ontario sediments, circulation simulation 80−26556
Moisie River, Quebec, gully flow development after heavy rainfall 77−5249
moraines, in Japan, rel. to late glacial age chronology 79−34872
movement behaviour, current, wave and wind effects *(French)* 77−78151
mudboils nature and genesis, Keewatin, Canada 79−5478
multilayered media, layer-indexed acoustic reflection model 80−43517
Musos Tyrelis (N.Lithuania) bog stratigraphy and palaeogeography *(Russian)* 78−49054
Nadym River, bottom sediments and sandwaves 77−78254
Namibian shelf, I and Br geochem. behaviour in recent sediments 78−32062
natural waters, suspended solids concs. rel. to spectral scatt. props. 80−72560
sediments continued
near-shore and lake sedimentation process, fallout radionuclide tracer obs. 80−81864
neutron activation anal., geochem. of genesis of ore deposits *(German)* 80−30301
neutron activation analysis, of deep ocean sediments *(Russian)* 79−29888
Newcastle-Port Stephens area of Australia late Quarternary deposits 79−88352
Newfoundland, depositional environments and benthos of the continental slope and rise 80−3987
Newfoundland, Late Wisconsinian glacitectonic struct. and post glacial permafrost 78−61440
Newfoundland fjords, gravel clasts rel. to glacial erosion of bedrock 77−17148
Niger delta, sedimentation rel. to struct. of continental margin 77−21693
Nile Cone, Lake Quaternary stratigraphy and sediment dispersal, climatic response 77−45040
Nile Delta, inner shelf sediment types and deposition 79−79868
Nipissing Great Lakes, radiocarbon dating of organic material, alluvial sediments 79−84251
nondestructive neutron activation analysis of environmental samples using low-energy photon spectrometry 78−3995
nonuniform suspended load, non-equilibrium transportation *(Chinese)* 80−8339
North American Atlantic continental margin, sedimentary basins 77−25666
W.North Atlantic Ocean, sediment cores laboratory and in situ compressional wave vel. meas. 79−57866
North Sea floor, lunar type features explanation 80−31028
Nova Scotia metasediments, melting rel. to geochemistry of tonalitic and granitic rocks 77−49064
NRM in deep sea sediments, time series anal. 79−29757
oblique anhysteretic remanent magnetisation 80−21717
ocean, neutron activated, gamma-ray scanning for elemental profile distribs. 77−17079
ocean, suspended sediment conc. and fluid vel. near-bottom meas., Long Island inner shelf 79−34838
ocean basins, thermal and subsidence history 78−49010
ocean bed carbonate sediments, acoustic stratigraphy 80−21709
ocean bottom, isotopes for oceanographic investigations *(Russian)* 77−60486
ocean bottom, O_2 penetration into coastal marine sediment 80−104952
ocean bottom in-situ soil testing, direct and indirect methods, trends 79−12307
ocean bottom profile form. mechanism under translational flow 79−29751
ocean bottom sediments, effects on sound attenuation in shallow water with rough boundaries 77−62091
ocean bottom transport, instrument system for studies on continental shelf 79−58113
ocean floor, refl. and attenuation obs. at 4 kHz 77−2140
ocean floor thermal cond. meas., pulse-probe method 79−53533
ocean sediment classification by seismic reflectivity meas. 77−5370
ocean sediment free-fall penetrometer with Doppler telemetry 80−46320
ocean sediment geotechnical prop. determ. instrumentation problems 79−12304
ocean sediment layer growth and diffusional flux 77−33047
ocean sedimentation rates and organic matter chemical reactions 77−64325
ocean sediments, experimental studies of acoustic wave attenuation 80−10067
oceanic aseismic ridges, sedimentary history rel. to subsidence rates 77−37162
oceanic heat flow meas. over E Canada continental margins 77−5144
oceanic model sediments, elastic wave propag. 77−44966
oceanic phosphorites, Fe, Ti and Al behaviour during initial form. stages 80−31029
oceanic sediments subduction mechanics in lithospheric plates underthrusting zone 77−53030
oceanic suspended particulate matter, chemistry, bottom sediment resuspension 79−12136
oceanic suspended sediment studies using acoustics 77−9523
oceans, Atlantic and Pacific, suspended particles rel. to chem. processes 78−36201
Odaka, Japan, Late Pleistocene sediments, reversed magnetozone 78−40486
offshore disposal of dredged material, sediment props. as tracers 77−5245
Okhotsk Sea, clay minerals distrib. in recent sediments 79−20804
old coast formations of E.Lithuanian upland *(Russian)* 78−16012
Oligocene sediments of Australian region, contrasts between oceanic and continental unconformities 78−73370
Oneida Lake, New York, Mn nodule growth rate 80−46208
opaline pelagic sediment, dissolution of silica into seawater 80−51419
Orca Basin brines and sediments, C isotope comps. 79−88369
Ord River, W.Australia, sedimentation in arid macrotidal alluvial system 79−44205
Ordovician Cap des Rosiers Formation, Quebec, deposits on submarine fan 79−25242
ores, sediments and metamorphism 77−86889
organic acids in Baltic and Black Seas 78−49007
organic matter, metamorphism degree as palaeo-geothermometer, appl. to Upper Rhine Graben 79−70800
organic matter in shales, subaerial weathering effects 78−57206
organic-rich shelf sediments, minor metal content 78−92853
Ottawa River, methylmercury equilib. concs. in sediments 78−11923
Otway sediments, S.E.Australia, analysis of concretions 78−20417
overburden mapping, from elec. cond. meas. via multifreq. airborne EM system 79−5446
S.E.Pacific, DSDP Site 319, metalliferous sedimentation history 78−7611
S.Pacific, neoformation and weathering of assoc. volcanosedimentary levels *(French)* 78−73353
N.Pacific, sediment core geotechnical and mineralogical props., appl. to coastal site for simulation *(French)* 79−34800
SW.Pacific basin, reverberant subbottom layers distrib. 80−8290
Pacific basin, sedimentation rates and sea levels 79−88365
N.Pacific Cenozoic sedimentation history 80−31027

sediments continued
N.Pacific deep sea sediments, ^{26}Al activity rel. to prod. by cosmic rays in atm. 77−5181
N.Pacific Mn nodule area, Recent metalliferous sediments 77−17076
Pacific Ocean, ^{10}Be dating compared with palaeomagnetic ages 78−32058
Pacific Ocean, box cores from Ontong-Java Plateau, radiometric obs. 80−61793
Pacific Ocean, Cd distrib. in bottom sediments surface layer 79−20809
Pacific Ocean, continuous seismic profiling, sedimentary mantle struct. and comp. 79−20806
Pacific Ocean, Sb in metalliferous sediments 77−78156
N.E.Pacific Ocean, sediment type effect on deep water ^{226}Ra concs. 77−5221
Pacific Ocean bottom sediments, interstitial waters B content 80−36289
Pacific Ocean floor, sedimentary contrib. to layer 2A 77−29260
N.Pacific Ocean sediments, 150000 yr ^{18}O-pollen record for palaeoclimate marine-continental correl. 79−80008
NW.Pacific oriented sedimentary cores, geomag. polarity transitions meas. 79−88243
Pacific Pleistocenes palaeoclimatic stratigraphies, comparative anal. of results 78−57295
Pacific Pliocene benthonic foraminifera, O isotopes for deep ocean temp. 80−56492
E.Pacific Rise, metalliferous sediments three-dimensional distrib. 80−21705
E.Pacific Rise, sulphide deposits obs., near 21°N 80−101361
E.Pacific Rise−Galapagos Rise system, sediment thickness rel. to heat flow meas. 78−73331
palaeoceanography, Santa Barbara Basin sediments, Radiolaria study 79−84297
palaeoclimate during last 600000 years, pollen anal. of 200 m core sample from Lake Biwa, Japan 78−24356
palaeoclimatic features, based on stable isotope compositions, Lake Biwa, central Japan 79−12230
palaeoclimatology and vegetation changes during 2000 years BP, from anal. of varved lake sediments 79−25279
palaeocurrent indicators in deep-sea sediments 80−3992
palaeohydrologic phenomena recorded by lake sediments 77−66936
palaeomagnetic intensity meas. of baked sediments, weathering effects 77−37135
palaeomagnetic polarities from cyclothermic sediments in Carboniferous Appalachian Basin, USA 79−70743
palaeomagnetism of late Precambrian and lower Palaeozoic sediments from W.Africa 78−65178
palaeomagnetism of Permian red sediments in Mehadia Basin, Rumania *(Rumanian)* 79−57855
palaeomagnetism of sediments from Nova Scotia, stratigraphic position of carboniferous mag. horizon marker *(French)* 77−78088
Panama Basin, E equatorial Pacific, Holocene sediment accumulation rates 77−81867
Par Pond, reactor cooling reservoir, seasonal cycling between water and sediment 79−100881
partial differential equations application, Rayleigh-Ritz method soln. 78−92878
peat of S.Long Island, New York, radiocarbon dates rel. to Holocene submergence 79−74881
Pee Dee River−Winyah Bay estuary, S.Carolina, sediments ^{226}Ra desorpt. rel. to dissolved ^{226}Ra behaviour 80−98360
pelitic sediments, Sr and Ar isotopic homogenisation during low grade regional metamorphism 79−62511
penetration into a sand sediment of difference-frequency sound generated by a parametric array 78−63227
penetration of highly directional acoustic beams 80−14511
periglacial cover formations in Lithuania *(Russian)* 80−98367
Permian sediments, Skrino anticline, strain var. determ. from deformed reduction spots 77−37184
W.Philippine Basin, DSDP sediments palaeomagnetism, mag. anomalies phase shifting and Basin rots. 77−86764
Philippine Sea, clay sediments comp. and accumulation rates 79−2221
phosphatic nodule beds in Victoria, correl. with late Miocene-Pliocene eustatic event 79−12105
E.Pilbara Block, W.Australia, Archaean shallow-water volcanic-sedimentary facies 79−57926
Pitt Lake, BC, sedimentation rates from ^{137}Cs measurements 80−4048
Pleistocene drift, ice-marginal sedimentary, glacitectonic and morphologic features, Newfoundland example 78−57233
Pleistocene ice fluctuations rel. to Earth orbit vars. 77−37346
Pleistocene sediments, palaeomagnetism and radiochemical age estimates for Late Brunhes polarity episodes 78−11797
Pleistocene-Holocene transition, W.Pacific, from stable isotopes anal. in deep sea carbonates 78−73354
Po river bed sediments, trace metal anal., sampling programme 78−69389
Point Pelee, SW.Ontario, sediments grain size rel. to geomorphology and origin 78−92857
pollen and spore concentration from fine grained sediments by sieving method 80−17402
pollution by ^{239}Pu, ^{241}Am, Ge monitor for in situ assay 77−9546
pollution by heavy metals, sedimentary record, Lake Erie 79−83644
pollution by Hg and As, instrumental neutron activation and atomic abs. spectrometric anal. 80−16890
Polomet River, stream kinematic struct., sandwaves 77−78255
polygonal patterned ground in central New Jersey, origin during Wisconsin glaciation 79−25248
polymodal sediments, interpretation 79−25273
pore water metal concs. in E. equatorial Pacific sediments 80−101358
pore water nutrients and carbonate in E. equatorial Pacific sediments 80−101357
porous deposits, NaCl mass transfer to stationary water region *(Japanese)* 77−25700
prebiotic oceans, soluble organic matter scavenging 77−64436
Precambrian sediments of Michigan Basin, densities from deep borehole gravimeter survey 79−39634
pressure solution thermodynamics, chem. and mech. forces interaction 77−60369
Proterozoic iron-formation, Labrador Trough, Canada, regional metamorphism rel. to mineralogy and chemistry 79−57916
quarks, search for occurrence in seawater, ocean sediment deposits and volcano lava *(Russian)* 77−64288
quartz grains of podzols, surface texture, SEM study 78−36151
sediments continued
Quaternary glaciolacustrine sediments in Val Tresa, collapse dislocations due to Wurm glacier melting *(Italian)* 79−8647
Quaternary sand deposits rel. to aridity in W. Australia 77−13113
Quaternary sediments and stratigraphy, continental shelf, N.Norway 79−84228
Quaternary sediments of N.America, pollen contents rel. to palaeotemps. and palaeoprecip. determ. 80−98438
Quaternary succession near Ottawa, mass flow deposits 77−53050
radioactive fallout effects of Nagasaki atomic bomb 78−85393
radioactivity, evolution in English Channel coastal sediments (1976-78) *(French)* 79−84219
radionuclide distribution among green alga, marine sediments and sea water 78−53534
radionuclide distributions in oceans and marine sediments from nuclear weapons testing 78−13344
radionuclide migration in seawater and marine sediments *(French)* 78−11916
radionuclides absorption through digestive tract of marine demersal fishes 79−92400
radiosotope behaviour in sediments in laboratory-scale aquatic ecosystem 78−3831
rapidly deposited sediments, geomag. secular vars. results for last 25000 years 77−32983
recent sediments, polycyclic aromatic hydrocarbons global distrib. 78−57192
Recent Texas continental shelf and slope sediments, light hydrocarbons meas. 79−2213
Recent tidal-flat sediments, post-depositional remanent magnetization 80−101320
Recent unconsolidated lacustrine, organic geochemical analysis 78−49016
Red Sea, sediments rel. to heat flow map 77−91083
regulation in reservoirs in silt-laden Chinese streams *(Chinese)* 77−70711
remanent magnetisation, acquisition by settling organic mud 80−61795
resedimented conglomerates of Huronian age, Lake Huron north shore, deposition from sediment gravity flow 78−36164
reservoir sediments, water and gas removal from Polesine area, surface subsidence study 78−28233
reservoir supplying major mining centre, water and sediments heavy metals content 80−30617
reservoir under random sediment yield, Bayes design 78−11933
reservoirs of Uttar Pradesh, sedimentation 80−31076
rigidity effects on ocean bottom underwater sound reflection loss in typical deep sea sediment 80−96083
Rimouski shelf region, lower Saint Lawrence estuary, sediments 79−62530
Rio Grande Rise, marine sediments and erosional canyons of late Cainozoic 80−56456
ripples formed by flowing water, size and origin 79−27628
river, from granitic rocks area, petrographical investigation, Yakuwa River, Japan *(Japanese)* 77−70694
River Almond, Scotland, sediment discharge measurements 79−88386
river bed load transport 77−73778
river bed material changes rel. to channel geometry, adaptive adjustment 77−45027
river bottom sediments, in situ neutron activation anal., pollution, mapping and prospecting appl. 77−87115
River Danube bottom sediments, radioactive pollution meas. by γ spectrometric anal. *(Bulgarian)* 79−88019
river flow and sediments to bed evolution *(Russian)* 77−29330
River Periyar, S.India, pollution profile 79−57510
river sediment transport meander of sand bedded stream 80−41466
river sediments, average Hg content in European Economic Community 79−8687
river sediments, P content, bonding form., in Elbe, Trave, Eider, Schwentine *(German)* 79−34868
river transport, fallacy of stream equilib. assumption in denudation studies 77−78236
rivers, sediment transport 77−86943
rivers, sediment yield of New Zealand S. Alps 80−21787
rivers, wind effects on sediment carrying capacity 77−21808
rivers suspended sediment rating curves, accuracy assessment for small basin 77−91170
Romanche fracture zone, limestones rel. to Neogene crustal emergence and subsidence 78−11857
Ross Ice Shelf project, glaciomarine mud 79−88366
Ross Ice Shelf Project in Antarctica *(German)* 77−70836
Rostherne Mere, Cheshire, ^{137}Cs dating confirmation by algal stratigraphy 79−12156
Rother catchment, W.Sussex, fine sediment mineralogy of source rocks and suspended sediment 79−20827
Rudnaya Bay, Sea of Japan, layer of storm network of sediments 79−2224
S-wave velocity versus depth in marine sediments 77−17034
Saguenay Fjord, suspended particulate matter geochemistry 78−92852
Saguenay fjord sediments, distrib. and partition of Co, Ni, Cr and V 77−33100
Sakhalin Island, grain size distrib. along underwater slope 77−64265
Salpausselka moraines, S.Finland, dating rel. to Baltic Ice Lake levels 79−20872
salt, diapirs distrib. and crustal models for E.Brazil margin 77−21698
sampling techniques for interplanetary particles 78−57459
sand, specularite-bearing, experimentally deposited, mag. declination and inclination errors 80−90075
sand grains, mobile, underwater detect. 78−96192
sand tracer dispersion under progressive water waves, laboratory and field obs. 80−46170
sand-wave motion of sediment along nonerodible bottom in open channel flow 78−16074
sandstones of Californiia Late Cretaceous fore-arc basin, petrofacies and petrologic evolution 79−2232
sandy beaches, rhomboidal lattice struct. 77−37178
sandy silts, liquefaction during Friuli 1976 earthquakes 78−24280
Santos Basin, Brazil, sediments of bordering continental rifts system 77−21768
Sao Paulo Plateau, Brazil continental margin sedimentary sequence and comparison with S Angola margin 77−21750
sapphirine-bearing rocks with sedimentary and volcanogenic protoliths from Arunta Block, Australia 79−44185

sediments continued
Saronikos Gulf, Greece, trace elements analysis by neutron activation 78−3825
E Saskatchewan, Pleistocene clays rel. to northern extent of Lake Agassiz 77−91161
sea bottom sediment motion, energy transfer from surface waves 78−73389
sea bottom sediments, machine classification 79−92626
sea floor south and west of Iceland, bottom sediment active redistrib. obs. 80−90068
Sea of Japan, geomorphological struct. and development of central bays 77−49058
Sea of Marmara, evidence for Late Quaternary water exchange 80−81916
sea-floor nodules, geological history 77−25674
seafloor, acoustical imaging of buried objects using focused US transducers 80−79036
seafloor sediments, scouring by drift ice 78−92822
Searles Valley, California, lacustrine sediment core chronology from palaeomagnetic data 80−89955
sediment-water interface in coastal zone, chem. exchange traced by ^{222}Rn obs. 80−101386
seismic velocities, sonobuoy meas. in Bengal Fan, Sunda Trench, Andaman Basin and Nicobar Fan 77−86852
seismite, occurrence in Precambrian rocks, Rajasthan, India 78−77227
seismogram inversion and pseudo velocity logs, lithology identification 77−87088
Seychelles-Mauritius Plateau, mag. anomalies, sediment thickness 78−3750
shallow lake, sediments transport and resuspension 79−70816
shear wave effects on ocean bottom refl. loss, ray path anal. 80−96084
shear wave transducer for use in marine sediment studies 78−63257
shear-wave meas. in laboratory sediments 78−51033
shelf sediments, rapidly accumulating, sonobuoy study 79−21042
shelf sediments off Bombay, geochem. study 79−48449
shelly beaches, Victoria, Australia 79−92525
silicate spherules in deep-sea sediments, extraterrestrial origin 79−48743
Siwalik Group, Dhok Pathan, Potwar Plateau, Pakistan, mag. polarity stratigraphy and age 79−29725
slope recession in Onefour Badlands, Alberta, Canada, rel. to moisture regimes 79−92552
slope stability and valley form. in glacial outwash deposits, Norfolk, England 79−20880
Solar Lake, Gulf of Elat, recent hot brine dolomitization 77−70634
solid solitary grains in water stream, saltation and suspension trajectories 77−44517
N Somerset Island, Arctic Canada, Upper Silurian rocks stratigraphy and sedimentology 77−91131
sonar mapping of lake bottom sapropel and sea shelf sediments *(Russian)* 77−9562
sonoprobe survey, automatic recognition of submarine sediments *(Japanese)* 79−39985
source identification, mag. meas. techniques 80−8348
South China Sea basin, sediments thickness from profiler-sonobuoy meas. 80−8291
South Prebetic Sierra de la Puerta, Spain, Middle Eocene to Miocene sequence 77−66920
south-east Baltic Sea silt granulometric and mineral composition *(Russian)* 79−96755
Spanish Sahara const., effects of arid climate and upwelling 77−60380
speleothems in N.America, stable isotope studies rel. to late Pleistocene palaeoclimates 78−57297
splash erosion, animal activity and sediment supply in forested catchment 77−81928
splash erosion and colluvium form. beneath deciduous woodland, Luxembourg Ardennes 77−81929
St. Lawrence Estuary turbidity maximum, sediment, salinity, suspended matter study 80−4015
stalagmite deposits, palaeomagnetism 79−84107
standard reference materials, based on river sediment and urban particulate matter (SRM 1645 and SRM 1648) 80−21831
Straits of Malacca, radioactivity in marine sediments 79−12135
stream sediment, deposition of trace metals downstream of Pb smelter 80−61475
stream sediment sources, use of metals as tracers, field expt. 78−81227
stream transport of solids, magnitude and freq. in Mississippi basin 77−78235
streams, Cd content determ., geochem. 78−36170
submarine canyon heads, relief development processes, Black Sea 78−44803
submarine landslides, North American east coast and upper rise 79−20815
submarine sediments, automatic recognition by sonoprobe survey, acoustic reflection pattern model *(Japanese)* 80−85776
subsurface water chemistry study, coring and squeezing technique 78−57332
sulphate evaporites, Middle Proterozoic, at Mount Isa mine, Australia 78−73371
sulphide deposits on E.Pacific Rise, assoc. with hot springs 80−101360
sulphide-rich sediment core, Fe diagenesis studies by Mossbauer spectroscopy 79−74917
sulphides and sulphates from DSDP Leg 37, S isotope comps 77−91101
supernova created sediment, γ-ray ablation of Moon 80−56731
surface charge 80−36331
suspended clastic material, in ocean, movement over shore slope under storm conditions 79−2223
suspended sediment load of estuarine and oceanic waters of old Mangalore port, seasonal vars. 80−41451
suspended sediment monitoring by remote sensing, universal multispectral algorithms 79−53558
suspended sediment sources identified by magnetic measurements 80−4052
suspended sediments, effects on dissolved pollutants photolysis rates 79−100546
suspended sediments in surface waters of Mississippi reservoirs 77−45041
suspended sediments in translational flow, vertical distrib. 78−3841
suspension in open channel flow, bed material load distinguishability from wash load *(Chinese)* 79−90338
Tarmanskii Marsh, peat-bed thermal props., influence of human activity 78−92864
sediments continued
telescopic alluvial fan complex, intersection points 79−20877
terrigenous and volcanogenic deep sea bottom sediments chem. comp., Sea of Japan 77−21758
Tertiary deltaic succession, palaeocurrents and sedimentary structure 77−17147
Tertiary sediments from North Sea area, O isotope palaeotemps. 78−88903
Texas shelf zone, sediments thickness from sonobuoy and ocean bottom seismograph data 79−5462
Thames Estuary, Flandrian sediments stratigraphy rel. to sea level changes and land subsidence 78−24304
thermal conductivity meas. using probes with semiconductor temp. sensors *(Russian)* 78−65431
thermoluminescence dating of sediments baked by Chaine des Puys lava flows 78−92808
Thunder Bay, Lake Superior, element conc. in post-glacial sediments 77−78237
Thunder Bay Late Quaternary sediments, palaeomagnetic record from remanent mag. meas. 80−17230
tidal embayment, dynamics and sediments 79−100841
tidal power schemes of West Bengal, siltation estimation 80−31059
tills, erosion and deposition by continental ice sheets 79−25276
tills deposited in arid polar environments, characts. 77−91160
titanomagnetite sand from New Zealand, density, elec. and mag. prop 80−98311
Tolaga Bay Flats basin, recent alluvial infilling estimation using tephra marker beds 78−11925
trace elements partition patterns in sediments from DSDP Site 219 78−36143
transport, erosion and deposition of cohesive sediments, modelling 78−15994
transport along Indian west coast rel. to wave refraction 77−91145
transport for desert watersheds in erodible materials 78−20442
transport mechanisms, alluvial rivers, braiding and meandering 78−36212
transport model for sandy river *(Chinese)* 79−96779
transport near breakwater, physical and numerical modelling 80−51401
transport near ocean bed, theoretical flow models 78−15996
travertine from archaeological sites, Nahal Zin, Israel, U series dating 79−34781
ungauged rivers, distributed numerical model development for estimating runoff and sediment discharge 77−91178
ungauged rivers, distributed numerical model for estimating runoff and sediment discharge 77−91177
ungauged rivers runoff and sediment discharge estimation, distributed numerical model 77−91179
unit sediment graph 79−79902
United States Atlantic continental shelf, US Geological Survey core drilling 80−72511
upper Keweenawan sediments, virtual geomag. pole position determ. 77−78089
Urazoko Bay, ^{239}Pu, ^{137}Cs and ^{60}Co distrib. and behaviour 80−97825
Urazoko Bay, ^{60}Co radioecology, levels in sargassoes and marine sediments 77−9448
urban hydrology and sediment control, symposium, Lexington (1976) 77−37266
urban stormwater and sediment discharge, deterministic model 77−37273
Vancouver Island, Wisconsin stratigraphy, climate reconstruction 80−8267
varved sediments from W.New England, palaeomagnetic recorder var. 79−70738
varved sediments from W.New England, secular var. 79−70739
Vema Channel, increased transport of Antarctic Bottom Water during last ice age 77−21798
Virginia Beach, Virginia, coastal currents and assoc. sand stream 78−73392
Visakhapatnam coast, Bay of Bengal, clay sediments derived from inland sediments 80−76959
viscous remanent magnetisation in sedimentary rocks, stability to AF demagnetisation, expt. results 79−79826
viscous sound attenuation in high-porosity marine sediments 80−74577
volcanic material alteration in marine sediments, SE.Pacific Ocean 80−3990
Vulcano Island neighbourhood, heritage and neoformation in volcanic and hydrothermal sediments *(French)* 79−62482
Wastwater, W.Cumbria, Pu and ^{137}Cs concs. in lake sediment samples 80−108817
water erosion characteristics in Siberia, Russian plains and central Asia 78−61449
water-sediment interface US reflection with bidirectional displacement 78−60017
watersheds of Eastern USA, ^{137}Cs distrib. 77−25701
watersheds sediment prod. long-term patterns following road construction and logging 79−84322
wave transport of sand sediment, by near bottom orbital motion 80−98306
wave-formed bars, sedimentation and equilib., review 79−92521
wedging out zones, separation via multiple seismic waves freq. selection *(Russian)* 79−8706
late Wisconsinan till sheets, Brantford-Woodstock area, S.Ontario, trend surface anal. 78−92858
Witwatersrand sediments in S.Africa, principal horizontal stresses 77−91093
X-ray fluorescence analysis, of ferromanganese nodules and marine sediments, use of semiconductor detectors *(Russian)* 79−29887
Y-5 ash layer in E.Mediterranean, age, origin and volcanology 80−56444
Yangtze delta, Holocene formation and development *(Chinese)* 79−16528
Yangtze River middle reaches, channel development after completion of aritficial cutoffs 79−44210
Yellow River, flow with heavy sediment concentrations *(Chinese)* 79−79886
Yellowstone and Jackson Lakes, mag. props. and secular var. in sediment cores 78−48968
Yellowstone Lake, seismic refl. and refr. surveys and palaeomag. study 78−49049
SE Yukon, unique stratigraphic record of late Tertiary-Quaternary events 79−62499

sediments continued
zircons, detrital, in N.Africa, no evidence of 500 Myr ages or Pan-African mountains 79−84213
Al, dissolved, in interstitial waters of recent marine sediments 79−92524
B abundance rel. to ocean palaeosalinity, implications of B loss from shells during weathering 77−78204
^{10}Be conc. vars. search in marine sediment core during geomag. reversal 80−26511
^{10}Be geochemistry in North Pacific during Pliocene 80−101356
^{10}Be in marine sediments rel. to geophysical events and cosmic ray var. 79−29748
^{10}Be var. in deep sea sediments, critical evaluation 78−7615
CO_3^{2-} sediments, Lawson's Bay area, Indian east coast, origin 79−25266
^{14}C age errors for recent deposits with fluvially transported charcoal 78−36172
^{14}C age of deep-sea sediments, rel. to vertical mixing 80−81865
^{14}C dating of geological and archaeological samples 78−92993
Ca, determ. in lake sediments, by atomic absorption spectroscopy 78−95970
$CaCO_3$ dissolution in deep sea sediments, rel. to palaeoceanographic reconstruction 79−25269
$CaCO_3$, radioactive dating via ^{41}Ca 79−21063
Cd sorption and accumulation in sediment of Tama River 79−74924
^{113}Cd^m, in marine organisms and sediment around Marshall Island nucl. test site 80−109174
Ce determination method for marine sediments 80−104543
Co and actinide adsorption by Mn and Fe oxides in soils and sediments 79−66422
^{137}Cs adsorption by sediments near water-cooled nuclear reactors 77−78281
^{137}Cs, contents in coastal sediments 79−57974
^{137}Cs fallout in arid watersheds, phys. and chem. parameters affecting transport 78−61461
^{137}Cs movement and loss in small lake 78−24317
Cu-Ni enriched ferromanganese nodules and assoc. crusts from Bauer Basin, NW. Nazca Plate 77−86851
Fe, characterisation in environmental samples by Mossbauer technique 79−66433
Fe formation, REE data rel. to seawater 79−66715
Fe precipitation in Vellar estuary, conc. determ. 80−77015
Fe-Mn deposits on abyssal sea floor, geochem. 79−12107
Fe-Mn nodules, todorokites new forms and cryst. structs. 79−48469
H_2S contaminated sediments composition, stagnation coeff. and appl. in palaeogeographic reconstruction 80−36291
^{3}H kinetics in freshwater marsh, simulation model 78−24318
Hg contamination of sediments in semienclosed bay, Norway 78−81220
Hg loss rate from contaminated estuarine sediments 80−85310
Hg pollution of Mediterranean sediments around Alexandria, Egypt 80−3538
K-Ar dating method for argillaceous sediments 79−8716
Li bearing metasediments, melting rel. to Li rich pegmatites petrogenesis 79−57918
Mn nodules, deep-sea, diffusion-controlled growth model 79−2212
Mn nodules, maintenance at surface by bioturbation of infauna 80−101359
Mn nodules, mineralogy and comp. changes from long-term seafloor mineral exposure expts. 79−5471
Mn nodules from N equatorial Pacific, post-depositional internal metal enrichment processes 79−34791
Mn nodulus and micronodules of NW.Atlantic, rare earth element study 80−46167
N fixation in Atlantic deep-sea and coastal sediments 78−81211
Nd isotope composition of ocean bed 80−21704
^{18}O in equatorial Pacific core, glacial time scales and climate 80−21817
^{18}O stratigraphy in deep-sea sediments, evidence for deglacial meltwater effect 78−85530
$^{18}O/^{16}O$ stratigraphy of deep sea sediments rel. to Eemian interglacial 79−29770
^{231}Pa, determ. in coastal sediments and seawater, activity ratios, disequilib. 78−27851
Pb determ. by atomic absorption 79−88035
Pb in subalpine pond sediments, anthropogenic source var. 80−85315
^{210}Pb chronologies of lake and marine sediments, problems 78−81122
^{210}Pb, dating, results from Lake Ipea and Lough Erne 78−28202
^{210}Pb dating of annually laminated Finnish lake sediments 79−74916
^{210}Pb determination in lake and marine sediments 79−48582
^{210}Pb determination in sediment core from ocean floor off Californian coast 80−72101
Pu accidental release at Thule, Greenland, environmental behaviour 77−56656
Pu, contents in coastal sediments 79−57974
Pu, industrial effluent, behaviour and transport in Great Miami River, Ohio 78−16061
^{222}Rn in biologically produced gas from reactor cooling pond 78−80976
S distribution in marine sediments 79−92523
S isotope studies, Isua, W.Greenland 79−92537
$^{87}Sr/^{86}Sr$ ratios of interstitital waters from DSPD sites rel. to sediment geochem. 79−34794

Seebeck effect
alloy, dil., thermoelectric effects 79−38054
alloy, dilute, thermoelectric effects, near cancellation of electron-phonon corrections 79−33283
amorphous semiconductors, appl. to thermoelec. generators 80−35704
anisotropic thermoelectric cooling unit, theory 78−47820
biopolymers, solid, apparatus for Seebeck coeff. meas. 78−21172
bipolymer, charge carriers origin and mobility, adsorbed water effects 79−92461
calorimetry, applications of thermoelectric devices in various types of calorimeters 80−105648
coefficient meas., 300 to 530K 78−91677
coefficient measurement of disc-shaped samples by AC method *(Japanese)* 80−73392
DH lasers, thermal-gradient enhanced current spreading 79−18416
dilute alloy, Seebeck coefficient, electron-phonon enhancement 80−70685
education, Joule heating, Peltier and Seebeck effects, Cu-Constantan thermocouple expt. 79−9056
electronic transport coeff., soln. between Mori-Green-Kubo formulae and Boltzmann approx. 78−79971

Seebeck effect continued
eutectics, HgTe-PbTe and Au-PbTe, prep. and thermoelectric behaviour characts. 80−107774
ferroelectric ceramic, elec. and thermoelec. props. of grains and grain boundaries 78−43382
fuel rod, simulated, for HTGR, pre- and postirradiational thermal transport and thermal expansion 79−6742
graphite, neutron irradiated, thermoelec. and thermomag. effects 77−59296
irreversible phenomena in homogeneous materials, and single and double bimetallic junctions *(French)* 78−95291
lattice parameters, mag. and elec. props. 80−100578
many-valley semiconductors, ellipsoidal energy surface, high field magnetoresist. and magnetothermal EMF 77−43621
metal, degree of deform. effect on thermophys. props. at high temps. 78−26694
metal, kinetic effects at high anisotropic strains, elec. transport props. meas. 78−54384
metals, diffusion thermopower, boundary scatt. effect 80−6817
metals, magnetic, Seebeck coefficient anomaly near spin ordering temp. 77−20302
$MgAl_{2-x}Fe_xO_4$ solid solution system, solid state properties study 80−93094
$(Pb_{0.95}Sr_{0.05})(Zr_{0.53}Ti_{0.47})O_3$+3% mol PbO, meas. and interpretation of effect *(Polish)* 79−4574
phosphate glasses: Ti^{3+}, $MO(M_2O)$-TiO_2-P_2O_5 M=K, Ca, Be, elec. resistivity *(Japanese)* 77−12719
polar semiconductors, magneto-Seebeck coeff., electron spin depend. 78−80011
polycrystalline substances, use of Hall and Seebeck effects in phys. parameter determ. 77−12023
rare earth compounds, R_2MoO_5, cryst. struct., IR spectra, elec. and mag. props. 80−33954
rare earth orthocobaltites, $R_{1-x}Sr_xCoO_3$ and $La_{1-x}M_xCoO_3$, itinerant electron ferromagnetism obs. 78−10660
rare earth pyrochlores, $R_2(V_{4/3}W_{3/3})O_7$, (R=Gd, Tb, Dy, Ho, Er, Tm, Xb, Lu), synthesis and elec. props. 80−29914
rare earth tungsten oxide bronzes, metallic, elec. props. meas. 78−30906
rare earth-CrO_3, elec. transport 80−70700
semiconductor, AC method of meas. using laser beam 78−76096
semiconductor, crystn. in constant electric field, thermoelectric parameters 77−44146
semiconductor, Seebeck and Hall coeffs. Lorenz number, anisotropy, theory *(German)* 80−65608
semiconductors, kinetic effects at high anisotropic strains, elec. transport props. meas. 78−54384
TCNQ salt, (1,2,-bis(di-n-alkyl-4-pyridinium) ethene)$^{2+}$ $(TCNQ)_x^{2-}$, cryst. struct. and elec. props. 79−56209
TCNQ salt, (1,3,-bis(di-n-alkyl-4-pyridinium) propane)$^{2+}$ $(TCNQ)_x^{2-}$, cryst. struct. and elec. props. 79−56209
TCNQ salt, $(TMA^+)_3(I_3^-)(TCNQ^-)_2(TCNQ^0)$, struct., phys. props. and lattice distortion evidence 78−6305
TCNQ salt, MeDABCO$(TCNQ)_2$, elec. cond. and IR and visible spectra meas. 79−42526
thermocell, solid electrolyte, twin, for entropy of O_2 in mixture determ. 78−27812
thermocouple, thermometers, voltage generation, calibration 80−57295
thermocouples, thermoelectric effects, reversibility, theory 77−59280
thermoelectric alloys, phase diagrams, and imperfection chemistry 80−108422
thermoelectric materials, B_4C_x and $(B,Si)_4C_x$ P-type LaS_x N-type alloys, fabrication and thermoelectric props. 80−107771
thermophysical measurements, sample shape determ. 79−30457
transition metal chalcogenophosphates, intercalation with n butyl-lithium, possible appl. in Li batteries 80−71446
volume component determination 80−49788
$Ag_{19}Sb_{29}Te_{52}$, single-phase, thermoelectric efficiency 80−107826
Al-TeO_2-Al, field-assisted cond. mechanism 80−11105
AlH_3, thermo-EMF meas. 80−39617
n-$BaTiO_3$, elec. transport props., theoretical discussion and expt. 78−84215
$BaTiO_3$, H_2-reduced, elec. cond. mechanism, EPR, resist. and Seebeck coeff. meas. 80−10976
$BaTiO_3$, semiconducting ceramic, AC thermopower measurement 80−44624
$BaTiO_3$, transport and optical props., small polaron hopping theory 79−47096
δ-Bi_2O_3, thermoelectric power, heat of transport of O^{2-} ions 80−92713
$Bi_{1-x}Sb_x$:Pb ($0.08 \leq x \leq 0.13$) Seebeck, magneto-Seebeck coeff., longitudinal Nernst coeffs. 78−56168
n-$(Bi_{1-x}Sb_x)_2Te_2$, magneto-Seebeck and Shubnikov-de Haas effect 79−42568
n-Bi_2Se_3, IR, reflectance, Seebeck coeff. and Hall voltage meas. 79−60692
n-Bi_2Se_3, single cryst., new aspect of carrier scatt. 80−49707
Bi_2Te_3, galvanothermomag. props. up to 14 kbar 77−47829
Bi_2Te_3-Sb_2Te_3 film, cond., galvanomag. Seebeck and Nernst-Ettingshausen effects under press., band model 77−47907
BiTeI, elec. props., crysts. grown from melt in excess iodine 79−4907
C fibres prepared from benzene, thermoelec. power, magneto-Seebeck effect 78−2507
Cd-Sb thin film prep. by vacuum deposition, elec. props. 78−92194
Cd_3As_2, band structure, Kane model, magneto-Seebeck and Hall data 77−62821
Cd_3As_2, band structure, pressure dependence of galvano- and thermomagnetic effects 80−6722
n-$CdCr_2Se_4$, single crystal, transport props. near Curie temp. *(Japanese)* 78−6406
Cd_3P_2, energy band struct. and electron mobility at low temp. 79−37984
Cd_3P_2, thermomagnetic transport effects and zero field Seebeck coeff. meas. 77−15883
a-CdS film, DC cond. Seebeck data 77−24626
CeO_{2-x}, conductivity and Seebeck coeff., small polaron and hopping mechanisms 77−76812
$CoMoO_4$, mag. susceptibility and electrical transport props. 79−56511
$Co_2Mo_6S_6O_2$, O-containing Chevrel phases, synthesis and props. 80−108368
$Co_{3-x}Ni_xO_4$, $0 \leq x \leq 1.1$, struct., semicond.-semimetal transition, Seebeck coeff. 78−87972
$CoSnTe_2$, thin films, metallic elec. props. 79−78212
Cr, high purity, 280-1000K 77−39816

Seebeck effect continued
Cr_2O_3 carrier mobility temp. dependence 77−35958
$Cr_2S_{3-x}Se_x$, elec. resist., thermal cond. and Seebeck coeff. meas. 80−24958
$CrSe_2$, layered, phys. and elec. props. 80−44594
Cs_xWO_3, normal phase and supercond. props 80−25035
Cu, stranded and solid wire, rel. stability of thermal EMF in cryogenic environment 78−60111
Cu-Constantan junction, elec. response to shock compression 79−95470
Cu-Fe wire, low-temperature measurements, undergraduate lab. project 78−54119
$Cu_{1-x}Fe_{2+x}O_4$, elec. resist., Seebeck coeffs., 20 to 900°C, cation distrib. 79−4575
$Cu_2Mo_6S_6O_2$, O-containing Chevrel phases, synthesis and props. 80−108368
Cu_xO, film, thermoelec. power, activation energy variation with electrode spacing in DC sputtering 78−76099
$EuO_{1-x}N_x$, ferromag. semicond., elec. and mag. props. *(French)* 78−79993
Fe-Si alloy, Si content determ. from Seebeck coeff. 77−56269
$Fe_{1-x}Cu_xCr_2S_4$, mag. semicond., mag. props. and elec. cond. *(Japanese)* 79−47111
Fe_2O_3-V_2O_5 system, elec. transport 79−51576
$Fe_3O_{4-x}F_x$ substituted magnetite, low temp. resistivity, Seebeck coeff., thermopower 80−20234
$Fe_{3-x}Ti_xO_4$, elec. transport near Verwey transition, thermoelec. power and cond. meas. 79−95455
Ge-Si alloy, quenching from high temp., thermal electric parameters, obs. 77−28165
Ge-Si alloys, n-type, phosphorous doped, precipitation effects due to heat treatment 80−107833
$GeBi_2Te_4$, Hall const., thermoelec. power, and elec. cond. 80−29407
$Ge_xNi_{1-x}O$, crystallographic and elec. props. 77−32011
HgSe, quantum oscills. in Seebeck effect in high mag. fields 77−72875
HgTe, magnetophonon oscills. of thermoelec. power 80−49789
In_2O_3, Seebeck coeff., density of states effective mass 78−56171
InSb, polar semicond., longit. magneto-Seebeck coeff. in quantising mag. field 79−56250
In_6Se_7, single cryst. prep. and electrophys. props. 79−43129
$KNbO_3$, elec. and thermoelec. singularities due to small polaron hopping motion cond. transition 79−42565
$KNbO_3$, thermoelec. effect and phase transitions 78−48123
$KTaO_3$, pure and Gd_2O_3 doped, elec. cond. and sp. ht. 79−78097
$KTaO_3$:Gd semicond., temp. depend. of thermal diffusivity and Seebeck coeff. 78−10481
$LaCO_{1-x}M_xO_3$, M = Mg, Ti, cryst. struct., elec. and mag. props. 79−86748
$LaNi_{1-x}Fe_xO_3$, semicond. and metallic phases, elec. and mag. props. 79−78102
$La_{1-x}Sr_xCoO_{3-y}$, Seebeck coeff. meas., small polaron hole conduction model 80−20233
$La_{1-x}Sr_xCrO_3$ ($0 \leq x \leq 0.4$), localised level hopping transport 80−10974
$La_{2-x}Sr_xNiO_4$, ($0 \leq x \leq 1$), cryst. struct. and elec. props. 78−2088
$Li[Mn_2]O_4$ spinels, crystallographic, electronic and mag. props. *(German)* 79−60324
MgO, $MgCl_2$ additions effect, ionic role 78−26895
MoO_3:Li, elec., catalytic props. 78−60122
Mo_6S_8 Chevrel phases with group IIIa metals, Nb, Hg, Pb and Cu, synthesis, stability and charact. 80−71608
$Mo_{0.5}W_{0.5}Se_2$ single cryst. vapour growth, characterisation 80−93466
$NaNbO_3$, elec. cond., Hall mobility, thermoelec. coeff. 79−82584
$NaNbO_3$, thermoelec. effect and phase transitions 78−48123
$NbSe_2$(2H), low field magnetoresist. and anomalous transport props. 80−65602
$NdTlO_3$, physicochem. props. 80−25625
Ni-Cr film, RF sputtered 77−63004
Ni-Cr-Si, thermocouple alloy, props. and thermoelec. reference data 79−26057
Ni-Si-Mg, thermocouple alloy, props. and thermoelec. reference data 79−26057
Ni-Zn ferrite, electrical cond., Seebeck coeff. and saturation magnetisation 77−20315
$Ni_2Mo_6S_6O_2$, O-containing Chevrel phases, synthesis and props. 80−108368
NiO catalyst, superparamagnetic, elec. props. 79−65506
NiO, localised charge carrier transport, Seebeck, resistivity meas. 78−72152
NiO, temp. and stoichiometry depend., antiferromag. T-domain influence 77−8332
Ni_xO, film, thermoelec. power, activation energy variation with electrode spacing in DC sputtering 78−76099
$PbMo_6S_6O_2$, O-containing Chevrel phases, synthesis and props. 80−108368
PbS:Tl, Hall and Seebeck coeffs., Hall mobility, impurity states 80−15545
$Pb_xSn_{1-x}O_2$:Sb films, DC sputtered, elec. props. 80−80426
$PbTiO_3$, thermoelectric effect and ferroelectric transition 78−48123
$Pb(Zr,Ti)O_3$ solid soln., elec. cond. and Seebeck coeff. 79−51564
$PbZrO_3$, thermoelec. effect and phase transitions 78−48123
$Pb(Zr_xTi_{1-x})O_3$, elec. props. effect of proportional composition, morphotropic phase boundary 78−35105
$Pb(Zr_xTi_{1-x})O_3$, elec. props. temp. and composition depend. 78−47817
$Pb(Zr_xTi_{1-x})O_3$ solid solns., elec. props. near morphotropic phase boundary 79−42566
Rb_xWO_3, phase transitions, supercond. transition temp. and elec. props. 79−28431
Rb_xWO_3, resistivity, Hall effect and Seebeck coeff. from 1.5 to 300K 80−6879
Sb_2S_3, elec. and mag. props., carrier transport mechanism 78−47792
Se, liq., pure and I doped, thermopower, temp. depend. *(French)* 77−69360
P-Si, highly doped, thermoelec. coeffs. meas. at semicond. solid-metallic liq. interface 77−39887
Si position-sensitive detector for CW and pulsed laser beams 80−78883
Si Seebeck effect position sensor for CO_2 laser beam alignment 80−5772
Si-Ge:Al(B)(P), hot-pressed alloy, thermoelec. props. 78−91711
Si-Ge:As,P, heavily doped, electron scatt., Hall coeff., Seebeck coeff. and resist. meas., 4-300K 77−4379
SiAs, cryst. growth from melt, elec. props. 80−76170
Sm, resistivity and thermopower anomalies at high temp. 78−64027
Seebeck effect continued
Sn-Pb (26%), liq. eutectic alloy Seebeck coeff. 80−84463
SnO_2 thermoelectrical properties, investigation 77−76852
Te thin film, thermoelec. EMF, Seebeck coeff., elec. cond. structural depend. 79−78230
$Te_{50-x}Se_{50}Sn_x$, thin films, elec. cond. and thermoelectric power meas. *(French)* 80−80335
TiO_2:Nb, rutile, Seebeck effect, 90-300K 78−43427
TiO_2:Nb, Seebeck coeff., Fermi level temp. depend. 79−11161
TiO_2-P_2O_5 reduced glasses, prep., elec. transport, chem. anal., DC, AC cond., seebeck coeff. 78−30924
TiO_2-Ti_2O_3-P_2O_5, glass form., struct. and elec. props. 80−44592
$Tl_xV_6S_8$, prep., struct., props. 77−19935
V, thermal cond., elec. resist. and Seebeck coeff. meas., 6-300K 77−39818
V_2O_5-BaO-K_2O-ZnO glasses, elect. props. and struct. 80−15547
V_2O_5-MoO_3 solid solns., small polaron cond., elec. resist. and thermoelec. power meas. 80−34447
V_2O_5-P_2O_5 (70-30), electrical cond. and thermoelectric meas., Au-glass-Au sandwich 80−29403
V_2O_5-V_2O_4-$BaZnO_2$ glass, V ion states, mag. and elec. props. 80−88556
$(Y,Eu,Tm,Ca)_3(Fe,Ge)_5O_{12}$, Ca, Ge substituted garnet LPE films, elec. props., charge imbalance, Seebeck effect 78−68101
$(Y,Sm)_3(Fe,Ge)_5O_{12}$, Ca, Ge substituted garnet LPE films, elec. props., charge imbalance, Seebeck effect 78−68101
YIG, elec. props. meas., 600-1500K 77−8098
YIG, nonstoichiometry and electronic defects, thermogravimetric expts. and anal. of elec. data 78−6050
$Y_2(V_{4/3}W_{2/3})O_7$ pyrochlore, synthesis and elec. props. 80−29914
Yb, semimetal-semicond. transition at high press., Seebeck coeff. meas. 77−62956
$Zn_xHg_{1-x}Se$, band struct. and scattering mechanism, determ. from transport coeffs. 77−59254

segregation
microstructural processes and features only
see also Guinier-Preston zones; spinodal decomposition
alkali halide, crystal, irradiation-induced defects 80−107316
alkali halides, divalent metal impurities, aggregation process, order of reaction, fractional time conc. depend. 80−107308
alloy, binary, crystallisation under parabolic stability *(Russian)* 79−70054
alloy, binary, magnetic, interface struct., Monte Carlo simultion 80−60317
alloy, binary, quenching, cluster growth, first order phase transition, computer simulation anal. 79−34039
alloy, binary, surface segregation prediction using bulk alloy variables 79−65300
alloy, binary, with curved solid-liq. interface, lateral solute segregation during unidirectional solidification 79−47692
alloy, chemical induced segregation, obs. by Auger fine struct. anal. 78−15416
alloy, cleaved, electronic theory, off-diagonal disorder 79−4596
alloy, disordered, bulk and surface density of states, effect of surface segregation 77−15729
alloy, FCC, Monte Carlo simulation of surface segregation 78−31413
alloy, lamellar multiphase, struct. and spatial comp. variation, analytical STEM 78−24011
alloy, solute redistrib. during in situ irrad. in HVEM 80−107324
alloy, surface segregation, appl. of quantification of atom-probe FIM data 78−62263
alloy, surface segregation, existence of surface miscibility gaps within regular soln. theory 78−71909
alloy, surface segregation prediction from bulk melting curve shape 77−12597
alloy constituents, segregation during irradiation 79−55791
alloy steel, rel. to special carbide formation *(Russian)* 77−21153
alloy surface, free energy of segregation 80−29256
alloy surface, theory of segregation 79−77886
alloy with two ferromagnetic components, surface excitations 80−25179
alloys, binary, surface composition, regular soln. theory 78−10265
alloys, binary, surface segregation kinetics 80−80044
alloys, clustering and ordering, radiation induced atomic rearrangements, conf. Atlanta, GA, USA (March 1977) 79−42099
alloys, complex, method for evaluating influence of each element on microsegregation of solidification *(French)* 79−74159
alloys, conc., theory of radiation-induced segregation 79−77633
alloys, definition for arbitrary duration and expt. temp. 79−51267
alloys, dilute, radiation induced solute segregation and precipitation study by means of Johnson-Lam kinetic model 79−43252
alloys, embrittling residuals categorisation by Auger electron spectroscopy 80−66739
alloys, irradiated, effect of defect trapping and solute segregation, on defect recombination rates and void swelling 78−47369
alloys, irradiated, segregation, inverse Kirkendall effect, effect of constitution on void swelling 78−91472
alloys, rapidly quenched crystalline, struct., and heat treatment effects 80−76292
alloys, temper embrittlement, impurities and alloying elements role, review 80−66649
bimetallic cluster, segregation and short range order props. at boundaries 79−29071
binary, segregating alloy, theory of surface effects 79−19435
binary alloy, concept of partial elastic energy in anal. of surface segregation *(French)* 79−77884
binary alloy, model quenched computer simulation of time evolution in nucleation region 79−82344
binary alloy, quenched, time evolution, computer-simulation of three-dimensional model system 77−48422
binary alloys, initial transient segregation during unidirectional solidification in a furnace with thermal damping 80−70146
binary alloys, surface conc. profile and surface energy 80−84350
binary liquid alloys, surface tension, compressibility and surface segregation 78−67889
binary liquid solutions, surface cluster functions 78−67631
binary melts, appl. of quasichem. method of cluster components *(Russian)* 77−80623
binary metal alloys, surface segregation correlation with bulk diffusion 80−54388
binary mixtures, liq. and solid, spinodal decomposition theory 78−71863

segregation continued
binary system cluster dynamics, critical diffusion and phase separation kinetics 77−61042
brass, α and $\alpha+\beta$ type, positron annihilation, short-range order, clustering and lattice defects influence 79−29107
brass, inface segregation in α/β two phase bicrystal and polycrystal *(Japanese)* 79−15675
α-β brass, interface segregation 80−89231
α-brass, quenched, secondary defect form. during ageing, TEM obs. 78−88482
brittle materials, influence of structural parameters on fracture toughness 79−96133
dl-camphene, self-diffusion, effect of impurities, radiotracer and plastic deform. study 78−43177
casting, dendrite remelting and macrosegregation in low-gravity 79−47669
cellular and cellular dendritic growth, general microsegregation eqn. 80−84921
ceramic, grain boundary segregation 78−15410
ceramics, glassy, struct. and electron beam sensitivity 80−79841
charged aggregates of divalent impurities in NaCl-type crysts. 77−84790
cluster model for transition state, electron diffr. study 78−10168
clustering, in melt, X-ray and neutron small-angle scattering determ., review 79−10752
concrete, fresh, behaviour under a vibr. action, large particle segregation *(Japanese)* 80−88329
crystal growth, macroscopic equilib. and transport concepts, book 80−27054
crystal growth from melt, reformulation of Burton, Prim and Slichter model of segregation 79−4909
Cunial MNA13-3, Mn addition effect on props. 80−21035
Czochralski growth, fluctuating growth rates effect on segregation, no backmelting 80−54161
Czochralski growth, fluctuating growth rates effect on segregation, backmelting 80−59413
dehydration kinetics in ferroelec. and paraelec. phases, surface acoustic waves influence 80−97204
diamond, natural, (110) and (210) defects, X-ray diffr. pattern weak extra reflections 79−82257
diamond, natural, $N_{S(111)}$ impurity segregation on diffuse X-ray scatt. 79−95046
diffusion phenomena, vacancy-impurity complexes effect, appl. to nonequilib. segregation near grain boundaries *(Russian)* 80−44350
dilute alloy, surface segregation, bond and strain energy effects, atomic calc. 79−69256
dilute alloys, time of flight atom-probe FIM exam. of surface segregation 79−19437
dilute solute-binary solvent activity coeffs., statistical mech. theory 80−59663
displacement spike annealing, Mont Carlo method computer expteriments 78−30672
dopant segregation during liq. phase electroepitaxy, theory and expt. 80−54384
electroslag remelting, steady state segregation and heat flow 79−11629
equilibrium segregation of dil. solutes to grain boundaries, free surfaces, interphase interfaces 78−31411
equilibrium upper limit, at grain boundaries 77−84763
extractive metallurgical processes, thermodynamic evaluations 80−11591
FCC crystal, interstitial and solute concentration gradients, flux expression derivation *(French)* 80−54219
FCC metals and alloys, grain boundary energy and self-diffusion, effect of solute segregation 78−15412
fission reactor materials, defect trapping and solute segregation in irradiated alloys 80−13603
garnet, Stockbarger-grown, impurity capture and distrib. 77−28713
garnets, concentrational inhomogeneities, appl. of vacuum decoration method 79−14835
glass fibre reinforced plastic, failure due to deform., optical investigation method *(Russian)* 80−35437
grain and phase boundaries between crystals, conf., Konigstein, Germany (Oct. 1977) 78−72762
grain boundaries, segregation-induced embrittlement 79−83318
grain boundary, equilib. impurity conc. *(Russian)* 80−103478
grain boundary, X-ray spectral analysis method, for element distrib. determination 80−21337
grain boundary cohesion, resulting from solute segregation, pair bonding theory 80−88166
grain boundary cohesion, segregation effects 78−15411
grain boundary decohesion, exchange type soft solute segregation in hard hosts 80−54258
grain boundary segregation, computer simulation using Mie type interatomic pot. 80−54259
grain boundary segregation, critical assessment 80−75362
grain boundary segregation, rel. to free surface segregation 80−71657
grain boundary segregation, T-t dependence of temper brittleness 77−36617
grain boundary segregation, two dimensional compd. form. and precipitation 78−15408
grain boundary segregation theory in terms of surface adsorption analogues 78−15407
grain growth, discontinuous, pore drag 77−44203
graphite catalytic gasification using Pt, Ir, Pt-Ir, small bimetallic particle identification by controlled atm. electron microscopy 79−83502
Guinier-Preston ellipsoidal zone model of X-ray scatt. *(French)* 77−84568
Hastelloy, H_2 embrittlement in H_2S environments, impurity segregation effects 80−71724
Hastelloy C-276, cold worked, annealed, surface segregation, Auger spectroscopy study 79−83204
horizontal macrosegregation during solidification with a heterogeneous zone *(German)* 78−15381
hydrocarbons decomposition reaction, with Ta and α-Hf, surface segregation influence of O_2 or N_2 80−55654
p-Hz:o-H_2, clustering rate and NMR obs., 25 mK-2K 78−47635
identification of segregating phases, single crysts., radiographs computer calc. 80−84934
impurity atoms diffusion and impurity-vacancy interactions *(Russian)* 80−19985
impurity ion clusters in a two-dimensional lattice 78−23047
Inconel 600, thermal treatment, grain boundary microstruct. and SCC resistance 80−71675
segregation continued
ingots, quenching technique, for studying formation of macrosegregations 78−52793
interface segregation, influence of cooling rate 78−72010
interface segregation through cooling 79−43294
interfaces, co-segregation of metallic and non-metallic impurities 80−60868
interfacial cohesion, adsorption-induced losses 80−65010
intergranular fracture energy, effects of segregated impurities 79−38928
interstitial cluster nucleation at the onset of irradiation 78−79635
irradiated dilute alloys, kinetic model for solute redistrib. to sinks and void growth 79−78973
irradiation-induced swelling, and creep, effects of pt. defect trapping and solute segregation 79−79040
Kh20N40 alloys, phase composition after quenching, tempering 78−60650
laser window degradation interactions and impurity clustering effects 79−14050
liquid-solid fluidised beds, particle segregation, transition regions 79−46379
low gravity experiment possibilities in electronic materials growth technology 79−47606
materials processing in space 78−35296
melt/solid segregation, rel. to eucrite parent body size and Earth low vel. zone stability 79−40144
metal, polycrystalline, binding energy spectrum approach to grain boundary segregation 78−15409
metal growth in space, theoretical models, comparison with ground expts. 78−84786
metal-H system, long wavelength density modes 78−79745
metals, atomic binding energy and surface energy rel. to prediction of physical props. 80−59434
metals, FCC and BCC, grain boundary struct., and segregated impurity sites, computer simulation 79−73173
metals, influence of a surface coating, on void formation 78−47416
metals, irradiated, solute segregation and annealing kinetics at sinks 79−23640
metals, residuals, impurities and props. 80−66521
metals and alloys, irradiated, solute segregation and precipitation effects on void swelling 78−67741
metals and alloys, non-equilib., review 80−66516
metals and alloys, segregation studies by imaging atom probe microscopy 80−66911
microsegregation and macrosegregation, relevance of processes in front of solidification front *(German)* 77−90342
microsegregation in crystals, anal. 80−59410
mixture, binary, off-critical, quenched, struct. functions and mobilities renormalisation 79−82343
molten polymers of different lengths, segregation below critical point 78−55801
monodispersed supersaturated solutions, fluctuation instability 78−18783
Nimonic alloy, effect of annealing on hardness, carbide phase strengthening *(Russian)* 79−34137
Nimonic PE16, neutron irradiated after heat treatment, solute segregation to pt.-defect sinks 79−78976
Nimonic PE16, Ni ion irradiated, Ni segregation to voids 79−28020
noble metal alloy, dil., solute segregation and subsequent film growth in corrosive environment, model 79−24649
nonequilibrium, during pulsed laser annealing, model 80−108451
opal glasses, phosphate opacified, phase comp. and struct. 80−64919
paramagnets, diluted solid, clustering of mag. ions, study method 80−11155
phase stability under irradiation, theory 79−77634
pipe, thick walled, increasing efficiency of automated ultrasonic inspection of segregate defects 79−11755
polyarylate-arylenesulfone oxide block copolymer, glass transition, melt and soln. viscosity *(Russian)* 79−55915
polyarylate-polyethylene oxide block-copolymers and mixtures, phase separation, DSC obs. *(Russian)* 79−55895
polyether-polyester elastomers, differential scanning calorimetry by using poly(oxy-1,4-butylene glycol) as soft segment *(Japanese)* 80−79916
polyisobutylene, impurity distrib. of tagged poly-cis-isoprene, individual and aggregate 79−68339
polymer blends, fluctuation dynamics, spinodal decomp. 80−79943
polymer mixture, molten, polydispersion effects, crit. behaviour *(French)* 78−42879
polystyrene blends, isotactic and atactic, small-angle X-ray scattering 78−55817
polyurethanes based on toluene di-isocyanate, struct.-prop. relns. inc. phase mixing and segreg. 78−80509
Pt-Au, chemisorption of H_2 and CO, effect of surface segregation 77−51601
quartz, ion-implanted layers, total X-ray reflection investig. of clustering 78−6081
radiation induced segregation of impurities to voids, kinetic model 77−43245
radiation-induced segregation in binary and ternary alloys 79−78970
rare earth oxides, segregation study by electron energy-loss spectroscopy 80−79953
refractory materials, contrib. of segregation and diffusion to heat cond. 80−20001
reversible temper embrittlement, book contrib. 78−11334
rotated remelted ingots, macrosegregation 79−52196
ruby, concentrational inhomogeneities, appl. of vacuum decoration method 79−14835
sapphire, concentrational inhomogeneities, appl. of vacuum decoration method 79−14835
secondary boundary formation during crystn. *(Russian)* 77−59767
semiconductor, polycrystalline, grain boundary effects, doping tech. for study and control 80−79815
semiconductor substrate surface, low loss electron and Auger images correl. 78−22944
on sintering of technical purity powders 77−63586
solid solutions, conc. tetragonal substitutional, dislocation impurity segregation *(Russian)* 79−65114
solid solutions, multicomponent, quasichem. variant of method of cluster components *(Russian)* 77−80622
solid surface, point defects, inclusion and separation zones, elastic energies determ. *(German)* 78−95054
solid-solid interface chemistry, characterisation, theory 80−75448

segregation continued
solidification, directional, processor-operated segregation of minority atoms 80−29941
solute, radiation-induced segregation, kinetic model, GEAR package of subroutines 78−30673
solutes, under irradiation 78−48407
solvophobic effect in simple fluid mixtures 77−31569
steel, 34KhN1MAR structural heterogeneity of 70 ton ingots γ to α transform, in dendritic section 77−70047
steel, alloy, cluster formation susceptibility in 40 KhN, influence of isothermal working in H_2 *(Russian)* 78−56643
steel, alloy, embrittlement during tempering *(Russian)* 77−90436
steel, alloy, HY130, temper embrittlement due to Si intergranular segregation, effect on H_2 induced cracking 78−76735
steel, alloy, Ni-Cr-Mn, type 4340 intergranular brittle fracture, exam. by impact testing and Auger spectroscopy 78−52978
steel, alloy, temper embrittlement, comp. influence 80−66658
steel, alloy, ultrahigh-strength, near threshold fatigue crack propag., microstructure effects 77−86168
steel, alloy Cr-Mn, exam. of phase composition and carbide form. *(Russian)* 79−20057
steel, austenitic, AISI 4340, effect of step quenching on microstruct. and fracture toughness 78−84834
steel, austenitic, Ni-Cr, neutron-irradiated solute segregation and void swelling 79−60407
steel, austenitic→pearlitic transformation, partitioning, atom probe microanal. 80−3079
steel, austenitic stainless, Cr-Ni-Mo (21,6,9 wt.%), N_2-strengthened, surface segregation of B, Auger and XPS spectra 79−90854
steel, austenitic stainless, grain boundary segregation studies, intergranular fracturing technique for stress corrosion cracking investigation 79−39057
steel, austenitic stainless, He implanted 1.4970, high temp. fracture 77−86186
steel, austenitic stainless, of H_2, microstructural distrib., autoradiography *(French)* 79−99234
steel, austenitic type 304, temper embrittlement and surface segregation an AES and ionization loss spectroscopy study 79−43372
steel, ball bearing with modified chem. comp., improved rolling contact fatigue 78−64732
steel, C, cementite formation and properties 80−45313
steel, C, hollow pipe body with internal crack pattern, ingot segregation, hot shortness 77−32693
steel, C (1 wt.%), intergranular segregation of C and P in as-quenched state, AES *(Japanese)* 78−19764
steel, C (1 wt.%), intergranular segregation of Cr, Mn, Sn in as-quenched state, AES *(Japanese)* 78−19764
steel, C martensitic, tempering induced decomposition and segregation, atom probe study 80−3112
steel, C-Mo-P, intergranular fracture and grain boundary segregation, P, H, Mo effects *(Japanese)* 79−15775
steel, C-Ni-Cr (0.6, 1, 1 wt.%), grain boundary segregation of S, N, P, As, Sb and Bi *(Japanese)* 78−15405
steel, cast, effect of non-uniform struct. on props. 78−84850
steel, CC Ni-maraging weld metal, increasing fracture toughness by heat treatment 78−72871
steel, Co-W-Mo-V-Ti-C (25.3, 12.8, 6.2, 0.5, 0.5, 0.05 wt.%), martensitically aged, structural transformation, and strengthening mech. *(Russian)* 79−15676
steel, continuously cast, macrosegregation, effect of electromagnetically induced fluid flow 77−73256
steel, continuously cast, segregation at halfway cracks 80−60869
steel, Cr (1.7 and 2.5 wt.%), segregation of S and P to prior austenite grain boundary, stress effect *(Japanese)* 77−55962
steel, Cr (40 wt.%), Sn and P segregation effects on impact toughness *(Chinese)* 77−73313
steel, Cr maraging, internal friction, 120 to 700K *(Polish)* 79−96075
steel, Cr-C, segregation of P, C, and Cr to γ-boundary and carbide/γ-interface *(Japanese)* 79−61593
steel, Cr-C (1, 1 wt.%), hot ductility and S segregation 80−66594
steel, Cr-Mn eutectoid, pearlite growth kinetics and partitioning 80−29963
steel, Cr-Mo:P (2.25, 1 wt.%), stress relief cracking, effect of P segregation 80−89324
steel, Cr-Mo, cast and forged, difference in mech. props. 77−48465
steel, Cr-Mo, ferritic, grain boundary segregation, X-ray microanal. by STEM 80−66740
steel, Cr-Mo (2.25, 1.0 wt.%), temper embrittlement, effect of P, Sn, comp. and carbide precip. 80−85036
steel, Cr-Mo (2.25, 1.0 wt.%), temper embrittlement, effect of Mn, Si, comp. and carbide precip. 80−85037
steel, Cr-Mo (2.25, 1 wt.%), SCC and temper brittleness, P grain boundary segregation effect 80−55571
steel, Cr-Mo (3 wt.%), temper embrittlement 77−36647
steel, embrittlement by impurity segregation 79−8367
steel, eutectoid, partitioning of Si during pearlite growth, electron microscopy study 79−83201
steel, ferritic, with interstitial N, continuous precipitation and clustering 80−7585
steel, grain boundary P segregation, effect after quenching and tempering *(Russian)* 80−81145
steel, grain boundary segregation of C, atom probe FIM study 80−37134
steel, graphite dissolution, segregation and diffusion *(Russian)* 78−11201
steel, hardenability, role of B and P segregation 80−97486
steel, high speed YXM62, heat treatment, mech. props., wear, fracture toughness for cutting tool 78−19864
steel, high strength, 300-M, slow fatigue crack growth, threshold behaviour, temper embrittlement, impurity segregation effects 77−86152
steel, high-strength, 80 kg/mm^2 class, effects of metallurgical factors on susceptibility of stress relief testing *(Japanese)* 79−43458
steel, impact and tensile props., Si effects 79−24614
steel, intergranular failure, role of grain boundary composition 79−20155
steel, killed, microsegregation and macrosegregation, relevance of processes in front of solidification front *(German)* 77−90342
steel, low alloy, crack form. during stress relief in heated zones *(German)* 79−74242
steel, low alloy, electron microprobes testing *(Croatian)* 77−36516
segregation continued
steel, low alloy, impurity and strength effect on H_2 induced cracking 78−27625
steel, low alloy, macrosegregation 80−11647
steel, low alloy, temper embrittlement, review 79−20154
steel, low alloy, temper embrittlement and ternary equilib. segregation 80−60958
steel, low alloy and C, reversible temper brittleness kinetics *(French)* 78−35498
steel, low alloy creep resisting, causes of weldment cracking 78−56760
steel, low C, cold rolled, graphite precip. and S segregation, AES investigation *(Japanese)* 80−89222
steel, low C, deep-drawing, mechanism of recrystn. texture formation 79−87658
steel, low C Cr-Ni, temper embrittlement by antimony, Ti addition effects 77−32683
steel, low-alloy, impurities, segregation and creep embrittlement 80−66653
steel, low-C, coherent precip. of VC 78−35392
steel, maraging, hardening mechanism of quenched samples, tempering *(Czech)* 79−78989
steel, maraging, Ni (18 wt.%), grain boundary precipitation, scanning Auger electron obs. 78−3132
steel, martensitic, alloying element effect on coarsening behaviour of cementite particles in ferrite 80−66518
steel, martensitic, Cr-Ni-Co-Mo-Ti, Kh12N8K5M3TYu, ageing of C free martensite *(Russian)* 79−1884
steel, martensitic 12% Cr, temper embrittlement 80−66650
steel, medium C, static and dynamic stress effect on hardenability and grain growth *(Korean)* 78−35404
steel, mild, surface analysis rel. to annealing *(French)* 77−32857
steel, mild, surface segregation induced by heat treatment *(French)* 77−59831
steel, Mn, tempered, sementite crystals, carbide phase segregation, X-ray study *(Russian)* 78−35391
steel, Mn-Ti-B-rare earth, distrib. of B *(Chinese)* 78−84811
steel, Mo-Cr (3 wt.%), CrC formation in isochronal tempering, electron microscope study 80−7584
steel, NC6, cementite network separation, kinetics *(Polish)* 80−25698
steel, Ni-B, B effect on temperability and microstructure 79−15710
steel, Ni-Cr, (4,1, wt.%), isothermal embrittlement, AES exam. of grain boundary segregation 78−60814
steel, Ni-Cr, cast, tempering embrittlement due to impurities, Auger spectroscopy exam. 80−11683
steel, Ni-Cr, intergranular segregation of P in austenite, grain boundary coherency depend. 78−84761
steel, Ni-Cr, P doped, tempered martensite embrittlement 80−30089
steel, Ni-Cr, Sb doped, solute segregation and brittle fracture 80−85033
steel, Ni-Cr, solute segregation and intergranular brittle fracture 80−108568
steel, Ni-Cr, temper embrittlement, intermediate tempering treatments 80−60944
steel, Ni-Cr, temper embrittlement by Sb, Ni, Cr effects 77−36628
steel, Ni-Cr temper embrittlement by P 77−40448
steel, Ni-Cr-Mo-U, ferritic, B segregation and high temp. embrittlement 78−7040
steel, Ni-Cr-Mo-V, temper embrittled, crack initiation strength *(Japanese)* 77−52474
steel, Ni-Cr-Ti-P, Ti and P solubility effect on free surface segregation 79−11628
steel, nonmetallic inclusion segregation during cooling *(Russian)* 80−100330
steel, of B, assessment 77−63627
steel, quenched, adsorption of P on austenite grain boundaries rel. to tendency to delayed fracture of type 18Kh2N4VA *(Russian)* 80−45378
steel, quenched, tempered, intergranular failure during fatigue crack growth 79−8357
steel, rimming, teeming and solidification *(French)* 80−16296
steel, segregation and adsorption of S, influence on carburisation and nitrogenation 80−66701
steel, Si, electron irrad. in HVEM, void swelling, Si role 80−54285
steel, Sn (1.5 wt.%) and Mn-Mo (3, 0.4 wt.%), specimen fracturing device for ion microprobe analyser, to grain boundary segregation 77−21341
steel, stainless, 410 type, surface segregation using atom-probe FIM 79−77883
steel, stainless, austenitic high Mn, thermally induced segregation 79−4971
steel, stainless, ferritic, mech. props., impurity effects *(Russian)* 77−52403
steel, stainless, He effects on microstruct. in ion-irrad. 80−29078
steel, stainless, high-strength 0Kh11N10M2T, phase transform. 77−70046
steel, stainless, sensitized, direct evidence of Cr depletion near grain boundaries 77−90358
steel, stainless, type 304 welded, low temp. sensitisation, nucleation of CR carbide nuclei along grain boundaries TEM, SEM study 79−38851
steel, stainless, type 304L, neutron irradiated, in-reactor precipitation and ferritic transformation 79−77644
steel, stainless, weld metal, segregation, S-TEM obs. 77−48431
steel, stainless AISI 316, Si and Ti effect in phase stability and swelling behaviour 79−78972
steel, stainless austenitic, low alloy 316, high temp. plasticity, B addition effects *(Russian)* 77−28852
steel, stainless casts, creep ductility, Auger spectroscopy study 80−60917
steel, temper embrittled, grain boundary failure model for intergranular fracture modes 80−25825
steel, temper embrittlement, fracture mech. of grain boundary segregated phases 78−48531
steel, temper embrittlement and embrittling intergranular segregates, Mo effects *(French)* 79−91788
steel, temper embrittlement control progress 78−72797
steel, tempered martensitic, type AISI 410, role of C in embrittlement phenomena 80−93652
steel, type 20 CND 10-10, temper brittleness and intercrystalline segregation *(French)* 77−81316
steel, undirectionally solidifying melt, horizontal macrosegregation during solidification with heterogeneous layer *(German)* 78−19733
steel, W-Cr (3 wt.%), CrC formation in isochronal tempering, electron microscope study 80−7584
steel alloy, austenite transformation in hot rolled strips 80−55407

segregation continued
steel cladding, 8 distrib. after Na exposure and high-temp. 77−57719
steel low C, Mn surface segregation during annealing, kinetic studies 78−27528
steel low C, surface segregation of Mn during annealing 77−36555
steel VNS-2, damping capacity, magnetomechanical, phase transform. effects 78−31445
steels, hot forming property and struct. *(German)* 80−25730
steels, low alloy, grain boundary anal.,, H_2 embrittlement, scanning AES 79−43256
steels, problematics of S additive segregation *(Czech)* 78−84818
steels, solute segregation and intergranular fracture 80−60957
steels, welded, types D36, D50, secondary ion anal. of segregation 80−7580
substitutionally disordered system in transition state, cluster model, electron diffr. patterns 77−20046
surface, point defects, inclusion and segregation zone, elastic energies *(German)* 78−95049
surface, surface energy and solute strain energy effects 77−72760
surface chemistry rel. to metallurgical props., SIMS, XPS and AES *(French)* 80−80045
surface deformation due to non-homogeneous distribution of solute atoms in crystals 79−33164
surface science in metallurgy, review 79−42388
surface segregation, bond and strain energy effects, Monte Carlo method 79−74161
surface segregation, quantitative theory 78−71910
surface segregation and bond strength-atomic size representation 80−20940
Surface segregation in alloys: existence of surface miscibility gaps within regular solution theory 78−18882
surface segregation kinetics, theory 80−11649
surface segregation of mixture, nonequilib. 80−88325
surface states, three-dimens. cryst. ab initio SCF LCAO calc., impurity clustering 78−56201
temper embrittlement kinetics, ternary and binary alloys, computer simulation 78−84953
thin film, microscopic electronic theory 77−85112
thin films, segregation effects at surfaces and interfaces 80−39475
transition metal alloy, surface segregation, electronic theory 77−43414
transition metal alloys, surface segregation 79−34044
transition metal compounds, $(M,M')Cr_2S_4$ and (M,M')S, where M,M' = Mo,Co,Zn,Cd, solid-state equilib. *(German)* 77−36486
transition metal dilute alloys, component segregation to interfaces 79−51398
ultradisperse particles, spinodal decomposition singularities, conc. profiles *(Russian)* 79−82340
undersaturated alloys, irradiated, solute segregation kinetics, via drift and defect-solute complexes 80−60872
void, and interstitial loop evolution in pulsed fusion reactors 80−84217
voids, coated, capture efficiency 80−96515
water-isobutyric acid (2,6-lutidine) mixtures, critically quenched, phase separation and coalescence 80−24581
web dendrites, dislocations, stacking faults, X-ray topographic study *(Chinese)* 80−88148
X-ray diffractometry, of superimposed twins and clusters, establishing UB matrices of single cryst. individuals 79−37586
Zircaloy-4, quenched and annealed, strain ageing 77−25071
ZnO-based varistor, grain-boundary segregation, thin film X-ray spectroscopy obs. 80−35185
Ag (110), adsorption of S, equilib. segregation isotherm, selvedge model 79−90883
Ag alloys, grain boundary energy and struct., solute atom effects 77−47465
Ag alloys, purification of solid metals by electrotransport *(German)* 78−51745
Ag composite, SiC whisker-reinforced, prep. aboard Skylab. 78−84741
Ag film on Mo, epitaxial growth, exam. of S impurity segregation at interface 78−84076
Ag-Au, surface layer, effect of Ar^+ bombardment, AES and SIMS 80−25504
Ag-Au, surface segregation, ion scatt. spectroscopy meas. 79−82423
Ag-Au alloy, ion irrad., surface segregation and selective sputtering, AES expts. 79−7740
Ag-Au system, surface segregation 79−69330
Ag-Cu, surface segregation, electronic theory, density of states, cluster-Bethe-lattice approx. 80−49369
Ag-Ni solid solution, reversible surface segregation, radioactive tracer, LEED, and AES expts. *(French)* 77−69155
Ag-Pd system, surface segregation 79−69330
Ag-S solid solution, grain boundary segregation and S diffusion in Ag 80−25700
Ag-Sn (0 to 6%), equilibrium intergranular segregation and diffusion 78−43130
AgBr:Cd^{2+}(Sr^{2+}), single cryst., stress-induced migration and aggregation of solute ions, internal friction 79−51200
AgBr:Pb, impurity segregation to surface, ion scattering spectroscopy obs. 77−19979
AgBr:Sr, stress induced anomalies in internal friction, logarithmic decrement 79−66095
Al, AES study of Sn diffusion and surface segregation in limit of small conc. 79−82384
Al alloy, weld metal structure and hot cracking susceptibility 79−24595
Al alloys, 7075-T6, H_2 effects and Cd segregation to grain boundaries 78−84764
Al, cast and directionally solidified, porosity 79−74145
Al, quenched, irradiated, and quenched plus irradiated, grain boundary hardening 80−3162
Al, resistivity decrement under torsional deform., impurity segregation at moving dislocations 77−4321
Al, vacancy distribution, interbonding atoms, heat peaks in scattered cascades *(Russian)* 80−39169
Al-Ag (up to 4 wt.%), creep, 570-630°C, influence of Ag addition *(Russian)* 79−5003
Al-Ag(Cu)(Zn), electrical resist. of Guinier-Preston zones during age-hardening 77−72848
Al-An (8-25 wt.%), solid solns., residual resist. during clustering 80−97483
Al-Cr, rapidly solidified, crystalline and amorphous structures 77−44274
Al-Cr(Mn), struct. form. and phase transform. kinetics *(Russian)* 78−15359
segregation continued
Al-Cu, cast and directionally solidified, porosity 79−74145
Al-Cu (Mg), vertically solidified, effect of fluid flow on solidification struct., and macrosegregation *(Japanese)* 78−48391
Al-Cu (10 wt.%), inverse segregation 78−52819
Al-Cu (1.9 at.%), solute fluctuations, EXAFS study 80−79949
Al-Cu alloy, cast, chilled zone composition and thickness obs. *(Japanese)* 80−7541
Al-Cu alloy, microsegregation *(Japanese)* 77−16589
Al-Cu dilute alloys, vein closing mechanism in fluidity tests 80−84924
Al-Cu(Mg), macrosegregation during solidification *(Japanese)* 79−100150
Al-Cu(Mg)(Cu-Mg), normal and gravity segregation in ingots, expt. study *(Japanese)* 79−24526
Al-In (40, 70 wt.%), liq. phase immiscible system, solidification in microgravity 78−84770
Al-Mg, homogenisation process, effect of solidification rate and alloying *(Polish)* 79−78949
Al-Mg (5.7 wt.%) alloy, pre-precipitation, elec. resist. investig. 77−32601
Al-Mg alloy, cast, chilled zone composition and thickness obs. *(Japanese)* 80−7541
Al-Mg alloys, distrib. of liquid Mg at liquid-solid interface *(Slovak)* 79−91637
Al-Mg-Fe-Mg-Si-Cr, alloys, dendritic segregation with Fe, Mg, Si and Cr additions *(Polish)* 79−56980
Al-Mg-Si alloys, dendritic non-homogeneity 78−56641
Al-Mg-Zn alloys, Al-rich, weld metal comp. effect on microsegregation and eutectic phase segregation *(German)* 80−108455
Al-Si, magnetic susceptibility and elect. resistivity, 500 to 1000°C, struct. sensitive props. *(Russian)* 78−15550
Al-Si eutectic alloy, banded struct., SEM and optical microscopy 80−104144
Al-Ti, solid soln., unidirectionally solidified, segregation patterns revealed by etching 79−47693
Al-Ti-B alloys, segregation of Ti, electron microscope exam. 78−52820
Al-Zn, ageing alloy, zonal decomposition stage, new effects in X-ray diffr. anal. *(Russian)* 79−4982
Al-Zn, Guinier-Preston ellipsoidal zone model of X-ray scatt. *(French)* 77−84568
Al-Zn (22 at.%), X-ray scatt. obs. of segregation *(French)* 79−96032
Al-Zn (40 at.%), resistance of homogenization in micro-segregation 79−100180
Al-Zn (6.8 at.%) alloy, elec. resist. temp. depend. rel. to ageing processes 77−77486
Al-Zn (7 at.%), liquid quenched, early stage phase separation, exam. 78−68698
Al-Zn changes in inner-electron binding energies during ageing, electronic spectra study 77−28816
Al-Zn-Mg, grain boundary surfaces, plasmon loss satellites in Auger spectra 78−15261
Al-Zn-Mg, grain boundary segregation, AES meas. 78−72781
Al-Zn-Mg alloy, welded, solute profiles at weld bead/parent metal interface 78−19942
Al-Zn-Mg alloy (6, 3 wt.%), grain boundary segregation, AES exam. 78−39783
Al-Zn-Mg alloys, decomp. kinetics from Young's modulus obs., microprocesses *(German)* 78−64522
Al-Zn-Mg alloys, grain boundary segregation, implications to stress corrosion cracking 80−84936
Al-Zr, interphases, formed during precipitation and solidification *(German)* 79−29062
Al_2O_3, dense, exposed to steam, influence of Ca migration on strength reduction 80−11797
Al_2O_3, dense, steam-enhanced Ca segregation, AES and SEM obs. 79−83352
Al_2O_3, dense, surface segregation of Ca under exposure to steam and steam-CO 78−85013
α-Al_2O_3, grain boundary segregation, electron microscopy 80−103361
Al_2O_3 polycrystalline, effects of space charge, grain-boundary segregation and mobility differences on conductivity 80−79979
Al_2O_3, sintered, electron microprobe anal. of impurity and additive distribs. 80−40359
Al_2O_3, sintered, MgO-enhanced densification, test of second phase and impurity segregation models 78−64511
Al_2O_3:MgO, grain boundary segregation of Ca and Mg X-ray spectrosc. and STEM study 80−107269
Al_2O_3-Ca (0.6 to 1.6 at.%), fracture behaviour, Ca segregation effect 80−40504
AlZn, homogenization processes, dendritic struct. 79−15700
Au, electron irradiated, interstitials and their clusters, diffuse X-ray scatt. study 80−33997
Au/Ti thin films, effect of Cl_2 on elec. resistance, Ti atom migration and preferred orientation 80−34530
Au-Ag, surface segregation 79−77873
Au-Ag(Cu), surface segregation, electronic theory, density of states, cluster-Bethe-lattice approx. 80−49369
Au-Cu, dil., electron irradiated, interstitials and their clusters, diffuse X-ray scatt. study 80−33997
Au-Cu, surface conc. profile and surface energy 80−84350
Au-Cu alloy, surface comp. as function of temp., AES expts. 78−95212
Au-Fe (17 at.%) alloy, fission fragment irrad., simulation of neutron effects 77−80549
Au-Ni, surface segregation, strain effects 80−80042
Au-Ni-Cu-Zn, white gold, metallographic struct., heat treatment and plastic working effect 80−40403
Au(111) and polycrystalline surfaces, O_2 adsorption, LEED, AES and energy loss spectra 80−34310
B, preparation and purification, physical characterisation *(French)* 80−16189
(Ba, Ca)(Ti, Zr)O_3, segregation of $CaTiO_3$ and effect on dielec. props. 78−38849
BaF_2:Er^{3+}, fluoresc. spectra of charge compensated cryst., multiphonon and energy transfer relax. 79−87496
$(BaF_2)_{1-x}(YF_3)_x$, crystal growth and struct. 77−12520
$(BaF_2)_{1-x}(YbF_3)_x$ and $(BaF_2)_{1-x}(NdF_3)_x$, crystal growth and struct. 77−12520
$BaFe_{12}O_{19}$, discontinuous growth, effect of equilib. segreg. at boundaries 77−51336
$BaTiO_3$ ceramics, PTC-type, grain boundary study using TEM 80−107267

segregation continued
$(Ba_{1-x}Y_x)TiO_3$ ceramic, resistivity rel. to donor dopant content 79−65474
Bi-Cu melts, struct., neutron scatt., conc. of segregated regions calc. 77−39528
Bi-Sn, superconductive microsegregations, 3.7K resist. drop 79−69646
Ca^{2+} impurity in Au, surface segregating, catalytic effect on chemisorption of O_2 on Au 79−15021
CaF_2, mixed cluster, doubly-doped with rare earths, elec. dipole relax. 79−82924
$CaF_2:Er^{3+}$, fluoresc. spectra of charge compensated cryst., multiphonon and energy transfer relax. 79−87496
$CaF_2:ErF_3$, clustering, defect struct., NMR study 78−80229
CaF_2:Eu, CaF_2:Eu,Mn(Gd), single crystal predisintegration phenomena, SEM cathodolum. obs. 80−59502
CaF_2:Mn, CaF_2:Eu,Mn, single crystal predisintegration phenomena, SEM cathodolum. obs. 80−59502
$CaF_2:YbF_3$, clustering, defect struct., NMR study 78−80229
$Ca_3Ga_2Ge_3O_{12}$, substrate, electron examination of microstruct. and microsegregation 78−67919
Cd-Zn (up to 1.57 at.%), single cryst., precip. hardening, 77-300K 78−60675
$CdF_2:Eu^{3+}$, luminesc. spectra conc. and annealing depend. 79−65917
$Cd_xHg_{1-x}Te$, vertically grown crysts., factors affecting segregation behaviour 79−55684
CdTe:Ge, dopant behaviour 78−22742
Cl^-Ar_{N-1} small ionic clusters, thermodynamic behaviour 79−77769
Co (100), clean and C-covered, LEED-Auger expts. 78−38921
Co-C, dil., C segregation to single cryst. surfaces 80−39301
Co-Nb alloys, segregation of Nb to stacking faults, field ion microscopy investigation 77−8816
Co-Ti(Hf)(Ta)(Mo)(Zr)(Al)(Fe)(Ni), dendritic segregation 80−76260
Co_2GeO_4-Mg_2GeO_4, solid solubility and cation distrib., free energy 77−35700
Cr, internal friction and segregation effects *(Russian)* 77−66669
25Cr-20Ni stainless steel dendritic solidification, growth morphology and solute redistrib. *(Japanese)* 80−81045
Cr-Fe, superparamagnetic clustering near critical conc., neutron scatt. study 79−11293
CsI, {100} faces, form. of etch pits of different size and morphology, segregation influence 78−2130
CsI, annealing effects on mech. and microstruct. props. 77−66686
CsI:Na^+(K^+)(Tl^{3+}), crysts., segregations detection 79−15748
Cu, (111) and (100) surfaces, Sn segregation 78−14554
Cu alloys, purification of solid metals by electrotransport *(German)* 78−51745
Cu, cold work, P effect on annealing 79−47707
Cu, crysts., absorbed H, strain anal., X-ray divergent beam method 78−15463
Cu ferrite films, Mn-, Ni- and Al-substituted, LPE growth 80−96752
Cu film on Mo, epitaxial growth, exam. of S impurity segregation at interface 78−84076
Cu matrix, coalescence of SiO_2 particles 78−92271
Cu polycrystals, Bi segregation embrittlement 79−83318
Cu-Ag, surface segregation of S, Auger spectral study diffusion 80−76549
α-Cu-Al, Al bulk segregation determ. by small angle neutron scattering 79−82127
Cu-Al, surface segregation during adsorption and low pressure oxidation *(French)* 78−75932
Cu-Al(Au)(Ga)(Ni)(Pd)(Rh)(Zn) (4 at.%), anneal hardening mechanism 80−60879
Cu-Au system, grain boundary adsorption thermodynamics *(Russian)* 80−44317
Cu-Be, dilute, electron irradiated, Be segregation 79−77637
Cu-Be, dynamic segregation, ESCA obs. 77−8718
Cu-Be, electrical resist. of Guinier-Preston zones during age-hardening 77−72848
Cu-Be (0.0182 at.%), radiation induced Be segregation 78−23710
Cu-Bi, grain boundary struct. intergranular fracture, segregation role 80−66648
Cu-Bi (0.0115 wt.%), embrittled, Bi segregation to grain boundaries, faceting, TEM study 79−27998
Cu-Bi alloys, grain boundary segregation 79−61596
Cu-Fe (0.2 at.%), clustering, precipitation, and oxidation, 298 to 919K, Mossbauer study 80−7242
Cu-Fe (1.5 wt.%), precipitation-effect on void formation during electron irradiation 80−84211
Cu-Fe alloy, cluster form., Fe solubility determ., 450 to 1000°C, Mossbauer spectra obs. *(German)* 79−29021
Cu-Mn (3, 5, 10 at.%) alloys, surface segregation of Mn and oxide film form., AES study *(French)* 79−66065
Cu-Mn alloys, Cu-rich, heat treated, segregation obs. *(Russian)* 78−27517
Cu-Mn-S, Mn surface segregation and Mn/S cosegregation 80−40367
Cu-Ni, clean surface, surface segregation and growth process of altered layer *(Japanese)* 80−24720
Cu-Ni, evaporation limited segregation 80−70513
Cu-Ni, liq., surface conc. profile and surface energy 80−84350
Cu-Ni, sputter-induced subsurface segregation, Auger electrons obs. 80−10757
Cu-Ni, surface layer, effect of Ar^+ bombardment, AES and SIMS 80−25504
Cu-Ni, surface segregation, comparison of low-energy ion-scatt. results with theory 78−38923
Cu-Ni (50 wt.%) alloys, estimation of sublimation energy of Cu atoms, evaporation rate and surface composition, AES meas. *(Japanese)* 80−49352
Cu-Ni alloys, surface segregation and in-depth profile, AES 77−31856
Cu-Ni dil. paramagnetic alloys, sp. elec. resist., effect of Ni clusters *(German)* 78−95293
Cu-Pd, surface struct. from LEED and AES meas. 79−77882
Cu-Pt, surface segregation, comparison of low-energy ion-scatt. results with theory 78−38923
Cu-Sb melt, eutectic struct. by neutron diffr., isotopic substitution 78−47233
Cu-Sb solid solution, dil., FCC, intergranular solid shortness mechanism *(Russian)* 79−5032
Cu-Sn, exam. of surface segregation equilibrium and kinetics, by Auger spectroscopy *(Russian)* 79−56981
segregation continued
Cu-Sn, Sn surface segregation in monolayer regime, model of kinetics and equilib., AES data explained 79−7739
Cu-transition metal alloy, internal adsorpt. and mag. susceptibility, grain size effects *(Russian)* 78−19759
$CuAl_2$, single cryst., embrittlement and subboundary hardening via interstitial segregation *(Russian)* 77−12679
CuNi alloys, electronic theory of surface segregation 79−23819
EuTe, high-temperature evaporation and reactivity 80−103469
Fe (100), equilib. surface segregation of dissolved C, N and S 77−62723
Fe, (100) surface, S segregation and 2D compounds precipitation *(Japanese)* 80−35188
Fe and steel, macrosegregation of S and form. of equiaxed crystals, autoradiographic study, cast struct. effect 77−63658
Fe, Armco, inter- and intragranular sulphidation 80−55570
Fe based alloys, solute segregation to grain boundaries 78−72780
Fe based binary and ternary alloys, intercrystalline internal adsorption exam. by electrolytic dissolution *(Russian)* 78−35390
Fe, C or N segregation, equilib. and struct. *(German)* 79−47690
Fe, cast, alloyed and unalloyed, microsegregation thermodynamics 80−76261
Fe, cast, Mg, despheroidising effect of Bi, Sn on graphite in alloy 78−56670
Fe, cast, Mo distribution 78−92269
Fe, cast, spheroidal, segregation investigation by X-ray spectral analysis *(German, English)* 77−63993
Fe, cast, unalloyed and alloyed, addition effects on struct., thermodynamics of microsegregation 79−8305
Fe, cast alloyed, struct., props., heat treatment 77−16623
Fe, diffusion and solid solubility of Sb, 773-873K, ion backscatt. anal., rel. to intergranular embrittlement 78−71880
Fe, free surface and grain boundary O_2 and S chemistry 80−75410
α-Fe, grain boundary segregation of C, N_2 and C Auger spectroscopy 78−72778
α-Fe, irradiation induced void swelling, Cr additions effect 80−55408
α-Fe, S and C diffusion, AES obs. 77−51543
Fe, segregation and adsorption of S, influence on carburisation and nitrogenation 80−66701
Fe, segregation of ^{119m}Sn at grain boundaries, Mossbauer effect 78−15414
Fe, segregation of impurities, physico-chemical aspects *(Czech)* 80−60866
Fe, segregation of S, O_2 and P at (100) surface in single crystal *(Japanese)* 79−61591
Fe, single cryst., segregation behaviour of S, O and P at (100) surface 80−100841
Fe, single crysts., absorbed H, strain anal., X-ray divergent beam method 78−15463
Fe, surface chemistry during annealing of soft magnet 78−48546
Fe, surface segregation of Sn, AES obs. 77−20172
Fe surfaces, adhesion, effect of adsorbed atoms, AES study 80−39456
Fe surfaces, adsorption, segregation and reactions of non-metal atoms, LEED and AES obs. 80−59783
α-Fe:He, impurity clustering in vacancies bound to edge dislocations 78−91358
α-Fe-(Ni,Mn,Cr,Mo,W)-P (1 wt.%). grain boundary segregation, temper brittleness, AES study *(Japanese)* 79−78981
Fe-C, graphitisation, interfacial segregation effects 77−52373
Fe-C (0.25 wt.%), austenitising temp. effect on proeutectoid ferrite reaction kinetics, scanning Auger microprobe exam. 78−44144
Fe-C (1.86 wt.%), exam. of C clustering in martensite, using Mossbauer spectroscopy 78−84821
Fe-Co, surface comp. and surface segregation 80−34280
Fe-Co-Cr, 25KKh15 alloy, nuclear γ-reson. investig. of atomic redistrib. during annealing *(Russian)* 77−12640
Fe-Co-Cr, alloy K25Kh15, phase tranforms., nucl. gamma reson. and X-ray diffr. meas. *(Russian)* 77−44241
Fe-Co-Ti-Al alloy type YuNDK magnets, metallographic method of distinguishing cracks 80−85096
Fe-Cr, grain-boundary segregation of carbon, electrochemical study 79−100147
Fe-Cr, irradiation induced void swelling, Cr additions effect 80−55408
Fe-Cr, of ^{121}Sb, Mossbauer spectroscopy 79−47698
Fe-Cr, surface segregation of impurities (C,N and S) *(French)* 77−56192
α-Fe-Cr alloys, recrystallised, C segreg. effects, TEM *(French)* 77−28828
Fe-Cr-Co martensite, ordering and segregation *(Russian)* 79−20052
Fe-Cr-Ni (12, 15 wt.%) austenitic alloy, Ni^{6+} irradiated, void swelling and phase stability, Si and Ti effects 80−65055
Fe-Cr-Ni-Cu-Sn, Cu and Sn effect on Cr and Ni segregation *(German)* 78−72777
Fe-Cr-Ni-Mo-V, Mo and V effects on segregation *(German)* 77−55942
Fe-Cr-(Co), decomposition of solid soln. in mag. field, neutron and X-ray diffr. study *(Russian)* 78−68694
Fe-Cr(55 wt.%), phase decomp. early stages and clustering *(Japanese)* 80−55403
Fe-Cu (0.34 wt.%), neutron irradiated, field-ion microscope detection of ultra-fine defects, existence of Cu/vacancy clusters, TEM obs. 79−42116
Fe-Cu-C, phase equilibria, 950 to 1500°C 80−60836
Fe-In, dil., hyperfine field of In, clustering effect, nucl. orientation obs. 77−16188
Fe-M-(I) (M≡Ni, Cr, V, Ti, Mo; I≡Sb, P), co-segregation at free surfaces studied by Auger spectroscopy 80−59767
Fe-Mn, as cast, pseudo-composite struct. resulting from interdendritic segregation, cryogenic materials appl. *(French)* 80−93556
Fe-Mn, dilute, short-range ordering and segregation ascending diffusion *(Russian)* 77−24406
Fe-Mn cast alloys, homogenisation annealing and chemical diffusion *(Czech)* 80−66551
Fe-Mo-C alloy, splat cooling, microstruct. changes 78−84855
Fe-Mo-P, P-induced temper embrittlement, Mo role 80−35316
Fe-N, single cryst., solid soln. softening, effect of interstitial N 80−97496
Fe-Ni, grain boundary segregation, X-ray microanal. by STEM 80−66740
Fe-Ni, of ^{121}Sb, Mossbauer spectroscopy 79−47698
Fe-Ni, segregation of inhomogeneities during crystallisation *(Russian)* 78−27521

segregation continued
Fe-Ni (3 wt.%), grain boundary segregation of Sn and P embrittling additions, STEM microanal. 78−76654
Fe-Ni (3 wt.%) alloys, embrittled, microanalysis of grain boundary segregation using STEM 78−35633
Fe-Ni (30 wt.%), Ni segregation singularities during dendrito-cellular solidification *(Russian)* 80−7542
Fe-Ni two-phase films, alloy component redistrib. during annealing, electron diffr. anal. *(Russian)* 79−20053
Fe-Ni-Al (10, 0.1 wt.%), clustering of Al_2O_3 inclusions 79−83205
Fe-Ni-C, martensitic, modulation of local C atom cumulation during ageing *(Slovak)* 78−19790
Fe-Ni-C, model alloy, intercrystalline brittleness caused by segregation and precipitation in austenite *(Slovak)* 79−70073
Fe-Ni-C martensite, autoradiographic evidence of C clustering 79−83203
Fe-Ni-C-Mn (3.56, 3.25, 0.6 wt.%), solid soln., quenched, changes during annealing to crystal structure, mech. props. *(Russian)* 79−34076
Fe-Ni-Cr, high Ni content, intergranular corrosion, effect of Cr *(French)* 80−7708
Fe-Ni-Cr-Al-Ti-W-Mo (35, 15, 2.4, 2.3, 2.2 wt.%) wrought superalloy, freckles *(Chinese)* 80−104137
Fe-Ni-Cr-C, ferritic, P segregation to free surface, 723 to 823K, AES 78−48411
Fe-Ni-Mn, martensite, aged, grain boundary embrittlement 79−96144
Fe-Ni-P, segregation kinetics, theory, and temper brittleness 80−11649
Fe-Ni-Sb (4, 0.0087 at.%), surface segregation 79−96031
Fe-Ni-Sb-S, S/Sb surface site competition in segregation 80−40366
Fe-Ni-V, nitrided austenitic alloys, modulated substitutional interstitial solute atom clustering 79−74160
Fe-P, P equilib. grain boundary segregation 79−38835
Fe-S system, segregation kinetics *(Japanese)* 79−61592
Fe-Sb-Ti(V)(Cr)(Mn)(Co)(Ni), interactions and segregations, Mossbauer and X-ray diffr. study 80−70415
Fe-Si, (3wt.%) alloys, grain boundary anal., scanning AES 79−43256
Fe-Si (2.35 wt.%), misorientation dependence of grain boundary segregation, Auger spectroscopy exam. 78−76629
Fe-Si (3 wt.%), containing B, grain boundary segregation, AES evidence 77−86046
Fe-Si-B-N-S, B, S, N effects on grain boundary segregation and grain growth inhibition, review 80−3047
Fe-Sn, grain boundary embrittlement by Sn segregation, Mossbauer study 80−7239
Fe-Sn, segregation of Sn, kinetics, theory 80−11649
α-Fe-Sn alloy, grain boundary hardening and segregation 80−55417
Fe-Sn system, Sn binding state, using segregated ^{119m}Sn, Mossbauer anal. *(Japanese)* 80−20525
Fe-Ti (0.15 wt.%), Ti distrib., segregation, FIM anal. 80−84200
Fe-Ti-Si-Ni-P-C-S, H_2 segregation kinetics *(Russian)* 78−18832
Fe-Zr, dilute solid solution, surface segregation, AES exam. 77−43413
$Fe_{40}Ni_{40}B_{20}$, amorphous alloy, ductile-brittle transition temp., relation to composition 78−52972
$FeB_5C_{15}SSi_{15}Cr_5$, amorphous, exam. of metalloid atom mobility by Auger spectroscopy 78−47575
$Fe_{40}Ni_{40}P_{20}$, amorphous alloy, ductile-brittle transition temp., relation to composition 78−52972
$Fe_{40}Ni_{40}P_{14}B_6$, amorphous alloy, ductile-brittle transition temp., relation to composition 78−52972
FeO-Fe_2O_3-SiO_2 -Al_2O_3-$CuO_{0.5}$/Cu slag-metal system, distrib. equilib. of Sn, Se, Te 78−44111
$FeP_{13}C_7$, amorphous, exam. of metalloid atom mobility by Auger spectroscopy 78−47575
FeTi, hydrogen energy storage, surface segregation *(German)* 79−77872
FeTi, hydrogenation, effect of surface segregation on mag. props. 78−84819
FeTi, surface and mag. props., heat treatment and hydrogenation effects 80−75447
FeTi, surface segregation and catalytic effect on hydrogenation, AES and XPS study 79−11626
GaAs layers, Cu segregation along grain boundaries, spectroscopy study 80−49234
GaAs, surface segregation of implanted alkali metals, photoemitter prep. and characts. *(French)* 78−60544
GaAs, surface studies during MBE growth 79−90899
GaAs:Cr, impurity conc. and segregation coeff., optical absorpt. meas. 79−56819
GaAs:Si, current-controlled growth, segregation and amphoteric behaviour 78−31346
GaAs:Sn, dopant segregation during liq. phase electroepitaxy 80−54384
GaAs:Sn, doping characts. during LPE 79−10866
GaAs:Sn, surface segregation of Sn during MBE, SIMS and AES 78−72031
$Ga_xIn_{1-x}P$, diffuse X-ray scatt. investig. of cation distrib., segregation 77−24409
GaP, impurity behaviour during crystallisation from melt 77−84772
$Gd_3Ga_5O_{12}$, substrate, electron examination of microstruct. and microsegregation 78−67919
Ge, crystal growth and segregation under zero gravity 79−43130
Ge, ion bombarded, radiation defect formation, atom-atom collision cascades modelling 80−10582
Ge single crystals, constitutional supercooling growth conditions, structural and chem. inhomogeneities 80−93473
Ge:Ga, appl. of heat pipe to Czochralski growth, segregational behavior 79−61511
Ge:Ga, effects of destabilising vertical thermal gradients on cryst. growth and segregation 78−52659
Ge:metal, polycrystalline film, electron transport props. 79−99642
Ge:O, Cu, amorphous thin film, impurity effects on struct. 80−107054
Ge:P, solubility and segregation of electrically active P 77−15442
Ge-Ga, segregation of Ga due to barometric mol. diffusion in gravitational, centrifugal fields 78−14472
Ge-metal film, polycryst., struct. props. determ. 79−4494
Ge-S-Cu, phase separation in melt centrifugal quenching 80−25701
Ge-Si-Sb, segregation of Si,Sb due to barometric mol. diffusion in gravitational, centrifugal fields 78−14472
Ge-Sn(In) melts, short-range order, radial atomic distrib. functions 79−86673
Hf-O(N), solid soln. hardening, impurity cluster and interstitial mechanisms 77−36523
Hg, inductively stirred, convective flow rate controlled by Lorentz's number rel. to solidified struct. 79−10444

segregation continued
$Hg_{2.86}AsF_6$, anisotropic supercond. caused by Hg extrusion, DTA 78−55953
$Hg_{1-x}Cd_xTe$, segregation, compositional characterisation 80−107434
$Hg_{2.91}SbF_6$, anisotropic supercond. caused by Hg extrusion, DTA 78−55953
In-Sb-Te, region of In-Sb-based solid solutions 77−36466
InAs, obtained by liquid-seal method, deviation from stoichiometry 77−40345
InP, effects of baking time on purity and morphology 78−6862
InP, growth and props., Fe segregation 79−1822
InSb, undoped and Te-doped, anomalous impurity segregation, Hall and mass spectrum meas. *(Chinese)* 80−59501
InSb-GaSb alloys, directionally solidified, influence of twinning on segregation, electron probe anal. 79−24513
interstitial cluster nucleation, effect of trapping at onset of irradiation 79−78974
Ir, brittle fracture, impurity segregation to grain boundary effects 78−64637
Ir-W (0.3 wt.%), P segregation to grain boundaries, effect on high temp. ductility 78−95754
Ir-W (0.3 wt.%): Al(Fe)(Th)(Ni)(Rh), effect of additions on grain boundary composition 79−83309
KBr:KCN, segregation during physical vapour transport 78−43992
KBr(Cl):Mg^{2+}, dopant aggregation and precipitation 80−107306
KCl:KCN, and KCl:KOH, segregation during physical vapour transport 78−43992
KCl:Pb, lead aggregation effect on yield stress, incoherent precipitates, solubility determ. method 80−50645
KCl:Pb, solid solution, electron microscope exam. of decomposition, of naturally aged specimens 79−96030
KCl-CuCl solid solution supersaturated, precipitation, impurity aggregation 80−29174
KCl-KBr, dislocation rosettes, diffusion origin 78−83820
KCl-NaCl, dislocation rosettes, diffusion origin 78−83820
$LaNi_5$, self restoring of active surface, photoemission, mag. susceptibility study 78−48280
$LaNi_5$, surface segregation induced by O_2, LEED and AES exam. 79−11009
$LaNi_5$ surface segregation, influence of O_2, H_2, H_2O, SO_2 *(German)* 80−51008
$(LaO)_2S$-$(LnO)_2S$ system (Ln=Y or Lu), TEM, X-ray diffr. and fluorescence spectroscopy 79−64957
Li-ND_3, near liq.-liq. crit. point, conc. fluctuations, neutron diffr. long wavelength thermodynamic limit 79−10948
LiF, alkali ion implantation, migration, segregation, effect on optical props. 80−100269
$LiY_{0.416}Er_{0.5}Tm_{0.067}Ho_{0.017}F_4$, Stockbarger single cryst., charact. of solidification behaviour 77−24948
MO-B, B effects, rolled, segregation of implanted elements, Auger spectroscopy exam. *(Russian)* 78−35389
Mg-Si-Al-O-N, grain boundary segregation, combined X-ray microanal. and lattice fringe imaging determ. 79−15681
Mg_2Cu polycrystals, surface study by AES, XPES and X-ray induced AES 80−65346
$MgFe_2O_4$:Ga, Sn, Cr, LPE film, segregation coeffs. 78−11136
MgO, boundary segregation of Ca, Fe, La and Si 79−70069
MgO, segregation of aliovalent solutes adjacent {100} surfaces 79−78979
MgO, technical powder purity, of technical purity powders 77−63586
MgO:Mn^{2+}, clustering of mag. ions, study method 80−11155
Mn-Cu, mag. and cryst. struct., neutron and X-ray diffr. meas. *(Russian)* 78−22694
$MnFe_2O_4$, discontinuous growth, effect of equilib. segreg. at boundaries 77−51336
Mo alloy, long-term ageing effects on ductility and microstruct. 77−44348
Mo, cast and low alloy, C distrib. between solid soln. and precipitate *(German, English)* 79−20059
Mo, competition between interstitial atoms during segregation at grain boundaries, AES obs. *(Russian)* 77−25008
Mo, doped, surface tension driven flow in electron beam floating zone expts. 80−19731
Mo, grain boundary segregation of O, atom probe FIM study 80−37134
Mo, internal friction and segregation effects *(Russian)* 77−66669
Mo ion incorporation into TiO_2 matrix, ESR, UV, and ESCA spectral anal. 79−43670
Mo, O segregation at grain boundaries, obs. by atom imaging probe 78−21276
Mo, segregation of impurities and alloy elements at surface *(French)* 79−47697
Mo sheet, conc. of interstitial elements on lamination surface 77−86038
Mo, sintered, grain boundary segregation of S and N 79−56982
Mo:C (110) surface, segregation, precip. and desorpt. of C, AES and LEED study *(French)* 80−103480
Mo-Fe metalloceramic alloy, brittle fracture investigation, segregation, morphology, struct. *(Russian)* 80−55503
Mo-Mn metalloceramic alloy, brittle fracture investigation, segregation, morphology, struct. *(Russian)* 80−55503
Mo-O system, grain boundary segregation and intergranular fracture 80−55516
Mo-O-C system, grain boundary segregation and intergranular fracture 80−55516
Mo-Ti (1 wt.%), fast neutron irradiated, direct obs. of solute segregation to voids 79−78971
Mo-Zr alloys, TsM-6, Zr segregation at grain boundaries, carbide precipitation, X-ray spectral anal. *(Russian)* 79−74154
NaBr:Tl, impurity segregation with Kyropoulos growth 78−9977
NaCl bicrystal, grain boundary segregation, Au decoration obs. 77−68982
NaCl, impurity precipitation and grain boundary diffusion 80−107567
NaCl:Ca, surface segregation and diffusion 77−43416
NaCl:Ca^{2+}, highly doped, aggregation of point defects, NMR and dielec. loss meas. 79−10847
NaCl:Eu, secondary Eu phase dissolution, EPR and optical absorpt. study 80−96655
NaCl:Mg^{2+}(Ba^{2+}), dopant aggregation and precipitation 80−107306
NaCl:Sr, dimer and trimer aggregate formation by NMR, ionic cond. and dielectric losses 80−15094
NaCl+Pb, Pb aggregation effect on yield stress, incoherent precipitates, solubility determ. method 80−50645

segregation continued
Na_2O-B_2O_3-Na_2SO_4, glass, exam. of chemical differentiation, using Cu ion segregation 78−87625
Na_2O-B_2O_3-SiO_2:Yb(Tb), luminesc. cooperative processes, glass struct. and comp. effect 80−16101
β-Na_2O-CaO-Al_2O_3, impurity conc. at grain boundaries, AES obs. 77−35570
Na_2O-GeO_2-Yb_2O_3, glass struct., Yb^{3+} ion segregation 78−87620
Na_xWO_3 bronzes ($0.4<x<1$), domain, surface and substrate structs. 80−34281
Nb (110) and (750), interaction with O_2, LEED, AES, SIMS, and EELS obs. 80−44408
Nb alloys, long-term ageing effects on ductility and microstructure 77−44348
Nb thin foils, surface segregation during sputtering at elevated temps., Auger study 80−54386
Nb-D, stability curve for phase separation of D, neutron small-angle scatt. study 79−15672
Nb-O, exam. of surface segregation equilibrium and kinetics, by Auger spectroscopy *(Russian)* 79−56981
Nb-O solid solution, interaction with O_2 at low press., segregation equilib. and chemisorpt. *(French)* 77−24483
Nb_3Ge sputtered films, Ge surface segregation exam. by AES 79−56084
Nd_2O_3-Y_2O_3 film, segregation obs. by EELS 80−79953
Ni, (110), surface relaxation and composition, medium energy ion scatt. spectra 78−63916
Ni (111), C monolayer phase condensation, LEED and AES obs. 79−46960
Ni base alloy, directionally solidified, fatigue crack propag. 77−36639
Ni, binary alloy, irrad. with heavy ions, non-equilib. segregation phenomena 80−19950
Ni binary alloys, constituent segregation during irradiation 79−55791
Ni dilute alloys, implant profiles modification by radiation enhanced diffusion and segregation 80−88217
Ni dilute alloys, mechanisms of radiation induced segregation 79−77649
Ni, dissolution and passivation in acid medium, effect of S in solid solution *(French)* 78−64771
Ni, integranular precipitation after annealing, ion imaging microanalysis *(French)* 79−61594
Ni, intergranular corrosion in dil. H_2SO_4 solns., S segregation effects 80−30152
Ni model material, defect buildup and solute segregation, in alloys under pulsed irradiation 78−71757
Ni, oxidation, high temp., effect of C on cavity form., SEM study 80−97638
Ni, segregation of C to (100) surface, isosteres 77−1282
Ni, stress corrosion susceptibility, S segregation effect, Auger spectrosc. study 80−61019
Ni:Cr, He^+ radiation-enhanced diffusion and segregation effects of point-defect trapping 79−77824
Ni-Al (6.35 wt.%) precipitate coarsening, redistribution and renucleation during ion irradiation 78−23709
Ni-Al-Ta (7.5, 2.0 wt.%), dendritic monocrystal, microsegregation and nonhomogenisation 79−37940
Ni-Al(Ti)(Mo)(Si), effect of solute misfit and temp. on irradiation induced segregation 78−72779
Ni-Au, dil., orientation depend. of surface segregation, AES and SEM obs. 78−71908
Ni-Au alloys, surface segreg., surface energy and solute strain energy effects 77−72760
Ni-B, hydrogen embrittlement, effect of B additions *(Japanese)* 78−84973
Ni-base binary alloys, solute segregation and precip. under heavy-ion bombard. 79−11623
Ni-Be system, radiation induced solute segregation and precipitation study by means of Johnson-Lam kinetic model 79−43252
Ni-Cr-Fe, Inconel, effects of heat treatment on surface segregation, Auger spectroscopic exam. 80−7602
Ni-Cr-Mg alloy, KhN70VMTYu, Mg effect on grain boundary struct., props. 79−19261
Ni-Cr-Ti rapidly solidified superalloys, surface segregation 80−76263
Ni-Cu, sputtering rate, radiation-induced segregation and preferential sputtering effects, kinetic model 80−40199
Ni-Cu, surface segregation using atom-probe FIM 79−77883
Ni-Cu, surface segregation, computerised atom-probe FIM study 80−75412
Ni-Cu(5%), absolute composition depth profile, surface segregation, field-ion microscope obs. 79−33166
Ni-Fe, (100) surface, O interaction, Fe segregation, LEED and XPS studies 79−82437
Ni-Ge , defect-solute interactions and radiation-induced segregation 80−25705
Ni-Mo, sputtering rate, radiation-induced segregation and preferential sputtering effects, kinetic model 80−40199
Ni-Pd (1 at.%), surface comp. and surface segregation, AES obs. 79−51404
Ni-Si, defect-solute interactions and radiation-induced segregation 80−25705
Ni-Si, intergranular segregation of Si, electron energy loss spectrometers, X-ray anal. *(French)* 79−8388
Ni-Si, ion beam irradiation induced Ni_3Si surface film segregation 78−38761
Ni-Si, proton irrad., γ' precipitation, early stages 80−34096
Ni-Si (1 at.%), dose depend. of ion irradiation induced segregation 79−42123
Ni-Si:Cr, He^+ radiation-enhanced diffusion and segregation effects of point-defect trapping 79−77824
Ni-Th (1 at.%), surface comp., temp. and O_2 exposure effects, AES study 80−80914
Ni-Ti (12 wt.%), dil. alloys, transform. early stages 78−3096
$Ni_{1-x}Al$ solid solution, vacancy ordering exam. by electron diffr. after annealing 78−3123
Ni_3Al and $Ni_3(Al, Ti)$, S segregation to grain boundaries 78−48410
Ni_3Al-B, $L1_2$ type intermetallic cpd. room temp. ductility improvement by B addition *(Japanese)* 80−35263
$Ni_{0.96}Sb_{0.04}$, surface segregation, XPS and AES obs. 80−76135
Ni_3Si coatings, form. and stability during high temp. irrad. 80−35088
Ni_3Sn_2, single cryst. embrittlement and subboundary hardening via interstitial segregation *(Russian)* 77−12679
Pb-Au, interstitial and substitutional distrib. 80−84204
Pb-Se-As-Ge, phase separation in melt centrifugal quenching 80−25701
segregation continued
Pb-Sn, undercooled eutectic, compositional variations at various gravity levels 77−52314
PbO/PbF_2 solvent, cluster forming, effect of B_2O_3 79−19985
$Pb_{1-x}Sn_xTe$ monocrystal and sinter thermoelec. inhomogeneity 78−91713
$Pb_{1-x}Sn_xTe$, segregation during solidification by Bridgman technique 79−38735
PbTe thermoelectric materials, microstructure anal. using SEM X-ray microanalysis 80−107211
Pd-Ag, ion bombarded, surface segregation, XPES obs. 79−77885
Pd-Ag, surface segregation, Auger studies 78−87849
Pd-Al(Si) melts, appl. of quasichem. method of cluster components *(Russian)* 77−80623
Pd-C, dil., C segregation to single cryst. surfaces 80−39301
Pt, quenched, coprecipitation of vacancies and C atoms 79−78978
Pt:C, C layer formation on (111) surface, temp. depend., LEED, AES study 78−71911
Pt/Fe solid solution crucibles, Fe segregation 80−61192
Pt-Au, surface segregation using atom-probe FIM 79−77883
Pt-Au, surface segregation, comp. depth profiles meas. using atom-probe field ion microscope 80−100380
Pt-C, dil., C segregation to single cryst. surfaces 80−39301
Pt-Cu, surface segregation, ion scatt. spectroscopy meas. 79−82423
Pt-Rh alloys, surface behaviour on heating in air, XPS and SIMS *(French)* 77−40327
Rh (111), co-adsorption of H_2 and CO segregation of co-adsorbed species 80−65361
S segregation on Fe(111) surface, LEED, AES and work-function change 80−15350
S-metal interactions 80−55710
Sc surface, single cryst., segregation of impurities 79−65299
Sc_2O_3-Ho_2O_3 (Dy_2O_3), solid solution, use of segregation phenomena to exam. solidification phase diagrams *(French)* 79−8293
Si (111), surface reproducibility and impurity segregation ion neutralisation spectra and UPS obs. 78−34688
Si, annealing, using laser pulses, impurity incorporation at melt-cryst. interface 80−59504
Si, As segregation, TEM obs. 77−63674
Si, crucible grown, virgin and implanted, laser irradiation effects on surface structure 80−92768
Si, Czochralski cryst. growth, faceted and nonfaceted, Sb microsegregation 80−45227
Si, Czochralski crystals, O microsegregation, swirl defect distrib., growth rate depend. meas. 80−39295
p-Si, Czochralski grown, microdistrib. of O, SEM and spreading resist. obs. 80−79830
Si Czochralski growth, large crystal, convection and segregation 78−6843
Si epitaxial layers, temp. dependence of P dopant inclusion in gas phase deposition *(German)* 79−52127
Si, ion bombarded, radiation defect formation, atom-atom collision cascades modelling 80−10582
Si, ion implanted, dopant depend. of oxidation rate 80−89384
Si, ion-implanted layers, total X-ray reflection investig. of clustering 78−6081
Si, melt grown cryst., impurity incorporation, calcs. 80−79718
Si, multigrained, impurity segregation to grain boundaries, AES and SIMS obs. 80−65027
Si, polycrystalline, As segregation at grain boundaries, elec. props. meas. 80−75259
Si, single-crystal, grown-in structural defects 79−10860
Si:As, ion-implanted, channelling anal. of CW Ar laser annealing 79−73186
Si:As, segregation and desorption kinetics for evaporation of As 79−99410
Si:As, shallow junctions by high-dose implants 80−96694
Si:As laser annealing, heat and mass transport model 80−92546
Si:As(B), heavy-doping effects and impurity segregation during high-press. oxidation 80−65014
Si:As(Pb), ion-implanted, impurity redistrib. during laser irrad. 80−100280
Si:B, near intrinsic ⟨100⟩ and ⟨111⟩ samples, inert and oxidising ambients, diffusion, segregation 78−75882
Si:B(P)(As)(Sb)(Cu)(Fe), ion implanted, doping profile, pulsed laser annealing effects 80−88197
Si:Co, implanted or diffused, and annealed, localisation of Co atoms, Mossbauer obs. 80−39140
Si:Cu, segregation effects after laser pulse melting 79−1843
Si:Fe^0, solid soln. decomp., Fe deposition on dislocations 77−51943
Si:Fe(Cu), impurity segregation and microstructural changes by pulsed laser irrad. 79−82254
n-Si:Ga laser doped, segregation, Rutherford backscattering 80−103483
Si:In, clustering and precipitation, time-dependent perturbed ang. correlation meas. 80−65234
Si:O, A centre, theoretical study 80−75521
Si:Pt, implanted and laser annealed, segregation and increased dopant solubility 80−65016
Si:Sb, dopant microsegregation rel. to crystal and crucible rotation 78−11106
Si:Sb crystal Czochralski growth, radial microsegregation analysis 78−11105
Si-Al-O-N, high-temp. fracture and diffusional deform. mechanisms 80−40509
Si-Al-O-N ceramic, grain boundary desegregation and intergranular cohesion 80−100872
Si-Al-O-N ceramics, grain boundary segregation determ. by X-ray microanal. and lattice fringe imaging 79−15681
Si-Fe(Cu), segregation to surface during laser annealing, model calc. 79−69148
SiC-B eutectic alloys, struct. of crystallising graphite 79−38829
SiO_2:B, B segregation during dry, nearly dry and wet O_2 oxidation 79−66178
$SmCo_5$, mag. props., effect of phase and struct. transforms. during liq.-phase sintering 79−100086
Sn, binding state of atoms segregated at boundary of Fe and Fe alloys, Mossbauer study 80−7232
Sn diffusion in Cu, via surface segregation 77−7905
Sn-Pb (5 wt.%) ingots, quenching technique, for studying formation of macrosegregations 78−52793
Sn-Pb alloys, dil., low-freq. phonon spectrum peculiarities 79−60463

segregation continued
Sn-Zn alloy, planar and cellular solidification interfaces, distrib. coeffs. and conc. profiles *(German)* 77−32568
$SrF_2:Dy^{3+}$, cluster form., IR absorption study *(French)* 80−108240
$SrF_2:Er^{3+}$, fluoresc. spectra of charge compensated cryst., multiphonon and energy transfer relax. 79−87496
steel, C, eutectic, YU8, effect of segregating structurally free ferrite *(Russian)* 79−15677
Ta-D, stability curve for phase separation of D, neutron small-angle scatt. study 79−15672
Ti alloy, H_2 embrittlement, directional diffusion of H_2 *(Russian)* 79−15763
α-β-Ti alloy, stress, H segregation, fracture 77−40450
Ti alloy, TA6V, surface segregation, AES exam. *(French)* 78−22941
Ti, and alloys, intergranular precipitation after annealing, ion imaging microanalysis *(French)* 79−61594
α-Ti, recrystallised commercial purity, Fe-rich precipitates obs. *(French)* 80−50637
Ti, surface impurity segregation, quantitative AES 78−19611
Ti-Al, surface segregation, AES exam. *(French)* 78−22941
Ti-Al (14.4 at.%), void form. and solute segregation under Ni ion irradiation 79−42122
Ti-alloys, liquation in microdendrites, cells and macrovolumes *(Russian)* 77−76561
Ti-V-Si (30, 1 at%), quenched and aged, hardness, tensile behaviour and phase transform. 79−11646
α_m-Ti-X (X=Ag, Au, Si), precipitation mechanisms and Meyrick theory of cellular reaction initiation 79−74163
TiO_2-SiO_2, submicron dispersion of impurity, chem. diffusivity and elec. cond. 79−1528
$(U,Pu)O_2$, mixed oxide fuel elements, Pu redistribution 78−78463
U-Pu carbides, advanced LMFBR fuels, equilib. thermodynamics 79−67862
U-Pu-C system, segregation and v.p. obs. 77−28793
UO_2, desintering of unrestructured UO_2 fuel during film boiling testing, grain boundary separation 80−22997
UO_{2+x}, configurational entropy of defect complexes, Mayer cluster theory calcs. 79−77591
V, neutron irradiated, saturable trap anal., of solute segregation applied to O_2 trapping 79−77645
V-Cr (15 wt.%), radiation-induced solute segregation 80−29086
V-Cr (wt.%), 3.5 MeV $^{51}V^+$ irrad. induced void swelling and solute segregation 79−7637
V-Pd, dil. alloys, surface segreg. 78−18883
V-Ti-C, elemental anal. of second phase carbides using electron loss spectroscopy 79−20500
V_3Ga, superconducting transition temp., metallurgical processing, struct. 77−63019
$(V_2O_5)_{0.93}(MoO_3)_{0.07}$ solid soln., struct. transform. in oxidizing and reducing gas atm. 79−23740
W (100), clustering of Kr, He desorption spectrometry 80−77908
W, competition between interstitial atoms during segregation at grain boundaries, AES obs. *(Russian)* 77−25008
W, distribution of C, effect of grain boundary free energy *(Russian)* 77−90351
W electrodes, C segregation and arc damage 80−64795
W, LEED and electron microscopic investigs., review *(Hungarian)* 77−47654
W, wire, exam. of grain boundary segregation, using Auger spectroscopy, new technique 78−80551
W-Cr alloys, segregation of Cr to gain boundaries, field ion microscope investigation 77−8816
W-Cu (92.8, 7.2 wt.%), liq.-phase sintered, embrittlement and interfacial impurity segregation 80−66647
W-Ni-Fe(Cu), liquid phase sintered, interfacial embrittlement 79−57101
WC_x, electrochem. separation from W alloys, phase anal. 78−60651
$Y_{2.3}Gd_{0.6}Fe_{4.7}Al_{0.4}O_{12}$ garnet, effect of Gd on magnetite exsolution in a garnet matrix 79−11624
YIG:(Si), liq. flux growth, SiO_2 segregation and cryst. defects 80−66416
YSmCaFeGe, mag. garnet films, segregation of Ca and Ge in LPE growth 80−29959
$(Y_{1-x}2Co_x)Co_5$, mag. props. annealing effects, phase segregation, EPMA 78−91898
YbTe, high-temperature evaporation and reactivity 80−103469
ZnO, segregation of Li_2O at grain boundaries 78−64513
ZnO-Bi_2O_3 varistor, grain boundary segregation, STEM study 79−78980
ZnS:Ag, struct. and mech. props. 78−22753
ZnS-MgF_2 alloy films, struct. and optical props. 79−90910
ZnTe, elec., SEM and TEM studies of impurity segregation during long annealing 80−30001
ZnTe, SEM and luminesc. study of Li segregation 79−38657
ZnTe:Li, impurity segregation during short annealing and quenching, SEM, TEM and elec. meas. 80−10676
Zr-Al (14 wt.%), transformation sequence from Zr-Al martensite to Zr_3Al phase 80−3027
Zr-Al-Fe (8.9, 0.001 to 0.006 wt.%) Fe partitioning to Zr_2Al during peritectoid transformation 78−39784
Zr-Ni, surface layer, segregation of ferromag. Ni, magnetooptic investigation 80−2256
Zr-Ni-H, surface segregation of Ni, influence on catalytic activity 80−30275
Zr-Ni-H_x(x=2.8 to 3), surface layer, segregation of ferromag. Ni, magnetooptic investigation 80−2256
ZrC_x, micro X-ray spectral anal. of boundary zones 79−8301
ZrNi, surface segregation of Ni, influence on catalytic activity 80−30275
ZrO_2-SiO_2, liquid immiscibility, microstruct. of plasma dissociated $ZrSiO_4$ 80−107429

Seidel theory *see aberrations*

Seignette salt *see Rochelle salt*

Seignettoelectric materials *see ferroelectric materials*

seismic waves
see also seismology
10 Hz wave attenuation in New Madrid seismic zone, time-domain study 79−12080
absorption coefficients of P- and L-waves 80−76915
absorption in partially melted medium 78−85488
absorption in petroleum and water *(Russian)* 77−70617
absorption inverse dynamic problem in seismic prospecting, controlling algorithm for soln. *(Russian)* 79−74859
seismic waves continued
absorption of longitudinal waves in upper mantle 80−46145
absorption-conditioned transition functions, estimation and props. *(Russian)* 79−53318
Acapulco earthquake, 1974 October 6, short-period surface waves, strong ground motion 79−84124
adaptive deconvolution of seismic signals 77−91062
E.African Rift valley, seismic wave travel times 80−98238
airborne sound coupling into earth, freq. dependence 80−74567
alabaster, US waves in crack preparation region rel. to seismic waves 77−9405
alluvial valley, ground motion due to plane SH waves 80−56383
Alpine orogeny, Europe, upper mantle horizontal inhomogeneities, P-wave obs. 80−98268
S.America, seismic wave propag. in Nazca plate, Altiplano and continental margin 80−36264
amplitude measurements, focal mechanisms of fore and aftershocks 79−20767
amplitude-distance realtion for Rayleigh waves 77−73651
anisotropic attenuation of mean-period Rayleigh waves 79−88259
anisotropic surface-wave dispersion, isotropic inversion significance 78−96156
anisotropy in isotropic media-horizontally layered, isotropy assumption anal. 80−12343
anomalous aftershock sequences, physical model 78−77194
anomalous Eurasian earthquakes, spectral and magnitude characts. 77−73656
anomalous propag. through shearing contact zone in New Hebrides Island Arc 80−3948
Appalachian Mountain topography and ground motions 80−56382
apparent velocities, meas. in oceanic lithosphere 77−2117
Arctic region, crustal vels. rel. to struct. 79−48439
arrival time differences of singly converted and longitudinal seismic waves *(Russian)* 77−70614
N. Atlantic, 1972 May 13, focal parameters from Rayleigh wave study *(Spanish)* 77−86823
attenuation, Earth as seismic absorpt. band 77−73689
attenuation, role of intrabed multiples 79−16393
attenuation and azimuthal depend. in SE United States 78−65185
attenuation coeffs. of acoustic normal modes in shallow water 77−86932
attenuation in aftershock region, example from Off-Izu Peninsula earthquake (1974 May 9) 80−76926
attenuation in core containing Fe slurry layers 78−44789
attenuation in dry and saturated rocks, lab. meas. 80−3998
attenuation in Massilon sandstone 79−44120
attenuation in nonresolvable cyclic stratification 78−7578
attenuation in N.Utah rel. to other regions of W.United States 77−91030
attenuation in partially saturated rocks 80−3997
attenuation in rocks, role of grain boundary friction 79−34755
attenuation mechanism for body waves using point defect increases *(Spanish)* 77−9376
attenuation mechanisms in dry and saturated rocks 80−3999
attenuation models 78−61367
attenuation of body waves, magnitude corrections for upper mantle 79−66642
attenuation of intensities in Iran 79−92497
attenuation of Lg phase and determ. of m_b, SE.USA 79−92487
axisymmetric disturbance due to shearing stress discontinuity propag. in elastic medium 78−67075
Baltic shield and Barents Sea, crust and upper mantle struct., Rayleigh waves dispersion 78−77204
basalts from Faeroe Islands, compressional and shear wave vels. at high temp. and press. 79−84244
Bengal Engineering College, Howrah, India, catalogue of disturbances, 1970 February 77−13063
Bengal Engineering College, Howrah, India, catalogue of disturbances, 1970 January 77−21684
Berea sandstone, effects of pore fluids on bulk and shear attenuation 80−51386
binary seismic holography, kinematic principle *(Russian)* 78−92795
Black Sea basin, crustal struct. from Love and Rayleigh waves dispersion *(Russian)* 78−28192
blind zone soln. to hidden layers in horizontal or dipping refractors 79−74839
body wave data and Earth models linear relationship 79−57885
body wave ground motion, generation of audible acoustic press. waves 77−9351
body wave propagation through anisotropic ground, seismic station problem *(Russian)* 80−31128
body wave seismograms, simple computational method 79−84492
body wave spectral structure from WWSSN stations long period records 78−28174
body wave theory, moment tensor representation of seismic source 80−36262
body waves, apparent phase vel. determ. 78−16177
body waves, attenuation from inversions of high freq. $Q_\gamma^{-1}(f)$ 77−33000
body waves, deep seismic zone as upper mantle reflector 78−44790
body waves, Earth-flattening approx. from geometric ray theory 77−64229
body waves, focusing at epicentres antipode 79−16399
body waves, matrices for equivalent models of seismic sources 77−78124
body waves, propagation in S. Kanto Region derived from earthquakes observed initial motion *(Japanese)* 80−94481
body waves, short period, propag., isotropic scatt. model including wave conversions 78−40510
body waves, short-period, conventional and spectral magnitudes 79−48417
body waves, spherical layer matrix technique for inhomogeneous media 77−78114
body waves attenuation in layered anelastic solid 77−25647
body waves due to general seismic source in layered Earth model 77−40985
body waves from intermediate and deep focus earthquakes, magnitude scale rel. to activity temporal var. 80−3943
body waves in anisotropic media, propag. through layer 77−49020
body waves in anisotropic media, refl. and refr. at plane interface 77−49019
body waves in anisotropic media, synthetic seismograms 77−49021
body waves in laterally inhomogeneous media, ray amplitudes calc. 79−44118

seismic waves continued
body waves in upper mantle, parameters in Crimea-Vrancha-Bohemia geological traverse *(Russian)* 79−53316
body waves spectra, free surface effects on moments and corner freqs. determ. 78−85492
body waves spectral anal., earthquake source parameters, Himalayan region 79−39660
body-wave magnitude, rel. to modified Mercalli intensity 80−36259
body-wave seismograms synthesis, modified first motion approximation 78−73315
Bonin Is. earthquakes, two-parameter scaling of source spectra of Love waves 77−73642
Borrego Mountain earthquake, 1968 April 9, source model from body wave data 77−25644
boundary conditions for the numerical solution of wave propagation problems 79−53310
boundary friction effects on elastic wave propag. 79−46242
S.British Columbia, upper mantle struct. from Love and Rayleigh wave obs. 77−78131
broad-band P-wave pulse, extraction and use for seismic event classification 77−81830
building-ground interaction by SH-waves *(German)* 77−72204
Burma-India border earthquake, 1970 July 29, source parameters from body waves 79−66649
S California, upper mantle seismic velocity, regional variations 80−109111
California rock P-wave velocity, high press. and temp. expts. 80−61783
camouflet source of transverse waves, theory 80−101344
cantilever cylindrical shells, seismic design, appl. to nuclear steam system 78−58339
Caribbean plate seismic wave attenuation near Lesser Antilles Island arc 77−40990
causal absorption, effect on synthetic seismograms 79−92486
CDP seismograms, two-dimens. time-variable analysis *(Russian)* 79−84161
cenotypal volcanogenic rocks under hydrostatic press., longitudinal wave vel. *(Russian)* 77−73722
W. China, seismic vel. anomalies before and after strong and moderate earthquakes *(Chinese)* 77−91009
classification of earthquakes 79−74851
coda waves from local earthquakes, spectral anal., decay characts. 79−66639
collocation formulation of wave equation migration 80−4126
colour TV display system 79−74995
common depth point effective velocities, critical values for stratified homogeneous forms *(Russian)* 79−39668
common depth point survey data, vel. characts. determ., refl. interfaces inclination angles *(Russian)* 78−53753
common depth point technique efficiency for inclined reflecting surfaces *(Russian)* 79−84527
complex propag., Earth anelasticity model constraints 78−88802
compressional and shear wave vels. in rocks, temp. depend. 78−7579
compressional and shear waves in saturated rock during water-steam transition 80−30995
compressional wave anisotropy in Pacific crust and upper mantle 77−17040
compressional wave attenuation in partially gas saturated porous rock 80−72434
compressional wave propagation in gas saturated porous rock 80−72433
compressional wave propagation in porous rock containing gas pockets 80−72432
compressional wave velocities in rocks at high temps. and press., rel. to crustal low-vel. zones 80−41435
compressional waves, laboratory and in situ vel. meas. in sediment cores from W.North Atlantic 79−57866
compressional waves, localised vel. decrease precursory to Kalapana (Hawaii) earthquake 78−65206
compressional waves in Mid-Atlantic Ridge N of Azores, obs. rel. to upper mantle struct. 77−73691
constant Q-wave propagation and attenuation 80−30996
continents and oceans, wave field assoc. with fine structured Moho 80−12361
converted PS waves, appl. to Earth crust and upper mantle struct. experimental study *(Chinese)* 79−12093
converted shear waves trapped in sediment layer ocean bottom seismometers and surface buoy meas. 78−44776
converted waves of nearby earthquakes, appl. to deep crustal struct. determ. 80−30999
convolution product, deconvolution problem *(French)* 79−44275
core and mantle elastic wave velocity at high-press., using Debye theory of sp. ht. 80−89979
core phases, Bangui obs. *(French)* 80−56396
core region, attenuation coeff. distrib. 80−90035
core-mantle transition zone, seismological significance *(Italian)* 77−70618
correlation of seismic events in time section, algorithm *(Russian)* 79−39962
correlograms, optically generated, noise resistance evaluation *(Russian)* 78−40699
coupled solid/fluid/surface wave dynamic interaction problem, improved fluid superelement 78−81108
crack anisotropy in NW.England Carboniferous Limestone, in-situ methods 80−17240
crack induced velocity anomaly, P-waves for crack estimation 80−98253
crack propagation theory, Lamb's problem for a point source 80−56375
critically refracted rays, numerical tracing 78−7783
crust and upper mantle regional studies, nonlinear interference anal. of seismic data 79−25217
crustal P-wave vels. in NORSAR area 78−3728
crustal rocks, exponential relationship between seismic vel. and radioactive heat prod. 79−70793
crustal thickness in N.Nevada from seismic refr. profiles 79−48425
crustal velocity anomalies determ. in Mugodzhary from seismic rays emergence angles and azimuths 79−25206
crustal velocity models in central United States, theoretical seismogram constraints 79−39693
crustal velocity structure, in Superior-Churchill boundary zone, S.Canada, cooperative surveys 80−89985
cumulative wave energies, in earthquake sequences 79−39672
cylindrical cavity surface, seismic radiation from point source 79−53308
seismic waves continued
damping in Crimean region of Black Sea, seismic coda appls. *(Russian)* 78−11824
deconvolution of data using homomorphic filtering 77−91063
deconvolution of seismic data, overview 77−91060
deep interior, magnetoviscoelastic wave refl. and refr. at welded contact 80−89967
deep reflections, unravelling via seismic stripping 79−34970
deep shear wave velocity meas. 79−88304
density profile determ. from dispersion of surface seismic waves *(Russian)* 77−53013
depth determ. from seismic refraction data, iterative method 78−96302
Diablo Range, California, P-velocity models from earthquake and explosion arrival times inversion 79−12094
differential travel times for later phases rel. to improved source depth determ. 77−81829
diffracted wave travel times determ. method 80−8432
diffraction at coal seams, approx. diffr. theory for transparent half-planes 80−89974
diffraction properties of crust, using Earth crust models 80−98239
diffractions for arbitrary source-receiver locations 78−28172
dip selective migration vel. determ. 77−41187
discontinuous vel. increase, full wave theory rel. to inner core boundary 77−73674
discrete wavenumber rep. of seismic source wave fields 77−73640
dislocation source in heterogeneous crust, propag. study using dislocation model 80−101340
dispersion, continuous representation technique 80−51334
dispersion curves, methods of computing partial derivatives 77−37149
displacement due to a uniformly moving line load over the plane boundary of an inhomogeneous elastic half-space 79−29716
displacement potentials for motion in homogeneous isotropic elastic medium 80−21649
distortions by refracting curved interfaces, correction algorithms *(Russian)* 79−58118
disturbances in viscoelastic medium due to impulsive forces on spherical cavity 78−67076
diving waves in multilayered medium, time-distance curve transformation 78−69472
dynamic field of Haskell's rectangular dislocation fault model 79−48403
dynamic parameters of seismic sources, explosions and earthquakes 79−84141
dynamic rupture on three-dimens. fault with near-field seismic waves 78−77186
dynamic spectral ratios with variable freq. bands as seismic discriminants 77−81834
Earth deformation, mag. field effects 80−109085
Earth reflectivity function, extraction via data deconvolution, book contrib. 79−92635
Earth strain response, bore-hole strainmeter meas. at Matsushiro Seismological Observatory *(Japanese)* 79−96745
Earth stretching approx. for Love waves 77−73664
earthquake, elastic energy release, heat prod., and Earth inertia tensor changes 79−44106
earthquake energy dissipation during propag., by solid friction 80−109106
earthquake fault plane soln. optimum search procedure using wave-amplitude data 78−45011
earthquake faulting, HF seismic waves from crack models 78−11821
earthquake focal mechanism effect on P-waves dynamic parameters and magnitudes from longit. waves 78−73318
earthquake foreshocks, waveform anal. rel. to differentiation from earthquake swarms *(Japanese)* 80−67342
earthquake magnitude calibration function for core phases, PKP1-PKP2 caustic 78−40509
earthquake magnitude determ. from surface and body waves, calibrating curves for different instruments 78−57173
earthquake magnitude scale structure from filtered broadband P-wave records 79−92509
earthquake magnitudes from ultralong period seismometer records 77−44928
earthquake modelled by centrifuge, seismic signal and stress change 78−81429
earthquake parameter determ. computer technique using wave phase data *(Chinese)* 80−77126
earthquake rupture velocity and radiation efficiency 77−9352
earthquake swarms, seismic waveform anal. rel. to differentiation from foreshocks *(Japanese)* 80−67342
earthquake wave analysis program WAVE, DEMOS-E library program 78−92800
earthquakes source spectrum determ. using code of seismic oscills. 79−48405
effective velocities, determ. in continuous seismic profiling with two receiver systems 80−31150
effective vels. for stratified-isotropic media with interfaces, ray technique *(Russian)* 79−62614
El Golfo earthquake, Mexico, 1966 August 7, seismic waves rel. to source mechanism 79−66627
elastic and acoustic wave equations, absorbing boundary conditions 78−59320
elastic half space response to realistic faulting model 78−85486
elastic prestress in Earth interior, effects 78−77202
elastic wave emission by small sources in heterogeneous elastic media 77−56599
elastic wave fields, discrete wave number representation in three space dimensions 80−3945
elastic wave propagation, point pulse source in anisotropic media 80−3939
elastic wave radiation expts. from fault models 80−3938
elastic wave source and receiver grouping in seismic exploration *(Russian)* 77−9563
elastic wave vel. before earthquakes 80−8256
elastic waves diffraction by finite crack, appl. to location of magma lens 79−16416
elastic waves from tensile cracks and shear faults 79−16411
elastic-acoustic system, response to press. source in acoustic medium 77−75833
elasticity inverse problem, soln. using amplitude and natural freq. data 77−2119
elastodynamic propag. matrices, stratified Earth models 78−77197
elastodynamic radiation from slip zone, ray method 78−73322

seismic waves continued
in ellipsoidally anisotropic media, refl. and transmission coeffs. 79−84136
emergence angle and azimuth, inclined interface effect *(Russian)* 78−11825
Epinal, France, focal zone, shear wave vel. anisotropy *(French)* 77−52990
Eurasia, travel time curve rel. to lateral var. in upper mantle struct. 77−33016
Eurasian earthquakes and explosions, discrimination using P codes spectral characts. 78−7576
W.Europe, upper mantle P-wave vel., large scale variations 80−109112
exchange waves produced by earthquakes, appl. to Cuba crust study *(Russian)* 79−44158
excitation function of elastic wave source, math. model *(Russian)* 78−53624
explosion seismic waves, appl. to Earth crust Q-factor beneath SW.Honshu, Japan 80−17242
explosion seismic waves, appl. to SW.Honshu, Japan, crustal struct. derivation 79−74862
explosion seismology primary signal form., effect of partial multiple refl. *(Russian)* 78−85484
explosive versus nonexplosive sources *(Russian)* 77−9377
extrapolation of seismic waveforms, by Fourier methods 79−34978
far field waves definition criteria *(Russian)* 79−39965
far-field body waves generated by slip faulting, theory for elliptically expanding rupture 77−81804
Fiji Plateau, underlying upper mantle struct. from second P-wave arrivals 77−60359
Fiji-Tonga deep focus earthquakes, relative teleseismic P-wave residuals interpetation 78−36111
finite difference and wave number migration 79−74842
finite-difference migration for steep dips 79−92620
first arrival of P-waves from quake, nonquadratic distrib. of signs 80−94474
first arrivals, automatic timing from microearthquake network data 78−81412
foreshocks spectral features 78−96147
Fourier and response spectra of seismic oscills. 77−56597
Franciscan rocks, dry, compressional wave vels. to 8 kbar and 300C 77−64273
free oscillations attenuation in viscoelastic Earth, theoretical contrib. 80−21652
free oscillations from Colombian deep earthquake (1970, July 31), and source mechanism 79−16394
frequency domain approach to two-dimensional migration 79−74841
frequency-filter anal. of surface waves, fast method, west Pacific region appl. 79−48573
frictional attenuation, amplitude depend. 80−31034
Friuli aftershocks, temporal var. of V_p/V_s ratio *(French)* 77−70600
Friuli earthquake, 1976, seismic response of different recording sites 80−41379
Friuli focal area, Italy, seismic body-wave dispersion 80−36267
G-type seismic waves generation 79−66624
Galway Lake earthquake, California, 1975, search for P-wave vel. variations before and after 77−40997
Garm region elastic wave vel. temporal changes in 80−104914
generalized ray and reflectivity methods of waveform synthesis, comparison 79−84501
generalized ray theory for dipping structures 78−7569
geological depth section, algorithm for tracing horizons *(Russian)* 77−66891
geomagnetic disturbance accompanying seismic wave propag. *(Chinese)* 79−88238
Goat Mountain earthquakes, California, 1975, search for P-wave vel. variations before and after 77−40997
Great Basin of Nevada and W Utah, struct. from seismic surface waves 78−73336
great circle Rayleigh waves attenuation and group vel. 79−2192
great earthquakes, stress drops, wave spectra and recurrence intervals 79−44116
Greece area, shallow earthquakes intensities attenuation with distance 79−44107
ground displacement vector, polarisation determ. rel. to seismic three-component registrations interpretation *(German)* 78−32017
ground motion amplification by topographic depressions for P-waves, acoustic approx. 77−73646
ground motion spectra, analysis 79−88311
ground response, seismic microzoning mapping from subsoil conditions 79−44108
ground response to weight dropping, wave amplitude and vel. 80−76914
group and phase vel. determ. and filtering of dispersed waves 79−35005
group vel. meas., error estimation 77−86805
group velocity, high resolution anal. appl. to explosion and earthquake 78−81111
group velocity and phase velocity relationships for finite discrete obs. 78−44774
Guatemala earthquake (1976, February 4), surface and body waves and siesmological aspects 78−85493
guide channels for seismic energy, transverse waves in upper mantle *(Italian)* 78−61355
Gulf of California transform fault aftershock sequences, sonobuoy and teleseismic study 77−25651
Haicheng earthquake, 1975 February 4, spectral changes of foreshocks and aftershocks *(Chinese)* 77−91010
Hawaii tsunami simulation, open boundary reflection interference 80−17232
head waves, screening in media with inclined boundaries *(Russian)* 78−92794
HF coda waves of local earthquakes, Stone Canyon, California, temporal trend in attenuation 79−57861
Hidaka mountain region, Hokkaido, Japan, unusual seismic waves from shallow quakes *(Japanese)* 80−94477
high freq. P_n and S_n phases in Western Pacific 77−86799
high velocity surface wave noise *(Russian)* 77−66892
high-frequency radiation from small earthquakes, directivity 79−66625
higher mode dispersion measurement, new method 79−39974
Himalayas adjoining Tibetan Plateau and Chinese mountains, crustal struct. 78−7600
Hindukush region, crustal struct. from body wave data 79−96752

seismic waves continued
hodographs of wave paths, imperfect knowledge appl. to seismic shocks location *(Russian)* 79−35009
horizontal ground motion, two-dimensional, evaluation for structs. design 79−48419
Hyderabad, India, peninsula shield crustal struct. from long period P-waves spectra 79−66667
Iberian Peninsula crustal structure from seismic wave dispersion *(Spanish)* 80−36269
Iceland, body wave vel. correl. with basaltic crust alteration 80−90015
impulsive waves, propag. in spherically symmetric model 79−74849
incident and reflected wave forms, inverse problem interpretation *(Russian)* 79−34762
inelastic media, propag. theory *(German)* 80−104885
infrasonic sea noise from underwater microearthquakes, meas. and experimental problems 78−11902
initial longitudinal waves of Friuli earthquake, 1976 May 6, polarities anal. and focal mechanism 80−85603
inner core PKIIKP wave detect. and damping 80−104925
integral spectrum parameters, appl. to geological section prediction *(Russian)* 79−8705
intense multiple waves, freq. selection for CDP method *(Russian)* 78−12012
interfacial waves launched by an explosive line-source in a submerged elastic half-space 78−75088
interference effects in thin layers 78−92780
interference Rayleigh waves (F-waves) appl. in coal forms. seismic tracing *(Russian)* 79−74858
interfering wave separation problem soln. *(Russian)* 77−91042
internal vels. in crustal layers from sonobuoy records of mantle reflections 78−28184
interval vel. estimation error and geological model 77−86790
inverse and spatial filtration by reflected wave method *(Russian)* 78−3970
inverse geometric seismology problem, seismic reflection data *(Russian)* 77−70613
inverse kinematic problems, correlations in model parameters *(Russian)* 77−70615
inverse normal mode problem for an elastic sphere *(French)* 79−41610
inverse problem appl. of control theory 79−2402
inverse problem for normal incidence waves to horizontal layered media 80−98252
inverse problem for seismic wave eqns. in one dimens. *(French)* 79−44138
inverse problem soln. using J-fraction expansion 78−11819
inversion of microseismic array cross spectra 80−98243
Iran, premonitory crustal vel. ratio changes 78−32029
isotropic scattering approx. for coda waves near hypocentre 78−11828
Iwate-Oki (Japan) earthquake, 1968, June 12, seismic waves rel. to focal mechanism 77−78123
Izu Peninsula, Japan, shear waves used to construct underground struct. *(Japanese)* 80−41387
Izu-Oshima-kinkai earthquake, Japan, 14 Jan. 1978, seismic waves anal. *(Japanese)* 80−41385
Izu-Oshima-kinkai earthquake, Japan, Jan. 1978, aftershocks and main shock ground accel. *(Japanese)* 80−41386
Japan area, surface wave group vels. 77−56603
Japan-Kurile Arc, upper mantle P-wave vel. model 77−78132
Kilauea Iki, shallow magma reservoir seismic props. 78−73338
kinematic mutuality of reflected and refracted waves, prospecting *(Russian)* 78−69298
kinematics and dynamics, statistical analysis determ. *(Russian)* 79−84533
Koyna earthquake, 1967 December 10, temporal var. of body waves travel time ratio 79−5456
L_g-phase propagation in E British Columbia, evidence from 1918 February 4 earthquake 80−3932
Lamb's problem, generalisation to class of inhomogeneous elastic half-spaces 78−32023
Lamb problem soln. for vertically inhomogeneous elastic halfspace 78−15971
late arrivals in E.Alps from Friuli aftershocks, focal depth determ. 78−24243
layered media, relative intensity of total multiply refl. waves *(Russian)* 78−28176
least-squares inverse filtering and wavelet deconvolution 78−61339
LF tunnel waves propag. through subcrustal lithosphere, numerical expt. 77−49025
Lg propagation and lateral variations in crustal structure in Asia 77−33008
Lg waves, N.E. United States and S.E. Canada earthquakes scaling 77−25646
limestone, dry and saturated, P and S wave attenuation, US obs. 80−72494
line migrated reflections, ray modelling and theory 78−40497
linearised multiple reflection model, for subsurface layered media parameter estimation 79−5691
Lipari, Eolian Islands, seismic response of local earthquakes rel. to crustal struct. 78−40494
lithosphere beneath New Madrid seismic zone, three dimens. vel. model 78−7573
lithosphere-asthenosphere boundary beneath S.America from converted phase wave obs. 77−64226
Lithospheric Seismic Profile in Britain (LISPB) rel. to N.Britain crustal struct. 78−73329
long period and surface waves, conf., Mamaia, Rumania, 1975, Sept. 77−37146
long period statics determ. by inverse filtering 77−41192
long wavelength static estimation in common depth point data 77−17032
long-period oscillations, meas. by borehole long-period seismometer (BELS type 79) with stable period *(Japanese)* 80−67417
long-period reflected and converted upper mantle phases 78−92786
long-period surface vels. and accels., dislocation source model 78−11829
long-period surface waves, inversion rel. to magnitude scale renormalization 78−15977
long-period surface waves dispersion obs., shield-like upper mantle struct. 77−56608
longitudinal and surface waves, mutual conversion 77−70610
longitudinal and transverse wave characts., shearing motion along pre-existing fracture 77−64220

seismic waves continued
longitudinal core waves, earthquake magnitude determ. *(German)* 77−70603
longitudinal incident wave directed from below onto inclined media interface, ground surface displacements calc. *(Russian)* 78−85485
longitudinal wave arrival directions rel. to crustal structure *(Russian)* 78−11850
longitudinal wave propag. from near earthquakes, Crimean obs. 77−70609
longitudinal wave vel. and hypocentre coords. determ. *(Russian)* 79−66623
longitudinal wave velocities in rocks, appl. to mineral comp. prediction for rocks at great depths *(Russian)* 80−104956
lossless wave eqn. in layered media, canonical Bremmer series decomposition 77−91064
Love and Rayleigh waves, possible mode conversion at continental margin 78−73314
Love and Rayleigh waves attenuation across Pacific Ocean, 15-110 s periods 77−9353
Love number changes during Earth model variations in static theory of tides 77−44951
Love wave data inversion for vel. and anelasticity 79−8604
Love wave dispersion curves for stressed stratum in isotropic elastic media 78−57169
Love wave dispersion in semi-infinite medium with inhomogeneous layers 77−49031
Love wave mode conversion at continental margin 77−40986
Love wave propag. in poroelastic medium 79−98653
Love wave scattering matrix for continental margin, theory 78−20360
Love wave scattering matrix for continental margin model 78−48982
Love waves, application of phase-matched filters 79−92602
Love waves, contribution to strong ground motions 79−88302
Love waves, in stratified magnetoelastic solid with material boundary 78−32015
Love waves, propag. in 3-dimens. structures, finite element techniques 80−21631
Love waves dispersion in continuously stratified layered Earth 79−20760
Love waves in infinite strip with surface step, transmission, reflection and diffraction 79−88260
Love waves in slowly varying layered media 77−37153
Love waves on an ellipsoidal Earth 77−37152
Love waves propagation in viscoelastic medium, effect of initial stresses 79−14299
Love waves transmission through laterally varying structure 77−56592
Love waves under initial stresses 79−29714
Love-type SH waves, propag. in nonhomogeneous internal stratum between two semi-infinite elastic media 78−32016
Love-type surface wave props. in frictionally bonded layer 80−21630
Love-type waves propagation in heterogeneous medium between semiinfinite homogeneous elastic media 79−18767
low-frequency seismic waves assoc. with volcanoes and glaciers, prod. by hydraulic transients 79−100816
lower mantle inhomogeneities characts. from scatt. waves, correction 77−49042
lower mantle large-scale heterogeneities from P wave travel times 77−33022
lower mantle seismic wave vel., meas. method using wide aperture array 80−105071
magneto-thermo-elastic surface waves in stressed conducting media, theoretical study 80−8253
magnetoviscoelastic solids under initial stress, surface waves 79−84140
magnitude corrections and group vel. dispersion from Simferopol obs. *(Russian)* 78−11826
mantle, method for quantitatively estimating vel. variations 77−44932
mantle attenuation, significance of ferroelectric phase transitions 77−53045
mantle base lateral heterogeneity from PKP phases amplitudes 80−21675
mantle base shear-wave velocity, by diffr. SH wave data 80−56380
mantle lateral variations from LF eigenspectra data 78−36123
mantle low velocity zone, interpretation in terms of thermally activated point defects 78−88806
mantle Rayleigh waves, phase velocity and Q 79−74846
mantle structure beneath Japan Sea 78−81118
mantle surface waves, vels. in SW flank region of Baikal Rift 80−94503
mantle under NW Pacific, HF P_n waveguide 77−91057
mantle velocity variations below E.Australia and SW.Pacific 80−36279
mantle waves, vel. anomalies rel. to single-cell mantle convection and geoid 77−60362
marine sediments, seismic vel., density and attenuation models from multibounce phases 79−57864
maximum entropy spectral analysis method *(Japanese)* 77−2260
meteorite explosion, Tunguska, Siberia, shock wave effects, model, computation 77−5507
Michigan Basin, in situ S-wave and P-wave vels. in deep borehole 79−39679
microacoustic signals assoc. with rock fracture, preliminary anal. 78−32070
microseismic vibration source position determ. 78−85489
microseisms at Palisades, source location and propag. 78−85495
microseisms in lakes, longitudinal waves, origin from atm. press. variations *(Italian)* 77−81798
microseisms influence on terrestrial quartz gravity meters, mechanism *(Russian)* 79−39967
microseisms meas. on Isle of Sylt *(German)* 77−86808
microseisms obs. at New York Rayleigh and Love wave characts., geologic control 80−26462
microvibration frequency analysis by 50 m interferometer 80−109276
Mid-Atlantic Ridge, amplitudes and travel times rel. to struct. at 45°N 78−73332
Mid-Atlantic Ridge, fault mechanisms and sub-crustal seismic vel. 80−36265
migration of seismic records, solution by phase shift method 79−84132
model sediments, elastic wave propag. 77−73672
models and wave eqns. *(French)* 79−74843
modified Merco Mercalli intensity scale, modification 80−36260
Mount Rainier, Washington, underlying struct. from teleseismic body waves 80−31011
multichannel subtracting filters *(Russian)* 78−3969
multidimensional velocity generalisation technique, appl. to Black Sea NW shallow and nearby land areas *(Russian)* 80−105068
seismic waves continued
multilayered elastic medium, reflection seismograms for explosive source, theory 80−17233
multiple ray reflections in spherical isotropic Earth model, normal mode representations 78−48981
multiple reflected signal attenuation, least squares estimation procedure 80−85596
multiple reflections, two-dimens. modelling 77−2264
multiple reflections and head waves in Gulf of Suez, obs. 80−56400
multiple reflections in multilayer absorbing medium *(Russian)* 79−20759
multiple scattering role in formation of seismogram coda 79−25205
multiple ScS differential travel times determ. by waveform correl., systematic bias 78−32019
multiple ScS waves, attenuation beneath Japanese Arc 79−92508
multiple seismic wave suppression on seismograms 80−46281
multiple wave parameter prognosis in velocity anal. *(Russian)* 77−70611
multiple wave suppression on seismic recordings, two methods of soln. 80−77147
multiple waves, appl. to freq. selection to wedging out zones separation *(Russian)* 79−8706
multiple waves, prediction filtering in non-ideal conditions *(Russian)* 79−44131
multiple waves suppression methods, comparative evaluation *(Russian)* 78−40515
Multiples in multilayered absorbing medium 79−34752
multipls ScS waves travel times, rel. to upper mantle lateral heterogeneity 77−29259
multiply reflected seismic ray, multi-segment traces deconvolution and synthesis 80−77162
multipolar source in layered media, seismic wave emission 80−81816
natural freq. spectra, information content of different angular numbers 78−61344
near-field Love waves synthesis by exact ray method 79−79750
near-field of seismic source in irregularly layered medium 77−78112
near-field waveforms from expanding transparent cavity in prestressed medium 79−25201
net downgoing energy and resulting minimum phase property 77−41004
Nevada Test Site, geology effect on absolute travel-time residuals 79−16391
New Hebrides earthquake, dispersion of first and second Rayleigh modes, periods greater than 50 s *(French)* 77−64212
New Hebrides earthquake (1969, January 19), waveforms rel. to fracture zone and aseismic ridge subduction 78−73342
New Madrid seismic zone, wave vel. determ., crustal model 77−73652
New Zealand, South Island, regional travel time ratio and near source V_p/V_s ratio 78−40500
noise level meas. at NORSAR 77−73657
nonlinear elasticity of geological media with phase microheterogeneities *(Russian)* 77−73719
normal mode attenuation, Q mode of mantle 78−61343
normal mode oscillations of Earth, asymptotic representation of multiplet spectra 80−94459
normal modes of rotating Earth model, excitation by earthquake fault 78−73312
North Sea region upper mantle struct. from Rayleigh wave dispersion 78−36122
Novaya Zemlya crust and upper mantle model from Rayleigh wave dispersion data 79−84187
Novaya Zemlya nuclear explosions, P-wave travel time residuals vars. in central California 77−25658
nuclear explosion generated body waves, time functions 80−56376
numerical seismogram dispersion curves computed by normal modes 79−16403
ocean bottom hydrophone array obs. of P and S waves, wave train characts. 80−104898
oceanic crust, continuous seismic profiling, diffr. waves travel time curves 78−3725
oceanic crust, seismic vel. evolution 79−5457
oceanic crust, vel. depth distribs. on E.Pacific Rise crest from travel time inversion 77−60357
oceanic crust, vel. in high-vel. layer indicating garnet comp. 80−17251
oceanic Lg phase search 79−25203
oceanic long-period Rayleigh group vel. dispersion curve from HF Doppler sounding of ionosphere 79−70756
oceanic Sa seismic waves 77−73670
oceanic upper mantle seismic anisotropy, evidence from ophiolite complex 80−21677
of R-waves from great earthquakes, initial phase anal. 80−41405
oil shale, dry and saturated, P and S wave attenuation, US obs. 80−72494
one-dimensional, in elastic inhomogeneous media, inverse solns. 78−40518
Onikobe earthquake, Japan, ground motion deduced from damage, source model *(Japanese)* 80−94479
onset detection, computing 79−80059
onset of waves, detection algorithm for automatic seismometer *(Japanese)* 80−94476
ophiolite complex of Point Sal, California, seismic vel. struct. 80−109110
ophiolites, seismic vels. and oceanic crustal struct. 78−77226
optimal estimation of wave field parameters *(Russian)* 78−28177
optimal freq. filtering for interference systems *(Russian)* 79−58117
Oroville, California, 1975 August 1, precursory P-wave travel-time vars. 77−56580
Oroville, California, crustal shear wave vel. struct. determ. from 1975 August 1 earthquake 79−16417
Oroville earthquake, California, 1975 August 1, focal mechanism 77−9346
Oroville earthquake, California, 1975 August 1, surface wave constraints on source parameters 77−56579
P_n vel. in USA, indicator of upper mantle anelastic quality factor 77−13064
P_n velocity anisotropy in a continental upper mantle. 77−49013
P_n velocity anisotropy studies in Britain and USA 79−53314
P_n velocity rel. to partial melting in upper mantle 78−3729
P'P' precursors, origin in mantle seismic scatt. 77−37144
P'P' precursors and upper mantle discontinuities 77−86806
P and pP waves, relative amplitudes rel. to fault plane solns. determ. 77−73669

seismic waves continued
P and S waves, vels. in oceanic crust rel. to ophiolites identification 78−81117
P and S waves beyond 95° 78−11818
P to SV wave conversion in mantle, detect. technique 77−81810
P wave travel times from Indian deep-focus earthquakes 79−2193
P wave/S wave ratios in foreshocks, rel. to faults premonitory slip and earthquake prediction 80−3944
P waveforms, surface layers effect, radial oscills. of multilayered elastic sphere and theoretical seismograms *(Japanese)* 79−66640
P- and S-wave demonstration with student participation 79−30177
P- and S-wave velocities in dry and saturated rocks, influence of cracks, model 78−20366
P- and S-waves decoupling in inhomogeneous elastic media 80−21650
P- and S-waves diffracted around core, attenuation 79−53312
P- and S-waves diffracted around core, rel. to mantle base vel. struct. 79−53313
P- and S-waves of deep interior, max. vel. amplitudes 80−98262
P- and S-waves spectral content, from Garm, Tadjikistan local earthquakes 79−48406
P- and SV-wave corner freqs., possible discriminant for earthquake source theories 77−56605
P-delays temporal var. in S.California, rel. to earthquake prediction 79−57873
P-phases, anal. of short-period waveforms, from deep focus earthquakes beneath Fiji Islands 79−25200
P-pulse propag. in elastic media, finite difference modelling 77−73868
P-residuals azimuthal var. in southern California, mantle structure 80−3954
P-signal complexity from nuclear explosions and upper mantle struct. 77−56596
P-wave, surface or interface, importance in near-earthquake studies 79−66628
P-wave abnormal delays in The Geysers-Clear Lake geothermal area, California 79−74860
P-wave amplitude anomalies, interpretation 80−56386
P-wave amplitudes, regional anomalies and focal regions tectonics 79−79751
P-wave amplitudes and magnitude corrections for deep focus earthquakes 77−86797
P-wave amplitudes and sources of scatt. in m_b obs. 77−86807
P-wave arrival-time differences for relative epicentre determ. 80−101328
P-wave coda, array anal. for Moho dip and strike determ. 79−66821
P-wave codas, spectral composition of earthquakes and explosions 80−21640
P-wave damping 77−2115
P-wave displacement in rectangular fault, spectral amplitude calcs. *(Chinese)* 80−76911
P-wave initial pulse widths rel. to anelastic props. and surface geology, central California 78−44778
P-wave interference recorded at Yellowknife Array 78−7586
P-wave model catalogue for upper mantle 77−17028
P-wave P vel. lateral inhomogeneities under lesser Himalayas from Tarbela array obs. 77−91027
P-wave reflection at non-vertical incidence, synthetic seismograms 80−56401
P-wave residuals, mantle vel. anomalies below Colorado Rocky Mountains 80−81853
P-wave seismograms complexity for deep earthquakes 77−52994
P-wave seismograms from continuously varying transition zones, acoustic media 78−20361
P-wave seismograms from continuously varying transition zones, elastic media 78−20362
P-wave signal, complex, from underground nuclear explosions, coda power and modulation characteristics 79−79757
P-wave signals, multivariate autoregressive model, short-period discrimination appl. 79−16385
P-wave signature of underground nuclear explosions, tectonic stress release effect 77−25642
P-wave source functions of large deep-focus earthquake, 1970 Aug. 30, Sea of Okhotsk 77−9372
P-wave spectra from Fiji-Tonga, 1957-71 deep-focus earthquakes 77−56600
P-wave spectra from remote earthquakes 77−64223
P-wave teleseismic delay times in major oceanic fracture zone 79−70754
P-wave three-dimensional velocity structure for Beijing upper mantle and crust *(Chinese)* 80−104894
P-wave time residuals, three-dimens. inversion 80−21849
P-wave travel time anomalies rel. to epicentral distance to African stations 80−98237
P-wave travel time residuals caused by dipping plate in Aegean Arc 77−33011
P-wave travel time stability in La Malbaie, Quebec region 80−21639
P-wave travel times and precursive spectral stability before 1975 June 30 Yellowstone earthquake 78−61352
P-wave travel times from deep earthquakes 77−25648
P-wave travel times from Nevada explosions to Oroville dam, 1970-76 period 77−56581
P-wave vel. determ. from Honshu local earthquake data 80−76937
P-wave vel. struct to depth of 150 km, Kanto District, Japan *(Japanese)* 80−94475
P-wave vel. structure of metamorphic belt of central California 80−98270
P-wave vel. structure of upper mantle of W.United States 78−61363
P-wave velocities, in uppermost mantle beneath Turkey and Iran 80−72462
P-wave velocities in Shikoku district, Japan, rel. to upper crustal struct. *(Japanese)* 80−94508
P-wave velocities in upper mantle, model for E. and S.Africa 79−44135
P-wave velocity anisotropy temporal stability before earthquakes in central California 78−7574
P-waveforms of deep Colombia earthquake (1970, July 31), rel. to spatio-temporal history 77−86813
P-waves, earthquake focus orientation effects 80−3940
P-waves, evidence of multiplicity in travel time curve beyond 30 degrees 77−81809
P-waves, evidence of vel. increase at about 770 km depth 77−2118
P-waves, from explosions, anisotropy in continental upper mantle 77−49014
P-waves, in situ vel. study at Stone Canyon well, California 79−57865
P-waves, initial, from microearthquakes, computer anal. 79−39987
seismic waves continued
P-waves, inversion of vel. anisotropy 77−49017
P-waves, long-period, diffracted, observed at Matsushiro, props. *(Japanese)* 79−96744
P-waves, long-period, spectral-ratio anal. rel. to Moho depth under NORSAR array 77−86814
P-waves, low-frequency, effects of crust spectrum charact. on station calibration *(Russian)* 78−49158
P-waves, mean travel time residuals, systematic variations 78−3727
P-waves, millisecond travel time vars. systematic monitoring near Palmdale, California 79−57863
P-waves, refl. delays beneath Cretaceous Fogo seamounts rel. to anomalous upper mantle struct. 78−85515
p-waves, residuals in Canada 77−91037
P-waves, short-period, anisotropic scatt. in upper mantle 79−16377
P-waves, short-period, attenuation in USA from P-wave spectra of SALMON nuclear explosion 77−25650
P-waves, short-period, for time-domain determ. of earthquake fault parameters 77−25643
P-waves, short-period, regional amplitude anomalies rel. to anelastic rel. to anelastic attenuation, North America 78−44777
P-waves, time and amplitude anomalies interpretation in terms of lithosphere heterogeneities 78−96153
P-waves, travel time residuals in United States rel. to continental and oceanic mantle struct. 77−29253
P-waves, travel time residuals rel. to continental plates ages 79−62439
P-waves, travel times in Europe and W.Russia 77−33001
P-waves, travel times in N.Australia in long-range seismic profile 79−16419
P-waves, travel times rel. to upper mantle lateral struct. vars. around India 77−49016
P-waves, vel. anisotropy meas. under high-press., high-temp. conditions 77−49059
P-waves, vel. anomalies rel. to Japanese subducting lithosphere 79−92489
P-waves, vel. determ. in area of unknown crustal parameters 78−7585
P-waves, vel.-depth model of subcrustal lithosphere beneath Fennoscandia 80−90009
P-waves anomalous vels. in outer core rel. to struct. 79−48436
P-waves coda, role of scattered waves 77−73684
P-waves diffraction at volcanic magmatic foci 79−25204
P-waves from Mindanao earthquake, 1976 August 16, preliminary seismological assessment 79−66635
P-waves from mining explosions near Centralia, Washington, search for time-depend. travel times 78−44788
P-waves from Rumania earthquake, 1977 March 4, obs. rel. to Moho vel. depth distrib. *(German)* 80−98256
P-waves from small earthquakes, anal. rel. to detailed spatial distribs. of foreshock and aftershock activities *(Japanese)* 80−94483
P-waves in Aegean region, rel. to dynamic model of Hellenic Arc 77−21734
P-waves in upper mantle, vels. in Japan using time-term method 77−37145
P-waves records, non-linear stochastic models with appls. in event identification 79−16396
P-waves records complexity appl. for discrimination of artificial and natural seismic sources 80−12340
P-waves refracted by mantle, hydrophone recordings of underground nuclear explosions 80−98257
P-waves signal character for focal depth determ. 77−9355
P-waves travel time anal. from underground nuclear explosions at Novaya Zemlya 79−84115
P/S-wave velocity ratio for rocks, statistical study *(Japanese)* 77−17036
W.Pacific, HF P_n and S_n phases obs. at great distances, spectral anal. 78−77195
W.Pacific, high shear vel. layer 78−3734
Pacific crust surface wave dispersion 77−56604
Pacific upper mantle regionalized shear vel. models from Love and Rayleigh wave dispersion 79−53321
Pamir-Hindu Kush intermediate depth earthquakes, spectral content rel. to upper mantle high-Q zone 77−86795
Pand S-phase data from local earthquakes, California, 1966-75 period 79−12088
parabolic wave theories and applications 80−51436
passing exchange wave effects on inclined interface *(Russian)* 80−85600
pattern recognition, preprocessing of signals prior to input to pattern recognition scheme 79−62631
PcP, long-period, amplitudes rel. to core-mantle boundary 77−37143
peg-leg multiples and dipping reflectors 78−7580
permafrost soil, compressional and shear wave vels. using US pulse technique 77−17081
perturbation matrix method for propag. in irregular stratification 77−73869
petrovelocity crustal model and M discontinuity along Shepetovka-Chernobyl seismic profile *(Russian)* 77−44948
phase vel. determ. of fundamental Love and Rayleigh waves 77−37148
Philippine earthquake, 1976 August 16 seismic waves rel. to subduction zone south of Mindanao 79−44117
PKIKP precursors rel. to lower mantle lateral vars., seismic array evidence 79−20781
PKIKP waves, calibration curve for earthquake magnitude determ. 77−64222
PKKP scattering, core-mantle boundary roughness 80−56437
PKP from deep-focus earthquakes, GH branch confirmed 78−61341
PKP precursor data comparison from seismic arrays 79−25208
PKP waves, times from Indian earthquakes 79−39674
planar dipping structure effect on source and receiver responses for const. ray parameter 78−7571
planar SH wave diffraction, density, rigidity bidimensional perturbation *(French)* 80−76917
plane SH waves, linearised direct and inverse problems for two-dimensional heterogeneities *(French)* 79−84131
plane wave, inversion of refl. data 77−21915
plane wave reflection and refraction at elastic interface, initial stress effects 79−62445
Pn waves, high freq., propag. in Central and South Pacific, rel. to lower lithosphere struct. 80−26459
point pulse source in elastic anisotropic half-space, propag. of vibrs. 78−57174

seismic waves continued
polarized waveform dectors, matrix and Stokes vector representations, teleseismic waves appl. 78−12008
PP waves refl. under E Canada, travel time residuals, crustal and mantle struct. 77−9354
Precambrian Earth crust, seismic refls. study 78−32034
precursors to PKKP, rel. to core-mantle boundary struct. 79−48409
predictive multiple wave filtering *(Russian)* 79−58115
prestressed Earth model, P- and S-wave radiation patterns 80−56404
propagation, effects of anisotropic layering, review 77−49012
propagation, Wiechert-Herglotz inversion, as integration on closed contour 80−61766
propagation and damping coeff. in electrically charged water-saturated rock 80−76921
propagation from moving normal point loads in layered media 77−37157
propagation in anomalous layers, variational approach 79−44260
propagation in cylindrical coord. systems 78−88798
propagation in highly scattering medium, diffusion approach 77−86804
propagation in layered transition zone between mantle and core *(Italian)* 79−12071
propagation in medium with randomly distrib. inhomogeneities, wave attenuation and scatt. *(Hungarian)* 77−86791
propagation in non-ideal elastic medium, spherical sources 80−3941
propagation in nonplanar struct., high-freq. glorified optics technique 79−66629
propagation in oil shale, dynamic modelling, Maxwell model 78−57196
propagation in two-phase media, interaction model 78−18213
propagation rel. under model and natural conditions, similarity criteria in comparative anal. 79−96742
propagation through cracked solid, polarisation rel. to dilatancy 78−61342
propagation through spherical body with linear vel. function, intensities and travel times 77−56582
propagation velocities in subsurface soil layers 79−62460
propagation velocities investigation, new methods using common-point obs. *(Russian)* 79−74981
PS-waves refl. from Moho 77−86809
pulse propag. in media with freq. dependent Q, theory 80−72438
pulse propag. in porous elastic solid 77−73677
PV waves station corrections for Cracow, Homogeneous Magnitude System 80−8254
Q_{ScS} frequency dependence 80−56381
Q-factor of Earth, body wave and surface wave studies 79−39682
Q-frequency depend. of coda, surface-body wave hypothesis 80−21660
Qiaojia and Shimian, China, small earthquakes source parameters and potential danger *(Chinese)* 77−9341
quasi P-SV waves in transversely isotropic media 80−36266
radial and spheroidal oscills. of elastic sphere 79−44130
radial velocity anomalies in lower mantle, identification using interference method 79−25209
radiation from a finite cylindrical explosive source 78−61340
radiation from spherical wave sources, seismic model 79−8612
randomly-structured layered medium, wave field neglecting multiple reflections 77−53000
Rat Island earthquake sequence, 1965, seismic scaling information 79−12076
ray amplitudes of compressional, shear, and converted body waves in laterally inhomogeneous media 80−56408
ray approx. for laminated heterogeneous media spectral charact. *(Russian)* 78−69482
ray paths and relative intensities in one- and two-dimens. vel. models 77−25649
ray series method and dynamic ray tracing system for three-dimensional inhomogeneous media 80−98456
ray tracing, three-dimens. methods 77−73870
ray tracing, through models of E.African Rift 78−11846
ray tracing with specified end points in constant vel. layers 77−64213
Rayleigh channel waves for reflection method, dipping coal seam discontinuity obs. 78−69471
Rayleigh channel waves propag. in coal seams, model seismic expt. *(German)* 78−40513
Rayleigh dispersion function computations for unlimited freq. values 80−21837
Rayleigh higher mode phase vels., regional var., spatial filtering 78−77187
Rayleigh in trench 80−98266
Rayleigh mode dispersion in upper mantle of W.Europe 77−73693
Rayleigh surface waves, interaction with structures 78−81109
Rayleigh surface waves, principal mode and harmonics obs. for earthquakes focal depth determ. 78−61351
Rayleigh wave amplitude attenuation across Eurasia 77−91028
Rayleigh wave amplitude meas. from earthquakes in distance range 0-150° 78−48979
Rayleigh wave attenuation in volcanic area of Massif Central, France 80−98264
Rayleigh wave dispersion along Reykjanes Ridge rel. to lithosphere age 79−88267
Rayleigh wave dispersion and rifting in Tyrrhenian Sea 80−56445
Rayleigh wave dispersion in visco-elastic solid *(Japanese)* 77−17035
Rayleigh wave dispersion over Canadian Shield 77−91029
Rayleigh wave dispersion rel. to mantle structure under north central Italy 80−3977
Rayleigh wave flattening corrections 77−40987
Rayleigh wave microseisms, geological control on three-component spectra 79−84122
Rayleigh wave phase velocities, intrinsic oceanic upper mantle heterogeneity effect 77−49022
Rayleigh wave phase vels. rel. to upper mantle struct. in Apennines 78−53618
Rayleigh wave scatt. from uneven topography or inclusion, theory 80−36263
Rayleigh wave signatures from Nevada Test Site (NTS) explosions, inferred crustal structs. 79−66632
Rayleigh wave study of crustal and upper mantle structure beneath Apennines 80−46153
Rayleigh wave transmission coeffs. through vertical interface 80−46144
Rayleigh waves, dispersion in Walvis Ridge rel. to lithospheric struct. 80−41412
Rayleigh waves, fundamental mode and harmonics, appl. to distant earthquakes focal depths determ. 80−21654
seismic waves continued
Rayleigh waves, great circle attenuation and group vel. for 150-600 s periods 77−49030
Rayleigh waves, great-circle, attenuation and group vel., regionalisation and pure path models 79−12091
Rayleigh waves, great-circle, inversion of global average group vels. and attenuation coeffs. 79−12090
Rayleigh waves, group vel. distribs. and upper mantle models, Pacific Ocean *(Japanese)* 79−70747
Rayleigh waves, higher mode, studied as individual seismic phases 79−62440
Rayleigh waves, inversions of high freq. $Q_\beta^{-1}(f)$ 77−33000
Rayleigh waves, long period, obs. phase vels. across Canadian shield 78−61346
Rayleigh waves, long-period fund. mode, global and regional phase vels. 77−73680
Rayleigh waves, modelling via broadband acoustic surface waves probe 78−23904
Rayleigh waves, phase vel. investigations in middle Europe 79−44136
Rayleigh waves, phase-matched filters appl. 78−45010
Rayleigh waves, regional differences in phase velocity and Q-factor 79−16413
Rayleigh waves, scatt. by ridge 77−78125
Rayleigh waves, sub-oceanic, amplitudes rel. to tsunami warning system 77−81806
Rayleigh waves, surface topography effects on propagation 77−37154
Rayleigh waves, teleseismic, anal. for S.California regional S-wave struct. determ. 79−92510
Rayleigh waves from point source in spherical medium with homogeneous layers 78−92790
Rayleigh waves group vel. in Cap Vert and Canarian Basins *(French)* 77−32999
Rayleigh waves higher modes to determine upper mantle struct. 80−104890
Rayleigh waves of period 50 seconds, group vel. distrib. in Pacific Ocean 78−65197
Rayleigh waves refr. and refl. in Tibet 77−78120
Rayleigh waves transmission and reflection through a step 78−44775
Rayleigh waves transmission prevention, trench performance, seismic model experiments 80−24727
Rayleigh waves under Pacific Ocean, group vels. and response 80−41398
raypath migration, using programmable pocket calculator 78−7784
raypath reflection model for layered media with source and receiver in different layers 80−83704
reactor struct. seismic response, modal response method 77−83059
real-time kinoform synthesis using chalcogenide glass films *(Russian)* 78−13669
reflected wave, appl. to cross seismic sounding data interpretation *(Russian)* 78−92796
reflected wave, time fields method for curved interfaces determ. in bidimensional inhomogeneous media *(Russian)* 79−35010
reflected wave method for media with variable vels., inverse case *(Russian)* 79−84525
reflected wave parameters, interpolation algorithm for vel. determ. *(Russian)* 79−88494
reflected wave recordings, allowance for vel. inhomogeneities in CDP data processing *(Russian)* 79−84526
reflected wave time-distance waves for laminated media *(Russian)* 79−84160
reflected wave travel times inversion 77−56595
reflected wave travel-time curve inversion theory 80−89968
reflected waves, spectral charact. in region of bright spot anomalies *(Russian)* 79−53319
reflected waves, travel-time curves, interpretation as head waves curves 77−9371
reflecting area parameters, estimation allowing for amplitude charact. correl. *(Russian)* 79−74856
reflecting areas, preassigned parameters rel. to boundary delineation *(Russian)* 79−74857
reflecting/refracting plane surface image, form. using two-point eikonal *(Russian)* 79−96740
reflection, refraction and diffraction in media with elliptical vel. depend. 79−5454
reflection amplitude rel. to oil well productivity 78−69295
reflection and transmission coeffs. in media with lateral inhomogeneities 77−37156
reflection at free surface appl. of Huygens' principle 78−7594
reflection at wide angles, travel times, interpretation method 78−65202
reflection coefficients, determ. from waves 79−44115
reflection coefficients, identification from noisy data 79−29718
reflection coefficients for layered media, fast computer program 77−49186
reflection coeffs. and response for horizontally layered media, direct and inverse problems 78−28173
reflection data inversion 78−96307
reflection seismograms, calc. in freq. domain 78−96152
reflection seismograms, simultaneous spherical divergence correction and optimal deconvolution 80−98258
reflection sounding in Precambrian rocks 79−79743
reflections and refractions from curved interfaces: model study 78−69294
reflector parameter estimation by virtual image technique 78−40681
refracted transverse, influence of adjoining media charact., on the amplitude 78−94614
refracted wave correlation method, interpretation accuracy *(Russian)* 80−85758
refracted wave field digital filtering allowing for ray diffraction *(Russian)* 79−88495
refracted wave hodographs, inverse problem interpretation *(Russian)* 79−34762
refraction delay time, appl. as weathering correction method 79−44255
refraction method appl. to faults prospecting, model expt. and features of seismograms *(Chinese)* 79−12286
refraction methods for tectonic dislocation detection *(Russian)* 78−12010
refraction parameters, nomogram for rapid computation 78−7785
refraction waves, time-distance curve analysis methods *(Japanese)* 77−17038
refractive index distribution, image reconstruction via iterative ray tracing between boreholes 80−98466
refractor velocity determ., cause and nature of errors 80−56621

seismic waves continued
regular wave detect. using similarity factor *(Russian)* 77−86819
regular waves with fluctuating parameters, separation efficiency of linear multichannel systems *(Russian)* 79−39922
residual statics anal., general linear inverse problem 77−17031
response of flexible cylindrical liquid storage tanks 79−31241
reverberation periodicities, appl. to Earth crust structure investigation 79−66820
ringing P-waves and submarine faulting 79−84158
rock elastic props., expts. on two-phase aggregates 80−56463
rock rupture by elastic shock wave superposition in multiple detonations *(Russian)* 77−35082
rock samples, dry and water-saturated, at high press., elastic wave vels. and v_P/v_S ratio 79−92529
rock seismic wave attenuation, role of crack and grain boundaries 80−72495
rocks, crystalline, from Michigan Basis, seismic vels. rel. to microcracks 79−39705
Rumania, 1977 March 4 earthquake, specific defect of area *(Rumanian)* 79−20768
rupture incoherence influence on seismic directivity 79−12077
S_n waves, propag. through Bering Sea and NW.Pacific Ocean 80−51346
S and ScS waves from Sea of Okhotsk earthquake, rel. to lithospheric slab penetration into lower mantle 77−73700
S times for deep-focus Indian earthquakes 78−77188
S-wave anisotropy in the upper mantle under a volcanic area in Japan 80−90024
S-wave far-field spectra, corner freqs. and pulse shapes 79−84153
S-wave propag. from explosion in transversely isotropic medium 78−81110
S-wave short-period attenuation under W.United States 80−98242
S-wave travel times for a spherically averaged Earth 79−8601
S-wave vel. meas. in soil and bedrock using down-hole method 80−98458
S-wave velocity, lateral var. in upper mantle, Rayleigh mode data 79−66643
S-wave velocity versus depth in marine sediments 77−17034
S-waves, from explosions, anisotropy in continental upper mantle 77−49014
S-waves, type II, refl. and refr. in elastic and anelastic media 77−52986
S-waves, vel. anomalies rel. to Japanese subducting lithosphere 79−92489
S-waves, vel. struct. of upper mantle in New Hebrides island arc convex side 79−74861
S-waves means free path under Kanto district, Japan 79−79748
S-waves travel times, resolving power of data simultaneous inversion 79−16699
S-waves vertical distrib. of vel. at Iwatsuki Deep Borehole Observatory, Japan 79−62457
S-waves with continental ray path integral over time along ray path of inverse Q, calc. 79−48408
Sainte-Marie-aux-Mines observatory, underlying crustal struct. from analysis of converted P_s waves *(French)* 77−73666
San Andreas Fault, vel. contrast, P-wave nodal plane distortion 78−65188
San Andreas fault zone, seismic vels. rel. to constitution at depth 79−12097
San Fernando earthquake, 1971, foreshock wave forms rel. to fault zone struct. heterogeneity 79−66626
San Fernando earthquake, 1971 Feb. 9, source finiteness, teleseismic body waves 78−92781
San Fernando earthquake, 1971 February 9, source mechanism and aftershocks anal. 77−49023
San Fernando earthquake, strong ground motion, ray models 80−61762
sandstone, dry and saturated, P and S wave attenuation, US obs. 80−72494
sandstone, propagation vel. 80−76915
scattering and diffraction by canyons 79−88300
scattering by rough core-mantle boundary 78−61345
scattering of horizontally-polarized shear waves by surface irregularities 78−77184
scattering of SH waves from harmonic point source by sphere 78−77185
screening effect of petroleum deposits *(Russian)* 77−44939
ScS multiple waves, attenuation operator 77−52995
ScS travel time residuals, rel. to differences between continental and oceanic mantle 77−29253
seafloor propagation of earthquake wave, theory 80−81843
seismic coda of local earthquakes, synthesis method 77−73683
seismoacoustic activity distrib. near coal bed face 78−73320
self-adaptive wave train subtraction, in linear and three-dimensional surveying *(Russian)* 78−40695
separation from records by interference system spectral synthesis *(Russian)* 77−91043
separation theory for quasiregular waves 77−9366
SH, of central California earthquakes in 1972, appl. to source parameters determ. 77−2112
SH channel wave attenuation in coal seams with discontinuities 78−69292
SH wave equation soln. for scattered field near plane boundary 77−86788
SH wave motion, connectivity theory, application to seismic wave scattering 79−88306
SH wave propag. in heterogeneous media, from line source 80−81842
SH wave propag. in medium with step-shaped discontinuity 77−56602
SH wave propag. in two-layered heterogeneous medium 78−48976
SH wave scattered by cavity of arbitrary shape 80−51341
SH waves, complete theoretical seismograms generation 77−45179
SH waves, complete theoretical seismograms generation 77−45180
SH waves, generation of complete theoretical seismograms 78−40498
SH waves, theory and obs. for epicentral distances greater than 90° 77−81811
SH waves diffraction by rectangular impenetrable wedge 77−86780
SH waves due to shearing-stress discontinuity in viscoelastic half-space, displacement 80−56405
SH waves in anelastic media, ray-synthetic seismograms 80−98241
SH waves in Earth models with single discontinuity, ray-mode duality 78−77183
SH waves in infinite monoclinic crystal plate with initial stress 77−86789
SH waves in layered transversely isotropic media, wave approach 80−30991
seismic waves continued
SH waves in multilayered, laterally heterogeneous media, dispersion eqn. 77−73645
SH waves propagating in layered transversely isotropic media 80−36250
SH waves refl. and refr. at plane boundary 80−12339
SH waves scattering, linearised inverse problem, density perturbation soln. *(French)* 80−51333
SH-motion in general viscoelastic material overlying hard elastic matter 79−29715
SH-wave generation by dislocation sources, numerical study 79−92485
SH-wave propag. in heterogeneous media over homogeneous half-space 79−62446
SH-wave travel times and amplitudes for two well-constrained earthquakes 79−48407
SH-waves incident on cylindrical tunnel dynamic stress anal. of elastic liner 80−79201
SH-waves propag. in stratified medium with local inhomogeneities, finite element treatment *(Russian)* 79−34763
SH-waves ray-mode duality in Earth models with crust and mantle discontinuities 79−25213
SH-waves refl. and refr. in presence of slip and friction 79−46243
shallow crustal vels., phase time inversions for Galway Lake earthquake aftershocks 80−21634
shear and compressional wave vels. in porous rocks rel. to saturation 77−2114
shear modes in anisotropic systems, dispersion curves 78−36107
shear velocity discontinuities, effect on asymptotic overtone struct. of Earth torsional eigenfreqs. 77−78111
shear wave generator in borehole, construction, expt. results 78−40692
shear wave propag. in double layer, applied mag. field effects 77−70605
shear wave recording with geophones 80−101447
shear wave travel time residuals from oceanic earthquakes 77−64224
shear wave velocity structure for spherically averaged Earth 79−92504
shear wave vels. from down-hole meas. 77−70849
shear waves, crustal, anal. for Lithospheric Seismic Profile in Britain (LISPB) 78−73313
shear waves, polarisation anisotropy in Pacific Basin 77−49018
shear waves, Q estimation from S-SS spectral ratios 77−64218
shear waves computation by ray method 79−53532
shear waves excitation and propag. from Melanesia and Banda arcs to Australia 80−104887
shear-wave attenuation in crust and upper mantle, 0.05-25 Hz 80−36268
shock waves, propag. in silicate rocks with allowance for phase transitions 79−88347
short period P-waves, crustal struct. from spectral ratio response 77−73688
shot grouping in marine seismic surveying, potential efficiency *(Russian)* 78−40702
sign coding in seismic data processing algorithms *(Russian)* 79−62616
signal filtering, distrib. theory appls. *(Rumanian)* 79−58122
signal processing, solution of two-dimensional wave eqns. using recursive phase filter 79−86295
signal processing using inverse diffraction technique 80−74608
signals amplitude and phase jitter, rel. to optimal multichannel filtering evaluation *(Russian)* 78−40697
signals in wave field, estimate of number *(Russian)* 78−49157
Sinfengkiang Reservoir impounding earthquake, precursory V_P/V_S variations *(Chinese)* 78−3720
SKS amplitudes and travel times, outer core struct. model 78−65208
small shocks in Friuli, Italy, signal total durations and local magnitudes 79−34750
Sn transverse component, Love waves normal mode propag. in oceanic struct. 77−56583
soil, shear wave vel. meas. during standard penetration test 78−48978
soil amplification functions, stochastic approach 77−9358
soil interaction with surface mounted struct. under excitation by plane SH wave 78−22292
soil layer amplifying plane waves arriving at surface 80−76929
soil profile fundamental period estimation 77−9359
soil subject to stress wave, cavitation effects 79−70792
Solenhofen limestone, US propag. at high press. 79−29756
source location by surface waves, reference point equalisation method 80−72648
sources spectral theory, determ. of earthquake foci parameters 77−21687
sP and P amplitudes for fault plane soln. of shallow quake 80−51335
Sp waves, from upper-lower mantle transition cone, seismogram calcs. 80−104901
space-time functions integral representations in seismic holography *(Russian)* 78−85483
Spanish deep-focus earthquake, 1954 March 29, body waves and source process 77−9375
spectra, explosion earthquakes assoc. with 1973 eruptions of Asama Volcano *(Japanese)* 80−67340
spectral analysis, total field structure anal., autocorrelation functions 80−4142
spectral composition of wave field, effect of multiple scatt. *(Russian)* 79−8607
spherical waves normally incident on plane parallel absorbing layers, synthetic seismograms calc. *(Russian)* 79−39667
spheroidal modes, classification and nomenclature 79−44129
spheroidal modes and upper mantle structure 79−8603
spheroidal modes from 1977 Indonesian earthquake, attenuation obs. 80−81815
SS shear-wave travel time for Earth struct. 80−81817
statistical algorithm for interfering seismic wave correl. *(German)* 77−25787
statistical algorithms for scaling geophysical fields 78−73527
Stonely waves, direct meas. at Ni-Pyrex rel. to crustal seismic waves 78−10268
stratified elastic half space response 79−66641
stratum velocities determination using seismic data, iterative method convergence *(Russian)* 79−74982
stress relaxation earthquake models, finite difference calc. rel. to waves radiation 77−73682
strong earthquake foci dynamic parameters, from longit. wave spectra 78−57171
strong earthquakes, precision in hypocentre and dimens. determ. 78−57172
strong ground motions at short epicentral distance, simulation 80−104906
strong motion seismology 79−88271

seismic waves continued
strong motion short period accel. and vel. using fault model 80−104918
structural foundations, excitation by seismic surface wave 80−10182
structure independent velocity estimation 77−17029
structure seismic design, probable simultaneous response by response spectrum method 77−83060
subducting lithosphere boundary determ. using ScS to P conversions 78−7572
subduction beneath W.South America, evidence from converted phases 80−26484
submarine lithosphere, geophys., geochem. and petrological model 80−3994
supercritical reflected waves from essentially nonplane siesmic boundary, props. and peculiarities of record *(Russian)* 79−8606
surface displacement, extended asymmetric surface source in elastic half-space 80−36251
surface displacements of stratified half space, theory 80−56403
surface Rayleigh waves, magnitude MLV depend. on travel paths 77−21681
surface response, complete microzonation procedure importance and existing methods reliability 79−34748
surface seismic waves dispersion curves, partial derivatives calc. *(Russian)* 79−34764
surface wave and free oscillation problems, physical dispersion due to anelasticity 77−64231
surface wave anelastic attenuation lateral var. across Pacific 79−84123
surface wave contrib. to dislocation source in superficial multi-layers 79−44126
surface wave crossing a vertical discontinuity, refl. and transmission coeffs. *(German)* 80−76931
surface wave data inversion 77−37147
surface wave data inversion in source mechanism studies 77−33204
surface wave dispersion, digital processing *(Chinese)* 78−24374
surface wave dispersion, resolving power of data simultaneous inversion 79−16699
surface wave dispersion from earthquakes, use in Reykjanes Ridge crest study 80−90021
surface wave dispersion function, computations for unlimited freq. values 79−74848
surface wave group vel. determ., optimum filter 77−56736
surface wave inversion problem and upper mantle density 77−17039
surface wave investigation of Southwestern Germany and Switzerland rel. to geothermics *(German)* 78−53633
surface wave phase vel., partial derivatives calc. algorithm 80−4140
surface wave phase vels. in isotropic laterally inhomogeneous media 77−37155
surface wave study of crustal structure beneath Tibetan Plateau 77−91068
surface waves, anal. using PDP-15 interactive graphics 78−81427
surface waves, correlation method, appl. to tectonic dislocations prospecting in complex media *(Russian)* 79−8605
surface waves, dispersion across Iceland Plateau rel. to deep struct. 80−41413
surface waves, dispersion in Marie Byrd Land inhomogeneous ice sheet 79−66631
surface waves, higher mode, polarisation rel. to anisotropy in Eurasia upper mantle 77−49015
surface waves, importance in strong ground motion 79−84185
surface waves, inversion of dispersion data with random errors 77−73681
surface waves, method for separation of interfering waves and dispersion comp. 77−73649
surface waves, of July 1905 Mongolian earthquakes, anal. rel. to source parameters 77−37142
surface waves, phase vel. and attenuation simultaneous inversion, Love waves in W North America 78−85491
surface waves, theory and obs., review *(German)* 77−64227
surface waves analysis, new techniques appl. to Adriatic subplate averaged model 79−44159
surface waves and Earth structure 78−73323
surface waves and free oscills., evidence for lateral vars. 78−88799
surface waves anomalous propagation in Barents Sea, from NORSAR data 79−25202
surface waves azimuthal anisotropy, physical model 78−65186
surface waves from E.North American earthquakes, rel. to focal mechanisms and tectonics 80−3942
surface waves from Labrador Sea earthquake, 1971, December 7, source parameters determ. 77−91040
surface waves in three-dimens. struct., finite element matrices 80−61765
surface waves in vertically inhomogeneous elastic halfspace with horizontal inhomogeneity 77−52998
surface waves influenced by gravity, effects of anisotropy 80−8252
surface waves initial phase and phase vel. from 1968 Jan. 29 Shikotan earthquake 78−92793
surface waves propag. in crystalline media 78−2350
surface waves propagation over liquid and crystalline layers, elastic consts. of crysts. 80−76924
surface waves propagation over liquid and crystalline layers, theory 80−76925
surface-wave phase vel. inversion for anisotropic structure 78−85482
surface-wave phase velocity and attenuation simultaneous inversion 79−92488
surface-wave ray tracing, appls. 79−66630
surfaces waves, effects of gravity and viscosity 77−81797
synthesis using prediction error filter 79−62630
T waves from Tonga earthquake (June 1977), human perception on Tahiti 80−61769
teleseismic body wave radiation from seismic source in layered medium 77−9363
teleseismic body-wave forms, crustal structure modelling 77−91283
teleseismic P- and S-waves at Corvallis, Oregon, crustal and upper mantle structure 77−91067
teleseismic P-residuals temporal var. for southern California stations 79−16383
teleseismic P-wave residual anal. at Shillong, India, earthquake prediction 80−104921
teleseismic P-wave residual variations before Haicheng earthquake *(Chinese)* 77−37139
teleseismic P-wave residuals prior to 1974 November 28 Hollister earthquake, California 77−9356
teleseismic PP-wave reflections, Newfoundland lithosphere struct. determ. 78−65210
seismic waves continued
teleseismic short-period P-waves propag. through crust 77−56590
teleseismic Sn, guided wave in upper mantle 78−11823
Tennessee, seismic characts., surface wave dispersion study 79−48426
Texas shelf zone, seismic vels. and crustal struct. from sonobuoy and seismograph data 79−5462
theoretical seismogram calc. for thinly-stratified absorbing media 78−15973
theoretical seismograms of core phases from freq.-depend. full wave theory 78−7581
Thomson-Haskell method extension to non-homogeneous spherical layers 77−9362
three dimensional US wave model for refractional diffracted waves *(Chinese)* 77−62080
threefold seismic or acoustic holographic interferograms for improved reconstructed-image definition and contrast 80−23844
Tibet earthquake, 14 July 1973, source mechanism and seismic wave attenuation 80−36252
Tokyo, base rock depth, seismic wave obs. from explosions *(Japanese)* 77−64232
Tokyo, base rock struct. from seismic waves from Yumenoshima explosions 79−66654
Tokyo, underground struct. from Yumenoshima explosions seismic waves obs. *(Japanese)* 77−41000
Tonga, island arc, vel. anomalies near deep inclined seismic zone 77−73661
torsional normal modes eigenfreqs., asymptotic overtone struct., model study 77−78110
torsional waves, computation of complete theoretical seismograms 79−12289
transfer function for horizontally stratified media, unification of seismic and magnetotelluric problems 80−56622
transient and impulse responses of one-dimens. linearly attenuating medium, analytical results 78−32687
transient and impulse responses of one-dimens. linearly attenuating medium, parametric study 78−32688
transient disturbance prod. in elastic half-space by impulsive shearing traction 78−57786
transverse waves, propag. in rocks, in situ meas. 77−21682
transversely isotropic layered media, reflection and transmission 77−91025
transversely isotropic media, P-, SH-, and SV-wave vels. computation 80−98249
transversely layered isotropic media, seismic wave vel. calcs. 80−12344
travel time inversion, for 3-D vel. struct., Backus-Gilbert method 80−21838
travel time inversion, geometrical approach 80−3946
travel time inversion 79−70891
travel time residuals at Gauribidanur seismic array (S.India), rel. to crust-upper mantle heterogeneities 78−32033
travel times, low-velocity zone parameters determ. as functions of focal depth 77−86828
travel times, meas. via method of seismically conjugate points 77−9368
travel times in plane layered media, computation 77−41191
travel-time anomalies, statistical anal., rel. to earthquake prediction 79−57868
travel-time curve analysis using computer *(Japanese)* 77−17226
traveltime data nonlinear least-squares inversion 80−4124
tsunami, 1978 June 12, Miyagi Prefecture, Japan *(Japanese)* 80−41401
tsunami, damping in stratified ocean with rough bottom *(Russian)* 80−21651
tsunami, due to Izu-Oshima-kinkai earthquake, Jan. 1978, source mechanism 80−41393
tsunami, generation and propag., simulation using shallow water eqns. 80−41407
tsunami, island of Hawaii, 1979 November 25, numerical anal. by finite-element method 80−72449
tsunami, response of bay water *(Japanese)* 80−41399
tsunami accompanying Tonankai earthquake of 1944, source model *(Japanese)* 80−67344
tsunami along Mie coast, central Japan, 1707 and 1854 records *(Japanese)* 80−41402
tsunami at Oshima (W.Hokkaido), 1741 August 29, religious monuments *(Japanese)* 80−67345
tsunami caused by Izu-Oshima-kinkai earthquake, Jan. 1978, source mechanism *(Japanese)* 80−41392
tsunami data, estimation of magnitude of great earthquakes, 1837-1974 period 79−79745
tsunami earthquakes and subduction processes near deep-sea trenches 79−84155
tsunami from Sanriku earthquake, 1933 March 2, initial motion rel. to dislocation model 80−31000
tsunami generation and propag. in ocean with real bathymetry, numerical simulation 78−40576
tsunami height rel. to earthquake mag., empirical relation 80−94461
tsunami prediction, overview and recommendations 79−8703
tsunami prediction and magnitude, coastal radar system appl. 80−82101
tsunami solitary wave, height vars. in near-shore zone 79−16507
tsunami source model from fault parameters, reliability 79−44128
tsunami type plane wave, Coriolis force effect *(Russian)* 78−77193
tsunami wave generation by finite bottom displacement *(Russian)* 80−109113
tsunami wave propagation anal.; 2-step explicit finite element method 78−40503
tsunami with Miyagiken-oki 1978 June 12 earthquake *(Japanese)* 80−41400
tsunamis, historical, in Japan Sea, behaviour and source areas 78−65198
tsunamis, large, occurring off Sanriku district coast, simulations *(Japanese)* 78−65199
tsunamis, local behaviour 78−40577
tsunamis, theoretical research, obs. in Japan 78−40575
tsunamis, transform. in coastal zone 78−77192
tsunamis from large thrust earthquakes, implications for fore arc basins development 79−57905
tsunamis in Kanto, 1677 and 1703, behaviour along Kujukuri-hama coast from old monuments *(Japanese)* 80−67339
tsunamis propagation, finite difference simulation, book contrib. 80−3956
W. Turanian platform, reflected and refracted seismic wave data rel. to crustal models *(Russian)* 78−40526

seismic waves continued
two-dimensional refl. time-delay curve, approximation for arbitrary refl. surface *(Russian)* 79−44132
S.Tyrrhenian Sea region, seismic wave study of crustal struct. 80−41380
underground explosions, seismic wave spectra forecasting from preliminary detonations 77−44930
underground nuclear explosions, T-phase recordings at Rarotonga, S.Pacific Ocean 79−84138
United States, attenuation of strong ground motion 80−81834
W.United States, horizontal ground accel. attenuation rel. to magnitude 80−104905
E.United States, Rayleigh and Love wave velocities 80−56385
United States, upper mantle seismic struct., inversion of body wave arrival times 79−53322
upper mantle, travel-time branches from Yellowknife seismic array data 78−65211
upper mantle S-wave velocity model, based on great circle Rayleigh waves 80−109107
US pulse transit times, simultaneous stress and strain monitoring 77−91046
USA east coast P-wave vels. 77−86792
USA Midwest, ellipticity of Rayleigh waves 77−73648
Ust'-Kamchatka earthquake, 1971 December 15, P-wave study 78−73317
V_p/V_s as a potential hydrocarbon indicator 77−17102
v_p/v_s ratio and hypercentre determs. for aftershocks from 1976 May 6 Friuli earthquake 78−24258
V_P/V_S ratio space-time distrib. in Chuyskiy depression and mountain framework 79−74853
V_P/V_S ratio spatial and temporal changes before earthquakes in Kamchatka 78−32027
v_P/v_S ratio spatial and temporal vars. prior to strong earthquakes, Kamchatka 79−39657
V_p/V_s variations, earthquake prediction, case history, Chinese earthquake 1976 November 79−57869
V_P/V_S variations before and after Haicheng earthquake *(Chinese)* 77−37140
variable angle seismic reflection-refraction profiles, oceanic upper crustal structure 79−70761
velocities, effective, in minerals, var. with press. and use in vel. prediction 79−44179
velocities, inaccurate data r.m.s. cubic spline approx. 80−17406
velocities, influence of lateral vars. on seismic refr. interpretation 77−21686
velocities in Aleutian crustal section, fine struct. 77−33017
velocities in geological strata with curvilinear boundaries, three-dimens. case *(Russian)* 79−39928
velocities in lower mantle, evaluation of finite strain eqns. of state using lattice models 80−96620
velocities in sediments, sonobuoy meas. in Bengal Fan, Sunda Trench, Andaman Basin and Nicobar Fan 77−86852
velocities in upper mantle of N.Cocos plate 79−57858
velocities inversion, for rock pore aspect ratio determ. 80−51387
velocities of compressional and shear waves in Earth lower mantle, radial var. 78−73316
velocities of Lewisian metamorphic rocks, high press., rel. to crustal layering in N.Britain 79−84137
velocity along Sanbagawa metamorphic belt in Shikoku area, SW.Japan 78−11830
velocity analysis, accuracy of determ. kinematic parameters of regular events *(Russian)* 79−39944
velocity anisotropy correl. with in situ stresses 77−91045
velocity anisotropy rel. to initial stress state in Armenia 79−44123
velocity anomalies, California, explanation 79−16384
velocity anomalies before and after earthquakes, curvature vars. of wadati diagrams *(Chinese)* 79−62435
velocity anomalies before and after strong and moderate earthquakes in W China *(Chinese)* 77−9340
velocity anomalies in dilatant rock 79−20821
velocity anomalies in lithosphere, P-time residual data inversion 77−73877
velocity anomalies in mantle under N.Atlantic 77−49024
velocity anomalies in Pamirs-Hindu-Kush upper mantle, mapping by graphical method 80−77146
velocity anomalies prior to rock failure and violent slip 79−16409
velocity anomalies rel. to local seismicity 80−3953
velocity calc. using reflection amplitude 78−69296
velocity change in S.Kanto area, study by Tateyama explosions *(Japanese)* 80−67338
velocity changes at pressure- and temp.-induced phase transitions 79−62447
velocity changes during fracture and frictional sliding 79−16408
velocity changes in deep interior, press. and temp. induced phase transitions 80−90034
velocity changes induced by rock dilatancy and fracture 79−16458
velocity data analysis using interference methods *(Russian)* 77−45193
velocity data used for rock mass quality classification 80−17248
velocity determ., allowance for intermediate and reflecting boundaries *(Russian)* 77−70612
velocity determ. by reflected wave method, thin stratification effects *(Russian)* 77−44936
velocity determ. from arrival times *(Spanish)* 77−86822
velocity determination, overlying sequence stratification effect *(Russian)* 79−39961
velocity determination in formations with curved interfaces *(Russian)* 78−53748
velocity dispersion and freq. depend. of rock elasticity 77−73727
velocity estimation, arrival time functions and max.-likelihood detector 78−45013
velocity estimation and downward continuation, wavefront synthesis technique 79−16392
velocity in unconsolidated sand reservoir, effect of brine-gas mixture 77−17030
velocity inversion in upper crust, for synthetic seismogram construction *(Japanese)* 80−94478
velocity profiles, synthesis from geotechnical data 79−88516
velocity profiles near Explorer Ridge (NE Pacific), deep sounding survey rel. to crustal struct. 79−39684
velocity structure below Hawaii island from local earthquake data 79−84195
seismic waves continued
velocity time variance from multiple explosive sources, Hollister, California 78−44779
velocity time vars. rel. to earthquake prediction problems 79−57870
velocity variations rel. to solid Earth tides 78−28183
velocity-density law, rel. to deep seismic sounding and gramimetry data combined interpretations 80−21845
vertical time-depth curve, automatic approximation via successive layer detect. *(Russian)* 78−40700
very long period, charact. of upper mantle *(French)* 77−78107
vibroseis signals with prescribed power spectrum 78−40495
Vladivostok earthquake 1973 September 29, seismic moment from P-waves and mantle Rayleigh waves 78−61354
volume and surface sources, due to laterally varying boundaries of elastic homogeneous layers 79−16397
Vrancea, Rumania, 1977 March 4 earthquake, seismic waves and intensity recorded in Poland 78−92779
Vrancea earthquake, 1977 March 4, recording peculiarities and source parameters 79−84170
wave fields and fronts reconstruction, numerical models appl. *(Russian)* 79−39923
wave groups arrival times and azimuth, minimum data technique for earthquakes global location *(German)* 80−56627
wave seismograms and earthquake focus fracture vel. 77−70606
wave-equation datuming technique, appls. and computations 80−51553
wavefront curvature in layered medium 79−29712
wavefront curvature theory, for laterally inhogeneous media 80−104908
wavelet estimation using short-time homomorphic signal 78−88930
wavetrain response to longitudinal excitation, US profiling 78−44786
weak explosion in deformed elastic material, elastic waves 77−56598
in weathered layer, wave front eqn. and travel time 77−78122
Weber function computation in the interference reflected-head wave amplitude 77−78117
Westerley Granite, changes in seismic vel. and attenuation during deformation 78−28221
xenoliths underlying Sierra Nevada batholith, anisotropic elastic vels. 77−64225
Zoeppritz's amplitude eqns. and Knott's energy eqns., computer program 77−40988
Fe alloy core containing slurry layers, motion and thermodynamics, seismic wave propag. 78−48993
Pn,Sn phases, high-freq., recorded on ocean bottom seismographs, spectral anals. 79−16400

seismographs *see seismometers*

seismology
see also earthquakes; lunar seismology; seismic waves; seismometers
abyssal fan sediment in Arabian Sea, acoustic velocity 80−72488
acoustic holography applied to seismic data processing 80−46268
acoustic imaging, source receiver coincident profiles 79−92615
acoustic impedance logs computed from seismic traces 80−56398
acoustic logging data, on-line computer interpretation techniques 80−90239
acoustic logging data averaging for seismic wave fields *(Russian)* 77−73673
acoustic reflection in discrete layered media, structure estimation accuracy 79−23108
acoustical imaging, US visualization and characterization, conf., vol.8, Key Biscayne, FL, USA (May-June 1978) 80−83720
active continental margins, earthquake foci three-dimensional projection 80−72453
active faults, aerial photographs interpretation *(Japanese)* 78−96124
active faults, research in urban areas, Japan 79−62471
Adak Canyon region, central Aleutians, seismicity and tectonics 80−61772
adaptive deconvolution, processing technique for time-varying seismic data 77−91287
adaptive deconvolution of seismic signals 77−91062
adaptive predictive deconvolution of nonstationary seismic data 77−87096
Aegean area, crustal struct. from deep seismic sounding 77−64239
Aegean region, crust and upper mantle struct. from deep seismic sounding 78−69308
Aegean region, geodynamics 78−69307
N.Aegean region, intermediate earthquakes rel. to crustal shortening 77−53028
Aegean Sea and surrounding regions, earthquakes rel. to active tectonics 78−96181
Afar region plate tectonics, seismic and volcanic evidence 80−21700
E.Afghanistan, shallow earthquakes and tectonic activity 80−72444
N.Afghanistan focal zone, statistical methods for seismic activity analysis 77−41201
southern Africa, seismicity and incipient rifting 77−81813
African lithospheric thickness from teleseismic delay times 78−11847
African plate, seismicity rel. to mantle convection pattern and stress system 77−81859
E.African Rift models, seismic ray tracing 78−11846
aftershock region of Off-Izu Peninsula earthquake, 1974 May 9, seismic waves attenuation 80−76926
aftershock sequences, implications of dilatancy-fluid diffusion theory 80−85604
aging and strain softening model for episodic faulting 79−79777
air gun array, high resolution or deep penetration survey, charact. 80−12557
air gun operational method, pulse generation 80−90234
air-gun arrays, efficient design 77−41193
air-gun arrays for marine prospecting, acoustic wave radiation 77−39177
Alaska, earthquake, 1964, March 28, static displacement data inversion anal. 80−30998
Alaska, earthquake periodicities rel. to lunar sidereal period 78−53621
N.E.Alaska, seismicity 77−64217
Alaskan Seismic Gap, effect of 1979 February 28 earthquake 80−109116
Alboran Sea, crustal seismic profiles 78−61370
Aleutian oceanic crustal section, fine struct. from seismic profile 77−33017
Aleutian subduction zone seismicity, volcano-trench separation, rel. to great thrust-type earthquakes 80−21655
central Aleutians, ocean bottom seismograph meas. 80−89978
central Aleutians, seismicity rel. to double Benioff zone and lithosphere unbending 78−32047

seismology continued
Alpine Longitudinal Profile 1975, first results 77−49172
E. Alpine region, seismicity and earthquakes assoc. with Bohemian Massif-Carpathians contact zone 80−104888
Alps, Longitudinal profile (Judenburg to Hozzupereszteg), refr. seismic meas. *(German)* 80−76916
E.Alps crusted struct., HD-profile (Vicenza to Innsbruck) preliminary interpretation 79−34765
S.America, earthquake migration, spectral anal. 80−85614
central America, earthquake periodicities rel. to lunar sidereal period 78−53621
N.America, effect of craton on distrib. of seismicity and intraplate stresses 80−98248
N.Anatolian fault zone, earthquake migration and seismic gaps 80−85613
Anchorage, Alaska, postseismic crustal uplift 77−86849
Ancona, Italy, seismological network 77−52989
Ancona (Italy) seismic area, strain meas. 77−86742
Ancona area, Italy, seismotectonics 78−65246
Ancona region, Italy, seismo-tectonic considerations *(Italian)* 78−40492
Andaman Sea crust, seismotectonics and tectonic history 80−8283
Andaman-Nicobar region, neo-tectonics and time-space seismicity 79−12082
Andean subduction zone, intermediate aseismicity and recent andesitic volcanism 77−49055
central Andes, seismic provinces rel. to Plio-Quaternary plate tectonics 77−29273
anelasticity of Earth interior, stress/strain relation 80−26471
anisotropy in continental upper mantle, evidence from explosion seismology 77−49014
anomalies associated with hydrocarbon bearing anticlines, location tool and theory 80−17234
anomalous seismicity changes prior to rock bursts rel. to earthquake prediction 77−91052
anomalous vel. zones, fan shooting and least-squares analysis 79−57857
E Antarctic craton sedimentary basins from seismic, mag., gravity and radar obs. 77−21733
Antarctica, seismicity meas. 77−86803
antipodal waves for Earth interior structure determ. 80−89972
antiseismic calc., stochastic model appl. 78−96139
NW.Apennines, seismicity and relation with surface structs. 79−34749
applied inverse problems, book 79−49017
AR method for seismic moment calcs. WWSSN instrument appl. 80−21828
Arctic basin, seismic and gravity profiles 77−33030
Arctic permafrost regions, seismic and resistivity obs. 77−41072
Arctic region, crustal studies by deep seismic sounding 79−48439
Arctic regions, seismicity (1908 to 1975) 79−48423
Argo Abyssal Plain, mag. anomalies, bathymetry and seismic struct. 79−29741
Armenian territory foundation, new struct. and age data *(Russian)* 79−74874
array anal. of surface waves, limits and possibilities 77−37150
array processor appl., advantages 79−70899
array recorded signals, apparent vel. and azimuth meas., computer programs 79−84522
Asal-Ghoubbet rift zone, Afar, 1978-9 geodetic survey after seismo-volcanic activity 80−46164
Asama Volcano, Japan, joint geophys. and geochem. obs. in 1977 *(Japanese)* 79−70771
central Asia, active faulting and Cenozoic tectonics of Tien Shan, Mongolia and Baykal 80−8278
Middle Asia, geomag. investigations rel. to seismic activity 80−26464
central Asia, seismic moments of major earthquakes and average slip rate 77−86796
central Asia, seismic risk zones from gravimetric data 77−70608
N.Atlantic, refraction studies of upper igneous crust and Layer 2 porosity estimates 78−53629
NE.Atlantic, upper crustal struct., seismic study 80−61784
Atlantic Ocean south of Bermuda, geophys. survey within Mesozoic mag. anomaly sequence 80−26492
Mid Atlantic plate boundary between Iceland and Azores, seismicity and earthquakes 79−88266
Mid Atlantic Ridge, 45°N, seismic vel. struct. of crust 79−25214
Atlantic S.E. of Azores, crustal struct. rel. to mag. anomalies and bathymetry 80−51384
Atlantic type continental margins, struct. from geophysical meas. 77−21702
Atotsugawa Fault, Japan, seismicity and focal mechanism of local earthquakes *(Japanese)* 80−94482
attenuation meas. of split normal modes for 1960 Chilean and 1964 Alaskan earthquakes 79−84120
attenuation of multiples in marine seismology by antiaveraging *(French)* 77−64215
Auburn Dam, case history for earthquake evaluation 79−88284
Aulneau batholith, Ontario, subcritical seismic crustal refl. survey 78−65213
NW.Australia, crustal profile across Archaean cratons 80−51352
SE.Australia, explosion seismic profiles and crustal evolution 80−51332
N.Australia, long-range controlled source seismic profile 79−16419
SE Australia, long-range seismic profile 77−44945
Australia, plate collision, seismic shear waves excitation and propag. 80−104887
Australia, siesmic risk estimates 77−53009
Australia, stress state of upper crust 77−9387
Australian seismological services 79−39915
Avalon zone, Atlantic Canada, extent determ. from mag., seismic and gravity data 80−12384
axisymmetric seismic response of thick circular plate supporting many rods, nuclear power plant appl. 80−1458
Azores, earthquake (1980 January 1), aftershock sequence and present day tectonics 80−104911
Azov-Kuban' oil-gas basin structure from seismic data *(Russian)* 80−85601
b-value changes during movement on cut surfaces in granite, lab. expt., rel. to earthquake prediction 79−12109
b-value time and space scanning, appl. to catastrophic earthquakes development monitoring *(Chinese)* 79−12072
b-values, vars. before large earthquakes in N.China *(Chinese)* 79−12073

seismology continued
b-values and seismic source models, tectonic stress vars. along active crustal fault zones 79−84150
Badra area, Iraq, microseismicity 80−56413
Baffin Bay continential margin and Lancaster Sound, seismic refr. meas., continental/oceanic crust boundary determ. 78−20368
Baikal and continental rift zones, deep struct. from seismic data 78−36130
NE.Baikal region, seismicity, interpretation 80−98217
SW Baikal Rift, crust and upper mantle struct. according to seismic data 80−94503
Baikal rift zone, seismic activity rel. to continental rift form. *(Russian)* 80−12364
Baikal rift zone, seismicity and earthquake focal mechanisms 78−36115
Baikal rift zone, seismotectonics 78−36134
Baja California, Mexico, microseismicity 77−40991
Balkan earthquake provinces, largest magnitudes third asymptotic distribs. 79−39669
Baltic Shield, lithospheric thickness from S-wave anal. 80−3978
Baltimore Canyon lease area, microzonation 79−84183
Banda Arc, seismic profiles rel. to continent-island arc collision 79−84211
Banda Sea, seismic refr. expt., crustal struct. 78−73335
Banda Sea (E.Indonesia), seismicity and fault plane solns. rel. to subducted lithosphere geometry 78−81131
Basilicata, seismic risk, geostructural map 78−65195
Bay of Biscay, seismic profiles rel. to rifting, crustal attenuation and subsidence 79−2209
Bay of Islands ophiolite complex, Newfoundland, seismic vel. struct 80−21688
Baykal regions, 1962-71 epicentre field structure 77−33006
beam forming with vibrator arrays, seismic field tests near Tulsa and Handy 78−61338
Beaufort Sea area, earthquake data, tectonic setting and stress study 80−3931
Bengal Engineering College, Howrah, India, catalogue of disturbances, 1970 February 77−13063
Bengal Engineering College, Howrah, India, catalogue of disturbances, 1970 January 77−21684
Benin Gulf, Africa, sedimentation and struct. of continental margin, seismic survey 77−21693
binary seismic holography, kinematic principle *(Russian)* 78−92795
Black and Azov Sea floors, seismic profiling, techniques and expt. results 80−89970
Black Sea continental platform, seismic prospecting method appl. *(Rumanian)* 78−20564
Black Sea transverse rise, geological and geophysical data 78−3754
Blanco fracture zone, microearthquakes location determ. using sonobuoy arrays 78−40504
blind zone problem with multiple refraction layer overburden, soln. 80−17241
blind zone soln. to hidden layers in horizontal or dipping refractors 79−74839
body force sources, gravitating Earth flattening approximations to propagators and Green matrices 77−33002
body-wave analysis of St. Elias, Alaska earthquake (1979 February 28) 80−104897
body-wave inversion method for Earth struct., using travel time and amplitude data 80−109108
body-wave seismograms synthesis, modified first motion approximation 78−73315
Bonin trench, landward seismicity rel. to seaward lithosphere flexure 79−57903
book 80−27055
bore hole explosion, elastic wave emitter model 77−33005
borehole acoustic velocity measurement system, within or between boreholes 80−51557
borehole explosions, mechanical impulse of plates *(Russian)* 79−62455
boundary delineation, with respect to reflecting areas preassigned parameters *(Russian)* 79−74857
boundary images reconstruction, numerical models appl. *(Russian)* 79−39923
S.Brazilian continental margin, seismic refr. and refl. study of struct. 77−21694
Bremmer series decomposition of solns. to lossless wave eqn. in layered media 78−53738
Brevard ductile deformation zone, N.Carolina, struct. and seismic refl. study 78−65289
British Columbia, crustal structure from seismic refr. profile 80−17236
British Columbia, seismic risk 77−13062
brittle rocks undergoing non-elastic deformation at high-press., elastic wave vel. *(German)* 80−36296
broadband recording and data processing system 77−49173
brontides associated with seismicity 80−12523
Bucharest, microzoning studies *(Rumanian)* 78−20365
Bucharest, seismic microzonation 79−88280
Burma and S China, seismicity and tectonics 80−89983
Caledonides of N.Britain, struct. contrast, seismic wave interpretation 80−3975
California, earthquake swarms and local crustal spreading along major strike-slip faults 79−66645
S.California, regional S-wave struct. from anal. of teleseismic Rayleigh waves 79−92510
S.California, teleseismic P-residuals rel. to mantle structure 80−3954
S California, upper mantle seismic velocity, regional variations 80−109111
California, zoning for surface fault rupture 79−88293
S.California coastal waters, risk evaluation 79−84184
S.California downwarping, tectonomagnetic anomaly and seismicity 80−21626
California earthquake parameters, statistics and model 80−104891
camouflet source of transverse waves, theory 80−101344
Canada, 1973 earthquakes, annual list 77−91059
Canada, 1975 seismograph operations 79−16414
Canada, seismic techniques for crustal struct. study 77−45169
W.Canada, seismicity, 1899-1975 period 79−5452
N.Canada, seismicity 77−81799
Canada, seismological research in Charlevoix region *(French)* 77−78116
E.Canada seismic risk, regional assessment 80−61774
E.Canada tectonically active region, magnetotelluric fields time depend. 80−26451

seismology continued
Canadian Rockies, seismic refraction survey and crust and upper mantle structure 77−53015
Canadian Seismic Array Monitor processing system 77−9517
Canadian seismic risk estimation, probabilistic methods 80−61773
Canadian seismograph operations, (1977) 79−66837
Canadian seismograph operations for 1974 period 77−25661
Cape Verde archipelago, underlying crustal struct. from seismic, mag. and gravity data 77−17052
carboniferous rock, cyclically layered, seismic response from synthetic seismograms 78−69293
Caribbean Sea floor, sedimentary cover struct. and thickness *(Russian)* 78−77212
Caribbean seismic network, preliminary results 80−61771
Caribbean seismotectonics, implications from Caracas, Venezuela 1967 earthquake 79−20761
Carpathian earthquake, 1977, March 4, precursory seismic processes rel. to prediction *(Russian)* 78−48985
Carpathian region, expected earthquakes, max. magnitude, seismo-tectonic anal. 77−53002
Carpathian region and Ukrainian shield adjacent slope, basic crustal surfaces, seismic obs. 80−89995
Caucasus, max. possible earthquake and shakeability maps 77−70607
S.E.Caucasus, young tectonic disturbances and seismicity 79−44165
cavity radius estimation for contained nuclear explosions 79−16712
Central Asia seismicity, historical and modern data 80−36254
Chagos-Laccadive Ridge, earthquake swarm and tectonic implications 79−16395
Chagos-Laccadive Ridge (Indian Ocean), geophysical study 77−44952
Chandler wobble, seismic excitation 80−26437
Charleston-Summerville area of South Carolina, Geological and geophysical studies of seismicity 78−11837
N.China, 1966 earthquake series, Joint Epicenter Determ. 77−40994
China, geophysical methods of seismology and earthquake prediction *(Rumanian)* 80−8257
China, seismicity and Quaternary faulting 77−40995
China, seismicity and seismotectonics charcts. *(Chinese)* 79−16406
NE China, seismicity rel. to physical interpretation of Haicheng earthquake prediction 77−49028
S China and Burma, seismicity and tectonics 80−89983
Chinese earthquake catalogue for evaluation of seismic risk 80−36258
Chinese earthquake history, point process anal. 80−85612
Chu depression basin, seismicity changes with time 77−53003
circular fault, slip and stress drop 77−73641
Claerbout equation, alternative derivation 79−84135
class 1E equipment, seismic qualification 78−78475
classification of rock mass qualities, vel. data 80−17248
coal formations seismic tracing, interference waves appl. *(Russian)* 79−74858
coal prospecting by seismic profiling, new technique testing 80−17404
coal seams, synthetic seismogram calc. with reflectivity method 79−74844
coal seams fault indication using acoustic array processor 80−85778
coherency weighting, suppression of long leg multiples 79−92613
Colima earthquake, Mexico, Jan. 1973, source mech. and aftershocks 80−81823
Colombia basin, Caribbean Sea, crustal struct. from profiler-sonobuoy meas. 78−28198
S.W.Columbia, active plate boundary dynamics, deep seismic sounding study 77−13074
combined spectral analysis of seismic records, for determ. of geologic section props. *(Russian)* 78−40696
common depth area algorithms in complex seismic conditions *(Russian)* 77−44937
common depth point effective velocities, critical values for stratified homogeneous forms *(Russian)* 79−39668
common depth point ray modelling in presence of three dimensional isovelocity layers 77−21914
common depth point seismic data stacking, weighting coeffs. *(Russian)* 77−86816
common depth point seismic profiles, arc-shaped line-ups nature anals. *(Russian)* 79−44134
common depth point seismogram, signal and noise separation in amplitude spectra *(Russian)* 78−15970
common depth point survey data, vel. characts. determ., refl. interfaces inclination angles *(Russian)* 78−53753
common depth point survey technique appl. in permafrost conditions *(Russian)* 78−53751
common depth point technique efficiency for inclined reflecting surfaces *(Russian)* 79−84527
common-depth-point method, prestack migration method for deformed refl. layer 80−98251
common-depth-point stacking, appl. of multirate digital filtering approach to interpolation 79−29876
complete microzonation procedure, importance and existing methods reliability 79−34748
complex trace analysis and colour encoded data display 80−21646
compression experiments on Gabbro, microcrack development and seismic vel. anal. 80−17250
compressional wave velocity and damping, minerals and rocks at high-press. *(German)* 80−31031
computer-aided seismic anal. and discrimination, bibliography 77−81832
computer-aided seismic anal. and discrimination 77−81815
computer-aided seismic analysis and discrimination 78−20530
computerised data processing, petroleum industry appl., automation level analysis 78−28327
computerised seismic data processing, Fourier transform wave filter appl. *(Chinese)* 79−96838
Concepcion Bank, off Morocco, crustal struct., tectonic unit of volcanic origin 79−39689
conference, New Delhi, India (March 1978), earthquake prediction 80−85602
conference, Nov. 1979, New Orleans, USA 80−81891
connectivity theory, application to seismic wave scattering, SH wave motion 79−88306
continental basement exploration by seismic reflection profiling 78−96172
continental crust, seismic refl. studies rel. to struct. and comp. 79−16420
continental tectonics and seismicity, review 79−44160
continents, deep seismicity rel. to epicentre distribs. *(Russian)* 79−39670

seismology continued
continuous seismic profiling with two receiver systems, effective vels. determ. 80−31150
contouring irregularly spaced data 77−64180
Coral Sea, crustal struct. from seismic data 80−72459
core boundary discovery, historical aspects 80−105486
core fluid oscillations, transverse motion, Earth rot. effects 80−89965
corrective gradient projection method applied to seismic array processing 77−17222
correlation of seismic events in time section, algorithm *(Russian)* 79−39962
Coso geothermal area, underlying low-vel. body, teleseismic evidence 80−90005
Coso Hot Springs, Known Geothermal Resource Area, model 80−90004
Coso Range, California, seismicity 80−89971
Coyote Lake, California (1979 August 6), local magnitude and seismic moment determ. 80−104904
crack anisotropy in NW.England Carboniferous Limestone, in-situ methods 80−17240
crack propagation theory, Lamb's problem for a point source 80−56375
Crimea, seismic processes rel. to tectonics *(Russian)* 78−3721
Crimean mountains, crustal structure from deep seismic sounding *(Russian)* 78−3732
cross seismic sounding, data interpretation via reflected wave method *(Russian)* 78−92796
crust and mantle, temperature-depth profiles, Poland, from geothermal and deep seismic sounding data 78−48988
crust deep structure, determ. via nearby earthquakes converted seismic waves 80−30999
crustal, deep structure to NW of Cape Verde Islands 79−2201
crustal deep structure model of East European platform *(Polish)* 77−21706
crustal deformation, viscoelastic, by finite quasi-static sources 79−39686
crustal dilatancy and short-period geomagnetic var. 77−2096
crustal low-velocity zones, compressional wave vels. meas. in rocks at high temps. and press. 80−41435
crustal movements, conf., Palo Alto, California, USA (July 1977) 79−79785
crustal seismic reflection studies, Canadian Shield, weighted vertical stacking 77−87089
crustal structure, investigation via seismic reverberation 79−66820
crustal structure along international DSS profile VIII from Russian to Poland 77−21705
crustal structure in Marcus Island Pacific Ocean 79−53331
crustal uplift prior to earthquakes 78−7575
crustal velocity model, from seismic data, Kurinian depression example 79−39678
crystalline basement, seismic anisotropy 77−64221
Cuba, seismic risk estimation 79−74852
Cuba crustal struct. study, earthquakes exchange waves method appl. *(Russian)* 79−44158
Cuvier Basin, off W.Australia, crust form. by rifting, seismic study 80−12368
data analysis, appl. of wavefront curvature expression in layered medium 79−29712
data analysis, random values separation *(Russian)* 79−74983
data collection and anal., detect. of possible violations of Nuclear Test Ban Treaty 79−39919
data compression in microprocessor-based data acquisition systems 79−12270
data deconvolution, review 78−53736
data filtering and smoothing, least-squared error, stationary and nonstationary 80−4158
data migration by Fourier transform 78−77341
data migration in two and three dimens., integral formulation 78−77342
data processing, Karhunen-Loeve transform. appl. *(French)* 79−44258
data processing, predictive deconvolution method appl. 79−8725
data processing hardware developments 77−60355
data reduction, approximate realisation, new techniques 79−70898
data simultaneous inversion, resolving power 79−16699
Dead Sea region seismicity over past 4000 years 77−73687
Dead Sea Rift and adjoining areas, gravity and seismic data rel. to density distrib. 79−57893
Dead Sea-Jordan Rift, archaeological evidence for Subrecent seismic activity 77−86810
deconvolution, for extraction of reflectivity function from seismic trace, book contrib. 79−92635
deconvolution, influence of phase prop. of random noise finite realisation 79−44254
deconvolution and wavelet estimation 78−20542
deconvolution of data using homomorphic filtering 77−91063
deconvolution of seismic data, overview 77−91060
deconvolution of seismic data using homomorphic filtering 77−81823
deconvolution with l_1 norm 79−88484
deep crustal structure beneath Wind River Range, Wyoming, USA 80−46141
deep earthquakes, brittle fracture model rel. to pore fluids and Q 79−39671
deep focus earthquakes, P-waves amplitudes and magnitude corrections 77−86797
deep interior, magnetoviscoelastic wave refl. and refr. at welded contact 80−89967
deep probing and refraction seismograms, computer processing *(Russian)* 79−84528
deep reflections, unravelling via seismic stripping 79−34970
deep seismic data processing, digital techniques appl. *(Italian)* 78−40719
deep seismic data processing procedure *(Russian)* 79−21036
deep seismic profiling, Atlantic Ocean, automatic processing of bottom seismograph records 78−45030
deep seismic sounding, automation of obs. and processing of ocean-bottom seismograph recordings 78−57339
deep seismic sounding and gramimetry, combined data interpretation 80−21845
deep seismic sounding for studying seismic anisotropy of crust and upper mantle 77−70855
deep seismic zone, Tohoku, Japan, freq.-magnitude obs. rel. to geochem. changes 80−72447
deep sounding, computer-aided data interpretation 77−41202
deformation, fracture and elastic wave vel. correls., Fourier anal. *(German)* 77−70604

seismology continued
Delaware River, evidence for former extension to Wilmington Submarine Canyon 77−37255
Delhi region, seismotectonics, earthquake data, strain distribs. 77−17044
Dellwood knolls, active seismicity rel. to role in triple junction tectonics off northern Vancouver Island 80−90067
depositional facies interpretation from seismic date 80−4122
depth determ. from seismic refraction data, iterative method 78−96302
depth migration after stack, finite-difference method 80−98254
depth migration before stack, finite-difference method 80−98255
depth sections from seismic time sections, regulated directional reception method *(Russian)* 77−45192
depth-time conversion with weighting *(Russian)* 77−45194
descending slab stress state, anal. of seismic source parameters 80−104946
detection probability for weak seismic events, theory 80−67347
detonation of ground vibrations from seismic detonation, ground vibrations 77−73667
Diablo Plateau region, W.Texas, preseismic deform. model for tectonic uplift 80−72481
diffraction properties of crust, using Earth crust models 80−98239
digital, seismic recordings, dynamic range compression *(Russian)* 79−39930
digital bandpass filters, filter type and operator parameters selection for instrumental realisation *(Russian)* 79−74984
digital filters for long and short period seismic signal extraction from noise 77−81824
digital generation of accurate synthetic seismograms 80−85779
digital processing of CDP seismic data for curvilinear reflecting boundaries *(Russian)* 79−84534
digital processing techniques for petroleum and natural gas 77−29469
digital seismic data processing, struct. anal. of graphs *(Russian)* 78−53749
digital seismic prospecting, in oil and gas bearing provinces of Ukrainian SSR 79−96836
digital signal detect. system *(Russian)* 77−29515
digital signal modelling and classification with the teleseismic data 78−73325
digital signal processing appls. 79−29915
digital time-domain finite length filter, exact wave-shaping 77−2266
dilatancy in dry rock, quantitative model and appl. to Westerly granite 79−16445
dilatancy induced fluid migration and vel. anomaly 77−33065
dilatancy induced seismogram polarisation anomalies, and earthquake prediction 80−101342
dip selective migration vel. determ. 77−41187
direct inversion procedure for Claerbout's eqns. 80−21645
discrete time series spectral estimation novel aspects 77−91336
discrimination between Eurasian earthquakes and explosions from P codas spectral characts. 78−7576
discrimination between explosions and earthquakes 78−11809
discrimination between induced and natural earthquakes in geothermal area 80−101332
dislocation modelling of creep-related tilt changes 78−92801
dislocation sources, gravitating Earth flattening approximations to propagators and Green matrices 77−33002
dislocation theory appl., book contrib. 80−109119
dispersion in seismic data, continuous representation technique 80−51334
displacement field close to focus of earthquake, calc. *(Russian)* 78−65204
display-equalised filter for freq.-time anal. 77−73650
diving waves in multilayered medium, time-distance curve transformation 78−69472
Dnieper-Donets depression, sedimentary cover struct. along Jagotin-Baturin profile *(Russian)* 78−92806
Dong-Xing Oil Field, seismic survey, three-dimens. interpretation of complex fault struct. *(Chinese)* 79−100833
double seismic zone in downgoing slabs and mesosphere viscosity 80−26472
down-hole meas. of shear wave vels. 77−70849
dynamic parameters of seismic sources, explosions and earthquakes 79−84141
dynamic poroelasticity, fundamental soln. rel. to pore fluid effects on seismic wave propag. 79−74847
dynamic problems in horizontally-layered media discounting multiple reflections *(Russian)* 77−91041
Earth core synthetic seismograms, full wave theory and reflectivity method 80−61777
Earth crust, seismic activity rel. to struct. and evolution 79−96749
Earth crust, tectonic deform. characts. from seismological data in China *(Chinese)* 80−76951
Earth crust and upper mantle structure, experimental study by converted waves *(Chinese)* 79−12093
Earth crust investigation, gravity and seismic methods combined appl. *(Russian)* 79−74987
Earth free oscill., radial mode Q-value using 1977 Indonesia earthquake data 80−67346
Earth free oscill. spectra, coupling and attenuation of near reson. multiplets 80−61778
Earth free oscillation data inversion, asymptotic approach 79−92624
Earth free oscillations, finite element modelling 80−51338
Earth free oscillations, unresolved split normal mode multiplets spectra 79−74845
Earth interior sounding iterative ray tracing between boreholes for underground image reconstruction 80−98466
Earth mantle, seismic discontinuities rel. to garnet lherzolite high-press. phase equilibria 79−66687
Earth models, seismic sections construction using stacked recordings of controlled directional reception *(Russian)* 79−39960
Earth oscillations, corrections to eigenfreqs. due to dynamic shear modulus 77−81800
Earth Q-factor, results from seismic studies 79−39682
Earth strain measurements by bore-hole strainmeter at Matsushiro, seismic waves response *(Japanese)* 79−96745
Earth structure model based on torsional oscill. eigenperiods 80−90044
Earth structure seismic investigation, new methods using common-point obs. *(Russian)* 79−74981
Earth tremors true velocities, determ. from seismograms 79−96743
earthquake, elastic energy release, heat prod., and Earth inertia tensor changes 79−44106

seismology continued
earthquake, prediction, interpretation of vertical crustal movements in time-space domain 79−80056
earthquake acceleration hazard map, sensitivity to input seismic parameters 79−44111
earthquake ages, determ. in central Asia via lichenometry 79−92505
earthquake control, appl. of hydrofracturing stress measuring method 79−29885
earthquake cycle, asthenosphere readjustment effects on free surface deform. 78−85490
earthquake detectability, estimates for 478 globally distributed seismograph stations 78−15976
earthquake energy dissipation during propag., by solid friction 80−109106
earthquake fault mapping in Japan *(Japanese)* 80−51348
earthquake fault plane solution using theoretical P-wave seismograms 78−11822
earthquake focal depth determination method 80−56389
earthquake focal mechanism consistency, new parameter describing seismic activity *(Chinese)* 79−12074
earthquake focal mechanisms, classical study techniques 80−76918
earthquake frequencies, stochastic modelling *(Japanese)* 80−94480
earthquake location accuracy depend. on number of seismic stations 78−32025
earthquake magnitude correl. with focal parameters, theoretical basis 80−101338
earthquake magnitude scale, renormalisation 78−15977
earthquake mechanisms, Izu Peninsula, Japan 80−12345
earthquake moments and corner freqs., effects of free surface on body waves 78−85492
earthquake motions, dynamic response of submerged hemispherical shells 78−51110
earthquake occurrence as stochastic event, theoretical models 78−40491
earthquake precursors, classification 79−88264
earthquake precursors, conf., Jan. 1977, Tokyo, Japan 80−46146
earthquake precursory seismicity burst, long-term prediction 80−72441
earthquake prediction, appl. of geodetic research *(German)* 80−101317
earthquake prediction, based on geochem. meas., conf., San Francisco, USA (Dec. 1980) 80−90606
earthquake prediction, biosystem behaviour as precursor 79−39673
earthquake prediction, bursts of aftershocks as strong earthquakes long-term precursors 80−41406
earthquake prediction, electrokinetic and magnetic anomalies associated with dilatant regions in a layered Earth 79−39658
earthquake prediction, foreshock activity of 1971 San Fernando earthquake, California 79−66626
earthquake prediction, from micro-earthquake obs. near Wakayama city, Kii Peninsula, Central Japan 80−31001
earthquake prediction, implications of crustal deform. migration 79−79800
earthquake prediction, implications of tectonomagnetic studies in Tajikistan 80−26446
earthquake prediction, precursory aerosol anomalies 79−16407
earthquake prediction, rocks stress cycling and inelastic volumetric strain rel. to remanent magnetisation 78−88820
earthquake prediction, search for time-depend. P-wave travel times from mining explosions 78−44788
earthquake prediction, use of seismic acoustics *(Chinese)* 79−34759
earthquake prediction, via mag. behaviour of magnetite and rocks stressed to failure 78−32068
earthquake prediction, workshop, Strasbourg, France, (1980 January 31 to February 1) 80−62396
earthquake prediction and warning, theoretical review 79−5455
earthquake prediction from pseudo-periodicity of strong after shocks *(Chinese)* 80−76913
earthquake prediction using scale invariant inclusion theory 77−49032
earthquake recurrence rate curves and Rautian K energy class 77−56601
earthquake response spectra 78−41871
earthquake response spectrum amplitudes, probabilistic computation 79−8610
earthquake response spectrum estimation from stimulated spectrum 79−686
earthquake risk maps for Western Central Europe *(German)* 79−8600
earthquake risk prediction, as stochastic process 77−49029
earthquake seismic moment tensor elucidation from teleseismic data 80−104915
earthquake seismic moments beneath island arcs, phase changes and subduction vels. 77−33007
earthquake shocks, location with imperfect knowledge of seismic wave path hodographs *(Russian)* 79−35009
earthquake similarity laws 77−81808
earthquake source development, model, rel. to precursory phenomena *(Chinese)* 77−9339
earthquake source mechanism model for thermo-visco-elastic Earth 80−104886
earthquake spatial distribution, two-point correl. function 80−89963
earthquake strength, seismic spectra anal., predictions *(Chinese)* 77−49009
earthquake swarms, differentiation from foreshocks via similarity of seismic waveform *(Japanese)* 80−67342
earthquake swarms, model 77−44934
earthquake-source parameters, relation to magnitude 78−96154
earthquakes, automatic recognition and timing from single traces 79−66822
earthquakes, intermediate and deep focus, temporal var. of activity 80−3943
earthquakes connected with human engineering activity, tectonic and tectonophysical conditions for occurrence 77−81802
distant earthquakes focal depths, determ. from fundamental mode and harmonic Rayleigh surface waves 80−21654
earthquakes global location using minimum information *(German)* 80−56627
earthquakes maximum magnitude prediction, geotectonic method and appl. to N.Italy area 78−40493
earthquakes occurrence time forecasting results of expt. 79−53315
earthquakes precursor swarm, appl. to long-range forecasting 78−15975
earthquakes recurrence relations 79−39672
Echzell/Wetterau, earthquake, 1975 November 4, seismotectonics 78−40512
effective seismic input through rigid foundation filtering 78−29659

seismology continued
effective vel. determ. in 3-dim. reflection surveys with multiple coverage *(Russian)* 77−86818
elastic moduli of two-component systems 78−59302
elastic prestress in Earth interior, effects 78−77202
elastic relaxation coefficients for spherical cavity in prestressed medium of arbitrary orientation 77−73692
elastic source model for 1 Mton explosion in tuff 77−44927
elastic wave applications 77−19470
elastic wave fields, discrete wave number representation in three space dimensions 80−3945
elastic wave propagation in anomalous layers, variational approach 79−44260
elastic wave vels. of metamorphic rock mass, seismoacoustic methods 77−81871
energy density, math. modelling 77−78118
energy release in great earthquakes 77−86798
energy spectra and data systems of earthquakes 77−41005
engineering seismology, two-dimensional horizontal ground motions during earthquakes rel. to structs. design 79−48419
epicentre location procedure for RESMAC seismic array 80−56616
Etna, 1973 November seismicity 77−44956
Eurasia, lateral var. in struct. of upper mantle 77−33016
Eurasia, upper mantle anisotropy from polarisation of higher mode seismic surface waves 77−49015
N.Europe, Benelux region, upper mantle struct. from seismic data 80−21691
Europe, seismicity rel. to heat flow from preliminary map 79−70765
W.Europe, upper mantle P-wave vel., large scale variations 80−109112
E. and central Europe, velocity-depth distribution in upper mantle 80−3980
event classification, extraction and use of broad-band P-wave pulse 77−81830
events identification, appl. of non-linear stochastic models 79−16396
exact and asymptotic synthetic multiplet spectra on ellipsoidal Earth 80−21673
excitation of Earth's normal modes 77−37158
exploration problems of complicated basins, S.China appl. *(Chinese)* 79−100961
exploration seismology, wave refl., refr. and diffr. in media with elliptical vel. depend. 79−5454
Explorer ridge, marine deep seismic sounding survey 77−17048
Explorer ridge, off W.Canada, marine geophys. survey 79−25224
Explorer Ridge (NE Pacific), crustal struct. from marine deep seismic sounding survey 79−39684
explosion in brittle rock, props. gas cavity expansion, soil dilatation 79−8608
explosion profiling of deep crust struct., 2-D scheme 80−72637
explosion radiation pattern, cavity creation in prestressed media, theory 80−61780
explosion seismology, appl. to rocks mineral comp. prediction at great depths *(Russian)* 80−104956
explosion seismology, data processing, predictive dynamic deconvolution *(Rumanian)* 80−8454
explosion seismology, residual static correction problem, iterative soln. anal. 80−101334
explosion seismology data analysis *(Hungarian)* 80−21841
explosion seismology data analysis method for wave eqn. migration 80−90233
explosion seismology in boreholes, multiple wave intensity at large explosion-seismometer distance *(Russian)* 80−30994
explosion seismology in Central Europe, book 77−25662
explosion seismology primary signal form., effect of partial multiple refl. *(Russian)* 78−85484
explosions, line-up axis time shift correction algorithm *(Russian)* 79−62613
explosive sink rates for marine seismology 79−34753
facies analysis concepts 78−96151
Fairbanks, Alaska seismic zone, earthquake migration 80−101330
far field waves definition criteria *(Russian)* 79−39965
Farallon Escarpment vicinity, seismicity and tectonics 78−32018
fast Walsh transform configuration program derivation, appl. to seismic data processing *(Chinese)* 80−21853
fault gouge composition effect on frictional sliding stability 78−3759
fault location in underground coal seams 80−94613
fault mechanics and earthquake prediction, conf., Stanford, California, USA (Dec. 1977) 79−84143
fault model, frictional, earthquake sequence 80−30992
fault motion, energy balance 77−56593
fault motion in presence of friction and inhomogeneous initial stress, rupture propag. 77−86835
fault rupture model for seismic risk anal. 78−11810
fault strain field, included rectangular fault in semi-infinite media 80−98261
fault with arbitrary shape, fast computation of theoretical seismograms 77−9373
fault zone with finite thickness, frictional heating, comment 79−25215
fault-plane soln. from geodetic data inversion 78−12016
faulting, acoustic fluidisation theory 80−85653
faulting, simulation, expt. thermal fragmentation 78−96160
faulting inception in rock mass with weakened zone 77−33064
faulting rupture process, plane shear faulting model of earthquake *(Chinese)* 80−104893
faults prospecting via seismic refr. method, model expt. and features of seismograms *(Chinese)* 79−12286
Fennoscandia, subcrustal lithosphere seismic investigations 80−90009
Fennoscandia seismic risk, by recurrence periods 80−21664
filtering by sliding mean in seismic data processing *(Russian)* 77−86821
finite difference techniques for computing synthetic seismograms 78−73326
fluid-saturated rocks, elastic dilatancy and earthquake dynamics 77−21683
Fogo seamounts, anomalous upper mantle struct. indicated by P-wave rel. delays 78−85515
folded and crystalline basements of deep cavities, determ. from seismic data *(Russian)* 79−39692
Foothills fault system of Sierra Nevada, seismicity 78−92792
forg-arc basins off S.America, seismic reflection profiles 77−44943
foreshocks, characts. rel. to earthquake prediction and premonitory slip on faults 80−3944
seismology continued
foreshocks, differentiation from earthquake swarms via seismic waveform variability *(Japanese)* 80−67342
Fort Ross, California, earthquake sequence, March-April 1978 80−81824
fractured zone dip-angle and width, seismic determ. *(Japanese)* 77−17228
Frank's method for obtaining crustal shear strains from survey data 77−41177
free modes excited by Indonesia earthquake, Aug. 19th 1977 obs. 80−61767
free oscillation of Earth, attenuation of radial modes 80−89966
free oscillation of Earth, radial mode, damping by bulk attenuation 80−76928
free oscillations, amplitudes of split normal modes 78−40508
free oscillations, attenuation data inversion, fundamental and first higher modes 77−78113
free oscillations, eigenspectral estimates from decaying time series, uncertainty estimation 80−30993
free oscillations, perturb. theory, surface waves group vel. formulae 78−61349
free oscillations, rot. and elliptical splitting 79−88257
free oscillations due to earthquake, complex eigenfreqs. improved resolution in analytically continued seismic spectra 78−36106
free oscillations in gross Earth models, effect of attenuation 77−53005
free surface effect on calculated stress drops 78−65193
frequency selection, appl. to wedging out zones separation with intensive multiple wave development *(Russian)* 79−8706
frequency-magnitude relations, in NGSDC earthquake data file 80−81838
Friuli, Italy, May 6, 1976, earthquake sequence 80−81822
Friuli, Italy, tilting vars. and seismicity preceding 1976 May 6 earthquake *(Italian, English)* 78−48971
Friuli aftershocks, temporal var. of V_p/V_s ratio *(French)* 77−70600
Friuli area, NE Italy, seismicity, rel. to 1976 May 6 earthquake 77−73690
Friuli area (NE.Italy), seismicity 78−24233
Friuli Venezia Giulia region seismicity 78−24234
Friuli-Venezia Giulia region, A.D. 365-1976 earthquake catalogue 78−24230
Fruili area, seismic activity rel. to neotectonic movements 78−24229
Fruili-Venetia Julia region, regional geodynamics and seismicity 78−24227
Fuji river, active faults anal. by track etch method *(Japanese)* 80−109127
fusion reactors, JT-60, seismic anal., design changes 80−95425
Gabilan Range, central California, pressure-induced seismic vel. gradient 80−21635
Garm region, weak earthquakes space-time sequence 80−21653
Gauribidanur seismic array in S.India, quantitative assessment of crust-upper mantle heterogeneities 78−32033
GCFR core and core support struct., seismic model test 78−41869
generalized reflection coefficients for a layered medium and asymmetrical source *(Chinese)* 79−100964
generally stratified media, matrix methods 77−2116
geological section local inhomogeneities determ. by reflected-wave probing method *(Russian)* 79−39947
geological section prediction, appl. of seismic waves integral spectrum parameters *(Russian)* 79−8705
geometrical inversion for boundary shape between two layer stacks 79−16684
geophones, electromechanical feedback for low freq. equipment *(Russian)* 79−62618
geophysical elastodynamics, group theoretical formulation, seismic sources 77−78126
Georges Bank, NW.Atlantic, seismic vel. of sediments to 1.4 km depth 80−21644
Georges Bank Basin, stratigraphy, seismic correl. to W.Scotian Shelf 78−28231
Georgia Strait, British Columbia, seismic risk maps 79−88274
geotechnical data at selected strong motion accelerograph station sites 79−88310
geothermal energy prospecting by geophys. methods, review 78−7803
geothermal gradient at 1000 km depth 80−8260
geothermal steam, ^{222}Rn emanations, rel. to seismic activity 78−11832
Geotraverse Rhenoherzynikum, fault zones investigation by seismic refl. and refr. studies 80−90046
Geysers geothermal field, California, explosions and microearthquakes study 80−3964
SE.Ghana, seismicity 79−88255
Gilbert Islands region, sedimentary mantle and basement struct. 79−2219
glaciers, hydraulic transients as seismic source 79−100816
global geodynamics, Canadian contribs., 1971-79 period. 80−8262
global network for seismic data teleprocessing 77−29255
global seismicity, aspects from earthquake catalogue 79−53320
Goban Spur, SW of Ireland, continental fault pattern, seismic reflection study 77−78152
Gorda Ridge spreading centre, active faulting meas. by sonobuoy array 78−85494
Gore Range (Summit County, Colorado), Quaternary geology, surface faulting and earthquake hazard 79−2238
granite terrain weathered zone, appl. of correl. refr. method 80−90230
Grass Valley, Nevada, USA, microseisms in geothermal exploration 80−21647
gravimetric and deep seismic sounding, data interpretation *(Russian)* 79−39937
gravimetric and seismic methods combination for initial seismic data crustal vel. sections 80−105070
gravitational radiation, seismometer detection possibility 80−86196
gravitational radiation of galactic supernovae, seismic detection *(Russian)* 77−13371
Great Barrier Reef, geological history and structure from seismic profile 79−84222
Great Barrier Reef, sedimentation trends in lee of ribbon reefs, seismic reflection profiling 79−84224
great earthquake occurrence, chaos theory of fault block behaviour 80−72448
great earthquakes, chaotic behaviour, coupled relax. oscillator model, billiard model and electronic circuit model 80−94462

seismology continued
great earthquakes, stress drops, wave spectra and recurrence intervals 79−44116
Greece area, shallow earthquakes intensities attenuation with distance 79−44107
Griffith crack-antiplane shear wave interaction at interface of two bonded elastic half-spaces, geophys., seismological appl. 80−92087
ground motion duration after nuclear explosions 79−48413
ground motion near ridge, due to Rayleigh waves scatt. 77−78125
ground motion prediction, fallacies in current methods 79−88292
ground motion simulation and spectral representation using non-stationary amplitude modulated mathematical model *(Spanish)* 80−56397
ground motion spectra, analysis 79−88311
ground movement reconstruction from earthquake recording 78−49165
ground response near Long Beach, California, near surface struct. 80−61775
ground surface displacements, for longit. incident wave directed from below onto inclined media interface *(Russian)* 78−85485
ground vibration caused by sonic boom from fireball over Japan, recorded on seismographs *(Japanese)* 79−66962
ground-response maps for Tonopah, Nevada 79−12086
Guadeloupe, seismic profiles of superficial structs. *(French)* 80−76932
Guatemala City, 1976 February 4 earthquake, landslides, implications for seismic hazard reduction 79−88276
W.Gulf of Mexico, sedimentary section, multichannel seismic refl. results 77−21749
W.Gulf of Oman, multichannel seismic refl. profiles rel. to tectonics 80−8279
Gulf of Oman, seismic refl. profiles, sediment deform. and plate tectonics 77−5176
Gulf of Papua, crustal struct. from seismic data 80−72459
Gulf of Sidra (Mediterranean Sea), seismic profiling rel. to sediment mantle geological struct. 80−36290
Gulf of Suez, multiple refls. and head waves obs. 80−56400
Gutenberg-Richter relation appls. problems 77−44923
Hawaiian Ridge seismicity from Makapuu ocean bottom seismograph 78−77190
hazard model for Reno, Nevada 79−88285
hazards warning, US Geological Survey's role 79−84488
Hebridean continental margin, seismic evidence for Mesozoic age sedimentary troughs 78−53643
Hellenic Arc, historical seismicity rel. to recent Quaternary tectonics 79−79797
Hellenic Arc, seismic data rel. to dynamic model 77−21734
Hellenic arc earthquakes, fault plane mechanisms rel. to E.Mediterranean area neotectonic evolution 80−56451
Hengill-Hellisheidi area, SW. Iceland, seismicity obs. 80−89976
N. Hida region, Japan, seismicity and focal mechanism of local earthquakes *(Japanese)* 80−94482
high sensitivity obs. in wells to avoid city noise 77−44931
high-resolution group vel. analysis, appl. to explosion and earthquake 78−81111
higher-order moveout spectra in refl. seismology, iterative computation procedure 79−92501
hills, seismic response 78−65194
Himalaya and Tibet Plateau region, tectonic history 80−72486
Himalayan mountain front NW termination, active tectonics from microearthquakes 78−40505
Himalayas, epicentre distrib. rel. to south-central Asia large-scale Cenozoic tectonics 80−17246
Himalayas, seismicity, earthquake mechanisms and tectonics 78−40514
Himalayas, seismotectonics, continental plate convergence 78−7593
Hindu Kush region, microearthquake seismicity and fault plane solns. 80−72446
Hindukush, Baluchistan arc, seismotectonics and struct. (1890-1970) 80−104922
Hokkaido and Tohoku, Japan, intraplate seismicity and large quakes 80−51337
Hollister area, S.Coast Ranges, California, earthquake focal mechanisms 79−79752
homomorphic and predictive deconvolution 77−29254
SW.Honshu, Japan, crust Q-factor derived from explosion seismic waves 80−17242
SW.Honshu, Japan, crustal struct. derived from explosion seismic waves 79−74862
Honshu, Japan, deep seismic zone and upper mantle struct. 80−8269
horizon recognition by factorial discriminant analysis *(French)* 77−41190
horizontal ground acceleration, Fourier amplitude spectra estimation 79−16389
horizontally layered media, reflection coeffs. and response 78−28173
horizontally stratified media sounding, geophysical problems unification 80−56622
HTGR core, seismic anal. 80−32327
hydrocarbon exploration, seismic signatures of sedimentation models using synthetic seismograms 77−21913
Iberian Peninsula, 1977 earthquakes and seismicity *(Spanish)* 80−36270
SW. Iceland, axial rift zone, seismic crustal study 80−90014
N.Iceland, major rifting episode with intense earthquakes, ground deform. and magmatism 77−37175
N.Iceland, plate boundary rifting, 1975-78 period 79−84210
Iceland, seismic structure along RRISP-Profile I 80−90018
Iceland, statistical anal. of damaging earthquakes and volcanic eruptions, (1550 to 1978) 80−89975
Iceland crust above layer three, seismic structure 80−90015
Iceland Plateau, deep crust and mantle struct. from surface waves dispersion 80−41413
N.Iceland rift zone, seismic study of crust struct. 80−90013
Iceland-Faeroe Ridge, crustal struct. 80−90016
imaging expt. 80−46130
Imperial Fault, California, large creep events, 1975-77 period 79−12096
impulse response data and inverse problem uniqueness 77−73678
inclined seismic zones rel. to age-length depend. of subducting margin 78−57175
N.E. India, and N. Burma, seismicity, gravity and tectonics 77−25654
NE India, higher seismicity related to lower premonsoon rainfall 79−79742
NE.India, seismicity and focal mechanisms rel. to faults and tectonics 78−24221
seismology continued
India, seismicity rel. to Holocene deform. and crustal movements 79−79793
NE.India, teleseismic P-wave residual anal. at Shillong, rel. to earthquake prediction 80−104921
India, upper mantle struct. lateral vars. from Gauribidanur seismic array data 77−49016
SW Indian coast, seismic and magnetic obs. 77−41018
Indian earthquakes, PKP times 79−39674
Indian geopotential anomaly, seismic and gravity data anal. 80−90037
S.W.Indian Ocean Ridge, earthquakes rel. to Africa-Antarctica present relative motion 77−29272
Indian Ocean triple junction region, microseismicity 78−32020
Indian Shield, deep seismic study 80−12358
Indo-Australian plate, intraplate seismicity rel. to plate internal deform. 80−109134
Indo-Gangetic Plains, shield-like upper mantle vel. struct. 77−29257
initial phase analysis, of R-waves from great earthquakes 80−41405
interference separation using least squares method *(Russian)* 78−15969
interfering signals in seismic records, combined separation *(Russian)* 78−12011
interpolation of digitized curves for seismograms 77−40999
intraplate seismicity, zones of weakness, alkaline magmatism and tectonism 79−74882
intraplate seismicity on bathymetric features, 1968 Emperor Trough earthquake 80−30997
intraplate seismicity rel. to gravity anomalies 78−53606
inverse dynamic problem in seismic prospecting, controlling algorithm for soln. *(Russian)* 79−74859
inverse filter which is optimum in error-distrib. sense, stability characts. 78−81424
inverse filter with optimum error distribution 77−81825
inverse filters rel. to recursive seismogram model *(Russian)* 77−86815
inverse problem, non-linearity effects 79−8704
inverse problem appl. of control theory 79−2402
inverse problem for normal incidence waves to horizontal layered media 80−98252
inverse problem for SH wave scattering *(French)* 80−51333
inverse problem for two-dimensional velocity variations 80−21833
inverse problem stability, one-dimens. wave eqn., seismic profiles appl. 79−84490
inverse problems, anal. *(Russian)* 79−34762
inverse problems soln. by method of dynamic models *(Russian)* 78−85714
inverse seismometry problem soln., limits of appl. 79−62606
inversion of long range seismic profiles 77−73878
Iran, attenuation of intensities 79−92497
Iran, seismic risk 80−76922
Iran, seismic waves from Iranian quakes, excitation and attenuation 80−104900
Iran, seismicity rel. to 1903 Sept. 25 Turshiz earthquake 77−49008
Iran, seismotectonic implications of relocated aftershock sequences 79−44119
Iran, seismotectonic provinces, discussion 79−92499
Iran, seismotectonic provinces 77−9357
Iran and Turkey, focal and seismicity depth determ. errors 80−61779
Iranian earthquakes, instrumental and relocated epicentres evaluation 79−88258
Iranian Plateau, quantitative seismotectonic study 79−88279
Iraq, Badra area, (1975 November-1976 March) microearthquake study 79−88268
Iraq, microearthquakes recording 77−21689
Iraq, seismicity and seismotectonics, 1900-72 period 77−73665
ISC seismological catalogue, geographical distrib. of detectability 80−109117
N.Italy, crustal structure and seismicity 78−24264
Italy, crustal structure from deep seismic soundings 80−56417
S.Italy, crustal structure from seismic refraction profile 77−33013
Italy, earthquake prone areas, pattern recognition 80−56411
Italy, fault-plane solns. and stress regime 78−69299
Italy, isoseismic area and earthquake magnitude relations 78−65196
Italy, precursory seismicity to strong earthquakes 80−104884
S.Italy, seismic risk map preliminary results 79−44113
NE.Italy, surface geology rel. to seismically active tectonic structures 78−24286
N.-central Italy, upper mantle structure from Rayleigh wave dispersion 80−3977
iterative identification of noninvertible autoregressive moving average systems 77−81816
Izu Peninsula, active faults anal. by track etch method *(Japanese)* 80−109127
Izu Peninsula, Japan, tidal effects on swarm activity, 1975-8 period *(Japanese)* 80−41389
Izu-Oshima kinkai earthquake, 1978, fore- and aftershock distrib. *(Japanese)* 80−41383
Izu-Oshima-kinkai earthquake, 14 Jan. 1978, aftershocks and crust struct. *(Japanese)* 80−41384
Izu-Oshima-Kinkai earthquake, 1978, foreshock and aftershock activity *(Japanese)* 80−51349
Izu-Oshima-kinkai earthquake, Jan. 1978, foreshocks of Oshima Volcano *(Japanese)* 80−46138
Izu-Oshima-kinkai earthquake, Jan. 1978, precursory mag. field changes *(Japanese)* 80−41395
Izu-Oshima-kinkai earthquake, Japan, 14 Jan. 1978, seismic waves anal. *(Japanese)* 80−41385
Izu-Oshima-kinkai earthquake, Japan, Jan. 1978, aftershocks and main shock ground accel. *(Japanese)* 80−41386
Izu-Oshima-kinkai earthquake of Jan. 1978, pre- and post-event seismicity *(Japanese)* 80−41382
Izu-Tokai District, Japan, tectonic activity rel. to earthquake prediction *(Japanese)* 78−96145
Jan Mayen fracture zone, Norwegian Sea, seismicity map 77−78127
central Japan, conductivity anomaly changes rel. to earthquake occurrences 77−2102
Japan, deep seismic zone cross-section beneath NE Honshu 80−3951
SW.Japan, major earthquake focal mechanisms rel. to tectonics 78−11827
Japan, regional distrib. of max. earthquake motions 79−62461
Japan, seismic activity research using catalogues of destructive earthquakes *(Japanese)* 77−17037
Japan, seismicity index maps, rel. to earthquake risk 78−36117

seismology continued
SW.Japan, Shikoku area, Sanbagawa metamorphic belt, seismic wave vel. 78−11830
Japan, statistical analysis of strong-motion acceleration records 79−88298
Japan, statistics of earthquakes energy release (1915 to 1978) 80−94471
Japan, strongest possible earthquake determ. 77−9365
N.E.Japan, upper mantle regionality from explosion seismic obs. 77−37167
NE.Japan Arc, deep seismic zone double-planed struct. 78−77203
NE.Japan Arc, double-planed deep seismic zone and upper mantle structure 78−77198
NE.Japan arc, seismic activity, earthquake prediction research 79−57875
Japan local earthquakes, JMA network epicentre detect. capability simulation *(Japanese)* 79−96844
Japan seismicity, 1885 to 1925, catalogue of M≥6 earthquakes and smaller, damaging, earthquakes *(Japanese)* 80−67341
Japan trench, microearthquake activity off Sanriku, ocean bottom seismographic network obs. 77−81803
Japan-Bonin trench, crustal and upper mantle changes 80−72466
Japanese earthquakes, 1901 to 1925, instrumental magnitudes *(Japanese)* 80−94484
Japanese Islands region, earthquakes and mechanisms data compilation *(Japanese)* 80−67332
Jocassee reservoir, South Carolina, stress distrib. 77−91047
Jordan Rift Valley, macroseismic study and structural damage of major earthquakes 78−65190
Jordan-Dead Sea Rift, crust and upper mantle struct. from seismic refr. data 80−26474
kaersutite, sound vels. and anisotropy, rel. to upper mantle seismic struct. 80−26501
Kamchatka active zone, Q-factor of upper mantle 77−44929
Kamchatka basin, W.Bering Sea, seismic refr. meas. 77−17053
Kane Fracture Zone of Atlantic, seismic study of crust struct. 80−104936
Kangzhuang-Dachang region near Peking, deep struct. and earthquake foci *(Chinese)* 80−56415
S.Kanto and Tokai districts, Japan, crustal plate dynamics *(Japanese)* 80−51382
S.Kanto area, seismic waves vel. change meas. from Tateyama explosions *(Japanese)* 80−67338
Kanto Distict, Japan, earthquakes rel. to countercurrent accompanying descending Pacific plate *(Japanese)* 80−94514
Kanto district, definition and characts. of seismically active regions *(Japanese)* 78−96148
S.Kanto district, Japan, crustal struct. by explosion seismology *(Japanese)* 80−51368
S. Kanto Region, Japan, body waves propag. derived from earthquakes observed initial motion *(Japanese)* 80−94481
Kenya rift valley, geophysics 77−86825
Kern County, earthquake, precursory seismicity and small quakes 80−104902
Kilauea Iki, shallow magma reservoir seismic props. 78−73338
Kilauea volcano, Hawaii, three-dim. crust and mantle struct. 78−28205
Kilawea Iki, Hawaii, sources of seismic events in cooling lava lake 79−84156
kinematic data, joint linear external inversion method 80−90240
King's Trough, NE.Atlantic Ocean, struct. from bathymetric, seismic and gravity data 78−49005
N.Kirgizia, crustal 79−44124
Krafla volcano, Iceland, 1978 July deflation, seismic activity rel. to magma intrusion 80−90054
Kuril Trench area, evidence for high vel. zone from ocean bottom seismometer obs. 78−48999
Kuril-Kamchatka trench, seismic study of crust 80−89982
Kurile Island earthquake, seismic quiescence precursory 80−85610
Kurile-Japan trench, low-vel. layer thinning 79−79782
Kusatsu-shirane Volcano, Japan, 1976 steam explosion, geophys. obs. *(Japanese)* 79−70773
La Malbaie, Quebec (1924-1978), epicentre relocation 80−104903
La Malbaie area, Canada, upper crustal struct. lateral vars., teleseisms meas. 78−28187
La Soufriere, Guadeloupe, seismic profiles of superficial structs. *(French)* 80−76932
Lachlan Fold Belt, SE.Australia, deep crust. struct. 80−56436
Lacq, France, petroleum exploitation rel. to non-natural earthquakes *(French)* 80−104892
lake, artificial, time evolution of stress, rel. to indúced seismicity 79−25272
Lake Baikal area, seismic profiling by converted earthquake waves *(Russian)* 77−66893
Lake Jocasse impoundment, S.Carolina, induced seismic activity, earthquake prediction model 79−62453
Lake Jocassee, S.Carolina, seismicity rel. to Rn content of groundwater 80−94466
Lake Jocassee area, S.Carolina, seismicity, earthquake prediction algorithms 80−51345
Lake Keowee, S.Carolina, USA, 1978 earthquake swarm 80−36255
Lake Mead, Nevada-Arizona region, earthquake monitoring 77−25653
Lake Oroville, reservoir-induced pore pressure and seismic activity 79−2190
land seismic reflection exploration data acquisition systems 77−29444
land seismology, appl. of mini-SOSIE 77−21917
Laramide orogeny, seismic profiles in Wyoming, USA 80−85626
Laramide Wind River uplift, Wyoming, USA, gravity and seismic refl. data 80−21679
large earthquakes, time-predictable recurrence model 80−85598
large scale network modelling, multiple covering problem appl. 78−69540
laser extensometer, comparative anal. with rod extensometers 77−64452
Lassen Volcanic National Park, California, 1976-8 seismic events 80−36257
lateral inhomogeneities affecting propag., computational approach 80−21661
layer pressures inferred from wave velocity *(Hungarian)* 80−21840
layered media lossless wave eqn. soln., Bremmer Series decomp. 80−89962
layered media with curvilinear boundaries, correction of seismic constructions *(Russian)* 79−88261
layered system, spectral function, waveform determ. at depth 78−16172

seismology continued
Lehmann discontinuity, mantle props. beneath continents 80−56425
lenticular low-vel. inclusion effect on wave pattern, US modelling 77−41006
Lesser Antilles island arc, crustal struct., seismic refr. expt. 79−84139
Ligurian Sea area, crustal and upper mantle structure from seismic and gravity data 78−65209
linear inverse theory with a priori data 79−53580
Lipari, Eolian Islands, crustal struct. from seismic response of local earthquakes 78−40494
lithosphere, heterogeneities rel. to P-wave time and amplitude anomalies interpretation 78−96153
lithosphere, isostatic disturbances rel. to elastic stresses 77−81842
lithosphere, lower, structure in USSR from explosion seismology 77−86836
lithosphere, review of seismic anisotropy 77−49011
lithospheric downgoing slabs, temps. rel. to seismic zone lengths 79−25212
Lithospheric Seismic Profile in Britain (LISPB), crustal shear waves studies 78−73313
Lithospheric Seismic Profile in Britain (LISPB) rel. to N.Britain crustal struct. 78−73329
local earthquakes, synthesis of seismic coda 77−73683
local magnitude, determination method from seismoscope records 80−56393
local seismicity rel. to vel. anomalies 80−3953
locally non-linear systems, peak harmonic response 78−51109
long period and surface waves, conf., Mamaia, Rumania, 1975, Sept. 77−37146
Los Angeles, application of seismic risk procedures to microzonation problems 79−88289
lossless layered media state space models 77−91065
lossless wave eqn. in layered media, canonical Bremmer series decomposition 77−91064
low-vel. zone inversion, Weichert-Herglotz integral 80−21829
low-velocity zone, parameters determ. as functions of focal depth 77−86828
lower continental crust, seismic refr. and refl. data rel. to model 77−81840
lower mantle Gruneisen parameter, seismic evidence for approximation $\gamma\rho$=const 80−3970
lower mantle seismic wave vel., meas. method using wide aperture array 80−105071
LWR plant, economic effect of increased seismic load on design and construction costs 78−66432
LWR power stations, R and D for improving seismic safety 80−99231
macroseismic aspects of event intensities 78−24232
macroseismic data processing and interpretation 78−61583
macroseismic intensity map of Friuli, 1976 May 6 earthquake 78−65203
Madonna di Buia area (Udine), microseismic zoning 78−24244
magnitude bias in network meas. rel. to identification criteria 77−40989
magnitude of seismic event, statistical models 80−51343
magnitude scale based on strong-motion horizontal particle vel. 80−81836
Makran coast, Iran and Pakistan, seismic harzards, regional tectonics and geology 79−88295
Makran region, seismicity var. rel. to large earthquakes 80−85611
Manic 3 reservoir, Quebec, induced seismicity 79−66636
Mantaro landslide, Peru, seismological and geological aspects 78−96248
mantle, density inhomogeneities beneath oceanic trenches, island areas and marginal seas from DSS data 80−21676
mantle, detect. of waves converted from P to SV 77−81810
mantle, lateral heterogeneity from multiple ScS waves travel times 77−29259
mantle, lower, compressional and shear vels. radial var. 78−73316
mantle, lower, lateral vars., seismic array evidence 79−20781
mantle, lower, radial vel. anomalies identification via interference method 79−25209
mantle, peridotite high-temp. anelasticity and elasticity at seismic freqs. 80−17256
mantle, seismic discontinuities rel. to radial and lateral temp. vars. in upper regions 77−5141
mantle, seismic vel. variations, origins 80−81854
mantle, siesmic discontinuity at 650 km depth 79−44143
mantle, upper, Rayleigh waves global average group vels. and attenuation coeffs. inversion 79−12090
mantle, upper, Rayleigh waves regionalisation and pure-path models 79−12091
mantle, upper, vel. cross sections from deep seismic sounding data 79−39677
mantle, velocity-depth structure, Central Europe 80−3976
mantle and crust seismic vel. struct., model 80−89990
mantle below Colorado Rocky Mountains, seismic vel. anomaly 80−81853
mantle convection pattern and subcrustal stress field under Asia, rel. to seismicity 78−57190
mantle earthquakes, spatial distrib. in Japan and Aleutian arcs 80−81820
mantle earthquakes near junction of Kurile and northern Honshu arcs, mechanism 77−81805
mantle isotropy assumption brought into question 80−90024
mantle of W.Pacific, multiple ScS travel times 80−72443
mantle partial melting and mineral-stability boundaries, rel. to seismic exploration of lithosphere, Canada 78−36121
upper mantle seismic discontinuities, implications of monticellite ($CaMgSiO_4$) high-press. phase transforms 80−17255
mantle seismic waves in Europe and Eurasia, inferences from higher mode data 80−72436
mantle upper structure of Caucasus and Carpathians from seismic data 77−41009
Mariana trench, landward seismicity rel. to seaward lithosphere flexure 79−57903
marine deep seismic sounding system 77−87083
marine geophysical exploration, review 77−41196
marine geophysical surveying, seismic techniques appl. 79−53560
marine profiling images, recording, signal amplitude preservation 78−36326
marine refraction seismology, interpretation techniques 77−64230
marine sediment classification, using broadband deep towed seismic system data 79−16721

seismology continued
marine sediments, acoustic anisotropy due to overburden press. 80−56455
marine seismic data for detrital sediments, petroleum exploration 78−96303
marine seismic exploration data acquisition systems 77−29445
marine seismic exploration ship 77−64449
marine seismic refl. data acquisition using extended arrays 78−77340
marine seismic survey off Canada west coast, crustal struct. 79−100820
marine seismic surveying, potential efficiency of shot grouping *(Russian)* 78−40702
marine source signatures, debubbling 79−16692
Markansu Valley earthquake, Tadjikstan, USSR, 1974 August 11, seismotectonics 80−21659
Massif Central, France, Rayleigh wave attenuation in volcanic area 80−98264
maximum entropy method for spectral analysis of digital data *(Japanese)* 77−17227
maximum ground acceleration determ. for large earthquakes *(Japanese)* 80−101453
E.Mediterranean, crustal struct., sedimentary layers 78−69311
E.Mediterranean, deep struct. and tectonics 78−69309
E.Mediterranean, struct. and tectonic setting of Levant continental margin 78−69310
Mediterranean area, surface wave and seismotectonic studies 77−37151
W.Mediterranean Basin, upper mantle structure from seismic profile 78−11841
Mediterranean earthquake catastrophes, statistics 80−3955
Mediterranean region, struct. and tectonics, conf., Haifa, Israel (Aug.-Sep. 1976) 78−69306
Mediterranean Ridge, submerged chain assoc. with Hellenic arc, struct. from refl. data 77−53014
E.Mediterranean Sea, seismic refl. data rel. to tectonic elements and crustal struct. 78−44801
meizoseismal shaking of long-period, for strike-slip event 80−81814
Melendy Ranch, Calif., San Andreas fault, search for resistivity variations 78−28185
methane outgassing from Earth interior, seismological implications 78−92809
trans-Mexican volcanic belt, seismic refl. and geomag., leg 17 of project CICAR *(Spanish)* 80−36280
Michoacan, Mexico, seismic gap, length of earthquake-free period 80−76919
microearthquake location using max. likelihood processor 77−17033
microearthquake network automatic data anal. 77−81820
microearthquake network data, automatic anal. 78−81412
microearthquake research, methods and meas. errors 79−39987
microearthquake survey in N.W. British Columbia and S.E. Alaska 77−25652
microearthquakes preceding Hollister, California, 1974 November 28 earthquake, fault-plane solns. 80−3936
microseism generation mechanism from sea floor obs. off Shikotan Island 78−73319
microseismic array cross spectra, inversion 80−98243
microseismic events in rocks at high confining press. and differential stress 77−73716
microtremours, 1 to 5 s, earthquake engineering appl., Tokachi-oki 1968 earthquake long-period accel. 79−16387
microzonation, application of regionalized variables 79−88288
microzonation, geological considerations 79−88272
microzonation, proceedings of international conf. (San Francisco, 1978 Nov. 26-Dec. 1) 79−88269
microzonation of continental shelf, high-resolution geophysical surveys 79−88515
microzonation of offshore areas, overview 79−84182
microzoning for earthquake risk reduction 79−88290
microzoning methods, need for experimental evidence 79−88514
Mid Atlantic Ridge, SW of Azores, deep seismic sounding results 78−3747
Mid Atlantic Ridge near 45°N, ocean bottom seismograph obs. 78−11875
Mid-Atlantic Ridge, struct. at 45°N 78−73332
Mid-Atlantic Ridge N of Azores, upper mantle struct. from compressional waves obs. 77−73691
Mid-Atlnatic Ridge, ocean-bottom seismograph obs. near 45°N, results 78−96157
Middle America Trench offshore Guatemala, seismic refr. and refl. meas. 80−26493
migration by phase shift-algorithm for array processor 80−72638
migration in terms of spatial deconvolution 79−88256
migration velocity estimation, problems *(Russian)* 79−66622
Mindanao earthquake, 1976 August 16, preliminary seismological assessment 79−66635
Mini-Sosie high resolution seismic reflection system, operational principles 78−85707
minicomputer based system for marine seismic data acquisition 77−82072
minimum entropy deconvolution, appl. to refl. seismic recordings 78−81423
minimum entropy deconvolution 77−81817
mining tremors, seismic moment and source size, Upper Silesia, Poland 78−48977
mining tremors, seismic moment and source size determ. 78−3717
mining tremors in anisotropic media, optimal recording 78−3718
Minnesota, crustal struct. and seismicity, rel. to historic earthquakes 78−11840
Miramichi Bay, New Brunswick, Canada, echo sounder and seismic profiling survey 78−61390
mislocation patterns for seismic networks and mantle heterogeneity 77−81843
Mississippi embayment, remote sensing appls. to tectonics and seismicity 77−81856
SE Missouri, seismic characts. from regional telemetered microearthquake array 77−40993
mixed Fourier Walsh transforms, appl. to seismic array processing 77−81819
Miyagiken-oki earthquake, June 1978, aftershock spectral anal. 80−109118
Modified Mercalli and JMA intensity scales, peak acceleration comparison 79−62443
seismology continued
Mogod, 1967 January 5, earthquake, focal mechanism and parameter determ. 80−3937
Moho, continental, throws and dips sounding by explosion seismology 80−85620
Moho, dip and strike determ. from array anal. 79−66821
Moho dip beneath Scotland, by PS reflections 80−41409
moment magnitude scale 79−84157
moment tensors of seismic sources, discontinuous displacements 77−2110
monitoring underground nuclear explosions, book 79−681
monofrequency borehole traveltime survey 78−28328
motion from seismic sources 80−36248
Mountain Crimea region, surface seismic Rayleigh waves, amplitude spectra 80−89969
Mozambique Channel, crustal struct., seismology study 80−51362
multi-segment seismic traces, deconvolution and synthesis 80−77162
multichannel observations, orthonormal lattice filter estimation 79−84497
multichannel subtracting filters, construction *(Russian)* 78−49156
multichannel telemetry system, design, seismic data processing *(Chinese)* 79−21033
multidimensional polarization analysis 78−73528
multidimensional velocity generalisation technique, appl. to Black Sea NW shallow and nearby land areas *(Russian)* 80−105068
multilayered seismic dynamic problem, admissibility of soln. without consideration of multiples 77−73668
multiple reflected signal attenuation, least squares estimation procedure 80−85596
multiple water reflections recorded at ocean bottom 78−57331
multiple waves, prediction filtering in non-ideal conditions *(Russian)* 79−44131
multiple waves suppression methods, comparative evaluation *(Russian)* 78−40515
multipolar source field transformation under a change of reference frame 77−5135
multipolar source in layered media, seismic wave emission 80−81816
multivariate autoregressive feature extraction and the recognition of multichannel waveforms 79−39878
Nankaido earthquakes correl. with Shikoku seismicity characts. 80−101339
Nazca plate off S. Peru, crustal model from ocean bottom seismometer obs. 78−32032
N.China, seismic gaps prior to large earthquakes *(Chinese)* 79−20755
near-earthquake studies, importance of surface or interface P-wave 79−66628
Nelson River gravity anomaly, SE.Saskatchewan, seismic survey 78−28153
Nemaha Uplift in Oklahoma, Kansas and Nebraska, geological survey of seismicity and tectonic rels. 78−7589
Nepal Himalaya, body waves from earthquakes, focal mechanism and tectonics 80−72455
Nevada Test Site region, seismic hazard 78−65189
New England, empirical study of seismicity (1727 to 1977) 79−92492
New England earthquake hazard based on 1725-1974 seismic data 77−37159
New Guinea-Solomon Islands region, seismicity maps 78−7592
New Hebrides Island Arc, anomalous propag. through shearing contact zone 80−3948
New Hebrides island arc, earthquakes precise relocation rel. to seismotectonics 79−16404
New Hebrides island arc, upper mantle struct. in arc convex side 79−74861
New York area, seismicity and lithospheric stress 78−36113
New York State, earthquakes related to hydraulic mining and natural seismic activity 78−48986
New York state, microzonation 79−88275
New Zealand (N.Island), plate boundary microearthquake study 80−109131
New Zealand seismograph network 79−39916
Newfoundland, Bay of Islands ophiolite complex, seismic vel. structure 78−40506
Newfoundland Basin, seismic surveys rel. to Mesozoic evolution 78−32045
Newfoundland Ridge, multichannel seismic refl. profiles of subsided continental crust 78−15980
Newfoundland Ridge, seismic structure, nature of crust, oceanic origin 79−25211
Ninetyeast Ridge, seismic sounding with bottom seismographs and air guns 78−3748
Ninetyeast Ridge area, seismicity and tectonics, Indian plate internal deform. 78−73343
noise effects on seismograms 77−45181
nonlinear interference systems for separation of waves with different vels. 77−78438
Nootka Fault Zone, new plate boundary off W.Canada 79−92518
normal incidence marine seismic profiles, reflection energetics 77−81821
normal incidence synthetic seismogram fine struct., inverse problems soln. 78−49152
normal mode excitation by collapsing cavity 78−7583
normal mode oscillations of Earth, asymptotic representation of multiplet spectra 80−94459
normal modes of laterally homogeneous Earth, one dimens. example 78−88797
normal modes of rotating Earth model, excitation by earthquake fault 78−73312
normal modes of simple Earth models, variational type finite element solution 78−11817
normal moveout difference curve improvement 77−17225
normal moveout velocity in 3D laterally inhomogeneous media with curved interfaces 80−101336
Norris Geyser, Yellowstone Park, USA, microseisms of geothermal area 80−104909
North America, S and P station anomalies 80−94460
NE. North America, spectral moments, magnitudes and intensities for 32 earthquakes 77−91020
E.North American earthquakes, surface wave focal mechanisms with tectonic implications 80−3942
North Sea, Buchan and Witchground Grabens, seismology study 80−51364
North Sea basin, seismic refr. expts., using Pull-Up Shallow Water Seismometer 78−45025

seismology continued
Novaya Zemlya nuclear explosions, P-wave travel time residuals vars. in central California 77−25658
nuclear explosion generated body waves, time functions 80−56376
nuclear plant, seismic testing motions anal. with instantaneous response spectra 79−22498
nuclear plant design, seismic response spectrum normalisation 78−50415
nuclear plant equipment, standardised seismic design spectra 78−41870
nuclear plant seismic anal., multicountry application 77−65306
nuclear plant seismic design, automated generation of spectrum compatible artificial time histories 78−29661
nuclear power plant, earthquake proof design of components 78−21733
nuclear power plant seismic floor response spectra 78−819
nuclear power plant siting, US midcontinent 78−85501
nuclear power plant siting 78−82481
nuclear power station, Caorso plant, dynamic tests and seismic records of RHR building 78−41872
nuclear power station, seismic anal., slab modelling 78−50414
nuclear power stations, seismic qualification of Class 1E eqpt. 80−99234
nuclear power stations, seismic qualification of systems, structures, equipment and components 78−41878
nuclear power stations, seismic qualification tests of elect. eqpt., damage severity factor concept 80−99235
nuclear power stations, seismic safety margins research program of the US Nuclear Regulatory Commission 80−99229
nuclear power stations, seismic safety of mechanical eqpt., R and D program 80−99232
nuclear reactor components, seismic amplification factors 79−597
nuclear reactor safety anal. 78−41834
nuclear spent fuel elements storage in large pools, seismic load anal. 78−17400
numerical seismograms for vertical point force in layered solid 78−92784
Oaxaca earthquake, Mexico, aftershocks in former seismic gap 80−98265
Oaxaca gap, Mexico prediction of earthquakes 80.−85609
observation network *(Japanese)* 78−28341
observatory network and seismic instrument construction in Poland *(Polish)* 77−21911
ocean bottom seismometry 78−65397
ocean crust layer 2, oblique seismic expt. on DSDP leg 52 80−36275
ocean crust sounding, computer processing method of seismograph records 80−85605
ocean crust studies, suppression of sea-floor multiples 80−90231
ocean sediment classification by seismic reflectivity meas. 77−5370
ocean-basin models, isotropic inversion of anisotropic surface-wave dispersion 78−96156
ocean-bottom seismograph observation system *(Japanese)* 80−94615
oceanic crust, evidence for low velocity layer at base 77−37164
oceanic crust, ophiolites identification 78−81117
oceanic crust, petrology and porosity, shear vel. struct. 80−72473
oceanic crust, structure from refraction expts. 80−3952
oceanic crust evolution, East Pacific Rise crest model from seismic refr. data 77−17054
oceanic crust seismological methods, expanded spread and const. offset profile 80−56632
oceanic crust studies, deep seismic profiling using refl. meas. *(Russian)* 79−39966
oceanic lithosphere, apparent seismic velocity meas. rel. to struct. 77−2117
oceanic long range explosion expt., preliminary report 77−73679
oceanic transform earthquakes, source parameters rel. to plate vel. and transform length 78−53620
oceanic trench earthquakes, props. rel. to plates bending at trenches 80−41426
oceanic type crust as a type of Earth crust 80−89997
oceanic upper mantle, seismic anisotropy of ophiolite peridotite 78−53645
oceanographic research techniques used in survey ships *(French)* 78−65434
offshore seismic refraction surveying, nonexplosive energy sources *(Russian)* 78−53752
offshore Texas seismic signals, hydrophone array effects 79−53309
oil exploration data processing, white-noise estimates 78−3973
oil prospecting, new seismic reflection techniques 78−73541
Okhotsk Sea and Kuril Islands, earthquake magnitude determination, body wave anal. 80−4139
Okhotsk Sea deep basin, seismic study of crust 80−89982
Olinghouse fault zone, Nevada, strike-slip fault 79−79840
Ondrejov laser satellite-tracking station, regional tectonics and seismicity 78−36418
Ontong Java and Manihiki Pacific oceanic plateaus, seismic struct. 80−21680
ophiolite complex of Point Sal, California, seismic vel. struct. 80−109110
optically processed seismic data, noise resistance *(Russian)* 77−86820
optimal config. of seismic recording stations for mining tremor analysis 78−20359
optimal inverse filtering parameters in deconvolution correction *(Russian)* 77−86817
optimal multichannel filtering, evaluation taking account of signals amplitude and phase jitter *(Russian)* 78−40697
optimal velocity analysis, in common depth point method *(Russian)* 78−40698
optimum mixed delay spiking filters appls. 78−77346
optimum stacking filters in suppressing uncorrelated noise 77−64216
optoelectronic analyzer for seismic data processing *(Russian)* 77−29516
Oroville, California, crustal stresses due to artificial lake rel. to seismicity 77−9347
Oroville, California, local magnitudes, seismic moments and coda durations 77−91021
Oroville earthquake, USA, foreshock identification 80−56379
Osaka region, microzoning in Japan 79−88283
oscillation sources, ground response and theoretical problems *(Russian)* 77−44938
oscillations, split normal modes, theoretical amplitude and Green's dyadics 80−101341
Oshima (W.Hokkaido), source area of 1741 tsunami from religious monuments *(Japanese)* 80−67345
Oslo Rift, crustal structure from seismic refr. study 78−32037

seismology continued
P_n velocity anisotropy in continental upper mantle, anal. by MOZAIC time-term method 77−49013
P-wave signals, multivariate autoregressive model, short-period discrimination appl. 79−16385
NW Pacific, seismic data rel. to upper mantle struct. and deep processes 77−37160
Pacific, W. edge, new $dt/d\Delta$ profile for lower mantle 77−9380
NW.Pacific attenuation from intensity data 80−21642
SW.Pacific basin, reverberant subbottom layers distrib. 80−8290
Pacific basin, seismic stratigraphy, sedimentation rates and sea levels 79−88365
Pacific Ocean crust, seismic props. of layer 2A 77−29260
Pacific plate subduction beneath Japan Islands, 3-D seismic struct. 80−51376
E.Pacific Rise, seismic sounding rel. to oceanic crust props. and origin 80−101360
E.Pacific Rise, synthetic seismic profile 79−12095
E.Pacific Rise crest, crustal struct. vars. from seismic travel time inversion 77−60357
E.Pacific Rise crest structure from multichannel seismic reflection 78−40523
Paicines Fault, Calaveras fault zone, California, slip meas. 79−48416
Pakistan and N.W. India, seismicity patterns assoc. with continental collision 77−25655
PAL, highly tutorial interactive, pattern recognition program for seismic anal. 77−81833
palaeoanisotropy in upper mantle 78−7602
Pamir-Himalayan deep fault zone description 79−39676
Pamir-Hindu Kush region, seismicity and fault plane solns. 80−72445
Pamirs-Hindu-Kush region, mantle intermediate seismic zone 77−53011
Panamint Valley fault zone, W.Basin and Range province, California, Holocene offset and seismicity 79−79802
NE.Pannonian Depression, seismogeological study *(Rumanian)* 79−57877
Papuan Ultramafic Belt, crustal structure 77−37166
parabolic wave theories and applications 80−51436
Parece Vela Basin, E.Philippine Sea, seismic refr. data rel. to evolution 80−41431
Parkfield earthquake, USA, foreshock identification 80−56379
Parkfield earthquakes, California, comparison of 1966 and 1934 sequences 80−56412
Pasadena magnitude scale of earthquakes, based on vertical ground accel. 80−51344
pattern recognition, fundamental problems 78−81428
peak acceleration, velocity, and displacement from strong-motion records 80−98246
Peking-Tientsin area, China, crustal struct. from gravity data, rel. to seismicity *(Chinese)* 78−61357
Peninsular Ranges of S.California, increased seismicity period rel. to early 20th century upwarping 79−79796
Peru, microzonation methods and techniques 79−88513
Peruvian earthquakes, seismic gaps and source zones 80−85607
petroleum deposits, screening effect on seismic exploration *(Russian)* 77−44939
petroleum prospecting, digital recording of ultrasonic signals [petroleum prospecting]. 78−73552
petroleum traps, synthetic seismic sections 79−53311
petrovelocity model of crust for Ukrainian Shield 78−7597
phase plane method for seismic signals anal. 79−66843
Philippine Islands, tectonic struct. revealed by seismicity and volcanicity 80−94511
Philippine Sea plate, lateral structural variations, surface wave anal. 77−33024
Philippines, ground motion attenuation 79−88278
Philippines, microearthquake survey of tectonic features 80−81827
Phlegraean fields, Italy, intercrustal hydrodynamic correlation with geodynamics 77−2138
physical source parameters determ. from free oscill. data, numerical method 78−11820
piping systems under seismic excitation, modal anal. 80−33512
plane SH waves, linearised direct and inverse problems for two-dimensional heterogeneities *(French)* 79−84131
plane shock wave propag. in nonhomogeneous water saturated soil 77−56607
planetary gravitational forces, effect on earthtides and earthquakes 79−100817
plate boundary quakes, magnitude-freq. relation 80−56390
plate boundary seismic pot., major boundaries 80−85606
Pocatello Valley earthquake, 1975 March 28, source model 80−104896
polarisation state of waves, theory 80−56525
power density spectrum estimation from finite length signal 77−91337
power spectrum estimation using maximum entropy method, data analysis appl. 80−37006
pre-seismic sound *(Chinese)* 79−34760
Precambrian Earth crust, seismic refls. study 78−32034
prediction error filter, quantitative evaluation 78−40496
prediction filtering by adaptive updating technique 79−92614
premonitory crustal deformations, strains and seismotectonic features (b-values) preceding Koyna earthquakes 79−79755
pressure amplitudes of seismic signals in offshore Louisiana 77−52991
prestressed thermoelastic media, seismic-dislocation theory 77−86811
propagating rectangular fracture in semi-infinite elastic medium 78−57168
propagating strike-slip fault in elastic half-space, near-field motions 78−7568
prospecting, effect of spatial deflection during longit. obs. *(Russian)* 79−39945
prospecting, instability of finite difference schemes due to boundary conditions in elastic media 77−21912
prospecting, iterative identification of non-invertible autoregressive moving-average systems 78−81422
pulse propag. in media with freq. dependent Q, theory 80−72438
Pyramid Lake fault zone, Walker Lane, strike-slip fault 79−79839
q estimates using the coda of local earthquakes 80−104899
Q frequency depend. in Earth rel. to mantle rheology and Chandler wobble 79−84190
quadrupole source cylindrical shear potentials giving equal displacements 78−92785
quality factor and effective viscosity relationship 80−12360
Quebec City, geomagnetic and telluric var. in seismic region 77−52974

seismology continued
W.Quebec zone, focal depth changes 80−26453
quiescence duration in seismic gap, empirical determ. method 80−26627
radial oscillations of multilayered elastic sphere and theoretical seismograms, surface layers effect on P waveforms *(Japanese)* 79−66640
radial overtones eigenfrequencies, pattern for specified Earth model 80−104889
radioactive waste deep geological repositories, seismic design considerations 80−23019
Raft River geothermal area, Idaho, seismic refr. study 80−3963
Ramganga reservoir, Kalagarh, India, filling rel. to seismic activity 77−25657
random oscills., RMS level estimation, fast method 77−70857
rapid convolution and correl. FFT procedure *(Russian)* 79−39959
Rat Island earthquake sequence, 1965, seismic scaling information 79−12076
ray method for theoretical seismograms, accuracy 80−67348
ray theoretical inverse methods in geophysics 79−53578
ray theoretical seismograms, construction methods 79−34761
ray theoretical seismograms of laterally inhomogeneous structs. 80−72450
ray tracing, three-dimens. methods 77−73870
ray tracing, two-point problem, adaptive finite difference method 80−98457
Rayleigh channel waves for reflection method, dipping coal seam discontinuity obs. 78−69471
Rayleigh waves, higher mode, studied as individual seismic phases 79−62440
Rayleigh waves, modelling via broadband acoustic surface waves probe 78−23904
Rayleigh waves from nucl. explosion, anomalous generation 80−81833
Rayleigh-wave radiation pattern, for small earthquake mechanism 80−61764
real time detect. and location of seismic events in central California 77−73654
recording station situated on anisotropic ground, body wave propagation *(Russian)* 80−31128
recursive derivation of reflection coefficients from noisy seismic data 78−73324
recursive multichannel max. entropy spectral estimation 78−53735
reflected and transmitted filter functions for simple subsurface geometries 77−44924
reflected wave complex spectra, composite processing appl. *(Russian)* 79−84531
reflected wave method for media with variable vels., inverse case *(Russian)* 79−84525
reflected wave recordings, allowance for vel. inhomogeneities in CDP data processing *(Russian)* 79−84526
reflected wave surveys for oil and gas in non-anticlinal traps *(Russian)* 78−12013
reflected wave travel-time curve inversion theory 80−89968
reflecting area parameters, estimation allowing for amplitude characts. correl. *(Russian)* 79−74856
reflection coefficient calc. from digital data *(German)* 77−70853
reflection coefficients, determ. from waves 79−44115
reflection data, inversion 77−21915
reflection data dynamic corrections, fast algorithm 78−3966
reflection method, high-resolution near surface, using vertical array technique 78−36306
reflection profile modelling system 77−52993
reflection profiles, suppression of long-decay long-delay multiple reflections by predictive deconvolution 79−84133
reflection profiles of marine sediments, statistical anal. 79−2385
reflection profiling on land with controlled source 77−64450
reflection records, homomorphic deconvolution by log spectral averaging 78−28329
reflection seismic method for Silurian reef detect. in N.Michigan 77−2265
reflection seismic recordings, control theory appl. to inverse problem *(French)* 77−87081
reflection seismograms, calc. in freq. domain 78−96152
reflection seismograms, simultaneous spherical divergence correction and optimal deconvolution 80−98258
reflection seismograms for explosive source in multilayered elastic medium, theory 80−17233
reflection seismograph data, maximum likelihood filtering 79−5453
reflection seismology, curved interfaces determ. in bidimensional inhomogeneous media via time fields method *(Russian)* 79−35010
reflection seismology, synthetic seismograms at non-vertical incidence 80−56401
reflection seismology, tool for energy resource exploration, book 78−96162
reflection seismology, use of kepstrum in signal anal. 78−81425
reflection seismology, wavefront synthesis for vel. estimation and downward continuation 79−16392
reflection seismology, waves spectral characts. in region of bright spot anomalies *(Russian)* 79−53319
reflection seismology south and west of Iceland, rel. to sea floor morphology and struct. 80−90068
reflection surveying, wave eqn. migration with absorbing boundary conditions 80−104907
reflection surveys, establishment of zero time 77−21916
reflection time contour maps, migration 77−64214
reflectivity method extensions 80−56640
refracted wave correlation method, interpretation accuracy *(Russian)* 80−85758
refraction data interpretation, time-term method to simulated crustal struct. 80−61768
refraction method, velocity inversion errors, computation and recognition 80−4132
refraction methods for tectonic dislocation detection *(Russian)* 78−12010
refraction parameters, nomogram for rapid computation 78−7785
refraction profiling at sea, sediments vel., density and attenuation models from multibounce phases 79−57864
refraction seismology, time term method anal. 79−66838
refraction survey, program for pocket calculator for depth determination 80−82088
refraction waves, time-distance curve analysis methods *(Japanese)* 77−17038
refractor velocity determ., cause and nature of errors 80−56621

seismology continued
regional seismic network optimum distrib., algorithm 78−32024
regional seismic network optimum extension, Upper Silesia 77−52985
regular waves separation with fluctuating parameters, linear multichannel systems comparative anal. *(Russian)* 79−39922
regularization method and uniqueness problems in study of regional flat-layered structs. 78−49161
residual static and crossdip corrections, simultaneous estimation 79−92500
RESMAC seismic array, interactive epicentre location procedure 78−65395
reversed reflection traveltime data, computerised method for effective vel. 80−21832
Reykjanes Ridge, crustal struct. at 63°N from seismic meas. 79−66661
Reykjanes Ridge, crustal struct. from seismic refr. 80−90020
Reykjanes Ridge, mid-Atlantic 59$^{1}/_{2}$°N, seismic crustal struct. 80−56423
Reykjanes Ridge, Profile I on SE. flank, seismic struct., RRISP 80−90019
Reykjanes Ridge, SE.flank, lithosphere evolution, seismic surface wave study 80−90022
Reykjanes Ridge at 59°N, microearthquake epicentres and seismic vel. 80−89964
Reykjanes Ridge Iceland Seismic Experiment (RRISP 77), for crust and upper mantle struct. 80−90017
Reykjanes Ridge Iceland Seismic Project 1977, first results 79−57889
Rhenish Massif/Rhenohercynian zone, W Germany, crustal struct., seismic refr. data 79−48435
Rhinegraben area, crustal struct. rel. to gravity anomalies and geothermal implications 80−104852
Rhinegraben rift system, Holocene movements and stress state rel. to seismicity 79−79801
risk anal., renewal process model *(Japanese)* 79−84159
risk analysis of lifeline networks 78−65192
risk in S.Europe through to India, using Gumbel's third distrib. of extreme values 80−21648
Rivera-Tamayo oceanic fractures, ocean bed renewal, photographic/seismographic obs. *(French)* 79−74887
rock fracture, assoc. microacoustic signals anal. 78−32070
rock layers, adjacent, material const. determ. using seismic refl. *(German)* 80−105054
rock masses seismic flows, deform. vels. calc. 79−74850
rock pore aspect ratio spectrum determ., seismic velocities inversion 80−51387
rock specimens impulse response estimation, numerical method and appl. to laboratory data 79−80049
Rockall Bank, N.Atlantic, seismic struct., synthetic reconstruction 80−21670
rocks, subsolidus attenuation at simultaneous high temp. and press. 78−3764
rocks, water-saturated, dynamic props. of seismoelec. effect 79−25233
Rocky Mt. Trench, Canada, depth limits on Mohorovicic discontinuity 77−73662
Roosevelt hot springs, Utah, seismic noise study 80−56399
Rumania earthquake, 1977 March 4, P-waves obs. rel. to Moho vel. depth distrib. *(German)* 80−98256
safety factor for nuclear siting in earthquake zones 78−11839
Sagami Bay and off Bose Peninsula, seismic activity during 1971, ocean bottom seismometer obs. 79−79749
salt deposits, seismic prospecting by well logging *(Rumanian)* 78−20566
Salt Lake City, ground response maps 79−88287
central San Andreas fault, creep. tilt, strain and water level var. 77−91023
San Andreas Fault, crustal strain obs. site for earthquake prediction 80−81832
San Andreas fault, microearthquake activity 79−92493
San Andreas fault, Parkfield, repeated creep events, strainmeter array meas. 79−20762
San Andreas fault, Rn emanation vars. meas. 78−32022
San Andreas fault (central California), mag. field local vars., creep rate changes and local earthquakes 80−26450
San Andreas fault aftershocks 80−36249
San Andreas fault quakes, precursory rainfall 80−85615
San Andreas fault zone, seismic vols. rel. to constitution at depth 79−12097
San Diego, 1934-74 seismicity 77−91031
San Fernando earthquake, California (1971), dislocation fault model, tectonic significance *(Japanese)* 80−104923
San Fernando region, California, recent seismicity and west-central Transverse Ranges tectonics 79−66634
San Fransisco Bay, seismic zonation 79−88273
San Gregorio-Hosgri trend, evidence for 115 km of dexteral movement 78−53641
San Jacinto fault, Riverside, California, strain accumulation 77−25633
sand seismic response, effect of stress condition on dynamic props. *(Japanese)* 80−17235
W.Santa Ynez fault system in S.California, seismology rel. to struct. and neotectonics 79−79774
Sao Paulo Plateau, Brazil continental margin seismic profiles, comparison with S Angola margin 77−21750
S.Saskatchewan, seismotectonics 79−20757
Scandinavia, Blue Road area, crustal model and isostatic state 77−64240
N.Scandinavia, compressional and shear wave anal. of lower lithosphere fine structure 80−3979
Schlegeis reservoir, water level var. and seismic microactivity 77−81807
NW.Scotland, Lewisian Units Seismic Traverse, vel. depth depend. 79−44179
screw dislocations in vertical slab with shear modulus contrast, shear stress, strain and displacement 77−56594
seabed acoustic impedance, normal incidence seismic profiles 77−81822
sedimentary rocks, anisotropy due to overburden press. 80−56455
seismic activity of Earth, Sun-induced vars. 77−90981
seismic attenuation in rocks, role of grain boundary friction 79−34755
seismic data inversion, appl. of revised Earth mass and moment of inertia 77−86735
seismic energy transmission in intensively scatt. environment, diffusion eqn. 77−73685
seismic events visual correlation quantitative estimates based on min. average risk criteria *(Russian)* 79−44133
seismic exploration, technique and processing, book 80−51975

seismology continued
seismic fields, decomposition algorithm from charact. numbers and vectors of spectral matrices 77−9370
seismic gaps, two types of definition 80−85608
seismic glut moments of total degree two or less, interpretation 77−91038
seismic hazard mapping, Bayesian model 80−56391
seismic imaging by holography, techniques and appls. 79−66831
seismic instrumentation for nuclear power plants in Germany, review 79−620
seismic microzoning, mapping method based on subsoil conditions 79−44108
seismic moment, method of determination from seismological bulletin data 80−89980
seismic moment tensor estimated by linear inversion method 80−31125
seismic noise sources mapping in geothermal regions 77−81828
seismic pattern, automatic recognition 77−81831
seismic prospecting, minimisation of distortion caused by geophone-ground coupling 79−44256
seismic prospecting techniques for oil resources *(French, English)* 80−21362
seismic recordings, information quality and data processing techniques efficiency *(Russian)* 79−39666
seismic refraction profiles, influence of vel. lateral vars. on interpretation 77−21686
seismic refraction technique for geophys. surveying, teaching 79−97161
Seismic Research Observatories, upgrading of worldwide seismic data network 77−5334
seismic response anal. of structures, new discrete models 78−67081
seismic risk in linear source regions, San Andreas fault appl. 77−56588
seismic risk map, new proposal for Japan 79−88281
seismic signals, detect. under conditions of limited information about signals and noise 77−9536
seismic signals deconvolution, adaptive filter structs. 80−98451
seismic sounding, weathering correction method 79−44255
seismic sources, equivalent models 77−78124
seismic sources with observable glut moments of spatial degree two 77−91039
seismic velocity profiles, synthesis from geotechnical data 79−88516
seismic wave field, estimate of number of signals *(Russian)* 78−49157
seismic waves propag. in medium with randomly distrib. inhomogeneities, attenuation and scatt. *(Hungarian)* 77−86791
seismic zoning, contrib. of geophysical methods, conference (Erice, Italy, 13-23 April, 1977) 79−44104
seismic zoning map, new elements 79−44105
seismic zoning problems, effect of earthquake freq.-magnitude statistical parameters 79−44112
seismicity, model and observed, represented in two-dimens. space 78−53619
seismicity 1897-1906, reevaluation 80−21656
seismicity and global tectonics as framework for microzonation 79−88270
seismicity associated with subduction zones, stereoviews 80−72452
seismicity fluctuations before major earthquakes 77−49027
seismicity from geological structure, seismic risk studies 79−92491
seismicity in deep-level mine, influence of mine geometry and closure volume 78−3723
seismicity increase prior to moderate rock burst 78−3722
seismicity space-time course, energetics model 77−9369
seismite, occurrence in Precambrian rocks, Rajasthan, India 78−77227
seismo-magnetic effect in 1964 Niigata earthquake 77−2093
seismo-magnetic induction, numerical theory of 3-dim. EM induction *(Chinese)* 77−64191
seismoelectric effect, intensification by steady elec. field 77−81790
seismoelectric effect in rocks, nature 77−44974
seismogram inversion, use of generalised Kunetz-type eqns. 80−101337
seismogram inversion and pseudo velocity logs, lithology identification 77−87088
seismogram synthesis in multilayered dissipative media 79−2382
seismograms, digital processing, kinematic corrections *(Russian)* 79−39929
seismograms, synthetic, lossless layered media, time-domain state space models 80−12342
seismograms and images, automatic transform. to seismic sections *(Russian)* 78−49155
seismograms and residual static corrections *(Russian)* 79−58116
seismology, vertical stacking as reflection filter 78−12007
seismomagnetic earthquake precursors, uniaxial stress effects upon rocks remanent magnetisation 80−26505
seismomagnetic effect during Gazly, 1976 May 17, earthquake, unsuccessful search 80−26463
seismomagnetic effects, space correl. method rel. to earthquake prediction *(Chinese)* 78−3719
seismotectonic map of France for appl. to antiseismic design of nuclear installations 80−860
self-adapting fan filters for seismic data 79−44265
self-adaptive wave train subtraction in linear and three-dimensional surveying *(Russian)* 78−40695
SH sudden crack, displacement far-field spectrum, earthquake appl. 77−25641
shallow earthquake source characts., Sanriku-Oki region, Japan 80−12346
shallow earthquakes, seismic efficiency, radiated seismic energy, fault motion energy balance 80−76927
shallow earthquakes occurrence, statistical study 78−96155
shallow focus earthquakes, implications of in situ seismic vel. study in San Andreas fault zone 79−57865
shallow refraction records reflections from overburden-bedrock interface 77−78115
shear displacement along pre-existing fault 79−16412
Shepetovka-Chernobyl seismic profile, petrovelocity crustal model and nature of M discontinuity *(Russian)* 77−44948
Shikoku district, Japan, upper crustal struct. from seismic anal. *(Japanese)* 80−94508
Shizuoka district, Japan, crustal struct., explosion seismology data 80−12359
Sierra Nevada-Walker Lane region, recent crustal movements, rate and style of deform. 79−79838
Sierran foothills near Oroville, California, regional seismicity 79−48411
sign coding in seismic data processing algorithms *(Russian)* 79−62616
seismology continued
signal amplitude digital auotmatic control system, instrumental realisation algorithm *(Russian)* 79−39924
signal detection and parameter estimation 79−92502
signal filtering, distrib. theory appls. *(Rumanian)* 79−58122
signal processing method for circular arrays 80−4123
signal separation by iterative stacking algorithm 79−92612
signals, adaptive deconvolution 78−53737
signals distortion by grouped piezoelec. receiver array *(Russian)* 79−39948
signals resolution from coherent and incoherent noise, operators efficiency *(Russian)* 79−39963
silicate minerals, relationship between phonon cond. and seismic parameter Φ 79−39707
similarity criteria, for comparative anal. of elastic waves propag. vel. under model and natural conditions 79−96742
simulator studies of cylindrical tanks 78−45027
single-channel white-noise estimators for deconvolution 78−77345
Sinkiang-Tibetan region, seismicity and tectonics 78−32030
site transfer functions, preliminary evaluation 79−88301
Sitka, Alaska, earthquake, 1972 July 30, changes in direction of mag. vector of short-period geomag. vars. 80−76923
S.Kivu, Zaire, basaltic flows on Idjwi Island *(French)* 77−64246
slashes on seismic records caused by electrical bursts 77−86794
slip monitoring along major faults in southern California 79−48388
W.Slovenia, tectonic structures, rel. to macroseismic effects 78−24254
small earthquakes, detailed spatial distribs. of foreshock and aftershock activities *(Japanese)* 80−94483
small shocks in Friuli, Italy, total durations and local magnitudes 79−34750
Snake Bay-Kakagi Lake greenstone belt, NW.Ontario, expanding spread seismic refl. survey 80−12356
Snyder, Texas, USA, 16th June 1978, seismic activity 80−56395
soil, shear wave vel. meas. during standard penetration test 78−48978
soil amplification functions, stochastic approach 77−9358
soil profile fundamental period estimation 77−9359
soil-structure interaction effects 79−92496
soils, non-linear seismic response and liquefaction 79−57862
solid-liquid model for explosion in ground 78−96158
Somali Basin, seismic profiling and bottom topography, possible fracture zone 78−28213
sounding for oil and gas-bearing structures *(Russian)* 77−45195
source depths, improved determ. using seismic coda 77−81829
source location by surface waves, reference point equalisation method 80−72648
source props. determ. by seismograms linear inversion 78−65394
source spectral theory and earthquake foci parameter determ. *(Rumanian)* 77−33010
source-receiver arbitrary locations, diffractions 78−28172
source-receiver nonzero separation, diffraction response 78−28171
W.South America, volcanism, seismicity and anelasticity interrelationships 77−33044
South China Sea basin, crustal struct. from profiler-sonobuoy meas. 80−8291
South Sandwich Islands, seismicity 78−7582
Soviet seismology evolution during 1917-77 period 79−84142
space-time functions integral representations in seismic holography *(Russian)* 78−85483
S.Spain, crustal struct. from deep seismic sounding *(Spanish)* 78−44795
Spain, dam and reservoir induced seismicity 80−61776
S.Spain, deep seismic soundings 78−7587
SE.Spain, Quaternary strike slip faults rel. to current seismicity 79−79798
Spain, seismicity and seismic risk map *(Spanish)* 78−44791
Spain during 1976, seismic activity *(Spanish)* 79−29717
spectral anal., recursive multichannel max. entropy method 77−91338
spectral anal. of natural seismic events using autoregressive techniques 77−29470
spectral analysis, maximum entropy spectra, choice of operator length 79−84134
spectral estimation techniques for discrete time series 78−53734
spectral shakeability maps 77−52997
spectral theory of seismic sources, appl. to determ. of earthquake foci parameters 77−21687
spheroidal eigenoscillations, freqs. and corrections to interior struct. 77−52996
split spheroidal and torsional free oscills. of 1960 Chilean earthquake, time-domain obs. 79−12079
spontaneous rupture propagation, two-dimens. model, numerical study 77−78159
spreading shear faults stabilization by coupled deform. diffusion effects 77−17056
St. Lawrence Valley, La Malbaie, Quebec, microearthquake survey 78−61337
station correction for Cracow, Homogeneous Magnitude System for PV waves 80−8254
station magnitude correction determ. with selected references 77−33202
steady-state seismic slip, precise recurrence model, rel. to earthquake prediction 77−33003
stick slip earthquake, rupture propag. and energy focusing in foam rubber model 80−3947
storm microseisms form. conditions on Shikotan Island, 1974 Feb. 8-11 period 77−53004
strains and stresses in seismically active regions, calc. 79−79744
stratigraphic sequences, differentiation by statistical anal. 79−92503
stratum velocities determination using seismic data, iterative method convergence *(Russian)* 79−74982
stress accumulation in lithosphere 77−17071
stress buildup detection by meas. of ^{222}Rn concs. in Earth using nuclear track technique 79−53574
stress concentration mechanism for intraplate earthquakes 78−81112
stress drop seismic sources, body force equivalents 77−40984
stress field around block segments immediately before strong shock *(Chinese)* 79−100814
strike slip fault, three dimens. viscoelastic model 77−56591
strike-slip failting, in crust of horizontally variable rigidity, model 80−56377
strong ground motion, prediction using small earthquakes 79−88297
strong ground motion characterisation, uniform risk functionals 78−92789

seismology continued
strong ground motion representation and simulation 79−16388
strong ground motions at short epicentral distance, simulation 80−104906
strong motion accelerographs, charact. of EM starters 78−65396
strong motion earthquake records, horizontal components duration charcts. 79−66637
strong motion observations, analysis of source and medium effects 79−88299
strong motion prediction for pot. earthquake fault, barrier model 80−105053
strong motions, estimation with regard to fault rupture 79−88307
strong-motion, status and recent results 79−88271
strong-motion accelerogram from horizontal component spectral max. 77−91034
strong-motion accelerograms, digitization errors and base line corrections 80−98245
strong-motion accelerograms, vertical component charcts. 79−62458
strong-motion autoregressive modelling of rock-site accelerogram 80−81835
strong-motion data management developments 79−62629
strong-motion displacements simulation using surface-wave modal superposition 79−48404
strong-motion duration, definition using r.m.s. accel. as parameter 80−56392
strong-motion Fourier spectra of bedrock 80−81839
structural and vibr. bedrock props. in Sweden, seismic events 79−16402
structural system under multiple support excitation, seismic response anal. 78−53623
Sturt Block, Australia, vel. determ. and error anal., seismic refr. obs. 80−90229
subcrustal lithosphere, seismic anisotropy rel. to dynamical processes in upper mantle 77−49039
subcrustal lithosphere structural variation, explosion seismic profiles 80−3974
subduction zone seismicity, Makran coast, Iran 80−85635
subduction zones, seismicity and seismic risk 79−88294
subduction zones, shallow seismicity meas. 79−16401
subsurface layered media parameters, estimation using linearised multiple refl. model 79−5691
S.Sulaiman Range, Pakistan, struct. and seismicity rel. to tectonics 79−39715
summation base, restriction in seismic section migration *(Russian)* 78−40701
Sunda and Banda Arcs, seismic studies of crustal struct. 77−70622
Sunda trench and forearc basin, seismic study 80−72470
supercritical reflected waves from essentially nonplane siesmic boundary, props. and peculiarities of record *(Russian)* 79−8606
Superior-Churchill provinces boundary zone, S.Canada, cooperative seismic surveys 80−89985
surface acceleration, relevance of one dimensional shear models 79−88303
surface ground motion generated by forced vibration of a building 77−73647
surface motion of layered half-space calc. by Laplace transform method 78−7570
surface multiple reflections, suppression on seismic records 80−56402
surface wave and free oscillation problems, physical dispersion due to anelasticity 77−64231
surface wave dispersion function, computations for unlimited freq. values 79−74848
surface wave inversion problem and upper mantle density 77−17039
surface wave processing using PDP-15 interactive graphics 77−81818
surface waves, correlation method, appl. to tectonic dislocations prospecting in complex media *(Russian)* 79−8605
surface waves propagation over liquid and crystalline layers, elastic consts. of crysts. 80−76924
survey data analysis, sequential anal. method 80−89981
surveying, features of time sections in two dimensionally inhomogeneous media 77−44933
surveys, optimum multichannel filters theory *(Russian)* 79−39921
central Sverdrup Basin, crustal struct. from seismic refr. data 80−12355
Swabian Jura earthquake of Sept. 1978, macroseismic field obs. 80−72451
Sweden, map of maximum seismic intensity using new determ. method 80−105089
Sweden, seismicity map, earthquake catalogue for 1951-76 period 78−96159
Sweden earthquakes (1951-76), error anal. of source parameters 80−104920
Swedish earthquakes, focal depth distrib. 79−79756
sweeps, nonlinear techniques 79−92616
synthetic seismogram computation, new method 78−85711
synthetic seismogram construction and reconstruction, weighting factors 78−28330
synthetic seismogram of layered media with explosive source 80−98250
synthetic seismograms, calc. for spherical waves normally incident on plane parallel absorbing layers *(Russian)* 79−39667
synthetic seismograms, computation for impulsive waves in spherically symmetric model 79−74849
synthetic seismograms, for body waves in anisotropic media 77−49021
synthetic seismograms, for case of receiver within reflectivity zone 77−86786
synthetic seismograms (one dimensional), effect of subsurface sampling 80−72435
synthetic seismograms and anisotropic attenuating medium response 77−78108
synthetic seismograms from model ocean bottoms 79−48420
synthetic seismograms of upper crust involving vel. inversion *(Japanese)* 80−94478
synthetic sonic logs, as process for stratigraphic interpretation 79−88483
T waves from Tonga earthquake (June 1977), human perception on Tahiti 80−61769
Tabas-e-Golshan earthquake, Iran, Sept. 1978, mechanism and aftershocks 80−81825
SW Tadzhikistan, earthquake energy rel. to lithosphere thickness, forecasting 77−9367
Taiwan, seismic zonation risk model 79−88277
Taiwan velocity risk mapping for seismic resistant building design 80−31002
Tamayo transform fault, E.Pacific Rise, deep tow study 80−51361
seismology continued
Tangshan earthquake, seismogenic models rel. to convection-generated stress concentration 79−92507
Tarbela array, P vel. lateral inhomogeneities under lesser Himalayas 77−91027
Tarbela reservoir, Pakistan Himalayas, seismicity during initial filling 80−56388
Tasmania University seismic net, electronic development 80−82073
Tataria, USSR, lithological data from seismic refl. of longit. and transverse waves *(French)* 80−101335
tectonic plate boundaries, seismic activity dynamic interaction along rising and sinking edges 77−73706
tectonic stress directions in Alpine regions, correl. with joint orientations 80−105052
tectonics conference on passive margins, Jun. 1978, Nova Scotia, Canada 80−36774
tectonoelectricity, review 78−36095
tectonomagnetic events, detect. using empirical transfer functions 79−16374
tectonomagnetics and small scale secular variation, symposium, Seattle, Washington (1977 August 22) 80−22133
tectonomagnetism, implications of magnetite mag. susceptibility under hydrostatic press. 80−26504
tectonomagnetism as earthquake precursor, piezomagnetism response depth depend. 80−26465
Tehran region, Iran, microearthquake survey 77−25656
telephony appls., underground cables laying, rocks location verification 80−72456
teleseismic magnitude relations, extension of Zurich magnitude recommendations (1967) 80−109105
S. central Texas, effect of Balcones Faults on groundwater movement 78−53672
Texas shelf zone, crustal struct. from sonobuoy and ocean bottom seismograph data 79−5462
Texas-New Mexico Permian Basin seismicity rel. to hydrocarbon recovery operations 80−36256
theoretical introduction, book 80−41962
theoretical problems, conf., Aug. 1978, Caracas, Venezuela 80−51400
theoretical seismograms calc., reflectivity method for buried source 79−48421
three dimensional seismic struct. of the lithosphere 77−33023
Three Forks Basin, Montana, USA, seismicity and tectonics 80−81829
three-component registrations, interpretation via orthogonal regression *(German)* 78−32017
Tibet and Himalaya, long-term premonitory seismicity 80−72442
Tibetan Plateau, Rayleigh wave attenuation 77−33028
N.Tien Shan seismic zone, fracture water radioisotope vars. and earthquake prediction 79−44204
Tien-Shan seismic zone, secular geomagnetic variations *(Russian)* 77−86777
Timano-Pechora province, USSR, seismic profile, upper mantle stratigraphy *(Russian)* 77−70616
time correlation using radio broadcast signals 80−90253
time section conversion to depth sections, weighted summation *(Russian)* 79−84532
time series alignment, new statistical approach 79−92623
time series filtering with time variant operators, convolution and Fourier transform 77−87082
time-to-depth conversion for layered medium 78−3962
time-variable curvilinear anal. of seismic recordings *(Russian)* 79−39946
Tohoku, Japan, intraplate seismicity correl. with interplate earthquakes 78−92787
Tokyo, base rock, seismic explosion obs. *(Japanese)* 80−41403
Tokyo, liquefaction of the ground during earthquakes 79−88309
Tokyo, seismic microzoning map 79−88282
Tokyo area deep shear wave velocity meas. 79−88304
Tonankai (Japan) earthquake, 1944, source model for accompanying tsunami *(Japanese)* 80−67344
N.Tonga region, earthquake distrib. geometry and complicated subduction closure model 80−90010
Tonga-Kermadec region, deep and intermediate earthquakes energy release rel. to mantle flow depth 80−41404
Tonga-Lau system, deep collision of subducted lithospheric plates 79−29736
topolgy of ray surfaces in low-velociy zones 80−21633
toroidal free oscillations, upper mantle discontinuity effects 79−29713
transfer function, for horizontally stratified Earth, prospecting appls. 77−21918
Transkei Basin, seismic refraction obs. 78−11831
transmission synthetic seismograms, direct inversion 79−29877
travel time interpretation method, for wide angle reflections from crust-mantle 78−65202
travel time inversion, computational methods 80−51340
travel time inversion, geometrical approach 80−3946
travel-time inversion method, for earthquake location and vel. struct. 80−109109
travel-time inversion problem, new approach 80−51339
tree ring growth, affected by Fort Tejon 'quake, California 80−98259
triangular networks relative performance in regional seismic sources location 79−84523
Tsengwen reservoir, Taiwan, seismicity due to fault and lake filling 80−81930
tsunami, scatt. at estuaries bordering continental shelf 77−78191
tsunami amplitude, correl. with sub-oceanic Rayleigh waves, appl. in tsunami warning system 77−81806
tsunami propagation, nonlinear dissipation effects *(Russian)* 79−8639
tsunami response for island system and surrounding underwater topography, calc. 77−86919
tsunamis effects at coastal sites due to offshore faulting, appl. to Israel 78−69300
tsunamis interaction with Hawaiian Islands, finite element numerical model 78−69361
tsunamis inundation in Kochi Prefecture, Japan, numerical expts. *(Japanese)* 78−96150
tsunamis of 1707 and 1854 along Shizuoko coast, Japan, field surveys *(Japanese)* 78−96149
W. Turanian platform, seismic crustal models of major structural zones *(Russian)* 78−40526
Turgen' Geophysical Observatory data for crustal deformations 80−76935

seismology continued
Turkey, earthquake epicentre and origin time determ. accuracy 77−41002
Turkey, local magnetic constant var. rel. to seismicity 77−2095
Turkey, seismic risk calc., preliminary approach 79−57878
Turkey, seismotectonic implications of relocated aftershock sequences 79−44119
two-dimensional profiles, dip-domain migration 78−77343
two-dimensional refl. time-delay curve, approximation for arbitrary refl. surface *(Russian)* 79−44132
two-dimensional strike-slip fault, static deform. of laterally inhomogeneous half-space 80−31012
two-point eikonal, appl. to seismic images form. systems *(Russian)* 79−96740
Udine area, Italy, seismic shakeability and seismic risk 78−24261
Ukrainian Precambrian Shield, deep fractures analysis *(Russian)* 79−20773
NW Ukrainian Shield, abyssal fractures obs. from deep seismic sounding data *(Russian)* 79−96746
Ukrainian Shield, deep crustal structure from seismic studies *(Russian)* 79−48428
Ukrainian Shield, deep seismic sounding profile reinterpretation 80−56407
Ukrainian Shield, deep seismic survey profile comparison with gravity and heat model *(Russian)* 78−48991
underground explosion source models 77−33004
underground nuclear explosion, far-field waveforms calc. 77−60356
underground nuclear explosions, complex P-wave signal coda power and modulation characteristics 79−79757
underground nuclear explosions, seismic source functions and magnitude determ. 77−56584
underground rock destruction seismic meas. method 77−9419
United Kingdom, estimation of probability of earthquake damage to nuclear power plants 79−93844
United Kingdom, perceptible earthquakes 78−77189
W.United States, 3-D mantle struct., P vel. study 80−85621
United States, attenuation of strong ground motion 80−81834
NE United States, crust and mantle struct. by seismic vel. 80−56429
W.United States, ground motion parameters for moderately strong earthquakes 79−88305
W.United States, horizontal ground accel. attenuation rel. to magnitude 80−104905
United States, national seismic hazard and zoning maps status and prospects 79−44109
eastern United States, seismic hazard estimates, seismicity uncertainty effects 77−91032
E.United States, seismic struct., shear wave vel. 80−56385
W.United States, short-period S-wave attenuation 80−98242
United States, western region, strain accumulation rates, 1970-78 period 80−21607
central United States crustal velocity models, theoretical seismogram constraints 79−39693
E.United States of America, seismicity, 1754-1972 data 80−36253
United States seismic hazard maps, prospects for geological data appl. 79−44110
Uordan-Dead Sea rift, crust and upper mantle seismic study, transition towards Mediterranean Sea 79−79766
Upper Amur region USSR, seismicity, tectonic features and earthquake epicentre confinement 80−101343
upper mantle, body waves parameters in Crimea-Vrancha-Bohemian Massif geological traverse *(Russian)* 79−53316
upper mantle, nonlinear stress propagation 77−17058
upper mantle, P-wave vel. profile, eastern USA 80−81818
upper mantle, struct. from inversion of surface wave dispersion data with random errors 77−73681
upper mantle physical conditions, Walsh's model 80−90047
upper mantle waveguides, rel. to possible density inversion 79−12099
Upper Rhine graben, seismic risk evaluation 79−25207
Urach region, Germany, seismic obs. rel. to temp. field investigation at great depths 79−48440
US, Eastern Mass., fault zones 78−85502
US, Missouri and S.Carolina seismic areas 78−85505
US, north-east, risk analysis 78−85503
US National Earthquake Information Service seismic data acquisition 77−29446
S.E.USA, earthquake activity data and seismic zones 78−11838
USA, East-Central, geological perspectives of earthquake hazards 78−11834
N.E.USA, rel. of seismicity to geology 78−11836
N.E.USA, seismic risk analysis in rel. to nuclear plant siting 78−11835
USA background seismic risk and incremental risk due to nuclear power stations 79−70757
USA-Japan studies on wind and seismic effects, conf., Tokyo, Japan (May 1975) 78−36252
USSR, correl. between seismicity and underground water regime *(Russian)* 80−104913
N.Utah, seismic attenuation rel. to other regions of W.United States 77−91030
Utah seismic refr. profile DELTA-W, crustal phases 80−56384
variable angle seismic reflection-refraction profiles, oceanic upper crustal structure 79−70761
Vela Seismological Network, use of Datacomputer 77−82013
Vela seismological network, use of datacomputer 78−81411
velocity data analysis using interference methods *(Russian)* 77−45193
velocity-depth structure, using waveform inversion method 80−105060
vertical motions, vel. during rock mass seismic flow 77−33035
vertical profiling, horizontal stacking technique *(Russian)* 79−62619
vertical seismic profiling, travel-time curves, theory 80−94473
vertical seismotectonic motions in Baykal rift zone 79−79783
vertical time-depth curve, automatic approximation via successive layer detect. *(Russian)* 78−40700
vibration generator for seismic surveys, electromagnetic motor type 80−90262
vibration sources at sea, charact., theory *(Russian)* 78−75154
vibrator exploration with non-sinusoidal signal 80−82086
vibroseis deconvolution 78−16171
Vibroseis deconvolution method, noise effects 80−90232
vibroseis operation, vibrator-ground forced oscillating system, reson. phenomena *(Hungarian)* 80−105074
vibroseis signal similarity, computerized anal. 78−20543
Vibroseis system, encoding techniques 78−69474

seismology continued
Vibroseis technique, signal design 77−41182
vibrosource, charact. in liq. layer 79−81905
Viljuy syneclise, common depth point data digital processing technique *(Russian)* 79−74875
Villalvernia-Varzi-Bobbia Line (N.Apennines), seismicity and geomorphology rel. to neotectonic deform. *(Italian)* 79−8624
Virgin Islands, tectonic struct. and earthquake swarms, seismic network obs. 80−89973
viscoelastic stiffness model of seismicity 79−20764
VLF vertical seismic noise 79−20763
Volcano Mihara tremors rel. to emitted gases 77−66899
volcanoes, hydraulic transients as seismic source 79−100816
volume and surface sources, due to laterally varying boundaries of elastic homogeneous layers 79−16397
Voronezh Crystalline Massif, seismic vels. significance of mineral substance inhomogeneous compression 80−94504
Vrancea, 1977 March 4, anomalous seismicity pattern, rel. to earthquake prediction 79−88263
Vranch earthquake seismic wave travel-time curves 80−89998
S.Wales, deep geologic struct. by explosion seismology 80−36261
Walvis Ridge, seismic refr. obs., crust and mantle struct. 77−78153
Warrnambool earthquake, 1903 July 14, isoseismal map 79−92506
wave field spectral composition, effect of multiple scatt. *(Russian)* 79−8607
wave front control method in seismic surveys and shooting data processing 80−90238
wave kinematics and dynamics; statistical analysis determ. *(Russian)* 79−84533
wave velocity determination, overlying sequence stratification effect *(Russian)* 79−39961
wave-equation datuming technique, appls. and computations 80−51553
wavefront curvature theory, for laterally inhogeneous media 80−104908
wavelet estimation, short-time homomorphic signal anal. appls. 78−81426
weathered layer, seismic wave front eqn. and travel time 77−78122
Weddel Sea, geomagnetic, bathymetric and seismic obs. of crust 80−104929
Wellington region, New Zealand, seismicity within plate convergence zone 79−16398
Western Cordillera, Colombia, upper crust seismic vel. 80−81819
white noise estimators for deconvolution 77−29472
wide angle refl. data from expendable sonobuoys, display and processing 79−39896
wide line profiling and two-dimens. version of CDP technique *(Russian)* 79−62615
wind and seismic effects, conf., Tokyo, Japan (May 1977) 79−62569
Wood-Anderson synthetic and actual seismograms comparison 79−48418
Yakataga Gap, Alaska, seismic history and earthquake pot. 80−109115
S.Yamanashi Prefecture, Central Japan, microearthquake activity *(Japanese)* 80−67343
Yamasaki fault, SW.Japan, seismic activity and crustal movement, predictions 79−57872
yearly seismic energy release, world totals versus ridge system total 77−2113
Yellowstone caldera, seismic evidence for chem. mantle plume 77−2105
Yellowstone Lake, seismic refl. and refr. surveys and palaeomag. study 78−49049
Yellowstone Lake, submerged hydrothermal explosion crater in Mary Bay, bathymetry, seismic and mag. surveys 78−49050
Yellowstone National Park, USA, teleseismic delay anal. mantle struct. 80−3981
Yellowstone volcanic plateau, conf., USA (1974) 78−49004
Yoshioka-Shikano Fault, Japan Sea SW coast, geomag. induction study rel. to seismic activity 80−26475
Zagros Mountains, Iran, seismicity depth 79−34751
Zambia, provisional seismicity map and interpretation 77−49026
zonation for critical facilities based on two-level earthquakes 79−88286
NWSyria, seismic risk to large quakes 80−72454

seismometers
see also seismology
accelerographs, mechanical-optical, cross-axis sensitivity and misalignment effects 77−91285
adaptive delay element for seismic noise cancellation 79−74994
amplitude and phase calibration, automated high-precision method 77−9519
arrays for marine seismic exploration, coherent noise attenuation 79−74840
Australian seismological services 79−39915
automatic seismic array and network detect. 77−9516
beamforming array, linear adaptive algorithm 80−21834
Blacknest ocean bottom seismograph operational experience 77−64473
borehole acoustic velocity measurement system, within or between boreholes 80−51557
borehole easy-operation long-period seismometer (BELS type 79) with stable period *(Japanese)* 80−67417
bubble tiltmeter as horizontal seismometer 78−85712
bubble tiltmeter use as horizontal seismometer, comment 80−21839
calibration, in situ, modified step method 77−87101
calibration using random binary signals 79−92604
Canada Seismological Service, instrumentation and data processing 79−39914
Canadian operations, 1976, report 79−34993
Canadian Seismic Array Monitor processing system 77−9517
Canadian seismograph network, station P-wave residuals 77−91037
Canadian seismograph operations, (1977) 79−66837
with damping factor correction, freq. charcts. anal. 78−7800
digital automatic amplitude controller with preliminary smoothing, parameter selection *(Russian)* 79−74985
digital bandpass filters, filter type and operator parameters selection for instrumental realisation *(Russian)* 79−74984
digital event recording ocean bottom seismometer 77−64472
direct recording ocean bottom seismometer 77−64469
double-pendulum vibration oscillator or seismograph 78−16200
earthquake detectability, estimates for 478 globally distributed seismograph stations 78−15976
earthquakes investigation, possibilities in development of equipment 77−53228
EDS 1, electronic seismograph *(German)* 79−84503

seismometers continued
electrochemical convertors for seismic registering device, data readout 77−2287
EM and hybrid instruments, developments 79−39906
feedback-controlled wide-band seismographs, design, rel. to undesired side effects 79−39909
field recorder, dedication of micro-computer to signal selection 77−82073
Finnish seismic array, data transmission, recording and handling 79−39917
free fall direct recording ocean bottom seismograph 77−64471
Gauribidanur seismic array for underground explosions monitoring 79−39913
Gauribidanur seismic array in S.India, quantitative assessment of crust-upper mantle heterogeneities 78−32033
geophone sensitivity in Chebyshev optimised arrays 80−21835
geophones for recording shear waves 80−101447
Graefenberg array, digital recording and anal. of broadband data 79−25348
gravimeter of Gs-11/12 type adapted to seismometer operation *(German)* 80−31127
gyroscopic, horizontal component meas. *(Japanese)* 77−5351
gyrotransducer instrument for vertical seismic motion meas. *(Japanese)* 79−96842
horizontal pendulum tiltmeters, recording device 78−40679
inertial seismographs, sensitivity and dynamic range 79−39910
instrumental response, parametric expression scheme 77−91286
instrumentation and data analysis, conf., Durham, England (Aug. 1977) 79−39905
intermediate-period field system 80−61910
International Deployment of Accelerometers, very long period network 77−33198
JMA seismic network, epicentre detect. capability simulation for local earthquakes *(Japanese)* 79−96844
laser interferometer, NBS system, for earthquake prediction 80−13125
linear multichannel systems employed in regular waves separation, efficiency comparative anal. *(Russian)* 79−39922
long period seismic wave obs. with 5s period seismometer *(Japanese)* 80−94627
long-period seismograph, temp. effects, transfer function determ. 77−9518
long-period seismographs, noises and generating mechanisms 78−12017
long-period seismometers, appl. to higher-mode dispersion meas. 79−39974
marine seismic survey, modified integrating A/D convertor *(Russian)* 78−49142
mechanical sensors, frequency charact., influencing factors *(Japanese)* 78−85722
Milne seismograph, reconstructed to assess effective magnification 80−21656
miniature wideband horizontal-component feedback seismometer 78−24382
miniature wideband siesmometers, design 79−16698
MIT ocean bottom seismometer system 77−64470
near-bottom quantitative seismic profiler 78−16196
New Zealand seismograph network 79−39916
ocean bed seismic station, self-contained system with mag. recorder *(Russian)* 80−36410
ocean bottom, with response from 25 Hz to 100 s, instrument design 79−21082
ocean bottom hydrophone 78−12020
ocean bottom hydrophone system 80−51582
ocean bottom multipurpose seismograph, design and shipboard operation 78−16187
ocean bottom networks, hypocentre location, resolution 78−85713
ocean bottom refraction seismograph, data telemetry to surface vessel 79−39892
ocean bottom seismograph, comparison with sonobuoy data rel. to Texas shelf zone crustal struct. 79−5462
ocean bottom seismograph development at Hawaii Inst. Geophysics 78−12019
ocean bottom seismograph using digital telemetry and floating-point conversion 77−41197
ocean bottom seismometers 78−65397
ocean-bottom seismograph observation system 80−98479
ocean-bottom seismograph system off Pacific coast of Honshu, Japan, research and development 79−62628
ocean-bottom seismometer capsule, operationally optimized 79−39911
offshore seismic exploration streamer cable connector design and programming 77−25803
optimum multichannel filters used in seismic surveys theory *(Russian)* 79−39921
parametric models, seismic system calibration 79−92603
PLL lock indicator and event alarm for multiplexed telemetry 79−62597
pop-up bottom seismic recorder for marine seismic refraction expts. 77−64468
portable easy-operation long-period seismometer, peripheral stabilising device 78−65399
Pull-Up Shallow Water Seismometer design and appls. 78−45025
quintuple strong motion seismograph *(Chinese)* 79−62591
receiver within seismic reflectivity zone, synthetic seismograms 77−86786
recording channel, input cct. parameters matching *(Russian)* 79−39920
recording equipment, digital automatic amplitude control unit parameters choice *(Russian)* 79−39964
recording network at Campotosto reservoir *(Italian)* 80−101446
reliability of standby instruments 78−61585
RESMAC, Mexican seismic array 77−5355
RESMAC seismic array, epicentre location procedure 80−56616
seafloor earthquake meas. system, development 79−5689
seafloor instrumentation systems development, multifunctional, USA project 79−53584
seismic moment tensor estimated by linear inversion method 80−31125
Seismic Research Observatories, upgrading of worldwide seismic data network 77−5334
Seismic Research Observatory, seismograph systems 77−41179
Seismic Research Observatory seismograph system transfer functions 79−12291
seismic stations calibration, appl. of crustal spectrum charact. *(Russian)* 78−49158
seismometers continued
seismoacoustic station ASS-1_1 construction, operation principles *(Polish)* 78−24377
seismograph operations during 1975 in Canada 79−16414
signal enhancement seismograph linked with graphics computing system description and application 80−4131
SL-1 long-period seismograph at Simferopol, sensitivity *(Russian)* 78−12009
soil-structure interaction effect on seismometer readings, seismogram correction 79−16685
strong motion, accelerometry, improvements and limits 79−80046
strong-motion accelerograph data management 78−36332
strong-motion accelerograph maintenance and data processing Japan 78−36330
strong-motion accelerograph network, USA, field operations 78−36331
Tasmania University seismic net, electronic development 80−82073
telemetered seismographic stations, appl. to seismicity meas. in N.E.Alaska 77−64217
triangular networks relative performance in regional seismic sources location 79−84523
triggering digital seismograph with microprocessor 78−96308
UK Institute of Geological Sciences seismograph networks 79−39918
US seismoscopes, pulse output generator 77−9537
USSR unified system of seismic obs. 79−39912
vertical component meas. using quasi-TDF gyroscope *(Japanese)* 78−4006
wave onset detection algorithm for automatic seismometer *(Japanese)* 80−94476
wide band recorders specification 79−39908
wide frequency band seismic station in Miechowice coal mine, Upper Silesia *(Polish)* 77−53218
wide-band feedback instrument 79−39907

selective dissemination of information *see information dissemination*

selenium
see also nuclei with .....
A1 type, supercond. destruction by mag. field 78−91825
additions to polyethylene, effect on mechanical and electrical strength *(Russian)* 79−11662
additive, to polyethylene and rubber, effect on mechanical and elec. strength, after mechanical and elec. ageing *(Russian)* 79−52396
adsorbed layer on Ni, photoelectron intensity modulation for binding site 79−47589
adsorbed layer on Ni (111) surface, bonding geometry and electronic struct. 79−77909
adsorbed on Ni, photoelectron diffr. data 80−29851
adsorbed on Ni(001), resonancelike peaks in angle-resolved UPS 79−69955
adsorbed on Ni(111), surface bonding mechanism for ang. resolved photoemission 79−69360
adsorbed on Ni (001), angle resolved UPS, resonancelike peaks 79−87562
adsorbed on Ni (001), photoelectron diffr. obs. 80−40223
adsorption, on Ni, photoemission intensities from core states 78−95654
adsorption on Ni (100), orbital identification in INS and UPS spectra 77−43427
adsorption on Ni (111), angle-resolved photoemission 80−40230
allotropic modifications, muonic X-ray intensities, computer analysis 80−23577
amorphous, AC cond. magnitude and variation *(French)* 79−47095
amorphous, acoustic behaviour in terms of model involving stochastic reson. 79−23681
amorphous, acousto-optic props., 10.6 μm 77−43966
amorphous, anomalous currents during electrodeposition 77−44486
amorphous, bulk, DC cond. expts., cond. mechanism 78−43401
amorphous, bulk, Raman scatt. near Tg 80−60596
amorphous, bulk, reson. Raman scatt. 80−60597
amorphous, carrier lifetime and drift mobilities 78−87985
amorphous, conducting channel temp., time depend., under monostable switching conditions 78−19109
amorphous, correl. between mol. struct. and props. 77−11484
amorphous, defect states, SCF pseudopot. and tight-binding calc. 79−65415
amorphous, density of surface states 77−76897
amorphous, diffusion and electrodiffusion of Ag and its role in switching effect 78−19163
amorphous, dipolar activity at glass transition temp., AC method 77−66454
amorphous, effect of doping on mol. struct. and valence alternation states 80−49249
amorphous, elastic props. at high press. 79−37753
amorphous, elec. cond., activation energy, density, cryst. Se effect 80−65548
amorphous, elec. cond. at room temp., contact effect 77−20354
amorphous, elec. cond. increase on addition of O, Cl, K impurities 77−11920
amorphous, elec. field effect on crystn. 77−15318
amorphous, electrical transport, activation energy 79−95406
amorphous, electron irrad.-induced paramag. centres, 77K 78−88187
amorphous, electronic props., xerographic use 80−20242
amorphous, electronic props. rel. to xerography, defects 79−97454
amorphous, electronic struct. and optical props., pseudopot. calc. 80−65428
amorphous, evap. layers, electrophotographic props. depend. on thermal treatment of initial material 77−76978
amorphous, far IR investigation of structure, ring and polymeric chain components *(Japanese)* 77−76311
amorphous, friction and wear under lightly loaded contact 78−64740
amorphous, high field transport, impact ionisation, carrier mobility 80−80286
amorphous, hole diffusion obs. 77−76828
amorphous, influence of O_2 on phase separation 77−47354
amorphous, interface with poly-N-vinyl carbazole, photoinsulator-air gap-dielectric system, charges on surfaces 79−67407
amorphous, kinematic transform. study by DTA 79−27921
amorphous, luminescence 80−80862
amorphous, memory and threshold switching effects 78−14774
amorphous, monostable switching, current noise 80−44682
amorphous, negative magnetoresist., doping depend. 78−56161
amorphous, nuclear spin-lattice relaxation 79−11354
amorphous, O impurity addition rel. to elec. cond. 79−38067

selenium continued
amorphous, photoconductivity quantum yield, experimental validation of fund. theory 80−6909
amorphous, photogeneration, thermalisation model calcs., band gap *(French)* 80−75595
amorphous, photoinjection of holes into triphenylamine doped bisphenol-A-polycarbonate polymer 78−72191
amorphous, press. depend. of AC cond. 77−76858
amorphous, relax of sound velocity, struct. determ. 78−38786
amorphous, sound propag. at low temps. 77−72657
amorphous, struct., DSC and X-ray diffr. expts. 78−22662
amorphous, struct. and elec. cond. transitions under high press. 79−42237
amorphous, struct. models 79−37628
amorphous, struct. relax. effects, obs. by mech. props. *(French)* 79−51201
amorphous, structure, random chain assembly model 78−6015
amorphous, theoretical calc. of defect states 80−49657
amorphous, theory of anomalous dispersion of photocurrent transients 78−6412
amorphous, thermal quenching of photocond. 78−23137
amorphous, transient electrical transport, general and unified treatment 80−59977
amorphous, trap-limited model for dispersive transport of holes 78−6378
amorphous, TSC, dielec. relax. modes 77−90090
amorphous, US attenuation at low temp., internal friction peak 80−65152
amorphous, US relaxation and retardation of deform. near T_g point 80−84256
amorphous, US wave attenuation and vel., near glass transition 77−89501
amorphous, vac. deposited on polymeric substrates, with dynamic coating device 80−100792
amorphous, viscosity meas. using holographic technique 79−37263
amorphous and liq. states, Raman scatt. meas. 80−50328
amorphous and liquid state, mol. structure, local atomic arrangement at intrinsic bonding defects 80−59374
amorphous and liquid state, Raman spectra, crystn. processes 80−60608
amorphous and partially crystallised layers, trap spectrum, TSC and I-V characts. 77−76981
amorphous evaporated layers, struct. inhomogeneities due to prep. technology fluctuations 77−76710
amorphous film, AC conductivity at radio and microwave frequencies 79−11248
amorphous film, between metal electrodes, switching mechanism 78−39172
amorphous film, crystn., tehrmal and photo-effects 77−47692
amorphous film, dark and photoconductivities 79−87173
amorphous film, dielec. activity obs. near glass transition temp. 80−75933
amorphous film, Hg activated, anomalous photocond. 77−43658
amorphous film, highly disordered, UPS study 80−76148
amorphous film, influence of wavelength on optical quenching of photoconductivity 80−60046
amorphous film, interference enhanced Raman scatt. 80−50326
amorphous film, inverse/combined photoadsorption and photodeposition, light-temp. interference 79−46977
amorphous film, photocond., dark cond., rel. to crystn. 80−88596
amorphous film, photodeposition by Selor process, kinetics 78−75963
amorphous film, photodeposition by Selor process, struct. and kinetics 78−75964
amorphous film, photodeposition by Selor process struct. 78−75962
amorphous film, spherulite formation and role of stresses due to volume changes in crystallisation 77−1083
amorphous film, stabilisation by thermal treatment *(French)* 79−47176
amorphous film, substrate effects on crystn. kinetics 77−1337
amorphous film, Te and Ag doped, elec. conduct. 300 to 350K, transition 77−4454
amorphous film, threshold and memory switching 79−82651
amorphous film, vac. evaporated, density meas., microcrystalline model of struct. 80−2313
amorphous film-metal system, contact pot. distrib. and photo-EMF, work function 77−76925
amorphous films, characts. determ., majority carrier eqn., exponential trap distribution 78−14760
amorphous films, evaporated, ageing and crystn., DTA 80−65413
amorphous films, structural relax., viscosity, creep, heat capacitors, and IR spectra meas. 79−42424
amorphous layer, localised states in band gap 80−59928
amorphous layer structure, influence of vacuum deposition conditions *(German)* 78−63957
amorphous layers, dielectric relax. in glass transition range, ageing 79−82923
amorphous layers, steady-state photocond. meas. 77−35961
amorphous layers, substrate range depend. on dielec. relax. in glass transition temp. 79−69773
amorphous solid dielectric loss meas. by submillimetric waveguide laser 79−33603
amorphous thin film, elec. noise, monostable switching 80−44684
amorphous thin film photodeposition from hydrosols 78−11109
amorphous vibr. props. calc. for models 77−84873
atom, 1897 to 9271 Å region spectrum 78−21869
atom, chemisorption on Cu, cluster theory 80−29264
atom, chemisorption on Ni, cluster theory 80−29264
atom, Doppler effects in X-ray spectra excited by accelerated ions 78−86808
atom, electron bombard., 300 to 600 keV, K_α/K_β X-ray intensity ratios, K-shell ionis. cross sections 78−37747
atom, electron impact ionisation, characteristic X-radiation ang. distrib. obs. 80−1069
atom, electronically excited, direct obs., quenching by inert gases 78−25461
atom, ionisation by proton-atom collisions, loss of K-electron calc. *(Russian)* 77−50523
atom, LMM Auger spectra, relative intensity and relaxation energy 80−69115
atom, photoionisation cross sections and ang. distribs., outer p subshell 80−9572
atom+$H^+(D^+)$, K shell ionisation, nuclear Coulomb effect 80−91650
Bijvoet intensity differences, prediction in noncentrosymmetric structs. 79−7574
bonded to Ni (100) surfaces, electronic orbitals 78−72224
bonding coordination defects 80−59927
carrier mean transit time superlinear depend. on material thickness 80−6894
cathodoluminescence of trigonal Se at 10K *(German)* 78−2923
charge density, self-constent OPW and pseudopot. calcs. 80−92813
chemical bonding in group V and VI elements and compounds with tetradymite structure 80−15036
chemisorption on Ni, Xα cluster model calcs. 79−65313
chemisorption on Ni(100), struct. and energy levels calc. 77−47663
coating, on Al thin film, effect on supercond. 80−7026
Compton profile, charge and momentum density 80−55220
Compton profile, charge density and momentum density determ. 77−63480
Compton profile, valence electron, self-consistent OPW calcs. 77−36307
covalent solid, struct. props. and valence force fields, non-empirical calc. 77−1096
crystallisation kinetics correlation with molecular structure 78−94998
cubic modification prepared by shock compression 78−34494
dark current relax., barrier cond. mech. 80−6904
Debye temperature, using elastic consts. and Kopp-Neumann relations 78−2220
determination, in complex alloy, by at. absorpt. 77−40582
determination, matrix effects in graphite furnace AAS 78−85230
determination in environmental water by preconc. on charcoal, neutron activation anal. 77−44551
dielectric function in trigonal phase, model calc., local-field corrections 78−39045
differential dosimetric characts. w.r.t. γ-radiation 80−32529
diffusion coefficient in Si, by sheet Hall coeff. meas. 79−46843
diffusion in GaAs 77−51547
diffusion into SnO_2 films *(Japanese)* 79−95218
diode surface states determ. by conductance and capacitance 77−85318
dislocations in undeformed rhombohedral crystals, obs. by electron microscopy *(French)* 78−51548
dissolved Se(VI) meas. of estuarine water in Solent area 78−57230
distribution equilibrium between FeO-Fe_2O_3-SiO_2-Al_2O_3-CuO/Cu slag/metal system 78−44111
effective charge tensor, microscopic treatment 78−59879
elastic and piezoelec. consts., US phase vel. meas. 79−86834
electrical conduction behaviour, 0-500 kbar 79−99589
electrical conductivity after X-ray irradiation 79−51567
electroconductivity, X-ray effects *(Russian)* 80−15519
electronic states, tight-binding model Hamiltonian for trigonal struct. 77−59250
electronic structure of cryst. phases, hydrostatic press. effects 80−59865
electrophotographic and electroradiographic image convertors with electronic readout 79−71554
electrophotographic characts. of films rel. to viscosity of bulk specimens *(Russian)* 80−73505
electrophotographic film, Se spheres embedded in polymer matrix, optical props. 78−83055
electrophotographic film current/density voltage characteristic rel. to substrate temp. *(German)* 77−55629
electrophotographic films, ageing effects on structure and properties 77−47699
electrophotographic films, surface potential microprofile meas. 77−45913
electrophotographic layers, amorphous, resolution parameters 80−31926
electroradiographic layer, radiographic contrast 80−12241
electrotransfer in liquid Te 77−11716
EM wave scattering from crowded Se sphere monolayer, migration imaging film appl. 80−99627
epitaxial growth on Te (1$\bar{2}$10) face, LEED and AES meas. 77−1328
epitaxial monocrystalline film, trapping, TSC meas. 77−85349
evaporation kinetics from temp. programmed large area source 77−69996
exciton luminesc. in trigonal form 79−33802
film, A1 type metallic phase, optical consts. and refl. 77−32455
film, amorphous, block formation during crystn., electron microscope obs. 79−11030
film, amorphous, crystallisation induced by corotron charging 77−35832
film, amorphous, density of localised states 78−34742
film, amorphous, empirical formula for temp. depend. of dielec. loss peaks 80−97197
film, amorphous, photocond. props. *(French)* 77−72886
film, amorphous, thermo-crystn. obs. 77−11810
film, crystallisation using org. catalysts, struct. and elec. props. 77−51613
film, effect of thermal history and substrates or crystn. by vac. condensation 77−15713
film, epitaxially grown on Te substrates, crystallinity, RHEED and SEM meas. 77−40373
film, gas-evaporated, selective absorpt. characts. and emissivity 80−50998
film, ion plated on thermally evap., ESCA interface study 78−43269
film, laser beam hole machining 80−30207
film, metal ion diffusion during memory switching 78−26976
film, noncryst., ageing and crystn. obs., tentative struct. model 80−2295
film, noncryst., controlled vapour deposition, crystn., and optical props. 78−39696
film, obliquely deposited, elec. resist. anisotropy 80−2486
film, resonance Raman spectrum 79−28760
film, switching characts. under pulsed bias 77−39979
film, trigonal, sputtered and evaporated, nucleation and growth processes 77−31920
film, vacuum deposited, struct. asymmetry, reflectivity elec. cond. 79−23855
films, Ag diffusion, effect on interferometric thickness meas. 80−96695
films, optical constants in visible region 80−97360
fluorescence pumped photolytic gas laser system for fusion plant 78−62606
foil, traversed by $H^+(He^+)$, energy loss and straggling meas. 78−95100
Fourier-transformed Compton profile as microstruct. probe 77−59636
Gaussian basis sets, Ga, Ge, As, Se, Br, and Kr, HF calcs. 77−38611
glass, catalytic crystallization in organic media at room temp. 77−84657
glass, flexural strength in transition range 77−56032
glass transition temp., enthalpy rel. to annealing, DSC 77−15561
glassy, localised electronic states, photoluminesc. and ESR studies 80−65501

selenium continued
glassy, pure and K-doped, photolum. and optically induced ESR 80−50398
glossy, structural excitation energies of defects, pseudopot. approach 80−107061
gravimetric determ. by reduction of H_2SeO_3 77−90683
hexagonal, resistivity depend. on applied elec. field freq. during crystn. 77−35938
hole drift mobility meas. by light pulse technique 78−19086
human tissue, Se determ. by thermal neutron activation analysis and atomic absorpt. spectrometry 79−88218
impurity in Nimonic 105, influence on creep and stress rupture props. 80−66602
ion implantation into $Ga_{1-x}Al_xAs$ *(French)* 77−68986
ion implantation into GaAs 78−55884
ion prod. in 2 MV Van de Graaff 80−14031
K shell photoelectric cross section, at 74.409 keV 79−72288
K-edge dispersion anomalies, meas. using X-ray interferometry 80−90956
$L_2M_{4,5}M_{4,5}$ Auger spectrum following photoionisation, post collision interaction, chemical shifts 79−22678
Lande factors measurement in $B\ ^3\Sigma_u^-$ state 77−34648
laser, auroral and transauroral transitions, high energy storage 77−10897
laser, OCSe photodissoc., forbidden at. transitions 78−79010
laser, photolytic, expts. for fusion research 78−63101
laser action from $Se(^1S_0)$, OCSe photolysis 79−31889
latent electrophotographic image, formation mechanism *(Russian)* 79−26157
layer crystallinity meas., combination microwave resonator method *(Russian)* 78−22652
layer in metal crucible, radiation emissive power theory 78−22874
liquid, and liq. Se-Na, elec. resistivity and phase separation 79−82573
liquid, Anderson transition, cond., at high temp. and supercrit. press. 78−34869
liquid, chain molecule struct. exam. by time-of-flight pulsed neutron diffr. 77−55228
liquid, compressibility 77−65997
liquid, correlation between switching and struct. 77−69388
liquid, dielectric relax. and elec. cond. 80−108150
liquid, electrical cond. transition at high temp. and press., Anderson localisation *(Russian)* 77−1462
liquid, electronic transport props., equation of state, to 1900K and 1800 bars 80−65574
liquid, electronic transport props. at sub- and supercritical conditions 77−51788
liquid, eqn. of state determ., crit. props. and mol. comp. 80−49336
liquid, estimate of self-diffusion coeffs. from viscosity data 77−55370
liquid, heat capacity, 500-700K, dynamic differential calorimeters comparison 78−89482
liquid, heat capacity and chem. equilib. 80−103486
liquid, metal-insulator transition, review 77−1367
liquid, pure and I doped, DC cond., temp. depend. *(French)* 77−69322
liquid, pure and I doped, DC cond. and thermoelectric power *(French)* 79−56223
liquid, pure and I doped, thermopower, temp. depend. *(French)* 77−69360
liquid, review of continuous metal-nonmetal transitions 77−51787
liquid, ring-chain transition, disordered chain model 78−59943
liquid, struct. factor determ. rel. to short-range correlations 77−1060
liquid, surface tension isotherms, struct. changes 79−37904
liquid, thermal cond. meas., resistive probe method 77−15636
liquid, US absorpt. meas. 78−2202
liquid, US rel. temp. depend., melting effects 78−38782
liquid, viscosity meas. by rot. cylinder method 80−88347
liquid and amorphous, struct. by pulsed neutron diffr. using an electron LINAC 77−51307
liquid and amorphous, struct. modelling using Monte Carlo method 80−59391
liquid-crystal phase transition, elec. cond. changes 79−33310
liquid-glass transition, P-V-T relations 77−24387
low-frequency coupled photocurrent and temp. oscillation 80−60044
magnetic susceptibility meas. rel. to heat treatment 78−34952
mass spectrometry in INS separator 77−38056
mean excitation energies from α-particle stopping power meas. 79−13615
metal-insulator transition induced by temperature 78−2529
metallic state, press. induced, elec. cond. meas. 80−96949
modulated photocurrent, analysed for trap-limited case *(Japanese)* 80−60030
molecular crystal, Se-Se nonbonded pot. parameters derivation from heat of sublimation 79−27945
molecular photolytic dissociation, obs. using inert gas halide lasers 80−11935
molecule, Lande factor meas. by Zeeman quantum beats *(French)* 79−45761
monoclinic, α-phase, heat capacities and thermodynamic properties, 3-300K 78−95162
monoclinic allotrope, thermal behaviour 78−67813
monoclinic to trigonal transform., DTA, X-ray diffr. and optical microscopy meas. 78−14461
monolayer, adsorbed on Al (111), angle resolved UPS of 2-dimens. band struct. 80−60059
muonic allotropes, muonic Roentgen intensities *(German)* 80−53168
nanosecond switching investigation 80−20263
neutron activation analysis determ. of Se in human urine 80−36079
neutron activation analysis of Se in TeO_2 77−86400
neutron irradiated single crysts. at high fluence, annealing 77−85266
NMR chemical shift, tight-binding calc., trigonal Se 78−2759
nonoclinic to trigonal conversion, thermodynamic stability and associated investigs. 80−24592
$(np)^4\ ^1S_0$-level photoionisation via autoionising levels 79−76398
overlayer, c(2×2), on Ni (001) surface, angular resolved UPS 78−76584
overlayer, on Ni (100), bonding, photoemission expts. 77−35819
overlayers on Ni(100), normal photoelectron diffr. of Se 3d level 79−11501
oxide glasses with Bi or Se granules, elec. props. and microstructure 78−2490
p-type film, photocond., phase-memory effect 78−91723
phonon dispersion curves, scaling formalism 80−54326
selenium continued
photoabsorption spectra for amorphous, trigonal and monoclinic samples 78−23551
photocell, high-gain amplifier cct. 78−4679
photocell optical vibration transducer 80−77768
photocells, temp. coeff. of sensitivity 78−82033
photoconducting film, phase memory effect and deep levels 79−82556
photoconductive film, field instability, Ar^+ ion irrad.-induced defects 78−87997
photoconductive layers, impedance-freq. characts. meas. *(Japanese)* 79−38120
photoconductor for KD_2PO_4 spatial light modulator, optical data processing appl. 80−9988
photodetector, linearity, stability, fatigue and light memory effects meas. *(Spanish)* 77−87837
photoelectronic behaviour, in glass transition region 80−60045
photoemission relax. energies *(French)* 77−36357
photographic migration images, liquid developed, fixing and abrasion resistance 80−4792
photoreceptors, phthalocyanine sensitized, elec. cond., charge decay characts. 80−15630
photosensitive particle migration, electrophotographic film structure and process 80−101863
physics, conf., Konigstein, Germany (May 1979) 80−51958
piezoelastic modulator for 10.6 μm radiation using Au clad amorphous Se optical waveguide 78−66956
plate, sensitivity exam. for xeroradiography appls. 77−45909
poly(N-vinyl carbazole) sensitisation with Se, purification effect on electrophotographic characts. 80−49825
polycrystalline trigonal layer, freq. depend. elec. behaviour and its relationship to xerographic performance of Se particle contact photoreceptors 79−82640
positron annihilation, of amorphous trigonal and α-monoclinic Se 79−11484
positron lifetime meas., comparison with theory 77−63483
positron lifetimes, positronium form. in trigonal and amorphous Se 80−60711
powder compacts, sintered, electrical cond. 80−70693
radiation damage expts. review, defect interactions 77−84800
red amorphous film, textural change, thermal and photo effects 78−63951
rhombohedral, IR absorpt. spectrum 80−103949
SAW vel. and electromech. coupling factor 80−75422
sea- and river water, Se (−II,0), -(IV), and -(VI) composition, by gas chromatography method 80−81928
semiconducting, and related materials, historical study, 1833-1919 78−57727
single crystal, behaviour in strong electric fields 77−62942
solid, chemical shift and nucl. spin-lattice relax., high temp behaviour 80−60445
solid solubility in GaAs, SIMS 78−67830
solubility in liquid Cu 77−21096
space group $C3_12$-$C3_22$, habit variation 80−107090
spectrochemical analysis, atomic absorption using vapour generation method 80−16745
steel, maraging, Se microalloying, machinability improvement 80−21116
surface, (10$\bar{1}$0) and (1$\bar{2}$10), LEED study *(French)* 79−14991
symmetry coordinate generation using multiplier representations of space groups 79−37646
thermal expansion and Gruneisen coeffs., 10-300K, trigonal or amorphous phase 78−22870
thermodynamic basis for generalisation of melting curves 78−2236
thin film selective absorber coatings, prod. using an oblique vacuum deposition technique 80−81488
threads in natural mordenite channels, optical absorpt., cond. *(Russian)* 80−89022
trace amount determ. by hydride generation-nondispersive flame at. fluoresc. spectroscopy 80−89553
trace impurities, after solvent extraction, spectral determ. 77−90676
transient photocurrent data, multiple-trapping model of anomalous transit-time dispersion, α-phase 78−34860
trigonal, acoustoelectric current saturation 80−60053
trigonal, behaviour of optical gap under press. 80−80171
trigonal, cryst. growth from CS_2 soln. 78−23596
trigonal, dielec. matrix calcs. 80−54630
trigonal, electronic props. under press. 77−31939
trigonal, electronic struct., near metal transition, press. depend. 78−34758
trigonal, force field calc. of phonon dispersion relations 80−54328
trigonal, indirect exciton ground states, photoluminescence 79−24361
trigonal, inverse dielec. tensor in static limit, local field corrections 77−51690
trigonal, luminesc. identification of indirect transition 80−55189
trigonal, model of lattice dynamics using long and short range interactions 78−59893
trigonal, normal mode calcs. 80−84259
trigonal, Raman scatt. at very high press. 80−60566
trigonal, reflectivity and density of states press. depend., self-consistent pseudopotential calc. 77−31931
trigonal, state-of-the-art review of model calcs. 80−54327
trigonal, surface lattice dynamics, mean square displacement spectra in long wavelength limit 80−54498
trigonal, transverse magnetoresistance meas., influence of illumination 80−65607
trigonal, vitreous and red amorphous, phonon density of states comparison 80−54329
trigonal and amorphous, electronic struct. and nonempirical calc. of struct. props. 80−59866
trigonal and vitreous, sp. ht. and thermal cond., 3 to 300K 80−59676
trigonal single crystal, peak in temp. dependence of elec. cond. 80−44663
US absorption and velocity, near first-order phase transition 77−20014
vacuum evaporated film, photoinduced amorphous-crystalline transition obs. *(German)* 79−82156
vapour, photolysis by UV lasers, appl. to kinetics of group VI laser systems 80−7807
vapour laser, operation by dissoc. of metal complex 77−54702
vitreous, crystn., optical microscope obs. 77−84659
vitreous, darkened films, thermal and optical bleaching, light transmission obs. 80−50447

selenium continued
vitreous, elastic coeffs. about glass transition temp. US study *(French)* 80−19865
vitreous, mech. props. at temps. <300K, uniaxial compression tests *(French)* 78−55908
vitreous, micromech. props., anelastic behaviour, internal friction *(French)* 77−72652
vitreous, sp. ht. excess rel. to far IR absorption 77−84874
vitreous, temp. depend. of sound vel. 77−84855
vitreous, time dependent thermal expansion 78−14485
wedge shaped film, photovoltaic effect 77−1454
X-ray K-emission satellites, HF and LF, origin 80−50465
X-ray K-shell absorpt. discontinuity in amorphous and cryst. Se 79−61467
X-ray sensitivity, induced photocurrents, xeroradiographic meas., pair creation energy 80−22490
xerographic photoreceptor on flexible Ni foil, NiO interface 78−29184
xerography applications 80−57415
xeroradiography films, photosensitivity recovery from X-ray induced fatigue 77−2709
Al:Se, anodic oxidation, mobility of foreign atoms 77−90494
Al-amorphous Se-Al struct., capacitance variation with illumination 79−87165
As:Se film, amorphous, chemical modification of props. 80−49250
As_2S_3-Se, glass-forming system, phase diagram 77−16551
BP:Se, epitaxial layers, ion implantation, defects and lattic locations, channelling obs. 80−88179
CdS:Se, heavily doped, defect struct. 78−22756
Cs-Se thermionic converter, output power, vap. source depend. 80−44000
GaAs pure and Se-doped, photoluminescence at dislocations, band gap electronic levels 79−99926
GaAs:Be,Se VPE layers, ion implanted, donor-acceptor pair radiative recomb. 79−91489
GaAs:Cr, Se, shallow impurity implantation, elec. props. after annealing 80−24465
GaAs:Cr, Se layers, ion implanted, ohmic contact form., contact resist. meas. 79−91158
GaAs:Cr,Se, ion implantation of Se, carrier conc. and mobility profiles 77−47479
GaAs:Cr,Se, ion-implanted, semi-insulating effects of Cr redistrib. on elec. characts. 80−59982
GaAs:Ge,Se transmutation shallow donor transition obs. 80−59925
GaAs:Se, and undoped sample, annealed, surface cond. change, n-p double layer 78−64095
GaAs:Se, fast diffusion of elevated temp. ion implantation, SIMS meas. 78−34527
GaAs:Se, Ga, dual species ion implantation, elec. characts. 80−103377
GaAs:Se, implantation and laser annealing 80−24476
GaAs:Se, implanted, annealing with O-free CVD Si_3N_4 encapsulant 78−83834
GaAs:Se, implanted, depth profile, SIMS obs. 78−30655
GaAs:Se, implanted, multilayered encapsulation using SiO_2:As and Si_3N_4 79−11715
GaAs:Se, ion implanted, evaluation by contactless mobility meas. 79−1448
GaAs:Se, ion implanted, laser annealing, appl. to microwave devices 79−69139
GaAs:Se, ion implanted, surface state study from photoreflectance 79−91465
GaAs:Se, ion implanted, Cr redistrib. during annealing, SIMS anal. 80−10570
GaAs:Se, ion implanted, laser annealing 80−24482
GaAs:Se, ion-implanted, capless annealing by melt-controlled ambient technique 80−75251
GaAs:Se, LPE growth, Ga-As-Se phase diagram 79−1849
GaAs:Se, laser annealed, donor implanted, elec. props. 79−4556
GaAs:Se, MBE grown, surface exchange doping using PbS(Se) captive sources 79−10864
GaAs:Se, multiple scatt. Xalpha cluster model, impurity electronic states, dangling bond effect elimination 79−99504
GaAs:Se, n-type layers, heavily doped, formation by multiple ion implantation 80−88187
n-GaAs:Se, nonalloyed ohmic contacts of TiPtAu by pulse-electron-beam annealed Se implants 80−2466
GaAs:Se, pulsed electron beam annealing, doping profiles 80−6421
GaAs:Se, recrystn. of implanted amorphous layers, TEM and channelling obs. 77−89459
GaAs:Se, VPE, high purity, residual donors, photocond. expts. 77−85174
GaAs:Se cathodoluminescence decay obs. with SEM and streak camera, 90 to 300K 80−97348
GaAs:Se depth profiles, Cs^+ SIMS anal. appl. 79−39265
GaAs:Se ion implanted samples, Q-switched ruby laser annealing, improvement in elec. props. 80−100460
GaAs:Se ohmic contacts, pulsed electron beam annealing donor density, mobility 80−65678
GaAs:Se polycrystalline film, Hall effect, resistivity meas. 80−96911
GaAs:Se^+, Cs^+-SIMS and negative ion spectrometry 79−12882
GaAs:Se^+, implanted semi-insulating, pulsed electron and laser beam annealing effects on elec. characts. 79−73196
GaAs:Se^+, ion implanted, laser annealing effect on elec. characts. 79−73195
GaAs:Se^+, TEM structural study, surface and interior damage 80−34025
GaAs:Zn, Se, double doping during LPE, exam. of elec. cond. and Hall effect 79−4923
GaP:S, Se, Te, Si, shallow donors, excitation spectra 77−81128
GaP:Se, donor bound exciton excited states 80−66284
GaP:Se, IR photocond. response spectra 79−56257
GaP:Se, pot.-depend. g-values and quenched diamag., props. of donor states 77−62861
GaP:Se, pot.-depend. g-values and quenched diamag., pseudoacceptors D^0, X 77−62862
n-GaSb:Se, forbidden optical band gap, Moss-Burstein effect 78−88335
n-GaSb:Se, resonant and bound impurity states, Hall effect and resistivity press. depend. 77−28143
GaSb:Se thermal sensitivity, −170 to +180°C, resist. meas. 77−39906
Ge:Se^+, energy spectra, multivalley effective mass calcs. 77−59266
He-Se, metal ion laser, noise props. *(Japanese)* 79−64209
He-Se, vapour laser, continuous wave, intensity fluctuations investig. 80−83593
selenium continued
He-Se laser, cataphoretic effects in power output 77−83863
He-Se laser, noise props. 77−83857
He-Se^+ three-colour laser engineering 78−46644
He-Se^+ white light laser 80−1226
HgSe-Se, photo-field model, rel. to anomalous photocond. in Se:Hg 77−43658
InAs:Te(Se)(S), intrinsic pt. struct. defects 80−33998
InAs:Zn,Se, exam. of microhardness, Hall effect as function of dopant 79−95038
InAs:Zn,Se, solubility and donor-acceptor interaction 80−54263
InP:Se, implantation and laser annealing 80−24476
InP:Se^+, ion-implanted VPE layers, laser annealing, elec. and struct. anal. 79−73199
InSb:Se, exam. of defects in crystal 80−6423
n-InSb:Se, Moss-Burstein effect, optical energy gap depend. on doping conc. 77−8581
InSb:Se, reson. states and reson. scatt. 80−49738
InSb:Se p-n tunnel diodes, influence of doping on characts. 79−73575
n-InSb:Se(Te), drift tunnel diode, prod., current ratio meas. *(Russian)* 77−8185
KBr:Se^{2-} single cryst., dielec. relax. of impurity-vacancy dipoles, ITC meas. 79−91349
KBr:SeO_4^{2-}, IR absorpt. spectra, vibr. splitting *(Russian)* 79−51995
KI:Se_2^-, reson. secondary emission, total spectrum *(Russian)* 78−19551
Na_2O-B_2O_3:Se, EPR, γ-ray effects *(Russian)* 78−31109
NaX-Se semiconductor superlattice absorpt. edge, light scatt. *(Russian)* 80−71438
Ni-Se interface, reactive diffusion, electronic struct., UPS study 78−51748
S^+ form., CSe_2 photoionis. obs., heat of form. and dissoc. energy calc. 77−46604
Se, amorphous, vac. deposition on polymer substrates, use of temp. gradient vac. coating device 80−35099
Se, atom positions, effect of press. 78−34465
a-Se, hole form. energy, heating time and cooling rate depend. 79−41958
Se I resonance lines, new meas. 78−938
Se IV, radiative lifetimes, calcs. and beam-foil spectra 77−75223
α-Se, multiple-trapping model and time-dependent random walk 78−34842
Se, trigonal, low temp. sp. ht. and elastic consts., piezoelec. effect influence on phonons 80−54404
Se VI, 2400 to 90 Å spectrum anal. 78−58616
Se VII, VIII, $3p^5 3d^{10}$ config., spectrum, 100-1200 Å 77−65431
Se XXVI, $2p^5$-$2p^4 3s(2p^4 3d)$ transitions in laser produced X-ray spectra 78−13460
Se XXVI, spectra and energy levels of F isoelectronic series 79−93948
Se XXVI, transitions between $1s^2 2s^2 p^5$-$1s^2 2s^2 2p^4 3d$ and $1s^2 2s^2 2p^5$-$1s^2 2s^2 2p^4 3s$ configs. 79−26925
Se^+, ionisation pot., periodic regularities, relativistic corrections calcs. 79−49950
Se:As, amorphous, pure and doped, photoelectronic preps. in glass transition region 79−4583
Se:As, amorphous film, dielec. activity obs. near glass transition temp. 80−75933
Se:As, continuous crystn. kinetics 77−24382
Se:As X-ray plates, electronic transport *(German)* 80−80290
Se:As(Cl), trigonal, defect and impurity electron levels, surface photovoltage spectra 78−72108
Se:Cd dilute liquid, perturbed ang.-correl. meas. of motional-correl. time 79−41930
Se:Ge(Si)(Sn), vitreous, crystn. kinetics study by elec. cond. meas. 79−65526
Se:Hg amorphous film, photocond. anomaly due to HgSe layer form. 77−66183
Se:Hg film, amorphous, anomalous photocond. and residual interelectrode photo-EMF 77−69376
Se:I, vitreous, crystn, kinetics determ. *(German)* 80−79936
Se:O, amorphous, photocond. spectrum impurity effect 77−76862
Se:P, vitreous, crystn. kinetics study by elec. cond. meas. 79−64998
Se:P, vitreous, stabilisation of cond. 77−11910
Se:Ta, electrophysical meas. rel. to control of conductivity type 77−24323
Se:Te, amorphous, conductivity and activation energy depend. on dopant conc. 77−69325
Se:Te, amorphous, pure and doped, freq. depend. of elec. cond., 150 to 310K 79−42545
Se:Te, liq., viscosity, impurity effect, chain length role *(French)* 78−51717
Se:Te multilayer solar cell 79−43762
Se:Tl, and undoped material, dielec. losses and permittivity meas. 77−28518
Se:U, cryst. and amorphous, impurity conc. and distrib., solid state nuclear track detection 79−46694
Se-Ag_2Se, heterojunction with memory, transient switching characteristics 80−44718
Se-Ag_2Se, heterojunction, electrically controlled negative differential conductance, mechanism 80−44720
Se-Ag_2Se, thin film polycrystalline heterostructure, exhibiting memory switching, noise level 78−84288
Se-Bi bilayers chemical reactions, differential scanning calorimetry technique and obs. results 78−2398
Se-binding agent electrophotographic film characteristics and sensitivity *(German)* 80−4789
Se-Ni-Mylar multilayered struct., interfacial bonding effect on adhesion, ESCA obs. 79−95274
Se-poly(N-vinylcarbazole), double layer polymeric photoreceptor, potential discharge kinetics 78−72194
Se-polystyrene hexylmethacrylate, interface photocurrent studies, charge transfer mechanism 79−99627
Se+H^+, K-shell ionisation cross-section determ. 80−48077
Se+inert gas, ^1S-^1D collision-induced transitions 78−33588
Se+O→SeO, chemiluminescent reaction, $B^3\Sigma \rightarrow X^3\Sigma$ band emission 79−79254
Se+Zn, π^- capture, radioactivity meas. 80−47831
Se_2, 3d absorption spectra, mol. damping of centrifugal barrier effects 77−61736
Se_2, $b^1\Sigma^+ \rightarrow X^3\Sigma^-$ near IR emission obs. 80−91556
Se_2, dissoc. energies determ. 78−33632
Se_2, laser induced fluoresc. in inert gas matrix 80−87161

selenium continued
$Se_{5,6}$, influence of source material and shape on sublimation props. 78−80474
Se_8, monoclinic, XPS and valence band struct., comparison with trigonal form and S_8 77−44124
Se_8^{2+}, electronic struct. and localised MOs, bonding nature and geom. struct. 80−18798
Se_n, properties of small aggregates rel. to metallic character of Te_n 78−86985
$(Se)_x$, crystn. and melting 80−40241
$Se(^3P_1)$+inert gas, gas phase flash photolytic deexcitation obs., 1000K *(Russian)* 78−50626
$Se(^1S)$, quenching of high concs. prod. by photolysis 79−6904
^{74}Se, L-shell X-ray prod. by H(He) ion bombardment 79−47548
^{73}Se, yield for various reactions and chem. processing 80−36131
^{75}Se labelled adenosyl selenomethionine, distrib. in rat and prostate scanning appl. 80−17132
^{75}Se, neutron activation anal., coincidence counting, biological and soot samples *(Japanese)* 80−97750
^{75}Se, tracer for Se conc. in seawater expts., ^{203}Hg tracer 80−21420
$^{80}Se_2$, $B\ ^3\Sigma_u^-$ state, Lande factor meas., mol. perturbations 79−45756
Se*+OCSe, radiation quenching rates 79−86050
Si:Se, detector for 3-5 μm appl. development 79−35825
Si:Se, energy levels, resistivity and Hall coeff. 79−69528
Si:Se, IR absorption and photocond., donor levels 77−55809
Si:Se, impurity states, A- and B-centres, electron, hole thermionic emission rates 80−96813
Si:Se,B(Ga)(Al)(In), diffusion of Se, solubility and ionization levels, Hall effect and photocond. meas. 79−42486
n-Si-Se, ion implantation studied by deep level transient spectroscopy 78−10392
Te lattice distortion and p-orbital bands 77−89405
Te-Se-Cd, sandwich structure, fabrication and characteristics 80−60089
Te-Se-Cd rectifying sandwich structs., elec. forming action, Schottky junction form. 80−80371
Te-Se-CdO struct., fabrication and charact. 78−76106
ZnP_2:Se, optical absorpt. spectra in range 0.5 to 2.2 eV 80−66250

selenium alloys
see also selenium compounds
steel, low C, type AISI 1010, effect of Se, Te additions on fatigue props. 78−92359
γ-Bi-Se phase, electronic props. 77−43493
Bi-Se system, high-temp. calorimetry *(French)* 77−44501
Co-Se, P-T diagram and structural study 78−56622
Cu-Se(-Ag-Sn), Ag, Se, and Sn effects, singly and together, on recrystallisation 79−100164
Fe-Se, low conc. binary system, Mossbauer spectroscopy meas. 79−24239
FeSe-MnSe phase relationships in presence of excess Fe 77−52291
Ge-Se-Fe films, metallic and semicond., amorphous, mag. and elec. props. 78−52319
Mo-Sn-Se system, supercond. crit. temp. and cryst. struct. *(Russian)* 80−107947
Na-Se system, liq., thermodynamic props. 80−21319
$Nb_{1-x}Mo_xSe_2$, supercond. transition temp. and mag. susceptibility 77−12043
$NbSe_2$ nonstoichiometry, electrical props. *(Japanese)* 78−10593
$NbSe_2$-Fe, dil. alloy, magnetotransport and superconductivity 77−55516
$NbSe_3$, electronic props. variation with struct. 79−42438
$NbSe_x$, nonstoichiometric, thermodynamic props. and crystal struct. *(Japanese)* 78−11206
$Nb_{1-y}Ti_ySe_2$, supercond. transition temp. and mag. susceptibility 77−12043
Ni-Se, dil., ferromagnetic, hyperfine field and relax. time obs. of impurity heavy nuclei 80−75533
Pd-Se, thin layers, phase identification and struct., electron diffr. 77−51615
Pd_7Se_4, cryst. struct. determ. *(German)* 78−75628
Rb-Se system, phase equilibria 78−44079
Se-Na, and Se, liqs., elec. resistivity and phase separation 79−82573
Se-Sb(Bi), liq., diamag. susceptibility, semicond./metal behaviour 78−14927
Se-Te, liq., localised impurity states, mag. susceptibility of Co and Mn solutes 77−51882
Se-Te, new material for granule microphone 79−3878
Se-Tl-S alloys, liq., dielectric relax. and elec. cond. 80−108150
Se-Tl(Bi)(Sb), liquid alloys, vapour phase effect on activity determ. *(German)* 79−43210
SeTe liquid alloy, effect of branched chain polymers on bond equilib. 80−24348
Sn-Se, melt, density, kinematic viscosity, struct., 900-1400K 78−14395
$TaSe_2$-Fe, dil. alloy, magnetotransport and superconductivity 77−55516
$TaSe_3$, electronic props. variation with struct. 79−42438
Te-Se liq. semicond., resist. meas. under high press. 77−51791
Tl-Se, liquid mixtures, press. effect on two-phase region 80−75347
Tl_xSe_{1-x}, liquid semiconductor, diamagnetism and paramagnetism, dangling bond paramag. centres, mag. susceptibility obs. 80−44797

selenium compounds
see also selenium alloys
alkyl Se compounds, in atmosphere, detect. via gas chromatograph-microwave plasma detector 78−68975
binary, with non-transition elements, at. vol. and semicond. props. 77−20089
chemical bonding in group V and VI elements and compounds with tetradymite structure 80−15036
inorganic, chemical bonds using $K\alpha_1$ line chem. shifts, Mossbauer isomer shifts 77−27089
LMM Auger spectra, relative intensity and relaxation energy 80−69115
muonic capture rates in elements of compounds, influence of chemical bond 78−58874
1,2,5-selenadiazole, partially oriented in mesophase, r_z struct. PMR obs. 78−58719
selenide systems, binary, glass transition behaviour, model, comp. depend. 78−26673
xerographic applications 80−57415
Ag-As-Se system, glass-forming 79−65001
As-Ge-Se, and As-Ge-Se-Sb glasses, acousto-optic props. 77−27327
As-Ge-Se based glasses, refr. index, 1-11 μm 78−39520
As-Ge-Se system glasses, alkali-free, optical absorpt. 79−65883

selenium compounds continued
As-S-Te, vitreous semiconductor, photoconductivity *(Russian)* 79−11172
As-Se, amorphous, glass transition and specific heat, intermolecular bond saturation 80−15011
As-Se amorphous film, density of upper valence band states, annealing effects, UPS obs. 80−29845
As-Se amorphous film, optical props. change under high-power light pulse action 79−47534
As-Se and As_2S_3 films, electron-stimulated changes in optical props. and dissolution rate 80−29709
As-Se based glasses, refr. index, 1-11 μm 78−39520
As-Se chalcogenide glass, semicond. film, laser stimulated refr. index change, writing/erase cycle 77−50677
As-Se chalcogenide glass, optical const. photoinduced changes mechanism 80−7321
As-Se glass, magnetic susceptibility meas. at room temp. *(Japanese)* 79−82748
As-Se glass film, MgF_2 coated, effectiveness for optical holographic recording *(Russian)* 77−71960
As-Se glass film, photoinduced absorpt. changes 79−87519
As-Se glass thin-film waveguide, for 10.6 μm range 77−50770
As-Se glasses, low temp. photocond. 80−49808
As-Se glassy system, mag. susceptibility 77−55657
As-Se system glasses, electronic props. and localised states, review 77−62871
As-Se system glasses, point defects, positron lifetime spectra meas. 78−88380
As-Se system glasses, thermal expansion coeff. and free vol. at transition temp. *(Japanese)* 79−55876
As-Se-Ge, amorphous film, relief-type hologram mode, hologram replication *(Japanese)* 78−78959
As-Se-Ge film, master for hologram copying 78−29912
As-Se-S-Ge chalcogenide glass films, appls. to passive optical waveguide components 79−37048
As-Se-S-Ge chalcogenide amorphous film, computer-generated holograms using electron beam irrad. 80−95846
As-Se-Sb, crystallised glasses, struct. from Mossbauer spectra 80−64917
As-Se-Te, amorphous, electron and hole drift mobilities 80−34442
As-Se-Te glasses, electron transport props. 78−10439
As-Se-Te system glasses, AC cond. and permittivity, freq. and temp. depend. 77−76857
As-Se-Tl system, chalcogenide glasses, NMR spin-lattice relax. time meas. 79−95671
As-Se(-Ge) chalcogenide glasses, mode-guiding layer in IR microwaveguides 80−28329
As-Se(Te)-Ge, fabrication of amorphous semicond. thin films with graded band struct. *(Japanese)* 77−55623
As_2-Se_3-Bi_x amorphous system, elec. and photocond. props. 79−51574
As_xS_{1-x}, chalcogenide, covalent non crystalline topology, short range order 80−15009
$As_{40}S_{25}Se_{25}Si_{10}$ glass film, transient photoinduced absorpt. 77−40295
$As_4Sb_2Se_9$ glassy semiconductors, electronic props. 80−103712
$As_2(Se,Te)_3$ glasses, X-ray absorption and photoelectron spectroscopy study 80−7463
$AsSe_{10}$, stable thermoelectret, effects of anisotropic external perturbation *(Russian)* 77−63361
$As_{1-x}Se_x$, amorphous, struct. models 79−37628
$As_{1-x}Se_x$ glass, refr. index comp. depend. and photo-induced variation 79−91398
As_2Se_3, amorphous, elec. cond. at room temp., contact effect 77−20354
As_2Se_3, thermal expansion at low temperatures 78−83982
As_xSe_{100-x} glasses, temp. depend. of mag. susceptibility and EPR 77−63073
$(As_2Se_3)_{1-x}(As_2Te_3)_x$ amorphous films, changes in optical props. under elec. fields and optical excitation 79−61455
$AsSe_{1.5}Bi_{0.05}$ glasses, soln. rate in alkali solns. 80−16531
$As_{10}Se_{67.5}Ge_{22.5}$, film as master for PVC copied holograms 77−23632
As_4Se_5Ge, glass, light irrad. induced changes in optical and elec. props. *(Japanese)* 78−68031
As_4Se_5Ge glass, struct. changes, Mn^{2+} EPR expts. 78−79534
$As_{40}Se_{50-x}S_xGe_{10}$ film strip-loaded waveguide formed in graded-index $LiNbO_3$ planar waveguide 78−74965
$AsSe_{1.5-x}Te_x$ glasses, physical props. 78−68028
As_2Se_2Te, electrical conductivity at strong elec. fields and high hydrostatic press. *(Czech)* 77−24560
$As_2Se_xTe_{3-x}$ chalcogenide glasses, cond. meas., field strength and temp. depend. 78−84225
$As_{60}Se_xTe_{40-x}$ glasses, crystallisation 77−35488
$As_xTe_yS_xSe_{100-3x}$ glasses, IR absorpt. spectra 77−12378
$AsTeSe_x$, chalcogenide glass, thin film crystallisation 79−7758
Ba-Se system, phase diagram 77−36472
CdSe thin-film solar cells 80−93970
Cu compounds, chemical shifts of X-ray electron and Auger lines 78−86912
Cu-As-Se glasses, recording and erasure by laser beam *(Russian)* 78−71170
$CuIn_{1-y}Ga_ySe_{2(1-x)}Te_{2x}$ pentenary alloy compounds for photovoltaic solar energy conversion 80−93971
Ga-Ge-Se chalcogenide glasses, rare earth element doped, elec. props. 80−96885
Ga-Se system, phase diagram and cryst. struct. of phases *(French)* 80−93544
GaSe, wave function symmetries of valence band states revealed by polarisation effects in angle-integrated photoemission spectroscopy 79−67395
$GaSe_{1-x}S_x$, magnetic susceptibility anisotropy, chemical bonds, electron density distribution *(Russian)* 80−50073
$GaSe_{1-x}Te_x$, Raman spectra, phonon freq. 80−97286
Ge-As-Se, amorphous film, condensation formation and struct. props. *(Russian)* 78−38629
Ge-As-Se, Se-As and Se-Ge glasses, for IR appl., prod. using H_2 distillation 77−32551
Ge-As-Se films, light irrad., heat treatment rel. to optical props. *(Russian)* 79−4858
Ge-As-Se glass, appl. to 8 to 12 μm thermal imaging system 78−25935
Ge-As-Se system glasses, thermal capacity, 300-600K 79−65210
N-Ge-Bi-Se glass, elec. and optical props. 80−65550
Ge-P-Se system glasses, penetration by indentor, activation parameters, microhardness 79−43419
Ge-S-Se, glass formation 80−103251

selenium compounds continued
Ge-Sb-Se glass, elec. props, comp. depend. 80−70697
Ge-Sb-Se glass, physical props., purification method for Sb, Se from surface oxides 78−46735
Ge-Sb-Se system glasses, thermal capacity, 300-600K 79−65210
Ge-Se, glassy, photoinduced photolum. fatigue *(Russian)* 78−60520
Ge-Se based glasses, refr. index, 1-11 μm 78−39520
Ge-Se glass, effect of Ag electrodiffusion on volt-ampere characteristics 79−7869
Ge-Se glass, elastic props. under press., US interferometry 78−79658
Ge-Se glass, vibr. props., Raman and IR spectra obs. *(Japanese)* 77−43989
Ge-Se glass film, photoinduced absorpt. changes 79−87519
Ge-Se glasses, radiative localised centres, photoluminesc. 79−83025
Ge-Se liquid solutions, glass-forming, viscosity 77−66036
Ge-Se-Fe films, metallic and semicond., amorphous, mag. and elec. props. 78−52319
Ge-Se-Fe phase system, amorphous films, mag. and elec. props. 79−51695
Ge-Se-Ga thin film, elec. cond., switching phenomena *(Polish)* 80−11120
Ge-Se-Ga(In) system glasses, vitreous phase struct. 77−76320
Ge-Se-Te amorphous alloys, prep. and calorimetric obs. 77−11675
Ge-Te-Se/Si amorphous film-cryst. heterojunction, electron-beam-induced current 79−24060
$Ge_xAs_yS_zSe_{(0)-3x}$ and $Ge_xTe_yS_xSe_{100-3x}$ glasses, IR absorpt. spectra 77−12378
$Ge_{30}As_{17}Te_{30}Se_{23}$, antireflection coating for KCl, design, prep. and performance 79−14063
$Ge_{30}As_{17}Te_{30}Se_{23}$-$As_2S_3$, two-layer antirefl. coating, error considerations in design 80−74477
$Ge_xAs_xTe_xSe_{100.3x}$, glassy, IR absorpt. spectra 78−23448
n-$Ge_{20}Bi_{10}Se_{70}$ glass, preparation and elec. props. 79−74126
$Ge_{20}Bi_xSe_{70-x}Te_{10}$, n-type semiconducting glasses, resistivity and thermoelectric power meas. 80−54695
GeSe, amorphous film, optical properties 78−39620
$GeSe_2$-$SnSe_2$-As_2Se_3, GeSe-SnSe-As_2Se_3, Mossbauer investigation 77−20052
$Ge_{0.08}Se_{0.92}$, molten semicond., pseudogap, elec. cond. and optical absorption meas. 77−8160
$Ge_{1-x}Se_x$, amorphous, struct. models 79−37628
$Ge_{1-x}Se_x$ glass, refr. index comp. depend. and photo-induced variation 79−91398
Ge_8Se_{92}, glassy and liq. states, elec. cond. freq. depend. 77−76856
Ge_xSe_{1-x}, amorphous, excitation spectra of photolum. fatigue and creation of paramag. centres 80−50402
Ge_xSe_{1-x}, amorphous, X-ray diffr. and local order modelling 80−49125
Ge_xSe_{1-x} amorphous film, photocrystn., elec. cond. and optical microscopy obs. 79−87024
Ge_xSe_{1-x}, chalcogenide, covalent non crystalline topology, short range order 80−15009
Ge_xSe_{1-x} chalcogenide glasses, trap-controlled carrier mobility, time of flight meas. 79−4557
Ge_xSe_{1-x} chalcogenide glasses, drift mobility of optically injected carriers 79−19627
Ge_xSe_{1-x} glasses, DC cond. and static dielectric const. meas. *(French)* 77−62925
Ge_xSe_{1-x} glasses, vibr. props. 78−2219
Ge_xSe_{1-x}, liq., kinematic viscosity, 300-600°C 77−31706
$(Ge_{1/3}Se_{2/3})_{100-x}Ni_x$, ESR, rel. to elec. cond. 80−7155
$Ge_{20}Se_{40}Te_{40}$ amorphous alloys, thermal crystn. study 78−26789
$Ge_3Se_2Te_4$ film, chalcogenide glass, freq. depend. of Hall effect 77−1436
$(Ge_{0.32}Se_{0.32}Te_{0.32}As_{0.4})_{100-x}Ni_x$, ESR, rel. to elec. cond. 80−7155
$Ge_{20}Te_2Se_{80-x}Si$, amorphous-cryst. heterojunctions 79−65546
H_2SeO_4, NMR of ^{77}Se, chemical shift and screening tensors *(Russian)* 78−64285
In-As-Se-I system, glass form. obs. 77−77466
$InGe_{1.5}Se_{1.5}$, new skutterudite relation compounds, prep. and charact. 78−52700
KCl:SeO_4^{2-}, IR absorpt. spectra, vibr. splitting *(Russian)* 79−51995
KH_2PO_4:SeO_4^{2-}, ferroelec., low freq. fluctuations, isotope effects, EPR, ENDOR, ESCA 77−73118
KH_2PO_4:SeO_4^{2-}, slowing down of fluctuations near T_c, EPR obs. 78−60403
Mo_6Se_8Sn, triple chalcogenide, NMR spectra in supercond. state *(Russian)* 80−93194
$NH_4H_2PO_4$:SeO_4^{3-}, antiferroelec., low freq. fluctuations, isotope effects, EPR, ENDOR, ESCA 77−73118
$(NH_4)_2SO_4$:SeO_3^-, γ-irrad., hyperfine interaction, ferroelec. transition effects, EPR expt. 78−15024
$NbSe_2Cu_x$, ordering study using electron diffr. and microscopy 80−39043
P-Se, amorphous, glass transition and specific heat, intermolecular bond saturation 80−15011
P-Se, phase diag. 77−52296
P-Se, phase diag. and crystallisation of glasses at high press. 77−52297
P-Se system, glass form. props., effect of P concentration *(Russian)* 78−2019
P-Se system glasses, magnetochem. investig. 77−51325
P-Se-Te system glasses, mag. susceptibility and opt. props. 80−25079
P-Se-Tl glasses, NMR of ^{31}P and ^{205}Tl 80−15812
$P_2Se_xS_y$ glass, thermophysical props., 303-413K, struct. interpretation 78−47615
P_2Se_xSy glass, vitrification temp., elec. props. and hardness meas. *(Russian)* 77−28177
$(PbSe)_{1-x}(SnTe)_x$, lattice dynamic props., Gruneisen parameters *(Russian)* 78−83984
$Pt(SeC(NH_2)_2)_4Cl_2$, crystal and mol. struct. 78−59794
S-Se, liquid semicond., bonding energies and entropies, mag. susceptibility meas. 80−49082
S-Se amorphous alloys, crystn. kinetics, elec. cond. meas. 78−34441
S-Se-Te semicond. glasses, mag. suscept. meas., refractive index 78−34952
SSe, dissoc. energies determ. 78−33632
SSe_{20}, crystalline phase growth in amorphous solid and liquid samples 78−43107
$SSe_{22.5}$, amorphous, photo-effect on crystn. kinetics, elec. cond. obs. 79−77522
$SSe_{22.5}$, amorphous-cryst. transition, light effect, rel. to polymer crystallisation 79−99076
SSe_{40}, amorphous alloy, crystn., elec. cond. meas. 78−34440
selenium compounds continued
SSe_9, stable thermoelectret, effects of anisotropic external perturbation *(Russian)* 77−63361
SSe_x (x=10, 15, 40), amorphous crystal transition, appl. of Kolmogorov-Avrami equation 78−67649
S_xSe_y, s=6-3, y=2-5, thermal behaviour 78−67813
Sb-Ge-Se system glasses, thermal capacity, 80 to 300K 79−42272
Sb-Ge-Se system glasses, activation energy of elec. cond. calc. 79−51568
Sb-Se-I system, exam. of glass formation, IR transmission spectra 78−88452
SbSe, amorphous thin film high field charge transport and quasi-Fermi level location 80−70863
$Sb_{35}Se_{65}$, polycrystalline, elec. cond. mech. 80−49705
Se-As, amorphous, dipolar activity at glass transition temp., AC method 77−66454
Se-As, photoelectronic behaviour, in glass transition region 80−60045
Se-As 36.4 at % amorphous alloy, heat treatment effect on acoustic props. 79−86843
Se-As film, evaporated, thickness, substrate temp. effects 79−15610
Se-As_2Se_3 system glasses, vibr. spectra and partial vols. of components 79−42973
Se-As-Ge, glass alloy system, annealed light irradiated, photoinduced absorption change, random network model 79−59773
Se-Bi-I, amorphous, high sensitivity visible-near IR photoconductor development and characterisation 78−39153
Se-Fe amorphous films, mag. and elec. props. 79−51695
Se-Ge, amorphous, elec. cond. at room temp., contact effect 77−20354
Se-Ge, amorphous, Raman spectra and average band gap 80−50327
Se-Ge, amorphous thin film, photocontraction rel. to surface struct. 80−49551
Se-Ge, chalcogenide glass, Raman scatt. and bond struct. 79−95772
Se-Ge amorphous films, obliquely deposited, photoinduced chem. changes 80−76385
Se-Ge amorphous system, AC elec. cond., near T_g, temp. depend. 80−49791
Se-Ge glass, lattice vibr. spectra, photostruct. change, far IR absorpt. 78−72494
Se-Ge glasses, extreme far IR absorpt. meas. 80−50318
Se-Ge system, amorphous, press. depend. of AC cond. 77−76858
Se-Ge-As, chalcogenide glass, self-diffusion, investigation using radioactive tracers 79−23770
Se-Ge-Sb alloy glass, crystn. kinetics 77−20057
Se-Ge-Te, chalcogenide glass, elec. cond. and dielec. const. 80−75567
Se-Ge-Te glass, dielectric meas. 79−87382
Se-S, glassy alloy, order-disorder transition kinetics 78−67650
Se-Si system glasses, vibr. IR spectra 80−20643
Se-Te, liq., electronic props., mag. susceptibility meas. 79−95567
Se-Te crystallised glasses, struct. transforms. and IR spectra 80−19712
Se-Te film, evaporated, drift mobility of holes, elec. field and comp. depend. 77−39977
Se-Te single crystals, chem. etching 80−96526
Se-Te solid solutions, ordering, diffuse X-ray scatt. 77−65965
Se-Te whisker crystals, growth 79−99464
Se-Te-As-Ge glasses, absorpt. spectra, diffuse reflectivity loss correction 79−82995
Se-Te-As-Ge glasses, elec. transport 79−60833
Se-Te-Ge, amorphous, off-state thermal switching 79−65524
Se-Te-Ge and Se-Sb systems, amorphous, electrical transport, activation energy 79−95406
Se-Te-Sb glasses, electronic transport 80−88579
$Se+H^+$, K-shell ionisation cross-sections calcs. 80−43165
Se_{90}-Te_{10} alloy crystals, growth and cleavage 78−88421
a-$Se_{97.5}As_{2.5}$, trapping, photo-stimulated and thermally-stimulated current obs. 77−28192
SeBr, X-ray diffr. study of crystalline modifications 77−89420
$SeBr_2$, He I photoelectron spectra, ionis. pots. calcs. 79−50080
$SeBr_2$, photoelectron spectra, visual assessment stripping program anal. 80−28062
$SeBr_4$, enthalpy of formation determ. 78−80777
$SeBr_4$, X-ray diffr. study of crystalline modifications 77−89420
$SeCF_2$, IR, Raman and matrix isolation spectra, isotopic shifts, anharmonicity consts. *(German)* 77−83600
SeCl, X-ray diffr. study of crystalline modifications 77−89420
$SeCl_2$, He I photoelectron spectra, ionis. pots. calcs. 79−50080
$SeCl_2$, photoelectron spectra 80−69186
$SeCl_4$, enthalpy of formation determ. 78−80777
$SeCl_4$, X-ray diffr. study of crystalline modifications 77−89420
$SeCl_4$-$SbCl_5$ systems, Raman spectra *(German)* 80−93324
$(SeCl_4)_4$, vibr. anal., cubane-like T_d model 78−66537
Se_2Cl_2, photoelectron spectra 80−69186
SeD, ground state, spin-orbit coupling const. vac. UV determ. 78−70847
SeD, isotope effects, Rydberg levels-ground state transitions, rot. consts., VUV spectra obs. 80−58279
SeF_2, He I photoelectron spectra, ionis. pots. calcs. 79−50080
SeF_6, electron affinities from collisional ionisation with alkali atoms 78−55226
SeF_6, electron affinity, MS Xα calc. 77−30778
SeF_6, IR photolysis, $NH_3^-+CO_2^-$ laser isotope separation and dissoc. enhancement 79−29377
SeF_6, IR vibr. band contours, isotope substitution, force consts. 78−17670
SeF_6, in Kr matrix, temp. reversible IR spectral changes, site struct. dynamics 80−102505
SeF_6, isotopically selective IR photodissociation 78−42142
$^{77}SeF_6^-$, radical, prep. and EPR comparison with other hexafluoride radicals 78−68381
$SeF_6+K(Cs)$, crossed beam reaction cross section 77−77740
$Se_{0.84}Ge_{0.16}$ glass, sp. ht. excess rel. to far IR absorption 77−84874
$Se_{1-x}Ge_x$, amorphous, AC cond. magnitude and variation *(French)* 79−47095
$Se_{1-x}Ge_x$, amorphous, IR absorption spectra *(French)* 77−73146
$Se_{1-x}Ge_x$ amorphous film, photocontraction effect 79−46975
$Se_{75}Ge_{25}$, obliquely deposited amorphous films, photo-induced optical effects 79−56871
SeH, ground state, spin-orbit coupling const. vac. UV determ. 78−70847
SeH, isotope effects, Rydberg levels-ground state transitions, rot. const., VUV spectra obs. 80−58279
SeH_2, atomisation in cool H_2-O_2 flame burning in quartz tube atomiser 80−76581
SeH_3^+, inversion barrier calc. 78−9271

selenium compounds continued
SeH($X^2\Pi$), IR LMR spectrum, spin-orbit coupling const. direct determ. 79−76429
SeH($X^2\pi_{3/2}$), far IR LMR spectrum 78−66564
$SeMoOCl_7$, prep., cryst. struct., characterisation *(French)* 78−63722
SeO, $A^3\pi$-XO^+, 1 band system 77−58039
SeO, $b^1\Sigma^+ \rightarrow X^3\Sigma^-$ near IR emission obs. 80−91556
SeO, IR bands of 10296 and 10491 Å, rot. struct. 78−5224
SeO, mol., mm wave spectra, $X^3\Sigma^-$ state 79−85959
SeO, molecular constants determ. from $b^1\Sigma$-$X^3\Sigma$ transition, nonlinear least squares procedure 79−798
SeO, pot. energy curves, dissoc. energies 78−50485
SeO, $X^3\Sigma^-$ state mol. parameters, Zeeman and EPR spectra 79−6966
SeO_2, free radicals, pulse radiolysis obs. 78−20040
SeO_2, HeI and II photoelectron spectrum, valence electronic struct. 77−61798
SeO_2, vapour, oxidation of metal selenides 77−52520
SeO_2+Ar(N_2)(CO_2), radiative lifetime and quenching rates 80−95685
SeO_3, rotational Raman spectrum, rot. consts. and bond lengths 79−18196
SeO_3^{2-}, SeO_4^{2-}, O K-emission spectra, electron struct. 80−87099
SeO_4^{2-} luminescence of ions in aqueous solns. of halides at 4.2-290K *(Russian)* 77−28624
$SeOCl_2$:Pr^{3+}(Nd^{3+})(Er^{3+}), $SbCl_5$ acidified, Racah and Judd-Ofelt parameters in laser liqs. 80−106516
$SeOCl_2$.dioxane, cryst. struct., secondary and multi-centre bonding 78−63751
SeS, $b^1\Sigma^+ \rightarrow X^3\Sigma^-$ near IR emission obs. 80−91556
SeS gas, thermodynamic props., quadrupole mass filter study 80−16716
Se_3S_5, cryst. struct. 78−42978
Se_4S_4, mol. chalcogenide, synthesis and struct. 79−33912
SeTe, dissoc. energies determ. 78−33632
SeTe/Se multilayer photoreceptor, transient photoconductivity *(Japanese)* 80−75596
$Se_{0.95}Te_{0.05}$, glass crystallisation, effect of an alternating electric field 80−88054
$Se_{1-x1}Te_{x1}$-$Se_{1-x2}Te_{x2}$ heterostructure, amorphous, rectification phenomena and photovoltaic effects 79−99610
$Se_{1-x}Te_x$, amorphous, optical and elec. props. 80−84506
$Se_{1-x}Te_x$, amorphous film, photo-crystallisation 80−59839
$Se_{1-x}Te_x$ amorphous films, sublinear and superlinear I-V charcts. 79−82695
$Se_{1-x}Te_x$, film, struct. and props. 79−99079
$Se_{1-x}Te_x$ systems, amorphous and liq. states, short range order, neutron scatt. study 80−49124
$Se_{1-x}Te_x$-$Se_{1-y}Te_y$ junctions, photovoltaic effects and rectification phenomena 80−84506
$Se_{90}Te_{10}$ whiskers, chem. and thermal etching 77−15417
Se_xTe_{1-x}, acoustoelectric current saturation 80−60053
Se_xTe_{1-x}, amorphous, structural relaxation and crystallisation kinetics study by DTA 80−59394
Se_xTe_{1-x}, growth of single crystals by Czochralski method 80−66423
Se_xTe_{1-x}, liq., thermoelec. transport at mobility edge 80−49787
Se_xTe_{1-x} melt, densities and surface tensions 79−86831
Se_xTe_{1-x} system melts, bonding system change obs. using density meas. 77−11456
$Se_{12}Te_{49}As_{29}Ge_{10}$ semiconductor amorphous films, field effect, trapping 80−84472
$Se_{60}Te_{30}Ge_{10}$, amorphous, neg. magnetoresist. 79−51603
Se_2TiO_6, cryst. struct. *(French)* 78−95023
SnSe-Se, p-T projection of phase diag. 78−27485
Te-Se, Debye temp. calcs. using elastic consts. and Kopp-Neumann relation 78−2220
Te-Se liquid mixtures, sound vel. meas., adiabatic compressibility determ. 80−65161
Te-Se mixtures, liquid, electrical conductivity and thermoelectric power, high temps. and pressures 80−39639
$TeSe_{12.5}$, amorphous alloy, thermal and elec. cond. during devitrification 78−26922
$TeSe_{20}$, vitreous alloy, elec. and thermal cond. during crystallisation 79−7550
$TeSe_{50}$, amorphous to cryst. transition, kinetics 79−73099
$Te_{43}Se_{30}Sn_7$ in MSM struct., switching effects 78−19164
$Te_{50-x}Se_{50}Sn_x$, thin films, elec. cond. and thermoelectric power meas. *(French)* 80−80335
Tl-Se liquid binary mixtures, phase separation under press. 80−34183
Tl-Se phase diagram, 73-100 at.% Se 79−96018
$Tl_2SeAs_2Te_3$, amorphous semicond., nuclear spin-lattice relaxation by localised electronic states, modification by spin diffusion 78−52372
$Tl_2SeAs_2Te_3$, glassy and liq. states, elec. cond. freq. depnd. 77−76856
$Tl_2SeAs_2Te_3$, molten chalcogenide semicond., temp. depend. of 10^{10} Hz elec. cond. 77−4388
$Tm_xSe_yTe_{1-y}$, magnetic ordering studies *(German)* 80−54882
Y_2Se_4 powder, prep. and optical props. 77−28771
Zn-Cu-Se system, condensed phase equilibria, 800-1000°C, vapour pressures of Zn, Se_2 77−16553
Zn-Cu-Se system, region of existence of ZnSe phase 77−16554

self-adjusting systems
see also learning systems
autoregulating pacemaker responsive to metabolic requirements 77−81726
gamma-ray spectrometer self-stabilising peak detector *(Russian)* 79−26814
nerve nets, fundamental theory, developmental plasticity anal. 80−67062
neural nets, Caianiello type, self-control 78−20167
neural network model, self-organising multilayered 77−40661
neural theory of association and concept-formation 77−52763
pH-neutralisation process, self-tuning control 80−30242
plasma grooved instability, feedback system for stabilisation *(Russian)* 77−68767
thermonuclear device control, automatic feedback parameter analogue simulation 78−26336

self-consistent field calculations *see SCF calculations*

self-diffusion
see also self-diffusion in gases; self-diffusion in liquids; self-diffusion in solids
activation of kinetic processes in condensed media 77−55368
coefficient at low densities 78−36950
crystal growth, stochastic models, diffusion and relax. kinetics 79−37642
electron gas, classical and two-dimens., self-diffusion theory 80−141

self-diffusion continued
electron gas, self-diffusion (spin diffusion) coeff., proper connected diagram expansion 78−21067
fluid, anisotropic, transport coeffs., perturbation theory 77−7497
fluid, rotational and translational diffusion, stochastic Liouville eqn. formalism 79−64971
hard-sphere fluid, eqns. of state, transport data, glass transaction 77−4182
ionic solution, uphill diffusion associated with a flux of extrinsic vacancies 79−65229
methane, transport coeffs., statistical mech. calcs. 77−7494
multicomponent self-diffusion measurement using spin echo expts. on standard Fourier transform NMR spectrometers 80−22401
NMR pulse-gradient meas. noise pulse generator 77−53965
plasma, one-component classical system, self-diffusion, microscopic theory 77−55131
polymethylsiloxane-toluene gels, light scatt., compression moduli, cooperative diffusion 78−23970
sine-Gordon chain, self diffusion via solitons 80−70443
spherical Brownian particle in flow, hydrodynamic model for attractive pot. self-diffusion 77−11293
square well fluid, self-diffusion coeff. density depend., repeated ring approx. 79−77326
suspension, particles self-diffusion in shear flow 77−24015
two-dimensional transport coefficients, self-diffusion, theory 78−32777

self-diffusion in gases
atoms in resonance cell, coeff. meas. using self-oscillating quantooptical magnetometer 77−76018
binary mixture, moderate density diffusive creep along flat surface 80−43822
n-butane-N_2(CO_2) mixtures, viscosity, diffusion coeffs. 80−1722
dense gases, vel. autocorrelation function, memory function 80−59154
dilute gas, transport props., simple pair pot. model 80−87835
dilute gas transport props., logarithmic term in softness expansion 80−83872
dilute hard sphere gas, vel. autocorrelation function, diffusion coefficient 77−62324
ellipsoidal molecular models, transport props. determ. 77−68725
ethane-CO_2(N_2)(SF_6)(tetrafluoromethane) mixtures, viscosity, diffusion coeffs. 80−1722
gas discharge with travelling mag. field, isotope separation by mass diffusion 80−44050
hard sphere gas mixture, vel. autocorrelation function calc. 80−75019
hard-sphere Boltzmann-Lorentz-Enskog kinetic equation, study of correl. functions 79−68894
isotope separation, HF stationary discharge, travelling mag. field, barodiffusion separation 80−44049
isotope separation by gaseous diffusion, aerodynamic effects 78−59469
Lennard-Jones mols., self-diffusion coeffs. at moderate densities, mol. dynamic simulation 78−38440
methane, liq. and gas, mol. dynamics simulation, thermodynamic props., struct. factors, etc. 79−50976
methane, self-diffusion coeffs. evaluation from expt. data 77−42953
monatomic gases, transfer coeffs., 100-3000K 79−82021
NMR with nonuniform RF field, appl. to self diffusion and liq. flow meas. 78−60343
optically oriented atoms in inhomogeneous RF fields, meas. method *(Russian)* 77−27004
propane-N_2(CO_2), mixtures, viscosity, diffusion coeffs. 80−1722
spherical drop combustion, asymptotic, drop shrinkage and flame movement, heat and mass transfer 77−81405
vapour deposition process, mass diffusion in two-dimens., perturbation method 79−2737
vapour mixtures, with or without inert gas, condensation, heat transfer coeff. calc. *(German)* 77−39724
velocity correlation functions, transport props. predictions, medium density 77−7500
Ar, interatomic pot. and transport props. 77−14519
Ar, transport props. with Lennard-Jones (12-6) pot., distance parameter 79−55437
Ar-SF_6, thermophysical props., second virial and diffusion coeffs., thermal diffusion factors 78−42699
Ar+Kr, binary diffusion coeff. pressure depend. meas. 80−43826
CO_2 gas, electron mobility to lateral diffusion coeff. ratio 80−43836
H, RF induction discharge breakdown, diffusion theory 77−84562
H_2, dense gas, self-diffusion, quasielastic incoherent neutron scatt. obs. 78−22451
H_2, gaseous, high density, enhanced self diffusion, incoherent neutron scatt. study 79−46417
H_2-O_2 gas mixture in chem. equilib., elemental diffusional separation in nonisothermal flow 79−55429
He, RF induction discharge breakdown, diffusion theory 77−84562
Kr, interatomic pot. and transport props. 77−14519
Kr, Lennard Jones (12,6) pot. distance parameter, transport props. calc. 80−79423
Kr, self-diffusion coeff. behaviour at low density, 293K 78−67302
Kr, self-diffusion coefficient, radioactive tracer meas. 77−13534
N_2+Ar, binary diffusion coeff. pressure depend. meas. 80−43826
N_2+O_2, binary diffusion coeff. pressure depend. meas. 80−43826
Ne, interatomic pot. and transport props. 77−14519
Ne, Lennard Jones (12,6) pot. distance parameter, transport props. calc. 80−79423
O_2 gas, electron mobility to lateral diffusion coeff. ratio 80−43836
O_2+Ar, binary diffusion coeff. pressure depend. meas. 80−43826
Si-Ge-Br system, diffusion mass transfer 80−33911
Xe, gas, diffusion enhanced by radioactivity 79−60094
Xe, Lennard Jones (12,6) pot. distance parameter, transport props. calc. 80−79423
Xe, self-diffusion coefficient, radioactive tracer meas. 77−13534

self-diffusion in liquids
acetonitrile, liq., rotational motions, diffusion coeffs., quasi-elastic neutron scatt. study 79−50979
alcohols, flow meas., 25-65°C 78−2278
alkali halides, molten, rigid sphere model 77−7946
alkali metals, liq., self-diffusion coeffs. calcs. 78−2274
p-alkanoyl-benzylidene-p'-aminoazobenzenes, liq. cryst., proton mag. relax., self-diffusion 77−84632
alloy, at. transport props., review 77−1248
automated measurement technique, using NMR spin echo 78−27114

self-diffusion in liquids continued
benzene, diffusion coeff. meas., Fourier transform NMR, pulsed field gradient system 80−57353
benzene, in benzene-d_6 soln., IR and Raman spectra, line breadths, rot. diffusion consts. 79−56772
benzene, isotope-mass effects in self-diffusion 80−92695
benzene, liq., mol. motion at high press. 80−103509
benzene, self-diffusion coefficients determ. by gel sectioning technique 80−92694
benzene, self-diffusivity data 78−6169
benzene-cyclohexane, solution, self-diffusion, capillary cell meas. 78−34637
benzene-toluene, solution, self-diffusion, capillary cell meas. 78−34637
binary liquid mixtures, diffusion coeffs., conc. depend., theory 77−89557
binary molten salt mixture, ionic and mol. mobilities, inter-diffusion and self-diffusion *(German)* 77−11720
binary systems with strong chem. interaction, spin echo obs. *(Russian)* 79−95197
n-butane, skeletal alkane fluid simulation, vibr., rot., torsional gauche/trans relax., diffusion const. 79−1378
n-butyl-4-(4′-phenylbenzylideneamino)cinnamate-d_9, smectic E, B and A phases, quasielastic neutron scatt. obs. 78−75539
carbon tetrachloride, liq., hard spheres diffusion, free vol. theory, Macedo-Litovitz eqn. 77−51530
carbon tetrachloride, liq., self-diffusion coeff., temp. and density depend. 78−91461
carbon tetrachloride, transport coefficients for a fluid of square-well rough spheres 79−55634
2-chloro-2-nitropropane, far IR-microwave estimation of binary collision approx. 80−55095
chlorobenzene, self-diffusivity data 78−6169
chlorotrifluoromethane, self-diffusion coeff. near crit. temp., density depend. obs. 78−95530
cholesteryl-m-fluorobenzoate, cholesteric liq. cryst., NMR, orientational order parameter 77−8429
cyclohexane, isotope-mass effects in self-diffusion 80−92695
cyclohexane, liquid, density effect on transport properties 80−65264
cyclohexane, self-diffusion coefficients determ. by gel sectioning technique 80−92694
cyclopropane, liq., mol. dynamics, self-diffusion, quasielastic neutron scatt. and NMR spin-echo meas. 78−10201
cyclopropane, liq., molecular motion, incoherent neutron scatt. study 79−50978
decane-water-Na p-octylbenzene sulphonate-1-pentanol-NaCl, microemulsion system, existence of bicontinuous zone 80−104466
dense hard core system, transport coeffs., entropy 77−62656
dextrane, aq. solns., H_2O diffusion, PMR investig. *(Russian)* 79−51290
di-(2-ethylhexyl)phthalate, ^{13}C and ^{1}H relax., reorientational correlation times 79−51869
2,2-dimethylpropane, liq., self-diffusion coeff., temp. and density depend. 78−91461
p-dodecanoylbenzylidene-p′-aminoazobenzene, smectic A mesophase, self- and impurity diffusion, NMR spin echo obs. 78−94975
EABAC, smectic A, nematic, and isotropic phases, NMR and quasielastic neutron scatt. obs. 80−88022
EBBA, isotropic phase, order fluctuations, self-diffusion, and rot. motion, proton spin relax. meas. 79−87328
EBBA, liq. cryst., isotropic phase, NMR pulsed field grad. study of self-diffusion 79−90814
electrolyte, and polyelectrolyte solns., apparent ionic charge 78−76875
electrolyte solns., 79−23753
electrolyte solns., particle-particle interactions, velocity correl. coeffs. 78−64852
electrolyte solution, Brownian dynamics approx., time evolution and transport props. 79−37604
electrolyte solution, tracer and mutual diffusion, open-end capillary method 79−28119
electrolyte transport, irreversible thermodynamics calcs. 80−3364
estimation method, empirical relationship 79−90808
ethanol-carbon tetrachloride, binary soln. with mol. assoc., interdiffusion anal. 79−55912
fluid of partially rough spheres, translational and rot. diffusion coeffs. 78−26404
fluid-like viscoelastic liquid, coupling of orientational and translational motions, LF depolarised (VH) scatt. 77−7642
free radical reactions, liquid phase, cage model, solvent effects 77−16811
glycerol, supercooled, Mossbauer effect and model of mol. motion 78−64301
haemoglobin, human and Lumbricus terrestris, conc. depend. of self-diffusion 78−68984
haemoglobin, mutual and tracer diffusion coeffs., photon correl. obs. 80−72123
hard sphere dense fluid, rel. to type of liquid 77−11715
hard sphere fluid in small pores, mol. dynamics simulation 80−24333
hard spheres, free vol. theory, Macedo-Litovitz eqn. 77−51530
hard-disc mixture, mol. dynamics simulation, self-diffusion coeffs. 77−89356
hard-sphere fluid, kinetic theory of self-diffusion 79−4225
hard-sphere fluid, viscosity and self-diffusion coeffs. 78−51716
heavy water, compressed, NMR spin echo obs., self-diffusion coeffs. 77−1250
hexafluorobenzene, liq., self-diffusion and denisty as functions of press. and temp. 80−92696
hexafluorobenzene-n-paraffins, binary liquid solns., self diffusion, spin echo meas. 80−65263
hexafluorobenzene-O_2, soln., NMR for translational O_2 diffusion 79−65749
p-hexanoylbenzylidene-p′-aminoazobenzene, smectic A mesophase, self- and impurity diffusion, NMR spin echo obs. 78−94975
hydrodynamic model, vibr. relax. 77−35734
IBPBAC, dynamics of smectic phases, quasi-elastic neutron scatt. meas. 79−86700
IBPBAC, smectic phases, self-diffusion coeffs., radiotracer meas. 80−49394
III-V compound crystal growth from solution, computer simulation 77−51332
inert gas, dense, depolarised Rayleigh scatt. 79−69851
inert gases, transport props. in mean spherical approx. 78−9927
intermolecular nucl. relax. by translational and rot. diffusion, effect of pair correl. functions *(French)* 79−19794
self-diffusion in liquids continued
latex spheres in H_2O, photon correlation spectroscopy, diffusion coeffs. determ. 80−93802
Lennard-Jones fluid, dense, memory function model for vel. autocorrelation function and self-diffusion coeff. 79−77472
Lennard-Jones fluid, self-diffusion 78−43163
Lennard-Jones liquid mixtures, mol. dynamics, particle mass and size depend. 78−22615
Lennard-Jones mixture, binary, equimolar, static (dynamic) props., mol. dynamics calc. 80−64857
liquid, simple, transport coeffs. and internal energy relation, hard sphere model 77−76284
liquid metals, diffusion mechanisms, and coeff. determ. *(Russian)* 80−34215
liquid rot. and transl. correl. time discrimination by ELDOR 77−1619
lithium perfluoro-octanoate-water system, liq. cryst. struct., self-diffusion, NMR 78−15036
low conductivity media, unipolar injection, forced diffusion model 80−92692
macromolecular dilute solutions, self-diffusion and momentum autocorrel. functions 78−33645
macromolecular solutions, review 80−15273
MBBA, isotropic phase, order fluctuations, self-diffusion, and rot. motion, proton spin relax. meas. 79−87328
MBBA, liq. cryst., isotropic phase, NMR pulsed field grad. study of self-diffusion 79−90814
MBBA, order fluctuations, self-diffusion, rot. motion, proton spin T_1 relax. 77−32285
mean spherical model approx. 78−75514
melt near solid-liquid interface, diffusion during crystallisation *(German)* 79−29046
metal, at. transport props., review 77−1248
metal, ionic transport coefficient calculation *(Rumanian)* 79−60533
metal, mechanism and coeffs. calc., model *(Russian)* 77−15610
metal, mol. motions from NQR, viscosity and sound damping 77−1615
metals, liq., self diffusion coeff. determ. using radial distrib. function 80−15280
metals and alloys, book 78−51406
methane, liq., compressed, self-diffusion coeff. temp. and density depend. calcs. 78−38864
methane, liq., mol. dynamics calcs. 77−19857
methane, liq. and gas, mol. dynamics simulation, thermodynamic props., struct. factors, etc. 79−50976
methane-Ar, liq. mixture, self-diffusion and nuclear mag. relaxation *(Russian)* 78−87799
methane-Kr, mixture self-diffusion of Kr, density depend. 77−76587
methane-Kr mixtures, rot. self-diffusion and spin-lattice relax. *(Russian)* 79−69745
methanol, liq., compressed, self-diffusion, NMR spin-echo meas. 77−77122
methanol-carbon tetrachloride, binary soln. with mol. assoc., interdiffusion anal. 79−55912
methyl iodide, liq., expt. comparison with rough sphere rot. diffusion model 78−30532
methylcyclohexane, dense liq., self-diffusion and viscosity 80−15278
microemulsion, H_2O-toluol-sodium dodecylsulphate-alcohol, diffusion coeff., light scatt. data 78−15722
microemulsion system, existence of bicontinuous zone 80−104466
mixture, binary, off-critical, quenched, struct. functions and mobilities renormalisation 79−82343
molecular liquids, corrected Enskog theory, transport props. 77−72538
molten salts, tracer diffusion coeffs., determ. methods 78−71873
multicomponent electrolyte systems, elec. cond. and diffusion 78−71872
nematic liquid cryst., rot. diffusion and freq. spectra 77−84631
nematic liquid crystal, molecular dynamics, self-diffusion and structure 77−65946
nematic liquid crystal, nuclear spin relax., translational self-diffusion 78−43670
nematic liquid crystals, orientation ordering, mol. dynamics obs. 78−91239
neutron scattering obs., book contrib. 77−89573
Nylon 12 melt, bulk diffusion coeff. and local diff. coeff. *(Japanese)* 79−46823
Nylon 12 melt, diffusion coeff. meas. by microspectrophotometry using dye-tagging *(Japanese)* 79−23756
PAA, homologous series, isotropic phase, mol. self diffusion by spin echo method 80−44109
PAA, selectively deuterated, proton spin-lattice relax. temp. freq. depend., diffusion 77−43132
perfluorocyclobutane, dense fluid, self-diffusion, shear viscosity, density, and temp. depend., NMR 77−36152
perylene, organic soln., picosec. fluoresc. for rot. diffusion 79−56839
PET, densification, cryst. perfection, mechanism 79−66082
polar liquid, computer simulation, thermodynamic props., diffusion coeffs. 79−90507
poly(methacrylic acid), aq. soln., gelation kinetics under shear stress 78−3387
polyadenilic acid, semi-dil. soln., slow modes 78−53319
polyatomic molecular, intermol. dipolar mag. interactions effect on nucl. relax. *(French)* 77−32277
polybutadiene-n-hexane-n-heptane soln., Rayleigh scatt., diffusion coeff., viscosity 78−15179
polydisperse systems, photon correlation spectroscopy, diffusion coeffs. determ. 80−93802
polyelectrolyte soln., small ion self-diffusion, Manning's limiting law derivation 80−54416
polyelectrolyte soln., small ion self-diffusion coeffs., cell model 79−19385
polyethylene oxide, NMR relaxation in melt, three component model 77−55723
polymer, spherical, in soln, long time tail in diffusion 80−88018
polymer chain dynamics in solns. trapped in slit 78−2276
polymer melt, entangled, reptation 78−22669
polymer melt, NMR relaxation, mol. motion, local defect component theory 77−55722
polymer melts, dynamics, self-diffusion const., relax. time and viscosity 80−64874
polymer self-diffusion, review 80−29193
polymer solutions, diffusion coefficients estimation methods, review 79−90807
polystyrene, benzene soln., self-diffusion, test for scaling and reptation 79−77789

self-diffusion in liquids continued
polystyrene, solns., diffusion coeffs. meas., Fourier transform NMR, pulsed field gradient system 80−57353
polystyrene solution, conc., diffusion and NMR relax. times 77−55725
polystyrene solutions, translational diffusion coeff., light-scatt. meas. 78−52519
pyridine, compressed liq., self-diffusion coeffs., viscosity, density, temp. press. depend., NMR spin-echo 79−37862
reaction rate increase in US cavitation, diffusion model 79−96312
in rectangular cross-sectional area, equiv. time constant *(Polish)* 77−65008
restricted self-diffusion measurement with gradient modulation 77−4568
rough hard spheres treatment of tracer diffusion 78−87798
seawater, self-diffusion coefficient for water molecules (1 to 7000 kg/cm^2, 0 to 60°C) *(Russian)* 77−64291
serum albumin, bovine, mutual and tracer diffusion coeffs., photon correl. obs. 80−72123
serum albumin, diffusion and sedimentation in conc. solns. 77−48749
serum albumin, human hydration, pH depend., water self-diffusion obs. *(French)* 79−34475
simple liquid, mol. dynamics study of effect of nonadditive interparticle interactions on transfer props. 77−43360
simple liquid, self-diffusion and viscosity near MP, hard sphere model *(Russian)* 77−66035
smectic A mesophase, self-diffusion and undulation modes, high resoln. neutron scatt. 77−11471
smectic liq. crystal, nuclear spin relax., effect of translational diffusion 78−63669
smectic liquid crystal, self-diffusion meas. by multiple pulse NMR 78−76352
smectic-A liquid crystals, nucl. spin relax. by translational self diffusion 80−60442
sodium cholate-decanol, soln., aggregate form., comp. and dynamics 80−45575
sodium valerate, mesophase, self-diffusion and spin-lattice relax. 79−69008
soft core model of simple liquids self diffusion, glass transition 78−67634
solution, electronic excited state transport, Green function soln. 79−68994
spherical particles, hydrodynamic interaction, translational, rot. and translational-rot. diffusion 78−26405
surfactant vesicles, low-ang. light scatt. and photon correlation spectroscopy 79−79484
TBBA, nematic liq. crystal, self diffusion coeffs., NMR spin echo 77−31789
TBBA, smectic, spin-lattice relax., self-diffusion, mol. rot. 78−35055
TBBA, smectic-A, self-diffusion, neutron incoherent scatt. law 78−83726
TBBA liquid crystal, self diffusion coeffs., neutron diffr. and NMR study 80−19689
tetramethylsilane, liq., self-diffusion coeff., temp. and density depend. 78−91461
toluene, diffusion, viscosity rel. to temp. *(German)* 79−42289
tracer diffusion meas., closed capillary method 78−14491
transport coefficients for a fluid of square-well rough spheres 79−55634
Van Hove self-correlation function, intermediate incoherent scatt. function, beyond Ficks law 80−6532
water, −31°C to 350°C 78−2275
water, diffusion const. in presence of large background gradients, modified pulsed gradient technique 80−31831
water, diffusive motions near 1°C 78−43156
water, flow meas., 25-65°C 78−2278
water, force bias Monte Carlo simulation 79−77487
water, H_2O and $H_2{}^{18}O$, self-diffusion, pressure and temp. depend., NMR spin-echo obs. 80−65266
water, self diffusion, high-press., low-temp. spin-echo NMR obs. 77−8446
water, self-diffusion coeff., pressure and temp. depend. meas. by proton spin echo 80−39328
water, self-diffusion coeffs. in pure water and aq. electrolyte solns., ^{18}O and ^2H tracers 78−95169
water, structure and motion at high pressure 78−87606
water self-diffusion in porous membranes, ionic solns., struct., props. 79−52765
Ag-In melt system, conc. depend. of component and impurity diffusion coeffs., radioactive isotope method *(Russian)* 80−107454
Al-Cu, melt near solid-liquid interface, diffusion during crystallisation *(German)* 79−29046
Al_2O_3, liquid, exam. of diffusion parameters, using Al^{26} 79−1518
Ar, liquid, binary non-additive particle interaction, self diffusion and at. motion, mol. dynamics method 80−59372
Ar, liquid, diffusion coefficient for model potentials through means square displacement 80−70098
Ar, mol. dynamics calc. 77−19857
Ar-Kr liq. and gas. solns., collision-induced dipole moment, far IR band obs., self-diffusion coeff. 77−38627
BeF_2, molten, symm. stretching freq. calc. using mol. dynamics method 77−71790
BeF_2-LiF molten mixtures, mass transport, chronopotentiometry 77−21391
CO, solid and liq., vibr. relax. and vibr. diffusion rates, 66-79K 78−17757
Ca diffusion in silicate melt 79−90809
$CaO-Al_2O_3-SiO_2$ melt, at 1723 to 1823K, determ. of inter diffusivities matrix 78−43161
$CaO-SiO_2$ melt, ^{31}Si tracer diffusivity at 1600°C 80−54418
$CaO-SiO_2-Al_2-O_3$, 1500°C, ion transport coeffs., interdiffusivities 77−11718
$CaO-SiO_2-Fe_xO$ system, liq., steel making slag, Ca and Fe tracer diffusivities, O_2 press. depend. 78−38863
CdI_2, aq. soln., isothermal transport props., 298.15K 78−18815
CdI_2, aq. soln., transport props., irreversible thermodynamic anal. 78−14490
CdI_2, aq. solns., ^{115}Cd isotopic diffusion coeffs. 78−47545
CdI_3, aq. solns., ^{115}Cd isotopic diffusion coeffs., expt. anal. 78−43160
Co-Ca, liq. alloy form. kinetics *(French)* 80−96652
Cs, transport coeffs., temp. and press. depend., Enskog theory 78−6170
Cu-Sn, self-diffusion of Sn, correl. with other props. *(Russian)* 79−23764
D_2, D_2-H_2 mixtures, coeff. determ., mechanism 77−35746
DCl, liq., self-diffusion coeffs., NMR spin-echo meas. 80−50223

self-diffusion in liquids continued
D_2O, compressed at low temp., mol. motions, spin-lattice relax., viscosity and self-diffusion 77−76287
D_2O-H_2O mixing, diffusion meas. using neutron radiography 77−15605
$FeO-Cr_2O_3$, melt, exam. of viscosity and self-diffusion 79−95198
FeS-MnS(MnO), melt, exam. of viscosity and self-diffusion 79−95198
Ga, self-diffusion coeffs. by radioactive tracer technique 80−49392
Ga, tracer diffusion studies using metallic ^{67}Ga 80−24629
Ga-GaAs melt, mutual diffusion from soln. kinetics, self-diffusion coeffs. 77−47608
H_2, H_2-D_2 mixtures, coeff. determ., mechanism 77−35746
H_2, review of neutron radiography results 78−59961
HCl aqueous solutions, diffusion coeffs. at 298K, conductimetric obs. 80−24628
HCl, liq., self-diffusion coeffs., NMR spin-echo meas. 80−50223
HCl, liq. struct. simulated by a Lennard-Jones pot. 80−1917
H_2O, self-diffusion coeff. meas. in aq. electrolyte solns., NMR spin-echo method 78−80243
^3He-^4He mixture, near absolute zero, holographic interferometry exam. of phase changes 78−38905
Hg, liq., self-diffusion coeffs. by radioactive tracer technique 80−49392
Hg, transport coeffs., temp. and press. depend., Enskog theory 78−6170
InAs, melt, mutual diffusion of components 80−88345
InGaAs, LPE, diffusion-limited step-cooling technique, layer thickness and composition 80−84402
InGaAsP, LPE, diffusion-limited step-cooling technique, layer thickness and composition 80−84402
KBr-LiBr, liq. mixture, struct. and diffusion 80−24344
KCl, molten, vapour-liq. interface, mol. dynamics model 80−54362
Kr, ^{85}Kr diffusion meas., precision apparatus 78−54520
La, liquid, viscosity from 940 to 1220°C *(German)* 79−28123
$(Li-K)NO_3$, molten, $K^+(Rb^+)(Cs^+)(Tl^+)$ diffusion, wavefront shearing interferometric obs. 79−60535
$LiBeF_3$, $LiBe_2F_4$, molten, self-diffusion of Li 80−54417
LiCl, aqueous, proton, deuteron and ^7Li relax. times, mol. motion obs. 79−28632
LiCl-KCl, molten mixture, struct., diffusion, cond., mol. dynamics calc. 80−64871
LiCl-RbCl, molten, Chemla effect, mol. dynamics simulation, self exchange vel. 80−79967
LiF-BeF_2, molten, self-diffusion coeff. of F *(Japanese)* 77−47610
Li_2O-SiO_2, cation interdiffusivity, electrochem. determ., 1100-1350°C 78−47544
N_2, liq., hard spheres diffusion, free vol. theory, Litovitz eqn. 77−51530
Na, liquid, diffusion coefficient for model potentials through mean square displacement 80−70098
Na, liquid, self-diffusion coeff., 127°C, from mol. dynamics data 77−76585
Na-K liquid alloy, self and mutual diffusion coeff. 78−22877
NaCl, aq. soln., Cl^- self-diffusion, using β-active tracers, plastic capillary method 77−50333
$^{22}NaCl$, tracer diffusion meas. in aq. NaCl soln., closed capillary method 78−14491
$NaNO_3$-$AgNO_3$, molten salt mixture, ionic and mol. mobilities, interdiffusion and self-diffusion *(German)* 77−11720
Na_2O-CaO-SiO_2, molten glass, self-diffusion of Ca ions 78−10202
Na_2O-K_2O-SiO_2 glass melt, interdiffusion coeffs. of Na^{2+}, K^{2+}, temp. depend. 80−44348
Na_2S_5-molten S interface, mass transport phenomena, rel. to Na/S battery 80−72026
Ne, mol. dynamics calc. 77−19857
Ne-Kr, partially miscible mixture, high press. mol. dynamics using Lennard-Jones pot. 79−41929
$NiCl_2$, aq. soln., diffusion and struct. 78−14488
Pb, vacancy motion from coordination statistics 77−1063
Pb-Bi, liquid alloy, chemical and intrinsic diffusion coeffs., exam. *(German)* 78−83987
Pb-Bi liquid alloy, Pb and Bi diffusivities, temp. and conc. depend. *(German)* 80−84311
PbO-K_2O-SiO_2, O tracer diffusion above transform. temp. 79−28120
PbO-$PbCl_2$-PbS, liquid system, elec. cond. meas. 78−43162
Rb, liq., computer-simulated, search for atomic vacancies 77−84620
Sb, liq., self-diffusion, long capillary method obs., using radioactive Sb 77−89564
Sn, $^{113,117m,125}Sn$ diffusion coeff. meas. *(Ukrainian)* 80−10690
Sn, diffusion coeff. of ^{113}Sn, ^{124}Sb, ^{110}Ag, and ^{195}Au 80−96676
Sn-Pb (38.1 wt.%) alloy, self-diffusion coeff. of Sn, 466 to 786K 77−69106
$TlNO_3$, molten, Tl^+ self-diffusion coeff., 230-330°C 78−22878
$TlNO_3$-$NaNO_3$, melt, cationic self-diffusion coeffs., temp. and conc. depends. 78−22879
$TlNO_3$-$RbNO_3$, melt, cationic self-diffusion coeffs., temp. and conc. depends. 78−22879
Tl_2Se, fused, diffusion of ^{204}Tl, ^{110}Ag, ^{112}Sn impurities 80−54415

self-diffusion in solids
see also diffusion creep
actinide carbides, lattice defects and rel. to phys. props., review 77−27874
activation energy of self diffusion, temperature dependence 78−91470
activity and steady-state diffusion 78−95176
adamantane, crystalline, lattice and sub-grain boundary self-diffusion coeffs. meas. 78−6179
β-Al_2O_3-Na_2O, diffusion and ionic cond. meas. 80−6542
β-Al_2O_3-Na_2O, mechanism of diffusion 80−2202
β-Al_2O_3-Na_2O, Monte Carlo calc. of Na diffusion 77−89579
alkali halide, diffusion of monovalent ions 78−30790
alkali halide, energy of movement of vacancies, zeroth order calc. 77−89571
alkali halide, migration enthalpy and entropy for cation vacancy motion 77−35750
alkali halide, migration enthalpy of cation vacancy correl. with MP 77−76606
alkali halides, ion migration, barrier heights, shell model calcs. 77−35742
alkali halides, mass transport, contrib. of vacancy defects 79−46831
alkali halides, matter transport rel. to point defect parameters 80−107488
alkali metal sheet phases, $A_x(L_xM_{1-x})O_2$, (A=Na,K; L=In,Sc; M=Ti,Zr,Hf,Sn), influence of A^+ ion environment *(French)* 79−65244

self-diffusion in solids continued
alkali metals, vacancy formation energies calc. 79−82197
alkali silicate and borate glasses, ionic motion, ^{7}Li NMR obs. 78−27107
alkaline earth fluoride, doped with trivalent rare earths, migration entropy for bound fluorine motion 80−71303
n-alkane, order-disorder phase transition bits. calc. 77−72684
alloy, binary, diffused layer growth kinetics, effect of interphase reaction rate 77−7888
alloy, binary, interdiffusion theory allowing for nonuniformity of inert marker displacement *(Russian)* 77−7889
alloy, binary, kinetic behaviour of vacancies and atoms 79−28129
alloy, binary, solid state second phase redistribution in applied field 78−51721
alloy, binary, solidification, transition from diffusion controlled to diffusionless, solute drag treatment 77−16563
alloy, binary, surface dehomogenisation during evaporation and ion sputtering 77−73207
alloy, binary, vol. changes during sintering, inter-ion interaction influence 79−28982
alloy, binary and ternary interdiffusion parameters, possibility of correl. with solidus temp. *(Russian)* 77−24426
alloy, diffusive phase transform., boundary conditions 77−11693
alloy, dispersion hardened, work hardening due to Orowan loops, temp. depend. *(Japanese)* 80−66534
alloy, hyperplastic, diffusion coeffs. determ. during deform. 79−51298
alloy, solid substitutional soln., diffusive creep *(Russian)* 79−55816
alloys, intergranular precipitate effect on diffusion growth of creep voids 79−34041
alloys, thermomigration, substitutional-vacancy and interstitial-vacancy mechanism 77−35744
amorphous metals, struct. imperfections, review of expt. evidence 79−37630
anisotropic NiAs-CdI_2 type structure, Mossbauer line broadening due to diffusion 77−12281
anomalous diffusion in omega forming systems 78−63873
atom flux inequality with vacancy counter flux 78−95178
atomic diffusion mechanisms *(Hungarian)* 78−38868
austenite, computer simulation of C diffusivity 79−77803
basaltic expt. study of cationic diffusion of alkali and alkali-earth ions 78−95180
BCC metals, anomalous 78−91474
BCC metals, stressed, computer simulation of vacancy and divacancy migration 78−47573
BCC structures, simulation of vacancy-thermotransport 78−47570
bimetal system, diffusion kinetics taking into account nondiagonal coeff. of Onsager matrix *(Russian)* 78−38871
binary alloy, phenomenological theory of interdiffusion, role of nonequilib. vacancies *(Russian)* 78−59966
binary alloys, ordered, self-diffusion kinetics 80−10698
binary alloys, preferential sputtering with diffusion, equilib. distrib. 78−68592
binary metallic solid solns., thermodynamic quantities rel. to vacancy and diffusion characts. 79−95204
binary solids, sputtered, influence of incident flux depend. radiation enhanced diffusion on composition changes 79−52067
binary substitutional solid solution, diffusion, correl. effects and jump freq. ratios 79−99350
α-brass, electron irradiated, defect production and interdiffusion 78−67739
α-brass, electron irradiated, vacancy migration props., effect on enhanced atomic mobility 79−46829
brass, plastically deformed, phase transforms. and diffusion phenomena *(Russian)* 79−20115
brass, two-phase α/β bicrystal, diffusion induced twins in α-phase 79−46967
α-brasses, cold worked, atomic diffusion kinetics to stacking faults, Laplace transformation method 80−19977
dl-camphene, self-diffusion, effect of impurities, radiotracer and plastic deform. study 78−43177
d-camphor, NO diffusion, ELDOR, self-diffusion 77−1618
d-camphor, plastic crysts., impurity size effect on self-diffusion 77−11727
Cationic conduction and diffusion and the compensation law 78−18822
choline salts, mol. motion, proton spin-lattice relax. 77−59474
classical model single particle Hamiltonian 80−39340
correlated self-diffusion in crystals, and quasielastic neutron scatt. 77−84967
creep crack growth, model based on vacancy diffusion along grain boundaries 78−75716
crystal, subjected to high-energy, particle flux, point defects, hopping freq. 79−7708
crystal vacancy migration induced by subthreshold collisions, computer simulation exam. 78−47365
cubic crystal, non-Arrhenius diffusional behaviour and high-field nuclear spin relax. 77−47611
cubic crystal, self-diffusion and melting 77−31803
cubic crystals, random motion, of vacancies, correl. factor and NMR diffusion parameters determ. 78−2284
cubic crystals, randomly migrating vacancies, computer simulation of correlated self-diffusion 78−2283
cubic lattice, self-diffusion via vacancy mechanism, correl. effect 80−59693
cyclohexane, dynamic props. investig. by Rayleigh scatt. of Mossbauer radiation *(Russian)* 77−69760
cyclohexane, FCC plastic phase, self-diffusion coefficient, 6 to −40°C, nucl. spin-lattice (spin) relax. 77−36144
cyclohexane, NO diffusion, ELDOR, self-diffusion 77−1618
defective solids, chemical diffusion, steady-state computer simulation method for lattice gas 80−49401
cis-dekalin, dynamic props. investig. by Rayleigh scatt. of Mossbauer radiation *(Russian)* 77−69760
1,2-difluorotetrachloroethane, mol. motions and Zeeman-quadrupole cross relax., NMR obs. 79−65751
dilute alloy, ternary, substitutional solute element effect on diffusivity of interstitial solute element 78−59969
dilute alloy in dissociative equilibrium, solute and solvent diffusion 77−76593
dislocation damping during electron irrad. 77−35632
dislocation loop diffusion growth in saturated soln. of point defects 77−68974
dislocation motion, effect of diffusion 79−27983
self-diffusion in solids continued
dislocation pinning, linear stress effect on diffusion, internal friction *(Russian)* 77−80505
n-eicosane, triclinic phase, self-diffusion, 295 to 309K 80−88359
elastic-diffusion interaction of closely situated pores *(Russian)* 77−76592
elasto-diffusive solids, singularity movement, appl. to fracture propag. 78−30235
elastomer, relaxation processes, statistical description *(Russian)* 79−23229
electromigration and diffusion, new examination technique 78−67852
enhanced diffusion mechanisms, review 78−67847
exact analysis of diffusion coefficients and correlation factors in crystals 78−59968
faulted dislocation loops induced by elastic interaction, climbing motion 80−75227
FCC crystal, interstitial and solute concentration gradients, flux expression derivation *(French)* 80−54219
FCC crystals, close packed vacancy clusters, enumeration of migration, growth and contraction mechanisms 78−47352
FCC lattice, correl. functions for simple hopping, diffusion coeffs. 79−95202
FCC metals, props. of vacancies and divacancies 80−10545
FCC metals, self-diffusion calc. 78−10212
FCC metals and alloys, grain boundary energy and self-diffusion, effect of solute segregation 78−15412
α-Fe, mag. ordering affecting homodiffusion coeff., 511-1200°C 79−73711
feldspars, of O_2, ion microprobe determ. 78−69325
ferrite-austenite (α-γ) interface, Fe self-diffusion compared with grain boundaries diffusion 80−65306
ferrite-austenite transition, C diffusion const. determ., rate const. of carburization and decarburization 78−48396
film, grain boundary electromigration, low temp. theory 77−31799
film, polycryst., nodule mechanism of diffusion-induced disintegration *(Russian)* 78−51829
fluorite lattices, $^{19}F^-$, self-diffusion, spin lattice relax., NMR techniques 80−34801
flux of vacancies and atoms, computer simulation 79−73332
glass, decomposition, phase separation processes, diffusion coeffs. determ. *(Germany)* 78−39736
glass, ion motion and mixed alkali effect analysis 78−30793
glass systems used for optical fibres, diffusion kinetics 79−90040
grain boundary cavities, star-shaped unstable growth 79−46679
grain boundary crack, diffusional growth 78−47471
grain boundary migration obs. using FIM 78−79617
grain boundary sliding and its accommodation during creep and superplasticity 77−40436
graphite, point defects and self diffusion 78−63758
graphite-DNO_3, intercalation cpd., mol. dynamics 79−28631
heat of transport in solids, computer simulation of a vacancy in FCC cryst. 79−14955
heterogeneous systems, self-diffusion, NMR pulsed field gradient *(German)* 78−60341
ice, cubic, D_2O isolated, H^+ exchange and Bjerrum defect migration, direct spectroscopic obs. 80−88356
ice, vacancy conc. calc. from self-diffusion const. 77−35553
III-V crystals, thermally enhanced diffusion of point defects near dislocations during device operation 79−90820
Inconel 600, Cr diffusion 77−20110
interdiffusion during anomalous phase growth, anal. *(Russian)* 78−55990
interface composition during diffusion controlled precipitate growth, model for ternary systems 77−36513
interstitial solid solutions, self-diffusion activation energy rel. to partial molar energy 80−15291
interstitialcy diffusion, correl. factor estimation 78−43167
ionic crystal defects, mag. reson. studies 80−108066
ionic crystals, nonstoichiometric, equilib. with gas phase in mech. vibr. field 78−43388
ionic solids, diffusion routes and thermal vibrs., calc. method 80−107462
lattice defects and diffusion processes in solids, book 80−107207
liquid crystal, thermotropic, diffusion and nucl. mag. relax. 80−24362
lunar regolith particles, volatile elements diffusion and volatilisation 77−9680
metal, Arrhenius plot of diffusion, curvature, disappearance under press. with single-vacancy model 79−10975
metal, creep movement of dislocations, effect of stress distrib. at grain boundaries *(Russian)* 78−27564
metal, diffusion, correlation with entropy of fusion 78−43109
metal, diffusion of interstitial atoms through crystal lattice interstices *(Russian)* 77−24425
metal, diffusional relaxation of stress conc. at second phase particles 79−1889
metal, dynamic study of defect mobility using HVEM 78−47327
metal, FCC, homovalent impurity migration energies, fluctuation theory model 79−95219
metal, FCC and BCC, self-diffusion along edge dislocations by vacancy mech. *(Russian)* 78−87810
metal, FCC and BCC, vacancy diffusion along single edge dislocations, computer modelling *(Russian)* 77−47612
metal, HCP, long-range interstitial migration rel. to c/a ratio 79−28125
metal, HCP, self-migration energies, elastic calc. 79−95205
metal, non-Arrhenius diffusion and NMR relax. relationship 78−47568
metal, pure, review 78−47561
metal, refractory, BCC, free migration of self-interstitials 78−47574
metal, self diffusion, effect of homogeneous plastic deformation *(Russian)* 77−89572
metal, self- and impurity diffusion, connection between preexponential factor and activation enthalpy 77−69111
metal, self-diffusion, atomic jump processes 78−47562
metal, self-diffusion acceleration by dissolved H_2 *(Russian)* 78−34647
metal, vacancy diffusion during plastic deform., possibility of stimulated electron emission obs. *(Russian)* 79−5007
metal carbide, magnetron-sputtered, solar selective absorbing surfaces 79−92079
metal layered contacts at low-temps. *(German)* 80−6538
metal oxide metaphosphate glasses, vibr. study of metal cation reduction at surface 78−56797
metal-H system, constitution diagrams and hydride struct. form. 79−24509

self-diffusion in solids continued
metal-H system, electro- and thermotransport of H, book contrib. 80−24644
metal-H system, neutron spectra, book contrib. 77−89573
metal-H system, NMR depend. on struct., H diffusion and electronic struct., book contrib. 79−82887
metal-H systems 79−82906
metal-H systems at high H press., physicochemical props., book contrib. 80−24535
metallic glasses, atomic transport behaviour, review *(Japanese)* 79−94907
metals, atomic mobility under pulsed loading conditions *(Russian)* 80−96684
metals, diffusion alloying conditions, deep chemical-heat treatment *(Russian)* 80−40393
metals, individual atomic events on surfaces, quantitative examination 80−75409
metals, light interstitials diffusion, multiphonon transition modes classification 80−70448
metals, point defect diffusion controlled reaction theory, book contrib. 80−103318
metals, point defect dynamic props. and diffusion controlled reactions, book 80−101674
metals, point defect simultaneous clustering during irrad. 79−95000
metals, pure and alloyed, grain boundary relaxation model, *(Russian)* 80−39107
metals, quenched, vacancy cluster form. process 80−92706
metals, radiation creep speed and swelling, self diffusion mechanisms *(Russian)* 80−92595
metals, sintering analysis using sintering maps 80−93513
metals, structural state and physical similarity criteria *(Russian)* 79−52298
metals, vacancy migration energy 78−51723
metals and alloys, NMR results, brief survey 79−73830
metals and alloys, protective oxide layer stress accumulation and perturbation of parabolic kinetics 79−5076
mica, stress-induced K^+ ion migration, X-ray fluoresc. anal. 77−4221
migration and formation energies rel. to Debye temp. and melting point 78−22710
migration energies of point defects, in pure metals and dilute alloys, calc. 78−47572
molecular crystals, diffusion and point defect struct., review 79−82373
Mossbauer line broadening, effect of diffusion by vacancy mechanism 77−40161
Mossbauer line broadening due to correlated diffusion 77−73097
Mossbauer line broadening due to Mossbauer atom diffusion via vacancies 79−73868
neutron irradiation effects *(Japanese)* 77−59048
neutron scattering techniques in applied research, medium-flux research reactors 79−13514
NMR apparatus for meas. of self-diffusion coeffs. in solids 79−217
NMR spin-lattice relax., effect of correlated atomic diffusion 80−107495
non-Arrhenius self-diffusional behaviour effect on quasielastic neutron scatt. and Mossbauer linewidth 78−67853
norbornylene and norbornane, HCP plastic cryst. phases, radiotracer self-diffusion obs., monovacancy mechanism 79−33111
nuclear fuel, MX type, self diffusion in- and out-of-pile 78−82457
nuclear fuel, transport phenomena under severe temp. gradient 80−615
nuclear fuel element, cylindrical analytical soln. to mass transport eqn. 78−21643
nuclear fuels, creep, irradiation induced, transient state, kinetic eqn. treatment 80−88251
nuclear spin relax., motion induced, orientation depend., point defect self-diffusion mechanism 77−48078
one-dimensional chains, diffusion of labelled particles, density fluctuations 79−4426
optical material, phototransport laser damage mechanism 77−63498
oxide compounds, binary, solid-phase reactions of form., direction of diffusion 79−43179
oxide glasses, elec. cond. and dielec. relax., correl. 78−79801
oxides, impurity diffusion and self-diffusion, review and bibliography 80−59719
oxides, point defects diffusion coeffs. calc. *(Japanese)* 80−15302
paramagnet system, low-temp. diffusive transport for polarons and defectons 78−43174
pivalic acid, plastic cryst., self-diffusion 79−46832
plastic crystals, self-diffusion parameters from anal. of NMR relax. data 79−42301
plastically deforming solid, creep cavitation by vacancy diffusion 78−48471
point defect diffusion in stress field of edge dislocation of irrad. solid 78−51720
point defect sink strength in irradiated materials 77−51368
polycomponent metallic solid soln., creep and diffusion of vacancies *(Czech)* 79−43340
polycrystalline materials, diffusion controlled stress rupture 79−14878
polycrystalline materials diffusion controlled stress rupture 79−14879
polyisobutane, relax. times, self diffusion, devel. and appl. of NMR data acquisition system 80−34807
polymer, NMR matrix technique 80−15806
polymer self-diffusion, review 80−29193
polymers, NMR, review 80−88888
porous structure, shrinkage kinetics, boundary slip and superplasticity 77−36611
powder, deforming, self-diffusion coeffs. in failure zones and percolation 80−76209
proton transport 80−79974
radiation effects, distrib. functions of point defects and moving gas filled holes 77−55302
rare earth metal silicide thin film formation on (100), (111)Si substrates, backscattering study 80−70542
rare earth metals, diffusion, review 79−69281
rare earth metals, thermodynamic props. determ. form US vel. meas. 78−55912
refractory composites, fibre reinforced, directionally solidified tensile tests, in HVEM, deform. and fracture *(French)* 78−68785
refractory metals, mech. props. and diffusion figures *(Russian)* 80−40436
ruby, rel. to temp.-time dependence of yield point by compression and extension 78−6988

self-diffusion in solids continued
sapphire, work hardening 77−16604
semiconductor, amorphous, diffusion phenomena, mechanisms and meas. 77−76608
semiconductors, atomic diffusion, review 79−4423
short-lived large energy fluctuations, semiphenomenological collective treatment, Arrhenius approx. 78−43168
silicate glasses, ion-microprobe determ. of Li diffusion 78−53649
silicate glasses, Na ion mobility, OH content effect 79−99359
silicides, of Si, obs. by ^{31}Si tracer and Rutherford backscatt. methods 79−4431
simple cubic lattice, vacancy, diffusion harmonic theory, heat of transport 77−84962
simple solid family of phase states *(Russian)* 80−15216
sintering, bulk transport morphology relations 77−70015
sintering, surface redistribution by grain boundary diffusion 80−84871
solid electrolyte, diffusion and ionic cond., correl. factor meas. problems 80−59709
solid electrolytes and solid soln. electrodes, NMR investigs., review 80−60432
solid solution, diffusion, influence of conc.-induced stresses *(Russian)* 78−55969
solid solution, grain boundary self-diffusion co-eff. meas. in single phase 77−7886
solid-phase reaction kinetics, intercrystallite diffusion role 79−33106
solute-induced jump correlations during diffusive processes 79−51297
steel, alloy, carburised, kinetic parameter determ. *(Rumanian)* 79−29259
steel, alloy, uphill diffusion during homogenization 77−90381
steel, austenitic, Cr-Ni, bulk and intergranular autodiffusion of ^{59}Fe *(French)* 79−55921
steel, austenitic, of Fe, Cr, and Ni *(Czech)* 80−107464
steel, austenitic, supercooled, decomposition by heat treatment, carbide particle morphology *(Russian)* 77−70076
steel, austenitic stainless, bulk and grain boundary diffusion of Fe, Cr, Ni, effect of Si content 78−38875
steel, austenitic stainless, Cr-Ni (18, 10 wt.%), ^{59}Fe self-diffusion in ferrite/austenite interface *(French)* 80−19975
steel, austenitic stainless, extrinsic grain boundary dislocation spreading 79−57004
steel, austenitic stainless AISI 321, Cr tracer diffusion coeffs. 80−2193
steel, austenitic stainless Cr-Ni, ^{51}Cr tracer diffusion coeffs. 80−34225
steel, C, rel. to effect of temp., deform. rate and stress state on ductility *(Russian)* 78−35428
steel, cementite migration in temp. gradient 78−44151
steel, CK10, structural, stress induced diffusion of carbon particle atoms at dislocations *(German)* 79−38888
steel, corrosion resistance, effect of diffusion Fe plating *(Russian)* 77−70208
steel, Cr (0.5 wt.%), austenite-pearlite transformation 80−97480
steel, Cr (4 wt.%), Cr_7C_3 precipitate growth during tempering, effect of Cr diffusion *(Russian)* 79−52219
steel, Cr-Mo, martensite to ferrite transform. by fatigue deform. *(French)* 79−66056
steel, ferrite-austenite transition, diffusion const. of C and carburisation rate consts., thermopower meas. 80−89216
steel, low alloy, coarsening at high temp. of small carbide particles dispersed in ferrite 77−52335
steel, low alloy and C, reversible temper brittleness kinetics *(French)* 78−35498
steel, low C, hysteresis loop initiation mechanism under repeated load *(Japanese)* 78−39851
steel, Mn, with varying Mn content, diffusion of ^{48}V and ^{59}Fe *(Czechoslovakian)* 77−35743
steel, of C, after high-temp. thermomechanical treatment *(Russian)* 78−39813
steel, stainless, 316, intergranular crack growth by diffusion 79−24608
steel, stainless, duplex alloy, Cr diffusion 77−20111
steel, stainless, thermal transfer of C *(Russian)* 78−6174
steel, stainless, type 316, point defect simultaneous clustering during irrad. 79−95000
steel, stainless, VHS-2USh, α to and from γ transformation investigation by thermomagnetic structural anal. *(Russian)* 79−83197
steel, stainless 304L, sintering, effect of grain growth and boundaries on shrinkage rate 77−36419
steel, stainless 316, creep under high stress 78−52892
steel, structural, fatigue softening, temp. and load freq. influence, C atom diffusion *(German)* 79−61614
steel low C, γ-α transform. kinetic rel. with self-diffusion charact. *(Russian)* 78−67850
steel VKS-210, α to and from γ transformation investigation by thermomagnetic structural anal. *(Russian)* 79−83197
steels, austenitic-C steel diffusion couple, diffusion of C, 773-1373K 79−19392
superionic conductor, effects of disorder and mobile particle interactions 80−107536
superionic conductor, Haven ratio, temp. depend., correl. effects role 80−107504
superionic conductor, hydrodynamic theory for collective excitations 80−107530
superionic conductor, interacting Brownian particles in periodic medium model 80−59712
superionic conductors, continuous stochastic models, book contrib. 80−24663
superionic conductors, lattice gas models, book contrib. 80−24661
tensor for atomic migration in crysts. 79−7705
theory, connection between D_0 and Q for self- and impurity diffusion 78−30777
thermosetting resin, estimation of diff. co-eff. distrib. and mol. wt. distrib. by computer *(Japanese)* 77−66042
tracer diffusion, effect of vacancy conc. on correlation factors 79−4425
transition metal-H system, exam. of excitation spectra and diffusion mobility of H using neutrons 80−29203
transition metals, group IV, diffusion mechanism *(Russian)* 79−73335
n-tritriacontane, non periodic molecular motions, neutron scatt. study 79−51024
vacancies, interpretation of data obtained by NMR and Mossbauer expts., mol. dynamics study 78−47567
vacancy diffusion correl. factors, Monte Carlo computer simulation 77−15615
vacancy formation energy, correl. with compressibility 78−2112

self-diffusion in solids continued
vacancy formation vol., stress-assisted diffusion theories 79−95201
vacancy migration vol. 80−10701
vacancy nonlinear diffusion in crystal 80−39338
voids, review of diffusional growth of creep voids 78−71720
Zircaloy-4 oxide, O diffusion during Zircaloy-4 oxidation in steam, 900-1500 degrees C 79−100288
$16Na_2O.12CaO.72SiO_2$, self-diffusion of Ca^{2+} ions *(Japanese)* 78−6173
$40CaO.20Al_2O_3.40SiO_2$ slag glass, self-diffusion of Ca^{2+} ions *(Japanese)* 78−6173
Ag, activation enthalpy determ., tracer diffusion method 79−28128
Ag, Ag-Cd(In) dil. alloys, electron irrad., stage I_E recovery 77−39616
Ag, electron irradiated, exam. of vacancy migration energies, and annealing kinetics 78−47571
Ag halides, matter transport rel. to point defect parameters 80−107488
Ag, low-temp. self-diffusion, comparison between microsectioning studies 79−19393
Ag, of ^{110}Ag in temp. gradient, local vacancy conc. determ. 78−87812
Ag, periodic precipitation, conc. depend. of diffusion coeffs. *(Russian)* 77−16584
Ag, spherical powder, sintering, study of initial stage 79−20004
Ag, surface self-diffusion coeff., O_2 potential effect 80−15354
Ag, vacancy and divacancy diffusion 79−82377
Ag-Cd dilute alloy, isotope effect and correlation factor for Cd diffusion 78−14501
Ag-Co, dil., binding and caging of impurities and trapped interstitials 78−39462
Ag-In-Sn, internal oxidation, solute element and O_2 behaviour *(Japanese)* 80−89479
Ag-Nb-Ga, phase relations, A15 phase diffusion layer formation 78−52764
Ag-Sn (0 to 6 wt.%) exam. of bulk diffusion of ^{113}Sn and ^{110}Ag 78−75864
Ag-Sn (0 to 6%), equilibrium intergranular segregation and diffusion 78−43130
α-Ag-Zn, electron irrad., atomic mobility enhancement by defects, dynamic characts. 79−37871
Ag-Zn, electron irrad. self-interstitials, migration and elimination characts. 79−37872
Ag-Zn (30 at.%), electron irrad., mobilities of self-interstitials and vacancies 77−84795
Ag-Zn (30 at.%), electron irradiated, atomic mobility, elastic after-effect meas. *(French)* 78−63874
Ag-Zn (30 at.%), neutron irrad., at. mobility enhancement, Zener relax. meas. 77−1157
AgBr, activation parameters of mass transfer processes *(German)* 80−38974
AgBr, Ag^+ migration vol. for vacancy and interstitial motion, influence of anharmonicity 79−14965
AgBr, Br^- diffusion plot, anomalous curvature 79−60548
AgBr, self-diffusion of ^{82}Br by both single vacancies and vacancy pairs 78−55978
AgBr(Cl), ionic transport, defect form. and migration energies, quasiharmonic model 80−107538
AgCl, activation parameter of mass transfer processes *(German)* 80−38974
AgCl, ionic mobility, diffusion coeffs., defect mobility energies 80−65284
AgF, diffusion, elec. cond. and ^{19}F relax. $T_{1\rho}$ meas. 80−92718
Ag_2Hg_3, grain-boundary and volume diffusion coeffs. of Hg 77−55385
α-AgI, diffusion dynamics, quasielastic neut. scatt. expt. 80−107484
α-AgI, diffusive motion of Ag^+ ions, quasielastic neutron scatt. 77−11726
α-AgI, dynamic cage effect 80−107541
α-AgI, I_2 diffusion obs. using ^{131}I radiotracers 78−18830
α-AgI, ionic motions nature, mol. dynamics calcs. 80−107533
α-AgI, molecular dynamics exam. of Ag diffusion 78−55981
AgI, position and dynamics of Ag ions using EXAFS, jump-diffusion cond. model 77−59643
β-AgI, self-diffusion of Ag, quasielastic neutron scatt. study 78−83999
α-AgI, structural and dynamical behaviour 80−107544
AgI type solid electrolytes, expt. props. 78−63877
$(AgI)_x(Ag_2O\ B_2O_3)_{1-x}$, amorphous superionic compound, ^{11}B lineshape and relaxation 80−108107
Ag_2Se, between metal electrodes, current-voltage characts *(French)* 80−97005
Ag_2Te, Ag movements, X-ray microanal. by SEM *(French)* 79−42304
α-Ag_2Te, of Ag^+, deviation from Einstein relation 77−76595
$Ag_xV_2O_5$, diffusion of Ag 77−20120
β-$Ag_xW_yV_{2-y}O_5$ bronzes, β-phase existence range, elec. cond. and Ag diffusion 78−35373
Al, Al-Ag(Mg) dil. alloys, electron irrad., stage I_E recovery, interstitial trapping 77−15405
Al, bicrystal, faceting of migrating ⟨110⟩ coincidence boundaries 79−46680
Al, diffusion in migrating interfaces 79−19390
Al, FCC, strain hardening and recovery by pure metal mode, high temp. deform. *(Japanese)* 78−52843
Al, pressure effect on diffusion, theoretical study 78−47566
Al, quenched, diffusion solution for point defects in stress field, steady state and transient 78−30780
Al, vacancy and divacancy diffusion 79−82377
Al, vacancy double jumps and atomic diffusion 78−6175
Al, vacancy double jumps at high temp. 78−47569
Al, vacancy formation energy and entropy, migration, quenched-in resist. meas. 77−11540
Al-Ag, discontinuous decomposition *(Polish)* 78−52808
Al-Al_3Ti, directionally solidified, thermal stability during annealing, 435-660°C 80−108393
Al-Al_3Ti, peritectic transform. 77−16564
Al-B, dil., diffusion of ^{12}B 79−60541
Al-Co, dil., binding and caging of impurities and trapped interstitials 78−39462
Al-Cr, thin film metal contact, sheet resistance changes 80−80356
Al-Cu (4 wt.%), non IPS geometric surface relief effects associated with diffusional phase transform. 77−32575
Al-Ga (10 wt.%), exam. of ^{27}Al diffusion by NMR technique 78−87813
Al-Ni, interdiffusion and intrinsic diffusion in NiAl δ phase 79−10988
Al-Sc, dil., thermomigration of Sc 79−69280
Al-Si, enhanced interdiffusion during Ar ion bombardment 79−99353

self-diffusion in solids continued
Al-Si (0.6, 0.9, 1.19 wt.%), interdiffusion coeffs. determ. by Matano's method 79−42295
Al-Si (1.2 wt.%), dispersion hardened, work hardening due to Orowan loops, temp. depend. *(Japanese)* 80−66534
Al-Zn, dil., grain boundary diffusion 78−91475
Al-Zn, dil. alloy, ^{65}Zn diffusion 77−51540
Al-Zn, discontinuous decomposition *(Polish)* 78−52808
Al-Zn (15 at.%), supersaturated alloy, growth and decomposition kinetics 80−29965
Al-Zn alloy, solid state eutectoid transformation 79−74146
Al-Zn alloys, cast, Zn diffusion during homogenization *(Polish)* 79−33108
Al-Zn solid soln., controlling creep mechanisms, role of diffusion 78−31469
Al-Zn solid soln., controlling creep mechanisms role of diffusion 78−31470
Al-Zn-Mg (Fe), dil. alloy, ^{65}Zn diff. 77−51540
β-AlO_3-$(Na,Li)_2O$, NMR, Raman and IR spectra, and X-ray diffr., heat treatment induced changes 80−107508
Al_2O_3, pure and Fe or Cr doped, polycryst., creep, diffusion mechanisms 78−11272
Al_2O_3, single cryst., O self diffusion, ion-probe meas. 80−59701
Al_2O_3, single cryst., self-diffusion of O, isotope exchange investig. 80−100348
Al_2O_3 single crystal, vapour-grown, self-diffusion coeff. of O 78−30792
β-Al_2O_3-$(Na,K)_2O$, model calcs. of cond. anomalies, pot. energies of cation arrangements 80−107510
β-Al_2O_3-$(Na,Li)_2O$, first-order quadrupole NMR obs. of cation distrib. and ion motion 80−108113
β-Al_2O_3-$(Na,Li)_2O$, ionic motion obs. using NMR and internal friction 80−108099
β-Al_2O_3-$(Na,Li)_2O$ solid electrolyte, Li motion and activation obs. using ^{7}Li NMR 80−108100
β-Al_2O_3-Ag_2O, Haven ratio, temp. depend., Ag diffusivity and ionic cond. 80−107503
β″-Al_2O_3-$Ag_2O(K_2O)(Li_2O)(Na_2O)(Rb_2O)$, single cryst. Raman scatt., cond. mechanism and cryst. struct. 80−66209
β″-Al_2O_3-$H_3O^+(Na_2O)$, struct. basis for superionic cond. 80−107498
β-Al_2O_3-NH_4^+ and β″-Al_2O_3-NH_4^+-H_3O, single cryst. PMR and proton motion 80−108101
β″-Al_2O_3-Na_2O, ^{23}Na NMR obs. of ionic diffusion, 180 to 800K, attempt freq. 80−108097
β-Al_2O_3-Na_2O, ^{23}Na NQR and two-dimens. diffusion, model analysis 80−108111
β-Al_2O_3-Na_2O, ^{27}Al NMR obs., Na motion and cond. characts. 80−108096
β-Al_2O_3-Na_2O, anomalous Na behaviour obs. using pulsed and CW NMR 80−108095
β-Al_2O_3-Na_2O, calculation of simultaneous ionic cond. and tracer diffusion 78−43178
β-Al_2O_3-Na_2O, diffusion of Na^+, effect of path tortuosity and anisotropy 79−28140
β-Al_2O_3-Na_2O, low-temp. ^{23}Na satellite spectra, Na ion motion 80−108112
β-Al_2O_3-Na_2O, motion of charge carrying ions, mol. dynamics simulation 80−107506
β″-Al_2O_3-Na_2O, NMR of ^{23}Na, elec. quad. interaction, 185 to 419K, ion motion obs. 80−108110
β″-Al_2O_3-Na_2O, nonstoichiometric, correl. effects in diffusion, Haven ratio, point defect interactions 80−107505
β″-Al_2O_3-Na_2O, polycryst. Na^+ ion diffusion rel. to cond. 77−72715
β-Al_2O_3.$Li_2O(Na_2O)(K_2O)(Rb_2O)(Ag_2O)$, low temp. sp. ht., tunnelling states and diffusion theory 77−43345
Ar, diffusion processes in plastic deform. *(Russian)* 80−92591
As_2S_3-Ag_2S glass, Ag diffusion, 50-120°C 78−18828
As_2Se_3 amorphous films, thermal relax. processes determ. by optical props. 77−15716
Au, electron irradiated, exam. of vacancy migration energies, annealing kinetics 78−47571
Au film, excess vacancy diffusion to free surfaces and voids, resist, decay 79−65237
Au, film, grain boundary electromigration, tracer meas. 77−31802
Au film, threshold current density and incubation time to electromigration 78−14643
Au, temp. depend. of isotope effect 78−47563
Au, vacancy and divacancy diffusion 79−82377
Au, vacancy props. 78−47326
Au-Ag, radiation damage and diffusion 80−24645
BaF_2, NMR relax., ionic cond. and self-diffusion 78−23362
BaF_2:$K^+(La^{3+})$, nuclear spin relax. orientation depend., point defect self-diffusion mechanism 77−48078
$BaFe^{2+}{}_2Fe^{3+}{}_{16}O_{27}$, metal deficient, hexagonal with W struct., chemical instability 78−27662
Ba_2MoO_5, Ba_3MoO_6, electrophys. props., effects of thermophys. props. of medium in synthesis 77−48375
$Ba(N_3)_2$, thermal decomp., role of defects 78−73033
$BaTiO_3$, ferroelec., susceptibility of eight site order-disorder model calcs. 77−8523
Bi_2Te_3-Sb_2Te_3 composite billet, diffusion during plastic deformation *(Russian)* 79−23767
β-CO, ^{13}C NMR, self-diffusion activation parameter, press. depend. 77−69719
CO, solid and liq., vibr. relax. and vibr. diffusion rates, 66-79K 78−17757
CaD_2, neutron diffr., NMR 77−15378
CaF_2, cation jump freq., isotope effect, lattice dynamical calc. 80−88357
CaF_2, F^- diffusion 79−14964
CaF_2, fast ion transport, computer simulation 80−107485
CaF_2, mol. dynamics studies of superionic conductors 80−107547
$Ca^{2+}F_2^-$, particle motions, ionic conduction, self-diffusion 77−15620
$CaMoO_4$, exam. of electrical conductivity, absorption spectrum 79−51301
Cd-Cd_3Ag, peritectic transform. 77−16564
CdF_2, polarisation phenomena due to vacancy migration 78−76377
$Cd_xHg_{1-x}Te$, epitaxial growth from stoichiometric melt, crystn. and diffusion 80−75475
$Cd_xHg_{1-x}Te$, long term stability at 300K, rel. to device appl. 80−59978
$Cd_xHg_{1-x}Te$, solid soln., pure and Ag(In) doped, defect struct. model, Hg self-diffusion coeff. 79−95213
CdSb, self-diffusion of Cd, radioactive tracer investig. 77−24428

self-diffusion in solids continued
$CeCo_2$, of Co, interdiffusion exam., growth kinetics of intermediate layers 78−2304
Co alloys, binary, and MAR-M322 type, influence of phase transform. on diffusion and mech. props. *(Russian)* 79−5000
β-Co, creep at low stresses 79−79028
Co, FCC, self-diffusion and isotope effect, influence of mag. order-disorder transition 80−29205
Co, low temp. electron irrad., elec. resist. recovery 77−35588
Co, thermomigration and electromigration in high-purity samples 79−55919
Co-Cu(Ti)(Fe), neutron radiation stimulated diffusion, electrical resistivity exam. *(Russian)* 79−14959
Co-Mn (10.24 at.%), Mn diffusion, 903-1148°C 77−24427
Co-Mn (5.22 at.%), Mn diffusion, 868-1200°C, mag. transform. effects 77−24427
Co-Zn, physical-chemical metallurgy *(German)* 80−108390
$CoFe_2O_4$, cation self-diffusion, 1231 to 1390°C, vacancy migration mechanism 77−1260
CoGa, diffusion coeffs. of ^{60}Co, 800-1050°C 77−84966
CoGa, ordered electronic cpd., self-diffusion of ^{60}Co and ^{72}Ga 79−65238
CoO, defect struct. and self-diffusion 78−63759
CoO, isotope effects in CoO diffusion rel. to vacancies 80−84319
CoO, polycrystalline, high temp. deform. 78−3174
CoO-ZnO-MgO ternary systems, solid solns., struct. charact. 80−60629
$Co_{1-x}O$, point defect struct., elec. cond. and Co tracer diffusion 79−10849
$Co_{1-x}O$ single crystal of controlled stoichiometry, ^{60}Co self-diffusion 77−43369
$Co_{1-y}O$, self-diffusion and defect struct. 78−22889
Cr, self-diffusion activation energies, positron trapping meas. 79−74015
Cr, thermal vacancies, energy of form. and conc. 80−29014
Cr_2O_3, O diffusion coeff. from creep meas. 78−18823
CsBr, self-trapped hole, hopping motion, electronic excitation energy, activation energy, calc. 78−10046
CsCl, self-trapped hole, hopping motion, electronic excitation energy, activation energy, calc. 78−10046
CsI, isotope diffusion 78−75875
CsI, self-trapped hole, hopping motion, electronic excitation energy, activation energy, calc. 78−10046
$Cs_2MFe(CN)_6$, M=Ba, Mg, Ca, Sr, lattice instabilities 77−72668
Cu, defect annealing around stage III, γγ ang. correlation expt. 79−14846
Cu, elastoresistivity of Frenkel pairs, defect migration *(French)* 80−2073
Cu, electron irradiated, exam. of vacancy migration energies, and annealing kinetics 78−47571
Cu, entropy factors for vacancy formation and migration 78−75866
Cu film, Gorsky effect, internal friction maxima, atom diffusional mobility *(Russian)* 80−70446
Cu film, polycryst., nodule mechanism of diffusion-induced disintegration *(Russian)* 78−51829
Cu, impurity diffusion of Vth period elements and self-diffusion 80−65301
Cu, monovacancy formation enthalpy 79−65217
Cu, μ^+ diffusion data anal., theory of incoherent direct and indirect multiphonon transitions 80−70448
Cu, nonlinear diffusion eqns., identification of thermal cond. and sp. ht. *(French)* 77−47614
Cu, radiation damage, vacancy migration induced by subthreshold focused collisions 77−19982
Cu, radiation damage and diffusion 80−24645
Cu, self diffusion at low temp., low energy ion beam sputtering 78−18821
Cu, self-diffusion of ^{64}Cu, 737-1079°C, monovacancy and divacancy contribs. 79−19394
Cu, sintering, contact resist. determ. of neck growth rate and mass transport mechanism 77−55899
Cu, vacancy and divacancy diffusion 79−82377
Cu, vacancy migration energy in FCC lattice by computer simulation 77−11722
α-Cu-Al, kinetic behaviour of vacancies and atoms 79−28129
Cu-Al, vacuum condensate, struct. and mech. props. depend. on deposition conditons 80−15417
Cu-Al (15 at.%), vacancy migration, and short range ordering, comparison of exp. results with theory 78−47356
Cu-Au solid soln., Cu rich, meas. of interdiffusion, intrinsic and tracer diffusion coeff. 78−47608
Cu-Be (6.2, 9.3, 13.4 at.%), cell growth of discontinuous precipitation *(Japanese)* 79−24525
Cu-Bi-Fe, Fe effects on embrittlement 77−28900
Cu-Co, dil., binding and caging of impurities and trapped interstitials 78−39462
Cu-Fe, dil., diffusion and ageing processes, Mossbauer study 80−7245
Cu-Fe, dil. alloy solubility and diffusion of Fe 78−43170
Cu-Fe, implanted, Mossbauer study, rel. to annealing temp. 78−31135
Cu-Ge solid soln., isotope effect for Ge diffusion 78−2285
Cu-Ir, dil., impurity diffusion, temp. depend. *(Russian)* 78−67851
Cu-Ni, Cu rich, chemical and intrinsic diffusion coeff. determ. 79−28130
Cu-Ni, diffusion of Ni, resistometric meas. 80−29222
Cu-Ni, neutron irradiation, enhanced diffusion, elec. resist. meas. 80−6440
Cu-Ni, neutron radiation stimulated diffusion, electrical resistivity exam. *(Russian)* 79−14959
Cu-Ni, sintered, props. and degree of nonhomogeneity 80−20848
Cu-Ni-Zn, multiphase couples, diffusion paths and struct. at 775°C 77−62666
Cu-Ni-Zn alloy, at 775 degrees C, diffusional and thermodynamic interactions 78−38883
Cu-Si, reaction diffusion, effect of compressive stress 77−28050
Cu-Sn, self-diffusion of Sn, correl. with other props. *(Russian)* 79−23764
Cu-Ti (0.9 at.%), age hardening effect on critical resolved shear stress 79−61603
α-Cu-Zn, whiskers, X-ray topography, substruct. 77−11831
Cu-Zn-Mn, steady-state diffusion of Zn and Mn 80−70445
CuBe, SIMS quantitative anal. of Be distrib. in vicinity of oxidation boundary *(French)* 80−11984
CuBr(Cl)(I), LF light scatt. spectra in superionic cond. phases, ion motion obs. 80−108217

self-diffusion in solids continued
CuCl(Br)(I), Raman spectra, Cu ions vibr. and diffractive motions 80−11412
CuI, ionic motions nature, mol. dynamics calcs., sp. ht. anomaly due to order-disorder transform. 80−107533
$CuInS_2(Se_2)(Te_2)$, thin films and photovoltaic devices, AES evaluation 78−67928
$Cu_xMo_6S_{8-y}$, mixed conductor, partial Cu ion cond. and chem. diffusion 80−84323
CuO-containing glass, Cu^+ diffusion and oxidation 80−79980
Cu_2O, self-diffusion of Cu 77−84983
$Cu_{2-\delta}S$, Cu chem. diffusion, and nonstoichiometry, 400°C, electrochem. determ. 79−28132
Cu_3VS_4, out of equil. mixed cond., chem. origin of mobile ions, spin-lattice relax. and NQR obs. 80−108104
Er_2O_3, pure and HfO_2-doped polycryst., Er self-diffusion 80−29207
Eu, BCC, self-diffusion coeff. meas. *(French)* 77−15616
Fe, adsorbed S effects on surface reaction kinetics and surface self-diffusion 78−7234
Fe alloys, ion-implanted, depth profile and diffusion coeff. 80−54277
Fe, Armco, discontinuous laser beam effect on mass transfer *(Russian)* 79−33109
Fe, atom mobility, laser irrad. effects *(Russian)* 77−59139
Fe, BCC, strain hardening and recovery by pure metal mode, high temp. deform. *(Japanese)* 78−52843
Fe, cast form. of surface graphitisation centres *(Russian)* 79−11720
Fe crystallites, vacancy diffusion and vacancy lattices semi-empirical mol. orbital calcs. 77−1121
Fe, effect of plastic deform. and martensite transformation on Fe atom mobility *(Ukrainian)* 78−55974
Fe, ferrite/austenite interface, prep. and charact. *(French)* 79−95272
2-Fe, ferromagnetic self-diffusion 78−6176
α-Fe, high purity, neutron and electron-irrad., interstitial migration at 200K 79−55920
α-Fe, O_2 potential effect on surface self-diffusion coeff. 80−15353
Fe-Al (50.5 at.%), ordered, neutron irrad. enhanced defect diffusion, resist. meas. 77−11598
Fe-Al-C, gamma irrad., crystal lattice parameter reversible changes *(Russian)* 80−10576
Fe-B metallic glasses, diffusion coeffs. from primary crystn. data 80−100345
Fe-C, ageing late stages, diffusional coalescence of precip. along dislocation lines *(Russian)* 77−25060
Fe-C interstitial solid solutions, self-diffusion activation energy rel. to partial molar energy 80−15291
Fe-Co(Cr), compositional diffusionally bonded alloy, mass transfer investigation *(Russian)* 80−39342
Fe-Cr, tracer diffusion meas. using tracer anal. 79−82376
Fe-Cr (9 wt.%), oxidation studied using $C^{18}O_2$ and D_2O tracers 80−71784
Fe-Cr-C, self-diffusion processes during homogenisation of heterogeneous systems *(Russian)* 79−60539
Fe-Cr-Ni, austenitic, self-diffusion and swelling under irradiation 80−39343
γ-Fe-Cu, lattice and grain boundary diffusion of Cu 79−23765
Fe-Mn, dilute, short-range ordering and segregation ascending diffusion *(Russian)* 77−24406
Fe-Mn cast alloys, homogenisation annealing and chemical diffusion *(Czech)* 80−66551
Fe-Mo (0.54 to 2.50 wt.%) ferromag. ordering effect on Fe diffusion *(Czech)* 77−62665
Fe-Mo system, rel. to phase relns. 77−4214
Fe-Mo-C, eutectoid transform. of δ-ferrite 77−16570
Fe-Ni, film, depth profiles, sputter etching obs. 79−83079
Fe-Ni alloy, effect of plastic deform. and martensite transformation on Fe atom mobility *(Ukrainian)* 78−55974
Fe-Ni Invar alloy, electron irrad. effects 79−56638
Fe-Ni Invar alloy, virtual miscibility gap and interdiffusion coefficient 79−55891
Fe-Ni system, Ni addition effects on activated sintering of Fe powder compacts 77−4756
Fe-Ni-C, self-diffusion processes during homogenisation of heterogeneous systems *(Russian)* 79−60539
Fe-Ni-Co, diffusion controlled phase growth 78−30782
Fe-Ni-P, interface composition during diffusion controlled precipitate growth 77−36513
Fe-Pd alloy, diffusion coeffs. of ^{59}Fe and ^{103}Pd meas. *(French)* 77−15617
Fe-Pd film, depth profiles, sputter etching obs. 79−83079
Fe-Pt alloy, diffusion of ^{197}Pt and ^{59}Fe *(Czech)* 79−77804
α-Fe-Si, single cryst., ^{59}Fe diffusion coeffs., 1013 to 1373K 77−69110
Fe-Si alloys, kinetics of spinodal decomposition in 2-phase region of B_2+DO_3 77−28806
Fe-Si-C, austenitic, C diffusivity *(German)* 80−92705
Fe-V, ^{59}Fe self-diffusion *(Czech)* 80−88352
α-Fe-V, dilute alloy, Mossbauer diffusion line broadening, exponential fitting evaluation 78−52379
Fe-V solid solution, diffusion of V 79−90817
Fe-Zn, physical-chemical metallurgy *(German)* 80−108390
$FeB_5C_{15}SSi_{15}Cr_5$, amorphous, exam. of metalloid atom mobility by Auger spectroscopy 78−47575
$Fe_{40}Ni_{40}B_{20}$ glass, ^{10}B self-diffusion, meas. by SIMS 80−49406
α-Fe_2O_3 film, formed on Fe in O_2 and CO_2 at 550°C, growth and struct. 77−52549
$Fe_{3-x}O_4$, vacancy diffusion from relax. of deviations from stoichiometry 79−23769
Fe_3O_4 film, formed on Fe in O_2 and CO_2 at 550°C, growth and struct. 77−52549
Fe_3O_4, magnetite, cation diffusion, correlation and isotope effects 80−96686
$FeP_{13}C_7$, amorphous, exam. of metalloid atom mobility by Auger spectroscopy 78−47575
$Fe_{1-\delta}S$ chemical diffusivity and nonstoichiometric props. 78−10217
Fe_9S_{10}, antiferro- to ferrimag. transition, Mossbauer and mag. exam., diffusion of Fe during transition 79−73716
Fe_9S_{10}, polytypism, Fe diffusion near antiferromag. to ferrimag. transition 80−44830
$Fe_{0.96}Se$, Mossbauer diffusional line-broadening 77−55734
Fe_3Se_4, Mossbauer diffusional line broadening 77−43370
$FeTiH_x$, (x=0.65 to 1.03) diffusion of H, neutron scatt. exam. 79−65243

self-diffusion in solids continued
Ga-In eutectic system, diffusion coeff. depend. on composition *(Russian)* 80−59695
Ga-Zn, eutectic system, diffusion coeff. depend. on composition *(Russian)* 80−59695
GaAlAs-GaAs heterostructures, electronic excitation effects on mobility of point defects and dislocations 78−2561
GaAs, degraded layer form. by annealing, photolum. obs. of defects 78−10968
GaAs, thermomigration of molten Ga 77−69118
GaAs VPE layers, role of diffused Ga vacancy in degradation 78−95050
β- and β''-Ga_2O_2-Na_2O, fast ion conductor, Na^+ self diffusion and Na-K exchange 79−28133
β-Gd, BCC, self-diffusion coeff. meas. *(French)* 77−15616
Gd_2O_3, polycryst. monoclinic, Gd self-diffusion 80−24655
Ge, activation energy and entropy factors 80−88353
Ge, creep and self-diffusion activation energies 78−38772
Ge, dynamical recovery and self-diffusion 79−82379
Ge, migration energy of intrinsic point defects in different charge states 77−89582
Ge, quenched n- and p-type, intrinsic defects migrating near 100°C 77−62670
Ge, self- and impurity diffusion 80−29213
Ge, self-diffusion, dynamical recovery 80−29215
Ge, self-diffusion mechanism 79−90824
Ge, vacancy paradox 78−59804
GeO_2, gamma-ray induced O diffusion, ESR measurement 79−99358
GeO_2, O self-diffusion theory 79−95214
GeS_2-GeS-Ag_2S glass, Ag diffusion, 50-120°C 78−18828
H_2, solid, enhanced quantum diffusion, below 0.3K 79−90845
α-$HCrO_2$, H^+ mobility investig. by nuclear relax. meas. 77−48076
$H_{0.36}MoO_3$ and $H_{1.71}MoO_3$ bronzes, NMR relax. obs. at 77<T<450K, H diffusion 80−108089
H_xMoO_3 (0.3<x<2.0), H mobility from NMR spin echo 79−1416
$HNO_3.H_2O$, devitrification crystallisation, fast Raman and wide-line NMR obs. *(French)* 79−73915
H_2SO_4:Fe^{2+}, frozen aq. soln., photolysis, H form., distrib. and diffusion 78−20044
$H(UO_2P(As)O_4)4H_2O$, H motion, PMR obs. 78−80239
$H_{0.4}WO_3$, inelastic neutron spectra 77−15287
H_xWO_3 films, proton diffusion coeffs. 80−6548
He, solid, vacancy tunnelling freq. calc. 77−80678
^{3}He solid, paramag., low-temp. diffusive transport for polarons and defects 78−43174
^{3}He, solid, spin diffusion at very low temp., multiple echo amplitudes 79−19423
^{3}He, solid, vacancy mobility *(Russian)* 77−85015
$HfV_2H_{2.1}$, proton NMR relax. time and Knight shifts, diffusional activation energies meas., sorption props. 80−75871
$Hg_{1-x}Cd_xTe$, long-term Hall-type conversion by vacancy diffusion at room temp. 79−65498
HgTe, of Hg, self diffusion and defect struct. 79−23775
HgTe, self-diffusion of Te, layer stripping technique 79−37873
IF_6, NMR and NQR of ^{127}I and ^{19}F, solid-solid transitions and mol. motions 79−99784
In, vacancy formation and activation volume, macroscopic model 80−54221
In-Ag, dil., TDPAC technique appl. to diffusion model 79−78589
In_2O_3-SnO_2 thin film, Hall mobility, temp. depend., grain boundary effects 80−75658
InSb, self-diffusion 79−65249
K, self-diffusion, high temp. bulk modulus determ. 80−79976
KBr, X-irrad., H-, and I-centre thermal diffusion 78−72606
KCl, and KCl:Ca^{2+}(Sr^{2+})(SO_4^{2-}), conductivity, self-diffusion coeffs., lattice defect props. 77−4216
KCl, ionic cond., defect parameters, diffusion coeffs. 80−79978
KCl, premelting due to thermal form. of dislocations 77−11671
KCl, X-irrad., H-, and I-centre thermal diffusion 78−72606
KCl:Sr^{2+}(SO_4^{2-}), ionic cond., defect parameters, diffusion coeffs. 80−79978
KCl-KBr-KCl, layered system, diffusion zone, pore form. and movement *(Russian)* 79−69282
KF, of K, new NMR technique for slow diffusion exam. 77−51970
KH_2PO_4, elec. cond. and diffusion, Co dopant effects 77−72716
$KHSO_4$:Co^{2+}, conduction and ^{3}H diffusion 77−15622
KN_3, migration of K^+ and N^0 interstitials, activation energies 79−77813
K_2O-SrO-SiO_2, O_2 self diffusion exam. by proton activation anal. 79−65241
K_2TiF_6, anion motion and phase transition, NMR spectra 79−99788
LaF_3, self diffusion studied with ^{19}F relaxation 78−6180
$LaH_{2.69}$ two-phase behaviour, ^{1}H-NMR evidence 80−93189
$LaMnO_3$, solid phase synthesis mechanism 80−21268
β-$LaNi_{5-y}Al_y$ hydrides, H diffusion, NMR studies 80−15298
$LaNi_5H_x$ (x=4.7, 4.9), NMR line width, spin-lattice relaxation time temp. depend., H self-diffusion *(Russian)* 79−61248
$LaNi_5H_6$, diffusion const. in presence of large background gradients, modified pulsed gradient technique 80−31831
$LaNi_5H_{6.6}$, $LaNi_5H_{6.2}$, H diffusion NMR spectra *(Russian)* 78−2287
$LaNi_5H_{\geq 3.0}$, H diffusion coeff., neutron scatt. obs. 80−24643
β-$LaNi_5H_x$, H_2 diffusion, NMR meas. 79−82378
$La_2Ni_7H_x$ (x=9.9, 11.4), NMR line width, spin-lattice relaxation time temp. depend., H self-diffusion *(Russian)* 79−61248
Li wire, NMR line shape, eddy current effect in presence of self-diffusion 80−54955
LiAl, β phase thermodynamic props., chem. diffusion coeff., electrochem. meas. 80−39308
LiAl, NMR relax. investig. of ^{7}Li self-diffusion 77−12217
$LiAlSiO_4$, β-eucryptite, of Li, one dimens. co-operative diffusion 78−2294
$Li_xFePS_3(Se_3)$, Li_xMnPSe_3 and $Li_xNiPS_3(Se_3)$, NMR and neutron diffr. obs., mag. props. 80−60433
LiH, anion and neutron diffusion, NMR relax. and linewidth obs., Schottky disorder 80−15815
LiH, self-diffusion of Li and H ions 78−59974
Li_3N, diffusion processes and struct. NMR study 80−108090
Li_3N, interstitial sites and anharmonic thermal vibrs. in cryst. struct., ionic cond. mechanism 80−107190
Li_3N, ionic hopping model, NMR relax. data anal. 80−92714
Li_3N layer structure with fast ion cond., ^{6}Li NMR obs. of diffusion 80−108102
$LiNbO_3$, diffusion of alkali metals and self-diffusion 77−84989
self-diffusion in solids continued
$LiNbO_3$-CdO, CdO addition effect on sintering 79−83157
$LiNbO_3$, Li_2O diffusion for chemical control of laser induced optical damage 78−46693
Li_xNiPS_3, antiferromag., mag. props. and ionic mobility, NMR meas. 79−24223
Li_2O, cation diffusion, NMR obs., MgO and LiF doping effects *(German)* 77−20112
Li_2O, Li^+ ion self-diffusion coeff., sectioning technique 80−15296
Li_2O-SiO_2 glass, thermotransport props. 80−79985
Li_2O-SiO_2 glasses, Li self-diffusion, mass spectrometric method 80−79982
$Li_2S(O)$, cation diffusion NMR investigation up to 800°C 80−108092
Li_2SO_4 based solid electrolytes, FCC phase transport mechanism studies and uses 80−107525
$Li_3Sb(Bi)$, evaluation as electrode material, electrochem. expts., 360-600°C 78−11526
Mg, grain boundary diffusion creep 78−11291
Mg-Al (5, 7, 9 and 11 at.%,) discontinuous precipitation growth kinetics 77−63677
$Mg_xFe_{1-x}O$, diffusion of ^{59}Fe and elec. cond. 80−59700
$MgMn_2O_4$, cation migration, neutron diffr. investig. 77−7896
MgO, subgrain boundaries form. obs. by TEM, diffusion coeff. determ. 80−79817
MgO, ultrafine grained Fe doped, high temp. creep 79−15727
MgO-Cr_2O_3, diffusion of Cr_2O_3 and Fe_2O_3 in gas phase during firing *(French)* 78−80495
2MgO.TiO_2, single cryst. and polycryst., O diffusion characts. 77−84968
Mg_2SiO_4, ^{18}O self-diffusion expts., high-temp. creep implications 80−81870
Mg_2SiO_4, forsterite, O_2 self-diffusion coeffs. 80−70457
Mn-Pt alloys, of ^{54}Mn, radioactive tracer study *(French)* 79−86915
MnS, phase transform. at 200°C, diffusive and deformational mechanisms 80−65216
Mo, 1360 to 2773K 79−86919
Mo, powder sintering, transition metal activators, 1000-1350°C, heterodiffusion model 78−44044
Mo, pure, 1100-1300°C *(Russian)* 77−47613
Mo, vacancy diffusivity from width of grain boundary void denuded zone 77−47615
Mo-Ni (40 at.%), exam. of ion transfer *(Russian)* 79−28127
Mo-Ni two phase alloys, elec. and mass transport *(Russian)* 78−76044
MoO_3, reduction at low temp., role of defects, electron microscope obs. 77−77755
Mo_5Si_3, layer electrotransfer of Si 80−92708
$NH_4H_2PO_4$, elec. cond. and diffusion, Co dopant effects 77−72716
Na, at. migration 79−69279
Na, atomic jump processes, quasi-elast. neutron scatt. study 80−84317
Na, diffusion data under press., anal. 78−55975
Na, localised density minima propag. mechanism 78−51722
Na, quasielastic neutron scatt. obs. 79−90818
Na, self-diffusion mech., NMR meas. 80−44356
Na, vacancy double jumps and atomic diffusion 78−6175
Na, vacancy thermal expansion coeff., lattice statics calc. 79−37698
Na_2CO_3+$CaCO_3$ solid state reactions, Hedvall effect 79−96300
NaCl, calc. of migration volume of vacancies 78−75872
NaCl, premelting due to thermal form. of dislocations 77−11671
NaI, transport processes, test of validity of Arrhenius law *(French)* 79−77808
NaI:Ca^{2+}, pure and doped, lattice defects, entropy and enthalpy of formation and migration 80−96687
$Na_xIn_xSn_{1-x}S_2$, ionic conductors, ^{23}Na NMR and complex impedance meas. 79−91314
$NaNO_3$, rel. to ^{23}Na spin-lattice relax. time −75.5 to +320°C *(Japanese)* 77−43897
Na_2O-B_2O_3 glass, Na and Ag diffusion, elec. cond. 79−51300
Na_2O-B_2O_3-Bi_2O_3-SiO_2, heterophase glass, diffusion and elec. cond. 78−67858
Na_2O-K_2O-SiO_2, Na diffusion 78−26724
Na_2O-SiO_2-SnO_2 (TiO_2) glass, exam. of Na^+ self diffusion, elec. conductivity, and viscosity 78−87819
$Na_2O.5Al_2O_3$, diffusion of Na, computer simulation based on Monte Carlo method 77−24431
$NaPO_3$ glass, Na diffusion 78−63875
$Na_2S(O)$, cation diffusion NMR investigation up to 800°C 80−108092
$Na_3Zr_2PSi_2O_{12}$, NASICON, ^{23}Na NMR obs. of ionic diffusion, 180 to 800K 80−108097
β''-$Na_2O.6Al_2O_3$, polycrystalline Na^+ ion drift and diffusion anomalies in elec. field 77−43372
Nb CVD coatings on graphite, grain struct. depend. on temp. 80−25574
Nb, diffusion of ^{95}Zr, diffusion coeff., effect on Nb self diffusion isotope effect 78−47602
Nb, Fe impurity diffusion effect 77−84992
Nb, meas., and enhancement by Fe addition 78−47590
Nb, radiotracer and electron microprobe meas. 77−76615
Nb, self diffusion, 1353 to 2693K, diffusion coeff. 78−47576
Nb, up to 2570K, temp. and O content effects 78−47564
Nb/Cu-Sn-Mg, superconductor, effect of Mg addition to Cu-Sn matrix 80−25028
Nb-Cu, neutron radiation stimulated diffusion, electrical resistivity exam. *(Russian)* 79−14959
Nb-H, spinodals and diffusion coefficients of H, sample shape depend. 78−19713
Nb-H interstitial alloy, props. and synthesis 79−69265
Nb-H interstitial alloys, prep. and props. 78−23669
NbC, exam. of temp., and composition effects, on diffusion coeff. in its homogeneity range 79−33115
NbC_x, near surface effect 79−42303
NbC_x, x=0.868, 0.834, 0.766, self-diffusion of ^{14}C 80−29206
$NbH_{0.02}$, diffusion of H, neutron scatt. study 79−60550
$NbH_{0.02}$, jump models for H diffusion, quasielastic scatt. of slow neutrons 79−95208
$NbH_{0.11}$, incoherent struct. factor of H, neutron scatt. exam., quasielastic energy spectrum 79−99186
NbH_x, diffusion of H atoms, quasielastic neutron scatt. obs., book contrib. 79−82383
α-NbH_xD_y, H diffusion, NMR spin echo obs. 80−34228
$NbH_{0.004}N_{0.007}$, H-diffusion, interstitial trapping, quasielastic neutron scatt. study 79−42298
NbN_xHy, diffusion of H, PMR obs. 79−69287

self-diffusion in solids continued
Nb_2O_5, diffusion of O_2, solid-gas isotope exchange method *(French)* 78−34650
$Nb_{28}O_{70-x}$, O diffusion, rel. to Nb_2O_5 nonstoichiometry *(French)* 78−47583
Nb_3Sn, multifilamentary conductors, stress-induced enhancement of critical currents 79−69644
Nb_3Sn-Cu multifilamentary composite wire, Nb_3Sn filament morphology and grain size 80−100855
Ne, of ^{21}Ne, ultraslow diffusion, adiabatic demagnetisation in rotating reference frame 77−73095
Ni (110), anisotropy of surface self diffusion 77−43367
Ni (110), surface self-diffusion, sinusoidal profile decay technique 79−99404
Ni alloy, Numonic 80A, grain boundary crack diffusional growth, high temp. rupture possibility 78−47471
Ni alloys, recrystallised, grain boundary inheritance and props. 77−59816
Ni crystallites, vacancy diffusion and vacancy lattices, semi-empirical mol. orbital calcs. 77−1121
Ni dilute alloys, implant profiles modification by radiation enhanced diffusion and segregation 80−88217
Ni, expt., 813-1193K 77−15618
Ni, hardness after-effect studied by anelastic relaxation 80−66570
Ni, mass transfer parameters, lattice defect effects under laser pulse action *(Ukrainian)* 80−6537
Ni, plastically deformed, recovery stages III and IV investig. by positron annihilation 77−31715
Ni, radiation damage and diffusion 80−24645
Ni, self interstitial migration and crowdion conversion, dislocation pinning expts. 77−84762
Ni, self-diffusion and vol. diffusion coeffs. of Co and W, 1050 to 1400°C *(Russian)* 79−28147
Ni surface, single-atom self-diffusion FIM study 80−103548
Ni, surface self-diffusion in presence of adsorbed halogens *(French)* 80−24723
Ni, vacancy and divacancy diffusion 79−82377
Ni, vacancy diffusivity from width of grain boundary void denuded zone 77−47615
Ni-Al, grain boundary diffusion in migrating boundaries 79−46830
Ni-Al(-Si), diffusion, lattice parameter, microhardness, and constitution, effect of Si additions *(Russian)* 80−84316
Ni-Co-Cr-Al-Ti-Mo superalloy IN738, casking porosity removal using hydrostatic press. sintering 80−55322
Ni-Cr (20 wt.%), volume and grain boundary diffusion of Ni and Cr, C effect *(French)* 79−95203
Ni-Cr (33 at.%), US deform. effect on short range order form. *(Russian)* 78−39839
Ni-Cr austenitic alloy, oxidation mechanism, intergranular diffusion effect *(French)* 80−81229
Ni-Cr-Al aluminised coating, diffusion paths for formation and degradation of oxidation resistant coatings 78−11431
Ni-Cr-Y, Y addition effect on intergranular and volumetric diffusion, oxidation reduction *(French)* 79−83382
Ni-Ta system, phase diagram diffusion relation *(Russian)* 77−52287
Ni-Ta-Al-Fe, Al and Fe effect on precipitation kinetics 79−20054
Ni-V, solid soln., diffusion and thermodynamic props. 80−65278
Ni-V system, conc. depend. of interdiffusion coeff., 810-1175°C, rel. to phase diagram *(Russian)* 79−4429
Ni-Zn, physical-chemical metallurgy *(German)* 80−108390
Ni-ZrB_2 powders, densification by hot pressing 80−25604
β'-NiAl, ordered, hardness after-effect studied by anelastic relaxation 80−66570
Ni_3Al based alloys, mean square atomic displacements, rel. to diffusion activation energy 79−28053
Ni_3Al, refractory transition metal alloying effects 78−26691
Ni_3Al-Ni_3Nb eutectic alloy, ^{63}Ni diffusion rate rel. to struct. defects *(Russian)* 78−2288
Ni_3Al-Ni_3Nb eutectic alloy, aluminide coated, diffusion processes 78−15593
$Ni(NH_3)_6I_2$, phase transition and rot. excitation 80−96642
NiO, chemical diffusion 79−60544
NiO, diffusion of ion-implanted ^{18}O 80−107494
NiO, diffusion of Ni in bulk and along dislocations 79−82381
NiO, elec. cond. and chem. diffusion coeff. at high temps. 79−23962
NiO, grain boundary thermal grooving, mass transport, self-diffusion coeffs. 80−44217
NiO, nonstoichiometric, near-surface and bulk chem. diffusion 80−80035
NiO, of Ni, 700-1400°C, rel. to Ni oxidation mechanism 78−27681
NiO, polycrystalline, high temp. deform. 78−3174
NiO single crysts., creep along ⟨100⟩, stresses 50 MPa-120 MPa, 950-1200°C, O diffusion *(French)* 79−20121
NiO, undoped and Al doped, Ni self-diffusion, vacancy-impurity complex effects 80−107493
NiO_2, elect. cond. under low O_2 press., kinetics interpretation 79−82587
β-Ni_3S_2, formed during sulphidation of Ni, defect struct. and chemical diffusion 78−2115
$Ni_{0.5}Zn_{0.5}Fe_2O_4$ coarse grain polycryst. ferrite, diffusional creep *(Japanese)* 80−104238
Ni(110), surface self diffusion, temp. depend. directional anisotropy 78−87851
P_2S_5-Ag_2S glass, Ag diffusion, 50-120°C 78−18828
Pb, electron irradiation at 4.7K and below 3K, annealing expts. 77−11595
Pb, grain boundary self diffusion, microtome serial sectioning anal. 80−79975
Pb, impurity diffusion and self-diffusion activation volumes 80−2209
Pb-In, FCC, In diffusivity, conc. depend. 77−39702
PbF_2, NMR relax. and self diffusion 78−80236
PbS_xSe_{1-x}, chalcogen interdiffusion, electron microprobe obs. 79−28145
PbTe-PbS, solid-phase solubility, use of diffusion couple 77−12602
Pd-H alloy, 50K transition, sp. ht. and thermal relax. meas., diffusion effects 77−15596
Pd-Ni, neutron radiation stimulated diffusion, electrical resistivity exam. *(Russian)* 79−14959
$PdH_{0.76}$, ^1H spin-lattice relax. meas. 78−43672
β-PdH_x diffusion of H, high resolution neutron scatt. meas. 79−60551
PdH_x, diffusion of H atoms, quasielastic neutron scatt. obs., book contrib. 79−82383
Pt (110), two-dimens. diffusion of Pt adatom 79−28183

self-diffusion in solids continued
Pt, Frenkel defect migration and reactions, by subthreshold recoil events, exam. 78−47364
Pt, point defect properties, damage curve anal. 78−47359
Pt, radiation damage, recovery of elec. resist., interstitial migration and clustering 77−11604
Pt, radiation damage recovery curves, evidence for two self-interstitial configs. 77−7773
Pt, self-diffusion of ^{197}Pt at low temp. 78−30789
Pt, vacancy and divacancy diffusion 79−82377
Pt-Au, ion-irradiated, self-interstitial migration in stage II recovery, FIM obs. 77−59140
Pt-Ba cathode, rel. to vaporisation 78−10272
Pt(Au), ion irradiated alloys, stage II recovery 78−47440
Pu, β-, γ-, δ-, δ'-, and ε-phases, self diffusion 393 to 886K 78−87811
Pu-Zr alloys, BCC, activation volumes, melting-diffusion correl. validity 77−20122
α-$RbAg_4I_5$, dynamic cage effect 80−107541
$RbAg_4I_5$, I_2 diffusion obs. using ^{131}I radiotracers 78−18830
$RbAg_4I_5$, nonequilibrium thermodynamic description, variation of ionic cond. with temp. 79−61391
$RbAg_4I_5$, solid electrolyte development, Ag^+ cond. 80−107532
$RbCu_4Cl_3I_2$, development of Cu^+ ion cond. 80−107532
Se-Ge-As, chalcogenide glass, self-diffusion, investigation using radioactive tracers 79−23770
Si, (p,γ) resonance broadening method 80−24646
Si, activation energy and entropy factors 80−88353
Si, carrier lifetime degradation at room temp. 78−95301
Si, creep and self-diffusion activation energies 78−38772
Si, diffusion of self-interstitials and As, B and P, radn.-enhanced 80−29216
Si, dynamical recovery and self-diffusion 79−82379
Si, dynamical recovery at high temps. 79−69284
Si, high temp., dominance of self-interstitials 77−80500
Si, intrinsic, self-diffusion, 885-1175°C 80−10700
Si inversion layers, magnetocond. in ground Landau level, defect diffusion in Wigner cryst. 77−39914
Si, ion implanted, interstitial generation and loop form. during annealing in oxidising medium 80−107225
Si, migration energy of intrinsic point defects in different charge states 77−89582
Si, rel. to O_2 partial press. depend. of oxidation-induced stacking faults 78−39922
Si, rel. to oxidation stacking faults and microdefects, growth behaviour during high temp. annealing 78−72901
Si, self diffusion entropy 80−29211
Si, self- and impurity diffusion 80−29213
Si, self-diffusion, dynamical recovery 80−29215
Si, self-diffusion coeffs. between 1320K and 1660K, extended-interstitial mechanism 77−84985
Si, self-diffusion mechanism 79−90824
Si, single crystals, dynamical recovery and self-diffusion 78−87816
Si, stacking fault growth, oxidation-induced, HCl and interstitial effects 80−49241
Si, thermal oxidation, ^{18}O study 79−52400
Si, tracer diffusion of ^{71}Ge and ^{31}Si in intrinsic and doped samples 80−29214
Si, vacancy paradox 78−59804
n-Si wafer, trap centres of self-interstitials 80−75516
Si:B(P), proton-irrad., impurity uphill diffusion, vacancy mechanism 80−92719
Si:P, interstitial supersaturation near P-diffused emitter zones 79−65541
Si:P(B)(As), proton enhanced diffusion and vacancy migration 78−67747
Si-SiO_2 interface, oxidation stacking faults, growth rel. to self-diffusion 80−49239
α-SiC, ^{30}Si self-diffusion, ion microprobe anal. 79−42309
SiC, high-temp. creep interpretation by deform. mapping techniques 77−21230
β-SiC, polycryst., ^{30}Si self-diffusion 80−100350
β-SiC, polycrystn., C^{14} self diffusion 80−2200
SiH_4, NMR linewidths and relax. times at 6.7 to 124K 77−85602
Si_3N_4, ^{15}N self-diffusion, isotope exchange meas. 77−11724
Si_3N_4, hot pressing with Y_2O_3 and Li_2O additives 78−92220
SiO_2, amorphous, ^{30}Si diffusion *(French)* 80−59696
SiO_2, amorphous, of ^{30}Si, SIMS *(French)* 80−107482
SiO_2 glasses, O self-diffusion theory 79−95214
SiO_2, non crystalline, exam. of O_2 transport phenomena correlations 78−47581
SiO_2, vitreous, O and Si diffusion-controlled processes 80−79981
SiO_2-Na_2O glass, Na^+ diffusion 78−91478
Sn, vacancy formation and activation volume, macroscopic model 80−54221
SnO_2 thin films, O_2 vacancy diffusion 80−107467
$SnSe_yTe_{1-y}$, semicond. chalcogen interdiffusion coeffs., antifrenkel defects, interstitials *(German)* 77−43375
SnTe, ^{117}Sn diffusion coeff. meas., stoichiometric deviation, SIMS 80−34236
SnTe, diffusion of ^{125}Te 80−84325
$SrCl_2$, anion diffusion mechanism 80−2201
$SrCl_2$, fast ion transport 80−107558
$SrCl_2$, ionic cond., self-diffusion, rel. to defect motion, mol. dynamics study 80−65282
$SrCl_2$, mass and charge transport 80−100347
$SrCl_2$, self-diffusion and ionic cond. 80−107489
SrF_2:Er, activation vol. for interstitial motion, dielec. const. meas. 80−49412
Sr_3MoO_6, electrophys. props., effects of thermophys. props. of medium in synthesis 77−48375
$Sr(NH_3)_6$, PMR linewidth, proton tunnelling and NH_3 rot., rapid NH_3 diffusion 78−35045
$SrTiO_3$ crystals, O ion diffusion, in single and polycrystalline structures 78−22892
Ta, vacancy formation and migration energies, positron annihilation meas. 77−84739
Ta-H, spinodals and diffusion coefficients of H, sample shape depend. 78−19713
Ta_2D, atomic displacements determ. by deuteron magnetic resonance *(Japanese)* 78−15035
$TaH_{0.13}$, diffusion of H, neutron scatt. study 79−60550

self-diffusion in solids continued
TaH_x, diffusion of H atoms, quasielastic neutron scatt. obs., book contrib. 79−82383
TaH_x, H diffusion and electronic struct., pulsed NMR obs. 80−54967
TaS_2-NH_3 intercalation complex, press. induced diffusion effects, NMR study 79−19797
Te, diffusion and cond. props., NMR investigation 79−78547
Te, electron irradiated, dose-depend. and recovery behaviour of transport props. 78−71761
Th_4D_{15}, NMR relax. expts., diffusion processes and hyperfine fields 79−8066
Th_4H_{15}, NMR investig. of proton environment and motion 77−48077
ThO_2, ^{18}O self-diffusion, isotope exchange meas. 77−11725
ThO_2, ceramic oxide, thermally stimulated depolarisation currents as probes diffused in ceramic bulk 79−65792
ThO_2 gel, morphology relations during bulk transport sintering 77−70015
ThO_2, O_2 self-diffusion and intrinsic p-type electronic conduction 79−90821
ThO_2-CaO, and ThO_2-$YO_{1.5}$, solid solns., defective oxides, ionic cond. 80−107548
Ti, α- and β-phases *(Russian)* 79−86916
β-Ti, BCC, anomalous diffusion behaviour 78−91474
Ti-Al-V (6,4 wt.%), surface and grain boundary free energy, zero-creep determ. 79−4313
Ti-Cr_3C_2 composite, TiC and struct. form. during sintering 79−29011
Ti-Fe-H system, H diffusion, neutron scatt. obs. *(German)* 79−56963
Ti-H, diffusion in hydride phase, exam. 80−29204
Ti-Nb BCC alloys, diffusion coeffs. of Ti and Nb, 950 to 1511°C 79−73333
Ti-Nb-H, proton spin-lattice relax. time, conc. depend., diffusion effects 77−4576
Ti-Ni-Co, constitution diagram, isothermal section, interdiffusion coeffs. *(Russian)* 80−89200
TiC_x, nonstoichiometric, densification during sintering 80−84895
$TiFe_2$, mechanism of mixing and reactive diffusion 79−7706
TiH_x, H diffusion, NMR obs. 80−34813
γ-TiH_x, interstitial H diffusion mechanism, NMR spin-lattice relax. study 80−103515
Ti_2Ni, determ. of H diffusion coeff., quasielastic neutron scatt. 78−30781
TiO_2, rutile, mass transport mech. determ. by sinusoidal profile decay method 78−6178
TiO_2, slightly reduced rutile, diffusion of Ti 78−79799
TiO_{2-x}, rutile, O chem. diffusivity, near stoichiometric ratio 77−11731
TiO_2(-Cr_2O_3), rutile, Cr_2O_3 effects on O_2 tracer diffusivity, depth profile meas. by SIMS 80−24651
TiO_2 electrodes, room temp. diffusions, capacitance, spectral response and volt-ampere characts. 80−15294
(U,Ce), U self-diffusion 80−92711
(U,La)C, U self-diffusion 80−92711
(U,Pu)(C,N) and (U,Pu)N, high burn-up simulated, Pu self diffusion 80−92712
(U,Pu)C, self-diffusion meas. 80−6544
$(U,Pu)C_{0.8}N_{0.2}$, self diffusion processes 78−50259
(U,Pu)N, self-diffusion meas. 80−6544
$(U,Pu)O_2$, mixed oxide fuel elements, Pu redistribution 78−78463
$(U,Pu)O_{2-x}$, chemical diffusion of O *(French)* 79−42300
$(U,Pu)O_{2-x}$, O_2 thermomigration described by cluster model 78−22888
$(U,Pu)O_{2\pm x}$, gradient of U, Pu and O at surface 77−18665
$(U,Pu)O_{2\pm x}$, O chemical diffusion coeff. 79−10977
$(U,Pu)O_{2\pm x}$, solid state transport as mechanism of O thermomigration 79−19395
(U,Y)C, U self-diffusion 80−92711
(U,Zr)C, U self-diffusion 80−92711
UC_x, computer simulation of C activity and transport 78−86618
UC_x, self-diffusion and nonstoichiometry, modified Monte Carlo method 77−69114
UC_xN_{1-x}, self diffusion processes 78−50259
UO_2, grain boundary diffusion, sintering and creep correlation, reinterpretation of creep mechanism 79−66111
UO_2, hyperstoichiometric, O_2 chemical diffusion coefficient 79−85608
UO_2, lenticular void migration rate in thermal gradient 78−21642
UO_2, O diffusion mechanism 78−33249
UO_2, quenched and neutron irrad., recovery processes, vacancy migration 77−28048
UO_2, Y_2O_3 stabilised, O self diffusion 79−28135
$UO_{2\pm x}$, O self and chem. diff. coeff. 78−71879
$U_{0.8}Pu_{0.2}N$, of ^{238}Pu, 1500 to 1800°C 78−78457
$(U_{0.8}Pu_{0.2})N$, self diffusion of ^{238}Pu 78−82461
$(U_{1-y}Pu_y)O_{2-x}$, thermodynamics 78−70593
V, electro- and thermo-self-transport, 1480-1822°C, effect of impurities 79−42297
V, polycryst., rel. to creep behaviour, 790-880°C 79−24578
V, self diffusion coeffs., 1170 to 1893°C *(German)* 79−86917
V, self diffusion meas. 77−89570
V-Fe, ^{57}Co Mossbauer spectra, diffusion mechanism of Fe 80−15292
V-H, NMR of anomalous diffusion of H and phase transition 77−16571
V-Ti, exam. of intrinsic diffusion and vacancy flow effects 79−4430
$VH_{0.07}$, diffusion of H, neutron scatt. study 79−60550
VH_x, diffusion of H atoms, quasielastic neutron scatt. obs., book contrib. 79−82383
VH_x, NMR, phase transition obs., activation energy for H diffusion meas. *(Russian)* 78−27506
W, fine tip microcrystal, thermal smoothing after critical remoulding 78−27381
W, meas. on thin surface layer by sectioning 78−47565
W, self-diffusion, high temp. bulk modulus determ. 80−79976
W, self-diffusion in range 1700 to 3400K 79−42296
W, self-diffusion parameters, depend. on degree of purity *(Russian)* 79−19391
W, self-interstitial diffusion, fully dynamic computer simulation 77−39687
W, surface, self-diffusion coeff., determ. from van der Mast's expt. data between 3000-3600K 79−11011
W surface self-diffusion, ion impact induced, FIM study 80−103549
W, surface self-diffusion by ion impact, protrusion formation 78−75938
W, vacancies, quenching and recovery invest., resist. and TEM study 80−39074
W, vol. self-diffusion, temp. depend. from radiometric anal. *(Russian)* 77−66040
self-diffusion in solids continued
WC, ^{14}C self-diffusion *(French)* 79−60542
WF_6, effect of high hydrostatic press. in reorientation and internal motion, ^{19}F NMR spectra 79−15364
WO_3M_x (M=H, Li, Na, K, Ag), bronzes, atom motion 78−75874
YIG, anal. of data using results of thermogravimetric analysis 78−6050
YIG:Ca, O diffusion depend. on defect conc. 78−67857
YIG:Ca films, rapid O diffusion at 25 to 250°C 77−85120
$YMnO_3$, solid phase synthesis mechanism 80−21268
Zn-Al (20 wt.%) superplastic alloys, Zn diffusion, strain influence *(Russian)* 79−37870
Zn-Cu system, sputtering during atomic diffusion, UPS meas. 78−92159
ZnO, vaporization from spinel solid solns. 77−76541
ZnSe:Al(As), and pure single cryst., defect struct., Hall effect and Zn self-diffusion meas. 79−1427
ZnTe, anomalous penetration of implanted ^{65}Zn and compensation zone build up 77−19975
ZnTe, self-diffusion profile and trapping of Zn 80−75381
ZnTe:Ag, real structure effect on luminescence and absorption spectra, dislocations 80−16085
β-Zr, BCC, anomalous diffusion behaviour 78−91474
β-Zr, temp. depend. of isotope effect 79−86918
Zr-Mn alloys, impurity and self-diffusion 79−60540
$ZrBrH_x$, PMR exam. of H-location and diffusion 78−56382
$ZrClH_x$, PMR exam. of H-location and diffusion 78−56382
ZrH_x, of T, autoradiographic study, energy of soln. in H sublattice *(Russian)* 80−2194
δ-Zr_xH_y, diffusion of H_2 *(Korean)* 77−20118
$ZrH_mCe_n(PO_4)_2.XH_2O$, cryst., self-diffusion of Ce^{3+} ions 78−34648
α-$ZrH_{0.74}La_{0.42}(PO_4)_2.4.6H_2O$ cryst., self-diffusion of La^{3+} ions 78−34648
$ZrMn_2D_3$, deuterated hexagonal Laves-phase, D atoms interstices and diffusion paths, positional disorder 79−73334
$ZrMn_2H_x$, proton NMR relax. time and Knight shifts, diffusional activation energies meas., sorption props. 80−75871
ZrN_x, $0.71 \leq x \leq 0.79$, ^{15}N tracer diffusion, short cct. mechanism 77−24429
ZrO_2, cubic, anion vacancy form. during electrolysis, density change 77−80648
ZrO_2-CaO, and ZrO_2-$YO_{1.5}$, solid solns., defective oxides, ionic cond. 80−107548

self-focusing
see also electrostriction; Kerr electro-optical effect; optical Kerr effect; optical self-focusing
acoustic system, rapid variation in focal length 79−81641
coaxial atomic and light beams, simultaneous self-focusing and self channelling *(Russian)* 80−28292
diamond, ultrarelativistic electron beam self acceleration probability 79−86819
education, plasma-laser beam self focusing using paint stripper flame 79−9066
electron beam, gas-neutralised self-focused, effect of self-elec. and mag. fields 78−50692
electron beam, pulsed high-intensity, low-press. gas obs. 80−32899
electron beam, relativistic, high-current, self-focused, energy dissipation at focus 80−5674
electron beam, self-focused, relativistic, filamentation instability 80−74289
electron beam, self-focusing in ferrodielectric channel, nonlinear eqn. anal. 77−61905
electron beam self-focusing decline by gas breakdown, avalanche and plasma cond. effects 78−18420
EM beam self-focusing in semiconductor 79−18488
EM excitation of plasma wave by two coaxial Gaussian beams 79−55511
EM wave self-action during thermal modulation instability of high hybrid oscills. *(Russian)* 80−53980
ethyl alcohol, stimulated Raman scattering of psec. pulse train, dynamics 79−64286
Gaussian laser beam, nonlinear self-focusing in plasma 79−27786
inhomogeneous absorbing solid, self-focusing of intense hypersonic and US beams 77−84038
ion-acoustic wave excitation by two Gaussian laser beams, density profile modification 79−19006
ionosphere, self-focusing of HF EM waves, striations 78−96347
liquid crystal, nematic, orientational acoustic nonlinearity 80−34143
magnetoplasma, plasma wave generation and SHG by Gaussian EM beam 79−37479
magnetoplasma, rel. to third harmonic generation by Gaussian EM beam 78−83572
nonaxisymmetric beam self focusing 77−75627
nonlinear dielectric slab, surface wave propagation characts. 77−42609
nonlinear focusing and Kelvin-Helmholtz instability 80−83785
particulate self-focusing and nonlinear-wave mechanics 80−105520
plasma, axially inhomogeneous, laser beam self-focusing 79−32778
plasma, EM beam self-focusing and harmonic generation 77−19714
plasma, EM wave beam self-focusing 78−75357
plasma, nonlinear quasioptics in DC mag. field *(Russian)* 79−98914
plasma, nonstationary thermal self-focusing of EM waves in low temp. plasma *(Russian)* 77−76086
plasma, opaque layer, e.m. wave self-focusing, expt. *(Russian)* 77−3949
plasma, self-focusing and filamentation of Gaussian whistlers 77−47206
plasma, self-focusing of EM wave propag. along conductor in plasma 79−19048
plasma, strongly ionised, self-focusing laser mode 78−59599
plasma, Thomson scatt. of EM pulses by random fluctuations, self-focusing effects 78−83573
plasma driftwaves, self-focusing and mag. field stabilisation *(Russian)* 77−47180
plasma flowing transverse to EM beam, kinetic approach 78−59602
plasma waves relativistic self-focusing in cold plasma 79−73009
plasma-wave excitation, self focusing, ponderomotive nonlinearity transient setting, carrier diffusion time 79−77387
pulsed electron beam, in Ar, He, and O_2, self-focusing, polyatomic additives effects 77−68164
relativistic electron beam, in conical diode, self-focusing 79−89840
relativistic electron beam focusing using axial loads 78−18464
semiconductor injection laser, intensity pulsation enhancement by self focusing 80−48253
simulation of self focusing of beams 77−75628

self-focusing continued
sound beam, self defocusing in presence of acoustic streaming 77−14833
third-harmonic generation in collisional plasma, self-focusing effect 77−7550
US nonstationary self-focusing in nonlinear media 77−27412
water, stimulated Raman scattering of psec. pulse train, dynamics 79−64286
wave beam self focusing with plateau-like intensity distributions *(Russian)* 79−89976
wave self-focusing in a nonlinear inhomogeneous medium 79−64293
He, superfluid, self-focusing of second sound *(Russian)* 79−10996

self-induced transparency
acrosol, plasma production by CO_2 laser beam, brightening channel 80−6272
antiferromagnet, acoustic nuclear resonance, self-induced transparency *(Russian)* 79−91304
breather generation, inverse scatt. technique 80−78913
coherent pulse propagation, 0π pulse generation from zero-area pulse 80−48352
coherent pulse propagation, soliton creation by chirped initial profiles 79−72632
Coulomb retarded interaction effect, impurity centre excitation into collective coherent states 79−55191
crystal, coherent optical pulse propag., polariton effects 77−42576
dense plasma clarification by strong EM wave self-action 78−75360
diffraction instability of light 2π pulses, numerical anal. 79−89975
diphenyl:pyrene, self induced transparency under nonreson. excitation, luminesc. and stimulated emission 80−11436
diphenyl with pyrene cryst., self induced transparency self stimulated excitation *(Russian)* 80−14403
EM wave self-action during thermal modulation instability of high hybrid oscills. *(Russian)* 80−53980
exciton part of spectrum self-induced transparency 78−33786
exciton system in pulsed field 77−42575
exciton transitions, intraseries and interseries, self-induced transmission and radiation echo 78−5528
excitons, dispersion law of steady-state exciton-photon pulses 79−27336
excitons, steady-state exciton-photon pulse dispersion law 78−30028
glass:Nd, self-induced transparency effect in two-quantum resonant absorption *(Russian)* 79−3750
initial-value problem for zero-area pulses, anal. props. 80−23756
interaction of light with phonon excitations in medium, coherent effects 79−15103
ionic insulating crystal, light pulse propag. 78−90462
Kerr nonlinearity 78−63155
microwave EPR self-induced transparency in free radical powder, waveguide propag. 77−24747
molecular crystal with spatially disperse media, exciton model 77−7162
optical-pumping wavefronts, inducing complete transparency during propagation 79−89974
pentacene, narrow band laser excitation, fluoresc. decay, optical free induction, dipole moment 78−21956
perturbed soliton solns., finite relax. time 80−58643
phonon generation by IR reson. radiation, nonlinear effects 78−50865
picosecond nonlinear optics, book contrib. 77−65609
pulse compression by two-photon self-induced transparency, feasibility 78−66870
pulse train propagation, two-level absorber, relax. effects 79−46011
quantum theory *(Russian)* 79−98448
relaxation effects 79−3749
resonant media, coherent optical pulse propag., transverse effects 77−65612
resonant media, transverse instability of one-dimens. transparent optical pulses 79−46010
resonant orientation of tunnelling centres, self-induced anisotropy 78−79075
resonant propagation of two concomitant optical pulses interacting with three-level atomic system, num. modelling 80−9942
retarding interaction allowance, dipole moment of transformation *(Russian)* 80−14402
semiconductor, nonlinear coherence phenomena in exciton region 80−99806
semiconductor, superlattice, EM field nonlinear penetration 78−25930
semiconductor 2π-pulse propagation in crossed elec. and mag. fields 78−79079
soliton wave packet propag., superfluidity of Bose condensed excitons and photons 78−22178
solitons, laser physics appls. 80−48333
solitons, lecture 78−24690
solitons in system of coherent phonons and photons 79−64291
third harmonic generation under 2-photon reson. conditions, ultrashort pulse propag. *(Russian)* 79−59768
three level absorber, two-photon transition, self-induced transparency 79−27337
three level medium, ultrashort pulse propag., transient processes 78−18024
three-level atom system, distortionless optical pulse propag. 78−22179
three-level equidistant degenerate system, dynamic Stark effect 78−50863
three-level medium, coherent transient pulse propag. in two-photon reson. 77−79904
three-level system, double-reson. self-induced transparency, numerical integration 80−28288
two-frequency pulse in resonantly absorbing medium 78−42390
two-level medium, coherent interaction with radiation, relax. processes effect 79−59774
two-level resonant medium, light pulses propag. 80−64119
two-photon resonance, coherence effects on summation of optical frequencies *(Russian)* 77−62012
two-photon resonance for inhomogeneous broadened line *(Russian)* 79−86221
two-photon resonant up-conversion, third harmonic generation 78−90453
ultrashort laser pulses, interaction with condensed matter *(German)* 79−27335
zero-area pulse output, initial conditions 79−41424
CO_2 laser nanosecond pulse coherent interactions with amplifying media *(Russian)* 80−14314
$CdS_{0.4}Se_{0.6}$, reson. excitation of excitons by ultrashort freq.-tunable light pulser 78−46728

self-induced transparency continued
Cu_2O, two-photon interaction of laser radiation with Frenkel excitons 78−25931
GaAs, two-photon absorpt. of Nd:glass laser radiation 78−87107
GaSe, absorpt. spectra, electron-hole system at high densities 77−69854
HF gas, self-induced transparency using HF chemical laser 77−88866
I atomic vapour, self-induced transparency and reson. self focusing 80−64114
$LiAl_5O_8:Cr^{3+}$, self-induced transparency and light echo *(Russian)* 77−62016
$LiNbO_3$, induced refl. and transparency increase *(Russian)* 78−59094
Na, vap., picosec. photon echo and self-induced transparency 79−46015
Na vapour, saturation of transient reson. nonlinear processes 77−68243
Na vapour, soliton interactions, self-induced transparency, numerical plane wave simulations 80−64117
Nd:glass, self-induced transparency on two-photon reson. line *(Russian)* 79−86221
Ne absorber discharge, 3 nsec laser pulse propag., self-induced transparency 77−10986
SF_6 10.5 μm spectrum, high-J assignments, identification of levels pumped by CO_2 P(12) and P(22) 78−70837

self inductance *see inductance*

self-optimising systems *see self-adjusting systems*

self-organising storage
visual cortex development model, mammal 78−3483

self-organising systems *see self-adjusting systems*

self-trapping
anisotropic resonance medium, radiation trapping 80−9970
atom or molecule, cooling and trapping by reson. light field *(Russian)* 77−46544
EM beam self-focusing in semiconductor 79−18488
envelope wave stability 80−43410
exciton motion depend. on lattice vibr., inner potential energy, ground state, effective mass *(Chinese)* 80−54610
filament of light form., self-focusing and trapping of intense laser beams 77−39001
Gaussian laser beam, transverse self-focusing and self-trapping investig., moment method 80−58652
hadrons, relativistic self-trapping 78−21405
ideal gas, self-trapping of electrons, nonlinear Schrodinger eqn. soln. 79−2662
inert gas discharge, reson. radiation imprisonment model 80−38756
lattice vibration TO and LO modes, role in self-trapping of powerful light pulses 80−99809
long-range interaction between CW laser beams in at. vap. 78−87110
magnetoplasma, collisionless, self-trapping and self-focusing of elliptical laser beam 80−53991
molecular rotational coherence, reson. collisional exchange, time resolved microwave obs. 80−23525
one-dimensional crystal lattice, nonlinear interaction of ps light pulses with lattice vibrations 78−30032
paraxial self focusing theory, EM wave propagation in plasma 79−94304
plasma, Gaussian ripple on uniform EM beam, growth in magnetoplasma 79−19041

selsyns *see synchros*

SEM *see scanning electron microscopy*

semi-insulating materials *see semiconductor materials*

semiconductor alloys *see semiconductor materials; semiconductors*

semiconductor counters
see also position sensitive particle detectors
1024-channel particle spectrometer power supply 79−68169
$\Delta E \times E$ counter telescope, improved mass resolution 77−54458
active volume, determ. from gamma ray interactions, Monte Carlo method 80−63448
alpha, surface-barrier Au(Si), protective glass walls 80−91374
alpha spectral line intensity gauge using semiconductor detector *(Italian, Spanish)* 78−86716
alpha-spectrometer with Si surface barrier detector 78−82565
automated correlation spectrometer with two Ge(Li) detectors 78−82562
avalanche radiation detector, large-area, high-gain, using transmutation doped Si 77−23367
backscattered electron detector, multi-purpose 80−102404
binary counter with controlled scaling factor, using ICs 79−3322
breakdown counter for fission fragments 77−38563
bronchoscopic tumour localisation, small radiation detector probes, scintillation and semiconductor detectors 80−61676
C-CD Si substrate ionisation trails prod. by cosmic ray background 80−51669
CdTe, detection characteristics in gamma-ray spectroscopy 78−41888
charge transfer device for particle detection 79−93883
charged particle beam homogeneity testing with surface barrier detector 78−25365
charged particle range and stopping power, new empirical relns. 77−61671
charged particle spectrometer telescope 80−42895
combination intermediate-image magnetic plus Si(Li) electron spectrometer for in-beam experiments 79−31308
conference on nuclear power systems, Washington, USA (1978) 79−41045
cosmic ray charge meas., minimum pulse selection method, energy levels 80−37712
cosmic ray spectrometer, for study of 6 to 50 MeV electrons 78−45235
dE/dx methods of particle identification, review 77−23377
deep water muon and neutrino detection using semiconductor photoreceivers *(Russian)* 78−55109
detector array for 4-dimens. reconstruction of radioisotopic activity in brain 78−11732
detector utilizing impact ionisation, resolution 77−6639
development of the semiconductor radiation detector 79−68153
diamond, elec. props and performance for α- and β-particles 79−36481
diamond, natural, hole trapping levels 79−76278
diamond detector use as immersed α counter 77−54461
diamond detectors, beta/gamma ratio 77−54431
diamond detectors, use as immersed alpha-counters 77−54432
diamond tissue-equivalent dosimeter, for X-rays and gamma-rays 77−56477
dielectric-breakdown, heavy-ion counters based on MOS structure 80−69032

semiconductor counters continued
dose measurement using radiation induced changes in semiconductor devices *(Japanese)* 78−78504
dosimeter for rectal dosimetry in treatment of cervical cancer using RALSTRON technique *(Japanese)* 77−73594
dosimetry in intense neutron-gamma fields 77−46460
efficiency curves of semicond. detector. *(Spanish)* 77−67935
electron spectrometers, pulse shape anal. in fosfich detector 77−65387
energy resolution of semicond. detectors with alternating bias 77−10553
epitaxial integrated E-dE silicon detector with a buried low-resistive diffused layer 80−58059
fabrication techniques for Si and Ge diode structs. 78−46219
field ionisation device for neutral particles, appl. to He^+ pulse height defect in Si 77−50330
fission chamber, absolute fission ratio measurement *(Japanese)* 77−67948
fission-fragment scattering kinematics multiparametric anal., TDF instrument with semiconductor detectors 78−78550
fission-fragment scattering kinematics multiparametric anal. electronic meas. system, semiconducting detectors 78−78551
flaw detection systems based on semicond. detectors and scintillation crysts. for hard bremsstrahlung 79−11748
fluctuation problems, computer simulation 77−3218
gamma camera, electronically collimated, for single gamma emission computed tomography 78−44603
gamma-flash suppressed solid state detector for fission fragments 79−26857
gamma-ray detectors, S/N ratio optimisation *(German)* 77−10534
gamma-ray four-detector counting system, computer controlled 79−9957
Ge, hyperpure, β end-point-energy meas. 78−78587
Ge control detector, dead layer minimisation for Compton-suppression spectrometer 80−99400
heavy ion identification, combined magnetic anal. time of flight and energy meas. 77−23359
heavy ion physics, expt. methods for radiation detection and meas., review *(Russian)* 79−49900
heavy-ion time-of-flight telescope, walk-free fast timing 77−404
high energy physics uses of semiconductor detectors *(Russian)* 77−50325
high-Z detectors, future prospects 77−54410
HPGe coaxial detectors, timing props. 78−50436
hybrid impedance matching circuit for surface barrier detectors *(French)* 78−90035
IEEE conf., scintillation and semiconductor counters and nucl. power systems 77−54389
immersible Si Li-drift alpha- and beta-radiation detector, fabrication 77−65386
immersible Si spectrometric alpha-particle detector, fabrication 77−65385
impact ionisation detectors, resolution power, fluctuation sources 77−54433
in-beam Ge(Li)-NaI(Tl) Compton suppression spectrom. 77−88325
internal pair formation high resolution in-beam studies with magnetic+Si(Li) spectrom. 79−18073
ion implantation, isotope separator, prep. of p-n junction particle detectors 80−34034
ion implanted, neutron detection 80−69030
ion-doped, coordinate detector for charged particles 79−26825
ionising radiation dosimetry, anisotropy of dose sensitivity 78−70705
IR radiation pulses meas. response characts. of AuSi detectors 80−52308
leading-edge spectrometer for current signals 77−6607
long-range charged particle detector, field effect investig. *(Russian)* 80−106234
low energy α and proton spectra, simultaneous detect. *(Russian)* 77−50332
low-background system for neutron activation anal. 77−36843
magnetic plus Si(Li)-Si(Li) sum coinc. technique for internal pair transitions 80−18752
microwave P-N avalanche diode as gamma-ray dosimeter 77−54408
MOS diode as low energy Xand γ-ray spectrum 79−36462
MOS dosimeters, series configuration, sensitivity increase *(Czech)* 79−36425
MOS rectangular vol., distrib. function for ion track lengths 79−85872
MOS thin film dielectric breakdown counters, heavy-ion detection props. 80−52827
mosaic, characts. and parameters, nuclear radiation detection 80−69031
multichannel semiconductor detectors for X-ray transmission computed tomography 80−58058
multicrystal detection system for localisation and meas. of photon emitters without external collimation 77−32959
multistrip β semicond. detectors for magnetic spectrometers 78−78545
neutron counter with time window, 10 to 1000 μsec, using integrated microcircuits 79−3321
neutron field detectors for critical assemblies 77−54430
neutron yield from D-T generator meas. *(German)* 77−23336
nondestructive neutron activation analysis of environmental samples using low-energy photon spectrometry 78−3995
nuclear radiation, large scale potential fluctuations 79−9966
nuclear radiation detectors, effect of trapping on response 80−5447
oriented radioactive nuclei, JINR investigs. using SPIN equipment *(Czech)* 77−42220
p-n junction detectors, low-level DC current amplifier 77−38573
p-n junction with inhomogeneous impurity distrib., space-charge layer 78−30982
peak identification in spectral analysis program 80−37706
photodiode radiation monitor with op-amps, cct. 78−78591
photovoltaic cells as fission product detectors 79−93873
PIN-photodiodes, comparison for X-ray spectrom. 78−74531
pocket radiation chirper, CdTe crystal and electronics 79−68165
position sensitive ΔE-E telescope for Z-identifications 77−30726
position sensitive semiconductor detector for gamma-rays 77−54435
position-sensitive, analog meter for signal ratio 79−97943
position-sensitive semiconductor detectors, principles of operation, performance, and appl. 79−68155
positron tomography, evaluation of semiconductor detectors 79−53221
principles of operation and appl., review 79−68154
protective surface coatings anal. 80−58057
proton-recoil telescope for in-line absolute neutron fluence measurements 79−18079
pulse height and time analyser for semiconductor detectors 78−78592

semiconductor counters continued
radiation detectors, with alternating bias, formation of signal 79−13608
radionuclide radiation precision spectrometry using semiconductor detectors *(Russian)* 79−31305
RAM, use as α-particle detector 80−37701
recoil spectrometer for 5 GeV pion-He interactions 78−90011
review of nucl. particle detectors 79−54740
scattering chamber, rotatable lid, vacuum sealed, with semicond. detector arrays, INS cyclotron accessory 77−6599
Si(Li) detector efficiency for 0.7-6 keV X-ray energy region 79−97928
Si(Li) detector-opto feedback FET system, time-variant filter performance in 1/f noise 77−57830
signal coupling of semiconductor detector to cold resistance preamplifier through cable or delay-line transformer 78−33401
single carrier charge collection 77−61657
solid-state integrated cct. micro-detectors for high energy experiments 77−30705
spectrometer, semiconductor mosaic type, amplification-conversion tract meas./monitoring automation 78−78547
spectrometer system, energy resolution, electronic aspects 78−46231
spectrometers, Fano factor determ. in semiconductors 80−47813
spectrometric and temporal characts. 79−97944
spectroscopy and applied phys. appls. 78−46218
spontaneous fission low background detection system 79−36475
stack gas monitor, β scintillation detector+Ge(Li) detector system, environmental γ dose *(Japanese)* 79−3246
state of art and future prospects for γ-ray detectors *(Hungarian)* 80−42890
surface barrier, detection probabilities for α-decay chain members 79−76315
surface barrier detector, peak changes under particle irrad. 80−58077
surface barrier detector, pulse height defects, heavy-ion detection 78−55093
surface barrier detector, suitability for solid surface layer anal. by ion backscatt. 79−4456
surface barrier detector for beta dosimetry 80−57973
surface barrier detector for detection of He-Ne laser beams 79−36485
surface barrier detectors, fabrication techniques for fast neutron spectrometry 79−18074
surface barrier detectors, props. determ. by temp. controlled spectrometer 77−83443
surface barrier detectors, pulse height defect and window energy loss of low energy ions 78−74541
surface barrier detectors for low energy heavy ions 79−68138
surface barrier particle spectrometer, testing by precise light pulser 77−79508
surface barrier spectrometers for fast neutron calibration in MeV range 79−9961
surface barrier TOF telescope, effects seen in fast timing 78−70683
surface-barrier photodetectors, registration of pulsed radiation 80−91373
telescopic setup for detection of heavy particles produced in electron-nucleus reactions at 4.5 GeV *(Russian)* 80−63461
thin window detectors for interplanetary particles, Compton-Getting effect complications 78−49269
three Ge(Li) Compton polarimeter with kinematic selection, for γ polarisation meas. 77−83456
time clamping to detector signals using universal discriminator 79−3323
time resolution, analytical expressions 77−54409
timing props. of detector-preamplifier system using laser pulser 77−54443
TOF spectrom., intrinsic time resolution of detectors 78−849
weak γ-ray transitions observed in coincidence with summed cascades 79−76264
whole-body counter, shadow-shielded, for detection, identification, and localisation of incorporated radionuclides *(German, English)* 78−20266
X-ray, for elemental anal. in electron microscope 79−11838
X-ray beam characteristic time vars. meas. using solid state devices 80−46048
X-ray detectors, energy depend. efficiency response modelling 79−45560
X-ray diffractometry uses and assoc. problems *(French)* 80−84031
X-ray imaging, MOS solid-state detector arrays 78−47180
X-ray semiconductor radiation detector, cooled preamplifier systems *(Slovak)* 78−21813
X-ray spectrometry at high count rates 79−31310
Zener diode, breakdown voltage, electron irrad. effects 79−95472
α, counting chamber, for use with surface barrier detectors 78−873
β-γ-γ coinc. spectrom. using GM-Ge(Li)-Na(Tl) counter combination 78−46210
γ spectrometers with CdTe detectors, pulse selection to improve energy resolution 79−22533
AlSb as high-energy photon detector 77−75026
^{41}Ar release from TRIGA reactor, comparison of γ-ray detectors 78−57309
Au-CdTe-Au structure, as spectrometric detector of nucl. radiation 77−54460
Au-Si detectors, pulse height defect meas. for 2 to 400 MeV/nucleon ions 78−86733
AuSi ionizing radiation detector, photosensitivity variation 79−36464
^{10}B, neutron cross section standards, detection techniques 79−9970
CdTe, biotelemetry of glomerular filtration rate in man by external detection of DTPA-(Sn)-$^{99}Tc^m$ 78−44591
CdTe, characterisation by light spot scanning 78−41894
CdTe, Cl compensated detectors, polarisation suppression methods 77−61661
CdTe crystal growth for γ-ray detectors 78−41889
n-CdTe, deep trapping levels in high resistivity films 77−72930
CdTe detector, Cl doped, for reentry vehicle appl., development electronics 77−45288
CdTe detector, performance compared to HgI_2 detector 80−58062
CdTe detector, use in γ-ray spectrometric study of VVER reactor spent fuel rods 79−76094
CdTe detector for personal radiation chirper 79−45557
CdTe detector for radionuclide tracer biotelemetry 77−86587
CdTe, detector grade semi-insulating crystals, determ. of product of mobility and carrier lifetime 80−39601
n-CdTe, detector material, single crysts., activation energy anal. of defect levels 78−6321
CdTe detectors, correlation between surface props. and detection characteristics 79−45539
CdTe detectors, depletion layer extension 78−41891

semiconductor counters continued
CdTe detectors, finite solid angle correction factors for 100 keV to 10 MeV γ-rays 77−61659
CdTe detectors, gamma and electron irradiation effects 78−41893
CdTe detectors, geometry variations 77−61663
CdTe detectors, international workshop 78−41887
CdTe detectors, nonlinear response 79−93878
CdTe detectors, photoscanning, determ. of crystal quality and contact behaviour 77−61664
CdTe detectors, portable miniature scanner, bone mineral meas. using ^{125}I X-rays 77−44750
CdTe detectors, props. 77−61658
CdTe detectors, small, props. uses in biotelemetry 77−44747
CdTe detectors, test of fuel enrichment *(Czech)* 77−50276
CdTe detectors, use in spectrometers, physical and electronic factors *(Czech)* 80−23259
CdTe detectors, X-ray fluorescence escape peaks in X-ray spectra 80−9448
CdTe detectors in nuclear medicine, capabilities, limitations, X-ray transmission tomography appl. 77−44748
CdTe detectors with small volume, high gamma-ray sensitivity, 100 to 150 keV 79−63865
p-CdTe diodes, X-ray escape peak variations 77−71723
CdTe, electron induced defect creation rates 78−41892
CdTe, film, theoretical models of impurity levels 79−82557
CdTe gamma backscatt. assay meter 80−58070
CdTe gamma radiation detectors, operation, energy resolution, efficient and appl. 79−68156
CdTe γ spectrometer, use in monitoring activity deposited in nuclear power stations 77−42193
CdTe γ-ray detector, resolution for 122 keV ^{57}Co and 59 keV ^{241}Am 77−75027
CdTe, high purity crystal, growth from soln., γ-ray detector appls. 77−14310
CdTe, irrad.-induced damage on γ-detector performance 80−23264
CdTe low-cost portable detector, 3D lung densitometer, diagnosis and evaluation 77−44749
CdTe, MIS contacted small portable detector head for X-ray spectrometry 77−61662
CdTe, MSM detectors, charge collection 77−61660
CdTe n-type low resistivity detectors, advantages and limitations 78−41890
CdTe photovoltaic mode γ- and X-radiation dosimeters 79−13594
CdTe, properties and appls., conf., Strasbourg, France (Jun-Jul 1976) 77−39832
CdTe semiconductor detector system, ^{133}Xe clearance meas., muscle blood flow in man 78−40305
CdTe sensors, review of medical appl. 77−64147
CdTe, single carrier charge collection 77−61657
CdTe spectrometers for hard X-ray astronomy 77−13206
n-CdTe surface barrier detectors, energy resolution 77−71724
CdTe, thermal neutron detection 78−17479
CdTe, use in ovum movement measurement in rabbit oviduct 78−36087
CdTe, use in X-ray detectors 78−86745
CdTe ventricular function monitor, ambulatory, cardiac ejection fraction meas. 80−61680
CdTe X-ray detectors, energy resolution 77−71722
p-CdTe:Cl, gamma-ray detector prep. and resolution 77−39802
CdTe:Cl, gamma-ray detector growth, travelling heater method improvement 77−40353
Ce(Li), fast neutron leakage spectrum determ. 80−32565
GaAs, epitaxial, appl. to surface barrier particle detectors 79−72203
GaAs radiation detector, characteristics 79−68139
GaAs, semi-insulating, VI characts., γ-ray sensitivity and performance 77−46467
n-GaAs surface barrier diodes for nuclear radiation detection, deep trapping centres 80−92849
Ge 2-D position sensitive orthogonal strip gamma-ray detector employing resistive charge division 77−10538
Ge, amorphous Ge contact for electron or hole blocking 77−54400
Ge and Si detectors, development, construction, operating principles, uses 78−46220
Ge and Si material props., purification, cryst. growth, ion implantation 78−47674
Ge camera, 2-detector, 512 element high purity prototype 78−40301
Ge camera, high purity, for nucl. medicine imaging 80−17113
Ge charged particle telescopes with ultra thin detector contacts 79−81130
Ge coaxial detectors, n-type high purity, construction and performance 79−41075
Ge coaxial detectors with reverse electrode, radiation damage resistance 79−41076
Ge detector, charge collection characteristics, influence on timing performance 80−47820
Ge detector, delayed coincidence summing, nucl. half life meas. 78−55088
Ge detector, high purity, fast neutron damage 80−59526
Ge detector, high purity, fast neutron damage, hole trapping and detrapping 80−63463
Ge detector, intrinsic, for meas. of soft X-ray spectra of Tokamak plasma 77−51232
p-Ge detector, responsivity comparison with p-GaAs photon-drag detector 79−11185
Ge detector as ^{239}Pu-^{241}Am monitor for in situ soil surface and pond bottom assay 77−9546
Ge detector in superconducting solenoid, semi-empirical beta-ray response function 79−13584
Ge detector system for inhaled radionuclide detection and meas. 80−57990
p-Ge, detector-grade single crysts., impurity background 79−11088
Ge detector; high-purity, effect of crystal growth direction on energy resolution 79−45541
Ge detectors, automatic anal. of gamma-ray spectra 77−3246
Ge detectors, calibration using precise relative γ-ray intensities 78−17469
Ge detectors, calibration using ^{152}Eu source uncertainties in peak area determ. 80−5436
Ge detectors, γ-γ linear polarisation direction correls., $^{110}Ag^{m}$ cascade decay *(Japanese)* 78−41903
Ge detectors, high purity, event timing, compared to Ge(Li) detectors 80−69018

semiconductor counters continued
Ge detectors, use at low temps. 77−65398
Ge detectors array, collimated, computer-driven scanning bed, clinical appls., tomography 78−40309
Ge detectors for X- and gamma-ray spectroscopy, high-purity preparation and properties 78−86723
Ge detectors in space, computer spectral anal. of cosmic ray proton induced radioactivity 79−12413
Ge diode, high purity, buffer ring for edge protection 80−63465
Ge diode detector telescope for particle spectroscopy, design and performance 78−13384
Ge diodes, γ-radiometric appl. 78−33385
Ge diodes as low-temp. β-ray detectors 77−30724
Ge, efficiency at very low energies by X-ray double method 79−3286
Ge, efficiency calibration in range 122-412 keV 80−37682
Ge, fast and slow quenching defects 78−39052
Ge γ-ray camera, calc. of picture element efficiency and side scatt. fraction 77−77968
Ge γ-ray detectors, materials props., appls., radiation damage 78−13392
Ge, high parity detectors, 6 GeV/c proton irradiation 78−37508
Ge, high purity, carrier trapping 79−47104
Ge, high purity, comparative study with Li drifted Si detector re. thyroid scanning 79−16275
Ge high purity planar detectors, contacts made by ion implantation 79−97949
Ge, hydrogen multivalent acceptor complexes 77−55491
Ge hyper-pure closed and coaxial spectrom., pulse height depend. on source position 77−54403
Ge, hyper-pure coaxial detectors, comparison with Ge(Li) detectors 77−54404
Ge, intrinsic, detection of Mossbauer gamma-rays from ^{73}Ge and ^{181}Ta 77−10530
Ge intrinsic detector, use in borehole sonde for U exploration 77−9547
Ge intrinsic detector and multichannel analyzer in 5.1 cm borehole probe 80−63451
Ge intrinsic detector appl. to determ. of photon energy distrib. of diagnostic X-ray beams 77−70530
Ge, intrinsic efficiency, calc. of expected detector efficiency 77−54405
Ge large intrinsic detectors, characteristics at elevated temp. 77−54402
Ge low energy X-ray detectors, entrance windows 77−71718
Ge on-line, hyperpure detector, radiation monitoring system 78−37493
Ge p^{+}-ν-n^{+} structures, charge transport under impurity freezeout conditions 80−92965
Ge p^{+}-ν-n^{+} structures, large-scale trap characts. 80−92966
Ge p-i-n diodes, deep level transient spectroscopy 79−47105
Ge planar detectors, high-resolution charged particle spectroscopy 77−54401
Ge position sensitive γ-ray detectors using resistive charge division readout 77−54420
Ge, purification by zone refining 78−39683
Ge radiation detectors, high-purity, ion implanted n-type contact 77−54416
Ge radiation detectors, recording power at 4.2K 77−67936
Ge shielded detector, cryostat cold-finger support 79−93868
Ge spectrom., intercomparison of ^{152}Eu gamma-ray emission rate meas. 78−82568
Ge spectrometer, energy and efficiency calibration in 100 keV to 3000 keV γ-ray energy range 78−17464
Ge spectrum, precise γ-ray energies for calibration up to 3.5 MeV 79−31311
Ge, total pair prod. cross section near threshold, meas. using variable energy source *(French)* 79−85866
Ge, trapping defects, deep level transient spectroscopy 79−47045
Ge, ultra pure, method to determ. composition and struct. of non-elemental acceptor and donor centres 78−39658
Ge, use in X-ray radiometric fluorescence analysis 77−52701
Ge X-ray detector, Au contact layer thickness meas. 80−62627
Ge, X-ray spectroscopy by Compton-scatter method, for diagnostic X-rays 77−2044
Ge:Li detectors in-beam gamma spectroscopic investigations of nanosecond iosmers 78−86506
Ge:O, intrinsic γ detector, deep level defect connection with O content *(Russian)* 78−43331
Ge-Li spectrom., re-evaluation of precise γ-ray energies for calibration 78−90015
Ge-Li total efficiency calc., algorithm for small calculators 79−9938
Ge(I) gas cooled high resolution mini-probe 79−22550
Ge(Li) 50 cm^3 detector, energy response for 4 to 10 MeV photons 78−46211
Ge(Li), American National Standards Institute quality assurance programme 77−38585
Ge(Li), analytic fitting of full energy peaks 77−71716
Ge(Li) and Ge spectrom., calibration using ^{228}Ra and ^{228}Th decay 79−85857
Ge(Li) and intrinsic Ge detectors in borehole sondes for U and coal exploration 77−37442
Ge(Li), anomalies in charge collection effects on time resolution *(French)* 77−57801
Ge(Li), automatic anal. of complex γ-ray spectra 78−33370
Ge(Li) balloon borne spectrom. for obs. of neutron star cyclotron line emissions 80−41721
Ge(Li), calc. of finite angle correction coeffs. and linear polarisation sensitivity 79−736
Ge(Li), calibration using linearly varying amplitude pulse generator 77−10526
Ge(Li) coaxial detector, triple const. fraction discriminator evaluation 78−70708
Ge(Li) coincidence detector system, meas. on ^{144}Ce decay 80−52605
Ge(Li) commercial coaxial large-volume detectors, time characts. 78−9029
Ge(Li), constant slope timing 79−76305
Ge(Li), constrained model-based representations of X-ray detector efficiency curves 79−49897
Ge(Li) detector, comparison with Ge(Li)-NaI(Tl) Compton suppression spectrometer for low level activity meas. *(Slovak)* 78−21814
Ge(Li) detector, fast neutron damage 80−59525
Ge(Li) detector, for in situ anal. of river bottom sediments 77−87115
Ge(Li) detector, gamma pulse pileup, random summing losses 80−58023
Ge(Li) detector, gamma spect., coincident sum peaks 80−63447
Ge(Li) detector, γ-spectra, noniterative method for fitting Gaussian to peaks 77−57840

semiconductor counters continued
Ge(Li) detector, rapid monitoring of ^{131}I in human thyroid gland 79−2134
Ge(Li) detector, use in activity determ. of gamma source with flat surface *(German)* 78−58528
Ge(Li) detector, use near 400 MeV proton beam in p-γ coincidence expt. 80−5452
Ge(Li) detector, well type, spectrum interpretation problems due to self absorption variations 79−31307
Ge(Li) detector and magnetic lens spectrometer, combined, for e-γ delayed coincidences 79−710
Ge(Li) detector efficiency determ. for gas bomb geometries 80−78486
Ge(Li) detector for precise meas. of ^{106}Ru 512 keV γ-ray 77−6610
Ge(Li) detector in anti-Compton spectrom. 79−26804
Ge(Li) detector pulse formation, Monte-Carlo anal. of multiple interaction processes 77−399
Ge(Li) detectors, anal. of monochromatic γ-ray and annihilation spectra 78−50429
Ge(Li) detectors, coaxial, zero cross-over timing 80−69017
Ge(Li) detectors, commercial, time parameters 79−728
Ge(Li) detectors, efficiency calibration using continuous external bremsstrahlung 78−46228
Ge(Li) detectors, energy meas. source position effect 79−13579
Ge(Li) detectors, gamma-ray intensity standards for calibration 80−74083
Ge(Li) detectors, precise environmental gamma-ray meas. 77−38568
Ge(Li) detectors, relative γ-ray intensities for calibration 79−49896
Ge(Li) detectors, use of annihilation radiation for precision energy calibration 77−10528
Ge(Li) detectors for environmental assay, calibration using NBS mixed-radionuclide gamma sources 77−38541
Ge(Li) detectors for γ-radioactivity in rocks and soils 80−67418
Ge(Li) diodes, teflon covered for fast neutron detection 78−25384
Ge(Li) efficiency, effect of counting rate and source-to-detector distance 79−68122
Ge(Li), efficiency curve dependence on detector shape 77−54449
Ge(Li) energy calibration using $^{13}C(\alpha,n)$ radioactive sources 79−13572
Ge(Li) gamma detectors, radial efficiency gradients 78−9034
Ge(Li), gamma spectra calibration problems in automatic processing *(Rumanian)* 80−5431
Ge(Li), gamma-ray activity of large vol. samples, determ. 77−90656
Ge(Li) gamma-ray spectrometer calibration for radioactive inert gas meas. 77−83442
Ge(Li), γ-ray energies of ^{40}K, ^{108m}Ag and ^{226}Ra decay chain 80−27865
Ge(Li) γ-ray spectra, NUKLID program for automatic line identification *(German)* 78−58536
Ge(Li) γ-spectrom. for environmental radionuclide meas. 79−6791
Ge(Li) high-resolution detector, role in neutron activation anal. of water 77−56324
Ge(Li) in situ environmental spectrometer, spectrum-to-exposure rate conversion function 77−65379
Ge(Li), in situ meas of fission product plateout in HTGR 80−73881
Ge(Li), in-beam γ-ray spectroscopy at tandem Van de Graaff accelerators 78−13373
Ge(Li) large detectors, timing improvement by pulse shape selection method 77−54457
Ge(Li), meas. of γ-ray elastic and Compton scatt. through small angles 79−718
Ge(Li), nondestructive assay of highly enriched spent fuel 79−89522
Ge(Li) not ideally compensated coaxial detectors, elec. field distrib. and charge collection process 78−94164
Ge(Li), peaks in gamma spectra analysis, analytic approx. 80−102395
Ge(Li) photon detectors, analytic fitting of full energy peaks 79−36458
Ge(Li) planar detector, in γ-γ polarised directional correlations set-up 77−34530
Ge(Li) planar detector efficiency curve obtained using K_β/K_α X-ray intensity ratio 80−880
Ge(Li), relative ang. efficiency meas., Q_k factors and Doppler broadening 79−54750
Ge(Li) semiconductor, used simultaneously with NaI(Tl) scintillation spectrometer, in neutron activation cross-section meas. 80−78485
Ge(Li), simple algorithm for Gaussian peaks best fit *(Italian)* 78−58538
Ge(Li) spectrom., balloon-borne, recent meas. 78−93107
Ge(Li) spectrom., precision energy meas. of gamma rays of ^{51}Cr, ^{103}Ru, ^{109}Cd, ^{144}Ce, and ^{203}Hg 78−58533
Ge(Li), spectrometer efficiency, dead time and pulse pile-up correction 78−50442
Ge(Li) spectrometry, pulser method limitations in pile-up and dead-time corrections 77−23384
Ge(Li) spectrum, ^{236}Ra as calibration standard 77−38543
Ge(Li) summing-up effects, optimisation of detector-target geometry for in-beam γ-spectroscopy 80−74070
Ge(Li) system for low level radioactive gas monitoring 78−9038
Ge(Li), timing resolution, comparison with hyper-pure Ge detectors 77−54404
Ge(Li) uncollimated detector, parametric representation of efficiency curves for X-rays 77−18740
Ge(Li) upward looking dip-stick type spectrom., in-situ environmental γ-ray meas. 78−37480
Ge(Li), well-type detectors for low-level radiochemical analysis 78−37119
Ge(Li) well-type semiconductor detector, γ-ray spectrometry *(Japanese)* 79−89521
Ge(Li)-NaI(Tl), Compton suppression spectrometer for in-beam expts., design and performance 78−78553
Ge(Li)-NaI(Tl) Compton suppression spectrom. for low-level activity meas. 78−9022
Ge(Li)-NaI(Tl) Compton suppression spectrometer for low level activity meas., rel. to Ge(Li) detector *(Slovak)* 78−21814
HPGe detector, gamma spect., coincident sum peaks 80−63447
HgI_2, characterisation by light spot scanning 78−41894
HgI_2, charge collection efficiency 80−32575
HgI_2, cryst. growth by multiple vacuum sublimation 80−7485
HgI_2 detector, performance compared to CdTe detector 80−58062
HgI_2 detectors, fabrication, appl. to X- and gamma-ray detection 77−83459
HgI_2 detectors, γ- and X-ray detection, solution grown crystals 80−63452
HgI_2 detectors, international workshop 78−41887
HgI_2, detectors, novel pulse processing system 78−41902
semiconductor counters continued
HgI_2 detectors, recent improvements 78−37507
HgI_2 detectors, state-of-art crystal growth and nucl. spectroscopic evaluation 78−41895
HgI_2, effects of dislocations and crystal defects on energy resolution and reponse uniformity 77−54412
HgI_2, energy response to ^{137}Cs photons, appl. to medical imaging 78−44592
HgI_2, gamma radiation detectors, operation, energy resolution, efficient and appl. 79−68156
HgI_2, high energy gamma spectrometers, room temp., appl. to ^{60}Co 77−65378
HgI_2, imperfections determ. by thermally stimulated currents method 77−54413
HgI_2 in vivo medical probe, DC and pulse counting meas. 78−44593
HgI_2 medical probe 79−66555
HgI_2 miniature probes for in-vivo medical appls., fabrication, spectroscopic evaluation 78−40308
HgI_2, nuclear detectors, high X-ray fluence irrad., DC currents 77−54415
HgI_2 nuclear detectors, bulk homogeneity, spectral response, performance 78−37524
HgI_2, nuclear radiation detector, status *(Japanese)* 78−33398
HgI_2 nuclear radiation detector, polarisation reduction 80−58060
HgI_2, photoelectronic props. 78−41897
HgI_2, radiotelemetry pill for biomedical meas. of ionising radiation 78−40318
HgI_2, resolution limit in room temp. low energy X-ray spectrom. 78−37479
HgI_2, scatter reduction in nuclear medicine and computed axial tomography 79−5368
HgI_2, single carrier charge collection 77−61657
HgI_2, soln. grown crystals, low-energy gamma-ray cond. type detectors 80−97418
HgI_2, thermally stimulated current meas. 78−41896
HgI_2 X-ray luminesc., emission band characts., use as X-ray detectors 77−55815
Hg_2I_2, cryst. growth by multiple vacuum sublimation 80−7485
In_2Te_3 type semiconductors, basis of ionising radiation detectors 78−86743
In_2Te_3-type semicond. radiation-resistant fast-electron detectors 78−78559
NaI(Tl) double crystal gamma ray spectrom., efficiency calibration 79−717
NaI(Tl) Polyscin module arrays, Monte Carlo code for design, use in γ-ray spectroscopy 77−54436
PbI_2, detector fabrication 77−54411
PtSi-Si, front contact to surface barrier detectors 77−65404
Rn, short lived daughters, detection method *(Chinese)* 80−42889
Si 2-D position sensitive orthogonal electrode surface barrier detectors 78−50437
Si, axially channelled protons, transmission meas. using two-dimensional position-sensitive detector 79−1471
Si α-particle spectrom., stopping power and straggling meas. in liquids 78−82563
Si barrier layer counter, reduction of noise level *(German)* 80−47809
n-typeSi breakdown heavy ion counters, MOS struct., physical props. determ. 79−732
Si, defect prod. by GeV muons, thermally stimulated current technique 78−5099
Si detection system for fusion products in migmacell II 77−83089
Si detector, anal. of ΔE,E particle identification 77−88348
Si detector, α-particle dense track charge losses 77−3233
Si detector, energy response differences for p and α particles 79−6805
Si detector, proton spectra, noniterative method for fitting Gaussian to peaks 77−57840
Si detector electrical contact at He temp. to evaporated Au film 78−37019
Si, detector response functions for radioisotopes complex β spectrometry *(Slovenian)* 78−21802
Si detector with p-i-n junction in pulse count mode for γ dosimetry 78−33386
Si detectors, automatic anal. of complex charged particle spectra 78−33370
Si detectors, CERN neutrino beam monitoring by μ flux in Fe shield meas. 78−37523
Si detectors, charge multiplication under dense irradiation 78−37506
Si detectors, fast neutron flux meas. and spectroscopy 77−30709
Si detectors, high resistivity p-type, for β-ray and X-ray spectrometry, advantages 77−88329
Si detectors, high resistivity n-type prod. by neutron transmutation doping 79−45540
Si detectors and Pb absorber plate, telescope structure, high energy muon flux measurement 80−58061
Si diffused junction detector for alpha air monitoring instrumentation 80−58083
Si diffused n-P^+ junction miniature for electron meas. 77−30718
Si diode as in vivo fast neutron dosimeter 77−73587
Si diode detectors in radiological physics, energy compensating shield development 78−24142
Si diode detectors in radiological physics, high-energy photon dosimetry 78−24143
Si diode heavy ion detector, all epitaxial, fabrication and performance 77−54414
Si diode neutron detector for meas. near high-energy accelerator, photon and electron response 78−35963
Si diodes, γ-radiometric appl. 78−33385
Si dosimeter, proton beam dosimetry in C, Al, Fe, mylar and H_2O 80−47733
Si epitaxial detector fabrication, crystal growth and preferential etching 78−37505
Si epitaxial detectors, chemical preferential etching 77−79509
Si epitaxial detectors, review 77−54406
Si heavy ion detectors, book contrib. 79−31335
Si heavy ion surface barrier detector, plasma delay times, electron backscattered from fission fragment or alpha particle 80−58095
Si high-resolution X-ray spectrocopy, portable system 79−81117
Si, ionisation energy for channelled 160 MeV α-particles 78−62680
Si junction detectors, low noise, fabrication 80−52820
Si live targets, transversal filter approach of trapezoidal pulse shaping 79−36487

semiconductor counters continued
Si microelectronic p-n junction photon detector 79−26815
Si p-n junction, radiation detector DC cct., transient processes 77−70556
Si p-n junction radiation detectors in DC mode, temp. response non-linearity 77−38565
Si p-n junction radiation detector behaviour in temp.-compensated cct. 78−33389
Si particle detection, use of dislocation-free Si 80−42893
Si photodiodes for neutron dosimetry 78−31907
Si posn. sensitive strip detector for image intensifier gamma camera 77−81565
Si, radiation detector, barrier heights, electron and hole currents, Schottky contact effects 79−33293
Si, radiation detectors ion-doped, effects of 5.5 MeV α-particle irradiation 77−65397
Si, response to relativistic pions, electrons and protons 79−13597
Si sandwich surface barrier detector with ^{6}LiF radiator, neutron spectrom. 77−57807
Si solid state detector telescopes, neutral particle background effects 78−28472
Si solid-state detector manufacture, modified etching method 77−28917
Si subnanosecond detector, charcts. 78−9027
Si surface barrier detectors, energy distrib. functions of low energy H and ^{3}He ions 77−6652
Si surface barrier detector, pulse height defect of fission products 77−18741
Si surface barrier detector, pulse height response to mass and energy separated fission fragments 77−57812
Si surface barrier detectors, dE/dx thin detector technology, n^{+} layer electrolytic removal *(Russian)* 77−57823
Si surface barrier detectors, direct meas. of plasma delays due to fission fragments and α-particles 78−58546
Si surface barrier detectors, meas. of plasma delay differences due to ^{252}Cf fission fragments and α-particles 78−58547
Si surface barrier detectors, charact. meas. *(Bulgarian)* 78−82592
Si surface barrier detector, pulse height-defect calibration 79−13602
Si surface barrier detector, Fano factor for protons 79−36480
Si surface barrier detector, operation in nitrate solns. 79−63873
Si surface barrier detector, fission fragment pulse height defect 79−76292
Si surface barrier telescope, for low energy π detection 79−13591
Si surface-barrier detectors with Sn electrodes, charcts. 78−5097
Si surface-barrier detector in lava or teflon housing, production 78−17481
Si surface-barrier detector, electron backscattering 78−55095
Si surface-barrier detectors, charcts. in Xe ion beam 78−78571
Si, surface-barrier detector, impurity distrib., influence on charcts. 80−18766
Si thin epitaxial dE/dx detectors 77−54407
Si, X-ray detector calibration in 183 to 932 eV range 77−71717
Si, X-ray fluorescence spectrum 77−46452
Si:Li detector, influence of distrib. of drift temp. on props. 77−3234
Si:P, B α-particle spectrum fabrication by ion implantation 78−33373
n-Si-^{119}Sn resonant detector for Mossbauer spectroscopy 80−883
p-Si-Al, barrier junction form., appl. as nucl. particle detector 77−12006
Si-Li surface-barrier detectors for electron and soft X-ray spectrometry 80−882
Si(Li), 2D position sensitive detector with 100 μm resolution 79−45544
Si(Li), analytic fitting of full energy peaks 77−71716
Si(Li), constrained model-based representations of X-ray detector efficiency curves 79−49897
Si(Li), detection of Mossbauer gamma-rays from ^{73}Ge and ^{181}Ta 77−10530
Si(Li) detector, appl. to Am and Pu low conc. meas. in earth samples 78−58505
Si(Li) detector, β-ray background removal in X-ray meas. 78−55091
Si(Li) detector, cooling system with liq. N_2 *(Rumanian)* 79−85867
Si(Li) detector, improvement of time depend. instabilities by IR and γ-irradiation 79−36477
Si(Li) detector, low power monoenergetic X-ray tube for trace element anal. 78−70686
Si(Li) detector efficiency meas. 78−55108
Si(Li) detector for energy dispersive analysis *(French)* 77−26445
Si(Li) detector in X-ray spectrometer, preamplifier with drain feedback 78−66448
Si(Li) detector probe with RFT radiation meas. unit for diagnosis of intraocular tumours *(German, English)* 78−20265
Si(Li) detector response function approach in least squares anal. of X-ray fluorescence spectra 80−11989
Si(Li) detector system, discrepancies in X-ray excitation efficiencies 80−9450
Si(Li) detector system response to microphonics 79−31333
Si(Li) detector window of aluminised mylar for X-ray fluorescence meas. 80−27894
Si(Li) detectors, efficiency for 0.05-1.25 MeV γ-rays 78−86744
Si(Li) detectors, electron counting, appl. to electron energy loss spectra, by high voltage electron microscopy *(French)* 78−54511
Si(Li) detectors, unfolding procedure for slowly varying pulse height spectra of β-particles 78−50430
Si(Li) detectors, X-ray detection efficiency at off centre point 77−57811
Si(Li), efficiency at very low energies by X-ray doublet method 79−3286
Si(Li) electron spectrometer on-line with an automatic irradiation apparatus 78−90014
Si(Li) gas cooled high resolution mini-probe 79−22550
Si(Li) high resolution spectrometer, with thermoelectric cooling 79−26813
Si(Li), in-beam γ-ray spectroscopy at tandem Van de Graaff accelerators 78−13373
Si(Li), non-dispersive X-ray spectrom. with high precision dead-time correction 77−54392
Si(Li), peaks in gamma spectra analysis, analytic approx. 80−102395
Si(Li) photon detectors, analytic fitting of full energy peaks 79−36458
Si(Li) photopeak efficiency meas., 0.52-8.04 keV 80−27889
Si(Li), relative photoionisation determ. from X-ray meas. 78−33369
Si(Li), simple algorithm for Gaussian peaks best fit *(Italian)* 78−58538
Si(Li) solid state detector appl. on modern single cryst. X-ray diffractometer 79−58855
Si(Li) spectrom. with ^{71}Ge source for energy dispersive X-ray fluorescence anal. *(German)* 77−86429

semiconductor counters continued
Si(Li) thin window detectors for NASA ISEE-C cosmic ray telescope 78−40819
Si(Li) uncollimated detector, parametric representation of efficiency curves for X-rays 77−18740
Si(Li), use in energy dispersive X-ray spectrometry of minerals *(French)* 80−85251
Si(Li), use in energy dispersive X-ray spectrometry of fracture surfaces *(French)* 80−89571
Si(Li) X-ray detector, Au contact layer thickness meas. 80−62627
Si(Li) X-ray detector, efficiency calib. in range 1-5 keV 77−79504
Si(Li) X-ray detector, efficiency calibration in 1.5 to 60 keV energy range 80−47823
Si(Li) X-ray spectrom., dead-time meas. system 77−79503
Si(Li) X-ray spectrometer, development, and interdisciplinary appl. *(Hungarian)* 80−18056
Si(Li)-emulsion shower counter for cosmic ray electron obs. 80−58033
SiO_2, current pulse counter for fission fragments 77−38564
^{A}Si(n,α), 14.8 MeV, A=28-30, cross section determ. for threshold detectors 79−17907
^{A}Si(n,p), 14.8 MeV, A=28-30, cross section determ. for threshold detectors 79−17907
Si(npn) detector with two surface-barrier junction 77−6635
Si(p) surface barrier detectors, energy resolution 78−90021
U stored in lung, meas. using NaI and solid-state detectors 78−28090

semiconductor defects *see crystal defects*

semiconductor device manufacture
Used for commercial manufacture only
conference, New York, USA (Oct. 79) 80−73093
CVD $SiHCl_3$ process, for low cost solar grade Si 79−62007
diode laser manufacture and test procedures 80−9895
diodes, use of Ag electroplating in manufacture 79−33952
epitaxial integrated E-dE silicon detector with a buried low-resistive diffused layer 80−58059
microelectronics and thin film components frontiers 80−73123
optical microscope, large field, for use in semiconductor manufacture 80−82812
oxidation with trichloroethylene additive to eliminate oxidation induced stacking faults 80−39118
photopile manufacture for terrestrial solar cells, review *(French)* 79−24895
plasma processing for device fabrication 78−63602
production equipment, high vacuum cryopumps optimisation using thermal design criteria 80−22377
solar cell, multiple Si ribbon growth by EFG 79−8245
solar cell, vertical junction, with high radiation resistance 79−48131
solar cell arrays, high capacity arc heater production of Si 79−11509
solar cells, concentrated, conducting grid, design rules *(French)* 79−24896
solar cells, dendritic web growth processes, computer modelling 79−11508
solar cells, Dow Corning process for Si, advances 79−8243
solar cells, polycrystalline Si, amorphous Si and CdS/CuS, function and construction *(Swedish)* 80−7940
solar cells, silane pyrolysis for Si production, process design and economics 79−8234
solar cells, thick film technology applic. 80−93903
solar cells automated production, with wraparound contacts 80−76635
substrate spin coating process, rheology and modelling 78−27655
surface contaminant anal. by plasma chromatography-mass spectroscopy 78−3433
surface-barrier photodetectors, GaP and GaAs with Au film deposition 77−77423
VPE, reduced pressure, advances 80−40242
Cd_xHg_{1-x} Te Ir detectors, props. and manufacture *(German)* 77−2693
CdS-Cu_2S thin-film solar cells, low-cost manufacturing process outline, economic anal. 80−93930
Cu_2S-CdS, heterojunction photocell, thin film structure, props. 77−51806
Cu_xS-CdS large-area solar cell production pilot line 79−61994
Ge p-n junction, high-grade, temp. gradient zone melting in production 77−4747
HgSe, highly-electronegative stable metallic contact for semicond. devices 77−24617
Si junction detectors, low noise, fabrication 80−52820
Si, single crystal solar cell manufacturing process, laser annealing of implanted area, energy saving 80−97791
$SiCl_4$ physical and thermodynamic properties, rel. to Si technology 79−65218
Si_3N_4 passivation planar plasma deposition system, productivity increase 80−40269
ZnO based varistors, evolution and role of chem. constituents rel. to prep. method, influence on elec. props. *(French)* 78−31367

semiconductor device models
1/f noise, theoretical analysis *(Polish)* 78−91737
abrupt p-n junction with one side heavily doped, elec. field max. formulation 80−75629
back surface field solar cells, theoretical design considerations 80−93961
bulk, negative-cond., transverse spreading of high-field domain, two-dimens. simulation and equivalent cct. model 79−1602
C-CD, surface channel, interface trapping noise calc. 80−11058
cascade solar cells design for high-temp. operation using computer modelling 80−81456
chalcogenide glass threshold switch, on-state model 79−56270
chalcogenide glasses, threshold switch, on-state model 79−99588
charge cameras, models for transport and accumulation 78−87975
charge flow analogue computation, attenuation-free upwind difference formula 77−28241
diode, with deep impurity levels, diffusion effect on negative resist. 78−56217
diode array SAW correlator model and expt. 78−9508
Electrochemical Society Meeting, Boston, USA, (May, 1979) 79−91959
electrode, charge injection, space charge region, digital simulation 77−15949
electrode, open-circuit photopotential, simulation 77−15950
electrode, photogenerated free carriers and photocurrent relax., simulation 77−15951
epitaxial diodes, influence of geometry on interpretation of current, model 77−11994
FET, alloy scatt., high field transport 78−30929

semiconductor device models continued
gain-guiding double-heterostructure laser transverse carrier diffusion effects 79−55139
glass diode with electrothermal instability in switching channel 79−78238
graded composition semiconductor, minority carrier transport, rel. to transistor 78−80022
heavily doped shallow-emitter p-n junction solar cells, diodes and transistors, Auger recombination 79−96445
heterojunction solar cell model, design and evaluation 80−93964
heterojunction theory, Anderson model review 80−6961
high-power p-n junctions, large-area inhomogeneous, I-V characts. theory 78−47859
hyperabrupt varactors, fabrication from vapour phase epitaxial GaAs 80−29288
IC, junction isolated, ionising radiation performance, black box modelling 77−83467
IC phototransistor static characteristics, effect of insulating p-n junction *(Russian)* 78−52069
IGFET, simulation of semiconductor transport using coupled and decoupled solution techniques 80−65695
inversion layer solar cells, numerical modelling 80−81444
ion sensitive FET, mechanism 77−48741
irradiated MIS device positive space charge formation kinetics 78−76155
J-FET noise model for low-noise photodiode amplifiers in optical fibre receivers 78−37997
junction diode, diffused, with deep level traps, negative capacitance 80−96976
large flexible solar array design analysis and verification 79−96459
large-area solar cell electrical characterisation accuracy 79−96454
metal-insulator-Si(n)-Si(p^+) device, switching voltage criteria 80−15610
MIM structure, analytical expressions for tunnel currents 80−60064
MIS capacitors, theory of nonequilibrium props. including charge exchange of interface states 79−42659
MIS capacitors with single-level traps in semicond. region, model 77−35991
MIS I-V characteristic with insulator opaque to tunnelling 78−80061
MIS inversion layer solar cells, two-dimensional model 80−89641
MIS Schottky barrier and conducting diodes with interface traps, capacitance and conductance 78−10564
MIS structures, analytical expressions for tunnel currents 80−60064
MIS structures with semiconductor layers of critical thickness, potential distrib. and capacitance calc. 78−95381
MIS transistor, mobility in inversion channel calc. *(German)* 80−6996
MNOS devices, transient charge and current distribs. calc. 77−55611
MNOS structure, model for degradation mechanisms 80−29477
MOS, charge build-up due to radiation, mathematical model 79−19667
MOS, electron mobility in inversion and accumulation layers on thermally oxidised Si surfaces 80−103753
MOS capacitors, dynamic model for e-beam irrad. 79−91147
MOS inhomogeneous transmission lines, analytical solutions for charge transport 79−91153
MOS inversion layers, freq. response of charge transfer 80−88638
MOS struct. with nonuniformly doped semiconductors, depletion approx. anal. of differential C-V characts. 79−99625
MOS structure, bulk lifetime determ. by voltage step response method 78−47882
MOS structure resistive gate, charge propagation, transmission line appl. 77−85325
MOS structures, quasistatic and nonequilibrium phenomena with constant gate-current bias 80−80385
MOS system photocapacitance, influence of surface charge fluctuations *(Russian)* 78−43480
MOS system surface charge inhomogeneity modelling and analysis *(Russian)* 78−43479
MOS tetrodes, analytical model for effect of impurity concentration *(Spanish)* 79−99624
MOS transistor, Au-doped, Au surface-state energy levels 80−11092
MOS transmission line, distributed model computer anal. of free charge transport 78−76150
MOS transmission line, resistive, free charge transport, simulation, distrib. model 78−68092
MOS transmission line models, differential eqn. solns. generalised to lossy cases 79−38182
MOSFET, flicker noise theory 80−11100
MOSFET, magnetoconductance and DC cond., influence of one-dimensional superlattice on two-dimensional electron gas 77−43683
MOSFET, n-type inverted surface channel, reproducibility of electronic props. 79−99628
MOST structure, using hybrid computing system, Poisson partial differential equation solution *(Slovak)* 80−75643
n^+-p-p^+ solar cell operation anal. for concentrated illumination 79−43761
n−n^+ low-high junctions, static circuit model 79−91132
negative differential mobility and geometrical magnetoresist. calc. 77−43624
one-dimensional phenomenological transport equation set 78−39102
p^+-n−n^+ pulsed diodes, forward pulsed case, voltage transient response 80−60071
p-n homojunctions, breakdown voltage for onesided abrupt junctions, anal. *(German)* 78−56210
p-n junction, breakdown voltage drift, walk-out phenomenon, model 77−80834
p-n junction, majority carrier flow model, diffusion effects in equilib. field distrib. 77−51808
p-n junction, majority carrier flow model, props. of forward conducting diode 77−35986
p-n junction devices, normal modes for material parameter determ. 77−4426
p-n junction solar cells, Si, importance of surface recombination and energy-bandgap narrowing 79−100520
p-n junctions, thermally assisted field emission near precipitates 78−14809
p-n junctions small signal equivalent circuit, finite carrier multiplication 80−65664
p-n structures, nonlinear small signal distortion, numerical anal. 77−11989
p-n-insulator (tunnel)-metal devices, switching theory; punchthrough mode 79−60926
p-n-insulator metal switching devices, avalanche mode operation 80−70838
p-n-n^+ junctions, epitaxial planar, two-dimensional anal. of breakdown 78−80045
photovoltaic solar energy, conference, Luxembourg (1977) 78−64106
quasi-monopolar semiconductors, I/V characts., effect of weak diffusion with metal contacts 80−70824
RC network model, based on percolation theory, for amorphous semiconductors 79−4560
SAW memory correlators, charge storage 79−64455
SAW p-n diode storage correlator, charging process 78−9500
SAW storage correlator equivalent circuit models 78−9506
Schottky barrier solar cell, doping density effect on efficiency 80−101100
secondary breakdown, hydrodynamic instability model *(Russian)* 78−43407
solar cell, rel. to optimisation 79−39297
solar cell, Si, p^+-n-n^+, edge-illuminated, analytical model 80−12018
solar cell, Si, tandem junction, operation and parameters, model 79−100521
solar cell, tandem, low-high junction model 80−89626
solar cell, tandem junction, Ebers-Moll transistor model 80−93911
solar cell, tandem junction, one-dimensional theoretical model 80−81450
solar cells, based on Si on ceramic 79−11511
solar cells, monolithic III-V compound two-junction cascade devices, computer modelling 80−81433
solar cells with distributed series resistance, simulation using single diode models 80−93962
static induction transistors, one-dimens. potential profile anal. 79−56290
surface CCDs, electron mobility surface diffuse scatt. model 78−47879
surface recombination, effect on steady-state relationships 78−39191
thin film struct., external circuit current calc. 77−39972
thin film transistor, quasi-equilibrium TSC process, model 77−36002
thin-oxide MIS thyristor devices, interface state charge 79−38172
tunnel MIS solar cells, grain boundary effect on performance 79−79394
(Al,Ga)As DH injection lasers, ambipolar transport 80−64025
Al-Si_3N_4-SiO_2-Si capacitors with optical data writing, relaxation obs. 78−76154
Al-SiO_2-Si Schottky barrier solar cells, recomb. effects 79−39310
$Al_xGa_{1-x}As$ LEDs, nonlinear distortions anal. 78−37992
$Al_xGa_{1-x}As$-GaAs LED design and characterisation for fibre-optic communications 78−46796
Au-n-GaAs Schottky diodes, interface state density model 77−39937
Au-Si-Al structure electrode mass transfer and switching with memory 78−95389
B diffusion in oxidised atmosphere, minicomputer model *(Rumanian)* 79−82247
$Cd_xHg_{1-x}Te$-metal contacts, schematic energy band diag., transport props. 77−47897
CdS-Cu_2S heterojunctions, photovoltaic mechanism, model 77−43715
CdS-Cu_2S solar cell photovoltaic effects, self-consistent model 79−61989
CdS-Cu_2S solar cells, role of diode exponential factor 79−61990
CdS-$CuInSe_2$ solar cells, grain boundary and interface recomb. effects 79−39311
CdSe, MIS thin film capacitance, theory 79−87156
Cr-SiO_2-n-Si tunnel diodes elec. characts. meas. and modelling 77−39955
Cu_2S-CdS heterojunction model 78−39205
Cu_2S-$Zn_xCd_{1-x}S$ heterojunction, improved model of electro-optic behaviour 80−94023
$Ga_{1-x}Al_xAs$/GaAs heterostructure solar cell design for space usage 79−96450
GaAs forward-biased diode structures, numerical anal. based on direct gap semicond. 79−65542
GaAs Gunn devices, maximum electric field in high-field domain 78−79996
GaAs LED modulation bandwidth, influence of inhomogeneous current density distrib. 80−9993
GaAs-$Al_xGa_{1-x}As$ heterostructures, real-space electron transfer by thermionic emission, analytical model 80−100512
n-GaAs-Au(Al) Schottky diodes, interface state density model 77−80840
GaAs-Ge, n-n isotype heterojunctions, fixed-interface-charge model 78−56215
$Ga_{1-x}As(Al,In)_x$, heterojunction solar cells, optimum bandgap, computer anal. 79−43767
GaP LED's, current/voltage and light/voltage characts. 77−8662
GaP-Si heterojunction solar cell, computer simulation 79−74529
n-Ge-n-GaAs isotype heterojunctions, modelling, characts. 80−103747
HgCdTe MIS structure, modelling and appl. to CCD IR imagery 78−80058
InP Gunn devices, maximum electric field in high-field domain 78−79996
InSb film cyclotron-frequency submillimetric oscillation generation model 77−80801
InSb, MIS thin film capacitance, theory 79−87156
PbSnTe IR detectors, spectral response depend. on surface carrier concentration *(Japanese)* 79−44929
Si, heavily doped, excess intrinsic carrier density, deionisation of impurities as explanation, bipolar transistor/solar cell models 80−96864
Si photovoltaic detector, quantum efficiency rel. to position and wavelength 79−75593
Si reverse-biased p-n junction DC characteristics interpretation *(Polish)* 78−91761
Si solar cell, device model for tandem junction cell 80−16813
Si solar cell I-V charact. meas., effect of voltage ramp, theoretical anal. using linear model 80−61354
Si solar cells, edge-illuminated p^+-nn$^+$, analytical model under concentrated sunlight 80−7942
Si solar cells, fundamental efficiency limitations 80−93963
Si solar cells, unified model of fundamental limitations 80−81448
Si substitutional diffusion model 78−71884
Si:Zn p-n junction diode, computer-aided study of carrier lifetimes 80−24999
Si:Zn p-n junctions, I-V characts. using exact DC circuit model 79−95476
n-Si-Ag Schottky barrier diodes, excess current mechanism under uniaxial press. 78−91771
Si_3N_4 MNS capacitors, elec. cond. 79−95499

semiconductor device testing
see also integrated circuit testing
acoustic microscopes, nondestructive testing appls. 80−48537
automatic display, CV and GV charcts. at HF 77−26329
avalanche photodiode receiver sensitivity, specification and testing *(German)* 78−38015
deep-level transient spectroscopy appl., using HP-IB instruments and desk-top computer 80−37091
defect birefringence detection by polarisation IR microscopy 79−83405
diode, thermal resistance meas. using temp. depend. of forward charcts. 77−47893
diode forward slope resistance, small resist. value meas. cct. 77−37941
diode laser manufacture and test procedures 80−9895
dislocations and microplasma sites, STEBIC/STEM/EELS correlation 80−96528
electron beam depth profiling, using carrier collection models 80−70723
electron beam induced current technique appl. to semicond. device charcts., review 78−21302
EM monitoring methods for thin film devices *(Russian)* 80−214
European nonreflective solar cell qualification 79−96477
intensified CCD test results 77−41318
intrinsic semiconductor IR detector array data acquisition system 78−77991
IR ellipsometry of polySi-SiO_2-monoSi structure thickness 79−56287
laser diode and transmitter unit lifetime tests *(German)* 78−37883
laser diode degradation modes and accelerated life tests 78−1233
laser measurement, of semiconductor materials and devices *(Rumanian)* 78−52035
MIS structure minority carrier generation time constant meas. 77−89873
MIS structures mobile charges determ., using triangular voltage sweep methods *(German)* 80−4740
MNOS P-channel switch, accelerated reliability testing *(German)* 80−6988
MOS, based on bulk dielectric charge calc., from C-V charcts. 79−56326
MOS, capacitors, SEM investigs. using electron beam induced current technique 78−23177
MOS capacitors, establishment of inversion layer in Si substrate under high oxide field conditions 77−66202
p-n junction, planar, nondestructive determ. of depth by SEM 78−19132
p-n junction potential step meas. by SIMS 80−34503
p-n junction thermal second breakdown prediction test 79−82668
pacemaker electrostatic discharge sensitivity grouping 80−30941
planar diode characterisation using SEM with movable Faraday cup, illuminator and backscatt. diode detectors 78−21292
poly Si gate MOS capacitor post-irradiation flat-band shift expts. 77−76939
power devices, stacked, thermal device for inspection of contact joints 78−76819
resistivity and lifetime inhomogeneities, laser scanning method detect. 79−30489
resistivity profile meas. using two-probe spreading resistance techniques 80−49742
scanning optical microscope for semicond. materials and devices 80−95136
SEM, electron beam induced cond. of defects, rel. to TEM 80−107027
SEM characterisation of semiconductor materials and devices 80−49064
SEM voltage contrast obs., electron beam current-recording relationship 80−73528
SEM-AES-IMA combination with SIM spectrometer, Si device anal. appls. *(Japanese)* 78−85249
solar array sample accelerated thermal cycling facility 79−96458
solar cell, automated electronic analysis system 80−93952
solar cell maximum power output determ. 79−74527
solar cells, electron beam induced currents appl. 80−3518
solar cells, polycryst., scanning optical microscopy examination of grain boundaries 78−79618
strain gauge resistors, characteristics in elastic waves 78−85097
surface barrier particle spectrometer, testing by precise light pulser 77−79508
temperature testing probes, accuracy and thermal charcts. 80−52201
terrestrial solar cell reliability, accelerated stress testing 79−74528
terrestrial solar cells, accelerated stress testing 79−92083
thyristor p-n-p-n structure turnon parameter meas. by optical probe 77−57358
transmission system, semiconductor device reliability tests 80−58573
(AlGa)As, CW laser diodes, long-term lifetests at room temp. 79−22963
AlGaAs-GaAs DH lasers, accelerated life test 78−66830
GaAlAs LED, operating life test and accelerated ageing, for fibre optical communication 77−79940
$Ga_{1-x}Al_xAs$ junction-up TJS laser electron injection efficiency improvement 80−48300
GaAs-$Al_xGa_{1-x}As$ DH laser, high-temp. degradation *(German)* 78−37884
GaAs-AlGaAs transverse junction stripe laser, single mode behaviour after 12000 hr ageing test 78−66831
GaAs-$Ga_{1-x}Al_xAs$ DH lasers, electron beam induced current microscopy 80−95899
$Ga_{1-x}In_xAs_{1-y}P_y$-InP DH lasers, 1000-hour CW operation 78−1265
Si ion-implanted laser-annealed solar cells 80−93881
Si solar cells with light concentrating lens *(Rumanian)* 80−89620
Si terrestrial solar cells, stress tested, contact integrity testing 80−94018
Si-SiO_2 structures, scanning analyser of electrophysical parameters of MOS transistors *(Polish)* 79−91145

semiconductor devices
see also field effect devices; Gunn devices; integrated circuits; semiconductor counters; semiconductor diodes; semiconductor junction lasers; space-charge limited devices; thermistors; thyristors; transistors; transit time devices; varistors
1/f fluctuations *(Japanese)* 78−43448
amorphous semiconductors, conference, Balatonfured, Hungary (Sept. 1976) 77−76802
amorphous semiconductors, props., principles, appls. review 77−4287
anemometer, cupless solid-state device 79−96832
applied solid state physics, book 80−94936
backscattered electron detector, solid state, operating at TV scan rates in scanning electron microscope 79−18089
band-narrowing electro-optical deflector 79−98483
biomedical pressure transducer *(Japanese)* 80−94394
cardiac pacemaker, reliability technology conf., Gaithersburg, USA, (Jul. '76) 78−57129
carrier lifetime meas. from transient photoresponses of pulsed laser *(French)* 79−24898
chalcogenide glass device developments and future trends 77−69386
charge carrier transport operator, soln. for device in cct. 77−39836
charged-particle detector manufacture 79−93886
computer-aided design using parallel computer in University research 79−54114
conference, New York, USA (Oct. 79) 80−73093
conference, nuclear and space radiation effects, San Diego, Calif., USA (July 1976) 77−20376
contact and interconnect form. by ionised-cluster beam deposition 77−32528
cooling device, rectangular monolithic infinite cascade thermojunctions 78−57944
crystal defects, appl. of STEM 78−23155
crystal defects, high voltage TEM obs. 78−10037
deep levels, detection in high power devices 79−28318
detector for testing SEM quality parameters 80−22484
detectors, determination of thickness of sensitive layer with aid of β and γ sources 80−22323
diamond, applications in electronics *(Czech)* 77−1414
dislocation effects 79−82221
dislocation electric barrier appl. in devices 79−82551
displacement damage, displacement energy determ. by electron beam induced conductivity 80−70097
electrical parameters determ. by electron probe method 79−9259
electronics for the physicist with applications, book 80−62403
elementary semiconductor physics, book 80−6824
ferroelectric-semiconductor system, illuminated, voltage redistrib. 77−40194
force transducer suitable for use with small muscles 80−72395
frequency breakdown, effect of freq. on applied voltage 80−75592
gas detector, for gas chromatograph, electroadsorption phenomena *(Russian)* 78−7307
gas sensors *(Japanese)* 80−31736
generation-recombination noise 79−24032
generator current control and stabilization appls. 78−21790
high-resistance specimen conductivity nonlinearity meas. instrument 79−67341
InSb subMM detector, fast response, for use in measuring electron cyclotron emission 80−27347
IR detector development and characteristics 78−77986
laser output control, monitoring 78−22137
laser radiation image recording, semicond. plate charge distrib. *(Russian)* 77−79951
longitudinal thermomagnetic amplifier using Bi or InSb-NiSb 77−47838
low temp. plasma in mag. field, periodic signal generation, I/V charcts. *(Russian)* 77−20352
low temperature, selections from 1977 Comments on Modern Physics, book 79−30181
magnetic field bipolar sensor using carrier domain rotation, proposed device design 77−2670
magnetic field bipolar sensor using carrier domain rotation, operation and performance 77−2671
microelectronics and thin film components frontiers 80−73123
micron scaled cathodoluminescence with SEM, review 78−23537
microwave transducer, thermoelectric using hot carrier semicond., reactive props. and equiv. cct. 77−10109
minority carrier conc. determ., integral eqn. approach to abrupt depletion approx. 77−32022
monolithic layered piezoelectric-semicond. structures, acoustoelectric coupling 77−32050
MOS gas sensor for combustible gas and vapour monitoring 79−16104
Nernst amplifier, feasibility with heat sink and magnet winding at liq. N_2 temp. 77−53932
noise, conference, Bad Nauheim, West Germany (Mar. 1978) 79−24031
noise, physical aspects *(French)* 78−19111
particle tracking chamber based on semiconductor detectors *(Russian)* 78−872
photoanodes, corrosion stability 80−21130
photoelectrochemical cells, energy conversion system, principles and appl. 80−89652
photomultiplier cooling by semiconductor microrefrigerators 78−57942
piezoelectric transducer, pre-energised nonuniform, delay rod loaded, subject to body force, mechanical response 77−27449
power devices, high frequency US testing 79−47851
pressure sensor, two-conductor pressure-to-current transducer appl. *(Czech)* 79−97374
pressure sensors, thin Si diaphragm form., piezoresistive and capacitive structs. 80−13065
pressure transducers and transmitters 77−30175
radiation effects, conf., Williamsburg, USA (July, 1977) 78−26594
radiation effects, dose rate dependent effects of total ionising dose irradiation, annealing 80−70249
recombination, conference, Southampton, England (Aug.-Sept. 1978) 79−38087
remanent deep impurities, capacitative spectrosc. 79−82628
reradiation effects in negative electron affinity photocathodes 80−55274
resistance thermometers, for low-temps. 78−223
scanning electron probe voltage contrast, device ground level floatation 80−73527
sensors development trends and appl. *(German)* 80−52186
sensors for high direct voltages meas. 79−44916
sensors properties and uses *(German)* 78−36991
solid state devices, conference, Montpellier, France (Sep. 78) 79−33333
solid state physics, book 80−101676
solid-state imaging, conference, Louvain-la-Neuve (Sept. 1975) 77−39073
STEM characterisation 78−34893
STEM spectroscopic techniques for simultaneous electronic and defect obs. 80−100145
strain gauge with elastic coating 79−7350
strain gauges, strain indicator 77−71313
superlattice microwave/infrared detectors 80−13138
temperature meas. devices developments *(German)* 80−8986
temperature regulators using Darlington cct. as sensor and controller *(German)* 79−30467

semiconductor devices continued
temperature sensors, probes for sediments thermal cond. meas. *(Russian)* 78−65431
tensoresistor use for extending operating temp. range of press. transducers 78−4608
ternary semiconductor device applications, review 78−39207
theoretical foundations 77−39835
thermomagnetic recording using semiconductor optical image transducers *(Russian)* 80−44833
thermometer, resistance, thin-film, Ti and Ge, for surface temperature meas., design, fabrication and appl. 78−24792
transducers, temp. range up to 1000°C *(Croatian)* 79−40569
two-layer systems with an air gap, interaction of Rayleigh waves with electrons 77−39901
UHF biased semicond., cylindrical resonator for photoconductivity investig. 78−21117
X-ray detector for industrial intensitometry 79−67452
CdS, sintered film, solar cell *(Chinese)* 79−74517
CdS, ultrasonic transducer, multilayer systems, amplitude-freqn. characts. *(Russian)* 77−23843
GaAlAs-GaAs heteroepitaxial devices, interstitial impurities and degradation, Auger obs. 80−99730
n-Ge sensor, resist.-temp. characts., 50-125K 77−41602
Ge sensors, He level gauge appl. 80−57277
HgI_2 detectors for X-ray, computerized tomography, evaluation 80−89837
InSb IR detector array, AES anal. of localised contaminants at interfaces 77−57391
PbS-Si heterojunction detector, direct injection readout 80−4765
PbTe detector arrays, planar oxide-insulated 79−40614
Si devices, obs. of carrier densities via IR emission 77−72707
Si digital Sun sensor electrical and optical props. *(Japanese)* 78−32313
Si, implanted layer anal. for semiconductor device processing 77−76447
Si, photovoltaic cell, absolute spectral sensitivity calibration, radiometry, photometry *(Chinese)* 80−86367
Si solar cells, carrier lifetime and its impact on solar cell characts. 79−74521
Si spectroscopic applications of structures produced by orientation-dependent etching 80−93668
Si strain-gauge device, two-component, for aerodynamic tests on thin assemblies 78−3263
Si:Li X-ray detector, escape peaks and internal fluoresc., general geometry case 77−18150
n-Si:P, etched, high sensitivity temperature sensor, 1-10K 77−13757
p-Si:P semiconductor detector in radiometric inspection problems 80−62819
Si/Li spectrometer, cooled with Peltier elements *(Czech)* 78−49947
SnO_2, gas sensor, CO, H_2O vapour, surface temp. effect on cond. 78−76067
SnO_2:ThO_2, selective detection of CO, hydrophobic and hydrophilic silica effect 79−97372

semiconductor diode light emitters *see light emitting diodes*

semiconductor diodes
see also avalanche diodes; BARITT diodes; charge storage diodes; light emitting diodes; photodiodes; Schottky-barrier diodes; solid-state rectifiers; tunnel diodes; varactors; Zener diodes
air gap diode acoustic imaging and scanning 79−50524
back diode amplifier, use at low temp. 80−57324
carrier mobility, carrier density depend., scaling law 77−8179
chemically sensitive devices for trace level anal. 77−52720
control circuits using diode switches with switching of nsec pulses 78−8415
deep centres in overcompensated semicond., isothermal relax. of current 78−52072
diffused p-n diode memory correlator 77−23831
DLTS for diodes with large leakage currents 80−34504
dosimetry diodes, irrad. by γ-rays and fast neutrons, lattice defect annealing *(Czech)* 79−45570
double injection p-i-n, negative resistance characts. 78−30983
drift-velocity saturation regime, dynamic characts. 79−19651
electric field effect on thermal emission of traps 80−11073
electron beam induced current technique appl. to semicond. device characts., review 78−21302
epitaxial diodes, influence of geometry on interpretation of current, model 77−11994
forward slope resistance, small resist. value meas. cct. 77−37941
gated diode, surface states, density and capture cross section determ. *(German)* 78−23173
glass diode with electrothermal instability in switching channel 79−78238
heavily doped planar diode, collection efficiency and surface recomb. vel. modulation 80−20291
heavily doped shallow-emitter p-n junction solar cells, diodes and transistors, Auger recombination 79−96445
heavily doped transparent-emitter devices, analytical treatment 79−96444
impedance of a p-n junction by direct currents *(Russian)* 78−84285
ion controlled chemically sensitive diodes 80−13066
junction diodes, fabrication by LPE on Si:B substrates, and characts. 80−80363
layer, HF characts. 79−7886
leak detector appl., sparking 80−31774
low temperature measurement in high mag. fields, instrumentation and methods, review 78−37003
magnetodiode, characts., expt. *(Slovak)* 77−8186
magnetodiode and magnetoconcentration effects, influence of field effect 80−107903
magnetodiodes, planar, weak alternating mag. field effects on characts. 79−38155
majority carrier camel diode 79−95471
manufacturing, use of Ag electroplating 79−33952
microwave p-i-n diode modulator, transient plasma instability meas. *(German)* 80−87942
minority and majority mobilities, transit time effects determ. 78−14753
minority carrier charge accumulation effects on semicond. diode parameters *(Russian)* 79−73569
MIS, electronic processes *(Russian)* 79−56312
n^+-n-n^+ and p^+-n-n^+ structures with strong carrier accumulation, current-voltage characts. theory 79−42626

semiconductor diodes continued
n-i-p-i-n, UHF channel for quasi-zero double-comprison spectrometer for 21 cm wavelength appl. *(Russian)* 77−29658
negative resistance, diffusion effect, for diode with deep impurity levels 78−56217
p^+-i-n^+, double-injection switching, effect of surface recomb. 78−88025
p^+-i-n^+, Si:Au, influence of trapped space charge on double injection switching 77−1473
p^+-i-n^+ Si:Au diode, I-V characts., recomb. centre influence 78−19134
p^+-n^--n^+ pulsed diodes, forward pulsed case, voltage transient response 80−60071
p^+-n, deep centre activation energy determ. by capacitance method 79−11215
p^+-n diode under forward bias, effects of radiation-induced deep levels on admittance 78−23157
p^+n diodes, minority carrier lifetime 78−91350
p^+np^+ reach-through structure, electronic cond. 78−64103
p-ν-n, CO_2 laser beam modulation 77−79873
p-ν-n Si, for CO_2 laser modulation 78−42364
p-ν-n Si diode, for CO_2 laser modulation, temp. and switching characts. 79−81467
p-i-n, analytical expressions for duration of initial step recovery phase 80−25000
p-i-n, cryogenically cooled C-band p-i-n diode integrated switch matrix for radio astronomy applications 78−96392
p-i-n, influence of high temp. processes on props. of high resistivity region 77−35988
p-i-n diode, design technique for specific reverse bias characts. 78−34890
p-i-n diode, low temp. field ionisation of localised impurity levels 79−47600
p-i-n subnanosecond Si detector 78−9027
p-n diode, 1/f noise calc., free carrier mobility interpretation 80−54774
p-n diode, cut-off freq. 77−39923
p-n diode minority carrier storage effect reduction by F ion implantation damage 78−72243
p-n junction, electrical parameters, optical derivative meas. 80−2455
p-n junction, majority carrier flow model, props. of forward conducting diode 77−35986
p-n junction, normal modes for material parameter determ. 77−4426
p-n junction diode, electron-beam annealing of ion-implantation damage 79−77622
p-n junction diodes, emitter and base lifetimes determ. 77−43701
p-n junction injection characts. in strong elec. fields 77−76913
p-n junctions, variation forward voltage with temp., use as linear temp. transducer 80−57293
p-n structure, microwave reflection *(Russian)* 79−95481
p-n structures, nonlinear small signal distortion, numerical anal. 77−11989
planar, metal-coated, binary memory device, laser writing 79−69593
planar diode characterisation using SEM with movable Faraday cup, illuminator and backscatt. diode detectors 78−21292
point contact, subMM wave mixing in metal-metal and metal-semiconductor diodes 80−4769
point-contact, submillimetre wave detection, sensitivity detn. 77−37984
pulse diodes, application of Pd for reducing recovery time of reverse current *(Russian)* 79−99226
radiation dose measurement using radiation induced changes *(Japanese)* 78−78504
radiation effects, damage coeffs. for fission neutron and gamma-ray irrad. 80−34058
review of semicond. heterostructures, elec. and optical phenomena, discrete devices 78−72250
S-diode, influence of light, semiconductor compensated in upper half of forbidden gap *(Russian)* 77−85303
S-diode, Zn-doped, for IR modulation radiometer 78−4694
S-type diode, role of deep trapping levels in form. of current-volt. characts. 77−76948
S-type diodes made from Ir compensated Si 78−56224
SAW memory correlators, charge storage 79−64455
second breakdown electro-thermal model, computer program 77−24561
semiconductor layers, thin, theory of lifetime meas. with SEM, transient anal. 80−88573
semiconductor-insulator-semiconductor solar cells, basic principles of operation theoretical characts. 80−50986
semiconductor-insulator-semiconductor solar cells, fabrication and performance characts. 80−45707
semiconductor-oxide-semiconductor diodes, tunnel-assisted transport at room temp. 80−92975
sensors for high direct voltages meas. 79−44916
single injection diodes, 1/f noise 78−60204
single-injection solid-state diodes with exponential trap distrib., elec. cond. of hot carriers 79−99556
spectral sensitisation, diode model 77−41716
sublinear I-V characts., theory 78−91763
surface flicker noise at high injection level 77−47892
surface recombination effect, dynamic relationships 79−82664
temperature measurement using double p-n junction diodes *(German)* 78−201
temperature sensor appls., mag. field depend. 78−45623
thermal resistance meas. using temp. depend. of forward characts. 77−47893
thermometer system sensor, for use in varying ambient conditions 80−73361
thermometric characts., 15 to 300K 78−8403
thin film glass based structures, surface electron states effect on switching *(Russian)* 80−107887
transient process calcs., minority nonequilibrium carriers, potinjection EMF 80−6971
whisker diodes sub-MM receivers, antenna characts. 78−12755
Al-SiO_2-Si, MIS diode, neutralisation of mobile ions in insulating film *(Japanese)* 79−73591
AlGaAs-GaAs mesa diode, deep level defects and hole diffusion length meas. in proton irradiated GaAs 80−60000
$CdIn_2S_4$-Au surface-barrier diodes, mech. of current flow 78−56228
CdS-InP n-p heterodiodes, junction props. using injection electroluminescence 79−82667
CdTe, generation-recomb. and ionisation processes, temp. depend. *(Russian)* 77−39942
GaAs diode temperature sensors, characts. obs. at 4.2 to 393K 80−47054

semiconductor diodes continued
GaAs, high temp. and freq. characts., made by gas-transport method 79−19654
GaAs MBE physical characteristics and applications *(German)* 79−7618
GaAs, p^+-ν-n, nonlinear transport phenomena *(Japanese)* 80−6850
n-GaAs planar diodes with intervalley carrier transfer, dynamics and captive processes 78−47864
GaAs, quantum efficiency and nonequilibrium carrier lifetime 77−12442
GaAs sensors for low temp. thermometry *(German)* 79−35762
n-GaAs surface barrier diodes for nuclear radiation detection, deep trapping centres 80−92849
GaAs thermionic diode, temp. meas. appl., 1-400°C range 77−37886
GaAs, wide-gap semiconds., HV diodes, current-voltage characts. 79−24068
GaAs:Cr, carrier transport in p^+-ν junction based on relaxation semiconductors 79−65543
GaAs:Cr, high magnetosensitivity of negative resist. region 78−26946
GaAs:Cu(Cr) S-type diodes, thermal quenching of injection currents and current-voltage characts. 78−26942
GaAs-AlAs heterojunction, recombination currents 78−14806
GaAs-GaAlAs-GaAs rectifying semicond. struct., prep. by MBE and characts. 80−65657
GaAs-$Ge_{1-x}(GaAs)_X$ n-p heterojunctions, hydrostatic press. effect on elect. and photoelectric props. 80−20304
$GaAs_{0.6}P_{0.4}$ p-i-n diode, behaviour of turnover voltage under pulsed conditions 77−20408
$Ga_xIn_{1-x}Sb$, with Au metallisation, interdiffusion effects of heat treatment 78−14820
p-GaP electrode, photoelectrochemical effect 80−55673
GaP, high temperature electronics for geothermal energy 80−11997
GaP, p^+-n diode junction, admittance meas. and carrier traps 78−91757
GaP:Fe, current-voltage characteristics p-i-n diodes, luminescence, absorpt. double injection methods 79−65407
Ge, influence of mechanical stresses on effective carrier diffusion length in base region 77−35987
Ge p-i-n diodes, deep level transient spectroscopy 79−47105
Ge sensors for low temp. thermometry *(German)* 79−35762
Ge:Hg, S-type diode, elec. props. 80−20299
Ge-GaAs, p-nn^+ junction, I-V characts., inverse branch, effect of dislocation defects *(Russian)* 79−15217
p-Ge-n-GaAs diode, microplasma breakdown 79−91140
$In_{1-x}Ga_xAs_xP_{1-y}$, p-n junction diodes, fabrication by Be ion implantation 79−47156
InP p-n junction diodes, fabrication by Be ion implantation 79−47156
InP:Cd, p^+-p^--n^- junction form. by diffusion doping 80−84504
InSb, reverse biased diode, negative resist. 78−19129
InSb:Zn p-n junctions, ion implantation and diffusion spreading, elec. and photoelec. props. 79−73573
$InSb/LiNbO_3$ gap-coupled convolver operation at 77K 79−50242
InSe, photovoltaic effect, appl. to solar energy conversion 79−29481
$LiNbO_3$-pn-diode airgap convolver struct. optical scanner using single SAW pulse 80−64144
PbS_xSe_{1-x} film, prep. by co-evaporation method, p-n junction diodes fabricated, props. meas. *(Japanese)* 78−64477
$Pb_{1-x}Sn_xSe(Te)$, elec. props. under high press. 77−47809
$Pb_{0.86}Sn_{0.14}Te/PbTe$, interface recomb. velocity in DH laser diodes 79−64222
Se diode surface states determ. by conductance and capacitance 77−85318
Si, as temperature sensor, thermometer features *(Croatian)* 78−89479
Si, cryogenic thermometer appl., 4.2-300K range 77−137
Si diode, Auger recombination coefficient at very high injection rates 78−47863
Si, diode, high dislocation density effect on charact. *(German)* 79−33336
Si diode as in vivo fast neutron dosimeter 77−73587
Si diode detectors in radiological physics, energy compensating shield development 78−24142
Si diode detectors in radiological physics, high-energy photon dosimetry 78−24143
Si diode heavy ion detector, all epitaxial, fabrication and performance 77−54414
Si diode storage correlator optical imaging and memory characteristics 77−23772
Si diode thermometer, anomalous behaviour, 11 to 16K 79−35738
Si diode with pulse height analyser as alpha-detector *(Danish)* 77−18732
Si diodes as low temperature sensors *(German)* 80−31744
Si double base magnetodiodes, current-voltage characts. 79−7889
Si, electron irrad. devices, dominant recomb. centres 77−72912
Si hole injection diode, drift and diffusion of hot holes 79−78110
Si, impurity profiles, scanning electron microprobe anal. 80−79832
Si, ion implantation with Li^+, characts. for thin film solar cell use *(Korean)* 77−51812
Si ion-controlled diodes, acid-base exposure effects, Si-SiO_2 interface state density 80−96984
n-Si, ion-implanted, elec. characts. after laser annealing, mesa diode fabrication 80−88562
Si junction diode, diffused, with deep level traps, negative capacitance 80−96976
Si, laser annealed, elec. props. 79−69609
Si, magnetodiode, effect of mag. field on current-voltage characts. at low temp. 79−91134
Si, magnetodiode with polar magnetosensitivity 79−73579
Si, minority-charge-carrier lifetime, rel. to abrasion of surface *(Russian)* 80−11805
Si, n-n^+ point junctions 80−44719
Si n-p planar diode, Al layer covered, laser beam produced alloy areas, characterisation 79−69594
Si, negative resist. permanently induced in reverse-biased p-n junctions 78−56214
Si, neutron irrad., displacement damage for monoenergetic neutrons 78−30670
p-Si, neutron irrad. effects, admittance meas. of n^+-p diode 78−51587
Si p-n junctions, spin depend. surface recomb., electron irradiation effect 80−88627
n-Si, *p*-type regrowth layer formed by brazing with metal support disc, diode appl. *(Japanese)* 79−15833
Si pin diode, current filament temp. and Au acceptor level capture cross section temp. depend. 78−95351

semiconductor diodes continued
Si planar diode temperature sensor, long-term stability for 70 to 420K digital thermometers *(Czech)* 77−67435
p-Si, proton irrad. magnetiodiode effect, heat treatment, photocond. spectra 79−69591
n-Si, recomb. parameters of heat treatment defects in diodes 79−56299
Si sensors for low temp. thermometry *(German)* 79−35762
Si, superconducting magnet quench protection system for ISABELLE 77−83233
p-Si surface barrier particle detectors 77−50326
Si, thermometric props. in temp. range 4.2-300K 77−17998
Si, transient switching duration, linear carrier lifetime, emitter efficiency and Auger recomb. coeff. determ. 79−11207
Si, uncompensated, influence of carrier transit time on small-signal admittance of SCLC diode 77−85305
Si:Al lamellar devices, surge protector, solar cell, HV diode and negative resistor appls. 78−10068
Si:Au, p^+-n junction, quantitative study of Au atoms by TSC method 80−2458
Si:Au diodes, diffused, influence of gamma irradiation, Au levels monitored 77−66199
Si:B, p-n junction diodes, scanning-electron-beam annealing, elec. characts. 79−79128
Si:BF_2^+, ion implanted, arc annealing by flash lamp 80−44223
Si:Co, diode minority carrier lifetime, Lax method meas., effect of Co diffusion 79−69525
Si:Ir, magnetosensitive diodes, characts. 79−24069
Si:O,P, N^+-p diode, influence of O on performance 79−23985
p-Si:P p-n junctions, dislocations investig. rel. to P diffusion, SEM, X-ray topography techniques 77−76433
n-Si:Re diode photocapacitance spectra, Re centre dissociation 79−90997
Si:S diode, ionisation energies of S levels, photocapacitance meas. 77−4432
Si:Sb vacuum deposited coating, p-n junction, pulsed electron beam annealing doping, diffusion 80−75480
Si:Zn, p-n junction diode, computer-aided study of carrier lifetimes 80−24999
Si-CdS heterojunction memory diodes, switching process 78−80046
n-Si-Pd diodes, chemical reduction process for fabrication 80−60082
Si-SiO_2-Al MOS surface channel influence on channel-to-contact diode charact. 80−92994
Si-Te structural changes rel. to memory effect *(Russian)* 78−71679
Si-W point diode, utilisation as radiation detector and mixer in sub MM band 79−89006
SiAs-Au surface barrier diodes, optical props. of SiAs 79−8145
SiC diodes, S-type, high-voltage switching 77−20421
SiC, vapour grown, elec. breakdown field 78−19135
p^+-$Si_{1-x}Ge_x$-nSi junction diodes, lattice misfit effects on I-V characts. 80−70804
Si_xGe_{1-x}-GaAs, p-nn^+ junction, I-V characts., inverse branch, effect of dislocation defects *(Russian)* 79−15217
ZnO Sezawa mode pn-diode array memory correlator 79−78178

semiconductor doping
see also doping profiles; ion implantation
acceptor-donor complex model 77−51695
adsorption rel. to dopant admixture 78−95596
amorphous semiconductor, substantially doped, electronic props., review 79−87175
amorphous semiconductors, conference, Balatonfured, Hungary (Sept. 1976) 77−76802
amorphous semiconductors, doped, electronic props. 78−19030
amorphous semiconductors, doped, electronic props. 80−80283
amorphous semiconductors, doping effect and nature of localised states 78−14696
amorphous semiconductors, impurity control *(Japanese)* 79−37722
amorphous semiconductors, thermopower, conductivity, statistical shift, doping effects 79−69537
amorphous tetrahedrally bonded cpds. 80−2361
amorphous tetrahedrally bonded semicond., As(P) doped, gap density of states 79−19545
anomalous diffusion from doped oxides due to dopant depletion effects 77−89461
a-As_2Se_3, diffusion of Ag and Au 77−51549
atomic diffusion in semiconductors, review 79−4423
borosilicate glass sputtered film, phys. and chem. props., B diffusion into Si, SiO_2 80−29040
capacitance-voltage profiling tech. 78−38749
cd CdTe, growth from In solvents, self-compensation 77−28144
chalcogenide amorphous semiconductors, ESR studies of doped Mn, review *(Japanese)* 77−90019
chalcogenide glasses, memory effect, local doping, switching 80−107873
channelled ion implantations, apparatus for spatially uniform doping 78−51569
combined doping 78−2147
computer controlled neutron irrad. system 80−19851
concentration calc. in weakly doped sample, iterative method, GaAs appl. *(French)* 77−72634
convertors, photoelectric, optical methods for checking parameters of semiconductor doped layer 80−93869
developments, late 1970s innovations 80−6666
diamond: Li, ion implantation doped, IR photocond. 80−20249
diamond:Li, ion implantation, Hall effect and elec. cond. meas. 80−15526
diamond:Sb, implanted, radiation damage and annealing study 80−100263
diamond:Sb, ion implanted under channelling conditions, depth profile, distribution tail 80−2057
diamond:Xe, quadrupole interaction of implanted Xe 79−61279
diamond, high temp. ion implantation 79−23623
diamond, ion implantation, review 78−87698
diamond, synthetic, p-n junction prod. and doping, I-V characts. 77−15943
diamond Ge(B)(B_4C), doping by diffusion at high temp. and press. 79−19273
diffusion into Si, in open tube, high vacuum system 78−91349
diffusion layer, method for determining dopant and defect distribs. using polishing agent 79−37727
diffusion process, built-in elect. field diffusion enhancement factor, anal. 78−55985
dopant impurity redistrib., Chen and Chen series method 79−1457

semiconductor doping continued
dopant surface concentration determ. by IR reflectance 80−34036
electron beam induced current technique appl. to semicond. device charcts., review 78−21302
electron inelastic tunnelling spectrometer, construction and operation 79−40646
electronic component and material improvement, ion implantation techniques *(French)* 78−18667
epitaxial films, model for autodoping lateral variation 80−103595
epitaxial layers and bulk material, SIMS characterisation *(French)* 80−50904
Fermi level, effect of random var. in impurity conc., n-Si appl. 79−51470
film, growth and doping by MBE 77−73239
n-GaAs:Cr(Si), deep-level extrinsic photocond. response, decay at 4.2K 80−2420
GaAs:O, growth, O_2 solubility determ. rel. to temp. 78−34624
p-GaAs:Zn, diffusional doping, photoluminesc. in mag. field 77−16384
Gaussian diffusion determ., alternative method to angle lap and strain anal. 79−86925
grain boundary effects, doping tech. for study and control 80−79815
Gunn diode, anode domain disappearance dynamics, computer simulation calcs. 80−6859
Gunn planar elements, stationary domains 79−56238
heavily doped semiconductors and devices, review 79−47039
heavy-dose implantation, defect centre study, amorphous phase profile 77−80531
heteroepitaxial vacuum deposited films, doping *(German)* 77−84779
high current ion implanter with hybrid scanning 80−79826
high-low junction, heavy doping effects on minority carrier reflecting props. 79−42623
highly doped, behaviour of buried O_2 implanted layers 80−59499
homogeneous doped semiconductor, influence of internal elec. field on diffusion of ionised impurity 79−55940
hyperabrupt junction, C-V index, junction parameters depend. 80−49876
II-V compounds, indirect doping method *(Czech)* 80−24468
II-VI compounds, indirect doping method *(Czech)* 80−24468
II-VI semiconductors, for optoelectronic appl. *(German)* 77−7745
III-V compounds, survey 77−76448
III-V compounds, vapour growth, element incorporation 78−30556
III-V compounds and alloys, MBE process and problem areas, review 80−10815
III-V semiconductor solid soln., LPE, doping with groups II and IV *(Russian)* 77−80705
III-V semiconductors, diffusion theory for impurities 79−82246
III-V semiconductors, ion implantation, effect of implantation 78−75683
III-V semiconductors VPE using organometallics and hydrides *(French)* 79−33936
implanted ion lateral spread *(Japanese)* 79−4322
impurities, conc. of C, O, Si 78−59832
impurity conduction, at very low temp. *(Japanese)* 80−20200
impurity distribution, calc., using multicomponent diffusion theory 79−1456
inhomogeneous semiconductor, impurity opt. absorpt. and photocond. spectral line profile variation 77−16352
intense ion beams for implantation 78−66004
ion implantation, high current and medium current implanter 77−11577
ion implantation, ion imaging for micromachining *(French)* 80−34027
ion implantation, radiation defect form. in presence of force fields 79−51126
ion implantation, recent progress 79−14831
ion implantation, research at Central Physical Research Institute in Hungary *(Hungarian)* 77−51395
ion implantation, semiconductor device processing 80−34031
ion implantation, Si prod. applications 79−51124
ion implantation angular sensitivity, controlled doping profiles 79−55770
ion implantation appls., survey 77−7750
ion implantation by laser annealing, characterisation, solar cell applications 80−70247
ion implantation dose meas. 78−2150
ion implantation process survey 78−87692
ion implantation systems, high throughput 80−34029
ion implantation technique 78−14371
ion implantation with arbitrarily shaped mask edges, implant distribs. 77−31689
ion implanted impurities, absolute dosimetry using colorimeter-Faraday cup system 78−26590
ion implanted layers, annealing by laser beam 80−24469
ion implanter, semiconductor device processing 80−31944
IV-VI semiconductors, crystal structure and symmetry of electron spectra, doping effects *(Russian)* 79−7696
laser annealing appl. to ion-implanted semiconductors 79−73202
laser annealing of ion implanted semiconductors *(Japanese)* 80−19821
lightly doped compensated, electric fields at impurity centres *(Russian)* 80−84198
MBE, doping impurity transport, free carriers effect 78−26793
MBE for precision doping 80−89156
metal-semiconductor contact, surface doping effect *(Russian)* 77−47896
metal-semiconductor contacts with thin interfacial films 80−96969
MOS p-channel transistors, ion implantation effect on threshold voltage 78−34903
MOS structure, flatband shift induced by electron beam radiation, Si dopant effects 77−32085
MOS tetrodes, analytical model for effect of impurity concentration *(Spanish)* 79−99624
n^+-p-p^+ bifacial back surface field solar cells, optimisation of p^+ doping level by ion implantation 80−97784
neutrality and equilibrium in semiconductors 79−65544
neutron transmutation doping, conf., Columbia, USA (April 1978) 80−12849
neutron transmutation doping, damage-energy distrib. 80−15137
neutron transmutation doping 80−15133
nonuniformly doped MOS devices with lateral symmetry 80−15606
nuclear transmutation method *(German)* 78−95066
ohmic contacts to semicond. based on graded amorphous-cryst. junction, model 77−76923
one-sided abrupt junctions, normalized representation of avalanche breakdown behaviour 80−65666
planar source diffusion system props. 77−7751
polyacetylene:AsF_5, mag. susceptibility, Fermi surface density of states, semicond.-metal transition 79−95566

semiconductor doping continued
polyacetylene:I, electric props. in semicond. and metallic regions 80−29432
polyacetylene, doping with AsF_5, mechanism, effect on elec. cond. and spectra 80−24473
polyacetylene, n- and p-type doping, and compensation, p-n junction formation 78−76070
polyacetylene, p-n junction, elec. props., review *(Japanese)* 80−29410
polyacetylene, pristine and acceptor doped isomers, EPR, DC cond., evidence against solitons 80−15782
polyacetylene film, $(CH)_x$, synthesis, struct. and elec. props., doped materials, review 80−15623
polyacetylene film, partially oriented, anisotropic elec. cond., quasi-one-dimens. behaviour of fully oriented doped material 80−11112
polyacetylene films, doping effect on elec. cond., chem. and optical props. 80−65572
polyacetylene films, doping investigation, insulator-metal transition, optical transmission meas. 80−103729
polyacetylene pure and doped films, anisotropic optical properties 78−92137
predeposition diffusion profiles, errors in iterative numerical calcs. 78−26591
pulse diodes, application of Pd for reducing recovery time of reverse current *(Russian)* 79−99226
redistribution of dopant impurities in oxidising ambients 79−90695
reduction doping using zone recrystn. with temp. gradient 80−104062
Schottky barrier, real and ideal, photosensitivity losses 80−2452
Schottky barrier height control using knock-on effect in ion implantation 77−76919
Schottky barrier solar cell, doping density effect on efficiency 80−101100
semiconductor epitaxial structures, atomic diffusion 77−85110
Si:Au, step junction, mathematical model *(Rumanian)* 79−87148
$Si_{1-x}H_x$:P(B) film, amorphous, RF sputtered, optical consts. 79−95866
Si, on sapphire, Schottky magnetodiode, integrated mag. sensor 80−68223
Si, single cryst. characteris. by SEM using Schottky barrier charge collection microscopy 77−4444
Si (111) face, cryst. film growth, transfer of impurity during condensation of mol. beams 78−10299
solar cell fabrication, laser-induced p-n junction formation 80−93880
solar cells, photovoltage source in photocond. materials due to comp. and doping var. 80−7938
solubility of group III and V elements 77−84928
static dielec. response using simple homogeneous and isotropic model 79−73460
superlattice doping, electronic states, elec. props. 79−95480
ternary semiconductor device applications, review 78−39207
tetrahedrally coordinated semiconductor, effect of doping on dislocation mobility 79−82550
thermomigration method, using molten wires, nonequilib. morphology of migrating liq. inclusions 78−38882
thermomigration of molten metal wires, p-n junction fabrication 78−67870
αTTF:Br, transport and mag. props., effect of doping 80−24934
uniformity, four-point sheet resist. meas. technique 77−47475
uniformity assessment using fully automated four point probe method 77−59040
VPE, mol. flow in vac., free carriers effect on doping impurity distrib. 78−47682
in VPE, retrodiffusion cell design and applic. 77−84773
VPE impurity profile computer-aided control 80−2962
Al/copper phthalocyanine/Au cell, photoexcitation, doping, energy loss mechanisms 79−99573
AlAs-GaAs LEDs, Ge or Zn-doped, mechanism of degradation 77−76911
AlAs-GaAs stripe heterojunction laser, O^+ implantation effect on threshold characts. 79−41383
AlAs-GaAs:Ge double heterojunctions, efficiency of radiative recombination 77−77286
p- (AlGa)As:Zn, MBE grown, elec. props., shallow junction solar cell use 79−91175
AlGaAs-GaAs:Mg heteroepitaxial wafers, surface morphology and photoluminesc. meas. laser applics. 77−3591
$Al_{0.36}Ga_{0.64}As$, LPE films, Te-induced defects 78−43037
$Al_{0.7}Ga_{0.3}As$ layers, diffusion of Zn, comparison with GaAs 78−26589
$Al_xGa_{1-x}As$ DH laser, rake-line form. in LPE growth, doping effects 80−2287
$Al_xGa_{1-x}As$, epitaxial layer, distribution of Te and Ge impurities 78−43046
$Al_xGa_{1-x}As$, graded-gap crystal, voltage-current characteristics 79−69613
$Al_xGa_{1-x}As$, LPE, effect of doping on interface morphology 77−81231
$Al_xGa_{1-x}As$ MBE layers, ionized beam doping, elec. and optical characts. 79−37721
$Al_xGa_{1-x}As$, solid soln., synthesis by ion implantation Al^+ ions 78−38741
p-$Al_xGa_{1-x}As$:Be layer, MBE growth, Be doping and diffusion 77−51397
$Al_xGa_{1-x}As$:Mg doping characteristics, elec. props., effective hole masses 79−78117
$Al_xGa_{1-x}As$:Zn epitaxial layers, composition and Zn carrier conc. 80−25585
$Al_xGa_{1-x}P$, Zn diffusion behaviour, device appls. 77−11741
AlGaSb, growth and characts. for 1.0-1.8 μm heterojunction devices 78−6870
$Al_xGa_{1-x}Sb$:Zn, impurity diffusion, p-n junction depth 80−24678
$Al_xGa_{1-x}Sb$:Zn(Si)(Ge)(Sn)(Pb), doping of solid solns. during LPE *(Russian)* 77−85087
AlN, impurity-doped film, cathodoluminescence spectra 79−83038
As:Ni(Ge)(S)(Se)(Te) film, amorphous, chemical modification of props. 80−49250
$As_{10}Ge_{15}Te_{75}Ag_x$ glass, elec. and dielec. props., Ag additions effect 80−65558
As_2S_3 chalcogenide glass films, photographic Ag photodoping to produce negative relief image 80−59490
As_2S_3, glassy, build-in mechanism of impurities, electronegativity influence 77−76313
As_2S_3, glassy, diffusion, elec. transport and first group impurities effect on elec. and opt. props. 77−76623
As_2S_3:Ag, vitreous, doping influence on photolum. at 77K 77−77293

semiconductor doping continued
As_2S_3:Ag film, Ag photodoping rate, localised struct. transform. effect, absorpt. meas. 77−31914
As_2S_3:Ag glassy films, optical transmission spectra, photodoping effect 80−66317
$As_2S_3(Se_3)$:Ag glassy films, doped by photodiffusion and thermodiffusion, photocond. 80−29441
As_2Se_3, glassy, influence of oxygen added in As_2O_3 and SeO_2 forms on phys. props. 77−76314
As_2Se_3, glossy, Cu, Ag and 0 impurities influence on electronic energy spectrum and mol. vibr. spectrum 77−90181
As_2Se_3:Ag, amorphous, doping effect of gap states and elec. cond., dielec. relax. and DC cond. meas. 79−47098
As_2Se_3:B:, devitrification kinetics, Bi impurity effects 77−35675
As_2Se_3:Fe, glassy, mag. susceptibility investig. of doping effect 77−77024
B, versatile diffusion process using water vapour press. to control B-glass vapour press. 77−7749
BP:Zn(Se)(Cd), epitaxial layers, ion implantation, defects and lattic locations, channelling obs. 80−88179
$Bi_{12}GeO_{20}$:Ga,Ca, photocond. suppression by simultaneous Ga and Ca doping, and appl. to electro-optic light valve 79−78134
Bi_2Se_3:Sn(Pb), dopant influence on elec. cond. 79−51569
Bi_2Te_3-Bi_2Se_3-Sb_2Te_3, solid solution, single crystal, elec. cond., thermoelectric props. 80−88550
$Bi_2Te_{2.88}Se_{0.12}$, solid soln., single cryst. growth and doping, thermoelec. efficiency and Hall coeff. 79−33921
C:H film, amorphous elec. props., chem. modifications by doping 80−84523
$CdCr_2S_4$ crystal growth, structural defects, physical properties 80−60759
$CdCr_2S_4$:Ag, mag. semicond., ferromagnet resonance angular and temp. depend. 79−69730
$CdCr_2S_4$:In, single cryst. prep. and elec. props. 79−38727
$CdCr_2S_4$:In(Ga), resist. and magnetoresist. meas., effect of donor impurities 79−19608
$CdCrSe_4$, ferromag. semiconductor, mag. props. near Curie pt., doping effects 79−1670
$CdCr_2Se_4$:Ag, magneto-electrical props. temp. behaviour depend. on dopant conc. *(Russian)* 80−11006
$CdCr_2Se_4$:In (Ga)(Ag), and undoped, elec. prop., vac. heat treatment effect 80−15518
$Cd_{1-x}Fe_xCr_2S_4$:Cu, effect of doping on elec. props. and Curie temp. 78−84214
$CdGeAs_2$, p-n junction form. by heat treatment, photosensitivity 77−28247
$(CdGeAs_2)_{1-x}D_x$ amorphous films, property control in common target sputtering, elec. cond. 80−7494
$Cd_xHg_{1-x}Te$, diffusion and struct. of defects 77−84775
$Cd_xHg_{1-x}Te$, dopants behaviour and p-n junction formation 80−44225
$CdInGaS_4$, pure and Cu-doped, electrophotography layers *(Russian)* 80−68282
CdS, diffusion of In, 729-1411K 78−22895
CdS film, doping and recrystn. effect on photocurrent relax. time. 77−4409
CdS film, high cond., high transmittance, growth by evaporation method, and characterisation 77−77386
CdS, indirect doping method *(Czech)* 80−24468
p-CdS, indirect doping technique, using short-life radioactive atoms 77−31688
CdS vacuum evaporated film photoconductivity and In doping effects *(Japanese)* 79−87174
CdS:$CuCl_2$, sintered film, dopant conc. effects on carrier mobility 78−2484
CdS:Cu(Ag), charge and transport mechanism of impurities, electrodiffusion doping 80−59725
CdS:Cu(Cl), thin layer, electron pulse induced cond. relax. 80−2501
CdS:Cu(Se)(Zn), heavily doped, defect struct. 78−22756
n-CdS:In, containing excess Cd, effects of In on elec. props. 79−56217
CdS:In film, flash evaporated, prep. and elec. props. 80−20792
CdS:Li lattice, location of implanted Li atoms 80−6428
CdS:N, P, As, Sb, Bi photoluminescence obs. 78−10965
n-CdS:Te, grown from Te soln., elec. props. 79−65475
CdS_xSe_{1-x}:In film, flash evaporated, prep. and elec. props. 80−20792
CdSb:Au, solubility, thermal anal., microhardness, microstruct., elec. charcts. 77−16557
CdSe:Cu surface layer of CdSe, microstruct., photoelec. props. 78−43221
CdSe:In, epitaxial layers, synthesis and elec. props. 77−47909
CdSe:In, epitaxial layer, effect of activator distribution on conductivity 78−43047
$CdSiP_2$:Na(Bi), single crystal, photocond. under laser excitation 80−44661
CdTe, amphoteric behaviour and solubility of Sn 79−33008
CdTe, diffusion and solubility of Ge, 630-800°C, prep. conditions depend. 80−103519
CdTe, diffusion of Cu at 250 to 500°C, interstitial process 77−11737
CdTe, diffusion of Sn and intrinsic defects role 79−33116
CdTe, obliquely deposited layers with reduced resist., photovoltaic props. and Cd doping effects 77−43755
CdTe, photoplastic effect, influence of plastic deform., heat treatment and doping 79−82277
CdTe, single cryst. IR laser window, low absorption at 10.6 μm 78−79081
CdTe:As^{2+}, photovol. props. of p-n junction prod. by ion implantation 78−43038
CdTe:Cl, grown by travelling heater method, carrier homogeneity investig. 77−39848
CdTe:Cu, doping effects on evaporation kinetics and electronic props. during high-temp. annealing in vacuum 78−22743
CdTe:Fe, dopant solubility 77−90334
CdTe:Fe(Ni), luminesc. and refl. spectra, high temp. annealing effects 80−24472
CdTe:Ge, dopant behaviour 78−22742
CdTe:Li(Cl), acceptor states study by donar acceptor pair excitation luminesc. 80−100683
CdTe:Tl, growth by travelling heater method, elec. and optical characterisation 77−40356
CdTe-Au system, phase diagram rel. to doping 80−16282
$CdTl_2Se_4$:Au, solubility meas. by microhardness method 80−96650
$CdTl_2Se_4(Te_4)$:Au, elec. cond., density, dielectric const., changes on fusion 80−88553

semiconductor doping continued
$Cd_{1-x}Zn_xSe$, epitaxial layer growth with Zn content from doping to solid soln. formation 77−85094
CeO_2:S, acceptor properties of S, free electron concentrations 80−34395
Co_3O_4:Li(Cr)(Al)(S), and pure Co_3O_4, elec. cond. and thermo-EMF 80−20231
$CuGaSe_2$, single cryst. growth from melt, doping 77−12522
$CuInS_2$, homogeneity region and intrinsic dopant mechanism 78−34630
$CuInSe_2$, photovoltaic props. and p-n junction form. 77−69371
$CuInTe_2$ single crystals, directional freezing growth and doping, resist. changes on annealing 80−60768
$CuInTe_2$:Zn, donor impurity in diffusion, elec. and optical props. 78−68504
Cu_2S:Cd(Zn), effects of doping on elec. and optical props. 78−38743
Cu_2S-CdS heterojunction interface, depth distribution profiles, Auger spectra 80−88622
Cu_2S-CdS thin film heterojunctions, base doping effect on elec. and photoelec. props. 78−80043
$Cu_{2-x}S$-CdS, solns. cell, photo-emf, depend. on degree of doping of CdS 79−52934
EuO:Gd, critical specific heat depend. on doping, microwave cond. 79−95602
Fe_2O_3, electrochem. doping 77−76430
GaAS, semi-insulating and n-type, doping by neutron transmutation 80−96553
GaAS, semiinsulating, heat treatment effects 78−6382
GaAlAs, native defects, stoichiometry, doping effect 77−11541
(GaAl)As, Zn diffused DH laser with twin transverse junctions, low threshold current 79−98393
(GaAl)As, Zn diffused proton bombarded stripe laser 79−98392
$Ga_{1-x}Al_xAs$, solid solution, synthesized by ion implantation, Raman scattering 79−42972
$Ga_{1-x}Al_xAs$, Zn diffusion, depend. on Al content 78−59981
$Ga_{1-x}Al_xAs$:Si p-n junction, doping in LPE, elec. and luminesc. props. *(Czech)* 78−47851
GaAs, active layers produced by high energy Se^{++} implantation, FET appls. 77−39605
GaAs, anomalous diffusion of Sn from doped oxides due to dopant depletion effects 77−89461
GaAs autoepitaxial structure on heavily Te-doped GaAs substrate *(Russian)* 80−49556
GaAs, CVD, S doping behaviour during growth, electron conc. 78−26784
n-GaAs carrier compensation by O ion implantation, C-V meas. 77−7747
GaAs, carrier conc. and compensation microprofiles 80−80820
GaAs cryst., creep and dislocation vel. at different doping and temps. 78−95783
GaAs deposition by molecular epitaxy, uncontrolled doping obs. *(Russian)* 80−2276
GaAs devices, ion implantation damage, characterisation and appl. 80−92551
GaAs, diffusion of Cr and Ag, radiotracer profiles 80−24680
GaAs, disordered, ion implanted, elec. props. 78−84212
GaAs, donor and acceptor concs. determ. by optical method 78−19525
GaAs, dopant atom charge effect on lattice parameter 77−31631
GaAs, doped with Group IV elements, etching, electron spectra, cathodoluminesc. study of inhomogeneities 77−11556
n-GaAs, electron and gamma ray irradiated, introduction and annealing of defects, rel. to doping 78−67736
GaAs, electron and neutron irrad., defect clusters, carrier lifetime changes, doping level depend. 80−2077
GaAs, epitaxial, impurity gradients caused by surface states and substrate doping 77−84784
GaAs, epitaxial, Si and Ge doping 80−24470
GaAs, epitaxial layer, effective doping density, comparison of Hall and magnetoresistance meas. 77−11938
GaAs, epitaxial layer, partition coefficients of impurities 77−15443
GaAs epitaxial layers, transient processes during doping for large conc. jumps. 80−39134
GaAs film, MBE, growth and doping kinetics 77−76682
GaAs, grown-in dislocation density, impurity effect 78−51543
GaAs heavily doped n-type layers, formation by multiple ion implantation 80−59491
GaAs, impurity anal. by photoluminescence *(Japanese)* 77−24888
GaAs, impurity density of states, effect of doping and injections, models and calc. method 79−73466
GaAs, interimpurity interaction effect on distrib. profiles of impurities diffusing simultaneously 77−76451
GaAs, ion implantation, survey 77−76448
GaAs, ion implantation, review 78−6080
GaAs ion implantation, semiinsulating materials, role of substrate in elec. props. 80−59488
GaAs, ion implantation 1978 state of art review 79−42089
GaAs, ion implanted, diffusion of Zn and Ag, profiles 80−24681
GaAs, ion implanted, laser pulse annealing 80−19825
GaAs LPE layers, effect of baking on mobility and doping conc. 79−99641
GaAs laser-annealing behaviour, Si_3N_4 encapsulation effect forming n-type layers 79−79131
GaAs, lateral spread of implanted ions *(Japanese)* 79−4322
GaAs, low temp. selective Zn diffusion process using anodic oxides 78−47399
GaAs, MBE, SnTe source of donor impurities 79−95035
GaAs, MBE, surface reaction steps, dopant incorporation 79−77941
GaAs, MBE, technology and epitaxial layers props. 79−33945
GaAs, MBE with ionised dopant 77−40338
GaAs, migration of liquid inclusions, effect of DC current and temp. 77−7910
GaAs, multilayer epitaxial growth with Sn doping 77−47690
n-GaAs, nature of low temp. field generation of carriers, liberation from surface states 80−92960
GaAs, neutron transmutation doping, shallow donors magneto-optical effects 80−20255
GaAs, open tube diffusion of Zn 80−84326
GaAs p-n junction formation, laser assisted, TEM and elec. props. 79−69138
GaAs, periodic doping structure, nipi superlattices, HBE growth and characts. 79−95484
GaAs, planar diffusion of Sn from doped SiO_2 films, for planar junction fabrication 79−69289

semiconductor doping continued
GaAs, positron annihilation depend. on doping 80−60710
GaAs, produced by VPE using trimethylgallium and arsine, controlled doping 78−6855
GaAs, semi-insulating, effects of heat treatment characterised by SIMS 78−6091
GaAs, sequential multiple layer VPE, method 77−12545
GaAs, Si ion implantation and annealing, damage recovery, surface carrier profile 77−4119
GaAs, site selective doping by ion implantation of radioactive nuclei 80−34023
GaAs, solid solubility of Se, SIMS 78−67830
GaAs structures produced by laser doping, recombination radiation, anomalous temp. depend. 80−2847
n-GaAs substrates, ion implanted, compensation 78−75680
GaAs, thermomigration of molten Ga 77−69118
GaAs thin layers, MBE, growth conditions and phys. props. *(German)* 80−55307
GaAs, transmutation doping by thermal neutrons 80−10581
GaAs unintentionally doped layer growth using MBE 78−72741
GaAs, VPE, hole diffusion lengths, effect of transition metal diffusional doping 80−15628
GaAs, VPE, incorporation of deep levels, effects of growth conditions 80−20111
GaAs VPE, residual donor impurities 77−76679
GaAs, VPE by Ga-$AsCl_3$-H_2 process, role of Si 77−40380
GaAs, VPE in CVD systems, anisotropic phenomena 80−54563
GaAs:Au, back surface gettering 80−10758
GaAs:B, deep levels, optically stimulated transient current method *(French)* 80−59919
p-GaAs:Be layer, MBE growth, Be doping and diffusion 77−51397
p-GaAs:C, ion implantation efficiency, elec. profile and compensation level meas. 77−27880
GaAs:Cd, time depend. of Cd diffusion from gaseous phase 79−46844
GaAs:Co, epitaxial layers and bulk, diffusion and elec. activity of Co 79−56333
GaAs:Cr, gettering by back surface mech. damage 80−10759
GaAs:Cr, ion implanted, implantation damage profiles, laser annealing, ellipsometry study 80−79819
GaAs:Cr, low temp. gettering 80−96549
GaAs:Cr, Se implantation, carrier conc. and mobility profiles depend. on dose and annealing temp. 77−47479
GaAs:Cr, Se layers, ion implanted, ohmic contact form., contact resist. meas. 79−91158
GaAs:Cr, Te implantation, electron conc. and mobility profiles depend. on dose and annealing temp. 77−39607
GaAs:Cr, VPE grown, exam. of doping GaAs using $Cr(CO)_6$ 78−72737
GaAs:Cr, VPE growth, carrier conc. profiles 79−74099
GaAs:Cr,O semi-insulating monocrystal development and four-level model 80−88191
GaAs:Cr,Se, ion-implanted, semi-insulating effects of Cr redistrib. on elec. characts. 80−59982
GaAs:Cr(Te)(Zn), dopant influence on hardness 77−84777
GaAs:Cu, Fe, Cr resistance thermometer expts., 0° to 200°C *(Russian)* 78−45627
GaAs:Cu melt grown, 1.36 eV band luminescence studies, edge emission 79−87510
n−GaAs:Fe, diffusion doped compensated layers 80−15125
GaAs:Fe, for FET, VPE and characterisation 78−19672
GaAs:Fe, LPE, phase diagram 77−16509
GaAs:Fe, static magnetis. rel. to doping method and heat treatment conditions 77−36092
n-GaAs:Ge, film, substrate temp. depend. of Ge incorporation during MBE 80−76196
GaAs:Ge, ion implanted, elec. props., comparison with Sn, Se and Te ion implanted samples 77−39879
GaAs:Ge, LPE growth, Ge incorporation 78−27423
GaAs:Ge, solubility and point defect-dopant interactions 79−90689
GaAs:Ge, vap. grown, diatomic complex donor and acceptor model 78−80003
GaAs:Ge,Se transmutation shallow donor transition obs. 80−59925
n-GaAs:Ge epitaxial layer, ion-implantation doped, anomalous behaviour of impurities 78−18669
GaAs:Ge film, MBE grown, heavily doped, elec. props. rel. to growth parameters 80−100537
GaAs:Ge MBE power FETs with Sn surface impurities 80−80374
GaAs:Ge(Sn), LPE layer growth, impurity effect on terrace form. 79−95288
GaAs:Li diffused, lattice imperfections, TEM 77−80521
GaAs:Mg, photoluminesc. temp. depend., 4.2-293K 77−69878
GaAs:S, depth profiling using Cs^+ bombardment and negative SIMS in UH vac. 79−99232
GaAs:S, implantation depth profiles of S^+ and S_2^+ using AES 79−55774
GaAs:S, ion implantation, expt. 77−11574
GaAs:S epitaxial layers, dopant conc. control method 77−1807
GaAs:S^+ film, ion implanted carrier characterisation by cyclotron reson. 77−20472
GaAs:S(Se), ion implanted, evaluation by contactless mobility meas. 79−1448
GaAs:S(Se), MBE grown, surface exchange doping using PbS(Se) captive sources 79−10864
GaAs:S(Si), ion-implanted, capless anneal in As controlled vapour 79−55767
GaAs:Se, low dose Se^+ ions implanted, DLTS study of laser annealing 80−80204
GaAs:Se(Sn), annealing kinetics of implanted donor ions 78−6079
GaAs:Se(Te), laser annealed, donor implanted, elec. props. 79−4556
GaAs:Si, accelerated growth rate effect on MBE, Hall mobility and photolum. meas. 80−104067
GaAs:Si, activation by multiply scanned electron beams 80−75246
GaAs:Si, Cr, carrier concs. from Hall effect, microscopy, localised vibrational modes absorption meas. 78−56104
GaAs:Si, current-controlled growth, segregation and amphoteric behaviour 78−31346
GaAs:Si, electrical activity of Si 79−15145
GaAs:Si, faulted and prismatic loops obs. 77−51386
GaAs:Si, ion implanted effect of anneal ambient and occurrence of compensated regions in Si implants 77−51394
GaAs:Si, ion-implanted, depth distrib. profiles of Si ions 77−43230
GaAs:Si, ion-implanted, elec. props. 79−46686

semiconductor doping continued
GaAs:Si encapsulated with AlN, Si_3N_4 layers, photolum., annealing effects 80−20681
GaAs:Si(Cr), LPE, spiral growth patterns, dopants role 77−72800
GaAs:Si(Sn), ion implanted, laser annealed, high doping levels 80−88181
GaAs:Si(s), generation of high mobility n layers, SIMS 80−103375
GaAs:Sn, doping characts. during LPE 79−10866
GaAs:Sn, effect of ambient As vapour press. on surface stability 80−2208
GaAs:Sn, influence of growth process in doping profile and mobility profile during LPE 79−70000
GaAs:Sn, LPE, growth rate and temp. depend. of impurity incorporation 78−3063
GaAs:Sn, nature and conc. of point defects over conc. range 10^{17} to 6.10^{18} cm^{-3} 79−14802
GaAs:Sn, solubility and point defect-dopant interactions 79−90688
GaAs:Sn films, MBE grown, doping profiles, carrier mobilities, RHEED and AES obs. 79−1447
GaAs:Sn films, MBE power MESFETs 80−50563
GaAs:Sn thermal diffusion from spin-on SnO_2/SiO_2 source 80−96691
GaAs:Sn(Te), epitaxial film, influence of impurities on stacking fault energy 80−103371
GaAs:Te, Ge, compensated, activated cond. 77−76968
GaAs:Te, LPE, Te induced defects, rel. to growth conditions 78−6067
GaAs:Te, solubility and point defect-dopant interactions 79−90687
GaAs:Te, superdilation and defects, lattice parameter meas. and carrier mobility 80−10569
GaAs:Te-implanted by laser-annealing, ohmic contacts 79−19658
GaAs:Zn, high surface conc. Zn diffusion for good ohmic contact 77−11575
GaAs:Zn, implanted, furnace annealed, electrical, Rutherford backscattering and TEM meas. 80−100272
GaAs:Zn, implanted, laser annealing, elect., Rutherford backscattering and SEM meas. 80−100273
GaAs:Zn, laser annealing of implanted layers 77−55296
GaAs:Zn, MBE with ionized beam doping 77−77418
GaAs:Zn, Se, double doping during LPE, exam. of elec. cond. and Hall effect 79−4923
GaAs:Zn, surface conc. control 79−55758
GaAs:Zn epitaxial layers, composition and Zn carrier conc. 80−25585
GaAs:Zn MBE layers, ionized beam doping, elec. and optical characts. 79−37721
n-GaAs:Zn substrate, ion implantation as predeposition process 79−19268
GaAs:Zn(Cr), As precipitation at dislocations, TEM study 80−79820
GaAs:Zn(S), LPE, and doping characts. 79−33948
GaAs:Zn(Si)(Sn), etching rel. to dopant and carrier conc. 77−16704
GaAs-$Al_xGa_{1-x}As$ modulation-doped heterojunction superlattices, electron mobilities 79−7877
GaAs-AlAs, epitaxial layer, partition coefficients of impurities 77−15443
GaAs-Br_2(-Zn) system, filamentary cryst. prep. 78−52650
GaAs-$Ga_{1-x}Al_xAs$ variable gap p-n junction, variable gap and photo EMFs 80−15596
GaAs-$Ga_{2.2}Al_{0.8}As$:Be, LPE, diffusion of Be into GaAs substrate 80−103517
GaAs-$Ga_xIn_{1-x}P$ multilayer epitaxial films, MBE technology and epitaxial layers props. 79−33945
GaAs-S VPE layers, thickness and carrier conc. variations 79−100060
GaAs-Si ion implanted, impurity profiles elec. props. 80−96550
$GaAs_{0.6}P_{0.4}$, VPE, hole diffusion lengths, effect of transition metal diffusional doping 80−15628
$GaAs_{0.6}P_{0.4}$:$Zn^+(Ar^+)$, ion-implanted, thermal degradation of mechanical surface perfection and surface photolum. 77−77271
$GaAs_{1-x}P_x$, N doping using ionised beam in MBE 78−47400
$GaAs_{1-x}P_x$, N implantation, characterisation by photolum. and channelling 80−54262
$GaAs_{1-x}P_x$, N^+ implantation photoluminesc. props. 77−68987
$GaAs_{1-x}P_x$, N^+ implantation, annealing props. 77−68988
$GaAs_{1-x}P_x$, solid soln., synthesis by ion implantation P^+ ions 78−38741
$GaAs_{1-x}P_x$, solid solution, synthesized by ion implantation, Raman scattering 79−42972
$GaAs_{1-x}P_x$, structural defects, optical props. effect 80−55208
$GaAs_{1-x}P_x$:N, photolum. and electrolum. study of N isoelectronic traps 80−89061
$GaAs_{1-x}P_x$-SiO_2:N,Zn ion-implanted multiple layers, ion range distribs., secondary ion microprobe meas. 79−42129
$GaAs_{1-x}Sb_x$:Te(Ge), LPE and elec. props. 77−55896
$Ga_{1-x}In_xAs$:Mn grown by LPE, elect. props. 80−100541
GaInAsP/InP lasers, LPE grown, effect of p-doping on carrier lifetime and threshold current density 80−99726
GaInAsP-InP Zn diffused stripe geometry DH diode laser fabrication 79−98386
$Ga_xIn_{1-x}P$, epitaxial film, diffusion of Cu(Au)(Zn), intrinsic impurity effects 78−87825
GaN and GaN:Zn epitaxial layers, doping effect on cathodoluminesc. 77−20935
p-GaN, doping in nonequilibrium conditions 77−62556
GaN, indirect doping method *(Czech)* 80−24468
GaN:Al, VPE grown, luminesc. and elec. props. depend. on doping conc., bound excitons 80−20688
GaN:Zn, VPE growth, photoluminesc. rel. to doping conditions 80−55159
GaN:Zn(Fe)(Ni)(Cr), lattice parameters, variation with stoichiometry and doping 79−73153
GaN-AlN, solid solution, epitaxial growth and electrical props. 77−73236
n-GaP, cryst. growth, synthesis solute diffusion method, elec. characts. *(Korean)* 78−52653
GaP, dopant dislocations, scanning electron micrographs, cathodoluminesc. 78−91340
p-GaP, epitaxial layers grown from liq., overcompensated, doping levels 78−91353
GaP, green LED, high efficiency, by Zn diffusion into n-LPE layers 77−80519
GaP, grown by SSD method, Zn diffusion for green LED fabrication 77−81208
GaP, impurity behaviour during crystallisation from melt 77−84772
GaP, interimpurity interaction effect on distrib. profiles of impurities diffusing simultaneously 77−76451
GaP, ion-implanted, form. and annealing of radiation damage 78−91363

semiconductor doping continued
GaP LED, N content by photovoltage meas. 77−11993
GaP, low temp. selective Zn diffusion process using anodic oxides 78−47399
GaP, n-type, Zn diffusion, p-n junction depth 77−89841
GaP, radiation defect accumulation due to ion bombardment, optical absorpt. meas. 77−76438
GaP, SEM, cathodoluminesc., impurity and defect detect. 78−83695
GaP, site selective doping by ion implantation of radioactive nuclei 80−34023
GaP:Au, diffusion, solubility, and electrotransport of Au 78−91489
GaP:Bi,N, photoluminesc., electroluminesc., 4.2 to 300K, excitons and hole traps 80−108275
GaP:Cr, diffusion parameters and solubility and influence on elec. and optical props. 79−73343
GaP:Cr_2O_3, growth, dopant distribution, elec. resist. 78−34531
GaP:Cu, elec. and optical props., rel. to doping and heat treatment 80−16056
GaP:Dy, photolumines. spectra 79−52015
n-GaP:In, LPE from In solvent, dislocation density reduction by doping 78−18919
GaP:N, epitaxial layer, determination of nitrogen concentration from cathodoluminescence spectra 78−38744
GaP:N, epitaxial layer doping 77−51396
GaP:N, epitaxial layers, N concentration determination by two independent methods 80−39142
GaP:N, Zn epitaxial layers for yellow-LEDs, prep. and props. *(Czech)* 78−48234
GaP:Ni, whisker growth on surface 79−33212
GaP:Sb(Bi), gap vibrs. and impurity conc. determ. 79−69869
GaP:Sn, LPE growth from Sn soln., elec. resist. and Hall coeff. meas. 78−2593
n-GaP:Te, doping parameters calc., by means of Hall data analysis 78−51925
GaP:Te, struct. imperfections, prep. and doping effects 77−89451
GaP:Zn, doping from gas phase during LPE 80−55312
GaP:Zn, Sn doped epitaxial layers, Hall const., hole mobility and conc. 80−15143
GaP:Zn, Te, epitaxial layers, determ. of Zn conc. 79−77614
GaP:Zn, thermodynamics of Zn doping by liquid phase expitaxy 78−83832
GaSb, effect of n-doping on Debye temp. 80−2175
GaSb high-purity and doped layers grown by LPE and VPE methods 78−6863
GaSb, migration of liq. inclusions, effect of DC current and temp. 77−7910
GaSb, separate and combined solubilities of donors and acceptors 77−15434
GaSb, site selective doping by ion implantation of radioactive nuclei 80−34023
GaSb:Cd(Te)(Zn), carrier density dependence on impurity conc., rel. to solubility limit 77−8047
GaSb:Gd(Yb), elec. props., dopant effects 79−87115
GaSb:Li, dopant behaviour 77−51696
n-GaSb:Te, elec. transport mechanism in cond. band from Hall mobility and transverse mangetoresist. meas. 79−73531
GaSb:Te,Zn(Te,Mn), prep. and electrophys. props. 79−87116
p-GaSb:Zn, hole transport props. from 77 to 300K 79−73530
GaSe, ^{110}Ag diffusion, temp. depend. and solution *(Russian)* 80−70467
GaSe:Sn, ^{113}Sn diffusion, temp. depend. and Sn solubility *(Russian)* 80−70466
GaTe, ^{110}Ag diffusion, temp. depend. and solution *(Russian)* 80−70467
Ge, amorphous, doping, Schottky barrier and p-n junction form. by RF sputtering 77−8187
Ge, diffusion of Ga along dislocations 79−82385
Ge epitaxial film, vac. deposited on GaAs, doping effect of annealed GaAs surface 80−65718
Ge far IR photoconductive detector speed, limitation 79−30550
Ge, growth from lightly doped melt, dopant distrib. 78−2039
Ge, heavily-doped single cryst., macroinclusions, annealing in elec. field 77−47474
Ge, hopping cond. at intermediate impurity concs. 80−6840
Ge, impurity determ. in very pure sample by photoelec. spectroscopy 77−39888
Ge, melt growth conditions and doping level influence on impurity distrib. ratio 77−12516
Ge, p-n junction, I-V curve for microplasma breakdown, at. size difference effect 78−2550
Ge, pure, degree of compensation, capacitance meas., 4.2-150K 79−7624
Ge:Al, limiting solubility, rel. to charge carrier conc. 80−24596
Ge:Al(Sb) film, amorphous, ion implantation, effect on cond. 78−83839
n-Ge:As closely compensated, photolum. of charge carriers localised in trails of density of states 77−77294
n-Ge:As(Sb)(Bi), irradiated with fast electrons at 77K, investigation of 300K annealing stage 79−51155
Ge:Au, Sb 79−69577
Ge:B, epitaxial film, exam. of doping during chemical deposition from gas phase 79−1446
Ge:B, ion implantation and depletion at low temps., radiation and DC characts. 79−60392
Ge:B, single crystals, grown by Czochralski method, exam. of B distribution ratio and diffusion coeff. 79−95042
Ge:Be single crystals, grown by Czochralski method, exam. of Be distribution ratios and solubility 79−95043
Ge:Ga photoconductor detector performance in low optical background 77−37999
Ge:Mg, diffusion and p-type cond. 80−6419
n-Ge:O, Czochralski growth, O content rel. to props., IR, Li precipitation determs. 77−15445
Ge:O ion implanted, O localisation determ. 79−95040
Ge:P, conc. depend. of diffusion coeff. at P diffusion 78−95185
Ge:P, doping of epitaxial layers, in chloride and hydride processes 78−43036
Ge:P, solubility and segregation of electrically active P 77−15442
Ge:P(Sb), growth atm. effect on struct. microdefect form. 80−20779
Ge:Pb, ion implanted, lattice reordering, channelling and sheet resist. meas. 77−35577
Ge:Sb, Czochralski growth, orientation depend. of impurity distrib. coeff. 79−69976
Ge:Sb, dopant distrib. rel. to direction of cryst. growth 77−51400
Ge:Sb, effect of degree of doping on surface state charact. 79−69577
semiconductor doping continued
Ge:Sb, limiting solubility, rel. to charge carrier conc. 80−24596
Ge:Sb, Ni(Mn), recombination wave spectrum, two-level traps 80−96906
Ge:Sb(As)(P), implantation doping, annealing and doping profile determ. 77−19972
Ge:Sn, ion implantation of radioactive ^{119}Sn 80−59495
Ge-Si alloys, Au+Sb dopant reactions 77−84774
Ge-Si:Sb, energy spectrum of Sb 80−34382
GeS:Si, elec. cond. and thermally stimulated currents 80−20194
$Ge_{30}S_{70}$ glass film, Ag photodoping sensitivity 80−39121
$Ge_{42}S_{58}$:Ag, amorphous, bulk and film forms, doping effect on elec. props. 80−103691
$Hg_{1-x}Cd_xTe$, doping props. of selected impurities, diffusion behaviour 77−72632
HgI_2, doped, vap. growth by temp. oscill. method 78−39674
HgSe:In, enrichment of doping substances at pseudo phase boundaries *(German)* 80−29036
HgTe, single crystal, diffusion of transition metals 79−77818
HgTe, vacancy doping by off-stoichiometry, influence on transport props. 78−55862
HgTe:Cu, effect of prep. conditions on impurity distrib., hole conc. 77−8743
HgTe:Cu(In), dopant interactions 77−47834
HgTe:In, enrichment of doping substances at pseudo phase boundaries *(German)* 80−29036
n-In Ar:Te(Sn), heavily doped, cathodoluminescence, doping effect on luminesc. band position and spectral profile 80−45153
InAs, band gap and effective mass, depend on impurity conc. 79−69412
n-InAs, edge luminescence band, shape depend. on degree of doping, band gap 80−7405
InAs, migration of liq. inclusions, DC current and temp. effects 77−7910
n-InAs, photoelectric props., inhomogeneous impurity distrib. 80−107867
InAs, site selective doping by ion implantation of radioactive nuclei 80−34023
InAs:Cd, Te, donor-acceptor interaction, elec. cond. and Hall coeff. meas. 80−59988
InAs:Cd,Te interaction between impurities, effect on elec. props., Hall effect. 80−19832
n-InAs:Cr, Czochralski growth of high-resist. single crysts. 77−66587
InAs:Zn,S,(Se)(Te), exam of microhardness, Hall effect as function of dopant 79−95038
InAs:Zn,S(Se), solubility and donor-acceptor interaction 80−54263
p-$In_{0.53}Ga_{0.47}As$:Zn on InP, elec. and optical props. 80−75662
InGaAsP, LPE growth, orientation depend. of incorporation of Ga, As, and Zn 78−6869
InGaAsP, LPE grown, impurity effect on surface morphology 80−29291
InGaAsP:Sn(Te)(Zn), LPE growth, influence of growth-solution dopants on distrib. coeffs. 79−47640
InGaAsP/InP DH lasers, Zn doping level 79−98373
InGaAsP-InP, Zn diffused DH structures, oxide defined transverse junction stripe lasers 79−98389
$In_{1-x}Ga_xAs_yP_{1-y}$:Be, ion implantation, hole conc. and mobility, junction depth 79−46685
$In_{1-x}Ga_xP_{1-z}As_z$:Zn, x∼0.12, z∼0.26, LPE, DH lasers, tunnelling involving defects 77−65594
In_2O_3, electro-conducting transparent film, props. rel. to production method *(Japanese)* 80−25557
InP, diffusion of Cd acceptors 79−82246
InP, epitaxial layer, effective doping density, comparison of Hall and magnetoresistance meas. 77−11938
InP, grown-in dislocation density, impurity effect 78−51543
n-InP, high resistivity layers produced by Fe^+ implantation 78−47404
InP, ion implantation damage compensation 77−84770
InP, ion implantation used to create n-type, p-type and high resist. layers 78−6076
InP, ion-implanted n- and p-type layers, characts. 78−6075
InP, LPE grown, impurity effect on surface morphology 80−29291
InP, n-type conductive regions produced by ion implantation 78−10067
InP p-n junction diodes, fabrication by Be ion implantation 79−47156
InP, planar Zn diffusion process for p-n junction formation 78−43040
p-InP, prep. of single and bi-crysts., epitaxial layer and polycryst. films 77−81211
InP, pure and S doped, VEP, exam. of molar fraction controlled impurity in In-PCl_2-H_2 78−56587
InP, Schottky diode, barrier height control by S diffusion 77−85309
InP, site selective doping by ion implantation of radioactive nuclei 80−34023
InP, terracing of LPE growth, doping effects 80−10846
InP VPE, growth kinetics and controlled doping 79−87569
InP, VPE growth for MESFET's 80−103602
InP, VPE using CVD 79−28927
InP:Be, ion implantation, hole conc. and mobility, junction depth 79−46685
InP:Be, LPE, Be distrib. coeff., carrier conc. 79−90694
InP:Cd, doping by UV laser photodeposition 80−84191
InP:Cd, p^+-p -n^- junction form. by diffusion doping 80−84504
InP:Co(Fe), diffusion solubility and elec. activity of Co and Fe 77−43240
InP:Fe, deep acceptor levels, photocond. meas. 80−20116
InP:Fe, deep levels 79−56166
InP:Fe, precipitate mixture 77−77485
InP:S, SSD growth of low dislocation density crystals 80−89135
InP:Sn film, mol. beam epitaxial growth 77−16505
InP:Zn, isoconcentration diffusion of Zn at 800°C 78−6186
p-InP:Zn, result of doping during film growth by close space vapour transport on acceptor conc. 79−28944
p-InP:Zn, vapour grown, prep. and props. 80−54268
InP:Zn(S)(Se), liquid encapsulated Czochralski cryst. growth, X-ray study 79−47619
p-InP-Cd(Zn), ohmic contact formation on InP by laser photochemical doping 80−80369
InP-metal Schottky barriers, effects of heat treatment characterised by SIMS 78−6446
n-InSb, doping and strain depend. of quantum props. 79−60690
InSb, ion implantation, anomalous radiation disordering 80−92553
InSb, low defect crystal growth by InN doping, IR detector appl. 80−20780
InSb, morphological and structural changes due to ion bombardment 80−79843

semiconductor doping continued
InSb, periodically doped cryst. prod. by Peltier effect, helicon diagnostics *(German)* 77−48338
InSb, site selective doping by ion implantation of radioactive nuclei 80−34023
InSb:Cd (Zn) (Ge), ion-irradiated, p-n conversion during heat treatment 80−96558
InSb:S, ion implanted, Hall effect meas. 77−20342
InSb:Se p-n tunnel diodes, influence of doping on charact. 79−73575
InSb:Sn, equilibrium distribution coefficient of Sn 79−10872
InSb:Zn p-n junctions, ion implantation and diffusion spreading, elec. and photoelec. props. 79−73573
InSb-NiSb, eutectic alloy, Te-doped, electrophys. props. 77−35955
InSe, ^{110}Ag diffusion, temp. depend. and solution *(Russian)* 80−70467
In_2Te_3-type semiconductor, mechanism of electrically inactive impurities 80−24834
Mn_3O_4:Li(Cr)(Al)(S), and pure Mn_3O_4, elec. cond. and thermo-EMF 80−20231
Ni-n-GaP:Si(Ge) contacts, doping effect in elec. props. 80−6983
PF_5 dopant for polyacetylene 80−88171
PH_3-doping, conc. meas. by vacuum UV absorpt. spectra 80−71972
PbI_2, photoelectromagnetic investigation, expt. 79−24010
PbO:Ag film, X-ray stimulated diffusion, current-voltage charact. 77−80653
n-PbSe, heterodiffusion of Sn 80−34245
$Pb_{1-x}Sn_xSe(Te)$:I epitaxial layers, photoelectric props., doping donor impurity behaviour 77−80810
$Pb_xSn_{1-x}Se(Te)$ film, Bi and Tl impurity dopant incorporation and diffusion during MBE growth 79−66012
$Pb_{0.8}Sn_{0.2}Te$:Cd, defect struct., Hall effect and solubility meas. 77−11571
$Pb_{0.82}Sn_{0.18}Te$:Cd, effective distrib. coeff. of Cd *(Russian)* 79−73203
$Pb_{1-x}Sn_xTe$, Cd-In diffusion, changes in elec. props. 78−91348
$Pb_{1-x}Sn_xTe$, epitaxial layers, In doping, donor impurity singularities, distrib. coeff. 77−80526
$Pb_{1-x}Sn_xTe$:Cd, Cd diffusion obs. using Hall mobility and Cd solubility expts. 78−26584
$Pb_{1-x}Sn_xTe$:In(Cd), photoconductivity 78−23129
$Pb_{1-x}Sn_xTe$:In(Ga)(Al), elec. props., dopant influence 79−51599
PbTe, carrier conc. inhomogeneity 78−52019
PbTe film, Bi and Tl impurity dopant incorporation and diffusion during MBE growth 79−66012
PbTe film, ion-implantation-induced lattice defects 77−68985
PbTe, ion implantation induced damage and reson. levels 80−49255
PbTe:As, hole conc. control, in LPE layers, plasma reflectivity and thermoelec. probe meas. 79−99640
PbTe:Cd, Cd diffusion obs. using Hall mobility and Cd solubility expts. 78−26584
PbTe:Cd, defect struct., Hall effect and solubility meas. 77−11570
PbTe:Zn, defect struct., Hall effect and solubility meas. 77−11572
$Pb(Zr,Ti)O_3$:$Nb_2O_5(Sc_2O_3)$, elec. cond. investigation with and without various dopants and stoichiometry 79−11120
Sb_2Te_3, $Sb_{1.5}Bi_{0.5}Te_3$, Te- and Se-doped cryst. growth and elec. props. 77−48334
Se, amorphous, effect of doping on mol. struct. and valence alternation states 80−49249
Se:Ge(Si)(Sn), vitreous, crystn. kinetics study by elec. cond. meas. 79−65526
Se:I, liq., DC cond., temp. depend. *(French)* 77−69322
Se:I, liq., thermopower, temp. depend. *(French)* 77−69360
Se:P, vitreous, crystn. kinetics study by elec. cond. meas. 79−64998
Se:P, vitreous, stabilisation of cond. 77−11910
Se:Ta, electrophysical meas. rel. to control of conductivity type 77−24323
p-Si, $^{49}BF_2$ ionised mols. obtained by implantation of 78−31003
Si, ^{75}As implantation, scanned CW electron beam annealing 79−99225
Si, amorphous, asymmetrical profile of ion implanted P 79−46693
Si, amorphous, doping, Schottky barrier and p-n junction form. by RF sputtering 77−8187
Si, amorphous, doping effects on cond. in hopping transport regime 79−28424
Si, amorphous, elec. and opt. props., review 78−23094
Si, amorphous, hydrogenation using DC and HF plasma treatment 80−59497
Si, amorphous, ion implantation method, B and P ions 80−100274
Si, amorphous, laser-induced epitaxial regrowth, substrate and doping effects 79−56082
Si, amorphous, p-n junction preparation, by SiH_4 decomposition *(Czech)* 77−63560
Si, amorphous, sputtered, resist. control by ion implantation 80−100262
Si, amorphous, substantially doped, electronic props., review 79−87175
Si amorphous evaporated film, doping 79−51127
Si amorphous film, heavy doping by alkali ion implantation 80−2045
Si, amorphous film prepared from glow discharge, quantitative H anal. 77−69188
Si, Ar(Xe) ion bombarded, sputtering yield energy and fluence depend. 79−78805
Si, As diffusion from As doped oxide film, stress effect on film roughening 78−2389
Si, As diffusion from doped polycryst., conc. depend. 78−34656
Si, As implantation *(Japanese)* 78−38738
Si, Au diffusion enhancement by photo- and electron irrad. 77−27901
Si, BN glass transfer process 80−107459
Si, bandgap narrowing model in moderately to heavily doped material 79−99477
Si, behaviour of B molecular ion implants 78−47405
Si buried-grid fabrication by LPE 79−78906
Si, by thermal neutron irrad., annealing charact. of bulk electron traps obs. 80−49244
Si, CC Si_3N_4 film formation by $^{14}N_2^+$ ion implantation into Si 79−99455
Si, CVD mechanism, book contrib. 79−69991
Si, CVD polycryst. solar cell, grain boundary effects rel. to dopant conc. 77−7744
Si, channelled-ion implantation of group III and group IV ions 78−75682
Si, complex doping effects on limiting electron conc. 78−22740
Si concentrator solar cells, new technology for fabrication 80−81457
Si, correl. between photolum. spectra and impurity conc. 78−23513
Si, Czochralski cryst. growth, faceted and nonfaceted, Sb microsegregation 80−45227
semiconductor doping continued
Si, Czochralski grown, dislocation free, swirl defect form., doping effect 80−92519
Si, Czochralski grown crystal, radial impurity distrib. improvement 77−73225
Si, Czochralski growth from heavily Sb doped melt, interface morphological instability 80−2939
n-Si, Debye temp., electronic effect 78−83901
Si, deep planar Ga and Al diffusion 79−69290
Si detectors, high resistivity n-type prod. by neutron transmutation doping 79−45540
Si devices, obs. of carrier densities via IR emission 77−72707
Si, diffusion of As, from As-doped oxide source 77−47477
Si, diffusion of B from CVD BN covered with Si_3N_4, appl. to master slice p-MOS IC 80−107564
Si, diffusion of B in oxidised atmosphere, minicomputer model *(Rumanian)* 79−82247
Si, diffusion of Ga in closed capsule, surface damage elimination 78−87691
Si, diffusion of Ga through SiO_2 layer, junction depth 78−51574
Si, diffusion of Na, retarding action of radiation defects 77−1140
Si, diffusion of nitrogen during annealing, effects on ion implanted layers 77−24436
Si, diffusion of Os, diffusion parameters using photocapacitance and four-probe methods 79−51314
Si, diffusion of P, 900-1150°C, controlled surface conc. condition 77−7746
Si, diffusion of P, dislocations, creation conditions 79−95039
Si, diffusion of P from spin-on SiO_2:P film 80−2050
Si, diffusion of self-interstitials and As, B and P, radn.-enhanced 80−29216
Si, diffusion of transition elements, anomalous behaviour 80−29044
Si, diffusion profiles, P and B diffusion determ. *(Rumanian)* 79−77615
Si, diffusion-induced lattice strain and dislocation obs. by X-ray diffraction *(Japanese)* 77−84753
Si, dislocation velocities as function of electronic doping 77−4117
Si, dopant striae, SEM obs. by Schottky barrier charge collection 77−31684
Si, dopant survey for IR detector appl., 2 to 2.7 and 3 to 5 μm 77−15433
Si, doped with metal impurities contact angle, water adhesion energy *(Russian)* 77−89620
Si, doping, low temp. radiation induced impurity diffusion 77−15439
p-Si, doping by Ti diffusion 78−18670
Si, doping impurity distrib., during cryst. growth by Czochralski method *(Russian)* 80−100276
Si, dynamic recoil implantation, of Au film 79−14833
Si, ESR in neutron transmutation doped samples 80−20462
Si, effect of disloc. density on diffusion process *(Hungarian)* 77−62553
n-Si, effect of random var. in impurity conc. on Fermi level 79−51470
Si, epitaxial, minority carrier lifetime and impurity conc. meas. *(Japanese)* 80−25025
Si, epitaxial film, dopant incorporation model 79−99228
Si, epitaxial film, dopant incorporation during growth, theory and expt. 79−99229
Si, epitaxial film, kinetics of doping, gas-phase decomposition of SiH_4 77−16499
Si epitaxial film dopant incorporation, transient response 77−76976
Si, epitaxial growth, adsorbed layer model for autodoping mech. 80−7505
Si, epitaxial growth, impurities incorporation kinetics *(French)* 78−22749
Si, epitaxial growth from vapour, dopant inclusion model *(German)* 79−42088
Si, epitaxial layer, incorporation conc. depend. of P from silane-phosphine-H_2 mixture 80−2053
Si epitaxial layer growth in vacuum, Ar, Xe ion bombardment effect 80−39463
Si epitaxial layers, doping the P cpds., process parameters effect on electrophys. charact. 78−38734
Si epitaxial layers, grown in vac. at low temps. P and Sb doping 80−88189
Si epitaxial layers, temp. dependence of P dopant inclusion in gas phase deposition *(German)* 79−52127
Si epitaxial layers, vacuum deposited, conditions for impurity migration from B, P, Sb doped sources *(Russian)* 80−107570
Si epitaxial reactor, doping system, transient steady state response, transfer function approach 79−42086
Si epitaxial wafer, impurity profile meas. by multilayer spreading resist. anal. 77−76449
Si epitaxy, autodoping effects 80−100259
Si epitaxy and oxidation, first-order process models 78−72049
Si, epitaxy lateral autodoping kinetics 78−6087
Si extrinsic photoconductive IR detector, counterdoping scheme 78−49896
Si film, MBE, cryst. defect props., substrate treatment effects 80−70551
Si film, sputtered amorphous, P and B doped, elec. cond. and thermopower meas. *(French)* 78−47403
Si, floatzone, P doping by thermal-neutron irradiation 78−22750
Si, Ga diffusion open-tube system 80−19822
Si gates ion implantation, without implanting ions into SiO_2 insulating layer 79−7619
Si, heavily doped, doping density striation effects in metal-nonmetal transitions studies 79−28383
Si, heavy ion induced disorder in surface and at shallow depths 80−59535
Si, homogeneous n-type doping by thermal neutrons 80−2051
Si, implanted layer anal. for semiconductor device processing 77−76447
Si implanted layers, utilisation coefficient of impurities after laser annealing 77−76437
Si, impurity conc. from MOS DC transfer charact. 78−2155
Si, impurity determ. in very pure sample by photoelec. spectroscopy 77−39888
Si impurity diffusion through SiO_2 layer, physicochemical processes *(German)* 78−2149
Si, interactions between sequential dopant diffusions, review 77−27900
Si, ion bombardment induced light emission, investig. of cpd. form. 77−48257
Si, ion implantation, investigation of radiation damage by pendellosung topography 79−51125
Si, ion implantation, off-axis channelling disorder anal. 77−24325

semiconductor doping continued
Si, ion implantation with Li^+, characts. for thin film solar cell use *(Korean)* 77−51812
Si, ion implantation-induced damage after Ar and P implantation, defect density and distrib. *(German)* 77−24337
Si, ion implanted, dopant depend. of oxidation rate 80−89384
Si, ion implanted, pulsed-laser annealed, Raman obs. 79−73189
Si, ion implanted, standard for TEM, EELS 80−99017
Si, ion implanted Kr migration during anneal 78−18834
Si, ion-implantation damage, annealing using pulsed-electron-beam 79−55768
Si, ion-implantation gettering effects, crit. microstructure 77−43229
n-Si, ion-implanted, elec. characts. after laser annealing, mesa diode fabrication 80−88562
Si ion-implanted dopant redistribution under laser annealing 80−70242
Si, ion-implanted layers, impurity profile meas. after laser annealing 78−87702
Si, laser annealing, nonequilib. incorporation of impurities during rapid solidification 80−55286
Si, laser assisted doping, ohmic contacts and p-n junction form. 78−79621
a-Si, laser induced crystallisation mechanism, epitaxial regrowth 80−84962
Si layer, neutron activation analysis, contamination and cross-contamination 78−83837
Si, Li ion implantation, depth distrib. variation after heat treatment 79−86814
Si, MBE, on n^+ Si, with wide range doping control 78−27402
Si MOSFET, conductance oscills., source-drain limited cond. 80−20316
Si, masking effects of Sb diffusion, from doped oxide source 77−15437
Si, migration of Au, electron bombardment effects 80−100362
Si, minority carrier lifetime degradation by $POCl_3$ emitter diffusion 78−2496
Si, minority carrier lifetime in neutron doped samples 80−20218
n-Si, mobility and resist. as functions of dopant density and temperature 78−2487
p-Si, monocryst., diffusion of As, Henry const., temp. depend., 1448 to 1523K 79−42399
Si n-p junction vertical solar cells, Al-plated, photovoltaic effect variation with impurity conc. 79−100522
p-Si, Na impurity diffusion, ion irrad., defect form. effects *(Russian)* 77−43386
Si, neutron bombarded homogeneous (NBH) P doping, power device appls. 77−1138
Si, neutron irrad., residual radioactivity meas. 80−19829
n-Si, neutron irradiated, annealing behaviour characterisation by electrochem. meas., transmutation doping 80−19847
Si, neutron irradiation installation for power thyristor production 77−65993
Si, neutron transmutation doping, detect. and identification of potential impurities activated 79−42090
Si, neutron transmutation doping, photoluminesc. characterisation 80−11453
Si, neutron transmutation doping, impurities 80−15134
Si, neutron transmutation doping, radioactivity form. 80−15135
Si, neutron transmutation doping for IR detector material 80−15136
Si, neutron transmutation doping in Harwell reactors 80−15138
Si, neutron transmutation doping, irrad. facilities 80−15139
Si, neutron transmutation doping, General Electric test reactor 80−15140
Si, neutron transmutation doping, automated irrad. facility 80−15141
Si, neutron transmutation doping, annealing, lattice damage 80−15163
Si, neutron transmutation doped, highly compensated, resistivity fluctuations 80−15531
Si, neutron transmutation doped, elec. props. 80−15532
Si, neutron transmutation doping, irrad. techniques 80−19827
Si, neutron transmutation doped, isochronal annealing of resistivity 80−19828
Si, neutron transmutation doping, ^{31}P conc. meas. 80−19833
Si, neutron transmutation doping, at. displacement effects 80−19852
Si, neutron transmutation doping, annealing, deep defect levels 80−20123
Si, neutron transmutation doping using nuclear reactor thermal neutron irrad., review 80−39161
Si, neutron transmutation doping, impediments to use in power device fabrication 80−96560
Si, neutron-transmutation doped, annealing behaviour, EPR obs. 79−86804
Si, nuclear transmutation appl. 77−84782
Si, open-tube P diffusion kinetics 79−33117
Si, oxidation-induced stacking faults, control by Cl implantation 79−46682
Si, oxidised surface, irregular growths of $B(OH)_3$ 78−39926
Si, P implanted, low temp. annealing characts. 77−11576
Si, P^+ implantation, induced disorders. 80−6422
Si p^+-n high efficiency solar cell, B diffusion process 77−85302
Si p-n junction formation, laser assisted, TEM and elec. props. 79−69138
Si, p-n junctions, neutron transmutation doping, breakdown process 80−15600
Si, phonon-phonon relaxation investigation for conventional and neutron doped crystals 80−96927
Si, planar technology, insulating thin film preparation and props. 78−10589
Si, polycryst., lateral diffusion of B, influence on submicron MOST fabrication 78−26588
Si, polycryst. film doping during deposition and with diffusion 78−6088
Si, polycryst. rods, p-n junction appls. and transport props. 79−99612
Si, positron annihilation, effect of doping 79−24385
Si, pyrolytic BN wafer as diffusion source characterisation 78−91352
Si, reaction of rare earth impurities with carbon during cryst. growth 79−38733
Si ribbon solar cells, var. of minority-carrier diffusion length with light intensity, heavy metal doping effects 80−93937
Si, shallow impurities, photolum. anal. 78−23512
Si, SiO_2 diffusion sources under oxidising ambient conditions, solar cell fabrication 78−2148
Si, single crystal, depth profile of radiation damage using lattice deform. study *(German)* 77−39618
Si solar cell, ion-implanted, effect of electrostatic drift field 77−24615

semiconductor doping continued
Si solar cells, diffusion fabrication process, low cost, highly automated 80−30487
Si solar cells, effects of metallic impurities 80−85278
Si solar cells, fabrication using continuous or pulsed lasers *(French)* 80−61350
Si solar cells, high open circuit voltage, P implantation 80−89642
Si solar cells, implanted layers characteristics, laser irradiation effects 80−35692
Si solar cells, ion implanted, from EFG Si ribbons 80−30485
Si solar cells, ion implanted grating type 80−101102
Si solar cells, junction formation techniques using spray-on polymer dopants, cost effective, high throughput 80−94014
Si solar cells, $POCl_3$ gettering of Ti, Mo and Fe-contaminated cells 80−94010
Si solar cells, realisation by laser induced diffusion of deposited Sb 80−93998
Si, solid solubility of Co, 1000-1270°C, radiotracer obs. 77−51500
Si, stress enhanced diffusion of B, using SiO_2 diffusion masks, photodiode fabrication 78−67865
Si surface, interaction of oxygen gas discharge plasma 78−83840
Si, surface, pulsed electron beam processing, doping, annealing 80−75254
Si surface layers, impurities, elec. and photoelec. props. 80−2298
Si surfaces, influencing microstruct. deform. process by impurity type *(German)* 79−65107
Si, technology and physics, review 80−34353
Si, thermal oxidation, high resolution Rutherford backscatt., implanted ions analysis 79−87911
Si, thermomigration of molten Ga 77−69118
Si thin film, polycryst., CVD, elec. props. 80−107934
Si, tracer diffusion of ^{71}Ge and ^{31}Si in intrinsic and doped samples 80−29214
Si, transmutation doped, deep trap level analysis 78−10471
Si, transmutation doped, stabilisation 78−10449
Si two-step impurity diffusion, effect of internal elec. field 77−76624
Si, VPE at reduced pressure, autodoping 77−77389
Si, vacuum deposition, combined with Sb ion implantation *(Japanese)* 78−88428
Si wafer, colour-band generation during high dose ion implantation 79−1449
Si wafer, migration of fine molten Al rich wires, vertical p-n function fabrication 78−68077
Si wafer, surface exam. of ion-implantation using SAW convolver 77−72897
Si wafer, thermal neutron irrad., charge carriers behaviour obs. *(Japanese)* 79−42484
Si wafer surface doping profile determ. by SIMS 79−77618
Si wafers, floating-zone, etch struct. on microdefects as affected by dopants and surface treatment 80−79773
Si:Al, diffusion, open-tube high-vacuum method 78−6084
p-Si:Al, diffusion and incorporation of dopant in closed system, elec. props. 77−59026
Si:Al effect of dopants on grain growth 80−54575
Si:Al film, low-temp. diffusion of Al 78−38878
Si:Al p-n lamellar structures, processing by molten Al rich wire thermomigration 78−10068
Si:Al(Ga), O_2 diffusion, conc. profile meas. 80−79990
Si:Al(Ga), spreading resist. calibration using Si:B 80−103690
Si:Al(Sb) film, amorphous, ion implantation, effect on cond. 78−83839
Si:Ar, As, ion implanted, laser annealing, doping profiles, channelling 80−97506
Si:Ar, ion implant gettering of MOS capacitors using linear voltage ramp and N^+ backscattering 79−95502
n-Si:Ar(P), single cryst., positron annihilation parameters, energy-band struct. on surface in free-electron approx. 79−15555
Si:As, amorphous, field effect and thermoelectric power 79−33289
Si:As, amorphous layers, laser induced As profile broadening 79−95045
Si:As, As implantation damage and atom location, channelling meas. 77−59032
Si:As, CVD, doping using SiH_4-H_2-AsH_3 system 80−79823
Si:As, depth profile detect. limit of 3×10^{15} atom cm^{-3} using Cs^+ bombardment negative SIMS 77−65988
Si:As, diffusion of implanted As induced by laser annealing 77−89590
Si:As, elec. activation of implanted As during low temp. anneal, Hall effect meas. 78−51571
p-Si:As, electrochem. doping, depth profile analysis 77−72630
Si:As, electrochemical doping 79−90684
Si:As, electrochemical doping profiles 79−90685
Si:As, epitaxy, lateral autodoping kinetics 78−39699
Si:As, heavily As-diffused, Hall mobility and resist. rel. to carrier conc. 80−107815
Si:As, high conc. diffusion from double-layer sources 78−10075
Si:As, implanted, laser annealing reduction in defect conc. 77−62559
Si:As, implanted As redistrib. during annealing in oxidising ambient, carrier distrib. meas. 79−19275
Si:As, ion implanted, annealing characts., elec. props. 77−19974
Si:As, ion implanted, anomaly of elec. activation by additional Ne irradiation 78−84211
Si:As, ion implanted, anomalous diffusion of As 79−14842
Si:As, ion implanted, formation of As complexes 80−59511
Si:As, ion implanted, glow discharge optical spectroscopy 78−22755
Si:As, ion implanted, low temp. thermal annealing 80−96552
Si:As, ion implanted, two-step annealing 78−18664
Si:As, ion implanted, two-step annealing, TEM study 79−82249
Si:As, ion implanted layers in device structures, boundary effects in laser annealing 79−73188
Si:As, laser annealing of implanted layers 77−55296
Si:As, melting by high power ns laser pulsing, As diffusion 78−79789
Si:As, planar and axial channelling of 800 keV As 77−19995
Si:As, relation between total and electrically active As conc. produced by diffusion 79−55773
Si:As, scanning electron beam annealing, spreading resistance, junction depth 80−75267
Si:As, solid solubility and thermal behaviour of metastable 80−75359
Si:As, solid solubility of As determ. by ion implantation, CW laser annealing 80−6517
Si:As ion implanted layers, annealing by CO_2 laser, doping profile shift 80−84965
Si:As thermal diffusion retardation by inert gas ion implantation 79−77616

semiconductor doping continued
Si:As$^+$, implanted, CW laser annealing, electron-beam induced current 80−100709
Si:As$^+$ sheet resistivity rel. to isochronal annealing and defect structures 77−76443
Si:As(B)(N)(P), conc. profiles of ions and recoiled N after implantation through Si_3N_4 films 79−55764
Si:As(P), depth profiling using Cs^+ bombardment and negative SIMS in UH vac. 79−99232
Si:As(P), oxidation-enhanced diffusion of impurities 79−46840
Si:As(Sb), MBE, n-type doping techniques 80−15126
Si:Au, autoradiographic detection of getter effect, Ar ion implantation 78−38739
Si:Au, diffusion, effect of C concentration 78−10076
Si:Au, p$^+$-n junction, quantitative study of Au atoms by TSC method 80−2458
Si:B, annealing mechanism of radiation change and dopants in pulsed laser irrad. ion implanted layers 79−46691
Si:B, autodoping during epitaxial growth from SiH_4 77−47476
Si:B, conc. depend. of B diffusion coeff. 80−39353
Si:B, conc. profile of implanted cryst., by $^{11}B(p,\alpha)$ chem. anal., annealing *(German)* 78−83843
Si:B, diffusion for very shallow defect free p$^+$-n junc. for solar cells 79−15218
Si:B, diffusion from BN source with H_2 injection, AES study 80−19986
Si:B, diffusion of As atoms from ion implanted layers, conc. profiles 77−43376
Si:B, diffusion of B atoms and growth kinetics of oxidation induced stacking faults, correlation 79−37720
Si:B, diffusion of B from B_2H_6-CO_2 system, lower temp. limit of 775°C 77−43232
Si:B, heavily doped, annealing characteristics obs., Ne^+ ions implantation for damage density control *(Japanese)* 78−18666
Si:B, heavily implanted wafers, secondary defect generation suppression by HCl oxidation 78−10069
Si:B, high conc. effects in ion implantation 80−75245
Si:B, highly-doped polycryst. thin film, growth kinetics and properties 78−44016
Si:B, implantation energy, rel. to dose, Szabo-Bogancs effect 78−38740
Si:B, implanted, effectiveness of charged vacancies in diffusion 80−34239
Si:B, influence of proton beam irrad. on concentration profiles *(French)* 77−51402
Si:B, ion implantation, anal. of disordered regions in crystal with Promiss protonograph 80−19823
Si:B, ion implantation, channelling and random distrib. of B ions meas. 77−47473
Si:B, ion implantation using B_2O_3-B mixture, Auger spectra, channelling anal. 79−4317
Si:B, ion implanted, comparison of range and range straggling 77−55293
Si:B, ion implanted, laser and thermal annealing compared, TEM obs. 78−75681
Si:B, ion implanted, laser annealed, Raman scatt., Fano interactions, lattice damage 79−78711
Si:B, ion implanted, localised defects, TEM study 78−87699
Si:B, ion-implantation doped, influence of radiation dose on diffusion processes 77−1141
Si:B, ionisation-assisted annealing 79−23628
Si:B, lateral effect of oxidation on B diffusion 80−29217
Si:B, lattice location of implanted ions after laser annealing 78−30660
Si:B, low conc. B diffusion using doped-oxide film 77−76431
Si:B, near intrinsic ⟨100⟩ and ⟨111⟩ samples, inert and oxidising ambients, diffusion, segregation 78−75882
Si:B, P, high temp. diffusion, effects of laser irrad. on diffused layer 79−14834
Si:B, p-n junction form. by B deposition and laser-induced diffusion 78−87690
Si:B, polycryst. film, piezoresistive gauge factor 77−12029
Si:B, polycrystalline, ion implanted, AES analysis 77−31690
Si:B, predeposition of B using BBr_3 78−55882
Si:B, proton-irrad.-enhanced diffusion 80−29227
Si:B, solubility and precip., and supersat. resulting by thermal predeposition 78−11232
Si:B, sputtering influence on distrib. profile of ion-implanted impurities 79−42091
Si:B, use of BN source to achieve high surface concentration of B *(Russian)* 80−107639
Si:B, using oxidised BN dopant source, sheet resist:, rel. to temp. and deposition time 77−43231
Si:B,As selective area simultaneous doping 80−34015
Si:B,P, anomalous diffusion 80−29229
Si:B,P, diffusion patterns obs., for SiO_2 deposited by means of centrifuge *(Bulgarian)* 77−76429
Si:B,P, high conc. diffusion without disloc. generation 78−10072
Si:B,P, simultaneous diffusion, radioactivation techniques 77−76622
Si:B amorphous film, CVD prep., EPR, elec. and optical props. 79−4558
Si:B deep diffusion at solid solubility limits for p-channel MOS IC 78−10070
Si:B deposition diffusion from B_2H_6, AES analysis 78−6085
Si:B diffusion at Si-SiO_2 interface, Auger spectra, Rutherford backscattering 80−70471
Si:B doping from BN sources, impurity transfer considerations 77−76441
Si:B effect of dopants on grain growth 80−54575
Si:B film, polycrystalline, deposition on Si wafer, doping effect on bending 79−95276
Si:B high-temp. diffusion, glass layer formation obs. 78−7069
Si:B ion implanted, strain profiles from X-ray rocking curves 80−107290
Si:B redistribution after oxidation, integro-differential eqn. 77−76453
Si:B_2O_3, analytic study of Si-B phase formed 79−19269
Si:B$^+$, TEM of lateral implantation effects near mask edges in wafers 79−37724
Si:BF_2^+, ion implantation appl. in semicond. device production 80−103383
Si:BF_2^+, recrystallisation of implanted amorphous layers, F migration 79−55763
Si:BF_2^+(Si^+,B^+), recrystallisation of implanted amorphous layers, elec. props. 79−55762
Si:B(Al), (P)(As)(In), ion implanted film, elec. prop. impurity depend. 80−24467
Si:B(As)(P), new paint-on diffusion source 77−4118
semiconductor doping continued
Si:B(BF_2), p$^+$-n junction form., ion implantation damage, leakage current 77−24334
Si:B(Be)(Li) ion implanted, channelling and random equivalent depth distrib. 80−100293
Si:B(P), diffusion induced imperfections, laser annealing, rel. to junction characts. 78−75678
Si:B(P), impurity-peak form. during proton-enhanced diffusion 79−55772
Si:B(P), ion implanted, polycryst. annealing characts. 77−24324
Si:B(P), ion implanted crystalline and amorphous laser annealing 80−97509
Si:B(P), ion implanted layers, carrier distrib. meas. precision 77−43603
Si:B(P), ion implanted processing parameters for diffusion redistribution 79−10871
Si:B(P), proton enhanced diffusion, vacancies diffusion length 80−29226
Si:B(P) polycrystalline thin film, plasma annealing, effect on elec. props. 80−7005
Si:B(P)(As), impurity diffusion from implanted layer, influence of radiation damage 77−76621
Si:B(P)(As)(Cu)(Fe), dopant profile changes induced by laser irrad. using SIM and backscatt. meas. 79−69148
Si:B(P)(Ge), strain distributions rel. to dopant conc., accurate determ. by X-ray Bragg reflection 77−19835
Si:B(Sb), deform. coeff. due to impurity diffusion 78−18671
Si:B(Sb)(P), microdefect formation depend on doping, Cu decoration, X-ray transmission topography, preferential etching 79−69120
Si:Ba, Geiger counter determ. of Ba by neutron activation 79−52816
Si:Be, ion implanted, correl. of atomic distrib. and implantation induced damage profiler 80−88199
Si:Bi, ion implanted, channelling obs. of pulsed Q-switched ruby laser annealing 80−59542
Si:Co, diffused distrib. and state of Co atoms 77−1146
Si:Co, diffusion coeff. of Co meas. 77−20126
Si:Co, diode minority carrier lifetime, Lax method meas., effect of Co diffusion 79−69525
Si:Co, high-temp. ion-implanted and diffused samples, Mossbauer spectra of ^{57}Co 79−51891
Si:Co, ion implanted, Co lattice location, channelling meas. 80−88201
Si:Co, study of impurity states 78−76020
n-Si:Cs, ion implanted, minority carrier lifetime and defect struct., annealing effect 78−6395
Si:D, ion implanted, D depth distribs., SIMS meas. 80−54279
Si:Fe(Au)(Pt)(Ag)(Ti), photoionisation cross-sections and energy levels 79−87060
Si:Fe(Cu), impurity segregation and microstructural changes by pulsed laser irrad. 79−82254
Si:Ga, As, sequential diffusion, radiotracer obs. 78−10073
Si:Ga, diffusion of impurity into cryst., doping profile 79−77621
Si:Ga, gettering of Au and Cu during Ga diffusion 78−91350
Si:Ga, LPE on Si, technique and characterisation 79−38751
Si:Ga, neutron irrad., Hall effect meas. of shallow donor levels 80−20124
p-Si:Ga, neutron transmutation counterdoped, shallow defect levels, Hall effect and photocond. obs. 79−87055
Si:Ga, sealed tube diffusion, Au and Cu gettering behaviour 77−76445
n-Si:Ga laser doped, segregation, Rutherford backscattering 80−103483
Si:Ga$^+$, impurity distrib. profiles using SIMS and Hall effect method 79−69152
Si:Ga(As) 80−19824
Si:Ga(Sb), epitaxial film, doping efficiency *(Japanese)* 79−73201
Si:Ge B, strain compensation, X-ray Bragg reflexion 80−39137
Si:H, amorphous, Brillouin scattering from acoustic bulk and surface waves 80−11425
Si:H, amorphous, model for variable gap intrinsic semiconductor 80−10988
Si:H, amorphous and crystalline, hydrogenation and dehydrogenation, luminesc. spectra 80−11477
Si:H, amorphous films, absorption edge and doping 80−29042
a-Si:H, depletion width determ. by analytical model 80−100445
Si:H, evaporated amorphous film, prep. elec. cond. and photocond. 79−38201
Si:H,Li, amorphous, DC electrical conductivity, absorption edge and IR meas., role of H 80−54694
Si:H,Li, amorphous, photoluminescence obs. 80−66280
Si:H amorphous film, sputtered in Ar-SiH_4 mixtures, props. 79−87023
a-Si:H film, glow discharge deposited, H profiles, doping level 80−84202
a-Si:H:F, depletion width determ. by analytical model 80−100445
Si:H(Li)(Ni), amorphous, vac. evaporated, doping, transport and optical props. 80−49715
Si:Ho(Gd)(Yb), impurities behaviour, dynamic nucl. polarisation 79−78568
Si:In, dopant energy levels, Hall meas. interpretation 80−107736
Si:In, doping conc., meas. by Hall, C-V and junction breakdown methods 79−14824
p-Si:In, ion implanted, doping profiles from capacitance-voltage characts. 80−88203
Si:In, neutron irrad. to compensate for residual B, photocond., IR focal plane array 78−67727
Si:In, new acceptor level determ. from Hall effect and photocond. meas. 77−66136
Si:In(Sb), incorporation of implanted impurities during amorphous layer regrowth 79−55761
Si:K, ion implanted, influence of doping and annealing on carriers 78−38742
Si:Li, amorphous, elec. cond. and thermopower 79−73537
Si:Li, amorphous, interstitial doping by in-diffusion and implantation and elec. characterisation 78−26585
Si:Li, amorphous, thermopower and cond. meas. 79−69142
p-Si:Li, dislocation free, minority carrier lifetime, effects of heat treatment *(Japanese)* 79−65492
p-Si:Li, electrolytical doping, depth-profile anal. 79−77623
Si:N, amorphous, prep. by RF sputtering and props. 80−44229
Si:N, high energy ion implantation of buried insulating layers 80−88188
Si:N, implantation at high doses, annealing conditions for homogeneous buried insulating layer *(French)* 80−59498
Si:N, ion implanted, oxidation characts. 80−89385
Si:Na ion implanted, Hall effect temp. depend., electron surface density and mobility 80−11018
Si:Na(K)(Cs), amorphous, ion implanted, control of cond. 79−60835

semiconductor doping continued
Si:Ni,Co,Mn, γ-irrad., interaction of deep-level impurity atoms with radiation defects 77−76457
Si:O, annealing behaviour of O donor, conc. reductions via resistivity meas. 79−51129
Si:O, CVD layer, RHEED study of surface crystallinity, annealing effect on structure 79−69371
Si:O, evaporated amorphous film, effect of O_2 on props., ESR spectra 80−11265
Si:O, implanted O location, channelling effect meas. 78−26593
Si:P, amorphous, CVD, defect compensation 80−54644
Si:P, amorphous, CVD, substitutional doping, electronic props. 79−23923
Si:P, amorphous, substitutionally doped CVD, electrical props. 79−99566
Si:P, and of P diffused layers 78−38736
Si:P, anomalous doping profiles, numerical anal. 79−73206
Si:P, Au, neutron irradiated, distrib. of P and Au determ. 78−79627
Si:P, Au gettering by P diffusion and P-induced dislocations 78−91346
Si:P, BF_2^+ ion implantation, anomalous carrier profiles 80−2048
Si:P, carrier mobility and distrib. rel. to annealing, 400-910°C 78−79995
p-Si:P, Cu, influence of Cu on diffusion of P meas. 77−1267
Si:P, Cu(Au) radiation-doped, influence of growth defects on elec. props. 79−69144
Si:P, Czochralski growth, dopant evaporation coeffs., resistivity distrib. 77−16487
p-Si:P, defect energy levels, ion implantation effects, Hall coeff., sheet resist. meas. 77−85173
Si:P, diffusion from ethylene glycol grown anodic oxide 77−76440
Si:P, diffusion of P, 900-1100°C, distrib. of excess vacancies 77−72631
Si:P, diffusion of P impurities stimulated by gas discharge Ar plasma, low temp. 80−6560
Si:P, diffusional doping, diffusion-induced strain and dislocation effects 79−42084
Si:P, diffusivity, strain-induced band gap narrowing, E-centres 80−29228
Si:P, diffusivity, versus Si oxidation rate 77−15436
Si:P, distrib. of implanted impurity after laser annealing, e.s.r. and neutron activation analysis 77−4122
Si:P, doped by neutron transmutation, lattice defects 80−34018
n-Si:P, doping, by zone melting using solid dopant source 78−43035
Si:P, doping by diffusion from phosphosilicate glass sheets *(German)* 77−39604
Si:P, doping by neutron transmutation, residual radioactivity 79−33009
Si:P, doping during growth from gas phase, thermodynamic analysis 80−59489
Si:P, electrostatic field on impurity atoms, heavy doping effects 78−51570
Si:P, emitter-misfit dislocation formation during P diffusion 78−91338
Si:P, epitaxial layer, vapour phase grown, temp. dependence of dopant inclusion, differential molar solution enthalpy *(German)* 79−52128
n-Si:P, etched, high sensitivity temperature sensor, 1-10K 77−13757
Si:P, excess vacancy generation by P diffusion *(Japanese)* 77−89460
Si:P, float-zone cryst. growth, shape of melt interfaces and radial P distrib. 77−24952
Si:P, Gd, optical orientation of ^{29}Si nucleus, effect of donor level implantation depth *(Russian)* 77−8452
Si:P, Ge, simultaneous diffusion processes, elastic stress influence 77−89591
Si:P, heavily doped, diffusion of Au 77−51550
Si:P, heavily ion implanted, polycrystalline, grain growth 79−19477
Si:P, homogeneous epitaxial layers, production, appl. of neutron transmutation doping 78−38737
Si:P, homogeneous nuclear transmutation technique, thyristors appl. 80−70236
Si:P, implanted low temp. annealed, elec. activation, damage depend. 80−88182
Si:P, impurity cond., hopping conduction and the Coulomb gap 80−44605
Si:P, incoherent light flash annealing, elec. props., backscattering spectra 80−97504
Si:P, ion implantation, effects of high dose rate 78−83835
Si:P, ion implanted, damage layer props. obs. using ellipsometric parameters *(Russian)* 77−43234
Si:P, ion implanted, ionisation enhanced annealing, resist. changes meas. 78−30667
Si:P, low energy and high dose ion implantation, through SiO_2 film 77−15435
Si:P, N implantation through Si_3N_4 film, depth distrib. of knock-on N, SIMS meas. 78−10066
Si:P, neutron transmutation doping distrib. by emitted β-radiation meas. 77−19977
Si:P, neutron transmutation doped, electron trap annealing, deep level transient spectra 78−14368
Si:P, neutron transmutation doped, EPR obs. of annealing behaviour 79−1453
Si:P, neutron transmutation doping, elec. props. rel. to neutron fluence 80−96555
Si:P, neutron transmutation doping, resist. homogeneity rel. to compensation ratio 80−96556
Si:P, polycryst., growth in epitaxial reactor at 800°C, using PH_3 doping 77−1815
Si:P, polycryst., neutron transmutation doped, elec. props. 78−34836
Si:P, polycryst. etching characts. in CF_4 plasma 78−76777
Si:P, polycryst. films, elec. props., EPR, defect states, doping effects 80−75660
Si:P, quantitative model for diffusion of P and emitter dip effect 77−76611
Si:P, secondary defect generation suppression and diffusivity restraint by HCl oxidation 79−70191
Si:P, SiP precipitation concomitant with P predeposition 77−24326
Si:P, solid planar source for diffusional doping, with SiP_2O_7 active component 77−1139
Si:P, spin-on borosilica diffusion source, doping uniformity factors 77−76442
Si:P, sputter-deposited polycryst. films, resist. meas. 78−14842
Si:P, stacking fault and dislocation growth induced by P predeposition 77−59023
Si:P, strain-induced band-gap narrowing effect on P diffusion 79−55935
Si:P, through-oxide implanted samples, anomalous residual defects after annealing 77−76432

semiconductor doping continued
Si:P, uniaxially deformed, multiparticle impurity complexes, luminesc. spectra *(Russian)* 79−4854
Si:P,B, wafer, long range enhancement of B diffusivity induced by high surface conc. P diffusion 79−46687
Si:P amorphous films, doping and annealing effects on localized states, ESR meas. 79−38380
Si:P Czochralski crystal donor homogenisation by thermal neutron irradiation 78−6108
Si:P film, polycryst. pulsed electron beam annealing 80−10566
Si:P non-Fickian diffusion, parameter depend. on doping level and impurity gradient *(German)* 80−54440
p-Si:P p-n junctions, dislocations investig. rel. to P diffusion, SEM, X-ray topography techniques 77−76433
Si:P polycrystalline layer, role in lattice defect reduction assoc. with P predeposition 80−70229
Si:P solar cell, minority carrier lifetime degradation during ion implanted processing, surface photovoltage 79−39305
Si:P^+, ions implanted through SiO_2 mask window, lateral spread 79−77627
Si:P^+, misfit dislocation net propagation due to osmotic forces 79−65108
Si:P^+ ion implanted single crysts., secondary defects development during annealing 80−44228
Si:$P^+(As^+)(Sb^+)$, implantation damage removal by laser irrad. and its thermal stability, TEM study 79−74024
Si:P(As)(B)-SiO_2 interface oxidation kinetics, high doping levels, experiment 80−11828
Si:P(B), high temp. impurity diffusion via vacancies and self-interstitials 80−24667
Si:P(B) effect of impurities on solar cell performance 80−55848
Si:P(O) p^+-n-n^+ solar cells, comparison rel. to resistance to 1.5 MeV electron irrad., majority carrier trapping 80−94087
Si:Pb, diffusion behaviour of Pb in high dose implanted Si layers during isothermal annealing 79−1525
Si:Pb, ion-implanted and annealed, dose depend. of residual lattice disorder 77−43228
Si:Sb, diffusional doping by doped oxide method 80−15127
Si:Sb, dopant implantation, activation analysis errors due to isotope comp. *(German)* 80−34037
Si:Sb, dopant microsegregation rel. to crystal and crucible rotation 78−11106
Si:Sb, epitaxial film, growth by mol. beam technique 80−2292
Si:Sb, implantation of Sb for buried layers appl. *(French)* 77−80527
Si:Sb, ion implantation combined with vacuum deposition of Si 79−47631
Si:Sb, ion implanted doping, isotopic composition shifts on neutron activation determination 80−24487
Si:Sb, MBE film, doping technique 80−79821
Si:Sb, produced by ion implantation and laser annealing, Sb behaviour above solid solubility 80−88200
Si:Sb,As, autodoping effect of Sb-As simultaneous diffusion 77−80522
Si:Sb,P, double implants, residual defect reduction after damage anneal 80−88170
Si:Sb crystal Czochralski growth, radial microsegregation analysis 78−11105
Si:Sb vacuum deposited coating, p-n junction, pulsed electron beam annealing doping, diffusion 80−75480
Si:Sb(Ga)(Bi)(In), dopant solubility limit, laser irrad. effects 80−84295
Si:Se, detector for 3-5 μm appl. development 79−35825
Si:Se, energy levels, resistivity and Hall coeff. 79−69528
Si:Te, laser melting, surface Te atom accumulation, profiles 80−100258
Si/surface porous oxide film, impurity distrib. during P diffusion 77−39944
Si-Au Schottky barrier solar cell fabrication, doping of a-Si 80−50969
Si-B, exam. of two stage diffusion of B, under a gas phase oxide film 79−95044
Si-B, P diffusion and activity after Ar ion bombardment 78−95192
Si-B, using BN, expt. *(Bulgarian)* 78−59824
Si-borosilicate glass, B impurity diffusion, separation factor estimation 79−86926
Si-F-H:P, film, dark cond., struct., Raman scatt. 80−88588
Si-Ge, solid solns., doping characts. 78−22745
Si-H, amorphous plasma deposited film, H content and density 79−82472
Si-H:As alloy, amorphous film, coordination of impurities, EXAFS of data 77−84780
n-Si-Se, ion implantation studied by deep level transient spectroscopy 78−10392
Si-SiO_2, Al-implanted, low-temp. annealing effect on charge and surface state density 77−85337
Si-SiO_2, interface, doping depend. of interface states and charges 80−92992
Si-SiO_2 interface, Au traps 80−20319
Si-SiO_2 interface oxidation kinetics, high doping levels, theory 80−11827
Si(:Au), gamma-induced trapping levels 79−87059
n-SiC (6H), doping effect on birefingence dispersion, effective electron mass 79−69807
SiC, crysts., tetrahedral bond deformation variation with hexagonality and doping degree of N 79−94977
SiC, N doping inhomogeneities due to growth conditions 78−22741
SiC:Al epitaxial layers, growth, Al distrib. and solubility 80−15391
SiC:Al^+ p-n junctions, elec. props., defect effects 80−15594
SiC:B(Be), dislocation induced deceleration of impurity diffusion 77−28043
SiC:Be, gas-phase equilib. comp., thermodynamic analysis rel. to cryst. growth and doping 77−85909
SiC:N, conversion factor at high doping levels 78−22744
SiO_2:P films, P content determ. by IR absorpt. and activation anal. 79−51139
SiTe:Ge(Sn), substitution of Si, thermoelectric props. *(Russian)* 80−11023
$^{30}Si(n,\beta)^{31}P$ transmutation doping 78−6107
$^{30}Si(n,\beta)^{31}P$ transmutation doping and electrical characterisation 78−10071
SnO_2, electro-conducting transparent film, props. rel. to production method *(Japanese)* 80−25557
SnO_2, film, diffusion of impurities *(Japanese)* 79−95218
SnO_2, film, effects of Sb and In additions on struct. and resist. 77−20469
SnO_2:As film, prep. and elec. cond. 80−2959

semiconductor doping continued
SnO_2:P, CVD films, elec. props., cryst. to amorphous transition effects 80−107933
SnO_2:P, CVD growth and etching charact., doping effects 80−107667
SnO_2:Sb, transparent cond. film prep. by thermal decomp. of Sn salt of organic acid *(Japanese)* 77−90269
SnO_2:ThO_2, exposed to H_2, temp. depend. of resistivity 79−56219
$SrTiO_3$:B layers, ion implanted, conductive props. Hall mobility, defect energy levels 79−82693
Te:I, semicond., elec. efficiency *(German)* 78−84166
TiO_2, doping processes, influence on photoelectrochem behaviour 80−79822
TiO_2, electrochem. doping 77−76430
n-TiO_2 photoelectrochemical electrodes, effect of Nb doping on quantum efficiency 80−101121
TiO_2:S, acceptor properties of S, free electron concentrations 80−34395
VO_2, thin films, doping by ions of Ar, B, P 77−84781
VO_2:Al(W), thin layer prep. by reactive DC sputtering doping effectiveness *(German)* 78−6847
VO_2:M^{3+}, M=Al,Ga,Fe, anisotropy of thermoelec. power, hole conductivity 77−11946
V_3O_5, metal-insulator transition, effect of doping *(German)* 78−30869
V_3O_5, Mo,Ti, and Ga doping effects on conductivity transition 77−11971
(W-Au)-SiO_2-Si:B MOS transistor, ion implantation effect on threshold voltage 78−34903
YIG:Si single crystals, liq. flux growth, obs. 80−66416
$Zn_xCd_{1-x}S$:Cu, photoluminescence 80−29783
ZnO, defect struct. calc., doping effects 80−107218
ZnO:$^{31}P^+$ implanted nonlinear resistor production and characteristics *(Russian)* 80−49252
ZnO:Ga sputtered films, props. rel. to deposition conditions 80−107935
ZnO-based ceramic microstructure and nonlinear props., B diffusion effects *(Russian)* 80−49423
Zn_3P_2, single crystal, growth, electronic and device props. 80−25551
ZnS, dependence of hexagonal layer formation on dopant conc. 79−19265
ZnS, low resistivity, prep. and characterisation for blue LEDs 77−81209
ZnS:Cu, film effect of Cu valency on cond. 79−11246
ZnS:Mn, dopant conc. effect on stacking fault energy 80−2041
ZnS:Ne, implanted single crysts., photolum. and bombardment effect, thermolum. curve obs. 80−55166
ZnS:Tl(Al)(Zn), UV spectra of donor-doped single crysts. 77−12404
ZnSe:Ag(In)(Cu), melt growth, dopant partition coeffs. 79−14837
ZnSe:Al, vapour phase doped, thermodynamics 79−90686
ZnSe:Al(Ga)(In), single cryst., doping, blue luminesc. 78−39584
ZnSe:Al(Mn), elec. and luminesc. props. 77−39844
p-ZnSe:As, ion implantation and heat treatment 78−87700
ZnSe:B(F), ion implantation, photocond. and cathodoluminesc. meas. 78−26586
ZnSe:Ga,As, charact. of simultaneous incorporation, by Mn^{2+} ESR and X-ray fluoresc. anal. 80−34017
ZnSe:Ga(As), edge luminesc. 80−20699
ZnSe:I, I vapour transport prep., conductive and photolum. cryst. 79−100035
ZnSe:In, single crysts., new vapour phase growth method, elec. cond. props. and photoluminesc. spectra 79−19982
ZnSe:In elec. transport props., effect of Zn-annealing, 300 to 77K 78−76075
ZnSe:In films, MBE growth, doping effect on photoluminesc. 80−10818
p-ZnSe:Li(Na)(N)(P), LPE layers, photocapacitance and photocond. meas. 79−99572
ZnSe:N, ion implanted cond. type conversion on annealing *(Korean)* 78−18668
ZnSe(:Ga)(Al), effect of thermal treatment and doping on elec. props. 77−85223
$ZnSiP_2$, effect of crystal growth method, on physical props., effect of doping on physical props. *(German)* 79−52094
ZnTe, anomalous penetration of implanted ^{65}Zn and compensation zone build up 77−19975
ZnTe, doping and intrinsic stoichiometric defects, self-compensation 80−59918
ZnTe, growth from In solvents, self-compensation 77−28144
ZnTe, optical identification of substitutional acceptors by low temp. photoluminescence 79−99940
ZnTe:Ag, doped during frowth and by diffusion, defect form. 80−15129
ZnTe:Cr(Mn)(Fe), exciton refl. spectra 80−2806
ZnTe:Cu, doping behaviour, SEM in cathodoluminesc. and photoluminesc. exam. 79−65927
ZnTe:Li, diffusion investigation by SEM and TEM 80−10706
ZnTe:Li, impurity segregation during short annealing and quenching, SEM, TEM and elec. meas. 80−10676
ZnTe:Li(Cl)(Al)(In), ion implanted and annealed, photoluminesc. meas. 78−15208
ZnTe:O,Zn, dual ion implantation, luminesc. spectra obs. 78−87697
ZnTe:P(As), ion implanted, cathodoluminescence emission spectrum 80−108281
ZnTe:P(Li), luminesc. transitions, quantum efficiency 79−1783
ZnTe:Sb, film, electrical props. 78−76172

semiconductor-electrolyte boundaries
anthracene, cryst., with electrolytic contacts, photocurrent anomalous behaviour, current-volt. charects. 77−39933
anthracene, cryst.-electrolyte system, pot. well, hole residence time 77−8190
anthracene, crystal-electrolyte interface, ionis. energy of uppermost cryst. mols. 78−27764
anthracene crystal, sensitised injection from surface oxidation products 78−76143
book contribution 79−1621
CdTe thin polycrystalline film for photoelectrochemical cell 78−23162
charge transfer via surface states, water photoelectrolysis anal. 80−75636
chrysene, crystal-electrolyte interface, ionis. energy of uppermost cryst. mols. 78−27764
compound semiconductor interfaces, conf., Los Angeles, USA (Jan. 1978) 78−91756
conduction noise *(French)* 80−20306
covalently-bound dyes on semiconductor surfaces in new type of photocell 77−69414

semiconductor-electrolyte boundaries continued
current flow, study of semicond. using electrochem. techniques 78−95356
current-voltage charects., effect of mechanical deform. 78−68082
defect doped semiconducting electrodes, ageing effects 79−69592
differential capacitance measurement by desk calculator controlled system 79−78170
digital simulation, charge injection, space charge region 77−15949
digital simulation, open-circuit photopotential 77−15950
digital simulation, photogenerated free carriers and photocurrent relax. 77−15951
doping inhomogeneity, meas. by low field electrorefl., in semicond.-electrolyte config. 77−11584
electrode, interpretation of selective etching, electrochem. props 80−7703
electrodes for light energy conversion and storage 78−14813
electroluminescence due to hole injection from electrolyte into n-type semicond. electrode 77−20926
electrolytic decomposition and photodecomposition 78−95357
electron injections from semicond electrodes liq. NH_3 80−6977
excited electronic state, photoelectrochemistry 78−76872
film-covered metal electrodes, electron transfer reactions 78−20024
flat band potential determ. *(French)* 79−99613
flat band potential from Mott-Schottky plot 78−34896
flatband, potentials, prediction from atomic electronegativities 78−40068
flatband potentials, temp. depend. 78−60201
hot carrier injection, tunnelling from semiconductor states in depletion region 80−75637
impedance measurement of boundary, ohmic drop correction *(French)* 79−70332
interfacial tension, elec. field depend. 78−87845
IR photographic methods 79−93243
molecular crystal/electrolyte interface, illuminated, space charge behaviour 78−84290
n-type semiconductor, thermodynamic pot. for anodic dissolution, rel. to photoelectrochem. cell efficiency 78−26948
n-type semiconductor anode, illum., charge transfer modes, digital simulation 80−2464
naphthalene, crystal-electrolyte interface, ionis. energy of uppermost cryst. mols. 78−27764
oxide electrodes, electron transfer reactions, tunnelling through a space charge barrier 78−80050
oxide O_2 electrode charects. 79−24073
oxide semiconductors in photoelectrochemical conversion of solar energy, use as cell anodes 80−101120
oxide-water, photoassisted electrolysis 77−69413
perylene, crystal-electrolyte interface, ionis. energy of uppermost cryst. mols. 78−27764
phenanthrene, crystal-electrolyte interface, ionis. energy of uppermost cryst. mols. 78−27764
photocharacteristics for electrolyte-semiconductor junctions 78−91764
photochemical diode using p-n heterojunction or Schottky barrier immersed in electrolyte 77−66201
photoelectrochemical cells, energy conversion system, principles and appl. 80−89652
photoelectrochemical cells, semiconductor based, interaction of light and transport control 80−12020
photoelectrochemical cells with semiconductor electrodes for solar energy conversion and storage *(French)* 80−61386
photoelectrochemical generation of H_2 at p-semiconds. 77−89844
photoelectrochemical processes, at semicond.-electrolyte interfaces, efficient electrode materials 79−29478
photoelectrochemical processes, hologram recording utilisation 77−88667
photoelectrochemical solar cells, semiconductor/redox electrolyte junctions, functions examples and problems 80−45714
photoelectrochemical solar energy conversion principles, review 80−35695
photoelectrode, appl. in reproducible photoelectrochem. imaging 80−14446
photoelectrode kinetics of H_2 evolution reaction at semicond. electrodes 78−44388
photoelectrolysis, role of semicond. props. 78−14816
photoelectrolysis, semicond. electrode requirements and props., book contrib. 79−65547
photoelectrolysis cell for solar energy conversion 77−20423
photoelectrolysis cells, props. of oxide-based heterostruct. photoelectrodes 80−12023
photoelectrolysis irreversibilities 78−23161
photoelectrolysis of water, appl. to solar energy conversion 79−29477
photoelectrolysis of water with semicond. materials 78−2562
photoelectrolysis of water with semicond. surface, review *(Japanese)* 78−6440
photoexcited semiconductor electrode, I-V curve 78−14811
photovoltaic cells, interface charge transfer, recombination rate, C-V charects. 80−70818
photovoltaic effect, phenomenological theory and expt. confirmation 80−15601
pyrene, crystal-electrolyte interface, ionis. energy of uppermost cryst. mols. 78−27764
semiconducting oxide electrode, O_2 reduction kinetics improvement 78−20029
semiconducting oxides, interband transitions determined from photoelectrolysis spectra 79−65378
n-Si-electrolyte junction, Schottky barrier height and reverse current 80−6979
solar cell, efficiency, electrochemical stability and surface preparation 78−14817
solar cell, minority carrier transfer, energy levels role 78−39209
solar cells, electrochem. liquid-junction, Schottky barrier height, photovoltage and photocurrent 80−26162
solar cells (Becquerel effect), fundamentals and appl. *(Spanish)* 79−96447
solar photoelectrolysis with semiconductor electrodes, photodecomposition of electrodes 79−74533
sulphide minerals, two-layer capacitance meas. *(Russian)* 78−10551
surface state charge transfer in photoelectrolysis of water 79−28405
TCNQ salt in aqueous media, electrochem. behavior 80−6976
thin film electrode, photosensitization by cyanine dye in lipid bilayer 80−75639
transfer of electrons and ions in and on semiconductors *(French)* 80−6935

semiconductor-electrolyte boundaries continued
transition metal, group VIa, layered dichalcogenides, hole reactions, electrochem. solar energy conversion appl. 79−7893
wet type solar cells with semiconductor electrodes dye sensitised, aspects 79−29474
zero bias electrodes, photosensitive props., correl. with electronegativity 77−44482
$BaTiO_3$ electrode, surface comp. changes during photoelectrolysis, XPS obs. 79−7894
$BaTiO_3$ electrodes, photocurrent efficiency, photo-oxidation of water 77−12000
CdS electrode, in aq. soln., flatband potential, effects of dissolved Cd^{2+} and S^{2-} ions 77−51815
CdS electrode, photoexcited, charge transfer in electrolyte with Na_2S additive 79−99618
n-CdS electrode in DMF solns., electrochem., photoelectrochem., redox. pot. determ. 79−96322
CdS, photoanode, flat band pot., depend. on surface ion effects 79−62013
CdS photoanode, for photovoltaic cells, prep. and characts. 78−14818
CdS, photoanodes in sulphide-polysulphide electrolytes, instability 78−80755
n-CdS, photoanodic behaviour in acetonitrile-iodide solns. 78−47868
CdS polycrystalline thin-film liq. junction photovolt. cell 80−50988
CdS, semicond. film, contoured anodic photodissolution 79−74277
CdS, single cryst. surfaces, diffr. gratings, electrochem. recording of holograms 80−32934
CdS:Te-based photoelectrochem. cell, luminesc., thermal manipulation of deactivation processes 80−81479
n-CdS-CdSe mixed polycryst. electrode for photoelectrochem. cell 78−47867
CdS-GaAs n-n voltage-enhanced photoanode, solar cell efficiency 78−14810
CdS-$NiCl_2$ interface, elec. props. using SAW techniques 79−56302
CdS-$NiCl_2$ interface, transverse acoustoelec. voltage spectroscopy 80−49828
CdS(Se) photoanodes, effect of S(Se) substitution, photoelectron spectroscopy obs. 80−2463
CdS(Se)-based photoelectrochem. cells, characts. 77−25287
n-CdS(Se)(Te) semicond. liq. junction solar cells, photocurrent spectra, carrier recombination 78−76142
CdSe, chemically sprayed thin films as photoanode in photoelectrochem. cells, power charact. meas. 80−85293
CdSe electrochem. photovoltaic cells, effect of thin film electrode prep. and conc. on efficiency 80−55847
CdSe film photoanodes for electrochem. photovoltaic cells, fabrication and evaluation 80−76641
CdSe photoanode improved efficiency by photoelectrochem. etching 80−104512
CdSe photoanodes, S substitution during operation and mech. of surface protection 80−107906
CdSe, photoanodes in sulphide-polysulphide electrolytes, instability 78−80755
CdSe photoelectrode, immersed in polysulphide soln., S/Se substitution, XPS obs. 79−19656
CdSe photoelectrode, polycrystalline, for solar energy conversion 78−19147
CdSe(Te)-electrolyte photovoltaic cells, solar cell appls. 77−35990
Cd_2SnO_4 and Cd_2SnO_4:CdO, thin film electrodes in H_2SO_4 electrolytes, reduction, AES and SEM 80−65674
CdTe, minority carrier diffusion length from photocurrent meas. in semicond.-electrolyte boundary 80−65584
n-CdTe, semiconductor electrode, electrochem. behaviour in nonaqueous media *(French)* 80−66808
n-CdTe-electrolyte solar cells, interface changes during operation, AES, electrolum. and electroreflectance meas. 79−100525
CdTe-$SnCl_2$ electrolyte heterojunction photoelec. props., feasibility as solar energy convertors 77−76918
Fe oxide films, semicond. electrode props. 79−91093
n-Fe_2O_3 electrodes, characterisation and behaviour in acetonitrile solns. 80−25004
n-Fe_2O_3 electrodes, enhanced photoeffects by electrocatalysis and peroxide effects 80−16815
Fe_2O_3, semicond. anode in aq. electrolyte, electrolum. and electrochem. 80−76080
Fe_2O_3, sintered semicond. electrode, photoeffects 79−51669
Fe_2O_3-water, photoassisted electrolysis 77−77771
Fe_xO_y electrodes, photoassisted electrolysis of water 78−15683
Fe_xO_y film, semicond. model for electronic struct., high electronic cond. 80−2493
Fe_xO_y thermal oxide film on Fe, capacitance, temp. and freq. depend., in aq. electrolyte soln. 80−54776
$FeTiO_3$, Fe_2TiO_4, and Fe_2TiO_5 anodes, appl. to photoelectrolysis of water 77−63920
$FeTiO_3$, Fe_2TiO_4, influence of cryst. struct. on photoresponse of electrodes 78−43471
$Ga_{1-x}Al_xAs$ electrodes, interface capacitance meas., flatband pot., conduction and valence band boundaries *(French)* 79−33339
GaAs, automatic electrochemical Hall mobility profiling 79−99615
p-GaAs electrode, flatband pot. determ. from differential stress meas. 80−75638
p-GaAs, electrode, photoemission into electrolyte solns. 77−24616
GaAs electrode in acetonitrile solns., photoelectrochem. behaviour 79−4600
GaAs electrodes, n- and p-type, freq. depend. of impedance 77−12001
GaAs electrodes, photo-induced electrogenerated chemilum. and up-conversion 79−91510
n-GaAs electrodes in acetonitrile solns., liq. junction photovolt. cell 79−99617
GaAs electrodes in aqueous electrolytes, localised avalanche breakdown 79−4599
n-GaAs in DMF solns., electrochem., photoelectrochem., redox. pot. determ. 79−96322
n-GaAs, metal filmed photoelectrochemical cell, energy conversion characts. 80−101118
GaAs photoanode, using n/n^+ struct., power conversion efficiency 80−50990
n-GaAs semicond. liq. junction solar cells, photocurrent spectra, carrier recombination 78−76142
n-GaAs, VPE, hi-lo, carrier conc. profiling by electrochem. methods 80−49958
semiconductor-electrolyte boundaries continued
p-GaAs/electrolyte soln., electrode photoemission, energy diagram, Volta pot. 77−62990
p-GaAs/heptyl viologen system, appl. in photoelectrochemical cells and photoelectrochromic displays 80−76640
n-GaAs/K_2Se-K_2Se_2-KOH/C solar cell, Ru (III) chemisorption on photoanode, effect on performance 80−3516
n-GaAs/K_2Se-K_2Se_2-KOH/C liq. junction cell, effect of Ru ion chemisorption on grain boundaries 80−55879
GaAs-electrolyte 79−19657
n-GaAs-electrolyte interface, surface pretreatment rel. to photocurrent, spectral response 80−3204
GaAs-electrolyte interface, surface barrier electroreflection anisotropy *(Russian)* 80−34895
GaAs-Ga interface immersed in electrolytic solns., elec. props. 78−95368
n-GaAs-K_2Se-K_2Se_2-KOH/C thin film solar cell, 7.3% cell efficiency 80−93931
GaAs-NaOH interface, inversion layer form. and surface states 80−2465
$GaAs_{1-x}P_x$ electrodes, interface capacitance meas., flatband pot., conduction and valence band boundaries *(French)* 79−33339
$Ga_xIn_{1-x}P$ electrode, in aqueous electrolytes, impedance meas. *(French)* 79−87153
$Ga_xIn_{1-x}P$, flat band pot., impedance meas. and photoelectrochemistry *(French)* 80−49894
n-GaP, Au-coated semicond. electrode, photoelectrochem. behaviour in water 77−21399
p-GaP, cathode of photoelectrochemical cell 78−10552
p-GaP electrode, for solar cell, differential capacitance meas. for flatband potential determ. 78−72256
n-GaP electrode, photoanodic dissolution rate, effect on surface electronic band energies 80−103748
p-GaP electrode, spectral response extension by metal adatoms 78−34895
n-GaP electrode in DMF solns., electrochem., photoelectrochem., redox. pot. determ. 79−96322
p-GaP electrodes with metal adatoms, surface states form. due to impregnated H 80−54778
p-GaP, irrad. by visible light, photoelectrolytic decomposition of water 77−77778
GaP, minority carrier quasi-Fermi level meas. in illuminated photoelectrolysis cell 77−85308
GaP, n-, p-type, electrode, impedance in alkaline medium *(French)* 79−43586
GaP photoelectrode, role of Au overlayers 78−14812
GaP photoelectrode, stability 77−20422
p-GaP semiconductor-electrolyte solar cells for photochemical reduction of CO_2 to organic fuel 80−55880
GaP, single cryst. electrode, impedance, effect of freq., voltage and electrolyte comp. 78−19146
plGaP:Zn-electrolyte interface, electrochemical LED, luminescence obs. 80−84507
p-GaP-aqueous CO_2 liq. junction solar cells, CO_2 photoelectrochemical reduction 78−88649
GaP-liq. NH_3 soln. junctions, elec. characts. *(French)* 80−2460
GaP-NH_3 electrolyte interface, photo-assisted electron injection 79−87152
p-GaP-NaOH interface, Schottky barrier model of photoelectrochemical effect 80−55673
Ge electrode, cathodic characts. rel. to halide ions 79−57238
Ge, electrodeposited, X-ray, electrochem., and electrorefl. characterisation 78−14624
Ge, electrodes, photoemission into electrolyte solns. 77−24616
N-Ge, electrorefl. spectra, light induced, electrolyte and Schottky barrier techniques of meas. 80−76046
p-Ge in DMF solns., electrochem., photoelectrochem., redox. pot. determ. 79−96322
Ge surface states, recomb. centres, regularities, electrolyte contact effects *(Russian)* 80−65652
Ge surface states, recombination centre formation *(Russian)* 80−29459
Ge/electrolyte soln., photoemission, energy diagram, Volta pot. 77−62990
Ge-$Na_2S_2O_3$ interface anodic oxidation electron transfer 79−56304
H_2, review 80−61453
HgS, photo-stable semicond. in electrolyte soln., photo-EMF and photocurrent obs. 79−42637
II-VI semiconductor-electrolyte boundaries, electrolyte boundaries, photo e.m.f. meas., semicond. energy bands 77−1481
In_2O_3 semiconductor electrode, sensitised photocurrent by energy and electron transfer in dye monolayers 79−38119
InP, automatic electrochemical carrier conc. profiling 79−99614
InP carrier profiling using liq. barrier contact 78−76087
InP electrode in acetonitrile solns., photoelectrochem. behaviour 79−4600
InP electrode-electrolyte interface, Schottky barrier obs. 78−52079
InP electrodes, photo-induced electrogenerated chemilum. and up-conversion 79−91510
InP, N- and p-type electrodes in acetonitrile solns., photoelectrochemical behaviour 79−99616
n-InP photoelectrode, stabilisation to photoanodic dissolution, in aqueous solutions of Te^{2-}/Te_2^{2-} 78−14814
n-InP photoelectrode, stabilisation to photoanodic dissolution in solns. containing Te^{2-} and Te_2^{2-} 78−19144
InP-electrolyte struct., field effect of photoluminesc. 79−99928
n-$MoSe_2$ based liq. junction solar cell, nonaqueous electrolyte system employing Cl_2/Cl^- couple 80−81432
$MoSe_2$ layer-type electrochem. solar cells, electrode material performance, doping effect 79−74532
$MoSe_2$-I^-, photoelectrode, time resolved photocurrent, nanosecond excitation 80−45708
n-Si, Fe_xO_y-coated, heterostruct. photoanode for photoelectrolysis of water 80−61384
NH_3 electrolyte-semiconductor interface, photo-assisted electron injection 79−87152
Nb_2O_5 electrodes, in aq. and acetonitrile solns., electrochromism 80−50298
NiO and lithiated NiO, thermally grown, electrochemical capacitance variations 80−29475
NiO electrode for photolysis 80−40696
PbS, nonstoichiometric, increase of rest pot. with p-type semicond. character 78−56170

semiconductor-electrolyte boundaries continued
Sb_2O_3 electrolyte boundary, semicond-props. of anodically formed layer 79−56303
Si, amorphous, in contact with electrolyte, Schottky barriers at interface 79−78169
Si, electrochemical carrier conc. profiling 80−2461
Si, ion implanted, in HF electrolyte, characterization by electrolytic reverse current 78−6078
Si, ion-implanted surface, profiling method 78−95075
Si, surface characterisation by Si-electrolyte interface impedance meas. 78−84291
Si, thermally oxidised-electrolyte system, features of cathodic breakdown *(Russian)* 80−107907
Si:H, amorphous, photoelectrochem. behaviour 80−81480
p-Si:P(P^+) photolytic props. in HF 80−89504
Si/SiO_2-electrolyte interface, electron exchange at surface of thermally grown SiO_2 80−16696
Si-aq. $NaNO_3$(LiI) electrolytes, anodic current meas., Si carrier conc. determ. 78−60200
Si-electrolyte 79−19657
n-Si-electrolyte boundary, selective anodic oxidation 78−15563
Si-electrolyte contact, implantation profile meas. from capacitance-voltage characts. *(German)* 77−1145
Si-$NaNO_3$ aq. soln., anodic polarisation of semicond. electrode 77−11999
Si-SiO_2-KCl_{aq}, interface, capacitance meas. 78−80051
Si-thermal SiO_2-electrolyte system, cond. in superhigh elec. field 78−52080
SiC, surface luminesc. in presence of anodisation 78−52579
Sn/Te/electrolyte system, interface processes 77−63923
n-SnO_2 pigmented solar cell for electrolysis of water, two-photon process 80−93932
n-$SrTiO_3$ electrode, flatband pot. determ. from differential stress meas. 80−75638
$SrTiO_3$, electrode, surface photovoltage expts. 78−72227
$SrTiO_3$, photoanode water photoelectrolysis at high current density 78−15679
$SrTiO_3$ photoelectrolytic electrodes, defect surface states obs. 78−14815
$SrTiO_3$, semicond. anode in aq. electrolyte, electrolum. and electrochem. 80−76080
$SrTiO_3$ semicond. electrode, electrochem., photoelectrochem. props. 80−3352
$SrTiO_3$ semicond. electrodes, electroreduction process kinetics, cathodic dark current meas. 80−66807
$SrTiO_3$, transition metal doped anodes for water photoelectrolysis, response to visible and UV 79−74531
$SrTiO_3$-H_2O, H_2O photoassisted decomp. 80−85202
Te, polarographic prewave, photo-effect 77−36833
TiO_2 (rutile) photoanode, corrosion suppression by high-energy redox reactions 78−23163
TiO_2 anodes, corrosion suppression by high energy redox reactions 77−77599
n-TiO_2, crystal, in aqueous soln., electrochemistry and electrolum. meas. 78−48665
TiO_2, doping processes, influence on photoelectrochem behaviour 80−79822
TiO_2 electrode, chem. modification for dye sensitisation, rel. to H_2O oxidation 79−91964
TiO_2 electrode, doping density dependent attachment of rhodamine B 80−54777
n-TiO_2 electrode, flatband pot. determ. from differential stress meas. 80−75638
TiO_2 electrode, sensitised, photoelectrolysis of water in sunlight 78−19143
n-TiO_2 electrode in $AlCl_3$-NaCl melt, electrochem. and photoelec. props. 80−81328
n-TiO_2 electrode in photoelectrochem. cell, anomalous photoresponse 77−11998
TiO_2 electrodes, chemically modified, nature of surface states 80−107905
TiO_2 electrodes, electron transfer from rose bengal, photoelectrochem. meas. 77−66758
TiO_2 electrodes, in aq. electrolytes, surface states, photocurrent obs. 80−49895
TiO_2 electrodes in photoelectrochem. cell, photothermal effect 80−7947
TiO_2 films as solar photocatalysts, preparation 79−74530
n-TiO_2 photoanode, band bending at surface used to dissociate water under solar illumination 78−91765
TiO_2 photoanode, water photoelectrolysis at high current density 78−15679
n-TiO_2 photoanodes, corrosion suppression mechanism 80−2462
n-TiO_2 photoelectrochemical electrodes, effect of Nb doping on quantum efficiency 80−101121
TiO_2 photoelectrode, stability 77−20422
n-TiO_2, rutile anode, water photolysis 78−2563
TiO_2, semicond. anode in aq. electrolyte, electrolum. and electrochem. 80−76080
TiO_2, sputtering defects, associated surface electron states, UPS, XPS and AES obs. 80−60755
TiO_2, transition metal doped anodes for water photoelectrolysis, response to visible and UV 79−74531
TiO_2:Al(Y), polycrystalline photoanode, improved solar efficiency 79−96479
n-TiO_2:Be electrodes, photoassisted oxidation of water 80−30502
TiO_2:Cu, anodic, effect of Cu on optical props., rel. to possible appl. in solar energy conversion 80−16115
TiO_2:Nb semicond. electrodes, electroreduction process kinetics, cathodic dark current meas. 80−66807
TiO_2-aqueous electrolyte interface, pot. distrib., Mott-Schottky plots 80−11084
n-TiO_2-electrolyte interface, electrolum. obs. 79−47520
n−TiO_2-electrolyte interface, equivalent circuit elements from impedance meas. 80−39669
n-TiO_2-electrolyte interface, charge-transfer-controlled photocurrent 80−50992
n-TiO_2-electrolyte interface, charge transfer via surface states, water photoelectrolysis anal. 80−75636
n-TiO_2-electrolyte interface impedance, freq. depend., equiv. cct. 80−100516
n-TiO_2-KOH-Pt cell, water photolysis, H_2 partial press. 78−64858
semiconductor-electrolyte boundaries continued
TiO_2-NH_3 electrolyte interface, photo-assisted electron injection 79−87152
TiO_2-O_2/OH^- photoelectrochemical cell, temp. effects on performance 79−92084
TiO_2-water, H_2 prod. using solar energy 77−11956
TiO_2 electrodes, effect of processing variables on photoelectrochem. props 80−6975
TiO_2 electrodes, room temp. diffusions, capacitance, spectral response and volt-ampere characts. 80−15294
WO_3 anode, props. and appl. to photoelectrolysis of water 77−66757
WO_3 electrodes, electrochem. and photoelectrochem. behaviour 78−26949
WO_3, semicond. anode in aq. electrolyte, electrolum. and electrochem. 80−76080
WSe_2 d-band semicond., photoelectrochem. props., electrochem. solar cell appl. 79−66411
n-WSe_2 electrode in aq. iodide medium, high efficiency photoelectrochemical solar cell 80−72069
$YFeO_3$ photoanode for photoelectrolysis of water 77−81409
ZnO (0001) surface, hardness, electrolyte pH and bias voltage effect 78−47654
ZnO ($10\bar{1}0$) surface bias voltage effect on hardness, charge exchange near dislocations 78−52078
ZnO accumulation layers, electrolytic contact quantisation effects, self consistent quantum calcs. 79−60920
ZnO electrode, in aq. soln., phototransition at 380 nm, anodic photocurrent obs. 78−19145
ZnO electrode, reson. Raman spectra of adsorbed rose bengal 78−76446
ZnO electrode, role of triplet states in xanthene dye sensitisation 78−76869
ZnO, sintered, for dye-sensitised solar photocell 80−16816
ZnO surface, photocell, enhancement of photoelec. effect by organic additives 79−57437
ZnO-electrolyte contact current-potential characts. 77−1482
ZnO-electrolyte interface, electron transfer sensitisation by salt additions 78−34894
n-ZnO-rubrene, radical cation reduction, triplet state formation, luminesc. 77−16825
ZnS crystals in electrolyte, electrolum. and elec. props. 80−93407
ZnSe:I/aqueous electrolyte junction, electrochem. behaviour in dark and under illum. 80−25003
ZnSe-electrolyte junction, current photoresponse 79−82669
p-ZnTe, interface impedance in KOH electrolyte soln. *(French)* 77−51814
ZnTe single crystal electrodes, non-intentionally doped, electrochem. props. *(French)* 79−96326
ZnTe-electrolyte interface, electrochem. behaviour of single crysts. 79−91138

semiconductor electron states *see band structure of crystalline semiconductors and insulators; electron energy states of amorphous solids; electron energy states of liquid semiconductors*

semiconductor epitaxial layers
anodic thinning below avalanche breakdown potential 78−10309
autodoping, lateral variation model 80−103595
binary compounds, LPE, book contrib. 77−12553
C GaP on GaAs substrate, heteroepitaxial layers, stuct. defects *(German)* 79−23865
carrier concentration profile, p-n junc. and Schottky barrier differential capacitance obs. 77−12036
carrier density and mobility meas. using a long gate MOSFET structure 79−47178
characterisation, on high resistivity substrates, by MESFET 79−87170
coeff. and surface conc. 80−39122
compound semiconductor, heteroepitaxial growth and characterisation, book contrib. 79−83133
CVD, appl. to Si, II-VI and III-V semiconductor growth 77−32530
CVD epitaxy, book contrib. 77−12544
deep level profile anal. by double deep level transient spectrosocpy 77−20378
deep level studies, growth by time difference method at controlled vapour pressure 80−39522
depth profiling by electron beam induced junction current meas. 80−96977
diamond:B, charge transfer and acceptor state 78−19169
diamond-like semiconductor film epitaxial growth, computer simulation 80−70560
direct-gap layers, optical compensation profiling 77−76450
dopant profile and Schottky barrier height determ. by second differential method *(Chinese)* 80−49257
doping profile using ellipsometric meas. 79−99453
doping reduction using zone recrystn. with temp. gradient 80−104062
electrodeless measurement of resist. and spherical curvature 79−49252
evaporated compound films, formation and structure *(Japanese)* 78−22979
film-substrate boundary, epitaxial interface form. and transition regions 80−10821
free carrier profile measurement on thin-layers, fast current pulse MOS deep-depletion technique 78−80075
free-carrier density determ. by Hall meas., surface and interface depletion corrections 79−91170
$Ga_{1-x}Al_xAs$ LPE growth: composition control and growth rate analysis 79−95946
n-GaAs, persistent photocurrents, Hall effect anal. 79−87130
GaAs MBE growth, deep levels effect on electron and hole trap densities 80−49652
GaInAsP quaternary alloys, orientation effects in LPE growth 78−92203
GaP/$In_xGa_{1-x}P$/GaAs:(Cs-O) high sensitivity transmission photocathodes, photosensitivity, electron diffusion length 79−78832
graded gap layer as broad range photodetector 78−74060
groove and tunnel growth mechanism 80−10804
growth and doping of films by MBE 77−73239
growth with ionised beams and surface imperfections 77−32529
heteroepitaxial, electrical characterisation, book contrib. 79−82699
heteroepitaxial, on insulating substrates, characterisation, book contrib. 79−82497
heteroepitaxial film deformation, causes and countermeasures *(Russian)* 80−49561
heteroepitaxial semiconductors for electronic devices, prep. and props., book 79−83116

semiconductor epitaxial layers continued
heteroepitaxial surface morphologies and misalignments *(Japanese)* 80−15411
heteroepitaxial vacuum deposited films, doping *(German)* 77−84779
heterojunction, band-edge discontinuities and interface pot. step, two-band narrow-gap approach 80−39665
heterojunction devices, double and triple layer, density of misfit dislocations 78−51850
heterostructure superlattice, props. in high mag. fields 79−73570
HgCdTe/CdTe, limited diffusion volume photodiode, characterisation 80−75627
I-III-VI_2 compounds, lattice parameters meas. using RHEED 79−90913
II-VI semiconductors, direct synthesis *(German)* 80−104070
II-VI semiconductors, heteroepitaxial, for SAW and electro-optic device appl., prep. and props., book contrib. 79−83134
III-V, electronic and struct. props., correlation 77−89835
III-V compound, dislocations nature, origin and effects 79−28232
III-V compound, vapour transport reactions and kinetics 79−28931
III-V compound heteroepitaxial interface mech. and crystallographic props. 77−76706
III-V compounds, lattice consts. determ. 79−19479
III-V compounds and alloys, MBE process and problem areas, review 80−10815
III-V epitaxial pseudobinary compounds, lattice deform. determ. by X-ray diffraction 78−6242
III-V heterojunctions, misfit dislocation banding, stress-induced birefr. 77−28542
III-V multilayer structure, as-grown, assessment of defects by differentiated cathodolum. topography 80−59819
III-V pseudobinary compound, growth and phase equilib. in vertical rotating LPE reactor *(French)* 77−77430
III-V semiconductor, MBE and applications 78−11135
III-V semiconductor based layered multielectronic systems, electronic process investig. survey *(Russian)* 80−107891
III-V semiconductor compound structures, TEM analysis 77−89836
III-V semiconductor compounds for optical devices in 1.0-1.6 μm region, crystal growth by LPE and CVD 79−43161
III-V semiconductor epitaxial structures as wide-gap substrates, minority carrier diffusion length determ. by photoluminesc. 80−103992
III-V semiconductor epitaxial ultra-thin layers, bevel cross sectioning 79−74275
III-V semiconductor ternary alloys, VPE growth lattice mismatch effects 79−28220
III-V semiconductors, electroliquid epitaxy, role of electrotransport 79−56095
III-V semiconductors, heteroepitaxial, for SAW and electro-optic device appl., prep. and props., book contrib. 79−83134
III-V semiconductors, heteroepitaxy *(Japanese)* 77−24968
III-V semiconductors, MBE, surface reaction steps 79−77941
III-V semiconductors, MBE developments in device fabrication 79−78902
III-V semiconductors for optoelectronic appls., review 78−30975
III-V semiconductors VPE using organometallics and hydrides *(French)* 79−33936
individual misfit dislocations, obs. by high voltage electron microscopy 79−82222
injection laser integration with Gunn oscillator on semi-insulating GaAs 78−71232
InP-InGaAsP-InP, low threshold laser, threshold density temp. depend., LPE method *(Russian)* 78−22133
ion implantation induced defects, annealing 80−24479
ion implanted semiconductor epitaxial regrowth, laser annealing dynamics 80−92548
ionised-cluster beam deposition and epitaxy, for electronic device fabrication 78−11133
laser annealing, optical constants, ellipsometry observation 80−34024
laser epitaxial growth with moulded reflectors 78−42347
laser material requirements, liq. heteroepitaxy of solid solns., review 77−14718
LPE, Peltier induced 78−48342
LPE, Peltier induced 78−48343
LPE method for batch growth of layers 77−77424
luminescence, spin-dependent, of donor-acceptor pairs 77−52173
MBE, doping impurity transport, free carriers effect 78−26793
MBE, new technique for growing crystal 77−66591
MBE, review and appls. *(German)* 78−68630
MBE manufacture 80−103593
minority carrier diffusion lengths in semicond. SEM meas. interpretation 78−80002
multicomponent epitaxial structure synthesis device 77−77414
multicomponent solid solutions, defect formation in heteroepitaxial structures 78−83825
multilayer epitaxial heterostructures, use of two-photon absorption in study 79−8185
multilayer systems, film growth, spectroscopic ellipsometry, review 80−103603
narrow-band semiconductor, growth, activation by UV and IR radiation 80−71598
nonhomogeneous semiconductor, galvanomagnetic effects 79−91077
nonstoichiometry and carrier concentration control in MBE of compound semiconductors 79−95941
optical constants meas. by far IR ellipsometry 78−93753
p-n-n^+ junctions, epitaxial planar, two-dimensional anal. of breakdown 78−80045
p-type epitaxial layer, thermalisation of electron-hole plasma, photolum. meas. 78−80408
periodic structures, props., prep., use 78−51982
photoeffect obs. with flying light spot 79−28401
phthalocyanine monolayers and vapour-grown films, surface struct., LEED 77−35830
piezoelectric, surface phonon amplification 77−31864
polySi and amorphous Si photovoltaic thin film developments 79−74524
potentially superior method of preparing semicond. devices *(Czech)* 78−44027
reduced pressure, advances 80−40242
resistivity and thickness monitoring, use of spreading-resistance method 80−47075
resistivity meas. using Hg−n-GaAs barrier contact 79−60945
semiconductor epitaxial structures, atomic diffusion 77−85110
semiconductor thin films, fabrication for device appls. 80−100418

semiconductor epitaxial layers continued
Si, stacking faults, development, structure and props. *(Russian)* 80−24461
Si epitaxy, vapour phase deposition technology 80−75472
SIMS characterisation *(French)* 80−50904
solar cell fabrication, laser-induced p-n junction formation 80−93880
SOS, cryst. perfection rel. to MOS transistor mobility 78−75956
SOS film, electron mobility 78−91792
sputter deposition, review 77−32521
superlattice doping, electronic states, elec. props. 79−95480
surface, {001} layer, dislocation etch pits revealed by molten KOH 78−63772
ternary semiconductors, measurement of lattice parameters of thin heteroepitaxial layers, RHEED technique 80−15406
thin epitaxial layer surface As concentration meas. 79−95037
transition regions 78−72294
transition regions in epilayer structures 79−78167
varizonal, parameter determ. by photoluminescence method *(Russian)* 80−108291
VPE, mol. flow in vac., free carriers effect on doping impurity distrib. 78−47682
VPE growth, book contrib. 79−69997
VPE growth of $A^{III}B^{V}$ compounds flow graph model 79−56088
VPE of III-V ternary layers, on-time comp. determ. 78−67915
(Al,Ga)As DH wafer, Al distrib. meas. 77−7994
Al-GaAs-$Al_xGa_{1-x}As$ Schottky barrier diodes, prep., charcts. 80−6948
(Al+Si)-Si thin films, struct. transitions and phase comp. 80−49537
AlAs epilayers, MBE growth on GaAs, self-terminating thermal oxidation 78−92374
AlAs-GaAs film heterojunction, VPE growth and charcts. 78−6439
AlAs-GaAs heterostructure, fabrication by selective liq.-phase epitaxy 79−15618
Al_xGa_{1-x}-GaP structure, LPE, double heterostruct. light modulator appl. 79−28963
AlGaAs, heteroepitaxial waveguides, far radiation field charcts. *(Russian)* 77−11038
AlGaAs, LPE layers, growth initiation and cathodoluminesc. irregularities 79−87010
AlGaAs layer, epitaxial, grown from pre-heated Ga soln., photolum. study 78−39591
AlGaAs p-n diodes, I-V charcts., tunnelling 80−100510
p- (AlGa)As:Zn, MBE grown, elec. props., shallow junction solar cell use 79−91175
(AlGa)As-GaAS DH lasers prep. by new LPE technique 77−40358
(AlGa)As-GaAs, large area high efficiency solar cell fabrication, LPE process 77−36410
AlGaAs-GaAs proton irradiated solar cells, deep-level defects, recombination mechanisms, performance charcts. 80−81459
AlGaAs-GaAs transverse mode stabilised plano-convex waveguide laser made by single step LPE 80−48274
$Al_{0.3}Ga_{0.7}As$:Te(SN), impurity effects on interface morphology of LPE films on corrugated GaAs substrates 78−88435
$Al_{0.36}Ga_{0.64}As$, LPE films, Te-induced defects 78−43037
$(Al_{0.42}Ga_{0.58})As$, LPE grown layer, optical absorpt. coeff. meas. 78−6801
$Al_{0.42}Ga_{0.58}As$-GaAs-$Al_{0.42}Ga_{0.58}As$, etalon, optical bistability and modulation 80−58628
$Al_xGa_{1-x}As$, DH, defect generation in active regions at high optical excitation rates 79−23845
$Al_xGa_{1-x}As$ epitaxial diode, neutron and γ-irrad. effects on cathodolum. in SEM 79−11473
$Al_xGa_{1-x}As$ epitaxial films, microanal. in photoemissive electron microscope 79−16068
n-$Al_xGa_{1-x}As$ epitaxial films, elec. cond. press. depend. 79−56337
$Al_xGa_{1-x}As$, epitaxial growth from limited vol. melt 79−70005
$Al_xGa_{1-x}As$, epitaxial layer struct., dislocation etching obs. 77−85095
$Al_xGa_{1-x}As$, epitaxial layer crystn. from soln. in melt, diffusion limited 78−35321
$Al_xGa_{1-x}As$, epitaxial layer, distribution of Te and Ge impurities 78−43046
$Al_xGa_{1-x}As$ epitaxial layers on GaAs, struct. study by scanning Auger electron microscopy 80−80110
$Al_xGa_{1-x}As$, graded-gap crystal, voltage-current characteristics 79−69613
$Al_xGa_{1-x}As$ grown by organometallic VPE, luminesc. efficiency 79−78892
$Al_xGa_{1-x}As$, growth of high-resistivity layers by liquid-phase epitaxy 79−70008
$Al_xGa_{1-x}As$, growth of uniform epitaxial layers 77−40393
$Al_xGa_{1-x}As$ heterojunction laser diode, technology and spectral charcts. 77−38885
$Al_xGa_{1-x}As$, high-resistivity film growth by LPE 77−44179
$Al_xGa_{1-x}As$, LPE, deep levels, photocapacitance obs. 77−15790
$Al_xGa_{1-x}As$, LPE, effect of doping on interface morphology 77−81231
$Al_xGa_{1-x}As$, LPE, quantitative analysis by AES 77−89667
$Al_xGa_{1-x}As$ layers, graded band gap, growth and properties 79−60645
$Al_xGa_{1-x}As$, MBE grown film, in situ surface characterisation by RHEED, SIMS and AES 77−43410
$Al_xGa_{1-x}As$ MBE layers, ionized beam doping, elec. and optical charcts. 79−37721
$Al_xGa_{1-x}As$, microstruct., effect on elect. charcts. of Schottky diode *(Russian)* 80−107671
n-$Al_xGa_{1-x}As$, nonradiative donor related defect centre obs. 78−23497
$Al_xGa_{1-x}As$ oxidised AlAs as multidielectric for GaAs MIS devices 79−65333
n-$Al_xGa_{1-x}As$, photolum. emission and excitation spectra 78−76526
$Al_xGa_{1-x}As$, pure and Ge doped, shallow acceptor photoluminescence 80−76064
$Al_xGa_{1-x}As$ semitransparent photocathode, LPE, quantum efficiency spectrum 80−76153
$Al_xGa_{1-x}As$ solid soln., epitaxial layer growth on GaAs by zone recrystallisation with temp. gradient 77−16510
$Al_xGa_{1-x}As$ thin graded band-gap layers, isothermal LPE growth 80−34325
$Al_xGa_{1-x}As$, VPE and LPE growth, electron mobility 79−91165
$Al_xGa_{1-x}As$, VPE growth and characterisation 78−35315
n-$Al_xGa_{1-x}As$, variable-gap solid solns., diffusion length, photolum. meas. 79−38659
$Al_xGa_{1-x}As$: Sn(Te), persistent photocond., due to donor-related centres, symmetry 80−15558

semiconductor epitaxial layers continued
p-$Al_xGa_{1-x}As$:Be layer, MBE growth, Be doping and diffusion 77−51397
$Al_xGa_{1-x}As$:Cr, exptl. verification of Cr^{2+} models of photoluminescent transitions 78−27320
$Al_xGa_{1-x}As$:Cr, high resist. film, photolum. and photocond. meas. 78−72596
$Al_xGa_{1-x}As$:Cu(Ag)(Au), LPE film, impurity levels, elec. and optical props. meas. 78−26862
p-$Al_xGa_{1-x}As$:Ge layer on GaAs substrate, Hall and elec. cond. meas., Hall mobility 80−2402
$Al_xGa_{1-x}As$:Ge(Te)(Zn), photo- and cathodolum., comp. depend. *(Russian)* 77−48215
$Al_xGa_{1-x}As$:Mg doping characteristics, elec. props., effective hole masses 79−78117
$Al_xGa_{1-x}As$:Mn epitaxial layers, Mn-O association, EPR meas. 77−69677
$Al_xGa_{1-x}As$:Te, elec. cond. and Hall coeff. rel. to donor levels 77−24630
$Al_xGa_{1-x}As$:Zn epitaxial layers, composition and Zn carrier conc. 80−25585
$Al_xGa_{1-x}As$/GaAs heterojunction laser, appl. of stress distrib. calc. for multilayer heteroepitaxial struct. 77−72798
$Al_xGa_{1-x}As$-$Al_yGa_{1-y}As$ DH IR-visible (0.89-0.72 μm) MBE grown lasers 80−64058
$Al_xGa_{1-x}As$-GaAs, epitaxial heterostructure, influence of defects on diffusive distrib. of group I impurities 78−43045
$Al_xGa_{1-x}As$-GaAs multilayer heterostructures, optical birefringence 78−64422
$Al_xGa_{1-x}As$-GaAs multilayers, LPE, using addition of GaCl vapour and new boat struct. 79−33950
$Al_xGa_{1-x}As$-GaAs n-n heterojunction, interface width determ. 80−49887
p-$Al_xGa_{1-x}As$-n-GaAs heterojunction solar cells, optical characts. study 77−24609
AlGaAsP(Sb), compositional grading by LPE 80−10844
AlGaAsSb LPE growth, lattice-matched to GaSb, characterisation 80−60794
AlGaAsSb, photodiode, lattice-matched to GaSb 79−71527
$Al_yGa_{1-y}As_{1-x}Sb_x$ LPE phase diagram 78−11137
$Al_xGa_{1-x}AsZn$-GaAs solar cells by LPE, open circuit voltage, fill factor 80−101108
$Al_xGa_{1-x}N$ epitaxial layers, growth and props. 79−11522
$Al_xGa_{1-x}P$, LPE, crystallographic obs. and electrolum. 80−88445
p-$Al_xGa_{1-}Sb$, cathodoluminescence investig. for varying x *(Russian)* 77−20931
$Al_xGa_{1-x}Sb$, compositional var. during LPE growth using ternary phase diagram 77−59761
$Al_xGa_{1-x}Sb$, photolum. intensity increase due to composition variation 79−15528
$Al_xGa_{1-x}Sb$, solid soln., epitaxial layer growth from liq. phase 77−85089
$Al_xGa_{1-x}Sb$, solid soln., depend. of forbidden-band width on composition 78−39602
$Al_xGa_{1-x}Sb$-Pd contacts, struct., preparation elec. props. 80−65684
AlN epitaxial films, optical props. in vac. UV region 79−56872
AlN film, epitaxial growth by reactive evaporation *(Japanese)* 78−23629
AlN, impurity-doped film, cathodoluminescence spectra 79−83038
AlN, refl. spectra, 5-12.5 eV 79−99967
AlN, VPE by closed space vapour process, and optical absorpt. edge 78−88371
AlSb solar cell material, epitaxy, ionicity and bond struct. 80−61367
AlSb, thin film growth on insulating substrates, by metal organics CVD 80−60786
$(AlSb)_x(GaSb)_{1-x}$, LPE growth 77−40392
BN, refl. spectra, 5-12.5 eV 79−99967
BP, CVD on Si substrate, cryst. imperfections 78−10294
BP, epitaxial growth using B_2H_6-PH_3-H_2 system 79−28937
BP, hardness meas. 77−11629
BP on Si substrates, epitaxial growth and device appls. 78−48333
BP:Zn(Se)(Cd), epitaxial layers, ion implantation, defects and lattic locations, channelling obs. 80−88179
$B_{13}P_2$, micro-Vickers hardness number 77−40444
Bi-Sb-Te system, epitaxial film prep. in closed-crucible 77−52230
$Bi_{1-x}Sb_x$ epitaxial thin films, galvanomag. props. in semimetal and semicond. regions 79−11254
$Bi_{1-x}Sb_x$ film, low temp. anomalies of elec. props. and quantum size oscillations 79−65571
(Cd,Hg)Te epitaxial structures, comp. profile depend. on deposition parameters 80−100795
Cd chalcogenides, film, on NaCl, preferential epitaxy induced by electron bombard. or elec. field 80−10824
$CdCr_2Se_4$ film, electron irradiated, struct. 79−15032
$CdCr_2Se_4$, spinel film, struct. SEM study, props. 78−79905
(CdHg)Te, ion implanted graded gap photodiodes 78−39192
$Cd_xHg_{1-x}Te$ epitaxial graded gap layers, plasma reflection and magnetoreflection 80−71391
$Cd_xHg_{1-x}Te$, epitaxial growth from stoichiometric melt, crystn. and diffusion 80−75475
$Cd_xHg_{1-x}Te$, epitaxial layer p-n junction, current-voltage characteristics of photovoltaic detectors, 1 to 15 μm 80−86407
$Cd_xHg_{1-x}Te$, film, optical props., struct. depend. 77−1751
$Cd_xHg_{1-x}Te$ films, epitaxial growth, optical, elec., and photoelec. props. 79−11512
$Cd_xHg_{1-x}Te$, graded gap epitaxial layers, elec. and photoelec. props. 77−85362
$Cd_xHg_{1-x}Te$, graded gap epitaxial layers, spectral characts. of photoelectromagnetic effect 80−60022
$Cd_xHg_{1-x}Te$, graded-gap, elec. transport props. 77−85358
$Cd_xHg_{1-x}Te$ graded-gap epitaxial layers, photocond. meas. 0.5 to 6 μm, detector appl. 79−60869
$Cd_xHg_{1-x}Te$, graded-gap layers, galvanomag. props. at low temp. and in weak mag. field 80−75664
$Cd_xHg_{1-x}Te$, isothermal growth of epitaxial layers 78−60577
$Cd_xHg_{1-x}Te$ solid solns., epitaxial growth under isothermal conditions 77−16504
$Cd_xHg_{1-x}Te$, tunnelling effect in p-n junctions 80−75630
$Cd_xHg_{1-x}Te$, VPE on CdTe *(Russian)* 78−11129
$Cd_xHg_{1-x}Te$, variable-gap struct., additional p-n junction in epitaxial film, photosensitivity 77−24588
$Cd_xHg_{1-x}Te$, variable-gap structures, galvanomagnetic effects 80−11014

semiconductor epitaxial layers continued
CdS, epitaxial film, conductivity control by S vacancy form., light modulation appls. 77−4455
CdS, epitaxial film, structural and electron transport props. 79−82481
CdS, epitaxial growth and nucleation, on monocrystn. ZnS, substrate real struct. influence 80−88455
CdS, epitaxial layers on (111) Ce, growth and defect struct. 78−18920
CdS, epitaxial layers on Cd single crystal, direct synthesis and struct. 78−68628
CdS epitaxial layers on sapphire, exciton struct. of absorpt., photoluminesc. and photocond. spectra 80−89027
CdS film preferred orientation, internal stress, and interface characteristics 78−26795
CdS, grown by vac. evaporation on Si 80−25567
CdS heteroepitaxial films on ZnS, surface-wave acoustoelectric domain excitation and probing 79−46904
CdS layers, epitaxial, deposited on InP substrates, vapour growth technique 77−21033
CdS, on Ge, morphology and six-pointed optic figures obs. 78−2390
CdS, on Si, structural and transport props. 78−6463
CdS, with grain-boundary barriers, field characts. of elec. cond. 77−55626
CdS:M, M=Zn, Te, doping and solid soln. prep. during VPE 77−85353
CdS/InP epitaxial thin films on NaCl, HEED and TEM study 80−88446
CdS-Al_2O_3-Al diodes fabricated by MBE, junction characts. 79−65550
CdS-CdTe double layers on various GaAs surfaces, morphology and crystallography 80−34326
CdS(Se)(Te), condensation from gas phase of controlled comp., and props. 80−54562
CdS(Se)(Te), evap. onto electron bombarded NaCl substrates, epitaxial growth and characts. 79−28948
CdSe, epitaxial film, gas-phase comp. effects on elec. props. 77−85354
CdSe, epitaxial films, carrier scattering temp. depend. *(Russian)* 78−10583
CdSe epitaxial layers, on GaP-CdS substrates, absorption and electroabsorption 80−40178
CdSe evaporated films, struct. and epitaxy, TEM, RHEED, and X-ray diffr. obs. 79−77939
CdSe, LPE growth on ZnTe, characterisation of heterojunction 77−4745
CdSe, monocryst. layers and bulk specimens, spectral comp. of impurity luminesc. 77−16364
CdSe:In, epitaxial layers, synthesis and elec. props. 77−47909
CdSe:In, epitaxial layer, effect of activator distribution on conductivity 78−43047
CdSe:Zn(Ga), impurity distrib., current transfer features *(Russian)* 77−47908
CdSe-Ge (111) heterojunctions, epitaxial, azimuthal rotation 78−84085
CdSe(Te) films, oriented, epitaxial growth by epitaxial nucleation in submicroscopic holes method 80−59834
$CdSe_xTe_{1-x}$, solid solns., epitaxial layer prod. 78−23619
CdTe epitaxial films, surface morphology, layer and spiral growth 80−10823
CdTe, film grown by hot wall epitaxy, elec. props. 79−82696
CdTe, film grown in quasi-closed volume, struct. *(Russian)* 78−75952
CdTe films, structural imperfections depend. on crystn. temp. 79−90661
CdTe, films grown by hot wall epitaxy, elec. props. 79−28420
CdTe, growth by photostimulated VPE, electrophys. props. 77−40390
CdTe homojunctions from VPE growth, solar cell appl. *(French)* 77−43453
CdTe, on CdS substrate, closed-tube vapour growth 80−55302
CdTe on GaAs, cryst. sfruct. and phys. props. 79−33202
CdTe, on mica, substrate defects effect on epitaxy 78−26794
CdTe, optical waveguide, fabrication by LPE using boat-slide technique 77−63570
CdTe p-n homojunction, elec. and photovoltaic props. rel. to solar energy conversion 79−51668
CdTe thin films, oriented, VPE growth, infrared transmission, photovoltaic cells 80−59825
CdTe-CdS heterojunctions, growth by closed-tube chem. transport, elec. props. 80−60070
CdTe-PbTe(InSb) superlattices, laser deposition of multilayer heteroepitaxial structs. 80−44450
CdTe-Si heterojunctions, epitaxy and electrical props. *(Japanese)* 77−32074
$Cd_{1-x}Zn_xS$ heteroepitaxial single-cryst. layers, photoluminesc. props. 80−100692
$Cd_{1-x}Zn_xS$-p-GaAs heterojunctions, elec. and photovolt. props. rel. to growth technique 80−29466
$Cd_{1-x}Zn_xSe$, epitaxial layer growth with Zn content from doping to solid soln. formation 77−85094
p-$CuGaS_2$, LPE on n-ZnS, heterojunction prep. and characterisation 79−1831
$CuGaSe_2$, lattice parameters meas. using RHEED 79−90913
$CuGaSe_2$ thin films, on GaAs substrates, structural and elec. props., photoluminesc. meas. 79−65564
$CuGaTe_2$, elec. props. as function of growth temp. 79−65565
$CuGaTe_2$ films deposited on GaAs substrates by flash evaporation, struct. and elec. cond. 80−24755
$CuIn_{0.7}Ga_{0.3}Se_2$ epitaxial layers, on GaAs substrates, struct. and elec. props. 80−107670
$CuInS_2$, epitaxial thin film on GaAs, exam. of growth, electrical props. 80−24754
$CuInSe_2$ epitaxial growth on GaAs 78−84104
$CuInSe_2$ film, MBE growth, AES and optical absorpt. obs. 79−78903
$CuInSe_2$, heteroepitaxy on {111} oriented Ge by flash evaporation, struct. 80−108333
$CuInSe_2$ on GaAs, epitaxy grown RHEED exam. of epitaxial overgrowth *(German)* 79−11042
$CuInTe_2$ epitaxial layers, on GaAs, growth and props. 80−108359
Cu_2S epitaxial films, reactive sputtering prep. and electronic props. 79−78885
EuSe, VPE by hot-wall technique 80−80958
(Ga,Al)As, LPE growth of multilayered struct., explanation for meniscus lines on surfaces 77−76681
(Ga,Al)As:Si (Ge), epitaxial layers, radiative recomb., compensation, cathodolum. study 80−66307
(Ga,In)As, growth of epitaxial layers 77−12542
Ga-In-As-Sb system LPE layers, pseudoquaternary phase diagram 78−10293

semiconductor epitaxial layers continued
Ga-P-Bi(Sb), liquidus isotherms, GaP solubility in Sb, Bi, rel. to epitaxial growth 78−34721
GaA-$Al_{0.27}Ga_{0.73}As$ DH lasers grown by MBE, growth conditions influence on threshold current density 80−32984
n-GaAS, electrical parameter determ. by graphical method *(Russian)* 77−15975
n-GaAS epitaxial film, radiative recomb. under influence of mech. stresses 80−66291
GaAS-AlGaAs LPE layers, defects formed by oxygen in ambient gas *(Japanese)* 77−70009
GaAlAs DH, optically-pumped, degradation at elevated temps. 79−50295
GaAlAs, SEM defect study, transmission cathodoluminescence 79−64964
(GaAl)As system, automated system for growth of multilayered structs. by LPE 79−38752
GaAlAs/GaAs heterostructures, ellipsometric assessment of epitaxial layer during growth in organometallic VPE system 79−37933
GaAlAs-GaAs, defects and degradation, transmission cathodolum. evaluation 80−65395
(GaAl)As-GaAs, double heterostructure laser, TEM study of dark line defect growth from dislocation clusters 79−33206
GaAlAs-GaAs epitaxial heterostructures for integrated optics functional elements 78−50948
GaAlAs-GaAs heteroepitaxial devices, interstitial impurities and degradation, Auger obs. 80−99730
GaAlAs-GaAs heterojunction prep., Zn conc. effect in epitaxial layer, high-power IR emission *(Spanish)* 77−39932
$Ga_{0.1}Al_{0.9}As$ LPE layers containing low-cond. regions, charging effects in SIMS anal. 80−66348
$Ga_{0.65}Al_{0.35}As$ epitaxial layer on GaAs, two-dimensional lattice mismatch parallel to interfacial boundary 79−51439
$Ga_{0.65}Al_{0.35}As$, LPE growth, wave morphologies on surface 77−40396
$Ga_{0.7}Al_{0.3}As$ epitaxial film, inclusion-generated dislocation clusters 77−89445
$Ga_{0.9}Al_{0.1}As$, nucleation morphologies on $Ga_{0.65}Al_{0.35}As$ surfaces grown by LPE 78−15323
$Ga_{0.9}Al_{0.1}As$:Ge(Si) epitaxial layers, defect obs. by TEM 77−51618
$Ga_{1-x}AlAs$, LPE layers, electron mobility, scatt. processes 80−84519
$Ga_{1-x}AlAs$:Zn, acceptor energy level and elec. props. 80−65482
$Ga_{1-x}Al_xAs$, alternate monolayer crysts., MBE and props. exam. 78−10289
$Ga_{1-x}Al_xAs$ based layer structures, optimum growth conditions, comp. and struct. perfection 80−104069
$Ga_{1-x}Al_xAs$ DH laser, LPE surface protective coating 78−35320
$Ga_{1-x}Al_xAs$, epitaxial, radiative deep states 80−76061
$Ga_{1-x}Al_xAs$, epitaxial layers on GaAs substrate, mismatch stress accommodated by tetrahedral distortion 77−55466
$Ga_{1-x}Al_xAs$, epitaxial layers, reflectivity meas. by wavelength modulation spectroscopy *(French)* 77−59632
$Ga_{1-x}Al_xAs$ epitaxial layers, spectroscopic technique for imaging spatial distrib. of nonradiative defects 78−23498
$Ga_{1-x}Al_xAs$, epitaxial layers, on GaAs substrates, X-ray double-cryst. diffractometry, state of strain 79−19480
$Ga_{1-x}Al_xAs$ epitaxial layer, absorpt. and transmission coeffs. *(French)* 80−2887
$Ga_{1-x}Al_xAs$ epitaxial layer, elec. cond., Hall effect, band struct. 80−49964
$Ga_{1-x}Al_xAs$, LPE, growth mechanism and morphology on channelled substrates 79−28960
$Ga_{1-x}Al_xAs$ LPE crystals for DH laser, LEDs, TEM obs. of Ge, Si-doped epitaxial layers 79−1556
$Ga_{1-x}Al_xAs$, LPE growth and characterisation 80−50566
$Ga_{1-x}Al_xAs$ LPE layer photoluminescence obs. *(Polish)* 77−77268
$Ga_{1-x}Al_xAs$, LPE layer thickness depend. on soln. comp. 78−10295
$Ga_{1-x}Al_xAs$ LPE layers, diffusion limited growth, thickness comparison with GaAs 78−87892
$Ga_{1-x}Al_xAs$ LPE layer on GaAs, lattice mismatch using X-ray source 79−82470
$Ga_{1-x}Al_xAs$ LPE layers, comp. and refr. index, ellipsometry meas. 79−87011
$Ga_{1-x}Al_xAs$, photoluminescence, deep level trap emission capture 80−29805
$Ga_{1-x}Al_xAs$, self-aligned three dimensional struct. MBE growth 77−59697
$Ga_{1-x}Al_xAs$, surface phonon polaritons, frustrated total internal refl. expts. 78−47656
$Ga_{1-x}Al_xAs$ transverse mode DH laser with inbuilt plano-convex waveguide 80−48296
$Ga_{1-x}Al_xAs$ VPE layers, X-ray diffr. 80−29296
$Ga_{1-x}Al_xAs$:Si, LPE, phase diagram, Hall effect meas., carrier conc., donor ionisation energies 77−72803
$Ga_{1-x}Al_xAs$:Si p-n junction, doping in LPE, elec. and luminesc. props. *(Czech)* 78−47851
$Ga_{1-x}Al_xAs$-GaAs, grown by LPE, direct obs. of dislocations 79−65087
$Ga_{1-x}Al_xAs$-GaAs, heteroepitaxial layers on GaAs(001), misfit dislocation asymmetry 77−47694
$Ga_{1-x}Al_xAs$-GaAs, injection lasers, defects, TEM anal. 79−23866
$Ga_{1-x}Al_xAs$-GaAs LPE multilayer heterostructure photovolt. solar cells, fabrication and performance 79−48128
$Ga_{1-x}Al_xAs$-GaAs p-n and p-p-n heterojunction solar cells, high efficiency, prep., eval. and characters *(Japanese)* 80−61342
$Ga_xAl_{1-x}As$, LPE, charge carrier conc. distrib. *(Russian)* 78−52694
$Ga_xAl_{1-x}As$-GaAs heteroepitaxial layer distortion characterisation by X-ray multiple diffr. 80−96754
$Ga_xAl_{1-x}As$, photodetector diode on GaAs substrate dark currents, tunnelling, energy gaps, effective masses 80−70805
$Ga_{1-x}Al_xAs_{1-y}P_y$ epitaxial film, nonradiative recomb. at dislocations 80−44213
$Ga_{1-x}Al_xAs_{1-y}P_y$ epitaxial layer heterojunction, nonradiative recombination at misfit dislocations 80−96901
$Ga_{1-x}Al_xAs_{1-y}P_y$ layer of uniform composition grown on GaAs by LPE, temp. diff. method appl. 79−23864
$Ga_{1-x}Al_xAs_{1-y}P_y$-GaAs quaternary heterojunction strains and IR laser diode performance 78−9385
$Ga_{1-x}Al_xAs_{1-y}P_y$-GaAs quaternary heterojunction, misfit dislocation charact. by synchrotron radiation white beam topography 78−63771
GaAlAsSb-GaSb low bandgap solar subcell for high efficiency multibandgap convertors, LPE growth 80−93927

semiconductor epitaxial layers continued
$Ga_{1-x}Al_xN$ heteroepitaxial films, photoluminesc., cathodoluminesc. 80−66292
$Ga_{1-x}Al_xN$, VPE growth on sapphire, RHEED obs.of orientation rels. 77−20208
$Ga_{1-x}Al_xP$, LPE grown, green electroluminescence 78−19571
$Ga_{1-x}Al_xP$:N epitaxial films, ion implanted, cathodoluminescence study 80−60684
$Ga_{1-x}Al_xSb$, LPE growth and phase diagram *(French)* 77−24974
$Ga_{1-x}Al_xSb$ p-n homojunction LPE and photovoltaic effect obs. *(French)* 78−64108
$Ga_xAl_{1-x}Sb$, VPE, closed tube transport technique 79−28935
$Ga_xAl_{1-x}Sb$, VPE with I_2 as transport agent 78−48325
GaAs, 1.06 μm two-photon absorption coeff., guided wave meas. 78−46707
GaAs (100), VPE, role of Cl, LEED, RHEED, and AES obs. 77−1327
GaAs, (100) surfaces, reconstructed, ang. resolved photoemission from surface states, adsorption and annealing effects 80−16143
GaAs, (100) surfaces, struct. and stoichiometry during molecular beam epitaxy, RHEED anal. 79−4921
GaAs (111) epitaxial film, adsorption of Cs, Cs+O ellipsometric study 80−29282
n-GaAs, alloyed in As_2 beam, metal-Ga contacts 79−95495
GaAs, anodic oxidation 77−16710
GaAs antireflecting MOS solar cells, epitaxial and polycryst. using OM-CVD techniques 80−94072
GaAs, appl. to surface barrier particle detectors 79−72203
GaAs, AuGe ohmic contact production by laser alloying 78−88026
GaAs, autoepitaxial layer, local impurity inhomogeneities *(Russian)* 79−23854
GaAs autoepitaxial structure on heavily Te-doped GaAs substrate *(Russian)* 80−49556
GaAs, back etching and growth by liq. phase epitaxy, surface morphology obs. 80−29287
GaAs base laminated epitaxial struct., surface plasmon phonon polaritons *(Russian)* 80−59905
n-GaAs, bulk and epitaxial film, IR reflectance meas. 77−32364
GaAs, bulk and epitaxial crysts., electron traps characterisation 77−39865
GaAs, bulk and epitaxial crysts., hole traps characterisation 78−6392
GaAs, bulk purification by chemical vapour transport 79−24437
GaAs, C distrib., anal. by quasichem. reactions 77−11803
GaAs, CVD, S doping behaviour during growth, electron conc. 78−26784
GaAs, CVD in Ga-$AsCl_3$-H_2 system with different input supersaturations *(Russian)* 78−68098
GaAs, characterisation Hall effect and Schottky diode profile meas. 78−91791
GaAs, chem. transport by water vapour, thermodynamic calcs. 77−12539
GaAs compensated VPE thin film, electron Hall mobilities 80−107932
GaAs contact pot. difference, rel. to Fermi level stabilisation 77−20403
GaAs, controlled electrochemical and selective etching, integrated optics appl. 77−14814
n-GaAs, conversion to p-type after 1 MeV electron irrad. 79−77636
GaAs, deep centre reson. charging, photocapacitance meas. on Schottky barrier 78−26908
GaAs, deep level photoionisation, absorpt. by derivative surface photovoltage spectroscopy 79−99575
n-GaAs, deep level traps, transient and thermally stimulated capacitance meas. *(Chinese)* 79−91072
GaAs, deep trap characts. by photocapacitance spectroscopy 78−6398
GaAs, deep traps exam. by capacitive method 77−11869
n-GaAs, defect clusters, charge-carrier mobility temp. depend. anal. 80−54701
GaAs, degraded layer form. by annealing, photolum. obs. of defects 78−10968
GaAs, direct-gap layers, optical compensation profiling 77−76450
GaAs, donor and acceptor concs. determ. by optical method 78−19525
GaAs donor characterisation by far IR photoconductive techniques 78−43501
GaAs, doping profile degradation due to ion implantation 80−84194
p-GaAs, electron minority carrier diffusion lengths 80−29807
GaAs, electron-beam excited, efficient generation of electron-hole plasma 80−76051
n-GaAs, epilayer, on semi-insulating substrate, elec. field distrib. *(French)* 80−20333
GaAs epilayers, high-quality, sharp-line transitions due to donor-acceptor recomb. 78−6768
GaAs epilayers and p-n junctions, anisotropic phonon generation 79−37784
n-GaAs, epitaxial, electron mobility calc. 77−69435
n-GaAs, epitaxial, high temp. carrier transport 80−65725
GaAs, epitaxial, impurity gradients caused by surface states and substrate doping 77−84784
n-GaAs, epitaxial, ionised donor pair spectrum 77−63477
GaAs, epitaxial, Si and Ge doping 80−24470
n-GaAs, epitaxial, thermoelec. power, temp. depend. in mm wavelength range 79−23996
GaAs, epitaxial deposition, growth kinetics *(French)* 80−2961
GaAs, epitaxial film, amorphous and polycrystalline, vol. plasmon energy and linewidth, electron scatt. obs. 80−50482
GaAs epitaxial film, enhanced electrodiffusion purification in mag. field 80−66409
n-GaAs epitaxial film, magnetoresist. at low temp., geometric effect 80−93015
GaAs, epitaxial film, photon transfer of excitation of nonequilibrium carriers, radiative recomb. 77−8639
GaAs epitaxial film, photo-EMF echo at 4.2K 80−60038
n-GaAs epitaxial film, potential barrier height, temp. depend. *(Russian)* 78−68070
GaAs, epitaxial film, positron annihilation, impurity centre study 79−15554
n-GaAs epitaxial film, pure and Cr doped, heavy electron trapping, Gunn oscills. 80−6857
GaAs epitaxial film on GaAs substrate, IR characterisation 78−23544
GaAs, epitaxial film on GaAs substrate, two-interface surface polariton modes 78−60180
GaAs epitaxial film recombination props. *(Russian)* 80−49812
GaAs epitaxial films, deep levels, impurity photocond. 80−20247

semiconductor epitaxial layers continued
n-GaAs epitaxial films, residual cond. meas., struct. perfection rel. to photomemory 80−7010
GaAs epitaxial films on strongly doped substrate, basic parameter meas. utilising magnetoresist. and SEM techniques under cathodoluminesc. conditions 80−65728
GaAs, epitaxial growth in $Ga(CH_3)_3$-AsH_3-H_2 system 78−35312
GaAs, epitaxial growth under different intake supersaturations in GaAs-$AsCl_3$ gas transport system *(Russian)* 78−26776
GaAs epitaxial III-V semiconductor thin film prep. by low temp. CVD 80−60789
GaAs epitaxial layer, Be, O, Si, S, Zn and Sn impurity concentrations 80−49260
GaAs epitaxial layer, comparison of compensation ratios determ. by photolum. and elec. methods 79−28818
GaAs, epitaxial layer, effective doping density, comparison of Hall and magnetoresistance meas. 77−11938
GaAs epitaxial layer, laser mag. photoelec. spectra 79−82635
GaAs, epitaxial layer, nondislocation etch pits 80−92535
n-GaAs epitaxial layer, planar diode, intervalley carrier transfer, dynamics of capture processes 78−47864
GaAs epitaxial layer, photoluminesc. defect complex 80−29804
GaAs, epitaxial layer, surface morphology 79−90852
GaAs epitaxial layer and Sn-doped bulk characterisation 79−82596
GaAs, epitaxial layer growth by chloride process, μ and subμ thickness 78−23624
GaAs epitaxial layer high power Gunn diode developement and fabrication 80−16199
GaAs epitaxial layers, electronic surface props., photoluminesc. exam. 77−20901
GaAs, epitaxial layers, high density electron-hole plasma luminesc. 78−19537
p-GaAs epitaxial layers, electron-hole plasma, quantum effects in magnetoluminesc. 78−72591
GaAs, epitaxial layers, low freq. current noise between 4.4 and 300K 78−95388
GaAs epitaxial layers, non-doped, from Ga-$AsCl_3$-H_2 system, TEM and RHEED study of micromorphology and defects 79−65340
GaAs epitaxial layers, from mixed Ga solns., C solubility 80−15392
GaAs epitaxial layers, structural defect and conc. inhomogeneities influence on barrier diode I-V characts. 80−15602
GaAs, epitaxial layers, MBE grown, Hall mobilities, substrate temps. 80−20335
GaAs, epitaxial layers, grain boundaries, deep level transient spectroscopy study 80−49234
GaAs epitaxial layers, meas. of doping profiles *(Hungarian)* 80−70545
GaAs epitaxial layers, surface impurity gradients, Schottky barrier capacitance meas. 80−70782
GaAs, epitaxial layers, electron irrad. deep level trap energy depend. 80−80205
GaAs, epitaxial layers on conductive substrate, elec. characterisation 78−91790
GaAs epitaxial layers on polycryst. GaAs substrates, LPE growth characts. 80−75471
GaAs, epitaxial multilayer, electron irrad. defect study by transient capacitance 79−99241
GaAs, epitaxial structures, impurity profile 77−39610
GaAs epitaxial thin films with neg. electron affinity, photoelectron energy distrib. 80−100755
GaAs epitaxial tunnel diode pressure sensors 78−57975
GaAs, epitaxially grown (001), (111) and $(\bar{1}\bar{1}\bar{1})$ surfaces, LEED, AES, photoemission 78−38924
GaAs, epitaxy by metallorganic and chloride depositions, defect characterisation at growth interface 80−59817
GaAs, epitaxy on semiinsulating GaAs, elec. props. of transitional layers rel. to growth conditions 77−15977
GaAs, epitaxy using TMG and AsH_3, chloride etching effect 78−76606
GaAs, etching by water vapour, rate 80−16519
GaAs, exciton effects in photocond., photoluminesc. 80−96797
n-GaAs, exciton luminescence, excitation intensity depend. 78−52554
GaAs FET buffers, high purity LPE growth by sliding boat method *(Japanese)* 79−28955
GaAs FET double layer production, study by sliding boat method *(Japanese)* 79−66014
GaAs fast characterisation, electroless plating of Au 79−33347
GaAs, fast electron irradiation, impurity distrib. profile obs. 77−76969
GaAs, field effect struct., elec. breakdown, negative resist. 77−12030
GaAs film, epitaxial deposition from gas phase, transient processes, elec. cond. 77−16501
GaAs film, MBE, growth and doping kinetics 77−76682
GaAs film, piezoelec. semicond., cascade capture of carriers by attractive impurity centres, cross sections 78−56157
GaAs, film, radiative relax. time, nonequilibrium carriers 78−84657
GaAs film, surface trap exam. by surface doping and field effect 77−76896
GaAs film on recrystallised Ge film, solar cell appl. 78−19671
GaAs film optical components, prep. by MBE using Si shadow masking technique 80−28358
GaAs film solar cell fabrication, substrate requirements 78−11125
GaAs films for solar cells appl., deposition and characterisation 80−84853
GaAs, gamma and electron irrad. defect formation depend. on interface, luminescence study 80−34057
GaAs, gas-phase epitaxy, step stopping centre form. kinetics 80−65407
GaAs grown by VPE using organometallic method, deep trap levels 80−10923
GaAs, growth kinetics for step-cooling LPE technique 77−40395
n-GaAs, heat treated, origin of 1.41 eV emission band, photolum. expt. 78−72579
GaAs, heavily doped, strongly compensated, hopping cond. 79−47180
GaAs, heteroepitaxial layers on Si substrates by LPE 79−1832
GaAs, heterogeneous reactions in chemical transport by water vapour, growth kinetics of epitaxial layers 77−16500
GaAs homoepitaxial interface, thermal degradation 77−11988
GaAs, hot carrier noise rel. to FET appl. 79−24035
n-GaAs, hot electron magnetophonon resonance, Fourier anal. 80−54718
GaAs, hydride VPE growth for FETs, and characterisation 78−27407
n-GaAs, impact ionisation initiated by acoustoelectric effect 78−52038
GaAs, impurity distribs. by chemical methods 77−43237
GaAs, impurity gettering by ion implantation damage 77−11579
GaAs, LPE, charge carrier conc. distrib. *(Russian)* 78−52694

semiconductor epitaxial layers continued
GaAs, LPE, deep levels, photocapacitance obs. 77−15790
GaAs, LPE, deep levels rel. to growth conditions 79−28314
n-GaAs, LPE, deep trapping centre characterisation by Hall and photo-Hall meas. 80−88578
GaAs, LPE, dislocations obs. by etching 79−95284
GaAs, LPE, gaseous impurity source and effect on purity 79−28959
GaAs, LPE, residual impurities and deep levels, FET fabrication 79−28964
GaAs, LPE, smooth, thin layers on nominally oriented substrate 78−44030
GaAs LPE (001) layer, etching by molten KOH 78−34515
GaAs LPE buffer layers for MESFET appls. 80−29887
GaAs LPE from Ga soln., carrier conc., growth condition depend. 80−71584
GaAs, LPE growth, electric current controlled, on n^+ and semi-insulating substrates 77−73240
GaAs, LPE growth, wave morphologies on surface 77−40396
GaAs, LPE growth from supercooled soln., thickness uniformity 80−54547
GaAs, LPE growth of high purity layers by sliding boat method 78−76610
GaAs, LPE growth on O-implanted GaAs substrates, surface morphology 77−28732
GaAs, LPE growth on O-implanted GaAs substrate, elec. props. 78−2592
GaAs, LPE growth surface, singular instabilities 77−24969
GaAs LPE in situ etchback calibration 79−83114
GaAs, LPE layers, ambient O_2 effect on defects and elec. props. 77−76683
GaAs LPE layers, dopant tracing of terrace growth 78−75948
GaAs LPE layers, effect of baking on mobility and doping conc. 79−99641
GaAs, LPE layers, outdiffusion of recomb. centres from substrate during growth 80−39466
GaAs, LPE layers, screw dislocations, optical microscope obs. 77−35561
GaAs, LPE layers, voids and depressions in facet and terrace growth 78−38974
GaAs LPE layers, X-ray topographic studies of defects 77−62772
GaAs, LPE layers, X-ray topographic exam. of defects 78−30844
GaAs LPE on polycrystalline Mo 79−43157
GaAs layer grown by MBE, directional coupler switch 79−76878
GaAs, layer growth by electroepitaxy, thickness profiles 79−4486
GaAs layers, electroepitaxy and thermal LPE growth, defect struct. and electronic characts. 80−2290
GaAs layers, grown by electroepitaxy and LPE, surface morphology 79−19478
GaAs layers, heteroepitaxy, grown on Si and Ge from multiple component solns. *(Russian)* 78−15319
GaAs layers, LPE from Au-Ge-Ni melts, elec. props. of Ni/Au-Ge/GaAs contacts obs. 77−77437
n-GaAs, longitudinal magnetophonon reson. and Fourier anal. 79−4569
n-GaAs, low temp. field generation of carriers, liberation from surface states 80−92959
GaAs, low temp. gamma irrad., donor-acceptor pair formation 79−69158
n-GaAs, MBE, correl. between electron traps and growth processes 80−65387
GaAs, MBE, growth temp. depend. and characts. 79−28946
GaAs, MBE, process anal. and appl. *(French)* 79−56937
GaAs, MBE, surface reaction steps 79−77941
GaAs, MBE, technology and epitaxial layers props. 79−33945
GaAs, MBE, undoped, growth and characterisation 80−10836
GaAs, MBE (001) layers, work function meas. 80−49870
GaAs MBE epilayers, photoluminesc. and elec. characterisation 80−11500
p-GaAs, MBE grown, As_2 and As_4 effects on photolum. 80−103974
GaAs, MBE grown film, in situ surface characterisation by RHEED, SIMS and AES 77−43410
GaAs MBE layer, Al_2O_3 film growth 78−39706
GaAs, MBE layers, H_2 effect on residual impurities, photolum. obs. and elec. characts. 79−47636
GaAs MBE physical characteristics and applications *(German)* 79−7618
GaAs, MBE with ionised dopant 77−40338
GaAs MESFET layers, low-temp. halide epitaxial growth 77−77403
GaAs MIS dynamic optically controlled transparencies 78−90523
GaAs MOS diodes, interface states, deep-level transient spectroscopy 80−44727
GaAs, magnetoplasma reflectivity, difference method, IR *(German)* 77−12363
GaAs, microstruct., effect on elect. characts. of Schottky diode *(Russian)* 80−107671
GaAs, minority carrier diffusion lengths, contact metal effects 78−72260
GaAs, multiexciton complex bound to neutral acceptors, photoluminesc. obs. 79−87503
GaAs, multilayer epitaxial growth with Sn doping 77−47690
GaAs, multilayer liquid phase epitaxy, transition to faceting 80−96750
GaAs multilayer photocathode structures, TEM obs. of dislocations generated 80−100241
GaAs, multiple layer LPE growth by controlled supercooling of Ga soln. 77−77429
GaAs n^+n^{2+} multilayers, carrier conc. from Fourier transform anal. of magnetoresist. signal 79−38205
GaAs, nonequilibrium carrier relax., recombination radn. 80−7416
GaAs, nonradiative capture, direct obs. of phonons 78−30976
GaAs, nonuniform electroconductivity *(Russian)* 80−70753
GaAs on GaAs and Ge, epitaxy, mechanism, effect of substrate surface struct. 77−51614
GaAs, optically pumped, absorption spectrum, band filling, hot electron effects 78−31199
GaAs, organometallic VPE, with varying As/Ga ratios, deep states 80−65480
GaAs, partition coefficients of impurities 77−15443
GaAs, photoconductivity, high field effects on carrier capture and recomb. 77−43646
GaAs, photoconductivity and photomagnetic effect spectra 79−11178
GaAs, photoconductivity meas. of cyclotron resonance 79−82638
GaAs, photoluminescence, deep level trap emission capture 80−29805
GaAs, photoluminescence, electron gas coding influence in ion-bombarded layers 80−108272

semiconductor epitaxial layers continued
GaAs, plastic deform. prod. by thermocompression bonding, elec. props. 77−76807
GaAs, polariton wave packet propag. in exciton reson. 80−2345
GaAs, proton irradiated, low energy, deep level defects and hole diffusion length meas. 80−60000
GaAs, qualitative anal. of oxygen in thin epitaxial layers by SIMS 79−5233
n-GaAs, real epitaxial surface, photoelec. spectroscopy, mechanisms 78−34858
GaAs, residual donor identification by far IR photocond. 80−60047
GaAs, residual donor identification by far IR photoconductivity meas. 80−103717
GaAs ribbons from Ga-$AsCl_3$-H_2 epitaxy 80−7498
GaAs, S and Se ion implantation 78−55884
GaAs, Schottky diode, trap levels, admittance spectroscopy 79−51672
GaAs Schottky-barrier diode submicron layer LPE reactor 77−77439
GaAs, selective growth, MBE and self-masking method 77−52256
GaAs, selective in situ vapour etch of substrate and growth 80−2958
GaAs, self-compensation due to shallow and deep levels 80−24837
GaAs, semi-insulating, LPE growth for FET buffer layers 79−66015
GaAs, semi-insulating, thermal conversion, Hall effect and luminesc. meas. 78−6405
GaAs, sequential multiple layer VPE, method 77−12545
GaAs, solar cell, thin film, prep. by Peeled Film Technology 79−29472
GaAs structures produced by epitaxy, recombination radiation, anomalous temp. depend. 80−2847
GaAs, substrate for epitaxial growth, backscatt. anal. of surface prep. and anodic oxidation 77−25175
GaAs, substrate prep. effect on surface morphology 78−26780
n-GaAs, surface mode phonon amplification, numerical analysis 78−34691
GaAs, surface studies during MBE growth 79−90899
GaAs, surface-mode acoustic wave amplification 79−46907
n-GaAs, switching time in low-temp. impurity breakdown 77−15923
GaAs thin layers, MBE, growth conditions and phys. props. *(German)* 80−55307
GaAs, time-resolved spectra, carrier relax. time, phonon lifetime 80−11433
GaAs, transient processes during doping for large conc. jumps. 80−39134
GaAs, transmutation doped, shallow donors, magneto-optical study, photocond. meas. 78−87996
GaAs, trapping levels obs. using deep level transient spectroscopy, laser irrad. effects 79−99499
GaAs type FET with buffer, bias effects due to deep centres in struct. *(French)* 80−107917
GaAs, ultrathin film growth by cracking of organometallic compounds at 40 to 100 torr *(French)* 78−44023
n-GaAs, undoped, correl. incorporation of donors, photocond. meas. at 4.2K 80−6898
GaAs, undoped, recomb. of non-equilib. carriers, steady-state photocond. 77−85357
GaAs, undoped epitaxial layer growth from nonstoichiometric solns., O_2 contamination sources 80−108362
GaAs unintentionally doped layer growth using MBE 78−72741
GaAs, unintentionally doped layer grown by MBE, elec. props. 79−91167
GaAs, VPE, electron Hall mobility meas., attempted correlation with growth parameters 78−43417
GaAs, VPE, fast growth at low temp. and high partial pressure 79−51446
GaAs, VPE, growth method at low H_2 press. 79−28936
GaAs, VPE, growth parameters effect 77−28726
n-GaAs, VPE, hi-lo, carrier conc. profiling by electrochem. methods 80−49958
GaAs, VPE, high purity, residual donors, photocond. expts. 77−85174
GaAs, VPE, hole diffusion lengths, surface prep. and heat treatment effects, etchant evaluation 80−15627
GaAs, VPE, hole diffusion lengths, effect of transition metal diffusional doping 80−15628
GaAs, VPE, incorporation of deep levels, effects of growth conditions 80−20111
n-GaAs, VPE, influence of growth conditions on incorporation of deep levels 77−4310
GaAs, VPE, multi-wafer growth technique using $AsCl_3$-Ga-N_2 system with horizontal reactor 79−28934
GaAs, VPE, partial press. diagrams use for thermodynamic represent. 79−33201
GaAs VPE, residual donor impurities 77−76679
GaAs, VPE, review of growth techniques *(French)* 79−33935
GaAs, VPE, surface defects rel. to technological parameters 78−44015
GaAs, VPE, thermodynamic factor influencing growth rate and layer purity in Ga-$AsCl_3$-H_2 system 79−28933
GaAs, VPE, thermodynamic analysis of Si contamination 79−28932
GaAs, VPE by CVD, vapour-solid interface, expt. anal. *(French)* 79−33940
GaAs, VPE by Ga-$AsCl_3$-H_2 process, role of Si 77−40380
GaAs, VPE by pyrolysis, producing power GaAs MESFETs 78−23623
GaAs, VPE film growth in Ga-$AlCl_3$-H_2 system, O_2 injection effect 79−100057
GaAs VPE growth, growth rate anal. 78−52680
GaAs VPE growth, in situ surface anal. 79−95937
GaAs, VPE growth, surface morphology study by optical microscopy 79−60651
p-GaAs, VPE growth and characterisation, doping levels 80−10841
GaAs, VPE growth by single flat temp. zone method, residual doping level 77−48352
GaAs, VPE growth on {110} cryst. plane 80−10840
GaAs, VPE growth rate variation with distance along substrate within const. temp. zone 78−2384
GaAs, VPE layer growth with abrupt doping profile 80−24746
GaAs, VPE layer on Ge, antiphase domain structures 77−69193
GaAs, VPE layer props. control using boundary layer characts. 80−50561
GaAs VPE layers, back surface gettering, Cr out diffusion 80−10802
GaAs VPE layers, elec. props., semi-insulating substrates effect 80−11123
GaAs VPE layers, electron irrad., electron traps 80−25026
GaAs, VPE layers, growth conditions effect on deep levels 79−95360
semiconductor epitaxial layers continued
n-GaAs VPE layers, Hall mobility, effect of Cu contamination, photolum. expts. 80−54810
GaAs VPE layers, role of diffused Ga vacancy in degradation 78−95050
GaAs VPE layers for FET devices, impurity characterisation 80−29491
GaAs, VPE on Ge substrate, and characterisation 78−72736
GaAs, VPE UV stimulated 78−35313
GaAs, VPE using low press. organometallics 79−100054
n-GaAs vapour phase epitaxial film electrophysical props. rel. to growth temp. *(Russian)* 80−49961
GaAs, vapour-phase epitaxial growth, transfer mechanism of Si 77−51616
GaAs:Be, annealing effect during MBE 78−79898
GaAs:Be, deep levels 80−29358
GaAs:Be,Se VPE layers, ion implanted, donor-acceptor pair radiative recomb. 79−91489
p-GaAs:Be layer, MBE growth, Be doping and diffusion 77−51397
GaAs:Be(C)(Ge)(Sn), MBE layers, photoluminesc. 80−29803
GaAs:Co, epitaxial layers and bulk, diffusion and elec. activity of Co 79−56333
GaAs:Co VPE layers, bound-exciton luminesc., Zeeman anal. 79−95818
GaAs:Cr, epitaxial layers, MBE grown, Hall mobilities, substrate temps. 80−20335
GaAs:Cr, exptl. verification of Cr^{2+} models of photoluminescent transitions 78−27320
GaAs:Cr, intracenter radiative transition in Cr^{2+} ions 79−11463
GaAs:Cr, ion implanted, Cr conc., depth distrib. and diffusion coeff. 80−49243
GaAs:Cr, Se layers, ion implanted, ohmic contact form., contact resist. meas. 79−91158
GaAs:Cr, semiinsulating, LPE and elec. props. 77−44178
GaAs:Cr, VPE growth, carrier conc. profiles 79−74099
GaAs:Cr semi-insulating substrate, photoluminescence obs. of surface degradation during LPE growth 78−6865
GaAs:Cr substrates and LPE layers, Au film deposition and annealing, Cr redistrib. 80−15312
GaAs:Cu, LPE, photoelec. meas. of electron density for different Cu introduction methods 78−43437
GaAs:Fe, for FET, VPE and characterisation 78−19672
GaAs:Fe LPE layers, negative resist. effects and deep acceptor model 77−72929
p-GaAs:Ge, (111) surface, LPE grown, cryst. struct., phys. and chem. props. by Auger obs. 79−73386
GaAs:Ge, cryst. and epitaxial layers, ion-implanted, elec. props. 79−99542
GaAs:Ge, LPE, on semi-insulating GaAs, film-substrate interface characterisation 78−72017
GaAs:Ge, LPE growth, Ge incorporation 78−27423
GaAs:Ge, MBE layers, complex free-carrier profile synthesis 80−54266
GaAs:Ge, mol. beam epitaxy of n- and p-types 80−10839
n-GaAs:Ge, substrate temp. depend. of Ge incorporation during MBE 80−76196
GaAs:Ge, VPE, doping, electrophysical characts. meas. 78−43493
GaAs:Ge, vap. grown, diatomic complex donor and acceptor model 78−80003
n-GaAs:Ge epitaxial layer, ion-implantation doped, anomalous behaviour of impurities 78−18669
GaAs:Ge film, MBE grown, heavily doped, elec. props. rel. to growth parameters 80−100537
GaAs:Ge MBE power FETs with Sn surface impurities 80−80374
GaAs:Ge(Sn), LPE layer growth, impurity effect on terrace form. 79−95288
GaAs:Mn, fabrication and electrical props. 77−80859
GaAs:Mn, LPE layer, near band edge photoluminescence, 2K, low excitation intensities 78−48218
n-GaAs:Ni(Zn), VPE, deep-level transient spectroscopy 80−34383
GaAs:O epitaxial film, impurity states, photocapacitance spectra 80−65625
GaAs:P films, epitaxial growth from melt with components introduced by ion bombardment 77−21044
GaAs:S, dopant conc. control method 77−1807
n-GaAs:S, Zn VPE film, LF current oscill., negative photocond. 77−80858
GaAs:S^+ ion implanted carrier characterisation by cyclotron reson. 77−20472
GaAs:S(Se), MBE grown, surface exchange doping using PbS(Se) captive sources 79−10864
GaAs:Si, accelerated growth rate effect on MBE, Hall mobility and photolum. meas. 80−104067
GaAs:Si, electron irradiated, LPE layers and Bridgman crysts., IR absorption and Hall meas. 77−16345
GaAs:Si, ion implanted effect of anneal ambient and occurrence of compensated regions in Si implants 77−51394
GaAs:Si, momentum distrib. of valence electrons, positron annihilation meas. 79−51530
GaAs:Si, transferred-electron devices by low-level ion implantation 80−92543
GaAs:Si epitaxial films, elec. and photoelec. props., impurity distrib. 80−7006
GaAs:Si LPE layers, surface morphology, substrate misorientation, initial supercooling effects 80−34329
GaAs:Si layers, MBE growth, elec. and optical props., doping characts. 80−10819
GaAs:Si p-n structs., effect of growing conditions on distrib. of recomb. parameters 80−39668
GaAs:Si(Ge) LPE layers, luminesc. props. rel. to substrate quality 78−52583
GaAs:Si(Mg), doped and undoped, sputtered epitaxial films, elec. props. 79−78234
GaAs:Si(S), ion implanted, capless anneal in As controlled vapour 79−55767
GaAs:Sn, 1.39 eV luminescence, injection level depend., freq. response and thermal quenching 78−19529
GaAs:Sn, doping characts. during LPE 79−10866
GaAs:Sn, electronic props. and epilayer-substrate interface props. 77−89886
n-GaAs:Sn, free carrier relax. time, transverse magnetoplasma ref. 77−90212
GaAs:Sn, influence of growth process in doping profile and mobility profile during LPE 79−70000

semiconductor epitaxial layers continued
GaAs:Sn, LPE, growth rate and temp. depend. of impurity incorporation 78−3063
GaAs:Sn, LPE layers, electronic props., depend. on Sn incorporation 78−87883
GaAs:Sn, surface segregation of Sn during MBE, SIMS and AES 78−72031
GaAs:Sn diode, LPE grown, electron irrad. effect on characts. 80−39667
GaAs:Sn films, MBE 80−50563
GaAs:Sn films, MBE grown, doping profiles, carrier mobilities, RHEED and AES obs. 79−1447
GaAs:Sn layers for MESFET, MBE growth 77−15952
GaAs:Sn(Be) MBE films, elec. characterization 79−91168
GaAs:Sn(Te), epitaxial film, influence of impurities on stacking fault energy 80−103371
GaAs:Te, Ge, compensated, activated cond. 77−76968
GaAs:Te, LPE, Te induced defects, rel. to growth conditions 78−6067
GaAs:Te diffused LED, electron irrad. effect on characts. 80−39667
GaAs:Te influence of fluctuations of impurity pot. on Burstein-Moss effect 78−48240
p-GaAs:Zn, luminescent, ion doped MBE growth 80−44436
GaAs:Zn epitaxial layers, composition and Zn carrier conc. 80−25585
GaAs:Zn films, VPE growth and photoluminesc. props. 79−38642
GaAs:Zn MBE layers, ionized beam doping, elec. and optical characts. 79−37721
GaAs:Zn(S), LPE, and doping characts. 79−33948
GaAs/AlGaAs DH wafers and lasers, defect struct., X-ray topography 79−50312
GaAs/GaInP DH, MBE grown, optically pumped laser action at 77K 80−95890
GaAs-Al, X-ray total-external-refl.-Bragg diffr. study 80−34321
p-GaAs-$Al_{0.3}Ga_{0.7}As$, cladded dielec. waveguide, loss meas. using Raman scatt. 79−81539
GaAs-$Al_{0.3}Ga_{0.7}As$ n-N heterojunction, LPE grown, cond. band discontinuity, C-V profiling meas. 80−70801
GaAs-$Al_xGa_{1-x}As$, optically pumped multilayer struct. and DH, laser oscillations 77−3589
GaAs-$Al_xGa_{1-x}As$ current injection multi-quantum-well heterostructure lasers, MBE grown 80−19042
GaAs-$Al_xGa_{1-x}As$ DH lasers, MBE grown, substrate temp. effect on current threshold 80−48243
GaAs-$Al_xGa_{1-x}As$ DH laser, MBE grown, CW electro-optical props. 80−102725
GaAs-$Al_xGa_{1-x}As$ films for optical devices, masked MBE 78−38100
GaAs-$Al_xGa_{1-x}As$ heterojunction, MBE, diffusion across interface, optical annealing expts. 78−2305
GaAs-$Al_xGa_{1-x}As$ heterojunctions, MBE grown, photocollection efficiency and interface charges 79−11199
GaAs-$Al_xGa_{1-x}As$ heterojunctions, LPE grown, 2D electron gas obs. 79−99606
GaAs-$Al_xGa_{1-x}As$ integrated injection lasers and detectors with etched reflectors 77−62074
GaAs-$Al_xGa_{1-x}As$ LPE heterojunction, interface states 78−19128
GaAs-$Al_xGa_{1-x}As$ multilayer struct., MBE, selective area growth using Si shadow masks 77−85946
GaAs-$Al_xGa_{1-x}As$ multilayers, two-dimens. transport at high mag. fields 80−65724
GaAs-AlAs, epitaxial layer, partition coefficients of impurities 77−15443
GaAs-AlAs, epitaxial struct. with alternate layer comp. modulation, fabrication and characterisation 77−1322
GaAs-AlAs, large area p-n heterojunctions, vapour phase epitaxially grown, elec. characterisation 77−11990
GaAs-AlAs, one-dimensional superlattice, X-ray diffr. 77−27860
GaAs-AlAs alternating epitaxial monolayers, Raman scatt. and zone-folding effects 77−90208
GaAs-AlAs alternating monolayers, zone folding effects on phonons 78−72510
GaAs-AlAs layered films, MBE prep., struct., rel. to optical props. 79−77950
GaAs-AlGaAs DH layers, tapered growth by wipingless LPE 77−66594
GaAs-AlGaAs LPE layers, baking effect on surface morphology 78−14625
GaAs-AlGaAs multilayer stack, optical surface wave propag. 78−38090
GaAs-AlGaAs photoelectroluminescent diodes, characts., radiant power 80−6972
GaAs-$Ga_{0.7}Al_{0.3}As$ (001), (211), threading dislocation in single layer heteroepitaxial struct., bowing 79−65341
GaAs-$Ga_{0.8}Al_{0.2}As$ layered struct., LPE, optical surface waves 78−48244
GaAs-$Ga_{1-x}Al_xAs$, DH, improved LPE growth method 77−4746
GaAs-$Ga_{1-x}Al_xAs$, semiconductor superlattices by MBE 79−95939
GaAs-$Ga_{1-x}Al_xAs$ heterostruct. superlattice, props. in high mag. fields 79−73570
GaAs-$Ga_{1-x}Al_xAs$ LPE wafer stress-free dislocation generation 77−75527
GaAs-$Ga_xAl_{1-x}As$ double heterojunction laser structures, LPE growth with double source method 79−28962
GaAs-$Ga_xIn_{1-x}P$ heterostructure, elastic stresses and substrate/epitaxial film mismatch, X-ray diffr. method 80−92794
GaAs-$Ga_xIn_{1-x}P$ multilayer epitaxial films, MBE technology and epitaxial layers props. 79−33945
GaAs-GaAlAs DH material, dislocation glide and climb, electron diffr. 78−83824
GaAs-GaAlAs heterostructures, growth by metal-alkyl hydride process 78−15313
GaAs-GaAlAs injection laser sources for fibre optic communications, design 79−31923
GaAs-GaAlAs LPE layers, laser material, shallow growth pits obs. 77−7985
GaAs-GaAlAs LPE layers, DH material, TEM obs. of crystal defects 78−6241
GaAs-GaAlAs laser, degraded, characterisation by selective etching and photoetching 80−48252
GaAs-GaAlAs superlattices, metalorganic VPE growth, in sites ellipsometry monitoring 80−70547
n-GaAs-GaAs:Cr, interface elec. props., substrate effects 78−6438
n-GaAs-GaAs:Cr. semiinsulating, low freq. current pulses 77−8176
GaAs-$GaAs_{0.5}P_{0.5}$ almost perfect epitaxial multilayers, TEM obs. 77−89668
GaAs-$GaAs_xSb_{1-x}$, heteroepitaxial structs., mismatch dislocation nets 79−10855
semiconductor epitaxial layers continued
GaAs-GaInAs structure, dislocation struct., TEM anal., appl. as IR LED 80−70206
GaAs-Ge, heterostructure, zincblende-on-diamond type systems, MBE growth, (110) orientation as preferred orientation 80−80099
GaAs-$Ge_{1-x}(GaAs)_x$ n-p heterojunctions, hydrostatic press. effect on elect. and photoelectric props. 80−20304
GaAs-on-sapphire spatially distributed thermal light modulator 79−59839
GaAs-S VPE layers, thickness and carrier conc. variations 79−100060
$(GaAs)_n(AlAs)_m$ multilayers, MBE, interdiffusion, X-ray diffr. study 80−70474
GaAsGa$_{1-x}$Al$_x$As DH laser material, rapid optical degradation obs. 77−75528
GaAsP epitaxial film, composition self modulation, defect struct. 80−34331
GaAsP epitaxial waveguide, electro-optic phase modulation of laser radiation 79−10417
GaAsP, misfit dislocation array obs. by TEM, nucleation and multiplication 77−39742
GaAsP, VPE, lattice forbidden band composition depend. *(Hungarian)* 80−6669
$GaAs_{0.6}P_{0.4}$, VPE, hole diffusion lengths, surface prep. and heat treatment effects, etchant evaluation 80−15627
$GaAs_{0.6}P_{0.4}$, VPE, hole diffusion lengths, effect of transition metal diffusional doping 80−15628
$GaAs_{1-x}P_x$ based structs., carrier conc., mobility calcs. from Hall effect meas. 78−60138
$GaAs_{1-x}P_x$ epi-wafer, comp. profile of heterogeneous struct., anodisation-electrorefl. meas. 78−26782
$GaAs_{1-x}P_x$ epitaxial films, VPE grown, photolum. spectra 79−73997
$GaAs_{1-x}P_x$ epitaxial layer prep. for electroluminescent diodes *(Czech)* 77−21032
$GaAs_{1-x}P_x$ epitaxial layers, charge carrier conc. determ. from low-field electrorefl. spectra 77−85320
$GaAs_{1-x}P_x$, MBE growth on GaP, and crystallographic evaluation 77−8762
$GaAs_{1-x}P_x$, modulation of direct and indirect gaps, piezotransmission meas. 77−24819
$GaAs_{1-x}P_x$, mol. beam epitaxial growth, cryst. quality, composition investig. *(Japanese)* 77−55895
$GaAs_{1-x}P_x$, N doping using ionised beam in MBE 78−47400
$GaAs_{1-x}P_x$, prep. and photoluminesc. and. electroluminesc. props. *(Czech)* 78−48233
$GaAs_{1-x}P_x$, solid soln. comp. control during gas-phase heteroepitaxy 77−85091
$GaAs_{1-x}P_x$, structural defects, optical props. effect 80−55208
$GaAs_{1-x}P_x$: N, absorption and photolum. spectra meas. 77−24894
$GaAs_{1-x}P_x$:Zn implanted, Zn diffusion 77−84993
$GaAs_{1-x}P_x$-GaP heterostructure, photomodulation spectroscopic exam. 77−40257
$GaAs_xP_{1-x}$, surface phonon polaritons, total internal refl. *(Russian)* 79−38688
$GaAs_xP_{1-x}$ epitaxial film nonlinear light absorpt., photoluminesc. meas. 77−66528
$GaAs_xP_{1-x}$, liquid phase epitaxial growth on GaP, growth and properties 79−47641
$GaAs_yP_{1-y}$ alloy, composition effects in growth by MBE 80−59816
$GaAs_{1-x}Px$, heteroepitaxial solid soln., defects of struct 79−28223
$GaAs_{1-x}Sb$, microprocessor controlled MBE growth 78−3058
$GaAs_{1-x}Sb_x$, cryst. growth by steady state LPE 78−44032
$GaAs_{1-x}Sb_x$ epitaxial n-n heterostructures, gap energies and interface pots., modulation electroabsorpt. meas. 79−11201
$GaAs_{1-x}Sb_x$ layer on GaAs, dislocation density reduction by improved LPE growth method 80−76202
$GaAs_{1-x}Sb_x$, MBE grown, surface struct. exam. by MEED 78−87847
$GaAs_{1-x}Sb_x$, narrow-gap film on wide-gap GaAs, energy gap grading, optical transmission meas. 77−20943
$GaAs_{1-x}Sb_x$ on GaAs, LPE growth of GaAs 79−61519
$GaAs_{1-x}Sb_x$ undoped epitaxial layers, photoluminesc. meas. 80−20703
$GaAs_xSb_{1-x}$, lattice-matched LPE growth in InP substrates 79−42402
$GaAs_xSb_{1-x}$ solid solution epitaxial layer, morphology and defect structure 77−1330
$GaAs_xSb_{1-x}$, struct. defects rel. to luminesc. 78−72040
$GaAs_xSb_{1-x}$-GaAs epitaxial films and multilayer heterostruct., SEM obs. under cathodolum. conditions 79−11023
$GaAs_{2-x-z}Sb_xP_z$, LPE growth, continuous comp. grading, use as secondary substrate 77−31913
$(GaAs)_{1-x}(ZnSe)_x$, LPE growth, resist., Hall effect and cathodoluminesc. meas. 77−28270
GaAs:Cu, epitaxial and bulk conductivities compared *(Russian)* 78−10585
GaInAs, electron-pumped laser, far-field radiation pattern, optical confinement effects 79−86181
GaInAs-InP, growth by low-pressure metalorganic CVD 80−71595
$Ga_{0.47}In_{0.53}As$, LPE growth and characterisation 80−10845
$Ga_{1-x}In_xAs$ epitaxial layer growth by organometallic pyrolysis, homojunction LED prep. 80−76194
$Ga_{1-x}In_xAs$, VPE grown, refractive index, reflectance meas. 79−4780
$Ga_{1-x}In_xAs$, VPE layers, main electron trap, transient capacitance spectroscopy obs. 78−34800
$Ga_{1-x}In_xAs$:Mn grown by LPE, elect. props. 80−100541
$Ga_{1-x}In_xAs$-GaAs epitaxial interface with small misfits, TEM image contrast 80−2275
$Ga_{1-x}In_xAs$-GaAs low-misfit epitaxial interface, electron microscope contrast 79−73416
$Ga_xIn_{1-x}As$, on (111)B InP, LPE growth, characterisation of high purity lattice 80−104082
$Ga_xIn_{1-x}As$ on InP, lattice matched LPE film growth and characts. 78−72033
$Ga_xIn_{1-x}As$, substrate orientation effect on liq.-solid distrib. coeffs., 600-700°C 80−2278
$Ga_xIn_{1-x}As$-InP, lattice matched LPE film growth and characts. 78−15320
$Ga_xIn_{1-x}As$-InP, MBE film growth, composition control obs. 80−84399
GaInAsP, VPE growth and props. 80−16194
GaInAsP-InP DH laser grown by newly designed vertical LPE furnace 78−9380
GaInAsP-InP DH laser, relaxation and delay in oscillations 78−13709
$Ga_{0.08}In_{0.92}As_{0.18}P_{0.82}$, band struct., optical studies 79−47013

semiconductor epitaxial layers continued
$Ga_xIn_{1-x}As_yP_{1-y}$, conduction band and phonons, Shubnikov-de Haas effect, magnetophonon resonance, Raman scattering 80−24795
n-$Ga_xIn_{1-x}As_{1-y}P_y$, photoluminesc. of epitaxial films, isovalent substitution 80−16097
$Ga_xIn_{1-x}As_{1-y}P_y$:Ge(Sn)(Te), epitaxial film, elec. and optical props. 79−11251
$Ga_xIn_{1-x}As_yP_{1-x}$, epitaxial layers on InP, expt. determ. of effective masses 79−65370
$Ga_xIn_{1-x}As_yP_{1-y}$, IR refl. spectra 80−60602
$Ga_xIn_{1-x}As_yP_{1-y}$, LPE layers, growth and characterisation 78−38983
$Ga_xIn_{1-x}As_yP_{1-y}$ LPE layers matched to InP, comp. and lasing wavelengths 78−71103
$Ga_xIn_{1-x}As_yP_{1-y}$-GaAs substrate, lattice matching 79−90901
$Ga_xIn_xAs_yP_{1-y}$-InP substrate, lattice matching 79−90901
$Ga_yIn_{1-y}As_xP_{1-x}$, LPE growth 80−66440
$Ga_{1-y}In_yAs_xSb_{1-x}$, LPE on GaSb, miscibility gap in liq. phase and lattice mismatch 80−15404
$Ga_xIn_{1-x}As_ySb_{1-y}$, epitaxial film and DH, luminesc. props. 77−686
$Ga_xIn_{1-x}P$, epitaxial film, diffusion of Cu(Au)(Zn), intrinsic impurity effects 78−87825
$Ga_xIn_{1-x}P$ MBE layers, comp., Rutherford scatt. and X-ray diffr. meas. 80−75457
$Ga_xIn_{1-x}P$ solid soln. epitaxial layers, stabilisation of composition 78−18933
$Ga_xIn_{1-x}P$ solid solns., isothermal liq. epitaxy 80−60793
$Ga_xIn_{1-x}P$, undoped liquid epitaxial layers, effect of heat treatment on photoluminescence 78−60512
$Ga_xIn_{1-x}P$:N, Delta lattice parameter model, correl. with electronic props. 78−91560
$Ga_xIn_{1-x}P$:N layers, LPE growth, luminesc. and direct exptl. obs. of band struct. effects 77−52157
$Ga_{1-x}In_xP_{1-y}As_y$, carrier compensation and alloy scatt. 80−29490
$Ga_xIn_{1-x}P_yAs_{1-y}$, (0.5<y<0.9), LPE on InP, Ga, As distrib. coeffs., lattice matching 78−47673
$Ga_{1-x}In_xSb$, LPE on GaSb by stepwise grading, and characterisation 78−72745
$Ga_{1-x}In_xSb$-GaSb, lattice parameter meas. in epitaxic layers 79−11040
$Ga_xIn_{1-x}Sb$, LPE, growth by vertical dipping method and elec. props. 77−85949
GaN and GaN:Zn, cathodoluminescence, doping effect 77−20935
GaN CVD layer props. rel. to Ga-GaCl conversion efficiency and HN_3 decompositon 77−77404
GaN, cathodolum., 78-300K 78−19575
GaN, characts. from cathodoluminesc. 78−35208
GaN, cryst. quality meas. by channelling 78−38986
GaN epitaxial films, cathodoluminesc. spectra 80−71496
GaN, epitaxial growth on sapphire substrates, elec. props., X-ray diffr. anal., photoluminescence spectra 79−4919
GaN, epitaxial layer prep. and elec. props. 77−85097
GaN epitaxial layers, exciton cathodolum. *(Russian)* 78−76543
GaN epitaxial layers, exciton cathode luminesc. 79−65933
GaN epitaxial layers for LED, X-ray diffr. topography and cryst. characterisation 79−65336
GaN epitaxy, sapphire substrate prep. 78−39929
GaN, high-press. VPE and elec. characts. 78−14627
GaN, magnetoplasma reflectivity, difference method, IR *(German)* 77−12363
GaN, photoluminesc. spectra, energy distrib. 80−97339
GaN, planar waveguides for integrated optics appls. 79−10416
GaN, preparation by pyrolysis of $Ga(CH_3)_3$ in NH_3, cathodoluminesc. 77−4691
GaN, pure and Zn-doped, luminesc. 78−10955
GaN, refl. spectra, 5-12.5 eV 79−99967
GaN, VPE, on sapphire, crystallographic aspects 78−2387
GaN, VPE, requirements and structural etching of Al_2O_3 substrates *(Polish)* 77−43440
GaN VPE for blue LEDs *(French)* 79−28928
GaN, VPE growth rate influence on elec. and luminesc. props. 80−100702
GaN:Al, VPE grown, luminesc. and elec. props. depend. on doping conc., bound excitons 80−20688
GaN:As(P), implanted single cryst. film, cathodolum. 78−60523
GaN:Zn, epitaxial layer, effective electroluminesc., blue regime *(Russian)* 77−77302
GaN:Zn, low voltage LED, epitaxial layer, growth and electrolum. *(Russian)* 77−77297
GaN:Zn epilayers, growth parameters effect on props., device struct. 78−26975
GaN:Zn epitaxial films, luminesc. spectra separation into individual bands by impurity absorpt. region excitation 79−74002
GaN-AlN, solid solution, epitaxial growth and electrical props. 77−73236
GaP, birefringence observations of strain and plastic deform. 80−50678
GaP, current controlled LPE from finite volume melt 80−20805
GaP, deep level profiles at substrate-epitaxial interfaces, photoionisation meas. 79−38025
n-GaP, electrical parameter determ. by graphical method *(Russian)* 77−15975
GaP, epitaxial growth from Sb and Bi melts 79−52131
GaP epitaxial growth from solution in melt, crystn. theory 80−16204
GaP, epitaxial layer, carrier recomb. at dislocations 77−20932
GaP, epitaxial layer prep. and elec. props. 77−85096
GaP, epitaxial layers, anisotropy of growth rate from soln. in melt 78−35322
GaP, epitaxial layers, dislocation recomb., SEM cathodoluminescence studies 79−42558
GaP epitaxial layers, stable growth conditions, by molten salt electrodeposition on Si and GaP substrates 79−20000
p-GaP, epitaxial layers grown from liq., overcompensated, doping levels 78−91353
GaP, epitaxial struct., cathodolum. in SEM 78−10991
GaP for yellow-LEDs, prep. and props. *(Czech)* 78−48234
GaP, grown in Ga-PCl_3-H_2 system, surface defects 77−7993
GaP, growth and props. of LPE layers on Si substrates 78−6864
GaP, heteroepitaxial CVD on Si, dual process, film characts. 77−16503
GaP, heteroepitaxial deposition on GaAs, Sn solvent inclusion, surface morphology *(German)* 79−28968
GaP, heteroepitaxial growth on Si, substrate misorientation effects 78−3055
semiconductor epitaxial layers continued
n-GaP, interface-recomb.-controlled minority carrier lifetime obs. 77−12027
GaP, ionised-cluster beam epitaxial growth on GaP and Si, characts. for LED 79−28951
GaP, LPE, cathodo- and electrolum., residual impurity and struct. defect effects 78−19570
GaP, LPE, LED fabrication and electroluminesc. characts. 77−28632
n-GaP, LPE, minority carrier bulk lifetime and diffusion coeff. meas. 77−11932
n-GaP, LPE, non-radiative recombination 78−19565
GaP, LPE, perfection, effect of dislocation loops in GaP substrate 78−30843
GaP, LPE at 650°C from In solvent, low Si contamination 78−80480
GaP, LPE layer for LED, photoluminesc. distrib. meas. *(Czech)* 78−48209
p-GaP, LPE layers, Hall effect 78−91704
GaP LPE layers, low temp. growth from In solvent 79−56924
GaP LPE layers and LEC substrates, correlation between dislocation pits 78−38706
GaP, LPE layers high purity, invest. *(German)* 78−31353
GaP layers, heteroepitaxy, grown on Si and Ge from multiple component solns. *(Russian)* 78−15319
GaP layers, LPE growth, elec. props., residual impurities 79−38202
GaP luminescence, crystal defects influence obs. 79−87511
GaP, MBE growth on GaP, and crystallographic evaluation 77−8762
GaP, minority carrier lifetimes at dislocations, SEM meas. using photon counting 78−23109
GaP, mol. beam epitaxial growth, cryst. quality composition investig. *(Japanese)* 77−55895
GaP, non-radiative recombination and structural defects 78−19566
GaP, thickness and diffusion length, photocurrent meas. 77−32096
n-GaP, transverse magnetoresist. *(Russian)* 77−76964
GaP, two-stage vapour/liq. epitaxial growth on Si 78−3054
GaP, VPE, background deep level defects, transient capacitance obs. 77−62854
GaP, VPE cryst., electrolum. characts. 77−28631
GaP, VPE layer on Si or Ge, antiphase domain structures 77−69193
GaP, VPE layer structures for LED's, SEM, and TEM obs. of dislocation density reduction expt. 80−100425
GaP VPE layers, precision lattice parameter meas. by Umweganregung method 79−65047
GaP, VPE Ni contaminant detection, IR photoluminescence of Ni 78−15212
GaP:Ce(Dy)(Pr) epitaxial films, photoluminesc. spectra 80−66294
GaP:Cr epitaxial layers, Cr conc. profile determ. 80−65029
GaP:Cu, LPE, photoconductive props. obs. 78−47836
GaP:Fe n-i-n epitaxial struct., photoconductivity, recombination scheme *(Russian)* 80−15569
n-GaP:In, LPE from In solvent, dislocation density reduction by doping 78−18919
GaP:N, determination of nitrogen concentration from cathodoluminescence spectra 78−38744
GaP:N, epitaxial layer doping 77−51396
GaP:N, epitaxial layers, N concentration determination by two independent methods 80−39142
GaP:N, N doping profiles in GaP grown by LPE, cathodoluminesc. data 79−23631
GaP:N VPE LED, deep level centres, DLTS studies 79−42493
GaP:N VPE layers, thermal emission energies, trapping, and carrier lifetimes, deep level capacitance spectroscopy 79−42487
GaP:N(N,O) epitaxial struct., luminesc. study of degradation during heat treatment 80−45139
GaP:Sb(Bi), gap vibrs. and impurity conc. determ. 79−69869
GaP:Sn, LPE growth from Sn soln., elec. resist. and Hall coeff. meas. 78−2593
GaP:Te, dopant distrib. obs. by amalgam polarography 77−39609
n-GaP:Te, LPE layers, Hall effect 78−91704
GaP:Te on GaAs, LPE growth fron Sn, exam. of impurity band conduction effects 79−11249
GaP:Zn, doping from gas phase during LPE 80−55312
GaP:Zn, Sn doped epitaxial layers, Hall const., hole mobility and conc. 80−15143
GaP:Zn, Te, epitaxial layers, determ. of Zn conc. 79−77614
GaP:Zn,O, epitaxial p-n junction, IR electroluminesc. exam. *(Russian)* 78−35207
GaP/Si heterostruct., differential thermal contraction, plastic deform., fracture 80−108494
GaP-GaAlP-GaP, lattice-matched, LPE layer growth under P vapour pressure and reduced O_2 contamination 79−51445
GaP-In LPE layers, carrier diffusion lengths and escape probabilities optical absorpt. and photoemission meas. 79−87559
GaP-Si, heterostructure, zincblende-on-diamond type systems, MBE growth, (110) orientation as preferred orientation 80−80099
$GaP_{0.9}As_{0.1}$/GaP, heteroepitaxial structs., refined formulation of relative orientation criterias 80−44448
GaP_xAs_{1-x} ($0 \leq x \leq 0.32$) epitaxial film, one-dimens. superlattice, X-ray spectrometer scanning, struct. variations 78−47681
GaP_xAs_{1-x}, N doped, alloying induced shift between excitation and luminesc. of N bound exciton 79−52013
GaP_xAs_{1-x} solid soln., specularly smooth epitaxial layers, superlattice struct. 77−24959
GaP_xAs_{1-x}, surface defects and comp. inhomogeneity during gas-phase heteroepitaxy 77−85090
$(GaP)_x(ZnSe)_{1-x}$/GaP, epitaxial heterostructures, chem. microinhomogeneity 77−80831
GaS, sputtering conditions effect on film struct. and optical absorption *(Russian)* 77−12525
GaSb, electroliquid epitaxial growth 80−89160
GaSb high-purity and doped layers grown by LPE and VPE methods 78−6863
n-GaSb:Te, IR refl. meas., carrier conc. and mobility determ. 80−80769
p-GaSb-Zn, lifetime of nonequilib. carriers, determ. from circular polarisation of luminesc. 77−24898
$GaSb_{1-y}As_y$, MBE-grown, substrate effect on lattice consts. 79−77942
$(GaSb)_{1-x}Ge_x$ films, single-cryst. metastable semicond., growth and phase stability 80−80115
Ga_2Se_3, vapour phase deposited films, struct. 78−2383
Ga_2Te_3, vapour phase deposited films, struct. 78−2383
Ge, amorphous, growth rate of crystallisation, Raman spectroscopy study 80−44227

semiconductor epitaxial layers continued
Ge, amorphous film, ion-implanted, regrowth 79−15043
Ge, amorphous layer, epitaxial recrystn. by electron irrad., solar cell appl. 78−84079
Ge, crystallographic imperfections 77−35826
Ge, epitaxial, in situ X-ray topography, misfit dislocations 78−47671
Ge, epitaxial and amorphous film growth, low energy ion beam deposition 77−28729
Ge epitaxial film, ion implantation and electron beam anneal effects on carrier conc. 80−75255
Ge epitaxial film, misfit dislocations, determination of Burgers vector *(Russian)* 79−33207
Ge epitaxial film, vac. deposited on GaAs, doping effect of annealed GaAs surface 80−65718
Ge, epitaxial film growth by hydride-iodide method 77−48343
Ge epitaxial films, structural perfection rel. to deposition conditions 78−43258
Ge, epitaxial growth from monogermane at 685°C 78−51833
Ge, epitaxial growth of very thin electron microscopy specimens 80−100793
Ge epitaxial layer on GaAs tetragonal distortion in heteroepitaxial layer, X-ray diffr. exam. 78−67922
Ge, epitaxial-diffusion p-n junction, inductive props. in secondary breakdown 80−15598
Ge, film, epitaxial growth on Si, interdiffusion, plasmon energy loss anal. 77−31916
Ge film on Si, influence of fragmentary struct. on galvanomag. effects *(Ukrainian)* 78−84327
Ge films, ohmic contacts for GaAs devices 78−88027
Ge films on semicondcuting substrates with diamond structure, computer model of autoepitaxial growth 79−95927
Ge films used in fabricating ohmic contacts for GaAs devices 78−47871
p-Ge, fragmented struct., elec. cond., Hall coeff. and magnetoresist. meas. 77−15979
Ge heteroepitaxial film, ethanol pulsed adsorption effect on elec. cond. 80−93014
P-Ge, heteroepitaxial film, galvanomagnetic effects, influence of mechanical stresses 79−91171
Ge, ion sputtering, growth mechanism, struct., props. 77−31917
Ge, ion-implanted amorphous layers, melting model for pulsing-laser annealing 79−56080
Ge, MBE, on GaAs, hetrojunction chemistry, photoemission expts. 78−95244
Ge, on GaAs, orientation depend. of interface dipole energies 78−39196
Ge, on GaAs substrate, misfit dislocation multiplication mechanism 78−87673
Ge, on n-GaAs, with Ni overlayer, smooth and continuous ohmic contact form. by solid-state diffusion 78−68086
Ge, on Si, misfit, strain and dislocations, book contrib. 79−82499
Ge p-n junction, high-grade, temp. gradient zone melting in production 77−4747
Ge, solid-phase epitaxial growth through PdGe layers, channelling and backscatt. obs. 77−85936
Ge^+, low energy mass analysed ion beam deposition on Ge and Si substrates 79−33946
Ge:B, epitaxial film, exam. of doping during chemical deposition from gas phase 79−1446
Ge:P, doping of epitaxial layers, in chloride and hydride processes 78−43036
Ge-$Ga_{1-x}Al_xAs$, MBE of ultra thin film superlattices on GaAs substrates, TEM study 79−37932
Ge-GaAs, heteroepitaxial systems, misfit dislocations obs. using HV electron microscopy 80−100242
Ge-GaAs heteroepitaxial system, dislocation struct. in stress measurements 80−29030
Ge-GaAs heterojunctions, electronic struct. 78−19138
Ge-GaAs inter faces, heteroepitaxial, misfit dislocations, TEM obs. 79−23610
Ge-Si, solid phase heteroepitaxy 80−6670
Ge-Si, UHV-produced epitaxial structs., electrophys. props. 78−3060
Ge-Si alloy, epitaxial growth by getter sputtering, charact. 79−28915
$Hg_{0.6}Cd_{0.4}Te$ LPE layer growth from Te-, Hg-, and HgTe-rich solns., comparison 80−76199
$Hg_{1-x}Cd_xTe$, epitaxial layer, vapour phase growth 79−1829
$Hg_{1-x}Cd_xTe$, epitaxial layers, elec. properties in the range 4.2 to 300K *(French)* 80−65721
$Hg_{1-x}Cd_xTe$ epitaxial layers, elec. props. 80−96910
$Hg_{1-x}Cd_xTe$, LPE growth and characterisation 80−50565
$Hg_{1-x}Cd_xTe$, LPE-grown and optically pumped crystal, continuous lasing at 2.79 μm 79−68397
$Hg_{1-x}Cd_xTe$, surface topographic stoichiometry variations, electrolyte electrorefl. obs. 78−27249
HgS, RF sputtering on NaCl, growth and struct., electron diffr. and TEM obs. 77−90271
HgSe, epitaxial growth on CdSe, struct. and electrophysical props. 77−12540
HgTe, conditions for oriented crystn. 79−52124
HgTe, heteroepitaxial growth by close-spaced technique of confined type *(Japanese)* 77−24967
HgTe-CdTe, form. by evap. and interdiffusion under isothermal conditions, book contrib. 77−12549
(In,GA)(As,P) binary, ternary and quaternary, hydride vapour phase epitaxy, cryst. growth and props. 80−66434
In-Ga-As-P, phase diagram rel. to lattice matched LPE 78−39708
$In_{1-x}Al_xP$:Bi(N)(Zn,O) radiative recombination at isoelectronic centres 79−52027
InAs, electron beam excitation, luminesc. and stimulated emission 77−16339
InAs, epilayer, MBE growth parameters, relationship with elec. props. 80−2296
InAs epilayers in MOS, carrier transport coeffs. determ. by multilayer model 78−2575
InAs, heteroepitaxial, far IR refl. and transmission meas., surface and interface effects 80−16044
InAs, heteroepitaxial film, orientation and struct. investigation 79−82480
InAs heteroepitaxial layers, VPE grown, effect of $AsCl_3$ mole fraction on elec. props. 79−11255
InAs, heteroepitaxial layers, $AsCl_3$ mole, fraction and substrate orientation effects on elec. parameters 80−39690
InAs, laser action mechanisms with electron beam excitation 80−28240
semiconductor epitaxial layers continued
InAs, on GaAs, charge transport obs. by gate-voltage-controlled meas. on MOS struct. 77−47912
InAs on GaAs, epitaxial-substrate system, far IR transmission and refl. 78−6802
InAs on GaAs, far IR reflectivity obs. 77−40251
InAs, on GaAs, heteroepitaxial layers, compositional profile, AES 77−20212
InAs, on GaAs substrate, electron diffr. and SEM exam., electronic props. 79−1552
InAs, organometallic VPE growth on InAs and GaSb 80−16193
InAs, possibility of local epitaxy in depressions on unmasked substrates 79−42415
n-InAs, VPE layers, on GaAs substrate, electronic profile 79−95525
InAs-GaSb heterostruct. superlattice, props. in high mag. fields 79−73570
$InAs_{1-x}P_x$, high field instabilities, press. and comp. depends. 78−26873
$InAs_{1-x}P_x$, sub-threshold velocity-field characts., intervalley separation 77−63010
$InAs_yP_{1-y}$ alloy, composition effects in growth by MBE 80−59816
$InAs_{1-x}Sb_x$, epitaxial film, carrier recomb., elec. and optical props. 79−15164
$InAs_{1-x}Sb_x$ on GaSb, LPE growth 80−29293
(InGa)As, growth kinetics for step-cooling LPE technique 77−40395
InGaAs, LPE, diffusion-limited step-cooling technique, layer thickness and composition 80−84402
InGaAs, transferred electron photoemission to 1.65μm 78−68600
InGaAs-GaAs heterojunction with low misfit, misfit dislocation struct. 77−62783
$In_{0.53}Ga_{0.47}As$, growth on (100)-oriented InP, from supercooled solution 79−70001
$In_{0.53}Ga_{0.47}As$, LPE layer on InP, electron mobility and energy gap 77−24627
$In_{1-x}Ga_xAs$, LPE, electron mobility and max. drift vel., microwave device appls. 77−77431
$In_{1-x}Ga_xAs$, LPE growth on InP substrate, quasi grown layers, photoluminescence meas. 79−23862
$In_{1-x}Ga_xAs$, LPE layer on InP substrate, phys., elec. and optical props. 78−39235
$In_{1-x}Ga_xAs$, LPE on InP substrate, comp. latching phenomenon and lattice mismatching effects 79−28961
$In_{1-x}Ga_xAs$, MBE-grown, substrate effect on lattice consts. 79−77942
$In_{1-x}Ga_xAs$-$GaSb_{1-y}As_y$, semiconductor superlattices by MBE 79−95939
$In_{1-x}Ga_xAs$-$GaSb_{1-y}As_y$, new heterostruct. characts. 78−72247
$In_xGa_{1-x}As$:Zn, lattice matching to InP, LPE growth conditions 80−70541
n-$In_xGa_{1-x}As$, epitaxial growth on GaAs 77−1812
$In_xGa_{1-x}As$, epitaxial solid soln. film, spectral depend. of transparency, absorpt. spectra calcs. 80−45161
$In_xGa_{1-x}As$, heteroepitaxial, MBE grown, props. 78−84328
$In_xGa_{1-x}As$, LPE growth on GaAs 79−61519
$In_xGa_{1-x}As$ layers, on GaAs substrate, MBE fabrication and laser operation 80−10820
$In_xGa_{1-x}As$, MBE layers on InP substrates, elec. props., photoluminesc., X-ray and Auger obs. 79−51450
$In_xGa_{1-x}As$ MBE layers on InP substrate, lattice deformation, misorientation 79−90896
$In_xGa_{1-x}As$, waveguiding at 1.06 μm, losses 78−18052
$In_xGa_{1-x}As$:Si, p-n junction form. in LPE layers, In content effect on inversion temp. 77−4266
$In_xGa_{1-x}As$-$InAs_xP_{1-x}$ VPE mixed crystal composition rel. to vapour pressure *(Japanese)* 77−55893
InGaAsP, anodic oxidation, refractive indices 80−97601
InGaAsP avalanche photodiodes, breakdown mechanism, donor conc. effect 80−70710
InGaAsP, epitaxial layer, defect evaluation by cathodoluminescence 80−2866
InGaAsP, expitaxial growth by chloride CVD process, thermodynamic anal. 80−64936
InGaAsP, high radiance CW LEDs emitting at 1.30 μm 78−22196
InGaAsP, LPE, diffusion-limited step-cooling technique, layer thickness and composition 80−84402
InGaAsP, LPE growth on InP, influence of lattice mismatch on surface morphology 79−1553
InGaAsP, LPE growth techniques influence on composition 79−52130
InGaAsP, LPE growth, impurity depend. of distrib. coeff. 80−10843
InGaAsP, LPE grown, impurity effect on surface morphology 80−29291
InGaAsP LPE heterostructs., interface grading, Auger depth profile 80−103585
InGaAsP LPE layers on InP substrate, material selective chemical etching 79−70188
InGaAsP, with and without InP cladding layers, low photolum. regions 79−33754
InGaAsP:Sn(Te)(Zn), LPE growth, influence of growth-solution dopants on distrib. coeffs. 79−47640
InGaAsP/InP, native oxide stripe laser 79−68405
InGaAsP/InP phototransistors, fabrication by LPE, photodetectors 80−95139
InGaAsP-InP, anomalous luminesc., near heterojunction interface 79−65932
InGaAsP-InP DH laser, 1.55 μm, low temp. LPE growth for room-temp. CW operation 80−64045
InGaAsP-InP DH lasers, perturbed InP growth, photoluminesc. study 80−106518
InGaAsP-InP heterojunction, LPE, lattice mismatch, Auger depth profile 79−87005
InGaAsP-InP layers, grown by LPE techniques, lattice const., bandgap, thickness and surface morphology meas. 80−59818
$In_{0.79}Ga_{0.21}As_{0.54}P_{0.46}$, LPE layer, electroreflectance meas. 79−24290
$In_{1-x}Ga_xAs_{1-y}P_y$ layers on InP substrate, LPE growth, quaternary phase diagram, and band gaps 79−42403
$In_{1-x}Ga_xAs_yP_{1-y}$ DH laser, low threshold current density, near equilibrium LPE growth 80−19040
$In_{1-x}Ga_xAs_yP_{1-y}$ epitaxial layer, far IR refl. spectra, lattice vibrs. 80−97282
$In_{1-x}Ga_xAs_yP_{1-y}$ far IR reflection spectrum 80−60612
$In_{1-x}Ga_xAs_yP_{1-y}$, hole mobility over temp. range 77 to 300K 80−60111
$In_{1-x}Ga_xAs_yP_{1-y}$, LPE growth on InP (100), lattice matched composition 78−87881
$In_{1-x}Ga_xAs_yP_{1-y}$ LPE layers, background carrier conc. and electron mobility. 79−95523

semiconductor epitaxial layers continued
$In_{1-x}Ga_xAs_yP_{1-y}$, lattice vibrs., Raman study 78−91391
$In_{1-x}Ga_xAs_yP_{1-y}$, lattice matched to InP, band gap vs. comp., and Vegard's law demonstration 79−7782
$In_{1-x}Ga_xAs_yP_{1-y}$, oscillatory magneto-transmission, band parameters 79−60707
$In_{1-x}Ga_xAs_yP_{1-y}$ quaternaries VPE 0.75 to 1.35 eV band gap range 79−69987
$In_{1-x}Ga_xAs_yP_{1-y}$, traps in device quality n- and p-type LPE material 80−10999
$In_{1-x}Ga_xAs_yP_{1-y}$/InP 1.5 μm room-temp. CW laser fabrication and operation 80−64070
$In_xGa_{1-x}As_{1-y}P_y$ epitaxial layers, characterisation and relation to lattice matching 80−100540
$In_xGa_{1-x}As_yP_{1-y}$ layers on InP, LPE and opt. props. characteris. 79−28849
$In_xGa_{1-x}As_yP_{1-y}$, on InP, heterojunction photodiode characts. 78−14800
$In_xGa_{1-x}As_yP_{1-y}$ photodetector diode on InP substrate dark currents, tunnelling, energy gaps, effective masses 80−70805
InGaAsSb, LPE growth, and appl. in GaSb/AlGaAsSb/InGaAsSb/AlGaAsSb/GaSb DH 80−16205
$In_{1-x}Ga_xAs_{1-y}Sb_y$, LPE growth on (111)B-oriented InAs, growth conditions and lattice matching 77−24973
InGaP/InGaAs struct. for transferred electron photocathodes, VPE growth and characterisation 80−76193
$In_{0.3}Ga_{0.7}P$, N free and implanted, photoluminescence study 80−97322
$In_{1-x}Ga_xP$, cathodolum. obs., recomb. mechanisms 78−72613
$In_{1-x}Ga_xP$, compositional inhomogeneity 80−88444
$In_{1-x}Ga_xP$, epitaxial growth from melt, optimisation of growth conditions 79−52132
$In_{1-x}Ga_xP$, epitaxial growth on GaAs substrate, formation of intermediate layers 80−2304
$In_{1-x}Ga_xP$, LPE, on $GaAs_{1-y}P_y$, photo- and cathodolum. 78−19559
$In_{1-x}Ga_xP$:Bi(N)(Zn,O) radiative recombination at isoelectronic centres 79−52027
$In_{1-x}Ga_xP$:N(Te), composition depend. of bound state luminesc. transitions 78−39595
$In_{1-x}Ga_yP$-GaAs heterojunction, VPE, energy band gap and lattice parameter, lattice mismatch effects 78−95345
$In_xGa_{1-x}P$, solid solns., gas phase epitaxy from Ga-In-HCl-PH_3-H_2 systems 78−34722
$In_xGa_{1-x}P$-GaAs heterojunction, interface recomb. velocity determ. 77−89838
InGaPAs LPE layers, compositional inhomogeneity, photoluminesc. obs. 80−75451
InGaPAs LPE multilayered DH lasers exhibiting quantum size effects 78−1227
InGaPAs, LPE-grown on (001)-InP, lattice mismatch study using X-ray double-cryst. diffr. 79−99440
$In_{1-x}Ga_xP_{1-y}As_y$ LPE films, hot electron and magnetotransport props. 78−26977
$In_{1-x}Ga_xP_{1-z}As_z$, lattice matched to InP, electroreflectance obs. 80−93416
$In_{1-x}Ga_xP_{1-z}As_z$ solid solution, radiative transitions 79−11476
$In_{1-x}Ga_xP_{1-z}As_z$, stimulated yellow-green emission under electron excitation, 80K 79−33846
$In_{1-x}Ga_xP_{1-z}As_z$:Zn, x∼0.12, z∼0.26, LPE, DH lasers, tunnelling involving defects 77−65594
$In_{1-x}Ga_xP_{1-z}As_z$-InP, LPE heterojunctions, lattice matching and dislocations 78−23150
$In_{1-x}Ga_xP_{1-z}As_z$-InP, single and multiple layer heterostruct., LEDs and lasers 78−46626
$In_uGa_{1-u}P_vAs_{1-v}$-InP, LPE, lattice matching, phase 80−54350
InN, epitaxial layer prep. using $InCl_3$-NH_3 system 78−3056
InN, epitaxial layer prep. and X-ray analysis 79−38747
InP (100) surfaces, chem. treatment effects on comp. and nature 79−47794
InP, (100)-orientated, vapour phase deposited in closed-tube system, surface comp. variation 80−24752
InP, current controlled LPE growth 77−77428
InP, deep trap characts. by photocapacitance spectroscopy 78−6398
n-InP, defects in homoepitaxial layers, on p-type substrate, accurate lattice parameters 78−47675
InP double cladded $Ga_{0.47}In_{0.53}As$/InP DH laser, 1.67 μm operation 79−50314
InP, effects of baking time on purity and morphology 78−6862
InP epitaxial films, grown on heavily doped substrates, carrier mobility study, magnetoresist. meas. 80−60116
InP, epitaxial growth, thermodynamic conditions 77−89661
n-InP, epitaxial layer, (100) surface chemistry, ESCA study 80−103552
InP, epitaxial layer, effective doping density, comparison of Hall and magnetoresistance meas. 77−11938
InP, excitons bound to neutral donors in VPE layers, luminesc. and absorpt. obs. 79−42460
InP, far IR LPE photodetector performance 79−30546
InP film, liquid-phase epitaxial growth on (100) and {111} substrates *(Slovak)* 79−15037
InP films, organometallic VPE grown, props. 80−96753
n-InP, Hall effect, electron mobility and density, temp. depend. 78−72288
n-InP, heat treatment effect on surface carrier conc. 77−11936
InP, heteroepitaxial, deposition on GaAs substrate, using close-spaced metod, X-ray analysis *(Czech)* 77−15710
InP, heteroepitaxy on CdS substrates using InI_3 as transport agent 79−56083
n-InP, hole traps by deep level transient spectroscopy and transient capacitance methods 79−51514
InP, homoepitaxial film by MO-CVD process, for heterojunc. solar cell fabrication 79−8250
InP, LPE grown, impurity effect on surface morphology 80−29291
InP, LPE grown, surface morphology 77−62771
InP layer growth method, model validity evaluation *(Slovak)* 80−54535
InP layers, grown by LPE from supercooled solns., thickness meas. 78−10307
InP layers, LPE growth from undercooled melts, numerical method 80−6665
InP, MBE, substrate temp. related degradation mechanisms 80−65385
InP, MBE growth, expt. *(Japanese)* 77−4743
InP, MBE growth on InP substrate, orient.-depend. faceting 77−24966
InP, MBE growth surface, singular instabilities 77−24969
semiconductor epitaxial layers continued
InP, organometallic growth by cracking of $In(C_2H_5)_3$ and PH_3 80−11575
n-InP, oscill. intrinsic photocond. 79−60871
InP, photoluminesc. of epitaxial films, isovalent substitution 80−16097
InP, planar reactive deposition on CdS, heterostruct. formation and elec. evaluation 78−72738
InP, relaxation LSA mode obs. 77−8102
n-InP, subthreshold velocity-field charact., 77K 78−64038
InP surface decomposition prevention in LPE growth 80−96749
InP, terracing of LPE growth, doping effects 80−10846
InP, thermal degradation and its control in LPE growth 79−100343
InP VPE, growth kinetics and controlled doping 79−87569
InP, VPE growth for MESFET's 80−103602
InP, VPE layer props. control using boundary layer characts. 80−50561
InP, VPE using CVD 79−28927
InP, vapour phase epitaxial growth in presence of O_2, elec. props. 79−46971
InP very high purity LPE layer growth 78−3061
InP:Be, LPE, Be distrib. coeff., carrier conc. 79−90694
InP:Bi, uniaxial stress effect on free and Bi-bound excitons 79−56854
InP:S^+(Se^+), ion-implanted VPE layers, laser annealing, elec. and struct. anal. 79−73199
InP:Si, vibr. modes of Si, IR absorpt. bands 78−55922
InP:Sn, LPE growth from Sn soln., elec. props., 80 to 300K 79−11250
InP:Sn film, mol. beam epitaxial growth 77−16505
p-InP:Zn, vapour grown, prep. and props. 80−54268
InP/InGaAsP/InP double heterostructure, grown on InP(111)B substrate, threading dislocation multiplication 80−54237
InP-$Ga_xIn_{1-x}As_yP_{1-y}$ systems, for optical devices in 1 to 1.6 μm region, LPE growth *(Japanese)* 79−28956
InP-$Ga_xIn_{1-x}As$-InP, DH fabrication, crack form. due to lattice mismatch 77−15104
InP-GaInAsP buried heterostructure lasers of 1.5 μm region, fabrication and characts. 80−74388
InP-$In_{1-x}Ga_xAs_yP_{1-y}$-InP 1.53 μm single-mode CW ridge-waveguide laser 80−64072
InP-$In_{1-x}Ga_xP_{1-y}As_y$, LPE for optoelectronic devices *(German)* 79−95280
InP(100) undoped homoepitaxial films grown by MBE, photoluminesc. props. 80−2809
InSb, epitaxial film, amorphous and polycrystalline, vol. plasmon energy and linewidth, electron scatt. obs. 80−50482
n-InSb film, low energy electron irrad. effect on elec. props. 80−7009
InSb film, MBE apparatus and AES 78−47875
InSb, heteroepitaxial film, orientation and struct. investigation 79−82480
InSb, LPE growth characteristics, substrate surface contamination dependence 80−39470
InSb thin films prepared by ion beam epitaxy system *(Japanese)* 78−22976
InSb-PbTe(CdTe) superlattices, laser deposition of multilayer heteroepitaxial structs. 80−44450
$InSb_{1-x}Bi_x$ films, single-cryst. metastable semicond., growth and phase stability 80−80115
$InSb_{1-x}Bi_x$, metastable epitaxial film, phase diagram 80−76238
$InSb_{1-x}Bi_x$, multitarget RF sputtering, metastable phase, conductivity transition 80−76178
InsB, heteroepitaxial, MBE growth and elec. props. 80−2301
PBS, moisture drift origin 77−20187
Pb chalcogenide films, epitaxial, orientation on fluorite struct. substrate 77−35824
$Pb_{1-x}Cd_xS$, metastable, optical props. and electronic struct. 79−15543
$Pb_{1-x}Cd_xS$, metastable epitaxial films, elec. props. 78−26979
$Pb_{1-x}Cd_xS$ metastable epitaxial films, growth and physical props. 78−27417
$Pb_{1-x}Cd_xS$, resist. and Hall coeff., substrate temp., thickness and comp. depend. 78−72290
$Pb_{1-x}Ge_xTe$ epitaxial layers, phase transition obs. by far IR reflectivity spectroscopy 79−33691
$Pb_{1-x}Ge_xTe$ magnetoplasma reflectivity and transmission spectra 80−71428
$Pb_{1-x}Hg_xS$ epitaxial films, electroless deposition and struct. props. 79−90915
PbS epitaxial film, struct., optical and elec. props. 78−19583
PbS, epitaxial layer, structural nonuniformities and dislocation struct. 79−23852
PbS, epitaxial layer on rock salt substrate, stresses, hydrostatic press. effects 78−51831
PbS, ion bombardment effects on struct., and annealing 79−10882
n-PbS, $PbS_{1-x}Se_x$ layers prepared by hot-wall epitaxy 77−16481
PbS, small-angle X-ray scatt. and electron density inhomogeneities 80−96758
PbS, struct. perfection, two cryst. X-ray spectrometry 78−26792
PbS-PbSe epitaxial bicrystals, direct scatt. of channelled He ions at dislocations 80−65110
PbS_xSe_{1-x} film prep. by co-evap., elec. props. *(Japanese)* 78−80470
PbS_xSe_{1-x}, Hall mobility meas., surface charge transport 77−20473
PbSe, film with pot. barrier, magnetoresistance anisotropy 79−91172
PbSe films, current carrier conc. and type control, elec. cond., synthesis process *(Russian)* 80−100412
PbSe, moisture drift origin 77−20187
PbSe, monocrystalline film prod. by laser pulse *(Russian)* 78−3059
PbSe on NaCl, epitaxial-substrate system, far IR transmission and refl. 78−6802
PbSe on NaCl, far IR reflectivity obs. 77−40251
PbSe, X-ray diffr. exam. of struct., and luminescence props. 80−55209
PbSe-PbS(Te) and PbS-PbTe epitaxial layers, electron microscope contrast of misfit dislocations 77−85113
$PbSe_xTe_{1-x}$, growth, struct., elastic strain and Hall mobility 77−15717
$Pb_{1-x}Sn_xSe$ epitaxial layers, radiative and nonradiative recomb. processes 80−60670
$Pb_{1-x}Sn_xSe$, film struct. and elec. props. 77−80708
$Pb_{1-x}Sn_xSe$, Hall mobility meas., surface charge transport 77−20473
$Pb_{1-x}Sn_xSe$ layers obtained by LPE, growth conditions correl. with morphology 80−104079
$Pb_{1-x}Sn_xSe$(Te) epitaxial layers, growth, phase diagram, p-n junctions, optical, elec. props. 78−44029
$Pb_{1-x}Sn_xSe$(Te):I, photoelectric props., doping donor impurity behaviour 77−80810
$Pb_{1-x}Sn_xSe_{1-y}Te_y$ optically pumped heterojunction laser with matched gratings, photolum. obs. 79−89909

semiconductor epitaxial layers continued
$Pb_xSn_{1-x}Se(Te)$ film, Bi and Tl impurity dopant incorporation and diffusion during MBE growth 79−66012
PbSnTe and PbSnTe, epitaxial-substrate system, far IR transmission and refl. 78−6802
PbSnTe film epitaxial growth on BaF_2 substrates 78−11134
$Pb_{0.78}Sn_{0.22}Te$:In epitaxial layers, dislocation density, Hall effect, conductivity, photoeffects 80−25024
$Pb_{0.79}Sn_{0.21}Te$ on $Pb_{0.79}Sn_{0.21}Te$, far IR reflectivity obs. 77−40251
$Pb_{0.8}Sn_{0.2}Te$, far IR refl. spectra, carrier density, Hall const., and plasma freq. 80−20629
$Pb_{0.8}Sn_{0.2}Te$, implantation of S^+ and In^+ ions 77−19973
$Pb_{0.8}Sn_{0.2}Te$, LPE layers, carrier conc. variation with annealing and growth temp. 77−39878
$Pb_{0.8}Sn_{0.2}Te$:In, implanted thin epitaxial films, laser annealing 79−65104
$Pb_{0.82}Sn_{0.18}Te$ epitaxial films, surface transport of carriers at 77K 79−28419
$Pb_{0.82}Sn_{0.18}Te$ films, VPE, hot wall technique, struct., elec. props. 79−37926
$Pb_{0.85}Sn_{0.15}Te$ homostructure diode laser, LPE growth, with controlled carrier conc. 80−95903
$Pb_{1-x}Sn_xTe$ epitaxial films, adsorption-induced accumulation layer form. on surface 80−60117
$Pb_{1-x}Sn_xTe$, epitaxial growth on $LiNbO_3$, electron diffr. and microscopy exam. 77−1331
$Pb_{1-x}Sn_xTe$, epitaxial layers, cond. *(Russian)* 77−24629
$Pb_{1-x}Sn_xTe$, epitaxial layers, carrier lifetime meas. 79−42559
$Pb_{1-x}Sn_xTe$, epitaxial layers, photolum. in mag. field 79−83033
$Pb_{1-x}Sn_xTe$, far IR magneto-optical meas. 79−61343
$Pb_{1-x}Sn_xTe$ film on BaF_2, electron beam delineation effect on MBE growth, LEED and AES obs. 79−99434
$Pb_{1-x}Sn_xTe$, grown by LPE, solid-liquid tie line determ. 78−64526
$Pb_{1-x}Sn_xTe$, heteroepitaxial film, fundamental absorpt. edge and Shubnikov-de Haas effect 79−24381
$Pb_{1-x}Sn_xTe$ heterojunction lasers, instantaneous vacuum evaporation grown, threshold current density 80−5759
$Pb_{1-x}Sn_xTe$, In doping, donor impurity singularities, distrib. coeff. 77−80526
$Pb_{1-x}Sn_xTe$, interband absorpt. edge for single cryst. epitaxial films 78−43948
$Pb_{1-x}Sn_xTe$ LPE film IR detector performance 80−86422
$Pb_{1-x}Sn_xTe$ LPE grown heterostructures, dislocation etch pitch, interfaces 80−2023
p-$Pb_{1-x}Sn_xTe$, LPE layer, carrier conc. and mobility 79−99639
$Pb_{1-x}Sn_xTe$ layers, LPE, phase diagram rel. to lattice const., distrib. coeffs. 79−37925
$Pb_{1-x}Sn_xTe$ layers, LPE growth on metal-etched substates 80−55313
$Pb_{1-x}Sn_xTe$, MBE, O_2 uptake, AES, XPS and UPS expts. 78−95227
$Pb_{1-x}Sn_xTe$ solid solution, radiative recombination 79−52016
$Pb_{1-x}Sn_xTe$, VPE crystals, X-ray diffr. data interpretation 77−15712
$Pb_{1-x}Sn_xTe$, x=0.2, monocrystal, photoelectric props. of p-n structures *(Russian)* 80−70808
$Pb_{1-x}Sn_xTe$:In epitaxial layers, growth, elec. props., and luminesc. 80−54542
$Pb_{1-x}Sn_xTe$-PbTe heterojunction, Sn diffusion and elec. effects of dislocations, elec. and metallurgical expts. 77−89839
$Pb_{1-x}Sn_xTe$-PbTe heterojunction, Sn diffusion profile, X-ray diffr. data interpretation 78−51832
$(Pb_{1-x}Sn_x)_{1+y}Te_{1-y}$ system, VPE parameters influence on epitaxial film props. 79−28229
p-$Pb_xSn_{1-x}Te$, on n-PbTe, junction elec. props. and photoresponse 78−56225
$Pb_xSn_{1-x}Te$, RF-sputtered epitaxial single-cryst. films, thermorefl. spectra 77−63476
PbTe (111) epitaxial films, localised electron irrad. effects on elec. props. and O_2 sorption 80−49472
PbTe, continuous epitaxial film, grain size, growth cond. depend. 78−26786
PbTe, crystallite size in epitaxial layers by X-ray diffraction rocking curves 80−20052
n-PbTe epitaxial film, magnetophonon and Shubnikov-de Haas oscills. 78−60234
PbTe, epitaxial film on fluorphlogopite, effects of annealing in Te vapour 77−80709
PbTe epitaxial films, carrier recomb. and deep levels, photocond., Hall effect, and luminesc. meas. 79−38024
PbTe epitaxial films, quantum size effect, optical meas. 80−11121
n-PbTe, epitaxial layers, elec. characts. rel. to explosive evap. in closed vol. 77−89885
PbTe, epitaxial layers, carrier lifetime meas. 79−42559
PbTe epitaxial layers, submillimetre spectroscopy 79−83048
n-PbTe, far IR magnetotransmission and refl., dielec. function 77−52091
PbTe, far IR spin flip reson. 79−82979
PbTe film, Bi and Tl impurity dopant incorporation and diffusion during MBE growth 79−66012
n-PbTe film, transverse magnetoresistance oscillations, depend. on film thickness 79−65567
PbTe, high field drift vel. and Hall coeff. 78−26875
PbTe, high mobility polycrystalline layer, mol. beam deposition 79−83138
n-PbTe, hot electron transport effects 77−12035
PbTe, ion implanted, magneto-optical expts. *(German)* 79−28848
n-PbTe, LPE layer, carrier conc. and mobility 79−99639
PbTe, many valley semicond., band population effects, intraband magneto-optical props. 79−78007
PbTe, microwave magnetoplasma exam. of lattice and electronic props. 77−69364
n-PbTe, noncubic (111) oriented epitaxial films, weak field magnetoresistance 80−75584
PbTe, nonstoichiometric, evap. and growth of epitaxial layers 80−104072
PbTe orientation on different faces of $LiNbO_3$ 78−79907
PbTe, patterns of diffuse bands on electron diffr. patterns 79−11021
PbTe, stimulated emission, absorption spectra and recombination 78−80409
PbTe, TO phonon mode softening, sub mm spectra 78−6665
PbTe, thick epitaxial film, laser deposition technique 78−68629
n-PbTe, time dependent negative weak field magnetoresist. 78−64151
PbTe, uncontaminated films prepared by mol. beam deposition, elec. props. meas. 78−15316
PbTe, VPE, on $LiNbO_3$, struct. and morphology obs. 80−54561

semiconductor epitaxial layers continued
PbTe, VPE film growth under near equilib. conditions 77−32526
PbTe very thin epitaxial films, transmission and refl. spectra, 1 to 5 eV 80−7430
PbTe:As, hole conc. control, in LPE layers, plasma reflectivity and thermoelec. probe meas. 79−99640
PbTe:Bi-PbSmTe-PbTe, epitaxial laser struct., growth, p-n junction position and lasing region 79−89908
PbTe-CdTe(InSb) superlattices, laser deposition of multilayer heteroepitaxial structs. 80−44450
p-PbTe-M, M=In, Pb, Zn, Cu, barrier props. 79−7898
PbTe-PbSnTe heterjunction, misfit dislocations, etch pit and electron probe study 79−77926
PbTe-ZrO_2 (SiO_2), epitaxial MIS struct., fabrication and elec. props. 80−2472
$Pb_{1-y}Te$-$Pb_{1-x}Sn_xTe$ (x,y≤0.3), double heterostruct., LPE growth, heterointerface morphology 80−70550
$PbTe_{1-x}Se_x$, epitaxial layers synthesis, cryst. struct. perfection and elec. characts. 79−87587
$PbySn_{1-x}Se$ epitaxial film narrow band photovoltaic detectors, detection at long wavelengths 78−8443
Sb_2Te_3 epitaxial films, growing conditions effect on elec. cond., thermo-EMF 80−39687
Se film, epitaxially grown on Te substrates, crystallinity, RHEED and SEM meas. 77−40373
Se, on Te(1$\bar{2}$10) face, LEED and AES meas. 77−1328
Se, SAW vel. and electromech. coupling factor 80−75422
Se, TSC meas., trapping effects 77−85349
n-Si (001) on sapphire, galvanomag. effect for holes, valence band 79−91166
Si (100)-Pd_2Si-Si system, Si epitaxy obs. by ^{31}Si tracer and Rutherford backscatt. methods 79−4431
Si, amorphous, epitaxial regrowth, structure and impurities effect 80−84401
Si, amorphous, substrate orientation effect on regrowth by laser pulses, channeling, backscatter 80−84409
Si, amorphous film, epitaxial laser crystallisation 78−84078
Si amorphous film, ion-implanted, regrowth 79−15043
Si, amorphous layer, epitaxial growth by laser annealing 78−79899
Si amorphous layer, solar furnace annealing to induce solid-phase epitaxy 80−2277
Si, autoepitaxy, displacement of microrelief 80−2307
Si beam epitaxy for epitaxial film growth and p-n junction formation in high vacuum 80−16187
Si, CVD film, stacking fault nucleation and growth 78−10064
Si, CVD growth, inelastic light scatt. as in situ probe of chem. reaction 77−40383
Si, CVD growth surface, singular instabilities 77−24969
Si, CVD mechanism, epitaxial growth, IR obs. 79−23859
Si, cryst. quality improvement by ion implantation, backscatt. and TEM obs. 79−42397
Si crystal, obtained by local epitaxial accretion, facing and shape meas. 77−4270
Si, dechannelling by stacking faults, channelling effect technique using He^+ and D^+ ion backscatt. 79−4361
Si, defects, electrically active, correl. of electrolytic etch and surface photovoltage methods 79−77929
Si, doping the P cpds., process parameters effect on electrophys. characts. 78−38734
Si, elec. activity of stacking faults, determ. using SEM in EBIC mode 77−43445
Si, electrodeposited film, appl. in solar cell fabrication 78−76611
Si electron beam deposited film, epitaxy by pulsed laser annealing 78−56055
Si, epitaxial and amorphous film growth, low energy ion beam deposition 77−28729
Si epitaxial detector fabrication, crystal growth and preferential etching 78−37505
Si epitaxial film, containing struct. defects formed during growth, positron annihilation 80−93433
Si epitaxial film, correlation between electrooptical and electrical props., IR absorpt. spectra *(Russian)* 78−60453
Si, epitaxial film, dopant incorporation model 79−99228
Si, epitaxial film, dopant incorporation during growth, theory and expt. 79−99229
Si, epitaxial film, struct. defects, effects on planar diffused p-n junction elec. props. *(Russian)* 78−60195
Si epitaxial film concentrated inhomogeneity detection by selective etching *(Russian)* 78−10298
Si epitaxial film dopant incorporation, transient response 77−76976
Si, epitaxial film growth by hydride-iodide method 77−48343
Si epitaxial film growth on sapphire in SiH_4-H_2 system, optimum deposition 77−77397
Si epitaxial film on sapphire, microtwins, TEM exam. 80−70555
Si, epitaxial growth, adsorbed layer model for autodoping mech. 80−7505
Si epitaxial growth, in $SiCl_4$-HCl-H_2 system, model based on flow graph 79−42405
Si, epitaxial growth, nucleation 77−62770
Si, epitaxial growth from vapour, dopant inclusion model *(German)* 79−42088
Si, epitaxial growth kinetics, experimental verification of theoretical model 79−95278
Si, epitaxial growth on ion-implanted Si:As 78−6243
Si, epitaxial growth on sapphire by partially ionised vapour deposition, RHEED-AES obs. 80−80985
Si epitaxial interface migration, theory and expt. test 80−29290
Si, epitaxial layer, growth mechanism from ion-molecular beams 80−2299
Si, epitaxial layer, incorporation conc. depend. of P from silane-phosphine-H_2 mixture 80−2053
Si epitaxial layer, minority carrier lifetime obs. *(Russian)* 80−49765
Si, epitaxial layer deposition by ion beam methods 80−100417
Si, epitaxial layer grown by saturated Sn melt undercooling, morphology 78−22969
Si epitaxial layer growth in vacuum, Ar, Xe ion bombardment effect 80−39463
Si, epitaxial layer on sapphire, shear strain, TEM 78−51835
Si epitaxial layer regrowth due to laser annealing mechanism, liquid and solid phase regimes 80−100712

semiconductor epitaxial layers continued
Si epitaxial layer substrate junctions, carrier lifetime and abnormal conduction phenomena *(Korean)* 78−47888
Si, epitaxial layer thickness meas. using phase correction function of substrate resistivity *(Rumanian)* 80−90812
Si epitaxial layers, grown by sublimation in vacuum, TEM study of surface 79−46982
Si epitaxial layers, grown in vac. at low temps. P and Sb doping 80−88189
Si, epitaxial layers, stacking defect distrib. anal. using ion channelling tech. 80−100294
Si epitaxial layers, temp. dependence of P dopant inclusion in gas phase deposition *(German)* 79−52127
n-Si epitaxial layers on oppositely conducting substrates, two layer Hall coeff. meas. technique 80−80297
Si, epitaxial layers on ribbon substrates, solar cell prod. and characterisation 77−77354
Si epitaxial p-i-n photoconvertor characteristic deterioration at high illumination 78−89536
Si, epitaxial regrowth of thin amorphised layers by laser annealing, absorpt. coeff. influence 79−46968
Si, epitaxial stacking faults, nucleation sites 77−20201
Si epitaxial stacking fault nucleation site identification, annihilation, and suppression 77−76705
Si epitaxial structures, junction layer width and impurity conc. estimates *(Russian)* 80−49893
Si epitaxial thin film growth on sapphire and spinel by MBE 80−76186
Si epitaxial wafer, impurity profile meas. by multilayer spreading resist. anal. 77−76449
Si epitaxial wafers, role of metallic contamination in formation of 'saucer' pit defects 77−39588
Si epitaxy, autodoping effects 80−100259
Si epitaxy and oxidation, first-order process models 78−72049
Si, epitaxy by solid phase crystn. of amorphous film 78−19663
Si, epitaxy lateral autodoping kinetics 78−6087
Si, etching by CF_4, plasma deposition reactor gas phase characts., mass spectra 80−70566
Si, evap. heteroepitaxial film, deep defect states obs. 78−72292
n-Si film, epitaxial, electrical activity of stacking faults 77−39744
Si film, epitaxial growth on Si, impurities, plasmon energy loss anal. 77−31916
Si film, MBE, cryst. defect props., substrate treatment effects 80−70551
Si film, solid phase epitaxy, Au and O distrib. 77−66095
Si film on sapphire, quality evaluation using soft X-ray rocking curve 77−80711
Si, graphoepitaxy on fused SiO_2 using surface micropatterns and laser crystn. 80−70554
Si, growth, submicrometer thickness 79−95932
Si, growth in Si-P-H system, depend. of doping element incorporation on temp. in CVD 80−45234
Si, growth on Si(111) and sapphire (1$\bar{1}$02), simultaneous RHEED/AES study 80−10833
Si, heteroepitaxial, prep. and props., book contrib. 79−83128
Si, heteroepitaxial early growth island morphology rel. to deposition conditions 78−6245
Si, heteroepitaxial films, photomagnetoelectric effect 77−85264
Si heteroepitaxial films on sapphire, vac. deposited, struct. and elec. props. 80−15390
Si heteroepitaxial growth using SiH_4 in He-H_2 atm. 77−77396
Si, heteroepitaxial growth using SiH_4 in H_2-He atm. 80−20049
Si, high electron mobility, grown on sapphire at high growth rate 77−81225
Si, homoepitaxy, local selective, at reduced temp. using Si-I transport system 79−24444
Si homoepitaxy in high vac., stacking fault nucleation, crit. temp. for SiC growth 78−14620
Si homogeneous epitaxial layers, production, appl. of neutron transmutation doping 78−38737
Si horizontal epitaxial reactor transport expt. and model 77−77399
Si, ion implanted, annealing by ion beam heating 80−103382
Si, ion implanted, CW laser annealing 80−92550
Si, ion-implanted amorphous layers, melting model for pulsing-laser annealing 79−56080
Si, ion-implanted amorphous, laser epitaxial recrystallisation threshold energy 80−70571
Si, ion-implanted layers, crystn. by ns laser pulses, TEM and RHEED 80−100421
Si, ion-implanted layers, epitaxial regrowth by laser beam and flash annealing 80−100420
Si, ionised-cluster-beam deposited, cryst. and elec. characts. 80−70553
Si junction diodes, fabrication by LPE on Si:B substrates, and characts. 80−80363
Si, kinetics of doping, gas-phase decomposition of SiH_4 77−16499
Si, LPE from Sn melt by dipping 78−6871
Si, LPE growth from supersaturated Sn melt 78−56592
Si LPE layers, dopant distrib., meltback effects 79−69151
Si, LPE using Ga_xAl_{1-x} solvent 77−36411
Si, laser measurement, of semiconductor materials and devices *(Rumanian)* 78−52035
Si layer growth by CVD on Sn-coated background *(Dutch)* 80−7502
Si, lifetime control through impact sound stressing 77−85238
Si, MBE, on n^+ Si, with wide range doping control 78−27402
Si, MBE growth and surface struct. 80−10816
Si MBE layer resistivity and carrier mobility obs. *(Russian)* 80−49962
Si MIS solar cells, spectral response and diffusion length 79−92077
Si, meas. of doping profiles *(Hungarian)* 80−70545
Si, metallurgical-grade, fabrication by epitaxial growth or direct diffusion 80−101104
Si, minority carrier lifetime and diffusion length meas., photocurrent technique 78−95302
Si, minority carrier lifetime and impurity conc. meas. *(Japanese)* 80−25025
Si, mol. beam and solid-phase epitaxies under ultrahigh vacuum 79−28945
p-Si, monocryst., diffusion of As, Henry const., temp. depend., 1448 to 1523K 79−42399
Si n/n^+ epitaxial layers, anomalies of Sb distrib. 80−65035
Si, on Czochralski sapphire, optimisation of deposition conditions in SiH_4-H_2 system 80−75464
Si, on metallurgical-grade polycryst. substrates, characteris. 79−28967
Si, on sapphire, characterisation, X-ray rocking curves 80−75458
semiconductor epitaxial layers continued
Si, on sapphire, early growth, TEM 77−24961
Si, on sapphire, early growth, models 77−24962
Si, on sapphire, epitaxial, crystalline quality improvement by ion implantation and furnace regrowth 80−88452
Si on sapphire, gettering effect by O implantation, Hall and Rutherford backscattering meas. 79−65103
Si on sapphire, laser annealing dynamics epitaxial regrowth, optical reflectivity 80−29285
Si, on sapphire, optical absorption and interface comp. profiles 77−12459
Si on sapphire, stacking faults and twins, TEM obs. at early stage of epitaxy 79−28233
Si, on sapphire, twin three dimens. distrib. 77−89666
Si, on sapphire or Si, misfit, strain and dislocations, book contrib. 79−82499
Si, on sapphire substrates, Al conc. as a function of depth using $^{27}Al(p,\alpha_0)$ reson. reaction 79−4328
Si, on Si ribbon substrate, dislocation density, X-ray topography obs. 77−85102
Si, optical reflectance rel. to surface damage 79−14985
Si p-n homoepitaxial junctions, elec. and struct. characts. 80−6662
Si, planarized solid state epitaxy for Schottky barrier diodes 78−35302
Si polycrystalline p-n junction deposition 78−10549
Si, power transistor and solar cell epitaxy from SiH_2Cl_2 source 77−77402
Si, saucer pit microdefects reduction by intrinsic gettering 80−75450
Si single-crystal thickness meas. using interference thickness gauges 79−97351
Si, solid phase epitaxial growth temp. depend. 78−10305
Si, solid phase epitaxial growth, crystalline qualities, ^4He backscatt. and TEM exam. 78−10306
Si, solid phase epitaxy, Si⟨100⟩/Pd_2Si system, dissoc. mechanism 77−7980
Si, solid phase grown, structural obs. 78−2397
Si, solid soln. of B, equilib. with B_2H_6 80−97721
Si, solid-phase epitaxial growth, rapid 77−21022
Si, solid-phase epitaxial growth stages in Si(crystal)-Pd_2Si-Si(amorphous) system 77−85114
Si, solid-phase-epitaxial, deposited above 380°C, defects obs. 78−63942
Si, solid-state epitaxial growth of amorphous layer 80−10803
Si, state of art of deposition 79−33937
Si surface layers, impurities, elec. and photoelec. props. 80−2298
Si, thickness and optical consts. meas. using IR laser ellipsometer 78−62219
Si, thickness meas. during deposition using diffraction *(German)* 79−97355
Si thin autoepitaxial layers low temp. growth mechanism in $SiCl_4$-H_2 system 80−20795
Si, ultra high vacuum epitaxy on Si substrates *(German)* 77−47702
Si, VPE, fine struct. formation *(French)* 78−43275
Si, VPE growth mechanisms 79−28929
Si, VPE layer props. control using boundary layer characts. 80−50561
Si, VPE tangential growth, thickness meas. 77−35836
Si, VPE using SiH_2Cl_2/H_2 as source for epitaxial films on insulators 78−48327
Si, VPE via SiH_2Cl_2 in barrel reactor 78−52685
Si, vacuum deposited, conditions for impurity migration from B, P, Sb doped sources *(Russian)* 80−107570
Si vacuum sublimated thin film structure impurity distrib. 78−95354
Si, vapour epitaxy, optimum growth conditions 78−76608
Si wafer, ion implanted, electron beam annealing, computer simulation 80−96569
Si, X-ray topographic study using Berg-Barrett techniques 79−28221
Si:AS, lateral autodoping kinetics 78−39699
Si:Ar, ion-implanted, epitaxial regrowth by laser annealing, microstruct. 80−84404
Si:As, ion implanted, laser annealed, lattice defects, epitaxial regrowth 80−103334
Si:As, ion-implanted, dislocation loops and etch pits, X-ray diffr. and TEM obs. 79−42068
Si:As(Sb), MBE, n-type doping techniques 80−15126
p-Si:B, proton-implanted, annealing characts., carrier conc. profiles 77−32097
Si:B epitaxial layer, B diffusion coeff. 79−99372
Si:Ga(Al), MBE, growth, struct. and elec. props. 77−89458
Si:Ga(Sb), doping efficiency *(Japanese)* 79−73201
Si:Ge, regrowth behaviour from backscatt. and channelling meas. 80−2300
Si:O, annealed, minority carrier lifetime 79−23985
Si:P, As, chem. etching, thick epitaxial layers prod. for dopant conc. investigations by neutron activation anal. 79−37728
Si:P, epitaxial layer, vapour phase grown, temp. dependence of dopant inclusion, differential molar solution enthalpy *(German)* 79−52128
Si:P epitaxial layer, strain distrib. at interface with substrate, obs. by X-ray double cryst. method 79−99461
Si:Sb, epitaxial film, growth by mol. beam technique 80−2292
Si:Sb, epitaxial layers, doping profile techniques 80−44231
Si:Sb, MBE film, doping technique 80−79821
Si:Sb (P) (B), interpretation of the temp. depend. of partition and sticking coeffs. 77−7756
Si:Ti substrate for epitaxial solar cells 80−61341
Si-Al interface, solid phase epitaxial growth of Si 80−34324
Si-Au-P system, partition coeff. of P, temp. depend. 79−43158
Si-$CoSi_2$Si, double heteroepitaxy, solid phase and MBE 80−104063
Si-Ge heteroepitaxial layers, Ge/Si ratio transfer curve from gas phase to solid phase obtained by epitaxial growth 77−73234
Si-Ge heteroepitaxial layers on Si substrate, lattice const. meas. 79−69382
Si-Ge heteroepitaxial system, imperfections and morphology, electron microscope and electron diffr. obs. 79−42420
Si-Pd_2Si heterostructure growth by solid-phase epitaxy from Si (111)-Pd-Si (amorphous) 77−51617
Si-Pd_2Si-Si, kinetic aspects of solid phase epitaxial growth of amorphous Si 79−4491
Si-sapphire interface charge trapping, effects of sapphire type and epi growth conditions 77−20447
Si-SiO_2, interface, doping depend. of interface states and charges 80−92992
n-SiC, 6H, saturated electron drift velocity meas. 78−19168

semiconductor epitaxial layers continued
n-SiC, 6H polytype, expitaxially grown, electronic props. meas. 77−39975
SiC, 6H polytype, LPE growth by dipping technique for prep. by blue LEDs 77−8769
SiC (6H), blue-emitting diodes by CVD 80−97439
SiC (6H), epitaxial film, electronic props. 79−60942
SiC, CVD film growth, morphological, chem. and cryst. struct. investig. 77−40385
SiC, energy distrib. in photolum. spectra, influence of synthesis conditions 79−52009
SiC, epitaxial growth by sublimation sandwich method, effect of impurities 80−25568
SiC epitaxial layer, vapour phase growth, investigations of kinetic and thermal conds. 79−42407
SiC epitaxial layer growth from sublimation in vac., kinetics 80−20791
SiC, epitaxial layer polytypism 77−62781
SiC, epitaxial layer polytypism 77−62782
SiC, exam. of N solubility, in epitaxial layers 80−6520
SiC film, growth on Si ribbon surface, TEM anal. 78−84094
SiC, growth techniques 80−108360
α-SiC, impurity macroincorporation, distrib. of Al, B, N and P 77−69192
SiC p-n junction, epitaxial, grown by sublimation, elec. and struct. props. *(Chinese)* 80−60067
SiC, VPE kinetics study in SiC-C system 79−37934
SiC, VPE layers, growth kinetics, polytypism 77−11809
SiC:Al epitaxial layers, growth, Al distrib. and solubility 80−15391
SiC:Be, film donor impurity, diffusion influence on elec. and optical props. 78−87942
SiC:N, conversion factor at high doping levels 78−22744
$Si_{0.92}Ge_{0.08}$ film on Si, elastic strain, misfit dislocation density 77−85119
p^+-$Si_{1-x}Ge_x$-nSi junction diodes, lattice misfit effects on I-V charact. 80−70804
Si⟨111⟩/Al/Si, growth kinetics of ⟨111⟩ Si through Al layer by solid phase epitaxy 79−28236
$Sn_{1-x}Pb_xSe(Te)$, Mossbauer effect of ^{119}Sn, spectral charact., conc. depend. 80−103903
$Sn_{1-x}Pb_xSe(Te)$, oxidation rel. to annealing temp. and time, Mossbauer spectra, X-ray and microstruct. obs. 80−104311
$Sn_{1-x}Pb_2Te$, elec. and struct. props. of epitaxial layers *(Russian)* 78−64147
$Sn_{1-x}Pb_xTe$, epitaxial layers synthesis, cryst. struct. perfection and elec. charact. 79−87587
SnTe, expitaxial film, early stages of growth, replication and TEM obs. 79−65348
p-SnTe, film and bulk, weak-field magnetoresistance 78−84236
SnTe-Sn epitaxial system, electron microscope contrast of misfit dislocations 77−85113
Te, ENSH method of oriented thin film growth 79−99443
Te, evaporated film epitaxial and amorphous-crystalline phase transition growth and struct. 79−51449
Te, on electron irrad. KBr, epitaxial growth and surface coverage 80−10825
$V_{1-x}Cr_xO_2$, VPE and elec. and optical characterisation 78−3053
VO_2, VPE and elec. and optical characterisation 78−3053
YIG, n and p-type, UPS, elec. struct. 77−4710
Zn chalcogenides, film, on NaCl, preferential epitaxy induced by electron bombard. or elec. field 80−10824
Zn_3As_2, solubility in Bi, LPE on $(Cd_xZn_{1-x})_3As_2$ 78−35324
$Zn_xCd_{1-x}S$ epitaxial layers, elec. resist. and luminescence obs. 78−19540
ZnO, CVD, highly conductive layer, cond. and Hall coeff. obs. 79−51696
ZnO, CVD of epitaxial films on sapphire, SAW interdigital transducer fabrication 80−66430
ZnO epitaxial film, nonuniform cond. due to H chemisorption *(Russian)* 80−65723
ZnO epitaxial film electrical props. rel. to substrate orientation and growth conditions 79−56339
ZnO epitaxial film on Al_2O_3 substrate, recombination radiation in intense single photon excitation 80−7410
ZnO epitaxial film with smooth surface from CVD onto a sputtered ZnO film on sapphire, waveguide appl. 78−56588
ZnO, epitaxial layers, influence of deposition conditions on luminescence, electrical props. 79−99924
ZnO epitaxial layers, rel. between elec. and photoluminesc. props. and their deposition conditions 79−95530
ZnO film, longit. elastic wave attenuation, 9.4 GHz 78−18888
ZnO film, optical waveguide fabrication, CVD on sputtered ZnO film on sapphire 79−86269
ZnO film, prep. by reactive ionized cluster beam deposition, and characterisation 80−10829
ZnO films, RF sputtered single-cryst., on sapphire, struct. and SAW props. 80−80105
ZnO heteroepitaxial film, orientation relations for growth on Al_2O_3 substrates, X-ray diffr. anal. 79−15049
ZnO heteroepitaxial films, grown on Al_2O_3 substrates, X-ray topographic study of struct. 79−15048
ZnO, high rate epitaxy on sapphire by planar magnetron RF sputtering 79−28916
ZnO, ionized-cluster beam and reactive ionized-cluster beam deposition, cathodolum. characterisation 80−16202
ZnO on Zn (0001), oxide film growth, at. and electronic struct. 78−15587
ZnO, piezoelec. films produced by gas transport reaction, US excitation efficiency 80−2700
ZnO, RF sputtered epitaxial film, appl. to integrated optics 77−14821
ZnO, UV luminesc. due to one-, two-photon excitation, laser possibility 79−11468
ZnS, epitaxial film, CVD growth and characterisation *(French)* 77−36403
ZnS, epitaxial growth, appl. to electronic devices, review *(Japanese)* 80−55281
ZnS epitaxial growth, in H_2, mass transport processes and effects of bypass flow 79−23860
ZnS, epitaxy in quasiclosed volume 77−85093
ZnS, growth on Si in ultrahigh vacuum, source nonstoichiometry effects 77−77387
ZnS, heteroepitaxial growth on GaP by closed space technique 79−28939
ZnS, VPE on GaP in open tube system 79−28938

semiconductor epitaxial layers continued
ZnS:Cu crystal, powder, epitaxial film, luminescence anomalous thermal 80−76077
ZnS-GaAs, n-p heterojunction, struct., multibeam electron microscopy obs. 79−11031
ZnS(Se), growth kinetics on CaF_2 by vapour phase transport *(French)* 80−54572
ZnS_xSe_{1-x}, epitaxial film, CVD growth and characterisation *(French)* 77−36403
ZnS_xSe_{1-x}, on CaF_2, comp. and temp. depend. of fund. band gap 80−11115
ZnS_xSe_{1-x}, VPE, characterisation of defect centres by photoelectronic meas. 80−10914
ZnS_xSe_{1-x}, VPE on CaF_2 substrate, in flowing H_2, growth and characterisation *(French)* 80−107678
ZnSb, epitaxial films, growing conditions effect on elec. cond., thermo-EMF 80−39687
ZnSb, orientated crystn. conditions during reaction diffusion *(Russian)* 80−70558
ZnSe, close-spaced technique, preparation and optical props. 79−47637
ZnSe, epitaxial growth on Ge substrate 80−75469
ZnSe epitaxial layers, prep. by chem. transport reactions 80−16192
ZnSe, evap. onto electron bombarded NaCl substrates, epitaxial growth and charact. 79−28948
ZnSe film, MBE and resistivity 79−100059
ZnSe film on GaAs substrate, transition layer form. kinetics 79−87007
ZnSe, grown on sapphire substrate, stimulated emission 79−78708
ZnSe, LPE from Zn-Ga soln., charact. 79−28965
ZnSe, LPE growth on ZnTe, characterisation of heterojunction 77−4745
ZnSe layers, LPE growth from Zn-Ga soln., photoluminesc. 79−56840
ZnSe MBE growth, growth rate and sticking coeff. 77−32532
ZnSe, organometallic CVD, on GaAs, and photolum. 79−8249
ZnSe, organometallic CVD prop., growth kinetics and luminescent props. 79−51458
ZnSe, single cryst. film, MBE, quality obs. using photoluminesc. 77−77419
ZnSe, VPE on GaAS, role of interaction between gas and solids *(French)* 77−62769
ZnSe:In films, MBE growth, doping effect on photoluminesc. 80−10818
ZnSe:Li(Na)(Ga) doped and pure cryst., donor-acceptor bands 80−11465
p-ZnSe:Li(Na)(N)(P), LPE layers, photocapacitance and photocond. meas. 79−99572
ZnSe-CdTl, epitaxial film, cond. transition, laser switched memory *(Russian)* 77−8182
ZnSe-Ge(GaAs)(mica) epitaxial heterostructs., growth struct. 78−43257
$ZnSe_xTe_{1-x}$, MBE, comp. ratio control 79−28947
$ZnSiAs_2$, synthesis and layer growth by CVD in open flow system 78−15312
ZnTe, epitaxial film growth initial stages 77−80707
ZnTe, epitaxial growth on GaAs by closed-tube chemical vapour transport method, elec. props. 79−99449
ZnTe film, prepared by single-source vacuum deposition method *(Japanese)* 80−6664
ZnTe films, residual conductivity, Kikuchi lines of electron diffr. pattern 79−91173
ZnTe, grown on sapphire substrate, stimulated emission 79−78708
ZnTe, LPE growth on ZnSe, characterisation of heterojunction 77−4745
ZnTe, MBE growth, growth rate and sticking coeff. 77−32532
ZnTe MBE thin film growth, elec. and optical props. 78−47887
ZnTe, on NaCl, ion deposited layers 77−32533
ZnTe-CdS(Se)(S_xSe_{1-x}) heterojunctions, prep. and electrolum. charact. 77−24610
ZnTe-CdSe single cryst. film heterojunctions, prep. and props. 79−19652
ZnTe(:In), single cryst. film, MBE, quality obs. using photoluminesc. 77−77419

semiconductor growth
$Al_xGa_{1-x}As/Al_yGa_{1-y}As$ heterostructure lasers, prep. charact., and CW reliability 80−58586
alloy semiconductor, for appl. in IR detector arrays, comp. control 80−31872
amorphous film formation by vacuum deposition review *(Japanese)* 77−66590
amorphous semiconductor, substantially doped, electronic props., review 79−87175
anthracene, prep. and growth of single cryst. 78−64463
binary semiconductors, cathodic deposition and characterisation 79−69998
C GaP on GaAs substrate, heteroepitaxial layers, stuct. defects *(German)* 79−23865
$Cd_xHg_{1-x}Te$, vertically grown crysts., effects of growth speed on comp. variations 79−55684
CdSe whiskers, growth in H_2 80−15425
chalcogenide glass, prep. by laser evaporation, and characterisation 77−12533
chalcogenide magnetic semiconductors, spinal-type, closed tube vapour transport method *(Japanese)* 80−25539
chalcopyrites, for electrolum. device appl., props. and technology, book contrib. 77−73175
compound semiconductor, heteroepitaxial growth and characterisation, book contrib. 79−83133
crucible shape effect on crystallisation front 80−16173
crystal growth and defects, appl. of analytical techniques for observation 80−73546
crystal growth and phase diagrams 80−66407
crystallisation in constant electric field, thermoelectric parameters 77−44146
CVD epitaxy, book contrib. 77−12544
CVD technology trends, use of low-pressure hot-wall reactor, plasma systems and computer control 78−19670
Czochralski bulk flow in parameter range appropriate for liquid semiconductors, digital simulation 78−31320
Czochralski growth system, time-depend. cryst.-melt interface shape 77−24280
detector materials, Ge and Si 78−47674
developments, late 1970s innovations 80−6666
device fabrication by ionised-cluster beam deposition and epitaxial techniques 77−81227
diamond, synthetic, p-n junction prod. and doping, I-V charact. 77−15943

semiconductor growth continued
diamond, temperature field dynamics during synthesis 79−38755
diamond-like semiconductor film epitaxial growth, computer simulation 80−70560
doping in VPE, retrodiffusion cell design and applic. 77−84773
Electrochemical Society Meeting, Boston, USA, (May, 1979) 79−91959
electronic materials 80−66405
epitaxial film growth by sputtering, review 77−32521
epitaxial groove and tunnel growth mechanism 80−10804
epitaxial growth, surface reconstruction effects, review 77−89669
epitaxial layer CVD, appl. to Si, II-VI and III-V semiconductor growth 77−32530
epitaxial reactors, transport phenomena meas. 78−39701
evaporated compound films, formation and structure *(Japanese)* 78−22979
ferromagnetic semiconductors, review 77−85923
FeS_2, thin films, prep. and charact. 80−16178
film, growth and doping by MBE 77−73239
film deposition technology, conf., Uppsala, Sweden (Aug-Sept. 1976) 77−90270
film vacuum deposition methods *(Polish)* 79−56932
flow-graph model 79−78893
Ga(AsP) on GaAs, LPE, growth with Ge and Sn solvents, phase diags. 78−88434
GaAlAs-GaAs heterostruct. solar cells, Al, P, Zn incorporation by LPE *(French)* 79−24899
GaAs MBE growth, deep levels effect on electron and hole trap densities 80−49652
GaInAsP quaternary alloys, orientation effects in LPE growth 78−92203
heteroepitaxial semiconductors for electronic devices, prep. and props., book 79−83116
α-HgS, cryst. growth from soln. at low temps. 80−7487
I_5-III-VI_4, synthesis and props. 77−52231
II-VI compounds, high intensity US effects on synthesis and growth 77−819
II-VI compounds, hollow crysts., morphology, review 77−11494
II-VI compounds, optimal synthesis conditions for single cryst. growth 80−100776
II-VI compounds, optimal synthesis methods for single cryst. growth 80−100764
II-VI cpds., solar cell applic. role of thin film growth morphology and grain size 77−77377
II-VI semiconductor, hot wall epitaxy, review 78−52678
II-VI semiconductor electroless film deposition with variable comp. and polymorphic structs. 79−95952
II-VI semiconductor film technology 78−23621
II-VI semiconductors, from melt, dependence of mass losses upon press. 80−25547
II-VI semiconductors, heteroepitaxial, for SAW and electro-optic device appl., prep. and props., book contrib. 79−83134
II-VI semiconductors, thin epitaxial layer, direct synthesis *(German)* 80−104070
III-V compound, vapour transport reactions and kinetics 79−28931
III-V compound crystal growth from solution, computer simulation 77−51332
III-V compound epitaxial layers, dislocations nature, origin and effects 79−28232
III-V compounds, CVD, crystal growth mechanisms *(French)* 79−33939
III-V compounds, vapour growth, using organometallic sources *(Japanese)* 80−16195
III-V compounds and alloys, MBE process and problem areas, review 80−10815
III-V materials bulk crystal growth, LPE and VPE methods *(Czech)* 80−89131
III-V nitride, preparation technology *(Czech)* 78−3037
III-V pseudobinary compound, growth and phase equilib. in vertical rotating LPE reactor *(French)* 77−77430
III-V quaternary alloys, melt and soln. growth of bulk single crysts. 80−35079
III-V semiconductor, MBE and applications 78−11135
III-V semiconductor compounds for optical devices in 1.0-1.6 μm region, crystal growth by LPE and CVD 79−43161
III-V semiconductor heterostructures, growth and dissolution kinetics by LPE 80−49543
III-V semiconductor solid soln., LPE, doping with groups II and IV *(Russian)* 77−80705
III-V semiconductor ternary alloys, VPE growth lattice mismatch effects 79−28220
III-V semiconductors, electroliquid epitaxy, role of electrotransport 79−56095
III-V semiconductors, heteroepitaxial, for SAW and electro-optic device appl., prep. and props., book contrib. 79−83134
III-V semiconductors, heteroepitaxy *(Japanese)* 77−24968
III-V semiconductors, MBE, surface reaction steps 79−77941
III-V semiconductors, MBE developments in device fabrication 79−78902
III-V semiconductors, props. and optoelectronic device appls. 79−74088
III-V semiconductors, VPE, recent advances, book contrib. 79−66011
III-V semiconductors, VPE 78−92195
III-V semiconductors, VPE by metalorganic CVD *(Japanese)* 80−50562
III-VI compound layered materials, prep. and growth, book contrib. 78−19661
ionised-cluster beam deposition and epitaxy, for electronic device fabrication 78−11133
IV-VI compound layered materials, prep. and growth, book contrib. 78−19651
IV-VI compound vapour growth and transport in microgravity 77−77400
IV-VI compounds, mixed, morphology and transport rates, in microgravity 77−77353
IV-VI film technology, review 78−3034
IV-VI material production and physical props. for microelectronics *(Russian)* 78−11108
IV-VI narrow gap semiconductors, fabrication, IR laser and detector appls. 77−77415
IV-VI optoelectronic devices, MBE techniques 79−95942
IV-VI semiconductor, hot wall epitaxy, review 78−52678
IV-VI semiconductor electroless film deposition with variable comp. and polymorphic structs. 79−95952
localised crystal growth and dissolution, morphology analysis 79−99089
low gravity experiment possibilities in electronic materials growth technology 79−47606
semiconductor growth continued
LPE, multilayer, technique 78−31345
LPE, Peltier induced 78−48342
LPE, Peltier induced 78−48343
LPE, wipingless method *(Japanese)* 78−27422
LPE apparatus for multiple layers using centrifugal forces 77−77433
LPE edge-growth reduction, by aux. heating of graphite slider side-walls 78−30848
LPE pure melt batch production in sliding apparatus 78−44028
materials science, current topics, book 79−69966
MBE, ang. distrib. of beam from modified Knudsen cell 78−60586
MBE, appl. to electron devices *(Japanese)* 79−38749
MBE, appl. to II-VI compounds *(Japanese)* 78−15317
MBE, device appls. 80−25570
MBE, doping impurity transport, free carriers effect 78−26793
MBE, new technique for growing crystal 77−66591
MBE, review and appls. *(German)* 78−68630
MBE, state-of-the-art 79−24450
MBE *(Japanese)* 80−55305
MBE crystal growth, review 78−39707
MBE for precision doping 80−89156
MBE in space 78−35317
MBE of injection lasers, integrated optics device fabrication 79−90042
MBE study of semiconductor surface and crystal physics 79−95289
MBE technique, analytical methods 78−72027
metal chalcogenides, electrodeposition, using nonaqueous solvents 80−76200
metallic substrate, temp. meas. during evap. 77−69997
microscopic mechanism of film growth from non-condensed phases, kinetic anal. 80−54565
molecular beam deposition apparatus, design and construction *(Japanese)* 78−23632
molecular beam epitaxy, review of recent progress *(Japanese)* 77−63566
molecular beam epitaxy for superlattices control 80−2283
multicomponent epitaxial structure synthesis device 77−77414
narrow band gap semiconducting alloy layers, electron-beam microzone refining, in space 78−35325
narrow-band semiconductor, growth of epitaxial layers, activation by UV and IR radiation 80−71598
nonstoichiometry and carrier concentration control in MBE of compound semiconductors 79−95941
oxide semiconductor crystals, with forbidden energy gap, review of spectroscopic props. 78−2876
periodic structures, props., prep., use 78−51982
potentially superior method of preparing semicond. devices *(Czech)* 78−44027
reactive closed-space vapour transport, simplified theory 80−15396
reproductive epitaxy, exam. 80−55303
ribbon growth using scanned focused CO_2 laser beams 80−66417
ribbon-to-ribbon growth method and sample characterisation Si 78−11103
selective lift-off for preferential growth with MBE 77−90281
shaped crystal growth from melt, meniscus-controlled process 80−107075
Si:In growth by Czochralski crystal pulling, characterisation for extrinsic IR detectors, focal-plane arrays 80−76168
Si epitaxy, vapour phase deposition technology 80−75472
β-SiC, 6H polytype, pure and doped, prep. by pyrolysis of silane cpds. 78−44018
solar cell materials research to reduce costs, book 78−15306
solid solutions, growth of homogeneous single crystals 77−12518
SOS early growth, island coalescence model 77−76704
SOS early growth, transmission electron microscope obs. 77−76703
sputtered amorphous film heterostructure solar cell and laser fabrication 78−64472
Stepanov method, semicond. shaping problem 78−3012
surface reconstruction, cryst. growth for screw dislocation free semiconductors 77−55251
ternary semiconductor crystals for nonlinear optical applics., review 78−33782
thermoelectric recrystallisation, epitaxial film growth rate 80−100424
V-VI-VII ferroelectric semiconductor film growth, effect of artificial nucleation centres 79−11032
vapour growth, element incorporation 78−30556
VPE, gas-flow dynamics in horizontal CVD reactor, book contrib. 79−82498
VPE growth of $A^{III}B^{V}$ compounds flow graph model 79−56088
VPE impurity profile computer-aided control 80−2962
VPE of III-V ternary layers, on-time comp. determ. 78−67915
zero gravity, Polish expts. in space *(Polish)* 79−56920
zone melting, process parameters influence on radial scatter of resist. 80−16174
$AgBiTe_2$-PbTe solid solution, prep. and thermoelec. props. 77−47839
$AgGaSe_2$, growth by Bridgman method, optical charact. 77−69980
$AgGaSe_2$, seeded Bridgman growth of crack-free crysts., thermal expansion coeff. 78−11101
$AgGa(Se_{1-x}S_x)_2$, crystal growth, phase studies, optical props. 78−48305
$AgInS_2$, and $AgIn_5S_8$, spray pyrolysis, film struct., elec. and optical props. 80−71592
Ag_2S film, vacuum deposition and struct. 77−73233
$Ag_2S(Se)(Te)$, thermodynamic props., growth of single cryst. by chem. transport reaction 77−36380
Ag_2Te, growth by chem. transport *(Russian)* 79−38728
(Al,Ga)As, growth imperfections effect on losing 77−3588
Al-Ga-As heterostruct. with confined current flow, fabrication 78−68081
Al-Ga-Sb ternary phase diagram, calc., DTA and LPE expts. 80−29931
n-AlAs, VPE on GaAs, for heterojunction devices 77−1814
AlAs-GaAs film heterojunction, VPE growth and charact. 78−6439
AlAs-GaAs heterostructure, fabrication by selective liq.-phase epitaxy 79−15618
AlB_{12}, preparation of single crystal 78−43997
Al_xGa_{1-x}-GaP structure, LPE, double heterostruct. light modulator appl. 79−28963
AlGaAs, LPE layers, growth initiation and cathodoluminesc. irregularities 79−87010
(AlGa)As-GaAS DH lasers prep. by new LPE technique 77−40358
AlGaAs-GaAs, DH laser material, singular instabilities of LPE growth surface 77−24969
(AlGa)As-GaAs, large area high efficiency solar cell fabrication, LPE process 77−36410

semiconductor growth continued
AlGaAs-GaAs transverse mode stabilised plano-convex waveguide laser made by single step LPE 80−48274
$Al_{0.3}Ga_{0.7}As$:Te(SN), impurity effects on interface morphology of LPE films on corrugated GaAs substrates 78−88435
$Al_{0.3}Ga_{0.7}As$-GaAs DH mesa stripe laser, metalorganic VPE growth and characterisation 79−98391
$Al_{1-x}Ga_xAs$, transient-mode LPE on GaP 78−72746
$Al_xGa_{1-x}As$ and GaAs planar local struct. synthesis by LPE 79−56097
$Al_xGa_{1-x}As$ DH laser, with constricted active region, fabrication and characts. 78−37895
$Al_xGa_{1-x}As$ epitaxial film, LPE growth and semi-insulating props. 77−44179
$Al_xGa_{1-x}As$, epitaxial growth, orienting substrates effects 77−43444
$Al_xGa_{1-x}As$, epitaxial growth from limited vol. melt 79−70005
$Al_xGa_{1-x}As$, epitaxial layer crystn. from soln. in melt, diffusion limited 78−35321
$Al_xGa_{1-x}As$, epitaxial layer, distribution of Te and Ge impurities 78−43046
$Al_xGa_{1-x}As$ grown by organometallic VPE, luminesc. efficiency 79−78892
$Al_xGa_{1-x}As$, growth of high-resistivity layers by liquid-phase epitaxy 79−70008
$Al_xGa_{1-x}As$, growth of uniform epitaxial layers 77−40393
$Al_xGa_{1-x}As$ layer, LPE, graded bond gap solar cell, composition profile, Rutherford backscatt. 78−76612
$Al_xGa_{1-x}As$ layers, graded band gap, growth and properties 79−60645
$Al_xGa_{1-x}As$, MBE grown film, in situ surface characterisation by RHEED, SIMS and AES 77−43410
$Al_xGa_{1-x}As$, organometallic VPE growth, and characterisation 79−78899
$Al_xGa_{1-x}As$ oxidised AlAs as multidielectric for GaAs MIS devices 79−65333
$Al_xGa_{1-x}As$ solid soln., epitaxial layer growth on GaAs by zone recrystallisation with temp. gradient 77−16510
$Al_xGa_{1-x}As$ thick epitaxial layer production, by zone recrystn. in temp. gradient 79−15619
$Al_xGa_{1-x}As$ thin graded band-gap layers, isothermal LPE growth 80−34325
$Al_xGa_{1-x}As$, VPE, recent advances, book contrib. 79−66011
$Al_xGa_{1-x}As$, VPE and LPE growth, electron mobility 79−91165
$Al_xGa_{1-x}As$, VPE growth and characterisation 78−35315
$Al_xGa_{1-x}As$, waveguide heterostruct. epitaxial growth with gradual composition change 79−42416
$Al_xGa_{1-x}As$:Zn epitaxial layers, composition and Zn carrier conc. 80−25585
$Al_xGa_{1-x}As$-GaAs heterostruct. lasers, metallorganic CVD 80−23692
$Al_xGa_{1-x}As$-GaAs multilayers, LPE, using addition of GaCl vapour and new boat struct. 79−33950
$Al_xGa_{1-x}As$-GaAs multiple-quantum-well injection lasers grown by metal-organic CVD, room temp. continuous operation 80−1218
$Al_xGa_{1-x}As$-GaAs photopumped quantum-well heterostructure lasers grown by metalorganic CVD 79−98390
$Al_xGa_{1-x}As$-GaAs quantum-well heterostructure laser, metalorganic CVD growth, CW operation 300 to 337K 79−10304
$Al_xGa_{1-x}As$-$Al_xGa_{1-x}As$ laser struct., for integrated optics, MBE 78−13817
AlGaAsSb LPE growth, lattice-matched to GaSb, characterisation 80−60794
AlGaAsSb, photodiode, lattice-matched to GaSb 79−71527
$Al_yGa_{1-y}As_{1-x}Sb_x$ LPE phase diagram 78−11137
$Al_xGa_{1-x-y}In_yAs$, LPE on InP, solid-liq. equilib. calcs. 78−84083
AlGaSb, growth and characts. for 1.0-1.8 μm heterojunction devices 78−6870
$Al_xGa_{1-x}Sb$, compositional var. during LPE growth using ternary phase diagram 77−59761
$Al_xGa_{1-x}Sb$, surface flatness depend. on LPE condition 79−15042
$Al_xGa_{1-x}Sb$:Zn(Si)(Ge)(Sn)(Pb), doping of solid solns. during LPE *(Russian)* 77−85087
$Al_xIn_{1-x}Sb$, DC sputtering and struct. 78−52674
$Al_2In_{12}Se_{21}$, cryst. growth from melt, elec. props. 79−56922
AlN, CVD from $AlCl_3/NH_3$, calc. of equilibrium yields 79−52121
AlN, epitaxial growth, by ammonolysis of $AlCl_3$, thermodynamics 77−8758
AlN film, epitaxial growth by reactive evaporation *(Japanese)* 78−23629
AlN film, thermodynamics and kinetics of CVD 80−108354
AlN films on glass substrate, prep. by reactive DC magnetron sputtering technique, c-axis orientation 80−89146
AlN, single cryst. growth by sublimation-recondensation technique 78−31310
AlN, VPE by closed space vapour process, and optical absorpt. edge 78−88371
AlSb film, laser-induced metal-semicond. transition in Al-Sb mixed film 80−6661
$(AlSb)_x(GaSb)_{1-x}$, LPE growth 77−40392
As-Ge-Se system, synthesis and phys. props. of amorphous layers 77−52252
As_2Se_3, vacuum evaporation, composition of condensates 78−44012
$AsTeS_x(Se_x)(Sb_x)(Bi_x)$, chalcogenide glass, thin film crystallisation 79−7758
BN film, high temp. reactive plasma deposition, struct., resist., and dielec. const. meas. 77−7988
BN, semicond. film, chemical deposition 80−71596
BP, cryst. growth from Cu-fluxed melt, and characterisation 77−85920
BP, epitaxial, CVD on Si substrate, cryst. imperfections 78−10294
BP, epitaxial growth on Si substrate, Si impurity profile, ion microanal. 78−87886
BP, epitaxial growth using B_2H_6-PH_3-H_2 system 79−28937
BP, VPE, diffused layers formed in Si substrates, device appls. 78−56585
BP-Si junctions epitaxial growth and device appls. 78−48333
Ba_2ZnS_3, prep. by solid state reaction and melt growth, X-ray anal. 77−73226
$Bi_{1-x}Sb_x$, growth by horizontal zone refining, low charge carrier conc. 77−21020
ρ-BiSe, single crystal, synthesis and elec. props. 77−16490
p-Bi_2Se cryst. growth, elec. props. 77−8748
$Bi_2TE_{3-x}Se_x$, solid solution films, prep. and props. 78−44013
Bi_2Te_3-based solid solns., decomp. kinetics under flux layer 77−81205

semiconductor growth continued
Bi_2Te_3-Bi_2Se_3 solid solns., bladed cryst. growth, electrophysical props. 78−43387
Bi_2Te_3-Bi_2Se_3 solid solns., single cryst. growth and thermocouple construct. 80−104056
BiTeI, elec. props., crysts. grown from melt in excess iodine 79−4907
BiTeI, melt and vapour grown, optical props. 80−84746
BiTeI-SbTeI solid solns., form., crystn., elec., thermal props. 78−44003
$Bi_2Te_{2.88}Se_{0.12}$, solid soln., single cryst. growth and doping, thermoelec. efficiency and Hall coeff. 79−33921
C, amorphous, prepared by glow discharge method, elec. and optical props. 77−21036
CC GaAs:Sn, solubility and point defect-dopant interactions, LPE growth 79−90688
CC GaP, improvements in synthesis, solute diffusion (SSD) growth 79−65992
$CaSO_4$:Dy, cryst. growth from soln., thermoelec. and thermoluminesc. props. 79−56923
(Cd,Hg)Te epitaxial structures, comp. profile depend. on deposition parameters 80−100795
Cd chalcogenides, film, on NaCl, preferential epitaxy induced by electron bombard. or elec. field 80−10824
Cd-Sb thin film prep. by vacuum deposition, elec. props. 78−92194
$CdAs_2$ single crystals, growth from vapour phase 78−88416
Cd_3As_2 film on NaCl substrate, vacuum deposition, growth morphology, microstructure 80−75479
Cd_3As_2 platelet, single vap.-grown cryst., passive annealing, Fermi energy variation 80−45223
Cd_3As_2, vapour phase single cryst. growth, X-ray topographic obs. of perfection 78−9976
$CdCr_2S_4$ crystal growth, structural defects, physical properties 80−60759
$CdCr_2S_4$, ferromagnetic semiconductor films, prep. and props. *(Japanese)* 79−47308
$CdCr_2S_4$, single cryst. prep. and elec. props. 79−38727
$CdCr_2S_4$, single crystal ferromagnetic semiconductor, vapour-liquid transport growth method 77−21013
$CdCr_2Se_4$, crystn. from high temp. soln., $CdCr_2Se_4$-$CdCl_2$ phase diagram 78−3009
$CdCr_2Se_4$, ferromagnetic semiconductor, single cryst. growth *(Japanese)* 79−47612
$CdCr_2Se_4$ film, ferromag. semicond., prep. by vacuum condensation 77−28724
$CdCr_2Se_4$, single cryst. growth by chem. transport reactions 80−16163
$CdGa_2S_{4(1-X)}Se_{4x}$, solid soln., crystallographic studies 78−15301
$(CdGeAs_2)_{1-x}D_x$ amorphous films, property control in common target sputtering, elec. cond. 80−7494
$CdGe(As_{1-x}P_x)_2$, crystal growth, phase studies, optical props. 78−48305
$CdGeP_2$, crysts., prep. by chem. vapour transport 80−55280
$CdGeP_2$, growth from melt solution in Cd, microhardness 77−44139
$CdGeP_2$ synthesis and cryst. growth 79−87577
$Cd_xHg_{1-x}Te$, cast-recrystallise-anneal growth 79−91578
$Cd_xHg_{1-x}Te$, epitaxial growth from stoichiometric melt, crystn. and diffusion 80−75475
$Cd_xHg_{1-x}Te$ films, epitaxial growth, optical, elec., and photoelec. props. 79−11512
$Cd_xHg_{1-x}Te$, homogeneous mixed crysts. with large segregation tendency, Bridgman growth *(German)* 79−33923
$Cd_xHg_{1-x}Te$, isothermal growth of epitaxial layers 78−60577
$Cd_xHg_{1-x}Te$ solid solns., epitaxial growth under isothermal conditions 77−16504
$Cd_xHg_{1-x}Te$, solubility in Hg, rel. to LPE 78−35359
$CdIn_2O_4$, crystal growth from flux, elec. and struct. props. 77−81206
$CdIn_2S_4$ film, vac. deposited, growth, struct., optical and photoelectronic props. 80−10831
$CdIn_2S_4$ single crystal growth by two-zone horizontal Bridgman technique 78−27400
$CdIn_2Se_4$, cryst. growth, photoresponse and optical props. 78−39165
CdP_2, large tetragonal single cryst. growth from vap. 77−69976
CdP_4 single crystal growth 80−35065
$Cd_3P_2(As_2)$, cryst., gas phase growth, morphology 79−10821
Cd(S, Se) film grown on InP substrate, mismatch dislocations and lattice distortion, dangling bond density 80−84406
CdS, CdSe, growth rate, sublimation rate and etching behaviour along polar axis 80−24387
CdS, chem. sprayed film, struct. and morphology 78−72020
CdS, chem. sprayed film growth using centrifugal disc atomiser 78−92189
CdS, cryst. growth from vapour by one-dimens. nucleation on (110) singular surface, model 78−2048
CdS, cryst. growth from vapour in sealed silica tubes, emission and mass spectra 79−43117
CdS, crystal growth from vapour phase, model for interface kinetics 77−76335
CdS crystal growth from vapour, preferential deposition, elec. field effects 80−84122
CdS crystal growth with strong long-lived polarisation echoes 79−43113
CdS, crystallisation and stability in high-temp. alkaline solns. 77−52240
CdS, electrocrystallisation of films on Cd 78−72014
CdS, epitaxial film, conductivity control by S vacancy form., light modulation appls. 77−4455
CdS, epitaxial layers on (111) Ce, growth and defect struct. 78−18920
CdS, epitaxial layers on Cd single crystal, direct synthesis and struct. 78−68628
CdS evaporated films, growth rate and resist. determ., in situ meas. technique 79−77940
CdS film, growth by chem. bath deposition, photocond. props. 77−59703
CdS film, high cond., high transmittance, growth by evaporation method, and characterisation 77−77386
CdS film, precipitation from solns., form. characts. 79−11524
CdS film, spray pyrolysis prep., elec. transport props. 78−2590
CdS film growth, with smooth surfaces through boundary layers 79−28244
CdS film spray fabrication, physical props., Cu_2S-CdS solar cell applications *(French)* 80−60113
CdS, film with high photocond. and good reproducibility, prep. by chemical deposition 79−66019
CdS films, chem. deposited, growth kinetics and polymorphism 80−75463
CdS films, from thermal decomp. of organometallics, growth kinetics and struct. 79−78895

semiconductor growth continued
CdS films, photosensitive, growth by reactive RF sputtering, props. *(French)* 78−35308
CdS, grown by vac. evaporation on Si 80−25567
CdS, heterojunctions with InP and GaAs, prep. by CdS CVD and etching 78−52062
CdS, hydrothermal crystal growth on seeds of various orientations 77−4730
CdS layers, by vacuum evaporation, formation mechanism of preferred orientation 79−56094
CdS layers, epitaxial, deposited on InP substrates, vapour growth technique 77−21033
CdS, oriented single cryst. growth method from vapour 77−8734
CdS photoanode, for photovoltaic cells, prep. and characts. 78−14818
CdS photosensitive film production from chelated metallo-organic compounds *(Russian)* 80−49813
CdS, seeded growth from vapour of large single crystals 78−64449
CdS single cryst., melt growth, improvement of elec. characts. 79−38734
CdS, single crystal, growth by modified Piper-Polich method, props. *(Japanese)* 79−100036
CdS smoke particle growth, prep. by evaporation in inert gases 77−24938
CdS, solution growth, using Te solvent 79−65993
CdS sprayed film, prep., optical props., struct. and comp. 79−78875
CdS sputtered film, photocond. props. 78−10586
CdS, thin films, deposition onto hot substances, vapour phase method 78−95694
CdS thin films, growth and evaluation for fabrication of high performance photovoltaic solar cells 80−93501
CdS thin layers, recryst. from CdS-Cr_2O_3 mixtures, phys. and photoelec. props. 80−96935
CdS, vacuum epitaxial growth on $CuInSe_2$ 78−92193
CdS, vap. phase grown cryst., stoichiometry control, elec. cond. 79−100034
CdS:In whiskers, prep. by vapour deposition 78−75969
CdS/InP epitaxial thin films on NaCl, HEED and TEM study 80−88446
CdS-CdSe bladed crystal prep. from gas phase 77−16478
CdS-CdTe double layers on various GaAs surfaces, morphology and crystallography 80−34326
CdS-CdTe solar cell, prep. by VPE, junction struct. and photovoltaic props. 77−73235
CdS-CdTe solar cells fabrication *(Japanese)* 79−87992
CdS-PbTe and CdS-Te heterojunctions, electron irrad. effect on electrophys. props., prep. conditions depend. 79−28421
CdS-Si n-p heterojunction photodetector, fabrication and characts. 78−52068
CdS(Se) films, electron irrad. effect on electrophys. props., prep. conditions depend. 79−28421
CdS_xSe_{1-x} photosensitive films, prep., props., and use for photodetectors 80−55298
CdS_xSe_{1-x} solid soln. film by spray pyrolysis 77−81214
$Cd_{1+y}(S_xSe_{1-x})$ single crysts., vapour phase transport and stoichiometry control 79−28940
CdS(Se)(Te), epitaxial, condensation from gas phase of controlled comp., and props. 80−54562
CdS(Se)(Te), evap. onto electron bombarded NaCl substrates, epitaxial growth and characts. 79−28948
CdS_xTe_{1-x}, recryst. from CdS_xTe_{1-x}-Cr_2O_3 mixtures, photocond. props. 80−96936
CdSb, monocrystalline film, prep., elec. props. 79−43159
CdSe, epitaxial growth by transport reactions in closed system 77−52232
CdSe evaporated films, photoconductivity and effect of deposition conditions 79−95442
CdSe film, effect of growth conditions on electrophysical properties 78−44024
CdSe film, soln. growth 80−66437
CdSe film, stimulated recrystn. influence on photocond. 77−43754
CdSe film, struct. props., influence of O_2 partial press. and substrate temp. during vapour deposition 77−39751
CdSe film deposition, and reaction sequence of H_2SeO_3 reduction 80−71603
CdSe films, growth kinetics and cryst. struct. during vacuum condensation 80−2305
CdSe, LPE growth on ZnTe, characterisation of heterojunction 77−4745
CdSe photosensitive film production from chelated metallo-organic compounds *(Russian)* 80−49813
CdSe, VPE on ZnTe (111), monocrystalline layers 78−14631
CdSe:In, epitaxial layers, synthesis and elec. props. 77−47909
CdSe(Te) films, oriented, epitaxial growth by epitaxial nucleation in submicroscopic holes method 80−59834
$CdSnO_3$ and Cd_2SnO_4, crystal growth by flux or high press. method, elec. and struct. props. 77−81206
Cd_2SnO_4 film, sputter deposition and characterisation 79−43146
$CdSnP_2$ crystal growth, DTA obs. of Cd-Sn-$CdSnP_2$ phase diagram 80−24394
$CdSnP_2$-$CdSnAs_2$, and $CdSnP_2$-$CdGeP_2$, solid solution form. and elec. characterisation 78−43125
$CdSnP_2$-InP, n-n heterojunctions, growth, elec. characts. 77−11992
CdTe and $Cd_xHg_{1-x}Te$, crystal growth by zone passing techniques 77−40360
CdTe and CdTe:Cl, grown by travelling heater method, EPR defect charact. 77−40125
CdTe cathodic deposition from aqueous electrolytes 78−64484
CdTe, cryst. growth from vapour 77−24936
CdTe crystal growth for γ-ray detectors 78−41889
CdTe epitaxial films, on CdS substrate, closed-tube vapour growth 80−55302
CdTe epitaxial films, surface morphology, layer and spiral growth 80−10823
CdTe epitaxial layers on GaAs, cryst. struct. and phys. props. 79−33202
CdTe film, growth by photostimulated VPE, electrophys. props. 77−40390
CdTe film, low-resist., prep. by multi-source evaporation method, and characterisation 80−25582
CdTe film formation on glass substrates, influence of sublayers of recrystn. stimulators 77−43455
CdTe, film grown by hot wall epitaxy, elec. props. 79−82696
CdTe, films grown by hot wall epitaxy, elec. props. 79−28420

semiconductor growth continued
CdTe, grown by chem. transport, morphology, struct. and microhardness *(Russian)* 78−22729
CdTe, growth by travelling heater method, high resistivity charact., γ-ray detector appl. 78−84707
CdTe, growth by vapour phase chem. transport in I_2 77−40342
CdTe, growth from Cd rich soln. by solvent evaporation 77−40355
CdTe, growth from In solvents, self-compensation 77−28144
CdTe, growth from soln. in fused $CdCl_2$ 77−44138
CdTe, growth from Te soln. by slow cooling or travelling heater method, Te inclusions 77−40352
CdTe, growth from Te-rich soln. by travelling heater method, cond. and luminesc. 77−40351
CdTe, growth from Te-rich soln. in vertical Bridgman furnace 77−40354
CdTe, growth on Te substrate by solid-state reaction 79−95287
CdTe, high purity crystal, growth from soln., γ-ray detector appls. 77−14310
CdTe, high-resistivity, grown by modified travelling heater method, trapping parameters 77−39871
CdTe, LPE in CdTe-$CdCl_2$ system 78−35323
CdTe, laser window material, vap. deposition 78−27391
CdTe layer deposition by ionised cluster beam technique 77−48351
n-CdTe layers, growth and characterisation, heterojunctions and Schottky barriers fabrication *(German)* 80−89151
CdTe, low temp. themal cond., growth parameter influence 80−92725
CdTe, melt-growth review, including liquid encapsulation method, defect charact. 77−40350
CdTe, on mica, substrate defects effect on epitaxy 78−26794
CdTe, optical waveguide, fabrication by LPE using boat-slide technique 77−63570
CdTe, properties and appls., conf., Strasbourg, France (Jun-Jul 1976) 77−39832
CdTe, purification, efficiency for extraction of Cu and Ag impurities, impurity scatt. meas. 77−8749
CdTe reactive close-spaced vapour transport, simplified theory 80−15396
CdTe, single cryst. sublimation growth, X-ray topographic characterisation 80−29866
CdTe, solubility in Hg, rel. to LPE 78−35359
CdTe, sputtered film, electrode effects in AC characts. from equivalence impedance meas. of metal-CdTe-Al struct. 79−82686
CdTe thin films, oriented, VPE growth, infrared transmission, photovoltaic cells 80−59825
CdTe, undoped, high-resist., grown by travelling heater method, characterisation 77−39801
CdTe:Cl, gamma-ray detector growth, travelling heater method improvement 77−40353
CdTe:Cl, grown by travelling heater method, carrier homogeneity investig. 77−39848
CdTe:Tl, growth by travelling heater method, elec. and optical characterisation 77−40356
$CdTe/Hg_{1-x}Cd_xTe$ multilayers, LPE growth 80−80104
CdTe-In system, equilib. phase diagram and liq. phase epitaxial growth of CdTe from In soln. *(Japanese)* 80−71634
CdTe-Te film, prep. by combined hot-wall-flash evaporation method, and characterisation 80−55296
CdTe-ZnSe pseudobinary system, phase diagram and equil., Bridgman single cryst. growth method 79−43213
$CdTl_2Se_4$, single cryst., preparation, elec. cond. 77−24554
CdZnS thin films, growth and evaluation for fabrication of high performance photovoltaic solar cells 80−93501
(CdZn)S-Cu_2S solar cell, film form. and characts. 78−68080
$Cd_{1-x}Zn_xS$, film, technical data, for low cost solar cell 79−48127
$Cd_{1-x}Zn_xS$-p-GaAs heterojunctions, elec. and photovolt. props. rel. to growth technique 80−29466
$Cd_{1-x}Zn_xSe$, epitaxial layer growth with Zn content from doping to solid soln. formation 77−85094
$Co_{3-x}Mo_xO_4$ films, prep., struct. and elec. characteris. 80−108353
$CrPr_2S_4$, synthesis, single crystal growth, mag. and elec. props. 79−78857
$CrPr_2Se_4$, synthesis, single crystal growth, mag. and elec. props. 79−78857
$(Cu,Ag)_2Se/(Bi,Sb)_2Te_3$, P type selenide segmented element fabrication, thermoelectric props. 80−107835
$CuCr_2Se_4$, cryst., preparation, elec. cond., thermo EMF 77−8125
$CuGa_xIn_{1-x}Se_2$, CVD, elec. and optical props., use as heterojunction solar cell absorber 79−52095
$CuGaS_2$, crystal growth and luminesc. *(Japanese)* 78−23515
$CuGaS_2$, crystal growth by solid phase crystallisation 80−25556
p-$CuGaS_2$, LPE on n-ZnS, heterojunction prep. and characterisation 79−1831
$CuGaS_2$-$CuGaSe_2$ system, forbidden-band width 78−35280
$CuGaSe_2$, film, spray pyrolysis prod. 79−95953
$CuGaSe_2$, single cryst. growth from melt, doping 77−12522
$CuGaTe_2$ film, flash evaporated, growth and optical props. 79−95296
$CuGaTe_2$ films deposited on GaAs substrates by flash evaporation, struct. and elec. cond. 80−24755
$CuInS_2$, crystals and thin films, growth, struct., and elec. props. 79−38729
$CuInS_2$ films prod. by RF sputtered Cu-In films exposure to H_2S 79−95926
$CuIn_5S_8$, single crystn. phase, CVD prep., X-ray cryst. struct. determ. 79−65990
$CuInS_2(Se_2)$, film, spray pyrolysis prod. 79−95953
$CuInSe_2$ film, MBE growth, AES and optical absorpt. obs. 79−78903
p-$CuInSe_2$ film, prep. from vac. evaporation of $CuInSe_2$, optical and elec. props. 79−82697
$CuInSe_2$, growth on CdS (0001) surface using MBE 79−56936
$CuInSe_2$, heteroepitaxy on {111} oriented Ge by flash evaporation, struct. 80−108333
$CuInSe_2$, large single crystals growth by iodine transport and Bridgman methods 78−35300
$CuInSe_2$, melt-grown, EPR characts. 78−35030
$CuInTe_2$ epitaxial layers, on GaAs, growth and props. 80−108359
$CuInTe_2$, grown from near stoichiometric comp., elec. and optical props. 78−68504
$CuInTe_2$ single crystals, directional freezing growth and doping, resist. changes on annealing 80−60768
$CuInTe_2$, vac. deposited film, growth, struct. and elec. characts. 77−69995
$(CuInTe_2)_{1-x}$-$(2ZnTe)_x$, phase diagram and cryst. growth of $CuZn_2InTe$ from $ZnCl_2$ flux 80−16287

semiconductor growth continued
Cu_2O, CVD from Cu-O-H-Cl-N system, thermodynamic anal. 78−39676
Cu_xO film, growth by anodisation, switching characts. 77−55898
Cu_2S epitaxial films, reactive sputtering prep. and electronic props. 79−78885
Cu_2S film, for CdS/Cu_2S photovoltaic devices, formation and props. 79−11257
Cu_2S film, on rough $Zn_xCd_{1-x}S$ substrate, film substrate lattice mismatch calcs. 78−43263
Cu_2S, film preparation for solar cells, elec., optical, struct. props. 78−76602
Cu_2S stoichiometric thin films for solar cells 79−61991
Cu_2S-CdS, photovoltaic junction, prep. by chemical deposition 79−66019
Cu_2S-CdS solar cells, prep. and stoichiometric control of Cu_2S film 78−2560
$Cu_{2-x}S$ on CdS, low temp. growth, AES obs. 79−28924
$Cu_{2-x}S$-CdS p-n heterojunction, copper sulphide growth features during formation *(Russian)* 80−107898
Cu_xS evaporated thin films, composition, prep. and characts. 80−25569
Cu_xS films, magnetron reactive sputtering deposition and elec. props. 79−78884
Cu_xS-CdS solar cells, Cu_xS transform. behaviour rel. to topotaxial growth, cell efficiency 77−11814
Cu_xS-CdS solar cells, cu_xS growth kinetics and composition analysis by absorbance transient and galvanic electrochemical measurements 80−92797
$CuSbS_2$ crystals, growth and characterisation 80−60770
Cu_2SnSe_3, single cryst. growth and morphology 77−85908
Er_2Te_3, films, prep., elec. props. 78−43494
EuGa(In)$_2X_4$, X=S,Se,Te, prep. and props. 77−85214
$Eu_{1-x}Gd_xO_{1-x}N_x$, ferromag. semicond., prep., ferromag. props. *(French)* 77−69550
EuS, film, anisotropic growth on amorphous substrate 77−12547
EuS_x film, vacuum deposited, composition depend. on substrate temp. and deposition rate 78−84107
EuSe, VPE by hot-wall technique 80−80958
$FeCr_2S_4$, ferrimag. semicond., elementary step growth on surface of vapour grown cryst. 77−76649
$FeCr_2S_4$, single crysts., vapour grown, growth of triple unit cell steps on surface 79−19984
$Fe(Sb_{1-x}Te_x)_3$ system cpds., prep., cryst. struct., elec. and mag. characteris. 80−108349
(Ga,Al)As, LPE growth of multilayered struct., explanation for meniscus lines on surfaces 77−76681
(Ga,In)As, growth of epitaxial layers 77−12542
Ga-Al-As(Sb) system, ternary phase diagrams, method for determ. of liquidus surfaces 77−28787
Ga-Al-Sb, liq. phase epitaxy, phase diagram, X-ray microanal. 79−19491
Ga-As-P system, ternary phase diagrams, method for determ. of liquidus surfaces 77−28787
Ga-In-As system, ternary phase diagrams, method for determ. of liquidus surfaces 77−28787
Ga-In-As-Sb system LPE layers, pseudoquaternary phase diagram 78−10293
GaA-$Al_{0.27}Ga_{0.73}As$ DH lasers grown by MBE, growth conditions influence on threshold current density 80−32984
GaAS-AlGaAs LPE layers, defects formed by oxygen in ambient gas *(Japanese)* 77−70009
GaAlAs based heterojunctions, integrated optics appl., technology advancements *(Slovak)* 80−33226
(GaAl)As, DH laser, LPE growth, meniscus lines as nucleation sites 77−15706
(GaAl)As DH laser, threshold current density, growth terraces effect 80−99723
(GaAl)As, LPE, GaAs dissolution kinetic in undersaturated isothermal solns. in Ga-Al-As system 80−80106
(GaAl)As low-beam-divergence CW DH laser, grown by low press. metallorganic CVD 80−74376
(GaAl)As system, automated system for growth of multilayered structs. by LPE 79−38752
GaAlAs/GaAs heterostructures, ellipsometric assessment of epitaxial layer during growth in organometallic VPE system 79−37933
GaAlAs-GaAs, high efficiency heterostruct. solar cell grown by metalorganic CVD 78−11118
GaAlAs-GaAs heterostructure laser fabrication, using horizontal and vertical LPE furnaces 77−42538
GaAlAs-GaAs lasers, channelled substrate, prepared by combination of organometallic pyrolysis and LPE 80−99745
$Ga_{0.65}Al_{0.35}As$, LPE growth, wave morphologies on surface 77−40396
$Ga_{0.7}Al_{0.3}As$ epitaxial film, inclusion-generated dislocation clusters 77−89445
$Ga_{0.9}Al_{0.1}As$, nucleation morphologies on $Ga_{0.65}Al_{0.35}As$ surfaces grown by LPE 78−15323
$Ga_{1-x}Al_xAs$, alternate monolayer crysts., MBE and props. exam. 78−10289
$Ga_{1-x}Al_xAs$, appl. of theory of electroepitaxy of multicomponent systems 80−65396
$Ga_{1-x}Al_xAs$ based layer structures, optimum growth conditions, comp. and struct. perfection 80−104069
$Ga_{1-x}Al_xAs$ heterostructure, LPE prep., growth and dissolution kinetics, thermodynamic and kinetic models 80−75456
$Ga_{1-x}Al_xAs$, LPE, growth mechanism and morphology on channelled substrates 79−28960
$Ga_{1-x}Al_xAs$, LPE growth and characterisation 80−50566
$Ga_{1-x}Al_xAs$, LPE layer thickness depend. on soln. comp. 78−10295
$Ga_{1-x}Al_xAs$, LPE layers, grown under const. cooling rate conditions, cryst. composition 78−39710
$Ga_{1-x}Al_xAs$, LPE layers, diffusion limited growth, thickness comparison with GaAs 78−87892
$Ga_{1-x}Al_xAs$ LPE layers, comp. and refr. index, ellipsometry meas. 79−87011
$Ga_{1-x}Al_xAs$ layer form. on GaAs during dissolution in Ga-Al-As soln. 80−10799
$Ga_{1-x}Al_xAs$, liquid and solid comp. variations during LPE growth 79−99445
$Ga_{1-x}Al_xAs$, Peltier LPE, absence of electromigration of As and Al 77−81230
$Ga_{1-x}Al_xAs$, self-aligned three dimensional struct. MBE growth 77−59697
$Ga_{1-x}Al_xAs$, solar cells appl., technology advancements 79−43776

semiconductor growth continued
$Ga_{1-x}Al_xAs$:Si p-n junction, doping in LPE, elec. and luminesc. props. *(Czech)* 78−47851
$Ga_{1-x}Al_xAs$-$Ga_{1-y}Al_yAs$ DH laser, grown by organometallic CVD, room temp. operation 78−29950
$Ga_{1-x}Al_xAs$-GaAs, abrupt quantum-well heterostruct. grown by metalorganic chemical vapour deposition 79−56933
$Ga_{1-x}Al_xAs$-GaAs, CVD laser diodes, operation and growth processes 78−46598
$Ga_{1-x}Al_xAs$-GaAs, heteroepitaxial layers on GaAs(001), misfit dislocation asymmetry 77−47694
$Ga_{1-x}Al_xAs$-GaAs, high efficiency solar cell, isothermal etchback-regrowth method 77−59701
$Ga_{1-x}Al_xAs$-GaAs, room temp. DH laser, CVD growth 78−37912
$Ga_{1-x}Al_xAs$-GaAs DH lasers grown by metalorganic CVD, room temp. operation 78−1248
$Ga_{1-x}Al_xAs$-GaAs heterostructure lasers grown by metalorganic CVD, prep. and props. 79−36918
$Ga_{1-x}Al_xAs$-GaAs injection laser, branching waveguide coupler fabrication by LPE 78−63202
$Ga_{1-x}Al_xAs$-GaAs laser, DH, grown by metalorganic CVD, room temp. operation 78−13702
$Ga_{1-x}Al_xAs$-GaAs low threshold room temp. DH lasers grown by metalorganic CVD 78−50804
$Ga_{1-x}Al_xAs$-GaAs p-n and p-p-n heterojunction solar cells, high efficiency, prep., eval. and characters *(Japanese)* 80−61342
$Ga_xAl_{1-x}As$, LPE, charge carrier conc. distrib. *(Russian)* 78−52694
$Ga_xAl_{1-x}As$, LPE, GaAs solubility in Ga-Al alloys investig. 78−52690
$Ga_{1-x}Al_xAs_{1-y}P_y$ layer of uniform composition grown on GaAs by LPE, temp. diff. method appl. 79−23864
GaAlAsSb/GaSb alloys, prep. and optoelectronic device appl. 80−25587
GaAlAsSb-GaSb low bandgap solar subcell for high efficiency multibandgap convertors, LPE growth 80−93927
$Ga_{1-x}Al_xP$ varigap structs., crystallation 80−80993
$Ga_{1-x}Al_xSb$, LPE growth and phase diagram *(French)* 77−24974
$Ga_{1-x}Al_xSb$, melt growth and elec. props. 79−65999
$Ga_{1-x}Al_xSb$ p-n homojunction LPE and photovoltaic effect obs. *(French)* 78−64108
$Ga_{1-x}Al_xSb$ variable-gap p-n struct., selective photoelec. effect 77−76912
$Ga_xAl_{1-x}Sb$, VPE, closed tube transport technique 79−28935
$Ga_xAl_{1-x}Sb$, VPE with I_2 as transport agent 78−48325
GaAs (100), VPE, role of Cl, LEED, RHEED, and AES obs. 77−1327
GaAs, (100) surfaces, struct. and stoichiometry during molecular beam epitaxy, RHEED anal. 79−4921
GaAs (111) substrate, and homoepitaxial layers, characterisation by divergent X-ray beam diffr. 78−31352
GaAs, and its alloys, as integrated optics materials, book contrib. 79−64362
GaAs and related cpds., conf., Edinburgh, Scotland (Sep 1976) 78−3039
GaAs and related cpds., conference, St. Louis, MO, USA (Sept. 1978) 80−8737
GaAs, back etching and growth by liq. phase epitaxy, surface morphology obs. 80−29287
GaAs, CVD, S doping behaviour during growth, electron conc. 78−26784
GaAs, CVD for solar cell applications 77−77412
GaAs, CVD in Ga-$AsCl_3$-H_2 system with different input supersaturations *(Russian)* 78−68098
GaAs, CVD mechanism, product catalysed reaction of Me_3Ga with AsH_3 77−48345
GaAs, CVD on W coated graphite, characterisation, and Schottky barrier solar cell characts. 79−28930
GaAs, CVD using Ga-As-H-Cl system, theoretical anal. of equilib. adsorption layers 79−23858
GaAs, concs. of C and O_2 in LEC grown cryst. determ. 77−39612
GaAs, cryst. growth from large Ga:As solns., critical cooling rate 80−64938
GaAs, cryst. prod. in strip and rod form., Stepanov method 78−3017
GaAs, crystal pulling of semi-insulating material, liquid encapsulated compounding and Czochralski growth 79−43136
GaAs, Czochralski growth, melting and regrowth, inclusion density and dislocation generation 77−21016
GaAs, device quality, epitaxial growth on Ge/Mo substrates 79−69988
GaAs diode, high temp. and freq. characts., made by gas-transport method 79−19654
GaAs, epitaxial, optical integrated circuits appl. 77−65644
GaAs, epitaxial, polycryst., monocryst. layers and whiskers grown by CVD, SEM obs. electron diffr. study *(French)* 79−43150
GaAs, epitaxial, Si and Ge doping 80−24470
GaAs, epitaxial deposition from organometallic cpds. 77−47689
GaAs epitaxial film, chem. transport by water vapour, thermodynamic calcs. 77−12539
GaAs epitaxial growth, CVD-organometallics method, reactional efficiency in solar cell elaboration 80−93498
GaAs, epitaxial growth and etching rate meas. method 77−35829
GaAs, epitaxial growth for microwave devices *(French)* 77−48360
GaAs, epitaxial growth in $Ga(CH_3)_3$-AsH_3-H_2 system 78−35312
GaAs, epitaxial growth under different intake supersaturations in GaAs-$AsCl_3$ gas transport system *(Russian)* 78−26776
GaAs, epitaxial layer, micron and submicron vap. phase growth, for FET 80−11577
GaAs, epitaxial layer growth by chloride process, μ-and subμ thickness 78−23624
GaAs epitaxial layer high power Gunn diode developement and fabrication 80−16199
GaAs epitaxial layers, substrate prep. effect on surface morphology 78−26780
GaAs epitaxial layers, growth below 700°C electrophysical props. 79−1827
GaAs epitaxial layers, from mixed Ga solns., C solubility 80−15392
GaAs epitaxial layers on polycryst. GaAs substrates, LPE growth characts. 80−75471
GaAs epitaxy, ultrathin film growth by cracking of organometallic compounds at 40 to 100 torr *(French)* 78−44023
GaAs, epitaxy by metallorganic and chloride depositions, defect characterisation at growth interface 80−59817
GaAs, epitaxy on semiinsulating GaAs, elec. props. of transitional layers rel. to growth conditions 77−15977
GaAs, epitaxy using TMG and AsH_3, chloride etching effect 78−76606

semiconductor growth continued
GaAs, expitaxial growth in Ga-$AsCl_3$-He_2 system, expt.-statistical analysis *(Bulgarian)* 78−60580
GaAs FET, continuous growth of LPE double layers 78−64487
GaAs FET double layer production, study by sliding boat method *(Japanese)* 79−66014
GaAs film, epitaxial deposition from gas phase, transient processes, elec. cond. 77−16501
GaAs film, growth kinetics for step-cooling LPE technique 77−40395
GaAs film, vapour-grown, effect of gas-phase stoichiometry on deep levels 78−10393
GaAs film on recrystallised Ge film, solar cell appl. 78−19671
GaAs film optical components, prep. by MBE using Si shadow masking technique 80−28358
GaAs film solar cell fabrication, substrate requirements 78−11125
GaAs films for solar cells appl., deposition and characterisation 80−84853
GaAs, gas-phase epitaxy, mass exchange during 79−78901
GaAs grown by VPE using organometallic method, deep trap levels 80−10923
GaAs, grown-in dislocation density, impurity effect 78−51543
GaAs growth dual-bubbler CVD system, characts., for MESFET applics. 78−6856
GaAs, heteroepitaxial layers on Si substrates by LPE 79−1832
GaAs homoepitaxy, vicinal surfaces of substrates, characterisation 77−20207
GaAs, hydride VPE growth for FETs, and characterisation 78−27407
GaAs, ion bombardment by alkali metal sputter ion source *(Japanese)* 79−54734
GaAs, LEC growth using pyrolytic BN crucibles 78−6841
GaAs, LPE, charge carrier conc. distrib. *(Russian)* 78−52694
GaAs LPE, current controlled for optimum doping profiles in LSA diodes 78−35318
GaAs, LPE, deep levels rel. to growth conditions 79−28314
GaAs, LPE, gaseous impurity source and effect on purity 79−28959
GaAs, LPE, growth mechanism and kinetics 78−34726
GaAs, LPE, residual impurities and deep levels, FET fabrication 79−28964
GaAs, LPE, smooth, thin layers on nominally oriented substrate 78−44030
GaAs, LPE, temperature instability effect, report 80−66446
GaAs LPE buffer layers for MESFET appls. 80−29887
GaAs LPE from Ga soln., carrier conc., growth condition depend. 80−71584
GaAs, LPE growth, electric current controlled, on n^+ and semi-insulating substrates 77−73240
GaAs, LPE growth, wave morphologies on surface 77−40396
GaAs, LPE growth 78−18924
GaAs, LPE growth on O-implanted GaAs substrates, surface morphology 77−28732
GaAs, LPE growth on O-implanted GaAs substrate, elec. props. 78−2592
GaAs, LPE growth surface, singular instabilities 77−24969
GaAs, LPE in graphite boat, total ionised impurity density 77−12550
GaAs, LPE layers, ambient O_2 effect on defects and elec. props. 77−76683
GaAs LPE layers, effect of baking on mobility and doping conc. 79−99641
GaAs, LPE layers, outdiffusion of recomb. centres from substrate during growth 80−39466
GaAs, LPE layers, screw dislocations, optical microscope obs. 77−35561
GaAs LPE layers, thickness comparison with $Ga_{1-x}Al_xAs$, for layers grown by linear cooling 78−87892
GaAs, LPE layers, voids and depressions in facet and terrace growth 78−38974
GaAs LPE layers, X-ray topographic studies of defects 77−62772
GaAs LPE on polycrystalline Mo 79−43157
GaAs, LPE with $AsCl_3$-saturated Ga/As solns. 78−63953
GaAs large-grained solar cell film recrystallisation 79−38737
n-GaAs layer, VPE, influence of growth conditions on incorporation of deep levels 77−4310
GaAs layers, electroepitaxy and thermal LPE growth, defect struct. and electronic characts. 80−2290
GaAs layers, from gas phase, impurity influence on growth micromechanism 80−45237
GaAs layers, high resistivity, growth for microwave device appl. 79−100056
GaAs layers, LPE from Au-Ge-Ni melts, elec. props. of Ni/Au-Ge/GaAs contacts obs. 77−77437
GaAs layers, LPE growth, graphite boat construction 78−31348
GaAs layers and p-n junctions grown by current-controlled LPE, elec. characts. 78−6436
GaAs, liquid-phase electroepitaxial growth kinetics, Peltier effect and solute electromigration 79−42401
n-GaAs, MBE, correl. between electron traps and growth processes 80−65387
GaAs, MBE, growth temp. depend. and characts. 79−28946
GaAs, MBE, process anal. and appl. *(French)* 79−56937
GaAs, MBE, SnTe source of donor impurities 79−95035
GaAs, MBE, surface reaction steps 79−77941
GaAs, MBE, technology and epitaxial layers props. 79−33945
GaAs, MBE, undoped, growth and characterisation 80−10836
p-GaAs, MBE grown, As_2 and As_4 effects on photolum. 80−103974
GaAs, MBE grown film, in situ surface characterisation by RHEED, SIMS and AES 77−43410
GaAs, MBE layers, H_2 effect on residual impurities, photolum. obs. and elec. characts. 79−47636
GaAs, MBE of autoepitaxial films, temp. range for growth, RHEED monitoring 78−44025
GaAs, MBE of doped cryst., thermodynamics and kinetics interplay 80−70144
GaAs, MBE prep., device props. 77−77417
GaAs, MBE with ionised dopant 77−40338
GaAs MESFET layers, low-temp. halide epitaxial growth 77−77403
GaAs MESFET layers, low temp. VPE growth by halide process 77−90279
GaAs, MESFET structure, buffered, LPE growth 80−40271
GaAs MM-wave and sub MM-wave receiver elements, Schottky-barrier resistive mixer devices LPE 80−11558
GaAs MOS device, new method of fabrication 78−47872
n-GaAs, melt-grown, stoichiometry, photolum. obs. 78−72583

semiconductor growth continued
GaAs, migration of liquid inclusions, effect of DC current and temp. 77−7910
GaAs, monocrystalline, lateral definition, prep. by MBE 80−108357
GaAs, multilayer epitaxial growth with Sn doping 77−47690
GaAs multilayer with abrupt carrier conc. profile, vapour growth technique 78−11123
GaAs, multiple layer LPE growth by controlled supercooling of Ga soln. 77−77429
GaAs, ohmic contact formation with thin film 77−8756
GaAs, optoelectronic devices, conf., Berlin, DDR 78−91755
GaAs patterned epilayer structures, MBE writing 78−56590
GaAs, Peltier induced growth kinetics of LPE 78−64485
GaAs, Peltier LPE, absence of electromigration of As and Al 77−81230
GaAs, polycryst. solar cells, thin film growth and grain size, effect on cell efficiency 80−81471
GaAs, polycrystalline, for solar cells 78−11124
GaAs polycrystalline film growth for solar cells 79−33941
GaAs, prep. of thin films by ionised-cluster beam deposition *(Japanese)* 80−25576
GaAs, produced by VPE using trimethylgallium and arsine, controlled doping 78−6855
GaAs ribbons from Ga-$AsCl_3$-H_2 epitaxy 80−7498
GaAs Schottky-barrier diode submicron layer LPE reactor 77−77439
GaAs, selective growth, MBE and self-masking method 77−52256
GaAs, selective in situ vapour etch of substrate and growth 80−2958
GaAs, semi-insulating, LPE growth for FET buffer layers 79−66015
GaAs, sequential multiple layer VPE, method 77−12545
GaAs, single crystal growth and heat treatment *(Chinese)* 77−73222
GaAs, solar cell, thin film, prep. by Peeled Film Technology 79−29472
GaAs, structural defects in single crysts., first order distribs. eval. *(German)* 78−6049
GaAs, substrate for epitaxial growth, backscatt. anal. of surface prep. and anodic oxidation 77−25175
GaAs surface, during vapour phase epitaxial growth, characterisation techniques and meas. *(French)* 77−1817
GaAs, surface studies during MBE growth 79−90899
GaAs synthesis, Ga+As reaction temp. determ. 77−24978
GaAs, synthesis by molten salt electrolysis 78−64486
GaAs, synthesis in pyrolytic BN boat 78−6840
GaAs technology, MBE growth, microwave, optoelectronic devices appl. 79−52129
GaAs thin layers, MBE, growth conditions and phys. props. *(German)* 80−55307
GaAs, transient-mode LPE on InP 78−72746
GaAs, travelling heater method growth, dislocation elimination 77−7684
GaAs, undoped epitaxial layer growth from nonstoichiometric solns., O_2 contamination sources 80−108362
GaAs unintentionally doped layer growth using MBE 78−72741
GaAs, unintentionally doped layer grown by MBE, elec. props. 79−91167
GaAs, VPE, fast growth at low temp. and high partial pressure 79−51446
GaAs, VPE, growth method at low H_2 press. 79−28936
GaAs, VPE, growth parameters effect 77−28726
GaAs, VPE, incorporation of deep levels, effects of growth conditions 80−20111
GaAs VPE, influence of growth parameters, $AsCl_3$ transport method 80−29881
GaAs, VPE, multi-wafer growth technique using $AsCl_3$-Ga-N_2 system with horizontal reactor 79−28934
GaAs, VPE, partial press. diagrams use for thermodynamic represent. 79−33201
GaAs VPE, residual donor impurities 77−76679
GaAs, VPE, review of growth techniques *(French)* 79−33935
GaAs, VPE, surface defects rel. to technological parameters 78−44015
GaAs, VPE, thermodynamic factor influencing growth rate and layer purity in Ga-$AsCl_3$-H_2 system 79−28933
GaAs, VPE, thermodynamic analysis of Si contamination 79−28932
GaAs, VPE by CVD, vapour-solid interface, expt. anal. *(French)* 79−33940
GaAs, VPE by Ga-$AsCl_3$-H_2 process, role of Si 77−40380
GaAs, VPE by pyrolysis, producing power GaAs MESFETs 78−23623
GaAs, VPE by single flat temp. zone method, elec. props. 79−95526
GaAs VPE growth, growth rate anal. 78−52680
GaAs VPE growth, in situ surface anal. 79−95937
GaAs, VPE growth, surface morphology study by optical microscopy 79−60651
p-GaAs, VPE growth and characterisation, doping levels 80−10841
GaAs, VPE growth by single flat temp. zone method, residual doping level 77−48352
GaAs, VPE growth on {110} cryst. plane 80−10840
GaAs, VPE growth rate variation with distance along substrate within const. temp. zone 78−2384
GaAs, VPE in CVD systems, anisotropic phenomena 80−54563
GaAs, VPE in Ga-$AsCl_3$-H_2 system at reduced temp. 79−11519
GaAs, VPE in inert gas-H_2 mixed carrier system, thermodynamic analysis 78−11120
GaAs, VPE layer growth with abrupt doping profile 80−24746
GaAs, VPE layer props. control using boundary layer characts. 80−50561
GaAs, VPE layers, growth conditions effect on deep levels 79−95360
GaAs VPE layers, role of diffused Ga vacancy in degradation 78−95050
GaAs, VPE on Ge substrate, and characterisation 78−72736
GaAs, VPE thin layers, thickness uniformity, main factor anal. 80−76197
GaAs, VPE UV stimulated 78−35313
GaAs, VPE using low press. organometallics 79−100054
GaAs, vapour phase epitaxy using computer control 79−38744
GaAs, vapour-phase epitaxial growth, transfer mechanism of Si 77−51616
GaAs, whisker growth by thermal decomp. 77−55875
GaAs:Be, annealing effect during MBE 78−79898
GaAs:Cr, semiinsulating, LPE and elec. props. 77−44178
GaAs:Cr, VPE grown, exam. of doping GaAs using $Cr(CO)_6$ 78−72737
GaAs:Cr, VPE growth, carrier conc. profiles 79−74099
GaAs:Fe, for FET, VPE and characterisation 78−19672
n-GaAs:Ge, film, substrate temp. depend. of Ge incorporation during MBE 80−76196
GaAs:Ge, LPE, on semi-insulating GaAs, film-substrate interface characterisation 78−72017

semiconductor growth continued
GaAs:Ge, LPE growth, Ge incorporation 78−27423
GaAs:Ge, mol. beam epitaxy of n- and p-types 80−10839
GaAs:Ge, VPE, doping, electrophysical characts. meas. 78−43493
GaAs:Ge, vap. grown, diatomic complex donor and acceptor model 78−80003
GaAs:Ge p-n junctions by mol. beam epitaxy 79−56289
GaAs:Ge(Sn), LPE layer growth, impurity effect on terrace form. 79−95288
GaAs:Mn epitaxial layers, fabrication and electrical props. 77−80859
GaAs:P films, epitaxial growth from melt with components introduced by ion bombardment 77−21044
GaAs:S epitaxial layers, dopant conc. control method 77−1807
GaAs:Se, LPE growth, Ga-As-Se phase diagram 79−1849
GaAs:Si, accelerated growth rate effect on MBE, Hall mobility and photolum. meas. 80−104067
GaAs:Si, current-controlled growth, segregation and amphoteric behaviour 78−31346
GaAs:Si, thick LPE layer growth and characterization 77−12511
GaAs:Si LPE layers, surface morphology, substrate misorientation, initial supercooling effects 80−34329
GaAs:Si layers, MBE growth, elec. and optical props., doping characts. 80−10819
GaAs:Si p-n structs., effect of growing conditions on distrib. of recomb. parameters 80−39668
GaAs:Si(Cr), LPE, spiral growth patterns, dopants role 77−72800
GaAs:Sn, doping characts. during LPE 79−10866
n-GaAs:Sn, heavily doped, nonalloyed ohmic contact form. by MBE and metallisation 79−7895
GaAs:Sn, influence of growth process in doping profile and mobility profile during LPE 79−70000
GaAs:Sn, LPE, growth rate and temp. depend. of impurity incorporation 78−3063
GaAs:Sn, LPE layers, electronic props., depend. on Sn incorporation 78−87883
n-GaAs:Sn, nonalloyed and in situ Ohmic contacts for FETs 79−56307
GaAs:Sn, selective LPE, orientation dependent growth, luminesc. 77−12551
GaAs:Sn, surface segregation of Sn during MBE, SIMS and AES 78−72031
n-GaAs:Sn, VPE growth, reactor design 80−2956
GaAs:Sn films, MBE 80−50563
n-GaAs:Sn-p-GaAs:Ge-p-$Al_xGa_{1-x}As$:Ge heterostructure solar cells, LPE growth techniques 80−66977
GaAs:Te, LPE, Te induced defects, rel. to growth conditions 78−6067
GaAs:Zn, diffusion during LPE, impurity gradients and annealing effects 80−29882
p-GaAs:Zn, luminescent, ion doped MBE growth 80−44436
GaAs:Zn, MBE with ionized beam doping 77−77418
GaAs:Zn, Se, double doping during LPE, exam. of elec. cond. and Hall effect 79−4923
GaAs:Zn epitaxial layers, composition and Zn carrier conc. 80−25585
GaAs:Zn films, VPE growth and photoluminesc. props. 79−38642
GaAs:Zn(S), LPE, and doping characts. 79−33948
GaAs-(Ga,Al)As heterostructure transmission photocathodes, characts. and epitaxial growth *(French, English)* 78−52616
GaAs-(GaAl)As channelled substrate buried heterostruct. injection laser, fabrication 77−7087
GaAs-$Al_{0.27}Ga_{0.7}$ $_3$As Dh lasers grown by MBE, influence of growth conditions on threshold current density 80−58587
GaAs-$Al_xGa_{1-x}As$ transverse junction lasers with low threshold current prep. by MBE on semi-insulating substrates 80−58588
GaAs-$Al_xGa_{1-x}As$, current transverse junction lasers, low threshold, MBE prep. 80−83614
GaAs-$Al_xGa_{1-x}As$ buried-heterostructure lasers, current injection confinement, MBE/LPE hybrid technique 80−74374
GaAs-$Al_xGa_{1-x}As$ DH lasers, MBE grown, low current threshold, high lasing uniformity 79−64223
GaAs-$Al_xGa_{1-x}As$ DH lasers, very low current threshold, MBE grown 80−43353
GaAs-$Al_xGa_{1-x}As$ DH lasers, MBE grown, substrate temp. effect on current threshold 80−48243
GaAs-$Al_xGa_{1-x}As$ films for optical devices, masked MBE 78−38100
GaAs-$Al_xGa_{1-x}As$ multilayer struct., MBE, selective area growth using Si shadow masks 77−85946
GaAs-$Al_xGa_{1-x}As$ structures for DH lasers, LPE *(Polish)* 79−4922
GaAs-AlAs, epitaxial struct. with alternate layer comp. modulation, fabrication and characterisation 77−1322
GaAs-AlAs layered films, MBE prep., struct., rel. to optical props. 79−77950
GaAs-AlAs layered superlattices, deposited by MBE, exam. of crystal growth kinetics 78−72739
GaAs-AlGaAs DH, improved LPE growth, lasing characts. 77−81229
GaAs-AlGaAs DH laser, improved lifetime by defects reduction during LPE 77−75547
GaAs-AlGaAs DH layers, tapered growth by wipingless LPE 77−66594
GaAs-AlGaAs LPE growth, wipinglass method for DH laser *(Japanese)* 78−48304
GaAs-AlGaAs LPE layers, baking effect on surface morphology 78−14625
GaAs-Au Schottky barrier diodes, fabrication using LPE 77−40357
GaAs-Br_2(-Zn) system, filamentary cryst. prep. 78−52650
GaAs-$Ga_{1-x}Al_xAs$, DH, improved LPE growth method 77−4746
GaAs-$Ga_{1-x}Al_xAs$, semiconductor superlattices by MBE 79−95939
GaAs-$Ga_{1-x}Al_xAs$ half-ring laser, fabrication by LPE over chemically etched channels 77−684
GaAs-$Ga_{1-x}Al_xAs$ laser, low threshold room temp. embedded DH, fabrication and characts. 77−681
GaAs-$Ga_{1-x}Al_xAs$ multilayer struct., growth over preferentially etched channels, MBE 77−40388
GaAs-$Ga_xAl_{1-x}As$ double heterojunction laser structures, LPE growth with double source method 79−28962
GaAs-$Ga_xAl_{1-x}As$ DH laser wafers, active layer inhomogeneities 79−74106
GaAs-$Ga_xIn_{1-x}P$ multilayer epitaxial films MBE technology and epitaxial layers props. 79−33945
GaAs-GaAlAs, inverted-ridge-waveguide DH injection laser with current and lateral optical confinement LPE growth 77−75540
GaAs-GaAlAs DH CW laser, growth by Peltier effect induced LPE 77−48357

semiconductor growth continued
GaAs-GaAlAs DH laser with low threshold current, metalorganic CVD 79−50293
GaAs-GaAlAs double heterostructures for CW injection lasers, LPE growth 79−31931
GaAs-GaAlAs heterostructures, LPE growth, Peltier effect *(Polish)* 78−6861
GaAs-GaAlAs heterostructure, growth by metal-alkyl-hydride process 78−15313
GaAs-GaAlAs LPE layers, DH material, TEM obs. of crystal defects 78−6241
GaAs-GaAlAs superlattices, metalorganic VPE growth, in sites ellipsometry monitoring 80−70547
GaAs-GaAlAs-GaAs rectifying semicond. struct., prep. by MBE and characts. 80−65657
GaAs-Ge, heterostructure, zincblende-on-diamond type systems, MBE growth, (110) orientation as preferred orientation 80−80099
GaAs-HBr chemical vap. transport system, thermochem. data 78−6854
GaAs-$In_yGa_{1-y}P$, CW room temp. DH lasers prep. by VPE 77−10942
n-GaAs-n^+-$Al_xGa_{1-x}As$ heterostructure production, by MBE *(German)* 80−44711
GaAs-S VPE layers, thickness and carrier conc. variations 79−100060
GaAs-ZnSe, solid solution crystals, grown by Bridgman method, exam. of resistivity and Hall effect 79−95919
GaAsP, VPE, lattice forbidden band composition depend. *(Hungarian)* 80−6669
$GaAs_{1-x}P_x$, chemical transport and crystal growth in closed tube *(Japanese)* 78−39673
$GaAs_{1-x}P_x$ epitaxial layers prep., photoluminesc. and electroluminesc. props. *(Czech)* 78−48233
$GaAs_{1-x}P_x$ heterostructure, LPE prep., growth and dissolution kinetics, thermodynamic and kinetic models 80−75456
$GaAs_{1-x}P_x$ layer, growth by isothermal LPE 77−40398
$GaAs_{1-x}P_x$, MBE growth on GaP, and crystallographic evaluation 77−8762
$GaAs_{1-x}P_x$, mol. beam epitaxial growth, cryst. quality, composition investig. *(Japanese)* 77−55895
$GaAs_{1-x}P_x$, molecular beam epitaxial, effect of substrate temp. on composition ratio 77−1811
$GaAs_{1-x}P_x$, N doping using ionised beam in MBE 78−47400
$GaAs_{1-x}P_x$, VPE on Ge substrate, and LED characts. 78−72736
$GaAs_xP_{1-x}$, liquid phase epitaxial growth on GaP, growth and properties 79−47641
$GaAs_xP_{1-y}$ alloy, composition effects in growth by MBE 80−59816
GaAsSb/GaAlAsSb DH lasers, growth and props. 80−69412
$GaAs_{1-x}Sb$, microprocessor controlled MBE growth 78−3058
$GaAs_{1-x}Sb_x$, cryst. growth by steady state LPE 78−44032
$GaAs_{1-x}Sb_x$, LPE,phase diagram meas. 77−20047
$GaAs_{1-y}Sb_y$ layer on GaAs, dislocation density reduction by improved LPE growth method 80−76202
$GaAs_{1-x}Sb_x$ on GaAs, LPE growth of GaAs 79−61519
$GaAs_{1-x}Sb_x$ ternary phase diagram, LPE, band gap and elec. props. 77−55896
$GaAs_{1-y}Sb_y$, organometallic VPE growth using trimethylantimony 80−60788
$GaAs_xSb_{1-x}$, lattice-matched LPE growth in InP substrates 79−42402
$GaAs_ySb_{1-y}$, miscibility gap, rel. to LPE 79−33090
$GaAs_{1-x-z}Sb_xP_z$, LPE growth, constant compositional grading 78−6867
$GaAs_xSb_yP_{1-x-y}$, continuously graded comp. layers, LPE 77−24970
$Ga_yIn_{1-y}As_xP_{1-x}$-InP heterostructure, lattice matching and cryst. perfection 78−6437
GaInAs-InP, growth by low-pressure metalorganic CVD 80−71595
$Ga_{0.47}In_{0.53}As$, LPE growth and characterisation 80−10845
$Ga_{0.47}In_{0.53}As$, MBE, InP/$Ga_{0.47}In_{0.53}As$/InP DH laser fabrication and room temp. operation 78−74906
$Ga_{1-x}In_xAs$ epitaxial layer growth by organometallic pyrolysis, homojunction LED prep. 80−76194
$Ga_{1-x}In_xAs$, organometallic VPE growth using trimethylarsenic 80−60788
$Ga_xIn_{1-x}As$, alloy film surface processes controlling growth by MBE RHEED and AES exam. 78−84084
$Ga_xIn_{1-x}As$, cryst. growth on (100) InP by LPE 78−56591
$Ga_xIn_{1-x}As$, on (111)B InP, LPE growth, characterisation of high purity lattice 80−104082
$Ga_xIn_{1-x}As$ on InP, lattice matched LPE film growth and characts. 78−72033
$Ga_xIn_{1-x}As$, substrate orientation effect on liq.-solid distrib. coeffs., 600-700°C 80−2278
$Ga_xIn_{1-x}As$, VPE growth, thermodynamic anal. 80−2933
$Ga_xIn_{1-x}As$-InP, lattice matched LPE film growth and characts. 78−15320
$Ga_xIn_{1-x}As$-InP, MBE film growth, composition control obs. 80−84399
$Ga_xIn_{1-x}As$-InP heterostructure, growth by MBE 79−8251
GaInAsP, diffusion-limited growth in LPE 80−10842
GaInAsP layers on InP substrate, conditions for lattice matching in LPE growth 78−6866
GaInAsP, VPE growth and props. 80−16194
GaInAsP/InP DH lasers, with (100) substrate, 1.2-1.5 μm, LPE growth conditions 79−15617
GaInAsP/InP DH lasers emitting at 1.3 μm, growth and characts. 80−64057
GaInAsP/InP DH stripe geometry lasers emitting at 1.3 μm, growth characterisation 80−69410
GaInAsP/InP DH lasers, 1.3 μm wavelength, LPE growth and characterisation 80−69411
GaInAsP-InP buried stripe DH laser, fabrication using meltback method and CW operation 79−3708
GaInAsP-InP DH laser grown by newly designed vertical LPE furnace 78−9380
GaInAsP-InP DH laser, LPE and wet chem. etching techniques for integration 79−98388
GaInAsP-InP DH lasers made by melt-back method, operating characteristics 80−48287
GaInAsP-InP DH injection lasers prep. by LPE, 1.11-1.67 μm operation 80−53321
GaInAsP-InP double heterostructure laser, prep. by LPE growth and laser operation 77−3590
$Ga_{1-x}In_xAs_{1-x}P_x$, VPE growth and characterisation 78−22970
$Ga_xIn_{1-x}As_yP_{1-y}$, LPE layers, growth and characterisation 78−38983
$Ga_xIn_{1-x}As_yP_{1-y}$/GaAs structure, LPE growth and lattice consts. matching conditions 80−59822

semiconductor growth continued
$Ga_xIn_{1-x}As_yP_{1-y}$/Inp DH laser emitting at 1.15 micron grown by low-pressure CVD 80−64052
$Ga_xIn_{1-x}As_yP_{1-y}$-InP, rib-waveguide injection lasers made by one-step LPE 79−59710
$Ga_yIn_{1-y}As_xP_{1-x}$, LPE growth 80−66440
$Ga_{1-y}In_yAs_xSb_{1-x}$, LPE on GaSb, miscibility gap in liq. phase and lattice mismatch 80−15404
$Ga_xIn_{1-x}P$ alloy films, surface processes controlling growth by MBE, RHEED and AES exam. 78−84084
$Ga_xIn_{1-x}P$, LPE producing coherent interface, model 77−59229
$Ga_xIn_{1-x}P$ solid soln. epitaxial layers, stabilisation of composition 78−18933
$Ga_xIn_{1-x}P$ solid solns., isothermal liq. epitaxy 80−60793
$Ga_xIn_{1-x}P$ solid solutions, single cryst prep. and props. 80−16162
$Ga_xIn_{1-x}P$, VPE, recent advances, book contrib. 79−66011
$Ga_xIn_{1-x}P$, LPE, with GaP saturation source wafer *(Polish)* 78−23633
$Ga_{1-x}In_xP_yAs_{1-y}$/InP DFB injection laser, one-step LPE 80−58575
$Ga_xIn_{4-x}PyAs_{1-y}$, In rich bulk single crysts. growth from melt via gradient freeze method, and characterisation 78−68618
$Ga_{1-x}In_xSb$, epitaxial, vapour-phase growth using open-tube flow system 79−33943
$Ga_{1-x}In_xSb$, LPE on GaSb by stepwise grading, and characterisation 78−72745
$Ga_{1-x}In_xSb$, temp. gradient zone melting 80−50550
$Ga_{1-x}In_xSb$, vapour phase epitaxial growth by open tube method 78−84109
$Ga_xIn_{1-x}Sb$, Ga-rich, prep. by Czochralski technique 80−60771
$Ga_xIn_{1-x}Sb$, growth by LPE 78−27421
$Ga_xIn_{1-x}Sb$, LPE, growth by vertical dipping method and elec. props. 77−85949
$Ga_xIn_{1-x}Sb$ p-n junction photodiode fabrication, sensitivity as 1 to 2.5 μm detectors *(Japanese)* 80−52311
GaN CVD layer props. rel. to Ga-GaCl conversion efficiency and HN_3 decompositon 77−77404
GaN, deposition from plasma reactor, organo-metallic and donor-acceptor complex exchange in HF plasma 80−38839
p-GaN, doping in nonequilibrium conditions 77−62556
GaN, epitaxial growth on sapphire substrates, elec. props., X-ray diffr. anal., photoluminescence spectra 79−4919
GaN epitaxy, sapphire substrate prep. 78−39929
GaN film, deposition by pyrolysis of gallium trichloride and triiodide ammoniates 77−36402
GaN film, heteroepitaxial deposition, growth kinetics and catalytic effects 79−4487
GaN film, preparation by pyrolysis of $Ga(CH_3)_3$ in NH_3, cathodoluminesc. 77−4691
GaN, growth and morphology of crystals *(Japanese)* 80−11548
GaN, high-press. VPE and elec. characts. 78−14627
GaN, initial growth, on Al_2O_3 and spinel *(German)* 80−107664
GaN on Si, form. with GaCl-NH_3-H_2(He), ESCA and RHEED meas. 79−90909
GaN, plasma deposition and elec. cond. 78−60585
GaN, preparation variables rel. to dielectric data, GaAs conversion 78−60591
GaN single crystals, by three methods, influence on morphology *(Japanese)* 79−43112
GaN, VPE, on sapphire, crystallographic aspects 78−2387
GaN, VPE, requirements and structural etching of Al_2O_3 substrates *(Polish)* 77−43440
GaN VPE for blue LEDs *(French)* 79−28928
GaN, VPE growth rate influence on elec. and luminesc. props. 80−100702
GaN:Mg, and undoped, epitaxial growth from vapour, orientation, elec. props. 77−4740
GaN:Zn, low voltage LED, epitaxial layer, growth and electrolum. *(Russian)* 77−77297
GaN:Zn epilayers, growth parameters effect on props., device struct. 78−26975
GaN-AlN, epitaxial growth and electrical props. 77−73236
GaP, CVD mechanism, product catalysed reaction of Me_3Ga with PH_3 77−48345
GaP, chem. vapour growth in closed system 78−35283
n-GaP, cryst. growth, synthesis solute diffusion method, elec. characts. *(Korean)* 78−52653
GaP, cryst. growth for green luminesc. diode manuf. 77−40346
GaP, current controlled LPE from finite volume melt 80−20805
GaP, effects of hydrogen incorporation during deposition by sputtering 79−69981
GaP electroluminescent diode struct. prep. by SSD and Czochralski methods, dynamic props. *(Czech)* 80−97425
GaP, epitaxial growth by $GaPO_4$-C system 79−99448
GaP, epitaxial growth from Sb and Bi melts 79−52131
GaP epitaxial growth from solution in melt, crystn. theory 80−16204
GaP, epitaxial layers, anisotropy of growth rate from soln. in melt 78−35322
GaP epitaxial layers, stable growth conditions, by molten salt electrodeposition on Si and GaP substrates 79−20000
GaP epitaxial layers for yellow-LEDs, prep. and props. *(Czech)* 78−48234
GaP epitaxial layers grown in Ga-PCl_3-H_2 system, surface defects 77−7993
p-GaP, epitaxial layers grown from liq., overcompensated, doping levels 78−91353
GaP film, polycryst., with negative affinity, secondary emission *(Czech)* 78−52604
GaP, growth and props. of LPE layers on Si substrates 78−6864
GaP, growth of dislocation free crysts. from stoichoometric melt. 77−81212
GaP, growth of epitaxial layers from limited of melt-soln. 78−19676
GaP, heteroepitaxial CVD on Si, dual process, film characts. 77−16503
GaP, heteroepitaxial deposition on GaAs, Sn solvent inclusion, surface morphology *(German)* 79−28968
GaP, heteroepitaxial growth on Si, substrate misorientation effects 78−3055
GaP, heteroepitaxial growth on Si substrate by MBE 78−64481
GaP high-pressure reaction synthesis 77−77372
GaP, impurity behaviour during crystallisation from melt 77−84772
GaP, ionised-cluster beam epitaxial growth on GaP and Si, characts. for LED 79−28951
semiconductor growth continued
GaP, LEC growth of dislocation-free crysts., microdefects and striations 78−9974
GaP, LPE, LED fabrication and electroluminesc. characts. 77−28632
GaP, LPE, solvent choice in In-Ga-P system 79−87589
GaP, LPE at 650°C from In solvent, low Si contamination 78−80480
GaP, LPE layers, comparison of growth rates with theoretical predictions 79−52134
GaP LPE layers, low temp. growth from In solvent 79−56924
GaP, LPE layers high purity, invest. *(German)* 78−31353
GaP, LPE method for green LED mass production 77−77422
GaP layers, LPE growth, elec. props., residual impurities 79−38202
GaP, MBE growth on GaP, and crystallographic evaluation 77−8762
GaP, mol. beam epitaxial growth, cryst. quality composition investig. *(Japanese)* 77−55895
GaP on GaAs, LPE, growth with Ge and Sn solvents, phase diags. 78−88434
GaP, optoelectronic devices, conf., Berlin, DDR 78−91755
GaP, plasma deposition and elec. cond. 78−60585
GaP ribbon waveguide, vapour-grown, phase-matched SHG 80−48339
GaP, SSD method, Zn diffusion for green LED fabrication 77−81208
GaP, soln. growth of bulk crysts., luminesc. and elec. props. 78−92181
GaP, solubility in fused Sb, Bi, thermodynamics, rel. to epitaxial growth 78−34721
GaP, synthesis by gas chemical transport reactions, exam. of kinetics 79−95933
GaP, two-stage vapour/liq. epitaxial growth on Si 78−3054
GaP, VPE layer structures for LED's, SEM, and TEM obs. of dislocation density reduction expt. 80−100425
GaP:Cr_2O_3, growth, dopant distribution, elec. resist. 78−34531
n-GaP:In, LPE from In solvent, dislocation density reduction by doping 78−18919
GaP:N, N doping profiles in GaP grown by LPE, cathodoluminesc. data 79−23631
GaP:Sn, LPE growth from Sn soln., elec. resist. and Hall coeff. meas. 78−2593
GaP:Te, struct. imperfections, prep. and doping effects 77−89451
GaP:Zn, doping from gas phase during LPE 80−55312
GaP-GaAlP-GaP, lattice-matched, LPE layer growth under P vapour pressure and reduced O_2 contamination 79−51445
GaP-Si, heteroepitaxial growth, electronic and optical props. 80−104075
GaP-Si, heterostructure, zincblende-on-diamond type systems, MBE growth, (110) orientation as preferred orientation 80−80099
GaP_xAs_{1-x} solid soln., specularly smooth epitaxial layers, superlattice struct. 77−24959
$(GaP)_x(ZnSe)_{1-x}$, solid solution, reaction of Zn with Se during Czochralski growth and LPE 79−8238
GaS(Se), growth by I_2 vapour transport using temp. oscill. method 77−77355
GaSb and $GaSb_xAs_{1-x}$ films, MBE growth and elec. props. 79−23863
GaSb, CVD using organometallics, epitaxial growth 80−29879
GaSb, electroliquid epitaxial growth 80−89160
GaSb film, ion bombard. effects on elemental Sb incorporation probability during sputter deposition 79−83120
GaSb films, elemental incorporation probability modification by ion bombard. during growth 80−80118
GaSb high-purity and doped layers grown by LPE and VPE methods 78−6863
GaSb, migration of liq. inclusions, effect of DC current and temp. 77−7910
GaSb, pulled crystal, microfacet obs. near irregularly remelted surfaces 78−91278
GaSb, single crysts., grown by vertical and horizontal travelling heater method, growth parameters and cryst. quality 79−24421
GaSb, sputtered films, on GaAs, growth, Hall effect, impurity levels 80−20334
GaSb thin layers, directed crystn. on sapphire, props. 80−35111
$GaSb_{1-x}As_x$, MBE RHEED meas. 78−18916
$GaSb_{1-y}As_y$, MBE-grown, substrate effect on lattice consts. 79−77942
$(GaSb)_{1-x}Ge_x$ films, single-cryst. metastable semicond., growth and phase stability 80−80115
GaSe, growth of crysts. with natural facets at large angles to layers 78−15305
Ga_2Se_3, sublimation growth, closed tube, mass flow and press. meas. 77−63550
$\alpha(\beta)$-Ga_2Se_3, cryst. growth, optical, X-ray diffr. and SEM study 80−71587
GaTe, single cryst. prep. and electroabsorpt. spectra investig. 80−103968
Gd_2Se_3/PbTe, N type selenide segmented element fabrication, thermoelectric props. 80−107835
Ge, amorphous film, post nucleation growth, computer simulation 78−34729
Ge, amorphous whisker growth 78−2400
Ge, crystal growth, O equilib. between Ge and gas over melt 80−2938
Ge, crystal growth and segregation under zero gravity 79−43130
Ge, Czochralski growth system, time-depend., cryst.-melt interface shape 77−24280
Ge detector; high-purity, effect of crystal growth direction on energy resolution 79−45541
Ge, epitaxial, in situ X-ray topography, misfit dislocations 78−47671
Ge, epitaxial and amorphous film growth, low energy ion beam deposition 77−28729
Ge, epitaxial film growth by hydride-iodide method 77−48343
Ge epitaxial films, structural perfection rel. to deposition conditions 78−43258
Ge, epitaxial growth of very thin electron microscopy specimens 80−100793
Ge, epitaxial layer deposition by vacuum pyrolysis 78−52676
Ge film, amorphous, vac. deposited, XPS and elec. props., evidence for polycryst. phase 77−28691
Ge, film, elec. props., prep. by DC sputtering *(Japanese)* 79−78237
Ge, film, epitaxial growth on Si, interdiffusion, plasmon energy loss anal. 77−31916
Ge film, growth on graphite substrate by thermal reduction 78−18934
Ge film, prep. by low press. reactive deposition process 79−24449
Ge films on semicondcuting substrates with diamond structure, computer model of autoepitaxial growth 79−95927
Ge, growth, chem. transport, transfer inversion using Mo catalyst 79−11517
Ge, growth from lightly doped melt, dopant distrib. 78−2039

semiconductor growth continued
Ge, heavily doped, vacuum hot-pressing thermal and electrical props. 77−40400
Ge, heavily-doped single cryst., macroinclusions, annealing in elec. field 77−47474
Ge, large shaped single cryst. prod., Stepanov method 78−3014
Ge, melt grown single crystals, preferred growth directions and perfection 79−77537
Ge, melt growth conditions and doping level influence on impurity distrib. ratio 77−12516
Ge, molten zone movement under influence of Peltier effect 78−44007
Ge, on n-GaAs, with Ni overlayer, smooth and continuous ohmic contact form. by solid-state diffusion 78−68086
Ge p-n junction, high-grade, temp. gradient zone melting in production 77−4747
Ge, polycrystalline epitaxial film, exam. of growth kinetics and props. 80−55304
Ge ribbon single crysts. grown from melt, dislocation struct. form. under thermal stress 80−107082
Ge, shaped crystals, grown by Stepanov method, struct. perfection 78−2123
Ge shaped single crystal, Stepanov method growth, temp. distri b. 78−2032
Ge, single cryst. growth, supercooling needed for Czochralski and Stepanov methods 78−3015
Ge single crystal of circular cross section, thermoelastic stresses 78−2033
Ge, solid-phase epitaxial growth through PdGe layers, channelling and backscatt. obs. 77−85936
Ge strips grown by Stepanov method, thermoelsatic stress calc. 78−2034
Ge, thin single crystal, (110) orientation, preparation technique 79−95930
Ge, vapour transport rate, Ge-I_2 equilib. 700 to 1300K *(French)* 78−64476
Ge:Ga, appl. of heat pipe to Czochralski growth, segregational behavior 79−61511
Ge:Ga, effects of destabilising vertical thermal gradients on cryst. growth and segregation 78−52659
n-Ge:O, Czochralski growth, O content rel. to props., IR, Li precipitation determs. 77−15445
Ge:P(Sb), growth atm. effect on struct. microdefect form. 80−20779
Ge:Sb, dopant distrib. rel. to direction of cryst. growth 77−51400
Ge-As-Se, amorphous film, condensation formation and struct. props. *(Russian)* 78−38629
Ge-$Ga_{1-x}Al_xAs$, MBE of ultra thin film superlattices on GaAs substrates, TEM study 79−37932
Ge-Si alloy, epitaxial growth by getter sputtering, characts. 79−28915
Ge-Si solid solution, equilib. gas phase comp. in Si-Ge-Br heterogeneous system 79−10820
Ge-Sn solid solution, cooling rate effect on partition coeff. of Sn between liq. phase and crysts. 77−12510
Ge-Sn-M, M=Cu, As, Sb, formation of Ge-based solid solns. during crystallisation 77−80625
GeC_x, amorphous, prepared by glow discharge method, elec. and optical props. 77−21035
GeS, conc. depend. of rate of formation on Ge surface 79−43152
GeS, gas-phase single-cryst. growth, photoelec. props. 77−36381
GeS, growth parameter meas. during cryst. growth from vapour in closed ampules 79−19168
$GeSe_2$, single cryst. growth 77−52305
GeTe, nonstoichiometric, homogenisation 78−44004
HgCdTe photodiodes formed by double-layer LPE 80−104078
HgCdTe-CdTe photodiode, 1.33 μm, grown by LPE, phys. props. 80−107892
$Hg_{0.60}Cd_{0.40}Te$, LPE growth from Te-rich soln. 80−7508
$Hg_{0.6}Cd_{0.4}Te$ LPE layer growth from Te-, Hg-, and HgTe-rich solns., comparison 80−76199
$Hg_{0.74}Cd_{0.25}Te$ thin film deposition on Si substrates by RF triode-sputtering, large-area photodetector arrays 80−80965
$Hg_{1-x}Cd_xTe$, for appl. in IR detector arrays, comp. control 80−31872
$Hg_{1-x}Cd_xTe$, high-pressure reflex growth technique, IR detector appl. 77−40347
$Hg_{1-x}Cd_xTe$, homogeneous single cryst., growth by modified Bridgman technique 78−39682
$Hg_{1-x}Cd_xTe$, LPE current controlled 80−40272
$Hg_{1-x}Cd_xTe$, LPE growth and characterisation 80−50565
$HgCr_2Se_4$, cryst., preparation, elec. cond., thermo EMF 77−8125
$HgCr_2Se_4$, vapour growth using $AlCl_3+Cl_2$ as transport components 78−35282
$HgCr_2Se_4$-$CdIn_2S_4$ heterojunction, prep. and photovoltaic prop. *(Japanese)* 78−34889
$HgCr_2Se_4$-$CdIn_2S_4$ heterojunctions, prep. and photovoltaic prop. 78−34892
HgI_2 detectors, fabrication, appl. to X- and gamma-ray detection 77−83459
HgI_2 detectors, recent improvements 78−37507
HgI_2 detectors, state-of-art crystal growth and nucl. spectroscopic evaluation 78−41895
HgI_2, doped, vap. growth by temp. oscill. method 78−39674
α-HgI_2, single cryst. growth from iodomercurate complexes 80−35069
HgI_2, soln. grown crystals, low-energy gamma-ray cond. type detectors 80−97418
HgI_2, thermally stimulated current meas. 78−41896
HgI_2, vap. growth by temp. oscill. method in horizontal furnace 78−39675
HgS, cinnabar, chem. vapour growth in closed system 78−35283
α-HgS, crystn. in NaHs solutions 77−8740
HgS film, deposition from colloidal solns. 78−92209
HgS film, RF sputtered, effect of K on cryst. modification 77−62773
HgS, RF sputtering on NaCl, growth and struct., electron diffr. and TEM obs. 77−90271
HgSe, Bridgman growth at hydrostatic press. to 3 kbar, free electron conc. and mobility 77−52245
HgSe, CVD crysts., electrophys. characts. 77−85910
HgSe, epitaxial growth on CdSe, struct. and electrophysical props. 77−12540
HgSe/CdSe lattice-matched heterostructs. as Schottky barriers, CVD epitaxial growth and elec. props. 80−49877
HgSe-CdSe pseudobinary alloy, phase diagram and cryst. growth 78−68620
HgTe, conditions for oriented crystn. 79−52124
semiconductor growth continued
HgTe, heteroepitaxial growth by close-spaced technique of confined type *(Japanese)* 77−24967
HgTe, high purity cryst. grown from soln. by travelling heater method 77−52243
HgTe single crystals, crystn. from vapour phase, thermodynamical conditions 79−33908
HgTe, VPE growth control by EM irrad. *(Russian)* 80−34338
HgTe:Cu, effect of prep. conditions on impurity distrib., hole conc. 77−8743
HgTe-CdTe, distrib. ratios of components during crystn. of melt 77−16485
HgTe-CdTe, epitaxy by evap. and interdiffusion under isothermal conditions book contrib. 77−12549
HgTe-MnTe, growth from two-phase melts, crystallisation characts. 77−36393
IN_2O_3:Sn, RF magnetron sputtered film, elec. and optical props. 80−104065
(In,GA)(As,P) binary, ternary and quaternary, hydride vapour phase epitaxy, cryst. growth and props. 80−66434
In-As-P system, ternary phase diagrams, method for determ. of liquidus surfaces 77−28787
In-Ga-As-P, phase diagram rel. to lattice matched LPE 78−39708
In-Ga-P ternary system, low temp. phase diagram rel. to epitaxial growth 80−84916
InAs, epilayer, MBE growth parameters, relationship with elec. props. 80−2296
InAs epitaxial layers, on GaAs substrate, electron diffr. and SEM exam., electronic props. 79−1552
InAs, heteroepitaxial film, orientation and struct. investigation 79−82480
InAs heteroepitaxial layers, VPE grown, effect of $AsCl_3$ mole fraction on elec. props. 79−11255
InAs, MBE growth, SEM, RHEED, optical microscopy and elec. meas. 78−18925
InAs, migration of liq. inclusions, DC current and temp. effects 77−7910
InAs, obtained by liquid-seal method, deviation from stoichiometry 77−40345
InAs, organometallic VPE growth on InAs and GaSb 80−16193
InAs, soln. in liq. Sn, vapour phase partial press. meas., rel. to LPE 78−34610
InAs:Cd,Te interaction between impurities, effect on elec. props., Hall effect. 80−19832
InAs-FeAs, eutectic, growth from melt, electrical props. 77−11911
$InAs_yP_{1-y}$ alloy, composition effects in growth by MBE 80−59816
$InAs_{1-x}Sb_x$, LPE on InAs substrate, $InAs_xSb_yP_{1-x-y}$ used as buffer layer 78−3065
$InAs_{1-x}Sb_x$ on GaSb, LPE growth 80−29293
$InAs_{1-x}Sb_x$, organometallic VPE growth on InAs 80−45233
$InAs_{1-x}Sb_x$-InAs stepwise-graded struct., steady-state LPE, etching, investig. 77−21042
$InAs_xSb_yP_{1-x-y}$, LPE on InAs substrate 78−3065
$In_{1.9}As_{0.1}Se_3$, growth by chem. vap. transport, characterisation as photoelectrode 78−43994
(InGa)As film, growth kinetics for step-cooling LPE technique 77−40395
InGaAs, LPE, diffusion-limited step-cooling technique, layer thickness and composition 80−84402
InGaAs, lattice-matched VPE on (100) InP, photodiode appl. 80−35102
InGaAs on (100) InP substrate, VPE 80−40267
InGaAs-$In_{1-x}Ga_xAs_yP_{1-y}$ DH laser, LPE fabrication, electroluminesc., lasing characts. 79−3709
$In_{0.53}Ga_{0.47}As$, growth on (100)-oriented InP, from supercooled solution 79−70001
$In_{0.53}Ga_{0.47}As$, incorporation of Ga during LPE growth on (111)B and (100)InP substrates 78−91557
$In_{0.53}Ga_{0.47}As$, LPE growth on (100) InP, for field assisted photocathode appl. 78−15318
$In_{0.53}Ga_{0.47}As$-InP heterostructure, LPE growth 80−11582
$In_{1-x}Ga_xAs$, LPE growth on InP substrate, quasi grown layers, photoluminescence meas. 79−23862
$In_{1-x}Ga_xAs$, LPE layer on InP substrate, phys., elec. and optical props. 78−39235
$In_{1-x}Ga_xAs$, LPE on InP substrate, comp. latching phenomenon and lattice mismatching effects 79−28961
$In_{1-x}Ga_xAs$ layer on InP, misfit dislocation free, LPE growth 80−108364
$In_{1-x}Ga_xAs$, MBE-grown, substrate effect on lattice consts. 79−77942
$In_{1-x}Ga_xAs$-$GaSb_{1-y}As_y$, semiconductor superlattices by MBE 79−95939
$In_{1-x}Ga_xAs$-$GaSb_{1-y}As_y$, superfine heterostruct., MBE 78−95348
n-$In_xGa_{1-x}As$ film, epitaxial growth on GaAs, using CVD system 77−1812
$In_xGa_{1-x}As$, LPE growth on GaAs 79−61519
$In_xGa_{1-x}As$, MBE layers on InP substrates, elec. props., photoluminesc., X-ray and Auger obs. 79−51450
$In_xGa_{1-x}As$ MBE layers on InP substrate, lattice deformation, misorientation 79−90896
$In_xGa_{1-x}As$, thick LPE growth, electrolum. obs. 78−60589
$In_xGa_{1-x}As$, VPE on (100), (111)A, and (111)B InP substrates 80−15382
$In_xGa_{1-x}As$:Si, p-n junction form. in LPE layers, In content effect on inversion temp. 77−4266
$In_xGa_{1-x}As$:Zn, lattice matching to InP, LPE growth conditions 80−70541
$In_xGa_{1-x}As$-$InAs_xP_{1-x}$ VPE mixed crystal composition rel. to vapour pressure *(Japanese)* 77−55893
InGaAsP, LPE, diffusion-limited step-cooling technique, layer thickness and composition 80−84402
InGaAsP, LPE growth, orientation depend. of incorporation of Ga, As, and Zn 78−6869
InGaAsP, LPE growth on InP, influence of lattice mismatch on surface morphology 79−1553
InGaAsP, LPE growth techniques influence on composition 79−52130
InGaAsP, LPE growth, impurity depend. of distrib. coeff. 80−10843
InGaAsP, lattice matched, LPE growth on (100) InP, for 1.15-1.31 μm spectral region 78−64483
InGaAsP/InP, DH laser, 1.5 μm, with optical waveguide structure, fabrication 79−72587
InGaAsP/InP DH, vapour phase growth by dual-growth-chamber method 80−50559
InGaAsP-InP CW lasers, 1.5-1.7 μm, VPE 80−78861

semiconductor growth continued
InGaAsP-InP DH laser, 1.55 μm, low temp. LPE growth for room-temp. CW operation 80−64045
InGaAsP-InP lattice-matched heterojunction, LPE growth and characterisation 77−21041
InGaAsP-InP lattice matched DH, growth by two-phase supercooled soln. technique 78−10296
InGaAsP-InP layers, grown by LPE techniques, lattice const., bandgap, thickness and surface morphology meas. 80−59818
$In_{0.8}Ga_{0.2}As_{0.5}P_{0.5}$, LPE growth 80−11557
$In_{1-x}Ga_xAs_{1-y}P_y$ layers on InP substrate, LPE growth, quaternary phase diagram, and band gaps 79−42403
$In_{1-x}Ga_xAs_yP_{1-y}$ DH laser, low threshold current density, near equilibrium LPE growth 80−19040
$In_{1-x}Ga_xAs_yP_{1-y}$ quaternaries VPE 0.75 to 1.35 eV band gap range 79−69987
$In_{1-x}Ga_xAs_yP_{1-y}$, vapour grown, alloy comp., thermodynamic calc. 79−99094
$In_{1-x}Ga_xAs_yP_{1-y}$/InP 1.5 μm room-temp. CW laser fabrication and operation 80−64070
$In_{1-x}Ga_xAs_yP_{1-y}$-InP DH lasers, fabrication and performance 78−5500
$In_{1-x}Ga_xAs_yP_{1-y}$-InP DH laser on InP (100) substrate 78−29965
$In_xGa_{1-x}As_yP_{1-y}$ layers on InP, LPE and opt. props. characteris. 79−28849
InGaAsSb, LPE growth, and appl. in GaSb/AlGaAsSb/InGaAsSb/AlGaAsSb/GaSb DH 80−16205
$In_{1-x}Ga_xAs_{1-y}Sb_y$, LPE growth on (111)B-oriented InAs, growth conditions and lattice matching 77−24973
InGaP/InGaAs struct. for transferred electron photocathodes, VPE growth and characterisation 80−76193
$In_{1-x}Ga_xP$, epitaxial growth from melt, optimisation of growth conditions 79−52132
$In_{1-x}Ga_xP$, epitaxial growth on GaAs substrate, formation of intermediate layers 80−2304
$In_{1-x}Ga_xP$, homogeneous bulk, growth from soln. with predetermined cryst. comp. 78−11097
$In_{1-x}Ga_xP$, LPE, conditions, reacts. in In-Ga-P system 79−11525
$In_{1-x}Ga_xP$, solid soln., evaporation of P during LPE 79−95948
$In_xGa_{1-x}P$, solid solns., gas phase epitaxy from Ga-In-HCl-PH_3-H_2 systems 78−34722
$In_{1-x}Ga_xP_{1-y}As_y$ lattice-matched epitaxial layers, LPE growth on GaAs(100), characterisation 80−75465
$In_{1-x}Ga_xP_{1-z}As_z$ DH lasers, multiple LPE, lattice matching 77−77421
$In_{1-x}Ga_xP_{1-z}As_z$ LPE DH laser with multiple thin layer active region 77−83887
$In_{1-x}Ga_xP_{1-z}As_z$ near IR DH laser, constant temp. LPE, external grating cavity 77−75550
$In_{1-x}Ga_xP_{1-z}As_z$, room temp. visible heterojunction lasers 78−5501
$In_{1-x}Ga_xP_{1-z}As_z$-InP, LPE heterojunctions, lattice matching and dislocations 78−23150
$In_{1-x}Ga_xP_{1-z}As_z$-InP, single and multiple layer heterostruct., LEDs and lasers 78−46626
InGaSb, LPE growth characteristics, substrate surface contamination dependence 80−39470
$In_{1-x}Ga_xSb$ film, epitaxial growth by multitarget RF sputtering 77−44157
$In_xGa_{1-x}Sb$, molecular beam epitaxy 79−47638
$In_xGa_{1-x}Sb$, vertical Bridgman Stockbarger growth, magnetic field effect 78−60565
$In_{1-x}GaxAs$, MBE, RHEED meas. 78−18916
InN, epitaxial layer prep. using $InCl_3$-NH_3 system 78−3056
InN, epitaxial layer prep. and X-ray analysis 79−38747
In_2O_3, electro-conducting transparent film, props. rel. to production method *(Japanese)* 80−25557
n-In_2O_3 film, RF sputter grown, substrate bias effect on elec. and optical props. 78−64150
In_2O_3 films, electron beam evaporation, elec. and optical props. *(Japanese)* 80−60784
In_2O_3, pure and Sn-doped, prep. by activated reactive evaporation, and characterisation 80−80989
In_2O_3:Sn, glass like thin film, electron evaporated, conductive transport *(Chinese)* 80−49960
In_2O_3:Sn, transparent conducting films, prep. by $InCl_3$ thermal decomp., transmittance, resistivity 79−33944
In_2O_3:Sn/n-Si heterojunction solar cell, fabrication and characts. 78−15314
InP (100) substrates, for MBE, ion-cleared, contamination, SIMS meas. 78−11353
InP (111) substrate, and homoepitaxial layers, characterisation by divergent X-ray beam diffr. 78−31352
InP, concs. of C and O_2 in LEC grown cryst. determ. 77−39612
InP, crystal growth by synthesis solute diffusion method 78−64454
InP, current controlled LPE growth 77−77428
InP, current-controlled LPE growth, Peltier cooling at In-InP interface 77−8770
InP cylindrical magnetron reactive sputtering, for solar cell appl. 78−39693
InP, effects of baking time on purity and morphology 78−6862
InP electrodeposition, solvent systems, low melting point comps. in alkali metal metaphosphate/fluoride systems 79−28079
InP, epitaxial, kinetics of VPE 80−60790
InP epitaxial growth, in vertical reactor, construction and expt. data *(Slovak)* 77−28081
InP, expt. studies on meltback morphology 78−31347
p-InP film, CVD, growth characts. and CdS/InP solar cell efficiency 77−1813
InP film, CVD on preferentially etched Mo, initial growth behaviour 78−51855
InP film, on rough $Zn_xCd_{1-x}S$ substrate, film substrate lattice mismatch calcs. 78−43263
InP film, prep. by low press. reactive deposition process 79−24449
p-InP film growth, by close space vapour transport 79−28944
InP films, organometallic VPE grown, props. 80−96753
InP grown by LPE, method for free In removal from surface 80−84860
InP, grown-in dislocation density, impurity effect 78−51543
InP growth from soln. and LEC, photolum. and elec. meas. 79−87575
InP, heteroepitaxy on CdS substrates using InI_3 as transport agent 79−56083
InP, high-purity bulk, prep. from soln. 78−6839
InP, high-purity VPE, by PCl_3/In/H_2 technique, progress in control 78−6857

semiconductor growth continued
InP, homoepitaxial film by MO-CVD process, for heterojunc. solar cell fabrication 79−8250
InP, LEC growth using pyrolytic BN crucibles 78−6841
InP, LPE, high purity, use of baking to reduce Si contamination 78−72744
InP, LPE, solvent choice, equilib. in In-Ga-P system 79−87589
InP, LPE grown, surface morphology 77−62771
InP, LPE growth 80−11557
InP, LPE growth on GaAs, etching and electron probe anal. 79−11526
InP, large size single crysts., synthesis, solute diffusion technique 79−33917
InP layer growth method, model validity evaluation *(Slovak)* 80−54535
InP layers, grown by LPE from supercooled solns., thickness meas. 78−10307
InP layers, LPE growth from undercooled melts, numerical method 80−6665
InP, liq.-seal growth, protective props. of B_2O_3 flux 77−12519
InP, MBE, substrate temp. related degradation mechanisms 80−65385
InP, MBE from In and P_2 beams, substrate temp. limits 80−15385
InP, MBE growth on InP substrate, orient.-depend. faceting 77−24966
InP, MBE growth surface, singular instabilities 77−24969
InP, molten stoichiometric, surface tension 78−39684
InP, organometallic growth by cracking of $In(C_2H_5)_3$ and PH_3 80−11575
InP, planar reactive deposition on CdS, heterostruct. formation and elec. evaluation 78−72738
p-InP, prep. of single and bi-crysts., epitaxial layer and polycryst. films 77−81211
InP, pure and S doped, VEP, exam. of molar fraction controlled impurity in In-PCl_2-H_2 78−56587
p-InP, RF sputtering on CdS and other substrates, and grain size obs. 77−90272
InP, soln. in liq. Sn, vapour phase partial press. meas., rel. to LPE 78−34610
InP substrates, control of thermal degradation in LPE growth with PH_2 partial pressure 79−33949
InP, synthesis solute diffusion grown, elec. props., photoluminesc., etch pit profiles 79−4914
InP, terracing of LPE growth, doping effects 80−10846
InP, thermal degradation and its control in LPE growth 79−100343
InP VPE, growth kinetics and controlled doping 79−87569
InP VPE, In-H_2-PCl_3 chemistry 80−11549
InP, VPE, thermodynamics of transfer by water vapour 78−43260
InP, VPE growth for MESFET's 80−103602
InP, VPE layer props. control using boundary layer characts. 80−50561
InP, VPE using CVD 79−28927
InP VPE with new metallorganic compound 80−55278
InP, vapour phase epitaxial growth in presence of O_2, elec. props. 79−46971
InP very high purity LPE layer growth 78−3061
p-InP:Cd(Zn), single cryst. growth by temp. gradient method 79−28907
InP:Sn film, mol. beam epitaxial growth 77−16505
p-InP:Zn, vapour grown, prep. and props. 80−54268
InP-$Ga_xIn_{1-x}As_yP_{1-y}$ systems, for optical devices in 1 to 1.6 μm region, LPE growth *(Japanese)* 79−28956
InP-$Ga_xIn_{1-x}As_yP_{1-y}$ DH, LEDs and lasers, fabrication and operation in 1.5 μm region 78−37893
InP-$Ga_xIn_{1-x}P_yAs_{1-y}$ heterostruct. lasers, growth and characterisation 80−23691
InP-GaInAsP buried heterostructure lasers of 1.5 μm region, fabrication and characts. 80−74388
InP-GaP, solid soln. crystallization from stoichiometric melt, solidus construction 77−85927
InP-$In_{1-x}Ga_xAs_yP_{1-y}$-InP 1.55 μm DH room-temp. CW laser fabrication and operation 80−64071
InP-$In_{1-x}Ga_xAs_yP_{1-y}$-InP 1.53 μm single-mode CW ridge-waveguide laser 80−64072
InP-$In_{1-x}Ga_xP_{1-y}As_y$, LPE for optoelectronic devices *(German)* 79−95280
InP-$In_{1-x}Ga_xP_{1-z}As_z$ heterostructure laser, single and multiple quantum-well, liquid-phase epitaxial growth 80−38031
InS, prep., and elec. and optical props. 77−77361
InSb, charact. and phys. props., review *(Japanese)* 80−39576
InSb, convection in melts, and cryst. growth under large inertial accelerations 80−66421
InSb, crystal growth from melt, facets and twin formation obs. *(Chinese)* 80−59409
InSb, Czochralski growth, thermoelec. monitoring of interface temp. 78−31331
InSb, dislocations due to thermal stress, single and composite crysts. 78−2124
InSb film, grown by MBE, RHEED study 80−100415
InSb film, heteroepitaxial, MBE growth and elec. props. 80−2301
InSb film, ion bombard. effects on elemental Sb incorporation probability during sputter deposition 79−83120
InSb film, prep. by rotary type flash method *(Japanese)* 77−40372
InSb film, synthesis by 2-source mol. beam technique and AES characterisation 78−72729
InSb films, elemental incorporation probability modification by ion bombard. during growth 80−80118
InSb films on $LiNbO_3$, prep. and props. 80−35093
InSb, growth angle determ. from cryst. lateral face shape and solidified separation drops 80−103282
InSb, heteroepitaxial film, orientation and struct. investigation 79−82480
InSb, horizontal zone melting in vacuum 79−47624
InSb, LPE growth characteristics, substrate surface contamination dependence 80−39470
InSb, low defect crystal growth by InN doping, IR detector appl. 80−20780
InSb, morphological instability under constitutional supercooling during cryst. growth from melt and stabilising thermal gradient 79−4910
InSb, periodically doped cryst. prod. by Peltier effect, helicon diagnostics *(German)* 77−48338
InSb, prep. of thin films by ionised-cluster beam deposition *(Japanese)* 80−25576
InSb, single crysts., grown by vertical and horizontal travelling heater method, growth parameters and cryst. quality 79−24421
InSb thin layers, directed crystn. on sapphire, struct. 80−35112
InSb thin layers, interface stability during crystn. 79−65326

semiconductor growth continued
InSb:Te, cryst. growth from melt, pulling method, US effects on facet growth 80−76169
InSb:Te, Czochralski cryst. growth, strain configuration study using X-ray anomalous transmission topography 79−23552
InSb/GaSb superlattice thin films, sputtered, ion-bombardment-enhanced diffusion during growth 78−87882
InSb-GaSb, compositionally modulated sputtered superlattice, growth and interlayer diffusion 79−56930
InSb-GaSb superlattice, interlayer diffusion 77−85086
InSb-$LiNbO_3$ layer structures, fabrication and use in SAW amplification 79−41540
InSb-NiSb, eutectic alloy, Te-doped, electrophys. props. 77−35955
$InSb_{1-x}Bi_x$, film, multitarget sputtering growth technique 78−84711
$InSb_{1-x}Bi_x$ films, single-cryst. metastable semicond., growth and phase stability 80−80115
$InSb_{1-x}Bi_x$, multitarget RF sputtering, metastable phase, conductivity transition 80−76178
$InSbS_3(Se_3)$, prep., polymorphism, cryst. struct. 78−44002
$InSbSe_3$, cryst. prep. and props. 79−15601
$In_{1.8}Sb_{0.2}Se_3$, cryst. prep. and props. 79−15601
InSe, large monocrysts., grown from nonstoichiometric melt., comp. and photovoltaic substrate 77−55882
InSe luminescent film, production and characterisation *(Russian)* 78−39581
InSe thin film, sputter growth and chem. anal. by XPS/ESCA 80−80976
In_2Se_3, chem. transport reactions with I, single cryst. growth 77−16480
In_6Se_7, single cryst. prep. and electrophys. props. 79−43129
In_2Te_3 film thermal deposition, transmission spectra and elec. cond. *(Russian)* 80−49555
In_2TeO_6, crystal growth by high press. method, elec. and struct. props. 77−81206
IrP_2, prep. and characterisation 78−39679
$LiInS_2$, single cryst. growth by directional solidification, photoluminescence meas. 79−61514
LiV_2O_5, needle cryst. form. by reduction of molten Li_2O-V_2O_5, semicond. props. *(Japanese)* 78−3030
$Mn_{15}Si_{26}$, growth by Bridgman method and chemical transport, X-ray structural analysis 79−100043
MoS_2, synthetic molybdenite single crystals, growth from vapour, elec. props. 80−34446
Pb chalcogenide films, epitaxial, orientation on fluorite struct. substrate 77−35824
$Pb_{1-x}Cd_xS$ metastable epitaxial films, growth and physical props. 78−27417
$Pb_{1-x}Hg_xS$, soln. growth, variable gap film for i.r. detector 77−1796
PbS, crystallisation and stability in high-temp. alkaline solns. 77−52240
PbS film, polycryst., chem. deposition from soln. and characterisation 78−72743
PbS, film condensation on amorphous substrate, struct. and growth 78−38981
PbS, low carrier conc., prep. and props. 77−39846
n-PbS, $PbS_{1-x}Se_x$ layers prepared by hot-wall epitaxy 77−16481
PbS, sublimation growth, using liq. encapsulation zone-refined source material 78−27399
PbS, vap. deposited film, island growth obs. by optical diffr. from electron micrograph 78−10291
PbS-PbSe-PbS DH laser, fabrication, CW operation up to 120K 77−23692
PbS-Si heterojunction, PbS film growth and struct. 80−96762
PbS_xSe_{1-x} film, prep. by co-evaporation method *(Japanese)* 78−64477
PbS_xSe_{1-x}, film prep. by co-evap., elec. props. *(Japanese)* 78−80470
PbSe, complex-composition film production method from vapour *(Russian)* 78−95702
PbSe film, 50 μ, prep. in double quasiclosed volume 79−38745
PbSe film, soln. growth 80−66437
PbSe films, synthesis charact. 80−35094
PbSe, monocrystalline film prod. by laser pulse *(Russian)* 78−3059
PbSe, vacuum evaporation, composition of condensates 78−44012
PbSe-flux, boundary interfacial tension, rel. to Czochralski growth 77−35797
PbSe(Te), single cryst. growth, reaction kinetics in binary melts of KCl, NaCl and $PbCl_2$ 77−16486
$Pb_{0.93}Sn_{0.07}Se$ crysts., sublimation growth, controlled carrier concs. for IR lasers and detectors 77−52237
$Pb_{1-x}Sn_xSe$ epitaxial layers obtained by LPE, growth conditions correl. with morphology 80−104079
$Pb_{1-x}Sn_xSe(Te)$ epitaxial layers, growth, phase diagram, p-n junctions, optical, elec. props. 78−44029
$Pb_{1-x}Sn_xSe(Te)$ single crystals, Bridgeman grown, X-ray exam. 79−56926
$Pb_xSn_{1-x}Se(Te)$ film, Bi and Tl impurity dopant incorporation and diffusion during MBE growth 79−66012
PbSnTe film epitaxial growth on BaF_2 substrates 78−11134
$Pb_{0.8}Sn_{0.2}Te$ film, growth in quasi-closed space, single and polycryst. 79−33930
$Pb_{1-x}Sn_xTe$, cryst. growth rel. to IR detector fabrication 77−85911
$Pb_{1-x}Sn_xTe$, epitaxial growth on $LiNbO_3$, electron diffr. and microscopy exam. 77−1331
$Pb_{1-x}Sn_xTe$ film on BaF_2, electron beam delineation effect on MBE growth, LEED and AES obs. 79−99434
$Pb_{1-x}Sn_xTe$, grown by LPE, solid-liquid tie line determ. 78−64526
$(Pb_{1-x}Sn_x)Te$, growth by sublimation technique *(German)* 77−73224
$Pb_{1-x}Sn_xTe$ LPE film IR detector performance 80−86422
$Pb_{1-x}Sn_xTe$, LPE grown heterostructures, improved nucleation and planar interface 79−95949
$Pb_{1-x}Sn_xTe$, large non-seeded single cryst. growth by sublimation method, and characterisation 79−78860
$Pb_{1-x}Sn_xTe$, large single crystal growth, on quartz surface, non-seeded 78−48293
$Pb_{1-x}Sn_xTe$ layers, LPE growth on metal-etched substates 80−55313
$Pb_{1-x}Sn_xTe$ optically pumped lasers, power output and wavelength, 4 to 30K 78−79035
$Pb_{1-x}Sn_xTe$, segregation during solidification by Bridgman technique 79−38735
$Pb_{1-x}Sn_xTe$ single crystals, selection using travelling solvent method *(German)* 80−2936
$Pb_{1-x}Sn_xTe$, Te-rich growth by ingot nucleation method, laser fabrication 77−77362
$Pb_{1-x}Sn_xTe$, temperature gradient LPE, PbTe substrate 78−3066
semiconductor growth continued
$Pb_{1-x}Sn_xTe$:In epitaxial layers, growth, elec. props., and luminesc. 80−54542
$Pb_{1-x}Sn_xTe$-PbTe heterostructures, MBE produced on mica and $LiNbO_3$, elec. props. study 80−88629
$(Pb_{1-x}Sn_x)_{1+y}Te_{1-y}$ system, VPE parameters influence on epitaxial film props. 79−28229
$Pb_xSn_{1-x}Te$, for appl. in IR detector arrays, comp. control 80−31872
$Pb_xSn_{1-x}Te$, grown by vap. transport in closed system, quality improvement 77−40341
$Pb_{1-x}Sn_xTe_{1-y}Se_y$, quarternary solid solns. with const. lattice parameter, cryst. growth and charact. 80−108332
PbTe, and $Pb_{1-x}Sn_xTe$, VPE growth control by EM irrad. *(Russian)* 80−34338
PbTe, complex-composition film production method from vapour *(Russian)* 78−95702
PbTe, continuous epitaxial film, grain size, growth cond. depend. 78−26786
PbTe film, 50 μ, prep. in double quasiclosed volume 79−38745
PbTe film, Bi and Tl impurity dopant incorporation and diffusion during MBE growth 79−66012
PbTe films grown from vapour, optimum conditions and elec. charact. 79−52117
PbTe, high mobility polycrystalline layer, mol. beam deposition 79−83138
PbTe IR diode, epitaxially grown and ion implanted, minority carrier lifetimes, efficiency 77−20411
PbTe, LPE, solvent choice, equilib. in Pb-Sn-Te system 79−87589
PbTe, nonstoichiometric, evap. and growth of epitaxial layers 80−104072
PbTe single crystals, growth from vapour phase under micro-gravity conditions 80−80957
PbTe, thick epitaxial film, laser deposition technique 78−68629
PbTe, uncontaminated films prepared by mol. beam deposition, elec. props. meas. 78−15316
PbTe, VPE film growth under near equilib. conditions 77−32526
PbTe-flux boundary, interfacial tension, rel. to Czochralski growth 77−35797
PbTe-$Pb_{1-x}Sn_xTe$-PbTe DH, LPE and VPE, stimulated emission 77−75526
PbTe-SnTe, solid soln. single crysts., TSM growth and elec. charact. 78−68625
PbTe-SnTe solid solns., directional solidification 77−44149
PbTe-ZrO_2 (SiO_2), epitaxial MIS struct., fabrication and elec. props. 80−2472
$Pb_{1-y}Te$-$Pb_{1-x}Sn_xTe$ ($x,y \lesssim 0.3$), double heterostruct., LPE growth, heterointerface morphology 80−70550
PbTe(Se) vacuum deposited thin films, struct. and growth 79−19482
$PbTe_{1-x}Se_x$, epitaxial layers synthesis, cryst. struct. perfection and elec. charact. 79−87587
RuP_2, prep. and characterisation 78−39679
$(Sb,Bi)_2(Se,Te)_3$ profiled crystalline ingot continuous elongation 79−69975
SbSI, crystal growth from SbI_3 flux 79−66000
SbSI, vapour phase growth on seeds 78−11090
$(Sb_2Se_3)_{0.7}(Bi_2Se_3)_{0.3}$, solid soln., prep. and elec. properties of layered crystals 80−70762
Sb_2Te_3, $Sb_{1.5}Bi_{0.5}Te_3$, Te- and Se-doped cryst. growth and elec. props. 77−48334
Sb_2Te_3-Bi_2Te_3 solid solns., bladed cryst. growth, electrophysical props. 78−43387
Sb_2Te_3-Bi_2Te_3 solid solns., single cryst. growth and thermocouple construct. 80−104056
Se, amorphous film, photodeposition by Selor process, kinetics 78−75963
Se, amorphous film, photodeposition by Selor process, struct. and kinetics 78−75964
Se amorphous thin film photodeposition from hydrosols 78−11109
Se, amouphous film, photodeposition by Selor process struct. 78−75962
Se, evaporation kinetics from temp. programmed large area source 77−69996
Se, film, effect of thermal history and substrates or crystn. by vac. condensation 77−15713
Se film, epitaxially grown on Te substrates, crystallinity, RHEED and SEM meas. 77−40373
Se film, trigonal, sputtered and evaporated nucleation and growth processes 77−31920
Se, trigonal, cryst. growth from CS_2 soln. 78−23596
Se_xTe_{1-x}, growth of single crystals by Czochralski method 80−66423
Si (111) face, cryst. film growth, transfer of impurity during condensation of mol. beams 78−10299
Si, amorphous, p-n junction preparation, by SiH_4 decomposition *(Czech)* 77−63560
Si, amorphous, prep. by glow discharge decomposition method *(Japanese)* 77−81226
Si, amorphous, prep. by reactive RF sputtering in Ar-silane mixtures, undoped, n-type and p-type targets 80−76182
Si, amorphous, production by glow-discharge method *(Japanese)* 77−90283
Si, amorphous, substantially doped, electronic props., review 79−87175
Si, amorphous CVD films for high temp. solar photothermal conversion 80−26161
Si, amorphous film, plasma-deposited, photoluminesc. and EPR meas. 79−4864
Si amorphous film, sputter-deposited, elec., optical, and photoelectronic props. 79−24433
Si, amorphous film deposition from silane glow discharge plasma 77−44173
Si, amorphous film prepared by CVD, optical props. and struct., solar absorber appl. 79−52035
Si, amorphous hydrogenated, manufacture of Schottky-barrier and MIS tunnel solar cells *(French)* 79−24897
Si amorphous layer, solar furnace annealing to induce solid-phase epitaxy 80−2277
Si, amorphous whisker growth charact. by SiH_4 thermal decomposition 80−34342
Si, annealing during Czochralski growth, influence on defect density 80−60769
Si beam epitaxy for epitaxial film growth and p-n junction formation in high vacuum 80−16187
Si bridging epitaxy from Si windows onto SiO_2, ruby laser pulse annealing 80−44441

semiconductor growth continued
Si buried-grid fabrication by LPE 79−78906
Si, CVD, characterisation and morphology 79−33938
Si, CVD, for appl. in high temp. photothermal conversion 79−79403
Si, CVD, gas phase diffusion and surface reactions 79−15614
Si, CVD, underlying oxide layer thickness effect on in-process thickness monitoring 80−6679
Si, CVD, using CO_2 laser for substrate heating 78−39698
Si, CVD crystal growth mechanisms *(French)* 79−33939
Si, CVD epitaxial growth, from $SiCl_4+H_2$, in vertical cylinder reactor, transport processes analysis 77−48344
Si, CVD from SiH_4-HCl-H_2 system, rate-determining reactions and surface species 80−84405
Si, CVD growth, high- and low-temp. models 78−6244
Si, CVD growth and film morphology, rel. to model of mass transport 77−59233
Si, CVD growth rate, temp. and conc. effects, mass transport model 77−59234
Si, CVD growth surface, singular instabilities 77−24969
Si, CVD mechanism, book contrib. 79−69991
Si, CVD mechanism, epitaxial growth, IR obs. 79−23859
Si CVD of polycrystal on liquid Sn layer 78−64479
Si, CVD on liq. Sn layers in HCl presence, enhanced crystallinity 78−6853
Si, CVD on SiO_2 and Si_3N_4, SEM study *(Dutch)* 80−2960
Si, CVD on SiO_2 and Si_3N_4 substrates, nucleation in SiH_4-HCl-H_2 system at high temp. 80−49538
Si, CVD polycryst. film, growth texture 77−7990
Si, CVD polycryst. solar cell, grain boundary effects rel. to dopant conc. 77−7744
Si, CVD using CO_2 laser 78−56589
Si, CVD using Si-H-Cl system, theoretical anal. of equilib. adsorption layers 79−23858
Si, coating of mullite ceramic substrate, for solar cell appl. 79−34432
Si continuous polycrystalline films on C substrates 78−64490
Si, cooling rates of large diameter crysts. 78−35291
Si, crack free ingots, by directional solidification using heat exchanger method 79−8242
Si, crucible-free growth, zone melting in combined heating system 78−3031
Si, cryst. growth, float zone, low ohmic seeds and dislocations 78−27398
Si, cryst. growth, temp. field, stresses rel. to dislocation density *(German)* 77−51335
Si crystal, high O_2 content, Czochralski growth parameters related to epitaxial stacking faults 79−4314
Si crystal, obtained by local epitaxial accretion, facing and shape meas. 77−4270
Si crystal, shape stability in float zoning 77−47362
Si crystal growth, for electronic devices 80−66419
Si, crystal growth conditions effect, on microdefect distrib. 80−50549
Si, crystal growth from melt in vac., origin of SiC impurities 80−2940
Si crystal production and perfection for photodetectors 78−11107
Si, crystalline sheets production, low cost, crystal growth techniques comparison 80−35083
Si, crystn. front face effect on at displacements *(Russian)* 78−67781
Si, Czochralski and web crystals, transition metal doped for solar cells 78−35297
Si, Czochralski crystal growth and charact., oxidation induced stacking faults 79−47621
Si, Czochralski crystal growth, low O content 80−40251
Si Czochralski grown, O distrib. meas. 77−11580
Si, Czochralski grown crystal, radial impurity distrib. improvement 77−73225
Si, Czochralski grown crystal, O precip., nucleation behaviour and dislocation loop form. *(Japanese)* 80−59664
Si, Czochralski grown crystals, swirl-type defect obs. 80−100236
Si, Czochralski growth, drop form. and crystn. rel. to dislocation struct. 78−2030
Si, Czochralski growth, equilib. of dissolved C and O with CO in ambient atm. 80−1949
Si Czochralski growth, large crystal, convection and segregation 78−6843
Si, Czochralski growth and characterisation *(Japanese)* 79−43125
Si, Czochralski growth from heavily Sb doped melt, interface morphological instability 80−2939
Si, Czochralski growth with automatic diam. control 78−52658
Si Czochralski wafer intrinsic gettering by oxide precipitate induced dislocations 78−6092
Si Czochralski wafer oxidation-induced stacking faults correl. with bulk defects 77−76428
Si Czochralski wafer oxide precipitate-dislocation complex characterisation 78−14357
Si, Czochralski-grown, oxide precip. form. process 80−49364
Si, Czochralski-grown cryst., swirl defect formation and defect migration 77−76405
Si, Czochralski-grown crysts., thermally induced microdefects, annealing temp. and starting material effects 80−49141
Si, defects, solid-phase epitaxy process, rel. to Si dissolution into Al 78−95188
Si, dendritic film growth on alumina, solar cell appls. 77−77432
Si dendritic web growth, correlation of solute and interface partition coeffs. 79−24427
Si, dendritic web growth processes for solar cells, computer modelling 79−11508
Si deposition by SiH_4 pyrolysis at low temps. and atm. press. 79−91595
Si, deposition on rotating disc, one-dimens. model 80−75461
Si devices, application of epitaxy technology, deposition techniques 80−7501
n-Si, dislocation free, process induced cryst. defects 80−24392
Si, dislocation-free crystal point defect condensation 78−6026
Si, dislocation-free single crystals, growth microdefects, etching and X-ray expts. 78−47385
Si, edge-defined film-fed growth of controlled shape crysts. 78−31327
Si, effect of C on dissolution of quartz in liq. Si, rel. to melt growth 80−70414
Si electron beam deposited film, epitaxy by pulsed laser annealing 78−56055
Si, epitaxial, impurities incorporation kinetics *(French)* 78−22749
Si, epitaxial and amorphous film growth, low energy ion beam deposition 77−28729

semiconductor growth continued
Si epitaxial detector fabrication, crystal growth and preferential etching 78−37505
Si epitaxial film, high electron mobility, grown on sapphire at high growth rate 77−81225
Si, epitaxial film, of submicrometer thickness 79−95932
Si epitaxial film deposition, vapour-phase, small-scale system design and operation 79−43151
Si, epitaxial film growth by hydride-iodide method 77−48343
Si epitaxial film growth on sapphire in SiH_4-H_2 system, optimum deposition 77−77397
Si, epitaxial film growth on Si(111) and sapphire ($1\bar{1}02$), simultaneous RHEED/AES study 80−10833
Si epitaxial films on Czochralski sapphire, optimisation of deposition conditions in SiH_4-H_2 system 80−75464
Si, epitaxial growth, adsorbed layer model for autodoping mech. 80−7505
Si epitaxial growth, in $SiCl_4$-HCl-H_2 system, model based on flow graph 79−42405
Si, epitaxial growth, novel reactor for high volume, low cost prod. 79−24442
Si, epitaxial growth by partially ionized vapour deposition, low temp. 77−40389
Si, epitaxial growth chambers cleaning, improved method using KOH solution 78−64478
Si, epitaxial growth from vapour, dopant inclusion model *(German)* 79−42088
Si, epitaxial growth kinetics in damp H_2 77−44171
Si, epitaxial growth kinetics, experimental verification of theoretical model 79−95278
Si epitaxial growth on porous Si layer, struct. 79−1557
Si, epitaxial growth on sapphire by partially ionised vapour deposition, RHEED-AES obs. 80−80985
Si epitaxial interface migration, theory and expt. test 80−29290
Si, epitaxial layer, growth mechanism from ion-molecular beams 80−2299
Si epitaxial layer, large-area uniform growth through Al film by solid epitaxy 78−3033
Si, epitaxial layer deposition by ion beam methods 80−100417
Si, epitaxial layer grown by saturated Sn melt undercooling, morphology 78−22969
Si epitaxial layer growth in vacuum, Ar, Xe ion bombardment effect 80−39463
Si epitaxial layer regrowth due to laser annealing mechanism, liquid and solid phase regimes 80−100712
Si epitaxial layers, temp. dependence of P dopant inclusion in gas phase deposition *(German)* 79−52127
Si epitaxial layers on metallurgical-grade polycryst. substrates, characteris. 79−28967
Si, epitaxial layers on ribbon substrates, solar cell prod. and characterisation 77−77354
Si epitaxial reactor, doping system, transient steady state response, transfer function approach 79−42086
Si, epitaxial regrowth of thin amorphised layers by laser annealing, absorpt. coeff. influence 79−46968
Si epitaxial solid-phase growth, rapid 77−21022
Si epitaxial thin film growth on sapphire and spinel by MBE 80−76186
Si epitaxial wafers, role of metallic contamination in formation of 'saucer' pit defects 77−39588
Si epitaxy and oxidation, first-order process models 78−72049
Si, epitaxy by solid phase crystn. of amorphous film 78−19663
Si, epitaxy lateral autodoping kinetics 78−6087
Si, failure in strong melt grown single crysts. 78−3205
Si, filamentary, grown by chem. transport reaction method, banded struct. 80−38978
Si filamentary crystals, grown from vapour, electron probe microanal. 79−77538
Si film, amorphous, structural comparison of evaporated and glow discharge samples 77−62778
Si, film, chemically deposited on amorphous SiO_2, influence of substrate temp. and SiH_4 to N ratio on struct. 79−65346
Si film, crystallographic orientation using surface relief grating and laser crystn. 79−95277
Si film, electron beam evaporation, for solar cell appl., heat exchanges and columnar growth 79−15609
Si film, epitaxial growth on Si, impurities, plasmon energy loss anal. 77−31916
Si film, epitaxial growth by partially ionised vapour deposition, RHEED-AES-QMS study 79−83136
Si film, glow discharge deposition, SiH_4 discharge parameters obs. 80−44030
Si film, MBE, cryst. defect props., substrate treatment effects 80−70551
Si film, on graphite, early growth by ion-beam sputtering 77−44158
Si film, polycryst., electron microscopic investigation of initial stage of growth 79−23849
Si film, polycryst., laser-induced CVD growth from $SiCl_4$ 80−84852
Si film, polycrystalline, struct. thickness relationships 77−62779
Si film, solid phase epitaxy, Au and O distrib. 77−66095
Si, film and p-n junction growth by ionised-cluster beam deposition 77−32527
Si, film deposition, growth kinetics under low H_2 press. 78−56586
Si film deposition, on quart z and MgO substrates, using double cathode sputtering system *(Japanese)* 77−55889
Si film deposition by CO_2 laser irrad. of SiH_4 80−16190
Si film on SiO_2 substrate, CVD by pyrolysis of SiH_4 77−89678
Si films, electron beam evaporated, for MIS solar cells 80−93490
Si films, electron-beam-deposited on W substrates, growth and struct., AES and SEM obs. 79−46972
Si films, ribbon-against-drop process, physical and chemical characterisation 80−92798
Si, float zone crysts., large diameter, growth parameters 78−31336
Si, float-zone cryst. growth, shape of melt interfaces and radial P distrib. 77−24952
Si, focused ion beam designs for sputter deposition 79−89841
Si, from Al-Si-Cu melt, faceted cryst., cellular hole growth 77−4061
Si, graphoepitaxy on fused SiO_2 using surface micropatterns and laser crystn. 80−70554
Si, growth and melting processes, origin of swirl defects 77−76407
Si, growth by thermal decomp. of SiH_4 79−69970
Si, growth conditions rel. to cryst. struct. perfection *(Russian)* 80−38971

semiconductor growth continued
Si, growth processes, in-situ obs. *(Japanese)* 80−35104
Si growth technology, erosion of graphite and vitreous C in molten Si 78−3244
Si, heteroepitaxial, prep. and props., book contrib. 79−83128
Si, heteroepitaxial early growth island morphology rel. to deposition conditions 78−6245
Si heteroepitaxial growth using SiH_4 in He-H_2 atm. 77−77396
Si, heteroepitaxial growth using SiH_4 in H_2-He atm. 80−20049
Si, heteroepitaxy, refractory oxides as substrates *(French)* 77−44181
Si, high capacity arc heater production for solar cell manufacture 79−11509
Si, high-meniscus ribbon growth, thermal balancing via distributed inert gas streams 78−31329
Si, high-purity, preparation by H_2 reduction of trichlorosilane *(Korean)* 77−21034
Si homoepitaxy in high vac., stacking fault nucleation, crit. temp. for SiC growth 78−14620
Si, inclusion type defects removal from bulk of single cryst. by elec. fields 79−43126
Si, interstitial swirl defect form. in dislocation free floating zone cryst. 77−7682
Si, introduction of defects during growth and processing 79−95925
Si junction diodes, fabrication by LPE on Si:B substrates, and characts. 80−80363
Si, LPE from Sn melt, kinetics 78−19675
Si, LPE from Sn melt by dipping 78−6871
Si, LPE growth from supersaturated Sn melt 78−56592
Si, LPE using Ga_xAl_{1-x} solvent 77−36411
Si, large single crystal production, using directional solidification tech. 78−35298
Si layer growth by CVD on Sn-coated background *(Dutch)* 80−7502
Si layers, solid phase epitaxial growth temp. depend. 78−10305
Si layers, solid phase epitaxial growth, crystalline qualities, ^4He backscatt. and TEM exam. 78−10306
Si, liquid, interaction with die material during edge defined film fed growth 80−104060
Si, local mechanical defects, annealing and effect on autoepitaxial growth *(Russian)* 80−7701
Si, low cost production for solar cells, growth from melt 78−3028
Si, low press. epitaxial reactor for multi-wafer growth 79−43153
Si, MBE, cryopumped ultra high vac. system 77−67448
Si, MBE, on n^+ Si, with wide range doping control 78−27402
Si, MBE for semiconductor devices 79−83141
Si, MBE growth and surface struct. 80−10816
Si, mechanism of cryst. growth during chemical reactions in Si-H-Cl system 78−2392
Si, melt and vapour growth for integrated circuits and solar cells 79−47609
Si, melt grown crysts., impurity incorporation, calcs. 80−79718
Si, melt surface boundary, mass transfer, influence on crystal habit during growth 79−14712
Si, metallurgical grade, purification and charact. 78−56573
Si, mol. beam and solid-phase epitaxies under ultrahigh vacuum 79−28945
p-Si, monocryst., diffusion of As, Henry const., temp. depend., 1448 to 1523K 79−42399
Si monocrystalline rod growth from gas phase 78−64453
Si monocrystalline sheet fabrication for solar cells, CLF Czochralski furnace and enhanced slicing technology 80−93476
Si multicrystalline solar cell material prep., fast-pulled float zone, CZ and cast ingot and foil methods 80−93483
Si, multiple ribbon growth by EFG 79−8245
Si on ceramic, coating with inverted meniscus (SCIM) technique, solar cell appl. 80−89163
Si on ceramic, from melt, for solar cell appl. 79−11511
Si, on sapphire, early growth, TEM 77−24961
Si, on sapphire, early growth, models 77−24962
Si on sapphire, stacking faults and twins, TEM obs. at early stage of epitaxy 79−28233
Si $p^+\pi p n \nu n^+$ structure form. by epitaxial growth 77−76906
Si, photocell, ionized cluster beam deposition and epitaxy, cell characts. 77−77416
Si photopile manufacture for terrestrial solar cells *(French)* 79−24895
Si, planarized solid state epitaxy for Schottky barrier diodes 78−35302
Si plasma deposited amorphous hydrogenated film, optical props., annealing effect 79−56874
Si plate prod. by Stepanov method, stability analysis *(Russian)* 78−52655
Si, polycryst., deposition as example of pyrolytic CVD process 80−84407
Si, polycryst., growth, props. and MIS appl. *(Slovak)* 78−92196
Si, polycryst., growth kinetics in low press. CVD reactor 79−91594
Si, polycryst., low press. CVD production processes 77−77395
Si, polycryst. film, ion plating on Al, growth from eutectic melt 77−8765
Si, polycryst. film doping during deposition and with diffusion 78−6088
Si, polycryst. film from low. temp. pyrolysis of SiH_4 78−31342
Si, polycryst. layers, ribbon-against-drop pulling process 79−8241
Si, polycryst. manufacturing methods for photovoltaic energy prod., solar cells, grain growth from melt *(Dutch)* 78−52661
Si, polycrystalline, ribbon to ribbon, using laser scanning, solar cell appl. 78−35299
Si polycrystalline layers on C substrates, RAD process, solar cells appl. 80−89635
Si, polycrystalline ribbon prep. by electron bombardment *(French)* 78−64474
Si, porous film, form. by anodic reaction in HF soln., struct. props. 77−24971
Si preparation by electrolysis of fluorosilicate solns. in molten alkali halide mixtures *(French)* 78−64491
Si, preshaped single crystal prep. by pendant drop method *(French)* 78−64466
Si, prod. of polySi vapour deposited coatings for solar cells, cost anal. 80−93495
Si production, low-cost low-energy processes 78−11126
Si, production by reduction of SiO_2 with C black in plasma reactor, feasibility 78−27426
Si purification, using silicon fluoride as transport 78−35316
Si, rapidly grown RTR sheet, props. and solar cell processing 79−100048
semiconductor growth continued
Si, reaction of rare earth impurities with carbon during cryst. growth 79−38733
Si, reactive close-spaced vapour transport, simplified theory 80−15396
Si ribbon, crystal characterisation, growth with dies 78−76598
Si ribbon, dendritic web growth, solar cell prod. and characterisation 77−77366
Si ribbon, dendritic web growth from melt, solar cell module fabrication 80−93478
Si, ribbon, edge-defined film-fed grown, orientation depend. of defect struct. 77−1134
Si ribbon, edge-defined film-fed growth, solar cell prod. and characterisation 77−77365
Si ribbon, edge-defined film-fed growth, melt temp. distrib. 79−52108
Si, ribbon, impurity distrib. in EFG 78−91280
Si ribbon, low angle sheet growth technique, direct shaping characts. 80−93480
Si ribbon crystal growth, 10 cm wide, temp. distrib. meas. in die 80−104059
Si ribbon crystals, edge-defined film-fed growth technique for solar cells 80−89633
Si, ribbon edge-defined film-fed growth control using C-CD imagers 78−68623
Si ribbon grown by capillary action shaping technique, electron channelling analysis 77−76418
Si ribbon growth, ribbon-to-ribbon process, thermal environment control 80−35116
Si ribbon growth, Stepanov technique, recent develop. 79−11510
Si ribbon growth, technology assessment 1978-1986, computer anal. using PECAN 79−8244
Si, ribbon growth, via RTR technique, process update and material characterisation 78−76597
Si ribbon growth by capillary action shaping technique 80−29888
Si ribbon growth by EFG, thermal sensitivity and stability 80−107080
Si, ribbon growth by edge-defined film-fed process, morphology, stability 77−24947
Si ribbon growth from melt, monitoring device for width and thickness uniformity 80−35077
Si ribbon parallel twinned structure development by shaped crystallisation 78−64465
Si ribbon-graphite in-situ thermocouple, calibration and meas. accuracies manufacture 79−97386
Si ribbons, dendritic web for solar cells 80−89634
Si ribbons, edge-defined film-fed growth technique for solar cells 80−89138
Si ribbons for solar cells, ultra high speed growth, elec. props. 80−89162
Si ribbons grown by capillary action shaping technique, surface quality and impurity distrib. 80−108343
Si, ribbons produced through capillary action shaping, elec. and struct. characts. 78−47804
Si, selectivity of deposition from $SiCl_4$ 77−24958
Si, self-supporting polycryst. film deposited by energy beam plasma, for terrestrial solar cells 79−11523
Si sheet, high speed growth, heat transport analysis 80−107669
Si sheet edge-defined film-fed growth, for photovoltaic cells 79−61982
Si, silicide forming systems, solid phase epitaxy 78−23613
Si, single cryst., temp. gradient meas. by photoelec. pyrometer 77−40359
Si, single cryst. growth in clear SiO_2 crucibles, heat exchanger method 79−33919
Si, single cryst. ribbon growth, thermal anal. 78−3029
Si single crystal, improved horizontal ribbon growth technique 80−108345
Si single crystal growth advances 78−6842
Si single crystal growth by heat-exchanger casting 78−11104
Si single crystal ingot growth from metallurgical grade Si, inhomogeneities 80−59416
Si, single crystal sheets grown from melt require no slicing or polishing 79−74079
Si, single-crystal, grown-in structural defects 79−10860
Si solar cell, fabrication using zone melting of CVD Si on graphite, and performance 77−85945
Si solar cell fabrication from multiple ingots using melt replenishment Czochralski method, cell anal. 80−93477
Si solar cells, capacitance transient spectra of processing- and radiation-induced defects 80−61340
Si solar cells, crystal growth, heat exchanger method, fixed abrasive slicing technique 80−35082
Si solar cells, growth of large grain polycryst. layers on graphite substrates by CVD on liquid layers 80−55849
Si, solar grade, advances in Dow Corning process 79−8243
Si, solar grade, by silane pyrolysis, process design and economics 79−8234
Si, solar grade, Czochralski growth, solar cell efficiency vs. metallic impurity conc. 78−31330
Si solar power cell production by capillary action shaping technique 79−34431
Si, solar-grade, directional solidification in carbon crucibles 80−45663
Si, solid phase epitaxial growth through Al film 79−24432
Si, solid phase epitaxy, Si⟨100⟩/Pd_2Si system, dissoc. mechanism 77−7980
Si solid phase grown, structural obs. 78−2397
Si, solid-phase epitaxial growth stages in Si(crystal)-Pd_2Si-Si(amorphous) system 77−85114
Si, solid-phase epitaxy in Si (100)/Pd_2Si/Si (amorphous) system, radioactive tracer obs. 77−89663
Si, solid-phase-epitaxial, deposited above 380°C, defects obs. 78−63942
Si, solid-state epitaxial growth of amorphous layer 80−10803
Si, square single crystals, Czochralski growth 80−97422
Si, strip-type crystals, growth mechanism, morphology 79−7559
Si strips, growth by Stepanov's method 79−78867
Si surface, reduction growth, autoepitaxy *(Russian)* 80−107672
Si technology, phys. and thermodynamic props. data for $SiCl_4$ 79−65218
Si, temp. distrib. in working zone of composite heater, heat transfer calc. 78−3016
Si thick-film growth using contiguous capillary coating on porous C substrates 80−93507
Si thin autoepitaxial layers low temp. growth mechanism in $SiCl_4$-H_2 system 80−20795
Si thin film for solar cells, thermal expansion shear separation technique 80−81439

semiconductor growth continued
Si thin ribbon grown at high speed, thermal stresses, reduced thermal buckling 80−107078
Si thin-film polycrystalline vacuum-deposited solar cells, TiB_2 bottom electrode, 10% efficiency 80−93489
Si tube growth by EFG process 80−108344
Si, VPE, gas-flow dynamics in horizontal CVD reactor, book contrib. 79−82498
Si, VPE, pattern shift comparison in vertical, horizontal, and cylindrical reactor geometries 78−27408
Si VPE, reduced pressure, advances 80−40242
Si, VPE, state of art 79−33937
Si, VPE, stationary model, appl. to $SiCl_4$-H_2 system 78−52679
Si, VPE at reduced pressure, autodoping 77−77389
Si, VPE growth, in process monitoring and control of doping gas conc. 79−24443
Si, VPE growth mechanisms *(French)* 77−59236
Si, VPE growth mechanisms 79−28929
Si, VPE layer props. control using boundary layer characts. 80−50561
Si, VPE tangential growth, thickness meas. 77−35836
Si, VPE using SiH_2Cl_2/H_2 as source for epitaxial films on insulators 78−48327
Si, VPE via Si H_2Cl_2 in barrel reactor 78−52685
Si, vacuum deposition, combined with Sb ion implantation *(Japanese)* 78−88428
Si vacuum deposition combined with Sb ion implantation, neutron activation anal. 79−47631
Si, vacuum deposition of polycrystalline film on metal substrate 79−91588
Si, vapour epitaxy, optimum growth conditions 78−76608
Si, vapour-liq.-solid growth, using Pt and Au liq. forming agents, kinetics and morphology 78−42935
Si, vapour-liq.-solid growth, using Pt and Au liq. forming agents, struct. perfection 78−42936
Si wafer prod., diffusion furnace temp. profile meas. systematic errors, theoretical model *(German)* 80−8989
Si, whisker, amorphous, growth method for field desorption mass spectrometry 79−28262
Si, whisker, growth by reduction of $SiCl_4$ in H_2 gas current 77−15726
Si, whisker growth in amorphous state, in SiH_4-Ar atmosphere, visual obs. 78−84112
Si wide ribbon, high speed edge-defined film-fed growth 80−104058
Si, wide ribbon crystal growth apparatus 78−48307
Si, zone melting, swirl defects A-type as source of dislocation generation on macroscopic scale 80−25554
Si:As, CVD, doping using SiH_4-H_2-AsH_3 system 80−79823
Si:As, epitaxy, lateral autodoping kinetics 78−39699
Si:As, MBE with simultaneous ion implant doping 80−66432
Si:As wafers, laser annealing, Rutherford backscatt., optical, and TEM obs. 79−1445
Si:B, autodoping during epitaxial growth from SiH_4 77−47476
Si:B, highly-doped polycryst. thin film, growth kinetics and properties 78−44016
Si:F, amorphous alloys, RF sputtering prep. in SiF_4-Ar gas mixture, spectra 80−80772
Si:Ga, LPE growth on Si substrate, melt-back approach 78−80481
Si:Ga, LPE on Si, technique and characterisation 79−38751
Si:Ga(Sb), epitaxial film, doping efficiency *(Japanese)* 79−73201
Si:H, amorphous, control and anal. of deposition, using plasma spectroscopy 80−45230
Si:H, amorphous, prod. by high temp. thermal decomp. of SiH_4, and photocond. 79−87585
Si:H, amorphous film, prep. by plasma decomp. of SiH_4 under mag. field, and characterisation 80−45239
Si:H, amorphous thin film, ion plating, IR absorpt. meas. 80−84857
Si:H amorphous films, effects of glow-discharge prep. conditions on H content 79−46969
Si:In, gradient transport soln. growth, IR monitoring, 950-1300°C 79−100040
Si:In extrinsic IR detector material with high responsivity compensated by neutron transmutation, float-zone growth 80−75597
Si:N, amorphous, prep. by RF sputtering and props. 80−44229
Si:Ne(Ar)(Kr), amorphous, implanted and sputtered, epitaxial regrowth, influence of noble gas atoms 80−2289
Si:O, C, impurity conc. profiles and process-induced defects 78−6094
Si:P, Czochralski growth, dopant evaporation coeffs., resistivity distrib. 77−16487
n-Si:P, doping, by zone melting using solid dopant source 78−43035
Si:P, doping during growth from gas phase, thermodynamic analysis 80−59489
Si:P, doping element incorporation, temp. depend. in CVD epitaxy 80−45234
Si:P, epitaxial layer, vapour phase grown, temp. dependence of dopant inclusion, differential molar solution enthalpy *(German)* 79−52128
Si:P, polycryst., growth in epitaxial reactor at 800°C, using PH_3 doping 77−1815
Si:P, RF sputtered polycryst. film, MOS compatibility 78−6455
n-Si:Sb, arbitrary doping profiles produced by MBE 79−7617
Si:Sb, dopant microsegregation rel. to crystal and crucible rotation 78−11106
Si:Sb, epitaxial film, growth by mol. beam technique 80−2292
Si:Sb, vacuum deposition combined with ion implantation *(Japanese)* 79−28005
Si:Sb crystal Czochralski growth, radial microsegregation analysis 78−11105
Si:Sb wafers, laser annealing, Rutherford backscatt., optical, and TEM obs. 79−1445
Si/Pd system, solid phase epitaxial growth control by C ion implantation 80−75466
Si-Al interface, solid phase epitaxial growth of Si 80−34324
Si-Al solid-phase epitaxial growth, substrate effects, SIMS and backscatt. spectra 79−42421
Si-Au-P system, partition coeff. of P, temp. depend. 79−43158
Si-$CoSi_2$Si, double heteroepitaxy, solid phase and MBE 80−104063
Si-Ge, heavily doped vacuum hot-pressing, thermal and electrical props. 77−40400
Si-Ge, variable-gap cryst. made from solid soln. 79−66003
Si-Ge heteroepitaxial layers, Ge/Si ratio transfer curve from gas phase to solid phase obtained by epitaxial growth 77−73234
Si-Ge single crystals, solid solutions, growth by electron-beam zone melting without crucible 79−4917

semiconductor growth continued
Si-In_2O_3:Sn heterojunctions for solar cells 78−64107
Si-Pd_2Si heterostructure growth by solid-phase epitaxy from Si (111)-Pd-Si (amorphous) 77−51617
Si-Pd_2Si Schottky barrier diode grown by solid phase epitaxy 77−80837
SiAs, cryst. growth from melt, elec. props. 80−76170
SiC, 6H polytype, LPE growth by dipping technique, electroluminesc. meas. 77−8769
SiC (2H), vapour grown, growth and deform. faults, X-ray obs. 78−30650
SiC (6H), blue-emitting diodes by CVD 80−97439
SiC (6H) epitaxial layers, growth by CVD, morphology 79−24446
SiC, CVD film growth, morphological, chem. and cryst. struct. investig. 77−40385
SiC, cryst. growth on oriented seeds by sublimation 78−35279
β-SiC, cryst. temp. variation during growth 77−40340
SiC, crystal growth from gas phase role of Si in mass transfer 79−8233
α-SiC crystals, broad-band semiconductors, growth in Acheson furnace 80−84841
β-SiC crystals, wetting by Si and growth by vap.-liq.-solid mechanism 78−3005
SiC, eccentric growth spirals 78−26470
SiC, epitaxial growth by sublimation sandwich method, effect of impurities 80−25568
SiC, epitaxial growth by direct synthesis in vacuum 80−40262
SiC epitaxial layer, vapour phase growth, investigations of kinetic and thermal conds. 79−42407
SiC epitaxial layer growth from sublimation in vac., kinetics 80−20791
SiC epitaxial layers, energy distrib. in photolum. spectra, influence of synthesis conditions 79−52009
SiC film, growth on Si ribbon surface, TEM anal. 78−84094
SiC, film, synthesized by RF reactive ion plating, struct. 77−40391
β-SiC, film prep by RF sputtering 77−44164
SiC film synthesis by plasma deposition process 78−11127
β-SiC form. on Si substrate in RF powered reactor 80−76173
SiC, growth from soln. in fused Si, temp. gradient method in Tb vap. 78−35301
β-SiC, growth kinetics by Van Arkel method 77−16479
SiC, H_2 effects on epitaxial growth rates 78−22968
β-SiC, heteroepitaxial growth on Si substrate using $SiCl_4$-C_3H_8-H_2 system 79−24445
SiC, LPE for blue LEDs 77−81228
SiC, N doping inhomogeneities due to growth conditions 78−22741
SiC, on Si and metal silicides, formation characteristics and mechanism, by ion backscattering techniques 79−60653
SiC p-n junction, epitaxial, grown by sublimation, elec. and struct. props. *(Chinese)* 80−60067
SiC, phys. props. and crystal growth, rel. to appl. in electrolum. devices, book contrib. 77−77299
β-SiC, polytype stability, $\alpha \rightarrow \beta$ phase transformation during growth 78−6028
SiC, single cryst. ingots, growth using seeds, 1800-2600°C 78−43993
n-SiC, single cryst. layers deposition on charact. substrates, morphology *(German)* 79−28943
SiC, synthesis by ion implantation of diamond, role of struct. imperfections 78−34529
SiC, VPE kinetics study in SiC-C system 79−37934
SiC, VPE layers, growth kinetics, polytypism 77−11809
SiC, vapour deposition, thermodynamics of Si-C-Cl-H system *(German)* 79−11520
SiC:Al(B)(Ga), 4H-, 6H- and 3C-polytypes, melt growth and photoluminesc. 77−24885
SiC:Be, gas-phase equilib. comp., thermodynamic analysis rel. to cryst. growth and doping 77−85909
SiC:N, conversion factor at high doping levels 78−22744
SiC-N_2 system, high temp.-processes, thermodynamics 77−85105
SiC_x, amorphous, prepared by glow discharge method, elec. and optical props. 77−21035
Si_xGe_{1-x}, Ge distrib. in single crysts. grown by zone refining without crucible 78−22754
Si_xGe_{1-x} multitip photofield emission cathode, fabricated by crystn. from vapour, emission characts. 78−2975
Si_2Te_3, growth by Bridgman technique and sublimation, cryst. struct. 77−1106
Si⟨111⟩/Al/Si, growth kinetics of ⟨111⟩ Si through Al layer by solid phase epitaxy 79−28236
SmS-based alloy, preparation and properties 78−44034
SnO_2 CVD film form. mechanism 78−38977
SnO_2, cryst. growth by chem. transport method 78−3004
SnO_2, electro-conducting transparent film, props. rel. to production method *(Japanese)* 80−25557
SnO_2 film, CVD using $SnCl_4$-H_2O and $SnCl_4$-H_2O_2 systems, elec. and optical props. 78−52686
SnO_2 film, growth by DC sputtering from compressed target, cond. and optical props. 77−59690
SnO_2 film, pure and Sb doped, transparent cond., prop., characts., stability, struct. *(Japanese)* 78−47889
SnO_2 film growth at room temp. 79−91592
SnO_2, two-step deposition process using DC sputtering and oxidation, and characterisation 78−95691
SnO_2:As film, prep. and elec. cond. 80−2959
SnO_2:Sb sprayed film, growth mechanism and cryst. struct. 80−89143
$Sn_{1-x}Pb_xTe$, epitaxial layers synthesis, cryst. struct. perfection and elec. characts. 79−87587
$Sn_{1-x}Pb_xTe$, film, production under quasi-equilibrium conditions 80−45241
SnS, single cryst. growth and struct. props. 79−52109
SnS_2, cryst. growth, photoconductivity 77−85912
SnS_2, crystal growth and optical props. in visible and IR regions 77−52114
SnSe, single crysts., growth by Bridgeman technique, electron diffr. anal., lattice consts., carrier conc. 79−47616
SnSe, sublimation growth, deviation from stoichiometry, elec. props. 78−76594
SnTe, annealed, iodide method of prep., props. meas. 80−71591
SnTe, complex-composition film production method from vapour *(Russian)* 78−95702
SnTe, expitaxial film, early stages of growth, replication and TEM obs. 79−65348
SnTe film, 50 μ, prep. in double quasiclosed volume 79−38745
SnTe, LPE, solvent choice in Pb-Sn-Te system 79−87589

semiconductor growth continued
SnTe-InTe system, solid soln. films prep. under quasi-equilibrial conditions 79−33931
SnTe-PbSe, semicond. film, growth, phase composition, condensation temp. rel. to cond. type 77−28266
Sr_2MNbO_6, (M=Ti, Zr, Nb), perovskite struct., synthesis, lattice constants and elec. props. 77−21369
Te, Czochralski growth of single crystals 79−4912
Te, ENSH method of oriented thin film growth 79−99443
Te, evaporated film epitaxial and amorphous-crystalline phase transition growth and struct. 79−51449
Te film, evaporated, predeposited Ag, Sn, Bi, Al and Se nucleation centres effect on grain growth 77−4739
Te film, from melt, between Ge and CdS substrates, heterojunction prep. and characterisation *(German)* 77−20413
Te film, on electron irrad. KBr, epitaxial growth and surface coverage 80−10825
Te film growth on KBr (111) on mica *(Japanese)* 78−79903
Te, growth of single crystals by Czochralski method 80−66423
Te, pure, prep. by combined method, vacuum distillation and double condensation 79−33956
Te, single cryst. growth by hydrothermal method *(French)* 78−11096
Te, single crysts., Czochralski growth, etch pit orientation study 79−43133
$Te-(Bi_xSb_{1-x})_2Te_3$ eutectic, electrophys. props., directed crystn. conditions influence and comp. depend. 80−107827
Te-As-Ge, RF sputtering, temp. and bias effects on comp. 77−40367
Te-based eutectics, crystn. rate effect on electrophys. props. mutual solubility effect 80−60774
Te-Se-Cd, sandwich structure, fabrication and characteristics 80−60089
TiO_2 films as solar photocatalysts, preparation 79−74530
Ti_nO_{2n-1}, cryst. growth and characterisation 78−31311
TiS_2, growth by chem. vapour transport using press.-temp.-comp. diagram 77−59764
Tl-Se-$TlInSe_2$, struct. and growth peculiarities, epitaxial heterojunctions *(Russian)* 79−11038
TlTe, elec. props., cryst. growth *(Japanese)* 79−33907
$V_{1-x}Cr_xO_2$, VPE, and elec. and optical characterisation 78−3053
VO_2, VPE and elec. and optical characterisation 78−3053
VO_2:Al(W), thin layer prep. by reactive DC sputtering doping effectiveness *(German)* 78−6847
V_2O_5 film, amorphous, CVD prep. method 80−55299
V_2O_5 film, amorphous, thickness, density and refr. index determ. from reflectance interference spectra 80−55206
V_nO_{2n-1}, cryst. growth and characterisation 78−31311
V_xO_y film, prep. by thermal decomp. of vanadium naphthenate, and elec. props. *(Japanese)* 78−88425
WSe_2, chem. vapour transport growth, microstruct. develop. 80−103278
WSe_2, single cryst. growth by sublimation method 78−11091
$YbGa(In)_2X_4$, X=S,Se,Te, prep. and props. 77−85214
Yb_2Te_3, films, prep., elec. props. 78−43494
Zn chalcogenides, film, on NaCl, preferential epitaxy induced by electron bombard. or elec. field 80−10824
$ZnAs_2$, single crystals, growth from vapour phase 78−88416
Zn_3As_2, solubility in Bi, LPE on $(Cd_xZn_{1-x})_3As_2$ 78−35324
Zn_3As_2:Cu(Te), single crysts., gas phase growth, elec. props. 79−15598
$Zn_xCd_{1-x}S$ film, prep. by soln. spray method, and struct., optical and elec. props. 78−52666
$Zn_xCd_{1-x}S$ film, prep. and use as heterojunction optical energy converters 79−95488
$Zn_xCd_{1-x}S$ layers on ZnS substrate, VPE growth 77−77420
$Zn_xCd_{1-x}S$ solid soln. film by spray pyrolysis 77−81214
$Zn_{1-x}Cd_xTe$ p-n junctions, LPE growth process, elec. props. 77−7981
$ZnGeP_2$ dissoc. press., vapour comp. and press., thermodynamic charact. 77−24934
$ZnGeP_2$, synthesis, charact., applic. to laser windows *(French)* 78−80467
$ZnIn_2S_4$ film, photoluminesc. and photocond. 78−52677
$Zn_{1-x}Mg_xTe$ alloys, high purity, metallurgical and analytical methods of prep. 80−40247
$Zn_{1-x}Mg_xTe$, cryst. growth conditions and luminesc. *(French)* 77−21019
ZnO, c-direction cryst. growth and crystallographic polarity 79−28902
ZnO film, growth rate and defectiveness, rel. to deposition conditions and substrate orientation 78−3057
ZnO film, Zn target, fabrication, properties 78−3040
ZnO films, amorphous and cryst., CVD growth and elec. props. 77−76973
ZnO films, RF sputtered single-cryst., on sapphire, struct. and SAW props. 80−80105
ZnO, high rate epitaxy on sapphire by planar magnetron RF sputtering 79−28916
ZnO, hollow crystals, growth by oxidation of ZnSe vapour, mechanism 78−34733
ZnO, rate of deposition and morphology 78−84719
ZnO, single cryst. growth in $ZnO-H_2-H_2O-O_2$ vapour, morphology, electrophys. and opt. props. 78−52649
ZnO thin film SAW device manufacture, sputtering system and film characterisation 78−95692
ZnO, ZnS, growth rate, sublimation rate and etching behaviour along polar axis 80−24387
ZnP_2, large tetragonal single cryst. growth from vap. 77−69976
Zn_3P_2 photovoltaic material and Schottky diode characteristics 78−64066
Zn_3P_2, single crystal, growth, electronic and device props. 80−25551
ZnS, Bridgeman growth under pressure, macroscopic inclusions and defects 80−45226
ZnS, cubic, gel growth, expt. conditions 78−68614
ZnS, epitaxial film, CVD growth and characterisation *(French)* 77−36403
ZnS, epitaxial growth, appl. to electronic devices, review *(Japanese)* 80−55281
ZnS epitaxial growth, in H_2, mass transport processes and effects of bypass flow 79−23860
ZnS, epitaxial growth by Zn-S-H_2 CVD method 78−27413
ZnS, epitaxial layers on Ge and GaAs substrates, exam. of growth 79−1828
ZnS, epitaxy in quasiclosed volume 77−85093
ZnS film, epitaxial, growth on Si in ultrahigh vacuum, source nonstoichiometry effects 77−77387
ZnS film, ion beam deposition 77−70008
semiconductor growth continued
ZnS, film, laser evaporation synthesis, surface struct. 79−28954
ZnS, film, vac. deposition onto NaCl cryst. in H_2S environment 78−63945
ZnS, film, vac. sputtering deposition by CW CO_2 laser beam *(Russian)* 77−21024
ZnS films, from thermal decomp. of organometallics, growth kinetics and struct. 79−78895
ZnS, growth from melt, impurity distrib. coeffs. 77−55298
ZnS, heteroepitaxial growth on GaP by closed space technique 79−28939
ZnS, horizontal epitaxial growth systems, transport kinetics 79−4920
ZnS, low resistivity, prep. and characterisation for blue LEDs 77−81209
ZnS, single cryst. vap. growth by sublimation and chem. transport 78−27390
ZnS, solution growth, using Te solvent 79−65993
ZnS, thin film deposition, by low pressure, high freq. induction plasma *(Russian)* 79−69992
ZnS, VPE on GaP in open tube system 79−28938
ZnS-CdS films, prep. by atomisation 80−16176
$ZnS-CuGaS_2$ heterodiodes, LPE, emission spectra 79−33335
ZnS(Se), growth kinetics on CaF_2 by vapour phase transport *(French)* 80−54572
ZnS_xSe_{1-x}, epitaxial film, CVD growth and characterisation *(French)* 77−36403
ZnS_xSe_{1-x} layer on ZnS, ZnSe, growth by solid-state diffusion technique 78−56578
$ZnS(Se)(S_xSe_{1-x})$, growth of cubic single crystal by I_2 transport 79−91572
ZnS(Se)(Te) film, on semicond. substrates, early stages of growth, electron microscope obs. *(Russian)* 78−38976
$ZnS_{1-x}Te_x$, polytype single cryst. grown from melt 79−14762
ZnSb, orientated crystn. conditions during reaction diffusion *(Russian)* 80−70558
ZnSe, amorphous thin film, prep. and electronic props. 77−85350
ZnSe, Bridgeman growth under pressure, macroscopic inclusions and defects 80−45226
ZnSe, Bridgman growth under Ar press., temp. distrib. in furnace 78−11100
ZnSe, epitaxial, organometallic CVD, on GaAs, and photolum. 79−8249
ZnSe, epitaxial growth, orienting semiconductive substrate effects 77−47688
ZnSe, epitaxial growth by vapour flow method 78−64482
ZnSe, epitaxial growth on Ge substrate 80−75469
ZnSe, epitaxial layers, close-spaced technique, preparation and optical props. 79−47637
ZnSe epitaxial layers, organometallic CVD prop., growth kinetics and luminescent props. 79−51458
ZnSe epitaxial layers, prep. by chem. transport reactions 80−16192
ZnSe, evap. onto electron bombarded NaCl substrates, epitaxial growth and charact. 79−28948
ZnSe, LPE from Zn-Ga soln., charact. 79−28965
ZnSe, LPE growth on ZnTe, characterisation of heterojunction 77−4745
ZnSe, MBE growth, elec. and optical props. 80−75462
ZnSe MBE growth, growth rate and sticking coeff. 77−32532
ZnSe, single cryst. film, MBE, quality obs. using photoluminesc. 77−77419
ZnSe, single cryst. vap. growth by sublimation and chem. transport 78−27390
ZnSe, single crysts., grown from melt under Ar pressure, defects form. 79−4312
ZnSe, solution growth, using Te solvent 79−65993
ZnSe, twinning on melt-growth under pressure 77−80515
ZnSe, VPE on GaAS, role of interaction between gas and solids *(French)* 77−62769
ZnSe, vapour phase single crystal growth 79−91573
ZnSe:Ag(In)(Cu), melt growth, dopant partition coeffs. 79−14837
ZnSe:I, I vapour transport prep., conductive and photolum. cryst. 79−100035
ZnSe:In films, MBE growth, doping effect on photoluminesc. 80−10818
ZnSe-GaAs solid solns., chem. transport cryst. growth, struct. 78−43991
$ZnSe_xTe_{1-x}$, MBE, comp. ratio control 79−28947
$ZnSiAs_2$, synthesis and layer growth by CVD in open flow system 78−15312
$ZnSiP_2$, conc. profiles during gas phase transport *(German)* 78−64452
$ZnSiP_2$ crystal growth, DTA obs. of Sn-Zn-$ZnSiP_2$ phase diagram 80−24394
$ZnSiP_2$, crystallisation from gas phase *(German)* 77−69977
$ZnSiP_2$, effect of crystal growth method, on physical props., effect of doping on physical props. *(German)* 79−52094
$ZnSiP_2$, growth under nonstoichiometric conditions in gas phase, microanalytical investig. *(German)* 79−33909
$ZnSiP_2$-Au(Ni) Schottky contact, production and props. 79−7901
$ZnSnAs_2$, LPE in open tube system 78−92206
$ZnSnP_2$, charact. of Zn-Sn-P phase diag. 77−44225
$ZnSnP_2$-$ZnSiP_2$, heterocombination simultaneous crystallisation 78−60560
ZnTE, MBE growth, elec. and optical props. 80−75462
ZnTe, cryst. growth under thermodynamically controlled conditions 77−48327
ZnTe, epitaxial growth on GaAs by closed-tube chemical vapour transport method, elec. props. 79−99449
ZnTe film, electron irrad. effect on electrophys. props., prep. conditions depend. 79−28421
ZnTe film preparation and props., by single-source vacuum deposition method *(Japanese)* 80−6664
ZnTe, growth from In solvents, self-compensation 77−28144
ZnTe growth from vapour, growth interruption 80−97416
ZnTe high-purity single cryst. growth by sublimation travelling heater method 79−28901
ZnTe, LPE growth on ZnSe, characterisation of heterojunction 77−4745
ZnTe, low temp. vapour growth, closed tube transport technique 77−85914
ZnTe, MBE growth, growth rate and sticking coeff. 77−32532
ZnTe MBE thin film growth, elec. and optical props. 78−47887
ZnTe, single cryst. vap. growth by sublimation and chem. transport 78−27390
ZnTe, vapour growth by closed tube method 78−39703
$ZnTe-CdS(Se)(S_xSe_{1-x})$ heterojunctions, prep. and electrolum. charcts. 77−24610

semiconductor growth continued
ZnTe-CdSe single cryst. film heterojunctions, prep. and props. 79−19652
ZnTe(:In), single cryst. film, MBE, quality obs. using photoluminesc. 77−77419

semiconductor-insulator boundaries
C-CD, insulator-semiconductor interface, electrostatic field, Green's function calc. 77−76933
capacitance meas. for Schottky barrier 80−39678
capture coeff. of neutral surface traps, influence of image forces 79−51683
charge transport in insulators, rel. to passivation of semicond. material 77−20452
charge transport kinetics in MISIM struct. 79−38188
conductor-insulator-semicond. (CIS) solar cells, noncrystalline (poly and amorphous), interface importance 80−81466
conference, Durham, England (July 1979) 80−90612
conference, on cpd. semicond. interfaces, Princeton, USA., (Feb, 1977) 77−85300
contact interaction mechanism, mech. and optical props. 78−88375
density of states determ. from field effect data 80−107688
dielectic-semiconductor systems, immersion ellipsometric obs. *(Russian)* 79−15548
dielectric-semiconductor interface, anal. of fast surface states 79−42648
dielectric-semiconductor structures, surface ion migration, theoretical analysis 80−65700
dual-dielectric charge storage cells, electron-electron effects in writing and erasing 78−34900
effective-mass approx. 79−99629
electrostatic interaction of charges with semiconductor-insulator interface 80−24996
ferrite-semiconductor structure, EM wave excitation and amplification 80−6891
ferrite-semiconductor structure, transverse galvanomag. effect *(Russian)* 77−24569
ferrite-semiconductor structure with volume magnetostatic waves, effect of convolution 80−54761
ferroelectric-semiconductor structure, effect of potential relief of ferroelectric substrate on props. 79−11235
ferroelectric-semiconductor system, illuminated, voltage redistrib. 77−40194
Ge-GeO_2, oxidation process rel. to elec. props. 77−76927
III-V oxide interface state and Schottky barrier form., unified mechanism 80−44724
III-V semiconductor anodic oxidation and applications 77−77598
III-V semiconductor-oxide interface states, photoemission obs. of energy levels induced by adsorpt. 80−93000
impurity electron states near interface 78−95320
impurity-band hopping conduction in surface layers 80−75649
interface electronic struct., microcomputer aided anal. 80−80383
interface states, thermally stimulated surface pot. in MIS struct. 78−68091
interfacial electronic props. 79−42662
interfacial polarisation effect on dielectric props., sandwich capacitor model 80−15614
inversion layer, EM modes 78−80030
inversion layer, interface barrier effects 77−89867
inversion layers, CDW mag. fields and stability 78−10533
inverted semiconductor surfaces near conduction threshold, mobility meas. technique 79−69602
ionic semiconductor-oxide interface, plasmon-phonon interactions 80−44730
light reflection and absorpt. control, boundary state population rearrangement 77−69795
localisation in two-dimens. systems 78−60213
MIS transistor, mobility in inversion channel calc. *(German)* 80−6996
MOS capacitor, Au-doped, bulk and interfacial prop. determ. using quasi-equilibrium and linear voltage ramp techniques 79−95501
MOS struct., minority carrier nonuniform generation, SEM obs. 78−72273
MOS structure, electron irrad. effects, pulsed CV charact. obs. 77−76935
MOS structure implanted with B ions, radiation defects and impurity activation 80−103757
MOS system photocapacitance, influence of surface charge fluctuations *(Russian)* 78−43480
passivated semiconductor surface, net surface charge determ. using floating field ring devices 78−88037
photocell, surface-channel photoelec. characts. 78−26909
photoemission and Auger spectroscopy for anal. of semiconductor-oxide interface and Schottky barriers 80−50536
photoresponse on electron beam scanning, video signal enhancement *(Russian)* 77−47863
polyacetylene-graphite, ohmic control *(Japanese)* 80−96888
polymer photolytic film on semicond., thickness modulation by p-n junction microfield 78−10561
richardson-Schottky type photoinjection current from photoconductor into insulating liquid 80−15608
semiconductor, amorphous, field effect and capacitance-voltage meas. anal., localised density of states 80−103686
semiconductor-ferrite layered structs., SHF spin wave interaction with electrons, review 79−95507
semiconductor-insulator boundary, space charge layers, HF magnetoconductivity 78−60231
semiconductor-oxide-semiconductor diodes, tunnel-assisted transport at room temp. 80−92975
SIS system, mutual drag of carriers 78−6430
solid-state device conference, Tokyo, Japan (Sept. 1976) 77−76901
SOS, cryst. perfection rel. to MOS transistor mobility 78−75956
SOS, quality evaluation using soft X-ray rocking curve 77−80711
SOS device structure, nonlinear B impurity redistrib., numerical soln. 79−1625
SOS film, electron mobility 78−91792
SOS films, cryst. quality improvement by Si ion channelling, annealing 80−44222
SOS MOST, electronic props. at Si-sapphire interface 80−96993
SOS quality determ. using IR and UV specular reflectance meas. 80−108684
SOS structure, radiation dose at interface due to electron beam aluminisation 78−68089
SOS structures, high-field electron transport, drift vel. meas. 80−80387

semiconductor-insulator boundaries continued
surface magnetoplasma wave spectrum in HF mag. field 80−24995
surface polaritons of LO-phonon-plasmon coupled modes 79−7792
surface properties, methods of influencing 77−15965
surface wave propagation, in presence of radial density gradient 79−7875
surface wave spectrum, theory 79−19674
tetrahedral semiconductor/oxide interface, continuous random network and tight-binding models 77−89866
trap filling differential equation, tunnel hopping current in insulating layers 79−65555
valve metal oxide-semicond. oxide, electron injection, interface reactions 77−76936
Al_2O_3-Si, insulator charges evaluation *(German)* 79−82682
Al_2O_3-SiO_2-Si, insulator charges evaluation *(German)* 79−82682
Bi_2O_3-based glass, in ZnO-glass-ZnO struct., current-voltage characts. and TSC *(Russian)* 77−69404
$Bi_{2/3}Te_{1-x}S_x$-epoxy-glass device, peaked struct. in single cryst. film 77−66207
$Bi_4Ti_3O_{12}$, ferroelec. film, on Si substrate, polarisation reversal and film struct. 79−91392
CdS-SiO_2-Si solar cell, I-V characteristics 80−89621
CdS-SiO_2-Si structures, elec. props., role of interface states 79−56286
CdSe-$LiNbO_3$ structure, acoustoelectronic interaction between SAW and transverse drift current 77−69424
CdSe-SiO_2 thin film transistors, fabrication and electronic characts. 79−33351
CdSe-SiO_2 thin film transistors, slow states, trapping state densities and cross sections 80−15613
CdTe film-ferroelectric TGS substrate system, influence of polarisation reversal on elec. cond. of CdTe thin film 80−65720
p-CdTe-Langmuir film interface, prep., characters. and MIS struct. 80−92998
$Ga_{1-x}Al_xAs$-SnO_2, rapid localised non-destructive optical charact. of ternary layer *(French)* 77−62725
GaAs anodic oxide film, direct current-voltage characts. 78−23186
GaAs film, plasma oxidation and oxide props. 78−95825
GaAs, film, selective anodisation, grain boundary edge passivation 79−11711
GaAs, film and solar cell on graphite, struct. and elec. props. 80−2286
GaAs, GaO_xN_y-passivated, surface state density 80−11809
GaAs interface with anodic and thermal oxides, comparison of AES and ESCA 78−95980
GaAs MIS diodes, interface states determ., by deep-level transient spectroscopy *(Japanese)* 80−49917
GaAs, multiple insulator layers studied by Auger anal. 79−83345
GaAs, oxidation, initial process and oxide/semicond. interface formation 80−50739
GaAs, plasma-grown oxides, in situ anal. using spectroscopic ellipsometer 79−79138
GaAs, polycryst., wet and dry oxides, comparative study by AES, SIMS and XPS 80−80116
GaAs, selective plasma oxidation, interface props. 80−100933
GaAs substrate, plasma polymerised polysiloxane film growth, dry etching process 80−25575
GaAs, surface passivation using composite Al_2O_3 and native oxide, MIS characts. 80−93004
GaAs, surface passivation using Si_3N_4, interface characts. 80−93005
GaAs, surface passivation using GaO_xN_y based multiple insulating layers 80−93006
GaAs:Si,Cr, under layer of SiO_2, effect of annealing, on electron concentration and mobility, and impurity distrib. 79−4323
GaAs/anodic oxide interface, characterisation of proposed model 80−103754
GaAs/oxide interface, interface states obs. by electrochem. method 79−99626
GaAs/SiO_2 substrate/film system, Ga content in SiO_2 after annealing at 730-940°C 78−43255
GaAs/SiON substrate/film system, interface formation during CVD, modelling 80−24764
GaAs-Al_2O_3, in MIS struct. surface states 77−85336
GaAs-Al_2O_3 interface, fabricated by interactive oxidation, props. 80−49935
n-GaAs-anodic oxide, C-V and I-V characts. 77−89863
GaAs-anodic oxide interfaces, struct. and chem. props., Raman scatt. obs. 79−47168
GaAs-GaAs oxide interface layer characterisation by spectroscopic ellipsometry 80−50738
GaAs-insulator film interface, evidence for growth-induced damage from photolum. expts. 78−75953
GaAs-insulator interface, elec. props. 78−95370
GaAs-insulator interface, processes of electron emission from traps 79−73598
GaAs-native oxide interface, electronic props. 79−73590
GaAs-oxide, interface layer determ. by spectroscopic ellipsometry 79−95275
n-GaAs-oxide, plasma-grown, surface states, modified DLTS meas. 80−11094
GaAs-oxide interface, field effect 79−87160
GaAs-oxide interface, physical struct. 79−60644
GaAs-oxide interfaces, local atomic and electronic struct., high resolution XPS 80−49927
GaAs-plasma grown oxide interface, new resonant ellipsometric technique for characterisation 79−40606
GaAs-Si_3N_4 layer struct., electron-hole liq. at interface 79−69434
GaAs-Si_3N_4 structure, photoluminesc. and collective effects 78−6727
GaAs-Si_3N_4 system, photoluminesc. edge line *(Russian)* 79−4852
n-GaAs-$Si_xO_yN_z$, C-V and I-V characts. 77−89863
GaAs-SiO_2 interface local props. *(Russian)* 78−10567
GaAs-Ta_2O_5 interface, fabricated by interactive oxidation, props. 80−49935
$GaAs_{1-x}P_x$-SiO_2:N,Zn ion-implanted multiple layers, ion range distribs., secondary ion microprobe meas. 79−42129
GaAs(Sb), Schottky barrier and semicond./insulator interface states formation 80−49906
n-GaP, inversion layers, broken-symmetry ground states 77−47873
GaP-anodic oxide devices, optoelectronic device, processing appl. 78−84304
$GaPO_4$ film growth on GaP, XPS exam. 78−31552
Ge (111)-amorphous SiO_2 or Si_3N_4 film, dislocation interactions, substrate bending and edge effects 80−39472

semiconductor-insulator boundaries continued
n-Ge inversion layers, broken-symmetry ground states 77−47873
Ge-dielectric layer interface discrete levels in Ge-metal contacts, surface treatment effects *(Russian)* 80−34497
Ge-GeO_2, optical charging memory, influence of doping GeO_2 with metal ions *(Russian)* 79−24077
Ge-GeO_2 boundary, electrophysical parameters *(Russian)* 77−85327
Ge-GeO_2 system, optical charge memory obs. 77−89871
Ge-metal oxide, elec. props., molecular deposition method 80−34525
Ge-pyrolytic SiO_2 system, carrier trapping, GeO_2 sublayer effect 78−91775
Ge-Si_3N_4 system, potential barriers determ. from photoinjection carriers trapping 80−103756
Ge-SiO_2-p^+Si tunnel junctions, for determ. of AC cond. of amorphous Ge 77−24608
$Hg_{1-x}Cd_xTe$ interface with native oxide, elec. props. 80−20318
$Hg_{1-x}Cd_xTe$-oxide interfaces, MIS capacitance characts. 80−49926
In_2O_3-SnO_2/SiO_x/Si diode solar cells, loss mechanisms, characts., band struct. 80−26135
In_2O_3-SnO_2-Si SIS solar cells, reverse current-voltage characts. under illumination 80−89622
InP, and $In_xGa_{1-x}As_yP_{1-y}$ binary and quaternary cpds., surface and dielec.-semicond. interface props. 80−93001
InP interface with anodic and thermal oxides, comparison of AES and ESCA 78−95980
InP, Schottky barrier and semicond./insulator interface states formation 80−49906
InP, surface passivation using composite Al_2O_3 and native oxide, MIS characts. 80−93004
InP/SiO_2 substrate/film system, interface formation during CVD, modelling 80−24764
InP-Si_3N_4 (SiO_2), interface props., plasma deposited dielectrics, n-channel MOSFET action 80−93003
InP-SiO_2, with reduced interface state density near cond. band 78−26954
InP-SiO_2 interface, CVD problems, ESCA profiles 80−93497
InSb, covered with thin oxide protective film, intrinsic photocond. 77−55578
InSb-anodic oxide MIS struct., electrophys. props. *(Russian)* 77−39961
InSb-insulator boundary, surface wave resonance in transversely magnetised semicond. plasma 78−30948
h-InSb-oxide system, interface recombination activity variation on annealing *(Russian)* 79−78199
InSb-oxide-electrolyte interface, electroluminesc. in anodic oxidation *(Russian)* 77−90201
$In_{2-x}Sn_xO_{3-y}$ solar cells, majority carrier conduction effects 80−97796
n-$In_{2-x}Sn_xO_{3-y}$/p-Si, semicond.-insulator-semicond. solar cell, performance and spectral response, fabrication 79−83596
$In_{2-x}Sn_xO_{3-y}$-insulator-poly-Si solar cells, photovoltaic conversion parameters 80−101093
$LiNbO_3$-p-Si, frequency doubling of the two-pulse and three-pulse echoes in surface acoustic waves 79−69335
$LiNbO_3$-Si, acoustoelectronic memory, effect of band-bending 80−70771
PbS-$(PbSO_4)_x(PbO.PbSO_4)_y$ heterosystem, cathodoluminescence spectra 79−24370
n-PbTe-oxide interface, quantized surface states in accumulation layer 80−20279
Se-polystyrene hexylmethacrylate, interface photocurrent studies, charge transfer mechanism 79−99627
n-Si (100), O_2 partial press. depend. of fixed surface state charge due to thermal oxidation 79−70179
Si (100)-SiO_2 inversion layers, exchange and correl. contribs. to subband energies 79−42654
Si, (111) surface, electronic density of states changes during O adsorption, AES obs. 79−65528
Si (111)-SiO_2 interfaces, sixth-valley state stability a priori calc. 80−49859
Si, CVD on SiO_2 and Si_3N_4 substrates, nucleation in SiH_4-HCl-H_2 system at high temp. 80−49538
Si, diffusion of Ga through SiO_2 layer, junction depth 78−51574
Si, diffusion of P from spin-on SiO_2:P film 80−2050
Si disc semiconductor-insulator structure, for liq. cryst. incoherent-coherent image convertor 80−28342
Si, epitaxial layer on sapphire, shear strain, TEM 78−51835
Si epitaxial layers on insulators, VPE using SiH_2Cl_2/H_2, expt. 78−48327
Si, film, chemically deposited on amorphous SiO_2, influence of substrate temp. and SiH_4 to N ratio on struct. 79−65346
p-Si film, on sapphire, elastoresist. coeffs., room temp. 80−34532
Si film on SiO_2 substrate, CVD by pyrolysis of SiH_4 77−89678
Si heteroepitaxial films on sapphire, vac. deposited, struct. and elec. props. 80−15390
Si, inversion layer, 1/f noise and percolation in impurity bands 79−24029
n-Si inversion layer, electronic bound states, theory 78−60217
n-Si inversion layer, resist. minima in surface quantum oscills. 78−60215
p-Si inversion layers, hot carrier effects in high mag. field, 1.25-20K 78−34908
n-Si inversion layers, in strong mag. field, quantum galvanomag. expts. 78−60214
Si inversion layers, random pair attractive interaction model of carrier correl., compared with expt. 78−60212
Si inversion layers, review 77−80842
Si inversion layers, stress effects on electronic props. 78−43476
n-Si ion implanted surface potential barriers, $LiNbO_3$ SAW obs. 77−28234
Si on sapphire in SOS technology, gettering effect by O implantation, Hall and Rutherford backscattering meas. 79−65103
Si on sapphire thin film, Hall effect, magnetoresistance *(French)* 80−65601
Si, oxidised in trichloroethylene-O_2, Cl incorporation and elec. props. 79−91827
Si, planar technology, insulating thin film preparation and props. 78−10589
Si shallow junction device, silicide contact 80−70819
Si substrate, crystn. of amorphous SiO_2, Si_3N_4 and $Si_xO_yN_z$ films 79−28225
Si substrate, stress field, induced by Si_3N_4 film edge, indentation-injected dislocation half-loops obs. 78−30839
Si substrate, struct. stability of dielec. film 80−54564
Si, surface emission of hot electrons 78−30998

semiconductor-insulator boundaries continued
Si, thin single crystal, MeV ion scatt. and channelling obs. of interfaces 80−50492
Si wafer, trichloroethane oxidation, effect on SiO_2 and Si props. 79−70193
Si:B, implanted, oxidation-induced stacking faults, EBIC and TEM expts. 78−39923
Si:B, with insulating coating, mechanical stress influence on B diffusion, strained surface layers 80−29224
p-Si:B-SiO_2 interface in MOS structures, carrier mobility and impurity distrib. 78−34902
Si:P(As)(B)-SiO_2 interface oxidation kinetics, high doping levels, experiment 80−11828
Si/Si_3N_4, charges at laser recrystallised poly Si/insulator interface 80−54789
Si/Si_3N_4 substrate/film system, implantation effects on substrate hardening and film stress reduction 78−71748
Si/SiO_2, charges at laser recrystallised poly Si/insulator interface 80−54789
Si/SiO_2 interface, transition region thickness, determ. by He^+ backscatt. 77−62762
Si/surface porous oxide film, impurity distrib. during P diffusion 77−39944
Si-Al_2O_3, inversion layer subbands, magnetocond. oscills. 78−64124
Si-Al_2O_3 interface, charge injection from surface depletion region 80−54797
Si-B, exam. of two stage diffusion of B, under a gas phase oxide film 79−95044
Si-BN interface, elec. characts., expt. 77−20459
Si-$BaTiO_3$ interface, elec. props., expt. 77−20460
Si-insulator interface, non-avalanche charge injection, expt. study, charge trapping effects 80−60099
Si-insulator structures, contact pot. meas., vibr. condensor method *(German)* 79−11232
Si-$LiNbO_3$ structure, acoustoelectronic interaction between SAW and transverse drift current 77−69424
Si-on-sapphire MOS devices, effects of planar defects near Si-SiO_2 interface on elec. props. 79−11231
Si-rare earth oxide interface in MOS struct., charge density 80−7013
Si-sapphire, interface radiation induced charge trapping, rapid anneal phenomena 79−19666
Si-sapphire interface charge trapping, effects of sapphire type and epi growth conditions 77−20447
Si-sapphire interface in SOS ICs, elec. investigation 80−11097
Si-sapphire interface states exam. by transient current anal. 77−43736
Si-sapphire interface structure, SIMS obs. 77−76675
Si-Si_3N_3, dielec. function calc. 79−95862
Si-Si_3N_4, anodisation into SiO_2, charge in electrophysical props. 78−2574
Si-Si_3N_4, hole conduction, shallow junction diode detection 77−8215
Si-Si_3N_4 interface, effect of F ions on props. and stability, expt. 78−64141
Si-Si_3N_4 interface in MNS capacitors, surface state density investigation 80−60100
Si-Si_3N_4(SiO_2) boundary, electrophysical properties, effect of ionic processes in dielectric layers *(Russian)* 78−10562
Si-SiO_2, Anderson transition in inversion layer, random field origin, substrate bias effect 77−28255
Si-SiO_2, angular-dependent X-ray photoelectron spectra 77−12485
Si-SiO_2, anodic polarisation in electrolyte containing fluoride ions, effect on oxide props. 80−39679
Si-SiO_2, bonding at (111) interface, stoichiometry and kinetics, synchrotron radiation photoemission spectroscopy 80−24744
Si-SiO_2, broken symmetry states obs. in inversion layers 78−95125
Si-SiO_2, CVD oxide, distributed fixed charge elimination using HCl 79−42661
Si-SiO_2, charge injection from polycryst. Si at low fields 77−39945
Si-SiO_2, cond. and trapping of electrons in highly stressed ultrathin thermal SiO_2 film 77−66216
Si-SiO_2, dielec. function calc. 79−95862
Si-SiO_2, distinction between donor and acceptor character of surface states 78−39216
Si-SiO_2, ESR centres, interface states and oxide fixed charge 80−2474
Si-SiO_2, effects of processing on radiation damage 78−39223
Si-SiO_2, electron injection, microplasma model 78−23176
Si-SiO_2, electron photoemission from Si, band struct. effects 79−19977
Si-SiO_2, electron tunnelling into thermally grown SiO_2 77−12018
Si-SiO_2, electron-beam annealing of ion-implantation damage 79−77622
Si-SiO_2, emission probability of hot electrons into oxide 77−32084
Si-SiO_2, film thickness and field depend. of saturation defect density 78−56250
Si-SiO_2, fitting stress and its effect on vacancy generation and distrib. 77−28087
Si-SiO_2, form. by reactive sputtering, effect of defects in Si wafer 77−89676
Si-SiO_2, Fowler-Nordheim tunnel injection into SiO_2, Si surface pot. effect 79−91151
Si-SiO_2, generation of interface states due to emission of leaky electrons 77−62972
Si-SiO_2, growth and thermal evaporation kinetics of oxide film 78−3246
Si-SiO_2, H_2 and D_2 ion bombardment effects 80−34086
Si-SiO_2, hot electron emission from Si under low level avalanche multiplication 77−80851
Si-SiO_2, hot electron emission into SiO_2 78−30997
Si-SiO_2, improved RF sputtering technique *(Croatian)* 78−48316
Si-SiO_2, impurity redistrib. during oxidation, numerical soln. including interfacial fluxes 80−25888
Si-SiO_2, influence of oxidation conditions on elec. props. of ultrathin SiO_2 layers 78−39226
Si-SiO_2, influence on frequency-temp. coeff. of SAW devices 80−79066
Si-SiO_2, interface, detection of SiO_2^- ions by SIMS 77−77848
Si-SiO_2, interface, morphology and electronic struct. 79−78194
Si-SiO_2, interface, reconstructing states 80−49925
Si-SiO_2, interface, stress meas. technique 80−84395
Si-SiO_2, interface defect states obs. by constant capacitance DLTS 80−49924
Si-SiO_2, interface free carrier mobility in inversion layer, influence of polar phonon scatt. 79−73597
Si-SiO_2, interface groups of states, C-V meas. 78−2541
Si-SiO_2, interface states from capacitance-voltage term spectra anal. 77−4446

semiconductor-insulator boundaries continued
Si-SiO_2, inversion layer, electronic ground state, stress, temp., mag. field and gate voltage depend. 78−60226
p-Si-SiO_2, inversion-channel photoelectric cell characteristic *(Russian)* 80−49941
Si-SiO_2, ion bombardment by H_2^+, D_2^+, changes in annealing behaviour 79−78185
Si-SiO_2, ion implantation effects on charges 77−32086
Si-SiO_2, irradiation behaviour anal. 78−26957
Si-SiO_2, MOS interface states density, meas. techniques and model development 80−92988
Si-SiO_2, mobile Na ion instability in SiO_2 film 79−82503
Si-SiO_2, n-Si inversion layer, exchange instabilities 78−52052
Si-SiO_2, neutralisation of Na^+ ions, trap states 79−38181
Si-SiO_2, obs. of chem. struct. 78−27654
Si-SiO_2, origin of interface states and oxide charges generated by ionising radiation 77−20380
Si-SiO_2, oxidation induced stacking fault growth, role of point defects 78−10061
Si-SiO_2, oxidation rate constants and role of H_2O 78−7072
Si-SiO_2, oxidation-induced stacking faults, O_2 partial press. depend. 78−39922
Si-SiO_2, oxide defect density depend. on appl. elec. field and thickness 80−19791
Si-SiO_2, oxide growth in HCl-O_2 mixture, ellipsometric meas. 78−7073
Si-SiO_2, polycryst. Si, surface asperity mechanism of cond., SEM obs. 78−19153
Si-SiO_2, polycrystalline Si gates ion implantation, without implanting ions into SiO_2 insulating layer 79−7619
n-Si-SiO_2, screening of charged impurity centre localised inside oxide and at interface of inversion layer 79−73563
Si-SiO_2, separation boundary charact., surface oxidation after Ar^+ bombardment *(Russian)* 79−15028
Si-SiO_2, Si lattice constraints on structure of interface states 77−20379
Si-SiO_2, Si oxidation, solubility and transport behaviour of water, dissolution 80−93801
Si-SiO_2, Si thermal oxidation, ^{18}O study 79−52400
Si-SiO_2, SiOH and SiH groups, in SiO_2 film, IR absorpt. results 78−26779
Si-SiO_2, surface state annealing 77−39946
Si-SiO_2, surface states, oxide charge centres, annealing effects 78−2570
Si-SiO_2, thermal growth mechanisms of vitreous oxide layers on Si 80−93675
Si-SiO_2, thermally oxidised, origin of fixed charge, Si diffusion in transition region 77−20381
Si-SiO_2, two layer system, P^+-ion penetration tails, expt. and computer anal. 80−75249
Si-SiO_2 (111) interface, H_2 effects, AES study 80−65688
Si-SiO_2 (111) interfaces, sixfold valley degeneracy in electron inversion layers 80−49936
Si-SiO_2 abrupt interface form. by very high dose O^+ ion implantation 80−75253
Si-SiO_2 barrier height in MOS tunnel struct., SiO_2 thickness depend. 78−14831
Si-SiO_2 bonding layer, EPR exam. 78−15022
Si-SiO_2 boundary, precipitation of Na *(Russian)* 80−49368
Si-SiO_2 boundary, relaxation of nonequilibrium capacitance in electrolyte in intense elec. fields 80−70845
Si-SiO_2 boundary, surface charge transport in valence band of Si 80−70789
Si-SiO_2 charge accumulation during low energy electron bombardment 78−64142
Si-SiO_2 double barriers, reson. tunnelling 77−80846
Si-SiO_2 electrode, electronic cond., luminesc obs. 80−61111
Si-SiO_2 film, crater-edge profiling in interface anal., ion beam etching and AES 77−1323
Si-SiO_2 in MOSFETs, inversion layer carrier mobility, theory 80−60094
Si-SiO_2 interface, (001) vicinal planes, minigaps in inversion layers, far IR absorpt. meas. 80−107919
Si-SiO_2 interface, amorphous, electronic states, Cayley trees appl. 79−65373
Si-SiO_2 interface, An influence studied using threshold voltage shift 79−82672
Si-SiO_2 interface, anal. of fast surface states 79−42648
Si-SiO_2 interface, anisotropic photoinduced ESR 78−23345
Si-SiO_2 interface, Au conc., effective impurity doping 78−52094
Si-SiO_2 interface, Au doping, trapping states 80−20319
Si-SiO_2 interface, Au surface state energy levels and Au diffusion 79−51652
Si-SiO_2 interface, Auger sputter profiling and photoelectron spectroscopy obs. 78−10287
Si-SiO_2 interface, Auger sputter profiling 78−43254
Si-SiO_2 interface, Auger-sputter profiling obs. of P pileup 78−95240
Si-SiO_2 interface, avalanche injection of charge carriers, oxide current decay 77−43728
Si-SiO_2 interface, backscattering-channelling study 80−34320
Si-SiO_2 interface, bias temp. treatment effect, stability, Cl oxides effect 77−69419
Si-SiO_2 interface, chem. struct. of transitional region 78−95824
Si-SiO_2 interface, cluster Bethe-lattice method appl. 80−49852
Si-SiO_2 interface, continuous random network and tight-binding models 77−89866
Si-SiO_2 interface, density of states, theory 80−80395
Si-SiO_2 interface, doping depend. of interface states and charges 80−92992
Si-SiO_2 interface, ESCA and ellipsometric study 79−82678
Si-SiO_2 interface, effect of thin transition layer on electron mobility and energy levels 77−20458
Si-SiO_2 interface, effect of ^{11}B and ^{19}F ion implantation on charge density 79−10865
Si-SiO_2 interface, effect of N_2 annealing on electron scatt. 79−42660
Si-SiO_2 interface, effect of high-temp., post-oxidation annealing on elec. props. 79−82673
Si-SiO_2 interface, effect of oxidation time and temp. using AES 80−35359
Si-SiO_2 interface, elec. props., rel. to SiO_2 layer struct., 200-600°C heat treatment effects *(Russian)* 77−15967
Si-SiO_2 interface, elec. props. and influence on service performance and stability 78−23171
Si-SiO_2 interface, electron injection into oxide due to mobile ion induced internal field 77−15963
Si-SiO_2 interface, electronic props. of n-Si inversion layers, stress and temp. depend 78−19113
Si-SiO_2 interface, electronic states, review 78−30992
Si-SiO_2 interface, electronic struct., EELS study 79−99596
Si-SiO_2 interface, electrically active paramag. centres detect., photocond. reson. obs. 80−50185
Si-SiO_2 interface, electronic struct. calc. 80−100531
Si-SiO_2 interface, evolution of surface states density during bias temp. treatment 78−14832
Si-SiO_2 interface, form. and struct., AES obs. 79−56314
Si-SiO_2 interface, formed by anodic oxidation, F^- and Cl^- ions effect obs., on electrophysical properties of interface 79−15842
Si-SiO_2 interface, Hg probe *(Chinese)* 77−89857
Si-SiO_2 interface, high-resolution electron microscopy study 78−56046
n-Si-SiO_2 interface, hot carrier surface thermo EMF depend. on surface band bending 80−44734
Si-SiO_2 interface, hot electron capture process, expt. method for study 79−38180
Si-SiO_2 interface, improved characterisation, refined quasistatic and cond. methods 80−96990
Si-SiO_2 interface, in MOS struct., fast surface states density, electron irrad. effects 78−88042
Si-SiO_2 interface, in MOSFET struct., electronic props. 79−42662
Si-SiO_2 interface, intermediate chem. state of Si during sputter profiling, Auger spectra 79−11230
Si-SiO_2 interface, interface-state parameters near band edge, MOS conductance meas. 79−11226
Si-SiO_2 interface, inversion layer transport, radiation hardness effects, review 79−19673
Si-SiO_2 interface, ion implantation induced interface states, effect of oxidation and N_2 annealing 77−39949
Si-SiO_2 interface, light induced reson. centres, photocond. reson., EPR obs. 80−50184
Si-SiO_2 interface, model for doped-oxide-source diffusion with chemical reaction 77−39954
Si-SiO_2 interface, N_2 gas reaction, elec. and structural charact. 77−39950
Si-SiO_2 interface, Na^+ drifted, impurity bands in inversion layers 78−60211
Si-SiO_2 interface, oxidation stacking faults, growth rel. to self-diffusion 80−49239
Si-SiO_2 interface, props. 78−23170
Si-SiO_2 interface, props. variation in SiO_x region 80−49548
Si-SiO_2 interface, rad. hardness, carrier localisation in inversion layer 77−85332
Si-SiO_2 interface, radiation damage coeffs. for fission neutron and gamma-ray irrad. 80−34058
Si-SiO_2 interface, relax. of injected charge, temp. depend. 78−72269
Si-SiO_2 interface, remote polar phonon scatt. in Si inversion layers 80−80095
Si-SiO_2 interface, sputter profiling, ion knock-on mixing model 79−83081
Si-SiO_2 interface, stacking fault-free region formation by annealing 78−51561
Si-SiO_2 interface, surface states and elec. defects obs. using ESR 78−23169
Si-SiO_2 interface, surface generation velocity study, gate-controlled diode structure application 80−6986
Si-SiO_2 interface, surface states characterization, expt. techniques review 80−49949
Si-SiO_2 interface, thermally oxidised, oxide thickness effects on electron scatt. 78−88033
Si-SiO_2 interface, thermally grown, inhomogeneities of surface potential 80−34524
Si-SiO_2 interface, thermal SiO_2 sputter induced roughness, Auger sputter profiling study 80−75424
Si-SiO_2 interface, thermally grown, surface pot. inhomogeneities after stress ageing 80−92993
Si-SiO_2 interface, thermally grown oxide, spectroscopic ellipsometric anal. 80−107659
Si-SiO_2 interface, trapping props. from electrochemical current-voltage behaviour 79−69597
Si-SiO_2 interface, unwanted effects of ions in SiO_2 layers, review 80−92985
Si-SiO_2 interface, valley degeneracy splitting in n inversion layer, effective-mass approx. 79−99629
Si-SiO_2 interface, with Cl^- incorporated, characterisation by low temp. cond. meas. 78−60220
Si-SiO_2 interface charge effects and related props. 78−10575
Si-SiO_2 interface charge inhomogeneities effect on surface state density meas. by MOS AC cond. technique 78−14833
Si-SiO_2 interface in IGFETs, anal. of CVD SiO_2 on (100) and (111) surfaces, near-ideal structs. 80−100528
Si-SiO_2 interface in MIS struct., B^+ ion implanted, elec. props. due to laser irrad. 78−72272
Si-SiO_2 interface in MIS structs., effects of crystal defects on generation process 80−65702
Si-SiO_2 interface in MOS structs. low-energy electron beam irrad., charge accumulation process anal. 80−65701
Si-SiO_2 interface in MOS capacitors, lateral diffusion of Na^+, neutralisation 80−92986
Si-SiO_2 interface in MOS device, indirect tunnelling involving intermediate states 80−92994
Si-SiO_2 interface in MOS solar cells, operational charact. and struct. 80−93901
Si-SiO_2 interface layer characterisation by spectroscopic ellipsometry 80−50738
Si-SiO_2 interface morphology, P pileup effect, Auger sputter profiling 78−72006
Si-SiO_2 interface of MIS/SIS solar cells, automated surface states anal. 80−93966
Si-SiO_2 interface oxidation kinetics, high doping levels, theory 80−11827
Si-SiO_2 interface props., electrolyte anode polarisation effect 77−80849
Si-SiO_2 interface state density in MNOS structures 78−47873
Si-SiO_2 interface state distribution, Br incorporation effects 80−11091
Si-SiO_2 interface state density, dependence on thermal oxidation process variables 80−15607
Si-SiO_2 interface state density in ion-controlled diodes, acid-base exposure effects 80−96984

semiconductor-insulator boundaries continued
Si-SiO_2 interface states, effect on memory charact. of thin-oxide MNOS devices 79−82681
Si-SiO_2 interface states, deposition of H containing layers and annealing 80−92991
Si-SiO_2 interface struct. by cross-sectional TEM, amorphous oxide layer 77−24487
Si-SiO_2 interface struct., transient region 77−85115
Si-SiO_2 interface study by XPS 80−50507
Si-SiO_2 interface traps energy distribution meas., in MOS devices, under non-steady-state *(Korean)* 78−64119
Si-SiO_2 interfaces, local atomic and electronic struct., high resolution XPS 80−49927
Si-SiO_2 interfaces, near ideal, props. 80−80382
Si-SiO_2 interfaces, surface state form. during bias-temp. stress aging 79−78193
Si-SiO_2 interfacial region, nature of fixed oxide charge 78−56047
Si-SiO_2 interfacial regions obs., by XPS ultrathin oxide films 79−15039
Si-SiO_2 interfacial region on TCE/O_2 and CCl_4/O_2 oxidised Si, struct. and comp. 80−50741
Si-SiO_2 interfacial transition layer thickness, XPS obs. 80−11540
Si-SiO_2 inversion layers, applied stresses, cyclotron masses and CDWs 77−55596
Si-SiO_2 inversion layers, bound states at interface 79−42655
Si-SiO_2 laminar ion-implanted systems, struct. change investig. by MSSI method *(Russian)* 80−107918
Si-SiO_2 layer formation by O_2^+ ion implantation, interface struct. and C-V charact. 77−1142
Si-SiO_2 layers, physics, electron and ion motion, Cl, Na and K ion effects *(Dutch)* 80−60093
Si-SiO_2 layers on Si substrate, ellipsometric meas. 77−69403
Si-SiO_2 MOS capacitors, irradiated and avalanche injected, trapping effects 79−19669
Si-SiO_2 MOS interface, surface-state density and minority carrier generation rate, meas. by DLTS, hot hole effect 80−100527
Si-SiO_2 MOS interface states density, transient capacitance meas. eval. 80−92989
Si-SiO_2 microsensor, surface conductivity effect of aliphatic alcohol molecule adsorption *(Russian)* 78−34887
Si-SiO_2 new type of interfacial charge 78−23168
Si-SiO_2 structure, mechanical stress at Si(111) surface 78−63921
Si-SiO_2 structure, oxide charge evaluation, appl. of Kelvin method 78−19157
Si-SiO_2 structures, AS77 scanning analyser for electrophysical props. *(Polish)* 79−95498
Si-SiO_2 structures, B ions implanted, energy spectra of shallow traps at various implantation energies 80−80392
Si-SiO_2 structures, ion implanted, surface charact. 77−80850
Si-SiO_2 structures, scanning analyser of electrophysical parameters of MOS transistors *(Polish)* 79−91145
Si-SiO_2 surface states, influence of $\Phi ms(T)$ 79−99597
p-Si-SiO_2 system, C-V meas. using Au/Hg probe, work function difference between probe and Si 80−2450
Si-SiO_2 system, implanted with N, P and Te ions, refl. spectra and interference fringes 79−23629
Si-SiO_2 system, structural defect formation rel. to thermal oxidation kinetics *(Russian)* 78−43478
Si-SiO_2 transition region width, SIMS depth profiling 80−39454
Si-SiO_2 wafer thinning for TEM 77−89352
Si-SiO_2:B structure, AES meas. 77−39951
Si-SiO_2-Si capacitor, polycryst., capacitance voltage characterisation 80−70794
Si-SiO_2-Si structures, P, As depth profiles, ion microanal. *(Japanese)* 78−85251
Si-SiO_2-Si_3N_4, surface states, density and spectrum 77−69423
Si-SiO_2-$Si_xO_yN_z$ waveguide model *(Russian)* 79−10374
Si-SiO_2-SnO_2 structure, switching props. 78−76138
Si-SiO_2-polySi thin film structures, dielectric props. *(Slovak)* 80−75934
Si-SiO_2-polycryst. Si structs., field strength degradation exam. 77−4445
Si-SiO_2-vacuum system, principal angle and azimuth determ. 78−11009
Si-SiO_2(Si_3N_4), interface layer determ. by spectroscopic ellipsometry 79−95275
Si-SiO_2(SiN)(Si_3N_4) boundaries, thermal stresses, and cracking resist. of insulating films 78−63958
Si-SiO_3, effect of Au recomb. centres on interfacial trapping states 79−38175
Si-SiO_x, evidence for superlattices, magnetocond. expts. 77−89868
Si-SiO_x interface, localisation in inversion layer due to states in gap of oxide 77−12012
Si-SiO_x-SiO_2 interface, energy gap variation 79−91148
Si-thermal SiO_2-electrolyte system, cond. in superhigh elec. field 78−52080
n-Si-V_2O_5 system, carrier transport mechanisms 77−62999
SiC-anodic oxide, IR spectra *(Russian)* 78−11376
SiC-SiO_2 interface, Auger anal. 78−95375
Si_3N_4 layers, on GaAs, encapsulation, low-energy ion beam sputtering 79−78882
Si_3N_4-Si, photocurrents obs. 79−24092
SiO_2 film, ion bombarded, attenuated total refl. method obs. of H capture 79−95863
SiO_2 film, on Si, radiation damage structures, EPR obs. 78−95097
SiO_2 film, preferential etching on Si substrate, plasma reactive sputter etching 77−20448
SiO_2 films, grown in presence of O_2-trichloroethylene, room temp. negative bias instability 80−60102
SiO_2 films, on Si, role of H_2 79−69376
SiO_2 layers, anodic oxidation growth on p-Si, transmission electron diffr. obs. 79−28241
SiO_2 on Si, thermally grown, breakdown, review 78−23172
SiO_2, on Si, viscous flow meas., 960 to 1075°C 77−39729
SiO_2/InP interface formation, thermodynamic considerations 80−100529
SiO_2-Si, cathodoluminesc. and AES rel. to struct. 78−43937
SiO_2-Si, Cs doped, distrib. of impurity and oxide depth 78−6395
SiO_2-Si, insulator charges evaluation *(German)* 79−82682
SiO_2-Si, low-energy neutral particle bombardment of SiO_2 film, degradation 80−54790
SiO_2-Si, P ion implantation, electrical transport props. 80−39130
SiO_2-Si (n-type) interface, electrochem. etching 77−11799
SiO_2-Si in MIS, interface states, thermally stimulated charge decay 77−12009

semiconductor-insulator boundaries continued
SiO_2-Si MOS capacitor, two-stage process for building up of radiation induced interface states 80−20313
SiO_2-Si stratified system surface charges, adsorption and desorption effects *(Russian)* 80−49942
SiO_2-Si structure P^+ bombardment damage, exoelectron emission obs. 78−95383
SiO_2-Si:A, effects of recoil-implanted O on elec. activation of As 79−99227
SiO_2-Si:P, P pile-up at interface 78−84303
SiO_x ultrathin oxide on Si, struct. obs. by high-resolution electron microscopy 80−103592
SiO_x-GaAs, vacuum evaporated system, acoustoelec. signal, interface props. 80−75646
$(SiO_2)_x(Si_3N_4)_{1-x}$ on GaAs, deposition method and props. 78−91796
Si(100), inversion layer, interaction induced transition at low density 80−15581
SnO_2-Si, solar cell, max. theoretical efficiency 79−83598
ZnO ceramic varistors, I-V charact., single grain junction meas. 79−15225
ZnO/Si SAW structs., anal. of charge injection 80−80049
ZnO-Bi_2O_3-ZnO structure, injection currents, SCL and TSC obs. *(Russian)* 77−32068
ZnO-binder system, reciprocity failure, photoconductivity 78−39151
ZnO-SiO_2-Si monolithic convolver, long time storage of surface-acoustic-wave signals 77−1287
ZnSe-mica epitaxial heterostruct., growth and struct. 78−43257

semiconductor integrated circuits *see monolithic integrated circuits*

semiconductor junction lasers
acoustic DFB laser, high speed repetitive Q-switching 78−83007
acoustic distributed feedback, resonant acousto-optic interaction in degenerate semicond. 80−19036
active mode locking, effect of noise 80−19030
ageing and modulation in optical fibre links *(German)* 79−32042
$Al_xGa_{1-x}As/Al_yGa_{1-y}As$ heterostructure lasers, prep. charact., and CW reliability 80−58586
AlGaAs laser array with Si detector array for stabilization 80−58817
analogue video transmission feasibility using laser diode, over 30 km at 1.3 μm 80−58737
apparatus and applications *(Japanese)* 77−68215
applications and development *(German)* 77−61962
asymmetric waveguide structure semicond. laser, anomalous stimulated emission, theory 79−64228
asymmetric waveguide structure semicond. laser using external resonator, anomalous stimulated emission 79−64227
atom displacement as result of nonradiative recomb., defect form. mechanism 79−10308
automatic bias control cct. for injection lasers 78−71110
bent Guide structure semiconductor lasers, optimal ICs, appl. 79−41462
bent guide structure semiconductor lasers *(Japanese)* 78−87062
book, quantum electronics 80−105442
Bragg mirror, corner-reflector type, laser beam divergence reduction 80−91822
branching waveguide stripe injection laser, beam scanning and wavelength modulation 79−7138
buried heterostructure, dynamic behaviour 77−3592
buried heterostructure DFB laser investigation 77−31102
buried heterostructure laser, DH multilayer LPE growth on etched substrate, optical read-out appls., longitudinal mode operation 80−99749
buried heterostructure laser, fund. transverse mode operation, current limitation 78−55353
buried heterostructure laser, sinusoidal modulation charact. 78−87054
buried heterostructures, discrete or DFB 78−5499
buried strip geometry DH injection lasers, first derivative of I-V charact. above threshold 80−58533
buried-heterostructure laser packaging for wideband optical transmission systems 78−74920
calibration by IR spectra of OCS 80−83363
CdS, single crystals, laser emission from surface diffraction grating 80−95900
coherence analysis, meas. system with Michelson interferometer *(Polish)* 78−33762
communication device research in Japan 77−75677
communication sources, 1 μm range, LED and laser diodes 80−48448
communications transmitter, multipurpose IR emitters 78−30053
compact high power semiconductor laser array 79−10319
composite waveguide laser with end-fire excitation, output charact. 80−23738
conference, laser and electro-optical systems, San Diego, CA, USA (Feb. 1980) 80−62392
conference, Nemunosato, Japan (1976) 77−75509
construction, characteristics and applications *(German)* 79−13976
consumer's guide to laser diodes 80−14356
correlative data processing system using semiconductor injection laser 80−74307
correlator, laser diode lensless MSF holographic optical element 80−102663
corrugated waveguides, effective index approach to distrib. feedback, TE polarisation 80−102859
corrugated waveguides and lasers, improved coupled mode analysis 78−46842
corrugated waveguides and lasers, improved coupled mode analysis for TM mode 78−83117
coupled multiple stripe diode lasers, exptl. and analytic studies 80−5752
coupling efficiency of semicond. laser beam into fibre, matching element misalignment influence 80−48432
coupling from semicond. laser into tapered hemispherical end single-mode fibre 80−99827
coupling from semicond. laser to single-mode fibres, cylindrical lens method 79−76807
coupling of radiation to thin-film and fibre waveguides 77−19426
coupling techniques, to optical waveguides *(German)* 77−42613
coupling to fibre using cylindrical lens 77−75661
coupling to II-VI waveguides, transition struct. fabrication 78−38029
coupling to single mode fibre, by optical transition structure 78−42449
curved-line grating form., use as reflectors and laser resonators 77−88971
CW injection laser, oxide-defined stripe-geometry, low threshold current 79−59712
CW injection lasers and LEDs for optical communications 77−7210

semiconductor junction lasers continued
CW lasers, DH, with specific growth defects, degradation charact. 78−13713
CW stripe lasers, thermal-impedance ageing characteristics 80−64018
defect formation in active zone of heterolasers *(Russian)* 77−54712
defect-forming resonance electron capture, theory 80−14341
degradation, lattice defects *(Japanese)* 77−34889
degradation, review of recent expts. 78−82970
degradation *(Japanese)* 80−19032
degradation due to dark line defects 77−75523
degradation mechanisms, review 77−28630
degradation modes and accelerated life tests 78−1233
DFB, operating in higher Bragg interaction orders 79−89933
DFB film laser tuning using acoustic wave 77−58359
DFB for diode structure improvement *(German)* 79−89920
DH, degradation, internal parameter variations obs. *(Russian)* 77−61956
DH, single and dual-filament self-sustained oscillations, theoretical model 80−64023
DH, stripe geometry injection lasers, monolithic passivated, fabrication by selective chemical etching 77−10925
DH, top and side emission 77−79819
DH devices, interface recomb. effects on transient response 77−88722
DH devices, interface recomb. effects on transient response anal. 78−22127
DH diode lasers, appl. of equivalent-index method 80−23772
DH I-bar mesa lasers, for integrated optical circuits, selective LPE 78−6868
DH injection laser coupling to optical fibre waveguide 78−33851
DH injection laser with coherent light injection, modulation behaviour 78−55352
DH laser, model for static props. 79−98360
DH laser, thermal resistance and temp. distrib. calcs. and obs. 79−98368
DH laser, threshold current rel. to interface recombinations vels. 79−98369
DH laser configuration with passive transverse field confinement 78−33746
DH laser diode, elec. saturation behaviour anal. *(Korean)* 79−64225
DH laser diode, second harmonic distortion for threshold current, anal. *(Korean)* 80−87394
DH laser diodes, impedance charact. 80−23690
DH lasers, charact. explanation, multimode field theory 78−37880
DH lasers, current-crowded carrier confinement 80−78854
DH lasers, effect of impurities on quantum shot noise reson. 78−22132
DH lasers, phase and group indices 80−64016
DH lasers, symmetric waveguide, near and far-field analytical approx. for fundamental mode 79−50296
DH lasers, thermal-gradient enhanced current spreading 79−18416
DH lasers, three dimensional thermal problems 77−75554
DH stripe geometry lasers, three-dimensional anal. of mode props. 80−64020
DH stripe laser light source to meas. Faraday effect in single-mode optical fibre 80−48245
DH stripe lasers, field model 79−7128
DH stripe-geometry lasers, thermal props., interpretation of thermal resistance measurements 80−64017
dielectric facet reflector of alternating Al_2O_3 and Si layers 78−66841
dielectric optical waveguide charact. determ., far-field radiation patterns, semiconductor laser structure appl. 80−48407
dielectric transverse mode confinement semiconductor laser intensity fluctuation limits 80−48258
diffusion and rooftop etching technique 80−1227
diffusion-type stripe-geometry injection laser using V-groove, structure, fabrication process and props. 79−27277
digital optical fibre communication link for 1 Gbit/s *(German)* 79−81565
diode, direct modulation charact. 77−19251
diode, modulated, with short external cavity, single mode operation 80−5756
diode and transmitter unit lifetime tests *(German)* 78−37883
diode degradation acceleration techniques 79−50320
diode for single-mode fibre transmission systems, connector and laser module as interconnecting device 79−50422
diode laser, appl. to IR spectra of NH_3 mols. 78−58689
diode laser, closed-cycle refrigerator shock isolator 78−50796
diode laser, light feedback suppression, from optical fibre 79−1004
diode laser, optical isolator struct. simplification 80−1209
diode laser, principle of operation *(Polish)* 80−53294
diode laser, thermal time constant meas. method 80−99731
diode laser, vibr.-rot. spectrum of spherical top mols. 78−82734
diode laser communications for remote utility meter reading 79−86195
diode laser facet protective dielectric coating optimisation 78−63144
diode laser with spatial thickness var., anal. 80−102723
diode lasers as transmitter source in optical communication, modulation, power consumption, optical links 80−102807
diode noise in FM fibre-optic transmission system 79−45968
diode-laser-fibre coupling, effects of fibre propagation loss 80−74484
direct modulation for optical fibre transmission *(Japanese)* 79−41402
direct PCM improvement by optical feedback 78−1287
directly modulated, suppression of reson. in light output 78−66853
distributed, Bragg-reflector laser amplifiers, analysis 77−19348
distributed Bragg mirror continuous injection laser, operation and construction *(Russian)* 78−29972
distributed Bragg reflector injection lasers for integrated optics 78−42472
distributed Bragg reflector lasers, tunability using electro-optic effect 77−38938
distributed Bragg reflector optical resonator, response to light pulses 78−63141
double heterojunction laser diodes, design curves 78−50776
double heterostructure type, US wave freq. modulation anal. 78−83009
double-current-confinement channelled-substrate struct., near-field and beam-waist position 80−106553
dynamic behaviour, lateral mode and carrier density profile effects 78−82968
dynamic characteristics, effects of spontaneous emission 77−14713
electrical characteristic for operation in threshold vicinity, analytic expressions 78−22131
electron beam pumped semiconductor laser, use of periodic structs. with special profiles 80−95923
semiconductor junction lasers continued
electron beam pumping efficiency, coating effect 80−91795
electron-beam-induced stripe waveguide laser 80−28237
electron-beam-pumped laser, variable-gap struct. 79−31902
electrooptic polarization modulated injection laser 80−58591
EM models, Epstein layer and dielec. slab 77−79829
emission characteristics of laser with composite waveguide 79−72592
end-fire coupling of laser diode into $LiNbO_3$:Ti waveguides 79−94368
energy photometry, meas. of parameters of pulsed and steady-state radiation 79−14007
epitaxial growth with moulded reflectors 78−42347
Epitaxial waveguide laser with distributed second-order feedback by electron excitation *(Russian)* 78−29973
excitation generator for GaAlAs semicond. injection lasers 78−33748
exponentially decaying gain medium, waveguiding 78−50774
external cavity, linearized theory 80−69391
External cavity operation with complete removal of sub-cavity effects for mode-locking injection lasers 80−58545
with external dispersive resonator as narrow-line tunable emission source *(Russian)* 77−83898
external optical feedback effect on props. 80−58535
external resonator coupled diode lasers, tutorial review 79−94231
external resonator injection laser, threshold temp. depend. at fixed wavelength 78−25882
external selective mirror ^{133}Cs vapour, 852.1 nm pulsed stimulated emission 79−45961
fabrication reproducibility of laser diodes *(French)* 78−42357
fast laser modulation with GaAs MESFETs 77−88797
ferromagnetic ordering, radiation polarisation *(Russian)* 78−9384
fibre bandwidth determination in time domain, OTF meas., laser diode source evaluation 80−79002
fibre communication, elimination of polarisation in optical isolators 80−5844
fibre communication devices, directional couplers, atennuators, switches development 79−3782
fibre communication lines, use of semicond. lasers and avalanche photodiodes 78−46793
fibre communication technology, state of art *(Czech)* 78−5575
fibre coupled diode lasers, LF noise meas. 80−58542
fibre optic communication link, 500 MHz, injection laser diode 77−79964
fibre optic communication systems, sources and detectors 78−42412
fibre optic communication systems, utilisation of optoelectronic devices 80−1328
fibre optics transmitter, improvements *(German)* 77−11008
fibre-optic LED and laser source and Si photodetector development 78−42430
fibre-optic transmission by laser diode analogue baseband modulation 80−58738
for fibre-optic transmission systems 77−19342
fluctuation phenomena, injection laser characteristics due to reflected optical power 79−81428
Fourier transform spectrosc., new developments−passive heterodyne spectrosc. and diode laser absorpt. spectrosc. 80−95148
frequency self-modulation interpretation 80−64028
gaAlAs diode sources for laser-doppler anemometry 79−14499
GaAs laser diode power supply control cct. *(German)* 80−78852
GaAs laser diodes for optical communication transmission *(German)* 80−28252
GaAs-$Al_xGa_{1-x}As$ DH laser for optical communication 77−50684
GaAs-$Al_xGa_{1-x}As$ strip buried heterostructure laser densely packed monolithic linear array 79−45956
GaAs-$Ga_{1-x}Al_xAs$ DH crystals, <110> oriented dark line defects 77−80510
gain suppression in injection lasers 79−98372
gain-guiding double-heterostructure laser transverse carrier diffusion effects 79−55139
gain-guiding stripe-geometry DH semiconductor laser oscillation characteristics 79−45945
gain-guiding stripe-geometry DH semiconductor laser small-signal modulation characteristics 79−45946
generalised expressions for turn on delay 79−94233
glass fibre long wavelength optical communication, materials and devices, review 80−99854
guided-wave optical signal processing, diode laser sources and photodetectors 80−48465
guided-wave optical systems and devices, seminar, Washington, USA (April 1979) 80−31418
harmonic distortion analysis of injection lasers 80−58537
harmonic distortion in direct modulation of injection lasers 79−68411
heteroepitaxial structures based on III-V compounds, appl. in optical electronics, defect form., review 78−23160
heterojunction, 40 ns 55 A pulse generator for driving, cct. *(Polish)* 79−3701
heterojunction laser and LED reliability rel. to facet damage and nonradiative centre formation 78−5472
heterojunction laser diodes, book contrib. 80−99733
heterojunction lasers, for fibre optic data systems 79−55149
heterojunction lasers, partially homogeneous broadening and saturation, non-oscillating mode suppression 80−99775
heterojunction lasers for fibre optic appls., technological advances 79−36933
heterolasers, active layer, photoluminesc., temp. depend. *(Russian)* 79−10310
heterolasers, degradation at high temp. *(Russian)* 79−50298
heterostructure laser, elec. characterisation 78−79020
heterostructure laser, quantitative characterisation using differentiated electron-beam-induced current 79−55137
heterostructure lasers, fundamental principles, book 79−36899
high resolution measurement of laser output spectrum 80−95891
high speed direct modulation methods 77−10965
high-power coupled-multiple-stripe phase-locked injection laser, beam charact. 79−50307
high-power radiation propagation, rel. to interband absorption or amplification 79−76727
high-speed optical systems at 0.85 μm, modal noise and optical feedback 80−87323
hologram recording using a visible single-mode GaA/As CW emitted diode laser 80−95839
holographic memory devices, optoelectronic ROM memory, injection laser appls. in construction *(Polish)* 80−19007

semiconductor junction lasers continued
holographic memory readin system parameter optimisation *(Russian)* 78−13670
holographic selector in external resonator 79−98406
holographic storage device appl., expt. *(Russian)* 78−37824
homo- and heterojunction, history and development, new constructions *(Polish)* 80−91794
homojunction, gradual degradation process, expt. *(Polish)* 77−68213
homostructure injection laser mode form., spatial, spectral and temporal meas. 77−79821
III-V semiconductor, MBE and applications 78−11135
III-V semiconductor epitaxial ultra-thin layers, bevel cross sectioning 79−74275
III-V semiconductors, electrolum. and related props., book contrib. 77−73173
III-V semiconductors, p-n heterostructures, epitaxial growth techniques, appl. to optoelectronics, review 80−54770
III-V semiconductors, radiative recomb. and related phenomena, conference, Prague, Czechoslovakia (Sept. 1979) 80−51940
index-guiding structure injection laser, single longit. mode operation 79−98362
injection, defect-induced pulsations, theory 80−91793
injection, performance characts., with external gratings, cavity mounted 78−1274
injection (Swan) laser, planar stripe-geometry with waist/notch 79−13975
injection hetero laser with low generation threshold current at room temp. *(Russian)* 77−38943
injection heterolaser coupling into fibre waveguide, operation regime influence on efficiency 79−59834
injection laser, bias quenching of relaxation oscillations 79−72570
injection laser, comprehensive model, current depend. of spontaneous and coherent emission 80−74361
injection laser, intensity pulsation enhancement by self focusing 80−48253
injection laser, matching to optical fibre, use of graded-index fibre 79−32069
injection laser, minimum line width meas. 79−68396
injection laser, optimum pulsed pumping conditions, for communications appls. 77−75525
injection laser, output instabilities related to optical gain and lasing conditions 80−1203
injection laser automatic level control by optoelectronic feedback *(German)* 78−33883
injection laser developments and prospects 77−68221
injection laser diode coupling to planar waveguide 80−33245
injection laser diode mode structure enhancement by backface plating 80−64056
injection laser diodes for fibre optic communication 78−33751
injection laser light sources for optical fibre transmission 77−54777
injection laser longitudinal mode stabilisation by temp. compensation 79−45964
injection laser modulation using diode cct. 77−79935
injection laser mounting in single heat cycle 78−82982
injection laser oscillators, pumping via generator producing rectangular pulses 77−27299
injection laser output regulation by NTC resistor cct. 80−14353
injection laser pumping by thyristor oscillator 79−13982
injection laser switching, effect of gain saturation 79−86180
injection laser transmitter module, emitter unit, driving and control circuits *(French)* 78−46636
injection laser with composite resonator, active region internal parameters determ. 80−106548
injection laser/optical waveguide connection module 78−59023
injection lasers, current depend. of spontaneous emission and junction resist. 79−59699
injection lasers, integrated optical components 79−36932
injection lasers, internal quantum efficiency, algorithm for meas. 78−66822
injection lasers, intraband electronic relaxation effect on relaxation oscillation 79−81433
injection lasers, optical ringing effects, internal loss modulation and direct modulation 78−87081
injection lasers, output depend. on inhomogeneous bonding 80−64015
injection lasers, stripe geometry, nonlinearity in power output-current characts. 77−83875
injection lasers, theoretical spontaneous emission factor in the rate eqn. using classical EM theory 78−9383
injection lasers and appls., fundamental aspects *(German)* 80−23688
injection lasers operated with HF modulation, intensity fluctuations calc. 78−22123
injection stripe lasers, current carrier conc. distrib. *(Russian)* 78−13712
injection-laser optial repeater, pump signal by Gunn diode *(Russian)* 77−83974
InP-InGaAsP-InP, low threshold laser, threshold density temp. depend., LPE method *(Russian)* 78−22133
integrated and guided-wave optics, conference, Incline Village, NV, USA, January 1980 80−58772
integrated optics uses of heterostructures 77−39112
integrated twin guide lasers, axial mode selectivities 77−75519
integration with Gunn oscillator on semi-insulating GaAs 78−71232
intensity modulation in GHz region, image tube streak camera obs. 80−87417
intensity self-pulsation simulation in CW lasers 79−94232
interval modulation semiconductor laser communication system 78−9331
intracavity absorption spectroscopy, using semicond. injection laser 79−7157
intrinsic noise in optical communication systems 80−69394
intrinsic resonant freq., near-threshold behaviour 79−98367
inverted-ridge-waveguide DH injection laser with current and lateral optical confinement LPE growth 77−75540
IR, for 16 μm range, review *(Rumanian)* 80−87408
IR, tunable, review 78−13724
IR analytical instrumentation using tunable diode lasers 80−16762
IR diode laser for double-beam spectrometer 79−17510
IR emitting diodes and injection lasers, optical communication appls. 80−58563
IR laser for optical fibre communication 77−88745
IR spectra, intermode calibration using tandem etalons 80−32982
IR torch using semiconductor DH laser diode 77−39101
IV-VI multicomponent solid solutions for improved lasing 78−1232

semiconductor junction lasers continued
IV-VI narrow gap semiconductors, fabrication, IR laser and detector appls. 77−77415
IV-VI optoelectronic devices, MBE techniques 79−95942
laser diodes for optical fibre transmission systems, reliability tests 80−43464
lasing characteristics, transverse modes *(Japanese)* 79−81432
lateral mode selection 77−79861
lecture on optoelectronic devices 78−25990
lens-coupled, hermetic packaged, for wideband optical-fibre transmission 79−45970
level-control circuit for high-bit-rate system using slope detector 79−18430
light sources, physical principle and appl. *(German)* 78−71108
light sources for optical communications *(Japanese)* 79−27406
light versus current characteristic simulation using optoisolator 79−22960
lightwave transmitter, output stability, beam displacement and front/back mistracking effects 78−79059
linearised LED and laser transmitters, for analogue fibre optical systems 78−46818
long lived diode laser manufacture and test procedures 80−9895
long range injection laser radar 78−5549
long wavelength light sources, 1.06 to 1.6 μm range, review 79−45969
longitudinal model structure, depend. on injected carrier diffusion 77−54710
low-threshold-current injection laser with built-in passive waveguiding 80−64029
Luneberg lens for laser diode coupling to graded-index fibre *(German)* 78−33875
magnetic birefringence influence on stimulated emission spectrum 78−17941
matching of semiconductor sources to thin-film planar and stripe waveguides 80−64174
material requirements, multicomponent solid solns. for 0.32 to 32 μm range, review 77−14718
materials technology, review *(Polish)* 80−19029
MBE, device appls. 80−25570
MBE growth *(Japanese)* 79−38749
MBE of injection lasers, integrated optics device fabrication 79−90042
mear and far field characterization 80−48242
meas. generators of optical pulses appl. 80−23711
memory disc appl., large capacity (ten billion bits), Philips development 79−81369
mode competition in homojunction and single-heterojunction injection lasers 79−31901
mode composition of injection laser, control with selective cavities 80−19037
mode deformation due to self-focusing, rel. to output charact. nonlinearity 79−13966
mode locking, simplified theory 80−64021
mode locking to external resonator, theory 80−106550
mode patterns display and recording, spatial and spectral resolution 78−29955
mode selection and control, radiation freq. modulation, self-focusing *(Polish)* 80−19035
modulated optical output, relax. oscills., superradiation effects 77−7150
modulation, high-bit-rate pulse regeneration and modulation using planar Gunn device 79−59731
modulation, non-linear distortions, communication systems appl. *(German)* 80−69395
modulation at high bit rates 77−7151
modulation with 1 ns pseudo-random impulses 78−50836
modulator using bipolar transistor, high speed 78−1288
monolithic integration of laser and laser amplifier or detector, using AlGaAs twin guide structure 78−38082
monolithic integration of LOC-DBR lasers and optical components 78−38081
monolithic laser-waveguide coupling by evanescent fields 77−39110
monolithically integrated lasers and amplifiers using cleaved substrate technique 80−58590
monomode injection laser, sideband upconversion 78−79047
MOS injection laser, single heterostruct. 78−59005
multi-mode diodes, dynamic mode interaction 78−55354
multichannel communications applic., characterisation 78−87165
multichannel GaAs laser array output synchronisation 78−42417
multilayered structures containing optically active medium, absorption and amplification of light *(Japanese)* 80−19052
multimode generation *(Russian)* 78−55357
multiple-quantum-well laser, optical analysis, three-region waveguide model 80−14337
narrow band gap semiconductor, props. and optoelectronic appls. *(German)* 77−20356
narrow band gap semiconductor IR devices, advances 80−48464
narrow double-current-confinement channelled-substrate-planar laser fabrication by double etching 80−64073
narrow gap semiconductors, stimulated emission characts. 79−31903
narrow planar stripe laser, lasing characts. 77−38891
narrow stripe geometry, non-Gaussian fundamental mode patterns, waveguide model 78−94394
narrow stripe injection laser, voltage and current spatial var. 78−17936
narrow stripe laser with widths down to 3 micron, characts. *(German)* 79−41381
near IR (1 to 2 μm) optical communications, colloquium, London, England (May 1980) 80−86040
near-zone radiation field delay fluctuations, HF AM 77−61987
noise phenomena 80−58538
noise properties of injection lasers due to reflected waves 79−36897
optical communication, components development *(German)* 79−81563
optical communication conference, Munich (1977) *(German)* 78−33854
optical communication log-normal device optimal burn-in time 80−58743
optical feedback effects in CW injection lasers, using external reflecting surface 78−79045
optical fibre communication, cabling, light source and receiver technology, review 78−59125
optical fibre communication appl., characteristics and state of art *(Italian)* 80−58569
optical fibre communication equipment 80−43459
optical fibre communication system components, state-of-the-art survey *(German)* 80−69538
optical fibre communication system device, review 79−76858

semiconductor junction lasers continued
optical fibre couple, lasing spectra 80—1202
optical fibre coupling, efficient coupling using taper-ended multimode optical fibres 77—3657
optical fibre coupling circuit using cylindrical lens and Selfoc lens combination 77—79931
optical fibre interconnection *(Danish)* 77—88911
optical fibre light sources for 1.0 to 1.2 μm emission, review 77—38894
optical fibre mode excitation *(German)* 78—50921
optical fibre sources and detectors *(Italian)* 80—69390
optical fibre transmission capability expansion 78—66914
optical fibre transmission system devices *(Japanese)* 80—58693
optical fibre-laser transverse coupling and front-mirror monitoring for feedback control of laser transmitters 80—33151
optical isolators for semiconductor laser, in laser-to-fibre coupling module 80—48267
optical mode spectra, photodetector scanning and IR photography 80—48257
optical radiation generators, for power pulse meas. 80—23710
optical systems using caustic region or antiwaveguide struct. 77—61972
optical transmitter laser diode module description and performance 80—64069
optical transmitters, laser diode switching dynamics and noise *(German)* 79—89919
optical waveguiding in semiconductor injection lasers and integrated optics 77—14807
optically pumped, elec. cond. calc. 77—15888
optically pumped, mode broadening due to transient heating 77—75517
optoelectric systems on injection lasers 78—42464
optoelectronic devices and optical imaging techniques, book 80—27059
output power and coherence length in incoherent feedback 79—98412
output relax. oscill. suppression by elec. reson. cct. 77—88798
output stabilisation by mirror close to laser facet 79—45954
output stabilization by bevelled-end fibre coupling 80—91806
oxide stripe heterojunction lasers, asymm. modes 78—59006
pattern effect minimization at high-rate pulse modulation 80—19059
PCM of injection laser radiation, optimal conditions 79—59733
phase-modulated optical carrier detection using conductor laser source 80—64159
photon spectrum and distribution function, analogy with nonideal Bose gas 80—23689
photopumped, III-V semiconductor, book contrib. 80—99732
photoresist microlens production 78—9398
picosecond pulse generation scheme for injection lasers 80—87418
picosecond pulse generation using reson. oscill. 80—87391
planar stripe laser with deep Zn diffusion, stable transverse mode oscill. 80—14338
planar stripe lasers, very narrow, reduction of quantum noise 78—37901
planar stripe-geometry injection laser, SWAN, mode control 80—48281
plano-convex waveguide transverse-mode-stabilised laser, optical quality, static and dynamic characts. 80—69419
polarisation control, mode competition 77—75515
pressure-tuned diode laser, appl. to high-resolution spectroscopy 80—82835
properties and appls., reliability *(German)* 80—19034
pulse radiation, coherence rel. to Fourier hologram recording 78—50738
pulsed diode simulators of solid lasers $Al_xGa_{1-x}As$ and $Ga_xIn_{1-x}P_{1-y}As_y$ solid solns. 80—91816
pulsed laser communications 79—22972
pulsed Pb salt tunable diode laser appl. to micrometer IR detect. 80—13148
pump for $LiNdP_4O_{12}$ laser 77—75552
pumping, pulse generator cct. parameters 78—74919
pumping thyristor current pulse generator 78—79024
pumping thyristor nanosecond current pulse generator 78—79025
pumping with nanosecond source 77—14746
Q-switching, using electro-optical props. of Bragg reflectors 77—19345
quantum noise, theory 78—1228
quantum noise of injection lasers in optical fibre communication systems 80—48259
radiation coherence, interferometric analysis methods *(Polish)* 80—19065
radiation pattern of diode-laser transmitter *(German)* 78—55367
radiation sources for 1.1 to 1.6 μm range, p-n heterojunctions based on III-V and II-VI semiconductors *(Czech)* 80—32983
recent advances at MIT Lincoln Lab. 78—82969
relaxation oscillation in laser diodes, electron-photon lifetime ratio effects 77—50673
relaxation oscillations, effects of external injection and diffusion of excited states 77—61950
relaxation oscillations, suppression, by chemical etching on cleaved facets 78—25881
resonancelike peak reduction in direct modulation due to carrier diffusion 78—74905
with restricted area contacts, characteristics and control 77—19324
review 77—38892
review of recent progress in cryst. growth, processing and characterisation for reproducibility 78—17938
review of semicond. heterostructures, elec. and optical phenomena, discrete devices 78—72250
review of semiconductor diode lasers, book contrib. 80—106525
room temperature DH laser, appls. 78—66844
scalable tunable IR laser operating characteristics and limitations 77—54713
scanning optical microscope using semiconductor laser with longitudinal electron pumping 80—18012
selection criteria, w.r.t. performance, mounting and appl. 80—69407
self pulsing due to deep level traps 79—22950
self-sustained pulsations 80—106522
SEM evaluation *(Japanese)* 77—71992
semiconductor-waveguide-laser amplifier, with anisotropic gain by drift carriers 77—79818
sender element for optical fibre systems *(German)* 77—75674
short injection lasers using pump pulses, unique lasing features 78—82971
short resonator injection heterojunction laser, construction and output radiation characteristics 79—98408
simultaneous feedback control of bias and modulation currents for injection lasers 80—43332
single frequency injection laser diodes for integrated optics and fibre optic appls. 80—1237
semiconductor junction lasers continued
single heterostructure, spatial distrib. of radiative recomb. rate, time delays and Q-switching 79—22953
single heterostructure laser diode, pulse operating, anal. of temp. decrease in active region 78—13706
single laser diode CW output power limitation *(German)* 78—37886
single longitudinal mode oscill. by optical coupling 78—22157
single mode, spontaneous emission spectrum dip observation, generation saturation *(Russian)* 79—76691
single mode, with planar stripe structure 79—89907
single mode criteria at high speed pulse modulation 79—10305
single mode semiconductor laser *(Japanese)* 80—14339
single-channel injection laser manufacture and characteristics 77—38893
single-mode, fabrication and oscillation characts. *(Japanese)* 80—28231
single-wavelength oscillation at high speed pulse modulation 79—7129
sinusoidally modulated laser, phase shift of light output 79—98365
slab waveguide, TE Mode dispersion rel. to DH semiconductor lasers 80—91886
spatial coherence and modal struct. 80—87531
spatial coherence studied with reversing front interferometer 80—32993
spectral dynamics, carrier diffusion, higher order transversal modes 77—75522
spectral modulation behaviour of injection lasers, theory 78—50775
spectrometer, diode laser dual-beam, long-term temporal and scanning characts. 80—90902
spontaneous emission factor calculations, DH junction laser with gain-induced waveguide, spontaneous emission factor calc. 79—81429
spontaneous emission linewidth, calcs. 77—10927
spontaneous-emission coupling on number of excited longitudinal modes 79—18417
sputtered amorphous film heterostructure solar cell and laser fabrication 78—64472
stabilisation of radiated power, electronic 80—23702
state of research, review *(German)* 79—7146
state-of-the-art injection lasers 80—1236
stimulated emission, principle of operation *(Polish)* 80—53293
stimulated emission threshold of semiconductor, surface recombination influence 79—10311
strip geometry DH with linear characteristics 77—75542
strip-buried heterojunction laser, high-power fundamental transfer mode 78—46618
stripe contact injection lasers, heterostructure model, lateral mode control 80—14342
stripe geometry, launching efficiency into optical fibre determination 78—42406
stripe geometry, longitudinal field control 77—38888
stripe geometry, self focusing dynamics 78—29954
stripe geometry, self focusing obs., comprehensive model 77—79826
stripe geometry diode laser, gain induced waveguiding 78—59007
stripe geometry injection laser, lateral transverse mode instability and stabilisation 79—98358
stripe geometry injection lasers, horizontal mode deform. and anomalous lasing props. 77—19252
stripe geometry injection lasers, mode deformation effects on modal gain 79—81434
stripe geometry injection lasers, rigorous boundary value soln., for lateral modes 78—71100
stripe geometry junction laser, waveguiding mechanism 77—75521
stripe geometry laser, device geometry effect on lateral mode content 79—98363
stripe geometry laser, oxide-insulated narrow stripe, lateral mode behaviour 79—98359
stripe geometry proton-isolated DH lasers, thermal resistance models 78—37881
stripe geometry semiconductor lasers, transverse mode stabilisation 80—99774
stripe injection DH laser, radiation emission kinetics 79—64229
stripe laser high-speed modulation, noise, and nearfield meas. *(German)* 78—37923
stripe lasers, multimode rate eqn. description of homogeneous spectral broadening 78—79018
stripe lasers, twin-transverse junction, dielec. const. of inbuilt waveguide, injection current effect 79—50294
stripe-contact heterolasers, watt-ampere characts. 80—14340
stripe-geometry, active waveguides modes with inhomogeneous gain profiles 78—79017
stripe-geometry, below threshold waveguiding 77—46720
stripe-geometry, cladded parabolic index profile waveguide model 78—22205
stripe-geometry DH laser, lateral waveguiding below lasing threshold 79—98361
stripe-geometry heterojunction lasers, review 80—53288
super-DFB single-mode laser with periodic stripe width variations 80—58574
supercondensate photon spectrum *(Russian)* 77—27289
superlattice structures of semiconductor thin films, laser appl. 80—100418
symmetric DH, TE_0 mode radiation confinement factor, analytical approx. 78—46603
symmetric DH laser, beamwidth approx. for fundamental mode 79—22952
technology and present status *(German)* 80—58561
telecommunication appl., development *(Italian)* 77—773
telecommunication line, fibre optical, using 1.3 μm emitting semicond. heterolaser 79—64346
temperature compensated semicond. junction laser module for optical fibre communications 80—5757
temperature-compensating drive circuit using Si bipolar transistor, for injection lasers used in optical communications 79—45971
ternary semiconductors, pot. practical appl., review 79—10344
terraced substrate DH laser, fundamental transverse mode oscillation *(Japanese)* 80—78856
thermal characteristics determ. method 80—91800
thermal compensator for closed-cycle refrigerator stabilisation 78—50797
thermal impedance measurement technique 78—13705
thin film lasers and waveguides with arbitrary refr. index distribs., optical processes 77—79971
thin-film periodic structures, optoelectronic devices appls. *(Polish)* 78—50947
thin-film waveguide laser amplifier with lossy cladding 80—64074

semiconductor junction lasers continued
threshold current density for DH diode lasers, optimal cavity design 79−94259
threshold current temperature dependence potential barrier height influence 80−53296
TJS, single mode oscill. with low threshold currents, for optical communication 80−14355
TJS single-mode junction-up lasers, accelerated life tests 80−19045
transient effects, time delay and Q-switching 77−75513
transient processes, external optical feedback influence 79−50297
transient response of DH devices approx. techniques 78−68078
transient stimulated emission from optically coupled lasers 77−23678
transients in injection lasers, phase-plane anal., effects of absorbing section 80−64022
transmission system, semiconductor device reliability tests 80−58573
transport phenomena, junction effects and devices, book 80−98766
transverse junction stripe injection laser structural improvement 80−23687
transverse junction stripe laser diodes, with low threshold current and single-mode operation *(Japanese)* 79−86188
transverse junction stripe laser with buried p-region, high temp. CW operation 78−71111
transverse junction stripe lasers, dynamic props. 77−75520
transverse mode control by strip loaded waveguide 77−75543
triggerable laser, light-coupled logic appl. 80−74360
tunable coherent light sources, nonlinear freq. mixing, Raman, and semicond. lasers 77−7131
tunable diode, construction and operating characts. 77−27304
tunable diode laser, for high resolution matrix IR spectroscopy 78−45739
tunable diode laser, saturated absorpt. in NH_3 78−94239
tunable diode laser for IR-spectroscopy *(German)* 80−43361
tunable diode laser instruments, appl. advanced meas. and anal. 77−75600
tunable diode laser spectrometer, rapid-scanning computer-controlled 80−101854
tunable diode laser spectrometry, noise reduction in appl. to hot gases 80−31909
tunable diode laser spectroscopy in IR, techniques and calibration with HCN ν_2-lines 79−71542
tunable diode laser-CO_2 laser, heterodyne spectrometer, meas. of 2sQ(1,1) in NH_3 $2\nu_2$-ν_2 79−75626
tunable diode lasers and applications 78−25886
tunable diode lasers for spectrochem. anal., construction, appls. 78−33745
tunable IR diode lasers appls. to high resolution spectroscopy 80−58562
tuning, electro-optical, wide band, using birefringent filter 77−23689
tuning using autonomous high-press. chambers 77−46742
twin-guide laser, narrow radiation angle for optical fibre coupling 78−46628
twin-guide lasers theory, oscillation conditions and efficiency calc. 77−62076
two-resonator systems as multivibrators and flip-flops 77−79839
ultra-short light pulse generation, review *(Japanese)* 79−45973
variable band gap heterojunction laser spectral characteristics *(Russian)* 79−94236
very narrow conducting stripe lasers, symm. and asymm. waveguiding 79−36896
wave-number stability of laser diode mounted in closed-cycle He refrigerator 80−31906
wavelength extension, difference freq. generation in nonlinear optical waveguide using IR generator 80−33084
wavelength monitoring using fibre interferometer 80−74413
window-stripe high power laser, deep Zn-diffused stripe region, characts. 80−69419
(Al,Ga)As, ageing-induced self-pulsation stabilisation and initial degradation elimination by facet coatings 80−43347
(Al,Ga)As, CW long-life laser, use of half-wave Al_2O_3 facet coatings 77−23688
(Al,Ga)As, channelled substrate planar struct. injection lasers 77−71996
(Al,Ga)As, DH, light-current-voltage characts., derivative measurements 77−3584
(Al,Ga)As, DH, threshold current var., optical scatt. losses 77−3588
(Al,Ga)As DH diode laser, double-dovetail constricted, single mode CW operation 79−22949
(Al,Ga)As DH injection lasers, internal quantum efficiency, algorithm for meas. 78−66822
(Al,Ga)As DH injection lasers, sustained oscills. depend. on DC current bias 79−68392
(Al,Ga)As DH injection lasers, ambipolar transport 80−64025
(Al,Ga)As DH laser, effect of mounting on pulsed threshold 78−13711
(Al,Ga)As DH laser, pulsations produced by saturable absorber Q-switching, possible model 79−81426
(Al,Ga)As DH laser degradation, facet oxide formation 79−86185
(Al,Ga)As DH lasers, temp. accelerated ageing and degradation characts. 78−22130
(Al, Ga)As DH lasers, water role in gradual degradation 80−74379
(Al,Ga)As DH lasers, superlinear emission characts., negative resist. obs. 80−95895
(Al,Ga)As, DH stripe-geometry CW laser, junction voltage saturation 77−23675
(Al,Ga)As DH wafer, Al distrib. meas. 77−7994
(Al,Ga)As double heterostructure, comparison of deep and shallow proton bombardment fabricated devices 80−99724
(Al,Ga)As double-heterostructure lasers degraded, deep-level changes during accelerated ageing at high temps. 80−74356
(Al,Ga)As injection lasers, pulsations and adsorbing defects 79−94234
(Al,Ga)As long-lived DH injection lasers for fibre optic communication, degradation exam. 78−50778
(Al,Ga)As proton-bomard. stripe-geometry DH lasers, optical nonliniarities and optical spikes 79−55138
(Al,Ga)As, stripe geometry DH, threshold for amplitude stabilised oscill. 77−7084
(Al,Ga)As:Zn planar stripe lasers with deep Zn diffusion, guiding mechanisms controlled by impurity concs. 80−78853
(Al,Ga)As-GaAs, transverse junction stripe, high temp. single mode CW operation 78−74918
Al-Ga-As heterostruct. with confined current flow, fabrication 78−68081
AlAs-GaAs, strip heterolaser, O^+ implantation optimisation, relative threshold current density *(Russian)* 78−1230
AlAs-GaAs heterostructure, fabrication by selective liq.-phase epitaxy 79−15618
AlAs-GaAs stripe heterojunction laser, O^+ implantation effect on threshold characts. 79−41383
AlGaAs buried heterostructure lasers, gain and absorpt. spectra meas. 80−91792
(AlGa)As, CW, accelerated ageing effect on optical props. 77−38898
AlGaAs CW heterolaser, hysteresis of output radiation power 79−64230
AlGaAs CW injection heterostructure laser, with second order distributed Bragg reflectors, exam. 78−37907
(AlGa)As, CW laser diodes, long-term lifetests at room temp. 79−22963
(AlGa)As CW narrow stripe injection laser with induced waveguide, expt. props. 80−32988
AlGaAs CW oxide defined stripe laser, optical feedback effects 78−79045
(AlGa)As CW oxide-defined stripe laser, reliability statistical study 79−76687
AlGaAs constricted DH diodes, stable single filament laser action obs. 78−55358
AlGaAs constricted DH laser with large optical cavity, CW high-power single-mode operation 80−48276
(AlGa)As DH, proton-striped, proton-induced defects, photoluminesc. study 80−48251
(AlGa)As DH, short wavelength, degradation 78−63119
(AlGa)As, DH, stripe geometry second derivatives of elec. characts. obs. 77−10923
(AlGa)As DH CW laser diodes modulation characts. 77−38965
AlGaAs DH diode laser, ps optical pulse generation with RF modulated 80−9882
AlGaAs DH injection phase-locked laser, coherence 80−102726
(AlGa)As DH laser, insulating C film deposition to prevent facet deterioration 78−87049
AlGaAs DH laser, self-pulsations due to proton bombarded region self-annealing during ageing 80−99728
(AlGa)As, DH laser, threshold current temp. depend. 79−81431
(AlGa)As DH laser degradation due to facet oxidation 78−42336
AlGaAs DH laser epilayer struct. optimization for integrated optical circuits 80−99879
AlGaAs DH laser mirror degradation mechanism and lasing characts. changes 80−9919
AlGaAs DH laser preamplifier to improve optical receiver sensitivity 80−53316
AlGaAs DH laser with external grating oscillation properties 80−48247
(AlGa)As DH lasers, catastrophic optical damage generation mechanism, TEM obs. of dark line defects 80−100239
(AlGa)As DH lasers, comparison of 'normal' lasers and lasers exhibiting light jumps 80−106519
(AlGa)As DH narrow stripe injection laser with rigid waveguide, expt. props. 80−32987
AlGaAs DH short wavelength lasers, internal stress and degradation 79−68393
AlGaAs DH stripe geometry lasers, spontaneous radiation, carrier conc., and threshold current, luminesc. meas. 79−36898
AlGaAs DH stripe laser, spontaneous emission factor 77−75514
AlGaAs DH stripe laser, side lobe suppression by Te facet coating 80−5744
AlGaAs double heterostruct. laser, 'window-stripe', high power emission 79−72566
AlGaAs, fractional spontaneous emission coupling, power fraction, expt. evaluation 79−959
AlGaAs, having optical waveguiding 77−42540
AlGaAs heterojunction laser, single transverse and longit. mode operation 78−37887
AlGaAs heterojunction laser diodes for optical analogue link, evaluation 79−68395
AlGaAs heterojunction diode as light source for fibre optical communication 80−58653
AlGaAs heterojunction laser, lightwave sources and detectors 80−64068
(AlGa)As heterostruct., proton irrad., photoluminesc. 80−29808
AlGaAs heterostructures in integrated optics 77−75713
AlGaAs high-power constricted DH diode laser, for optical recording 80−43351
AlGaAs injection lasers, undoped, estimation of intra-band relax. time 80−43335
AlGaAs injection laser, large optical cavity, with multiple active regions 80−106538
AlGaAs, integrated twin-guide laser, mode selectivity 77−88723
AlGaAs integrated twin guide laser with distributed Bragg reflectors 77−88744
AlGaAs laser array on Si heat sink, optical power detection 80−74383
AlGaAs laser diode, interference and polarisation characts., using single mode fibre cable 79−81535
(AlGa)As laser system, VPE growth and degradation mechanisms 80−99748
AlGaAs lasers, CW high-power single-mode constricted DH lasers with large optical cavity 80−64076
(AlGa)As lasers, facet protection using SiO_2 sputter deposition 79−81444
AlGaAs lasers, relaxation oscillation rel. to carrier diffusion length, spontaneous emission 80−32986
AlGaAs leaky-mode buried heterostruct. injection lasers 77−68209
AlGaAs mode-locked diode laser, optical pulse generation 80−95907
AlGaAs, monolithic integration of laser and amplifier/detector by twin-guide struct. 78−42466
AlGaAs multimode laser, longitudinal modes intensity fluctuations effect on high bit-rate optical transmission 79−68415
(AlGa)As oxide-defined strip lasers, self-sustained oscillations, ageing effects 80−32991
AlGaAs, principle of operation *(Hungarian)* 80−53295
AlGaAs pulse modulate DH laser, oscillatory longitudinal mode competition 79−81427
AlGaAs resonant laser amplifier, gain and saturation power 80−53315
(AlGa)As self-pulsing junction laser, saturable absorpt. effects 79−72568
AlGaAs semiconductor lasers, single-mode stabilisation by traps 80−95893
AlGaAs, strip buried heterostruct. laser, linear light-current characts. 78−37908
(AlGa)As strip buried heterostructure lasers, mode locking using external cavity 80−91791

semiconductor junction lasers continued
(AlGa)As, stripe geometry DH laser, emission nonlinearities 77−685
(AlGa)As stripe geometry, proton-bombardment delineated DH laser, lifetime 80−106520
AlGaAs stripe-geometry DH laser, filament displacement and refr. losses 80−58536
AlGaAs transverse junction stripe lasers, single longit. and fund. transverse mode oscill. 78−22124
(AlGa)As, transverse junction stripe single mode oscillating laser, gain spectra 78−55356
AlGaAs transverse junction stripe laser with distributed Bragg reflector 80−106535
(AlGa)As, visible CW heterojunction laser diodes, room temp. operation 77−38895
AlGaAs, Zn diffused window structure laser, high optical power density emission 79−98394
(AlGa)As-GaAS DH lasers prep. by new LPE technique 77−40358
AlGaAs-GaAs, DH, with bent guide of planar struct. 78−1256
AlGaAs-GaAs, DH laser material, singular instabilities of LPE growth surface 77−24969
AlGaAs-GaAs, DH semiconductor laser, influence of struct. parameters on lasing characteristics 79−45942
AlGaAs-GaAs, defects and degradation *(Japanese)* 79−31899
AlGaAs-GaAs CW injection heterolaser, single freq., tunable by external dispersive resonator 80−28236
AlGaAs-GaAs DH laser, bent-guide struct. 77−75544
AlGaAs-GaAs DH lasers, accel. life test 77−79828
AlGaAs-GaAs DH laser, impurity effects on relaxation oscillations 78−13710
AlGaAs-GaAs DH laser, carrier leakage, physical mechanisms 78−66824
AlGaAs-GaAs DH lasers, accelerated life test 78−66830
AlGaAs-GaAs DH lasers, coupling efficiency between gain-induced guides 79−23094
AlGaAs-GaAs double heterostructure laser lifetime, point defect generation model calcs. 80−32992
AlGaAs-GaAs heteroepitaxial wafers, Mg doping, surface morphology and photoluminesc. meas. 77−3591
AlGaAs-GaAs injection laser, spectral band homogeneous broadening and narrow band emission 79−98364
AlGaAs-GaAs lasers for optical fibre transmission, defects and degradation 79−41382
AlGaAs-GaAs multimode laser, intensity fluctuations in each longit. mode 77−75512
AlGaAs-GaAs remote junction heterostructure laser, recomb. enhanced annealing effect 79−98355
AlGaAs-GaAs ring laser, injection type, laser oscill. 77−75570
AlGaAs-GaAs transverse mode stabilised plano-convex waveguide laser made by single step LPE 80−48274
n-$Al_{0.3}Ga_{0.7}As$, layer of (AlGa)As DH laser, deep levels 78−46605
$Al_{0.3}Ga_{0.7}As$-GaAs DH mesa stripe laser, metalorganic VPE growth and characterisation 79−98391
$Al_{1-x}Ga_xAs$, transverse junction stripe, with low threshold current and high efficiency 78−82985
$Al_xGa_{1-x}As$ CSP laser, analytical waveguide study 79−10302
$Al_xGa_{1-x}As$, as transmitter for fibre optical transmission lines 77−7134
$Al_xGa_{1-x}As$ buried heterostruct. laser, fabrication, optical props. and reliability 80−53322
$Al_xGa_{1-x}As$ CW heterolaser, 10000 hr. lifetime tests, degradation of mirror surfaces 80−106542
$Al_xGa_{1-x}As$, CW low threshold, high efficiency injection laser props. 78−22126
$Al_xGa_{1-x}As$ CW multiwavelength TJS laser, MBE, single-longitudinal modes 80−64049
$Al_xGa_{1-x}As$, DH, defect generation in active regions at high optical excitation rates 79−23845
$Al_xGa_{1-x}As$ DH laser, threshold current, stripe width influence 77−61952
$Al_xGa_{1-x}As$ DH laser, linear light output power depend. on effective gain width 77−75553
$Al_xGa_{1-x}As$ DH laser, accelerated ageing and uniform mode of degradation 77−83874
$Al_xGa_{1-x}As$ DH laser, with constricted active region, fabrication and characts. 78−37895
$Al_xGa_{1-x}As$ DH laser, rake-line form. in LPE growth, doping effects 80−2287
$Al_xGa_{1-x}As$ DH laser diodes, temp. rise under transient state conditions 77−68211
$Al_xGa_{1-x}As$ DH laser material, Ar laser induced catastrophic damage 79−86178
$Al_xGa_{1-x}As$ DH lasers, deep-level luminesc. 79−65913
$Al_xGa_{1-x}As$ DH lasers continuously operated, with 70°C lifetimes as long as two years 78−17952
$Al_xGa_{1-x}As$ DH p-n junction, surface recomb. effects on current, luminesc. expts. 78−72246
$Al_xGa_{1-x}As$ DH stripe-geometry lasers, degraded, capacitance spectroscopy 77−14715
$Al_xGa_{1-x}As$ DH superluminesc. diode, with unpumped region, time-delayed laser oscill. 77−54711
$Al_xGa_{1-x}As$ double heterostructure laser, CW optical power 77−14716
$Al_xGa_{1-x}As$ double heterostruct. lasers, optical pulsations 79−98354
$Al_xGa_{1-x}As$ heterojunction laser diode, technology and spectral characts. 77−38885
$Al_xGa_{1-x}As$ heterojunction laser diode, accelerated step-temperature ageing 78−46599
$Al_xGa_{1-x}As$ heterostructure laser, improved light-output linearity by antireflective coating 78−17953
$Al_xGa_{1-x}As$, indirect-gap, optical pumping, laser oscill. involving N isoelectronic impurities 77−10919
$Al_xGa_{1-x}As$ laser diode, reliability 80−53320
$Al_xGa_{1-x}As$ laser-alloyed stripe-geometry lasers 80−5745
$Al_xGa_{1-x}As$, metalorganic-CVD, photopumped laser operation meas. GaAs quantum well 79−10303
$Al_xGa_{1-x}As$, mode-stabilised injection laser, longitudinal-mode behaviour 79−962
$Al_xGa_{1-x}As$, modified-strip buried-heterostructure lasers, CW electro-optical properties 80−74359
$Al_xGa_{1-x}As$ pulsating DH laser, spectral broadening 80−23686
$Al_xGa_{1-x}As$ solid solution, pulsed diode laser simulator of solid laser 80−91816
$Al_xGa_{1-x}As$, spectral, threshold, power and time charac.s. 77−715

semiconductor junction lasers continued
$Al_xGa_{1-x}As$ stripe geometry DH lasers, proton bombarded, intensity pulsations 79−94235
$Al_xGa_{1-x}As$, transverse mode stabilized injection lasers 78−29964
$Al_xGa_{1-x}As$ triggerable semiconductor lasers made by deep proton bombardment 80−69408
$Al_xGa_{1-x}As$:N, indirect band-gap, visible laser oscill. at 77K 77−79820
$Al_xGa_{1-x}As$:N, luminescent material, appl. in optically pumped lasers and electrolum. diodes *(Japanese)* 77−44069
$Al_xGa_{1-x}As$:Zn DH laser, stripe geometry, horizontal transverse mode stabilisation, lasing characts. 77−19313
$Al_xGa_{1-x}As/Al_yGa_{1-y}As$ DH lasers grown by metalorganic CVD, CW operation in wavelength range 760-780 nm 80−64053
$Al_xGa_{1-x}As/GaAs$, appl. of stress distrib. calc. for multilayer heteroepitaxial struct. 77−72798
$Al_xGa_{1-x}As$-Al_yGa_{1-y} DH laser, threshold current temp. depend., potential barrier height influence 80−53296
$Al_xGa_{1-x}As$-$Al_yGa_{1-y}As$ DH IR-visible (0.89-0.72 μm) MBE grown lasers 80−64058
$Al_xGa_{1-x}As$-GaAs, CW 300k quantum-well heterojunction laser, optical and injection pumping operation 80−5735
$Al_xGa_{1-x}As$-GaAs, DH integrated optics development 80−33240
$Al_xGa_{1-x}As$-GaAs, p-n heterojunction laser, low temp. operation 80−1204
$Al_xGa_{1-x}As$-GaAs, p-n heterostruct. laser, tunnel injection and phonon-assisted recomb. 80−5733
$Al_xGa_{1-x}As$-GaAs, quantum-well MO-CVD heterostructure lasers, band-filling props. 79−22954
$Al_xGa_{1-x}As$-GaAs, quantum-well heterostructure laser diode, temp. depend. of threshold current 80−87395
$Al_xGa_{1-x}As$-GaAs DH injection laser, active region internal parameters determ., composite resonator use 80−106548
$Al_xGa_{1-x}As$-GaAs DH laser, short cavity, performance characts. 77−83889
$Al_xGa_{1-x}As$-GaAs DH lasers, metalorganic CVD growth and performance characts. 80−53312
$Al_xGa_{1-x}As$-GaAs DH laser diode, I-V characts., variation of ideality factor 80−64027
$Al_xGa_{1-x}As$-GaAs DH laser operation, phonon contrib. 80−102724
$Al_xGa_{1-x}As$-GaAs heterostructure, nonradiative large dark spots rel. to minority carrier transport 78−9378
$Al_xGa_{1-x}As$-GaAs heterostructures, MO-CVD, phonon assisted recomb. and stimulated emission 80−1205
$Al_xGa_{1-x}As$-GaAs heterostruct. lasers, metallorganic CVD 80−23692
$Al_xGa_{1-x}As$-GaAs large-quantum-well heterostructures, induced phonon-sideband laser operation 80−95888
$Al_xGa_{1-x}As$-GaAs laser, made by organometallic CVD, continuous room temp. operation 80−1201
$Al_xGa_{1-x}As$-GaAs long life laser, initial degradation, minority carrier lifetime reduction 77−71984
$Al_xGa_{1-x}As$-GaAs multilayers, LPE, using addition of GaCl vapour and new boat struct. 79−33950
$Al_xGa_{1-x}As$-GaAs multiple-quantum-well injection lasers grown by metal-organic CVD, room temp. continuous operation 80−1218
$Al_xGa_{1-x}As$-GaAs phonon-sideband metalorganic-CVD quantum-well heterostructure laser 79−64244
$Al_xGa_{1-x}As$-GaAs photopumped quantum-well heterostructure lasers grown by metalorganic CVD 79−98390
$Al_xGa_{1-x}As$-GaAs quantum-well heterostructure laser, metalorganic CVD growth, CW operation 300 to 337K 79−10304
$Al_xGa_{1-x}As$-GaAs quantum-well heterostructure laser diode, threshold current temp. depend. 80−43331
$Al_xGa_{1-x}As$-GaAs quantum well heterostructure lasers, operation 80−53292
$Al_xGa_{1-x}As$-GaAs quantum-well heterostructures, phonon-assisted recomb. and stimulated emission 80−74358
$Al_xGa_{1-x}As$-GaAs single-quantum-well heterostructure laser diodes grown by metalorganic CVD, continuous 300K operation 79−50309
$Al_xGa_{1-x}As$-GaAs-$Al_xGa_{1-x}As$ photopumped quantum-well laser, room temp. CW operation 78−74908
$Al_xGa_{(1-x)}As$-$Al_yGa_{(1-y)}As$ DH optically pumped laser, room temp. single pass gain 77−75511
$Al_yGa_{1-y}As$-$Al_xGa_{1-x}As$ laser struct., for integrated optics, MBE 78−13817
AlGaAsSb-GaSb heterojunction injection laser, radiative props. 1.4 to 1.8 μm range 80−91798
n-AlGaAsSb-GaSb-p-AlGaAsSb binary heterostructure injection laser, room temp. operation 78−9381
CC GaInAs-InP injection lasers with longer wavelengths for optical fibre communications, review *(Japanese)* 78−25892
CdS, combined pulse transformer for electronic pumping 78−1255
(Ga,Al)As CW diode laser, L(J) charact., external cavity induced nonlinearities 77−79824
(Ga,Al)As DH lasers used for optical recording; hole machining in Te films 79−89954
(Ga,Al)As injection laser parameters, homogeneous degradation calc. from initial rates 79−22951
(Ga, Al)As laser diode, operation and gain meas., importance of gap shrinkage effects 80−66257
(Ga,Al)As narrow double-current-confinement channelled-substrate planar laser fabrication, double etching technique 80−74371
(Ga,Al)As transverse mode stabilised laser, direct obs. of saturation behaviour of spontaneous emission 78−46600
(Ga,In)(As,P) DH lasers, 1.55 μm, low-threshold current densities 80−1221
GaA-$Al_{0.27}Ga_{0.73}As$ DH lasers grown by MBE, growth conditions influence on threshold current density 80−32984
GaAS-$Al_xGa_{1-x}As$, DH laser and modulation developments *(German)* 78−37903
GaAS-GaAlAs, DH laser, correlation between optical output characts. and time depend. behaviour 77−68210
(GaAl) As/GaAs five layer heterostructure narrow beam laser, characts. 77−10920
GaAlAs actively mode-locked laser, bandwidth limited picosecond pulses 80−95905
GaAlAs, baseband fast modulation, p-i-n photodetector unit characterisation 77−11025
GaAlAs based heterojunctions, integrated optics appl., technology advancements *(Slovak)* 80−33226
GaAlAs, buried-heterostructure injection lasers, threshold current reduction 77−10924

semiconductor junction lasers continued
(GaAl)As buried-heterostructure laser with buried optical guide, highly efficient operation 80−1219
GaAlAs CW DH diode lasers, optical emission and current noise obs. in LF range 77−3585
GaAlAs CW DH diode lasers, 1/f noise behaviour 78−1226
(GaAl)As CW DH lasers with stripe geometry, LF intensity noise obs. 77−38887
GaAlAs CW diode laser, external cavity control, 32 MHz single axial mode 78−1271
GaAlAs, CW radiation, high freq. intensity noise spectra of axial mode groups 77−34890
(GaAl)As, DH, LPE growth, meniscus lines as nucleation sites 77−15706
GaAlAs DH, optically-pumped, degradation at elevated temps. 79−50295
GaAlAs DH, SiO_2 insulated, characteristics and near field 80−64019
GaAlAs, DH CW diode laser, picosecond pulse generation 78−83002
(GaAl)As DH diode laser, microscale degradation absorpt. centres 78−13704
GaAlAs DH injection laser transmitter, for long distance fibre optics communication 78−42355
GaAlAs DH injection laser, half-ring, room temp. operation 80−58558
GaAlAs DH laser, broadband single mode tuning system 79−27256
(GaAl)As DH laser, gradual degradation accel. as exponent of driving current value 80−32990
GaAlAs DH laser, In solder deterioration, Au diffusion in In 80−33019
(GaAl)As DH laser, low-current, proton-bombarded, design and charact. 78−87059
GaAlAs DH laser, narrow stripe geometry, spontaneous carrier lifetime 80−87392
GaAlAs DH laser, optimum p-n junction depth, photoluminesc. method 79−4598
GaAlAs DH laser, stripe geometry, spatially resolved emission 79−27257
(GaAl)As DH laser, threshold current density, growth terraces effect 80−99723
GaAlAs DH laser coherent light, propagating in multimode optical fibre, speckle contrast 80−78978
GaAlAs DH laser coupled to $LiNbO_3$ Ti-diffused optical waveguide, anal. 80−58706
GaAlAs DH laser diode, deep level associated with slow degradation 78−87050
GaAlAs DH laser diodes, catastrophic degradation 79−50290
GaAlAs DH laser diodes, long-lived high-power at 70°C, using Al_2O_3 film coating 79−50321
GaAlAs DH laser diodes, small signal modulation, junction capacitance effect 80−83625
GaAlAs DH laser diode, edge coupling to planar $LiNbO_3$:Ti waveguide 80−87559
(GaAl)As DH laser wafer, photoluminesc. improvement with buffer layer 80−64014
GaAlAs DH laser-diode-to-diffused-waveguide coupling calcs., Gaussian beam model 79−94372
(GaAl)As, DH lasers, degradation mechanisms, temp. depend. 78−66825
GaAlAs DH lasers, electron-hole recomb. effects 79−45944
GaAlAs DH lasers, nonlinearity, second and third harmonic distortion 79−31898
GaAlAs DH lasers, proton-bombard., nonradiative recomb., luminesc. time-response meas. 79−98371
GaAlAs DH lasers, self-sustained pulsation suppression, effect of SiO_2 facet coating films 80−95894
GaAlAs DH p-n junction laser, construction and operating charact. 78−9377
GaAlAs DH pump laser for photoluminescence lifetime meas. 78−74085
(GaAl)As DH stripe contact injection lasers, local attached data fibre link appls. 80−19044
GaAlAs DH stripe geometry lasers, degradation phenomena 80−53290
GaAlAs DHS laser, direct modulated from 260 Mbit/s to 1.4 Gbit/s, monomode operation 78−46601
GaAlAs diode laser, communication by TDM pulse analogue modulation, computer simulation exam. 78−55455
GaAlAs embedded DH stripe laser with GaAsP strip-waveguide modulator 78−66957
(GaAl)As heterojunction laser with distributed Bragg refl., mode switching 80−43336
GaAlAs heterostructure fabrication, using horizontal and vertical LPE furnaces 77−42538
GaAlAs heterostructure lasers, fine-structure in spectra 80−19033
(GaAl)As high performance diode laser, high-reflectivity cavity mirrors 78−82994
GaAlAs injection DH laser and GaAs Schottky-gate FET, monolithic integration 80−58593
GaAlAs injection laser transmitter in optical fibre communication system 77−27382
(GaAl)As injection lasers, optimisation of power efficiency 77−42539
(GaAl)As injection lasers, self-pulsations, Q-switching and mode-locking effects 78−66827
GaAlAs injection lasers, AM charact. 79−50330
GaAlAs injection laser, long wavelength radn. spatial distrib. 79−76686
GaAlAs injection lasers, stability in single transverse mode operation 80−38027
GaAlAs injection laser, monolithic integration with Schottky-gate FET 80−48275
(GaAl)As injection lasers operating with optical fibre external resonator, charact. 80−58544
(GaAl)As injection laser operating in external cavity, intensity self-pulsations 80−64013
(GaAl)As injection lasers operating with optical fibre resonators 80−91812
GaAlAs, LPE edge-growth reduction by aux. heating in side-walls of graphite sliders 78−30848
GaAlAs laser, CW operation, self coupling phenomena caused by optical fibre, exam. 78−55355
GaAlAs laser, coherent pulse generation by active modelocking 79−89941
GaAlAs laser, used in Sagnac fibre-ring interferometer gyro with electronic phase sensing 79−17472
GaAlAs laser coupling to fibre, high efficiency 77−7173
GaAlAs laser diode, CW, ps pulse generation 79−50329
semiconductor junction lasers continued
GaAlAs laser diode, for heterodyne communication systems, high frequency stability 80−99727
GaAlAs laser nonlinearities, harmonic distortion 80−74357
GaAlAs laser power control loop, optical path electronic simulator *(German)* 78−82987
GaAlAs laser transmitter for optical fibre communication, features 78−90423
GaAlAs laser transmitters using optical tap for feedback control, output power stability 79−64241
(GaAl)As lasers, low threshold proton isolated, spectral and transient response 78−87052
GaAlAs lasers, return-beam-induced noise generation model 80−48244
GaAlAs lateral injection laser, low threshold, single mode operation 77−75545
(GaAl)As low threshold current proton isolated DH lasers 78−1258
(GaAl)As low-beam-divergence CW DH laser, grown by low press. metal-lorganic CVD 80−74376
GaAlAs mode stabilised separated multiclad layer stripe geometry DH laser, optical waveguide 80−64051
GaAlAs mode-stabilised semiconductor lasers 78−46638
GaAlAs, modulation behaviour in Gbit/sec range 79−31900
GaAlAs, native defects, stoichiometry, doping effect 77−11541
GaAlAs novel DH lasers fabrication 78−50803
(GaAl)As oxide-stripe geometry DH laser, cavity length effect on output 79−50323
GaAlAs stripe laser, longit. and transverse mode dynamics on junction plane 77−38890
(GaAl)As, stripe struct. for horizontal transverse mode stabilisation 77−79859
(GaAl)As system, automated system for growth of multilayered structs. by LPE 79−38752
GaAlAs terraced substrate laser, visible-light-emitting, charact. 80−106523
(GaAl)As, Zn diffused DH laser with twin transverse junctions, low threshold current 79−98393
(GaAl)As, Zn diffused proton bombarded stripe laser 79−98392
(GaAl)As:Be DH stripe geometry lasers with current confinement structure 80−58592
(GaAl)As:Be implanted DH stripe geometry laser 80−64044
GaAlAs/GaAs kink-free narrow-stripe proton-isolated injection DH lasers 80−58534
(GaAl)As/GaAs-heterostructure, degradation studies of sawn cavity lasers under pulsed operation 78−29953
(GaAl)As-GaAs, DH laser, degradation in water due to facet deterioration 79−22970
(GaAl)As-GaAs, double heterostructure laser, TEM study of dark line defect growth from dislocation clusters 79−33206
(GaAl)As-GaAs, long life lasers, initial degradation mode 77−14712
(GaAl)As-GaAs, low temp. threshold behaviour 78−46604
(GaAl)As-GaAs DH laser, anomalous emission intensity, cavity competition 77−79823
GaAlAs-GaAs DH laser diodes, long-life diodes for optical fibre communication 80−48246
GaAlAs-GaAs DH lasers, degradation caused by growth of dislocation networks 80−53289
(GaAl)As-GaAs deep proton-isolated lasers 79−36923
(GaAl)As-GaAs heterostruct. lasers, factors affecting catastrophic degradation 77−75524
(GaAl)As-GaAs heterostructure lasers, factors affecting catastrophic degradation 78−17942
GaAlAs-GaAs heterostruture, optical waveguide characteristics, mode spectrum, universal dispersion curves 79−72706
GaAlAs-GaAs heterostruc. lasers, interstitial impurities and degradation, Auger obs. 80−99730
GaAlAs-GaAs lasers, channelled substrate, prepared by combination of organometallic pyrolysis and LPE 80−99745
(GaAl)As-GaAs narrow stripe laser, improved optical communication system performance 80−102733
(GaAl)As-GaAs twin-transverse-junction stripe laser with linear light/current characteristic and low threshold 79−36893
(GaAl)As-heterostruct. stripe lasers, light/current charact. and near field shifts, waveguide self focusing effects 78−29952
$Ga_{0.65}Al_{0.35}As$, laser material, LPE growth, wave morphologies on surface 77−40396
$Ga_{0.7}Al_{0.3}As$-GaAs chemically etched mirror lasers, optical coupling effect 77−72000
$Ga_{0.9}Al_{0.1}As$, nucleation morphologies on $Ga_{0.65}Al_{0.35}As$ surfaces grown by LPE for DH lasers 78−15323
$Ga_{1-x}Al_xAs$ DH injection laser diode, long-term-degraded, TEM obs. 78−71102
$Ga_{1-x}Al_xAs$-GaAs DH lasers, very low threshold, grown by metalorganic CVD 78−55365
$Ga_{1-x}Al_xAs$, buried heterostruct., stable operation during accelerated ageing at 70°C 79−7125
$Ga_{1-x}Al_xAs$ buried heterostruct. injection laser, degradation rate, optical flux density depend. 79−50313
$Ga_{1-x}Al_xAs$ buried heterostructure lasers for analogue communication 80−48297
$Ga_{1-x}Al_xAs$, channelled substrate, planar struct. and DFB lasers 78−79032
$Ga_{1-x}Al_xAs$, DH, enhanced localised degradation and anomalous emission spectra 77−680
$Ga_{1-x}Al_xAs$ DH catastrophically degraded laser, TEM obs. of defects 80−32989
$Ga_{1-x}Al_xAs$ DH injection laser, FM at microwave freq. rates 80−58610
$Ga_{1-x}Al_xAs$ DH laser, LPE surface protective coating 78−35320
$Ga_{1-x}Al_xAs$ DH laser, accelerated ageing test 79−76688
$Ga_{1-x}Al_xAs$ DH laser diode, long-lived, high-power, facet coated 80−58564
$Ga_{1-x}Al_xAs$ DH laser hybrid device, reliability 79−27281
$Ga_{1-x}Al_xAs$, DH stripe geometry laser, lasing-induced change in differential resistance 79−45943
$Ga_{1-x}Al_xAs$, deep level-dislocation interactions, DLTS meas. 80−29357
$Ga_{1-x}Al_xAs$ double heterostruct. lasers, aging charact. 79−72569
$Ga_{1-x}Al_xAs$ feedback-stabilised injection laser for fibre-optic data transmission 77−19343
$Ga_{1-x}Al_xAs$ injection laser automatic bias control cct. 78−5498
$Ga_{1-x}Al_xAs$ junction-up TJS laser electron injection efficiency improvement 80−48300

semiconductor junction lasers continued
$(Ga_{1-x}Al_x)As$ LOC DBR laser integration with p-n junction detector 78−38066
$Ga_{1-x}Al_xAs$, LPE, growth mechanism and morphology on channelled substrates 79−28960
$Ga_{1-x}Al_xAs$ LPE crystals for DH laser, LEDs, TEM obs. of Ge, Si-doped epitaxial layers 79−1556
$Ga_{1-x}Al_xAs$ laser, SHG with $KNbO_3$ 80−74431
$Ga_{1-x}Al_xAs$ laser diode end facet protection by parylene coating 79−36921
$Ga_{1-x}Al_xAs$ lasers, processing stresses effect on residual degradation 79−72567
$Ga_{1-x}Al_xAs$ low threshold stripe geometry DH laser, Be implanted, on semi-insulating substrate 80−69409
$Ga_{1-x}Al_xAs$ pulsed injection laser, SHG in $KNbO_3$ 80−5785
$Ga_{1-x}Al_xAs$, room-temperature CW laser structures and characteristics 77−19323
$Ga_{1-x}Al_xAs$ stripe laser with stable transverse mode structure 80−48298
$Ga_{1-x}Al_xAs$, stripe-geometry DH, improved light output linearity 77−682
$Ga_{1-x}Al_xAs$ symmetrised epitaxial variable-gap waveguide, coherent radiation generation 80−38018
$Ga_{1-x}Al_xAs$, temp. sensitive, enhanced degradation rates 77−79825
$Ga_{1-x}Al_xAs$ transverse mode DH laser with inbuilt plano-convex waveguide 80−48296
$Ga_{1-x}Al_xAs$ visible diode lasers, transverse-mode stabilised, nonstigmatic laser beams 79−76694
$Ga_{1-x}Al_xAs$ visible diode lasers, degradation 80−43330
$Ga_{1-x}Al_xAs$ visible diode lasers, degradation mechanisms 80−64026
$Ga_{1-x}Al_xAs$ visible diode lasers, degradation due to macroscopic defects (<730 nm) and facet oxidation (>740 nm), life tests 80−99729
$Ga_{1-x}Al_xAs$-$Ga_{1-y}Al_yAs$, for 500 MHz fibre optic link 77−75704
$Ga_{1-x}Al_xAs$-$Ga_{1-y}Al_yAs$ DH laser, grown by organometallic CVD, room temp. operation 78−29950
$Ga_{1-x}Al_xAs$-GaAs, CVD laser diodes, operation and growth processes 78−46598
$Ga_{1-x}Al_xAs$-GaAs, DH, grown by metalorganic CVD, room temp. operation 78−13702
$Ga_{1-x}Al_xAs$-GaAs, heteroepitaxial layers on GaAs(001), misfit dislocation asymmetry 77−47694
$Ga_{1-x}Al_xAs$-GaAs, injection lasers, defects, TEM anal. 79−23866
$Ga_{1-x}Al_xAs$-GaAs, room temp. DH laser, CVD growth 78−37912
$Ga_{1-x}Al_xAs$-GaAs channel guide laser grown by metalorganic CVD 79−10317
$Ga_{1-x}Al_xAs$-GaAs DH injection lasers grown by metalorganic CVD, props. 80−99751
$Ga_{1-x}Al_xAs$-GaAs DH lasers grown by metalorganic CVD, room temp. operation 78−1248
$Ga_{1-x}Al_xAs$-GaAs heterostructure lasers grown by metalorganic CVD, prep. and props. 79−36918
$Ga_{1-x}Al_xAs$-GaAs injection laser, branching waveguide coupler fabrication by LPE 78−63202
$Ga_{1-x}Al_xAs$-GaAs laser, degradation, appl. of dislocation climb model 77−1125
$Ga_{1-x}Al_xAs$-GaAs laser, distributed Bragg confinement, room temp. operation 78−74907
$Ga_{1-x}Al_xAs$-GaAs low threshold room temp. DH lasers grown by metalorganic CVD 78−50804
$Ga_{1-x}Al_xAs$-GaAs narrow stripe laser for improved communication performance 80−48299
$Ga_{1-y}Al_yAs$, hetero-isolation stripe geometry for IR and visible radiation *(Japanese)* 80−83607
$Ga_xAl_{1-x}As$ channelled-substrate planar struct. injection laser 77−88742
$Ga_xAl_{1-x}As$ DH laser, suppression of output nonlinearities by use of misaligned mirrors 78−17954
$Ga_xAl_{1-x}As$ diode laser, modulation characts. 77−83903
$Ga_xAl_{1-x}As$ embedded stripe DH laser monolithically integrated with strip waveguide 78−59025
$Ga_xAl_{1-x}As$ injection heterojunction distributed output laser, exptl. study 80−43369
$Ga_xAl_{1-x}As$ stripe-geometry laser, current carrier conc. distrib. and threshold props. 77−68212
$Ga_xAl_{1-x}As$-GaAs DH laser, degraded, nature of ⟨110⟩ dark-line defects, TEM 77−89439
$Ga_xAl_{1-x}As$-GaAs DH laser, continuous room temp. operation 78−55363
$Ga_xAl_{1-x}As$-GaAs double heterostructure laser diode, temp. depend. of photolum. 80−5734
$Ga_xAl_{1-x}As$-GaAs heterostructure laser, suppression of internally circulating modes, effect on catastrophic degradation and efficiency 77−83896
GaAlAsP-GaAs T-Q DH laser, light induced misfit dislocation motion 77−75518
$Ga_{1-x}Al_xAs_{1-y}P_y$-GaAs quaternary heterojunction strains and IR laser diode performance 78−9385
GaAlAsSb/GaSb, for LW optical communication systems 80−10043
GaAlAsSb/GaSb alloys, prep. and optoelectronic device appl. 80−25587
Ga(As,P)/(In,Ga)P DH laser, red-emitting, optical and elec. characts. 78−66826
GaAs, 100 ps risetime pulse drive circuit 77−7149
GaAs, and its alloys, as integrated optics materials, book contrib. 79−64362
GaAs and related cpds., conf., Edinburgh, Scotland (Sep 1976) 78−3039
GaAs based laser diodes, comparison with Nd^{3+} based lasers 77−7088
GaAs, broadening mechanism, limitations to single mode power emission 79−961
GaAs CW DH laser, inherent oscillations and subharmonic resonances obs. in light output 78−74910
GaAs CW injection laser diode specification for integrated optical circuits 80−33034
GaAs, CW laser, sinusoidal modulation 9 MHz to 1.1 GHz, appl. for fibre meas. 77−10966
GaAs, comments on host dispersion in ultra-short pulse generation 80−64024
GaAs, crystals with nipi superstructures appl. *(German)* 78−95064
GaAs, current research, fibre optic appl. 80−83613
GaAs DH, for data recording on optical disc 80−19001
GaAs DH distributed Bragg reflector laser design, waveguide struct. 77−27306
GaAs DH injection laser, modulation behaviour, appl. in high bit-rate fibre optical communications 78−1281
semiconductor junction lasers continued
GaAs DH laser, alloying of ohmic contacts, Nd:YAG laser irrad. 80−43357
GaAs DH laser, high speed direct modulation, multimode operation effects 78−13738
GaAs DH laser, life test at room temp. 78−17937
GaAs DH laser, self-induced modulation, noise, instability 80−48250
GaAs DH laser diodes stabilised using self-apertured facet coatings 80−58609
GaAs DH laser/fibre transmission system modulation and injection 77−50764
GaAs DH lasers, review of fibre optical communication devices 77−58446
GaAs DH stripe geometry laser, horizontal mode deform. and anomalous lasing props. 77−19253
GaAs degraded heterojunction lasers, TEM obs. of dark defects 78−14355
GaAs degraded lasers, climb asymmetry, TEM obs. 80−79802
GaAs, digital modulation for optical communication systems *(German)* 78−37919
GaAs diode, IR radiation effects on human eye evaluation *(German)* 78−20241
GaAs diode laser, behaviour in optical feedback mode *(Dutch)* 79−76689
GaAs diode laser in communication system using PPM methods *(Rumanian)* 77−68260
GaAs diode lasers coupled to short external resonators, reson. amplifier model 77−31110
GaAs, distrib. Bragg reflector laser, highly collimated broadside emission 78−13721
GaAs distributed Bragg reflection lasers, large optical cavity, optimal design 80−38028
GaAs double and narrow stripe laser structures 80−64062
GaAs double cavity laser, with branching output waveguides, exam. 78−37918
GaAs double hetero stripe-geometry laser, two-dim. anal. 78−1231
GaAs double-cavity laser with branching output waveguides 78−63128
GaAs, electron-beam-pumped, transient waveguide effects and lasing time delays 78−37882
GaAs electrooptically tuned external-cavity CW injection laser, FM optical communication appl. 80−14351
GaAs, fabrication and characts. *(Korean)* 79−7144
GaAs, fabrication using double-etching technique 80−74387
GaAs, freq. retuning using electron beam excitation *(Russian)* 77−716
GaAs heterojunction, degradation, electron-hole recomb. at dislocations, point defect generation 79−37699
GaAs heterojunction, origin of dislocation climb during laser operation 77−51380
GaAs heterojunction diode as light source for fibre optical communication 80−58653
pnpn-GaAs heterostructure laser, barrier controlled low threshold 77−61966
GaAs homojunction lasers active layer in steady state, thermal conditions *(Polish)* 77−14717
GaAs homojunction laser diodes, in transient state conditions, analysis of junction temp. rise 77−38889
GaAs injection laser, active region effect on single-freq. stimulated emission conditions 80−9884
GaAs injection laser, intensified luminesc. *(Russian)* 78−90416
GaAs injection laser, output instabilities related to optical gain and lasing conditions 80−1203
GaAs injection laser, single heterostruct., mode competition effects, tuning characts. 80−48255
GaAs, injection laser with localisation of injection current, design and characts. 80−106543
GaAs injection lasers, spectral output, influence of diffusion and spontaneous emission 79−13965
GaAs injection lasers, amplified luminesc. 80−2824
GaAs injection lasers, direct modulation enhancement effect of HF noise 80−83608
GaAs, injection lasers with filament, junction current and carrier-conc. profiles *(Chinese)* 79−50292
GaAs integrated optical circuits by wet chemical etching 79−32092
GaAs laser, spectral depend. of gain calc. 77−23677
GaAs laser, spontaneous emission reduction at lasing with long delays 79−64226
GaAs laser array, integrated, Si substrate package fabrication 79−18555
GaAs laser array source package, with collimating lens and fibre lightguides 77−84007
GaAs laser array to channel groove waveguide coupling prism 78−38067
GaAs laser arrays, Si substrate packaged, thermal performance and limitations 78−46613
GaAs laser arrays 80−69393
GaAs laser convex micromirror mode control 79−36920
GaAs laser diode, SEM electron beam induced current study, contamination effect 79−43773
GaAs laser diode, spontaneous emission reduction 80−95904
GaAs laser diodes, absorption edge effects on temp. depend. of threshold currents 77−58328
GaAs laser diodes, coupling light efficiency into parabolic-index fibres 78−94435
GaAs laser diodes, junction temp. meas. method 79−36895
GaAs laser facsimile printer 80−30207
GaAs, laser material, LPE growth, wave morphologies on surface 77−40396
GaAs laser material, secondary dislocation climb during optical excitation 78−75672
GaAs laser reliability, protective facet coatings 79−81452
GaAs laser source package for multichannel optical links 78−1266
GaAs laser with integrated interferometric reflectors 77−65642
GaAs lasers, at room temp., modulation at X-band frequencies 78−87079
GaAs, long time delays, internal Q-switching 77−79822
GaAs, longitudinal mode spectrum, effect of carrier diffusion 78−71099
GaAs low-current-threshold strip-buried-heterostructure lasers with self-aligned current injection stripes 79−72581
GaAs, MBE prep., device props. 77−77417
GaAs narrow-channel double-current-confinement CSP lasers, current distrib. effect on performance 80−58539
GaAs, one-sided heterostructure injection laser, stability of output pulse power 77−83876

semiconductor junction lasers continued
GaAs, operation characteristics *(Rumanian)* 78−87053
GaAs, optically pumped laser, two-dimensional distributed Bragg reflectors, oscillation *(Japanese)* 78−42350
GaAs, optically pumped laser with acoustic distributed feedback 78−82977
GaAs, oxide-insulated stripe-geometry DH laser, low degradation rate at room temp. 77−23674
GaAs, periodic surface corrugation generation by holography 78−55469
GaAs, permittivity at laser transitions freq., excess carriers effect 77−14719
GaAs, photopumping of quantum well heterostruct. $Al_xGa_{1-x}As$-GaAs-$Al_xGa_{1-x}As$ 79−22956
GaAs planar stripe geometry and channelled substrate DH laser, lateral current confinement 78−66823
GaAs pulsed laser terrain profiler 77−91297
GaAs pulsed laser terrain profiler 78−49145
GaAs, radn. coupling to thin-film and fibre waveguides 77−19426
GaAs, refractive-index profile and resonant modes 79−86179
GaAs rib-waveguide laser, propag. and radiation charcts. 77−79933
GaAs, semi-insulating substrates, monolithic integration of optical and electronic devices, review 80−58543
GaAs, semi-insulating substrates, whispering gallery lasers 80−69405
GaAs, $Si_{1-x}C_x$ protective coating 80−5753
GaAs, single heterostruct. laser, transient effects 79−98366
GaAs single-channel injection laser, radiative charcts., single longit. mode 79−10309
GaAs single-channel injection laser, polarisation charcts. 80−48256
GaAs single-freq. injection laser, CW operation 78−46606
GaAs single-frequency injection laser, coherence of emitted radiation 79−31904
GaAs, spectral hole burning 79−50291
GaAs, stripe geometry laser, optical losses of O^+ and B^+ implanted layers 77−79827
GaAs, stripe-geometry, interaction and spectral distrib. of lateral modes *(Russian)* 78−22134
GaAs stripe-geometry laser, nonlinear temp. characteristics *(Chinese)* 80−43337
GaAs, striped DH lasers, anomalous behaviour at low temp. *(Chinese)* 80−87390
GaAs, surface temp. distrib. *(Russian)* 78−74909
GaAs, theory on long time delays and Q-switching 77−3587
GaAs transverse light coupling, into optical fibres 78−18045
GaAs, transverse modes, mirror reflectivity dependence 79−68404
GaAs, two dimensional DFB laser with distributed Bragg and acousto-optic reflectors 77−10946
GaAs, wavelength depend. of gain saturation 78−1229
GaAs/(Ga,Al)As, DH laser diode, electroluminescence near 1 eV 80−60682
GaAs/(GaAl)As channelled substrate narrow stripe lasers, with quarter-wavelength facet coatings 80−99746
GaAs/AlGaAs, DH, defect struct., X-ray topography 79−50312
GaAs/AlGaAs, DH laser, degradation under Ar laser irrad. 79−98375
GaAs/AlGaAs integrated twin guide injection lasers prepared by LPE, coupling coeff. and coupling length meas. 79−81458
GaAs/GaAlAs, distributed feedback for integrated optics 77−46721
GaAs/GaAlAs crowding effect lasers using whispering gallery mode on semi-insulating GaAs substrates 80−58589
GaAs/GaInP DH, MBE grown, optically pumped laser action at 77K 80−95890
GaAs-(Ga,Al)As light modulators and distributed Bragg reflector laser, monolithic integration 78−50944
GaAs-(GaAl)As, DH, injection enhanced dislocation glide under uniaxial stress 77−27885
GaAs-(GaAl)As, SiO_2 stripe geometry, for wide band optical communication systems 78−42358
GaAs-(GaAl)As channelled substrate buried heterostruct. injection laser, fabrication 77−7087
GaAs-(GaAl)As DH injection laser with pillbox resonator, charcts. and fabrication 80−58581
GaAs-(GaAl)As DH lasers, automated LPE growth, CW reliability tests 80−20804
GaAs-(GaAl)As DH stripe lasers, CW life tests 79−98383
GaAs-(GaAl)As epitaxial layers and DH lasers, deep centre 1.02 eV luminesc. 78−80387
GaAs-(GaAl)As injection lasers with circular resonator 80−74377
GaAs-(GaAl)As LOC-DBR laser, high differential quantum efficiency 78−79031
GaAs-(GaAl)As terraced-substrate injection lasers, fabrication and output charcts. 79−50310
GaAs-(GaAl)As terraced substrate laser, fundamental transverse and longit. mode oscill. 79−98357
GaAs-$Al_{0.27}Ga_{0.7}$ 7_3As Dh lasers grown by MBE, influence of growth conditions on threshold current density 80−58587
GaAs-$Al_{0.3}Ga_{0.7}$As laser diode, spontaneous radiation transfer 80−91796
GaAs-$Al_{1-x}Ga_xAs$, PbO-SiO_2 glass optical coating 78−71113
GaAs-$Al_xGa_{1-x}As$ transverse junction lasers with low threshold current prep. by MBE on semi-insulating substrates 80−58588
GaAs-$Al_xGa_{1-x}As$, optically pumped multilayer struct. and DH, laser oscillations 77−3589
GaAs-$Al_xGa_{1-x}As$, integrated twin-guide laser with distrib. Bragg reflectors 77−19310
GaAs-$Al_xGa_{1-x}As$, DH laser, lateral current confinement by reverse biased junction 77−58339
GaAs-$Al_xGa_{1-x}As$, optically pumped taper coupled laser, second order Bragg reflector 78−50788
GaAs-$Al_xGa_{1-x}As$, DH laser, effect of bulk nonradiative recombination 78−82967
GaAs-$Al_xGa_{1-x}As$, film waveguide, heterojunction lasers with Bragg mirrors, threshold charcts. 79−23095
GaAs-$Al_xGa_{1-x}As$, current transverse junction lasers, low threshold, MBE prep. 80−83614
GaAs-$Al_xGa_{1-x}As$ buried-heterostructure laser, wideband optical sources *(German)* 78−37904
GaAs-$Al_xGa_{1-x}As$ buried-heterostructure lasers, current injection confinement, MBE/LPE hybrid technique 80−74374
GaAs-$Al_xGa_{1-x}As$ CW-diode laser, coupled to freq.-selective external cavity, self-pulsing 77−61982
GaAs-$Al_xGa_{1-x}As$ channelled-substrate-planar-struct. laser with lateral-evanescent-field distributed feedback 79−98398
semiconductor junction lasers continued
GaAs-$Al_xGa_{1-x}As$ current injection multi-quantum-well heterostructure lasers, MBE grown 80−19042
GaAs-$Al_xGa_{1-x}As$ DH laser, high-temp. degradation *(German)* 78−37884
GaAs-$Al_xGa_{1-x}As$ DH laser, modulation with coherent light injection *(German)* 78−37922
GaAs-$Al_xGa_{1-x}As$ DH laser structures, high-resolution composition profiling with photolum. 78−71101
GaAs-$Al_xGa_{1-x}As$ DH laser, room temp. threshold current 78−79019
GaAs-$Al_xGa_{1-x}As$ DH lasers, LPE *(Polish)* 79−4922
GaAs-$Al_xGa_{1-x}As$ DH lasers, MBE grown, low current threshold, high lasing uniformity 79−64223
GaAs-$Al_xGa_{1-x}As$ DH broad contact pulse lasers, second-order coherence props. 80−23685
GaAs-$Al_xGa_{1-x}As$ DH lasers, very low current threshold, MBE grown 80−43353
GaAs-$Al_xGa_{1-x}As$ DH lasers, MBE grown, substrate temp. effect on current threshold 80−48243
GaAs-$Al_xGa_{1-x}As$ DH laser, MBE grown, CW electro-optical props. 80−102725
GaAs-$Al_xGa_{1-x}As$ electro-optic frequency- and polarisation-modulated injection laser 80−91810
GaAs-$Al_xGa_{1-x}As$ integrated injection lasers and detectors with etched reflectors 77−62074
GaAs-$Al_xGa_{1-x}As$ integrated lasers and detectors fabricated by wet chemical etching 77−88961
GaAs-$Al_xGa_{1-x}As$ injection laser, direct modulation and spectral props. *(German)* 78−37921
GaAs-$Al_xGa_{1-x}As$ multilayer struct., MBE, selective area growth using Si shadow masks 77−85946
GaAs-$Al_xGa_{1-x}As$ proton-isolated DH laser, threshold current optimisation *(German)* 78−37905
GaAs-$Al_xGa_{1-x}As$ single heterostructure laser diode, pulse operating, anal. of temp. decrease in active region 78−13706
GaAs-$Al_xGa_{1-x}As$ stripe geometry DH laser, threshold current density, effect of optical mode losses 78−59008
GaAs-$Al_xGa_{1-x}As$ strip-buried heterostruct. laser with distributed feedback 79−76696
GaAs-$Al_xGa_{1-x}As$ strip buried heterostructure lasers 79−81425
GaAs-$Al_xGa_{1-x}As$ strip buried heterostructure laser with passive DBR 80−14352
GaAs-$Al_xGa_{1-x}As$ transverse junction stripe laser, single-mode oscillation *(German)* 78−37885
GaAs-AlAs multilayer heterostructure laser, power and photoelectroluminescence charcts. 80−53297
GaAs-AlGaAs, fabrication, cleaving process for GaAs wafers 78−37915
GaAs-AlGaAs CW laser coupled to external cavity, multimode operation, output intensity low freq. pulsations 79−68394
GaAs-AlGaAs DH, improved LPE growth, lasing charcts. 77−81229
GaAs-AlGaAs DH, wipinglass LPE growth *(Japanese)* 78−48304
GaAs-AlGaAs DH injection laser, emission energy, wavelength depend. in strong mag. fields 80−48248
GaAs-AlGaAs DH injection laser with stripe contacts, radiation pulse stepped shape 80−91799
GaAs-AlGaAs DH laser, rapid degradation caused by process-induced defects 77−71985
GaAs-AlGaAs DH laser, improved lifetime by defects reduction during LPE 77−75547
GaAs-AlGaAs DH laser, impedance meas. 78−17939
GaAs-AlGaAs DH lasers, multipeak freq. response obs. 78−17940
GaAs-AlGaAs DH laser with buried facet 78−55373
GaAs-AlGaAs DH laser, degradation rate rel. to photocurrent 80−28233
GaAs-AlGaAs DH laser structure, defect assessment by differentiated cathodolum. topography 80−59819
GaAs-AlGaAs distributed Bragg reflector integrated twin-guide laser, temp. charcts. 78−87064
GaAs-AlGaAs double heterostructure, optically induced dislocation glide, cooperative phenomena 78−74911
GaAs-AlGaAs half-ring laser, fabrication by deep Zn diffusion 78−17960
GaAs-AlGaAs laser array packaged with fibre lightguide array on Si substrate 78−46611
GaAs-AlGaAs transverse junction stripe laser, single mode behaviour after 12000 hr ageing test 78−66831
GaAs-$Ga_{0.7}Al_{0.3}As$ channelled substrate buried heterostructure injection lasers 77−38932
GaAs-$Ga_{1-x}Al_xAs$, low threshold room temp. embedded DH laser, fabrication and charcts. 77−681
GaAs-$Ga_{1-x}Al_xAs$, monolithically integrated DFB diode laser, freq. multiplexing 77−702
GaAs-$Ga_{1-x}Al_xAs$, DH distributed Bragg reflector laser, room temp. operation 77−7085
GaAs-$Ga_{1-x}Al_xAs$, DH, Al_2O_3 facet coating effect on degradation 78−13722
GaAs-$Ga_{1-x}Al_xAs$, DH, charcts. exam. for communication appl. 78−37891
GaAs-$Ga_{1-x}Al_xAs$, single-heterostructure laser diode with short current pulses, heat spreading analysis 79−76690
GaAs-$Ga_{1-x}Al_xAs$ buried DH diode laser fabrication 77−75565
GaAs-$Ga_{1-x}Al_xAs$ DH lasers, X-ray topographic obs. of lattice defects rel. to degradation 77−15420
GaAs-$Ga_{1-x}Al_xAs$ DH lasers, long-term degradation due to facet erosion 77−50672
GaAs-$Ga_{1-x}Al_xAs$ DH strip CW laser for optical transmission *(German)* 77−68222
GaAs-$Ga_{1-x}Al_xAs$ double heterostructure LED and injection laser transmitters 77−68282
GaAs-$Ga_{1-x}Al_xAs$ DH injection laser, curved junction stabilized filament, struct. and charcts. 78−33744
GaAs-$Ga_{1-x}Al_xAs$ DH laser, curved stripe, operation and appl. 78−42341
GaAs-$Ga_{1-x}Al_xAs$ DH lasers, electron beam induced current microscopy 80−95899
GaAs-$Ga_{1-x}Al_xAs$ half-ring laser, fabrication by LPE over chemically etched channels 77−684
GaAs-$Ga_{1-x}Al_xAs$ LPE wafer stress-free dislocation generation 77−75527
GaAs-$Ga_{1-x}Al_xAs$ optically pumped, longit. mode broadening due to transient heating 77−61953

semiconductor junction lasers continued
GaAs-$Ga_{1-x}Al_xAs$ single heterostructure laser diode, anal. of temp. rise under transient-state conditions 77−61949
GaAs-$Ga_{1-x}Al_xAs$ stripe geometry lasers 79−94245
GaAs-$Ga_xAl_{1-x}As$, SiO_2 insulated, for optical communication 77−10949
GaAs-$Ga_xAl_{1-x}As$, degradation, TEM obs. 77−51625
GaAs-$Ga_xAl_{1-x}As$, magn. birefr. influence on stimulated emission spectrum 78−17941
GaAs-$Ga_xAl_{1-x}As$, injection laser with external resonator, mirrors of Michelson interferometer 79−81455
GaAs-$Ga_xAl_{1-x}As$ CW stripe geometry laser fabrication and performance 77−38933
GaAs-$Ga_xAl_{1-x}As$ DH diode lasers, single longitudinal mode operation 78−1243
GaAs-$Ga_xAl_{1-x}As$ double heterojunction laser structures, LPE growth with double source method 79−28962
GaAs-$Ga_xAl_{1-x}As$ DH laser wafers, active layer inhomogeneities 79−74106
GaAs-$Ga_xAl_{1-x}As$ DH lasers, dislocation effects 79−82221
GaAs-$Ga_xAl_{1-x}As$ DH laser material crystal cathodoluminescence, SEM analysis 80−97349
GaAs-$Ga_xAl_{1-x}As$ injection laser, external resonator, radiative characts. 77−23703
GaAs-$Ga_xAl_{1-x}As$ injection laser, large-optical-cavity, with low-loss distributed Bragg reflectors 78−1244
GaAs-$Ga_xIn_{1-x}P$ heterostruct., MBE layers, photolum. props., assessment as laser struct. 80−20705
GaAs-GaAlAs, DH laser material, rapid optical degradation 77−7083
GaAs-GaAlAs, double heterostruct. injection laser, curved junction stabilised filament, exam. 78−37911
GaAs-GaAlAs, grating coupled with distributed Bragg reflectors 78−17934
GaAs-GaAlAs, heterostructure laser diode, lasing threshold calc. 80−28232
GaAs-GaAlAs, injection laser and MESFET monolithic integration on GaAs substrate 79−64242
GaAs-GaAlAs, optical repeater using PFM at 1 GHz 79−98395
GaAs-GaAlAs, stripe geometry laser, simplified fabrication process, characts. 79−76697
GaAs-GaAlAs, transverse Bragg-reflector injection lasers 78−74926
GaAs-GaAlAs 13 μm wide stripe CW DH lasers linear to more than 10 mW 78−42344
GaAs-GaAlAs bipolar transistor and heterostruct. laser, monolithic integration 80−102858
GaAs-GaAlAs CW diode laser, lateral mode stabilization using apertured facet reflectors 80−23708
GaAs-GaAlAs CW injection laser, stripe geometry DH, temporal coherence 80−38016
GaAs-GaAlAs channelled-substrate narrow-stripe lasers, low threshold currents 80−23706
GaAs-GaAlAs DFB and distributed Bragg reflector lasers, historical review 77−31102
GaAs-GaAlAs DFB diode lasers with separate carrier and optical confinement, room temp. operation 77−10926
GaAs-GaAlAs DH CW laser, growth by Peltier effect induced LPE 77−48357
GaAs-GaAlAs DH diode lasers with angled pumping stripes, operation 78−46602
GaAs-GaAlAs DH injection laser, integrated optics techniques 80−33033
GaAs-GaAlAs DH injection lasers, external cavity operated angled-stripe geometry, CW operation 80−64078
GaAs-GaAlAs DH internally striped planar laser with flat freq. response up to 2 GHz 78−66829
GaAs-GaAlAs DH laser on semi-insulating substrate using carrier crowding 77−83886
GaAs-GaAlAs DH laser material, secondary dislocation climb in optical degradation 78−17935
GaAs-GaAlAs DH lasers, optical studies of defects and degradation 78−18654
GaAs-GaAlAs DH lasers, single longit. mode operation 78−22125
GaAs-GaAlAs DH laser, unsaturated optical gain spectra above threshold 78−29951
GaAs-GaAlAs DH laser diode, lateral modes 78−59009
GaAs-GaAlAs DH laser, beam scanning with twin-stripe injection lasers 79−10334
GaAs-GaAlAs DH laser with low threshold current, metalorganic CVD 79−50293
GaAs-GaAlAs DH lasers, strain-enhanced luminesc. degradation, photoluminesc. obs. 80−69392
GaAs-GaAlAs DH laser, O^+ isolation compared with SiO_2 isolation 80−74382
GaAs-GaAlAs DH stripe lasers, incremental efficiency enhancement and RF response 77−3586
GaAs-GaAlAs double heterostructures for CW injection lasers, LPE growth 79−31931
GaAs-GaAlAs embedded stripe DH laser with polycryst. GaAsP, cleaved mirrors 77−75548
GaAs-GaAlAs embedded stripe DH laser with polycryst. GaAsP, etched mirrors 77−75549
GaAs-GaAlAs grating coupled lasers, output power efficiency 77−79858
GaAs-GaAlAs heterostructure injection lasers, room temp. operation with curved stripe waveguides 78−37909
GaAs-GaAlAs heterostructure lasers on semi-insulating substrates 79−13977
GaAs-GaAlAs injection lasers, on semi insulating substrates, using laterally diffused junctions 78−37910
GaAs-GaAlAs injection laser, branching waveguide directional coupler, fabrication and operation 78−38047
GaAs-GaAlAs injection laser sources, for fibre optic communications 78−46637
GaAs-GaAlAs injection lasers on semi-insulating substrates using laterally diffused junctions 78−55364
GaAs-GaAlAs injection laser sources for fibre optic communications, design 79−31923
GaAs-GaAlAs injection laser, radiation divergence reduction by non-waveguide mode excitation 80−91797
GaAs-GaAlAs injection lasers, narrow-stripe proton-implanted, high bit-rate modulation 80−91824
GaAs-GaAlAs LPE layers, laser material, shallow growth pits obs. 77−7985
semiconductor junction lasers continued
GaAs-GaAlAs LPE layers, DH material, TEM obs. of crystal defects 78−6241
GaAs-GaAlAs laser, degraded, characterisation by selective etching and photoetching 80−48252
GaAs-GaAlAs laser, high-spectral radiance source using integrated optics 79−36931
GaAs-GaAlAs laser, practical appls. 80−1212
GaAs-GaAlAs laser with integral light intensity detector 79−89917
GaAs-GaAlAs lasers, recent advances in integrated optics 77−75712
GaAs-GaAlAs monolithically integrated DFB lasers as freq. multiplexing source 77−34958
GaAs-GaAlAs multiple-stripe phase-locked laser array, behaviour 79−45955
GaAs-GaAlAs nonplanar large optical cavity laser, pulsed room temp. operation 80−28244
GaAs-GaAlAs optically pumped DFB laser, wavelength tuning effect 78−82979
GaAs-GaAlAs planar stripe DH laser, origin of dark line defects 77−75510
GaAs-GaAlAs room temp. DBR lasers, highly collimated broadside emission 78−1428
GaAs-GaAlAs stripe injection laser, high performance, design and characts. 79−31932
GaAs-GaAlAs stripe injection laser, CW double heterostruct., technology 79−31933
GaAs-GaAlAs TJS lasers, high power density single mode operation, Si_3N_4 facet coating 79−86186
GaAs-$In_yGa_{1-y}P$, CW room temp. DH lasers prep. by VPE 77−10942
GaAs-InP heterojunction laser output wavelength control 80−74384
GaAs-metal junctions, thermal stability improvement, using transition and near noble metals 79−7143
$GaAsAl_xGa_{1-x}As$ heterostruct., anomalous elec. and optical characts. 80−2865
$GaAsGa_{1-x}Al_xAs$ DH laser material, rapid optical degradation obs. 77−75528
GaAsP/InP diodes for 1.56 μm CW operation 80−48254
$GaAs_{0.7}P_{0.3}$-$In_{0.34}Ga_{0.66}P$, CW heterojunction laser, visible, laser operation 77−38886
$GaAs_{1-y}P_y$-$In_{1-x}Ga_xP_{1-z}As_z$, DH, low threshold visible spectrum 78−5471
GaAsSb/GaAlAsSb DH lasers, growth and props. 80−69412
GaAsSb-AlGaAs, optimum wavelength emission for fibre guides 77−7086
GaAsSb-AlGaAsSb DH laser, LPE growth of $GaAs_{1-x-z}Sb_xP_z$ 78−6867
$GaAs_{1-x}Sb_x$, DH, LPE growth of $GaAs_{1-x-z}Sb_xP_2$ secondary substrate 77−31913
$GaAs_{1-x}Sb_x$, DH, laser operation between 0.9 and 1.1 μm 77−10922
$GaAs_{1-x}Sb_x$-$Al_yGa_{1-y}As_{1-z}Sb_z$, DH, threshold characts. and extended wavelength operation 78−9379
$GaAs_{1-x}Sb_x$-$Ga_{1-x}In_xP_{1-y}As_y$ multilayer structure, continuously tunable electron beam pumped laser 78−50802
$Ga_{0.47}In_{0.53}As$/InP DH lasers double cladded with InP by LPE technique, 1.67 μm operation 79−50314
$Ga_xIn_{1-x}As$-InP heterostructure, growth by MBE, laser action obs. 79−8251
GaInAsP DH laser diode CW modelocking 79−7126
GaInAsP DH laser emitting at 1.55 μm, threshold currents 80−83609
GaInAsP diode lasers, self-sustained pulsations in light output 80−64012
GaInAsP/InP, DH laser, low threshold current density, 1.3 μm emission 79−94249
GaInAsP/InP 1.5-1.6 micron integrated twin-guide lasers with distributed Bragg reflectors 80−74380
GaInAsP/InP buried heterostruct. laser, 1.6 μm, fabrication and room temp. CW operation 80−58568
GaInAsP/InP DH lasers, with (100) substrate, 1.2-1.5 μm, LPE growth conditions 79−15617
GaInAsP/InP DH lasers, direct modulation charact. meas. by sharp pulse method 80−1245
(GaIn)(AsP)/InP DH 1.27 micron lasers, nonradiative carrier loss and temperature sensitivity of threshold 80−43333
GaInAsP/InP DH lasers, room temp. CW operation at 1.5 to 1.6 micron range, fabrication 80−58585
GaInAsP/InP DH lasers emitting at 1.3 μm, growth and characts. 80−64057
GaInAsP/InP DH stripe geometry lasers emitting at 1.3 μm, growth characterisation 80−69410
GaInAsP/InP DH lasers, 1.3 μm wavelength, LPE growth and characterisation 80−69411
(100)GaInAsP/InP DH lasers, 1.5-1.6 μm wavelength, two phase soln. LPE technique using anti-meltback layer 80−99750
GaInAsP/InP integrated twin-guide lasers with first order distrib. Bragg reflector, room temp. operation at 1.3 μ 80−64077
GaInAsP/InP integrated twin-guide lasers with distributed Bragg reflector, spectral behaviour 80−74381
GaInAsP/InP lasers, 1.5 μm emitting, high temp. CW operation 80−95889
GaInAsP/InP lasers, LPE grown, effect of p-doping on carrier lifetime and threshold current density 80−99726
GaInAsP/InP narrow planar stripe lasers, lasing characts. 80−95897
GaInAsP/InP system, chemical etching, fabricating laser diodes and integrated optical circuits 80−38030
GaInAsP/InP terraced substrate DH lasers, fabrication and single transverse mode operation 80−58580
GaInAsP-InP, broad-area and stripe-geom. DH laser, for fibre optic communication 78−42356
GaInAsP-InP buried stripe DH laser, fabrication using meltback method and CW operation 79−3708
GaInAsP-InP buried heterostructure laser with mesa substrate, linear light/current characts. 79−36894
GaInAsP-InP buried heterostructure lasers, 1.6 μm wavelength 80−64055
GaInAsP-InP DH laser, 1.3 μm CW operation at room temp. 77−71986
GaInAsP-InP DH laser grown by newly designed vertical LPE furnace 78−9380
GaInAsP-InP DH laser, relaxation and delay in oscillations 78−13709
GaInAsP-InP DH layers, lattice deform. and misfit dislocations 79−19473
GaInAsP-InP DH lasers with low threshold, narrow-beam divergence 79−36892

semiconductor junction lasers continued
GaInAsP-InP DH lasers, for fibre optic communications 79−31924
GaInAsP-InP DH laser, LPE and wet chem. etching techniques for integration 79−98388
GaInAsP-InP DH lasers, 1.1 to 1.3 μm, fibre optics communications 80−14360
GaInAsP-InP DH laser, room temp. CW laser 80−28235
GaInAsP-InP DH lasers made by melt-back method, operating characteristics 80−48287
GaInAsP-InP DH lasers, LPE growth and operational charact. 80−53313
GaInAsP-InP DH injection lasers prep. by LPE, 1.11-1.67 μm operation 80−53321
GaInAsP-InP double heterostructure, prep. by LPE growth and laser operation 77−3590
GaInAsP-InP facet lasers with chemically etched end mirrors 80−1228
GaInAsP-InP integrated twin-guide lasers with first-order distributed Bragg reflectors, 1.3 μm 80−58567
GaInAsP-InP lasers and detectors, for fibre optic communications at 1.0-1.6 μm 79−3803
GaInAsP-InP mesa substrate buried heterostruct. injection laser, fabrication and lasing props. 80−53319
GaInAsP-InP planar stripe lasers, sputtered SiO_2 film as Zn-diffusion mask 80−48249
GaInAsP-InP stripe-geometry monolithic laser with etched mirror and monitoring detector 80−64054
GaInAsP-InP stripe laser, etched mirrors fabricated by wet chem. etch 80−99744
GaInAsP-InP surface emitting injection laser, fabrication and lasing props. 80−28234
GaInAsP-InP Zn diffused stripe geometry DH diode laser fabrication 79−98386
$Ga_{1-x}In_xAs_{1-y}P_y$-InP DH laser, carrier lifetime meas. 77−61955
$Ga_{1-x}In_xAs_{1-y}P_y$-InP DH lasers, 1000-hour CW operation 78−1265
$Ga_xIn_{1-x}As_{1-y}P_y$-InP, room temp. electron-beam-pumped laser with dielec. waveguide, output charact. 80−5761
$Ga_xIn_{1-x}As_yP_{1-x}$-InP buried-stripe DH diode laser, room temp. CW operation 77−50671
$Ga_xIn_{1-x}As_yP_{1-y}$ LPE layers matched to InP, comp. and lasing wavelengths 78−71103
$Ga_xIn_{1-x}As_yP_{1-y}$/Inp DH laser emitting at 1.15 micron grown by low-pressure CVD 80−64052
$Ga_xIn_{1-x}As_yP_{1-y}$-InP, CW stripe-geometry lasers, fabrication and props. 77−10943
$Ga_xIn_{1-x}As_yP_{1-y}$-InP injection laser, partially loaded with distributed Bragg reflector 78−82986
$Ga_xIn_{1-x}As_yP_{1-y}$-InP, rib-waveguide injection lasers made by one-step LPE 79−59710
$Ga_xIn_{1-x}As_yP_{1-y}$-InP injection laser partially loaded with first-order distributed Bragg reflector 79−98387
$Ga_xIn_{1-x}As_yP_{1-y}$InP, DH, 1500 h continuous CW operation 77−42537
GaInAsSb/GaSb DH lasers, 2 micron CW operation at 80K 80−53291
$Ga_xIn_{1-x}As_ySb_{1-y}$, efficient room temp. stimulated emission, 1.8 to 2.4 μm spectral range 79−10307
$Ga_xIn_{1-x}As_ySb_{1-y}$, epitaxial film and DH, luminesc. props. 77−686
$Ga_xIn_{1-x}As_ySb_{1-y}$ tunable electron-beam-pumped laser parameters 80−106524
GaInPAs, CW strip heterolaser, charact. 78−9382
GaInPAs multicomponent solid soln., room temp. operation 77−75516
GaInPAs, narrow-band tunable injection laser, 1.06 μm 79−76713
GaInPAs/InP heterostructure DFB laser under optical pumping, lasing charact. 80−87396
$Ga_{1-x}In_xP_yAs_{1-y}$/InP DFB injection laser, one-step LPE 80−58575
$Ga_xIn_{1-x}P_{1-y}As_y$ solid solution, pulsed diode laser simulator of solid laser 80−91816
$Ga_xIn_{1-x}P_yAs_{1-y}$-InP(GaAs), DH integrated optics development 80−33240
GaP semiconductor Raman laser 80−78864
n-GaP_xAs_{1-x}-p-$Ga_{1-y}Al_yP_xAs_{1-x}$ single sided heterolaser, visible emission 78−46607
(InGaAs)/(InGa)P, DH laser, threshold current temp. depend. 79−81431
InGaAs-$In_{1-x}Ga_xAs_yP_{1-y}$ DH laser, LPE fabrication, electroluminesc., lasing charact. 79−3709
InGaAs-InGaP vapour-grown ternary heterojunction laser struct., reliability 79−98385
$In_{0.53}Ga_{0.47}As$-InP, 1.7 μm heterojunction lasers and photodiodes fabrication 78−25880
$In_xGa_{1-x}As$ layers, on GaAs substrate, MBE fabrication and laser operation 80−10820
$In_xGa_{1-x}As$-$In_yGa_{1-y}P$ DH laser, CW room temp. operation at 1.06 μm 77−19250
InGaAsP buried stripe laser, modulation charact. 79−98418
InGaAsP DH laser charact., temp. depend. 80−1223
InGaAsP DH lasers with etched reflectors, fabrication, current density 80−64050
InGaAsP InP DH lasers, optical power and wavelength stabilisation 80−38036
InGaAsP, injection heterojunction laser at 1.3-1.5 μm 79−89910
(InGa)(AsP) laser system, VPE growth using metal organic sources or halide transports 80−99748
InGaAsP low-threshold 1.25-μm vapour grown CW lasers, emission charact. 79−50308
InGaAsP single-mode CW ridge waveguide laser emitting at 1.55 micron for optical fibre links 80−9883
InGaAsP single-mode CW ridge-waveguide laser emitting at 1.55 micron 80−58584
InGaAsP strip-buried-heterostructure high-output power laser 80−58540
InGaAsP strip-buried heterostructure laser, high output power, operation 80−58559
InGaAsP, with and without InP cladding layers, low photolum. regions 79−33754
InGaAsP/InP, DH laser, 1.5 μm, with optical waveguide structure, fabrication 79−72587
(InGa)(AsP)/InP, DH laser, threshold current temp. depend. 79−81431
InGaAsP/InP, for LW optical fibre communication 80−9885
InGaAsP/InP, for graded-index fibre cables, transmission meas. in 1.2 to 1.6 μm range 80−10037
InGaAsP/InP, for LW optical communication systems 80−10043
InGaAsP/InP, native oxide stripe laser 79−68405

semiconductor junction lasers continued
InGaAsP/InP buried heterostructure laser diodes for transmission loss meas. of graded-index fibres 80−87486
InGaAsP/InP DFB injection lasers 80−5746
InGaAsP/InP DH lasers, Zn doping level 79−98373
InGaAsP/InP DH laser, self-aligned struct. 80−9893
InGaAsP/InP DH lasers, temp. depend. charact. 80−58541
InGaAsP/InP DH stabilised 1.3 μm laser diode-isolator module for hybrid optical integrated cct. 80−58583
InGaAsP/InP heterostruct. lasers as optical source, CW operation at room temp. 80−1220
InGaAsP/InP injection lasers for long wavelength (1.1 to 1.6 μm) optical communication 80−58582
InGaAsP-InP, double heterostructure laser, temp. sensitive threshold current 79−59700
InGaAsP-InP, double heterostructure laser lifetime, point defect generation model calcs. 80−32992
InGaAsP-InP, LPE, 1.5 μm range, effects of double cladding struct. 80−48290
InGaAsP-InP, Zn diffused DH structures, oxide defined transverse junction stripe lasers 79−98389
InGaAsP-InP 1.27 μm CW DH injection lasers, 1.1 Gb/s pseudorandom PCM 78−55390
InGaAsP-InP buried crescent injection laser emitting at 1.3 μm with low threshold current 80−87404
InGaAsP-InP buried heterostructure lasers emitting at 1.3 μm, accelerated ageing charact. 80−95898
InGaAsP-InP CW lasers, 1.5-1.7 μm, VPE 80−78861
InGaAsP-InP DH, non-repeatered 50 km transmission experiment using low-loss optical fibres 78−79108
InGaAsP-InP DH laser emitting at 1.27 μm, fast pulse behaviour, high speed direct modulation 77−23676
InGaAsP-InP DH laser, room temp. operation, 1.27 μm emission 77−88743
InGaAsP-InP DH lasers, direct modulation 78−42363
InGaAsP-InP DH lasers, carrier lifetimes meas. 78−66828
InGaAsP-InP DH laser, threshold depend. on active layer thickness 79−7127
InGaAsP-InP DH lasers, threshold characteristic 79−81430
InGaAsP-InP DH laser, optical gain meas., low-intensity luminesc. and absorpt. spectra 79−98356
InGaAsP-InP DH lasers, low temp. behaviour of threshold current and carrier lifetime 79−98374
InGaAsP-InP DH lasers, degradation by In solder 79−98402
InGaAsP-InP DH laser with self-aligned struct., oscillation charact. 80−38017
InGaAsP-InP DH laser, 1.55 μm, low temp. LPE growth for room-temp. CW operation 80−64045
InGaAsP-InP DH lasers, interfacial recomb., influence on oscill. charact. 80−87393
InGaAsP-InP DH lasers, spatial hole burning, spontaneous emission saturation, direct obs. 80−95892
InGaAsP-InP DH lasers, temp. dependence of threshold and elect. charact. 80−99725
InGaAsP-InP DH lasers, perturbed InP growth, photoluminesc. study 80−106518
InGaAsP-InP DH laser, threshold current, temp. depend. 80−106521
InGaAsP-InP embedded mesa strip lasers 80−14350
(InGa)(AsP)-InP laser system, 1 μm wavelength, lattice matching techniques 80−99748
InGaAsP-InP lattice matched DH, growth by two-phase supercooled soln. technique 78−10296
InGaAsP-InP vapour-grown quaternary heterojunction laser struct., reliability 79−98385
$In_{0.84}Ga_{0.16}As_{0.46}P_{0.54}$, refractive index, at laser oscillating wavelength of 1.2 μm 79−64224
$In_{1-x}Ga_xAs_yP_{1-y}$, DH laser material, spatially resolved photolum. characterisation and optically induced degradation 79−47486
$In_{1-x}Ga_xAs_yP_{1-y}$ DH laser, low threshold current density, near equilibrium LPE growth 80−19040
$In_{1-x}Ga_xAs_yP_{1-y}$ DH lasers for 1.3 and 1.5 μm optical fibre communications 80−91817
$In_{1-x}Ga_xAs_yP_{1-y}$/InP 1.5 μm room-temp. CW laser fabrication and operation 80−64070
$In_{1-x}Ga_xAs_yP_{1-y}$-InP DH laser, fabricated on (100)-InP substrate, 500-hr CW operation 77−83890
$In_{1-x}Ga_xAs_yP_{1-y}$-InP DH lasers, fabrication and performance 78−5500
$In_{1-x}Ga_xAs_yP_{1-y}$-InP DH laser on InP (100) substrate 78−29965
$In_{1-x}Ga_xAs_yP_{1-y}$-InP DH laser, 10000 h continuous CW operation, dark-line and dark-spot defects 79−98384
InGaAsSb based injection heterolaser, 1.9 μm stimulated emission 79−18420
InGaAsSb, LPE growth, and appl. in GaSb/AlGaAsSb/InGaAsSb/AlGaAsSb/GaSb DH 80−16205
InGaAsSb-AlGaAsSb DH laser, room temp. operation at 1.8 μm wavelength 80−43358
$In_xGa_{1-x}As_ySb_{1-y}$ laser, nonequilibrium carrier recombination, luminesc. study 80−50431
$In_{1-x}Ga_xP$ electron-beam-pumped, LPE and VPE growth 80−2281
$In_xGa_{1-x}P$-GaAs lattice mismatched heterojunction, recomb. props. 78−13707
InGaPAs LPE layers, compositional inhomogeneity, photoluminesc. obs. 80−75451
InGaPAs LPE multilayered DH lasers exhibiting quantum size effects 78−1227
InGaPAs-InP DH laser, threshold current temp. depend., potential barrier height influence 80−53296
$In_{1-x}Ga_xP_{1-z}As_z$, DH, operated in external grating cavities, inhomogeneous and homogeneous line broadening 77−10921
$In_{1-x}Ga_xP_{1-z}As_z$, DH, diode and laser performance, limitations of direct-indirect transition 77−39927
$In_{1-x}Ga_xP_{1-z}As_z$ DH lasers, pulsed room temp. operation 77−10941
$In_{1-x}Ga_xP_{1-z}As_z$ DH laser, effective index of refr., wavelength depend. 77−61954
$In_{1-x}Ga_xP_{1-z}As_z$ DH lasers, multiple LPE, lattice matching 77−77421
$In_{1-x}Ga_xP_{1-z}As_z$ DH laser diode, defect and phonon assisted tunnelling 78−13708
$In_{1-x}Ga_xP_{1-z}As_z$ electron-beam-pumped, LPE and VPE growth 80−2281
$In_{1-x}Ga_xP_{1-z}As_z$ LPE DH laser with multiple thin layer active region 77−83887

semiconductor junction lasers continued
$In_{1-x}Ga_xP_{1-z}As_z$ near IR DH laser, constant temp. LPE, external grating cavity 77−75550
$In_{1-x}Ga_xP_{1-z}As_z$, room temp. visible heterojunction lasers 78−5501
$In_{1-x}Ga_xP_{1-z}As_z$ single thin active layer visible spectrum heterostruct. lasers 78−63120
$In_{1-x}Ga_xP_{1-z}As_z$, stimulated yellow-green emission under electron excitation, 80K 79−33846
$In_{1-x}Ga_xP_{1-z}As_z$ thin well in InP p-n junction, confined carrier luminesc. and laser modes 78−13703
$In_{1-x}Ga_xP_{1-z}As_z$, visible spectrum laser diode, continuous operation, 6280 Å, 77K 79−960
$In_{1-x}Ga_xP_{1-z}As_z$:Zn, x∼0.12, z∼0.26, LPE, DH lasers, tunnelling involving defects 77−65594
$In_{1-x}Ga_xP_{1-z}As_z$-$In_{1-x}Ga_xP_{1-z}As_z$ visible spectrum multiple-quantum-well heterostruct. lasers 80−106537
$In_{1-x}Ga_xP_{1-z}As_z$-InP, single and multiple layer heterostruct., LEDs and lasers 78−46626
$In_{1-x}Ga_xP_{1-z}As_z$-InP coupled multiple quantum-well heterostructure laser diodes, threshold current temp. depend. 80−78855
InP injection laser, strong mag. field effect on emission 77−58329
InP/$Ga_{0.47}In_{0.53}As$/InP DH, lattice matched, MBE and room temp. operation 78−74906
InP-$Ga_xIn_{1-x}As_yP_{1-y}$, DH, fabrication and operation in 1.5 μm region 78−37893
InP-$Ga_xIn_{1-x}As$-InP, DH fabrication, crack form. due to lattice mismatch 77−15704
InP-$Ga_xIn_{1-x}P_yAs_{1-y}$ heterostruct. lasers, growth and characterisation 80−23691
InP-GaInAsP buried heterostructure lasers of 1.5 μm region, fabrication and characts. 80−74388
InP-GaInPAs DH lasers, misplaced p-n junctions due to Zn contamination 78−87051
InP-$In_{1-x}Ga_xAs_yP_{1-y}$, DH lasers, dielectric-constant step 79−18418
InP-$In_{1-x}Ga_xAs_yP_{1-y}$-InP 1.55 μm DH room-temp. CW laser fabrication and operation 80−64071
InP-$In_{1-x}Ga_xAs_yP_{1-y}$-InP 1.53 μm single-mode CW ridge-waveguide laser 80−64072
InP-$In_{1-x}Ga_xP_{1-z}As_z$ quantum-well LPE heterostructure lasers, band filling and gain 79−22955
InP-$In_{1-x}Ga_xP_{1-z}As_z$ laser, phonon-assisted recombination 79−89906
InP-$In_{1-x}Ga_xP_{1-y}As_y$, LPE for optoelectronic devices *(German)* 79−95280
InP-$In_{1-x}Ga_xP_{1-z}As_z$ heterostructure laser, single and multiple quantum-well, liquid-phase epitaxial growth 80−38031
InP-InGaAsP-InP DH diode lasers, room temp. CW operation 80−1222
InP-InGaPAs heterojunction lasers and LEDs, 1.0 to 1.2 μm 80−74362
(Pb,Sn)Te, grating coupled emission 77−79860
Pb chalcogenide diode lasers, recent advances 80−5732
Pb salt, tunable IR diode lasers 78−59030
Pb salt DH lasers for IR gas spectroscopy 77−19325
Pb salt semiconductor laser, low freq. noise characts. 79−59698
Pb salt tunable diode lasers, wavenumber calibration using etalons 78−45738
Pb salt tunable diode laser-integrating sphere system, output intensity characts. 80−78881
Pb salt tunable laser diodes, for IR spectroscopy 77−82630
Pb-salt tunable diode lasers, beamshaping and polarisation control props. of flexible hollow metallic rectangular pipes in mid-IR 79−76856
Pb-SnSe diode laser, appl. to IR spectra of NH_3 mols. 78−58688
PbS current tunable p-n junction laser *(Polish)* 80−32985
PbS-$PbS_{1-x}Se_x$-PbS DH diode laser props., comparison of theory with expt. 78−22128
PbS-PbSe-PbS, DH, fabrication, CW operation up to 120K 77−23692
PbS-PbSe-PbS, DH, Peltier cooled, IR gas spectroscopy appl. 77−23690
$PbS_{1-x}Se_x$ (X=0.18) homojunction injection lasers, near-field emission 80−95896
$PbS_{1-x}Se_x$ diffused homojunction diode lasers, 140K operation 79−18415
$PbS_{1-x}Se_x$ diode laser, contact degradation due to diffusion 80−102734
$PbS_{1-x}Se_x$, single heterostruct. laser, wide tunability 77−79846
$Pb_{1-x}Sb_xTe$ DFB laser, CW operation 77−58338
PbSe diode laser correlation spectrometer, low SO_2 conc. meas. 77−91301
PbSe, diode laser spectrometer, for air pollution monitoring and mineral prospecting 77−82044
PbSe, pressure tunable CW injection laser, emission spectra 79−18419
PbSnSe, for IR heterodyne radiometry 78−267
PbSnSe tunable diode laser local oscillator, for heterodyne radiometer 77−91300
$Pb_{0.93}Sn_{0.07}Se$ crysts., sublimation growth, controlled carrier concs. for IR lasers and detectors 77−52237
$Pb_{0.995}Sn_{0.045}Se$ pulsed laser for high-resolution NH_3 spectroscopy 79−64252
$Pb_{1-x}Sn_xSe$ and $PbS_{1-x}Se_x$, single heterostructure tunable diode lasers formed by compositional interdiffusion 77−38896
$Pb_{1-x}Sn_xSe$ CW and pulsed diode laser spectroscopy of $^{14}NH_3$, $^{15}NH_3$ mols. 79−26980
$Pb_{1-x}Sn_xSe$ diode laser absorption spectrometer, pollution detection equipment 78−40672
$Pb_{1-x}Sn_xSe$ laser, optical feedback effects on performance, external cavity modes 80−32981
$Pb_{1-x}Sn_xSe$, single heterostruct. laser, wide tunability 77−79846
$Pb_{1-y}Sn_ySe$-PbSe, (0≤y≤0.08), lasing props. investigation 78−10990
$Pb_{1-y}Sn_ySe$-PbSe, prep. and emission characts., tuning 10.6-15 μm 77−58346
$Pb_{1-y}Sn_ySe$-PbSe pulse laser diode, temp. tuning of modes 78−50777
$Pb_{1-x}Sn_xSe_{1-y}Te_y$ optically pumped heterojunction laser with matched gratings, photolum. obs. 79−89909
PbSnTe, DH, anodic oxide film to avoid degradation by thermal cycling 78−50809
PbSnTe, tunable emission, 5-15 μm 77−50686
PbSnTe versus CO_2 laser for long path monitoring of ambient gases 79−16682
$Pb_{0.85}Sn_{0.15}Te$ homostructure diode laser, LPE growth, with controlled carrier conc. 80−95903
$Pb_{0.86}Sn_{0.14}Te$/PbTe, interface recomb. velocity in DH laser diodes 79−64222
$Pb_{0.93}Sn_{0.07}Te$ tunable diode laser for IR spectroscopy 78−33511
$Pb_{1-x}Sn_xTe$, DH, gain-freq.-current relation, k.p band model 77−61951

semiconductor junction lasers continued
$Pb_{1-x}Sn_xTe$ DH laser, minority carrier lifetimes and lasing thresholds 80−19031
$Pb_{1-x}Sn_xTe$ diode laser, appl. to high resolution IR spectroscopy *(Japanese)* 79−49306
$Pb_{1-x}Sn_xTe$ diode laser, contact degradation due to diffusion 80−102734
$Pb_{1-x}Sn_xTe$, distributed feedback DH lasers, design fabrication and characts. 77−10944
$Pb_{1-x}Sn_xTe$ heterojunction lasers, instantaneous vacuum evaporation grown, threshold current density 80−5759
$Pb_{1-x}Sn_xTe$ heterostructure laser, fabrication and props. 79−10306
$Pb_{1-x}Sn_xTe$ homojunction laser, increased freq. tuning range 77−75546
$Pb_{1-x}Sn_xTe$, injection laser, use in high-resolution spectroscopy 79−76714
$Pb_{1-x}Sn_xTe$ optically pumped lasers, power output and wavelength, 4 to 30K 78−79035
$Pb_{1-x}Sn_xTe$, small-gap, recomb. mech., rel. to DH laser threshold current 79−38099
$Pb_{1-x}Sn_xTe$, Te-rich growth by ingot nucleation method, laser fabrication 77−77362
$Pb_{1-x}Sn_xTe/PbTe_{1-y}Se_y$ lattice-matched buried heterostructure lasers with CW single mode output 80−74386
$Pb_{1-x}Sn_xTe$-PbTe, (0≤x≤0.2), lasing props. investigated 78−10990
$Pb_{1-x}Sn_xTe$-PbTe heterojunctions, interface recombination velocity reduction with decreasing lattice parameter mismatch 79−98370
$Pb_{1-x}Sn_xTe$-PbTe pulse laser diode, temp. tuning of modes 78−50777
PbTe, freq. tuning using press. and temp. combination 78−17978
PbTe, MBE homostructure diode lasers with CW operation up to 100K 78−22129
PbTe tunable laser diode IR absorption spectroscopy 79−75628
PbTe:Bi-PbSmTe-PbTe, epitaxial laser struct., growth, p-n junction position and lasing region 79−89908
PbTe-(Pb,Sn)Te DH laser, CW operation over 1500 h at 77K 78−17950
PbTe-$Pb_{1-x}Sn_xTe$-PbTe, DFB laser, coupling coeff. calcs. 77−14714
PbTe-$Pb_{1-x}Sn_xTe$-PbTe DH, LPE and VPE, stimulated emission 77−75526
SiO_2 insulated $Ga_xAl_{x-1}As$ laser, CW, 3-5 mW optical communication appl. 77−3656
ZnSe film, grown on sapphire substrate, stimulated emission 79−78708
ZnSe-GaAs narrow junction lasers 80−43334
ZnSe-ZnS semiconductor waveguide laser, electron beam excited, blue emission 79−18447
ZnTe film, grown on sapphire substrate, stimulated emission 79−78708

semiconductor junctions
see also p-n junctions
amorphous/crystalline heterojunction, energy-band diagram construction 77−55602
breakdown voltage, temp. effects 79−7882
chalcogenide glass/n-GaAs heterojunctions, elec. props. and band diagram 79−99609
charge flow analogue computation, attenuation-free upwind difference formula 77−28241
compound semiconductor interfaces, conf., Los Angeles, USA (Jan. 1978) 78−91756
depletion region of junction barriers, capture from free-carrier tails 80−70802
depth profiling by electron beam induced junction current meas. 80−96977
DH, nonequilib. carrier distrib., local excitation of active region, influence of diffusion of luminesc. 79−73574
doping profile using ellipsometric meas. for semicond. substrate-semicond. epitaxial layer system 79−99453
effective-mass approx. in presence of interface 79−99629
electric field effect on thermal emission of traps 80−11073
electrogradient EMF, V-I characts. *(Russian)* 78−47852
electron beam induced current technique appl. to semicond. device characts., review 78−21302
electron-phonon scatt. 80−24997
EMF in semiconductors, thermal injection of electrons, obs. 79−23994
forward biased junctions, excess noise sources due to defects 79−38154
$Ga_{1-x}In_xSb$, inverted diode, electron irradiation effect on props. *(Russian)* 78−14378
graded n-n$^+$ heterojunction, barrier height reduction 77−47891
grain boundary and interdiffusion studies, AES and SIMS 79−77842
heterojunction, band-edge discontinuities and interface pot. step, two-band narrow-gap approach 80−39665
heterojunction, compositionally graded, misfit dislocation energy calc. 77−59237
heterojunction, electronic struct. calcs. 79−1613
heterojunction, energy barriers and interface states 79−56295
heterojunction, impact ionisation 80−65663
heterojunction, model of anomalous photocond. 77−76914
heterojunction band-edge discontinuities, LCAO theory 77−89840
heterojunction interfaces, carrier transport 79−47158
heterojunction interfaces energy band discontinuities nontransitivity 80−44714
heterojunction properties analysis and control, cathodolum. appls. *(French)* 79−69892
heterojunction solar cells 80−61344
heterojunctions, between narrow-gap semiconds. interface states 77−55603
heterojunctions lineup, appl. of interstitial PD, electronegativity diff. and effective ionic charges 77−76766
heterostructure, potentials supporting continuum-embedded positive-energy eigenstates 77−47894
III-V heteroepitaxial interfaces, correl. of electronic and struct. props. 77−89835
III-V semiconductor *(Slovak)* 80−88620
III-V semiconductor compound structures, TEM analysis 77−89836
interface and surface phenomena, conference, Pacific Grove, USA (Jan.-Feb. 1979) 80−46725
isotype heterojunction barriers, cond. band discontinuity, C-V profiling meas. method 80−70801
isotypic heterojunction under transient depletion conditions, information-carrying charge 78−26944
laser processing of semiconductors, bibliography 79−74028
magnetic semiconductor, photomagnetisation, photoinduced heterojunctions 77−63259
multilayer heterojunction struct., impurity and phonon scatt. 80−2456
multilayer semiconductor structures, plasma-wave beams 80−49795

semiconductor junctions continued
multilayer structures, reversal junctions, voltage cutoff criterion *(Russian)* 78−72244
n^+-ν-n^+ structure, HF impedance of compensated semicond. 79−15212
n^+-n contact, electron transport, topological anal. 79−15209
n^+-n junction, elec. field screening 77−55605
n^+-n linear-gradient junction, thermoelectric effects 79−73577
n−n^+ low-high junctions, static circuit model 79−91132
n-n^+ junction point contacts, I-V charact. 77−1480
n-n^+ point contacts, current-voltage charact. 78−26940
n-n^+ step homojunction, theory 79−24056
n-n homojunction, calc. of free carrier density profile in a semicond. near ohmic contact 80−70810
n-p-i structure, exclusion effects on I-V charact. 77−15945
neutrality and equilibrium in semiconductors 79−65544
noisy transient meas., optimum correlation method 78−62205
one-sided abrupt junctions, normalized representation of avalanche breakdown behaviour 80−65666
p^+-ν-p^+ structure, expt. determ. of lateral spreading vel. of electron-hole plasma 77−4428
p^+-n-n^+ heterostructure, variable gap base, carrier injection, quasielectric field, transient process anal. 80−44716
p-i-p structure, two-dimensional carrier transport at high injection rate 79−15213
photovoltaic solar energy, conference, Luxembourg (1977) 78−64106
polar semiconductor, optical phonon-magnetoplasmon interface oscills. 78−43467
polar semiconductor-polar semicond. interface, optic-phonon-magnetoplasmons 78−23146
polycrystalline, X-ray diffractometric study 77−20406
relaxation semiconductor, theory of carrier transport in p^+-ν junction 79−60914
relaxation semiconductors, junction behaviour 78−30977
SEM, induced conductivity mode expts., apparatus requirements 79−9260
semiconductor-ferroelectric heterostruct. junction, nonvolatile polarised memory 79−78164
shallow junction devices, minority carrier diffusion lengths 78−72168
step l-h junction, elec. struct. analytical methods, review 80−100507
strongly degenerate plasma, double injection, vol. controlled current regime 79−51658
sublinear current-voltage charact., field-opposed diffusion of free carriers 78−47862
sublinear I-V charact., theory 78−91763
superlattice, electronic props. 79−95490
superlattices, optical and transport props., review *(Slovak)* 80−20288
ternary semiconductor device applications, review 78−39207
thin film Congress Loughborough, England, (Sept. 1978) 79−77949
transition regions in epilayer structures 79−78167
tunnel-effects in junctions generating burst-noise *(Rumanian)* 80−6960
AlAs-GaAs heterostructure, fabrication by selective liq.-phase epitaxy 79−15618
n-$Al_xGa_{1-x}As$, variable-gap crystal, magnetoresistance 78−34850
$Al_xGa_{1-x}As$:O-n-GaAs heterojunction for MIS device, capacitance voltage meas. 79−87157
$Al_xGa_{1-x}As$-GaAs, heterojunction, interface width, AES obs. 80−20290
$Al_xGa_{1-x}As$-GaAs abrupt LPE heterojunction, Auger profiling 77−85101
$Al_xGa_{1-x}As$-GaAs DH photodetector, optical power conversion at 8500 Å and I-V charact. 77−87833
$Al_xGa_{1-x}As$-GaAs n-n heterojunction, LPE, Auger profiling and absence of rectification 78−95349
$Al_xGa_{1-x}As$-GaAs n-n heterojunction, interface width determ. 80−49887
$Al_xGa_{1-x}As$-GaAs-$Al_xGa_{1-x}As$ quantum well, carrier collection 79−15211
AlN-Si, capacitance meas. 77−55468
As_2S_3-HgSe structure, anomalous photocond., relax. curves 77−55567
$As_{50}Te_{50}$, amorphous films, metal and semicond. contacts, threshold switching, IR emission 80−49831
Au-n-$Ga_{1-x}Al_xAs$-n-GaP narrow-band variable-gap surface-barrier photoedetector 80−96944
C, amorphous, struct. and semicond. props. and heterojunction form. with single cryst. Si 80−25002
CdS, electron traps, admittance spectra on hetero- and Schottky junctions 79−56159
CdS-GaAs n-n voltage-enhanced photoanode, solar cell efficiency 78−14810
CdS-ZnTe, acoustoelectric domain injection across interface, propag. loss, Brillouin scatt. 77−51778
CdSe-As_2S_3($AsSbS_3$) heterostructure, energy bands and interface props., photoelectron spectroscopy 78−2551
$CdSnP_2$-InP, n-n heterojunctions, growth, elec. charact. 77−11992
CdTe-HgTe ideal superlattice, electronic props. calc. 80−49885
GaAlAs/GaAs heterostructures, ellipsometric assessment of epitaxial layer during growth in organometallic VPE system 79−37933
GaAlAs-GaAs heterostructures, electronic excitation effects on mobility of point defects and dislocations 78−2561
GaAlAs-GaAs n-n heterojunction, rectification 79−28402
$Ga_{0.5}Al_{0.5}As$-GaAs(:Ge) DH structure, minority carrier lifetime and internal quantum efficiency of surface-free GaAs 79−43013
$Ga_{1-x}Al_xAs$ LPE layer on GaAs, lattice mismatch using X-ray source 79−82470
$Ga_{1-x}Al_xAs$ n-p_3-p_2-p_1-p_0 struct., degradation electrolum. 80−50428
$Ga_{1-x}Al_xAs$-GaAs, abrupt quantum-well heterostruct. grown by metalorganic chemical vapour deposition 79−56933
GaAs epitaxial layers, structural defect and conc. inhomogeneities influence on barrier diode I-V charact. 80−15602
n-GaAs epitaxial wafers, IR reflectance and elec. charact. 79−56293
GaAs, intrinsic, on degenerate n-Ge, surface polaritons, hydrodynamical model 80−6752
GaAs n-i-n junction, photoelec. props. investig., 77 to 300K 77−28248
GaAs, n-i-n junctions, simulation of long-term relax. of nonequilib. conductivity 79−38156
GaAs n-n^+ epitaxial structure for CW microwave electroacoustic amplifier 78−59235
GaAs:Sn epitaxial layer, electronic props. and epilayer-substrate interface props. 77−89886
n-GaAs/N-GaAlAs heterojunctions, microwave detection 79−54186
GaAs-$Al_{0.3}Ga_{0.7}As$ n-N heterojunction, LPE grown, cond. band discontinuity, C-V profiling meas. 80−70801
GaAs-$Al_xGa_{1-x}As$ heterojunctions, inelastic light scatt. 79−65867

semiconductor junctions continued
GaAs-$Al_xGa_{1-x}As$ modulation-doped heterojunction superlattices, electron mobilities 79−7877
GaAs-AlAs superlattice, folded acoustic phonons obs., Raman scatt. 80−88996
GaAs-$Ga_{0.7}Al_{0.3}As$ (001), (211), threading dislocation in single layer heteroepitaxial struct., bowing 79−65341
GaAs-$Ga_{0.7}Al_{0.3}As$ n-n heterojunction, LPE, rectification 80−49888
GaAs-$Ga_{1-x}Al_xAs$, n^+-i-n heterojunction, radiative recombination under double injection *(Russian)* 77−77298
GaAs-$Ga_{1-x}Al_xAs$, variable band gap, photo-EMF 80−20296
GaAs-$Ga_{1-x}Al_xAs$ n^+-ν-n junction, avalanche carrier multiplication *(Russian)* 78−76140
GaAs-$Ga_{1-x}Al_xAs$ repeated monolayer heterostructure, electronic struct. 77−66197
GaAs-$Ga_{1-x}Al_xAs$-$Ga_{1-y}Al_yAs$ n^+-i-n heterostructure, electroluminesc. charact., 80 to 330K *(Russian)* 79−28404
GaAs-GaAlAs heterostructures, saturation of free exciton absorption 79−61454
GaAs-GaAlAs-GaAs rectifying semicond. struct., prep. by MBE and charact. 80−65657
n-GaAs-GaAs:Cr, interface elec. props., substrate effects 78−6438
GaAs-$GaAs_xSb_{1-x}$, heteroepitaxial structs., mismatch dislocation nets 79−10855
GaAs-Ge interface, photoemission 80−25530
n-GaAs-n-$Al_xGa_{1-x}As$ rectifying heterojunction, cond. props. study 80−88626
n-GaAs-n-GaN, diffusion growth kinetics, morphology and electrical properties 80−20294
n-GaAs-n-GaP, in MIS structures, elec. controlled optical transparencies, optical processing use 77−85339
n-GaAs-n^+-$Al_xGa_{1-x}As$ production, by MBE *(German)* 80−44711
$GaAs_{1-x}Sb_x$ epitaxial n-n heterostructures, gap energies and interface pots., modulation electroabsorpt. meas. 79−11201
$GaAs_xSb_{1-x}$-GaAs epitaxial films and multilayer heterostruct., SEM obs. under cathodolum. conditions 79−11023
GaP:Fe n-i-n epitaxial struct., photoconductivity, recombination scheme *(Russian)* 80−15569
GaP:H/GaAs, amorphous film/crystal junction, optical and elec. props. 79−99611
GaSb, inverted diode, electron irradiation effect on props. *(Russian)* 78−14378
GaSb-InAs system, (110) surface and interface electronic struct. 80−100494
Ge, graded n-n^+ junction, hot-electron diffusion coefficient 78−87982
Ge, high purity, nature of large traps, expt. on p^+-n-n^+ struct. 78−19051
Ge Lo-Hi junctions, avalanche injection delay and ionization rate at low electric field 79−95475
Ge p^+-n-m structure, current-voltage charact. 77−1476
Ge p^+-n-n^+ and p^+-i-n^+ structures, inhomogeneous, influence of longitudinal mag. field 77−1479
Ge-$Ga_{1-x}Al_xAs$, MBE of ultra thin film superlattices on GaAs substrates, TEM study 79−37932
Ge-GaAs, n-n isotype heterojunctions, fixed-interface-charge model 78−56215
Ge-GaAs (110), heterojunction chemistry, photoemission expts. 78−95244
Ge-GaAs (110) interface, relax., self-consistent pseudopotentials 78−30981
Ge-GaAs (110) junction, interface states and electronic struct. 77−69408
Ge-GaAs interface, surface and interface states of (111) surfaces 79−15206
n-Ge-n-GaAs isotype heterojunctions, modelling, charact. 80−103747
a-Ge-Si crystal interface, low resist. elec. behaviour 77−89843
Ge-Si n-n heterojunctions, photovoltaic response 78−14804
Ge_xSi_{1-x} on nn$^+$ Si substrates, imperfections and morphology, electron microscope and electron diffr. obs. 79−42420
InAs-GaSb (001) superlattice, electronic struct., tight binding calc. 78−95350
InAs-GaSb (001) superlattices, two-dimens. effects and effective masses 80−49883
InAs-GaSb (100) superlattice, electronic struct., self-consistent pseudopot. method 80−49884
InAs-GaSb superlattice, electronic struct., self-consistent pseudopot. calc. 80−29470
InAs-GaSb superlattice, semiconductor-semimetal transition obs. 80−44710
InAs-GaSb superlattices, crystallography, Rutherford backscatt. and channelling obs. 80−49533
InAs-GaSb superlattices, semicond.-semimental transition obs. 80−49882
InAs-GaSb superlattices, mag. field induced semimetal-semicond. transition 80−65656
$InAs_{1-x}Sb_x$-InAs backside-illum. narrow band photodetectors 77−61118
InGaAs-GaAs heterojunction with low misfit, misfit dislocation struct. 77−62783
$In_{1-x}Ga_xAs$-$GaSb_{1-y}As_y$ heterostructure devices 79−42624
InGaP/InGaAs struct. for transferred electron photocathodes, VPE growth and characterisation 80−76193
InGaP-GaAs junction, effect of elastic strain on energy band gap and lattice parameters 79−24057
$In_xGa_{1-x}P$-GaAs heterojunction, interface recomb. velocity determ. 77−89838
$In_uGa_{1-u}P_vAs_{1-v}$-InP, LPE, lattice matching, phase 80−54350
In_2O_3:Sn/n-Si heterojunction solar cell, fabrication and charact. 78−15314
InP/InGaAs/InP field assisted photocathode, minority carrier electron transport across p-p heterojunction 78−95651
InSb-GaAs semiconductor plasmas, surface wave instabilities, temp. effects 79−78125
InSb-GaSb, compositionally modulated sputtered superlattice, growth and interlayer diffusion 79−56930
InSe based heterojunctions, props. 79−11210
InSe-SnO_2 n-n heterojunctions, photoelec. props. 80−96945
$In_{2-x}Sn_xO_{3-y}$-Si solar cells, SiO_2 detection of interface, Auger anal. 79−87991
$In_{2-x}Sn_xO_{3-y}$[SnO_2]-CdSe-CdS:Cd,Cl sandwich photoconductor injection obs. *(Russian)* 80−54773
PbS-Si heterojunction, PbS film growth and struct. 80−96762

semiconductor junctions continued
Se-Ag_2Se, thin film polycrystalline heterostructure, exhibiting memory switching, noise level 78−84288
$Se_{1-x1}Te_{x1}$-$Se_{1-x2}Te_{x2}$ heterostructure, amorphous, rectification phenomena and photovoltaic effects 79−99610
$Se_{1-x}Te_x$-$Se_{1-y}Te_y$ junctions, photovoltaic effects and rectification phenomena 80−84506
Si, between ion-bombarded amorphous and crystalline layers, insulating props. 77−59327
Si, Lo-Hi junctions, avalanche injection delay and ionization rate at low electric field 79−95475
Si, n-n^+ junction, influence of internal field on its elec. props. 79−56297
Si, n-n^+ point junctions 80−44719
n^+nn^+Si planar device, hot electron flicker noise at 78K 80−103732
p-Si surface barrier particle detectors 77−50326
Si:Cd n^+-n-n^+ structs., photoresist. props. under exclusion conditions 80−39666
Si:Cd(Zn), n^+-n-n^+ structure, photocond. lifetimes, deep level occupancy in exclusion region 78−72253
Si:P, through-oxide implanted samples, anomalous residual defects after annealing 77−76432
Si:Rh, p^+-n-n^+, n^+-n-n^+, p^+-n-p^+, structs., S- and N-type I-V charact. 77−43706
Si:Zn, p-n-n^+ and p-n-p struct., reson. characts. of impedance near excitation threshold of recomb. waves 80−20301
Si/In_2O_3-SnO_2 thin film junctions, polarity dependent memory switching effects 80−70814
Si/Si-Ge alloy, amorphous, solar cell, multijunction structure, increased conversion efficiencies, low cost 80−45677
Si-$As_2Se_3Ge_4$ heterojunction, elec. props. 78−6434
Si-CdSe n-n heterojunction, photovoltage sign reversal, energy band profile *(Korean)* 80−29469
Si-Ge heterojunction form., microscopic aspects, EELS meas. 80−80368
Si-Ge junction, Si monocryst. and Ge film, elec. props. 79−51660
Si-In_2O_3:Sn heterojunctions for solar cells 78−64107
Si-PbS heterojunction, effect of Si substrate orientation on struct. and interface props. 80−80097
Si-Pd_2Si heterostructure growth by solid-phase epitaxy from Si (111)-Pd-Si (amorphous) 77−51617
Si-Si interface, elec. cond. rel. to interface state population 80−65672
n-Si-SiC film junction device, elec. props. 80−15591
Si-SiC p-n and n-n heterojunctions, prep. by ion implantation, tunnelling cond. 77−43710
Si-SnO_2, barrier height meas. by HF capacitance method 77−69406
Si-SnO_2 heterojunctions, complementary Schottky barriers 79−78166
Si-ZnSe n-n heterojunction photovoltaic effect, freq. meter in visible wavelength *(Korean)* 79−60915
SiC, α-β heterojunctions, spectral characts. *(Russian)* 77−63467
SiC, point contact, stable elec. oscill. generation by high field strength *(Russian)* 77−62989
n-SiC-n-CdS heterojunctions, photoelec. and elec. props. 78−80042
SiC-Si struct. formation on ^{12}C ion implantation in Si, optical and photoelectric props. 79−91136
SnO_2/n-Si solar cells, fabrication and characterisation 79−79393
SnO_2-InSe n-n heterostructures, photoelec. props., 80 to 300K 80−20297
SnO_2-Si heterojunction solar cell, elec. props. *(Korean)* 80−45665
SnO_2-Si heterojunctions, elec. and photovoltaic props. 80−26141
SnO_2-Si n-n photodiode, 5.4 MeV electron irrad. effects 77−80806
Tl-Se-$TlInSe_2$, isomorphic pairs, struct. and growth peculiarities 79−1421
Tl-Se-$TlInSe_2$, struct. and growth peculiarities, epitaxial heterojunctions *(Russian)* 79−11038
ZnO/Si acoustoelectric devices, magnetron discharge sputtering prep. 80−80332
ZnO-Bi_2O_3, heterojunction, current-voltage characts. 79−56291
ZnO-CdSe thin film n-n heterojunctions, prep. elec. and optical props. *(Korean)* 77−28244
ZnP_2, α-β heterojunction, I-V characts. and photoresponse 78−64105
ZnS-Si, n-n, epitaxial, elec. props. *(Russian)* 78−88023
ZnS(Se) heterojunctions, with tetragonal BiOBr, BiOCl, ErOCl, LaOCl 79−60919
ZnSe:Mn/n-GaAs low threshold thin film DC electrolum. cell, pulse-excited characts. 80−76081
ZnSe:Mn-n-GaAs, single cryst. substrate low threshold DC electrolum. 77−63465
ZnSe-Ge (100) interface, electronic struct. calc., scattering theoretic approach 80−6940
ZnSe-ZnTe heterojunction, epitaxial, photosensitive, photoelec. props. 79−11203
ZnTe-ZnSe, MBE, photoluminesc. efficiency 77−77419

semiconductor materials
see also amorphous semiconductors; degenerate semiconductors; elemental semiconductors; heavily doped semiconductors; II-VI semiconductors; III-V semiconductors; III-VI semiconductors; IV-VI semiconductors; liquid semiconductors; magnetic semiconductors; many-valley semiconductors; narrow band gap semiconductors; organic semiconductors; polar semiconductors; semiconductors; ternary semiconductors
Cd_3As_2, energy band parameter calc., temp. and press. depend. 77−31943
ceramic, low resistance contacts 77−1483
chalcogenides of ABX_2 type comp., cybernetic prediction of form. possibility 80−101004
compound semiconductors, quantitative anal. with ion microanalyser *(Japanese)* 78−7292
copper quaternary thiospinels, mag. and elec. props. *(French)* 80−65771
galvanomagnetic effects, measurement cryostat *(Hungarian)* 77−17986
graphite intercalation acceptor lamellar cpds., charge distrib. and transport props. 79−95411
history, solid state research to semiconductor electronics 80−68015
I-VII semiconductors, excitonic polarons, Pollmann-Buttner variational method, donor and exciton binding energies 79−42469
II_3-V_2 compounds polymorphic modifications, low temp., genetic rel. between cryst. struct. 79−60302
II_3V_2 semiconductors, spin-orbit and cryst. field splittings of valence band 78−63980
inhomogeneous, impurity opt. absorpt. and photocond. spectral line profile variation 77−16352
layered semiconductors, transport props., book contrib. 77−43587
light absorption, amplification and luminescence, saturation effects *(Russian)* 78−13771
magnetospectroscopy, HCN CW laser source *(German)* 77−10948
minority carrier diffusion length meas. using electron microprobe 77−39867
α-MnS, elec. props. meas. 78−87971
multicompositional compound semiconductor materials *(Japanese)* 80−107778
oxide semiconductors in photoelectrochemical conversion of solar energy, use as cell anodes 80−101120
PbI_2, trapping levels, TSC meas. 78−23107
phthalocyanine compounds, UPS valence band studies 77−52221
pyrrhotite, complex refractive indices rel. to comp. of Saturn's rings 77−29716
rare earth chalcogenides, cond. mechanism and thermoelec. efficiency 79−38110
rare earth compounds, R_2MoO_5, cryst. struct., IR spectra, elec. and mag. props. 80−33954
rare earth monophosphides, K-emission bands, electronic struct. 78−15250
rare earth oxides, perovskite-like, synthesis, struct., elec. props. 80−65554
rare earth pyrochlores, $R_2(V_{4/3}W_{3/3})O_7$, (R=Gd, Tb, Dy, Ho, Er, Tm, Xb, Lu), synthesis and elec. props. 80−29914
rare earth sulphides, $EuRs_4$, R=La, Ce, Pr, Nd, Sm, Gd, elec. cond. meas. 80−65555
rare earth vanadites, RVO_3, extrinsic p-type cond. 77−11919
rubrene-in-benzene, excited state migration and charge transfer 77−55559
n-SiC, 6H and 15R polytypes, (0001) plane, influence of uniaxial mechanical stress on resist. anomaly 78−10445
β-SiC, 6H polytype, pure and doped, prep. by pyrolysis of silane cpds. 78−44018
spin splitting and effective g-factor of T-holes *(Russian)* 77−51643
sulphides of nonmagnetic transition metals, semicond. props. rel. to at. vol. 78−64037
transition metal, group VIa, layered dichalcogenides, hole reactions, electrochem. solar energy conversion appl. 79−7893
transition metal pnictides, atomic volume, semicond. props. 78−59780
transition metal vanadates, elec. and mag. props., stoichiometry 78−51991
troilite, complex refractive indices rel. to comp. of Saturn's rings 77−29716
V_2VI_3 compounds, electronic struct., X-ray emission, XPS, UPS obs. 78−52638
vibrational IR excitons, spectra *(Russian)* 78−15173
zinc blende structure, cond. band nonparabolicity and cyclotron reson. linewidth *(German)* 78−75993
zinc blende-type semiconductors, interstitial PDs, electronegativity diff. and effective ionic charges 77−76766
AgBr, electron-hole liquid, RPA calcs. 80−6743
AgBr, frequency dependent optical phonons contrib. to small radius excitons binding energy 77−69236
Ag_8MSe_6, M=Ge,Sn,Si, absorpt. edge under hydrostatic press. 77−85740
AgN_3, high-resist. explosive cpd., elec. and galvanomag. props., temp. depend. 80−103728
Ag_2O, forbidden energy gap oxide semicond. crystals, review of spectroscopic props. 78−2876
Ag_2O, photoconductivity of crystals grown under hydrothermal conditions 78−14765
$(Ag_{x/2}Pb_{1-x}Bi_{x/2})$Te solid solution, preparation and thermoelectric props. 77−47839
$(Ag_{x/2}Pb_{1-x}Sb_{x/2})$Te solid solns., Hall coeff., thermoelec. power, and thermal cond., 100 to 500K 79−82614
Ag_2S, changes in elec. cond. and thermoelec. power at melting point 79−15147
Ag_2S layers, quenching of photocond. by UV radiation 78−68047
Ag_2S, transport props., 700-1500K 78−47796
Ag_2Se, between metal electrodes, current-voltage characts *(French)* 80−97005
Ag_2Se, changes in elec. cond. and thermoelec. power at melting point 79−15147
Ag_2Te, changes in elec. cond. and thermoelec. power at melting point 79−15147
p-Ag_2Te, electrophysical props. 77−39842
Ag_2Te, growth by chem. transport *(Russian)* 79−38728
Ag_2Te-Ag_2S system, elec. and thermal props. at 300K 78−64044
$Ag_2Te_xSe_{1-x}$ system, solid solns. of substitution existence, X-ray phase obs. 79−43217
Al-Fe_2O_3-Al, space charge limited current, current density as function of elect. field and temp. 79−51688
Al-Ge-SiO solar selective absorber surfaces, optical behaviour at high temp. 80−101130
AlB_{12}, α- and β-forms, elec. props. at high temps. and in strong elec. fields, thermistor appls. 80−92903
AlB_{12}, preparation of single crystal 78−43997
AlH_3, dark electrical cond., exam. 80−39624
AlH_3, photocond., photocurrent carrier-type 78−34855
AlH_3, polycrystalline, photoconductivity and photochemical decomp. 80−44638
$Al_2In_{12}Se_{21}$, cryst. growth from melt, elec. props. 79−56922
AlN-Si_3N_4 mixture film, CVD, characterisation of film props. 78−43496
$Al_{2+x}O_3$, nonstoichiometric, DC and AC cond., 20 to 1200°C 77−51740
β-Al_2O_3-$H^+(H_2O)_n$, p-type conductor, stability *(French)* 79−38063
β-Al_2O_3-NH_4^+, p-type conductor, stability *(French)* 79−38063
As chalcogenides, deep levels, photoluminesc. and photocond. 80−70641
As-Se(S), glassy and crystalline, point defect exam. by positron annihilation 78−72637
AsI_3, photopolarisation, photoelectret state, electron-hole transitions 77−12300
As_2O_3 crystalline and amorphous, EXAFS study of struct. 80−19776
As_2O_3, X-ray emission spectrum and XPS, electronic struct. calcs. using scattered wave method 79−11502
As_2S_3, cryst., vitreous or amorphous, nonlinear light absorption, temp. depend. *(Russian)* 77−48199
As_2S_3, cryst. and glassy, two-photon spectrum at room temp. 79−24334
As_2S_3, crystalline, two phonon vibrational spectra 78−35142
As_2S_3, crystalline and vitreous, nonlinear absorption of ruby laser radiation *(Russian)* 78−22165
As_2S_3, electron drift mobility temp. depend., transient photocond. obs. 77−66164

semiconductor materials continued
As_2S_3 film, vacuum deposited, selective etching characts. obs. *(Russian)* 80−3207
As_2S_3, temp.-independent mobilities, phonon-induced electron hopping 79−28347
As_2S_3, two photon light absorpt. dispersion, induced linear light absorpt. *(Russian)* 80−66231
As_2S_3, two-phonon vibrational spectra, crystalline and amorphous forms, Raman and IR spectra 78−39537
As_2S_3-Ag system, activation energy for photochem. conversion, 80-340K, radiation intensity depend. *(Russian)* 78−3356
As_2S_3-CdSe heterostructure, energy bands and interface props., photoelectron spectroscopy 78−2551
As_2S_3-HgSe structure, anomalous photocond., relax. curves 77−55567
$AsSbS_3$-CdSe heterostructure, energy bands and interface props., photoelectron spectroscopy 78−2551
As_2Se_3, cryst. and amorphous, optically induced absorption in band gap, picosec. dynamics 79−87439
As_2Se_3, crystalline, electron drift mobility and DC cond., trapping model 77−47815
As_2Se_3, monoclinic, chem. bonds rel. to electronic and vibr. states 80−64951
As_2Se_3, photosensitive layer, in metal-photosemiconductor-insulator multilayered struct., optical image recording 80−42286
As_2Se_3, single crysts., fine struct. of direct gap from electrorefl. spectra 80−93280
As_2Se_3-HgSe double-layer system detector for temp. meas. 79−88952
$As_2(Se_{1-x}Te_x)_3$, thermal cond., temp. and press. depend. 79−82396
B-based semiconductors, props. review 79−42532
B-Si compounds, thermoelec. material, prep. by pyrolysis of BBr_3-$SiBr_4$ mixture 80−20862
$B_{12}C_x$, phonon energies and electronic props., x depend., refl. spectra and thermoelec. power meas. 80−16052
$B_{14}Si$, β rhombohedral, conduction mechanism, thermoelectric props. 80−24932
$B_{14}Si$ elec. props., medium range disorder model 80−15522
BaF_2 solid electrolyte, n-type electronic cond., 700-900°C 80−29448
$Ba_3Sc_4O_9$, $Ba_3Sc_2WO_9$ and Ba_2ScTaO_6, elec. cond. nature, depend. on comp. and medium thermodynamic parameters 80−70773
$Ba_{1-x}Sm_xS$, electron config. of Sm ions, X-ray L-absorpt. spectroscopy 80−60715
$Ba_{0.5}Sr_{0.5}Nb_2O_6$, electronic props. and photoresponses 80−92925
$BaTiO_3$ and $BaTi_{1-x}Fe_xO_{3-x}F_x$, electrical, optical and mag. props., photoelectrolysis 77−47856
n-$BaTiO_3$, grain boundary resistivities 77−80782
n-$BaTiO_3$, ohmic contact form. 80−92969
Ba_2ZnS_3, prep. by solid state reaction and melt growth, X-ray anal. 77−73226
(Be, Al)B_{12}, elec. cond., refl. and absorpt. spectra 80−20188
$(Bi,Sb)_2(Te,Se)_3$ thermoelectric alloys, phase diagrams, and imperfection chemistry 80−108422
(Bi, Sb)$_2Te_3$ solid soln., semiconductor film, oxidation, electrophysical props. 80−45407
Bi-Sb, semiconduct., e.m. wave propag. perpendicular to mag. field 79−82517
Bi-Sb, semiconducting solid solution, forbidden band width Sb-conc. depend. 77−66117
Bi-Sb alloy film, elec. resist., magnetoresist., Hall coeff., 4.2K, conc. depend., anomalous size effect *(Russian)* 77−89884
Bi-Sb alloys, lattice dielec. const., comp. depend. 80−39516
Bi-Sb solid soln., crystallisation in capillaries *(Russian)* 78−44006
Bi-Sb solid soln., thermoelectric props., 80 to 300K *(Russian)* 78−43425
$Bi_{12}GeO_{20}$ crystals, principal carriers obs., in dark and under laser illumination *(Russian)* 80−80312
$Bi_{12}GeO_{20}$, hopping cond., carrier mobility and density 78−19040
$Bi_{12}GeO_{20}$, photocond. spectra, current-voltage charact., photoelectret effect 79−69552
BiI_3, doped, IR photolum. and EPR spectra 78−19558
BiI_3, excitonic shifts of quasiatomic optical core to cond. band transitions, UPS obs. 78−11079
BiI_3, layered semicond., valence bands UPS and XPS obs. 78−11078
BiI_3, octahedrally coordinated, layer cpd., electronic struct. using synchrotron-radiation photoemission spectroscopy 79−74058
BiI_3, photopolarisation, photoelectret state, electron-hole transitions 77−12300
BiI_3, UV reflectivity meas. 78−72545
BiI_3-Sb(As)I_3, phase diags. 78−6905
Bi_2O_3, film, resist. and current controlled negative resist. 78−39238
Bi_2O_3, thermoelec. props., 500-1500K 80−29423
BiOCl-ZnS electroluminesc. heterojunction phys. props. 77−66198
BiOCl-ZnSe, electroluminesc. heterojunction phys. props. 77−66198
$Bi_{12}RO_{20}$, R=Ge, Si, photoinduced birefringence, dynamic transparency prod. 78−90472
Bi_2S_3, photostimulated electron emission, cryst. growth conditions depend. 77−44135
Bi_2S_3-Bi_2Se_3 and Bi_2Te_3-Bi_2Se_3 systems, thermal cond. change during phase transitions 80−100368
Bi_2S_3-$CuPbBi_5S_9$, solid solution, semiconductor and dielectric props. 79−69511
BiSb, hybrid resonance in a quantising magnetic field 78−67933
$Bi_{0.88}Sb_{0.12}$, semiconducting transport props., 2 to 100K 80−59989
$Bi_{0.89}Sb_{0.11}$, effect of band structure on the dispersion of magnetoplasma waves 77−47845
$Bi_{0.9}Sb_{0.1}$, magnetophonon effect on hot electrons *(Russian)* 80−107814
$Bi_{0.91}Sb_{0.09}$, magnetoresistance anisotropy in strong magnetic field 79−82613
$Bi_{0.91}Sb_{0.09}$, thermomag. power in strong mag. field, temp. and field depend. 78−43421
$Bi_{0.924}Sb_{0.076}$, doped, optical, oscillation and galvanometric effects *(Russian)* 77−85247
n-$Bi_{0.924}Sb_{0.076}$, one-ellipsoid to two-ellipsoid fermi surface transition in extended cryst. *(Russian)* 78−14657
$Bi_{1-x}Sb_x$, band inversion under press., Fermi surface anisotropy, galvanomag. meas. 77−51637
$Bi_{1-x}Sb_x$, deformation calculations, band struct. variation, electron phase transitions due to deform. *(Russian)* 80−65137
n-$Bi_{1-x}Sb_x$, determ. carrier dispersion relation parameters 79−38107
$Bi_{1-x}Sb_x$, EM wave propag. in direction perpendicular to mag. field 79−60687
semiconductor materials continued
$Bi_{1-x}Sb_x$, EM wave propag. for rot. of mag. field from Faraday to Voigt config. 80−84419
$Bi_{1-x}Sb_x$, far IR transmittance meas. *(Russian)* 77−44006
$Bi_{1-x}Sb_x$ film, low temp. anomalies of elec. props. and quantum size oscillations 79−65571
$Bi_{1-x}Sb_x$, galvanomag. props., energy spectrum *(Russian)* 79−56248
n-$Bi_{1-x}Sb_x$, Hall effect in strong mag. fields 79−69532
$Bi_{1-x}Sb_x$, magnetoresist., mag. field and ang. depend. 78−19063
$Bi_{1-x}Sb_x$, non-ellipsoidal Fermi surface, cyclotron reson. meas. at 35 and 70 GHz 77−62804
$Bi_{1-x}Sb_x$, semicond., photoconductivity *(Russian)* 79−7857
$Bi_{1-x}Sb_x$, semicond. alloy, mag. freeze-out effect, superlow temps. *(Russian)* 77−89775
$Bi_{1-x}Sb_x$, semicond.-semimetal transition, temp. and press. depend. of transport props. 78−76120
$Bi_{1-x}Sb_x$ semiconducting alloy, band struct. study, Shubnikov-de Haas effect *(Russian)* 80−80181
$Bi_{1-x}Sb_x$, semiconductor, anomalous conductance in strong electric and longit. quantised mag. field *(Russian)* 78−76084
$Bi_{1-x}Sb_x$ thin films, elec. props., 4.2-300K *(Russian)* 79−24087
$Bi_{1-x}Sb_x$:Pb ($0.08 \leq x \leq 0.13$) Seebeck, magneto-Seebeck coeff., longitudinal Nernst coeffs. 78−56168
$Bi_{100-x}Sb_x$, lattice dielec. const. meas. 78−10490
$Bi_{86}Sb_{14}$:Te, single crystal, dispersion of magnetoplasma waves *(Russian)* 80−70739
$(Bi_{0.25}Sb_{0.75})_2Te_3$, opt. props. of bulk and films 78−27206
$Bi_{0.5}Sb_{1.5}Te_3$ film, effect of struct. on thermal cond. 79−28257
$(Bi_{1-x}Sb_x)_2Te_3$, highest valence band struct., Shubnikov-de Haas effect 78−14661
n-$(Bi_{1-x}Sb_x)_2Te_3$, magneto-Seebeck and Shubnikov-de Haas effect 79−42568
n- $(Bi_{1-x}Sb_x)_2Te_3$, magnetoresist. in quantising mag. field 80−24953
$Bi_xSb_{2-x}Te_3$, 2-dimens. cryst. interface props. of Bi overlayer UPS obs. 78−34881
$Bi_{2-x}Sb_xTe_{3-y}Se_y$, elec. cond. and thermoelec. props., neutral defects influence 80−60017
$Bi_{2-x}Sb_xTe_{3-y}Se_y$ solid solution, density-of-states effective mass, carrier mobility temp. depend. 80−24931
p-Bi_2Se cryst. growth, elec. props. 77−8748
n-Bi_2Se_3, cryst. nonparabolic cond. band., IR refl. and Hall voltage meas. 77−31940
Bi_2Se_3 film, partly oriented, electron diffr. dynamic effects 77−7996
Bi_2Se_3, mechano-caloric energy conversion 80−10962
n-Bi_2Se_3, nonparabolicity of cond. band and anisotropy of electron effective mass 79−60692
Bi_2Se_3:Sn(Pb), dopant influence on elec. cond. 79−51569
n-$Bi_2(Se_xTe_{1-x})_3$, Shubnikov-de Haas oscills., 1.7-4.2K 77−15874
$Bi_{12}SiO_{20}$ film, photoelectric props. obs., UV illumination effects *(Russian)* 80−80313
$Bi_{12}SiO_{20}$ in insulator-semicond.-insulator struct., induced birefr., influence of kinetics of transient processes 79−24294
$Bi_{12}SiO_{20}$, visible and UV refl. and absorpt. spectra 80−34950
n-$Bi_2(Te,Se)_3$ semiconducting solid solns., plastic deform. during hot extrusion 79−20143
Bi_2Te_3, anodic film form., in situ ellipsometric study 80−104318
Bi_2Te_3, anodic oxide films, two-dimens. nucleation and growth 80−11807
Bi_2Te_3, chemical bonding models, correctness test using mag. susceptibility, and chemical substitution 78−67680
Bi_2Te_3, constant current anodisation, representation of layer periodicity 80−3218
Bi_2Te_3, crystallisation in constant electric field, thermoelectric parameters 77−44146
Bi_2Te_3 film, effect of struct. on thermal cond. 79−28257
Bi_2Te_3, galvanothermomag. props. up to 14 kbar 77−47829
Bi_2Te_3, lattice vibrs. coherent inelastic neutron scatt. meas. 78−34576
Bi_2Te_3, layered semiconductor, angle resolved photoemission 79−28893
n-Bi_2Te_3, magnetoresist. under uniaxial stress 77−35956
Bi_2Te_3, mechano-caloric energy conversion 80−10962
Bi_2Te_3, p- and n-type, free charge carrier mag. susceptibility, 90-650K 78−10643
Bi_2Te_3, Shubnikov-de Haas effect, high press. effect on band struct. 77−51767
Bi_2Te_3 single crystal, thermoelec. power anisotropy 77−55554
Bi_2Te_3 single crystals, melt grown, structural perfection 80−15101
Bi_2Te_3, surface prep. by etching for electroplating elec. contacts 80−108647
Bi_2Te_3, thermoelectric p-n junction, pulse refrigeration 78−23156
Bi_2Te_3 thermoelements, reliable bonding to Pd electrodes, radioisotope thermoelectric generator for biomedical appl. 79−52952
Bi_2Te_3-based solid solns., decomp. kinetics under flux layer 77−81205
Bi_2Te_3-Bi_2Se_3 solid solns., single cryst. growth and thermocouple construct. 80−104056
Bi_2Te_3-Bi_2Se_3 thermoelectric alloys, diffusion and evaporation of volatile component during prep. 80−35118
Bi_2Te_3-Sb_2Te_3, Bi:Sb=1:2, 2:1, solid soln. deviation from stoichiometric cross section 79−43221
Bi_2Te_3-Sb_2Te_3, plastically deformed by hot extrusion, diffusion meas. using micro-X-ray spectrum anal. 79−14954
p-Bi_2Te_3-Sb_2Te_3 semiconducting solid solns., plastic deform. during hot extrusion 79−20143
Bi_2Te_3-Sb_2Te_3 solid soln., deviation from stoichiometric cross section 78−35362
Bi_2Te_3-Sb_2Te_3:Cu, electrical cond. and thermopower, disorder effects *(German)* 77−1422
Bi_2Te_3-$SbTe_3$, ordered structure formation, heat treatment effect on thermal cond. 80−54448
BiTeI, melt and vapour grown, optical props. 80−84746
$Bi_2(Te_{1-x}S_x)_3$, quasi 2-D cryst., I-V and magnetocond. meas. 77−85360
$Bi_2(Te_{1-x}S_x)_3$, thin cryst. two-dimens. system, electronic props. 78−60181
$(Bi_2Te_3)_{0.9}(Sb_2Te_3)_{0.5}(Sb_2Se_3)_{0.05}$ n-type alloy for thermogenerators, thermo-EMF, elec. cond. and thermoelec. efficiency factor, 300-600K 80−70735
$Bi_2Te_{2.7}Se_{0.3}$ magnetoresistance and Hall EMF meas., using AM method 80−52278
n-$Bi_2Te_{2.88}Se_{0.12}$, extrusion deformed, powder dispersion degree influence on thermal and elec. props. *(Russian)* 80−39366
$Bi_2Te_{2.88}Se_{0.12}$, solid soln., single cryst. growth and doping, thermoelec. efficiency and Hall coeff. 79−33921
$Bi_2Te_{3-x}Se_x$ films, surface band struct. and scatt. mechanism 80−34535

semiconductor materials continued
$Bi_2Te_{3-x}Se_x$ films, thermal cond. depend. on grain size, phonon-boundary scatt. 79−69304
$Bi_2Te_{3-x}Se_x$ solid solution, Hall effect anisotropy parameter, thermoelectric power, depend. on carrier density 79−69536
$Bi_2(Ti_{1-x}S_x)_3$, thin crysts., adsorpt. effects on elec. cond. 78−19034
$Ca_{0.2}Ba_{0.8}TiO_3$:Nb, conductive single cryst. growth by Verneuil method 77−85928
CaF_2-Ge(Si), cosputtered composite semiconductors, selective solar energy absorbers 79−56876
$CaIr_xRe_{1-x}O_3$, (0<x<1), sintered, exam. of mag. and electrical props. 78−80135
$CaSO_4$:Dy, cryst. growth from soln., thermoelec. and thermoluminesc. props. 79−56923
$Ca_{1-x}Sm_xS$, electron config. of Sm ions, X-ray L-absorpt. spectroscopy 80−60715
Cd-Ge-As system, quenched samples, phase diagram, DTA after annealing 79−69226
Cd-Sb (53-100%), elec. resist. temp. depend. 77−59285
Cd-Sb thin film prep. by vacuum deposition, elec. props. 78−92194
$Cd_{1-x}Mn_xTe$, exchange interaction, magneto-optical spectra 80−25348
$CdAs_2$, cryst. struct. and vitrification capacity 80−88126
$CdAs_2$ single crystals, growth from vapour phase 78−88416
$CdAs_2$, synthesis, microstruct., hardness and elec. cond. 79−51268
$CdAs_2$, thermoelec. props., anisotropy 80−34470
Cd_3As_2, amorphous to crystalline transform. 79−77519
Cd_3As_2, anisotropy of electronic g*-factor 80−44483
Cd_3As_2, band structure, Kane model, magneto-Seebeck and Hall data 77−62821
Cd_3As_2, depend. of g-factor on electron conc. at low temps. 77−69218
Cd_3As_2, elec. resist. and HF dielec. const. calcs. *(French)* 77−59284
Cd_3As_2, electron conc. temp. depend. heavy hole-cond. band energy gap 79−69410
Cd_3As_2, electron effective mass. temp. depend., Hall effect and thermoelec. power meas. 80−39613
Cd_3As_2, electronic g-factor, effective mass and density of states 79−60691
Cd_3As_2, energy band structure calc. 80−75504
Cd_3As_2 film, crystalline and amorphous films, band structure, optical properties 78−11013
n-Cd_3As_2 film, vac. evaporated, Shubnikov-de Haas effect 79−99644
Cd_3As_2 film on NaCl substrate, vacuum deposition, growth morphology, microstructure 80−75479
Cd_3As_2 films, nucleation processes, on NaCl substrates 80−59813
Cd_3As_2, inverted band struct. 79−90958
Cd_3As_2, ionised-impurity mobility and static dielec. const. at 4.2K 77−32017
Cd_3As_2, low-temp. energy band struct. and depend. of direct gap on press. and temp. 77−62822
Cd_3As_2 platelet, single vap.-grown cryst., passive annealing, Fermi energy variation 80−45223
Cd_3As_2, Shubnikov-de Haas effect 80−11020
Cd_3As_2, thermal dissoc., 550-850°C 80−35512
Cd_3As_2, thermoelectric power and transverse Nernst Ettingshausen coefficent 79−38104
Cd_3As_2 type crystals, symmetry props. of energy bands 80−39500
Cd_3As_2, vapour phase single cryst. growth, X-ray topographic obs. of perfection 78−9976
$Cd_3(As_xP_{1-x})_2$, $0 \leq x \leq 1.0$, band struct. calc. near Brillouin zone centre 80−107703
$Cd_3(As_xP_{1-x})_3$, thermoelectric power and Hall effect., mag. field depend. 78−10484
CdF_2, conversion into semicond. by heating in H_2 atm., resist. meas. 80−20978
CdF_2: $YF_3(YbF_3)$, photoconversion from insulating to semicond. state, IR absorption and elec. cond. 78−14759
CdF_2:Eu(Gd)(Nd), semicond., symmetry of optical centres, optical and elec. props. 77−59592
CdF_2:Ge^{4+}, Ce^{3+}, in semicond. state, elec. cond. and Hall meas. 78−10443
CdF_2:In, shallow versus deep donors 77−85176
CdF_2:Mn, Y, deconversion due to vacuum heat treatment, elec. resist. and electron probe meas. 79−24025
CdF_2:Mn,Y, in MIS struct., blue-green electrolum. 79−52025
CdF_2:NaF(AgF), colour centres, IR absorpt. and photocond. after UV irrad. 80−79784
CdF_2:RF_3 films, R=Pr, Nd, Sm, Eu, Gd, Tb, Er, Dy, Ho, electroluminesc. meas. *(French)* 79−11471
CdF_2:YbF_3, conversion processes into semiconductor 78−14730
CdF_2-Au metal-semiconductor contact, capacitance and photocurrent, barrier height 77−85321
Cd_2GeO_4, n-type, prep. and photoelectronic props. 80−39628
CdI_2, ang. depend. electron energy loss meas. 79−95884
CdI_2, optical phonon anisotropies and intralayer bonding forces from IR refl. 77−59573
CdI_2, UV reflectivity meas., band struct., LCAO calcs. 78−72545
$Cd_xMg_{1-x}Se$ single crystals, melt grown, struct. and microhardness anisotropy 79−86836
$Cd_{1-x}Mg_xTe$:P, luminescence centres, photoluminesc. meas. 78−31236
$Cd_{1-x}Mn_xSe$, fundamental optical props. 80−84751
CdMnTe crystals, exciton binding energy, magnetoabsorption and magnetoreflectivity 79−38523
CdMnTe, exciton ground state, magnetic field influence 80−54616
$Cd_{0.6}Mn_{0.6}Te$ crystals, Mn($3d^5$) band, photoemission evidence 80−11535
$Cd_{1-x}Mn_xTe$, acceptor photoionisation and light-to-heavy hole absorpt. 79−65908
$Cd_{1-x}Mn_xTe$, effect of Mn $3d^5$ states on band struct., exciton refl. struct. in mag. field 79−11094
$Cd_{1-x}Mn_xTe$, magneto-optical props. of free excitons rel. Mn^{2+} ions spin alignment 79−47419
$Cd_{1-x}Mn_xTe$ mixed cryst., giant exciton Faraday rotation 78−27260
$Cd_{1-x}Mn_xTe$ mixed crystals, Raman spectra 80−103961
CdO-SnO_2 DC reactively sputtered films, elec. and optical props. 80−103763
CdO-SnO_2 film, DC sputtering prep., visible and near IR transmission, resist. 78−88049
Cd_3OF_4, electrical conductivity temp. quasi-independ., novel semiconductor 77−43589
CdP, electron mobility, carrier density depend. calc. 79−56229
CdP_2, birefringence and optical activity 78−15143
CdP_2, large tetragonal single cryst. growth from vap. 77−69976
semiconductor materials continued
CdP_2, light polarisation, self-induced optical rotation 79−19860
CdP_2, Raman spectra, mode symmetry 79−91441
CdP_2, reson. interaction of vibr. states, polarised Raman spectra meas. 77−15521
CdP_2, role of metal d states in valence band formation 79−65380
CdP_2:Bi,Zn, photolum. and photocurrent stationary charact. 78−27317
CdP_2:Cu, photoluminescence and photocond. charact., interimpurity recomb. of carriers 77−8637
CdP_4, λ-modulated photoemission spectra 79−87565
CdP_4, role of metal d states in valence band formation 79−65380
CdP_4 single crystal growth 80−35065
CdP_4, thermodynamic functions, 55-300K 80−34203
Cd_2P_3, role of metal d states in valence band formation 79−65380
Cd_3P_2, band struct., D_{4h}^{15} space group symmetry props. 80−34357
Cd_3P_2, band struct., X-ray spectra determ. 78−35225
Cd_3P_2, Cd_3As_2, sp. ht., thermodyn. props. 78−22863
Cd_3P_2, energy band structure for real D_{4h}^{15} symmetry 79−56124
Cd_3P_2, free carrier and interband absorption 78−23446
Cd_3P_2, role of metal d states in valence band formation 79−65380
Cd_3P_2, thermomagnetic transport effects obs. 77−15883
$Cd_3P_{2-x}As_x$ solid soln., US wave prop. velocity, composition depend. 77−20013
$Cd_3P_2(As_2)$, cryst., gas phase growth, morphology 79−10821
$Cd_xPb_{1-x}I_2$, photoluminescence comp. and energy depend., band gap 77−44045
p-CdSb, elastic moduli depend. on hydrostatic press. up to 17 kbar 79−37755
CdSb, elastic moduli temp. depend. 77−51430
CdSb, energy spectrum, influence of chem. bonds, LCAO calc. 80−34356
CdSb, Hall coeff. and resist. 79−56216
CdSb heterojunction, formation by laser irradiation, photoelec. meas. *(Russian)* 77−76915
CdSb, monocrystalline film, prep., elec. props. 79−43159
CdSb, phase diagram, region of homogeneity, elec. cond. 79−43219
p-CdSb, photoconductivity and absorpt. in submm region, electroluminesc. 77−32046
p-CdSb, photomagnetic and transverse Dember effects, 90 to 300K 77−4400
CdSb resistance thermometer, charact. of cryogenic temps. 79−21760
CdSb single crystals, surface layer melting and recrystallisation due to laser irradiation *(Ukrainian)* 79−46699
CdSb, thermodyanmic props. 79−77767
CdSb:Al, p-n junction formation by laser emission, photoelectric effects *(Russian)* 80−70815
CdSb:Al(In)(Ga)(Te), p-n junction formation by laser radiation 80−96983
CdSb:Au, solubility, thermal anal., microhardness, microstruct., elec. characts. 77−16557
CdSb:Fe, self absorpt. edge, impurity effect *(Russian)* 80−97316
CdSb:Ge, anisotropy of elec., mag. props. 78−34829
CdSb:Te, photoconductivity charact. 77−43653
Cd_2Se_3, elec. resist., thermoelectromotive force, temp. depend., 300 to 1400K *(Russian)* 78−84243
Cd_2SnO_4 and Cd_2SnO_4:CdO, thin film electrodes in H_2SO_4 electrolytes, reduction, AES and SEM 80−65674
Cd_2SnO_4 film, RF sputtered from powder targets, props. 77−43759
Cd_2SnO_4 film, sputter deposition and characterisation 79−43146
CdTe-InAs quasi-binary system, temp.-comp. diagram, physicochem. and thermodynamic analysis 80−104127
$(2CdTe)_x$-$(In_2SnTe)_{1-x}$, x=0.25, 0.5, 0.75, tetrahedral semiconductor, chem. interaction of Sn atoms, Mossbauer study 80−39977
$CdTm_2Se_4$, mag. susceptibility meas. 4.2 to 300K cryst. field approx. 77−66246
Cd_3X_2, X=P,As,Sb, phys. props. 78−26527
$Cd_{3-x}Zn_xAs_2$, cryst., two-band and impurity conduction, 1.8 to 370K 78−19057
$Cd_{3-x}Zn_xAs_2$, electron mobility and carrier density calc. 77−80780
$Cd_{3-x}Zn_xAs_2$ press. and temp. depend. of Hall coeff. 77−69349
$Cd_{3-x}Zn_xAs_2$ solid soln., US wave prop. velocity, composition depend. 77−20013
CeO_2 in O_2 atmos., adsorption and elec. cond. props. 79−23836
CeO_2, nonstoichiometric, defect struct. and elec. props. 79−60827
CeO_2:Nb_2O_5, sintered, elec. cond. and solid solubility, 800 to 1329°C 79−99546
CeO_2:S, acceptor properties of S, free electron concentrations 80−34395
CeO_2:S, in $O_2+CO_2+SO_2$ atmosphere, elec. cond. study 80−39583
CeO_2:S, influence of S on elec. props. *(Russian)* 79−51566
CeO_{2-x}, conductivity and Seebeck coeff., small polaron and hopping mechanisms 77−76812
CeO_{2-x}, small polaron mobility, elec. cond. and nonstoichiometry meas. 78−47785
$Ce_{3-x}S_4$, $Ce_{3-x}Sm_xS_4$, elec. cond. mechanism, thermoelec. power, Hall and absorpt. coeffs. 77−24559
$CoMoO_4$, mag. susceptibility and electrical transport props. 79−56511
Co_2NiO_4, powder prep. by freeze drying of solid solutions, solvent choice 80−11583
Co_3O_4:Li(Cr)(Al)(S), and pure Co_3O_4, elec. cond. and thermo-EMF 80−20231
Co_3O_4:S, defect struct. and elec. props., electron, hole conc. 80−44601
CoP_3, prep. and characterisation 77−77356
$Cr_{1-x}Mn_xSi_2$, semicond. props. 78−79992
$Cr_2S_{3-x}Se_x$, elec. resist., thermal cond. and Seebeck coeff. meas. 80−24958
$CrSi_2$, semicond. props. 78−79992
CsAu, band struct. and charge distrib., semicond. and metallic behaviour 77−20238
CsAu, semicond. and metallic, NMR line shape, Knight shift, X-ray diffr. study 78−68402
Cs_3Sb vacuum deposited photoemitter, XPS study 80−89122
$Cs_{0.3}V_2O_5$, cryst. struct., semicond. behaviour 77−35516
$Cs_{0.35}V_3O_7$, cryst. struct., semicond. and antiferromag. behaviour 77−35515
$(Cu,Ag)_2Se$, p-type, thermoelectric, vaporisation suppression, using inert and reactive coatings 79−48149
$(Cu,Ag)_2Se/(Bi,Sb)_2Te_3$, P type selenide segmented element fabrication, thermoelectric props. 80−107835
Cu-Tl-S, phases, semiconductor and metallic behaviour *(French)* 79−96011

semiconductor materials continued
CuB_{24}, elec. props. at high temps. and in strong elec. fields, thermistor appls. 80−92903
CuBr, 1S exciton triplet state, magneto-optical props. 80−25345
CuBr, direct gap semiconductors, charged excitons 77−62840
CuBr, exciton absorpt. band shape, dielectric const. real part derivatives *(Russian)* 80−25413
CuBr, P exciton fine struct. 80−20091
CuBr, piezo-optical effects on excitons, importance of k-linear terms 79−95802
CuBr, single oriented crystals., electroreflectance, exciton transitions 77−66517
CuBr, surface exciton polariton, ATR meas. 77−77236
CuBr, theory of photoelectric consts. 79−61335
CuBr(Cl)(I), energy bands, relativistic KKR method, UV absorpt. spectra 80−39501
CuBr(I), reflectance and thermoreflectance spectra, electronic struct. 80−71444
$CuCd_2GaTe_4$, semiconductor, physicochem. and transport props. 77−59762
CuCl, absorpt. coeff., 0.4-25 μm, band struct. determ. 77−73155
CuCl, band struct., OPW calc. and X-ray spectra meas. 80−75506
CuCl, biexciton resonant two-photon absorption 78−23491
CuCl, biexcitons existence, review 77−69239
CuCl, direct-gap semiconductors, charged excitons 77−62840
CuCl, donor-acceptor recomb. spectra 80−45131
CuCl, electron-hole pairs behaviour in energetic ion tracks 80−65457
CuCl, electronic struct. by LCAO and LMTO methods, direct gap semiconductor 80−59868
CuCl, energy bands and effective mass 80−10859
CuCl, exciton energy determ., electron beam excited luminesc. 79−38680
CuCl, exciton spatial dispersion determ., two-photon Raman scatt. via excitonic mol. state 80−60595
CuCl, excitonic polariton, picosecond time of flight meas. 80−29337
CuCl, excitons bound to neutral donor impurities, magneto absorption spectra 79−56816
CuCl, frequency dependent optical phonons contrib. to small radius excitons binding energy 77−69236
CuCl, phonon-assisted two-photon absorpt. of excitonic mol., bare-exciton approach 79−78702
CuCl powder compacts, DC voltage depend. resist. under press. 80−80334
CuCl, propagation process of polaritons *(Japanese)* 80−24809
CuCl, psec time resolved spectroscopy, excitonic mols. 79−47500
CuCl, reson. Raman scatt. and luminesc. under two-photon excitation 79−95765
CuCl, resonant emission, lifetime of excitons 77−69887
CuCl, surface exciton polariton, ATR meas. 77−77236
CuCl, theory of photoelectric consts. 79−61335
CuCl, two-photon absorpt. and luminesc., biexcitons 80−11434
CuCl, XPS and Auger spectroscopy, elec. struct. 80−29852
CuCl-Ag system, photosensitivity spectrum in region of CuCl exciton absorpt. *(Russian)* 79−78707
CuCl(Br), charged excitons, band struct., electron-hole exchange interaction 77−69233
CuCl(Br)(I), electron-exciton inelastic collision cross sections 79−90967
CuCl(Br)(I), luminesc. due to exciton-electron scatt., calc. 77−16379
CuCl(Br)(I), photoelasticity theory, strain polarisability effect 78−10868
Cu_5FeS_4, bornite, AES investig. of surface struct., oxide layer form. 77−15669
CuI, theory of photoelectric consts. 79−61335
$Cu(Mo_2Re_2)S_8$, synthesis and electrical props. of mixed tetrahedral cluster phases 80−2971
CuO, on Al or Cu, solar selective coating, figure of merit 80−72082
Cu_2O, CVD from Cu-O-H-Cl-N system, thermodynamic anal. 78−39676
Cu_2O, cond. filament props. and bistable switching effect *(German)* 78−2532
Cu_2O, Cu inclusions and annealing, optical and IR absorpt. obs. 80−60630
Cu_2O, defect levels, TSC 77−66138
Cu_2O, electro-optic effects due to the Stark splitting of energy bands 79−82950
Cu_2O, electron-exciton inelastic collision cross sections 79−90967
Cu_2O, electron-exciton scatt. cross sections, central field and exchange approxs. 77−62919
Cu_2O, energy band interactions under uniaxial compression 80−25412
Cu_2O, excitons and structural defects at low temp. 78−84255
Cu_2O film, reactively-sputtered, phase comp., resist. and optical consts. 79−95534
Cu_2O, forbidden energy gap oxide semicond. crystals, review of spectroscopic props. 78−2876
Cu_2O, front wall solar cells, chemical origin of space-charge layer 79−70449
Cu_2O, growth by melting, photocond. spectra 78−52029
Cu_2O, hole mobility, scatt. mechanisms, elec. field effect 77−80786
Cu_2O, odd photomag. effect. meas. 77−89805
Cu_2O, optical absorpt. due to paraexciton in strong mag. field 77−28596
Cu_2O, photoconductivity of crystals grown under hydrothermal conditions 78−14765
Cu_2O, photomemory effect, EPR expts. 78−52353
Cu_2O, photosensitive etching in nonoxidising etchants 80−78813
Cu_2O, positive and negative photomemory, IR luminesc. spectra, illum. effect 79−69557
Cu_2O, pure and Fe doped, carrier cyclotron resonance impurity scattering effects, polar mass extrinsic origin 79−56614
Cu_2O, relationship between interband transitions and spectrum of diagmagnetic excitons in moderate mag. fields 79−91412
Cu_2O, residual conductivity, role of vacancies, photoluminesc. and photocond. 77−15901
Cu_2O, reson. Raman scatt. from stress-split forbidden excitons 80−93332
Cu_2O, resonant Raman and Brillouin spectroscopy, review, book contrib. 80−49624
Cu_2O, sample thickness depend. of exciton polariton absorption coeff. 80−34941
Cu_2O, self-consistent energy bands 80−59869
Cu_2O single cryst. diodes, IR electroluminesc. 79−83034
Cu_2O single crystals, photomemory effect, kinetics of excitation and deexcitation processes 77−85262
semiconductor materials continued
Cu_2O solar cells, electrical and optical props., photocurrent anal. 80−101116
Cu_2O, theory of large-radius excitons 78−47710
Cu_2O, uniaxial stress effects on excitons 80−60589
Cu_2O, with impurities, exciton absorpt. line shape calc. *(Russian)* 78−10934
$Cu_2O:Ag^+$, exciton-neutral and exciton-charged impurity scatt. cross sections 80−70618
$Cu_2O:Cd^{2+}$ implanted, reson. Raman scatt., annealing effect 77−24838
Cu_2O:He(Na)(Cd), ion-implanted, resonance Raman studies of annealing 79−55765
Cu_2O:Mn, photomemory mobility components, charged centre conc. 80−103725
Cu_2O-Au(Mg)(Mn)(Yb) Schottky barrier solar cells, surface anal. using AES 79−43759
Cu_2O-Cu diode junction, Schottky barrier, electronic structure and minority carrier diffusion length *(French)* 80−65682
Cu_xO film, growth by anodisation, switching charcts. 77−55898
$Cu_{1.8}S$ film, vacuum evaporated, props. rel. to elec. cond. 77−36001
Cu_2S, defect models of different allotropic varieties, thermal reactions of Hall coeff. *(French)* 77−47448
Cu_2S, diffusion length meas. using scanned laser beam tech. 80−93886
Cu_2S, electromechanical props. *(Russian)* 79−11117
Cu_2S epitaxial films, reactive sputtering prep. and electronic props. 79−78885
Cu_2S film, on rough $Zn_xCd_{1-x}S$ substrate, film substrate lattice mismatch calcs. 78−43263
Cu_2S films, prpe. methods, appl. to Cu_2S-CdS solar cells 80−80980
Cu_2S layer spray preparation and CuCl-thiourea complex formation 78−64471
Cu_2S, low temp. modification, elec. props. 77−8092
Cu_2S, on Cu, solar selective coating, figure of merit 80−72082
Cu_2S, optical and calorimetric meas. of thin films for Cu_2S-CdS solar cells 80−55863
Cu_2S, polycryst. thin films, struct., optical and elect. props. for solar energy appl. 80−10837
Cu_2S, S and S^{2-} states, identification from Auger line shapes 79−92034
Cu_2S, thermoelectric props. 80−54726
Cu_2S:Cd(Zn), effects of doping on elec. and optical props. 78−38743
Cu_2S/CdS heterojunction solar cells, diffusion length determ. using minority carrier SEM 80−61359
Cu_2S/CdS solar cell, design and fabrication 80−30481
$Cu_2S/Zn_xCd_{1-x}S$ heterojunction solar cells, junction anal. 79−92080
Cu_2S-CdS heterojunction, influence of surface recomb. on photoelec. props. 77−43711
Cu_2S-CdS heterojunction, elec. and photoelec. charcts., effect of etching of CdS 78−80048
Cu_2S-CdS heterojunctions, electron trap characterisation by capacitance transient meas. 79−78163
Cu_2S-CdS heterojunction diodes, barrier model estimated from photovoltage and cathodoluminesc. spectra 79−78165
Cu_2S-CdS heterojunction solar cell, interface recomb. vel. determ. by capacitance/collection efficiency variation 80−50959
Cu_2S-CdS heterojunction solar cells, carrier transport, nonmonotonic band profiles 80−61361
Cu_2S-CdS heterojunction interface, depth distribution profiles, Auger spectra 80−88622
Cu_2S-CdS heterophotocells based on CdS films of stoichiometric composition, elec. and photoelec. props. 80−93873
Cu_2S-CdS solar cell, interface recombination and junction field studies, exptl. technique 80−45683
Cu_2S-CdS solar cell fabrication by magnetron reactive sputtering deposition 80−61363
Cu_2S-CdS solar cells, EBIC and capacitance measurements, stability problems 80−45684
Cu_2S-CdS solar cells, interface recombination phenomena and tunnel effect 80−66978
Cu_2S-CdS solar cells, optical absorption coefficient changes in Cu_2S 80−93980
Cu_2S-CdS solar cells, prep. and stoichiometric control of Cu_2S film 78−2560
Cu_2S-CdS thin film planar junction devices, quantitative photon loss anal. 80−61362
Cu_2S-$Zn_xCd_{1-x}S$ heterojunction, improved model of electro-optic behaviour 80−94023
$Cu_{2-\delta}S$, thin films, determ. of stoichiometry from optical props. 79−60656
$Cu_{2-x}S$, carrier mobility rel. to x 78−43389
$Cu_{2-x}S$ in chem. formed $Cu_{2-x}S$-CdS heterojunction, photosensitivity charcts. 78−72199
$Cu_{2-x}S$ on CdS, low temp. growth, AES obs. 79−28924
$Cu_{2-x}S$, single cryst., as p-component of heterojunction, props. 77−39926
$Cu_{2-x}S$ single cryst., struct. and elec. props. 77−24302
$Cu_{2-x}S$/CdS heterostructures, heat treated, capacitance voltage meas. anal. 80−20292
$Cu_{2-x}S$-CdS ceramic solar cells, solar batteries operating charcts. 80−93874
$Cu_{2-x}S$-CdS heterojunction, current flow charcts. and energy band struct. 77−43709
Cu_xS, diffusion length determ., resolution limit of EBIC technique 79−21865
Cu_xS evaporated layer growth in vacuum, compositional and optical characterisation, solar cell appls. 80−97437
Cu_xS evaporated thin films, composition, prep. and charcts. 80−25569
Cu_xS film for Cu-Cd-S solar cell, cathodolum. spectrum rel. to prod. method 79−56866
Cu_xS films, magnetron reactive sputtering deposition and elec. props. 79−78884
Cu_xS layer, on CdS, electron diffr. obs. of phases 78−51847
Cu_xS, photon and electron excitation phenomena 79−7865
Cu_xS-CdS heterojunctions produced by RF sputtering, for thin film solar cells 79−100053
Cu_xS-CdS solar cell, minority carrier diffusion length, SEM determ. 77−72911
Cu_xS-CdS solar cells, cu_xS growth kinetics and composition analysis by absorbance transient and galvanic electrochemical measurements 80−92797
Cu_xS-CdS solar cells, screen printed, prep. and photovoltaic props. 80−40863

semiconductor materials continued
Cu_xS-CdS solar cells, SCL current 80−76634
$Cu_2S(Se)(Te)$, thermal cond. changes on melting 77−7848
$Cu_{1.8}Se$, I-V characts., switching effects, nonstoichiometry effects *(Russian)* 78−84266
Cu_2Se-GeSe quasibinary system, phase diagram and struct. 77−8802
$Cu_{2-x}Se$, carrier mobility rel. to x 78−43389
$Cu_{2-x}Se$, elec. props. and band struct. 79−73513
$Cu_{2-x}Se$, electric, thermal and magnetic props. investigation in low temp. phase *(Croatian)* 79−11299
$Cu_{2-x}Se$, electrical activity of Cu vacancies 80−39606
$Cu_{2-x}Se$, single cryst., as p-component of heterojunction, props. 77−39926
$Cu_{2-x}Se(Te)$ crystals, struct. 79−90608
$(Cu_2SnS_3)_x(3CdS)_{1-x}$, second co-ordination sphere atoms effect on ^{119}Sm Mossbauer spectra *(Russian)* 77−63348
$(Cu_2SnS_3)_x(3ZnS)_{1-x}$, second co-ordination sphere atoms effect on ^{119}Sn Mossbauer spectra *(Russian)* 77−63348
$Cu_{1.7}Te$, and Cu_2Te, I-V characts., switching effects, nonstoichiometry effects *(Russian)* 78−84266
Cu_2Te-Ag_2S, kinetic props. of solid solutions 79−7827
$Cu_{2-x}Te$, carrier mobility rel. to x 78−43389
$Cu_{2-x}Te$, electrical activity of Cu vacancies 80−39606
$Cu_{2-x}Te$, single cryst., p-component of heterojunction, props. 77−39926
$Cu_{2-x}Te$, x=0 to 0.3, elec. cond., Hall const., carrier mobility, conc., thermoelec., density, lattice parameter 77−11915
Cu_3VS_4, conducting ions as mobile donors 80−11055
p-Cu_3VS_4, mixed conduction due to cationic interstitials 80−70772
Cu_3VS_4, out of equil. mixed cond., electronic cond. decrease in ionic soln. 80−107874
Cu_3VS_4, Raman active modes 80−11414
$CuWO_{4-x}$ prod. from $CuO+WO_3$ solid state reaction 80−66796
Er_2Te_3, films, prep., elec. props. 78−43494
EuB_6, correlation between mag. struct. and elec. props. 77−63192
$EuGd_2S_4$, nonstoichiometric, elec. transport props., semicond. and metallic cond. 80−107786
$Eu_2Ir_2O_7$, pyrochlore, sp. ht. below 20K, Debye temp. 80−65241
Eu_2Sb_3, cryst. struct., elec. and mag. props. 80−33958
$Eu_{1-x}Sm_xS$, electron config. of Sm ions, X-ray L-absorpt. spectroscopy 80−60715
$Eu_xSr_{1-x}M_4O_{11}$, M=Nb, Ta, electrophys. and mag. props. 77−89760
Eu_2VO_4, prep. and props. 77−15379
$Eu_3V_2O_7$, prep. and props. 77−15379
Fe oxide films, semicond. electrode props. 79−91093
$Fe_xCo_{1-x}Rh_2S_4$, spinel struct., X-ray, mag., elec. and Mossbauer spectra meas. 77−12278
$Fe(Mo_2Re_2)S_8$, synthesis and electrical props. of mixed tetrahedral cluster phases 80−2971
$Fe_xNb_xV_{2-2x}O_4$, NMR analysis of semiconductor transitions 78−52367
$Fe_{1-x}O$, wustite, thermoelec. power coeff. rel. to O_2 press. at high temp. *(French)* 77−76850
α-Fe_2O_3 ceramics, gas sensor for city gas appl. *(Japanese)* 80−61498
α-Fe_2O_3, elec. resist. and phase transition under shock compression 80−72496
α-Fe_2O_3, electrical conductivity 77−69365
Fe_2O_3, electrochem. doping 77−76430
n-Fe_2O_3 electrodes, characterisation and behaviour in acetonitrile solns. 80−25004
α-Fe_2O_3, polycryst., pure and TiO_2 doped, flatband potentials, donor densities, photocurrent meas. 78−76089
Fe_2O_3, semicond. anode in aq. electrolyte, electrolum. and electrochem. 80−76080
n-Fe_2O_3, sintered and flame-oxidised, photoelectrochemical props. 79−70355
Fe_2O_3, sintered semicond. electrode, photoeffects 79−51669
Fe_2O_3-V_2O_5 system, elec. transport 79−51576
Fe_xO_y thermal oxide film on Fe, capacitance, temp. and freq. depend., in aq. electrolyte soln. 80−54776
α-FeP_4, diamag., semicond., Mossbauer study 80−50243
$FePS_3$, layered semiconductors, optical and electronic props. 80−70761
$FePb_4Sb_6S_{14}$, photosensitive semiconductor, with high permittivity, elec. props. 79−65518
FeS_2, ionisation loss spectra, density of unoccupied states 80−55241
FeS_2, mag. susceptibility press. depend., bandstruct. calcs. 78−19212
FeS_2, natural pyrite, photocond. spectra 80−70758
FeS_2, pyrite, magnetokinetics of oxidation, appl. to mag. separation from coal 77−12161
FeS_2, pyrite, semiconducting props., energy gap press. and lattice parameter depend., Mossbauer obs. 80−44494
FeS_2, thin films, prep. and charact. 80−16178
$Fe(Sb_{1-x}Te_x)_3$ system cpds., prep., cryst. struct., elec. and mag. characteris. 80−108349
FeSi, inner level ESCA spectra, many particle effects, hole lifetime *(Russian)* 79−91560
$FeSi_2$, inner level ESCA spectra, many particle effects, hole lifetime *(Russian)* 79−91560
$FeTiO_3$, Fe_2TiO_4, and Fe_2TiO_5 anodes, appl. to photoelectrolysis of water 77−63920
$FeTiO_3$, Fe_2TiO_4, influence of cryst. struct. on photoresponse of electrodes 78−43471
θ-$Fe_xV_2O_5$, spin glass and paramag. props., susceptibility, EPR and Mossbauer studies 80−75782
GaAs-Si eutectic alloy, effect of crystallisation rate on microhardness 79−96110
GaAs-ZnSe, solid solution crystals, grown by Bridgman method, exam. of resistivity and Hall effect 79−95919
$(GaAs)_x(ZnSe)_{1-x}$ single crystal, visible cathodoluminesc. spectra 80−20716
$Ga(Mo_2Re_2)S_8$, synthesis and electrical props. of mixed tetrahedral cluster phases 80−2971
Ga_2O_3:Mg(Zr) single crystals, quenched, ionic and elec. props. 78−30922
GaP-ZnSe solid solutions, spectral studies *(Russian)* 79−91498
GaS-SmS system, phase diagram 79−78939
α-Ga_2S_3, defect semicond., optical absorption meas. 78−15186
αGa_2S_3, single crystal, lattice phonon exam., Raman and IR spectra of polycrystalline samples *(French)* 78−27229
Ga_2S_2Te, single cryst. X-ray data, struct. determ. *(French)* 79−60316
GaSb-GaAs-Ge system, props. and struct. 80−20232
GaSb-Ge eutectic alloy, effect of crystallisation rate on microhardness 79−96110

semiconductor materials continued
Ga_2Se_3, evaporation, thermodynamic props. 80−54365
Ga_2Se_3, film, electrical and optical props. 77−1505
Ga_2Se_3, single cryst., bistable cond. switching effect 77−51783
Ga_2Se_3, vapour phase deposited films, struct. 78−2383
Ga_2Se_3-In_2Se_3, semiconducting props. of four stable phases 77−55528
Ga_2Se_3-In_2Se_3 solid solution system, X-ray diffr. exam. 77−63639
Ga_2Te_3, single cryst., elec. cond. meas. 79−11124
Ga_2Te_3 single crystals, switching effect., carrier trapping 80−6919
Ga_2Te_3, vapour phase deposited films, struct. 78−2383
Ga_2Te_3:Sn, impurity atom electron shell compression by matrix *(Russian)* 77−28146
Gd_2S_3, resonance excitation of Nd^{3+}, luminescence, absorption spectra *(Russian)* 80−50381
α-Gd_2S_3:Nd^{3+}, spectroscopic props. from absorpt., photoluminesc. and excitation spectra 80−34968
$(Ge,Pb)_{1-x}Mn_xTe$, mag. and elec. props. meas. 80−29534
Ge-GaAs, crystallisation at superhigh cooling rates 80−54349
Ge-GaSb, metastable continuous solid solutions 79−8284
Ge-metal films codeposited, amorphous and polycryst., struct. and elec. props. 80−24766
Ge-Se-Ga thin film, elec. cond., switching phenomena *(Polish)* 80−11120
Ge-Si, electronic structure, short-range order effects, calc. 80−92861
Ge-Si, heat treated, carrier heating by strong microwave elec. field 77−69366
Ge-Si, imperfect homopolar cryst., lattice dynamics, IR spectra calc. 80−59601
Ge-Si, single crysts., photocond. 79−87126
Ge-Si alloy, epitaxial growth by getter sputtering, characts. 79−28915
Ge-Si alloy, phonon boundary scatt., reduction of lattice thermal cond. 78−55921
Ge-Si alloys, defect modes and optical spectra 80−11413
Ge-Si alloys, hot-pressed, fine-grained, boundary scatt. of phonons, lattice thermal cond. 80−107583
Ge-Si alloys, hot-pressed, fine-grained, boundary scatt. of phonons, theory 80−107584
Ge-Si cpds., short-range order, effect on valence band and direct optical gap 77−59252
Ge-Si single crystals, heat treated, hot carrier thermo-EMF 77−24575
Ge-Si solid solution film, elec. props. in range 4.2 to 500K 77−8214
Ge-Si system, diffuse scatt. of X-rays by single crysts. *(German)* 78−30517
Ge-Si thermoelectric alloys, phase diagrams, and imperfection chemistry 80−108422
Ge-Si:Sb, energy spectrum of Sb 80−34382
Ge-Si-Sb solid soln., prod. by 'Universal Furnace' expt. Sb and Si distrib. *(Russian)* 78−23692
GeAsS, X-ray photoelectron spectra, valence electrons density of states *(Russian)* 79−15583
$Ge_{1-x}(GaAs)_x$, metastable solid solution, fine struct. *(Russian)* 79−27960
$Ge_{1-x}(GaSb)_x$, metastable solid solution, fine struct. *(Russian)* 79−27960
GeO_2, band struct., tight-binding calc. 80−24796
GeO_2, forbidden energy gap oxide semicond. crystals, review of spectroscopic props. 78−2876
GeP, dissociation kinetics rel. to volatile component sublattice 77−84917
GeP, thermodynamic characts. 10-300K, interatomic bond elasticity 80−59677
GeS_2, energy gap and optical props. in IR region 79−51948
GeS_2, single cryst., IR polarised reflectivity spectra, 79−56775
$GeSe_2$, exciton absorpt., transmission spectra of cryst., glasses and amorphous samples 79−15485
$GeSe_2$, far IR reflectivity meas. 77−28565
$GeSe_2$, far IR reflectivity spectrum, dielec. const. and lattice vibrs. 77−52069
$GeSe_2$, IR and Raman spectra 78−95585
$GeSe_2$, optical absorption edge 78−43901
$GeSe_2$, photoluminescence at 77K 77−63456
$GeSe_2$, single cryst., IR polarised reflectivity spectra, 79−56775
$GeSe_2$, single crysts., 3 polymorphic forms, DTA, photolum., IR and Raman sepctroscopy 80−33923
Ge_xSe_{1-x}, bonds and band struct. determ., tight-binding model 78−18959
$Ge_{0.8}Si_{0.2}$, elec. cond., density of states, impurity and temp. depend 80−65568
p-$Ge_{1-x}Si_x$, $0.004 \leq x \leq 0.08$, hole mobility and hopping cond. rel. to composition fluctuations 77−76819
$Ge_{1-x}Si_x$, with Si implanted ions, optical and photoelec. props. 79−24014
$Ge_{1-x}Si_x$:Ga,As, interimpurity radiative recombination, composition depend. 79−11465
Ge_xSi_{1-x}, Si X-ray emission spectra obs. *(Russian)* 77−1767
Ge_xSi_{1-x}, solid solution, single crystal, photoconductivity *(Russian)* 79−11170
Ge_xSi_{1-x}:Cu, solid soln., single cryst., photocond. spectra 79−24015
GeTe-MnTe, heat treatment effect on struct., elec. props. 80−54725
GeTe-MnTe-SnTe system, compds., GeTe phase transition temp., elec. props., thermal cond. 79−43220
$(GeTe)_x$-$(AgSbTe_2)_{(1-x)}$, thermoelectric characts., temp. depend. 300 to 750K 79−78123
$Ge_{1-x}Te_x$, elec. cond., Hall effect in phase transition region 79−11113
H_xWO_3 bronzes, Anderson transition, XPS 80−107705
HfS_2, intercalation-induced shift of absorpt. edge 79−82999
HfS_2, optical props., modulation spectroscopy 77−52117
HfS_2, optical props. modulation spectroscopy, indirect absorpt. edge 77−52117
HfS_3, one-dimensional semicond., Raman spectra meas. 80−50345
$HfSe_2$, layer type dichalcogenides, reflectivity 6 to 40 eV, electronic deep level excitation 77−55801
$HfSe_{2-x}Te_x$, elec. resist. and mag. suscept. studies 80−44599
Hg-Ar quench condensed system, annealing effects on elec. cond. 79−60880
HgI_2, and photomagnetoelectric and photocond. meas., carrier lifetimes 77−55562
HgI_2 crystals, native defect compensation, doping, mobility-lifetime and TSC meas. 77−55492
HgI_2, doped, vap. growth by temp. oscill. method 78−39674
HgI_2, electrons and holes cyclotron reson. 78−72061
HgI_2, emission spectra in highly excited state 77−52167

semiconductor materials continued
HgI_2, exciton study by wave length modulated reflectivity, band parameters 77−51667
HgI_2, IR lattice vibr. and dielec. dispersion 80−76018
HgI_2, layered, photoelectromag. effect meas. of transport parameters 77−59301
HgI_2, mobility anisotropy determ. by photoelectromag. effect and photocond. 79−38126
HgI_2, phonon struct. in wavelength modulated refl. spectra and mag. circular dichroism 79−8125
HgI_2, phonon-assisted recomb. of free electron-hole pair 78−23521
HgI_2, photo-EM effect and photocond., trapping effects 77−32042
HgI_2, photoexcited, Hall effect, magnetocond., and cyclotron reson., carrier mobility and effective mass 77−59294
HgI_2, photomagnetoelectric effect anisotropy, photocond. 77−15897
α-HgI_2, Raman scatt. at room temp., improved polarisation spectra 80−25368
HgI_2, red, luminesc., excitation spectra on M-band 79−28822
HgI_2, red, reson. Raman scatt. and luminesc. 78−84579
HgI_2, red anisotropic polariton dispersion, reson. Brillouin scatt. 80−7366
α-HgI_2, single cryst. growth from iodomercurate complexes 80−35069
HgI_2, soln. grown crystals, low-energy gamma-ray cond. type detectors 80−97418
HgI_2, stimulated emission and optical gain, 80K 78−33738
HgI_2, stimulated emission at high exciton density, temp. depend. 78−84608
HgI_2, stimulated photoluminesc. excitons role 77−48201
HgI_2, vap. growth by temp. oscill. method in horizontal furnace 78−39675
HgI_2:Ag, trapping effects, TSC, photocond. and photolum. meas. 77−32023
HgI_2-CdS mixed system, photocond. depend. on composition and binder content 79−51625
$Hg_{1-k}Mn_kTe$, impurity magnetoabsorpt. 79−91473
$Hg_{1-x}Mn_xTe$, energy levels at Γ-point in intense mag. fields, Shubnikov-de Haas effect meas. 80−24951
$Hg_{1-x}Mn_xTe$, exchange interaction effect on $\Gamma_8 \rightarrow \Gamma_8$ magnetoabsorption 79−61351
$Hg_{1-x}Mn_xTe$, far IR interband absorption obs. 79−33696
$Hg_{1-x}Mn_xTe$, far IR studies of lattice and free carrier effects 78−39544
$Hg_{1-x}Mn_xTe$, indirect exchange interaction 79−61094
$Hg_{1-x}Mn_xTe$, magnetooptical and impurity effects 80−6721
$Hg_{1-x}Mn_xTe$ mixed crystals, zero gap, effect of exchange on interband magneto-absorption 78−23443
$Hg_{1-x}Mn_xTe$, non-parabolic zero-gap semicond., indirect exchange interaction 80−80498
n-$Hg_{1-x}Mn_xTe$, quantum transport phenomena, exchange interaction influence 78−76093
$HgSb_4S_8$, photosensitive semiconductors with high permittivity, elec. props. 79−65518
I_2:Li(Na) (K) (Cs) (Be) (mn) (Fe) (Cr), doping effect on elec. cond., semicond. props. 80−49732
IN_2O_3:Sn, RF magnetron sputtered film, elec. and optical props. 80−104065
In-Sb-Bi system, solid solns., solubility limits, microhardness, microstruct. investig. 78−35368
$(InAs)_{1-x}(CdSe)_x$ solid solution, elec. props. 79−15146
$In_{1.9}As_{0.1}Se_3$, growth by chem. vap. transport, characterisation as photoelectrode 78−43994
InO_3:Sn film, prep. by spray hydrolysis, struct., elec. and optical props. *(Japanese)* 79−42678
In_2O_3 film, evaporated, on ferroelec. ceramic, switching characts. 78−19107
n-In_2O_3 film, on Pb(Zr,Ti)O_3 ceramic, ferroelec. field effect 79−47177
n-In_2O_3 film, RF sputter grown, substrate bias effect on elec. and optical props. 78−64150
In_2O_3 films, electron beam evaporation, elec. and optical props. *(Japanese)* 80−60784
In_2O_3, In_2O_3-SnO_2, transparent thin films for satellite temp. control 79−80187
In_2O_3, lattice defects, optimum prep. conditions w.r.t. stoichiometry 79−27974
In_2O_3, polycrystalline, electron conc. and mobility, 25 to 700°C, O_2 partial press. depend. 77−76811
In_2O_3, Seebeck coeff., density of states effective mass 78−56171
In_2O_3, thermally evaporated film, struct. and elec. props. 80−104066
In_2O_3 thin film on polyester substrate, struct. determ. by TEM 80−6674
In_2O_3, transparent heat mirror formation by ion plating on ambient temp. substrates and props. 80−25578
In_2O_3:Sn, film, HF sputtered, cond., Hall mobility, oxidation, charge carrier density 78−72287
In_2O_3:Sn film, electroreflectance effects 79−43055
In_2O_3:Sn films, CVD prep. and elec. resist. meas. 79−52120
In_2O_3:Sn films, doping profiles and elec. props., appl. to optoelectronic devices 79−38203
In_2O_3:Sn films, elec. and optical props., solar energy conversion appl. 79−65945
In_2O_3:Sn films, pure and doped, prod. by ion plating, elec. and optical props. 80−2488
In_2O_3:Sn films, RF reactive sputtered, optical props. rel. to band struct. 79−91515
In_2O_3:Sn films; vac. deposited, elec. props. 80−100542
In_2O_3:Sn transparent cond. films, hydrolysis deposition, elec. and optical props. 79−43144
In_2O_3:Sn/n-Si heterojunction solar cell, fabrication and characts. 78−15314
In_2O_3:Sn-Si heterojunctions, current mechanisms and barrier height 80−11083
In_2O_3:Sn-Si solar cell, characterisation *(French)* 79−39306
In_2O_3-Si(Ge)(GaAs)(InP) heterostructure solar cells, photovoltaic and rectifying props., electron affinity determ. 79−1618
In_2O_3-SnO_2 film on Si, heterojunction, photovoltaic effect, sunlight induced 77−1470
In_2O_3-SnO_2-CdTe:P, p-n homojunction solar cell, elec., photovoltaic props., photoluminescence 80−81463
In_2O_3-SnO_2-Si SIS solar cells, reverse current-voltage characts. under illumination 80−89622
$In_{1-x}Pb_xTe$, single crystals, mag. susceptibility 79−51738
In_6S_7, absorpt. band edge investigation 79−69840
In_6S_7, TSC at various cooling rates *(Russian)* 80−11000
semiconductor materials continued
InSb-Ge eutectic alloy, effect of crystallisation rate on microhardness 79−96110
InSb-HgTe system solid solutions, elec. cond. and thermo-EMF 79−51570
InSb-NiSb, 8 mm band noise generation *(Russian)* 78−39175
InSb-NiSb eutectic, struct. and optical props., IR polariser appl. 80−45078
InSb-NiSb plate, nature of transverse photo-EMF 79−15186
InSb-NiSb plate, transverse EMF due to modulated illumination 77−55572
InSe, layer single crystal, infrared and Raman spectra 78−92070
$InSe_{1,2}$, In_2Se_3, solar heat capacity and enthalpy of transition, 129 to 920K range 77−29030
n-In_2Se, influence of hydrostatic press. on elec. cond. and Hall coeff. 77−55552
In_2Se with p-n junctions produced by laser radiation, photoelec. characts. *(Russian)* 78−56226
In_2Se_3, cryst. struct. determ. by X-ray diffr. *(French)* 78−26501
α-In_2Se_3, far infrared optical study of ordered and disordered forms 78−84572
α-In_2Se_3, X-ray diffr. line broadening 80−49047
In_2Se_3-Cu_2S system, electrophys. props., influence of 1-4% Cu_2S 80−20219
In_4Se_3 layer crystal, three-dimensionalization of transport effects 79−73514
In_4Se_3, layered cryst., sp. ht. rel. to phonon spectrum *(Russian)* 79−90794
p-In_6Se_7, electrophysical props. 110 to 400K *(Russian)* 77−35867
In_6Se_7, single cryst. prep. and electrophys. props. 79−43129
In_6Se_7 single crystals, absorpt. edge 79−87459
$(In_{1-x}Sn_x)_2O_2$-Si-N solar cell efficiency and elec. props. 80−35676
$In_{1.9}Sn_{0.1}O_3$ laser-damage-resistant transparent conductive coatings, appl. in Pockels cells 79−50333
$In_{2-x}Sn_xO_{3-y}$ solar cells, majority carrier conduction effects 80−97796
n-$In_{2-x}Sn_xO_{3-y}$/p-Si, semicond.-insulator-semicond. solar cell, performance and spectral response, fabrication 79−83596
$In_{2-x}Sn_xO_{3-y}$-CdTe(InP) photovoltaic heterojunctions, surface and interface studies, efficiency 80−45691
$In_{2-x}Sn_xO_{3-y}$-$Ga_xIn_{1-x}P(-InP_yAs_{1-y})$ heterojunction solar cells, chemistry and prep. 80−94073
$In_{2-x}Sn_xO_{3-y}$-insulator-poly-Si solar cells, photovoltaic conversion parameters 80−101093
$In_{2-x}Sn_xO_{3-y}$-Si solar cells, SiO_2 detection of interface, Auger anal. 79−87991
$(In_2SnTe)_x$-$(2InSb)_{1-x}$ system, semicond., Mossbauer absorption line of ^{119}Sn 78−27146
In_2Te, molten SRO 77−65945
In_2Te_3 defect semicond., photoconductivity kinetics 80−11035
In_2Te_3 film thermal deposition, transmission spectra and elec. cond. *(Russian)* 80−49555
In_2Te_3, low temp. ordered phase and transition state, TEM obs. 79−28095
In_2Te_3, photosensitivity on γ- and neutron-irrad., γ-ray dosimeter mat. applic. 77−85258
α-In_2Te_3 single crysts., elec. and photocond., temp. depend., linear thermal expansion coeff. 79−42541
In_2Te_3-PbTe system, phase diagram, elec. props. 78−35361
In_2Te_3-type semicond. radiation-resistant fast-electron detectors 78−78559
In_2Te_3-type semiconductor, mechanism of electrically inactive impurities 80−24834
In_2Te_5 (II), cryst. struct. determ. 78−26510
In_2Te_5, photocond. and absorption spectra, polarisation dependences 80−20642
$(In_2Te_3)_{1-x}(In_2Se_3)_x$, thermal cond. exam. 79−28160
N-$KTaO_2$, light and heavy cond. electrons at zone centre 79−73426
$KTaO_3$:Gd, temp. depend. of thermal diffusivity and Seebeck coeff. 78−10481
$LaCo_{1-x}Ti_xO_3$, cryst. struct., elec. and mag. props. 79−86748
La_2CuO_4, high pressure phase transformation, small polaron cond. to semicond. transition 78−6156
La_3NbO_7, weberite-type, elec., mag. and opt. props. 77−85212
$La_{1-x}Sr_xCoO_{3-y}$, Seebeck coeff. meas., small polaron hole conduction model 80−20233
$La_{1-x}Sr_xCrO_3$, x=0-0.2, AC and DC cond., 77-1300K, hopping of polarons 78−2477
$La_{1-x}Sr_xVO_3$, high-temp. transport meas., band model 77−11917
$La_{1-x}Sr_xVO_3$, semiconductor-metal transition, Anderson localisation, Hall mobility and 1/f noise meas. 79−78142
$Li_{2.33}Si$, cryst. struct. and electrochem. anal. *(German)* 80−88132
LiV_2O_5, needle cryst. form. by reduction of molten Li_2O-V_2O_5, semicond. props. *(Japanese)* 78−3030
$Lu_2Ir_2O_7$, pyrochlore, sp. ht. below 20K, Debye temp. 80−65241
$LuRhO_3$, elec., mag. and photoelectrochemical props. 80−96925
$Mg_xCd_{1-x}Te$, electroreflection spectra, comp. depend. 80−66230
Mg_2Ge, L, electron-phonon interaction and phonon cond. at low temp. L n-type semicond. 79−14903
Mg_2Ge, phonon cond. 4-1000K 78−79826
Mg_2Ge, semicond., electronic band struct., reson. Raman scatt. meas. 77−12384
Mg_2Ge, valence band, XPS meas. 77−8018
MgO porous layers, conductivity, conditions for lag and dark current 77−20476
MgO, prerededured surfaces, room temp. activity for oxygen isotopic exchange 79−91998
Mg_2Si, charact. X-ray temp. and thermal expansion coeff. 77−15599
Mg_2Si, phonon cond., 3-500K 78−79826
Mg_2Si, semicond., electronic band struct., reson. Raman scatt. meas. 77−12384
Mg_2Si, stress effects on Raman spectra 77−20851
Mg_2Si, valence band, XPS meas. 77−8018
Mg_2Sn, L, electron-phonon interaction and phonon cond. at low temp. L n-type semicond. 79−14903
Mg_2Sn, lattice dynamics, angular force model 77−4166
Mg_2Sn, phonon cond., 4-1000K 78−79826
Mg_2Sn, semicond., electronic band struct., reson. Raman scatt. meas. 77−12384
Mg_2Sn, stress effects on Raman spectra 77−20851
Mg_2Sn, valence band, XPS meas. 77−8018
$Mg_xZn_{1-x}Te$, band struct. refl. spectra meas. 80−80813

semiconductor materials continued
$Mg_xZn_{1-x}Te$, spin orbit splitting, of electron energy levels, reflectivity meas. 79−69479
$Mg_xZn_{1-x}Te$, temp. depend. of energy gap, near band gap reflectivity spectra 79−28786
$MnAs_{0.95}P_{0.05}$, anisotropy of elec. cond. and Hall effect 80−92908
$Mn_xCd_{1-x}Se$ single crysts., photoluminesc., composition depend. 80−80854
$Mn_xCd_{1-x}Te$, far IR refl. spectra, phonon spectra 78−52497
$Mn_xCd_{1-x}Te$, lattice vibrs., Raman and IR spectra meas. 80−93311
$MnCo_2O_4$ DC sputtered films, struct. and elec. props. 80−54812
MnO-CoO-O_2, semicond. solid solns., ageing effects on elec. cond. 78−23085
MnO_2, DC cond., water content depend. 77−80774
Mn_3O_4:Li(Cr)(Al)(S), and pure Mn_3O_4, elec. cond. and thermo-EMF 80−20231
Mn_3O_4:S, defect struct. and elec. props., electron, hole conc. 80−44601
α-MnS, defect energetics and range of homogeneity 78−47317
MnSe, and $MnSe_2$, thermodynamic props. 80−19958
MnTe film, elec. props. 78−43498
$(MnTe)_{1-x}$-$(As_2Te_3)_x$ solid solns., thermoelec. props. 79−42567
$(MnTe)_{1-x}(Bi_2Te_3)_x$ ($x \leq 0.05$) solid solution, electrophys. props. 80−24925
MoO_3, EPR investig. of defect centres 77−59457
MoO_3:Li, elec., catalytic props. 78−60122
$Mo_4Ru_2Se_8$, synthesis, struct., and elec. props. 80−92877
MoS_2 (2H), elec. cond. press. depend. 78−43394
MoS_2 (2H), low energy electron energy loss spectra 79−95885
MoS_2, clean surface, AES and LEED exam. 80−10762
MoS_2, elec. cond. and Hall coefficient temp. depend. 77−28180
MoS_2, electronic struct. by photoelectron spectroscopy using line and synchrotron sources 79−87560
MoS_2, factor-group analysis of high-symmetry layer dynamics 79−42160
2HMoS_2, far IR optical and magneto-optical absorpt. 77−52078
MoS_2, layer dynamics of high-symmetry crystals with atom-atom interactions 78−71799
MoS_2 molybdenite band structural props. rel. to supercond. and semicond. 80−96781
MoS_2, spatial symm. of valence band struct. by angularly resolved XPS 77−69961
MoS_2, surface electronic struct., slow electron reflection, total current spectroscopy *(Russian)* 80−54759
MoS_2, synthetic molybdenite single crystals, growth from vapour, elec. props. 80−34446
$MoS_2(Se_2)$, layer type dichalcogenides, reflectivity, 6 to 40 eV, electronic deep level excitation 77−55801
$MoS_2(Se_2)(Te_2)$(2H) polytypes, Kramers-Kronig anal. of reflectivity spectra, 0-30 eV, band model 79−51976
MoS_2(2H), electro-absorpt. edge spectra, cryst. thermal modulation, exciton state field ionisation 79−61395
n-$MoSe_2$ based liq. junction solar cell, nonaqueous electrolyte system employing Cl_2/Cl^- couple 80−81432
$MoSe_2$, elec. cond. and Hall coefficient temp. depend. 77−28180
$MoSe_2$, imperfections from TEM study 80−79800
$MoSe_2$ layer-type electrochem. solar cells, electrode material performance, doping effect 79−74532
$MoSe_2$:Nb(Re), layered, elec. props., semicond.-metal transition 77−11922
$MoSe_2$-I^-, photoelectrode, time resolved photocurrent, nanosecond excitation 80−45708
$MoSe_{2-x}$, transport meas. and band structure 77−69361
$MoSi_2$ sputtered films, protective layer form. on oxidation, Auger anal. and backscatt. meas. 79−15029
α-$MoTe_2$, band struct. photoelectron spectroscopy 77−51653
$MoTe_2$, elec. cond. and Hall coefficient temp. depend. 77−28180
$MoTe_2$, elec. cond. and thermoelec. power 79−91047
α-$MoTe_2$, electronic struct. by photoelectron spectroscopy using line and synchrotron sources 79−87560
$MoTe_{2-x}$, thermal switching mechanism 77−15920
$MoTe_{2-x}$, thermoelec. power and resist. meas., band struct. 77−1438
$Mo_{0.5}W_{0.5}Se_2$ single cryst. vapour growth, characterisation 80−93466
$NaNbO_3$, elec. cond., Hall mobility, thermoelec. coeff. 79−82584
$Na_{1.9}V_{12}O_{29.7}$, press. depend. of elec. cond., semicond.-metal phase transition obs. 78−64072
Na_xVS_2, intercalation cpd., mag. phase transitions 77−69558
$Na_xVS_2(Se_2)$, mag. and elec. props. rel. to struct. transitions 78−91848
Na_xVSe_2, intercalation cpd., mag. and structural phase transitions 77−69558
$NaZnGeO_4$:Mn, electrolum., ionisation domains 80−84787
Nb chalcogenides and chalcogenide halides, geometrical struct. and metal-metal bonding 80−80172
NbO_2, on-state decay rel. to recomb. and nonlinear props. 80−84492
NbO_2, semicond., thermal expansivity 80−34213
NbO_2, semicond. cryst., elastic props. 79−19308
NbO_2, semiconducting, elastic const., press. depend. at 296K 79−23672
NbO_2, threshold switching recovery curve, distribution trapped carrier lifetime 80−20258
Nb_2O_5 electrodes, in aq. and acetonitrile solns., electrochromism 80−50298
NbS_3, cryst. struct., X-ray diffr. obs. 79−1412
NbS_3, electronic struct. and predicted cond. props. 80−92815
NbS_3, phase transitions and elec. props. 80−20178
NbS_3, transport props. 80−20175
$NbS_2Cl_2(Br_2)(I_2)$, absorpt. edge spectrum, fine struct. 80−66219
Nd-Gd-Te alloys of R_2Te_3-T_3Te_4 region, physicochem. props. 78−52017
$Nd_2(MoO_4)_3$, mag. susceptibility, elec. cond. and thermoelec. power 78−88091
$NdNbO_7$, weberite-type, elec., mag. and opt. props. 77−85212
Ni-Ge-SiO, solar selective absorber surfaces, optical behaviour at high temp. 80−101130
$Ni_{1-x}Co_xS_2$, anomalous elec. props., polaron transport in highly correl. narrow bands 77−85222
$Ni(Mo_2Re_2)S_8$, synthesis and electrical props. of mixed tetrahedral cluster phases 80−2971
NiO and lithiated NiO, thermally grown, electrochemical capacitance variations 80−29475
NiO, elec. cond. and chem. diffusion coeff. at high temps. 79−23962
NiO, elec. cond. meas. at 1000°C 78−10451
NiO, elec. cond. variation with temp. *(French)* 79−60829
NiO, Hall effect anomaly, sign reversal at 600K 80−100471
semiconductor materials continued
NiO, thermodynamic study of point defects, anal. of elec. cond. results 79−23963
NiO:Li_2O-ZnO p-n heterojunction, contact resist., effects of water vapour 80−34506
$NiPS_3$, layered semiconductors, optical and electronic props. 80−70761
NiS, semiconductor-metal transition, UPS and XPS 79−23896
NiS_2, weak ferromagnet, galvanomagnetic effect 79−11148
$Ni_{1-x}S$, and $Ni_{1-x}S_{1-y}O_y(Se_y)$, mag. state in metal-semicond. transition region, neutrnon diffr. obs. *(Russian)* 77−89926
$NiSO_4$:Li (10 at.%), powder, semiconducting, exam. of freeze drying rate in cryochemical prep. method 78−52706
$NiS_{2-x}Se_x$, first-order Raman scattering 80−108206
OsB_2, possibility of semicond. props., rel. to atomic volume 77−69317
Pb chalcogenides, spectral depend. of internal quantum efficiency 77−4402
$Pb_{1-x}Cd_xS$ epitaxial layer, metastable, optical props. and electronic struct. 79−15543
PbI polytypes, phase transforms. and electrical behaviour 78−47839
PbI_2 (2H), electronic transport and cyclotron reson. 79−28369
PbI_2 (2H), layer cpd., band parameter determ. 79−95332
PbI_2 (2H), multi-phonon scatt. near direct absorpt. edge, resonant Raman obs. 79−87448
PbI_2, complex dielectric and optical consts., ellipsometric determ. 78−23425
PbI_2 crystals, exciton condensation, excitation and luminesc. study 80−55182
PbI_2, defect levels, TSC meas., photoconductor models, trap level capture cross section 79−69463
PbI_2 direct gap semiconductor, exciton lifetime and condensation threshold, luminescence spectra 80−34981
PbI_2, elec. props. rel. to polytypically modulated structs. 79−94971
PbI_2, emission spectra, 80K, high excitation intensity effects at different pump wave lengths 77−52170
PbI_2, exciton absorpt., band shape, dielectric const. real part derivatives *(Russian)* 80−25413
PbI_2, exciton magneto-optical spectra 80−25347
PbI_2, exciton states, high field magnetoabsorption 77−52130
PbI_2, excitonic shifts of quasiatomic optical core to cond. band transitions, UPS obs. 78−11079
PbI_2, factor-group analysis of high-symmetry layer dynamics 79−42160
PbI_2 film, highly excited, oscillator strength of excitons, absorpt. and emission spectra 78−76001
PbI_2, film, reflectance meas., optical consts., humidity effects 80−34994
PbI_2, first-order 2H-4H polytype transition, exciton spectroscopic study 80−59647
PbI_2, layer dynamics of high-symmetry crystals with atom-atom interactions 78−71799
PbI_2, layered, electronic band struct., direct evaluation by angle resolved photoemission 77−51652
PbI_2, layered, photoelectromag. effect meas. of transport parameters 77−59301
PbI_2 layered cryst. under uniaixal compression, low temp. thermal cond. *(Russian)* 80−44374
PbI_2, layered semicond., valence bands UPS and XPS obs. 78−11078
PbI_2, luminescence excited by high-intensity two photon pumping 77−44038
PbI_2, octahedrally coordinated, layer cpd., electronic struct. using synchrotron-radiation photoemission spectroscopy 79−74058
PbI_2, optical phonon anisotropies and intralayer bonding forces from IR refl. 77−59573
PbI_2, phase transition of first kind by exciton spectroscopy *(Russian)* 79−82334
PbI_2, photocond. induced by polaritons at band-edge 79−95450
PbI_2, photoelectromagnetic investigation, expt. 79−24010
PbI_2, photoexciton interaction, luminescence spectra, polariton dispersion diagram 80−93397
PbI_2, photolum. and reflectivity temp. depend., cryst. anisotropy effect on electron-phonon interaction *(Russian)* 78−15225
PbI_2 polytypes, elec. cond., band gap reduction due to stacking fault levels 77−32015
PbI_2, press. depend. of band-gap excitons, 77K, optical absorpt. spectra 79−8157
PbI_2, semicond., band struct., angle resolved photoemission meas. 78−15296
PbI_2 single crysts., resonant and nonresonant Raman spectra 77−69823
PbI_2, stimulated photoluminesc. excitons role 77−48201
PbI_2, TSC meas., localised levels in energy gap, depend. on purity and history 77−15856
PbI_2, thin cryst. barrier, reson. and inelastic tunnelling 80−44739
PbI_2, three-photon absorpt. coeff. determ. by nonlinear luminesc. expt. 80−14384
PbI_2, two-photon absorpt. spectrum 77−52118
PbI_2 two-photon absorpt. cond. and luminesc. meas. 77−52166
PbI_2, two-photon photoemission 79−28890
PbI_2, UV reflectivity meas., band struct., LCAO calcs. 78−72545
PbI_2, visible exciton spectrum, exciton-phonon interactions, dielectric const. and oscill. strengths 80−25405
PbI_2-Ag, light sensitivity for high exposure densities *(Russian)* 79−6212
PbI_2-Ag system, effect of bound and free exciton states on light sensitivity *(Russian)* 78−71169
PbI_2-Ag(Au)(Cu), light sensitive, internal photoelectric emission 80−107910
$Pb_{1-x}In_xTe$, $0.01 \leq x \leq 0.2$, elec. cond., Hall coeff. liquid He temp. 78−47815
$Pb_{1-x}In_xTe$, impurity-state conduction and temp. depend. of transport coeffs. 78−47795
$Pb_{1-x}Mn_xTe$ ($x = 0.005, 0.001, 0.05$), solid solns., exam. of electrical and thermal props. 79−1599
$Pb_{1-x}Mn_xTe$, photovoltaic effect, p-n junction, energy gap determ. 80−92931
$Pb_{1-x}Mn_xTe$, single cryst., mag. susceptibility 79−73672
PbS, phase transitions under action of high press., elec. cond. meas. 77−4196
PbS-Sb_2S_3 semicond., optical and photoelec. behaviour 80−96938
PbTe-InTe system, phase interactions and solid soln. form., physicochem. and elec. characteris. 80−104129
PbI_2, thermal cond., 2 to 30K, Umklapp processes and phonon boundary scatt. *(Russian)* 79−10991
PdO, semiconductivity and stability, optical props. 78−43497
Pr_2NiO_4, elec. props., 300 to 1000°C 78−91694

semiconductor materials continued
$PrFeO_3$, elec. props., 300 to 1000°C 78−91694
$PtCl_3Pt(NH_3)_4$, Magnus' Green Salt, extended localised holes charge distrib. 77−55496
$Pt_{0.97}S_2$, optical props. at absorption edge 78−35140
$RbMnF_3:Er^{3+}$, absorption, emission, excitation and lifetime meas. 80−71460
$RbSbS_2$, cryst. struct., space groups 79−7592
ReB_2 possibility of semicond. props., rel. to atomic volume 77−69317
RuB_2, possibility of semicond. props., rel. to atomic volume 77−69317
$Ru_xTi_{1-x}O_2$ films, elec. props. and IR spectra 79−38207
$Ru_xTi_{1-x}O_2$ films, percolation elec. cond. in strong electric fields *(Russian)* 80−84471
SMS, band struct. and semicond. metal phase transition 80−80180
$(Sb_{1-x}Bi_x)_2Te_3$, δ phase, equilib. state, electrophysical props. 79−52178
$p\text{-}Sb_{1.48}Bi_{0.52}Te_3$, extrusion deformed, powder dispersion degree influence on thermal and elec. props. *(Russian)* 80−39366
$Sb_{1.48}Bi_{0.52}Te_3$, obtained by zone crystallisation, effect of extrusion and annealing on elec. props. 79−96038
$Sb_{1.5}Bi_{0.5}Te_3$ solid solution, electrical, thermoelectric and thermal properties, temp. influence obs. *(Slovak)* 78−30946
$p\text{-}Sb_xBi_{2-x}Te_3$ *(German)* 79−51618
SbI_3, photopolarisation, photoelectret state, electron-hole transitions 77−12300
SbI_3, valence band, UPS meas. with synchrotron radiation 79−56914
$SbI_3\text{-}AsI_3$, phase diags. 78−6905
Sb_2O_3 anodic layers on Sb, semicond. props. 79−56303
Sb_2O_3, thermoelec. props., 500-1500K 80−29423
$p\text{-}Sb_2S_3$, bistable switching 79−73553
Sb_2S_3, defect drift in elec. fields and bistable switching 80−92947
Sb_2S_3, elec. and mag. props., carrier transport mechanism 78−47792
Sb_2S_3 film, amorphous and crystalline, optical props. 79−95867
Sb_2S_3 film, coevaporated, elec. cond. meas. 80−65726
Sb_2S_3 film, struct., influence of laser beam 79−7761
Sb_2S_3, galvanomag. props. and elec. resist., temp. depend. 78−43419
Sb_2S_3, hopping cond. in cryst. subjected to strong elec. fields 79−95456
Sb_2S_3, influence of temp. on NQR spectra of $^{121,123}Sb$ 78−60354
Sb_2S_3 layered biaxial cryst., surface phonon polaritons *(Russian)* 78−60021
Sb_2S_3, switching mechanism 77−15921
SbSI, phonon echoes *(French)* 77−51461
Sb_2Se_3, energy gap, light absorpt., elec. cond., photocond. meas. 78−47826
Sb_2Se_3, monostable switching effect *(Russian)* 79−33316
Sb_2Se_3, photocond., photo-EMF and photodielectric effect, expts. 80−20245
Sb_2Se_3 single crysts., phys. prop. anomalies, 400-450K *(German)* 79−38072
Sb_2Se_3-CdSe heterojunction, photoelec. props. 80−70816
$(Sb_2Se_3)_x\text{-}(Bi_2S_3)_{1-x}$ single crystals, elec. and photoelec. props., stoichiometry deviations influence 79−60870
$Sb_{35}Se_{65}$, polycrystalline, elec. cond. mech. 80−49705
$(Sb_2Se_3)_{0.7}(Bi_3Se_3)_{0.3}$, solid soln., prep. and elec. properties of layered crystals 80−70762
Sb_2Te_3, crystallisation in constant electric field, thermoelectric parameters 77−44146
Sb_2Te_3 epitaxial films, growing conditions effect on elec. cond., thermo-EMF 80−39687
Sb_2Te_3, free charge carrier mag. susceptibility, 300-600K 78−10644
Sb_2Te_3, mag. and elec. props., carrier excitation 78−43395
Sb_2Te_3, mechano-caloric energy conversion 80−10962
Sb_2Te_3, optical props. determ. via Kramers-Kronig transform. 77−8537
Sb_2Te_3, stoichiometric, Hall effect and thermoelec. power studies 80−100470
$p\text{-}Sb_2Te_3$, thermopower anisotropy, temp. depend. 77−15884
$Sb_2Te_3\text{-}Bi_2Te_3$ and $Sb_2Te_3\text{-}Sb_2Se_3$ systems, thermal cond. change during phase transitions 80−100368
$Sb_2Te_3\text{-}Bi_2Te_3$ solid solns., single cryst. growth and thermocouple construct. 80−104056
$Sb_2Te_3\text{-}Sb_2Se_3$, ordered structure formation, heat treatment effect on thermal cond. 80−54448
$Sb_2Te_3\text{-}Sb_2Se_3$ thin layers, struct., phase comp., and elec. cond. 80−15389
ScN_x, region of homogeneity, physicochem. props. 78−52018
Sc_2O_3, heat treated, elec. cond. rel. to O_2 partial press. 77−15845
$Sc_{2/3}\square_{1/3-y}Sc_yS$, elec. props. variation at high temps. *(French)* 79−82649
$Se_{90}Te_{10}$ whiskers, chem. and thermal etching 77−15417
Se_xTe_{1-x}, growth of single crystals by Czochralski method 80−66423
Si-Ge, heavily doped, reversal of precip. 80−2409
Si-Ge, high temperature thermoelectric materials 80−89659
Si-Ge, variable-gap cryst. made from solid soln. 79−66003
Si-Ge (22 at.%) alloy, thermoelec. props., time and temp. dependence 78−91712
Si-Ge heteroepitaxial layers, Ge/Si ratio transfer curve from gas phase to solid phase obtained by epitaxial growth 77−73234
Si-Ge single crystals, solid solutions, growth by electron-beam zone melting without crucible 79−4917
Si-Ge solid solns., p-n junctions, photoelec. props. obs. 77−1471
Si-Ge solid solution, thermal neutron monochromators 80−49053
SiAs, cryst. growth from melt, elec. props. 80−76170
SiAs, monoclinic, band struct., OPW calc. 77−59255
SiAs-Au surface barrier diodes, optical props. of SiAs 79−8145
$SiAs_2$, electron charge density calc., nature of bonding determ. 77−1098
α-SiC, ^{30}Si self-diffusion, ion microprobe anal. 79−42309
SiC, 2H→6H transform. mechanism, X-ray diffr. theory 78−30575
n-SiC, 6H, epitaxial layer, saturated electron drift velocity meas. 78−19168
α-SiC, 6H, excited states, photoluminesc. efficiency 78−39604
SiC, 6H polytype, elec. and thermal cond., carrier concentrations 80−2223
SiC, 6H polytype, LPE growth by dipping technique for prep. by blue LEDs 77−8769
SiC (2H), vapour grown, growth and deform. faults, X-ray obs. 78−30650
n-SiC (6H), anisotropy, of thermoelec. power and transverse Nernst-Ettingshausen effect 77−69362
n-SiC (6H), anisotropy of thermoelectric power *(Russian)* 78−91710
n-SiC (6H), density of states effective mass determ., high temp. meas. of elec. props. 79−15073

semiconductor materials continued
n-SiC (6H), doping effect on birefingence dispersion, effective electron mass 79−69807
α-SiC (6H), dynamic hologram high-speed recording and erasure mechanism 80−5710
SiC (6H), IR absorpt., UV illumination effects, defect levels 80−66251
α-SiC (6H), paramag. N impurity levels, IR absorpt. and ESR expts. 77−59598
SiC (6H), phonon drag and phonon-electron interaction *(Russian)* 78−79701
SiC (6H), semicond. with one-dimens. electron superlattice, interband optical absorpt. 79−15483
SiC (6H) (000$\bar{1}$), Ar^+ ion bombard., defect form., LEED obs. 79−69165
SiC (6H) epitaxial layers, growth by CVD, morphology 79−24446
α-SiC (6H) laser excited thermostimulated luminescence light sum dose depend. *(Russian)* 80−16111
SiC, anodised, IR spectra *(Russian)* 78−11376
SiC, α- and β-phases, isomer shift in Mossbauer spectra of implanted ^{129}I 78−15067
SiC, α- and β-types, electroreflection spectra of natural and low-energy ion-bombard. surfaces 79−61340
SiC, α-β heterojunctions, spectral charact. *(Russian)* 77−63467
SiC, B diffusion, polytype struct. effect 78−59983
SiC, CVD film growth, morphological, chem. and cryst. struct. investig. 77−40385
SiC, cathodoluminescence, comparison with other materials 78−92130
SiC, cryst. growth on oriented seeds by sublimation 78−35279
β-SiC, cryst. temp. variation during growth 77−40340
SiC, crystal growth from gas phase role of Si in mass transfer 79−8233
α-SiC crystals, broad-band semiconductors, growth in Acheson furnace 80−84841
β-SiC crystals, wetting by Si and growth by vap.-liq.-solid mechanism 78−3005
SiC, crysts., tetrahedral bond deformation variation with hexagonality and doping degree of N 79−94977
β-SiC, cubic, conduction band minima location and shape determ. 77−85141
β-SiC, cubic, elec. props. 78−51996
SiC, cubic, magnetoresistance and Hall mobility, field and orient. depend. *(Russian)* 77−69346
SiC, cubic, photo EMF on microtwinning lamella *(Russian)* 78−60165
n-SiC, cubic, piezoresistance meas. under hydrostatic compression 77−4344
α-SiC, deep centre levels, IR photoluminescence 77−16387
β-SiC, deform. potential and effective mass anisotropy, Hall constant 79−90949
SiC, determ. of size and conc. of crit. clusters in vapour phase in homogeneous nucleation process 79−94951
SiC devices, epitaxial layer growth techniques 80−108360
SiC, diffusion of B, elec. cond. meas. 80−96696
A-SiC, dimensions of muonium atoms, depolarisation of positive muons 79−11374
SiC diodes, S-type, high-voltage switching 77−20421
6H-SiC, dislocation etching 78−22721
SiC, donor exciton satellites, multiple bound excitons 77−11857
SiC, eccentric growth spirals 78−26470
SiC, electron trap depth, additional IR absorption induced by UV excitation *(Russian)* 79−78721
SiC, electron-hole liquid, RPA calcs. 80−6743
SiC, epitaxial growth by sublimation sandwich method, effect of impurities 80−25568
SiC, epitaxial growth by direct synthesis in vacuum 80−40262
α-SiC, epitaxial layer, impurity macroincorporation, distrib. of Al, B, N and P 77−69192
SiC epitaxial layer, vapour phase growth, investigations of kinetic and thermal conds. 79−42407
SiC epitaxial layers, energy distrib. in photolum. spectra, influence of synthesis conditions 79−52009
SiC film, growth on Si ribbon surface, TEM anal. 78−84094
SiC film electron beam preparation technique, diffraction pattern anal. *(German)* 80−55297
SiC, film growth by reaction of acetylene with Si (111) surface 79−100441
β-SiC, film prep by RF sputtering 77−44164
β-SiC form. on Si substrate in RF powered reactor 80−76173
SiC, growth from soln. in fused Si, temp. gradient method in Tb vap. 78−35301
β-SiC, growth kinetics by Van Arkel method 77−16479
β-SiC, heteroepitaxial growth on Si substrate using $SiCl_4\text{-}C_3H_8\text{-}H_2$ system 79−24445
p-SiC, inequivalent sites of IR luminescence centres *(Russian)* 77−1722
SiC, influence of plastic deform. on struct. of photoluminesc. spectra 77−55824
SiC LEDs, current-voltage and brightness-current charact. under prebreakdown conditions 79−51667
SiC, LPE for blue LEDs 77−81228
α-SiC, laser monopulse energy meas. using ruby laser SHG *(Russian)* 79−94272
SiC, laser Raman spin-flip scatt. from excitons, luminesc. 80−80786
β-SiC layer synthesized by C ion implantation in Si, IR absorpt. 78−56492
SiC, luminesc., electron-hole drop 79−38606
SiC luminophor powders, SAW nonlinear acoustoelectro-luminescence 80−45143
SiC, momentum density, Compton profile 77−20235
SiC, N doping inhomogeneities due to growth conditions 78−22741
β-SiC, n-type, thermoelectric efficiency at high temps. 80−35706
SiC, negative photoconductivity and photoconductivity quenching 78−6414
SiC, nonlinear refr. index meas. by nonlinear lens method *(Russian)* 79−26111
SiC, on Si and metal silicides, formation characteristics and mechanism, by ion backscattering techniques 79−60653
SiC, optical props. determ. via Kramers-Kronig transform. 77−8537
β-SiC, optical quenching of luminesc., acceptor ionisation energy 80−55178
SiC, p-n homojunction breakdown voltage for onesided abrupt junctions *(German)* 78−56210
SiC p-n junction, electroluminesc. 80−97343

semiconductor materials continued
SiC p-n junction, epitaxial, grown by sublimation, elec. and struct. props. *(Chinese)* 80−60067
SiC, p-n junction, vapour grown elec. breakdown fields 78−19135
SiC p-n junction photodetector, spectral characts. 77−41685
SiC p-n junctions, current-voltage characts. 80−60073
SiC p-n junctions, electrolum. spectra and kinetics 80−66305
SiC particles in EFG ribbon solar cells, EBIC and ion microprobe anal. 80−93838
SiC, periodical step system vibr. modes in step trains, rhythmical bunching 79−41996
SiC, phys. props. and crystal growth, rel. to appl. in electrolum. devices, book contrib. 77−77299
SiC, point contact, stable elec. oscill. generation by high field strength *(Russian)* 77−62989
SiC polymorphs, widths of first minibands and effective masses, resist. anisotropy 80−20071
SiC, polytypes, birefr. meas. 77−43963
SiC polytypes, free exciton luminesc. meas., phonon energies 80−80852
n-SiC, polytypes, temp. depend. of piezoresist. constants 79−11125
SiC polytypes deformed, resist. anisotropy in (0001) plane 80−20198
β-SiC, pyrolytic, optical and elec. props. 79−78093
SiC, radiation defect annealing, recovery of LEED maxima 80−65075
SiC, refractive index dispersion, 0.4-50 μm, 105-297K 78−84548
β-SiC, residual photocond. meas. 77−4408
SiC reverse biased p-n junctions, prebreakdown violet luminesc. 80−7420
n-SiC, saturation of electron drift velocity in strong electric field 77−76840
SiC, self-bonded polycryst., electrophys. props. 80−10980
SiC, self-focusing of ruby laser radiation, free carrier conc. depend. *(Russian)* 77−42579
SiC, semi-insulating in struct. with injecting contacts, cond. in strong elec. field 78−19160
α-SiC, short-wavelength photocond. and capacitance photo-EMF meas. 78−26906
SiC, single cryst. ingots, growth using seeds, 1800-2600°C 78−43993
n-SiC, single cryst. layers deposition on charact. substrates, morphology *(German)* 79−28943
SiC single crysts., polytypism obs. by high temp. oxidation expts. 78−59797
SiC, spin-flip scatt. of laser light from photoexcited excitons 80−93330
SiC, sputtered, comp. and struct. props., effect of target materials 80−54549
SiC, struct. of spectrum of excitons bound to neutral B atoms 78−19523
SiC, synthesis by ion implantation of diamond, role of struct. imperfections 78−34529
SiC, thermal oxide layers, AES depth-profiling anal. 79−43454
SiC, thermal S-N switching 79−24027
SiC, thermolum. excited by light outside fundamental absorpt. region 79−24375
SiC thin-film thermistors with high thermal response *(Japanese)* 80−105629
SiC, VPE kinetics study in SiC-C system 79−37934
SiC, VPE layers, growth kinetics, polytypism 77−11809
SiC, vapour deposition, thermodynamics of Si-C-Cl-H system *(German)* 79−11520
β-SiC whisker, atom-probe FIM expts. 78−35275
SiC with dielectric coating, surface polaritons, waveguide modes 80−80195
α-SiC, wurtzite type cryst., temp. depend. of one phonon Raman spectra, Gruneisen parameters 77−66500
SiC:Al, g-values, spin temp., determ. from Raman spectra 78−43856
B-SiC:Al, ion implanted, elec. props. and luminesc. meas. 77−12443
SiC:Al,N (6H), ODMR for effective-mass-like acceptor 80−93213
SiC:Al epitaxial layers, growth, Al distrib. and solubility 80−15391
SiC:Al^+ p-n junctions, elec. props., defect effects 80−15594
SiC:Al(B)(Ga), 4H-, 6H- and 3C-polytypes, melt growth and photoluminesc. 77−24885
SiC:Al(Ga)(B) (6H) LEDs, fabrication by rotation dipping technique, electrolum. mechanisms 80−50426
β-SiC:B, diffused structures, current-voltage characts. 78−47865
SiC:B, electroabsorption, 0.35-0.45 eV, under UV illumination 79−4831
SiC:B, impurity distribution determ. by neutron activation anal. 77−76452
SiC:B, ionisation energy of deep centres from absorpt. spectra, electron-phonon coupling 77−4663
p-SiC:B (4H), absorption spectra of bound excitons 78−88338
β-SiC:B p-n junction, IR electroluminesc. spectrum 77−44067
SiC:B(Be), dislocation induced deceleration of impurity diffusion 77−28043
α-SiC:B(Be)(Ga), piezoresist. rel. to acceptor levels 78−60129
p-SiC:Be, Fermi level, Fermi distrib. and activity coeff. calc. 77−1365
SiC:Be, gas-phase equilib. comp., thermodynamic analysis rel. to cryst. growth and doping 77−85909
β-SiC:Ga, donor-acceptor pair emission 77−4682
4H-SiC:Ga(Al), photoluminesc. spectra 77−66530
α-SiC:H, prepared by reactive sputtering, layer props. *(Japanese)* 80−60695
SiC:N, impurity effect on stress gradients and dislocation development 77−4116
n-SiC:N, O, cathodolum. spectra meas. 78−19573
SiC:N(Al)(Ga) (6H), photoluminesc., site-depend. donor and acceptor levels 79−61421
α-SiC:Sc, quasiline luminesc. spectrum 77−4686
SiC:Tb(Sc), various polytypes photolum. meas., identification of 4H and 6H polytypes 77−63459
SiC:Ti (6H), absorpt. spectra of n- and p-type cryst. 79−38581
SiC-n-Si junction device, elec. props. 80−15591
SiC-Si composite, bulk resist. of technical SiC powders 79−28350
SiC-Si n-n and n-p htheterojunctions, prep. by ion implantation, tunnelling cond. 77−43710
SiC-Si struct. formation on ^{12}C ion implantation in Si, optical and photoelectric props. 79−91136
SiC-SiO_2 interface, Auger anal. 78−95375
n-SiC(6H), donor ground state splitting, IR spectra *(Russian)* 78−92104
α-SiC(6H), electron bombardment, formation of defects on (000$\bar{1}$) surface 80−19844
α-SiC(6H), two stage transitions, nonlinear absorpt., thermoluminesc. method 80−7425
SiGe, matrix isolated cluster, optical absorpt. 80−16045
semiconductor materials continued
SiGe, ultra high vacuum epitaxy on Si substrates *(German)* 77−47702
$Si_{1-x}Ge_x$ system, lattice energy and consts., virtual cryst. approx., pseudopot. calc. 80−44166
Si_xGe_{1-x}-Si(GaAs) heterodiodes, interfacial structural defects effect on avalanche breakdown 79−42644
SiP, thermodynamic charact. 10-300K, interatomic bond elasticity 80−59677
SiP_2, electron charge density calc., nature of bonding determ. 77−1098
SiP_2, pyrite structure, density of states 77−15733
SiP_2 with pyrite struct., Fermi surface calc. 80−65427
$SiTe_2$, dislocations and stacking fault energy 78−47378
Si_2Te_3, fundamental absorption and Franz-Keldysh effect meas. 77−1694
Si_2Te_3, passivated single cryst., elec. conductivity 78−95299
p-Si_2Te_3, photoelectric props., luminesc., hole lifetime and trapping 77−39892
Si_2Te_3, surface exam. by Auger spectroscopy 77−69150
Si_3Te_3, photoconductivity of cryst. with clean surface 77−4395
$(SiTe)_{1-x}(ATe)_x$, A=Ge, Sn, Pb, solid soln. with small substitution, mag. susceptibility *(Russian)* 80−70933
Sm monochalcogenides, semicond.-metal phase transition 79−47017
$Sm_{1-x}Gd_xS$, calorimetric exam. of metal-semiconductor transition 78−18967
$Sm_{1-x}Gd_xS$, resistivity investig. of metal-semicond. transition, press. effects 77−62829
$Sm_{1-x}Gd_xS$ system, semicond. to metallic isomorphous phase transition mechanism 80−2338
$Sm_{1-x}M_xS$, M=Eu,Ca,Yb, valence transition under high press. 79−73551
$Sm_{1-x}Nd_xSe$, Nd substitution effect on lattice const., resist., and colour 79−56763
$Sm_{1-x}R_x^{3+}S$, (R is rare earth metal), semicond.-metal phase transition 79−47017
SmS, anomalously high magnetoresist., Hall coeff. and elec. resist. meas. 78−10479
SmS, cryst. struct. in homogeneity region 78−91334
SmS, defect struct., precipitate colonies, dislocation loops, TEM obs. 80−44214
SmS, divalent and trivalent ion doped, electronic struct., Mossbauer spectroscopy 78−39022
SmS, energy of metal-semicond. phase transition and threshold recording energy density 79−28386
SmS, f-d hybridisation, valence fluctuation and phonon spectrum, Raman scatt. expts. 78−60464
SmS film, semicond. and metallic modifications, elec. props. 77−32098
SmS, LO phonon freq. softening in semicond. and metallic phases 80−96619
SmS, mag. susceptibility in semicond. phase, in homogeneity region 79−28502
SmS, optical props. and electronic struct., Kramers-Kronig model anal. 79−69859
SmS, piezoresistance at 80K 80−59990
SmS, press. effect on lattice parameter, mag. susceptibility, and reflectivity 79−56272
SmS, relative intensity of optical bands calc. 77−8603
SmS, semicond., photocond. meas. 78−60164
SmS, semicond. phase, cond. band model, elec. and thermal cond. meas. 77−39854
SmS, semicond. thin film, absorpt. and refl. spectra, fine struct., cond. band extremum 79−69897
SmS, semicond.-metal transition, phase struct. determ. 78−91618
SmS, semicond.-metal transition, cond. band type, deform. pot. determ. 79−69417
SmS, trivalent rare earth substituted, stability of Sm^{2+} 80−65508
SmS type cpd., fd mixing effect on impurity levels, local valence transition 80−24831
SmS type semiconductors, electronic struct., influence of point defects 80−70650
SmS, valence transition, two band model 80−65507
SmS, vol. changes at press. up to 20 kbar 78−71791
SmS:P, neutron irrad., semiconductor-metal transition 80−24975
SmS-based alloy, preparation and properties 78−44034
SmS-CdS system, T-p-X diagram, semicond.-metal transition 79−69421
SmSe, pressure-induced reflectivity changes and semiconductor-metal transition 79−56763
SnAs, Sn_3As_2, and Sn_4As_3, mag. susceptibility components 78−43551
SnI_2 band struct., layer model 80−44501
SnO_2, band struct., tight-binding calc. 80−24796
SnO_2 CVD coating on glass, elec. resist. rel. to cryst. microstruct. 80−84520
SnO_2, CVD semicond. film, surface and bulk cond., process parameters effect 77−1502
SnO_2 coated glass, surface elec. breakdown 80−25303
SnO_2, correl. between simultaneous thermally stimulated cond. and thermlum. transients 79−91073
SnO_2, cryst. growth by chem. transport method 78−3004
SnO_2, doped, appl. as propane gas detector 79−29426
SnO_2 doped films for spectral-selective surfaces, refl. and elec. props. meas. 79−74013
SnO_2 electrodes, dye-modified, erythrosin, attachment, X-ray photoelectron, photocond. investigs. 79−43600
SnO_2 far IR photoconductivity response obs. 77−38000
SnO_2, film, diffusion of impurities *(Japanese)* 79−95218
SnO_2 film, doped, electron effective mass and elec. props., carrier density depend. 77−43750
SnO_2, film, effects of Sb and In additions on struct. and resist. 77−20469
SnO_2 film, growth by DC sputtering from compressed target, cond. and optical props. 77−59690
SnO_2 film, mobility limitation by intercrystalline potential barrier, tunnelling effect 77−66210
SnO_2 film, reactive ion-plasma sputtered, elec. and opt. props. 79−42677
SnO_2 film, reactor irrad. induced changes in elec. props. 77−28267
SnO_2, forbidden energy gap oxide semicond. crystals, review of spectroscopic props. 78−2876
SnO_2 gas sensor, fast-detecting, prep. 80−61497
n-SnO_2, high resist., photoelectronic processes 78−60157
SnO_2, O chemisorption, elec. cond. and EPR meas. correlation 80−84369
SnO_2, optical props., review 77−1673

semiconductor materials continued
SnO_2, rare earth ion doped, luminesc. and charge compensation 78−76532
n-SnO_2, semicond. electrode, electrolum. due to wide injection from electrolytes 77−20926
SnO_2, semiconductor, photoluminescence, depend. on lattice temp. and excitation intensity 80−45137
SnO_2 surface, interactions with O_2, H_2O and H_2, desorpt., ESR and cond. meas 80−10790
SnO_2 thermoelectrical properties, investigation 77−76852
SnO_2 thin films, O_2 vacancy diffusion 80−107467
SnO_2, transparent conductive film, prep. by magnetron sputtering and elec., optical and structural props. *(Japanese)* 79−8247
SnO_2, two-step deposition process using DC sputtering and oxidation, and characterisation 78−95691
SnO_2:As film, prep. and elec. cond. 80−2959
SnO_2:F films, elec. and optical props., solar energy conversion appl. 79−65945
SnO_2:P, CVD growth and etching characts., doping effects 80−107667
SnO_2:Sb, transparent cond. film prep. by thermal decomp. of Sn salt of organic acid *(Japanese)* 77−90269
SnO_2:Sb, transparent cond. films, hydrolysis deposition, elec. and optical props. 79−43144
SnO_2:Sb film, DC sputtered, substrate temp. effect on cond. 77−39971
SnO_2:Sb sprayed film, growth mechanism and cryst. struct. 80−89143
SnO_2:ThO_2, selective detection of CO, hydrophobic and hydrophilic silica effect 79−97372
SnO_2/n-Si solar cells, fabrication and characterisation 79−79393
SnO_2/n^+-pSi heterojunction solar cells, fabrication by paint-on-diffusant method 80−94048
SnO_2/V_2O_5-P_2O_5/Si heterojunction, static optoelectronic characts. 79−87146
SnO_2-based gas sensors, resist. temp. depend. on exposure to CO, H_2, and propane 80−103694
SnO_2-copper phthalocyanine-Ag systems, elec. and electroluminescent behaviour 80−80864
SnO_2-GaSe heterojunction, elec. props. and electrolum. spectra 77−59328
SnO_2-GaSe heterojunction photocell, fine struct. of photo-EMF spectra 80−6967
SnO_2-GaTe(GaSe)(InSe) heterojunctions, photoelec. props. 80−96945
SnO_2-InP heterojunctions, elec. and photovoltaic characts. 80−75628
SnO_2-InSe n-n heterostructures, photoelec. props., 80 to 300K 80−20297
SnO_2-polySi solar cells, fabrication, grain size effects on device parameters 80−94045
SnO_2-$Sb_xS_{1-x}Sn$ structures, photovoltaic effects *(Korean)* 80−44647
SnO_2-Si heterojunctions, elec. and photovoltaic props. 80−26141
SnO_2-Si solar cells, electron-beam-deposited, fabrication, angle-of-incidence effects 79−52931
SnO_2-Si solar cells, electron-beam deposited, struct., photovolt. props. 80−50956
SnO_2-ZnO-Bi_2O_3, ceramic semiconductor, injection currents 79−11141
SnO_x films, passivation effect on Si solar cells 80−61360
SnO_x films reactive DC sputtering prep., phase comp., X-ray diffr. and Mossbauer meas. 79−90914
SnS_2 (2H), band struct. press. depend. 78−43292
SnS_2, band struct., effect of polytypism 78−43293
SnS_2, cryst. growth, photoconductivity 77−85912
SnS_2, crystal growth and optical props. in visible and IR regions 77−52114
SnS_2, octahedrally coordinated, layer cpd., electronic struct. using synchrotron-radiation photoemission spectroscopy 79−74058
SnS_2, optical props., modulation spectroscopy, indirect absorpt. edge 77−52117
SnS_2 polytypes, electronic bandgap meas. 80−34358
SnS_2 press. effects on optical absorpt. edge 77−52119
SnS_2, refl. using Kramers-Kronig anal., optical functions 79−95798
SnS_2, single cryst., far IR reflectivity 79−56774
SnS_2, UV reflectivity meas., band struct., LCAO calcs. 78−72545
Sn_2S_3, mixed valence semicond., long wavelength phonons, full space group theoretical anal. 79−65873
Sn_2S_3 mixed valence semiconductor, far IR refl. spectra 80−108191
$SnS_{2-x}Se_x$, electron mobility elec. resist. and Hall constants 79−28346
$SnS_{2-x}Se_x$, layer cryst., Raman active modes 80−80767
$SnS_{2-x}Se_x$, Raman spectra 79−28763
$SnS_{2-x}Se_x$, solid soln., resistivity, lattice parameter, comp. and temp. depend. 78−91693
$SnS_2(Se_2)$, optical phonon anisotropies and intralayer bonding forces from IR refl. 77−59573
$SnS_2(Se_2)$, optical transitions from d core levels 80−45105
$SnSe_2$, band struct., angle resolved photoelectron spectra meas. 78−72680
$SnSe_2$, layer struct., acoustic phonon dispersion curves, propag. modes 77−51462
$SnSe_2$, mag. susceptibility components 78−43551
$SnSe_2$, optical props., modulation spectroscopy, indirect absorpt. edge 77−52117
$SnSe_2$, press. effects on optical absorpt. edge 77−52119
$SnSe_2$, refl. using Kramers-Kronig anal., optical functions 79−95798
$SnSe_2$, single crystal, reflectivity, XPS, UPS, and band struct. 78−6701
$SnSe_2$ spatial symm. of valence band struct. by angularly resolved XPS 77−69961
$SnSe_2$, thermorefl. spectra 77−90168
$SnSe_2$, UV reflectivity meas. 78−72545
SnTe-In_2Te_3 system, thermoelec. props., phase diagram, transitions 78−43424
SnTe-InTe system, solid soln. films prep. under quasi-equilibrial conditions 79−33931
Sr_2MNbO_6, M=Ti,Zr,Hf, semiconductors, elec. cond. 77−51748
$Sr_2Nb_2O_7$, electronic props. and photoresponses 80−92925
$Sr_3Re_2O_9$, cryst. struct., mag. and semicond. props. 79−10836
$Sr_{1-x}Sm_xS$, electron config. of Sm ions, X-ray L-absorpt. spectroscopy 80−60715
$SrTiO_3$, semicond. anode in aq. electrolyte, electrolum. and electrochem. 80−76080
$SrTiO_3$ surface, photosensitizer for water photoassisted decomp. 80−85202
TaS_2, 1T, anomalous magnetoresist., CDW state 78−72173
$Ta_xTi_{1-x}Se_2$, cryst. struct. and elec. props. 79−47133
$Tb(NO_3)_3$-$Fe(NO_3)_3$-$(NH_4)_2CO_3$-H_2O system, cpd. form., comp. and props. 80−100832
semiconductor materials continued
TcB_2, possibility of semicond. props., rel. to atomic volume 77−69317
Te-$(Bi_xSb_{1-x})_2Te_3$ eutectic, electrophys. props., directed crystn. conditions influence and comp. depend. 80−107827
Te-based eutectics, crystn. rate effect on electrophys. props. mutual solubility effect 80−60774
TeO_2, band struct., tight-binding calc. 80−24796
TeO_2 thin film, Al-TeO_2-Al, field-assisted cond. mechanism 80−11105
Th_3As_4, prep. and semicond. props. 78−23087
Th_3As_4-U_3As_4 solid soln., electronic props. 80−34469
TiO_2 (rutile), (001) and (110) faces, UPS and LEED obs. 80−45206
TiO_2 (rutile), (001) and (110) surfaces, surface and bulk density of states calcs. 80−49858
TiO_2 (rutile) photoanode, corrosion suppression by high-energy redox reactions 78−23163
TiO_2, chemisorption of O_2 and H_2O, electron stimulated desorption, AES and charact. loss spectra 78−22963
n-TiO_2, crystal, in aqueous soln., electrochemistry and electrolum. meas. 78−48665
TiO_2, deform. pot. meas. of direct forbidden transition 79−95806
TiO_2, doping processes, influence on photoelectrochem behaviour 80−79822
TiO_2, elec. cond., temp. depend. resistivity meas. at 77 to 600K, unwsitched samples 80−20262
TiO_2, electrochem. doping 77−76430
TiO_2 electrode, carrier density determ. by optical absorpt. and photoelectrolysis spectra 80−71462
TiO_2 electrode, doping density dependent attachment of rhodamine B 80−54777
n-TiO_2 electrode, flatband pot. determ. from differential stress meas. 80−75638
n-TiO_2 electrode, photo-oxidation of acetate and iodide 80−81331
TiO_2 electrode, sensitised, photoelectrolysis of water in sunlight 78−19143
TiO_2 electrode, silanisation effects on semicond. props. 79−96364
TiO_2 electrode, surface comp. changes during photoelectrolysis, XPS obs. 79−7894
n-TiO_2 electrode in $AlCl_3$-NaCl melt, electrochem. and photoelec. props. 80−81328
TiO_2 electrodes, chemically modified, nature of surface states 80−107905
TiO_2 electrodes, electron transfer from rose bengal, photoelectrochem. meas. 77−66758
TiO_2 electrodes, in aq. electrolytes, surface states, photocurrent obs. 80−49895
TiO_2, electrodes, solar energy conversion, photocatalytic prod. of H_2 77−1932
TiO_2 electrodes in photoelectrochem. cell, photothermal effect 80−7947
TiO_2 film, optical inhomogeneity, rel. to struct. 79−83047
TiO_2 films as solar photocatalysts, preparation 79−74530
TiO_2, fine struct. in intrinsic absorpt. edge 79−42987
TiO_2, indirect forbidden transitions, band struct. enhancement 80−44503
TiO_2, non-stoichiometric rutile, LO phonon-plasmon coupling, IR refl. spectrum 77−32376
n-TiO_2 photoanodes, corrosion suppression mechanism 80−2462
TiO_2, photodesorption of H_2O, pulsed-laser-dynamic-mass-spectrometer study 80−35568
n-TiO_2 photoelectrochemical electrodes, effect of Nb doping on quantum efficiency 80−101121
TiO_2 photoelectrode, stability 77−20422
TiO_2, prereduced surfaces, room temp. activity for oxygen isotopic exchange 79−91998
TiO_2, resolved quadrupolar transition, absorpt. spectra obs., 1.6K 78−27259
TiO_2, rutile, oscills. in elec. resist. induced by solid/gas interactions 79−91068
TiO_2, rutile ceramics, space charge effects 80−24945
TiO_2, semicond. anode in aq. electrolyte, electrolum. and electrochem. 80−76080
TiO_2 sputtered film, photocond. and TSC meas. 80−15560
TiO_2, sputtering defects, associated surface electron states, UPS, XPS and AES obs. 80−60755
TiO_2, stoichiometric single crysts., anisotropy of ion transport 80−2206
n-TiO_2, thermodynamic pot. for anodic dissolution, rel. to photoelectrochem. cell efficiency 78−26948
TiO_2, transition metal doped anodes for water photoelectrolysis, response to visible and UV 79−74531
TiO_2, two photon spectra, quantitative investigation, temp. depend. 80−50373
TiO_2, uniaxial stress depend. of direct-forbidden and indirect-allowed transitions, absorpt. edge obs. 79−42990
TiO_2:Al(Y), polycrystalline photoanode, improved solar efficiency 79−96479
n-TiO_2:Be electrodes, photoassisted oxidation of water 80−30502
TiO_2:Cu, anodic, effect of Cu on optical props., rel. to possible appl. in solar energy conversion 80−16115
TiO_2:H(D)(T), IR spectra, 300, 77 and 8K 78−35175
TiO_2:Nb, rutile, Seebeck effect, 90-300K 78−43427
TiO_2:Nb semicond. electrodes, electroreduction process kinetics, cathodic dark current meas. 80−66807
TiO_2:Nb_2O_5, preparation method, effect on semiconductive props. and sintering temp. 77−16527
TiO_2:S, acceptor properties of S, free electron concentrations 80−34395
TiO_2:S, in O_2+CO_2+SO_2 atmosphere, elec. cond. study 80−39583
TiO_2:Sb(Fe), Mossbauer effect exam. of impurities 78−31140
TiO_2:Si(Fe)(Ni)(Mn)(Cr), anodes, performance in photoelectrolysis of water 79−74407
TiO_2:Zr, electronic conduction, temp. depend. 77−8099
TiO_2-aqueous electrolyte interface, pot. distrib., Mott-Schottky plots 80−11084
n-TiO_2-electrolyte interface, electrolum. obs. 79−47520
n-TiO_2-electrolyte interface, charge-transfer-controlled photocurrent 80−50992
n-TiO_2-electrolyte interface, charge transfer via surface states, water photoelectrolysis anal. 80−75636
n-TiO_2-electrolyte interface impedance, freq. depend., equiv. cct. 80−100516
TiO_2-NH_3 electrolyte interface, photo-assisted electron injection 79−87152
TiO_2-Pd Schottky barrier, work function depend. on adsorbed species 80−54782

semiconductor materials continued
TiO_2-Si solar cell hybrid electrodes for photoelectrochem. H prod. 80−45775
TiO_{2-x}, comparison of photoelec. props. with system $TiO_{2-x}F_x$ 79−28371
TiO_{2-x}, reduced, cond. between elec. props. in equil. at 1100°C and after quenching, defects role *(French)* 80−44582
TiO_{2-x}, slightly reduced semiconducting, channelling expts. with 6 MeV protons, defect structs. 78−2117
Ti_2O_3, electronic structure from single crystal thermoreflectance spectroscopy 79−87420
Ti_2O_3, piezoresistivity and semiconductor-semimetal transition 79−42595
Ti_2O_3, semicond., effect of stress on elec. resist. 78−34832
Ti_3O_5-V; semicond.-metal transition, resist., enthalpy and mag. susceptibility changes obs. 77−62965
Ti_4O_7 and $(Ti_{1-x}V_x)_4O_7$, metal-insulator transitions, EPR, elec. and mag. props. 80−2336
Ti_4O_7, semicond.-semicond. transition, lattice gas model 77−1364
Ti_nO_{2n-1}, cryst. growth and characterisation 78−31311
$TiO_{2-x}F_x$ comparison of photoelec. props. with system TiO_{2-x} 79−28371
$(Ti_2O_3)_{1-x}(V_2O_3)_x$, lattice polarisability, electronic contribs. IR refl. obs. 78−59904
TiP_2, synthesis and characts. 77−85953
TiS_2 (IT), electronic and vibronic struct. 80−44500
TiS_2, band struct., angle-resolved photoemission studies 80−70610
TiS_2, electronic struct. and props., self consistent numerical basis set LCAO calc. 77−89698
TiS_2, evidence for semicond. props., Hall coeff., refl., cond., thermoelec. power 80−20220
TiS_2, growth by chem. vapour transport using press.-temp.-comp. diagram 77−59764
TiS_2, LEED, single-reflection layer scatt. theory 80−49059
TiS_2 layer compound, electronic ground state, band struct. calcs. 77−51651
TiS_2, layer cpd., metal-insulator transitions, energy gap calcs. 79−78009
TiS_2, semicond. charact. under press., in-plane resist. and Hall coeff. meas. 78−23086
TiS_2, semimetallic charact. 77−62926
TiS_2, transport props. under press. 79−95410
$TiSe_2$ layer compound, electronic ground state, band struct. calcs. 77−51651
$TiSe_2$, layer cpd., metal-insulator transitions, energy gap calcs. 79−78009
$TiSe_2$, semimetallic charact. 77−62926
$TiSe_2$, transport props. under press. 79−95410
$TiTe_2$, layer type cpd., reflectivity meas., 6-40 eV 77−55801
$(Ti_{1-x}V_x)_2O_3$, semicond. to semimetal electrical transition, lattice parameter changes 79−60714
TiO_2 electrodes, effect of processing variables on photoelectrochem. props 80−6975
TiO_2 electrodes, room temp. diffusions, capacitance, spectral response and volt-ampere characts. 80−15294
Tl-Sn-Te system equilibria, polythermal and isothermal cross sections obs., ternary cpd. form. 80−104128
Tl_3AsSe_3, refractive index, thermal expansion temp. depend. 80−97223
TlCl, band structure and optical spectra, local field and exchange effects 80−24798
TlCl, ground-state props., Wannier functions, and electronic struct., ab initio self-consistent calc. 80−80178
TlCl, self-consistent electronic struct. and ground state props. 80−15451
TlCl(Br), electron-hole liquid, RPA calcs. 80−6743
$TlCl_xBr_{1-x}$, $TlBr_xI_{1-x}$, polymorphous mixed cryst. layers, opt. props. 78−23490
$TlGaS_2(Se_2)$ film, elec. and photoelec. props. *(Russian)* 78−52109
Tl_2S(Ge), molten, SRO 77−65945
$TlSbS_2$, phase transitions under action of high press., elec. cond. meas. 77−4196
Tl_2Se, diamag., thermal expansion rel. to temp. at cryst.-melt transition 78−34954
Tl_2Se_3, diamag., thermal expansion rel. to temp. at cryst.-melt transition 78−34954
$(Tl_2Se)_{3x}$-$(Sb_2Se_3)_{1-x}$ system, phase diagram 77−16558
Tl_2Te_3, exam. of electrical props., density and viscosity, for solid or liquid states 79−95431
Tl_2Te_3, exam. of electrical props., in solid, liquid state 80−54686
Tl_2Te_3:Ag(Sn), effect of dopant on electrical props., density and viscosity, for solid or liquid states 79−95432
$Tm_{1-x}Eu_xSe$, semicond. with valence instabilities, cryst. chem. considerations 80−100213
Tm_2Se_3, mag. susceptibility meas. 4.2 to 300K cryst. field approx. 77−66246
$TmSe_{1-x}Te_3$, semicond. with valence instabilities, cryst. chem. considerations 80−100213
TmTe, far IR refl. and DC resist., 1-300K, interconfig. fluctuation effects 78−35136
UO_2, electronic contribution to thermodynamics, sp. ht. 79−7699
$V_{1-x}Cr_xO_2$, VPE, and elec. and optical characterisation 78−3053
$V_{1-x}Fe_xO_{2-x}F_x$, $0<x<0.20$, magnetic susceptibility and electron cond. *(German)* 80−39754
$V_{1-x}Ga_xO_2$, M1→T phase transition, X-ray and mag. meas. 77−11692
$V_{0.96}M_{0.05}O$, (M=Ni, Co, Mn), solid solutions, exam. of thermal conductivity 78−79827
VO_2, cylindrical specimen, thermal switching 80−44679
VO_2, elec. cond. and dielec. props. 79−11379
VO_2 film, negative resist. region, applic. as oscillator element and transducer *(Russian)* 77−85359
VO_2, film, optical consts. and electrical props. near phase transition *(Russian)* 77−59631
VO_2 film, optical props. meas. near semicond.-metal transition 77−1742
VO_2, film, semiconductor-metal phase transition, fast laser kinetic studies 79−69419
VO_2 film, sensitivity to heat perturbation and current noise, effect of temp. 77−66215
VO_2 films, elec. cond. near metal-semicond. phase transition 77−1503
VO_2 metal-insulator transition, technical appls. possibilities *(German)* 79−99587
VO_2, metal-insulator transition and electronic struct., ion bombard. effects 80−92948
VO_2 needles, switching, voltage oscills. 79−15199
VO_2, nonstoichiometry influence on electron struct. and metal-insulator phase transition 80−44507

semiconductor materials continued
VO_2, semicond. phase, optical spectrum, CNDO CI calc. 78−27258
VO_2, semicond.-metal phase transition, fast laser excitation, kinetics obs. 79−47018
VO_2 single cryst., noise in presence of current filament 80−92952
VO_2 single cryst., switching, visual obs. of metallic and semicond. domains 78−52041
VO_2 single cryst. film, ion-irrad., 'splitting' of semicond.-metal transition 80−11053
VO_2 single crystal, elec. switching 80−92946
VO_2, single crystal, fluctuations of current and switching time 79−38137
VO_2 single crystal, positron annihilation, metal-insulator transition obs. 77−85830
VO_2, single crystal and polycrystalline, synthesis and resist. near metal-semicond. phase-transition 80−44680
VO_2, switching effect, temp. depend. 80−20259
VO_2, V_2O_3 and V_3O_5, film prep. under equil. conditions, struct. and elec. props. 80−108352
VO_2, VPE, and elec. and optical characterisation 78−3053
VO_2, X-ray determ. of lattice constants and thermal expansion coeffs. near transition temp. 79−86747
VO_2:Al(W), thin layer prep. by reactive DC sputtering doping effectiveness *(German)* 78−6847
VO_2:Ga, Mo, conductivity transitions 78−76121
VO_2:M^{3+}, M=Al,Ga,Fe, anisotropy of thermoelec. power, hole conductivity 77−11946
$VO_{(2n-1)/n}$, metal-semicond. transition temps. 80−59876
VO_x, mag. susceptibility temp. depend. 79−47229
V_2O_5 crystal, photoinduced threshold switching in VO_2 channel 80−29450
V_2O_5 single crystals, contact-limited conduction 79−95493
V_2O_5, switching mech. 78−60175
V_2O_5, thermoelec. props., 500-1500K 80−29423
V_2O_5:Na(Li), pure and doped, elec. cond. and thermoelec. power meas. 80−10987
V_2O_5-BaO-K_2O-ZnO glasses, elect. props. and struct. 80−15547
V_2O_5-Si, sandwich system, photocond. in range 380-1000 nm 77−32034
V_2O_5-water, EPR of VO_{aq}^{2+} formed by solar light photoreduction, electrolysis appl. 78−11540
V_3O_5, electrical, thermodynamic and mag. props. at metal-semicond. transition, homogeneity range 77−4413
V_3O_5, Mo,Ti, and Ga doping effects on conductivity transition 77−11971
V_3O_5, resistivity switching due to phase transition, 154°C 79−19642
V_3O_5, steady-state elec. switching characts., simple thermistor model 77−8159
V_3O_7, ESR spectra of V^{4+} ions 77−28437
V_6O_{13}, semicond., IR vibration spectra 80−88997
V_nO_{2n-1}, cryst. growth and characterisation 78−31311
V_xO_y film, prep. by thermal decomp. of vanadium naphthenate, and elec. props. *(Japanese)* 78−88425
$V_xTi_{1-x}Se_2$, cryst. struct. and elec. props. 79−47133
WO_3 anode, props. and appl. to photoelectrolysis of water 77−66757
WO_3 electrodes, electrochem. and photoelectrochem. behaviour 78−26949
WO_3 layers, semiconductor electrodes, electrochromism and photoelectrochemistry 80−35544
WO_3, semicond. anode in aq. electrolyte, electrolum. and electrochem. 80−76080
WO_3 semiconducting electrode, influence of surface states, impedance meas. *(French)* 77−1468
WS_2 films, exciton peaks in absorpt. spectra, press. and temp. depend. 79−51496
WSe_2 (2H), elec. cond. press. depend. 78−43394
WSe_2, chem. vapour transport growth, microstruct. develop. 80−103278
WSe_2 d-band semicond., photoelectrochem. props., electrochem. solar cell appl. 79−66411
WSe_2, elec. cond. and Hall coefficient temp. depend. 77−28180
WSe_2, Raman spectrum, long wavelength optical phonons 77−40218
WSe_2, single cryst. growth by sublimation method 78−11091
Y oxides, perovskite-like, synthesis, struct., elec. props. 80−65554
Y-H film, temp., thickness and comp. depend. of elec. resist. 79−78221
YIG, magnetoresistance of bulk and epitaxial films 78−91706
δ-Y_2S_3:Nd^{3+}, spectroscopic props. from absorpt., photoluminesc. and excitation spectra 80−34968
Y_3Se_4 powder, prep. and optical props. 77−28771
$Y_2(V_{4/3}W_{2/3})O_7$ pyrochlore, synthesis and elec. props. 80−29914
YbS_x, thermo-EMF, elec. and thermal cond., 300 to 1000K, comp. depend. 79−38111
$Yb_{1-x}Sm_xS$, electron config. of Sm ions, X-ray L-absorpt. spectroscopy 80−60715
Yb_2Te_3, films, prep., elec. props. 78−43494
Zn silicates:Mn, sintered, photocond. *(German)* 79−51627
Zn-Ga-P-S quaternary system, p-type conductive alloys 78−39105
$ZnAs_2$, homogeneity region and electrophys. props. 80−60833
$ZnAs_2$, λ-modulated photoemission spectra 79−87565
$ZnAs_2$ Schottky diodes, elec. and photoelec. props., excitons 80−65653
$ZnAs_2$, single crystals, growth from vapour phase 78−88416
Zn_3As_2, optical band-gap, absorption meas. 80−25372
Zn_3As_2, p-type semiconductor, absorption edge spectra, energy gap 79−56793
Zn_3As_2, solubility in Bi, LPE on $(Cd_xZn_{1-x})_3As_2$ 78−35324
Zn_3As_2:Cu(Te), single crysts., gas phase growth, elec. props. 79−15598
Zn_3As_2-ZnSe(ZnTe) solid solutions, single cryst., phase equilib. and props. 80−16283
p-$Zn_{0.1}Cd_{0.9}Sb$, thermoelec. anisotropic semicond., carrier kinetics at low temps. 80−92893
$Zn_{0.1}Cd_{0.9}Sb$, thermoelectrically isotropic semicond., carrier kinetics in intrinsic cond. range 80−92894
ZnF_2:Mn, thin films, electroluminescence, brightness voltage characts. hysteresis 80−20709
$Zn_{1-x}Mg_xTe$ alloys, high purity, metallurgical and analytical methods of prep. 80−40247
$Zn_{1-x}Mg_xTe$ alloys, luminesc. and elec. props. 80−2813
$Zn(Mo_2Re_2)S_8$, synthesis and electrical props. of mixed tetrahedral cluster phases 80−2971
ZnO-SnO_2-M_xO_y, M_xO_y=glass-forming additive, I-V characts., heat treatment effects 77−43595
ZnP_2, α-β heterojunction, I-V characts. and photoresponse 78−64105
ZnP_2, birefringence and optical activity, dispersion 78−2821
ZnP_2, Brillouin scattering and optical props. meas. 80−76041

semiconductor materials continued
ZnP_2, cathodoluminesc. 4.2 to 200K 79−52028
α-ZnP_2, doped, single crystal, electrical properties 80−92892
ZnP_2, large tetragonal single cryst. growth from vap. 77−69976
ZnP_2, light polarisation, self-induced optical rotation 79−19860
ZnP_2, monoclinic, cathodoluminesc. spectra exam. 79−15534
ZnP_2, pure and doped, carrier mobility and conc., donor and acceptor energy levels, 190 to 380K 78−84217
ZnP_2, reson. interaction of vibr. states, polarised Raman spectra meas. 77−15521
α-ZnP_2, resonant Brillouin scatt. near indirect band gap 80−93350
ZnP_2, rotation of plane of polarisation of light 79−15432
ZnP_2 Schottky diodes, elec. and photoelec. props., excitons 80−65653
ZnP_2, second-order vibr. spectra and dispersion of phonon branches 80−25376
ZnP_2, sublimation 80−34181
ZnP_2 tetragonal crystals, polarisation study of photocond. 80−96942
ZnP_2 tetragonal crysts., light scatt. by optic phonons 80−55116
ZnP_2, trapping levels, TSC and thermolum. meas. 79−15115
ZnP_2:As, local vibrs. of impurity ions, Raman study 80−29745
ZnP_2:In(Ga)(Ge)(S)(Se), doped and undoped, optical absorpt. spectra in range 0.5 to 2.2 eV 80−66250
p-ZnP_2:S(Se)(Te), photocond., carrier generation and recomb. at high excitation levels *(Russian)* 78−64059
Zn_3P_2, absorption edge meas. 78−80380
Zn_3P_2 bulk and thin film, UV reflectivity spectra, photovoltaic effects, optical consts. 80−25472
Zn_3P_2, characteristics for photovoltaic appl. 79−7839
Zn_3P_2, direct and indirect optical transitions, metal-Zn_3P_2 contact photovoltage response 80−25402
Zn_3P_2, elec. cond., Hall effect, P interstitial effects 80−84465
Zn_3P_2, photocond. and Dember effect meas., 0.5 to 1.2 μm, possible detector appl. 78−91721
Zn_3P_2, photoluminesc. spectra 79−87502
Zn_3P_2 photovoltaic material and Schottky diode characteristics 78−64066
Zn_3P_2, single crystal, growth, electronic and device props. 80−25551
Zn_3P_2, stoichiometry deviation from phase diagram 80−35164
p-Zn_3P_2, temp. dependence of resistivity and Hall constant 77−35937
Zn_3P_2 thin polycrystalline films for solar photovoltaic cells 80−97797
Zn_3P_2, Zn_3As_2, sp. ht., thermodyn. props. 78−22863
Zn_3P_2-metal contacts, photoelectric props. 80−92930
ZnSb, band struct. calc. 78−39015
ZnSb, epitaxial films, growing conditions effect on elec. cond., thermo-EMF 80−39687
ZnSb, orientated crystn. conditions during reaction diffusion *(Russian)* 80−70558
ZnSb, thermodynamic props. 79−77767
ZnSb, thermoelec. anisotropic semicond., carrier kinetics at low temps. 80−92893
Zn_3X_2, X=P,As,Sb, phys. props. 78−26527
ZrC-C composite system, negative magnetoresist. 80−60008
ZrO_2-CeO_2, semiconducting ceramics, electronic conductivity and oxido-reduction *(French)* 78−26919
ZrS_2, intercalation-induced shift of absorpt. edge 79−82999
ZrS_2 layer compound, electronic ground state, band struct. calcs. 77−51651
ZrS_3, excitonic transition, reson. Raman spectra, Franck-Condon factors 80−97252
ZrS_3, one-dimensional semicond., Raman spectra 79−87447
ZrS_3, photolum. from excitons 80−66274
ZrS_3, quasi one-dimens. semicond., elec. transport props. 80−107790
$ZrSe_2$, layer type cpd., reflectivity meas., 6-40 eV 77−55801
$ZrSe_2$, photo-intercalation: possible application in solar energy devices 80−108803
$ZrSe_3$, electronic props, variation with struct. 79−42438

semiconductor-metal boundaries
see also Schottky-barrier diodes
absorption coefficient of semicond. detem., photo-EMF meas. 79−11224
amorphous semiconductors, barrier controlled charge carrier transport in structures *(German)* 79−47162
atomic mixing and preferential sputtering effect on depth profiles and interfaces 79−78806
Auger depth profiling 79−78177
barrier height and theoretical considerations, book contrib. 79−1621
barrier height rel. to metal at. number 77−12902
barrier heights, chemical trends 78−84293
barrier heights, photoelectric meas., correction diagram 79−33343
book 78−52090
bulk states in semiconductors and insulators in contact with metals, charging 80−54781
capacitance, temp.-depend., by space-charge methods 78−91758
chalcogenide glass-metal light sensitive systems with barrier layer, new photographic materials 77−75635
compound formation in metal-semicond. interactions 79−28217
compound semiconductor interfaces, conf., Los Angeles, USA (Jan. 1978) 78−91756
compound semiconductor-metal reactions, book contrib. 79−1622
conference, on cpd. semicond. interfaces, Princeton, USA., (Feb, 1977) 77−85300
contact, frequency relationships of photocurrent and photo-EMF *(Russian)* 80−107908
contact barrier inhomogeneities, characterisation by scanned internal photoemission 80−49915
contact investigation by photoelectron spectroscopy 80−100517
contact junction formation by ion evaporation 77−90285
contact resistance, method for analysing influence of extrinsic parameters 80−25007
contact resistance and bulk resist. of semicond. samples, pulse method 78−52083
contact resistance and resistivity meas. 80−105672
contacts, theory and appl. 78−2566
convergent beam electron microscopy obs. 80−108689
degenerate semiconductor-metal Schottky barriers, low temp. capacitance 80−60075
depletion depth, acoustic determ. 79−99621
deposition and post-deposition treatment effects on electrical props. 77−89853
diamond Schottky barrier, electronic struct., pseudopot. calc. 78−95364

semiconductor-metal boundaries continued
diamond Schottky barrier, electronic struct., pseudopotential method, jellium model 79−38162
diamond-Ag, photocond. and internal photoemission meas. 79−69546
differential photovoltage spectrum at Schottky barrier, wavelength modulation method *(Korean)* 79−11220
diffusion barrier formation, Au film, using laser annealing 80−80373
disordered interface, supercond. transition temp. enhancement by bipolaron interface centres 80−84528
doping inhomogeneity, meas. by low field electrorefl., in Schottky-barrier config. 77−11584
double injection structure, V-I characteristics and contact effects *(Russian)* 80−49911
dynamic cathode contacts., pinned cathode and cond. current density calc. 77−20427
electrical characteristics, interfacial reaction effects, book contrib. 79−1623
electron bombarded, energy dissipation 78−87732
electron microscopic observations of metal-semicond. contacts, new phases struct. 78−34899
electron-hole liq. near semiconductor-metal interface, binding energy 78−30985
electronic cond., temp. depend. review 80−59975
electronic structure, self-consistent pseudopot. method 77−20428
film-covered electrodes, electron transfer reactions, mechanisms, theory 78−20023
film-covered metal electrodes, electron transfer reactions 78−20024
flat band potential from Mott-Schottky plot 78−34896
III-V oxide interface state and Schottky barrier form., unified mechanism 80−44724
III-V semiconds., ohmic contacts *(Japanese)* 78−47869
III-V semiconductor, $(SN)_x$ and HgSe as contact materials, compared with Au 77−85312
III-V semiconductor Schottky barrier formation, Fermi-level pinning, defect mech. 78−95358
III-V semiconductor-metal surface barrier structures, chem. precipitation and props. *(Russian)* 78−84298
inhomogeneous slab with disc electrode, spreading resistance treated as mixed boundary value problem 79−87154
p-InSb-Au, surface barrier, structure, photosensitivity spectrum 79−51674
interface electronic struct., book contrib. 79−42619
interface electronic struct. 78−72261
interfacial film effects on elec. characts. of metal-semiconductor contact 80−96969
interfacial reaction, AES study *(Japanese)* 80−96701
interfacial reaction, dynamical obs. at room temp. using AES 80−10798
intrinsic surface states and Fermi-level pinning 78−95319
junction layer charge migration with localised state participation *(Russian)* 80−49913
junction photoelec. phenomena, effect of dielectric gap and surface states *(Russian)* 78−84299
Kane semiconductors, parametric excitation of surface waves 79−38014
layer semiconductor system, theory of Hall effect 79−69589
lead phthalocyanine:O_2(I), Schottky barrier effect on AC current response 80−75623
LEDs using II-VI semiconductor with wide energy gap materials *(Polish)* 79−91501
light sensitive systems for holographic gratings, characts. 78−13810
liquid metal-semiconductor structure electrocapillarity effects 79−73588
localised electronic states at interfaces 77−32081
luminescence due to photoinduced injection 78−10939
magnetoplasma polaritons at the interface 79−38163
mechanical metal-semiconductor contacts, I-V characts., press. effects 78−2564
metal silicide formation, induced by scanning CW laser, reaction rates, analytical model 80−66334
metal-amorphous Si barrier, electronic props. 80−11089
metal-diamond interface, Schottky barrier theory, ionicity depend. 78−52086
metal-InP contacts, intermediate adsorbed layer effect on electronic props. 80−39674
metal-InP contacts, metal beam epitaxy, struct. and elec. props. of films on ion bombarded InP 79−28922
minority carrier injection through injecting contact in strong elec. field 77−55609
molecular crystal-metal interface, exciton decay, random-walk model 78−10356
ohmic contact in two-carrier regime, avalanche injection model 77−55607
ohmic contact on n-type semiconductor with shallow n^+-surface layer 79−38164
ohmic contact props., factors affecting contact resistance of semiconductors, theoretical model 80−60076
ohmic contacts to semicond. based on graded amorphous-cryst. junction, model 77−76923
organic semiconductor Schottky barriers, capacitance meas. 79−82659
photochemical transformations rate rel. to light-stimulated diffusion coeff. 77−76626
photoelectron emission from metal into semiconductor 80−6984
photoelectron injection, quantum mech. transmission and optical phonon scatt. 80−84511
photoelectron injection, theory and expt. 77−85314
phthalocyanine-metal interfaces, surface photovoltage 80−20308
planar devices, contact resistance derivation 78−60205
polariton propagation between semiconductor-metallic screen interface *(Spanish)* 80−84510
poly-2-chloro-p-xylylene, photoinjection of holes from metal electrodes, barrier height 78−76145
polyacetylene-Au, ohmic contact *(Japanese)* 80−96888
preparation under UHV conditions 78−72733
quasi-monopolar semiconductors, I/V characts., effect of weak diffusion with metal contacts 80−70824
rectifier, theory, technology and appl. 78−52089
rectifying barrier formation with metal-semiconductor junction *(Russian)* 78−84296
rectifying contact, method for determ. of pot. barrier height 77−1486
residual conductivity, cathode quenching 79−7902
Schottky, barrier height modification by interfacial oxides 79−47163
Schottky, non-degenerate diode, current-voltage characts., analytical approx. 79−95494

semiconductor-metal boundaries continued
Schottky barrier, Au with III-V and II-VI semiconds., barrier height 77−20430
Schottky barrier, charge carrier conc. determ. from low-field electrorefl. spectra 77−85320
Schottky barrier, chemical reaction and charge redistrib. 78−95365
Schottky barrier, electronic struct. calcs. 79−1613
Schottky barrier, forward-biased, 1/f noise 79−82666
Schottky barrier, theory and complex band struct. 79−15220
Schottky barrier, tunnel effect theory, random field contrib. 77−43727
Schottky barrier form., chem. mechanisms 80−49869
Schottky barrier form., transition with chemical reactivity 78−30986
Schottky barrier formation, chemical effects 78−91753
Schottky barrier formation, microscopic model 78−52087
Schottky barrier height approaching semicond. band gap, minority carrier injection effect 77−20434
Schottky barrier height variation techniques 80−20284
Schottky barrier heights, semi-empirical tight-binding calc. 79−28408
Schottky barrier heights for low ionicity semiconds. 79−42640
Schottky barrier interfaces in pairing model, covalent-ionic trend 78−95367
Schottky barrier junction, characterisation and appl. 80−92971
Schottky barrier junction, fabrication aspects 80−88632
Schottky barrier ohmic contacts, recomb. beneath, and adjacent oxide covered regions 79−47164
Schottky barrier structure, characterisation by electron beam induced current, charge collection process 79−17580
Schottky barrier theory at jellium-semicond. interface, role of ionicity, pseudopot. method 77−47888
Schottky barriers, Bardeen and Schottky limits of interface index 80−49868
Schottky barriers, chemical trends 78−95363
Schottky barriers, photocurrent, recomb. losses *(Russian)* 80−2470
Schottky barriers, resonant tunnelling through traps, theory 78−10553
Schottky barriers, T_0 anomaly, comparison of Levine and Bardeen models 77−39938
Schottky barriers at metal-covalent semiconductor interfaces, independence of work functions *(Japanese)* 77−69417
Schottky contacts, submicron, high-field pulsed electroplating technique 80−49899
Schottky diode, thermionic emission-diffusion theory validity, thermodynamic conditions 77−12003
Schottky diodes with high series resitance, modified forward I-V plot 79−95491
Schottky layers, homogeneous avalanche breakdown instability mechanism, microplasma form. 78−72262
Schottky mesa diode, axial pressure effects on surface-state density redistrib. *(Russian)* 77−89847
Schottky model, ionised mixture effects, I-V characts. *(Russian)* 77−24622
Schottky-barrier diode wavelength-modulated photoresponse spectra *(Russian)* 78−84300
Schottky-barrier diodes, resonant tunnelling spectroscopy, deep centre detection 80−96968
Schottky-barrier formation, electronic structure of semiconductor surfaces 79−95466
Schottky-barrier metal-semiconductor junction carrier migration and equivalent cct. analysis *(Russian)* 78−84294
Schottky-barrier structs., surface barrier current instability, uniaxial crystal compression 80−20310
semiconductor, spin injection, carrier polarisation, luminesc. polarisation 77−15957
n^+-Si-Al ohmic contacts, metallisation structs. for very shallow n^+/p junctions 80−60084
silicide fabrication, surface resist. meas. for control 77−89854
silicide formation in thin layers of W or Mb *(German)* 80−7859
silicide Schottky barriers, elemental description 80−60085
SIMS characterisation *(French)* 80−50904
single injection diodes, 1/f noise 78−60204
solar cells, collection vel. of excess minority carriers 77−15954
solid surface, theory, book 80−36787
space charge effects of semicond. coatings on metal substrate, on triboelec. charge exchange 80−54763
substrate surface damage induced by RF-diode sputtering 77−90274
superconductivity at disordered interface 80−20347
surface barrier structures, two-photon photoelec. effect 80−88594
surface barrier volume wave transducer 80−33403
surface channel, quasitwo dimens. excitons and plasmons at different carrier conc. 78−60063
surface doping effect, neutralisation by SiO layer *(Russian)* 77−47896
surface exciton modes for plane and spherical interfaces 78−64113
surface states in (111) covalent faces, effect of alkali adsorbates 79−42601
surface-barrier photodetectors, GaP and GaAs with Au film deposition 77−77423
thermoelectric heterophase material with artificial anisotropy of thermo EMF 77−89781
thermoelement with deliberately induced anisotropy, optimisation of figure of merit 79−95433
transparency of metal films on semicond. substrates 77−16411
tunnelling spectroscopy, review *(German)* 78−91776
variable-gap metal-semiconductor structure, differential optospectrometric effect 77−62994
variable-gap surface barrier structures, photoelec. effect 79−7903
variable-gap surface-barrier structs., photoelec. effect, theoretical anal. 80−15564
volume and contact parameter determ. from V-I characteristic *(Russian)* 80−49912
Ag-In-Ge alloyed contacts to GaAs 79−78174
Ag-InP contact in InP Gunn device, relationship between microwave efficiency and metallurgical state of cathode contact 80−6981
Ag-InP interface, AgP_2 formation during sintering 80−65309
Ag-Si interfaces, solar cell contacts 80−92973
Ag−(100)InP, metal-semicond.cathode contact, metallurgical, physical, chemical processes 80−107911
Al contact of p-type Si surface-barrier diode, ageing 77−32077
Al/III-V interfaces, photoemission 80−25526
Al/tetracene/nesatron cell, electroabsorption and electrorefl., interfacial elec. fields 79−65548
Al-amorphous Ge-nSi, photoelectric props. 80−70822

semiconductor-metal boundaries continued
Al-chalcogenide glass thin layer struct., EMF in elec. field *(Russian)* 77−39936
Al-Ge (100) interfaces, MBE prep. and geometrical struct., total refl. X-ray diffr. study 80−49531
Al-InP Schottky barrier, increase 80−15603
Al-n-n^+-GaAs, deep centre reson. charging, photocapacitance meas. on Schottky barrier 78−26908
Al-Si, ion plated contacts *(Rumanian)* 78−88029
Al-Si contacts, effect of vacuum ambience 77−43718
Al-Si contacts, electromigration and diffusion of Cu in Al film 79−77820
Al-Ta-poly-Si interdiffusion, Ta barrier effect, Auger anal. 78−71888
Al-$TiSi_2$-n-Si struct., elec. props., charge transfer mechanism across $TiSi_2$-Si interface *(Russian)* 80−34515
(Al+Si)-Si thin films, struct. transitions and phase comp. 80−49537
$Al_xGa_{1-x}As$-Au, Auger depth profiling 77−89657
$Al_xGa_{1-x}Sb$ solid soln., electrochem. deposition of Ni and Pd 80−93505
$Al_xGa_{1-x}Sb$-Pd contacts, struct., preparation elec. props. 80−65684
$Al_xGa_{1-x}Sb$-Pd contacts, band gap depend. of barrier height 80−65685
As-Te-Si-Ge amorphous chalcogenide semiconductor, thin film interface, elec. charact. *(Korean)* 80−97014
As_2S_3, glassy, interface with metal, photoelec. props. 79−73589
As_2S_3-Ag, light sensitivity for high exposure densities *(Russian)* 79−6212
As_2S_3-Ag, resistance meas. during form., supersensitivity *(Russian)* 77−80839
As_2S_3-Ag interface, photodissolution kinetics of Ag in amorphous films 77−15955
As_2S_3-Ag photosensitive film systems, hologram recording 78−1194
As_2S_3-Ag system, photosensitivity depend. on As_2S_3 thickness *(Russian)* 80−54784
As_2S_3-Ag system, photosensitivity depend. on metallic layer thickness *(Russian)* 80−54785
As_2Se_3-Ag photosensitive semiconductor-metal systems, effect of AsS_3 barrier layer *(Russian)* 80−62777
As_2Se_3-Au sandwich cell, origin of dark currents 77−76920
a-As_2Se_3-metal system, time-resolved dark injection 79−91139
Au contact films, dissociation of GaAs and $Ga_{0.7}Al_{0.3}As$ during alloying 79−79357
Au films on Si substrate, solid-solid reactions 78−95369
Au/GaSb (110) interface, heat-treated, struct. and chem. state, angle-resolved XPS 80−97400
Au/Si interface, X-irradiated, dose profiles 79−24388
Au/ZnSe:Mn/n-GaAs low threshold thin film DC electrolum. cell, pulse-excited characts. 80−76081
Au-Al/GaAs interfaces, atomic interdiffusion, soft XPS studies 80−65302
Au-As_2Se_3 contact, model of charge injection 78−68088
Au-CdS junction diodes, chemically etched CdS cryst. surfaces effect on barrier layer 80−44722
Au-$Ga_{1-x}Al_xAs$ Schottky diodes, band struct. from I-V, C-V meas. 80−96989
Au-$Ga_{1-x}Al_xSb$ Schottky barriers, barrier height 80−96986
Au-GaAs, photosensitivity losses, field and spectral depend. 80−2452
Au-GaAs Schottky barrier solar cells, effect of interfacial oxide layer on cell characts. 80−61365
Au-GaS, Schottky-barrier electroreflectance spectra under uniaxial stress 79−56767
Au-Ge thin film couples, activation energy for interdiffusion, accelerated ageing studies 79−82671
Au-InS Schottky-barrier diode, tunnelling current due to thermionic-field emission 79−33340
Au-n-$Al_xGa_{1-x}As$-n-GaAS Schottky barrier solar cells, prep. and props. 80−26140
Au-n-$Ga_{1-x}Al_xAs$-n-GaP narrow-band variable-gap surface-barrier photoedetector 80−96944
Au-n-Si-p-Si structure with wavelength depend. photocurrent sign, photodetector 79−12849
Au-semiconductor system, room temp. interfacial reaction, AES obs. 78−18913
Au-Si, spatial origin of electrons in internal photoemission struct. *(French)* 78−91770
Au-Si interface, critical Au-film thickness obs. for room temp. interfacial reaction 80−75390
Au-Si interface, electron energy loss and AES meas. 80−89096
Au-Si interface, valence band and core levels, Si diffusion, alloy form., photoelectron spectra obs. 80−45205
Au-Si internal photoemission struct., spatial distrib. of excited electrons *(French)* 78−23166
Au-Si Schottky barrier solar cell interface props. and stability 79−61984
Au-Si Schottky contact elec. props. rel. to AES 77−85322
Au-Si system, transition layer struct. form. and heat treatment influence, amorphisation obs. 80−54529
Au-Si thin film double layer, silicide form., electron diffr. study 80−80005
Au-W-GaAs Schottky barrier, elec. and chem. props., AES 80−96973
AuGe/n-GaAs, SIMS study Au behaviour during annealing 78−75947
CdF_2-Au, capacitance and photocurrent, barrier height 77−85321
CdF_2-Au Schottky barrier diodes, degradation 79−23969
$CdGa_2S_4$ double surface-barrier diodes, current-voltage characts. 80−92972
$Cd_{0.96}Ga_2Te_{4.1}$ film-metal sandwich, switching effect 77−43753
$Cd_{0.175}Hg_{0.825}Te$-Au(In) contacts, photo-effect in the 77-300K range, barrier height estimation 80−107850
p-$Cd_xHg_{1-x}Te$-metal contact, negative resist. effects, impact ionisation 77−4440
$Cd_xHg_{1-x}Te$-metal contact, transport mechanism, thermionic and field emission processes 77−20425
$Cd_xHg_{1-x}Te$-metal contacts, schematic energy band diag., transport props. 77−47897
$CdIn_2S_4$-Au surface-barrier diodes, mech. of current flow 78−56228
CdS, Au deposition, Schottky diodes and MIS devices, surface treatment effects, SEM obs. 80−54794
CdS, deep level electron trap characts. 79−78036
CdS, electron traps, admittance spectra on hetero- and Schottky junctions 79−56159
CdS Schottky barrier diode with evaporated Au-Ti blocking contact, rectification props. 77−85319
CdS-Al, ohmic contact stability improved by annealing 78−6443
CdS-Al(Au) interfaces, bonding and interdiffusion, XPS obs. 80−80000

semiconductor-metal boundaries continued
CdS-Au, Schottky junction, surface defects, photovoltaic, piezoelectric and V-I characteristics *(French)* 80−49898
CdS-Au contacts, electronic states, vacuum UV photoelectron spectra 80−70827
CdS-Au Schottky diode, elec. props. under stress 79−15222
CdS-Au structure, work function of {0001} faces of CdS, contact pot. difference meas. 78−23164
CdS-metal interface, chemical reactions and local charge redistrib. 79−19661
CdS-Pb(Ag)(Pd), electrolytic deposition of metal films 77−77425
CdS(Se)-Al function formation, coupled interface plasmons, low energy electron energy loss spectra 77−24621
CdSe-Au contacts, electronic states, vacuum UV photoelectron spectra 80−70827
CdSe-metal interface, chemical reactions and local charge redistrib. 79−19661
CdSe-Mo, Schottky barrier, characts. study 79−51673
$CdSnAs_2$-Au(Al), surface barrier junction, elec. props., temp. depend. 80−65686
p-CdTe, barrier heights of metals on etched surface 80−80378
p-CdTe ohmic contact with Pd and Pt, I-V characts., temp. depend. of cond., activation energy 78−39211
p-CdTe, surface barrier struct., internal photoelec. emission 77−15958
CdTe-Ag diode, Schottky type, elec. and photoelec. props. 77−43719
CdTe-Au contacts, electronic states, vacuum UV photoelectron spectra 80−70827
CdTe-Au Schottky barriers, quantum photoelectric yield, theoretical anal. 77−39939
CdTe-Au(Al) Schottky barriers, defect effects 79−60921
CdTe-Au(In) contacts, photo-effect in the 77-300K range, barrier height estimation 80−107850
CdTe-metal, diode contact, elec. characts., generation-recombination space charge region *(Russian)* 78−39214
CdTe-metal contact, surface barrier exam. 78−64111
Co-Si interface, glassy layer, ellipsometric charact. 80−103589
Cr-GaAs, metal-nn^+ Schottky diode, I-V characts., inverse branch, effect of dislocation defects *(Russian)* 79−15217
Cr-GaAs, Schottky-barrier diode, surface electron states 79−73578
Cr-Si, cleaved junction, interface states, capacitance meas. 79−91118
Cr-Si, ion implanted, inert-gas-bubble form., TEM and Rutherford back-scatt. anal. 79−90682
Cr-Si, metal-nn^+ Schottky diode, I-V characts., inverse branch, effect of dislocation defects *(Russian)* 79−15217
Cr-Si interfaces, metallurgical and electrical props. 80−60081
Cr-Si(GaAs) Schottky barriers, interfacial structural defects effect on avalanche breakdown 79−42644
Cu-CdS, Schottky barrier, Cu diffusion and photovolt. mechanism 80−6980
Cu-CdS, Schottky barrier, reverse differential capacitance, diffusion of Cu, solar cell appl. *(French)* 80−15424
Cu-CuGaSe Schottky barriers, electrical and photovoltaic props. 80−92940
Cu-n-Si diodes, fabrication by electroless deposition method, characts. 80−100520
CuCl-Ag system, photosensitivity spectrum in region of CuCl exciton absorpt. *(Russian)* 79−78707
Cu_2O solar cell, low barrier heights, Auger spectra obs. 79−15224
$Cu_{2-x}S$/CdS heterostructures, heat treated, capacitance voltage meas. anal. 80−20292
EuS-metal contact, electrical switching exam. 78−68085
EuS-W emitter junction, energy loss of field emitted electrons 77−81201
EuS-W interface, electron spin polarisation in field emission 78−35265
Ga-As-Au, alloying behaviour at substrate-film interface, electron microscopy 79−60652
$Ga_{1-x}AlAs$ (110) oxide-free Schottky barriers, surface comp. and characts., AES obs. 79−82661
$Ga_{1-x}Al_xAs$, intervalley energy gaps, temp. junction, exptl. determ. using metal-semicond. contacts 80−80179
$Ga_{1-x}Al_xAs$ Schottky barrier, oxide free, surface composition and fabrication 78−68084
n-$Ga_{1-x}Al_xAs$-Au, Schottky barrier height as function of AlAs content 79−65535
$Ga_{1-x}Al_xAs$-Au variable-gap surface-barrier struct., photoelec. effect 80−39634
GaAs (001)-Ag contact, surface stoichiometry and struct., and electronic surface states 78−95361
GaAs (110), chemisorption of Al, electronic struct., tight binding calc. 80−49842
GaAs (110), chemisorption site geometry and interface electronic struct. of Al and Ga, photoelectron spectra 80−49843
GaAs (110), with Al or Ga overlayers, interfacial electron states, UPS and LEED obs. 80−80377
GaAs (110)-Al interface, XPS study of interface interaction, Al proximity effects and replacement reaction 79−100019
GaAs (110)-Al(Ga) interface, interface states, photoemission study 78−95359
GaAs (110)-Al(Ga)(In), Schottky barrier form., defect mechanism 80−49902
GaAs (110)-Au Schottky barriers on ordered and disordered GaAs surfaces, props. 78−95360
GaAs, alloyed contacts using Au-Ge-Ni metallisation scheme 77−43726
GaAs, alloying with Au and Au alloy ohmic contact metallisations, SEM and optical study 80−70820
GaAs, annealed, surface cond. change, Schottky barrier meas. 78−64095
GaAs, chemisorption of Al, surface barrier formation, localised orbital theory 79−51671
GaAs, epitaxial growth of Al/GaAlAs by hot. vac. deposition, and characterisation 79−56085
GaAs epitaxial layer, AuGe ohmic contact production by laser alloying 78−88026
GaAs, laser alloying of Au-Ge ohmic contacts 79−73583
GaAs, laser-annealed ohmic contacts for microwave devices 79−73584
GaAs MESFET struct., high-resolution deep level meas., photo-FET method 80−44531
GaAs MOS and Schottky systems, electromodulated reabsorption of luminesc. 79−15524
GaAs, minority carrier diffusion lengths, contact metal effects 78−72260
GaAs, ohmic contact form. to n- and p-type samples by MBE, characts. 79−47159

semiconductor-metal boundaries continued
GaAs ohmic contacts wtih Au-Ge, SEM and TEM obs. of struct. 80−100522
GaAs Schottky barrier, Auger de-excitation of metastable state 79−65410
n-GaAs Schottky barrier diode, electron processes at interface *(Russian)* 78−84301
GaAs, Schottky barrier electrorefl. meas. by sample rotating technique 80−60544
GaAs Schottky barrier function capacitance meas., determ. of deep electron traps 77−39797
GaAs Schottky barrier with Au and Au-Ga contacts, high temp. annealing behaviour 77−43725
n-GaAs, Schottky barriers, minority carrier trap meas. 78−26951
p-GaAs, Schottky barriers on polar (111) and ($\bar{1}\bar{1}\bar{1}$) surfaces 80−88631
n-GaAs Schottky diode, impurity photoluminesc. 80−29781
GaAs Schottky diode, influence of γ- and electron irradiated on recomb. characts. near GaAs surface 80−71478
GaAs Schottky-contact, influence of surface states and hole traps *(Bulgarian)* 80−25006
GaAs, temp. depend. of intervalley gap from Schottky diodes meas., thermionic emission theory generalization 79−73586
GaAs thin Schottky barrier metallisation, thermal reactions 79−78176
n- GaAs, ultra low resistance ohmic contacts 80−20307
GaAs, vacuum deposited Shottky barrier metallisation 79−78153
GaAs:Ar^+-metal, capacitor, capacitance-voltage and current-voltage meas., assuming intermediate dielec. layer 79−56316
GaAs:Cr substrates and LPE layers, Au film deposition and annealing, Cr redistrib. 80−15312
GaAs:Cr-Au Schottky barrier, local level near valence band, photocapacitance 79−11080
n-GaAs:Cu-Au, electron-phonon interaction in optical transitions between deep impurity level and allowed bands 79−42591
GaAs:Se ohmic contacts, pulsed electron beam annealing donor density, mobility 80−65678
GaAs:Te, ion implanted, ohmic contacts produced by laser-annealing 79−73585
p-GaAs:Zn, Mn, degenerate, tunnel p-n junction and semicond.-metal struct., I-V characts. 78−72252
GaAs/Au-Ge/Au structure, ohmic contact behaviour, alloying time effect 79−19659
GaAs/Au-Ge/Ni, Schottky barrier energy var. with interdiffusion 77−20435
GaAs/Au-Ge/Ni contact system, alloying behaviour, microprobe AES and X-ray diffr. 80−54548
GaAs/Au-Ge-Ni alloy metal-semiconductor thermoelectric coolers, effects of contact resist. and dopant conc. 80−81481
GaAs/In-Ge-Ag, semiconductor surface condition, effect on ohmic contact barrier height 77−4435
GaAs/metal contacts, recent developments in investigations of preparation and props. *(French)* 80−107909
GaAs/Ni-Ge-Au cathode struct., with enhanced injection efficiency, contact resist. 77−20431
n-GaAs/Pt/Cr Schottky contact, barrier height change due to heat treatment 79−47165
p-GaAs/rare earth metal contacts, surface pot. barrier 80−60086
GaAs-$(SN)_x$ semiconductor-polymer solar cell 79−15219
GaAs-Al (Ni-AuGe) contacts, elec. characts. 80−29476
GaAs-Al interdiffusion, 250-450°C, AES meas. 77−1263
GaAs-Al interface, ellipsometric anal. methods, correl. between optical props., thickness and surface roughness meas. *(German)* 80−55215
GaAs-Al interface, metal overlayer effect on semicond. (110) surface states 77−4441
p-GaAs-Al interface, produced by diffusion method using heavily doped GaAs, rectifying props. 79−28409
GaAs-Al interface, struct. study by X-ray total-external-refl.-Bragg diffr. 80−34321
GaAs-Al interface, thermal ageing of Al films, optical microscopy and SEM obs. 77−20203
GaAs-Al interfaces, chemically induced charge redistrib. 79−33342
n-GaAs-Al surface barrier diodes, influence of exciton effects on photo-EMF spectrum 78−10557
GaAs-Al(Au), MBE and field emission deposition of metal, comparative study, I-V meas. 79−87016
GaAs-Al(Ga)(Ge), surface reactions and interdiffusion, photoemission study 80−49532
GaAs-Au, electronic struct., photoemission meas. 77−20385
GaAs-Au, quenching of exciton luminesc. by surface elec. field 80−29801
GaAs-Au, Schottky barrier energy var. with interdiffusion 77−20435
GaAs-Au interface, atomic modulation of interdiffusion, effect of reactive Al monolayers 80−49432
GaAs-Au polycrystalline Schottky barriers, transition with grain size from electrode-limit to bulk-limited cond. 80−65676
GaAs-Au Schottky barriers, PES and depth profiling obs. 79−42641
GaAs-Au Schottky barrier, photocurrent, recomb. losses *(Russian)* 80−2470
GaAs-Au Schottky diode, electroless plating of Au, fast characterisation of epitaxial layers 79−33347
n-GaAs-Au-Mo, RF sputtering, elec. props. of contacts, compensating damage centres form. 80−34507
GaAs-Au(Ag) Schottky barrier solar cells, interface problems, AES, SIMS and XPS study 80−89627
GaAs-disperse metal film, photoluminesc. at interface 78−26953
GaAs-Ga, (110) interface electron states, photoemission study, chemical shift, surface charge redistrib. 78−72259
GaAs-Ga interface immersed in electrolytic solns., elec. props. 78−95368
GaAs-In Schottky barrier interface, covalent bonding of metal atoms 77−20429
GaAs-metal contacts, excess capacitance, depend. on nonlinear dielectric susceptibility 78−43475
GaAs-metal contacts, intervalley scatt. effect on current-voltage characts. 77−89845
GaAs-metal contacts, use of Ga to eliminate large As loss peaks 80−80370
GaAs-metal interface, metal-induced chem. reactions and surface states 80−20311
GaAs-metal interface form., chem. and electronic struct. 80−25009
GaAs-metal junction stabilisation by intermetallic diffusion barrier 79−38160

semiconductor-metal boundaries continued
GaAs-metal junction stabilisation by transition metal diffusion barrier 79−38161
GaAs-metal junctions, thermal stability improvement, with and without near noble metals 79−7143
GaAs-metal ohmic contacts, solid phase epitaxy formation, AES and channelling meas. 79−60658
GaAs-metal Schottky barrier, surface states and barrier height, I-V (C-V) characts. meas. 77−85310
GaAs-metal Schottky barrier diodes, impedance, freq. and voltage depend. 78−64114
GaAs-metal Schottky barrier contacts, interface chemistry 79−74049
GaAs-metal Schottky barrier height rel. to chem. reactivity 80−25008
n-GaAs-metal Schottky barrier, ultrathin native oxide, thickness determ. from C-V and photoresponse meas. 80−70821
GaAs-metal struct., photoresponse spectra, electron thermalisation *(Russian)* 79−15221
n-GaAs-Pb(Ag)(Pd), electrolytic deposition of metal films 77−77425
GaAs-Pd junction, contact reactions 79−56308
GaAs-Pt interface states energy distrib. and relaxation time 79−33345
GaAs-Pt-air system, far IR propag. distances of surface EM waves 79−42616
n-GaAs-W contact, Schottky barrier 78−39213
p-GaAs(P)/Au-Be ohmic contact form. by ionised-cluster beam deposition 77−32528
n-$GaAs_{0.6}P_{0.4}$, reproducible ohmic contacts 79−73587
$GaAs_{1-x}P_x$ epitaxial layers, charge carrier conc. determ. from low-field electrorefl. spectra 77−85320
$GaAs_{1-x}P_x$-Au, surface-barrier struct., photodetectors of visible and UV radiation 77−20437
GaAs(Sb), Schottky barrier and semicond./insulator interface states formation 80−49906
GaInAsP, rectifying and ohmic contacts 80−80376
p-$Ga_xIn_{1-x}PyAs_{1-y}$/Au-Zn, specific contact resist. 80−84509
$Ga_xIn_{1-x}Sb$ diode, with Au metallisation, interdiffusion effect of heat treatment 78−14820
GaP, electron traps around dislocations in p-n junction and metal-semicond. structs. 80−34388
GaP photoelectrode, role of Au overlayers 78−14812
n-GaP, Schottky barrier height data for several contact systems 80−60080
GaP Schottky barriers, voltage fluctuations, meas. 80−15604
p-GaP, Schottky barriers on polar (111) and ($\bar{1}\bar{1}\bar{1}$) surfaces 80−88631
GaP surface barrier structure, breakdown voltage exam., effect of proton irradiation 79−11225
GaP:Cu-Ni, Schottky barrier, TSC meas., trap levels 78−91709
n-GaP-(Ge-Au)/Ni, specific contact resistance calc. 78−43474
GaP-Ag(Au), Schottky barrier, stress effects on elec. props. 80−34512
n-GaP-Au, Au overlayer potential on photoelectrodes, I-V curves 77−89848
GaP-Au, Schottky barrier, layer formation, elec. and optical props. 78−91766
GaP-Au Schottky diode, elec. props. under stress 79−15222
GaP-Hg, elec. props. using Schottky barrier capacitance techniques 78−47870
GaP-metal Schottky barrier height rel. to chem. reactivity 80−25008
n-GaP-Pb(Ag)(Pd), electrolytic deposition of metal films 77−77425
GaP-Pd contact system, low temp. alloyed contact formation 80−100519
n-GaSb:S-metal surface barrier struct., elec. and photoelec. props. 78−56229
GaSb-Au contacts, interface struct., technology rel. to elec. props. *(German)* 77−72915
GaSb-Au Schottky barriers, PES and depth profiling obs. 79−42641
GaSb-Au structure, metal-semicond. interaction, soft XPS meas. 78−60203
GaSb-Pb junction, Ar ion bombard. effect on tunnelling props. 80−54783
GaSb;Au overlayer, adatom interactions, photoemission obs. 79−33898
GaSe, semiconductor-metal contact, photovoltaic props. 77−59330
Ge, amorphous, -metal junction, current-voltage charact., contact material effect 80−44725
Ge amorphous evaporated film, study of metal contact resistance and microstruct. 77−89880
Ge, electron-hole drop motion at low exciton densities 77−47865
Ge powder/Au electrode contact pot. difference, grain size depend. 80−44723
Ge, Schottky barrier, electronic struct., pseudopot. calc. 78−95364
Ge Schottky barrier, electronic struct., pseudopotential method, jellium model 79−38162
Ge/Al thin film couples, accel. ageing 80−44726
Ge-Au diode, deformed, dislocation energy band width 77−11874
Ge-Au(Sn)(In), twin lamellas formation due to deposition of metal contacts 78−10060
Ge-Ge (Sn) friction pairs, elec. cond. of Ge tribolayers at He temp. 79−87140
p-Ge-In injecting contact, sign of developed hot-carrier thermo-EMF 77−55606
Ge-In Schottky barrier interface, covalent bonding of metal atoms 77−20429
Ge-metal contacts, surface electron state spectrum surface treatment effects *(Russian)* 80−34497
Ge-metal interface, internal photoemission mechanisms 80−60077
Ge-metal Schottky barrier junction, surface electron states spectrum *(Russian)* 78−84297
Ge-metal Schottky barrier photodetectors, near IR interband transitions and optical parameters 80−73449
n-Ge-metal Schottky barrier contacts, IR optoelectronic props., quantum detector appls. 80−75640
Ge-Pd system, kinetics of formation of Pd_2Ge and PdGe films 77−69197
Ge-transition metal interfaces, planar, first phase to nucleate 77−62764
GeSe amorphous films, blocking metal contacts characteris. and photo/EMF obs. 77−76924
Hg-InP Schottky-barrier diode, contact times, I-V characts. 80−96971
n-$Hg_{1-x}Cd_xTe$, photoconductor, contact noise at 77K 78−88028
$Hg_{1-x}Cd_xTe$-In contact, diffusion of In 80−103520
HgSe, highly-electronegative stable metallic contact for semicond. devices 77−24617
II-VI semiconductor, $(SN)_x$ and HgSe as contact materials, compared with Au 77−85312
p-InAs, characts. of Pb supercond. contact 79−38254
semiconductor-metal boundaries continued
n-InAs, tunnelling spectra in mag. field, dispersion law *(Russian)* 79−60923
p-InAs-Au contacts, influence of free surface on elec. behaviour 78−95362
InGa-GaSe interface, microplasma electrolum. at 300K 79−11469
$In_xGa_{1-x}As$-Au Schottky contacts, interfacial oxide layers used to increase effective barrier height 79−7896
p-InGaAsP-Au, Schottky barrier height comp. depend., photoelec. meas. 77−20433
$In_{1-x}Ga_xSb$ alloy system, interband magnetooptical study using Schottky barrier 79−8124
$In_{1-x}Ga_xSb$-Au, photovoltaic effect and Schottky barriers 80−49897
InP (001)-Ag, contact, surface stoichiometry and struct., and electronic surface states 78−95361
InP, cleaved surface, metal contact props. and influence of intermediate adsorbed layers 80−49905
p-InP, ohmic contact using Be-Au metallisation, low contact resist. 80−65677
InP ohmic contacts 79−28406
InP, Schottky barrier and semicond./insulator interface states formation 80−49906
n-InP Schottky barriers, photocapacitance effects of deep traps 78−43325
InP surface, interaction with Cl, rel. to Schottky barriers at metal-InP interface 78−56036
InP surface preparation for Schottky barrier and ohmic contact formation 80−39671
n-InP/Au-Zn Schottky barrier diodes, fabrication and elec. props. 79−33348
p-InP/In-Zn(Cd) contact evaluation 77−24619
InP-Ag, MBE deposited Ag, struct. using TEM and RHEED 79−82492
InP-Ag, struct. of Ag contacts, TEM 77−62765
InP-Ag contact fabrication by at. beam epitaxy of metal, elec. props. 77−59691
InP-Ag contact system, evaluation of Auger depth profiling technique 79−56893
InP-Ag Schottky barrier, hot electron attenuation length 80−49904
InP-Al interface struct., low temp. interaction, AES study 80−107661
InP-Al(Au), MBE and field emission deposition of metal, comparative study, I-V meas. 79−87016
n-InP-Al(Hg), Schottky barrier height and stability characterisation 80−54786
InP-Au, O, Cl, interfacial layers, effect on Schottky barrier height 78−14824
InP-Au, Schottky barriers, electroreflectance spectra 77−43698
InP-Au contacts, conditions of fabrication that control interfacial microstruct. 79−42643
InP-Au Schottky barriers, PES and depth profiling obs. 79−42641
InP-Au(Ag)(In), electronic structure 78−10554
InP-Cu contact system, low temp. alloyed contact formation 80−100519
InP-metal ohmic contacts, elec. and metallurgical props., heat treatment effects 80−34514
n-InP-metal Schottky barriers, effective lowering using thin VPE n^+ lasers 77−43717
InP-metal Schottky barriers, effects of heat treatment characterised by SIMS 78−6446
n-InP-metal surface barrier struct., props. 79−11223
InP(100)-Ag contacts, interface struct. 79−60922
InSb surface, Cu deposition, ohmic contact formation, SEM obs. 77−51817
InSb, surface magnetoplasma waves, reson. spectrum and dispersion charcts. 79−38148
InSb-Au contact system, low temp. alloyed contact formation 80−100519
InSb-Au Schottky barrier, photovoltaic spectra and magneto-optical transitions, Landau levels and excitons 77−47858
InSb-Au Schottky barrier, photovoltage, temp. effects 77−69415
InSe, semiconductor-metal contact, photovoltaic props. 77−59330
In_xSe_{1-x}, amorphous film, in metal-In_xSe_{1-x}-SnO_2 system, photovoltages 77−28215
Mo-Si, non-volatile memory switching 80−54814
Mo-Si junctions, metallurgical boundary props. and elec. resistivity 78−2568
Nb-Si, bridge, crit. current 80−20359
Ni/GaAs film contact system, alloying reaction 80−96747
Ni-n-GaP:Si(Ge) contacts, doping effect in elec. props. 80−6983
Ni-Se interface, reactive diffusion, electronic struct., UPS study 78−51748
Ni-Si, ion implanted, inert-gas-bubble form., TEM and Rutherford backscatt. anal. 79−90682
Ni-Si(111), interface, reactivity and struct., ion channelling meas. 80−92788
Pb-CdS-In junctions, Josephson effect through 80−100558
Pb-Si:Sb Schottky tunnel junction, variable range hopping assisted tunnelling 80−39670
PbI_2-Ag system, effect of bound and free exciton states on light sensitivity *(Russian)* 78−71169
PbI_2-Ag(Au)(Cu), light sensitive, internal photoelectric emission 80−107910
$PbS_{1-x}Se_x$ diode laser, contact degradation due to diffusion 80−102734
$Pb_{0.8}Sn_{0.2}Te$-Pb, Schottky barrier form., Auger depth profiling and I-V meas. 80−49903
$Pb_{1-x}Sn_xTe$ diode laser, contact degradation due to diffusion 80−102734
PbTe-Au Schottky barrier junctions, Landau level oscills. in tunnelling data 80−49945
PbTe-based structures, zero anomaly of tunnel cond. 79−24107
PbTe-In contacts, fabrication and props. 80−60078
p-PbTe-M, M=In, Pb, Zn, Cu, barrier props. 79−7898
PbTe-metal barrier device, I-V and C-V characts., barrier energies, and depletion widths 77−85316
Pd coated Si wafers, interference effects on irrad. with laser beam 80−66333
Pd, film form. on Si surface by ion beam plating 77−90284
Pd/Si, Schottky-barrier type devices, chemical and polarisation characteristics, comparative study 79−78173
Pd/Si interface, chem. and struct. props. during silicide form., AES and TEM obs. 80−49430
Pd-Si, ion implanted, inert-gas-bubble form., TEM and Rutherford backscatt. anal. 79−90682
Pd-Si (111) interface, microscopic Pd_2Si form., UPS obs. 80−24743

semiconductor-metal boundaries continued
Pd-Si structure, epitaxial silicide growth, LEED and AES study 80−103590
Pd_2Si film on Si, substrate temp. effect on microstruct., TEM obs. 78−14621
Pt-Cr, shallow silicide contact 80−70819
Pt-GaAs contacts, sintered, eval. of W, Ti, Mo and Hf barrier metals 77−8193
Pt-Si:As, silicide form. during laser irrad., p-n junctions and ohmic contacts 80−84397
Pt-$SrTiO_3$ (100) interface, struct. and electronic props., AES, LEED, EELS, and UPS study 80−24986
Pt-$SrTiO_3$ (100) interface, Auger and photoemission studies, relax. and chem. shift effects 80−54749
PtSi film, on (001) Si, crystallography 78−75955
PtSi-n-Si, photoelec. barrier height and elec. props. 79−33344
Sb_2S_3, glassy, interface with metal, photoelec. props. 79−73589
Se, amorphous film-metal system, contact pot. distrib. and photo-EMF, work function 77−76925
Se diode surface states determ. by conductance and capacitance 77−85318
Se-Ni-Mylar multilayered struct., interfacial bonding effect on adhesion, ESCA obs. 79−95274
Si (111), with chemisorbed Al, electronic struct., self-consistent pseudopotential calc. 78−34880
Si (111) 7×7 surface, Schottky barrier formation, photoemission, exam. of filled surface states and band bending 77−28250
Si (111) surface, Al overlayers, theoretical study 78−95366
Si (111) surface with Al overlayers, electronic struct., self-consistent pseudopotential method 79−4595
Si (111)-Au interface, chemically driven intermixing, UPS study 80−50533
Si, amorphous, interface with V, V silicide formation, backscattering, diffraction meas. 80−2285
Si, amorphous, photovoltaic characts., rel. to appl. in solar cells 78−84253
Si, amorphous, Schottky barrier and p-n junction props. 79−28407
Si, amorphous, Schottky barrier solar cell, large-area RF sputtered, contact form, scaling and optimisation 80−45679
Si, amorphous, thin film reaction with Pd, metal-rich silicide formation 80−2284
Si amorphous film, crystn. on annealing at low temps. in contact with Al 80−24765
n-Si, bipolar ohmic contact with macroscopic recomb. centres. 80−80379
Si, chemically etched, metal contact, electron and hole currents correl. 78−91769
Si, cleaved surface, metal contact props. and influence of intermediate adsorbed layers 80−49905
Si device technology, thin film interaction effects, book contrib. 79−1620
Si intermixing with Pt, Ni and Hf films, ion-beam induced silicide form. 79−46718
Si, ion implantation, channelled, through metal silicide film 80−70231
n-Si, low noise ohmic contact prep., transport props. 77−43723
Si, metal contacts to O_2 contaminated surfaces, Schottky diodes 79−56309
Si, moderately doped, ohmic contact electron emission, quantum calc. 78−68087
Si n-p planar diode, Al layer covered, laser beam produced alloy areas, characterisation 79−69594
Si, Pd-Al metallisation, Cr thin film used as barrier to interaction of Pd_2Si with Al 77−43724
Si planar diode, Al coated, binary memory device, laser writing 79−69593
Si, polycrystalline-metal contacts, minority carrier injection 80−103750
Si polycrystalline-metal Schottky barrier solar cells, elec. and photovoltaic contact props. 80−93936
n-Si Schottky barrier, electron-irrad., surface defect distrib., deep-level transient spectroscopy 79−1459
Si Schottky barrier metallisation characteristics 77−76922
Si solar cells, all-plate low cost contact system 80−93992
Si solar cells, Ni-Cu conductor system 80−93991
Si solar cells, semiconductor thick film cell contacts, all metal 80−30489
Si substrate, reaction with Ti film, backscatt. anal. of silicides 79−69377
Si substrate, silicide formation with large bilayers of Pd-Pt, Pd-Ni and Pt-Ni 79−51444
Si, thin single crystal, MeV ion scatt. and channelling obs. of interfaces 80−50492
Si:H, amorphous, Pt film growth, AES and LEED study 80−88447
Si:H, amorphous, Schottky diodes, elec. props., light-induced effects 80−103741
Si/Al and Si/Al-Si(Cu), Si regrowth minimisation through overlying Al or Al alloy film 80−70569
Si/Al interfaces, chemical bonding states, low energy AES 80−6985
Si/Al thin film couples, accel. ageing 80−44726
a-Si/Au barrier, capacitance and cond. 80−2469
Si/Au interface, X-ray dose enhancement, Monte Carlo calcs. 79−22484
a-Si/metal barrier, capacitance and cond. meas. interpretation 80−49909
Si/NiSi/Al system, high temp. interaction study, elec. and struct. characts. 79−24075
Si/Pd-W, contact reactions, backscattering, X-ray diffr. meas. 80−20040
p-Si/rare earth metal contacts, surface pot. barrier 80−60086
Si/refractory metal-Ni(Pd)(Pt) interactions, phase separation 80−65303
Si-Ag, electronic and cryst. struct. of Ag adsorbed on Si (111), Schottky barrier form. obs. 78−84091
n-Si-Ag(Au) evaporated contact photoelectric props. *(Russian)* 78−43473
Si-Al, contact resist. response surface of sintered Al film on Si(100) 79−78175
Si-Al, current-voltage characts., oxide film effects 80−70841
Si-Al, long-term tests on Al film 79−33346
p-Si-Al, ohmic contacts, Si dissoln. and recrystn. effects, computer calc. 80−103749
Si-Al, solid phase epitaxial growth of Si 80−34324
Si-Al (Na) interface, barrier height anal. including virtual surface states 77−69416
p-Si-Al barrier junction form. 77−12006
Si-Al devices, thickness meter for Al contacting layers *(Russian)* 80−36980
Si-Al interface, dissolution rate of amorphous Si 78−95188
Si-Al interface, ellipsometric anal. methods, correl. between optical props., thickness and surface roughness meas. *(German)* 80−55215

semiconductor-metal boundaries continued
Si-Al interface in semiconductors, electronic parts, electromigration aspects 80−39355
Si-Al Schottky diode, type II localised interface states, Si surface prep. effects 78−39210
Si-Al system, Si regrowth minimisation methods in Al films 80−15384
Si-Al(Ga)(In) interface, electron energy loss spectra of Schottky barrier states 77−48290
Si-Al(Ni) structure, contact resist. and bulk resist. of Si, pulse method 78−52083
Si-Au, interface study using EELS 80−97391
Si-Au, O determ. by SIMS, nuclear reaction and Rutherford backscatt. anal. 79−4482
p-Si-Au, Schottky barrier IR detector 77−37985
Si-Au, thin oxide, O, Cl, interfacial layers, effect on Schottky barrier height 78−14824
Si-Au interface, algorithm for energy deposition of X-rays 77−28648
n-Si-Au Schottky barrier, role of surface states in appearance of photo EMF 79−11222
Si-Au Schottky diodes, role of O in formation mechanics 79−42639
Si-Au Schottky-barrier, formation process anal., V-I characts. *(French)* 78−91768
n-Si-Au surface barrier diode, photosensitivity in spectral range, 1-6 eV 77−89850
Si-Au(Ag) contacts, Schottky barrier heights and interface states 77−85317
Si-Au(Cr)(Pd), contact reactions between amorphous Si and metallic films, TEM, transmission electron diffr. obs. 79−23846
Si-Co interface metal-semiconductor transition, rel. to first compound nucleation 80−24771
Si-$CoSi_2$Si, double heteroepitaxy, solid phase and MBE 80−104063
n-Si-Cr, Schottky barrier IR detector 77−37985
n-Si-Cu Schottky contacts, electrochem. deposition, barrier height and ideality factor 80−75641
Si-In Schottky barrier interface, covalent bonding of metal atoms 77−20429
p-Si-In Schottky barrier structure, optical quenching of photovoltaic effect 77−55608
Si-Ir, silicide form., He ion backscatt., X-ray diffr. study 79−82471
Si-IrSi interface microstructure and Schottky barrier height 80−34508
Si-metal contact, transport theory of Schottky barriers 80−80372
Si-metal contacts, analytical techniques, review 80−80120
Si-metal contacts, low temp. reactions 78−2567
Si-metal interface, silicide formation, interface marker technique obs. 80−59734
Si-metal rectifying interface, reactively sputtered ultrathin metal oxide layer effect on current transport 79−78887
Si-metal Schottky barriers, surface states and barrier heights 77−80838
p-Si-metal Schottky contact surface state spectra and current transport mechanism *(Russian)* 78−43472
Si-metal systems, interfacial reaction and Schottky barrier 80−39672
p-Si-metallic liquid interface, thermoelec. coeff. meas. 77−39887
Si-Mg, laser induced formation of Mg_2Si_2 80−35011
p-Si-Mn contact, barrier height 80−34510
Si-Mo, silicide formation kinetics determ. 78−43261
Si-Mo diffusion couples, $MoSi_2$ or Mo_3Si/Mo_5Si_3 form. 79−77836
Si-Mo Schottky barrier diode, sputtering damage effects on I-V and C-V characts. 77−39940
Si-Mo sputtered contacts, contact resistance 80−92970
Si-Mo substrate-film interface, reaction on heat treatment, silicide formation 80−79999
n-Si-Ni, Schottky barrier, thermal annealing effect on props. 79−69596
n-Si-Ni, Schottky-barrier, I-V characts. of elec. contact 79−19662
Si-Ni, substrate-film, annealing effects on transmission electron diffr. patterns, silicide form. 78−91562
Si-Ni Schottky barriers, thermionic field emission at room temp. 78−6445
Si-Ni Schottky diode, type II localised interface states, Si surface prep. effects 78−39210
n-Si-Ni structure formed by elec. explosion of metal, rectifying barrier 78−72263
n-Si-Ni surface barrier junction, rectifying, struct. and elec. characts., effect of low temp. annealing 78−14821
Si-Ni surface barrier struct., surface electronic states, annealing effects *(Russian)* 78−6441
Si-$NiSi_2$, ion implantation damage in silicide layer, channelling obs. 78−30676
Si-Ni(Pd)(Pt) film struct., silicide form. He^+ back scatt. and X-ray diffr. obs. 79−51442
Si-Pb heterojunction, RHEED, Mossbauer spectroscopy and I-V characts. 80−70828
n-Si-Pd diodes, chemical reduction process for fabrication 80−60082
Si-Pd_2Si, resist. and Hall mobility meas. 78−47886
n-Si-Pd_2Si contact, interface struct. and Schottky barrier height, correl. obs. using TEM 80−100504
Si-Pd_2Si ion implantation damage in silicide layer, channelling obs. 78−30676
Si-$Pd_{80}Si_{20}$, amorphous, Pd_2Si layer form., shallow contact 80−103586
Si-Pd-Ti, silicide form. in evaporated films 80−80006
Si-Pd(Pt), substrate-film system, ion-induced intermixing 80−15420
Si-Pt, silicide layer, struct. and elec. props., sputter etching and annealing ambient effects 77−62991
Si-Pt contact, annealed in H_2 ambient, elec. props. 78−64110
Si-Pt Schottky barrier, laser formation and characts. 80−60079
Si-Pt Schottky diode, type II localised interface states, Si surface prep. effects 78−39210
Si-Pt(Ni)(Pd), laser-induced reactions of metal films with Si, surface struct. obs. 79−19471
n-Si-Re(Os) Schottky contact barrier height meas. 80−65675
Si-refractory metal contacts, thermally cleaned surfaces 80−100521
Si-refractory metal structs., interface modification by ion implantation 80−70475
Si-Sn heterojunction, RHEED, Mossbauer spectroscopy and I-V characts. 80−70828
Si-Sn tunnel structure, differential cond., density of states in heavily doped Si 79−15072
Si-transition metal interface, silicide formation, book contrib. 79−1530
Si-transition metal silicide Schottky barrier, effect of glassy membrane 77−85311
Si-transition metal silicide, chemical states, AES expts. 78−91767
SiAs-Au surface barrier diodes, optical props. of SiAs 79−8145

semiconductor-metal boundaries continued
SiC film, amorphous, reactively sputtered, effects of S/C ratio and H content on elec. and optical props. 79−90906
SiH_x amorphous films, internal photoemission, metal contacts 80−96964
SiH_x amorphous reactively sputtered films, in Pd Schottky barrier devices, photovoltaic props. 80−49910
$Si_{1-x}H_x$, amorphous, gap states, DLTS 80−49656
$Si_{12}Te_{48}As_{30}Ge_{10}$-Au, Schottky barrier props. 79−7897
SnO_2-Pb(Ag)(Pd), electrolytic deposition of metal films 77−77425
$SrTiO_{3-x}$-In contacts, differential capacitance, elec. field depend. permittivity effect 80−54779
T-metal, thin film contact, time evolution of photovoltaic effect 80−65687
Te/Ag double films, interdiffusion and struct. modifications *(French)* 77−62682
Te-Ag, thin film system, stress-relief appearance conditions 80−65416
Te-Au thin film interface, evolution, switching effects *(French)* 80−6660
Te-Se-Cd, sandwich structure, fabrication and characteristics 80−60089
Te-Se-Cd rectifying sandwich structs., elec. forming action, Schottky junction form. 80−80371
Ti-Si, ion implanted, inert-gas-bubble form., TEM and Rutherford backscatt. anal. 79−90682
TiO_2-Pd Schottky barrier, work function depend. on adsorbed species 80−54782
V-Si, ion implanted, inert-gas-bubble form., TEM and Rutherford backscatt. anal. 79−90682
V_2O_5-metal Schottky barrier, contact-limited conduction 79−95493
W-EuS, amorphous, memory effect in field emission 80−89126
$ZnIn_2S_4$ diode struct., photoelec. props. *(Russian)* 77−43720
$ZnIn_2S_4$-Ni diode, electric and photoelectric characts. 77−12005
ZnO-Pb(Ag)(Pd), electrolytic deposition of metal films 77−77425
Zn_3P_2, evaporated metal contact barrier heights 80−80375
Zn_3P_2-Au surface barrier diode, wavelength-modulated photoresponse spectra 77−12004
Zn_3P_2-Au(In) photovoltage response, optical transitions in Zn_3P_2 80−25402
Zn_3P_2-metal contacts, photoelectric props. 80−92930
ZnS metal interface, barrier height anal. including virtual surface states 77−69416
ZnS with Au film coating, calc. of defect conc. 78−95052
ZnS-metal interface, metal-induced chem. reactions and surface states 80−20311
ZnS-metal Schottky barrier height rel. to chem. reactivity 80−25008
ZnS-ZnSe mixed powders, hot-pressed polycrystalline, photolum. and electrolum. 77−32426
ZnSe, high-resistance layers, effect of electrode materials on switching 79−65549
ZnSe, low resistance ohmic contacts using In-Ga liquid alloy, LED fabrication appl. 80−70823
ZnSe/metal, dielectric phonon-metal electron interaction, effect on optical props. *(Russian)* 79−19663
ZnSe-metal contact, elec. props. 78−14826
ZnSe-metal Schottky barrier height rel. to chem. reactivity 80−25008
$ZnSiP_2$-Au(Ni) Schottky contact, production and props. 79−7901
ZnTe based metal-semicond. struct., spectral photosensitivity obs. 79−95492
ZnTe single crystal, Schottky-barrier diodes and ohmic contacts props. 80−96987
p-ZnTe surface barrier structures, photo-EMF 77−89851
ZnTe-Al, conduction mechanisms in non-ohmic off-state 77−72932
ZnTe-metal structures, photosensitivity spectrum *(Russian)* 78−76147

semiconductor-metal transition *see electrical conductivity transitions; metal-insulator transition*

semiconductor processing *see semiconductor technology*

semiconductor storage devices
see also integrated memory circuits
amorphous semiconductors appl. *(Japanese)* 79−23979
binary memory device laser writing on surface of metal coated semicond. planar diode 79−69593
cardiopulmonary monitoring of high-risk infants using microprocessor-controlled memory 78−31962
conference, ferroelectric materials and their applications, Kyoto, Japan, Nov. 17-19, 1977 79−19846
diffused p-n diode memory correlator 77−23831
digital data store for radio monitoring of patients *(German)* 78−80998
diode array SAW correlator model and expt. 78−9508
dual-dielectric charge storage cells, electron-electron effects in writing and erasing 78−34900
graded and stepped energy band-gap MIS structures 80−2473
linear accelerator calibration monitor with a memory 80−3821
MAOS memory element, stored charge volatility 78−52100
memory-correlator cells employing acoustically induced charge hologram in piezoelectric semiconductors 78−86290
metal-TiO_2-SiO_2-Si structure, dielectric props. and charge storage characts. 78−52098
MIOS memory structs., degradation 79−38179
MIS memories, tunnelling and photoionisation of states 80−11099
MIS structure, radiation induced charge storage 80−6997
MISM structure, photoresponse of residual conductivity 77−15968
MNMOS structure, with Pt interposed at Si_3N_4-SiO_2 interface, charge storage props. 77−51821
MNOS, on GaAs substrate, as optically controlled memory element 77−35995
MNOS capacitors, retention and endurance characts., annealing and oxidation effects 79−74274
MNOS devices, switching characts. at low fields 79−56311
MNOS diode, trap distribution, memory characteristics 77−85326
MNOS memory device, charge distrib. of nitride 78−2571
MNOS memory device, charge retention by Frenkel-Poole detrapping 78−47874
MNOS memory device, trapped charge behaviour, UV light effects 77−12014
MNOS p-channel transistor, memory characts., H_2 anneal effects 80−80388
MNOS structures, discharge behaviour 79−38174
MNOS thin-oxide devices, effects of Si-SiO_2 interface states on memory characts. 79−82681
MOS structure switching and memory effects 79−78197

semiconductor storage devices continued
multichannel analog memory, using MOS transistors for data transmission to M6000 computer 79−26043
nonvolatile memories, book 77−78906
pn diode MZOS memory devices, storage mechanisms 79−18611
SAW space-charge coupled signal processor with storage 78−9507
SAW storage correlator equivalent circuit models 78−9506
semiconductor-ferroelectric heterostruct. junction, nonvolatile polarised memory 79−78164
Ag-SiO-Ag sandwich structures, elec. props. and nonvolatile memory effect 79−87164
Ag_2O-P_2O_5, amorphous metaphosphate, memory cell with low switching fields *(German)* 79−19641
Al-Si-SiO_2-Al structure switching and memory effects 78−95385
$BaTiO_3/SiO_2$ charge storage memory films for IGFETs 80−11566
GaAs based MIS structures as possible optical memory elements 79−65556
GaAs p^+-p(i)-n^+ structures, S-shaped I/V characteristics based on laminated semicond. cryst. structures *(Russian)* 79−42628
Ge slow surface states, optical image storage for $LiNbO_3$ SAW readout 77−23773
$LiNbO_3$-p-Si, frequency doubling of the two-pulse and three-pulse echoes in surface acoustic waves 79−69335
Si diode storage correlator optical imaging and memory characteristics 77−23772
Si-CdS heterojunction memory diodes, switching process 78−80046
Si-SiO_2 systems, spectral characts. and photomemory effect *(Russian)* 79−42657
Si_3N_4 MNS capacitors, elec. cond. 79−95499
Si_3N_4-SiO_2:As, graded and stepped energy band-gap MIS struct. 80−2473
TiO_2/SiO_2 charge storage memory films fo IGFETs 80−11566
VO_2, laser induced metal-insulator transition, thermal switching dynamics 77−76885
V_2O_5-P_2O_5 glass, switching and memory behaviour, Pt point contact effects 77−11970
ZnO Sezawa mode pn-diode array memory correlator 79−78178
ZnO-SiO_2-Si monolithic convolver, long time storage of surface-acoustic-wave signals 77−1287

semiconductor storage systems
see also integrated memory circuits
biotelemetry radionuclide tracer data storage appl. 77−90877
electromyography and nerve conduction recorder 79−43999
high speed disc, for storing body surface pot. maps 77−78014
holographic memory photodiode matrix readout system *(Russian)* 77−58266
multichannel analyser buffer store, 4096 channel sequential memory, control circuitry 77−57829
photodiode storage matrix control system *(Russian)* 77−58263
SAW information storage and correlation in semiconductor diode arrays 78−9505

semiconductor switches
amorphous chalcogenide switching devices, reliability 79−11238
amorphous covalent semiconductors, choice and fabrication for switching applications 78−2415
amorphous device, transient on characts., filament model 77−15917
amorphous thin film chalcogenide semicond. *(French)* 77−72710
avalanche transistor switchout, high performance, for external pulse selection at 1.06 μm 79−7158
chalcogenide film, threshold switching mechanism, review 78−76122
chalcogenide glass, threshold switch, high resist. state 77−15924
chalcogenide glass device developments and future trends 77−69386
chalcogenide glass threshold switch, on-state model 79−56270
chalcogenide glass threshold switch response to pulse burst waveforms 78−10523
chalcogenide glass-GaAs(InP) p-n junction, fabrication, characterization, switching 80−49892
chalcogenide glasses, memory effect, local doping, switching 80−107873
chalcogenide glasses, threshold switch, on-state model 79−99588
chalcogenide switches, relaxation processes 78−60172
CMOS analogue gate, small DC voltage meas., at low temp. 79−35776
control circuits using diode switches with switching of nsec pulses 78−8415
cryogenically cooled C-band p-i-n diode integrated switch matrix for radio astronomy applications 78−96392
diodes, thin film glass based structures, surface electron states effect on switching *(Russian)* 80−107887
fast IR switch, ultrafast photography, with 10.6 μm radiation 78−38035
HF CRO design, using cold switching for front panel operation 78−93672
intracavity transmission switch, nsec. pulse selection in CO_2 oscillator 79−98382
laser diode modulator using current switching bipolar transistors 78−1288
light controlled switch with picosecond precision, appl. to high-speed Kerr cell 78−1327
metal-semi-insulating-n-p^+ Si devices, switching expts. 78−26965
metal-semi-insulator-n-p^+ Si device, switching theory 78−26964
MIS structure switching characts., theory, appls., expt. 78−68093
MNOS devices, switching characts. at low fields 79−56311
MNOS P-channel switch, accelerated reliability testing *(German)* 80−6988
MOS structure switching and memory effects 79−78197
MOSFET electrometer amplifier type MDM 77−79106
nondispersive IR analysers, programmable switching device for semiautomated multichannel gas analysers 77−77830
on-state behaviour and degradation effects 77−11967
optical waveguide switches, and modulators, review of development progress 78−38045
optoelectronic ps switch using pulsed lasers and photoresistive semiconductor *(German)* 77−72066
optoelectronic sampling with picosecond Auston switch, oscilloscope and photodiode testing appl. 77−58451
p-n-insulator (tunnel)-metal devices, switching theory; punchthrough mode 79−60926
p-n-insulator metal switching devices, avalanche mode operation 80−70838
p-n-p-I-M structure, tunnel cathode thyristor, theory of switching effect 77−39930

semiconductor switches continued
pnp switching transistors, anomalous breakdown regions, laser scanning obs. 80−34854
pulse shaping using laser-excited solid-state plasmas in Si, expt. 77−19397
pulsed electron accelerator current density distrib. multichannel recorder 78−58520
RF switch, linear, MOS transistors, analogue signals, NMR and nuclear quadrupole resonance pulse spectrometer appl. 77−10078
superconducting coil energy storage power supply 79−34442
switch, laser-activated, high-power switching with ps. precision 80−2416
temperature control of electrometer varactor-bridge amplifiers 79−9219
temperature regulator circuits, using thyristors and triacs *(Spanish)* 79−6115
ternary semiconductors, pot. practical appl., review 79−10344
thyristor magnetising current switch for magnetic flaw detector 78−44311
thyristor p-n-p-n structure turnon parameter meas. by optical probe 77−57358
triac TDA 1024 static interruptor cct., thermostatic, lighting control appl. *(Italian)* 78−73984
two-phase servo master-slave manipulators, triac output control system 79−9213
Ag-Cu_2O-Ag bistable switching devices, freq. distrib. of threshold voltage 77−32091
Ag_2Se thin film, switching and Ag movement, point contact technique 80−60107
Al-Si-SiO_2-Al structure switching and memory effects 78−95385
$Al_yGa_{1-y}As$-$Al_xGa_{1-x}As$, electrooptic rib waveguide modulators and switches 78−38046
$As_{10}Ge_{15}Te_{75}$, thermal memory switch development 78−89468
As_2Se_3, chalcogenide glass threshold switches, turn-on state, maintenance mechanism *(Russian)* 77−85271
$As_{50}Te_{50}$, amorphous films, metal and semicond. contacts, threshold switching, IR emission 80−49831
$As_{50}Te_{50}$ amorphous switches, light emission charact. 79−78139
$As_{0.3}Te_{0.48}Ge_{0.1}Si_{0.12}$, amorphous film, transient switching processes 78−84232
Au-Si-Al structure electrode mass transfer and switching with memory 78−95389
a-CdAs thin film fabrication for switching applications 78−2415
$Cd_{23}Ge_{12}As_{65}$, amorphous, threshold switching, expt. 80−49830
$CdS_{0.5}Se_{0.5}$, picosecond optoelectronic switching 80−54734
CuO-CaO-P_2O_5 glass devices, memory switching 78−56192
Cu_2O, switching channel electron probe microanalysis, switching cycle number (life) 77−32056
EuS, amorphous, on W, memory effect in field emission 80−89126
GaAs, control of fast Pockel cell for active pulse shaping in ps domain 80−28257
GaAs directional couplers and electrooptic switches, wavelength depend. 78−79143
GaAs electro-optic rib waveguide directional-coupler switch with stepped $\Delta\beta$ Schottky electrodes 79−98507
GaAs ion-irradiated layers switching conduction 78−34868
GaAs MESFET, for fast pulse modulation of semiconductor laser 77−88797
GaAs, photoconductive carrier lifetime meas. by optoelectronic gating technique 77−47857
GaAs switch, laser-activated, high-power switching with ps. precision 80−2416
GaAs-$Al_xGa_{1-x}As$, single-mode rib waveguide switches electro-optical modulation 78−46839
Ge-As-Te, thin chalcogenide glass film, high-field switching effects 77−32052
Ge-S-Ga amorphous thin film, memory switching effects 80−88605
$Ge_{10}As_{40}Te_{40}I_{10}$, chalcogenide glass film, switching delay time 78−26926
GeO_2 films, memory switching phenomena 79−82650
$Ge_{10}Si_{12}As_{30}Te_{48}$, monostable chalcogenide glass threshold switch, temp. meas. *(German)* 77−4412
$Ge_{15}Te_{81}X_4$ amorphous semicond. switches, fabrication technology *(German)* 80−7493
In-GaAs:Cu-In structure, phototrigger effect 78−56238
Se-Ag_2Se, thin film polycrystalline heterostructure, exhibiting memory switching, noise level 78−84288
Si laser activated switch, synchronisation jitter reduction in streak cameras 80−53440
Si light-controlled switch, appl. to high speed Kerr and Pockels cells 78−26925
Si MIS switch diode, charge storage effects, threshold depend. on driving voltage pulse freq. 80−49939
Si switching diode, thermometric props. 77−37889
Si/In_2O_3-SnO_2 thin film junctions, polarity dependent memory switching effects 80−70814
Si-SiO_2-SnO_2 structure, switching props. 78−76138
$Si_{12}Ge_{10}As_{30}Te_{48}$ chalcogenide glass threshold switches, turn-on state, maintenance mechanism *(Russian)* 77−85271
$Si_{12}Ge_{10}As_{30}Te_{48}$, chalcogenide glass film, switching delay time 78−26926
$Si_{12}Ge_{10}As_{30}Te_{48}$ chalcogenide glass threshold switch conductivity in high ohmic state *(Russian)* 78−43502
$Si_{12}Ge_{10}As_{30}Te_{48}$ chalcogenide glass, switching in thin layers with semicond. electrodes 79−4586
$Te_{40}As_{35}Ge_7Si_{18}$ film, threshold switching in relax. oscill. mode 77−69389
$Te_{40}As_{35}Ge_7Si_8$, amorphous, threshold switching, expt. 80−49830
TeO_2-V_2O_5 glass threshold devices, reversible monopolar switching 80−2434
VO_2, fluctuations of current and switching time 79−38137
VO_2, laser induced metal-insulator transition, thermal switching dynamics 77−76885
VO_2 thin film semiconductor-metal transition applications 80−49835
V_2O_5-$NaPO_3$-P_2O_5 threshold switches, elec. props. 77−35974
V_2O_5-P_2O_5 glass, switching and memory behaviour, Pt point contact effects 77−11970

semiconductor technology
See also under specific device headings
see also semiconductor doping; semiconductor growth
amorphous Si preparation, hydrogenated 80−80956
anisotropic etching by $CCl_4(+O_2)$ gas plasma 77−32701
anodic oxidation for Si film removal and determination of active impurity distrib. 80−40583

semiconductor technology continued
background heating for laser annealing 79−96047
boundary layer theory application, introduction 80−66431
capacitance methods for minority and majority carrier trap characterisation 77−51692
cathodoluminescence, bibliography of papers till 1977 79−21482
charge-conversion meas. of nonlinear capacitance 77−79115
charged-particle detector manufacture 79−93886
chemical etching of Si, Ge, GaAs, GaP, review 78−95832
conference, Brighton, England (Mar. 1976) 77−27898
conference, ion implantation equipment, Povo-Trento, Italy (Aug., 1978) 80−31413
conference on electron, ion and photon beam technology, Palo Alto, CA, USA (May 1978) 78−74827
contact and interconnect form. by ionised-cluster beam deposition 77−32528
contactless measurement of sheet conductivity and mobility of semiconductor wafer by using eddy current 80−62693
crystal growth and defects, appl. of analytical techniques for observation 80−73546
defect spatial distribution in Si, transient capacitance meas. of MOSFET 77−11973
device fabrication by MBE 79−43154
dielectric films on semiconductor devices, review of deposition techniques 78−23611
dielectric thin films, accurate meas. by symmetric prism wave couplers *(Chinese)* 80−2885
dielectric-isolated substrates, deform., and control by multilayer poly Si support struct. 80−107681
diffusion barrier formation, Au film, using layer annealing 80−80373
edge etch process for minimum geometry windows on poly Si surface 78−31550
Electrochemical Society Spring Meeting, Philadelphia, USA (1977) 78−6837
electron interactions with solids, conf., Southampton, England (Apr. 1976) 77−44570
electron speed, techniques for doubling in crystals 79−38076
electronic material and device characterisation using surface-sensitive analytical techniques 80−65341
ellipsometry for semiconductor process control, dielec. layers meas. 78−49887
etching characts. by plasma reactive sputter etching of semicond. device materials 78−27661
etching method using Au pellets, Si solid-state detector manufacture 77−28917
etching of SiO_2, DryOx process using anhydrous HF 77−77606
field emitter electron beam exposure system for semiconductor fabrication 79−30624
film processing, electron beam scatt. and energy loss during processing 77−27930
fine pattern etching by RF sputtering *(Japanese)* 77−70196
free carrier profile measurement on thin-layers, fast current pulse MOS deep-depletion technique 78−80075
n-GaAs-Ge laser alloying to from ohmic contacts 80−58546
glassy passivation films on Si substrates, appl. of silicates to flaw detection 77−39745
high dose Sb ion implantation, buried layer appls. 80−88186
high pressure pyrogenic oxidation in the production environment 78−35547
history, solid state research to semiconductor electronics 80−68015
history and development in USSR, brief survey 78−54142
III-V nitride materials preparation, powder, thin film and volume crystals *(Czech)* 78−3037
III-V semiconductor based layered multielectronic systems, electronic process investig. survey *(Russian)* 80−107891
impact sound stressing, appl. to lifetime control in Si 77−85238
inert gas ion milling processes, etch-rate ratio of oxides to nonoxides, increase using halocarbon gases 80−93663
insulating coatings on Si, dissolution and corrosion in high temp. water and moisture 77−48564
insulating thin films on Si, instability phenomena, review 77−12037
integrated circuit, plasma-removal of polymeric layers 80−1851
interleaved glass layer prism for semiconductor mask testing 80−43425
ion beam, plasma and reactive ion etching 80−108621
ion implantation, semiconductor device processing 80−34031
ion implantation with controlled nonuniformity 80−100261
ion implanter, semiconductor device processing 80−31944
ion milling, string segment motion algorithm 80−71779
ionised-cluster beam deposition and epitaxy, for electronic device fabrication 78−11133
LAMEL activities *(Italian)* 80−60026
large monocrystal X-ray reflection/scanning and transmission topographic methods 80−96415
laser annealing, review and anal. 80−25741
laser annealing of ion-implanted defects, and other processing 80−55431
laser applications in materials processing, seminar, San Diego, CA, USA (Aug. 79) 80−90609
laser processing, bibliography 79−74028
light detectors, multicolour *(Czech)* 79−26126
LPCVD-type plasma-enhanced deposition system [for semiconductor wafer processing] 80−60791
magnetron sputtering of SiO_2, compared with CVD 77−77381
metal silicide growth on Si 78−10230
metal-semiconductor Schottky barrier junctions, fabrication aspects 80−88632
metal-semiconductor thermoelectric coolers, effects of contact resist. and dopant conc. 80−81481
microelectronics, conf., Calcutta India (Jul. 79) 80−96755
microstructure fabrication, using STEM and X-ray lithography and reactive ion etching, appl. 79−15844
microwave plasma etching of Si wafers, role of ions and neutral active species 80−3217
MNOS structures, high temp. H anneal, effects of fast surface states 79−38178
MOS capacitor, filament-metallised, effect of K contamination of W 79−51679
MOS structures, radiation-induced positive charge, thermal annealing 80−75648
MOSFET, near-ideal Si-SiO_2 interfaces using CVD, props. 80−80382
MOSFETs, short channel, fabrication by ion implantation and laser annealing 80−20312

semiconductor technology continued
multilayer ellipsometry, layer thickness and refr. index determination of layers 80−95121
narrow double-current-confinement channelled-substrate-planar laser fabrication by double etching 80−64073
negative photoresist, RF O_2 plasma stripping, visible spectra 77−40591
negative photoresists, RF O_2 plasma stripping, optical detect. systems 77−40585
ohmic contacts to semiconductor, meas. of contact resistance using transmission line model 80−70826
optoelectronic devices development 80−91902
oxidation, effect of chlorinated ambients 79−100278
oxidation, high press. techniques, review 79−100279
oxidation, oxidation-induced lattice defects, review *(Japanese)* 78−39931
oxidation with trichloroethylene additive to eliminate oxidation induced stacking faults 80−39118
oxide thickness measurement in monolithic ICs, scanning electron microscope appl. 79−30619
p-n junction struct., X-ray topography visualisation during prep. *(Russian)* 78−26386
packaging hermetically sealed, moisture calibration and anal. by gas mass spectrometry 80−90928
passivation films, advances in deposition processes, review 78−23620
phosphosilicate glass flow mechanism, and appl. in MOS devices 77−77393
photopile manufacture for terrestrial solar cells, review *(French)* 79−24895
photoprojection method of image formation of submicron patterns 78−71180
photoresist residual film on thermally oxidised Si, ellipsometric meas. 77−48266
planar technology, insulating thin film preparation and props. 78−10589
plasma chemistry, appl. to IC fabrication 79−79252
plasma etching, loading effect 77−90475
plasma etching, mech., review 79−83348
plasma etching, process development and monitoring via mass spectrometry 78−35546
plasma etching characts., effect of dark space in RF glow discharge, photoresist ashing characts. 79−15830
plasma etching methods for semicond. struct. and devices *(Slovak)* 80−40564
plasma etching techniques in semiconductor manufacture 79−20238
plasma processing for device fabrication 78−63602
plasmatron for semiconductor surface treatment *(Russian)* 79−77428
plate cutting by electron beam 78−21268
positive photoresist, formulation, photochem. props., teaching appls. 78−89284
production processes, vacuum technique problems *(German)* 80−86330
protection of GaAs, $Ga_{1-x}Al_xAs$ and $GaAs_{1-x}P_x$ by reactively sputtered AlN *(French)* 78−23849
purification, by electrodiffusion in mag. field, GaAs epitaxial film appl. 80−66409
resistivity measurement of thin square sample with square four-probe array 77−41654
RF plasma etching, optical emission obs. 77−51226
RF plasmas for semiconductor device processing, spectroscopic anal. 78−63589
sapphire, etching of arrays of orifices using Pt-Cr composite layer mask 80−3216
silicate glass film, etching characts. in CF_4 plasma 77−90474
silicate glasses, carbon tetrafluoride plasma etching characteristics 77−77616
solar array repair, adhesive bonding, and interconnector developments 79−96455
solar cell, fabrication process, Si single cryst. cells 79−61977
solar cell fabrication, laser-induced p-n junction formation 80−93880
solar cell fabrication, preliminary 'test case' manufacturing sequence for 50 cent/watt solar photovoltaic modules in 1986 80−55858
solar cell fabrication, Si wafer prep., anti-refl. coatings and metallisation, efficiency *(Spanish)* 80−72059
solar cells, degradation processes of electrophysical characts. during long-term operation 80−89617
solar cells, ultra-thin, for high-performance panel appl. 79−52938
solar grade Si economic commercial production, problems in cost reduction *(Spanish)* 80−72058
solar-cell grade Si prod., recent developments, low-cost processes *(Spanish)* 80−72061
solid state devices, conference, Montpellier, France (Sep. 78) 79−33333
spreading-resistance meas. for doping profile determ., preprocessing of data for resistivity calcs. 80−57265
sputtered insulator film contouring over substrate topography 77−8752
substrate, surface quality determ. by optical reflectance methods 78−43862
substrate surface, low loss electron and Auger images correl. 78−22944
superlattice structures of semiconductor thin films, laser appl. 80−100418
surface, AB etch reappraisal 78−6065
surface, RF etch sputtering under controlled atmosphere 77−44397
surface deformation meas. in manufacturing, interferometric method 78−32793
surface testing, interf. method with quarter-wavelength sensitivity 78−32870
thermoelastic two-layer cylinder deform., rel. to microelectronic device manufacture 79−41561
thin sample etching for electron microscope exam. 80−86272
V-groove multijunction solar cell 79−100519
VLSI multilayer metallisation interlayer dielectrics, CVD films 80−45235
wafer C impurity IR absorption spectrometry, thickness fringe elimination 80−55132
wafer defect level detection using variable temp. apparatus 79−88951
wafer deformation *(Japanese)* 78−43064
wafer diagnostics, using computer automated scanning low-energy electron probe 79−4214
wafer exposure camera, optical, step-and-repeat, with dark field automatic alignment 80−68283
wafer O interstitial IR absorption spectrometry, multiple reflection correction 80−55131
wafer probing, four-point sheet resistance correction factors for thin rectangular samples 77−82547

semiconductor technology continued
wafers, scribing and subsequent fracture 80−11743
water impurity conc., from MOS DC transfer characts. 78−2155
X-ray lithography using synchrotron radiation, resist sensitivity 80−62820
Al etching surfactant evaluation 77−77646
Al film on GaAs, plasma oxidation, AES and TEM 77−77621
Al pattern etching, reactive ion etching, by discharge impedance monitoring end-point determ. 79−83372
Al plasma etching, undercutting phenomena 80−97635
Al_2O_3 films for Si devices, surface and bulk elec. conduction obs. 77−43761
Ar purifier, portable, 0.3 m^3/h, design and appl. *(Polish)* 79−12781
As_2S_3, inorganic resist, optical monitoring of etching 79−52412
CdS, chemical polish for Cd and S faces 77−73355
CdS-CdTe solar cells fabrication, thin film *(Japanese)* 79−87992
CdS-Cu_2S heterojunction, pilot line production 78−2525
CdTe, surface layers formed by etchants, XPS meas. 78−44240
CdTe-CdS heterojunctions, growth by closed-tube chem. transport, elec. props. 80−60070
Cr films, photoresist film on reverse gas plasma etching 80−97634
Cr-Au film structure, on Si interdiffusion 77−39698
$Cu_{1-y}Ag_yInS_{2-x}Se_{2x}$, for solar photovoltaic cells 80−10982
Cu_2S-CdS integrated thin film solar cell generators, fabrication techniques 80−55857
Cu_2S-CdS solar cell, fabrication using solid state reaction 77−16498
Cu_xS-CdS solar cell improvement by Cu treatment and front contacting 79−61987
Cu_xS-CdS solar cell junction formation and open-circuit voltage 79−61986
GaAlAs injection DH laser and GaAs Schottky-gate FET, monolithic integration 80−58593
GaAs and related cpds., conf., Edinburgh, Scotland (Sep 1976) 78−3039
GaAs anodic oxide, quantitative chem. depth profiles 77−72799
n-GaAs, AuGe contact formation 78−76146
GaAs, chem. etched surface, Auger characterisation 77−25169
GaAs, device compatible anodic oxidation technique 78−44236
GaAs, epitaxial and metallic thin-films, anodic oxidation anal. 78−80673
GaAs, etching soln. system H_3PO_4-H_2O_2-H_2O for MESFET fabrication 78−11379
GaAs, impurity gettering by ion implantation damage 77−11579
GaAs, ion implantation, trends 80−39132
GaAs, laser-induced microscopic etching 80−76379
n-GaAs MIS structs., native oxide, effect on interface props. and removal by sputter etching 79−11228
GaAs, ohmic contact formation with thin film 77−8756
GaAs, polishing dislocation etch 78−6066
n-GaAs, preferential photoelectrochemical dissolution in Fe(III) based etches 78−7066
GaAs, thermal oxidation in wet and dry atm., 470-830°C 77−86204
GaAs wafer, H_3PO_4-H_2O_2-H_2O etching solution system and its kinetics 79−20229
GaAs wafers, for semicond. lasers, cleaving process 78−37915
GaAs:Cr,Se, ion-implanted, semi-insulating effects of Cr redistrib. on elec. characts. 80−59982
GaAs:Cr wafers, semi-insulating, surface degradation by heat treatment at 900°C 77−80820
GaAs:Zn, pulsed laser annealing, expt. 78−34828
GaAs-$Ga_xAl_{1-x}As$ CW stripe geometry laser fabrication and performance 77−38933
GaAs-GaAlAs heterostructure, GaAs preferential etching, using O_2 and CCl_2F_2 mixture 79−8373
GaAs-metal junctions, thermal stability improvement, with and without near noble metals 79−7143
GaAs(Sb), electrochemical sectioning and surface finishing 80−108611
$GaAs_{1-y}Sb_y$, organometallic VPE, use of trimethyl As and trimethyl Sb 80−45238
$Ga_{1-x}In_xAs$ organometallic VPE, use of trimethyl As and trimethyl Sb 80−45238
GaP, polishing dislocation etch 78−6066
Ge, microdefect distrib. due to dislocation injection, selective etching 78−2122
Ge surface, wetting by Sn, Pb rel. to cryst. orientation 78−43211
$Hg_{1-x}Cd_xTe$ IR detector technology 78−77989
$Hg_{1-x}Cd_xTe$ photodiodes, implanted n^+-p, improved performance using insulated field plates 80−52309
InP, laser-induced microscopic etching 80−76379
InP substrates, chem. etching by H_2O_2-H_2SO_4-H_2O soln. 80−35360
InP substrates, HCl etching speed and polarity obs., with aid of laser beams *(Slovak)* 78−56575
InP substrates preparation, etching and polishing in Br-methyl alcohol solution *(Slovak)* 78−56576
p-type InP/Langmuir film MIS diodes, characts. 80−80384
InSb, ion bombard. and defect annealing, n- and p-type cond. layer prod. 78−26606
p-InSb, low-resistivity n-type layer form. by laser pulse irrad. 77−69944
$LiNbO_3$-InSb amplifier production, role of protective films 78−95220
N_2 purifier appl., 2.5 m^3/h *(Polish)* 79−12782
Ni-Cr/Au films, interdiffusion processes and oxidation phenomena 80−59735
Si 80−44200
Si, (100) and (110), anisotropic etching 79−15827
Si, (100) and (110), anisotropic etching for fabrication of 3-D microstructures 79−15826
Si, amorphous, hydrogenated, recent advances 79−28103
Si, carrier lifetime degradation at room temp. 78−95301
Si, chem. etching, comp. selection, geometry effects 77−21299
Si, clean SiO_2 film prep., use of poly-Si oxidation tubes 78−39924
Si device metallisation, TiN and TaN as diffusion barriers 80−65304
Si device processing, viscous flow of SiO_2 above 960°C 77−39729
Si, dislocation generation in local oxidation 80−107245
Si epitaxial wafer, saucer pit microdefects reduction by intrinsic gettering 80−75450
Si etch rate uniformity in CF_4+4% O_2 plasma 80−40568
Si, etching characts. using reactive ion etching with tetrafluoromethane-Cl_2 gas mixture 80−104313
Si, gettering by ion damage, minority carrier lifetime and backscatt. study 80−100286
Si, HCl etching, effect of O_2 traces 79−91818
Si high-pressure oxidation process *(Japanese)* 79−29249
Si, hyperpure, large scale prod. and prep. *(German)* 78−95704

semiconductor technology continued
Si, ion implanted, scanning CW and pulsed laser annealing 80−92549
Si ion-implanted laser-annealed solar cells 80−93881
Si, joining and recrystallisation using thermomigration process 80−65298
Si material processing, point defect thermodynamics 78−6054
Si, microdefect distrib. due to dislocation injection, selective etching 78−2122
Si, microwave O^+ plasma, magnetoactive, for oxidation of Si 80−38831
Si, n- and p-type (100) wafers, oxidation induced stacking faults 77−32699
Si, near (111) slices, scratches made by diamond stylus 77−12726
Si, optical reflectance rel. to surface damage 79−14985
Si, oxidation, use of new high press. steam apparatus 77−63818
Si, oxidation in presence of Cl and Cl cpds. 78−53009
Si, oxidation of dry O_2, revised model 78−92373
Si oxidation rate constants and role of H_2O 78−7072
Si, oxidation without stacking fault form. 78−7062
Si, plasma etching in Freon plasma, for microelectronics appls. 80−3080
Si, plasma etching using microwave discharge 78−11361
Si, polycryst., charges at laser recrystallised poly Si/insulator interface 80−54789
Si, polycryst., physical-chemical properties *(Slovak)* 78−92196
Si polycrystalline films, characts. 80−80988
Si, porous layer, struct. and heat-treatment effect 79−1557
Si preparation, by SiO_2 reduction by C in plasma, thermodynamic anal. 77−40530
Si, process stress analysis by IR photoelastic meas. 78−11488
Si, process-induced in-plane distortion, correl. with wafer bowing 80−54579
Si processing technology, appls. of scanning CW lasers and electron beams 80−100932
Si production from rice husk ash for solar cells 79−62008
Si, purification technology for the development of low cost solar cells 80−50976
Si, reactive ion beam etching expts., selectivity, anisotropy 80−104308
Si single crysts., mech. polishing with reagent, activation energy effects *(Japanese)* 80−89379
Si solar cell design and fabrication for concentrated light 79−61995
Si solar cell production, Union Carbide Corporation Silane Process, cost analysis 80−21403
Si solar cells, low-cost fabrication processes *(Japanese)* 79−83600
Si solar cells, photovoltaic energy conversion efficiency, photoacoustic spectra 79−15178
Si, solar cells, prospects *(Italian)* 80−60024
Si, sputter cleaning using Ar^+ ions, temp. depend. of residual damage, 25 to 800°C 77−48558
Si, stacking-fault nuclei gettering by trichloroethylene oxidation 77−43226
Si, steam oxidation at any elevation, improved theoretical predictions 79−20230
Si surface, wetting by Pb, Sn, Ge in H_2+HCl 78−43210
Si, surface cleaning by pulsed laser irrad. 80−45173
Si surface formation during etching of thin thermally grown oxide layers, ellipsometric control *(Russian)* 80−104315
Si, surface treatment by the low-energy ions of plasma accelerators 80−97608
Si, technology and physics, review 80−34353
Si, thermal oxidation at 1200°C, effects of trichloroethylene addition 78−27660
Si, thermal oxidation in O_2-H_2O and O_2-Cl_2 mixtures 78−44239
Si thermal oxidation kinetics in O_2/HCl mixtures 77−77617
Si, V-grooves formed by etching, phosphosilicate glass bridge struct. 80−104312
Si wafers, Czochralski, gettering of surface and bulk impurities 78−64456
Si wafers, process-induced in-plane distortion and wafer bowing 79−11048
Si wafers, saw damage reduction in lubricant environment 80−108585
Si:Ga, gettering of Au and Cu during Ga diffusion 78−91350
Si:P implanted, multiscanning electron beam annealing 80−75242
Si-based technology for hemispherical laser fusion target fabrication 79−89495
Si-Si_3N_4 system, anodisation into SiO_2, change in electrophysical props. 78−2574
Si-SiO_2:B structure, AES meas. 77−39951
Si-SiO_2(SiN)(Si_3N_4) boundaries, thermal stresses, and cracking resist. of insulating films 78−63958
6H-SiC, dislocation etching 78−22721
SiN_x films, plasma enhanced CVD, props., meas. and interpretations 80−80987
SiN_x films, plasma-deposited, radial wafer-to-wafer uniformity 80−104073
SiN_x films plasma deposition, process and props. 80−80986
SiN_x, plasma deposited, H content meas. 78−63949
SiN_x, plasma deposited dielectric film, elec. props. 78−68103
Si_3N_4 film, CVD, etching in acidic fluoride media 78−39927
Si_3N_4 film, prep. by reaction of active N with SiI_4 vapour 77−24963
Si_3N_4 film, thermal oxidation rate and masking effect against Si oxidation 78−64749
Si_3N_4 films for Si devices, surface and bulk elec. conduction obs. 77−43761
Si_3N_4 on Si, optical monitoring of etching using grating 78−76775
Si_3N_4 ultra-thin film composites of FET wafers and devices, thickness determ. by microprobe technique 77−36397
Si_3N_4:Ge films, intrinsic stress rel. to deposition conditions, use as Si oxidation mask 80−39467
Si_3N_4(SiO_2) plasma etching, plasma processes involved in dry processing using CF_4 active etchant species 80−79581
SiO_2 film, 10-22 Å, on Si wafer, production 77−76690
SiO_2 film deposition from SiH_2Cl_2 on Si 77−77407
SiO_2 film growth technology *(Japanese)* 77−40381
SiO_2 films, bibliography 77−12038
SiO_2 films, produced by thermal oxidation of Si, control of oxide defects 77−20477
SiO_2, HF vapour phase etching, prod. viability for semicond. manufacturing and reaction model 80−81219
SiO_2 layer prod., by oxid. of silane 78−3038
SiO_2 layers, anodic oxidation growth on p-Si, transmission electron diffr. obs. 79−28241
SiO_2 layers, passivating, deposition by plasma decomp. in planar reactor 78−88430

semiconductor technology continued
SiO_2 MOS structures, removal of electron traps by RF annealing 80−44728
SiO_2, masking film in alkaline etching 80−71771
SiO_2 nonporous film, plasma deposition method, appl. to semicond. device manufacture *(Russian)* 80−16197
SiO_2 on Si, optical monitoring of etching using grating 78−76775
SiO_2, oxide growth in HCl-O_2 mixture, ellipsometric meas. 78−7073
SiO_2, plasma-chemical etching, spectroscopy 80−85243
SiO_2, reactive ion beam etching expts., selectivity, anisotropy 80−104308
SiO_2, reduction by RF induction plasma torch., Si form. 78−11186
SiO_2 relief, plasma etching, tapered wall prod. 80−97606
SiO_2 separation below 500°C, state and tendency of chemical gas phase separation *(German)* 80−100794
SiO_2 substrate reaction with thin metal films obs. 78−51851
SiO_2 thin films, radiation-induced trapping centres, rel. to MOS transistor technology 80−107804
SiO_2 ulra-thin film composites of FET wafers and devices, thickness determ. by microprobe technique 77−36397
SiO_2:B implanted, thin films, props. *(Polish)* 80−39692
TiP_2, synthesis and characts. 77−85953
WSi_2 film, FET gate electrode, oxidation mechanism, SiO_2 overlayer formation 78−76773
YAG laser trimmer for wafer level products 80−87428
ZnSe, hot-pressed powder LED fabrication and characts. 78−23639
ZnSe, low resistance ohmic contacts using In-Ga liquid alloy, LED fabrication appl. 80−70823

semiconductor thin films
for electronic conduction in crystalline and amorphous films, see "electronic conduction in crystalline semiconductor thin films" and "electrical conductivity of amorphous semiconductors and insulators", respectively see also amorphous semiconductors; semiconductor epitaxial layers
$A_{1-x}B_xC$, rapid localised non-destructive optical charact. of ternary layer *(French)* 77−62725
acoustic wave amplification with paramag. admixture under EPR conditions *(Russian)* 77−63266
amorphous, effect of ion bombardment on cond. *(Russian)* 80−49969
amorphous, hologram recording 77−88677
amorphous, ion bombardment effect on electronic props. 79−65125
amorphous, vac. evaporated, doping, transport and optical props. 80−49715
amorphous film formation by vacuum deposition review *(Japanese)* 77−66590
amorphous semiconductor, substantially doped, electronic props., review 79−87175
amorphous semiconductor film, density of localised band tail states, transient photoconductivity 77−15898
amorphous semiconductor film, laser induced nucleation, long wavelength instability 80−84126
amorphous thin films, crack networks of voids 78−2399
anodic passive films, semicond. props. 77−36003
anthracene, evaporated films, fluoresc. 77−85777
anthracene, high field effects and switching, local centres importance 79−73548
anthracene derivative, Langmuir-Blodgett multilayer film, semiconducting props., optical and elec. meas. 80−11122
anthracene film, effect of struct. on luminesc. quenching *(Russian)* 80−7411
anthracene film, electroabsorption spectra obs. 80−50301
anthracene-tetracene amorphous films, host-guest energy transfer 78−60505
band structure, appl. of extended rigorous cellular method 78−52055
bound states of electrons and optical phonons 78−39038
carrier redistribution in strong crossed elec. and mag. fields *(Russian)* 77−72927
carrier temperature and density self-oscills. near instability threshold 80−11118
CdS thin films, slow electron mean free path 79−99998
CdTe thin polycrystalline film for photoelectrochemical cell 78−23162
chalcogenide glass, drift and thermal diffusion of Au electrodes, α-particle backscatt. meas. 79−4434
chalcogenide glass, kinoform optical element prod. *(Russian)* 77−14670
chalcogenide glass, kinoform optical elements and integrated optics elements prod. 77−75634
chalcogenide glass, opt. inform. recording uses 77−75633
chalcogenide glass, prep. by laser evaporation, and characterisation 77−12533
chalcogenide glass, reversible photostructural change obs. in IR absorption spectra 78−10897
chalcogenide glass film as master for PVC copied holograms 77−23632
chalcogenide glass films, high field, short pulse cond. expt. 80−49751
chalcogenide glass films, photostructural changes, photodarkening 80−49121
chalcogenide glass films, threshold switching 80−96950
chalcogenide glass films nonlinear current voltage characts., Poole-Frenkel effect 80−7007
chalcogenide glass switching phenomena 77−39976
chalcogenide glass thin film, thermal diffusion of Au electrode layer, α-particle backscatt. obs. 78−10228
chalcogenide glasses, photoconductivity dependences applied elec. field 80−107857
chalcogenide glassy semiconductors, positive photorecording effect on layers *(Russian)* 79−59781
chalcogenide switching device, on-state behaviour and degradation effects 77−11967
chalcogenide vitreous films, photoinduced optical anisotropy, spectral responses 79−65948
chlorophyll-a, crystalline film, energy levels and carrier generation by photocond. and fluoresc. 77−16909
coated Mo tips characterised by atom probe FIM, atomic clusters, voids 80−33863
coating on piezoelectric, Bleustein-Gulyaev wave amplification 79−61309
cobalt phthalocyanine, sorption of O_2 and water, AES obs. 78−91531
condensed, on supercond. film, effect on T_c and residual resist. 78−47900
conference, Masnuy-St-Jean, Mons, Belgium, Oct. 1979 80−82570
conference, New York, USA (Oct. 79) 80−73093
confining substrate for micron thick liquid films, semicond. films 80−96722

semiconductor thin films continued
copper phthalocyanine, elec. transport phenomena, charge carrier conc. and current-voltage characts. 77−1421
copper phthalocyanine, photoelectrochem. behaviour on SnO_2 electrodes 80−15626
copper phthalocyanine film, electroconductivity, effect of adsorption 77−85356
Coulomb interaction depend. on film thickness, exciton binding energies *(Russian)* 79−78027
crystallisation, elec. cond. determ. model and its verification for Ge 77−20475
cubic semiconductor, polarisation of edge luminesc. arising from quantum size effect calc. 77−16390
current filamentation on switching, analytical theory 77−15922
CVD films for solar energy conversion 77−32531
cyclotron-phonon absorption singularities 77−51955
cytochrome c_3 film, anhydrous, elec. cond. 79−66439
degenerate semiconductor, film, with unlike surfaces, theory of kinetic effects *(Russian)* 79−51694
degenerate semiconductor film, quantized, screening of elec. field and Coulomb interaction in strong mag. fields 79−69611
degenerate semiconductor film, with different surfaces, transport effects in weak mag. fields 79−73607
deposition with periodically pulsed CO_2 laser, film characts. 79−28926
diamond, hard conducting C ion implanted layer, resistivity 77−15974
diodes, thin film glass based structures, surface electron states effect on switching *(Russian)* 80−107887
diphenanthra[4,5,6-abcd, 4,5,6-jklm]perylene, high photoresponse, O_2, N_2 and SF_6 effects 77−32036
dislocation superstructures and conduction electron kinetics *(Russian)* 79−19678
dispersive properties, effect of multilayer dielec. medium, anal. *(Russian)* 78−31004
dispersive transport, trap-limited model 78−6378
donor-acceptor pairs, polarisation of recomb. radiation in presence of quantum size effect 79−11462
effective electron mass determ. 77−1506
electric-field-induced anisotropy, differential carrier mobility tensor derivation 77−39973
electrodeless measurement of resist. and spherical curvature 79−49252
electroluminescent, activating impurity diffusion coeff. *(Russian)* 77−84995
electron-phonon interactions in quantizing mag. field 79−69610
energy spectrum in mag. field, size effect, calc. 80−70865
enhanced conductivity in plasma hydrogenated films, thermionic emission 80−70692
epitaxial layer surface As concentration meas. 79−95037
exciton complexes, form. and dissoc. 79−95343
exciton light absorption coefficient *(Russian)* 80−71504
exciton oscillator strength, EM wave-polariton propagation , reflective power *(Russian)* 79−99491
exciton polariton attenuation, spatial dispersion effect 80−20097
exciton-donor complex, neutral, dissoc. energy 77−55488
excitons, Bose-Einstein condensation 77−28127
external circuit current calc. 77−39972
Fabry-Perot nonlinear interferometer for optical pulse shaping 79−89945
ferrite-semiconductor film struct., cyclotron resonance in static elec. mag. fields 80−29624
ferroelectric properties, quantum size effect 80−97201
FeS_2, thin films, prep. and charact. 80−16178
field emission through semiconductor and dielectric layers on metal 77−12501
field-effect controlled, carrier mobilities and doping conc., Hall meas. in MISIM struct. 77−76975
films, amorphous, prep., struct., props., review, book contrib. 78−48321
free exciton polaritons, energy dissipation 79−95870
glassy-crystalline, with switching channel, electrothermal instability 80−15576
grain boundary and interdiffusion studies, AES and SIMS 79−77842
grain boundary barriers, sudden change in current 78−56246
heavily doped film, laser irradiation, spontaneously broken gauge symmetry 79−47531
heterojunction thin film solar cells, survey or semiconductor combinations 80−50974
HF conductivity of films with macroscopic surface defects, size depend. 77−89888
II-VI cpds., solar cell applic. role of thin film growth morphology and grain size 77−77377
II-VI semiconductor electroless film deposition with variable comp. and polymorphic structs. 79−95952
III-V nitride, preparation technology *(Czech)* 78−3037
III-V semiconductor based layered multielectronic systems, electronic process investig. survey *(Russian)* 80−107891
III-V semiconductor thin film prep. by low temp. CVD 80−60789
III-V semiconductors, film, sample preparation for TEM studies 78−14258
inhomogeneous, transverse magnetoresist., size effects 78−72293
inhomogeneous thin amorphous chalcogenide films, reversible switching, thermal stability criteria 80−70856
InP film, prep. by low press. reactive deposition process 79−24449
intraband light absorption by degenerate electron gas in semiconductor films and wires *(Russian)* 77−44077
ion beam milling, amomalous sputter yield behaviour 80−108624
ion beam uses in thin film analysis and technology *(Czech)* 77−47478
ion-implanted, laser pulse annealing, TEM and channelling study 80−100264
ionised-cluster beam deposition and epitaxy, for electronic device fabrication 78−11133
iron phthalocyanine film, electroconductivity, effect of adsorption 77−85356
IV-VI film technology, review 78−3034
IV-VI semiconductor electroless film deposition with variable comp. and polymorphic structs. 79−95952
IV-Vi semiconductor film, quantum efficiency 79−75596
Josephson contacts with semicond. layer, critical current *(Russian)* 79−99661
laminar piezodielectric-dimensionally quantised semiconductor film struct., acoustoelectronic effects 80−75607
laminated systems, two dimensional and surface plasmon mixing *(Russian)* 80−15466

semiconductor thin films continued
laser beam induced synergetic phenomena in impure semicond. 79−74021
laser crystallisation, for production of large grained sheets for solar cells 80−93570
laser radiation recording using anomalous photovoltage 77−37989
laser-induced transmittance oscills. and struct. phase transitions 79−87516
lattice parameter measurement method 78−59720
layer semiconductor system, theory of Hall effect 79−69589
lead phthalocyanine:O_2(I), Schottky barrier effect on AC current response 80−75623
light absorption by film with surface states under superhigh vac. *(Russian)* 78−72618
light absorption in film with impurity centres, quantum size effect 78−27274
magnesium phthalocyanine, depletion layer studies, temp. depend. of LF capacitance 80−65617
magnetoresistance four-probe method for free carrier density and mobility meas. 77−43626
many-valley semicond., electric field absorpt. coeff., self consistent film pot. determ. possibility 79−69612
many-valley semiconductor, light absorpt. 79−83043
microelectronics, conf., Calcutta India (Jul. 79) 80−96755
microelectronics and thin film components frontiers 80−73123
Mott exciton spectrum in mag. field 78−34780
multilayer semiconductor structure, current noise 80−20302
multilayer semiconductor structures, plasma-wave beams 80−49795
multilayer spreading resistance anal., high-speed implementation and expt. evaluation 79−4324
multilayer structure of semiconductor, dielectric and mag. film, constant EMF 79−69583
multilayer systems, film growth, spectroscopic ellipsometry, review 80−103603
multilayer thin film struct. thermoelec. props. 80−92964
multitarget sputtering using decoupled plasmas, appl. to semicond. alloys 77−12529
narrow band gap semiconducting alloy layers, electron-beam microzone refining, in space 78−35325
narrow gap semiconductor, boundary conditions, energy spectrum, and optical transitions 79−42614
oblique cut production by etching 80−104309
octaethylporphin in Al-Ag sandwich cell, electroluminesc. 77−59615
one- and two-dimensional periodic superstructures, possibility of formation 79−11044
optical absorptance calc. 77−90207
optical characterization 80−50352
optical coatings, photoacoustic spectroscopy study 80−64124
optical frequency mixing and detect. by interaction of radiation 77−75614
optical integrated circuits, SEM written gratings in chalcogenide films 79−32087
optical properties of polycrystalline semiconductor films, grain boundary effects 80−80890
organic, optical constant determination, by reflection and transmission, errors 77−16414
organic, Schrieffer effect 80−60118
organic films, heating, electrode barrier presence, polarisation and depolarisation currents obs. 80−49764
pentacene layers, photogeneration, charge carrier transport *(Russian)* 78−56181
phase relief hologram recording on semiconductor films *(Russian)* 78−50741
phonon spectrum under one-dimens. quantisation conditions 77−66007
photoconductor, thermal-density hysteresis 79−51631
photogalvanic effect calcs., electron mean free path, size effect 80−34487
photovoltaic and photodiffusion mechanisms responsible for anomalously high photovoltages 78−26910
photovoltaic convertor, heterojunction phenomena and interfacial defects, review 79−74523
photovoltaic solar energy, conference, Luxembourg (1977) 78−64106
phthalocyanine film, surface photovoltage, central ligand effect 79−78231
phthalocyanine films, metal-free, adsorbed o-chloranil effect on surface photovoltage 80−34485
phthalocyanine thin films, transient photocond. obs. technique, freq. depend. 77−76860
phthalocyanine-halogen complex, influence of halogen on elec. and optical props. *(Japanese)* 79−51586
piezoelectric, mobility of hot electrons 78−56247
piezoelectric, quantum acoustoelec. interaction, thickness depend. *(Russian)* 79−47126
piezoelectric, Rayleigh wave amplification, quantum theory approach 77−69158
piezoelectric, surface mode phonon amplification theory 78−34691
piezoelectric semiconductor film, quantum acoustoelectric interaction 79−15197
polar semiconductor crystalline thin films, surface vibr. states, IR absorpt. spectra obs. *(Russian)* 80−60606
polaron near-threshold spectrum 80−65471
poly-N-epoxypropylcarbazole layers, optical and photoelec. props. 77−39896
poly-N-vinylcarbazole, drift mobility of photocarriers, polymerisation method influence 77−76986
polyacetylene, and derivatives, thin polycryst. film, solar cell applic. 80−92899
polyacetylene pure and doped films, anisotropic optical properties 78−92137
polycrystalline film, photocond. probe studies 80−80326
polymer, in MSM struct., thermionic field emission from metal 79−1629
polymethine semiconducting films, surface photovoltage 80−70857
polynaphthol, trap depth and trapping cross section from TSC curves 79−51700
potential relief of ferroelectric substrate effect on props. 79−11235
preparation and characterization, review 78−2598
quantised, indirect interband absorption rel. to surface irregularity 78−39618
quantised, one-phonon light absorption 78−60527
quasistatic and helicon wave propagation 79−56338
p-quaterphenyl oriented layers, field depend. mobility 79−91169

semiconductor thin films continued
review *(Japanese)* 80−107936
sapphire film, substrate for Si, laser annealing non-thermal theory expt. test 80−89273
semiconductor film, size-quantised, EM wave absorpt. coeff. in coherent hypersonic wave field 80−29819
semiconductor thin films, ion implanted, optical and luminesc. props. 80−60699
sheet resistance meas. by four point probe technique *(Chinese)* 80−52262
a-Si:H_x structure, effect of H-Ar plasma contact on elec. props., and optical gap 80−34533
single crysts. and thin films, absorpt. edge temp. depend., gap energy changes 79−42991
size-quantised films with tilted valleys, two-photon absorpt. 79−95869
size-quantised thermomagnetic coeffs. *(Russian)* 78−56249
solar cells, low cost fabrication utilising polycryst. and amorphous thin films 80−50972
solar cells, semiconductors, direct gap 79−92075
solar cells, thin film, performance analysis employing loss minimisation of essential characteristics 80−45682
SOS films, carrier recomb. props., magnetosensitive method 79−38186
SOS films, impurity conc. meas. technique using C-V plots 77−11585
SOS films, surface recomb. profile and transport parameters 79−33357
SOS single crystal films, struct. and elec. props., review *(Japanese)* 77−63009
sound propagation, in strong EM wave field *(Russian)* 80−39483
space charge effects of semicond. coatings on metal substrate, on triboelec. charge exchange 80−54763
spectrochemical analysis of film on dielec. backing 80−66904
sphalerite materials, complex, spray pyrolysis 79−43574
spin relaxation due to electric fields 77−62928
sputtered films, optical props. and appls. 78−72623
sputtered layers, EPMA of inert gas content 80−3443
Stoneley wave amplification between two piezoelecs. separated by thin semicond. film 79−14998
structure, influence of laser beam 79−7761
sulphide black, on Al, solar selective coating, figure of merit 80−72082
superconductor-semiconductor contact amplification props. 79−7941
superlattice structures and properties 80−100418
surface resistivity calc. 78−91751
switching components, amorphous thin film chalcogenide semicond. *(French)* 77−72710
symposium, American Vacuum society, Chicago (Sep. 1976) 77−39722
TEM 90° cross-section and 1° angle-lap specimen prep. 80−71881
tetrabenzo-[a,cd,j,lm]perylene thin films, high photoresponse, O_2, N_2 and SF_6 effects 77−32036
tetracene, amorphous film, TSC meas., carrier traps 80−2496
tetracene, depletion layer studies, temp. depend. of LF capacitance 80−65617
tetracene, layers, photogeneration, charge carrier transport *(Russian)* 78−56181
tetracene, polycryst. film, thermoelec. absorpt. spectroscopy 79−61451
thin film heterostructure, energy spectrum study 80−70787
thin sandwich film photovoltaic analyzer for wavelength meas. in 2000-7000 Å range *(French)* 79−95441
transition metal complexes, dimethylglyoxymate films, prep. and physical props. 79−90923
transmission and reflection spectra, surface roughness effect 77−77310
transparent conducting coatings, book contrib. 78−10587
transparent conductors, figure of merit 77−1741
transverse conductivity due to scatt. by acoustic phonons in quantizing mag. field 78−2594
TTT film, hopping cond. AC and DC meas. and EPR 80−11111
TTT film, Schrieffer effect 80−60118
two-photon absorption, exciton effects *(Russian)* 80−40174
two-photon absorption, optically induced diffr. 77−7154
two-photon interband absorpt., quantum size effects 79−43054
uracil, far vacuum UV transmission spectrum 77−8671
US propagation in quantised elec. field *(Russian)* 80−60050
V-VI-VII complex ferroelec. semiconductor monocrystalline film production 79−78905
V-VI-VII ferroelectric semiconductor film growth, effect of artificial nucleation centres 79−11032
vacuum deposition *(Polish)* 79−47630
vacuum deposition methods *(Polish)* 79−56932
violanthrene-A film, amorphous and crystalline, carrier mobility differences 78−60125
wafer thickness meas., contactless SHF method 79−67264
Wannier-Mott exciton states *(Russian)* 78−79943
work function var. meas. using single pulses 77−76898
X-ray and electrical characteristics meas. chamber 78−86396
X-ray diffraction in thin cryst. with linear variation of lattice period 78−26373
zero gap semiconductor, thin layer, dielec. response 80−103635
ZnS:Mn,Cu, thin-film phosphors, LV DC electroluminescence 79−11472
a-Si:H, effect of H conc. on photovoltaic props. 79−99577
Ag (112) chalcopyrite films, lattice mismatch with (0001)CdS substrates 79−87012
Ag-Se system, formation of FCC thin films *(French)* 77−4267
$AgInS_2$, and $AgIn_5S_8$, spray pyrolysis, film struct., elec. and optical props. 80−71592
Ag_2O, film, photocond., annealing and time effects *(French)* 78−23135
Ag_2O film, prep. and effect of O_2, Ar and H_2 gases *(French)* 78−14637
Ag_2S film, vacuum deposition and struct. 77−73233
Ag_2S, oriented growth by vacuum evaporation 77−21028
Ag_3SbS_3 film prep. 77−52250
Ag_2Se thin film, switching and Ag movement, point contact technique 80−60107
Al-amorphous GeSe-Al junctions, electrical contact effects on properties *(German)* 80−93010
Al-As_2Se_3-Al, photographic process based on electrochem. reactions *(Russian)* 79−6213
Al-CdSe-Ag dry air stabilised struct., elec. cond. mechanism, breakdown phenomena 80−34527
$Al_{0.36}Ga_{0.64}As$, LPE films, Te-induced defects 78−43037
$Al_xGa_{1-x}As$, electron mobility illumination, compensation, space charge regions, carrier scatt. 80−70691
$Al_xGa_{1-x}As$ film, hot photoluminescence spectrum, polarisation depend. 78−31254
semiconductor thin films continued
p-$Al_xGa_{1-x}As$ film, variable-gap photo-EMF 80−65626
$Al_xGa_{1-x}As$, Raman spectroscopy, characterisation of thin films and heterostructures 78−76439
$Al_xIn_{1-x}Sb$, DC sputtering and struct. 78−52674
AlN film, oriented c-axis, low temp. deposition by reactive magnetron sputtering 80−76180
AlN films on glass substrate, prep. by reactive DC magnetron sputtering technique, c-axis orientation 80−89146
AlN, nonlinear optical susceptibility, SHG expts. 78−30012
AlN, on Si and Ge, growth struct. and props. 77−55468
AlSb, laser pulse annealing, induced nucleation, crystal growth 80−84966
AlSb, thin film growth on insulating substrates, by metal organics CVD 80−60786
As, amorphous, photoluminescence, bulk and sputtered thin films 80−25457
As amorphous films, interference enhanced Raman scatt. 80−50326
As:Ni(Ge)(S)(Se)(Te) film, amorphous, chemical modification of props. 80−49250
As-Ge-S(Se), glass films, photostruct. changes 77−85822
As-Ge-Se system, synthesis and phys. props. of amorphous layers 77−52252
As-S amorphous film, photo-induced optical changes, annealing effect 78−27345
As-S glassy film, photobrightening effect 80−11498
As-S semiconducting glass film holographic recording media *(Russian)* 77−10864
As-Se, amorphous film, kinetics of photo-induced processes *(Russian)* 79−69896
As-Se, glassy, photostimulated changes in microhardness 77−15723
As-Se amorphous film, density of upper valence band states, annealing effects, UPS obs. 80−29845
As-Se amorphous film, optical props. change under high-power light pulse action 79−47534
As-Se amorphous films, photo-induced changes in IR vibr. spectra 79−91514
As-Se and As_2S_3 films, electron-stimulated changes in optical props. and dissolution rate 80−29709
As-Se films, chalcogenide vitreous semiconductors, reversible photoinduced changes in optical, physicochem. and contact props. 79−24378
As-Se glass, photoinduced absorpt. changes 79−87519
As-Se system, chalcogenide vitreous semiconductors, darkened films, thermal and optical bleaching, light transmission obs. 80−50447
As-Se-Ge, amorphous film, relief-type hologram mode, hologram replication *(Japanese)* 78−78959
As-Se-Ge(-S), photostructural change in Urbach tail 80−76021
As-Se-S-Ge chalcogenide amorphous film, computer-generated holograms using electron beam irrad. 80−95846
As-Se-Te, laser induced crystn. kinetics 77−76317
As-Se(Te), laser-beam recordings by thermal creation of holes 80−35010
As-Se(Te)-Ge, fabrication of amorphous semicond. thin films with graded band struct. *(Japanese)* 77−55623
As-Te-Ge chalcogenide films, thermally induced transformations, TEM obs. 79−94917
As-Te-Si-Ge amorphous chalcogenide semiconductor, thin film interface, electrical charact. *(Korean)* 80−97014
As-Te-metal amorphous film, switching, memory effects 80−44677
AsGe amorphous film, far IR absorpt. spectra, refractive index 80−80785
$As_{2-x}S_{3+x}$, hydrogenated chalcogenide glasses, prep. by plasma decomposition 80−49735
As_2S_3, amorphous, laser radiation induced struct. changes, electron microdiffr. obs. 79−10874
As_2S_3, amorphous, opt. const. changes under illumination 77−77316
As_2S_3, amorphous film, light enhanced vaporisation, photolithographic process, photographic appls. 77−5949
As_2S_3, amorphous film, photodissolution of Ag, struct. changes 77−11815
As_2S_3, amorphous film, photooxidation, substrate depend. 78−64866
As_2S_3 amorphous films, photo-induced changes in IR spectrum 79−52033
As_2S_3, amorphous Raman scatt. investig. of irreversible thermostruct. transform. 77−48163
As_2S_3, amorphous thin films resonant Raman scattering 78−68505
As_2S_3 and As_4S_4 vapour-deposited films, valence states, thermal and photo-induced changes UPS study 80−93459
As_2S_3 chalcogenide glass films, photographic Ag photodoping to produce negative relief image 80−59490
As_2S_3, evaporated, elec. cond. mech. obs. *(Japanese)* 80−11028
As_2S_3, evaporated, switching effects 80−96952
As_2S_3 evaporated film, optical props., depend. on light exposure and heat cycling 78−68572
As_2S_3 film, amorphous, deposited at different temps., IR spectra 80−40102
As_2S_3 film, amorphous, photo-induced dynamical changes 80−66142
As_2S_3 film, hologram recording using total-internal-refl., polarisation depend. 80−106491
As_2S_3 film, optical recording, light scatt. enhancement due to coherence 80−97362
As_2S_3 films, amorphous, structural implications from Raman spectra of As_4S_4 polymorphs 79−61385
As_2S_3 films, kinetics of light-enhanced vaporisation rel. to photocond. 77−84919
As_2S_3, inorganic resist, optical monitoring of etching 79−52412
As_2S_3, on Ag, light activated reactive diffusion of metal into chalcogenide 77−55393
As_2S_3 thin films for integrated optics, photodetector elements, relief-type diffraction gratings 79−32094
As_2S_3 thin glassy films, hole drift mobility, interaction with deep localised levels 80−11117
As_2S_3:Ag film, Ag photodoping rate, localised struct. transform. effect, absorpt. meas. 77−31914
As_2S_3:Ag glassy films, optical transmission spectra, photodoping effect 80−66317
As_2S_3-Ag interface, photodissolution kinetics of Ag in amorphous films 77−15955
As_2S_3-Ag photosensitive film systems, hologram recording 78−1194
As_xS_{100-x} amorphous film, composition depend. of photo-induced refr. index changes 79−78644

semiconductor thin films continued
As_xS_{100-x} amorphous film, photoinduced changes in optical props. 80−50445
As_xS_{100-x} amorphous films, optical props. and photoinduced changes 80−60700
As_xS_{100-x}, chalcogenide glass, absorption in range of large optical densities *(Russian)* 80−11428
As_xS_y, bulk and vapour deposited films, comparison of struct., X-ray diffr. meas. 77−69195
As_xS_y vapour deposited film, struct. determ., X-ray and neutron diffr. correl. functions 79−60654
$(As_2S_3)_{0.55}(Sb_2S_3)_{0.45}$ vitreous film, dispersive charge transport, time-of-flight meas. 79−19594
$As_2S_3(Se_3)$ evaporated films, optical absorpt. and thermally induced effects 79−42989
$As_2S_3(Se_3)$ evaporated films, struct. and thermally induced effects 79−41963
$As_2S_3(Se_3)$, vitreous, photodecomp. and photostruct. changes 77−76318
$As_2S_3(Se_3)$:Ag glassy films, doped by photodiffusion and thermodiffusion, photocond. 80−29441
$As_{40}S_{25}Se_{25}Si_{10}$ glass, transient photoinduced absorpt. 77−40295
AsSe, light-induced light absorption changes 77−73181
$As_{2-x}Se_{2+x}$, hydrogenated chalcogenide glasses, prep. by plasma decomposition 80−49735
As_2Se_3, amorphous, hole emission defect states 80−49759
As_2Se_3 amorphous film, comp. ratio variation by annealing and laser irrad., ESCA meas. 79−99447
As_2Se_3 amorphous film, pulse hologram recording 79−55091
As_2Se_3 amorphous thin films, illumination-induced change in contact pot. 80−20251
As_2Se_3, AsSe and As_3Se_2 films, photostimulated changes in opt. and elec. props. 77−76979
a-As_2Se_3 film, metallic impurity effect on transport props. 80−49963
As_2Se_3 glassy films, current-voltage charact., temp. depend., SCL current 80−92902
As_2Se_3, photodarkening and photostructural effects, Raman, IR and NQR studies 80−16036
As_2Se_3, vacuum evaporation, composition of condensates 78−44012
As_2Se_3 vitreous films, crystn. stimulated by org. subst. and electrophotographic parameters 77−76319
As_2Se_3:Mn^{2+} film, reversible photostructural change, ESR obs. 77−32411
As_2Se_3-Ge glassy thin films, flash photoresponse 80−107863
As_2Se_3-HgSe double-layer system detector for temp. meas. 79−88952
As_2Se, vitreous, optical transparency, photostimulated changes *(Russian)* 79−65941
As_3Se_2 amorphous film, photocond., TSC, light-induced changes 80−49810
As_3Se_2 chalcogenide semicond. film, thermoptical transitions with photostructural transformations *(Russian)* 80−16016
$As_{60}Se_{40}$, amorphous films, spectral charact. of photodarkening 78−76494
As_7Se_3 amorphous films, thermal relax. processes determ. by optical props. 77−15716
$(As_2Se_3)_{1-x}(As_2Te_3)_x$ amorphous films, changes in optical props. under elec. fields and optical excitation 79−61455
$As_2Se_3(S_3)$, glassy film, photostructural effects, NQR study 80−49549
As_2Te_3, amorphous, defect and impurity states, hopping cond. obs. 80−54650
As_2Te_3 and As_2Te_3Ge, amorphous, AC cond. at low temps. 80−80269
$As_{0.3}Te_{0.48}Ge_{0.1}Si_{0.12}$, amorphous film, transient switching processes 78−84232
$AsTeS_x(Se_x)(Sb_x)(Bi_x)$, chalcogenide glass, thin film crystallisation 79−7758
$As2S_3$ amorphous chalcogenide film inorganic photoresists, holographic resolution evaluation 79−76629
Au-amorphous GeSe-Au junctions, electrical contact effects on properties *(German)* 80−93010
Au-Si thin film double layer, silicide form., electron diffr. study 80−80005
B, amorphous, elec. cond. in strong elec. field 77−11928
B amorphous film, interference enhanced Raman scatt. 80−50326
B:H amorphous CVD films, IR, visible, and near UV optical props. 80−50442
BN, high temp. reactive plasma deposition, struct., resist., and dielec. const. meas. 77−7988
BP film, high temp. thermoelec. power, scattering processes 80−80305
$(Ba_xSb_{1-x})TiO_3$, ferroelectric films, dielectric and semicond. props. 79−91388
$(Bi, Sb)_2Te_3$ solid soln., semiconductor film, oxidation, electrophysical props. 80−45407
Bi-Te thin thermoelectric films prep. by solid state reaction method 80−108361
BiI_3 film, exciton-phonon interaction, optical consts., Faraday effect., permitt. 80−59884
Bi_2O_3, transmission spectra of thin films 78−76440
$Bi_{1-x}Sb_x$, semiconductor film, X-ray diffraction in thin cryst. with linear variation of lattice period 78−26373
$(Bi_{0.25}Sb_{0.75})_2Te_3$, opt. props. of bulk and films 78−27206
$Bi_{0.5}Sb_{1.5}Te_3$ film, effect of struct. on thermal cond. 79−28257
$Bi_{2-x}Sb_xTe_3$, solid soln. film on mica substrate, effect of stresses on elec. cond. 78−51859
Bi_2Se_3, amorphous, charge transport at high fields *(Rumanian)* 79−60841
Bi_2Se_3, partly oriented, electron diffr. dynamic effects 77−7996
$Bi_{12}SiO_{20}$, photoelectric props., obs., UV illumination effects *(Russian)* 80−80313
$Bi_2TE_{3-x}Se_x$, solid solution films, prep. and props. 78−44013
Bi_2Te_3 film, effect of struct. on thermal cond. 79−28257
Bi_2Te_3-Sb_2Te_3 film, residual cond. 78−52110
BiTeI-SbTeI, solid solns., phase diagrams, photocond., elec. props. 79−38125
$Bi_{2/3}Te_{1-x}S_x$, single cryst. film, field effect mobility, peaked struct. 77−66207
$Bi_2Te_{3-x}Se_x$ films, surface band struct. and scatt. mechanism 80−34535
$Bi_2Te_{3-x}Se_x$ films, thermal cond. depend. on grain size, phonon-boundary scatt. 79−69304
C, amorphous, prepared by glow discharge method, elec. and optical props. 77−21036
C, amorphous, struct. and semicond. props. and heterojunction form. with single cryst. Si 80−25002

semiconductor thin films continued
C, amorphous elec., struct. and optical props. 77−20474
C, film, amorphous, two-dimensional variable range hopping cond. 80−10977
C:H amorphous films, elec. cond. and optical absorpt. 80−49723
C:H films, amorphous, elec. props., chem. modifications 80−84523
CaF_2-Ge(Si), cosputtered composite semiconductors, selective solar energy absorbers 79−56876
Cd chalcogenides, thin films, VPE, needle-like cryst. growth 80−80148
a-CdAs thin film fabrication for switching applications 78−2415
Cd_3As_2, amorphous and cryst., transmission spectra, 0.6-15 μm and band struct. 78−11013
Cd_3As_2 film, optical absorption edge 80−50450
Cd_3As_2 film on NaCl substrate, vacuum deposition, growth morphology, microstructure 80−75479
$CdCr_2S_4$ ferromag. semicond. film, props. 78−76175
$CdCr_2S_4$, ferromagnetic semiconductor films, prep. and props. *(Japanese)* 79−47308
$CdCr_2S_4$, polycrystalline films, mag. semicond., spinel-type, magneto-optical effects *(Japanese)* 79−47415
$CdCr_2Se_4$, energy structure, magnetooptic effects 80−71394
$CdCr_2Se_4$ films, mag. hysteresis, domain struct., mag. viscosity 80−25169
$CdCr_2Se_4$, mag. linear and circular dichroism and Faraday rot. 79−99966
CdF_2:Mn films, electroluminesc. meas. *(French)* 79−11471
CdF_2:NaF thin films, electroluminescence obs. at 77K *(French)* 80−80866
$CdGa_2S_4(Se_4)$, optical absorpt., and energy gaps 78−11012
$CdGa_2Te_4$, effect of thermal annealing on struct., optical absorpt. and photocond. 79−65342
$Cd_{0.96}Ga_2Te_{4.1}$, amorphous film crystallisation and conductivity switching 77−4459
$Cd_{0.96}Ga_2Te_{4.1}$, switching effect 77−43753
$Cd_{23}Ge_{12}As_{65}$, amorphous, threshold switching, expt. 80−49830
$(CdGeAs_2)_{1-x}D_x$ amorphous films, property control in common target sputtering, elec. cond. 80−7494
$CdGe(P_xAs_{1-x})_2$, glasses, static current-voltage characteristics *(Russian)* 77−15925
$Cd_{0.1}Hg_{0.9}Te$, correl. between structure and 1/f noise 78−39234
$Cd_xHg_{1-x}Te$, comp. determ. by electroreflection method 77−52708
$Cd_xHg_{1-x}Te$ films, growth by cathodic sputtering in Hg vapour plasma 80−97431
$Cd_xHg_{1-x}Te$, vac. evap. film struct. rel. to carrier scatt. 77−85116
CdI_2, ang. depend. electron energy loss meas. 79−95884
$CdIn_2S_4$ films, vac. deposited, struct. and photoelec. props. 79−87006
$CdIn_2S_4$, vacuum deposited, growth, struct., optical and photoelectronic props. 80−10831
CdO, aqueous-deposited films, struct. and electronic props. for solar cell appls. 80−100797
CdO, electrophysical properties *(Russian)* 77−63008
CdO, magnetoresistance, temp. depend. of degenerate, narrow and broad samples 78−95306
CdO-P_2O_5 glass, thin film, elec. cond., high and low fields 80−80427
CdO-SnO_2 film, DC sputtering prep., visible and near IR transmission, resist. 78−88049
CdO-SnO_2 film, prep. by RF sputtering, elec. cond. and transparency 80−7492
Cd(S, Se) film grown on InP substrate, mismatch dislocations and lattice distortion, dangling bond density 80−84406
CdS, aqueous-deposited films, struct. and electronic props. for solar cell appls. 80−100797
CdS, chem. sprayed film, struct. and morphology 78−72020
CdS, chem. sprayed film growth using centrifugal disc atomiser 78−92189
CdS, chemically sprayed film, prod. by centrifugal disk atomizer, struct. 79−65343
CdS, cryst. and electronic surface struct., stimulated recrystn. effects 79−78151
CdS, dark cond., negative temp. depend. 78−47892
CdS, deposition onto hot substances, vapour phase method 78−95694
CdS, diffusion of Cu, 20 to 200°C *(French)* 80−15424
CdS, effect of heat treatment on photosensitivity *(Japanese)* 78−39237
CdS, electrocrystallisation of films on Cd 78−72014
CdS, electrolessly deposited, annealing effect on optical spectra 80−2884
CdS, epitaxial film, conductivity control by S vacancy form., light modulation appls. 77−4455
CdS evaporated films, growth rate and resist. determ., in situ meas. technique 79−77940
CdS evaporated films, O chemisorpt. kinetics, effects on elec. cond. 78−6464
CdS, evaporated forms n-type layer, substrate ordinary glass with silver layers 78−2525
CdS, exciton exhibiting spatial dispersion, reflectivity, polariton standing-wave struct. 79−4865
CdS fabrication for greatest conductivity for $Cu_{2-x}S$-CdS solar cell *(Korean)* 79−60916
CdS film, anomalous noise rel. to photomemory effect 77−20374
CdS film, chemically sprayed, elec. and photocond. props. 78−34913
CdS film, crystallinity and optical props., effect of cation-anion ratio 77−76689
CdS film, double-layered polycrystalline, on $LiNbO_3$ substrate, fabrication and props. rel. to SAW appl. 78−64480
CdS film, frozen-in conductivity, nature of recomb. barriers 79−56245
CdS film, Hall effect meas. 79−65570
CdS film, polycrystalline, photosensitive, struct., pseudoreplica method, using electron microscopy and microdiffr. 79−15030
CdS film, precipitation from solns., form. charact. 79−11524
CdS film, prep. by hot wall technique, morphology and semicond. props. 79−95292
CdS film, second harmonic generation by transverse acoustic wave 77−51782
CdS film, strain-induced modulation of photoconductivity 79−24009
CdS film, surface energy levels, thermally stimulated contact pot. difference method 79−99601
CdS, film, surface struct. and elec. props. 80−34531
n-CdS film, transient photoconductivity effects *(French)* 78−87994
CdS film and heterojunctions, grain boundary and interdiffusion studies, AES and SIMS 79−77842
CdS, film electrolytically deposited, surface and bulk photocond. props. 78−60154

semiconductor thin films continued
CdS film growth, with smooth surfaces through boundary layers 79−28244
CdS, film prep. from aqueous soln. of thiourea 77−8767
CdS film solar cell yield rel. to crystallite column statistics 79−62005
CdS film spray fabrication, physical props., Cu_2S-CdS solar cell applications *(French)* 80−60113
CdS, film with high photocond. and good reproducibility, prep. by chemical deposition 79−66019
CdS films, chem. deposited, growth kinetics and polymorphism 80−75463
CdS films, chemically deposited, phase comp. and photoelec. props. 77−40394
CdS films, from thermal decomp. of organometallics, growth kinetics and struct. 79−78895
CdS films, growth, residual cond., inclusions 78−43492
CdS, films, photovoltaic effect in wedge shaped film 79−56331
CdS films, precip. from soln., phase comp. change during annealing in air at 200-600°C 80−15393
CdS films, prep. by reactive pulverisation, chemical, crystallographic and electronic props. *(French)* 80−60112
CdS films, vac. evaporation from CdS.Cr_2O_3 system, photoelec. props. 78−80074
CdS, for solar cells, struct. and elec. props., thickness depend. 78−72289
CdS, granulated films, optical reson. 79−4863
CdS, growth and evaluation for fabrication of high performance photovoltaic solar cells 80−93501
CdS, growth by chem. bath deposition, photocond. props. 77−59703
CdS, inhomogeneities responsible for residual cond., microinclusions 77−28269
CdS layers, by vacuum evaporation, formation mechanism of preferred orientation 79−56094
CdS optical waveguide polariser 80−33180
CdS photoanode, for photovoltaic cells, prep. and charact. 78−14818
n-CdS, photocond. film, phase memory effect and deep levels 79−82556
CdS photosensitive film production from chelated metallo-organic compounds *(Russian)* 80−49813
CdS, piezoelec. polycryst. film layer struct., acoustic harmonic generation 77−89812
CdS, polycryst., optical spectra, 0.5-6.5 eV 80−55212
CdS, polycryst. films, microstruct. and X-ray cond. 79−56336
CdS polycrystalline film, pot. barrier at grain boundaries from Hall effect *(Russian)* 77−32094
CdS polycrystalline layers, electron trapping depend. on preparation conditions 79−78232
CdS polycrystalline thin-film liq. junction photovolt. cell 80−50988
CdS, polycrystn. films, recrystn. accompanying annealing *(Russian)* 80−20948
CdS, pure and Al doped vacuum deposited film, photoelectric props. and optical absorption 78−60162
CdS sintered film, photolum. and recomb. photocurrent noise spectra 78−6743
CdS, sintered film, solar cell *(Chinese)* 79−74517
CdS solar photovoltaic panels, deposited by spray pyrolysis, film and junction structure studies 80−45689
CdS spray pyrolysis film prep. and characterisation 78−64492
CdS sprayed film, heat treatment effect on props. 79−7916
CdS sprayed film, prep., optical props., struct. and comp. 79−78875
CdS sprayed films, elect. and optical props. 78−39241
CdS sprayed layers for solar cell prod. *(French)* 79−24901
CdS sprayed thin films for CdS-Cu_2S heterojunction solar cells 79−61988
CdS sputtered film, photocond. props. 78−10586
CdS, sputtered film, Rayleigh wave propag. *(French)* 77−62727
CdS, surface states, surface photovoltage spectroscopy meas. 77−1504
CdS, surface stoichiometry, vapour deposition 78−2956
CdS, thermal desorption of O_2, photopot. and surface pot. changes 77−11795
CdS thin film solar cell fabrication, HCl etching 80−81474
CdS thin-film Lamb wave delay line characteristics and strain effects 77−31185
CdS thin-film polycrystalline solar cell development 79−61993
CdS vacuum evaporated film photoconductivity and In doping effects *(Japanese)* 79−87174
CdS:Ag, vacuum deposited, recrystn. by H_2S heat treatment 80−34328
CdS:Bi film, implantation and post annealing, superlinearity 78−52028
CdS:Bi film, spectral response charact. 78−2512
CdS:Cu, dynamic quenching of photocapacitance, deep levels obs. 77−85175
CdS:Cu, In, Ga, spray deposited, struct., X-ray obs. 78−71713
CdS:Cu,Cl, photocond., applied voltage freq. effect on props. 80−39635
CdS:Cu films IR quenching of photocapacitance, deep level detection 79−56258
CdS:$CuCl_2$, sintered film, dopant conc. effects on carrier mobility 78−2484
CdS:Cu(Cl), thin layer, electron pulse induced cond. relax. 80−2501
CdS:Cu(Cl) polycrystalline films with residual conduction, kinetic phenomena *(Russian)* 77−15981
CdS:In, flash evaporated, prep. and elec. props. 80−20792
CdS:In, high cond., high transmittance, growth by evaporation method, and characterisation 77−77386
CdS:In, vacuum deposited, growth, elec. and optical props. 79−51460
CdS:Li, chemical bath deposited, photocond. and optical props. 80−2426
CdS:Li film, optical props. 80−2886
CdS:Li film, photocond., effects of annealing, S vacancies, and O_2 adsorption 78−34854
CdS:Mn, vacuum deposited film, Mn migration, EPR and X-ray study 80−65411
n-CdS/p-$ZnIn_2Se_4$ thin film solar cell, photovoltaic props. 80−89628
CdS-CdTe sintered film, prep. and photocond. props. 77−28220
CdS-CdTe thin film photoresistors, optimum photoelec. performance *(German)* 79−60941
CdS-Cu_2S, thin film heterojunction, dark J-V charact. and heat treatment 79−56294
CdS-Cu_2S junctions, carrier trap density, deep level defects 80−107801
CdS-Cu_xS heterojunctions produced by RF sputtering, for thin film solar cells 79−100053
CdS-Cu_xS solar cells, screen printed, prep. and photovoltaic props. 80−40863
CdS-CuI film heterojunction photocells, prep., photoelec. props. 78−80044
semiconductor thin films continued
$CdS_{1-x}Se_x$ film, resonance between Se atom dipole vibr. and interference modes, IR spectra obs. *(Russian)* 80−2888
CdS_xSe_{1-x}, flash evaporated, prep. and elec. props. 80−20792
CdS_xSe_{1-x} photosensitive films, prep., props., and use for photodetectors 80−55298
CdS_xSe_{1-x} solid soln. film by spray pyrolysis 77−81214
CdS_xSe_{1-x} triode cathode sputtered films, electrophysical props. *(Russian)* 79−42642
CdS_xSe_{1-x}, triode sputtered films, photoelec. props. *(Russian)* 79−15179
CdS(Se)(Te), vacuum condensed, growth and struct., HEED obs. 80−29292
CdS(Se)(Te), vacuum deposited film, orientation axis tilt rel. to vapour angle of incidence 80−88456
CdSb, monocrystalline film, prep., elec. props. 79−43159
CdSe, as-deposited and recrystallised, struct. and fund. optical absorpt. 77−1753
CdSe, chemically sprayed thin films as photoanode in photoelectrochem. cells, power charact. meas. 80−85293
CdSe, comp. and evap. kinetics on vacuum heating, effects on deposited film charact. 77−85940
CdSe, conductivity instability when exposed to the atmosphere 77−15980
CdSe electrochem. photovoltaic cells, effect of thin film electrode prep. and conc. on efficiency 80−55847
CdSe film, current noise due to thermal field ionisation 79−91110
CdSe film, effect of growth conditions on electrophysical properties 78−44024
CdSe film photoanodes for electrochem. photovoltaic cells, fabrication and evaluation 80−76641
CdSe film polycryst., thermal diffusion of Cr, 240-400°C 80−80001
CdSe films, effect of annealing on resistivity and charge carrier mobility 77−8209
CdSe films, growth kinetics and cryst. struct. during vacuum condensation 80−2305
CdSe films, solar energy conversion using electrodeposited films for photoelectrochemical cell 80−94093
p-CdSe layers, ion implantation prep., elec. props. 79−51699
CdSe, oriented single-crystal films, edge luminescence at high excitation levels 77−1720
CdSe, photocond. film, plasma reson., IR refl. obs. 80−11037
CdSe, photodetector, limiting sensitivity 79−63309
CdSe, photoelectron spectroscopy 78−2551
CdSe photosensitive film production from chelated metallo-organic compounds *(Russian)* 80−49813
CdSe, polycryst. film, photocapacitance, inductive effect and US oscills. *(Russian)* 77−8142
CdSe, polycrystalline, for solar energy convertors 80−93870
CdSe, stimulated recrystallisation 77−4272
CdSe, struct. props., influence of O_2 partial press. and substrate temp. during vapour deposition 77−39751
CdSe thin film transistor and MISM struct., effect of annealing on electron mobility and conc. 79−78198
CdSe thin film transistor on Cr substrate, cryst. struct., substrate defect effects 80−70563
CdSe, thin films, exciton piezotransmission 79−24380
CdSe:Cu surface layer of CdSe, microstruct., photoelec. props. 78−43221
CdSe-$LiNbO_3$ structure, electroacoustic effects and signal convolution 80−10098
$CdSe_xTe_{1-x}$ polycrystalline, deposition and physical props. 77−4741
$CdSe_xTe_{1-x}$, triode sputtered films, photoelec. props. *(Russian)* 79−15179
$CdSe_yTe_{1-y}$ triode cathode sputtered films, electrophysical props. *(Russian)* 79−42642
$CdSiAs_2$ chalcopyrite photovoltaic material 79−74526
$CdSn_xO_y$, DC reactively sputtered film, elec. and optical props. 79−87022
Cd_2SnO_4, film, spinel struct., X-ray diffr. study 78−75644
Cd_2SnO_4, RF sputtered from powder targets, props. 77−43759
CdTe, applications review 77−72894
n-CdTe, deep trapping levels in high resistivity films 77−72930
CdTe, film, anomalous-photovoltage, current-voltage charact. 79−69549
CdTe film, cathode sputtered, chemical composition and struct. 78−84100
CdTe film, excitation by H of anomalously high voltage *(Russian)* 78−60235
CdTe film, exciton spectra, press. and temp. depend. 80−80886
CdTe film, photogenerated carrier transport props. 80−88590
CdTe film, photopolarisation 80−25286
CdTe, film, theoretical models of impurity levels 79−82557
CdTe films, structural imperfections depend. on crystn. temp. 79−90661
n-CdTe films, uniform trap distrib., transient photocond. effects 79−28423
CdTe, growth on Te substrate by solid-state reaction 79−95287
CdTe, hexagonal film, effective birefringence 80−16004
CdTe layer deposition by ionised cluster beam technique 77−48351
n-CdTe layers, growth and characterisation, heterojunctions and Schottky barriers fabrication *(German)* 80−89151
CdTe layers, on CdS substrate, cryst. perfection and defects, X-ray diffr. obs. 79−56081
CdTe, low resist., prep. by multi-source evaporation method, and characterisation 80−25582
CdTe, obliquely deposited layers with reduced resist., photovoltaic props. and Cd doping effects 77−43755
CdTe single-crystal film, switching and memory effects 78−76174
CdTe, sputtered film, electrode effects in AC charact. from equivalence impedance meas. of metal-CdTe-Al struct. 79−82686
CdTe sputtered films, deposition conditions effects on struct. and props. 77−43452
CdTe sputtered films, struct., photocond., and trap distrib. 80−29489
CdTe, switching obs. in sandwich structures 77−43752
CdTe, thin film, stopping power for protons and alpha particles, proton energy straggle values 77−89489
CdTe thin film on ferroelectric TGS, influence of polarisation reversal on elec. cond. 80−65720
CdTe:Ag, with microscopic p-n junction, photopolarisation in anomalous photovoltage 79−11175
CdTe:Ag film, photoelectret effect *(Russian)* 79−28676

semiconductor thin films continued
CdTe:Cu films, impurity behaviour, Hall mobility and hole density meas. 80−80420
CdTe-Te film, prep. by combined hot-wall-flash evaporation method, and characterisation 80−55296
$CdTe_{1-x}Se_x$ solid solution films, prep., struct., and photocond. 80−54541
CdZnS, growth and evaluation for fabrication of high performance photovoltaic solar cells 80−93501
$Cd_{1-x}Zn_xS$ 10 μm film optical and electrical characterisation *(French)* 78−64153
$Cd_{1-x}Zn_xS$, electro-optical multilayer film, for data storage and display 78−71176
$Cd_{1-x}Zn_xS$, RF sputtered electro-optical film for data storage and display 78−83047
$Cd_{1-x}Zn_xS$ reactively sputtered phtoconductive films for high field applications *(German)* 78−39154
$Cd_{1-x}Zn_xS$ solar cell thin films, microprobe characterisation *(French)* 80−61349
$Cd_{1-x}Zn_xS$, spray deposited, for low cost solar cells 79−7915
$Cd_{1-x}Zn_xS$, technical data, for low cost solar cell 79−48127
$Cd_{1-x}Zn_xS$, use of parallel and monochromatic beams for comp. determ. by X-ray fluorescence 79−48000
Cds, doping and recrystn. effect on photocurrent relax. time 77−4409
Cds film on metal substrate, resistivity 79−95522
$Ci(Ga_xIn_{1-x})(S_ySe_{1-y})_2$, spray pyrolysis 79−70004
Cs_3Sb vacuum deposited photoemitter, XPS study 80−89122
Cu, (112) chalcopyrite films, lattice mismatch with (0001)CdS substrates 79−87012
Cu-S, thin film, phase formation conditions *(Russian)* 79−56078
Cu-Sb-S-I amorphous film formation and stimulated crystallisation, electrophysial props. *(Russian)* 78−30838
CuBr, exciton absorpt. band shape, dielectric const. real part derivatives *(Russian)* 80−25413
CuBr(I), reflectance and thermoreflectance spectra, electronic struct. 80−71444
CuCl film, exciton absorption bands *(Russian)* 79−51985
CuCl film tunnel conductivity *(Russian)* 79−51726
$CuGaSe_2$ film, optical props. near and above fundamental absorption edge 78−35215
$CuGaSe_2$, film, spray pyrolysis prod. 79−95953
CuGaTe, flash evaporated, growth and optical props. 79−95296
$CuGaTe_2$, refr. indices meas. 80−93259
$CuIn_{0.7}Ga_{0.3}Se_2$ epitaxial layers, on GaAs substrates, struct. and elec. props. 80−107670
$CuInS_2$ films prod. by RF sputtered Cu-In films exposure to H_2S 79−95926
$CuInS_2$ single phase thin film prep. by flash evaporation 80−100796
$CuInS_2(Se_2)$, film, spray pyrolysis prod. 79−95953
$CuInS_2(Se_2)$ films and heterojunctions, grain boundary and interdiffusion studies, AES and SIMS 79−77842
$CuInS_2(Se_2)$, vacuum-deposited, absorpt. coeff. 78−72621
$CuIn(S_xSe_{1-x})_2$, spray pyrolysis 79−70004
$CuInS_2(Se_2)(Te_2)$, electron and X-ray diffr. 77−11819
$CuInS_2(Se_2)(Te_2)$, thin films and photovoltaic devices, AES evaluation 78−67928
$CuInSe_2$ amorphous thin film, flash evaporation, struct., stoichiometry 80−89150
$CuInSe_2$, evaporation source temp. effect, on comp. 80−39478
p-$CuInSe_2$ film, prep. from vac. evaporation of $CuInSe_2$, optical and elec. props. 79−82697
$CuInSe_2$ polycrystalline thin film anomalous photovoltaic effect *(German)* 78−68102
$CuInSe_2$, refr. indices meas. 80−93259
$CuInSe_2$ semicond. films, optical props., 1-3 eV 78−27346
$CuInSe_2$, spray pyrolysis 79−70004
$CuInSe_2$ thin film fabrication by RF-sputtering for solar cell appls. 80−100786
$CuInSe_2$ thin films, prep. by spray pyrolysis, struct., elect. and optical props. for solar cell appls. 80−100781
$CuInTe_2$ epitaxial layers, on GaAs, growth and props. 80−108359
$CuInTe_2$, refr. indices meas. 80−93259
$CuInTe_2$, vac. deposited film, growth, struct. and elec. characts. 77−69995
CuO, on Al or Cu, solar selective coating, figure of merit 80−72082
Cu_2O, reactively sputtered, photovoltaic props. rel. to solar cell applic. 79−7914
Cu_2O, reactively-sputtered, phase comp., resist. and optical consts. 79−95534
Cu_xO, growth by anodisation, switching characts. 77−55898
Cu_2S, deposited by cylindrical magnetron reactive sputtering, for solar cell appl. 79−11258
Cu_2S films, prpe. methods, appl. to Cu_2S-CdS solar cells 80−80980
Cu_2S, for CdS/Cu_2S photovoltaic devices, formation and props. 79−11257
Cu_2S layer spray preparation and CuCl-thiourea complex formation 78−64471
Cu_2S, on Cu, solar selective coating, figure of merit 80−72082
Cu_2S, on rough $Zn_xCd_{1-x}S$ substrate, film substrate lattice mismatch calcs. 78−43263
Cu_2S, optical and calorimetric meas. of thin films for Cu_2S-CdS solar cells 80−55863
Cu_2S, polycryst. thin films, struct., optical and elect. props. for solar energy appl. 80−10837
Cu_2S stoichiometric thin films for solar cells 79−61991
Cu_2S-CdS film junction formation by dry-barrier process 78−64109
Cu_2S-CdS heterojunction photocell, props., manufacture 77−51806
Cu_2S-CdS integrated thin film solar cell generators, fabrication techniques 80−55857
Cu_2S-CdS solar cell fabrication by magnetron reactive sputtering deposition 80−61363
Cu_2S-CdS solar cells, prep. and stoichiometric control of Cu_2S film 78−2560
Cu_2S-CdS solar cells, thin film fabrication processes and conduction mechanism, review 79−74522
Cu_2S-CdS solar photopiles, tunnel conduction mechanism *(French)* 79−29480
Cu_2S-CdS thin film planar junction devices, quantitative photon loss anal. 80−61362
Cu_2S-CdS thin film solar cells, Cu_2S layer separation, struct. 79−95282
Cu_2S-CdS thin film solar cell fabrication by electrophoresis 80−55862
semiconductor thin films continued
Cu_2S-$Zn_xCd_{1-x}S$ solar cells, thin film photovoltaic solar energy conversion 80−61379
$Cu_{2-\delta}S$, thin films, determ. of stoichiometry from optical props. 79−60656
$Cu_{2-x}S$ films, vacuum deposited, electrical conduction and phase transitions 78−84332
$Cu_{2-x}S$ on CdS, low temp. growth, AES obs. 79−28924
$Cu_{2-x}S$/CdS heterostructures, heat treated, capacitance voltage meas. anal. 80−20292
$Cu_{2-x}S$-CdS fabrication for greatest conductivity for $Cu_{2-x}S$-CdS solar cell *(Korean)* 79−60916
Cu_xS chalcocite, solar cell fabrication appl., characts. 78−39240
Cu_xS, deposited on Si and CdS, props. rel. to solar cell applic. 79−15240
Cu_xS evaporated layer growth in vacuum, compositional and optical characterisation, solar cell appls. 80−97437
Cu_xS evaporated thin films, composition, prep. and characts. 80−25569
Cu_xS films, magnetron reactive sputtering deposition and elec. props. 79−78884
Cu_xS, layers produced by reactive RF sputtering, struct., elec. and optical props. 79−90908
Cu_xS, on CdS, electron diffr. obs. of phases 78−51847
Cu_xS, reactively sputtered, photovoltaic props. 79−11256
Cu_xS, thermally induced changes, and effect on CdS-Cu_xS solar-cell response 77−8181
Cu_xS/CdS, sequential evaporation, for solar cell applic. 80−93902
$Cu_{2-x}Te$-CdSe heterojunction, elec. and opt. props. *(Korean)* 77−51811
Er_2Te_3, films, prep., elec. props. 78−43494
EuO, light scatt. from spin waves and magneto-optic hysteresis meas. 80−97244
EuO, nonstoichiometric film with excess EU, optical, magneto-optical and elec. props. 79−8204
EuO nonstoichiometric film, ESR spectra and exchange interaction 80−93176
EuO, rotation of polarisation plane in very high mag. field 78−92054
$EuO_{1-\delta}$ films, Faraday effect dispersion rel. to electronic struct., visible and IR spectra 80−45162
EuS, anisotropic growth on amorphous substrate 77−12547
EuS, ferromag. semicond. film, Hanle effect, optical orientation time consts. meas. 77−40214
EuS, film, intrinsic demagnetising fields 78−10735
EuS films, ferromag., optical spectra and light scatt. from spin waves 80−16116
EuS, light scatt. from spin waves and magneto-optic hysteresis meas. 80−97244
EuS, struct., elec. and opt. prop. changes during annealing in air 77−7983
EuS, thermoreflectance spectra below Curie temp. 77−66550
FeO_x, anodic passive film on Fe, semicond. props. 77−36003
α-Fe_2O_3, photochem. props. of sintered and doped samples for solar photoelectrochem. cell appls. 80−89651
Fe_xO_y thermal oxide film on Fe, capacitance, temp. and freq. depend., in aq. electrolyte soln. 80−54776
$Fe(OH)_3$ thin films, elec. cond. var. with temp., amorphous struct. 80−75566
GaAS, photoluminescence in polycrystalline samples at 5K, possible solar cell material 79−99929
$Ga_{1-x}Al_xAs$ layer form. on GaAs during dissolution in Ga-Al-As soln. 80−10799
$Ga_xAl_{1-x}N$ film, growth and props. 78−39702
GaAs (100), VPE, role of Cl, LEED, RHEED, and AES obs. 77−1327
GaAs, amorphous, composition, study by nondispersive X-ray anal. *(French)* 79−8457
GaAs, amorphous, switching obs. 79−11190
GaAs amorphous film, EXAFS, optical and elec. props. 80−49547
GaAs amorphous film, effective medium theory and freq. depend of conductivity 79−24090
GaAs amorphous film/cryst. junctions, optical and elec. props. 79−99611
GaAs, amorphous layers, ion-implanted, low-temp. epitaxial regrowth 80−92790
GaAs, amorphous sputtered films, hydrogenated, photoinduced optical absorpt. 80−50362
GaAs anodic oxide system, multiple angle incidence ellipsometry, meas. at λ=632.8 nm 79−63294
GaAs base laminated epitaxial struct., surface plasmon phonon polaritons *(Russian)* 80−59905
GaAs, CVD on W coated graphite, characterisation, and Schottky barrier solar cell characts. 79−28930
GaAs, differential mobility anisotropy effect on wave propag. 78−88050
GaAs, effect of O on thin film compositions obtained by secondary ion emission 80−26079
GaAs epitaxial thin films with neg. electron affinity, photoelectron energy distrib. 80−100755
GaAs film, electron scatt., cathodoluminesc. meas., energy depend. of electron deposition depth determ. 80−104023
GaAs film, electroreflectance effects 79−43055
GaAs, film, solar cell on large grains 79−100528
GaAs, film and solar cell on graphite, struct. and elec. props. 80−2286
GaAs, LPE layers, X-ray topographic exam. of defects 78−30844
GaAs large-grained solar cell film recrystallisation 79−38737
GaAs layers, from gas phase, impurity influence on growth micromechanism 80−45237
GaAs, photovoltage anomaly investig., p-n-p microjunction model 77−4398
GaAs, plasma oxidation and oxide props. 78−95825
GaAs, polycryst. for terrestrial photovoltaic energy conversion 79−15242
GaAs, polycryst. solar cells, thin film growth and grain size, effect on cell efficiency 80−81471
GaAs polycrystalline film growth for solar cells 79−33941
GaAs, polycrystalline films, meas. of effective diffusion length by SEM 80−80424
GaAs, prep. of thin films by ionised-cluster beam deposition *(Japanese)* 80−25576
GaAs, RF sputtered, ESCA, surface chemistry suitability for photovolt. appl. 80−7476
GaAs, Raman spectroscopy, characterisation of thin films and heterostructures 78−76439
GaAs sandwich-type sputtered film, between Al electrodes, electrical props. 78−91780

semiconductor thin films continued
GaAs solar cells on Ge substrates, thin film shallow homojunction struct., quantum efficiencies 80−35677
GaAs thin films, reactively sputtered, ESCA/XPS study 80−97430
n-GaAs thin films carrier wave amplification, external medium stratification effects *(Russian)* 78−34905
GaAs:H amorphous sputtered films, high field cond. props. 80−44607
GaAs:Se(Zn) polycrystalline film, Hall effect, resistivity meas. 80−96911
GaAs:Si, film, conversion of type of conduction stimulated by ion bombardment 77−4457
GaAs-AlAs, epitaxial struct. with alternate layer comp. modulation, fabrication and characterisation 77−1322
GaAs-Cs-O film, polycryst., secondary emission props., activating coating effects 78−2957
$GaAs_{1-x}P_x$:N, film, optical absorpt. from photoluminesc. meas. 78−92134
$Ga_{1-x}In_xAs$, photocathode, work function depend. of photoelectric emission 78−68071
$Ga_xIn_{1-x}As_{1-x}P_x$ film, energy band struct., photolum. meas. 79−7784
GaN, deposition by pyrolysis of gallium trichloride and triiodide ammoniates 77−36402
GaN, film, secondary ion mass spectrometric qualitative anal. 78−7265
GaN on Si, form. with GaCl-NH_3-H_2(He), ESCA and RHEED meas. 79−90909
GaN, plasma deposition and elec. cond. 78−60585
GaN:Mg, and undoped, epitaxial growth from vapour, orientation, elec. props. 77−4740
GaP amorphous film, EXAFS, optical and elec. props. 80−49547
GaP anodic oxide system, multiple angle incidence ellipsometry, meas. at λ=632.8 nm 79−63294
GaP, deposited by RF sputtering, struct. and elec. props. obs. *(Czech)* 78−52667
GaP, effects of hydrogen incorporation during deposition by sputtering 79−69981
n-GaP films, reduced work function, energy spectra of secondary electron emission 79−28867
GaP films on Si, epitaxial crystallisation by nanosecond laser pulses 80−107674
GaP, plasma deposition and elec. cond. 78−60585
GaP, polycrystalline, with negative affinity, secondary emission *(Czech)* 78−52604
GaP, vac. deposited film, structural, elec. and photoelectric props. 79−82698
GaP/GaAs and GaP:H/GaAs amorphous film/cryst. junctions, optical and elec. props. 79−99611
$GaP_{0.1}As_{0.9}$, gas-transport condensate with superlattice, structural and chemical inhomogeneity 77−85088
GaSb amorphous film, elec. props. *(French)* 78−14843
GaSb and $GaSb_xAs_{1-x}$ films, MBE growth and elec. props. 79−23863
GaSb film, gamma-irradiated, struct., TEM and SEM obs. 79−15033
GaSb film, ion bombard. effects on elemental Sb incorporation probability during sputter deposition 79−83120
GaSb film, polycrystalline, Hall mobility 80−97015
GaSb, sputtered films, on GaAs, growth, Hall effect, impurity levels 80−20334
GaSe, far IR refractive index 80−80799
GaSe films, optical props. at lattice vibr. freqs., IR and Raman spectra 80−60696
ϵ-GaSe films, optical props. in IR region, metal substrate effect 80−71502
GaSe, photoelectrical props. at high electric field *(Russian)* 79−11247
GaSe thin films, electroabsorpt. spectra, exciton line splitting 80−107716
Ga_2Se_3, film, electrical and optical props. 77−1505
GaTe, hexagonal, vacuum deposited, physical parameters and substruct. 78−2393
$Ga_{0.25}Te_{0.75}$, amorphous, off-state recovery after nonosecond switching 80−44681
$Ga_{0.25}Te_{0.75}$ amorphous film, nanosecond switching, resist. fluctuations in low-resist. state 80−44676
$Ga_{0.25}Te_{0.75}$ time evolution of nanosecond switching 80−6921
$Ga_{1-x}Te_x$ amorphous films, elec. cond., optical absorpt. and transparency, band gap energy 79−56335
Ge, (110) orientation, preparation technique 79−95930
Ge, absorbing surface of solar collector, vacuum deposited coatings, deposited on metal surfaces 78−5580
Ge, amorphous, ^{74}Ge ion implanted, defect struct. obs. 78−51848
Ge, amorphous, 1 MeV electron irrad. influence on kinetics of crystallisation 77−89476
Ge, amorphous, complex refractive index and reflectance 77−52121
Ge, amorphous, crystallisation study 80−33889
Ge, amorphous, elec. cond. obs. of crystn., expt. verification of model 77−20475
Ge, amorphous, fast crystn. and void precipitation in laser pulse annealing, TEM exam. 79−56086
Ge, amorphous, freq. response characts. 79−56334
Ge, amorphous, high resolution electron microscopy, digital processing use 78−37116
Ge, amorphous, in situ meas. of thermal EMP, by ultrahigh vacuum electron microscopy 79−26184
Ge, amorphous, influence of deposition parameters on e.p.r. 77−1586
Ge amorphous, LF vel. of sound for Young's modulus mode 77−35636
Ge, amorphous, laser pulse annealing 80−15006
Ge, amorphous, O_2^+ ion implanted, influence on electrical and optical props. 77−89891
Ge, amorphous, prep. conditions influence on supernetwork struct. 77−76709
Ge, amorphous, prepared by evap. or sputtering, AC loss meas. 80−65560
Ge, amorphous, thermally induced reversible switching, effect of change in thermal resist. 77−20371
Ge, amorphous, thermoelec. power and structural investigs. using in-situ electron microscopy 77−76983
Ge, amorphous, vac. deposited, XPS and elec. props., evidence for polycryst. phase 77−28691
Ge, amorphous, vac. evaporated, density meas., microcrystalline model of struct. 80−2313
Ge, amorphous and crystalline, optical props. 77−16412
Ge, amorphous and crystn. films, contamination behaviour, XPS examin. 79−1815
semiconductor thin films continued
Ge, amorphous and polycryst. layers, sputtered, elec. cond. and thermoelec. power 78−2586
Ge, amorphous evap., structural aspects in electronic transport data interpret. 77−76977
Ge amorphous evaporated film, to metal contact resist. diffusion and microstruct. 77−89880
Ge, amorphous film, annealing, effect on localised states 79−4535
Ge amorphous film, crystn. front velocity during scanned laser crystn. 80−107662
Ge, amorphous film, DC sputter deposited, effect of trapped Ar on minimum temp. for impulse stimulated explosive crystallisation 80−100422
Ge amorphous film, effective medium theory and freq. depend of conductivity 79−24090
Ge amorphous film, effects of ion implantation on structure 78−55881
Ge amorphous film, effects of alloying chalcogen atoms 80−49670
Ge amorphous film, high freq. phonon scatt. 80−49328
Ge, amorphous film, high freq. cond., AC loss 80−49792
Ge, amorphous film, large aligned grain solid-phase growth during scanned laser crystallisation 80−49100
Ge amorphous film, O depth profiling by SIMS 80−39480
Ge, amorphous film, optical consts. in near IR range *(Korean)* 79−8137
Ge, amorphous film, persistent photoconductivity, dangling bonds 80−84487
Ge, amorphous film, post nucleation growth, computer simulation 78−34729
Ge, amorphous film, temp. thermal conductivity 78−22994
Ge amorphous film, ultra high vac. prep., DC elec. cond. 80−49721
Ge amorphous films, high elec. field cond. and magnetoresist. at 4.2K 80−49748
Ge amorphous films, self-ion bombard., electronic props. 79−28422
Ge amorphous films, structural relaxation and crystallisation 80−100170
Ge, amorphous layer on Ge bulk, photoemission during X-ray Bragg diffr. 78−47209
Ge, amorphous sputtered films, hydrogenated, photoinduced optical absorpt. 80−50362
Ge amorphous thin films prepared by vac. evaporation, density meas. 77−80714
Ge, crystal struct., influence of implanted O ions, electroreflection method 77−84783
Ge, electrical resistance, long term stability rel. to ambient atmosphere changes 78−2597
Ge, electrodeposited, X-ray, electrochem., and electrorefl. characterisation 78−14624
Ge, electron transmission, 1-5 keV, electron MFP 77−15472
Ge, electronic struct. charge on ordering, double beam photoemission 78−19634
Ge, evaporated amorphous, angle of deposition effects, electron microscopy 77−43451
Ge, evaporated film, lattice parameters and phase transition temp., surface influence of glass substrates 78−94996
Ge, film, amorphous, contamination anal. by AES 77−36828
Ge film, amorphous, O implantation effects on absorpt. edge and elec. cond. 77−39970
Ge film, amorphous, two-dimensional variable range hopping cond. 80−10977
Ge film, amorphous and crystalline, effects of Al and Cu alloying on elec. transport props. 79−51689
Ge film, amorphous to crystalline transform. 77−20206
Ge, film, dense electron-hole plasma, negative differential resistance 77−89794
Ge, film, elec. resist. and struct., post-deposition heat treatment effects 79−78229
Ge film, electroreflectance effects 79−43055
Ge film, growth on graphite substrate by thermal reduction 78−18934
Ge film, polycrystalline, structural and elec. props. 78−76173
Ge film, prep. by low press. reactive deposition process 79−24449
Ge film, radiation damage in electron microscope 77−84794
Ge film black, solar selective absorber surface 79−29484
Ge film bolometer, radiation loss from JFT-2 Tokamak, meas. 80−95141
Ge films, adhesion to substrates, effect of Ar^+ ion irrad. 79−11047
Ge films, evaporated, oxide layers 77−76927
Ge foil, thinning for electron microscopy 79−49217
Ge, inert gas ion refl., semiempirical analysis, compared with expt., 10-30 keV 78−6823
Ge, laser pulse annealing, induced nucleation, crystal growth 80−84966
Ge, optical characterisation, inversion method 78−11008
Ge thin films on glass substrates, annealing by Ar ion bombardment 80−80136
p-Ge, transverse magnetoresist. meas. 78−72293
Ge, volume plasmons, EELS, line shape 79−90984
Ge:Al(Sb) film, amorphous, ion implantation, effect on cond. 78−83839
Ge:Au film strain gauges, press. sensor *(Japanese)* 80−105631
Ge:Fe, amorphous film or ion-implanted, comparison of ^{57}Fe Mossbauer data 77−40159
Ge:H, amorphous, H content determ. by IR absorpt., gas evolution and nuclear reaction methods 80−44130
Ge:H amorphous films, photoemission spectra 80−50517
Ge:Mn, amorphous, cond. increase by Mn doping 78−72155
Ge:O, Cu, amorphous thin film, impurity effects on struct. 80−107054
Ge:Sb, amorphous, electronic transport props. 80−44589
Ge:Sb(In), film, electronic props. 78−84330
Ge-Al, elec. resist. and IR transmission, comp. and substrate temp. depend. 78−52112
Ge-Al (Sb) amorphous film junction, I-V and C-V characts. 77−85307
Ge-As-Se films, light irrad., heat treatment rel. to optical props. *(Russian)* 79−4858
Ge-Fe system, amorphous films, mag. and elec. props. 79−51695
Ge-Ga amorphous alloy, co-evaporated elec. and optical props. 80−70860
Ge-S amorphous film, defect states, ESR 80−49670
Ge-S film, amorphous, photo-induced ESR and optical absorption edge shift 78−88374
Ge-S-Ga amorphous thin film, memory switching effects 80−88605
Ge-Se glass, photoinduced absorpt. changes 79−87519
Ge-Se-Fe phase system, amorphous films, mag. and elec. props. 79−51695
Ge-Se-Te amorphous alloys, prep. and calorimetric obs. 77−11675

semiconductor thin films continued
Ge-Se(Te), laser-beam recordings by thermal creation of holes 80−35010
Ge-Si, amorphous, freshly-evap. and ion-bombarded, struct. differences 79−55666
Ge-Si amorphous film, ferromagnetic interaction between spins 78−2710
a-Ge-Si crystal interface, low resist. elec. behaviour 77−89843
Ge-Si junction, Si monocryst. and Ge film, elec. props. 79−51660
Ge-Si solid solution film, elec. props. in range 4.2 to 500K 77−8214
Ge-Te alloy films, amorphous, semicond. props., refr. index, struct. study 78−26978
Ge-Te-Se/Si amorphous film-cryst. heterojunction, electron-beam-induced current 79−24060
$Ge_{33}As_{27}S_{15}Te_{25}$, chalcogenide thin films, coupled carrier theory test, high field conditions 80−100466
GeC_x, amorphous , prepared by glow discharge method, elec. and optical props. 77−21035
GeO amorphous film, hologram recording, photochem. props. 79−64186
GeO amorphous semicond. films, photostructural changes by photomodulation ellipsometry 79−71510
GeO_2-SiO_2, pyrolytic film prep. 77−81223
GeP, thin films, vacuum-deposited, struct. characterisation 77−47691
GeS, conc. depend. of rate of formation on Ge surface 79−43152
GeS, deposited on Ge (110) surface, sublimation, LEED meas., structural transitions 77−59195
GeS, film, effective electron mass determ. 77−1506
GeS, photocond. kinetics 77−39897
GeS, thin layer cryst., far IR transmission spectra 79−56870
GeS_2, amorphous film, reversible and irreversible photostructural changes 79−74061
Ge_2S_3-Ag contact, photoinduced diffusion of Ag in amorphous semicond. film 80−49418
$Ge_{30}S_{70}$ glass film, Ag photodoping sensitivity 80−39121
$Ge_{42}S_{58}$, amorphous, bulk and film forms, elec. props. and ESR study 80−103691
GeS(S_2) amorphous films, photostructural changes, UPS study 80−49550
$Ge_{100-x}S_x(Se_x)(Te_x)$, amorphous film, effect of alloying chalcogen atom on elec. cond., optical transmission and ESR 79−78101
GeSe, amorphous, film, thermally induced effects, UPS study 80−104042
GeSe, amorphous film, optical properties 78−39620
GeSe, amorphous film, photocond. meas. 77−43647
GeSe amorphous films, blocking metal contacts characteris. and photo/EMF obs. 77−76924
GeSe amorphous films in Al-GeSe-Al structs., AC cond. and capacity, thickness depend. 79−65566
GeSe amorphouse sputtered film, DC and AC behaviour, effect of contact material 79−95513
$GeSe_2$, amorphous, film, thermally induced effects, UPS study 80−104042
$GeSe_2$ amorphous film, laser induced light absorpt. oscillation, exciton model 80−50446
$GeSe_2$ amorphous film, laser induced oscillatory phenomena 80−84711
$GeSe_2$, amorphous film, photocond., photo-induced ESR, optical edge shift 80−49809
$GeSe_2$ evaporated films, struct. and thermally induced effects 79−41963
$GeSe_2$ evaporated films, optical absorpt. and thermally induced effects 79−42989
$GeSe_2$ film, glassy, self-controlled laser-beam chopping effect 78−60528
$GeSe_2$ film, light induced transmittance oscillations 77−81171
$GeSe_2$, light-induced light absorption changes 77−73181
$GeSe_4$ film, self-controlled laser beam chopping effect 78−31266
$Ge_{1-x}Se_x$ film, EPR, elec. and optical props. meas. 78−48038
Ge_xSe_{1-x}, $0<x<0.2$, crystallisation in amorphous bulk and thin films 78−55813
Ge_xSe_{1-x} amorphous film, photocrystallisation, elec. cond. meas. 79−32911
Ge_xSe_{1-x} amorphous film, photocrystn., elec. cond. and optical microscopy obs. 79−87024
Ge_xSe_{1-x}, thin film Schottky diode, photovoltaic effect 77−15895
Ge_ySe_{1-y}, glass, bulk and film, IR transmission and reflectivity meas., struct. mode assignments 78−79537
GeSe(Se_2) amorphous films, photostructural changes, UPS study 80−49550
$Ge_{20}Se_{40}Te_{40}$ amorphous alloys, thermal crystn. study 78−26789
$Ge_3Se_2Te_4$, chalcogenide glass, freq. depend. of Hall effect 77−1436
Ge_4Se_5Te amorphous layers, prep. and elec. props. 80−97436
$Ge_7Si_9As_{39}Te_{35}Ga_{10}$, chalcogenide thin films, coupled carrier theory test, high field conditions 80−100466
$Ge_{0.5}Sn_{0.5}Te$ film, elec. and optical props. 77−12028
$Ge_{1-x}Sn_xTe$ film, amorphous, elec. cond. 80−93016
GeTe, amorphous, specific current noise power 77−66190
GeTe, amorphous and crystalline, electron diffr. meas. 77−39748
GeTe, amorphous film, annealing effects on resistivity, comparison with SnTe 77−66212
GeTe amorphous films, annealing effect on optical props. 77−72931
GeTe film 79−43055
GeTe films, elec. props. and struct., influence of annealing and condensation conditions 80−15388
GeTe, local order, electron diffraction study 79−77485
Ge_xTe_{1-x} amorphous matrix with Te crystallites, effect of annealing 77−24274
$Ge_{15}Te_{81}X_4$ amorphous semicond. switches, fabrication technology *(German)* 80−7493
$Hg_{0.74}Cd_{0.25}Te$ thin film deposition on Si substrates by RF triode-sputtering, large-area photodetector arrays 80−80965
$Hg_{1-x}Cd_xTe$ films, Tamm surface states, Kane model 79−28395
HgS, deposition from colloidal solns. 78−92209
HgS, RF sputtered, effect of K on cryst. modification 77−62773
HgS, RF sputtering on NaCl, growth and struct., electron diffr. and TEM obs. 77−90271
HgSe film, anomalous photocond., electron microscope study 80−65623
HgTe thin film Hall sensor fabrication 80−2951
HgTe-HgSe film, optical spectra in fundamental absorption edge 79−74012
IN_2O_3:Sn, RF magnetron sputtered film, elec. and optical props. 80−104065
InAs amorphous film, DC sputtered, optical absorpt. 78−19589
InAs, CVD H_2O transport method, Hall element preparation 77−40377
InAs film, DC sputtering, struct. and elec. props. 77−66567

semiconductor thin films continued
InAs, thin film prep. and elec. props. 79−1633
$In_{0.53}Ga_{0.47}As$, interband magnetoabsorption study, quasi-Ge model application 80−50304
$In_xGa_{1-x}As$ (x=0.03 and 0.05), grown as GaAs substrate, with InGaAsP buffer layer, exam. of dislocation density 80−44447
InGaAsP avalanche photodiodes, leakage current, shot noise, quantum efficiency, gain saturation 79−67381
$In_xGa_{1-x}P$, TEM foil preparation, using polishing set 'Elypovist' *(German)* 79−9264
$In_{1-x}Ga_xSb$ films, elec. props., preparation 80−100473
$In_{1-x}Ga_xSb$, multitarget sputtering using decoupled plasmas 77−12529
InN film, refl. and transmission spectra, band struct. 78−72625
InN film, specular reflection spectra, lattice parameters 80−7428
InN film growth by reactive sputtering in Ar-N_2 discharge, mechanism 80−89107
InN, thin film, characterisation using XPS electron energy loss spectra 79−87561
InO_3:Sn, thin films, prep. by pyrolitic method, charact. by SEM, electron diffr. and SIMS, solar energy appl. 79−43143
In_2O_3, conductive, transparent, optimal reactive sputtering conditions for prep. 79−95295
In_2O_3, elec. conducting film on glass substrate, measurement of optical constants and thickness 78−60525
In_2O_3, electro-conducting transparent film, props. rel. to production method *(Japanese)* 80−25557
n-In_2O_3 film, RF sputter grown, substrate bias effect on elec. and optical props. 78−64150
In_2O_3 films, electron beam evaporation, elec. and optical props. *(Japanese)* 80−60784
In_2O_3 layers, chemically sprayed, prep. and intrinsic absorpt. in band edge 77−81169
In_2O_3 semiconductor electrode, sensitised photocurrent by energy and electron transfer in dye monolayers 79−38119
In_2O_3, thermally evaporated film, struct. and elec. props. 80−104066
In_2O_3, thin film, characterisation using XPS electron energy loss spectra 79−87561
In_2O_3, thin film, sputter deposition form., optical and elec. props. 80−60123
In_2O_3 thin film on polyester substrate, struct. determ. by TEM 80−6674
In_2O_3, transparent films, state of art *(Chinese)* 79−73610
In_2O_3:Sn, film, HF sputtered, cond., Hall mobility, oxidation, charge carrier density 78−72287
In_2O_3:Sn, glass like thin film, electron evaporated, conductive transport *(Chinese)* 80−49960
In_2O_3:Sn, HF sputtered films, temp. depend. studies of the elec. transport props. 78−76170
In_2O_3:Sn, transparent conducting films, prep. by $InCl_3$ thermal decomp., transmittance, resistivity 79−33944
In_2O_3:Sn film, electroreflectance effects 79−43055
In_2O_3:Sn film, RF sputtered, effect of O_2 press. during deposition on props. 78−19664
In_2O_3:Sn films, CVD prep. and elec. resist. meas. 79−52120
In_2O_3:Sn films, doping profiles and elec. props., appl. to optoelectronic devices 79−38203
In_2O_3:Sn films, elec. and optical props., solar energy conversion appl. 79−65945
In_2O_3:Sn films, prep. at low deposition temps. by ion-beam sputtering, elec. and optical props. 79−66004
In_2O_3:Sn films, RF reactive sputtered, optical props. rel. to band struct. 79−91515
In_2O_3:Sn transparent cond. films, hydrolysis deposition, elec. and optical props. 79−43144
In_2O_3-InN film growth by reactive sputtering in N_2-O_2 discharge, mechanism 80−89108
In_2O_3-SnO_2, reactive DC diode sputtering, using large scale system 78−72723
In_2O_3-SnO_2, thin films deposited on cold substrates, life stability 79−23867
In_2O_3-SnO_2 film on Si, heterojunction, photovoltaic effect, sunlight induced 77−1470
In_2O_3-SnO_2 thin film, effects of heat treatment on resist. and optical absorpt. 78−43495
InO_xN_y, thin film, characterisation using XPS electron energy loss spectra 79−87561
p-InP, CVD, growth characts. and CdS/InP solar cell efficiency 77−1813
InP, CVD on preferentially etched Mo, initial growth behaviour 78−51855
InP cylindrical magnetron reactive sputtering, for solar cell appl. 78−39693
InP film, electron-beam annealed, surface conduction 80−84500
p-InP film growth, by close space vapour transport 79−28944
p-InP, on foreign substrates, prep. and solar cell characterisation 77−81211
InP, on rough $Zn_xCd_{1-x}S$ substrate, film substrate lattice mismatch calcs. 78−43263
n-InP, polycryst., deposited on Mo sheets, elec. props. obs., w.r.t. varying deposition conditions 79−4608
p-InP, RF sputtering on CdS and other substrates, and grain size obs. 77−90272
InP solar cells, thin film growth tech. and characterisation 80−89631
In_2S_3, film struct. and props. 77−80706
InSb amorphous film, effective medium theory and freq. depend of conductivity 79−24090
InSb, charact. and phys. props., review *(Japanese)* 80−39576
InSb, depletion layer, plasma and vibr. plasma type guided polaritons *(Russian)* 80−96933
InSb evaporation kinetics of InSb, rel. to film growth 78−3050
p-InSb, excess In, polycryst. thin film, elec. transport props., non-stoichiometric effect 79−95528
InSb, film, analysis by attenuation of substrate X-ray fluoresc. 78−27872
InSb film, degenerate, concs. and ionisation energies of defect levels, Hall effect meas. 79−91087
InSb, film, E_0, E_1 absorption edge size quantisation, optical and electroreflectance spectra 80−34998
InSb film, gamma-irradiated, struct., TEM and SEM obs. 79−15033
InSb film, ion bombard. effects on elemental Sb incorporation probability during sputter deposition 79−83120
InSb film, magneto-concentration effects *(Russian)* 79−47113

semiconductor thin films continued
InSb film, threshold singularity on quantising mag. fields 78−87904
InSb, film, transverse 1/f noise and signal-to-noise ratio of related Hall elements, comment 79−99593
InSb, film, transverse 1/f noise and signal-to-noise ratio of related Hall element 79−99594
InSb film cyclotron-frequency submillimetric oscillation generation model 77−80801
InSb films, transverse 1/f noise and S/N ratio of related Hall elements 79−42597
InSb, films, X-ray fluoresc. anal. method, long-term stability 80−61212
InSb films on $LiNbO_3$, prep. and props. 80−35093
InSb, Hall mobility of carriers at room temp. 79−65568
InSb, light scatt. from surface polaritons 79−8202
InSb, phase transition dynamics, investigating device 78−22967
InSb, photoconductive and photoelectromag. effect spectral distrib., sample thickness depend. 77−4394
InSb, prep. by rotary type flash method *(Japanese)* 77−40372
InSb, prep. of thin films by ionised-cluster beam deposition *(Japanese)* 80−25576
InSb, Raman scattering study of unoxidised Sb in anodic oxide films 80−88985
InSb, synthesis by 2-source mol. beam technique and AES characterisation 78−72729
InSb thin film element having non-linear galvanomagnetic effect 80−34534
InSb, thin film prep. with remelting, elec. props. 77−52255
InSb, thin films, electrophysical props. obs. 80−103765
InSb thin layers, interface stability during crystn. 79−65326
InSb thin layers, melt grown, mag. field depend. of PEM effect 79−95445
InSb, volume plasmon dispersion, anisotropy 78−56090
InSb/GaSb superlattice thin films, sputtered, ion-bombardment-enhanced diffusion during growth 78−87882
InSb-GaSb superlattice, interlayer diffusion 77−85086
$InSb_{1-x}Bi_x$, film, multitarget sputtering growth technique 78−84711
InSe film, photochem. production of holograms on surface *(Russian)* 79−7101
InSe luminescent film, production and characterisation *(Russian)* 78−39581
InSe, photovoltaic effect, appl. to solar energy conversion 79−29481
InSe thin film, sputter growth and chem. anal. by XPS/ESCA 80−80976
In_xSe_{1-x}, amorphous film, in metal-In_xSe_{1-x}-SnO_2 system, photovoltages 77−28215
In_xSe_{1-x}-SnO_2 amorphous film-SnO_2 system, photovoltic spectra, annealing effect *(Japanese)* 80−92926
$In_xSi_yO_z$, thin film, sputter deposition form., optical and elec. props. 80−60123
$In_{1.9}Sn_{0.1}O_3$ laser-damage-resistant transparent conductive coatings, appl. in Pockels cells 79−50333
$In_{2-x}Sn_xO_{3-y}$ film, deposited from organometallic composition, transparent cond. appl. 78−91793
InTe thin films, flash evaporation, electrical props. 80−65722
$In_{0.25}Te_{0.75}$, amorphous, off-state recovery after nonosecond switching 80−44681
$In_{0.25}Te_{0.75}$ amorphous film, nanosecond switching, resist. fluctuations in low-resist. state 80−44676
$In_{0.25}Te_{0.75}$ time evolution of nanosecond switching 80−6921
$In_{1-x}Te_x$ amorphous films, elec. cond., optical absorpt. and transparency, band gap energy 79−56335
In_2Te_2 amorphous film, pulse hologram recording 79−55091
Mo-amorphous GeSe-Mo junctions, electrical contact effects on properties *(German)* 80−93010
MoO_3, film and cryst., long range potential centres 78−30920
$MoSi_2$ sputtered films, protective layer form. on oxidation, Auger anal. and backscatt. meas. 79−15029
$NaSbSe_2$ films, struct., photoelec. and opt. props. 78−51834
Nb-Al_2O_3 cermet-type film, thermoelec. power and annealing effects 77−47911
Nb-Al_2O_3 composite, semicond. films, cond. on localised states 77−24628
Nb_2O_5 amorphous films, switching phenomena and dielec. breakdown 77−24594
Nb_2O_5, polycryst. film, switching processes, dielec. breakdown 77−39981
PbCl2:NaCl, trapped exciton states, absorption spectra 80−50383
p-$Pb_{1-x}Ge_xTe$ film, cyclotron reson. above and below struct. phase transition 80−88879
$Pb_{1-x}Hg_xS$ electroless-deposited films, optical and elec. props. 80−7011
$Pb_{1-x}Hg_xS$, IR detector material, struct. and IR props. 78−26775
$Pb_{1-x}Hg_xS$, soln. growth, variable gap film for i.r. detector 77−1796
$Pb_{1-x}Hg_xS$, solution-grown, struct., lattice parameters and optical band gap var. 77−69201
PbI_2, exciton absorpt. band shape, dielectric const. real part derivatives *(Russian)* 80−25413
PbI_2, film, reflectance meas., optical consts., humidity effects 80−34994
PbI_2, film exciton spectrum, Faraday rot. 77−20944
PbI_2, highly excited, oscillator strength of excitons, absorpt. and emission spectra 78−76001
PbI_2:KI, trapped exciton states, absorption spectra 80−50383
PbO, reactively evaporated photoconductive film, phase transform. induced by water vapour 79−78233
PbO, reactively evaporated, photocond., H_2O induced phase transform. 80−60122
PbO thin films, elec. props. *(Korean)* 79−60943
PbO:Ag film, X-ray stimulated diffusion, current-voltage characts. 77−80653
PbO-In_2O_3 two-phase film, quantitative analysis, use of internal calibration technique developed by AES 77−36834
PbS, absorbing surface of solar collector, vacuum deposited coating, deposited on metal surfaces 78−5580
PbS, chem. deposited thin film, effect of morphological struct. on photosensitivity 80−70760
PbS, chemically deposited film, photosensitivity, effect of morphological struct. 79−82647
PbS film, appearance of EPR centres in initial form. stage *(Russian)* 77−63283
PbS film, photosensitivity, role of surface oxide and ion bombardment 77−24631
PbS, film condensation on amorphous substrate, struct. and growth 78−38981
semiconductor thin films continued
PbS, film prep. from aqueous soln. of thiourea 77−8767
PbS film surface with oxysulphate layer, photoelec. memory effect 77−55584
PbS islands, vacuum deposited, electron microscope obs. 80−103601
PbS, polycryst., chem. deposition from soln. and characterisation 78−72743
PbS, polycryst., small-angle X-ray scatt. and electron density inhomogeneities 80−96758
PbS, soln.-grown on Si, struct. and comp. of heterojunction 80−54530
PbS, thin film, photoconductivity expts. 79−78130
PbS, thin film comp. and struct. rel. to precip. by allyl thiourea 77−48356
PbS, vacuum deposited film, orientation axis tilt rel. to vapour angle of incidence 80−88456
PbS, vap. deposited film, island growth obs. by optical diffr. from electron micrograph 78−10291
PbS-Al coatings, absorptivity, emissivity, as function of PbS thickness 78−46731
PbS-Si heterojunction, space charge capacitance, PbSn film thickness depend. 80−88630
PbS-Si heterojunction, PbS film growth and struct. 80−96762
PbS(Se), valence band struct. determ. by optical absorpt., size quantization effects 80−59871
$PbS_{1-x}Se_x$ thin film, stimulated emission, temp. depend. 80−66232
PbSe, complex-composition film production method from vapour *(Russian)* 78−95702
PbSe, film with pot. barrier, magnetoresistance anisotropy 79−91172
PbSe films, current carrier conc. and type control, elec. cond., synthesis process *(Russian)* 80−100412
PbSe films, synthesis characts. 80−35094
PbSe, partly oriented, electron diffr. dynamic effects 77−7996
PbSe, polycryst. film, low temp. illumination, residual cond. 77−43756
PbSe, stimulated photoluminesc. characts. meas., room temp. 77−90193
PbSe, vacuum evaporation, composition of condensates 78−44012
$Pb_{1-x}Sn_xSe$ epitaxial layers, radiative and nonradiative recomb. processes 80−60670
$Pb_{1-x}Sn_xSe$, film struct. and elec. props. 77−80708
$Pb_{1-x}Sn_xSe$, thin film, opt. props. *(Japanese)* 77−1750
$Pb_{1-x}Sn_xSe$, X-ray spectral investigation of solid solution 77−16477
$Pb_{1-x}Sn_xSe$, X=0.03-0.07, monocrystal film, edge of intrinsic absorpt. *(Russian)* 80−71368
$Pb_{0.8}Sn_{0.2}Te$, growth in quasi-closed space, single and polycryst. 79−33930
$Pb_{0.8}Sn_{0.2}Te$:La, evaporated thin films, low carrier conc. 80−65414
$Pb_{0.82}Sn_{0.18}Te$, effect of hydrostatic pressure on props. 80−70862
$Pb_{0.82}Sn_{0.18}Te$ films, piezoresist. effect 79−38197
$Pb_{0.82}Sn_{0.18}Te$, layers on mica substrate, Hall constant peculiarities 80−75588
$Pb_{1-x}Sn_{1-x}Te$, Burstein-Moss effect, absorpt. and photocond. spectra 78−18961
$Pb_{1-x}Sn_xTe$ film, pure and Bi doped, polycryst., struct., elec., optical props. 79−42542
$Pb_{1-x}Sn_xTe$ films, size quantisation, optical orientation of free carriers 80−20725
$Pb_{1-x}Sn_xTe$, heteroepitaxial film, fundamental absorpt. edge and Shubnikov-de Haas effect 79−24381
$Pb_{1-x}Sn_xTe$, sputtered, for IR detector appl. elec. and optical props. 80−35084
$Pb_{1-x}Sn_xTe$:In film, anomalous elec. props. 78−10477
$Pb_xSn_{1-x}Te$, oxidation, appl. of Mossbauer method 80−45410
$Pb_xSn_{1-x}Te$, RF sputtered films, struct., lattice parameter, stoichiometric comp., RHEED 78−38975
PbTe (001), two-photon transition rate calc. 79−95869
PbTe, complex-composition film production method from vapour *(Russian)* 78−95702
p-PbTe film, for IR magneto-optics, 8-30K 78−23543
PbTe film, light absorpt. 79−83043
n-PbTe film, magnetophonon reson., 55-90K 79−7913
PbTe film, optical consts., support roughness effect 80−2882
PbTe film, struct. anal. and sensitisation 78−22982
PbTe, film photodiodes, quantum efficiency 79−75596
PbTe films, thermal cond. and elec. props., 4.2 to 300K 79−28162
PbTe films grown from vapour, optimum conditions and elec. characts. 79−52117
PbTe, ion implantation induced damage and reson. levels 80−49255
PbTe, ion-implantation-induced lattice defects 77−68985
PbTe layers, quality control of carrier conc. using Hall effect graphical representation 77−1500
p-PbTe, magneto-optics of free and bound carriers 79−82985
p-PbTe, magnetophonon effect obs. 78−23115
n-PbTe, noncubic (111) oriented epitaxial films, weak field magnetoresistance 80−75584
PbTe, on NaCl and TGS substrates, photo-EMF investig. of induced elec. inhomogeneity 77−15909
PbTe, polycryst. film, RF sputtered, time stability 77−43758
PbTe, semiconductor polycrystalline thin films, low-frequency 1/f noise meas. 80−15629
PbTe, uniformly varying thickness, photovoltaic effects 77−51774
PbTe, wedge shaped film, photovoltaic effect 77−1454
Pb_xTe_{1-x}, highly absorbant, complex index of refr. determ. method 78−54445
PbTe(Se) vacuum deposited thin films, struct. and growth 79−19482
PdO, semiconductivity and stability, optical props. 78−43497
Pt-Si:As, silicide form. during laser irrad., p-n junctions and ohmic contacts 80−84397
$Ru_xTi_{1-x}O_2$ films, percolation elec. cond. in strong electric fields *(Russian)* 80−84471
S-based amorphous semicond. film, prep. by plasma decomp. of H_2S-N_2-NH_3, and characterisation 80−80422
SB-S, laser-beam recordings by thermal creation of holes 80−35010
(SN)x, halogen-doped, temp. depend. of elec. cond. 79−65563
Sb_2O_3 anodic layers on Sb, semicond. props. 79−56303
Sb_2S_3, amorphous and crystalline thin films, optical consts. 79−91518
Sb_2S_3, amorphous layer, scattering of visible light, rel. to substrate temp. during deposition 79−65950
Sb_2S_3, defect struct., electron microscope mode 79−28224
Sb_2S_3 film, amorphous and crystalline, optical props. 79−95867
Sb_2S_3, vacuum deposited films, struct. and photoelec. props. 77−85092
SbSI-BiSI, solid solns., phase diagrams, photocond., elec. props. 79−38125

semiconductor thin films continued
$(Sb_2S_3)_{0.95}(Na_2S)_{0.05}$, condensate, local states and switching effect 80−20336
$Sb_2S_3(Se_3)$, IR spectra rel. to bonding, amorphous film and cryst. 77−16410
Sb_2Se_3 film, struct. and photoelec. props. 77−85257
Sb_2Te_3-Sb_2Se_3 thin layers, struct., phase comp., and elec. cond. 80−15389
Se, Ag diffusion, effect on interferometric thickness meas. 80−96695
Se, amorphous, block formation during crystn., electron microscope obs. 79−11030
Se, amorphous, crystallisation induced by corotron charging 77−35832
Se, amorphous, crystn., thermal and photo-effects 77−47692
Se, amorphous, density of localised states 78−34742
Se, amorphous, evap. layers, electrophotographic props. depend. on thermal treatment of initial material 77−76978
Se, amorphous, influence of wavelength on optical quenching of photoconductivity 80−60046
Se, amorphous, localised states in band gap 80−59928
Se, amorphous, struct. and crystn., far IR transmission spectrum and DSC obs. 77−85106
Se, amorphous, substrate effects on crystn. kinetics 77−1337
Se, amorphous, thermo-crystn. obs. 77−11810
Se, amorphous, vac. evaporated, density meas., microcrystalline model of struct. 80−2313
Se, amorphous electrophotographic layers, resolution parameters 80−31926
Se, amorphous evaporated layers, struct. inhomogeneities due to prep. technology fluctuations 77−76710
Se, amorphous film, AC conductivity at radio and microwave frequencies 79−11248
Se, amorphous film, dark and photoconductivities 79−87173
Se, amorphous film, dielec. activity obs. near glass transition temp. 80−75933
Se, amorphous film, highly disordered, UPS study 80−76148
Se amorphous film, interference enhanced Raman scatt. 80−50326
Se, amorphous film, inverse/combined photoadsorption and photodeposition, light-temp. interference 79−46977
Se, amorphous film, photocond., dark cond., rel. to crystn. 80−88596
Se, amorphous film, photodeposition by Selor process, kinetics 78−75963
Se, amorphous film, photodeposition by Selor process, struct. and kinetics 78−75964
Se amorphous film, spherulite formation and role of stresses due to volume changes in crystallisation 77−1083
Se amorphous film, stabilisation by thermal treatment *(French)* 79−47176
Se amorphous film, threshold and memory switching 79−82651
Se, amorphous film-metal system, contact pots. distrib. and photo-EMF, work function 77−76925
Se, amorphous films, evaporated, ageing and crystn., DTA 80−65413
Se amorphous layers, dielectric relax. in glass transition range, ageing 79−82923
Se amorphous layers, substrate range depend. on dielec. relax. in glass transition temp. 79−69773
Se, amorphous thin film, elec. noise, monostable switching 80−44684
Se amorphous thin film photodeposition from hydrosols 78−11109
Se, amouphous film, photodeposition by Selor process struct. 78−75962
Se electrophotographic films, ageing effects on structure and properties 77−47699
Se electrophotographic film current density/voltage characteristic rel. to substrate temp. *(German)* 77−55629
Se film, amorphous, empirical formula for temp. depend. of dielec. loss peaks 80−97197
Se, film, effect of thermal history and substrates or crystn. by vac. condensation 77−15713
p-Se film, photocond., phase-memory effect 78−91723
Se film, resonance Raman spectrum 79−28760
Se, gas-evaporated, selective absorpt. characts. and emissivity 80−50998
Se, Hg activated amorphous film, anomalous photocond. 77−43658
Se, noncryst., ageing and crystn. obs., tentative struct. model 80−2295
Se, noncryst., controlled vapour deposition, crystn., and optical props. 78−39696
Se, optical constants in visible region 80−97360
p-Se photocond. film, phase memory effect and deep levels 79−82556
Se, photoconductive film, field instability, Ar^+ ion irrad.-induced defects 78−87997
Se, red amorphous film, textural change, thermal and photo effects 78−63951
Se sphere monolayer, multiple EM wave scatt., migration imaging film appl. 80−99627
Se, switching characts. under pulsed bias 77−39979
Se, thin film selective absorber coatings, prod. using an oblique vacuum deposition technique 80−81488
Se, trigonal, sputtered and evaporated, nucleation and growth processes 77−31920
Se, vacuum deposited, struct. asymmetry, reflectivity elec. cond. 79−23855
Se, vitreous, darkened films, thermal and optical bleaching, light transmission obs. 80−50447
Se:As, amorphous film, dielec. activity obs. near glass transition temp. 80−75933
Se:Hg, amorphous, anomalous photocond. and residual interelectrode photo-EMF 77−69376
Se:Hg amorphous film, photocond. anomaly due to HgSe layer form. 77−66183
Se:Te(Ag), amorphous film, elec. cond., 300 to 350K, transition 77−4454
Se:U, cryst. and amorphous, impurity conc. and distrib., solid state nuclear track detection 79−46694
Se-As, evaporated, thickness, substrate temp. effects 79−15610
Se-Bi bilayers chemical reactions, differential scanning calorimetry technique and obs. results 78−2398
Se-Fe system, amorphous films, mag. and elec. props. 79−51695
Se-Ge, amorphous thin film, photocontraction rel. to surface struct. 80−49551
Se-Ge amorphous films, obliquely deposited, photoinduced chem. changes 80−76385
$Se_{1-x}Ge_x$ amorphous film, photocontraction effect 79−46975
$Se_{75}Ge_{25}$, obliquely deposited amorphous films, photo-induced optical effects 79−56871
semiconductor thin films continued
$Se_{1-x1}Te_{x1}$-$Se_{1-x2}Te_{x2}$ heterostructure, amorphous, rectification phenomena and photovoltaic effects 79−99610
$Se_{1-x}Te_x$, amorphous, photo-crystallisation 80−59839
$Se_{1-x}Te_x$ amorphous films, sublinear and superlinear I-V charcts. 79−82695
$Se_{17}Te_{49}As_{29}Ge_{10}$ semiconductor amorphous films, field effect, trapping 80−84472
Si, amorphous, acoustic study using Rayleigh waves 80−75312
Si, amorphous, analytical techniques, review 80−80120
Si, amorphous, as photo-receptor for electrophotography 80−47126
Si, amorphous, control of dihydride bond density using RF sputtering, dark anal. and photocond. 80−34327
Si amorphous, crystallisation study 80−33890
Si, amorphous, crystn. on annealing at low temps. in contact with Al 80−24765
Si, amorphous, discharge produced, reversible cond. changes 77−85256
Si, amorphous, discharge produced, optical and photocond. props. 78−39147
Si, amorphous, doped, density of states determ. from transport meas. 80−49720
Si, amorphous, EELS microanalysis 80−100722
Si, amorphous, film, hydrogenation by H diffusion, effect on elec. cond., band gap *(Korean)* 80−45326
Si, amorphous, formed by CVD, crystallisation 77−39746
Si, amorphous, glow-discharge, optical props. *(Japanese)* 79−65946
Si, amorphous, glow-discharge, optically detected mag. reson., annealing and substrate temp. effects 80−20519
Si, amorphous, high resolution electron microscopy, digital processing use 78−37116
Si, amorphous, hydrogenated film, struct. determ. using electron microscopy 80−10806
Si, amorphous, hydrogenated, soft H plasma effect, IR absorpt. *(French)* 80−45054
Si, amorphous, hydrogenated, electron drift mobility meas. 80−75565
Si, amorphous, hydrogenated preparation by SiH_4 decomposition 80−80956
Si, amorphous, hydrogenated film, electroreflectance study 80−88967
Si, amorphous, LF vel. of sound for Young's modulus mode 77−35636
Si, amorphous, optical absorption at high press. 78−35216
Si, amorphous, photostructural changes, photodarkening 80−49121
Si, amorphous, plasma-deposited, H_2 evolution, mass spectrometry and RHEED obs. 78−72050
Si, amorphous, prep. by RF sputtering, photoconductivity determ. 77−73231
Si, amorphous, prep. conditions influence on supernetwork struct. 77−76709
Si, amorphous, RF-sputtered, influence of O_2 and deposition conditions, elec. cond., IR absorpt. and ESR 80−2949
Si, amorphous, sputtered, resist. control by ion implantation 80−100262
Si, amorphous, structural comparison of evaporated and glow discharge samples 77−62778
Si, amorphous, substantially doped, electronic props., review 79−87175
Si, amorphous and polycrystallised, localised states, elec. and optical props. 78−64008
Si, amorphous CVD film photodetector for picosecond pulses 80−47101
Si, amorphous CVD films for high temp. solar photothermal conversion 80−26161
Si, amorphous evap., structural aspects in electronic data interpret. 77−76977
Si, amorphous evaporated, picosecond optoelectronic detect., sampling and correlation meas. 80−100478
Si amorphous evaporated film, doping 79−51127
Si amorphous film, AC conduction 77−66213
Si amorphous film, anisotropic etching phenomenon, appl. as solar selective absorber surfaces 80−72054
Si amorphous film, crystallisation kinetics and morphology, TEM obs. 78−84093
Si amorphous film, dangling bond ESR, light-induced quenching 80−50162
Si amorphous film, EPR rel. to elec. cond. 77−69692
Si, amorphous film, ESR, cond. secular change on annealing *(Japanese)* 79−15238
Si, amorphous film, Fermi energy shift with substitutional doping 79−46998
Si amorphous film, film, glow discharge deposited, refl. spectra and dielec. function 80−50360
Si, amorphous film, glow discharge deposition, rate enhancement by mag. field 80−65412
Si, amorphous film, heavily doped, glow discharge, AC cond. 80−49718
Si amorphous film, heavy doping by alkali ion implantation 80−2045
Si amorphous film, hole carrier transport 80−2500
Si, amorphous film, hole drift mobility, temp. depend. 79−23973
Si, amorphous film, in Ti-Si-Ti struct., elec. cond. processes and threshold switching 79−78207
Si, amorphous film, interface charge, influence on transfer meas. 79−15237
Si amorphous film, optical props., electronic states 80−25475
Si, amorphous film, plasma preparation 78−72740
Si, amorphous film, plasma-deposited, photoluminesc. and EPR meas. 79−4864
Si, amorphous film, RF plasma deposition from $SiCl_4$-H_2, characterisation 80−66435
Si amorphous film, saturation meas. on ESR signals 79−33535
Si, amorphous film, selective laser recrystn. over heavily doped lines 80−84947
Si amorphous film, sputter-deposited, elec., optical, and photoelectronic props. 79−24433
Si, amorphous film, sputtering by 0.5 to 5 keV Ar^+ ions 79−91550
Si, amorphous film, TSC, density of localised states distrib. 80−65587
Si amorphous film, vacuum deposited, microscopic voids, gas absorpt., crystn. study 80−49534
Si, amorphous film deposition from silane glow discharge plasma 77−44173
Si amorphous film effect of gas exposure on EPR signal 78−84475
Si, amorphous film prepared from glow discharge, quantitative H anal. 77−69188
Si, amorphous film prepared by CVD, optical props. and struct., solar absorber appl. 79−52035
Si, amorphous films, characterisation by Rutherford backscatt. spectrometry 80−50498

semiconductor thin films continued
Si, amorphous films, halogenated and hydrogenated, elec. and optical props. 80−97016
Si, amorphous films, ion implanted, elec. and photocond. props. 80−49717
Si amorphous films, RF sputtered, appl. as Schottky barrier solar cells 79−34434
Si, amorphous films, RF sputtering prep. at high Ar press., props. obs. 80−80418
Si amorphous films, self-ion bombard., electronic props. 79−28422
Si amorphous films, switching, electrothermal model 80−80407
Si, amorphous glow discharge films, H_2 content, elec. props., and photostability 80−25577
Si, amorphous layer crystn., effect of ^{16}O, ^{12}C, ^{14}N and inert gases 78−14623
Si amorphous layers, laser annealing, photoluminesc. study 80−2049
Si, amorphous sputtered film, elec. cond. and photocond. 79−87097
Si, amorphous sputtered films, hydrogenated, photoinduced optical absorpt. 80−50362
Si, amorphous sputtered thin film, US anomalies, 0.5-300K 80−34145
Si, amorphous thin films, appl. in solar cells, recent developments 78−80016
Si, amorphous ultrahigh vacuum evaporated films, ESR obs., deposition effects 79−33534
Si, and Si:H, amorphous, sputter deposited, O_2 incorporation during and after fabrication 80−49541
Si and Si:H amorphous films, porosity and oxidation of evap., sputtered and plasma-deposited films 80−10838
Si, anodic oxidation for abrading thin layers from wafers *(German)* 77−25176
Si, Ar(Xe) ion bombarded, sputtering yield energy and fluence depend. 79−78805
Si, CVD, amorphous and polycryst., microscopic surface roughness, effective-medium models, ellipsometric expts. 80−24756
Si, CVD, underlying oxide layer thickness effect on in-process thickness monitoring 80−6679
Si, CVD amorphous films, effect of surface characts. on visible and UV optical props. 80−60698
Si CVD film on amorphous substrate, CW laser recryst. 79−90894
Si, CVD growth and film morphology, rel. to model of mass transport 77−59233
Si, CVD growth rate, temp. and conc. effects, mass transport model 77−59234
Si, CVD on liq. Sn layers in HCl presence, enhanced crystallinity 78−6853
Si, CVD on SiO_2 and Si_3N_4 substrates, nucleation in SiH_4-HCl-H_2 system at high temp. 80−49538
Si, CVD or evaporated, covered with Al layer, solid-phase crystn. obs. 77−85100
Si, CVD polycryst. film, growth texture 77−7990
Si, chemically deposited on amorphous SiO_2, influence of substrate temp. and SiH_4 to N ratio on struct. 79−65346
Si, coating of mullite ceramic substrate, for solar cell appl. 79−34432
Si continuous polycrystalline films on C substrates 78−64490
Si deposition by SiH_4 pyrolysis at low temps. and atm. press. 79−91595
Si deposition using solar furnace 80−89148
Si, diffusion layers, B distrib. 77−7753
Si, dopant distrib. in mono- and polycryst. samples, C-V technique 80−6425
Si, doped amorphous, transport props., conductivity, thermopower, temp. depend. 79−73512
Si, effect of O on thin film compositions obtained by secondary ion emission 80−26079
Si, electrical conduction in amorphous semiconductors, mechanisms 79−56214
Si, electrodeposited film, appl. in solar cell fabrication 78−76611
Si, electron beam deposited, elec. and struct. props. 79−1632
Si, electron beam evaporation, for solar cell appl., heat exchanges and columnar growth 79−15609
Si, electron-beam-deposited on W substrates, growth and struct., AES and SEM obs. 79−46972
Si, electron-beam-evaporated amorphous thin films, noise meas. 79−24091
Si, electroreflectance spectra, 2.8 to 5.0 eV, ion bombard. effects 77−1752
Si film, amorphous, effects of annealing of gap states 78−72115
Si film, amorphous, glow discharge deposited, for low cost solar cells 80−61355
Si film, amorphous, hopping cond. control by ion bombard. induced struct. modification 80−92898
Si, film, amorphous, two-dimensional variable range hopping cond. 80−10977
Si film, amorphous and crystalline, optical properties 77−24906
Si, film, CVD, low press., struct. and stability, X-ray diffr. and TEM obs. 78−91559
Si film, critical surface tension, aligning props. of nematic MBBA mols. 79−90846
Si film, crystallographic orientation using surface relief grating and laser crystn. 79−95277
Si film, growth on SiO_2 substrate by pyrolysis of SiH_4 77−89678
Si film, hydrogenated amorphous, Brillouin scatt. 78−72538
Si film, low press. CVD prep., struct., elec. and optical props. 80−70548
Si film, optical characterisation from guided wave optics 78−48245
Si film, polariton resonance obs. from reflectivity meas. 77−69251
Si film, polycryst., grain struct. and surface roughness, TEM study 80−70556
Si film, polycryst., laser-induced CVD growth from $SiCl_4$ 80−84852
Si film, prep. by plasma-induced CVD from $SiCl_4$-H_2 79−83132
Si film, sputtered, physical props. 79−77938
Si film deposition, on quart z and MgO substrates, using double cathode sputtering system *(Japanese)* 77−55889
Si, film on Al-Cu, ellipsometric meas. technique, comparison to X-ray fluoresc. anal. 78−51840
Si, film on Si substrate, stress meas., X-ray topography technique 78−5710
Si film thickness meas. from visible refl. spectra 79−99960
Si films, electron beam evaporated, for MIS solar cells 80−93490
Si films, polycryst., annealing of paramag. vacancy-type defects, EPR obs. 79−10848
Si films, RF sputtered, Ar conc. as function of operation frequency and discharge pressure 80−65393
semiconductor thin films continued
Si films, ribbon-against-drop process, physical and chemical characterisation 80−92798
n-Si films on sapphire, crystalline defects effect on elec. props. 77−20470
Si, foil, thinning for electron microscopy 79−49217
Si, glow discharge amorphous film, reflectance and transmittance *(Japanese)* 80−34995
Si, glow discharge deposited, optical spectra, reflectance, dielectric function and oscillator strength 80−11492
Si, glow discharge deposition, SiH_4 discharge parameters obs. 80−44030
Si, glow discharge film decomposed from silane, on amorphous substrate, elec. cond., RHEED study 80−20044
Si, growth by ionised-cluster beam deposition 77−32527
Si, growth of large grain polycryst. layers on graphite substrates by CVD on liquid layers 80−55849
Si, hydrogenated amorphous film, XPS and UPS 78−19636
Si implanted with ^{31}P, ^{75}As, ^{11}B, amorphous layer reordering 78−14622
Si, ion bombarded, crystalline-to-amorphous transition, defect-rich film prep. 80−65071
Si, ion implantation with Li^+, characts. for thin film solar cell use *(Korean)* 77−51812
Si, ion-implanted polycrystalline film, defect build-up efficiency 80−2054
Si large grain films on metallurgical Si substrates, chem., struct., elect. and photovoltaic props. 80−61357
a-Si, laser induced crystallisation mechanism, epitaxial regrowth 80−84962
Si, laser pulse induced amorphous to cryst. transition, thickness depend. 78−47678
Si layers, carrier profiling using four-point probe method 79−37732
Si noncrystalline film, struct., interatomic distances, SRO 80−107053
Si, on Al_2O_3, quantitative electron microprobe analysis 77−9150
Si, on graphite, early growth by ion-beam sputtering 77−44158
Si, on sapphire, defect struct., TEM obs. 77−47693
Si on sapphire, deposition kinetics and interface characteris. 79−28234
Si, on sapphire, quality determ. using IR and UV specular reflectance meas. 80−108684
n-Si on sapphire magnetoresistance anisotropies and electronic struct. obs. 77−20471
Si, on SiO_2, fitting stress and its effect on vacancy generation and distrib. 77−28087
Si, on W (100), struct. and work function, LEED meas. 77−66096
Si photoconducting films, amorphous, undoped, I-V characts. of vacuum deposited films 80−60049
Si plasma deposited amorphous hydrogenated film, optical props., annealing effect 79−56874
Si, plasma etching, role of chemisorpt. of CF_4, CF_3H, CF_3Cl, CF_2Cl_2 and CCl_4 79−11714
Si, polycryst, CVD, electron beam recrystn. 80−24759
Si, polycryst., energy distrib. of trapping states, from impedance of MOSS struct. 80−65691
Si, polycryst., growth kinetics in low press. CVD reactor 79−91594
Si, polycryst., layer structure dependence on carrier gas moisture and O_2 content *(Bulgarian)* 80−59811
Si, polycryst., thinning using plasma etching *(Slovak)* 80−45405
Si, polycryst. CVD film electrical props. 78−6466
Si, polycryst. film, ion plating on Al, growth from eutectic melt 77−8765
Si polycryst. film, ion-implanted, pulsed laser annealing 79−77612
Si, polycryst. film doping during deposition and with diffusion 78−6088
Si, polycryst. film from low. temp. pyrolysis of SiH_4 78−31342
Si, polycryst. films, transport props. and grain boundary charact. by TEM 80−50980
Si, polycryst. on Si, disloc. config. under periodic stress field 78−10312
Si, polycrystalline, As segregation at grain boundaries, elec. props. meas. 80−75259
Si, polycrystalline, electron microscopic investigation of initial stage of growth 79−23849
Si, polycrystalline, film thickness meas., visible spectral reflectance analysis 78−32786
Si, polycrystalline, glow discharge deposited below 250°C, struct. and morphology 80−49535
Si, polycrystalline, parameters in two absorbing layers effect on reflected light polarisation *(Polish)* 78−21095
Si, polycrystalline, struct.-thickness relationships 77−62779
Si, polycrystalline, substruct. 79−23848
Si polycrystalline CVD film optical props. 77−77315
Si polycrystalline CVD film formation and props. 77−77401
Si polycrystalline CVD films, non-volatile memory switching 80−54814
Si polycrystalline film, effect of defects/grain boundaries on photovoltaic mech. 80−93883
Si polycrystalline films, anomalous etching effects 77−77613
Si polycrystalline films, texture formation study 79−87662
Si, polycrystalline films, meas. of effective diffusion length by surface photovoltage method 80−80424
Si, polycrystalline layer, laser-induced single cryst. transition, RHEED and backscatt. obs 78−87704
Si, polycrystalline self-supporting, thermal expansion shear separation technique, solar cell appl. 80−81439
Si, polycrystalline structure stability, stacking defects, twins grain struct. *(Russian)* 80−100248
Si, porous, form. and oxidation by anodic reaction 79−28966
Si, porous film, form. by anodic reaction in HF soln., struct. props. 77−24971
Si, post-annealed amorphous layer, twinning struct. by transmission electron diffr. 77−76685
Si, prod. of polySi vapour deposited coatings for solar cells, cost anal. 80−93495
Si, RF sputtered amorphous film, high temp. metal induced crystn. 77−11825
Si, recrystallisation of CVD-grown polycryst. Si and influence of B, Al dopants on grain growth 80−54575
Si resistors, polycryst., elec. props. in nonlinear regime, grain boundary trapping model 79−38204
Si scattering surface layer, optical props. *(Russian)* 80−11419
Si, selective etchant for defect density distrib. profile 79−86793
Si, self-supporting polycryst. film deposited by energy beam plasma, for terrestrial solar cells 79−11523
Si, semi-insulating polycrystalline CVD layers, AES and XPS characterisation 80−16129

semiconductor thin films continued
Si, semicrystalline layer, deposited on stainless steel and Pyrex glass, growth conditions and props. 79−82482
Si, solar cell, from film on foreign substrate 77−77390
Si solar cell fabrication, R and D on low-cost processes, effect of impurities on cell performance 80−50978
Si solar cells, fabrication using continuous or pulsed lasers *(French)* 80−61350
Si solar cells, perform. parameters of amorphous and polycryst. thin film cells 80−93882
Si solar cells, polycrystalline, from recrystallized plasma deposited thin films 80−104509
Si, sputtered film, in Al-Si-Al(Mo), photovoltaic props. 77−24623
Si, surface layer, thin, density meas. by total external X-ray reflection 78−14635
Si thin epitaxial dE/dx detectors 77−54407
Si, thin film, evaporated amorphous, hydrogenation by plasma treatment 78−91555
Si, thin sub-monolayer film, Auger emission coeffs. meas. 80−55236
Si vacuum deposited polycryst. films, p-n junctions investigation 77−28249
Si, vacuum deposition, combined with Sb ion implantation *(Japanese)* 78−88428
a-Si, vapour species rel. to amorphous film deposition 78−14641
Si volume plasmons, EELS, line shape 79−90984
Si wafer, deformation *(Japanese)* 78−43064
Si wafer, shrinkage and annihilation of stacking faults 77−39598
Si wafers, n- and p-type (100), oxidation-induced stacking faults 77−39599
Si wafers, preparation of preselected areas for TEM 78−24887
Si, zone refined, prep. of solar cells 78−64475
Si:Al, polycryst. film, grain boundary diffusion, Auger sputter profiling 80−75388
Si:Al film, low-temp. diffusion of Al 78−38878
Si:Al(Sb) film, amorphous, ion implantation, effect on cond. 78−83839
Si:As(B)(P), ion-implanted polycrystalline films, laser annealing 79−73181
Si:As(P) film, polycryst. laser annealed, resistivity changes during thermal annealing 79−91163
Si:Au, O(H), film, amorphous, elec. cond. meas. 80−80423
Si:B, highly-doped polycryst. thin film, growth kinetics and properties 78−44016
Si:B, polycryst., effect of laser annealing on struct. and elec. props. 79−11243
Si:B, polycryst. film, piezoresistive gauge factor 77−12029
Si:B, use of BN source to achieve high surface concentration of B *(Russian)* 80−107639
Si:B amorphous film, CVD prep., EPR, elec. and optical props. 79−4558
Si:B ion implanted layers, light refl. and transmission coeffs., computer program 80−66316
Si:B(Al), (P)(As)(In), ion implanted film, elec. prop. impurity depend. 80−24467
Si:B(P), ion implanted layers, carrier distrib. meas. precision 77−43603
Si:B(P) polycrystalline thin film, plasma annealing, effect on elec. props. 80−7005
Si:F, amorphous, heat resistant, prep., elec. cond., IR absorpt., annealing 80−65719
Si:F, amorphous film, effect of F on elec. cond. 80−34444
Si:H, amorphous, control and anal. of deposition, using plasma spectroscopy 80−45230
Si:H, amorphous, dopant conc., glow discharge optical spectroscopy 80−49546
Si:H, amorphous, glow discharge deposited, laser annealing 80−49104
Si:H, amorphous, H content determ. by IR absorpt., gas evolution and nuclear reaction methods 80−44130
Si:H, amorphous, plasma deposited, cond. adsorbate and insulating layer effects 80−49749
Si:H, amorphous, plasma-deposited, effect of DC elec. field superimposed during deposition 80−44643
Si:H, amorphous, prep. by RF glow discharge decomp. of SiH_4, optical props. and H conc. 80−15416
Si:H, amorphous, prod. by high temp. thermal decomp. of SiH_4, and photocond. 79−87585
Si:H, amorphous, RF sputtered, suitability as solar cell material 80−40864
Si:H, amorphous, reactively sputtered, H content effect on props. 80−49714
Si:H, amorphous, refr. index, temp. depend., implications for thermoreflectance and electroreflectance 80−50290
Si:H, amorphous, sputtered on $Gd_2(MoO_4)_3$, ferroelec. domain wall motion, image scanning 80−83663
n-Si:H, amorphous, thickness depend. cond. 80−49724
Si:H, amorphous film, anal. of intrinsic photocond. spectrum 79−73541
Si:H, amorphous film, prep. by plasma decomp. of SiH_4 under mag. field, and characterisation 80−45239
Si:H, amorphous films, plasma-deposited, defect states, IR, ESR, and refractive index meas. 79−65944
Si:H, amorphous hydrogenated film, decomp. kinetics 79−100342
Si:H, amorphous Schottky solar cells, prep. and characts. of diode RF reactive cathodic sputtered films *(French)* 80−61347
Si:H, amorphous sputtered, excitation spectra and photoluminesc. 80−50396
Si:H, amorphous thin film, ion plating, IR absorpt. meas. 80−84857
Si:H, amorphous thin film solar cells 80−81478
Si:H, amorphouse film, optical and elec. props. 79−82694
Si:H, Cl(F), amorphous, photocond., dark cond. and photoluminesc. 80−49802
α-Si:H, discharge produced, electronic props. rel. to solar cell characts. 79−15241
Si:H, plasma-deposited amorphous film, proton mag. reson. 80−44931
Si:H,F,O amorphous, plasma deposited, comp. and optical props. 80−50441
Si:H,P, amorphous, heavily hydrogenated, high gap state densities 80−49803
Si:H,P amorphous film, elec. cond., thickness and temp. depend. 80−65559
a-Si:H alloys, sputter deposited thin film coatings, property-comp. relationships 80−80975
Si:H amorphous film, ^1H quantitative depth profiling by nuclear reactions and SIMS 78−14373

semiconductor thin films continued
Si:H amorphous film, plasma-deposited, growth morphology and defects 80−44128
Si:H amorphous film, plasma-deposited, elec. and comp. heterogeneity 80−44745
Si:H amorphous film, prop. by glow discharge deposition, and plasma parameter effects on props. 80−45240
Si:H amorphous film, sputtered in Ar-SiH_4 mixtures, props. 79−87023
Si:H amorphous film, sputtered IR vibr. spectra and photolum., effects of partial evolution of H 80−44413
Si:H amorphous films, conductivity and temp. dependence of optical gap 80−100462
Si:H amorphous films, ESR, optical gap and elec. cond. meas. 80−75842
Si:H amorphous films, effects of glow-discharge prep. conditions on H content 79−46969
Si:H amorphous films, IR spectrum and struct. 80−97277
Si:H amorphous films, interference enhanced Raman scatt. 80−50326
Si:H amorphous films, optoelectronic behaviour depend. on impurity incorporation during plasma deposition 80−49804
Si:H amorphous films, photovoltaic and photocond. spectra, photoluminesc. 80−44645
Si:H amorphous films, photoinduced optical absorpt. and photocond. 80−50361
Si:H amorphous films, role of Ar in deposition process, IR absorpt. and photocond. meas. 80−50321
Si:H amorphous films for solar cells, optical and elec. props. of RF glow discharge deposited films 80−54576
Si:H amorphous glow discharge film, optical absorpt., near IR region 79−87518
Si:H amorphous layer as passivant for p-n junction in crystalline Si 79−47155
Si:H amorphous layers, ion bombard., AES study, $L_1L_{23}V$ Coster-Kronig transition 79−99992
Si:H amorphous semiconductors, prep. from SiH_4 and characts. 78−48326
Si:H amorphous sputtered film, photoluminesc., photocond. 80−20729
Si:H amorphous sputtered films, optical gap, IR absorpt. meas. 80−50320
Si:H film, amorphous, bombarded, defects, luminesc. and ESR meas. 80−34977
Si:H film, amorphous, H-associated disorder modes, PMR spin-lattice relax. time meas. 80−93202
Si:H film, amorphous, photocond. imaging 80−1300
Si:H film, amorphous, plasma-deposited, small angle X-ray and neutron scatt. studies 80−59826
a-Si:H film, glow discharge deposited, H profiles, doping level 80−84202
Si:H plasma deposited film, amorphous, microstruct., TEM and SEM obs. 80−10801
Si:H sputtered amorphous film, luminesc. and non-radiative decay 80−50395
Si:H(B)(P), amorphous, UV absorpt. spectra 80−25420
Si:H(D), amorphous films, CVD, post-hydrogenation 80−54552
Si:In amorphous films, EPR, elec. cond., and magnetoresist. 80−50160
Si:Li, amorphous, elec. cond. and thermopower 79−73537
Si:Li(Na)(K)(F)(Cl), amorphous, implantation effects on elec. props. 80−49716
Si:Mn, amorphous, cond. increase by Mn doping 78−72155
Si:Mn(Fe)(Ni) amorphous films, ESR and elec. cond. 80−50171
Si:O, amorphous, sputtered, influence of O and deposition conditions 80−54693
Si:O, CVD layer, RHEED study of surface crystallinity, annealing effect on structure 79−69371
Si:O, evaporated amorphous film, effect of O_2 on props., ESR spectra 80−11265
Si:O,H amorphous, plasma-deposited, electronic and struct. props. 80−50391
Si:O film, near IR absorption, O impurity states 78−88333
Si:O film, near IR reflectivity at high temps. 78−56532
Si:O film, thermally deposited, semi-insulating, crystallographic study 78−75954
Si:P, amorphous, CVD, defect compensation 80−54644
Si:P, amorphous, CVD, substitutional doping, electronic props. 79−23923
Si:P, heavily doped, glow-discharge-produced, elec. and optical props 80−2497
Si:P, heavily ion implanted, polycrystalline, grain growth 79−19477
Si:P, polycryst. etching characts. in CF_4 plasma 78−76777
Si:P, polycrystalline laser recrystallised film on Si substrate, cryst. struct., thermal oxidation 80−65391
Si:P, RF sputtered polycryst. film, MOS compatibility 78−6455
Si:P film, CVD polycrystalline, low press. and atmos. press., oxidation 80−3214
Si:P film, polycryst. pulsed electron beam annealing 80−10566
Si:P(B), film, electronic props. 78−84330
Si:Sb, amorphous, electronic transport props. 80−44589
Si:Sb vacuum deposited coating, p-n junction, pulsed electron beam annealing doping, diffusion 80−75480
Si/Au films, laser-irrad., phase transform. study 80−49536
Si/Pd system, solid phase epitaxial growth control by C ion implantation 80−75466
Si/Si-Ge alloy, amorphous, solar cell, multijunction structure, increased conversion efficiencies, low cost 80−45677
Si-absorbing film system, ellipsometry 79−99964
Si-Al-Al_2O_3 system, solid phase Si regrowth on sapphire 80−100413
Si-Au amorphous film, metal-nonmetal transition, elec. cond., thermoelectric power meas. 79−47132
Si-Au amorphous system, optical absorpt., IR photocond. 79−42582
Si-Au-Si, Auger line intensity, contrib. of backscattered electrons 79−65962
Si-Au(Cr)(Pd), contact reactions between amorphous Si and metallic films, TEM, transmission electron diffr. obs. 79−23846
Si-B amorphous film, plasma deposited, characterization 79−69828
Si-B-O film, electron probe microanal., Monte Carlo calcs. 79−83533
Si-C:H, amorphous film, vibr. spectrum 79−61450
Si-F-H:P, film, dark cond., struct., Raman scatt. 80−88588
Si-Ge, amorphous, ESR line intensity anal., rel. to cond. mechanism 78−43645
Si-Ge amorphous films, effects of annealing and crystn., ESR microstruct. and elec. meas. 78−26790

semiconductor thin films continued
Si-H, amorphous, on Nb or W, spectrally selective absorber, IR spectra 80−26164
Si-H, amorphous, sputtered, photolum. obs. 80−80856
Si-H, amorphous, thermal stability and decomp. kinetics 80−24758
Si-H, amorphous plasma deposited film, H content and density 79−82472
Si-H, RF sputtered amorphous alloy, influence of Ar press. on elec. props. and photoluminesc. 79−91585
Si-H amorphous film, reactively sputtered, prep. and props. 79−78889
a-Si-H sputtered solar cells, temp. depend. of Schottky barrier charact. 80−45669
Si-H:As alloy, amorphous film, coordination of impurities, EXAFS of data 77−84780
Si-H:P amorphous film, dark cond., struct., Raman scatt. 80−88588
Si-H(-D), film, IR and Raman spectra, H bonding effects 78−72515
Si-metal contact, transport theory of Schottky barriers 80−80372
Si-Mo diffusion couples, $MoSi_2$ or Mo_3Si/Mo_5Si_3 form. 79−77836
Si-Ni(Pd)(Pt) film struct., silicide form. He^+ back scatt. and X-ray diffr. obs. 79−51442
Si-Pd-Si structure, epitaxial growth, backscattering and transmission electron microscopy studies of layered structures 80−80123
$Si-Si_3N_4-SiO_2$ non absorbing double layers, optical parameters reflectivity by liquid immersion method 80−71503
$Si-SiO_2$, film refr. index and thickness meas. 77−82589
$Si-SiO_2$-vacuum system, principal angle and azimuth determ. 78−11009
Si-transition metal metastable films as temp. independent resistors 78−68097
Si(:B), polycrystalline, deposition on Si wafer, bending effect 79−95276
$Si_xAs_{1-x}:H$, amorphous system, struct. and defects, Raman and EPR meas. 80−49103
$Si_{1-x}Au_x$ amorphous films, IR absorpt. spectra 80−16034
SiC, amorphous, reactively sputtered, effects of S/C ratio and H content on elec. and optical props. 79−90906
SiC amorphous film, elec. props. and hopping transp. 77−66211
SiC, film, synthesized by RF reactive ion plating, struct. 77−40391
SiC film electron beam preparation technique, diffraction pattern anal. *(German)* 80−55297
β-SiC, film prep by RF sputtering 77−44164
SiC film synthesis by plasma deposition process 78−11127
β-SiC form. on Si substrate in RF powered reactor 80−76173
SiC, on Si and metal silicides, formation characteristics and mechanism, by ion backscattering techniques 79−60653
n-SiC, single cryst. layers deposition on charact. substrates, morphology *(German)* 79−28943
SiC, sputtered, comp. and struct. props., effect of target materials 80−54549
SiC, sputtered amorphous film, struct., elec. and optical props. 79−78236
SiC, synthesis by ion implantation of diamond, role of struct. imperfections 78−34529
α-SiC:H, prepared by reactive sputtering, layer props. *(Japanese)* 80−60695
SiC:H amorphous reactively sputtered film, H content effect on film props. 80−75459
SiC_x, amorphous, prepared by glow discharge method, elec. and optical props. 77−21035
$Si_{1-x}C_x:H$ glow discharge films, local atomic struct., XPS and AES study 80−93448
$Si_{1-x}C_xH_z$, amorphous, H content determ. by nuclear reaction analysis 80−59821
$Si_{1-x}C_xH_z$ film, H content determ. by nuclear reaction analysis 80−59821
$Si_{1-x}Ge_x$, amorphous, ESR centres, effect of annealing 77−55701
$Si_{12}Ge_{10}As_{30}Te_{48}$ chalcogenide glass threshold switch conductivity in high ohmic state *(Russian)* 78−43502
$Si_{12}Ge_{10}As_{30}Te_{48}$ surface, heat treatment and electron bombard. effects. SEM obs., rel. to switching filament form. 77−47700
$SiH_{0.16}$ amorphous films, optical props. and photocond. near optical gap 80−50443
SiH_x amorphous reactively sputtered films, optical props. 80−50444
SiH_x polymer film, struct. rel. to amorphous solid 78−72048
SiH_z, amorphous, H content determ. by nuclear reaction analysis 80−59821
SiH_z film, H content determ. by nuclear reaction analysis 80−59821
$Si_{1-x}H_x$, amorphous RF sputtered, pure and P(B) doped, optical consts. 79−95866
$a\text{-}Si_{1-x}H_x$, oxygenated thin film, sputtered, elec. cond. and optical props. 79−15239
$Si_{1-x}H_x:Al$, amorphous, co-sputtered Al modification, electronic and optical props. 80−100461
Si_3N_4, film on Si substrate, stress meas., X-ray topography technique 78−5710
Si_3N_4, unsteady cond. in high elec. fields 78−76152
SiO_2, film on Si substrate, stress meas., X-ray topography technique 78−5710
SiO_2, oxide damage due to ion processing 79−24088
$Si_{12}Te_{48}As_{30}Ge_{10}$ amorphous film, current-voltage charact. 79−87104
SmS, absorpt. and refl. spectra, fine struct., cond. band extremum 79−69897
SmS, energy of metal-semicond. phase transition and threshold recording energy density 79−28386
SmS film amplitude-phase hologram recording *(Russian)* 79−94192
$Sn_{1-x}Ge_xTe$, evaporated thin films, charact. 79−60944
SnO_2 CVD film form. mechanism 78−38977
SnO_2, CVD using $SnCl_4-H_2O$ and $SnCl_4-H_2O_2$ systems, elec. and optical props. 78−52686
SnO_2, diffusion of impurities *(Japanese)* 79−95218
SnO_2, effects of Sb and In additions on struct. and resist. 77−20469
SnO_2, elec. conducting film on glass substrate, measurement of optical constants and thickness 78−60525
SnO_2, electro-conducting transparent film, props. rel. to production method *(Japanese)* 80−25557
SnO_2 film, mobility limitation by intercrystalline potential barrier, tunnelling effect 77−66210
SnO_2 film, orientating action of solid substrates, on liq. cryst. layer exam. 80−44111
SnO_2 film, pure and Sb doped, transparent cond., prop., charact., stability, struct. *(Japanese)* 78−47889
SnO_2 film growth at room temp. 79−91592
semiconductor thin films continued
SnO_2 films, selective, optical characterisation by thermodynamical method 80−84796
SnO_2 gas sensor, fast-detecting, prep. 80−61497
SnO_2, gas sensor, prep. 80−39691
SnO_2, growth by DC sputtering from compressed target, cond. and optical props. 77−59690
SnO_2, heat treated film, electrical conductivity 77−8211
SnO_2, O chemisorption, elec. cond. and EPR meas. correlation 80−84369
SnO_2, optical and elec. props., rel. to stoichiometric deviation and struct. 77−47701
SnO_2, optical characterisation, inversion method 78−11008
SnO_2, optical props., review 77−1673
SnO_2, reactive ion-plasma sputtered, elec. and opt. props. 79−42677
SnO_2 thin films, O_2 vacancy diffusion 80−107467
SnO_2 thin films, solid state gas sensor 80−40790
SnO_2, transparent conductive film, prep. by magnetron sputtering and elec., optical and structural props. *(Japanese)* 79−8247
SnO_2, transparent films, state of art *(Chinese)* 79−73610
SnO_2, two-step deposition process using DC sputtering and oxidation, and characterisation 78−95691
$SnO_2:F$, thin films, prep. by pyrolitic method, charact. by SEM, electron diffr. and SIMS, solar energy appl. 79−43143
$SnO_2:F$ films, elec. and optical props., solar energy conversion appl. 79−65945
$SnO_2:P$, CVD growth and etching charact., doping effects 80−107667
$SnO_2:Sb$, amorphous, electrotransport phenomena obs., under DC electric field 80−59840
$SnO_2:Sb$, transparent cond. film prep. by thermal decomp. of Sn salt of organic acid *(Japanese)* 77−90269
$SnO_2:Sb$, transparent cond. films, hydrolysis deposition, elec. and optical props. 79−43144
$SnO_2:Sb$ DC sputtered, heat treatment effects, expt. 77−28719
$SnO_2:Sb$ film on glass substrates, elec. props. 80−88652
$SnO_2:Sb$ sprayed film, growth mechanism and cryst. struct. 80−89143
$SnO_2:Sb$ transparent conductive coatings for Cu_2S-CdS solar cells 79−61992
SnO_x films, passivation effect on Si solar cells 80−61360
SnO_x films reactive DC sputtering prep., phase comp., X-ray diffr. and Mossbauer meas. 79−90914
Sn_xO_y, equipment for chemical vapour deposition on cylindrical objects 77−40378
$Sn_{1-x}Pb_xSe(Te)$ thin films, resistance to oxidation, Mossbauer study 80−39986
$Sn_{1-x}Pb_xTe$, production under quasiequilibrium conditions 80−45241
SnS(Se), electron diffr. struct. anal. 80−44449
SnTe, complex-composition film production method from vapour *(Russian)* 78−95702
SnTe film, electroreflectance effects 79−43055
SnTe, film, heat treatment in air, effect on struct., props. 79−11037
SnTe-InTe system, solid soln. films prep. under quasi-equilibrial conditions 79−33931
SnTe-PbSe, semicond. film, growth, phase composition, condensation temp. rel. to cond. type 77−28266
SnZ films, from thermal decomp. or organometallics, growth kinetics and struct. 79−78895
Sr-Te-O system, amorphous thin film, vacuum deposited, elec. cond., current cut-off *(Japanese)* 77−24625
T-metal, thin film contact, time evolution of photovoltaic effect 80−65687
Te, electrodeposit on Cu substrate 77−48355
Te, electronic struct. charge on ordering, double beam photoemission 78−19634
Te, evaporated, crystallinity and electronic props., annealing effect 77−85107
Te, evaporated deposition, absorptivity and emissivity 80−25473
Te, evaporated film, predeposited Ag, Sn, Bi, Al and Se nucleation centres effect on grain growth 77−4739
Te, evaporated film epitaxial and amorphous-crystalline phase transition growth and struct. 79−51449
Te evaporated film nucleation on Au oriented islands, grain growth 78−2388
Te, film, AES, LEED, XPS, energy loss spectra studies oxidation effects 78−73086
Te film, elec. props. effect of deposition rate 78−14844
Te film, electrodeposition on Sn in Sn/Te/electrolyte system, interface processes 77−63923
Te film, Hall consts., thickness depend. of mobility 79−87171
Te film, stability in moist air, rel. to information storage capability, atmospheric corrosion model 80−71774
Te film, surface morphology depend. on vacuum deposition angle 80−103553
Te film and trilayer antireflection structure for optical recording 79−94329
Te film condensed on mica, struct. and electrophysical props. 80−39688
Te film growth on KBr (111) on mica *(Japanese)* 78−79903
Te films, elec. props., 77 to 450K, thermal width of band gap 79−51698
Te, gas-evaporated, selective absorpt. charact. and emissivity 80−50998
Te, growth from melt, between Ge and CdS substrates, heterojunction prep. and characterisation *(German)* 77−20413
Te, hexagonal film vac.-evaporated at normal incidence, X-ray Fourier line shape anal. 79−99454
Te, interference enhanced Raman scatt. 80−42273
Te, oriented films, semiconducting props., Hall coeff., band structure 80−70854
Te, piezoresistance 79−95524
Te, polycrystalline, hole mobility, influence of tunnelling through barriers on grain boundaries 77−43748
Te, Seebeck coeff., elec. cond., structural depend. 79−78230
Te textured thin films, prep., high solar absorptivity by multiples refl. 80−11568
Te, thin evaporated films, 130 Å, temp. depend. of elec. props. 79−95529
Te thin film, optical props. *(French)* 77−44076
Te, thin film selective absorber coatings, prod. using an oblique vacuum deposition technique 80−81488
Te, vacuum deposited, growth and morphology of crysts. 80−96766
Te, vacuum deposition, effects of electron irradiation on surface coverage *(Japanese)* 79−82477

semiconductor thin films continued
Te/Ag double films, interdiffusion and struct. modifications *(French)* 77−62682
Te-Ag, thin film system, stress-relief appearance conditions 80−65416
Te-As-Ge, RF sputtering, temp. and bias effects on comp. 77−40367
Te-Au thin film interface, evolution, switching effects *(French)* 80−6660
Te-Bi thin film system, stress-relief appearance conditions 80−65416
Te-Ge-As-Si amoprhous film, voltage controlled negative resistance type characts. 79−69614
Te-Se-CdO struct., fabrication and characts. 78−76106
$Te_{40}As_{33}Ge_7Si_{18}$ film, threshold switching in relax. oscill. mode 77−69389
$Te_{40}As_{35}Ge_7Si_8$, amorphous, threshold switching, expt. 80−49830
$Te_{48}As_{18}Ge_6Si_{28}$ amorphous film, I-V curve, memory switching 79−69615
$Te_{39}As_{36}Si_{17}Ge_7P_1$ amorphous film, electroluminescence from on state 79−8188
TiO_2 film, electron diffr. exam. 78−79906
TiO_2, optical inhomogeneity, rel. to struct. 79−83047
TiO_2 semicond. films for water photoelectrolysis 80−26146
TiO_2 sputtered film, photocond. and TSC meas. 80−15560
$TlGaS_2(Se_2)$, elec. and photoelec. props. *(Russian)* 78−52109
VO_2, amorphous thin films, phase transition, resistivity and opt. transmission discontinuities 77−47871
VO_2, elec. cond. near metal-semicond. phase transition 77−1503
VO_2, film, IR induced metal-semicond. phase transition *(Russian)* 77−15769
VO_2 film, metal-dielec. transition, refl. after 40 keV ion bombardment 79−23899
VO_2, film, optical consts. and electrical props. near phase transition *(Russian)* 77−59631
VO_2, film, semiconductor-metal phase transition, fast laser kinetic studies 79−69419
VO_2 film, sensitivity to heat perturbation and current noise, effect of temp. 77−66215
VO_2, film, visualisation of microwave and IR radiation 80−5839
VO_2, nonlinear wave generation in system with metal-semicond. transition, wave propagation velocity *(Russian)* 79−73549
VO_2, nonstoichiometry influence on electron struct. and metal-insulator phase transition 80−44507
VO_2, optical characts. of phase transition, ion bombardment effects 79−28281
VO_2, optical props. meas. near semicond.-metal transition 77−1742
VO_2 pyrolytic film, phase transition and electrical cond. 77−89890
VO_2, resist.-temp. characts. and structure at phase transition temp. *(German)* 77−28265
VO_2, semicond.-metal phase transition, fast laser excitation, kinetics obs. 79−47018
VO_2 single cryst. film, ion-irrad., 'splitting' of semicond.-metal transition 80−11053
VO_2, sputtered, switching effects in four-electrode structures 78−2596
VO_2, thermochromic film, visualisation of microwave radiation using metal-semiconductor phase transition 79−65845
VO_2 thin film semiconductor-metal transition applications 80−49835
VO_2, thin films, doping by ions of Ar, B, P 77−84781
VO_2, V_2O_3 and V_3O_5, film prep. under equil. conditions, struct. and elec. props. 80−108352
VO_2:Al(W), thin layer prep. by reactive DC sputtering doping effectiveness *(German)* 78−6847
V_2O_4 films, characterisation using XPS, metal-semiconductor transition 79−28900
V_2O_5, amorphous, CVD prep. method 80−55299
V_2O_5, amorphous, thickness, density and refr. index determ. from reflectance interference spectra 80−55206
V_2O_5 amorphous film, photochromism and thermochromism 80−93254
V_2O_5 amorphous layers, gel deposited, semicond. props. 80−92887
V_2O_5 electrochromism obs. and mechanism, thin film growth *(Russian)* 77−77249
V_2O_5-ZnO-B_2O_3 glass, sputtered, optical absorpt., band gap and Urbach tail 77−8597
V_xO_y, film, preparation by calcining vanadium naphthenate, formation process exam. *(Japanese)* 78−30849
V_xO_y, prep. by thermal decomp. of vanadium naphthenate, and elec. props. *(Japanese)* 78−88425
WS_2 films, exciton peaks in absorpt. spectra, press. and temp. depend. 79−51496
Yb_2Te_3, films, prep., elec. props. 78−43494
Zn chalcogenides, thin films, VPE, needle-like cryst. growth 80−80148
Zn-In-S thin layers, ternary phases, optical props. near long-wavelength intrinsic absorpt. edge 80−80887
$Zn_xCd_{1-x}S$ film, prep. and use as heterojunction optical energy converters 79−95488
$Zn_xCd_{1-x}S$, film, single-thermal-source form. 80−2492
$Zn_xCd_{1-x}S$, film for heterojunction solar cell 77−8208
$Zn_xCd_{1-x}S$, granulated films, optical reson. 79−4863
$Zn_xCd_{1-x}S$, optimal synthesis conditions for single cryst. growth 80−100776
$Zn_xCd_{1-x}S$, prep by soln. spray method, and struct., optical and elec. props. 78−52666
$Zn_xCd_{1-x}S$ solid soln., reactive cosputtering, struct., comp. and opt. absorpt. edge *(French)* 78−6237
$Zn_xCd_{1-x}S$ solid soln. film by spray pyrolysis 77−81214
$Zn_xCd_{1-x}S$, thin solid soln. films, vapour deposited, elec. and optical characts. 80−60110
$Zn_xCd_{1-x}Se$, vacuum condensates, forbidden band width determ. from transmission spectra 77−8670
$Zn_xCd_{1-x}Te$ films, absorpt. spectra in 3.0 to 5.8 eV range 79−52034
ZnF_2:Mn, thin films, electroluminescence, brightness voltage characts. hysteresis 80−20709
$Zn_xHg_{1-x}Se(Te,S)$ film preparation and props. *(Russian)* 78−11122
$ZnIn_2S_4$ (I), one-packed polytype, resist., photocond. and luminesc. 79−1608
$ZnIn_2S_4$ film, photoluminesc. and photocond. 78−52677
ZnO, amorphous and cryst., CVD growth and elec. props. 77−76973
ZnO, aqueous-deposited films, struct. and electronic props. for solar cell appls. 80−100797
ZnO, CVD films on sapphire substrates, use as optical waveguide 78−90500
ZnO crystalline films, deposition techniques *(Japanese)* 79−74098
ZnO, DC diode sputtering, prep. and characterisation 78−3040
semiconductor thin films continued
ZnO film, chemisorption of H, electrical cond. exam. adsorption centres 78−67913
ZnO film, prep. by reactive ionized cluster beam deposition, and characterisation 80−10829
ZnO, film for solar cell appl. structural, optical and elec. props. 80−2294
ZnO films, DC reactive magnetron sputtering technique, quality study 79−78877
n-ZnO, highly degenerate, IR absorption by free polarons 77−4697
ZnO interdigital transducer, efficient bulk-wave excitation in layered media 77−69156
ZnO on Zn (0001), oxide film growth, at. and electronic struct. 78−15587
ZnO, piezoelec. films produced by gas transport reaction, US excitation efficiency 80−2700
ZnO RF sputtered films, post deposition annealing behaviour 80−100416
ZnO sputtered films, vertical electrode config. to avoid contamination 79−69982
ZnO, thin Zn or O rich layers, thermolysis, photolysis, SEM, XPS 77−11821
Zn_3P_2 bulk and thin film, UV reflectivity spectra, photovoltaic effects, optical consts. 80−25472
Zn_3P_2, elec. cond., Hall effect, P interstitial effects 80−84465
Zn_3P_2, optical props., transition energies from transmission and refl. meas. 80−60532
Zn_3P_2 thin polycrystalline films for solar photovoltaic cells 80−97797
ZnS, effect of fabrication parameters on electroluminescence and related props. *(Japanese)* 80−76083
ZnS electroluminescent films, low energy Mn implantation system 78−30658
ZnS evaporated film optical props. 160 to 2000 A 79−15544
ZnS film, defect form. and development 80−96759
ZnS, film, intrinsic stress meas. 80−71696
ZnS film, Joule heating, I-V characts. 78−2599
ZnS, film, laser evaporation synthesis, surface struct. 79−28954
ZnS, film, vac. deposition onto NaCl cryst. in H_2S environment 78−63945
ZnS film free carrier absorption for laser beam modulation *(Japanese)* 79−7164
ZnS film on Si, fused quartz substrates, H_2O absorpt., IR anal. 80−75446
ZnS films, electrolum., bistable excitation 80−93406
ZnS, granulated films, optical reson. 79−4863
ZnS, ion beam deposition 77−70008
ZnS, optical inhomogeneity, rel. to struct. 79−83047
ZnS, photovoltaic effects under illum. from above and below 78−52031
ZnS, RF sputtered film, stoichiometry, chem. comp. 78−34727
ZnS, thin film deposition, by low pressure, high freq. induction plasma *(Russian)* 79−69992
ZnS, vacuum deposited, origin of mech. stress 79−90925
ZnS, vacuum-evaporated conducting films, prep. and props. 79−66007
ZnS:Ag, IR quenching of photocapacitance, deep levels obs. 78−56180
ZnS:Ag film, photocapacitance IR quenching, hole photoionisation energy and spectral distrib. 79−87127
ZnS:Cu, Br based electroluminesc. cells, light, const. field effects on electroluminesc. 78−84658
ZnS:Cu, Cl, Mn film, AC electrolum. 80−60680
ZnS:Cu, film effect of Cu valency on cond. 79−11246
ZnS:Cu,Er,Cl film, ageing and forming, DC electroluminesc., impact excitation 79−47522
ZnS:Cu,Pb film, sublimated, pulse electrolum. meas. *(Russian)* 77−85806
ZnS:Mn, AC thin film electroluminesc., filamentary emission and memory effect 79−38672
ZnS:Mn, AC thin-film electrolum. devices, electrolum. efficiency profiles 79−65931
ZnS:Mn, Cu, Cl films, AC electrolum. 80−60679
ZnS:Mn, electrolum. film, direct impact excitation of Mn centres 77−24900
ZnS:Mn, electrolum. films, activating impurity diffusion coeff. *(Russian)* 77−84995
ZnS:Mn, photoluminesc. and electroluminesc., excitation mechanism of luminesc. centres 79−11459
ZnS:Mn, spectral and electro-optical props. 77−1736
ZnS:Mn AC electrolum., memory effect 78−15228
ZnS:Mn AC electrolum. device, filament behaviour 80−20712
ZnS:Mn AC thin film devices, domain electrolum. 80−66303
ZnS:Mn co-deposited electrolum. device, phys. and elec. characterisation 80−20713
ZnS:Mn electroluminescent films, amplification factor during electric field excitation, population inversion *(Russian)* 79−78757
ZnS:Mn film, AC electrolum., memory effects 79−38673
ZnS:Mn film, current conduction and light emission, physical mechanism 78−14840
ZnS:Mn film, electroluminescence theory 79−11470
ZnS:Mn film, emission centres of DC electrolum. 78−68564
ZnS:Mn film, luminesc. of highly efficient DC diodes 77−8630
ZnS:Mn film device, laser modulation of electrolum. 78−52576
ZnS:Mn film in SnO_2-ZnS-Cu_xS-ZnS:Mn-Al_2O_3-Al struct., electrolum. 79−33837
ZnS:Mn films, surface struct., microrelief rel. to morphology of SnO_2 transparent cond. support 79−56092
ZnS:MnF_2 films, effect of Mn conc., XPS obs. 79−33886
ZnS:RF_3 film, AC electrolum., memory effects 79−38673
ZnS:RF_3 in Ta-Ta_2O_5-ZnS:RF_3-Au struct., electrolum. and cathodolum. meas. *(French)* 77−16398
ZnS:Tb^{3+}, NdF_3, vac. deposited, electrolum. energy transfer 80−2861
ZnS:Tb^{3+}, sputtered film, DC electroluminesc. and host-excited photoluminesc., Tb^{3+} content depend. 77−85807
ZnS:TbF_3, between semicond. Y_2O_3 layers, bright green electrolum. 80−2859
ZnS-CdS films, prep. by atomisation 80−16176
ZnS-metal interface in MIM struct., photoexcitation level assignment *(French)* 80−15622
ZnS_xSe_{1-x} layer on ZnS, ZnSe, growth by solid-state diffusion technique 78−56578
ZnS(Se)(Te), on semicond. substrates, early stages of growth, electron microscope obs. *(Russian)* 78−38976
ZnSe, amorphous thin film, prep. and electronic props. 77−85350

semiconductor thin films continued
ZnSe, CVD, delayed failure 79−99462
ZnSe, film, hopping cond. 80−2499
ZnSe film, thermostimulated polariton emission 78−2436
ZnSe films, long wavelength IR polariton emission band thermal shift and broadening 80−92833
ZnSe films, reson. Raman spectra 80−80888
ZnSe, high conductivity films appl. to p.n. heterojunctions 78−68100
ZnSe, rare earth fluoride doped, electrolum. meas. 77−16397
ZnSe, single cryst. and film, long wave IR emission by lattice vibrs. 77−51528
ZnSe:In, optical absorpt. spectrum, 0.4 to 0.7 μm 77−81136
ZnSe:Mn thin film, AC electrolum. 79−47519
ZnSe/metal, dielectric phonon-metal electron interaction, effect on optical props. *(Russian)* 79−19663
$ZnSiAs_2$, synthesis and layer growth by CVD in open flow system 78−15312
ZnTe film, exciton spectra, press. and temp. depend. 80−80886
ZnTe film, prepared by single-source vacuum deposition method *(Japanese)* 80−6664
ZnTe films, grown on glass using atomic layer evaporation 80−44453
ZnTe films, internal stress effect on fund. refl. spectra 80−60701
ZnTe, stopping power for protons and alpha particles, proton energy straggle values 77−89489
ZnTe thin film, model for off-on transition 80−54742

semiconductors
Generalities and properties of unspecified materials only. For specific materials see semiconductor materials.
see also amorphous semiconductors; degenerate semiconductors; heavily doped semiconductors; magnetic semiconductors; many-valley semiconductors; narrow band gap semiconductors; polar semiconductors; thermoelectric effects in semiconductors and insulators
1/f noise, two electron centres as possible source 79−24030
1/f noise origin 80−11060
1/f-noise in Hall voltage 79−24039
2π-pulse propagation in crossed elec. and mag. fields 78−79079
absorption line profile in static elec. field, effect of impurities 78−92101
absorption of EM and sound waves in strong coupling case, effect of acoustic superlattice 78−26630
absorption of strong EM waves, weak electric field effects 79−95400
AC response, influence of states in gap and generation-recomb. effects 77−4362
AC thermopower measurement 80−44624
acceptor binding energies 77−69270
acceptor spectra, interpretation 78−43332
acoustic domain injection *(Japanese)* 80−91945
acoustic studies progress *(Japanese)* 80−49310
acoustoelectric absorpt. in semicond. with energy-dependent relax. time 79−56268
acoustoelectric current at moderate US freq. 80−29444
acoustoelectric effect at medium US freq. and anisotropy compensation effect 77−55588
acoustoelectric effects, electron absorption and amplification of sound at intermediate freqs. 80−54740
acoustoelectric effects, nonlinear 77−69382
acoustoelectric phenomena in variable elec. field *(Russian)* 79−51637
acoustoelectronic phenomena in alternating elec. field, theory 79−11187
acoustomagnetoelectric effects in inelastic scatt. of electrons by optical phonons 77−4372
adsorption, boundary layer and electron theories *(German)* 78−95236
alloys, reson. light scatt., luminesc. and Raman spectra 79−38615
ambipolar, even galvanomagnetoconcentration effect 78−26889
ambipolar diffusion, electron-hole scatt. effect 80−59976
ambipolar diffusion meas. using nonlinear transient gratings 78−80000
ambipolar hot-carrier size effect kinetics 80−107799
ambipolar photoelectric current in semiconductor with traps 79−91101
amorphisation by high-energy ion irrad. 79−51172
amorphous, Mossbauer spectrometry *(French)* 80−80660
amorphous zone accumulation under ion irrad., composite model 79−51169
anisotropic, absolute instability for locked packet of sound waves *(Russian)* 77−35969
anisotropic, binding energy of exciton complexes 79−15088
anisotropic, bulk photovoltaic effect and transverse Dember effect 77−55573
anisotropic, electron-hole fluid energy calc. *(Russian)* 77−1379
anisotropic, voltage fluctuations associated with carrier drift 79−51644
anisotropic, with traps, kinetic theory of acousto-electrical effect in non-hydrodynamic collision region *(Russian)* 79−24019
anisotropic carrier energy spectrum, quantum cyclotron reson. line width 77−8008
anisotropic conductivity, elec. and photoelec. props., review 78−10447
anisotropic conductivity and ambipolar drift noise 77−20375
anisotropic electrical conductivity, use in thermometry *(Russian)* 79−63211
anisotropic p-Ge type, carrier scatt. by ionised impurities, theory *(Russian)* 78−39103
anisotropic semiconductors, light reflection in interband transition freq. *(Russian)* 80−88945
anisotropic size effects, review 77−32032
anisotropic thermoelement used as heat pump, transverse Peltier effect 78−39098
anodic etching, physicochemical parameters for maximum resolution 79−74276
anomalous photoconductivity model 79−7860
antiresonance states of diamagnetic excitons in semiconductors with optically anisotropic energy bands 79−51500
apparent ageing, caused by defect migration, dark and photocond. 78−11169
applied solid state physics, book 80−94936
atomic displacement threshold energy determ. from defect creation by electron irrad. 80−19799
Auger and radiative recombination of acceptor bound excitons 79−47023
Auger recombination, phonon-assisted, transition probability 77−44064
Auger recombination cross sections associated with deep centres 78−47810
Auger recombination in semicondutors involving taps 80−49763
Auger recombination processes 79−38091
Auger recombination rate, nonequilib. carrier distrib. 80−65578
Auger transition probability, phonon-assisted 79−15120

semiconductors continued
avalanche breakdown field, approx. formula 80−11025
avalanche process, intrinsic response time and effective ionisation rate anal. 77−69329
avalanching, carrier drift vel. effect on meas. ionisation coeffs. 79−69516
band states temp. depend., book contrib. 80−80182
band structure under high stress, nonperturbative calc. 78−10344
barrier conductivity mechanism, effects due to emptying of local levels by electric field 79−65468
Benard effect, conditions for existence *(Russian)* 78−84122
Benard effect, influence of external elec. field *(Russian)* 79−1750
Benedicks effect in carrier heating by microwave field 79−15173
biexciton luminescence, influence of free excitons on profile 77−4684
biexcitons, coherent, two-photon nutation in semiconductors 80−80191
biexcitons, one-photon radiative recomb. 80−70621
biexcitons, optical transform. 77−62844
binary, cone formation during sputtering 77−44389
binary, estimation of heats of formation from melting temp. 78−27810
binary, solubility of third component, and thermo-EMF 78−43124
binary alloy, conduction band edge shift near precip. point, order parameter fluctuations 77−24517
binary semiconductors, cathodic deposition and characterisation 79−69998
binary semiconductors, general model pseudopot. 77−62800
birefringence in presence of electroabsorpt. 77−32351
bound exciton recombination, phonon replicas 79−38649
bound excitons, review, book contrib. 80−44519
bounded, transport effects when a current passes along an energy inhomogeneity 79−7845
bounded samples, phonon heating influence on volt-ampere characts. 77−39863
bounded samples, volt-ampere characts., nonequil. phonons influence on thermal dimensional effects 77−43611
Bourgoin mechanism, method for determ. 77−43534
Bragg X-ray diffr. in elastically bent cryst. 80−24310
broad-band, meas. setup with GDM 1000 grating double monochromator 78−21226
broadband Faraday rotation, spectral contour for strong exciton bands 78−27194
bulk, I-V characts. based on impact ionisation, model 77−11925
bulk, negative-cond., transverse spreading of high-field domain, two-dimens. simulation and equivalent cct. model 79−1602
bulk and interface imperfections, techniques for detecting trapped charges 77−11934
Burstein-Moss effect, photostimulated absorption of light 80−29757
capacitive profilometry, accuracy 80−9005
capture of carriers by attractive centres 79−7836
capture probabilities of two deep impurity levels, photoconductivity decay analysis 77−89808
carrier capture by attractive centres in strong elec. fields 79−11144
carrier capture cross section by attractive Coulomb centres, piezoelec. scatt. 78−72170
carrier collisions with impurity ions 80−34434
carrier concentration distribution by scanning IR absorption 79−61356
carrier distribution function 78−26856
carrier distribution function in inhomogeneous regions 79−11146
carrier distribution function in presence of external electric field, anal. 77−1415
carrier effective lifetime modulation, surface recomb. and mag. field effects 77−28193
carrier generation, recomb., trapping and transport in semiconductors with position depend. composition 77−43613
carrier generation lifetime profiles meas. in diffused layers 78−47803
carrier heating, optical temp. waves 77−89770
carrier intrinsic conc. and effective mass determ. by IR refl. 79−51580
carrier lifetime meas. by photoconductivity null apparatus 78−56184
carrier lifetime modulation, effective 78−47807
carrier lifetime modulation, effective 78−47808
carrier lifetime profiles meas. in diffused layers 78−47811
carrier mobility, free, associated with dislocation strain fields 77−51738
carrier mobility for semicond. with disordered regions, theory and expt. on Ge 78−56166
carrier mobility-meas. technique on inverted surfaces near cond. threshold, appl. to Si 79−69602
carrier multiplication, noise due to avalanche processes, theory 80−6865
carrier relaxation process in quantising mag. field, elastic scatt. mechanisms, relax. matrix 79−15166
carrier relaxation time and effective masses determ. by microwave photocond. meas. *(Russian)* 78−19071
carrier relaxation time anisotropy effect on free carrier dispersion studies 80−84474
carrier scattering by impurity potentials with spatially variable dielec. functions 79−69507
carrier scattering by ionized impurity potentials incorporating spatially variable dielec. functions 79−42535
carrier transport in presence of temp. gradient, flux method 78−72144
catalytic kinetics, excitation-complex mech. *(Chinese)* 77−70337
cathodoluminescence, bibliography of papers till 1977 79−21482
cathodoluminescence, effect of surface space charge region 78−43939
cathodoluminescence, viewing in stroboscopic SEM 77−20936
cathodoluminescence analysis in SEM 78−32949
cathodoluminescence analysis using STEM 78−32950
cathodoluminescence high-resolution anal. system 77−13806
cathodoluminescence meas. of minority carrier lifetime, appl. to GaP 78−19572
ceramic, meas. cell and setup for elec. resist. meas. 300-1400°C 79−30488
chalcogenide, density of valence-alternation centres, influence of additives 78−47733
channelling-blocking measurements, (n,α) method for B-depth profiling 80−70276
charge carrier capture by attractive centres 79−82602
charge carrier density determ. calibrated polarimeters and the Faraday magnetooptical effect 80−60551
charge carrier diffusivity in strong elec. fields 77−35950
charge carrier scattering by dislocations 79−82583
charge carrier transport operator, soln. for device in cct. 77−39836
charge carrier UHF heating using lumped-capacitance resonators 80−20203
charge carriers, models for transport and accumulation 78−87975

semiconductors continued
charge defects, screened interaction 78−39042
charge neutrality produced by impurity diffusion 80−59724
charged dislocation, hole capture cross section *(Russian)* 78−23108
charged impurity diffusion 80−6563
charged-impurity scatt. formulae, third-body interference 77−55520
chemical energy, direct conversion to elec. energy 80−66984
chemical thermodynamics, review 80−55692
chemiluminescence heterogeneous excitation, ionisational mechanism 80−40173
chemisorption of H_2, Anderson model, including correlation and overlap effects 77−76662
chemisorption of H_2, effect of surface states 78−51823
chemisorption of mol. complexes, bond orbital model *(German)* 80−59807
chemisorption on semiconductor surfaces, review, book contrib. 80−107648
coated semiconductor spheres, surface modes, plasmon oscills. 80−54730
coherent biexcitons, two-photon nutation effect *(Russian)* 80−59892
cold semiconductor, Mott transition, external excitation 78−91616
collective excitations of electrons and holes in strong EM field and absorpt. of light *(Russian)* 78−79945
collective magnetoexciton transition under action of light *(Russian)* 78−79939
combined resonance, basic mechanisms 79−61229
compensated, electron capture probability by Coulomb centre in case of optical phonon emission 80−20214
compensated, influence of carrier heating on exclusion 77−8110
compensated, phase transition of impurity electrons interacting with lattice 77−24535
compensated, photoresponse, spectral depend. 80−15562
compensated, solid-state inductance, theory and expt. 78−56138
compensated semiconductor, theory of transient processes 80−24930
compensated semiconductors, low temp. mobility, unscreened charged impurities effects calcs. 80−75562
complex band structure, two-component electron-hole liquid 79−15099
complex dielectric constant measurement of SHF, waveguide methods 78−95542
complex dielectric permittivity, meas. in H_{01n} cylindrical cavity 79−93160
complex energy band under optical excitation, high-frequency negative cond. and population inversion 80−107858
composite semiconductor-ferrite struct., surface magnetostatic spin wave interactions *(Russian)* 80−88739
composition profile in semicond. alloy, second derivative wavelength modulation 80−103967
composition variation determ. using electrolyte electroreflectance 78−80809
compound semiconductor, electronic polarisability rel. to energy gap 80−10524
compound semiconductor, plastically deformed, electronic transport and optical props. of dislocations 80−80212
conduction electrons spin relaxation in semicond. without inversion centre *(Russian)* 78−52355
conduction in materials with position depend. band struct. 78−43377
conduction mechanism in strong elec. field, method for determ. 77−1430
conductivity, anomalous temp. depend. 77−20319
conductivity field depend. meas. by coaxial line method *(Russian)* 77−85206
conference, condensed matter physics, Sarajevo, Yugoslavia (Oct. 1976) 77−51629
contact emission limited current with weak harmonic distortion of steady bias 78−39127
contact potential and conductivity simultaneous automatic meas. 78−21118
contact potential difference and surface cond., combined meas. method 77−18042
contamination equilibrium assessment 79−51134
core excitons, binding energies 79−73439
core excitons, binding energy in effective mass approx. 80−24808
core level spectra, electronic polaris. effects 79−90985
Coulomb collisions between nonequilibrium electrons during interband interaction of high-power optical pulses with semiconductors and insulators 80−76049
Coulomb screening in presence of two EM waves 79−15107
Coulomb screening in semicond. with superlattice 78−14684
covalent, cancellation effects in localised orbital theories 80−84445
covalent, charge density, struct. props. electron-electron interactions 78−47725
covalent, displacement correlations, adiabatic bond charge model 80−70350
covalent, electronic and struct. energies calc. 78−59874
covalent, molecular cluster model 78−43283
covalent, non-orthogonal tight-binding approach 80−2442
covalent, optical absorption by acoustic phonons related to shallow impurity levels 77−4665
covalent, phonon spectra calc. using dielectric matrix approach 79−4381
covalent, quantum mechanics of dislocation kinks 77−19951
covalent, single vacancy, relax. energy and form. vol. calcs. 78−38691
covalent, structural props. using electron-ion Hamiltonian using density-fundamental methods 79−82177
covalent, surface (110) atomic struct. 79−69331
covalent, tight binding analysis of step-depend. density of (111) surface states 77−59321
covalent, violation of Vegard's law 77−27847
covalent radii, tetrahedral and octahedral 77−31632
covalent semiconductor, heating of charge carriers, energy dissipation 80−49755
covalent semiconductors, electronic interface states in intrinsic stacking-faults 80−75522
covalent semiconductors, low temp. galvanomag. effects, shallow attractive traps 80−88575
covalent semiconductors, substitutional deep traps, theory 80−54651
covalent semiconductors, vacancy screening, dielec. const., exchange correl. pot., Thomas-Fermi description 80−44528
critical points for electron-hole system 80−44511
crystal defects induced by radiation, review 79−55776
crystal field coefficient of point defect 77−43537
crystal growth aspects of electronic materials 80−66405
crystal growth in zero gravity, Polish expts. in space *(Polish)* 79−56920
semiconductors continued
crystal structure stability of morphotropic and isomorphic series 77−51353
crystal surface discrete dipole layer effect on surface barrier shape 79−95468
crystal surfaces props., structural, chemical and electronic, use of LEED methods *(Italian)* 80−49467
crystalline, local field effects on static dielec. const. 77−59264
cubic, Debye temp., elastic consts. averaging 80−54332
cubic, exchange splitting of excitons 79−42467
cubic, in mag. field, exciton states 80−24807
cubic, noncentrosymmetric, electrooptic effect 79−69812
cubic, Seitz coefficients calc. for resistivity 80−6880
cubic, Zeeman split acceptor levels, calc. method 79−28322
cubic semiconductors, bulk hot-electron props., review 79−99553
current and voltage fluctuation determ. by noise spectral density meas. 80−15577
current fluctuation anisotropy, electron diffusion, quasielastic scatt. *(Russian)* 80−107882
current fluctuations in quantizing elec. field *(Russian)* 77−28175
current instabilities in semiconductors, theory and expts. *(Hungarian)* 77−39857
current instability, bifurcation and stability of dynamical structs. 79−91071
current instability due to Bragg scatt., travelling dipole domains, fluctuations 78−26874
current-voltage characts. of hot electrons under phonon heating and recomb. conditions 79−51591
current-voltage characts. of semicond. with two types of hot carriers under overheating stability conditions 77−62943
cyclic queue models of semiconductor noise and vehicle fleet operations 80−80336
cyclotron resonance, high frequency differential cond., needle shaped distribution model 79−65509
cyclotron resonance, theory 79−73817
cyclotron resonance fine struct. *(Russian)* 79−4727
cyclotron resonance linewidth, quantum-limit 80−7171
cyclotron resonance width due to electron-charged impurity interaction 77−55475
cyclotron resonances, transport and surface phenomena 78−6575
cyclotron-phonon reson., review 79−56615
cyclotron-phonon resonance due to polarisation scatt. from photons 79−95649
D^- centres, binding in mag. field 79−38019
D^--state in semiconductors *(Japanese)* 77−85178
dangling-bond states theory 80−24840
DC electron scattering, by spherical macroscopic pot. including screening 77−51739
de Haas-van Alphen effect, in semicond. with superlattice 77−85132
deep bound states, temp. depend. of ionisation energies 77−31975
deep centres, wave functions and optical cross sections 78−34801
deep defects, contrib. to binding energy 80−70634
deep impurities, book contrib. 78−10403
deep impurities, exptl. techniques *(Japanese)* 80−15476
deep impurities, photoionisation 78−39061
deep impurity centre, excited state energies calc. 78−18997
deep impurity centre photoionisation cross-section, freq. depend. 77−55494
deep impurity centres, elastic light scattering 80−97315
deep impurity centres, ionisation by elec. field 77−8053
deep impurity centres, multiphonon thermal field ionisation *(Russian)* 78−14690
deep impurity centres, spin relax. by exchange scatt. 77−43870
deep impurity centres, two-electron model 79−65411
deep impurity state characterisation 80−6776
deep level, laser monopulse energy meas., time-resolved spectroscopic method *(Russian)* 79−94272
deep level capture, two stage model 78−10396
deep level carrier trapping and emission, transient spectroscopy, book contribution 80−80216
deep level impurities spectrometry, transient capacitance instrumentation 77−51816
deep level impurity photoionisation cross-section 80−65485
deep level parameters, TSC meas., rel. to photocurrent techniques 78−72249
deep level profile anal. by double deep level transient spectroscopy 77−20378
deep levels, detection in high power materials 79−28318
deep levels, electronic struct. using, LCAO, SCF method 79−82555
deep levels, review 80−103640
deep levels, self consistent LCAO MO calcs. 80−29353
deep levels associated with 60° dislocations *(French)* 80−29352
deep transition metal impurity states, SCF CNDO cluster calcs. 80−100442
deep trap activation energy, effect of non-exponential transients, DLTs method 80−20115
deep traps, injection filament 77−76837
deep traps, nonradiative multiphonon carrier-capture cross-section, temp. depend. approx. 78−43415
deep-level centre discrimination from capacitance versus time transients 78−10395
deep-level impurities, insulating props. 78−39124
defect and impurity centre detection, junction capacitance and current techniques 78−10550
defect cluster annealing, kinetics 80−84209
defect electronic struct., SCF method 80−80208
defect electronic structure and lattice config., MO approaches 80−65495
defect fermion properties, ionic cond. calcs. 80−59457
defect images obs., SEM, charge-collection, contrast formation 80−70087
defect interactions, radiation physics *(Russian)* 79−46702
defect processes, electronic stimulation 80−24665
defect recombination, di-pair model, diffusion-controlled, incorporating Coulomb interaction and annihilation 78−23044
defect semiconductor, or insulator, carrier densities, elec. cond. and Fermi level 77−43532
defect state microscopy, review 79−94856
defect tetrahedral cpd. semiconductors, band struct. trends 79−90956
defect-density profiles, constant-capacitance DLTS meas. 79−95361
defective surface layer, surface positron states 80−75526
defects, electron microscopy study 79−95021

semiconductors continued
defects, electronic props. study by spectroscopic techniques 80−84446
defects, electronic structure and lattice distortion, Green's function methods *(French)* 80−59917
defects, entropy of ionisation and temp. variation of ionisation levels 77−11871
defects, noise models for investigation *(German)* 78−87661
defects, SEM in EBIC mode vs. HVEM images 78−9923
defects and radiation effects, conf., Nice, France (Sept. 1978) 80−22140
deformation potential, possibility of screening by free carriers 77−72826
degenerate electrons, relax. of spin and energy 80−10965
degenerate four-wave mixing near band gap 80−5782
Dember and photomagnetic effect, spectral characteristics, heterogeneous semicond. *(Russian)* 77−89809
Dember effect in superficially illuminated sample, space charge effect 77−8133
density of Wannier-Stark states, calc. 77−11885
density waves in one, two and three dimensions 79−95353
design, ionic microanalysis 79−40648
DFB laser pumped by electron beam, temporal and spectral characts. 79−94238
diamagnetic excitons, odd states, oscillator strengths and optical absorption line positions 79−11072
diamagnetic excitons in strong elec. field 79−38002
diamagnetic susceptibility of excitonic molecules *(Russian)* 80−7074
diamagnetism of deep impurities 79−23931
diamond-like, adiabatic pot. in quasimol. model 78−2063
diamond-structure semiconductor, Compton profile interpretation 80−29820
diamond-type, doped, US attenuation and electron-phonon scatt. 79−46771
dielectric electric-hole liquid form. 77−43508
dielectric function, freq.- and wave-vector-depend., of model semicond. 79−33253
dielectric function, modulation spectroscopy and elec. field effects book contrib. 80−80201
dielectric polarisation and Kohn effect in strong mag. field 77−4279
dielectric response, local field effects in phonon-induced density change 79−51510
dielectric response function, local field effect 79−51505
dielectric response of solids, approxs. for treatment of local field effects 79−47033
dielectric screening, Thomas-Fermi model 80−49648
differential conductivity with inelastic electron scatt. *(Russian)* 80−2399
differential thermal EMF measurement device for solid, fusion region and melt states 78−12716
diffusion, recoil and field enhanced mechanisms 77−89567
diffusion from limited source 80−70444
diffusion length, meas. by surface photovoltage method effects of optical beam size 80−60002
diffusion processes, elastic stresses effect 78−10226
dimerized interrupted strand model, optical absorption 77−16271
dipole impurities 79−28796
direct band gap, electronic Raman scatt. of polarised light on donor levels 80−93309
direct band gap type, polariton theory of reson. electronic Raman scatt. on neutral donor levels 80−108194
direct band-gap, polariton emission spectrum, exciton kinetics influence 78−14676
direct gap, final state interactions in gain and absorpt. spectra of electron-hole liq. 78−43305
direct gap, one-photon Keldysh absorption 77−8599
direct gap semiconductors, electron-hole droplet condensation 80−103630
direct gap semiconductors, exciton energy determ., electron beam excited luminesc. 79−38680
direct semiconductors, picosecond absorption spectroscopy 79−47482
direct-gap, gain spectrum of electron-hole liquid 80−66279
direct-gap, oscillator strengths for electron-hole complexes (A^0X) 77−35869
direct-gap, two-photon absorpt. 80−50292
direct-gap, under strong excitation conditions, exciton gas model 77−8650
direct-gap crystals, one-photon absorpt., Keldysh and perturbation formulas 80−20607
direct-gap semiconductor, absorpt. coeff. of light due to indirect transitions 79−91400
direct-gap semiconductors, charged excitons 77−62840
dislocation conduction process at low temperature 79−99551
dislocation density determ. with Kontrast automatic mineralogical analyser 79−51111
dislocation structure, optical microscopy obs. techniques 80−24458
dislocations, SEM charge-collection image contrast and resolution 79−46662
dislocations, structures and elec. props. 80−70201
dislocations, TEM/SEM observations comparing diffr., elec. and luminesc. contrast 78−38714
dislocations studied by weak beam electron microscopy 79−82216
disorder effects on electronic props. of pseudobinary system *(Japanese)* 80−49709
disorder scattering in semicond. alloys, Green's function calc. 77−11906
disordered, constrained cond. in powerful field *(Russian)* 77−55536
disordered, Coulomb gap in energy spectrum 78−14648
disordered, electroabsoprtion, contact excitons influence 80−10882
disordered, hopping thermoelec. power, temp. depend. 79−23995
disordered, light induced stationary non-equilibrium distribution of electrons, balance equation 80−39528
disordered, mobility edge exam. by new perturbation theory 78−47790
disordered, optical magnetoabsorption coeff. calc. in strong mag. field 80−16011
disordered, photon-phonon-assisted hopping, theory 80−44642
disordered, rate eqns. in hopping transport, DC phonon assisted hopping in mobility gap 79−60826
disordered, resonance Raman scatt. 79−11419
disordered, theory of photon-induced DC hopping cond. 78−30952
disordered, with random field, new photocond. type *(Russian)* 77−11961
disordered, with soft Coulombic aperture, screening and absorpt. of long EM waves *(Russian)* 78−23001
disordered semicond. elec. heat cond. calc. *(Russian)* 77−32009
semiconductors continued
disordered system, low-freq. cond. due to variable range hopping, cluster approx. 80−92886
dispersive energy rel. to covalent and ionic energies *(French)* 79−99478
displaced Maxwellian distribution function and warm electrons problem 78−26864
displacement damage, displacement energy determ. by electron beam induced conductivity 80−70097
dissociated dislocations, statistics of kink formation 79−82207
donor minus ion, binding energy determ. 80−70645
donor van der Waals interactions, spectral lineshapes 80−11450
donor-acceptor complexes and interactions, physicochem. nature 80−15472
donor-acceptor energy transfer, reabsorpt. mechanism 79−78041
donor-acceptor pair in elec. field, anomalous Stark shift of ground state energy 79−19564
donor-acceptor pair luminesc. band maximum position 77−52177
donor-acceptor pair luminesc. polarisation with optical orientation 77−24895
donor-acceptor pairs, polarisation of recomb. radiation in presence of quantum size effect 79−11462
donor-acceptor system, weak wave absorpt. in reson. laser radiation field 80−66252
dopant distribution from carrier distrib. in high elec. field 79−51140
doped, cluster model of impurity states 80−20117
doped, coexistence of insulating and metallic electronic phases 79−65385
doped, Coulomb repulsion term in Hubbard model for impurities 79−42492
doped, impurity band density in atomic limit 80−107735
doped, insulator-metal transition, dielec. const. enhancement on insulating side 80−20087
doped, insulator-metal transition, dielec. constant enhancement on insulating side 80−20088
doped, ionised centre diffusion accel. by electrostatic fields 80−70473
doped, lattice thermal cond., role of electron-phonon interactions and peripheral phonons, appl. to Ge:P 78−79702
doped, metal-insulator transition, anal. 80−88478
doped, metal-insulator transition, density functional approach 79−11067
doped, photoemission, calc. of escape probability of electrons *(Russian)* 79−24408
doped, radiation defect, form. mechanism associated with electron transitions 79−69155
doped, shallow impurity states, Hubbard bands and donor excitonic states, HF calc. 80−100443
doped, static dielec. response using simple homogeneous and isotropic model 79−73460
doped, variable range hopping, computer simulation 80−24929
doped, with neutral impurities, exciton spectrum, conc. depend. *(Russian)* 78−2894
doped and strongly compensated, fluctuation pot. and density of states *(Russian)* 79−95366
doped semiconductor, potential fluctuations, random impurity distribution 80−88512
doped semiconductors, correlation effects on Anderson localised states 79−95337
doped with magnetic impurity, ordering mechanism 80−2572
doping profile determ., interpretation of C-V meas. 80−59510
double injection characteristics under high voltages 79−51590
double injection currents in semiconds. with deep impurities 77−55543
double injection of holes and electrons, semicond. with carrier mobility gradients *(Russian)* 77−35948
drift mobility and Hall factor, nonpolar optical scatt. mechanism 79−51579
drift velocity relation to low-field mobility and high-field saturation velocity 80−75563
dynamic polarisation of nuclei due to optical orientation of conduction electrons 78−19376
dynamical effective charges, pseudopotential calc. 78−30881
dynamics of surface melting and resolidification during laser annealing 79−69918
effective masses, multiband calcs. by pseudopot. method 77−51644
Einstein relation for degenerate carrier concentrations 78−72143
elastic constants, resonance method for determ. within 80-300K temp. range 78−46918
elastic constants, second-order, of solids with ZnS struct., many-body effects 78−10116
electric field induced nonequilib. phase transitions 80−10879
electric field numerical soln. *(Slovak)* 78−66710
electric parameters at microwave frequencies, waveguide meas. method, review 79−93170
electric resistance, temp. depend., qualitative anal. by audible demonstration 80−46775
electric-dipole paramag. relax. due to carriers in quantising mag. fields 79−38381
electrical characterisation, review 78−60120
electrical conduction in strong elec. fields, percolation mechanism 80−20206
electrical conductivity and Hall mobility in disordered systems, theory 80−54697
electrical conductivity and magnetoresistance of semiconductor with charged defects 80−20225
electrical conductivity in quantising mag. field, and electron heating, mutual electron-phonon drag 77−69355
electrical conductivity measurement near inhomogeneities, four-probe meas. *(Russian)* 77−79104
electrical conductivity of excitonic and optical insulators with nonequilibrium distrib. of quasiparticles 77−15888
electrical instability, negative differential cond., electron heating by static and alternating elec. fields 79−11165
electrical parameters determ. by electron probe method 79−9259
electrical properties, mag. field effect determ., method 80−44623
electrical properties calculated from thermophysical and thermomagnetic effects 79−73535
electrical properties examination, polarity reversing control current magnet power supply with triangular waveform 79−12827
electrical resistance, exam at high temp. using inductive heating 79−7816
electrical resistivity, Hall coeff. of samples dual to van der Pauw samples 79−88984
electrical response, transient and AC, solid with recombining space charge 77−51737

semiconductors continued
electrical transport measurements, kinetic effects at high anisotropic strains 78−54384
electrical transport properties, effect of temp. depend. band shifts 77−55522
electro-optic effects anisotropy and hot electron cond., free carrier-impurity scatt. 77−4626
electroabsorption, interband, in semicond. with complex valence band, polarisation props. 80−66152
electrodes, charge distrib. and chemisorpt. processes *(German)* 79−52689
electron abs. and amp. of sound, validity criteria of phenomenological theory 78−91733
electron absorpt. and transmission charact., 5 to 30 keV, film-massive block method 78−88387
electron absorption and amplification of HF ultrasound, kinetic theory 77−32051
electron absorption of ultrasound in strong elec. field, oscills. 79−69563
electron beam depth profiling using SEM 80−70723
electron beam prod. of plasma oscillation instabilities *(Ukrainian)* 79−33318
electron conductivity, temp. and freq. depend., two band model *(Russian)* 80−75564
electron correlation and bound excitons 77−85150
electron distribution function, temp. gradient effect 78−72145
electron drag by photons during intraband absorption of light 79−51633
electron drift vel. and phonon multiplication 80−6848
electron emission from surface subband, reduced work function 80−60757
electron energy spectrum, influence of strong inelastic scatt. 79−23959
electron excitation spectra in field of two travelling waves 80−65514
electron excitation spectrum in resonance field of standing EM wave *(Russian)* 77−63386
electron heating by constant electric field, magnetoplasma wave instabilities 77−43639
electron heating by phonons, acoustic absorpt. and acoustoelectric current quantum oscills. *(Russian)* 79−19639
electron heating by strong static and HF elec. fields 77−8112
electron irradiation, low temp., multipurpose cryostat 79−35755
electron irradiation produced displacement defects 77−80543
electron microscopy, developments in high resolution imaging 80−99001
electron microscopy, semiconductor appls., advances 80−101911
electron mobility in quantising mag. field, effect of overlap function 78−43374
electron momentum distribution, anisotropy, positron annihilation *(Russian)* 78−84676
electron multiphonon capture by edge dislocation *(Russian)* 79−86861
electron multiplication, phonon scatt., ionisation rate calcs., Markov processes 80−50267
electron quantum states, nonequilibrium current fluctuations in quantised mag. fields *(Russian)* 80−107704
electron relaxation, electron hole interaction effect 78−10437
electron runaway and quasi-stationary states in electric field 77−4359
electron scattering by deep level impurities 80−10968
electron scattering by layer of dislocation lines 79−78091
electron scattering by layer struct., geometrical resonances, plasmon and free carrier freq. 79−56212
electron spectra in mag. and US fields *(Russian)* 77−62801
electron spectroscopy techniques, review *(Japanese)* 80−49061
electron states at planar and stepped surfaces 78−10531
electron states of point defects 80−39526
electron temperature superlattice, nonlinear theory *(Russian)* 79−78112
electron transport phenomena, high-field transport and quantum transport in strong mag. fields *(Japanese)* 77−55526
electron trap, positively charged, hot electron capture coeff. 78−52003
electron-donor recombination, Monte Carlo studies of transitions between excited donor states 79−38093
electron-electron collision effect on current voltage charact. in quantising mag. field 80−103705
electron-electron relaxation in ultraquantum mag. fields, electron-phonon interactions 77−4371
electron-hole drop, moving, temp. determ. *(Russian)* 78−67953
electron-hole drop, shape change during motion 80−20093
electron-hole drop formation, phonon wind influence *(Russian)* 80−92825
electron-hole drop in rapid motion *(Russian)* 79−60727
electron-hole drop nucleation, Fokker Planck treatment 80−6732
electron-hole droplet, US absorption 77−89814
electron-hole droplet cloud, role of thermalisation phonons 80−49617
electron-hole droplet condensation, phase diagrams 79−38001
electron-hole droplet nucleation and stability, hydrodynamic approach 78−72080
electron-hole drops, basic principles *(Russian)* 78−72081
electron-hole drops, effect of Coulomb interaction on mobility 79−15096
electron-hole drops under microwave radiation, kinetics of instabilities 78−60059
electron-hole liquid, 'neutrality' question of impurities 80−92822
electron-hole liquid, ground state energy and excitation spectrum 77−89713
electron-hole liquid, prod. and props. at low temp. 79−82527
electron-hole liquid, RPA calcs. 80−6743
electron-hole liquid droplets, theory 80−44689
electron-hole pair condensation and liquefaction in strong mag. field, RPA and variational calcs. 78−63984
electron-hole plasma and elec. field, stratification at low temp. 80−60020
electron-hole plasma current layering, electron cooling length, momentum scatt. 80−6890
electron-hole plasma drift due to carrier mobility gradients 78−26896
electron-hole plasma in crossed fields, renormalised diffusion coeffs. 79−87123
electron-hole plasma instabilities under impact ionization and microwave emission 79−65508
electron-hole plasma phase transition in direct and indirect gap semiconductors 80−24803
electron-hole system, two-dimens., phase diagram for plasma to liq. transition 79−95342
electron-hole system thermodynamics 78−43304
electron-hole-droplet condensation, scaling relations 79−99484
electron-hole-plasma, instability in heating elec. field 80−15552
electron-phonon interaction anal. using photoacoustic cell 78−68027

semiconductors continued
electron-phonon interactions, combined phonon resonance *(Russian)* 80−75321
electron-phonon interactions, dispersion law in van Hove critical point region 80−70344
electron-phonon interactions, phonons and localisation at impurities 80−24812
electron-phonon mechanism of cyclotron absorpt. hysteresis 79−69726
electron-stimulated absorption of bulk spin waves 80−70992
electronic absorption and amplification of acoustic waves 78−39166
electronic band shape, k.p perturbation theory *(Korean)* 78−23020
electronic cond., temp. depend. review 80−59975
electronic density of states in mag. and US wave fields *(Russian)* 78−72056
electronic elementary excitations in far UV and X-ray region, appl. to GaAs(P)(Sb) 79−95346
electronic polarizability as function of Penn gap 80−49638
electronic properties, rel. to chem. bonding and lattice dynamics 80−44169
electroreflectance, crystal termination effects, field reversal 77−69802
electrostrictive effect of hot electrons spherical energy band model 79−69778
elementary semiconductor physics, book 80−6824
EM beam self-focusing 79−18488
EM field nonlinear penetration in superlattice semicond., self-induced transparency 78−25930
EM generation of ultrasound 79−51639
EM oscillations in electric field, transport theory 79−69521
EM properties, general lecture 78−27173
EM radiation gain, semicond. subjected to mag. and US fields 80−48201
EM wave absorpt. by free carriers, high freq. quantum transport eqn., for semicond. with superlattice 78−60148
EM wave excitation and amplification under negative differential cond. conditions 77−15865
EM wave interaction in weakly nonlinear medium with superlattice 80−93257
EM wave propagation in semiconductor plasma, hot carriers, Hall effect, calc. 80−39620
EM wave propagation in semiconductors with superlattices, magnetic field effect 80−70745
EMF production by shock compression 77−31719
energy spectrum, optimisation of parameters of neutrality equation *(Russian)* 78−6320
energy spectrum of discrete centre in high inhomogeneous electric field of space charge region 80−10873
energy spectrum restructuring and light absorption in intense EM field 79−56111
energy transfer due to dynamical self diffraction of light beams of same freq. *(Russian)* 77−58397
energy-balance eqn. for hot electrons 79−73521
enhanced diffusion mechanisms, review 78−67847
entropy of fusion, electronic component 78−47503
entropy of fusion allowing for dissociation at melting point 77−55348
epitaxial structures, atomic diffusion 77−85110
EPR, optical detection in excited state *(Japanese)* 77−81029
evanescent states and complex bound structure 80−34387
evaporation, injection of nonequilibrium vacancies 80−39273
exchange and correlation energies, local field effects 78−39044
exchange interactions in semiconductors and insulators, mean free path and energy gap effects 80−88522
excitation spectrum and optical props. in field of standing EM wave and homogeneous field 78−91625
excited, extended phase diagrams, review 80−44521
exciton absorption, electric field effect *(Russian)* 78−43902
exciton and domain luminesc., book 80−82588
exciton and impurity states, unified theory, for arbitrary mag. field 80−39511
exciton and impurity states theory 79−82526
exciton binding to neutral donor 77−31949
exciton condensation, microwave cond., book contrib. 80−11043
exciton condensation and electron hole liquids, state-of-the-art 80−49625
exciton condensation and pairing, interacting boson theory without anomalous propagators 77−33942
exciton damping by phonons, appl. to Ge 77−1373
exciton effect in interband electronic Raman scattering 80−103946
exciton levels 77−69247
exciton light absorpt. band formation, linear and quadratic exciton acoustic photon interactions *(Russian)* 80−34368
exciton light absorpt. spectra depend. on crystal anisotropy *(Russian)* 80−50386
exciton luminescence, free carrier effect 78−48226
exciton physics, review, book contrib. 80−44517
exciton reflection of light for arbitrary surface pot. 79−38568
exciton states in semiconds. with polytype layers 78−26819
exciton-exciton and exciton-electron interactions in luminesc. spectra of two-dimensional cryst. 77−52179
exciton-impurity state with low binding energy 80−103646
exciton-impurity systems, binding energy of excitons, Haynes rule 79−15112
exciton-phonon energy transfer 78−18715
exciton-plasma transition 79−28295
exciton-polariton interactions, Green's function approach for semiconductors with direct band gaps 80−92831
exciton-polaritons, resonant Raman scattering *(Japanese)* 80−50349
excitonic dielectric liquid, Wannier-Mott 80−65458
excitonic molecular, exciton luminescence in longitudinal optical phonon sideband 79−61438
excitonic molecule creation by two-photon absorpt. 77−20247
excitonic molecules, two-polariton decay at 2K 79−95339
excitonic surface potential 78−76000
excitons, book 80−41951
excitons, condensation effects, review 78−2427
excitons, exciton-phonon interaction, resonant Raman and Brillouin spectroscopy, review, book contrib. 80−49624
excitons, multiple bound, binding energy calc. 78−51900
excitons and nonlocal optical props. 79−95345
excitons in semi-infinite crystals, microscopic calc. of optical refl. 79−69430
exoelectron emission, review 77−52228
exotic atoms, conf., Erice, Sicily, (1979) 80−67939

semiconductors continued
extrinsic, carrier concs. and Fermi levels 77−66112
extrinsic, defect level analysis, n(1/T) characts. 79−73464
extrinsic, parametric reson. of acoustic and optical phonons at low temps. 78−10519
extrinsic, photocurrents anal. 79−42588
extrinsic, resonance transitions between ground states of donor and acceptor impurities 80−45126
extrinsic covalent, Raman scatt. of light by phonons 77−73147
extrinsic semiconductor, Fermi level eqns. 79−99472
extrinsic semiconductors, impurity interaction and metal-nonmetal transition 80−29325
extrinsic semiconductors, negative magnetoresist., Hubbard model *(Russian)* 78−47816
Fabry-Perot interferometer retuning by optical excitation *(Russian)* 80−98970
Fano factor determ. 80−47813
far IR spectroscopy, appl. of far IR lasers 80−31914
Faraday effect meas. using IR magneto-optic polarimeter 77−34014
Faraday rotation in presence of attractive traps 78−76081
Faraday rotation in the presence of deep repulsive traps 80−29724
fast particle irrad., Frenkel defect formation threshold energy 80−6404
Fermi energy, empirical approx. for semicond. with parabolic bands 79−7770
Fermi level, monotonous shift with increasing temp. 80−92809
ferrite-semiconductor hybrid struct., magnetoelastic wave interaction with drifting carriers 80−54934
ferrite-semiconductor layer struct., with negative differential cond., spin wave instability 80−25118
ferrite-semiconductor layer structure, EMF created by spin-wave, effect of current 80−11072
ferrite-semiconductor layer structure, influence of Hall effect on spin wave spectrum and amplification by current 79−11308
ferrite-semiconductor layered struct., interaction of spin waves with hot carriers 79−15291
ferrite-semiconductor structure, nonlinearity and conditions of existence of convective instability 78−72241
ferrite-semiconductor structure, resonance galvanometric phenomena in semicond. 78−87989
ferrite-semiconductor structure, surface magnetostatic wave instability 78−76235
ferromagnet-semiconductor contact, spin-depend. recomb. and scatt. on electron injection 80−65654
ferromagnet-semiconductor structure, periodic, surface magnetostatic waves 78−27070
ferromagnet-semiconductor structure, surface wave gain, ang. depend. 77−51938
field penetration and band bending for simple geometries in high elec. fields 79−87106
filament, phonon drag contribution to thermoelectricity 78−19069
film, Wannier-Mott exciton states *(Russian)* 78−79943
FIM, possible role of surface states, Kronig-Penney model 77−47883
flicker noise, not true bulk effect 79−24028
fluctuation spectra near the threshold of a current instability 79−24037
forbidden gap width, relation to refractive index, single oscillator calcs. *(Russian)* 80−71372
force variation due to charged defects 80−92634
four-photon transitions, perturbation theory calc. 80−96786
Fourier transformed X-ray Compton profiles 80−35004
free carrier optical props., book contrib. 80−80738
free carrier scatt. by nonhydrogenic charged impurity centre 79−11110
free carrier scattering, due to screw dislocation strain field 77−1416
free electron scattering and dynamical cond. 78−2476
free-carrier concentration contactless meas., IR polarimeters, Faraday effect 77−73135
Frenkel pair defect formation threshold energy during particle irrad. 79−90647
Frenkel pair formation threshold energy during particle irrad. 79−90646
frequency dependent dielectric function of gapless semiconductors in a magnetic field 78−63994
frequency shift of combined resonance, influence of plasma oscills. of conduction electrons 79−7850
frozen-in conductivity, nature of recomb. barriers 79−56245
galvanomagnetic effects, small 77 to 400K cryostat 77−30149
galvanomagnetic effects in high mag. fields, for electron scatt. by optical phonons 80−2405
galvanomagnetic phenomena, model, transport phenomena in presence of medium range disorder *(French)* 78−56162
galvanomagnetic phenomena, quantum theory, cond. rel. to migration of cyclotron orbit centres *(Russian)* 77−66153
gap, energy simultaneous determination and identification using piezo-reflection-retrotransmission technique *(French)* 77−28545
gapless, bottleneck effect at low temp., hole heating 78−10470
gapless, current-voltage charact. in longit. quantizing mag. fields 77−55524
gapless, magnetophonon reson. for hot electrons and holes *(Russian)* 79−4565
gapless, nucl. spin relax. due to interaction with electrons 78−56398
gapless, with impurities, energy spectrum 78−67979
Gaussian diffusion determ., alternative method to angle lap and strain anal. 79−86925
generation-recombination noise 79−24032
graded-gap, internal photo-effects, excess carrier distribs. 80−107847
graded-gap, photoelectromagnetic effect 78−43445
grain boundary barriers, thermal breakdown 78−39171
grain boundary resistance, DC voltage depend. 79−82597
grain-boundary barrier semicond., boundary states' energy struct. influence on elec. cond. 79−11147
Gunn diodes, multidomain mode due to charge inhomogeneities 80−70714
Hall current, theory for flow in sample of arbitrary shape 79−73532
Hall current method generalisation to arbitrary magnitude mag. fields *(Russian)* 80−29421
Hall effect, anomalies under interband scattering conditions 78−6403
Hall effect, influence of nonhomogeneous mag. field 77−39882
Hall effect in finite specimens of arbitrary lifetime and trap content 78−72175
Hall effect in semiconductor with superlattice 80−39612
Hall effect noise explained as carrier mobility fluctuations 77−62949
Hall voltage, transverse magnetoresist. effects, theory 77−72870
heat pulse absorpt. in nonquantising mag. fields 80−60054
semiconductors continued
heating photoconductivity in semicond. with superlattice 79−19622
heavy hole spectrum in mag. field 79−15079
helical wave, low freq., nonlinear propag., for weak ellipticity of incident wave polarisation 77−62958
helicon damping in quantum limit 77−28205
helicon propagation, nonlinear effects 77−66180
heterogeneity refractive index meas., interferometric method 79−6172
heterogeneous, anisotropic, Hall coeffs., Hall mobility, carrier density *(Russian)* 80−70734
heterojunction superlattice, energy spectrum 78−6259
HF EM effects, nonquadratic dispersion law of carriers 78−19078
HF field energy absorpt. in strong parallel mag. and elec. fields 79−73801
HF wave dispersion for complex wave numbers, ordinary waves 80−70740
high density excitons and biexcitons, recomb. radiation bands profiles, time depend. 80−45140
high field transport, balance eqns., in finite collision duration regime 79−60843
high magnetic field semiconductor physics, review *(Japanese)* 80−50192
high-field electrical conduction, instabilities 77−24562
high-frequency ballistic electron transport, AC impedance meas. 80−80306
high-power radiation propagation, rel. to interband absorption or amplification 79−76727
high-pressure effects, conf., Moscow, USSR (May 1975). 77−43279
high-resistivity, SCL current, inhomogeneity effects 78−19047
highly excited, Auger coefficients 79−19606
highly excited photomagnetoelec. effect under Auger recomb. 80−44664
highly excited states, ps spectroscopy 77−48245
highly photoexcited semiconductors, picosec. luminesc. spectrosc. 79−47517
history of hot electron physics 78−26869
hole drag current in two-photon transitions due to EM wave momentum 79−15187
hole polaron self energy 77−43519
hole scattering, from impurity pots. in spherical-band approx. 77−76803
hologram recording by photosensitive etching, attainable spatial frequencies 80−69343
hologram recording on semiconductor, photochem. etching control 80−28179
homogeneous, Hall effect noise 78−39173
homogeneous, nondegenerate, single-level Schockley-Read-Hall recomb. centres, flicker noise 80−70779
homogeneous doped, influence of internal elec. field on diffusion of ionised impurity 79−55940
homologous series, semicond.-metal transitions, homeomorphous, polymorphous and morphotropic transitions 79−37988
hopping conduction anisotropy, percolation theory 78−72156
hopping conduction influence of HF elec. field 78−52025
hopping promoted by electron-electron coupling 80−59987
hopping transport theory for strong elec. field 77−8106
hot carrier noise, exptl. and theoretical aspect, survey 79−28389
hot carrier oscillatory magnetoresistance phenomena studies, mag. field modulation technique 78−4657
hot carrier phenomena, optical obs. 79−95845
hot carriers, conf., Denton, USA (July 1977) 78−26868
hot carriers, spreading and noise diffraction coeffs., identity 78−64047
hot electron current voltage curves, in transverse mag. field, account of phonon heating 78−6384
hot electron distrib. in strong electric and quantised mag. fields 79−95417
hot electron distribution functions, expts., review 78−27231
hot electron energy tails, Monte-Carlo, calcs. 77−62931
hot electron fluctuations with displaced Maxwellian distribution 80−29418
hot electron kinetic equation in semiconductor with quasirelativistic band struct. 78−84222
hot electron maximum mobility in longitudinal quantising mag. fields 79−69519
hot electron phenomena, calc., review 78−26870
hot electron physics, review *(Japanese)* 80−49754
hot electron quantum magnetotransport, review 78−30940
hot electron recombination at impurity centres 80−10995
hot electron semiconductor, capture of charge carriers rel. to I-V curves, phonon heating 79−51589
hot electron transverse escape galvanomagnetic effects *(Russian)* 80−80289
hot electron waves in transverse mag. field 77−4387
hot electrons, mobility in mag. field 77−4368
hot electrons, photoexcited in quantizing mag. field, energy distrib. calcs. 79−42586
hot electrons in longitudinal quantising mag. fields 80−39593
hot electrons in quantizing mag. field and impact ionization of impurities 78−6386
hot plasma, wave instability 78−84245
hot-electron energy distrib. in strong mag. field 78−43400
hydrogen embrittling effects from acoustic emission meas. 80−11742
hypersound amplification in quantising elec. field in semicond. with narrow cond. bands 77−89811
impact ionisation, Auger recombination involving traps 80−80912
impact ionisation of deep impurity centres 79−73470
impact ionisation theory 80−49752
impact ionization, review 80−65577
imparting states, transition metal, EPR linewidths calc. 80−80599
implanted layer, effectiveness of annealing by millisecond laser pulses 78−55885
impure, exciton absorpt. line shape calc. *(Russian)* 78−10934
impure, Wigner cryst., electron chain and CDW in strong mag. fields 78−60067
impurities, localised, transition metal, lattice relaxation in optical transition *(Polish)* 80−70345
impurities, trace element anal. 80−81399
impurities, visible and far-infrared laser spectroscopy 77−74524
impurities and other point defects, electronic struct., review 79−7803
impurity acoustoconduction, nonlinear theory 77−15914
impurity anal. by photoelectric spectroscopy, review 77−24584
impurity band, matrix elements in Matsubara-Toyozawa theory 79−33261
impurity band, molecular model 78−76018

semiconductors continued
impurity band density of states 77−31979
impurity band shift and width in mag. field calc. 78−6329
impurity bands, one-dimens. AMO-MT model validity 79−33256
impurity bands in doped semiconds., density of states, effect of nonorthogonality 77−59243
impurity breakdown in mag. field 77−24564
impurity centres, shallow, ground state energy calc. 77−4314
impurity centres in semiconductors containing screw dislocations 78−72111
impurity characterisation from thermal carrier meas. 80−65595
impurity complexes, H^--H^+ type, spectra, and pseudointeractions of mol. energy levels *(Russian)* 78−92100
impurity conduction phenomena, review of exptl. work *(Japanese)* 80−49737
impurity determination, neutron activation analysis program for multielement analysis with abs. counting 77−21439
impurity electron scatt., resonance scatt., Hall and drift mobility 80−65487
impurity interaction and donor-acceptor recombination 80−16094
impurity ion pot., approx. equivalence of Csavinszky and Resta models 80−59901
impurity ion pot., nonlinear Poisson eqn. soln., var. principles 80−29350
impurity ion pot., nonlinear Poisson eqn. soln., variational principles 78−67976
impurity ion pot., nonlinear Poisson eqns. 77−20265
impurity ion pot., screening charge density expansion convergence 79−7799
impurity ion potential, asymptotic corrections 77−47769
impurity ion screening charge density expansion 80−107780
impurity ions screening 79−87062
impurity levels, localised, low temp. field ionisation 79−47600
impurity levels of transition metal ions in cryst. field 78−23059
impurity molecules, shallow hydrogenic donor interaction 77−31977
impurity optical absorption in mag. field and resonant laser radiation 77−52145
impurity optical spectra, p-phonon processes 80−16061
impurity photoconductivity, monopolar injection *(Russian)* 79−24004
impurity photoconductivity, temp. elec. field and impurity centre conc. effects 78−56190
impurity photoconductivity for nonuniform impurity distrib. 79−82632
impurity photoionisation, quantum-defect, billiard-ball model comparison 80−65486
impurity profile determ., multilayer spreading resistance anal. using image method 77−68993
impurity screening in strong mag. fields 79−47054
impurity states, ionisation by elec. field 78−47738
impurity-level assisted two-photon interband absorption of laser radiation 78−23464
indirect band gap semiconductors, excitonic absorption band shape calc. 79−78015
indirect-gap semiconductors, tightly bound impurities, electromodulation symmetry sensitivity 77−66477
individual misfit dislocations, obs. by high voltage electron microscopy 79−82222
induced current obs. using stroboscopic SEM 77−19855
induced-current signal, semicond. with high quantum yield and recomb.-radiation reabsorpt. in SEM 79−11140
inductively heated, computer simulation of temperature and EM fields 78−55961
inelastic biexciton-biexciton collision, effect on radiative recombination of biexcitons 79−15529
influence on Auger transitions depend. of impact ionisation on electron energy impact ionisation, influence of scatt. on Auger transitions 80−44608
inhomogeneous, anomalous elec. props. in mag. field 80−44621
inhomogeneous, carrier statistics and thermal relax. *(Russian)* 77−4333
inhomogeneous, elec. cond. 77−8087
inhomogeneous, EM waves under elec. and mag. fields 80−20237
inhomogeneous, negative photocond. and IR quenching of resiual cond. 77−24587
inhomogeneous, photocond. spurious effects 77−55583
inhomogeneous, theory of residual cond. 78−14739
inhomogeneous anisotropic, spectral characts. of transverse Dember effect 78−39161
inhomogeneous electric fields in oscillatory photoconductivity 80−2421
inhomogeneous film, transverse magnetoresist., size effects 78−72293
inhomogeneous impurity distrib. semicond., irrad. effects 79−10875
inhomogeneous semiconductor, nonequilibrium carrier mobility 77−15879
inhomogeneous semiconductor structure with p-n junction, nonlinear current-voltage characts. 77−11929
inhomogeneous semiconductor structures, instability of plasma oscills. 79−11167
inhomogeneous semiconductor with nonequilibrium carriers, EM wave propag. 78−52024
inhomogeneous strain field scatt. deform. potential, theory 77−35905
inhomogeneous struct., transverse acoustoelectric effect 80−39638
inhomogeneously doped, computed IR refl. spectra 78−27205
inhomogenous, eigenoscills, of hot electrons in classically strong mag. field 79−73520
integrated optics and thin-film technology 77−54815
interband absorpt. in strong parallel mag. and elec. fields 79−78063
interband absorption in strong parallel mag. and elec. fields 80−6799
interband light scattering in semimetals and semiconductors *(Russian)* 78−60485
interband optical absorption with one-dimensional electronic superlattice 79−15483
interband resonant spectroscopy, review 79−61224
interband tunnelling of semiconductor in constant elec. and mag. fields 78−43405
interface and overlayer electronic struct., review 80−49841
interface and surface phenomena, conference, Pacific Grove, USA (Jan.-Feb. 1979) 80−46725
interface and surface physics, review 80−49872
interface between two semiconductors, magnetoplasmon-type surface polaritons 77−85292
interface formation, initial steps, surface states and thermodynamics 80−49503
interface with transversely magnetised ferrite slab, mag. surface wave amplification 78−72339
semiconductors continued
interfaces, conf., San Diego, Calif., USA (Feb. 1976) 77−20377
interimpurity absorption in strong EM wave field *(Russian)* 80−60631
interimpurity radiative recombination, intermediate exciton state *(Russian)* 80−49621
intermediate valence states, metal-insulator transition 78−51897
internal friction, simple recording system using electronic circuit 79−37260
intervalley acoustoimpurity resonance 80−107868
intrinsic, helicon nonlinear propag. 77−4385
intrinsic, indirect exchange interaction, finite temp. effects 80−71003
intrinsic, indirect interactions between localised mag. moments 78−43578
intrinsic, nonlinear theory of EM wave propagation *(Russian)* 78−60150
intrinsic, quantum theory of transverse galvanomag. phenomena, model of two standard bands *(Russian)* 77−62945
intrinsic, recombination induced nonequilib. phase transitions, thermodynamic and stochastic theory 77−49680
intrinsic and injected electron-hole plasmas, one-dimensional drift and diffusion of carriers 79−11163
intrinsic semiconductor, indirect exchange 77−80924
inversion layer, EM modes 78−80030
inversion layers, spectroscopy in high mag. fields, review 79−60889
inverted hot electron states and negative cond. *(Russian)* 77−43612
ion implanted, laser annealing 80−65023
ion implanted, ruby laser pulse effects 79−69125
ion irradiation produced amorphisation, disorder-ion fluencce functions, disorder mechanisms 80−29090
ion-implanted, laser annealing dynamics 79−69121
ion-induced kinetic electron ejection, pot. emission, semiconductors and insulators, review 77−44109
ionic, nonlinear intraband absorpt. and harmonic generation 78−33779
ionic, surface (110) atomic struct. 79−69331
ionic semiconductors, cyclotron resonance, elec. cond., electron-phonon interactions 80−93180
ionisation coeffs. of electron and hole multiplication, empirical fit to Baraff's curves 80−96897
ionisation energy of deep centres from absorpt. spectra, electron-phonon coupling 77−4663
ionisation rate, kinetic approach including acoustic phonon contrib. 79−56211
ionised impurity scatt. 78−51984
ionised impurity scatt. limited mobility in semiconductors with spatially variable dielec. function 78−51986
ionised impurity scattering, theory 80−20181
ionization and subthreshold effects in defect creation and annihilation 77−84811
IR absorpt. and optical relax. time of free carriers 80−66206
IR absorpt. of light by polarons 79−56799
IR modulation by free carrier confinement 78−25969
IR plasma reflectivity spectra analysis 78−52480
IR radiation ultra-fast switching by laser-produced carriers 79−98417
IR switching, ultrafast optically controlled, in semiconductors 80−58626
IR thermometry, semiconductor material temperature measurement *(Spanish)* 80−47062
irradiated, Hall mobility, dark and photo-conductivity calc. 78−47835
isothermal and non-isothermal C-V deep level meas. using Schottky contacts 80−88515
isotropic, differential relax. times and diffusivities of hot carriers 77−62936
isovalent impurity long range potential, role in electron scatt. 80−10966
Kane semiconductor, thermoelec. power and thermomag. effects of hot electrons 78−56174
Kane semiconductor films, thermomag. and thermoelec. effects, theory 80−70864
Kane semiconductors, parametric excitation of surface waves 79−38014
Kane semiconductors, transport props., kinetic integrals method 77−55525
Kerr effect, high-freq. 79−64294
kinetic fluctuations, global estimation 78−43376
large-band-gap, self-compensation, role of impurities 80−92850
laser annealing after ion implantation, temp. distrib. 80−54265
laser beam induced synergetic phenomena 79−74021
laser damage, role of carrier diffusion 79−19954
laser irradiation effects on struct. and props. *(Russian)* 78−30665
laser residual lattice absorpt., freq. and temp. depend 78−25910
laser stimulation of light interstitial diffusion in semiconds. and insulators, theory 77−15630
laser-induced damage 77−20961
laser-induced gratings, method for study of optically excited solids, forced light scatt. 79−41408
laser-modulated photoemission, technique for band struct. determ. 77−28686
laser-photoinduced etching, photodissociation of dissolved complexed halogens in soln. 80−100929
lasing action, exciton Bose condensate charact. function 79−64233
lattice thermal conductivity, high temp., role of optical phonons 79−33129
lattice vibration amplification in field of EM wave 77−76511
layer and defect structures, characts. of photocond. in strong absorption region 77−66184
layer crystals, exciton absorption of light 80−70623
layer crystals, light absorption by shallow impurity centres 79−15503
layer structure, dimens. depend. of elec. cond. *(Russian)* 77−51804
layer structure, laser-induced photolum. and collective effects *(Russian)* 79−95830
layer type, electron-hole pancake form. 77−47743
layered, constant current anodisation, representation of layer periodicity 80−3218
layered, DC hopping cond. due to stacking disorder and electron localisation 77−47819
layered, direct and indirect two photon processes 77−40261
layered, electron-hole liq. and metal-dielec. transition *(Russian)* 78−2425
layered, exciton spectra in case of strong anisotropy 77−51666
layered, exciton spectrum calc. *(Russian)* 77−1378
layered, high pressure effects on electronic structure and vibr. props. 77−51654
layered composite, magnetostatic Love waves by interaction with carrier waves 79−28577

semiconductors continued
layered compound, collective electron cond. in strong mag. field 79−42525
layered medium, electron dragging by spin wave *(Russian)* 79−78124
layered semiconductor, anodisation as layer counting method 78−76776
lifetime of carriers recombining in disordered regions, injection depend. 78−14742
light absorption, fundamental, in field of strong EM wave 77−52032
light absorption, temp. depend., exciton-exciton and -phonon interactions *(Russian)* 77−40265
light absorption, temp. depend., threshold flux density semicond. plate 77−83937
light absorption, two-photon, by excitons in static elec. field 80−11364
light absorption by deep impurity electrons 77−69871
light absorption due to electron-electron interaction of electrons occupying Landau levels 78−27195
light absorption in semiconductor with impurities *(Russian)* 79−47484
light beam dynamic conversion by phase shifted free-carrier holograms 78−46547
light diffr. by sound in doped semicond. 79−11404
light induced electron drift, two-photon transitions *(Russian)* 80−107853
light pulse, high-power, propag. under interband interaction conditions 79−10366
light pulse propagation, high-power, transitions between bands with different effective masses 80−34871
light scattering by phonon zero sound 79−56145
light scattering spectra, interference effects 79−82977
light transient scattering by free carriers 80−102766
light transmission, anomalous, phonon induced, below plasma edge 78−80368
lightly doped, 1/f noise for hopping conduction, theory 80−44683
linearised transport equations, explicit solns. 78−43375
linearized Boltzmann equation for semicond. plasma, carrier wave phase vel. 77−43634
local centre parameter determ. from thermally stimulated excitation curve derivative singularities 80−11004
local density of electron states for system with defects or impurities 80−92857
local fields, nonuniform charge distrib. 80−24826
local level parameters from thermally stimulated excitation curves, influence of variations of rate of heating 80−6769
localised electron states associated with transition metal impurity 79−56164
localised magnetic moment of transition metal impurities 80−60192
localised states, anomalous press. effects 77−51693
localised states near displacive transition 80−70644
lone-pair, localised gap states valence alteration model 77−8040
longitudinal isothermal Nernst-Ettingshausen effect in a quantising magnetic field 79−51617
low gravity experiment possibilities in electronic materials growth technology 79−47606
low resistance struct., visual obs. of V-I characts. 78−4646
low-dimensional materials, cond. temp. depend., metal-insulator transition, supercond. and semicond. behaviour 79−95391
low-symmetry, modelling of elec. props. 78−19036
luminescence, coherent conversion of excitons and photons to biexcitons *(Russian)* 79−47508
luminescence, due to exciton-electron scatt., calc. 77−16379
luminescence, high-conc. exciton and biexciton emission 78−6725
luminescence, PH band profile, exciton-electron interactions 80−20702
luminescence, spin-dependent, of donor-acceptor pairs 77−48223
luminescence, spin-dependent, of donor-acceptor pairs 77−52173
luminescence and luminescent devices, lecture 78−27323
luminescence emitted from excited acceptor-donor complexes subject to external electric field 77−66544
luminescence in presence of intense laser field 79−38621
luminescence parameters, absorpt. parameter effects *(Russian)* 78−80419
luminescence quenching by charged defects 78−23531
luminescent semiconductor electron-hole pair creation and migration 77−77304
magnetic circular dichroism at E_1 edges 78−92051
magnetic freezeout in ultraquantum limit, appl. to GaAs 78−76017
magnetic moment, spin splitting in strong electric fields 79−56175
magnetic oscillation of momentum distribution of hot photoexcited electrons *(Russian)* 80−2854
magnetic phase transitions in impurity band *(Russian)* 80−50097
magnetic susceptibility of hot electrons 78−10648
magnetised plasma, theory of EM surface waves 80−88584
magnetism and magnetic materials, conference, Cleveland, USA (Nov. 1978) 79−73651
magneto-microwave Kerr effect, K-band interferometer 80−52263
magneto-optic effects due to optical alignment of electrons and nuclei 78−6654
magneto-optic instability, overheating 77−1661
magneto-optical effects and cyclotron reson. in high mag. fields 80−27321
magneto-optical spectra, relax. and reson. struct. 80−29723
magneto-optical spectroscopy, MG field production and appl. 79−71491
magnetoabsorption, impurity-induced free-carrier 79−42950
magnetoabsorption, interband, in mixed semicond. with composition fluctuation and imperfect semiconds. 78−15152
magnetoconcentration effect, use of Boltzmann formalism *(French)* 77−32025
magnetoconcentration effect in variband struct. *(Russian)* 78−60143
magnetoconductivity, practical approx. to integrals 77−15870
magnetodiode and magnetoconcentration effects, influence of field effect 80−107903
magnetodiode effect 78−6401
magnetophonon oscillation separation techniques, advanced methods 78−2499
magnetophonon resonance due to two-phonon scatt. by acoustic phonons 77−69356
magnetophonon resonance oscills., peak shape, theory 80−107824
magnetoplasmon-polariton surface modes, Voigt geometry 78−43451
magnetoresistance, high field longitudinal, and bound states 78−23113
magnetoresistance, longitudinal, in quantising mag. field, var. calc. 77−43630
magnetoresistance, magnetic field modulation meas. technique *(Japanese)* 79−51614
semiconductors continued
magnetoresistance, odd, in HF elec. field 77−28198
magnetoresistance, superoperator theory 80−49776
magnetoresistance, transverse, quantum limit behaviour 77−4366
magnetoresistance coeff., anisotropic electron scatt., weak mag. field 77−76844
magnetoresistance four-probe method for free carrier density and mobility meas. 77−43626
magnetoresistance in narrow energy bands, Hubbard model 77−32029
magnetoresistance meas., transverse diffusion currents on source of error 79−7843
magnetoresistance quantum limit for impurity scatt. 79−91083
magnetostatic wave instability in ferrite-semicond. composite struct., theory 77−12186
many-phonon impurity absorpt. in external elec. field 77−52144
many-photon absorption by intraband transitions in mag. field 78−27261
many-photon magneto-optical absorption 78−19451
MCD due to free carriers 78−56462
micron scaled cathodoluminescence with SEM, review 78−23537
microplastic strain, low temp., physical nature *(Russian)* 79−65094
microwave absorption, near optical phonon creation threshold 78−47823
microwave conductivity meas. by eddy current loss method 78−8417
microwave magnetoconductivity in large quantising mag. field, effect of band non-parabolicity 79−47112
microwave noncontacting measurement techniques 77−2668
minority carrier conc. determ., integral eqn. approach to abrupt depletion approx. 77−32022
minority carrier exclusion 79−42561
minority carrier injection 78−60136
minority carrier injection in trap free semicond. 80−96904
minority carrier lifetime determ. by relative amplitude method 77−72869
minority carrier lifetime meas. for crysts. with high quantum efficiency *(Japanese)* 80−54711
minority-carrier injection into semicond. containing traps 78−60137
mixed, containing paramag. atoms, Landau levels and interband Faraday rot., appl. to $Cd_{1-x}Mn_xTe$ 79−61348
mixed, effective mass theory for carriers, spin effects 77−85208
mixed, EPR theory 78−39402
mixed semiconductor with comp. fluctuation, kinetics of intraband absorpt. and magnetoabsorption coeff. 79−19865
MM wave guiding and control by surface plasmons 80−103713
mobility anisotropy determ. by photoelectromag. effect and photocond., method and appl. to HgI_2 79−38126
mobility due to point defect scatt. calc. 78−19029
mobility-fluctuation description of 1/f noise 80−84496
modulation spectroscopy, two-ray methods, appl. to band struct. determ. *(Russian)* 78−54469
modulation spectroscopy in far UV, electroreflectance and thermoreflectance 77−66516
Moss formula, refr. index rel. to energy gap 80−108173
Moss relation between refr. index and energy gap of semiconductors 80−11357
Mossbauer spectra of implanted ^{83}Kr, line widths, isomer shifts 80−39899
Mott exciton formation in two-dimensional systems in high mag. fields *(Russian)* 80−65467
multicharged defects, screening of electrostatic fields 78−79959
multicomponent exciton gas, composition calc. 80−49618
multicomponent solid solutions, defect formation in heteroepitaxial structures 78−83825
multiexciton complexes, binding energy *(Russian)* 78−10372
multilayer semiconductor, exciton Stark effect 79−19528
multilevel generation-recomb. noise spectra, appl. of equivalent network methods 77−43674
multiphonon capture rate 79−38022
multiphonon electron-hole recomb. processes 78−6750
multiphonon electron-hole recomb. processes 78−6751
multiphonon IR absorption in highly transparent semicond. crysts. 78−10885
multiphonon nonradiative transition rate for electrons in semicond. and insulators 78−60503
multiphonon recombination processes 79−38643
multiphoton absorption by charge carriers in mag. field 77−28553
multiphoton absorption of intense EM waves 77−1648
multiphoton spectroscopy, IR tunable laser *(French)* 80−82836
multiphoton Stark effect, in quantized mag. field *(Russian)* 78−72541
multiple bound excitons, density functional calc. 80−10889
multiple-charge impurity states of transition and noble metal ions 79−33259
multiple-phonon scattering, statistical theory 78−67794
multiplication photoemission in strong field 77−85891
muon diffusion and trapping 80−71283
muon spin rotation research 79−56672
n-type, carrier waves instabilities, electron relax. time 77−4382
n-type, donor-polarizability enhancement as the insulator-metal transition is approached from the insulating side 80−80184
n-type, electron-phonon drag in longit. quantising mag. field 77−76805
n-type, free carrier absorpt., ionized impurity scatt. 79−42999
n-type, inelastic light scatt. from magnetoplasma oscills. 77−12385
n-type, influence of light on S-diode *(Russian)* 77−85303
n-type, inhomogeneous, nonequilib. carrier diffusion and lifetime 80−60005
n-type, lightly doped, hopping acoustoconductivity mechanism 80−65635
n-type, mag. and elec. dimens. reson., gyrotropic sphere problem 79−42570
n-type, metal-insulator transition, electronic phase diagram 77−8022
n-type, metal-insulator transition and negative resist. effects 79−24026
n-type, microwave induced emission of hot electrons, secondary emission study 79−69964
n-type, nonequilibrium photoelectron distribs. and absolute negative cond. in quantising mag. fields 80−65622
n-type, plasmon-local phonon mode interaction, RPA, CPA theory 78−87932
n-type, surface wave SHG 79−60860
n-type, thermionic emission, quasisteady noise effect 78−2974
n-type, unipolar cryst., intrinsic magnetoresist. in heating elec. field 78−72180
narrow-band, nonlinear anisotropic photoresistive effects 78−72202
narrow-band indirect-gap, exciton instability 77−8029

semiconductors continued
natural EM oscillations excitation by stream of electrons or EM field 80−34378
near intrinsic, magnetoresist. effect, determ. of carrier density and mobility 78−2501
negative conductivity, optically stimulated 77−4357
negative conductivity due to hot electrons transfer in geometric space *(German)* 78−56150
negative currents caused by injection-controlled polarization 79−28675
negative cyclotron resonance of hot carriers 78−2492
negative differential conductance, possible appearance at microwave freq. 79−11164
negative differential conductance, surface EM wave excitation, helicon and Alfven waves 79−69543
negative differential conductance media, amplification of HF waves 79−15177
negative electron diffusivity in high fields 78−30935
negative injection conductivity 79−69517
negative photoconducting materials, photovoltaic effects 80−96943
Nernst-Ettingshausen effect, thermopower, strong elec. field 78−23122
NMR of optically oriented nuclei in semicond. solid solns., quadrupole effects *(Russian)* 77−85592
noise, conference, Bad Nauheim, West Germany (Mar. 1978) 79−24031
non-equilibrium, acoustic plasma oscills. generation 80−96811
non-equilibrium phase transitions, formal conditions 79−47049
non-equilibrium phase transitions due to impact ionisation from traps 79−51520
non-linear optical props. of band charge carrier gas 78−33775
non-linear transport theory, field depend. of carrier screening 80−29415
non-polar cpd. semiconductor surfaces, chemisorption of O, π-bonding contrib. 80−6631
non-radiative de-excitation of deep centres 79−38644
non-radiative multiphonon carrier-capture cross-sections of deep traps, high-temp. limit 77−90191
non-radiative processes, multiphonon recomb. 78−6752
noncentrosymmetric crystals, subjected to strong elec. field, theory of transport phenomena 79−11136
noncoherent interaction of a light pulse 80−106561
nondegenerate, band electrons at arbitrary electron-phonon coupling, transport props. 80−39592
nondegenerate, flicker noise, mobility fluctuation possibility 79−91108
nondegenerate, free carrier absorpt. in quantising mag. fields 80−45044
nondegenerate, magnetophonon reson. in acoustic relax. of hot electron energy 78−26892
nondegenerate, quantum correction of Einstein reln. at high freqs. 78−19072
nondegenerate, thermomagnetic phenomena in quantising mag. field *(Russian)* 80−60014
nondegenerate, with ionised impurity scatt., acoustic wave amplification 77−11965
nondegenerate nonpolar, quantum theory of magnetophonon reson. 77−28200
nondegenerate plasma, polarisation description 78−56176
nondegenerate semicond. plasma carrier wave energy characts. *(Russian)* 79−7849
nondegenerate semicondcutor, three exciton radiative recomb. producing biexcitons 78−39603
nondegenerate semiconductors, effect of nonparabolicity on transverse magnetoresist. 77−51763
nonequilibrium acoustic phonons, generation by interband light absorption 80−96607
nonequilibrium carriers, diffusion in alternating elec. field 79−11133
nonequilibrium electron and phonon fluctuations *(Russian)* 77−80770
nonequilibrium electrons in semicond. excited by strong EM waves, self-polarisation 77−69910
nonequilibrium fluctuations in quantized mag. field *(Russian)* 79−95426
nonequilibrium optical phonons generated by electrons in laser radiation field 78−71802
nonequilibrium phase transitions, stability and dissipation, teaching 80−105479
nonequilibrium processes exam. by method of transient holograms 78−23105
nonequilibrium semiconductor, periodic stratification by diffusion 77−55544
nonequilibrium semiconductor with electron-hole pairing, mag. moment quantum oscills. *(Russian)* 77−28131
nonhomogeneous, dimens. localisation of electrons *(Russian)* 78−19000
nonhomogeneous hot solid state plasma, transverse EM instabilities 77−66177
nonhomogeneous semiconductor, galvanomagnetic effects 79−91077
nonlinear amplification of EM oscillations 79−51623
nonlinear coherence phenomena in exciton region 80−99806
nonlinear conductivity, vortex waves, carrier mobility and lifetime 80−96893
nonlinear conductor, odd-symmetry two-dimens. Hall effect in alternating elec. field 80−80303
nonlinear current density, theory 78−56149
nonlinear effects, induced by lasers 79−94300
nonlinear electroacoustic echo 80−92943
nonlinear equation, asymptotics of spectral boundary-value problem 80−6851
nonlinear HF conductivity in inhomogeneous EM field 77−51773
nonlinear impurity screening 78−67977
nonlinear intense EM wave absorpt. theory *(Russian)* 80−29425
nonlinear light absorption, influence of transitions via deep impurity centres 77−63446
nonlinear light absorption in presence of laser wave field 78−13747
nonlinear optical properties 80−25333
nonlinear optical props., book contrib. 80−78899
nonlinear optical props., non-stationary density matrix of electron-phonon system 78−71818
nonlinear plasma oscillations in superlattice semicond. 78−26897
nonlinear polarisability and self-action effects in binary and mixed semiconductors 80−99786
nonlinear refractive index under many-photon resonance conditions 78−90449
nonmagnetic, paramag. waves travelling near the paramag. resonance freq. 78−88168
nonohmic hopping conduction, theory 77−20328
nonohmic transport fluctuations 79−24034

semiconductors continued
nonparabolic, inelastic acoustic phonon scatt., in longit. quantising mag. field 77−28196
nonparabolic band semiconductor, diamag. excitons, optical absorpt. in mag. field 77−55487
nonparabolic bands, in mag. field, many photon Franz Keldysh effect 78−92055
nonparabolic generalised Franz-Keldysh effect in high freq. elec. field 77−59555
nonpolar, empty surface states and surface order effects on sorption 77−85281
nonpolar, normalised theory of impact ionisation and vel. saturation using Markov chain 79−91067
nonradiative multiphonon carrier capture and ejection props. of deep traps 78−35190
nonradiative multiphonon carrier capture by deep neutral traps 80−6871
nonradiative multiphonon carrier capture props. of deep charged and neutral centres 77−15866
nonradiative multiphonon carrier-capture cross section of deep traps, low temp. depend. 78−10469
nonradiative recombination, combination of Auger and many-phonon processes 79−87111
nonspherical band, optical absorpt. in crossed elec. and mag. fields 77−40264
nonspherical energy band, diamag. excitons and Franz-Keldysh effect 78−72554
nontrapping isoelectronic impurities, trapping in mag. fields 78−9097
nonuniform band structure materials, Shockley like equations for current density and carrier density 80−60001
nonuniform diffusion length and elec. field determ. 78−72166
nonuniformity monitoring by relative thermoEMF meas., limits by applicability 77−36702
normal transverse waves in longitudinal mag. field 80−80309
nuclear polarisation due to anisotropic size effect in weak elec. field 80−71199
nuclear relaxation due to interaction with excitons 78−56399
numerical integration of macroscopic semiconductor equations, applications *(German)* 77−69319
odd magnetophotoresistive effect 77−15908
ODMR appl. to recombination processes 79−42871
one dimensional, nonlinear optical props. 78−46708
one-dimensional semiconductor, delocalisation and superalternation effects in nonlinear susceptibilities 77−11840
one-dimensional systems, optical props. 77−43472
one-dimensional with deep levels, ambipolar transport of carriers 77−4356
opaque, inelastic dynamical light scatt. 80−25399
opaque, light scatt. from surface acoustic phonons 78−76484
optical absorption, Coulomb screening influence 78−72568
optical absorption of diamagnetic excitons in crossed mag. and elec. fields 78−10874
optical and IR characterisation 79−95846
optical generation of carriers under Franz-Keldysh effect conditions, instability 79−24017
optical heating, coupled diffusion eqns. for heat and excess carrier density 80−60718
optical heating of semicond. plate with temp. depend. absorption coeff. *(Russian)* 77−54867
optical investigations, vacuumless cryostat 80−73370
optical lattice vibrs., photostimulated enhancement 79−55845
optical non-locality phenomena near exciton reson. 79−95794
optical nonuniformity, spatial distrib. determ. 80−13116
optical orientation and spin system cooling *(Russian)* 78−88229
optical orientation of electronic and nuclear spins 78−79928
optical orientation of electrons, surface quality effects 79−11466
optical parameters in strong EM field, effects of finite wavelength of light 77−44050
optical phonon amplification by EM wave field in presence of mag. field 80−65181
optical properties, book 80−77554
optical properties, determ. via Kramers-Kronig transform. 77−8537
optical properties, equivalence of local field corrections and dynamical screeening 79−33250
optical properties, review 80−45106
optical properties above band edge, book contrib. 80−84425
optical properties due to phonons, book contrib. 80−80805
optical properties under press., book contrib. 80−84715
optical properties with electron temp. superlattice *(Russian)* 80−34879
optical props. under intense laser field 79−43040
optical props. under intense laser fields 78−72513
optical saturation for high carrier recomb. freq. *(Russian)* 80−88585
optical SHG, elec. field induced, theory 80−69457
optical thermal breakdown, fluctuations and wave processes 80−20587
optical thermal breakdown, semicond. plate-laser interaction, hysteresis 79−56889
optical transitions between deep impurity centre levels 79−61410
optical waveguide, semiconductor clad, attenuation and propagation coeffs. 80−79004
optically anisotropic, effect of modulation of mag. field on absorption 80−34898
optically anisotropic, magnetoabsorpt., light freq. modulation effect 80−66162
optically anisotropic, modulation of direction of mag. field 79−73911
optically anisotropic, orientation, use of polarisation depend. of photo-EMF and photoconductivity 77−89807
optoelectric effect and oscillations near surface 77−8172
optoelectric effect in semicond. with superlattice, theory 80−70768
oxide, gas adsorption effect on cond. *(Japanese)* 79−95408
oxide-cathode emission anal. by semiconductor theory *(German)* 78−88401
p-type, effective mechanism of hot electron energy relax. 78−26878
p-type, Faraday effect due to free holes 80−97247
p-type, field emission theory, surface states and recomb. processes 77−85901
p-type, g-values, spin temp., determ. from Raman spectra 78−43856
p-type, intervalence-band transitions, saturation, theory 80−75997
p-type, luminesc. parameters, reabsorpt. influence 79−95826
paramagnetic impurities, contrib. of collective excitations to mag. relax. 77−12190
paramagnetic phonon resonance, theory 80−50187

semiconductors continued
parametric conversion of acoustic/optical phonons, ultrasonic pumping 80−15209
parametric resonance of acoustic and opt. phonons 77−15915
parametric resonance of acoustic and optical phonons at low temp. 77−51779
parametric wave excitation in semiconductor electron plasma *(Russian)* 79−33252
partially disordered, density of states calcs., forbidden gap energy depth *(Russian)* 80−34347
particle complexes, N=1 to ∞, book contrib. 80−80194
partly disordered, with mobility threshold, transport props. and thermoelec. parameters 80−34449
Penn gap, energy gap, and dielec. function 79−82520
percolation level, Monte Carlo calc. for lightly doped compensated semicond. 80−59923
periodic potential with slowly varying envelope, effective Hamiltonian theory 79−23880
periodic structures, props., prep., use 78−51982
permittivity of crystal in strong EM field, light absorpt. and emission effect 80−15938
phase diagram interpret. using cryst. chem. formulae 77−81251
phase diagrams, exam. of compilation activity 79−8288
phase lines and thermodynamic props., quantitative filling of exptl. data to model parameters 79−11593
phase rule for semiconductor-vacuum interface 78−52049
phonon assisted electron impact ionisation and Auger recombination, theory 80−39591
phonon cond., three-phonon N- and U-processes 80−65313
phonon conduction and relaxation times 80−107585
phonon fluorescence stimulated by laser radn. 79−87504
phonon generation by EM wave 80−96606
phonon generation on intraband absorpt. of EM radiation *(Russian)* 77−48235
phonon induced hopping between Stark levels 80−92900
phonon replicas of bound exciton recombination 79−52008
phonon spectrum in mag. field, renormalisation 79−28060
phonon two-stage drag of electrons, thermoelectric power, scatt. mechanism 80−92919
phonon-assisted cyclotron reson., single and two-phonon pinning, review 79−15356
phonon-assisted nonradiative recombination phenomena *(Polish)* 77−69339
photo-EMF during charge carrier trapping *(Russian)* 79−42574
photo-excited electron momentum distrib., hot luminesc. polarisation 77−16396
photochemical etching mechanism 77−16709
photoconductivity, anomalous props. and appearance mechanism 78−95313
photoconductivity, low-temp., effect of electron-phonon interactions 77−66186
photoconductivity, nonequilibrium, in materials with nonequilib. distrib. of traps *(French)* 78−43433
photoconductivity, photoelec. effects, book contrib. 80−84488
photoconductivity and Dember effect, theory, allowance for long-range fields of charged impurities 79−24013
photoconductivity due to phonon scatt. and emission 78−10514
photoconductivity in conductivity locked relaxation semiconductor 79−73541
photoconductivity in highly excited state, thermodynamic theory 77−47742
photoconductivity measurement at UHF and at high excitation levels 80−65627
photoconductivity persistent impurity, in cpd. semicond., large-lattice-relax. model 77−85261
photoconductivity study using SAW convolver 79−42587
photoconductor, electron trapping kinetics at broadened levels, transient behaviour 77−47826
photoconductor-air gap-semiconductor system, calc. of surface charges under voltage in darkness 80−6905
photoconductors with deep impurities, resist. inhomogeneity effects on photoelec. props. 77−8151
photodesorption, review 79−51424
photodesorption, role of C 77−36787
photodielectric effect 78−6413
photodielectric effect associated with impurity excitation 79−82630
photoelectret state form. by IR light quenching photoelec. current *(Russian)* 79−91345
photoelectric conductance submicrosecond relaxations meas. *(Czech)* 80−31804
photoelectric fatigue 77−80808
photoelectric fatigue 78−10513
photoelectric Hall effect 78−91708
photoelectric spectra, conf., Moscow, USSH, (May 1977) 79−82622
photoelectric spectra of impurities 79−82623
photoelectrodes in electrolysis of water, appl. to solar energy conversion 79−29477
photoelectron spectra and band struct., book contrib. 80−16155
photoemission characteristics of semicond. with s-like valence band and p-like cond. band *(Russian)* 77−81195
photoemission in solids, book 80−12860
photoemission meas. of surface and bulk states 80−25527
photoexcitation, electron lifetime and capture by trapping centres *(Russian)* 77−32047
photoexcitation, high intensity, hot electrons and phonons 78−26905
photoexcitation phenomena, low density 78−27319
photoexcited hot electrons energy relaxation in near-surface region of semiconductors 80−92928
photoexciton waves, restrictions imposed on nature of additional boundary conditions 79−28789
photofield emission cathode, potential distrib. and model 78−2977
photogalvanic effect for free carriers in crysts. without symmetry centre *(Russian)* 78−87999
photographic stabilisers, reaction with yellow colloidal Ag, semiconductor props. *(German)* 78−86369
photography, semiconductor-photoemulsion system, characts. 77−87863
photoinjection characteristics 77−43654
photoinjection current kinetics in high resistivity semicond. 78−47834
photoionisation cross section of deep impurity centres for semicond. with highly anisotropic bands 78−56510
photoionisation cross-sections and phonon coupling 79−51518

semiconductors continued
photoionisation of deep impurity centres, drag of electrons 78−51938
photoionisation of deep impurity centres of quantising mag. field 78−6330
photoionisation of deep impurity levels 80−34386
photoluminescence, deep level recombination temp. depend. 79−47497
photoluminescence, temp. modulated, induced by photoexcitation 78−95605
photoluminescence, temp. modulated 79−38623
photoluminescence in crossed electric and magnetic fields 79−11464
photomagnetoelectric effect, contactless measurement apparatus, operation analysis using equiv. cct. 77−41655
photomagnetoelectric effect, expt. parameters rel. to material props. 79−99584
photomagnetoelectric effect, injection-level dependent lifetime 80−80319
photon drag effect, semicond. with elliptical isoenergetic surfaces 77−1443
photon enhanced field ionisation 79−83109
photoresistor noise measurement, determ. of drift mobility of semiconductors 77−4414
photosemiconductor-dielectric systems, two-component, photoelectret state 80−25287
photosensitive area localisation in semiconductors, expt. apparatus 80−75599
photosensitive etching in nonoxidising etchants 80−78813
photosensitive semiconductor element, discharge process, capture of carriers *(Russian)* 77−69343
photosensitivity of semicond.-metal system, theory *(Russian)* 78−3357
photostimulated impurity absorpt. of US 77−62962
photostimulated light absorption in Burnstein-Moss effect *(Russian)* 79−28706
photostimulated odd magnetoresist. 77−15910
photostimulated transport effects 79−11182
photovoltage for doping factor, mobility ratio and excess conc. determ. extreme band bendings 78−91726
photovoltaic effect, solar energy convertor theory with p-n junction 78−72201
photovoltaic effects, semicond. with internal elec. short circuits, calc. 80−65620
physics and technology, history and development in USSR, brief survey 78−54142
physics of semiconductors, conf., Edinburgh, Scotland (Sept. 1978) 79−95303
picosecond spectroscopy, nonlinear optical interactions 79−93230
piezoelectric-semiconductor, layer struct. transverse acoustoelectric effect 79−69565
piezoelectric-semiconductor interface, periodically irregular, electron absorp. and acoustic wave amplification 79−42361
piezoelectric-semiconductor struct., nonlinear acoustoelectric effects for large amplitude SAW 80−92942
piezogalvanomagnetic effects at low temp., meas. installation 77−41625
piezogalvanomagnetic effects measurement at low temps., apparatus with stabilised dynamic load 77−67458
pinch effect in solid-state plasma, review 77−1441
pinning struct. of cyclotron reson. lines 78−72414
planar acoustomagnetoelec. effect, theory 80−60052
plasma, EM wave instability, effect of density gradient 79−1607
plasma, EM wave propag., temporal instability in crossed elec. and mag. fields 79−4577
plasma, EM wave propag. in external alternating mag. field 77−20350
plasma, extraordinary electron cyclotron waves, transverse propag. in quantising mag. field 77−59298
plasma, inhomogeneous, radiation from a line source 77−66178
plasma, isotropic heated, temp. plasmon oscills. 78−26898
plasma, longitudinal oscillations with small number of carriers in perpendicular fields 80−88583
plasma, magnetically active, longit. propag. of surface waves 77−15934
plasma, oscillatory overheating instability 77−76855
plasma, single carrier, EM wave propag. in elec. field 77−43636
plasma, solitons in radiophysics 80−48124
plasma, surface-helical instability *(Russian)* 77−15885
plasma anodisation, model 79−28952
plasma effects, strongly elongated electron distrib., normal oscills. 80−60021
plasma self-oscillations within submillimetre freq. range 80−84473
plasma surface states of electrons in semiconductor in quantizing mag. field 79−11195
plasma surface waves 79−1612
plasma wave divergence criteria 77−4389
plasma waves propagation *(Russian)* 77−1439
plasmons, general theory 78−26826
plastic deformation, TEM obs. *(French)* 77−44303
plastic deformation under pulse action 77−76486
plate, light irradiation, heating and thermoelastic stress 80−25499
point defects, basis sets for study using Green's function methods 79−90994
point defects, high energy radiation effects, new developments 77−19980
point defects, review 77−7709
Poisson's equation, linear and nonlinear numerical solution including spatially variable dielectric const. 80−6825
Poisson's equation for impurity ion in medium with strongly variable dielec. constant, variational principle 77−69271
polar, free carrier magnetoabsorpt. by photon-ionised impurity magneto-plasmon processes 79−38117
polarisation in light oriented electron and nucl. spin system *(Russian)* 77−85619
polarised light nonlinear rotation 80−93268
polariton dispersion change by virtual biexciton form. under laser irrad. 79−38607
polariton structure of interband transitions 79−87048
polaritons, classical and quantum mechanical aspects *(French)* 80−103634
polaritons, two-phonon Brillouin scattering 80−20656
polaritons in mixed crystals, dispersion relation 78−18977
polaron mechanism of narrow band form. in quantising mag. field 77−76759
polaron transport eqn. soln. in strong alternating elec. field 80−39596
polaron transport in long phonon waves approx. 79−90975
polarons in degenerate-band case, weak to intermediate hole-phonon coupling 77−66126
polycrystalline, elec. cond. model 77−11908

semiconductors continued
polycrystalline, electron processes at grain boundaries under optical illum. 77−55561
polycrystalline, opto-electronic processes at grain boundaries 77−43667
polycrystalline, phenomenological theory of Hall effect 79−11160
polycrystalline, with low angle grain boundaries, residual cond. 80−15525
polydispersed, surface elec. cond. of particles influence on dielec. charcacts. *(Russian)* 77−16270
polypeptides, electronic struct., side-chain disorder effect 80−76706
Poole-Frenkel effect, grain boundary barriers 79−11137
population inverted, resonant Brillouin scatt., photoelastic consts. 80−89015
position-dependent band gap and electron affinity, current densities 77−85210
positron annihilation with electrons bound in edge dislocations 79−47539
positron lifetimes, causes of single short lifetime 79−28861
positronium atom, small-radius, anomalous props., exciton state 78−2433
potential barrier height, temp. depend. *(Russian)* 78−68070
potential calculations in non-homogeneous conducting layers, second-order perturbation method 77−15844
potential contrast appearance in SEM 79−27883
powder, prep., freeze drying of solid solutions, solvent choice 80−11583
powdered, EPR, effect of mag. field depend. of elec. parameters 79−99749
powders, semiconducting, band-gap energies, photoacoustic meas. 80−70579
powders, semiconducting, exam. of freeze drying rate in cryochemical prep. method 78−52706
power reflection spectroscopy, analytical techniques 80−62714
probe point characterisation by footprint in porous Si 79−96243
product analysis, defect finding by scanning electron microscope, electronic beam analysis *(German)* 79−94854
proton energy losses, Bohr equipartition rule 77−15467
proton semiconductors, with H-bonds, quantum theory of proton cond. 80−65641
proximity effects in transitions to exciton phases 79−28296
pseudobinary, electronic density of states, cluster-Bethe-lattice method 79−90939
pseudobinary, energy band calcs., comp. disorder effect determ. 79−42442
pseudopotential calculation of bending parameters 78−26813
pulsed electron beam processing 79−69159
pure, carrier mobility and electron state damping at low temps. *(Russian)* 80−15530
pyroelectricity, primary and secondary, review 80−93243
quadratic nonlinearity of semiconductors with zero forbidden band 79−10345
quantised inversion layer, hot carrier transport 78−30993
quantum diffusion in crystals, radiation enhancement conditions 78−47607
quantum electron-phonon system, theory of parametric excitation 78−10489
quantum insulator, plasma oscillation spectrum charges, continuum approx. free electron surface state binding energy 79−69575
quantum magnetoresistance results, using pulsed fields up to 35 T 79−73528
quantum oscillation amplitude, depend. on spin splitting 79−15066
quantum transport theory under high elec. field 78−23099
quasi elastic hot electron impurity scatt. in quantising mag. field 80−24938
quasi monopolar, integrally weak diffusion effect of I-V characts. 78−2491
quasi-one-dimensional, light absorpt. and Raman scatt., large exciton form. 77−16272
quasi-one-dimensional, many-exciton instability condition 77−43507
quasi-one-dimensional and quasi-two-dimens., exciton self-localisation *(Russian)* 77−31956
quasi-two-dimensional, crit. conc. of hot carriers 77−35977
quasi-two-dimensional, theory of collective phenomena 77−1376
quasi-two-dimensional semiconductor, warm carrier relax. via acoustic phonons 77−43694
quasi-two-dimensional semiconductors, electron scatt. by polar optical phonons 78−72237
quasienergy spectrum, polarisation depend. in field of strong EM wave 79−69415
quasilocal acceptor states, effects on band gap and electron mobility *(Russian)* 78−60082
quasiunipolar, elec. field screening 77−55605
quaternary, solid solutions with nearly perfect sublattices, stoichiometry invariants 79−51270
radiation damage, mechanisms, review 80−107315
radiation damage production, ionisation effects 77−7772
radiation damage studies on implanted Te, Sb and Sn by Mossbauer spectroscopy 78−2176
radiation damaged, residual defects rel. to back reaction annealing kinetics 78−3161
radiation defects, formation kinetics, successive capture of vacancies by impurities 79−10873
radiation dose for amorphisation, max. point defect conc. 77−55301
radiation effects, conference, Dubrovnik, Yugoslavia (Sept. 1976) 77−80540
radiation effects, role of nonequilibrium state 80−39152
radiationless Auger-recombination of electrons on three centres *(Russian)* 79−78114
radiative and nonradiative recomb. at metal ions, core struct. effects, review 79−4834
radiative and nonradiative recombination, spontaneous and stimulated emission *(Polish)* 80−53293
radiative recombination, book contrib. 80−84784
radiative recombination at donors and acceptors, majority impurity config. average calcs. 80−40154
radiative spectra from hot photocarriers 78−31249
radiative two-electron transitions 79−43026
Raman scattering, free carriers effect, complex band struct. 77−44001
Raman scattering, one-phonon final states and many-body effects 80−34913
Raman scattering by Landau levels, influence of impurities 77−1668
Raman scattering from impurities 78−56468
Raman scattering from impurities 78−56469
Raman spectroscopy *(German)* 79−28729

semiconductors continued
recombination, conference, Southampton, England (Aug.-Sept. 1978) 79−38087
recombination, three electron processes 78−43413
recombination at deep traps, review 79−38100
recombination centre distribution, scanning photocurrent microscopy 79−35822
recombination effect, spin depend. 78−34841
recombination of nonequilib. carriers in presence of dislocations 79−82607
recombination processes, review 79−38088
recombination radiation mag. depolaris., spin level quadrupole splitting of lattice nuclei *(Russian)* 79−38666
recombination radiation transfer effect on diffusion of nonequilibrium charge carriers 77−76843
recombination wave instability threshold, external load, boundary condition depend. 78−19053
recombination wave modes in case of several trap levels 80−39602
recombination-enhanced defect reactions 77−51377
refractive index dispersion for diamond and zinc blende struct. materials 79−24280
refractive index meas. using continuously recording spectrograph, instrum. 79−17467
relativistic electron spectrum, bound and reson. states 77−51701
relaxation of nuclear spins interacting with holes 78−48073
relaxation regime, generalised transport eqns. 78−56139
remanent deep impurities, capacitative spectrosc. 79−82628
resistivity and Hall effect meas., nondestructive four-electrode characterization 80−49743
resistivity meas., appl. of multiprobe measuring head 79−49253
resistivity meas., geometric factor in perpendicular four-point-probe technique 77−67475
resistivity meas., influence of space charge 78−23076
resistivity meas., two dimensional plotting by SEM 77−39852
resonance secondary radiation emission, theory 78−60452
resonance two-photon absorption, theory 80−28268
resonances in fundamental absorpt. region, quasi-mol. model interpretation 78−76490
resonant Brillouin scatt. as form of modulation spectroscopy 79−91456
resonant Brillouin scattering of exciton polaritons 80−93357
resonant Raman scatt., book contrib. 77−36251
resonant Raman scattering at indirect gap 79−73931
resonant Raman scattering in semiconductors *(Japanese)* 78−76459
RKKY interaction between localised mag. moments, conduction electrom MFP m model 77−66296
role of excitons in dispersion effects, band gap determ. 79−65393
runaway electron-heating dynamics 80−39597
saturated, dielectric response 78−10384
saturated, state, interaction with weak EM wave in quantising mag. field 77−16288
SAW amplification by transverse current in semiconductor with negative differential conductivity 79−7741
scalar electrodynamic pot., convolutional functional *(Polish)* 79−50205
Schottky barrier, charge carrier conc. determ. from low-field electrorefl. spectra 77−85320
screened impurity in mag. field ground state energy of bound electron 78−72107
second harmonic generation by hot-electron and electron transfer effects, optimum conditions 79−41491
secondary breakdown, hydrodynamic instability model *(Russian)* 78−43407
Seebeck coefficient, AC method of meas. using laser beam 78−76096
self-oscillatory medium, modelling 77−20811
self-oscillatory semiconductor medium, coupled temp. and carrier density self-oscills., photoelectron heating, microwave field 79−11166
SEM, high-resolution charact. 78−64794
SEM, induced conductivity mode expts., apparatus requirements 79−9260
SEM characterisation of semiconductor materials and devices 80−49064
SEM electron beam induced conductivity obs. of semicond. using Schottky barriers 78−34898
SEM electron beam induced current images of dislocations and stacking faults, computer simulation 80−70198
SEM meas. of diffusion const., lifetime and surface recomb. vel. 78−91701
semiconducting surface inversion layer, cyclotron reson. of interacting electrons 78−34885
semiconductor:transition metal, Anderson model localised impurity states *(Russian)* 80−6788
semiconductor, carrier number and effective bandwidths *(Spanish)* 78−18954
semiconductor, conduction electron paramag. relax., Coulomb mechanism 78−88191
semiconductor, drift mobility temp. depend. in presence of trap-recombination centres *(Russian)* 78−26880
semiconductor, localised defects, theory of SEM charge-collection imaging 79−1374
semiconductor, photo-field ionisation of deep centres allowing for Coulomb action *(Russian)* 78−27376
semiconductor, surface properties, investigation by laser and photovoltages *(Russian)* 78−23130
semiconductor, switching under impact ionisation 78−72215
semiconductor surface eval. using SAW convolver 80−97677
semiconductor-ferrite structure, surface spin waves, current-induced amplification, effect of static state inhomogeneity 79−28519
semiconductor-piezoelectric structure, vol. acoustic wave excitation in nonlinear interaction with surface waves 80−69582
semiconductors, elementary excitations in disordered systems with localised electrons, polarons *(Russian)* 80−49632
semiconductors, free carrier density in strong electric and quantised mag. fields 80−6860
semiconductors, with nonspherical bands, exciton absorpt. in crossed fields 79−69432
semiinsulator, minority carrier injection effect on TSC 78−10466
sensitised photolysis and latent image structure 79−24768
shallow and deep level evaluation using Schottky contacts, conc. and distrib. 80−49669
shallow donor states exam. by two photon spectroscopy 79−23925
shallow impurity centre spectra, isotopic shift of zero-phonon lines 80−66249
shallow impurity levels, effective mass approx. 80−6781

semiconductors continued
shielding by electron gas in magnetic field 80—107727
short range impurities in two band model 78—34803
single crystal polishing, vibratory polisher construction 78—80659
single crystals, melt grown, dislocation creation by thermal stresses 78—83825
single-valley, current instability and domain propag. due to Bragg scatt. 77—28187
sintering, cold, under high pressures, correlation to plastic props. and diffusion 79—38757
size effect, influence of space-charge regions on boundary conditions 77—89790
size quantised, superlattice state 78—39142
size-quartised wires, two-photon interband absorpt. 80—93256
small signal electrical response theory, generation-recomb. and trapping kinetics 77—89772
soft X-ray induced secondary-electron emission, models and meas. 79—74034
solid films and surfaces, conference, Tokyo, Japan (Jul. 78) 80—10739
solid solutions, influence of lattice disorder on elec. props. 77—8100
solid state physics, 1933-40, contrib. of Sir Nevill Mott 80—57055
solid state physics, conf. Munster, Germany (March 1979) 80—41941
solid state physics, historical aspects, symposium, London, England (Apr.-May 1979) 80—56999
solid-state plasma, current-convective instability kinetics 77—32031
sound absorption and amplification at intermediate freq. *(Russian)* 77—55586
sound absorption at very low temps. 79—95089
sound propagation, HF, nonlinear effects 80—88279
space charge, surface region, semiconductor with arbitrary energy spectrum of trapped states 80—107811
space charge region thickness, deep level props., determ. by γ-ray absorpt. 80—59995
spatially inhomogeneous, effect of heating field on reflection of EM waves 79—15157
spatially inhomogeneous magnetic field effect on semiconductor carriers 80—92916
spatially periodic, natural oscillations of nonequilibrium plasma 77—20355
spatially variable dielectric functions, ionized impurity limited mobility 79—42534
specific heat rel. to energy gap temp. depend. 80—54403
spectra, impurity electro- and magnetoabsorpt. coeffs., deep levels 79—24340
spectral noise meas. between 30 and 400 MHz, pulse technique device *(German)* 79—47134
spectroscopic techniques, anal. with STEM for electronic anal. and obs. of defects in semiconductors 79—14812
sphalerite, hydrothermal single crysts., feasibility of optical methods for quality control 80—89065
spin dependent recomb., theory 80—103708
spin glass, indirect exchange interaction of localised spins 80—88768
spin glasses, conduction electron produced exchange interactions between localised spins *(Russian)* 79—82799
spin injection, carrier polarisation, luminesc. polarisation 77—15957
spin orientation, violation of σH invariance *(Russian)* 78—35068
spin orientation by optical pumping, review 79—38410
spin polarisation induced by optical pumping 79—95681
spin relax., in quantising mag. field, effect of carriers 78—72388
spin relaxation due to electric fields 77—62928
spin-dependent recomb. and scatt. in presence of optical orientation of electrons 80—96908
spin-phonon interaction, dynamic screening by carriers, effect on paramag. relax. times 77—16150
spin-polarised electron-hole liquid, theory 78—43307
spreading resistances, multilayer analysis, errors in resistivities 80—10964
sputtering in multicomponent targets, surface binding and mass difference effects 79—83077
sputtering yield, energy depend., semiempirical formula 80—100736
stable electron-hole plasma, diffusion in magnetic field 79—24001
Stark and photoabsorption spectra, density of oscillator strengths 80—83318
Stark effect in quantising mag. field *(Russian)* 77—73126
Stark effect of localised electronic centres, impurities in semiconds. 77—66476
static conductivity change under quantum cyclotron reson. 78—39143
stationary recombination equations, analytical solutions in source limiting cases 80—44662
STEM spectroscopic techniques for simultaneous electronic and defect obs. 80—100145
stepped surface, electron states 78—95327
stimulated emission, highly excited excitation induced optical absorption 77—44025
stimulated scattering by light from free carriers created by light absorption 78—88330
strong electron-lattice interaction, review *(Japanese)* 80—49664
strong EM wave interaction 80—6852
strong EM wave interband absorption, saturation dynamics 79—992
structural transformation, at semiconductor-metal transition 79—23897
submillimetric magneto-optical props., strip line technique 80—60554
submillimetric-wave spectroscopy 79—33221
substrate, work function rel. to AES *(French)* 80—50479
subsurface strain, reconstruction induced, theory, appl. to Si (100) 78—63914
subthreshold effects, influence of electronic excitation on atom displacement 78—2158
superlattice, cond.-valence band interactions, subband struct. 77—72815
superlattice, EM wave absorption in quantising electric field 80—108182
superlattice, EM wave propagation, solitons *(Russian)* 78—79999
superlattice, geometrical and physical props. of constant-energy surface 77—69213
with superlattice, high freq. cond. 79—69542
superlattice, nonlinear EM wave amplification 77—88835
superlattice, nonlinear HF conductivity 77—15889
superlattice, nonlinear interaction of two waves 78—10494
superlattice, optical absorpt. by impurities 79—69867
superlattice, optical phonon excitation by light absorpt., impurity photoionisation 80—44275
superlattice, phonon spectrum, effect of strong elec. field, parametric reson. 80—44273
superlattice, plasma oscills. in strong elec. field 80—44637
semiconductors continued
superlattice, plasma resonant interaction with Stark oscills. 80—107842
superlattice, semicond.-dielec. high freq. electromagnetic response 78—19073
superlattice, soliton propagation 78—72162
superlattice, third harmonic generation *(Russian)* 77—27315
superlattice, transverse electron effective mass 80—100429
superlattice impurity photoconductivity electron spectrum reconstruction 80—24966
superlattice semiconductor, odd photomagnetoresistance effect 79—95425
superlattice semiconductors, cond. in strong elec. fields 77—55539
superlattices, electroplasmon parametric resonance 80—34475
superlattices, optical and transport props., review *(Slovak)* 80—20288
superlattices, Stark-cyclotron resonance, Larmour freq. *(Russian)* 80—60421
superradiant phase transition 77—44047
supersaturated solid solns., decomp., surface impurity content 78—51681
superstructured, weakly bound states of elementary excitations 79—60733
surface, 2-dimens. plasma formed by quantising surface channel *(Russian)* 77—15936
surface, atomic and electronic struct. 78—72223
surface, atomic geometry, ELEED meas. 79—51399
surface, cyclotron reson., projection operator formalism 80—88524
surface, depth profiling, optoacoustic technique 80—65337
surface, effects of ion sputtering, ion implantation 78—88395
surface, electron-electron interaction and electronic props. of space charge layers 78—60210
surface, electronic struct. rel. to sorption 78—14784
surface, field ionisation and field evaporation mechanisms 79—15594
surface, H recomb., nonequilib. charge carrier generation *(Russian)* 79—91126
surface, heterogeneous, slow relaxation kinetics 77—85288
surface, macroscopic recomb. centres 80—6933
surface, photoemission, book contrib. 78—95671
surface, plasmon dispersion, appl. to INSb 77—1464
surface, prereduced, room temp. activity for oxygen isotopic exchange 79—91998
surface, reson. inelastic light scatt. by charge carriers 80—20655
surface, review of electronic struct. calcs. 77—28226
surface, theory, book 80—36787
surface analysis by ion beam backscattering *(Chinese)* 79—82425
surface analysis by SIMS *(Czech)* 80—90927
surface and adsorbate states, charge injection into space charge layers 80—100496
surface and interface electronic struct., book contrib. 79—42619
surface and interface electronic structure, scattering theoretic approach 80—6940
surface and interface states, meas. *(Japanese)* 80—20269
surface Brillouin scattering from acoustic phonons 80—55113
surface characterisation using SAW 80—11069
surface depletion and inversion, arbitrary doping profile, theory 80—107912
surface electron states, calc. based on chemical pseudopotential 77—69393
surface electron states, empirical tight-binding method, critique 80—49854
surface electronic props., optical spectroscopic techniques, review 80—11070
surface electronic structure, low energy electron loss spectroscopy *(Japanese)* 78—88007
surface energy level determ., thermally stimulated contact pot. difference method 79—99601
surface evaluation by electroreflectance *(Japanese)* 79—82949
surface final-state effects on core electron transition energies 78—91745
surface galvanomag. props. and relax. time energy depend. 78—43459
surface helicon waves in Faraday geometry, existence 80—44703
surface helicons in semiconductor plasma, theory 80—60019
surface inversion layers, exchange and correl. 80—75618
surface magnetoplasma wave spectrum in HF mag. field 80—24995
surface magnetoplasmon type polaritons, LF, existence criterion in Faraday config. 80—96961
surface magnetostatic wave, travelling-wave amplification anal. using Maxwell equations *(Japanese)* 78—6560
surface melting during laser annealing 79—74023
surface parameters of semicond. with surface doping 77—15933
surface phenomena and optics, book 79—42428
surface photoelectric effects, influence of excitation rates 79—69547
surface photoemission of model system, book contrib. 78—95665
surface physicochemical processes, ellipsometric installation for kinetics study 77—18071
surface physics, conf., Eindhoven, Netherlands (June 1976) 77—62708
surface plasma, van der Waals interaction with neutral atom, mag. field effects 77—59316
surface plasmon polariton modes, struct. induced, using ATR, theory 79—60890
surface potential distrib. meas. using mirror electron microscope 79—35784
surface potentials using electron energy anal., SEM study 80—15582
surface recombination, effect on excess charge carrier distrib. and on base current 77—39866
surface reconstruction, dynamical theory 80—10773
surface reconstruction, theory 77—85282
surface reconstruction-induced subsurface strain, theory 78—91516
surface space charge layer spectroscopy 77—20386
surface space charge layer study using SAW convolver 77—46871
surface space charge layers, subband struct., perturbation theory 80—84497
surface spectroscopy, exciton effects, theory 80—49856
surface state excitons 77—51799
surface state interband transitions, electron-hole effects 77—66192
surface steps, electronic struct., Bethe-Peierls approx. 77—39911
surface structure and properties, review *(Japanese)* 80—49483
surface structure of cpd. semiconds., review 77—85032
surface subjected to chem. excitation, nonequilib. electron effects 78—72238
surface subjected to chem. excitation, nonequilib. electron effects 78—72239
surface superstructure, excitonic wave-phonon coupling 77—15775
surface-state props., using field effect anal. 79—24053

semiconductors continued
surface-states concentration profile and capture cross section determ. using SAW convolver 80−80341
surfaces, optical props., book contrib. 80−80737
surfaces, relaxation time spectrum of slow traps *(Russian)* 77−15937
surfaces and interfaces, electronic struct. calcs. 79−1613
temperature dependence of energy gap 80−2321
temperature dependences meas., of electric conductivity, Hall coeff. and magnetoresistance, automated installation 80−31792
temperature rise due to nonlinear heat generation 78−87983
temperature sensitive semiconductors, AC thermal theory 79−11131
temperature superlattice, in semiconductor with hot electrons, transport props. effects *(Russian)* 78−34839
temperature superlattice with hot electrons 80−20202
temperature waves in nonequilib. conditions 77−43397
ternary chalcopyrite, microhardness, empirical bond approach 77−69031
tetrahedral, bond orbital model on CNDO basis 77−47720
tetrahedral, electronic struct. of point defects, surfaces and interfaces, Green's function scatt. theoretic method 79−33258
tetrahedral, lattice thermal cond., ionicity depend. 79−37884
tetrahedrally bonded, microhardness, empirical bond approach 77−69030
tetrahedrally bonded, quasipolycryst. approx. for electronic states 79−77975
tetrahedrally coordinated, dislocation struct. 79−82206
tetrahedrally coordinated, dislocations, symposium, Hunfeld, Germany (Sept. 1978) 79−82214
tetrahedrally coordinated, effect of disorder and long range strain field on electron states 79−82545
tetrahedrally coordinated, effect of doping on dislocation mobility 79−82550
tetrahedrally coordinated, models of dislocation struct. 79−82205
tetrahedrally coordinated, temp. depend. of diamagnetic susceptibility *(Rumanian)* 80−88717
tetrahedrally coordinated covalent semiconductor point defects, multiple scatt. Xα model 80−54636
tetrahedrally coordinated electron states associated with dislocations 79−82544
tetrahedrally coordinated semiconductors, electronic nature of vacancies 77−62863
tetrahedrally coordinated semiconductors, electronic struct. and Fourier transformed Compton profiles 79−38689
thermal conductivity, calc. using numerical soln. of Boltzmann eqn. 80−44373
thermal conductivity, exciton-phonon drag 77−15640
thermal conductivity, rapid meas. method *(French)* 78−12689
thermal conductivity meas., cryostat design for 90 to 450K 79−76957
thermal conductivity on pulse heating, nonlinear *(Russian)* 77−43391
thermal conductivity theory *(Russian)* 79−37889
thermal domain investigation, Joule heating, current-voltage characts. 80−70711
thermal EMF measurement, thermal cell and copper blocks method, more accurate treatment of results 80−77812
thermal instability in semicond. based on effective thermal time const. 79−15155
thermal ionisation of an impurity in strong electric fields *(Russian)* 78−43410
thermal switching phenomenon 77−39904
thermally stimulated and isothermal discharges of capacitor across semicond. with grain-boundary barriers 78−2582
thermally stimulated conductivity luminescence, defect levels, traps, book contribution 80−80296
thermally stimulated relaxation processes, book contribution 80−80295
thermocouples, selection of semicond. materials *(Russian)* 78−73990
thermoelectric amplification of sound 80−2427
thermoelectric and thermomagnetic effects, heat transfer due to quasiparticle subsystems *(Russian)* 80−24959
thermoelectric figure of merit, direct meas. in transverse mag. field 78−10485
thermoelectric materials, thermal stability 79−19611
thermoelectric power, meas. using analogue subtraction 78−244
thermoelectric power, transverse, in anisotropic media, influence of anisotropy of thermal cond. 77−8127
thermoelectric power in high magnetic fields 79−60858
thermoelectrically anisotropic inhomogeneous media, eddy thermoelec. currents 77−55555
thermoelectromagnetic waves in conductors in a mag. field *(Russian)* 80−49695
thermoluminescence and TSC, evaluation of model, reliability of trap depth determ. 77−32451
thermoluminescence and TSC interpretation of expts., extensions of conventional model 78−27335
thermomagnetic effects, longitudinal, odd in respect of mag. field 77−89780
thermomagnetic photoeffect 79−23991
thermophysical props. determ. from Ettingshausen effect meas. method 80−44376
thin film semiconductors *(Japanese)* 80−107936
thin foils from multilayer heterostructures, prep. and ion etching 79−12779
thin layers, double injection in transverse mag. field, theory 80−80421
thin layers, resistivity meas. by four point contacts arbitrarily spaced on circumference 78−51983
Thomas-Fermi dielectric screening eqn. 78−10388
three-band, absorpt. of weak EM wave in presence of intensive one 79−61325
three-impurity clusters, ionisation energies and electron affinities 80−65496
time resolved reflectivity of ps pulses 78−31217
total electronic energy, force consts., and phonon dispersion curves, tight-binding calc., covalent 79−60747
transient and alternating currents, influence of deep traps 79−73525
transient donor recombination, adiabatic approx. 80−49761
transient injection currents, charge transport allowing for trapping 78−26884
transient SCL current problem 77−69331
transition into excitonic phase, boundary effects 78−76003
transport, quantum kinetics eqns. for finite collision duration regime 79−73519
transport equation and photocurrent of electrons, in EM field 78−26913
transport equations, generalised 79−95398
transport equations, initial approxs. for numerical soln. 78−14741
semiconductors continued
transport equations for junction behaviour of relaxation semiconductors 78−30977
transport equations formulations 77−43585
transport properties, Fermi-Dirac integral, approx. by 12th order polynomial *(French)* 79−11109
transport properties, Seebeck and Hall coeffs. Lorenz number, anisotropy, theory *(German)* 80−65608
transverse conductivity in quantising mag. fields, finite radius scatterer neutral impurities *(Russian)* 80−29400
trap parameters, calc. method from TSC under monomolecular recomb. conditions 77−8495
trap-free lifetime and relaxation, bulk boundary conditions for injection and extraction 78−72169
trapping of nonequilib. carriers by centres localised in disordered regions 77−43618
traps, spatial distrib. obs. with SEM *(Russian)* 77−32449
TSEE, role of surface pot. 77−8732
tunnelling, bound levels and band struct,, rel to inelastic electron tunnelling spectroscopy 79−4597
tunnelling and negative resistance phenomena, book 78−26947
two-band system, acoustic scatt., appl. to hole transport props. 79−60823
two-dimensional electron gas, CDW 80−65476
two-dimensional electron-hole systems in high mag. fields, phase transitions 80−49608
two-dimensional excitonic phase in strong mag. field 78−43308
two-level medium, coherent interaction with radiation, relax. processes effect 79−59774
two-phonon Raman scatt. by longitudinal optical phonons, double reson. 77−24852
two-photon absorption, free carrier storage by deep centres *(Russian)* 78−23131
two-photon absorption in crossed elec. and mag. fields 77−85693
two-photon absorption in semiconds. with superlattice 77−16331
two-photon absorption under reson. conditions 77−90170
two-photon conductivity calc., nano-pico sec. pulse excitation 78−72188
two-photon interband optical transitions involving deep impurity centres, photon drag 80−16069
two-photon interband transitions, carrier drag 79−7858
two-photon resonance absorption *(Russian)* 77−61997
ultrasound absorption, intermediate frequency, nonlinear effects 79−28380
uniaxial, with hot carriers, EM instability 77−32021
unijunction transistor transition critical exponents, negative resistance phenomena 80−44713
unipolar, n-type, field-effect mobility, energy spectrum of surface states 80−39657
unipolar, theory of acoustophotoelectric effect 77−55577
unipolar high-resistivity, directionality of longitudinal photocurrent 79−11177
US absorption and amplification moderate freq. 78−19102
US attenuation by impurities 77−69047
valence, conduction electron scattering by vibrating impurities 78−95297
valence band calc. using many-electron theory 80−15434
valence bond test, for validity of structure 79−10830
valence conduction band transitions, appl. of modulation spectroscopy with synchrotron radiation 78−4710
valence electron crystal pot. and pseudopot. components determ. from X-ray scatt. factors 79−65032
Van der Pauw structure with finite contacts, anal. of Greek cross, sheet resistance meas. 80−22387
variable band, recomb. radiation polarisation oscills. in mag. field *(Russian)* 77−77283
variable gap, photolum. emission and excitation spectra 78−76526
variable gap, photomagnetic EMF exam. 78−10510
variable gap semiconductor, photoluminesc. 78−48222
variable gap semiconductors, carrier transport and fluctuation effects due to changes in gap width 80−107793
variable gap thin structs., radiative recomb. photoluminesc. spectra 79−43036
variable-gap, exciton drift length 77−28129
variable-gap, photoluminesc. under transient excitation conditions 80−20698
variable-gap, with high band-gap gradient, characts. of radiative recomb. 79−56858
variable-gap semiconductors, anal. of drift of recombination radiation 80−16096
very pure, mobility calcs. including low impurity conc. limit 77−28173
VPE growth, book contrib. 79−69997
wafer, influence of discontinuous resist. distrib. on results of four-point probe method meas. 77−39841
Wannier excitons, fine structure, lineshape and dispersion, review 80−44520
Wannier-Mott polaritons in mag. fields, review 78−2437
Watkins-type radiation defects, low temp. form. mechanism 80−15153
weak heating of electrons, cyclotron reson. conditions, quantising mag. field 78−39141
weak helical waves, excitation and amplification by strong waves in strong mag. field 78−19077
weakly doped, compensated, IR light absorption by small scale fluctuations *(Russian)* 80−66255
weakly doped compensated, hopping photoconductivity in disordered systems *(Russian)* 80−65573
weakly inhomogeneous, impurity absorpt. and impurity photocond. line profiles 78−19098
weakly polar, free polaron IR absorpt. effect of DC field 77−81132
weakly polar, IR absorption by optical polaron in mag. field 77−66127
wide gap, recomb.-trap barriers 77−8119
wide gap monocrystalline semiconductor, determ. of bulk and surface absorption coeffs., photoacoustic spectroscopy 80−4781
wide-gap, electroluminesc. effects, population inversion of distant donor-acceptor pairs 79−99944
wide-gap, extrinsic, injection currents, theory 78−19052
wide-gap semiconductors, thermionic emission current, surface states effects 79−15581
wire, quantised monochromatic wave absorpt., indirect transitions due to surface roughnesses *(Russian)* 79−91397
wire, two-photon interband absorpt., quantum size effect *(Russian)* 79−95721
wires, Wannier-Mott exciton scatt. by phonons *(Russian)* 78−72074

semiconductors continued
work function, absolute determ. method for metals and semiconductors 77−28697
wurtzite structure, effect of local strain fields on shallow acceptor states 80−96821
wurtzite structure, natural optical activity *(Russian)* 79−78647
wurtzite-type, emission lineshape of excitonic mols., polariton states 77−20918
wurtzite-type semiconductor, with electron-hole exchange interaction, energy levels of A and B excitons 79−51494
X-ray diffraction by semicond. with p-n junctions, photoelec. EMF produced *(Russian)* 79−8225
X-ray K-absorpt. edge shift and electronegativity diff. 77−16424
X-ray photoelectron spectra struct., single and polycrysts., one-electron approx. 78−64445
X-ray topography camera, high speed, lattice defects exam. appl. 77−11443
XPS, core electron line shapes 78−11082
Zener tunnelling in mag. and elec. fields 79−91082
zero gap, collisionless, anomalous Hall effect 79−23988
zero gap, indirect exchange interaction 79−61094
zero gap semiconductors, electron scatt., thermoelec. power and Hall effect at low temp. 80−44628
zero-gap semiconductor, reson. scatt. of electrons 80−10938
zero-gap semiconductors, anisotropy of IR absorpt. coeff., k.p. calc. 80−97285
zero-gap semiconductors, dynamic dielec. function in mag. field, appl. to magnetoreflection spectra 79−15108
zero-gap semiconductors, electronic energy spectrum 77−66118
zero-gap semiconductors of α-Sn group, impurity states model, appl. to HgSe(Te) 79−60758
zero-phonon Raman scatt. of light 79−69843
zinc blende type, electronic charge density of valence electrons 77−1094
zinc blende type ionic semiconductors, vacancies, bound state energy level calcs., tight binding approx. 80−44694
zinc-blende struct., shallow acceptor contribution to near-resonance spin-flip Raman scatt. 79−95754
zincblende compounds, (111) face, dangling bond surface state 78−84278
zincblende compounds, electronic struct. and atomic config. at cleavage surface 77−62974
Zincblende struct., localised vibrs. due to defect complexes, Green's function study 80−79896
zincblende structure, dislocation climb model, appl. to degradation of lasers and LED's 77−1125
zincblende structure, phonon attenuation in presence of internal strains and mag. field 78−76118
zincblende structure, uniaxially stressed, band edge Landau levels 79−60706
zincblende type, building-up of covalent bonding, quadratic response of Fermi gas 77−28132
zincblende type, valence band effective mass strain depend. 78−51880
zincblende-type, exchange splitting of donor-acceptor pairs 77−20263
zone melting process, math. simulation *(German)* 79−28913
Ag halide photography, semiconducting models 79−19630
Au wire-semiconductor, elec. contacting by spark welding *(German)* 79−49215
CuCl, dielectric function for semiconductors with high exciton conc. 80−84443
Ge-type, light scatt. from zero-sound 78−43857
He^3/He^4 high isotope ratio in technical-grade metals and semiconductors 79−86080
^{129}I impurities implanted in semiconductors, isomer shift 80−20522
$In_{1-x}Ga_xP_{1-z}As_z$ DH lasers, multiple LPE, lattice matching 77−77421
$Mg_xCd_{1-x}Te$:P, vibr. modes of defects, IR absorpt. expts. 77−62601
Si, solar-grade, directional solidification in carbon crucibles 80−45663
Si-Al(Ni) structure, contact resist. and bulk resist. of Si, pulse method 78−52083
$Zn_xCd_{1-x}Te$-P, vibr. modes of defects, IR absorpt. expts. 77−62601

semileptonic decays
baryon octets, SU_3 theorems 80−32030
baryon resonances, EM transitions, multipole moments in single quark transition model 80−62985
Cabbibo fit, generalised, appl. to quark mixing angs. in sequential Weinberg-Salam model 79−17655
charm particles, obs. of $\mu^+\mu^-$ prod. in $\nu(\bar{\nu})N$ 78−89697
charm particles, sum rules for four-body semi-leptonic decays 79−36067
charmed baryon semi-leptonic decay and quark effective masses, SU_4 symmetry 78−58185
charmed baryons, semileptonic decays, SU(4) breaking, mag. moments, suppression factors 79−387
charmed baryons, weak decays, quark model framework 80−62976
charmed meson, possible semileptonic decay to K's in ν interactions 77−2819
charmed meson pair decay obs. in $pp\rightarrow e^{\pm}\mu^{\mp}$ 78−89759
charmed meson semileptonic decay, effective chiral Lagrangian method 78−74254
charmed meson semileptonic decay effects of hadron multiplicity on distribs. 78−4856
charmed mesons, semileptonic decays, charged weak current struct. 80−102042
charmed mesons and other heavy particles, inequalities for decay rates and lepton polarisations 79−89147
charmed mesons pairs produced in γN collisions, semileptonic decay spectra 77−49952
charmed particle decays, semileptonic, nonleptonic, isospin restriction on charge distibs., branching ratios 77−54099
charmed particle semileptonic decay to K_s^0e in e^+e^- 77−2853
charmed particle semileptonic decays 79−63473
charmed particle weak semileptonic decays, free parton model 79−75766
charmed particles, formalism using helicity amplitudes 78−4852
charmed particles, inclusive semileptonic decay, struct. functions, scaling limits 78−82165
charmed particles lifetime, semileptonic decay rate calc. 79−9366
charmed pseudoscalar mesons, quark model 77−61281
charmed quark semileptonic decay, gluon corrections to charged lepton spectrum 79−75765
charmed-meson decay, massive quark model 78−33067
D-mesons, spectrum generating SU(4) 77−54098
flavour-changing meson semileptonic decays 80−22553

semileptonic decays continued
free neutron decay, e^--ν ang. correl. coeff., determ. from proton recoil spectrum 79−22242
free neutron decay, fundamental phys. expts. with reactor neutrons and neutrinos, summary 79−67543
hadron electromag. and weak form factors, SU(6) scheme of relativistic quark model 78−41500
heavy b and t quarks, weak decay, lifetimes and branching ratios 79−97588
heavy meson inclusive semileptonic decays, lifetime estimates, quark-parton model difficulties 80−86704
heavy meson nonleptonic and inclusive semileptonic decay, lepton spectrum calc. 79−3018
heavy quark, next, semileptonic decay distribs. 79−45066
heavy quark semileptonic decay, gluon radiative corrections 79−75743
heavy quark semileptonic decays, gluon corrections 79−17688
heavy vector meson weak decays 79−13110
hyperon decay anal., Λ' existence, ninth $I=0$ $J^P=1/2^+$ baryon, asymptotic level realisation of SU(3) 77−18245
hyperon semileptonic decay, model with spectrum generating SU(3) symm. 77−38167
hyperon semileptonic decay, SU(3) spectrum generation, Cabibbo angle 80−9119
meson decay, effect of symmetry breakdown *(Russian)* 79−6337
neutral currents as higher order effects in Fermi-type charged current theory 78−41474
neutrons, ultracold, use for lifetime meas., collision loss calcs. *(Russian)* 80−52504
proton semileptonic decay in nuclei, pion attenuation 80−47286
pseudoscalar mesons, muonic double β-decay, tree and box diagram approx., K^- and F^- 79−17717
sequential charged lepton, semileptonic branching ratio and lifetime 80−57578
straton model of $1/2^+$ baryon semileptonic decays and high energy neutrino-nucleon reactions *(Chinese)* 78−12873
$SU_4\times U_1$ and the origin of the Cabibbo angle, charged gauge boson mixing 80−73639
SU(3) rules for semileptonic weak decay of charmed and strange mesons 78−45916
B-meson decay, partial unification of strong, weak and EM interactions 80−18106
$B_c\rightarrow e^+e^-$ + hadrons, decay due to weak neutral currents *(Russian)* 79−22146
D(1865), charmed meson semileptonic decays 78−4854
$D(1865)\rightarrow e\nu K^*(890)$, right handed current, eK* ang. correl., energy spectra 78−74248
D(1.87) mesons semileptonic decay, multiplicity effects 77−49953
D charmed meson weak decays, tests via parity violation, strangeness violation and semileptonic decays 77−30368
$D\rightarrow e+X$, anomalous electron prod. from D meson decay at $\psi(3772)$ 78−37203
$D\rightarrow K^*\mu\nu$, in e^+e^- annihilation, T-odd asymmetry in CP violation model *(Russian)* 80−105885
$D\rightarrow Kl\nu$, D meson weak decay const. determ. 79−93407
$D\rightarrow Kl\nu$, $K^*l\nu$, lepton spectrum anal. 78−4855
$D\rightarrow K\pi l\nu$, charm-changing weak hadronic current, models 80−57585
$D\rightarrow K\pi l\nu$, current algebra calcs., form factors and decay distribs. 80−42447
D meson decay, semileptonic and leptonic modes, electron momentum spectrum 78−8657
D meson decay in massive quark model 79−93376
D mesons, contrib. to single lepton spectra and dilepton invariant mass distribs. 77−2820
D mesons, semileptonic decay const., D and F decay const. ratio determ. 78−62392
$D\rightarrow\nu eK(K^*)$ at $\psi''(3770)$ from e^+e^- interaction 78−89693
D semileptonic branching ratio at $\psi''(3770)$ in $e^+e^-\rightarrow$hadrons 78−45934
D semileptonic branching ratio and lifetime from $e^+e^-\rightarrow e^{\pm}X$ 80−4983
D-meson semi-leptonic decay, current algebra treatment, rel. to charmed current quark mass 79−97577
D-meson semileptonic decays, K-e correl. anal. 78−78179
D^0, lifetime difference from D^+ 80−91084
$D^{\pm}$, nonleptonic and semileptonic decays, isospin selection rule tests 80−73700
DD production in large p_T hadronic collisions, eμ and eK correlation study 79−40772
$e\rightarrow\nu_e+\gamma$, lower bound of 3.5×10^{23} years *(Russian)* 79−40827
e^+e^-, anomalous e-μ events, semi-leptonic explanation 77−248
$e^+e^-\rightarrow\mu3\pi$, above 6 GeV, inference of τ decay 78−50042
$\eta(\eta')\rightarrow(\pi\pi\gamma)$, nonet mixing and gluon effects in current quark framework 79−80799
$\eta\rightarrow\pi^0\nu\bar{\nu}$, presence of second class neutral currents 79−26284
F mesons, semileptonic decay const., D and F decay const. ratio determ. 78−62392
F-meson semileptonic decay modes, explanation of inclusive electron spectra 78−37202
$F^+\rightarrow\pi^+e^+e^-$, enhancement due to π^+ EM form factor, generalised PCAC applicability 78−82164
$K\rightarrow l\nu_e\gamma(l\nu_e l'^+l'^-)$ in review of weak-EM decays *(Russian)* 77−2818
$K\rightarrow\pi^+\pi^-e^+\nu$ decay form factors, relativistic quark model 77−38160
$K\rightarrow\pi^+\pi^-\mu\nu$ decay rate 77−6113
$K\rightarrow\pi e(\mu)\gamma$, quark mass ratios 80−105884
$K\rightarrow\pi e(\mu)\nu$, form factors, SU(3) σ-model one loop calc., chiral symmetry breaking 80−52506
$K\rightarrow\pi e\nu$, radiative correction amplitudes from Ke_4 decay anal. 78−86451
$K\rightarrow\pi l\nu$ strangeness changing suppression factor, $SU(3)_E$-invariant form factor 77−61288
$K\rightarrow\pi\pi e\nu$, Ke_4 decay, radiative correction amplitudes 78−86451
$K^-\rightarrow\pi\mu\nu$, μ polarisation and T-odd correlations, Weinberg model of CP violation *(Russian)* 80−62969
$K^+\rightarrow\pi^0\mu^+\nu$, $K^+_{\mu3}$ decay spectrum and form factors 80−57587
$K^+\rightarrow\pi^+e^+e^-$, decay amplitude using simple model with PCAC 80−9162
$K^+\rightarrow\pi^+e^+e^-$, neutral-current process, strong interaction corrections 80−62968
$K^+\rightarrow\pi^+e^+e^-$, pole contribs., test of theory by comparison with expt. 78−70360
$K^+\rightarrow\pi^+e^+e^-$, quantum chromodynamics *(Russian)* 77−2822
$K^+\rightarrow\pi^+\mu^+\mu^-$, radiative corrections in Weinberg model *(Russian)* 77−38163

semileptonic decays continued
$K^+ \to \pi^+ \nu\bar{\nu}$, calc. of number N_ν neutrino types 79−26321
$K^+ \to \pi^+ \pi^- e^+ \nu$, $\pi\pi$ energy, phase shift difference, hadronic current form factors, scatt. length 77−41840
$K^{\pm} \to \pi^0 l^{\pm}(\bar{\nu}_l)$, decay form factors in relativistic symmetry SO(4,2)⊗SU(3)⊗SU(3) 79−36068
$K_{e3}{}^0$ decays, vector form factor slope parameter *(Russian)* 79−67547
$K_L \to \gamma\nu\bar{\nu}$, calc. of number N_ν neutrino types 79−26321
$K_L{}^0 \to (\pi\mu)\nu$, prod. and detect. calcs. 79−81306
$K_L{}^0 \to \pi^- \mu^+ \nu_\mu$, transverse polarisation of μ, violation of time-reversal invariance 80−68448
$K_L{}^0 \to \pi^{\pm} e^{\mp} \nu$, vector form factor meas. in large H bubble chamber 78−93875
$K_L{}^0 \to \pi^{\pm} \mu^{\mp} \nu$, form factors 4-momentum depend., μe universality *(Russian)* 80−68449
$K_L{}^0 \to \pi e \nu_e$, Dalitz plot anal., form factors 78−37204
$K_L{}^0 \to \pi\mu^- \nu_\mu$, form factor from μ polarisation meas. 77−38161
$K_L \to \pi\mu\nu$, Dalitz plot anal., vector and scalar form factors 79−71744
$K_L{}^0 \to \pi\mu\nu_\mu$, anomalous short-range $\pi\mu$ interaction anal. 78−8660
K_{l3}, struct. constants of mesons in quark diagram model *(Russian)* 79−30717
K_{l3} decay, scalar form factor, quark mass ratio determ. 79−93409
K_{l4} decay in relativistic quark model, axial vector form factors and decay rate 78−66109
K_{l4} decay vector form factor *(Russian)* 80−105900
$\Lambda \to pe^- \bar{\nu}_e$, $|g_A/g_V|$ calc. in quark model, 56-70 octet mixing 79−389
$\Lambda^0 \to pe^- \bar{\nu}$, absolute rate, $\Lambda(\Gamma^0 \to pe^- \bar{\nu})/\Gamma(\Lambda^0 \to p\pi^-)$ precise meas. 80−57593
Λ^+ decay, four body semileptonic decay rates of charmed baryons 78−8665
$\Lambda_c{}^+$ lifetime, semileptonic branching fractions, nonspectator quark interactions 80−37260
$\mu \to e\gamma$, gauge theory with lepton mixing, decay probability, neutrino oscillations 77−49940
μ production by decay of hadronic shower, EM production of trimuons in deep inelastic muon scatt. 80−22619
n, decay, weak interaction meas., coincidence type ion electron converter detector obs. 80−58100
$n \to ep\bar{\nu}$, H atom spectra and metastable state *(Russian)* 80−37262
$n \to H\bar{\nu}$, atomic decay, scalar and tensor interaction effects *(Russian)* 80−68455
$n \to pe^- \bar{\nu}$, neutron lifetime, expt. determ. using storage of decay protons 79−58959
$n \to pe\bar{\nu}$, experimental determination of the neutron lifetime 79−58958
$n \to pe\bar{\nu}$, expt. determ. of correlation coefficients in neutron β-decay 79−58960
$\nu_\mu(\bar{\nu}_\mu)$N, charm meson prod. and decay, lepton inclusive distrib., c-quark fragmentation function *(Russian)* 80−52493
νN, high energy, dilepton events, D meson semileptonic decay 80−42446
$\omega \to \pi^0 \mu^+ \mu^-$, branching ratio determ., dis. in π^-p collisions 79−67556
$\omega \to \pi^0 \mu^+ \mu^-$ decay, mass spectrum and branching ratio *(Russian)* 79−67546
$\Omega^- \to \Theta e(\mu)\bar{\nu}$ or $\Theta^* e(\mu)\bar{\nu}$, branching ratios and lepton energy spectra 80−73701
$\Omega^- \to \Xi^* \pi(\Xi^0 l^- \nu_l)$, nonleptonic hyperon decays, QCD description, PCAC anal. 80−95269
p, baryon number nonconservation, expt. status 80−57594
p, decay, confirmation of unification of forces, book contrib. 80−42383
p, decay, search techniques for lifetimes of order 10^{34} years 80−47287
p decay, flavour gonimetry 80−99100
p decay modes in SU(5) and SO(10) theories 80−13301
$\bar{p} \to e\pi^0$, lifetime meas. using counter technique at ICE 79−93413
$\pi \to e\nu_e\gamma$, isospin-breaking, chiral limit, conserved-vector-current violation, σ model 80−62988
$\pi \to e\nu\gamma$, SU(3)×SU(3) σ-model predictions, comparison with expt. 77−10243
$\pi \to l\nu_e\gamma(l\nu_e l'^+ l'^-)$ in review of weak-EM decays *(Russian)* 77−2818
$\pi \to \nu_\tau \rho\pi$, A_1 resonance, $\rho\pi$ mass distrib. 78−45902
$\pi^- \to \pi^0 e^- \bar{\nu}_e$, σ-model with quarks of π decays 79−22100
$\pi^+ \to e^+ \nu\gamma$ calculation using field-current identity *(Chinese)* 77−34149
$q\bar{q} + l^+ l^-$ + hadrons, probe of OZI suppression 79−17680
$\Sigma^- \to \Lambda e^- \nu$, branching ratio meas., Monte Carlo prediction 78−54631
$\Sigma^- \to \Lambda e^- \nu$, μ 80−42458
$\Sigma^- \to ne^- \bar{\nu}_e$, g_A/g_V ratio 77−26522
$\Sigma^- \to ne^- \bar{\nu}_e$ $|g_A/g_V|$ calc. in quark model, 56-70 octet mixing 79−389
$\Sigma^0 \to \Lambda e^+ e^-$, parity violating effects, standard and pure vector Weinberg Salam model 79−36075
$\Sigma^+ \to p\mu e$, flavour changing neutral current search 80−105836
t-quark, obs. in $\nu N \to \mu^- \bar{t} X$ 80−13297
τ, decay modes, masses, spin, lifetimes and τ-ν_τ coupling 79−85348
τ, semileptonic decay, polarisation near Z^0 pole 79−97644
$\tau \to A_2 \nu_\tau$, branching ratio calc. for possible A_2 decay mode of a spin 3/2 heavy lepton 79−6357
τ decay, $\nu_\tau(\bar{\nu}_\tau)N \to \tau^{\pm} X$, beam-dump experiment, observation of ν_τ interactions 80−22601
$\tau \to \nu_\tau$+hadron(s), decay modes and ν_τ-mass 80−63057
$\tau \to \nu_\tau n\pi$, T-violation effects, neutrino mass *(Russian)* 80−95294
$\tau \to \nu_\tau \rho\pi$, ang. correlations in τ decay 79−63567
$\tau \to \nu\pi\omega$, decay width and form factor calc. using vector dominance hypothesis *(Russian)* 80−47271
$\tau \to \nu\rho^0\pi$, spin parity anal. 80−105941
$\tau \to \nu\rho\pi$ decay parameters from PCAC and current algebra, A_1 characts. 80−37314
$\tau \to \pi K\nu$, energy and angular correl. meas. 79−89214
$\tau \to \pi\nu_\tau$, branching ratios 79−17703
$\tau \to \pi\nu_\tau$, spin 3/2 heavy leptons, decay suppression, weak current *(Chinese)* 78−82192
$\tau \to \rho\nu\pi$, halflife and mass determination from e^+e^- interactions 78−89765
$\tau \to \rho\pi\nu_\tau$, quark model, current algebra model, divergence of axial vector current 80−57655
τ three particle semileptonic decays, leptonic weak current *(Russian)* 79−97643
$\tau^- \to \nu_\tau \pi^- \gamma$, π form factors, axial-vector and structure dependent, vector meson dominance model 80−62989
$\tau^- \to \rho^- \nu$, branching fraction meas. 80−13296
$\tau^{\pm} \to \nu_\tau A_1{}^{\pm}(\to \rho^0 \pi^{\pm})$, inclusive distribs. of ρ^0 mesons from cascade decays of τ heavy leptons *(Russian)* 79−9390
$\tau^{\pm} \to \nu_\tau \rho^0 \pi^{\pm}$, possibility of observing A_1 meson current algebra anal. 79−13176

semileptonic decays continued
$V \to p\mu^+ \mu^-$, vector meson decay EM form factors in bag model *(Russian)* 80−62982
W-signal in p$\bar{p}$ collisions, t- and b-quark decays 79−13012
$\Xi^- \to \Lambda e^- \nu$, μ 80−42458
$\Xi^- \to \Lambda e^- \nu$ branching ratio meas., Monte Carlo prediction 78−54631
$D \to K\pi l\nu$, hadronic current form factors, ($\bar{c}$,s) weak current and symmetry props. 79−67545
$\eta \to \pi^0 e^+ e^-$, presence of second class neutral currents 79−26284
$K \to \pi e^+ e^-$, six-quark model, CP violation 80−78055
pN, 350 GeV in Ne, $D^{\pm}$ prod. cross section and lifetime 80−68494

semimetallic thin films
1/f fluctuations *(Japanese)* 78−43448
condensed, on supercond. film, effect on T_c and residual resist. 78−47900
Coulomb interaction depend. on film thickness, exciton binding energies *(Russian)* 79−78027
dislocation superstructures and conduction electron kinetics *(Russian)* 79−19678
film photopot detector characteristics for adaptive optical systems 79−59741
multilayer thin film struct. thermoelec. props. 80−92964
pressure induced transition to state with strongly anisotropic electron-hole pairing 77−47735
quantised, in high mag. field, thermodynamics of electrons *(Russian)* 79−56341
size-quantised thermomagnetic coeffs. *(Russian)* 78−56249
surface resistivity calc. 78−91751
Wigner crystal in high magnetic field 79−73456
As, bulk and sputter-deposited amorphous, vibr. props., Raman spectra meas. 77−63411
As, condensed layers, low temp. allotropic phase transition *(Russian)* 80−54553
As, sputtered film, density of valence states by XPS and UPS 77−24926
Bi, amorphous film, temp. dependence of SAW attenuation 80−75679
Bi, amorphous metal films, crystallisation with and without mag. field 80−70570
Bi, carrier conc. and mobility, resist., galvanomag. and thermoelec. meas. 78−52111
Bi, cryst., orientation dependence on substrate struct. 77−1335
Bi, deposition props. on specially prepared substrate, desorption energy and surface diffusion 79−90917
Bi, disordered and amorphous, quench-condensed, optical cond. and band struct. 77−1746
Bi, EM wave excitation *(Russian)* 77−32093
Bi, elec. cond., obs. of epitaxial growth mechanism *(French)* 78−84329
Bi, ellipsoidal model of textured specimens with uniaxial symm. *(Russian)* 80−80100
Bi, ellipsometric obs. of optical props. 79−78776
Bi, epitaxial, magnetoresist., EM meas. in mag. fields up to 85 kG 77−32095
Bi epitaxial film, twinning, electron diffr. 77−35838
Bi, epitaxial films, grain boundary struct., electron microscopy obs. *(Russian)* 79−46671
Bi epitaxial films, size effect in elec. props. 80−54813
Bi, evaporated film, nuclei size distrib. 77−11802
Bi film, adatom surface diffusion at low temps., elec. resist. study *(French)* 80−65376
Bi film, carrier conc., mobility and 1/f noise 80−44748
Bi, film, evaporated, elect. and elastoresistance props. 79−33367
Bi film, evaporated, lattice distortion spectrum, elec. resistance temp. variation 80−54806
Bi film, initial stages of growth and orienation, TEM study 79−28237
Bi film, optical props., inverse problem of phenomenological theory 79−43053
Bi film, oxidation kinetics and interfacial bonding using final states 77−56127
Bi, film, quantum size effect, electric field effect, Thomas-Fermi approx. energy surfaces, cond. 78−47890
Bi film, quantum size effect and band struct. Bi-dielec.-metal system obs. 80−54811.
Bi film, size effect on electrical cond. 78−84331
Bi film, transparency meas. in mag. field, electronic isoenergetic surface cross section *(Russian)* 79−47532
Bi film, vap. deposited, effect on deposition parameters and substrate condition on crystallinity 78−10290
Bi film, X-ray diffr. anal., {001} textured growth 78−72016
Bi film deposition by vacuum evaporation on $NaNO_3$ single cryst. cleavage 80−35091
Bi film fast-response photodetector, employing charge carrier photon entrainment 80−73462
Bi films, texture rel. to deposition conditions 79−60660
Bi, Hall effect, magnetoresist., resist. and TCR 78−2589
Bi, high-mobility, quantum size effects, struct. and kinetic characts. improvement 79−91174
Bi, in mag. field up to 40 kOe, microwave skin effect 77−12032
Bi island films, effect of surface press. on lattice spacings 79−11045
Bi, kinetic props. of electrons, resist., cond., magnetoresist., Hall effect 77−63011
Bi, non-extremal cross sections of isoenergy surfaces, tunnel spectroscopy determ. *(Russian)* 77−8011
Bi, on Sb_2Te_3, mean scatt. length of low energy electrons meas. 77−36370
Bi, on Si(111) substrate, MBE deposition kinetics 80−10817
Bi, optical, magneto-optical and struct. props. 77−1664
Bi, optical props. as function of wavelength *(Russian)* 78−52591
Bi, orientation on mica, effect of deposition parameters 77−28085
Bi, oxidation, UPS, valence band, cond. band and 5d core states 77−20995
Bi, oxidation process rel. to X-ray diffraction *(Japanese)* 79−29273
Bi, polycrystalline film, elec. resistivity, thickness depend., temp. coeff. 78−14839
Bi, spheres, mean inner pot., elec. biprism and interf. electron microscopy 80−49063
Bi, structure and elec. props. 77−1339
Bi, surface defects and struct., electron microscopy and elec. props. *(French)* 80−15415
Bi, thermoelec. power in transverse mag. field *(French)* 78−23183
Bi, thin film, 1/f noise, boundary scatt. effect 80−49836

semimetallic thin films continued
Bi thin film, structural evolution 8 to 573K, supercooling effects *(French)* 79−90921
Bi thin film, structure and electronic props. 80−70562
Bi thin wire, resist. anomaly, possibility of one-dimensional quantum size effect 80−54809
Bi, transverse mag. field depend. of thermoelec. power *(French)* 78−2587
Bi, vapour deposited on NaCl cleavages, crystallinity depend. on deposition parameters 78−63955
Bi:N, ion-implanted, struct. X-ray obs. 77−76692
Bi-Sb alloy, amorphous nature, AC and DC cond. and Hall coeff. obs. 80−11114
Bi-Sb alloy film, elec. props. *(Russian)* 79−11245
Bi-Sb alloy films, quantum size effect *(Russian)* 77−85351
Bi-Sb film thermopiles for radiation pyrometry 78−214
Bi-Sb interface, film, thermoelectricity, ageing differential efficiency *(German)* 78−60146
Bi-Te, thin film system, stress-relief appearance conditions 80−65416
$Bi_{0.9}Sb_{0.1}$, epitaxial film, defect struct. and galvanomagnetic props. 77−89889
$Bi_{1-x}Sb_x$ alloy films, quantum resistance oscills. at low temps., surface band distortion *(Russian)* 80−11110
$Bi_{1-x}Sb_x$ epitaxial layers, effect of film thickness on elec. props. *(Russian)* 79−11244
$Bi_{1-x}Sb_x$ epitaxial thin films, galvanomag. props. in semimetal and semicond. regions 79−11254
$Bi_{1-x}Sb_x$ thin film, elec. props., composition variations *(Russian)* 79−7841
$Bi_2(Te_{1-x}S_x)_3$, quasi 2-D cryst., I-V and magnetocond. meas. 77−85360
Sb, amorphous film on glass substrate, effect of substrate temp. on crystallisation 80−39468
Sb, amorphous sputter-deposited film, vibr. props., Raman spectra meas. 77−63411
Sb, amorphous to crystalline phase transition *(German)* 77−69196
Sb, critical thickness observations for crystallisation in amorphous thin films 79−69379
Sb, elec. cond., grain boundary scatt. effects 80−103766
Sb electrode, pH sensitivity and electrode potential *(Japanese)* 79−39159
Sb electrodeposit, amorphous, explosive crystn., semicond-semimetal transition and IR absorpt. 78−51849
Sb, electron microcopy, identification criteria of dislocations *(French)* 77−76411
Sb, epitaxial growth of electrodeposits on oriented single crystal Au and Ag 78−43267
Sb, epitaxial growth on Bi substrate 78−95246
Sb, evaporated, crystallite struct., texturisation 77−7991
Sb evaporated film crystallisation rel. to substrate temp., −50° to 170°C 78−47680
Sb film, elec. cond., and struct., thickness depend. 78−26974
Sb film, electroreflectance effects 79−43055
Sb film, initial stages of growth and orienation, TEM study 79−28237
Sb, film, microrelief, electron microscope obs., grain size and condensation rate 77−55469
Sb film, X-ray diffr. anal., {001} textured growth 78−72016
Sb, film growth mechanism, action of residual gases rel. to deposition conditions 79−23850
Sb, on NaCl, effect of ion irradiation on form., struct. and props. 77−36408
Sb, splat-cooled and vapour-deposited, metastable structs. 79−87018
Sb, thermoelec. power, thickness depend. 77−1501
Sb, thin films, IR absorpt. and intraband transitions 80−16114
Sb, thin plates, electron conduction, 4-293K, surface reflection ang. depend. *(Russian)* 78−19170

semimetals
see also antimony; arsenic; bismuth; semimetallic thin films
acoustic cyclotron reson., sound interaction with cyclotron waves *(Russian)* 77−35959
acoustic plasma wave excitation 78−10520
Alfven wave of finite amplitude, modulational instability 79−47118
anisotropic, electron-hole fluid energy calc. *(Russian)* 77−1379
anisotropic size effects, review 77−32032
beat effect of sp. ht. due to impurities, in external mag. field 78−10401
compensated, hydrodynamic cond., surface scatt. and phonon drag *(Russian)* 77−8088
degenerate, anisotropic scattering at low temp. *(Russian)* 78−95298
degenerate, conduction electron acoustic spin resonance, oscillations of absorbed power 80−108075
degenerate, heat conduction, thermal EMF, Lorenz number anisotropy at low temp. 80−75549
degenerate, quantum theory of transverse galvanomag. phenomena, model of two standard bands *(Russian)* 77−62945
doped, interband transition, effect on Curie temp. of ferromagnetic phase transition 79−7994
electric current distribution, by diffusion size effect 79−23987
electron drag by phonons, two-stage, in semimetals with equal electron and hole densities 77−15843
electron heating by phonons, acoustic absorpt. and acoustoelectric current quantum oscills. *(Russian)* 79−19639
electron heating due to acoustic phonon scatt. in Bi type semimetals *(Russian)* 80−10991
electron-hole pair condensation and liquefaction in strong mag. field, RPA and variational calcs. 78−63984
electronic phase transitions in strong magnetic field 79−60718
EM excitations in strong mag. fields, review 77−8130
EPR line shape, magnetoresist. effect 80−84638
exciton phase, transport effect in strong mag. fields 78−87977
excitonic phase and gas-liquid transition in strong mag. field 79−4514
giant quantum attenuation of sound, fluctuation effect of gas-liq. type transition 78−39168
Hall coefficient and magnetoresist. of interacting two carrier system 79−69530
higher sound harmonic generation in momentum nonlinearity regime *(Russian)* 78−38783
interband light scattering in semimetals and semiconductors *(Russian)* 78−60485
interband resonant spectroscopy, review 79−61224
intrinsic, dielec. and supercond. phase transitions 77−66111

semimetals continued
laminar, superconducting props., Coulomb electron interaction considerations 79−87185
layered, nonlinear screening 79−60746
longitudinal conductivity in extremely strong mag. field 77−89779
magnetic freeze out of extrinsic carriers 77−59268
magneto-quantum oscillations obs., new method 77−62946
many-valley degenerate semiconds., supercond. transition temp. *(Russian)* 78−56254
metal-semimetal system, local and total density of states determ. *(Russian)* 80−54586
mixed superconducting-excitonic insulator phase, diamagnetism, virtual intraband transitions 80−2520
phase transitions in strong mag. field, HF approx. 78−23028
phonon drag, role of surface in thermo EMF *(Russian)* 78−47819
phonon spectrum, influence of mag. field induced quasi-local levels 78−18946
photo-magneto-electric effect 79−56260
powdered, EPR, effect of mag. field depend. of elec. parameters 79−99749
pressure induced transition to state with strongly anisotropic electron-hole pairing 77−47735
proximity effects in transitions to exciton phases 79−28296
Raman scattering of sound in quantising mag. field 78−60171
simultaneous Cooper and insulating pairing, physical states 80−93036
spin-phonon interaction, dynamic screening by carriers, effect on paramag. relax. times 77−16150
superconductivity and dielectrisation in semimetallic systems *(Russian)* 79−65578
superradiant phase transition 77−44047
thermal diffusivity by laser flash technique 78−6189
thermoelectromagnetic waves in conductors in a mag. field *(Russian)* 80−49695
transition into excitonic phase, boundary effects 78−76003
two-dimensional, electron-hole rearrangements in high mag. fields 79−87028
two-phonon sound absorption in quantising mag. field 79−28382
US attenuation in strong mag. field, theory 77−11844
US propagation, nonlinear effects 77−59305
XPS, core electron line shapes 78−11082
As_xSb_{1-x}, thermopower, thermomagnetic power, 4.5 to 77K 80−107825
Bi whiskers, thermopower, temp. depend., 77 to 300K phonon drag effect 79−82615
Bi:Te(Sn) , elec. resist., 1.8 to 77K, electron-phonon scatt. mechanism 79−15144
Bi-Sb, magnetic susceptibility, 4.2 to 270K, field and band parameter depend. 77−36051
Bi-Sb, magnetoplasma effects at 300 GHz in Voigt configuration 80−39619
Bi-Sn(Pb), electrical cond. and thermal EMF at press. up to 12 kbar 77−47806
BiSb (>20 wt.%), electronic band struct. 80−107698
p-$Bi_{0.9}Sb_{0.1}$, Fermi surface anisotropy var. on press. induced transition to gapless state *(Russian)* 77−43483
$Bi_{1-x}Sb_x$, elec. resist., 1.8 to 77K, electron-phonon scatt. mechanism 79−15144
$Bi_{1-x}Sb_x$, Shubnikov-de Haas effect, Abrikosov-Falkovskii treatment of Fermi surface anisotropy *(Russian)* 78−43285
EuB_6, mag., transport and thermal props. 79−73738
$Hg_{1-x}Cd_xSe$, zinc blende structure, optical and electronic properties 80−6723
$Hg_{1-x}Cd_xTe$, Hall coeff., anomalous temp. depend., 4.2 to 70K 80−65604
$Hg_{1-x}Cd_xTe$, optical absorpt., quasilocal acceptor level effects, theory 80−92853
$Hg_{1-x}Cd_xTe$, quasi-local acceptor levels and electron mobility 78−67974
$Hg_{1-x}Cd_xTe$, semimetallic state, magneto-optical investig. of Landau levels and band parameters 77−63410
$Hg_{1-x}Cd_xTe$, zero-gap semicond. with nonparabolic band struct., hot electron mobility and conc. 78−76080
$Hg_{1-x}Cd_xTe$-type semimetals, kinetic props., local acceptor level effects 80−65557
$Hg_{a-x}Cd_xTe$, (x<0.16), semimetallic phase, acceptor states and galvanomagnetic effects 80−6882
$Hg_{a-x}Cd_xTe$, single-LO-phonon and -plasmon recombination channels narrow-bandgaps 78−91728
$Hg_{1-x}Mn_xTe$, semimetallic, giant spin splitting induced by exchange interactions 77−28150
LiAl, anomalous elec. resistivity near critical composition 80−103673
$NbSe_3$, chemical bonding and dimensionality 78−75992
PbPo, electronic struct., relativistic band struct. calc. 79−4510
PbS-Ni, phase diag., cpd. formation and electrophys. props. 77−85997
$Pb_{1-x}Sn_xTe$, Mossbauer investig. of phonon softening at semicond.-semimetal transition 77−43908
$TiSe_2$ (1T), electronic and vibronic struct. 80−44500
$TiSe_2$, band struct., angle-resolved photoemission studies 80−70610
$TiSe_2$ impurity effects on elec. props. 80−80263
$TiSe_2$, optical refl. spectra obs., suppression of antiferroelectricity by excess carriers 77−59536
$TiSe_2$, semimetal, electronic props., superlattice form. 77−15532
$TiSe_2$, semimetal, IR props. 79−24318
$TiSe_2$ Young's modulus and internal friction obs., 1.3 to 300K 79−46750
$TiSe_2$:Ta(V), transport props. and phase transition 78−72149
$Ti_{1+x}Se_2$, superlattice form. and phase transition, IR reflectivity meas. 79−24322
$(Ti_{1-x}V_x)_2O_3$, semicond. to semimetal electrical transition, lattice parameter changes 79−60714
UAsS(Se)(Te), positron annihilation ang. distrib., valence electrons and Fermi surface 77−28093
$UP_2(Sb_2)(As_2)$, positron annihilation ang. distrib., valence electrons and Fermi surface 77−28093
$Zn_xHg_{1-x}Se$ semimetal-semicond. transition, thermo-EMF in mag. field and Hall expts. *(Russian)* 77−15881

Senftleben-Beenakker effect
atom-diatom kinetic cross section, ES, CS and IOS approx. with translational-internal coupling, viscomag. effect 80−63764
o- and n-D_2, viscomag. effect, temp. depend. 78−9745
p- and n-H_2, viscomag. effect, temp. depend. 78−9745

Senftleben-Beenakker effect continued
linear mol. gas thermal cond. Senftleben-Beenakker effect, effective collision cross section 80−24117
methyl cyanide, anomalous Senftleben effect *(Russian)* 78−71415
methyl cyanide-Ar mixture, thermal cond. in mag. field 80−100058
polyatomic gas-inert gas mixture, viscomag. diffusion flux 78−47087
polyatomic gases, Senftleben-Beenakker effects, inverse operator calcs. 77−15152
polyatomic Knudsen gas, kinetic thermomag. phenomena 78−75246
shear viscosity SBE collision integrals, linear mol. gas, Liouville algebra 80−10353
shear viscosity Senftleben-Beenakker effect, in atom-diatom system, theory 79−86556
symmetric top molecules, thermal cond., Senftleben-Beenakker effect 80−100049
thermal conductivity of gases, ang. momentum polarisation contrib. 79−37435
thermal conductivity of gases meas. apparatus 78−81989
Ar-acetonitrile mixture, anomalous thermal cond. in const. elec. field 77−7505
Ar-O_2, diffusion, search for Senftleben-Beenakker effect 77−15155
CO_2+O_2(NO), Senftleben-Beenakker effect, saturation field, Kohler-Raum theory and obs. 80−28596
HD+He, relax. and kinetic cross-sections, DWBA calcs. 79−41782
He-O_2, diffusion, search for Senftleben-Beenakker effect 77−15155
NF_3, thermal cond. in parallel const. and alternating elec., mag. fields, parametric reson. 78−83515
NH_3-Ar mixture, thermal cond., viscosity, Senftleben-Beenakker effect 80−100054
NH_3-He mixture, viscosity, Senftleben-Beenakker effect 80−100054
NO, thermal cond. Senftleben effect meas. 79−18985
NO-Ar(He), thermal cond. Senftleben effect meas. 79−18985
NO-$N_2(H_2)$ mixtures, thermal cond., mag. field effect 79−94764
NO_2, thermal cond. in parallel const. and alternating elec., mag. fields, parametric reson. 78−83515
O single layer on Au, thermomag. effect, thermomag. props. *(Russian)* 78−64256
O_2, gas, thermal cond., mag. field effects 78−34255
O_2 interacting with Au or Pt surface, thermomag. effect *(Russian)* 77−11302
O_2 on Pt surface, thermomag. effect, temp. depend. *(Russian)* 78−60034
O_2-Ar, gas, thermal cond., mag. field effects 78−34255
O_2-He, thermal cond. Senftleben effect meas. 79−18985
O_2-$N_2(H_2)$, gas mixture, mag. field effect on thermal conductivity 78−59533

sensing devices *see detectors*

sensing devices, electric *see electric sensing devices*

sensing devices, nonelectric *see nonelectric sensing devices*

sensitivity
140 keV γ position-sensitive multiwire proportional chamber characteristics 79−54749
absolute radiometer instrumental correction theory improvement 77−82585
acoustic emission detection system sensitivity, direct comparison method 78−56848
acoustic emission transducer construction principles evaluated 78−59239
acousto-optic parallel channel wideband receiver 80−48447
aerial reconnaissance film interrogation by optical matched filtering 77−78484
airborne particulate detection by metal-coated Nuclepore filters 77−37463
annular photoelectric goniometer sensitivity calc. 78−41327
Apollo-Soyuz Test Project EUV telescope, 584 Å sensitivity rel. to local interstellar He density 79−92834
avalanche photodiode receiver sensitivity, specification and testing *(German)* 78−38015
biodynamic subminiature piezoresistive accelerometer performance evaluation 78−20340
brain impedance scanner principles and exptl. results 79−57804
bridge ccts. for differential resist. meas., resist. thermometry appl. 77−79126
cancer X-ray sensitivity increased by 434 MHz EM irradiation 78−24180
Cherenkov counter photomultiplier, sensitivity to gamma quanta 78−9032
chromatographic compound column, sensitivity regulation method 78−35752
current-to-frequency transducer systematic error and sensitivity threshold 77−79117
diagnostic radiology, detector sensitivity and image conversion improvement 77−25546
dichromated PVA specific wavelength sensitisation for laser beam recording 78−5531
differential absorption lidar system sensitivity with heterodyne reception 79−27310
digital weighing systems, error estimation *(German)* 77−74365
eddy current pressure transducer elastic elements characts. optimisation *(Russian)* 78−77890
electrocutaneous stimulation, energy threshold meas. and channel capacity estimation *(Japanese)* 78−53573
electron-sensitive materials, apparatus for measuring sensitivity and data-density 79−35893
EM distance measurement (EDM), single-wavelength, data ratios rel. to line length changes resolution 80−4143
environmental effects on microphones and Type II sound level meters 77−62127
EPR cavity sensitivity improvement 78−54419
ESR/ENDOR spectrometer sensitivity enhancement by microwave preamplifier 78−82014
ether wind first-order expt. with stabilised lasers 77−5665
Explorer 35 spacecraft magnetometers sensitivity rel. to lunar mag. permeability study 77−56846
fault detection by scanning acoustic microscopy 77−80040
fibre-optic system repeater error rate calc. approaches compared 77−54672
fluid anemometric microthermistor sensor sensitivity curves *(Russian)* 78−34219
fluorometric techniques and instrumentation 80−45845
focal plane IR detector arrays for planetary missions 80−85862

sensitivity continued
galactic plane survey at 5 GHz, point sources detect. limit 78−81686
gamma-ray detector, nonhydrogenous organic liquid scintillator sensitivity function calc. 78−78572
gamma-ray dosimeters with Si detectors, energy dependence of spectral sensitivity 79−68146
gas chromatograph-microwave plasma detector for alkyl Pb and Se compounds, detect. limits 78−68975
geomagnetic field local changes determ., narrow line ^{87}Rb, magnetometers accuracy and noise reduction 80−26636
gravimeter, HF, calibration and sensitivity 78−7812
gravimeters, sensitivity determ. rel. to gravity tidal changes at Poltava *(Russian)* 78−88782
gravitational radiation detectors, implications of extension to noise theory for RF SQUIDs 77−87685
gravitational wave astronomy, detectors' sensitivity 77−67368
gravitational-wave antenna, small, cryogenic, meas. and sensitivity at 1.5K 79−21646
gravitational-wave resonant antennas, optimum filtering and sensitivity 80−8545
gravity antenna small perturbation meas., optimum strategy 77−82438
Hall effect transducer, for weak magnetic field meas., features 77−57370
high-current photomultiplier with disc electrode leads 78−58032
high-sensitivity multipurpose remote sensor 78−40684
high-speed dual-lag photon-correlation signal processor development 77−18095
holographic laser beam deflector performance characteristics 77−19287
hot-film shear probes, position sensitivity 80−101286
hot-wire anemometer, sensitivity to stream temp. fluctuations, end cond. effects 78−34215
human visual system spatial sinewave/squarewave grating contrast threshold difference 79−57662
hydrophone, interferometric fibre optic, static press. sensitivity amplification 80−38094
hydrophone, multimode fibre optic, frustrated total internal reflection, testing 80−38096
image isocon, threshold and contrast sensitivities rel. to appl. in astrophysical obs. *(Russian)* 80−12671
image sensors for spaceborne astronomy 77−87268
induction inspection unit with spaced windings, increasing sensitivity over magnetising and measuring length 78−56864
inductive-capacitive transducers, information conversion sensitivity study 79−6113
integrated focal plane arrays for thermal imaging 77−19448
intensified CCD photon counting array photometer 77−37964
interferometers, Michelson-type, for anomalous dispersion meas. *(Russian)* 79−93211
ion chromatography for sulphate and nitrate assay in aerosols, sensitivity 78−68974
ion cyclotron resonance spectroscopy, sensitivity calibration of marginal oscillators 78−21177
ion microprobe analysis, calibration using matrix ion species ratios, appls. 78−61070
IR detector system limitations 78−77988
Josephson contact microwave detector sensitivity and cutoff frequency rel. to capacitance 78−49902
Lampard-type electrostatic system, appl. of sensitivity criterion in capacitance meas. 80−98942
laser cavity interferometer, for phase changes $<10^{-5}$Å 77−18087
laser-Raman spectrometer for ambient sulphate aerosols monitoring, sensitivity 78−69532
lateral motion analyser sensitivity stabilisation along ranging line 79−72694
LF spectral analyser with HF SQUID, threshold sensitivity 78−41328
LMFBR boiling acoustic detection sensitivity, PFR commissioning expts. 79−13452
low-level microwave power detector 79−54189
magnetic field measurement, max. sensitivity 79−17455
magnetic sensor, high permeability metal core solenoid absolute sensitivity calibration 80−31133
magnetic susceptometer, high sensitivity, based on SQUID magnetometer 78−49872
magnetoencephalography, sensitivity distrib. 80−101246
mammographic X-ray screen sensitivity and resolution 78−7449
manometers, liq., sensitivity, wetting hysteresis effect 80−98926
measuring instruments, gyroscopic and electrical, compound suspensions for improving sensitivity 79−35707
metallurgical analysis by atomic absorption spectrophotometry *(French)* 79−5241
microinterferometer limiting sensitivity and accuracy characteristics 77−79142
microphones, electret, ceramic and condenser types, environmental effects 77−39180
miniature pressure-frequency convertor with pulse output 78−57926
Moire projection topography accuracy and sensitivity 78−45677
mouse sensitivity to curariform drug. 2.45 GHz irradiation effect *(French)* 80−3717
multihole SQUID, miniature, with preset point contact, sensitivity 77−37952
multiple-beam array antenna for supernova radio pulse searches, sensitivity 78−40975
NMR, metal single crystal meas. 78−43659
NMR imaging of biological objects, sensitivity, performance time 79−96718
NMR spectrometers, SQUID-based sensitivity limit 80−98961
NMR wideband detectors, R-LC and autodyne types, performance comparison 77−74473
nuclear NDT methods, sensitivities and detection limits 77−32756
nucleonic dual charge sensitive preamplifier 78−55110
ocean acoustic model inputs/sensitivity 79−5492
ophthalmological diagnosis, US contact stabilisation method 77−25523
optoelectronic system, symmetrical input, direction-finding sensitivity control 79−50401
optoelectronic system threshold sensitivity calc., background spatial charact. determ. errors 79−26134
phase meter sensitivity improvement by use of pulse spectra 77−71344
photocells, temp. coeff. of sensitivity 78−82033
photoconductor slab space-time light modulator sensitivity enhancement *(Russian)* 77−58427

sensitivity continued
photodetector nonlinearity determ. by relative differential sensitivity meas. 79−71530
photoelectric colorimeter reconditioning methods 79−39618
photographic exposure prediction techniques, still, motion-picture photography appl. 80−66817
photometric analysis, reproducibility and lower detection limit 79−87899
photomultiplier absolute spectral sensitivity in photon-counting mode 79−67383
photomultiplier tube, RCA 4522, spectral sensitivity meas. 78−21818
photoreceiver sensitivity nonlinearity determ. by high-speed raster device 77−79150
photoreceiver system, photodiode-FET, achievable threshold limit calc. 79−49292
piezoelectric receivers, amplitude-freq. response determ. for acoustic emission 80−87699
piezoelectric sound receivers, impedance method appl. 77−11104
piezoelectric sound receivers, sensitivity determ. by impedance method 77−11104
piezoelectric transducers, long, experimental investigation of field 78−49822
point contact microwave detector/receiver 77−79153
point-contact diode, submillimetre wave detection, sensitivity detn. 77−37984
pressure transducer, miniature implantable, biomedical appl. IC fabrication techniques 80−76849
pulse counter, high-speed DC coupled, sensitivity and performance 79−89524
pulse counting measurement systems, optimum parameters determ. 79−89523
PVF_2 film pyroelectric radiation detector sensitivity *(Japanese)* 79−93222
PWR movable in-core neutron detectors *(Japanese)* 79−26722
quadrupole mass filter specification and calibration *(Japanese)* 78−12784
quantitative IR spectral analysis, background and overlapping of absorpt. bands influence on accuracy 80−55748
radiation monitor, thermoluminescent TDP-2 instrument, improved sensitivity 79−89504
λ 8-cm radioheliograph at Toyokawa, sensitivity and phase stability improvement project 79−101066
radiometer, sensitivity normalisation 78−86335
radiometer, wide-band, for short millimetre range wavelengths, limiting sensitivity 79−62750
Raman scattering spectrometer, sensitivity improvement via multiple transmission attachment 77−38036
rare earth phosphor intensifying screen speed gain 78−7447
retinal photoreceptor and horizontal cell synaptic connections 77−90787
RF and photodetection techniques at 10 μm, comparison 78−89539
SAW transmitting hydrophone development and performance 79−53586
scintillation counters for gamma-ray burst astronomy, critical comparison of sensitivities 77−64648
SEASAT radar altimeter, resolution capability preliminary estimates 80−72645
second-generation ion microanalyser description and performance *(French)* 80−101055
semiautomated thin-layer chromatography with scanning flame ionisation detector 79−74466
SIMS detector sensitivity improvement 79−26172
smoke density meter maximum sensitivity determination, flue gas optical density spectral analysis appl. 78−69500
sound detector using fibre optics 78−13871
sound level meter meas. accuracy 78−59211
space applications of LF supercond. sensors inc. SQUID devices 80−56691
Space Telescope spectrograph Digicons 80−85858
spark source and sputter-ion mass spectrometric analyses *(Japanese)* 77−86413
spark source mass spectrography, geochemical appl., element sensitivity, precision and accuracy 78−20544
spark-source mass spectrometry of metals, relative sensitivity coeff. 79−92045
spark-source mass spectroscopic anal. of Al, Al alloys, sensitivity calibration 78−68962
spatial light modulator with CCD address 80−48445
spectropyrometers, threshold sensitivity 80−8990
spectroscopic cooled and intensified array detectors 78−65983
square-wave modulation radiometer limiting sensitivity formula correction *(Russian)* 78−58030
submillimetric heterodyne receiver with laser local oscillator 77−38042
superconducting chopper amplifier, improved sensitivity 77−26306
superconducting film, illuminated, heating model and spectral characts. of phonon emission 79−28442
superconducting susceptometer, automatic, sensitivity calibration, biological appl. 78−57154
thermochemical analyser, continuous flow, high sensitivity 79−92022
tilt meter at Berezovaya Rudka station, obs. and sensitivity vars. *(Russian)* 78−88783
transducer, force measuring, EM, design and appl. *(Russian)* 78−16784
triaxicardiometric system polarcoordinate sensitivity 79−39587
tube flaw detection by annular US transducers 78−60971
underwater sound transducers, parabolic reflector as nearfield calibration device 80−48528
US bulk wave electromagnetoacoustic excitation 79−57195
US flaw detect., tolerance on operating freq., sensitivity standardisation 78−53089
US transducer design rel. to vibration geometrical effects 79−83871
vacuum emission detector sensitivity to γ-rays 77−54462
vacuum gauge, vibr. vane, sensitivity 78−49793
vectorcardiogram parameter sensitivity to digital filtering 79−39576
VHF resonator radiant energy meas. *(Russian)* 78−77944
vidicon contrast sensitivity reduction for short pulse exposures 78−86254
voltammetric analysis, micromolar, ring electrode shielding at rot. ring-disc electrode 79−92018
volume compression sensors, sensitivity under cyclic load 79−29315
Wheatstone bridge, optimisation 77−26330
zeugmatography, rotating frame 79−93186
$CaWO_4$ and rare-earth X-ray intensifying screen sensitivity to scattered radiation 78−7450
$Cd_xHg_{1-x}Te$ thin film Hall probes for high mag. fields 79−30452
Gd neutron radiographic amplifying screen sensitivity 78−7448
sensitivity continued
Ge spectrometers, for X-ray and gamma-ray astronomy, energy resolutions and sensitivities 77−5438
Ge(Li) detectors, precise environmental gamma-ray meas. 77−38568
InSb charge injection device IR imaging arrays 77−79962
KCl:OH mag. field-independent capacitance thermometers, sensitivity 78−4623
NaF:OH mag. field-independent capacitance thermometers, sensitivity 78−4623
Pd+Cr+Ru/Au+Fe thermocouple for 2-200K range, sensitivity 77−26293
Si accelerometer, batch fabricated 80−73328
Si intensifier target camera, expt. *(Japanese)* 78−89085
Zn-In-S ultraviolet detector *(Russian)* 80−18014
sensitivity analysis
see also control system analysis; dynamic response; frequency response; transient response
aquifer characteristics, sensitivity anal. rel. to linear programming management model 78−11936
BWR, fuel cycle cost sensitivity anal. 79−31104
BWR power plant, direct cycle, low sensitivity optimal controller study 78−8947
Calvin photosynthesis cycle parameter identification 79−92186
catchment model parameters anal. 78−77288
dielectric constant meter, Tangens-2M, static characts. 78−45651
dosimeter neutron/gamma sensitivity determ., comparison of spectral difference and Pb filtration methods 77−90915
dynamic system, two representations of sensitivity and error analysis 77−60900
elastic mechanical systems, design sensitivity analysis, adjoint variable methods 78−90706
elliptic problems, representations of first variations, appl. to optimisation and sensitivity anal. 78−77674
EM water current nonlinearity and sensitivity 77−5383
environmental assessment for air pollution abatement, diffusion model evaluation 79−57547
fast reactor fuel cycle cost 79−26501
FBR thermal hydraulics, sensitivity theory for general systems of nonlinear equations 80−86954
FFTF dynamic modelling and sensitivity analysis 79−605
fission reactor thermal hydraulics analysis, differential sensitivity theory for nonlinear equations with nonlinear responses 80−47551
fission reactor transient analysis, appl. of statistical methods to sensitivity anal. of Problem 2 79−31058
gapped pot core and Permalloy foil pressure transducer 79−75520
gravitational antenna sensitivity, quantum mech. anal. *(Russian)* 79−75436
HF hygrometry, modulated and unmodulated, comparative anal. *(Russian)* 77−67444
hydrophone quartz transducer stability analysis 77−11102
inertial seismographs, sensitivity and dynamic range 79−39910
interferometer, double-beam, computer analysis program 79−71520
laser rangefinder radiometric efficiency, optomechanical tolerance analysis 79−21705
measurement data processing system error analysis 78−41288
minicomputerized automatic radiocardiogram analysis *(Japanese)* 79−29614
myocardial fibre shortening velocity dependence on inotropic and haemodynamic conditions 78−31833
nonlinear, of multiparameter model systems 78−28931
nonlinear algebraic eqns. with constraints 78−21086
nuclear fuel component, PHWR, CANDU 78−54832
parametric acoustic receiving array vibration sensitivity anal. 78−66971
photoelectric inclinometer, sensitivity stabilization by negative feedback *(Russian)* 78−4012
planetary boundary layer equations soln. using sensitivity analysis 77−54957
PWR reliability prediction in design, empirical and Monte Carlo techniques 78−54827
quantum collision theory, generalised sensitivity anal. 80−31542
quartz resonator, influence of cryst. supports on acceleration sensitivity *(French)* 77−87753
radiation shielding, cross section sensitivity analysis 78−21778
radioisotope meas. instruments, output transducer as intensimeter, sensitivity and scale parameters calc. 79−11747
reactor airborne plume deposition estimation model evaluation 78−94148
receiving optical antenna, angle-distance sensitivity variation anal. 78−33841
resonant EM transducer, two-circuit system for elec. cond. meas. *(Russian)* 79−213
river quality study appl. of Streeter-Phelps models 77−70715
saccadic and vergence eye movements, reciprocal innervation model 78−31811
SAW filter transmission characts. manufacturing inaccuracies influence 79−10434
Schottky-barrier solar cell sensitivity computation 79−62004
secondary radiation dosimeters, prep., sensitivity anal. and calibration 80−74034
solar collector tilt, orientation, and overshadowing sensitivity rel. to Netherlands urban design 79−62073
strain-gauge transducer sensitivity to directional thermal gradient error 77−74382
structural fatigue life rel. to element uncertainty 79−27593
thermistor ebullioscopes, uncertainty in sensitivity 78−12695
thermographic meas., three-dimensional signal detection, expt. 78−3662
torsional vibration natural freq. calc. using eigenvalues and eigenvectors derivatives 77−74218
US flow detection, mirror shadow method sensitivity expression and analysis 78−53088
Wheatstone bridge, optimisation of sensitivity 78−86298
^{241}Am 60 keV γ backscatter meas. of solid powder mixture composition 77−52695
sensors, nonelectric *see nonelectric sensing devices*
sensory aids
see also contact lenses; hearing aids
acoustic aid for the blind 80−104810
acoustic seeing aid for blind *(Polish)* 80−8215
artificial sight and hearing, appl. of microcircuits 78−20311
blind aid, image conversion to a tactile presentation 80−94414
blind aids, Spanish electronic devices *(Spanish)* 79−39613

sensory aids continued
blind children's CW FM sonar 79−70708
blind mobility aid, computerised instrumentation system for simulation and evaluation 79−12045
blind reading aid, vibrotactile stimulation, using electrical and mechanical stimuli 77−5109
blind reading aid using conversion of optical images into vibrotactile 80−85533
Braille display cassette tape recording for text reproduction *(Spanish)* 79−39612
car drivers, work spectacles and functional visual fields *(Italian)* 80−108875
communication interface for non-vocal physically handicapped using 3-electrode EOG 77−25603
contact lens/spectacle system for altering retinal image movement to eye rotation relation 79−53281
deaf speech and hearing aids, vocoders, frequency lowering and lipreading cues 80−12309
deaf-blind communication, electromech. hand 78−48943
deafness categories and communication aids 77−40927
depth perceptor, hand held, tactile information transfer system 77−78059
devices for blind and visually impaired 78−11775
eikonic lens design for minus prescriptions 80−46095
electrocutaneous codes for prosthesis/orthosis sensory feedback 78−44715
electrocutaneous sensory aid based on two-point discrimination thresholds 77−81652
electrocutaneous stimulation, energy threshold meas. and channel capacity estimation *(Japanese)* 78−53573
electrocutaneous tracking, evaluation of sensory feedback codes 79−25004
electrotactile code evaluation 77−40932
Elektroftalm, optoelectronic instrum. with tactile display for blind people *(Polish)* 78−81073
eye refractive error, simplified anal. of meridional refr. data 78−65149
eyeglass lipreading aid system 77−25602
eyeglasses, conventional, value for X-ray protection 79−88202
focused US for input of auditory information into aural labyrinth 78−40275
formant based speech code for severely impaired hearing subjects 77−64051
gait trainer for hemiplegic patients with lower limb sensory loss 78−48940
glass lenses, effectiveness in reducing eye exposure 79−92394
handicapped persons technical aids, R&D in Sweden *(Japanese)* 78−48934
hearing and seeing aids, electronic developments 80−51285
Heliotrop for blind people, photoelec. set of instrums. *(Polish)* 78−81074
image intensifier aid for chronic night blindness 77−60288
intelligent communication device, design parameters 77−52928
intraocular lens implant evaluation 78−81061
intraocular lenses, literature review 1976-1977 79−96707
lens, Schott S-1005, static fracture resist. rel. to thickness 78−81063
lenses, low-power plus, perceptual effects in emmetropic observers 80−67084
lenses of TiO glass, and astigmatism of oblique rays *(Italian)* 80−56278
measuring cup for the blind, electronic, 50 ml indications 77−78054
MESA, multipoint electrotactile speech aid, reception of connected discourse 79−50529
microcomputer-based multiboard communication system for nonverbal handicapped children 78−57126
mobility aid for blind, passive optical system 77−25604
mobility aid for blind, quantitative depth perceptor 77−25605
Multipoint Electrotactile Speech Aid 78−40407
multispectral image visual interpretation aided by colouring 77−58281
night vision aid, second-generation intensifier monocular 77−40936
night vision equipment matching to human observer 77−40937
non-vocal communication encoded as eye movements, display board 77−52927
nonvocal communication aid improvement by microprocessor technology 80−8217
ophthalmic correcting cylinder axis, ophthalmometric prediction 80−98174
ophthalmic lens, choosing the base curve 79−29664
ophthalmic lenses, basic principles of fracture testing 79−96233
ophthalmic lenses, thin, chemtempered, static load strength testing 80−5812
ophthalmic lenses, thin, chemtempered, strength meas. by drop-ball testing 80−5811
ophthalmic materials evaluation 79−92426
ophthalmolscopic and vision function meas. instruments 79−96689
optical reading machine, multifont adaptable automatic, for blind people 80−104814
optical-to-tactile convertor 80−57041
optical-to-tactile convertor of wide images, blind aid 80−26414
pattern display using sound localising effect 79−53284
polycarbonate ophthalmic-prescription lens series 79−81501
prescription lenses, attenuation of diagnostic X-rays 79−92395
prosthetic hand pinch force, sensory-feedback system compatible with myoelectric control 80−41324
prosthetic sonar for congenitally blind children 77−70568
reading aid, portable, for partially-sighted 79−29665
reading aid using automatic recognition of printed characters *(French)* 77−48933
reading machines for blind 77−81654
rehabilitation engineering *(Japanese)* 80−12304
rehabilitation of severely disabled, microcomputer environmental control and communication system 80−8216
semantically accessible communication aid development trends 80−8218
spectacle lens blanks, grinding and polishing using automatic and semi-automatic machines *(French)* 80−58822
spectacle lens test facility complex 79−39603
spectacle lenses, eye testing using screen image divider 78−57114
spectacle lenses, hard resin, comparative study of bitoric effect 80−91877
spectacle lenses, scatt. light meas. *(German)* 78−46746
spectacle test lenses, large set 79−92427

sensory aids continued
speech parameter encoding using vibrotactile freq. discrimination 78−11772
tactile aids and equipment for physical science course for visually impaired students 78−8183
tactile artificial sensory communications, space and freq. optimal displays 78−36049
tactile perception, artificial skin, planary distributed transducers 77−81661
tactual sound localizer for deaf *(Japanese)* 77−86707
tactual vocoder, max. information transmission, time-invariant stimulation *(Japanese)* 80−41317
Tadoma vibrotactile speechreading, preliminary results 78−28127
telephone handling aids for handicapped people 80−36196
telescopes, light vergence and accommodation 78−24065
text TV display for visually handicapped *(German)* 79−2162
touch-sensitive audio tablet for blind access to digital memory 79−76916
US, mobility aid for blind people 80−56290
vibrotactile pattern perception extraordinary observers 77−64065
vibrotactile recorder, speech sound identification 77−78055
vision, artifical vision machine for blind people *(Korean)* 79−66583
vision, new Russian technical aids for compensating defective vision and blindness 78−85451
vision aids, training and practice effects on performance 78−11770
vision correction lens, hyperopic eye functional visual acuity at intermediate range 78−48791
vision sharpness improvement, optical devices and apparatus *(Hungarian)* 78−15823
visual aid for patients with retinitis pigmentosa and night blindness, Generation II 77−21660
visual angle increase, optical devices, geometrical and physiological optics *(Hungarian)* 78−20312
visual field expander for patients with retinitis pigmentosa 78−65148
visual optical systems, aberration tolerances 77−73529
visual perception, spatial Fourier transform model 79−11940
visual prosthesis, processing and tactile stimulation of images *(French)* 79−100788
visual prosthesis design, human factors and electrophysiological considerations 78−53583
visual prosthetic device, bioengineering and biomedical aspects of focal surface model 78−48942
writing aid for motor handicapped, microprocessor-based device, LOGOS 78−81077

separation
see also desalination; distillation; drying; filtration; isotope separation; magnetic separation
actinide elements, solvent extraction by trilaurylammonium nitrate carboxylic acid mixtures 79−22444
aerosol particle separation efficiencies of wire grids 78−87381
automated radiochemical separation systems use in destructive neutron activation analysis 77−90691
binary gas mixtures, separation and isotope separation in curved shock wave 79−94753
biological materials, radioactivation analysis, separation of U, Th, Cr, Mn and S *(French)* 77−90700
block copolymers, chromatographic separation on porous adsorbents *(Russian)* 79−66392
boric acid solutions, extractive purification from radioactive corrosion and fission products 80−18458
capillary isotachophoresis, principle, instrumentation and appl. 77−90607
carbon tetrachloride-I_2-water system, mass transfer in pulsed perforated plate column 78−71385
carrier-mediated extraction, development 80−66870
cell separation, local conc. gradient determ. by conductivity meas. *(German)* 79−5411
cement kiln dust emission control by electrostatic precipitator, meas. 79−52989
centrifugal separators, two-phase flow distribs., nuclear power appl. *(German)* 77−6574
CHISA international conference, Prague, Czechoslovakia (Aug. 1978) 80−62372
chromatographic column, effluent detector for volatile solvent systems 78−92529
Clusius separation column, appl. to catalytic prod. of highly conc. H_2 79−24832
colloid, fractionation and size analysis using flow field-flow fractionation 78−61062
colloid particle separation by potential barrier chromatography 77−73474
colloids, field separation with hydrodynamic amplification 78−27779
concrete, leachability determ., radioactive tracer method 78−61135
counter current extraction column, efficiency, using nonlinear PD model *(Russian)* 79−64808
cryogen separation of Kr and Xe from dissolver off-gas in fuel reprocessing plant 77−61590
cycling zone adsorption, travelling wave, continuous flow equilib. staged model 78−64874
dialysis device, high-speed 80−17205
distillation deoxidation during electron beam melting *(Russian)* 79−70306
electrolytic ion separation, by ion exchange membranes 78−53247
element mass separation mechanism in plasma discharge in intersecting fields *(Russian)* 80−14943
erythrocyte high gradient magnetic separation 78−53585
extractive metallurgy, fluidised bed electrode system appl. 79−57249
field flow fractionation, macromolecule separation, characterisation studies appl. 78−90327
filtration, dynamic, hybrid simulation, use of electrically conducting paper with discretely distributed capacitance *(Russian)* 78−88850
fission reactor materials management, using dynamic materials accounting methods 79−85738
flotation, noninertial, effect of particle aggregation 80−55719
flotation of fine particles, effects of size and charge 77−16865
flotation of hydrophobic minerals, US activation of non-polar collectors 78−63250
flow field-flow fractionation, for macromol. seperations 77−960
fluidised bed, continuous gas-solid, min. carrying vel. of particles prediction 80−33670
gas, in vortex tube, theory and expts. *(Japanese)* 79−4021

separation continued
gas discharge, DC, time-depend. cataphoretic gas separation with end volumes 80−79603
gas mixture, flowing, separation by thermal diffusion 79−68755
gas mixture, separation in travelling mag. field in discharge 79−64927
gas mixture separation by membranes *(Japanese)* 78−48691
gas mixtures, separation using variable-temp. cryogenic trap 79−16026
gas permselective membranes, irrad. effects on permeation and separation performances 78−29591
gas separation, energetic, influence of vortex-tube configurations and length 77−7400
gas separation by permeation, calc. methods and parametric anal. 78−80784
gas separation by permeation, permeate press. drop effect 78−80785
gas stripping column, periodically cycled, feedback control, simulations 79−1231
gaseous mixture separation, with asymmetric dense polymeric membranes 78−9696
gaseous mixtures, diffusion, laser separation 79−77331
geological materials, radioactivation analysis, separation of U, Th, Cr, Mn and S *(French)* 77−90700
giant planet interiors, dense fluid mixture of nuclei, phase separation calcs. 77−56849
high-temperature centrifuge construction 78−57938
homogeneous solids, leachability determ., radioactive tracer method 78−61135
immiscible liquids, separation kinetics in low gravity environment, computer simulation study 78−34629
industrial processes, appl. of radioisotope tracer method 78−76896
inertialess charged particles, collection on circular cylinders by elec. forces and gravitation 78−44400
inertialess charged particles, collection on elliptical and irregular cylinders by elec. forces and gravitation 78−68924
ingot formed in EM crystalliser, control of metal melt circulation *(Russian)* 78−84790
ion beams, mass separation in EM field, model mass separator 78−9855
ion exchange membrane selectivity w.r.t. dialysis prospects 80−45560
ionic mixtures, phase separation 80−77279
isobutyric acid-water mixtures, phase separation, light scatt. 78−84592
isobutyric acid-water mixtures, spinodal decomposition, light scatt. 77−72688
isocyanate polymers, partitioning between isotropic and anisotropic phases 80−24343
leukocytes of human blood, gravity sedimentation anal. 80−98197
Linderstrom-Lang vortex tube, gas separation perform. 77−27536
Linderstrom-Lang vortex tube, gas separation performance 77−47019
liquid membranes, emulsion-type, pertraction appls., comparison with double liq.-liq. extraction 80−66869
liquid membranes, separation and reaction appls. 80−66871
liquid mixture, crit. soln. point, sedimentation and density gradients in high gravit. field 77−59121
liquid mixture, shallow, laser separation, thermal mechanism 80−5925
liquid mixtures, separation by facilitated transport through liquid membrane 78−76920
liquid mixtures, thin layer separation by laser heating 79−29404
liquids, impurity separation, laser thermal method *(Russian)* 77−7859
low-boiling compound separation by low-temp. gas chromatography 79−70397
2,6-lutidine-H_2O, phase separation, hydrodynamic effects 78−83960
magnetic, dynamics of particle attracted by magnetised wire, theory 77−84307
magnetic reconnection, plasma accel., heating and shock form. 78−40773
magnetic separation, review of current activity 77−63961
magnetochemical, separatory motions of dia-/paramag. solns. and ferrimag. suspensions in mag. field 77−20628
mass-diffusion element, anal. of separative power 79−41039
membrane separation processes, principles, practice and prospects 78−92505
metal ammine complexes, metal extraction by adsorption, using low rank coals 79−11530
metal and alloy crystallisation, apparatus for decanting solid and liquid phases 78−56597
metal extraction kinetics, from deep-sea Mn nodules, pore diffusion controlling case 77−28984
metal extraction kinetics, from deep-sea Mn nodules, pore diffusion with chemical reaction 77−28985
metal ions, heavy, using vinylbenzyl gluconate acrylonitrile copolymer membrane 79−74418
metal refining by crystallisation and reflux, three component Raoultian behaviour 77−28799
mixtures, physical-chemical separation and thermodynamics, review *(German)* 78−18774
multicomponent polymer system, liq.-liq. phase separation, thermodynamic aspects of polymer compatability 78−14469
multigranular suspensions, aqueous, sedimentation in oblique plate separator under laminar flow conditions *(German)* 77−44513
multistage multicomponent separation, calc. using thermodynamic props. from SRK/PR eqn. of state 79−34346
nonequilibrium parametric pump, steady state predictions 77−49736
nuclear fuel elements extraction reprocessing, apparatus for solns. clarification 77−54348
ore, flotation extraction, thermoelectric power, extraction yield depdnd. 78−19686
organic cations, extraction from acid soln. by elec. field, mass spectrometric anal. 79−66390
partial condensation methods, thermodynamics *(German)* 78−20054
partially ionised inert gases in travelling HF mag. field 78−75474
particle separation, high-resolution, by sedimentation field-flow fractionation 77−73473
particle separation property of impactor stage with nonstationary flow *(German)* 78−18335
particulate materials, vibrated bed electrostatic separation 80−16641
perturbation chromatography theory, model independent aspects 79−8463
phase separation, competitive statistical and chem. mixing effects *(German)* 77−52665
photochemical separation of metals in aq. soln. 77−60082
pigment separation and deposition, electron sensitive, by electrophoresis *(German)* 80−108365
separation continued
plasma, rot. ternary, element separation, degrees of ionis. effects 77−15174
plasma centrifuges, fluid flow analysis, third-order differential equation solution *(Japanese)* 80−53949
plasma convection in force-free mag. field, mechanism for chem. separation in cosmic plasmas 79−35125
plasma impurity separation, in channel of magnetoplasma compressor, numerical investig. *(Russian)* 79−37467
plastics, leachability determ., radioactive tracer method 78−61135
poly-4,4-diphenylphthaleinterephthalamide, mol. mass distrib., sedimentation and fractionation method meas. *(Russian)* 80−71957
polyleucine membrane, water and water vapour permeation and solute separation *(Japanese)* 78−31701
polymer solution, complex coacervation, virial expsn. method 79−77750
polynuclear aromatic compounds, HPLC separation using aminosilane stationary phase 78−35747
powder, disintegration of powder particle agglomerates under the action of an alternating electric field 78−68642
powder, mixing/segregation behaviour, 2 powders of different density, quantit. anal. 78−84733
powder classification in electric field of plane capacitor 77−12775
powder particle motion and segregation by density difference in V-type mixer 80−45250
powders, fine, electrogravitation classification by particle mass 79−61531
powders, spark elutriation into plasma spectrochem. anal. *(German)* 78−68959
preparative scale thin-film dialysis apparatus 80−101296
pulsed extraction column, with perforated plates, efficiency 79−64809
racemic liq. soln., mirror isomeric mol. separation by RF rot. polarisation elec. field 78−80317
radioactive Kr and Xe in nuclear power station fuel cycle *(Czech)* 79−49707
radionuclide corrosion and fission products, ion exchange separation 80−18460
radionuclide corrosion and fission products, liquid-liquid extractions with metal diethyldithiocarbamates 80−18459
radionuclides, use of $^{140}Ba/^{140}La$ source *(German)* 77−25298
rare earth element separation from clay, complexation method 80−3442
rare earth metal impurities in PuO_2, PuO_2-UO_2 determ. by chem. separation, at. emission anal. 77−52723
rare earth purification, laser induced photochem. separation methods, review 79−61883
rare earths, purification, laser methods 80−16712
refractory metal refining, at. absorpt. spectroscopy for continuous process control *(Russian)* 77−56302
rhodamine Zh, isomer separation, identification and emission efficiencies *(Russian)* 77−83871
rotating plasma, separation of metals 78−75436
selective laser photophysics and photochemistry, applications 77−56243
sieving of fine powders by sonic oscillating air column *(Japanese)* 78−95712
slag and metal flow in ESR process, mathematic model 77−73249
solid-liquid extraction, diffusion processes, general soln. 78−20136
solvent extraction device using radioactive tracers 77−32819
solvent extraction processing of mixed actinide residues, air sparge batch contactor 77−46369
solvent-polymer system, liquid multi-phase separation 78−14468
styrene-ethylbenzne system, separation by liq. membrane permeation, operating parameters influence on selectivity 79−87871
sulphides, direct leaching 77−29033
superheavy elements, group separation procedure using diethyldithiophosphoric acid 77−26953
supersonic, two-phase flow, phase separation 79−23358
suspensions, dielectric separation of solid particles 80−16213
T separation from Li at low conc. using Y for fusion-reactor appls. 80−83219
thermodiffusion separation column, theory according to Frazier scheme 78−5842
thermoosmotic concentration difference meas. for gaseous mixtures across membranes 79−83508
trace elements, in acid solns., solvent extraction, chelation and thermodynamic activity *(French)* 78−27816
transactinides, gas phase separation methods 77−26954
two-phase flow, separation by solenoid *(Russian)* 77−7466
velocity sedimentation, mammalian cells 80−101293
virtual impactor for particle classif. and generation of test aerosols with narrow size distribs. 80−30626
volatile trace organics, aqueous environmental samples, head space anal. 80−40763
water turbulent heat transfer downstream of unsymmetric blockage in tube 79−55377
weakly conducting fluid, separation by thermal diffusion in elec. field *(Russian)* 79−16117
Z>103 transactinides, method for rapid separation and identification 77−26952
Ag recovery from laboratory wastes, teaching appl. 79−84912
Am, production by US irrad. in reactor, chem. separation, yield 77−63986
Ar purification system and electronegative impurity conc. meas. instrument 80−32571
Ar purifier, portable, 0.3 m^3/h, design, appl. *(Polish)* 79−12781
Ar-N_2 plasma, diffusion separation N_2 dissociation 77−76036
Be, determ. in biological materials, flameless atomic absorption spectrometry *(Japanese)* 80−26428
C-O eutectic, form. in C-O white dwarfs 80−77405
Cd-Pb(Sn)(Bi) alloy, molten, EMF meas. of liquid separation 78−39747
Cl_2-CO_2 system, vapour-liquid equilib. *(Japanese)* 79−42258
Cm, production by US irrad. in reactor, chem. separation, yield 77−63986
Co based alloy, distillation deoxidation during electron beam melting *(Russian)* 79−70306
Co based alloys, distillation deoxidation during electron beam melting *(Russian)* 79−70306
Co, extraction with 2-(2-thiazolylazo)-4-methyl phenol by chelate form. 77−60063
Cu alloys, determ. of Cu, Sb, inverse voltamperometry method 78−61099
Cu electrorefining process, quantitative evaluation of Ag transfer 80−30246

separation continued
Cu, extraction by Kelex 100, meas. and correl. of solvent extraction equilibria 77−29034
^{64}Cu, extraction from reactor-irrad. α-phthalocyanine target 80−35563
Fe, purification, removal of C, N, and O by dry H_2 method *(Japanese)* 78−11234
GeO_2-Na_2O borosilicate glass fibre prod. by phase separation and leaching 80−69558
H, thermochemical production, irreversibility anal. of separation schemes from binary gas mixtures 80−35767
H/He separation in interior of Saturn, rel. to energy release 80−77307
H_2-O_2 gas mixture in chem. equilib., elemental diffusional separation in nonisothermal flow 79−55429
H_2SO_4=Br cycle, separation processes simulation 79−74413
He recovery and recycling system, for CO_2 lasers 78−82974
He, superfluid, liquid-vapour porous-plug separators for cryogenic space system 79−54142
He-Ar mixture, mass separation with rot. plasma 79−13842
He-Ar mixture, mass separation during molecular beam sampling process 80−31937
Hf, from Zr, new process 78−6875
^{131}I, dynamic sorption from gas phase of dissociating N_2O_4 *(Russian)* 78−58356
Ir, recovery from laboratory residues 78−81957
Kr-N_2(He) gas mixtures, separation by silicone rubber, cellulose acetate membranes 77−36791
Kr-Xe, isotopic mixtures, separation in high-freq. discharge in mag. field *(Russian)* 77−75317
N_2, liq., impurity separation, laser thermal method *(Russian)* 77−7859
N_2 purifier, 2.5 m^3/h *(Polish)* 79−12782
Na coolant in EBR II, purification by cold trapping, effectiveness 77−14225
Na_2O-CaO-SiO_2, refining in glassmelting process 78−27467
^{210}Po determ. in air, radiochem. separation and α-counting method 78−73113
Pu, production by U_xS_y irrad. in reactor, chem. separation, yield 77−63986
Pu safeguarding, automated ion-exchange system for rapid Pu separation from impurities 80−78383
Pu, separation, by MnO_2 coprecipitation from fresh and saline water 78−27814
Rb, separation from potash salts, ion exchange methods *(German)* 78−23940
Ru determ. in silicate rocks, preseparation procedure for neutron activation anal. 77−44547
S-benzene systems, liq.-liq. phase separation 80−96658
Sb, A=131, 133 prod. by ^{232}Th reactor induced fission, yield, radiochem. separation, anal. 78−89923
Sr, separation from potash salts, ion exchange methods *(German)* 78−23940
T, removal from liq. K and Li by sorption onto Y, fusion reactor breeder blanket 78−66411
Te separation, determ. in inert gas, H_2 mixtures, oscillograph polarography method 78−61100
U determ. in natural water by ion exchange separation, delayed neutron counting 77−36847
U from sea-water by interfacial electrolysis *(Japanese)* 77−1931
U production by U_xS_y irrad. in reactor, chem. separation, yield 77−63986
U(VI) extraction from sea water using hydrous metallic oxide binded with hydrophilic polymers *(Japanese)* 79−48102
W alloys, phase anal., electrochem. separation of carbides 78−60651
Xe-He(Ne), gas mixture, element and isotope separation in impulse plasma centrifuge *(Russian)* 80−38725
Y impurity in PuO_2, PuO_2-UO_2 determ. by chem. separation, at. emission anal. 77−52723
Zn, extraction with 2-(2-thiazolylazo)-4-methyl phenol by chelate form. 77−60063

sequential circuits
atrioventricular sequential demand pacemaker, R-wave sensing methods *(Japanese)* 79−5406

sequential machines
X-ray fluorescence spectrometer for industrial quality assurance 79−70398

series (mathematics)
acoustics, approach *(Japanese)* 80−87658
amplitude transmittance expansion in Taylor series, for holography *(Spanish)* 78−50732
analytic continuation of the Fourier Series on connected compact Lie groups 78−93511
analytic iterability of formal power series vectors *(German)* 77−53736
Appell function F_1, generating functions 77−17777
artificial satellite, Vinti problem, extended phase space representation, luni-solar perturbations 79−35101
asymptotic expansions in mathematical physics *(Russian)* 78−28908
asymptotic series coefficient, generalised calculus using steepest descent method *(Rumanian)* 78−89304
asymptotic series expansion and complex classical trajectories 78−93557
beam mode function series approximating beam field *(Japanese)* 77−22427
beams flexural-torsional problem by series expansion in eigenfunctions 80−83732
Bertaut series convergence for extended cryst. lattice electrostatic energy calc. 79−55693
binary lattice gas, crit. phenomena, series anal. 80−4671
biorthogonal series convergence, biharmonic and Stokes flow edge problems 78−81847
blackbody function efficient computation, two-series approach 80−79128
Born series generalisation, sparse-matrix version 78−77751
Born series in scatt. theory, rearrangement, convergence improvement, orthogonal projections basis 77−60974
Born series rearrangement in model space, resolvent operator expansion 80−13422
Bosi's method for solving Laplace's equation in investigation of electrostatic mirrors 79−68347
boundary layer problem, unsteady, extended series expansion 80−83781
Bremmer series concepts, appl. in EM propag. slab geometry problem approximate solns. 79−64152
Bremmer series decomposition of solns. to lossless wave eqn. in layered media 78−53738

series continued
celestial mechanics, planetary motion, Taylor-Steffensen series appl. *(Russian)* 78−49352
celestial mechanics, regularised numerical method based on Taylor-Steffensen power series *(Russian)* 78−49300
charge density functions, Bertaut series, convergence props. study 80−27104
chemical kinetics, modelling, numerical method based on Taylor series expansion 78−48629
continued fractions method for Mie scatt. calcs. 78−82914
convection, free, in saturated porous medium boundary layer with lateral mass flux 79−27689
convergent expansion about mean field theory, mean field cluster expansion 77−5706
convergent expansion about mean field theory, nearly Gaussian quantum field theory 77−5705
convolution product, deconvolution problem *(French)* 79−44275
critical exponents in three dimensions, derivation from ϕ^4 field theory with Gaussian propagator 80−4686
cubic crystals, elastic strip, moving stress sources, boundary-value problem soln. *(German)* 78−38702
Debye lattice, thermal props., WINIMAX approx. appl. 80−49333
density series, analysis of tail for Coulomb crystal energy 78−91300
diffusion, linear eqn., improved series soln. method 80−8939
digital time series error detect. and correction 78−3963
Dini and trigonometric series summation, appl. to classical mechanics *(Polish)* 79−63032
direct gravity formula for 1967 Geodetic Reference System 78−92775
Dirichlet problem for semilinear eqn. $\Delta^k u = f$ on a disc, approx. techniques 79−40377
Dirichlet problem for semilinear eqn. $\Delta^k u = f$ on a disc, series soln. 79−40376
divergent series summation by order depend. mappings 79−88819
divergent series summing formula 77−53734
dual trigonometric series, appl. to mixed elasticity theory problems *(Russian)* 77−71189
education, conditionally divergent series, rearrangement, induced charge on parallel plates 77−87599
eigenfunction expansions assoc. with vector-matrix differential eqn., convergence 78−69965
elastic scattering, of atoms and mols., angular distribution, in complex angular momentum theories, calc. method 79−76483
electrical engineering dimensional unification *(Italian)* 80−27266
electron microscope, 3-dimens. imaging, curved axis electron optics *(German)* 79−13889
EM wave, of sinusoidal ring current, diffr. by cond. cone 79−27140
EM waves diffraction at surfaces with inhomogeneous admittance 80−69296
exospheric temperature, representation by sum of series in Legendre polynomials 78−45063
expansion technique for square lattices 77−57283
ferromagnetic classical vector model, extension of high temp. free energy series 80−7062
flow between concentric rot. spheres, nonlinear, axisymmetric 80−19412
flow rate transducer dynamic error determ. 77−72386
fluid, diat. symmetric mols., truncation of infinite series 79−90508
formal series solutions, rational solns., soliton eqns. 78−57747
FORTRAN function writer, FURI, polynomial expansion 78−16631
Fourier, convergence solution by infinite and finite integral transforms 77−75773
Fourier, strong (J, p_n) summability 79−58525
Fourier analysis of eclipsing binary light curves, series expansions 79−75248
Fourier expansions for anomalous geophysical fields *(Russian)* 79−62624
Fourier series, concept of basic number 80−4513
Fourier series, recursive evaluation, for teachers 79−35477
Fourier series and communication theory techniques for river water temp. forecasting 77−25718
Fourier series convergence rate, graphical illustrations, for teaching 79−80399
Fourier series in celestial mechanics, fast evaluation 80−56711
Fourier-Bessel series soln. of exterior Dirichlet boundary-value problem with rot. symm. 80−1103
Fourier-Bessel series summation *(Polish)* 78−12544
Fourier-Bessel series summation *(Polish)* 78−77818
Fraunhofer diffraction symmetry, series expansion of Fourier transform 79−50212
free-electron laser, relationship between mean and mean squared radiated energy and spontaneous power spectrum 79−50277
Gaussian integrals, evaluation by backwards recursion or Taylor expansion 80−31488
geomagnetic field, expansion using orthonormalised polynomials 77−29248
grating profile description, Rayleigh hypothesis in reflection theory by grating 79−50195
Haar series use in constructing difference schemes for meteorological appl. 79−58125
heat equation involving moving phase boundaries, analytic soln. 78−90694
heat transfer, nonlinear, iterative-variational method 78−94511
heat transfer in laminar freely convecting boundary layer, series soln. predictive capability 78−71335
heavy ion-induced multistep multinucleon transfer reactions, grazing collisions, quantal theory 79−6698
helical axisymmetrical motion, of perfect fluid through diffuser, function series soln. 78−49669
hierarchical model ε-expansion, numerical test of Borel summability 78−12650
hypergeometric functions asymptotic series calcs. 78−45468
image reconstruction from projections, freq. domain techniques 78−58935
inequality between arithmetic and geometric mean, comment on thermodynamic proof 79−67241
infinite series evaluation using physical analogues, for teaching 79−25803
integral approx. methods, appl. to Ising model susceptibility 79−71392
irrotational waves and convergence of Levi-Civita's series 77−58711
Ising model, critical temperature, modulated Pade approximant 80−84605
Ising model with free surface, series anal. 80−25062

series continued
Jacobian theta functions, evaluation of lattice sums 77−26245
Karman vortex street behind circular cylinder, series truncation method, Navier-Stokes eqns. solns. 78−79325
Lagrange's inversion formula, soln. 80−31484
Laguerre series, absolute Norlund summability 79−84935
Lane-Emden problem, series soln. 78−36559
lattice equivalent neighbour model, high-temp. series expansions 79−44877
Legendre Pade approximants, and appl. to pot. scatt. 78−28982
Legendre Pade approximants, convergence, to Coulomb and other scatt. amplitudes 78−28983
Legendre series summation, recursive procedure, gravit. potential evaluation 80−31486
Lie groups with discrete series, comment on conjecture of Wolf and Moore *(French)* 79−53960
Lie series and invariant functions for analytic symplectic maps 77−22373
Lie series use in studying nonlinear Hamiltonian systems 79−8811
linear systems, response to square wave force, transients, teaching appl. 80−31467
lossy plasma half-space, transient refl. for TM polarisation 79−98916
low-temperature series expansions, algebraic techniques 79−17352
magnetically dilute two-dimensional ferromagnet, concentration expansion, derivation of series *(Japanese)* 77−16019
matched asymptotic expansions method, asymptotic matching principle for higher approx., boundary layer problems appl. 78−94642
metal, electron momentum distrib. in truncated Fourier series form 79−56883
Morse function normalisation, Gamma function series summation 79−76477
multicomponent systems, comput. techniques for thermodynamic data treatment and equil. calc. 78−10172
multiple Fourier series, convergence of rectangular partial sums 78−73831
Navier-Stokes eqns., steady flow prod. by rot. disc, series soln. anal. 78−71308
neutron spectrum in heavy gas moderator, series methods, Runge Kutta integration 77−34365
neutron transport equation for slabs, power series solns. comparison 78−13190
nonorthogonal, numerical study of EM wave diffr. *(Russian)* 77−58237
nozzle, Laval, vortical helical ideal gas flow, asymptotic series soln. 79−81943
numerical coeffs. of series expansions, computation through pattern recognition 77−71199
numerical integration, error estimation by means of Fourier series *(Japanese)* 79−2612
open electron optical system with rotational symmetry, Fourier-Bessel series soln. for pot. and field intensity 79−76570
optimal control, differential eqn., canonical, functional relation expressed by Volterra series *(French)* 80−73159
Orr-Sommerfeld eqn. eigenvalues, series representation 78−38280
orthogonal polynomials expansions, summation procedure 78−81805
Pade and Pade-Borel perturbation theory series summation methods *(Russian)* 79−2663
Pade approximant, modulated, applied to Ising model critical temperature 80−84605
Pade approximants, nonperturbative analytic approach in plasmas 78−20951
Pade approximants used for sequential term prediction, appl. to lattice and death statistics 78−57866
Pade-Borel summation of perturbation series, Gell-Mann-Low function 78−86416
partial differential approximants for multicritical singularities 77−85466
Percus-Yevick eqn., orthonormal series expansion soln. 80−49065
perturbation series in quantum mechanics and field theory, Borel summation 78−16683
Planck integral, non evaluation in terms of finite series of elementary functions 80−31563
plane restricted three body problem, asymptotic solns. *(Russian)* 77−22049
plasma radiation emission spatial distrib. reconstruction in torous 80−103123
Poisson sum formula evaluation of infinite sums 79−86377
polymer chain, infinite, trigonometric series evaluation 79−7041
polymers, rectilinear on square lattice, series expansion 80−5646
polynomials, series conversion by five term recurrence formula 77−13594
Potts model, four state, series studies 79−85088
power series, class of algorithms for obtaining rational approximants 78−54169
power series, inhomogeneous differential approximants 79−92919
power series expansions by computer 79−84679
quadruple sequence equations involving orthogonal polynomials 79−35531
quantum system, intermediate states spectrum, Sturm expansions of Green's functions 79−9132
recurrence technique for confluent singularity analysis of power series 80−73277
rivers annual average discharge processes, long-range intraseries couplings 77−78260
rivers annual discharge variations, long-range intraseries couplings for ultralong range forecasting 77−78261
Schrodinger equation, nonseparable, series solns. and variational principle, appl. to H_2^+ and He 79−36504
Schumann resonance problem, convergence of zonal harmonic series 79−2348
sequence of series of one-dimensional random variables with arbitrary depend. character, limit theorems *(Russian)* 77−49571
solar storage tank, buried, hemispherical, heat cond. to environment, series soln. 79−3891
spherical delta functions, multipole expansions for fields, using Cartesian Taylor series 78−86118
spinless particles through one dimens. pot. barrier, formal series method, refl. coeff. 78−32700
standing waves of finite amplitude on surface of ideal liquid of finite depth 79−81906
Stark effect, perturbation and variation treatments, appl. to H(1s) reson. 80−14105
Stokes series, computed extension, circular boundary flow 78−42583
series continued
summing series and their derivatives, algorithm 77−9879
superconducting transition temp. theory, soln. of series expression for T_c and its radius of convergence 79−78251
suspension, Brownian rotational-translational particles, at finite conc., dynamics and hydrodynamics 79−7401
Taylor series method for two-body shell model matrix elements 80−32212
Taylor series method for two-nucleon reduced widths in symmetric two-centre shell model 80−32213
Taylor series methods for point reactor kinetics equations soln. 78−13201
Taylor-Fourier series, appl. in new exact method for Hill's eqn. of celestial mechanics *(Chinese)* 80−105152
thermal conductivity, nonlinear problems, temp. fields with variable thermophys. props., calc. method 79−86324
thermal consts. determ., inverse heat cond. problem soln. 79−37142
transport problem stationary, generalised, Laplace operator eigenfunction series soln. *(Russian)* 78−81931
truncated series expansion, for correl. function of permanent and induced depolarised Rayleigh bonds 77−61752
tube, circ., entrance region, mass transfer, asymptotic expansion soln. 78−87392
turbulent flows, two-point moments calcs., use of series expansions *(German)* 77−14997
two-centre expansion in molecular theory of solns., comment 77−60920
U(p,q), matrix elements and Casimir operators of discrete series representations 79−97238
wave equations, spatially nonhomogneous, nonmonochromatic solns. based on WKB approx. 78−86179
wave propagation in inhomogeneous media, backscatter folding series *(Russian)* 78−73862
X-ray scattering by electrons, basic theory 78−71623

serrated yielding
α-brass, Portevin-LeChatelier effect *(Japanese)* 80−11724
α-brass, single crystal, deform. and ductility at elev. temps. *(Japanese)* 79−5012
Incoloy 800H, high temp. low cycle fatigue, ageing and cold working effect 79−43277
Inconel 600, mechanisms of dynamic strain ageing and jerky flow 79−79024
Inconel 718, plastic deform., accelerated evolution of H_2 77−36594
Portevin-Le Chatelier effect and inverse strain-rate sensitivity 79−1476
steel, Cr-Ni and Cr-Mn, laws governing discontinuous yield under tensile strain in liquid He 77−63760
steel, low C, pressurised, strain rate sensitivity prior to serrated yielding onset 78−48482
steel, low C and alloy, serrated flow and thermomechanical treatment *(Korean)* 80−30026
steel, manageing 300 grade, serrated flow in austenitic state 80−30041
steel, stainless 304L, plastic deform., accelerated evolution of H_2 77−36594
strain ageing, dynamic, and serrated yielding, mechanism 80−88245
Al alloy, laws governing discontinuous yield under tensile strain in liquid He 77−63760
Al alloy 5086, plastic deform., accelerated yielding of H_2 77−36594
Al alloy 7075, serrated flow and thermomechanical treatment *(Korean)* 80−30026
Al-Cu alloy, Portevin-Le Chatelier effect, influence of specimen dimensions and machine stiffness 77−70128
Al-Mg, discontinuous deform. under various conditions 77−63716
Al-Mg (0.3 wt.%) single cryst., dislocations obs. by high voltage electron microsc. 80−79796
Al-Mg (1 wt.%), mechanisms of dynamic strain ageing and jerky flow 79−79024
Al-Mg (5 wt.%), serrated flow 79−43343
Al-Mg-Si (0.7, 0.4 at.%), effect of precipitation hardening on strain rate behaviour and yield behaviour 79−29075
β-brass, nonisoaxial bicrystal, simultaneous hardening and softening 77−36606
α-brass, serrated yielding, tensile tests and TEM obs. 79−34110
Cu-Ni, Portevin-Le Chatelier effect, during tensile deform. *(German)* 79−8330
Fe, cast, ductile, strain rate and temp., influence on strength, elongation and deformation *(Japanese)* 80−45356
Fe-Mo (3 wt.%), substitutional solid soln. with cubic faced symmetry, Portevin-Le Chatelier effect *(French)* 78−23785
Fe-N, neutron irrad. effects on mech. props. 79−4338
Nb, single crystal, surface oxide softening, TEM obs. 77−40462
Nb, surface oxide softening, anisotropy 78−60716
NbTi, dynamic stress effects, supercond. magnet training problems 78−49870
NbTi, superconducting, serrated yielding meas. via dynamic stress test facility 77−77698
Ni, plastic deform., accelerated, evolution of H_2 77−36594
Ni-Cr-Ti-Al/Au-Ni brazed joint, high temp., AE under elev. temp. and loading *(German)* 78−31597
Ni-Ti (1 wt.%), 77 to 723K 77−32649
Ni_3Fe alloy, step-like deformation *(Russian)* 78−27559
NiO, doped and pure single crystals, plastic deform. 77−36578
$Pd_{80}Si_{20}$ amorphous alloy, skip deform. and crit. shear stress, using tensile testing machine 80−89321
Ti alloy, yield, discontinuous, under tensile strain in liquid He, governing laws 77−63760
Ti, commercial-purity, Portevin-Le Chatelier effect, mechanism 77−8886
TiO_2 rutile single crystals, stoichiometric, dynamic strain ageing 80−50661
V-Nb, mech. props., −196-1000°C, comp. depend. 78−39847
V-Ta, mech. props. 79−61682
α-Zircaloy, strain ageing at 1000K 79−47725
α-Zr, strain ageing at 1000K 79−47725

service programs *see utility programs*
services, information *see information services*
servo systems *see servomechanisms*

servomechanisms
acoustooptic modulator intensity servo, optical isolation and amplitude noise reduction 79−98472
adaptive laser resonator, intracavity phase variations 77−88793
adaptive laser resonator techniques for CO_2 laser, phase error correction 79−59729

servomechanisms continued
arterial O tension servocontrol in preterm infants 80−17183
artificial arm, externally pneumatic powered controlled, features 77−90961
blood pressure or flow control system for unanaesthetised animal 77−48983
blood pump, experiences with miniaturised press.-controlled servo *(German)* 78−88762
blood pump regulation electropneumatic servo operation *(German)* 79−8579
blood pump regulation with pressure controlled servo-drive *(German)* 79−84003
chart recorders, technology improvements 79−88933
Cocatron, servo valve for liq. He II level control, superfluidity and supercond. applic. 78−18855
compact servo master-slave manipulator 79−9214
compensation densitometer servosystem using integrated operational amplifiers 78−89525
concentrator solar cell with tracking control information 79−29470
coronary perfusion pressure programmable control circuit 79−92278
Czochralski crystal growth, automatic, weighing method 77−85930
deformable mirror adaptive optical system 77−46796
dual capstan drive tape recorder *(German)* 80−95092
electro-optic modulator, servo controlled, for CW laser power stabilisation and control 80−19060
electroconvulsive therapy, servo-controlled volt. machine 78−77148
fatigue servo-hydraulic testing machines 80−108649
Fermilab master slave servo-manipulator, control system 77−83309
force plate for patient equilib. function study *(Japanese)* 79−74775
hand prosthesis myoelectric aid *(Spanish)* 79−84011
insulin delivery to diabetics, by computer controlled pulsed insulin infusion 77−37099
internal friction meas. servo system 77−39265
isobaric contraction system for left ventricular performance analysis *(Japanese)* 79−29677
laser frequency stabiliser using electronic servocontrol system 78−1240
linear servo-loop, increasing efficiency at low frequencies *(French)* 80−86280
master slave manipulator SM-229, compact servo system 79−45454
master-slave manipulator power-assisted grip system 79−9212
metrology, Cs beam freq. standard, servo-control system anal. 80−42201
microprocessor-controlled tape drive 79−93123
microscope objective, piezoelec. and electrodynamic automatic focusing servo mechanisms 80−73445
monochromator drive, using high-speed digital servo 78−36992
moving material fault test rig *(German)* 80−11855
multidither adaptive optics system, speckle interactive effects 77−46797
multidither coherent optical adaptive techniques 77−46793
muscle length reflex control, servosystem simulation 79−57639
nonlinear, for self-balancing AC potentiometer, design *(Russian)* 78−70156
optical screw, path difference meas. and control device, anal. of periodic errors 78−77972
optoelectronic, for correcting nonrectilinearity of ruling engine carriage 78−87174
phase control of HF chemical lasers 79−72580
photogrammetric automaton 'Zenit' positioning, electromechanical system *(Russian)* 78−21101
pion beam, hydraulic servomechanism for shifting range 77−83358
pion range shifter for clinical therapy hydraulic servomechanism 77−32953
plethysmograph with servo-control of hydrostatic press. 77−5118
polyvinylidene fluoride film, piezoelec. coupling factor meas. servo system 78−60397
prosthetic arm, hydraulically powered, with seven degrees of freedom 78−40404
radome and backstructure design improvements 78−57449
remote manipulation in reactors by MA-23 bilateral servomanipulator system 77−50314
resonant electromagnetic fatigue tester, strain control *(French)* 78−56870
respirator, constructed from positive-press. ventilator 77−13041
respirator, servo control of end-tidal CO_2 in paralysed animals 79−39607
river system, robust decentralised control of water quality 79−57522
scanning microscope stage for microdensitometry, computer-controlled 79−26117
servocontrolled hydraulic hot-torsion machine for hot working studies 78−27698
solar energy tracking system 79−57433
tilt meters, photoelectric, with negative feedback, servo devices transfer functions *(Russian)* 78−88948
tunable laser linear scan control by Fabry-Perot interferometer 79−76693
wave follower system, electromech., for wind-wave tank probe control 78−85734
wideband optical disc data recorder systems 80−102751
HF chemical laser phase control servo system 80−33063

servomotors
atrial and/or arterial blood pressure servo control in expt. animals 78−31986
automatic rotating disc viscometer *(Russian)* 77−19649
DC, brushless, pen recorder appl. 79−40552
error monitor for photoelectric tracking systems 79−97373
gyrostabilized platform, nonlinear response to transient input 78−30219
two-phase servo master-slave manipulators, triac output control system 79−9213

servos *see servomotors*

set theory
algebras, normal varieties of Ω-algebras *(Russian)* 80−68019
Boolean-valued models and independence proofs in axiomatic set theory, book 78−32649
chemical compounds, complete set, chiral subset, algebraic props. 77−70282
crystals, cubic-tetragonal transitions, symmetry anal. 80−10636
entropy of density matrix, definition with respect to observable 78−45586
evolution eqns. with given set of conserved densities, algorithm 79−71257
foundational studies, A. Mostowski, book 80−57014

set theory continued
foundational studies, A. Mostowski, book 80−57015
function processes, vector lattices, Riesz decomposition and characts. *(French)* 80−8908
fuzzy set theoretic approach to systems analysis, nuclear energy system appl. 78−17352
fuzzy set theory review *(German)* 77−67240
Gaussian cylinder set measures and abstract Wiener spaces mixtures as models for detection 78−89306
GM and GL type spaces, basic props., future appls. to physical axiomatics 78−45458
Herbrand theorem for ω^+-valued logic 78−57731
lattice, orthocomplemented quasi modular, quantum logic interpretation 80−12950
lattices, regular, isoperimetric problems, convex-set theory and lattice symmetry 80−46988
mixing distance 78−77662
Neumann's operator in potential theory, contractivity 78−69966
nilpotent Lie algebra, prime spectra of an enveloping algebra *(French)* 80−8777
nonstatistical parameter estimation adaptive algorithms 80−91995
partial inner product spaces, compatibility relns. 80−46855
partitioning and covering problems, appl. and algorithms *(French)* 77−17747
physical system, model of space-time from set theory concepts 80−82660
polygraphic sleep recordings, computerised scoring method 80−109049
quantum logic, props. of states 80−12947
random moires processes, densities of Minkowski measures *(German)* 77−64932
selective families of sets 80−98784
set of point sources determ. 79−88816
shock waves, global structure anal. 80−8800
supersonic plane flow, past a curved wedge, quasi-linear hyperbolic systems *(French)* 80−10261
thermal interaction between thermally homogeneous systems 78−57882
topology of molecular bonds 78−46253
transfinite ordinals as axiom no. symbols for unification of quantum and EM wave functions 77−5688
Voronoi polyhedra 79−9073

sets (mathematics) *see set theory*

sferics *see atmospherics*

shadow universe *see cosmology*

shape memory effects
acceleration waves in binary elastic materials, effect of memory, diffusion, multiple temp. 79−50640
alloy, martensite boundaries, lattice imaging study 80−107359
alloy, memory effects, props., phenomenological theory and appls. *(German)* 77−1864
alloy, props. and appl. 80−30049
alloy, recovery stress determ. 79−15665
alloy connector for optical fibres 80−53475
alloy with shape memory effect, working medium in heat engine *(Russian)* 78−48449
alloys, device for testing in bending 80−66723
alloys, unidirectional memory effect *(French)* 80−66606
brass, Cu-Zn (39(40) wt.%), shape memory effect and martensitic transform. depend. on heating-cooling cycles *(Russian)* 80−97482
brass, single crystal, two-way shape memory effect and other training phenomena 77−48505
β_1 brass containing α-precipitates, reversible shape memory effect *(Japanese)* 78−60711
brass single crystal, martensite form. and shape memory effect mech. 78−19744
Carnot cycles, transform. temp. and latent heat under applied stress, rel. to shape memory effect 77−28874
criteria for efficiency assessment *(Russian)* 80−21015
engine, memory alloy, efficiency 80−71648
marmem engines, martensitic transform. and shape memory effect 78−6920
martensitc transformations, inheritance of dislocations *(Russian)* 79−52211
martensite, shape memory, crystallographic similarities 79−66102
martensitic memory alloy composite, for prefabricated constructions *(Russian)* 77−21059
metal, martensitic memory mechanism *(Russian)* 77−21217
mica glass-ceramics, near perfect shape-memory solid 77−48492
Nitinol memory material for solid-state engine 78−59288
ordered cubic alloys, reversible martensitic transformations 78−27516
polyethylene, ionising radiation effects crosslinking with accelerated electrons, ageing, SCC *(Polish)* 79−52701
practical appls. of shape-memory alloys 80−45307
premartensitic phenomena, nucleation, shape memory effect, review 80−3041
pseudoelastic body, model for first-order phase transition 80−92642
shape memory alloys temperature entropy diagram of solid state engines and solid state heat pumping system 77−7785
shape memory effect, review 77−4144
steel, Mn, plastic deformation, shape recovery during γ to and from ϵ, ϵ' transformations *(Russian)* 79−83196
steel, stainless, ϵ-martensite, direct obs. of reverse transform. 77−55967
steel, stainless, reversibility of plastic strain during fatigue with martensitic transform. 78−31526
temperature waves in rigid materials with memory 79−17238
thermal efficiency, of ideal shape-recovery cycle 80−108445
Ti-Ni, electron emission and shape memory effect 80−50687
Ag-Cd (45 at.%) martensite, shape memory mech. and related phenomena 80−30009
Ce and Ce-Nd, reversible mech. memory effect, α to γ transition *(Russian)* 78−15396
Cu-Al-Ni(Mn), duplex shape memory effect after nonuniform plastic deform. *(Russian)* 80−25759
Cu-Zn-Al, β_1' martensite crystal crossing rel. to reversible shape memory effect *(Japanese)* 80−108499
Cu-Zn-Al, reversible shape memory effect obtained by heating under constraint *(Japanese)* 79−43335
Cu-Zn-Al, reversible shape memory effect associated with $\beta_1 \rightleftarrows \beta_1' \rightleftarrows \alpha_1'$, transform. *(Japanese)* 79−43242
Cu-Zn-Al, reversible shape memory effect *(Japanese)* 80−108500
Cu-Zn-Al (35.45, 1.72 wt.%), memory effect and martensitic transform. *(Russian)* 79−43320

shape memory effects continued
Cu-Zn-Ga alloy, configs. of martensite variants, shape deform. matrices 77−12620
Cu-Zn-Ga(Al), martensites, internally faulted, shape memory mechanism 80−30010
Cu-Zn-Si, deform. close to martensitic transform. temp. 77−63714
β-Cu-Zn-Si, premartensitic instability 77−12625
Fe-C-Mn-V, austenite microstruct. memory *(German)* 80−84977
Fe-Ni alloy, reverse martensitic transform., shape deform. reversibility 80−66506
Fe-Ni alloys, shape memory effect, martensite fine struct. effect *(Russian)* 79−52215
Fe-Ni-Co-Ti, shape memory effect after appl. of bending moment *(Russian)* 80−45305
Fe-Ni-Ti, shape recovery depend. on hardening *(Russian)* 79−83259
Fe-Ni-Ti (30, 3 wt.%), reverse martensitic transform. and memory effect *(Russian)* 79−87627
Fe-Ni(Mn) alloy, shape memory effect *(Russian)* 78−38771
Fe-Pd (31.2 wt.%), thermoelastic FCC-FCT martensitic transformation 80−104156
Fe_3Pb, reversible shape memory effect, rel. to microstruct. memory and residual stresses 77−90419
Fe_3Pt, stoichiometric composition, internal friction, microdeform. and memory effect, rel. to martensitic transform. *(French)* 77−52323
In-Cd, shape memory *(Japanese)* 79−43243
In-Sn alloy crystals, phase changes and shape memory effect *(Japanese)* 80−108502
$K(D_xH_{1-x})_3(SeO_3)_2$, ferroelastic, anelastic and elastic infra-low freq. props. 80−70304
KH_2PO_4, struct. memory effects in low temp. changes 79−28700
Mn-Cu, shape-memory effect at martensitic transform., cryst. and mag. struct. 77−36610
Mn-Cu alloy, plastic deform. mechanism and shape-memory effect, mag. struct. obs. *(Russian)* 78−60705
Mn-Cu-Al alloy under torsion, anomalous elasticity and transformation plasticity obs. *(Russian)* 78−75834
Mn-Ga (24.1 wt.%), reversible memory of form, X-ray diffr. expts. *(Russian)* 79−5006
Mn-Ge (10.3 to 15.5 wt.%), reversible memory of form, X-ray diffr. expts. *(Russian)* 79−5006
Mn-Ni, shape memory effect 78−35386
NaCl, plastic deformation influence on shape recovery effects 80−6684
NbTi, dynamic stress effects, supercond. magnet training problems 78−49870
Ni-Ti, Nitinol memory material heat engine, comment on efficiency 80−3529
Ni-Ti, Nitinol memory material heat engine, reply to comments on efficiency 80−3530
Ni-Ti (49.7 at.%) alloy, deform. behaviour and shape memory effect 77−32638
Ni-Ti (51.5 at.% Ni) metallide, thermal cond., elec. resistivity, 90-450K 78−68009
Ni-Ti alloy, shape memory effect mechanism 77−28865
Ni-Ti alloys, criteria for efficiency assessment *(Russian)* 80−21015
Ni-Ti mech. memory alloys, tensile props. *(Korean)* 77−63724
Ni-Ti shape memory alloy processing and medical applications *(German)* 80−17203
Ni-Ti shape memory alloy trigger for space satellite boom latch and release mechanism 80−7575
$(Ni_{1-x}Cu_x)Ti$, martensitic, shape memory effect kinetics and thermodynamics 80−3021
NiTi martensite, struct. characts., TEM $2^1/_2$ D imaging obs. 80−108446
NiTi, martensitic, shape memory effect kinetics and thermodynamics 80−3021
NiTi, premartensitic transformation of B2 phase, shape memory 80−84931
NiTi shape memory effects, substitution of Cu for Ni 79−61661
NiTi, stacking faults prod. by martensite transition, lattice imaging electron microscopy obs. 79−96026
PLZT ceramics, stress-induced ferrelec. transition, pseudoelasticity and shape memory, bending meas. 79−24274
Ti-Fe-Ni (67, 30, 3 wt.%), reversible shape alteration *(Russian)* 80−71647
Ti-Ni, hysteresis-free 'memory' effects 78−35385
Ti-Ni, reversible shape changes during martensitic transform., dislocation struct. stability *(Russian)* 77−63666
Ti-Ni (50.4 wt.%), thermal conversion efficiency of ideal thermoelastic marmem cycle 79−66057
Ti-Ni (51 at.%), plastic deform., two reversible form change effects *(Russian)* 77−8881
Ti-Ni-Co(Fe) alloys, shape memory temp., alloying effect 79−38912
Ti-Ni-Cu (44.5, 10 wt%), opposing stress effect on shape memory and martensitic reversion 78−44185
TiNi alloys, structural transform., physical props. and memory effects *(Russian)* 79−1856
TiNi, shape memory effect, spontaneous EMF generation 77−32637
TiNi-TiCu, exam. of shape memory effect, specific work 79−100216
U-Nb-Zr (7.5, 2.5 wt.%), texture development role in shape memory effect 79−87661
Zr-Nb (2.5 wt.%), memory effect in hydride precipitation 78−11227

shear *see crystallographic shear*

shear flow
see also shear turbulence
accelerating, internal gravity waves 79−32628
aerodynamic effects of inviscid parallel flow 78−1680
algebraic disturbances in stratified shear flows 79−50766
aniline-cyclohexane, crit. mixture with shear flow, light scatt. obs. 80−6521
anisotropic micropolar fluid theory 80−31515
aortic shear stress reduction by cardiac pacing 78−40239
aortic valve prosthesis, wall shear stress in Bjork-Shiley and Starr-Edwards types in vitro *(German)* 78−81067
approximations of unidirectional flow, unification using stress tensor 80−27139
arterial flow lipid transport model 78−44552
asthenosphere, thermal stability or instability of shear flow 78−20370
atmosphere, finite amplitude Kelvin-Helmholtz billows, evolution 78−81293
atmosphere, gravity waves generated by shear layers 77−2195
atmosphere, numerical method for stratified shear flows over long obstacle, numerical method 77−33157
atmosphere, stably stratified, resonant parallel shear instability 77−2200
atmosphere shearing instability mechanism model, effect of horizontal differencing 80−26578
average flow model, appl. to lubrication between rough sliding surfaces 80−16497
axisymmetric air free shear layer, effect of initial fluctuation level 78−90843
barotropic waves, large amplitude, interaction with ambient shear flow, critical modes 77−80175
BBOA, pretransitional shear viscosity divergence near smectic A-smectic B transition 79−33077
blood, rheological props. in transient regime to low velocity shear flow 79−79582
blood droplet deformation in Courette flow suspension, expt. *(German)* 79−16227
blunt body problem in nonuniform flow fields 78−5748
boundary layer in stratified medium, shear flow 79−64736
boundary layer shear stress distribution calc. 79−98701
boundary-value problems in stratified shear flows with a nonlinear critical layer 78−79357
Brownian motion in shear flow, exact solution by operator formalism 80−17874
Brownian motion in shear flow 78−5786
Brownian particle diffusion in shear induced convection, Poiseuille flow 80−33591
bulk dispersion coefficient in bounded skewed shear flow, tensor form 78−73393
buoyant surface jet, 2-D flow props. *(Japanese)* 80−48762
bursting phenomenon in bounded turbulent shear flow, streamwise vortices 80−1600
butadiene acrylonitrile copolymer, raw elastomer, containing crosslinked particles, flow behaviour 79−37359
carboxymethyl cellulose, aqueous soln., diffusion and mass transfer from rotating disc 80−83827
cardiotomy circuit, factors affecting haemolysis 78−36073
cascades, annular, secondary flow, shear flow turning or departure of exit flow 80−69842
Casson fluid flow between approaching discs, plug flow region 78−67230
cement paste, mathematical model relating flow curve to water/cement ratio 78−34100
cement pastes, flow behaviour, specific surface and conc. of solids influence 80−65132
charge particle electric double layer, large distortion by shear flow 79−68818
charged macromolecule soln., effective viscosity low-shear limit 79−69274
charged sphere elec. double layer deform., bulk stresses 78−48669
chiral smectic C_3 distortion under shear, optical study 77−39536
cholesteric liquid crystal, oriented, Newtonian capillary shear flow, effective viscosity 79−18957
cholesteric liquid crystals, steady low shear rate flow normal to helical axis 80−96443
cholesterics, shear flow induced propagating domains 80−54131
cholesterics, shear flow induced propagating domains 80−64887
circular jet, turbulent shear layer, shear fluctuations 79−81936
classical fluid near critical point, nonequilib. steady state fluctuations with laminar shear flow 79−81844
COC, cholesteric liq. cryst., shear flow, helix distortion, optical meas. 78−94982
colloidal dispersions, microrheology, Brownian diffusion of doublets of spheres 77−4942
colloidal dispersions, microrheology, chains of spheres in shear flow 77−7354
colloidal dispersions, microrheology, pairs of interacting spheres in shear flow 77−7352
colloidal dispersions, primary and secondary doublets of spheres in shear flow 77−7353
colloidal dispersions, stability in flow fields, trajectory anal. 78−5782
colloidal particles, Poiseuille flow, total particle conc. axial change 80−108752
compressible atmosphere, vertically rotating, critical levels 80−6073
concentrated disperse systems, non-Newtonian shear viscosity in steady flows 79−81957
conducting liquid, plane-parallel shear flow, elec. current and mag. field effects *(Russian)* 78−75221
conducting non-Newtonian liq., shear disturbance propag., mag. field effect *(Russian)* 77−65809
constant flow part cylinder with four leaved rose cross section 79−37283
convection, laminar mixed forced/free, about sphere, buoyancy effects 77−75907
convection, past hot porous circ. cylinders, of 2nd order liq. 79−14476
convective heat transfer theory 79−77094
Couette flow, striated boundary effect on viscous drag 78−59367
counter gradient flow downstream of two different diameter cylinders *(French)* 80−43693
critical fluctuations, shear flow effects 77−20045
critical fluids, light scatt. in presence of uniform shear flow 79−78693
critical fluids, non-Newtonian effect and normal stress effect 80−49396
critical fluids under shear flow, nonequilib. steady state, renormalisation group approach 80−6026
critical mixtures, shear and critical fluctuations, instantaneous mapping of velocity gradients 80−79420
curved shear flow, model consts., second order closure 78−38265
curved tube, wall shear rates in entry region, vortex struct. 79−81972
5-cyano-biphenyl, nematic phase, effect of elec. field on flow alignment angle 79−10792
cyanobiphenyls, liq. crysts. flow alignment 79−50988
cyclohexane-aniline mixture, shear induced transition to mean-field crit. behaviour 80−7364
cylinder, circ., separated wake stagnation pt., 2nd order boundary-layer soln. 78−63432
cylinder in viscous fluid, circular oscillations 79−14387
cylinder with elliptic limacon cross-section, stagnation points 80−23984
deagglomeration in viscous fluids, size distrib. response to shear stress 77−42903
density stratified reservoir, selective withdrawal from line sink 77−14980
die entry flow, kinematics and stability 79−60026
dilatant liquids, propag. of shear perturbations 80−6103

shear flow continued
dilatant media, shear perturbation propag., nonlinear effects in mag. field *(Russian)* 77—27612
directed fluid sheets and gravity waves in compressible and incompressible fluids 80—14714
direction measurement, anal. of errors 78—22436
disperse system, orthokinetic phenomena 77—32838
dispersion, kinetics, doublets of rigid spheres, calc. method 77—72344
dispersions, kinetics, doublets of rigid spheres, simple shear expt. 77—72345
drop, deformable, motion in second-order fluid 79—64754
drop deformation and orientation in shear and extensional flow fields, dynamic interfacial props. 80—107611
drop dynamics in shear fields, role of dynamic interfacial effects 80—107612
drop in shear flow, deform. and burst of drop 79—32645
drops, long and slender, slow viscous motion 80—79365
duct with sudden expsns., asymmetric flows and instabilities 78—22425
ducts, rapidly rot., variable area, rectangular, steady flow, inertial perturbations for small divergences 80—59112
ducts, sound propagation in parallel sheared flow mode estimation 80—79026
dumbbell kinetic problem, rheology, Langevin approach 78—42633
dynamic simple shear expt., deviation by velocity gradient profile from gap loading and surface loading 77—72257
Earth asthenosphere, frictionally heated shear flows stability 79—44164
Earth interior, shear heating as explanation for lithosphere-mantle decoupling 79—20790
Earth mantle, non-Newtonian corner flows press. rel. to plate subduction angle 79—39695
edgetone and instability of free shear layer 78—94672
EHD with asymmetric stress tensor fluid 80—19520
elastic polymer solution, shear flow, rel. to rheologic theory 77—55051
elastohydrodynamic oil film, shear behaviour 77—68635
ellipsoid freely suspended, rotation about a slow viscous flow's vorticity axis 78—38386
entangled monodisperse polymers kinetic network model for nonlinear viscoelastic flow props. 80—28538
extruded polymer soln. through capillary, flow instability and electrostatic effects 79—60035
falling coaxial cylinder viscometer for wide range of shear rates 78—79393
falling film flow, spatially growing three dimens. wave, annular-froth flow transition 78—14071
ferromagnetic suspension, heat transfer for shear flow conditions 79—46394
ferrosuspensions, mag. field effects on mech. props. 78—87321
fibrinogen, liq. cryst., layer, shear orientation 77—27807
film, liq., flowing down inclined plane with heat transfer, interfacial shear, stability 79—37290
fine particles aggregation, mechanism and rate at uniform shear field 80—101046
flow fields in plate and cone viscometers with small gap angles 80—19516
fluctuating free convection flow on horizontally magnetised plate 80—33683
fluid fluctuations about hydrodynamic nonequilibrium steady states, Langevin method calcs. 80—53761
fluidised, open channel flow 80—14826
forced oscillations of separated shear layer, appl. to cavity flow-tone effects 80—64256
forming limit curve for bending processes 80—7627
free coating of viscoelastic and viscoplastic fluids onto vertical surface 78—42576
free conducting shear layers, stability in transverse mag. field *(German)* 77—15132
free round cold subsonic jet, noise from axisymmetric shear flow, numerical results 79—77206
free round cold subsonic jet, noise from axisymmetric shear flow, analytical results 79—77207
free shear, channel and turbulent flows, finite element anal. 79—68808
free shear flow, effects of stream turbulence 78—59378
free shear layer, compressibility effect on stability 80—33562
free shear layer in viscous critical layer regime, nonlinear stability 80—33576
free-forced convection from a heated cone, cross flow transition, similarity soln. 78—90892
fully developed turbulent pipe flow, low Mach number wall turbulence—sound interaction 80—6148
gas, nonlinear shear viscosity in steady Couette flow 80—28588
glass-fibre reinforced PET, order-disorder transitions during extrusion 80—50633
granular cohesionless material, gravity flow in chutes and channels 79—64753
granular material flow from parallel sided bins, thickness of shear zone 80—81279
gravity wave, internal, propag. in shear layer, discontinuity form. 79—32543
gravity waves, shape and breaking in stratified shear flow 78—34147
gravity waves on rot. fluid, numerical method 77—51071
hard-sphere fluid, shear viscosity, nonequilib. molecular dynamics calcs. 79—68996
heat conducting viscoelastic fluids, nonlinear temp. depend. 79—41675
heat or mass transfer rate from freely suspended particle 80—79313
heterogeneous, infinitesimal stability 78—30262
homogeneous rotating fluid, topography/shear flow interaction 79—55354
hot film in reversing shear flow, heat transfer 77—15014
hot-wire measurement errors in shear flows 77—55119
hurricanes, shearing environmental steering current rel. to spiral bands excitation 80—56538
hydromagnetic free shear layers in rotating flows 79—14493
hydromagnetic thermal shear flow stability 79—32690
impinging free shear layers, self sustained oscillations, book contrib., review 80—19466
incompressible Kramers problem, direct simulation 79—94666
incompressible two dimensional slow flow, finite deform of viscous ellipsoidal inhomogeneity 77—51013
instability, Howard's semi-circle reduction 78—90833
instability, vortex nutation, amplitude oscill. 78—51171
instability of compressible fluid layer 77—80177
integral constitutive eqn., critical tests 77—72338
shear flow continued
interface displacement for free shear layer 77—72271
internal gravity wave reflection from shear layer 77—42854
inviscid, rotating, compressible fluid, linear stability 80—92161
inviscid flow, 2-D, weakly sheared, past circular cylinder 80—74893
inviscid shear flow over flexible membranes, stability 80—14658
ionosphere turbulent polar cusp, Kelvin-Helmholtz instability in low-energy proton flow 78—96343
jet, axisymmetric free shear flow with Reynolds stress closure 80—19469
jet, circ., free shear layer transition wave development 78—94643
jet, horizontal five-layer, instability 78—79348
jet exhaust noise, shear layer instability effect 78—94791
Jupiter, Great Red Spot, atmosphere baroclinic model, solitary waves on unsymmetric shear flow 80—82266
kaolin, aq. suspension, flocculated and dispersed, rheological behaviour in pipe flow 79—37361
Kelvin-Helmholtz instability waves and breaking gravity-waves 79—81847
Kelvin-Helmholtz-like instability of a shear layer subject to free boundary conditions 79—68726
laminar flow over shallow cavities, oscills. 77—89091
laminar shear layer on oscill. plate 79—32454
laminar to turbulent boundary layer shear flow, three-dimens., stability eqns. 78—38284
laminar water boundary layer on heated cones, variable viscosity effect, heat transfer, shear stress 79—32520
leading edge signal on flat plate in uniform shear 78—30259
Lennard-Jones fluid, nonlinear viscous flow 80—24060
lifting surface, varying thickness shear layer, soln. using kernel function 77—89137
linear, characterisation of acoustic disturbances 80—69848
linear flow past porous particle 77—15094
liquid crystal, reentrant nematic, oriented, capillary shear flow 80—49344
liquid crystal shear flow instability, model eqns. 79—41664
liquid thin film, evaporation and breakdown driven by shear stresses 80—38410
lorenz attractor behaviour in a continuously stratified baroclinic fluid 80—83806
macromolecules, coiled linear, effective diffusion tensor of chain mol. in shear flow 77—50579
magnetic-velocity shear, hydromag.-intertial-gravity waves propag. 79—55422
magnetic-velocity shears, linear wave motions 77—58799
magnetorheological systems, heat transfer 79—81988
maltrose syrup, separation of elastic and shear thinning effects in capillary rheometer 78—42691
MBBA, homeotropic nematic layer, torsional shear flow in normal elec. field 79—82155
MBBA, with chiral impurities, cholesteric struct. shear flow normal to helical axis 79—86689
MBBA/CC mixtures, cholesteric phase, torsional shear flow in elec. and mag. fields 79—86697
MHD boundary layer flow on flat plate, effect of transpiration 77—24028
MHD film flow, porous-walled squeeze film, slip effect in transverse field 79—77262
MHD shear flow, energy transfer from turbulent to mean motion 77—35252
MHD shear flow stability 78—51244
MHD shear invisual flow, vortex sheet stability 80—28571
MHD-gravity waves, over-reflection in stratified flow 77—11207
near wall vel. meas. for wall shear inference in turbulent flow 78—34234
near-field jet entrainment, overlaid viscous/inviscid model, BOAT computational model 80—19457
nematic film, phase grating produced by shear flow induced instability 78—9945
nematic liq. cryst., nonlinearities and fluctuations at hydrodynamic instability threshold 78—87614
nematic liquid, oscillatory convective instability *(French)* 79—1279
nematic liquid crystal, viscometric flow, apparent viscosity 79—60265
nematic liquid crystals, apparent viscosity during simple shear flow 77—72549
nematic liquid crystals, continuum theory 77—68920
nematic liquid crystals, effect of mag. fields and boundary conditions, PAA example 77—7668
nematic liquid crystals, homogeneous instabilities 78—63674
nematic liquid crystals, MHD instabilities 77—27828
nematic liquid crystals, shear flow in presence of electric AC field, elastic and viscous const. determ. 77—43144
nematic liquid crystals, shearing flow solns., stability and dissipation 80—49288
nematic liquid crystals, sinusoidal shearing and temporal sinusoidal standing twist wave 80—84053
nematic liquid crystals, viscosity, rel. to order parameter *(Russian)* 78—91242
Newtonian calibrating oil, stress transient data obtained from cone and plate flow 77—31407
non-axisymmetric small particles, rot. in simple shear flow 79—68722
non-linear model, constitutive equation testing with free. vol. relax. spectrum 80—6011
non-Newtonian effect and long-range correlation 79—46349
non-Newtonian effect near crit. point 78—22377
non-Newtonian fluid, quadratic shear flow, rigid sphere and drop migration 77—84309
non-Newtonian fluid, rot. liq. film, free surface instability 79—37294
non-Newtonian fluid film flow along vertical oscillating plate *(German)* 78—59431
non-Newtonian fluids oscillating pipe flow, shear dependent viscosity effects 79—77190
non-Newtonian liqs., origin of hole press. in slit die apparatus 78—63462
non-Newtonian liquid, isothermal Couette flow in slowly converging channel with complex shear 77—15069
non-Newtonian liquid with power-law behaviour, flat submerged jet theory 80—59078
non-Newtonian nonisothermal flow, in slowly converging channel 77—89168
non-Newtonian shear flow, eqns. of state 79—23344
non-Newtonian sheared coagulated sols, energy dissipation during sheared flow 78—63461

shear flow continued
non-stationary capillary-gravity waves in a shear flow *(Russian)* 79−34849
nonlinear split-disc problem for free shear layers in rot. fluid 77−42851
nonlinear viscoelastic fluid, steady shearing flow instability 79−32461
nonlinear viscous flow, in two and three dimens., kinetic theory 78−71372
nonlinear viscous flow in 2-D and 3-D, kinetic theory 79−50694
nonNewtonian flow model, for anisotropic viscosity tensor 78−90938
nonNewtonian fluid, shear rate calc. in coaxial viscometer, method comparison 79−4048
nonsteady plane stagnation point flow with hard blowing 80−33579
normal stress difference, estimation from shear stress data in polymer rheology 79−64506
nozzle boundary layer, hypersonic, static press. variation and Reynolds stress 77−84294
nylon 6.6 in 100% H_2SO_4, primary normal-stress difference coeff., dependence on molecular wt. 80−87752
ocean, abyssal shear zone obs. 78−73386
ocean, rel. shear microstructure and energy dissipation meas. adjacent to island 78−85573
ocean, stationary surface and internal waves generated in flow with vel. shear *(Russian)* 78−77252
ocean, vel. fluctuations scaling in surface mixed layer 77−45009
ocean internal short-period waves generation by shear flow instability 79−2273
optical fibre coating with conical shape applicator 80−58820
Orr-Sommerfeld eqn., continuous spectrum and eigenfunctions 78−67176
Orr-Sommerfeld problem, approx. to eigenvalue reln. 79−3995
parabolic, forces on neutrally buoyant disc, creeping flow approx. 80−92105
parallel or swirling stratified shear flow, internal gravity and axisymmetric waves 79−86446
particulate beds, sheared, mass transport kinetics, Markov chains appl. 79−60057
pathological synovial fluids, viscoelastic props. at different shear rates 79−32430
pentyl-cyano-biphenyl, nematic, hydrodynamic parameters meas. with and without applied elec. field 80−100297
perfect fluids expanding with both vorticity and shear, cosmological appl. 79−48669
phase interfaces, balance eqns. and struct. models 78−59453
pigment dispersion rheology, kinetic model, expt. results 79−7361
pipe flow, turbulence props. in core 77−68576
plane Couette flow, finite amplitude, instability shear layer parallel flow, cellular motion 80−1601
plane parallel flow, free convection in Couette and Poiseuille flows, numerical simulation 80−99995
plane shear flow, exterior Dirichlet problem for quasilinear elliptic boundary value problem 78−22317
plane shear waves in viscoelastic fluids as motions with proportional stretch history 79−64613
plasma shear flow, electrostatic instability theory and appl. to magnetopause and solar wind 80−96359
plate, with suction, three-dimens. fluctuating flow, heat transfer, skin friction 78−87389
plate, with temp. and vel. profile nonuniformities, laminar flow and heat transfer 77−75913
pneumatic transmission line transient response anal. by characteristic curve method 79−77244
Poiseuille channel flow, finite amplitude, instability shear layer parallel flow, cellular motion 80−1601
polyacrylamide, very dil. drag reducing soln., nonlinear viscoelastic props. 79−7355
polyacrylamide Separan MG200, aq. soln., rheological props. 80−64507
polyacrylamides-water-glycerol, streaming birefringence in extensional flow 80−6013
polybutadiene, high cis-1,4, orientation effects induced by shear rate in capillary rheometer 77−51014
polybutadiene soln., rheological behaviour of flow patterns around agitators 77−31269
polyethylene, high-density, polymer melt, shear stress at wall 80−19450
polyethylene, low density melts, temp. depend. of the elongational behaviour 80−6012
polyethylene, low- and high-density, melt, extensional flow 77−72259
polyethylene melt, nonlinear shear behaviour, strain-dependent memory function 78−67161
polyethylene melt, rheology in shearing and extensional flow 77−72256
polyethylene melts, low-density, viscosity and viscoelasticity, filler effect 80−10222
polyethylene oxide, aq. soln., mech. props. in parallel superposed flows, geometric effects 80−19448
polyethylene oxide, aq. soln., nonlinear dynamic viscoelasticity 79−94576
polyethylene oxide melts, viscoelasticity meas. 78−87324
polyisobutylene soln., start-up tests, relaxation meas. of shear and normal stress *(German)* 78−67166
polyisobutylenes, shear behaviour of Vistanex LMMH and L 100 80−1443
polymer, filled, solution, normal stresses and hyperelasticity under simple shear flow 80−1506
polymer crystallisation from solns. and melts, deform. effects 80−10504
polymer flow, birefringence meas. of normal and tangential stresses 77−58625
polymer melt, birefringence build up and relax., Lodge's rubberlike liquid model 77−54946
polymer melt, shear stress over wide shear rate range, in falling coaxial cylinder, rheometer 79−7363
polymer melt, viscoelastic, 2-dimens. nonisothermal processing between calender rolls, mathematical model 79−68670
polymer melt containing suspension, cell model theory of shear viscosity 80−103048
polymer melt flowing through duct, heat transfer 80−103049
polymer melt in intermittent shear flow, transient birefringence 78−63457
polymer melts, annular flow, secondary normal stress difference 80−106816
polymer melts, flow indices *(Japanese)* 80−79360
polymer melts, isothermal and non-isothermal stress relaxation following steady state shear flow *(German)* 79−77044
polymer melts, normal stresa and Barus effect 80−64589
shear flow continued
polymer melts, shear flow, network theory in nonlinear region *(German)* 79−77050
polymer melts and solutions, rheological equations, review 79−86391
polymer solns., constitutive relns. determ. using stiffened Weisenberg rheogoniometer for uniaxial shear flow 77−80188
polymer solns., dilute, Hartree self-consistent field analysis 80−5648
polymer solns., shear and normal stress behaviour in steady shear flow *(German)* 78−67165
polymer solution, conc., constitutive eqn. applic. to shear and elongational flow 79−90292
polymer solution, conc., rheological props. rod-like mol. model 78−75114
polymer solution, dilute, aq., appl. of Hildebrand's fluidity model, apparent viscosity temp. depend. *(German)* 79−37366
polymer solution, nonlinear response to uniaxial shear flow histories 80−59084
polymer solution elongational flow, wet spinning process for fibres 78−72760
polymer solution rheology based on a finitely extensible bead-spring chain model 80−83775
polymer solutions, aqueous, diffusion and mass transfer from rotating disc 80−83827
polymer solutions, dil., dynamics, model 79−73086
polymer solutions, dilute, normal stress difference and shear rate 80−83776
polymer solutions, flow behaviour in porous media *(German)* 78−55666
polymer solutions, liquid cryst., rheo-optics of shear and elongational flow, quiescent and flow birefringent characts. 80−83773
polymer solutions, plane polygonal, normal stress under oscill. shear flow 78−34420
polymer solutions, single-relaxation-time constitutive model 77−11156
polymer solutions and melts, flow under const. and periodic deform. 78−47004
polymer spheres, colloidal suspension, steady state shear flow coupled to conc. fluctuations 80−61170
polymeric, liq., spike-strain test relevance for network connectivity destruction by deformation 80−6001
polymeric liquid, steady shear flow, parallel superposition of oscillatory motion 79−18919
polymers, conc. solns. in volatile solvents, high temps., method for viscosity meas. 80−19535
polymers, flexible, solns., shear flow, dielec. anisotropy, appls. 79−15393
polymers, unsteady flow in rotary devices 80−24061
polymers solutions, zero-shear viscosity estimates from falling sphere data 80−19306
Polyox, drag reduction meas. in square duct, anomalous effects due to polymer degradation 80−83824
polypropylene, melt, extensional flow 77−72259
polypropylene-polyethylene blends, capillary flow, rheology and morphology 80−59088
polypropylene-polyethylene blends, flow behaviour in capillaries 80−59087
polystyrene, 7% in tricresyl phosphate and Arochlor, stress transient data obtained by cone and plate flow 77−31407
polystyrene, melt, extensional flow 77−72259
polystyrene, solns., nonlinear viscoelasticity, stress development at start of shear flow 77−3800
polystyrene melts, low mol. mass, dynamic viscoelastic behaviour, alternating shear expts. 77−62226
polystyrene monomer, high purity, soln., rheological behaviour of flow patterns around agitators 77−31269
polystyrene soln., rheological behaviour of flow patterns around agitators 77−31269
polystyrene solns., correlations of network model parameters 80−106772
polystyrene solution, constitutive models, exptl. tests based on birefringence data 80−100015
polystyrene solution, internal viscosity, model for Lamb-Matheson-Philippoff increment 77−62284
polystyrene-Aroclor 1254, streaming birefringence in extensional flow 80−6013
polystyrene-decalin solns., flow irregularity obs. in theta conditions 80−38453
polystyrene-mineral oil mixture, viscosity and normal stress coeff. 80−44349
polysytrene melts, stresses and birefringence in intermittent shear flows 80−19308
polythene melts of high density, viscosity meas., entropy and compressibility *(German)* 78−67162
power law liquid, flow between eccentric rotating cylinders 77−65766
power-law liquid, dil. suspensions of dipole dumbbells, rheological eqns. of state and shear flow in elec. field 79−86473
power-law liquid, shear flow, general soln. for mag. rheology *(Russian)* 78−47003
PPT in 100% H_2SO_4, primary normal-stress difference coeff., dependence on molecular wt. 80−87752
primary normal stress function from shear viscosity data 77−68548
protein solution, propagation of surface shear waves 79−77146
pulsatile laminar flow, velocity meas. for flow in 90° branch, appl. to atherogenesis 78−38277
pump with fixed and moving wall, steady shear flow *(German)* 78−87367
PVC cpds., rigid, plasticised, capillary flow 79−4046
PVC plastisol, flow behaviour at high shear rate *(German)* 80−92186
PVC plastisol, steady shear rheological behaviour 79−37274
PVC plastisols, high resin level, rheological behaviour, discontinuous viscosity 80−23980
radio double sources (astronomical), beam and cloud stability, shear layers, two dimens. computations 80−67893
Rayleigh stability in relaxing media 77−80141
rectangular duct, acoustic wave propag. in shear flow with temp. gradient, investigation using finite-element analysis 79−94379
Reynolds equation at very low spacing, compressible, numerical soln., factored implicit scheme, mag. recording appl. 80−92183
Reynolds stress transport eqns. 80−19320
rivers, stable numerical model of local scour 77−21809
Rossby wave critical layer, evolution 78−79329
Rossby wave forced on uniform shear, critical layer evolution 78−42622
rotating Boussinesq viscous fluid, inertial instability, appl. to atm. 80−90131
rotating disc, spin up, fluid motion, analytical-numerical anal., shear wave trains 77−15040

shear flow continued
rotating disc with axisymmetric surface heat source distrib., in laminar flow, heat transfer 79−46314
rotating stratified fluid, parallel shear flow, baroclinic and baratropic instability 80−98328
rotation effects on flow past porous plate 80−10256
rotational rheometry, edge effects and related error sources 80−19536
rubber and crumb mixtures from scrap pneumatic tyres, rheological behaviour 78−55619
rubber toughened plastics, ABS- and AAS-resin, flow props., effect of heating and shearing hysteresis *(Japanese)* 79−94685
second moment turbulence closure to heat and mass transport in two-dimens. thin shear flow 80−24010
second-order fluid, migration of spheres in two-dimens. unidirectional shear flow 77−940
secondary flow effects on decaying torsional oscills. of sphere and plane 77−3808
Separan, 1.5% in 50/50 glycerine water, stress transient data obtained by cone and plate flow 77−31407
separated supersonic boundary layer, moderate injection with reattachment, shear layer 79−32562
separation in flow past cylinder and plane 77−68567
separation of slow linear flow from cylindrical ridge or trough in plane 77−72290
shear layer, impingement upon corner or cavity edge, organised nature 79−81840
shear stress determination, in laminar and Taylor vortex flows using flush-mounted hot film probe 80−28486
shock wave structure close to wall, book contrib. 80−1650
silicon oil, separation of elastic and shear thining effects in capillary rheometer 78−42691
silicone oils, props. determ. by harmonical shear vibr. *(German)* 78−67164
simple fluid shear depend. viscosity, central force interactions 80−79970
simple shear flow of dilute fluid suspension, orthokinetic collisions of hard spheres 77−35199
small inviscid disturbance, evolution to marginally unstable stratified shear flow 78−83453
small sphere in slow viscous flow, shear and rot. flow, forces calc. 79−37282
smectic liquid crystal, flow inducing layer ordering, hydrodynamic theory 79−77731
soluble matter initial dispersion in three-dimensional flow 79−37387
sound attenuation in low Mach no. nozzle flow 79−50721
spheres, porous, in a linear flow field, motion and rupture 79−64755
spherical cap, free translation and rot. in linear shear flow, Stokes resistance 78−26095
spherical Couette flows, loss of stability between two rotating spheres 80−1527
spherical particle, lateral migration in 2-dimens. shear flow 77−15100
spheroids in shear flow, light scatt., orientation correlation 78−76481
stability, modified Tietjens function for asymptotic anal. 77−65733
stability, weakly nonlinear, of free shear layer 77−35118
stability and mixing of non-parallel shear flow 79−10547
stability investigation and secondary flows in rotating spherical layers at arbitrary Rossby numbers 79−18899
stability of aligned, stratified, compressible magnetoatmospheric shear flow 78−26197
stability of thermal flows 78−34110
stably stratified shear flow in channel, internal gravity wave packet mean flow 79−98740
stagnation points on cycloidal boundary in flow with const. shear 80−87755
steady flow in tubes of slowly varying cross section 79−32680
steady rotating flow over topography, steady β-plane channel, quasi-linear theory 80−92159
steam-water, flow characts. at high press. 78−94805
Stokes flow, attached and free eddies 80−48679
Stokes flow, separation, appl. of bipolar coordinates to two-dimensional creeping motion of liquid 79−14375
Stokes flow past slender body of revolution 77−14986
stratified, Stewartson vertical layers 80−48772
stratified, wave breakdown 77−31358
stratified compressible atmosphere with shear MHD wave-energy flux 78−93053
stratified currents with vel. shear, influence on forced wave motion *(Russian)* 78−77255
stratified flow, stress-driven entrainment expts. scaling 79−50768
stratified flow, weakly nonlinear stability theory 78−18331
stratified flow past three-dimens. obstacles 78−71383
stratified fluid, shear-induced instabilities, modal struct. 77−68662
stratified fluid confined between horizontal planes, flow due to object motion 77−51097
stratified fluid in sheared motion, over-reflection instabilities 79−60048
stratified fluid with shear, instability and turbulence 79−77216
stratified shear flows, internal solitary waves 80−69856
streaklines in a shear layer perturbed by two waves 80−59055
streamline patterns and eddies in low-Reynolds-number flow 80−33612
streamlines around single spheres and trajectories of pairs of spheres in two-dimens. creeping flows 78−22316
stress near rigid boundaries 77−80200
strip in shear flow, heat and mass transfer 78−51163
styrene-butadiene copolymer, soln., rheological behaviour of flow patterns around agitators 77−31269
styrene-butadiene-styrene block copolymer, stress relax. following steady-state flow, residual shear stress development 80−83772
styrene/acrylic terpolymers, viscoelastic props. 80−64509
supersonic thin turbulent layer, hot-wire anemometry, error reduction 78−34235
suspension, Brownian rotational-translational particles, at finite conc., dynamics and hydrodynamics 79−7401
suspension, conc., of aggregable particles, viscosity calc. 79−7362
suspension, effective thermal conductivity 77−7436
suspension, memory impairment, Brownian rotation of spheroids 80−79386
suspension, memory impairment, expt. 79−41736
suspension, nonuniform shear effects 79−96372
suspension, particles self-diffusion in shear flow 77−24015
suspension, rigid ellipsoids, rheological props., specific viscosity in shear flow *(Russian)* 78−75187
suspension of prolate spheroids in shear flow, bulk heat flux 79−46370
shear flow continued
suspension of rods in silicone oil, interactions between rods in shear flow 77−55075
symmetrical wake calc., two-dimens. laminar and turbulent flows 80−14707
Taylor column, vortex shedding 79−14407
Taylor column for hemisphere, nonlinear effects 77−11199
temperature boundary layer on rotating curved surface, constant wall temp. case 79−81903
temperature gradient effects on sound propag., thin shear layer expansion 77−14826
thermally driven shear flow heated from below, stability 78−67177
thermosphere, lower, thin shear turbulent layers induced by tides and gravity waves non-linear interaction 78−65444
thin film shear-stress gauge for three dimensional flow 78−55702
thixotropic fluid, shear flow, oscillatory Couette flow, apparent viscoelasticity 79−90288
thixotropic fluid, shear flow *(Russian)* 78−87365
thixotropic materials, characterisation via extrusion rheometer 77−63876
three dimensional laminar flow in curved pipes, Navier-Stokes eqn. numerical soln. technique 79−10611
three dimensional parallel shear flows, stability and transition for rot. disc 80−74887
three dimensional turbulent boundary layers, turbulence meas. c.f. shear stress hypothesis *(German)* 78−94664
Tolmin-Schlichting waves, nonlinear interaction in shear flow *(Russian)* 77−58708
transendothelial albumin transport in steady state pipe flow at high shear rates 77−32939
transient flow problems, Lagrangian soln. using triangular mesh 79−64678
transient free convection from an isothermal horizontal circular cylinder *(German)* 79−77115
transient viscosity determination method 80−43746
turbine impeller stream flow, turbulence props. in core 77−68576
turbomachine annuli with swirl, small shear disturbance propag. 77−84258
turbulence, grid generated, plane strain appl., Reynolds stress tensor in shear flow 79−81858
turbulent boundary layers, streamline curvature effects, anal. 78−59382
turbulent diffusion, stochastic model 79−18880
turbulent plane mixing layers, growth rate, structure measurements 79−50716
two dimensional steady flow problems, numerical soln., finite element method 79−23296
two layer shear flow, radiation field and baroclinic eddy development in β-plane 79−81897
two layer system with baroclinic mean shear flow, solitary Rossby waves theory 80−17293
two-dimensional shear flow, viscosity effects, microscopic model 77−89085
two-dimensional shear layer, instability wave excitation by sound 79−32541
two-dimensional soft-disc systems, nonlinear viscous flow 80−92102
uniform shear flow past a cylinder of section bounded by two circular arcs 78−94658
universe expansion, primordial shearing vel. fields vel. to cosmological element form. inhomogeneity 79−21471
unstable flow past cavities, shear layer oscill. freqs. 77−84228
unsteady motion on transversely sheared mean flows, scatt. and distortion 79−59997
unsteady transversely sheared mean flow characts., gusts 78−26142
viscoelastic droplet break-up, in nonuniform shear flow 80−64588
viscoelastic fluid, circular and elliptic polarised shear waves 79−60024
viscoelastic fluid, homogeneous shear flow, rigid particle slow motion 77−84308
viscoelastic fluid, nonlinear stress relax. after steady shear flow 77−51015
viscoelastic fluid, stability of steady shearing flows, energy method and parabolic maximum principle 80−74926
viscoelastic fluid flow between parallel plates, inertia elasticity and shear thinning props. *(German)* 78−55665
viscoelastic fluid theory, entropy effects 77−14971
viscoelastic fluids, Weissenberg rheogoniometer, R-17, axial compliance reduction 80−106859
viscoelastic incompressible fluid, accel. influence on shear initiation 77−54943
viscoelastic materials, time-depend. non-linear stresses, constitutive eqn. 77−35178
viscoelastic materials, time-depend. nonlinear stresses, memory function nonlinearity 77−35180
viscoelastic materials, time-depend. nonlinear stresses, shear and uniaxial elongation 77−35179
viscoelastic properties, direct meas. method using channel flow 79−37265
viscoelastic solutions, first and second normal stress differences in steady laminar shearing flows 79−46348
viscometric data from Brookfield RVT viscometer, conversion to shear stress-shear rate relationship 80−1495
viscometric flows and corotational stress relations 79−90212
viscous electrically cond. fluid, laminar free shear flow, transverse mag. field effect 80−48811
viscous fluid in rotating channel pulsatile flow 80−10311
viscous fluid under cyclic deform., self-heating, hydrodynamic thermal explosion 80−58993
viscous stratified shear flow, stability eqns., completeness obs. 80−64519
vortex ring evolution in stratified and shearing environment 78−30303
vortex shedding from inclined flat plate in shear flow, simulation 77−80170
vortex shedding from inclined flat plate in uniform flow 77−80169
vortex sheet, Helmholtz instability in uniform shear flow 79−37328
vortex streets from bluff bodies in flow, model 79−59987
vortex stretching, due to shear layer instability 77−65776
vortex-edge interaction, low frequency component generation mechanisms 80−53795
wall shear stress meas. in shock wave-boundary layer interaction, comments 80−14670
water, surface gravity water propag., wave action and set-down on shear current 78−90920
wave evolution, nonlinear, in free shear layers, effects of critical layer structure 80−83809

shear flow continued
wavelets, initial generation by coupled shear flow instability wind wave evolution 79−94635
Weissenberg effect, higher order theory 79−68766
Weissenberg rheogoniometer, computerised calib. and meas. of Newtonian fluids 78−87323
wind, strong shear obs. using pulse compression radar 78−32193
wind tunnel, for industrial aerodynamics, atm. shear flow simulation 77−55110
wind tunnel production using curved wire gauze screen 77−3805
Al, numerical smoothing of flow patterns 80−7625
Al plastic flow in plain strain extrusion, photographic appl. 80−7626
Fe_2O_3, flocculated suspension in ethylene glycol, intrinsic viscosity rel. to shear rate 80−1502
He, liq., surface, macroscopic electron lattice formation 79−77861
NaBr in hexantriol-1.2.6, structural relaxation shear and compressional viscous processes, electrolyte effects 79−94686
NaBr in hexantriol-1.2.6, shear relaxation 79−94687
$PbCrO_4$, paste, anomalous viscous flow 79−64617

shear modulus
A15 compounds, elec. struct., 3-D k.p model 78−2405
abietic acid, transverse US wave propag., glass and liquid transition region 80−79883
acrylic bone cement containing second phase dispersions, strength 77−81663
acrylic bone cement-stainless steel interface, shear strength 77−86706
adatoms, elastic interaction between, near distortive phase transition 80−80080
alkali halide crystal, vol. damage anisotropy under laser irrad. 77−89469
alkali halides, shear moduli near melting point rel. to cooperativity in dislocation theory 78−59934
alloy, overaged and dispersion hardened, dislocation bowing computed from Orowan relations 77−19949
anisotropic cantilever plate with variable rigidity, stress and deflection anal. 79−59927
aramid fibre reinforced epoxy resin, shear props. 77−81354
arch, cylindrical, heat resistant material, exam. of thermoelastic stress problem 78−63306
articular cartilage of normal rabbit, viscoelastic shear behaviour 77−36973
bar, rectangular, torsion crack problem, harmonic function continuation technique soln. 80−99969
beam subjected to gravity loading, Timoshenko shear coeff. 80−79159
biomembrane material, increase in rigidity during morphogenesis 80−94249
bitumous mixes, complex modulus calc. *(French)* 79−20092
bone, elastic props. of cortical bone of female human femurs, noninvasive meas. 77−21552
β-brass (40 to 50 at.% Zn), elastic shear consts., comp. depend., pseudo-pot. calc. *(Russian)* 80−24525
bulk material in centrifugal installations, capacitive transducer for rigidity determ. 78−19977
butyloxybenzylidene octylaniline, liq. cryst. film, smectic B-A transition, mech. meas. 80−79918
cap, cracked, transverse shear and material orthotropy effects 80−10144
carotid artery, human, shear modulus determ. 80−26253
cellulose film, meas. of shear modulus and damping in a torsion pendulum 79−4989
chain networks, static and dynamic entanglements, contrib. to equilib. shear modulus 80−28126
chitin (poly-N-acetyl-D-glucosamine), dynamic mech. behaviour, effect of water 80−97522
chitosan (poly-D-glucosamine), dynamic mech. behaviour, effect of water 80−97522
clay soft, increase in shear strength and rigidity due to Fe^{3+} addition *(Japanese)* 78−31463
composite, elastic props. meas., reliability establishment 77−52574
composite at uniform thickness, analysis of determ. methods 77−63873
composite elastic medium, effective bulk and shear moduli 80−99927
composite material models, three phase sphere and cylinder models soln. for effective shear props. 80−25749
composites, circular specimens, shear modulus determ. 80−25752
composites, fibre reinforced, fatigue damage under pulsating tensile stress 79−100237
composites, three-dimensional structure, mech. characts. 80−38266
concrete, porosity determ. from combined US and gamma absorption meas., mech. props. 79−29295
cord reinforced rubber laminate, interlaminar-shear-strain meas. 79−57043
crack development kinetics, with varied rigidity under low cycle loading 77−90464
crystalline material, melting criterion based on dilatation depend. of shear moduli 77−35673
cubic crystals, response to (111) loading, internal energy, elastic moduli 80−84230
cubic crystals at arbitrary pressure, shear moduli and relative elasticity 79−42132
cubic metal, temp. depend., Morse pot. calc. 78−10118
curved structural members, large displacement theory, applic. to lateral-torsional buckling anal. of circular arches 80−23924
cylindrical shell, circumferentially cracked, transverse shear effect 80−28472
cylindrical specimens, measurement of dynamic shear modulus using closed-loop vibration system with PLL 79−61827
cylindrical tubes, compressible, wire-layer reinforced, inflation and extension 79−3922
diamond, compressive strength for [111] loading 79−79036
diethylamine melanin, sound wave anomalous absorption and dispersion 79−77688
Earth, dynamic shear modulus and corrections to oscills. eigenfreqs. 77−81800
elastic constants determ. by resonant vibr. in thin disk, apparatus 77−56182
elastic deformation, thermodynamics of, eqn. of state for solids 80−96589
elastic-viscoplastic materials delayed behaviour of double shear perturbations 78−45483
elastohydrodynamic contact, rheological model 80−33544
elastohydrodynamic traction, granular behaviour 80−103008

shear modulus continued
elastohydrodynamic traction, non-Newtonian thermo-viscoelastic, from combined slip and spin 80−103043
elastomeric network, finite linear viscoelastic theory, time-depend. deform. behaviour 80−38292
electrolyte solutions, fluctuations rel. to shear modulus dispersion 77−15497
electron solid, two-dimens., shear modulus and melting, temp. depends. 80−158
Epon 828-Z, acoustical determ. of shear relax. functions 78−76686
epoxide resin cured with aliphatic dicarboxylic acids, fatigue behaviour *(Japanese)* 79−79092
epoxy resin, exam. of shear stress-strain characts. 78−60691
epoxy resin with various fillers, filler effect on relaxation time spectra 77−52390
ferromagnets, easy plane, containing dislocations, static props. 79−95626
fibre reinforced composite failure analysis by acoustic emission 78−80691
fibre reinforced composites, weakened by periodic system of cracks, longitudinal shear 80−35323
fibreglass, mechanoluminescence during monoaxial stretching 78−68742
filled polymer, elastic moduli, effect of particle shape 78−15444
filled polymer, mathematical model of strengthening *(German)* 78−63279
filled polymers, dynamic shear modulus and acoustic velocity, filler content depend. 80−60900
first normal stress difference prediction and dynamic moduli from steady flow viscosity 77−75868
gelatin gels, coloured component addition, struct. form., dynamic shear modulus, viscosity meas. *(Russian)* 80−7871
glass, C and glass/C hybrid reinforced plastics, fatigue props. and flexural rigidity *(Japanese)* 80−55510
glass, laser, elastic, elasto-optic consts. and extinction coeffs., Brillouin scatt. meas. 79−11429
glass bead-reinforced epoxy resin composite, bulk and shear elastic props. 78−6959
glass beam, rectangular, flexurally vibrating, Timoshenko's shear coeff. 78−83866
glass fibre reinforced composite, random short fibres, elastic props. 77−70090
glass fibre reinforced composite, shear fatigue 78−15493
glass fibre reinforced epoxy, as electrical insulation for Tokamak toroidal field coils, mech. props. 78−64610
glass fibre reinforced epoxy-phenolic, cyclically deformed under shear, energy dissipation, static tensile-compressive stress effect 80−104225
glass fibre reinforced plastic, dynamic stress conc. around defects, discrete model 80−30024
glass fibre reinforced plastics, ageing by boiling in water, effect on physicomech. props. 80−60892
glass fibre reinforced polyester resin laminate cantilever, bending fatigue strength, cyclic freq. effect *(Japanese)* 80−55507
glass reinforced plastic, thermal activity, prediction of struct. charact. and physicomech. props. 77−63872
glass with frozen structure, viscous flow, valence configuration flow theory 80−39335
glass-plastic, unidirectional, torsion strength and shear modulus 80−99948
graphite, irradiated, stored at room temp., neutron damage annealing and C_{44} shear modulus 80−2080
graphite, new force const. model 77−72643
graphite, pyrolytic, elastic and inelastic scatt. of Mossbauer γ quanta *(Russian)* 79−61287
graphite reinforced epoxy angle ply laminates, statistical fatigue in shear 79−11690
graphites, pyrolytic, compressed, annealed, low temp. electron irrad., elastic const. meas. *(French)* 78−43050
hard-disc solid, free vol. props. 79−46534
hexagonal crystal, anisotropic behaviour of Poisson's ratio, Young's modulus, shear modulus 77−11622
Hypalon 40, chlorosulphonated polyethylene, mech. props., press. effects 77−32618
internal fixation plate, effect on long bone remodelling 77−48935
internal fixation plates, evaluation of 1-, 2- and 3-dimens. finite element and exptl. models 77−48934
ionic solids, anal. of press. derivatives of shear moduli 78−18698
isotropic circular cylinder, periodic shearing stress, torsional vibration 78−75087
Kevlar 49 fibre reinforced composite, shear fatigue 78−15493
Kroner limits of technically important materials, low order limit comparison *(German)* 79−33029
lamellar liquid cryst. phases, form. at liquid-liquid interface, rheological props. 79−99063
laminate, deform. charact., pliability and rigidity 78−23798
laminated anisotropic shells, nonlinear eqns. of Timoshenko-type theory 80−69669
latex, monodisperse, mechanical props. 78−48701
liquids, complex shear modulus meas. by Ni-tube resonator in kHz range 80−17936
liquids, relation between viscoelasticity and shear-thinning behaviour 80−19307
low frequency shear modulus meas. during tension creep *(French)* 78−23913
lung, shear modulus and pleural membrane tension, improved meas. 80−30746
magnetostrictive core dimens., influence on internal friction and shear modulus 'defect' 78−95506
matrix analysis of composed bar of open cross section 80−83736
MBBA, shear modulus and viscosity relax. near isotropic-nematic phase transition *(Russian)* 77−39543
measurement by fully automated torsional pendulum, in range −180 to 250°C *(German)* 80−17935
metal, FCC, ratio of shear and Young's moduli 77−25088
metal, thermodynamic properties, outer electron contributions *(French)* 78−43091
metallic glasses, structures based on disclination-dislocation model 79−82159
metals, constitutive model at high strain-rate, shear modulus, yield strength 80−75292
metals, polycryst., relations between shear modulus, bulk modulus and Young's modulus 80−97540

shear modulus continued
metals, radiation effects on elasticity and elastic moduli, yield stress 80−2078
metals, simple, interion interaction and interion force constants, effective pots. in nonlocal pseudopot. method *(Russian)* 78−22684
mixtures and suspensions, flow rate meas., ultrasound propagation and scatt. approach 80−43806
multilayer cylindrical shell, theory in inhomogeneous temp. field 80−1434
Neoprene WB, polychloroprene rubber, mech. props., press. effects 77−32618
nylons, exam. of frictional behaviour *(Japanese)* 78−64714
nylons, glass transition temp., thermal, mech. meas. 77−31758
orthotropic laminates, torsion strength and shear modulus determ. 80−92587
phenolformaldehyde resin moulding compounds, dynamic testing *(German)* 78−76699
phenolic resin filled and unfilled, mech. relaxation behaviour, effects of temp. and time *(German)* 78−6963
phosphor bronze, beam, cylindrical, flexurally vibrating, Timoshenko's shear coeff. 78−83866
photoemulsions, gels, coloured component addition, struct. form., dynamic shear modulus, viscosity meas. *(Russian)* 80−7871
phthalocyanine polymer, dynamic mech. props. and fracture energy 80−100866
plasma coatings, elastic properties, acoustic meas. *(Russian)* 80−97519
plastic, glass-reinforced bottoms with a filler, rigidity 80−15183
plastic, with wide range of moisture content, mech. props. determ. with conic plastometer 78−11270
PMMA, acoustical determ. of shear relax. functions 78−76686
PMMA, nonlinear dynamic mech. moduli 78−60693
PMMA and PPMA, glassy state, cyclic loading effects on internal damping, shear modulus, heat capacity and density 77−43275
poly(di-n-heptyl itaconate), alkyl side chain independent relax., double glass transition 80−59636
poly-4-methylpentene-1, elastic parameters, US velocity meas. at 2.1-240K 80−40415
poly-n-benzamide, mols. in soln., dynamic birefringence and rigidity *(Russian)* 77−32349
polyacrylamide gel, audiofrequency very slow propagating mode 79−74429
polyamidoimide film, thermomech. props. rel. to mol. struct. *(Russian)* 79−57029
polycarbonate, nonlinear dynamic mech. moduli 78−60693
polycrystal, elastic deform., effect of Young's modulus, shear modulus, Poisson's ratio 77−24344
polycrystalline materials, effect of grain boundary sliding on anelasticity 80−96592
polyester resin, POLIMAL 190, influence of MgO, BeO and TiO_2 on dynamical mechanical props. *(Polish)* 79−96074
polyethylene, highly oriented, fibre composite model 78−3183
polyethylene, linear, γ-loss band, stress relax. 77−21201
polyethylene, low density, meas. of shear modulus and damping in a torsion pendulum 79−4989
polyethylene melt, nonlinear shear response during periodic deformation 79−100202
polyethylene oxide, dil. aqueous solns., dynamical shear characts. *(Russian)* 79−86393
polyisobutylene, Aerosil-filled, solution, periodic and unidirectional deform. effects 77−42791
polyisobutylene, low molecular weight, melt, nonlinear shear response during periodic deformation 79−100202
polyisobutylene melt, transient shear and elongational data 77−58631
polymer, foamed, rigidity 78−95769
polymer, glass transition due to plastic deform., high-molecular linear polymer of narrow molecular mass distrib. 79−96065
polymer, glassy, power law relationship between yield stress and shear modulus 78−15467
polymer, oriented, dynamic shear modulus determ. by acoustic method 78−23911
polymer, plasticizer effect on mech. props. *(German)* 80−92467
polymer materials, NDT, rigidity and hardness from acoustic, thermal, optical and dielectric props. *(Russian)* 77−48601
polymer network formation, pre-gel intramol. reaction and gelation, shear moduli and glass transition 80−45501
polymer network formation, relaxational props. variation 80−38961
polymer-metal laminate, bone fixation plate fabrication, flexural rigidity 79−79685
polymers, temp. depend. under dynamic conditions, linear theory of thermoviscoelasticity 79−61642
polymers solutions, zero-shear viscosity estimates from falling sphere data 80−19306
polymers with periodic deform., longitudinal flow 80−6008
polymethylsiloxane liquids, complex shear modulus determ. from shear wavelength meas. 79−14871
polyoxymethylene, effects of hydrostatic press. on shear deform. 78−15457
polyphenylquinoxaline cyclotriphosphazine hexaisothiocyanate networks, dynamic mech. props. *(Russian)* 78−72809
polypropylene, audio freq. shear and Young's modulus determ. from torsional vibr. of laminated bar 77−62218
polypropylene, effects of hydrostatic press. on shear deform. 78−15457
polystyrene, cyclically deformed under shear, energy dissipation, static tensile-compressive stress effect 80−104225
polystyrene, monodisperse latex, shear US meas. 78−31711
polystyrene, oriented high-molecular, physicocomech. props. *(Russian)* 79−33028
polystyrene latex, ordered monodisperse, lyotropic liq. cryst., mech. props. 79−98676
polytrivinyl benzene, thermal and mech. props. rel. to high-press. polymerisation conditions 79−70326
porous solid, shear stress enhancement of void compaction 79−69182
PVC, hard, flow zone effect on degradation, rigidity, deformation, under fatigue *(German)* 78−15471
PVC, sintered powder, elastic props. and porosity 77−63619
PVC, suspensions, melts, rheological props. rel. to struct. 79−3983
PVC, uniaxial tension, deep drawing, rigidity *(German)* 78−64556
rare earth Co Laves phase cmpds., elastic props. rel. to temp., mag. field 79−51834
relaxation time spectrum determ. from components on complex shear modulus, iterative method 77−50965
shear modulus continued
rigidity and indeformability, in spherical relativity *(Spanish)* 79−80429
rubber, natural, crosslinked by dicumyl peroxide, modulus, swelling relations 80−59551
rubber, rigidity and loss facter, meas. under steady vibr. 80−55602
rubber, Schallamach waves, rel. to friction of elastomers 79−29225
rubber elasticity, molecular aspects book contrib. 78−84886
rubber hydrochloride, meas. of shear modulus and damping in a torsion pendulum 79−4989
sand, dynamic properties w.r.t. seismic risk prediction, stress condition effect *(Japanese)* 80−17235
scragged torsion bar, residual shear stress meas. 79−59954
silicate glasses, elastic moduli calc. 78−60696
silicate glasses, industrial, elastic and shear moduli depend. on temp. 78−11254
smectic-A liquid crystal, layer rigidity, stress relax. 78−18545
sodium polystyrene sulphonate, solns., infinite dilution viscoelastic props. 79−14363
spinal cord, dog, in vivo dynamic material props. 77−40706
static, determ. method 78−7111
steel, 300 grade maraging low temp. elastic props. 78−27555
steel, austenitic, Mn-Cr-C(20, 4, 0.5 wt.%), intrinsic stacking fault energy, temperature variation 77−31679
steel, austenitic stainless, N-alloyed 80−108490
steel, Cr-Mn (13, 19 wt.%), elastic const. behaviour, anomalous, low temp. 80−97521
steel, elastic consts., meas. app. 77−33739
steel, elastic moduli, temp. depend. *(Japanese)* 77−59840
steel, low C, close coiled helical spring, corrosion under axial deflection and const. load 79−52428
steel, stainless, Cr-Ni-Mn, N strengthened, low-temp. elastic props. 79−70109
steel, stainless AISI 316, neutron irradiated, rel. between irradiation . induced swelling and shear modulus 80−15157
steel, stainless type 304, elastic const. variability, US vel. meas. 80−55446
4-sulphone diglycidyl ether, on Al alloy D16T alloy base, dynamic shear modulus determ., −80 to −180°C 78−60916
superconducting surface sheath, dynamic pinning model of elec. dissipation 77−28320
superconductor, type II, critical current density, depend. on past history of mag. field and temp. 78−6491
superplastically formed sandwich cores 79−32286
test machine rigidity, effect on superplasticity of Al-Zn eutectoid 79−70250
test machines, elastic yielding determ. 79−70251
tetragonal crystal, elastic moduli, anisotropic behaviour, cryst. symmetry effects 78−51604
thin shell, 9-node Lagrangian element 80−23888
torsional pendulum, for rigidity modulus meas. 79−84894
TORUS II Tokamak, toroidal field coil, fatigue test results 80−13928
trigonal crystal, elastic moduli, anisotropic behaviour, cryst. symmetry effects 78−51604
two-phase media, effective shear modulus and struct., rel. to seismic wave propag. in mantle 77−50949
Viton B, vinylidene fluoride-hexafluoropropylene copolymer, press. effects on mech. props. 77−32618
voids, coated, capture efficiency 80−96515
Zerodur, glass-ceramic, thermoelastic props. 78−27550
Ag, halides, strain derivatives of elastic and dielectric consts. 79−60421
Ag, pressure effect on shear modules and internal friction, EM reson. technique 77−31709
Ag, wires, polycryst., internal friction and rigidity modulus, O removal from grain boundaries 78−3160
Al alloy, elastic moduli, temp. depend. *(Japanese)* 77−59840
Al alloy, precipitation hardened 2014 and 2219, temp. depend. of elastic constants 77−66673
Al bar, meas. using holographic interferometry 77−31073
Al, pressure effect on shear modulus and internal friction, EM reson. technique 77−31709
Al, rigidity modulus, neutron irrad. and quenched, point defects 78−27546
Al, shear constants, press. effect up to 2500 atm., −196 to 25°C 77−31710
Al, surface strengthening of single crysts. on coating with evaporated films 77−8972
Al-Ga alloy, internal friction and shear modulus, temperature and concentration dependence 77−86077
Al-Ge, internal friction and shear modulus after neutron irrad. at 80K 79−1468
Al-Mg, single and polycrystal, variations 78−11263
Al-Ni (63.6 at.%), elastic softening and electron diffr. anomalies prior to martensitic transform. 77−86078
Al-SiC cermet elasticity, porosity meas. by US means 80−81101
Al_2O_3 ceramics, elastic props. meas. in 100 to 300°C range 80−55445
Al_2O_3 refractories, fracture, J-integral meas. 80−108537
Al_2O_3-Y_2O_3-SiO_2 containing TiO_2, La_2O_3, exam. of elastic moduli and refractive indices 78−80502
Al_2O_3+TiC system, elastic and fracture charact. at elev. temp. *(German)* 79−43299
$Al(PO_3)_3$-LiF system glasses, microhardness and US vel. 79−99274
$Al(PO_3)_3$-NaF system glasses, microhardness and US vel. 79−99274
Ar, liq., elastic modulus and stress relaxation 79−19304
a-As, second and third order elastic consts., ultrasonic velocity meas. 80−103408
B filament, uncoated and SiC coated, high temp. physicomech. props. 79−20140
Ba, elastic properties, Debye temp., 20°C, 20 to 70 kbar, US wave velocity meas. 78−87735
C fibre reinforced Al composite, C-Al contact interaction kinetics 79−20007
C fibre reinforced composite, shear fatigue 78−15493
C fibre reinforced plastic, effects of flaws and voids 77−44334
C fibre reinforced plastic, modulii meas. *(Russian)* 80−39199
Ce, elastic properties up to 84 kbar, US vel. meas. *(Russian)* 79−60434
$CeH_{1.98}$, $CeH_{2.98}$, elastic props. at high press. 77−84825
Cr-Fe, elastic moduli, electron conc., pulse echo overlap meas. 80−59550
Cr-Fe alloys, polycrystalline, antiferromag., elastic moduli and thermal expansion meas. 77−43860
Cu alloy, precipitation hardened, anomalous elastic props. 77−86071
Cu, elastic moduli second press. derivatives 79−96058

shear modulus continued
Cu, electron irradiated, dia- and paraelastic effects 77−76482
Cu, electron-irradiation internal friction behaviour, shear modulus and damping meas. 80−55444
Cu, pressure effect on shear modulus and internal friction, EM reson. technique 77−31709
Cu-Au solid soln., Cu rich, elastic const. 79−87681
Cu-Cd-Cr, precipitation hardened, low temp. elastic props. 77−73299
(Cu-Au)-Co, single crysts., solid soln. and particle strengthening, superposition 80−97495
Cu_2MnAl, dislocation structure, antiphase boundary energies, deformation behaviour prediction *(Russian)* 79−65085
Fe alloys, elastic props., texture correction formulae *(German)* 78−15439
α-Fe, polycrystalline, shear modulus, H_2 effects 77−36561
Fe-B(P) amorphous alloys, anomalous thermal expansion, ΔE effect, Invar and Elinvar characts., delay time 80−80589
Fe-C, effect of H on elastic props., due to internal microcracking *(Russian)* 79−24561
Fe-Cr, damping capacity *(Japanese)* 79−70104
Fe-Cr alloys, damping capacity 79−100206
Fe-Cr-Al (12, 3 wt.%), strain amplitude-depend. damping and modulus *(Japanese)* 80−92606
Fe-Cr-Ni, neutron irradiated, rel. between irradiation induced swelling and shear modulus 80−15157
Fe-Ni, FCC, anomalous props. at high temp. and new phase *(Japanese)* 78−80520
Fe-Ni (33.7 wt.%), γ-phase stability near martensitic transform., shear modulus obs. *(Russian)* 79−4966
Fe-Ni base metallic glass, annealing embrittlement 78−64635
Fe-Ni solid solution, deformation mechanism, softening phenomena, dislocation-solute atom interactions *(French)* 80−45344
Fe-Ni-Mn-C (5.9, 4.4, 0.48 wt.%) alloy, elastic moduli near martensitic transform. 80−7619
Fe-P-C, amorphous, at 0.5 Hz, room temp. to 550°C 77−25085
$Fe_{80}B_{20}$, $Fe_{78}Mo_2B_{20}$ glasses, internal friction and shear modulus 79−52287
$(FeCo)_{80}B_{20}$, glass, elastic consts. 79−83249
Fe_2MnAl, dislocation structure, antiphase boundary energies, deformation behaviour prediction *(Russian)* 79−65085
$Fe_{78}Mo_2B_{20}$, Elinvar-type behaviour 79−66091
$(FeNi)_{80}B_{20}$, glass, elastic consts. 79−83249
$Fe_{40}Ni_{40}P_{14}B_6$, $Fe_{29}Ni_{49}P_{14}B_6Si_2$ glasses, internal friction and shear modulus 79−52287
Ge, amorphous, random network model, calc. 78−6119
Ge-As-Se glasses, US vel. and reson. freq. meas. 78−23756
GeS_2 glass, temp. and press. depend. of elastic props. 77−15476
HFO_2, polycrystalline, monoclinic, elastic props. at room temp. 78−27548
^4He, HCP, pulse echo expts. 78−38910
In-Cd alloys, elastic-phase transition, US study 78−6919
KBr:divalent cations, minimum work-hardening rates in compression and shear 79−74175
$K(D_xH_{1-x})_3(SeO_3)_2$, ferroelastic, anelastic and elastic infra-low freq. props. 80−70304
$KH_3(SeO_3)_2$, ferroelastic, low-frequency elastic props., −190 to 50°C 79−37759
K_2O-PbO-SiO_2, glass, mech. and optical props. *(Russian)* 77−20860
K_2O-SrO-SiO_2, glass, elastic constants 77−16630
LC-440, shear modulus and viscosity relax. near isotropic-nematic phase transition *(Russian)* 77−39543
$LaH_{2.96}$, elastic props. at high press. 77−84825
LiF, inverse moduli, up to temp. of 650°C 78−14397
MgF_2, polycrystalline, elastic moduli, press. and temp. depend. US meas. 77−21202
Mn-Ga, Elinvar charact. *(Japanese)* 79−61638
Mn-Ni alloys, γ-phase antiferromag., lattice distortion and elastic props., ΔE effect interpret. 77−20671
Mn-Ni-Ti (Zr) systems, and mech. props. thermal expansion for different heat treatments *(Japanese)* 79−29123
Mn-Ni-Ti(Zr), non-ferromagnetic Elinvar-type alloys 79−24566
MnBi, mictomag. alloys, elastic props. *(Russian)* 80−7141
Mo, pure, temp. depend. of Young's modulus, and shear modulus 78−27553
Nb, elastic constants up to melting point, US meas. 77−86081
Nb, mixed state, Abrikosov vortices orientation depend. of elastic props. *(Russian)* 77−40007
Nb-H single crystal, temp. and H conc. depend. 78−39823
Nb-H(D)(T) system, BCC, US vel. changes caused by H isotope dissolution 80−65117
NbO_2, semicond. cryst., elastic props. 79−19308
Nb_3Sn, martensitic transition, lattice anharmonicity 79−8300
$Nb_{53}Ta_{47}$, elastic const. charge caused by H addition, hydrostatic press. effect 80−75287
NbTi filament reinforced Cu, superconducting composite, elastic const., temp. depend. 78−68717
Ni, electroplated layers, internal friction and ΔG effect, rel. to bath comp. and annealing 78−19296
Ni, grain boundaries, mobility, effect of impurities *(Polish)* 79−96073
Ni, pure, temp. depend. of Young's modulus, and shear modulus 78−27553
Ni, strain amplitude-depend. damping and modulus *(Japanese)* 80−92606
Ni-Al, neutron irradiated, rel. between irradiation induced swelling and shear modulus 80−15157
β_2-Ni-Al (47.6 to 60.5 at.% Ni), elastic stiffnesses −196 to 400°C 78−27556
Ni_3Al, substitutional soln. and defect hardening mechanisms 77−21155
$Ni_3B_7O_{13}I$, shear modulus anomalous temp. depend. 78−43061
Nichrome, plasma spray coatings, relaxation phenomena 80−19876
α-Np, bulk and shear moduli, 77 to 373K 77−20009
$Pb_{0.95}Sr_{0.05}(Zr_{0.53}Ti_{0.47})O_3$, low temp. internal friction in ferroelectric ceramic 77−21200
Pd, elastic consts. 4 to 300K 80−6455
Pd-Si, amorphous, at 0.5 Hz, room temp. to 550°C 77−25085
β-$PdH_{0.66}$, elastic consts. 4 to 300K, Debye temp. 80−6455
Pt, pure, temp. depend. of Young's modulus, and shear modulus 78−27553
Pt, rel. to high temp. dilation correction to sp. ht. at const. vol. 79−14940
α-Pu, sound vel. meas., press. to 50 kbar 77−20015

shear modulus continued
Pu-Ga (1 wt.%) alloy, polycryst. consts. calc. from single cryst. data 77−20005
Rb halides, photo-elastic constants and pressure derivatives of shear moduli 80−75284
$SbGe_xSe_y$ glasses with const. Sb content, heat capacity, thermal expansion, US vel. and elastic moduli 77−76574
Sc_2O_3, polycrystalline, elastic props., porosity and temp. depend. 77−52384
Se, vitreous, elastic coeffs. about glass transition temp. US study *(French)* 80−19865
Si, amorphous, random network model, calc. 78−6119
Si filler reinforced polyethylene, calc. of increase of shear modulus *(German)* 77−32613
Si_2N_2O, elastic props. 79−29122
SiO_2 vitreous fibres, relax. props. near glass transition interval 80−34137
SiO_2-Al_2O_3-MgO-TiO_2 glasses, internal friction during crystn. 79−52285
$SiTe_2$, dislocations and stacking fault energy 78−47378
$SrGa_2Si_2O_8$-$SrGa_2Ge_2O_8$, solid solution, exam. of elastic and electrical props. 79−96057
Ta, bamboo struct., wire, high-temp. rheology 77−1851
$Tb_{0.27}Dy_{0.73}Fe_2$, LF magnetoelastic effects 78−68348
$Tb_{0.3}Dy_{0.7}Fe_2$, sound velocity mag. field and temp. depend. elastic moduli calcs. 80−39839
Ti, deform. mech. map 77−77546
Ti-Mo alloys, elasticity moduli, 80-300°C *(Russian)* 78−80574
Ti-Mo-V-Al-Cr-Fe (4.8, 4.7, 5.2, 1.1, 1.0 wt.%), structural changes during heating up to 1000°C, DTA study *(Russian)* 80−93552
Ti-V, elastic moduli, electron conc., pulse echo overlap meas. 80−59550
TiC_xO_y, elastic characts. 77−80568
Tl halides, strain derivatives of elastic and dielectric consts. 79−60421
$TlSe.As_2Se_3$, $Tl_2Se.As_2Se_3$, γ-irrad. effects on mech. props. 77−80567
Tm_2O_3, polycrystalline, elastic props., porosity depend. 77−52384
α-U, martensitic behaviour 79−29058
α-U, martensitic behaviour 79−29059
V, elastic const. change caused by H addition, hydrostatic press. effect 80−75287
V-H(D)(T) system, BCC, US vel. changes caused by H isotope dissolution 80−65117
V_3Ge, low temp. props., mag. suscept. and resistance 78−19213
V_3Si, appl. of new three-dimens. k.p model for A-15 cpds. 78−23015
V_3Si, CDW instability and anharmonicity 78−79734
W, plasma spray coatings, relaxation phenomena 80−19876
WC-Co, elastic moduli and their press. derivatives 79−83248
ZnSb, thermodynamic props. and elastic moduli 79−77767
α-Zr, 4.2 to 1133K *(Russian)* 79−57034
Zr alloy, elastic props. of fuel cladding and press. tubing material 79−15711
Zr_3Al, $L1_2$ phase, work hardening 78−23718

shear strength
acrylic bone cement containing second phase dispersions, strength 77−81663
acrylic bone cement-stainless steel interface, shear strength 77−86706
adhered lap-shear and double cantilevered beam specimens, cyclic stress testing 79−15820
adhesive joint strength testing under normal rupture and shear stresses 79−52500
adhesive materials 77−16638
adhesives, thermosetting acrylic, electron beam curing 80−16634
adiabatic plastic deformation, shearing phenomena, review 80−50692
adiabatic shear in metals, explanation 77−14924
angle ply laminate, fibre reinforced, interlaminar strength test for delamination 78−88523
anisotropic elliptical layered plates, deflection, interlayer shear effects 79−98622
aramid fibre reinforced epoxy resin, shear props. 77−81354
arches stability analysis, flat, sandwich-type 80−48570
bar, homogeneous isotropic, shearing stress in Saint-Venant torsion, integral eqn. method 79−80445
beams, optimal layouts, allowance for cost of shear and bending 79−68566
body with period system of cracks laminar plastic zone development during longitudinal shear *(Russian)* 77−68442
bone, human compact, longit. shear, constituents and failure mech. 77−81518
bone strength, rel. to mineral supplemental diet in young rabbits 77−36986
bone-cement interface bond enhancement technique 78−31980
boride coating on stainless steel, elec., mech. props., boronising sintering method investig. 78−60594
α-brass, with few inclusions, shear mode of ductile fracture 77−36652
bulk solids, strength and flow props., vibrations effect 79−37237
cell membrane nuclear hydrodynamic shear, non-equil. Ising model, master eqn. 78−61146
cement mortar, deform. charact., expt. study *(Japanese)* 78−56704
clay soft, increase in shear strength and rigidity due to Fe^{3+} addition *(Japanese)* 78−31463
clays, heat treatment, effect on rheological props. of enamel slips 80−60809
clays, remoulded, shear stress path, stress history rel. to shear strength characts. 78−77219
colloids, model, elastic moduli, Monte Carlo methods 80−108754
composite, flexible spherical shell, dynamic and static loss in stability 77−52439
composite, metal-based fibre-type, designing for structural integrity 79−83155
composite beam, multilayered, anisotropic, exam. of shear stress distrib. under transverse loading 79−18731
composite cylindrical shells, reinforced, stability loss under isotropic external pressure 78−42554
composite material, in-plane shear charact. 80−35251
concrete, beam with mixed type of reinforcement, shear and bending strength 79−20124
concrete, plasticity theory anal. of shear 78−83270
concrete, prestressed beams without web reinforcement 79−52318
concrete, reinforced deep beams, with web opening, structural idealization 79−20125
concrete, reinforced slabs, punching shear strength under in-plane biaxial tension 80−100876
concrete beams, reinforced, shear strength calc. 80−99942

shear strength continued
concrete reinforced rectangular membranes, torsional stiffness 80−65131
cord reinforced rubber laminate, interlaminar-shear-strain meas. 79−57043
cord-rubber laminates, two-ply balanced, interlaminar-shear strain study 80−97526
Cosserat theory of crystal plasticity, appl. to anal. of lattice rotations under constrained deform. *(Japanese)* 78−2189
crack growth, at rubber springs bonds, energy calc. and meas. 79−83316
cross-plied factors controlling transverse cracking 77−77566
curved sandwich beam, five point loading test, bending and shear stiffness determ. *(German)* 77−16765
cyclic simple shear testing apparatus for granular materials 77−90578
cylinder, plastic flow rules and Bauschinger effect parameters 78−6984
cylindrical shell, transverse shear effect on axial crack 78−67090
cylindrical shell with circular cut out, uniform bending, strength and flexural rigidity 78−87282
dental crown restoration fixation, dynamic shear testing 78−36068
disperse system, plastoviscous, cone plastometer for strength props. determ. 80−76426
epoxide resin, tensile, compressive and shear yield strengths, pyramidal criteria 77−8884
epoxy Al bonded, adhesive joints under complex loading, development of failure criterion 78−92344
epoxy based structural adhesives, time-temp. cure behaviour, torsional braid anal. 80−55621
epoxy resin, exam. of shear stress-strain charact. 78−60691
epoxy resin, shear strength determ., anal. of methods 77−86107
epoxy resin adhesives, capillary flow and bond strength 80−71883
epoxy resin based composites, superconducting magnet insulators, gamma-ray radiation effects 80−24495
fayalite (Fe_2SiO_4), shear strength and press. distrib. in diamond anvil press 78−12710
fibre reinforced composite, discontinuous, surface treatment effect analysis and obs. *(Japanese)* 77−77596
fibre reinforced composite, shear props., test method eval. 77−81353
fibre reinforced composites, intralaminar-shear charact., 10 deg off axis test 78−35422
fibre reinforced composites, Monte Carlo study of strength 80−25844
fibre reinforced composites, stress redistribution dynamics during fibre rupture 80−64394
fibre reinforced epoxy, laminate, static and impact props. 77−63725
fibre-reinforced rigid-plastic plates transverse impact anal. 78−38211
fibreglass, mechanoluminescence during monoaxial stretching 78−68742
fine ceramic masses, organic plasticizer, plasticity model and plastic behaviour meas. by cyclic shear test *(German)* 79−96080
glass, strength under linear tension, bending, torsion and compression of type K8 79−14062
glass fibre reinforced composite, fatigue failure, role of shear deform. 78−15494
glass fibre reinforced composite, shear fatigue 78−15493
glass fibre reinforced composites, influence of form of reinforcement on spread of strength data *(Japanese)* 79−11672
glass fibre reinforced epoxy, as electrical insulation for Tokamak toroidal field coils, mech. props. 78−64610
glass fibre reinforced epoxy, deterioration in water, hydraulic press. effect *(Japanese)* 80−55470
glass fibre reinforced epoxy, deterioration in water, immersion time effect *(Japanese)* 80−55471
glass fibre reinforced epoxy, exam. of interlaminar shear stress distribution 79−43308
glass fibre reinforced epoxy, struts for superconductive storage magnets, mech. props. 80−25824
glass fibre reinforced epoxy, wound, strength in twisting, stretching and transverse bending 80−11622
glass fibre reinforced epoxy laminates, exp. determ. of nonlinear shear behaviour 80−66575
glass fibre reinforced epoxy resin, cryogenic tensile, compressive and shear props. 78−6983
glass fibre reinforced epoxy resin interlaminar shear strength determ., anal. of methods 77−86107
glass fibre reinforced plastic, dynamic stress conc. around defects, discrete model 80−30024
glass fibre reinforced plastic, fatigue strength in shear in plane of reinforcement 77−32690
glass fibre reinforced plastic, fracture dynamics 80−100906
glass fibre reinforced plastic, punching shear tests under static and impact loadings *(Japanese)* 80−55512
glass fibre reinforced plastic, unwinding resistance of hardening layers, fibre tension effect 77−32691
glass fibre reinforced plastics, cyclic strength in complex stressed state 80−3181
glass fibre reinforced plastics, shear characteristics of tubular specimens, strain gauge and clamp 80−85114
glass fibre reinforced poly- and vinyl ester thermoset moulding, cure cycle effect on mech. props. 80−45369
glass fibre reinforced polyester, epoxy-polyamide, single lap joint, tension-shear strength *(Japanese)* 78−11494
glass fibre reinforced polyester, single lap joint, tension-shear strength *(Japanese)* 78−11494
glass fibre reinforced polyester, struts for superconductive storage magnets, mech. props. 80−25824
glass fibre reinforced polyester resin, interfacial bond strength, effect of surface treatment 77−21303
glass fibre reinforced resin, shear strength determ., comparison of methods 77−90527
glass reinforced plastic, thermal activity, prediction of struct. charact. and physicomech. props. 77−63872
glass-epoxy laminate, superconducting magnet insulators, gamma-ray radiation effects 80−24495
granular material, particle crushing under high triaxial stresses *(Japanese)* 78−15466
granular materials deformation, microscopic and macroscopic exam., stress/strain charact. calc. *(Japanese)* 80−11691
graphite fibre epoxy composites, exposed to high temp., degradation of tensile and shear props. 80−81113
graphite fibre filled polyimide composite laminates, space environment, phys. and mech. response 80−81140
graphite fibre filled polyimide composite prepreg laminates, room-temp. ageing effect 80−81093

shear strength continued
graphite fibre reinforced epoxy resin, cryogenic tensile, compressive and shear props. 78−6983
graphite fibre reinforced polyester, pultruded fibres, interlaminar shear fatigue 78−56742
graphite fibre reinforced polyimide, correl. of US attenuation and shear strength 78−19968
graphite reinforced epoxy angle ply laminates, statistical fatigue in shear 79−11690
graphite-epoxy composite, hydrothermal ageing 77−21189
haemolytic characteristics of polydimethylsiloxanes 77−60290
hydrodynamic contacts, films, elastic properties 80−88239
ice, shear strength temperature depend. 80−24523
ice single crystal, friction of WC ball, slider size effect *(Japanese)* 78−88538
ice single crystal, rel. to friction of steel ball *(Japanese)* 78−88537
index, permissible values 78−63324
joints, double adhesive bonded, loaded in shear tension *(French)* 80−23968
junction growth mechanism during friction *(Japanese)* 79−32391
Kevlar 49 fibre reinforced composite, shear fatigue 78−15493
laminate, simple shear charact., comparison of test methods 78−44283
laminate, strength anal. and distribution, failure prediction 78−88522
laminated plates, optimum design under shear 80−23925
layered orthogonally reinforced plastics, strength and stiffness prediction in interlaminar shear 77−9025
linear elastic incompressible solid, stability of void growth under uniaxial tension and shear 79−76972
lubricant, shear rheological behaviour at high press. 80−35342
machining theory, strain rate predictions in chip formation zone of intense shear 77−70277
magnesial refractory concretes, cast. props. 80−89306
meas. installation for solids meas., at 120 to 300K and up to 100 kbar 80−50787
metal, cubic, heavily rolled, shear band occurrence 79−34058
metal-polymer, ply-separation resist. polymer polarity effect *(Russian)* 80−61064
metal-sapphire interface, effect on shear strength of adsorbed species 80−49485
metallic fibre knitted gauze permeable materials, mech. props. 80−66607
metallic glass, shear deform., mechanism involving dislocation glide 78−15462
metallic glasses, friction coeff. determ. using sliding friction rig 80−89355
metallic glasses, strength and stiffness 77−8899
metals, surface pretreatment effect on joint bond strength by cyanoacrylate adhesive Kanokonlit-E *(German)* 79−57202
metals and alloys, diffusion layers, effect of chemicothermal treatment on struct., surface energy, and bulk props. 79−96207
natural slopes materials, shear strength rel. to failure surfaces propag. 79−39719
Nylon 6, unidirectionally reinforced, mech. props. and fracture 77−21252
ocean sediment free-fall penetrometer with Doppler telemetry 80−46320
organic glass, creep under shear with superposition of hydrostatic press. 78−31482
organic glass, shear strength behind the front of a plane shock wave 79−15752
organoplastics, fracture charact., effect on strength 80−66642
organotextolite, in plane state of stress, temp. depend. variant of strength 80−40449
orthotropic laminates, torsion strength and shear modulus determ. 80−92587
orthotropic sandwich plates, simply supported shear stiffness rel. to forced vibrs. 77−46861
particulate materials, dynamic shear strength and flow behaviour, shear cell meas. 78−53048
plane shearing stress meas. with wired strain gauges *(German)* 78−89471
plastic, fibre-glass reinforced, flat stressed state, strength and deformation props. function of reinforcement struct. 80−19866
plastic flow round crack under friction and combined stress 78−79280
plastic laminates, glass- and fibre-reinforced, strength anisotropy comparative anal. 80−19872
PMMA, critical stress-intensity factor, determ. under mixed mode loading conditions by shadow optics 78−68868
polycarbonate, glassy, fatigue crack initiation in high strain fatigue tests 80−97564
polycarbonate, plane strain fracture energy instability and mixed mode crack propag. 78−68775
polyester resin, creep, temp. and humidity effects under shear and tensile strains 77−86105
polyethylene, branched, frictional props., normal force/shear for relationship 79−47785
polyethylene, creep during shear deform. with applied hydrostatic press. 80−76324
polyethylene, low density, shear and tensile creep at finite strains 78−52903
polyethylene terephthalate, crazing and shear deformation on stretching in air and liquids *(Russian)* 78−88558
polyethylene terephthalate, preoriented sheet, plastic deform., anisotropic behaviour 79−8335
polyethylene/Cu(Zn) adhesion, role of surface topography 80−35500
polymer, filled, rheology, steady state shear flow and periodic deform., relaxation time, spectra, viscosity 79−96066
polymer film, dynamic loading influence on sliding friction 79−50675
polymer film, semicrystalline, tear resist. 77−52488
polymer films, between contacting surfaces, effect of contact pressure and temp. 78−60842
polymer films, superconducting magnet insulators, gamma-ray radiation effects 80−24495
polymer systems for adhesive applications, radiation curing, lap shear strength props. 80−66842
polymer-metal adhesive bonds, shear resist., polymer crystn. effect 80−89462
polymers, friction and wear, role of mech. props. 78−52998
polymers, shear strength and friction 78−39913
polypropylene, isotactic, shear induced β-form crystallisation 78−18555
polypropylene, preoriented isotactic sheet, mol. behaviour in uniaxial drawing *(Japanese)* 77−68928
polypropylene, shear and tensile creep at finite strains 78−52903

shear strength continued
polystyrene, angle of intersection of coarse shear bands, optical obs. 79−66110
polystyrene, coarse shear bands and fracture, SEM study, craze fracture surfaces 79−29191
polystyrene, cryogenic foam insulators, low temp. props. 80−25818
polyurethane, cryogenic foam insulators, low temp. props. 80−25818
polyurethane cement, viscosity and shear strength, components influence *(German)* 80−93729
powder, tensile strength data and failure loci from Jenike shear cell tests 78−31476
prefluorinated polymer, DuPont Krytox 143-AB, viscoelastic and dielectric props. 80−1503
prosthetic intramedullary implants pre-coated with bone study, fixation study 80−7587
PTFE, partly crystalline, viscoelastic props., stressed state estimation 79−66099
PVC, glassy, fatigue crack initiation in high strain fatigue tests 80−97564
reinforced axisymmetric shells stratified by shear, bearing capacity 79−3979
reinforced concrete curved beam, expt. investigation of collapse 77−90404
reinforced ring, shear failure mechanism in bending 77−72189
rock and rock joints, empirical laws of friction and fracture 77−21762
rock parameters, drillability *(German)* 79−74888
rocks, effect of normal stiffness 77−17089
sand, cyclic liquefaction strength 80−3996
sand, shear strength at const. vol. 77−63865
scaling relations in mag., mechanical and superconducting pinning theory 77−76403
shaft, circular, with surface traction, perturbation of shear stresses 79−41577
shear lag problem, finite element anal. 79−32246
shearing process, basal section profile effect 79−47754
sheet metals, ductile, shearing process 78−84841
sheet metals, shearing test using pressure sensitive pin *(Japanese)* 77−48602
shell and plate, reinforced, viscoelastic and elastic, with transverse shear strain, stability 77−84171
simple shear generation *(German)* 77−44432
slab, semi-infinte, stress amplitudes and fatigue damage resulting from cyclic Hertzian compression 77−19567
soil, sliding masses, residual strength and frictional resist. *(Japanese)* 78−11919
spheres, porous, in a linear flow field, motion and rupture 79−64755
spheroplastic, spherical shells, supporting capacity 80−87723
steel, C, brazed butt joint, static torsional deform. 77−16657
steel, Cr-Mo-V, high-temp. cumulative damage for stage I crack growth 78−19883
steel, double-layer, adhesion strength determ. method 77−63857
steel, forged axle spindle, fractographic anal. of shear fracture 78−68821
steel, low alloy, acoustic emission during ductile fracture, isothermal tempering effect 79−83241
steel, maraging, ageing study by internal friction meas. 77−12660
steel, non-alloy, work hardening due to shearing *(French)* 78−15423
steel, rails of DIN 15087E, shear stress distribution caused by transverse force *(German)* 79−61647
steel, stainless, with Ni base filler metals, brazed joint strength *(Japanese)* 80−16636
steel granular model material, equipment for shear deform. investigation *(German)* 80−35449
steel sheets, overlapped, glued with nonuniform epoxy resin layer, strength tests *(German)* 78−15647
stress state of structural elements of vessels under external hydrostatic press. 77−14908
struct. changes, through simulated multiple layer welding, micro-tensile and shearing tests *(German)* 80−35215
suspension, conc., of aggregable particles, viscosity calc. 79−7362
Teflon, creep in shear, hydrostatic pressure effect 79−57065
Textolite, shear strength behind the front of a plane shock wave 79−15752
thermally sprayed coating adhesive strength testing method 79−83432
tibial plateau fixation, biomech. factors 77−56534
transversely isotropic plate with hole, edge supported, shear compliance in bending and torsion 77−2543
Tresca type plastic material, simple shear deform. with combined work hardening *(Japanese)* 80−35206
tuff, deform. charact., expt. study *(Japanese)* 78−56704
viscoplastic medium, flow between two noncoaxial circular cylinders under pure shear 80−99938
weathered Athenian schist, drained shear strength correl. with mineralogy 78−61408
wedge adhesive joint, nonuniform stress distrib. under combined normal and shear stresses 79−18837
AL, laminate, free-free plates, predicted and expt. natural modes 79−10520
Al, 6061-T6, pressure shear impact in transverse displacement interferometer, plastic flow 80−81137
Al, [111] single crystal, in situ deform., HVEM obs. 78−52886
Al, annealed, subjected to torsional impact loading strain-rate effects 78−92303
Al-Ag alloys, critical resolved shear stress 80−49296
Al-Cu alloy RR58, high strain fatigue life, prior treatment effect 78−60835
Al-Zn-Mg alloy 7075, unstable shear failure 77−48516
Al_2O_3, semisintered, shear strength at high press. 80−76308
B fibre reinforced Al, fracture mechanical study, unidirectional composites 78−88520
B fibre reinforced Al composite, strength of fibre-matrix interface and tensile strength *(Russian)* 80−21005
B fibre reinforced Al laminate, unidirectional, interlaminar shear strength exam. 78−35434
B fibre reinforced epoxy, fracture mechanical study, unidirectional composites 78−88520
B fibre reinforced epoxy and Al, cryogenic tensile, compressive and shear props. 78−6983
C fibre composite, interlaminar shear strength, effects of fibre surface treatment, resin type and fabrication process 78−35346
C fibre reinforced Al, formed by ion plating and vacuum hot pressing 78−11165

shear strength continued
C fibre reinforced C, processing, room temp. mech. props., and low temp. expansion 80−25820
C fibre reinforced composite, whisker coating of fibres to improve strength 78−3093
C fibre reinforced composite, shear fatigue 78−15493
C fibre reinforced composite, oxidation of C fibre effect on shear strength *(French)* 78−44238
C fibre reinforced epoxy, activated C, storage life effect on shear strength *(Russian)* 78−35483
C fibre reinforced epoxy, epoxy matrix, strength in twisting, stretching and transverse bending 80−11622
C fibre reinforced epoxy, deterioration in water, hydraulic press. effect *(Japanese)* 80−55470
C fibre reinforced epoxy, deterioration in water, immersion time effect *(Japanese)* 80−55471
C fibre reinforced phenol resin, karbovoloknits, improving transverse tensile, interlaminar shear and compressive strengths 79−87691
C fibre reinforced plastic, effects of flaws and voids 77−44334
C fibre reinforced plastic, ±45° orientation, creep, fatigue, repeated loading and crack growth 78−68729
C fibre reinforced plastics, use in orthopaedic implants, exam. of mech. props. 79−20706
C fibre reinforced plastics with mixed fibres, exam. of fracture toughness and shear strength 79−20151
C fibre reinforced plastic, shear strength of glued joint, combined effect of temp. environment moisture, fibre orientation 79−96100
C fibre reinforced plastics, strength props., effect of SiC coating on fibre 80−104224
C fibre reinforced polymers, strategic reinforcement of hybrid, impact props. 78−15502
C fibre reinforced polymer, strength props., fibre surface treatment effects 78−27636
C fibre-Kevlar 49 fibre epoxy laminate, impact props. 78−44164
C fibres with large breaking strain, prep., mech. props., struct., appl. 78−44077
C-C composite, structure model, Rosen model with fractional matrix 80−11719
C-fibre reinforced epoxy resin, laminated structs. mech. props. 80−50672
C-fibre reinforced plastic insert molding strength *(Japanese)* 80−66588
$CaSiO_3$ fibrous crystal reinforced matrix, unidirectional crystallization, anisotropic properties 79−56969
Cd-Ag (0.015 to 0.25 at.%), critical resolved shear stress at low temp. 77−69035
Cd-Zn (up to 1.57 at.%), single cryst., precip. hardening, 77-300K 78−60675
CdTe, single crystals, plastic deformation and dislocation struct. 79−8321
CsCl crystal, BCC and BCC ordered, core struct. of ⟨100⟩ dislocations, atomistic calc. 78−30637
Cu and Cu-Cr (0.6 wt.%), electron microscope obs. of shear bands *(German)* 77−48454
Cu, brazed butt joint, static torsional deform. 77−16657
Cu, mechanical twinning in (110)[$\bar{1}$12] single crystal under plane strain compression *(German)* 77−36616
Cu, rolling textures and texture inhomogeneities, exam. of development in single- and poly-crystals 79−11637
Cu, shear mode of ductile fracture 78−31525
Cu-Al_2O_3 extruded bars, strength anisotropy 77−16597
Cu-Be (2 at.%), plastic deform. and dislocation substruct. 80−76307
Cu-O single crystals, shear stress measurement, solid solution strengthening 79−52225
Fe and related compounds, hdyrostatic compression expts. 78−83862
Fe, plastic deform. of single crystal with shear tests in {110}⟨111⟩ and {11$\bar{2}$}⟨111⟩ slip system 77−48509
Fe-Cr-Ni, single crystal anomalies in curve of critical shear stress versus temp. at low temps. 77−16656
Fe-Mo, damping capacity *(Japanese)* 78−11259
$Fe_{32}Ni_{36}Cr_{14}P_{12}B_6$, shear band form. 78−68756
Fe_2O_3, semisintered, shear strength at high press. 80−76308
KH_2PO_3, mechanically treated single crystal, depth and struct. of disturbed layer *(Russian)* 78−23839
LiF, US attenuation, 4.2 to 300K 77−47513
Mg alloys, strain rate effects during reverse torsional shear 77−4143
MgO, semisintered, shear strength at high press. 80−76308
Mo single crystal dislocation interactions during parallel shear in (011) plane *(French)* 78−43029
Na_2O-CaO glass, shear deform. under pyramidal indentations 80−84989
Nb, stress differential in surface oxide softening of single crystals 77−86116
Ni sintered permeable materials with bidisperse structure, pore-forming additions effect 80−84885
Ni-Cr alloy (20 wt.%), on steel, plasma-sprayed coating 79−96222
$Ni_{49}Fe_{29}P_{14}B_6Si_2$ glass, flow and failure 80−40438
Pb, deformed by torsion, stored energy and recrystallization 79−34069
$Pd_{80}Si_{20}$, shear band form. 78−68756
Ti, neutron effects on thermally activated tensile props. 77−62567
Ti, shear bands in cup and cone fracture in pure plate *(Japanese)* 79−15773
$(U,Th)O_2$ fuel rods, analytical stressing in hot cell 80−18566
V, polycrystalline, strength, ductility, 4.2 to 400K, O_2 effect 77−36529
W, plasma coating, thick, struct. and mech. props. 77−28716
W, polycryst., loss of shear strength under shock compression 77−11635
W-Cu fibre reinforced composites, interface shear strength, critical aspect ratio 77−4826
WC-Co, size factor effect on strength in complex stressed state 78−31483
WC-Co particle-matrix composite, fracture and cleavage strength 77−73342
Zn single crystals, temp. and strain rate effects on strength, slip and twinning 80−16373
Zn-Al (22 wt.%), superplastic, eutectoid alloy, ductility and fracture 78−60819
ZrO_2, semisintered, shear strength at high press. 80−76308

shear turbulence
acoustic noise, convective amplification, jet noise appl. 77−23943
aerosol particles, turbulent migration phenomenon 80−53836
air-water film flow, transport phenomena, wary interface motion 77−35213

shear turbulence continued
airfoil, leading-edge separation bubbles, shear layer and transitional reattaching flow 77−27580
anal. using Lagrangian similarity hypothesis 77−42809
anisotropic homogeneous turbulence, numerical anal. 79−27626
annular conduit, wall suction, turbulent flow *(French)* 78−18343
arteriosclerotic flow models, velocity fluctuation and shear stress obs. *(German)* 79−16226
astrophysical plasmas, mirror instability, mag. field first adiabatic invariant breaking 80−67546
asymmetric mean profile flow, negative production 78−94666
atmosphere, turbulent shearing layers, dominant eddy scale, growth, limiting thickness 77−87022
atmosphere, turbulent shearing layers, growth, limiting thickness, dominant eddy scale 78−92955
axial turbomachine, cascade and through-flow theories as inner and outer expansions 78−75148
axisymmetric air free shear layer, effect of initial fluctuation level 78−90843
axisymmetric free shear layer, effects of initial momentum thickness 78−71325
axisymmetric supersonic turbulent base pressures 78−94764
axisymmetric turbulent jet initial region, annular free shear layer 80−106826
binary mixture, thin shear flow layer, momentum, heat and mass transfer *(German)* 77−39293
bluff bodies immersed in turbulent boundary layers, flow patterns, press. forces acting on inclined plates 77−58662
bluff body, turbulent near wake, vel. correlation struct. 78−30298
bottom settling of solid particles in turbulent shear flow, distribution statistical properties *(Japanese)* 80−19344
boundary layer, calc. on spinning and curved surfaces 77−65737
boundary layer, compressible, Reynolds number effects on turbulence field 80−19434
boundary layer, hyperbolic system of eqns., Keller-Cebeci 'box' scheme 80−79274
boundary layer, Reynolds stresses meas. 77−42807
boundary layer, struct. and development in oscill. external flow 80−19353
boundary layer, turbulent external turbulent shear flow 77−3817
boundary layer in stratified medium, shear flow 79−64736
boundary layer shear stress distribution calc. 79−98701
boundary layer transition on a flat plate considered as cascade of instabilities 79−41676
boundary layers, interacting, in duct 77−19597
boundary layers, vorticity transfer theory *(Russian)* 79−50719
bounded flow, coherent motion mechanism 78−90854
bounded turbulent shear flows, pattern-recognised coherent structures 78−22334
buoyancy and extra strain effects, mathematical modelling 78−94674
buoyant plumes behaviour on release at ground level, lab. wind tunnel obs. 80−30624
buoyant surface jets analysis for heated plume characts. prediction 77−15087
bursts in turbulent shear flow 77−11178
calculation methods, book contrib. 77−58655
cavity flow, broadband noise generation, vortex model 77−75900
channel, with stepwise change in wall roughness, relax. processes 78−90861
channel flow, smooth-rough surface discontinuity with zero press. gradient 77−51121
channel flow, velocity and eddy viscosity distribs. for turbulent shear flow 77−89104
chemically reacting nonequilibrium turbulent shear flow, prediction model *(German)* 79−18973
chemically reacting turbulent shear layer between two streams obs. 80−6163
chemically reactive flow struct. 78−1754
circular channel with centrifugal forces, laser Doppler meas. of vel. field 78−34225
coaxial jets, correl. covariance meas. in initial region 77−84289
coherent structure, by ramp model 78−94670
coherent structure, stereoscopic camera obs. 79−32485
complex flows, multiply interacting shear layers, distortion by extra rates of strain 77−68580
compressible turbulent shear layers, reviews, book contrib. 77−47034
computational modelling by finite elements 79−1163
convection, forced, turbulent, in square cavity, shear effect 79−1180
convective turbulent heat transfer from rough surfaces 79−27638
corner flow, Reynolds stress model 78−46954
counter gradient flow downstream of two different diameter cylinders *(French)* 80−43693
critical points in unsteady flow, functional anal. 80−33571
curved streamline algebraic stress-heat flux model 79−27625
curved wall flow turbulence, integral method calc. *(French)* 77−54984
cylinder wake, external turbulence effects 78−94665
cylinders, rot., intervening turbulent flow struct., model eqns. calc. 78−90852
cylinders placed in turbulent plane mixing layer, time-averaged aerodynamic forces 80−28524
discrete frequency sound generation by fluid flows 80−69812
disturbances effect, weak and strong, on axisymmetric turbulent layer 78−90857
duct, square, developing turbulent flow computation 80−1554
duct, turbulent air flow, small streamline curvature effects 79−60064
duct flow, wall shear stress fluctuation props. 78−38304
duct with rough walls, turbulent shear flow, stability anal. 80−38496
edgetone and instability of free shear layer 78−94672
electrodiffusive flow and shear transducer electrical anal. 80−48824
extended pressure strain correlation models for turbulent shear flows 80−69777
final self preserving state of disturbed large 2-dimens. shear layer 78−90851
finite difference techniques accuracy in complex geometries 80−19357
finite element model of flow behind prolate spheroid 79−23304
flow fields, multidimensional, of any turbulence intensity, analysis 79−27720
flow in plane channel, least energy dissipation rate principle 80−33577
flow measurements using hot-wire probe, effects of orientation 79−27722
flow over rectangular cavities, induced tones and press. oscills. meas. 79−32493
shear turbulence continued
fluctuations in shear stress of turbulent flow near wall *(German)* 80−19345
forced convection with chemical reactions, turbulent shear flow mixing, numerical modelling 79−1272
forward facing step, neutrally stable atmospheric flow, shear layer, separation, vortices 80−48685
free flows, turbulent stress modelling using tubulence distortion linear statement 80−1538
free shear flow, appl. of multiscale transport model *(French)* 79−50763
free shear flow, critical Reynolds number model 77−39279
free shear flow, effects of stream turbulence 78−59378
free shear flow, spatial interactions in the mean 78−22335
free shear layer, Reynolds stress closures systematic modelling rules 80−1552
free shear layer behavior in rotating systems 80−1545
free shear layer tone phenomenon, probe interface 78−71324
free stream turbulence and shear effects on boundary layer and wake structs. 78−26112
free turbulent shear flow, acoustic pressure fluctuations due to large scale coherent structs. 80−14677
free turbulent shear flow, initial condition effect, appl. to plane jet and axisymmetric shear layer 78−90850
free turbulent shear flows with strong density fluctuations 80−19342
free turbulent stratified shear flow, buoyancy effects on large scale struct. 78−90849
free-shear plane stationary computer simulated turbulence struct., discretized Navier-Stokes eqns. 78−26111
fully developed, local closure condition *(German)* 77−11179
gas, turbulent boundary layer vel. distrib., probabilistic statistical approach, vortices 80−92123
gas, with variable physical props., pipe flow, turbulent momentum and heat transfer calc. 78−90869
gas-solid turbulent shear channel flow, particulate motion, numerical simulation 80−53863
glycerol, shear relaxation, KCl or NaBr additive effects 79−60537
heat transfer, turbulent water film, different initial flow conditions, high temp. gradients 78−90862
heated air stream, parallel to ambient fluid, temp. fluctuations 78−94668
heated grid flow, temp. derivative skewness, alleviation 78−46951
heated homogeneous flow, instantaneous temp. meas. using electronic cct. 78−21137
heated planar jet, turbulent diffusion, second-order closure anal. 77−39364
heterogeneous liquid stream, stress diffusion effect, molar diffusion coeff. 78−79338
homogeneous, nearly, strongly sheared flow 80−79283
homogeneous turbulence under rigid rotation and uniform mean vel. gradient *(French)* 79−23306
homogeneous turbulence with const. shear and buoyancy effect, linear correls. *(French)* 77−75893
hydroacoustics, role of surface shear stress fluctuations 80−69808
hypersonic boundary layer over slender sharp cone, turbulent shear stresses, heat transfer 77−23989
incompressible turbulence, statistical investigation of eddy viscosity 80−14675
incompressible turbulent flow, numerical prediction 79−1171
incompressible viscous fluid, frictional flow through straight diffusor *(German)* 78−94662
instability waves, radiation of sound 80−79341
interactions between large-scale struct. and fine-grained turbulence 77−7378
interface displacement for free shear layer 77−72271
intermittency in free turbulent shear flows 80−19348
inviscid parallel shear flow, instability 80−79265
jet, axisymmetric, turbulent bulge struct. 78−90955
jet, axisymmetric, vel. distrib. and swirl effects, low speed results 79−46351
jet, axisymmetric free shear flow with Reynolds stress closure 80−19469
jet, circ., controlled perturbation, smoke visualisation 78−90956
jet, free, round, initial region flow struct. 79−50765
jet, large scale flow struct. 79−72923
jet, mixing layer, axisymmetric, influence of initial and boundary conditions 79−94689
jet, self-preserving turbulent flow over convex surface 77−58754
jet, structure functions of temp. fluctuations 78−71380
jet, turbulent, quasi-periodic structure 79−81935
jet, turbulent axisymmetric, spatial waves 77−19630
jet exhaust noise, role of shear-layer instability waves 77−47054
jets, flat and axisymmetric, submerged in incompressible fluid, calc. using turbulent energy balance eqn. 77−47051
jets, wakes, and shear layers, turbulent, power laws, rel. to marginal instability principle 79−32458
jets and boundary layers, irrotational strain dissipation eqn. sensitisation 80−106794
jets discharging into quiescent ambient, finite difference anal., turbulence modelling 78−30332
kaolin suspensions, aq., flocculated and dispersed, rheological behaviour in pipe flow 80−64510
Lagrangian turbulence characteristics meas. using photographic techniques 77−58811
laminar separation bubbles, airfoil performance effects, turbulent shear layer reattachment 80−48774
laminar source flow between parallel porous discs with equal suction and injection, in mag. field 77−84331
large eddy simulation 80−38390
large scale structure 78−90847
large scale structure and fine grained turbulence interactions 80−33575
large-scale coherent structure, and acoustic noise 78−94671
laser-Doppler technique, local size and vel. probability distrib., two-phase suspension flow 78−59517
layer attachment near Mach 6, peak heating 78−26153
linear shear flow and around cylinder, velocity gradient effects *(Japanese)* 79−23305
liquid, forced channel flow with surface boiling, analogies between heat and momentum transfer 77−47014
liquid, in rot. system, shear stress depend. on Hall parameter 79−41681
liquid film, heat transfer predictions for nonsheared and sheared films 77−15024

shear turbulence continued
LMFBR triangular rod array, flow resistance wall shear stress in interior subchannel 80−63244
longitudinal blunt circular cylinder, axisymmetric separated and reattached flow, turbulence 80−79285
low speed shear layer, turbulent mixing of passive and reactive species 77−75989
lubrication, turbulent, eqn. derivation using friction law 79−98694
MHD flow, shear turbulence with transverse mag. field 79−32695
MHD shear flow, struct. turbulence, anomalous impulse transfer *(Russian)* 77−27610
MHD turbulence stream with 2-dimens. struct. perturbation, shear region momentum transfer *(Russian)* 78−5812
mixing, model 78−1650
mixing layer, asymm. temp. distrib. expt. 79−32487
mixing layer, free, axisymmetric, turbulent spot, data processing 80−79280
mixing layer, free, axisymmetric, turbulent spot, vorticity and Reynolds stress 80−79281
mixing layer vortices, numerical simulation 78−90853
modelling methods, in physical and spectral space 78−42594
molecular Prandtl number, influence on turbulence in shear flow, book contrib. 80−1541
Navier-Stokes equation for numerical simulation 78−94743
near-wake phenomena, with and without external compression, axial and radial air injection effects 80−10273
nearly homogeneous flow, expts. 77−72286
noise generation on both sides of double layer jet 77−47056
nonequilibrium flow, turbulent length scales 79−1269
nozzles, plug, turbulent shear layers, mixing 77−89182
omnidirectional wall shear stress meter 80−106860
one-equation turbulence model, finite element anal. 79−7371
open wind tunnel jet flow, convection and refraction of acoustic waves *(French)* 77−24007
passage, arbitrary cross-section, fully developed flow prediction method 79−1254
perforated plate generators in wind tunnels, wake, shear flow and isotropic turbulence prod. 80−69770
periodic surge flow in circular tube, wall shear stress vel. distrib. *(German)* 79−10613
phenomenological theories for computation, Navier-Stokes eqns., Reynolds stress modelling 78−46955
pipe flow, correlations among turbulent shear stress, kinetic energy and axial intensity 79−3996
pipe flow, Reynolds shear stress, roughness effects 78−22426
pipe flow, turbulent, past rectangular roughness element 80−1555
pipe flow, turbulent, perturbed by sudden enlargement 80−19354
pipe flow, wall and shear turbulence during bursting periods 78−1743
plane mixing layer, two-point LDV meas., vorticity distrib. 80−38506
polymer admixtures influence on origin of vortices in wake behind cylinder 77−58744
polymer solution, dil., turbulent flow behaviour in annulus 80−33633
polymer solution, turbulent flow investig. using laser Doppler velocimeter 77−58822
polymeric additives, effect on submerged jets and wakes 79−77084
pseudoplastic fluid flow in pipes, press. loss 79−98765
quasi-standing-wave phenomenon due to oscillating internal flow, vortices in shear layer 80−106809
quasilinear approximation model 78−13997
reactive gas flows, two-dimens., nonequil. processes analysis 77−51129
recirculating flow behind backward-facing step, mean vel. and Reynolds stresses meas. 80−19355
recirculating jet flow, initial mixing region meas. 77−27570
relaxation in developed turbulent flow 77−89105
relaxing wakes behind surface-mounted obstacles in rough wall boundary layers 79−94625
Reynold's stress tensors, rot. probe meas., in 3-dimens. boundary layer 78−94656
Reynolds mean uw shear stress gradient meas., press. driven boundary layer 77−54986
Reynolds shear stress, turbulent flow over a periodic rough surface 78−71326
Reynolds shear stress in equilib. range, turbulence spectral props. *(Japanese)* 78−18284
Reynolds shear stress to total intensity ratio, response to additional distortion 80−79282
Reynolds stress production, compressible turbulent flow, analysing method *(French)* 79−7370
Reynolds stress tensor, direction of principal axes, transverse shear 78−67185
Reynolds stress tensor rot. in axisymmetric flow 78−26108
rod-bundle in nuclear fuel element, mathematical model for transient subchannel analysis 77−79430
roll-cell instability, rot. laminar and turbulent channel flows 77−946
rotating disc, local heat transfer, Prandtl's mixing length hypothesis 77−27540
round heated jet, heat and momentum transport, intermittency, entrainment 79−32608
scalar and vel. dissipation time scales ratio 79−18879
scalar field evolution equation, for conditioned probability density function 78−94669
separated flow, free shear layer behaviour in rotating systems 79−77137
separated flow behind double step at duct entrance, turbulent fluctuations and heat transfer 77−42829
separating boundary layer, subsonic, integral prediction method 80−1623
separating turbulent shear layers, flow field prediction 78−71321
shear layer instability noise produced by various jet nozzle configurations 80−69791
shear stress generation models, three-dimens. boundary layers 80−19360
shock-wave boundary-layer interaction, wall shear stress meas. 79−1212
small-scale, expt. 79−64643
small-scale turbulence, expt. *(Russian)* 77−89106
sound and aircraft noise spectral broadening by turbulent shear layer 79−37076
sound generation and simulated emission by vortex flows 80−69797
sound transmission through turbulent shear layer 79−37075
spectral theory of stratified turbulent shear flow, interactions between motion fields 80−90114
square cylinders, smooth/turbulent lift, drag, vortex shedding 77−89109
stable stratification expts. 77−27576
step, rearward-facing, downstream turbulent flow 78−59380
shear turbulence continued
stratified fluid, shear-induced turbulence spectrum 77−68661
stratified layer, thermally, turbulence structure and stability *(Japanese)* 79−41731
stratified shear flow, turbulence and entrainment *(Japanese)* 78−55674
stream, movement of cohesionless grain on bed, relative protrusion effect, shear stress 77−13094
stress transport closures, overview 80−19359
structure problems, new developments 77−31286
structures and mechanisms of turbulence, conference, Berlin, Germany (Aug. 1977) 78−94647
submerged jets impinging on baffle, flow and mass transfer, polymer additive effects 80−92194
subsonic turbulent flow past a downstream facing annular step, flow separation 80−43696
suction-induced asymptotic boundary layers, exptl. and predicted props. 80−1553
supersonic boundary layer, prediction by hybrid marching integration procedure 77−65761
supersonic boundary layers interacting with cooling wall jets, turbulent and optical characteristics 80−106792
supersonic flows, freq. response of constant temp. hot-wire anemometers 80−59149
supersonic round jet, flow characts. of large scale wave-like struct. 77−89178
supersonic turbulent flow, turbulence production 78−94767
surface jets, heated, three-dimens., modelling 80−24065
surface-mounted cube in uniform and turbulent streams 77−27535
symposium, University Park, PA, USA (April 1977) 80−17720
Taylor column for hemisphere, nonlinear effects 77−11199
Taylor-Gortler instability in turbulent shear flows and boundary layer transitions 78−90836
temperature derivative skewness, large scale struct. 78−30275
temperature derivative skewness 77−15002
temperature fluctuations, local isotropy 79−1191
temperature fluctuations, ramp model 77−3819
temperature fluctuations, struct. functions 78−30274
temperature ramps characterisation by two length scales 79−10560
thermal and dynamic fields analogy, with wall suction *(French)* 79−1249
thin shear flows, ratio of scalar-to vel. fluctuation time scales 78−46950
three-dimensional flow, in orthogonal curvilinear coordinates 77−23940
three-parameter model of shear turbulence 79−90231
triple correlation of the pressure in subsonic circular jets and nonlinear interaction of instability waves 80−69893
tube bank, heat transfer and flow around second cylinder of three cylinders in cross flow 77−15025
tube flow, longitudinal turbulent dispersion of dye pulse, asymptotic stage, Taylor conditions 77−51050
turbulence wakes behind isolated circular cylinder, determination of probe-length requirements for wind-tunnel investigations 79−68688
turbulent boundary layer, supersonic, wall temp. effect 78−94765
turbulent boundary layer, wall shear stress, small amplitude perturbations 78−14000
turbulent boundary layer on a moving surface, integral and numerical methods 78−63421
turbulent boundary layer with separated flow, integral method 80−1547
turbulent core of boundary layer 79−1168
turbulent correlation equations, by method of separation of variables 78−94673
turbulent diffusion 79−68690
turbulent jet, in coflowing stream, vel. and temp. profiles 77−27569
turbulent shear stress, correl. turbulent kinetic energy 78−94660
turbulent shear stresses in compressible boundary layers 80−14736
two viscous incompressible fluids in parallel uniform shearing motion, hydrodynamic stability 80−59010
two-dimensional free shear flow, modified one-equation model 80−6034
two-dimensional turbulence, in plane channel, in azimuthal mag. field *(Russian)* 77−47101
two-stream mixing layer, turbulence obs., hot-wire meas. system 79−32488
unsteady flow past semi-infinite porous flat plate with suction, velocity profiles 80−92129
velocity and temp. fields 78−22338
velocity decomposition method, pot./complex-lamellar method, turbulent shear layers 79−32481
velocity distrib., wall friction in rotational turbulent laminar boundary flow *(German)* 80−1526
viscous incompressible fluid, turbulent cocurrent flow, similitude postulates 79−98698
vorticity transfer theory, re-examination 77−31291
wake, for turbulent shear layers, modified law 77−35146
wake, of circ. cylinders, in nearly homogeneous turbulent stream 79−1197
wall jet, algebraic Reynolds stress model calc. 80−1668
wall jet over convex surface, turbulent flow characts., Reynolds shear stress 77−42890
wall jets, with cylindrical streamwise surface curvature 77−35193
wall shear stress meas. with hot film device in var. temp. flow 77−51142
wall shear stress prediction in three-dimensional turbulent boundary layers 78−67184
water pipe flow, turbulent shear struct. 77−3872
water pollutant dispersion in turbulent shear flow 77−41090
water wave interaction on turbulent struct. 77−47028
wavy boundary, shearing flow, heat, mass, momentum transfer, turbulence model 78−87335
CO_2 IR laser velocimetry, processing techniques and applications 80−87831
$N_2+N_2O_4 \rightarrow N_2+2NO_2$, turbulent mixing in shear layer 77−75989

shear turbulent flow *see shear turbulence*

sheathing, cable *see cable sheathing*

sheaths, plasma *see plasma sheaths*

shell model (nuclear) *see nuclear shell model*

shielding
see also magnetic shielding; radiation protection
14 MeV neutron generator, concrete shielding dose transmission factors 77−71702
14 MeV neutrons using iron-water combination 77−61614
accelerator shielding problems *(Japanese)* 80−99343

shielding continued
accumulation dose factor for scattered γ-radiation in two-layer cylindrical shielding blocks 79−18058
acoustic wave diffraction, study of efficiency of thin screen *(French)* 78−87188
activation detectors for neutron flux and spectrum determination 77−71727
actively shielded hard X-ray telescope 78−81540
AGR, internal radiation shields, design and performance evaluation 80−5373
AGR pressure vessels, radiation protection for shutdown man-access 80−5374
air-over-ground neutron and gamma spectroscopy 80−23161
analyses crystal of neutron spectrometer 80−42887
basalt, compressed, appl. to shielding against soft X-ray radiation 78−41865
benchmark gamma-ray skyshine expt. 79−59274
benchmark problems by CSEWG 80−47736
benchmark shielding problems, American Nuclear Society Standards Committee, documentation of computational methods 80−47737
benchmark shielding problems obtained from integral tests of neutron cross sections 80−47740
biological shield removal, associated radiological protection problems 80−9431
biological shield wall for Caorso nuclear plant, design, construction and erection 78−86694
BN-350 reactor shielding studies 78−21667
boral shielding material, neutron transmission calc. 80−854
bremsstrahlung distrib. in water, Al, Fe and Pb, 22 MeV electron bombardment 78−59840
bremsstrahlung in bulk media, shielding study, Monte Carlo anal. of thick target spectra 78−59839
bremsstrahlung influence on γ dose buildup factors rel. to penetration depth *(Russian)* 79−13542
bremsstrahlung spatial distribution in water and water-iron by 22 MeV electron bombardment, meas. with activation detectors 77−57754
build-up factors for 6.2 MeV photons penetrating multilayered shields 79−81093
BWR, shield design against neutron streaming in pressure vessel vicinity 80−13678
BWR feedwater nozzle cladding removal ALARA approach 79−59224
BWR power plant shielding concept 80−18712
BWR shield wall penetrations, radiation shielding 80−13679
cables insulated with Al_2O_3 and MgO, resistance to high-temp. and intense gamma radiation 78−25332
channel-type reactors, γ-ray dose rate spatial distrib. over entire thickness of side shield 78−86697
clay, compressed, appl. to shielding against soft X-ray radiation 78−41865
Clinch River Breeder Reactor primary coolant pipe chaseway neutron streaming analysis 79−9661
Compton scattering, Monte Carlo simulation including γ-ray polarisation 77−34476
concrete, albedo for low energy γ-radiation 80−32534
concrete, high density, radiation shielding below 1 MeV 79−13535
concrete, high-resolution gamma-ray spectra 77−50309
concrete, meas. of albedo number using ^{60}Co, ^{137}Cs sources 79−26768
concrete, neutron number and dose albedo 79−93681
concrete, neutron reflection characteristics 77−71633
concrete buildup factors based on the American National Standard for flux-to-dose-rate conversion 80−47732
concrete Eisenhauer-Simmons γ-ray build-up factors, Taylor coeffs. 77−34394
concrete with increased H content, shielding calc. 79−71922
concrete-equivalent materials, shielding calcs. below 100 kVp 79−29637
conference, radiation physics, Calcutta, India (30 Nov. to 4 Dec. 1974) 77−54128
controlled fusion expt. shielding and earth loop elimination using fibre optics 80−74007
cosmic-ray shielding for manned interstellar arks and mobile habitats 77−49264
cyclotron, variable energy, shielding calcs., concrete and earth shield design 77−61622
cylindrical source shielding eqns. including buildup, lateral dose rate, compact function use 78−89982
Darmstadt linear accelerator high resolution scatt. facility 78−70653
data file for reactor shielding calculations, ENDF/B-V 78−13398
Debye screening and electron conc. nonuniformity effects on cylindrical antenna on satellite 78−69563
deep penetration shielding problems, calc. of contribution flux and current spatial distrib. 79−59283
deep-penetration radiation transport, event and point value in Monte Carlo importance sampling 78−8869
deep-penetration transport calculations and neutron transport eqn. forms 78−8868
diagnostic X-ray rooms, simplified shielding 79−16313
dielectric trapping, bremsstrahlung shielding meas. 78−78507
earphone shielding effectiveness for artifact control, auditory evoked pots. meas. 79−57790
electrodynamic soln. for monochromatic field and thin shield, boundary conditions 77−54647
electron accelerator, shielding for high energy neutron dose 79−54609
electron accelerator systems, shielding and safety 77−67904
electron microscopy, dielectric support film screening effects 80−86504
EM field penetration and shield performance calc. 78−82885
EM field penetration through gaskets and seams, simple model 77−42464
EM shielding theory of metallic enclosures with apertures 78−55282
ENDF/B-V cross section data for shielding appls., Monte Carlo MCNP integral calcs. 80−47744
ENDF/B-V nuclear data for shielding appls., energy balance anal. 80−47745
epithermal 1/V self-shielding of reactor poisons using Nordheim integral method 78−17306
eye, effectiveness of ophthalmic lenses against beta radiation 77−66862
eye protection shield for the fluoroscopist 79−92398
eye shields, individualised, for electron beam therapy and low-energy photon irrad. 80−109040
fast neutron albedo for Fe, concrete and Fe-covered concrete radiation shields 79−76151

shielding continued
fast neutron pulses, time distrib. of doserate behind polyethylene/Fe layers *(German)* 77−26886
fast neutron transport through laminated Fe-H_2O shield 80−13931
fast reactor design data adjustments 79−9695
FBR, commercial demonstration reactor, radiation damage shielding 80−23178
FBR fuel reprocessing plant, radiation protection, containment and shielding 80−23179
fibre type light shield with absorbing cladding, Fraunhofer diffr. 78−90521
fifth international conference on reactor shielding, review 78−29599
finite element methods for radiation transport calcs. 78−13196
fission reactor, multigroup libraries from radiation shielding information centre 78−13399
fission reactor, sensitivity-based cross-section data assessment 78−9048
fission reactor, techniques survey and appl. *(German)* 78−29638
fission reactor fuel, mixed oxide, suitability of spent fuel shipping casks 80−27757
floating nuclear plant, shield design features 78−21777
fuel reprocessing plant, radiation protection design considerations 77−46416
fusion reactor, advanced fuel type, bundle divertor design 77−38413
fusion reactor, Doublet III, vacuum vessel neutral beam armour 80−95462
fusion reactor, ISSEC selection and PKA spectra, use of fission reactor test facilities 80−57950
fusion reactor, multigroup libraries from radiation shielding information centre 78−13399
fusion reactor, sensitivity-based cross-section data assessment 78−9048
fusion reactor irradiation test facility, higher energy neutrons, shielding calcs. 80−13786
fusion reactor Li liq., deuteron activated, shielding 80−99286
fusion reactor LOCA, performance of shield and magnet 77−67880
fusion reactor materials, neutronics analysis using ENDF/B-V cross-section covariance data 80−47710
fusion reactor radiation attenuation meas., sensitivity response of liquid scintillator detector 79−67951
fusion reactor shielding concretes, neutron activation props. 80−13787
fusion reactors, quantitative cross-section data assessment 78−9047
fusion reactors, shielding and maintainability in an experimental Tokamak 80−99287
gamma ray coherent scatt., semiempirical formulation 77−55846
gamma ray spectral penetration through radiation shields, review 80−5343
gamma rays, 6 MeV, penetrating shielding materials, energy and ang. flux density spectra 80−63393
gamma-ray albedo data, removal of negative albedo terms 80−5347
gamma-ray buildup factors for Pb/H_2O stratified radiation shields 80−86994
gamma-ray shielding, concrete wall cavities, compensation by Fe plates *(German, English)* 77−83109
gamma-rays due to reactor accident, shielding by vehicles and structs. 78−13251
GCFR, design of deep penetration integral expt. for ThO_2 blanket and radial shield mockup 80−23167
GCFR benchmark shielding expts. 79−9902
GCFR grid plate shield design, anal. of confirmation expt. 80−23166
GCFR shielding expts. at Tower Shielding Facility, ORNL 80−47739
granite, compressed, appl. to shielding against soft X-ray radiation 78−41865
graphite, neutron penetration, Monte Carlo calculations for 30, 45 MeV *(Japanese)* 80−18677
graphite, proton bombardment at 52 MeV, neutrons and photons penetration 80−27821
ground screening factor evaluation to protect systems from interference *(French)* 78−49071
health physics research reactor, neutron spectra meas., various shielding conditions 80−63396
heat, two-phase porous cooling system, hydrodynamic and thermal characts. 77−10012
heat radiation screening from hypersonic shock layer in boundary layer *(Russian)* 79−32497
high-speed cassette film fogging and shielding 78−8460
hot cell, shielding slab thickness calcs. 79−6752
HTGR refuelling, equipment safety, gamma dose meas. 80−47668
improved radiation shielding using packed mixed size Pb particles, nuclear plant maint. appls. *(Japanese)* 80−106207
inductive dipole sounding anomaly, low-impedance overburden screening *(Russian)* 78−81106
information centre on radiation shielding, international technology resource 78−17543
interplanetary electron shield anal. 77−78604
irradiation sources in reactor technology *(German)* 78−46180
KS-150 reactor, radial shielding model, neutron and γ-ray spectra meas. *(Slovak)* 78−21624
leakage effects in self-shielding factor methods, consistent treatment 77−50227
LF EM shielding props. of arbitrary cross-section conducting cylindrical shells 78−55283
linear accelerator, local absorber in accelerating section to reduce radiation level 80−83229
Lipowitz metal shielding thickness for dose reduction of 6-20 MeV electrons 80−76842
LMFBR, heat and mass transfer behind heated reactor cell liner following hot Na spill 78−17388
LMFBR, neutron elastic removal cross sections, interference effect of strong scattering resonances 80−68658
LMFBR, physics problems of fast reactor shielding 79−67873
LMFBR shielding calculations, accuracy of ENDF/B-IV cross sections 78−13401
LWR concrete shielding, ANS coupled cross-section standards 79−59281
LWR irradiated fuel transport flasks, shielding and engineering aspects 80−27831
LWR shielding, neutron transport anal. comparison of several multigroup libraries 80−23168
matrix methods for radiation transport 78−13198
metal shielded optical fibre transmission characteristics 78−1369
Millstone Unit No.2 neutron spectra and fluence determ. 79−9907

shielding continued
mixed oxide fuel fabrication, radiation protection and shielding 77−46417
Monte Carlo method modification for radiation field calc. behind thick shields 79−93760
Monte Carlo methodology for shielding of structures against initial nuclear radiation 80−47741
multigroup cross section calculation, self-shielding, subgroup method *(Rumanian)* 78−46140
multigroup transfer coeffs., efficient eval. for shielding appls. 80−47747
multilayer radiation shielding optimisation, conversational procedure 77−14273
neutron activation analysis, 14 MeV, screening effect of sample on standard calc. 77−56282
neutron bomb radiation protection, calc. of rad. penetration in air and shielded human tissue dose equiv. 80−47743
neutron flux self-shielding in activation anal. 80−93835
neutron information at National Neutron Cross-Section Center 78−13403
neutron leakage spectra from critical assemblies, depth dose, dose equiv. and quality factor 78−58504
neutron medium-energy radiotherapy, shield design 79−12016
neutron primary beam and shielding radiation quality and absorbed dose obs. 80−12281
neutron radiative capture, prompt gamma-ray spectra in keV region, rel. to reactor shielding 77−26761
neutron radiotherapy, 14 MeV, skin-sparing, effect of metal sheets 78−35923
neutron scatt., random sampling technique for choosing scatt. angle from ang. distrib. 77−61619
neutron shielding benchmark expts. 78−29655
neutron shields, homogeneous slabs, computer calcs. of transmitted, reflected spectra 77−3067
neutron shutter for cyclotron facility 78−21794
neutron transport numerical methods, recent work at LASL 78−13195
neutron-induced cross sections at 14 MeV for reactor and shield design 78−13103
neutrons, scattering materials effect on average neutron energy, spectral index, hardness parameter 77−26816
new waste calcining facility, radiation shield integrity testing 80−13940
N.S. Mutsu, primary shield, mock-up experiments, analysis 78−21782
N.S. Mutsu, radiation streaming, repair plan 78−21781
nuclear data for shielding calc. and influence of its uncertainty *(Japanese)* 79−71982
nuclear power stations containing VVER-440 reactors, radiation safety of personnel and local population 77−71700
nuclear reactor, large-scale steel melt/concrete interactions test 78−17387
nuclear reactor, thermal decomp. of concrete in hypothetical fuel meltdown accident 78−17386
nuclear reactor concrete shield, interaction with molten core material, heat flux determ. 78−17385
nuclear reactor shielding anal., spatial channel theory, appl. to FFTF 77−6569
nuclear reactor stainless steel and Na shield radiation heating expt. 79−9903
nuclear ship streaming neutron meas. by two-detector method 77−46408
organ shielding and localisation in a diverging treatment beam, simple method 80−94317
particle accelerators, radiological safety in design and operation, American National Standard 79−89511
particle accelerators ionising radiation produced during operation, dosage and shielding *(Czech)* 79−89505
particle transport in finite slabs, orders-of-scatt. anal. 77−22502
PBHTR, space-shielding cross sections 78−25274
PDX Tokamak, neutron skyshine Monte Carlo calcs. 80−47711
perturbation theory, higher order generalised 80−47731
perturbation theory developments for anal. and design, review 77−14227
PFR Dounreay, radiation and contamination control 80−27834
PFR Dounreay, utilisation of neutrons meas. for shielding calcs. 80−32538
photon attenuation coeffs. in heterogeneous media, nuclear geophysics methods 79−39708
polyethylene, neutron penetration, Monte Carlo calculations for 30, 45 MeV *(Japanese)* 80−18677
power reactors, coolant circuit contamination 78−21666
proton attenuation lengths in paraffin, concrete and iron around targets 80−102412
PWR, cavity streaming problem, shield config. optimisation 80−9352
PWR, low-pressure drop reactor cavity shield system 80−13677
PWR, shielding against neutron and gamma streaming, computational methods 78−21783
PWR, St. Lucie 850 MWe, neutron streaming meas. and shielding recommendations 78−70608
PWR cavity shield design, radiation streaming, calc., appl. of Monte Carlo and discrete-coordinates technique 79−89364
PWR containment building, design and anal. of cavity shield system 80−18713
PWR radiation shielding design 80−5372
PWR reactor cavity shield system, design and anal. 79−89366
PWR shield configs., concrete attenuation effectiveness, numerical studies 77−38356
PWR spent fuel calcs., neutron multiplication and shielding problems 77−74951
PWR spent-fuel shipping, neutron multiplication and shielding 77−46418
radiation, calc. of half-value layers for multiple sources 77−9274
radiation, profile optimisation, use of penalty functions 79−97909
radiation facilities, external exposures control, designer-health physicist collaboration 77−81586
radiation field functional calc. method for shielding parameters 79−71928
radiation protection and monitoring of personnel handling Pu reactor fuels 80−5389
radiation protection/shield design, systematic approach 78−21779
radiation shield design objectives selection, optimisation calcs. 77−6565
radiation shield integrity testing 80−5390
radiation shielding, cross section sensitivity analysis 78−21778
radiation shielding, in 3-D direct-coupled-ray method 78−21785
radiation shielding, Monte Carlo calcs., event-value path-length biasing 77−38421
shielding continued
Radiation Shielding Information Centre, available computer codes and data 77−65343
Radiation Shielding Information Centre 78−21784
radiation shielding standards in USA, development 77−54374
radiation streaming, shield design problems 78−21780
radiation therapy, neutron source shielding for Be(*d*,*n*) reaction 79−20617
radiation transport theory, tracklength biasing in Monte Carlo methods 80−5335
radioactivation of shielding materials Fe, Benelex by fast neutrons, γ-ray spectra, decay rates 79−682
radioactive samples, appl. of SEM with X-ray spectrometer, shielding design 77−189
radiotherapy, organ shielding using Pb-Sn-Bi-Cd low melting point alloy block *(Korean)* 80−36154
radiotherapy linear accelerator use factors 77−9275
radiotherapy neutron leakage charact. rel. to room shielding 80−51273
radiotherapy shielding, comparison of photoneutron and ^{252}Cf neutron spectra 79−59273
reactor, 6 MeV gamma photons penetration through Al, concrete and graphite determ. 80−5256
reactor cavity neutron shield design at Millstone Unit No.2 80−47748
reactor cavity radiation streaming, albedo Monte Carlo methods 79−89363
reactor fuel reprocessing plant, radiation protection and shielding 77−46415
reactor radiation streaming anal. using spherical harmonics expansion of albedo data 79−89367
reactor shielding, current status and future prospects 78−25328
reactor shielding computation methods and programs in Poland *(Russian)* 79−26767
reactor shielding methods, development in USA 78−21776
reactor shielding methods, evolution, data 78−21775
reactor thermal shielding for GCFR, development programmes 77−18648
resonance neutron self shielding factors for Au and Ag, expts. and calcs. 77−42008
response matrix doubling equations for particle distribs. calcs. improved formulations 77−6480
SCAP-BR, multilegged duct γ streaming computer program 79−9906
secondary neutron polarization via penetration through a ferromagnetic shielding wall 80−47742
SEM stray field reduction for voltage contrast meas. 79−67431
Serpukhov proton synchrotron shield, mixed radiation dose equivalent outside 80−32530
shield integral expts. at ORNL 80−47709
SNR-300, coolant outlet duct design from neutron transport experiments *(German)* 78−29566
SOLASE laser fusion reactor, Monte Carlo shielding calc. for mirror-laser beam duct system 80−23174
solid neutron shield development, materials eval. for spent fuel shipping cask 80−13939
source definition for head shielding requirements in linear accelerators, effect on room shielding design 80−46068
space station, radiation protection design considerations for man in geosynchronous orbits 78−28096
spacecraft thermionic reactors, neutron leakage control using boronated reflector drums leading to lower shielding mass 80−47663
statistically stationary traffic noise shielding by simple obstacles 78−90590
steel slab, scattered radiation intensity of ^{192}Ir gamma rays 77−30673
Super Phenix fuel fabrication for Creys-Malville station, core controls *(French)* 79−31089
tandem, nuclear safety facility at Daresbury, shielding methods for insulators, ICs, other components 78−33318
TFTR neutral-beam injectors, shielding calcs. 80−23172
thermal radiation shield, for cryogenic apparatus, thermodynamic optimisation 78−81982
thermal vacuum chamber shield, heat-absorbing, natural thermal radiation calc. 77−65666
thermoluminescent dosimeter monitoring post, concrete shielding to reduce background 78−817
thymic region shielding in radiobiology expts., dosimetry in irrad. mouse cadavers 78−61257
Tokamak experimental power reactor, shielding of major penetrations 77−34455
Tokamak reactor, radiation shielding 78−25323
Tokamak reactor blankets, effects of neutral beam injection tubes, shielding calcs. 80−23173
Tokamak reactor shielding requirements, penetration size effects 79−9875
tokamak reactors, radiation shielding of major penetrations, theory 79−36412
tomography, multi-slice positron emission-computed, design criteria, shielding 80−61673
toroidal geometry effects in neutron transport eqn., discrete ordinate S_N method 78−13327
transuranic element meas. in vivo at CRNL 77−77993
two-dimensional discrete ordinates calc. charact. for shielding design *(Japanese)* 79−93744
UK reactor fuel reprocessing plant remote handling experience 79−9839
Varian Clinac 4 MeV linear accelerator, radiation from U collimators, and shielding 78−24135
variance reduction techniques using adjoint Monte Carlo method in shielding problem 79−63759
water, neutron number and dose albedo 79−93681
Windscale nuclear fuel reprocessing, shielding and radiation protection 80−18714
X-ray attenuation measurements on Y tong shielding material *(German)* 80−98145
X-ray screening glass antireflection surfaces 77−21601
X-ray shielding arrangement, for diffr. equipment 80−849
X-ray shielding device, Pb glass, for use with ceiling mounted tube 79−92397
X-ray tubes, rotary anode, HV insulation, discharges due to back scattered electrons elimination *(German)* 80−105758
X-rays, high energy photon absorption cross section for matter, review *(Japanese)* 78−74506
d-d neutral beam facility neutron yield meas., shielding and diagnostics 79−9878

shielding continued
γ 6 MeV scalar leakage flux spectra through Pb-Al and Fe-Al shields 79−85871
Ag, resonance self-shielding factors, depend. of Doppler factor 78−17439
Al, meas. of albedo number using ^{60}Co, ^{137}Cs sources 79−26768
Al target inside magnet, hadron cascades prod. by 300 GeV protons 77−10566
Al-graphite two-dimensional shield, neutron penetration meas. 79−3245
Al-steel radiation shields, build-up factors for 6.2 MeV photons 79−81093
Au, resonance self-shielding factors, depend. of Doppler factor 78−17439
B_4C reflector-shield concept for fusion reactor designs 80−102293
B_4C-304 stainless steel cermet for nuclear shielding appls. 80−102352
B_4C-Cu cermet fabrication for neutron shielding appls. 80−102354
B_4C-phenolic fibre reinforced composite for nuclear shielding appls. 80−102353
^{10}B shields, transport calcs. and transmission factors for activation detectors 78−78434
^{252}Cb, polyethylene pellets in design, construction of storage safe, transport vessel, portable shield 79−5380
^{252}Cf, heavy metal shielding for neutron sources 79−9892
Fe, natural, neutron total cross section minima 78−37387
Fe, neutron number and dose albedo 79−93681
Fe radiation shielding, computational benchmark for deep penetration 80−47738
Fe radiation shielding, TLD meas. of neutron and gamma-ray energy deposition 80−23163
Fe shield, meas. of neutron and gamma ray penetration 80−47730
Fe shielding thickness effect on (n,2n) reactions and fission rates in ^{238}U, hybrid reactor situation 77−50122
^{2}H-^{2}H molten-salt-cooled fusion reactor blankets, nuclear heating and radiation leakage 78−78490
^{127}I, shielding of *(Japanese)* 80−63404
LiF tile and sheet for thermal neutron shielding *(Japanese)* 78−74510
MgO, GCFR shielding material, anal. of shielding effectiveness 80−47746
Pb shield, effects of thickness and geometry var. on neutron spectra 78−33300
Pb-Al radiation shields, build-up factors for 6.2 MeV photons 79−81093
Pu, high burnup fuels, shielding and handling problems 80−27833
Rn barrier to reduce indoor airborne Rn progeny 78−73262
Si diode detectors in radiological physics, energy compensating shield development 78−24142
Si, natural, neutron total cross section minima 78−37387
W, radiation shielding material, integral tests of ENDF/B-IV high-energy neutron cross-section data 80−23162

shielding, magnetic *see magnetic shielding*

shift register sequences *see binary sequences*

shift registers
see also logic circuits
cross-tie shift register memory device 79−78484
dynamic PMOS for self-scanned photodiode array, evaluation for integrated optics spectrum analyser 80−58806
electronically variable delay using a SAW tapped delay line and digital shift register 78−63241
fast event recorder utilizing a CCD analog shift register 79−45578
photon flare centre determ., online optoelectronic convertor *(Russian)* 79−75111
reliability assessment by scanning electron microscope 78−29215
whistler detection, multichannel filter and shift register obs. system 78−93031
PtSi Schottky-barrier monolithic IRCCD focal plane 80−86427

ships
see also navigation; radio direction-finding
accompanying waves of a ship, explicit approx. from slender body theory *(French)* 78−59408
acoustic beam output noise due to shipping, statistical meas. 79−3836
acoustic radiation from hull, theory for point excited rib-reinforced plate 77−80003
Argo Merchant wreck site, oil and sediment hydrocarbons, gas chromatography 79−83645
Batfish active towed body system development 77−5374
bilge water oil pollution monitoring system development 77−5246
boat wake effects on shoreline of Lake Manapouri 79−25278
computer-aided ship structural design for diploma and undergraduate courses 79−35494
correlation sonar for ship's velocity meas. 79−27474
corrosion rate of basal layers, cathodic protection meas. methods *(Dutch)* 78−3297
course speed and lateral drift, acoustical determination 80−5892
deep sea mining ship, telemedical treatment system development 78−77147
deep submergence vehicle development and reliability 77−5376
diesel-engined ships, noise in cabins and engine room, reduction by abatement at source *(Japanese)* 80−79052
Doppler sonar for ship's velocity meas. in deep water 79−27475
drill ship positioning, acoustic meas. system 78−45057
flat ship, low-aspect-ratio, planing at infinite Froude number 78−32684
heave and pitch motions in shallow water, forward speed effects 77−47126
hull form evaluation by wake pattern analysis and compilation *(Japanese)* 79−27644
hulls, three-dimens. turbulent boundary layer eqn. soln., exact integral method *(Japanese)* 77−54985
icebreakers, noise accompanying breakup of ice by hull 79−94402
infrasonic sea noise, contrib. of distant shipping 78−11902
infrasound, effect on people, exptl. study of levels 78−88726
magnetism, rel. to mag. compass, history, Airy-Scoresby controversy 78−4451
marine corrosion, and its prevention 80−104333
marine seismic exploration ship 77−64449
for microcystis removal in lake, Japan *(Japanese)* 77−56753
Mikhail Lomonosov, research vessel, review of 20 years of scientific results *(Russian)* 78−69485
mirror sight stabilisation using microcomputer 79−27369
model, hydrodynamic resistance, analytic calc. *(Russian)* 78−75123
Morning, Cloud, loss of yacht in English Channel, 1974 September 2, storm surge 78−88895
navigational almanacs for small computers, calculators 79−62726

ships continued
Navy vessel fracture mechanics and flow separation, instability phenomena 80−99971
noise control problems 79−32134
noise reduction using viscoelastic materials 78−22226
nonconservative system resonance, modal analysis 78−42557
nuclear, streaming neutron meas. by two-detector method 77−46408
nuclear merchant ship propulsion, operation experience 79−26745
nuclear propulsion, report on 1977 IAEA conference *(Dutch)* 77−83069
nuclear reactor, ^{16}N activity in water from ^{16}O(n,p)^{16}N, computer code and expt. 78−13192
nuclear vessels, probabilistic model for assessment of collision likelihood 78−5063
OCCULT laser system operating in marine boundary layer 78−5565
ocean, shipping noise ambient levels, freq.-freq. correls. 77−64302
ocean ambient noise, source level model for propeller blade rate radiation 80−43513
ocean internal ship waves, development caused by shifting press. in multi-layer fluid *(Russian)* 78−77256
oceanographic integrated research, with data acquisition and processing systems 79−34969
oceanographic research techniques used in survey ships *(French)* 78−65434
oceanographic research vessels, shipbaord minicomputers appl. 79−53562
oceanographic robot submarine with computer control 77−5375
offshore operations, LEO I submersible reliability and safety 77−5373
PISCES submersible scientific equipment and data acquisition system 77−5381
planing hulls, model tests using recirculating water channel, resistance characts. 79−18978
pollution monitoring system, automatic Beckman Model 915 organic carbon analyzer 79−16521
propeller induced underwater acoustic disturbance obs. 79−68463
propellers, acoustic wave generation, non-uniform liq. stream 80−96094
propulsion, fission reactor appl. *(German)* 78−29638
R/V 'Akademik Vernadsky', information exchange between oceanographic probe and computer *(Russian)* 78−77363
R/V Athena, high speed ship for towing research 77−41213
reduction of structure-borne sound, model tests 79−32133
resin selection, w.r.t. mechanical strength retention 79−96035
screening from bora wind in the port of Novorossiisk 77−78365
sea ice cover nonuniform thickness effects on navigability 77−78222
ship model wake meas. in wind tunnel, laser anemometer autocorrelation *(German)* 79−60085
ship propeller shaft dynamics, forces between shaft and bearings, root bearing rigidity depend. 79−81801
shipboard meteorological data system 80−46299
slender body potential flow between closely spaced walls 77−89095
small nuclear reactors for power production and ship propulsion appl., prospects 77−10485
small submersible, acoustic communications system design 79−5666
speed determ., new acoustical method 79−14178
steel, Ni, welded joints on LNG carriers mech. props. and fracture toughness 80−85017
streamlined, ray theory of ship waves 79−59994
structure, stress fields hybrid simulation 79−41637
structure borne sound attenuation 78−33947
submarine periscope optical design for laser rangefinding compatibility 80−78987
submarines, aero/hydrodynamic forces and moments 77−89094
submersible data acquisition system SCRIBE 80−46266
submersibles, acoustic navigation for precise underwater surveys 79−5683
submersibles for underwater research, commercially available vessels 80−82104
supertanker radiated noise spectra in deep ocean, origin 78−33959
surface effect, noise control design problems 80−74598
survey vessels, multiple use 79−53561
tanker oily discharge at sea, deballasting monitoring system appl. 77−45020
typhoon havens research program at the Naval Environmental Prediction Research Facility 79−5616
US echo sounder Koden SR651 *(Italian)* 79−14168
U.S. oceanographic research vessel fleet 77−91325

shock, thermal *see thermal shock*

shock control
gyroscope, forced vibrations shock absorber selection parameters 80−43659
shock absorber, elastic damping props. determ. unit 78−5703

shock measurement
cross-sectional shock shape meas. using columnar and plane discharges 79−27666
dielectric and magnetic pickups, signals comparison for waves up to 100 kbar intensity 78−5707
dynamic shock position measurements using microprocessor-controlled time-domain reflectometer 80−79248
effective intermittent shock testing *(German)* 78−77887
electron inertial effect, shock loaded rod, meas. of strain produced 78−51139
Fourier analyser signal processing system 77−68335
gas gun expts. for two-dim. strain meas. 78−5709
impedance match at low pressures 78−51264
K-band microwave interferometry for measurements of high surface vels. 80−77761
laser driven shock waves vel., risetime, luminosity struct. meas. using shocks own luminosity 78−59857
laser-produced shock wave optical diagnostic system 80−79421
meas. via Michelson field-widened interferometer plates diffuse back surfaces, vel. 77−61050
mechanical shock-test stand for repeated impact acceleration effect 79−80611
nanosecond hydrodynamic diagnostics, streaking camera, fibre optic probes 78−37096
piezoelectric transducer systems, noise suppression and prevention for shock and vibration meas. 80−22353
speed of shock wave, continuous recording in porous metal 78−5708
spherical blast wave, high-speed photogrammetry of real and ideal reflections 78−42694
steel, dielectric and magnetic pickup signals comparison 78−5707

shock measurement continued
temperature meas. of shock compression of solids by optical means 80−86304
velocity determ. by laser schlieren method 77−39370
C piezoresistive gauges, shock loading and unloading behaviour up to 5 GPa 80−87750

shock tubes
see also shock waves
acetylene-NO-O_2, combustion products, 1400-2600K, minimisation of NO, computer model 78−85161
airfoils, transonic testing at high Reynolds number in shock tube 80−14852
aqueous fog form. 80−19531
boundary layer instability, transition evolution 79−64642
boundary layer obs., unsteady, behind moving shock wave 78−46998
boundary-value problem global soln. *(French)* 78−63449
chemical kinetics, elem. gas reaction rate coeffs. meas., review 80−3299
choking phenomena, of flows in shock tubes 77−89152
combustion driving technique improvement 79−37350
detonation wave propagation, investigations on suitability of piezoelectric and magnetoelastic detectors *(Polish)* 80−79351
diaphragm opening process, model for inelastic diaphragm 79−7384
diaphragm rupture, initial flow model 78−14045
diffraction and reflection from open end, shock waves, numerical computation *(Chinese)* 80−43735
driver gas flow with fluctuations 80−96282
dynamic discharge arc driver, computer-aided circuit simulation 77−24219
EM shock tube for obtaining short pulses of visible radiation, plasma flow anal. 78−1909
expansion tunnel performance with and without an EM opened tertiary diaphragm 77−89211
fast-acting valve, construction and characts. 77−72372
flow field in large shock tube of variable cross sectional area *(Chinese)* 79−72908
flow parameter meas. in ϕ800 shock tube *(Chinese)* 79−37336
flow uniformity in variable area shock tube 79−10590
flows, unsteady non-equilibrium, discretisation of boundary layer terms ionisation relaxation as example 80−14742
gases, characterisation, reactive flow in shock tubes, laser absorpt. spectroscopy 80−45618
Hartmann-Sprenger tube, gas temperature calc., using Lagrange equations *(Japanese)* 79−4041
heat transfer gauge, thin film, use in shock tube *(Japanese)* 77−19654
high-speed shock generation, using explosives 78−26156
hypersonic shock tunnel, development for aerospace simulation 79−41777
ionising shocks reflection on end wall, finite difference analysis *(Japanese)* 78−42629
Langley expansion tube, operating characts. 78−63447
Ludwieg tube, steady flow duration extension 80−1700
Mach wave radiation of hot supersonic jets 80−69894
mass flow measurement using thermocouple-anemometer 79−77300
methane, shock-tube oxidation, equilibrium and nonequilibrium radiation emission 78−27760
moving plasma in an electric shock tube with pulsed gas injection 79−77355
for nuclear blast duration simulation appl. 79−18907
piston structure and gas distrib. in strong shock wave 80−10265
plasma source for high-temperature MHD generator 77−35372
pressure driven, shock formation distance 77−19623
pulse-pressure generator, quasistatic method for stepped pressure transducer testing 80−62678
pulsed gasdynamic shock-tube laser, working time extension 80−99696
spectroscopy of shock wave heated gases, using tunable diode laser 77−71890
tailored contact surface region, anal. 78−5832
temperature, concentration, and velocity in jets, flames, and shock tubes 79−68778
thermal boundary layer interactions in shock tube sampling for kinetic obs. 80−104420
transient jet of propelling gas during diaphragm rupture in shock tube, holographic images 79−77181
valveless shock tube pumping mechanism 79−14337
valves, fast-acting, formation of shock waves 80−24052
wall supported shock precursor obs. 80−100011
Ar, ionising boundary layer in shock-tube side-wall flow 79−60144
Ar, radiative level lifetime, photoionisation and photoexcitation rates, in shock tube 77−34594
B II, Stark shift, shock tube meas. 77−50403
CO_2 gasdynamic laser power, free-piston shock tube expts. *(Japanese)* 79−76661
CO_2-N_2 mixture, shock tube, operating channel humidity determ., apparatus *(Russian)* 77−7057
Fe+Ar, Fe I reson. line, collisional broadening at high temp. *(German)* 80−106298
H_A line width in at. H atmosphere, shock tube absorption meas. 79−64834
HBO_2, band strengths, shock tube IR spectrosc. meas. 80−106358
$H_2(D_2)$-Ne-He(Ar) plasma, combustion driven shock tube, H_β central struct., ion mass effect 78−26327
Kr plasma, shock-heated, continuum radiation emission coefficient meas. 79−64835
Mg+O_2=MgO+O, shock-tube study of evap. and oxidation kinetics 80−16651
MgO, electronic transition strengths, shock tube meas. 80−87183
NO γ-bands at 2259 Å, shock wave effective absorption coeffs., empirical determ. 79−64799
NO, in exhaust gas, direct optical detect., transverse sensitivity *(German)* 78−35751
N_2O ν_3-fundamental at 4.52 μ, shock wave effective absorption coeffs., empirical determ. 79−64799
NaCl+Ar, dissoc.-ionis. process rates in shock tube 78−35674
O_2, singlet states, quenching by $O_2(N_2)$, shock tube study 80−23511
OBF, band strengths, shock tube IR spectrosc. meas. 80−106358
Pb I and II, transition probabilities, Stark broadening parameters 80−23367
Xe, continuum absorpt. coeff., in shock tube, determ. 77−39463
Xe, s-p transitions, Stark consts. and oscill. strengths, shock tube meas. 80−18822

shock wave effects
acceleration of energetic charged particles by interplanetary and supernova shock waves 80−31189
achondrite meteorites, mag. effects of brecciation and shock 80−8603
alkali halide, Frenkel defect generation in cation sublattice, shock recomb. mechanism *(Russian)* 77−31656
alkali halide crystal, permittivity and polarisation behind shock wave front 77−52013
andalusite, shock-loaded, deform. 80−19873
anhydrite, shock compressed, vel. of sound meas. 78−10123
astrophysical plasmas, particle acceleration in collisionless shocks 80−31208
astrophysical shocks, particle accel. 78−49241
atmosphere, meteoroids ballistic shock waves and explosion geomag. disturbances prod. 77−13139
beams, transient response prediction by Laplace transform techniques 78−1596
Blair dolomite, shock wave expts. 80−67362
bleeding, inner-ears of chinchillas, caused by simulated sonic boom 79−16247
boundary layer, shock wave interactions 77−89151
boundary layers, shock-separated flows, turbulence models 78−71365
brittle solid, framgentation mechanism by explosion 77−84843
brittle solid deformation, review of theory 80−72493
Bruderheim meteorite, L6 chondrite, 500 Ma shock event effects on U-Pb age 80−98616
bubble breakdown, gas-in-liq. bubble, gas density 78−42653
buried obstacle, interaction of shock wave rel. to bulk viscosity of subsoil *(Russian)* 77−89054
3C 310, 326, relaxed double radio sources, in situ shock wave accel. model 80−51891
Canyon Diablo, iron meteorite, shock effects in phosphide and carbide phases 77−56879
cavitation, acoustic, threshold conditions for onset 78−59433
cavitation bubble collapse in water shock tube 78−67231
cavitation-produced stress in solid 77−24354
cavity, cylindrical in compressible liq., dynamics, underwater explosion appl. 79−7385
chains, one-dimensional, shock wave effects, mol. dynamics study 79−4371
charged particle acceleration to relativistic energies in interplanetary shock waves 79−80123
charged particles acceleration, role of mag. mirrors in shock waves 79−80122
charged particles acceleration on shock front, temporal characts. 79−80121
chemical laser, electronic phototransition, with thermal initiation by shock wave 80−53283
chemical reaction obs. shock tube unsteady expansion wave technique, applic. 78−61011
chemical shock tube flow, laminar to turbulent boundary layer transitions 77−48642
chemically reactive MHD flow near slender wing with supersonic leading edge *(Italian)* 79−14495
chemically reactive MHD flow parameter distrib. near weak shock wave *(Italian)* 79−14494
chondritic meteorities, L-group, incipient melting rel. to shock classification 79−88629
circular cylinder pressure rise caused by surface explosions *(Japanese)* 79−76994
compression expts. on materials, measurement of spectral radiance using multiwavelength optical pyrometer 80−52229
compression of constructional materials at speeds up to 1000 m/s 77−1860
concrete slab, explosive shock resist., tensile fracture 80−85065
condensing media, shock compression, relax. processes kinetics 78−94610
conductor-dielectric conductor system, electric signal rel. to plane load wave parameter 77−90105
conical shell, buckling in response to shock load 78−5679
containment vessel, cylindrical, submerged, dynamic plastic response, design formulae 80−83759
cosmic ray acceleration by supernova shocks in interstellar medium 80−31179
cosmic rays short-period variations, interplanetary shock wave struct. determ. 79−80125
cosmology, shock damping and entropy prod. in relativistic simple waves 77−17725
Crab Nebula filaments, shock waves hydrodynamics effects on spectra 78−85997
crack response to impact by caustics 78−56724
cycloheptatrienes, highly vibr.-excited thermal isomerisation in shock waves 79−79236
Cygnus Loop, H I shock excitation rel. to high-rel. gas Hα emission 80−41873
cylindrical shell in supersonic flow, response to shock load 77−42771
detonation, shock propagation, spallation, computer simulation 79−64554
detonation wave front, heating of contained particles, residual cryst. defects anal. *(Russian)* 79−68749
diamond, form. by shock compression of graphite, cryst., surface struct. 78−44060
diamond, mechanical strength depend. on thermal working parameters, microcracks *(Russian)* 80−55501
diamond, shock synthesis *(Japanese)* 80−29918
diamond, synthesis, shock loading from graphite-metal mixtures *(Russian)* 77−90298
diamond, synthesis and characterisation 80−50580
diatomic gas, dissociation past strong shock waves 78−42683
dislocation generation mechanism in shock wave deform. 78−43018
dispersed media, shock compressibility, brittle destruction 80−49303
dolomite, shock compressed, vel. of sound meas. 78−10123
drag, supersonic wave, of planar singularity distrib. 78−83430
dunite, elec. cond during shock compression from 12.5 to 45 GPa 78−85536
dust erosion by shock wave in air 78−42648
Earth atmosphere blow-off mechanism rel. to Van Allen belt populations 77−29524
elastoplastic relaxing media, shock waves struct., distribution model 80−58961
electrical conductivity of high temp. imperfect gas *(Russian)* 80−100072

shock wave effects continued
electrical response of relaxing dielectrics compressed by shock waves, axial mode problem 78−80280
elements, generalised shock adiabats 79−86839
EM waves generated by compression shocks, in weak mag. field 79−77292
EMF production by shock compression of solids 77−31719
emission nebulae with strong S II forbidden lines in LMC 77−29891
epoxy, Al_2O_3-filled, shock-wave compression, 0.4-3.7 GPa 78−59856
ESR, particle size and lattice microdistortions 80−97140
explosions in liquids, slow detonation, vapour explosions and bubble reson. explosions *(German)* 78−34150
Fe, twinning under influence of plane shock wave *(Russian)* 80−92538
Fermi acceleration of charged particles in astrophysical plasmas 80−31207
ferrite powders, mag. props., explosive shock treatment effects 79−52395
ferroelectric ceramic, shock induced polarisation 77−48133
ferroelectrics, converters of shock wave mech. energy into elec. power 80−61429
flow initiated by sudden motion of wedge, nonlinear anal. 77−80183
flow separation in transonic turbulent boundary layer, shock wave causing separation *(French)* 79−77186
fluorite-like structures of CaF_2 and BaF_2, elec. cond. of shock-compressed monocrystals 77−9404
foamed plastics, shock absorbing capacity determ. *(German)* 80−19877
fracture, computational models for one and two dimens. wave propag. 77−11628
frame, plane, impulsively loaded, large deflections, mode approx. technique extension 80−83757
Galaxy central region, vacuum cleaner effect of shock waves in stellar bar 77−45565
gas, ideal dissociating, differential effects of shock waves on flow parameter behind shock 77−15135
gas, oscills. in tubes at reson. freq., shock wave heating *(Russian)* 79−32570
gas centrifuges, shock-induced pressure recovery at high Mach number rotation 79−22480
gas mixture, binary, spherical expansion into flooded space, components separation 79−81948
gas pressure transients due to weak shock waves, measurement using reflectivity of glass/gas interface 79−63297
gas pumping arrangement, for relativistic electron-beam pumped lasers 77−701
gasdynamic disturbances, small amplitude, in exploding atmosphere 79−32574
gasdynamics of explosions, reactive systems, conf., Stockholm, Sweden (Aug. 1977) 79−64690
generation and application in solids *(Japanese)* 79−68475
geomagnetic disturbances produced by large meteoroids shock waves 77−49231
glass panel, dynamic stresses and failure under inertial loading 77−56073
Goat Paddock cryptoexplosion crater, W.Australia struct. and shocked rocks petrology 80−98322
graphite, self focusing high current relativistic electron beam for structural and chemical transformations *(Russian)* 80−15190
graphite, shock compression, polymorphic transform. kinetics 79−86838
graphite to diamond transition under shock wave loading *(Chinese)* 79−82337
graphite-diamond, shock induced transform. anal., post shock graphitisation 80−79933
graphite/epoxy laminates, stress wave damage 80−93611
gravitating gas, spherically symm. motion in presence of shock wave 77−11221
Gurney equations for multilayer metal fragments 79−86367
head-on interaction of two shock waves 78−67216
heterogeneous solid explosives, spin detonation 79−14429
hydrocarbons, shock compression, dynamic high press. eqns. of state 80−6450
hydrodynamical acceleration of particles in supernovae and extragalactic radio sources 80−31313
hypersonic flow, conical wing-body combination, thin shock layer theory appl. 79−46339
hypersonic flow, ice crystal-shock layer interaction 78−30317
IC 443, supernova remnant, H I shock excitation rel. to high-rel. gas Hα emission 80−41873
ice VI, shock compression expts. for Hugoniot function 80−84248
intergalactic medium, shock waves generated by galaxies and quasars at large redshifts 79−21442
interplanetary shock waves, effects on $^4He/H$ ratio vars. in energetic storm particle events 77−9636
interplanetary shock waves, inclination rel. to transient north-south anisotropy of cosmic rays 77−9634
interplanetary shock waves, influence on solar particle events 77−49250
interplanetary shock waves interaction with cometary atmospheres 77−22032
interstellar H_2 cooling, dissociation and IR emission in shocked clouds 78−41009
interstellar magnetic field amplification in collisionless shock waves 77−49459
interstellar medium, heating due to weak shock waves dissipation 78−81674
interstellar medium, mechanical heating rate by supernova blast waves 80−36682
interstellar medium, shock enhancement of HCO^+ in supernova remnant (IC 443) 80−82464
interstellar medium, star form. in shock-compressed layers 78−40919
interstellar molecular clouds, shock front propag. rel. to subgroups form. in OB associations 77−60800
interstellar molecular line emission, shock chemistry in Orion 79−21391
interstellar molecule formation and IR emission in shocks, physical processes 80−62219
interstellar molecules, collision-induced dissociation 80−17632
interstellar shock waves, CH^+ prod. in diffuse clouds 80−56898
interstellar shock waves, massive stars births induction 79−2542
isentropic explosion compression of matter, profiling of explosion shock waves 77−56228
isentropic explosion compression of matter nonhomogeneous transition layer for shock wave profiling 77−56229
kidney stone destruction by US shock wave focusing 77−32946
kidney stone non-contact destruction appl. *(German)* 78−7517
shock wave effects continued
laminate, shock wave propag., stress history recording 78−38242
laser interferometry, high speed meas. of two dimens. shock wave effects 77−79145
laser shock production rel. to material damage 77−90221
laser-induced breakdown, time-evolution of light emission 77−58836
liquid drop aggregate breakup in shock waves 80−24084
liquid surface wave due to shock wave interaction, viscosity effect 77−11202
liquid-vapor system, shock compression, equilib. states *(Russian)* 78−9687
liquid-vapour system, shock wave effect on thermodynamic equilib. 79−64746
liquids, shock excitation for diffuse-field reverberation studies 80−88267
LMFBR shock-induced fragmentation and detonating thermal explosions 79−13475
longitudinal and shear particle velocity histories in-material determ. in single inclined plate impact expt. 78−79289
magnetic field generation by detonation waves 80−24533
manganin foil like gauge calibration in planar shock wave expts. 80−95091
manganin pressure gauges, effects of shock compression and relief *(Russian)* 78−70149
Manicouagan impact structure, Quebec, shock waves rel. to melt rock petrogenesis 78−81166
materials under pressure, eqn. of state *(French)* 79−95117
media with bulk viscosity under shock loading, nonstationary plane wave propag. 78−94611
metal, equation of state, isentropic expansion method 78−91414
metal, Gruneisen ratio, rel. to Poisson ratio press. depend. and shock data 77−11712
metal, polycrystalline, elastic precursor wave model in shock loading 78−1601
metal, porous, shock compression calcs. using approx. eqn. of state 77−35657
metal, spallation on emergence of shock wave on free surface, pulse X-ray photography exam. 77−51439
metal powder explosive pressing, shock compression parameters *(Russian)* 77−52260
metal systems, mech. prop. improvement by pulsed laser generated shock wave 77−48443
metal tube, dynamic lateral compression, strain rate effects 80−83758
metal-ceramic containing diamond, impact hardening 79−15828
metallic shell, explosive expansion, deform. and rupture modes and mechanisms 80−85064
metallic shell, explosive expansion, rupture behaviour 80−85063
metallic target, laser produced shocks rel. to material damage 78−31285
metals, constitutive model at high strain-rate, shear modulus, yield strength 80−75292
metals, dislocations and shock compression, thermodynamics 80−100235
metals, FCC, plane shock wave loading, microdistortion X-ray anal. *(Russian)* 77−52399
metals, fracture due to laser irrad. and shock compressed plasma *(Russian)* 80−55500
metals, shock wave compression, reduced Hugoniot curve and eqn. of state *(Chinese)* 80−44259
metals and alloys, shock wave effect on martensitic transform. *(Russian)* 80−96595
meteorite explosion, Tunguska, Siberia, shock wave effects, model, computation 77−5507
methyl radicals, reactions behind shock waves, UV absorpt. obs. 78−46362
MHD waves, particle refl., energy spectrum and pitch angle distrib. 79−35126
minerals, dislocations and shock compression, thermodynamics 80−100235
minerals, eqns. of state for metastable phases 77−70639
minerals, post-shock temps. meas. 79−92527
minerals pressure-density path, effect of viscosity on release adiabat meas. 80−51388
molecular clouds, expanding H II region effects 79−5880
molecular dynamical studies of energy transport in crystalline solid 78−30803
molecular process kinetics, IR absorption meas. installation 79−70389
monatomic BCC lattice under intense excitation, energy transport 78−59922
monatomic three dimensional FCC lattice, solitary wave effect on shock profile 80−79874
monomethylamine, dilute mixtures, decomposition, shock tube studies, IR emission obs. 79−96301
nitromethane, shock-induced elec. polarisation *(French)* 79−11381
non-Newtonian liquid, shock-induced spreading of film between two colliding surfaces 77−7419
noncubic crystals, eqn. of state model, shock wave studies appl. 79−14883
oblique shock wave, interaction with flat plate *(French)* 79−14433
obstacle in shock tube, axisymmetric unsteady interaction 79−32575
olivine, shock induced high-pressure transformation 78−11883
one-dimensional chains, thermalization behaviour behind shock front, mol. dynamics calcs. 79−73253
one-dimensional lattice, shock propag., soliton like behaviour 78−59859
optical absorption wave propagation in gases, struct., propag., effects 79−10629
organic glass, shear strength behind the front of a plane shock wave 79−15752
Orion Nebula, high-vel. features driven by stellar wind from θ^2 Orionis A 79−8978
paraboloids of revolution, internal fractures due to stress wave focusing 80−83762
paraffin, shock compressed, vel. of sound meas. 78−10123
particle acceleration by propagating interplanetary shocks 80−31188
phase transitions under shock-wave loading 77−84888
photorecombination kinetics and lower mode waveguide amplification *(Russian)* 79−96313
photorecombination laser, shock wave triggered, waveguide mode optical gain 80−5730
photorecombination laser theory thermally induced behind a shock wavefront 79−76682
photorecombination reactions initiated by shock wave, light amplification *(Russian)* 80−38011

shock wave effects continued
plasma heating and radiation due to gas layer impact against obstacle at very high vel. 80−19602
plastic relaxation in shock wave, slip mechanism 79−41605
plastic-layer under shock, extrusion and heating 78−34064
plate, nonlinear struct. response to sonic booms 79−32322
plate contiguous to fluid, shock loading, bending 78−90765
plate under the effect of a spherical shock wave, stresses and deflections 80−79204
plates on elastic foundation subjected to shock waves, dynamic response 77−72217
plates with irregular shock response, sound power level and noise reduction parameters *(German)* 79−81616
Plexiglas, rod, breakdown charact. by longitudinal stress waves 78−38773
plexiglas, shock compressed, vel. of sound meas. 78−10123
Plexiglas 80−66592
plexiglass, shock loading, method for producing isentropic compression 77−44424
PMMA, shock induced polarisation, dielec. const., dipole lifetime rel. to particle velocity *(French)* 77−69776
PMMA, shock loaded, lateral compressive stresses meas. using Yb piezoresist. gauges 80−103007
PMMA, shock-wave compressed, dielectric props. 78−80281
point defect formation in weak shock wave front *(Russian)* 80−6401
polar material, PMMA-type, polaris. induced by shock waves *(French)* 77−62583
poly(pyromellitimide), shock-induced electrical activity, mechanically induced bond scission model 80−50256
polyatomic molecules, vibr. relax. behind shock wave 78−42177
polyethylene, shock compressed, vel. of sound meas. 78−10123
polyethylene prostheses, radiation crosslinking improvement of shock- and abrasion-resistance 77−60307
polymeric solids, shock-induced electrical activity, mechanically induced bond scission model 80−50256
polymorphic detonation 79−42147
polystyrene, Rankine-Hugoniot relation for shock waves 78−83317
porous media, Rankine-Hugoniot relation for shock waves 78−83317
porous samples, shock wave compression, expt. and model 78−63807
porous solid, generalised p-α model, eqn. of state, sound vel. 80−65154
powders, brittle, shock wave disintegration test method 80−66744
power type spectrum for particle accel. at spherical shock wave *(Russian)* 80−72730
props. gas cavity expansion, soil dilatation after explosion in brittle rock 79−8608
protostellar cloud and formation of solar-type stars in spherical symmetry, accretion shock effects 80−62107
PTFE, shock compressed, vel. of sound meas. 78−10123
pulsating star, atm. expansion due to periodic shock waves *(Russian)* 78−93244
PVC cases for Pb-acid batteries, pneumatic shock test *(German)* 78−85093
QSOs, shock waves in colliding gas cloud system rel. to spectrum 78−28836
quartz, impact structs., peak shock press., X-ray diffr. investig., lunar rock bombard. appls. 78−7002
quartz, porous, Hugoniot synthesis at high pressures 79−95080
quartz, shock compressed, phase equilib. and kinetics 77−62584
quartz, shock-loaded, y-cut shear-wave particle vel., interferometer technique 79−99268
α-quartz 80−72490
quartzite, shock compressed, vel. of sound meas. 78−10123
radiation damage, imitation by action of shock waves *(Russian)* 78−95107
rare earth sulphides, polymorphic transforms. on impact compression 77−47575
refractory grain destruction in low-velocity shocks 79−17041
retrograde vapour, shock wave induced condensation 80−34177
rigid body collisions, spalling, tensile stresses on target, appls. 79−7324
rigidly plastic media with hardening, shock-loaded, dislocation model and elastoplastic waves 79−86379
Rochechouart crater, Massif Central, France, shock zoning study 77−81897
rock half-space, impact of steel cylinder and effects 80−85649
rock magnetism in hypervel. impact expt. 79−29755
rock rupture by elastic shock wave superposition in multiple detonations *(Russian)* 77−35082
sapphire, shock compressed, refractive index, density, and polarisability behaviour 80−50295
shaped charge jet formation, Pugh-Eichelberger-Rostoker solution representation 79−94692
shear in shock-loaded solid, internal meas. 77−11633
shear resistance determ. behind shock-wave front 77−47511
shells with internally attached structures, transient response 79−3941
shock compression-pulse heating working process, apparatus design 80−16357
shock-shock interaction in hypersonic flow 79−94673
silica, fused, temp. in high-press. shock state 80−72490
silicate rocks, quartz-stishovite transitions, shock wave processes 79−88347
single crystals under large loads, theoretical elastic behaviour, review and appl. 80−71681
solar atmosphere, shock heating and emission lines form. 77−56889
solar chromosphere, shock heating 77−29745
solar chromosphere heating, acoustic shock waves dissipation and H^- radiation 78−96454
solar corona, fast electron tails form. in type II radio bursts 77−33439
solar flares, proton and electron accel. by shock waves 80−21974
solar UV line intensities brightness fluctuations during shock wave passage 79−66990
solar wind, energetic particles shock accel. in corotating, interaction regions 80−82159
solar wind, ion acceleration to 40 keV by shock wave disturbances 80−72738
solid, mol. dynamic simulation of shock wave propagation, kinetic energy and temp. profile 79−14882
solid, shock adiabatics at ultrahigh press. *(Russian)* 77−27941
solid, shock compression, review 80−24534
solids, equations of state determ. *(German)* 78−59858
solids, expansion after passage of shock waves 78−43068
shock wave effects continued
solids, practical applications of shock wave treatment *(Russian)* 79−55820
sonic boom, pressures inside room with open window, effect on plaster/wood walls 80−69602
sonic boom induced window response and damage 79−81604
sonic booms, simulated, influence of habituation, boom level and background noise on startle reactions 79−39326
star formation through accretion shock, model for H II blisters 80−21994
steel, C, rod, breakdown charact. by longitudinal stress waves 78−38773
steel, heat resistant, explosive loading effects on struct. and mech. props. *(Russian)* 78−39787
steel, high-strength, dynamic yield strengths, phase transition press. and Hugoniot parameters 80−75331
steel, low C, quenched, hardening during explosive forming 79−87650
steel, low C, surface shot blasting, prep. for plasma deposition 80−16586
steel, low-C, fatigue strength, low-cycle, effect of shock wave press. 79−29205
steel, low-temperature tempered, shock wave loading effects on mech. props. *(Russian)* 77−59857
steel, mild, plate, explosive hardening of one end of metallic block 77−36531
steel, spall investigations, pressures up to 100 kbar, failure and strength *(Ukrainian)* 77−73317
steel, St3 and KhVG, strength variation under influence of shock waves *(Russian)* 78−92299
steel, stainless, 304, post-shock temp. meas. 79−92527
steel, stainless, austenitic, explosively welded, orientation relationship in martensitic transform. 80−104158
steel, stainless, shock loaded, peak press. and press. pulse duration effect on crystallographic transform. 78−67769
steel, stainless, shock loaded, residual martensite obs. 80−104414
steel, stainless, shock loading parameter effect on substruct. and mech. props. 79−52360
steel, stainless 304, shock loading response, grain size effect 77−36601
steel, TRIP, hydrostatic extrusion shock treatment rel. to strength and plasticity 77−44281
steel St3 plates, mass transfer of C under influence of shock waves *(Russian)* 78−91380
stellar atmospheres, early B-type, radial shock effects 79−53807
stellar coronae, shock wave heating rel. to two-parameter models 80−8619
stellar winds, shock heating rel. to turbulent mixing with interstellar gas 80−67701
stream containing gasdynamic disturbances, variation in inversion 77−15137
stroboscopic method for pizosecond diagnostics of rapid processes 78−47159
strong curvilinear shock wave, with arbitrary profile, evolution in inhomogeneous medium 79−14428
structural member, dynamic loading and plastic response, review 80−83756
suction effects on shock wave-boundary layer interaction, numerical Navier-Stokes soln. 79−1243
supernova remnants, optical emission from shocks 79−5890
supernovae, effects of core eqn. of state on outcome of stellar collapse 80−85928
supernovae, self-similar oscillations of gas *(Russian)* 79−17001
supersonic, turbulent boundary-shock wave interaction, aerodynamic heating 78−26155
terrestrial planets atmospheres, origin by shock degassing during accretion stage *(Russian)* 79−101099
terrestrial rocks magnetism, shock effects 78−85538
tetrafluoroethylene, high temp. oxidation behind refl. shock waves 77−36743
Textolite, shear strength behind the front of a plane shock wave 79−15752
Textolite 80−66592
thermal energy relaxation in shock compressed solids, anal. of Cu, Al, Pb, Au, NaCl, Fe 77−69043
thermal explosions, fragmentation requirements for detonation 78−71368
thermodynamic relations, material with linear shock wave-particle vel. relation 77−69042
thick-plate technique for measuring ejecta from shocked surfaces 79−37760
Tishomingo Fe meteorite, microstructural study rel. to shock deform. 79−16898
transparent material, small particle impact, high speed photomicrographic recording of shock wave 78−44342
1,3,5-trinitro 1,3,5,-triazacyclohexane, shock-induced intramol. bond-breaking, XPS and EPR study 80−76512
trinitrotoluene, shock-induced intramol. bond breaking, XPS and EPR study 80−76512
tube flow initiated by expansion wave, viscous effects 78−26192
Tunguska catastrophe, computational modelling 80−41779
turbulent boundary layer on curved wall with vertical compression shock, separation onset criterion *(German)* 79−14431
turbulent boundary layer-transonic shock wave interaction, integral computation method 79−1213
underwater shock at a free surface, refl. effects, rel. to fast reactor safety 79−68751
unsteady flow of supersonic gas stream past a slender profile, asymptotic expansion of nonlinear effects 80−69863
ureilite meteorites, mag. effects of brecciation and shock rel. to strong nebular mag. fields 80−8602
urinary calculi in vitro destruction by laser-induced stress waves 78−77100
Uwet hexahedrite meteorite, shock event effects on platelike schreibersite habit planes 78−65572
Venus atmosphere, NO prod. by thunder shock waves 80−98587
viscoelastic rod, shock rel. to hard obstacle *(Russian)* 80−23911
viscoelastically damped beams, shock response 78−38232
wall shear stress measurements in a shock-wave boundary-layer interaction 79−1212
wall supported shock precursor obs. 80−100011
water, viscosity meas. behind shock wave front *(Russian)* 77−31707
water vapour, in rarefaction waves, condensation, heterogeneous nucleation 77−58731
white dwarf-main sequence star collision, shock waves prod. and effects 77−64758

shock wave effects continued
Wilson Cloud form. by low altitude nuclear explosions, water aerosol and droplets characts. 78−53704
wing moving with subsonic vel., shock wave effect 79−64684
yield strength estimate, self-consistent technique 78−80692
Al 2024 alloy, Young's modulus under shock loading, heat treatment effects 77−32611
Al 6061-T6 alloy, shock-compressed, reshock and release 77−32732
Al aircraft alloy, fatigue resistance improvement by laser shock 80−93654
Al alloy, 2024, shock-loaded, recovery of Young's modulus 78−23751
Al alloy 2024, post-shock temp. meas. 79−92527
Al alloy rod, wave profiles generated by short shock pulse 78−6125
Al alloys, surface shot blasting, prep. for plasma deposition 80−16586
Al and its alloys, dynamic determ. of Gruneisen coeff. 77−24418
Al, elasto-plastic stress wave propag. *(Czech)* 80−108507
Al, fracture due to shock waves leaving surface, shear stresses 78−51128
Al plate, explosive hardening of one end, X-ray back reflection meas. 77−36531
Al, porous, Hugoniot synthesis at high pressures 79−95080
Al rods, waveform variation of reflected acoustic shock pulse due to work hardening 77−21167
Al, shock compression at high press., neutron irrad. *(Russian)* 80−88264
Al, shock compression at high press. *(Russian)* 80−92608
Al, shock wave data, 'solid Hugoniot' rel. to 'fluid Hugoniot' 80−65155
Al-PMMA laminated composites, shock wave propag., flash radiographi obs. 79−4370
Al-steel mixture, wear resistant, produced by compaction by discrete shock waves 80−84882
AlN, powder shock wave compression prior to sintering 77−66615
Al_2O_3, dynamic deform., stress-wave response 80−21020
Al_2O_3 phase transformations, γ to α, produced by shock wave working 80−16305
$Al_2O_3:Cr^{3+}$, shock compression, absorpt. spectra 80−20675
Al_2O_3-epoxy mechanical mixtures, stress-wave propag. model, dynamic response expts. 79−1477
Al_2O_3-loaded epoxy, shock-wave compressed, dielectric props. 78−80281
Al_2O_3-SiO_2 system, andalusite and kyanite powders, shock induced transformations 80−45301
Ar crystal, laser breakdown as model of fast high-energy processes, shock waves motion 79−91541
Ar, ionising shock waves, stability, H impurities effect 78−22371
Ar, liq., shock wave compression, 400 to 910 kbar 80−29101
Ar liquid, shock compression temp., detonation front glow 80−43737
Ar+HCl(O_2), shock-heated, collision induced dissoc. 79−34290
Ar+HF(HCl)(CO), shock heated steady state dissoc. rate consts. calc. 78−40039
$^{40}Ar/^{39}Ar$ radiometric age determ. of rocks, shock press. effects 77−60360
BN powder, shock wave compression prior to sintering 77−66615
BN, self focusing high current relativistic electron beam for structural and chemical transformations *(Russian)* 80−15190
BN, shock compression, polymorphic transform. kinetics 79−86838
BN, shock synthesis *(Japanese)* 80−29918
BN, shock-compressed pyrolytic and hot-pressed, phase transitions to 120 GPa 77−70048
BN, structural changes occurring during shock compression in presence of H_2O 80−16301
BN structure after high temp. shock compression 80−39220
BN wurtzite-sphalerite phase transition, stacking fault role 80−6418
BN, wurtzite-type, lattice distortions 77−11636
β-BaF_2, (111) single cryst., behaviour under room temp. shock compression 77−62585
β-BaF_2, stress wave profiles 80−96593
Bi, shock loading and unloading, 293 and 473K 77−84840
Br_2 recombination in supersonic expansion in nozzle *(Russian)* 78−1757
Br_2, vibrational relaxation and dissoc. behind a shock front, absorpt. spectroscopy *(Russian)* 77−88536
C, glassy, migration into steel during shock compression 80−24679
C, noncrystalline conversion to diamond, diffusion conversion enhanced rate due to shock compression 80−39221
C-H-O(-N) gas mixtures, high temp. emissivity, 4.8 μ region, shock waves 77−76027
CH^+ formation in hot gas behind interstellar shock fronts 78−61910
CO_2, dissoc. in shock tube, interferometric meas. 77−9071
CO_2 pulsed laser system, acoustic suppression 80−74378
CS+O→CO+S, shock tube reaction, chemiluminescence and lasing 77−16824
CS_2, shock heated, visible emission 80−58274
Cl+Cl, radiative recomb., behind incident shock wave front *(Russian)* 77−65525
Cu, crystal lattice behaviour under intense unidimensional compression *(Russian)* 78−6123
Cu, explosive loading, depend. of struct. on deform. *(Russian)* 78−3177
Cu, fracture due to shock waves leaving surface, shear stresses 78−51128
Cu powder, two layered medium dynamic compaction 80−35138
Cu, residual temperature, meas. during quasi-isentropic compression *(Russian)* 77−89495
Cu, shock compressed, release isentropes, eqn. of state at high energy density *(Russian)* 80−54340
Cu, shock loaded, work hardening and press. depend. of dislocation arrangement and density 78−48429
Cu, shock wave compression, reduced Hugoniot curve and eqn. of state *(Chinese)* 80−44259
Cu, shock wave data, 'solid Hugoniot' rel. to 'fluid Hugoniot' 80−65155
Cu surface shot blasting, prep. for plasma deposition 80−16586
Cu-concentration junctions with solder, shock-induced elec. response 80−75626
Cu-Constantan junction, elec. response to shock compression 79−95470
Cu-Ga porous solid formed by shock compression 80−29905
Cu-Ge (8.7 at.%), pulse duration effects in shock hardening 77−12644
Cu-Mn alloy, manganin, hysteresis-corrected calibration under shock loading 80−74818
Cu-Ni, melt, accel. by shock wave treatment, crystallisation *(German)* 77−86022
$CuFeS_2$, explosive-shock deform. 78−95108
Fe, BCC, shock wave simulation using Morse pot. 78−2196
Fe, cast, structural changes, due to pulsed action of high temps. and pressures *(Russian)* 80−7554

shock wave effects continued
Fe, cast rod, breakdown charact. by longitudinal stress waves 78−38773
α-Fe, exam. of structural defects due to shock waves, and induced hardness 78−48427
Fe, fine particle dispersions, shock induced mag. effects 79−82832
Fe, first order shock induced mag. transitions characts. and discrimination from TRM 78−64205
Fe, shock wave compression, reduced Hugoniot curve and eqn. of state *(Chinese)* 80−44259
Fe-Cr-Ni alloy, shock loading effect on phase equilib. *(Russian)* 79−29017
Fe-Ni-C (21, 0.6 wt.%), stress assited and strain induced martensite morphologies 78−3187
Fe-Ni-C (31, 0.1 wt.%), kinetics of deform. induced martensite, shock loading and grain refinement effects 78−15395
$Fe_{50}Co_{50}$, disordering by laser irradiation, Mossbauer transmission spectroscopy and electron microscopy study *(French)* 79−23639
α-Fe_2O_3, elec. resist. and phase transition under shock compression 80−72496
Fe_2SiO_4, fayalite, elec. cond. obs. under shock compression 80−81873
n-Ge, elec. cond., effect of shock waves *(Russian)* 78−87979
H II regions, ion recomb. initiation by shocks 77−64825
p-H_2, FCC, equation of state and lattice dynamics, temp. depend. 77−76521
H_2, liquid, shock compression obs., various geometries 77−58732
H_2+Ar, 4500K shock wave expt. simulation, vibr. state changes and dissoc. 79−61850
H_2+inert gas, vibr. relax. mechanism, master eqn. anal., density changes 79−76493
HN_3, decomposition and ionisation in shock tube *(Russian)* 78−7182
$HNO_2+OH \rightarrow H_2O+NO_2$ react. kinetics, at high temps. behind shock waves 77−44477
H_2O, condensation via rarefaction wave 78−71847
H_2O, shock compression at high press. *(Russian)* 80−92608
He, excitation and ionisation, by instationary shock fronts 78−59540
I_2, recomb. shock heating in unsteady Ar expansion, vibr. relax. effect 77−16794
I_2, solid, metallic, insulating-metal transition at high-press., exptl. and theoretical shock-compression curves 77−39781
I_2, vibrational relaxation and dissoc. behind a shock front, absorpt. spectroscopy *(Russian)* 77−88536
$KAlSi_3O_8$, orthoclase, impact structs., peak shock press., X-ray diffr. investig., lunar rock bombard. appls. 78−7002
KCl, laser produced shocks rel. to material damage 78−31285
KI, soln. in organic solvents, elec. cond., shock compression effects 79−46822
Kr-Ar mixture, shock-heated, ionisation relax. processes 77−84277
Kr-H_2, ~5 torr, ionisation by Mach 15+shock waves, shock struct. and stability 77−75938
$LaCrO_3$-Cr cermet, effect of explosive compacting on props. 77−12557
LiF, dynamic strength, cryst. orientation effects 78−39846
LiF, precursor decay, stress threshold 77−4156
$LiNbO_3$, shock loaded above Hugoniot elastic limit, elec. and mech. response 78−19411
$LiNbO_3$, shock-wave compression, 2.4-44 GPa 80−34139
$(Mg,Fe)_2SiO_4$, shock deform. expts., Hugoniot data implications 80−94497
Mg, heating by shock compression, of porous material, vap. form. *(Russian)* 78−2195
Mg, melting temp. under shock loading 77−47553
Mg, shock wave compression, reduced Hugoniot curve and eqn. of state *(Chinese)* 80−44259
MgO briquets, prep. by shock compaction and characteris. 79−43178
Mg_2SiO_4, forsterite, single-cryst., shock wave compression 79−84242
Mg_2SiO_4, temp. in high-press. shock state 80−72490
Mo, laser irradiation, shock wave formation relationships, surface propagation, elastoplastic wave effects 79−55825
Mo powder, struct. changes under action of high-powder pulses 79−70018
Mo sheet, shock-induced intergranular cracks 79−57087
Mo, shock compression to 2.0 TPa, by nuclear explosion 77−84841
Mo, shock deformation twinning, shock press., pulse duration and grain size effects 79−5021
Mo, shock-deformation twinning, shock loaded BCC and FCC metals comparison 80−104413
Mo, shock loaded, peak press. and press. pulse duration effect on crystallographic transform. 78−67769
Mo wire, laser shock induced microstructural changes, rel. to explosive shock induced phenomena 78−67768
N liquid, shock compression temp., detonation front glow 80−43737
N_2, cryogenic, shock wave-boundary layer interaction *(German)* 78−71370
N_2 molecular beam generation, parameters rel. to stream perturbation before skimmer 79−86468
NF_3, shock induced decomposition in Ar, IR emission, reply 77−63907
NF_3 shock-induced decomposition in Ar, IR emission, comment 77−63906
NF_3, thermal decomp. in shock waves, rate consts. meas. 77−16810
NH_4NO_3, shock-induced intramol. bond breaking, XPS and EPR study 80−76512
NO_2, shock heated, visible emission 80−58274
N_2O-N_2-He, population inversion of N_2O vibr. levels behind shock wave front 79−31886
Na, anomalous laser fluoresc. scatt. in shock tube 77−10627
NaCl, finite strain isotherm and vels. for single crystal and polycrystalline samples 78−53646
NaCl, shock compressed, vel. of sound meas. 78−10123
NaCl, single cryst., shock wave compression, flash X-ray diffr. obs. 78−83877
$NaN0_3$, fine structure changes on interaction with weak shock waves *(Russian)* 80−54313
Nb_3Si, supercond. phase, formation by explosive compression 79−82701
Ni, shock loaded, work hardening and press. depend. of dislocation arrangement and density 78−48429
Ni, shock loaded, work softening 78−27537
Ni, shock loading parameter effect on substruct. and mech. props. 79−52360
Ni, shock-loaded, residual strengthening, effect of grain size, dislocation cell size and deform. twin spacing 79−91744
Ni-Cr alloy KhN70VMTYu, heat resistant, explosive loading effect on struct. and mech. props. *(Russian)* 78−39787

shock wave effects continued
O_2, dissociation relax. behind oblique shocks 77−548
O_2, vibrational relaxation and dissoc. behind a shock front, absorpt. spectroscopy *(Russian)* 77−88536
Pb, evaporation in shock compression release waves *(Russian)* 78−18761
Pb, shock compressed, release isentropes, eqn. of state at high energy density *(Russian)* 80−54340
Pb, shock compression at high press. *(Russian)* 80−92608
$(Pb_{0.715}Ba_{0.285})_{0.991}(Zr_{0.707}Ti_{0.293})_{0.981}Bi_{0.019}O_3$, slim loop ferroelec. ceramic, shock wave compressed, elec. response 78−80293
$Pb_{0.98}Nb_{0.02}(Zr_{0.95}Ti_{0.05})_{0.98}O_3$, PZT 95/5, ferroelec. ceramic, resist. meas. under shock wave compression 78−19031
$Pb(Zr,Ti)O_3$ ceramics, shock depoling, pulse charging of nanofarad capacitors 79−42913
$Pb(Zr, Ti)O_3$, ferroelectric ceramic discs, axial-current-mode shock depoling 79−78631
$Pb(Zr,Ti)O_3$ piezoceramic, phase transition under shock loading *(Russian)* 77−69041
$Pb(Zr,Ti)O_3$, shock wave compressed, dielec. props. 77−48139
$PbZr_{0.95}Ti_{0.05}O_3$, impact loading, mech. and elec. response, elec. state effect 78−64317
$Pb(Zr_xTi_{1-x})O_3$, ferroelectric energy generation by shock compression, modes 77−55757
$Pb(Zr_xTi_{1-x})O_3$, meas. of Hugoniot curve with commercial manganin stress gauges 80−70362
S, electrical conductivity under shock compression *(Japanese)* 78−26923
S, shock wave method observation of transition to highly conducting state 80−4738
SO_2, shock heated, visible emission 80−58274
SO_2+Ar, dissoc. rate meas. behind shock wave, laser Schlieren method 80−81296
$SO_3+Ar \leftrightarrow SO_2+O+Ar$, rate const. of spin forbidden dissoc. in shock wave 79−57214
Se, cubic modification prepared by shock compression 78−34494
p-Si, elec. resist., shock wave compression effects 80−80265
Si on sapphire film, laser annealing non-thermal theory expt. test 80−89273
Si p-n junction, compressed by shock wave, rectifying props. 77−4429
SiO_2 film, amorphous, shock crystn. obs. 80−10828
SiO_2, fused, shock compressed, refractive index, density, and polarisability behaviour 80−50295
SiO_2, shock compression at high press. *(Russian)* 80−92608
$Si_xO_yN_z$ film, amorphous, shock crystn. obs. 80−10828
$SmCo_5$ single crystals, magnetisation, creation of high-coercivity state *(Russian)* 77−66384
Ta_3Si, superconducting, shock synthesis *(Russian)* 77−85957
Ti alloy RMI 38644, shock loaded, residual strength 78−27574
Ti-Al alloy, VT5-1, strength variation under influence of shock waves *(Russian)* 78−92299
Ti-Al-V-Cr-Zr-Mo-Fe (3.4, 8.3, 5.8, 3.9, 4.2, 0.06 wt.%), shock loaded, residual strength 77−36589
Ti-M-V-Cr-Mo, RMI 38644, shock loaded, age hardening 79−29112
Ti-Nb, phase transformation due to shock wave treatment *(Russian)* 79−91641
TiO_2, rutile phase, shock induced phase transition anisotropic behaviour 80−103475
U, liquid, electronic density of states, shock vaporization technique 80−29300
UO_2, clustering phenomena effect, anal. based on shock wave model 78−21652
W, polycryst., loss of shear strength under shock compression 77−11635
W, porous, room temp. shock compression expts., Hugoniot states, 0.6-7.6 GPa 77−84842
W, shock compression, 1223K, re-exam. of expt. data 77−55320
W wire, laser shock induced microstructural changes, rel. to explosive shock induced phenomena 78−67768
WC-Co hard alloy, preheating influence on explosive shock hardening *(Russian)* 79−29083
Xe, electrical conductivity beyond critical point, intermediate density between gas plasma and solid *(Russian)* 80−20265
Zn, crystalline, wave formation during oblique collision *(Russian)* 77−89494
ZrO_2 shock wave treatment of powders *(Russian)* 77−44186

shock waves
see also detonation; explosions; plasma shock waves; shock tubes; shock wave effects; supersonic flow
1-dimensional shock wave propagation after explosion, calculation using BKWAVE 80−38448
absorption, fluid-saturated porous solids 80−53726
absorption by docked spacecraft after coupling 77−33317
acceleration of particles in astrophysical plasma 80−82192
acceleration waves in radiating gases, local and global behaviour 80−1618
acoustic discontinuous waves in nonlinear media, characts. 78−5601
acoustic shock pulse reflection at solid-solid interface 77−19466
acoustic shock pulses in Al rods, amplitude-dependent attenuation 78−55503
acoustic velocity, shock-compressed uniform solid, lateral discharge ang. semiempirical formula *(Russian)* 78−55910
acoustic wave-shock wave interactions in elastic solids 79−32370
acoustic wave-shock wave interactions in elastic solids 79−98521
activation regions behind shock waves, potential theoretic simulation *(German)* 78−90934
adiabatic perturbations of solitons and shock waves 80−46830
adiabatic self-similar blast waves, radial instability, appl. to supernova remnants 78−8089
aerocolloidal suspension of solid particles, shock wave entering aerocolloid domain 78−51227
aerofoil, dynamic forces acting, subsonic instabilities *(French)* 78−67213
air, atmospheric, cylindrically converging blast waves 80−92180
air, photoionisation kinetics ahead of strong shock fronts 79−7438
air, radiative cooling behind strong shock waves 78−91030
air, shock waves interferometric investig. 79−64695
air, strongly reflected shock wave trajectories, vel. parameters *(Russian)* 77−23993
air, untreated, laser velocimetry in shock, Teflon seeding technique 77−84348

shock waves continued
air, variable energy blast wave, shock trajectories, flow field densities 77−68620
air, weak nonlinear waves, struct. and propag., effect of vibr. relaxation 79−64683
air flows in triple point shock configurations, anal. thermodynamics *(Russian)* 79−32569
air in supersonic nozzle, shock activation with overexpansion, jet form. 78−18330
air-water bubbly mixtures, press. wave propag. *(French)* 78−22402
airfoil, wave drag in transonic flow, shear interferometry obs. 79−77165
airfoils, oscillating, power-law shocks, Newtonian flow theory appl. 79−41706
airscoops, vortex filament-shock front interference, vortex dissipation 80−10253
Alfven shock evolution is classical MHD *(French)* 78−18352
amplification in nonequilibrium system of liq. and solvent gas bubbles 79−18936
AO 0235+164, BL Lacertae object, relativistic blast-wave model for rapid flux vars. 79−9017
applied mechanics computing, conference, New York (1976) 77−67285
arbitrary strength, with viscosity and heat conduction, stability 80−59076
arterial blood flow, one-dimensional unsteady eqns., soln. by method of characts. 79−92251
arterial blood flow, shock wave formation, math. model 79−5305
artificial diffusion parameter, χ, improved form 79−64649
astrophysical media, relativistic and nonrelativistic gas flows, low press. limit 77−9655
asymmetric double exponential waveform, weak-shock soln. for nonlinear propag. 80−10061
asymmetrical explosions, blast wave propag. 77−75939
atmosphere, influence of aqueous fog on shock wave propag. 80−19531
attenuation by single transverse slit 77−3845
axially symmetric explosion in magnetogasdynamics 80−62007
Baneberry nucl. explosion, numerical simulation 80−841
bar semi-infinite prismatic, elastoplastic wave propag., intense load-release wave existence *(Russian)* 78−24671
beam, higher modal plastic response 77−50948
bifurcation on refl. from shock tube end wall 79−46346
binary gas mixtures, separation and isotope separation in curved shock wave 79−94753
blades in transonic flow, shocks and boundary layers, time marching method 79−4036
blast loaded prestressed flat plates, dynamic response 79−50637
blast loading on three-dimensional structures, transient, computational simulation 77−68624
blast wave, variable energy, perturbation solns. 78−51192
blast wave, with transport props., self-similar soln. 77−68621
blast wave computations using the flux-corrected transport algorithm 79−77184
blast wave problem in conducting gas 79−37414
blast waves, magneto-gasdynamic radiative, cylindrical, similarity soln. 79−37338
blast waves, phase space method 79−46344
blast waves, spherical, time-depend. energy deposition 78−9655
blast waves with heat transfer 77−35166
blunt biconic at incidence, laminar viscous shock layer, supersonic/hypersonic flow 78−30313
blunt body in supersonic flow, Navier-Stokes eqns. numerical computation 80−10263
blunted solid of revolution in gradient flow, shock wave form *(Russian)* 79−64697
Boltzmann equation, nonlinear, hierarchy kinetic model 79−98758
boundary layer, nonstationary, with self-induced press. 78−34164
boundary layer, oblique shock wave interactions *(Japanese)* 78−55662
boundary layer, unsteady, similarity problems 78−1633
boundary layer effects on weak shock wave and sound wave refl. at shallow incidence 78−22373
bow wave formations around blunt bodies in flow behind moving shock 79−68744
breakdown of continuous multidimensional gasdynamic flow from weak discontinuity theory 77−51075
brightness, in air with reduced density 80−86371
bubble, spherical, pressure waves produced by collapse *(Japanese)* 80−100027
bubble-liq. mixture with nonsteady interphase heat transfer, shock struct. 78−83424
bubbles in liquid, nonsteady shock waves 79−68792
bubbly, two-phase mixtures, numerical anal. of press. transients by explicit-implicit method 78−34185
bubbly liquids *(French)* 78−26183
bubbly mixtures, shock wave form. by compression wave steepening 78−38390
Burgers' equation for nonlinear shallow water waves, Galerkin method soln., expansion of B-splines 78−87352
Burgers equation, sawtooth soln. decay 80−31529
Burgers turbulence, asymptotic props., Burgers eqn. shocks 79−81852
3C 310, 326, relaxed double radio sources, shock waves prod. by fine scale struct. 80−51891
cascade shock loss location and magnitude by high speed smoke visualisation 80−24051
cavitation, investigation by coherent optical methods 78−38431
cavitation bubbles, amplitude distrib. of pulses produced by shock waves 80−64252
cavitation shock pressures in venturi, 10 kHz-1 MHz 77−24002
cavitation zone, shock wave theory rel. to acoustic and hydrodynamic cavitation 77−27567
cavity in viscous liquid, action of press. pulse 79−68769
channel, shock wave stationary motion for axial blowing and two-layer detonation 80−92177
channel, with varying cross section, shock wave proag. 79−23339
channel flow, unsteady, of compressible gas with shock waves, appl. to gasdynamic laser 77−72327
Chapman-Jouget curved detonation wave, existence conditions *(Russian)* 77−51084
Chapman-Jouget detonation wave near surface curvature rupture line *(Russian)* 78−46996
chemical explosion induced, nuclear power plant protection 77−38351
chemical reaction rate increase in US cavitation, diffusion model 79−96312

shock waves continued
chemically frozen multicomponent boundary layer, thermal diffusion effects behind strong shock 80−53772
chemically reactive flow, aerodynamic heating of blunt bodies 80−74998
chemically reactive flow, shock wave form. 77−62309
chloroform, variable energy blast wave, shock trajectories, flow field densities 77−68620
choking phenomena, of flows in shock tubes 77−89152
chromosphere, thermal shock waves rel. to pulsed microwave bursts with quasithermal spectrum 77−78762
chromospheres of late type stars acoustic wave heating and temp. minima heights 78−20818
chromospheres of late type stars temp. minima and shock form. heights 78−20818
Circinus X-1, binary star model with mass transfer and expanding shock fronts 79−75296
classical nonlinear scalar field, solns. with props. of shock waves 78−81865
cold plasma, Alfven shock waves in presence of effective electron-ion collisions 78−26286
collapsing gas, self-similar problem of strong explosion 79−90284
collisionless shock, in nonlinear LC circuit, asymptotic behaviour 79−23338
collisionless shocks, extended Rankine-Hugoniot relations 78−75209
collisions, anal. theory, vel., incidence angle and mag. field effects 77−7415
combined bodies, supersonic inviscid flow, shock interactions *(Chinese)* 80−6084
compact double radio sources, relativistic blast-wave model for superlight motion 78−28807
compact stars, attached shocks in axisymmetric accretion 77−33334
completely dispersed, in relaxing mixtures, struct. obs. 80−59072
compressible flow, Navier-Stokes solutions using Stetter's method 79−32551
compressible flow around expanding cylinder and sphere 77−35158
compressible flow fields, two-dimensional, computation by modified local stability scheme 78−1681
compressible gases interface, turbulent mixing 78−1683
compressible hyperelastic solids, spherical wave propag. analysis 77−58588
compression shock stability in streams of spontaneously condensing vapour 80−28563
concave corners, Whitham theory of shock-wave diffr. 80−100012
concentric impact of pointed bodies 79−41604
concentric shock wave, const. speed, in nonhomogeneous medium, thermonuclear microfusion 78−83281
concentric shock wave self-similarity exponent approximation 78−75169
concentric shock waves in inhomogeneous medium, self-similarity exponent 78−75168
Concorde sonic booms as probe of atm. temp.-wind parameters 77−91323
condensing injector, optimal diffusor throat cross section dimensions 77−31356
conducting, magnetisable, incompressible media, explosion interactions *(Russian)* 77−55037
cone, slender, at high incidence, supersonic flow 78−90932
cones, axisymmetric impingement of supersonic air jets, shock pattern 80−48741
cones at large incidence in supersonic flow, floating shock fitting method 78−71367
confined perfect gas, thermal disturbance response, slow transients 79−81976
confluence of three shock waves in three-dimens. flow 78−59422
conical gas flows, two-dimens. unsteady problems 77−51085
conical shell exposed to weak shock wave 77−58596
conical supersonic flow around yawed circular cones in the transonic region *(German)* 79−77175
conservative implicit method for shock wave calculations 79−77179
conservative scheme for eqns. of gas dynamics *(Russian)* 79−50755
convergent cylindrical wave parameters meas. in metals by elec. methods 79−46407
convergent shock wave in ideal elastic nonhomogeneous medium 77−55036
converging, self-similar solns. nonuniqueness 77−19624
converging, stability calcs. by computer 79−41715
converging, stability criteria as function of perturbation parameters amplitude and centre angle 79−1207
converging cylindrical detonation waves in magnetogasdynamics 79−77265
converging cylindrical shock problems, soln. by four step finite difference method *(Japanese)* 79−77185
converging cylindrical shock wave prod. 80−48748
converging shock and thermal waves, numerical study 77−62282
converging shock waves generated by instantaneous energy release over cylindrical surfaces 79−94640
converging spherical and cylindrical shocks with zero temp. grad. in rear flow field 77−80182
corner interaction of boundary layer and shock wave, flow separation 80−96287
cosmic ray acceleration in shock waves, energy loss effects *(Russian)* 80−17449
cosmic rays accel. on front of shock wave, regular mechanism 78−36410
cosmology, shock form. and shock struct. in radiative era 80−4463
cratering by meteorite impact 79−21244
curvature behaviour close to shock tube wall 77−51082
curved fluid-solid interface, shock wave front propagation 77−46962
curved shock waves in ideal fluid mixtures with multiple temps., theory of singular surfaces 80−28533
curvilinear shock wave smearing in particle in cell method calcs. 79−64693
Cygnus Loop, fast shock wave detection, optical spectra 80−82467
Cygnus Loop, forbidden Fe XIV emission radial distrib. rel. to shock front model 78−32545
Cygnus Loop, supernova remnant, filaments and high vel. gas rel. to shock waves *(Russian)* 78−41028
Cygnus Loop, X-ray image rel. to expanding blast wave 79−25663
cylinder, nonhomogeneous anisotropic, wavefront propag. analysis 77−68492
cylinders, elliptic 2-D, cavitation shock-noise measurement for different eccentricities 80−79368
cylindrical implosion, flow development, numerical anal. 79−4040
shock waves continued
cylindrical MHD shock wave propag. 79−98815
cylindrical relativistic shock waves, propag. in presence of mag. field 79−53708
cylindrically/spherically symmetric flow, numerical study of converging cylindrical shock 78−22370
decay, Maxwell-like relations in condensed materials 79−41702
decay in elastic rods 79−41603
delta wing, oscillating, with attached shock wave, flowfield theory 77−84276
delta wings in supersonic flow, crossflow shocks 80−48749
density distribution in a non-stationary bow wave in a transonic flow, book contrib. 80−1631
detached bow waves around bodies at slightly greater than sonic speed, book contrib. 80−1630
detonation, slow burning, starvation kinetics 78−64841
detonation sputtering, interaction between detonation waves and gas and powder flows *(Russian)* 80−16182
detonation wave, turbulent, boundary-layer treatment 80−106791
detonation wave magnification by pulsation energy 80−59075
detonation wave propag. with allowance for radn. and mag. field 79−64796
detonation waves, heterogeneous, propagation and blast wave initiation 80−74915
detonation waves, radiative MHD flow *(Russian)* 77−89207
detonation waves, stochastic phenomena 79−77180
diagnostics using laser interferometer, appl. to Al plate 79−64814
diatomic gas flow during shock wave diffr. at right angles *(Russian)* 77−27559
diatomic radiating low density gas, shock wave struct., vibrational energy 80−38504
dielectric deformable materials with memory, one dimens. shock 77−1170
difference schemes from fluid mechanical integral theorems 78−14032
differential analysers of shock waves, theory 77−15059
diffraction, by compression corner, regular reflection 77−58730
diffraction, nonlinear problem soln. *(Russian)* 78−75171
diffraction and reflection from shock-tube, numerical computation *(Chinese)* 80−43735
diffraction at small angles in ideal compacting medium *(Russian)* 78−67082
diffraction by compression corner, single Mach refl. 78−38370
diffraction by cones, critical semi-apex angle determ. 78−79335
diffraction of plane shock wave at angle in ideal compacting medium *(Russian)* 78−63357
diffraction on plane with semicircular cylindrical roughness, numerical integration *(Ukrainian)* 80−22201
diffraction over concave corners, von Neumann paradox, Mach reflection 80−28535
diffusion flame in turbulent boundary layer on liq. propellant surface behind shock wave 80−53763
dilatant (nondilatant) media, shock wave propagation 80−14608
discontinuity formation, phase velocities role 80−19440
discontinuity waves, reflection and transmission through shock wave, general theory, characteristic shocks 79−76908
disparate mass mixture flows, phys. mechanisms, shock wave struct. 79−94657
dispersed supersonic two-phase flow, shock characts., droplet size depend. at nozzle 80−106815
dispersion on plane layer *(Russian)* 80−33628
dissipative gasdynamic system, nonlinear interaction model *(French)* 79−14427
dissipative lattice, approx. solns. for max. shock response 78−6124
dissipative rubberlike material rod, nonisothermal nonlinear waves 79−86380
dissociating gases, shock wave form. 79−60004
distensible tubes, fluid-filled, biological appl. 80−94272
distribution theory use *(Rumanian)* 78−34046
disturbance wave-head amplification in homogeneous explosion in chem. reacting atm. 79−27658
droplet motion induced by weak shock waves 80−33627
droplet-vapour flow, normal shock waves 79−32651
duct, supersonic flow downstream oscillations from abrupt cross section increase, nozzles 80−74976
ducted and exhaust plume flow fields, computer anal. 79−7397
ducted flow, velocity and temperature development behind shock wave 78−34161
duralumin, shock-compressed, compression and rarefaction waves obs., 150-250 kbar 77−77535
dust entrainment in shock-induced turbulent air flow, dust entrainment 80−43763
dust laden gas, three-dimens. shock waves 79−68788
dusty gases, fully dispersed wave struct., Navier-Stokes eqns. 80−69875
dynamic and static high-pressure event differences 79−21557
Earth bow shock, conference, Strasbourg, France (1978 August 31 to September 1) 80−82573
Earth bow shock, DC mag. field obs. 80−90306
Earth bow shock, first evidence and early studies, historical introduction 80−85816
Earth bow shock, initial ISEE mag. field obs. 80−90307
Earth bow shock, obs. of backstreaming protons in upstream solar wind 80−90309
Earth bow shock, orientation and shape in three dimensions 79−101030
Earth bow shock, protons pitch angle distribs. transform. from solar wind into magnetosheath 77−87216
Earth bow shock, rel. to interplanetary and magnetosheath features of solar proton event 77−87215
Earth bow shock, review of upstream energetic-particle meas. 80−90308
Earth bow shock, solar wind upstream deceleration rel. to diffuse upstream ions origin 80−98528
Earth bow shock, three-dimensional shape 80−85832
Earth bow shock, upstream particle events obs. close to shock and 200 R_E upstream 80−77247
Earth bow shock and Pc 3-4 micropulsations, effects of interplanetary mag. field orientation and solar wind vel. 79−53672
Earth bow shock ions in upstream solar wind, two distinct populations obs. 79−21124
Earth bow shock plasma, possible generation mechanisms of low-freq. waves ($\lesssim$50 Hz) 80−90312
Earth bow shock vicinity, low-freq. waves obs. 80−90311

shock waves continued
Earth hour shock, assoc. with magnetosheath electrostatic turbulence 79−66881
EHD, shock adiabatic *(Russian)* 77−65812
EHD shock wave struct., anal. with complete charged component impulse eqn. *(Russian)* 78−42674
elastic bars, phase boundary propagation, dynamic elastic bar theory, sound wave interactions 80−69706
elastic fluids, thermodynamic effects on shock waves and vorticity jump 77−15061
elastic gas filled tube, pressure waves *(German)* 78−87295
elastic rods, linear, nonhomogeneous, propag. and decay of shock and accel. waves 78−83278
elastic rods, wave propag. 77−60939
elastic sphere, interaction with weak shock waves, hydrodynamic forces 77−58595
elastic wave propagation in isotropic space 80−28448
elastic waves on circular wire, nonlinear mode coupling rel. to shock wave 77−79990
elastoplastic half-spaces interface, oblique refr. of plastic wave, self-similarity problem *(Russian)* 78−20974
electrically exploded etched Cu mesh, impulse loading 80−64428
electron-hole drops, Cherenkov acoustic emission at supersonic vel. *(Russian)* 79−19529
EM shear stress gauge for large amplitude shear waves 78−70113
EM wave generated by compression shock, in weak mag. field 79−77292
end wall reflection of shock in ionising gas, numerical calcs. 77−89160
endochronic theory of viscoplasticity, steady waves in impacted plate, Al numerical calc. 78−83282
energy spectrum characts. of shock processes in fluid 80−103041
evolution rel. to dissipative phenomena 77−42857
exceptional wave propagation in continuous medium, finite deform., evolution of discontinuities, elastic pot. determ. *(Italian)* 78−54202
expansion corner effect on shock-wave and boundary layer interactions 80−14737
exploding atmosphere, compression pulse evolution, initial behaviour 79−94651
exploding wire, underwater, form. and propag. of compression wave *(Japanese)* 77−72329
exploding wire cylindrical blast wave high-speed photography for material impact testing 79−79189
explosion, thermal wave propag., effect of mass released 79−41713
explosion containment vessel research 77−58594
explosion due to inertial plate drive by pressure pulse 80−53811
explosion in atmosphere, 2D calcs. 79−46345
explosion shock wave propagation in hollow circular cylinder *(Japanese)* 80−10175
explosion wave, reflection from a plane, peculiarities 79−90281
explosion waves, atmospheric attenuation 77−31155
explosion waves, vibrational relaxation effects on atmos. attenuation and rise times 79−7244
explosive charges of finite radius, shock wave, energy hypothesis 78−55658
explosive instability upon interaction of localized and nonlocalized waves 80−31530
explosive shock wave on elastic plate 77−89060
explosives, volume of activation, shock initiation 80−16683
fast-slow gas interface, plane shock waves 78−51194
ferromagnetic material, nonlinear EM wave propag. and strong discontinuities *(Russian)* 78−74819
finite elasticity, equilibrium shocks, dissipation inequality 79−68634
flow computation, appl. to turbine blade profile design *(French)* 77−62281
flow oscillations in duct 77−35241
flow past an arbitrary body, extended variational principle, local pot. method 77−89089
flows with higher-order eqns., MacCormack's method extension 79−3987
fluid filled elastic tubes, effect of governing eqns. nonlinearity 77−89055
flux-corrected transport algorithm, rezoning technique 80−31516
foam, explosive charge detonation, shock wave parameters 77−15062
formation and decay for conservation law in several dimens. 77−53788
formation distance in press. driven shock tube 77−19623
freon gas flow around blunt object, bow shock instability 80−10266
frozen shock wave in two-dimensional steady flow past thin wedge *(Japanese)* 78−26212
fuel mixture stream, regular reflection of shock wave from solid wall 79−77291
fusion, inertial confinement, implosion of black body radiation 80−73990
fusion ignition cumulated shock waves, coming to free surface, optimal conditions 79−45414
galactic, properties, density wave theory *(Chinese)* 77−71145
galactic centre region, shock wave model of expanding ring 78−4365
galactic centre region, shock wave model of kinematic features of H I and molecules 77−91629
galactic nuclei, compact X-ray sources model rel. to giant elliptical galaxy (M87) 78−28847
galactic shocks in barred spiral galaxies, steady-state gas-dynamical study 80−12819
galaxies, barred spiral, large-scale shock wave formation 77−2470
galaxies, density wave shocks rel. to wave energy and lifetime and galaxies spiral struct. 80−98715
galaxies, shock wave formation mechanism and conditions for existence 79−101206
galaxies, shock waves rel. to stochastic star form. and spiral struct. 78−93395
galaxies, two-arm spiral shock prod. by non-linear corrugation waves 80−67859
Galaxy, MHD shock wave rel. to origin of 3 kpc arm and North Polar Spur 77−87547
Galaxy, spiral shocks model rel. to H I regions 21 cm line spectra 78−54042
Galaxy, stability of one-dimensional spiral shocks 77−64849
Galilean invariance of balance eqn. for singular surface in continuum 77−75792
gas, dissociating, relativistic flows, growth and decay of weak waves, shock wave formation 80−69949
gas, dissociating, sonic wave propagation, formation of shock waves 80−64672
gas, ionising shock wave in transverse mag. field, theory *(Russian)* 77−89161
shock waves continued
gas, isothermal, straight compression wave due to pressure pulse driven flat piston 80−69873
gas, laser absorpt. wave propag., shock waves 80−28597
gas, magneto-radiative, shocks 79−37423
gas, polytropic, synchronous shock waves overtaking each other, disintegration of arbitrary discontinuity 80−69871
gas, pressure wave resulting from heating wire *(French)* 77−926
gas, shock wave under continuous energy supply 80−103042
gas blown from cylinder end in hypersonic flow, shocks and blowing parameter 80−33624
gas bubble-liquid system, shock wave refl. 79−81952
gas bubble-liquid system, struct. of weak shock waves 79−86492
gas bubble-water mixture with polymer additive, shock wave propag. 78−47021
gas compression in heavy piston, hypersonic speed, shock waves 80−69869
gas detonation wave, calculation of equilibrium flow *(Russian)* 78−1690
gas dynamic ionising shock wave, appl. of computational method 78−38447
gas dynamic parameters, calc., termination of regular reflection 79−81910
gas expansion into near vacuum, contact front-primary shock regime, particle path formulation 80−59070
gas in closed tube, resonant oscills., Chester's eqn. soln. 77−3869
gas jet, interaction with plane barrier *(Russian)* 77−27571
gas jet, nonstationary, wave structure and density distrib. 77−62286
gas mixtures, detonating, symmetric piston motion 80−59073
gas motion near symmetry centre for energy release on the periphery, shocks 80−33626
gas of variable density, channel flow, discontinuity evolution 77−58734
gas pipe lines, decompression waves following rupture 79−68807
gas shock adiabats, props. near Jouguet points 80−92178
gas unsteady expansion into nonuniform near-vacuum 77−72265
gas vibrations in tubes under action of periodically varying pressure 79−94718
gas-hard particle mixtures, nonstationary waves, shock wave interactions *(Russian)* 77−27587
gas-liquid film interface stability behind slipping shock wave front *(Russian)* 78−55630
gas-liquid mixture, press. perturbations propag. 78−34186
gas-particle flow in shock tube, finite difference calc. *(Japanese)* 80−79390
gas-particle flows in shock waves, radiant interchange among suspended particles *(Japanese)* 77−15063
gas-particle mixture, particle specific heat, Boltzmann eqn. 78−14072
gas-particle mixtures, effect of thermal radiation on shock wave 78−91032
gas-particulate fluidised beds, bubble formation and shock front 79−90318
gas-radiating particle mixture, shock wave struct. numerical investigation 80−10298
gasdynamic disturbance in chem. reacting gas mixture, shock wave formation 80−74999
gases, shock wave radiation, low inertia pyroprobe meas. *(Russian)* 77−31333
general relativity, geometrical struct. of shock waves 79−71297
general relativity, self-similar solns. with divergent and collapsing shock waves *(Russian)* 77−74290
general relativity, self-similar solutions with spherical shock waves *(Russian)* 78−8284
generation and application in solids *(Japanese)* 79−68475
global analysis of shock waves *(Chinese)* 79−64699
global geometry of shock curves 77−65750
global structure anal. 80−8800
granular material, uniformly distributed, 1-dimens. shock waves, porosity discontinuity 78−83285
granular solid, one-dimens., small amplitude wave behaviour 78−59339
granular solids bed, shock wave attenuation 77−51110
graphite, shock wave, prod. by explosion, vel. meas. 80−59074
gravitational and EM in general relativity, detection 77−5710
gravitational compression of a body within the approximation of the special theory of relativity 80−4611
gravitational shock waves from Einstein eqns. eikonal approx. 78−116
growth function for human response to large-amplitude impulse noise 79−16222
Gyugonio's eqn. rel. to heat exchange *(Russian)* 77−68625
H II region globules, time evolution 77−17661
hard-core fluid, struct. of shock wave front, mol. dynamics study 78−1970
Hartmann-Sprenger tube, gas temperature calc., using Lagrange equations *(Japanese)* 79−4041
Hartmann-Sprenger tube, thermal effects, finite difference method for analysis 80−14771
head-on collision, appl. to nonlinear interaction and diffraction *(Russian)* 78−22372
heat front in weak mag. field, EM field perturbation *(Russian)* 78−94835
heat pipe, supersonic flow and shock waves 79−32568
heat transfer in shock interaction with turbulent boundary layer 77−23994
heavy-ion high energy inelastic collisions, cascade evaporation model of shock waves *(Russian)* 78−41766
Herbig-Haro object 1, shock wave model rel. to far UV spectrum 80−67714
Herbig-Haro objects, shock wave interpretation of individual condensations 78−45324
Herbig-Haro objects, spectrophotometry and radiating shock waves 78−85936
Herbig-Haro objects, stellar wind model 80−85985
Herbig-Haro objects in Gum Nebula, spectrophotometry rel. to shock wave model 78−36565
high density nuclear Mach shock waves, central heavy ion collisions, compressed nuclear matter, meson condensation 78−46089
high Reynolds number supersonic flow, compression corner flowfields, turbulent boundary layer separation 80−14735
holographic shearing interferometer with narrow ref. beam for flow investig. in reflecting nozzle of shock wave 77−47118
homogeneous explosives, electrical polarisation with initiation of shock wave detonation 79−100378

shock waves continued
homothermal shock, prod. by instantaneous monochromatic radiation 80−59159
Hugoniot eqn. corollaries, impact heat transfer and shock waves. 80−92132
hydraulic shock during tube filling by liquid *(Russian)* 80−24053
hydrodynamic cumulation regimes during lining collapse, cumulative jet 80−69891
hyperbolic system, simple wave growth, charact. shock instability, fluid appl. *(French)* 77−68623
hyperbolic systems, increasing entropy-like generating functions *(French)* 77−13573
hyperdetonation eccentric shock wave, approx. soln. 78−67070
hyperdetonation shock wave passage through jump like nonhomogeneity 78−67069
hyperdetonation shock wave propagation in a nonhomogeneous medium 79−23236
hypersonic aerodynamics, limiting shock layer *(Russian)* 78−30316
hypersonic axisymmetric flow with const. momentum, shock wave, ideal and laminar regions *(Russian)* 77−55033
hypersonic blunted sphere cones, viscous shock layer solns. 78−51186
hypersonic bow shock interaction with ice crystal, aerodynamic shattering criterion 77−27558
hypersonic conical nozzle, boundary layer separation from compression shock 80−48766
hypersonic flow, bodies at high attack angle, shock-layer eqns. 79−4042
hypersonic flow, shock layer separation, asymptotic soln. *(Russian)* 80−33625
hypersonic flow around blunt bodies, surface friction, physiochemical processes in shock layer 78−46997
hypersonic flow around three-dimensional wing 77−19621
hypersonic flow in converging conical channel 77−39310
hypersonic flow over blunt body, viscous shock-layer eqns. 79−60002
hypersonic flow past blunt axisymmetric body, shock layer 78−9654
hypersonic flow past blunt bodies, aerodynamic heating, effect of chemical reactions of injected gas *(Japanese)* 79−94739
hypersonic flow past blunted cones, shock waves 78−1684
hypersonic flow through body wall 80−38447
hypersonic flow with attached shock waves over plane delta wings 77−27556
hypersonic nonstationary flow past wedge and cone, thin shock wave method *(Russian)* 77−80180
hypersonic shock layer, screening of selective heat radiation in boundary layer *(Russian)* 79−32497
hypersonic streams in mag. field, secondary shock waves *(Russian)* 78−87401
hypersonic two-dimens. flow behind compression shock, entropy layer 78−1691
hypersonic viscous flows over sphere cones at high angles of attack 79−98746
hypersonic viscous shock layer, leeward vortex-induced heat transfer 77−80179
hypersonic viscous shock layer, three-dimens., numerical calc. on sharp cone at incidence 77−47041
hypersonic viscous shock layer equations, num. soln. scheme 79−90280
hypersonic viscous shock-layer equation, method for successive approximations for integration *(Russian)* 78−59421
hypersonic viscous state stability of sharp cone at incidence 77−23987
hypersonic wedge flow, dusty gas effect 80−6083
hypervelocity particle-surface impact simulation, using high-power pulsed laser 77−44094
ideal compressible media, elastoplastic thin walled constructional elements and shock wave interaction *(Russian)* 79−68618
ideal electrically conducting gas, weak discontinuities in singular surface theory 80−43736
ideal gas flow, arrival of a shock wave at the expanding part of a channel 80−6088
ideal gas supersonic flow around blunt wedge, sonic line shape 80−64577
ideal radiating gas, sonic discontinuities, shock development 80−43802
ignition of metal powders, pre-ignition processes 77−40546
impact response, two degrees of freedom system, effect of damping 80−74587
impacted solid, expt. facility to produce and measure compression and shear waves 80−59581
impacted solids, compression and shear wave propag., modelling 80−83755
implicit dissipative schemes for solving systems of conservation laws, shock regions 79−72909
implicit divergent difference formulation *(Russian)* 77−51022
imploding cylindrical shock waves, ideal gas, gasdynamic eqns. 79−32572
implosive spherical, produced by laser pulses, shadowgraphic detection 80−87529
incompressible elastic solids, thermodynamic theory 77−68508
industrial explosions, causes, propagation, and suppression methods 80−31725
inert gases, weak shock wave struct. investig. 79−94679
inertial motion of continuum, shock waves form. 79−18861
inertial motion of fluid, shock formation 78−13985
infinite circular cylinder, moderately strong shock wave interaction 80−92176
inhomogeneous atmosphere, shock wave propag., appl. to meteorite explosion 77−66973
inhomogeneous granular solid, one dimens. accel. waves, speed, amplitude 78−87288
initial shock parameters for explosion in rarefied gas 80−53815
instability in a relaxing medium 80−100013
insulator, transparent, laser breakdown, acoustic charact. 80−50269
integral momentum eqn. for flows with entropy gradients across inviscid streamlines 77−11214
interaction, compression areas buildup *(German)* 79−81921
interaction in gas of $\gamma=3$, mutual penetration approach 79−14432
interaction with free surface 79−2287
interaction with triangular acoustic pulses with discontinuous edges 77−50802
interactions, regular and irregular, props. 79−68745
interactions with boundary layers, review, book contrib. 80−96283
intergalactic medium, shock waves rel. to giant ellipsoidal shells around normal elliptical galaxies 80−86000
internal resonances 78−1627

shock waves continued
internal state variables materials, thermomech. wave propag., isotropic linear theory 77−3760
interplanetary, caused by 1972 August solar flares, Pioneer 9 obs. 77−2317
interplanetary, cosmic ray distrib. 77−17304
interplanetary, energetic solar flare particles 78−49276
interplanetary, generated emission in 100-700 kHz range, Prognoz obs. 78−69636
interplanetary, generation by solar flares *(Italian)* 78−96377
interplanetary, interaction with low-energy protons, 1975 January, Helios 1 obs. 78−20609
interplanetary, MHD soln. of disturbances generated by simulated vel. perturbations 77−29615
interplanetary, solar flare assoc., from radiosource scintillation obs. 77−2318
interplanetary, three-dimens. geometry 77−22033
interplanetary acceleration of electrons and ions by shocks 78−49285
interplanetary collisionless shock waves, thickness 80−90314
interplanetary flux from flare of August 4, 1972, hydromagnetic struct. 78−28475
interplanetary plasma flows from strong flares, props. and nature of mag. regions 77−91397
interplanetary shock, assoc, plasma wave turbulence obs. 79−53700
interplanetary shock followed by large solar wind He^+ flux, Imp 7 obs. 80−101520
interplanetary shock wave, 1978 January 3 to 4, Prognoz-6 energetic particle and solar wind meas. 80−90315
interplanetary shock wave, He^+ obs. in driver gas 80−72735
interplanetary shock wave in flare plasma flow, 1972 August 4 to 5, struct. rel. to mag. storm 79−53653
interplanetary shock wave in solar wind, thermal electrostatic noise, LF obs. from ISEE 3 80−101519
interplanetary shock waves, 1973, April 29-30, anal. of complex solar particle event 78−20593
interplanetary shock waves, during August 1972, vels. from solar wind plasma obs. 77−25902
interplanetary shock waves, flare generated, during second STIP interval (1976, March 15-May 15), obs. 78−81514
interplanetary shock waves, in time-depend. two-fluid solar wind model with thermal cond. 79−92643
interplanetary shock waves, ISEE magnetic field profiles 79−58196
interplanetary shock waves, parameters correl. with energetic storm particle events 79−35079
interplanetary shock waves at large heliocentric distances, Pioneer 10 studies 79−84621
interplanetary shock waves during August 1972, directions rel. to cosmic rays N-S anisotropies 78−89018
interplanetary shock waves during August 1972, rel. to high-energy cosmic ray obs. 77−25894
interplanetary shock waves during August 1972, summary of solar/interplanetary events 77−25991
interplanetary shock waves during August 1972 solar-terrestrial events, mag. field obs. and vels. 77−25903
interplanetary shock waves in August 1972, meas. by radio source scintillation obs. 77−25901
interplanetary shock waves in outer solar system, mag. fields and plasma effects 79−58213
interplanetary shock waves in turbulent medium, energetic particles interaction 80−4210
interplanetary shock waves interaction with bow shock-magnetopause system 80−26712
interplanetary shocks, identification by computer on board HELIOS-1 and (HELIOS-2) 79−92679
interplanetary shocks during August 1972, obs. at 2.2 AU 77−45276
interplanetary shocks interaction with Earth's magnetosphere, computer simulation 78−16243
interplanetary travelling phenomena, symposium (Tel Aviv, 1977 June 7-10) 78−49275
interplanetary two-fluid shock waves propag., model 80−26711
interstellar bright rimmed molecular clouds, evidence for CH emission from postshock gas 80−62238
interstellar cloud, shocked gas dynamics rel. to sequential form. of subgroups in OB associations 80−98696
interstellar medium, H II region shock fronts rel. to interstellar clouds form. 80−109506
interstellar medium, radiation from shocks 79−48899
interstellar neutral H, weak R-type ionisation front approaching a contact discontinuity 78−49510
interstellar radiative shocks, thermal instability rel. to maser condensations form. 80−67821
interstellar radiative shocks and UV precursors, theoretical models 79−25660
interstellar shock wave in IC 1805, assoc. IR object radio identification 78−93369
interstellar shock wave models 79−58389
interstellar shock wave towards ζ Ophiuchi, evidence from OH obs. 79−97052
interstellar shock waves, post-collisional propag. and amplification *(Russian)* 79−44360
interstellar shock waves, rel. to intermediate-vel. gas obs. 78−36655
interstellar shock waves, vel. determ. from high vel. H I absorpt. features 79−48891
interstellar shock waves structure, first stages 79−88714
interstellar shocks, analytical results for post-shock gas temp., density, vel. and comp. 80−56911
interstellar shocks, mol. diagnostics 80−56899
interstellar shocks from presupernova stellar wind, rel. to supernova remnant filamentary struct. 80−62249
ionisation by shock waves in transverse magnetic field, finite-difference methods 78−51249
ionisation fronts, weak D-type, departures from equilibrium 77−49288
ionised, equilibrium zone behind shock wave *(Russian)* 77−89154
ionising Ar flows, shock wave and laminar boundary layer coupled interaction 80−59071
ionising shock wave interaction with transverse mag. field, numerical anal. 77−84279
ionising shock waves, in monatomic gas, large Mach numbers 80−6096
ionising shock waves in EM field in supersonic flow *(Russian)* 77−89155

shock waves continued
ionising shocks reflection on end wall of shock tube, finite difference analysis *(Japanese)* 78−42629
isomagnetic shock waves, conducting medium 77−89205
isothermal, propagation in nonhomogeneous medium 77−55017
isothermal, propagation in perfect gas, density increase 77−55016
isothermal, reflection from rigid wall 77−55035
isothermal, reflectionless passage across jump-like nonhomogeneity 78−30210
isothermal blast waves, one-dimens. in mag. field, mathematical theory 80−28532
isothermal flows behind shock wave in water 77−89159
isothermal gas, closed form soln. to nonstationary plane shock wave propagation 78−51195
isothermal self-similar blast waves, one-dimensional flow and its stability 78−45214
isothermal self-similar blast waves, two-dimensional flow and its stability 78−49307
isotropic elastic medium, finite deformation shock waves, centric cumulation 80−53673
jet, axisymmetric, counterflow problem, num. soln. procedure 77−58757
jet, free, streamlines and local velocities in rarefied atm. 77−42884
jet, supersonic, flowing onto infinite perpendicular barrier, limiting expansion ratio 78−59439
jets, adiabatic, spatial form 79−46284
jets, colliding supersonic coaxial underexpanded, investigation of flow 78−67237
jump-inhomogeneous medium, homogenisation by a reflectionless shock-wave 78−83568
Kaprolon, compressibility, elec. cond., sound vel. behind shock front 78−95105
Kelvin-Helmholtz instability in supersonic and super-Alvenic fluids 80−87816
Korteweg-de Vries-Burgers equation, time evolution, stability, of shock soln. 77−37743
Kortweg de Vries (Burgers) nonlinear long waves, mathematical modelling 80−8791
Lagrangian hydrodynamics meshes, discrete rezoning algorithm, hot interacting bubbles calcs. 78−42628
laminar to turbulent boundary layer transition, effect on current flow 79−41709
laminar wake formation in shock wave prod. from plate edge 79−77120
laser impact on transparent dielectric, shock wave dissipation from imperfections 79−69925
laser irradiated freely falling glass microballoon, hemispherical shock wave 79−63809
laser supported detonation wave, Whitham's rule anal. 78−59423
laser-liquid interaction, air shock wave generation at surface 78−19608
laser-produced shock wave optical diagnostic system 80−79421
layered hyperelastic half-space, one-dimens. propag. of weak discontinuities 78−30226
leading shock wave front in front of blunt object with recess instability *(Russian)* 77−75940
Lennard-Jones 6-12 crystal, shock wave mol. dynamics, nonsteady to steady wave transition 80−15189
lightning, expanding return stroke channel diameter and shock waves 77−70751
lightning channels radial expansion and shock wave form. 80−12530
linear charge explosion *(Ukrainian)* 79−76901
liquefaction shock waves, shock tube expt. study 80−19439
liquid, laser breakdown, photoacoustic and photohydrodynamic parameters 78−52597
liquid, laser induced shock wave 77−7413
liquid containing gas bubble, structure *(Russian)* 77−35224
liquid containing gas bubbles, struct. of supersonic waves and cavitation development 80−33643
liquid foams, shock wave dispersion 79−46359
liquid fuel film, combustion behind shock wave, heat and mass transfer in turbulent boundary layer *(Russian)* 78−71401
liquid in elastic pipe, press. wave pattern 79−46387
liquid pool boiling, shock form., dissipation interactions, fission reactor safety appl. 77−31341
liquid-gas bubble mixtures, shock wave disturbances 78−22411
liquid-liquid interface, with temp. discontinuity, shock wave generation 78−51197
liquids, practical microphone developments *(German)* 79−82001
liquids, response to dynamic tension, conf., Ispra, Italy (Sept. 1977) 79−69175
localisation, by shock-capturing results of computation of gas dynamics problems 80−83815
long period variable stars atmospheres shock wave periodicity rel. to mass loss 79−44487
longitudinal shock-waves in an elastoplastic medium *(French)* 79−46249
Ludwieg tube, steady flow duration extension, reservoir orifice method, variable opening area effect 80−64579
RR Lyrae, UV light curve rel. to atmospheric shock waves 77−45435
Mach reflection transition, steady (unsteady) flow, with (without) relax. 79−50752
Mach reflexion transition for strong shocks 80−6091
Mach to regular reflection transition *(Russian)* 77−51083
Mach wave radiation of hot supersonic jets 80−69894
Mach waves, kinematics inside and outside supersonic jets, book contrib. 80−1640
Magellanic Cloud supernova remnants, optical emission from shocks 79−92831
magnetised relativistic continuum, shock invariants *(French)* 79−25944
magneto-radiative gas, spherical shock, exact similarity soln. 79−16815
magneto-radiative shocks, axisymmetric, equatorial propagation 80−79349
magnetoelastic medium shock loading, linear and nonlinear problems *(Russian)* 77−39246
magnetogasdynamic shock wave, variable strength, plane 79−98813
magnetogasdynamic spherical shock waves, propag. in exponential medium 79−84664
magnetosheath, form. due to SSC 78−45147
magnetosonic wave propag. in warm plasma, appl. to solar atm. MHD fluctuations 80−77275
magnetosphere, double layers and electrostatic shocks review 80−36460
magnetosphere, electrostatic shock waves rel. to ULF elec. field fluctuations in dayside auroral oval 80−98505
shock waves continued
magnetosphere, electrostatic shocks, double layers and anomalous resistivity 78−45152
magnetosphere, electrostatic shocks as source of discrete auroral arcs 78−45153
magnetosphere, V-shock mechanism for discrete aurora 79−8737
magnetosphere stand-off shock front, passage of low-freq. wave packet 78−45138
Manicouagan Impact Structure, Canada, formation *(French)* 79−88355
Mars bow shock, positions, rel. to Mars mag. field, Mars 5 evidence 78−49362
Maxwell gas, shock struct., numerical integration of Burnett eqns. 79−94677
metagalactic shock waves, thermal processes 80−46678
metal, attenuating shock waves following meteoroidal impact *(Russian)* 77−71068
metal body, obliquely impacted at high velocity, wave formation *(Russian)* 77−68478
metals, shock adiabats, weak shock wave profiles 79−7651
metals under contact explosion loading, shock damping process 80−54309
meteorite atmospheric entry, expansion, decel. and intense shock wave emission 77−37584
MHD, Brinkley-Kirkwood method, appl. to shock waves in stellar atm. *(Russian)* 78−93102
MHD, generalised polar diagrams of plane-parallel stationary simularity flows, waves 80−96314
MHD, nonsimilarity solns. for cylindrical blast waves 77−39357
MHD, oblique shock waves calc. 79−77263
MHD, solitary fluid transient compression wave in rectangular duct in transverse mag. field 78−59503
MHD asymptotic shock wave propagation in EM field 77−75982
MHD axisymmetric shocks, equatorial propag. 77−75985
MHD blast wave in gravitational field 78−83496
MHD generalized equation of state, charact.-shock and struct. exceptionality 79−10614
MHD shock, axisymmetric, equatorial propag. 77−19640
MHD shock wave propag. and growth in inhomogenous fluid 78−67272
MHD shock wave propag. in non-homogeneous media 77−7459
MHD shock wave propagation at conducting gas boundary 78−79383
MHD shock wave propagation in inhomogeneous atmosphere 79−55426
MHD shock wave refl. from conducting wall *(Russian)* 77−80223
MHD shock wave refraction 78−1749
MHD shock wave smoothing with artificial heat conduction 78−67271
MHD shock waves, oblique propag. *(Russian)* 79−14483
MHD shock waves with heat addition 79−55427
microplastic regime in elastic-plastic media, shock layer struct. 79−76997
micropolar elastic media, anisotropic, propag. of shock and acceleration waves 79−30242
minimized sonic boom waveforms, subjective loudness 79−16221
mobile load on ideally packed material layer 80−99952
model for heavy ion high energy collisions 79−54402
model optimization of detonation-wave description on consideration of combustion kinetics 79−91955
molecular rotational distribution, exponential gap law 77−89156
monatomic gas, non-stationary oblique shock wave reflexions, domains and boundaries 80−48750
monatomic three dimensional FCC lattice, solitary wave effect on shock profile 80−79874
monotone, Korteweg-de Vries-Burger equation, asymptotic soln. and generalisation 79−35568
Mott-Smith method for shock waves in supersonic compressible flow, modification 79−50754
MSH 11-54, supernova remnant, adiabatic shock wave model rel. X-ray obs. 80−82463
multicomponent gas mixture, transport eqns. and distrib. functions 80−64581
multicomponent media, cylindrical detonation wave propag. 79−86287
multicomponent medium, non-homogeneous plane shock wave propagation 78−46908
multicomponent nonlinear viscous media, plane waves 78−51228
multidimensional fluid dynamic calcs., artificial viscosity use, Navier-Stokes viscosity 80−92181
multidimensional magnetogasdynamic flows, shock wave propagation and breaking 79−98818
multiframe shadow photography using optical delay like 77−764
multilayered spherical vessel, elastoplastic response to intermittent internal blast loading 77−65705
multishock problem in cylindrical symm., particle trajectory method, explosion near ground 78−1692
N-wave sonic booms, subjective loudness tests 79−16220
natural and man-made shock waves on Earth and in space 78−3897
natural flow and US cavitation erosion comparison 78−59435
Navier-Stokes eqns. of shock wave struct., stability of solns. 77−75874
Navier-Stokes equations, for front struct. in liq. 79−64702
nebulae ionisation-shock fronts hydrodynamic linear theory 80−17625
NGC 281, H II region, obs. of shock in region of shock-induced star form. 79−25688
NGC 7027, planetary nebula, shock model for H_2 emission generation 80−98698
non-asymptotic shock-detachment distance of slender cones in transonic flow, book contrib. 80−1632
nonadiabatic, shock heat exchange *(Russian)* 78−75170
nonconservative hyperbolic systems, gradient catastrophe in soln. 78−69992
nonequilibrium gas flow, growth of discontinuities 80−48734
nonhomogeneous medium, reflectionless shock wave 78−54197
nonhomogeneous medium, shock wave refl. from movable partition 79−7327
nonhomogeneous plastic polytropic medium, plane shock wave propagation, closed form soln. *(Polish)* 79−32350
nonlinear compressible medium, shock propag. 79−14329
nonlinear deformation waves in nonhomogeneous medium *(Russian)* 79−50642
nonlinear elastic media 80−48629
nonlinear heat conduction effect on shock wave fronts *(Russian)* 80−79352
nonlinear hydrodynamic shock propagation, finite element anal. and method of weighted residuals 80−53813

shock waves continued
nonlinear mechanics eqns. and entropy growth across a shock, symmetric form 80−69705
nonlinear reflection from hard wall, law of similarity *(Russian)* 77−80181
nonlinear resonance effects in closed shock tubes with varying cross section 77−50803
nonlinear self-dual network eqn., shock wave and hole type soliton 78−27
nonlinear viscoelastic rods, shock wave front definition *(Russian)* 79−50635
nonlinear wave effects in a closed tube 79−90332
nonlinear wave phenomena in a closed tube *(Russian)* 78−87353
nonlinear wave propagation, analytic solns. for accel. waves, non-equilib. effects 78−94890
nonlinear wave propagation and unsteady transonic flow, variational formulations 78−55660
nonlinear waves, wavefronts in vibr. relax. gas 78−83431
nonreflecting boundary conditions for nonlinear hyperbolic systems 79−50748
nonstationary oblique reflections, actual isopycnics and numerical expts. 79−41712
nonsteady two-dimens. transonic flow, numerical solns., shock waves 80−53808
novae flare-ups theory, exact analytic self-similar solns. 79−35269
nozzles, high enthalpy supersonic flow conversion to hypersonic flow 80−74937
nuclear, detonation waves, initiation and propagation conditions 79−93834
nuclear matter, phase transitions and shock waves 79−49594
nuclear matter, shock wave matter, shock wave dynamics, phase transition effects 78−21509
nuclear matter, width of compression wave front *(Russian)* 77−34242
nuclear matter props. at high densities *(German)* 77−38237
nuclear power plant blast effects due to gas cloud explosions 77−38350
nuclear reactor, structural shock tests, prototype FBR MONJU scale models, computer code verification 77−3131
numerical shock structure, nonlinear corrections for difference schemes in conservation form 80−36878
oblique waves, interactions with compressor blades in subsonic flow *(French)* 79−14434
ocean blast wave propagation, theory for stratified ocean *(Russian)* 80−81904
oceanic warm front propagation, shock wave model with appl. to Sagami Bay Kyucho phenomenon 80−94538
off-centre point explosion in spheroid 78−63450
one dimensional, in gas dynamics with low viscosity and heat conductivity 79−64698
one-dimensional lattice, shock propagation at nonzero initial temp. 78−75724
one-dimensional nonstationary problems of gas dynamics, estimates of shock wave motion 79−18912
one-dimensional quiescent lattices, shock profiles, end condition effects 80−34138
one-dimensional unsteady flow, numerical solution of hyperbolic initial-boundary value problem *(German)* 80−6095
one-mass vibroshock system, forced random oscills., treatment by Markov process methods 79−14335
open tubes, resonant oscillations of gas 77−68628
organic fluids, liquefaction shock wave obs. 77−51484
Orion Nebula, shock vel. from search for H_2 ground state S(2) line 79−8961
oscillatory shock waves in soliton system under perturbation *(Russian)* 79−92959
outer shock struct., partially ionised gases 78−9656
overtaking interaction in ideal gas 78−71369
oxyacetylene, critically-initiated detonation waves, quasi-steady regime 78−90930
panels, cylindrical, failure under gasdynamic periodic shock waves 80−14611
paper membrane sound generation by impulsive tension 78−90581
parabolic, strong blast theory 77−35164
particle acceleration by MHD shock turbulence 80−87894
perfect fluid, irrotional stationary flows, unicity condition *(French)* 78−87356
permanent one-dimens. flow, small unsteady perturbations *(French)* 77−51024
Perspex spheres, times to fracture due to point explosive loading 77−50989
perturbed solitons, interaction, and struct. of oscillatory shocks 79−64868
piezoelectric semiconductor, shock waves and acoustoelec. domains 77−32049
piezoresistive C gauge for low shock pressure meas. 79−1278
piston, magnetic field effect, self-similar magnetogasdynamic problem with radiative heat transfer 80−64578
piston problem, one-dimens., in gasdynamics 78−34162
piston problem, shock formation, Boltzmann eqn. 77−31334
piston produced shock waves in nonisentropic medium, Riemann wave soln. *(Russian)* 77−68626
piston structure and gas distrib. in strong shock wave 80−10265
planar detonation waves, diffraction at an abrupt area change 80−14744
planar sonic nozzle, three dimens. wave struct. of nonstationary gas outflow 77−55068
plane acoustic wave normal and oblique interaction with plane shock, wavenumber jump conditions 78−1466
plane converging duct, separation zone for turbulent boundary layer and oblique shock interaction 80−14759
plane hyperdetonation shock wave reflection from rigid wall 78−75167
plane hyperdetonation wave generation, optimum conditions 78−67068
plane nonstationary self-similar gas flow with energy liberation in shock waves 79−77182
plane obstacles, weak shock wave reflection in air 80−48751
plane relativistic shock waves, propag. 79−53707
plane relativistic shock waves, propag. in slowly moving medium 80−62005
plane shock impinging on wavy contact surface, results *(German)* 80−14747
plane shock thermal layer interaction flow props. and temp. profiles 77−58735
shock waves continued
plane sound waves in air, finite-amplitude saturation and shocks 78−1465
plane wave-plane shock interaction in magnetofluiddynamics 80−69931
plane-layered medium, shock form. during strong sound wave propag. 77−34980
plasma sheet, electrostatic shock waves assoc. with auroral electron precip., model 77−9616
plasmas, soliton damping 79−64869
plastic wave, two-dimensional, propagation in nonlinearly compressed half-plane 79−7325
plates colliding, shock front determ., damping, hydrodynamic approx. 78−9595
point explosion in arbitrary atmosphere with radiative heat transfer 78−53708
polymorphic phase transitions induced by shock waves, review 80−15188
polytropic gas, initial pressure effect on stationary shock wave propagation 79−50753
polytropic media, shock waves formation processes, boundary condition effects 79−46347
polytropic medium, nonstationary plane shock wave propagation, local closed form soln. 79−68747
polytropic medium, shock compression using absorbing layer 80−6092
polytropic medium layer on linear elastic substrate, mass-impact generated shock waves 80−69870
polytropic plastic gas, nonstationary shock wave propag., closed form soln., thermonuclear microfusion 80−28534
porous rocks, dry and water-saturated, plane shock wave studies 80−21714
porous solids, sound velocity *(Russian)* 78−71788
post shock expansion behind normal shock on curved wall, flow separation, book contrib. *(German)* 80−1628
potential theory model for separation regions behind shock waves *(German)* 80−1636
precursor, probe meas. 79−64701
pressure discontinuity system with 1 or 2 triplets, supersonic object, air equilib. physicochem. transforms. 79−90350
pressure shock in gases at high temp. 79−18910
pressure wave, two dimens. cylindrical, excited by moving load, propag. in acoustic medium 77−68300
pressure waves in compressible liquid, one-dimens. anal., LMFBR fuel-coolant interaction 77−88235
pressure waves interaction with combustion field 78−63504
profile about hemispherical nose, low supersonic Mach nos. 77−89149
profiles of shock waves in shock-loaded solids 79−94564
profiling pressure pulse by rarified gas layer 77−68631
propagation, in smoothly-varying density condensed medium, thermodynamic description 77−75844
propagation across deflagration, radiative and chemical 77−3846
propagation along 90 degree bends, curvature effects on stability 78−18314
propagation in channel in nonuniform EM field *(Russian)* 77−58798
propagation in general relativity, stationary approx. 80−86172
propagation in inhomogeneous medium using finite differences 77−7414
propagation in solid, atomistic model 77−47509
propagation in two-phase mixture *(Russian)* 78−51196
propagation investigations on suitability of piezoelectric and magnetoelastic detectors *(Polish)* 80−79351
propagation of strong plane waves in optically thin grey atmosphere 80−53810
propagation of strong wave in channel 77−89157
propulsion system, pulsed laser, fluid mech. model, real gas effects 79−60089
pseudo-shocks in cylindrical duct 77−58722
pseudo-steady single-Mach reflection, reconsideration of shock polar soln. 80−99893
pseudoshock, friction in channel 77−27546
pulse wave propagation in arteries 80−41099
pulsed discharge, air, elec. wind and sonic wave (350 m/s) initial growth, Schlieren obs. 78−87587
punch-elastic body dynamic contact, superseismic stage, exact soln. 78−55614
quasars, two-dimensional relativistic blast waves, solns. for adiabatic case 80−22108
quasars and active galactic nuclei, magnetic flare model, magnetised accretion disc around massive black hole 80−22113
quasars and active galactic nuclei radiation from relativistic blast waves 77−74156
quasi-one-dimensional flow equations, exterior differential form represent. *(Japanese)* 78−8243
quasilinear hyperbolic system of gas dynamics *(Russian)* 80−33629
quasilinear hyperbolic systems, propag. of weak discontinuities when charact. shock occurs 78−79153
radiating gas, weak stationary shock wave formation *(Russian)* 77−35259
radiating gases, flow parameter vorticity and gradients for an optically thin gas 79−4089
radiating gases, sonic wave propag., wave front curvature effects, shocks 80−87784
radiating gases, sonic wave propagation 77−47114
radiating laminar boundary flow over flat plate at large free stream Mach no. 79−1270
radiative boundary shock wave struct. 80−10264
radiative gas, boundary shock waves 79−64694
radiative transfer in shock layer, spectral lines calc. 78−5641
radiative viscous-shock-layer analysis for equilib. flow about blunt axisymm. body, effect of coupled ablation injection 77−24033
radio galaxies, double source structs. form. and superluminal expansion 78−8141
radio sources, compact, emission from moving shock wave in relativistic jet 80−4448
radiogalaxy M87 jet, internal shocks in plasma beam 78−93416
radiosources, extended, particle accel. and radiative losses effects on source dynamics 80−46687
Rankine-Hugoniot jump conditions, viscous and thermal effects 78−59418
rapidly rot. gas, free jet expansion, Newtonian thin shock layer approx. 80−74888
rarefaction shock waves generated by moving thermal sources 79−7386
rarefied flow by kinetic theory, closure relations 79−98757

shock waves continued
rarefied shock wave existence near thermodynamic critical point of a substance *(Russian)* 80−88263
ray method for solving gas dynamics equations *(Russian)* 79−27659
reaction-diffusion eqns., slowly varying waves and shock structures 77−66747
real gas, blast wave, effects of compressibility, vibr. excitation, dissoc. and ionisation 77−68622
real gas effects in cryogenic wind tunnels 78−94760
recompaction waves, propagation calcs. 79−68752
reflected shock tunnel, driver gas contamination 78−63448
reflected shock wave at wall, press. change meas. 80−53812
reflection, regular to Mach transition, Monte Carlo simulation 77−75936
reflection from concave surface, numerical simulation 79−18913
reflection from concave wall, cumulative effect 77−89158
reflection from cylindrical surface, transition from normal to Mach refl. 80−64582
reflection from rigid walls *(Russian)* 79−32576
reflection from solid moving partition in non-elastic medium, loading process behind front 78−46907
reflection from sphere or cylinder, gas parameter distrib. in initial stage 80−96281
reflection from wall in stream of burning mixture *(Russian)* 79−14496
reflection of detonation waves from a wall 80−53885
reflection of explosion waves from plane surface *(Russian)* 78−87361
reflection of nonlinear shock waves in lattice 77−24355
reflectionless passage through region of jump-like nonhomogeneity 77−42870
reflectionless shock wave in stratified medium 78−51193
refraction, at slow-fast gas interface 79−32573
refraction at oblique shock, tensors and polars 78−30318
region behind shock surface, point explosion in axisymm. media flow variables 79−68736
relativistic, damping 77−75994
relativistic, propag. in presence of transverse mag. field 78−75207
relativistic blast waves that accelerate 80−67534
relativistic flow in homogeneous medium, similarity soln. 79−98826
relativistic fluid mechanics and shock waves, basic results 77−42933
relativistic fluid with vibrational relaxation, growth and decay of weak discontinuities 80−69948
relativistic gas conducting heat, shock relns., and conservative form of hyperbolic eqns. 79−14498
relativistic gravitating gas in presence of strong shock, spherically symm. motion 78−12629
relativistic infinite electrically conducting fluids, strong shock waves 77−39365
relativistic MHD, plasma and condensed medium 77−24035
relativistic nucleus-nucleus collisions, high density nuclear Mach shock waves 78−633
relativistic shock waves, anal. approaches *(French)* 80−96317
relaxing gas, sonic discontinuities 80−28531
relaxing gas flow, discontinuity growth 80−28525
resonance tube, jet flow and heating, unsteady complex shock struct. 80−6115
resonant three-wave process, Backlund transform. 77−68609
rods, simple orthotropic elastic, shock waves and wave-type instability 80−48622
rotating gas, strong diverging cylindrical shock propagation 80−79350
rotating gaseous disc with gravitation, shock waves, spiral galaxy model *(Russian)* 79−88749
rotating shock and detonation wave anal. 80−53792
rotational shock waves as bow and return shock waves in interplanetary plasma flows 77−17315
scalar partial differential eqns., variational principles 79−30255
schlieren probe method for measurement of refractive index profile of shock wave in fluid 80−23785
Schrodinger nonlinear coupled eqns. with complex coeffs., analytical and numerical anal. of wave-wave interaction 78−54220
second Hugoniot relationship 77−35659
secondary shock waves, detonation of heterogeneous systems *(Russian)* 77−931
Sedov-Taylor blast wave solns. stability 79−35104
segmented explosive charges, co-acting detonation and shock waves 77−927
selective radiative heat exchange screening in shock boundary layer 79−90283
self-similar explosion waves of variable energy at the front 80−103040
self-similar shock and rarefaction waves in polarizable continuous media 78−47047
semicone body, hypersonic inviscid flow, shock shape calc. methods 77−89150
separated turbulent boundary layer at compression corner, mean flow meas. 77−42867
shell, cylindrical, viscous, explosive squeezing and effects 79−86378
shell, shallow spherical, plastic deformation under explosive loading 80−14589
shell deformation by supersonic gas flow, drag 80−96279
shell fracture by periodic shock waves 77−89068
shells, cylindrical, subjected to localised perturbations, equilib., states 79−18850
shells, two fluid-coupled cylindrical elastic, transient response to incident press. pulse 80−58966
shock boiling, liq. discharge through short nozzles, flow blocking 79−86491
shock capturing application of the finite element method 79−27665
shock formation distance in real air 79−37351
shock separated boundary layer, suction effects, compressible Navier-Stokes eqn. solns. 80−24050
shock tubes, use of fast-acting valves, shock wave formation 80−24052
shock wave propagation, steady state, Navier-Stokes eqns. 77−68615
shock-boundary layer interaction flows, multieqn. turbulence modes for duct and channel 80−24093
shock-front loading method for dynamic photoelasticity studies 77−7349
silica shock adiabat, rel. to specimen size 77−81873
simple gases, relativistic shock wave struct., Boltzmann eqn. soln. 80−1644
simple wave description by particle displacement 79−12623
singular hypersurfaces, asymptotic regularisation as alternative to distrib. 80−36923
shock waves continued
singular nonlinear differential eqns., boundary flow behind shock wave 78−63413
slurry explosives, layered medium with liquid-polytropic gas structure, pressure pulse propagation 80−69872
soil, nonhomogeneous water saturated, plane shock wave propag. 77−56607
soil model, viscoplastic, eqns. and expt. determ. *(Russian)* 78−7619
soil subject to stress waves, cavitation effects 79−70792
solar atmosphere, acoustic shock waves rel. to chromosphere temp. rise 79−16911
solar atmosphere, August 1972 flares shock waves, ground-based radio obs. 77−25993
solar atmosphere, chromospheric boundary layer structure influence on solar wind 79−53788
solar atmosphere, propag. of MHD shockwaves 78−24503
solar chromosphere, acoustic shock waves dissipation and H^- radiation 78−96454
solar corona, shock wave propag. rel. to type II radio burst with reverse freq. drift 80−17567
solar corona and transition region, shock wave dissipation 77−60740
solar corona shock waves and magnetic field above an active region 77−53512
solar corona streamer, drift pair radio burst theory 79−25558
solar coronal expansion, hydrodynamic blast wave theory with radiation heat flux 80−90377
solar flare, 1973 September 5, radio data and theoretical model for fast-mode MHD shock wave 79−92734
solar flare generated shock wave, plasma enriched by O^{6+} and He^{++} 80−72740
solar moving type IV radio bursts, shock and plasmoid models 79−40174
solar wind, evolving streams and shocks beyond 1 AU, Pioneer 10 and 11 obs. 78−49283
solar wind, magnetoacoustic solitons ahead of near Earth shock wave front 80−4217
solar wind, shock-associated energetic proton events at large heliocentric distances 78−77451
solar wind magnetic fluctuations, Helios 1 search-coil magnetometer expt. 78−20607
solar wind shocks and assoc. wave-particle interactions 78−49284
solid, compression wave interaction, pulsed electron beam initiation 80−79877
solid, dimensionless Hugoniot eqn. of state 79−69191
solid, energy transport, molecular dynamical calc. 78−95117
solid, heavy ion bombard., Mach shock electron distrib. 80−45194
solid, shock induced free surface velocity and postshock sp. volume 78−43074
solid, shock wave profile 78−55911
solid bodies, high speed collisions, dynamic pressures, shock wave parameters 77−68491
solid body-microparticle impact, cratering, viscous effects 79−66255
solid matter behind wave front, eqn. of state *(Chinese)* 79−82308
solid undergoing phase transitions, finite amplitude waves *(Russian)* 79−28100
solid undergoing phase transitions, shock wave propag. 79−14331
solids, resist to shock front propag., wall of dislocations model 79−90728
solids, simulations of shock waves 79−33035
sonic bang, review 77−42858
sonic boom, infrasound generated by Concorde used to monitor stratospheric winds 80−51492
sonic boom, nonlinear propag., including asymm. effects, numerical soln. program 77−72326
sonic boom induced window response and damage 79−81604
sonic boom of supersonic transport aircraft, effects on ecological environment 80−106661
sonic boom propag. in thermosphere 80−33305
sonic booms focusing conditions 77−50804
sonic discontinuities propagation through thermally conducting and dissociating gases 78−30311
sonic flow simulation, permeability law study *(French)* 79−32567
sonic wave propagation, thermally conducting and radiating gases 78−42679
sonic-boom press. signature distortion by high-speed jets 78−79156
sound pulse propag. in inhomogeneous atm., flow struct. near intersection between shock and caustic 79−14139
sound wave interaction with shock waves 79−27457
spark channel, high-conducting, shock wave degeneration to sound waves 80−38428
spark channel, highly-conducting, shock wave degeneration to sound waves 80−38429
spark channel shock wave detection 78−87586
sphere at supersonic speeds, impulsive motion, shocks, subsonic flow at stagnation point 80−106814
sphere in supersonic and hypersonic flows, shock stand-off distance, formula 77−55030
spherical blast wave, high-speed photogrammetry of real and ideal reflections 78−42694
spherical blast waves generated by spherical flames, anal. 80−16686
spherical detonation waves in media with volumetric viscosity 79−14332
spherical imploding shocks, pressure extremes 80−64580
spherical shell, internal weak shock wave action *(Russian)* 77−68497
spherical shock, interaction with plate 80−38446
spherical shock waves from explosion in homogeneous water 79−77183
spherical shocks reflected from real and ideal surfaces, photogrammetry 77−72328
spherically blunted cone with massive surface blowing, laminar and turbulent flows, shocks 80−38445
spherically imploding shocks 79−10591
spinning detonation mechanism 78−22362
spiral galaxies, shocks, in hydrodynamic flows in regions of Lindblad resons. 78−96527
sprays, blast wave propag. 79−34367
sputtering yields, hydrodynamical approach to non-linear effects 80−66374
square shaped fluid shock wave pulses with variable time duration 80−74593
stability in gas-dynamic context *(Russian)* 80−6093
stability of an ionizing shock wave in an electromagnetic field 80−6076
stars, radial gas oscills. after explosion shock wave passage *(Russian)* 79−8903
stars, solns. for dynamical rupture of equilib. 77−56913

shock waves continued
steady homenergic compressible flow with finite shocks, variational principle 80−69874
steel, shock transition rise-time meas., limiting viscosity coeffs. 79−77680
stellar atmospheres, radiative shock dynamics and H continua 78−40918
stellar atmospheres, soln. for one-dimensional piston problem in non-ideal gas 80−82185
stellar collapse, adiabatic hydrodynamics and shock wave propag. 80−56861
stellar collapsing core, shock struct. and neutrino radiation, rel. to supernova explosions 78−49427
stellar explosion models, new solns. 80−12751
stellar photospheres of cool Mira variables, shock wave accel. 77−13352
stellar wind, shocked cloudlet model for Herbig-Haro objects 78−89196
stellar winds, polytropic fluid flow in central gravitational field 77−45301
step-wavefronts, reflection from perforated and flared tube extensions rel. to railway tunnels 79−14426
strained coordinate method for transonic flows 80−69861
stratified medium, reflectionless shock wave passage 78−54196
stress measurements in severe shock-wave environments using low-impedance Mn gauges 80−38367
stress wave propagation calcs., effect of material constitutive models 78−90769
stress waves, high amplitude, laser generated in materials 79−78797
strong shock wave in nonuniform medium, front propag. 78−83422
strong shock waves, motion in nonuniform density medium 78−42630
strong shock with radiation near stellar surface 78−32442
structure close to wall, book contrib. 80−1650
sub and transonic flow over wing, flow separation, vortex struct., shock wave shape *(French)* 80−14733
supernova, remnants, O, N and S abundances, optical emission from shock waves 77−49447
supernova, shock accelerated galactic cosmic rays 80−82154
supernova blast wave, Lagrangian coordinate transforms. in self-similar model 77−57072
supernova blast wave instabilities, adiabatic and isothermal models 80−67814
supernova blast waves, propag. rel. to interstellar medium mechanical heating 80−36682
supernova blast waves and the interstellar medium *(Italian)* 79−53845
supernova remnant optical emission spectra, effect of shock wave intermediate zone radiative cooling 80−109517
supernova remnants, cosmic rays accel. in shock fronts 78−32302
supernova remnants, cosmic rays in dense shell 77−33599
supernova remnants, fast shock wave optical emission 80−46631
supernova remnants, Hα emission of optical filaments, shock waves interaction with interstellar medium 78−8103
supernova remnants, isothermal blast wave model 77−9778
supernova remnants, isothermal self-similar blast wave theory 77−82295
supernova remnants, pulsar-driven isothermal blast-wave models 77−78847
supernova remnants, self-similar flow behind blast wave 77−53415
supernova remnants, two-fluid blast-wave model 79−80345
supernova remnants in Magellanic Clouds, cloudlet shocks model 79−75259
supernova remnants optical emission, diagnostic diagrams 77−64816
supernovae, MHD shock wave model 80−46588
supernovae, shock steepening and prompt thermal emission 79−16998
supernovae, shock wave model for radiation dynamics, envelope ejection and light curves 77−64783
supernovae, shock-accelerated cosmic rays early radiation spectrum, cooling and escape 79−48626
supernovae, type II, nonequilib. processes in evolution 80−46586
supersonic, flow through body wall 80−38447
supersonic cascade with strong in-passage shocks, unsteady flow 78−14041
supersonic conical flow, without axial symmetry, numerical method 77−89147
supersonic diffuser with surface cooling, flow and heat transfer meas. in pseudo-shock region 77−42868
supersonic flow, finite difference method calcs. *(French)* 78−34157
supersonic flow, inviscid, over external axial corner, shock wave and vortical singularities 77−42866
supersonic flow, self-induced oscills. 78−67215
supersonic flow, steady two- and three-dimensional, shock discontinuities detection method 77−58736
supersonic flow around circular cone, shock and combustion waves 78−26154
supersonic flow around wings with attached shock wave on leading edge, num. soln. 77−51080
supersonic flow field meas. of slender cone at high angle of attack 79−77177
supersonic flow of inverted population gas flow round blunt bodies, amplification factor 78−5828
supersonic flow over cones with near-critical and supercritical vertex angles 79−81918
supersonic flow past blunt body, radn. effect on flow field and heat flux 77−47113
supersonic flow past slender body, wave system 78−34155
supersonic gas particle flows over wedge *(German)* 80−43731
supersonic inviscid conical corner flowfields, complex shock interactions 80−48739
supersonic jet, nonsteady interaction with barrier, math. model of oscillatory cycle 80−19462
supersonic jet, shock layer ahead of barrier 79−64723
supersonic jet, two-dimens., impingement on flat plate, shock-interference heating 79−94688
supersonic jet, two-dimensional, impingement on normal ground surface 77−24003
supersonic jet-barrier interaction, shock layer flow near axis 79−90282
supersonic local zone near wing profile of infinite span, flow calcs. 79−32565
supersonic Ludwieg tube with downstream valve, starting process 79−72965
supersonic nozzle, pulsed jet wave struct. in nonstationary flow stage 80−59094
supersonic separation flow, 2- and 3-dimens., turbulent boundary layer and shock wave 80−100017
shock waves continued
supersonic shock-wave boundary-layer interaction, appl. laser anemometer 77−35275
supersonic shock-wave-turbulent boundary layer interaction, appl. photon correlation anemometry 77−35277
supersonic turbulent boundary layer 79−41711
supersonic underexpanded jet, press. pulsations on flat plate 78−94778
supersonic velocity and turbulence, appl. Doppler velocimeter with Fabry-Perot interferometer 77−39377
surface velocity measurement, interferometric laser technique 77−50972
surface waves generated by shallow underwater explosions 79−2288
switch on shocks, hydromagnetic 77−84337
symmetrical airfoil, transonic flow, inviscid and turbulent flow props., wake 80−48736
symmetrical flow past double wedge at subsonic Mach nos. 78−51182
tangential shock, stability in inhomogeneous medium 79−14430
tension waves, propagation calcs. 79−68752
terrestrial and cosmic, review 78−15967
terrestrial bow shock, ISEE magnetic field profiles 79−58196
thermal boundary layer interactions in shock tube sampling for kinetic obs. 80−104420
thermal radiation effects on shock wave incident on wall 78−5823
thermal reactor, steam explosion propagation phenomena, multidimensional aspects 79−89420
thermal shock in chemically active medium *(Russian)* 79−32709
thermally conducting gas, point explosion 79−41714
thermoelastic fluids, stability of motion anal. 80−10221
thermoelastic solids, weak shock waves 77−75849
thermoelastic-plastic coupled medium, accel. and shock wave propag. 77−58578
thin walled sphere in contact with elastic or acoustic media, interior dynamics 80−5981
thin-shock-layer approximation, restriction on soln. procedures 77−62279
thread, nonlinear elastic, cone-induced shock, self-similar problem soln. *(Russian)* 80−53677
three dimensional interactions with obstacles 80−53814
three dimensional separated turbulent flows at supersonic speeds 80−19435
time analysis of shock flow, dual microwave and dual schlieren systems 77−15143
torus, axially symmetric, transonic flow 80−28527
tracking, subgrid resolution of fluid discontinuities 80−105506
train tunnel pressure jump reduction by slotted portals 77−62097
transient, differential equations 79−64696
transient cavitation, on marine propellers, high-speed photography 78−38432
transient jet of propelling gas during diaphragm rupture in shock tube, holographic images 79−77181
translational relaxation at shock wave front in gas mixture 80−74917
translational rotational shock detachment, relaxation effects, subsonic layer, length scale 79−81923
transonic channel flow, unsteady, with shock waves 77−23991
transonic channel flows, two-dimensional, shock-wave motion 79−60005
transonic diffuser flow, shock wave oscillations 80−14729
transonic flow, bow shocks comput. method 77−55027
transonic flow, discontinuous 78−38362
transonic flow, parabolic regularisation of nonlinear mixed elliptic hyperbolic eqn., finite element anal. 80−83814
transonic flow, plane, weak shock wave solns. 78−38364
transonic flow, shock wave interaction with turbulent boundary layer, pressure distrib. 80−74918
transonic flow, shock wave interaction with turbulent boundary layer, wall shear stress 80−74919
transonic flow, turbulent boundary layer-shock wave interaction *(French)* 78−34163
transonic flow, two- and three-dimens., perturbation soln. method 79−1208
transonic flow, unsteady, implicit shock-fitting computational scheme 78−94763
transonic flow, unsteady, turbulence modelling, compression waves developing into shock wave 80−74909
transonic flow, unsteady perturbations 79−4033
transonic flow around lifting round-nosed airfoil, extended integral eqn. method 77−62271
transonic flow multidimens. imbedded shocks 77−3841
transonic flow numerical calculation methods and problems, review 77−58723
transonic flow over airfoil, steady and unsteady, shock-induced separation 79−59999
transonic flow with shocks, finite element method appl., shock-fitting 80−14730
transonic flows, exact shock-jump conditions, numerical solns. 79−41704
transonic indicial method, shock motion effect 78−94769
transonic integral eqn. method with curved shock waves 79−68739
transonic nonseparating normal shock-turbulent boundary layer interaction, approx. anal. theory 77−23992
transonic normal shock-turbulent boundary layer interaction, Reynolds no. and mass transfer effects 79−37353
transonic profile flow at incidence with shock 79−4031
transonic profile flow with shock, supercritical flow 77−15056
transonic shock wave-boundary layer interaction, dual-scatter laser velocimeter meas. 77−39376
transonic shock-boundary layer interaction, shock obliquity effect 78−90933
transonic shock/boundary-layer interaction subject to large pressure fluctuations 80−38433
transonic small-disturbance eqns., shock-fitting appl. to relax. solns. 77−84275
transonic streamline shape, influence of nonconservative differencing 77−23983
transonic turbulent boundary layer, shock pentration 78−14044
transonic unsteady flow in two-dimens. diffuser 78−71361
transonic unsteady flows calc. using integral eqn. method, aerodynamics 79−32554
transonic wind tunnel laser velocimeter meas. interpretation 77−31324
transparent stagnation point shock layers, non-iterative solution of energy eqn. 79−18911
transverse shocks in detonation waves, strength var. 78−26157
trapped nonlinear waves near sonic type singularity 80−24041
Tunguska meteorite, possible mechanism of event 77−78728

shock waves continued
turbulence separation, subsonic and supersonic, ultra-short duration visualisation *(French)* 78−75128
turbulent boundary layer at permeable plate with shock waves, heat transfer 79−81922
turbulent boundary layer interaction, numerical simulation, Navier-Stokes eqns. soln. 77−31332
turbulent boundary layer interaction 80−74916
turbulent boundary layer interactions, Reynolds no. effect 78−1689
turbulent boundary layer separation at curved wall with shock 79−46343
turbulent boundary layer/shock-wave interaction sweep effect on separation conditions 77−62280
two degree of freedom nonlinear vibratory system, shock spectrum 77−27421
two dimensional shockwave−turbulent boundary layer interaction, flow separation 80−14758
two-dimensional steady transonic flow, nonlinear wave propag. 77−75935
two-dimensional supersonic viscous in reactions near walls, prediction method 77−58726
two-dimensional turbulent blunt body flows with impinging shock 80−38444
two-phase detonation front compression waves, solid particle oxidation reaction *(Russian)* 78−34207
two-phase reactive particle flow through normal shock waves 78−42676
two-phase shock wave 77−68674
Tycho supernova remnant, shock front rel. to radio remnant struct. 80−56919
ultrahigh press. (TPa) shockwave from underground nuclear explosion 80−59580
underwater electrical discharge, compression wave calc. and obs. *(Russian)* 79−1354
underwater explosion, commnet on weak shock soln. 79−90068
underwater explosion generation of sound wave pulse, nonlinear region 80−56493
underwater explosions, scaling law for shock waves 77−14838
underwater explosions, shock wave interactions 80−14746
underwater explosions, surface effects, review 80−14745
underwater explosive shock waves, formulation of weak shock soln. 80−10070
underwater explosive shock waves, weak-shock soln. 78−26003
underwater spark induced axisymmetry unsteady motion betweeen shock wave front and contact surface *(Russian)* 79−77323
underwater wire explosion, shock wave propag. *(German)* 77−76244
unidimensional gas flow prod. by piston in nonmonotonic motion *(Russian)* 77−42871
unsteady boundary layer, behind moving shock waves 77−23995
unsteady flow, space-time motion of shock waves *(French)* 77−65763
unsteady flow fields with detonation, num. modelling 77−55107
unsteady flow in radial channel, incident shock wave 78−1744
unsteady hypersonic gas-dynamic eqns., approx. solns. *(Russian)* 77−35165
unsteady laminar boundary layers behind blast waves, num. soln. 80−69776
unsteady supersonic flow around wings with detached shock wave, numerical soln. 79−94647
unsteady transonic flows with shock waves in an asymmetric channel 78−71366
unsteady transonic shock motions in two-dimens. flow 80−14731
upwind second-order difference schemes for transonic flow with embedded supersonic and shock regions 77−23975
US shock waves emitted by cavitation at rotating perforated plate, wear, thickness effects 77−27565
variable area ducts, shock propag. with phase changes, extended Chisnell's method 77−68627
velocity meas. in liquid H_2 77−75999
velocity measurement, generation by pulse chamber ignited by HV ignition spark 77−24039
Venus bow shock, attachment to ionosphere 77−37541
Venus bow shock, Pioneer magnetometer obs. 80−36535
vibration relaxation time in nozzle and shocktube expansion flows, physical model 80−24067
viscoelastic biological tube dynamic rheology 79−62274
viscoelastic media, shock profiles, elastic discontinuities struct. 79−14330
viscoelastic medium, eqn. of state for shock-wave struct. 78−9594
viscoelastic rod, nonlinear waves and finite rod impact on rigid obstacle 79−41606
viscoplastic medium, plane wave propag. and scatt., similarity condition 77−35072
viscoplastic shock profile analysis 77−72203
viscoplasticity, wave problems, appl. of methods of characteristics and perturbation 79−68614
viscoplastoelastic material, plane wave propagation anal., upon shock loading 79−14336
viscous compressible flow, hybrid integration scheme, shock tube problem 80−69868
viscous compressible flow at high Reynolds number, global approach and coupling approach 80−48742
viscous heat-conducting gas, numerical simulation methods 80−38449
viscous materials, heat-conducting, with hidden variables, shock waves and acceleration waves 80−74788
viscous shock layer flow over highly cooled sphere, coupled eqns. anal. 78−51189
viscous supersonic flow over external axial corners, shock and bubble generation computation 80−14734
viscous-inviscid flow matching, separation, shock waves *(French)* 78−34105
visualisation, at few torr, holographic technique 77−55038
visualisation, by elec. discharge radiation 77−72371
volcanic eruption column, Tolbatchik area 77−56612
Volterra soliton, collapse into weak monotone shock wave 78−49673
vortical ring, interaction with shock wave 79−94650
W1, supernova remnant, shock wave refl. from small dense cloud rel. to radial vel. field 80−62250
wake formation caused by shock wave descending from plate edge *(Russian)* 79−14402
wall shear stress meas. in shock wave-boundary layer interaction, comments 80−14670
wall shock decay in large abrupt area change, expt. 79−32571
water, cavitation expts. using shock tube 80−87789
water, explosive shock wave propagation, energy hypothesis 80−92179
water, tension pulse transmission 79−68750
shock waves continued
water column, shock wave generation by impinging piston, waveform, propag. mode and state change 77−58733
water vapour condensation in rarefaction waves, homogeneous nucleation case 77−42869
water vapour-N_2, nonstationary rarefaction wave, nonequilib. condensation obs. 77−75937
wave diagrams, weak shock wave diffraction and reflection *(Chinese)* 79−64692
wave fronts of nonlinear waves in vibr. relaxing gas, comments and reply 80−1645
weak, in mechanics, short-wave asymptotics 77−37763
weak detonation waves 79−41710
weak discontinuities in high temp. phenomena, relativistic theory 80−53889
weak plane waves at wedge, reflection, diffr. 77−72111
weak shock propagation in liquid-filled tubes 78−26004
weak shock wave focusing at an arete 79−37352
weak shock waves in chemically reacting gas *(Russian)* 78−42681
weak spherical shock waves, propagation from arbitrary piston motions 80−22204
weak-shock transmission coefficient via harmonic generation 77−68294
weakly dissipative system, higher order approx. in reductive perturbation method, shock wave appl. 80−14743
weakly ionised gas, heavy ion seeded, theory 79−60006
weakly nonlinear wave propagation due to dispersion and dissipation. long wave approx. 80−57104
wedge, intense supersonic gas blowing through wall, dividing static press. determ. 77−84273
wind tunnel calibration by shock standoff distance computation up to Mach 1.2, schlieren method 77−27557
wing, oscillating, in transonic flow, unsteady airloads and flow linearisation 80−19426
X-ray densitometer with high sensitivity and quantum flux for density meas. 79−26031
X-ray induced shocks in stellar winds of massive binaries 80−94784
Zemplen's studies on shock waves *(Hungarian)* 80−31476
Al foil, with Au overlay, impedance-match expts. using laser-driven shock waves 80−29119
Al foil in quartz dust, electrical explosion for accelerator application 80−6314
Al, laser driven shock waves vel., risetime, luminosity struct. meas. using shocks own luminosity 78−59857
Al, shock transition rise-time meas., limiting viscosity coeffs. 79−77680
Al, shock-waves, ultrahigh-press., laser-driven 79−55823
Ar, electrical conductivity, behind detached shock wave 79−10592
Ar, gas, temp. behind strong shock front, M=8-30 79−72910
Ar, gas in planar nozzle, shock-wave propag., effect of transverse mag. field 80−6094
Ar, precursor shock waves, electron density and assoc. ionisation 78−67217
Ar, reflected shock wave, press. anal. at Mach numbers of 10 to 35 77−15060
Ar, shock-tube end-wall boundary layer 80−79348
B fibre, reinforced epoxy angle-ply laminate wave propag. during transverse impaction 79−83295
Br_2, dissoc. and recomb. rate consts. meas., 1200-3000K, techniques comparison 77−63892
CO, vibr. relax. in unsteady expansion wave, vibr. temp. distrib. 77−68096
$CO+CO_2$, exchange rates behind reflected shock waves for $C^{18}O$ and ^{13}CO 79−29363
$CO+O+M \rightarrow CO_2+M$, time-resolved and flame-band emissions in shock tube expts. 77−36729
CO_2, 10.6 μm reson. absorpt. behind shock front 78−42707
CO_2 laser, high repetition rate-pulsed, weak shock wave effect 78−90409
CO_2 laser, Lamberton and Pearson type, shock wave detect. 79−36946
CO_2, viscous hypersonic flow over blunted cone, numerical anal. 79−77171
CO_2, weak nonlinear waves, struct. and propag., effect of vibr. relaxation 79−64683
CO_2-F_2-Ar mixture, vibr. relax. in shock wave, 4.3 μm radn. 78−1062
CO_2-He-N_2, gas dynamic laser, gain coeff. numerical estimates, book contrib. 80−1183
CO_2-N_2-He, coefficient of optical amplification behind an axisymmetric shock wave *(Russian)* 77−89153
CS_2-O_2 mixture, stimulated emission of CO behind overdriven detonation wave front *(Russian)* 77−23668
$Cl_2+Ar(He)(Cl_2)$, dissoc. in shock wave, density gradient meas. 77−83682
ClF+Ar, shock wave, vibr. relax., laser schlieren meas. 78−90267
Cu, deformation hardening by shock front, quasiisentropic compression, front width effects 79−100209
Cu, shock transition rise-time meas., limiting viscosity coeffs. 79−77680
Cu, shock-compressed, compression and rarefaction waves obs., 150-250 kbar 77−77535
DT plasma in biconical system, neutron generation by shell implosion 79−37524
Fe, Armco, dyuamic $\alpha \rightleftarrows \varepsilon$ transform., stress gauge meas. 80−96594
Fe, Armco, shock front phase transition kinetics 78−10122
Fe, thermal props. at high-press. (150 GPa), from shock-wave expts., Earth core struct. 80−21683
Fe-Cr-Al, attenuation and vel. of acoustic shock waves, amplitude depend. 78−63810
Ge:Sb, shock polarisation anisotropy in elastoplastic compression range 77−16244
H II regions, weak shocks props. 78−93348
H II regions ionization front time evolution 77−17654
H, ionisation rates, shock tunnel meas. 80−75022
H_2-O_2 mixture, explosion limits as stochastic phenomenon 77−21387
H_2O, acoustic rad. from ionising particles 78−71793
H_2O foams, shock wave propagation 79−64737
H_2O vapour, shock waves, in pure vap. vibr. relax. time at low density 79−98761
H_2O-H_2 mixtures, vibr. energy transfer in shock waves, population inversion 80−37996
He-N_2-CO_2 mixture in supersonic nozzle, shock activation with overexpansion, jet form. 78−18330
^{4}He, liquid, first sound nonlinear wave distrib. *(Russian)* 80−107588
^{4}He, superfluid, second sound shock waves, pulse characts. and temp. depends. 78−67876

shock waves continued
^{4}He, superfluid, second sound shock waves, detection by superconducting thin film probe 79−73355
^{4}He, superfluid, second sound discharge and compression shock wave propagation *(Russian)* 80−103529
KBr, shock adiabatic, nonparametric equation of state 78−10121
KNO_3, aq. solns., laser induced breakdown 79−87530
KOH, aq. solns., laser induced breakdown 79−87530
LiBr, shock adiabatic, nonparametric equation of state 78−10121
LiF(:Mg), shock waves in (111) direction, elastic precursor amplitudes 80−54314
Mn-Cu alloy, acoustic shock pulse charact., stress amplitude and temp. depend. 79−19323
Mn-Cu alloy, high-damping, acoustic shock pulse attenuation and vel., stress amplitude and temp. depend. 77−15503
Mo single crystal surface, shock wave form. due to laser radiation interaction 77−81180
N_2 gas, domains and boundaries of non-stationary oblique shock wave reflexions 79−68746
N_2 in supersonic nozzle, shock activation with overexpansion, jet form. 78−18330
N_2, oscillatory-dissoc. relax. in hypersonic shock layer at moderate Reynolds number *(Russian)* 77−39311
N_2, rot. relax. in viscous shock layer *(Russian)* 77−89162
N_2, rotational relax. in shock layer 79−64703
NF_3, thermal dissoc. behind shock waves, rate meas. 78−61002
N_2O, weak nonlinear waves, struct. and propag., effect of vibr. relaxation 79−64683
Na+N_2, Na excitation in non-equilib. conditions behind shock wave 77−23539
NaBr, shock adiabatic, nonparametric equation of state 78−10121
NaCl(I), aq. solns., laser induced breakdown 79−87530
Ni, deformation hardening by shock front, quasiisentropic compression, front width effects 79−100209
O_2 dissociation relaxation behind regular reflected and stationary oblique shocks 78−85159
$Pb(N_3)_2$-He system, high-velocity two-layer detonation 77−84278
RbF(Cl)(Br), shock adiabatic, nonparametric equation of state 78−10121
SO_2, thermal decomposition in shock waves, infrared measurements 79−47903
Ti+C(B)(Si) self-propagating, high-temp. synthesis wave, radiating power 79−100377
Xe, condensed at high press., electron-band theory and fluid theory calcs. 80−59875
Xe gas, supersonic radiation waves generated by CO_2 laser radiation 79−10593
Yb stress transducer, piezoresistive effects 77−68539

shocks, electric *see electric shocks*

short-circuit currents
battery, thermal, using Ca anode, electrolyte composition improvement *(Japanese)* 79−83584
flameproof coating for PVC insulated cables, composition, tests *(Russian)* 78−68828
HV electron gun power supply protection 79−44989
insulators, HV for transmission lines, power arcs occurring in networks and laboratories, comparisons 80−87983
LV short-circuit testing station, equipment and measurement methods *(Polish)* 80−77773
minority carrier diffusion length determ., using angle-lapped p-n junctions 79−42631
n-p junction solar cell, anal. of short circuit currents generated by electron beam 79−39308
p-n junction minority carrier diffusion length meas. 80−31849
semiconductor, bounded, transport effects when a current passes along an energy inhomogeneity 79−7845
solar cell, fabrication process, Si single cryst. cells 79−61977
solar cells, defects, rel. to elec. parameters, SEM electron beam induced current investig. 79−43772
turbogenerator, short circuits, stator end windings deformation *(Japanese)* 78−11465
CdS-$CuInSe_2$, solar cell, grain boundary effects on performance 79−83603
$CuInSe_2$ polycrystalline thin film anomalous photovoltaic effect *(German)* 78−68102
Cu_xS-CdS solar cell, minority carrier diffusion length, SEM determ. 77−72911
$Ga_{1-x}Al_xSb$ p-n homojunction LPE and photovoltaic effect obs. *(French)* 78−64108
GaAs polycrystalline film growth for solar cells 79−33941
GaAs shallow junction solar cells damaged by electron irrad., recovery of short cct. current 79−29471
n-GaSb:S-metal surface barrier struct., elec. and photoelec. props. 78−56229
p-GaSe, back wall Schottky barrier cells, diffusion length, RT spectral response meas. 80−107806
In_2O_3:Sn/n-Si heterojunction solar cell, fabrication and charact. 78−15314
Si n-p junction vertical solar cells, Al-plated, photovoltaic effect variation with impurity conc. 79−100522
Si Schottky barrier solar cell, V-I charact. and efficiency 78−14828
Si solar cells, analysis of short-circuit current 80−85285
Si-In_2O_3:Sn heterojunctions for solar cells 78−64107
SiH_x, amorphous, solar cells, short circuit-currents and collection efficiencies 80−94028

short-range order
see also order-disorder transformations
adsorbed layers, order-disorder transition, effect on work function 80−59791
alkali metal:inert gas, optical absorpt. by impurity, short-range order effects 77−8612
alkali metals, liq., collective excitations and short-range order 78−63665
alloy, activity coeffs. and short-range order, correl. *(Russian)* 78−56614
alloy, binary, conc., with short and long range order, computer simulation of diffusion 78−30778
alloy, binary, elec. resist. depend. on LRO, SRO and composition, inhomogeneous order effects 79−60781
alloy, binary, short range order calc. using equilib. diagram *(Russian)* 79−87610
short-range order continued
alloy, binary substitutional, short-range ordering kinetics, vacancy behaviour 78−55867
alloy, disordered, energy band struct. and elec. cond., effect of short-range order 80−10860
alloy steel, rel. to special carbide formation *(Russian)* 77−21153
alloys, anisotropic binary, HCP struct., influence of spatial nonuniformity of short-range order on interdiffusion *(Russian)* 78−6187
alloys, binary, constitution diagrams, computer calc. *(Russian)* 80−84909
alloys, binary substitutional, determ. of local atomic configurations 79−86739
alloys, binary with long and short range order, electron energy spectrum calcs. *(Russian)* 79−99471
alloys, definition for arbitrary duration and expt. temp. 79−51267
alloys, density of electronic states, dressed-cluster approx. 78−95249
alloys, disordered, residual resistivity due to clustering, ageing effects 80−65521
alloys, DO_{22} and $L1_0$ superstructures, atomic ordering, multicluster approx., order-disorder transition 80−38990
alloys, electronic theory using pseudopot. approx., review 79−47004
alloys, phase transition premonitory phenomena, exam. by electron diffr. and microscopy *(French)* 80−59651
alloys, substitutional, electrical resist., long and short range orders effect 80−107761
alloys, substitutional disorder description within supercell model 78−26479
amorphisation due to ion bombardment, SRO struct. 80−79844
amorphous alloy, struct. relax., compositional SRO 78−79538
amorphous alloys, at. order effects on mag. props. 77−73006
amorphous intertransition metal alloys, short-range struct. 79−50995
amorphous materials, Mossbauer effect, props. and investigation methods *(French)* 80−80652
amorphous metals, struct. imperfections, review of expt. evidence 79−37630
amorphous semiconductor, local order as determined by electronic and vibrational spectroscopy 79−37627
amorphous solid, structural defects, computer simulation study 80−88040
amorphous solids, symmetry of short-range order, polyhedra model 78−42913
anisotropic liquid, rel. to integral eqn. for ang. distrib. function, quasi-chem. approx. *(Russian)* 78−6147
antiferromagnet, short range order effects on EPR frequencies 77−69669
antiferromagnetic heavily doped semiconductors, Faraday light depolarisation in mixed mag. states 80−29726
antimonates, columbite or trirutile struct., force fields rel. to cryst. struct. *(French)* 80−107104
asperomagnetic alloy, amorphous, spin-wave theory including short range order 79−38313
austenitic steel, pearlitic transformation incubation effect, Mossbauer spectra *(Russian)* 79−70061
p-azoxyanisole, nematic eqn. of state, incorporating short-range orient. order. 77−55237
bimetallic cluster, segregation and short range order props. at boundaries 79−29071
binary, segregating alloy, theory of surface effects 79−19435
binary alloy, electron theory, two particle interaction, perturbation theory 78−10390
binary alloy, ordered BCC to disordered FCC transition 77−43327
binary alloy, short range order effect on density of states *(Russian)* 78−67929
binary alloy, thermal EMF, short-range order effects *(Russian)* 77−15835
binary alloys, concentration derivatives and correlation functions of intrinsic variables 77−17937
binary alloys, diagrams of state, component interaction parameters *(Russian)* 80−55354
binary alloys, FCC, with short-range order, electron theory, pair interaction and third-order perturbation theory 79−69404
binary alloys, FCC lattice, mean distrib. of vacancies, computer program 77−62444
binary BCC and FCC solid solns., short range order rel. to comp.-prop. relations *(Russian)* 78−47280
binary linear chain, electronic props. 80−96769
binary liquid system, colligative prop., composition diagram *(Russian)* 79−14663
binary melts, short-range order, X-ray and neutron scatt. *(German)* 78−14272
binary ordering alloy, gas absorption, correl. effects *(Russian)* 78−47525
binary ordering alloy, theory of surface effects 79−19434
brass, α and $\alpha+\beta$ type, positron annihilation, short-range order, clustering and lattice defects influence 79−29107
brass, γ-phase region, X-ray and electron diffr. obs. 79−61562
brass, martensitic transform., short range order effect 79−61586
tert-butanol, mol. dynamics, liq. and cryst. states, neutron inelastic scatt. obs. 78−75599
CBOOA, with cholesterol decanoate, short range smectic A order in nematic phase, NMR meas. 77−28475
chemical reaction rate constants, in solution, short-range caging effects 79−96286
chemical reactions rate constants, in solution, escape probability and time-depend. reactivity 79−96287
classification by electron microscopy 78−38623
cluster model for transition state, electron diffr. study 78−10168
copolymer globule model, orientationally-ordered liq. cryst. state *(Russian)* 80−59389
copper formate tetrahydrate, model two-dimensional ferroelec., short-range order, neutron scatt. 78−68458
copper formate tetrahydrate, short-range order, diffuse neutron scatt. 78−15124
crystallisation, percolation theory, Lindemann melting criterion and thermodynamic props. 79−28081
dense fluid, hydrodynamics, high freq., small wavelength 77−19860
diamond, covalent semicond., depend. of energy gap on short-range order 78−84142
dilute simple cubic lattice, short-range quadrupolar order 79−65681
disordered alloy, short range order effect on electron states 77−15732
disordered alloys, electronic struct., CPA calcs., short-range order 78−63964

short-range order continued
disordered alloys, short range order diffuse electron scatt. 78−87595
disordered chains with short-range order, freq. spectra 78−10148
disordered multicomponent solid solutions conc. fluctuation waves, microscopic theory 80−44327
disordered structures, two-dimensional, computer program for modelling *(French)* 80−59337
disordered system with correls., density of states at band tail 80−80154
disordered system with short range order, elementary excitations 78−23000
disordered systems, coarse-grained quantities and short-range order 78−75787
disordered systems, short-range order and off-diagonal randomness 78−75782
disordered transition alloys, generalized perturbation calcs. of ordering energies 77−4282
distance dependence restrictions, Cowley short-range order parameters 80−103294
electron gas, many electron effects on characteristics of short range order, pseudopotential calc. 78−79954
electron gas, two dimensional, classical, hypernetted chain solns. 78−67963
electron liquids, two-dimens., short-range order onset, thermodynamic props. 78−43454
electronic theory, pseudopotential approach 77−80717
Elinvar, γ to γ' transformation and γ' phase form. kinetics, lattice consts. 80−35191
ethylammoniumtetrachlorochromate, optical absorption intensity, short-range spin correlation 80−108185
FCC binary alloys, short-range order diffuse scattering, Fermi surface imaging *(Japanese)* 79−7776
ferroelectric and first and second order structural transitions, model theory 79−51915
ferromagnetic alloys, disordered crystalline and amorphous, dipole field distribution 80−25101
ferromagnetic binary alloy, short-range and long-range ordering 78−76206
ferromagnetic sol, relaxation of mag. birefr. and dichroism 79−57301
ferromagnetism, itinerant electron model, spin quantization direction fluctuations, short range order. 80−34582
fluid, classical, short-range struct. universality, bridge functions 80−10478
fluid, near liq.-gas crit. pt., local order effects on dynamic props., US and light scatt. 78−67806
fluid, of isotropic mols., DID Rayleigh and Raman depolarised scatt., lattice-gas model 80−10356
fluorite ceramics, doped, short range order anal. by electron diffr. 78−83672
glasses, polymerised, statistical thermodynamics, short and long range props. 77−27834
Heisenberg ferromagnet, spin wave excitations at finite temp., CPA calc. 77−32142
Heisenberg magnets, pure and pseudo-one-dimens. temp. depend. of EPR freqs. 78−6563
Heisenberg model, nearest-neighbour spin-spin correl. functions calc. 80−80537
Heisenberg paramagnet, electronic spin dynamics, NMR 78−76266
hollandites, cryst. growth and structural props. 80−89129
II-IV-V_2 semiconductors, amorphous, SRO 77−84653
Ising chain, in transverse field, variational treatment, static props. at zero temp. 79−4642
Ising paramagnet, impure, influence of spatial short range order 78−43542
Ising square lattice, phase transitions, next nearest neighbour interactions 80−50128
itinerant magnetism, quasispin model, effect of short-range order 78−68144
Krieger-James approx. of short range order effects, antiferro- and ferromag. 78−56276
latex, monodisperse, order-disorder phase transitions, short-range order 77−29056
latex, monodisperse, short-range order, spectroscopic study 78−85208
linear Ising mixture, frozen system, thermodynamic props. 77−40064
liquid, Debye temp., short-range order, theory 78−2264
liquid alloy, dil. binary, partial interference functions, short range chem. order effects 79−7541
liquid crystal, ferroelec., helicoidal, smectic-C, dynamics 79−1396
liquid crystal, rel. to molecular-statistical theory of translational transitions *(Russian)* 77−15564
liquid metals, atomic radial distrib. curve anal. *(Russian)* 80−14996
liquid metals, structure factor modelling using quasi-crystallised model *(Russian)* 80−54118
liquid semiconductor, metal-insulator transition model 77−1368
liquids, triplet correlations, book contrib. 79−60251
liquids and amorphous solids, similarity and short range order parameters 78−83730
magnetic cluster pinning by localised optical excitation 78−68279
magnetic materials, transparent, optical studies of phase transitions 77−66481
magnetic soft and hard materials, garnets, magnetic properties and applications, structural props. 80−65760
MBBA, shear modulus and viscosity relax. near isotropic-nematic phase transition *(Russian)* 77−39543
melts, of a congruently melting substance, single struct. model 80−103233
metal, amorphous, struct. model and SRO characts. *(Japanese)* 77−84654
metal-H systems 79−82906
metallic glass, short-range order, hyperfine field distrib. determ. by Mossbauer spectroscopy 80−39962
metallic melts, three-component, enthalpies of form. *(Russian)* 79−51277
metals, amorphous, structure model, structural changes 80−92462
methylammoniumtetrachlorochromate, optical absorption intensity, short-range spin correlation 80−108185
microdiffraction obs. of SRO, applic. to quenched Cu-Pt alloy 77−76360
mixed crystal, coexistence of different spin structures, computer simulation 77−8276
mixed diatomic system, depend. of fine struct. on short-range order parameter 79−51991
short-range order continued
mixed semiconductor with comp. fluctuation, kinetics of intraband absorpt. and magnetoabsorption coeff., influence of short-range ordering 79−19865
mixed valence systems, Falicov-Kimball model, mag. short- and long-range order 80−15480
mixed-valence systems; short-range-order model 79−78049
mobility edge, analogy with spin glass problem 77−85164
modulated structures, review 79−94929
multicomponent system of nonspherical molecules, statistical thermodynamics in quasichemical approximation *(Russian)* 78−5995
nematic liquid crystal, eqn. of state, incorporating short-range orient. order 77−55237
nematic liquid crystals, continuum theory of disorder, comparison with lattice models 80−54126
nematic mesophase, statistical model, orientational order parameters 80−28910
nematic-isotropic phase transition and short range orientational order 77−27832
nematic-isotropic transition, permanent dipoles effect 77−20054
niobates, columbite or trirutile struct., force fields rel. to cryst. struct. *(French)* 80−107104
nonlinear cooperative system, kinetic Ising model in Bethe approx. 77−13709
nonstoichiometric compounds, physicochem. props. depend. on short-range order struct. 80−100227
one dimensional mixed crystal short range order, frequency spectrum 79−95093
one-dimens. ionic conductor, modulation and incommensurability 80−19980
one-dimensional amorphous solid, short-range order effect on spectral density of excitations 77−76514
one-dimensional disordered system withshort-range order, struct. and model and config. entropy 77−80422
one-dimensional disordered systems, electron transmission and wave propag. 80−24907
order-disorder transformation effect on valence electron spectrum, XPS (X-ray emission) obs. 78−52639
PAA, isotropic-nematic transition, appl. of integral eqn. for ang. distrib. function *(Russian)* 78−6147
PCP, oriented swollen soln., IR dichroism, short-range orient. order *(Russian)* 79−51941
pentacene, disordered solid layer, absorpt. spectra 80−93417
p-n-pentyl-p′-cyanobiphenyl, nematic liq. cryst., Raman depolaris. ratios, order parameters 79−28733
Permalloy, order-disorder transform. and magnetic props. obs., by neutron diffraction method *(Slovak)* 79−4963
phonon density of states in linear disordered system with short-range order 77−69062
phonons in cellular system with strong short range order, effect of off-diagonal randomness 77−47531
photoemission technique for meas. of magnetic order and spin depend. of electron scatt. 80−60748
polyethylene, hydrostatically compensated, SRO in precrystallisation phase 79−69033
polymer, amorphous, bulk, structure models and exptl. methods, review 78−22671
polymer, amorphous, segmental distrib., light-, neutron- and X-ray scatt., piezooptical and dielec. meas., review 78−51444
polymer, amorphous, stress-optical investig. of short-range order 78−22672
polymer, short-range order, radial distrib. functions from X-ray diffr. 77−76330
polymer glasses and melts, struct., review of expt. results 79−37636
polymer solution, short-range order and solvent crystallisation; spectroscopic and microcalorimetric, methods *(Russian)* 78−26416
polymer solution, short-range solvent orientational order, IR dichroism and photoelasticity obs. *(Russian)* 78−26415
Raman spectra of liq. phase weak H-bonds, short range order and anharmonicity effects 78−64357
random alloy with short-range order, iterative calc. of energy levels 77−66104
random anisotropy model in Ising model, Monte Carlo simulation 80−80546
rare earth oxide film, short-range order to long-range order transition 78−10288
rare earth sulphides-1.8 Ga_2S_3 glasses, vibr. spectra, electronic transitions, short range order 77−69820
rare earth-gallium sulphide glass, R_2S_3-1.8Ga_2S_3, vibr. and electronic spectra, short-range order 78−27228
rare earth-transition metal alloys, disordered, magnetisation behaviour 80−71099
semiconductor, crystal-glass transition influence on local struct., Mossbauer and X-ray spectra 77−36163
semiconductor glass, tetrahedral, disorder 78−51423
semiconductors, amorphous, short-range order, theory and probes 80−79698
size effect in electron theory, static conc. waves approximation *(Russian)* 78−39049
size effect in electronic theory *(Russian)* 77−15339
smectic B, liq. cryst., positional short-range order 79−10790
solid solution, heterogeneous short-range order parameters, Mossbauer meas. *(Russian)* 79−4418
solid solutions, AC-BD, X-ray diffr. determ. of short-range order parameters 80−38875
solid solutions, BCC, SRO and LRO 77−43178
spin glasses, relax. of magnetisation and order parameter 78−27043
steel, austenitic, Al-C, microstruct., Mossbauer obs. *(Russian)* 80−29655
steel, maraging, ageing study by internal friction meas. 77−12660
steel transformer, Mossbauer atomic struct. anal., decarburising annealing, cold rolling *(Russian)* 80−11294
structural phase transformations, static critical behaviour 80−92640
substitutionally disordered binary systems, existency domain 80−88068
swollen rubber network, stress-optical coeff. and amorphous order 77−77169
swollen semirigid polymer, short-range orientational order *(Russian)* 77−84662
tantalates, columbite or trirutile struct., force fields rel. to cryst. struct. *(French)* 80−107104
TCNQ salt, TSeF-TCNQ, CDWs, X-ray study 79−28301

short-range order continued
TCNQ salt, TSeF-TCNQ, short-range ordering investigated by XDE 80−59652
temperature dependence, linear approx., nonlinear term *(Russian)* 78−63840
temperature dependence, linear approx. *(Russian)* 78−63839
ternary alloy ordering, correlation effects, Kirkwood method calcs. *(Russian)* 79−66038
ternary BCC alloys, ordering process, effect of short-range order *(Russian)* 80−84908
ternary oxides, short-range order and superstructures 80−49159
tetrabromomethane, plastic phase, neutron diffr. obs. and theory 79−77533
tetracene, disordered solid layer, absorpt. spectra 80−93417
thin disordered film, electronic energy spectrum calcs. extended Halpern Green's function technique 80−20066
TiO, single cryst., short range ordering of vacancies, X-ray anal. 79−73163
tolan-mercury diphenyl, energy characts. determ. of mol. interaction and short range order parameters 79−14794
tolan-mercury diphenyl solid soln., anal. of diffusely scatt. intensity distrib. of X-rays 78−95048
transition metal alloys, amorphous, mag. props., chem. short-range order 80−75739
transition metal alloys, binary, state density curves, relation between short-range order and Fermi level position, CPA calculations 80−107687
transition metal alloys, ferromag., with atomic short range order, local environment effects on electronic struct. 78−67936
transition metal carbides and nitrides, solid soln. formation, elastic lattice deform. energy 77−84927
transition metal-metalloid glasses, short range order of dense-random-packing models 80−64907
transition metal-metalloid glasses, struct. end plastic flow, review 80−84090
TTF-TCNQ, short-range and long-range order of phason clusters 77−35874
water, liq., internal press. isobars, anomaly short-range order influence 77−65944
β'-NiAl, Ni rich, electron diffr. pattern anomalies, rel. to martensitic transform. and short range ordering 78−6926
Ag chalcogenide melts, changes in short-range order struct. during heating 79−50973
Ag-Al, short-range order, X-ray and electron diffr. study 80−54173
Ag-Al, ζ-phase *(Japanese)* 80−15256
Ag-Au system, surface segregation 79−69330
Ag-Ge alloys, liq., thermodynamics and short range order, mass spectra meas. 79−52740
α-Ag-Mg, disordered, shaft range order diffuse scatt., electron diffr., interpretation 77−84596
Ag-Mg (15 at.%), disordered, short-range order, X-ray diffr. obs. 79−95176
Ag-Pd system, surface segregation 79−69330
α-Ag-Zn, atomic short-range order determ., X-ray scatt. and pseudopot. calc. 78−2067
α-Ag-Zn, short-range order calc. by pseudopotential method *(Russian)* 77−43175
Ag-Zn (30 at.%), electron irrad., mobilities of self-interstitials and vacancies 77−84795
AgAu, quenched, short range order effects on specific heat 80−29181
$AgSbSe_2(Te_2)$, exam. of kinematic viscosity of melts, and short range ordering 79−1383
Al-Li alloy, annealing of vacancies and ageing, resist. and TEM obs. 77−21172
Al-Zn (10 at.%), short-range order parameter calc. in pseudopot. approx. *(Russian)* 80−49183
$Al_2Mn_3Si_3O_{12}$ glass, mag. ordering effects at low temps., Mossbauer and neutron diffr. meas. 77−16047
Al_2O_3 amorphous films, struct., electron diffr. investigation 80−20046
β-Al_2O_3-Ag_2O, stoichiometric A phase, X-ray diffuse scatt. obs., sublattice phase transition 80−64944
$AlPO_4$, amorphous, struct. determ. by radial distrib. functions derived from X-ray diffr. 77−43151
AlZn, disordered, residual resistivity due to clustering, ageing effects 80−65521
Ar, liq., short range order parameter 78−83712
As, amorphous, intermediate range order from polarised features of Raman spectrum 80−49113
As, amorphous, neutron diffr. investig. of local order 77−35480
AsI_3, molten, X-ray intensity curve, short-range order 77−4034
As_2O_3, glassy, intermediate range order from polarised features of Raman spectrum 80−49113
$As_x(S,Se)_{1-x}$, chalcogenide, covalent non crystalline topology, short range order 80−15009
As_2S_3, amorphous, laser radiation induced struct. changes, electron microdiffr. obs. 79−10874
As_2S_5, amorphous, struct., vibr. and electronic spectra 80−64908
As_2Se_3, glassy defect electron states, tight binding calc. 80−96818
As_2Se_3, vitreous, neutron diffr. in high momentum transfer region 77−4045
Au-Ag, surface segregation 79−77873
Au-Ag alloys, SRO and ordering energy *(Russian)* 77−65964
Au-Ag-Cd, γ-ray PAC of ^{111}Cd, nearest neighbour contrib. to elec. field gradient 77−36161
Au-Cu alloys, short-range order and energy of ordering, diffuse X-ray diffr. meas. *(Russian)* 77−43174
Au-Fe (22 at.%), ferromag. phase, AC susceptibility near T_c 78−43575
Au-Pd (1(50) wt.%), quenched, vacancy annihilation and short-range order formation, elec. resist. 80−108487
Au-Pd(Zn), disordered, shaft range order diffuse scatt., electron diffr., interpretation 77−84596
Au_4Mn, heat treated, short-range order, diffuse X-ray diffr. study *(German)* 80−88092
Au_xSi_{1-x} amorphous films, phys. studies 80−75476
Ba-Cd system, short-range order calc. *(Russian)* 79−23566
Be, X-ray emission spectra, effect of short range order and deep vacancy screening, multiple-screening theory 77−28651
BeP_2, tetrahedral struct. of order-disorder type, coordination rule for short-range order 77−15370
C, vacuum condensed film, SRO from radial-distrib. curve analysis 77−89662

short-range order continued
Cd-Pb-Sn melt, enthalpies of form. *(Russian)* 79−51277
Cd-Pb-Sn melts, enthalpies of form. *(Russian)* 79−51277
$CdB^4C^5_2$, chalcopyrite struct., surface energy and compressibility, rel. to glass form. 79−51417
$CdGeAs_2$, amorphous and cryst., Mossbauer expts. 78−22648
CdSn(Ge)As_2, amorphous, SRO 77−84653
$Ce_{0.73}Ho_{0.27}Ru_2$:Co, spontaneous mag. order below superconducting transition temp., Mossbauer study 80−39701
Co-Os, short-range order parameters, ordering energy on first coordination sphere *(Russian)* 79−69058
Co-P, amorphous electrodeposited foils, struct. characterisation by X-ray scatt. 79−77932
Co-P, amorphous foil, complex permeability and eddy currents, annealing induced short-range order 77−8360
$CoCl_2.2NC_5H_5$, quasione dimens. Ising system, thermodynamic props. 78−27042
$Co(N_2H_5)_2(SO_4)_2$:Co, Mossbauer effect and paramag. relax., superparamag. behaviour of correl. spin domains 77−69756
$Co_{0.9}P_{0.1}$ noncrystalline ferromagnet, electroless deposited, struct. and microscopic mag. props. 80−88063
Co_2SnO_4, CoMg(Zn)SnO_4 and $Co_{2-x}Mg_2TiO_4$, magnetic props., short-range ordering 77−32155
Co_xZrS_2, ($0<x\leq0.50$), intercalation compounds, ordered phases obs. 80−33962
Cr-Ge liquid and amorphous alloys, struct. props., cond., viscosity, surface tension *(Russian)* 80−54119
$Cr_{11}Ge_8$, CrGe, and $Cr_{11}Ge_{19}$ amorphous films, short-range order, electron diffr. obs. *(Russian)* 78−56050
Cr_3Ge amorphous films, short range order struct. *(Russian)* 78−30841
Cr_5Ge_3, amorphous film, short-range-order struct., electron diffr. meas. 79−15047
Cs, liq., short range order parameters, from information theory 78−83730
Cs-Au alloy, liq., electronic struct., effects of short-range order 77−15755
$CsLi_{0.5}(Al,Fe)_{1.5}F_6$ pyrochlore, Mossbauer contrib. to exam. of cationic order *(French)* 80−93224
$CsLi_{0.5}Fe_{1.5}F_6$ pyrochlore, Mossbauer contrib. to exam. of cationic order *(French)* 80−93224
$CsMnCl_3.2H_2O$, Heisenberg antiferromag., linear mag. birefringence meas. 77−16277
$CsMnFeF_6$, mag. short-range ordered, neutron scatt. meas. 77−16048
$CsNiF_3$, one-dimensional ferromagnet, optical absorpt. and static spin correlation functions 80−71415
$CsNiF_3$, quasielastic neutron scatt. around Neel-point 80−75768
$CsNiFeF_6$ pyrochlore, Mossbauer contrib. to exam. of cationic order *(French)* 80−93224
α-Cu-Al, binary substitutional, short-range ordering kinetics, vacancy behaviour 78−55867
Cu-Al, short range order and static distortion contribution to residual elec. resistivity *(Russian)* 80−70672
α-Cu-Al, short range order effect, atomic potential appl. 77−27850
α-Cu-Al, short range ordered, struct. and new superlattice phase 78−52756
Cu-Al (15 at.%), vacancy migration, and short range ordering, comparison of exp. results with theory 78−47356
Cu-Al (15 wt.%), residual resistivity, influence of short range order and size effect *(Ukrainian)* 79−99528
Cu-Al (21 at.%) transition state, tempered and quenched alloy *(French)* 80−55392
α- Cu-Al (6 to 17 at.%), short-range order investigated by diffuse X-ray scatt. *(Russian)* 80−104187
α-Cu-Al (9.13, 13.56, 14.76, wt.%) short-range ordered, characterisation of locally ordered regions 80−79747
α- Cu-Al alloy, short range order structure 78−91303
Cu-Al(Au) alloys, HV electron microscopy, crit. voltages depend. on comp., temp. and short-range order 80−100146
Cu-Au, elec. resist., pseudopot. calc. *(Russian)* 78−2460
Cu-Au alloys, vacancy and divacancy migration activation energies, elec. cond. meas. 80−88140
Cu-Ga (17 wt.%), elec. resist. and TEM studies 80−108604
Cu-Mn (15 at.%), mictomagnetic, short-range ordering, neutron scatt. polarisation anal. 80−50110
Cu-Mn (7 at.%), magnetic susceptibility, clustering, band model of heterogeneous magnetics 77−43823
Cu-Ni, mag. ordering temp. depend. on atomic short-range order from susceptibility meas. 79−61159
Cu-Ni (20-80 at.%), clustering, diffuse neutron scatt. study, conc., temp. depend., miscibility gap location 78−47529
Cu-Ni alloys, magnetic diffuse neutron scatt. 78−14931
Cu-Pd(Pt), disordered, shaft range order diffuse scatt., electron diffr., reinterpretation 77−84596
Cu-Pt, quenched, microdomain model anal. of diffuse X-ray scatt. 79−52276
Cu-Pt alloy, quenched, SRO, microdiffr. obs. 77−76360
Cu-Si (6.5 at.%), plastic deformation, HVEM study *(French)* 80−66605
Cu-Zn-Al, martensitic transform., short range order effect 79−61586
α-CuAl, kinetic study of short-range ordering 78−23726
CuAu, order-disorder transform., band theory for internal energy 79−19539
Cu_3Au, ordered and disordered, cavitation induced erosion 77−16743
CuAu(Pt), quenched, short-range order X-ray diffuse scatt., microdomain model anal. 79−96043
Cu_3Ga, interpretation of diffuse contours in electron diffr. *(French)* 79−19377
Cu_3Ga, transition state between long range order and short range order, model, computer simulation *(French)* 80−49371
$CuGaTe_2$, exam. of kinematic viscosity of melts, and short range ordering 79−1383
$Cu_{1/2}In_{1/2}Cr_2S_4$, transition from long-range to short-range mag. ordering 77−36087
$CuInTe_2$, exam. of kinematic viscosity of melts, and short range ordering 79−1383
Cu_xMS_2, ($0<x\leq0.50$) (M=Zr, Hf), intercalation compounds, ordered phases obs. 80−33962
r-CuMn, annealing ordered phase study by neutron diffr. 80−89265
γ-$Cu_{15}Mn_{85}$, antiferromag., neutron diffr. 80−2550
Cu_3Mn, atomic short-range order, TOF neutron diffraction 79−10831

short-range order continued
$Cu_{75}Mn_{25}$, concentrated spin glass, variation of short-range atomic order 79−69685
$Cu_2MnIn_{1-x}Sn_x$ alloy, compositional SRO, hyperfine interactions 80−71065
$Cu(NO_3)_2.2^1/_2H_2O$, singlet ground-state system, mag. props., short-range ordered state 78−23289
$Cu(NO_3)_2.2^1/_2H_2O$, singlet ground state system, mag. props. 80−44850
CuPt, quenched, state of local order 79−47722
ErO, vac. deposited films, struct. changes due to annealing 79−77741
ErO_x films, phase transforms. 77−62784
ErO_x, nonstoichiometric film, short-range order characts. and its effect on elec. behaviour 79−99435
Fe, liq., short-range order struct., O impurity influence *(Russian)* 80−38901
Fe, liquid, structure factor near transform. to amorphous solid, X-ray diffr. *(Russian)* 77−31579
Fe, liquid and amorphous states 77−1069
Fe-Al, residual elec. resist., contrib. from static lattice distortions and short-range parameters *(Russian)* 79−51548
Fe-Al (15 at.%), short range order form. kinetics *(Russian)* 78−3146
Fe-Al alloy, short range order, neutron scatt. meas. 77−19907
Fe-Al(Si), disordered, obs. of Kohn singularities in X-ray diffuse scatt. 79−27874
Fe-B, amorphous, short-range order, Mossbauer meas. 80−44986
Fe-B, amorphous alloys, compositional study on short-range struct. 80−84095
Fe-B metallic glasses, short-range orders 79−65002
Fe-B metallic glasses, short range order 79−77528
Fe-B(Si) amorphous alloys, Mossbauer spectra, struct. 80−15840
Fe-based alloy, effect of sp-3d impurity interactions in resistivity 79−46696
Fe-C, liquid, C content effect on short-range order struct., X-ray diffr. obs. 80−6351
Fe-C, pre-eutectic melt, struct. anomalies *(Russian)* 77−28794
Fe-C melt, mag. susceptibility and short range order, 900-1800°C 78−84382
Fe-C melts, short-range order, neutron scatt. obs. *(German)* 78−71669
Fe-C molten alloy, short range order *(Russian)* 79−90521
Fe-C system, mixing variables, activities and entropies calc., short range order model *(German)* 80−25655
Fe-Co-Cr, Cr effect on struct. of ordering 78−35407
Fe-Co-Ni, liquid, solubility of H, 1400 to 1800°C, short-range order effects 77−1231
Fe-Cr-C solid solns., ordering and γ to α transforms, effect of heat treatment *(Russian)* 79−24520
Fe-Cr-Co martensite, ordering and segregation *(Russian)* 79−20052
Fe-Ge, amorphous, atomic struct., neutron diffr. study 80−59392
Fe-Mn, dilute, short-range ordering and segregation ascending diffusion *(Russian)* 77−24406
Fe-Ni (29.3%), N29, martensitic tranform. kinetics and morphology, ordering role 77−63673
Fe-Ni alloy, disordered, short-range order study by time-depend. PAC method 78−6618
Fe-Ni alloy, martensitic transform., influence of thermal and electron irrad. treatment of austenite *(Russian)* 80−66509
Fe-Ni alloy, ordered, low temp. $\alpha \rightarrow \gamma$ transform. *(Russian)* 78−19740
Fe-Ni alloys, γ- and α-phase struct. in supercooled austenite *(Russian)* 77−66642
Fe-Ni alloys, ordering on annealing and electron irrad., mech. props. change *(Russian)* 80−29981
Fe-Ni melt, short-range order, m.p. to 1750°C *(Russian)* 78−94966
Fe-Ni system, ferro-antiferromag. transition, γ phase mag. struct. 79−91231
Fe-Ni-Cr, mag. props. in weak mag. fields *(Russian)* 80−75771
γ-Fe-Ni-Mn alloys, spin glass state, short and long range order investigation 80−65808
Fe-P-B, amorphous alloy, Mossbauer effect and short-range order 80−2675
Fe-P-C, amorphous alloy, Mossbauer effect and short-range order 80−2675
Fe-P-C amorphous alloys, Mossbauer spectra, struct. 80−15840
Fe-P(Ga)(As)(Sb), dil., short range order, NMR study 80−71237
Fe-Pd, mag. moment, comp. depend. *(Russian)* 78−47280
Fe-Sb-Ni(Cr), dil., short range order, NMR study 80−71237
Fe-Si (10 wt.%), effect of short range order on yield stress *(German)* 78−52932
Fe-Si (3% wt.) polycrystalline, short-range order and induced anisotropy *(Russian)* 79−51772
Fe-Sn liquid alloy, conc. depend. of enthalpy of form., conc. depend. *(Russian)* 78−44081
Fe-V (10 to 50 at.%), solid soln., tempered, exam. of long and short-range order, using Mossbauer effect *(Russian)* 79−29105
$Fe_{84}B_{16-x}C_x$, amorphous alloys, short range order, Mossbauer and DSC study 80−39960
$Fe_2Ca_3Si_3O_{12}$ glass, mag. ordering effects at low temps., Mossbauer and neutron diffr. meas. 77−16047
Fe_3Ge amorphous films, short-range struct., electron diffr. obs. 77−24267
Fe_5Ge_3 film, electron diffr. study of struct. and microheterogeneity 77−85108
Fe_xGe_{1-x}, amorphous alloy, short range order anal. 77−80423
FeI_2, first order mag. phase transition, neutron scatt. study 80−50090
$Fe_{10.92}K_{1.55}O_{17}$, ferrite, cryst. struct., nonstoichiometry, ion-ion correlations 80−88130
$FeMo_2S_4$, Mossbauer spectra, 79-300K, Neel pt. determ. 78−60360
$Fe(N_2H_5)_2(SO_4)_2$:Co, Mossbauer effect and paramag. relax., superparamag. behaviour of correl. spin domains 77−69756
Fe_xNbS_2, ordering of Fe atoms 78−38650
$Fe_{70}Ni_{30}$, short range order, diffuse elastic neutron scatt. study 78−52219
$(Fe_{1-x}Ni_x)_{75}B_{25}$, amorphous and cryst., short range order, Mossbauer study 80−39961
$Fe_{27}Ni_{53}P_{14}B_6$, amorphous, Hall resist. and mag. props., short range order effects 80−34422
$Fe_{40}Ni_{40}P_{14}B_6$, amorphous, resistometric study of short-range ordering rel. to heat treatment 80−70140
FeO-FeS, mag. susceptibility, eutectic phase diagram *(Russian)* 80−15682
FeP(Ga)(As)(Sb), dil., short-range order, neutron diffuse scatt. and spin echo NMR 80−50106

short-range order continued
$Fe_xZn_{1-x}F_2$, Neel point and short range order, dilution effects, mag. birefr. obs. 80−71019
Fe_xZrS_2, ($0<x\leq0.50$), intercalation compounds, ordered phases obs. 80−33962
GaAs, (110), correl. of short-range order and sputter dose, using vidicon-based LEED system 79−83082
GaAs:Te, ion implanted optical transitions in modulated reflectivity spectrum 79−73972
$Ga_{0.67}Cr_2S_4$, semiconducting thiospinelide, spin glass type mag. ordering *(Russian)* 80−50123
$Ga_xIn_{1-x}P$, diffuse X-ray scatt. investig. of cation distrib., segregation 77−24409
GaP_xAs_{1-x}:N, luminesc. of N bound state excitons, local-environment effects 80−100691
Gd, mag. short range order, 80 to 425K 79−42784
^{160}Gd, ferromagnetic, isotopically enriched single crystals short-range order 79−4653
Gd-Co amorphous films, annealed, short-range order and perpendicular mag. anisotropy 80−15765
Gd-Co film, amorphous, Ar sputtered, struct. 78−63946
Gd-Co film, amorphous ferrimagnet, anisotropic short range order effects on mag. props. 79−1691
Gd-Co-Mo alloy film, amorphous, mag. props., ion implantation damage effects 77−89991
Gd-Co-Mo film, amorphous, Ar sputtered, struct. 78−63946
$Gd_3Ga_5O_{12}$, magnetic interactions and short range order 79−78401
Ge-Sb liq. alloys, SRO 78−22632
Ge-Si, electronic structure, short-range order effects, calc. 80−92861
Ge-Si cpds., influence on valence band and direct optical gap 77−59252
Ge-Sn(In) melts, short-range order, radial atomic distrib. functions 79−86673
Ge-Te, As-Te, Ge-As-Te molten systems, metal-semicond. transition, cond. obs. *(German)* 77−1457
GeO_2, vitreous, struct., contrasted with EXAFS obs. of $ZnCl_2$ liq. and glass struct. 80−70133
$Ge_x(S,Se)_{1-x}$ chalcogenide covalent non crystalline topology, short range order 80−15009
GeS_2, cryst. and glass, Raman spectra, struct. *(Russian)* 79−51966
$GeSe_2$, cryst. and glass, Raman spectra, struct. *(Russian)* 79−51966
Ge_xSe_{1-x} melts, short-range order change with comp. and temp., anomalous density behaviour 77−11676
H_2, quantum cryst. short-range corre. and motional renormalisation of anisotropic interactions as function of density 80−34272
^4He, liq., short range order parameters, from information theory 78−83730
^4He, liquid, Raman intensity, depend. on short-range struct. 79−56801
^4He, normal and superfluid, short range order parameter 78−83712
^4He, temp. depend. of spatial correls. 78−71896
HfV_2D_4, disordered solid solution, order-disorder transition 80−88321
HgTe-CdTe, mixing energy and short-range order, diffuse X-ray scatt. 77−28006
HgTe-CdTe(ZnTe) solid solns. form., equil. vacancy conc. changes 77−43208
HoP, flopside mag. struct. to ferromag. transition, elastic neutron scatt. obs. 80−50058
In-Sn-Sb, liquid state, structure of eutectic alloy 78−42890
InP, fused, SRO structure changes on heating 77−89367
InTe, In_2Te_3, molten III-VI semiconductors, SRO 77−65945
K_2CoF_4, obs. of short range order by optical birefringence 79−11318
K_2CoF_4, two-dimensional Ising-like antiferromag. birefringence, short-range order effect 77−81081
$K_{1.54}Mg_{0.77}Ti_{7.23}O_{16}$, hollandite, cationic short range order, ion-ion interaction 77−11729
$KReO_4$, vibr. spectrum, Raman and IR spectra obs. 80−55104
Kr.$2SiO_2$, vitreous short-range atomic packing rel.to Kr entrapment 78−22664
LC-440, shear modulus and viscosity relax. near isotropic-nematic phase transition *(Russian)* 77−39543
La_2NiO_4, La_2CuO_4, magnetic properties obs. 80−70937
Li-Ag, liq. alloy, density, compressibility and diffr. data 77−47336
Li-Na, liq., short-range order, neutron diffr. obs., near crit. composition 78−22639
Li_2O-LiX-B_2O_3 glass, X=halogen, high anionic cond. of new solid electrolytes 80−107546
Li_2O-TeO_2 glasses, struct., IR reflection spectra 78−68516
$LiTbS_2$, long and short range order 78−38667
Mg-Bi (30 at.%), molten, short range order and partial struct. factor, neutron and X-ray diffr. 78−9941
Mg-Cd melts, atomic struct., short range order and melting *(German)* 78−14273
Mg-In, short-range order, temp. and conc. depend. *(Russian)* 77−43173
MgO-ZnO-Fe_2O_3-Cr_2O_3 system spinels, IR absorpt. spectra, short-range order 79−42957
Mn-Bi mictomagnetic alloy, mag., elec. and elastic props. *(Russian)* 80−108028
Mn-Ga, mag. and cryst. struct. in conc. region of gamma phase, temp. depend. *(Russian)* 79−65649
Mn-Ge amorphous films, short-range order, electron diffr. obs. 80−39473
$Mn_{46}Co_{54}$, amorphous alloy prep. by high-rate sputtering, struct. and prop. characteris. 79−24462
MnF_2, magnetic, thermal, elastic refraction of light, mag. order influence on refractive index *(Russian)* 80−34880
Mn_3Ge_2, $Mn_{11}Ge_8$, amorphous thin films, quasieutectic model, electron diffr. investigation of short range order 79−69013
MnO, neutron diffr. meas., 100 to 700K, spin correls, above and below T_N 77−59390
MnOOH, mag. ordering, fine struct. and crit. behaviour, neutron diffr. meas. 80−65800
$Mn_{1-c}Zn_cF_2$, Heisenberg antiferromag., linear mag. birefringence meas. 77−16277
$Mn_xZn_{1-x}F_2$, Neel point and short range order, dilution effects, mag. birefr. obs. 80−71019
Mo-permalloy, magnetic permeability and order form. kinetics under annealing, conc. depend. 77−8356
Mo-W system, short-range order calc. *(Russian)* 79−23566
Nb-H, ordering of hydride phases 77−19902
Nb-Ta system, short-range order exam. by diffuse X-ray scatt. *(Russian)* 77−31644

short-range order continued
Nb-V system, short-range order exam. by diffuse X-ray scatt. *(Russian)* 77−31644
$Nb_3Ge(Si)$, amorphous films, thermally-activated internal friction peaks, structural obs. 80−80147
$Nb_3Ge(Si)$, RF sputtered films, amorphous atomic scale struct. 80−84064
Nb_2O_5-TiO_2, splat cooled, crystallization and ordering 77−68953
Nb_2O_5-WO_3 system complex cpds. with TTB type subcells, HV superhigh resolution electron microscopy obs. of struct. 80−103311
Nb_3Sn, A15 cpd., normal state, low temp. resist., disorder effects 80−107762
Nd_2NiO_4, Nd_2CuO_4, magnetic properties obs. 80−70937
Ne, liq., short range order parameter 78−83712
Ni, paramagnetic, mag. form factors in Stoner-like model 80−97061
Ni-Al, melt, short-range order and microinhomogeneity, rel. to NiAl form. 77−35466
Ni-Al (6.3 at.%), influence of localised order on thermo-EMF and Hall-EMF *(Russian)* 78−6951
Ni-Co (25 wt.%), short range order parameters from Mossbauer data 79−56645
Ni-Cr, (30 wt.%), collective dislocation movements, in situ study 80−100243
Ni-Cr (33 at.%), plastic deformation, HVEM study *(French)* 80−66605
Ni-Cr (33 at.%), US deform. effect on short range order form. *(Russian)* 78−39839
Ni-Cr-Mn-Fe-Nb (20,3,3,2.5 wt.%), short-range order effects on tensile behaviour 80−25793
Ni-Cu, electron-irrad., neutron-scatt. studies 80−75268
Ni-Cu alloys, short-range atomic clustering, residual resist. meas. 80−29386
Ni-Fe, influence of atomic ordering on spin waves 79−7987
Ni-Fe(Pd)(Pt)(Cu), ferromag., influence of local ordering on spin wave stiffness const. 77−89937
Ni-Ge, amorphous, atomic struct., neutron diffr. study 80−59392
Ni-Mn, permeability, diffusion and solubility of H 80−107573
Ni-Mo, short range order considerations and development of long range order 77−16574
Ni-Mo (10.7 wt.%) alloy, ordering energy calc. 80−10522
Ni-Mo (5.8-24 at.%) solid soln. struct. and strength charcts. *(German)* 79−4975
Ni-Os, short-range order parameters, ordering energy on first coordination sphere *(Russian)* 79−69058
Ni-P-B alloy, amorphous, giant moments and short-range orders 77−4499
Ni-Pt, short-range order parameter calc. in pseudopot. approx. *(Russian)* 80−49183
Ni-Pt alloys, magnetic-moment distrib. neutron study 80−97066
Ni-Ta(7 at.%), short-range order, pseudopot. calc. and diffuse X-ray scatt. *(Russian)* 77−28008
Ni-Zn, γ-phase region, X-ray and electron diffr. obs. 79−61562
Ni_2Cr, neutron irrad., point defect prod. and annealing 78−87718
$Ni_{1-x}Fe_x$, short range order exam. allowing for formation of structural domains *(Russian)* 78−6888
Ni_3Fe alloys, low-temperature specific heat, long and short range order effects 80−100339
Ni_3Fe, atomic order, Mossbauer effect obs. 77−69736
Ni_3Fe, short range order determ. after heat treatments 79−96044
Ni_3Fe, short-range order, diffusive elastic neutron scattering 80−24400
Ni_3Fe, short-range order parameter calc. in pseudopot. approx. *(Russian)* 80−49183
Ni_3Fe-Sn, dil., atomic order detection by ^{119}Sn spectroscopy 80−39993
$NiFe_2O_4$ precipitation process from silicate glass, ESR study, effective g value, transition temp. 80−25194
NiGe, and Ni_2Ge, amorphous film, electron diffr. exam. of struct. 77−35828
Ni_3Ge, amorphous film, electron diffr. exam. of struct. 77−35827
Ni_4Mo, quenched, short-range order, electron diffraction study 77−39560
Ni_4Mo, stoichiometric and quenched, short range order and order-disorder transform. 79−78955
NiPt, short-range order, effect of plastic deform., electron diffr. anal. *(Russian)* 80−24403
$Ni_{40}Ti_{60}$, amorphous, chem. short-range-order, X-ray and neutron scatt. obs. 80−96447
Ni_xZrS_2, ($0<x\leq0.50$), intercalation compounds, ordered phases obs. 80−33962
NpC_{1-x}, nonstoichiometric, atomic short-range order obs. by diffuse neutron scatt. 77−24315
O, solid, magnetic props. theory for Heisenberg system *(Russian)* 80−54900
P, amorphous, prepared by chem. transport in low-press. H_2 plasma, radial distrib. function 80−64899
P-Se system glasses, magnetochem. investig. 77−51325
Pb, liq., short range order parameters, from information theory 78−83730
Pb, liquid, short range order amongst cond. electrons 80−107040
Pb-Tl-Cd(Sn) melt, short-range order struct. 80−49088
$PbMg_{1/3}Nb_{2/3}O_3$, short-range ordering, electron microscope and diffr. study 80−10469
Pd-Ce alloy, SRO determ. 77−7738
Pd-Ge glass, short range order obs. for $Pd_{80}Ge_{20}$ and $Pd_{78}Ge_{22}$, EXAFS expts. 78−55815
Pd-Si, amorphous, compositional study on short-range struct. 80−84095
Pd-Ti, hydrogenation, lattice spacings, microhardness and mag. susceptibility meas. 79−77557
Pd-W (20 wt.%), permeability, diffusion, and solubility of H_2, elec. resist., heat treatment effects *(Russian)* 79−51307
Pd-Zn, γ-phase region, X-ray and electron diffr. obs. 79−61562
$Pd_{1-x}Ag_{1-x}$-Au, dil., electron density at Au, Mossbauer reson. 78−39473
$Pd_{0.775}Cu_{0.06}Si_{0.165}$ alloys, glassy and crystallised, low-temp. specific heat 79−60516
PdH_x-Au, dil., electron density at Au, Mossbauer reson. 78−39473
$Pd_{0.8}Si_{0.2}$ alloy, liquid and amorphous states 77−1069
$Pd_{1-x}W_x$, calc. of short-range order parameters from X-ray scatt. data *(Russian)* 80−75367
Pr_2NiO_4, Pr_2CuO_4, magnetic properties obs. 80−70937
PtCr, AC susceptibility near percolation limit, ordered and disordered alloy 80−65900

short-range order continued
Rb_2CrCl_4, optical absorption intensity, short-range spin correlation 80−108185
S-Se-Te semicond. glasses, mag. suscept. meas., refractive index 78−34952
Sb-Au amorphous film, quench condensed, struct. and stability 79−99459
SbI_3, molten, X-ray intensity curve, short-range order 77−4034
Sc-Zr(Mg), low-temp. heat capacity 80−75370
Se, amorphous, effect of doping on mol. struct. and valence alternation states 80−49249
$Se_{1-x}Te_x$ systems, amorphous and liq. states, short range order, neutron scatt. study 80−49124
short range order amongst cond. electrons Al, liquid, short range order amongst cond. electrons 80−107040
Si film, amorphous, structural comparison of evaporated and glow discharge samples 77−62778
Si noncrystalline film, struct., interatomic distances, SRO 80−107053
Si, short range order in surface layers, electroreflection exam. 78−6703
Si(-H), amorphous, H atom effect on Si-Si atomic short-range order, X-ray diffr. obs. 79−64996
$Si_{1-x}H_x$, noncrystalline film, struct., interatomic distances, SRO 80−107053
Si_3N_4 amorphous films, struct., short-range order, and crystn. kinetics 79−28240
Si_3N_4 films, struct. 80−54545
Si_3N_4, non-stoichiometric films, struct. 79−42412
SiO_2, chemical bond and related props. 77−43171
SiO_x, dielec. and optical props., chemical disorder effects 80−80815
$Si_xO_yN_z$, non-stoichiometric films, struct. 79−42412
Sm_2CuO_4, magnetic properties obs. 80−70937
$Sr_{1-x}Eu_xS$, dilute spin glass, mag. props. 79−78386
$SrTiO_3$, structural phase transition, intrinsic and extrinsic central peak properties 80−34168
Ta-V system, short-range order exam. by diffuse X-ray scatt. *(Russian)* 77−31644
$Tb(OH)_3$, powder and single crystal, mag. props. 80−2558
Te-Si glassy alloys, IR transmission and sp. ht. changes in glass interval, vibr. modes, struct. models 78−23474
TeO_2-P_2O_5 system, glass struct., neutron diffr. study 80−70128
ThC_{1-x}, nonstoichiometric, atomic short-range order obs. by diffuse neutron scatt. 77−24315
Ti-Fe, equiatomic, heats of form., influence of short-range order *(Russian)* 80−81354
Ti-Mo, lattice parameter and Debye temp., comp. depend. *(Russian)* 78−47280
TiN_x, cryst. and internal structs., electron diffr. and microscopy 77−27861
$Ti_{1+x}S_2$, short-range ordering, electron and X-ray diffuse scatt. 77−19936
$Tl_2S(Se)$, molten III-VI semiconductors, SRO 77−65945
$Tl_{1-x}Se_x$, amorhpous, IR spectra, structure 77−77194
Tl_xSe_{1-x}, amorphous and cryst., IR transmission spectra and struct. interpret. 78−23471
$UC_{1-x}N_x$,nonstoichiometric, atomic short-range order obs. by diffuse neutron scatt. 77−24315
V-Fe, ferromagnetism to mictomagnetism at low Fe conc. 78−91878
V-Fe, mag. ordering temp. depend. on atomic short-range order from susceptibility meas. 79−61159
V-Rh alloys, short range atomic order exam. *(Russian)* 78−63696
V_2D, BCC α-phase, metal atom-induced diffuse X-ray scatt. from short range order 79−60358
V_2D, short-range interstitial order above crit. temp., diffuse X-ray scatt. obs. 79−95159
VI_2, MCD spectra, interpretation rel. to mag. struct. 80−66222
VI_2, mag. struct., long- and short-range order and Mossbauer spectroscopy 80−65803
$VO_{1.23}$, electron diffr. study of diffuse scattering due to atomic displacements 79−99327
$VO_{1.30}$, ordered phase, X-ray anal. of defect struct. 79−99177
V_2O_5-P_2O_5 glass, splat-cooled, EPR of V^{4+}, polaron hopping and carrier localisation 77−28436
V_nO_{2n-1} ($3\leq3\leq9$), Magneli phases, mag. susceptibilities at low temp. 80−20389
V_nO_{2n-1}, insulating Magneli phases, mag. susceptibility and sp. ht. meas. 80−34604
Y-Si melts, enthalpy of formation and dissolution, microinhomogeneous struct., interatomic interactions *(Russian)* 80−34206
$(Y_{3-x}Ca_x)(Fe_{2-x}Sn_x)(Fe_3)O_{12}$, long and short range magnetic order 79−38419
$ZnB^4C^5_2$, chalcopyrite struct., surface energy and compressibility, rel. to glass form. 79−51417
$ZnCl_2$, glassy and liq, EXAFS obs. of struct., comparison with vitreous GeO_2 80−70133
$ZnCr_2Se_4$:In, magnetoresist. and elec. resist. above and below Neel temp. *(Russian)* 80−88576
$Zr(Ca,Y)O_{2-x}$, local ionic arrangement, X-ray diffr. study 80−100203
$Zr_{1-x}S$, short- and long-range ordering of vacancies, rel. to supercond. transition temp. 77−19945

shot noise *see random noise*

showers, cosmic ray *see cosmic ray showers and bursts*

Shpolskii spectra
acenaphthene in n-alkane matrices, Shpolskii spectra fluorescence 78−9190
anthracene, in n-hexane, Shpolskii absorpt. spectra at 77K, vibronic struct. *(German)* 79−59507
anthracene, in n-paraffin matrices, luminesc. spectra, depend. of inhomogeneous broadening *(Russian)* 79−10145
anthracene, Shpolskii spectra, vibronic struct., fluoresc. *(German)* 79−22754
anthraquinone, in Shpolskii matrices, triplet state spin-lattice relax. rates 78−21952
9,10-anthraquinone, Shpolskii quasi-line phosphoresc. spectra, electronic-vibrational interactions 78−55196
aromatic compounds luminesc. polarisation, quasilines and bands in Shpolskii spectra *(Russian)* 79−31592
aromatic hydrocarbons, $S_0\rightarrow T_1$ phosphoresc. under Shpolskii effect conditions 77−83643
aromatic hydrocarbons in Shpolskii matrices, $S_0\rightarrow T_1$ absorpt. spectra 79−85995

Shpolskii spectra continued
azulene, Shpol'skii matrix, $S_2 \rightarrow S_1$ fluoresc., spectral anal. 77−18956
benzenoid aromatics, triplet zero field splitting parameters, ODMR obs., struct. effects 80−78636
1,12-benzperylene, in benzene, 77K, quasi-line luminesc. spectra obs., Shpolskii's method 77−69894
1,2-benzpyrene, in cyclohexane, 77K, quasi-line luminesc. obs., Shpolskii's method 77−69894
chloroquinolines, photophys. behaviour, substituent and solvent effects 80−106342
coronene, in cyclohexane, 77K, quasi-line luminesc. spectra obs., Shpolskii's method 77−69894
coronene, multiplet struct., insertion modes, Shpol'skii spectra 79−13752
coronene, triplet mol. in n-heptane Shpol'skii sites, distortion and orientation meas. by MIDP 78−37668
4,10-diazachrysene, absorpt. spectra and luminesc. in cryst. and glassy matrices, 77K 78−37650
dihydroporphin, single crystal Shpolskii matrix, fluoresc. anisotropy 79−85994
9,10-dimethylanthracene, in n-hexane, Shpolskii absorpt. spectra at 77K, vibronic struct. *(German)* 79−59507
9,10-dimethylanthracene, Shpolskii spectra, vibronic struct., fluoresc. *(German)* 79−22754
dinaphtho-(2′.3′:1.2);(2″3″:6.7)-pyrene, triplet state, phosphoresc. and ODMR obs. 79−27013
2,5-distyrylpyrazine, absorpt., Raman and fluoresc. spectrosc. 80−28049
haloacenaphthenes in n-heptane, quasi-line phosphoresc. spectra, vibronic spin-orbit interaction 80−43096
hexahydrohexahelicene, in Shpolskii matrix, absorpt., fluoresc., phosphoresc. spectra 79−76463
identification and struct. anal. of unknown compounds in organic mixture 79−87891
indigoid dyes, Raman, IR and Shpolskii spectra 79−65866
isoquinoline, quasilinear absorpt. spectrum, in Shpolskii system 77−46571
9-methylanthracene, in n-hexane, Shpolskii absorpt. spectra at 77K, vibronic struct. *(German)* 79−59507
9-methylanthracene, Shpolskii spectra, vibronic struct., fluoresc. *(German)* 79−22754
3-methylisoquinoline, quasilinear absorpt. spectrum, in Shpolskii system 77−46571
multisite luminesc. spectrum deconvolution, vibr. struct. anal. 80−58304
naphthalene, and deutero derivatives, fluoresc., absorpt. spectra under Shpolskii conditions 80−2825
napthalene-$d_{0\text{-}8}$, fluoresc. and absorpt. Shpolskii spectra *(Russian)* 78−90208
organic donor-acceptor solns., triplet-triplet energy transfer under Shpolskii effect conditions 79−64031
organic molecules in Shpolskii matrices, phosphoresc. site selection spectrosc., ODMR 79−36687
perylene in n-paraffin crystal matrices, effect of heat pulses on fluoresc. 78−88360
phenanthrolines, in Shpolskii matrices, phosphoresc. spectra 78−94276
phenazine, triplet state, ^{14}N quadrupole tensor, optical detection of NQR 79−18218
phenazine, zero field studies of spin lattice relaxation in excited triplet states 79−18219
phosphorescence, sensitised, in Shpolskii systems, triplet-triplet energy transfer *(Russian)* 78−76527
phthalocyanine, in n-alcanes and polyethylene, absorpt. and fluoresc. spectra, 4.2 and 77K 78−976
polyaromatic hydrocarbons, quasi-linear fluoresc. spectra, temp. effect 79−22745
polyatomic mol. quasi line spectrum in paraffin matrix, electronic-vibr. interaction 79−85971
polycyclic aromatic hydrocarbons, matrix isolated, quasilinear Shpol'skii fluoresc. spectra 78−9189
porphin, single crystal Shpolskii matrix, fluoresc. anisotropy 79−85994
porphins orientation in n-aikane Shpolskii hosts, spectra 80−48035
porphyrin in n-octane Shpolskii matrix, defect props., Monte Carlo obs. 80−63533
pyrazine, zero field studies of spin lattice relaxation in excited triplet states 79−18219
pyrimidine, zero field studies of spin lattice relaxation in excited triplet states 79−18219
quinazoline, in n-pentane (isooctane) Shpolskii matrices, luminesc. props., vibr. struct. 79−22739
quinoxaline, zero field studies of spin lattice relaxation in excited triplet states 79−18219
quinoxaline in Shpolskii-type hydrocarbon matrices, vib. struct. of electronic spectra 77−85773
transition metal porphyrins, quasiline absorpt. spectra, metal and substituent effects 77−34628
sym-tribenzotridehydro [12] annulene, electronic spectra in Shpolskii type hydrocarbon matrices, electronic struct. and fluoresc. 78−66589
triphenylene, multiplet struct., insertion modes, Shpol'skii spectra 79−13752
triphenylene in Shpolskii matrix, orientation, ESR and fluoresc. spectra 79−36688
triplet-triplet excitation energy transfer, sensitised-phosphoresc. spectra, cryst. solns., 77K 79−815
zinc porphin, in anthracene, triphenylene, n-octane, fluoresc. and optical absorpt. spectra 79−68240
zinc porphin in n-octane, population hole-burning using triplet reservoir 79−87491

shrinkage
alloy powder, two component, sintering 80−20847
borides, metallic, sintering, review, book contrib. 78−48359
brittle elastic body, stability and post-critical growth of system of cooling or shrinkage cracks 80−1486
clays and ceramics, plasticity determ. using drying process and shrinkage 79−20307
coke, shrinkage kinetics during calcination 80−93572
concrete, creep, long term prediction and shrinkage from short term tests 79−20122
concrete, creep during drying and wetting 79−52319
concrete, drying shrinkage due to wind action *(Japanese)* 79−61838
concrete, flowing, expt. studies *(Japanese)* 80−89298
concrete, high strength, made with a special cement admixture, mech. props. *(Japanese)* 80−89297
shrinkage continued
concrete, strength, shrinkage strain and deterioration down to −160°C *(Japanese)* 80−100886
dilatometer, high-temp., for meas. shrinkage kinetics of liquid-containing ceramic materials 79−17396
ethylene-vinyl alcohol copolymer, drawn samples, annealing effect around T_g temps. on shrinkage and mol. orientation 80−79712
ferrite, hot pressed, powders, influence of CoO and CuO alloying on physicomechanical characts. *(Russian)* 77−66600
fibre reinforced composites, elastic moduli and shrinkage factors, calc. taking account of anisotropy 79−52291
fibre reinforced composites, transverse plane, elastic, failure behaviour *(Japanese)* 78−48510
fibre reinforced composites, viscoelastic thermal shrinkage stresses 80−38287
fibre reinforced plastic, regular struct., shrinkage stress calc. 77−70125
glass fabric reinforced phenol resin, effect of thermal loading on physicomech. props. 79−24622
graphite, neutron effects on shrinkage 80−37456
graphite, polygranular, flexural strength after heat treatment porosity correl. 80−84996
holograms, 3-dimens., emulsion thickness change effects 78−78968
holographic binary information image reconstruction, aberrations, shrinkage effects 78−78967
kaolin bodies, effect of mineralizers on firing shrinkage, microstruct. and strength 80−97488
magnesite artifacts, roasted, props., filler porosity effect 80−104099
mullite ceramic rollers, heat treatment effects 79−61616
nuclear fuel compacts for HTR, irrad.-induced creep 78−44168
Nylon 6 fibre, shrinkage, influence of chain rupture during tensile deform. 79−34055
organosilicon ladder polymers, struct. and phys. props., book contrib. 79−65012
PMMA, biaxially oriented, shrinking kinetics in transform. range 78−27588
PMMA, uniaxially drawn, shrinkage, continuum model *(German)* 78−76722
polyethylene, shrinkability, orient. 79−11660
polyethylene, ultra-oriented high density, shrinkage as meas. of deformation efficiency 80−40398
polyethylene flow crystallisation, in extensional flow developed by convergent capillaries, props. 80−84111
polyethylene terephthalate, oriented, amorphous, stress-induced crystn., shrinkage meas. 80−92466
polystyrene melt, carbon-black filled, rheological study 80−48665
porous structure, shrinkage kinetics, boundary slip and superplasticity 77−36611
stress, semicircular inclusion in semi infinite plane, experiment and analysis *(Japanese)* 77−65672
thermoplastic elastomers, crosslinked by secondary valence interactions, elasticity and processing, crosslinking behaviour 80−40320
Ag, loosely packed powder, sintering SEM and dilatometry obs. 80−20843
Al binary alloys, exam. of dislocation structure, using diffraction electron microscopy *(Russian)* 79−10857
Al-Mg alloys, relationship between props. and nonequilib. phase diagram 79−96000
AlN powder, plasma synthesized, sintering behaviour, props. and struct. 79−100097
Al_2O_3, initial sintering, method for obtaining surface diffusion coeffs., appl. to shrinkage data 78−95713
Al_2O_3, sintering behaviour and props. of 24 aluminas *(German)* 79−4932
Al_2O_3-glass mixture, microstructural changes and shrinkage during sintering 80−25640
Al_2O_3-SiO_2, mullite, powder, synthesis using silicic acid, clay and $AlCl_3$ *(German)* 79−4933
Al_2O_3-SiO_2 fibre/mineral wool fibre composites, exam. of strength and shrinkage characts. rel. to Al_2O_3-SiO_2 fibre content effects 79−20105
Al_2O_3-SiO_2-MgO, cordierite, powder, synthesis using silicic acid, clay and $AlCl_3$ *(German)* 79−4933
$BaFe_2O_4$, $BaFe_{12}O_{19}$, formation, dilatometric investigs. 78−27459
$BaTiO_3$, chemically precipitated, exam. of sintering behaviour by isothermal shrinkage *(German)* 79−4935
Be, porous, shrinkage during sintering, kinetics, photographic method 79−15622
C, polygranular, flexural strength after heat treatment porosity correl. 80−84996
C reinforced plastic, degraded, study of strain, 20 to 1000°C 80−71680
C, stripper foils under 4.8 MeV Ar^{++} ion bombardment, shrinkage, rupture, lifetime 78−33352
CrC-Ni alloys, exam. of activated sintering 80−16241
Cu compact, exam. of anisotropic shrinkage as function of pressure 79−8257
Cu, loosely packed powder, sintering SEM and dilatometry obs. 80−20843
Fe, carbonyl pore struct. orientation, shrinkage anisotropy effect 80−20845
Fe ore, sintering, agglomeration charge layer shrinkage *(Russian)* 80−16224
Fe powder compacts, pressed under static or vibr. load, shrinkage anisotropy during sintering 80−50574
Fe sintered compact, shrinkage and mech. props., admixed zinc stearate lubricant effect 80−45402
Fe, vacancy mobility determ., HVEM expts. 80−33993
Fe-B_4C sintered material, mech. props. and struct. characts. 79−100084
Fe-C (2. wt.%), sintering shrinkage kinetics 80−20829
GdCu, electrical resistivity and length changes with temp., hysteretic behaviour 80−97600
Si, defect form. during high press. low temp. steam oxidation 79−29238
Si, oxidation-induced stacking faults, influence of annealing ambient on shrinkage kinetics 80−29035
SiAlON, prepared from siliceous sand and Al powder, hot pressing, steatite contamination effects *(Japanese)* 80−93528
α-SiC, sintered, influence of B, C additives on microstructure, SEM exam. 79−8262
Ti-Al (Sn), porous, effect of Al and Sn on sintering 80−20830
W-Ni, liquid phase sintering 80−25613
W-WC, activated sintering, mech. props. *(Koreqn)* 78−60622

shrinkage continued
YIG, substituted, magnetite nucleation in transitional zone, ionic process, lattice imaging 80−107424
ZrO_2-CaO(Y_2O_3) ceramics with grainy structure, props., effect of heating to 2000°C 80−104194
Shubnikov-de Haas effect *see magnetoresistance*
Si-Ge alloys *see Ge-Si alloys*
SIC *see monolithic integrated circuits*
signal acquisition *see signal detection*
signal coding *see encoding*
signal delay lines *see delay lines*
signal detection
acoustic, dead-zone limiter, conditional tests appl. in nonparametric detect. 77−7262
acoustic, detect. of LPM signals with estimation of their vel. and arrival time 78−90604
acoustic, Fourier series method appl. to signal in noise background, comments 80−106671
acoustic, underwater passive detection and spatial coherence testing 79−46113
acoustic arrays, spatial aliasing of broadband signals, frequency wavenumber analysis 79−1031
acoustic emission, time-domain deconvolution technique for signal identification 79−20306
acoustic emission monitoring difficulties overcome by optical detectors 78−60968
acoustic logging, channel requirements for elastic waves recording *(Russian)* 79−39955
acoustic signals, freq. shift arrival time determ. 79−3875
acoustic signals, narrowband in noise, robust sequential detection 79−59869
acoustic signals, robust sequential detection of weak signals in undefined noise using acoustic arrays 80−58861
acoustic signals in noise background, Fourier series method for detect. and localisation 79−3861
acoustic tonal signal lateralization and detection of interaural differences of time 79−43930
analogue signal fast acquisition, for large particle detectors, CYCL-OP 78−17534
auditory detection of intensity increments of narrowband noise signals, amplitude model 80−61591
auditory evoked cortical potential online detector 78−31952
automatic device for radiowaves refl. or scatt. from ionosphere 77−49179
biological, use of voice key *(Czech)* 77−5124
biological signal time averaging, digital Wiener filtering and detection statistical aspects 78−35979
biosignal processing, spurious signal detection method *(German)* 78−92722
clock random perturbations, absolute continuity theorem *(French)* 78−62150
coherent detection of partially coherent sources 80−47109
colour vision models, vector magnitude operation, derivation from signal detect. theory 80−101174
computerised tomography, detectability in CT images 80−3806
CW signals in white noise, influence of data window shape 80−64300
deadtime perturbed doubly stochastic Poisson counting system, information, error and imaging 79−22901
delay parameter estimation following robust detection 79−55267
destabilising factors, evolution of influence 80−9825
diagnostic imaging systems, image quality assessments 77−90890
digital FM detector, multichannel, EEG appl. *(Danish)* 78−35980
digital modulator and synchronous demodulator system: an alternative to the analog phase detector 78−70107
digital moving target indicator system for detection of intracranial arterial echoes 80−17035
direct reception method of swept-frequency topside sounder signals from ISIS-II 77−21923
ECG P-wave recognition, using adaptive correlating filter *(Japanese)* 78−28119
EEG preamplifier for surgical appls. 77−40916
EEG spike detection using combined inverse and matched filter techniques 78−61267
electron-optical convertor detection characteristics, multielectron scintillation effect 79−72686
electroretinogram, photopic, freq. response characts. meas. with synchronous detect. 77−48796
exercise ECG analysis, noise-impervious pattern recognition approach 78−7515
eye movement monitoring, signal detect. via phase-locked sampling in mag. search coil 79−25124
fibre optic laser gyro signal detection and processing technique 79−37037
fibre optic rotation sensor, signal detection and processing, inertial reference device 79−54111
fibre optic rotation sensor 79−37034
fluctuating signal, detector threshold and saturation effects on statistics 79−31803
fluorescence lifetime measurement using time correlation method with CW He-Cd laser 79−50072
foetal ECG adaptive real-time noninvasive extraction using near-orthogonal functions 78−28110
foetal ECG detection, real-time system using near-orthogonal basis functions 77−21638
Gaussian acoustic signal detection using array processors, performance eval. 80−83696
geomagnetic pulsations, cross-correlation and cross-spectral analyses *(French)* 79−70928
grating detectability, aberration effect evaluation in visual instruments 79−55073
gravity prospecting, accuracy, meas. spacing and contour intervals rel. to anomaly detect. *(Russian)* 79−44272
hearing, detection of signals with identical energy spectra but different waveforms under conditions of signal uncertainty 80−51125
hearing, detection of temporally uncertain signals 80−67094
hearing, theory of FM detection for low modulation freqs. 80−61586
heterodyne detection of random gaussian signals, pulse duration optimisation 79−12848
holographic processing, space-frequency equivalence 79−76646
homodyne detection at 100 GHz with a pyroelectric detector 80−105650
signal detection continued
image detection in the presence of speckle 79−45909
image quality descriptor relationships using signal detect. theory 78−71050
incoherent complex signal detection, spatial filtering technique 79−3639
intra-auricular P wave monitor, experience, performance evaluation 78−11764
ionosphere LF signals, modulated reception method for refl. coeff. determ. 78−45114
IR heterodyne detect. 10.6 μm, using (Hg,Cd)Te photodiodes in CO_2 laser system 80−9042
IR sky survey by Air Force Geophysics Laboratory, extended source extraction 79−101088
isotope radiometry, nonlinear information processing in random signal detection *(Russian)* 80−22428
laser beam wandering in turbulent atm., error probability in binary signal reception 79−10337
laser Doppler velocimeter, optimisation of receiving optical system for sampling volume reduction 77−72379
laser signal distortion for chopped beam, due to beam pointing error 78−37937
LF source localization and polarization determination using satellite radioastronomy *(French)* 79−70940
lidar return signals, coaxial and noncoaxial systems with central obstruction 79−76744
logarithmic detection of signals with high noise background, luminesc. spectra recording *(German)* 77−37904
low-level imaging, optical signal detection and meas. 79−94350
m-distributed optical signals, statistical props. and photoelectron counting distrib. 77−38809
magnetotellurics, lock-in signal detect. appl. 78−81104
matched filter, realisation, electronically tunable *(Russian)* 79−98538
memoryless nonlinear functional of random process in Gaussian white noise, Volterra expansion 79−86296
multi-channel integrator for plasma magnetic-probe meas. 78−75413
multichannel audio monitor for detecting electrical signals, neurophysiological expt. appl. 79−20694
multichannel synchronous detector for NQR signals 77−61098
multispike signal detection and sorting hardware 79−79711
NMR signal detection at high freqs., use of slotted tube resonator as probe head 77−30192
noiselike optical signals, photoelectron counting statistics and error rate characteristics 78−1178
nonlinear detector effects on statistics of fluctuating signal 78−24735
nonlinear filtering technique for identification of biological signals 78−40438
nonwhite noise, S/N ratio and detail detection 80−102648
NQR spectrometers, continuous-wave scanning, signal recovery system 78−74039
nuclear imaging of tumour, optimum detector spatial resolution performance study 78−73223
nuclear medicine, image processing clinical quality meas. 77−86626
optical, quantum problems 77−42488
optical communication receiver, direct detection, performance for intensity subcarrier FSK 77−39033
optical discrete PPM signal reception accuracy *(Russian)* 79−94171
optical fields, heterodyne detection, optimum conditions 77−2694
optical heterodyne receiver arrays in turbulent atm., joint signal current probability distrib. 79−81368
optical heterodyne receivers in turbulent atm., signal current probability distrib., theory 78−78916
optical heterodyne receivers in turbulent atm., signal current probability distrib., expt. 78−78917
optical homodyne detection in turbulent atm. 77−34839
optical image, simultaneous detection and intensity estimation 79−46040
optical matched filters, performance 79−90012
optical PCM with envelope modulation, pulse detection characteristics 77−11010
optical pulsed signals of variable length in correlated interference, S/N ratio 78−37816
optical radar, S/N ratio statistics 78−17866
optical radar pulsed systems using photodetectors with lag, characts. 79−13918
optical radiation source with rectangular intensity profile, estimate of coordinates 79−31819
optical signal discrete reception in turbulent atm. 78−73511
optical signal waveform optimisation 79−76618
optical system with storage, sweep parameters optimisation 77−39059
optical target detection, background suppression using double-beaming technique with selective modulation interferometric spectrometer 79−97445
optical vs digital Fourier transform. computers, tradeoff anal. 79−27181
optical/digital components evaluation in hybrid processor 78−63026
optimum detect. in non-Gaussian noise 78−38149
optoelectronic devices with matching filter, scanning rate effect on S/N ratio 79−7223
optoelectronic system with rectilinear scanning, optimal meas. of optical signal parameters 78−17865
orthogonal signal detection, 1 of M, asymptotic equiv. of likelihood ratio and multiband models 78−71045
P wave detection and identification using statistical signal analysis 80−8202
P-wave, a new method of detect. in electrocardiograms 79−48360
P-wave detection in noise, consecutive vectorcardiogram external product technique 77−9289
partially coherent radiation, optical heterodyne detection 80−77871
partitioned signal detection by discrete cross-spectrum analysis 80−91966
Pc 1 geomagnetic pulsation sources, location using ULF goniometer techniques *(French)* 79−70890
periodic magnetic signal detection by magnetoresistance sensor *(Japanese)* 78−57997
phase fluctuations statistical anal., instrument design 77−45861
phase-coherence detector and estimator, formed via overlapped FFT 79−59870
phase-sensitive detection, representation of observable signals in Chebyshev polynomials 79−89857
photodetector with automatically adjustable threshold level, design considerations 80−62724
photodetectors, highspeed, performance testing, optical communication appl. 79−26129

signal detection continued
photoelectric pulse signals, precision loss meas. using microcomputer 80−13142
polarization modulated light, freq. mixing detection using periodic analyzers 78−5433
polyphase envelope detection for physiological signals *(Korean)* 79−66565
proportional chamber, electronic device using K405KhP1 IC (USSR) 80−91376
psychoacoustics, signal detect. theory 78−3514
Pull Up Shallow Water Seismometer, signal detect. and recording systems 78−45025
pulse-echo experiments, using pulse generator and coupled fast signal averager 78−21188
pulsed NMR spectrometer, signal amplitude meas. via digital integrator 77−26372
quantum optical fields, discrimination 77−10879
quantum signals, close, methods of distinguishing 77−7044
radar, passive detection system for wide class of illuminator signals 79−64408
radar signals refl. from mesosphere, VHF signal detection 80−46274
radiation detectors pulses, position meas. methods review 77−65410
radio astronomy, interference-excising correlator 79−75110
radiographic observer performance meas. and characterisation, free response approach 78−69200
radiographic observer performance meas. and characterisation, free-response approach 79−74752
radiography, medical diagnostic decision making and image quality 78−28059
radiography, threshold detection in visible noise 77−86624
radiological imaging systems, unified view using Schade aperture theory, noisy images 77−73563
radiotelescope sensitivity optimisation, deterioration coeff. *(Italian)* 78−85845
random phase modulated signal, nonlinear medium *(Russian)* 77−75606
random signal in noise Bayes detector, accounting for polarisation 77−61672
rank-order speech classification algorithm (RASCAL) 79−64426
repetitive image visibility, two-dimensional Fourier spectrum description 77−58282
resolution enhancement by deconvolution of detected signal 79−71440
ripple noise pitch detection by human, adaptive model 78−73166
sampled/raster displays, assessment of information visibility using signal detection model 80−19002
SAW filters for signal sorting, identification in military high density signal receivers 79−18615
sea surface scattering channel and undersea communications, modelling 79−1022
seismic digital signal detect. system *(Russian)* 77−29515
seismic regular wave detect. using similarity factor *(Russian)* 77−86819
seismic signals, detect. under conditions of limited information about signals and noise 77−9536
seismic signals anal. by phase plane method, explosion technology 79−66843
seismic signals distortion by grouped piezoelec. receiver array *(Russian)* 79−39948
seismic surveys, optimum multichannel filters theory *(Russian)* 79−39921
seismic waves definition in far field, criteria *(Russian)* 79−39965
seismology, signals resolution from coherent and incoherent noise, operators efficiency *(Russian)* 79−39963
shape variation detection, two-component chromatographic peaks resolution 80−71971
signal register, IC, for pulsed two-freq. NQR spectrometer 77−61099
single-threshold detection of random signal in noise, appl. to optical communications 79−18353
SIT vidicon detector system, for Palomar 1.5 metre telescope 79−92674
sonar adaptive beamformer for optimal directional spectra 79−18621
sonar output fluctuation modelling, stochastic process 78−66981
SonoChromascope, US B-scan image acquisition, display and recording 80−30818
Space Shuttle/Orbiter S-band communication development problems 78−45197
spectral line recording in presence of intense background, techniques, appls. *(Russian)* 77−40613
spectrum analyser, frequency overlap requirements and detectability 79−1032
STEM, multi-signal detection and processing 80−73552
stochastic signal locally optimum detect. in non-Gaussian noise 78−38148
tectonomagnetism, improved signal discrimination and volcanomag. effect at Kilauea, Hawaii 79−92629
three level coincidence-correlator detectors, underwater sound appls. 78−63245
threshold detection equivalence with and without dead time 80−32580
time position accuracy determ. of optical pulsed signals for correlated noise types 78−12761
time signal multifreq. transmission ambiguity detection 77−87741
time-varying signal coherent detection using multiple obs. 80−43553
ULF magnetospheric waves, identification using cross-spectral matrix *(French)* 79−70929
ultrashort time resolved photodetection theory 79−89003
underwater, adaptive detection processor in non-stationary noise, for narrowband signals 79−59868
underwater passive detection, adaptive approach 78−5607
underwater sound, broadband detection system, anal. 79−3827
visual, by simultaneous observation through multiple channels, decision behaviour 77−90791
VLF signals, time-varying, determination of wave normal directions *(French)* 79−70927
weak optical signal meas. in strong interference *(German)* 77−65623
weak signal detection, circuits for resistance meas. and temp. control *(Chinese)* 79−30451
zero-crossing statistics utilization 80−74609
Cu-Be search coil for measurement of magnetisation and susceptibility in pulsed magnetic field 79−63281

signal generators
see also function generators; noise generators; ramp generators; swept-frequency oscillators
AC voltage standard GK-10A 77−10055

signal generators continued
code generator to identify time, date, and events in physiologic event recording 77−86674
combined instruments provide several test functions DMM, oscilloscopes, frequency counters, signal generators 77−34000
cosmic-plasma diagnostics 79−90469
digital sinewave generator, for wattmeter calibration at zero power factor 77−18039
ECG arrhythmia simulator, cct. description 77−73608
electronic sector scanning sonars, signal generation 79−18622
FM signal modulated by smoothed random telegraph signal, generation and appl. to underwater acoustic meas. 78−18130
HV generator for accelerator beam control 79−26797
interference fringe signal generator for testing fringe shift measuring system 78−65962
laser Doppler velocimeter calibration burst generator 79−77321
LMFBR safety testing, scram signal generator for fluid motion monitoring 80−18551
mean-time value signal, digital, plug-in module printer controller appl. *(German)* 77−67414
output measurement, correction coefficient for waveforms, standard instruments *(Polish)* 77−53957
pacemaker interference test signal generator, operation and cct. *(Spanish)* 78−20315
primary meas. transducer error twin-circuit correction *(Russian)* 79−71404
programmable power supply, as gating signals source for multichannel analyser 77−42218
reference voltage, testing with B3-24 compensation valve voltmeter *(German)* 79−54155
resursive digital filter, generation of 1/3 octive data 78−87211
RF automatic test equipment, synthesised signal generator design 77−53875
RF signal level calibration source 77−115
SAW device analogue signal processing appl. 77−27437
sawtooth wave generator, amplitude stabilised, for space plasma probe 77−56807
stochastic, theoretical fundamentals and applic. *(German)* 77−53956
student apparatus using IC chip 79−48998
time meas. system adjustment and calibration signal generator 78−57903
two-part, detachable synchronizer, 10 kHz to 120 MHz 77−87790
VLBI, Japanese domestic system, recording signal generator *(Japanese)* 80−21924
VLF oscillator providing variable freq. between 0.1 and 10 Hz, teaching appl. 79−62977
wattmeter calibration, (3+3)-phase voltage and current source of high stability 77−18038

signal processing
see also bandwidth compression; correlation theory; data compression; filtering and prediction theory; picture processing; signal detection; signal synthesis; Walsh functions
A/D convertor, two-phase, processes small analogue signals *(German)* 78−61572
abdominal foetal ECG and VCG recording/processing systems 78−31947
AC Kerr effect meas. in conducting liquids 78−23431
acoustic, allowance for temporal variablity of random inhomogeneities of a medium in connection with the local method 79−32144
acoustic, analysis of fill time effects on cylindrical hydrophone arrays 80−19163
acoustic, analytic expansion technique for ambient-noise directionality determination 79−90088
acoustic, band elimination processor for experimental parametric acoustic receiving array 79−90086
acoustic, bispectrum and its appl. *(Japanese)* 80−91965
acoustic, broadband directional reception, US transducer arrays 80−96126
acoustic, detect. of LPM signals with estimation of their vel. and arrival time 78−90604
acoustic, echolocation in bats 80−108906
acoustic, eigenvector decomposition of correlation matrices 80−96118
acoustic, element failure and random errors effect on sidelobe level for linear array 80−106670
acoustic, energy processing technique for stress wave emission signals, comments 80−48520
acoustic, estimating bearing of source endfire to array 79−50515
acoustic, estimation of differential Doppler shifts 80−19162
acoustic, estimation of source motion from time delay and time compression measurements 80−58860
acoustic, for sound decay measurement using integrated-impulse method 79−94406
acoustic, Fourier efficiency using analytic translation and Hilbert samples 80−48519
acoustic, gain limitations of passive vertical line array in shallow water 80−96117
acoustic, maximum a posteriori estimation of narrow-band signal parameters 80−96120
acoustic, maximum entropy array processing for estimating bearing and strength of source 79−90087
acoustic, maximum likelihood detection and estimation for harmonic sets 80−96116
acoustic, maximum likelihood estimation of position of radiating source in waveguide 79−90085
acoustic, multiple input/output problems anal. 80−96122
acoustic, optimal array processing for case of strong localized interference using appl. of adaptive beamforming 79−41521
acoustic, optimum range and bearing estimation with randomly perturbed arrays 80−96119
acoustic, passive range estimation using subarray parallax 79−72759
acoustic, passive source location with array meas. 79−64410
acoustic, performance estimates for Hunt transit detector 79−68494
acoustic, phonon echo, recent trends in physical acoustics *(Japanese)* 80−79889
acoustic, remote measuring techniques, three-channel correlation *(German)* 79−50512
acoustic, resolving directions of sources in correlated field incident on array using adaptive beamforming algorithm 80−64297
acoustic, robust formulation of optimum cross-spectral beamformer for linear array of hydrophones 79−68495

signal processing continued
acoustic, schemes for filtering signals propagating through random multipath medium 80−58862
acoustic, simplified approach to optimum quadrature sampling 80−79061
acoustic, source extraction in random field 79−50514
acoustic, super-reduction imaging using sequential estimation of hologram 79−68499
acoustic, time windows and DFTs *(Japanese)* 80−87658
acoustic, triangulation ranging using beta density angular errors 79−72758
acoustic, underwater sound, average array signal response in two-path medium 80−87657
acoustic, unreliability of coherence estimates based on amplitudes of signals reradiated by rough sea surface, unreliability 80−58847
acoustic adaptive array processing, time and frequency domains 79−59874
acoustic array, optimal processing for case of strong localized interference, comments on rapid approximation 79−90084
acoustic array beam scanning, phase decorrelation effects 79−3860
acoustic array gain for signals and noise having amplitude and phase fluctuations 80−43548
acoustic array processing, comments on errors 80−19164
acoustic array processing, errors concerning calc. of max. likelihood estimator 79−41523
acoustic array processing using freq.-wavenumber approach 78−66974
acoustic arrays, irregular, amplitude shading coeffs., steering, beam pattern generation 78−83178
acoustic arrays, spatial aliasing of broadband signals, frequency wavenumber analysis 79−1031
acoustic billboard array, high resolution cross-sensor beamforming 79−41520
acoustic bispectral holography, theory 77−84086
acoustic convolution in hybrid piezodielectric-semiconductor system 79−7268
acoustic diagnosis using nonlinear effects, asymptotic feasibility anal., props. of layer on halfspace object 78−63248
acoustic diffraction field, B-scan viewing using backward wave propagation 80−33352
acoustic electronic signal processing devices, photoelastic materials, nonlinear elastic interactions *(French)* 79−41525
acoustic emission, time-domain deconvolution technique for signal identification 79−20306
acoustic emission anal., signal recovery technique for martensitic transformation study 78−60965
acoustic emission signals interpretation during tensile testing 77−9030
acoustic filter components for ANSI standard psychoacoustic testing 78−83198
acoustic holography, wideband signals, ang. resolution, image intensity 78−83182
acoustic holography system, Sonoscan using microprocessor 80−38184
acoustic imaging, multiplicative and additive processing comparison 80−64303
acoustic intensity meas. with sound level meter and microphones 78−83194
acoustic log primary signals recording, synchronous orthogonal detect. appl. *(Russian)* 79−88498
acoustic logging, channel requirements for elastic waves recording *(Russian)* 79−39955
acoustic logging, errors of statistical signal processing *(Russian)* 79−39939
acoustic logging, phase-freq. charact. effect on transmission accuracy of analogue signals *(Russian)* 79−39940
acoustic motional source transfer function characts., ocean profile anal. appl. 78−66982
acoustic multipath signal, individual pulse resolution, maximum likelihood procedure 78−83176
acoustic narrow band signals, bearing estimation via FFT and Prony algorithms 77−46855
acoustic noise in speech, nonstationary, reduction using LMS adaptive noise cancellation 79−64414
acoustic noise in speech, suppression using spectral subtraction algorithm 79−64413
acoustic noise source contribution to observed noise estimation digital signal processing techniques appl 79−18617
acoustic noise sources, time delay bias errors in estimating frequency response and coherence functions 79−18614
acoustic passive bearing estimation, removal of bias and 2π ambiguities 78−38150
acoustic performance sensitivity of array detectors to a priori spatial knowledge 78−55524
acoustic processor in conversational speech recognition system 79−46130
acoustic processors, experimental, recognition results 79−64421
acoustic radiation and scatt. anal., use of linear system theory 77−75729
acoustic real-time and frequency-domain processor simulation 79−81643
acoustic reflection in discrete layered media, structure estimation accuracy 79−23108
acoustic signal, pulsed, mathematical models *(Russian)* 80−38180
acoustic signal characterization using spectral microanalysis 80−74607
acoustic signal coherence limits in random ocean environment 80−46193
acoustic signals, degenerate parametric amplification 77−27414
acoustic signals, matrix formulation of multiple and partial coherence 77−46831
acoustic signature anal. for noise source identification 77−68336
acoustic sounding of ocean-bottom subsurface layered media, spatial parameter estimation 80−77134
acoustic sparse array technique, min. output variance, S/N ratio 78−83177
acoustic spectral inspection unit piezoreceiver, operation conditions 79−64465
acoustic surface waves and devices, book 79−50518
acoustic transfer function of the ocean for motional source 79−14140
acoustic using nonlinear interaction of bulk and surface waves in piezoelectric crystals *(Russian)* 77−3703
acoustic wave, using HF strain transducer 77−88991
acoustic wave convolver based on semi-conductor-airgap-piezoelectric structure 77−7260
acoustical communication theory, computation of modulation and carrier functions of an arbitrary audio signal 80−79064
acoustical holography, digital reconstruction and computer graphics display 80−23842

signal processing continued
acoustics, correlation coeff. meas. for signals with stationary additive noise 78−94489
acoustics, homomorphic deconvolution, reverberant and distortional channels 78−90606
acoustics, influence of time- and space-varying random filters 78−5615
acoustics, lagged signal power spectrum in cross correl. 78−9502
acoustics, optimum detection of signals in non-Gaussian noise 79−7260
acoustics, speech and signal processing, conf., Tulsa, USA, 1978, April 78−63242
acoustics, speech and signal processing, IEEE international conf., Washington, DC, USA, 1979 Apr. 79−55275
acoustics, time delay estimation in presence of source or receiver motion 77−88977
acousto-optic memory correlator using acousto-photorefractive effect 78−71248
acousto-optic multichannel signal processor 78−66990
acousto-optic planar guided-wave Bragg modulators, RF signal processing appls. 80−38131
acousto-optical processors based on light polarization discrimination techniques 80−74310
acousto-optics, conf., San Diego, Calif., USA (Aug 1976) 77−58463
acousto-optics, guided-wave, with appls. to wideband communications and signal processing, progress review 80−58801
adaptive cross-sensor beam forming with planar arrays 78−18121
adaptive detection processor in non-stationary noise, for narrowband signals 79−59868
aerospace systems and electronics, IEEE conference, Washington D.C., USA, 26-29 Sept (1976) 77−5420
analog, instrumentation, book 80−86047
analogue cct. for fast-response frequency measurement, used for foetal heart rate 79−21708
anemometer, hot wire, signal processing, technique for dynamic calibration 77−19644
anemometer, three-dimensional signal smoothing in simulated tornado flow meas. 77−17244
aneurysm detection using bioacoustic signal processing techniques 78−28120
array processor for noise and interference suppression 77−23815
array processors for noise and interference suppression and signal-to-noise resolution enhancement, error corrections 78−30132
astronomical images, PDS microdensitometer processing for astrometry 78−16306
atmosphere radar signal processing, for SOUSY-VHF-radar, using preprocessor 80−85774
atmosphere submillimetre emission and absorpt., freq. spectrum of fluctuations 77−41308
audio, compensating circuit for audio system functions *(Japanese)* 80−53566
audio, hearing, application of communication theory 80−79063
audio, with transversal filters 79−64406
audio digital signal processing, spurious signals and their suppression *(Czech)* 79−98555
audio spectrum analyser HP3582A using digital signal processing 80−43567
audition, compound PST histogram rel. to neural activity in cochlear 80−94148
audition, freq. following pot., appl. of least-square-fit technique 80−94149
audition, signal anal. by Hopf bifurcation in cochlear fluid 80−26241
auditory evoked brain stem pots., effects of analogue and digital filtering 80−89878
auditory frequency measurement based on neural timing 77−5011
auditory models and signal processing, conf., Munster, Germany (Sep. 1978) 80−90610
Auger lineshape determ. by numerical integration background subtraction 79−74469
aural signal central spectral pattern anal. based on cochlear neural timing and freq. filtering 79−5300
automatic coded digital speech transmission, pitch extractor appl. 79−41530
automatic device for radiowaves refl. or scatt. from ionosphere 77−49179
autoregressive model order selection applied to physiological signals 80−104780
bandpass filters, technique, construction, appl. *(German)* 79−50544
beamforming a towed line array of unknown shape 78−63230
beamforming when the sound velocity is not precisely known 80−96123
binary data, holographic coding methods investig. 77−68192
bio-signal processing, ECGs and patient safety using opto-electronic appls. 79−44016
bioelectric signal measurement and processing instrument trends *(Croatian)* 78−44665
bioelectric signal recording using surface electrodes, methods of reducing movement interference *(German)* 78−85405
bioelectric signals, time-connectivity patterns quantification of point processes 80−21564
bioengineering and medical instrumentation, symposium, Laramie, USA, (May '76) 77−25571
biological signal conditioning for system identification 77−44578
biomechanical impact data, digital filtering 77−78070
biomedical Doppler signal processing, swept-frequency transient signal filtering 78−48848
biomedical equipment instruction using modularised signal processor 78−41131
biomedical MEFV curves, smoothing by digital filtering 80−98157
biomedical recording system, TDM multiplexing system for multichannel signal averaging of visually evoked responses 80−36165
biomedical signal and image processing, digital techniques *(Croatian)* 78−44623
biomedical signal conditioning CCD transversal filter 77−52901
biomedical signals, development of common struct. for filters, correlators and Fourier analysers *(German)* 78−88748
biomedical signals, short-length, maximum-entropy correlation and spectral analysis 79−66577
biomedical ultrasonics, signal processing aspects 78−7418
biotelemetry techniques for studies of brain elec. activity 77−60310
bispectral passive imaging system for machine-system diagnosis 78−63239
bispectral synthesizer for acoustic signals 79−50513

signal processing continued
bistable optical device development from integrated two-arm interferometer, appls. *(French)* 80−69555
blind children's CW FM sonar 79−70708
blood velocity waveform display by spectrum analysers, direction Doppler signal preprocessing 79−34611
blood vessel bubble detection and flow evaluation 79−34612
body control mechanism, human, investigation using analysis of body's period signals 79−66576
broadband target classification using bionic sonar 78−18123
C-CD and SAW analogue signal processing 77−27439
C-CD and SAW devices, survey of component technologies 79−32160
C-CD and SAW in signal processing, comparison with digital devices 79−32145
C-CD appls. in sonar systems 80−53535
C-CD/SAW devices for signal and image processing, conf., Ottawa, Canada, 1977, Oct. 79−32159
cardiac arrhythmias, automatic detection in long term ECG monitoring 80−3850
channel vocoder based on CCD discrete Fourier transform processors 80−53568
charge transfer inefficiency affecting modulation transfer function of CCD 79−94175
Cherenkov radiation from large air showers, image reconstruction 79−25420
chirp transform processors using US strip dispersive delay lines, implementation 80−53577
CLEAN deconvolution algorithm, radioastronomy appl. 79−8844
code delta-modulation for standard hydrophysical information compression *(Russian)* 78−65432
coherent Doppler anemometer for turbulent vel. meas., potential accuracy anal. *(Russian)* 78−71406
coherent microwave imaging of limited fields of view, angular and aperture noise, optimum procedure 77−67045
coherent optical defectoscopy, correlation, materials testing appl. *(German)* 78−7110
coherent optical implementation of generalized two-dimensional transforms 79−94174
common depth point seismogram, signal and noise separation in amplitude spectra *(Russian)* 78−15970
composite signals, by cepstral inverse filtering, biomedical appl. 78−69243
composite strip piezoceramic US receiving array 78−42511
compound PST histograms, deconvolution 80−94146
computerized hearing aid test system, signal processing techniques 78−30131
conditional sampling, detection and data signal phase relation, turbulent boundary layer appl. 78−24772
conference, Paris, France (June/July 1978) 79−59864
conference, Portovenere, Italy (Aug./Sept. 1976) 78−5614
conference on acoustics, speech and signal processing, Denver, CO, USA (Apr. 1980) 80−83689
conformal array beam patterns and directivity indices 78−55523
constant-Q spectral analysis and Mellin transforms 79−98551
Continental Shelf sediment sonar signal processing 78−61622
continuous noisy signal analysis by autoregression time-series model 79−3209
convolution by membrane waves, using transversal piezoelectric effect of PVF_2 film 79−3859
convolution effect in volume magnetostatic waves in ferrite-semiconductor structure 80−54761
convolution equation solution, problems arising, auditory appl. 80−94147
correlation methods, signal parameter meas. 80−57241
correlator, investigation of optimum and sub-optimum filters, time delay estimation 79−59866
cross correlator, wide bandwidth, construction and appls. 78−4658
cyclical data collection, linear method for second degree interpolation 78−45473
data reduction, approximate realisation, new techniques 79−70898
degenerate SAW elastic convolver, theory 80−74628
delay line signal processors using acousto-optic interactions, real time system 80−28384
delay parameter estimation following robust detection 79−55267
digital, transfer function estimation for acoustic system with sharp resonances 79−18616
digital, used for analysis of forestry data obtained by remote sensing, book contrib. 79−92634
digital images, numerical filtering, Conf. on Earth resources electronics Rome, Italy (Mar.77) *(Italian)* 77−82056
digital optical fibre communications multilevel signals theory 79−22900
digital processing of radiograph for vessel edge detection in angiograms, appl. of Wiener filter, book contrib. 79−92357
digital signal modelling and classification with the teleseismic data 78−73325
digital sound spectrograph for speech signal anal. 78−63251
digital speech processing, book 79−72767
digitising error from period and freq. counting techniques 78−61570
digitizer for use with pulsed depth sounders 79−21065
discrete integration, optimum filter design, geophys. appl. 80−200
displacement transducers, for use below 50 mm, review 79−63200
disturbed measuring systems, estimation of signal parameters, autoregressive linear models *(German)* 80−68165
doppler lidar processing for atmospheric turbulence measurements 78−73554
Doppler microscope for flow velocity meas. in areas $<10\ \mu$ dia., signal-analysing system *(Japanese)* 78−22441
Doppler sonar, digital processing of signals 77−46856
double sample-and-hold circuit for deep-level trap spectroscopy 77−87789
dual-gate depletion-mode FET/piezoelectric film transducer 79−50563
Dutch vowels, anal. using fast Fourier transform 79−3858
Earth conductivity, model for quantitative interpretation of towed-bird airborne EM system meas. 79−5447
Earth transient EM sounding, meas. errors anal. in computer processing *(Russian)* 79−44269
ECG, automatic analysis of 24 hr recordings, optimum ECG morphology and quality 79−70664
ECG, digital filter for the QRS complex detection 80−36166
ECG, His-bundle activity detect., theoretical anal. of error during signal averaging 80−94392
ECG, homomorphic anal. and modeling 79−74768
signal processing continued
ECG, QRS detection accuracy rel. to anal. of HF components 80−17158
ECG, R-wave enhancement for heart rate determ., abdominal-lead fetal ECG 80−67264
ECG atrioventricaulr transmission intervals, automatic recording and processing 77−25568
ECG fine structure analysis by noise reduction *(German)* 78−73268
ECG frequency spectrum anal., clinical usefulness 79−25147
ECG linear filtering artifacts 77−44810
ECG optimum data processing and storage design 78−57118
ECG signal automatic evaluation using analogue circuits *(German)* 78−92717
ECG signal distortion reduction by statistical deconvolution 78−28118
ECG signal recognition and anal. *(Slovenian)* 79−83958
ECG/vector cardiogram interpretation modular system 78−7484
echotomograph, ultrafast, using optical processing of US signals 80−51180
ecological system model sampling/identification, input signal anal. 78−69267
EEG, by spatial deconvolution 80−94391
EEG, deconvolution procedure for information extraction from average evoked response signals 80−61724
EEG, detect. of intermittent transient patterns of brain elec. activity of unknown waveshape 78−31958
EEG, infant, ordinary and partial coherences of bipolar and quasi-unipolar derivations 77−44828
EEG discriminant function classification from renal patients, methods 78−28115
EEG features extraction by adaptive segmentation 77−44794
EEG frequency analyser, real-time, microprocessor monitored 78−57092
EEG signals, analyser-integrator model ANIEG-8 for frequency analysis 80−41295
EEG signals with changing spectra, anal. using Kalman estimator 78−24167
electrical charge injection methods for CCD 77−39082
electron diffraction patterns convergent-beam type, obtained by beam-rocking method 80−70085
electron micrograph optical and digital spatial freq. filtering 78−70231
electron microscope image enhancement, digital processing method *(German)* 78−89599
electronic sector scanning sonars, signal generation 79−18622
EMG, surface-recorded, stabilisation of isoelec. line using high-pass filter 78−31917
EMG filtered signal in isometric muscle contraction, S/N ratio anal. *(German)* 77−81490
EMG motor command extraction by pulse counting method *(Japanese)* 78−53546
EMG signal processing rel. to human locomotion, optimality criterion 78−92612
EMG signal processor, sequential multistate 79−100763
EMG/electrocorticogram automated anal. of sleep in rat 77−90969
evoked potential averaging, cross correlation and latency-corrected averaging comparison 79−53268
evoked potential estimation, method for evaluation of Wiener filtering method 78−24190
evoked potential optimal filtering in sequential range *(German)* 78−85401
evoked responses, statistical detect., evaluation of Woody's adaptive filter 77−81757
evolution systems, meas., rel. to master eqn., Bayesian anal. 80−90782
exercise ECG computer analysis 78−7516
exercise ECG computer processing expts. 78−7510
exercise ECG processing, influence of heart rate and coronary artery disease 78−7512
exercise ECG processing principles and multivariate analysis results 78−7511
external gravity field calc., signal processing approach 78−24708
extraterrestrial civilisation radiocommunication, efficiency of signals associated with natural phenomena *(Russian)* 78−40842
fast signal averager and coupled pulse generator, for pulse-echo expts. 78−21188
fault detection by scanning acoustic microscopy 77−80040
FFT analysers, high real time, applications 79−1041
fibre optic laser gyro signal detection and processing technique 79−37037
fibre optic rotation sensor 79−37034
filter functions, Savitzky-Golay, freq. response plots 77−53741
flash chambers as 'active' detectors and a special processor for fast decision making 79−26832
flow meas. with hot-wire probe, simultaneous and instantaneous temp. and vel. meas. 78−34236
flowmeter, ultrasonic cross correl. flowmeter 78−30393
fluorescence lifetime measurement using time correlation method with CW He-Cd laser 79−50072
foetal heart rate non-invasive registration by transabdominal ECG *(German)* 78−85418
foetal heart rate variability anal. using spectral anal. 78−28111
frequency method of signal averaging in ionosphere 79−53628
frequency response testing in noisy environment, time domain averaging 77−14856
frequency-time filtering of ULF signals and magnetospheric channel characterisation *(French)* 79−70920
gastro-intestinal electrical rhythms, freq. estimation using auto-correlation and auto-regressive modelling 77−44875
Gaussian signals in Gaussian noise transmitted over digital channel, degradation of S/N ratio 80−64298
geographic information processing *(Japanese)* 79−74978
geomagnetic D_{st} variations analyses, comparison using distortion free filter 80−17419
geomagnetic fluctuations, spectral stacking and smoothing rel. to Earth global elec. cond. character 80−17231
geomagnetism inverse problem, interval estimation of geophysical parameters via identification methods 77−82024
geophysical potential field data, interpretation methods 77−73861
geophysics, complex exponentiated data digital correl. *(German)* 79−44279
haemodynamic research, human, physiological signal acquisition and processing 77−44768
hand prosthesis myoelectric aid *(Spanish)* 79−84011
Hankel transform computation using projections 80−96124

signal processing continued
HEAR acoustic processor, performance statistics 79−59873
hearing, acoustic integration for lateralisation at high freqs. 77−90802
hearing, direct use of time information, place clues in white-spectra stimuli 77−90803
hearing, humans, binaural analyser detector charact., correlometer comparison 77−86506
hearing, two-tone suppression in nonlinear model of basilar membrane 77−48811
heart beat rate, sampled data analysis by fast Fourier analysis 77−81595
heart rate meas. (foetal), adaptive correlation ratemeter, US signals 78−88732
heterodyne holographic interferometry, electronic circuitry used for signal preprocessing 80−87352
heterodyne interferometers, quasilinear filtration theory appl. to signal processing *(Russian)* 80−82807
HF radar sea-echo Doppler spectra, extraction of wave height and period 77−78474
high counting rate spectrom. 77−44788
holographic passive imaging systems, effective utilisation of spectral spread 78−71250
holographic radio data aperture synthesis reconstruction 79−21191
homomorphic and predictive deconvolution in seismology 77−29254
hydroacoustic scatterers identification, system optimisation *(German)* 78−42487
hydrophone array response calc. errors due to two dimensional beam pattern assumption 78−66972
hydrophone arrays, optimum turbulent boundary layer induced noise suppression with suboptimum realizations 80−19161
hydrophone passive bearing estimation in unequal S/N ratio, optimum element placement 78−87210
image formation, perception and measurement, conference, Leeds, England (Mar. 1976) 77−86561
image processing appl. of multiple bandpass filters 80−109002
image reconstruction from incomplete and noisy data, examples and appls. 78−53837
Image Transform computerised transfer system, videotape signal processing, cinefilm appl. 78−45742
imaging systems, methods and terminology 79−66580
information processing methodologies, conference, Trieste, Italy (1979 February 23 to 24) *(Italian)* 80−94917
integrated and guided-wave optics, conference, Incline Village, NV, USA, January 1980 80−58772
integrated optic spectrum analyser, design of Bragg cells 80−74515
interaction of determinate packet with random noise, in Burgers' equation 80−106650
interferometer signal processing by acoustooptic correlation devices, radio astronomy applications 80−8543
ion beam co-ordinate monitor, induced noise-like signals processing 80−102607
ion-specific electrode output volt. linearisation 78−35991
ionosphere electron content data, mixing freq. components identification by multiplicative homomorphic filtering 79−29929
ionosphere sounding, filtering effect on drift parameters determined by full correl. anal. 78−65450
IR astronomy, data processing 79−101087
IR imagery, CCD, modelling and appl. of HgCdTe MIS struct. 78−80058
IR sensors and assoc. signal processing, performance evaluation 77−49313
isotope radiometry, nonlinear information processing in random signal detection *(Russian)* 80−22428
isotropic reconstruction of track-type airborne geophysical surveys, 2D filter design 79−66844
Josephson ultrahigh resolution sampling system 80−90828
Kalman filter design for estimating human blood-flow velocity, Doppler ultrasonic meas. 79−62325
LANDSAT data multivariate distribution relative normality measure 77−78506
large time-bandwidth acousto-optic signal processors 79−46118
laser anemometer Doppler system, optics and signal processor for turbulent low speed flows *(French)* 78−59521
laser anemometry, flow statistics retrieval via photon correl. 77−3896
laser beam interferometric wavelength measurements through post-detection signal processing 80−42254
laser burst-like Doppler signals, digital freq. meter 77−72376
laser Doppler anemometers, sensing volume and biasing corrections for dual counter processors 79−77314
laser Doppler velocimeters, signal processing using counters, biasing elimination method 78−1773
laser Doppler velocimeters 78−59520
laser flash absorption change kinetics spectroscopy at 820 nm, photosynthesis study appl. 78−92769
laser light pulse detection appl. to air pollution detection, Walsh transform appl. *(Japanese)* 77−78449
laser transit anemometer signals, semiclassical processing 80−59145
laser velocimeter, differential Doppler system, transverse vel. meas. at remote point 77−65816
laser velocimeter for wind tunnel meas. appl. 77−80252
laser velocimetry, photon correlation signal processor 77−62035
laser-Doppler velocimeter signals digital processing *(German)* 78−83510
latency meter, digital, for evoked pots. 77−60322
LED analogue video signal transmission, LED linearisation by predistortion 78−37993
lensless acouto-optical convolver using SAW device with polarisation discrimination detect. 78−79170
LF signal optical processing procedure 78−9343
LF signals, correl. function high-speed meas. using US delay line 77−75757
linear array acousto-optical modulator devices 77−39072
linear dichroism measurement, fictitious signal elimination via polarisation scrambling 78−4683
linear feedback AGC with input-level-invariant response times for sonar signal processing 78−30130
linear sonar array processor finite impulse response digital filter design 80−43549
linear vibratory system, multivariate joint probability density function 78−59329
linguistic processor in conversational speech recognition system 79−46131
signal processing continued
liver pathology characterisation, clinical appl. of a US attenuation coeff. estimation technique 80−76813
local circulatory system characterisation by CW Doppler US flow meas. 78−57109
loudspeaker free-field meas. in normal room using digital signal processing 78−66995
Macquarie University lectures, signal amplification via microphone amplifier for tape recording 79−71210
magnetophonon oscillation separation techniques, advanced methods 78−2499
magnetosphere chorus and hiss observed by GEOS, automatic recognition using coherence function 79−44307
marine profiling images, recording, signal amplitude preservation 78−36326
marine seismograms, source signatures debubbling 79−16692
matched filter device development using monolithic integration of SAW and semiconductor ccts. 79−32164
maximum entropy spectral analysis, power estimation method 79−16691
maximum entropy spectral analysis, prediction filter error length determ. for artificial samples 79−66829
maximum-likelihood estimation of source parameters from time-sampled outputs of linear array 77−75751
mechanical speech processing, new results *(Hungarian)* 80−69604
mechano-receptors, model for stimulus processing 79−74633
medical US, spread energy method, use of time gain control 80−108988
medical US imaging technology status 78−24174
memoryless nonlinear functional of random process in Gaussian white noise, Volterra expansion 79−86296
metal defect meas. using US cepstral processing 78−73010
meteorological radar equipment, pulse-wise interpretation of echo-signals *(Russian)* 80−67432
meteorological satellite NOAA digital signals *(Japanese)* 78−24424
metrological research on prospective measuring techniques, conf. Wroclaw, Poland, Sept. 1978 *(Hungarian)* 80−86247
microearthquake network automatic data anal. 77−81820
microearthquake network data, automatic anal. 78−81412
microoptic signal processing research, review 78−38073
microphone signals, cross-spectral density for acoustic intensity meas. 78−9514
microwave spectrometer baseline suppression using FM and harmonic detection 78−82866
Mills' cross array antenna, digital baseband processing 80−36500
minimum entropy deconvolution 77−81817
MM wave signals in radio astronomy using acousto-optical spectrometer 80−4253
modal anal. of vibrating structures using transient excitation 77−62220
modular chirp Z transform equivalent to two-lens optical Fourier transform 78−78943
multibeam sonar systems, data flow requirements 77−3697
multicomponent noise signal decomposition 79−3210
multimicrophone technique for room reverberation removal from speech signals 78−9501
multiple Markov sequences of interpoint intervals, inverse density modulation, rel. to removal spike trains 79−20529
multispike signal detection and sorting hardware 79−79711
multivariate and conventional ECG analysis programs compared 78−7492
musical acoustics, Fourier anal., phase determ. *(French)* 79−90100
myoelectric multistate channel for multifunction powered prosthesis, signal processing 77−44837
myoelectric multistate channel signal processing, prosthesis control 78−88768
myoelectric processor sampling rate selection 79−96713
myoelectric signal processing, expt. demonstration of optimal myoprocessor performance 80−89882
myoelectric signal processing, optimal myoprocessor derivation 80−89881
myoelectric signals, improved processor 80−104800
narrowband digital, meas. transfer charact. of acoustic systems with long reverberation *(Japanese)* 80−64304
NDT betatron flaw detection, signal processing algorithm 77−81375
NDT betatron flaw detection 77−81375
NDT probe array using 4 transducers 80−35499
nerve conduction velocity variability, effect of averaging and limb warming 77−60274
nerve spike trains, interleaved, in a noisy channel, separation system 80−94424
nerve trunk multifibre activity quantitation 80−76853
neurological, detection of pathological conditions in humans 79−83993
neurophysiological activity in olfactory system of rabbits, and pheromones 77−90816
new technology assessment seminar, Aviemore (1976) 77−39166
NMR image recovery under nonuniform magnetic fields 78−40282
noise and vibration analysis, Cranfield Institute of Technology, SPAG minicomputer system 80−96162
noise field in a wedge, mode representation 79−86299
noise intensity meas., nonstationary, using modulation radiometer 77−61048
noisy acoustic signal sources, optimal meas. of coords. by group of acoustic arrays 80−87659
nonlinear acoustoelectro-luminescence excited by SAW poss. processing appl. 80−45143
nonlinear friction element output with stochastic input 79−50674
nonstationary data, dynamic spectral comparisons, EEG anal. 77−44827
nuclear medicine images, controllable parameters affecting number of false positives and negatives 78−69191
numerical digital filter for on-line processing of wind tunnel data *(French)* 80−19537
ocean acoustic background noise, detection of sinusoids 80−33347
ocean acoustic transfer function impact on coherence of undersea propag. 80−58842
ocean internal waves, spatial spectra autoregression evaluations using reference sensor *(Russian)* 78−61578
ocean mapping, bottom return signal model and signal processor 77−2272
ocean wave spectra derivation by integral inversion of second order radar echoes 77−78475
on-chip signal processing to overcome IR detector nonuniformities 77−79154
optical, clip-level crossing rates in photon correl. and analogue signal processing 77−88650

signal processing continued
optical and acoustic integration in high speed signal processing, overview 78−51012
optical fibre data bus systems, for electrical control TDM signals *(German)* 78−25968
optical fibre testing using digital processing oscilloscope 78−22188
optical sensor array systems for astronomic longitude determ. 77−82023
optically processed seismic data, noise resistance *(Russian)* 77−86820
optimum estimation of signal parameters in non-Gaussian noise 79−14164
optimum resolution of signals with varying freq. 78−13862
optoelectronic analyzer for seismic data processing *(Russian)* 77−29516
optoelectronic device S/N ratio optimisation 79−26133
optoelectronic meas. system, comparison of pulsed and continuous modulation and pseudorandom coding 77−71374
parametric acoustic receiving array vibration sensitivity anal. 78−66971
passive coherence processing sonars, near-field performance 80−33346
passive sonar system adaptive processor 78−5622
period analysis at high noise level 80−73263
phase retrieval from modulus data 77−3540
phase-coherence detector and estimator, formed via overlapped FFT 79−59870
phase-matched filters appl. to Rayleigh waves from seismic sources 78−45010
photometer-bichromator, elec. ratio system with phase separation of signals 78−270
photomultiplier, digital signals processing via SAW spectrum analyser 78−26007
photon pulse delay estimation, nonregularity 78−29157
piecewise-linear approximated ECG waveform recognition 78−57119
Pioneer Venus occultation expt., bandwidth reduction for radio science data generation 80−67492
polarography, differential pulse, improved signal to noise ratio 77−29072
post-detection data load prediction for passive sonars 80−96125
pressure sensor, catheter-tip, with on-chip compensation and signal processing 77−44818
probe current modulation, electron distrib. determ., finite amplitude distortion, instrumental function 78−47168
programmable transversal filtering using baseband compatible SAW processors 79−98548
prosthesis, multifunctional upper extremity, control signal generation using EMG signal processing 80−8219
prosthetic fitted below-knee amputees, pylon transducer signal variability anal. 79−74715
psychoacoustic and sound recording, book 77−826
pulse compression using SAW components *(German)* 79−81639
pulse echo US and freq. domain deconvolution, for tissue anal. 77−40720
pulsed laser radiation beams, energy flux density meas. based on thin-film thermometry 79−81472
pulsed NMR spectrometer, signal multiple averaging via digital integrator 77−26372
pyroelectric vidicons for thermal imaging 77−19449
quantification of stochastic process, principles of quantification noise *(Spanish)* 80−57190
quantisation and averaging auditory appl. 80−94145
quartz piezoelectric crystal, electron-acoustic signal processing *(Russian)* 77−62111
radar pulse Doppler processing with low-loss SAW delay line 77−31184
radar signal reflection from sea surface, spatial intensity fluctuations 80−109170
radar symposium, London (Oct. 1977) 78−24395
radio antenna arrays, incoherent optical 1-bit cross-correlators, radioastron. appls. 80−98555
radio astronomy, multidimensional power spectral anal. 79−12406
radioastronomy, phaseless aperture synthesis technique 78−32353
radioastronomy receiver for LF planetary radio emission meas., Voyager spacecraft mission 78−4075
radioisotope imaging, digital low-pass filtering, random noise removal 77−5065
radiosources, two-dimensional max. entropy reconstruction of radio brightness 78−28534
random path detection, Gaussian noise hypotheses testing 78−58551
random pulse train inputs, use of digital filters *(Japanese)* 78−53547
random signal analysis, conf., London (April 1977) 77−44822
random signal mean power meas. error *(Polish)* 78−89425
real 1D signal convolution and correlation by freq. plane filtering 80−32919
real time phaseless filter with delay circuit, ECG appl. *(Japanese)* 80−56253
real-time Fourier transform. via acousto-optics 79−46112
recursive derivation of reflection coefficients from noisy seismic data 78−73324
reflection seismic recordings, minimum entropy deconvolution 78−81423
reflection seismograms, simultaneous spherical divergence correction and optimal deconvolution 80−98258
reflection seismograms signal anal., use of kepstrum 78−81425
reflection seismograph data, maximum likelihood filtering 79−5453
reflective acoustic microscope, signal processing, image enhancement 78−75022
remote sensing of Earth from space, role of 'smart sensors', book 80−62402
remote sensors, signal correction optimisation considering internal noises *(Russian)* 78−16191
remote transducer optimal signal correction with internal fluctuating white noise *(Russian)* 79−6107
removal of periodic waves from reflecting signals, moving target indicator 80−69585
repetitive signal, signal processing via surface acoustic wave recirculation loops 78−22228
resolution enhancement by deconvolution of detected signal 79−71440
response function relaxational frequency spectra, simultaneous meas. by digital signal processing 80−15959
reverberation meas., integrated impulse response method 78−59175
river, dissolved oxygen and biochemical oxygen demand, random signal anal. applic. 77−45047
room reverberation decay curve meas., FFT methods and errors *(Japanese)* 79−27468
rotating machinery diagnostics, signal extraction and filtering 80−23840
sampling considerations and FM compression system, correlators using split-electrode CCDs 79−18625

signal processing continued
SAW, physical props. and communication signals processing applications and devices 80−38162
SAW chirp filter FFT processor 78−87209
SAW components fabrication process 79−32162
SAW components review for signal processing equipment *(French)* 78−51013
SAW convolver, convolution voltage enhancement due to carrier transverse drift 80−1381
SAW correlator, storage mechanisms in ZnO monolithic device 79−18611
SAW device analogue signal processing appl. 77−27437
SAW device analogue signal processing technology, transversal filters and resonators 80−87656
SAW devices, fundamental aspects, book contrib. 79−50521
SAW devices, review 80−38204
SAW devices and appls. review, book contrib. 79−50519
SAW edge bonded transducer design and application 79−55304
SAW EM transducer model and flexible design for NDT 77−23844
SAW filter appls. in consumer electronics, review 80−74675
SAW filter design for TV, CATV and radar appls. 80−53579
SAW filters, design, construction, appl., book 80−1393
SAW metallic gratings, equivalent circuit of step discontinuity, rel. to SAW devices 80−33389
SAW monolithic storage correlator, appl. to adaptive filter 78−87208
SAW signal convolution using acoustooptic interaction in film waveguide 77−27428
SAW signal processor theory and production method *(German)* 80−58867
SAW space-charge coupled signal processor with storage 78−9507
SAw/CCD accumulating correlator for analogue signal processing 79−72757
SAW/CCD hybrid signal processor 79−32163
scanning background-limited IR sensor with adaptive threshold signal processing logic, performance 80−37082
scanning electron microscopic appl. 78−78040
scanning signal, influence of resonance filter on wave form *(Russian)* 79−55265
Schottky diode/$LiNbO_3$ acoustoelectric integrating correlator 77−88990
sea bed mapping by acoustic method, signal processing technique *(Dutch)* 77−64478
search for extraterrestrial intelligence, signal processing equipment 78−69709
sediment classification by ocean subbottom acoustic Q meas. 80−46168
seismic, solution of two-dimensional wave eqns. using recursive phase filter 79−86295
seismic, using inverse diffraction technique 80−74608
seismic broad-band P-wave pulse, extraction and use for event classification 77−81830
seismic coda of local earthquakes, synthesis method 77−73683
seismic data, deconvolution techniques for extraction of reflectivity function from seismic trace, book contrib. 79−92635
seismic data, nonlinear interference anal., crust and mantle regional studies 79−25217
seismic data, optimum mixed delay spiking filters appls. 78−77346
seismic data, self-adapting fan filters 79−44265
seismic data, single-channel white-noise estimators for deconvolution 78−77345
seismic data deconvolution 78−53736
seismic deconvolution, influence of phase prop. of random noise finite realisation 79−44254
seismic deconvolution and wavelet estimation 78−20542
seismic digital processing techniques for petroleum and natural gas 77−29469
seismic events correlation in time section, algorithm *(Russian)* 79−39962
seismic events visual correlation quantitative estimates based on min. average risk criteria *(Russian)* 79−44133
seismic exploration, deep refls. unravelling via seismic stripping 79−34970
seismic exploration, iterative identification of non-invertible autoregressive moving-average systems 78−81422
seismic exploration, signal processing method for circular arrays 80−4123
seismic exploration, technique and processing, book 80−51975
seismic field recorder, dedication of micro-computer to signal selection 77−82073
seismic linear multichannel systems employed in regular waves separation, efficiency comparative anal. *(Russian)* 79−39922
seismic multiple waves, prediction filtering in non-ideal conditions *(Russian)* 79−44131
seismic observations digital processing, steady numerical solns. *(Russian)* 79−53317
seismic P-waves, effects of crust spectrum characts. on station calibration *(Russian)* 78−49158
seismic pattern recognition, fundamental problems 78−81428
seismic recordings, information quality and data processing techniques efficiency *(Russian)* 79−39666
seismic records, surface multiples suppression 80−56402
seismic signals, adaptive deconvolution 78−53737
seismic signals, optimal multichannel filtering evaluation taking account of amplitude and phase jitter *(Russian)* 78−40697
seismic signals, preprocessing of signals prior to input to pattern recognition scheme 79−62631
seismic signals, stability characts. of optimal inverse filter 78−81424
seismic signals adaptive deconvolution 77−91062
seismic sounding, weathering correction method 79−44255
seismic surface wave dispersion, digital processing *(Chinese)* 78−24374
seismic surveys, optimum multichannel filters theory *(Russian)* 79−39921
seismic time profiles, processing for seismic sections construction as Earth pictures *(Russian)* 79−39960
seismic wavelet estimation, short-time homomorphic signal anal. appls. 78−81426
seismic wavelet estimation using short-time homomorphic signal 78−88930
seismic waves with different velocities, separation using nonlinear interference systems 77−78438
seismograms, digital processing, kinematic corrections *(Russian)* 79−39929

signal processing continued
seismograms and images, automatic transform. to seismic sections *(Russian)* 78−49155
seismology, comparative evaluation of methods for multiple waves suppression *(Russian)* 78−40515
seismology, deconvolution and synthesis of multi-segment seismic traces 80−77162
seismology, estimate of number of signals forming wave field *(Russian)* 78−49157
seismology, transmission synthetic seismograms direct inversion 79−29877
SEM, signal treatment, backscattered electron spectral distrib. *(French)* 80−42305
sensitivity of optical metrology using time modulation, electronically generated limitation 78−16828
shape variation detection, two-component chromatographic peaks resolution 80−71971
side-scan sonar with selective textural enhancement 77−5371
sideways-looking radar using synthetic aerial, remote sensing appl. 78−69537
siesmic multiple waves signal, seismology, multiple waves freq. selection appl. to wedging out zones separation *(Russian)* 79−8706
signal parameter trend anal. 78−15920
solar flares, principal component anal. in soft X-ray flux 80−41781
solar spectra, correction function for granulation mean vertical vel. determ. 80−62094
sonar, A-scan data for object pattern classification 78−66980
sonar, adaptive beamforming introduction 79−18620
sonar, rel. resolution with linear-period-modulated pulse 77−54825
sonar, synthetic-aperture sonar systems in turbulent medium 80−96080
sonar, technology development, review 78−55500
sonar beam steering, time delay and integrate CCDs 79−18623
sonar data, testing for multivariate normality 79−59865
sonar for smaller ships, clutter spatial correlation signal processor 79−3833
sonar ranging systems, pulse compression techniques 80−33350
sonar signal processing, conf., London, England, 1978, Nov. 79−18618
sonar system design, beamforming and signal processing systems 80−33325
sonar system design requirements 77−27441
sonar systems, digital beam forming 80−91950
sonar transducer arrays, image prod., signal processing methods comparison 78−18122
sound and vibration monitoring, signal processing developments 78−83181
SPAC, speech processing using the autocorrelation function, noise reduction in speech communication *(Japanese)* 80−33371
SPAC speech processing system using autocorrelation function, operation and characts. 79−68510
space research, signal preprocessing on spacecraft 77−64609
space-time signal processing, optimal versus conventional detectors 79−27467
spatial electric filters, 2-D image formation book contrib. 77−79772
speaker recognition, minicomputer based signal processing facility 79−18667
speckle reduction in US B-mode images of human tissue 80−74634
spectral analysers, amplitude accuracy limitations 79−1042
spectral analyzers, survey of currently available models 79−1040
spectral line recording in presence of intense background, techniques, appls. *(Russian)* 77−40613
spectrograms, detection, estimation and classification 80−64296
spectrometer, diode laser dual-beam, long-term temporal and scanning characts. 80−90902
spectrometer data conditioning by digital averaging 79−12867
spectrophotometers automatic processor for atomic absorption signals 80−105694
spectroscopy, noise reduction by low pass filter for DC signal, appl. chlorophyll-a fluoresc. 80−87249
spectrum analyser, frequency overlap requirements and detectability 79−1032
spectrum expander for multichannel filter spectromers 79−35790
spectrum width estimtes for weather echoes 80−12477
speech, amplitude and frequency distribs. of levels of processed signal 77−16942
speech, equalizer in spectral domain for speech processing by autocorrelation function 80−1383
speech, maximum likelihood parameter estimation of noisy data 79−64418
speech, microprocessor based real-time speech processor 79−64437
speech, parallel processor for real-time speech signal processing 79−64436
speech, phoniatric diagnostics of speech organ disorders, objective acoustic methods 80−104598
speech, pitch extraction from corrupted harmonics of the power spectrum 79−43936
speech, preservation of phase 79−59875
speech, two-dimensional discrete Hilbert transform and computational complexity aspects in its implementation 79−84937
speech communication systems, narrowband, frequency domain noise cancelling preprocessor 79−68511
speech enhancement, reduction of acoustic noise based on spectral noise subtraction method 79−64415
speech intelligibility improvement in the presence of noise to combat hearing impairment 77−11091
speech processing, automatic, approaches, models and appls. *(German)* 79−50532
speech processing, linear amplification, AF peak clipping and HF carrier clipping 77−17007
speech processing system using autocorrelation function, 8 kbits/sec. 79−59893
speech samples of deaf children, effect of timing errors on intelligibility 80−19167
speech signals, instantaneous value, statistical depend. represented as analytic signal *(German)* 79−94409
speech synthesizer, software linear predictive coding k-parameter synthesizer via dynamic programming 79−64443
speech training aid system tri-normalized speech processor 79−70700
statistical time interval analyser with visual display 77−37850
steel, cold rolled strip, surface defects, online automatic system, design study 79−34231
STEM, multi-signal detection and processing 80−73552
signal processing continued
stochastic-ergodic meas. instrument technology, student laboratory experiments *(German)* 77−49705
storage convolution, correlation using SAW, piezoelectric devices *(French)* 79−32146
strain gauges, self-conditioning transducers for long cable runs, operation 77−5827
stress-wave emission signals anal. to determ. relative energy released by materials under stress 79−86297
strip-coupled varactor SAW convolvers, parametric cct. anal. 78−71245
structural material defect characterisation by US signal processing 79−52614
surface texture assessment, Walsh function method 80−36995
surface wave random signals, for level and velocity meas. in rivers and open channels 77−45205
synchronous filter for signal shape reconstruction from derivative 77−37870
synthetic aperture sonar in turbulent media 79−90058
tagging flowmeter, signal processing 80−10328
thermal images, data processing and optimal projection to human eye 78−38038
Three Array Processor beamforming system 80−43550
time delay and integrate CCD device for pulse sector scanning in sonar 79−18624
time delay estimation using parameter estimation of FIR filter 79−59867
time selector for acoustic spectrosc. 80−87660
time signal from Loran-S station, propagation path effect on locking error 77−87742
time-domain reflectometry, signal separation for overlapping time windows, homomorphic deconvolution 77−18019
tissue structures characterisation, method of obtaining an acoustic impedance profile 80−67171
tomography, emission, compensation of tissue absorption 79−70686
towed-line array, iterative technique for ambient-noise horizontal-directionality est. 78−55525
transducer, stroboscopic, dynamic characteristics determining, correlation method 77−5824
transducer signals, flow noise rejection using coherence function method 77−84067
transionospheric propagation from a satellite, observations on the beyond-the-horizon statistics 77−25825
TV pupillometer, anal. of dynamic performance *(Japanese)* 79−39545
two-phase flow meas., digital processor for real-time anal. 77−80235
ultrasonic symposium, Phoenix, AZ, USA (Oct. 1977) 79−46096
ultrasonics, signal processing, conf., London, England, Jan. 1980 80−33351
undersea platform location by acoustic signature processing 80−43519
underwater acoustic pulse compression system, source and receiver methods 80−56630
underwater acoustic scatterers, classification, experimental appls. involving fish 79−41502
underwater acoustic signals, classification using environmentally adaptive approach 79−46114
underwater acoustic time delay estimation, cross-correl. and smoothed coherence transform methods compared 80−96086
underwater Doppler tracking using optimization techniques 78−55526
underwater passive listening, influence of spatial coherence of background noise 79−64387
underwater sound, ambient sea noise directionality meas. and processing techniques 78−16025
underwater sound, cancellation of turbulent boundary-layer press. fluctuations 77−88978
underwater sound, Confidence bounds for magnitude-squared coherence estimates 78−66979
underwater sound, general formulation of source extraction problem 77−84043
underwater sound, range information from approximate ray angle diagram 77−46843
underwater sound, source location in random dispersive media using generalised reduction methods 80−43509
underwater sound channel bandlimited impulse response display 78−66983
underwater sound measurement, FM signal correl. Methods 77−62086
US, broadband, pulsed, meas. of attenuation of soft tissues 78−77094
US, pulsed Doppler meas. of turbulent blood flow 77−40871
US, random signal, transducer limitations 77−25536
US, transcutaneous CW Doppler signals, for arterial physio/pathological data 77−44731
US abdominal scanners survey, clinician's viewpoint 79−66582
US data, digital processing by deconvolution 80−106669
US digitiser/processor for extraction of clinical parameters from Doppler-shift waveforms 80−36042
US Doppler blood velocimeters, max. freq. detector 79−53201
US Doppler device in detect. of fat particles in blood, digital signal processing 77−25525
US Doppler flowmeter average frequency processor 79−83873
US Doppler returns from foetal heart, processing, valvular timing information extraction 80−101238
US Doppler shift signal processing, maximum frequency follower 79−62320
US Doppler signal time-domain frequency analyser, numerical assessment 79−92314
US Doppler-shift arterial flow signals, Fourier anal. 77−29187
US flowmeter, correlation and spectral props. of flow modulated US signals 77−42948
US flowmeter for measuring rapidly changing gas flows, freq. range, excitation and signal processing *(German)* 78−83502
US frequency analysis, Fourier model 77−40504
US imaging system using random phase mask, processing by stationary-point receiver 77−80035
US impediography, deconvolution and processing procedures and corrections 77−64122
US in patient diagnosis 80−36049
US pulsed Doppler techniques for cardiovascular meas. 77−77947
US real-time two-dimensional ECG images, direct conversion 77−60233
US return signals, correlation with bipolar digital representation of broadcast waveform 80−99897
US signals, physiological measurements and numerical analysis 77−86577
US testing, axial resolution by signal processing *(German)* 80−7736

signal processing continued
US tissue characterisation, clinical spectrum anal. techniques 80−45998
US tomography, signal processing for improved directivity 77−44729
US transmission/reception system with single crystal, principle, biomedical appl. *(Japanese)* 77−84093
velocity meas. sonar system, transfer function model 77−7275
Very Large Array, phase switching, Walsh function appl. in radioastronomy 78−81539
vibration and pressure transducer design for nuclear reactor environment 78−823
vibration-acoustic diagnostics, random signal patterns recognition, with aid of computer *(Slovak)* 79−18612
vibroseis deconvolution 78−16171
vibroseis signal similarity, computerized anal. 78−20543
vibrotactile speech training deaf aid, frequency analysis system 77−29214
visual evoked cortical potential, removal of alpha by selective averaging 77−81766
visual evoked cortical potential meas., signal optimisation using Kalman filter *(Japanese)* 80−72348
visual evoked potentials, transient, real-time filtering 78−31940
visual evoked response, digital inverse filtering 79−53098
visual function assessment, electrophysiological responses, signal averaging technique 77−44655
visual system, hyperacuity decision model 79−5294
visual system spatial and temporal information separation model 78−40167
Walsh spectral estimates with appls. to classification of EEG signals 80−104789
white noise estimators for deconvolution 77−29472
wide bandwidth analogue correlator, appl. to mode-locked ion laser meas. 79−88983
wideband, with acoustoelectric SAW devices 77−27442
Wien bridge oscillator, AC signal control rel. to continuous recording of elec. resist. changes 77−53931
wind velocity meas. system, computerised 77−56742
wind-driven wave parameters determ. at automated buoy stations 79−21064
X-ray astronomy, risetime discrimination appl. to pressurised Xe gas proportional counter for hard X-ray detect. *(Japanese)* 79−80219
Cu-Be search coil for measurement of magnetisation and susceptibility in pulsed magnetic field 79−63281
He speech unscrambler using charge-transfer devices 79−98559
InSb-$LiNbO_3$ SAW convolver, efficient struct. realisation, Hall mobility meas. 80−83705
$LiNbO_3$, diffused waveguide for acoustooptical signal processing 79−90029
$LiNbO_3$ low-loss high-coupling volume mode 79−51409
$LiNbO_3$ SAW plate convolvers at 1 GHz 80−1382
$LiNbO_3$, Y-cut, SAW right angle reflection coeff. from metal strip array meas. 77−23814
Ni-Fe polycrystalline film cross-tie memory for shipborne radar/sonar 80−42204

signal processing, computerised *see computerised signal processing*

signal sources
see also signal generators
biomedical, ccts., galvanic separation *(Dutch)* 77−90939
digital laser-Doppler-velocimeters signal processor accuracy testing *(German)* 78−86242
explosive signals in shallow water, computer simulation 78−79160
LORAN-C type standard freq. signal, time and freq. calibration standard comparison *(Rumanian)* 79−40542
sinusoidal signal source with variable phase shift, teaching apparatus 78−36782
GaAs homojunction LED signal source for fibre-optic communication 78−1413

signal synthesis
acoustic, detect. of LPM signals with estimation of their vel. and arrival time 78−90604
bispectral synthesizer for acoustic signals 79−50513
cardiac system pressure pulse LF wave synthesizers, mammalian cardiac system 77−9301
complex exponential signal representation for calibration of underwater acoustic transducers 78−79183
complex representation of polarised signal rel. to ULF wave anal. 77−53236
computer-synthesized noise, signal detection 80−21476
digital waveshaping synthesis for musical sound generation 79−68526
harmonic waves, introduced through Fourier synthesis, for teaching 80−27080
matched electromagnetic pulse transmission, for good conducting media 79−36823
remote sensing, error anal. of ill-conditioned data, inversion technique 77−66992
resursive digital filter, generation of 1/3 octive data 78−87211
RF automatic test equipment, synthesised signal generator design 77−53875

signal transformers *see high-frequency transformers; pulse transformers*

signalling
see also alarm systems
coaxial coils, for signalling between surface and buried coils, max. induced voltage calc. 79−12299
stars and point sources, visibility estimate using visual instruments, search coeffs. 79−7089

silica minerals *see minerals*

silicate glasses *see glass*

silicate minerals *see minerals*

silicon
see also nuclei with .....
(1,1,0) direction, channelled particle radiation spectra, emitted quanta angular distrib. 80−96578
(001)2×1 surface, LEED spectra calc. 79−37910
(001) (2×1) reconstructed surface, dimer model self consistent calcs. 80−88613
(001) substrate for Pd_2Si epitaxial islands 80−96748
(100), (111) substrates for rare earth metal silicide thin film formation, backscattering study 80−70542
(100) inversion layer, electromigration in two dimensional electron gas, driving force 80−84441

silicon continued
100 kW peak photovoltaic power system, design, construction and capabilities 80−45705
(110) plane, quantum state observation during fast electron channelling *(Russian)* 80−59541
(111) surface, annealing of scratches 79−60609
(111) surface, proton dechannelling under channelling, blocking and double alignment conditions 80−88235
(111) surface structure phase transform, screw dislocations RHEED study 80−88153
(111) surface substrate for Al film, struct., props. depend. on vapour flow *(Russian)* 80−75453
(111) surface substrate for $NiSi_2$ epitaxial film, interfacial order, backscatter, channelling study 80−65390
n-type, *p*-type, regrowth layer formed by brazing with metal support disc, diode appl. *(Japanese)* 79−15833
A-centre, theoretical study 80−75521
A-centre formation by vacancy-O_2 recomb., acceptor impurity conc. effect 77−43243
A-centre ionisation energy change due to uniaxial deform. 78−71733
A-centres, photoionisation cross section 78−39063
absorption constants, interband and free carrier, at high-level photoinjection 79−38514
acceptor levels, ionis. energy and IR absorpt. 79−78033
acceptor spectra, interpretation 78−43332
acceptors, bound exciton lifetimes 77−80738
accumulation layer, intersubband-cyclotron combined resonance, theory 80−20278
accumulation layers, temp. depend. of inter-subband transitions, many-body effects 79−60899
acetone chemisorbed layer on Si, CH radical production by sputtering, rot. and vibr. population distrib. 78−64436
acoustic phonon geometric propag., anisotropic continuum acoustics 77−4170
additive to fluoride-oxide slags, influence on elec. cond. *(Russian)* 80−39572
adsorbed metal atoms effect on surface electron props. 77−55597
adsorbed Pd impurity, effect on surface electronic props. *(Russian)* 79−91124
adsorption, of organic solvents *(Russian)* 78−91537
adsorption of Al on (111) 7×7 surface, electron energy loss spectroscopy and LEED 77−43432
adsorption of Au+Ag, dispersed struct. formation 78−22952
adsorption of C_2H_2 and O_2, low-energy electron loss spectroscopy obs. 77−1303
adsorption of Cs, (100)2×1 surface, LEED 77−62747
adsorption of Cs on (111) surface, LEED, work function and thermal desorpt. 78−14590
adsorption of gases, electron energy loss spectral study of surface vibrs. 77−69160
adsorption of $H_2S(H_2O)(O_2)$, electron energy loss spectra exam. 77−39736
adsorption of H, kinetics of H generation and adsorption, UPS 77−55450
adsorption of H on (100), MeV ion scatt. study 80−80071
adsorption of HBr(Cl), AES, electron energy loss spectra and electron impact desorption exam. 78−43243
adsorption of O_2, early stages, AES, LEED, and XPS obs. 79−46937
adsorption of O_2, EPR, comparison with free mol. 77−69176
adsorption of O_2, UPS, new adsorption state 78−34702
adsorption of O_2 on ion-bombard. (111) surfaces, SIMS study 80−70522
adsorption of O on (111), and stimulated oxidation by electron bombardment, AES 78−14599
adsorption-desorption kinetics of H_2, O_2 and other gases, catalysis 77−47684
advanced material for space solar cell 80−94007
AES, backscattering factor, Monte Carlo method calc. 80−7449
AES, convolution and deconvolution 78−52601
AES, $L_{2,3}$ VV, local probe of atomic charge 78−48261
AES, lineshape, one-electron theory for $L_{23}VV$ and $L_1L_{23}V$ 78−72645
AES, obtaining density of states information from self-deconvolution of Auger band-type spectra 78−92150
AES examination of Ar^+ ion retention during Ar sputtering 78−56552
AES quantitative anal. of impurities *(Japanese)* 78−91356
air pollution neutron activation anal. using 14 MeV neutrons 77−91257
alignment chips for optical fibre cable connector 78−1411
alpha-particle, multiple scatt., ang. distrib. meas. 78−29720
ambient effect of O precipitation, self interstitial mechanisms, IR spectra, TEM study 80−66510
amorphisation by $^{31}P^+$ ion irrad. 79−51172
amorphisation by bombardment with O ions 78−10098
amorphisation by ion implantation, energy depend. 77−7769
amorphisation by ion implantation, energy depend. 78−2175
amorphisation by ion implantation, homogeneous or heterogeneous nucleation 77−11578
amorphisation dependence on low-energy irrad. conditions 79−60408
amorphisation due to irradiation with heavy ions 77−11606
amorphised by ion implant., localised states and cond., irrad. and heat treatment, doping 80−39529
amorphised by ion implantation, EPR obs. of mag. ordering 79−24186
amorphous, anomalous magnetoresist., hopping model 78−23117
amorphous, anomalous magnetoresistance 80−6877
amorphous, Ar^+ bombardment induced ripple topography 77−77336
amorphous, as photo-receptor for electrophotography 80−47126
amorphous, asymmetrical profile of ion implanted P 79−46693
amorphous, chemical effects on freq. of Si-H vibrations 79−51227
amorphous, clean and O_2 adsorbed, light sensitive electron loss meas. 79−24396
amorphous, co-sputtered doped, photovoltaic material appl. 80−93488
amorphous, control of dihydride bond density using RF sputtering 80−34327
amorphous, Coulomb gap and hopping cond. 80−44583
amorphous, crystallisation study 80−33890
amorphous, CVD, retarding crystn. by alloying with C,N,B or Ge 80−44129
amorphous, CVD, substitutional doping, electronic props. 79−23923
amorphous, defects, band gap states 80−80215
amorphous, diamagnetism temp. depend. 78−47940
amorphous, diffraction intensities, chem. bonding effects 77−72557
amorphous, discharge produced, electronic density of states 79−46992
amorphous, discharge produced, optical and photocond. props. 78−39147

silicon continued
amorphous, discharge produced, reversible cond. changes 77−85256
amorphous, dissolution into Al 78−95188
amorphous, doped, density of states determ. from transport meas. 80−49720
amorphous, doped, drift and Hall mobility, photocond. 79−65477
amorphous, doped, electronic props. 77−1418
amorphous, doped, electronic props. 78−19030
amorphous, doped, electronic props. 80−80283
amorphous, doped, non-polaronic, cond. and thermopower near band edge 80−49719
amorphous, doped, optically induced ESR, correl. effects 77−40115
amorphous, doped, photoconductivity and recomb. meas. 77−89800
amorphous, doping, Schottky barrier and p-n junction form. by RF sputtering 77−8187
amorphous, doping and absorption edge 80−29042
amorphous, doping effect and nature of localised states 78−14696
amorphous, doping effects on cond. in hopping transport regime 79−28424
amorphous, effective mass theory, impurity states in band gap 79−77992
amorphous, elastic moduli, random network model, calc. 78−6119
amorphous, elec. props., ion implantation effects 80−79828
amorphous, electrical conduction in amorphous semiconductors, mechanisms 79−56214
amorphous, electrical transport and photocond. 77−85355
amorphous, electronic and optic props. 78−39013
amorphous, electronic density of states, mol. liq. model 80−49581
amorphous, electronic props. and localised states, review 77−62871
amorphous, electronic struct., far infrared absorption 80−45051
amorphous, electronic struct. and optical dielec. function, LCAO calc. 79−42478
amorphous, electronic structure and molecular liquid model 80−54133
amorphous, epitaxial regrowth, structure and impurities effect 80−84401
amorphous, epitaxial regrowth by pulsed laser beam 78−91554
amorphous, EPR 78−88167
amorphous, EPR and spin-dependent effects 80−80592
amorphous, ESR and DC cond. 77−48032
amorphous, ESR linewidth, exchange interaction effect 79−61216
amorphous, film, hydrogenation by H diffusion, effect on elec. cond., band gap *(Korean)* 80−45326
amorphous, first order transition to metallic liquid, calc. of transition temp. 79−69227
amorphous, glow discharge, fatigue effect in luminesc., recovery by annealing 80−50416
amorphous, glow discharge deposited, mobility edge calc. 80−80220
amorphous, glow discharge deposited, photolum. decay 78−72590
amorphous, glow discharge produced, defect creation, high optical excitation 80−97327
amorphous, glow-discharge deposited, ODMR spectrum, deposition temp. and annealing effects 80−50229
amorphous, glow-discharge produced, fast photoconductor coupled liquid crystal light valve 79−59805
amorphous, H atom effect on Si-Si atomic short-range order, X-ray diffr. obs. 79−64996
amorphous, H isotope backscattering, trapping, and depth profiles, model 79−99233
amorphous, heavy ion ranges, He^+ backscatt. obs. 78−63796
amorphous, highly photoconductive, prep. by RF sputtering 77−73231
amorphous, hopping conduction, semiclassical theory 79−91052
amorphous, hopping model for activated charge transport 79−87099
amorphous, hydrogenated, diffusion of D_2, SIMS anal. 78−75877
amorphous, hydrogenated, electron drift mobility meas. 80−75565
amorphous, hydrogenated, electronic density of states determ. from Schottky diode meas. 80−49907
amorphous, hydrogenated, electronic struct., SCF Xα calc. 80−49580
amorphous, hydrogenated, H configs., Cayley trees appl. 79−65373
amorphous, hydrogenated, pure and B doped, effect of annealing on transport props. *(Korean)* 79−15142
amorphous, hydrogenated, recent advances 79−28103
amorphous, hydrogenated, small angle X-ray scatt., void distrib. 80−15087
amorphous, hydrogenated, soft H plasma effect, IR absorpt. *(French)* 80−45054
amorphous, hydrogenated, spin depend. photoluminesc. 78−72589
amorphous, hydrogenated, stacked solar cells 80−55842
amorphous, hydrogenated, work function and Auger spectroscopy of initial oxidation 78−76132
amorphous, hydrogenated and deuterated, struct. 80−103245
amorphous, hydrogenated film, electroreflectance study 80−88967
amorphous, hydrogenated film, struct. determ. using electron microscopy 80−10806
amorphous, hydrogenated photolum., heating effects 78−15204
amorphous, hydrogenation and density of defect states, hopping cond. 79−60757
amorphous, ideal network struct., electronic struct., tight-binding model 80−44485
amorphous, ideal surface, definition and characts. 80−107623
amorphous, implanted, recrystn. induced by scanning CW laser, reaction rates, analytical model 80−66334
amorphous, implanted, struct. transition under laser irrad. 79−50992
amorphous, impurity effects on hopping conductivity 79−65485
amorphous, in contact with electrolyte, Schottky barriers at interface 79−78169
amorphous, interface with V, V silicide formation, backscattering, diffraction meas. 80−2285
amorphous, ion bombard., etch pit and ripple struct. formation mechanisms 80−66366
amorphous, ion bombardment, controlled hydrogenation at low temps. 79−69119
amorphous, ion implantation, negative magnetoresist., localised mag. states 80−70731
amorphous, ion implantation method, B and P ions 80−100274
amorphous, ion implanted, laser annealing, reflectivity meas. 80−29039
amorphous, ion irradiated, elec. cond. 79−11127
amorphous, ion-implanted, hopping parameter at natural phonon freqs. 79−15152
amorphous, IR absorpt., first-order effective charges due to at. displacements 77−48164
amorphous, $L_{2,3}$ threshold spectra 77−69934
amorphous, large vacancy cluster annealing by ion bombard., EPR investig. 77−68965

silicon continued
amorphous, laser-induced epitaxial regrowth, substrate and doping effects 79−56082
amorphous, Lifshitz constant for calc. of van der Waals force between two solids *(French)* 80−107658
amorphous, luminesc. of diode structures 77−8656
amorphous, luminescence 80−80862
amorphous, mag. field depend. of luminesc. 79−43034
amorphous, MIS diode I-V characts. 78−43485
amorphous, monolithic solar cell appl. 80−45666
amorphous, opaque, surface phonon attenuation, Brillouin scatt. 80−80808
amorphous, optical absorpt. edge shape, band edge fluctuations 77−20880
amorphous, optical props., appl. as solar absorber review 79−74519
amorphous, optically detected ESR obs. 78−84500
amorphous, p-n junction devices, barrier profile effect on elec. props. 80−49890
amorphous, p-n junction prep. by vapour deposition *(Czech)* 77−63560
amorphous, phonon interaction in luminescence 78−43927
amorphous, photo-induced changes in elec. props., defect states 79−82553
amorphous, photoconductivity, mag. field depend. 78−80023
amorphous, photogeneration of charge carriers and recomb. 77−81147
amorphous, photoluminesc. and radiative lifetimes 79−61419
amorphous, photoluminesc. spectra from 77K to room temp. 77−20916
amorphous, photoluminescence, fast radiationless recombination 79−99939
amorphous, photostructural changes, photodarkening 80−49121
amorphous, photovoltaic behaviour, solar cell appl. 80−94051
amorphous, photovoltaic cell, plasma deposited, horizontally multilayered struct. 80−50964
amorphous, photovoltaic characts., rel. to appl. in solar cells 78−84253
amorphous, photovoltaic diodes, influence of mag. field on charge transport 80−49891
amorphous, position of Fermi level, spectroscopic and transport determ. 80−6706
amorphous, possible ABB-type excitonic superconductor *(Chinese)* 80−7029
amorphous, prep. by glow discharge decomposition method *(Japanese)* 77−81226
amorphous, prep. by reactive RF sputtering in Ar-silane mixtures, undoped, n-type and p-type targets 80−76182
amorphous, presence of acceptor states around Fermi level 78−2445
amorphous, production by glow-discharge method *(Japanese)* 77−90283
amorphous, ps. relax., optically induced absorpt. 80−48325
amorphous, pure and doped, photolum. meas. 77−36285
amorphous, pure and H doped, picosecond relax. of optically induced absorption 80−97302
amorphous, pure and hydrogenated, far IR absorption coeff. meas. 80−108213
amorphous, pure and hydrogenated, Raman spectra 79−61358
amorphous, radiative and non-radiative tunnelling, photoluminesc. decay meas. 79−83026
amorphous, Raman spectra, vibrational properties 79−99881
amorphous, random-network model, charge-density variation 80−80165
amorphous, recomb. centre study by spin-depend. photocond. 80−49805
amorphous, reduced intensity functions, thermal vibr. coupling 78−42910
amorphous, rehydrogenation, photoluminesc. recovery 78−72571
amorphous, rel. to SiH_x polymer film struct. 78−72048
amorphous, scanning TEM studies of cryst. inclusions 80−79699
amorphous, scatt. intensity and radial distrib. function, random stacking model 79−27919
amorphous, Schottky barrier and p-n junction props. 79−28407
amorphous, Schottky barrier solar cell, large-area RF sputtered, contact form, scaling and optimisation 80−45679
amorphous, short-range order, theory and probes 80−79698
amorphous, Si implanted, substrate-orientation depend. of epitaxial regrowth rate 78−79900
amorphous, small dia. laser beam annealed, temp. distrib. and microstructure 79−73098
amorphous, solar cell appl. *(Chinese)* 80−45671
amorphous, solar cells, and photovoltaic devices *(Japanese)* 80−50965
amorphous, solar cells, barrier props. determ. by differential I-V characts. meas. 80−94053
amorphous, solar cells, current collection and electrical shorting problems 80−93969
amorphous, solar cells, efficiency, transport props. 80−50961
amorphous, solar cells *(Japanese)* 79−57430
amorphous, solar cells design considerations 80−85277
amorphous, spin depend. recomb., luminesc. and light induced ESR 80−50393
amorphous, spin-pairing at defect centres, mechanism in terms of chem. bonding 79−23928
amorphous, sputter deposited, O_2 incorporation during and after fabrication 80−49541
amorphous, sputter-deposited, electrical and optical props. 79−47181
amorphous, sputtered, Auger surface spectroscopy 80−50472
amorphous, sputtered, resist. control by ion implantation 80−100262
amorphous, struct. and growth kinetics, topological principles 80−49123
amorphous, struct. models 79−37628
amorphous, structural and electronic props., review 80−64901
amorphous, structural defects EPR 80−25208
amorphous, structural disorder rel. to electronic props. 78−34756
amorphous, substantially doped, electronic props., review 79−87175
amorphous, substrate orientation effect on regrowth by laser pulses, channeling, backscatter 80−84409
amorphous, thermoelec. power in phonon-assisted hopping regime, Coulomb effects 78−76097
amorphous, time resolved photoluminesc. near band gap 80−25445
amorphous, time-resolved ODMR and luminesc. 80−25254
amorphous, transient electrical transport, general and unified treatment 80−59977
amorphous, transport results, interpretation 80−80260
amorphous, transport results interpretation 80−44590
amorphous, tunnelling states simulation and sp. ht. 79−37791
amorphous, UHV evaporated, annealing behaviour of spin density 80−93163
amorphous, undoped, photocond., continuous illum. effect 80−84486
amorphous, undoped and B doped, ESR-linewidth temp. depend. meas. 80−20459

silicon continued
amorphous and cryst., optical absorpt. at λ=1.06 μm, temp. depend. 79−82939
amorphous and cryst. K X-ray spectra of band struct. 79−87525
amorphous and crystalline, heating by Q-switched laser radiation 80−84963
amorphous and crystalline, hydrogenation and dehydrogenation 78−51677
amorphous and crystalline, ion implanted, UPS meas. 80−97411
amorphous barrier with metal, capacitance and cond. meas. interpretation 80−49909
amorphous CVD fabrication for solar photothermal conversion appl. 80−7504
amorphous CVD film photodetector for picosecond pulses 80−47101
amorphous deposited, laser induced epitaxy 79−69372
amorphous electron and hole drift mobility, meas. 78−19027
amorphous evaporated, picosecond optoelectronjc detect., sampling and correlation meas. 80−100478
amorphous evaporated film, doping 79−51127
amorphous film, AC conduction 77−66213
amorphous film, acoustic study using Rayleigh waves 80−75312
amorphous film, analytical techniques, review 80−80120
amorphous film, anisotropic etching phenomenon, appl. as solar selective absorber surfaces 80−72054
amorphous film, annealing behaviour of void network 78−18551
amorphous film, dangling bond ESR, light-induced quenching 80−50162
amorphous film, drift mobility and photocond. 79−15143
amorphous film, EELS microanalysis 80−100722
amorphous film, effect of gas exposure on EPR signal 78−84475
amorphous film, electron beam evaporated, freq.-depend. dielec. behaviour 79−99549
amorphous film, electron-beam-evaporated, noise meas. 79−24091
amorphous film, epitaxial laser crystallisation 78−84078
amorphous film, EPR rel. to elec. cond. 77−69692
amorphous film, ESR, cond. secular change on annealing *(Japanese)* 79−15238
amorphous film, Fermi energy shift with substitutional doping 79−46998
amorphous film, glow discharge deposited, for low cost solar cells 80−61355
amorphous film, glow discharge deposited, refl. spectra and dielec. function 80−50360
amorphous film, glow discharge deposition, rate enhancement by mag. field 80−65412
amorphous film, glow-discharge, optical props. *(Japanese)* 79−65946
amorphous film, glow-discharge, optically detected mag. reson., annealing and substrate temp. effects 80−20519
amorphous film, heavily doped, glow discharge, AC cond. 80−49718
amorphous film, heavy doping by alkali ion implantation 80−2045
amorphous film, hole carrier transport 80−2500
amorphous film, hole drift mobility, temp. depend. 79−23973
amorphous film, hopping cond., thickness depend. 77−89887
amorphous film, hopping cond. control by ion bombard. induced struct. modification 80−92898
amorphous film, hydrogenated, fabrication method 80−80956
amorphous film, in Ti-Si-Ti struct., elec. cond. processes and threshold switching 79−78207
amorphous film, interface charge, influence on transfer meas. 79−15237
amorphous film, ion-implanted, regrowth 79−15043
amorphous film, IR and Raman spectra of Si-H bonds 78−19482
amorphous film, LF vel. of sound for Young's modulus mode 77−35636
amorphous film, optical props., electronic states 80−25475
amorphous film, plasma preparation 78−72740
amorphous film, plasma-deposited, photoluminesc. and EPR meas. 79−4864
amorphous film, reflectance and transmittance *(Japanese)* 80−34995
amorphous film, RF plasma deposition from $SiCl_4$-H_2, characterisation 80−66435
amorphous film, RF-sputtered, influence of O_2 and deposition conditions, elec. cond., IR absorpt. and ESR 80−2949
amorphous film, selective laser recrystn. over heavily doped lines 80−84947
amorphous film, sputter-deposited, elec., optical, and photoelectronic props. 79−24433
amorphous film, sputtered, photovoltaic properties as Al-Si-Al(Mo) 77−24623
amorphous film, sputtering by 0.5 to 5 keV Ar^+ ions 79−91550
amorphous film, TSC, density of localised states distrib. 80−65587
amorphous film, vacuum deposited, microscopic voids, gas absorpt., crystn. study 80−49534
amorphous film, variable range hopping 78−76176
amorphous film deposition from silane glow discharge plasma 77−44173
amorphous film prepared from glow discharge, quantitative H anal. 77−69188
amorphous films, characterisation by Rutherford backscatt. spectrometry 80−50498
amorphous films, crystallisation kinetics and morphology, TEM obs. 78−84093
amorphous films, halogenated and hydrogenated, elec. and optical props. 80−97016
amorphous films, ion implanted, elec. and photocond. props. 80−49717
amorphous films, laser beam annealing, optical information storage possibilities 79−87515
amorphous films, porosity and oxidation of evap., sputtered and plasma-deposited films 80−10838
amorphous films, RF sputtered, appl. as Schottky barrier solar cells 79−34434
amorphous films, RF sputtering prep. at high Ar press., props. obs. 80−80418
amorphous films, switching, electrothermal model 80−80407
amorphous foil, electronic energy, straggling of light ions, at. number depend. 77−11612
amorphous glow discharge films, H_2 content, elec. props., and photostability 80−25577
amorphous hydrogenated, manufacture of Schottky-barrier and MIS tunnel solar cells *(French)* 79−24897
amorphous hydrogenated film, plasma deposited, optical props., annealing effect 79−56874
amorphous hydrogenated Si use as solar cell material 78−2565
amorphous hydrogenated solar cells, field depend. quantum efficiency, electron-hole recombination 80−66971
silicon continued
amorphous implanted ion trajectory and spatial distrib., Monte Carlo simulation 77−11611
amorphous laser effects 79−69921
amorphous layer, comparison of laser and electron beam pulsed annealing 79−69374
amorphous layer, epitaxial growth by laser annealing 78−79899
amorphous layer, inhomogeneity formed by ion bombardment 77−69017
amorphous layer, ion-beam induced epitaxial regrowth 79−69378
amorphous layer, ion-implanted, spatially controlled cryst. regrowth by laser irradiation 78−55810
amorphous layer, post-annealed struct. and twinning by transmission electron diffr. 77−76685
amorphous layer, solar furnace annealing to induce solid-phase epitaxy 80−2277
amorphous layer crystn., effect of ^{16}O, ^{12}C, ^{14}N and inert gases 78−14623
amorphous layer prod. by ion implantation, diffusion broadening, ESR study 80−92552
amorphous layer recrystallisation by laser beam 80−93566
amorphous layer reordering, implanted with ^{31}P, ^{75}As, ^{11}B 78−14622
amorphous layers, glow-discharge, laser-annealed, elec. props. 80−75661
amorphous layers, laser induced As profile broadening 79−95045
amorphous layers, on Si substrates, deposited and ion-implanted, laser-annealing behaviour 79−69373
amorphous layers, oxidised, supercond. tunnel junction barriers 80−93040
amorphous layers, recrystallisation, pulsed laser annealing 80−65404
amorphous layers, RF-sputtered on sapphire, crystallisation by CW ion laser annealing 80−80109
amorphous p-n junctions, high current, characts. 80−70807
amorphous Schottky barrier solar cells, deep hole traps, spectral response and TSC meas. 80−50962
amorphous Si region obs. in Si-rich CVD SiO_2 films 80−84400
amorphous silicon absorber, high efficiency, for solar energy utilisation 77−39907
amorphous sputtered film, elec. cond. and photocond. 79−87097
amorphous sputtered film, solar energy selective absorber, spectral emissivity 78−83045
amorphous sputtered films, hydrogenated, photoinduced optical absorpt. 80−50362
amorphous sputtered thin film, US anomalies, 0.5-300K 80−34145
amorphous thin films, appl. in solar cells, recent developments 78−80016
amorphous ultrahigh vacuum evaporated films, ESR obs., deposition effects 79−33534
amorphous-implanted laser induced struct. changes related to pulse shape 79−69123
amorphous/cryst. interface, supercond. mechanism 80−44783
anisotropic etching by $CCl_4(+O_2)$ gas plasma 77−32701
anisotropic etching of (100) and (110) Si 79−15827
anisotropic etching of (100) and (110) Si for fabrication of 3-D microstructs. 79−15826
annealed, photoluminesc. anal. of defects 80−80836
annealed, TEM and EELS identification of oxide precipitates 80−100723
annealed crystal, oxide precipitates identification by electron loss spectra 78−83952
annealing, impurity film form., energy loss anal. 77−31916
annealing, in elec. field, behaviour of second phase inclusions *(Russian)* 79−23779
annealing, using laser pulses, impurity incorporation at melt-cryst. interface 80−59504
annealing during Czochralski growth, influence on defect density 80−60769
annealing with 1.06 μm laser pulses 79−69913
anodic oxidation, high electronic current density 80−89386
anodic oxidation, mobile ion identification, Rutherford backscatt. analysis 77−44381
anodic oxidation at constant voltage, mechanism 79−70184
anodic oxidation for abrading thin layers from wafers *(German)* 77−25176
anodic oxidation in RF induced O plasma 80−100931
anodic oxide films, space charge, TSC obs. 77−32326
anodic oxide superficial layer, X-ray emission spectrometry and ion backscattering *(French)* 80−49482
anodisation at low substrate temp. by low pressure O_2 plasma 80−104314
anodisation in HF soln., proous layer form. mechanism 80−71769
anodised layers on clean and ion bombardment Si surfaces, ellipsometry *(Russian)* 79−24382
anomalous avalanche breakdown 80−80284
anomalous muonium states, time behaviour of μ spin polarisation 79−11371
antireflection coating, 100 ns pulsed laser damage at 2.7 and 3.8 μm 80−33057
antireflection coating, two given wavelength design method 78−59102
arc heater production, high capacity, for solar cell manufacture 79−11509
as-grown Czochralski crystal, multiple p-n junction structure obtained by heat treatment, appl. to solar cells 80−101099
atom, $^3P \rightarrow {}^1D$ electron impact excitation, distorted wave approx., exchange and polaris. effects 77−34764
atom, ab initio effective valence shell Hamiltonian for neutral and ionic valence states 80−74117
atom, and ions, two and three-electron Auger transition, with vacancies in 2p-shell 79−63972
atom, chem. environent effect on Kα satellites intensity, heavy-ion collision 77−54527
atom, density functional theory, energy calcs., core effects 78−72106
atom, elastic scatt. of slow electrons 77−88564
atom, excited states, quadrupole moments, Sternheimer shielding factors 78−82630
atom, excited states lifetimes, fluoresc. decay curves 80−58175
atom, first order density matrix, effective core pot. valence electron UHF method 77−30786
atom, foil excitation, K-vacancy bearing metastable states yield, 30-50 MeV 77−54600
atom, Gaussian basis sets, quality studies 79−59345
atom, He-like, 2^3P_1 state lifetime, X-ray emission 77−18851
atom, highly ionised, beam foil lifetimes 77−57934
atom, highly ionised, beam-foil lifetime obs. 80−32670

silicon continued
atom, K-shell ionis., X-ray prod. cross section for incident H^+, ^4He and ^{14}N ions 78−70923
atom, L X-ray emitting levels, lifetimes 78−66493
atom, MINDO parameters 78−86786
atom, Rydberg series electronic struct. 79−22614
atom, Rydberg series electronic struct. 79−22615
atom, SCF electron-gas local-spin-density model including correlation 80−9488
atom, two electron one photon transitions, K$\alpha\alpha$ X-rays 77−30813
atom+heavy ion, X-ray spectra, one-photon two-electron rearrangements 77−6712
atomic displacements damped by chemical bonds, computer calc. 78−47370
atomic Kα X-ray satellite spectra, gas phase meas. 78−66496
atomic scattering factor, anomalous X-ray scatt. obs. 77−55204
atomically sharp cracks, TEM study 80−71729
Auger band-to-band recomb. temp. depend. 80−29416
Auger electron emission, ion induced and secondary ion emission 80−71546
Auger electron emission 3-15 keV Ar^+ induced 77−59654
Auger electron prod. by Ne^+ bombard. 80−7460
Auger emission from (100) surface, ang. depend., overlayer effects 78−39637
Auger line shape $L_{2,3}$ VV, energy band theory 79−43074
Auger processes, role in electron emission due to 1-10 keV H^+, He^+ irrad. 79−15579
Auger recombination, localized and free carrier comparison 79−38090
Auger recombination 78−26883
Auger recombination coefficient, temp. depend. 80−24942
Auger spectra, ion-excited L-shell, characts. 79−87533
Auger spectra, KLL and KLV, screening effects and plasmon gains 80−80913
Auger spectra induced by 100 keV Ar^+ impact 80−84820
Auger spectra intensity var. due to diffr., (111) surface 77−85849
Auger transitions, $L_{2,3}$VV, struct. meas., rel to soft X-ray spectra 78−2953
autoepitaxial growth, low temp., using $SiCl_4$-H_2 system 80−20795
autoepitaxy, displacement of microrelief 80−2307
avalanche photodiode, lightwave sources and detectors 80−64068
avalanche photodiode, reach-through, temp. depend. characts. 79−95482
avalanche radiation detector, large-area, high-gain, using transmutation doped Si 77−23367
avalanche regime, carrier drift vel. effect on meas. ionisation coeffs. 79−69516
axial channelling, fast electron bound states *(Russian)* 77−80562
axially channelled protons, transmission meas. using two-dimensional position-sensitive detector 79−1471
back surface field solar cell degradation at high intensity due to base cond. modulation loss 80−94085
band narrowing and lifetime meas., in p-n junc. solar cell 79−7892
band structure, appl. of nondiagonally screened model potential 78−14651
band structure, atomic wave functions localisation, LCAO calcs. 77−51648
band structure, cluster type effect 77−28109
band structure, modulation spectroscopy, two-ray methods *(Russian)* 78−54469
band structure, self-consistent pseudopotential *(Japanese)* 77−43491
band structure, semi-empirical APW calc. 80−84424
band structure, use of two-centre approx. with Hartree-Fock eqns. 77−76726
band structure and valence charge density, self consistent pseudopot. method with Gaussian orbitals 79−90928
band structure of diamond like crystals, cluster-Bethe lattice model calc. 80−6713
band structure selfconsistently determined with X_α potentials using MAPW method 79−33227
band structure under high stress, nonperturbative calc. 78−10344
band structure using modified Vejkovic, Slavic pseudopot. form factor 79−56121
bandgap narrowing in heavily doped material 80−15479
bandgap narrowing model in moderately to heavily doped material 79−99477
bars, generation-recombination noise at 77K 79−60883
beam foil spectra in extreme UV 77−6711
beam splitter for CdSe optical parametric oscillator 77−88851
bent crystal, γ-radiation beam deflection due to 900 MeV channelled electrons 80−84223
bent crystal, X-ray Laue diffraction, integrated intensity 79−23492
bent single crystal, proton beam trajectory control *(Russian)* 80−19859
bevelled p-n junction in Si power device, elec. field in controlled region and blocking capabilities determ. 77−1474
bicrystals, grain boundary states and varistor characts. 80−24829
biexcitons, photoluminesc. spectrum exam. 78−47705
birefringence of dislocation lines in (111) wafers 79−61332
blazed holographic grating fabrication by selective etching 80−74320
blistering by plasma focus discharge deuterons, statistical anal., plasma diagnostics 77−35351
blistering due to 400 to 1800 keV $^4He^+$ ions, modal range determ. 80−100289
Bloch waves, corresponding atomic and mol. orbitals, in HEED 79−27880
blocking effect, backscatt. method *(Chinese)* 79−90708
bolometers, low-temperature far and middle IR 79−71529
bombardment of N_2^+ ions, form. of Si_3N_4 films 77−16705
bonding electron distribution 79−90594
Bormann effect, multiwave, expt. detect. 79−14648
Borrmann effect, enhanced, in heat treated Czochralski grown cryst. 80−70191
bound multiexciton complexes, luminesc. 80−10888
bound-exciton spectral lines, conc. broadening at high impurity concs. 80−80826
Bragg diffraction from crysts., Mo K_α radiation polarisation 80−1893
Bragg-case X-ray thin cryst., rocking curves, theory and expt. comparison 78−55785
bremsstrahlung spectra for 1 GeV electrons and positrons, planar and axial channelling *(Russian)* 77−32465
bridging epitaxy from Si windows onto SiO_2, ruby laser pulse annealing 80−44441
brightening and darkening wave generation by Nd:glass laser 78−18023

silicon continued
Brillouin scattering from surface waves, appl. of surface Green's function mapping method 80−40125
brittle, deform. during static indentation in single crystals 79−87714
brittle fracture in axisymmetric bending, study at room temp., for single cryst. 80−81180
brittle-ductile transition rel. to covalent bond metallisation *(Russian)* 77−56071
bulk and surface equlib. props., self-consistent pseudopotential calcs. 79−60750
bulk hot-electron properties, review 79−99553
bulk moduli, temp. variation 79−73237
bulk modulus from local Heine-Abarenkov model potential 78−42949
bulk plasmon dispersion, electron energy loss spectra meas. 80−59899
buried-grid fabrication by LPE 79−78906
c Si-SiO_2 layers, physics, electron and ion motion, Cl, Na and K ion effects *(Dutch)* 80−60093
C-CD imager, edge enhancement using 3×3 pixel neighbourhood operator functions 80−102644
C-CD Si substrate ionisation trails prod. by cosmic ray background 80−51669
capture of carriers by attractive centres 79−7836
carrier capture at amphoteric deep level defects 80−88569
carrier conc. determ., electrochem. method 78−60200
carrier concentration distribution by scanning IR absorption 79−61356
carrier concentration variations using electrolyte electroreflectance, topographical features 79−99562
carrier distribution function 78−26856
carrier generation in depletion layer, effect of stacking faults 79−23983
carrier lifetime, comparison of meas. by photocond. decay and surface photovoltage 78−68038
carrier lifetime and its impact on solar cell characts. 79−74521
carrier lifetime depth distrib. due to Ar ion implantation 80−70232
carrier photogeneration high level, determ. of absorption and free carrier distrib. 79−33309
cast, growth structure and photovolt. props. of solar cells 80−94008
cast polycrystalline, hydrogenation effects, rel. to p-n solar cells 80−93916
cast polycrystalline, laser annealed for solar cells 80−93918
catalyst for water photolysis, I-V model 80−108721
CdS:N, Mn, ion implanted, anomalous enhancement of EPR signal of Mn^{2+} 78−27080
cell for precise measurement of thermal expansion, at low temps., results for Cu, NaF 80−37027
n-channel MOSFET, Si inversion layer, negative differential resistance 78−30996
channeled ion implantation, of B and P ions 78−22739
channelled α-particles, 160 MeV, stopping power, expt. 78−26613
channelled energy loss 79−3332
channelled ion implantations, apparatus for spatially uniform doping 78−51569
channelled particles, quantum oscills. of spatial density 77−39620
channelled protons, energy loss to valence electrons, dielec. calc. 77−55312
channelled protons, theory of energy loss 78−38765
channelled-ion implantation of group III and group IV ions 78−75682
channelling of 1 MeV He ions with greater-than-random energy loss 77−80564
channelling of π^- and π^+ 79−60414
channelling of electrons and protons, correspondence between classical and quantal descriptions 78−18682
channelling of fast electrons, flux redistrib. meas. 80−19856
channelling of fast electrons, temp. depend. of anomalous Rutherford scatt. *(Russian)* 78−83857
channelling of H^+ and He ions, backscatt. particles ang. distrib. 79−51174
channelling of positrons, 56 MeV, producing radiation 79−51176
channelling of relativistic protons in bent crysts., theory 80−96581
channelling spectra of relativistic electrons, 28 and 56 MeV 80−24516
channelling surface peak rel. to thin film anal. 78−43966
characterisation and analytical techniques *(Japanese)* 77−84735
characterisation by photolum. method *(Japanese)* 79−38638
characterisation by photoluminescence method *(Japanese)* 78−80404
characterisation techniques and trends 78−11487
charge carrier UHF heating using lumped-capacitance resonators 80−20203
charge densities with hard-core and soft-core pseudopots. 79−33266
charge density, struct. props. electron-electron interactions 78−47725
charge disturbance around neutral defect, simple new method, appl. to ideal vacancy 79−82554
charge transfer by SAW in ZnO 77−27415
charge transport properties, review 77−39851
chemical etching, comp. selection, geometry effects 77−21299
chemical staining due to suboxide form. 78−35540
chemisorbed Al monolayer on (111) surface, local density of states 79−47142
chemisorbed H_2(Cl), conduction-band surface resonance 78−52051
chemisorbed H on surface, relation of Si-H vibr. freq. to surface bonding geometry 80−49502
chemisorbed O_2 on (111) surface, bonding geometry, electron yield EXAFS meas. 80−50461
chemisorbed O_2 on (111) surface, electronic struct. tight-binding calc., XPS and UPS meas. 80−49845
chemisorbed on Ni(100), LEED and angle-resolved AES obs. 79−95258
chemisorption of Cl_2, photoemission polarisation effects with synchrotron radiation 78−14580
chemisorption of Cl, chemisorpt.-site geometry from polarised photoemission 77−15684
chemisorption of Cl, cluster model calc., iterative EHT 77−32062
chemisorption of Cl in surface vacancies 79−77910
chemisorption of CO(Cl), surface photoemission, adsorption gate geometry 78−73079
chemisorption of Ga on (111) surface, Ga-induced surface states 79−19644
chemisorption of H_2, atom-probe FIM obs. 78−71968
chemisorption of H_2, magnetic-sector atom-probe field ion microscopy exam. of hydride form. 77−80699
chemisorption of H, new type of chemisorptive bond, theory 78−26930
chemisorption of H on (111) surface, localised model, ab initio HF-LCAO calc. 80−6930
chemisorption of H on (111) surface 77−62743

silicon continued
chemisorption of O_2, AES and photoelectron spectra exam. of early stages of oxidation 79−74272
chemisorption of O(1s), XPS investigation 77−69170
chemisorption of XeF_2 and SiF_4, XPS and Auger spectra, surface chemistry 80−81358
chemisorption on Al_5, core hole induced electronic relax. 79−90874
chemisorption on semiconductor surfaces, book contrib. 80−107648
chip manufacture for fibre alignment in lightguide cable connectors 80−64188
chromosphere, Si II and Si III lines spectral synthesis 78−36543
cleavage, (111), Kikuchi pattern, 40 keV incident electrons, electron energy loss spectra *(French)* 78−87594
cleaved surface, metal contact props. and influence of intermediate adsorbed layers 80−49905
coated by insulating film, dissolution and corrosion in high temp. water and moisture 77−48564
coated with copper phthalocyanine dye, optical modulation of low energy electron transmission 79−69939
coated with Pd, interference effects on irrad. with laser beam 80−66333
coating of mullite ceramic substrate, for solar cell appl. 79−34432
coating on C fibre, mech. props. 77−70197
coating on glass ceramic, surface prop. 78−11367
coherent twin boundaries, struct. by TEM 80−75238
colar cell arrays, for earth orbital and orbit transfer missions 80−94044
collision cascade following ion bombard. 80−65069
compensated, ^{29}Si dynamic polarisation by optical pumping in weak mag. field *(Russian)* 77−40152
compensated, ^{29}Si nuclei optical polarisation, nucl. relax. effects *(Russian)* 77−43907
compensated by thermal defects, recomb. and optical props. 80−64989
complex permittivity and cond., microwave meas. 79−65784
complex reflectivity determ., absolute method 79−30584
complexing mechanism, effect of ion etch rate 79−70197
composite materials, survey 78−56609
composition of inclusions, single cryst. 77−15441
compressed, polycrystalline, deform. and recrystallisation texture 78−27538
compression, effect of press. on lattice defects up to 90 kbar *(Japanese)* 77−72654
compression to 8 GPa, meas. with WC-anvil X-ray apparatus and epoxy press. medium 77−89496
Compton profile, expt., one dimens. Fourier transform 77−73187
Compton profile anisotropy, pseudopot. calc. 79−28854
Compton profiles, anisotropic momentum densities 77−48268
Compton profiles, directional, X-ray scattering factors and 1-electron density matrix 80−10458
concentration determ. in atm. and rainwater in Vizcaya, Spain *(Spanish)* 78−57264
concentrator solar cells, effects of nonuniform illumination 80−93942
concentrator solar cells, high efficiency, state-of-the-art design and processing 80−93958
condensation of Au on (111), AES obs. of very first stages 78−14633
conductivity, study with supercond. metal contacts 80−15621
conductivity of holes at low temp., electric field depend. 77−28179
conductor-insulator-semiconductor solar cells, automated production, outlook 80−94021
contact angle, surface doped with metal impurities, water adhesion energy *(Russian)* 77−89620
contacts to single cryst. Si, O distrib. profile, from emitted α-particle energy anal. of $^{16}O(\alpha,\alpha)$ 79−5213
contaminant in GaP grown by synthesis solute diffusion method 79−65992
continuous polycrystalline films on C substrates 78−64490
continuum-exciton effect in optical spectrum 80−25416
controlled dislocation formation, struct. density *(Russian)* 80−107244
controlled etching in catalysed ethylenediamine-pyrocatechol-water solns. 80−3223
core and valence electron excitations, AES, chemical shift and line shape 80−2365
core exciton binding energies 80−80188
core level spectra, electronic polarisation effects 80−6765
core levels, 2p, and core exciton binding energies, for pure and heavily-doped Si 78−76583
core levels, chem. shift and relaxation energy, temp. dependence 80−39520
core levels, temp. depend. of conduction band and core exciton energies 80−24828
covalent semiconductor, electronic response to high symmetry lattice vibr. 80−10619
crack free ingots, by directional solidification using heat exchanger method 79−8242
crack-tip dislocation pattern, X-ray topography *(French)* 80−107253
creep and dislocation structure under tension *(Russian)* 78−19839
creep and self-diffusion activation energies 78−38772
critical resolved shear stress, 800 to 1050°C indentation dislocation rosettes 79−24577
cross-slip of isolated dislocations at surface and in bulk 80−70215
cross-slip of single dissociated screw disclocations, double etching and X-ray topography studies 80−15104
crucible grown, laser irradiation effects on surface structure of virgin and implanted Si 80−92768
crystal, desorption of SiO_2 films, ellipsometric obs. 80−100410
crystal, electron and hole effective mass, intrinsic conc., temp. depend. 80−107692
crystal defect obs. by TEM *(Japanese)* 77−84752
crystal defects, interaction with impurities, electron microscopy obs. 80−65003
crystal defects, X-ray step scanning section topography, lattice imperfection characterisation automatic Bragg angle control 79−60221
crystal defects in integrated circuits, review 78−88547
crystal film growth by condensation of mol. beams, transfer of impurity 78−10299
crystal growing technology *(Korean)* 80−50538
crystal growth, float zone, low ohmic seeds and dislocations 78−27398
crystal growth, for electronic devices 80−66419
crystal growth, improved horizontal ribbon growth technique 80−108345
crystal growth, reaction of rare earth impurities with carbon 79−38733
crystal growth, temp. gradient meas. by photoelec. pyrometer 77−40359
crystal growth conditions effect, on microdefect distrib. 80−50549

silicon continued
crystal growth from Al-Si-Cu melt, faceted cryst., cellular hole growth 77−4061
crystal growth from melt in vac., origin of SiC impurities 80−2940
crystal growth mechanism during chemical reactions in Si-H-Cl system 78−2392
crystal microcrack detection by ultrasonoprobe 80−66733
crystal orientation determ. by Laue method, computer calc. *(Chinese)* 79−32853
crystal production and perfection for photodetectors 78−11107
crystal structure and lattice imperfections 80−24398
crystal structure images of diamond structure, electron microscope obs. 78−14256
crystal structure stability, P-T diagrams 78−51886
crystal whiskers for use as photoconvertors 79−67386
crystalline, regrowth into amorphous layers 79−69040
crystallisation front face effect on at. displacements *(Russian)* 78−67781
crystallisation in Si-H-Cl system, adsorpt. layer comp. 77−15697
crystallised layers by laser annealing, ⟨100⟩ and ⟨111⟩ self-implanted samples, struct. 78−47644
crystallographic electron distribution re-evaluation 78−38657
crystals, deformed, strain distrib. characterisation, annealing response 77−70140
crystals, dislocation free, floating zone method growth in Spacelab 79−78872
crystals, rapidly grown RTR sheet, props. and solar cell processing 79−100048
current instabilities in semiconductors, theory and expts. *(Hungarian)* 77−39857
curved crystals, neutron diffr., comparison with theory, for Laue geometry 78−14248
CVD, amorphous and polycryst., solar thermal absorber, temp. variation of absorpt. edge 80−12028
CVD, characterisation and morphology 79−33938
CVD, gas phase diffusion and surface reactions 79−15614
CVD, plasma stream transport method 78−52684
CVD, surface anal. during growth using RHEED and Auger spectroscopy 80−66433
CVD, underlying oxide layer thickness effect on in-process thickness monitoring 80−6679
CVD, using CO_2 laser for substrate heating 78−39698
CVD amorphous films, effect of surface characts. on visible and UV optical props. 80−60698
CVD amorphous films, for high temp. solar photothermal conversion 80−26161
CVD based on pyrolytic reaction, polycryst. Si deposition as example 80−84407
CVD crystal growth mechanisms *(French)* 79−33939
CVD epitaxial growth, from $SiCl_4+H_2$, in vertical cylinder reactor, transport processes analysis 77−48344
CVD epitaxy, book contrib. 77−12544
CVD film electrical props. 78−6466
CVD film on amorphous substrate, CW laser recryst. 79−90894
CVD films, polycryst., elec. and optical props., electronic density of states model 79−56332
CVD films, polycryst., non-volatile memory switching 80−54814
CVD for appl in high temp. photothermal conversion 79−79403
CVD from SiH_4-HCl-H_2 system, rate-determining reactions and surface species 80−84405
CVD grown polycrystal recrystallisation 78−64560
CVD growth, high- and low-temp. models 78−6244
CVD growth and film morphology, rel. to model of mass transport 77−59233
CVD growth rate, temp. and conc. effects, mass transport model 77−59234
CVD growth surface, singular instabilities 77−24969
CVD layers, change of etch rate associated with amorphous to crystalline transition 78−7064
CVD mechanism, book contrib. 79−69991
CVD mechanism, epitaxial growth, IR obs. 79−23859
CVD of polycrystal on liquid Sn layer 78−64479
CVD on liq. Sn layers in HCl presence, enhanced crystallinity 78−6853
CVD on SiO_2 and Si_3N_4, SEM study *(Dutch)* 80−2960
CVD on SiO_2 and Si_3N_4 substrates, nucleation in SiH_4-HCl-H_2 system at high temp. 80−49538
CVD polycrystalline film, growth texture 77−7990
CVD polycrystalline layer, on oxide-covered single cryst. Si substrate, deform. 78−26778
CVD using CO_2 laser 78−56589
CVD using Si-H-Cl system, theoretical anal. of equilib. adsorption layers 79−23858
cyclotron reson. linewidth in quantizing mag. field 77−15752
cyclotron resonance absorptions due to excitonic ion and excitonic mol. ion 77−73082
Czochralski and web crystals, transition metal doped for solar cells 78−35297
Czochralski cryst., hillock etching of microdefects, TEM obs. 78−87678
Czochralski cryst. growth, faceted and nonfaceted, Sb microsegregation 80−45227
Czochralski crystal growth, low O content 80−40251
Czochralski crystal growth and charact., oxidation induced stacking faults 79−47621
Czochralski crystals, O microsegregation, swirl defect distrib., growth rate depend. meas. 80−39295
Czochralski grown, inhomogeneous O precip. and stacking fault form. 79−14820
Czochralski grown, intrinsic gettering by oxide precipitate induced dislocations 77−27903
Czochralski grown, O distrib. meas. 77−11580
Czochralski grown, oxide precip. homogeneous nucleation 80−65221
Czochralski grown crystal, O precip., nucleation behaviour and dislocation loop form. *(Japanese)* 80−59664
Czochralski grown crystal, radial impurity distrib. improvement 77−73225
Czochralski grown crystals, swirl-type defect obs. 80−100236
Czochralski grown wafer, precip. during high temp. oxidation 78−11381
Czochralski grown wafers, minority carrier transport props., laser beam scan for homogeneity anal., photovoltaic cell appls. 80−92905
Czochralski growth, equilib. of dissolved C and O with CO in ambient atm. 80−1949

silicon continued
Czochralski growth, large crystal, convection and segregation 78−6843
Czochralski growth, small-angle dislocation boundary form. anal. 80−89136
Czochralski growth and characterisation *(Japanese)* 79−43125
Czochralski growth from heavily Sb doped melt, interface morphological instability 80−2939
Czochralski growth of dislocation-free (110) crystals 79−100042
Czochralski growth parameters related to epitaxial stacking faults, high O_2 content 79−4314
Czochralski growth with automatic diam. control 78−52658
Czochralski wafer intrinsic gettering by oxide precipitate induced dislocations 78−6092
Czochralski wafer oxidation-induced stacking faults correl. with bulk defects 77−76428
Czochralski wafer oxide precipitate-dislocation complex characterisation 78−14357
Czochralski wafers, oxidation induced stacking fault sources 77−7737
Czochralski wafers, thermally oxidized, stacking fault distrib., O conc. depend. 80−2042
Czochralski-grown, oxide precip. form. process 80−49364
Czochralski-grown crysts., thermally induced microdefects, annealing temp. and starting material effects 80−49141
damage in electron bombardment, threshold voltage 77−27910
damage profile after H_2^+-ion irradiation, proton backscatt. exam 79−60410
dangling bonds, EPR, localised states and unpaired electrons on microcrack surfaces 78−52351
dangling-bond surface states 78−43452
DC sputtered, amorphous, dark conductivity and photocond. obs. *(French)* 78−64155
Debye temperature, influence of temp. and alloying on integral X-ray intensities *(German)* 77−69066
dechannelling, of MeV He ions by twinned regions in implanted crystals 78−75700
dechannelling by twins, ^{4}He backscatt. spectra 78−18691
dechannelling of H^+, generalised Fokker-Planck eqn. calc. 77−19999
deep amorphous layer implantation, laser effects, channelling diffr. study 80−25494
deep centres, continuous energy spectrum, isothermal capacitance relaxation method 80−107741
deep centres, wave functions and optical cross sections 78−34801
deep centres associated with plastic deform. and quenching *(French)* 77−28145
deep centres due to transition metals, model 79−78045
deep diffusion of B at solid solubility limits 78−10070
deep dislocation states 80−24836
deep donor character of muons and protons 80−10911
deep impurity levels, activation energy 80−107742
deep level defects, struct. bonding, amphoteric centres 80−88506
deep level determ. using deep depletion MOSFET test structure 78−10571
deep level transient spectroscopy *(French)* 79−11079
deep levels, detection in high power materials and devices 79−28318
deep planar diffusion of Al and Ga 79−69290
deep-level point defects, effective-mass nature 80−59922
defect annihilation depth by pulse laser annealing 80−16128
defect density studies, by ASLEEP, SEM and scanning AES 79−19256
defect evaluation, new preferential etch for (100) and (111) oriented n- and p-type cryst. 77−59954
defect form. under radiation-accelerated diffusion conditions 80−19854
defect formation, high temp. treatment, growth-band influence *(Russian)* 79−4299
defect formation kinetics during charged particle irrad. 80−29096
defect generation and annealing by intense subthreshold electron beam bombardment 79−51149
defect production by GeV muons, thermally stimulated current technique 78−5099
defect spatial distribution in annealed ion-implanted Si, transient capacitance meas. 77−11973
defect states produced by electron bombardment, capacitance transient analyses 77−80545
defect storage kinetics during neutron irrad. 80−24505
defect studies status 77−84742
defects, divacancy and split 100 interstitial, electronic structure calc. 80−65494
defects, electrically active, correl. of electrolytic etch and surface photovoltage methods 79−77929
defects, form. and annihilation after irrad. with Cr^+, ESR investigation 79−90707
defects, introduction during growth and processing 79−95925
defects, small, in Czochralski grown and zone-floated monocrystals, TEM identification 79−95001
defects detect. by EPR superheterodyne spectrometer 77−43885
defects in surface due to oxidation, exam. using double crystal back reflection topography *(German)* 79−51098
deformation, annealing characts., X-ray study 78−75713
deformed, annealed and recrystallized, struct., implications for solar cells 80−60922
deformed, defect states associated with dislocations, capacitance transient spectroscopy 79−42483
deformed, ENDOR of dislocation centre 78−72434
deformed, faulted dipole, TEM obs. 78−38712
deformed, recomb. radiation from electron-hole drops and free excitons 77−8641
deformed crystal, Czochralski and float zone growth, Luder's bands 79−79025
deformed crystal, faulted dipoles 78−59814
deformed surface, defect struct. rel. to elec. props. 78−72231
degenerate four wave mixing of 1.06 μm laser radiation 80−5794
dendritic film growth on alumina, solar cell appls. 77−77432
dendritic web for solar cells 80−89634
dendritic web growth, computer modelling and material charact., solar cell appl. 79−11508
dendritic web growth, correlation of solute and interface partition coeffs. 79−24427
dense plasma dynamics during pulsed laser annealing, carrier density, recombination 80−84479
deposition by SiH_4 pyrolysis at low temps. and atm. press. 79−91595
deposition diffusion from B_2H_6, AES analysis 78−6085
deposition on rotating disc, one-dimens. model 80−75461
silicon continued
depth profiling by electron beam induced junction current meas. 80−96977
depth profiling of ^{3}He ion implantation 78−59830
depth profiling of As and P, SIMS, high sensitivity 77−7742
desorption kinetics of two-dimens. phases on single cryst. substrate, Au and Ag on (111) surface 78−14598
destruction mechanisms by intense IR laser radiation *(Russian)* 78−39633
detector, α-particle dense track charge losses 77−3233
detector, energy loss of H and ^{3}He ions 77−6652
detector for γ-ray dosimeter, energy dependence of spectral sensitivity 79−68146
determination, by neutron activation anal., 14 MeV *(Czech)* 79−24862
determination, in Fe-Si alloy by X-ray fluorescence spectrometry *(Japanese)* 79−57324
determination, in steels, by spectrographic method using combined discharge 79−57327
determination in bauxite by neutron activation anal. 79−24858
determination in high alloy steel, by 14 MeV neutron activation-high resolution γ-ray spectroscopy 77−1967
determination in metals, by deuteron irrad., nucl. microprobe anal. 78−7285
determination in optical waveguide glass by DC plasma emission spectroscopy 80−87446
determination of P, As by ion microanal. *(Japanese)* 78−85250
determination with Al in atmospheric aerosols by neutron activation anal. 80−72116
deuteron, multiple scatt., ang. distrib. meas. 78−29720
deuteron bombardment and implantation 77−59033
device starting material, crystal defects, high voltage TEM obs. 78−10037
device technology, thin film interaction effects, book contrib. 79−1620
diamagnetic and dielectric susceptibility, temp. depend. 78−10646
diamagnetism of excitons and biexcitons, recomb. spectra *(Russian)* 80−7412
diamond:Si, paramag. centres, ESR spectra 77−36132
diamond:Si, substitutional impurities 79−87056
diamond-Si heterostructure, Auger spectra electron microscopy study 80−34340
dielectric band structure calc. 79−47034
dielectric function, effective, and exchange interaction effects, calc. 79−99494
dielectric function spectra, ellipsometric determ., many-particle effects at E_1-transition 80−93363
dielectric matrix, microscopic inverse, local field correction and acoustic sum rule 77−84863
dielectric polarisation calcs., microscopic local fields 80−20582
dielectric properties, mean point value calc. 78−87930
dielectric screening, microscopic theory, phonon dispersion, moment expansion calcs. 79−55839
dielectric screening and zone-centre phonons 78−67785
diffracted X-ray channelling by special deform. fields 80−100295
diffraction grating, rectangular profile, fabricated from single cryst. 80−38093
diffusion, in amorphous SiO_2 *(French)* 80−107482
diffusion and power spectral density and correl. function of vel. fluctuation for electrons 80−65576
diffusion coefficient determ. from carrier conc. depth profile 80−107566
diffusion coefficient of Se, by sheet Hall coeff. meas. 79−46843
diffusion coefficients for O impurity, determ. from optical absorpt. 79−69294
diffusion in Au-refractory thin film systems obs., by combination of scattering techniques 80−65308
diffusion in liq. Al-Sn(Ag)(Cu)(Au) alloys *(Russian)* 79−28118
diffusion in Mn steel, electron probe microanalysis *(Czech)* 77−59149
diffusion in Ni, ion radiation effect on redistrib. 78−34551
diffusion into liq. Fe *(Russian)* 78−79791
diffusion layers, B distrib. 77−7753
diffusion mechanism of P, migration channels along vacancies and interstices 80−79996
diffusion of ^{71}Ge and ^{32}P, effect of dislocation struct. on migration rate 77−51551
diffusion of Al, open-tube high-vacuum method 78−6084
diffusion of Al in open tube high vacuum system 78−91349
diffusion of As, from As-doped oxide source, mechanism 77−47477
diffusion of As from doped oxide film, stress effect on film roughening 78−2389
diffusion of As from doped polycryst., conc. depend. 78−34656
diffusion of Au, enhancement by photo- and electron irrad. 77−27901
diffusion of B, in oxidised atmosphere, minicomputer model *(Rumanian)* 79−82247
diffusion of B,P and Sb, implantation damage effects 78−55988
diffusion of B and P, influence of dislocations 78−18840
diffusion of B from CVD BN covered with Si_3N_4, appl. to master slice p-MOS IC 80−107564
diffusion of B impurity, separation factor estimation 79−86926
diffusion of Ga, using open-tube system 80−19822
diffusion of Ga in closed capsule, surface damage elimination 78−87691
diffusion of Ga through SiO_2 layer, junction depth 78−51574
diffusion of impurities accelerated by γ rays 77−55394
diffusion of Na, retarding action of radiation defects 77−1140
diffusion of Ni below 475°C, role of defects 79−51319
diffusion of nitrogen during annealing, effects on ion implanted layers 77−24436
diffusion of Os, diffusion parameters using photocapacitance and four-probe methods 79−51314
diffusion of P, 900-1150°C, controlled surface conc. condition 77−7746
diffusion of P, dislocations, creation conditions 79−95039
diffusion of P, elastic deform. relax. and dislocation generation 80−79997
diffusion of P, excess vacancy generation by E-centre dissociation 77−72720
diffusion of P from spin-on SiO_2:P film 80−2050
diffusion of Sb, along dislocations, 1165-1320°C 77−15631
diffusion of self-interstitials and As, B and P, radn.-enhanced 80−29216
diffusion of transition elements, anomalous behaviour 80−29044
diffusion profiles, P and B diffusion determ. *(Rumanian)* 79−77615
diffusion through Au films at low temp., Co effect 80−100361
diffusion-induced lattice strain and dislocation obs. by X-ray diffraction *(Japanese)* 77−84753

silicon continued
diffusive mass transfer in closed bromide system 77−44169
digital Sun sensor electrical and optical props. *(Japanese)* 78−32313
diode, Auger recombination coefficient at very high injection rates 78−47863
diode, high dislocation density effect on charact. *(German)* 79−33336
diode, impurity profiles, scanning electron microprobe anal. 80−79832
diode, thermometric charact., 15 to 300K 78−8403
diode, transient switching duration, linear carrier lifetime, emitter efficiency and Auger recomb. coeff. determ. 79−11207
diode radiation detector, stabilisation of radiation damage 80−91377
diode storage correlator optical imaging and memory characteristics 77−23772
diode thermometer, anomalous behaviour, 11 to 16K 79−35738
diodes, temp. and mag. field depends., appl. as thermometers 78−45623
diodes as low temperature sensors *(German)* 80−31744
dip-coated on graphite substrate, photovoltaic effects 80−29442
directional Compton profile meas., structural information 79−28855
dislocation behaviour, low temp. relax. of local stresses, X-ray obs. 79−69110
dislocation centres, exchange-coupled, spin-depend. recomb. 77−89725
dislocation core, electron states, EHT calc. 77−35887
dislocation defect states 79−82549
dislocation density, effect on C-V charact. of MOS struct. *(Russian)* 78−6447
dislocation density of slices determ., using ellipsometer *(Hungarian)* 79−99198
dislocation detection by divergent polychromatic beam method 77−35568
dislocation dipole lattice image, stacking fault energy 79−60375
dislocation dissociation and mobility of partial dislocations 77−68980
dislocation dynamics during plastic deform., stress-strain charact. 79−27996
dislocation dynamics in plastic deform., theoretical anal. 79−42077
dislocation electronic states, Schottky diode meas. 79−82548
dislocation energy spectrum, appl. of EPR and elec. meas. 79−82547
dislocation ensembles motion in neutron irradiated covalent crystals *(Ukrainian)* 80−10579
dislocation etch pits on various cryst. planes 77−24317
dislocation formation, under high stress, low temp. 78−47386
dislocation free, C and O impurity clouds, heat treatment influence on light scatt. 80−6427
dislocation free, O_2 precipitation, stacking fault form. 78−38731
dislocation free crystal growth 79−100030
dislocation generation, influence of film stress and thermal oxidation 79−23609
dislocation generation in local oxidation 80−107245
dislocation growth during laser melting and solidification 80−2022
dislocation images, comparison of SEM and scanning optical obs. 79−51112
dislocation loop, of hexagonal interstitial Frank type, dissoc. 77−35556
dislocation loops, creation in region of interface, after annealing 79−82210
dislocation loops motion, nonconservative model anal. 78−18647
dislocation luminescence obs. 78−15217
dislocation mobility 77−76413
dislocation mobility and mech. behaviour 79−82208
dislocation motion from indentation rosette 80−79798
dislocation motion near surface 79−82219
dislocation multiplication *(German)* 78−38721
dislocation observation by electron channelling imaging in SEM 80−10471
dislocation processes, during high temp. deform., in-situ HVEM obs. in single crysts. 80−103342
dislocation reactions, obs. by X-ray topography 78−75691
dislocation structure, effect of induction heating *(Russian)* 77−21180
dislocation study by high voltage electron microscopy and SEM 79−82217
dislocation velocities as function of electronic doping 77−4117
dislocation velocities meas. 79−82230
dislocation velocity, thermal activation exam. of applied stress and temp. depend., expt. methods *(French)* 80−59474
dislocation-free, deep centres formed after high temp. treatment 80−96824
dislocation-free, O_2 precip., IR and TEM obs. 80−29173
dislocation-free crystal O precipitation obs. 78−6095
dislocation-free Czochralski-grown, detection of microamounts of O *(German)* 78−26592
dislocation-free single crystals, growth microdefects, etching and X-ray expts. 78−47385
dislocation-free single crystals, microdefect type by anomalous X-ray transmission 79−95019
dislocation-induced elec. pots. appl. 79−82551
dislocationless plates, microdefect dissolving due to high temp. annealing *(Russian)* 80−54378
dislocations, associated electron states 79−82544
dislocations, computer simulation methods in X-ray topography 79−23484
dislocations, depth distrib. planar channelling anal. with 2 MeV He backscattering 79−7640
dislocations, dynamic behaviour *(Japanese)* 78−38722
dislocations, EPR meas. 79−82871
dislocations, extended glide, motion obs. by high voltage electron microscopy 80−10555
dislocations, extinction fringes and Burgers vector determ. single-cryst. interferometric techniques 79−95013
dislocations, HVEM struct. images of extended 60° and screw dislocations 80−59466
dislocations, luminesc. spectra *(Russian)* 77−90197
dislocations, noise spectrum 80−107881
dislocations, stacking faults, swirl defects, production and mechanisms *(Chinese)* 79−46684
disorder depth distrib. prod. by N^+ irrad. 79−73227
disorder distribution extraction, semiempirical method of applying dechannelling correction 78−22781
disorder produced by high-dose implantation, channelling meas. 77−11573
disordered, effect of disorder on H content 80−75258
dispersion law of indirect excitons 80−24805
displacement of group III, IV, V, and VI impurities in Si by He^+ and H^+ analysing beam 79−4330
dissociated dislocations, statistics of kink formation 79−82207

silicon continued
dissolution rates in KOH, orientation effects 77−36674
distribution in alloy steel welds, laser emission microanal. method 78−61110
divacancies due to proton irrad., IR absorpt., annealing effects 80−20673
divacancies orientation induced by IR light, EPR spectra 80−25209
divacancy, hyperfine interactions from ENDOR meas. 79−42868
divacancy, positive, EHT calcs. 79−99184
divacancy, positive, extended Huckel theory calc. of hyperfine interactions 77−89742
divacancy, positive, extended Huckel theory calculations 78−87938
divacancy charge states, photoconductivity spectra 77−15899
divancancy photoionisation cross section, photocapacitance meas. 80−6901
donor bound excitons and bound multiexciton complexes 77−40282
donor ground state wave functions 78−87937
donor ion pot., small r behaviour of nonlinear Poisson eqns. 80−54652
donor polarizability, multivalley effective mass calc. 80−96817
dopant distrib. in mono- and polycryst. samples, C-V technique 80−6425
dopant in GaAs, role during VPE 77−40380
dopant segregation by pulsed-laser annealing, test case for thermal melting concept 80−24489
dopant striae, SEM obs. by Schottky barrier charge collection 77−31684
dopant survey for IR detector appl., 2 to 2.7 and 3 to 5 μm 77−15433
doped, basis functions for studying intervalley effects 79−69442
doped, $L_{2,3}$ threshold spectra 77−69934
doped, many-valley semiconductor, effective mass theory of intervalley mixing 77−47763
doped amorphous, transport props., conductivity, thermopower, temp. depend. 79−73512
doped and intrinsic, chemomech. effect 78−64751
doped n- and p-type, thermoreflectance spectra 79−24296
doped polarisability of donors 78−14693
doped semiconductor devices, obs. of carrier densities via IR emission 77−72707
doping, complex, effects on limiting electron conc. 78−22740
doping, interactions between sequential dopant diffusions, review 77−27900
doping, low temp. radiation induced impurity diffusion 77−15439
doping, pyrolytic BN wafer as diffusion source characterisation 78−91352
doping by ion implantation, atomic collision theory and range-energy relations 78−71753
doping by neutron transmutation doping, detect. and identification of potential impurities activated 79−42090
doping by nuclear transmutation 77−84782
doping by thermal neutron irrad., annealing charact. of bulk electron traps obs. 80−49244
doping impurity distrib., during cryst. growth by Czochralski method *(Russian)* 80−100276
doping process, effect of disloc. density *(Hungarian)* 77−62553
doping using SiO_2 diffusion sources solar cell fabrication 78−2148
double polycrystalline VLSI devices, low temp. differential oxidation 80−16521
double-mesa reach-through avalanche photodiode with large gain-bandwidth product 79−12845
double-sided free polishing 78−11380
drop shape on Czochralski grown cryst. surface, dislocation struct. 78−2030
dry etching induced surface contamination, SIMS, AES, and XPS obs. 80−11810
dry pressure-oxidation for low-temp. IC processing 78−7068
ductile-brittle transform. hypothesis and temp. depend. of charge bond *(Russian)* 78−35484
dynamic nuclear polarisation and mag. relax. of ^{29}Si in optically pumped samples 78−48081
dynamic polarisation of ^{29}Si nuclei, impurity centre photoionisation, extrinsic light absorpt. *(Russian)* 79−15378
dynamical recovery and self-diffusion 79−82379
early oxidation stages, AES study *(French)* 79−8379
edge dislocation, crystal surface interception, X-ray diffr. obs. in Bragg case 80−49228
edge dislocation struct., lattice distortion and surrounding vacancy distrib. 77−19954
edge dislocations, energy spectra 80−70637
edge etch process for minimum geometry windows on poly Si surface 78−31550
edge-defined film-fed growth of controlled shape crysts. 78−31327
edge-type dislocations, energy spectrum 80−24842
education, forbidden energy gap meas. in Si and Ge p-n junctions 80−57027
effective mass, transverse, of E_1 and $E_1+\Delta_1$ transitions, rel. to band struct. 77−80725
effective mass from Kramers-Kronig analysis for various doped crysts. 77−31942
effective masses of heavy and light holes, from ohmic mobility data 80−80160
effective potentials, ab initio calc. 77−69222
effective supersystem cryst. simulation method, geometrical parameters, bulk moduli, impurity levels calcs. *(French)* 80−15430
EHT calcs. of energy bands and pressure dependences *(Japanese)* 78−34747
Einstein force constants, harmonic and cubic, calc. 77−47515
elastic constants, third-order 79−51184
elastically bent cryst., intensity of diffracted beams in general case of diffr. 79−50935
elastically bent crystal, with large strain gradient, X-ray diffraction study 80−44073
elasto-optic constants, real and imaginary, direct absorpt. and Raman scatt. meas. 80−97234
electrical and mechanical props., influence of heat treatment on high O conc. cryst. 77−35934
electrical characterisation, review 78−60120
electrical cond. at low temps., γ-ray induced 78−52002
electrical conductivity, inertia of electron heating, expt. and theory 80−65613
electrical conductivity between 500 and 1200°C 77−11923
electrical properties, plastic deform. and annealing temp. depend., dislocation effects *(Russian)* 77−89765

silicon continued
electrical properties of single crystal, dislocation effects *(Rumanian)* 79−73504
electrical props. affected by heat treatment *(Russian)* 78−11352
electrical recomb. behaviour at dislocations 79−82606
electrical resistivity four-point probe meas. error factors, SEM obs. 79−71484
electrical resistivity of crystals after reactor neutron irrad., impurities determ. 80−65563
electrochemical carrier conc. profiling 80−2461
electrodeposited film, appl. in solar cell fabrication 78−76611
electroless codeposition of Si and Ti on Ni superalloy 77−16513
electrolytic buffing using non-abrasive electrolyte *(Japanese)* 77−4862
electron beam, relativistic, channelled, anal. of low-energy bremsstrahlung meas. 77−36304
electron beam annealing, beam voltage effect modeling 80−75275
electron beam annealing of ion implanted layer, computer simulation 80−96569
electron beam evaporated Si films for MIS solar cells 80−93490
electron beam induced current technique appl. to semicond. device characts., review 78−21302
electron beam irrad., {113} faults, nature and origin 80−70258
electron beam irrad. at 31 GeV, polarised photon emission *(Russian)* 80−29811
electron beam irradiation, 2.3 MeV, positron annihilation exam. of radiation defects *(Russian)* 78−34542
electron beam scan annealed, deep levels 80−65481
electron bombardment, absorption of energy 79−14847
electron channel pattern linewidth measurements 80−62805
electron channelling patterns, contrast mechanisms, lattice-defect images, in SEM 79−27884
electron density distribution, 80−49189
electron diffraction, ang. distrib. of electrons, beyond single cryst. 78−1962
electron diffraction axial channelling Kossel patterns, Bloch wave model, obs. 78−42869
electron diffraction Kossel pattern anal. 78−83676
electron diffraction on single-cryst. slabs at 2.27 MeV 79−50962
electron diffraction study, ECP contrast, Bloch wave model 80−96419
electron distribution, forbidden Bragg refl. 77−51265
electron drift in high elec. fields, long-time tail of autocorrelation function 80−103702
electron emission coeffs. for electron and hole traps 79−91075
electron energy loss spectra, direct nonvertical interband transitions 77−85856
electron energy losses, anisotropy of excitation probability 78−15265
electron field emission statistics 77−1791
electron impact ionisation, direction depend. of threshold energy 79−42550
electron inelastic mean free paths and energy losses, electron gas statisitcal model 79−46733
electron inversion layer, minigaps 80−20282
electron irrad., limiting position of Fermi level, elec. cond. and optical absorpt. meas. 79−65484
electron irrad., resistivity-fluence relation 80−54700
electron irrad., rod-shaped defects, electron microscopy and IR spectra obs. 80−39159
electron irrad., two-vacancy defect EPR 80−29619
electron irrad. damage, capacitance meas. 80−24935
electron irrad. induced defects, bulk photo-EMF meas. 80−39160
electron irradiated, EPR of C-O divacancy complex 77−69691
electron irradiated, high resist. surface layer, Schottky barrier meas. 78−64093
electron irradiated, multivacancy-O complexes, EPR expt., correl. with IR absorpt. data 77−28443
electron irradiated, O-vacancy pair, EPR of optical absorption 77−16173
electron irradiated, photolum. due to interstitial complex 77−44048
electron irradiated devices, dominant recomb. centres 77−72912
electron irradiation induced corrosion 77−59960
electron irradiation induced defects, carrier density, mobility and lifetime changes 77−43250
electron irradiation induced defects, thermally stimulated capacitance 77−11933
electron irradiation induced displacement defects 77−80543
electron mean free path, stopping and straggling 78−91367
electron mean free paths and stopping powers calc. using statistical model 77−19996
electron microprobe local anal. of light elements, ultrasoft X-ray spectroscopy 80−99027
electron microscope exam., spatial measurement using images corres. to different reflexes 77−55216
electron microscopic examination, high resolution, images of atoms projected onto (110) plane 79−32866
electron microscopy, single-electron excitations, image contrast from delocalised excitations 79−46529
electron mobilities on inverted surfaces near cond. threshold, appl. of meas. techniques 79−69602
electron mobility anisotropy anomaly in plastically deformed Si with low dislocation density *(Russian)* 77−80777
electron mobility is semiconductors based on dielectric function modification of Dingle pot. 79−60836
electron momentum distribution, anisotropy, positron annihilation *(Russian)* 78−84676
electron optical conditions for struct. image form. in (110) orientation 80−75131
electron recombination, role of intervalley scatt. *(Russian)* 79−19605
electron scattering anisotropy, Hall mobility calcs. 77−24552
electron scattering by atomic planes in single crysts., and band struct., with intrinsic values of transverse energy *(Russian)* 78−39639
electron scattering energy distrib., channelling effect *(Russian)* 78−2183
electron states associated with core region of 60° dislocation 78−39057
electron transmission and absorpt. in bulk solids, 5 to 30 keV 77−89491
electron transmission at 15 MeV 78−83671
electron transport and ionisation at high fields 78−30933
electron trapping, donor state generation, photo I-V study 80−20210
electron traps due to electron irrad. induced divacancies 77−4126
electron-exciton elastic scatt. cross sections, central field and exchange approxs. 77−62919
electron-exciton inelastic collision cross sections 79−90567
silicon continued
electron-hole drop luminescence, hysteresis effect and surface energy 78−2907
electron-hole drop transition to metallic condensed state, Hartree-Fock theory 79−56136
electron-hole droplet, effect of nonlocal contributions to energy 77−69246
electron-hole droplet condensation, crit. point 80−49612
electron-hole droplet condensation, phase diagram and surface tension 79−19521
electron-hole droplet condensation model, phase diagram and surface tension 80−6734
electron-hole droplet luminesc., laser excitation threshold meas. 79−33821
electron-hole droplet spatial distrib., luminesc. obs. 80−49615
electron-hole droplets, large uniaxial stress 78−47703
electron-hole droplets, nonequilib. orientation of electrons in mag. field *(Russian)* 77−36294
electron-hole droplets nucleation at swirl defects 79−15095
electron-hole drops, Auger recomb. 77−48240
electron-hole drops, Auger recomb. 78−39600
electron-hole drops, far IR absorpt. spectrum 78−47706
electron-hole drops, near and far IR emission spectra 77−48242
electron-hole drops, nonequilib. paramagnetism 80−6749
electron-hole drops, nucleation, luminesc. threshold obs. 79−33822
electron-hole drops, nucleation, time resolved luminesc. spectroscopy 78−6280
electron-hole drops, surface struct. 78−60058
electron-hole drops, thermodynamical parameter determ. from luminescence data 80−2845
electron-hole drops formation, nucleation theories 79−33239
electron-hole drops radius, luminesc. meas. 80−50415
electron-hole liquid, free excitons, biexciton gas, luminesc. 80−6750
electron-hole liquid, RPA calcs. 80−6743
electron-hole liquid, spatial condensation of strain-confined excitons and excitonic mols. 78−39592
electron-hole liquid and exciton and biexciton gas in elastically deformed cryst. *(Russian)* 78−34782
electron-hole liquid theory, generalised RPA 78−87914
electron-hole nonequilibrium system, gas-liq. phase diagram *(Russian)* 77−43509
electron-irradiated, {113} loops obs. 79−82225
electron-irradiated, annihilation of positrons 77−55847
electron-irradiated, positron annihilation 78−48256
electron-phonon interaction, internal strain and impurity elec. field effect 78−14418
electron-phonon interaction anal. using photoacoustic cell 78−68027
electronic and optic props. 78−39013
electronic and struct. props., nonlocal pseudopot. calc. 80−34349
electronic defect levels in self-implanted CW laser annealed samples 79−87053
electronic energy bands of diamond-type crysts., appl. of EHT method 78−87907
electronic energy levels strain depend., pseudopot. method 77−39775
electronic interface states in intrinsic stacking-faults 80−75522
electronic properties, rel. to chem. bonding and lattice dynamics 80−44169
electronic properties, temp. depend. *(German)* 77−76822
electronic screening of lattice vibrs. 78−59875
electronic states associated with 60° edge dislocation 77−20261
electronic states of isolated negative donor ion, binding energy 79−65404
electronic struct. from SCF calc. using intersecting spheres model 78−51888
electronic structure, ab initio self consistent calcs., charge density and band struct., Wannier function scheme 79−69409
electronic structure, non-spherical local pseudopotential calcs. 80−39496
electronic structure, self consistent local description 80−20067
electronic structure, with non-spherical pots. for two basis atoms 78−72069
electronic structure at high press. near semicond.-metal transition 80−49586
electronic structure of surface (111), atomic geometry effects, photoemission and electron energy loss spectra 77−85283
electronic vacancy states by chemical pseudopot. method 79−23929
electrophysical props. of single crysts. with and without dislocations 77−47812
electroreflectance, dielec. function, ellipsometric meas. 79−4790
electroreflectance, low-field, symmetry analysis of E_2 structs. 77−40209
electroreflectance and thermoreflectance spectra, line-shape anal. 79−24296
electroreflectance spectra, polarisation dependent, surface phenomena 78−68479
electroreflection exam., short range order in surface layers 78−6703
electrotransfer, in Mo_5Si_3 80−92708
EMF appearance under action of thermal field pulses with high temp. gradients 79−56252
emission spectra, excitons bound to isoelectronic trap 79−33772
emission spectra of ultrarelativistic collimated positrons 80−7434
emitter for field desorpt. mass spectrometry 79−79323
ENDOR, hyperfine interaction of divacancies 77−4579
energy band gap dilation and vibr. contrib. determ. 79−60703
energy bands and wavefunctions, localised orbital description 78−18942
energy deposition in heavy-ion path using Monte Carlo transport anal. of delta rays in track 80−39185
energy gap, impurity conc. depend., calc. 80−80170
energy gap of intrinsic Si, temp. depend. as thermodynamic problem *(German)* 77−43488
energy loss and multiple scattering of non-channelled α-particles *(German)* 80−59544
energy loss of 120 keV heavy ions, range and range straggling determ. 79−45595
energy losses on C contaminated surfaces, secondary electron spectra, AES, and SEM 79−99997
energy spectrum of Fe group impurities 79−23932
energy spikes due to heavy ion bombardment, semiempirical model 78−47453
enhanced conductivity in plasma hydrogenated films, thermionic emission 80−70692
entropy of fusion anomalies, deviation from Richard's rule 77−47601
epitaxial, elec. activity of stacking faults, determ. using SEM and EBIC mode 77−43445

silicon continued
epitaxial, minority carrier lifetime and impurity conc. meas. *(Japanese)* 80−25025
epitaxial, on sapphire, characterisation, X-ray rocking curves 80−75458
epitaxial, on Si or sapphire, misfit, strain and dislocations, book contrib. 79−82499
epitaxial, optical constants meas. by far IR ellipsometry 78−93753
epitaxial (111) surface, etching observation of stacking faults, dislocations, S-pits, etch pits *(Chinese)* 80−70197
epitaxial crystal, facing and shape meas. following local epitaxial accretion 77−4270
epitaxial deposition from $SiCl_4$, selectivity 77−24958
epitaxial detector fabrication, crystal growth and preferential etching 78−37505
epitaxial film, containing struct. defects formed during growth, positron annihilation 80−93433
epitaxial film, correlation between electrooptical and electrical props., IR absorpt. spectra *(Russian)* 78−60453
epitaxial film, dopant incorporation during growth, theory and expt. 79−99229
epitaxial film, dopant incorporation model 79−99228
epitaxial film, electrical activity of stacking faults 77−39744
epitaxial film, ionised-cluster-beam deposited, cryst. and elec. charact. 80−70553
epitaxial film, kinetics of doping, gas-phase decomposition of SiH_4 77−16499
epitaxial film, struct. defects, effects on planar diffused p-n junction elec. props. *(Russian)* 78−60195
epitaxial film concentrated inhomogeneity detection by selective etching *(Russian)* 78−10298
epitaxial film CVD growth, inelastic light scatt. as in situ probe of chem. reaction 77−40383
epitaxial film deposition, vapour-phase, small-scale system design and operation 79−43151
epitaxial film dopant incorporation, transient response 77−76976
epitaxial film growth and p-n junction formation by Si beam epitaxy in high vacuum 80−16187
epitaxial film growth by hydride-iodide method 77−48343
epitaxial film growth on sapphire in SiH_4-H_2 system, optimum deposition 77−77397
epitaxial film growth on Si(111) and sapphire ($1\bar{1}02$), simultaneous RHEED/AES study 80−10833
epitaxial film on sapphire, microtwins, TEM exam. 80−70555
epitaxial film on sapphire, optical absorption and interface comp. profiles 77−12459
epitaxial film on sapphire, stacking faults and twins, TEM obs. at early stage of epitaxy 79−28233
epitaxial films on Czochralski sapphire, optimisation of deposition conditions in SiH_4-H_2 system 80−75464
epitaxial growth, adsorbed layer model for autodoping mech. 80−7505
epitaxial growth, in $SiCl_4$-HCl-H_2 system, model based on flow graph 79−42405
epitaxial growth, mechanism, impurities incorporation kinetics *(French)* 78−22749
epitaxial growth, novel reactor for high volume, low cost prod. 79−24442
epitaxial growth, nucleation 77−62770
epitaxial growth, of submicrometer thickness 79−95932
epitaxial growth, solid-phase, in Si(crystal)-Pd_2Si-Si(amorphous) system, growth stages 77−85114
epitaxial growth by partially ionized vapour deposition, low temp. 77−40389
epitaxial growth chambers cleaning, improved method using KOH solution 78−64478
epitaxial growth from vapour, dopant inclusion model *(German)* 79−42088
epitaxial growth in Si-P-H system, depend. of doping element incorporation on temp. in CVD 80−45234
epitaxial growth kinetics, experimental verification of theoretical model 79−95278
epitaxial growth kinetics in damp H_2 77−44171
epitaxial growth of amorphous layer 80−10803
epitaxial growth on ion-implanted Si:As 78−6243
epitaxial growth on porous Si layer, struct. 79−1557
epitaxial growth on sapphire by partially ionised vapour deposition, RHEED-AES obs. 80−80985
epitaxial growth via SiH_2Cl_2 in barrel reactor 78−52685
epitaxial interface migration, theory and expt. test 80−29290
epitaxial layer, CVD, stacking fault nucleation and growth 78−10064
epitaxial layer, growth mechanism from ion-molecular beams 80−2299
epitaxial layer, incorporation conc. depend. of P from silane-phosphine-H_2 mixture 80−2053
epitaxial layer, large-area uniform growth through Al film by solid epitaxy 78−3033
epitaxial layer, minority carrier lifetime and diffusion length meas., photocurrent technique 78−95302
epitaxial layer, minority carrier lifetime obs. *(Russian)* 80−49765
epitaxial layer, on sapphire, twin three dimens. distrib. 77−89666
epitaxial layer, on Si ribbon substrate, dislocation density, X-ray topography obs. 77−85102
epitaxial layer CVD, appl. to Si, II-VI and III-V semiconductor growth 77−32530
epitaxial layer deposition by ion beam methods 80−100417
epitaxial layer grown by saturated Sn melt undercooling, morphology 78−22969
epitaxial layer growth in vacuum, Ar, Xe ion bombardment effect 80−39463
epitaxial layer on sapphire, shear strain, TEM 78−51835
epitaxial layer regrowth due to laser annealing mechanism, liquid and solid phase regimes 80−100712
epitaxial layer substrate junctions, carrier lifetime and abnormal conduction phenomena *(Korean)* 78−47888
epitaxial layer thickness meas. using phase correction function of substrate resistivity *(Rumanian)* 80−90812
epitaxial layers, anomalies of Sb distrib. 80−65035
epitaxial layers, cryst. quality improvement by ion implantation, backscatt. and TEM obs. 79−42397
epitaxial layers, development, structure and props. of stacking faults *(Russian)* 80−24461
epitaxial layers, doping with P cpds., process parameters effect on electrophys. characts. 78−38734
silicon continued
epitaxial layers, grown by sublimation in vacuum TEM study of surface 79−46982
epitaxial layers, grown in vac. at low temps. P and Sb doping 80−88189
epitaxial layers, homogeneous, production, appl. of neutron transmutation 78−38737
epitaxial layers, meas. of doping profiles *(Hungarian)* 80−70545
epitaxial layers, solid phase grown, structural obs. 78−2397
epitaxial layers, stacking defect distrib. anal. using ion channelling tech. 80−100294
epitaxial layers, temp. dependence of P dopant inclusion in gas phase deposition *(German)* 79−52127
epitaxial layers, thickness and optical consts. meas. using IR laser ellipsometer 78−62219
epitaxial layers, thickness meas. during deposition using diffraction *(German)* 79−97355
epitaxial layers, vacuum deposited, conditions for impurity migration from B, P, Sb doped sources *(Russian)* 80−107570
epitaxial layers, X-ray topographic study using Berg-Barrett techniques 79−28221
epitaxial layers on metallurgical-grade polycrysts. substrates, characteris. 79−28967
epitaxial layers on ribbon substrate, solar cell prod. and characterisation 77−77354
epitaxial p-i-n photoconvertor characteristic deterioration at high illumination 78−89536
epitaxial photoconvertors, p-n and p-i-n structures, props. 77−51807
epitaxial reactor, doping system, transient steady state response, transfer function approach 79−42086
epitaxial regrowth and grain struct. of Al metallisation on ⟨100⟩Si 78−79901
epitaxial regrowth of thin amorphised layers by laser annealing, absorpt. coeff. influence 79−46968
epitaxial solar cell substrate prep., low-cost, unidirectional solidification process 80−93924
epitaxial solid-phase growth, rapid 77−21022
epitaxial stacking fault nucleation site identification, annihilation, and suppression 77−76705
epitaxial stacking faults, nucleation sites 77−20201
epitaxial structures, junction layer width and impurity conc. estimates *(Russian)* 80−49893
epitaxial thin film growth on sapphire and spinel by MBE 80−76186
epitaxial wafer, impurity profile meas. by multilayer spreading resist. anal. 77−76449
epitaxial wafer, saucer pit microdefects reduction by intrinsic gettering 80−75450
epitaxial wafers, role of metallic contamination in formation of 'saucer' pit defects 77−39588
epitaxially grown on sapphire substrates, Al conc. as a function of depth using $^{27}Al(p,\alpha_0)$ reson. reaction 79−4328
epitaxy, autodoping effects 80−100259
epitaxy, low pressure multi-wafer growth system 79−43153
epitaxy and oxidation, first-order process models 78−72049
epitaxy by solid phase crystn. of amorphous film 78−19663
epitaxy in high vac., stacking fault nucleation, crit. temp., for SiC growth 78−14620
epitaxy lateral autodoping kinetics 78−6087
epitaxy on sapphire, cryst. perfection rel. to MOS transistor mobility 78−75956
epitaxy technology, application to Si devices, deposition techniques 80−7501
EPR and cyclotron resonance of laser annealed Si 80−34773
EPR and spin-lattice relax. of dislocation spin chains *(Russian)* 79−91291
EPR of quenched-in defects 80−29620
EPR of radiation damage due to complete stopping of 30 MeV protons 77−65994
EPR of radiation defects, temp. depend. 78−15023
EPR of thermally induced defect 77−81005
EPR study of annealing characts. for irrad. Si 78−10771
equation of state, under press. 78−75801
etch rate uniformity in CF_4+4% O_2 plasma 80−40568
etching, anomalous etch structures using ethylenediamine-pyrocatechol-water based etchants and their elimination 80−81217
etching, gas phase, model 79−96165
etching, HF ion-plasma, cryst. surface layers treatment and study *(Russian)* 80−16517
etching, of Si monocryst., by Br, Ar laser beam initiation *(Russian)* 77−73358
etching by CF_4, plasma deposition reactor gas phase characts., mass spectra 80−70566
etching by CF_4 plasma, mechanisms 78−72907
etching by tetrafluoromethane plasma, mechanism 79−15832
etching characts. using reactive ion etching with tetrafluoromethane-Cl_2 gas mixture 80−104313
etching in fluorocarbon glow discharge, chemical aspects 79−86631
etching in He-F_2 plasma, etch rates, mass spectra, direct ion sampling study 80−79510
etching in reactive plasmas 80−71778
etching using XeF_2 vapour, adsorption/desorption process 79−43449
etching with CF_4 in diode system 79−61759
EUV beam foil spectra, highly resolved, fine struct. splittings 79−31448
exchange and correlation pot., band struct. calc. 78−56068
exciton and deformation pot. fine struct. 78−88301
exciton emission, phonon-assisted, temp. depend. of relative integrated intensities 77−1375
exciton ground state splitting 80−6736
exciton lifetime, temp. depend., photoluminesc. meas. in high-purity Si 80−44508
exciton luminescence in mag. field or under uniaxial stress 78−27322
exciton mol. by phonon-assisted two-photon absorpt., theory 78−48197
exciton-dopant bound states, Auger lifetimes 78−18970
exciton-impurity complexes, emission spectra, Zeeman splitting *(Russian)* 78−64413
exciton-plasma Mott transition, luminescence spectra 77−62836
exciton-plasma transitions, dense electron-hole system portrait composition *(Russian)* 80−49622
excitonic molecules, thermodynamics, luminesc. 80−25442
excitons, 1s, splitting, derivative spectra of optical absorption 77−69249
excitons, far IR absorption 78−31201

silicon continued
excitons and electron-hole drops, phonon assisted luminescence lineshape 79−99942
excitons and electron-hole liquid, luminesc. 80−6746
excitons bound to acceptors, Auger transition rates 78−34778
extrinsic IR detectors, As doped, low-level γ-ray irrad. effects 80−37085
extrinsic IR monolithic focal plane array detectors, I-V characts. of p^+-p-p^+ and n^+-p-p^+ structs. 80−77863
extrinsic photoconductive IR detectors, VLF behaviour 78−81542
extrinsic stacking faults, core struct., TEM obs. 78−55878
f-type, degenerate, Raman effect, interacting elementary excitations 78−43846
Fabry-Perot couplers for optically pumped far IR lasers 80−69404
Fano factor for protons 79−36480
far IR complex refr. index spectra determ., new method, for transparent solids 77−28566
far IR impurity spectra, effects of high uniaxial stress 78−56508
Faraday rotation and ellipticity, interband transitions, comparison with Ge 77−52048
fast electron channelling, quantum-mechanical approx. 78−87731
fast electron planar channelling in single cryst. 78−2178
fast particle irrad., Frenkel defect formation threshold energy 80−6404
Fermi level, minority carrier conc., effective intrinsic conc., Einstein relation in n- and p-type 77−85209
ferromagnetism induced by ion irrad., e.p.r. investig. *(Russian)* 77−1595
fibre growth and struct. 79−69970
field effect characts. rel. to surface inhomogeneity 78−26933
field emission photocathodes, emission current noise characts. 80−100746
field evaporation, anomalous 79−15596
field penetration in FIM, band bending 79−87567
filamentary, grown by chem. transport reaction method, banded struct. 80−38978
filamentary crystals, branching and bending obs. 77−7954
filamentary crystals, grown from vapour, electron probe microanal. 79−77538
filamentary piezoresistor for pulsed wave process meas. 78−57980
film, (001), on sapphire galvanomag. effect for holes and valence band 79−91166
film, amorphous, crystn. on annealing at low temps. in contact with Al 80−24765
film, amorphous, effects of annealing of gap states 78−72115
film, amorphous, formed by CVD, crystallisation 77−39746
film, amorphous, optical absorption at high press. 78−35216
film, amorphous, oxidised, vacuum deposited, cond. change due to electron irrad. 78−10089
film, amorphous, plasma-deposited, H_2 evolution, mass spectrometry and RHEED obs. 78−72050
film, amorphous, prep. conditions influence on supernetwork struct. 77−76709
film, amorphous, saturation meas. on ESR signals 79−33535
film, amorphous, structural comparison of evaporated and glow discharge samples 77−62778
film, amorphous, two-dimensional variable range hopping cond. 80−10977
film, amorphous and crystalline, optical properties 77−24906
film, amorphous and polycrystallised, localised states, elec. and optical props. 78−64008
film, amorphous evap., structural aspects in electronic data interpret. 77−76977
film, chemically deposited on amorphous SiO_2, influence of substrate temp. and SiH_4 to N ratio on struct. 79−65346
film, critical surface tension, aligning props. of nematic MBBA mols. 79−90846
film, crystallographic orientation using surface relief grating and laser crystn. 79−95277
film, CVD, amorphous and polycryst., microscopic surface roughness, effective-medium models, ellipsometric expts. 80−24756
film, CVD, low press., struct. and stability, X-ray diffr. and TEM obs. 78−91559
film, CVD or evaporated, covered with Al layer, solid-phase crystn. obs. 77−85100
film, elec. props., effect of amorphous to polycryst. transition 79−28425
film, electron beam evaporation, for solar cell appl., heat exchanges and columnar growth 79−15609
film, electron-beam-deposited on W substrates, growth and struct., AES and SEM obs. 79−46972
film, electroreflectance spectra, 2.8 to 5.0 eV, ion bombard. effects 77−1752
film, epitaxial growth by partially ionised vapour deposition, RHEED-AES-QMS study 79−83136
film, epitaxial growth from noncondensed phases, kinetic anal. 80−54565
film, epitaxial growth on Si, impurities, plasmon energy loss anal. 77−31916
film, evaporated amorphous, hydrogenation by plasma treatment 78−91555
film, focused ion beam designs for sputter deposition 79−89841
film, glow discharge deposition, SiH_4 discharge parameters obs. 80−44030
film, grown on Al from eutectic melt following ion plating 77−8765
film, growth on SiO_2 substrate by pyrolysis of SiH_4 77−89678
film, high electron mobility, grown on sapphire at high growth rate 77−81225
film, ion bombarded, crystalline-to-amorphous transition, defect-rich film prep. 80−65071
film, low press. CVD prep., struct., elec. and optical props. 80−70548
film, low press. CVD techniques, IC fabrication process anal. 79−100058
film, MBE, cryst. defect props., substrate treatment effects 80−70551
film, on Al_2O_3, quantitative electron microprobe analysis 77−9150
film, on graphite, early growth by ion-beam sputtering 77−44158
film, on sapphire, defect struct., TEM obs. 77−47693
film, on sapphire, etching method 78−7070
film, on sapphire, Hall mobility, carrier distrib. effects 77−51818
film, on sapphire, laser annealing dynamics epitaxial regrowth, optical reflectivity 80−29285
film, on W (100), struct. and work function, LEED meas. 77−66096
film, optical characterisation from guided wave optics 78−48245
film, plasma etching, role of chemisorpt. of CF_4, CF_3H, CF_3Cl, CF_2Cl_2 and CCl_4 79−11714
silicon continued
film, polariton resonance obs. from reflectivity meas. 77−69251
film, polycryst., electron microscopic investigation of initial stage of growth 79−23849
film, polycryst., for photovoltaic appl., grain size effects 78−72034
film, polycryst., grain struct. and surface roughness, TEM study 80−70556
film, polycryst., ion-implanted, pulsed laser annealing 79−77612
film, polycryst., laser-induced CVD growth from $SiCl_4$ 80−84852
film, polycryst., meas. with ellipsometrical methods *(Polish)* 78−21095
film, polycryst., substruct. 79−23848
film, polycryst., thinning using plasma etching *(Slovak)* 80−45405
film, polycrystalline, annealing of paramag. vacancy-type defects, EPR obs. 79−10848
film, polycrystalline, glow discharge deposited below 250°C, struct. and morphology 80−49535
film, polycrystalline, low press. CVD, resist. meas. 80−2494
film, polycrystalline, struct. thickness relationships 77−62779
film, porous, form. and oxidation by anodic reaction 79−28966
film, prep. by plasma-induced CVD from $SiCl_4$-H_2 79−83132
film, removal using anodic oxidation, determination of active impurity distrib. 80−40583
film, selective etchant defect density distrib. profile 79−86793
film, semi-insulating, with 40 at.% O, AES and PES study 80−107939
film, single-layer, 2.8 μm and 3.8 μm absorpt. meas. 78−90463
film, solid phase epitaxy, Au and O distrib. 77−66095
film, solid-phase-epitaxial, deposited above 380°C, defects obs. 78−63942
film, sputtered, physical props. 79−77938
film, sputtered amorphous, P and B doped, elec. cond. and thermopower meas. *(French)* 78−47403
film, transport props. 79−24089
film, volume plasmons, EELS, line shape 79−90984
film and p-n junction growth by ionised-cluster beam deposition 77−32527
film deposition, growth kinetics under low H_2 press. 78−56586
film deposition, on quartz and MgO substrates, using double cathode sputtering system *(Japanese)* 77−55889
film deposition by CO_2 laser irrad. of SiH_4 80−16190
film doping during deposition and with diffusion 78−6088
film growth, epitaxial and amorphous, low energy ion beam deposition 77−28729
film on Al-Cu, ellipsometric meas. technique, comparison to X-ray fluoresc. anal. 78−51840
film on Fe foil, EM excitation of sound, Mossbauer study *(Russian)* 79−99795
film on sapphire, deposition kinetics and interface characteris. 79−28234
film on sapphire, early growth, models 77−24962
film on sapphire, early growth, TEM 77−24961
film on sapphire, electron mobility 78−91792
film on sapphire, quality evaluation using soft X-ray rocking curve 77−80711
film on sapphire, residual strain effect on elec. props. *(Japanese)* 80−84522
film on sapphire, stress-relieved regrowth by laser annealing 80−65389
film thickness meas. from visible refl. spectra 79−99960
films, amorphous, hopping conduction, dangling bond generation by high temp. annealing 80−60115
films, electron beam deposited, elec. and struct. props. 79−1632
films, polycrystalline elec. props., grain size and dopant conc. influence 80−29492
films, polycrystn., texture formation study 79−87662
films, RF sputtered, Ar conc. as function of operation frequency and discharge pressure 80−65393
films, ribbon-against-drop, physical and chemical characterisation 80−92798
films on Si substrate, stress meas., X-ray topography technique 78−5710
fine pattern etching by RF sputtering *(Japanese)* 77−70196
fine structure of lowest exciton state *(Russian)* 80−96801
fission fragment irradiated, carrier removal rate, spreading resist. meas. 77−51418
float zone, meas. of deep levels by photovoltage spectroscopy 80−103723
float zone, process-induced effects on carrier lifetime and defects 80−81216
float zone crystal, dislocation creation and elimination 80−107072
float zone crystal growth, growth parameters for large diameter crysts. 78−31336
float zone growth, maximum stable zone length 79−91582
float zoning, shape stability of solidifying crysts. 77−47362
float-zone growth, shape of melt interfaces and radial P distrib. 77−24952
floating zone growth limitations in using KHz radio frequencies 79−19989
floating zone melting, forced and free convection, computer simulation 78−88423
floating zone melting, forced convection, computer simulation 78−88422
floating zone structural perfection changes by high temp. treatment, dendrites, dislocation interactions 80−29049
floating-zone method crystals, temp. distrib. anal. 79−74082
fluorocarbon ion beam etching characts. 80−35363
foil, computer simulation of high resolution images of defects 80−107208
foil, thinning for electron microscopy 79−49217
forbidden 200 diffr. spots 78−47214
foreign interstitial atoms rel. to thermal intrinsic defects 80−29018
formation of Al-SiO_2 film-substrate interface 78−91571
Fourier transform interferometry, visible reflectivity spectra 77−33765
fracture, of single crysts., under several liq. environments 80−81157
fracture by painted indenter, on near (111) surface 80−71734
free carrier and interband absorpt. at 1.06 μm, temp. depend. 80−2783
free exciton luminesc. band, resolved splitting 79−73995
free excitons, drift and diffusion, luminesc. obs. 80−84434
free-carrier holograms recording by ultrashort pulses *(Russian)* 77−14680
fused, SiC cryst. growth from soln., temp. gradient method in Tb vapour 78−35301
n-GaAs:Cr(Si), deep-level extrinsic photocond. response, decay at 4.2K 80−2420
GaAs, back-wall Schottky barrier solar cell with interfacial layer 77−62993

silicon continued
galactic cosmic rays, Ne, Mg and Si isotopes high resolution meas. 80−51631
galvanomagnetic effect for hot electrons 77−32028
gamma radiation angular distribution of channelled 900 MeV electrons *(Russian)* 80−19858
gas-sensitive microtransducer, cond. variation with pulsed ethanol adsorption *(Russian)* 80−50915
gate controlled surface doped channels, quantum galvanomagnetic effects 78−64134
gettering by ion damage, minority carrier lifetime and backscatt. study 80−100286
gettering effects, of P ions and P induced dislocations for Au impurities 78−91346
gettering effects *(Japanese)* 79−83356
glide-set 90° and 30° partial dislocations, core struct. 80−96523
glow discharge deposited, optical spectra, reflectance, dielectric function and oscillator strength 80−11492
glow discharge film decomposed from silane, on amorphous substrate, elec. cond., RHEED study 80−20044
graded index films appl. to solar absorbers 77−62042
grain boundaries, high resolution TEM 80−103364
grain boundaries, TEM obs. 80−15118
grain boundary elec. props./impurity correl. using surface anal. of multi-grained samples by SIMS and AES 80−79816
graphite-Si powder mixture, reaction hot pressing 78−60592
graphoepitaxy on fused SiO_2 using surface micropatterns and laser crystn. 80−70554
gray Fe, Mg-bearing, reverse liquation, eutectic grain determ. 79−15886
ground state props. in density-functional pseudopot. approach 80−92803
growth, crucible-free, zone melting in combined heating system 78−3031
growth, dislocation-free crystal point defect condensation 78−6026
growth, from melt on ceramic, for solar cell appl. 79−11511
growth, temp. field, stresses rel. to dislocation density *(German)* 77−51335
growth and characterisation of polycrystalline ingots from metallurgical grade source material 79−87576
growth and etching vectors, adsorption and step reconstruction 79−23548
growth and melting processes, origin of swirl defects 77−76407
growth conditions rel. to cryst. struct. perfection *(Russian)* 80−38971
growth from melt, temp. distrib. calc. in working zone of composite heater 78−3016
growth kinetics of low-temperature SiO_2 films by oxidation of SiH_4 77−8763
growth mechanisms of single crysts. with and without dislocations 77−89395
growth of Ag on Si(111), cohesive energy and 2-dimens. phase diagram, AES exam. 78−43246
growth of sheet Si, coating with inverted meniscus (SCIM) technique, solar cell appl. 80−89163
growth of single crystal sheets from melt requiring no slicing or polishing 79−74079
growth of strips by Stepanov's method 79−78867
Gruneisen coeff. from stress-induced phonon energy meas., inelastic neutron scatt. 79−82298
Gruneisen constant, temp. depend. 77−72667
guided-wave acousto-optical devices 80−102864
half wavelength and stopping power of planar channelled protons 80−65087
Hall effect, influence of dislocations 79−82611
heat treated, minority carrier lifetime, effect of swirl defects 77−39868
heat treated, spin-depend. recomb. at dislocations 79−47122
heavily damaged ion implanted (100) and (111), development of secondary defects 79−51166
heavily doped, approx. of Einstein relation, carrier diffusivity to mobility ratio 79−65494
heavily doped, bandgap narrowing and diffusion length meas. 79−7781
heavily doped, carrier diffusion coeff. 79−47099
heavily doped, carrier mobility calc., 300K 79−56215
heavily doped, carrier recomb. through shallow donor and acceptor states 80−15535
heavily doped, charcts. of distrib. of density of states 79−15072
heavily doped, doping density striation effects in studies of metal-nonmetal transition 79−28383
heavily doped, electronic effects on dislocation velocities 77−62531
heavily doped, electronic effects on dislocation velocity 77−62532
heavily doped, energy gap 77−43489
heavily doped, excess intrinsic carrier density, deionisation of impurities as explanation 80−96864
heavily doped, intraband Raman scatt. by free carriers 78−19483
heavily doped, microcreep breakdown 80−97549
heavily doped, minority carrier injection, model 77−39874
heavily doped, minority-carrier transport parameters meas. 80−80291
heavily doped, negative magnetoresistance model, spin-up spin-down electron effective mass variations 79−95423
heavily doped films, electromigration obs. 80−65295
heavily doped implantation layers, laser beam annealing 78−88481
heavily doped layer, electronic charcts., electron beam induced current obs. 78−10473
heavily implanted, lattice defects and strains after high temp. annealing 78−10077
heavy ion ranges, 120 keV Pb ions backscatt. obs. 80−19855
HEED, Bloch functions rel. to at. or mol. orbitals 78−83662
HEED, virtual inelastic scattering estimated 78−26390
heteroepitaxial, prep. and props., book contrib. 79−83128
heteroepitaxial early growth island morphology rel. to deposition conditions 78−6245
heteroepitaxial film, evaporated, deep defect states obs. 78−72292
heteroepitaxial films, photomagnetoelectric effect 77−85264
heteroepitaxial films on sapphire, vac. deposited, struct. and elec. props. 80−15390
heteroepitaxial growth using SiH_4 in H_2-He atm. 80−20049
heteroepitaxial growth using SiH_4 in He-H_2 atm. 77−77396
heteroepitaxial vacuum deposited films, doping *(German)* 77−84779
heteroepitaxy, refractory oxides as substrates *(French)* 77−44181
heterogeneities meas. *(Japanese)* 77−35549
hexagonal form existence in Si_3N_4 77−1112
HF field effect meas. 77−55556
high field electron transport, effect of ionised impurities 77−28186

silicon continued
high press. appl. by spherical diamond indentor, plastic deform. obs. method 78−35619
high resistivity, local IR refraction and transmission 79−15429
high resistivity, specific resistance depend. determ. using impedance freq. depend. *(Czech)* 80−15536
high-pressure oxidation process *(Japanese)* 79−29249
high-purity, preparation by H_2 reduction of trichlorosilane *(Korean)* 77−21034
high-resistance, contactless method of meas. resistivity 77−90518
high-resistivity, characterisation by Hall meas. 78−10480
high-resistivity layer form. during electron irrad. 80−80352
high-resistivity structure, photoelec. props. 78−91730
hole diffusivity, time-of-flight and noise meas. 79−56233
hole localisation, solid solubility, excitonic Auger lifetime of acceptors 80−20216
hole mobility temp. depend., valence bandstruct. 77−80771
hole-hole-electron Auger recombination 80−70720
hologram recording time and diffraction efficiency *(Russian)* 77−58286
homoepitaxy, local selective, at reduced temp. using Si-I transport system 79−24444
homogeneous plates, theory of arising longitudinal photoeffect *(Russian)* 79−19614
horizontal epitaxial reactor transport expt. and model 77−77399
horizontal ribbon growth from melt, theoretical anal. 78−75604
hot electron diffusivity, theory 77−62940
hot electron distrib. function, response to step changes in elec. field 80−24937
hot electron repopulation at 77K, electron-electron scatt. effect 78−10456
hot exciton dissociation by long-wavelength acoustic phonons, photocond. spectra 77−4300
hot hole diffusion and white noise, microscopic Monte Carlo model 78−30937
hot holes, drift and diffusion 79−78110
hot holes negative Hall effect 79−87118
hot-electron diffusion, Boltzmann eqn. 77−51757
hydrogenated, amorphous, theoretical calc. of defect states 80−49657
hydrogenated, discharge produced amorphous film, gap state role in carrier transport 79−73608
hydrogenated amorphous, gap states, comparison of photoemission and photocond. results 80−103724
hydrogenated amorphous, laser annealing 80−100713
hydrogenation of a-Si using DC and HF plasma treatment 80−59497
hyperfine interactions from β-ray spectra of recoil nuclei polarised by fast polarised beams 77−28502
hyperpure, large scale prod. and prep. *(German)* 78−95704
I-V impurity profiling under Schottky barrier 78−19148
ideal vacancy, self consistent Green's function calc. 78−91640
IGFET, velocity-field curves for surface-free carrier in Si 80−60095
immersible Si Li-drift alpha- and beta-radiation detector, fabrication 77−65386
impact ionisation, threshold energies calcs. for electrons and holes 77−62933
imperfections, influence on microplasma formation in p-n junctions 77−8177
implantation, microstruct. fabrication, ion channelling effects 80−70230
implantation damage for low-energy heavy-ion bombard., spike effects 77−59055
implantation induced strains, X-ray interferometry and topography 78−43039
implantation of Pb, channelling and RHEED anals. 78−30657
implantation of Si, Al, Hf, Ta into InP and GaAs, form. of protective oxide 78−79622
implantation on Cr-Ni Nb stabilized austenitic stainless steel surface, effect on oxidation behaviour 80−71791
implantation profile for As, calc. comparison with expt. 78−38748
implanted, annealed layers, amorphised structure formation mechanism and crystallographic nature 80−29091
implanted, standard for TEM, EELS 80−99017
implanted ^{16}O, lattice location of ^{16}O by α-particle backscatt. method 78−10080
implanted ^{222}Rn TIPAC measurements 78−43732
implanted amorphous, comparison of laser and thermal annealing 79−70084
implanted and annealed, effect of twins on dechannelling charged particle beam 79−4315
implanted Bi distrib., planar oscills. effects, low angle He^+ backscatt. obs. 78−34534
implanted crystal, laser induced annealing and diffusion behaviour 80−88202
implanted ion detection by X-ray emission anal. in TEM 78−51575
implanted layers, interaction of defects and impurities stimulated by induced ionisation, ESR 80−11270
implanted layers, utilisation coefficient of impurities after laser annealing 77−76437
implanted Li atoms, depth profiles and sputtering anal. by optical spectra 77−35579
implanted Ne, depth profiling using $^{20}Ne(p,\gamma)$ 79−7621
implanted semiconductors, laser annealing, review 80−107301
implanted with low solubility dopants, laser annealing, TEM study 80−70233
impurities displacement by H^+ or He^+ irrad. 79−86824
impurities of O, N, C, trace anal. by proton activation *(Chinese)* 80−81403
impurities rel. to lattice parameters, dislocation density, stresses *(German)* 77−51403
impurity anal. by photoelectric spectroscopy, review 77−24584
impurity at glass-metal seal interface, composition and conc. determ. by AES 80−76587
impurity concentrations, correlation with photolum. spectra 78−23513
impurity content characterisation, exciton luminesc. 80−60653
impurity determ. in very pure sample by photoelectron spectroscopy 77−39888
impurity determination, by neutron activation analysis 78−11586
impurity diffusion, models for irradiation effects 77−80654
impurity diffusion through SiO_2 layer, physicochemical processes *(German)* 78−2149
impurity distribution, optical inhomogeneities obs. by spectral modulator 78−59144

silicon continued
impurity doping, by thermal neutron irradiation, charge carriers behaviour obs. *(Japanese)* 79−42484
impurity doping influence on free-exciton absorpt. 77−69861
impurity interstitials, EHT calcs. 80−24845
impurity ion potential, asymptotic corrections 77−47769
impurity ion potential, in spatially varying dielec. const. semicond., variational calc. 79−7800
impurity levels of H and muons 79−56162
impurity penetration depth, chemical-spectral determ. 80−19830
impurity precipitation from solid soln., neutron irrad. effect 80−29177
impurity redistribution during single oxidation step, computer program calc. 80−2060
impurity screening, local-field effects 79−60759
impurity solubility limit after laser induced melting 80−107426
impurity stabilised by Te deposition, atomic arrangement, LEED exam. 77−11770
impurity states, localised orbital approach 80−92851
impurity states and core excitons, binding energies, perturb. theory 80−49659
impurity-doped cryst. plate, as an X-ray monochromator, strain distribs. for 220 reflections 80−100126
impurity-ion potential, electron-conductivity mobility, spatially variable dielectric function calcs. 79−78105
impurity-vacancy complexes, many-electron approach 78−67980
inclusion type defects removal from bulk of single crysts. by elec. fields 79−43126
inclusions, microscopic, nondestructive monitoring 79−55749
indentation hardness and semiconductor-metal transition 78−35499
indirect free exciton, ground state, magneto-optical investigation 77−51670
indirect gap semiconductor, valley-orbit interaction and effective-mass theory 78−23043
inelastic X-ray scatt. cross section accompanied by intermediate momentum transfer 79−24387
inelastic X-ray scattering cross-sections, energy-integrated separation of components 78−38587
integrated circuit technology for hemispherical laser fusion target fabrication 79−89495
integrational etching composition and method 78−10055
interface structural model between amorphous and crystalline phase 78−63941
interface with electrolyte, energetic barrier height hypothesis 79−19657
interimpurity radiative recomb. with phonon cooperation 77−16385
intermixing with Pt(Ni)(Hf) films, ion-beam induced silicide form. 79−46718
internal photoelectric effect, quantum efficiency 80−20254
internal photoelectric effect, spectral depend. of quantum efficiency 78−39150
internal strain rel. to strain tensor, group theory anal. 79−86835
interstellar Si, chemistry in diffuse clouds 77−45507
interstitial H-related defects, vibr. and electronic struct., extended Huckel theory 77−62604
interstitial swirl defect form. in dislocation free floating zone cryst. 77−7682
interstitials and lattice vacancies 78−10038
interstitials in radiation defect formation 77−15461
intrinsic, phonon replicas of electron-hole liq. luminesc. line 79−28831
intrinsic, radiative recombination probability *(German)* 79−61441
intrinsic, self-diffusion, 885-1175°C 80−10700
intrinsic, two-phonon assisted free exciton recomb. radiation 78−2922
intrinsic radiative recombination probability *(German)* 78−95608
inversion and accumulation layers, (100), effective mass and collision time of electrons 78−34909
inversion layer, 1/f noise and percolation in impurity bands 79−24029
inversion layer, Γ and X electric breakthrough interference effect 79−47137
inversion layer, cyclotron resonance in extreme quantum limit, collective ground state 80−50191
inversion layer, dynamic conductivity of electrons, temp. depend. 78−19115
inversion layer, elec. break-through, exactly solvable model 78−56234
inversion layer, elec. cond., freq. depend. 78−72270
inversion layer, far IR photoresponse 77−38002
inversion layer, Hall effect meas. 78−56199
inversion layer, high freq. cond., Drude relax., 2D plasmons and minigaps in surface lattice 78−60230
inversion layer, impurity scatt., self-consistent calc. 79−28415
inversion layer, in strong mag. fields, electron localisation 78−60219
inversion layer, influence of natural superlattice on 2-dimens. electron gas spectrum *(Russian)* 78−68064
inversion layer, inter-subband optical absorpt. in mag. field 77−32375
inversion layer, interacting electron system, cyclotron reson. 78−87902
inversion layer, IR spectrum, 10°G field effect 78−946
inversion layer, magnetoplasmon reson. lineshape theory 79−1615
inversion layer, n-channel, electron mag. suscept. 78−52009
inversion layer, n-channel (100), theory of valley splitting, electric break through 77−85330
inversion layer, n-channel (100), valley splitting, formulation by extended zone effective mass theory 77−85329
inversion layer, n-channel (100), valley splittings, enhancement by many-body effects 77−85331
inversion layer, n-channel (100), valley splittings due to elec. break through 79−4592
inversion layer, negative differential resist. 78−60225
inversion layer, obs. of localisation in two-dimens. system 78−60213
inversion layer, on vicinal plane, band structure 80−24994
inversion layer, photoconductivity meas. 78−10498
inversion layer, polaron model for localisation 80−20280
inversion layer, press. depend. of struct. of field effect mobility 78−60216
inversion layer, random attractive electron-electron interactions in two-dimens. systems 78−60183
inversion layer, surface quantum oscillation under pressure 78−60228
inversion layer, temp. depend. of subband energies, exchange and correlation effects 80−20281
inversion layer, theory of impurity-shifted intersubband transitions 80−20324
inversion layer, transient response of hot electrons, calc. 80−49747
inversion layer, transient response under hot electron conditions 78−60223
silicon continued
inversion layer, two-dimensional magnetoplasmon 78−2440
inversion layer, valley splitting, effects of misorientation 79−73564
inversion layer, voltage tunable far IR emission 80−25018
inversion layer (100), hot electron drift velocity, Monte Carlo calcs. inc. 3 subbands 78−91752
inversion layer (100), two-dimensional electron fluid, spin density, valley density waves 77−69400
inversion layer electronic transitions for voltage-tunable far IR emission 77−39962
inversion layer electrons, temp. depend. cyclotron reson. lineshape 78−10568
inversion layer in MOS struct., carrier-phonon interaction, nonohmic transport 80−49943
inversion layer in quantising mag. field, Einstein relation 78−19156
inversion layer mobility depend. on intersubband scatt. at low temps. 79−95506
inversion layer surface cyclotron resonance, temp. and stress effects 78−60229
inversion layer warm electrons 78−60222
inversion layers, (100), effective masses, Shubnikov-de Haas oscills. under mechanical stress 77−43625
inversion layers, (100), magnetoelec. and piezoresist. evidence for mobility domains 77−4447
inversion layers, (100), wavevector, depend. of the 2D plasmon disp. relationship 78−76101
inversion layers, (111), CDW induced cyclotron reson. harmonics 78−64085
inversion layers, Anderson transition, random field origin, substrate bias effect 77−28255
inversion layers, angular dependent negative magnetoresist. 78−80062
inversion layers, CDW mag. fields and stability 78−10533
inversion layers, CDWs, effect of four valley interaction terms 79−33324
inversion layers, cyclotron and subband emission 78−64128
inversion layers, discrepancies between absorption and photocond. meas. 78−6451
inversion layers, effective mass variation 79−24050
inversion layers, effects of uniaxial stress on cyclotron reson. 80−20322
inversion layers, electronic g-factor, spin-split Landau levels 80−80346
inversion layers, far IR cyclotron emission 79−61226
inversion layers, far IR emission from hot electrons 78−30995
inversion layers, far IR reson. magnetotransmission, temp. and band gap light depend. 78−64363
inversion layers, far IR transmission spectra, two-dimensional plasmons 77−76931
inversion layers, first order intervalley scatt. 80−29484
inversion layers, Hall effect, consistency with presence of macroscopic inhomogeneities 79−51681
inversion layers, high field magnetocond. 77−32020
inversion layers, intervalley transitions and subband splitting 77−20455
inversion layers, low density, far IR resonant magnetoabsorption 77−55789
inversion layers, magnetic localisation of electrons 78−43481
inversion layers, magnetocond. in ground Landau level, defect diffusion in Wigner cryst. 77−39914
inversion layers, mobility temp. depend., Coulomb and surface roughness scatt. 80−80390
inversion layers, multivalley effective mass theory 79−47136
inversion layers, near threshold at low temps., cond. anomalies and electronic states 77−59333
inversion layers, nonmetallic cond. at low temp. 80−70833
inversion layers, phase diagram in strong mag. fields. 80−88492
inversion layers, piezoresistance 77−35935
inversion layers, prep. domain studies of intersubband optical transitions 80−20637
inversion layers, quantum magnetoresist. results, using pulsed fields up to 35 T 79−73528
inversion layers, random pair attractive interaction model of carrier correl., compared with expt. 78−60212
inversion layers, resist. temp. depend. at liq. He temps. 80−80391
inversion layers, resolution of Shubnikov-de Haas paradoxes 80−39648
inversion layers, review 77−80842
inversion layers, stress and intersubband correlation 78−60227
inversion layers, stress and temp. depend. of subband struct., plasmon-pole approx. 79−95461
inversion layers, stress effects on electronic props. 78−43476
inversion layers, submillimeter cyclotron reson. at low electron density 79−60925
inversion layers, two-subband screening and transport 78−64126
inversion layers on high-index surface of Si, valley-valley splitting 78−39219
inversion layers under stress, density functional calc. of subband struct. 80−20321
inversion-layer electrons, temp. depend. cyclotron reson. lineshape, theory 78−64086
ion and electron emission following ion impact 80−100729
ion backscattering, H^+, H_2^+, and He^+, energy spectra and charge fractions 80−35046
ion beam irrad., defects prod. by individual displacement cascades, TEM study 80−70265
ion beam milling, amomalous sputter yield behaviour 80−108624
ion bombarded, projectile energy depend. and line shape of Ar-L AEs 80−16139
ion bombarded, radiation defect formation, atom-atom collision cascades modelling 80−10582
ion bombardment, amorphous surface layer produced, insulating props. of interfacial layer 77−59327
ion bombardment, anomalous surface damage from channelling-backscatt. meas. 80−84222
ion bombardment, energy distrib. of positive secondary ions and sputtered atoms 77−32485
ion bombardment, low energy Ar, evidence for spike-effects 79−19292
ion bombardment effect on surface struct., RHEED and Au decoration 80−2096
ion bombardment induced buildup of disordered material, model 77−47496
ion bombardment induced defect distrib., IR and electron diffr. study 80−65074
ion bombardment induced light emission, investig. of cpd. form. 77−48257

silicon continued
ion bombardment induced residual stress in amorphous implanted surface layers 77−35610
ion damage, TEM study of laser annealing 80−88215
ion damage critical gettering doses, elec. characts. 78−10085
ion damage critical gettering microstructures 78−6098
ion etching using Ar, carbide form. 80−81222
ion implantation, appl. in Si technology 79−51124
ion implantation, channelled, through metal silicide film 80−70231
ion implantation, channelling, alignment effects 80−88183
ion implantation, damage obs. by X-ray double refl. 77−15463
ion implantation, electrical profile of double damage layers using electron microscope 78−2169
ion implantation, energy deposition profiles from range data, simple method for calc. 77−39619
ion implantation, heavy, MeV region, damage profiling, electron microscope determ. 78−75686
ion implantation, high current and dose, visible interf. effects 77−7743
ion implantation, high dose, solid phase epitaxial regrowth 80−103380
ion implantation, high-dose Ar, X-ray topographic obs. of strains and damage 80−59496
ion implantation, in crystals of diamond struct., computer modelling 77−43235
ion implantation, investigation of radiation damage by pendellosung topography 79−51125
ion implantation, neutron activation analysis, contamination and cross-contamination 78−83837
ion implantation, off-axis channelling disorder anal. 77−24325
ion implantation, problems and techniques 77−59029
ion implantation, ranges of implanted B^+ and B^{2+} 77−31687
ion implantation, recent progress 79−14831
ion implantation, semiconductor device processing 80−34031
ion implantation, target heating, temp. measurement 80−34032
ion implantation, TSC meas. of coupled levels 78−84165
ion implantation and pulsed laser annealing of group III and group V dopants, supersat. alloy form. 80−54267
ion implantation by laser annealing, characterisation, solar cell applications 80−70247
ion implantation causing surface defects, electroreflectance 79−19274
ion implantation damage, annealing, role of stresses 78−75679
ion implantation damage in Si devices, review 77−27899
ion implantation doping and laser processing 79−69127
ion implantation for InP n-type doping 78−91351
ion implantation gettering effects, crit. microstructure 77−43229
ion implantation in natural diamond, He backscatt. and IR absorption 77−89466
ion implantation induced disorder in surface and at shallow depths 80−59535
ion implantation of B and Ar, effect on cond. 77−80779
ion implantation of B molecular ions 78−47405
ion implantation of diamond, SiC synthesis and struct. characterisation 77−76434
ion implantation of N, Si_3N_4 film formation 79−90692
ion implantation of noble gases, high fluence retention 79−23627
ion implantation radiation damage, SEM electron beam absorpt. meas. 78−75696
ion implantation systems, high throughput, appl. to Si 80−34029
ion implantation using $^{14}N_2^+$, Si_3N_4 film form. 79−99455
ion implantation with Si^+, high dose spatial correl. of primary and secondary defect profiles 80−59536
ion implantation-induced damage after Ar and P implantation, defect density and distrib. *(German)* 77−24337
ion implanted, amorphous to crystalline transition due to laser irrad. 80−103451
ion implanted, annealing by ion beam heating 80−103382
ion implanted, annealing of heavy ion cascade damage, channelling meas. 80−89255
ion implanted, complex annealing behaviour of amorphous layers, TEM obs. of defect struct. 80−107299
ion implanted, CW laser annealing 80−92550
ion implanted, damage profiles, Rutherford backscattering 80−100733
ion implanted, damage struct. obs. using TEM and cross section specimens 80−107298
ion implanted, defect struct., dislocation loops and elongated defects 80−107300
ion implanted, difference between ruby and Nd:YAG laser annealing 79−37723
ion implanted, dopant depend. of oxidation rate 80−89384
ion implanted, dynamic behaviour of pulsed-laser annealing, time depend. optical reflectance meas. 79−60393
ion implanted, electron beam annealing, surface struct. study using SEM 80−70235
ion implanted, EPR line shape exam. of amorphous centres 79−28587
ion implanted, extent of annealed or melted regions as function of pulsed laser irrad. energy 79−74025
ion implanted, interstitial generation and loop form. during annealing in oxidising medium 80−107225
ion implanted, laser annealed, deep levels study 79−69457
ion implanted, laser annealed, elec. characterization 79−69137
ion implanted, laser annealed, elec. props. and annealing kinetics 79−69508
ion implanted, laser annealed microstructure 79−74027
ion implanted, laser annealing, periodic regrowth phenomena 78−67724
ion implanted, laser annealing 79−69124
ion implanted, laser annealing 79−69126
ion implanted, laser-annealed, theoretical anal. of thermal and mass transport 78−91364
ion implanted, mode-locked Nd:YAG laser annealing, recrystn. 80−19817
ion implanted, photovoltaic effect related to annealing 78−76111
ion implanted, pulsed electron and laser beam annealing, comparison 79−52256
ion implanted, pulsed electron beam annealing 79−52254
ion implanted, pulsed ruby laser annealing 79−52255
ion implanted, pulsed-laser annealed, Raman obs. 79−73189
ion implanted, radiation defect production at different temps. 80−103398
ion implanted, ruby laser pulse effects 79−69125
ion implanted, scanning CW and pulsed laser annealing 80−92549
ion implanted, scanning electron beam annealing 80−6420
silicon continued
ion implanted, self implanted, self annealing using high ion current density treatment 80−89254
ion implanted, SiO_2 antireflection coating effect on CW laser annealing 80−49242
ion implanted, spin density effect on laser annealing 80−11517
ion implanted, surface characterisation by Si-electrolyte interface impedance meas. 78−84291
ion implanted, transient optical reflectivity study of laser annealing, thresholds and kinetics 79−60390
ion implanted, voids, electron microscopy 78−67757
ion implanted amorphous layers, free carrier plasma effects 77−73133
ion implanted and laser annealed, characterisation 80−29043
ion implanted by high energy C ions, structural and optical props. 80−107292
ion implanted electrodes in HF electrolyte, characterization by electrolytic reverse current 78−6078
ion implanted films, optical and luminesc. props. 80−60699
ion implanted Kr migration during anneal 78−18834
ion implanted layers, complex refr. index profile, ellipsometric meas. 80−93262
ion implanted layers, laser annealing 78−67732
ion implanted layers, pulsed electron beam annealing, He^+ backscatt. and TEM study 79−51152
ion implanted layers, pulsed electron beam annealing, TEM and particle backscatt. meas. 79−69134
ion implanted single crystal, depth profile of radiation damage using lattice deform. study *(German)* 77−39618
ion implanted wafer, colour generation model 77−85868
ion inelastic stopping cross-sections, channelling meas. 77−59058
ion irrad., temp. and dose depend. of defect profiles 80−29097
ion irradiated, 100 keV Sb, disorder accumulation, saturation and sputter limitation 78−67753
ion irradiated, Auger electron spectra struct., possible surface diagnostic methods 79−69946
ion irradiated, B ions, long-range damage to crystallinity, X-ray diffr. meas. 78−2171
ion irradiated, room temp., depth distrib. of disorder 79−37745
ion irradiated by 50 keV N^+ and P^+, depth distrib. of struct. defects, secondary emission obs. 78−2168
ion irradiation damage, strain effect contrib., channelling meas. 78−67752
ion irradiation prod. of stable vacancy-interstitial pairs 77−27925
ion penetration, computer program 80−88185
ion range of 100 keV Pr^{2+} and Tb^{2+}, M-shell X-ray cross-sections 77−35614
ion scattering energy spectra by TOF and electrostatic analyser methods, comparison 79−2895
ion sputter cleaning, in EM 80−101895
ion-bombarded by Cs, surface Cs concs., AES meas. 79−83073
ion-controlled diodes, acid-base exposure effects, Si-SiO_2 interface state density 80−96984
ion-implantation damage, annealing using pulsed-electron-beam 79−55768
ion-implanted, annealing using scanning CW laser system 80−100265
ion-implanted, cryst. to amorphous transform., ESR expts. and composite model 78−59825
ion-implanted, defect struct., SEM, TEM and X-ray topography expts. 77−51399
ion-implanted, disorders, nature and annealing behaviour, review 78−83836
ion-implanted, effect of free-carrier absorpt. on annealing by pulsed laser 79−55757
ion-implanted, impurity activation monitoring by SAW techniques 80−65020
ion-implanted, lapping and staining techniques, junction depth determ. 80−29468
ion-implanted, laser annealing, appls. 79−73202
ion-implanted, laser annealing dynamics 79−69121
ion-implanted, laser irrad., characterisation by X-ray topography 79−74026
ion-implanted, laser pulse annealing, TEM and channelling study 80−100264
ion-implanted, low-fluence, primary defects, transient capacitance spectroscopy 80−44238
ion-implanted, period surface struct. in laser annealing, new expt. evidence 80−29836
ion-implanted, pulsed-laser annealing, dynamic behaviour by optical reflectance meas. 79−69122
ion-implanted, secondary defects development, three-stage model 78−87725
ion-implanted, thermally oxidised, Rutherford backscatt. analysis 78−19910
ion-implanted amorphous, laser epitaxial recrystallisation threshold energy 80−70571
ion-implanted amorphous layers, melting model for pulsing-laser annealing 79−56080
ion-implanted dopant redistribution under laser annealing 80−70242
ion-implanted laser-annealed solar cells 80−93881
ion-implanted layers, crystalline-to-amorphous transition, radiation defect prod. 78−87696
ion-implanted layers, crystn. by ns laser pulses, TEM and RHEED 80−100421
ion-implanted layers, epitaxial regrowth by laser beam and flash annealing 80−100420
ion-implanted layers, impurity profile meas. after laser annealing 78−87702
ion-implanted layers, residual defects after high temp. annealing 78−87695
ion-implanted layers, total X-ray reflection investig. of clustering 78−6081
ion-implanted polycrystalline film, defect build-up efficiency 80−2054
ion-implanted semiconductor, annealing, crystallisation, laser pulse energy depend. 78−34528
ion-implanted structure annealing, defect behaviour obs. *(Russian)* 80−49281
ion-implanted surface, profiling method 78−95075
ion-induced Auger electron emission, depend. on ion energy 79−78814
ionisation energy loss of electrons with large Lorentz factors 78−55117
ionised impurity scatt. limited mobility in semiconductors with spatially variable dielec. function 78−51986

silicon continued
ions, dielectronic recomb. and ionization equilib., autoionization and excitation influence 78−1077
ions, H-like, He-like and Li-like, X-ray spectra after foil excitation 79−59545
ions, multiply-charged, beam-foil obs. of $1s2p^3P_1$ lifetime 80−14114
IR absorption spectra, Fourier transform obs. 80−60644
IR absorption spectra, Si-H bonds, crystal defects *(Chinese)* 80−55073
IR detector, extrinsic photoconductive, counterdoping scheme 78−49896
IR detector, free carrier absorpt. 78−37060
IR emission under α-irrad. *(Russian)* 77−85811
IR photoresponse at 1.15 microns 79−7864
irradiated, nature of 0.97 eV A band luminesc. 77−44049
irradiation induced crystalline to amorphous transition, Gibbs energy 80−70371
isoelectronic sequence, CI calcs. of oscillator strengths, L-S framework 80−14089
isolated dislocation motion, velocity determ. *(Chinese)* 80−107243
isomer shift values of implanted $^{133}Xe/^{133}Cs$, Mossbauer spectra 80−7240
isotope abundances in lunar samples 77−60676
Jahn-Teller distorted vacancy, electronic struct. 80−10869
Jahn-Teller Mn^0 centre ESR spectrum, depend. on axial press. 80−44911
joining and recrystallisation using thermomigration process 80−65298
junction diode, diffused, with deep level traps, negative capacitance 80−96976
junction diodes, fabrication by LPE on Si:B substrates, and characts. 80−80363
junction FET, annealing of neutron induced defects, transductance meas. 78−43052
junction field effect structures, 2-D subbanding 78−64125
Kikuchi diagrams, by electron diffr., temp. depend. 80−1904
Kikuchi electron diffraction lines, forbidden, formation mechanism 80−44081
Kikuchi electron patterns, unindexable and forbidden lines 79−94850
Kikuchi patterns, contrast depend. on primary electron beam energy *(Russian)* 80−64844
Kikuchi patterns due to plasmon and phonon excitations 77−76264
Kikuchi structures, energy analysis by intensity profiles *(German)* 79−7528
Kikuchi structures, phonon scatt. and thermal diffuse scatt., transmission electron diffraction study *(German)* 80−44082
L-shell ionisation by 80 keV electrons, transmission electron energy loss spectrometry 80−60721
large monocrystal X-ray reflection/scanning and transmission topographic methods 80−96415
large single crystal production, using directional solidification tech. 78−35298
large unit cell semiempirical mol. orbital approach to props. of solids 79−87036
laser, atomic, pulsed microwave discharge of SiH_4 source gas 80−48233
laser and thermal annealing, elec. cond. and Hall effect meas. 79−69145
laser annealed, charge collection microscopy, carrier lifetime determ. 79−69136
laser annealed, defect luminesc. 80−50388
laser annealed, elec. props. 79−69609
laser annealed, nonequilibrium solubility and segregation 80−84296
laser annealed, solubility of impurities 79−69247
laser annealed ion implanted, elec. props., melting threshold 80−10969
laser annealing, nonequilib. incorporation of impurities during rapid solidification 80−55286
laser annealing, nonlinear dynamic transport processes 80−93437
laser annealing, optical constants, ellipsometry observation 80−34024
laser annealing, optical refl. meas. of melted layer 79−78796
laser annealing, surface layer temp. distrib. 79−74029
laser annealing after ion implantation, temp. distrib. 80−54265
laser annealing at 1.06 μm, free carrier absorpt. role 80−24964
laser annealing at 1.06 μm of ion implanted solid, computer simulation 79−47556
laser annealing for improved stacked-struct. oxide quality 80−65386
laser annealing mechanisms, disordered overlayers, crystalln. 80−84967
laser annealing of ion bombardment damage 80−25502
laser annealing of Si on sapphire film, non-thermal theory expt. test 80−89273
laser annealing of SiO_2 layers 80−97505
laser assisted doping, ohmic contacts and p-n junction form. 78−79621
laser beam induced temp. rise, nonlinear heat cond. 79−11487
laser crystallisation, for production of large grained sheets for solar cells 80−93570
laser damage, 10.6 μm CW CO_2 beam 77−63497
laser damage statistics rel. to structural defect statistics 80−91829
laser heating of lightly damaged material, carrier diffusion effect 80−84809
laser induced damage, effect of applied electric field 77−40310
laser induced dense plasma, dynamics 80−65612
laser induced elec. damage, carrier removal, mobility degradation 77−80791
laser induced formation of metal silicides 79−70366
laser induced reactions with metal films, silicide formation 79−70365
laser induced surface deforms. 79−82262
laser irradiated, anisotropic melting and epitaxial regrowth, surface struct. 79−33163
laser irradiation effect on cohesion 80−50470
laser irradiation of furnace preannealed (111) ion implanted Si 80−65015
laser measurement, of semiconductor materials and devices *(Rumanian)* 78−52035
laser plasma X-ray spectroscopic diagnostics using high-quality quartz and Si crystals 79−68953
laser pulse induced amorphous to cryst. transition, thickness depend. 78−47678
laser pulse train shaping for polycrystal recovery in self-ion implanted samples 79−47555
laser pulsed annealing, carrier diffusion role in lattice heating 80−45172
laser pulsed heating, lattice temp., Raman meas. 80−80780
laser residual lattice absorpt., freq. and temp. depend 78−25910
laser window material, surface and bulk absorpt., photoacoustic meas. 78−25912
laser-induced bulk breakdown and free carrier generation, photocond. meas. 80−35018

silicon continued
laser-pulse-control, self-diffr. effects 78−18022
lateral diffusion of B, influence on submicron MOST fabrication 78−26588
lattice constant, press. depend., X-ray diffr. meas. effect of nonhydrostaticness of press. 77−35439
lattice constants anomalous temp. depend. 79−46821
lattice constraints on structure of interface states 77−20379
lattice damage, influence of laser annealing 79−23608
lattice dynamical calc. using extended Born-von Karman scheme 78−59889
lattice dynamics, inversion matrix, approx. inversion 78−71797
lattice dynamics of diamond type crysts., Keating's valence force field 78−79687
lattice dynamics of group IV elements with the local Heine-Abarenkov model potential 78−63821
lattice dynamics under press 80−92627
lattice dynamics using Born-van Karman model 79−73271
lattice energy, pseudopotential calc. 78−23002
lattice energy, strong orthogonality, requirement in calcs. dealing with crysts. by geminal method 78−14307
lattice images of defects and radiation damage applics. 80−107210
lattice parameter determ. by X-ray multiple diffr. study *(Russian)* 80−10460
lattice parameters and perfection *(Japanese)* 79−4300
lattice parameters and topographic meas., using double-beam triple-cryst. X-ray spectrometer 80−77915
lattice scattering mechanism in quantised inversion layers 79−78187
lattice stability, pseudopotential theory and problem of covalent bonding 77−55490
lattice strains induced by localized oxidation, high temp. real-time X-ray topographic studies 80−108489
lattice thermal conductivity, 2-1400K, phonon scatt. calcs. 78−2311
layer growth by CVD on Sn-coated background *(Dutch)* 80−7502
layers, solid phase epitaxial growth, crystalline qualities, ^4He backscatt. and TEM exam. 78−10306
layers, solid phase epitaxial growth temp. depend. 78−10305
layers amorphized by molecular ions, laser annealing 80−103379
LEED, (111) clean surface, internal pot., interplanar spacing 77−89627
LEED exam. of (001)2×1 surface struct. 79−19438
LEED intensity-energy spectra of (100) surface 77−47653
LEED patterns, intensity dynamics 78−10267
lifetime control through impact sound stressing 77−85238
lifetime of free vacancies 79−10851
light beam extinguishment device, without scatter 78−87126
light energy transfer by semiconductor in crossed elec. and mag. fields *(Russian)* 77−75453
light reflection, effect of repeated oxidation 79−52402
light scattering due to microdefects 78−27248
lightguide connector component characts. 80−69544
lightly doped, movement of dissociated dislocations in diamond cubic struct. 78−59806
limited topogram technique for investigation of dislocation distrib. 79−23496
liquid, dissolution of quartz, effect of C, rel. to melt growth 80−70414
liquid, interaction with die material during edge defined film fed growth 80−104060
liquid, mag. susceptibility 78−95415
liquid, sound vel. meas. 79−77684
liquid, wetting and reactions on α-Al_2O_3 77−85022
liquid inclusion migration in temp. gradient field 78−18842
liquid solubility in metallic solvents *(French)* 77−27978
Lo-Hi junctions, avalanche injection delay and ionization rate at low electric field 79−95475
local electron irrad., Frankel pair separation, influence on photo EMF 80−44203
local field, microscopic electronic polarisation 80−25283
local pseudopotential, Gaussian band charge model 80−88477
localised defect, self consistent Green's function calc. 80−10919
localised states due to isocoric donor impurities 77−76768
longitudinal intervalley EMF due to inhomogeneities 78−19045
low angle boundary formation, in single crysts., effect of impurities on cryst. growth conditions 80−11555
low resistivity, field emission, role of surface electron states 78−2993
LPE from Sn melt, kinetics 78−19675
LPE from Sn melt by dipping 78−6871
LPE growth from supersaturated Sn melt 78−56592
LPE Layers, dopant distrib., meltback effects 79−69151
LPE using Ga_xAl_{1-x} solvent 77−36411
luminescence, simultaneous kinetics of drops and excitons during drop formation 77−48222
luminescence centres, fast electron irradiation 77−81153
luminescence emitted as a result of carrier heating 77−52185
luminescence induced by MeV region O^+ implantation 78−6788
luminescence of multiparticle exciton-impurity groups 79−83003
lunar basalts and regolith, anal. of var. in Al, Mg and Si abundances 78−16320
lunar regolith, reduction of Fe, Ti, Si in H atom., X-ray photoelectron spectra 79−25527
LVV Auger spectra 79−52055
magnetic circular dichroism at E_1 edges 78−92051
magnetic susceptibility of light and heavy holes 79−42734
magnetodiode, effect of mag. field on current voltage characts. at low temp. 79−91134
magnetodiode effect, expt. *(Slovak)* 77−8186
magnetodiode with polar magnetosensitivity, voltage-induction and current-voltage characts. 79−73579
magnetotransistor, single-junction, characts. 79−24066
manufacturing methods for photovoltaic energy prod., solar cells, grain growth from melt *(Dutch)* 78−52661
many-valley cubic semiconductor, elec. conductivity tensor, warm electron range 78−39123
many-valley semiconductor, large binding due to dispersive screening and Bloch function interference 79−51525
many-valley semiconductor, linear galvanomag. effects of hot electrons 79−11154
masking effects of Sb diffusion, from doped oxide source 77−15437
mass-anisotropy exciton splitting determ. 78−6685
material processing, point defect thermodynamics 78−6054
materials, advanced, preliminary evaluation for space solar cells 80−94006

silicon continued
matrix isolated cluster, optical absorpt. extended Huckel calcs., electron energy levels 80−16045
MBE, cryopumped ultra high vac. system 77−67448
MBE, doping impurity transport, free carriers effect 78−26793
MBE, on n^+ Si, with wide range doping control 78−27402
MBE, state-of-the-art 79−24450
MBE and solid-phase epitaxy under ultrahigh vacuum 79−28945
MBE growth and surface struct. 80−10816
MBE growth for semiconductor devices 79−83141
MBE layer resistivity and carrier mobility obs. *(Russian)* 80−49962
mean excitation energy based alpha particle stopping power meas. 78−30678
mechanical defects, local, annealing and effect on autoepitaxial growth *(Russian)* 80−7701
mechanical Q meas., low temps. 78−48118
mechanical strength, origin of difference in Czochralski grown and float-zone-grown cryst. 80−44212
mechanically damaged surfaces, EPR meas., role of microcracks 79−42836
mechanically treated surface, chem. state *(Russian)* 80−11805
mechano-chemical polishing rate *(Japanese)* 80−89379
melt, structural factors, at. distrib. curves, thermodynamic and neutron diffr. study *(German)* 80−19687
melt, structural factors, tetrahedral concs., neutron diffr. study *(German)* 80−19688
melt and vapour growth for integrated circuits and solar cells 79−47609
melt grown crysts., impurity incorporation, calcs. 80−79718
melt surface boundary, mass transfer, influence on crystal habit during growth 79−14712
melting and resolidification, laser-induced, surface morphology 79−87529
melting by high power ns laser pulsing, As diffusion 78−79789
in metal grain from Murchison type 2 carbonaceous chondrite 80−77363
metal-amorphous Si barrier, electronic props. 80−11089
metal-polymer-Si structure, elec. props., tunnel current 77−28256
metal-semiconductor contact, surface doping effect *(Russian)* 77−47896
metal-Si, polycryst., Schottky barrier solar cells, elec. and photovoltaic contact props. 80−93936
metal-Si contacts, low temp. reactions 78−2567
metal-TiO_2-SiO_2-Si structure, SiO_2 growth under TiO_2 film during postdeposition high temp. annealing 80−15400
metal-ZnO-SiO_2-Si structures, charge injection 80−49919
metallic, eqns. of state under high press. 79−60475
metallic, superconducting transition temp., press. effects, elec. cond. 80−103777
metallic state, press. induced, elec. cond. meas. 80−96949
metallisation, Pt_2Si and PtSi form. with high-purity Pt films 77−76676
metallisation, TiN and TaN as diffusion barriers 80−65304
metallurgical grade, impurity gettering of polycrystalline solar cells 80−81441
metallurgical-grade, solar cells 80−101104
microcrack detection using US sonoprobe 80−76462
microdefect density, in dislocation free crystals, quantitative determ. by preferential chem. etching 80−65001
microdefect distribution due to dislocation injection, selective etching 78−2122
microdefect obs., using double cryst. X-ray topography 77−4105
microdefects, diffuse X-ray scatt. obs. 80−34014
microdefects, X-ray topography 79−86797
microdefects induced by heat treatment, appl. of X-ray channeling technique using anomalous transmission 79−19124
microdot standards, ion implanted, SIMS anal., detection limits 79−39264
microhardness exam. using static indentation on single crystal 79−52517
microwave oxidation, negative role of fast electrons 78−64744
migration energy of intrinsic point defects in different charge states 77−89582
migration of Au, electron bombardment effects 80−100362
miniature biomedical piezoresistive pressure transducer *(German)* 80−37016
minority carrier diffusion length, Schottky barriers, electron bombard. investigation 78−68037
minority carrier diffusion lengths, surface photovoltage meas. 78−72168
minority carrier lifetime, effect of low dose ion implantation *(Japanese)* 80−54715
minority carrier lifetime, effect of SiO_2 coating deposited by sputtering 80−11003
minority carrier lifetime and diffusion length meas. contactless nondestructive technique 77−80789
minority carrier lifetime and surface recomb. vel. determ. 77−89771
minority carrier lifetime and surface recomb. vel. meas. 77−28194
minority carrier lifetime and surface recombination velocity meas. by photocurrent 78−10515
minority carrier lifetime degradation by $POCl_3$ emitter diffusion 78−2496
minority carrier lifetime degradation effect of $POCl_3$ emitter diffusion 77−76917
minority carrier lifetime improvement through laser damage gettering 80−65589
minority carrier lifetime in neutron doped samples 80−20218
minority carrier lifetime meas. by contactless technique 78−23102
minority carrier lifetime meas. methods and results *(Hungarian)* 79−56241
minority carrier lifetime profiles meas. 77−39873
minority carrier MIS solar cells, AM1 efficiencies 80−93975
minority-carrier diffusion length, and drift mobility determ. using a modulated SEM beam 79−19607
MIS, photocurrent spectra investig. of fund. absorpt. edge 77−4397
MIS, Si solar cells, effects on performance 78−76153
MIS capacitors, C-V curves, outer oxide surface conditions effects 80−97000
MIS negative barrier contact for induced back surface field solar cell 80−101101
MIS photocapacitive IR detector 78−62223
MIS phototransistors, photoelec. props. at high illum. intensities 80−60101
MIS Si solar cell, I-V curves, open circuit voltage 77−8196
MIS solar cell, general theory, expt. on Si 77−8197
MIS solar cells, 655 mV open-circuit voltage 79−79391
MIS solar cells, comparison of majority and minority-carrier 80−85280
silicon continued
MIS solar cells, computer simulation studies rel. to interface state meas. 80−72048
MIS solar cells, spectral response and diffusion length 79−92077
MIS solar cells with Cr, Hf, Be, Sc and Y as barrier forming metals, expt. investigation 80−94077
MIS structure, photoelectric characts. carrier injection levels *(Russian)* 80−96946
MIS structure using LaF_3 insulator 79−78182
MIS switch diode, charge storage effects, threshold depend. on driving voltage pulse freq. 80−49939
MIS/inversion layer solar cells 80−94075
misfit dislocations removal by laser irrad. 79−83063
MNOS structures with tunnelling-thickness SiO_2 films, surface channel hole mobility obs. 78−95380
model pseudopotential, band struct. calcs., liquid semicond. resistivity calcs. 80−20075
moderately doped, ohmic contact electron emission, quantum calc. 78−68087
moderator for slow positron beams 79−71888
momentum density, Compton profile 77−20235
monochromators, harmonic-free single crysts., neutron and X-ray physics appl. 78−75493
monocrystal, channelling of 5 MeV protons *(Rumanian)* 79−14863
monocrystal peripheral fusion channelling under HF heating *(Russian)* 80−59627
monocrystalline, effect of notch root radius on fracture behaviour 78−76751
monocrystalline plates, purification by thermal diffusion impurity migration anal. 80−25553
monocrystalline rod growth from gas phase 78−64453
monolayer adsorbed on W(100) face, LEED, dynamic props. 77−89634
monolithic US transducer array 79−3877
MOS, capacitors, SEM investigs. using electron beam induced current technique 78−23177
MOS capacitor, direct current/voltage relns. as function of oxide doping 80−88635
MOS capacitor, interface state parameter determ. by DLTS 80−65642
MOS capacitor, minority carrier lifetime, effects of swirls and stacking faults 77−32088
MOS capacitor, nondestructive of P^+ and He^+ induced damage, doping profiles 80−34087
MOS capacitor, SiO_2 precipitation in Si, effect on generation currents 79−78188
MOS capacitors, establishment of inversion layer in Si substrate under high oxide field conditions 77−66202
MOS capacitors, pulse response anal., lateral depletion region around gate area 79−38187
MOS capacitors, scanning photovoltage investigation 80−80396
MOS charge layer n-channel (001) surface induced valley splitting 79−28414
MOS device, electron optical identification of precipitations 80−16309
MOS device, subject to linear voltage ramp, non-steady-state studies 79−78189
MOS device, thermally oxidised surfaces, electron mobility in inversion and accumulation layers 80−103753
MOS device irradiation with γ-rays, minority carrier generation, C-V characts. 80−88637
MOS devices, Anderson localisation in Landau level tails, anal. of Shubnikov-de Haas cond. minima 77−76947
MOS devices, SEM, electron beam induced currents, Si stacking fault investig. appl. 79−42665
MOS devices, Si-on-sapphire, effects of planar defects near Si-SiO_2 interface on elec. props. 79−11231
MOS diode, bulk traps and interface states determ., deep-level transient spectroscopy appl. *(Japanese)* 79−42645
MOS diode, dependence of minority carrier bulk generation on HCl concentration 80−88639
MOS diode characts. obs., electron irradiation damage effects *(Japanese)* 79−42646
MOS diodes, P^+ implanted, DLTS of bulk traps and interface states 79−33350
MOS diodes interface trap states obs., due to electron beam lithography using DLTS *(Japanese)* 80−54787
MOS interface states, capture cross-sections 78−64129
MOS inversion layer, Anderson localisation and Wigner crystal form. *(Japanese)* 77−69425
MOS inversion layer, magnetoconductance oscillations 80−20325
MOS inversion layer, subband struct., many body effects 78−64131
MOS inversion layers, Hall effect 78−64118
MOS inversion layers, negative magnetoresist. 80−49922
MOS structure, low leakage, determ. of surface- and bulk-generation currents 79−24055
MOS structure, p-channel, effect of isotropic stress on Si valence band struct., press. transducer appl. 80−25011
MOS structure, p-channel, stress effects on elec. props., press. transducer props. 80−100526
MOS structure, Si-SiO_2, specific memory effect, radiation effects 79−51680
MOS structure, space-charge generation props. of Au 80−2475
MOS structure, surface charge, effect of process induced defects in Si 78−72274
MOS structure Pt diffused, hysteresis and memory props. 80−96992
MOS structure two-layer dielectric interface In doping effect 79−56324
MOS structure with Al_2O_3 grown by molecular beam reaction under UV excitation 79−60927
MOS tunnel junctions, processing condition depend. of props. 80−80380
MOS-structure, with adjoining reversed biased p-n junction, charge pumping current and reverse current *(German)* 80−88636
MOSFET, conductance oscills., source-drain limited cond. 80−20316
MOSFET, electron and hole drift velocities in high elec. field, Monte Carlo calc. 78−60224
MOSFET, far IR emission on high index surfaces 78−48232
MOSFET, intersubband reson. photoresponse, mechanism 79−82677
MOSFET, method to determine effective channel length 79−69601
MOSFET, n-channel, Hall meas. on trap states at 77K 80−44732
MOSFET, n-type inverted surface channel, reproducibility of electronic props. 79−99628
MOSFET, spin orbit interaction and many body effects in surface states 78−64132

silicon continued
MOSFET, voltage tunable far IR emission from inversion layers 77−12440
MOSFET dopant profile determ., DC method 80−70244
MOSFET fabricated on MBE Si layer 79−78179
MOSFET inversion layers, IR photocond. and absorption 78−64123
MOSFET structures, photocond. rel. to intersubband transitions 78−64127
MOSFETS, n-channel ⟨100⟩ Shubnikov-de Haas oscills. in mag. fields up to 35T 79−91154
MOSFETs, Shubnikov-de Haas oscills. from electron irrad. induced two-dimens. leakage channel 79−19671
Mossbauer effect, ^{57}Fe isomer shift, quadrupole coupling and interat. distance correl. 78−52408
Mossbauer spectroscopy of defects, radiation damage and deep levels 80−59533
MOST, comparison of Shubnikov-de Haas effect and cyclotron reson. under uniaxial stress 80−20320
MOST structure, determ. of hole mobility in Si 77−66204
muffin-tin phaseshift parametrization, position of energy states 77−55473
multiband and multivalley effective mass theory for impurities 79−65409
multigrained, grain boundary elec. and compositional props., surface anal. 80−76575
multigrained, impurity segregation to grain boundaries, AES and SIMS obs. 80−65027
multilayer structure dopant distrib. and minority carrier diffusion length, SEM obs. *(Russian)* 78−10543
multiparticle exciton-impurity complexes, induced by uniaxial deform., polarisation of recombination radiation *(Russian)* 79−78754
multiphonon IR absorpt. expt. 78−60461
multiphonon IR absorption in highly transparent semicond. crysts. 78−10885
multiple band excitons, binding-energy calc. 78−34775
multiple bound exciton states, valley-orbit splitting 79−60725
multiple bound excitons, uniaxial stress effects and excited states 78−6281
multiple ribbon growth by EFG 79−8245
multiple tip field emission photocathode, photokinetics 80−100480
multiply charged impurity centers, energy spectrum 79−69469
multivalley structure, helical instability *(Russian)* 79−47101
muon depolarisation, diamag. and paramag. states obs. *(Russian)* 79−87370
muon depolarisation 79−56675
muon spin rotation, spin Hamiltonian and anomalous muonium states 80−71286
muon state, muon spin rot. exam. 78−60373
muonic K-shell X-ray transitions, nuclear charge radius 78−66195
muonium, deep and shallow levels, electronic struct. 78−39051
muonium state, anomalous, μSR 79−56674
muonium state, anomalous 79−56673
muonium states, form. probability meas. 79−11370
n^+pp^+ solar cells, back illuminated, internal quantum efficiency 79−34435
n^+-p diffused diode, optical lifetime meas. in heavily doped diffused regions 77−80829
n^+-p diode, γ-radiation defects, annealing and recomb. props. 80−65045
n^+-p junction, microplasma sites, SEM and TEM characterisation 77−43702
n^+-p junction, surface peripheral leakage currents 78−26939
n^+-p solar cell, forward and reverse bias tunnelling 80−85274
n^+-p-π-p^+ avalanche photodiodes, carrier multiplication and noise in avalanche devices 80−15579
n^+p junction, spin dependent recombination *(French)* 78−80047
n^+p solar cells, effect of elec. bus during 1 MeV electron irrad. and isochronal annealing, elec. characts. and deep level pop. 80−94086
n-channel inversion layers, mag. susceptibility of electrons in presence of quantising mag. field 80−75650
n-n^+ junction, influence of internal field on its elec. props. 79−56297
n-n^+ point junctions, elec. props. in microwave electric fields 80−44719
n-p junction vertical solar cells, Al-plated, photovoltaic effect variation with impurity conc. 79−100522
n-p planar diode, Al layer covered, laser beam produced alloy areas, characterisation 79−69594
n-p-n heterojunction transistor 80−6959
n-type, 300 keV proton irrad., temp. depend. of defect prod. 78−6113
n-type, 77K hot electron repopulation and anisotropy *(Japanese)* 79−82600
n-type, γ-irrad., galvanomagnetic effect anisotropy rel. to layer inhomogeneity 79−33299
n-type, γ-irrad. (E_{max}=100 MeV), carrier recomb. 78−56158
n-type, (100) inversion layers on sapphire, surface quantum oscills. 78−19158
n-type, (111) inversion layers, valley splitting, Shubnikov de Haas oscills 80−65698
n-type, (11$\bar{1}$) MOS charge layer, optical spectrum of inter-subband transition 78−64133
n-type, anisotropy of differential conductivity and transverse diffusion coefficient 78−76078
n-type, bipolar ohmic contact with macroscopic recomb. centres. 80−80379
n-type, bound excitons and bound multiexciton complexes, excitation spectra 80−96792
n-type, capture cross section and generation lifetime determ. of Au, MOS expts. 78−91772
n-type, carrier recomb. and photoionisation via E-centre resonance state 79−60847
n-type, carrier relax. time, mag. field effects, rel. to Hall effect 80−39608
n-type, complex defect production rate introduced by high energy electron irradiation 77−72635
n-type, cond. in warm electron region, phenomenological theory 77−43586
n-type, cond. in warm electron region, temp. depend. of anisotropy of nonlinearity coeff. 77−43610
n-type, current load capacity of contacts with Au, Ni_xSi, and Al *(Czech)* 77−89846
n-type, current-volt. characts. along ⟨110⟩ 79−78111
n-type, current-voltage characts., static high field domains 78−84223
n-type, Debye temperature, electronic effect 78−83901
silicon continued
n-type, deep levels in p-n junctions or Schottky barriers determ., hybrid method 79−24067
n-type, defect charge states, complex form., gamma-ray effects 80−96564
n-type, degenerate, density of states from elastic consts. 80−6690
n-type, diode with Au traps, negative differential conductance 79−11221
n-type, dislocation free, memory effect associated with appearance of prismatic dislocation loops 77−1130
n-type, dislocation free, process induced cryst. defects 80−24392
n-type, donor energy and polarisability in weak mag. field, rel. to hydrogenic atoms 79−3594
n-type, drag thermoelec. power, anisotropy parameter determ. 80−20235
n-type, edge dislocation and stacking fault defect electrical recombination efficiency 80−15106
n-type, effect of random var. in impurity conc. on Fermi level 79−51470
n-type, effective mass from intraband Faraday rot. and Hall effect 77−52049
n-type, efficiency of radiation defect generation by electron bombardment, influence of Fermi energy 77−11596
n-type, elec. cond. control by hot electron intervalley transfer 80−59993
n-type, elec. cond. in weakly heating alternating elec. field 79−23977
n-type, elec. props., in strong elec. fields 79−95416
n-type, electron heating by static elec. field 80−96894
n-type, electron irrad., defect energy levels, energy depend. 79−33262
n-type, electron irrad., positron annihilation, effect of high-temp. annealing 78−76552
n-type, electron irradiated, elec. props. 77−8041
n-type, electron radiation defect annealing, negative stage, Hall coefficient, defect levels 79−90701
n-type, electron-irrad., surface defect distrib., deep-level transient spectroscopy 79−1459
n-type, electron-phonon scatt. and high-field transport 79−42552
n-type, electron-two phonon scatt. 77−47527
n-type, EPR linewidth, Orbach relax. process, conc. depend. 80−44901
n-type, exoelectron emission, effect of surface polishing rel. to defect distrib. in surface layer 80−40239
n-type, Faraday rot. temp. depend., effective mass determ. 80−71392
n-type, Fe_xO_y-coated, heterostruct. photoanode for photoelectrolysis of water 80−61384
n-type, field and current domains, at low temp. 80−6868
n-type, Hall effect appl. in coaxial power meter 78−238
n-type, heavily doped, carrier conc., comparison of expt. and theory, screening effects 77−85216
n-type, heavily doped, extrinsic sp. ht. in metallic regime 78−59956
n-type, heavily doped, meas. of minority carrier transport parameters 80−15537
n-type, heavily doped, Raman phonons, interband excitation effects 78−52501
n-type, heavily doped, self energy of phonons interacting with free electrons, Raman scatt. 78−64366
n-type, heavily-doped, EPR near metal-nonmetal transition 77−28446
n-type, HF plasma oscills. in external mag. field 80−54731
n-type, high-field domain appearance in pinch channel 78−26900
n-type, high-temp. vacuum etching, p-n junction photodetectivity 78−95355
n-type, hot carrier noise and generation-recomb. noise 79−38140
n-type, hot-electron diffusion, effect of ionised impurity scatt. 78−56151
n-type, hot-electron diffusion noise, meas. using radiometric method in X-band region 77−39905
n-type, impurity-assoc. magnetophonon reson. 80−20221
n-type, in MOSFET inversion layer, Gunn instability 78−84305
n-type, influence of deform. on capture of electrons by divacancies 77−1449
n-type, inhomogeneous impurity distrib., elec. props. efect of γ-irradiation 77−55550
n-type, interaction of disordered regions with point defects 79−19296
n-type, internal stress effect on electron-phonon interaction 79−42468
n-type, inversion layers, broken symmetry states 79−15229
n-type, inversion layers, many-valley electron-phonon interactions, piezoresistance, anisotropic cond., Shubnikov-de Haas oscillations 78−52096
n-type, inverted MOSFET surface, evidence for Lande factor g=2, finite valley splitting 80−6989
n-type, inverted MOSFET surfaces, quantum oscills., valley splitting, lineshape in state density effects 79−56318
n-type, ion implanted surface potential barriers, $LiNbO_3$ SAW obs. 77−28234
n-type, ionisation of low donor levels and recomb. of hot electrons at low temp. 79−51596
n-type, irrad, with 1.2 GeV electrons, form. of radiation defects 79−51156
n-type, irradiated with large neutron doses, defect annealing 80−19849
n-type, lattice vibr. excitation conditions, vol. charge redistrib. effect *(Russian)* 80−103427
n-type, low noise ohmic contact prep., transport props. 77−43723
n-type, magnetoresistance, growth layer influence, effect of randomly distributed inhomogeneities 80−20229
n-type, many-valley semicond., current-voltage characts., with multivalued depend. of current on elec. field 78−26876
n-type, many-valley semiconductor, relative displacement of D_1 and D_2' bands under shear deform. influence 79−15080
n-type, meas. of recomb. rates of non-equilib. carriers, absorption modulation method 77−55575
n-type, microwave and far IR hot carrier mobility, Monte Carlo calc. appl. to mm. transit time oscill. efficiency 78−72184
n-type, mobility and resist. as functions of dopant density and temperature 78−2487
n-type, Mott transition, dielec. enhancement and conduction electron screening 78−72073
n-type, multivalued Sasaki effect 80−107795
n-type, negative absolute conductance, electrothermal mechanism 79−69518
n-type, neutron irradiated, annealing behaviour characterisation by electrochem. meas. 80−19847
n-type, neutron irradiated, characts. of changes in mobility 78−39135
n-type, new small donors, energy spectra, photoionisation energy *(Russian)* 80−34391
n-type, noise, small signal conductivity and diffusion in strong elec. fields 79−11192
n-type, noise and hot carrier diffusion in mag. fields 79−11193
n-type, noise at high elec. fields 77−8163

silicon continued
n-type, nonlinear birefr. and dichroism at microwave freqs. and intervalley scatt. 79−19602
n-type, O_2 partial press. depend. of fixed surface state charge due to thermal oxidation 79−70179
n-type, passive, complete activation initiation by local photoactivation 79−100403
n-type, phenomenological energy relaxation time, temp. depend. 78−43409
n-type, photoionisation of doubly charged divacancies 79−51526
n-type, piezoresist. effect, influence of temp. and impurity conc. *(German)* 77−62924
n-type, piezoresist. rel. to piezothermoelec. power, electron-phonon drag region 80−70737
n-type, plastically deformed, donor action of dislocations, elec. props. 79−11126
n-type, quantum magnetoresist. results, using pulsed fields up to 35 T 79−73528
n-type, Re-compensated, photoconductivity 77−15902
n-type, recomb. parameters of heat treatment defects in diodes 79−56299
n-type, relaxation of electron energy, carrier-density dependence 80−107809
n-type, rod, placed in rectangular waveguide, microwave field distrib. 80−39622
n-type, selective anodic oxidation after P implantation *(German)* 79−52411
n-type, shallow impurity states for far IR heterodyne detection 77−38005
n-type, size-induced magnetoresist. in strong elec. fields 80−65582
n-type, sputtering-induced defects, elec. characts. 78−51941
n-type, strained cryst., role of phonon reson. scatt. in phonon cond., appl. to Si:Li 79−19407
n-type, surface, photocond. and photo-emf spectra 79−73544
n-type, surface (100), oxidation-induced stacking faults, O_2 partial press. depend. 78−39922
n-type, surface conductivity anisotropy in accumulation layers 78−10536
n-type, surface electron states, props. determ. at 77K 77−55598
n-type, surface polaritons in DC current 80−34369
n-type, surface quantum oscills. in inversion layers under uniaxial press. 78−88041
n-type, surface space-charge layer, intersubband-cyclotron combined reson. 78−68063
n-type, surface-barrier electroreflection, polarisation anisotropy 79−24295
n-type, thermally oxidised, natural inversion layer, UV photodiode construction 79−30559
n-type, uniaxially deformed, intervalley scatt., 78-300K 77−20330
n-type, V-I response in epithermal electron range 77−4361
n-type, wafer, trap centres of self-interstitials 80−75516
n-type 80−11010
n-type crystals, phonon-phonon relaxation 80−96609
n-type current instability due to temp.-elec. domain pulsations 77−43608
n-type dislocation images, electron beam induced current, charge collection process 79−17580
n-type doping, homogeneous, by thermal neutrons 80−2051
n-type epitaxial layers on oppositely conducting substrates, two layer Hall coeff. meas. technique 80−80297
n-type films on sapphire, crystalline defects effect on elec. props. 77−20470
n-type gamma ray irrad., impurity composition influence on recombination centre formation 80−6872
n-type intervalley electron-phonon deform. pot.-consts. from high-field transport props. 77−62938
n-type inversion layer, electronic bound states, theory 78−60217
n-type inversion layer, exchange instabilities 78−52052
n-type inversion layer, resist. minima in surface quantum oscills. 78−60215
n-type inversion layer, thermal activation of two-dimens. Shubnikov de Haas cond. extrema 78−60218
n-type inversion layers, many-body effects, excitation to higher subbands, MOS struct. 77−62997
n-type inverted (100) MOSFET surfaces, valley splitting quantitative determ. 79−51678
n-type inverted MOSFET surface, mag. field depend. of valley splitting 79−19650
n-type layer impurity distrib., γ-ray and neutron irradiated, transverse magnetoresist. and Hall effect meas. 78−19058
n-type neutron and electron irrad., isochronous annealing influence on edge absorpt. 80−11449
n-type on sapphire, magnetoresistance anisotropies and electronic struct. obs. 77−20471
n-type plate, effect of nonequilibrium carriers on IR transmission 79−38548
n-type plate, internal friction, illumination effects, 50-250°C *(Russian)* 77−20010
n-type solar cell and concentrator manufacture *(French)* 79−83602
N-type switching, thermal mechanism 77−85273
n-type warm-electron magnetoresistivity 79−65503
n-type with ^{11}B implanted ions, high-temp. treatment effect on distrib. profile *(Russian)* 77−89454
n-types, IR spectra of surface photocond. and photo-EMF 77−76868
natural, neutron total cross section minima 78−37387
negative conductivity due to hot electrons transfer in geometric space *(German)* 78−56150
negative differential mobility and geometrical magnetoresist. calc. 77−43624
negative electron affinity, statistics of transmission secondary emission 77−48287
negative electron affinity (100) surface, electron emission 77−52215
negative electron affinity surface, with Cs and $Cs+O_2$ overlayers, thermal stability of work function 78−92167
negative electron diffusivity in high fields 78−30935
neutral undistorted vacancy 78−91638
neutral vacancy, generalised valence band. calc. 77−55493
neutral vacancy electronic struct. 77−62865
neutron and electron bombard., radiation defect recomb., photoelec. props. meas. 80−60039
neutron angular deviations meas., of order of 10^{-3} sec of arc 79−37593
neutron Bragg-case rocking curves from front and back surfaces of a Si crystal plate 78−91202
silicon continued
neutron damage, displacement and ionis. fractions of fast neutron kerma 78−30669
neutron diffraction by curved crystal, evidence for Fankuchen effect 77−55209
neutron diffraction by perfect cryst., mag. field effects 79−73071
neutron diffraction examination, white beam technique 77−31565
neutron displacement cross section, radiation effects intercalibration, damage coeff. 79−23653
neutron doped, γ-irrad. influence on elec. props. 80−6845
neutron irrad., point defects photopopulation and photoionis., IR spectra meas. 80−25423
neutron irrad., residual radioactivity meas. 80−19829
neutron irrad., small angle neutron scatt. meas. 80−29073
neutron irrad. effects, admittance meas. of n^+-p diode 78−51587
neutron irradiated, changes in lattice period, X-ray meas. 77−7767
neutron irradiated, characts. of defect form. 78−14382
neutron irradiated, direct band gap transition, IR absorpt. 79−73980
neutron irradiated, displacement damage for monoenergetic neutrons 78−30670
neutron irradiated, EPR, ⟨100⟩ split di-interstitial positive charge state 77−20698
neutron irradiated, Hall effect and magnetoresist. meas. 80−6883
neutron irradiated, heavily disordered, electronic excitation bands 78−2448
neutron irradiated, influence of defects and temp. on positron annihilation 77−4699
neutron irradiated, internal friction obs. of defects 78−51597
neutron irradiated, intrinsic defect exam. by IR spectra 78−52534
neutron irradiated, resistivity and minority carrier lifetime, radial inhomogeneity *(Russian)* 78−26881
neutron irradiated and annealed, EPR centre (S=1), characts. 80−71177
neutron irradiation effects on lattice parameter and anomalous X-ray transmission 79−86821
neutron irradiation installation for power thyristor production 77−65993
neutron transmutation doped, elec. props. 80−15532
neutron transmutation doped, ESR 80−20462
neutron transmutation doped, highly compensated, resistivity fluctuations 80−15531
neutron transmutation doped, isochronal annealing of resistivity 80−19828
neutron transmutation doped, zero-bias resist. of grain boundaries 78−76072
neutron transmutation doping, ^{31}P conc. meas. 80−19833
neutron transmutation doping, annealing, deep defect levels 80−20123
neutron transmutation doping, annealing, lattice damage 80−15163
neutron transmutation doping, at. displacement effects 80−19852
neutron transmutation doping, automated irrad. facility 80−15141
neutron transmutation doping, General Electric test reactor 80−15140
neutron transmutation doping, impediments to use in power device fabrication 80−96560
neutron transmutation doping, impurities 80−15134
neutron transmutation doping, irrad. facilities 80−15139
neutron transmutation doping, irrad. techniques 80−19827
neutron transmutation doping, photoluminesc. characterisation 80−11453
neutron transmutation doping, radioactivity form. 80−15135
neutron transmutation doping for IR detector material 80−15136
neutron transmutation doping in Harwell reactors 80−15138
neutron transmutation doping using nuclear reactor thermal neutron irrad., review 80−39161
neutron-produced defects, deep level transient spectroscopy 79−47047
neutron-produced defects, investigation by transcond. meas. of junction FETs 77−15455
neutron-transmutation doped, annealing behaviour, EPR obs. 79−86804
nitridation, effect of BaF_2 80−81359
nitridation, effect of Fe alloy additions 78−48650
nitridation, effect of Fe and H 79−57129
nitridation, effects of Fe and Al additions 77−16708
nitridation, fluoride accelerated 80−7705
nitridation, H_2 effects 79−57128
nitridation, metal additives effects, comparative study 77−44511
nitridation kinetics, combined effect of Fe and H_2 78−95722
nitridation mechanism, Fe-contaminant effects 78−80496
nitridation to form α- or β-Si_3N_4 80−50609
nitriding, reactions *(German)* 79−74414
nitriding kinetics and mechanisms 79−70190
NMR of ^{29}Si in weak mag. fields 79−65746
noble-gas ion bombardment, secondary ion emission 80−35042
non thermal laser induced ordering, plasma life time, phonon interactions 80−84481
noncrystalline film, struct., interatomic distances, SRO 80−107053
nonequilibrium carrier density relax., lifetime determ. using light absorption 78−15170
nonequilibrium carrier excitation by CO_2 laser radiation 77−89803
nonequilibrium carriers generated by Nd laser, relax. rate temp. depend. 78−26911
nonlinear optical susceptibility, tight binding bonding orbital model 80−5784
nonpolar semiconductor, IR free carrier absorpt., two short wavelength phonon scattering 79−78665
nonradiative deexcitation in O_2 atmos., using differential meas. of excited state lifetime 78−2920
nonradiative recombination and luminesc. 79−33770
nonsingle crystalline, solar cells, book contrib. 79−43771
nuclear collision effects of He ions, appl. to surface-barrier detector 77−10546
nuclear polarisation due to optical pumping, weak mag. field *(Russian)* 79−19805
nuclear radiation detectors, effect of trapping on response 80−5447
nuclear spin-lattice relax. in weak mag. fields *(Russian)* 79−51879
O and B stars, theory of Si spectra 78−57539
ohmic contacts, two carrier operation 77−43716
ohmic point contact, noise meas. 77−4443
one-sided abrupt junctions, distinction between avalanche and tunnelling breakdown 78−56211
optical absorption by acoustic phonons related to shallow impurity levels 77−4665
optical constants, heavily doped crystals, Kramers-Kronig analysis 77−85676
optical constants at 5461 Å 78−92043

silicon continued
optical constants by unpolarised incident radiation 80−76044
optical critical point structures, symm. anal. by low-field electroreflectance 77−66478
optical demultiplexer using Si echelette grating 80−53422
optical excitations, many particle effects 79−87046
optical fibre, drawn at high temp., preform method *(Italian)* 77−3646
optical fibre ribbon-splicing injection-moulded connector with Si chip insert 78−1412
optical properties, absorpt. spectrum red shift, spectrum temp. depend. 79−78699
optical properties, scatt. surface layer *(Russian)* 80−11419
optical properties of monocrystal by electron energy loss meas. *(German)* 79−24283
optical properties of Si polymorphs, orthogonalized LCAO calc. 78−10345
optical reflectance rel. to surface damage 79−14985
optical spectroscopy, absorpt. coeff., lattice vibr. modes, band gap, acoustic approach 77−69822
optical spectrum, many particle effects, band struct. 80−89024
optical surface modes calc. 77−59200
optical waveguides along both sides of groove 80−96006
optically pumped, distrib. of polarisation of electrons and nuclei 77−59485
optically stimulated ESR, dielec. effects 77−73080
optoelectronic devices for optical signal processing and communications 79−37056
order-disorder transformation, pulsed UV laser induced 79−60400
orientation anal. of polycrystalline samples 79−1438
overabundance in chemically peculiar stars and oblique rotator model 79−30067
Overhauser effect in optically pumped compensated samples 79−73857
oxidation, AES photoelectron spectra exam. of early stages 79−74272
oxidation, Auger spectra 78−14600
oxidation, chem. stability of SiO_2 produced in catalytic reaction 77−86353
oxidation, CL conc. profiles in SiO_2 using SIMS anal. 79−65110
oxidation, clean SiO_2 film prep., use of poly-Si oxidation tubes 78−39924
oxidation, dopant redistrib., Cs^+ SIMS anal. appl. 79−39265
oxidation, effect of chlorinated ambients 79−100278
oxidation, electron diffr. obs. of oxide film struct. 79−15050
oxidation, film defect equilibria and growth reactions 78−11377
oxidation, growth of vitreous SiO_2 films, role of defect struct. of film 80−65403
oxidation, high press. techniques, review 79−100279
oxidation, high-pressure pyrogenic, in the production environment 78−35547
oxidation, in dry O_2 and H_2O ambients, initial oxidation regime obs. 79−29240
oxidation, in O_2/N_2 mixture, kinetics, 950-1100°C 77−86202
oxidation, in steam, high press. and low temp., defect formation 79−29238
oxidation, masking effect of thermal oxidation rate of covering Si_3N_4 film 78−64749
oxidation, oxidation-induced lattice defects, review *(Japanese)* 78−39931
oxidation, oxide growth kinetics for SiO_2 films in low O_2 partial press. *(Japanese)* 78−27665
oxidation, phase comp. of SiO_x, electron spectroscopy obs. 78−60042
oxidation, selective, in high press. steam, using Si_3N_4 mask 79−38997
oxidation, stress in thermal SiO_2 during growth 79−91812
oxidation, thermal growth kinetics, SiO_2 profile meas. 78−88551
oxidation, thermal growth mechanisms of vitreous oxide layers 80−93675
oxidation, use of new high press. steam apparatus 77−63818
oxidation, X-ray photoelectron spectra 77−18971
oxidation *(Chinese)* 79−52401
oxidation at 1000°C, Na contamination and furnace cleaning procedures 77−59955
oxidation comparison with O_2 adsorption, SIMS 78−15273
oxidation expanded defects, effect on MOS parameters 78−19152
oxidation in flow conditions at 1000 to 6000K 78−11445
oxidation in HCl, conditions for stacking fault nuclei gettering and undesirable etching 78−68830
oxidation in HCl-O_2 atms., Si etching and SiO_2 bubble form. 77−63823
oxidation in HCl/O_2 ambients, phase separation and Na passivation in thermal oxides 80−3219
oxidation in high press. O_2, residual stress, chemical etch rate, ref. index and density meas. 80−71768
oxidation in high-press. steam, 800 to 1000°C rate consts. 77−48565
oxidation in O_2-H_2-HCl mixture, kinetics, and SiO_2 film elec. props. 80−40569
oxidation in presence of Cl and Cl cpds. 78−53009
oxidation in UHV, growth and thermal evaporation kinetics of oxide film 78−3246
oxidation induced by ion or electron bombardment, AES-SIMS study 80−108606
oxidation induced stacking fault retrogrowth, O_2 press. depend. 78−64747
oxidation induced stacking faults, n- and p-type (100) wafers 77−32699
oxidation induced stacking faults, surface vs. bulk nucleation 77−62545
oxidation mechanism and kinetics 78−95833
oxidation of dry O_2, revised model 78−92373
oxidation of Si, magnetoactive O^+ plasma 80−38831
oxidation of surface, in wet O_2 environment 80−3410
oxidation rate, initial 79−91817
oxidation rate constants and role of H_2O 78−7072
oxidation solubility and transport behaviour of water, dissolution 80−93801
oxidation stacking faults, shrinkage and growth, bulk O_2 effects 80−96546
oxidation stacking faults and microdefects, growth behaviour during high temp. annealing 78−72901
oxidation struct. and comp. of oxides grown in HCl/O_2 ambients 79−42404
oxidation without stacking fault form. 78−7062
oxidation-induced Frank sessile dislocation loops, struct. change 80−75228
oxidation-induced stacking fault form., by high press. steam oxidation 78−83830
silicon continued
oxidation-induced stacking faults, control by Cl implantation 79−46682
oxidation-induced stacking faults, distinction between clean and decorated faults by etching 80−79818
oxidation-induced stacking faults, influence of annealing ambient on shrinkage kinetics 80−29035
oxidation-induced stacking faults, nucleation mechanism 80−15122
oxidation-induced stacking faults, refl. X-ray topography 77−84767
oxidations, Cl incorporation in O_2-HCl ambients 78−11378
oxidative vaporisation, thermochemical analysis 78−11447
oxide formation in microwave discharge 79−52406
oxide growth, ambient water vapour trace effects 77−77618
oxide growth, trichloroethylene and HCl grown oxides compared 77−76988
oxide growth in HCl-O_2 mixture, ellipsometric meas. 78−7073
oxide layer, vibration of adsorbed molecules, effect on electron capture by deep centres 80−29458
oxide layer anodically grown on high resistivity n-Si wafer, improved homogeneity 79−24642
oxide layer form., crystallisation, structural props. rel. to annealing 78−34724
oxide layer form. by O^+ ion implantation, Rutherford backscatt. and IR transmission obs. 79−51141
oxide layer formation on O_2^- ion implantation, phase comp. 77−90470
oxide precipitate diffusion limited growth in Czochralski Si 80−97484
oxide scale microstruct. of oxidised single cryst. 80−108613
oxide structure obs. by high-resolution electron microscopy 80−103592
oxidised, angular-dependent X-ray photoemission at low X-ray incidence angles 77−32492
oxidised in trichloroethylene-O_2, Cl incorporation and elec. props. 79−91827
oxidised on one side, elastically flexed, dynamic X-ray scatt. *(Russian)* 77−43115
oxidised surface, irregular growths of $B(OH)_3$ 78−39926
$p^+\pi pn\nu n^+$ structure form. by epitaxial growth 77−76906
p^+-i-n^+ diode, double-injection switching, effect of surface recomb. 78−88025
p^+-n contaminated junction, precip.-induced and generation-recomb. currents 78−2555
p^+-n diode, neutron irrad., defect levels, G-T and C-T curves obs. 77−62986
p^+-n diode under forward bias, effects of radiation-induced deep levels on admittance 78−23157
p^+-n high efficiency solar cell, B diffusion process 77−85302
p^+-n junction 80−24509
p^+-n junction diodes, flow fluence S implanted unequal defect densities, dynathermal obs. 80−20293
p^+-n-n^+ back surface field concentrator solar cells 80−93939
p^+-n-n^+ back-surface-field solar cells, physics underlying performance 80−85283
p^+-n-n^+ high efficiency back surface field solar cells, design and fabrication 78−84283
p^+nn^+ reverse-bias struct. with confined space-charge region, field profile 79−73581
p-i-n avalanche photodiode, temp. depend. characts. 79−35835
p-i-n laser detector, wavelength and temp. depend. characts. 80−13134
p-i-n photodiode meas. of X-ray tube kVp *(German)* 79−232
p-i-n photodiode with internal reflection 78−37059
p-i-n structure, ESR of conduction electrons 80−93179
p-i-n structures, pinch effect expt. obs. 79−90971
p-n diode, 1/f noise calc., free carrier mobility interpretation 80−54774
p-n function local temp. meas. using pulsed SEM, induced-current mode 80−54775
p-n heterojunction, DC sputtering growth, photocond. and photovoltaic effects 79−33337
p-n homoepitaxial junctions, elec. and struct. characts. 80−6662
p-n homojunction, radiation detector appl., for integrated optics *(Czech)* 80−33227
p-n homojunctions made by ruby laser pulses *(Polish)* 78−84286
p-n junction, alpha-particle effects, photoelec. parameters determ. *(Russian)* 77−31702
p-n junction, As-diffused, ion implantation effects on leakage current 77−62555
p-n junction, avalanche multiplication factor and reverse current 77−11991
p-n junction, avalanche multiplication of electron beam generated carriers 77−80833
p-n junction, breakdown voltage drift, walk-out phenomenon, model 77−80834
p-n junction, characts. linearisation for temp. meas. 77−53904
p-n junction, charge carrier recomb. at dislocations, combined SEM and TEM study 80−15105
p-n junction, compressed by shock wave, rectifying props. 77−4429
p-n junction, current-voltage characts., misfit dislocations, high press. effects 80−65671
p-n junction, DC characts. at avalanche breakdown including selfheating 79−42629
p-n junction, dielectric props., freq. depend. of capacitance and conductance 78−43469
p-n junction, dopant conc. diffusion length and lifetime variations, SEM obs. 79−82604
p-n junction, effect of elec. and struct. parameters on avalanche breakdown localisation 77−11926
p-n junction, electrolytic anodic oxidation method of decoration 80−60069
p-n junction, ellipsometric method of temp. meas. rel. to secondary breakdown *(Russian)* 80−11074
p-n junction, energy loss and escape depth of hot electrons 79−78159
p-n junction, high-voltage, microplasma characts. 77−11997
p-n junction, ion implanted, cryst. damage influence on elec. props. 78−56219
p-n junction, mesoplasma formation, light-emitting properties of secondary breakdown region *(Russian)* 79−91131
p-n junction, microplasma characts. 77−4430
p-n junction, microplasma instability, effect of space-charge field of mobile carriers 78−19140
p-n junction, negative annealing of γ-radiation defects 77−43246
p-n junction, passivation by amorphous Si:H layer 79−47155
p-n junction, passivation by slightly conductive chalcogenide film 78−2556
p-n junction, plasmon mechanism for secondary breakdown 78−95352

silicon continued
p-n junction, polycryst.-single cryst., elec. characts. 80−11077
p-n junction, quantum efficiency as absolute radiometric standard 79−49284
p-n junction, reverse bias high voltage, secondary surface breakdown 80−70813
p-n junction, small signal equivalent circuit, finite carrier multiplication 80−65664
p-n junction, spin-depend. recomb. at dislocations revealed at reverse current 79−24062
p-n junction, subnanosec. current drops in delayed breakdown 80−75633
p-n junction, subnanosec. current drops in delayed breakdown 80−75634
p-n junction, thermally associated field emission near precipitates 78−14801
p-n junction, through oxide As implantation, Ar implantation gettering 78−14802
p-n junction, unified approach to breakdown phenomena 79−42630
p-n junction, voltage-current characts., fast neutron irrad. effects *(Russian)* 80−65659
p-n junction, with hot carriers, amplification 78−39203
p-n junction depletion layer, electron beam damage inhibition 80−70817
p-n junction depth, electron probe determ. *(German)* 78−2552
p-n junction diodes, reversed-biased, permanently induced negative resist., expt. 78−56214
p-n junction diodes and solar cells, minority carrier diffusion length 80−107894
p-n junction formation, laser assisted, TEM and elec. props. 79−69138
p-n junction formation in B implanted wafers, enhanced annealing behaviour 77−43233
p-n junction I-V reln. calc. 77−43704
p-n junction in surface region obtained by evaporation in UHV 78−39198
p-n junction pressure transducer characteristics *(Polish)* 77−89832
p-n junction sensor for high intensity solar flux mapping 78−40720
p-n junction solar cells, photon degradation effects 79−92078
p-n junctions, avalanche breakdown anisotropy 80−70811
p-n junctions, current-voltage relation 79−42632
p-n junctions, depletion layer recombination theory 77−80828
p-n junctions, electron emission from depletion layers 80−100509
p-n junctions, high-voltage, elec. props. by optical scanning 80−6969
p-n junctions, microplasma characts., temp. depend. 77−4430
p-n junctions, neutron transmutation doping, breakdown process 80−15600
p-n junctions, polycryst., solar cell appls. 78−56220
p-n junctions, spin depend. surface recomb., electron irradiation effect 80−88627
p-n junctions, thermal emission rates and capture cross sections of majority carriers at V centres 80−96980
p-n junctions in vacuum deposited polycryst. films 77−28249
p-n step junctions, temp. depend. of capacitance 79−15210
p-n-n^+ structure, external resistance effect on current-mode second breakdown 78−56216
p-type, $^{49}BF_2$ ionised mols. obtained by implantation of 78−31003
p-type, (111) surface inversion layer, Cs covered, negative magnetoresist. in 2D impurity band 78−64135
p-type, achievement of negative electron affinity 78−2980
p-type, anodic etching for discriminating between elec. active and inactive defects 80−108605
p-type, compensated by radiation defect centres, photoresistors 77−62961
P-type, conductivity and carrier, lifetime, high injection effects 80−70719
p-type, Czochralski grown, microdistrib. of O, SEM and spreading resist. obs. 80−79830
p-type, defect form. due to multiple N^+ and B^+ irrad. 79−90706
p-type, defect-associated photoconduction bands, piezo-spectroscopy *(Russian)* 77−28607
p-type, deformed, 1/f noise, resist., mobility, and carrier density 77−8161
p-type, deionisation effect on hole mobility evaluation 77−35945
p-type, delineation of n-type ion implant 79−77619
p-type, doping Ti diffusion 78−18670
p-type, elec. props. and thermal defects, influence of high temp. treatment 79−69531
p-type, electron irrad., influence of acceptor impurity conc. and irrad. temp. on defect formation 79−19281
p-type, electron irrad. effect on Hall mobility temp. depend. 80−60011
p-type, energy spectrum and thermal stability of radiation defects 77−4406
p-type, fast electron irrad., energy levels determ. by photocapacitance meas. 79−51531
p-type, fast electron irrad., Hall mobility, temp. depend. 78−56165
p-type, galvanomagnetic effects 79−33297
p-type, heavily doped, intra- and interband Raman scatt. 79−95788
p-type, heavily doped, intra- and interband Raman scatt. by free carriers 80−108208
p-type, heavily doped contact layers on IR detectors, IR transmissivity 80−108190
p-type, high-resistivity, ISC and photo-EMF in p-n junction, deep levels 77−72913
p-type, highly deformed, hole scattering 77−20309
p-type, hole drift vel. in high field 79−95415
p-type, interband transitions, contrib. to conductivity at submillimetre wavelengths 80−34473
p-type, interstitial Fe and thermal defects, Hall effect and resist. meas. 79−82200
p-type, inversion layer, screening effect and quantum transport in strong mag. fields 78−19155
p-type, inversion layers, intersubband spectroscopy by photocond. and absorpt. 78−10566
p-type, laser irrad., accumulation of defects, effect on elec. props. 80−107317
p-type, low temp. defect prod., obs. by thermally stimulated capacitance technique 77−84801
p-type, low temp. depend. of elastic const. c_{44} 77−84831
p-type, millimetric and far IR cond., evidence for interband transitions 78−52022
p-type, millimetric and far-IR cond., freq.-depend. carrier relax time 80−34460
p-type, monocryst., diffusion of As, Henry const., temp. depend., 1448 to 1523K 79−42399
silicon continued
p-type, Na impurity diffusion, ion irrad., defect form. effects *(Russian)* 77−43386
p-type, neutron irradiated, elec. props. 78−51939
p-type, odd magnetoresist. under weak carrier heating conditions 80−96917
p-type, ohmic contact formation method 78−76137
p-type, phonon conductivity and attenuation 77−4167
p-type, photoabsorpt. associated with divacancies 79−15502
p-type, photon drag detector, performance in 2 to 33 μm range 79−35834
p-type, photosensitivity of elastic moduli and surface tension 78−83864
p-type, positron annihilation, effects of applied elec. field *(German)* 78−72634
p-type, proton irrad. magnetodiode effect, heat treatment, photocond. spectra 79−69591
p-type, radiation defects by annealing, kinetics anal. 79−33018
p-type, Raman spectra, pseudopot. calc. of discrete-continuum interference 80−2747
p-type, self-interstitials, influence of white light on annealing process *(German)* 79−19245
p-type, surface elec. behaviour after chem. treatment 80−20185
p-type, US attenuation by impurities 77−69047
p-type, US attenuation due to donors and acceptors 77−28223
p-type, X-irradiation, subthreshold defect prod. 77−89470
p-type and n-type, temp. coeff. of resist. calc. 78−91698
p-type elec. resist., shock wave compression effects 80−80265
p-type film, on sapphire, elastoresist. coeffs., room temp. 80−34532
p-type inversion layers, hot carrier effects in high mag. field, 1.25-20K 78−34908
p-type inversion-channel photoelectric cell characteristic *(Russian)* 80−49941
p-type photoresistor, compensated with radiation centres, current responsivity and detectivity 79−17492
p-type polycrystalline films on graphite substrates *(French)* 78−64154
p-type single crystal whisker for thermoanemometers 78−3975
p-type wafer, self-interstitials form. during chemicomech. polishing *(German)* 79−34175
p-type X-ray bombard. effects on elec. resist., and carrier density, annealing effect 77−4125
packing defects, change in size during heat treatment 80−39079
paramagnetic defects produced by electron irrad., EPR 79−19779
paramagnetic state (μ^+e^-) at high temp. 79−56676
partial dislocation electron states 79−60760
partial dislocations, motion 79−82229
particle detection, use of dislocation-free Si 80−42893
particle detectors, high resistivity n-type, prod. by neutron transmutation doping 79−45540
particle reinforced Al, internal stresses, X-ray diffr. meas. *(Russian)* 78−23765
particles, grown in Ar gas, cryst. struct. and habit, electron microscope study 79−74071
Pendellosung fringes, meas. of real part of anomalous scatt. 78−26381
Pendellosung fringes in synchrotron X-ray topographs 79−32858
perfect crystal, dispersion surface of X-ray radiation, X-ray acoustic resonance method 79−41908
perfect crystal, disturbed surface layer, X-ray diffr. 77−85038
periodic stepped structure, on vicinal planes, LEED obs. 80−24725
phase gratings in semiconductors with one- and two-photon excitation 77−8546
phase transformation, lattice dynamics, microscopic theory 80−107387
phonon assisted Auger recomb. in indirect gap semiconductors 78−39126
phonon assisted free exciton luminesc. 79−33833
phonon boundary scatt., reduction of lattice thermal cond. 78−55921
phonon dispersion calc., dielectric screening theory, closure approx. 79−77700
phonon dispersion curves, pseudopotential calc. 80−10620
phonon dispersion relation, adiabatic bond charge model 77−69057
phonon induced intervalley transitions, violation of selection rules 78−30875
phonon scattering at low-angle grain boundary 79−77708
phonon spectra calc. using dielectric matrix approach 79−4381
phonon spectroscopy, amorphous versus crystalline material 78−83898
phonon transmission from incoherent radiator into cryst., anisotropic continuum acoustics 77−47521
phonon viscosity tensor 78−34570
phonon-assisted Auger recomb., direct calc. of overlap integrals 80−107808
phonon-phonon relaxation investigation for conventional and neutron doped crystals 80−96927
phonons, directional depend. of boundary scatt. mean free path 79−73354
phonons, TO and TA, electronic and struct. energies calc. 78−59874
photo-EPR of dislocations in deformed sample 80−11267
photo-field cathode, ageing and surface state effects *(Russian)* 77−28703
photoacoustic effect, free flexural vibrs. damping 77−89813
photoacoustic signal changes assoc. with crystallinity, recrystallisation after laser annealing 80−16127
photocapacitive MIS IR detector, spectral response, noise characts. 80−75644
photocathode, negative electron affinity process obs. by laser beam scanning *(Japanese)* 80−55262
photocell, with field-induced p-n junction, inversion layer solar convertor 77−15906
photoconducting films, amorphous, undoped, I-V characts. of vacuum deposited films 80−60049
photoconductivity, extrinsic, contrib. by hopping through excited states of donors 78−6411
photoconductivity, influence of surface recombination rate and carrier diffusion 80−44660
photoconductivity, temp. dependence, excitation with laser pulses *(Russian)* 80−11031
photoconductivity, two-step, by dislocations 78−14761
photoconductivity and Dember effect, theory, allowance for long-range fields of charged impurities 79−24013
photoconductivity and electrical resistivity of Si with thermal defects 80−6837
photoconductivity kinetics, effect of exciting illumination *(Russian)* 80−11032

silicon continued
photoconductivity of negative donor ion states, for far IR detect. 77−59299
photoconductivity polarisation effects appl. of exptl. technique 79−4581
photoconvertor, short-circuit current and load current depend. on angular sensitivity 79−83594
photoconvertors, p-i-n structure, high resistivity, operational parameters theoretical and experimental analysis 79−96441
photocurrent in diffused junction, back surface field effect 78−91762
photodetector, for improved short-wavelength quantum efficiency 80−31874
photodetector, linearity, stability, fatigue and light memory effects meas. *(Spanish)* 77−87837
photodetector, shallow junction type, internal quantum efficiency meas. model fits, visible quantum yield 80−267
photodetector optimisation for radiation environments 78−29158
photodetector storage-mode operation 77−39075
photodetectors, pin- and avalanche diodes, characts. *(Swedish)* 78−89545
photodetectors, surface-barrier 80−4771
photodetectors, vac. UV performance, 500-2000 Å 77−26397
photodetectors with increased blue sensitivity *(Rumanian)* 80−62720
photodiode, 1.06 μm range, neutron and γ-irrad. effects 79−97433
photodiode, as position sensing detectors for precision measurement and control 79−86273
photodiode, avalanche, $n^+p\pi p^+$-type, primary photocurrent anal. by noise measurements *(French)* 80−88624
photodiode, correcting absorber selection for flash photometry 79−72699
photodiode, diffused junction, performance characts. 80−80367
photodiode, in combination with PbS and PbSe photocells, multicolour detectors *(Czech)* 79−26126
photodiode, multidecade linearity meas. 79−75592
photodiode, semiconductor junctions, dark currents *(Russian)* 77−24612
photodiode, shallow junction n^+-p, spectral response limitation mechanisms 78−37058
photodiode, violet and near UV sensitive, prep. and expt. study *(Chinese)* 79−49285
photodiode absolute spectral response self-calibration 80−73448
photodiode array detector for at. emission spectroscopy *(German)* 79−87926
photodiode array for integrated optical spectrum analyser 80−33241
photodiode array for position-sensitive X-ray detector 80−52831
photodiode array for radiation detection in AES and analytical appl. *(German)* 80−11992
photodiode for optical channel waveguides 80−102805
photodiode imaging array design factors 77−39085
photodiode internal quantum efficiency basis for absolute radiometric standard 80−86410
photodiode photodetector, UV enhanced responsivity 77−74499
photodiode saturation at high modulation freq. 78−54453
photodiodes, linear arrays, use for high-energy electrons detection, SEM assessment 78−32951
photodiodes, reach-through type, avalanche buildup time 77−15892
photoelectret effect, plastic strain induced dislocation relax. time enhancement *(Russian)* 79−15397
photoelectric cell, characteristics, for various solar radiation incidence angles 79−83593
photoelectric convertors, bilateral sensitivity, optical characts. anal. 80−40858
photoelectric convertors, p-n mesa structure for investigating optical and energy characts. of solar and radiant energy concentrators 80−97783
photoelectric convertors, photoelectric parameters under illumination 80−40857
photoelectric spectra of remanent impurities 79−87125
photoelectric-yield spectrum in 3d transition metal silicides 77−28680
photoelectron emission due to Bragg diffr. of X-rays 79−69960
photoelectron escape depths determ. from X-ray photoelectron spectra 78−27368
photoelectron yield variation under asymmetric diffr. condition of X-rays 79−65972
photoemission, primary and secondary yields using low-energy monochromatic X-rays 80−35053
photoemission electron microscopy in high vacuum region, image brightness and contrast 78−55791
photoemission relax. energies *(French)* 77−36357
photoemission spectroscopy of surface states and oxidation 77−55863
photoemission study of energy depend. of bulk plasmon loss intensity 79−47035
photoexcited, highly stressed, electronic Raman scatt. and antireson. 80−29737
photofield cathode, BaO adsorbed layer, work function and emission props. *(Russian)* 78−68608
photofield emission cathodes, single-tip and multitip, fabrication and emission characts. 78−2976
photoillumination effect on field ion microscopy 79−78850
photoionisation cross-sections of valence s- and p-electrons *(Ukrainian)* 77−73211
photoionisation of Group III acceptors, model 78−35174
photoluminescence due to biexcitons, uniaxially deformed *(Russian)* 77−59611
photoluminescence of annealed cryst., defect anal. 79−87500
photoluminescence of electron-hole drops under uniaxial stress 79−91491
photoluminescence of thermal donors after annealing 79−87499
photon drag and radiation press. in refractive media, subMM wavelength 80−60048
photon drag detection 78−43440
photon emission due to Ar^+ ion bombard., adsorbed and recoil-implanted O effect 80−80872
photopassivation kinetics in alkali soln., spectral depend. 77−1886
photopile manufacture for terrestrial solar cells *(French)* 79−24895
photostimulated thermal diffusion of Li using concentrated solar rays 77−51544
phototransistors, slow contamination and fast surface state effects, SEM study 80−107896
photovoltaic and photomagnetic effects, rel. to intervalley electron transfer 80−60034
photovoltaic cell, absolute spectral sensitivity calibration, radiometry, photometry *(Chinese)* 80−86367
photovoltaic cells using silicone materials, encapsulation 80−94019
photovoltaic concentrator cell for high intensity appl. 80−93940

silicon continued
photovoltaic concentrator cells development project, developments, performances and future trends 80−45699
photovoltaic detector, quantum efficiency rel. to position and wavelength 79−75593
photovoltaic detector, radiometric meas. description 78−29140
photovoltaic generators using optical concentration, current status and development trends review 80−45697
photovoltaic industry, environmental control, economic and ecological requirements 80−94026
photovoltaic solar energy conversion [conf. Berlin, West Germany, April 79] 80−30482
photovoltaic technology, conf., San Diego, CA, USA (Jan. 1980) 80−86041
piezo−spectroscopic study of ratio of electron−TO phonon to hole−TO phonon interaction 79−24289
piezo-optical consts., Raman meas. 78−65951
piezobirefringence above fundamental edge, Raman scatt. meas. 79−42941
piezobirefringence in opaque region 80−60541
piezoresistance, energy and momentum relax. of charge carriers 78−47786
piezoresistive accelerometer power transfer factor *(German)* 80−37017
piezoresistive coefficient calc. and meas. *(German)* 80−39571
piezospectroscopic determ. of electron-phonon to hole-phonon interaction 79−95783
piezospectroscopic effect on zero-phonon luminescence lines 80−50406
pin diode, current filament temp. and Au acceptor level capture cross section temp. depend. 78−95351
pionic atom, 2p level shifts and widths 78−46469
planar bipolar devices, dislocation effects 79−82221
planar channelling of fast electrons, 0.8-2.0 MeV 77−59059
planar dechannelling of protons, (100) direction 77−20000
planar diode, Al coated, binary memory device, laser writing 79−69593
planar semiconductor junctions, disruptive voltage calc., ionisation coeff. *(Rumanian)* 80−103746
planar structures, Haynes-Shockley expt. for students 78−28888
planar technology, insulating thin film preparation and props. 78−10589
plasma, dense, nondegenerate, electron transport, thermal cond. *(Russian)* 79−98865
plasma, laser-heated, bremsstrahlung spectra, Gaunt factor calcs. 77−3968
plasma, of laser-irradiated glass shell, electron temp. and density X-ray emission diagnostics *(Chinese)* 80−38718
plasma effects during pulsed laser annealing 80−84480
plasma etching, control of relative etch rates 77−44390
plasma etching, effect of O_2 additions to CF_4 plasmas 78−72908
plasma etching, etch rate loading effect and temp. depend. in CF_4 plasma 79−34167
plasma etching, loading effect 77−90475
plasma etching, mass spectroscopic exam. 78−72909
plasma etching, using CF_3^+, ion-surface interactions 77−90473
plasma etching, using tetrafluoromethane plasma, O_2 addition effects 78−75363
plasma etching characts., effect of dark space in RF glow discharge 79−15830
plasma etching in Freon plasma, for microelectronics appls. 80−3080
plasma etching using microwave discharge 78−11361
plasma growth of native layers, F-enhanced, Auger profiles 80−93662
plasmon dispersion relation, local microscopic field effects 80−20103
plasmon sideband exam. by synchrotron radiation tuning of electron escape depths, UPS 77−47755
plasmons, influence of cryst. orientation on intensity, electron energy loss meas. *(German)* 79−23921
plastic deformation, dislocation density in yield point area *(German)* 78−38720
plastic deformation of single crystals *(German)* 79−52316
plastic flow, initial stages obs. 78−64602
plastic properties, internal friction, dislocation motion *(Russian)* 80−54305
plastically deformed, dislocation structure with different sample orientation 80−70207
plastically deformed, EPR spectra of point defects, temp. depend. 77−90033
plastically deformed, high dislocation density crystals, photoelectret state investigation 80−97191
plastically deformed, hot-exciton luminesc. as function of strain 78−88361
plastically deformed, spin-depend. charge transport 80−6895
plastically deformed monocrystal, X-ray topographical study *(German)* 78−59813
plate, internal friction temp. depend. 77−15491
plate prod. by Stepanov method, stability analysis *(Russian)* 78−52655
plates, semicond., scribing marks rel. to sclerometric microhardness 79−15891
pn-product calc. as function of temp. and impurity conc. 77−35891
point charge impurity screening 80−6783
point defect aggregates, high resolution diffuse X-ray scattering study 80−49211
point defect clusters identification by TEM 77−43210
point defect trapping in stainless steel, anal. from interstitial loop growth rate temp. depend. obs. 80−49270
point defects, H passivation 80−75515
point defects, laser annealing 80−107224
point defects, multiple scatt. Xα model 80−54636
point defects, negative-U props. 80−49660
point defects, review of characts. *(Japanese)* 77−89428
polished plate, internal friction *(Russian)* 78−15441
poly-oxide-poly struct., elec. cond., charge distrib. in SiO_2 films 80−92984
polycrystalline, anisotropic plasma etching 80−85069
polycrystalline, Ar segregation at grain boundaries, elec. props. meas. 80−75259
polycrystalline, CVD, electron beam recrystn. 80−24759
polycrystalline, CVD, recrystn. on heating 80−80107
polycrystalline, elec. and photovolt. props., grain size effects 80−49800
polycrystalline, electrode shape effects on oxide conduction 80−96890
polycrystalline, electronic behaviour of grain boundaries, solar cell appl. 80−92859
polycrystalline, end point detection in plasma etching by optical emission spectroscopy 80−50733

silicon continued
polycrystalline, energy distrib. of trapping states, from impedance of MOSS struct. 80−65691
polycrystalline, for efficient low cost solar cells 80−21405
polycrystalline, grain boundary effects on minority-carrier diffusion length and solar-cell efficiency 79−48124
polycrystalline, grain boundary obs. by TEM, solar cell appl. 80−72057
polycrystalline, grain growth study 78−92188
polycrystalline, growth kinetics in low press. CVD reactor 79−91594
polycrystalline, Hall mobility 80−60006
polycrystalline, in semiconductor engineering, physical-chemical properties *(Slovak)* 78−92196
polycrystalline, large grain size, gross defects effect on effective carrier lifetime 77−80793
polycrystalline, laser recrystallised poly Si/insulator interface, charges at interface 80−54789
polycrystalline, layer structure dependence on carrier gas moisture and O_2 content *(Bulgarian)* 80−59811
polycrystalline, layers on C substrates, RAD process, solar cell appl. 80−89635
polycrystalline, lightly doped film, cond. mechanisms, correl. with SEM examination of film 79−1634
polycrystalline, low cost conversion into sheet by heat exchange method and fixed slicing technique 80−93479
polycrystalline, low press. CVD production processes 77−77395
polycrystalline, neutron transmutation doped, grain boundary zero-bias resistance 79−15153
polycrystalline, oxidation, morphological aspects 80−76388
polycrystalline, p-n junction solar cell, grain-boundary and intragrain recombination currents 80−81442
polycrystalline, passivation of grain boundaries 79−56158
polycrystalline, phenomenological model for mobility 80−65564
polycrystalline, recrystn. after plastic deform. and annealing 80−3145
polycrystalline, solar cells, grain-boundary hydrogenation technique for improvement 80−85273
polycrystalline, thermal oxide anomalous stress 80−93661
polycrystalline and amorphous, sputtering with keV Ar^+ ion, meas. and Monte Carlo calc. of sputtering yield 79−95886
polycrystalline barrier heights and passivation of grain boundaries 80−93890
polycrystalline CVD film formation and props. 77−77401
polycrystalline CVD film optical props. 77−77315
polycrystalline Czochralski-grown, MIS solar cell characterisation using scanned laser response exam. 80−93884
polycrystalline film, on Si, disloc. config. under periodic stress field 78−10312
polycrystalline film resistivity reduction by Nd:YAG laser annealing 80−100539
polycrystalline films, anomalous etching effects 77−77613
polycrystalline films, characts. 80−80988
polycrystalline films, meas. of effective diffusion length, by surface photovoltage meas. 80−80424
polycrystalline films 80−50980
polycrystalline gates ion implantation, without implanting ions into SiO_2 insulating layer 79−7619
polycrystalline layer, laser-induced single cryst. transition, RHEED and backscatt. obs 78−87704
polycrystalline layer growth, ribbon-against-drop pulling process 79−8241
polycrystalline layers, O doped, on Si p-n junction, charge transport and passivation 79−38206
polycrystalline multilayer support struct., control of deform. in dielec. isolated substrates 80−107681
polycrystalline p-n junction deposition 78−10549
polycrystalline rods, p-n junction appls. and transport props. 79−99612
polycrystalline Si-Al Schottky barrier solar cell, grain boundary effects on elec. behaviour 80−85279
polycrystalline solar cell base material characterisation, defect states 80−50979
polycrystalline solar cells, ion implantation method and results 78−63784
polycrystalline solar cells fabricated from refined metallurgical-grade Si, impurity gettering 80−94011
polycrystalline structure stability, stacking defects, twins grain struct. *(Russian)* 80−100248
polycrystalline thin films for solar cells, thermal expansion shear separation technique 80−81439
polycrystalline thin-film solar cells 79−57426
polycrystalline with columnar struct., crystn. using casting technique and microstruct., book contrib. 79−43137
polycrystalline-metal contacts, minority carrier injection 80−103750
polymorphism under high press. *(Russian)* 78−59947
porous, form. during anodic treatment in aq. HF 80−35369
porous, formation during anodic treatment in HF aq. soln., growth kinetics and density 80−20059
porous film, form. by anodic reaction in HF soln., struct. props. 77−24971
porous layer, oxidation, and oxide film props. 80−55556
porous layer, struct. and heat-treatment effect 79−1557
position-sensitive detector for CW and pulsed laser beams 80−78883
positron annihilation, effect of doping 79−24385
positron annihilation, mag. field effect, positronium states 77−16417
positron annihilation rel.to surface treatment *(Russian)* 77−44081
positron anomalous passage mechanism *(Russian)* 77−85836
positron anomalous passage obs. 79−95052
positron channelling, possible tunable X-ray source 79−69167
positron implantation profile and mobility, elec. field effects 77−48273
positron mobility, drift vel. meas. 78−6808
positron trapping in electron-irradiated Si crystals, temp. depend. 80−104009
positronium formation at surface, positron beam irrad. 79−13845
postimplantation damage profiles, backscatt. meas. 78−47402
postimplantation defect annealing in samples heavily damaged by 140 keV Si^{2+} ions 77−11602
powder, effect of Fe and $FeSi_2$ on nitriding 79−33985
powder, nitridation, effect of Fe_2O_3 addition *(Japanese)* 77−60123
powder, nitridation to Si_3N_4, factors affecting α- and β-phase formation 78−52738
powder, reaction with HF and HF+H_2SO_4 mixture 79−11821
powder, X-ray K_α doublet diffr. peak position rel. to lattice const. precision 77−68891
powder compact, Ar-sintering, microstruct. changes 77−90306
silicon continued
powder compact nitriding, growth of α and β phases of Si_3N_4 78−95717
powder heap, thermal cond., effect of temp., press., and atmospheric composition, sintering appls. 78−80487
powder semicond., microwave propagation, Rayleigh limit 79−78126
powdered, microwave propag. 78−56175
powders, laser synthesis using SiH_4 79−74119
power devices, high frequency US testing 79−47851
power transistor and solar cell epitaxy from SiH_2Cl_2 source 77−77402
precipitation of Au from supersaturated soln., Hall effect 77−89465
precipitation of O, 1000°C TEM, IR absorpt. and X-ray studies 80−34194
precipitation of O, 650°C, IR absorpt. and X-ray diffr. 80−76258
precipitation of O, annealing, IR spectra meas. 80−24606
preparation by electrolysis of fluorosilicate solns. in molten alkali halide mixtures *(French)* 78−64491
preparation by SiO_2 reduction by C using a plasma, thermodynamic anal. 77−40530
preshaped single crystal prep. by pendant drop method *(French)* 78−64466
prismatic dislocation loops, (g.b)s product sign determ. *(Russian)* 78−38705
process stress analysis by IR photoelastic meas. 78−11488
production, low-cost low-energy processes 78−11126
production by reduction of SiO_2 with C black in plasma reactor, feasibility 78−27426
production from rice husk ash for solar cells 79−62008
production process effect on fracture strength 80−93656
profile analysis using anodisation and stripping, computer algorithm 77−43241
proton, energetic, range distribs., Monte Carlo computer simulation 78−22777
proton beam uniaxial channelling-blocking and single-alignment channelling-backscatt. anal. 77−84816
proton damage, depth profile anal. by channelling 78−43054
proton energy loss, 0.1-1.0 MeV 80−42909
proton energy staggling in ion backscatt. expt. 79−37750
proton feeding-in and blocking, 1 MeV, simple diffusion model 78−22782
proton impact, electron capture cross-section calcs. 78−95623
proton irradiated, efficiency of form. and nature of defects, Hall meas. 80−6444
proton irradiated, IR absorption 79−33742
proton irradiation, energy depend. of rate of degradation of cond. 77−62944
proton irradiation damage 78−34556
proton multiple scatt., ang. distrib. meas. 78−29720
proton random and aligned stopping powers, 80 to 300 keV, backscatt. meas. 77−27931
proton small-angle backscatt. at grazing incidence 79−83085
proton stopping power, channelled and random, 30-1000 keV 78−67760
pseudo-Kikuchi patterns in refl. expts. during scanning of single cryst. by intermediate energy electrons 78−1964
pseudodiffusion of Ni in single crystal Si during RF sputtering 78−2396
pseudopotentials, nonlocal 77−11848
pseudopotentials for band struct. and cryst. energy calcs. 79−82514
pulsed laser annealing, mechanism 80−25739
pulsed laser annealing, nonthermal, plasma annealing 80−25498
purification, plasma melting zone technique, optimisation *(French)* 80−89142
purification, plasma melting zone technique *(French)* 80−89141
purification and transport, using SiF_2 78−35316
purification technology for the development of low cost solar cells 80−50976
purity for semicond. appls., neutron activation anal. 80−71979
pyrographite, Si-containing, high-temp. treatment effects 77−40429
quadratic piezoresistance, ang. depend. *(Russian)* 78−47782
quantised inversion layers, hot electron effects 77−28188
quantised inversion layers, hot electron microwave cond. calc. 77−43734
quasi-two dimensional space charge layers, transport phenomena 79−95508
quasimonolithic and hybrid integrated optical circuits on Si substrates 80−64218
radiation damage by 0.5 to 10 keV ions 80−100285
radiation damage effects on characts. *(Korean)* 79−60402
radiation damage rate distrib. with depth on 6 MeV electron bombard. 77−31694
radiation defect clusters, form. kinetics and parameters 77−11545
radiation defects, influence of dislocations on accumulation, elec. props. 80−92558
radiation defects due to 30 MeV proton irrad. 78−71776
radiation detector, barrier heights, electron and hole currents, Schottky contact effects 79−33293
radiation detector, ionisation energy for channelled 160 MeV α-particles 78−62680
radiation detectors ion-doped, effects of 5.5 MeV α-particle irradiation 77−65397
radiation energy loss of impurity atoms in hot plasma 78−18441
radiation induced defects, IR absorpt. bands 80−25424
radiation induced defects in high-voltage electron microscope 80−65048
radiation pressure, photon drag effect in far-IR 80−50452
radiation-induced migration of Sn, Mossbauer obs. 77−15462
radiation-stimulated dissociative diffusion of Au, model 79−23785
radiative band to band recomb. lifetime meas., Auger coeffs. 77−85764
radiative electron capture by channelled O ions 79−77658
radiative recomb. centre accumulation due to high temp. electron irrad. 80−93394
radiative recombination centres, fast neutron and ion irradiation 77−81152
radiative recombination in hydrogen containing complexes 77−24896
radiative recombination involving silane mols. 79−73998
radiometer for storage ring synchrotron radiation 80−86411
Raman cross section and its press. depend., theoretical study 79−91448
Raman scattering, free carriers effect, complex band struct. 77−44001
Raman scattering absolute cross-section 80−11410
Raman scattering by phonons and electrons, interference effects 78−60469
Raman spectrum, two-dimens. tensile stress effects 78−48173
reaction kinetics of liquid with B_4C 80−84344
reactions with metal oxides, general features, glass form. 79−11819
reactions with spray coated metal oxides, IR investig. 79−39197

silicon continued
reactive close-spaced vapour transport, simplified theory 80−15396
reactive diffusion in $MoSi_2$, kinetics and mechanism 77−35751
reactive ion beam etching expts., selectivity, anisotropy 80−104308
reactive ion etching, high rate 80−85070
reactive plasma etching with CF_4, mag. field control 80−11796
reactive sputtering, current-voltage charact. 79−95888
reactivity with organic nitrogen compound, rel. to polishing *(Russian)* 79−70192
recombination at dislocations 79−38023
recombination centres and carrier lifetimes after γ-irrad. of n-Si 80−60004
recombination characteristics used in design of semicond. devices *(Russian)* 79−42557
recombination luminescence, electron-hole drop, excitons orientation in mag. field 78−88362
reconstructed (001)2 x 1 surface structure, LEED intensity calcs., dimer model variations 79−77875
reconstructed surface physics, review 80−10766
reconstructed surfaces 78−95214
recrystallisation of CVD-grown polycryst. Si and influence of B, Al dopants on grain growth 80−54575
recrystallised amorphous layer, self-ion irradiated, defect structures, TEM obs. 78−75688
reflectivity time dependence during pulsed laser annealing 80−66214
refractive index, 95-298K, 2.5-12 μm 77−8535
refractive index dispersion 79−24280
regrowth under laser irrad. 80−24481
removal by plasma etching process, from thin oxides and thin metal films 80−76384
residual stacking-fault-type contrast after unfaulting reactions 79−82243
residual stress and defects induced by scribing 80−60990
resistivity and carrier mobility effects of dissolved interstitial O_2 77−76824
resistivity and deep impurity levels at 300K anal. 77−43591
resistivity depth profiles calcs. from spreading resist. meas. using math. algorithm 80−2393
resistivity meas., instrument *(German)* 79−12824
resistivity meas. simplified temp. corrections 77−26338
resistivity measurement, application of capacity gauges *(Polish)* 79−2784
resistors, polycryst., elec. props. in nonlinear regime, grain boundary trapping model 79−38204
resonance dechanneling of fast protons in axis to plane transitions 79−14861
resonant interaction of acceptor states with optical phonons 77−1394
resonant interaction of optical phonons with acceptor continuum states 78−35178
resonant Raman scattering at indirect gap 79−73931
reverse-biased p-n junction DC characteristics interpretation *(Polish)* 78−91761
RF plasma etching for IC processing, mechanistic considerations for selective etching 78−64754
RF sputtered amorphous film, high temp. metal induced crystn. 77−11825
ribbon, dendritic web growth, solar cell prod. and characterisation 77−77366
ribbon, dendritic web growth from melt, solar cell module fabrication 80−93478
ribbon, edge-defined film fed grown, orientation depend. of defect struct. 77−1134
ribbon, edge-defined film-fed growth, melt temp. distrib. 79−52108
ribbon, edge-defined film-fed growth, solar cell prod. and characterisation 77−77365
ribbon, EFG, C contaminant conc. determ. by nuclear techniques and SIMS 80−59506
ribbon, EFG, characterisation by ion beam tech. 80−79833
ribbon, high speed edge-defined film-fed growth 80−104058
ribbon, impurity distrib. in EFG 78−91280
ribbon, low angle sheet growth technique, direct shaping charact. 80−93480
ribbon, prep. by rapid quenching 79−33957
ribbon crystal evaluation for solar cells 77−76813
ribbon crystal growth, 10 cm wide, temp. distrib. meas. in die 80−104059
ribbon crystal growth, capillary action shaping tech., lifetime charact. 78−34847
ribbon crystals, edge-defined film-fed growth technique for solar cells 80−89633
ribbon edge-defined film-fed growth control using C-CD imagers 78−68623
ribbon grown by capillary action shaping technique, electron channelling analysis 77−76418
ribbon growth, high-meniscus, thermal balancing via distributed inert gas streams 78−31329
ribbon growth, ribbon-to-ribbon process, thermal environment control 80−35116
ribbon growth, technology assessment 1978-1986, computer anal. using PECAN 79−8244
ribbon growth, via RTR technique, process update and material characterisation 78−76597
ribbon growth by capillary action shaping technique 80−29888
ribbon growth by edge-defined film-fed process, morphology, stability 77−24947
ribbon growth by EFG, thermal sensitivity and stability 80−107080
ribbon growth by laser zone melting 80−93482
ribbon growth from melt, monitoring device for width and thickness uniformity 80−35077
ribbon growth Stepanov technique, recent develop. 79−11510
ribbon growth using scanned focused CO_2 laser beams 80−66417
ribbon parallel twinned structure development by shaped crystallisation 78−64465
ribbon prep. by electron bombardment *(French)* 78−64474
ribbon solar cells, defect anal. using laser scanner 80−94089
ribbon solar cells, var. of minority-carrier diffusion length with light intensity, heavy metal doping effects 80−93937
ribbon surface, vapour-deposited SiC film growth, TEM anal. 78−84094
ribbon to ribbon growth, using laser scanning tech., solar cell appl. 78−35299
ribbon-form material, rapid quenching from melt *(Japanese)* 78−92210
ribbon-to-ribbon growth method and sample characterisation 78−11103
silicon continued
ribbons, edge-defined film-fed growth technique for solar cells 80−89138
ribbons, roller quenching method of prep., grain sizes and carrier conc. 80−40275
ribbons for solar cells, ultra high speed growth, elec. props. 80−89162
ribbons grown by capillary action shaping technique, surface quality and impurity distrib. 80−108343
ribbons produced through capillary action shaping elec. and struct. characts. 78−47804
ring photodiode reflectometer for cavity reflectance 80−86376
rough surface, polarisation angles, ellipsometric meas. 78−56449
RTR ribbon, impact of defects on photovoltaic potential 79−11186
rubber, dimensional stability, surface roughness testing by interferometric gauge 79−21807
sapphire-Si interface structure, SIMS obs. 77−76675
Schottky barrier diodes, temp. anomalies 78−14823
Schottky barrier formation, photoemission exam. of filled surface states and band bending 77−28250
Schottky barrier height approaching band gap, minority carrier injection effect 77−20434
Schottky barrier height control using knock-on effect in ion implantation 77−76919
Schottky barrier height meas. on clean-cleaved samples 78−52081
Schottky barrier metallisation characteristics 77−76922
Schottky barrier photovoltaic IR detector 80−9040
Schottky barrier solar cell, V-I charact. and efficiency 78−14828
Schottky barrier structs., proton bombarded, defect states 80−29356
Schottky barrier to transition metal silicide, effect of glassy membrane 77−85311
Schottky barriers, silicide contacts, elemental description 80−60085
Schottky diode aging, influence of metal electrode O diffusion coeffs. 79−99620
Schottky diodes on sputtered amorphous Si:H, light induced ageing effects, interpretation of photovoltaic stability 80−54780
Schottky magnetodiode, integrated mag. sensor 80−68223
scratches on near (111) slices 77−12726
screened donor impurities, binding energy calc., anisotropic mass effect 78−10399
screening of donor ions by delocalised electrons 79−69466
screening of ions, band struct. calcs. with screening variants 78−67938
screw and 60° dislocations velocities 79−86798
screw dislocation networks, TEM study 80−70204
secondary electron emission on low energy primary electron irrad. 79−69934
secondary electron energy spectra due to He^+, Ar^+ ion impact 78−11049
Seebeck effect position sensor for CO_2 laser beam alignment 80−5772
selective anodic oxidation of Si in O_2 plasma 80−108610
self diffusion entropy 80−29211
self implanted, and additional impurity implanted laser induced recrystn., threshold power density 79−69131
self- and impurity diffusion 80−29213
self-consistent pseudopotential cal. of electronic states associated with reconstructed vacancy 79−73465
self-diffusion, activation energy and entropy factors 80−88353
self-diffusion, dynamical recovery 80−29215
self-diffusion, probed by (p,γ) resonance broadening method 80−24646
self-diffusion and dynamical recovery at high temps. 79−69284
self-diffusion and dynamical recovery in single crystals 78−87816
self-diffusion coeffs. between 1320K and 1660K, extended interstitial mechanism 77−84985
self-diffusion mechanism 79−90824
self-implanted, defect-density profiles, constant-capacitance DLTS meas. 79−95361
self-implanted layer, grain size, laser irrad. energy density depend. 78−72012
self-interstitials, vacancies of their clusters 77−80500
self-ion implanted, amorphous to polycrystalline transition induced by laser beam 77−84771
self-ion implanted, laser annealing, channelling and TEM meas. 80−24466
self-scanned photodiode array, evaluation for integrated optics spectrum analyser 80−58806
self-supporting polycryst. film deposited by energy beam plasma, for terrestrial solar cells 79−11523
SEM, contrast of electron channelling patterns, estimation from low index refl. 78−9921
SEM, electron channelling patterns 78−83697
SEM characterisation of single cryst. using Schottky barrier charge collection microscopy 77−4444
SEM exam., ultra-high vacuum, secondary electron emission dependence on electron beam dose, surface interactions from AES and ELS 80−61209
semi-insulating polycrystalline CVD layers, AES and XPS characterisation 80−16129
semiconductor detector material, purification, cryst. growth, ion implantation 78−47674
semiconductor pulse diodes, application of Pd for reducing recovery time of reverse current *(Russian)* 79−99226
semiconductor-insulator structures, contact pot. meas., vibr. condensor method *(German)* 79−11232
semiconductors, defect processes, electronic stimulation 80−24665
semicrystalline layer, deposited on stainless steel and Pyrex glass, growth conditions and props. 79−82482
semicrystalline vs. single crystal, for photovoltaics 80−93917
semivacancy and pair of semivacancies calc. by CNDO/2 method 78−51537
shadow mask etching for ion implantation 78−6086
shallow contact formation substrate temp. depend., Pd-W alloys 80−96963
shallow contact formation substrate temp. depend., Pt-W alloys 80−96963
shallow donor states, substitutional donors 79−65403
shallow donors, Zeeman interaction, relativistic corrections and very small g-shifts, contrib. to EPR 78−72393
shallow impurities, photolum. anal. 78−23512
shallow impurity bound states, IR spectroscopic obs. 77−39806
shallow junction devices, silicide contact 80−70819
shaped crystal growth from melt, meniscus-controlled process 80−107075
shear deformed, Smith-Herring and mobility change piezoresistance 80−6842

silicon continued
sheet, high speed growth, heat transport analysis 80−107669
sheet casting for solar cells 80−89139
sheet edge-defined film-fed growth, for photovoltaic cells 79−61982
sheet-form solar cells, efficiency improvement, minority carrier diffusion length limitations 80−93925
sheets production, low cost, crystal growth techniques comparison 80−35083
Si:Au, step junction, mathematical model *(Rumanian)* 79−87148
n-Si:B, ion implanted, rapid identification of faulted loops 79−19254
Si:B, isolated A^+ states under high compressive stress, long wavelength photocond. spectra 79−60765
a-Si:H_x structure, effect of H-Ar plasma contact on elec. props., and optical gap 80−34533
Si:In growth by Czochralski crystal pulling, characterisation for extrinsic IR detectors, focal-plane arrays 80−76168
Si:P(As)(Sb)(Bi), high resolution study of group V impurities absorption 80−7388
Si surface, line tension induced dislocation motion 79−82212
Si-Al_2O_3-SiO_3 in MIS struct., charge accumulation and spreading *(Russian)* 78−64116
n^+-Si-Al ohmic contacts, metallisation structs. for very shallow n^+/p junctions 80−60084
n-Si-electrolyte junction, Schottky barrier height and reverse current 80−6979
Si-quartz boundary, mech. of contact interaction, mech. and optical props. 78−88375
SIMS quantitative anal. 80−101052
single cryst., chem.-mech. polishing of low-scatt. optical surface 80−96040
single cryst. growth in clear SiO_2 crucibles, heat exchanger method 79−33919
single crystal, appl. as thermal neutron filter 79−45512
single crystal, inelastic neutron scatt. study using uniaxial press. 77−35442
single crystal growth advances 78−6842
single crystal growth by heat-exchanger casting 78−11104
single crystal ribbon growth, thermal anal. 78−3029
single crystal solar cell manufacturing process, laser annealing of implanted area, energy saving 80−97791
single-crystal, grown-in structural defects 79−10860
single-crystal clocks and frequency standards 78−57915
slice resistivity var. meas. using automated photovoltaic systems 80−52274
slip, room temp., TEM obs. 80−79804
slip dislocation nucleation during laser annealing 80−84179
small-diameter cryst. grown by pedestal technique, investigation of microdefects using X-ray topography 79−55683
snowflake defect due to annealing in H at 1000°C X-ray topography study *(Chinese)* 80−49227
SOC (Si on ceramic) continuous coating for solar cells 80−93904
soft X-ray electroreflectance, final state effects on Si(2p) optical transitions 77−66553
solar, cell high-intensity, fabrication and AM1 efficiency 79−43760
solar cell, amorphous, technological development trends for low cost energy requirements 80−26136
solar cell, CVD layers, grain boundary effects rel. to dopant conc. 77−7744
solar cell, device model for tandem junction cell 80−16813
solar cell, EFG ribbon, diffusion length enhancement under illum. 78−14756
solar cell, elec. characts. of Pd_2Si and PtSi Schottky barriers 78−14825
solar cell, fabrication using zone melting of CVD Si on graphite, and performance 77−85945
solar cell, I-V charact. meas., effect of voltage ramp, theoretical anal. using linear model 80−61354
solar cell, ion implanted drift field device 77−24615
solar cell, laser annealing, conversion efficiency improvement *(French)* 80−66976
solar cell, minority carrier excess charge and time const. 78−30938
solar cell, minority carrier lifetime *(Korean)* 78−23103
solar cell, n^+-p, degradation mechanisms associated with Ti impurities 80−81465
solar cell, open-circuit voltage at ultrahigh light intensities, plasma reflection effects 80−96928
solar cell, p^+-i-n^+, field induced junction, conversion efficiency limit in concentrated sunlight 80−85282
solar cell, photovoltaic energy conversion efficiency, photoacoustic spectra 79−15178
solar cell, tandem junction, operation and parameters, model 79−100521
solar cell, thin film prep., in orbiting ultrahigh vac. facility 78−7855
solar cell application, characterisation of nonideal material by lifetime and diffusion length 79−15192
solar cell array with concentration, design and development 80−45700
solar cell arrays, Si, fixed-base, flat panels, possible developments for more competitive power production 80−72050
solar cell arrays, technological and economic barriers to be overcome for competitive power production 80−72049
solar cell fabrication, R and D on low-cost processes, effect of impurities on cell performance 80−50978
solar cell fabrication developments using Si on ceramics and minute spherical cells 80−55839
solar cell fabrication from multiple ingots using melt replenishment Czochralski method, cell anal. 80−93477
solar cell from film on foreign substrate 77−77390
solar cell multicryst. material prep., fast-pulled float zone, CZ and cast ingot and foil methods 80−93483
solar cell parameters, grain size dependence 80−94049
solar cell processing, pulsed laser techniques for annealing ion-implantation damage 80−81453
solar cell production, Union Carbide Corporation Silane Process, cost analysis 80−21403
solar cells, Al-thin oxide-Si, Schottky barrier, degradation effects, ion beam induced nuclear reactions 80−30488
solar cells, all-plate low cost contact system 80−93992
solar cells, amorphous, glow discharge produced 80−12013
solar cells, amorphous and polycryst. thin film solar cells, perform. parameters, review 80−93882
solar cells, analysis of short-circuit current 80−85285
solar cells, appl. to electronic equipment and appliances *(Japanese)* 79−83599
silicon continued
solar cells, base resist. influence on temp. characts., temp. cycling 80−89618
solar cells, calculations of absorption coefficient 80−7944
solar cells, capacitance transient spectra of processing- and radiation-induced defects 80−61340
solar cells, carrier lifetime meas. from transient photoresponses of pulsed laser *(French)* 79−24898
solar cells, concentrated, conducting grid, design rules *(French)* 79−24896
solar cells, concentrator, new technology for fabrication 80−81457
solar cells, crystal growth, heat exchanger method, fixed abrasive slicing technique 80−35082
solar cells, design, fabrication and evaluation of a 2″ high efficiency cell for concentrator systems 80−55854
solar cells, design for limit conversion efficiency 80−93960
solar cells, developments, appls., and economics of solar photovoltaic conversion *(German)* 80−26132
solar cells, developments *(French)* 80−55845
solar cells, developments and trends for automatic interplanetary stations, Venus-9 and Venus-10, and mooncar program 80−89613
solar cells, diffused horizontal homojunction, effects of junction depth and impurity conc. 80−55877
solar cells, diffused junction, n^+pp^+ or p^+nn^+, prep. using solid diffusion sources 80−35689
solar cells, diffusion fabrication process, low cost, highly automated 80−30487
solar cells, edge-illuminated p^+-nn^+, analytical model under concentrated sunlight 80−7942
solar cells, effect of Ti, Cu and Fe 80−72064
solar cells, effects of metallic impurities 80−85278
solar cells, efficiency limits, comprehensive explanation 80−35688
solar cells, experimental efficiency optimisation of n^+pp^+ and p^+nn^+ cells 80−30486
solar cells, fabrication using continuous or pulsed lasers *(French)* 80−61350
solar cells, for satellite solar power systems, developments and future trends 80−45694
solar cells, fundamental efficiency limitations 80−93963
solar cells, grain boundary defects in thin semicrystalline material 80−93889
solar cells, grating minority carrier, design and expt. results 80−81445
solar cells, growth of large grain polycryst. layers on graphite substrates by CVD on liquid layers 80−55849
solar cells, high open circuit voltage, P implantation 80−89642
solar cells, HV, multijunction, characts. 80−89615
solar cells, implanted layers characteristics, laser irradiation effects 80−35692
solar cells, inhomogeneities and their influence on cell performance 80−93967
solar cells, ion implantation and annealing technology 80−93996
solar cells, ion implanted, from EFG Si ribbons 80−30485
solar cells, ion implanted grating type 80−101102
solar cells, ion-implanted, expt. study of efficiency controlling factor 80−93997
solar cells, ion-implanted, factors controlling efficiency 80−81451
solar cells, ion-implanted 80−81452
solar cells, junction formation techniques using spray-on polymer dopants, cost effective, high throughput 80−94014
solar cells, large grain films on metallurgical Si substrates, chem., struct., elect. and photovoltaic props. 80−61357
solar cells, laser annealing, reviews 80−93976
solar cells, light-enhanced diffusion length obs. by DC photocurrent meas. 79−39301
solar cells, limit efficiency evaluation 80−93973
solar cells, low cost, Ni contacts 80−94017
solar cells, low cost processes for fabrication 80−94013
solar cells, low cost Si production, growth from melt 78−3028
solar cells, low mass space blanket using 50 μm cells 80−30498
solar cells, low-cost, starting materials technology and economics 80−30483
solar cells, low-cost fabrication processes *(Japanese)* 79−83600
solar cells, low-cost sheet fabrication 80−50977
solar cells, manufacturing cost anal. of flat plate vs. concentrator solar cells 80−93949
solar cells, minority carrier lifetimes determ. from spectral and transient meas. 79−100533
solar cells, monocryst. sheet fabrication, CLF Czochralski furnace and enhanced slicing technology 80−93476
solar cells, MOS and oxide-charge-induced BSF structs., open-cct. voltage >700 mV, 20% conversion efficiencies 80−81435
solar cells, multi-bandgap concentrator cells, Si and $Al_xGa_{1-x}As$ systems, operation with spectrum splitting filter 80−45698
solar cells, n^+-p junction, electron irrad., DLTS spectra and defect effects 80−93999
solar cells, Ni-Cu conductor system 80−93991
solar cells, output power and sunshine conditions, correlation 80−97785
solar cells, p-n junction, importance of surface recombination and energy-bandgap narrowing 79−100520
solar cells, photoelectric effect and principles of operation and efficiency 80−50983
solar cells, photoreactance of p-n junction diodes 80−81464
solar cells, $POCl_3$ gettering of Ti, Mo and Fe-contaminated cells 80−94010
solar cells, polycryst. surface barrier cells, eval. for terrestial appls. 80−61376
solar cells, polycrystalline, from recrystallized plasma deposited thin films 80−104509
solar cells, polycrystalline film, effect of defects/grain boundaries on photovoltaic mech. 80−93883
solar cells, polycrystalline n^+/p, computer model of spectral response and photocurrent 80−55853
solar cells, polycrystalline p-n junctions, recombination currents, physical models 80−93892
solar cells, preparation using laser processing 80−81454
solar cells, production problems of polycryst. Si cells *(Rumanian)* 80−21398
solar cells, RAD polysilicon sheets, photovoltaic potentialities, conversion efficiencies, limitations 80−30484
solar cells, radiation damage annealing mechanisms and low temp. annealing 80−94003

silicon continued
solar cells, radiation damaged, origin of reverse annealing 80−76630
solar cells, realisation by laser induced diffusion of deposited Sb 80−93998
solar cells, review and current developments 80−108801
solar cells, review of physics underlying recent improvements 80−93974
solar cells, screen printed, effect of double exponential on efficiency and yield 80−55851
solar cells, SEM electron beam induced current study, contamination effect 79−43773
solar cells, semiconductor thick film cell contacts, all metal 80−30489
solar cells, solid source diffusion process for fabrication 80−93994
solar cells, spray-on TiO_2 antireflection coatings 80−80963
solar cells, technological developments of single crystal cells and cost-effective cells 80−50984
solar cells, technology development of 50 μm cells for space power systems 80−30499
solar cells, terrestrial photovoltaic systems, historical developments and current research and development trends 80−45702
solar cells, thin cell with back surface reflector, and controlled optical absorptance 80−35691
solar cells, TiO_2 AR coating by spray deposition 80−104511
solar cells, ultrathin, electron and proton effects 80−94002
solar cells, undergraduate teaching expts. 77−74177
solar cells, unified model of fundamental limitations 80−81448
solar cells, updating limit efficiency 80−81447
solar cells, upgraded metallurgical grade substrates, epitaxial growth 80−93905
solar cells appl. minority carrier MIS diodes *(Slovak)* 80−97792
solar cells effects of B and P impurities on cell performance 80−55848
solar cells for cathode protection of submerged marine structures 80−40859
solar cells proton irradiated, processing influence on elec. performance 80−94001
solar cells using minority carrier MISS 80−101103
solar cells with concentrating collectors and integrated heat use system 80−45701
solar cells with fire through contacts printed on anti-reflection coating 80−93993
solar cells with screen printed diffusion and metallisation 80−94015
solar concentration cells, concentrated sunlight effects, experimental results, interpretation 80−35690
solar concentrator cell, effects of nonuniform illumination and temp. profiles under concentrated sunlight 80−93941
solar concentrator cells with high efficiency 80−93938
solar energy conversion, Si film selective absorber 78−25954
solar grade, advances in Dow Corning process 79−8243
solar grade, by $SiHCl_3$ CVD process, low cost 79−62007
solar grade, Czochralski growth, solar cell efficiency vs. metallic impurity conc. 78−31330
solar grade, silane pyrolysis, process design and economics 79−8234
solar grade Si prod., using Dow Corning process 80−29894
solar power cell production by capillary action shaping technique 79−34431
solar selective absorbers, Si on Al, interf. films deposited on diffr. gratings 79−14103
solar-grade, directional solidification in carbon crucibles 80−45663
solid, electron rearrangement after inner shell ionisation by heavy charge particle impact 80−87043
solid phase epitaxial growth through Al film 79−24432
solid phase epitaxy, Si(100)/Pd_2Si system, dissoc. mechanism 77−7980
solid phase epitaxy in silicide forming systems 78−23613
solid solubility of Co, 1000-1270°C, radiotracer obs. 77−51500
solid solution, of B, equilib. with B_2H_6 80−97721
solid thermal cond. and interface resistance meas. by radiation thermometry 80−86289
solid-phase epitaxy in Si (100)/Pd_2Si/Si (amorphous) system, radioactive tracer obs. 77−89663
solubility in Al-Au melt *(Russian)* 77−66024
solubility in $Ga_xAl_{1-x}m$ melts *(French)* 77−51498
solubility in Mg, depend. on impurity inclusions *(German, English)* 80−97492
solubility of Au, gettering by P 78−83961
solubility of group III and V elements 77−84928
solute loss on laser annealing, solute out diffusion 80−100840
solution-melt Ge-Au drops, periodic instability of motion over cryst. surface 78−47260
SOS early growth, island coalescence model 77−76704
SOS early growth, transmission electron microscope obs. 77−76703
SOS epitaxial layer, gettering effect by O implantation, Hall and Rutherford backscattering meas. 79−65103
SOS films, cryst. quality improvement by Si ion channelling, annealing 80−44222
SOS films, surface recomb. profile and transport parameters 79−33357
SOS MOS devices, hole mobility under residual stress, Hall meas., valence band struct. 78−88039
SOS single crystal films, struct. and elec. props., review *(Japanese)* 77−63009
SOS structure, radiation dose at interface due to electron beam aluminisation 78−68089
SOS structures, high-field electron transport, drift vel. meas. 80−80387
SOS wafer for beam profile monitoring in high-current ion implantation systems 80−13182
spatial distribution of temperature rise induced by Gaussian laser beam 79−69917
specific heat at constant volume, leading anharmonic contribs. 77−89549
spectrochemical anal. of semiconducting Si for traces of Br and Cl using hollow cathode of special design *(Russian)* 77−29083
spectrochemical analysis, atomic-absorption, tubes design with hollow cathode *(Bulgarian)* 80−85232
spectroscopic applications of structures produced by orientation-dependent etching 80−93668
spherical effective impurity electron mass 77−24532
spin dependent effects, theory 78−23342
spin dependent recomb. at dislocations, EPR and photocond. 79−38095
spin dependent recombination and photoconductive resonance 78−43439
spin effects in electron transitions via dislocation states 79−82642
spin polarons, mag. props. of dislocations 79−82531
spreading resistance calibration, effect of specimen preparations 78−10450
spreading resistivity rel. to load applied to meas. probe 73−4647

silicon continued
sputter cleaning using Ar^+ ions, temp. depend. of residual damage, 25 to 800°C 77−48558
sputter yields, anomalous, due to cascade mixing 80−76122
sputter-machined surface, Ar^+ ion, lattice disordering obs. *(Japanese)* 80−3228
sputtered, cluster formation, influence of HF plasma interaction 78−64441
sputtered amorphous film, photocond. and electronic props., effects of annealing in plasma gas 80−44644
sputtered atom ang. distribs. for keV Ar^+ bombard. 80−84819
sputtered layers, EPMA of Ar content 80−3443
sputtering, low energy, H, D and He ions 80−100734
sputtering by Ar^+ ions, energy depend. of excitation 79−56906
sputtering by low energy Ar ions, temp. depend. of sputtering coefficient 79−15578
sputtering process study on Au, Al, Si targets, Rutherford backscatt. technique 77−8703
sputtering rate on Ar ion bombard. 80−55245
sputtering yield, Ar(Xe) bombarded, energy and fluence depend. 79−78805
square single crystals, Czochralski growth 80−97422
stacking fault annihilation by impurity diffusion 77−19968
stacking fault energies, dislocation struct. models 79−82205
stacking fault energies, intrinsic and extrinsic, by TEM 80−10562
stacking fault form. model during oxidation and ageing, defect clustering 77−24322
stacking fault formation, elimination by preoxidation annealing in $N_2/HCl/O_2$ mixtures 78−88550
stacking fault growth, oxidation induced, role of point defects 78−10061
stacking fault growth, oxidation-induced, HCl and interstitial effects 80−49241
stacking fault nucleation at oxide precipitate-dislocation complexes, TEM 77−19967
stacking faults, dynamic processes associated with deform. twins, HVEM in-situ obs. 80−103369
stacking faults, elimination in CCD processing 78−10065
stacking faults, generation and annihilation during oxidation 77−76419
stacking faults, MeV He ion irrad., TEM obs. of defect clusters 77−89483
stacking faults, oxid. induced, oxygen content influence in Czochralski wafers 78−10062
stacking faults, oxid. induced, wafer orientation and ion implantation effects 78−10063
stacking faults, preoxidation gettering by reverse side P diffusion-induced misfit dislocations 80−60988
stacking faults, weak-beam contrast in TEM 80−75132
stacking faults and precipitates, elec. props. in heated-treated dislocation-free crysts. 77−39796
stacking faults growth by Bardeen-Herring mechanism 79−99222
stacking faults induced by oxide precipitates 78−67723
stacking-fault nuclei, gettering by trichloromethylene, oxidation 77−43226
static compression in [100] and [111] directions, elec. resist. obs. 80−65637
static dielectric function, local field correction, tight-binding model 79−95355
stationary creep depend. on deform. stabilisation of material struct. *(Russian)* 80−100300
steam oxidation, low temp., high press., oxide growth kinetics and props. 80−16523
steam oxidation at any elevation, improved theoretical predictions 79−20230
steel:Si alloy formation kinetics at solid cathodes, metal electrodeposition from molten salt electrolytes 80−26028
steels, Si determination by at. emission spectroscopy using steeloscope 79−57330
STEM and TEM, limiting factors in specimen thickness 77−19852
stimulated Raman scattering using Q-switched single mode Nd:YAG laser 79−94289
strain distributions rel. to dopant conc., accurate determ. by X-ray Bragg reflection 77−19835
strain gauge for cryostatic temp. 78−24782
strain meas. by Pendellosung effect after P ion bombard. 78−55773
strained, crit.-point for electron-hole droplets 79−4516
strained crystal, annealing effect, recrystn. and struct. *(Russian)* 80−89252
stress enhanced diffusion of B, using SiO_2 diffusion masks, photodiode fabrication 78−67865
stress measurement, appl. of photoelastic technique 80−48656
stress relaxation, analysis of expt. results 77−84835
stressed, one- and two-component electron-hole liq. at T=0 80−80189
stretched, lattice vibr. anharmonicity, influence of stress on elastic moduli, Raman spectra 80−80791
strip mass flowmeter 79−77302
strip-type crystals, growth mechanism, morphology 79−7559
strongly-doped monocrystal Josephson junctions 79−56400
structural defects on (115) plane 78−87675
structural properties, self-consistent calc. 80−28947
structural props. using electron-ion Hamiltonian using density-fundamental methods 79−82177
structurally related bulk and surface props., self-consistent pseudopot. method 80−54632
structure factors, determ. by intersecting-Kikuchi-line method 80−14971
subnanosecond detector, characts. 78−9027
substitutional diffusion model 78−71884
substrate, Ag film growth modes and nucleation, SEM study 80−100423
substrate, Au film oriented crystn., formation of coincidence orientations on interphase boundary 79−90922
substrate, crystn. of amorphous SiO_3, Si_3N_4 and $Si_xO_yN_z$ films 79−28225
substrate, doped oxide film formation mechanism, X-ray spectral anal. 79−87008
substrate, doubler layers of Ni and Pt, silicide formation 78−84010
substrate, effect of surface conditions on plasma sprayed metal coatings 80−21145
substrate, effect on liq. cryst. mol. alignment 77−7663
substrate, for Au film, interphase coincidence boundaries 79−1560
substrate, heteroepitaxy of deposited amorphous Ge layer by laser annealing 79−77952

silicon continued
substrate, implantation effects on hardening and Si_3N_4 film stress reduction 78−71748
substrate, ion induced intermixing of Pd or Pt film 80−15420
substrate, low temp. migration into Au/Pt film, with interposed Cr layer 79−10981
substrate, Nb thin film intermixing with substrate, ion induced silicide formation 80−34101
substrate, nucleation controlled interaction with metal film, silicide form. 80−10711
substrate, polycryst. Al_2O_3 anodisation, MAOS struct. form. and props. 77−48563
substrate, process-induced in-plane distortion, correl. with wafer bowing 80−54579
substrate, reaction with Ti film, backscatt. anal. of silicides 79−69377
substrate, Si_3N_4 growth using anhydrous NH_3 79−43141
substrate, silicide formation with bilayers of Pd-Pt, Pd-Ni and Pt-Ni 79−51444
substrate, silicides formation on Mo-W bilayer films, marker expt. 79−99376
substrate, solid state reaction with Ti film, backscatt. anal. 80−34257
substrate, stress field, induced by Si_3N_4 film edge, indentation-injected dislocation half-loops obs. 78−30839
substrate, struct. stability of dielec. film 80−54564
substrate, thermally oxidised, interface props., sputter deposition parameters effects *(German)* 80−40257
substrate, thin films of Ag or Al, work function *(French)* 80−80353
substrate, vitreous SiO_2 film defect struct. comparison with crystalline SiO_2 and Si-O bond nature 80−54557
substrate (111), MBE deposition kinetics of Bi film 80−10817
substrate for Ag, UHV-SEM studies of Stranski-Krastanov growth 80−79722
substrate for Al film, annealing effect on eutectic point *(Russian)* 80−100850
substrate for Au film, use of sputtering for layer removal 79−78813
substrate for epitaxial crystn. of GaP films by ns laser pulses 80−107674
substrate for Pb, Sb, and Bi silicate films, form. kinetics and props. 80−35358
substrate for Pb thin film, residual strains 78−18915
substrate for Pb ultrathin films, supercond. transition temp. 77−66220
substrate for Pd and Pt, silicide formation by laser, electron beam annealing 80−84849
substrate for PMMA electron sensitive layer, 400 Å linewidth electron beam lithography 80−65392
substrate for Pt-Ni vacuum condensates, X-ray anal. *(Russian)* 80−70559
substrate for RF sputtered ferroelectric $BaTiO_3$ films, ferroelectric props. 80−80697
substrate for SiO_2 film, ellipsometric spectra, thickness determ. *(Chinese)* 80−86379
substrate for Ta or Ta_2O_5 film, film-substrate interaction obs. 77−1324
substrate for W film, properties and kinetic parameters for deposition 78−91570
substrate for wet thermal oxide film, trap emptying kinetics 80−92983
substrate for ZnS, Na_3AlF_6 films, H_2O absorpt., IR anal. 80−75446
substrate package for integrated GaAs laser arrays, fabrication 79−18555
substrate surface, low loss electron and Auger images correl. 78−22944
substrate thinness, device design, solar cell processing, empirical study of interaction 80−93995
substrates, action of plasma in capacitive electrode HF discharge *(Russian)* 78−95818
substrates, appl. of silicates to detection of flaws in glassy passivation films 77−39745
substrates, growth and props. of GaP liquid phase epitaxial lqyers 78−6864
substrates, reactive ion etching 79−83351
substrates, review of defects 77−39597
substrates, semicond., stress meas. in deposited thin films, X-ray topography techniques 78−5710
substrates for integrated optics high quantum efficiency waveguide coupled photodetectors 80−58805
superconducting film, A1-type, critical mag. field 78−31023
superconductor-semicond. device research, future prospects 79−28467
superlattice, natural orientational, and 2D electron gas 79−99598
superlattice and 2-D electron gas 78−64080
support, effect on transverse modes in gap-coupled surface-wave devices 79−46138
surface, 100, reconstructed, atomic and electronic struct. 79−73381
surface, {100}, defect etch for evaluation 79−90657
surface, {111}, 2×1 reconstruction mechanism 77−66079
surface, (001), clean, double diffr. spots in RHEED patterns 79−90855
surface, (001), energy gaps in inversion layer band struct., spectroscopic determ. 79−82658
surface, (001)-(2×1), reconstruction-induced mean-square displacements 80−15343
surface, (100), (1×1)H struct., averaged LEED 77−62720
surface, (100), accumulation layer, subband struct. and inter-subband absorption in strong mag. field 78−39177
surface, (100), diffr. of He atoms obs. 78−52609
surface, (100), dimer reconstruction, photoemission obs. 80−80939
surface, (100), effect of H adsorption on surface struct., LEED meas. 78−14602
surface, (100), intersubband optical absorption in space-charge layers 77−35984
surface, (100), inversion layer, interaction induced transition at low density 80−15581
surface, (100), LEED meas. 78−60016
surface, (100), models of (2×1) surface struct., quasidynamical calc. of LEED intensities 78−71921
surface, (100), pairing model, electronic pot., charge density, Fermi energy and surface density of states 77−47875
surface, (100), space-charge layer, intersubband cyclotron combined resonances 79−69571
surface, (100), struct., LEED study, atomic arrangement model 78−71922
surface, (100), temp. depend. of electron intersubband reson. 78−14783
surface, (100) 1×1, H monolayer, electronic props., self-consistent calc. 77−43690
surface, (100) (2×1) clean, struct. using averaged LEED 77−59194
silicon continued
surface, (111)2×1, surface electron states detected by external reflectivity 78−80036
surface, (111)2×1, surface states, reflectivity obs. 80−50368
surface, (111)7×7, electronic struct. calc. 80−24993
surface, (111), Al overlayers, theoretical study 78−95366
surface, (111), anal. by ion-electron spectroscopy 78−72670
surface, (111), ang.-resolved photoemission, matrix element effects 79−69957
surface, (111), atomic and electronic struct. 78−72223
surface, (111), atomic and electronic struct. 80−54746
surface, (111), atomically clean, diffusion of adsorbed Au 78−72037
surface, (111), clean, ESCA obs., Ni(Au) surface impurities 78−52640
surface, (111), clean, new diffr. phenomena in RHEED 78−63910
surface, (111), clean and O_2-chemisorbed, electron states by AES 80−54747
surface, (111), Cu phthalocyanine dye deposition, low energy electron optically modulated transmission increase 79−78133
surface, (111), electron energy loss spectroscopy of NO, O_2 and NH_3 78−2374
surface, (111), electron inversion layers, obs. of sixfold valley degeneracy 79−38176
surface, (111), electronic density of states changes during O adsorption, AES obs. 79−65528
surface, (111), energy states, computer renormalisation-group calc. 80−75617
surface, (111), H chemisorbed, electronic struct. 78−39182
surface, (111), heating effects on ellipsometric parameters 77−72764
surface, (111), high resolution photoemission yield, surface states 77−69392
surface, (111), ideal and relaxed surface, electronic struct. 79−60901
surface, (111), interaction with Ag, AES 78−14589
surface, (111), interpretation of intrinsic surface states 78−6423
surface, (111), ion bombard., struct. changes, AES obs. 80−79842
surface, (111), LEED intensity measurement by photographic method with digital image processing 79−60234
surface, (111), low energy H^+ and He^{++} ion refl., computer simulation 80−11524
surface, (111), low press. baked, dominant interactions and average distances between paramag. centres 80−15783
surface, (111), MEED, secondary electron emission under surface state reson. 78−84688
surface, (111), metastable 2×1 reconstructed, dangling bond mediated attractive electron-electron model 78−91520
surface, (111), non-orthogonal tight-binding approach to surface states 80−2442
surface, (111), O_2 adsorption, atomic steps and residual gas effects 80−54517
surface, (111), oxidation stage, EXAFS 79−95876
surface, (111), oxide formation, AES and EELS meas. 80−3232
surface, (111), oxidised, energy depend. of photoelectron attenuation length 78−52643
surface, (111), relax. of surface atoms, Si_4H_9 clusters 77−35980
surface, (111), surface energy bands, and atomic position of chemisorbed Cl 78−56041
surface, (111), UHV cleaved, adsorbed O, electronic transitions 78−39183
surface, (111), with Al overlayers, electronic struct., self-consistent pseudopotential method 79−4595
surface, (111), with and without H chemisorption, Auger surface spectroscopy 80−50472
surface, (111) 2×1, cleaved, O_2 adsorption, low-energy electron loss spectra 79−15840
surface, (111) 2×1, LEED theory and expt. 79−46895
surface, (111) 7×7, energy- and ang.-depend. secondary electron emission, surface state reson. 79−69930
surface, (111) 7×7, interaction with H_2S, LEED and AES 78−38966
surface, (111)-(7×7), and impurity stabilised Si(111)-(1×1) surface, photoemission studies 80−104041
surface, adatom indirect interaction, theory 80−44696
surface, adsorbed Br, X-ray standing waves obs. 80−96417
surface, Al-coated, surface phonon Brillouin spectra 79−78694
surface, ang. variations of backscatt. yield with 20 keV proton bombardment, for single cryst. 79−4879
surface, Ar^+ and e^- excited Ar Auger electron emission 79−47560
surface, Ar^+ ion bombardment, O_2 enhancement of sputtered ion yields 79−38705
surface, Ar bombarded, blistering effects, SEM obs. 78−67745
surface, atomically pure, optical consts. and temp. depends. 79−65823
surface, Auger spectrum, high energy plasmon satellites 78−2955
surface, band structure, minigaps, magnetoresistance, cond. space charge layers 80−92980
surface, bonding states of adsorbed O_2, photoemission obs. 78−92170
surface, CF_3^+ ion bombardment, XPS and Auger study 79−70367
surface, chem. deposition of Au film, reacts. 78−34723
surface, chemical aspects of fluorocarbon plasma etching 79−83350
surface, chemical reaction with H, contact with low-press. plasma 79−47968
surface, chemically etched, struct. transforms. during thermal oxidation 78−79557
surface, chemisorption of H, UPS spectra meas. 77−20186
surface, clean, geometrical struct. rel. to electronic props. 77−62719
surface, clean and gas (O_2 and H_2O) covered, appl. of UPS ultrahigh vacuum apparatus *(Japanese)* 80−37125
surface, cleaved (111), electronic structure following Al adsorption 80−75610
surface, cluster model approach for electronic struct. 78−56205
surface, controlled stripping, automated system 78−31557
surface, decontamination of Au impurities by etching 80−55559
surface, depth profiling, optoacoustic technique 80−65337
surface, electron states, surface photovoltage spectroscopy study, doping effects 80−49860
surface, electronic struct. at semicond.-vacuum and semicond.-metal interfaces 77−20428
surface, electronic struct. rel. to sorption 78−14784
surface, energy-minimisation approach to atomic geometry 78−95213
surface, etched and heat-treated, optically stimulated ESR investigation 80−11245
surface, field penetration and band bending in high elec. fields 79−42613

silicon continued
surface, giant core-exciton effects, electron energy loss spectra and XPS 77−24600
surface, He^+ bombardment, damage production, defect diffusion 80−39181
surface, high index, theory of inversion layers 80−44697
surface, ideal and 2xl chain-reconstructed, electronic struct. determ. 78−52050
surface, influence of mech. treatment, charact. by ellipsometry 78−15141
surface, interaction of oxygen gas discharge plasma 78−83840
surface, inversion layer, crit. conc. of hot carriers 77−35977
surface, ion bombardment enhanced mixing of Ag layers, Rutherford backscatt. meas. 80−65034
surface, KLL Auger peaks, bremsstrahlung-induced 80−45199
surface, laser-annealed, characterisation by ellipsometry 80−103544
surface, local density of states method and bond orbital model calc. 77−8165
surface, Lyman-α emission from proton bombard. 79−91503
surface, metal doped, recomb. of nonequilib. carriers at high excitation rates 79−7835
surface, morphology and electronic struct. 79−78194
surface, $MoSi_2$ form. in Mo films *(French)* 78−43270
surface, N_2^+ bombardment, 500 eV chem. reactions, XPS and UPS 78−48265
surface, near (III), dislocation movement at annealed scratches, X-ray topography obs. 80−2029
surface, negative electron affinity activation treatment, laser beam scanning obs. 79−4890
surface, optical modulation of low energy electron reflection and transmission 78−88388
surface, oxide overlayer, angular-depend. XPS exam. 77−55864
surface, photon excited field emission 79−78851
surface, plasma etching as diagnostic technique 77−44385
surface, plasma etching in CF_4-H_2 glow discharge, AES meas. 79−98922
surface, plasma etching using CF_4 78−39921
surface, pulsed electron beam processing, doping, annealing 80−75254
surface, pulsed laser atom-probe FIM, expts. 80−66402
surface, pure, oxidised element determ. by SIMS 78−85247
surface, pure and with adsorbed Al(Au), thermal expansion and at. vibr. 77−89635
surface, reactive ion etching, reactant supply 79−83349
surface, reactive ion etching in CF_4 plasma, competitive mech. 79−91816
surface, reconstructed, (111)2×1, polarization depend. of optical absorpt. spectrum 79−28396
surface, reconstructed {001}2×1 struct., LEED intensity analysis 77−28068
surface, reconstructed Si(111) 7×7 surface superlattices, microdomain model 80−107625
surface, reduction growth, autoepitaxy *(Russian)* 80−107672
surface, relax. of surface atoms, Si_4H_9 clusters 77−8171
surface, selectively roughened, polarimetry of specular and non-multiple scatt. EM radiation 79−13904
surface, spin-depend. carrier recomb., photocond. expt. 78−19096
surface, sputter etched, damage, contamination, ion backscatt. obs. 79−33167
surface, stacking fault generation due to mech. damage, preoxidation annealing influence 80−54261
surface, stressed, n-inversion layers, Hartree calc. 78−68066
surface, thermal oxidation induced defects, origin and growth *(Chinese)* 80−66681
surface, valence band Auger line shape, corrected numerical results 78−52602
surface, wetting by Pb, Sn, Ge in H_2+HCl 78−43210
surface (001), Debye temp. meas. by HEED 77−89633
surface (001), high energy ion scatt. study 80−59772
surface (001), RHEED, expt. compared with calcs. 78−91523
surface (100), atomic and electronic structs., energy minimisation calcr. 80−49480
surface (100), chemisorption of H, pairing model calcs., compared with expt. 78−34719
surface (100), electronic struct., scattering-theory formulation 79−42607
surface (100), N_2^+ active ion bombardment, SIMS obs. 79−16034
surface (100), oxides formed in Cs-O adsorbed films, ionisation loss spectra, Auger spectra 79−69365
surface (100), P implanted, edge dislocation obs. by backscatt. spectrometry and TEM 79−4308
surface (100), reconstructed, struct. study using thermal energy He diffr. 80−60731
surface (100), reconstruction induced subsurface strain, appl. of theory 78−63914
surface (100), reflection of high freq. phonons 79−65304
surface (100), slow electron elastic scatt. threshold effects 79−100002
surface (100), vicinal, LEED obs. of stepped surface 80−59773
surface (100), vicinal plane surface band struct. electron inversion layers, minigaps 78−68062
surface (100)(1×1)H struct., LEED study 78−67910
surface (110), intrinsic surface states, photoemission study 80−50514
surface (110) atomic struct. 79−69331
surface (111)7, In submonolayer growth, superstruct. 79−77930
surface (111)7×7, dangling-bond surface states and O_2 adsorption, reflectometric study 79−99600
surface (111)7×7, electronic struct., angle-resolved UPS study 80−40226
surface (111), 1-3 keV He^+, Ne^+, Ar^+, Xe^+ bombard., AES obs. 79−33877
surface (111), 2×1 reconstructed, self-consistent anal. 78−91518
surface (111), 2×1 to 7×7 struct. transition during annealing, LEED obs. 79−42352
surface (111), 2-dimens. condensed layer, isothermal desorption spectroscopy 77−69181
surface (111), 500 eV Ar^+ bombard., high temp. annealing, recovery, RHEED obs. 78−87723
surface (111), 7×7 and 1×1 chemisorption of Cl_2, UPS obs. 78−34704
surface (111), (e,2e) reactions, theory 78−39640
surface (111), adsorption of Cl, electronic energy states, cluster-type calcs. 79−47149
surface (111), adsorption of CO, AES, SEM, ESD, flash desorption mass spectra 78−63934
surface (111), chemisorbed Cl layer, SCF LCAO band struct. calcs. 78−88010
surface (111), chemisorpt. of Cl, electronic states tight-binding method appl. 80−49564
surface (111), chemisorption of Cl, LCAO calcs., Auger line shapes, localized density of states 78−56202
surface (111), Cl_2 chemisorption, ang. resolved UPS and LEED meas. using Vidicon intensity processor 78−71972
surface (111), cleaved, geometrical struct., LEED expts. 78−91517
surface (111), covalent, pot. and charge distribs. and dangling-bond state 78−2537
surface (111), density of states from soft X-ray absorpt. spectra 80−40187
surface (111), dynamic effective charge and surface reconstruction, soft-mode theory 79−4460
surface (111), electronic states and initial steps in oxidation 78−91534
surface (111), geometric struct., LEED obs. 80−49479
surface (111), H atoms chemisorption, formation of monohydride and trihydride phases, LCAO model appl. 79−15004
surface (111), induced by Ag evaporation, struct. investigation by RHEED 79−23814
surface (111), intermediate oxidation state, core photoelectron absorpt. vs. chemical shifts 80−81220
surface (111), LEED, Auger spectra, PES study, Ag monolayer electronic props. 79−77934
surface (111), low-pressure-baked, EPR study 79−82860
surface (111), nitridation, AES and LEED results 80−80041
surface (111), O and CO sorption, ion scatt. obs. 80−59810
surface (111), partial monolayers of H, UV photoemission, disordering effect 77−1308
surface (111), reaction with acetylene and NH_3, 1225 to 1380°C 79−100441
surface (111), relax., EHT and cluster calcs. *(Chinese)* 80−59762
surface (111), relax., mol. SCF calcs. 78−91522
surface (111), relax. and reconstruction using Si_4H_9 clusters, MINDO/3 calc. 79−42356
surface (111), struct. depend. oxidation, high resolution photoemission yield spectroscopy 77−1305
surface (111), surface states and surface struct., angle-resolved PES 79−28390
surface (111), water vap. and O_2 interactions, EELS 78−14571
surface (111), with Al overlayers, electronic states 80−11061
surface (111), with chemisorbed Al, electronic struct. self-consistent pseudopotential calc. 78−34880
surface (111), with chemisorbed Cl, angle resolved secondary emission and electron energy loss study of electronic struct. 79−61477
surface (111), with chemisorbed Cl and F, electronic energy struct. calcs. 79−78144
surface (111)(7×7) struct. models, LEED anal. 80−75418
surface (111) 7×7, chemisorption of H_2O 80−10792
surface (111) 7×7, clean and O chemisorbed, valence band density of states from $L_{23}VV$ AES 80−100717
surface (111) 7×7, electronic struct., angle-resolved UPS study 80−50513
surface (111) 7×7, struct., LEED, theory and expt. 77−85033
surface (111) 7×7, structure model from anal. of RHEED patterns 80−49471
surface (111) 7×7, the at. beam diffr. obs. 79−33165
surface (111) 7×7 struct. determ. using RHEED 80−96723
surface (111) (7×7) structs., LEED anal. and energy minimisation calcs. 80−49478
surface (111) reconstruction, milk-stool model, quantum chem. ab initio calc. 80−49477
surface (111) structure, LEED seventh order diffr. beams interpretation 77−62716
surface (111)-1×1, electronic struct. of surface, model pseudopot. calc. 80−65651
surface and films on sapphire quality determ. using IR and UV specular reflectance meas. 80−108684
surface barrier detectors, dE/dx thin detector technology, n^+ layer electrolytic removal *(Russian)* 77−57823
surface barrier detectors for 4π alpha spectrometer 78−82565
surface Brillouin scatt. from acoustic phonons 80−55113
surface characterisation using SAW 80−11069
surface charging during illumination, effect of various surface treatments 79−51651
surface cleaning by pulsed laser irrad. 80−45173
surface cond. mechanism in Si covered by ultra thin oxide layer 79−38149
surface contamination during high dose ion implantation, AES obs. 79−70374
surface crystal damage due to RF sputter etching, spectroscopic ellipsometry obs. 80−103538
surface cyclotron resonance, freq. depend. 77−8170
surface defects, influence on MOS radiation sensitivity 77−20445
surface diffusion of Al 79−28184
surface electrical props. by SAW meas. 77−20387
surface electron beam deposited silicide formation using scanning CW laser beam 80−66862
surface electron states, appl. of surface photovoltage spectroscopy 77−69391
surface electron states, review of optical methods of detection 77−66191
surface electron states comparison with Ge 77−47880
surface electron states using discontinuous potential model 79−69574
surface electrons, (100), effective mass and collision time 78−64081
surface emission of hot electrons 78−30998
surface energy evaluation, by a microindentation method 80−16473
surface final-state effects on core electron transition energies 78−91745
surface formation during etching of thin thermally grown oxide layers, ellipsometric control *(Russian)* 80−104315
surface interacting with adsorbed gases, paramag. props., EPR study 80−34772
surface inversion layers, harmonic generation due to hot electrons 80−65694
surface inversion layers, intersubband optical absorpt., Auger-type transition 80−29741
surface layer, on buried SiO_2 layer formed by high-dose, O ion implantation, TEM, AES, and XPS obs. 80−88172
surface layer defects, influence of multiple oxidation *(Russian)* 78−47650

silicon continued
surface layer structure changes following α-particle irrad., X-ray investig. 78−6114
surface layers, impurities, elec. and photoelec. props. 80−2298
surface layers, ruby laser pulse effects 79−69920
surface microstructural deformation, influencing process by impurity type *(German)* 79−65107
surface morphology of HCl etched wafer, gas phase comp. effect 78−11360
surface oxidation, after Ar^+ bombardment *(Russian)* 79−15028
surface passivation in solar cells by SnO_x films, effect on cell transport props. and short circuit current 80−61360
surface peak anal. by 100-350 keV protons 80−55247
surface phase transition, order-order type *(Russian)* 77−39728
surface photovoltage, effects of atomic steps on clean cleaved surfaces 78−19120
surface porous oxide film, impurity distrib. during P diffusion 77−39944
surface potential, influence of metal impurities, surface photo-EMF obs. 78−19122
surface potential spread rel. to chemical treatment *(Russian)* 78−11363
surface props. using SAW attenuation in adjacent $LiNbO_3$ 79−87131
surface quality estimation after polishing, Kikuchi reflection obs. *(German)* 77−86208
surface radiation damage cross sections, influence of distortions 80−6442
surface reaction with organic N cpds., struct. obs. of surface film 79−87009
surface reconstruction, cryst. growth for screw dislocation free semiconductors 77−55251
surface reconstruction-induced subsurface strain, theory 78−91516
surface reproducibility and impurity segregation ion neutralisation spectra and UPS obs. for Si (111) 78−34688
surface resistivity, effect of hydrofluoric acid treatment 78−10537
surface roughness and surface defects during thermal oxidation 77−7956
surface roughness evaluation by UV refl. 80−39393
surface selective etching relative to SiO_2 by $CBrF_3$ plasma without undercutting 80−76380
surface self-diffusion, investigation by slow electron diffr. method *(Russian)* 78−51808
surface Si reinforced type U8 steel, metastable phase composition, struct. *(Russian)* 80−92599
surface space charge layer, anisotropic and tilted valley systems, absorption 77−85726
surface space charge layer, electron subbands, mag. field effect 77−20393
surface space charge layer, inter-subband optical transitions 77−15931
surface space charge layers, cyclotron reson. of electrons 77−8169
surface space charge layers, cyclotron reson. of holes 77−76932
surface state distrib. after treatment with HF and H_2O using photovoltage pulses 79−60888
surface states, step depend., self-consistent pseudopot. calcs. 77−20384
surface states and photoemission 77−72900
surface states on (111) 7×7, low-energy electron loss spectroscopy 79−60891
surface steps, electronic struct., Bethe-Peierls approx. 77−39911
surface structural transitions, LEED obs. of clean (110) surface 78−6203
surface structure, (111), induced by Ag evaporation, RHEED meas. 78−22942
surface structure, (111) 7×7, LEED intensity calc. 78−34683
surface structure, coincidence site superpositions 77−69154
surface structure, LEED and spot photometric meas. 79−23811
surface structure, Si (111)7×7, Si (111) $\sqrt{19}\times\sqrt{19}$ Ni, Si (111)5×1 Au, RHEED 77−62452
surface structure changes by laser pulses 78−14548
surface structures after pulsed laser annealing, LEED obs. 80−54494
surface topography changes due to pulsed laser annealing 80−84348
surface transition layer form., band struct., electroreflectance 77−16333
surface treatment by the low-energy ions of plasma accelerators 80−97608
surface treatment quality control of semicond. plates, using Al spraying technique 80−60989
surface-barrier detector, electron backscattering 78−55095
surface-barrier detector, impurity distrib., influence on characts. 80−18766
surface-barrier detectors with Sn electrodes, characts. 78−5097
surfaces, amorphous, hydrogenated, and monocryst., AES and LEED, comparative study *(French)* 80−44398
surfaces, electronic struct., tight-binding calc. 80−54755
surfaces (001) and (111), geometrical and electronic struct., review 80−80039
surfaces (111), (100) and (110), valence-band Auger lineshape theory 77−48286
surfaces etched in CF_4 or CF_4-O_2 plasma, morphology 80−93671
swirl defect characterisation in floating-zone cryst., comment 77−4098
swirl defect formation, doping effect, Czochralski grown dislocation free cryst. 80−92519
swirl defect formation and defect migration in Czochralski-grown cryst. 77−76405
swirl defect formation in floating-zone cryst., role of interstitials, reply to comments 77−4099
swirl defect in single crystals, formation model 79−94999
swirl defects, formation by agglomeration of self interstitials 77−80507
swirl defects, gettering effects, obs. by photoluminesc. meas. 78−84623
swirl defects in single crysts. 80−44200
swirl type defects in float-zone and Czochralski single crysts. 79−27992
switch, laser-activated, high-power switching with ps. precision 80−2416
switch, light-controlled, appl. to high speed Kerr and Pockels cells 78−26925
technology, phys. and thermodynamic props. data for $SiCl_4$ 79−65218
technology and physics, review 80−34353
temperature during CW laser heating, Raman scatt. meas. 80−76109
temperature field determ. under laser irradiation *(German)* 80−25496
temporary trap characteristic after heat treatment *(German)* 80−34459
terrestrial solar cells, stress tested, contact integrity testing 80−94018
textured wafer, selective absorber for solar thermal conversion 80−30544
thermal annealing study of Au-$Ti_{0.3}W_{0.7}$ metallisation 80−80134
thermal conductivity, calc. using numerical soln. of Boltzmann eqn. 80−44373
thermal conductivity at high temperature 79−55857
thermal conductivity calculation for single crystals *(Hungarian)* 80−65311
silicon continued
thermal conductivity variation with temperature 79−23793
thermal donor energy levels, Hall effect meas. 78−6335
thermal donor generation in temp. range 600-800°C 79−11121
thermal expansion coeff., optical mode Gruneisen const. 79−46820
thermal expansion coefficient and Gruneisen const. 77−59128
thermal expansion meas., 6 to 340K, using linear absolute capacitance dilatometer 77−47603
thermal expansion reference data: 1-1000K 80−96669
thermal neutron cross sections, in single crysts. 80−19672
thermal oxidation, ^{18}O study 79−52400
thermal oxidation, high resolution Rutherford backscatt., implanted ions analysis 79−87911
thermal oxidation, in O_2-HCl mixture, Cl incorporation in SiO_2 films 79−70186
thermal oxidation, in presence of oxides of group III metals 77−12722
thermal oxidation, role and effect of Cl 80−108622
thermal oxidation, role of H_2O, ellipsometry expts. 78−27656
thermal oxidation, SiO_2 amorphous film form., struct., mechanism 77−12725
thermal oxidation at 1200°C, effects of trichloroethylene addition 78−27660
thermal oxidation in Cl-H-O ambient, gas phase comp. considerations 77−48562
thermal oxidation in HCl-O_2 gas mixture, mobile Na ion passivation 79−70187
thermal oxidation in O_2-H_2O and O_2-Cl_2 mixtures 78−44239
thermal oxidation in O_2-trichloroethylene mixture, 900, 1000 and 1100°C 80−3221
thermal oxidation in wet O_2/trichloroethylene mixtures at 1200°C 80−16522
thermal oxidation kinetics, steady-state transport anal. 80−71773
thermal oxidation kinetics, theoretical perspective 80−76387
thermal oxidation kinetics in O_2/HCl mixture, rate consts. 77−59953
thermal oxidation kinetics in O_2/HCl mixtures 77−77617
thermal oxidation kinetics in pyrogenic water and HCl-H_2O mixture 78−64748
thermal oxidation technology, improved using 1,1,1-trichloroethane as optimised additive 79−29239
thermally induced donors due to heat treatment and Fe contamination 79−78035
thermally induced microdefect form., C and O role 80−11439
thermally induced microdefects, effect of C, TEM obs. *(Japanese)* 80−54244
thermally oxidized, chemical shift meas. by ESCA *(Japanese)* 79−61761
thermionic electron emission, from defect states at grain boundaries 79−91559
thermo-EMF, bulk differential meas. 77−4380
thermocouple, in-situ graphite-Si ribbon, calibration and meas. accuracies manufacture 79−97386
thermomigration of molten Ga 77−69118
thermoreflectance near $L_{2,3}$ soft X-ray threshold, temp. depend. 78−35224
thermosprayed, bonding to glass ceramic 78−23848
thick-film growth using contiguous capillary coating on porous C substrates 80−93507
thin crystal, electron backscatt. in electron microscope 78−75510
thin crystal foil, large angle electron scattering by dependent Bloch wave model 79−99257
thin film, effect of O on thin film compositions obtained by secondary ion emission 80−26079
thin film, polycryst., CVD, elec. props. 80−107934
thin film deposition using solar furnace 80−89148
thin film on sapphire, Hall effect, magnetoresistance *(French)* 80−65601
thin foil cells, technology developments 80−35693
thin foil thickness meas. using ^{148}Gd and ^{241}Am alpha-particles 79−30417
thin layers, carrier profiling using four-point probe method 79−37732
thin p-n junction solar cells, minority carrier mirrors and optical confinement for high efficiency (27%) 80−93933
thin single crystal, MeV ion scatt. and channelling obs. of interfaces 80−50492
thin slabs, vibr. freq. calcs., dimens. effect 80−60585
thin sub-monolayer film, Auger emission coeffs. meas. 80−55236
thin-film polycrystalline vacuum-deposited solar cells, TiB_2 bottom electrode, 10% efficiency 80−93489
thin-film reactions with metal, solid-phase, laser annealing 79−70364
thinly oxidised wafer reflectance at normal incidence, calc. 79−78641
three-dimensional electron-positron pair momentum density from positron annihilation meas. 79−43059
threshold energy for displacement of atoms 78−47428
thyristors, high-output, air cooling intensification design method *(Chinese)* 80−19229
time dependent phonon irrad. of detector area from pulsed incoherent phonon radiator 78−38790
total energy calcs. by r-space method, Wannier functions 80−88503
tracer diffusion of ^{71}Ge and ^{31}Si in intrinsic and doped samples 80−29214
transfer from gas phase to molten Fe in blast furnace 77−4930
transfer mechanism in vapour-phase epitaxial growth of GaAs 77−51616
transformation, order-disorder, repeatable, using intense laser beam 80−39150
transistor, defect obs. using stroboscopic SEM 79−9261
transistor, microwave Stark effect spectrometer, with electric molecular modulation *(Russian)* 80−9003
transistor damage characts. by neutron displacement cross section 79−42118
transistors, damage by fast burst reactor neutrons, Pb, paraffin shields 77−23172
transition density of states from $L_1L_{2,3}V$ and $L_{2,3}VV$ Auger spectra 77−40314
transmutation doped, deep trap level analysis 78−10471
transmutation-produced in Al, by neutron irrad., effects on positron annihilation 80−20732
transport phenomena in strong elec. fields, intervalley electron scatt. 79−56240
TSC, deep centres, majority carrier thermal capture cross section 78−10468
tube growth by EFG process 80−108344

silicon continued
twinned, neutron diffr. topographic obs. 78−38727
two dimensional impurity bands, Hall mobility 79−95509
two-dimensional electrons in superlattice, HF cond. 78−64055
two-dimensional inversion layer on surface, minigap and conductivities 80−20267
two-photon transitions from deep neutral impurity centres, light absorpt. and drag effect 79−91478
two-step impurity diffusion, effect of internal elec. field 77−76624
n-type, many-valley semicond. anisotropic acoustoelectric effect, thermo-EMF anisotropy fluctuation depend. on ultrasound freq. 79−69562
ultra high vacuum epitaxy on Si substrates *(German)* 77−47702
ultrafine particles prep. by gas evaporation in Ar 78−34455
uncompensated, influence of carrier transit time on small-signal admittance, of SCLC diode 77−85305
uniaxially stressed, excitonic molecule emission spectra, electron valley degeneracy effects 80−60669
US eval. of Si wafers using SAW 80−76470
US Propagation in pure and n-type crysts., velocity and attenuation, second and third order elastic moduli 80−70325
UV detectors coated with thin film scintillators 80−86412
V-grooves formed by etching, phosphosilicate glass bridge struct. 80−104312
vacancies and interstitials 80−29015
vacancy, charge states, Jahn-Teller stabilisation energy 80−80209
vacancy, defect electronic energy levels calc., optimisation 79−28315
vacancy, electron states, Anderson negative-U system 80−96820
vacancy, ideal, electronic struct., tight-binding calc. 79−4529
vacancy, isolated, electronic struct., SCF method 80−80208
vacancy, local energy levels in Wannier approx. 77−20264
vacancy, possible Anderson negative-U system 80−2358
vacancy, self consistent Green's function method 80−24843
vacancy, self-consistent electronic states 80−29354
vacancy, tight-binding calc. 80−24844
vacancy cluster props., effect of natural anisotropy *(Russian)* 77−62522
vacancy clusters produced by ion bombardment, annealing 77−89485
vacancy complexes, annealing kinetics 78−87666
vacancy diffusion, radiation-stimulated mechanisms 77−55396
vacancy electronic states, covalent states 79−23926
vacancy electronic struct., self-consistent approach 79−78043
vacancy electronic struct., self-consistent Koster-Slater method 80−10920
vacancy formation and stability due to noncentral force 80−70192
vacancy formations, entropy and enthalpy, comparison of theory with quenching expts. 77−11872
vacancy paradox 78−59804
vacancy screening, dielec. const., exchange correl. pot., Thomas-Fermi description 80−44528
vacuum deposition, combined with Sb ion implantation *(Japanese)* 78−88428
vacuum deposition combined with Sb ion implantation, neutron activation anal. 79−47631
vacuum deposition combined with Sb ion implantation technique *(Japanese)* 79−28005
vacuum deposition of polycrystalline film on metal substrate 79−91588
vacuum deposition source, with two independent filaments 80−76190
vacuum sublimated thin film structure impurity distrib. 78−95354
vacuum-crushed surface, adsorption of H_2 and Cl_2, EPR meas. 79−46957
valence band Auger spectrum, cluster approach, comparison with experimental spectrum 80−40191
valence band model, nonlocal exchange and correl. pot. 77−43492
valence band relaxation energies during XPS 78−39657
valence bands, XPS excited by Zr $M\zeta$ radiation 80−40236
valence bond Wannier functions calcs. 78−60053
valence charge density calc. 78−34463
valence electron radial and momentum distribs., X-ray form factors and Compton profiles 79−65956
valence electrons, energy-depend. photoionisation probability calc. 77−16462
valence electrons XPS spectrum, OPW calc. 77−4715
valence force model for lattice vibr. 77−20026
van der Waals electron correlation energy, bond polarisability model 78−95013
Van der Waals interaction, between two samples, influence of optical absorpt. 79−95273
vapour deposited coatings for solar cells, prod. by $SiCl_4$ reduction, cost anal. 80−93495
vapour phase epitaxy technology 80−75472
vapour species rel. to amorphous film deposition 78−14641
vapour-liquid-solid growth, using Pt and Au liq., forming agents, struct. perfection 78−42936
vapour-liquid-solid growth, using Pt and Au liq. forming agents, kinetics and morphology 78−42935
vertical etching, at very high aspect ratios, review 80−50744
very perfect crystals, topography and goniometry 78−30516
vibrational properties of the ⟨001⟩ split interstitial 78−91405
vicinal surface struct., LEED exam. 79−60611
voltage-current curves, specimens of variable cross-section 77−8113
volume plasmon dispersion at large wave vectors, EELS 78−56094
VPE, deposition mechanisms *(French)* 77−59236
VPE, gas-flow dynamics in horizontal CVD reactor, book contrib. 79−82498
VPE, growth processes, in-situ obs. *(Japanese)* 80−35104
VPE, pattern shift comparison in vertical horizontal, and cylindrical reactor geometries 78−27408
VPE, reduced pressure, advances 80−40242
VPE, state of art 79−33937
VPE, stationary model, appl. to $SiCl_4$-H_2 system 78−52679
VPE at reduced pressure, autodoping 77−77389
VPE growth, in process monitoring and control of doping gas conc. 79−24443
VPE growth 79−28929
VPE layer props. control using boundary layer characts. 80−50561
VPE tangential growth, thickness meas. 77−35836
VPE using SiH_2Cl_2/H_2 as source for epitaxial films on insulators 78−48327
wafer, (001), pyramidal hillocks, TEM obs. during chemical etching 80−70508
wafer, anomalously transmitted X-ray intensity enhancement by asymmetric diffr., appl. to microstructure 79−14647
silicon continued
wafer, automatic meas. system for resist. profiles 80−39574
wafer, B predeposited, anal. by combined ion beam techniques and X-ray microanal. 79−5238
wafer, bending by thin polycrystalline Si film deposition and by film doping using B diffusion 79−95276
wafer, chemically etched, surface roughness by gas adsorption techniques 80−15398
wafer, colour-band generation during high dose ion implantation 79−1449
wafer, colour-banded, sheet resist. variation following high dose implantation at high dose rates 78−95074
wafer, contaminated, Au redistrib. during wafer, growth of oxide or phosphosilicate glass 77−4121
wafer, Cu-decoration technique, for lattice imperfection characterisation *(Japanese)* 79−65069
wafer, Czochralski grown, interstitial O gettering 77−86196
wafer, deformation *(Japanese)* 78−43064
wafer, dislocation propagation and emitter edge defects, appl. to transistors 77−1128
wafer, high resolution SIMS 78−56929
wafer, interaction with Mo film, silicide formation kinetics determ. 78−43261
wafer, ion etching, secondary ion monitoring 79−91551
wafer, migration of fine molten Al rich wires, vertical p-n function fabrication 78−68077
wafer, nondestructive method for meas. of spatial distrib. of minority carrier lifetime 80−13098
wafer, photovoltaic technique for meas. resistivity variations 79−21783
wafer, shrinkage and annihilation of stacking faults 77−39598
wafer, slotted mask, direct deposition of metal contact pattern on MIS solar cells 80−97786
wafer, stress meas. in film, X-ray method 78−51860
wafer, stresses generated by thermomigration of liquid inclusions 79−37875
wafer, suppression of oxidation stacking fault generation by preannealing in N_2 atm. 78−30648
wafer, surface characterization by ellipsometry 79−90853
wafer, surface exam. of ion-implantation using SAW convolver 77−72897
wafer, Ta sputtered induced stress meas., X-ray transmission topography 79−24434
wafer, thermal characts. of H_2SO_4-H_2O_2 cleaning soln. 80−3225
wafer, thermally oxidised, stress and strain meas. *(Russian)* 78−11375
wafer, thin surface layers, amorphous to cryst. transform., obs. technique 80−107288
wafer, trichloroethane oxidation, effect on SiO_2 and Si props. 79−70193
wafer C impurity IR absorption spectrometry, thickness fringe elimination 80−55132
wafer characterisation by photonic injection+microwave meas., appl. to Si *(French)* 78−23106
wafer creep testing using stress provided by deposited Si_3N_4 film 77−66000
wafer defect level detection using variable temp. apparatus 79−88951
wafer diagnostics, using computer automated scanning low-energy electron probe 79−4214
wafer O interstitial IR absorption spectrometry, multiple reflection correction 80−55131
wafer processing, CO_2 laser heating dynamics 80−76106
wafer prod., diffusion furnace temp. profile meas. systematic errors, theoretical model *(German)* 80−8989
wafer stacking fault formation model 77−76426
wafer surface doping profile determ. by SIMS 79−77618
wafer surface sputtering, secondary postive ion mass and kinetic energy anal. 78−88391
wafer thermal gradient induced slip, effect of starting cooling temp. 78−10057
wafers, Au contamination during plasma etching 80−19831
wafers, channelling dips for K and L X-ray prod., PIXE and Rutherford backscatt. anal. 79−4363
wafers, Czochralski, gettering of surface and bulk impurities 78−64456
wafers, Czochralski grown, crystal defects, photoluminesc. topographic obs. 79−1432
wafers, Czochralski-grown, lifetime improvement by two-step annealing 80−49916
wafers, dislocation dynamics during annealing, X-ray topography system obs. 77−76261
wafers, etched in HCl, exam. of bunch formation 78−68831
wafers, floating-zone, etch struct. on microdefects as affected by dopants and surface treatment 80−79773
wafers, HCl etched, surface morphology, etch pit origin 79−96166
wafers, microwave plasma etching, role of ions and neutral active species 80−3217
wafers, MOS structs. formed on stain films, electrophysical props. *(Russian)* 78−52095
wafers, N heat-treatment effects, stacking faults formation 78−85016
wafers, n- and p-type (100), oxidation-induced stacking faults 77−39599
wafers, preparation of preselected areas for TEM 78−24887
wafers, process-induced in-plane distortion and wafer bowing 79−11048
wafers, saw damage reduction in lubricant environment 80−108585
wafers, scribing and subsequent fracture 80−11743
water impurity conc., from MOS DC transfer characts. 78−2155
waveguide photodetector matrix, appl. in integrated-optics demultiplexer 79−32095
weak heating of electrons, cyclotron reson. conditions, quantising mag. field 78−39141
web dendrites, dislocations, stacking faults, X-ray topographic study *(Chinese)* 80−88148
web dendritic ribbon growth, thermal analysis of solidification 78−72770
wetting of self-bonded polycryst. α-SiC, base plate surface roughness effect 79−23809
whisker, (111) oriented, FIM and atom-probe FIM obs. 80−10473
whisker, amorphous, growth method for field desorption mass spectrometry 79−28262
whisker, amorphous, Young's modulus meas. 78−83865
whisker, growth by reduction of $SiCl_4$ in H_2 gas current 77−15726
whisker coated C fibres for composites, shear strength improvement 78−3093
whisker for field desorption ion source for isotope abundance ratios 80−11975
whisker growth characts. by SiH_4 thermal decomposition 80−34342

silicon continued
whisker growth in amorphous state, in SiH_4-Ar atmosphere, visual obs. 78−84112
whisker indirectly-heated thermoresistor 78−86255
whiskers, polytypism and amorphousness 78−26801
whiskers, shadow electron microscopy study of steps of {112} faces 79−60666
whiskers as basis for low-temp. sensors of temp. and deformation 79−5095
whiskers as basis for strain resistors 79−5094
whiskers nucleation, effect of machining support surface *(Russian)* 79−65352
wide ribbon crystal growth apparatus 78−48307
work function and Auger spectroscopy of initial oxidation 78−76132
X-irradiated, photoconductivity spectrum 77−15903
X-ray absorption K-edges in crystalline Si, SiO, SiO_2, SiC, Si_3N_4 *(Russian)* 79−47541
X-ray acoustic reson., Borrmann effect reson. suppression by transverse US vibrs. 79−32852
X-ray acoustic reson. in perfect crystal 79−27873
X-ray attenuation coeff., anomalous scattering factors and dispersion corrections rel. to photoeffect cross section 79−99980
X-ray attenuation coeffs. 25 to 50 keV, energy dispersive method 77−66557
X-ray continua emission, proton and ^{14}N bombard. 78−23559
X-ray data, refinement using a generalised aspherical-atom formalism 79−7516
X-ray diffraction, extremely asymmetric, Laue case of grazing incidence 78−51392
X-ray diffraction, three and four wave, comparison of diamond type crysts. 78−67608
X-ray diffraction characterisation, highly collimated beam 78−9912
X-ray diffraction contrast by 60° dislocations, section topography 78−83819
X-ray diffracton, meas. of dynamical and kinematical components with triple cryst. diffractometer 79−50948
X-ray emission and fluorescence yields under F^{q+} ion irradiation 79−83060
X-ray emission spectra, high energy plasmon satellite intensities 78−64430
X-ray emission spectra formation, role of nonequilibrium electron density *(Russian)* 77−63490
X-ray intensity anomalously transmitted, ε_{220} values 78−83650
X-ray interferometry preliminary results for crystallography, Si lattice constant 79−7522
X-ray K_α emission spectra, Si, SiC, SiO_2 and Si_3N_4, chemical shifts, linewidths and intensities 78−13461
X-ray K-spectra, fine struct. intensity, temp. depend. *(Ukrainian)* 77−55850
X-ray $L_{2,3}$ emission spectrum, high energy plasmon satellite 79−82538
X-ray linear absorpt. coefficients, in energy range 5 to 50 keV 79−73066
X-ray linear absorption coeff. 78−26384
X-ray mass attenuation coeff. meas. 77−31556
X-ray monochromator for high-angle double-cryst. diffr. 77−43111
X-ray multiple diffr., Bragg. refl. theory 79−94842
X-ray photoelectron spectra and density of states, strong-coupling method 77−28679
X-ray photoelectron yield, effect of asymm. Bragg diffr. *(Japanese)* 77−43110
X-ray plane wave topography, observation of dislocation in Si single cryst. 78−91342
X-ray polarisation, ang. depend. of curve of 111 Bragg reflection 79−46509
X-ray resonance Raman scattering, solid target, proton bombarded 79−61465
X-ray scattering, and temp. depend. of Debye-Waller factors, shell model calcs. 79−99022
X-ray scattering cross sections, inelastic, in case of small momentum transfer 77−27786
X-ray scattering from small defects in very perfect crysts. 78−47395
X-ray section topography in the Bragg case 80−79637
X-ray source, Kα, sensitivity factors, cross section and resolution data 80−77920
X-ray topography and double-crystal diffraction 80−92534
X-ray triple-crystal diffractometer appl. to dynamical and kinematical diffr. from perfect and damaged crysts. 78−55784
XPS, single cryst. and polycryst. comparison 77−12493
yield strength calc. 78−43062
yield stress from Hugoniot elastic limit and elastic consts. 79−83261
zincblende structure group IVA covalent crystals, Murnaghan parameter estimates from Morse pot. 78−95014
zone melting, swirl defects A-type as source of dislocation generation on macroscopic scale 80−25554
zone refined, prep. of solar cells 78−64475
β-ray and X-ray spectrometry by high resistivity p-type Si detector 77−88329
μ^+ spin relaxation in longitudinal mag. fields *(Russian)* 78−88245
μ^+-meson depolarisation, spin relax. *(Russian)* 78−52416
Si:P, sheet resistance of Gaussian n-type ion-implanted layers 79−87103
a-Si:H, effect of H conc. on photovoltaic props. 79−99577
Ag-BN-Si-Al sandwich, humidity sensitive threshold switching 78−88046
Ag-In_2S_3-Si layered struct., Hall effect, I-V characts., surface states *(Russian)* 80−97001
Ag-Si interfaces, solar cell contacts 80−92973
Al:Si, film deposition by reactive sputtering 79−66005
Al/NiSi/Si system, high temp. interaction study, elec. and struct. characts. 79−24075
Al/SiO_x/p-Si contacts for IMS solar cells, high temp. lifetesting 79−87988
Al-Al_2O_3-Si structure, study of charge trapping 80−60097
Al-Al_2O_3-SiO_2-Si capacitors, physical and elec. props. of RF plasma grown Al_2O_3 80−100530
Al-AlN-SiO_2-Si capacitors, physical and elec. props. of RF plasma grown AlN 80−100530
Al-amorphous Ge-nSi, photoelectric props. 80−70822
Al-Cu-Mg(:Fe,Si) alloys, double-ageing, resist., hardness meas. 77−28822
Al-In_2S_3-Si layered struct., Hall effect, I-V characts., surface states *(Russian)* 80−97001
silicon continued
Al-nSi-Al, p^+np^+ reach through structs., electronic cond. mechanism 78−64103
Al-sapphire-Si capacitor, effect of electron-beam aluminisation on Si-sapphire interface 77−89856
Al-Si, contact resist. response surface of sintered Al film on Si (100) 79−78175
Al-Si, ion plated contacts *(Rumanian)* 78−88029
Al-Si contacts, effect of vacuum ambience 77−43718
Al-Si contacts, electromigration and diffusion of Cu in Al film 79−77820
Al-Si interface in semiconductors, electronic parts, electromigration aspects 80−39355
Al-Si MIS solar cells, depth conc. profiles, elec. and optical props. of Al films 80−94076
Al-Si Schottky barrier solar cell, metallurgical reactions 77−72914
Al-Si_3N_4-Si struct., surface energy bands under step function illumination 80−49840
Al-Si_3N_4-SiO_2Si, MNOS structures degradation under UV irradiation effect 80−107923
Al-Si-Al contact current response to 100 keV neutron irrad. *(Russian)* 80−49956
Al-Si-SiO_2-Al structure switching and memory effects 78−95385
Al-SiO_2-Si, charge measurement in MIM and MIS struct., MOS system appl. 78−2572
Al-SiO_2-Si, MOS struct., lateral photovoltaic effect 79−4601
Al-SiO_2-Si, pyroelectricity 80−100524
Al-SiO_2-Si, void form. in Al interconnection lines at Si-SiO_2 boundaries 80−2476
Al-SiO_2-Si capacitor C-V characteristic determ. of surface minority carrier lifetime *(Polish)* 77−89855
Al-SiO_2-Si capacitors, transient capacitance temp. depend., −40 to 70°C 79−47167
Al-SiO_2-Si Schottky barrier solar cells, recomb. effects 79−39310
Al-SiO_2-Si struct., mobile ion neutralisation in SiO_2 layer, TSC and C-V characts. meas. 79−95503
Al-SiO_2-Si structs., implanted B^+ ions, high-freq. CV characts. *(Russian)* 78−80056
Al-SiO_2-Si structure, Auger depth profiling and ion sputtering of interfaces 77−20200
Al-SiO_2-Si structure, location of positive trapped charge by internal photoemission 77−51820
Al-SiO_2-Si structure, photon-assisted tunnelling 77−89865
Al-SiO_2-Si structure, photocurrents, 1.4 to 3.1 eV 79−65514
Al-SiO_2-Si structure, positive interface charge, exciton and H diffusion models 80−2471
Al-SiO_2-Si structure, small signal HF photo EMF meas. 78−52097
Al-SiO_2-Si system, EMF origin in pulsed UHF field 77−4448
Al-SiO_2-Si system with reactively sputtered SiO_2, work functions difference 80−6987
Al-SiO_2-Si:B ions, annealing effect on energy spectrum of radiation defects *(Russian)* 78−88488
Al-SiO_2-Si-Pb, MIS system, photocurrent, effect of supercond. to normal transition in Pb 78−72271
Al-SiO_2Si, mobile ion kinetic behaviour 79−56315
Al-SiO_x-Si MIS solar cells, short-wavelength response 79−57428
Al-SiO_x-Si MIS solar cells, I-V characts. temp. depend. 80−7935
Al-SiO_x-Si MOS solar cells, open-cct. voltage var. with oxide layer thickness 80−81434
Al-SiO_x-Si minority-carrier MIS photodiodes, elec. characts. 79−51676
Al-SiO_x-(p-)Si barrier structs., minority carrier injection ratio meas., MIS solar cell model 80−93007
Al-SiO_x-p-Si MIS solar cells with back surface fields 80−12006
Al-Ta-poly-Si interdiffusion, Ta barrier effect, Auger anal. 78−71888
Al-$TiSi_2$-n-Si struct., elec. props., charge transfer mechanism across $TiSi_2$-Si interface *(Russian)* 80−34515
Al-ZnO-SiO_2-Si monolithic MIS struct., charge-transfer device using SAW 79−11229
(Al+Si)-Si thin films, struct. transitions and phase comp. 80−49537
$Al_xGa_{1-x}As$:Si, charge state of impurity atoms, positron annihilation meas. 78−39062
$Al_xGa_{1-x}Sb$:Si, doping of solid solns. during LPE *(Russian)* 77−85087
n-$Al_xGe_{1-x}As$:Si-GaAs heterojunctions, selectively doped, FET 80−80364
AlN film, Si doping by DC glow discharge 78−19674
Al_2O_3:Si, gamma-irrad., low temp., induced absorpt. spectra 79−56820
Al_2O_3:Si, Ti, pure and doped, luminescence, optical absorpt. and colour centres 79−87501
Al_2O_3:Si,Ti photostimulated thermolum., and appl. to UV dosimetry 78−53511
Al_2O_3:Si thermoluminescent phosphor, annealing characts. and nature of traps 77−85817
Al_2O_3:Ti(Si), annealing, electron irrad., absorpt. spectra 77−20890
Al_2O_3-Si, alternating layers, dielec. facet reflector for semiconductor lasers 78−66841
Al_2O_3-Si-Te-Al_2O_3 layered apertured facet reflector, for lateral mode stabilisation of diode lasers 80−23708
Ar^+ ion implant damage gettered Si, generation lifetime meas. 80−75247
As implantation *(Japanese)* 78−38738
As segregation, TEM obs. 77−63674
Au diffusion, and elastic strain, influence on O_2 state in Si *(Russian)* 79−69181
Au/Si interface, X-irradiated, dose profiles 79−24388
Au-Mo-Si multiple layer structure, bombarded with P ions, calc. of P ion profile in substrate *(Russian)* 79−55771
Au-n-Si Schottky barrier solar cells, recombination in space charge region 80−61351
Au-n-Si-p-Si structure with wavelength depend. photocurrent sign, photodetector 79−12849
Au-p-n-Si Schottky barrier solar cell, photovoltaic characts., barrier heights, carrier mobility 79−83601
Au-Si, spatial origin of electrons in internal photoemission struct. *(French)* 78−91770
Au-Si interface, electron energy loss and AES meas. 80−89096
Au-Si interface, valence band and core levels, Si diffusion, alloy form., photoelectron spectra obs. 80−45205
Au-Si internal photoemission struct., spatial distrib. of excited electrons *(French)* 78−23166
Au-Si Schottky contact elec. props. rel. to AES 77−85322

silicon continued
Au-Si system, transition layer struct. form. and heat treatment influence, amorphisation obs. 80−54529
Au-Si thin film double layer, silicide form., electron diffr. study 80−80005
Au-Si-Al structure electrode mass transfer and switching with memory 78−95389
Au-SiO_2-nSi, tunnelling MIS struct. 80−92995
Au-Ti/SiO_2/p-Si MOS struct., interface state distrib., DC tunnelling spectra determ. 80−75611
B high-temp. diffusion, glass layer formation obs. 78−7069
Be-SiO-p-Si, MIS solar cell, performance figures 78−88030
Bi implanted, elimination of He^+ beam effect on channelling dips 80−54292
Bi:Si, mag. field dependent electron and hole scatt., quantum limit 77−15878
C^+ ion implantation, SiC synthesis and struct. characterisation 77−76434
n-CdS:Cu, Si, photocond., carrier lifetime, X-ray effects 77−59300
CdS-SiO_2-Si structures, elec. props., role of interface states 79−56286
CdTe:Si, force variation due to charged defects 80−92634
Co-Si film system, diffusion marker expts. 78−79824
Co-Si film system, interaction kinetics 78−79823
Co-Si interface, glassy layer, ellipsometric charact. 80−103589
^{57}Co ion implantation, Mossbauer spectra, dose depend. 79−82899
Cr-(Pd_2Si)-Si, $CrSi_2$ form. kinetics 77−24492
Cr-MIS solar cells, on polycryst. Si, grain boundary effect and conduction mech. 80−93894
Cr-Si, cleaved junction, interface states, capacitance meas. 79−91118
Cr-Si, metal-nn^+ Schottky diode, I-V characts., inverse branch, effect of dislocation defects *(Russian)* 79−15217
Cr-Si interfaces, metallurgical and electrical props. 80−60081
Cr-SiO_2-Si structure, solid-phase interaction between Cr and SiO_2, X-ray spectral obs. 78−10560
Cr-SiO_2-n-Si tunnel diodes elec. characts. meas. and modelling 77−39955
Cr-SiO_x-Si MIS solar cell, current cond. 80−7936
Cr-SiO_x-Si MIS solar cells, photovoltaic performance and interface states, nucl. radiation effects 80−94004
$CrSi_2$ formation on Pd_2Si and PtSi, radioactive Si tracer obs. 78−60578
Cu-n-Si diodes, fabrication by electroless deposition method, characts. 80−100520
Cu+X^{n+}, X=F, Al, Si, S, K X-ray production, target thickness depend. 77−75280
D implanted, trapping of D, calibration for particle energy meas. in plasma boundary of Tokamaks 79−98983
(Ga,Al)As:Si, epitaxial layers, radiative recomb., compensation, cathodolum. study 80−66307
$Ga_{0.9}Al_{0.1}As$:Ge(Si) epitaxial layers, defect obs. by TEM 77−51618
$Ga_{1-x}Al_xAs$:Si, LPE, phase diagram, Hall effect meas., carrier conc., donor ionisation energies 77−72803
n-$Ga_{1-x}Al_xAs$:Si, room-temp. cond. and band struct. 80−96869
$Ga_{1-x}Al_xAs$:Si, Si determ., spectrochem. method, photoluminesc. spectra, Hall effect meas. *(German)* 77−77851
$Ga_{1-x}Al_xAs$:Si p-n junction, reemission effects 78−15230
$Ga_{1-x}Al_xAs$:Si p-n junction, doping in LPE, elec. and luminesc. props. *(Czech)* 78−47851
$Ga_{1-x}Al_xAs$:Si photoelectric convertors, broadband varizone creation 80−40856
$Ga_{1-x}Al_xAs$-GaAs:Si, momentum distrib. of valence electrons, positron annihilation meas. 79−51530
GaAs, C, O, Si impurities 78−59832
GaAs, Si contamination in VPE, thermodynamic analysis 79−28932
GaAs, Si ion implantation and annealing, damage recovery, surface carrier profile 77−4119
GaAs:Cr, Si, deep centre photoluminescence spectra 78−95601
GaAs:Si, accelerated growth rate effect on MBE, Hall mobility and photolum. meas. 80−104067
GaAs:Si, activation by multiply scanned electron beams 80−75246
n-GaAs:Si, B, IR absorpt. spectra, reson. and localised modes 80−66172
GaAs:Si, charge state of impurity atoms, positron annihilation meas. 78−39062
GaAs:Si, Cr, carrier concs. from Hall effect, microscopy, localised vibrational modes absorption meas. 78−56104
GaAs:Si, current-controlled growth, segregation and amphoteric behaviour 78−31346
GaAs:Si, donor-acceptor pair defects absorpt. bands 80−16064
GaAs:Si, doped and undoped, sputtered epitaxial films, elec. props. 79−78234
GaAs:Si, electrical activity of Si 79−15145
GaAs:Si, electron irradiated, LPE layers and Bridgman crysts., IR absorption and Hall meas. 77−16345
GaAs:Si, encapsulated by SiO_2 and Si_3N_4, ion-implanted As profiles 79−4319
GaAs:Si, epitaxial layers, photo- and cathodoluminesc. 77−77285
GaAs:Si, faulted and prismatic loops, TEM obs. 77−51386
GaAs:Si, film, conversion of type of conduction stimulated by ion bombardment 77−4457
GaAs:Si, generation of high mobility n layers, SIMS 80−103375
GaAs:Si, hardening by solute-vacancy pairs 77−4794
GaAs:Si, heteroface solar cells, diffusion lengths 78−47849
GaAs:Si, IR absorpt. bands, localised modes, Si-related defects 80−76054
GaAs:Si, influence of stoichiometry on recomb. processes 80−93396
GaAs:Si, ion implantation, thermal annealing, Hall meas., SIMS atomic profile meas. 80−75243
GaAs:Si, ion implanted, capless anneal in As controlled vapour 79−55767
GaAs:Si, ion implanted, laser annealing, appl. to microwave devices 79−69139
GaAs:Si, ion implanted, photoluminesc. 79−69887
GaAs:Si, ion implanted, laser annealed, high doping levels 80−88181
n-GaAs:Si, ion implanted and/or annealed, As vacancy form., photolum. line 77−27875
GaAs:Si, ion implanted effect of anneal ambient and occurrence of compensated regions in Si implants 77−51394
GaAs:Si, ion-implanted, depth distrib. profiles of Si ions 77−43230
GaAs:Si, ion-implanted, elec. props. 79−46686
GaAs:Si, ion-implanted, annealing with Nd:glass laser 79−73194
GaAs:Si, ion-implanted, capless anneal, effect of As partial press. 80−29038
silicon continued
GaAs:Si, ion-implanted, capless annealing by melt-controlled ambient technique 80−75251
GaAs:Si, Li, IR absorpt., microstruct., charge compensation 80−107565
GaAs:Si, momentum distrib. of valence electrons, positron annihilation meas. 79−51530
GaAs:Si, n-type layers, heavily doped, formation by multiple ion implantation 80−88187
GaAs:Si, neutron irrad., strain detection by local mode IR absorpt. meas. 77−69828
GaAs:Si, positron lifetime temp. depend. 80−29826
GaAs:Si, pulsed laser annealing of implanted layers, defect structure and Hall effect meas. 79−69118
GaAs:Si, quantitative anal. with ion microanalyser *(Japanese)* 78−7292
GaAs:Si, radiative recomb. *(Russian)* 79−91499
n-GaAs:Si, radiative transitions induced by modest annealing, photoluminesc. spectra 80−55158
GaAs:Si, single crysts., asymmetric deform. 79−23616
GaAs:Si, stacking fault prod. during heat treatment in As vapour 80−96547
n-GaAs:Si, thermally treated, photolum., acceptor levels obs. 79−38587
GaAs:Si, thick LPE layer growth and characterization 77−12511
GaAs:Si, transferred-electron devices by low-level ion implantation 80−92543
GaAs:Si, VPE, high purity, residual donors, photocond. expts. 77−85174
GaAs:Si, VPE film growth, effect of O_2 injection 79−100057
GaAs:Si,Cr, under layer of SiO_2, effect of annealing, on electron concentration and mobility, and impurity distrib. 79−4323
GaAs:Si encapsulated with AlN, Si_3N_4 layers, photolum., annealing effects 80−20681
GaAs:Si epitaxial films, elec. and photoelec. props., impurity distrib. 80−7006
GaAs:Si LED, with anti-Stokes phosphor 79−11204
GaAs:Si LED p-n structures, speed *(Russian)* 79−43044
GaAs:Si LEDs grown from restricted soln.-alloy bulk, props. *(Russian)* 79−43043
GaAs:Si LPE layers, luminesc. props. rel. to substrate quality 78−52583
GaAs:Si LPE layers, surface morphology, substrate misorientation, initial supercooling effects 80−34329
GaAs:Si layers, MBE growth, elec. and optical props., doping characts. 80−10819
GaAs:Si p-n junction, electrolum. power, injection current and temp. depend. *(Russian)* 77−16401
GaAs:Si p-n junction LED, electroluminesc. efficiency 80−71491
GaAs:Si p-n light-emitting structs., soln. of general minority carrier transport eqn. 80−15597
GaAs:Si p-n structs., effect of growing conditions on distrib. of recomb. parameters 80−39668
GaAs:Si p-n structure, radiative recombination region 78−52071
GaAs:Si substrate, VPE growth, photoluminesc. and emission spectra 80−29774
GaAs:Si(Cr), LPE, spiral growth patterns, dopants role 77−72800
GaAs-AlGaAs:Si heterojunction interface, two-dimens. electron gas, Hall effect and cyclotron reson. meas. 79−65530
GaAs-Si heterojunction, IR quenching of photocapacitance 80−92968
GaAs-Si ion implanted, impurity profiles elec. props. 80−96550
$GaxIn_{1-x}P$:Si, solid soln., splitting of ground state 79−51527
GaP, chemical etching processes, review 78−95832
GaP:C,Si, LPE, cathodo- and electrolum., residual impurity and struct. defect effects 78−19570
GaP:S, Se, Te, Si, shallow donors, excitation spectra 77−81128
GaP:Si, donor centre struct. and conduction band nonparabolicity 78−14695
GaP:Si, IR photocond. response spectra 79−56257
GaP:Si p-n struct., on n-$Ga_{1-x}Al_xP$ and n-GaP substrates, electrolum. spectra 79−24368
GaP/Si heterostruct., differential thermal contraction, plastic deform., fracture 80−108494
GaP-Si, heteroepitaxial growth, electronic and optical props. 80−104075
GaP-Si, heterostructure, zincblende-on-diamond type systems, MBE growth, (110) orientation as preferred orientation 80−80099
Ge, growth, chem. transport, transfer inversion using Mo catalyst 79−11517
Ge:O(Si), effect of impurities on mech. strength in brittle fracture region 79−87682
Ge:Si, impurity lattice modes due to single and paired defects 78−75780
Ge:Si, impurity modes and IR absorption 78−76506
Ge:SiO_2 optical fibres, total dispersion in step-index monomode fibres 79−68427
Ge/Si ratio vars. along Reykjanes Ridge and Iceland 79−8617
p-Ge-nn^+-Si, heterojunction, γ-radiation effect on forward I-V characteristics *(Russian)* 78−72255
Ge-Si, solid phase heteroepitaxy 80−6670
Ge-Si, solid soln., local IR transmission 80−7357
Ge-Si, UHV-produced epitaxial structs., electrophys. props. 78−3060
Ge-Si and Ga-Al fractionation in Hawaiian volcanic rocks 79−12112
a-Ge-Si crystal interface, low resist. elec. behaviour 77−89843
Ge-Si heterodiode, interfacial structural defects effect on avalanche breakdown 79−42644
Ge-Si n-n heterojunctions, photovoltaic response 78−14804
Ge-Si sandwich structure, sputter profiling, combined Auger-X-ray anal. 80−66909
Ge-SiO_2-p^+Si tunnel junctions, for determ. of AC cond. of amorphous Ge 77−24608
Ge-Te-Se/Si amorphous film-cryst. heterojunction, electron-beam-induced current 79−24060
GeO_2:Si, optical props. IR absorpt., UV reflection spectra 78−84619
GeS:Si, elec. cond. and thermally stimulated currents 80−20194
$Ge_{20}Te_2Se_{80-x}Si$, amorphous-cryst. heterojunctions 79−65546
H^+ and H_2^+ ion implantation profiles determ. by SIMS 79−4334
H^++Si collisions, charge exchange 77−6921
HCl etching, effect of O_2 traces 79−91818
^1H ion implantation at 0.5 to 300 keV, range parameter meas. 80−44242
He, Ne isotopes and radionuclides prod. cross sections induced by 12-45 MeV protons 77−17310
He-like ion, spectral broadening in plasma, theory 80−6223
In electrodeposition from glycerine soln., rapid method 77−32534
$In_xGa_{1-x}As$:Si, p-n junction form. in LPE layers, In content effect on inversion temp. 77−4266
$In_xGa_{1-x}As$:Si p-n structs., electrolum. spectra, 77 to 300K 80−93408

silicon continued
In_2O_3-Si highly photosensitive diodes, and their appl. 78−23152
In_2O_3-SnO_2/Si solar cells, antireflection props. of oxide film 80−3513
In_2O_3-SnO_2/polySi, solar cell response exam. using electron-beam-induced current and scanning light spot tech. 80−81477
In_2O_3-SnO_2-Si heterojunctions, elec. and photovoltaic characts. 78−52070
In_2O_3-SnO_2-Si SIS heterojunction solar cells 80−85281
In_2O_3-SnO_2-Si SIS solar cells, reverse current-voltage characts. under illumination 80−89622
InP:Si, implantation at high temp., elec. mobilities 79−99541
InP:Si, ion implantation and PH_3 ambient annealing under VPE conditions 79−42085
InP:Si, pulse electron annealing, carrier activation and mobility 80−15124
InP:Si, vibr. modes of Si, IR absorpt. bands 78−55922
$(In_{1-x}Sn_x)_2O_{3-y}$-Si solar cells, degradation 80−94047
$(In_{1-x}Sn_x)_2O_2$-Si-N solar cell efficiency and elec. props. 80−35676
n-$In_{2-x}Sn_xO_{3-y}$/p-Si, semicond.-insulator-semicond. solar cell, performance and spectral response, fabrication 79−83596
$In_{2-x}Sn_xO_{3-y}$-insulator-poly-Si solar cells, photovoltaic conversion parameters 80−101093
$In_{2-x}Sn_xO_{3-y}$-n-Si, electron deposited solar cell, photovoltaic props. 79−96446
$In_{2-x}Sn_xO_{3-y}$-Si solar cells, SiO_2 detection of interface, Auger anal. 79−87991
$In_{2-x}Sn_xO_{3-y}$-SiO_x-Si SIS solar cells, loss mechanisms study for improvement of efficiency to above 12% 80−94080
n-inversion layers, (001), $K_{\|}$-depend. of subband energies 80−103738
Li-Si, electrode pot., Li utilisation determ. 80−81427
LiF:Si, injection electrolum., fields up to 10^4 V cm^{-1} 77−12445
LiF:Si^{4+}, impurity effect on elec. cond. 79−7709
Li_2GeO_3:Si,Mg, impurity effects on elastic and piezoelec. props. 79−47388
$LiNbO_3$-Si, acoustoelectronic memory, effect of band-bending 80−70771
MgO:Si^{4+}, short-wave luminesc., V-centre electron recomb., impurity effects *(Russian)* 77−20921
MnSi, amorphous, sputtered, mag., elec., struct. and thermal props., spin glass behaviour 80−50124
Mo-n-Si Schottky barrier, sputtered, freq. cond. charact. 77−20426
Mo-Si diffusion couples, $MoSi_2$ or Mo_3Si/Mo_5Si_3 form. 79−77836
Mo-Si junctions, metallurgical boundary props. and elec. resistivity 78−2568
Mo-SiO_2-Si, Mo-Si pelicular structures, struct. transitions during vacuum thermal treatment *(Russian)* 78−95238
Mo-SiO_2-Si, R/MOS struct., heat treatment effects 78−76683
Mo-SiO_2-Si, thermally stimulated ionic cond. 78−10565
n-type, passivation, photoactivation kinetics in conc. alkali, ellipsometric investig. 77−1885
n-type inversion layers, in strong mag. field, quantum galvanomag. expts. 78−60214
N_2^++Group IV elements and oxides, XPS and UPS prod. determ. 78−73084
Nb-Si, bridge, crit. current 80−20359
Ni based superalloys 713C and Mar-M200, Si effect on oxidation, hot corrosion and mech. behaviour 78−39950
Ni-Cr-Mn alloy solidification, effects of Si, Mo and Co alloying 79−83193
Ni-Cr-W-Mo-Al-Ti (15,6,3,2,2, wt.%), wrought, Si effect on transition brittleness *(Chinese)* 80−55491
Ni-n-GaP:Si contact, doping effect in elec. props. 80−6983
Ni-Si film system, silicide first phase form., reaction kinetics 78−79821
Ni-Si(111), interface, reactivity and struct., ion channelling meas. 80−92788
O content determ. by spectral analysis, phonon absorpt. effects *(Russian)* 77−48177
O depth profiling, comparison of techniques 80−29048
P doped Czochralski crystal donor homogenisation by thermal neutron irradiation 78−6108
P ion implantation, processing parameters for diffusion redistribution 79−10871
Pb-Si:Sb Schottky tunnel junction, variable range hopping assisted tunnelling 80−39670
$Pb_5Ge_3O_{11}$:Si, switching velocity, increase over that of undoped crysts. 79−51922
$Pb_{1-x}Hg_xS$-Si heterojunctions, elect. props. 80−100513
PbS-Si, photosensitive p-n heterojunction, energy band diagram 79−95489
PbS-Si heterojunction, chem. struct., AES anal. 80−76115
PbS-Si heterojunction, related optical and IR detector props. 80−77866
PbS-Si heterojunction, space charge capacitance, PbSn film thickness depend. 80−88630
PbS-Si heterojunction, PbS film growth and struct. 80−96762
PbS-Si heterojunction detector, direct injection readout 80−4765
PbS-Si p-n heterojunctions, AC admittance meas. 80−96979
Pd/Si, Schottky-barrier type devices, chemical and polarisation characteristics, comparative study 79−78173
Pd-amorphous Si thin film interaction, metal rich Pd-silicide formation 80−2284
Pd-Si Schottky barrier chemical sensor, for H_2 detect. 78−44646
Pd-Si structure, epitaxial silicide growth, LEED and AES study 80−103590
Pd_2Si-Si Schottky barrier diode grown by solid phase epitaxy 77−80837
Pt-Si contact, annealed in H_2 ambient, elec. props. 78−64110
Pt-Si film system, silicide first phase form., reaction kinetics 78−79821
Pt-Si interface, low-temp. diffusion, ambient effects 80−100355
Pt-Si Schottky barriers on Si, laser formation and characts. 80−60079
Pt-Si:As, silicide form. during laser irrad., p-n junctions and ohmic contacts 80−84397
Rh-Si thin film interaction, interdiffusion, temp. depend. 80−54443
S V, spectral lines, 460-3604 Å 77−27011
S:P, ion implanted, defect annealing 450-800°C, deep-level transient spectroscopy 79−47042
S:Si, implanted, defect signature by thermally stimulated meas. 78−91643
S_3^-, photodetachment cross section, 0.5 to 3.0 eV photonenergy *(German)* 77−65518
SI II, Stark broadened linewidths, plasma diagnostics and stellar spectra appls. 77−84496
SI III, electron impact excitation of $3s^2\ ^1S$-$3s3p\ ^3P^0$ transition 80−102578
silicon continued
SOS, epitaxial, crystalline quality improvement by ion implantation and furnace regrowth 80−88452
Se:Si, vitreous, crystallisation kinetics study by elec. cond. meas. 79−65526
Si, ^{75}As implanted, comparison of effects of pulsed ruby laser and pulsed electron beam annealing 79−69135
Si $3p^2(^1D_2)$ state collisional quenching 79−22806
Si (III), excitation thresholds and oscillator strength calc. using CI wavefunctions 80−91496
Si (001)-SiO_2, n-inversion layer, valley splitting without effect mass approx. 80−15586
Si (100)-Pd_2Si-Si system, Si epitaxy obs. by ^{31}Si tracer and Rutherford backscatt. methods 79−4431
Si (100)-SiO_2 inversion layers, exchange and correl. contribs. to subband energies 79−42654
Si (111)-Au interface, chemically driven intermixing, UPS study 80−50533
Si (111)-Pd interface, microscopic Pd_2Si form., UPS obs. 80−24743
Si (111)-SiO_2 interfaces, sixth-valley state stability a priori calc. 80−49859
Si (111)($\sqrt{31}\times\sqrt{31}$)R ± 9°-In struct., RHEED obs. 79−60612
Si, amorphous, hydrogenated bonding 78−19636
Si amorphous films, self-ion bombard., electronic props. 79−28422
Si, Auger recomb. coeff. meas. using laser excitation 79−38654
n-Si, bulk, high field characts. *(Japanese)* 78−34837
Si, carrier lifetime degradation at room temp. 78−95301
n-Si channel ⟨100⟩ inversion layer MOSFET, valley splitting, conductivity 80−70840
Si, cooling rates of large diameter crysts. 78−35291
n-Si, current carrier-dislocation interactions, resistance in UHF range *(Russian)* 80−54732
n-Si, deformed, thermal treatment effect on elec. cond. and dislocation mobility 80−107265
Si, drift mobility and Hall coeff. factor of holes 78−43379
Si, dynamic recoil implantation, of Au film 79−14833
Si, elastically bent, strain canc. determ. by microfluorescent densitometry of X-ray topography 80−79245
Si, failure in strong melt grown single crysts. 78−3205
Si, floatzone, P doping by thermal-neutron irradiation 78−22750
Si, gamma-irradiated, number of Frenkel defects 78−14377
p-Si, high ohmic material, deep level investigation, vacuum growth *(Russian)* 80−54654
Si, highly excited, theory of electron-hole plasma 78−10363
Si I CI calcs. of oscillator strengths, L-S framework 80−14089
Si I lines in far UV spectra of G-type dwarf stars 80−56829
Si I sequences for elements Cr to Zn, n=3→n'=4 transitions 79−26922
Si I UV spectrum, series from 3000 to 1200 Å, identifications in solar spectrum 77−56882
Si II, interstellar, fine struct. levels population ratios 79−35351
Si II, oscillator strength meas. and trends in group IV homologous ions 80−42991
Si II, reson. transitions, radiative lifetimes, astrophys. appls. 78−62767
Si II, transition probabilities between excited states, SCF treatment 78−82658
Si II 1533 Å identifications in QSO spectra rel. to absorption redshift 79−35417
Si II and III, UV line spectrum of active chromosphere star ε Eridani, models 80−77394
Si II homologous ions series, Stark broadening trends 80−105157
Si II lines in A-type star α Lyrae (Vega), Copernicus UV obs. 80−8627
Si II lines in shell spectrum of ζ Tauri 77−60774
Si II solar lines 1808-1817 Å, observed and theoretical profiles 78−49412
Si II spectrum calc. for quasistellar objects 77−60844
Si III, $^3F^0$ Rydberg series, energy levels, multiconfigurational HF procedure 80−47882
Si III, EUV spectra in solar transition zone rel. to energy balance and press. 80−21957
Si III, IV, beam foil spectra, radiative lifetimes, oscillator strengths 77−30973
Si III, IV, Stark line broadening in pulsed arc, plasma diagnostics 78−944
Si III 1892 Å emission line obs. of solar atmosphere 80−31277
Si III 1892 Å emissivity in solar spectrum, effect of charge transfer rel. to spectral diagnostics 80−41717
Si III and IV, electron impact width of plasma lines, approximative semiclassical formula 80−43972
Si IV, 1122 and 1128 Å lines in solar spectrum 78−4170
Si IV, V, VI, beam-foil level populations, charge state fractions 80−52913
Si IV interstellar column density towards early-type stars 80−73018
Si IV interstellar lines in Wolf-Rayet star spectra, IUE obs. 80−67748
Si IV radial wave functions of discrete spectrum calcs., dipole and quadrupole polarisation 80−5476
Si IV spectra, nonrelativistic oscillator strengths calc. 77−83538
Si IV/C IV ratio for Be-stars, Skylab UV obs. 77−56987
Si IX, UV lines, theoretical intensity ratios 78−90108
Si IX and X solar line intensities, OSO-7 obs. of limb brightening 78−69759
Si, ion beam damaged, minority carrier lifetime distribs., electron beam meas. 79−87108
n-Si, ion-implanted, elec. characts. after laser annealing 80−88562
a-Si, laser induced crystallisation mechanism, epitaxial regrowth 80−84962
Si, laser irradiated, positron annihilation crystal struct. imperfection monitoring 80−11506
Si MIS grating solar cells on minority carrier blocking back surface field substrates 80−94078
n-Si MOS inversion layers, Hall cond. meas. 80−39676
Si, metal contacts to O_2 contaminated surfaces, Schottky diodes 79−56309
Si, neutral point defect electronic struct., self consistent method 78−91641
Si, P diffused sample, stacking faults and dislocations formation from interstitials 78−95059
a-Si p-i-n and c-Si p-n junction solar cells, design concept differences 80−94031
Si p-n junctions, secondary breakdown, pre-mesoplasma state expsn. *(Russian)* 79−56723

silicon continued
n-Si, passive, complete activation initiation by local photoactivation 79−100403
n^+nn^+Si planar device, hot electron flicker noise at 78K 80−103732
Si, planarized solid state epitaxy for Schottky barrier diodes 78−35302
n-Si, quenched, fast electron irradiated, annealing of defects 80−89259
Si, radiation-doped and annealed, carrier density and mobility meas. 78−56145
a-Si, resonant and non-resonant photoconductivity changes 80−49814
a-Si, resonant and non-resonant luminesc. changes theory 80−50410
Si ribbon, crystal characterisation, growth with dies 78−76598
Si rich SiO_2-SiO_2-Si rich SiO_2 layers for dual electron injector struct. 80−96991
Si, simple scheme for describing dislocation motion 79−65259
Si single crystals, nearly perfect, high resolution diffuse X-ray scattering study 79−32854
Si, solar grade, directionally solidified using C crucibles, TEM study 79−47617
Si, stressed, at high mag. field, submillimeter cyclotron res. of electrons 77−81012
n-Si, substrate surface damage induced by RF-diode sputtering 77−90274
p-Si surface barrier detectors, charact. meas. *(Bulgarian)* 78−82592
Si, surface layer, thin, density meas. by total external X-ray reflection 78−14635
p-Si, thermal noise, effects of hot carriers 79−24036
Si thin ribbon grown at high speed, thermal stresses, reduced thermal buckling 80−107078
Si, transmutation doped, stabilisation 78−10449
Si type semiconductor, interimpurity zero-phonon radiative transitions 78−15222
Si V, transition probabilities and radiative lifetimes 79−98041
Si V, VI, beam-foil meas. of lifetimes, 500 to 1300 Å 78−9118
Si VI, $2p^43s$, $2p^43p$ and $2p^43d$ configs., UV spectrum anal. 78−21868
Si VI-XIV, line strengths, collision strengths and excitation rates, calcs. 78−5174
Si VII, excited level populations, line intensity ratios, solar corona appl. 80−32637
Si VII, O I like ion, solar emission lines density depend. 79−40165
Si, VPE, fine struct. formation *(French)* 78−43275
Si, vapour epitaxy, optimum growth conditions 78−76608
Si wafer, heat treatment behaviour of microdefects and residual impurities, X-ray diffr. and IR absorpt. study 80−49214
Si X, low lying levels, excitation equilib. and line intensities 79−12401
Si, X-ray diffuse scatt. close to reciprocal lattice points, high-resolution technique 77−39511
Si, X-ray rot. polarisation, absorpt. crystal orientation effects 78−47206
Si XI, $2s2p(^3P_1^0)\rightarrow 2s^2(^1S_0)$ transition probabilities, CI calcs. 79−36544
Si XI, allowed transitions, radiative lifetimes and oscill. strengths meas. 78−78797
Si XI, beam-foil obs. of oscillator strengths for E1 transitions 80−14112
Si XI, wavefunctions and oscill. strengths, CI calcs. 80−23317
Si XI 303 Å, solar line profiles 79−12452
Si XII, allowed transitions, radiative lifetimes and oscill. strengths meas. 78−78797
Si XII, in plasma, ion electron collisional radiative recomb. coeffs., bottleneck calc. 80−53942
Si XIII, $1s2s\ ^3S$-$1s2p\ ^3P$ transitions, Lamb shift, VUV beam foil spectra obs. 80−52919
Si XIII, ground-state electron impact excitation strengths, close-coupling calcs. 80−23561
Si XIV, H-like ion, anal. of satellites to reson. lines in X-ray region 77−88421
Si XIV, X-ray spectral lines profile evolution due to Comptonisation, Monte Carlo computations 79−66916
Si^-, ground state, photodetachment cross section calc., low energy 79−63970
Si^- opacity source in stellar atmospheres 78−53930
Si^+, and isoelectronic ions, excited-state energy level k-ordering, l-patterns 77−88406
Si^+ lines, from plasma, Stark broadening 79−4189
Si^+, reson. line regularities in plasma Stark widths and shifts 80−43881
Si^+, Stark broadening, shock tube meas. 78−17614
Si^{12+}, $1s2s\ ^3S_1$-$1s2p\ ^3P_{0,2}$ transition wavelengths, by beam-foil 80−32649
Si^{12+}, $1s2s\ ^3S$-$1s2p\ ^3P$ transitions 79−22632
Si^{2-}, parameters for analytical radial orbitals, total and binding energies 77−6668
Si^{2+}, static dipole quadrupole polarisabilities and shielding factors calc. using HF scheme 80−99450
$^{28}Si^+$, stopping power in Au at 50-500 eV 77−76478
Si^{4+}, ionic size rel. to Koopmans' ionisation pot. 79−85892
Si^{6+}, $2s2p^5$-$2s2p^43s$ transitions, spectroscopic investig. 79−59384
Si^{n+}, excited state population density in p and p^5 configs., temp. depend. 80−31273
Si^{n+}, foil excited, satellite lines in X-ray spectrum 79−85929
Si^{q+} electron loss, forward peak oscill. struct. 78−78796
Si: (B, P, Ge), impurity-pair diffusion, influence of elastic stresses 78−87824
Si: As(Pb), high-dose ion implanted and annealed, implant redistribution 80−107309
Si: Li, absorpt. and luminesc. transitions involving exciton excited hole states 79−78038
Si:^{119m}Sn, impurity lattice dynamics, Mossbauer spectra, Debye temp. 80−84262
Si:^{119}Te(^{119}Sb), implanted atom site changes with time, Mossbauer obs. 77−20757
Si:^{11}B, amorphous, calc. of implanted-ion range and energy-deposition distrib. 77−7748
Si:$^{31}P^+$, implanted layers, characterisation by ellipsometry 79−90683
Si:^{57}Co, ion-implanted, Mossbauer study, annealing effects 80−7231
Si:^{57}Co/^{57}Fe, Mossbauer spectra, deep level Co impurity study 80−29666
Si:^{57}Co(^{57}Fe), implanted, Mossbauer spectra, study of dose dependence 80−75900
Si:^{57}Fe, electric quadrupole coupling at Fe nuclei 78−27137
Si:^{57}Fe, quadrupole interac. 78−92005
Si:^{57}Fe study via conversion electron Mossbauer spectroscopy 77−55735
Si:^{85}Kr, ion-implanted, impurity distrib. 80−15145
Si:O, electrical activity due to heat treatment, Hall effect meas. 80−15543
Si:Ag, photoexcitation of electrons from ionised AG acceptors 78−2519
silicon continued
Si:Ag, surface layer, ellipsometry 78−19121
Si:Ag (Zn,Fe), diffusion mechanism of fast impurities, distrib. in surface layers 77−11735
Si:Al, absorpt. line broadening 78−95594
Si:Al, bound exciton and bound multiexciton complexes, electronic structure, luminesc. obs. 79−56139
Si:Al, bound exciton and multiple bound electron luminesc., fine struct. 77−48221
Si:Al, bound-exciton absorption 78−56507
p-Si:Al, diffusion and incorporation of dopant in closed system, elec. props. 77−59026
Si:Al, electron irrad. induced defects, transient capacitance study 80−59516
Si:Al, localised exciton bound to isoelectronic trap 80−66283
Si:Al, P-diffused, recomb. centres, thermally stimulated capacitance meas. 77−72834
Si:Al, polycryst. film, grain boundary diffusion, Auger sputter profiling 80−75388
Si:Al, radiation defects by annealing, kinetics anal. 79−33018
Si:Al, recomb. enhanced migration of interstitial Al 79−82201
Si:Al, thermally induced deep levels, TSC meas. 77−31974
Si:Al, valley-orbit splitting of bound exciton states 79−28290
Si:Al epitaxial layers, nuclear microanalysis of Al impurities $^{27}Al(d,\alpha)^{25}Mg$ 80−61193
Si:Al film, low-temp. diffusion of Al 78−38878
Si:Al p-n lamellar structures, processing by molten Al rich wire thermomigration 78−10068
Si:Al ribbon, edge-defined film-fed growth, Al redistrib. 80−29873
Si:Al(B)(P), bound multiexciton complexes, work function thermodynamic determ. 78−72078
Si:Al(Ga), O_2 diffusion, conc. profile meas. 80−79990
Si:Al(Ga), spreading resist. calibration using Si:B 80−103690
Si:Al(In), acceptor levels, IR spectra 78−67972
Si:Al(Sb) film, amorphous, ion implantation, effect on cond. 78−83839
Si:Ar, As, ion implanted, laser annealing, doping profiles, channelling 80−97506
Si:Ar, ion implant gettering of MOS capacitors using linear voltage ramp and N^+ backscattering 79−95502
Si:Ar, ion implanted, amorphous, epitaxial regrowth 79−10868
Si:Ar, ion-implanted, epitaxial regrowth by laser annealing, microstruct. 80−84404
Si:Ar, ion-implanted, high resolution LMM Auger spectra 79−83066
Si:$Ar^+(Si^+)$, implantation effect on carrier lifetime, damage obs. by TEM 79−65493
Si:Ar(B), implantation doped, electroreflection spectra 79−51983
Si:Ar(Ne)(O)(N), ion-implanted, defect reverse annealing, 550-650°C 80−88875
n-Si:Ar(P), single cryst., positron annihilation parameters, energy-band struct. on surface in free-electron approx. 79−15555
Si:As, ^{75}As implantation, scanned CW electron beam annealing 79−99225
Si:As, 1.5 MeV H^+ and He^+ irradiations of As diffused layers 78−47447
Si:As, amorphous, appl. of EXAFS methods for struct. determ. 79−37624
Si:As, amorphous, field effect and thermoelectric power 79−33289
Si:As, annealed, dopant profile parameter contactless probing by IR spectroscopy 79−77629
Si:As, anomalous tail generation, As ion channelling 80−49246
Si:As, As implantation damage and atom location, channelling meas. 77−59032
Si:As, CVD, doping using SiH_4-H_2-AsH_3 system 80−79823
Si:As, CW CO_2-laser annealing, comparison with thermal annealing 80−84193
Si:As, CW laser annealing mechanism, annealed spot size, solid phase epitaxial regrowth 79−78798
Si:As, conc. profiles of As and recoiled O atoms after ion implantation into SiO_2-Si, SIMS obs. 79−51138
Si:As, depth profile detect. limit of 3×10^{15} atom cm^{-3} using Cs^+ bombardment negative SIMS 77−65988
Si:As, diffused, laser irrad., stability study 80−65547
Si:As, diffusion model, degeneracy and partial ionisation effects 80−96693
Si:As, diffusion of implanted As induced by laser annealing 77−89590
Si:As, displacement effect beam energy depend., vacancy trapping 80−33996
Si:As, dose depend. in laser annealing 78−91354
Si:As, dual wavelength, laser ion implantation damage annealing 79−69117
Si:As, effects of recoil-implanted O on elec. activation of As 79−99227
Si:As, elec. activation of implanted As during low temp. anneal, Hall effect meas. 78−51571
p-Si:As, electrochem. doping, depth profile analysis 77−72630
Si:As, electrochemical doping 79−90684
Si:As, electrochemical doping profiles 79−90685
Si:As, electron induced displacement, channelling study 80−29058
Si:As, electron irrad. induced defect levels, annealing, deep level transient spectroscopy obs. 77−59044
Si:As, electron irradiated, majority carrier trap prod., effect of O_2 enhanced annealing 77−1151
Si:As, H, amorphous system, struct. and defects, Raman and EPR meas. 80−49103
Si:As, heavily As-diffused, Hall mobility and resist. rel. to carrier conc. 80−107815
Si:As, high conc. diffusion from double-layer sources 78−10075
Si:As, high-dose implanted, irrad. time and subsequent heat treatment effects on laser annealing 80−29041
Si:As, implantation into polycryst. Si and diffusion into Si substrate 77−59025
Si:As, implanted, laser annealing reduction in defect conc. 77−62559
Si:As, implanted, residual defects after one- and two-step annealing 78−6083
Si:As, implanted, spatially varied activation during regrowth of amorphous layers, sheet resist. and backscatt. obs. 78−71749
Si:As, implanted, thermal diffusion of As 80−39352
Si:As, implanted As redistrib. during annealing in oxidising ambient, carrier distrib. meas. 79−19275
Si:As, implanted through SiO_2 films, elec. props., defect struct. 80−54264

silicon continued
Si:As, ion implantation system, high current, design of end station 80−34030
Si:As, ion implanted, amorphous-cryst. transition induced by multiple-pulsed ruby laser 79−90555
Si:As, ion implanted, annealing characts., elec. props. 77−19974
Si:As, ion implanted, anomaly of elec. activation by additional Ne irradiation 78−84211
Si:As, ion implanted, anomalous diffusion of As 79−14842
Si:As, ion implanted, beam techniques 80−24474
Si:As, ion implanted, formation of As complexes 80−59511
Si:As, ion implanted, glow discharge optical spectroscopy 78−22755
Si:As, ion implanted, laser scanning apparatus for annealing 78−34526
Si:As, ion implanted, laser annealed, lattice defects, epitaxial regrowth 80−103334
Si:As, ion implanted, low temp. thermal annealing 80−96552
Si:As, ion implanted, pulsed ion beam annealing 80−103395
Si:As, ion implanted, pulsed laser annealing, partial solid-state regrowth 80−103591
Si:As, ion implanted, recrystallisation by free running ruby laser 79−73185
Si:As, ion implanted, scanning-electron-beam annealing 79−60391
Si:As, ion implanted, two-step annealing 78−18664
Si:As, ion implanted, two-step annealing, TEM study 79−82249
Si:As, ion implanted layers in device structures, boundary effects in laser annealing 79−73188
Si:As, ion-implanted, CW IR laser annealing 80−34022
Si:As, ion-implanted, channelling anal. of CW Ar laser annealing 79−73186
Si:As, ion-implanted, dislocation loops and etch pits, X-ray diffr. and TEM obs. 79−42068
Si:As, ion-implanted, laser annealing, channelling obs. of As cluster form. 79−69128
Si:As, ion-implanted, laser recrystallisation by freq.-doubled Nd:YAG laser 79−77613
Si:As, ion-implanted and post-annealed, dislocation loops, TEM obs. 77−84776
Si:As, ion-implanted layers, ellipsometric anal. of laser annealing 79−73190
Si:As, laser annealing, channelling, optical obs., and resist. meas. 79−1444
Si:As, laser annealing of implanted layers 77−55296
Si:As, laser induced diffusion and annealing processes 77−69943
Si:As, laser-doped, impurity distrib., Rutherford backscatt. and channelling anal. 80−59507
Si:As, MBE with simultaneous ion implant doping 80−66432
Si:As, neutron damage mechs. in IR detectors 78−30668
Si:As, Orbach spin-lattice relax. rate, uniaxial stress depend. 78−72391
Si:As, p-n junction form. by laser annealing, space charge region, effects on reverse current 80−54772
Si:As, planar and axial channelling of 800 keV As 77−19995
Si:As, relation between total and electrically active As conc. produced by diffusion 79−55773
Si:As, SIMS, energy distrib. of sputtered ions 79−38706
Si:As, scanning electron beam annealing, spreading resistance, junction depth 80−75267
Si:As, segregation and desorption kinetics for evaporation of As 79−99410
Si:As, shallow junctions by high-dose implants 80−96694
Si:As, solid solubility and thermal behaviour of metastable 80−75359
Si:As, solid solubility of As determ. by ion implantation, CW laser annealing 80−6517
Si:As, thermal oxidation in wet ambient from 650°C to 850°C 79−61758
Si:As, time-resolved reflectivity during laser annealing 78−92086
Si:As,Sb, amorphous, damage depend. of epitaxial regrowth during annealing 78−47679
Si:As detector, high-low junction contact at low temp. 77−39925
Si:As epitaxy, lateral autodoping kinetics 78−39699
Si:As high-dose implanted single crysts., pulsed electron-beam annealing 80−103373
Si:As implanted emitters, oxidizing drive-in ambient deleterious effect 80−2044
Si:As ion implanted, laser induced diffusion modelling 80−24672
Si:As ion implanted layers, annealing by CO_2 laser, doping profile shift 80−84965
Si:As ion implanted shallow junction 80−70228
Si:As ion implanter system, high current, architecture and control 80−31942
Si:As laser annealing, heat and mass transport model 80−92546
Si:As photoconductive detector for IR astronomy, responsivity and system noise 80−51665
Si:As sputter rate meas. SIMS combination with Rutherford backscatter 80−21334
Si:As thermal diffusion retardation by inert gas ion implantation 79−77616
Si:As wafers, laser annealing, Rutherford backscatt., optical, and TEM obs. 79−1445
Si:As^+, annealing by scanning Ar ion laser, dislocation loop density comparison 78−47438
Si:As^+, implanted, CW laser annealing, electron-beam induced current 80−100709
Si:As^+ ion implanted, sheet resistivity rel. to isochronal annealing and defect structures 77−76443
Si:$As^+(P^+)$ ion implanted, laser annealed, correlation of struct. and elec. props 80−70855
Si:$As^+(P^+)(Sb^+)$, implantation damage removal by laser irrad. and its thermal stability, TEM study 79−74024
Si:As(B), heavy-doping effects and impurity segregation during high-press. oxidation 80−65014
Si:As(B), implanted CW laser annealing, elec. props., cryst. struct. and limitations 80−39131
Si:As(B), ion implanted, pulsed laser annealing appl. to device fabrication 79−73180
Si:As(B), ion-implanted, scanned laser and electron beam annealing 79−73182
Si:As(B)(Ga)(In)(P)(Sb), mean square dynamic displacement of atoms, effect of electron-phonon interactions *(Russian)* 78−10145
Si:As(B)(N)(P), conc. profiles of ions and recoiled N after implantation through Si_3N_4 films 79−55764
silicon continued
Si:As(B)(P), ion-implanted polycrystalline films, laser annealing 79−73181
Si:As(Li)(P), luminesc., stress effects on donor exciton satellites 77−85786
Si:As(P), depth profiling using Cs^+ bombardment and negative SIMS in UH vac. 79−99232
Si:As(P), ion implanted, TEM study after laser and furnace annealing 80−70234
Si:As(P), oxidation-enhanced diffusion of impurities 79−46840
Si:As(P) film, polycryst. laser annealed, resistivity changes during thermal annealing 79−91163
Si:As(P)(Sb), donor-polarizability enhancement as the insulator-metal transition is approached from the insulating side 80−80184
Si:As(P)(Sb) film, implanted, elec. cond., sheet resist. as function of ion dose and temp. 79−78235
Si:As(Pb), ion-implanted, impurity redistrib. during laser irrad. 80−100280
Si:As(Sb), implanted, pulsed ruby-laser annealing, Rutherford backscatt., TEM and ion channelling study 79−86805
Si:As(Sb), ion implant lattice location after pulsed ruby laser annealing 79−73204
Si:As(Sb), ion implanted, lattice location of impurities after pulsed laser annealing 80−88196
Si:As(Sb), ion-implanted, thermally assisted Xe-flash annealing, Rutherford backscatt. meas. 79−10881
Si:As(Sb), ion-implanted, CO_2 laser annealing 79−73183
Si:As(Sb), MBE, n-type doping techniques 80−15126
Si:As(Sb)(Bi)(P), luminescence associated with transitions from bound exciton excited states 78−23534
Si:Au, amphoteric centre, struct. bonding of deep level defects 80−88506
Si:Au, autoradiographic detection of getter effect, Ar ion implantation 78−38739
Si:Au, C-V curves of MIS diode used to examine trapping levels 80−65697
Si:Au, carrier capture cross-section at low temp. *(Rumanian)* 79−15163
Si:Au, deep impurities, book contrib. 78−10403
Si:Au, degeneracy factor of acceptor level 78−51927
Si:Au, diffusion, effect of C concentration 78−10076
Si:Au, diffusion of Au anal. 79−23786
Si:Au, EPR spectrum, strong nucl. quadrupole effect 80−93172
Si:Au, electron capture cross section, energy level of Au acceptor centre 78−51926
Si:Au, IR absorption and elec. resist. meas., impurity centres 79−38580
Si:Au, impurity diffusion and distribution obs. by neutron activation analysis *(Japanese)* 77−84787
Si:Au, impurity induced internal friction, impurity centre symmetry 79−73252
Si:Au, impurity photocond., for IR electrophotographic system 77−24589
Si:Au, influence of carrier heating on exclusion 77−8110
Si:Au, method of determining content of impurities with deep levels 80−2056
Si:Au, neutron irradiated, penetration of Au into Si 78−59984
Si:Au, nonequilib. population of electron states and photomemory of surface pot. 78−56206
Si:Au, O(H), film, amorphous, elec. cond. meas. 80−80423
Si:Au, p^+-n junction, quantitative study of Au atoms by TSC method 80−2458
Si:Au, P-induced point defects influence on Au gettering mechanism 80−65030
Si:Au, precipitation of solid soln., effect of gamma irradiation 80−59515
Si:Au, thermally stimulated capacitance method fitting anal. 79−47107
Si:Au Ar ion implant gettering obs. by MOS and Rutherford backscatt. techniques 80−39119
Si:Au deep level parameter determ. by isothermal capacitance transient spectroscopy 80−88507
Si:Au diodes, diffused, influence of gamma irradiation, Au levels monitored 77−66199
Si:Au donor and acceptor centre obs. using IR absorpt. and dynamic nucl. polarisation with optical pumping 80−54639
Si:Au n^+p diodes, deep level transient spectroscopy, system effects and data anal. 79−99501
Si:Au p^+-i-n^+ diode, double injection switching, effect of trapped space charge 77−1473
Si:Au p^+-i-n^+ diode, I-V characts., recomb. centre influence 78−19134
Si:Au p^+-n junction, small area, acceptor level conc., determ. from TSC curves 80−75631
Si:Au planar extrinsic IR detector, use of multiple internal refl. for increased sensitivity 80−77862
Si:Au surface, electronic props. 77−66194
Si:Au use in weakly absorbed nucl. radiation detectors 77−67947
Si:Au(Hg), photomag. effect 77−4401
Si:Au(P)(B) whiskers, impurity inhomogeneity 80−39145
Si:Au(Pt), electron and hole capture, DLTS obs. 80−49661
Si:Au(Pt), heavily doped, gradual p^+-n junctions, trap levels *(French)* 80−34392
Si:Au(Zn) deep-level impurities, insulating props. 78−39124
Si:B, annealing mechanism of radiation change and dopants in pulsed laser irrad. ion implanted layers 79−46691
Si:B, anomalous B profiles prod. by BF_2 implantation 80−75252
Si:B, antiferromagnetic ordering of holes, recombination radiation polarisation *(Russian)* 80−45121
Si:B, As, first and second order Raman scatt. by pair modes 79−65869
Si:B, autodoping during epitaxial growth from SiH_4 77−47476
Si:B, B segregation during dry, nearly dry and wet O_2 oxidation 79−66178
Si:B, bound many-exciton complexes, luminescence spectra, mag. props. 80−103994
Si:B, bound multiexciton luminesc., recomb. kinetics 79−38591
Si:B, conc. depend. of B diffusion coeff. 80−39353
Si:B, conc. profile of implanted cryst., by $^{11}B(p,\alpha)$ chem. anal., annealing *(German)* 78−83843
p-Si:B, defect energy levels with 1 MeV electron irrad. and annealing, transient capacitance spectra 77−62860
Si:B, detection of atomic plane displacement in near-surface layers, ang. depend. of photoemission during X-ray Bragg diffr. 78−47207
Si:B, diffusion for very shallow defect free p^+-n junc. for solar cells 79−15218
Si:B, diffusion from BN source with H_2 injection, AES study 80−19986
Si:B, diffusion length, SEM-EBIC/Schottky diode 79−82605

silicon continued
Si:B, diffusion of As atoms from ion implanted layers, conc. profiles 77−43376
Si:B, diffusion of B atoms and growth kinetics of oxidation induced stacking faults, correlation 79−37720
Si:B, diffusion of B from B_2H_6-CO_2 system, lower temp. limit of 775°C 77−43232
Si:B, diffusion of randomly implanted ions during high temp. processing 77−24439
Si:B, diffusion with BN, expt. *(Bulgarian)* 78−59824
Si:B, diffusional impurity redistrib., elastic stress field effect *(Russian)* 77−72719
Si:B, dislocation net form. during annealing 77−51385
Si:B, distrib. profiles, high temp. treatment effects 79−69150
Si:B, dopant density and temp. depend. of hole mobility and resistivity 79−38075
Si:B, dopant density determ. by nucl. track technique 78−55886
Si:B, ESR at zero and small external stress, interpreted in spin Hamiltonians 78−43641
Si:B, ESR at zero and small external stress, elastic strengths for point defects 79−19764
p-Si:B, Fe, 0.45 eV majority carrier trapping level after quenching 78−18990
Si:B, He^+ irradiation-induced diffuiion, effect on impurity distrib. 80−70470
Si:B, heat treatment centres changes, EPR obs. 80−29601
Si:B, heavily doped, annealing characteristics obs., Ne^+ ions implantation for damage density control *(Japanese)* 78−18666
Si:B, heavily doped, paramagnetic props., anomalous hole spin susceptibility *(Russian)* 80−54861
Si:B, heavily implanted wafers, secondary defect generation suppression by HCl oxidation 78−10069
Si:B, high conc. effects in ion implantation 80−75245
p-Si:B, high temp. treatment, effects on ion implanted impurity distrib. profile 78−79625
Si:B, highly-doped polycryst. thin film, growth kinetics and properties 78−44016
Si:B, hole mobility calc. for dopant density and temp. var., resistivity meas., effective mass calcs. 80−54703
Si:B, hole trapping by B atoms at low temps. 79−7837
Si:B, hot-carrier scatt. and recomb. characts. 79−91069
Si:B, IR spectra of acceptor levels 80−34953
Si:B, implantation distribution determ. using ion bombardment 80−44230
Si:B, implantation energy, rel. to dose, Szabo-Bogancs effect 78−38740
Si:B, implanted, effectiveness of charged vacancies in diffusion 80−34239
Si:B, implanted, free carrier conc. and impurity location, Raman scatt. obs. 77−55295
Si:B, implanted, laser-annealed, lattice dilatation 79−46690
Si:B, implanted, oxidation induced precipitate defects, TEM 78−31556
Si:B, implanted, oxidation-induced stacking faults, EBIC and TEM expts. 78−39923
Si:B, implanted, radiation damage and minority carrier lifetime, SEM-EBIC obs. 80−96573
Si:B, implanted, shrinkage of rod shaped defects 78−6061
Si:B, implanted laser annealed, lattice strain, X-ray study 80−96554
Si:B, implemented laser annealed samples, unidirectional contraction 78−71747
Si:B, impurity conc. from photoluminesc. anal. 78−63785
Si:B, impurity excited state lifetimes 78−60083
Si:B, impurity range distrib. determ. by $^{10}B(n,\alpha)^7Li$ reaction 78−11585
Si:B, influence of proton beam irrad. on concentration profiles *(French)* 77−51402
Si:B, inhomogeneous surface layer, diffusion and implanted, X-ray rocking curves 80−6603
Si:B, interstitial Si atom formation by light ion bombardment 78−47406
Si:B, ion implantation, anal. of disordered regions in crystal with Promiss protonograph 80−19823
Si:B, ion implantation, channelling and random distrib. of B ions meas. 77−47473
Si:B, ion implantation using B_2O_3-B mixture, Auger spectra, channelling anal. 79−4317
Si:B, ion implanted, comparison of range and range straggling 77−55293
Si:B, ion implanted, depth and lateral profiles of B atoms, Monte Carlo simulation 77−55297
Si:B, ion implanted, ellipsometric study for low doses, cryst. damage parameter 79−65105
Si:B, ion implanted, laser annealing 78−34525
Si:B, ion implanted, laser and thermal annealing compared, TEM obs. 78−75681
Si:B, ion implanted, laser annealed, thermal annealing effect 79−73191
Si:B, ion implanted, laser annealed, IR and Raman spectra 79−73914
Si:B, ion implanted, laser annealed, Raman scatt., Fano interactions, lattice damage 79−78711
Si:B, ion implanted, localised defects, TEM study 78−87699
Si:B, ion implanted, radiation defect accumulation and annealing, X-ray diffr. obs. 79−37726
Si:B, ion implanted, SOS device struct., nonlinear impurity redistrib. 79−1625
Si:B, ion implanted, struct. of rod defects, TEM obs. 78−71744
Si:B, ion implanted, structure defects formation and behaviour under annealing in various ambients 80−65033
Si:B, ion-implantation doped, influence of radiation dose on diffusion processes 77−1141
Si:B, ion-implanted, annealing by incoherent light source 79−19267
Si:B, ion-implanted, dislocation climb, TEM obs. 78−6062
Si:B, ion-implanted, influence of US waves on charged particle channelling 79−23668
Si:B, ion-implanted, rod-like defects, TEM obs. 77−68975
n-Si:B, ion-implanted damage, positron annihilation and sheet resist. meas. 80−35003
Si:B, ionisation-assisted annealing 79−23628
Si:B, irrad. with fast neutrons true profiles of impurity photocond. bands from piezodichroisms 79−91103
Si:B, laser damage obs. by DLTS 78−76023
Si:B, lateral effect of oxidation on B diffusion 80−29217
Si:B, lattice location of implanted ions after laser annealing 78−30660
Si:B, layer resist. depend. on implanting and annealing conditions *(German)* 80−96551
Si:B, low conc. B diffusion using doped-oxide film 77−76431
silicon continued
Si:B, low noise avalanche photodiode fabrication by channelling implantation 79−35827
Si:B, many-body exciton-impurity complexes, stress depend. of photolum. meas. 79−28833
Si:B, N-implanted junction capacitance meas., appl. of dynamic lateral photovoltaic effect 77−85304
Si:B, near intrinsic ⟨100⟩ and ⟨111⟩ samples, inert and oxidising ambients, diffusion, segregation 78−75882
Si:B, P, deep diffusion of B and P, expt. results 80−54437
Si:B, P, first and second order Raman scatt. by pair modes 79−65869
Si:B, P, high temp. diffusion, effects of laser irrad. on diffused layer 79−14834
Si:B, P, long range enhancement of B diffusivity by P diffusion 80−103386
Si:B, p-n junction diodes, scanning-electron-beam annealing, elec. characts. 79−79128
Si:B, p-n junction form. by B deposition and laser-induced diffusion 78−87690
Si:B, photoconductivity, impact neutralisation of H^--like centres 77−69377
Si:B, photolum. of heavily doped p- and n-type 80−20708
Si:B, piezothermoelec. power 78−56173
Si:B, polycryst., effect of laser annealing on struct. and elec. props. 79−11243
Si:B, polycryst., N_2 heat treated, anomalous resist. change due to Bn form. 78−2591
Si:B, polycryst. film, piezoresistive gauge factor 77−12029
Si:B, polycrystalline, depth profiles of implanted B atoms, meas. by secondary ion mass spec. *(Japanese)* 78−67734
Si:B, predeposition of B using BBr_3 78−55882
Si:B, proton-irrad.-enhanced diffusion 80−29227
Si:B, RF glow discharge sputtering damage centres, barrier formation 79−33329
Si:B, radiation defects by annealing, kinetics anal. 79−33018
Si:B, redistrib. of B during thermal oxidation, numerical and analytical calcs. 80−49259
p-Si:B, reduction of vibration noise, suitable orientation of element, rel. to crystallographic axes 79−11123
Si:B, resonant scattering of phonons by bound holes in temp. range 1 to 5K 80−75393
Si:B, SEM obs. of dislocations using Schottky barrier EBIC technique 78−79614
Si:B, selective etching by NaOH soln. 79−70189
Si:B, self-interstitials location by Rutherford backscatt. of channelled ions 80−2101
Si:B, solubility and precip., and supersat. resulting by thermal predeposition 78−11232
Si:B, sputtering influence on distrib. profile of ion-implanted impurities 79−42091
Si:B, TEM study of stacking fault form. and annealing 78−51566
p-Si:B, thermoelec. power, 20-300K 78−19067
p-Si:B, total piezoresist. tensor, 20 to 300K 78−19037
p-Si:B, trace determ. of U impurity by fission track method 79−79354
P-Si:B, US spectroscopy, energy splitting of acceptor ground state 79−33260
Si:B, use of BN source to achieve high surface concentration of B *(Russian)* 80−107639
Si:B, using oxidised BN dopant source, sheet resist., rel. to temp. and deposition time 77−43231
Si:B, with insulating coating, mechanical stress influence on B diffusion, strained surface layers 80−29224
Si:B,As selective area simultaneous doping 80−34015
Si:B,In, sharp line series in near-band-edge photolum. 80−16092
Si:B,P, anomalous diffusion 80−29229
Si:B,P, diffusion patterns obs., for SiO_2 deposited by means of centrifuge *(Bulgarian)* 77−76429
Si:B,P, double implanted layer, n-p-n struct., single pulse laser annealing 80−49247
Si:B,P, high conc. diffusion without disloc. generation 78−10072
n-Si:B,P, radiative recombination at thermal defects, luminescence centre electron struct. 79−91496
Si:B (0.2 wt.%) ion implanted, B atom displacement due to low temp. irrad. 80−88234
Si:B amorphous film, CVD prep., EPR, elec. and optical props. 79−4558
Si:B diffusion at Si-SiO_2 interface, Auger spectra, Rutherford backscattering 80−70471
Si:B doping from BN sources, impurity transfer considerations 77−76441
Si:B effect of elec. field on carrier capture by attractive centres. 79−11145
Si:B epitaxial layer, B diffusion coeff. 79−99372
p-Si:B epitaxial layer, proton-implanted, annealing characts., carrier conc. profiles 77−32097
Si:B film, sputter-deposited, elec. props., struct., SEM and TEM obs. 79−95298
Si:B implanted wafers, ionis. assisted annealing and effects 80−100257
Si:B impurity conc. profile determ. by anodic oxidation 79−28010
Si:B ion implanted, strain profiles from X-ray rocking curves 80−107290
Si:B ion implanted, X-ray topographical images at different absorption conditions 80−2052
Si:B ion implanted grating-type solar cells, var. of junction depth, collection efficiencies 80−93934
Si:B ion implanted layers, light refl. and transmission coeffs., computer program 80−66316
Si:B MOS structures, implanted laser beam irrad. effects on interface electrophys. props. 79−1627
Si:B photodiode front region collection efficiency models 80−96899
Si:B recombination emission polarisation of bonded multiple-exciton complexes in mag. field *(Russian)* 78−2905
Si:B redistribution after oxidation, integro-differential eqn. 77−76453
Si:B sputtering by Ar^+, computer simulation of sputter broadening in impurity depth profiling 80−2908
Si:B_2O_3, analytic study of Si-B phase formed 79−19269
p-Si:B-SiO_2 interface in MOS structures, carrier mobility and impurity distrib. 78−34902
Si:B^+, ion implanted, lateral spread of B^+ ions through SiO_2 mask 79−51130
Si:B^+, TEM of lateral implantation effects near mask edges in wafers 79−37724

silicon continued
Si:BF_2^+, anomalous migration of F and electrical activity of B 78−34654
Si:BF_2^+, ion implantation appl. in semicond. device production 80−103383
Si:BF_2^+, ion implanted, arc annealing by flash lamp 80−44223
Si:BF_2^+, recrystallisation of implanted amorphous layers, F migration 79−55763
Si:BF_2^+ implanted, low-temp. annealing characts. 79−55759
Si:BF_2^+(Si^+,B^+), recrystallisation of implanted amorphous layers, elec. props. 79−55762
Si:B(Al), (P)(As)(In), ion implanted film, elec. prop. impurity depend. 80−24467
p-Si:B(Al), radiation defect form. and annealing study using Hall effect, cond. and carrier diffusion length 80−84214
Si:B(Al)(Ga)(In)(Tl), high resolution recomb. radiation, investigation, electron excited 78−15233
Si:B(Al)(Ga)(In)(Tl), binding energy, excited state spectra, photolum., semi-empirical short range pot. 80−44534
Si:B(As), polycrystalline, ion implanted, AES analysis 77−31690
Si:B(As)(P), doping, new paint-on diffusion source 77−4118
Si:B(As)(Sb) devices, anal. using SEM-AES-IMA combination with SIM spectrometer *(Japanese)* 78−85249
Si:B(BF_2), p^+-n junction form., ion implantation damage, leakage current 77−24334
Si:B(Be)(Li) ion implanted, channelling and random equivalent depth distrib. 80−100293
Si:B(Ga), even-parity acceptor excited states, bound exciton two hole transitions 77−85793
Si:B(Ga), heavily doped, form of occurrence of acceptor impurities 77−11581
Si:B(Ga)(Sb), plastic deform. and formation of dislocation loops, effect of Au atoms 79−69184
Si:B(Li)(P), piezospectroscopic studies of bound multiexciton complexes 80−16006
Si:B(P), amorphous, photo- and dark conductivity 77−28216
Si:B(P), deformed, EPR fine struct. spectrum of dislocation 77−66422
Si:B(P), diffusion induced imperfections, laser annealing, rel. to junction characts. 78−75678
Si:B(P), dislocated crystals, DC conductivity, Hall effect, energy spectrum 78−10400
Si:B(P), dislocated crystals, microwave cond., localised electron energy spectrum 78−14694
Si:B(P), dislocations under high stress, stacking fault energies, TEM study 80−70202
a-Si:B(P), Hall effect and impurity cond. 77−72871
Si:B(P), heavily diffusion-doped layers, Co diffusion 78−59982
Si:B(P), impurity-peak form. during proton-enhanced diffusion 79−55772
Si:B(P), ion implanted, polycryst. annealing characts. 77−24324
Si:B(P), ion implanted crystalline and amorphous laser annealing 80−97509
Si:B(P), ion implanted layers, carrier distrib. meas. precision 77−43603
Si:B(P), minority carrier diffusion coeffs. 79−99559
Si:B(P), photocond. spectra of H^--H^+-type complexes 79−95451
Si:B(P), positron annihilation in 100 and 111 orientation 77−44083
Si:B(P), proton enhanced diffusion, vacancies diffusion length 80−29226
Si:B(P), proton-irrad., impurity uphill diffusion, vacancy mechanism 80−92719
Si:B(P), recombination spectra of bound multiexciton complexes, Zeeman splitting *(Russian)* 79−38526
Si:B(P), simultaneous diffusion, radiactivation techniques 77−76622
Si:B(P), single crysts., oxidation investigations, 780°-1150°C 79−5068
Si:B(P), uniaxially stressed, impurity-assisted intervalley scatt., photoluminesc. obs. 80−34979
Si:B(P) implanted layers as strain sensors 77−35098
Si:B(P) polycrystalline thin film, plasma annealing, effect on elec. props. 80−7005
Si:B(P)(As), impurity diffusion from implanted layer, influence of radiation damage 77−76621
Si:B(P)(As), ion implantation, 20-2800 keV, obs. of X-rays produced 78−14367
Si:B(P)(As)(Cu)(Fe), dopant profile changes induced by laser irrad. using SIM and backscatt. meas. 79−69148
Si:B(P)(As)(Sb), ion implanted, redistrib. of dopants by pulsed laser annealing 79−7620
Si:B(P)(As)(Sb)(Cu)(Fe), ion implanted, doping profile, pulsed laser annealing effects 80−88197
Si:B(P)(Sb), multiparticle impurity complexes *(Russian)* 78−72601
Si:B(P)(Sb), single cryst., transmission characts. for IR optical components 77−27325
Si:B(Sb), deform. coeff. due to impurity diffusion 78−18671
Si:B(Sb)(P), microdefect formation depend on doping, Cu decoration, X-ray transmission topography, preferential etching 79−69120
Si:Ba, Geiger counter determ. of Ba by neutron activation 79−52816
Si:Be, ion implanted, correl. of atomic distrib. and implantation induced damage profiler 80−88199
Si:Bf_2^+ layers, ion-implanted, anomalous carrier tail generation mechanism 80−19819
Si:Bi, ion implanted, channelling obs. of pulsed Q-switched ruby laser annealing 80−59542
Si:Bi, ion-implanted, solid phase epitaxial growth during annealing, supersaturated solid soln. form. 80−103384
Si:Bi(,As), optical polarisation of ^{29}Si nuclei, nucl. relax. due to optical pumping 80−2665
Si:C, disorder profiles by proton backscattering, proton bombardment annealing 78−47449
Si:C, electron irrad., C interstitial, photo EPR 77−16175
Si:C, H^+ and He^+ beam impact phemomena, damage annealing rates 78−47450
Si:C, impurity determ. by IR absorpt. spectroscopy, room temp. and low temp. meas. comparison 80−108237
Si:C(O), photoluminescence spectra, radiation damage investig. 77−28620
Si:C(O)(Sb), striated impurity distrib. calc. in melt-grown crystals 80−24488
Si:Cd n^+-n-n^+ structs., photoresist. props. under exclusion conditions 80−39666
Si:Cd(Zn), n^+-n-n^+ structure, photocond. lifetimes, deep level occupancy in exclusion region 78−72253
Si:Co, diffused distrib. and state of Co atoms 77−1146
silicon continued
Si:Co, diffusion coeff. of Co meas. 77−20126
Si:Co, diode minority carrier lifetime, Lax method meas., effect of Co diffusion 79−69525
Si:Co, high-temp. ion-implanted and diffused samples, Mossbauer spectra of ^{57}Co 79−51891
Si:Co, implanted or diffused, and annealed, localisation of Co atoms, Mossbauer obs. 80−39140
Si:Co, ion implanted, Co lattice location, channelling meas. 80−88201
Si:Co, minority carrier lifetime investigation 80−80292
Si:Co, study of impurity states 78−76020
Si:Co, substitutional Co and Co precipitates, identification by Mossbauer spectroscopy 79−11631
Si:Cr, ion implanted, Cr conc., depth distrib. and diffusion coeff. 80−49243
Si:Cr, photoconductivity exam. 77−20361
Si:Cr, specific resistance, activation energy of deep levels, and carrier mobility *(Russian)* 78−72146
Si:Cr, spin-lattice relax. of Jahn-Teller Cr^0 centre *(Russian)* 78−72402
Si:Cr^0(Mn^+, spin-lattice relax. of Jahn-Teller centres, coexistence of minima with different symmetries 80−80602
Si:Cr^+ EPR spectra and spin state population inversion with unpolarised optical lighting *(Russian)* 80−44909
Si:Cs, high dose implantation profiles, determ. using low angle Rutherford He ion backscatt. 79−4327
n-Si:Cs, ion implanted, minority carrier lifetime and defect struct., annealing effect 78−6395
Si:Cs-O photocathodes negative electron affinity electron emitting devices, reson. transmission 77−90240
p-Si:Cu, Cn precipitation effects, for solar cells appl. 79−69249
p-Si:Cu, influence of Cu on diffusion of Au 77−62679
Si:Cu, interaction between vacancy emitting absorbing precipitates and dislocations, TEM obs. 78−71755
Si:Cu, parameters of Cu levels determ. by photocapacitance meas. 77−62869
Si:Cu, photocond. spectra and IR quenching 77−55568
Si:Cu, precipitate morphology, IR microscopy study *(Chinese)* 80−103539
Si:Cu, segregation effects after laser pulse melting 79−1843
Si:Cu extinction of X-ray topographic images of Cu precipitates 80−45310
Si:Cu(Au), recoil implantation from thin surface films, backscatt. obs. 78−63783
Si:D, amorphous, thermal stability, comparison with Si:F 80−49542
Si:D, ion implanted, D depth distribs., SIMS meas. 80−54279
Si:D, ion implanted, struct. of impurity centre 79−7623
Si:F, amorphous, heat resistant, prep., elec. cond., IR absorpt., annealing 80−65719
Si:F, amorphous, pure and doped, vibr. excitations at defect sites, IR and Raman spectra calc. 80−49329
Si:F, amorphous, thermal stability, comparison with Si:D 80−49542
Si:F, amorphous alloys, RF sputtering prep. in SiF_4-Ar gas mixture, spectra 80−80772
Si:F, amorphous film, effect of F on elec. cond. 80−34444
Si:F, H amorphous films, optical props., photoconductivity, photostructural changes 80−11034
Si:F,H, amorphous, elec. and optical props. 80−60031
Si:F,H, amorphous, glow discharge deposited elec. props. and device aspects 80−44744
Si:F,H, amorphous efficient carrier generation for solar photovoltaic energy conversion 80−92906
Si:F(,H), amorphous, electronic struct., orthogonalised LCAO calc. 80−44486
Si:Fe, anisotropic broadening of linewidth in EPR spectra of Fe^0 77−66417
Si:Fe, B, Fe reaction with ion implanted B 79−77620
Si:Fe, B thermally activated Fe interstitial, elec. and kinetics props. *(German)* 80−34035
Si:Fe, EPR and neutron activation anal. of thermal defects 78−91355
Si:Fe, ESR, cryst. field under stress, C_{11} and C_{44} meas. 77−12194
-Si:Fe, effect of γ-irradiation, photocapacitance meas., impurity centre conc. 78−18993
Si:Fe, implanted, annealing and stripping, Mossbauer expts. 80−39141
Si:Fe, implanted, Mossbauer spectra, conversion electron, temp. dependence 80−40025
Si:Fe, interstitial form., Au dopant effect 80−29611
Si:Fe, ion implanted, laser annealing studies using Mossbauer spectroscopy 80−79827
Si:Fe, laser annealing of implanted ^{57}Co sources, Mossbauer obs. 80−39139
Si:Fe, laser implantation, Mossbauer obs. 80−39125
Si:Fe, photoconductivity and Hall effect 79−4579
Si:Fe, solubility study by EPR and neutron activation anal. 80−75361
n-Si:Fe 79−28312
Si:Fe group ion, energy spectrum of deep centres, ESR spectrum 77−90023
Si:Fe^0, solid soln. decomp., Fe deposition on dislocations 77−51943
Si:Fe^0, spin relax. rate ang. depend. for pulsed saturation of inhomogeneously broadened ESR line 79−65721
Si:Fe^0 interstitial localisation, EPR spectrum 79−1582
Si:Fe(Al), compensated substrates for solar cells, effects of Fe and Al 80−94009
Si:Fe(Au)(Pt)(Ag)(Ti), photoionisation cross-sections and energy levels 79−87060
Si:Fe(Cr), EPR line intensity and widths, temp. depend. 79−28604
Si:Fe(Cu), impurity segregation and microstructural changes by pulsed laser irrad. 79−82254
Si:Fe(Cu)(Pt), implant redistrib. and enhanced solubility following laser irrad. 79−69129
Si:Ga, As, sequential diffusion, radiotracer obs. 78−10073
Si:Ga, bound-exciton absorption 78−56507
Si:Ga, diffusion of impurity into cryst., doping profile 79−77621
Si:Ga, electron irrad.-induced defects, DLTS meas. 80−24499
Si:Ga, gettering of Au and Cu during Ga diffusion 78−91350
Si:Ga, heavily damaged, channelling investigation of diffusion behaviour 79−37877
Si:Ga, IR absorption of dopant centres, spectral depend. on doping, impurity conc. and temp. 80−76053
Si:Ga, IR spectra of acceptor levels 80−34953
Si:Ga, LPE growth on Si substrate, melt-back approach 78−80481
Si:Ga, LPE on Si, technique and characterisation 79−38751

silicon continued
Si:Ga, laser-doped, impurity distrib., Rutherford backscatt. and channelling anal. 80−59507
Si:Ga, luminescence fine struct. from bound exciton and multiexciton complexes 77−32430
Si:Ga, neutron irrad., Hall effect meas. of shallow donor levels 80−20124
p-Si:Ga, neutron transmutation counterdoped, shallow defect levels, Hall effect and photocond. obs. 79−87055
Si:Ga, possibility of use in fabrication of fast response photodetectors 79−15184
Si:Ga, sealed tube diffusion, Au and Cu gettering behaviour 77−76445
Si:Ga,P(As), sequential diffusions, comparison of interactions 77−80655
Si:Ga (Al)(In) extrinsic detector material props. 77−89797
n-Si:Ga laser doped, segregation, Rutherford backscattering 80−103483
Si:Ga^+, impurity distrib. profiles using SIMS and Hall effect method 79−69152
Si:Ga(Al), edge luminesc. spectra of acceptors, multiexciton complexes 78−56517
Si:Ga(Al), MBE, growth, struct. and elec. props. 77−89458
Si:Ga(As) 80−19824
Si:Ga(Sb), epitaxial film, doping efficiency *(Japanese)* 79−73201
Si:Ga(Zn), impurity ground states 79−28313
n-Si:Gd, depth of energy levels of As and P from impurity photocond. 79−90996
p-Si:Gd, irradiated, elec. props. 79−51613
Si:Gd, magnetic props. and interaction of impurities 79−11286
Si:Gd, radiation defect form., effect of Gd impurities, elec. and optical meas. 78−71764
Si:Gd, radiation defects effect on elec. props. 77−28184
Si:Gd(Pr), photoconductivity anomalies due to mag. impurities *(Russian)* 80−103722
n-Si:Ge, electron induced defects, room temp. instability 80−29052
Si:Ge, recryst. after implantation using different temp. and energy sequences 80−84196
Si:Ge, regrowth behaviour from backscatt. and channelling meas. 80−2300
Si:Ge,Sn, role of interelectronic correl. in paramag. props. of impurity-vacancy complex 77−62858
Si:Ge B, strain compensation, X-ray Bragg reflexion 80−39137
Si:H, 50-250 keV H^+ irrad. damage distrib., $^4He^+$ channelling obs. 78−26587
Si:H, amorphous, 2p level shift, XPS obs. 80−97401
Si:H, amorphous, Auger electron spectrosc. obs. 80−76112
Si:H, amorphous, band tail absorpt., photocurrent meas. for Schottky barrier solar cell 80−60032
Si:H, amorphous, Brillouin scattering from acoustic bulk and surface waves 80−11425
n-Si:H, amorphous, bulk density of deep states, DLTS meas. 80−88518
Si:H, amorphous, control and anal. of deposition, using plasma spectroscopy 80−45230
Si:H, amorphous, defect creation and H evolution 80−50392
Si:H, amorphous, defect photoluminesc. meas. 80−97334
Si:H, amorphous, defect states, luminesc. and ESR obs. 80−76075
Si:H, amorphous, density of states determ. using field effect 80−49937
Si:H, amorphous, depletion width determ. by analytical model 80−100445
Si:H, amorphous, discharge prod., optically induced cond. changes 80−96937
Si:H, amorphous, dopant conc., glow discharge optical spectroscopy 80−49546
Si:H, amorphous, doped, Fermi level position, photoelectron spectra 79−47592
Si:H, amorphous, effect of gap state density on photocond. and photolum. 79−91096
Si:H, amorphous, electronic states of hydrogenated Si, theory 79−42494
Si:H, amorphous, electronic struct. calc., rel. to UPS data 80−39527
Si:H, amorphous, excess carrier thermalisation and recomb., luminesc. decay and photocond. 80−50397
Si:H, amorphous, exodiffusion of H, EPR expts. 80−49102
Si:H, amorphous, geminate recombination model for photoluminescence decay 80−71481
Si:H, amorphous, glow discharge deposited, thermal dehydrogenation, IR spectra 80−44442
Si:H, amorphous, glow discharge deposited, laser annealing 80−49104
Si:H, amorphous, H content determ. by IR absorpt., gas evolution and nuclear reaction methods 80−44130
Si:H, amorphous, HV photovoltaic cells, design parameters 80−101105
Si:H, amorphous, horizontal cascade type integrated photovoltaic cell module 80−94091
Si:H, amorphous, image pickup devices 80−100481
Si:H, amorphous, in p^+-i-n^+ struct., hole diffusion length meas. 80−44712
Si:H, amorphous, light-induced ESR and photoluminesc., dangling bonds with positive correl. energy 80−50161
Si:H, amorphous, luminesc., band tail states and thermalization 80−25455
Si:H, amorphous, mobility edge position using continuous random network model for struct. 80−44544
Si:H, amorphous, model for variable gap intrinsic semiconductor 80−10988
Si:H, amorphous, optical studies of excess carrier recomb., evidence for dispersive diffusion 80−76059
Si:H, amorphous, p^+-i-n^+ struct. solar cells, material parameters and deposition condition optimisation study for higher efficiencies 80−45676
Si:H, amorphous, photoelectrochem. behaviour 80−81480
n-Si:H, amorphous, photoelectromagnetic effect 80−107845
Si:H, amorphous, plasma deposited, cond. adsorbate and insulating layer effects 80−49749
Si:H, amorphous, plasma-deposited, effect of DC elec. field superimposed during deposition 80−44643
Si:H, amorphous, prod. by high temp. thermal decomp. of SiH_4, and photocond. 79−87585
Si:H, amorphous, ps. relax., optically induced absorpt. 80−48325
Si:H, amorphous, Pt film growth, AES and LEED study 80−88447
Si:H, amorphous, RF sputtered, suitability as solar cell material 80−40864
Si:H, amorphous, RF sputtered, Schottky barrier solar cells, photovoltaic props. and capacitance-voltage charact. 80−45678
Si:H, amorphous, radiative recomb. by diffusion and tunnelling, photocond. quantum efficiency 80−50394
silicon continued
Si:H, amorphous, radiative recomb. and luminescent processes 80−55152
Si:H, amorphous, refr. index, temp. depend., implications for thermoreflectance and electroreflectance 80−50290
Si:H, amorphous, Schottky diode, spectral response and hole drift mobility 80−39673
Si:H, amorphous, Schottky barrier solar cell, degradation mechanisms affecting stability and operation 80−45680
Si:H, amorphous, Schottky barrier solar cell, deposition parameter effects on elec. props. 80−45681
Si:H, amorphous, Schottky diodes, elec. props., light-induced effects 80−103741
Si:H, amorphous, solar cell struct., photocurrent meas., absorpt. coeff. 80−50960
Si:H, amorphous, solar cells, carrier generation, recombination, and transport 80−55844
Si:H, amorphous, solar cells, trap spectroscopy using transient current techniques 80−104508
Si:H, amorphous, solar-cells, charge collection and spectral response 80−85275
Si:H, amorphous, sputter deposited, O_2 incorporation during and after fabrication 80−49541
Si:H, amorphous, sputtered, Auger surface spectroscopy 80−50472
Si:H, amorphous, sputtered on $Gd_2(MoO_4)_3$, ferroelec. domain wall motion, image scanning 80−83663
Si:H, amorphous, sputtered Schottky barrier solar cells, conduction mechanism 80−104506
Si:H, amorphous, stacked solar cells, development 80−94050
Si:H, amorphous, structural model 80−49105
Si:H, amorphous, surface activated, photoemission spectra, minority carrier diffusion length 80−40235
Si:H, amorphous, surface states distribution using MOS tunnel junctions 80−103735
Si:H, amorphous, temp. depend. of photolum. 80−89063
n-Si:H, amorphous, thickness depend. cond. 80−49724
Si:H, amorphous and crystalline, hydrogenation and dehydrogenation, luminesc. spectra 80−11477
Si:H, amorphous defect model 80−24363
Si:H, amorphous field induced and quenched-in excess cond. 80−24968
Si:H, amorphous film, anal. of intrinsic photocond. spectrum 79−73541
Si:H, amorphous film, prep. by plasma decomp. of SiH_4 under mag. field, and characterisation 80−45239
Si:H, amorphous films, plasma-deposited, defect states, IR, ESR, and refractive index meas. 79−65944
Si:H, amorphous Schottky barrier solar cells, depletion region, capacitance study 80−50963
Si:H, amorphous Schottky solar cells, prep. and charact. of diode RF reactive cathodic sputtered films *(French)* 80−61347
Si:H, amorphous sputtered, excitation spectra and photoluminesc. 80−50396
Si:H, amorphous thin film, ion plating, IR absorpt. meas. 80−84857
Si:H, amorphous thin film solar cells 80−81478
Si:H, amorphouse film, optical and elec. props. 79−82694
Si:H, Cl(F), amorphous, photocond., dark cond. and photoluminesc. 80−49802
Si:H, correlations between elastic energy transferred by implanted H ions and H trapping 78−14370
Si:H, defects in monovacancy Si cluster, semi-empirical calc. 78−43329
α-Si:H, discharge produced, electronic props. rel. to solar cell charact. 79−15241
Si:H, electron states 80−29355
a-Si:H, electronic states and bonding config. 80−64900
Si:H, evaporated amorphous film, prep. elec. cond. and photocond. 79−38201
Si:H, H^+ sputtered as result of ion bombardment, ionis. mechanism 79−100009
Si:H, implanted, annihilation of free excitons, inelastic scatt. by SiH_4 mols., photolum. obs. 78−19561
a-Si:H, influence of H on optical props., H conc. and H bonds 80−76098
Si:H, interstitial electronic struct., self-consistent pseudopotential calcs. 79−73469
Si:H, ion implanted, anal. of methods used for H profiling in materials using ion beams 79−5197
Si:H, ion implanted Monte Carlo calcs. of profiles of H ions 78−55889
Si:H, ion-implanted, photoluminesc. spectrum 80−45129
Si:H, new IR absorpt. bands 79−87472
Si:H, plasma-deposited amorphous film, proton mag. reson. 80−44931
a-Si:H, spin defect and recombination influence on electronic transport 80−50409
a-Si:H, structural interpretation of vibr. spectra 79−69864
Si:H,B, amorphous, field effect and thermoelec. power 80−96924
Si:H,F,O amorphous, plasma deposited, comp. and optical props. 80−50441
Si:H,Li, amorphous, DC electrical conductivity, absorption edge and IR meas., role of H 80−54694
Si:H,Li, amorphous, photoluminescence obs. 80−66280
Si:H,P, amorphous, heavily hydrogenated, high gap state densities 80−49803
Si:H,P, amorphous, in MOS tunnel junction, electron tunnelling charact. 79−73592
Si:H,P amorphous film, elec. cond., thickness and temp. depend. 80−65559
Si:H alloy, amorphous, dihydride model of vibrational spectra 80−80827
Si:H amorphous, cooperative charge disproportionation of defects, rel. to photolum. 80−54649
Si:H amorphous, plasma-deposited, luminesc. decay 79−73989
Si:H amorphous, solar cell structure, optical absorption by gap states 80−94052
Si:H amorphous film, H quantitative depth profiling by nuclear reactions and SIMS 78−14373
Si:H amorphous film, plasma-deposited, growth morphology and defects 80−44128
Si:H amorphous film, plasma-deposited, elec. and comp. heterogeneity 80−44745
Si:H amorphous film, prep. by RF glow discharge decomp. of SiH_4, optical props. and H conc. 80−15416
Si:H amorphous film, prop. by glow discharge deposition, and plasma parameter effects on props. 80−45240
Si:H amorphous film, sputtered in Ar-SiH_4 mixtures, props. 79−87023

silicon continued
Si:H amorphous film, sputtered IR vibr. spectra and photolum., effects of partial evolution of H 80−44413
Si:H amorphous films, conductivity and temp. dependence of optical gap 80−100462
Si:H amorphous films, ESR, optical gap and elec. cond. meas. 80−75842
Si:H amorphous films, effects of glow-discharge prep. conditions on H content 79−46969
Si:H amorphous films, IR spectrum and struct. 80−97277
Si:H amorphous films, interference enhanced Raman scatt. 80−50326
Si:H amorphous films, optoelectronic behaviour depend. on impurity incorporation during plasma deposition 80−49804
Si:H amorphous films, photoinduced optical absorpt. and photocond. 80−50361
Si:H amorphous films, reactively sputtered, prep. and characterisation 80−100785
Si:H amorphous films, role of Ar in deposition process, IR absorpt. and photocond. meas. 80−50321
Si:H amorphous films for solar cells, optical and elec. props. of RF glow discharge deposited films 80−54576
Si:H amorphous glow discharge film, optical absorpt., near IR region 79−87518
Si:H amorphous layer as passivant for p-n junction in crystalline Si 79−47155
Si:H amorphous layers, ion bombard., AES study, $L_1L_{23}V$ Coster-Kronig transition 79−99992
Si:H amorphous MIS solar cell, loss mechanisms and photovoltaic parameters, overview 80−93923
Si:H amorphous semiconductors, prep. from SiH_4 and characts. 78−48326
Si:H amorphous sputtered film, photoluminesc., photocond. 80−20729
Si:H amorphous sputtered films, optical gap, IR absorpt. meas. 80−50320
Si:H film, amorphous, bombarded, defects, luminesc. and ESR meas. 80−34977
Si:H film, amorphous, elec. cond., effect of adsorbed gases and illumination 78−88048
Si:H film, amorphous, H-associated disorder modes, PMR spin-lattice relax. time meas. 80−93202
Si:H film, amorphous, photocond. imaging 80−1300
Si:H film, amorphous, plasma-deposited, small angle X-ray and neutron scatt. studies 80−59826
Si:H film, amorphous, reactively sputtered, H content effect on props. 80−49714
a-Si:H film, glow discharge deposited, H profiles, doping level 80−84202
a-Si:H highly homogeneous, for low-cost solar cell fabrication 80−72053
a-Si:H MIS junction, electronic struct. study by tunnelling 80−44729
Si:H plasma deposited film, amorphous, microstruct., TEM and SEM obs. 80−10801
a-Si:H Schottky barrier diodes, capacitance studies 80−49908
a-Si:H solar cells, photoexcited carrier collection efficiency 79−100526
Si:H solar cells, photovoltage source in photocond. materials due to comp. and doping var. 80−7938
Si:H sputtered amorphous film, luminesc. and non-radiative decay 80−50395
a-Si:H sputtered films, ohmic contacts by H depletion, H diffusion 80−34511
Si:H:F, amorphous, depletion width determ. by analytical model 80−100445
a-Si:H/Pt, Schottky diode, influence of prep. conditions on forward bias currents 79−78171
Si:H(B)(P), amorphous, UV absorpt. spectra 80−25420
Si:H(D), amorphous films, CVD, post-hydrogenation 80−54552
Si:H(D), H-related defects, channelling and IR meas. 80−25422
Si:H(F), amorphous, Schottky barrier profiles, depletion region width 80−49871
Si:H(Li)(Ni), amorphous, vac. evaporated, doping, transport and optical props. 80−49715
Si:He, B ion implantation 80−96559
Si:He, He impurity props. investigation by EHT calcs. 79−99183
Si:Ho(Gd)(Yb), impurities behaviour dynamic nucl. polarisation 79−78568
Si:In, absorpt. spectra, impurity excited state lines 80−108243
Si:In, backward wave phonon spectroscopy 80−2357
Si:In, bound exciton photolum. obs. 78−95607
Si:In, bound-exciton absorption 78−56507
Si:In, C, 0.111-eV acceptor level, X-level defect conc. from IR absorpt. and Hall meas. 79−51512
Si:In, capture cross section of excitons on neutral In impurities, photoluminesc. decay 78−6760
Si:In, clustering and precipitation, time-dependent perturbed ang. correlation meas. 80−65234
Si:In, dopant energy levels, Hall meas. interpretation 80−107736
Si:In, doping conc., meas. by Hall, C-V and junction breakdown methods 79−14824
Si:In, electron irrad., Hall effect meas. 80−2401
Si:In, gradient transport soln. growth, IR monitoring, 950-1300°C 79−100040
Si:In, implanted, laser annealing 79−52050
Si:In, ion implanted, annealing behaviour, time differential PAC obs. 77−89455
p-Si:In, ion implanted, doping profiles from capacitance-voltage characts. 80−88203
Si:In, MIS structure, determ. of deep level parameters in surface layer of semiconductor 80−15612
Si:In, MOSFET device structure for characterising imperfection centres 79−73595
Si:In, neutron irrad. to compensate for residual B, photocond., IR focal plane array 78−67727
Si:In, new acceptor level determ. from Hall effect and photocond. meas. 77−66136
Si:In, obs. of long lifetime lines in photolum. 79−47512
Si:In, photoelec. props. meas 77−89804
Si:In, photoluminesc., In acceptor excited level 79−47506
Si:In,P, photoinduced IR absorpt. and luminesc. 79−33828
Si:In amorphous films, EPR, elec. cond., and magnetoresist. 80−50160
Si:In extrinsic detectors, compensation of residual B by neutron transmutation 78−281
Si:In extrinsic detectors in IR imaging systems, focal plane temp. stability requirements 79−94324

silicon continued
Si:In extrinsic IR detectors with closely compensated residual impurities, model of responsivity temp. depend. 80−73453
Si:In extrinsic IR detector material with high responsivity compensated by neutron transmutation, float-zone growth 80−75597
Si:In(Sb), incorporation of implanted impurities during amorphous layer regrowth 79−55761
Si:Ir, Ir diffusion and solubility 77−15448
Si:Ir, magnetosensitive diodes, characts. 79−24069
Si:Ir, precipitation of solid soln., photocapacitance, electrical resistivity meas. 78−47833
Si:Ir S-type diodes, characts. 78−56224
Si:K, bound exciton luminescence in mag. field *(Russian)* 80−108278
Si:K, ion implanted, influence of doping and annealing on carriers 78−38742
Si:l, obs. of donor exciton in far IR transmission meas. 79−91477
Si:Li, amorphous, elec. cond. and thermopower 79−73537
Si:Li, amorphous, interstitial doping by in-diffusion and implantation and elec. characterisation 78−26585
Si:Li, bound exciton complexes associated with Li, photolum. meas. 79−28823
Si:Li, bound-exciton excited states, uniaxial anal. 80−71475
Si:Li, defect electronic struct. and config., semi-empirical calc. 80−107739
p-Si:Li, dislocation free, minority carrier lifetime, effects of heat treatment *(Japanese)* 79−65492
Si:Li, EPR in mechanically affected sampler 78−39385
p-Si:Li, electrolytical doping, depth-profile anal. 79−77623
Si:Li, electron-phonon scatt., in intermediate conc. region 80−65180
Si:Li, ion implantation, effect of heat treatment on distrib. profile 79−86814
Si:Li, luminesc. of bound exciton and bound multiexciton complexes 79−28821
Si:Li, nonrandom strain, EPR of thermally excited donors 78−43629
Si:Li, photolum. of bound exciton and bound multiexciton complex, Zeeman effect 80−108265
Si:Li, precipitation centres, elec. cond., Hall effect meas. 78−48417
Si:Li, strongly doped, piezoresist., gas-liq. type transition 77−43600
Si:Li, thermal cond., low temp. phonon scatt., internal strain effects 80−96706
Si:Li amorphous, thermopower and cond. meas. 79−69142
Si:Li n^+-p solar cells, electron beam irrad. damage 80−94000
Si:Li P/N type solar cells, irradiation obs. 79−66406
Si:Li radiation detector, influence of distrib. of drift temp. on props. 77−3234
Si:Li X-ray detector, escape peaks and internal fluoresc., general geometry case 77−18150
Si:Li(Na)(K)(F)(Cl), amorphous, implantation effects on elec. props. 80−49716
n-Si:Mg, energy levels and degeneracy ratios determ. by Hall effect meas. 79−90993
Si:Mg, Zeeman effect of excitation spectrum of neutral donors 77−63439
Si:Mn, amorphous, cond. increase by Mn doping 78−72155
Si:Mn, amorphous, EPR meas. 77−85559
Si:Mn, characts. of residual cond. 79−15188
p-Si:Mn, defect levels, transient capacitance spectroscopy 78−6322
p-Si:Mn, giant residual cond. 80−20250
Si:Mn, negative photoconductivity 79−38132
Si:Mn, photosensitivity, residual cond. effects 78−19099
p-Si:Mn, temp.-elec. instability, photocond. meas. 77−1448
Si:Mn,Bi, standard, doubly implanted, Rutherford backscattering meas. at MeV energies, screening corrections 80−88204
Si:Mn(Fe)(Ni) amorphous films, ESR and elec. cond. 80−50171
Si:N, amorphous, DC sputtered, enhanced, photocond. 78−56183
Si:N, amorphous, prep. by RF sputtering and props. 80−44229
Si:N, high energy ion implantation of buried insulating layers 80−88188
Si:N, implantation at high doses, annealing conditions for homogeneous buried insulating layer *(French)* 80−59498
Si:N, interstitial Si atom formation by light ion bombardment 78−47406
Si:N, ion implantation, photon emission studies of mol. synthesis, interstellar process simulation 77−70297
Si:N, ion implantation, refractive index, IR spectra, ion range and straggling meas. 80−34020
Si:N, ion implanted, oxidation characts. 80−89385
Si:N, laser-annealed, Jahn-Teller distorted donor, EPR meas. 80−84642
Si:N, struct. defects formed by 50 keV N^+ irrad., depth distrib. 78−18688
Si:N wafers, Si_3N_4 layer growth by high dose implantation and annealing, elec. props. 80−70227
p-Si:N_2^+ implanted, anneal behaviours of lateral photovoltaic method 79−14825
Si:N^+ ion, implantation, disorder profiles meas. by Rutherford backscatt. and channelling 80−54270
Si:N(P), ion implanted, IR transmission and rel. spectra study 80−108244
Si:Na, quantitative analysis of residual impurities with SIMS 78−87688
Si:Na ion implanted, Hall effect temp. depend., electron surface density and mobility 80−11018
Si:Na^+, inversion layer, far IR optical spectroscopy 80−20680
Si:Na^+, variation of cond. in two-dimensional impurity band with Fermi level position 79−95510
Si:Na(K)(Cs), amorphous, ion implanted, control of cond. 79−60835
Si:Ne, amorphous, implanted, cond. change 78−23097
Si:Ne ion implanted, channelling anal. of disorder struct., ^4He ions, 0.7 to 2.2 MeV 79−4321
Si:Ne(Ar)(Kr), amorphous, implanted and sputtered, epitaxial regrowth, influence of noble gas atoms 80−2289
Si:Ne(Ar)(Kr), ion implantation damage, annealing, comparative study 79−10867
Si:Ne(Kr), ion implanted, amorphous, epitaxial regrowth 79−10869
Si:Ni, capture probabilities of two deep impurity levels by photocond. decay 80−49799
Si:Ni, low temp. annealing effect on behaviour of Ni 79−10862
Si:Ni,Co,Mn, γ-irrad., interaction of deep-level impurity atoms with radiation defects 77−76457
Si:Ni,O, interaction of Ni with O, influence of heat treatment, IR absorption meas. 77−4667
Si:Ni deep impurity levels, electron capture probabilities rel. to temp. 78−2523

silicon continued
Si:Ni p^+n and n^+p diodes, thermally stimulated capacitance obs. of Ni acceptor levels 78−19137
Si:Ni(Co)(Mn), influence of neutron irradiation as elec. props. 78−55895
Si:O, 9 μm absorpt. band attributed to dissolved O, from expts. on quartz particles 79−19914
Si:O, amorphous, sputtered, influence of O and deposition conditions 80−54693
Si:O, annealed, minority carrier lifetime 79−23985
Si:O, annealed, precipitates, dislocation and stacking fault loops, TEM characterisation 77−4111
Si:O, annealing behaviour of O donor, conc. reductions via resistivity meas. 79−51129
Si:O, C, impurity conc. profiles and process-induced defects 78−6094
Si:O, CVD layer, RHEED study of surface crystallinity, annealing effect on structure 79−69371
Si:O, carrier recomb. processes, role of vacancy-O complexes 80−65592
n- Si:O, charge carrier scattering on neutral centres 80−49762
Si:O, crit. stress of dislocation movement, determ. new method 77−80503
Si:O, cryst., annealed, struct. defects 78−75673
Si:O, cryst., donor form. during annealing, elec. resist. study 80−49653
Si:O, Czochralski crystal, oxygen striation and thermally induced microdefects 80−100275
Si:O, dislocation-free, Si-O complexes, heat treatment effects 77−62557
Si:O, EPR spectra of heat treatment centres 78−48039
Si:O, effect of interstitial O on elec. props. 77−76846
Si:O, electrial and infrared spectroscopic investigations 80−34389
Si:O, evaporated amorphous film, effect of O_2 on props., ESR spectra 80−11265
Si:O, heat treated, excess carrier recomb. rate, defect levels 80−75579
Si:O, high temp. annealing effect on impurities 78−38745
Si:O, IR absorpt. at low temp. *(Chinese)* 80−108228
Si:O, IR absorpt. spectra of Si:O complexes 78−19520
Si:O, implanted O location, channelling effect meas. 78−26593
Si:O, impurity conc. profiles, scanning IR absorpt. using semicond. laser 80−50376
Si:O, impurity solubility and diffusion props. 78−6093
Si:O, incorporation of O during pulsed-laser irrad. 80−96557
Si:O, interstitial Si atom formation by light ion bombardment 78−47406
Si:O, ion-implanted between 2 and 20 MeV, range and range straggling 80−44241
Si:O, kinetics of donor formation, under heat treatment in 450-900°C range 80−75523
Si:O, O content and depth profiling, $^{16}O(\alpha, \alpha)^{16}O$ reaction method obs. 79−34408
Si:O, O rich polycryst. film, carrier transport 78−80076
Si:O, semi-insulating polycryst. film, cond. through localised and extended states 77−28268
Si:O, specific resist. rel. to annealing, Si-O complex form., O_2 distrib. *(German)* 77−72863
Si:O, Xe, ion implanted, Xe retention, Rutherford backscatt., comparison with SiO_2+Xe 79−4320
Si:O,C, electron irradiated, indirect vacancy-interstitial recomb., IR absorpt. meas. 77−43209
Si:O,H, amorphous plasma-deposited, electronic and struct. props. 80−50391
Si:O,H amorphous, time resolved luminesc. 80−66288
Si:O film, near IR absorption, O impurity states 78−88333
Si:O film, near IR reflectivity at high temps. 78−56532
Si:O film, thermally deposited, semi-insulating, crystallographic study 78−75954
Si:O wafer, annealed, surface- and inner-microdefects, TEM obs. 80−54236
Si:O wafer, dislocation pinning effect of O atoms 77−89437
$Si:O_2^+$, in-depth distrib., Cs^+ SIMS anal. appl. 79−39265
Si:O(C), implant redistribution, annealing effects, SIMS meas. 80−96561
Si:O(C) wafers, impurity meas. by Fourier transform IR spectra 80−89030
Si:O(C) wafers, impurity meas. by Fourier transform IR spectra at low temp. 80−89031
Si:O(Gd), radiation-produced vacancies and interstitials, annihilation processes 77−89432
Si:Os, P, photoelec. props., depend. on P conc. 79−91099
Si:Os, photocapacitance meas. of impurity levels 77−55579
Si:P, absorpt. due to creation of bound excitons 78−23025
Si:P, acceptor bound multiexciton complex recomb., shell model, luminesc. line splitting 78−6275
Si:P, amorphised by Ne^+ implantation, high fluence P implants, plasma region obs. 79−86807
Si:P, amorphous, CVD, defect compensation 80−54644
Si:P, amorphous, elec. cond. and thermoelectric power 77−89783
Si:P, amorphous, substitutionally doped CVD, electrical props. 79−99566
Si:P, amorphous, thermoelectric power and conductivity 77−89782
Si:P, and of P diffused layers 78−38736
Si:P, annealing after ion implantation, ellipsometric study 80−65018
p-Si:P, annealing behaviour, recovery, surface carrier density and Hall mobility meas. 77−32012
Si:P, annealing characteristics at low temp., elec. props. 78−63781
Si:P, anomalous doping profiles, numerical anal. 79−73206
Si:P, As, chem. etching, thick epitaxial layers prod. for dopant conc. investigations by neutron activation anal. 79−37728
Si:P, Au, neutron irradiated, distrib. of P and Au determ. 78−79627
Si:P, B, α-particle spectrum fabrication by ion implantation 78−33373
Si:P, BF_2^+ ion implantation, anomalous carrier profiles 80−2048
Si:P, bound exciton and multiexciton complex struct., luminesc. obs. 77−81138
Si:P, bound multiexciton complexes, shell model 77−31953
Si:P, CVD amorphous film, electronic density of states 79−46993
Si:P, carrier mobility and distrib. rel. to annealing, 400-910°C 78−79995
Si:P, characterisation by IR reflectivity 78−56501
Si:P, conc. profiles of P and recoiled O atoms after ion implantation into SiO_2-Si, SIMS obs. 79−51138
p-Si:P, Cu, influence of Cu on diffusion of P meas. 77−1267
Si:P, Cu(Au) radiation-doped, influence of growth defects on elec. props. 79−69144
Si:P, Czochralski growth, dopant evaporation coeffs., resistivity distrib. 77−16487
silicon continued
Si:P, defect annealing, ionisation effects, DLTS meas. 80−24483
p-Si:P, defect energy levels, ion implantation effects, Hall coeff., sheet resist. meas. 77−85173
Si:P, defects, SEM in EBIC mode vs. HVEM images 78−9923
Si:P, depth of melting produced by pulsed-laser irrad. 79−55756
Si:P, determ. of P content in high-purity Si using meas. of Mo in 12-molybdophosphoric acid by NAA and AAS 80−15148
Si:P, dielec. susceptibility meas., polarisation catastrophe at metal-insulator transition 80−59873
Si:P, diffusion eqn. numerical soln. 79−51311
Si:P, diffusion from ethylene glycol grown anodic oxide 77−76440
Si:P, diffusion of P, 900-1100°C, distrib. of excess vacancies 77−72631
Si:P, diffusion of P impurities stimulated by gas discharge Ar plasma, low temp. 80−6560
Si:P, diffusion-doped laser irradiation effects, electrical reactivation of P 80−39124
Si:P, diffusional doping, diffusion-induced strain and dislocation effects 79−42084
Si:P, diffusivity, strain-induced band gap narrowing, E-centres 80−29228
Si:P, diffusivity, versus Si oxidation rate 77−15436
Si:P, dislocation dissoc. mode obs. by weak-beam TEM 80−107259
Si:P, disorders produced during high-current and high-dose P ion implantation 80−6422
Si:P, distrib. of implanted impurity after laser annealing, e.s.r. and neutron activation analysis 77−4122
Si:P, donor excited state lifetime, delayed avalanche breakdown 77−85231
Si:P, doped by neutron transmutation, electron traps 78−84164
Si:P, doped by neutron transmutation, lattice defects 80−34018
n-Si:P, doping, by zone melting using solid dopant source 78−43035
Si:P, doping by diffusion from phosphosilicate glass sheets *(German)* 77−39604
Si:P, doping by neutron transmutation, residual radioactivity 79−33009
Si:P, doping during growth from gas phase, thermodynamic analysis 80−59489
Si:P, E-centre formation mechanism 77−72614
Si:P, EPR line shift, 0.56 to 4.2K, investig. of interacting donor clusters 77−77084
Si:P, EPR of interacting donor centres, Overhauser effect and ENDOR 77−77085
Si:P, ESR-induced changes in DC resistance 78−35037
n-Si:P, edge dislocation energy level, differential capacitance meas. 79−23927
Si:P, effect of annealing on charge carrier conc. on floating zoned crystals 78−47805
Si:P, electrical conductivity oscillation, effect of dislocations 78−6388
n-Si:P, electron mobility and resist., dopant density and temp. depend. 77−76816
Si:P, electronic states, NMR of metallic and intermediate samples 79−4511
Si:P, electrostatic field on impurity atoms, heavy doping effects 78−51570
Si:P, emitter-misfit dislocation formation during P diffusion 78−91338
Si:P, epitaxial layer, vapour phase grown, temp. dependence of dopant inclusion, differential molar solution enthalpy *(German)* 79−52128
n-Si:P, etched, high sensitivity temperature sensor, 1-10K 77−13757
Si:P, excess vacancy generation by P diffusion *(Japanese)* 77−89460
Si:P, excitation density depend. of cathodoluminesc. from bound multiexciton complexes 78−72609
Si:P, excitation spectrum of P donors introduced by neutron transmutation, high resolution study 79−47460
Si:P, exciton complexes bound to impurities, resolved fine structure 77−62843
Si:P, exciton two-electron luminesc., temp. and impurity-conc. depend. 78−39585
Si:P, expt. evidence against shell model of bound multiexciton complexes 78−10368
n-Si:P, fast neutron irrad., defect clusters and defect build-up kinetics 79−33019
Si:P, Gd, optical orientation of ^{29}Si nucleus, effect of donor level implantation depth *(Russian)* 77−8452
Si:P, Ge, simultaneous diffusion processes, elastic stress influence 77−89591
Si:P, Hall effect 78−72176
n-Si:P, heavily depend., spin-lattice relax. at high temp. 78−39403
Si:P, heavily doped, 100 GHz ESR of impurity band 79−95631
n-Si:P, heavily doped, carrier conc., Hall coeff. and elec. cond. meas. 77−8094
Si:P, heavily doped, degenerate electron gas, Friedman effect, review 77−20242
Si:P, heavily doped, diffusion of Au 77−51550
Si:P, heavily doped, EPR spectra of electron irradiation induced defects 77−81008
n-Si:P, heavily doped, elec. cond. and Hall effect meas., impurity effects 78−19032
Si:P, heavily doped, electron-hole droplets, photolum. obs. 1.5 to 80K 77−36289
Si:P, heavily doped, electronic sp. ht. meas., rel. to metal-nonmetal transition 78−6162
Si:P, heavily doped, electron mobility carrier conc. relationship 79−65470
Si:P, heavily doped, glow-discharge-produced, elec. and optical props 80−2497
Si:P, heavily doped, IR bound-exciton luminesc. spectra 78−15211
Si:P, heavily doped, influence of impurities and crystalline defects on electron mobility 79−78095
Si:P, heavily doped, mag.-field depend. of sp. ht. 80−29183
Si:P, heavily doped, metallic region, resist. decrease due to ESR 77−16178
Si:P, heavily doped, origin of photoluminesc. 79−56856
Si:P, heavily doped, paramagnetic spin susceptibility 79−78306
Si:P, heavily doped, sp. ht. near metal-nonmetal transition, generalized Matsubara-Toyozawa theory 79−73321
Si:P, heavily doped, sp. ht., calc. using AMO-MT scheme for impurity bands 79−95182
Si:P, heavily doped, thermal oxidation 78−56793
Si:P, heavily doped semicond., scatt. mechanism, resist, and Hall coeff. maxima 80−75586
Si:P, heavily doped wafer, anomalous bending obs. 78−10074
Si:P, heavily ion implanted, polycrystalline, grain growth 79−19477

silicon continued
Si:P, high dose implantation, outside dislocation generation 78−87672
Si:P, high fluence ion implantation, layer thickness and refr. indices, IR refl. meas. 79−82248
Si:P, homogeneous nuclear transmutation technique, thyristors appl. 80−70236
Si:P, IR absorpt. and D^--band 78−52533
Si:P, impact excitation of P at low temps. 78−23098
Si:P, implantation damage of channelled P ions, elec. activity recovery stages 77−59034
Si:P, implantation depth distrib. meas. by neutron activation anal., SIMS, junction depth method 77−31693
Si:P, implanted, pulsed electron beam annealing, Hall effect and sheet resist. meas. 80−34467
Si:P, implanted, SiO_2-film-covered, laser annealing behaviour 79−86808
Si:P, implanted, two-stage laser annealing of lattice disorder 79−1452
Si:P, implanted layers, ionisation-enhanced crystallisation 79−51151
Si:P, implanted low temp. annealed, elec. activation, damage depend. 80−88182
Si:P, impurity band states calc. and photoluminesc. meas. 77−8046
Si:P, impurity conc. from photoluminesc. anal. 78−63785
Si:P, impurity conductivities 78−91691
Si:P, impurity doped, electron lifetime and transport in upper Hubbard band 79−95452
Si:P, impurity redistrib. by Ar ion hot implantation 77−72633
Si:P, incoherent light flash annealing, elec. props., backscattering spectra 80−97504
Si:P, interstitial supersaturation near P-diffused emitter zones 79−65541
Si:P, ion implantation, effects of high dose rate 78−83835
Si:P, ion implantation defect annealing investig. by CESR 77−8404
Si:P, ion implantation doped, positron annihilation meas. 78−14380
Si:P, ion implanted, damage layer props. obs. using ellipsometric parameters *(Russian)* 77−43234
Si:P, ion implanted, ionisation enhanced annealing, resist. changes meas. 78−30667
Si:P, ion implanted, irrad. by laser of different wavelengths, annealing behaviour 79−69132
Si:P, ion implanted, lattice damage and electrical activation correlation 78−67726
Si:P, ion implanted, regrowth of damage structs. by laser annealing 80−107289
Si:P, ion implanted, resist. changes induced by ESR 78−68377
Si:P, ion implanted, selective annealing of amorphous layers by Nd^{3+}:YAG laser irrad. 79−14823
Si:P, ion implanted, sheet resistance variations at elevated temps. 78−43041
Si:P, ion implanted, subsurface damage, TEM and channelled Rutherford backscatt. study 80−107337
Si:P, ion implanted and unimplanted, laser annealing, photoluminesc. study 80−2049
Si:P, ion implanted low temp. elec. cond. 79−56225
Si:P, ion implanted with small doses, defect annealing by nanosecond laser pulses 80−107297
Si:P, ion-implanted, carrier conc. reduction caused by wet O_2 oxidation 80−10565
Si:P, ion-implanted, damage-dependent elec. activation 79−55793
Si:P, ion-implanted, laser annealing 80−10564
Si:P, ion-implanted, optical refl. obs. of damage 78−55883
Si:P, ion-implanted layers, CESR meas., impurity distrib. inhomogeneity 78−2738
Si:P, low energy and high dose ion implantation, through SiO_2 film 77−15435
n-Si:P, low-compensated, Hall factor, electron-phonon interactions 79−4570
Si:P, luminesc. lines, multiexciton complexes and unaixial stress 78−92114
Si:P, luminescence circular polarisation, emission by many exciton complexes 80−93398
Si:P, many-valley semicond., donor binding energies, variational calc. 78−23041
Si:P, measurement techniques for determining P densities 80−75262
Si:P, mechanism of diffusion of P 77−7906
Si:P, metal-nonmetal transition, Anderson localisation 79−95335
Si:P, metallic, heat treatment effects, EPR and photoluminesc. 77−77262
Si:P, model for exciton bound to donor pair, photolum. data anal. 79−51498
Si:P, N implantation through Si_3N_4 film, depth distrib. of knock-on N, SIMS meas. 78−10066
Si:P, neutron irrad. crysts., qualitative distrib. of P using autoradiography 80−24486
Si:P, neutron irradiated, influence of growth defects on change in cond. 78−39117
Si:P, neutron transmutation doping distrib. by emitted β-radiation meas. 77−19977
Si:P, neutron transmutation doped, electron trap annealing, deep level transient spectra 78−14368
Si:P, neutron transmutation doped, radiation damage exam., elec. props. 78−95080
Si:P, neutron transmutation doped, EPR obs. of annealing behaviour 79−1453
Si:P, neutron transmutation doped, EPR, electron trapping 79−73179
Si:P, neutron transmutation doping, elec. props. rel. to neutron fluence 80−96555
Si:P, neutron transmutation doping, resist. homogeneity rel. to compensation ratio 80−96556
Si:P, optical excess charging $D^0 \rightarrow D^-$, photoelectron spin relaxation *(Russian)* 79−78572
n-Si:P, optical orientation of ^{29}Si and its depend. on pumping light intensity *(Russian)* 77−4581
Si:P, optically induced divacancy reorientation, EPR spectra 78−80216
Si:P, Orbach spin-lattice relax. rate, uniaxial stress depend. 78−72391
Si:P, phonon cond., electron-phonon relax. rate 79−46771
Si:P, photodielectric effect associated with impurity excitation 79−82630
Si:P, photolum. obs. of donor pairs 79−52014
Si:P, photoluminesc. associated with impurity clusters 79−38656
n-Si:P, piezoresist. under strong uniaxial elastic deform. 77−15858
n-Si:P, piezothermoelec. power in electron-phonon drag region, anisotropy 80−70738
Si:P, polycryst., CVD, elec. activation of impurities, EPR obs. 80−34774
silicon continued
Si:P, polycryst., channelling of implanted P during MOS device processing 80−65017
Si:P, polycryst., growth in epitaxial reactor at 800°C, using PH_3 doping 77−1815
Si:P, polycryst., neutron transmutation doped, elec. props. 78−34836
Si:P, polycryst. etching characts. in CF_4 plasma 78−76777
Si:P, polycryst. films, elec. props., EPR, defect states, doping effects 80−75660
Si:P, polycrystalline, thermal oxidation in wet O_2 78−92376
Si:P, polycrystalline laser recrystallised film on Si substrate, cryst. struct., thermal oxidation 80−65391
Si:P, quantitative model for diffusion of P and emitter dip effect 77−76611
Si:P, RF sputtered polycryst. film, MOS compatibility 78−6455
p-Si:P, random and aligned implants, Rutherford backscatt. and TEM exam. 78−47454
Si:P, satellite of bound excitons, transient decay 80−11466
n-Si:P, Sb, reson. four wave mixing, valley orbit splitting 79−89960
Si:P, secondary defect generation suppression and diffusivity restraint by HCl oxidation 79−70191
n-Si:P, secondary defects produced by high-temp. electron irrad. 79−33017
Si:P, shallow strain distrib. near cryst. surface, asymmetric X-ray Bragg reflexion 77−76252
Si:P, SiP precipitation concomitant with P predeposition 77−24326
Si:P, solid planar source for diffusional doping, with SiP_2O_7 active component 77−1139
Si:P, spin relax. time of electrons determ., dynamic polarisation of ^{29}Si nuclei 77−55730
Si:P, spin-on borosilica diffusion source, doping uniformity factors 77−76442
Si:P, sputter-deposited polycryst. films, resist. meas. 78−14842
Si:P, stacking fault and dislocation growth induced by P predeposition 77−59023
Si:P, strain-induced band-gap narrowing effect on P diffusion 79−55935
Si:P, strongly compensated, temp. depend. cond. meas. down to 1K 77−72865
Si:P, submillimetre wave study of metal-insulator transition 79−95336
Si:P, temp. depend. of anomalous struct. in wavelength-derivative absorption spectra 77−52143
Si:P, thermal cond., electron-phonon interaction at low temps. 80−92730
Si:P, thermally annealed, high dose, ion-implanted, dislocation array prevention by prior laser annealing 79−73187
Si:P, through-oxide implanted samples, anomalous residual defects after annealing 77−76432
Si:P, uniaxially deformed, multiparticle impurity complexes, luminesc. spectra *(Russian)* 79−4854
Si:P, variable range hopping conduction, in lowest temp. region 79−73511
Si:P, variable range hopping at very low temp. 80−49736
Si:P,B, amorphous, localised level density 79−56168
Si:P,B, wafer, long range enhancement of B diffusivity induced by high surface conc. P diffusion 79−46687
Si:P,Sb(Te), impurity implantation effect on CESR, spin-orbit interactions 77−36133
n-Si:P,V, degeneracy ratios and impurity levels of V, resist. and Hall effect meas. 77−20260
Si:P amorphous films, doping and annealing effects on localized states, ESR meas. 79−38380
Si:P bipolar transistors, interstitial supersaturation and misfit dislocation climb, TEM study 80−70203
Si:P bound multiexciton complexes, expt. evidence for shell model 78−39036
Si:P CVD films, ion-implanted, doping effect on elec. props. 80−2495
Si:P diffused solar cells, laser treatment to dissolve diffused P precipitates 80−45667
Si:P dislocation p-n junctions, capacitive props. 80−20300
Si:P epitaxial layer, strain distrib. at interface with substrate, obs. by X-ray double cryst. method 79−99461
Si:P film, amorphous, unusual temp. depend. of thermoelec. power 77−59343
Si:P film, CVD polycrystalline, low press. and atmos. press., oxidation 80−3214
Si:P film, polycryst., heavily doped, mobility and carrier conc., optical determ. 80−66314
Si:P film, polycryst. pulsed electron beam annealing 80−10566
Si:P heavily-doped, photoluminescence 78−72572
Si:P implantation profiles, neutron activation anal. 78−7284
Si:P implanted, low temp. annealing characts. 77−11576
Si:P implanted, multiscanning electron beam annealing 80−75242
p-Si:P implanted films, piezoresist. stress tensors, ion dose depend., −80 to 120°C 80−100538
Si:P impurity conc. profile determ. by anodic oxidation 79−28010
Si:P non-Fickian diffusion, parameter depend. on doping level and impurity gradient *(German)* 80−54440
p-Si:P p-n junctions, dislocations investig. rel. to P diffusion, SEM, X-ray topography techniques 77−76433
Si:P photochronic detector, IR detect. using delayed breakdown 79−58786
Si:P polycrystalline layer, role in lattice defect reduction assoc. with P predeposition 80−70229
p-Si:P semiconductor detector in radiometric inspection problems 80−62819
Si:P solar cell, minority carrier lifetime degradation during ion implanted processing, surface photovoltage 79−39305
Si:P solar cells, improved P diffusion using laser treatment 80−55850
Si:P spherical defect cluster and dislocation loop analysis 78−14356
$Si:P^+$, highly implanted, two step annealing effect on crystallinity 77−31683
$Si:P^+$, ion-implanted, annealing characts., X-ray diffr. exam. 78−14372
$Si:P^+$, ions implanted through SiO_2 mask window, lateral spread 79−77627
$Si:P^+$, misfit dislocation formation mechanism, effect of implantation temp. 78−38708
$Si:P^+$, misfit dislocation net propagation due to osmotic forces 79−65108
$Si:P^+$, Zeeman energy transfer at surface layer 80−11247
$Si:P^+$ ion implanted single crysts., secondary defects development during annealing 80−44228

silicon continued
Si:P(As)(B), nonequilibrium solid solutions obtained by heavy ion implantation and laser annealing 80−92544
Si:P(As)(B)-SiO_2 interface oxidation kinetics, high doping levels, experiment 80−11828
Si:P(As)(Sb) donors, polarisability binding energy in mag. field 79−1581
n-Si:P(B), elec. cond. oscills., electron instability effects due to dislocations 80−103704
Si:P(B), film, electronic props. 78−84330
Si:P(B), high temp. impurity diffusion via vacancies and self-interstitials 80−24667
Si:P(B), multiple-particle exciton-impurity complex form. *(Russian)* 78−43925
Si:P(B)(As), proton enhanced diffusion and vacancy migration 78−67747
Si:P(O) p^+-n-n^+ solar cells, comparison rel. to resistance to 1.5 MeV electron irrad., majority carrier trapping 80−94087
p-Si:P(P^+) photolytic props. in HF 80−89504
Si:P(Sb), electron-nucl. interaction under optical pumping, ^{29}Si optical polarisation meas. 79−95680
n-Si:P(Sb)(As), characts. of piezoresist. 77−51750
Si:Pb, diffusion behaviour of Pb in high dose implanted Si layers during isothermal annealing 79−1525
Si:Pb, He^+ Rutherford backscatt. and TEM exam., implant species effect on recrystn. 78−47452
Si:Pb, high dose implantation profiles, determ. using low angle Rutherford He ion backscatt. 79−4327
Si:Pb, implanted, laser annealing 78−75685
Si:Pb, implanted and annealed, impurity redistrib. 78−75689
Si:Pb, ion-implanted and annealed, dose depend. of residual lattice disorder 77−43228
Si:Pb, lattice location of dopant and amorphous zones, by Rutherford backscatt. 77−68990
Si:Pb, low-solid solubility ion-implanted, pulsed and continuous laser annealing and furnace annealing comparison 79−73184
Si:Pb implanted layers, recrystn. on annealing, backscatt. and TEM obs. 77−51421
Si:Pb oxides, thermal oxidation, kinetics and mechanism 77−36673
Si:Pd, deep levels, conc., activation energies, thermal emission rate 79−51524
Si:Pd, energy levels obs. 77−35890
n-Si:Pd, surface, photocond. and photo-emf spectra 79−73544
n-Si:Pd Schottky diodes photocapacitance meas., photon and carrier capture cross sections 80−20309
Si:Pt, deep level, exam. by thermally stimulated current and capacitance techniques 79−1579
Si:Pt, depth depend. of atomic mixing by ion beams 80−29837
Si:Pt, elec. props., deep-level transient spectroscopy and thermal emission meas. 79−82542
Si:Pt, hole capture cross-section at E_v+0.34 eV, capacitance meas. *(French)* 80−65493
Si:Pt, implanted and laser annealed, segregation and increased dopant solubility 80−65016
Si:Pt, photoionisation cross-sections, photocurrent and photocapacitance meas. 78−10497
Si:Re, diode, barrier capacitance and photocapacitance, uniaxial press. effect 77−20416
n-Si:Re, photon-capture cross sections of Re levels, spectral depend. 77−89726
Si:Re diode, photocapacitance and induced photocapacitance spectra 77−4404
n-Si:Re diode photocapacitance spectra, Re centre dissociation 79−90997
Si:Rh, p^+-n-n^+, n^+-n-n^+, p^+-n-p^+, structs., S- and N-type I-V characts. 77−43706
Si:Rh(Pd), Schottky diode, capacitance characts., donor and acceptor levels 77−43697
Si:Ru, photon- and carrier-capture cross sections of Ru levels 79−90995
Si:S, deep level characterisation, implantation predeposition technique 80−100444
Si:S, electron-nuclear interactions during pumping, influence of mag. field 79−95378
Si:S, existence of isotope shift for S deep level, isothermal transient capacitance meas. 78−63999
Si:S, γ-irrad. influence on elec. props. 80−6845
Si:S, i.r. photodetector, background-limited operation near 77K 77−122
Si:S, two-electron donor centre, photoionisation cross sections meas. 77−8044
Si:S diode, ionisation energies of S levels, photocapacitance meas. 77−4432
Si:S IR detectors, performance and elec. transport props. 78−45702
Si:S p^+-n junction, optical props., photocurrent meas. 77−4425
Si:S(Se), IR absorption and photocond., donor levels 77−55809
Si:Sb, amorphous, electronic transport props. 80−44589
n-Si:Sb, arbitrary doping profiles produced by MBE 79−7617
Si:Sb, diffusional doping by doped oxide method 80−15127
Si:Sb, dopant implantation, activation analysis errors due to isotope comp. *(German)* 80−34037
Si:Sb, dopant microsegregation rel. to crystal and crucible rotation 78−11106
Si:Sb, electron irrad. damage, electron trapping centres 77−39798
Si:Sb, epitaxial film, growth by mol. beam technique 80−2292
Si:Sb, epitaxial layers, doping profile techniques 80−44231
Si:Sb, epitaxial regrowth of amorphous layers created by high-dose Sb implantation 78−30654
Si:Sb, heavily doped, TEM obs. of impurity effects in dislocation motion 77−43220
Si:Sb, high dose implanted, orientation dependent annealing effects 78−18665
Si:Sb, high dose Sb ion implantation, buried layer appls. 80−88186
Si:Sb, implantation of Sb for buried layers appl. *(French)* 77−80527
Si:Sb, in solar cell struct., heavily doped, dopant striation, SEM 79−39312
Si:Sb, ion implanted, annealing behaviour of stress 78−63778
Si:Sb, ion implanted, Sb diffusion during oxidation, snow-plough effect 80−88366
Si:Sb, ion implanted and annealed, influence of implantation temp. on dislocation generation 80−88158
Si:Sb, ion implanted doping, isotopic composition shifts on neutron activation determination 80−24487
silicon continued
Si:Sb, laser doping, evaporation loss and diffusion of Sb, under pulsed laser irrad. 80−59508
Si:Sb, low energy ion implantation, profile determ. 80−88176
Si:Sb, low energy ion implantation Schottky barrier diodes and resistors 80−88177
Si:Sb, MBE film, doping technique 80−79821
Si:Sb, Mossbauer spectra of ^{119}Sn defect struct. 80−97174
Si:Sb, polarisability of Sb donors in mag. field 79−95368
Si:Sb, produced by ion implantation and laser annealing, Sb behaviour above solid solubility 80−88200
Si:Sb, redistribution of thin impurity layers after laser annealing, theoretical model and expt. results 79−69147
Si:Sb,As, autodoping effect of Sb-As simultaneous diffusion 77−80522
Si:Sb,P, double implants, residual defect reduction after damage anneal 80−88170
Si:Sb crystal Czochralski growth, radial microsegregation analysis 78−11105
Si:Sb vacuum deposited coating, p-n junction, pulsed electron beam annealing doping, diffusion 80−75480
Si:Sb wafers, laser annealing, Rutherford backscatt., optical, and TEM obs. 79−1445
Si:Sb(As)(P), bound excitons and bound multiexciton complexes for shallow donors, luminesc. meas. 79−24363
Si:Sb(Ga)(Bi)(In), dopant solubility limit, laser irrad. effects 80−84295
Si:Sb(P) (B) homoepitaxial film, interpretation of temp. depend. of partition and sticking coeffs. 77−7756
Si:Sb(P)(As), shallow donor states with strong central cell perturbation theory 78−51933
Si:Sb(P)(As), shallow donor electrons, hyperfine interactions, reply to Onffroy's calcs. 78−51934
Si:Sc, photocapacitance and photoconductivity 80−107859
Si:Se, detector for 3-5 μm appl. development 79−35825
Si:Se, energy levels, resistivity and Hall coeff. 79−69528
Si:Se, impurity states, A- and B-centres, electron, hole thermionic emission rates 80−96813
Si:Se,B(Ga)(Al)(In), diffusion of Se, solubility and ionization levels, Hall effect and photocond. meas. 79−42486
Si:Sm, implanted impurity location, Mossbauer and channelling expts. 80−39128
n-Si:Sm,P, carrier conc. and mobility, electron irrad. effects *(Russian)* 77−66168
Si:Sn, Mossbauer spectra of ^{119}Sn impurity atoms 80−15935
Si:Sn, Mossbauer study of defects due to ^{119}In implantation 80−80641
Si:Sn, thermal conductivity, Hall mobility depend. on Sn conc., phonon-defect scatt. 80−29232
Si:Te, implanted impurity location, Mossbauer and channelling expts. 80−39128
Si:Te, ion implanted, laser annealed, lattice location of Te 78−67725
Si:Te, laser melting, surface Te atom accumulation, profiles 80−100258
Si:Te, Mossbauer spectra of ^{119}Sn defect struct. 80−97175
Si:Te implanted, laser annealing, Mossbauer obs. 80−39127
Si:Th, ion implanted, meas. of stopping power of channeled B ions 79−28025
Si:Ti, deep level impurity, Hall meas. 80−6768
Si:Ti substrate for epitaxial solar cells 80−61341
Si:Tl, energy level, deep level transient spectroscopy 79−19541
Si:Tl, IR excitation spectra 78−88289
Si:Tl, ion implantation, indirect doping method 80−10568
Si:Tl, optical absorption and photolum. of bound exciton 78−88359
Si:transition metal, electronic states of impurities 77−43531
Si:Y, photoelectric props. 80−107860
Si:Zn, implanted atom diffusion during laser annealing 79−37725
Si:Zn, minority carrier lifetime investigation 80−80292
Si:Zn, P^+-n-n^+ struct., deep doubly ionized centres, impedance calc. 79−11202
Si:Zn, photoionisation of deep impurity levels 80−34386
Si:Zn, recombination waves threshold parameters in microwave field 77−28206
Si:Zn, resist. inhomogeneity effects on photoelec. props. 77−8151
Si:Zn, reson. characts. of impedance near excitation threshold of recomb. waves 80−20301
Si:Zn, trapping struct., analysis of TSC meas. 77−8045
n-Si:Zn,P, local deform. of cryst. lattice, charact. parameters or recomb. waves 77−4386
Si:Zn (Mn) (In), surface characterised by negative electrochemical pot., electronic props. 80−44695
Si:Zn p-n junction diode, computer-aided study of carrier lifetimes 80−24999
Si:Zn p-n junctions, I-V characts. using exact DC circuit model 79−95476
p-Si:Zn^-, deep levels, optical-phonon-assisted capture of carriers 79−51597
Si/Al and Si/Al-Si(Cu), Si regrowth minimisation through overlying Al or Al alloy film 80−70569
Si/Al interfaces, chemical bonding states, low energy AES 80−6985
Si/Al thin film couples, accel. ageing 80−44726
Si/Al-Si systeym, vacuum deposition, rate controlling and composition anal. by electron impact emission spectroscopy 79−91591
n-Si/As-Te-Ge film, heterojunction, elec. and photovolt. props. 80−100514
a-Si/Au barrier, capacitance and cond. 80−2469
Si/Au films, laser-irrad., phase transform. study 80−49536
a-Si/$In_{2-x}Sn_xO_{3-y}$, p-i-n heteroface solar cell, device physics and design 80−101113
n-Si/In_2O_3:Sn heterojunction solar cell, fabrication and characts. 78−15314
Si/In_2O_3-SnO_2 thin film junctions, polarity dependent memory switching effects 80−70814
Si/In(-Cd), Si/Cd Schottky contacts, electrochemically deposited 80−88633
Si/metal system, silicide form. by thin film interactions, review 80−49429
Si/Ni, Stoneley waves at (001) interface between cubic symm. cryst. 80−100388
Si/Pd interface, chem. and struct. props. during silicide form., AES and TEM obs. 80−49430
Si/Pd system, solid phase epitaxial growth control by C ion implantation 80−75466
Si/Pd-W, contact reactions, backscattering, X-ray diffr. meas. 80−20040
p-Si/rare earth metal contacts, surface pot. barrier 80−60086

silicon continued
Si/refractory metal-Ni(Pd)(Pt) interactions, phase separation 80−65303
Si/Si-Ge alloy, amorphous, solar cell, multijunction structure, increased conversion efficiencies, low cost 80−45677
Si/Si-Ge junction, elec. and photoelec. props. 78−10545
Si/SiC ceramic composite, room temp. props., effect of SiC content and orientation 78−27599
Si/SiO_2, adsorbed methanol, light scatt. from clusters 79−33721
Si/SiO_2, CCD, incomplete charge transfer, fringing fields and interface states effects 77−15964
Si/SiO_2 interface, precise wet-chemical etching, using rapidly rotating sample 80−93669
Si/SiO_2 interface, slow-trapping instability, kinetics 78−76151
Si/SiO_2 interface, transition region thickness, determ. by He^+ backscatt. 77−62762
n-Si/SiO_2 solar cells, fabrication and characterisation 79−79393
Si/SiO_2-electrolyte interface, electron exchange at surface of thermally grown SiO_2 80−16696
Si/SiO_2/In_2O_3-SnO_2 diode solar cells, loss mechanisms, charact., band struct. 80−26135
Si/V_2O_5-P_2O_5/SnO_2 heterojunction, static optoelectronic charact. 79−87146
n-Si-^{119}Sn resonant detector for Mossbauer spectroscopy 80−883
Si-^{3}He interface, phonon reflection 78−84043
Si-^{4}He boundary superfluid, quantitative meas. of phonon energy transmission coeff. 77−66084
Si-absorbing film system, ellipsometry 79−99964
Si-Ag boundary, electronic and cryst. struct. of Ag adsorbed on Si (111), Schottky barrier form. obs. 78−84091
n-Si-Ag Schottky-barrier diodes, excess current mechanism under uniaxial press. 78−91771
Si-Ag-Si heat mirror on plastic sheet for radiation insulation of visible windows 80−95985
n-Si-Ag(Au) evaporated contact photoelectric props. *(Russian)* 78−43473
Si-Al, composite, simulation of tensile behaviour and fracture void initiation *(Japanese)* 78−52948
Si-Al, film, quantitative anal. by DC arc optical emission spectroscopy 78−68940
p-Si-Al, ohmic contacts, Si dissoln. and recrystn. effects, computer calc. 80−103749
Si-Al (Na) interface, barrier height anal. including virtual surface states 77−69416
p-Si-Al barrier junction form. 77−12006
Si-Al devices, thickness meter for Al contacting layers *(Russian)* 80−36980
Si-Al interface, ellipsometric anal. methods, correl. between optical props., thickness and surface roughness meas. *(German)* 80−55215
Si-Al interface, solid phase epitaxial growth of Si 80−34324
Si-Al optically thick, plasma, use of multiple photoexcitation to obtain lasing at 44 Å 79−3684
Si-Al Schottky diodes, with Ti contact, voltage-current charact., appl. to ignition circuits 80−11088
Si-Al solid-phase epitaxial growth, substrate effects, SIMS and backscatt. spectra 79−42421
Si-Al system, Si regrowth minimisation methods in Al films 80−15384
Si-Al_2O_3, inversion layer subbands, magnetocond. oscills. 78−64124
Si-Al_2O_3, MIS structure, with dielectric film, from UV irradiation converted metalorganic compounds *(Russian)* 80−45245
Si-Al_2O_3 interface, charge injection from surface depletion region 80−54797
Si-Al-Al_2O_3 system, solid phase Si regrowth on sapphire 80−100413
Si-Al-Si, isothermal version of the moving solvent method 79−1824
Si-Al(Ga)(In) interface, electron energy loss spectra of Schottky barrier states 77−48290
Si-Al(Ni) structure, contact resist. and bulk resist. of Si, pulse method 78−52081
p-Si-As_2S_3 isotype crystalline-amorphous heterojunctions, electrophysical props. 79−24063
Si-$As_2Se_3Ge_4$ heterojunction, elec. props. 78−6434
Si-As(Sb) temp. depend. of irradiation-induced displacement of impurities, backscattering meas. 78−26605
Si-Au, interface study using EELS 80−97391
Si-Au, ohmic contact to GaP, metallurgical struct. 77−1485
p-Si-Au, Schottky barrier IR detector 77−37985
Si-Au boundary, Schottky barrier height, interfacial layer effects 78−14824
Si-Au contact, O determ. by SIMS, nuclear reaction and Rutherford backscatt. anal. 79−4482
Si-Au interface, algorithm for energy deposition of X-rays 77−28648
Si-Au interface, critical Au-film thickness obs. for room temp. interfacial reaction 80−75390
Si-Au Schottky barrier solar cell fabrication, doping of a-Si 80−50969
Si-Au Schottky diodes, role of O in formation mechanics 79−42639
Si-Au Schottky-barrier, formation process anal., V-I charact. *(French)* 78−91768
Si-Au substrate-film system, relax. effects, internal friction meas., temp. range 20 to 900°C 78−18886
n-Si-Au surface barrier diode, photosensitivity in spectral range, 1-6 eV 77−89850
Si-Au-Si, Auger line intensity, contrib. of backscattered electrons 79−65962
Si-Au(Ag) contacts, Schottky barrier heights and interface states 77−85317
Si-Au(Cr)(Pd), contact reactions between amorphous Si and metallic films, TEM, transmission electron diffr. obs. 79−23846
Si-Au(Rb)(In), Schottky diode, X-ray effects on elec. props., irrad. induced diffusion 77−4439
Si-B, diffusion-free annealing, use of scanning CW Kr laser 78−91345
Si-B, exam. of two stage diffusion of B, under a gas phase oxide film 79−95044
Si-B, P diffusion and activity after Ar ion bombardment 78−95192
Si-B crystal, Bond method, of meas. lattice parameters, asymmetric Bragg reflections appl. 80−38861
Si-borosilicate glass, B diffusion from sputtered glass film into Si 80−29040
Si-borosilicate glass, Van der Waals interaction meas., influence of optical absorpt. 79−95273
Si-C, one-bond couplings, orbital and spin dipolar contribs., INDO approx. 79−31552
silicon continued
Si-C interface on polycryst. Si ribbon, effect on solar cell efficiency *(French)* 80−54531
Si-C-O-Ar, high temp. plasma, prod. quenching mol. dynamics simulation 78−39711
Si-CaF_2, cosputtered composite semiconductors, selective solar energy absorbers 79−56876
Si-CaF_2 film, dielectric constant and selective solar absorption 78−2937
Si-CdS heterojunction memory diodes, switching process 78−80046
Si-CdS p-n heterojunction photodetector fabrication and charact. 78−52068
Si-CdSe n-n heterojunction, photovoltage sign reversal, energy band profile *(Korean)* 80−29469
Si-chalcogenide cryst. amorphous heterojunction, energy band diagram construction 77−55602
Si-Co interface metal-semiconductor transition, rel. to first compound nucleation 80−24771
Si-$CoSi_2$Si, double heteroepitaxy, solid phase and MBE 80−104063
n-Si-Cr, Schottky barrier IR detector 77−37985
Si-Cr Schottky barriers, interfacial structural defects effect on avalanche breakdown 79−42644
Si-Cr_2O_3Al, current-voltage charact., oxide film effects 80−70841
Si-CsSe p-n heterojunction, vacuum deposition, photovoltaic effects *(Korean)* 77−28243
n-Si-Cu Schottky contacts, electrochem. deposition, barrier height and ideality factor 80−75641
n-Si-electrolyte boundary, selective anodic oxidation 78−15563
Si-electrolyte contact, current-voltage charact., effect of mechanical deform. 78−68082
Si-electrolyte contact, implantation profile meas. from capacitance-voltage charact. *(German)* 77−1145
Si-F-H amorphous solar cells, DC glow discharge fabrication 80−72041
Si-F-H:P, film, dark cond., struct., Raman scatt. 80−88588
Si-GaAs heterojunction photothyristor, spectral charact. 78−10546
Si-GaP, heterojunction, photosensitivity spectrum, charact. 79−24071
Si-GaSe n-p heterojunction, elec. charact., interface states 80−70812
Si-Ge heteroepitaxial system, imperfections and morphology, electron microscope and electron diffr. obs. 79−42420
Si-Ge heterojunction form., microscopic aspects, EELS meas. 80−80368
Si-Ge junction, Si monocryst. and Ge film, elec. props. 79−51660
Si-H, amorphous, energy gap negative-U states, Si-H-Si three centre bond model 78−91606
Si-H, amorphous, H three-dimens. distrib., ion-induced AES and Rutherford backscattering 80−44132
Si-H, amorphous, plasma-deposited, H evolution and defect creation 80−44914
Si-H, amorphous, random network model 80−1932
Si-H, amorphous, sputtered, photolum. obs. 80−80856
Si-H, amorphous, struct. and press. induced transition 80−44131
Si-H, amorphous film, in situ prepared, photoemission studies 80−35060
Si-H, amorphous plasma deposited film, H content and density 79−82472
Si-H (up to 15 at.%), amorphous, ion implanted, laser annealing obs. 79−69133
Si-H amorphous film, reactively sputtered, prep. and props. 79−78889
a-Si-H sputtered solar cells, temp. depend. of Schottky barrier charact. 80−45669
Si-H:P amorphous film, dark cond., struct., Raman scatt. 80−88588
Si-In Schottky barrier interface, covalent bonding of metal atoms 77−20429
p-Si-In Schottky barrier structure, optical quenching of photovoltaic effect 77−55608
p-Si-$In_{2-x}Sn_xO_{3-y}$ solar cells, thermal degradation mechanisms 80−55841
Si-$In_{2-x}Sn_xO_{3-y}$ SIS heterostructure solar cells, spray-deposited 80−101106
Si-In_2O_3 heterojunction solar cells, photovoltaic and rectifying props. 79−1618
n-Si-In_2O_3:Sn, solar cell characterisation *(French)* 79−39306
Si-In_2O_3:Sn heterojunctions for solar cells 78−64107
Si-In_2O_3:Sn heterojunctions, current mechanisms and barrier height 80−11083
Si-In(Rh)(Au) Schottky diodes, X-ray irradiated, radiation-accelerated diffusion of impurities in Si 78−26952
Si-insulator interface, non-avalanche charge injection, expt. study, charge trapping effects 80−60099
n-Si-$IrSi_x$, Schottky diode, rectifying barrier height meas. 79−99619
p-Si-$LiNbO_3$, frequency doubling of the two-pulse and three-pulse echoes in surface acoustic waves 79−69335
Si-$LiNbO_3$ layer struct., acoustoelectronic phenomena 77−55556
Si-$LiNbO_3$ structure, acoustoelectronic interaction between SAW and transverse drift current 77−69424
Si-Li(Au)(Cu), diffusion-induced defects, X-ray triple cryst. diffractometry 80−2213
Si-liquid He interface, refl. of high frequency phonons, role of phonon focusing 77−80691
Si-liquid N_2 system, kinetics of switching effect and electrothermal memory 79−51641
Si-metal contact, transport theory of Schottky barriers 80−80372
Si-metal contacts, analytical techniques, review 80−80120
Si-metal interface, silicide formation, interface marker technique obs. 80−59734
a-Si-metal Schottky barrier, I-V charact., barrier heights 77−8191
p-Si-metal Schottky contact surface state spectra and current transport mechanism *(Russian)* 78−43472
Si-metal systems, interfacial reaction and Schottky barrier 80−39672
p-Si-metallic liquid interface, thermoelec. coeff. meas. 77−39887
Si-MgO film, dielectric constant and selective solar absorption 78−2937
p-Si-Mn contact, barrier height 80−34510
Si-Mo sputtered contacts, contact resistance 80−92970
Si-Mo substrate-film interface, reaction on heat treatment, silicide formation 80−79999
Si-MoO_3 photodiode, fabrication as function of O_2 partial press. 80−29464
Si-N-H gaseous system, deposition ranges of Si_3N_4 and Si *(French)* 77−36405
Si-NH_3 electrolyte interface, photo-assisted electron injection 79−87152
Si-$NaNO_3$ aq. soln., anodic polarisation of semicond. electrode 77−11999
n-Si-Ni, Schottky barrier, thermal annealing effect on props. 79−69596
n-Si-Ni, Schottky-barrier, I-V charact. of elect contact 79−19662

silicon continued
Si-Ni interface, NiSi formation from Ni_2Si, Pt marker study 78−87830
Si-Ni Schottky barriers, thermionic field emission at room temp. 78−6445
n-Si-Ni structure formed by elec. explosion of metal, rectifying barrier 78−72263
Si-Ni substrate-film interface, annealing effects on transmission electron diffr. patterns, silicide form. 78−91562
n-Si-Ni surface barrier junction, rectifying, struct. and elec. characts., effect of low temp. annealing 78−14821
Si-Ni surface barrier struct., surface electronic states, annealing effects *(Russian)* 78−6441
Si-Ni wafer-thin interface, marker motion in Ni_2Si formation 77−89593
Si-Ni(Pd)(Pt) film struct., silicide form. He^+ back scatt. and X-ray diffr. obs. 79−51442
Si-O bonds, cryst. chem. at high press., rel. to Earth mantle mineralogy 79−48470
Si-O system, modern view 78−10045
Si-on-ceramic solar cells, short-circuit current density meas. using light-beam-induced-current tech. 80−93887
Si-P, dislocation networks due to ion implantation, TEM exam. 77−35563
Si-P, excess carrier recomb., photocond. 79−65495
Si-P dust, electrification and cond. 79−82662
Si-P MOS devices, time dependence of depletion region formation at cryogenic temp. 80−34522
Si-Pb heterojunction, RHEED, Mossbauer spectroscopy and I-V characts. 80−70828
Si-PbS heterojunction, characts. and operation, IR detector appls. 78−52075
Si-PbS heterojunction, effect of Si substrate orientation on struct. and interface props. 80−80097
Si-PbS heterojunction, struct. and comp. 80−54530
n-Si-Pd diodes, chemical reduction process for fabrication 80−60082
n-Si-Pd_2Si contact, interface struct. and Schottky barrier height, correl. obs. using TEM 80−100504
Si-Pd_2Si heterostructure growth by solid-phase epitaxy from Si (111)-Pd-Si (amorphous) 77−51617
Si-Pd_2Si-Si, kinetic aspects of solid phase epitaxial growth of amorphous Si 79−4491
Si-$Pd_{80}Si_{20}$, amorphous, Pd_2Si layer form., shallow contact 80−103586
Si-Pd-Si structure, epitaxial growth, backscattering and transmission electron microscopy studies of layered structures 80−80123
Si-Pd-Ti, silicide form. in evaporated films 80−80006
Si-polymer interface states in MOS structure, capacitance and cond. meas. 77−20438
Si-Pt contact, silicide layer struct. and elec. props., effect of processing conditions 77−62991
Si-PtSi interface, impurity effects 80−80037
Si-Pt(Ni)(Pd), laser-induced reactions of metal films with Si, surface struct. obs. 79−19471
n-Si-Re(Os) Schottky contact barrier height meas. 80−65675
Si-refractory metal contacts, thermally cleaned surfaces 80−100521
Si-refractory metal structs., interface modification by ion implantation 80−70475
Si-Rh interface, RhSi form. by lattice diffusion 78−71891
Si-saphhire, Si ion implanted wafer, laser annealing 79−99989
Si-sapphire, interface radiation induced charge trapping, rapid anneal phenomena 79−19666
Si-sapphire interface charge trapping, effects of sapphire type and epi growth conditions 77−20447
Si-sapphire interface in SOS ICs, elec. investigation 80−11097
Si-sapphire interface states exam. by transient current anal. 77−43736
n-Si-Se, ion implantation studied by deep level transient spectroscopy 78−10392
Si-Si interface, elec. cond. rel. to interface state population 80−65672
Si-Si_3N_3, dielec. function calc. 79−95862
Si-Si_3N_4 interface, effect of F ions on props. and stability, expt. 78−64141
Si-Si_3N_4 interface in MNS capacitors, surface state density investigation 80−60100
Si-Si_3N_4-Al, electrical strength, effect of struct. defects in Si_3N_4 *(Russian)* 78−26955
Si-Si_3N_4-Al, photoexcitation of emission currents, I-V characts. *(Russian)* 77−72917
Si-Si_3N_4-SiO_2 non absorbing double layers, optical parameters reflectivity by liquid immersion method 80−71503
Si-Si_3N_4-SiO_2-Si multilayer structs., impurity distrib., activation anal., autoradiography techniques 77−16881
Si-Si_3N_4(SiO_2) boundary, electrophysical properties, effect of ionic processes in dielectric layers *(Russian)* 78−10562
Si-SiC chemical interaction in rarefied O_2 under pulsed action of concentrated solar radiation 80−71930
Si-SiC composite film, optical props., appls. 77−754
n-Si-SiC film junction device, elec. props. 80−15591
Si-SiC p-n and n-n heterojunctions, prep. by ion implantation, tunnelling cond. 77−43710
Si-SiC struct. formation on ^{12}C ion implantation in Si, optical and photoelectric props. 79−91136
Si-SiN mixtures, X-ray diffr. powder anal. method, integrated intensities peak height approx. 77−56323
Si-SiO_2, Al-implanted, low-temp. annealing effect on charge and surface state density 77−85337
Si-SiO_2, angular-dependent X-ray photoelectron spectra 77−12485
Si-SiO_2, anodic polarisation in electrolyte containing fluoride ions, effect on oxide props. 80−39679
Si-SiO_2, bonding at (111) interface, stoichiometry and kinetics, synchrotron radiation photoemission spectroscopy 80−24744
Si-SiO_2, charge injection from polycryst. Si at low fields 77−39945
Si-SiO_2, dielec. function calc. 79−95862
Si-SiO_2, ESR centres, interface states and oxide fixed charge 80−2474
Si-SiO_2, effects of processing on radiation damage 78−39223
Si-SiO_2, electron photoemission from Si, band struct. effects 79−19977
Si-SiO_2, electron tunnelling into thermally grown SiO_2 77−12018
Si-SiO_2, electron-beam annealing of ion-implantation damage 79−77622
Si-SiO_2, emission probability of hot electrons into oxide 77−32084
Si-SiO_2, film refr. index and thickness meas. 77−82589
Si-SiO_2, flat-band voltage due to fixed surface charge density, modified expression 79−56317
Si-SiO_2, Fowler-Nordheim tunnel injection into SiO_2, Si surface pot. effect 79−91151
silicon continued
Si-SiO_2, generation of interface states due to emission of leaky electrons 77−62972
Si-SiO_2, hot electron emission from Si under low level avalanche multiplication 77−80851
Si-SiO_2, hot electron emission into SiO_2 78−30997
Si-SiO_2, impurity redistrib. during oxidation, numerical soln. including interfacial fluxes 80−25888
Si-SiO_2, influence of oxidation conditions on elec. props. of ultrathin SiO_2 layers 78−39226
Si-SiO_2, influence on frequency-temp. coeff. of SAW devices 80−79066
Si-SiO_2, intentionally contaminated interface, transient capacitance meas. 79−33349
Si-SiO_2, interface, distinction between donor and acceptor character of surface states 78−39216
Si-SiO_2, interface, doping depend. of interface states and charges 80−92992
Si-SiO_2, interface, electronic ground state of inversion layers 77−43731
Si-SiO_2, interface, hopping conduction, anal. in impurity bands in inversion layers 79−47171
Si-SiO_2, interface, morphology and electronic struct. 79−78194
Si-SiO_2, interface, props. of surface states reviewed 77−20449
Si-SiO_2, interface, reconstructing states 80−49925
Si-SiO_2, interface, stress meas. technique 80−84395
Si-SiO_2, interface defect states obs. by constant capacitance DLTS 80−49924
Si-SiO_2, interface free carrier mobility in inversion layer, influence of polar phonon scatt. 79−73597
Si-SiO_2, interface groups of states, C-V meas. 78−2541
Si-SiO_2, interface states from capacitance-voltage term spectra anal. 77−4446
Si-SiO_2, interface states, new model 80−29478
Si-SiO_2, inversion layer, electronic ground state, stress, temp., mag. field and gate voltage depend. 78−60226
Si-SiO_2, ion bombardment by H_2^+, D_2^+, changes in annealing behaviour 79−78185
Si-SiO_2, ion implantation effects on charges 77−32086
Si-SiO_2, ion implantation through SiO_2 film, recoil implantation of O, EPR study 80−88180
Si-SiO_2, MOS interface states density, meas. techniques and model development 80−92988
n-Si-SiO_2, MOS structures, radiation states 80−103758
Si-SiO_2, nitridation, formation and growth rate of Si_2ON_2 *(Japanese)* 79−91574
Si-SiO_2, oxide defect density depend. on appl. elec. field and thickness 80−19791
Si-SiO_2, P ion implantation, elec. transport props. 80−39130
Si-SiO_2, recoil implanted O profile after ion implantation through SiO_2 80−88198
n-Si-SiO_2, screening of charged impurity centre localised inside oxide and at interface of inversion layer 79−73563
Si-SiO_2, SiO_2 layer charging in UV irrad. of MISS struct., photoinjection currents *(Russian)* 80−39680
Si-SiO_2, surface and interface phonons in bonded solids 78−71931
Si-SiO_2, surface state annealing 77−39946
Si-SiO_2, surface states, oxide charge centres, annealing effects 78−2570
Si-SiO_2, thermally oxidised, origin of fixed charge, Si diffusion in transition region 77−20381
Si-SiO_2, two layer system, P^+-ion penetration tails, expt. and computer anal. 80−75249
Si-SiO_2 (111) interface, H_2 effects, AES study 80−65688
Si-SiO_2 (111) interfaces, sixfold valley degeneracy in electron inversion layers 80−49936
Si-SiO_2 abrupt interface form. by very high dose O^+ ion implantation 80−75253
Si-SiO_2 barrier height in MOS tunnel struct., SiO_2 thickness depend. 78−14831
Si-SiO_2 bonding layer, EPR exam. 78−15022
Si-SiO_2 boundary, origin of interface states and oxide charges generated by ionising radiation 77−20380
Si-SiO_2 boundary, precipitation of Na *(Russian)* 80−49368
Si-SiO_2 boundary, relaxation of nonequilibrium capacitance in electrolyte in intense elec. fields 80−70845
Si-SiO_2 boundary, surface charge transport in valence band of Si 80−70789
Si-SiO_2 charge accumulation during low energy electron bombardment 78−64142
Si-SiO_2 double barriers, reson. tunnelling 77−80846
Si-SiO_2 electrode, electronic cond., luminesc obs. 80−61111
Si-SiO_2 film, crater-edge profiling in interface anal., ion beam etching and AES 77−1323
Si-SiO_2 in MOSFETs, inversion layer carrier mobility, theory 80−60094
Si-SiO_2 interface, (001) vicinal planes, minigaps in inversion layers, far IR absorpt. meas. 80−107919
Si-SiO_2 interface, amorphous, electronic states, Cayley trees appl. 79−65373
Si-SiO_2 interface, An influence studied using threshold voltage shift 79−82672
Si-SiO_2 interface, anal. of fast surface states 79−42648
Si-SiO_2 interface, anisotropic photoinduced ESR 78−23345
Si-SiO_2 interface, Au conc., effective impurity doping 78−52094
Si-SiO_2 interface, Au doping, trap distribution 80−20319
Si-SiO_2 interface, Au surface state energy levels and Au diffusion 79−51652
Si-SiO_2 interface, Auger sputter profiling and photoelectron spectroscopy obs. 78−10287
Si-SiO_2 interface, Auger sputter profiling 78−43254
Si-SiO_2 interface, Auger-sputter profiling obs. of P pileup 78−95240
Si-SiO_2 interface, avalanche injection of charge carriers, oxide current decay 77−43728
Si-SiO_2 interface, backscattering-channelling study 80−34320
Si-SiO_2 interface, barrier height in MOS tunnelling structures 80−88644
Si-SiO_2 interface, bias temp. treatment effect, stability, Cl oxides effect 77−69419
Si-SiO_2 interface, chem. struct. of transitional region 78−95824
Si-SiO_2 interface, cluster Bethe-lattice method appl. 80−49852
Si-SiO_2 interface, continuous random network and tight-binding models 77−89866
Si-SiO_2 interface, defects, intimate valence attenuation pairs 80−54132
Si-SiO_2 interface, density of states, theory 80−80395
Si-SiO_2 interface, ESCA and ellipsometric study 79−82678

silicon continued
Si-SiO_2 interface, effect of thin transition layer on electron mobility and energy levels 77−20458
Si-SiO_2 interface, effect of ^{11}B and ^{19}F ion implantation on charge density 79−10865
Si-SiO_2 interface, effect of N_2 annealing on electron scatt. 79−42660
Si-SiO_2 interface, effect of high-temp., post-oxidation annealing on elec. props. 79−82673
Si-SiO_2 interface, effect of oxidation time and temp. using AES 80−35359
Si-SiO_2 interface, effect of hot electron injection on interface charge density 80−49921
Si-SiO_2 interface, elec. props., rel. to SiO_2 layer struct., 200-600°C heat treatment effects *(Russian)* 77−15967
Si-SiO_2 interface, elec. props. and influence on service performance and stability 78−23171
Si-SiO_2 interface, electron injection into oxide due to mobile ion induced internal field 77−15963
Si-SiO_2 interface, electronic struct., field depend. internal photoemission probe 77−20450
Si-SiO_2 interface, electronic props. of n-Si inversion layers, stress and temp. depend 78−19113
Si-SiO_2 interface, electronic states, review 78−30992
Si-SiO_2 interface, electronic struct., EELS study 79−99596
Si-SiO_2 interface, electrically active paramag. centres detect., photocond. reson. obs. 80−50185
Si-SiO_2 interface, electronic struct. calc. 80−100531
Si-SiO_2 interface, evolution of surface states density during bias temp. treatment 78−14832
Si-SiO_2 interface, fitting stress and its effect on vacancy generation and distrib. 77−28087
Si-SiO_2 interface, form. and struct., AES obs. 79−56314
Si-SiO_2 interface, γ-ray irradiated thin oxide, MOS struct. *(Russian)* 78−84302
Si-SiO_2 interface, Hg probe *(Chinese)* 77−89857
Si-SiO_2 interface, high-resolution electron microscopy study 78−56046
n-Si-SiO_2 interface, hot carrier surface thermo EMF depend. on surface band bending 80−44734
Si-SiO_2 interface, improved characterisation, refined quasistatic and cond. methods 80−96990
Si-SiO_2 interface, impurity electron states near interface 78−95320
Si-SiO_2 interface, in MOS structure, effect of irrad. with low energy electrons *(French)* 77−55617
Si-SiO_2 interface, in MOS struct., fast surface states density, electron irrad. effects 78−88042
Si-SiO_2 interface, in MOSFET struct., electronic props. 79−42662
Si-SiO_2 interface, intermediate chem. state of Si during sputter profiling, Auger spectra 79−11230
Si-SiO_2 interface, interface-state parameters near band edge, MOS conductance meas. 79−11226
Si-SiO_2 interface, inversion layer transport, radiation hardness effects, review 79−19673
Si-SiO_2 interface, ion implantation induced interface states, effect of oxidation and N_2 annealing 77−39949
Si-SiO_2 interface, light induced reson. centres, photocond. reson., EPR obs. 80−50184
Si-SiO_2 interface, local at. struct., XPS obs. 80−20042
Si-SiO_2 interface, MeV backscatt. channelling meas. of Si monolayers 79−11020
Si-SiO_2 interface, model for doped-oxide-source diffusion with chemical reaction 77−39954
Si-SiO_2 interface, N_2 gas reaction, elec. and structural charact. 77−39950
Si-SiO_2 interface, Na^+ drifted, impurity bands in inversion layers 78−60211
Si-SiO_2 interface, new type of interfacial charge 78−23168
Si-SiO_2 interface, O_2 plasma effects on elec. props. 80−100523
Si-SiO_2 interface, optical props. of CDW ground states in Si inversion layers 77−43732
Si-SiO_2 interface, optical props. 79−99908
Si-SiO_2 interface, oxidation stacking faults, growth rel. to self-diffusion 80−49239
Si-SiO_2 interface, props. 78−23170
Si-SiO_2 interface, props. variation in SiO_x region 80−49548
Si-SiO_2 interface, quasistatic capacitance-voltage determ. of interface state density, sources of error 77−12011
Si-SiO_2 interface, rad. hardness, carrier localisation in inversion layer 77−85332
Si-SiO_2 interface, radiation damage coeffs. for fission neutron and gamma-ray irrad. 80−34058
Si-SiO_2 interface, radiation hardness eval. using elec. meas. technique 80−34516
Si-SiO_2 interface, relax. of injected charge, temp. depend. 78−72269
Si-SiO_2 interface, remote polar phonon scatt. in Si inversion layers 80−80095
Si-SiO_2 interface, sputter profiling, ion knock-on mixing model 79−83081
Si-SiO_2 interface, stacking fault-free region formation by annealing 78−51561
Si-SiO_2 interface, surface states and elec. defects obs. using ESR 78−23169
Si-SiO_2 interface, surface generation velocity study, gate-controlled diode structure application 80−6986
Si-SiO_2 interface, surface states characterization, expt. techniques review 80−49949
Si-SiO_2 interface, thermally oxidised, oxide thickness effects on electron scatt. 78−88033
Si-SiO_2 interface, thermally grown, inhomogeneities of surface potential 80−34524
Si-SiO_2 interface, thermal SiO_2 sputter induced roughness, Auger sputter profiling study 80−75424
Si-SiO_2 interface, thermally grown, surface pot. inhomogeneities after stress ageing 80−92993
Si-SiO_2 interface, thermally grown oxide, spectroscopic ellipsometric anal. 80−107659
Si-SiO_2 interface, trapping props. from electrochemical current-voltage behaviour 79−69597
Si-SiO_2 interface, two-dimensional impurity bands, carrier-density dependence of activation energies associated with hopping 80−88561
Si-SiO_2 interface, valley degeneracy splitting in n inversion layer, effective-mass approx. 79−99629
silicon continued
Si-SiO_2 interface, with Cl^- incorporated, characterisation by low temp. cond. meas. 78−60220
Si-SiO_2 interface as electrode for electrical and ellipsometric meas. of adsorbed organic molecules 80−15366
Si-SiO_2 interface charge effects and related props. 78−10575
Si-SiO_2 interface charge inhomogeneities effect on surface state density meas. by MOS AC cond. technique 78−14833
Si-SiO_2 interface formation, by anodic oxidation, F^- and Cl^- ions effect obs. 79−15842
Si-SiO_2 interface in IGFETs, anal. of CVD SiO_2 on (100) and (111) surfaces, near-ideal structs. 80−100528
Si-SiO_2 interface in MIS struct., B^+ ion implanted, elec. props. due to laser irrad. 78−72272
Si-SiO_2 interface in MIS structs., effects of crystal defects on generation process 80−65702
Si-SiO_2 interface in MOS structs. low-energy electron beam irrad., charge accumulation process anal. 80−65701
Si-SiO_2 interface in MOS capacitors, lateral diffusion of Na^+, neutralisation 80−92986
Si-SiO_2 interface in MOS solar cells, operational charact. and struct. 80−93901
Si-SiO_2 interface layer characterisation by spectroscopic ellipsometry 80−50738
Si-SiO_2 interface morphology, P pileup effect, Auger sputter profiling 78−72006
Si-SiO_2 interface of MIS structure, generation-recomb. charact., effect of γ-irradiation *(Russian)* 77−76938
Si-SiO_2 interface oxidation kinetics, high doping levels, theory 80−11827
Si-SiO_2 interface props., electrolyte anode polarisation effect 77−80849
Si-SiO_2 interface state density in MNOS structures 78−47873
Si-SiO_2 interface state spectrosocpy using MOS tunnelling strucures 80−6991
Si-SiO_2 interface state distribution, Br incorporation effects 80−11091
Si-SiO_2 interface state density, dependence on thermal oxidation process variables 80−15607
Si-SiO_2 interface states, effect on memory charact. of thin-oxide MNOS devices 79−82681
Si-SiO_2 interface states, deposition of H containing layers and annealing 80−92991
Si-SiO_2 interface struct. by cross-sectional TEM, amorphous oxide layer 77−24487
Si-SiO_2 interface struct., transient region 77−85115
Si-SiO_2 interface study by XPS 80−50507
Si-SiO_2 interfaces, local atomic and electronic struct., high resolution XPS 80−49927
Si-SiO_2 interfacial region, nature of fixed oxide charge 78−56047
Si-SiO_2 interfacial regions obs., by XPS ultrathin oxide films 79−15039
Si-SiO_2 interfacial region on TCE/O_2 and CCl_4/O_2 oxidised Si, struct. and comp. 80−50741
Si-SiO_2 interfacial transition layer thickness, XPS obs. 80−11540
Si-SiO_2 interlayer, optical evidence 79−69800
Si-SiO_2 inversion layer, n-channel, anomalous magnetoresist., model 80−96996
Si-SiO_2 inversion layers, applied stresses, cyclotron masses and CDWs 77−55596
Si-SiO_2 inversion layers, bound states at interface 79−42655
Si-SiO_2 laminar ion-implanted systems, struct. change investig. by MSSI method *(Russian)* 80−107918
Si-SiO_2 layer formation by O_2^+ ion implantation, interface struct. and C-V charcts. 77−1142
Si-SiO_2 layers on Si substrate, ellipsometric meas. 77−69403
Si-SiO_2 MIS systems, dynamic props. of switching, appl. to charge transfer devices 80−92997
Si-SiO_2 MOS capacitor, two-stage process for building up radiation induced interface states 80−20313
Si-SiO_2 MOS capacitors, relationship between trapped holes and interface states 80−70830
Si-SiO_2 MOS interface, surface-state density and minority carrier generation rate, meas. by DLTS, hot hole effect 80−100527
Si-SiO_2 MOS interface states density, transient capacitance meas. eval. 80−92989
Si-SiO_2 metal structure, ponderomotive force effect on dielec. breakdown 79−15230
Si-SiO_2 microsensor, surface conductivity effect of aliphatic alcohol molecule adsorption *(Russian)* 78−34887
Si-SiO_2 structure, alkali metal ion migration and accumulation, interface struct. 80−107574
Si-SiO_2 structure, electrophysical props. after B^+ ion bombardment 77−12013
Si-SiO_2 structure, mechanical stress at Si(111) surface 78−63921
Si-SiO_2 structure, oxide charge evaluation, appl. of Kelvin method 78−19157
Si-SiO_2 structure, SAW device, appl. to integrated oscillators 78−83186
Si-SiO_2 structures, AS77 scanning analyser for electrophysical props. *(Polish)* 79−95498
Si-SiO_2 structures, B ions implanted, energy spectra of shallow traps at various implantation energies 80−80392
Si-SiO_2 structures, ion implanted, surface charcts. 77−80850
Si-SiO_2 structures, scanning analyser of electrophysical parameters of MOS transistors *(Polish)* 79−91145
Si-SiO_2 surface states, influence of $\Phi ms(T)$ 79−99597
p-Si-SiO_2 system, C-V meas. using Au/Hg probe, work function difference between probe and Si 80−2450
Si-SiO_2 system, implanted with N, P, and Te ions, reflectance spectra and interference fringes 79−23629
Si-SiO_2 system, structural defect formation rel. to thermal oxidation kinetics *(Russian)* 78−43478
Si-SiO_2 systems, spectral charcts. *(Russian)* 79−42657
Si-SiO_2 transition region width, SIMS depth profiling 80−39454
Si-SiO_2 wafer thinning for TEM 77−89352
Si-SiO_2:B structure, AES meas. 77−39951
Si-SiO_2-Al, interface barrier energies for tunnel oxides, internal photoemission meas. 80−84512
Si-SiO_2-Al, internal photoemission, pot. barrier height determ. 80−65699
Si-SiO_2-Al MOS surface channel influence on channel-to-contact diode charact. 80−92994
Si-SiO_2-Al structure, mechanical stress at Si(111) surface 78−63921
Si-SiO_2-Al structure, neutralisation of mobile ions in insulating films *(Japanese)* 79−73591

silicon continued
Si-SiO_2-Al structures, SiO_2 thin dielec. film elec. props. with DC voltage *(Slovak)* 80−88634
Si-SiO_2-Al with thick dielec. layer, photoelec. props. 80−92979
Si-SiO_2-Au Schottky barrier solar cells, back-illuminated, theoretical performance 80−61345
Si-SiO_2-Au system, oxide film 16-36 Å thick, tunnel currents 80−70842
Si-SiO_2-CdS solar cell, I-V characteristics 80−89621
Si-SiO_2-KCl_{aq}, interface, capacitance meas. 78−80051
Si-SiO_2-Mg-Cu powder compact, nitridation to form Si_2ON_2 whiskers *(Japanese)* 80−93674
Si-SiO_2-Mo-Si_3N_4-Al MNOS structures with metal grains, charge transport at SiO_2-Si_3N_4 interface 80−65693
Si-SiO_2-Si capacitor, polycryst., capacitance voltage characterisation 80−70794
Si-SiO_2-Si structures, P, As depth profiles, ion microanal. *(Japanese)* 78−85251
Si-SiO_2-Si thin film MOS structures, elec. props. with applied DC voltage *(Slovak)* 80−92977
Si-SiO_2-Si_3N_4, internal photoemission 80−7475
Si-SiO_2-Si_3N_4, surface states, density and spectrum 77−69423
Si-SiO_2-Si_3N_4 MNOS structure, chem. comp. and electronic states, Auger and energy loss spectra obs. 80−92999
Si-SiO_2-Si_3N_4 system, internal photoelec. emission and residual photoelec. effects 79−73599
Si-SiO_2-$Si_xO_yN_z$ waveguide model *(Russian)* 79−10374
Si-SiO_2-Sl MOS structures, charge motion, TSC meas. 80−100534
Si-SiO_2-SnO_2 structure, switching props. 78−76138
n-Si-SiO_2-SnO_x SIS solar cell, transport props., 14% efficiency realisation 80−94079
n-Si-SiO_2-ZnO-Al, SAW convolver in monolithic MIS struct. 77−23791
Si-SiO_2-metal structures, tunnelling probabilities for electrons and holes in ultrathin SiO_2 79−99631
Si-SiO_2-polySi thin film structures, dielectric props. *(Slovak)* 80−75934
Si-SiO_2-vacuum system, principal angle and azimuth determ. 78−11009
Si-SiO_2(Si_3N_4), interface layer determ. by spectroscopic ellipsometry 79−95275
Si-SiO_3 interface, effect of Au recomb. centres on interfacial trapping states 79−38175
Si-SiO_x interfaces, carrier transport processes, electron states, conference, Durham, England (July 1979) 80−90612
Si-SiO_x interface, evidence for superlattices, magnetocond. expts. 77−89868
Si-SiO_x interface, localisation in inversion layer due to states in gap of oxide 77−12012
Si-SiO_x-Al photodiode experimental verification of theoretical predictions 80−29485
Si-SiO_x-SiO_2 interface, energy gap variation 79−91148
Si-silicide-Al systems with $CoSi_2$, $Pt_xNi_{1-x}Si$, and $MoSi_2$ as silicide, diffusion, compound form., and microstructure 80−34253
n-Si-silicide-Al systems with $CoSi_2$, $MoSi_2$, and $Pt_xNi_{1-x}Si$ as silicide, Schottky-barrier height 80−34520
Si-Sn heterojunction, RHEED, Mossbauer spectroscopy and I-V charact. 80−70828
Si-SnO_2, p-n heterojunction, prep., elec. and optical props., expt. *(Korean)* 77−4427
Si-SnO_2 heterojunction, barrier height meas. by HF capacitance method 77−69406
Si-SnO_2 heterojunctions, complementary Schottky barriers 79−78166
Si-SnO_2 heterojunctions, elec. and photovoltaic props. 80−26141
Si-SnO_2 highly photosensitive diodes, and their appl. 78−23152
Si-SnO_2 n-n photodiode, 5.4 MeV electron irrad. effects 77−80806
Si-Te, laser and thermal annealing, Mossbauer resonance lines 79−99810
Si-thermal SiO_2-electrolyte system, cond. in superhigh elec. field 78−52080
Si-TiO_2-Al, current-voltage charact., oxide film effects 80−70841
Si-TiO_x-Ni, MIS amorphous solar cell, increase in open-circuit voltage and short-circuit current on addition of TiO_x layer 79−57425
Si-transition metal interface, silicide formation, book contrib. 79−1530
Si-transition metal metastable films as temp. independent resistors 78−68097
Si-transition metal silicide interface, chemical state, AES expts. 78−91767
Si-undoped poly Si interface, in oxidation process, defects generation 80−40571
Si-V_2O_5 p-n heterostructure, photocond. *(Russian)* 79−42622
n-Si-V_2O_5 system, carrier transport mechanisms 77−62999
Si-V_2O_5-Al, current-voltage charact., oxide film effects 80−70841
Si-ZnO interface, XPS and Auger LMM anal. 79−90893
Si-ZnS n-n heterojunction, epitaxial, elec. props. *(Russian)* 78−88023
Si-ZnSe, IR segmented composite window design 80−106621
Si-ZnSe n-n heterojunction photovoltaic effect, freq. meter in visible wavelength *(Korean)* 79−60915
Si+$2XeF_2$→SiF_4+2Xe, surface reaction, IR chemiluminesc. 79−83504
Si+Co(Fe) recoil, transient mag. field 78−29838
Si+F_2, chemilum., at. absorption, and laser-induced fluoresc. obs. 80−3315
Si+F_2, fast flow reactor, second order rate coeff. determ. 78−80723
Si+F^-, inner-shell ionisation, X-ray cross sections 80−58369
Si+F^{q+}, q=3-9, Si K-shell ionis., electron transfer cross sections, solid targets 79−10192
Si+Ga^+ ion implantation at high current density, lattice disorder, proton backscattering 80−34085
Si+$H_2(O_2)$(He)($SiCl_4$), $3p^2(^1D_2)$ state behaviour, at. absorpt. spectra 78−29846
Si+H^+, K-shell ionisation cross sections for 15-65 keV protons 78−90284
Si+H^+(^{3}He) ion collisions, K-shell ionisation cross sections 77−23555
Si+$HF_{(g)}$, reaction kinetics 77−86288
Si+He$^+$, X-ray spectra, two-electron one-photon transition in solid target, 2 MeV 78−94209
Si+He(C)(O)(Ne), K-shell ionising collisions, average L-shell ionisation probability, K_α spectra 79−72408
Si+La_2O_3, reduction in solar furnace *(French)* 80−16784
Si+N_2O, flame chemiluminesc., SiO emission, $A^1\Pi$, $b^3\Pi$ and $a^3\Sigma$ states 77−77767
Si+NH_3, surface nitride form., XPS excited by Zr Mζ radiation 80−40236
Si+O_2(NO)(N_2O), reaction rate consts. at 350K 78−53186
silicon continued
Si+OCS, SiS multiple collision chemiluminesc., intercombination systems and SiS* collisional quenching 80−45505
Si+SF_6, IR laser induced surface reaction, mol. vibr. and mol. dissoc. obs. 80−93798
Si+Ti, self-propagating, high-temp. synthesis wave, radiating power 79−100377
Si+XeF_2, surface reaction, IR chemiluminesc. 79−43633
Si+$XeF_2(F_2)(Cl_2)$ plasma etching, electron or ion bombardment, Ar^+ enhancement 79−82073
Si^++benzene, energy-rich collision complex form. 77−9068
Si^{12+}+He, K X-rays for population in $^3S_1$ metastable state, Si^{12+} from C, Au foils 78−17776
Si^{14+}+H, charge transfer, total and partial cross-sections calcs. 80−23542
Si^{2+}+H, charge transfer reactions in interstellar medium 77−9789
Si^{n+}+Ar, n=10,11,12 79−31674
Si^{n+}+S(Ar)(Al)(Cu), K-shell vacancy sharing ratio, foil or gas target 78−42198
Si^{q+}+Ar, electron capture to continuum states, forward ejected electron spectra 79−45831
Si^{q+}+He, q=2-11, K-shell fluoresc. yields, charge-state depend. 78−55231
Si_2, charge density and pseudo charge density, pseudopot. and SCF calcs. 78−70740
Si_2, density functional theory, energy calcs., core effects 78−72106
Si_2, electronic struct. and bonding, atomic effective pot. appl. 80−95745
Si_2, multiplet struct. and charge distrib. 79−26881
Si_2, pseudopotential charge densities calcs. 79−31367
Si_2, SCF Xα calcs. using pseudopots. and PW basis set 77−34558
Si(:Au), gamma-induced trapping levels 79−87059
β-SiC/Si abrasive resistant material, prep. and props. 80−20878
SiC-Si composite, bulk resist. of technical SiC powders 79−28350
p^+-$Si_{1-x}Ge_x$-nSi junction diodes, lattice misfit effects on I-V charact. 80−70804
Si_xGe_{1-x}-Si heterodiode, interfacial structural defects effect on avalanche breakdown 79−42644
SiH_1-like centres, in cryst. Si, vacancies and chem. trapping obs. 79−99916
$Si_{1-x}H_x$, amorphous, atomic struct., X-ray study 80−49106
$Si_{1-x}H_x$, amorphous, gap states, DLTS 80−49656
a-$Si_{1-x}H_x$, oxygenated thin film, sputtered, elec. cond. and optical props. 79−15239
SiIX, solar emission lines, density dependence 80−21963
Si(Li), 2D position sensitive detector with 100 μm resolution 79−45544
Si(Li) detector, cooling system with liq. N_2 *(Rumanian)* 79−85867
Si(Li) detectors, escape peak losses 80−27383
Si(Li) electron spectrometer with superconducting transporting magnets 80−27376
Si(Li) X-ray detector, Au contact layer thickness meas. 80−62627
SiN powder formation, in high-temp. N flow *(Russian)* 80−100818
Si_3N_4:Si amorphous film, optical and electrical props. 77−76987
SiO, role of O in phonon conductivity 79−42326
SiO_2, electronic energy, structure calc. using tight binding approximation 77−69215
SiO_2, reduction by RF induction plasma torch., Si form. 78−11186
SiO_2-Si, cathodoluminesc. and AES rel. to struct. 78−43937
SiO_2-Si, film-substrate, single reflection retarders for different Hg spectral lines 78−79122
SiO_2-Si, low-energy neutral particle bombardment of SiO_2 film, degradation 80−54790
SiO_2-Si (n-type) interface, electrochem. etching 77−11799
SiO_2-Si boundaries, insulator charges evaluation *(German)* 79−82682
SiO_2-Si in MIS, interface states, thermally stimulated charge decay 77−12009
SiO_2-Si interface, interaction of point defects, electron microscope exam. 77−7979
SiO_2-Si interfaces, surface state form. during bias-temp. stress aging 79−78193
SiO_2-Si structure P^+ bombardment damage, exoelectron emission obs. 78−95383
SiO_2-Si:A, effects of recoil-implanted O on elec. activation of As 79−99227
SiO_2-Si:P, P pile-up at interface 78−84303
SiO_3-Si, B ion implanted MOS struct., form. and annealing of radiation damage 79−56321
SiSb impurity profile eval. in p-n diffusion junction by anodisation and resist. meas. 79−46695
Si(Si^+), static quadrupole polarisability and shielding factor, Hartree-Fock calc. 78−41950
Si(Si^+)(Si^{2+})(Si^{3+}), excited levels, radiative lifetimes, beam foil spectra 80−58368
^{28}Si, $3d_{5/2}$-$2p_{3/2}$ muonic X-ray transition, energy, wavelength meas. 78−66695
$^{28}Si^{n+}$+Sc(Ti)(Cu)(Ge), K-shell ionisation, projectile charge state depend., theory 78−17786
^{28}Si+^{60}Nd(^{67}Ho)(^{79}Au), target Lα X-ray prod., projectile charge state depend. 79−47549
^{28}Si+H(H_2), single electron capture cross sections 78−58812
^{29}Si, NMR signal intensity enhancement by polarisation transfer 79−94013
^{29}Si, nucl. mag. screening in SiH_4, pseudopot. calcs. 79−6879
^{30}Si(n,β)^{31}P transmutation doping 78−6107
^{30}Si(n,β)^{31}P transmutation doping and electrical characterisation 78−10071
Si*+He(H_2)(N_2)(O_2)(Cl_2)(CO)(NO)(C_2H_2)(C_2H_4), collisional quenching, reson. line absorpt. expt. 78−46297
Si(100)-SiO_2 interface, mobility in Si inversion layers, screening and neutral impurity effects 79−28412
Si(111), conduction-band surface resonance 78−52051
Si(111):Pb ion implanted amorphous layers, recrystallisation, impurity out-diffusion model *(Chinese)* 80−88363
Si(111)/Pt/Ni Schottky diodes, current-voltage charact. and comp. profiles 80−84508
Si(111)-$\sqrt{3}\times\sqrt{3}$-Ag structure, atomic arrangement, low energy ion scatt. spectroscopy 80−96724
Si($3p^2(^1S_0)$)+He($SiCl_4$)(O_2)(N_2O), attenuation of reson. radiation, time-resolved kinetic obs. 78−5329
Si:O, effect of displacement upon impurity levels, pseudopotential calc. 77−39803

silicon continued
Si(111)/Al/Si, growth kinetics of (111) Si through Al layer by solid phase epitaxy 79−28236
Sn:O, matrix O_2 precipitation and stacking fault formation 77−76427
SnO_2/n-Si solar cells subjected to different weathering conditions, stability 79−52936
SnO_2/n-Si spray-deposited solar cells 80−12007
SnO_2/n^+-pSi heterojunction solar cells, fabrication by paint-on-diffusant method 80−94048
SnO_2-polySi solar cells, fabrication, grain size effects on device parameters 80−94045
SnO_2-Si, heterojunction solar cells, anomalous photocurrent 80−3515
SnO_2-Si, solar cell, max. theoretical efficiency 79−83598
SnO_2-Si heterojunction, elec. and photoelec. props. 77−1477
SnO_2-Si heterojunction solar cell, elec. props. *(Korean)* 80−45665
SnO_2-Si solar cells, electron-beam-deposited, fabrication, angle-of-incidence effects 79−52931
SnO_2-Si solar cells, electron-beam deposited, struct., photovolt. props. 80−50956
$SrTiO_3$-Si junction, photoresponse 78−72254
Su-SiO_2 interface states, exptl. study of charge model 79−65554
surface (111), high temp. RHEED Obs. using metal-backed fluoresc. screen 80−75126
Ti-Si film thin film interaction, metallisation, X-ray diffr. and sheet resist. 80−54442
TiO_2-Si, MIS capacitor, C-V characts. meas. 78−60208
V_2O_5-Si, sandwich system, photocond. in range 380-1000 nm 77−32034
V_3Si film, superconducting props. 79−38215
W siliciding, in vacuum, diffusion saturation, effect of NaCl, kinetics 79−15859
W:K-Al-Si, state of bonding, distribution of impurities 78−92212
YIG: Si single crysts., mag. props. 80−107981
YIG:Si, EM wave effects on mag. and optical props., lecture 78−27031
YIG:Si, effects of nontrigonal cryst. field on spectroscopic props. of Fe^{2+} ions 80−92864
YIG:Si, enhanced photoinduced mag. circular and linear dichroism 77−52053
YIG:Si, Fe^{2+} spectroscopic props., nontrigonal cryst. field effects 80−44553
YIG:Si, photo-induced low freq. mag. permeab. *(Russian)* 78−39368
YIG:Si, relative Fe^{2+} ion conc. depend. 77−48150
YIG:Si, thermomagnetic processing and illum. effects on mag. props. *(Russian)* 77−8410
YIG:Si^{4+}, mag. permeability, illumination and impurity depend. *(Russian)* 78−64220
YIG:Si^{4+}, X-ray induced change in initial permeability 78−19280
ZnO/Si acoustoelectric devices, magnetron discharge sputtering prep. 80−80332
ZnO/Si SAW structs., anal. of charge injection 80−80049
ZnO-Si p-n diode monolithic storage correlator 78−18119
ZnO-SiO_2-Si monolithic convolver, long time storage of surface-acoustic-wave signals 77−1287
ZnO-SiO_2-Si SAW device, interface transduction 80−102949

silicon alloys
see also Ge-Si alloys
A-15 superconductor, dHvA effect 78−75985
Al-Si (2.4 wt.%), liq. fluidity, solid-liq. coexisting zone *(Japanese)* 80−15175
alkaline earth-Si, M_2Si, occurrence struct. 78−38663
alumel, B versus H measurement from 25 to 180°C 78−23297
Alumel, thermocouple alloy, heat treatment effects on thermoEMF and mag. flux 77−63235
amorphous ribbon, saturation magnetostriction, and electronically controllable delay line 79−1700
binary alloys, detection of compositional homogeneities using ion-induced Auger electron spectroscopy 80−25514
coatings, for high temp. alloys, process development and props. 80−40614
Colmonoy, self-weldability in high temp Na *(Japanese)* 80−89392
Colmonoy hardfacing materials, friction characts. in high temp. Na *(Japanese)* 80−89356
dilute, irradiation softening effect on yield stress 80−76319
hardness, elec. cond., photo emission, and mag. props. *(Norwegian)* 79−32909
Hastelloy N, Si additions, comp. of eta carbide after ageing 78−52816
Hayes alloy no.716, Fe-Cr-Ni-Co-W-Mo-Si-C-B (26, 22, 12, 3.5, 3, 1.2, 1.1, 0.4 wt.%), hardfacing alloy 80−100802
irrad., surface effects on precip. morphology 80−104168
Magnico alloy, with Si, Nb, Ti and La, low-temp. thermomag. treatment 77−63812
Magnico alloy, with Si, Nb, Ti effect of Ub on mag. props. and grindability 77−63811
metal silicides, fabrication technique and characterisation *(Japanese)* 80−60779
metal-silicide coating system, thermal stresses *(Russian)* 78−13891
neutron irrad., elec. resist., temp. depend. 79−91024
Nicrosil-Nisil, thermocouple appl. for digital furnace control system 78−49831
Nimonic alloy, effect of annealing on hardness, carbide phase strengthening *(Russian)* 79−34137
NK, thermocouple alloy, heat treatment effects on thermoEMF and mag. flux 77−63235
plasticity due to superimposed macrosonic and static strains 78−60719
rare earth alloys, RM_2Si_2 (M=Rh,Pd,Ag,Ir,Pt,Au), cryst. struct. 80−1964
rare earth alloys, RPt_2Si_2, struct. determ. 77−89407
rare earth intermetallics, RMn_2Si_2, cryst. struct. 78−59782
rare earth intermetallics, $RNiSi_3$, mag. susceptibility, 80-1200K *(Russian)* 77−66281
rare earth iron silicides, $R_2Fe_4Si_9$ and $RFeSi_3$, cryst. struct. and mag. suscept., temp. depend. *(Russian)* 78−34957
rare earth silicides, RFe_2Si_2, mag. props. 4.2 to 950K 77−20544
rare earth silicides, RMn_2Si_2, magnetisation, 4.2-1200K 77−8285
rare earth-Fe(Co)-Si, $ThCu_2Si_2$ type, lattice parameters 78−51469
rare earth-transition metal alloys, $RM_2Si_{2-x}Ge_x$, magnetism and hyperfine interactions, magnetisation and Mossbauer effect studies 80−75892
SA, thermocouple alloy, heat treatment effects on thermoEMF and mag. flux 77−63235
Sendust alloy, magnetic head wear resistance and surface characts. against mag. tape *(Japanese)* 80−35335

silicon alloys continued
Silumin, AlSi10Mn, struct. and mech. props., Na modification effects 77−63786
Silumin, CsSi phase form. due to Cs diffusion 79−38798
steel, alloy, cluster formation susceptibility in 40 KhN, influence of isothermal working in H_2 *(Russian)* 78−56643
steel, alloy, Fe-Cr-Mo-Si-V, various steels, short rod stress intensity factor tests up to 700K, exam. 78−60815
steel, alloy, Fe-Ni-Mn-Si-Cr-Ni-Mo, effect of metallurgy on stress corrosion cracking, and hydrogen embrittlement 78−60885
steel, alloy, Mn-Si-C, exam. of fracture toughness for sheets, using linear elastic fracture mechanics 78−56762
steel, alloy, Si-Mn(Mn-Cr), heat treated, exam. of microfractographic aspects of fatigue cracks *(Japanese)* 78−52959
steel, alloy, softening process in deformed type 15GYuT, metallographs *(Russian)* 78−52840
steel, alloy cyclic strength after strain hardening and tempering, precip. hardened 40FT and 40 78−52988
steel, austenitic stainless, bulk and grain boundary diffusion of Fe, Cr, Ni, effect of Si content 78−38875
steel, austenitic stainless, metastable, Si effects, unlubricated adhesive wear, oxidation resistance, solid soln. hardening 77−59949
steel, B-Si, grain-oriented, high induction, Cu impurity effects 80−89366
steel, Cr-Mn-C-Si (20, 14, 0.2, 0 to 3 wt.%), high-temp. oxidation *(Russian)* 80−25904
steel, Cr-Mo, Mn and Si effect on temper embrittlement, comp. and carbide precip. effects 80−85037
steel, Cr-Ni (16,14 wt.%), Si effect on texture, grain growth after rolling or recrystallisation *(French)* 77−55986
steel, Cr-Si, oxidation resist. in high pressure CO_2, Si effect 80−66704
steel, eutectoid, partitioning of Si during pearlite growth, electron microscopy study 79−83201
steel, ferrite and dual phase, mech. props., effect of Si and P 79−57063
steel, high permeability grain-oriented, AlN precip. study 79−83337
steel, high speed S6-5-2 Si content effect on solidification *(German)* 78−11213
steel, highly-oriented, domain and grain patterns obs., using ferromagnetic colloid technique 80−11856
steel, impact and tensile props., Si effects 79−24614
steel, low C, impact and tensile props., effect of Si 77−36526
steel, low C, Si effect on gas nitriding, surface hardness *(Japanese)* 77−48582
steel, Mn-Si, St 52-3, cleavage fracture toughness, temperature and notch sharpness influence *(German)* 80−35291
steel, Mn-Si, St 52-3, fracture toughness determ. from yield strength and cleavage fracture strength *(German)* 80−35292
steel, nonoriented elec. sheet, solute oxidation effect on mag. props. 79−83335
steel, Si, commercial, ordering after heat treatment, Mossbauer meas. 80−7556
steel, Si, electron irrad. in HVEM, void swelling, Si role 80−54285
steel, Si, grain-oriented, high permeability, dissoln. and precip. of AlN and MnS 80−89223
steel, Si, metallography of bainitic transform., carbide precipitation 78−27527
steel, Si, nonoriented sheet prod. with texture of {100} ⟨ovw⟩ 80−89246
steel, Si, textured, alloying addition inhibition effects on grain orientation and growth *(Japanese)* 79−43270
steel, Si, upper bainite morphology *(Czech)* 78−64537
steel, Si, with coating, grain-oriented, domain pattern measurements *(Japanese)* 79−38353
steel, Si (6.5 wt.%) Mn, Ni and Al additions influence obs., on mech. and magnetic props. *(Slovak)* 79−5064
steel, Si and Si-Mn, non-magnetic, minimum electroresistivity, −268 to 0°C *(Russian)* 79−91021
steel, Si-Al, non-oriented elec., internal oxidation and nitridation effects on mag. props. 79−83336
steel, Si-Cr-Mo-W-V (2,4,1,3,2 wt.%), heat treatment and props. 80−16349
steel, Si-Mn, 27SG, heat treated sheets, underwater explosive forming *(Polish)* 79−34052
steel, Si-Mn, ferrite-pearlite structs., fatigue crack propagation *(Russian)* 79−34126
steel, Si-Mn-C (1.6-2.0, 0.4-0.6, 1.1-1.4 wt.%), cast graphitised, heat treatment effects on mech. props. and wear resist. 79−96050
steel, Si-Mn-Ni-Cr-Mo, acoustic emission during stress corrosion cracking appl. to materials testing 78−53042
steel, stainless, austenitic, Cr-Ni-Mn-Si-Mo-C alloy, 13Khi8N10G3S2M2, elastic moduli exam. after thermomechanical treatment *(Russian)* 79−24558
steel, stainless, deoxidation in melting with Si *(Korean)* 78−19947
steel, ultrahigh strength, Si addition and retain austenite effect on SCC, quenched and tempered 78−48567
Stellite, self-weldability in high temp Na *(Japanese)* 80−89392
stellite hardfacing materials, friction characts. in high temp. Na *(Japanese)* 80−89356
supercooled, struct. refinement mech. *(Russian)* 80−20975
ternary silicides, (Cr, Nb or Ta)$_{11}$Si$_8$, (Mn,Mo)$_{11}$Si$_8$, cryst. struct. *(French)* 78−38675
thermally degenerated Schottky diodes, resonant tunnelling 80−100503
Ticonal with Sm, magnetic props., phase transform. after thermomagnetic treatment 78−3155
transition metal disilicides, chem. linkage, enthalpy, above 1200K 77−90324
transition metal silicide, interface with Si, chemical state, AES expts. 78−91767
transition metal silicide, Schottky barrier to Si, effect of glassy membrane 77−85311
transition metal silicides, NMR and μSR, microscopic mag. props. *(Japanese)* 78−52368
transition metal silicides, V(Nb)(Ta)(Cr)(Mo)(W)-Si-Cu, struct. and supercond., Cu influence 80−50592
transition metal-Si, coupled phase diagram and thermochemical data 79−95997
transition metal-Si systems, Si stabilised C14 Laves phases 78−84777
transition metal-Si-B ternary and quaternary amorphous alloys, effect of comp. on crystn. *(Japanese)* 79−94910
78 a/o Si-22 a/o Ge alloy, time and temp. behaviour 77−22543
Ag-Si eutectic alloy, X-ray spectral exam. *(Russian)* 77−63489
Al bronze, G, Si additions, corrosion resistance 77−16714

silicon alloys continued
Al/NiSi/Si system, high temp. interaction study, elec. and struct. charcts. 79−24075
Al-Ag-Si alloys, phase equilibria at 500°C *(Russian)* 78−56612
Al-Cu-Mg-Mn-Fe-Si, alloy D16, effect of mechanisothermal treatment on mech. props. 78−56674
Al-Cu-Mg-Mn-Si-Fe, endurance with cyclic bending, effect of loading conditions 80−50724
Al-Cu-Mg-Mn-Si-Fe, subcritical crack growth under static plane stress 80−55528
Al-Cu-Mg-Mn-Si-Fe, torsional vibrations decrement, deformed vol. effect 80−76326
Al-Cu-Mg-Si, inclusions, oriented distrib. metallography and effects on anisotropy *(Russian)* 78−80589
Al-Cu-Mg-Si-Fe-Mn-Ti, Si, Fe, Mn and Ti effect on precipitation in solid soln. *(Korean)* 79−66064
Al-Cu-Mg-Si-Mn (2.5, 0.7, 0.7, 0.5 wt.%), alloy AK6, US inspection of heat treatment quality 78−76681
Al-Cu-Mg-Si-Mn alloy AK8, fatigue strength, effect of residual stresses and cold working 77−56101
Al-Cu-Mn-Mg-Fe-Si, corrosive environment effect on fatigue crack growth rate 80−55584
Al-Cu-Mn-Mg-Fe-Si (4.48, 0.66, 1.55, 0.43, o.23 wt.%), alloy D16, relationship between intercrystallite corrosion depth, and elec. cond. 79−20220
Al-Cu-Mn-Mg-Fe-Si-Zn alloy D16, surface layers chem. composition rel. to fatigue resist., corrosion-fatigue resist. 79−29275
Al-Cu-Mn-Zr-Fe-Si (6,0.3,0.18,0.3,0.1 wt.%) experimental evidence of Mn enrichment in Al_2Cu precipitates by EDS in TEM 78−15415
Al-Cu-Si, Al rich, unidirectionally solidified, microstruct. 79−34021
Al-Cu-Si, effect of sample conditions on sputtering and intensities, emission spectrochem. anal. using glow discharge *(Japanese)* 80−21349
Al-Cu-Si-Mg, deform. simulation using torsional test, elastoplastic constitutive eqn. 80−93594
Al-Cu-Si-Mg (4, 0.8, 0.8 wt.%), GPB zone formation during room temp. ageing 77−44263
Al-Cu-Si-Mn, type 2017S-T4, crack initiation at root of circumferential notch of round bar specimens *(Japanese)* 80−60947
Al-Fe-Si, eutectic alloy growth, by twinning plane propagation *(French)* 78−60667
Al-Fe-Si, Fe phase form., solidification condition effects *(French)* 77−70030
Al-Fe-Si commercial alloy, elevated temp. low cycle fatigue behaviour under rotating bending 79−47766
Al-Fe-Si(0.5, 0.2 wt.%), cast, phase determ. 77−70032
Al-Fe-X-Si (X=transition metal), struct. and comp. by electron microscopy 80−88093
Al-Mg, Si alloy, void form. under different precip. conditions, after Al ion irrad. 80−59529
Al-Mg_2Si, ageing sequence study by electron microdiffr. 80−81068
Al-Mg_2Si, STEM microdiffr. obs. of precip. struct. 80−104167
Al-Mg_2Si (0.95 wt.%), excess Si effect on ductility 78−27580
Al-Mg_2Si (1 wt.%), precipitation reactions 80−11652
Al-Mg_2Si (1 wt.%) secondary recrystallisation by grain boundary unsewing 79−1886
Al-Mg_2Si(1.42 wt.%), aged, dislocation structs. caused by plastic deformation 80−25786
Al-Mg-Cu-Si-Cr (1,2.7,0.6,0.2wt.%), laser shock hardening of weld zones 78−39800
Al-Mg-Fe-Mg-Si-Cr, alloys, dendritic segregation with Fe, Mg, Si and Cr additions *(Polish)* 79−56980
Al-Mg-Li-Si system, phase diag. *(Russian)* 78−80515
Al-Mg-Si, brittleness and heat treatment, statistical design of expts. 77−73349
Al-Mg-Si, cast, precip.-rich zones on grain boundaries, soln. heat treatment conditions effect on mech. props. 80−104176
Al-Mg-Si, DTA exam. after small and medium deform. 80−21002
Al-Mg-Si, deformed, orientation of recrystallisation nuclei 79−91681
Al-Mg-Si, dendritic non-homogeneity 78−56641
Al-Mg-Si, dil. alloy, Mn additions and heat treatment effect on $\beta \rightarrow \alpha$ transformation 80−7566
Al-Mg-Si, dispersoid effect on fatigue crack propag. 79−43420
Al-Mg-Si, effect of quenching on recrystn. after hot working 79−43289
Al-Mg-Si, electron probe microanalysis, depleted zone formation in air and vacuum 79−57013
Al-Mg-Si, Guinier-Preston zones, inception and effect on ageing, review *(Hungarian)* 79−11627
Al-Mg-Si, heavily rolled, electron microscope obs. of cube oriented region, rolling texture 79−29093
Al-Mg-Si, heterogeneous precipitation studies using differential scanning calorimetry 80−3062
Al-Mg-Si, Mg loss, mass spectrometry/thermogravimetry 77−16620
Al-Mg-Si, nucleation and precipitation growth on dislocations, electron microscope studies 80−3064
Al-Mg-Si, Portevin-Le Chatelier effect, effect of precipitation hardening 77−32585
Al-Mg-Si, precipitation of cube-shaped phases, electron diffr. study using TEM *(Japanese)* 79−43251
Al-Mg-Si, thermomechanically treated, age-hardening 78−11236
Al-Mg-Si, type 6010, microstruct. charcts. influence on formability, heat treatment 80−81090
Al-Mg-Si, type 6061-T6, 6063-T6, effective stress range factor in fatigue 80−100924
Al-Mg-Si, under ion irradiated, modification of precipitate interface and effect of precipitates stability 79−77651
Al-Mg-Si (0.52, 0.58 wt.%), ductile fracture intergranular mechanism 79−15784
Al-Mg-Si (0.7, 0.4 at.%), effect of precipitation hardening on strain rate behaviour and yield behaviour 79−29075
Al-Mg-Si alloy, descriptive method for alloy creep tests by nonstationary loadings 78−23759
Al-Mg-Si alloy, Mg_2Si dispersion hardened US waveguides, concentrators *(Polish)* 80−89237
Al-Mg-Si alloy, Mn additions, effect on deform. 77−8876
Al-Mg-Si alloys, DTA exam. of zone form. and other solid phase conversions 77−86057
Al-Mg-Si alloys, DTA meas. of struct. changes in zones after quenching and isothermal heat treatment 79−52248
Al-Mg-Si alloys, ductile intergranular fracture mechanisms, void formation and nucleation 80−108578

silicon alloys continued
Al-Mg-Si alloys, effects of dispersoids upon micromechanism of crack propagation 79−83286
Al-Mg-Si core, deformation behaviour contrib. in rod drawing *(German)* 80−11684
Al-Mg-Si liquid alloy, exam. of thermodynamic props at 780-820°C *(Czech)* 79−91626
Al-Mg-Si rod, extruded and cold drawn, annealing *(German)* 78−39804
Al-Mg-Si-Cu, cold plastic deformation, stress/strain relations 79−56991
Al-Mg-Si-Cu, tube drawing, tensile forces, plastic deformation *(French)* 79−70130
Al-Mg-Si-Mn, Mn addition effects on fracture 78−60791
Al-Mg-Si-Mn foil, planar defect spacing meas. by TEM 78−2135
Al-Mg(Cu)(Si), (5.0(4.5)(11.8) wt.%), ingots, vibr. effect during solidification on porosity formation 80−108426
Al-Mn-Si, recrystallisation and precipitation 78−52824
Al-Ni-Si, directionally solidified eutectic, morphological and mech. props. *(Russian)* 80−30057
Al-Ni-Si, eutectic, unidirectional solidification 77−16565
Al-Ni-Si sintered SAS-1 alloy, struct. *(Russian)* 79−52135
Al-Ni(Cd)(Fe)(Si), cold worked, struct. and props. 80−71666
Al-Pd_2Si contacts on Si, elec. and structural characterisation 77−43695
Al-Si, AC colour anodisation 79−20283
Al-Si, acoustic emission signals in plastic deform., amplitude distrib. *(Japanese)* 78−6978
Al-Si, and Al-Si-Na eutectic melts, struct. determ. *(Russian)* 77−80408
Al-Si, DC magnetron-sputtered, residual gas influence on props. 80−80968
Al-Si, deformed, local lattice rotations at second phase particles 80−25709
Al-Si, dil., Dingle temp. calc. 78−39005
Al-Si, dil., mechanism of dissolution of Si 79−19375
Al-Si, dilute, anomalous primary creep behaviour, precipitate form. 80−7646
Al-Si, effect of irrad. on the nucleation of incoherent precipitates 79−8303
Al-Si, enhanced interdiffusion during Ar ion bombardment 79−99353
Al-Si, eutectic, quasiisotropic, rheological deformation theory 80−79165
Al-Si, eutectic colonies morphology by stereometric microanal. *(Russian)* 77−81247
Al-Si, graphite dispersed, wear charcts. *(Korean)* 80−93658
Al-Si, hypereutectic Ostwald ripening of Si crystals during solidification *(Japanese)* 79−4962
Al-Si, hypereutectic silumins, P and Na modification 78−84792
Al-Si, inoculated with NaCl+KCl+NaF, effect on morphology of eutectic columns *(Russian)* 79−15684
Al-Si, internal friction and Si precipitate nucleation 78−60690
Al-Si, liq., dissoln. and diffusion of alloying components, 700-1000°C *(Russian)* 80−15275
Al-Si, liq. alloy, chem. diff. coeff. determ. 77−1249
Al-Si, liquid, thermodynamic props. 79−91619
Al-Si, liquid alloy, compressibility and struct. factors at zero wavevector 79−23515
Al-Si, magnetic susceptibility and elect. resistivity, 500 to 1000°C, struct. sensitive props. *(Russian)* 78−15550
Al-Si, molten, Na determ. using β-Al_2O_3 probe 77−48714
Al-Si, neutron small angle scatt. study 79−43255
Al-Si, off-eutectic alloy growth from stirred melt 77−8809
Al-Si, optical emission spectrographic analysis of some binary alloys by a glow discharge of Grimm lamp *(Japanese)* 79−99015
Al-Si, penetrability coeffs. for two-phase zone of solidifying castings *(Russian)* 77−55956
Al-Si, preferred sputtering on surface, mass difference and chemical bonding difference effects, AES obs. 79−83078
Al-Si, rapid quenching, struct. and decomp. 80−76244
Al-Si, recrystallization texture 79−91679
Al-Si, thermal control of interphase microstresses and mech. props. 77−12654
Al-Si, three dimensional dry cutting, with sintered diamond tool *(Japanese)* 80−25917
Al-Si, unidirectionally solidified eutectic alloy grow at different rates, Vickers hardness 77−36654
Al-Si (0.57 at.%), Si precipitate dissolution kinetics 80−84935
Al-Si (0.6, 0.9, 1.19 wt.%), interdiffusion coeffs. determ. by Matano's method 79−42295
Al-Si (1 wt.%) hardness-flow stress rel. during strain-controlled bending fatigue 79−74245
Al-Si (16 wt.%) melt, fivefold twinned Si cryst. growth, crytallographic study 80−2942
Al-Si (1.2 and 0.6 wt.%), single crystal, dispersion hardened with SiC, Bauschinger effect and work hardening 79−43360
Al-Si (1.2 wt.%), dispersion hardened, temp. depend. of work-hardening due to Orowan loops 79−91668
Al-Si (1.2 wt.%), dispersion hardened, work hardening due to Orowan loops, temp. depend. *(Japanese)* 80−66534
Al-Si (25.4 wt.%), solidification, high press. effects 80−66499
Al-Si (2.4 wt.%), liq. fluidity in solid-liq. zone 80−108429
Al-Si (35 wt.%), Cr, Co, Si addition effects on strength of powder 77−24983
Al-Si (8 wt.%), threshold H_2 for pore form. during solidification 78−52794
Al-Si (9 wt.%), precipitation hardening during isothermal ageing 80−29969
Al-Si alloy, as-cast binary, wear characteristics against steel 79−96156
Al-Si alloy, compression, effect of press. on lattice defects up to 90 kbar *(Japanese)* 77−72654
Al-Si alloy, dilute, electron irradiation, interstitial dislocation loop obs. 78−18681
Al-Si alloy, hot shortness, rheological model *(Russian)* 77−56072
Al-Si alloy, rod, tensile loaded, internal friction and Young's modulus measuring equipment, inelastic phenomena exam. *(Hungarian)* 79−52546
Al-Si alloy 6061, extraction and phase anal. 79−15673
Al-Si alloys, modification by Na-containing agents, ^{24}Na radioisotope investigation *(Russian)* 77−40567
Al-Si alloys, neutron irrad., precip. processes, neutron small-angle scatt. obs. 77−4131
Al-Si alloys, phosphorus content determ. by neutron activation anal. *(Russian)* 77−40614
Al-Si alloys, surface tension *(Czech)* 79−77865

silicon alloys continued
Al-Si cast alloy, flank wear of carbide tool during machining *(Japanese)* 78−19900
Al-Si casting alloys, graphite-dispersed, mech. props. and wear resist. 77−4857
Al-Si coatings, form. and behaviour under particle bombard. 80−35029
Al-Si crystals, work hardened, softening and creep rates on annealing 80−11663
Al-Si eutectic, depend. between min. creep rate and time of beginning of secondary creep *(Czech)* 80−35267
Al-Si eutectic, directionally solidified, tensile props. 78−64531
Al-Si eutectic, high temp. creep, two regimes of flow, modified Dorn eqn. anal. 79−74215
Al-Si eutectic, irregular, branching limited growth 80−81042
Al-Si eutectic, Na, Sb and Sr alloying addition effects on microstructure *(French)* 78−64548
Al-Si eutectic, pressure effect on metal-die heat transfer coeffs. during solidification 80−7544
Al-Si eutectic alloy, banded struct., SEM and optical microscopy 80−104144
Al-Si eutectic alloy, hardness rel. to tensile and compressive strength 79−52354
Al-Si eutectic alloys, superplasticity 80−11710
Al-Si eutectic alloys in screened ohmic contacts for solar cells 80−94090
Al-Si eutectics and hypoeutectics, mech. props. and thermal cond., P impurity effect 79−83271
Al-Si film, ion-implanted, percolation and superconductivity 78−26982
Al-Si film, magnetron sputtered deposition, charcts. 79−91587
Al-Si film, preferred sputtering on surface, mass and bonding difference effects, AES obs. 79−87552
Al-Si foil, alloying effect on strength charcts. and weldability 80−55475
Al-Si hypereutectic alloy, dissolution and primary crystallization of Si *(French)* 77−59832
Al-Si hypereutectic alloy, wear resistance 77−77593
Al-Si ion-implanted, enhancement of supercond. transition temp. 77−32103
Al-Si melt, microheterogeneity *(Russian)* 80−103238
Al-Si melts, hypoeutectic, eutectic, hypereutectic structural factors, atomic radial distrib. functions *(Russian)* 79−73091
Al-Si melts, spreading behaviour on Fe 80−84345
Al-Si melts, struct. factors, at. distrib. curves, thermodynamic and neutron diffr. study *(German)* 80−19687
Al-Si-Cn-Mg, alloy AL32, ageing of castings produced by pressure die castings 78−56650
Al-Si-Cu, fracture resistance at low temps. 80−104284
Al-Si-Cu, granules, energy conditions of rolling 77−12578
Al-Si-Cu, LM30, crack propag. rates in air and salt soln. 80−21063
Al-Si-Cu casting alloy, optimum selection of chem. contents for optimum strength *(Czech)* 79−15625
Al-Si-Cu-Be alloys, phase equilib. *(Russian)* 77−59748
Al-Si-Cu-Mg-Ni, piston, depend. between min. creep rate and time of beginning of secondary creep *(Czech)* 80−35267
Al-Si-Cu-Mg-Ni cast alloy, fractography *(German, English)* 79−87809
Al-Si-Cu-Ni alloy casting, thermal props. 78−95814
Al-Si-Cu-Zr, ageing kinetics *(Russian)* 80−76274
Al-Si-Li system, Al-rich, phase comp., limits of solid solubility *(Russian)* 77−21097
Al-Si-Mg, corrosion inhibition in 0.1 N NaOH soln. 78−19924
Al-Si-Mg, Si content and Mg addition effect on mech. props., Na treatment *(Korean)* 79−38901
Al-Si-P (19, 0.02 wt.%), primary Si crystals in Al melt, Ostwald ripening and solidification growth 80−35179
Al-Si-Sr phase diagram *(Russian)* 78−15363
Al-Si-Y alloy, phase equilibria in Al rich region *(Russian)* 80−93537
Al-Si-Zn alloy, creep rates, pre-torsional deformation effect 79−96096
Al-Si(-Mg), dimensional changes in heat treatment. 80−89271
Al-Si(0.1 at.%), μ^+ depolarisation 79−56697
Al-Si(7 wt.%), anodically oxidised, sunlight absorber, struct. and thermal efficiency 77−125
Al-Si(9.3, 12) with graphite particles seizure resistance study using Hohman wear tests 80−89360
Al-Ti-Si, nucleation entropy and grain refinement 79−91627
Al-Ti-Si phase diagram, calc., interpretation of grain refinement results 78−84781
Al-TiB_2-Si, Si effect on grain refinement *(German)* 79−91656
Al-Zn, Si effect on transport props., GP zones 77−16588
Al-Zn-Fe-Si, Fe and Si effects on precip., TEM and X-ray diffr. obs., ageing at 90°C 77−48439
Al-Zn-Si, thermodynamic props., meas. by EMF method *(Czech)* 77−59753
(Al-Mg-Si)-Al_2O_3, SAP type, ageing 79−96055
(Al-Si)/Si system, Si regrowth minimisation through overlying Al or Al alloy film 80−70569
α-AlFeSi, crystal struct., anomalous dispersion methods 78−9998
AlMgSi, adhesive jointing, acoustic anal. *(German)* 78−7168
Au-Ge-Si, influence of struct. on elec. resist. of glass forming alloys 80−65518
Au-Si, amorphous sputtered film, elec. props. 78−68006
Au-Si, liq. alloy, thermodynamic activity meas. by Knudsen-cell mass spectrometry *(French)* 80−10684
Au-Si, melt, thermodynamic study of phase diagram *(French)* 78−27482
Au-Si eutectic melt, wetting of quartz 77−31840
Au-Si film, elec. resist. decay and struct. change on exposure to air 77−72924
Au-Si formation at thin film interface, electron diffr. study 80−80005
Au-Si interface, valence band and core levels, Si diffusion, alloy form., photoelectron spectra obs. 80−45205
Au-Si-Mn, amorphous spin glass film, mag. susceptibility 79−42775
$Au_{77}Ge_{13.5}Si_{9.4}$, heat of crystn. and viscous behaviour 80−75166
AuSi, wetting and reactions on α-Al_2O_3 77−85022
$Au_{1-x}Si$ amorphous metallic films, optical props. as function of composition 79−95865
$Au_{1-x}Si_x$, amorphous film, spectra 0.01-6.2 eV, $0.13 \leq x \leq 0.5$ 78−68574
$Au_{1-x}Si_x$, liquid, elec. resistivity as function of temp. and comp. 79−56188
Au_3Si, room temp. dissociation 78−35672
$Au_{35}Si_{65}$, amorphous vacuum-deposited and liquid-quenched films, diffusion and crystn. 80−84094
Au_8Si_{19}, optical refl., 0.5 to 6 eV, hall coeff. and elec. resist. 80−29755

silicon alloys continued
$Au_{81.4}Si_{18.6}$, glass forming alloy, Gibbs free energy change on crystallisation 80−25676
Au_xSi_{1-x} amorphous alloy, crystallisation, elec. cond. study 80−103246
Au_xSi_{1-x} amorphous films, phys. studies 80−75476
$Au_{75}Si_{19}Fe_6$, apparatus for measurement of initial paramagnetic susceptibility 79−54160
Au_4Si.m, metastable phase, substruct. unit cell *(German)* 80−88091
$Au_{1-x}Sn_x$ liq./solid alloy, resist. and percolation 80−6804
B fibre reinforced Al-Si, calc. of thermodynamic interaction potential between B fibre and matrix 80−11627
B-Si, (0 to 14.3 at.%), phase charact., regions of existence *(French)* 80−104117
B-Si, diffusion coatings on alloy steel U8, wear resistance 78−56823
B-Si alloys, B-rich, prep., anal. and cryst. growth *(French)* 80−104091
B-Si alloys prep., struct., phys., chem. props., appls., review, book contrib. 78−48388
Ba-Al-Si, exam. of phase diagram, confirmation of $BaAl_2Si_2$ and $Ba(Al,Si)_2$ *(Russian)* 79−29019
Ba-Al-Si system, phase diagrams construction by simplex designing method 78−6899
Be-Si, solubility of Cu at low temps. 77−62646
Bi-Si, dil., mag. field depend. electron scatt. rates, de Haas-van Alphen meas. 78−10436
Ca-Si, deoxidation of steel, thermodynamics *(Russian)* 80−16268
Ce-Co-Si, thermoelectromotive force and electrocond. *(Ukrainian)* 80−54670
Ce-Co-Si system, mag. props. in 77-300K range *(Russian)* 78−56290
Ce-Fe-Si, thermoelectromotive force and electrocond. *(Ukrainian)* 80−54670
Ce-Fe-Si system, mag. props. in 77-300K range *(Russian)* 78−56290
Ce-Nd-Si, phase diagram, X-ray anal. *(Ukrainian)* 79−38792
Ce-Ni-Si, thermoelectromotive force and electrocond. *(Ukrainian)* 80−54670
Ce-Ni-Si system, mag. props. in 77-300K range *(Russian)* 78−56290
$CeAg_2Si_2$, ^{29}Si NMR and mag. susceptibility 79−61246
$CeAu_2Si_2$, ^{29}Si NMR and mag. susceptibility 79−61246
$CeCoSi_2$ film, Hall effect and magnetoresist. *(Russian)* 80−11109
$CeCu_2Si_2$, collective phenomena 80−65933
$CeCu_2Si_2$, local mag. moments, neutron scatt. study 79−61058
$CeCu_2Si_2$, resistivity, thermal conductivity and thermopower between 1.5 and 300K 78−87963
$CeCu_2Si_2$, strong Pauli paramagnetism, superconductivity obs. 80−29499
$CeCu_2Si_2$, transport anomalies 80−20148
$CeCu_2Si_2$, tunnelling anomalies due to intermediate valence phenomenon 77−62873
$CeCu_2Si_2$, valence fluctuations, ^{29}Si NMR and mag. susceptibility 79−61246
$CeMg_2Si_2$ type structure, role of elongated rhombic dodecahedron in alloy structs. 79−32946
$CeMn_2Si_2$, cryst. and mag. struct. determ. 78−52225
$CeMn_2(Si_xGe_{1-x})_2$, $Ce(Mn_{1-x}B_x)_2Si_2$, (B=Fe, Cu) mag. props. 80−25134
$CeNi_{8.5}Si_{4.5}$, X-ray cryst. struct. determ. 80−88089
$Ce_2Sc_3Si_4$, X-ray cryst. struct. determ. 80−92480
$(Co,Fe,M)_{78}Si_8B_{14}$ amorphous alloys (M=V,Nb,Ta,Cr,Mo,W,Mn or Ni), zero magnetostriction and low field mag. props. 80−34741
Co-B-Si, mag. props. different in amorphous and cryst. phases 77−69617
Co-B-Si amorphous alloy, liq. quenched, elec. resist. and cyclic deform. 80−59949
Co-B-Si ternary system, partial phase diagram, Co rich region 77−52293
Co-Cr-Mo-Ni-Fe-Si-Mn-C, protective coatings by B diffusion, microstruct. and mech. props. 78−11427
Co-Cr-Si alloy hot corrosion and oxidation expts. for ionic conducting scale 78−11446
Co-Fe-Ni-Si-B glasses, soft mag. props. 79−73774
Co-Fe-Si-B, amorphous alloys, substitution effect on mag. props. 79−69695
Co-Fe-Si-B, decomp. of amorphous state during annealing below recryst. temp., electron microscope study *(Russian)* 80−75164
Co-Fe-Si-B, ferromag., magneto-optical spectra in amorphous and cryst. states *(Russian)* 80−84749
Co-Fe-Si-B amorphous alloys, mag. props. 77−16055
Co-Mn-Ni-Fe-Si-B amorphous alloys, mag. props., low magnetostriction 80−75832
Co-Mo-Cr-Si, plasma and detonation coatings, Laves- and carbide-strengthened, comparative props. 78−15562
Co-Mo-Cr-Si Laves phase, sputter deposited, struct. and wear props. 77−40477
Co-Nb(W)(Mo)(Ti)-Si, directionally solidified eutectics 79−61575
Co-Ni-Fe-Si, amorphous ribbon, magnetostriction meas. 80−15778
Co-Si, band model of high temp. magnetism 78−26809
Co-Si, directionally solidified eutectic composite alloy, form. and strength 77−90294
Co-Si, liquid alloy, optical charact. *(Russian)* 77−24810
Co-Si, surface physicochemical state, Auger electron spectroscopy study 80−100715
Co-Si alloy, secondary ion mass spectrometry *(Dutch)* 79−1809
Co-Si film system, diffusion marker expts. 78−79824
Co-Si film system, interaction kinetics 78−79823
Co-Si-B, amorphous ribbon, saturation magnetostriction meas. by small-angle magnetisation rot. 80−60391
Co-Si-B, embrittlement by crystallisation *(Japanese)* 78−48513
Co-Si-B amorphous alloys with metalloid elements, embrittlement/crystn. relationship *(Japanese)* 79−96134
Co-Si-B-Fe alloy magnet, Al_2O_3 particle embedded surface, amorphous mag. anal. using electron diffr. 79−56568
Co-Si-Ge system, X-ray diffr. exam., band struct. *(Russian)* 78−56623
Co-Si-Nb(Zr), eutectic alloys, charact. by melting, oxidation resistance and composition 78−52768
$(Co_{1-x}Fe_x)$-B-Si, amorphous mag. props. *(Japanese)* 77−85433
$(Co_{0.93}Fe_{0.07})_{75-x}Cr_xSi_{15}B_{10}$ amorphous alloy, thermal stability, Cr conc. effects, DTA expts. 80−59395
$(Co_{0.89}Fe_{0.11})_{72}Mo_3Si_{15}B_{10}$, metallic glass, strain- and field-induced mag. anisotropy 80−108004
$Co_{57}Fe_5Ni_{10}(Si,B)_{28}$, amorphous, soft mag. props., switched-mode power supply appls. 80−88850
$(Co_{1-x}Fe_xNi_y)_{80}(Si_{1-z}B_z)_{20}$, amorphous films, spin wave spectra 80−34777

silicon alloys continued
$Co_{1-x}Fe_xSi$, solid solution, optical props. 78−72556
$Co_{70}Fe_5Si_{15}B_{10}$, amorphous, crystn. and thermal stability 80−107057
$Co_{70.4}Fe_{4.6}Si_{15}B_{10}$, amorphous, mag. aftereffect spectra and annealing props. 80−88831
$Co_{75-x}Fe_xSi_{15}B_{10}$, quenched ferromag. ribbon, Brillouin spectra 80−2776
$Co_{1-x}M_xSi$ (M=Fe, Ni), elec. field gradient, quadrupole splitting of ^{59}Co 80−29641
$Co_2Mn_xFe_{1-x}Si$, hyperfine fields of Fe impurities, Mossbauer effect meas. 78−31130
CoMnSi, $CoMnSi_{0.85}Ge_{0.15}$, mag. props. 79−42758
Co_2MnSi, ferromag. Heusler alloy, spin echo NMR meas. 77−63319
$Co_3Mn_3Si_2$, Curie-Weiss law depend. of susceptibility, mag. props. *(Russian)* 79−65655
$CoMnSi_{1-x}Ge_x$, amg. props. 80−60270
$Co_{73}Mo_2Si_{15}B_{10}$, metallic glass, strain- and field-induced mag. anisotropy 80−108004
$Co_{50}Ni_{20}Fe_6Si_{12}B_{12}$, amorphous, mag. props., effects mech. deform. 80−39840
$Co_{1-x}Ni_xSi$, IR refl. spectra in plasma refl. region 78−27233
$Co_{1-x}Ni_xSi$, solid solution optical props. 78−72556
$Co_xPd_{80-x}Si_{20}$, amorphous, low field susceptibility near transition temp. 77−66359
$Co_xPd_{80-x}Si_{20}$, amorphous, structural and mag. heterogeneities 80−80484
CoSi, and TiCoSi, electronic struct., X-ray K- and L-spectra obs. *(Russian)* 78−11022
CoSi, IR refl. spectra in plasma refl. region 78−27233
CoSi, plasma refl., 80 to 300K, energy overlap of valence and conduction bands 79−28366
CoSi solid solution, optical props. 78−72556
CoSi, X-ray emission spectra obs. of valence band states *(Ukrainian)* 77−69935
$CoSi_2$, interface struct. and growth mechanism from melt 79−14715
Co_2Si, struct. comparison with Co_2P, $PbCl_2$, and SbSI *(French)* 80−84155
$Co_{74}Si_{10}B_{16}$ amorphous toroidal core, switching charcts. and domain structs. 78−95477
$Co_{74}Si_{10}B_{16}$, amorphous ferromagnetic alloy, isothermal annealing effect on static magnetic props. *(Japanese)* 79−52398
$Co_{75}Si_{15}B_{10}$, amorphous, crystn. and thermal stability 80−107057
$Co_{75}Si_{25-x}B_x$ glass, mag. moment, Curie temp., and microhardness, metalloid comp. depend. 77−55665
Cr-Fe-Ni-Si, ternary phase equilibria for Cr-Fe-Ni rich portion, lattice stabilities 80−71628
Cr-Fe-Si, mag. excitation, neutron spectrometry 79−4654
Cr-Fe-Si, sp. ht., 1.4-4.2K 77−20079
Cr-Fe-Si, spin density wave, neutron diffraction studies 79−1664
Cr-Si, amorphous sputtered film, material for kilo-ohm sheet resistances, prep. and props 79−78227
Cr-Si, corrosion and failure mechanisms of coatings for gas turbine applications 79−29284
Cr-Si, dil., latent heat exam. of magnetic transitions 79−61156
Cr-Si, dilute alloy, mag. susceptibility and Neel temp. meas. 80−71017
Cr-Si, first order transition of spin density wave state, thermal expansivities meas. 77−85453
Cr-Si, magnetically insensitive Invar-type alloys *(Japanese)* 79−8034
Cr-Si, press. depend. of Neel temp. 77−69555
Cr-Si, thin films, deposition method, for controllable comp. with given elec. props. 80−35087
Cr-Si (1.37 at.%), thermal and elec. props. 79−78071
Cr-Si alloys, antiferromag.-ordering, neutton diffr. 77−69492
Cr-Si-Fe, mag. moment of Fe, mag. suscept. meas. 79−61079
Cr-Si-V, (2, 0.1 at.%), paramag. to commensurate spin density wave transition 80−65875
Cr-Si-V, dil., V effect on para- to incommensurate and commensurate transitions 78−68260
$CrSi_2$ film, kinetics of growth 77−43454
Cr_3Si, band theory, semiself-consistent band calcs. 78−2406
Cr_3Si, charge distrib. X-ray diffr., rel. to supercond. V_3Si 77−68944
Cr_3Si, mag. susceptibility, 2 to 300K, rel. to electron energy spectrum 80−60185
Cr_3Si type phases, A-15, crystallographic interpretation of atomic volumes 79−10833
Cu-Al-Si, Si effect on mech. props. and microstructure *(Korean)* 79−38903
Cu-Al-Si-C (95, 2.8, 1.8, 0.4 wt.%) fracture charcts. of superplastic single phase, exam. 78−48500
Cu-Al-Si-Co (2.8, 1.8, 0.4 wt.%), superplastic phase, exam. of mech. props. 78−52891
Cu-Co-Si (0.36, 0.11 wt.%), surface layer struct. on annealing, SIMS and AES exam. 80−88415
Cu-Ni-Si, cast, strength and hot ductility, Si effect 80−66595
Cu-Si, change in force constant due to volume effects 78−75778
Cu-Si, deformation and fracture under dynamic loading 78−35442
Cu-Si, dil., chemical etching and X-ray topography obs. of cellular struct. *(French)* 79−96249
Cu-Si, dil., optical props. and electronic struct. 78−35164
Cu-Si, dil., oxide film form. in ammoniacal Cu(II) solns., AES obs. 80−45415
Cu-Si, dissoc. dislocations pinning by Suzuki effect *(French)* 79−100223
Cu-Si, high dislocation density alloys and oxide precipitated struct., NMR, spin echo 80−39892
Cu-Si, impurity concentration effects 78−75777
Cu-Si, mech. of formation of martensitic struct. *(Russian)* 78−23702
Cu-Si, melt, enthalpy of formation at 1370K 80−26042
Cu-Si, phase transform, exam. *(Russian)* 77−8822
Cu-Si, preferred crystallographic orientation of melt grown single crystals *(Czech)* 79−43134
Cu-Si, preferred crystallographic orientation of unidirectionally solidified polycrystals *(Czech)* 79−43233
Cu-Si, reaction diffusion, effect of compressive stress 77−28050
Cu-Si, Si effect on stainless steel embrittlement during soldering 79−47773
α-Cu-Si, solid soln., ductility, comp. effect *(Japanese)* 79−43334
Cu-Si, stacking fault energy meas. by tensile deform. of polycrystalline samples 78−95060
α- Cu-Si, superconducting transition temp. depend. on electrons per atom ratio, lattice deform. 77−8222

silicon alloys continued
Cu-Si (0.7 to 3.3 at.%), stacking fault energies, weak beam method of electron microscopy 77−19971
Cu-Si (6.5 at.%), CC Cu-Al(Si), single crysts., latent hardening study by meas. of flow stress on secondary systems *(Japanese)* 79−24538
Cu-Si (6.5 at.%), plastic deformation, HVEM study *(French)* 80−66605
Cu-Si (6.5 at.%) alloy, easy glide deform., obs. and mechanism 77−8887
Cu-Si (7 at.%), dislocation interactions, influence of jogs on extension of dislocation nodes 80−84176
Cu-Si (8 wt.%), intrinsic struct. in grain boundaries and boundary mobility 80−103368
Cu-Si (up to 4.75 wt.%), exam. of high temp. oxidation in low O_2 and pure CO_2 atmospheres, by thermogravimetry 78−88574
Cu-Si alloy, FCC→HCP transition mechanism 77−77479
Cu-Si correl. of periodicities in diffr. patterns and images from grain boundary 78−14362
Cu-Si-, microconductors, cast, struct. and physical props. exam 78−44232
Cu-Si-S, stirred at different speeds under reduced press., evap. of Si 77−47555
Cu-Si-Zn wire, silicon bronze, magnetoresist. upper limit 77−43567
Cu-SiO_2 alloy, fracture at elevated temp. 78−39896
Cu-Ti-Si, struct. and coalesc. of oxide particles during internal oxidation *(Russian)* 79−90781
Cu-V-Si, supercond. props. 80−107945
Cu-V-Si, two-step supercond. transition 80−34539
Cu-Zn-Si, deform. close to martensitic transform. temp. 77−63714
β-Cu-Zn-Si, premartensitic instability 77−12625
$Cu_{0.9}Si_{0.1}$, chemical effect on valence electronic states, AES and SXAPS meas. 79−47558
η-Cu_3Si precipitates in Si, cryst. struct. 78−91304
DyM_2Si_2, (M=Mn, Fe, Co, Ni, Cu), Mossbauer spectra 80−20558
$EuCu_2Si_2$, fluctuating valence system, quadrupole interaction temp. depend. 80−54972
$EuCu_2Si_2$, interconfiguration fluctuation, NMR expts. 80−66069
$EuCu_2Si_2$, valence fluctuation and temp. depend. of Cu nuclear quadrupole interaction 80−15818
$EuCu_2Si_2$, XPS studies, valence band, 4-f region 78−6831
FE-Si, ordering studied by Mossbauer effect 77−63342
(Fe,Co,Ni)-Si, amorphous alloy, magnetostriction rel. to soft mag. props. 80−84633
(Fe, Ni, Co)-Si-B, amorphous, compositional effect on struct. changes, after heating up to 700°C, exam. *(Japanese)* 78−48433
Fe, cast, C and Si effect on spheroidal graphite *(Korean)* 79−38839
Fe, cast, grey Al-Si, eutectoid decomp. of austenite 80−29951
Fe, cast, Si, ferrite heterogenisation, phase separation and embrittlement, Si effects 79−96125
Fe-Al-Si, bending test, mech. props. under high press. and temp. *(Japanese)* 78−76711
Fe-Al-Si (6.22, 9.63 wt.%), bending test under high press., high temp. 80−85057
Fe-Al-Si alloy, order-disorder transform. exam. by Mossbauer spectroscopy 77−63334
Fe-As-Si, Si additions to Fe-As melts, influence on surface tension and density *(Russian)* 80−15337
Fe-As-Sn-Si, melts, As and Sn distrib., Si, Cr, and Mn influence *(Russian)* 80−16274
Fe-B-Si, amorphous alloy, anelastic relaxation 79−4997
Fe-B-Si, amorphous ferromag. alloys, mag. struct., Mossbauer study 80−39746
Fe-B-Si, glassy, field-induced mag. anisotropy near eutectic comp. 80−93110
Fe-B-Si amorphous alloy, liq. quenched, elec. resist. and cyclic deform. 80−59949
Fe-B-Si amorphous alloys, crystallisation temp., Curie temps., saturation magnetisation 79−82820
Fe-B-Si amorphous ribbon, strain induced anisotropy, and toroid diam. effect on mag. props. 80−34623
Fe-B-Si amorphous ribbons, effect of annealing conditions on magneto-mechanical props. 80−34740
Fe-B-Si-C amorphous alloys, prep. and props. 80−88748
Fe-C-Mn-Si (4, 2, 1.5 wt.%), cast wire, influence of B addition on struct. and elec. cond. *(Russian)* 80−55391
Fe-C-Si, cast, graphite nodularization during annealing, Mg and S effects *(Japanese)* 80−81087
Fe-C-Si, effects of Si on matrix struct. of spheroidal graphite cast iron *(Korean)* 78−60666
Fe-C-Si, eutectoid alloy, Si addition effects on pearlite growth rate 77−16575
Fe-C-Si, graphitisation during heat treatment *(Russian)* 80−20971
Fe-C-Si, high purity, vacuum melted, nodular graphite form. 80−108452
Fe-C-Si, S effect on graphite morphology, formed during annealing *(Japanese)* 78−15434
Fe-C-Si, spheroidization 77−66665
Fe-C-Si, splat cooled, formation of metastable crystalline phases and glasses 78−88461
Fe-C-Si, splat quenched, electron diffr. and Mossbauer study of retained ε-phase 77−52354
Fe-C-Si, struct. and constitution on quenching from liquid state *(Russian)* 77−52309
Fe-C-Si (0.62, 2.0 wt.%), interfacial struct. of broad faces of ferrite plates 79−46660
Fe-C-Si alloy, lattice parameters of cementite after quenching 78−11198
Fe-C-Si system, liq.-solid equilib. at high press., influence of graphitising elements *(Russian)* 78−56613
Fe-C-Si-Mn, cast, high C, K_1 phase formation due to peritectoid transitions *(Russian)* 79−11548
Fe-C-Si-Mn (1.5-2.9, 2.4-3.4, 0.54-31.7 wt.%), discontinuous decomp. of supersaturated austenite *(Ukrainian)* 79−38788
Fe-Ci, high permeability, mag. props., applied stress effects 80−34726
Fe-Ci (3 wt.%), commercially produced, grain-oriented, mag. props., stress coating effects 80−34727
Fe-Ci (3 wt.%), local magnetisation losses, grain orientation effect 80−88817
Fe-Co-Cr-Si, structural transform. and mag. props. following heat treatment *(Russian)* 77−81274
Fe-Co-Ni-Al, Si alloying of mag. hard alloys *(Russian)* 79−73765
Fe-Co-Ni-Si-B amorphous alloy, magnetostriction and permeability, effect of annealing 79−1701

silicon alloys continued
Fe-Co-Si, BCC solid soln. interchange energies, high temp. neutron diffr. 80−29166
Fe-Co-Si (4,1.5 wt.%), textured, mag. props. 80−35200
Fe-Co-Si solid solutions, BCC, atomic configs., Mossbauer study 80−39006
Fe-Co-Si-B, amorphous, rapidly quenched, mag. heads appl. *(Japanese)* 80−54922
Fe-Co-Si-B, amorphous soft ferromagnet with high mag. induction 80−84619
Fe-Co-Si-B, zero magnetostrictive amorphous alloy with high saturation induction, mag. annealing 80−60362
Fe-Co-Si-B sputtered amorphous thin film, coercivity, galvanomagnetic props., resistivity 80−29578
Fe-Co-Si(B), amorphous ferromagnet, mag. after effect on soft mag. props. 80−84626
Fe-Cr-Co-Si alloy, interaction domains after heat treatment in mag. fields *(Russian)* 78−68286
Fe-Cr-Co-Si-Mo, plastic deform. influence on structure and mag. props. *(Russian)* 79−70176
Fe-Cr-Mo-Si, amorphous films, corrosion resist. and ion plating use 80−89423
Fe-Cr-Ni (12, 15 wt.%) austenitic alloy, Ni^{6+} irradiated, void swelling and phase stability, Si and Ti effects 80−65055
Fe-Cr-Ni-Si, austenitic, oxidation behaviour on addition of Si 77−12740
Fe-Cr-Ni-Si, sintered, carbide coated, crack propag. energy in impact bending 79−66162
Fe-Cr-Si, heat resistive films prepared by sputtering, lifetime meas. 80−80132
Fe-Cr-Si, oxidation resist. in high pressure CO_2, Si effect 80−66704
Fe-Cr-Si film heater, lifetimes for 800 to 1000°C temp. range 78−215
Fe-Hf (Si) (Ti) (V), molten, gaseous O_2 absorption 80−11836
Fe-Mn-C-Si alloy, G20 type, vol. effects during $\gamma \rightarrow \varepsilon$ transform., lattice parameters of γ-and ε-phases, Si and Mn effects *(Russian)* 78−6918
Fe-Mn-C-Si alloy G20, effect of Si and Mn additions on phase composition in multiple $\gamma \rightleftarrows \varepsilon$ transitions *(Russian)* 78−95743
Fe-Mn-Si, mag. contribs. to $\gamma \rightarrow \varepsilon$ phase transforms 80−25694
Fe-Mn-Si, struct. and props., Si alloying effects *(Russian)* 77−90360
Fe-Mn-Si-C, cast, Mn effect on struct. during solidification 79−83191
Fe-Mn-Si-C, minimum of elec. resist. near LNT *(Russian)* 77−66707
Fe-Ni-B-Si, amorphous, mag. props., heat treatment effects 80−89370
Fe-Ni-Co-B-C-Si, amorphous, room-temp. saturation induction 78−95476
Fe-Ni-Cr-Si, superalloy, Cr and Si effect on mech. props. and microstruct. *(Chinese)* 79−100207
Fe-Ni-Cr-Si (35, 18, 2 wt.%), heating element wire, failure and oxidation 79−83378
Fe-Ni-Cr-Si alloy 800, Si effect on creep and age hardening 77−48444
Fe-Ni-Si, austenite, annealing effect on atom redistrib., Mossbauer anal. *(Russian)* 80−66529
Fe-Ni-Si, double spontaneous reversible deformation during thermal cycling 78−84942
Fe-Ni-Si, ordered, low temp. $\alpha \rightarrow \gamma$ transform. *(Russian)* 78−19740
Fe-Ni-Si-B, amorphous paramag. alloys, hyperfine field distrib., Mossbauer study 80−39958
Fe-Ni-Si-Mn-Cr(Co-Mo), effect of prolonged aging on mag. props. 80−16513
Fe-P-Si, amorphous alloy, anelastic relaxation 79−4997
Fe-P-Si alloys, electrothermal-grade, thermoelec. characts. in region 273 to 573K 78−23834
Fe-Si, 180° Bloch wall motion, Barkhausen jumps *(French)* 78−23294
Fe-Si, 6.3-25 at.% Si, single crysts., adiabatic elastic consts., room temp. US pulse echo meas. 77−48467
Fe-Si, (110) [001] oriented, mag. props., compressive stress effects 80−60392
Fe-Si, (3 wt.%), nonuniform elastic deform. in grains *(Russian)* 78−35415
Fe-Si, (3wt.%) alloys, grain boundary anal.,, scanning AES 79−43256
Fe-Si, amorphous film, mag. props. 77−1575
Fe-Si, atomisation of melt, charact. of metal powder 78−19688
Fe-Si, BCC, cyclic cleavage crack growth model for fatigue 80−55519
Fe-Si, Bloch wall motion, irreversible processes 79−78431
Fe-Si, Bloch wall motion self-similarity *(French)* 79−82810
Fe-Si, coated, effective domain and grain obs. methods and Fe losses 80−34675
Fe-Si, crack propag. kinetics, effect of current pulses 78−31531
Fe-Si, determ. of chem. and magnetic interchange energies 77−80925
Fe-Si, determ. of Si by X-ray fluorescence spectrometry *(Japanese)* 79−57324
Fe-Si, dil., mag. hyperfine fields, Curie temp. and Mossbauer meas. 77−63190
Fe-Si, dil., Mossbauer spectra meas. 77−63344
Fe-Si, dil., XPS meas. 77−63538
Fe-Si, dislocation struct. of plastic relax. zone at tip of brittle crack 77−77582
Fe-Si, dislocation wall form. in contact with surface active melt, stacking fault energy *(Russian)* 77−72626
Fe-Si, disordered, obs. of Kohn singularities in X-ray diffuse scatt. 79−27874
Fe-Si, dissolution rate into molten Al, convection mass transfer *(Japanese)* 78−71858
Fe-Si, domain struct., influence of insulating coating, high voltage SEM obs. 77−1565
Fe-Si, domain struct. obs. by high voltage SEM 77−1564
Fe-Si, domain structure of Neel oriented samples 77−69601
Fe-Si, dynamically strained, temp. depend. of twinning characts. *(Russian)* 79−46673
Fe-Si, effect of alloying additions on magnetoelastic effects 78−43624
Fe-Si, elastic consts., temp. depend., 77 to 300K 77−70089
Fe-Si, electron density distrib. vs. at. order 79−60309
Fe-Si, etch figure method appl. *(Chinese)* 80−21194
Fe-Si, fatigue crack propag., low temp. 80−35311
Fe-Si, fatigue fracture fractography in broad strain-amplitude range, in air and vacuum 80−81186
Fe-Si, ferritic, precipitation of AlN *(French)* 78−23711
Fe-Si, ferromag., magnetisation in high fields, influence of internal field nonuniformity 79−51819
Fe-Si, glissile and twinning dislocation motion temp. depend., influence of grain boundaries *(Russian)* 77−47452
Fe-Si, grain oriented, core losses *(Japanese)* 78−60303
Fe-Si, grain oriented, effect of tensile stress on domain struct. 78−95462
silicon alloys continued
Fe-Si, grain oriented, fatigue crack direct obs. by SEM, propag. mechanism *(Japanese)* 79−20164
Fe-Si, grain oriented, misorientation effects on mag. props 80−88792
Fe-Si, grain oriented, phosphate coating anal. by IR spectroscopy 80−89570
Fe-Si, grain oriented, with unique inhibition system for texture development 77−90366
Fe-Si, grain oriented sheet, grain struct. by computer mapping 80−88168
Fe-Si, grain oriented sheet, AC hysteresis, surface struct. and elastic stress effects 80−88791
Fe-Si, grain oriented transformer sheets, permeability and magnetostriction, tensile stress effects 80−88843
Fe-Si, grain-oriented, AC magnetostriction at high temp., mag. annealing effects 77−20672
Fe-Si, grain-oriented, magnetostriction, and domain struct. 79−1703
Fe-Si, grain-oriented, surface coating effect on transverse magnetostriction 77−66402
Fe-Si, grain-oriented sheets, high permeability, low losses, review 80−88790
Fe-Si, H_2, induced cracking, crystallographic and fractographic studies 79−5052
Fe-Si, hyperfine fields, Mossbauer meas. 80−40024
Fe-Si, hysteresis loops described by 180° Bloch wall *(French)* 79−15322
Fe-Si, influence of stress on rotational loss, lamination appl. 78−35384
Fe-Si, internal friction, domain boundary area *(Russian)* 79−24562
Fe-Si, internal friction anisotropy, dynamic magnetostriction *(Russian)* 78−2194
Fe-Si, irreversible Barkhausen jumps *(French)* 77−1568
Fe-Si, layers formed by reaction with molten Al, X-ray, EMPA and hardness meas. *(Japanese)* 78−72926
Fe-Si, liq., thermodynamic characts. calc. *(Russian)* 80−15264
Fe-Si, liq. alloys, surface tension, sessile drop method meas. *(French)* 78−84029
Fe-Si, liquid, surface tension model using surrounded atom concept 77−15665
Fe-Si, liquid diffusion of H_2 *(German)* 78−14487
Fe-Si, loss meas. at high flux densities 80−88799
Fe-Si, low frequency power losses 78−95466
Fe-Si, low-temperature fatigue crack propagation 78−72876
Fe-Si, mag. losses, depend. on stress and orientation 77−1882
Fe-Si, mag. method for rapid analysis 77−44540
Fe-Si, mag. props., stress and reannealing effects 80−88844
Fe-Si, magnetic domain obs. by SEM 77−69606
Fe-Si, magnetic props., material for electrical engineering *(German)* 77−21293
Fe-Si, magnetostatic couplings between 180° Bloch walls 77−69613
Fe-Si, maze domains upon appl. of horizontal mag. field or mech. tension 80−11218
Fe-Si, microflow and strain hardening under cyclic loading 80−104182
Fe-Si, microplastic deform. and amplitude depend. of internal friction *(Russian)* 80−45349
Fe-Si, Mossbauer study of mag. ordering 79−24245
Fe-Si, non-oriented sheets, production and props. 80−88797
Fe-Si, oxide layer form. during annealing, AES in-depth anal. *(German)* 80−16576
Fe-Si, plastic deform., synchrotron X-ray topography dynamic expts. 78−67621
Fe-Si, plastic deformation mechanism, meas. of microplasticity 78−60720
Fe-Si, polycrystalline, domain struct. at grain boundaries *(Russian)* 77−51917
Fe-Si, polycrystalline, exam. of stress-strain state of individual grains 78−80580
Fe-Si, power loss and permeability meas. by means of Hall probes and stochastic ergodic correl. 80−86350
Fe-Si, rapid cracks self-arrest potential, −196-0°C 80−100911
Fe-Si, recrystallisation study 79−91275
Fe-Si, recrystallization, in situ studies, appl. of X-ray synchrotron topography 78−35610
Fe-Si, ribbon, prep. by rapid quenching 79−33957
Fe-Si, ribbon-form material, rapid quenching from melt *(Japanese)* 78−92210
Fe-Si, simple domain structs., magnetisation jumps 77−69624
α-Fe-Si, single cryst., ^{59}Fe diffusion coeffs., 1013 to 1373K 77−69110
Fe-Si, single cryst., lattice parameter determ., ratio method 77−43106
Fe-Si, single cryst., mag. domain wall motion, X-ray topography study 80−65953
Fe-Si, solid and liq. paramag. props. *(Russian)* 77−66247
Fe-Si, spin- and charge-density oscillations 77−11886
Fe-Si, spreading behaviour of liq. Al 80−84345
Fe-Si, stator core, grain-oriented and non-oriented, magnetic flux and loss distrib. 80−88798
Fe-Si, steel sheet static mag. props., elastic tensile stress effect 78−47999
Fe-Si, strain hardening and rate-sensitivity, effect of ductile-brittle transition temp. 78−39900
Fe-Si, stress and plastic deform. effect on Barkhausen effect, instrumentation 78−52313
Fe-Si, strips and rods, spatial extent of flux due to irreversible changes of mag. polarisation 79−33506
Fe-Si, temp. depend. of twinning intensity, development of deform. *(Russian)* 79−51116
Fe-Si, temperature dependence of the twin growth rate *(Russian)* 79−27999
Fe-Si, thermally activated motion of 180° Bloch wall 78−95457
Fe-Si, thin cryst., domain struct. behaviour during magnetisation *(Russian)* 78−2697
Fe-Si, transformer steel, high-temp. heat treatment, resist. of refractories in contact 80−66554
Fe-Si, twinned annealing, plastic deform., and recrystallisation *(Russian)* 77−28829
Fe-Si, type B_1 domain struct., Mossbauer exam. 77−51931
Fe-Si, yield stress, temp. depend. *(Russian)* 78−56691
Fe-Si (0-25 at.%), composition depend. of elastic consts. at 0K 77−84830
Fe-Si (0-6 wt.%) melts, viscosity *(Russian)* 80−15285
Fe-Si (1-5 wt.%), optimum sintering conditions and mag. props. 77−85958

silicon alloys continued
Fe-Si (1%), LEED-Auger exam. of (1$\bar{1}$0) surfaces 78−71915
Fe-Si (10 wt.%), effect of short range order on yield stress *(German)* 78−52932
Fe-Si (110)[001] sheet, normal stress effect on magnetostriction 77−40102
Fe-Si (2-8 wt.%), single crysts., growth striations, X-ray studies 80−79774
Fe-Si (2.35 wt.%), misorientation dependence of grain boundary segregation, Auger spectroscopy exam. 78−76629
Fe-Si (2.4 wt.%), ductile fatigue crack growth mechanism in single crystals, in situ SEM obs. 79−61695
Fe-Si (2.4 wt.%), simulation of X-ray topographies of ferromag. domains *(French)* 77−77070
Fe-Si (2.5%), Bloch wall zig-zag struct., neutron small angle scatt. 77−16099
Fe-Si (2.5%), mag. stray fields above stripe domains, electron optic meas. 80−15755
Fe-Si (2.6 wt.%) single cryst., crack propag., controlled plastic crack tip opening rate 80−60943
Fe-Si (2.9 wt.%), spatial orientation of grain boundaries *(Russian)* 77−11567
Fe-Si (3 at%), deformation and electron bombardment, influence on dislocation struct., 20-500°C *(Russian)* 80−92536
Fe-Si (3 at.%), acoustic emission response 79−87801
Fe-Si (3 to 5 wt.%) sinters, mag. props., Si and Fe-Si additions effect 80−71104
Fe-Si (3 wt.%), (110)[001] oriented single crystal, form. of rolling and annealing texture 77−16608
Fe-Si (3 wt.%), Al-bearing, grain-oriented, N_2-H_2 annealing effect on texture, mag. props. 77−12714
Fe-Si (3 wt.%), AlN-inhibited, Se effect on primary grain recrystallisation 77−12715
Fe-Si (3 wt.%), anisotropy induced by rolling in (001) and (111) planes *(Russian)* 77−80931
Fe-Si (3 wt.%), BCC, crystallographic depend. of fatigue crack propag. *(Japanese)* 77−48528
Fe-Si (3 wt.%), BCC, transcrystal fatigue crack propag. mechanism *(Japanese)* 77−48529
Fe-Si (3 wt.%), Barkhausen effect meas. 77−85492
Fe-Si (3 wt.%), behaviour of disperse inclusions, influence of recrystn. processes *(Russian)* 80−66519
Fe-Si (3 wt.%), breaking stress grain size and grain boundary energy during onset of reversible temper brittleness *(Russian)* 77−32673
Fe-Si (3 wt.%), chemical comp. and hot rolling effect on brittleness *(Czech)* 80−50712
Fe-Si (3 wt.%), cold rolled, effect of primary recrystallisation texture, on behaviour of secondary recrystallisation 78−39802
Fe-Si (3 wt.%), containing B, grain boundary segregation, AES evidence 77−86046
Fe-Si (3 wt.%), cube-on-edge oriented, high permeability, mill processing and mag. props. 77−86045
Fe-Si (3 wt.%), current pulse effects on structure at crack tip *(Russian)* 77−44332
Fe-Si (3 wt.%), deform., effect of superimposed US oscillatory stress *(Japanese)* 78−31461
Fe-Si (3 wt.%), degeneration of slip on ($\bar{2}$11) planes *(Russian)* 78−80587
Fe-Si (3 wt.%), directional, power loss anomalies temp. depend., effect of intrinsic parameters 77−12156
Fe-Si (3 wt.%), domain struct. rel. to cryst. size *(Russian)* 80−29568
Fe-Si (3 wt.%), domain wall spacing and losses, orientation depend. 78−56343
Fe-Si (3 wt.%), domain wall drift due to nucleation during cyclic magnetisation 78−95461
Fe-Si (3 wt.%), domain wall spacing and core loss, forsterite and stress coatings effect 80−88780
Fe-Si (3 wt.%), EM losses, effect of bending of 180° domain boundaries *(Russian)* 78−39357
Fe-Si (3 wt.%), eddy current and hysteresis losses, role of domain struct. *(Russian)* 77−80961
Fe-Si (3 wt.%), eddy current losses, domain structure influence obs. and calc. *(Slovak)* 79−4693
Fe-Si (3 wt.%), effect of heating rate during primary recrystn. on props. after secondary recrystn. 78−84837
Fe-Si (3 wt.%), elec. field gradient by trigonal and tetragonal distortions 77−8474
Fe-Si (3 wt.%), electron irradiated, yield strength and elongation 80−76325
Fe-Si (3 wt.%), exam. of plastic deformation, slip band dislocation, under hydrostatic pressure 78−56695
Fe-Si (3 wt.%), fatigue crack propag. work coeff. 80−16422
Fe-Si (3 wt.%), ferromag. domains, imaging by neutron interferometry 80−71087
Fe-Si (3 wt.%), Goss oriented, stress effects 78−91916
Fe-Si (3 wt.%), grain growth inhibition by MnS spherical particles with size distrib. 80−35218
Fe-Si (3 wt.%), grain oriented tape-wound core, dynamic domain size var. and Fe losses 77−12146
Fe-Si (3 wt.%), grain oriented, MnS-AlN-inhibited, precipitate morphology 77−12648
Fe-Si (3 wt.%), grain oriented, lowest core loss 78−91887
Fe-Si (3 wt.%), grain orientated, negative magnetostriction, theory 78−91917
Fe-Si (3 wt.%), grain oriented, domain wall variation throughout magnetisation cycle 78−95459
Fe-Si (3 wt.%), grain oriented, power loss depend. on domain wall bowing 78−95460
Fe-Si (3 wt.%), grain oriented, MnS precipitate distribution, electron microscope observation *(Chinese)* 78−95751
Fe-Si (3 wt.%), grain oriented, mag. domain movements 79−82815
Fe-Si (3 wt.%), grain oriented, mag. props., effect of decarburizing *(Chinese)* 80−103821
Fe-Si (3 wt.%), grain-oriented, effect of forsterite coatings in domain struct. 78−23293
Fe-Si (3 wt.%), grain-oriented, domain struct. regulation and power loss reduction 80−88779
Fe-Si (3 wt.%), grain-oriented, domain wall profiles throughout magnetisation cycle 80−88781
Fe-Si (3 wt.%), grain-oriented, stacking effect on power loss, mag. props. 80−88795

silicon alloys continued
Fe-Si (3 wt.%), grain-oriented, power loss and domain wall variation with lamination thickness 80−88814
Fe-Si (3 wt.%), grain-oriented, energy loss reduction by lowering sheet thickness 80−88816
Fe-Si (3 wt.%), high induction grain oriented, metallurgical treatment and mag. props. 77−86044
Fe-Si (3 wt.%), high permeability, use in transformer cores 80−88793
Fe-Si (3 wt.%), hot rolled sheet steel, ductile-brittle transition temp. *(Chinese)* 78−31498
Fe-Si (3 wt.%), hysteretic losses, domain struct. and cryst. defects 79−19747
Fe-Si (3 wt.%), internal friction, instantaneous, depend. on phase of torsional oscills. *(Russian)* 80−71142
Fe-Si (3 wt.%), loss contribs. from correlations among irreversible movements of Bloch walls 77−85483
Fe-Si (3 wt.%), loss prediction, from distorted waveforms 78−76273
Fe-Si (3 wt.%), losses, demagnetisation freq. and grain orientation depend. 80−88796
Fe-Si (3 wt.%), mag. anisotropy induced by rolling in (110) plane *(Russian)* 78−34978
Fe-Si (3 wt.%), mag. anisotropy induced by cold rolling *(Russian)* 80−84595
Fe-Si (3 wt.%), mag. domain wall contrast in synchrotron X-ray topographs 80−75792
Fe-Si (3 wt.%), mag. loss and magnetostriction, DC flux alternation effects 80−88794
Fe-Si (3 wt.%), mag. props., stress coating effects 80−34728
Fe-Si (3 wt.%), magnetisation variation during bending oscills., rel. to ΔE effect *(Russian)* 80−65983
Fe-Si (3 wt.%), Mossbauer spectra, domain magnetisation vector rotations, domain struct. 79−69761
Fe-Si (3 wt.%), nonoriented sheets, magnetisation, tensile stress effects 80−88845
Fe-Si (3 wt.%), orientation distrib. in primary recrystallised textures, mag. permeability 77−12712
Fe-Si (3 wt.%), orientation development during secondary recrystallisation, primary matrix effect, magnetic props. *(Czech)* 78−60679
Fe-Si (3 wt.%), oriented, losses and domains, mech. stress effects 80−88852
Fe-Si (3 wt.%), polycryst. (110), synchrotron radiation topographs and mag. domain obs. 78−67620
Fe-Si (3 wt.%), polycrystal in mag. field, stress induced magnetisation, synchrotron Bragg refl. topography obs. 80−50139
Fe-Si (3 wt.%), power losses at extremely low freqs. 80−88815
Fe-Si (3 wt.%), prediction of magnetisation hysteresis loops for distorted waveforms 79−47303
Fe-Si (3 wt.%), pulsed laser induced deform. 77−36605
Fe-Si (3 wt.%), recrystallisation along grain boundaries *(Russian)* 78−6942
Fe-Si (3 wt.%), rotational power losses, freq. depend. 78−91888
Fe-Si (3 wt.%), scratching effects on mag. losses in single crysts. with orientation near (110)[001] 79−51802
Fe-Si (3 wt.%), secondary recrystn., struct. inhibition, permeability improvement 77−12713
Fe-Si (3 wt.%), secondary recrystn., role of solutes 77−86043
Fe-Si (3 wt.%), secondary recrystallisation, effect of composition and original orientation 78−68707
Fe-Si (3 wt.%), single crystal, colour etching of striations 77−70253
Fe-Si (3 wt.%), single crystal, plastic deform., 473 to 1000K 77−73310
Fe-Si (3 wt.%), single crystal growth by floating zone melting at various rates, growth striation obs. 79−95914
Fe-Si (3 wt.%), single crystals, cyclic deformation oriented for single glide 79−100224
Fe-Si (3 wt.%), single crysts. and polycrysts. strain rate influence on low cycle fatigue props. 80−3126
Fe-Si (3 wt.%), singularities in geometry of slip, point temp. depend. *(Russian)* 79−24574
Fe-Si (3 wt.%), solubility of MnS, 950-1200°C *(Russian)* 77−16541
Fe-Si (3 wt.%), square etch pit characts., subgrain misorientation and mag. domain patterns 77−25199
Fe-Si (3 wt.%), strain aged polycrystalline samples, AE study of deform. 77−63696
Fe-Si (3 wt.%), strain distribution near notch tip under mixed plane stress-plane strain condition *(Japanese)* 77−8891
Fe-Si (3 wt.%), stripe domain structure, dynamic behaviour at high max. induction values *(Russian)* 80−80553
Fe-Si (3 wt.%), struct. and preferred orientation, annealing parameters influence *(Czech)* 80−89248
Fe-Si (3 wt.%), temp. depend. of migration rate of secondary recrystallisation grain boundaries *(Russian)* 79−1436
Fe-Si (3 wt.%), tertiary products from deoxidation, electron emission microscope study *(Russian)* 78−11214
Fe-Si (3 wt.%), texture, Mossbauer expts. 80−71262
Fe-Si (3 wt.%), texture form., plastic strain effect, hot rolled 79−79002
Fe-Si (3 wt.%), total losses under tensile stress, rel. to orientation near (110)[001] 78−76272
Fe-Si (3 wt.%), transformer steel, grain-oriented, magneto-optical domain obs., magnetisation mechanism 77−12364
Fe-Si (3 wt.%), transformer laminations, processing and props. 78−52325
Fe-Si (3 wt.%), triaxial ferromagnets, spontaneous magnetisation distrib., plane stress state influence *(Russian)* 79−61071
Fe-Si (3 wt.%), US oscillatory stress superimposition effects on deformation 80−35287
Fe-Si (3 wt.%), yielding phenomena at high temp. *(Japanese)* 77−48489
Fe-Si (3 wt.%) (001) [100] single crystal, cold rolled texture *(Japanese)* 77−21169
Fe-Si (3 wt.%) (110), domain size depend. on crystal thickness *(Russian)* 79−69692
Fe-Si (3 wt.%) alloy, H containing, H influence on internal friction *(Russian)* 79−38877
Fe-Si (3 wt.%) alloy, mag. domain movements prod. by mech. stress 79−87284
Fe-Si (3 wt.%) BCC single crystals, low cycle fatigue *(French)* 79−20177
Fe-Si (3 wt.%) cores with insulative coatings, morphological and struct. SEM characteris. 78−23881
Fe-Si (3 wt.%) domain struct., tensile load effects *(Russian)* 78−47995

silicon alloys continued
Fe-Si (3 wt.%) grain-oriented transformer sheet, effect of phosphate coating containing Cr_2O_3 and CaO 77−16135
Fe-Si (3 wt.%) high-permeability grain-oriented steel, quenching effect on primary recrystn. texture development 80−84956
Fe-Si (3 wt.%) laminations, orientation and stacking influence on losses obs. *(Slovak)* 79−4696
Fe-Si (3 wt.%) laminations, isotropic and cube-on-face, magnetostriction behaviour 80−39843
Fe-Si (3 wt.%) laminations, magnetostriction behaviour associated with closure domain spikes 80−75834
Fe-Si (3 wt.%) laminations, grain oriented, plastically deformed, anomalous losses 80−88853
Fe-Si (3 wt.%) layers, with ceramic coating, interface struct., electron microscopy and Mossbauer obs. *(Russian)* 79−28216
Fe-Si (3 wt.%) locally deformed, EM loss depend. on cryst. struct. and orientation *(Russian)* 80−7694
Fe-Si (3 wt.%) mag. domain motion quasi-lifetime topography using white synchrotron radiation, mag. field effects 79−42797
Fe-Si (3 wt.%) sheet, obs. through surface coating of domain struct., SEM 77−85482
Fe-Si (3 wt.%) single crysts., rolling-induced mag. anisotropy *(Russian)* 78−19243
Fe-Si (3 wt.%) steel, high permeability, grain oriented 78−91886
Fe-Si (3 wt.%) steel, high permeability, magnetostriction, stress inducing coating effects 80−34730
Fe-Si (3 wt.%) steel, oriented, stress depend. mag. props., coating effects 80−34729
Fe-Si (3 wt.%) struct. and texture changes during repeated deform.-recrystn. *(Russian)* 78−88474
Fe-Si (3% wt.) polycrystalline, short-range order and induced anisotropy *(Russian)* 79−51772
Fe-Si (3%), power loss, domain wall motion depend. 77−16100
Fe-Si (3%), spikn related contrast effect, visibility of 180° ferromag. domain walls 78−43612
Fe-Si (3%wt.), dynamics of 180° domain boundaries and electromag. losses *(Russian)* 79−51801
Fe-Si (3.1 wt.%), anisotropy of electromigration of substructure of polygonisation *(French)* 77−28047
Fe-Si (3.1 wt.%), solubility product of BN 79−10955
Fe-Si (3.12 wt.%), brittle fracture, work hardening effect at notch tip 78−44220
Fe-Si (3.2 wt.%), single cryst., prism-shaped closure domains on (110) surface 79−69690
Fe-Si (3.22 wt.%), topographic and type-2 magnetic contrast, effect of collector position in SEM 79−12909
Fe-Si (3.25 wt.%), Burgers vector identification from electron microscope images 80−2030
Fe-Si (3.25 wt.%), dislocations in twin boundaries, electron microscopic images 80−34006
Fe-Si (3.25 wt.%), mag. props., influence of struct. and chemical composition of surface oxide layer 78−2700
Fe-Si (3.25 wt.%), single crystals and polycrystals, cutting surface texture 79−20291
Fe-Si (3.25 wt.%), single cryst. with (007) planes, domain struct. influence on mag. torque 80−108034
Fe-Si (3.5 wt.%), Barkhausen noise, strain depend., interaction of dislocations and domain walls 77−12155
Fe-Si (3.5 wt.%), cutting of bicrystal to compare mechanism for large crystals and polycrystals *(Japanese)* 78−60871
Fe-Si (3.5 wt.%), dynamic neutron depolarisation meas. of ferromag. domain struct. 79−82812
Fe-Si (3.5 wt.%), magnetisation reversal and domain walls 78−84451
Fe-Si (3.5 wt.%), static neutron depolarisation meas. of ferromag. domain struct. 78−14978
Fe-Si (3.5 wt.%) picture frame cryst. , domain wall bowing dynamic neutron depolarisation 78−56344
Fe-Si (3.5 wt.%) picture frame, domain wall bowing, time-depend. neutron depolarisation 78−95458
Fe-Si (3.5 wt.%) plastic deform., slip initiation, X-ray topography study 79−47750
Fe-Si (3.72 wt.%) fatigue failure in vacuum and air 78−68789
Fe-Si (3wt.%), grain-oriented, secondary recryst., grain growth inhibition 80−89245
Fe-Si (3wt.%), hardening under dynamic load, grain boundary effect 77−12674
Fe-Si (3wt.%), notched sheet under tensile loading, notch tip opening/contraction, J-integral relationship *(Japanese)* 77−4840
Fe-Si (3wt.%), quantitative determ. of grain orientation and textile by etch figure method *(Chinese)* 78−11233
Fe-Si (4 at.%), Bloch wall thickness determ. by neutron small-angle scatt. 80−15754
Fe-Si (4 wt.%), coercive force, influence of stabilisation of domain struct. on temp. depend. *(Russian)* 77−52513
Fe-Si (4 wt.%), freq. depend. of Fe losses in single crysts. with (100) [001] 79−51803
Fe-Si (4 wt.%), neutron crit. scatt., experimental anisotropy 78−38590
Fe-Si (4%), (110)[001] and (100)[001], dynamic domain struct., AC excitation 77−16097
Fe-Si (5.8 at.%), mech. behaviour in microplastic strain region *(Russian)* 78−39838
Fe-Si (6.5 wt%) filament, formation by modified Taylor technique, and mag. props. 80−75795
Fe-Si (6.5 wt.%), ductility and mag. props., Ni and Mn addition effects 78−76704
Fe-Si (6.5 wt.%), effect of ordering on mag. props. 79−51833
Fe-Si (6.5 wt.%) ribbon, splat-cooled, mag. props. 80−88805
Fe-Si (6.5%), struct. and rolling texture 79−79006
Fe-Si (7.5, 14.3 at.%), mag. moments and form factors, neutron diffr. obs., d-band electron redistrib. 79−51751
Fe-Si (up to 8 wt.%), magnetostriction temp. and comp. depend. 77−66405
Fe-Si alloy, deformed by slip, polygonal boundary form. *(Russian)* 79−24534
Fe-Si alloy, Si content determ. from Seebeck coeff. 77−56269
Fe-Si alloys, kinetics of spinodal decomposition in 2-phase region of B_2+DO_3 77−28806
Fe-Si alloys, liq., refractive index, absorpt. coeff., elec. cond. 78−43830
Fe-Si alloys, recrystn. while carburising, interphase boundaries movement 79−52208
Fe-Si amorphous alloys, Mossbauer spectra, struct. 80−15840
silicon alloys continued
Fe-Si amorphous film, conversion electron Mossbauer effect 78−72440
Fe-Si amorphous film, crystallisation, Mossbauer studies 80−33900
Fe-Si amorphous film, Hall const. and magnetoresistive effect 78−52105
Fe-Si amorphous film, struct. and crystallisation, Mossbauer study 80−11300
Fe-Si amorphous films, mag. and magnetoelastic props. 79−99746
Fe-Si as grown crystal, dislocation study by etching and X-ray topography 78−47377
Fe-Si binary alloys, anodic behaviour using cyclic voltammetry 79−52417
Fe-Si cast alloy with spheroidal graphite, transform. investigation during tempering *(Russian)* 80−97479
Fe-Si crystal, neutron depolarisation studies of ferromagnetic domain structures 80−25155
Fe-Si ferromag. film, props. 79−4709
Fe-Si film, amorphous, conversion electron Mossbauer study 78−84507
Fe-Si gas-flame spray deposited protective coating, for C steel heat exchanger 80−61025
Fe-Si layer, growth kinetics and morphology 78−95700
Fe-Si melts, high Si, O solubility *(Russian)* 80−15252
Fe-Si plate, ferromag. domain structure obs. by neutron diffr. topography 77−69645
Fe-Si protective oxide film form. 80−11818
Fe-Si sheets, grain oriented, with insulating coating, nondestructive grain identification methods *(Slovak)* 79−5090
Fe-Si single crystals with cube-on-edge orientation, iron-loss-domain-struct. correls. *(Japanese)* 80−7534
Fe-Si single crysts., interaction of {110} 90° walls with lattice imperfections 80−39807
Fe-Si steel, high permeability, processing effect on recrystn. and deform. 77−12716
Fe-Si system, melting equilibria study *(German)* 80−66473
Fe-Si transformer steel, supplementary domain struct. of misoriented grains *(German)* 78−14979
Fe-Si-Al, high temp. oxidation resist., comp. depend. 77−12739
Fe-Si-Al, Sendust, 12 μ thick film prep. by sputtering, mag. and other props. 77−55888
Fe-Si-Al, Sendust, ribbon-form, prep. by rapid quenching, mech. and mag. props. 80−71611
Fe-Si-Al, surface oxide layer struct., AES study 80−89396
Fe-Si-Al (2.8-3.4, 0-0.86 wt.%) oxidation, annealing 80−89395
Fe-Si-Al (5,10 wt.%) struct. anal. by electron microscopy and electron diffr. *(Chinese)* 79−11618
Fe-Si-Al (6,4 wt.%), Sendust alloy, effect of Ni content on mag. props. 78−72897
Fe-Si-Al (6.5 wt.%, up to 0.5 wt.%), elongation, cold workability and mag. permeability meas. 77−12667
Fe-Si-Al (9.6, 5.4 wt.%), ribbon-form Sendust alloy, mag. props., annealing effects 80−88800
Fe-Si-Al alloy, cryst. lattice deform. at antiphase boundaries, theoretical electron images exam. 77−11448
Fe-Si-Al ribbon-form Sendust alloy made by rapid roll quenching, mag. props., recording head appls. 80−81001
Fe-Si-Al Sendust alloy ribbon form, rapid quench prepared, elec. cond., coercive field, permeability 79−83151
Fe-Si-Al sendust type alloys, Co preferred substitution sites, Mossbauer spectra 79−91328
Fe-Si-Al-Ni alloy, Super Sendust, Ni content and thermomag. treatment effects 77−4861
Fe-Si-B, embrittlement by crystallisation *(Japanese)* 78−48513
Fe-Si-B, high induction, hot rolling treatment 80−89266
Fe-Si-B, high induction alloy, improving mag. props. by adding B to coating 79−83338
Fe-Si-B, magnetic metallic glasses, mag. props. 80−84620
Fe-Si-B, melt C content effect on grain growth and induction 80−35351
Fe-Si-B, surface tension, density, and oxidation kinetics 80−20028
Fe-Si-B alloy filaments produced by glass-coated melt spinning 80−76213
Fe-Si-B amorphous alloys, metalloid content effects on Curie temp. and mag. moments 78−14956
Fe-Si-B amorphous alloys, Mossbauer spectroscopy *(French)* 80−80653
Fe-Si-B amorphous alloys with metalloid elements, embrittlement/crystn. relationship *(Japanese)* 79−96134
Fe-Si-B amorphous films, mag. props. 80−34710
Fe-Si-B amorphous powder, production by spark erosion, and mag. props. 77−90290
Fe-Si-B ferromagnetic amorphous alloys, Young's modulus and delay time characts. *(Japanese)* 77−85543
Fe-Si-B glassy alloys, mag. props., comp. effects 80−88752
Fe-Si-B magnetic powder, amorphous, prep. by atomisation technique 78−92213
Fe-Si-B metallic glass, magnetisation meas. 78−23252
Fe-Si-B metallic glasses, mag. props., depend. on metalloid content 77−85485
Fe-Si-B metallic glasses, crystn., differential scanning calorimetry obs. 79−82160
Fe-Si-B sputtered amorphous films, mag. props. and corrosion resist. 79−28567
Fe-Si-B-N-S, B, S, N effects on grain boundary segregation and grain growth inhibition, review 80−3047
Fe-Si-B-S, grain-oriented, high induction, B and S addition effect on magnetic props. *(Slovak)* 79−4697
Fe-Si-C, austenitic, C diffusivity *(German)* 80−92705
Fe-Si-C, cast, spheroidal graphite, metallography of solidification 78−19737
Fe-Si-C, liquid alloy, activity of Si and C *(Russian)* 78−11203
Fe-Si-C (2.86, 0.07 wt.%), internal friction peak at about 300°C *(Russian)* 77−81284
Fe-Si-C melt, Si and C activity *(Russian)* 77−55364
Fe-Si-C mixed powder, cast Fe powder sintering study *(Japanese)* 80−108373
Fe-Si-Cr magnetic films, sputtered, corrosion reduction, effect of Cr obs. 80−80573
Fe-Si-Mn, effect of Mn addition on mag. props. and elec. resist. 78−91890
Fe-Si-Mn (3, 0.004 to 0.1 wt.%), Mn effect on oxidation in H_2O-H_2 atmos. 78−31560
Fe-Si-Mn (6.5 wt.%, up to 0.12 wt.%), elongation, cold workability and mag. permeability meas. 77−12667

silicon alloys continued
Fe-Si-MnS-Al, Al effect on hot rolling struct., recrystallization, texture magnetic props. *(Chinese)* 78−11237
Fe-Si-N alloy, BCC→FCC transform., martensitic character obs. *(Russian)* 78−48397
Fe-Si-Ni (6.5 wt.%, up to 2 wt.%), elongation, cold workability and mag. permeability meas. 77−12667
Fe-Si-S melt, S evaporation *(Russian)* 78−19716
Fe-Si-Ti(Zr)(V)(Nb), eutectic alloy, exam. of eutectic temp., composition, and oxidation resistance 78−52767
Fe-Si-Zn, influence of trace elements on morphology *(German)* 80−108390
Fe-Si(3 wt.%), ferromag. alloy, mag. anisotropy induced by cold rolling 80−30114
Fe-Si(3.25 wt.%), crack nucleation depend. on twins during intense slip *(Russian)* 79−100239
Fe-Si(4 wt.%), (110) and (100)[001] oriented, simulation of domain wall bowing 80−44854
Fe-Si(6.5 wt.%) ribbon, prep. by rapid quenching and mag. props. 80−45251
$(Fe\text{-}Co\text{-}Ni)_{78}Si_8B_{14}$, amorphous, low coercivity and zero magnetostriction 78−23299
$Fe_3Al_xSi_{1-x}$, DO_3 structured, ferromag., lattice parameters 79−42010
$Fe_{73}Al_xSi_{27-x}$, DO_3 structured, ferromag., lattice parameters 79−42010
$(Fe_{100-x}B_y)_{1-x}Si_x$ thin film glasses, mag. props. and corrosion resist. 80−80576
$Fe_{78}B_{12}Si_{10}$, amorphous, continuous versus discrete hyperfine field distrib., Mossbauer spectra 79−33583
$Fe_{78}B_{12}Si_{10}$, amorphous, Mossbauer study of hyperfine interaction and mag. anisotropy 80−40027
$Fe_{78}B_{12}Si_{10}$, amorphous ferromagnet, long and short range exchange interactions, Mossbauer spectra and interpretation 79−56526
$Fe_{80}B_{15}Si_5$ metallic glass, large uniaxial magnetostrictive anisotropy, magnetisation reversal 80−34736
$Fe_{80}B_{20-x}Si_x$, amorphous, mag. saturation, spin wave stiffness, temp. depend. 80−75741
$Fe_{80}B_{20-x}Si_x$, amorphous, size effect of metalloids on mag. props. 80−84594
$Fe_{80}B_{20-x}Si_x$ glass, magnetisation, Curie and crystn. temps. 79−87289
$Fe_{80}B_{20-x}Si_x$, metallic glass, mech. and mag. props., depend. on metalloid content 79−91213
$Fe_{80}(B_ySi_{1-y})_{20}$, amorphous, saturation magnetostriction, comp. effects 80−34735
$Fe_{81.5}B_{14.5}Si_4$, amorphous metal ribbon, stresses, magnetoelastic anisotropy and zero-field mag. domain struct. 80−44896
$Fe_{82}B_{15}Si_3$, metallic glass, low temp. specific heat, metalloid effects 80−34654
$Fe_{82}B_{18-x}Si_x$ glasses, soft mag. props. 79−73774
$Fe_{83}B_{16.5}Si_{0.5}$, amorphous, spin waves, inelastic neutron scatt. meas. 79−73701
$Fe_{84}B_{13}Si_2$, metallic glass, electrical resistivity and crystallisation 80−88526
$Fe_{35}Co_{32}B_{20}Si_{10}Al_3$, stress-induced variation in magnetisation and dynamic magnetostrictive charact. 80−88855
$(Fe_{0.07}Co_{0.93})_{75-x}Cr_xSi_{15}B_{10}$, amorphous, disaccommodation of mag. permeability and induced anisotropy 80−88741
$(Fe_xCo_yNi_{1-x-y})_{78}Si_8Bi_{14}$ amorphous ribbons, saturation magnetostriction and vol. magnetostriction 77−85538
$FeCo_2Si$, Heusler type materials, mag. props. 77−40042
$(Fe_{0.5}Co_{0.5})Si$, weak itinerant ferromag., polarised neutron scatt. exam. 77−4503
$Fe_{1-x}Co_xSi$, mag. props., sp. ht., n.m.r. and Mossbauer effect meas. 77−12129
$Fe_{3-x}Co_xSi$, structural, mag. moment, and hyperfine field behaviour, local environment model 79−65762
$Fe_xCo_{1-x}Si$ alloys, disordered, hydrostatic pressure effects on mag. props. 77−32175
$Fe_xCo_{1-x}Si$, mag. props., effect of hydrostatic press. 77−12101
$Fe_xCo_{1-x}Si$, mag. props. 79−56532
$Fe_xCo_{1-x}Si$, mag. props., sp. ht. and resist. meas. 79−61120
$(Fe_{0.05}Co_{0.95})_{78}Si_8B_{14}$ amorphous ribbon, anomalous mag. aftereffect 80−100602
$(Fe_{0.9}Co_{0.1})_xSi_yB_z$, $(Fe_{1-x}Co_x)_{78}Si_8B_{14}$ amorphous ribbons, magnetomech. coupling and saturation magnetostriction 78−68353
$(Fe_{1-x}Co_x)_{77}Si_{10}B_{13}$ alloys, amorphous, induced mag. anisotropy by mag. annealing 79−4671
$(Fe_{1-x}Co_x)_{77}Si_{10}B_{13}$, amorphous, mag. moments at 0K, Curie temp., mag. interactions 79−4670
$(Fe_{1-x}Co_x)_{77}Si_{10}B_{13}$, amorphous magnetic alloys, density meas. 80−1934
$(Fe_{1-x}Co_x)_{78}Si_{10}B_{12}$, amorphous Hall effect and magnetoresist. *(Japanese)* 77−85199
$(Fe_{1-x}Co_x)_{78}Si_{10}B_{12}$, amorphous alloys, magnetic anisotropy meas. 80−2570
$(Fe_{1-x}Co_x)_{78}Si_{10}B_{12}$, amorphous, roll mag. anisotropy 80−75757
$(Fe_{1-x}Co_x)_{78}Si_8B_{14}$ ribbon, magnetostriction exam. 79−73794
$Fe_{4.7}Co_{70.3}Si_{15}B_{10}$, amorphous ferromag., roll mag. anisotropy 79−51773
$Fe_5Co_{70}Si_{10}B_{15}$ amorphous magnetic alloy, decrease of permeability after demagnetisation, disaccommodation 80−39814
$Fe_5Co_{70}Si_{15}B_{10}$, amorphous ribbon, zero magnetostriction, low residual mag. loss 77−12157
$Fe_5Co_{70}Si_{15}B_{10}$, amorphous ribbon, HF mag. characts., magnetostriction role 77−66408
$Fe_5Co_{70}Si_{15}B_{10}$ amorphous ferromag. ribbons, change of permeability by heat treatment 77−85493
$Fe_5Co_{70}Si_{15}B_{10}$, amorphous, change of mag. props. by low temp. annealing 78−27058
$Fe_5Co_{70}Si_{15}B_{10}$, amorphous toroidal core, switching characts. and domain structs. 78−95477
$Fe_5Co_{70}Si_{15}B_{10}$, amorphous ferromagnetic alloy, isothermal annealing effect on static magnetic props. *(Japanese)* 79−52398
$Fe_5Co_{70}Si_{15}B_{10}$, amorphous, crystn. effect on mag. props. *(Russian)* 80−44858
$(Fe_xCo_{1-x})_{100-y}(Si_{0.4}B_{0.6})_y$ amorphous alloy zero magnetostrictive, mag. props. 79−99743
$(Fe_xCo_{1-x})_{78}Si_8B_{14}$, amorphous, saturation magnetostriction, strain modulated FMR obs. 80−75863
$(Fe_xCo_{100-x})_{100-(y+z)}Si_yB_z$ amorphous ribbon, mag. moment and Curie temp., comp. depend. 78−95421
$Fe_{78-x}M_xSi_{10}B_{12}$ (M=refractory metal), glass form. and thermal stability 80−79703

silicon alloys continued
$(FeMn)_3Si$ alloys, mag. and crystallographic props. by diffr., resist. and magnetisation meas. 77−59393
$(Fe_{1-x}Mn_x)Si$, US vel. rel. to mag. struct. and phase transforms *(Russian)* 77−47976
$(Fe_{1-x}Mn_x)_3Si$, $(Fe_{1-x}Co_x)_3Si$, order distrib., hardening effect *(Russian)* 77−89410
$(Fe_{1-x}Mn_x)_3Si$, mag. phase diagram determ. 77−24697
$(Fe_{1-x}Mn_x)_3Si$, sp. ht. at low temps., mag. transitions *(Russian)* 77−32189
Fe_2MnSi, antiferro- and ferromag. props. 77−12104
$Fe_{2.45}Mn_{0.05}Si$, slow neutron polariser, by single cryst. (111) refl. 80−49052
$Fe_{3-x}Mn_xSi$, evidence for the ang. depend. of the hyperfine interactions 78−76241
$Fe_{3-x}Mn_xSi$, Mossbauer and NMR exam. of site substitution and mag. struct. 77−12092
$Fe_{3-x}Mn_xSi$, struct., magnetisation, and spin echo expts., rel. to local environment model 77−20518
$(FeNi)_{80}Bi_{17.5}Al_2Si_{0.5}$, stress-induced variation in magnetisation and dynamic magnetostrictive charact. 80−88855
$Fe_{40}Ni_{40}(Mo,Si,B)_{20}$, amorphous, soft mag. props., switched-mode power supply appls. 80−88850
$Fe_{29}Ni_{49}P_{14}B_6Si_{12}$, Metglas fibre reinforced mortar, fracture props. 79−70159
$Fe_{29}Ni_{49}P_{14}B_6Si_2$ glass, crystn. kinetics, DSC expts. 78−26444
$Fe_{29}Ni_{49}P_{14}B_6Si_2$ glasses, internal friction and shear modulus 79−52287
$Fe_{29}Ni_{49}P_{14}B_6Si_2$, Metglas 2826B, Hall, elec. resist., magnetisation and heat capacity meas. 78−68019
$(Fe_{1-x}Ni_x)_{77}Si_{10}B_{13}$, amorphous magnetic alloys, density meas. 80−1934
$(Fe_{1-x}Ni_x)_{77}Si_{10}B_{13}$ amorphous alloy system, saturation mag. moment, Curie temp., mag. susceptibility 80−39753
$(Fe_{1-x}Ni_x)_{77}Si_{10}B_{13}$, amorphous, Landau-Ginzburg theory, magnetisation and Curie temp. 80−75700
$(Fe_{1-x}Ni_x)_{78}Si_{10}B_{12}$, amorphous Hall effect and magnetoresist. *(Japanese)* 77−85199
$(Fe_{1-x}Ni_x)_{78}Si_{10}B_{12}$ amorphous alloys, cold rolled and as-quenched, mag. anisotropy 80−97089
$Fe_{62.4}Ni_{15.6}Si_7B_{15}$ amorphous ferromagnetic alloy, anomalous magnetisation possible reasons, Mossbauer spectra *(Russian)* 79−78441
$Fe_{80}(P_{13}C_7)_{20-y}Si_y$, density, microhardness, and crystn. temp., comp. depend. 80−84093
$Fe_{80}P_{20-x}Si_x$, amorphous, effect of metalloids on mag. props. 79−11304
$Fe_{80}P_{20-x}Si_x$, amorphous, size effect of metalloids on mag. props. 80−84594
$Fe_xPd_{80-x}Si_{20}$, amorphous, structural and mag. heterogeneities 80−80484
$Fe_xPd_{80-x}Si_{20}$, low field susceptibility near transition temp. 77−66359
$Fe_xPd_{82-x}Si_{18}$, amorphous, magnetisation, magnetoresist., spin glass and ferromag. phases 80−34697
$Fe_xPd_{82-x}Si_{18}$ metallic glass, long range interaction and spin wave interactions 80−65949
$Fe_xPd_{82-x}Si_{18}$ metallic glass, mag. transitions, weak ferromagnetism 80−100583
FeSi, (110), Neel cryst., refr. of neutrons in Bloch walls using double cryst. arrangement 79−24191
FeSi, domain struct. and magnetisation reversal, time depend. neutron depolarisation 80−50138
FeSi, hyperfine fields about μ^+ 79−56664
FeSi, nearly ferromag. semicond. mag. and thermal props., spin fluctuation theory 79−65687
FeSi picture frame single cryst., domain wall motion and magnetisation reversal, time-depend. neutron depolarisation study 80−88782
FeSi, single cryst., orientation of pieces of zigzag Block walls, neutron small-angle scatt. determ. 79−24190
FeSi, single crystals., domain struct., temp. and field depend. 80−71085
FeSi-Ca-V complex alloy oxidation of steel, nonmetallic additions *(Russian)* 80−93685
$FeSi\text{-}Fe_2Si_5$ eutectic, $FeSi_2$ formation, annealing temp. and time effects 79−24512
FeSi-graphite-SiC refractory, oxidation loss and wettability of inorganic fluxing materials *(Japanese)* 78−84755
$FeSi_2$, effect on nitriding of Si powder 79−33985
$FeSi_2$ films, Mossbauer investig. of struct. 79−87341
$FeSi_2$ films, structural and Anderson transitions, cond. and IR reflectance meas. 79−15200
$\alpha\text{-}FeSi_{2.33}$, interface struct. and growth mechanism from melt 79−14715
$\alpha\text{-}Fe_{1-x}Si_2$, many-body atomic correlations, Mossbauer spectroscopy study 80−15934
$\alpha\text{-}Fe_{1-x}Si_2$, vacancy ordering, cryst. stabilisation energy aspects 80−103325
$Fe_{1-x}Si_x$ film, optical and magneto-optical characts., mag. preps. 79−82956
$Fe_{100-x}Si_x$ ribbon, magnetostriction exam. 79−73794
Fe_2Si-transition metal alloys, Heusler type materials, mag. props. 77−40042
$\alpha\text{-}Fe_2Si_5\text{-}\varepsilon\text{-}FeSi$ eutectic, orientation relationships 78−31397
Fe_3Si, 3d transition metal substituted, limits of solubility, mag. props. and electron conc. 78−10670
Fe_3Si, elastic consts., elec. resist. 77−39815
Fe_3Si, electronic structure, X-ray spectra comparison with band struct. calcs. 80−97383
Fe_3Si, electronic structure, magnetic moments 80−107695
Fe_3Si, etching of slip produced antiphase domain boundaries 78−63769
Fe_3Si hardening and softening during absorption fatigue in surface active medium, governing laws 77−86230
Fe_3Si, ordering energy, electron micrography determ. 78−14353
Fe_3Si, transition metal impurities, hyperfine fields 77−59365
Fe_3Si-based alloy, dil., cond. electron polarisation and moment perturbations 78−68224
Fe_3Si-based dil. alloys, conduction electron polarisation, moment perturbations 78−68225
$Fe_{3+x}Si_{1-x}$, electron transport 78−91669
$Fe_{95}Si_5$, thermal and elec. cond., heat transport by spin waves 79−38047
Fe_xSi_{1-x}, amorphous, high field magnetisation meas. 78−39367
Fe_xSi_{1-x}, amorphous, mag. behaviour, rel. to Fe_xSn_{1-x} and Fe_xGe_{1-x} amorphous, alloys 78−95478
Fe_xSi_{1-x}, amorphous, struct. and mag. props., giant moment form. at mag. ordering 78−68192
Fe_xSi_{1-x} amorphous alloys, magnetisation meas. showing crit. conc. at x=0.4 77−59429

silicon alloys continued
Fe_xSi_{1-x}, amorphous film, magneto-optic Kerr effect 80−66158
Fe_xSi_{1-x}, struct. exam. by electron diffr. and resist. meas. 77−89409
$Fe_3Si_{1-x}Al_x$, hyperfine interactions and structural disorder, spin echo, X-ray and magnetisation meas. 77−32289
$Fe_3Si_{1-x}Al_x$, hyperfine-field distrib. 79−69732
$Fe_3Si_xAl_{1-x}$-Co, dil., site preference of ^{57}Co impurities, Mossbauer study 80−39999
$Fe_xSi_yAl_z$ ribbon, magnetostriction exam. 79−73794
Fe_5SiB_2, Mossbauer spectra, 140-784K, spin rotation 78−52409
$Fe_{75}(Si_{0.5}B_{0.5})_{25}$ film, amorphous, sputtered, ferromag., thermal stability 78−76280
$Fe_{75}Si_{15}B_{10}$, amorphous ferromag. ribbons, US rel. meas. 77−80582
$Fe_{75}Si_{15}B_{10}$, amorphous ferromagnetic alloy, isothermal annealing effect on static magnetic props. *(Japanese)* 79−52398
$Fe_{75}Si_{15}B_{10}$, duplex ferromag. alloy, thermoremanent magnetization 79−73778
$Fe_{75}Si_{15}B_{10}$, mag. behaviour rel. to magnetostatic interactions 80−11224
$Fe_{78}Si_{10}B_{12}$ amorphous ferromag. ribbons, change of permeability by heat treatment 77−85493
$Fe_{78}Si_{10}B_{12}$, amorphous toroidal core, switching characts. and domain structs. 78−95477
$Fe_{78}Si_{10}B_{12}$ amorphous ribbons, magnetomechanical coupling constant and Young's modulus, mag. annealing 79−15333
$Fe_{79.5}Si_{1.5}B_{19}$, evaluation of hyperfine parameter distribs. from overlapped Mossbauer spectra at room temp. 79−99804
$Fe_{80}Si_5B_{15}$, amorphous, soft mag. props. and potential uses 80−88807
$(Fe_{1-x}Si_x)_{1-y}By$, metallic glass, mag. props., crystallisation 80−65885
$Fe_{3-x}V_xSi$, Fe hyperfine fields 79−78055
$Fe_{3-x}V_xSi$, selective site substitution and spin polarisation 79−78583
$Fe_{3-x}V_xSi$, struct., magnetisation, and spin echo expts., rel. to local environment model 77−20518
Gd-Fe-Si, phase diagram 79−52158
Gd-Si amorphous films, spontaneous Hall effect and elec. resist. 80−80251
$GdCu_2Si_2$/Mo, point contact spectroscopy of magnons 79−38312
$Gd_xPd_{82-x}Si_{18}$ amorphous alloys, mag. susceptibility, 4.2-300K 77−66248
$(Ge,Si)_{1-x}Y_x$, Y=H,F,B,P,..., amorphous struct., kinetically determined topological model 79−55666
Ge-Si alloy, quenching from high temp., thermal electric parameters, obs. 77−28165
Ge-Si-Sb solid soln., distrib. of components in universal furnace expt. in Soyuz-Apollo programme *(Russian)* 78−31381
GeSi alloy, composition determ. by ellipsometry 79−83537
$HfFe_{2-x}Si_x$, Laves pseudo-binary compound, cubic C15 phase stabilisation 77−39559
$HfFe_{2-x}Si_x$, Mossbauer spectra, hyperfine interactions 80−15862
$HfFe_2Si_2$, cryst. struct. 77−31633
$Hf_3Ni_2Si_3$, struct., lattice consts., space group, X-ray Weissenberg camera data 78−47284
$IrSi_x$, formation, Ir films on Si, He ion backscatt. X-ray diffr. study 79−82471
$LaAg_2Si_2$, ^{29}Si NMR and mag. susceptibility 79−61246
$LaAu_2Si_2$, ^{29}Si NMR and mag. susceptibility 79−61246
$LaCu_2Si_2$, ^{29}Si NMR and mag. susceptibility 79−61246
$LaCu_2Si_2$, resistivity, thermal conductivity and thermopower between 1.5 and 300K 78−87963
Li-Si, eval. as negative electrodes for Li-FeS_2 cells, thermodynamic props. 77−16547
LiSi/Fe$S(S_2)$ battery developments for electric vehicle propulsion and load levelling appls. 80−61325
Mg-Si, unidirectional solidification, method for determ. of diffusion and thermal diffusion coeffs. in molten Mg 78−30772
Mg-Si (5 wt.%), thermally induced strains, X-ray line broadening 77−4809
$MgSi_2$, laser irrad. induced form., cryst. microstruct. 80−35011
Mg_2Si, semicond., electronic band struct., reson. Raman scatt. meas. 77−12384
Mg_2Si, stress effects on Raman spectra 77−20851
Mg_2Si, valence band, XPS meas. 77−8018
Mg_2Si, valence band density of states, pseudopot. calc. 78−72067
Mn-(Fe)-Si-C, activity determ. by vapour press. meas. *(Japanese)* 77−63631
Mn-Fe-Si-C, melts, activities of Mn at 1673K 80−50597
Mn-Si, activity determ. by vapour press. meas. *(Japanese)* 77−63631
Mn-Si, liq. alloys, equilibria between MnO-SiO_2-CaO-MgO slags 80−10639
Mn-Si, liq. thermodynamic props., rel. to alloy form. 77−7875
Mn-Si, melt, activation determ. by vapour press. meas. 80−16279
Mn-Si (62.5 to 63.8 wt.%), phase anal. and cryst. struct. *(Japanese)* 80−15049
Mn-Si liquid alloy, vapour-pressure meas. using torsion effusion method 79−42215
Mn-Si-C, melts, activities of Mn at 1673K 80−50597
MnCoSi, effect of press on mag. transition temp. *(Russian)* 80−25137
MnCoSi, mag. struct. *(French)* 78−39323
$(Mn_{0.95}Cr_{0.05})_3Si$, sp. ht. at low temps., mag. transitions *(Russian)* 77−32189
$Mn_{1-x}Fe_xSi_{1.7}$, solid soln. system, temp. depend of conductivity and thermo-EMF, conc. depend of Hall const. 77−11913
$Mn_{77}Fe_4Si_{19}$, cryst. struct. and superstruct. 77−35511
β-$Mn_{66}Ni_{20}Si_{14}$, X-ray crystal struct. refinement 79−14735
$MnNiSi_{1-x}Ge_x$, mag. props. 77−12118
MnSi, amorphous, spin glass transition, AC susceptibility meas. 80−75779
MnSi, amorphous magnetisation meas. 80−34599
MnSi, crit. transverse US attenuation, spin fluctuations 78−48022
MnSi, electronic energy band struct., self-consistent APW calc. 80−65433
MnSi, helically ordered state, ^{55}Mn and ^{28}Si NMR 78−43655
MnSi, itinerant electron system, helical spin structure 78−23234
MnSi, itinerant electron system, neutron scatt. 78−68194
MnSi, itinerant ferromag. spin dynamics field depend. 79−38315
MnSi, low field mag. studies 78−23255
MnSi, mag. anisotropy exam., ferromag. to antiferromag. transition 79−73708
MnSi, mag. phase diagram, crit. US attenuation 77−12122
MnSi, mag. phase diagram, US attenuation meas. 77−63188
MnSi, μ^+ Knight shift, temp. depend. 78−80270
MnSi, μ^+ probe, itinerant electrons spin fluctuations 79−56671
silicon alloys continued
MnSi, μ^+ spin relax. 79−56670
MnSi, NMR and susceptibility above T_c 78−43665
MnSi, weak itinerant ferromagn., mag. excitations, neutron scatt. obs. 78−34969
MnSi, weak itinerant ferromagnet, mag. excitations 79−7985
MnSi-CoSi solid solution, mag. props. 78−56403
MnSi-Si system, striations and cryst. struct. of matrix 80−103292
$MnSi_{\sim 1.73}$ crystal growth and characterisation 80−93474
Mn_3Si, electronic structure, X-ray spectra comparison with band struct. calcs. 80−97383
Mn_5Si_3, interface struct. and growth mechanism from melt 79−14715
Mn_5Si_3, polycrst., mag. struct., 66-100K *(Russian)* 78−68161
Mn_5Si_3-Mn_5Ge_3, electrical resistivity meas., order-disorder transition 80−10945
$Mn_{85.5}Si_{14.5}$, R-phase, cryst. struct. 78−42953
$Mn_5(Si_{1-x}Ge_x)_3$, magnetic and cryst. struct., ferromag. props. 77−59391
$Mn_5(Si_xGe_{1-x})_3$ solid solution, mag. ordering, magnetisation and neutron scatt. meas. 78−27023
Mo fibre reinforced AlSi, SEM study *(Slovenian)* 78−84923
Mo film on Si surface, $MoSi_2$ form. conditions *(French)* 78−43270
Mo-Co-Si, cryst. struct. and defects, high resolution electron microscopy obs. 79−94961
Mo-Mn-Fe-Si/Al_2O_3 ceramic seal, interfacial phases 78−72011
Mo-Ru-Si, amorphous superconductors, prep. by electron beam evaporation and liq. quenching, crit. temp. 80−103776
Mo-Si, amorphous supercond. alloy, produced by coevaporation, struct. and supercond. 79−91179
Mo-Si coating on Nb and Nb alloys, protection against high temp. oxidation *(Russian)* 79−39029
$(Mo_{0.6}Ru_{0.4})_{80}Si_{10}B_{10}$, amorphous supercond. matrix, flux pinning by MoRu precips. 80−65756
$MoSi_2$, diffusion grown layers, texture 79−74095
$MoSi_2$, effect of Al on oxidation behaviour *(German)* 78−31587
$MoSi_2$, SiO_2 coating effect on oxidation, AES study *(German)* 79−74298
$MoSi_3$, high temp. material, coatings, powder metallurgy, review *(German)* 79−74295
Mo_3Si, layer growth, effect of DC density, temp. 79−43160
Mo_3Si, Mo_5Si_3 and $MoSi_2$, ultrasoft X-ray emission bands, empirical band schemes 78−15249
Mo_3Si, $MoSi_2$, form., Mo thin film on Si, He^+ backscattering, X-ray diffr. study 78−43261
Mo_5Si_3 layer growth, effect of DC density, temp. 79−43160
$Mo_{70}Si_{20}B_{10}$, amorphous alloys obtained by liq. quenching, superconductivity 80−75670
Monel, Norton-Bailey parameters, from creep rupture data 80−30098
Nb-Al-Si, supercond. transition temp., Si conc. depend. 78−84339
Nb-Ge-Si, A15 struct. superconductor, high field transport props. TEM study 80−34574
Nb-Ge-Si, compounds with A15 structure, films, TEM study *(French)* 80−80135
Nb-Ge-Si, Si effect on raising superconducting transition temp. in pelicular specimens *(Russian)* 78−23188
Nb-Ge-Si, supercond. state transition temp., influence of Si on alloy constitution *(Russian)* 79−78244
Nb-Ge-Si film, CVD, struct., comp., stability and homogeneity 80−15421
Nb-Si, amorphous supercond. alloy, produced by coevaporation, struct. and supercond. 79−91179
Nb-Si, compounds with A15 structure, films, TEM study *(French)* 80−80135
Nb-Si amorphosamorphous thin film tunnel junctions 79−28473
Nb-Si and Nb-Ge-Si, A15 cpds., CVD prep. and supercond. crit. temp. 79−60949
Nb-Si compounds, CVD, struct. and supercond. props. 79−24447
Nb-Si diagram of state, melting temp., polymorphic transform. temp. *(Russian)* 80−50594
Nb-Si film, superconductivity close to A15 stoichiometric phase 79−95540
Nb-Si liquid quenched alloy, metastable A-15 and amorphous phases, interstitials 80−54394
Nb-Si-C, phase equilib. and supercond. 80−50593
Nb-Si-Sn(Pt)(Ir), A15 cpds. prod. by liq. quenching, phase stability and supercond. props. 79−95538
Nb-Si(−V)(Zr)(Mo)(Ta)(W)(C)(B)(Ge), ductile amorphous, superconductivity 80−60131
Nb-Sn-Si, ternary A15 phase regions, solubility 77−44215
Nb_3(Al,Si), liq. quenched, supercond. props. 80−84580
Nb_3(AlSi), electronic characts. from thermomodulation spectra 79−87421
Nb_3(AlSi) film, thermomodulation spectra, 1.1-2.8 eV 78−48250
Nb_3(AlSi), ternary supercond. alloy films, T_c, props. *(Russian)* 78−88055
$Nb_3Al_{0.2}Si_{0.8}$, A-15 alloy synthesis by ion implantation 78−80489
$NbFe_{2-x}Si_x$, crystalline struct., electron microscopy determ. *(French)* 80−54174
$Nb_{78}Fe_{40}Si_{80}$, X-ray cryst. struct. determ. *(French)* 80−15048
Nb_3(Ge,Si) A15 film, supercond. and structural props. 79−87177
Nb_3(Ge, Si) CVD tapes, supercond. props. at high mag. fields 79−38279
$Nb_3(Nb_{1-x}Si_x)$, impurity stabilised A15 supercond., transition temp., lattice consts., specific heat 80−93026
$NbSi_2$, superconducting transition temp. meas. of sputtered films and bulk 80−7019
Nb_3Si, A-15 diffusion layers, influence of additions of growth and supercond. props. *(German)* 80−11130
Nb_3Si A15 phase from amorphous Nb-Si alloys, high-press. synthesis 80−93516
Nb_3Si A15 struct., high press. synthesis *(Chinese)* 80−70917
Nb_3Si, A15 struct., synthesis at high press., preferable conditions *(Chinese)* 77−48363
Nb_3Si, amorphous films, thermally-activated internal friction peaks, structural obs. 80−80147
Nb_3Si, electronic struct. calcs. 79−47005
Nb_3Si, electronic struct., electron-phonon interactions, and low temp. anomalies 79−60701
Nb_3Si epitaxial layers, ion implantation synthesis, supercond. transition temp. optimization 79−38218
Nb_3Si film, quasiamorphous, supercond. phase formation by heat pulse 77−63017

silicon alloys continued
Nb_3Si film, supercond., obtained by vaporisation in vacuum, props. 78−14865
Nb_3Si films, form. of A15 phases by DC sputtering 79−38740
Nb_3Si, high press. phase, prod. by recrystn. of metastable sputter deposits, struct. and supercond. props. 78−60571
Nb_3Si, high T_c, supercond. props. from extrapolation of sp. ht. meas. on A-15 Nb-Si 80−25045
Nb_3Si, high T_c supercond., anal. of X-ray traces 79−56098
Nb_3Si, hypothetical, electronic struct., lattice parameters and possible supercond. transition temp. 79−23891
Nb_3Si, metastable A-15 struct. synthesis by ion implantation, supercond. transition temp. 80−55319
Nb_3Si, RF sputtered films, amorphous atomic scale struct. 80−84064
Nb_3Si, structural and supercond. props. press. effects 80−39700
Nb_3Si, substituted, splat cooling influence on supercond. T_c and stoichometry 80−80439
Nb_3Si, supercond., A15 film, electron beam evaporation 80−29284
Nb_3Si, supercond. phase, formation by explosive compression 79−82701
Nb_3Si, supercond. transition temp., rel. to A15 phase stability 78−52137
Nb_3Si, superconducting, high transition temp., sputtering 78−15309
Nb_3Si, superconducting A-15 type compounds, transition temp., radii ratio and structure *(Chinese)* 80−44752
Nb_3Si type with A15 struct., supercond. transition temp., depend. on stoichiometry *(German)* 77−69444
Nb_4Si, Nb_5Si_3 and $NbSi_2$, ultrasoft X-ray emission bands, empirical band schemes 78−15249
Nb_5Si_3, supercond. props. and cryst. struct. 79−78245
NdSi mag. struct. and mag. moments, neutron diffr. meas. 77−85424
Ni-Al-Si, β-phase stability *(Russian)* 78−39738
Ni-Al-Si, diffusion, lattice parameter, microhardness, and constitution, effect of Si additions *(Russian)* 80−84316
Ni-Be bronze, Fe and Si alloying addition effect on phase composition *(Russian)* 78−15360
Ni-Cr-B-Si, hard faced with WC, exam. of abrasion and wear props. 79−34202
Ni-Cr-B-Si-Fe alloy, Cr content by X-ray fluoresc. 79−43654
Ni-Cr-Fe-Si-B wear-resist. and corrosion-resist. coatings by furnace melting 80−35428
Ni-Cr-Si, corrosion and failure mechanisms of coatings for gas turbine applications 79−29284
Ni-Cr-Si, thermocouple alloy, props. and thermoelec. reference data 79−26057
Ni-Cr-Si (10, 1.8 wt.%), Zr, Hf, La or Sm alloying additions effect on oxidation resist. 77−63831
Ni-Cr-Si alloy system, oxidation resist. 79−24661
Ni-Cr-Ta-Ti-Si, EP557 precipitation hardening alloy, mech. props., heat treatment effect 80−60877
Ni-Cr-W-C-Si, hardness, corrosion resistance, wear resistance tests in 10% HCl *(German)* 78−92368
Ni-Cr-W-C-Si, struct. and props. of corrosion and wear resistant alloys 79−24627
Ni-Cu-Si, Si effect on structural changes during ageing, TEM and X-ray obs. 78−15438
Ni-Cu-Si (37.6, 6.1 at.%), spinodal decomposition, morphology of microstructure, elastic strain energy anisotropy effect 78−15354
Ni-Cu-Si (38,5 at.%), changes in modulated struct. during ageing early stages *(Japanese)* 79−100183
Ni-Mn-Al-Si-Co, Alumel, Ettingshausen-Nernst coeff. and transport props. from 200 to 473K 80−44573
Ni-Mo-Cr-Si, plasma and detonation coatings, Laves- and carbide-strengthened, comparative props. 78−15562
Ni-Pd-Si, amorphous, low-field mag. susceptibility meas., 4.2-580K 79−61057
Ni-Pd-Si, phase composition, isothermal section at 800°C *(German)* 77−16544
Ni-Si, band model of high temp. magnetism 78−26809
Ni-Si, Cs ion-bombarded, surface Cs concs., AES meas. 79−83073
Ni-Si, defect-solute interactions and radiation-induced segregation 80−25705
Ni-Si, dil., mag. props. at elevated temps. 77−63089
Ni-Si, effect of solute misfit and temp. on irradiation induced segregation 78−72779
Ni-Si, intergranular segregation of Si, electron energy loss spectrometers, X-ray anal. *(French)* 79−8388
Ni-Si, ion beam irradiation induced Ni_3Si surface film segregation 78−38761
Ni-Si, liquid, surface tension model using surrounded atom concept 77−15665
Ni-Si, magnetoresistivity anisotropy, spin mixing 80−88538
Ni-Si, proton irrad., γ' precipitation, early stages 80−34096
Ni-Si, solidified from supercooled condition, Si conc. influence on struct. *(Russian)* 77−16567
Ni-Si (1 at.%), dose depend. of ion irradiation induced segregation 79−42123
Ni-Si (12.7 at.%), heterogeneous precipitation at internal and external surfaces during Ni ion irradiation 79−77647
Ni-Si (12.7 wt.%) Ni^+ ion irradiation, precipitate restructuring, mechanisms and kinetics 79−77650
Ni-Si film system, silicide first phase form., reaction kinetics 78−79821
Ni-Si liquid alloys, thermodynamic props., enthalpy of mixing *(Russian)* 80−34207
Ni-Si melt, ultra acoustic study *(Russian)* 78−15613
Ni-Si melt refining by electric fields, ionic conduction of Ni, Si *(Russian)* 80−65273
Ni-Si solid soln., radiation, induced precipitation dose rate effects 78−6936
Ni-Si solid soln., radiation-induced solute redistribution and precipitation, model 79−19277
Ni-Si solid solution alloys, γ phase precipitation under irrad. 77−1839
Ni-Si:Cr, He^+ radiation-enhanced diffusion and segregation effects of point-defect trapping 79−77824
Ni-Si-B, amorphous, thermal stability of ductility 80−76327
Ni-Si-B, embrittlement by crystallisation *(Japanese)* 78−48513
Ni-Si-B amorphous alloys with metalloid elements, embrittlement/crystn. relationship *(Japanese)* 79−96134
Ni-Si-B powder, oxidation at 850°C, SEM, ESCA, and elec. cond. meas. 80−7717
Ni-Si-Mg, thermocouple alloy, props. and thermoelec. reference data 79−26057
Ni-Si-Mn(Al) alloy systems, oxidation resist. 79−24661

silicon alloys continued
Ni-SiC, electrodeposited, oxidation 78−64756
Ni-SiC coating, heat treated, as plated, electrochemical study of corrosive wear 80−16536
$Ni_{0.7}Cu_{0.3-x}Si_x$, magnetic props., 4.2 to 800K 77−8290
$Ni_{78-x}M_xSi_{10}B_{12}$ (M=refractory metal), glass form. and thermal stability 80−79703
$(Ni_{0.75}Mn_{0.25})_{82}Si_{10}B_8$, amorphous, exchange anisotropy, mag. susceptibility meas., 4.2K to room temp. 80−11186
NiSi, dissociation in presence of Ni film 79−47892
NiSi, partial sputtering yields 77−8696
NiSi-Si:As(Sb), implanted dopant redistrib. after silicide form., appl. to ohmic contacts 79−37729
$NiSi_2$, epitaxial film on Si, ^4He ion channelling meas. and RHEED anal. 80−10834
$NiSi_2$, layer, on Si, ion implantation damage, channelling obs. 78−30676
$NiSi_2$ layer, on Si, struct. modelling, using axial and phase channelling techniques 79−4489
$NiSi_2$, substrate ion implantation, channelled, through metal silicide film 80−70231
$NiSi_x$, cryst. struct. of phase *(German)* 79−99119
$Ni_{1-x}Si_x$, electronic states of Si NMR study 80−50216
Ni_2Si formation at Ni film/Si wafer interface, marker motion obs. 77−89593
Ni_2Si formation from Ni-Si sample, obs. by ^{31}Si tracer and Rutherford backscatt. methods 79−4431
Ni_2Si coatings, form. and stability during high temp. irrad. 80−35088
$Ni_{76}Si_{24}$, ordered BCC phases at high temp. 79−32948
Ni_3Si contact for n-type Si, current load capacity meas. *(Czech)* 77−89846
$Ni_{78}Si_{10}B_{12}$, amorphous, struct. factor temp. depend., X-ray diffr. study *(Japanese)* 79−51005
Np intermetallics, NpM_2Si_2, (M=Cr, Mn, Fe, Co, Ni, Cu), Mossbauer and magnetization expts. 78−31138
$NpCo_2Si_2$ and $NpFe_2Si_2$, itinerant magnetism obs. 77−28406
$NpCo_2Si_2$, mag. props., high press. studies with $^{237}Np(60)$-resonance 80−39924
$NpCo_2Si_2$, mag. struct., neutron diffr. determ. 80−93084
$NpCu_2Si_2$, mag. struct., neutron diffr. determ. 80−93084
$NpFe_{2-x}Co_xSi_2$, mag. and hyperfine props. 79−51887
$NpFe_{2-x}Co_xSi_2$, mag. and hyperfine props. 80−7247
Pb-Ni-Si, metallic glass, electron irrad., positron annihilation radiation, angular correlation study 78−84678
Pb-Si amorphous films, supercond. transition temp. and residual elec. resist. *(Russian)* 79−19680
Pb-Si-Sb amorphous alloys, electrical resistometric detection of relaxation 79−60278
Pd-Ag-Si alloys, amorphous, crystn. kinetics, DSC meas. 80−1933
Pd-Au-Si, amorphous films, RF sputter deposition, composition and thermal behaviour 80−55292
Pd-Au-Si, influence of struct. on elec. resist. of glass forming alloys 80−65518
Pd-Cu-Si, glass form., crit. cooling rate 80−75169
Pd-Cu-Si, laser melting and splat quenching to form foils for TEM obs. 80−29986
Pd-Cu-Si, metallic glass, miscibility limits, computer study 79−65198
Pd-Cu-Si glass, cold drawn, serrated plastic flow, optical and SEM study 79−79052
Pd-Cu-Si metallic glass, energy loss spectra and Auger spectra 78−23563
Pd-Ni-Si amorphous alloys, crystn. process during isothermal ageing 80−89275
Pd-Si, amorphous, compositional study on short-range struct. 80−84095
Pd-Si, amorphous, neutron irradiated, small angle X-ray scatt. study 79−14850
Pd-Si, amorphous, struct., crystn. and Hall effect meas. 80−75178
Pd-Si, amorphous, US velocity, freq. and temp. depend. 78−63812
Pd-Si, amorphous alloys, elastic props. and temp. coeff. of delay time, appl. to US delay lines *(Japanese)* 79−96069
Pd-Si, amorphous metallic, sound propag. at low temps. 77−72656
Pd-Si, amorphous metallic glass, with defined local coordination, struct. model 80−84092
Pd-Si, amorphous $Pd_{0.8}Si_{0.2}$, struct. anal. by dense random packing model 79−51003
Pd-Si, amorphous viscoelastic behaviour *(Japanese)* 77−86110
Pd-Si, glassy, phonon transport below 100K 78−14422
Pd-Si, liq., mag. susceptibility 78−95415
Pd-Si, melt, struct. and physical-chemical props., thermodynamic props. *(Russian)* 78−18536
Pd-Si, metallic glass, phonon propagation at low temp. 78−87756
Pd-Si, metallic glass, theoretical studies on structural models 79−37633
Pd-Si, metallic glasses, XPS and UPS studies 79−74062
Pd-Si, struct. obs. by X-ray diffr., low temp. annealing and deform. effects 79−56995
Pd-Si alloys, metallic glass, structural model 79−14690
Pd-Si amorphous, internal friction and shear modulus 77−25085
Pd-Si amorphous alloy, heat treated, low temp. lattice sp. ht. 80−75368
Pd-Si amorphous alloy, neutron irradiation effects *(Japanese)* 77−84806
Pd-Si amorphous alloy, positron annihilation exam. of crystallisation 79−43061
Pd-Si amorphous alloys, anal. of crystallisation kinetics 79−32912
Pd-Si amorphous films, RF and DC sputter deposition, composition and thermal behaviour 80−55292
Pd-Si glass, thermal cond., 01.-30K 77−20286
Pd-Si glasses, changes in density of states with alloys comp., UPS obs. 80−50531
Pd-Si layers, form. by laser irrad. of Pd film on Si substrate 79−99438
Pd-Si melts, appl. of quasichem. method of cluster components *(Russian)* 77−80623
Pd-Si metallic glass, high-resolution electron microscopy 80−84097
Pd-Si-Cu metallic glass tips, appl. as electron field emission source 79−8229
Pd-Si-Fe amorphous alloy, Mossbauer spectra, struct. and bonding 80−7224
Pd-Si-H(D) alloys, superconductivity in solid solution and amorphous phase regions, isotope effect 79−56347
Pd-Si-Sb, amorphous, phase separation and crystallisation 79−51002
Pd-Si-Sb, mostly crystalline, rapidly quenched, mech. props. 79−61610
Pd-Si(-Cu), amorphous, Hall effect meas. and electronic struct. 80−75551

silicon alloys continued
Pd-Si(-Cu) amorphous ribbons, low temp. sp. ht., density of states trends 80−79957
Pd-Si(−Cu), glassy, liq. and cryst., mag. and elec. props. 77−66249
$Pd_{78}Ag_4Si_{18}$, amorphous, crystallisation kinetics 77−35487
$Pd_{82-y}Ag_ySi_{18}$, amorphous, roller-quenching conditions determ. 77−21051
$(Pd_{80}Au_7Si_{13})/Fe_{30}$, compositionally modulated amorphous film, diffusion, struct. relax. 80−103518
$Pd_{0.775}Cu_{0.06}Si_{0.165}$ alloys, glassy and crystallised, low-temp. specific heat 79−60516
$Pd_{0.775}Cu_{0.06}Si_{0.165}$ glass, optical props. in energy range 0.67 to 5.6 eV 80−34872
$Pd_{68.5}Cu_{15}Si_{16.5}$ glass, elec. resist., struct. and mag. props. 79−65423
$Pd_{77.5}Cu_6Si_{16.5}$, cold drawn wires, surface markings, fracture stresses 79−56997
$Pd_{77.5}Cu_6Si_{16.5}$, heat of crystn. and viscous behaviour 80−75166
$Pd_{77.5}Cu_6Si_{16.5}$ metallic glass, diffusion of Au 78−55983
$Pd_{77.5}Cu_6Si_{16.5}$, metallic glass, composition, mech. props., simulation 80−49117
$Pd_{77.5}Cu_6Si_{16.5}$ metallic glass wire, cold drawing 80−50650
$Pd_{77.5}Cu_6Si_{16.5}$, ternary miscibility gap, simulation, dispersed phase composite form. 80−54379
$Pd_{77.5}Cu_{6.0}Si_{16.5}$ metallic glass, glass transition temp., cooling rate depend. 80−75181
$Pd_{77.6}Cu_6Si_{16.5}$, metallic glass, viscosity meas. from rates of thermal transformations 78−26713
$Pd_{781}Cu_{55}Si_{164}$ glass, erosion craters produced by spark machining, scanning microscopy obs. 78−44268
$Pd_{781}Cu_{55}Si_{164}$, liquid quenched metallic glass, wear resistance 79−66079
$Pd_{70}Fe_{10}Si_{20}$ alloy, amorphous to cryst. transition, 350 to 450°C, Mossbauer spectra 78−59758
$Pd_{60}Ni_{20}Si_{20}$, amorphous, struct., high resolution electron microscopy 80−1969
$Pd_{81}Si_{19}$ and $Pd_{84}Si_{16}$, metallic glasses, optical refl. spectra and optical consts. 79−87464
PdSi alloys, amorphous thermal behaviour and crystallisation kinetics 78−26446
PdSi, amorphous, crystn. kinetics 79−99078
PdSi, amorphous, structural relaxation enhancement following stress reduction 80−3118
PdSi films, on Si, stress obs. 80−80145
PdSi, formation by Xe ion beam bombard. of Pd film on Si substrate 80−10800
$a\text{-}Pd_{0.8}Si_{0.2}$ alloy, struct. factor determ. rel. to short-range correlations 77−1060
$Pd_{0.8}Si_{0.2}$, amorphous, He^{2+} ion irradiation effect on structure 79−42120
$Pd_{0.8}Si_{0.2}$, amorphous ribbon, struct. factor anisotropy, pulsed neutron diffr. study 78−87619
$Pd_{0.8}Si_{0.2}$, liquid and amorphous states, short-range order comparison 77−1069
$Pd_{0.81}Si_{0.19}$, amorphous, partial densities of states, XPS, UPS and AES meas. 79−95315
Pd_2Si, Cs ion-bombarded, surface Cs concs., AES meas. 79−83073
Pd_2Si, epitaxial film on Si, ^4He ion channelling meas. and RHEED anal. 80−10834
Pd_2Si film, on Si, metallic, resist. and Hall mobility meas. 78−47886
Pd_2Si film on Si, substrate temp. effect on microstruct., TEM obs. 78−14621
Pd_2Si films, on Si, stress obs. 80−80145
Pd_2Si films on Si, lattice imaging obs. of structural details 80−103604
Pd_2Si, form. in Si-Pd-Ti evaporated films 80−80006
Pd_2Si, formation at Pd-Si (111) interface, UPS obs. 80−24743
Pd_2Si formation from Pd-Si sample, obs. by ^{31}Si tracer and Rutherford backscatt. methods 79−4431
Pd_2Si layer, on Si, ion implantation damage, channelling obs. 78−30676
Pd_2Si layer 79−4489
Pd_2Si, on Si substrate, thermally induced Si accumulation, AES study 80−24718
Pd_2Si, solid-phase epitaxy in Si (100)/Pd_2Si/Si (amorphous) system, radioactive tracer obs. 77−89663
Pd_2Si-Si, Schottky barrier, for solar cell appl., elec. characts. 78−14825
Pd_2Si-Si, substrate ion implantation, channelled, through metal silicide film 80−70231
Pd_2Si-Si Schottky barrier diode grown by solid phase epitaxy 77−80837
Pd_2Si-Si:As(Sb), implanted dopant redistrib. after silicide form., appl. to ohmic contacts 79−37729
$Pd_{80}Si_{20}$, amorphous, electronic struct. calc. 79−87032
$Pd_{80}Si_{20}$, amorphous, elec. resist. and magnetoresist. 80−49693
$Pd_{80}Si_{20}$, amorphous, structural changes by neutron irradiation, X-ray scatt. meas. 78−6104
$Pd_{80}Si_{20}$, amorphous, struct. factor temp. depend., X-ray diffr. study *(Japanese)* 79−51005
$Pd_{80}Si_{20}$, amorphous, structural changes with neutron irrad., X-ray scatt. obs. 80−33898
$Pd_{80}Si_{20}$, amorphous alloy crystn., high press. effect 78−95001
$Pd_{80}Si_{20}$, amorphous alloy, partial struct. functions, X-ray, electron and neutron diff. studies *(Japanese)* 80−88050
$Pd_{80}Si_{20}$ amorphous alloy, skip deform. and crit. shear stress, using tensile testing machine 80−89321
$Pd_{80}Si_{20}$, glass, deform. localisation, plastic instabilities and fracture 80−89320
$Pd_{80}Si_{20}$ glass, struct. simulation 78−38624
$Pd_{80}Si_{20}$ metallic glass, struct. relax., X-ray expts. 79−1400
$Pd_{80}Si_{20}$ metallic glass, vibrational spectrum, inelastic neutron scatt. meas. 79−60465
$Pd_{80}Si_{20}$ metallic glass, high-resolution XPS study, electronic state struct. 80−29846
$Pd_{80}Si_{20}$, metallic glass, composition, mech. props., simulation 80−49117
$Pd_{80}Si_{20}$ metallic glass, inelastic deform., free energy spectra 80−71699
$Pd_{80}Si_{20}$ metallic glass, tensile deform., shear band form., high-speed cinematographic obs. 80−89322
$Pd_{80}Si_{20}$, plastic flow, fracture, slanted necking and elongation at high temps. 79−57057
$Pd_{80}Si_{20}$, shear band form. 78−68756
$Pd_{80}Si_{20}$, vapour quenched amorphous alloy, atomic arrangements 80−100173
$Pd_{82}Si_{18}$ glassy, long term creep tests, isoconfigurational viscosity rel. to annealing treatment 79−66122
$Pd_{82}Si_{18}$, stress/strain rate depend. of homogeneous flow 80−71687
$Pd_{82.5}Si_{17.5}$, amorphous and liq. alloys, struct., X-ray diffr. 77−24275
silicon alloys continued
$(Pd_{86}Si_{15})_{61}/(Fe_{85}B_{15})_{39}$, compositionally modulated amorphous film, diffusion, struct. relax. 80−103518
PdSiCu, amorphous, US attenuation and vel. studies 80−19881
PdSiCu, amorphous, US attenuation and vel. studies at low temps. 80−88278
$Pd_{0.775}Si_{0.165}Cu_{0.06}$, glassy alloy, resist. minimum associated with mag. impurities 79−56187
$Pd_{0.775}Si_{0.165}Cu_{0.06}$, metallic glass, intensity-depend. US attenuation at low temps. 78−79671
$Pd_{0.775}Si_{0.165}Cu_{0.06}$, metallic glass, 0.01-10K, relax of tunnelling systems by conduction electrons, US expts. 79−14889
$Pd_{0.78}Si_{0.16}Cu_{0.06}$, phonon propagation below 1K 78−71824
$Pd_{1-x-y}Si_xCu_y$, glassy, low temp. specific heat 78−83969
$Pd_{18}Si_{14}Cu_6$, glass, changes in density of states with alloys comp. UPS obs. 80−50531
$Pd_{77}Si_{17}Cu_6$, amorphous, struct. changes due to cold rolling and low temp. annealing 79−66072
$Pd_{77.5}Si_{16.5}Cu_6$ amorphous, indentation recovery, defect struct. produced by deformation 79−43275
$Pd_{80}Si_{17}Cu_3$, glass, changes in density of states with alloys comp., UPS obs. 80−50531
$Pd_{100-x-y}Si_xFe_y$, amorphous, ^{57}Fe Mossbauer spectra, X-ray diffr., ageing behaviour 79−28651
$Pd_{80-x}Si_{20}Fe_x$, amorphous, low x, hyperfine interactions and mag. ordering temp. 79−15303
$Pd_{82-x}V_xSi_{18}$, amorphous, effect of structural relax. on elec. resist. 79−56186
$Pd_{82-x}V_xSi_{18}$, metallic glasses, effect of press. on elec. resist. 80−6805
PrSi, mag. struct. and mag. moments, neutron diffr. meas. 77−85424
Pt-Si, constitution 79−29054
Pt-Si, Cs ion-bombarded, surface Cs concs., AES meas. 79−83073
Pt-Si film system, silicide first phase form., reaction kinetics 78−79821
Pt-Si layers, form. by laser irrad. of Pt film on Si substrate 79−99438
Pt-Si melts, surface tension and density *(Russian)* 80−39388
Pt-Si system, formation of Si enriched metastable cpds. using ion bombardment and post annealing 79−69143
Pt-Si thermally degenerated Schottky diodes, resonant tunnelling 80−100503
Pt-Si:As, silicide form. during laser irrad., p-n junctions and ohmic contacts 80−84397
PtSi, 10-160 keV Ar ion sputtering, Rutherford backscatt. obs. 79−15574
PtSi, Ar bubble formation after 20 to 160 keV sputtering, TEM and backscatt. spectrometry obs. 78−64435
PtSi, dissociation in presence of Pt film 79−47892
PtSi, epitaxial film, cryst. perfection and thermal stability, channelling and backscatt. meas. 79−99255
PtSi, epitaxial film on Si, ^4He ion channelling meas. and RHEED anal. 80−10834
PtSi film, on (001) Si, crystallography 78−75955
PtSi film formation by ion sputtering and annealing, form. and exam. problems 80−100782
PtSi films, on Si, stress obs. 80−80145
PtSi, form. kinetics, AES, SIMS, EPMA 77−11800
PtSi, growth rate for form. by Pt film deposition under ultrahigh vac. and controlled impurity atm. 80−65388
PtSi, partial sputtering yields 77−8696
PtSi Schottky-barrier monolithic IRCCD focal plane 80−86427
PtSi, substrate ion implantation, channelled, through metal silicide film 80−70231
PtSi surface, and interface with Si, impurity effects 80−80037
PtSi thin film structures, preferential sputtering meas. Rutherford backscatt. 79−43087
PtSi-n-Si, photoelec. barrier height and elec. props. 79−33344
PtSi-Si, Schottky barrier, for solar cell appl., elec. characts. 78−14825
PtSi-Si:As(Sb), implanted dopant redistrib. after silicide form., appl. to ohmic contacts 79−37729
Pt_2Si film formation, AES exam. to characterise impurity effects 79−15054
Pt_2Si formation from Pt-Si sample, obs. by ^{31}Si tracer and Rutherford backscatt. methods 79−4431
Pt_2Si, growth rate for form. by Pt film deposition under ultrahigh vac. and controlled impurity atm. 80−65388
Re-Al-Si , X-ray determ.of system *(Russian)* 78−19763
Re-Al-Si system, phase equilibria, $ReAl_{1.2}Si_{0.8}$, $ReAl_{1.25}Si_{0.75}$ prod., struct. 78−35357
$ReSi_2$, atomic volume deviations and supercond. T_c and elec. cond. 80−75203
Re_5Si_3, X-ray cryst. struct. determ., microhardness rel. to Re content 80−84142
Rh-Si, melts, surface props. *(Russian)* 78−26750
Rh-Si thin film interaction, interdiffusion, temp. depend. 80−54443
Rh_xSi_y-n-Sn Schottky diodes, rectifying barrier height meas. 80−49896
Sc-Co-Si, phase equil. and atomic struct. *(Russian)* 77−77462
Sc-Fe-Si system, phase obs. at 800°C *(Russian)* 78−23661
Sc-Rh-Si system, partial phase diagram, X-ray diffr. and microprobe anal. 80−25659
Sc_2M_3Si, M=Fe, Co, Ni, struct. determ. by X-ray powder method *(Russian)* 77−55261
$Sc_{(3)}Re_2Si_3$, X-ray cryst. struct. determ. 80−39009
Si:H, amorphous, solar cells using ultrathin active layer to increase conversion efficiency 80−94030
a-Si:H alloys, sputter deposited thin film coatings, property-comp. relationships 80−80975
a-Si:H highly homogeneous, for low-cost solar cell fabrication 80−72053
Si/Al-Si systeym, vacuum deposition, rate controlling and composition anal. by electron impact emission spectroscopy 79−91591
Si-Al, silumin, crystn. of eutectic phases *(Russian)* 80−29942
Si-Al C fibre composite technological coatings, liquid phase method preparation *(Russian)* 80−108375
Si-Al electrical steel, surface oxidation during annealing 78−68838
Si-Au, (LMM) Auger electron emission by keV Ar^+ bombardment 79−95880
Si-Au, amorphous, ESR linewidth var. with temp. and comp. 77−48033
Si-Au, solid soln., influence of precip. on relax. of ^{29}Si nucleus 80−11287
Si-Au alloys, direct synthesis by inplantation of Au^+ *(Japanese)* 79−28006
Si-Au amorphous film, metal-nonmetal transition, elec. cond., thermoelectric power meas. 79−47132

silicon alloys continued
Si-Au amorphous system, optical absorpt., IR photocond. 79−42582
Si-Au eutectic alloys, field ion sources 80−97414
Si-Au films, quenched condensed, elec. resist. and supercond. 80−54669
Si-Au system, ion implanted induced giant gettering, annealing effects 80−88221
Si-B amorphous film, plasma deposited, characterization 79−69828
Si-B based CVD coating for gas turbine blading, props. 80−40615
Si-C, coupled phase diagram and thermochemical data 79−95997
Si-C:H, amorphous film, vibr. spectrum 79−61450
Si-$CoSi_2$Si, double heteroepitaxy, solid phase and MBE 80−104063
Si-Cr, dil., spin density wave under high press., neutron diffr. study 80−65798
Si-Cu, (LMM) Auger electron emission by keV Ar^+ bombardment 79−95880
Si-Cu alloys, direct synthesis by implantation of Cu^+ *(Japanese)* 79−28006
Si-Fe, domain and grain obs. using ferromag. colloid technique 80−11219
Si-Fe, ferromagnetic domains and their junctions, simulation of X-ray topographs 79−78434
Si-Fe, freq. spectrum of Barkhausen noise of moving 180° domain wall 77−16115
Si-Fe-W, dil. alloy, compositional changes on sputtering, projectile energy depend. 80−66362
Si-Ge, solid soln., vol. effect on bulk modulus 80−24526
Si-H, amorphous, energy gap negative-U states, Si-H-Si three centre bond model 78−91606
Si-H, amorphous, sputtered, photolum. obs. 80−80856
Si-H, amorphous, struct. and press. induced transition 80−44131
Si-H, amorphous, structural and electronic props., review 80−64901
Si-H, RF sputtered amorphous alloy, influence of Ar press. on elec. props. and photoluminesc. 79−91585
Si-H:As alloy, amorphous film, coordination of impurities, EXAFS of data 77−84780
n-Si-$IrSi_x$, Schottky diode, rectifying barrier height meas. 79−99619
Si-Mn(Fe)(Co)(Ni), liquid alloys, thermodynamic charact. calc. *(Russian)* 78−27475
Si-Ni, (LMM) Auger electron emission by keV Ar^+ bombardment 79−95880
Si-Ni(Fe,Co,Cu,Ti) powder based composite, high temp. strength of W reinforcing fibres 79−70021
Si-Pd, (LMM) Auger electron emission by keV Ar^+ bombardment 79−95880
Si-Pd, preferred sputtering on surface, mass difference and chemical bonding difference effects, AES obs. 79−83078
Si-Pd film, preferred sputtering on surface, mass and bonding difference effects, AES obs. 79−87552
n-Si-Pd_2Si contact, interface struct. and Schottky barrier height, correl. obs. using TEM 80−100504
Si-Ti-Cr system, plasma coating on Nb, alloy substrates, radiating power 79−60529
$Si_{100-x}Al_x$, RF sputtered, amorphous, props. 80−34754
$Si_{1-x}Au_x$ amorphous films, IR absorpt. spectra 80−16034
$Si_{100-x}Au_x$, amorphous, dielec. anomaly, rel. to nonmetal-metal transition 78−2791
$Si_{1-x}B_x$:H, amorphous films, thermopower and cond. for mixed band and broad tail state cond. 80−49786
SiC, (LMM) Auger electron emission by keV Ar^+ bombardment 79−95880
SiC fibre reinforced Al-Si alloy, liq. phase process prep. effect on mech. props. 79−70020
SiC-B eutectic alloys, struct. of crystallising graphite 79−38829
$Si_{1-x}Co_x$ film, metastable impurity band, conductivity meas., semiconductor-metal transition 77−76884
SiFe sheets, grain-oriented, stray field meas. 80−88775
Si_xFe_{100-x} polycryst. ribbon, prep. by rapid quenching, and props. 80−75803
SiGe, ultra high vacuum epitaxy on Si substrates *(German)* 77−47702
Si_xGe_{1-x}, amorphous, vibr. props. 79−23693
SiH, (LMM) Auger electron emission by keV Ar^+ bombardment 79−95880
$Si_{1-x}H_x$, amorphous, gap states, DLTS 80−49656
$Si_{1-x}H_x$ film, amorphous, RF sputtered, pure and P(B) doped, optical consts. 79−95866
$Si_{1-x}Ni_x$ film, metastable impurity band, conductivity meas., semiconductor-metal transition 77−76884
Sr-Al-Si system, phase diagrams construction by simplex designing method 78−6899
Ta-Cr-Si-Al, heat resistive films prepared by sputtering, lifetime meas. 80−80132
$TaSi_2$, superconducting transition temp. meas. of sputtered films and bulk 80−7019
Ta_3Si, superconducting, shock synthesis *(Russian)* 77−85957
Ta_5Si_3, supercond. transition temp. meas. *(Russian)* 77−20485
$TbSi_2$, γ-γ ang. correl. obs. of polymorphic transition, 200-900°C 80−29653
Ti-(Al)-Zr-Si (5, 0.5 wt.%), creep 77−36595
Ti-Al-Cr-Fe-Si alloy AT6, and weldments, mech. and corrosion props. 77−90409
Ti-Al-Mo-Sn-Si(4,4,2,0.5 wt.%), fracture toughness and crack propag. 78−39892
Ti-Al-Mo-Zr-Si (6.6, 3.3, 1.8, 0.3 wt.%)-SiC fibrous composite, component interaction kinetics *(Russian)* 80−55364
Ti-Al-Sn-Zr-Mo-Si (6, 2, 4, 2, 0.1 wt.%), effect of elevated temperature and environment on fatigue crack growth 80−40486
Ti-Al-Sn-Zr-Mo-Si-O-H, Si, O, H effects on fatigue, fracture and creep charact. 79−11697
Ti-Al-Zr-Mo-Si (6,5,0.5,0.25 wt.%), fracture toughness and crack propag. 78−39892
Ti-Be-Si glass ribbons, physical and mech. props. 78−95767
Ti-Cu-Si system, transforms. in Ti-Ti_5Si_3-TiCu region, 800-1600°C *(Russian)* 77−21099
Ti-Mo-Zr-Sn-Fe-C-Si alloy, β-III, cold deform. and annealing, effect on struct. and mech. props. *(Russian)* 79−24533
Ti-Nb-Si, amorphous alloy, supercond. props. and crystn. behaviour, TEM and DTA study *(Japanese)* 80−84536
Ti-Ni-Si metallic glass, prep., thermal and mech. props. 78−64497
Ti-Si, binary inclusions, interaction with diamond in polycryst. diamond sintering *(Chinese)* 78−80484
Ti-Si, existence of β to α_m phase transformation 78−44123

silicon alloys continued
Ti-Si, thermodynamics and kinetics of β to α_m transformation 78−84795
Ti-Si amorphous alloy, melt-quenched, transform. studies and mech. props. 80−100838
Ti-Si cosputtered films, silicide form., X-ray diffr. and resist. study 80−54546
Ti-Si film thin film interaction, metallisation, X-ray diffr. and sheet resist. 80−54442
Ti-$TiSi_2$, metal-silicide coating system. thermal stresses *(Russian)* 78−13891
Ti-V-Si, equlibrium silicide, X-ray and electron diffr. obs. 78−27483
Ti-V-Si, Si effects on precipitation and strengthening 77−55970
Ti-V-Si (30, 1 at%), quenched and aged, hardness, tensile behaviour and phase transform. 79−11646
βTi-V-Si (40, 1 at.%), Si effect of precipitation and age hardening 77−63676
Ti-Zr-Nb-Si, Nb and Si surface alloying effects on wear and corrosion resistance *(Russian)* 77−25191
TiSi, and TiCoSi, electronic struct., X-ray K- and L-spectra obs. *(Russian)* 78−11022
$TiSi_2$, form. in Si-Pd-Ti evaporated films 80−80006
transition metal silicides, elec. struct., X-ray spectra *(Russian)* 77−28106
U-Si-Al fuel rods, Zr-Nb cladding, irradiation behaviour with peripheral voidage 78−54835
$U_{10}Co_{51}Si_{33}$, crystal struct., dimensions, space group and coord. *(Russian)* 80−88085
$U_2Co_3Si_5$, cryst. struct. 78−47285
$U_6Co_{30}Si_{19}$, X-ray cryst. struct. determ. 80−107111
UIr_2Si_2, cryst. struct. 80−1964
$U_3Ni_4Si_4$, X-ray cryst. struct. determ. 80−33931
UPd_2Si_2, magnetic phase transition, neutron diffr. meas. 79−47284
$U_4(Re_{0.17}Si_{0.83})_{13}$, X-ray diffraction anal. of crystal struct. *(Ukrainian)* 78−83773
$U_4Re_7Si_6$, X-ray diffraction anal. of crystal struct. *(Ukrainian)* 78−83773
USi_3, thermoelectric power, 5-300K 79−65444
U_3Si, crystalline elec. field studies using neutron inelastic scatt. at NRCN 80−10931
U_3Si, heat capacity and thermodynamic props., 1 to 1203K 77−72697
U_3Si, reversible twinning, in-situ obs. 80−104241
U_3Si, tensile ductility from 25 to 320°C 79−74225
U_3Si, X-ray diffr. exam. 78−75629
$(V,Fe)_3Si$, solid soln. form. and supercond. T_c *(Russian)* 78−80512
$(V,Nb)_3Si$ solid solns., supercond. T_c, absolute thermal EMF, microhardness 77−36006
$(V,Nb)_3Si$ type with A15 struct., supercond. transition temp., depend. on stoichiometry *(German)* 77−69444
V Si, supercond. alloy, electron distrib. vel. to Cr_3Si 77−68944
V-Si, A15 compounds, Hall coeffs. 79−33281
V-Si, fast quenching of A15-phases *(German)* 77−36014
V-Si, strengthening by internal oxidation 80−55424
V-Si-C, phase equilib. and supercond. 80−50593
V-Si-C film, superconductivity 78−72299
$(V_{1-x}Cr_x)_3Si$, elastic moduli, 4.2 to 290K, softening near supercond. transition *(Russian)* 80−92582
$(V_{1-x}Cr_x)_3Si$, mag. susceptibility, 4.2 to 320K, density of states model 80−7035
$(V_{1-x}Cr_x)_3Si$, single cryst., elec. resistivity, temp. depend. 79−56193
$V_{3-x}Cr_xSi$, x=0 to 3, struct., supercond. and mag. props. 80−1962
V(Nb)-Si-Cu, rapidly quenched, comp. and phase equilib. 80−76235
VSi_2 thin film growth rel. to annealing environment and interposed layers 78−2395
VSi_3, cubic-tetragonal phase transition, two-band (s-d) model 79−56193
$V_{1-x}Si_x$, A-15 cpds., nucl. mag. relax. in normal and supercond. state 80−49993
V_3Si, ^4He induced damage, channelling effect meas. 77−62570
V_3Si, A 15 compound, Raman scatt. and phonon density of states 79−28768
V_3Si, A-15 compounds, interlattice displacements, elastic consts. 78−55906
V_3Si, A-15 struct. supercond., microhardness, bonding 78−76199
V_3Si, A-15 supercond. cpd., martensitic transform. 79−60499
V_3Si, A15 compound, exam. of deformation processing, review 78−39864
V_3Si, A15 compound, microscopic model of supercond. and martensitic transform. 77−8226
V_3Si, A15 cpd., hydrogenation effects on supercond. transition temp., lattice parameters 80−103772
V_3Si, Anderson-Gruneisen parameter, from 3rd order elastic const. data 79−33059
V_3Si, anharmonic contrib. to mode softening 79−73241
V_3Si, band theory, semiself-consistent band calcs. 78−2406
V_3Si based ternary solid soln., supercond. T_c and paramag. susceptibility *(Russian)* 77−59348
V_3Si bridge contacts, nonstationary props. 80−103793
V_3Si, CDW instability and anharmonicity 78−79734
V_3Si, channelling, at displacements and electron phonon/defect interactions 77−84815
V_3Si, chemical composition effect on phase transition and transition temp. 78−14860
V_3Si, coherence parameter, nonlinear high temp. supercond. elements with A-15 lattice *(Russian)* 80−60127
V_3Si, complex refr. index and reflectivity of thin film, microscopic charcts. and superconductivity 78−31267
V_3Si, Czochralski growth, supercond. behaviour 79−74080
V_3Si, d-spacing fluctuations above Martensitic phase transition 80−7570
V_3Si, de Haas van Alphen meas. of Fermi surface for H≤40 T 79−73424
V_3Si, de Haas-van Alphen oscills. in normal state 79−56116
V_3Si, dislocations, obs. by TEM 77−59012
V_3Si, E_g optical phonon, Raman scatt. meas. 79−24316
V_3Si, EFG and band struct. 77−35861
V_3Si, elec. resist. below 77K, phonon assisted interband scatt. 78−14703
V_3Si, electrical resistivity, saturating contrib. from electron-phonon interactions 80−2376
V_3Si, electron charge distrib., martensitically transforming single cryst., X-ray diffr. meas. 78−75631
V_3Si, electron energy loss spectra, AES and HEED investig. of surface 77−24635

silicon alloys continued
V_3Si, electron spectrum characts., mag. susceptibility depend. on resistivity ratio 79−95320
V_3Si, electron-phonon coupling and supercond. crit. temp. 79−33379
V_3Si, electronic props. calc. 79−7780
V_3Si, electronic struct., electron-phonon interaction and high temp. superconductivity, APW calc. 78−14871
V_3Si, electronic struct., charge distrib. and X-ray emission spectra 79−51481
V_3Si, electronic struct., electron-phonon interactions, and low temp. anomalies 79−60701
V_3Si electronic struct. from three-dimens. k.p model 78−84139
V_3Si, electronic struct. calcs. 79−47005
V_3Si embedded in resin, composite supercond., high transition temp. 80−88660
V_3Si, exam. of superconductivity and props. 79−1649
V_3Si, far IR transmission spectrum 77−38041
V_3Si, Fermi surface, positron annihilation study 79−4869
V_3Si, Fermi surface, positron annihilation meas. 79−87039
V_3Si, Fermi surface determ. by positron annihilation 80−2326
V_3Si, Fermi surface studies by the positron annihilation technique 79−82515
V_3Si, Fermi surface topology, positron annihilation meas. 79−56117
V_3Si film, far IR reflection and transmission spectra, room temp. 77−55792
V_3Si film, optical props. *(Russian)* 80−93418
V_3Si film, quasiamorphous, supercond. phase formation by heat by heat pulse 77−63017
V_3Si film, sputtered, high press. induced shifts in supercond. transition temp. 77−85374
V_3Si film, superconductivity 78−72299
V_3Si film, T_c var. with ^4He irrad. induced defects 77−8220
V_3Si formation by bronze process 77−86032
V_3Si, grain size in A-15 reaction layers 78−14911
V_3Si, grown-in dislocations, diffr. contrast behaviour 79−86794
V_3Si, Gruneisen parameter and thermal expansion eval. at room temp. 80−70351
V_3Si, H_{c2} anisotropy in high field, grain boundary flux pinning 78−43532
V_3Si, Hall effect, 77K to superconducting transition temp. 78−43359
V_3Si, He irrad., computer simulation of channelling 79−55800
V_3Si, heat capacity rel. to temp. *(Russian)* 78−52152
V_3Si, high T_c supercond., electron-phonon coupling, effect of electronic density of states sharp struct. 78−14877
V_3Si, intra-atomic Coulomb interaction effect on band type of Jahn-Teller effect 79−78057
V_3Si, ion irradiated, influence on struct., resist., and supercond. transition temp. 80−54823
V_3Si, lattice defect, high voltage electron microscopy *(French)* 79−27993
V_3Si, lattice dynamics, inelastic coherent neutron scatt. 78−26645
V_3Si, low fluence neutron irradiation, behaviour of supercond. transition temp. 78−43509
V_3Si, low temp. irrad. with 20 MeV S ions, effect on supercond. props. 79−38223
V_3Si, martensitic transform. coupling with supercond. transition 78−44126
V_3Si, martensitic transform., thermal expansion meas. in normal and supercond. states 79−56381
V_3Si, mixed state, ultrasonic anomaly 77−55644
V_3Si, mixed state A15 struct., Gibbs free energy and lower crit. field temp. depend. 77−55643
V_3Si, Mossbauer spectra of ^{57}Fe *(Russian)* 79−24235
V_3Si, NMR meas. near struct. transform. *(Russian)* 80−44942
V_3Si, NMR of ^{51}V above and below 21K struct. transition *(Russian)* 80−34796
V_3Si, neutron irrad., grain boundary pinning, field-depend. change of crit. current density 80−65759
V_3Si, neutron irrad., neutron diffraction studies 78−88076
V_3Si, neutron irrad., sound velocity, magnetic susceptibility and upper critical field 78−88074
V_3Si, neutron irrad., volume pinning force, summation and saturation behaviour 79−95554
V_3Si, neutron irrad. effects on transition temp. *(Japanese)* 79−82707
V_3Si, neutron irradiated, A15 compound, recovery of T_c by annealing 78−52132
V_3Si, neutron irradiated single crystal, superconducting transition temp. widths, resistivity and heat capacity meas. 78−91802
V_3Si, neutron-irrad., ht. capacity and resistivity 78−88075
V_3Si, nontransforming, press.-induced phase transformation 78−80084
V_3Si, normal, mixed and supercond. state, specific heat meas., thermodynamic and superconducting props. 80−49987
V_3Si, normal state, Fermi surface, de Haas-van Alphen oscills. 79−65369
V_3Si, normal state resistivity as function of neutron irrad. 79−56194
V_3Si, nuclear magnetic relaxation, near T_c *(Russian)* 79−42852
V_3Si, phase transition and transition temp., chemical comp. effects, defect struct. exam. 78−18651
V_3Si, phonon densities of states and Debye temp. calcs. 79−51212
V_3Si, phonon density of states at 300K, mode softening 77−11648
V_3Si, phonon density of states, temp. depend. 79−42183
V_3Si, phys. props., appl. of new three-dimens. k.p model for A-15 cpds. 78−23015
V_3Si, plasma energies, tight-binding energy-band model 78−84159
V_3Si, plastic deform. effect on supercond. props. 80−29500
V_3Si, positron annihilation lifetime meas. 79−19946
V_3Si, powdered, Debye-Waller factors and lattice consts., 25-1000K, X-ray diffr. obs. *(German)* 79−33060
V_3Si, press. depend. of positron lifetimes 78−11015
V_3Si single cryst., A-15 compound supercond., plastic deform., at high temp. 79−20104
V_3Si, single cryst., anharmonicity determ. from X-ray refl. intensities 79−73284
V_3Si, single cryst., computer simulation of channelling meas. 79−51180
V_3Si single cryst., creep deform. 80−71695
V_3Si, single cryst., double supercond. transitions 79−28430
V_3Si, single cryst. growth by electron beam melting 78−64467
V_3Si single crystal, radiation damage and superconductivity 78−52129
V_3Si single crystals, channelling effect studies using He ions and $^{28}Si(d,p_8)$ reaction 79−4362
V_3Si, single crystals, supercond. tunnel characts. 80−7044

silicon alloys continued
V_3Si single crysts., elec. resist. and Hall coeff., temp. depend., 17-300K *(Russian)* 77−69292
V_3Si, soft mode sound vel. in mag. field rel. to density of states 78−14647
V_3Si, sp. ht. anomaly at struct. transform. 78−14426
V_3Si, static compressibility, up to 20 kbar 77−43281
V_3Si, supercond., crit. fields Pauli paramag. limiting and material parameters 79−78277
V_3Si, supercond., sp. ht. meas., internal heating effect obs. in mixed state 77−12067
V_3Si, supercond. and struct. transitions *(Russian)* 78−52118
V_3Si, supercond. film, electron beam codeposition, synthesis and props. 78−72296
V_3Si, supercond. mixed state, low temp. tetragonal-domain-reorientation phenomena, US expts. and thermal props. 80−60141
V_3Si, supercond. props., effect of neutron irrad. 80−80463
V_3Si, supercond. structure and properties *(German)* 80−93631
V_3Si, supercond. tape, growth technique via amorphous state 78−84708
V_3Si, supercond. transition temp. and phase transform. at press. up to 45 kbar 79−56352
V_3Si, superconducting, optical props. and electron-phonon interactions 80−2510
V_3Si superconducting bridge junctions, vortex model appl. *(Russian)* 79−60986
V_3Si superconducting props. and structural transition *(Russian)* 77−12052
V_3Si, superconducting thin films, energy gaps from tunnelling meas. 80−25050
V_3Si, superconducting transition temp. press. depend., for shear-stress induced tetragonal phase 77−36010
V_3Si, superconducting transition temp., correl. with resist. anomalies and defect struct. 77−47920
V_3Si superconductor film, Fourier and laser spectroscopy comparison in far IR-sub. mm. range 79−93237
V_3Si, temp. depend. of mag. susceptibility *(Russian)* 77−36053
V_3Si, thermal expansion, 20-300°C, using differential push-rod dilatometer 80−39320
V_3Si, thermal expansion meas., 4.2 to 293K 79−56382
V_3Si, thermodynamic props. determ. using ternary phase equilibria 78−91449
V_3Si, thermodynamic study, intrinsic type II superconductivity 79−47193
V_3Si thin film far IR laser thermal spectroscopy 80−60144
V_3Si thin films, Holstein processes and electron-phonon spectral function, far IR meas., 19K 79−87445
V_3Si, thin films in supercond. and normal states, far IR laser spectroscopy 79−61453
V_3Si, third order elastic consts. 78−88490
V_3Si, transforming and nontransforming, high press. effects 78−80086
V_3Si tunnel junctions, energy gap investigation 80−84569
V_3Si, US anomaly when cooled below martensitic and supercond. transition temps. 80−20354
V_3Si volume changes during phase changes, meas. low temp. differential scanning dilatometer *(Russian)* 79−34224
V_3Si, X-ray emission spectra, electron struct. 77−48278
V_3Si, XPS and APS of valence band 77−20994
V_3Si-Fe, mag. impurities effect on supercond. props. 77−1524
V_3Si-SiO_x-Mo_3Re_2, supercond. tunnel junctions 80−107961
V_5Si_3, thermodynamic props. determ. using ternary phase equilibria 78−91449
$V_3(Si_{1-x}C_x)$, bulk, effect of C on supercond. transition temps. and microstructure 80−54824
$V_3Si_{1-x}Ge_x$, elastic props., 77 to 290K, rel. to supercond. transition temp. *(Russian)* 80−66560
$V_3Si_{1-x}Ge_x$ solid soln., longitudinal and transverse US wave propag. rate, 4.2 to 300K *(Russian)* 80−103423
$V_3Si_xOs_{1-x}$, supercond. transition temp. and paramag. susceptibility 79−28436
W-K-Si-Al doped wires, heavily drawn, fibre struct., annealed 79−56993
W-Ru-Si-B glass, struct. obs. 80−1938
WSi_2 based silicide and borosilicide coatings on W substrate, serviceability at elevated temps. 79−87751
WSi_2, diffusion grown layers, texture 79−74095
WSi_2 film, FET gate electrode, oxidation mechanism, SiO_2 overlayer formation 78−76773
$W_{70}Si_{20}B_{10}$, amorphous alloys obtained by liq. quenching, superconductivity 80−75670
Y-Fe-Si alloys, phase diagrams 79−52158
Y-Si melts, enthalpy of formation and dissolution, microinhomogeneous struct., interatomic interactions *(Russian)* 80−34206
YFe_2Si_2, mag. props. 4.2 to 950K, diamag. Fe atoms 77−20544
$YbCu_2Si_2$, interconfiguration fluctuation, NMR expts. 80−66069
$YbCu_2Si_2$, local mag. moments, neutron scatt. study 79−61058
$YbCu_2Si_2$, mag. 4f Zeeman-level power spectrum using diffuse mag. neutron scatt. 79−60775
$YbCu_2Si_2$, tunnelling anomalies due to intermediate valence phenomenon 77−62873
$YbCu_2Si_2$, valence fluctuation and temp. depend. of Cu nuclear quadrupole interaction 80−15818
Zr-Nb-V-Si superconductor, struct. determ. by optical microscopy and electron diffraction *(Russian)* 77−16628
ZrCoSi, crystal struct. *(Ukrainian)* 78−83774
ZrSi and $ZrSi_2$, ultrasoft X-ray emission bands, empirical band schemes 78−15249

silicon compounds
see also quartz; silicon alloys; silicones
21.2 km graded-index VAD fibre with low loss and wide bandwidth 80−53414
additive method of analysis, Fe determ. by flame emission and absorption spectrometry *(German)* 79−39235
Aerosil, diffusion coeffs. and characterisation by photon correl. spectrosc. *(German)* 79−29418
AES quantitative anal. of impurities *(Japanese)* 78−91356
Al_2O_3-SiO_2 refractories, using neutron-2 equipment 80−45612
alumino-silicate melt, Monte Carlo calc. of ionic struct. 79−60256
aluminosilicate refractory, wetting by molten steel 79−82415
basalt, cement reinforcing fibre, alkali resist. 80−89377
binary, with chalcogenides and pnictides, at. vol. and semicond. props. 77−20089

silicon compounds continued
bis-methyldisilyl chalcogenide, ^{1}H and ^{13}C NMR study, chemical shifts 80−71201
bitumen-silica composites, dynamical mechanical props. 80−58996
borosilicate cladding compatibility with Nb, W, Mo *(Russian)* 77−66741
borosilicate glass film, vapour-deposited, structural model, IR spectra meas. 77−1084
borsic fibre reinforced Ti, unidirectional, K-calibration and compliance curves 78−88518
borsic fibres, fibre, metallisation by continuous casting in Al and Al alloys *(Russian)* 78−35538
cabal glass:$SiO_2(TiO_2)$, microheterogeneity, and elec. cond. 78−83997
CaO-SiO_2, wollastonaite, exam. of synthesis by hydrothermal sintering *(German)* 79−4934
CaO-SiO_2-MgO melt, elec. cond. meas., MgO behaviour *(Japanese)* 78−75857
carborundum, oxidation protection via phosphate impregnation 77−44374
ceramics, stepped temperature stress rupture testing 79−61804
chloromethylsilane, polycryst., proton spin-lattice relax. times meas. 78−39430
chlorosilanes, adsorption on quartz crystal 79−4466
chrysotile, cryst. struct. rel. to milling, X-ray diffr. 77−55278
clay, Al_2O_3 and SiC recovery by C reduction 80−108704
corundum refractories, dense production and performance 80−20866
CVD in hot-wall diffusion system 79−19996
diatomic molecules, linear, substituted fragment series, electronic struct. transferability, mutual at. influence 78−9066
diphenylsilanediol, recrystallized, cell const. refinement precision powder data 79−10841
electron trapping, donor state generation, photo I-V study 80−20210
ESCA using Au M_α X-rays (2123 eV) 78−72683
eucryptite-cordierite binary system, sintering of polycrystalline bodies *(Japanese)* 77−12588
films, formed by reaction of Si with organic compounds of N, struct. investigation 79−87009
fission reactor Na system, deposition and effects of Si compounds 78−86599
fusion reactor material, 0.6, 3.5 MeV He^+ irrad., surface erosion, porosity effects 77−35602
glass, alkali silicate, oxidation reduction equilibria and optical absorption of Cu ions *(Japanese)* 77−12824
glass, tunnelling systems, intrinsic elec. dipole moment, coherent elec. echo obs. 80−29705
halomethylsilanes, internal torsion modes, inelastic neutron scatt. 77−19105
high-silica fibre-optic waveguide, sensitivity to low-dose radiation *(German)* 78−33869
hot-pressed with crystn. grain boundary phases 78−95716
interstellar Si-containing molecules, chemistry and abundances 77−45507
Jupiter, atmosphere coloration due to Si compounds 80−51689
kaolinite rare-earth complexes, relax., molar free energy of activation for dipole relax. 80−88919
kaolinite to mullite reaction series, reexam. of solid state phase transformations 78−64535
Kovar-silicon oxynitride-aluminium cathode, local electron emission and electroluminesc. patterns obs. 80−108327
mag. limiter plate, electron irrad. and thermal shock 78−66416
materials for thermoelectric conversion of solar energy *(French)* 80−89660
metal-ZnO-SiO_2-Si structures, charge injection 80−49919
methylhydropolysiloxanes, equilibration by catalysts *(German)* 78−35722
methylsilylene, closed shell states, isomerisation, config. calcs. 78−35652
MIS structures, photoelectric conversion *(Czech)* 79−83595
mixed-chain silicates, new ordering schemes 79−99142
monochalcogenides, crysts., interaction of outer s states 79−10825
monochalcogenides interaction of internal s states 79−10826
mullite, crystallisation from SiO_2-Al_2O_3 melts 78−47243
mullite, quantitative X-ray anal., standardisation, texture *(German)* 78−11176
mullite fibre reinforced mullite, in vitro degradation, bending strength, Young's modulus, density meas. 78−85011
mullite-corundum ceramics, thread-like crystals reinforced, props. 80−108525
neutron radiation damage of graphite rods and vitreous silica blocks 80−29070
nitrides, bridging bond angle variations, mol. orbital calc. 78−55125
opal, ordered arrangements of SiO_2 spheres of two different sizes 78−87658
opals, crystal struct. and IR spectra 80−40117
optical fibres, 800 Mbit/s optical transmission experiments with dispersion-free fibres at 1.5 μm 80−58680
optical fibres, ultratrace impurities determ., and behaviour during production by CVD process *(Japanese)* 80−87505
organic and inorganic free mol. chemical shift, binding energy and Auger spectra 80−32782
organic silicone, bending with acrylic for permanent antistatic props. 79−1839
organosilicon ladder polymer, vel. meas. of longitudinal and shear US waves 78−95114
organosilicon ladder polymers, struct. and phys. props., book contrib. 79−65012
organsilicon films for waveguide structure, optical props. *(Russian)* 79−98481
orthosilicates, determ. of electronic polarisabilities of ions 79−7570
oxide melts, specific weight, electrical conductivity, viscosity and surface tension meas. methods survey *(Slovak)* 80−47079
oxide precipitates, TEM and EELS identification 80−100723
oxide thickness measurements up to 120 Å on silicon and aluminium using the chemically shifted Auger spectra 78−23586
oxides, grown in Cl-containing ambients, correl. between elec. and material props. 80−39479
oxides, steam grown, index of refr. ellipsometric meas. 80−75995
oxidised surface, bonding of cadmium arachidate monolayers, XPS 79−15011
Permalloy-SiO_2-Schott glass, bubble propagation struct. 80−34719
phosphosilicate glass film, vapour-deposited, structural model, IR spectra meas. 77−1084

silicon compounds continued
phthalocyanine, elec. cond. temp. depend. 80−80271
phyllosilicates, new types, in carbonaceous chondrite matrix 79−80285
plasma etching, gas flow-rate depend. 80−97603
plasma etching in Freon plasma, for microelectronics appls. 80−3080
polymorphism, electron diffr. and optical simulation *(French)* 77−39519
polyorganosiloxane-talc composites, high-temp. transitions 79−52152
polysilicic acid, IR spectra, struct., crystallisation effects *(Russian)* 78−72528
porcelain, crack propag. data applicability to failure prediction 80−81154
protosilicate particles, IR laboratory spectra rel. to interstellar silicate absorption bands 80−56907
quasi-linear molecules, low frequency anharmonic vibrations, pot. function determ., Raman and IR spectra obs. 80−52997
rubber-silica mixtures, natural ageing effects on dielec. props. 77−24778
salt toxic effect on activated sludge micro-organisms *(Chinese)* 79−24919
serpentine minerals, milling rel. to cryst. struct., X-ray diffr. 77−55278
Si_3N_4-Ce_2O_3-SiO_2 materials: phase relations and strength 80−97465
Si poly-oxide leakage current and conductivity reduction expts. 77−76990
Si-Al_2O_3-SiO_3 in MIS struct., charge accumulation and spreading *(Russian)* 78−64116
Sialon, high resolution electron microscopy 79−90501
β-Sialon, high strength, reaction sintering 80−7525
sialon, high temp. creep 77−77530
sialon, oxidation 77−56126
Sialon, prep. and charact. of ultrafine powders 80−11604
Sialon, reaction sintered, mech. props., effect of composition and X-phase 77−56013
β′-Sialon, sintering kinetics and rates of microstructural changes 79−100102
β′-sialon compositions, reaction sintering obs. 80−55337
SiAlON X-phase, X-ray diffr. data 80−49198
sialons, ceramic material fracture mechanics, review 80−45373
n-SiC, 6H and 15R polytypes, (0001) plane, influence of uniaxial mechanical stress on resist. anomaly 78−10445
β-SiC, optical quenching of luminesc., acceptor ionisation energy 80−55178
SiC (6H) thermal oxide layers, AES *(Japanese)* 79−96386
SiH_5, SCF calcs. including polaris. functions 80−87034
silaethylene, closed shell states, isomerisation, config. calcs. 78−35652
silane, coupling agent on E-glass fibre, structure, Fourier transform infrared spectroscopy 78−60643
silane, coupling agent on porous silica, Fourier transform infrared spectroscopy 78−60642
silane layers, reactive ion etching and Auger electron spectra 79−24394
silane molecules, substituted, chemical effects on freq. of Si-H vibrations 79−51227
silica, colloidal, liquid imbibition characteristics *(Japanese)* 78−95963
silica, hydrated, adsorbed $^{205}Tl^+$ NMR relax., chem. shift 78−72427
silica, stepwise multilayer adsorpt. of water vapour, 130-150°C 78−14574
silica, vitreous, effects on viscosity of impurity alkali oxide, OH, Al_2O_3 and Ga_2O_3 78−64580
silica, vitreous, Nd^{3+}-activated, multitype opt. centre 78−68558
silica, vitreous, vapour-synthesized, viscous flow 78−64581
silica, windows, in IR cell, appl. in wavelength calibration of UV-visible spectrophotometer 77−33808
silica (metallised) gels, thermal cond., 10-200K, cryogenic appls. 78−79828
silica colloid fractionation and size analysis using flow field-flow fractionation 78−61062
silica colloidal dispersion, submicroscopic struct. determ. using very-slow-neutron transmission 77−62448
silica fibre, high efficiency tunable CW Raman oscillator 77−14773
silica gel, elec. cond. on surface, effect of impurity adsorption *(German)* 78−30971
silica gel, fixed substance identification using Raman spectroscopy *(French)* 78−88664
silica gel, infrared absorpt. spectra *(Russian)* 77−55794
silica gel, ion exchanger, isotope separation appls. 78−86961
silica gel, IR spectra of dry transparent plates, surface struct. study 79−87884
silica gel, microporous amorphous toroidal, spectroscopic and thermal analysis, adsorption properties 79−57305
silica gel, Mn^{2+} adsorption rel. to H_2O adsorpt., EPR study 79−5180
silica gel, polymer adsorption into surface pores, computer simulation, phase transition *(Russian)* 78−51824
silica gel, pore struct., effect of washing with aq. solns. containing Mg^{2+}, Ca^{2+} ions 79−52786
silica gel, skeletal struct. modification with alcohols and water vap., thermal analysis obs. 78−88659
silica gel, struct., dielec. polarisation, IR spectral investigs. *(French)* 77−81427
silica gel for low temp. regenerator of cryogenic refrigerator 77−17994
silica gel regeneration by adiabatic desorption mathematical model 79−1967
silica gel with benzene submonolayer PMR and DMR dynamics and surface heterogeneity 79−69735
silica gels, surface treatment, adsorption properties *(Japanese)* 78−95855
silica hard coating for magnetic surfaces 80−7715
silica mass balance and dynamic response to eutrophication in Lake Superior 79−74912
silica optical fibres, surface flaws obs., fracture strength 77−14793
silica paricle filled epoxy resin, mech. props., fracture by slow crack growth 77−40443
silica reflectors, ageing under flash lamp light pulses *(Russian)* 77−54737
silica surface, adsorption of I_2, reson. Raman spectrum 78−42066
silica surface, amorphous, with adsorbed ammonia, Raman scatt. 80−11948
silica-alumina hard coating for magnetic surfaces 80−7715
silica-plastic fibres, propag. characts. and fabrication for short-medium distance appls. 78−66892
silicaalumo gels, Na-K, crystn. and characts. of A-type zeolites 79−52780
silicate, effect on Magnox AL 80 corrosion 77−70230

silicon compounds continued
silicate, fundamental study on quantitative anal. of O^0, O^-, O^{2-} ions by XPS *(Japanese)* 77−48710
silicate, interstellar 10 μm absorpt. band equivalent widths and dust temps. in IR sources 78−57614
silicate, polymerised binary melts, activities and free energy of mixing 77−47596
silicate, quantitative analysis using SIMS 77−56285
silicate+$Ca(OH)_2$, reaction rates 80−26006
silicate+Portland cement, reaction rates 80−26006
silicate gardens, growth morphology, mechanisms 80−100765
silicate glass, nonactivated, far UV image recording, colour centre formation *(Russian)* 77−5950
silicate glasses, polyalkali effect 77−24270
silicate glaze, diffusion of Sn(IV) 80−49417
silicate grain condensation, laboratory expt. 78−54015
silicate melt, cavities in random close packed struct., applic. as model exam. 78−55802
silicate melt, effect of CoO, MnO, NiO impurities on elec. cond. *(Ukrainian)* 77−69104
silicate melt, Monte Carlo calc. of ionic struct. 79−60256
silicate minerals, Mossbauer anal. of Fe chem. state 80−20547
silicate minerals, phonon cond. and mean sound vel., linear relationships 77−21761
silicate rocks, Br determ. by epithermal neutron activation anal. 78−35741
silicate rocks, X-ray spectral fluoresc. anal. 78−3762
silicate thermoplastic pigments for glassware, chem. resist. 79−61755
silicates, amorphous, IR extinction meas., rel. to interstellar dust 77−12352
silicates, bridging bond angle variations, mol. orbital calc. 78−55125
silicates, core-level XPS peak intensity ratio ang. variations rel. to surface anal. and chemisorption 80−40225
silicates, elec. field gradient at Fe^{2+} sites, Mossbauer spectra 80−15484
silicates, elemental concentration, estimations, in small particles using X-ray anal. in SEM 79−16098
silicates, emission and extinction in 4-14 μ range 79−44581
silicates, ion bombardment, secondary positive mono-atomic ion emission, cation conc. depend and matrix effects *(French)* 80−50487
silicates, layered, cylindrical crystallite layer disorder, X-ray diffr. intensity effect 80−39113
silicates, layered, not containing Al, synthesis and cryst. chem. 78−51495
silicates, liquid, thermodynamic props., calc. model 79−34804
silicates, molten, struct. and stat. interpret. of Masson theory *(French)* 80−49078
silicates, molten, with high and medium Si contents, stat. theory *(French)* 80−49079
silicates, non-porous, powder geometric surface meas., chemical planimetric method *(German)* 79−88915
silicates, nonstoichiometry influence on plasticity *(German)* 79−24592
silicates, radiation effects rel. to diffuse interstellar bands origin 77−13432
silicates and aluminosilicates, thermodynamic props. determ. by Monte Carlo calc. 77−47597
silicates dissolved in deep water of Bering Sea 80−31061
silicates in anoxic pore waters, effects of oxidation during sampling 78−61394
silicides, oxidation and hot corrosion resistance kinetics 80−25896
silicon oil, separation of elastic and shear thining effects in capillary rheometer 78−42691
silicon rubber model for design and stress analysis of large parts 77−7350
silicon sands, water drainage, by capillary flow *(Japanese)* 78−95208
silicone, B_4C filled, neutron shielding materials, long term radiation effects 80−9413
silicophosphate melts, diffusion 79−46824
siloxane rubber, energy investigation of softening during deform. 77−4819
silyl radical, conform., hyperfine struct., nonempirical calcs., vibr., effects 79−97998
silylcarbene, closed shell states, isomerisation, config. calcs. 78−35652
SiN, hot-pressed, creep 80−16380
sitall coating, control of phase composition, microstruct. and props. 77−32545
soda-lime-silicate glass, dynamics of fracture mirror boundary formation 77−86132
steel, structural, addition of solid SiO, effect on ductile fracture 80−16465
submicron particle, size distrib. in colloidal suspension FODA 78−61057
sulphide compounds of Si, Ge and Sn, struct. and chem. bonding *(French)* 78−30580
sulphides, bridging bond angle variations, mol. orbital calc. 78−55125
synthesis by ion implantation of diamond, role of struct. imperfections 78−34529
systems Ni ions anal. by ESCA *(Japanese)* 80−40787
tetrahalides, isotope shifts, Coriolis coupling and force consts., isotope substitution and matrix isolation 77−42322
tetrahalides of Gp.IV elements, M-X bond flexibility, by compliance scheme 80−37805
tetramethyl silicon, methyl reorient., lattice vibrs., neutron scatt. obs. 79−51016
tetramethylsilane, liq., electron mobility up to crit. point 77−76809
thin film deposition using solar furnace 80−89148
tremolite asbestos, fibrous. elec. anisotropy 78−80273
triatomic molecules, linear, substituted fragment series, electronic struct. transferability, mutual at. influence 78−9066
tricalcium silicate paste, composition of solution in contact 77−81423
tridymite, low, synthetic, struct. refinement, Si-O bond lengths and Si-O-Si bridging angles 77−80456
trimethylsilyl azide, vibr. spectra, normal mode assignment 78−86867
trimethylsilyl isocyanate, vibr. spectra, normal mode assignment 78−86867
trimethylsilyl isothiocyanate 78−86867
tris(trimethylsilyl)phosphine, gamma irrad., free radicals, struct. and EPR spectra 80−29623
zeolite, adsorbed amino radical extra coupling with ^{23}Na 77−7963
zeolite, powdered synthetic, crystn. of supercooled fog 77−37296
zeolite L-D, prep. and props., from crystn. of obsidian 79−100067
zeolite surfaces, bonding of Cu^{2+}, Cr^{3+}, Co^{2+} ions, EPR, optical spectroscopy investig. *(German)* 79−95266
silicon compounds continued
zeolites, coordination of Al and Si from X-ray spectra 78−11021
zeolites, matrix isolation of homonuclear diatomics, induced IR spectra 78−46333
zeolites, synthetic, effect of sintering on elec. cond., porosity and microstruct. 79−29009
Zircon ceramic, exam. of development and fabrication 80−11608
$3Al_2O_3$-GeO_2-SiO_2, reduction by C, mixed diffusional-kinetic regime *(Russian)* 80−66771
Ag-SiO_2 cermet film, optical props., comparison of effective medium theories 79−24379
Ag-SiO_2 composite film, optical props., appls. 77−754
AgBr-SiO_2, field effect potentiometric sensors 78−35691
Ag_8SiSe_6, absorpt. edge investigs. at phase transitions 78−35149
Al film+vitreous silica substrate, reaction 77−86380
Al/SiO_x/p-Si contacts for IMS solar cells, high temp. lifetesting 79−87988
Al/SiO_x/pSi MIS solar cells, stabiiity 80−85287
Al/SiO-B_2O_3/Au *(French)* 80−39681
Al-Al_2O_3-SiO_2-Si capacitors, physical and elec. props. of RF plasma grown Al_2O_3 80−100530
Al-AlN-SiO_2-Si capacitors, physical and elec. props. of RF plasma grown AlN 80−100530
Al-Ge-SiO solar selective absorber surfaces, optical behaviour at high temp. 80−101130
Al-Si_3N_4-Al thin film cathode, pulsed emission obs. 77−8728
Al-Si_3N_4-Si struct., surface energy bands under step function illumination 80−49840
Al-Si_3N_4-SiO_2-Ge structure, small signal HF photo EMF meas. 78−52097
Al-Si_3N_4-SiO_2Si, MNOS structures degradation under UV irradiation effect 80−107923
Al-$Si_xN_yO_z$-Al thin film cathode, physical model from expt. study 80−100535
Al-Si_xNyO_z-Al systems, mechanism of current transfer *(Russian)* 77−69427
Al-Si-N-O system, comps. corresponding to β′-sialon phase reaction hot-pressing 80−84891
Al-Si-SiO_2-Al structure switching and memory effects 78−95385
Al-SiC cermet elasticity, porosity meas. by US means 80−81101
Al-SiO_2, Al-SiO_2(SiO)-Si, solid-state reaction mechanism 77−52623
Al-SiO_2, film system, kinetics of interaction 77−44459
Al-SiO_2, surface reactions and interdiffusion, photoemission study 80−49532
Al-SiO_2 (2wt.%), dispersion hardened particulate composite, prep. 80−7588
Al-SiO_2 film-substrate interface, obs. of Al_2O_3 and free Si 78−91571
Al-SiO_2 interface, chem. struct., deposition conditions depend. 78−72007
Al-SiO_2 interface, internal photoemission and photon-assisted tunnelling 80−6982
Al-SiO_2 interface, stress and microstruct. via TEM 78−26797
Al-SiO_2 interface in MOS capacitors, conductivity effects of oxidation temperatures 80−100518
Al-SiO_2-Au, thin layer struct., electroluminesc. *(French)* 78−76531
Al-SiO_2-Si, charge measurement in MIM and MIS struct., MOS system appl. 78−2572
Al-SiO_2-Si, MOS struct., lateral photovoltaic effect 79−4601
Al-SiO_2-Si, pyroelectricity 80−100524
Al-SiO_2-Si, TSC due to trapped electrons, rate-determining process 77−59290
Al-SiO_2-Si, void form. in Al interconnection lines at Si-SiO_2 boundaries 80−2476
Al-SiO_2-Si capacitors, transient capacitance temp. depend., −40 to 70°C 79−47167
Al-SiO_2-Si Schottky barrier solar cells, recomb. effects 79−39310
Al-SiO_2-Si structs., implanted B^+ ions, high-freq. CV charact. *(Russian)* 78−80056
Al-SiO_2-Si structure, Auger depth profiling and ion sputtering of interfaces 77−20200
Al-SiO_2-Si structure, photon-assisted tunnelling 77−89865
Al-SiO_2-Si structure, photocurrents, 1.4 to 3.1 eV 79−65514
Al-SiO_2-Si structure, positive interface charge, exciton and H diffusion models 80−2471
Al-SiO_2-Si structure, small signal HF photo EMF meas. 78−52097
Al-SiO_2-Si system, EMF origin in pulsed UHF field 77−4448
Al-SiO_2-Si system with reactively sputtered SiO_2, work functions difference 80−6987
Al-SiO_2-Si:B ions, annealing effect on energy spectrum of radiation defects *(Russian)* 78−88488
Al-SiO_2-Si-Pb, MIS system, photocurrent, effect of supercond. to normal transition in Pb 78−72271
Al-SiO_2-TiO_2 interference mirror coatings, high mech. strength 78−30043
Al-SiO_2-p-Si solar cells, comparison of majority- and minority-carrier silicon MIS solar cells 80−85280
Al-SiO_2Si, mobile ion kinetic behaviour 79−56315
Al-SiO_x-Au, MIM struct., electroformed, struct. and elec. props., 4-300K 79−78206
Al-SiO_x-Au cathode, emitted electron energy distrib. 78−52645
Al-SiO_x-GaAs, C-V characteristics 79−65553
Al-SiO_x-Si MIS solar cells, short-wavelength response 79−57428
Al-SiO_x-Si MIS solar cells, I-V characts. temp. depend. 80−7935
Al-SiO_x-Si MOS solar cells, open-cct. voltage var. with oxide layer thickness 80−81434
Al-SiO_x-Si minority-carrier MIS photodiodes, elec. characts. 79−51676
Al-SiO_x-(p-)Si barrier structs., minority carrier injection ratio meas., MIS solar cell model 80−93007
Al-SiO_x-p-Si MIS solar cells with back surface fields 80−12006
Al-SiO_x(+SiO_2)-Si structures, I-V and C-V characts., current and capacitance kinetics 78−88043
Al-silicon oxynitride-Al cathode, LF noise sources and reduction 80−108328
Al-Sio-Al structure, with amorphous SiO, VLF behaviour 77−76946
Al-ZnO-SiO_2-Si monolithic MIS struct., charge-transfer device using SAW 79−11229
Al_4C_3-Be_2C-SiC system, phase equilibria 80−45284
Al_4C_3-Be_2C-SiC system, phase analysis and TEM struct. obs. 80−108420
AlN-Si_3N_4 CVD film preparation and props. 77−77408
AlN-Si_3N_4 mixture film, CVD, characterisation of film props. 78−43496
AlN-Si_3N_4-Be_3N_2 system, phase equilibria 80−60844

silicon compounds continued
Al_2O_2-SiO_2, mullite 2:1 cryst., dielectric tensor components 77−48142
Al_2O_3-$4SiO_2$-H_2O, pyrophyllite, thermal diffusivity meas. using const. rate heating method *(Japanese)* 77−87759
Al_2O_3-B_2O_3-SiO_2 system, liq. phase calc. for commercial quartzite powders 80−25671
β-Al_2O_3-Na_2O-SiO_2, solid electrolytes, exam. of microstruct. ionic resistivity 78−80566
Al_2O_3-Si_3N_4 preparation, compressive strength 80−25634
Al_2O_3-SiO_2, derived from metalalkoxides, sintering behaviour 79−29005
Al_2O_3-SiO_2, mullite, powder, synthesis using silicic acid, clay and $AlCl_3$ *(German)* 79−4933
Al_2O_3-SiO_2, sillimanite, lattice defects, crystallo-chemical model, TEM obs. *(French)* 78−26570
Al_2O_3-SiO_2, thermomech. props., dependence on struct. and composition 78−84748
Al_2O_3-SiO_2 (3 wt.%), J-integral meas. at high temps. *(German)* 80−93624
Al_2O_3-SiO_2 fibre/mineral wool fibre composites, exam. of strength and shrinkage characts. rel. to Al_2O_3-SiO_2 fibre content effects 79−20105
Al_2O_3-SiO_2 heat insulating refractories, prep., physical, thermal, structural props. 78−68662
Al_2O_3-SiO_2 melt, exam. of surface tension and density 79−1541
Al_2O_3-SiO_2 powder, plasma-prepared, glass form. and phase transforms 77−44208
Al_2O_3-SiO_2 refractory, SiO_2-rich glassy phase, deconvolution of microprobe conc. profiles 77−52606
Al_2O_3-SiO_2 refractory, creep, viscosity, resist. to inelastic deform. 80−89309
Al_2O_3-SiO_2 refractory concrete, elastic props. 80−89280
Al_2O_3-SiO_2 system, evidence for metastable miscibility gap 80−71632
Al_2O_3-SiO_2 system, solid state transform. of andalusite to mullite 80−16281
Al_2O_3-SiO_2-CaO-B_2O_3(1,1,1 wt.%) chemical analysis by photocolorimetry and titration 79−20483
Al_2O_3-SiO_2-Fe_2O_3-CaO-MgO-TiO_2, refractory, corrosion and mech. behaviour correlations 80−40563
Al_2O_3-SiO_2-MgO, cordierite, powder, synthesis using silicic acid, clay and $AlCl_3$ *(German)* 79−4933
Al_2O_3-SiO_2-MgO-CaO, blast furnace slag, viscosity, MP *(Russian)* 77−25039
Al_2O_3-SiO_2-TiO_2-B_2O_3-Fe_2O_3, exam. of porous structure, using a combinational method 79−29303
Al_2O_3-SiO_2-ZrO_2, liquidus surface, discussion 77−44231
Al_2O_3-SiO_2-ZrO_2 refractories, corrosion behaviour in glassmelting furnaces *(Polish)* 80−71783
Al_2O_3-ZrO_2-SiO_2, fusion cast refractory, effects of glassy phase on thermal cycling resist. 78−84956
$Al_2O_3.SiO_2.H_2O$, new materials from pianlinite minerals *(Chinese)* 79−95982
$3Al_2O_3.2SiO_2$ as intermediate cubic phase in kaolinite-mullite thermal sequence 80−25652
$3Al_2O_3.2SiO_2$, mullite, synthesis by freeze drying 80−16252
$3.5Al_2O_3.2SiO_2$, mullite, decomposition by SiO_2 volatisation 80−61082
$3Al_2O_3.2SiO_2$-ZrO_2 composites, sintered, in situ-reacted, fracture props. 80−81158
As-Te-Ge-Si sandwich type amorphous films with metal electrodes, space-charge-limited switching, pre-breakdown characts. *(Japanese)* 77−69385
As-Te-Si-Ge amorphous chalcogenide semiconductor, thin film interface, elec. charact. *(Korean)* 80−97014
$As_{40}S_{25}Se_{25}Si_{10}$ glass film, transient photoinduced absorpt. 77−40295
$As_{35}Te_{28}Ge_{16}S_{21}$, chalcogenide semiconductor study of electric properties *(French)* 80−29414
$As_{0.3}Te_{0.48}Ge_{0.1}Si_{0.12}$, amorphous film, transient switching processes 78−84232
As_4Te_5Si glass, struct. changes, Mn^{2+} EPR expts. 78−79534
$As_{30}Te_{48}Si_{12}Ge_{10}$, chalcogenide glass film, charge screening length 79−23974
Au-Si_3N_4-GaAs-GaP structures, as elec. controlled optical transparencies, optical processing use 77−85339
Au-SiO_2-Si system, oxide film 16-36 Å thick, tunnel currents 80−70842
Au-SiO_2-n-Si solar cells, comparison of majority- and minority-carrier silicon MIS solar cells 80−85280
Au-SiO_2-nSi, tunnelling MIS struct. 80−92995
Au-SiO_x-Au diode and triode struct., angular distrib. of emitted electrons 77−69429
Au-SiO_x-Au evaporated thin film sandwich, circulating and emission currents 80−11102
Au-SiO_x-Ge, sandwich structure, exam. of image structure using mirror electron microscopy *(German)* 79−11019
Au-SiO-Au structure AC conductivity, bulk and interface effects 80−54798
Au-Ti/SiO_2/p-Si MOS struct., interface state distrib., DC tunnelling spectra determ. 80−75611
B-Si system, phase diagram review, book contrib. 78−48388
BN-SiO_2 composites, sintered, oxidation kinetics 79−96171
B_2O_3-Na_2O-SiO_2-Al_2O_3, effect of alumina dispersions on the thermal cond./diffusivity/stress resist. 80−39368
B_2O_3-SiO_2 optical fibres, exposed cladding technique, birefr. and polarization props. 79−14094
$(B_2O_3)_x$-$(SiO_2)_{1-x}$, spontaneous Raman scattering *(French)* 79−78674
$B_{14}Si$, switching and high field effects, cond. mechanism 78−64048
$BaAl_2Si_2O_8$-SiO_2, celsian solid solns., effects on polymorphic transform. kinetics 78−68677
BaO-Al_2O_3-SiO_2-H_2O system, phase transitions during hydrothermal treatment 79−43216
BaO-CaO, amorphous film, Cu-electrodes, elec. props. 77−35997
BaO-K_2O-VO_2-SiO_2, glass, elec. cond. rel. to ion polarisability, polarons 80−49729
BaO-$La_{0.6}O$-VO_2-SiO_2, glass, elec. cond. rel. to ion polarisability, polarons 80−49729
BaO-SiO_2, and KF-BeF_2 systems, complex ionic liquids, corresponding-state principle *(Japanese)* 77−56245
BaO-SiO_2, molten, corresponding state principle with KF-BeF_2 and appl. 79−11589
BaO-SiO_2-TiO_2, molten, ionic elec. cond., TiO_2 effects *(Japanese)* 77−51532
$BaSi_{2-y}Ge_y$, solid solution with type $SrSi_2$ struct., lattice parameters at high press. 80−54203
$Ba_5SiO_4Cl_6$:Eu, blue-emitting phosphor high quenching temp. 80−16076

silicon compounds continued
Be-Si-N system polytypes, struct. obs. using TEM 80−107192
Be-Si-O-N polytypes, X-ray study 78−27496
Be-SiO-p-Si, MIS solar cell, performance figures 78−88030
$Be_9Si_3N_{10}$, TEM, direct obs. of cryst. struct. 79−60339
Bi-SiO_2 cermet films, elec. and optical props. 79−78775
Bi_2O_3-SiO_2, melt struct. model 80−33870
Bi_2O_3-SiO_2, metastable phases form., crystn. conditions, melt viscosity and density effects 80−35167
$6Bi_2O_3.SiO_2$, stable γ-phase cryst. form. from supercooled melt, metastable δ-phase precip., surface contamination role 79−91635
$Bi_4Si_3O_{12}$, eulytine, change in band structure on transition to amorphous state 79−15081
C-O-H-N-Si-Ar, computer calculations of heterogeneous equilib. 79−66044
C-Si, amorphous, localised gap states, variable range hopping 77−72866
CSiH, matrix Hartree-Fock calcs. 79−5874
$CaAl_2Si_2O_8$, anorthite, quenched from 1530°C, struct. refinement 77−15355
CaF_2-MgO-SiO_2, melts, elec. cond., surface tension, viscosity, density *(Russian)* 80−92758
CaF_2-SiO_2, melts, elec. cond., surface tension, viscosity, density *(Russian)* 80−92758
$CaF_2.SiO_2$, dehydration product of fluorapophyllite, X-ray powder and cryst. data 79−37686
CaO-Al_2O_3-Fe_2O_3-SiO_2, phase relations 77−12610
CaO-Al_2O_3-SiO_2 based glasses, kinetic parameters of glass ceramic form. 77−24385
CaO-Al_2O_3-SiO_2 diffusion triangular diagram, diffusion between lime and sintered kaolinite *(French)* 79−69296
CaO-Al_2O_3-SiO_2 glass, remanent magnetisation, log t low 78−68300
CaO-Al_2O_3(B_2O_3)-SiO_2 glass-forming additive, effect on Al_2O_3 ceramics sintering 80−89187
CaO-Fe_2O_3-SiO_2 glass, struct. behaviour at melting, Mossbauer exam. 79−10802
CaO-MgO-Al_2O_3-Cr_2O_3-Fe-O_2-SiO_2 system, exptl. determ. of periclase and spinel comps. 78−6906
CaO-MgO-Cr_2O_3-Al_2O_3-ZrO_2-SiO_2 system, subsolidus region characts. 80−97466
CaO-MgO-SiO_2, diopside, exam. of synthesis by hydrothermal sintering *(German)* 79−4934
CaO-MgO-ZrO_2-SiO_2, phase study, SiO_2 compatibility relationship 78−95734
CaO-MgO-ZrO_2-SiO_2, phase study, ZrO_2 compatibility relationship 78−95735
CaO-MgO-ZrO_2-SiO_2 refractories, phase diagram 80−11634
CaO-SiO_2, and NaF-BeF_2 systems, complex ionic liquids, corresponding-state principle *(Japanese)* 77−56245
CaO-SiO_2, arc electrode processes, thermodynamic approach *(Russian)* 77−27755
CaO-SiO_2, cements, effect of additives on compressive strength, carbonisation shrinkage, frost resistance 79−1897
CaO-SiO_2, melt, effect of cooling rate upon glass transition, X-ray analysis 79−27920
CaO-SiO_2, molten binary, X-ray exam. of struct. 78−38610
CaO-SiO_2 DC arc plasma, meas. of conc. ratio of component atoms *(Russian)* 77−27754
CaO-SiO_2 melt, ^{31}Si tracer diffusivity at 1600°C 80−54418
CaO-SiO_2 melt, tracer diffusivity of Ca^{45} and elec. cond. 79−60532
CaO-SiO_2 melt, viscosity and polymerisation *(Russian)* 78−26712
CaO-SiO_2 slags, containing CaF_2 and B_2O_3, SO_2 capacity determ. by encapsulation method 80−11944
CaO-SiO_2/GeO_2-H_2O system, phase relations, influence of Si/Ge isomorphous substitution 79−52180
CaO-SiO_2-Al_2-O_3, 1500°C, ion transport coeffs., interdiffusivities 77−11718
CaO-SiO_2-Al_2O_3, metallurgical slag, dissolution of N_2 77−21109
CaO-SiO_2-Al_2O_3, slag phase, activity of components at 1873K *(Polish)* 78−52775
CaO-SiO_2-Al_2O_3, wollastonite, low dielec. loss factors, fabrication *(Japanese)* 80−55032
CaO-SiO_2-Al_2O_3-Fe_2O_3 mix, liquid phase sintering 79−91610
CaO-SiO_2-Al_2O_3-MgO, phase equilibria 77−86011
CaO-SiO_2-Fe_2O_3(MgO), melt, CaO dissolution *(Japanese)* 78−6909
CaO-SiO_2-Fe_xO system, liq., steel making slag, Ca and Fe tracer diffusivities, O_2 press. depend. 78−38863
CaO-SiO_2-MnO molten mixtures, struct. and phys. props. *(French)* 80−24635
CaO-SiO_2-MnO system, melts, densities, molar vols., thermal expansivity *(French)* 79−51183
CaO-SiO_2-MnO systems, melts, elec. cond., struct. *(French)* 79−51287
CaO-SiO_2-NiO melt, viscosity and elec. cond., effect of NiO conc. *(Japanese)* 79−23760
CaO-V_2O_5-SiO_2 system, compatibility triangles 80−81037
$(CaO)_3SiO$ cement pastes, electron microsc. anal. 80−108761
$(CaO)_3SiO_2$, effects of polymorphism on hydration, X-ray and TEM obs. *(Japanese)* 79−20046
β-$2CaO.SiO_2$, carbonation reaction kinetics, with CO_2 and H_2O vap. 79−79219
β-$CaO.SiO_2$, parawollastonite, rel. between structs. proposed 80−15056
$ZCaO.SiO_2$-$2CaO.Na_2O.P_2O_5$ system, polymorphism and solid soln. 78−19731
$(CaO)_3.SiO_2$, adsorption of H_2O, NMR exam. 78−48354
$CaO.SnO_2.SiO_2$, tin sphene, lattice parameters 77−7697
$Ca_x(Si,Al)_{12}(O,N)_{16}$, α'-Sialon ceramics, prep. and characterisation 78−84750
β-Ca_2SiO_4-CaO-SiO_2 paste, hydration, compression strength and composition 80−50584
$3Ca.SiO_2$, carbonation reaction kinetics, with CO_2 and H_2O vap. 79−79219
CdS-SiO_2 layered system, characts. of phase-velocity dispersion and struct. of surface waves 80−59775
CdS-SiO_2-Si structures, elec. props., role of interface states 79−56286
CdSe-SiO_2 layered system, characts. of phase-velocity dispersion and struct. of surface waves 80−59775
$CdSiAs_2$, electron irrad., defects, elec. and optical props. 79−19282
p-$CdSiAs_2$, electron irrad. elec. props. annealing, lattice defects 80−100465
$CdSiP_2$, birefringence meas. 78−56455
$CdSiP_2$, birefringence, effects on hydrostatic pressure and temp. 80−45033

silicon compounds continued
$CdSiP_2$, bond strengths and bond lengths, thermal expansion coeff. meas. 78−87651
$CdSiP_2$, optical activity near isotropic point, absorpt. spectra 79−69804
$CdSiP_2$, PAC examination of deuteron irrad. damage, annealing effects 78−47446
$CdSiP_2$, pseudodirect chalcopyrite semicond., electronic band struct. 80−20079
$CdSiP_2$:Fe, EPR and optical absorpt. of Fe^+, Fe^{2+}, Fe^{3+} and Fe^{4+} on tetragonal sites 77−8397
$3Ce_2O_3.2Si_3N_4$, ceramic, prep. by cold compaction and firing, struct. anal. 77−21070
$Ce_2O_3.2Si_3N_4$, preferred unit cell for indexing powder diffr. pattern 80−49200
$Cl^{n+}+Ne(SiH_4)(H_2S)(HCl)(Ar)$, K X-ray cross section, projectile charge depend. 77−19029
$Cl_nSi(CH_3)_{4-n}$, ^{35}Cl NQR, geminal and vicinal interactions on substituents electronic effect 80−63663
$Cl_nSi(OCH_3)_{4-n}$, ^{35}Cl NQR, geminal and vicinal interactions on substituents electronic effect 80−63663
$Cl_3SiOSiCl_3$, normal vibs. and force field, calcs. using electron diffr. struct. determ. *(Russian)* 78−46317
$CoO-Al_2O_3-SiO_2$ glass, mag. ordering, Mossbauer exam. 77−24764
$CoO-SiO_2$ systems high press. phases stability and $MO-SiO_2$ systems phase diagrams code 79−90779
Cr-SiO, thin film, laser beam-treated, emission mode of SEM 79−28226
Cr-SiO cermet film, silicide form. during deposition 77−12535
Cr-SiO cermet thin films, thickness effect on density, resist., adhesion and annealing coeff. 77−69432
Cr-SiO film, elec. props., effect of P^- and Ar^+ implantation 79−11239
Cr-SiO films, sputtered, elec. and struct. props. 80−39694
Cr-SiO_2 cermet film, deposition by RF sputtering of powder target, elec. resist. and TCR 79−78890
Cr-SiO_2-Si structure, solid-phase interaction between Cr and SiO_2, X-ray spectral obs. 78−10560
Cr-SiO_2-n-Si tunnel diodes elec. characts. meas. and modelling 77−39955
Cr-SiO_x-Si MIS solar cell, current cond. 80−7936
Cr-SiO_x-Si MIS solar cells, photovoltaic performance and interface states, nucl. radiation effects 80−94004
Cs-SiO_2-Al_2O_3 system interactions, getter development for radiocaesium 80−83208
Cs_2O-SiO_2(-GeO_2) system glasses, X-ray diffr. anal., electron radial distrib. curves 78−87622
$Cs_2O.Al_2O_3.4SiO_2$ (pollucite) for long term-storage of $^{137}CsCl$ 80−37467
$CsSiF_6$:Mn^{4+}, splitting of vibronic levels 78−60496
Cs_2SiF_6, lattice dynamics from neutron scatt., Raman and IR absorpt. meas. 79−60449
Cu-Cr-SiO_2 single crysts., yield and pre-yield behaviour rel. to aging time 80−81103
Cu-Cr-SiO_2 system, age and dispersion strengthened, dislocation struct. around SiO_2 particles 80−108468
Cu-Si-Te, phase equilib., DTA and metallographic anal. *(French)* 79−52182
Cu-SiO/B_2O_3-Cu thin film, amorphous, conductance and capacitance, effect of electroforming 80−34537
Cu-SiO_2, cavity nucleation at particle poles 79−29127
Cu-SiO_2, deformed, lattice rotations at second phase particles 80−25709
Cu-SiO_2, dispersion hardened, surface plasticity effect 78−52832
Cu-SiO_2, dispersion hardened single crystal, cyclic deform. *(French)* 79−1893
Cu-SiO_2, low-temp. recovery creep, Orowan loop accumulation 80−81126
Cu-SiO_2 (0.0052 vol. fraction), work hardened, low temp. softening, particle size effects 77−52342
Cu-SiO_2 single crystals, dispersion hardened, exam. of yield stress between 77 to 1200K 78−76720
Cu-SiO_2-alloys, internally oxidised, plastically deformed, influence of particle form on primary loop nature *(French)* 80−103344
Cu_2O-PbO(NiO)-SiO_2, equilibrated with liquid Cu, Pb and Ni distrib. 77−28790
D_3SiNCO, low freq. bending mode, pot. function 78−82728
D_3SiNCS, IR and Raman spectra, vibr. anal., LF bending mode 78−70842
F_3SiAsH_2, liq. Raman, gas phase IR spectra, normal coord. anal., assignments *(German)* 77−6778
$F_3SiOSiF_3$, vibr. bands, normal coord. calcs. *(Russian)* 78−70814
Fe-Cr-SiC-B_4C powder mixture, compressibility and elec. cond. in cold pressing under low press. 78−60609
Fe-Fe_2O_3-SiO_2-Si melt, interacting system, oxidation products *(Russian)* 78−19728
Fe-M-SiO_2 (M=Ru,Pt), supported catalysts, Mossbauer spectra 80−11296
Fe-P-Cu-SiO_2-$FeAl_3$-asbestos composite, thermal and elec. conds., temp. and composition depends. 77−66609
Fe-SiO multilayer film, interface magnetisation, neutron Bragg refl. 78−56355
Fe-SiO multilayer film, interface magnetisation 80−7135
Fe-SiO multilayer films, interface magnetisation 80−88858
Fe-SiO_2, granular compund, superpara- to ferromag. transition temp. meas. 77−69633
Fe-SiO_2 cermet film, solar absorbing, production by dual cathode DC magnetron sputtering 80−16186
Fe-SiO_2 granular film, interface props., Mossbauer spectroscopy 80−34336
Fe-SiO_2 granular films, superparamag., Mossbauer effect 80−7131
Fe-SiO_2 supported catalysts, Mossbauer spectra 80−11296
Fe-SiO_2-Al_2O_3 Lisakovskii concentrate mixture, sintering process, temp. thermal treatment *(Russian)* 80−55317
$(Fe-Ni)_{1-x}(SiO)_x$, cermet film, internal strsses *(Russian)* 78−75951
$Fe(H_2O)_6SiF_6$, pressure-induced orbital ground state inversion, Mossbauer study 80−39979
$(Fe_yNi_{1-y})_{1-x}(SiO)_x$, dielec. effect on magnetisation and Faraday rot. *(Russian)* 78−39298
FeO-Fe_2O_3-SiO_2-Al_2O_3-$CuO_{0.5}$/Cu slag-metal system, distrib. equilib. of Sn, Se, Te 78−44111
FeO-Fe_2O_3-SiO_2 system, molten, struct. using high temp. X-ray method *(Japanese)* 80−14992
FeO-Fe_2O_3-SiO_2 system, molten, struct. by high temp. X-ray diffr. 80−49084
silicon compounds continued
FeO-Fe_2O_3-SiO_2-Al_2O_3-$CuO_{0.5}$ slag, and Cu, distribution equilibria of Sn, Se, Te 77−51502
FeO-MnO-SiO_2 system, melts, viscosity rel. to temp., composition *(Czech)* 79−19387
FeO-SiO_2, molten, viscosity and density 78−59965
FeO-SiO_2, molten, X-ray diffr. exam. of struct. 79−46543
FeO-SiO_2 melt, viscosity and polymerisation *(Russian)* 78−26712
FeO-SiO_2 system, high press. phases stability and MO-SiO_2 systems phase diagrams code 79−90779
$2FeO.SiO_2.2MnO.SiO_2$ melt, free energy of mixing 79−61572
$FeSiF_6.6H_2O$, dielec. props., 100-270K, rel. to $NiSiF_6.6H_2O$ 78−35088
$FeSiF_6.6H_2O$, phase transform. exam. by X-ray and DSC methods 78−83948
GaAs-Si eutectic alloy, effect of crystallisation rate on microhardness 79−96110
GaAs-Si_3N_4 system, photoluminesc. edge line *(Russian)* 79−4852
n-GaAs-SiO_2 interface, MOS capacitors, surface states from conductance and capacitance meas. 80−100533
GaAs-SiO_2 interface local props. *(Russian)* 78−10567
Ge-pyrolytic SiO_2 system, carrier trapping, GeO_2 sublayer effect 78−91775
Ge-Si, electron irradiation and annealing 77−55305
Ge-Si, influence of short-range order on valence band and direct optical gap 77−59252
Ge-Si single crystals, heat treated, hot carrier thermo-EMF 77−24575
Ge-Si solid solution film, elec. props. in range 4.2 to 500K 77−8214
Ge-Si system alloys, growth by Czochralski method, morphology 77−15329
Ge-Si_3N_4 system, potential barriers determ. from photoinjection carriers trapping 80−103756
Ge-Si-S system, glass formation, transition temp., crystallisation and melting 80−100178
Ge-SiO_2, MIS struct., electrophysical characts. 79−82680
Ge-SiO_2-Si_3N_4, MIS struct., electrophysical characts. 79−82680
Ge-SiO_2-p$^+$Si tunnel junctions, for determ. of AC cond. of amorphous Ge 77−24608
GeH_4:$SiHD_3$, symmetries of GeH_4 cryst. phases, IR spectra meas. 79−19886
GeO_2-P_2O_5-SiO_2 graded index optical fibres optimised for 1.3 μm wavelength region, fabrication techniques *(Japanese)* 80−99888
GeO_2-SiO_2, reduction by C, mixed diffusional-kinetic regime *(Russian)* 80−66771
a-GeSi film with Mo contacts, AC performance *(German)* 77−63012
Ge_xSi_{1-x}, Si X-ray emission spectra obs. *(Russian)* 77−1767
$Ge_{10}Si_{12}As_{30}Te_{48}$, monostable chalcogenide glass threshold switch, temp. meas. *(German)* 77−4412
$Ge_7Si_9As_{39}Te_{35}Ga_{10}$, chalcogenide thin films, coupled carrier theory test, high field conditions 80−100466
H_3SiCl, mol., valence and core ionis. energy, RHF-SCF and PNO-CEPA calc. 79−85890
$HSiCl_3$($DSiCl_3$), Raman and IR spectra, mol. motion 78−64353
H_3SiNCO, low freq. bending mode, pot. function 78−82728
H_3SiNCS, IR and Raman spectra, vibr. anal., LF bending mode 78−70842
H_2SiO, electronic struct., dipole moments, mol. polarisability, force fields, ab initio calcs. 80−78531
$H_3SiOSiH_3$, pot. function governing low freq. bending mode 77−58016
HfO_2/SiO_2 mirror coatings, light scatt. and optical strength in UV range 80−106595
HfO_2-SiO_2, layer for dielectric mirror, for KrF excimer laser *(Japanese)* 79−72588
In_2O_3-SnO_x/SiO_x/Si diode solar cells, loss mechanisms, characts., band struct. 80−26135
n-InP/SiO_2 capacitors, minority carrier generation 79−95496
InP-SiO_2 interface, CVD problems, ESCA profiles 80−93497
InSb-SiO-Al MIS structure, prep. and characts. *(Italian)* 78−84715
$In_{2-x}Sn_xO_{3-y}$-SiO_x-Si SIS solar cells, loss mechanisms study for improvement of efficiency to above 12% 80−94080
KF-PbO-SiO_2 glass shear wave velocity and its temp. depend. *(Japanese)* 78−30702
$KO_{0.5}$-$AlO_{1.5}$-SiO_2 system, activities calc. from vapour press. meas. and known data 79−91985
$K_2O-B_2O_3-SiO_2$, glass, crystallisation range *(German)* 80−38934
K_2O-BaO-SiO_2-Ti(Ce)O_2 laser glasses, TiO_2 and CeO_2 antisolarisation additive effects 79−94309
K_2O-CaO-SiO_2 glass, composition-density relationship 77−90326
$K_2O-Fe_2O_3-SiO_2$, subsolidus sector of phase diagram, X-ray obs. 80−40335
$K_2O-Na_2O-BaO-SiO_2$ glass, corrosion kinetics in aqn. KOH, transition metal oxide addition effects 77−56125
K_2O-PbO-PbF$_2$-SiO_2 glass shear wave velocity and its temp. depend. *(Japanese)* 78−30702
K_2O-PbO-SiO_2, glass, mech. and optical props. *(Russian)* 77−20860
K_2O-PbO-SiO_2, structural units, Raman spectroscopy 77−20847
K_2O-SiO_2, glass, influence of electric charge phenomena on AES *(French)* 80−50478
K_2O-SiO_2, vap. press., thermodynamic props. and phase diagram at high temps. 78−83932
K_2O-SiO_2 glasses, IR reflection spectra, computer resolution *(Japanese)* 77−69832
K_2O-SrO-SiO_2, glass, elastic constants 77−16630
K_2O-SrO-SiO_2, solid glass, influence of composition on electrical conductivity 77−11723
$K_4Sc_2(OH)_2Si_4O_{12}$, crystal struct., X-ray diffr. study 80−79763
$Kr.2SiO_2$, props. of vitreous deposits 78−22664
La-Si-O-N, comments on new apatite phase 80−15255
La-Si-O-N system, new compound form. with fluorapatite struct. 79−4941
La_2O_3-SiO_2, gels, microstruct. and crystallisation, prep. method and thermal treatment effect 79−61913
$La_4Si_2O_7N_2$ single cryst. growth by floating zone method with SiO_2-Si_3N_4 additions 80−93481
LiO_2-Al_2O_3-SiO_2, bonding of Si-O exam. by X-ray emission spectra 78−52594
LiO_2-Al_2O_3-SiO_2-TiO_2:Sn^{3+}, ESR and X-ray phase anal. 79−99752
Li_2O-Al_2O_3-SiO_2, kinetics of glass-ceramic formation, by modified broken total internal reflection method 77−36444
Li_2O-Al_2O_3-SiO_2 glass, crystn. aggregation and migration of ion-implanted Ag 77−55240
Li_2O-Al_2O_3-SiO_2 glass, He migration, struct. effects 77−55389

silicon compounds continued
Li_2O-Al_2O_3-$4SiO_2$, glass-ceramic, tensile creep and high temp. fracture 78−52914
Li_2O-BeO-SiO_2, X-ray diffr. exam. of phase equilibrium 78−80522
Li_2O-Fe_2O_3-SiO_2 glass, struct. and crystallisation behaviour 78−83738
Li_2O-SiO_2, cation interdiffusivity, electrochem. determ., 1100-1350°C 78−47544
Li_2O-SiO_2, glass ceramics, phase transformation processes 80−3025
Li_2O-SiO_2 glass, crystallisation and phase separation 79−10803
$Li_2O.2SiO_2$ ceramics unidirectionally solidified, porosity *(Japanese)* 79−38816
$Li_2O.2SiO_2$, directionally solidified, thermal and mech. props. *(Japanese)* 80−16295
$Li_2O.2SiO_2$, polycrystalline, oriented, fabrication by unidirectional solidification from melt *(Japanese)* 78−31371
$Li_2O.2SiO_2$, prep. from film forming soln. 80−60811
$100(Li_2O.2SiO_2).3B_2O_3(3Na_2O)(3MgO)(3Al_2O_3)(3SiO_2)(3P_2O_5)$, directionally solidified, thermal and mech. props. *(Japanese)* 80−16295
$100(Li_2O.2SiO_2).3SiO_2$, directionally solidified, thermal and mech. props. *(Japanese)* 80−16295
$Li_2O.nAl_2O_3(7.3-n)SiO_2$, metastable solid soln., Al^{3+} vacancy incorporation 77−12593
$Li_x(Si,Al)_{12}(O,N)_{16}$, α'-Sialon ceramics, prep. and characterisation 78−84750
Mg-Si-Al-O-N, grain boundary segregation, combined X-ray microanal. and lattice fringe imaging determ. 79−15681
$MgO:CaO(SiO_2)(B_2O_3)(Cr_2O_3)$, effective of impurities on high temp. creep 80−40455
$2MgO$-$2Al_2O_3$-$5SiO_2$, cordierite, synthesis rel. to WC addition 77−8787
MgO-$(Cr_2O_3)(AP_2O_3)(Fe_2O_3)(SiO_2)$, vaporization 79−99308
MgO-Al_2O_3-Fe_2O_3-SiO_2, cordierite, in ceramic, effect of heat treatment on cordierite content 79−20039
MgO-Al_2O_3-SiO_2, exam. of microstructure and crystallisation kinetics 78−80501
MgO-CaO-Fe_2O_3-Al_2O_3-SiO_2, clinker production from dolomite and magnesite 80−55339
MgO-CaO-FeO-Fe_2O_3-SiO_2-Cr_2O_3-Al_2O_3 spinel refractories, physicochem. prod. conditions 80−89185
MgO-CaO-SiO_2-Al_2O_3-$Na_2O.P_2O_5$, effect of $NaPO_3$ on phase composition rel. to basic refractories 78−80528
MgO-CaO-SiO_2-C, equilibrium partial press. of Mg, SiO, Ca and CO 77−36482
MgO-Ga_2O_3-SiO_2 system, subsolidus phase equilib. 78−44106
MgO-Si_3N_4, hot-pressed, electrical props. 78−39136
MgO-SiO_2, and LiF-BeF_2 systems, complex ionic liquids, corresponding-state principle *(Japanese)* 77−56245
MgO-SiO_2, melt, effect of cooling rate upon glass transition, X-ray analysis 79−27920
MgO-SiO_2, molten binary, X-ray exam. of struct. 78−38610
MgO-SiO_2 system, high-press. phase transistions calcs. rel. to mantle discontinuities 79−90780
MgO-SiO_2-Si_3N_4-Mg_3N_2, phase relations 77−63614
$Mg_2Si_xGe_ySn_{1-x-y}$ composite Te material with high figure of merit 77−28164
$MgSiO_3$, vaporization 79−99308
Mg_2SiO_2:SiO_2, elec. and dielec. props. 400-900°C 80−104953
Mg_2SiO_4, ionic transport model 79−69285
Mg_2SiO_4, NMR of ^{29}Si and ^{25}Mg with dynamic polarisation technique 78−56405
Mg_2SiO_4:(Fe)(H), elec. cond. meas. 79−69285
Mg_2SiO_4-Fe_2SiO_4-$CaAl_2Si_2O_8$-SiO_2 system phase relations rel. to lunar basalts origin 78−65512
$Mg_3Si_4O(OH)_2$, ball mill grinding, rate constant determination *(Japanese)* 78−95828
$MgSiP_2$, elec. props. and diode struct. exam. 79−51665
Mn-Si, liq. alloys, equilibria between MnO-SiO_2-CaO-MgO slags 80−10639
Mn-Si-O, phase equilibrium *(Russian)* 77−66630
Mn-SiO, annealed cermet films, elec. resist., composition depend. 80−97007
Mn-SiO cermet film, silicide form. during deposition 77−12535
Mn-SiO cermet films, DC and AC resist. 80−54804
Mn-SiO cermet films, elec. resist., annealing behaviour 80−54803
Mn-SiO cermet thin film, DC resist., activation energy, thickness depend. 80−84518
MnO-Al_2O_3-SiO_2 glass, optical spectra 78−68528
MnO-SiO_2 melt, viscosity and polymerisation *(Russian)* 78−26712
MnO-SiO_2 slag, SiO_2 solubility and MnO activity 79−52184
MnO-SiO_2-TiO_2 melt, electrical cond. meas. and electrolytic anal. *(Japanese)* 78−38861
MnO-SiO_2-ZrO_2 molten slag system-molten steel interface, wetting angles, surface tension *(Czech)* 79−19432
MnO_2 porous powders, Al_2O_3 and SiO_2 coated, changes in surface free energy for N adsorption 80−84363
$MnO.Al_2O_3.SiO_2$, spin glass materials, mag. field dependence of susceptibility peak 80−103840
Mo/SiO_2, supported catalyst, EPR and UV-visible spectra of $Mo_6O_{19}^{3-}$ 79−99764
Mo-Mn-SiO_2 mixture, premetallizing of high alumina ceramics 79−47792
Mo-SiO_2-Si, R/MOS struct., heat treatment effects 78−76683
$Mo_5(B,Si)_3$, stability of heatproof coating 77−86201
$MoSi_2$-$TiSi_2$, high-temp. oxidation 79−83341
NaF-MgF_2-MgO-SiO_2, phase formation 78−27460
$Na_2Mg_6Si_8O_{22}F_2$, fluoramphibole, fibrous, crystn. from gas phase, mechanism 78−34451
Na_2O-$2SiO_2$, melt, effect of cooling rate upon glass transition, X-ray analysis 79−27920
Na_2O-Al_2O_3-SiO_2 glass, He migration 77−7902
Na_2O-Al_2O_3-SiO_2-TiO_2-NiO glass, paramagnetic centres, form. during crystn., ESR study 79−65710
Na_2O-B_2O_3-SiO_2 glass, fracture toughness, effect of microheterogeneous struct. 80−104256
Na_2O-CaO_2-SiO_2 glass, stressed, chemical reaction in water vapour 79−91819
Na_2O-CaO-SiO_2, corroded glasses, electron microprobe analysis 77−4956
Na_2O-CaO-SiO_2, expt. errors in estimating time to failure 77−16666
Na_2O-CaO-SiO_2, multicomponent liq. state diffusion 78−55962
Na_2O-CaO-SiO_2 glass, K_{IC} eval. by double torsion technique 77−90444
Na_2O-CaO-SiO_2 glass, electronic struct. and optical props. 80−2790

silicon compounds continued
Na_2O-CaO-SiO_2-Cr_2O_3 glass, redox equilibria of Cr ions, impurity effects 80−89477
Na_2O-CaO-SiO_2-Fe_2O_3 molten glass, optical props., temp. depend. *(French)* 80−100667
Na_2O-CaO-SiO_2-H_2O system gels, metastable nature 80−71952
Na_2O-CaO(Al_2O_3)-SiO_2 glass, composition-density relationship 77−90326
Na_2O-Fe_2O_3-SiO_2, Mossbauer spectra, crystallisation study *(Russian)* 79−19816
Na_2O-Fe_2O_3-SiO_2 glass and crystals, leucite type, Mossbauer ESR study of Fe^{3+} distrib. 79−65774
Na_2O-K_2O-$Al_2O_3SiO_2$-H_2O system A-type zeolites, crystn. from Na-K silicaalumo gels, and characts. 79−52780
Na_2O-NaF-CaO_xZnO_{1-x}-Al_2O_3-SiO_2, opal glasses, strength, surface composition 80−30066
Na_2O-PbO-SiO_2, activity of PbO, EMF meas. 77−47595
Na_2O-PbO-SiO_2, molten glass, reactions with conducting materials 80−85186
Na_2O-PbO-SiO_2, PbO activity 78−44112
Na_2O-Si_2O glass, high-temp. peak of internal friction 80−39218
Na_2O-SiO_2, aqueous solns., Raman and IR spectra, pH depend., species at equilib. identification 79−87866
Na_2O-SiO_2, melt, EMF meas., partial molar enthalpy and entropy 80−6525
Na_2O-SiO_2, thermal expansion at low temperatures 78−83982
Na_2O-SiO_2 glass, electronic struct. and optical props. 80−2790
Na_2O-SiO_2 glass containing halogens glass formation 80−103254
Na_2O-SiO_2 melt, diffusion coeffs., electron microanal. meas. of Na and Si concs. 77−31790
Na_2O-SiO_2-CoO glass, Co^{2+} ion activated, magneto-opt. study 79−65844
Na_2O-SiO_2-CuO, γ-irrad., CuO effects on EPR 80−84645
Na_2O-SiO_2-Fe_2O_3, glass, X-ray absorpt. spectra, effective co-ordination charges 80−84805
Na_2O-SiO_2-MgO melt, elec. cond. meas., MgO behaviour *(Japanese)* 78−75857
Na_2O-SiO_2-NaF, elec. cond. of melt, and IR absorpt. spectra of glassy phase *(Japanese)* 77−62657
Na_2O-SiO_2-NiO melt, viscosity and elec. cond., effect of NiO conc. *(Japanese)* 79−23760
Na_2O-SiO_2-NiO systems Ni ions anal. by ESCA *(Japanese)* 80−40787
Na_2O-TiO_2-SiO_2, phase relations 79−61567
$(Na_2O)_{0.3}(SiO_2)_{0.7}$, nuclear spin lattice relax. in amorphous state, review 79−11354
$5Na_2O.Fe_2O_3.8SiO_2$, glass crystallisation study by Fe^{3+} EPR and Mossbauer spectra 80−64904
$Na_2O.SiO_2$, prep. from film forming soln. 80−60811
Na_2S-SiS_2, glass forming region, struct. and ionic cond. 80−88358
Na_2S-SiS_2, synthesis, structure and ionic conduction *(French)* 80−65291
$Nb_5(B,Si)_3$, stability of heatproof coating 77−86201
NbO_2-Na_2O-SiO_2, amorphous films, characteristics of monostable switching 77−80817
Ni/SiO_2, adsorption of CO, scavenging effect of H_2, in situ Fourier transform IR spectra obs. 80−39410
Ni/SiO_2 methanation catalysts, nonreduced, IR spectra 78−88288
Ni-Ge-SiO, solar selective absorber surfaces, optical behaviour at high temp. 80−101130
Ni-SiC, dispersion hardened coating, chemically deposited using electroless baths, protection props. 79−34208
Ni-SiC coating adhesion to Al alloy, metal interdiffusion *(Russian)* 80−66697
Ni-SiC composite coatings, phase composition calc., wear resistance *(Russian)* 79−11709
Ni-SiO cermet film, elec. resist., percolation effects 77−76954
Ni-SiO composite film, acoustic damping capacity and struct. *(Russian)* 77−59070
Ni-SiO multilayer film, interface magnetisation 80−7135
Ni-SiO multilayer films, interface magnetisation 80−88858
Ni-SiO_2, granular film, hopping cond., magnetoresist. 78−56240
Ni-SiO_2, high temp. plasticity, oxide inclusion effect 80−50681
Ni-SiO_2 composite film, influence of hardening phase on yield stress *(Russian)* 79−5001
Ni-SiO_2 supported catalysts, particle size, H_2 chemisorption, Mossbauer study 80−7219
$NiSiF_6.6H_2O$, dielec. loss and relax., 100-270K, reorient. mech. 78−35088
$NiSiF_6.6H_2O$, single cryst., EPR, 77-300K, Debye temp. 77−85551
$OSiF_2$ prod. from $SiO+F_2$ matrix reactions, IR spectra and force consts. calcs. *(German)* 80−97718
P-SiO_2, film, quantitative anal. by DC arc optical emission spectroscopy 78−68940
P_2O_5-SiO_2 clad low-loss monomode fibres for 1.2 to 1.6 μm, modified CVD prep. 80−48479
$(P_2O_5)_x$-$(SiO_2)_{1-x}$, spontaneous Raman scattering *(French)* 79−78674
Pb-SiO_2-Au tunnel junction, obs. of conductance anomalies 78−26968
Pb-SiO_2-$Pb_{1-x}Ge_xTe$, semicond. band struct., tunnelling obs. 80−54795
Pb-Zn-SiO melt, mathematical model of thermal C reduction *(Russian)* 78−15663
PbO-B_2O_3-SiO_2, molten mixture, microprobe state anal. by X-ray OK and BK emission band spectra *(Japanese)* 78−19606
PbO-MO-SiO_2 (M=Ca,Mg,Ba,Ni,Co) system, melt, viscosity meas. in temp. range 950 to 1250°C *(Japanese)* 79−77663
PbO-SiO_2, molten, activity of PbO, effect of CaO, Al_2O_3, MgO and ZnO 78−60663
PbO-SiO_2 glass, electronic struct. and optical props. 80−2791
PbO-SiO_2 glasses, elec. cond. and dielec. behaviour 80−44361
PbO-SiO_2 melt, behavior of MgO and NiO *(Japanese)* 79−52746
PbO-SiO_2 melts, ionic transport, tracer diffusion and chem. interdiffusion 79−77785
PbO-SiO_2-Fe_2O_3(0,2,10 wt.%), conduction process 77−8096
PbO-SiO_2-(CaO)(MgO)(BaO)(NiO)(CoO), melt, PbO activity *(Japanese)* 78−6907
PbO-SiO_2-(CaO)(SrO)(BaO)(NiO), melts, density *(Japanese)* 78−6908
2PbO-SiO_2-xSiO_2 melts, crystn. 80−59400
$(PbO)_x(SiO_2)_y$ glass, vibrational spectroscpic exam. 79−11417
PbTe-ZrO_2 (SiO_2), epitaxial MIS struct., fabrication and elec. props. 80−2472
Pd/SiO_x/Si, Schottky-barrier type devices, chemical and polarisation characteristics, comparative study 79−78173

silicon compounds continued
Pd-Si, amorphous thin films, laser irrad., metastable phases 80−96622
Pd-SiO_2 interface, H induced interfacial polarisation, internal photoemission meas. 77−1490
Pd-SiO_2 interface, work function changes due to adsorbed H_2, surface and interface dipoles 80−96972
Pr_2O_3-Si_3N_4, prep. by sintering and X-ray diffr. data 79−77570
Pt-Si, amorphous thin films, laser irrad., metastable phases 80−96622
Pt-SiO_2 cermet films, struct. and props. 80−96956
S^{++}+Ne(SiH_4)(H_2S)(HCl)(Ar), K X-ray cross section, projectile charge depend. 77−19029
SIO, Franck-Condon factors rot. depend. 80−58319
Si_3N_4 film on Si wafer, provided stress for creep testing 77−66000
SO_2 emission meas., Baden-Wurtemberg network *(German)* 79−52977
Sb_2O_3-SiO_2(GeO_2)-Na_2CO_3-H_2O, crystallisation 77−12605
Sc_2O_3-Bi_2O_3-SiO_2, three-layer antirefl. coatings, form. and props. 77−58420
Se-Si system glasses, vibr. IR spectra 80−20643
Si (001)-SiO_2, n-inversion layer, valley splitting without effect mass approx. 80−15586
Si (100)-SiO_2 inversion layers, exchange and correl. contribs. to subband energies 79−42654
Si (111)-SiO_2 interfaces, sixth-valley state stability a priori calc. 80−49859
Si biradical, six-coordinate, mol. mobility two-spin probe investig. 80−102529
Si oils, free convective heat transfer from horizontal cylinder, correlation eqns., viscous dissipation 78−5632
Si oxide, photoresist residual film, ellipsometric characterisation 77−48266
Si rich SiO_2-SiO_2-Si rich SiO_2 layers for dual electron injector struct. 80−96991
Si rubber as electro-optic material for optical hydrophones 80−43412
Si, thermally oxidised-electrolyte system, features of cathodic breakdown *(Russian)* 80−107907
p-Si:B-SiO_2 interface in MOS structures, carrier mobility and impurity distrib. 78−34902
Si:H, amorphous hydrogenated film, decomp. kinetics 79−100342
Si:In, p-n junction, spin-dependent recomb. at dislocations, revealed at reverse current 79−24062
Si:P(As)(B)-SiO_2 interface oxidation kinetics, high doping levels, experiment 80−11828
Si/SiC ceramic composite, elastic moduli and bend strength meas., anisotropy 77−59838
Si/SiC ceramic composite, room temp. props., effect of SiC content and orientation 78−27599
Si/SiO_2, adsorbed methanol, light scatt. from clusters 79−33721
Si/SiO_2, CCD, incomplete charge transfer, fringing fields and interface states effects 77−15964
Si/SiO_2 interface, precise wet-chemical etching, using rapidly rotating sample 80−93669
Si/SiO_2 interface, slow-trapping instability, kinetics 78−76151
Si/SiO_2 interface, transition region thickness, determ. by He^+ backscatt. 77−62762
Si/SiO_2-electrolyte interface, electron exchange at surface of thermally grown SiO_2 80−16696
Si-Al-B-O-N, calc. of phase diagrams from data set 80−55362
Si-Al-Be-C-N system, phase equilibria 80−60839
Si-Al-O-N, ceramics, thermal decomposition 79−91936
Si-Al-O-N, compression creep, comparison with SiC and Si_3N_4 79−15728
β′-Si-Al-O-N, Mg-containing phases, crystn. 80−39297
Si-Al-O-N, mullite like cpd. comp., EPMA, X-ray and chem. anal. obs. *(Japanese)* 80−35175
Si-Al-O-N, oxidation mechanisms 80−40570
Si-Al-O-N ceramic, grain boundary desegregation and intergranular cohesion 80−100872
Si-Al-O-N ceramic, single-phase, prep. by hot-pressing, microstruct. investig. 77−8792
Si-Al-O-N ceramic, single phase form. using hot pressing *(Japanese)* 79−70031
Si-Al-O-N ceramic systems, layer struct. 80−6382
Si-Al-O-N ceramics, elec. and therm. cond. 79−86934
Si-Al-O-N ceramics, grain boundary segregation determ. by X-ray microanal. and lattice fringe imaging 79−15681
Si-Al-O-N composites, dense direct prep. from naturally occurring SiO_2 and Al powder 78−11187
Si-Al-O-N compounds, decomposition in N_2 atm. at high temp. 79−57226
Si-Al-O-N polytypes, direct lattice resolution using high resolution electron microscopy 78−38682
Si-Al-O-N polytypes, hot-pressed, microstruct. 80−3023
Si-Al-O-N sintered ceramic, microstruct., phase composition and transformation mech., mech. props. 80−40309
Si-Al-O-N system, behavioural diagrams 79−24507
Si-Al-O-N system, exam. of compounds and properties 78−48387
Si-Al-O-N system, ionic cond. from 850 to 1400°C 80−2203
Si-Al-O-N system, phase analysis and TEM struct. obs. 80−108420
Si-Al-O-N system, stable phase cryst. struct. and microstruct. obs. using TEM 80−108421
Si-Al-O-N system, TEM exam. of X phase structure 78−56606
Si-Al-Zr-O-N, calc. of phase diagrams from data set 80−55362
Si-Al(Ti)C, sintered, exam. of props. 80−25644
Si-As-Te glass, thermoelec. power and DC cond., temp. depend. 77−62955
Si-As-Te glasses, crystallisation kinetics under influence of water vapour 78−59762
Si-B amorphous film, plasma deposited, characterization 79−69828
Si-B system, DTA, X-ray diffr. and metallographic study *(German)* 80−66484
Si-B system, liq., surface tension, density, and oxidation kinetics, 1410-1700°C 80−20011
Si-B-O film, electron probe microanal., Monte Carlo calcs. 79−83533
Si-C amorphous wear-resistant coating 79−34165
Si-C films, plasma deposition with neutralisation 78−88429
Si-C-Al-O-N system, behavioural diagrams 79−24507
Si-containing deposit layers on Ni alloys, appl. methods *(German)* 78−85025
Si-F-H amorphous alloy for electronic appls. 79−15627
Si-Ge, temp. depend. of ESR line intensity of surface centres 77−32246
Si-Ge alloy, hot-pressed, thermal cond., effect of grain size 77−31813
silicon compounds continued
Si-Ge solid solns., p-n junctions, photoelec. props. obs. 77−1471
Si-Ge:As,P, heavily doped, electron scatt., Hall coeff., Seebeck coeff. and resist. meas., 4-300K 77−4379
Si-Ge-Br, heterogeneous system, equilib. gas phase composition, Si-Ge cryst. growth appl. 79−10820
Si-Ge-Br system, diffusion mass transfer 80−33911
Si-Ge-Te system glasses, structural and electronic transitions 77−76890
Si-H, amorphous, H atom effect on Si-Si atomic short-range order, X-ray diffr. obs. 79−64996
Si-H, amorphous, on Nb or W, spectrally selective absorber, IR spectra 80−26164
Si-H, amorphous, random network model 80−1932
Si-H, amorphous, struct. anomalies, theoretical interpretation 79−90556
Si-H, amorphous, thermal stability and decomp. kinetics 80−24758
Si-H, amorphous film, optical and elec. props. 79−82694
Si-H, amorphous plasma deposited film, H content and density 79−82472
Si-H amorphous, defect model, light-induced ESR obs. 79−69721
Si-H amorphous film, reactively sputtered, prep. and props. 79−78889
Si-H:As alloy, amorphous film, coordination of impurities, EXAFS of data 77−84780
Si-H(-D), film, IR and Raman spectra, H bonding effects 78−72515
Si-N film, passivation layer, density comp., and ref. index, Lorentz-Lorenz correl. 78−39697
Si-N films, reactive plasma deposited for MOS-LSI passivation 78−56584
Si-O compounds, X-ray photoelectron spectra 77−18971
Si-O cpds., bond lengths rel. to force consts. 77−46653
Si-O fibres, parametric excitation of anti-Stokes coherent stimulated scatt. *(Russian)* 80−58637
Si-O system, disordered, coordination props., electronic struct. 77−15755
Si-O_2-N_2 system, Si_2N_2O, corrosion in O_2, sintered in the presence of magnesia *(French)* 78−23837
Si-Si_3N_3, dielec. function calc. 79−95862
Si-Si_3N_4, interface layer determ. by spectroscopic ellipsometry 79−95275
Si-Si_3N_4 interface, effect of F ions on props. and stability, expt. 78−64141
Si-Si_3N_4 interface in MNS capacitors, surface state density investigation 80−60100
Si-Si_3N_4-Al, electrical strength, effect of struct. defects in Si_3N_4 *(Russian)* 78−26955
Si-Si_3N_4-Al, photoexcitation of emission currents, I-V characts. *(Russian)* 77−72917
Si-Si_3N_4-SiO_2 non absorbing double layers, optical parameters reflectivity by liquid immersion method 80−71503
Si-Si_3N_4-SiO_2-Si multilayer structs., impurity distrib., activation anal., autoradiography techniques 77−16881
Si-Si_3N_4(SiO_2) boundary, electrophysical properties, effect of ionic processes in dielectric layers *(Russian)* 78−10562
Si-SiC chemical interaction in rarefied O_2 under pulsed action of concentrated solar radiation 80−71930
Si-SiC composite, high temp. time depend. strength 77−56083
Si-SiC composite film, optical props., appls. 77−754
Si-SiO_2, Al-implanted, low-temp. annealing effect on charge and surface state density 77−85337
Si-SiO_2, angular-dependent X-ray photoelectron spectra 77−12485
Si-SiO_2, anodic polarisation in electrolyte containing fluoride ions, effect on oxide props. 80−39679
Si-SiO_2, bonding at (111) interface, stoichiometry and kinetics, synchrotron radiation photoemission spectroscopy 80−24744
Si-SiO_2, charge injection from polycryst. Si at low fields 77−39945
Si-SiO_2, dielec. function calc. 79−95862
Si-SiO_2, ESR centres, interface states and oxide fixed charge 80−2474
Si-SiO_2, electron tunnelling into thermally grown SiO_2 77−12018
Si-SiO_2, electron-beam annealing of ion-implantation damage 79−77622
Si-SiO_2, emission probability of hot electrons into oxide 77−32084
Si-SiO_2, flat-band voltage due to fixed surface charge density, modified expression 79−56317
Si-SiO_2, hot electron emission from Si under low level avalanche multiplication 77−80851
Si-SiO_2, influence on frequency-temp. coeff. of SAW devices 80−79066
Si-SiO_2, intentionally contaminated interface, transient capacitance meas. 79−33349
Si-SiO_2, interface, distinction between donor and acceptor character of surface states 78−39216
Si-SiO_2, interface, electronic ground state of inversion layers 77−43731
Si-SiO_2, interface, hopping conduction, anal. in impurity bands in inversion layers 79−47171
Si-SiO_2, interface, morphology and electronic struct. 79−78194
Si-SiO_2, interface, props. of surface states reviewed 77−20449
Si-SiO_2, interface, reconstructing states 80−49925
Si-SiO_2, interface, stress meas. technique 80−84395
Si-SiO_2, interface defect states obs. by constant capacitance DLTS 80−49924
Si-SiO_2, interface free carrier mobility in inversion layer, influence of polar phonon scatt. 79−73597
Si-SiO_2, interface layer determ. by spectroscopic ellipsometry 79−95275
Si-SiO_2, interface states, new model 80−29478
Si-SiO_2, inversion layer, electronic ground state, stress, temp., mag. field and gate voltage depend. 78−60226
Si-SiO_2, ion bombardment by H_2^+, D_2^+, changes in annealing behaviour 79−78185
Si-SiO_2, ion implantation effects on charges 77−32086
Si-SiO_2, ion implantation through SiO_2 film, recoil implantation of O, EPR study 80−88180
Si-SiO_2, MOS interface states density, meas. techniques and model development 80−92988
n-Si-SiO_2, MOS structures, radiation states 80−103758
Si-SiO_2, nitridation, formation and growth rate of Si_2ON_2 *(Japanese)* 79−91574
Si-SiO_2, oxide defect density depend. on appl. elec. field and thickness 80−19791
Si-SiO_2, recoil implanted O profile after ion implantation through SiO_2 80−88198
n-Si-SiO_2, screening of charged impurity centre localised inside oxide and at interface of inversion layer 79−73563
Si-SiO_2, SiO_2 layer charging in UV irrad. of MISS struct., photoinjection currents *(Russian)* 80−39680
Si-SiO_2, surface and interface phonons in bonded solids 78−71931
Si-SiO_2, surface state annealing 77−39946

silicon compounds continued
Si-SiO_2, surface states, oxide charge centres, annealing effects 78−2570
Si-SiO_2, thermally oxidised, origin of fixed charge, Si diffusion in transition region 77−20381
Si-SiO_2 (111) interface, H_2 effects, AES study 80−65688
Si-SiO_2 (111) interfaces, sixfold valley degeneracy in electron inversion layers 80−49936
Si-SiO_2 abrupt interface form. by very high dose O^+ ion implantation 80−75253
Si-SiO_2 barrier height in MOS tunnel struct., SiO_2 thickness depend. 78−14831
Si-SiO_2 bonding layer, EPR exam. 78−15022
Si-SiO_2 boundary, origin of interface states and oxide charges generated by ionising radiation 77−20380
Si-SiO_2 boundary, precipitation of Na *(Russian)* 80−49368
Si-SiO_2 boundary, relaxation of nonequilibrium capacitance in electrolyte in intense elec. fields 80−70845
Si-SiO_2 boundary, surface charge transport in valence band of Si 80−70789
Si-SiO_2 charge accumulation during low energy electron bombardment 78−64142
Si-SiO_2 double barriers, reson. tunnelling 77−80846
Si-SiO_2 electrode, electronic cond., luminesc obs. 80−61111
Si-SiO_2 film, crater-edge profiling in interface anal., ion beam etching and AES 77−1323
Si-SiO_2 interface, (001) vicinal planes, minigaps in inversion layers, far IR absorpt. meas. 80−107919
Si-SiO_2 interface, amorphous, electronic states, Cayley trees appl. 79−65373
Si-SiO_2 interface, anisotropic photoinduced ESR 78−23345
Si-SiO_2 interface, Au conc., effective impurity doping 78−52094
Si-SiO_2 interface, Au doping, trapping states 80−20319
Si-SiO_2 interface, Au surface state energy levels and Au diffusion 79−51652
Si-SiO_2 interface, Auger sputter profiling and photoelectron spectroscopy obs. 78−10287
Si-SiO_2 interface, Auger sputter profiling 78−43254
Si-SiO_2 interface, Auger-sputter profiling obs. of P pileup 78−95240
Si-SiO_2 interface, avalanche injection of charge carriers, oxide current decay 77−43728
Si-SiO_2 interface, backscattering-channelling study 80−34320
Si-SiO_2 interface, barrier height in MOS tunnelling structures 80−88644
Si-SiO_2 interface, bias temp. treatment effect, stability, Cl oxides effect 77−69419
Si-SiO_2 interface, chem. struct. of transitional region 78−95824
Si-SiO_2 interface, cluster Bethe-lattice method appl. 80−49852
Si-SiO_2 interface, continuous random network and tight-binding models 77−89866
Si-SiO_2 interface, defects, intimate valence attenuation pairs 80−54132
Si-SiO_2 interface, density of states, theory 80−80395
Si-SiO_2 interface, ESCA and ellipsometric study 79−82678
Si-SiO_2 interface, effect of thin transition layer on electron mobility and energy levels 77−20458
Si-SiO_2 interface, effect of ^{11}B and ^{19}F ion implantation on charge density 79−10865
Si-SiO_2 interface, effect of N_2 annealing on electron scatt. 79−42660
Si-SiO_2 interface, effect of high-temp., post-oxidation annealing on elec. props. 79−82673
Si-SiO_2 interface, effect of oxidation time and temp. using AES 80−35359
Si-SiO_2 interface, effect of hot electron injection on interface charge density 80−49921
Si-SiO_2 interface, elec. props., rel. to SiO_2 layer struct., 200-600°C heat treatment effects *(Russian)* 77−15967
Si-SiO_2 interface, elec. props. and influence on service performance and stability 78−23171
Si-SiO_2 interface, electron injection into oxide due to mobile ion induced internal field 77−15963
Si-SiO_2 interface, electronic struct., field depend. internal photoemission probe 77−20450
Si-SiO_2 interface, electronic states, review 78−30992
Si-SiO_2 interface, electronic struct., EELS study 79−99596
Si-SiO_2 interface, electrically active paramag. centres detect., photocond. reson. obs. 80−50185
Si-SiO_2 interface, electronic struct. calc. 80−100531
Si-SiO_2 interface, electron mobility in inversion and accumulation layers 80−103753
Si-SiO_2 interface, fitting stress and its effect on vacancy generation and distrib. 77−28087
Si-SiO_2 interface, form. and struct., AES obs. 79−56314
Si-SiO_2 interface, γ-ray irradiated thin oxide, MOS struct. *(Russian)* 78−84302
Si-SiO_2 interface, Hg probe *(Chinese)* 77−89857
Si-SiO_2 interface, high-resolution electron microscopy study 78−56046
Si-SiO_2 interface, improved characterisation, refined quasistatic and cond. methods 80−96990
Si-SiO_2 interface, impurity electron states near interface 78−95320
Si-SiO_2 interface, in MOS structure, effect of irrad. with low energy electrons *(French)* 77−55617
Si-SiO_2 interface, in MOSFET struct., electronic props. 79−42662
Si-SiO_2 interface, intermediate chem. state of Si during sputter profiling, Auger spectra 79−11230
Si-SiO_2 interface, interface-state parameters near band edge, MOS conductance meas. 79−11226
Si-SiO_2 interface, inversion layer transport, radiation hardness effects, review 79−19673
Si-SiO_2 interface, ion implantation induced interface states, effect of oxidation and N_2 annealing 77−39949
Si-SiO_2 interface, light induced reson. centres, photocond. reson., EPR obs. 80−50184
Si-SiO_2 interface, local at. struct., XPS obs. 80−20042
Si-SiO_2 interface, MeV backscatt. channelling meas. of Si monolayers 79−11020
Si-SiO_2 interface, metallisation induced stress meas., X-ray transmission topography 79−24434
Si-SiO_2 interface, model for doped-oxide-source diffusion with chemical reaction 77−39954
Si-SiO_2 interface, Na^+ drifted, impurity bands in inversion layers 78−60211
Si-SiO_2 interface, O_2 plasma effects on elec. props. 80−100523

silicon compounds continued
Si-SiO_2 interface, optical props. of CDW ground states in Si inversion layers 77−43732
Si-SiO_2 interface, optical props. 79−99908
Si-SiO_2 interface, oxidation stacking faults, growth rel. to self-diffusion 80−49239
Si-SiO_2 interface, props. 78−23170
Si-SiO_2 interface, props. variation in SiO_x region 80−49548
Si-SiO_2 interface, rad. hardness, carrier localisation in inversion layer 77−85332
Si-SiO_2 interface, relax. of injected charge, temp. depend. 78−72269
Si-SiO_2 interface, remote polar phonon scatt. in Si inversion layers 80−80095
Si-SiO_2 interface, stacking fault-free region formation by annealing 78−51561
Si-SiO_2 interface, surface generation velocity study, gate-controlled diode structure application 80−6986
Si-SiO_2 interface, surface states characterization, expt. techniques review 80−49949
Si-SiO_2 interface, thermally oxidised, oxide thickness effects on electron scatt. 78−88033
Si-SiO_2 interface, thermally grown, inhomogeneities of surface potential 80−34524
Si-SiO_2 interface, thermal SiO_2 sputter induced roughness, Auger sputter profiling study 80−75424
Si-SiO_2 interface, thermally grown oxide, spectroscopic ellipsometric anal. 80−107659
Si-SiO_2 interface, trapping props. from electrochemical current-voltage behaviour 79−69597
Si-SiO_2 interface, two-dimensional impurity bands, carrier-density dependence of activation energies associated with hopping 80−88561
Si-SiO_2 interface, valley degeneracy splitting in n inversion layer, effective-mass approx. 79−99629
Si-SiO_2 interface, with Cl^- incorporated, characterisation by low temp. cond. meas. 78−60220
Si-SiO_2 interface as electrode for electrical and ellipsometric meas. of adsorbed organic molecules 80−15366
Si-SiO_2 interface charge effects and related props. 78−10575
Si-SiO_2 interface formation by anodic oxidation, F^- and Cl^- ions effect obs. 79−15842
Si-SiO_2 interface in IGFETs, anal. of CVD SiO_2 on (100) and (111) surfaces, near-ideal structs. 80−100528
Si-SiO_2 interface in MIS struct., B^+ ion implanted, elec. props. due to laser irrad. 78−72272
Si-SiO_2 interface in MIS structs., effects of crystal defects on generation process 80−65702
Si-SiO_2 interface in MOS structs. low-energy electron beam irrad., charge accumulation process anal. 80−65701
Si-SiO_2 interface in MOS capacitors, lateral diffusion of Na^+, neutralisation 80−92986
Si-SiO_2 interface in MOS solar cells, operational characts. and struct. 80−93901
Si-SiO_2 interface layer characterisation by spectroscopic ellipsometry 80−50738
Si-SiO_2 interface morphology, P pileup effect, Auger sputter profiling 78−72006
Si-SiO_2 interface oxidation kinetics, high doping levels, theory 80−11827
Si-SiO_2 interface state spectrosocpy using MOS tunnelling strucures 80−6991
Si-SiO_2 interface state distribution, Br incorporation effects 80−11091
Si-SiO_2 interface state density, dependence on thermal oxidation process variables 80−15607
Si-SiO_2 interface struct. by cross-sectional TEM, amorphous oxide layer 77−24487
Si-SiO_2 interface struct., transient region 77−85115
Si-SiO_2 interface study by XPS 80−50507
Si-SiO_2 interfaces, local atomic and electronic struct., high resolution XPS 80−49927
Si-SiO_2 interfacial region on TCE/O_2 and CCl_4/O_2 oxidised Si, struct. and comp. 80−50741
Si-SiO_2 interfacial transition layer thickness, XPS obs. 80−11540
Si-SiO_2 interlayer, optical evidence 79−69800
Si-SiO_2 inversion layer, n-channel, anomalous magnetoresist., model 80−96996
Si-SiO_2 inversion layers, bound states at interface 79−42655
Si-SiO_2 laminar ion-implanted systems, struct. change investig. by MSSI method *(Russian)* 80−107918
Si-SiO_2 layer formation by O_2^+ ion implantation, interface struct. and C-V characts. 77−1142
Si-SiO_2 layers on Si substrate, ellipsometric meas. 77−69403
Si-SiO_2 MIS systems, dynamic props. of switching, appl. to charge transfer devices 80−92997
Si-SiO_2 MOS capacitors, relationship between trapped holes and interface states 80−70830
Si-SiO_2 MOS interface, surface-state density and minority carrier generation rate, meas. by DLTS, hot hole effect 80−100527
Si-SiO_2 metal structure, ponderomotive force effect on dielec. breakdown 79−15230
Si-SiO_2 microsensor, surface conductivity effect of aliphatic alcohol molecule adsorption *(Russian)* 78−34887
Si-SiO_2 structure, alkali metal ion migration and accumulation, interface struct. 80−107574
Si-SiO_2 structure, electrophysical props. after B^+ ion bombardment 77−12013
Si-SiO_2 structure, mechanical stress at Si(111) surface 78−63921
Si-SiO_2 structure, oxide charge evaluation, appl. of Kelvin method 78−19157
Si-SiO_2 structure, SAW device, appl. to integrated oscillators 78−83186
Si-SiO_2 structures, AS77 scanning analyser for electrophysical props. *(Polish)* 79−95498
Si-SiO_2 structures, B ions implanted, energy spectra of shallow traps at various implantation energies 80−80392
Si-SiO_2 structures, ion implanted, surface characts. 77−80850
Si-SiO_2 surface states, influence of Φms(T) 79−99597
p-Si-SiO_2 system, C-V meas. using Au/Hg probe, work function difference between probe and Si 80−2450
Si-SiO_2 system, structural defect formation rel. to thermal oxidation kinetics *(Russian)* 78−43478
Si-SiO_2 systems, spectral characts. *(Russian)* 79−42657
Si-SiO_2 transition region width, SIMS depth profiling 80−39454
Si-SiO_2 wafer thinning for TEM 77−89352

silicon compounds continued
Si-SiO_2-Al, interface barrier energies for tunnel oxides, internal photoemission meas. 80−84512
Si-SiO_2-Al, internal photoemission, pot. barrier height determ. 80−65699
Si-SiO_2-Al MOS surface channel influence on channel-to-contact diode charact. 80−92994
Si-SiO_2-Al structure, mechanical stress at Si(111) surface 78−63921
Si-SiO_2-Al with thick dielec. layer, photoelec. props. 80−92979
Si-SiO_2-Au Schottky barrier solar cells, back-illuminated, theoretical performance 80−61345
Si-SiO_2-CdS solar cell, I-V characteristics 80−89621
Si-SiO_2-KCl_{aq}, interface, capacitance meas. 78−80051
Si-SiO_2-Mg-Cu powder compact, nitridation to form Si_2ON_2 whiskers *(Japanese)* 80−93674
Si-SiO_2-Mo-Si_3N_4-Al MNOS structures with metal grains, charge transport at SiO_2-Si_3N_4 interface 80−65693
Si-SiO_2-Si capacitor, polycryst., capacitance voltage characterisation 80−70794
Si-SiO_2-Si structures, P, As depth profiles, ion microanal. *(Japanese)* 78−85251
Si-SiO_2-Si thin film MOS structures, elec. props. with applied DC voltage *(Slovak)* 80−92977
Si-SiO_2-Si_3N_4, internal photoemission 80−7475
Si-SiO_2-Si_3N_4, surface states, density and spectrum 77−69423
Si-SiO_2-Si_3N_4 MNOS structure, chem. comp. and electronic states, Auger and energy loss spectra obs. 80−92999
Si-SiO_2-Si_3N_4 system, internal photoelec. emission and residual photoelec. effects 79−73599
Si-SiO_2-$Si_xO_yN_z$ waveguide model *(Russian)* 79−10374
Si-SiO_2-Sl MOS structures, charge motion, TSC meas. 80−100534
n-Si-SiO_2-SnO_x SIS solar cell, transport props., 14% efficiency realisation 80−94079
n-Si-SiO_2-ZnO-Al, SAW convolver in monolithic MIS struct. 77−23791
Si-SiO_2-metal structures, tunnelling probabilities for electrons and holes in ultrathin SiO_2 79−99631
Si-SiO_2-polySi thin film structures, dielectric props. *(Slovak)* 80−75934
Si-SiO_2-vacuum system, principal angle and azimuth determ. 78−11009
Si-SiO_3 interface, effect of Au recomb. centres on interfacial trapping states 79−38175
Si-SiO_x interfaces, carrier transport processes, electron states, conference, Durham, England (July 1979) 80−90612
Si-SiO_x interface, evidence for superlattices, magnetocond. expts. 77−89868
Si-SiO_x interface, localisation in inversion layer due to states in gap of oxide 77−12012
Si-SiO_x-Al photodiode experimental verification of theoretical predictions 80−29485
Si-SiO_x-SiO_2 interface, energy gap variation 79−91148
Si-Te structural changes rel. to memory effect *(Russian)* 78−71679
Si-Te system, phase diagrams 80−89209
Si-Te system glasses, local struct., ^{119}Sn Mossbauer obs. 79−41968
Si-thermal SiO_2-electrolyte system, cond. in superhigh elec. field 78−52080
Si+carbon tetrafluoride, reaction, metastable C phase prod. 79−29393
$Si+H_2(O_2)(He)(SiCl_4)$, $3p^2(^1D_2)$ state behaviour, at. absorpt. spectra 78−29846
Si_3N_4, low press. CVD production processes 77−77395
Si_5-Al-O-N_7, hot pressed, exam. of fracture mechanisms 78−72879
$Si_{(6-z)}Al_zO_zN_{(8-z)}$, sialons, hot-pressed, dielec. props. 78−10822
β'-$Si_2Al_4N_4O_4$, combined X-ray and IR analyses 78−79579
SiAlON ceramic, pressureless sintering 78−27449
SiAlON, oxidation 77−56130
SiAlON powder, prod. by reaction clay+C+N_2 80−40295
SiAlON, prepared from siliceous sand and Al powder, hot pressing, steatite contamination effects *(Japanese)* 80−93528
SiAlON, pressureless sintered with low amounts of sintering aid 79−66029
SiAlON system, β', 15 R phases, oxidation resist. *(French)* 78−72899
$Si_{6-x}Al_xO_xN_{8-x}$, x=1.5, 3, 4, Sialon ceramics, elec., thermal cond. 79−33124
$Si_{6-z}Al_zO_zN_{8-z}$, β-Sialon, form. from Si_3N_4-SiO_2-AlN system *(Japanese)* 80−45261
$Si_{6-z}Al_zO_zN_{8-z}$, hot pressed, DC elec. props., 18-500°C, fields up to 1.1×10^4 V cm^{-1} 78−26860
$Si_{(6-z)}Al_zO_zN_{(8-z)}$ 78−39136
SiAs, cryst. growth from melt, elec. props. 80−76170
SiAs, deterioration in air, product identification 77−36675
SiAs, monoclinic, band struct., OPW calc. 77−59255
SiAs-Au surface barrier diodes, optical props. of SiAs 79−8145
SiAs+$Cl_2(Br_2)(I_2)$, high temp. Raman spectra, cryst. growth mechanism *(French)* 79−26999
$SiAs_2$, electron charge density calc., nature of bonding determ. 77−1098
Si_xAs_{1-x}:H, amorphous system, struct. and defects, Raman and EPR meas. 80−49103
SiB_{12-x}, thermam cond., temp. depend., up to 2000K *(French)* 80−70484
SiB_4, mech. and thermal props. 80−21083
Si_xB_{1-x} films, anal. of H ratios and profiling using nucl. techniques and Rutherford backscatt. 80−61202
Si_xB_y formed when Bi_2O_3 is diffused in Si, anal. study 79−19269
SiBr, $B^2\Sigma^+\rightarrow X^2\Pi$ transition, rot. anal. *(French)* 79−50013
$SiBr_4$, electronic struct., Xα SW calcs. 80−102447
$SiBr_4$, fine struct. resolution in Raman-active fundamentals 79−42967
$SiBr_4$, vac. UV absorpt. spectra, 130-270 nm 77−75183
$SiBr_4$, X-ray absorpt. spectra struct. 80−37819
$SiBr_4+H_2$, SiH_nBr_{4-n} heat of form., mass spectrometric determ. 79−20455
$SiBr_m$, (n=1,2,3) heats of formation, mass spectrometric determ. 80−89511
$SiBr_x$, x=1,2,4, diffusive mass transfer of Si, calc. for closed system 77−44169
Si_6Br_{12}, and Si_6Cl_{12}, vibrational spectra and force constants, rel. to Si_5Cl_{10} and Si_5Br_{10} *(German)* 79−22716
α-SiC ^{30}Si self-diffusion, ion microprobe anal. 79−42309
SiC, 10 keV H^+ irrad., C deposition, surface swelling, surface morphology changes 77−35608
SiC, 102R polytype struct, and localisation, by RHEED *(French)* 77−65966
SiC, 126R polytype, struct. determ., use of lattice imaging in electron microscope 78−26498

silicon compounds continued
SiC 147$R_{(b)}$ polytype, crystal structure by X-ray diffraction method *(Chinese)* 80−54206
SiC, 2H disordered single crystal, X-ray diffr. stacking fault exam. 77−89452
SiC, 2H→6H transform. mechanism, X-ray diffr. theory 78−30575
n-SiC, 6H, epitaxial layer, saturated electron drift velocity meas. 78−19168
α-SiC, 6H, excited states, photoluminesc. efficiency 78−39604
SiC, 6H polytype, elec. and thermal cond., carrier concentrations 80−2223
n-SiC, 6H polytype, expitaxially grown, electronic props. meas. 77−39975
SiC, 6H polytype, LPE growth by dipping technique for prep. by blue LEDs 77−8769
β-SiC, 6H polytype, pure and doped, prep. by pyrolysis of silane cpds. 78−44018
SiC (1 OH), phonon spectrum, dispersion curves energy discontinuity and vibr. modes, IR spectra obs. 80−44274
SiC (15 R), polytype, many valleyed polar semicond., electron-hole-liquid, obs. from excitation and time delayed spectra 79−28289
n-SiC (6H), anisotropy, of thermoelec. power and transverse Nernst-Ettingshausen effect 77−69362
n-SiC (6H), anisotropy of thermoelectric power *(Russian)* 78−91710
SiC (6H), blue-emitting diodes by CVD 80−97439
n-SiC (6H), density of states effective mass determ., high temp. meas. of elec. props. 79−15073
n-SiC (6H), doping effect on birefingence dispersion, effective electron mass 79−69807
α-SiC (6H), dynamic hologram high-speed recording and erasure mechanism 80−5710
SiC (6H), epitaxial film, electronic props. 79−60942
SiC (6H), IR absorpt., UV illumination effects, defect levels 80−66251
α-SiC (6H), paramag. N impurity levels, IR absorpt. and ESR expts. 77−59598
SiC (6H), phonon drag and phonon-electron interaction *(Russian)* 78−79701
SiC (6H), piezoresist. meas. 78−2090
SiC, (6H), radiation damaged, luminesc. 80−25462
SiC (6H), semicond. with one-dimens. electron superlattice, interband optical absorpt. 79−15483
SiC (6H), slip systems and plastic deform. at high temp., Knoop hardness meas. 79−87683
SiC (6H) (000$\bar{1}$), Ar^+ ion bombard., defect form., LEED obs. 79−69165
SiC (6H) epitaxial layers, growth by CVD, morphology 79−24446
α-SiC (6H) laser excited thermostimulated luminescence light sum dose depend. *(Russian)* 80−16111
SiC, abrasion of polymers, metal surfaces, mechanism rel. to groove sizes, shapes 79−20216
SiC, abrasive, evaluation of brittleness, contact endurance by cyclic microhardness 79−15890
SiC, abrasive, wear in simulated hot grinding 78−56784
SiC, abrasive grains, single, wear on steel, exam. *(Japanese)* 78−44230
SiC, abrasive paper, variables affecting degradation 79−43444
SiC abrasive papers, frictional force amplitude effect on degradation 79−74264
SiC, absorption of US waves 78−72210
SiC, acoustic props. study at 9.43 GHz 80−65169
α-SiC, afterglow stimulated by IR radiation *(Russian)* 80−89066
SiC, amorphisation induced by ion bombardment, Raman spectroscopy 77−80551
SiC, amorphous, localised gap states, hopping cond. and chem. bonding 78−23052
SiC, amorphous, reactively sputtered, effects of S/C ratio and H content on elec. and optical props. 79−90906
SiC amorphous film, elec. props. and hopping transp. 77−66211
SiC and IR excess of C stars 78−16413
SiC and Si_3N_4, hot pressed, comparison of high-temp. thermal fatigue resistance 77−36623
SiC and Si_3N_4 sintered bodies with polyborodiphenylsiloxane binder 77−40401
SiC, anodised, IR spectra *(Russian)* 78−11376
SiC, appl. of replica electron fractography 79−60237
SiC, atomically sharp cracks, TEM study 80−71729
SiC, α- and β-phases, isomer shift in Mossbauer spectra of implanted ^{129}I 78−15067
SiC, α- and β-types, electroreflection spectra of natural and low-energy ion-bombard. surfaces 79−61340
SiC, α-β heterojunctions, spectral charact. *(Russian)* 77−63467
SiC, B diffusion, polytype struct. effect 78−59983
SiC base material, electrical props., heat treatment effect 77−12645
SiC, blistering and flaking due to light ion bombardment *(Japanese)* 80−70264
SiC, blue-LED for stimulation of visual cells of insects *(German)* 79−39623
SiC brittle coating for B fibres, critical thickness effect on strength *(Russian)* 80−40426
SiC, $\beta\rightarrow\alpha$ transformation, interfacial energetics 79−8296
SiC, $\beta\rightarrow\alpha$ transformation, microstructural aspects 79−8295
SiC, CVD, microstruct. obs., optical and TEM 79−7560
SiC, CVD, polished, total integrated vac. UV scatt. 77−62029
SiC, CVD anisotropic thick hollow cylinder, residual stress due to uniform cooldown 79−42423
SiC, CVD film growth, morphological, chem. and cryst. struct. investig. 77−40385
SiC CVD substrate, Cu mirror vapour deposition, pulsed laser damage characts. 80−48314
SiC, cathodoluminescence, comparison with other materials 78−92130
SiC cavity radiator, spectral emissivity and radiance 77−83939
SiC ceramic, high performance, for load-bearing engineering applics. 77−8785
SiC, ceramic, mass loss in inert gas stream *(Russian)* 79−7686
SiC ceramic heat exchanger, cost-effective design 80−95341
SiC, ceramic material fracture mechanics, review 80−45373
SiC ceramics, fireproof, direct energy conversion appl. *(Czech)* 79−70455
SiC, chem. stability, mech. and thermal props. rel. to appls. 80−21103
SiC cladding possibility for gas-cooled fast breeder reactor fuel 77−18667

silicon compounds continued
SiC coated B filament, uncoated and SiC coated, high temp. physicomech. props. 79−20140
SiC coated C fibres, effect on strength props. of C fibre reinforced plastics 80−104224
SiC coated fuel particles, failure during thermal excursion above 2000°C 79−36317
SiC, coating, vapour deposition by plasma activated process 79−57125
SiC coating corrosion by fission product Pd in HTGR coated particle fuels 80−102237
SiC, coating for C fibres in glass composites, hot pressing production method *(German)* 78−95724
SiC, coating for oxidation resistance 77−32704
SiC coating on C fibre, chemical vapour deposition, relation between surface morphology and coating conditions *(Japanese)* 78−39704
SiC, coating on graphite, by reactive magnetron sputter deposition *(Japanese)* 80−16185
SiC coating on Mo, CVD and stability under thermal cycle conditions 80−7500
SiC coatings, CVD on microspheres in fluidised bed, parametric investig. 77−40457
SiC coatings for first-wall candidate materials by RF sputtering 80−25563
SiC coatings for HTR nuclear fuels, characterisation by small-angle X-ray scatt. 80−44451
SiC, combustion-heated thermionic diode appl. 79−48157
SiC, compression creep, comparison with Si_3N_4 and sialon 79−15728
SiC, constituent of ceramic moulding material, moisture content meas. in UHF range 79−34404
SiC containing material, deform. props. investigation by pure bending 78−19823
SiC, continuous fibre synthesis with high tensile strength and Young's modulus 79−15633
SiC continuous fibres, mech. props. depend. on testing conditions *(Russian)* 80−35297
SiC, controlled nucleation thermochemical deposition, charact. and props. 80−108355
α-SiC, corrections for crystal-to-film distance variations in Laue photographs 77−43114
SiC, corrosion in gases and alkaline melts 77−8967
SiC corrosion in HTGR fuel particles 77−67817
SiC corrosion in HTGR fuel particles 77−74932
SiC, corrosion resist. in residual fuel oil fired environment 79−39010
SiC, cryst. growth on oriented seeds by sublimation 78−35279
β-SiC, cryst. temp. variation during growth 77−40340
SiC crystal, energy band struct. and optical spectra 78−18962
SiC, crystal growth from gas phase role of Si in mass transfer 79−8233
SiC crystals, 2H to 6H solid-state transformation, X-ray diffraction study 80−28943
α-SiC crystals, broad-band semiconductors, growth in Acheson furnace 80−84841
α-SiC crystals, dynamic holographic grating recording 77−79785
β-SiC crystals, wetting by Si and growth by vap.-liq.-solid mechanism 78−3005
SiC, cubic, atomic displacement energy determ. by bracketing technique 80−49272
β-SiC, cubic, conduction band minima location and shape determ. 77−85141
β-SiC, cubic, elec. props. 78−51996
SiC, cubic, electron-hole liq., luminesc. obs. 78−31239
SiC, cubic, electron-hole liq., ground state props. calc. 79−69429
β-SiC, cubic, electronic props. of vacancies and divacancies 77−76767
SiC, cubic, magnetoresistance and Hall mobility, field and orient. depend. *(Russian)* 77−69346
SiC, cubic, photo EMF on microtwinning lamella *(Russian)* 78−60165
n-SiC, cubic, piezoresistance meas. under hydrostatic compression 77−4344
α-SiC, deep centre levels, IR photoluminescence 77−16387
β-SiC, deform. potential and effective mass anisotropy, Hall constant 79−90949
SiC, dense, joining by hot pressing, and bond strength 80−66458
SiC, desorption of D, activation energies 79−65330
SiC, determ. of size and conc. of crit. clusters in vapour phase in homogeneous nucleation process 79−94951
SiC devices, epitaxial layer growth techniques 80−108360
SiC, dielectric coating effect on surface polaritons, optical consts. *(Russian)* 80−88489
SiC, dielectric hard transparent coatings 77−36678
SiC diffraction grating for vac. UV, fabrication 77−79920
SiC, diffusion behaviour of fission products, 1650 to 1850°C 78−79814
SiC, diffusion of B, elec. cond. meas. 80−96696
SiC, diffusion tracer deposition, using travelling solvent zone 78−51742
A-SiC, dimensions of muonium atoms, depolarisation of positive muons 79−11374
SiC diodes, S-type, high-voltage switching 77−20421
6H-SiC, dislocation etching 78−22721
SiC, dissociation in silicate bonded refractories, X-ray obs. *(German)* 79−47893
SiC, dissolution rate in molten Si, Fick's law calc. 79−99319
SiC distribution profiles of 30 keV Al ions using Lindhard-Scharff-Schiott model *(German)* 80−15172
SiC, donor exciton satellites, multiple bound excitons 77−11857
SiC, eccentric growth spirals 78−26470
α-SiC, effect of cryst. shape and size on plastic deform. to rupture and strength 77−56043
SiC, effect of crystallographic anisotropy on Knoop microhardness 80−66626
SiC, electrodeposition mech., onto metal electrodeposit, cermet prop. 79−33992
SiC, electron microscopical fractography *(Russian)* 77−25146
SiC, electron trap depth, additional IR absorption induced by UV excitation *(Russian)* 79−78721
SiC, electron-hole liquid, RPA calcs. 80−6743
SiC, ellipsometric exam. of polytypes 78−92044
SiC, energetic deuteron irradiated surface struct. quantitative meas. 78−95210
SiC, energetic H and Ar ion sputtering, AES-SIMS-FDS combined obs. 78−80444
SiC, energetic ion sputtering, appl. of AES-SIMS (IMA)-FDS combined systems to physical and chemical processes 78−95636
SiC, engng. ceramic, lattice resolution studies 78−27510

silicon compounds continued
SiC, epitaxial film, effect of impurities on polymorphism during growth 80−15414
SiC, epitaxial growth, appl. for solid state devices *(Japanese)* 80−11579
SiC, epitaxial growth by sublimation sandwich method, effect of impurities 80−25568
SiC, epitaxial growth by direct synthesis in vacuum 80−40262
α-SiC, epitaxial layer, impurity macroincorporation, distrib. of Al, B, N and P 77−69192
SiC epitaxial layer, vapour phase growth, investigations of kinetic and thermal conds. 79−42407
SiC epitaxial layer growth from sublimation in vac., kinetics 80−20791
SiC, epitaxial layer polytypism 77−62781
SiC, epitaxial layer polytypism 77−62782
SiC epitaxial layers, crystallographic orientation effects on polytype stabilization and transform. 79−42413
SiC epitaxial layers, energy distrib. in photolum. spectra, influence of synthesis conditions 79−52009
SiC, epitaxial layers on diamond, electron diffr. patterns 77−15720
SiC, exam. of N solubility, in epitaxial layers 80−6520
SiC, exam. of T_2 diffusion coeffs. and D_2 solubility 78−79816
SiC, extremely large-period polytypes, X-ray diffr. and TEM 77−31636
SiC, failure prediction technique derived from fracture mech. 77−7343
SiC fibre, development from organosilicon polymers by heat treatment 80−81014
SiC, fibre, metallisation by continuous casting in Al and Al alloys *(Russian)* 78−35538
SiC fibre development using organosilicon polymer precursor 78−60627
SiC, fibre growth kinetics in laser-heated system 77−81203
SiC fibre reinforced Al-Si alloy, liq. phase process prep. effect on mech. props. 79−70020
SiC fibre reinforced Al interaction between components and compatibility, mech. props. effect 80−11761
SiC fibre reinforced Al-Mg, heat treatment effect on struct., tensile strength 80−55487
SiC fibre reinforced Al, thermophys. props. 80−59745
SiC fibre reinforced Al, plasma-formed semifinished products, props. 80−84890
SiC fibre reinforced Al, synthesis by liquid pressing method 80−100816
SiC fibre reinforced Ti, effect of Al, Zr and Mo alloying additions on reaction rate of Ti with fibres 80−16249
SiC fibre reinforced Ti-Al-Mo-Zr composites, matrix selection *(Russian)* 80−35192
SiC fibre reinforced Ti-Al-Mo-Zr-Si (6.6, 3.3, 1.8, 0.3 wt.%) composite, component interaction kinetics *(Russian)* 80−55364
SiC fibres, continuous, tensile strengths and Young's moduli, 600-1400°C 77−59885
SiC fibres, microcrystalline state anomalous charact. 79−74122
SiC fibres, plasticizing and wettability-enhancing coatings 79−29252
SiC fibres obtained from polycarbosilane fibre 80−50582
SiC fibres reinforced Ni complex alloy, influence of TiN coating on fibre matrix interaction *(Russian)* 78−95820
SiC fibres with protective Al_2O_3 coatings in Ni-Cr alloy based composites, IR investigation 78−60623
SiC filament, W, TaC and HfC CVD coatings, effect on high temp. mech. props. 78−15347
SiC filament reinforced phosphate foam ceramics, bending strength 80−11716
SiC filamentary crystals, dia. determ. by X-ray extinction method 79−97343
SiC film, growth on Si ribbon surface, TEM anal. 78−84094
SiC, film, synthesized by RF reactive ion plating, struct. 77−40391
SiC, film growth by reaction of acetylene with Si (111) surface 79−100441
β-SiC, film prep by RF sputtering 77−44164
SiC film synthesis by plasma deposition process 78−11127
β-SiC, fluidised bed deposited coatings for nucl. fuel granules, microstructural obs. by SEM 77−14233
SiC, form. from SiO_2 flour and coke breeze, kinetic and mechanistic study 79−15979
β-SiC form. on Si substrate in RF powered reactor 80−76173
SiC formation on polycryst. Si ribbon, effect on solar cell efficiency *(French)* 80−54531
SiC fracture stress effects of coated nuclear fuel particle failure 80−73920
SiC, fracture toughness specimen, appl. of wedge indentation technique for precracking 78−85087
SiC, fuel particle, coating meas. of strength and Young's modulus, brittle ring test 77−8868
SiC, further polytypes discovered using Laue diffraction *(Chinese)* 80−10535
SiC, fusion reactor first wall appl., radiation damage 79−86822
β-SiC, gas phase comp. effects on growth kinetics 77−52233
SiC, grinding, effect of grinding wheel material, particle size, temp. *(German)* 79−43173
SiC, grinding material, grain shape optimization *(Polish)* 80−29916
SiC, ground state of electron subsystem, quasimolecular model 79−69055
SiC, growth by C ion implantation of Si 80−107292
SiC, growth by reaction of ethylene with Si(100) and (100) 79−47981
SiC, growth from soln. in fused Si, temp. gradient method in Tb vap. 78−35301
β-SiC, growth kinetics by Van Arkel method 77−16479
SiC, H_2 effects on epitaxial growth rates 78−22968
SiC, H^+, D^+, He^+ ion bombardment, Raman scatt. and SEM anal. 77−35609
SiC, H^+, D^+ and He^+ ion implanted, Raman scatt. obs. of localised vibr. modes 78−6689
SiC, HF, ion-plasma etching, cryst. surface layers treatment and study *(Russian)* 80−16517
SiC, HVEM obs. of various polytypes 80−76248
SiC heat-exchanger tubing, IR techniques for evaluation 80−76435
SiC heating element, $MoSi_2$ protective coating 80−21137
SiC heating element, resistance meas. instrument 77−71349
SiC heating elements for elec. furnaces, elec. cond. 79−69510
β-SiC, heteroepitaxial growth on Si substrate using $SiCl_4$-C_3H_8-H_2 system 79−24445
SiC, high density, development for heating elements using planning method 77−12584
SiC, high period polytype at interface of two interacting spirals 80−20041

silicon compounds continued
SiC, high temp. creep. 77−77530
SiC, high-temp. creep interpretation by deform. mapping techniques 77−21230
SiC, high-temp. oxidation in glow discharge oxygen plasma, oxide scale struct. 77−25174
SiC, hot pressed, bending strength *(German)* 79−24571
SiC, hot pressed, brittle fracture and subcritical crack growth 78−72885
SiC, hot pressed, K_{Ic} and delayed fracture meas. 79−61701
SiC, hot pressed, oxidation *(German)* 79−96161
SiC, hot pressing, role of grain boundaries, addition of B, B_4C and Al_2O_3 77−24999
SiC, identation plasticity and microfracture 79−70158
SiC, impact resistance, instrumented drop weight test 78−11265
p-SiC, inequivalent sites of IR luminescence centres *(Russian)* 77−1722
SiC, influence of plastic deform. on struct. of photoluminesc. spectra 77−55824
SiC, instrumented Charpy impact testing 77−36719
SiC, ion bombard. induced light emission 77−48257
SiC ion implanted, laser induced ordering and defects 80−84754
SiC LED, defect luminesc. 80−89069
SiC LEDs, current-voltage and brightness-current characts. under prebreakdown conditions 79−51667
SiC LEDs prepared by overcompensation method, photon assisted tunnelling 80−97341
SiC, LPE for blue LEDs 77−81228
α-SiC, laser monopulse energy meas. using ruby laser SHG *(Russian)* 79−94272
SiC, laser Raman spin-flip scatt. from excitons, luminesc. 80−80786
α-SiC, lattice absorpt. bands in IR spectra, surface treatment effects 77−52071
β-SiC, lattice dynamics, phonon dispersion curves 77−89509
β-SiC layer synthesized by C ion implantation in Si, IR absorpt. 78−56492
SiC limiter for JFT-2 Tokamak 79−85768
SiC, low blow Charpy impact 79−34122
SiC, luminesc., electron-hole drop 79−38606
SiC luminophor powders, SAW nonlinear acoustoelectro-luminescence 80−45143
SiC, meas. of critical stress intensity factor and subcritical crack propag. rates 78−72880
SiC, mechanical props. charact. by dynamic elastic modulus meas. up to 1400°C *(German)* 79−70101
SiC, mechanoluminesc., Mn impurities role 78−39612
SiC, microrelief of fracture failures *(Ukrainian)* 77−32729
SiC microtubes, formation by carburisation of Si whiskers 80−81011
SiC, momentum density, Compton profile 77−20235
SiC, monocryst., and epitaxial layer growing, temp. distrib. study in high temp. furnaces 79−65989
SiC, monocrystalline bars, grown from gas phase, exam. of growth process 79−95912
α-SiC monocrystalline grains, mech. props. and grain separation *(Polish)* 80−40554
SiC, N doping inhomogeneities due to growth conditions 78−22741
β-SiC, n-type, thermoelectric efficiency at high temps. 80−35706
SiC, negative photoconductivity and photoconductivity quenching 78−6414
SiC nonlinear lens, with variable focal length 79−81511
SiC, nonlinear refr. index meas. by nonlinear lens method *(Russian)* 79−26111
SiC, on Si and metal silicides, formation characteristics and mechanism, by ion backscattering techniques 79−60653
SiC, one dimensional disorder 78−51492
SiC, optical second-order nonlinear polarisability 78−25919
SiC, oxidation and corrosion behaviour, formation of protective SiO_2 coatings *(German)* 80−25885
SiC, oxidation and hot corrosion resistance kinetics 80−25896
β-SiC, oxidation in CO-CO_2 mixture *(German)* 78−23844
SiC, oxidation protective coating on C fibres *(Polish)* 79−52408
SiC, oxide scale microstruct. of oxidised single cryst. 80−108613
SiC p-n junction, electroluminesc. 80−97343
SiC p-n junction, epitaxial, grown by sublimation, elec. and struct. props. *(Chinese)* 80−60067
SiC, p-n junction, vapour grown elec. breakdown fields 78−19135
SiC p-n junction photodetector, spectral characts. 77−41685
SiC p-n junctions, current-voltage characts. 80−60073
SiC p-n junctions, electrolum. spectra and kinetics 80−66305
SiC particles in EFG ribbon solar cells, EBIC and ion microprobe anal. 80−93838
SiC, pellet, rise in temp. involving reaction sintering 77−12555
SiC, periodical step system vibr. modes in step trains, rhythmical bunching 79−41996
SiC, permeability and solubility of H_2, 1200-1450°C 80−39351
SiC, phase transition under isostatic press., microhardness meas., −196 to 1700°C 79−19318
SiC, phys. props. and crystal growth, rel. to appl. in electrolum. devices, book contrib. 77−77299
α-SiC, plastic deform. 77−12673
SiC, point contact, stable elec. oscill. generation by high field strength *(Russian)* 77−62989
SiC, polar semiconductor, electron-hole liquid, electron-phonon interactions 80−6739
β-SiC, polycryst., ^{30}Si self-diffusion 80−100350
SiC, polycryst., high resolution TEM study of $\beta \rightarrow \alpha$ transform. 80−84928
SiC, polycrystalline, quantitative phase analysis, statistical estimation and mathematical splines *(Bulgarian)* 78−39753
β-SiC, polycrystn., C^{14} self diffusion 80−2200
SiC polymorphs, widths of first minibands and effective masses, resist. anisotropy 80−20071
SiC polytype 6H, space group 80−1956
SiC, polytype relative stabilities, entropy contribs. 80−100197
β-SiC, polytype stability, $\alpha \rightarrow \beta$ phase transformation during growth 78−6028
SiC, polytypes, birefr. meas. 77−43963
SiC polytypes, contribution of ionic bonding to thermal stability 80−28946
SiC polytypes, elastic moduli, effect of degree of hexagonality 77−59845
SiC polytypes, electrolum. in anodic oxidation, band model *(Russian)* 80−50429
SiC polytypes, free exciton luminesc. meas., phonon energies 80−80852

silicon compounds continued
SiC polytypes, high resolution TEM observations 79−23621
SiC polytypes, lattice imaging studies on intergrowth structs. 80−107025
SiC polytypes, localisation of cond. band minima in Brillouin zone 80−20082
SiC polytypes, quantitative calcs. from X-ray diffr. peak intensities 79−82174
SiC polytypes, stacking sequences by high resolution electron microscopy 80−15054
n-SiC, polytypes, temp. depend. of piezoresist. constants 79−11125
SiC polytypes deformed, resist. anisotropy in (0001) plane 80−20198
SiC, polytypic forms determ. from Kikuchi electron diffr. patterns 77−31566
SiC, polytypic transform. during hot pressing 78−52739
SiC, polytypic transform., interface struct. exam. by TEM 80−15033
SiC, polytypism, effect of furnace temp. and contamination *(Polish)* 79−27969
SiC, polytypism, phase and growth aspects 78−83764
SiC, polytypism, reflection electron diffr. 78−83694
SiC, pot. curves, ab initio MRD-CI method 80−83293
β-SiC, powder, synthesis by chemical vapour phase reaction from methylsilane, exam. of props. *(German)* 79−4938
β-SiC powder compact, microstruct. changes and β to α transform., Si vapour influence 78−19738
SiC, powder mixtures, composition vs. apparent density diagrams construction, model 78−60633
SiC powders, form. by vapour phase method 80−25623
SiC, power, electroluminesc. excitation by SAW, nonlinear effects 80−16104
β-SiC, prep. by siliconisation of C black, sinterability *(Japanese)* 79−78921
SiC, pressureless-sintered, high temp. strength *(Japanese)* 80−104299
SiC protective coatings, on graphite for HTR, corrosion *(German)* 78−3248
SiC, pyrolitic coating for nuclear fuel particles 77−79465
SiC, pyrolytic, on C fibres, rate of oxidation 78−60857
β-SiC, pyrolytic, optical and elec. props. 79−78093
SiC pyrolytic coatings for HTGR fuel particles, props. rel. to deposition conditions 79−31088
SiC, pyrolytic particles for high temp. reactor fuel, X-ray and SEM study *(French)* 78−22734
SiC, REFEL, strength parameters 77−1830
SiC, radiation damage, review 77−80553
SiC, radiation defect annealing, recovery of LEED maxima 80−65075
SiC, radiation resistant substrate materials, for X-ray gratings 80−90960
SiC, reaction bonded, microstruct. characterisation 78−48353
SiC, reaction bonded, microstructural characterization 79−100093
SiC, reaction densified, controlled surface flaw initiated fracture 77−8919
SiC, reaction sintered, microstruct. *(Japanese)* 77−1825
SiC, reaction sintered, TEM exam. of recrystallisation, phase transformation 78−80567
SiC, reaction sintered transform. interface morphology 78−31364
SiC, reaction-bonded, impact erosion by ang. Al_2O_3 particles 80−89362
SiC, reaction-bonded , 'REFEL', microstruct. characterization 80−97490
SiC, reactions with oxidising atms. 80−11812
SiC, reactive RF sputtering in N_2, Si_3N_4 film deposition 79−78886
SiC, refractive index dispersion, 0.4-50 μm, 105-297K 78−84548
SiC reinforced Al, thermal stresses in unit cell 80−10160
β-SiC, residual photocond. meas. 77−4408
SiC, resist. to oxidation and corrosion at high temps. *(German)* 80−35357
SiC reverse biased p-n junctions, prebreakdown violet luminesc. 80−7420
n-SiC, saturation of electron drift velocity in strong electric field 77−76840
SiC, self bonded, exam. of fracture 79−20149
SiC, self bonded, wetting by Si, effect of phase composition 79−33161
SiC, self-bonded, fracture characts. and rupture strength, temp. effects 79−96136
SiC, self-bonded, microstruct., electrical props., sintering effects 77−1822
SiC, self-bonded, statistical distrib. of values of apparent density 78−68657
A-SiC, self-bonded polycryst., wetting by Si, base plate surface roughness effect 79−23809
SiC, self-bonded polycryst., electrophys. props. 80−10980
SiC, self-focusing of ruby laser radiation, free carrier conc. depend. *(Russian)* 77−42579
SiC, semi-insulating in struct. with injecting contacts, cond. in strong elec. field 78−19160
SiC, semiconductor, optical props. determ. via Kramers-Kronig transform. 77−8537
α-SiC, short-wavelength photocond. and capacitance photo-EMF meas. 78−26906
SiC, Si X-ray absorption K-edges, charact. parameters *(Russian)* 79−47541
SiC, Si_3N_4, (Si,Al)N, vapour deposition, feasibility of fusion reactor first wall regeneration in situ 77−18701
SiC, SiO_2, Si_3N_4, Si K_α X-ray emission spectra chemical shifts , linewidths and intensities 78−13461
SiC, single cryst., friction and wear behaviour in sliding contact with various metals 80−21112
SiC single cryst., reaction-bonded and hot pressed, hardness and wear behaviour 79−38970
α-SiC, single cryst. growth rel. to polarity 77−52235
SiC, single cryst. ingots, growth using seeds, 1800-2600°C 78−43993
n-SiC, single cryst. layers deposition on charact. substrates, morphology *(German)* 79−28943
SiC single crystal, fracture toughness 78−7019
SiC single crystal, friction and fracture in contact with itself and Ti 80−11780
SiC single crystal, hot hardness and creep behaviour 79−100247
SiC single crystals, friction, deform., and fracture, crystal orientation effect 79−96150
α-SiC single crystals, liq. Ni spreading 79−86962
SiC single crysts., polytypism obs. by high temp. oxidation expts. 78−59797
α-SiC, single crysts. phase struct. rel. to heat treatment, nucleation 80−38991
B SiC, sintered, effect of Al trace amounts on specimen props. 79−83289

silicon compounds continued
SiC, sintered, electrode and container material in Na/S cell 80−35355
α-SiC, sintered, influence of B, C additives on microstructure, SEM exam. 79−8262
SiC, sintered with three dimensional crosslinked polycarbosilane 78−56601
β-SiC, sintering, B transport and lattice parameter change 80−108370
SiC smokes, vapour-condensed, 800 to 130 nm extinction and interstellar extinction curve 80−82180
SiC, solid-state ^{13}C NMR spectra 79−24220
SiC, solubility, partition coeff. of Be 79−10951
SiC, sound absorption 78−88000
lett-SiC, space group refinement, P3 ml 78−47299
SiC, specimen preparation for TEM by ion beam thinning *(German, English)* 80−11861
p-SiC, spin-flip Raman scattering, review 80−108209
SiC, spin-flip scatt. of laser light from photoexcited excitons 80−93330
SiC, spiral growth of polytype struct. from faulted matrix, 15R and 4H struct. 77−4778
SiC, spray dried agglomerates, compaction response, fracture, deform. 79−43172
SiC, sputtered, comp. and struct. props., effect of target materials 80−54549
SiC, sputtered amorphous film, struct., elec. and optical props. 79−78236
SiC, sputtering, low energy, H, D and He ions 80−100734
SiC, sputtering, physical and chemical, by H_2 and He, 600 to 7500 eV 77−36340
SiC, sputtering processes by energetic ions, combined SIMS-AES study 80−40201
SiC, sputtering yield, use as first wall material 78−95629
SiC, strength assessment by Young's modulus meas. up to 1400°C *(German)* 78−11253
SiC, strength-grain size relation, surface finish effects 77−81333
SiC, struct. of $L_{2,3}VV$-Auger lines, rel. to soft X-ray spectra 78−2953
SiC, struct. of spectrum of excitons bound to neutral B atoms 78−19523
SiC, struct. of thin seam obs. by optical microscopy 77−39596
SiC, subcrit. crack growth, in corrosive environment, 600-850°C 77−56080
SiC, subjected to thermal shock, study of substruct. and surface morpholoy, X-ray diffr. and TEM study 79−43292
β-SiC, submicron powder, prep. by siliconization of C black, props. *(Japanese)* 79−66192
SiC substrate with SiO_2 film, ellipsometric meas., accuracy and sensitivity 80−77840
SiC surface, H^+, D^+ and Ar^+ bombardment, 5 to 15 keV, meas. of erosion yield 78−79647
SiC surface, roughness factor measurement, energetic D^+, He^+, Ar^+ irradiation 80−39172
SiC, surface characterisation by combined AES-IMA system, for first wall material of fusion devices *(Japanese)* 79−74039
SiC, surface defect annealing, following Ar ion and electron irrad. 80−7603
SiC, surface defects due to Ar ion bombardment, 100-1000 eV 80−6445
SiC surface irregularity statistics for laser component materials 79−14057
SiC, surface luminesc. in presence of anodisation 78−52579
SiC, synthesis by ion implantation of diamond and silicon, struct. charcts. 77−76434
SiC, TEM investigation using C replicas 80−61034
SiC, tensile strength distrib. 80−40471
n-SiC, thermal defects, ESR study 80−88876
SiC, thermal diffusivity measurement, constant rate heating method *(Japanese)* 80−6572
SiC, thermal oxide layers, AES depth-profiling anal. 79−43454
SiC, thermal S-N switching 79−24027
SiC, thermally thin solids, photoacoustic effect 80−75304
β-SiC, thermodynamic props., temp. depend., 5 to 300K 80−96666
β-SiC, thermoelectric material, thermal cond. meas., 1100-2000K 78−24798
SiC, thermolum. excited by light outside fundamental absorpt. region 79−24375
SiC, thin film, effect of O on thin film compositions obtained by secondary ion emission 80−26079
SiC thin film, RF-sputtered, highly reliable temp. sensor 80−224
SiC thin-film thermistors with high thermal response *(Japanese)* 80−105629
SiC thread-like crystals reinforced mullite-corundum ceramics, props. 80−108525
β-SiC, twinned crystals, fracture charcts. 80−3193
SiC, US comminution of refractory compound powders 78−23656
SiC, uncommon mode of morphological development among coherent phases, optical and electron microscope exam. 78−80544
β- SiC, undoped compact, microstruct. development during heating 80−25746
α-SiC, uniaxial compressive damage at low homologous temps., AE and SEM obs. 79−91736
SiC, VPE kinetics study in SiC-C system 79−37934
SiC, VPE layers, growth kinetics, polytypism 77−11809
SiC, vapour deposition, thermodynamics of Si-C-Cl-H system *(German)* 79−11520
SiC, wetting by Cu-Ti and Cu-Sn-Ti melts 78−68664
β-SiC, wetting by fused Ge, Sn and Pb 77−85016
β-SiC whisker, atom-probe FIM expts. 78−35275
β-SiC whisker, failure and defects 79−96145
SiC whisker coated C fibres for composites, shear strength improvement 78−3093
SiC whisker reinforced Ag composite, prep. aboard Skylab, and characterisation 78−84741
SiC whiskers, wetting of surface by Fe-Si-C melt and its influence on growth stability 77−39756
SiC with dielectric coating, surface polaritons, waveguide modes 80−80195
α-SiC, wurtzite type cryst., temp. depend. of one phonon Raman spectra, Gruneisen parameters 77−66500
B-SiC, X-ray diffr. study of anisotropic layers in twinned seams 80−107274
SiC, X-ray diffuse scattering 80−14964
SiC:Al, g-values, spin temp., determ. from Raman spectra 78−43856
B-SiC:Al, ion implanted, elec. props. and luminesc. meas. 77−12443
SiC:Al,N, blue cathodolum. spectra obs. 78−19574

silicon compounds continued
SiC:Al,N (6H), ODMR for effective-mass-like acceptor 80−93213
α-SiC:Al diodes, ion implanted, transient charcts. of electrolum. 79−24369
SiC:Al epitaxial layers, growth, Al distrib. and solubility 80−15391
SiC:Al^+ p-n junctions, elec. props., defect effects 80−15594
SiC:Al(B)(Ga), 4H-, 6H- and 3C-polytypes, melt growth and photoluminesc. 77−24885
SiC:Al(Ga)(B) (6H) LEDs, fabrication by rotation dipping technique, electrolum. mechanisms 80−50426
β-SiC:B, diffused structures, current-voltage charcts. 78−47865
SiC:B, electroabsorption, 0.35-0.45 eV, under UV illumination 79−4831
SiC:B, impurity distribution determ. by neutron activation anal. 77−76452
SiC:B, ionisation energy of deep centres from absorpt. spectra, electron-phonon coupling 77−4663
SiC:B, p-n junction, LED with new low-temp. alloy 79−73582
4H-SiC:B, very slow decays of luminesc., 2-300K 77−1718
p-SiC:B (4H), absorption spectra of bound excitons 78−88338
β-SiC:B p-n junction, IR electroluminesc. spectrum 77−44067
SiC:B(Be), dislocation induced deceleration of impurity diffusion 77−28043
α-SiC:B(Be)(Ga), piezoresist. rel. to acceptor levels 78−60129
p-SiC:Be, Fermi level, Fermi distrib. and activity coeff. calc. 77−1365
SiC:Be, film donor impurity, diffusion influence on elec. and optical props. 78−87942
SiC:Be, gas-phase equilib. comp., thermodynamic analysis rel. to cryst. growth and doping 77−85909
β-SiC:Ga, donor-acceptor pair emission 77−4682
α-SiC:H, prepared by reactive sputtering, layer props. *(Japanese)* 80−60695
SiC:H amorphous reactively sputtered film, H content effect on film props. 80−75459
SiC:N, conversion factor at high doping levels 78−22744
SiC:N, impurity effect on stress gradients and dislocation development 77−4116
n-SiC:N, O, cathodolum. spectra meas. 78−19573
SiC:N(Al)(Ga) (6H), photoluminesc., site-depend. donor and acceptor levels 79−61421
α-SiC:Sc, quasiline luminesc. spectrum 77−4686
SiC:silumin, LED, highly stable *(Russian)* 77−8183
SiC:Tb(Sc), various polytypes photolum. meas., identification of 4H and 6H polytypes 77−63459
SiC:Ti (6H), absorpt. spectra of n- and p-type cryst. 79−38581
β-SiC/Si abrasive resistant material, prep. and props. 80−20878
SiC-2H, structure parameters and polarity, X-ray diffr. meas. 80−19781
α-SiC-Al_2O_3, sintering 80−11611
SiC-AlB_2 (0.61 to 1.2 wt.%), hot pressed, microstruct. 80−93563
SiC-AlN, solid solns. series rel. to new materials in Si-C-Al-O-N system 78−95159
SiC-B_4C (B+1 wt.% C), sintering 77−36432
SiC-B_4C eutectic, directional solidification, growth and mech. props. 79−91638
SiC-Bn composite, polymorphic transforms. 77−81259
SiC-C, sputtering and blistering from H^+ and He^+ bombardment 78−79649
SiC-ceramic, nondestructive evaluation, scanning photoacoustic microscopy 80−85115
SiC-coated C fibre, compatibility with Al *(Japanese)* 80−71700
SiC-fibre reinforced glass, fabrication, thermal expansion, flexural and fracture toughness 80−40319
SiC-fission product isothermal reactions in HGTR TRISO UC_2 and UC_xO_y fuel 80−42744
SiC-fission product reaction kinetics in HTGR TRISO UC_2 and UC_xO_y fuel in thermal gradient 80−47570
SiC-graphite-FeSi refractory, oxidation loss and wettability of inorganic fluxing materials *(Japanese)* 78−84755
SiC-H_2 system, thermodynamic analysis 77−86347
SiC-N_2 system, high temp.-processes, thermodynamics 77−85105
n-SiC-n-CdS heterojunctions, photoelec. props. 78−80042
SiC-n-Si junction device, elec. props. 80−15591
SiC-Si, wear resist., props. under abrasion and corrosion 80−100927
SiC-Si composite, bulk resist. of technical SiC powders 79−28350
SiC-Si n-n and,n-p htheterojunctions, prep. by ion implantation, tunnelling cond. 77−43710
SiC-Si struct. formation on ^{12}C ion implantation in Si, optical and photoelectric props. 79−91136
SiC-SiO_2 interface, Auger anal. 78−95375
SiC+BaO+$BaCO_3$ react., contact phenomena at SiC grain boundary 79−43193
SiC+carbon tetrafluoride, reaction, metastable C phase prod. 79−29393
SiC+CeO_2(Pd), high temp. chem. reactions, products obs. by X-ray diffr. 78−17312
SiC_x, amorphous, prepared by glow discharge method, elec. and optical props. 77−21035
$Si_{1-x}C_x$ protective coating for GaAs laser 80−5753
$Si_{1-x}C_x$:H glow discharge films, local atomic struct., XPS and AES study 80−93448
Si_xC_{1-x}, amorphous, luminescence 80−80862
Si_xC_{1-x}, amorphous, photoluminesc., comp. depend. 78−68541
Si_xC_{1-x}, ion beam synthesis for photodetector fabrication 79−46688
Si_xC_{1-x}:H reactive sputtering deposition, compositional and structural props. 79−99077
SiCH, matrix Hartree-Fock calcs. 79−5874
SiCH, nucl. spin-spin coupling consts. to H, INDO calcs. 77−83621
$Si_{1-x}C_xH_y$ amorphous film, H content determ. by nuclear reaction analysis 80−59821
$Si_xC_{1-x}H_z$ amorphous films, IR absorpt. bands 80−100705
$Si_xC_yH_z$ films, reactive plasma deposited, comp., IR anal., and optical props. 79−95945
$SiCH_3H_3$, core Auger shifts, ab initio LCAO MO SCF calcs. 78−904
$Si(CH_3O)_4$, prep. from metal alkoxide, props. as precursor of oxide glass 78−48700
n-SiC(6H), donor ground state splitting, IR spectra *(Russian)* 78−92104
α-SiC(6H), electron bombardment, formation of defects on (000$\bar{1}$) surface 80−19844
SiC(6H), ion-implanted, laser-induced recrystallization and defects 80−44221
α-SiC(6H), radiation defect distrib. anisotropy near (000$\bar{1}$) surface, LEED study 80−96577

silicon compounds continued
α-SiC(6H), two stage transitions, nonlinear absorpt., thermoluminesc. method 80−7425
SiCl, ($A^2\Sigma^+$-$X^2\Pi$) transition, rot. anal., equilib. consts. 78−37648
$SiCl_2$, band system reassignment to PO and P_2 radicals 77−23505
$SiCl_2$, enthalpy of formation, thermochem. stability 77−58185
$SiCl_4$, convective instabilities in closed vertical cylinder heated from below 79−77072
$SiCl_4$, conversion to $SiCl_3$ in unipolar HF discharge 80−1855
$SiCl_4$, electron bombardment and thermal dissoc., thermochem. stability 77−58185
$SiCl_4$, He(II) photoelectron spectra, spectral intensity patterns 79−98152
$SiCl_4$ hydrolysis and oxidation kinetics for graded-index fibre vapour phase axial deposition 80−48477
$SiCl_4$, liq. struct., oscill. amp., neutron diffr. study 79−46544
$SiCl_4$, liq. struct. by neutron diffr. 79−73089
$SiCl_4$ liquid, angular momentum relaxation, effective collision numbers 80−64873
$SiCl_4$ molecule, NMR relaxation expts. to study molecular reorientation 80−63673
$SiCl_4$, oxidation kinetics 78−92380
$SiCl_4$ physical and thermodynamic properties, rel. to Si technology 79−65218
$SiCl_4$, vac. UV absorpt. spectra, 250-115 nm 77−79628
$SiCl_4$, X-ray absorpt. spectra struct. 80−37819
$SiCl_4^-$, ESR of radical in adamantane matrix, γ-irrad. of $SiCl_4$ in adamantane matrix 79−27011
$SiCl_4$:H_2 binary gas mixture convective instabilities in closed vertical cylinder heated from below 79−72880
$SiCl_4$-$GeCl_4$-BCl_4 particulate layers consolidation, in fabrication of optical fibre preforms 80−60787
$SiCl_4$-$TiCl_4$, liq. struct., oscill. amp., neutron diffr. study 79−46544
$SiCl_4$-$TiCl_4$ liq., beat effects, neutron diffr. studies 80−38897
$SiCl_4$+Na, rainbow scatt. at thermal energy, anisotropic pot. 78−29837
$SiCl_4+O_2$ in modified CVD process for optical fibre prod., reaction IR spectra 78−80472
$SiCl_4$+Si*, collisional quenching, reson. line absorpt. expt. 78−46297
$SiCl_4$+Si($3p^2(^1S_0)$), attenuation of reson. radiation, time-resolved kinetic obs. 78−5329
Si_5Cl_{10}, and Si_5Br_{10}, vibrational spectra and force constants, rel. to Si_6Cl_{12} and Si_6Br_{12} *(German)* 79−22716
$(SiCl_3)_2O$, IR matrix isolation spectrum, Raman spectrum 78−82730
SiCl(g), heat of formation, mass spectrometric determ. 78−15694
$SiCl_2$(g), heat of formation, mass spectrometric determ. 78−15694
$SiCl_3$(g), heat of formation, mass spectrometric determ. 78−15694
SiD_3^++benzene, energy-rich collision complex form. 77−9068
SiD_3F, microwave spectrum, rot.-vibr. interaction consts., Coriolis reson., E1 moment 77−6766
SiF, $A^2\Sigma(v'=0)$ state, radiative lifetime meas. 77−27110
SiF, chemilum. obs. of $A^2\Sigma^+$ and $a^4\Sigma^-$ states 78−66816
SiF, D-X transition, rot. anal. 79−72331
SiF, heat of form. mass spectrometric determ. 78−76900
SiF, use in chemical lasers 80−64004
SiF_2, force fields using Redington method 77−18899
SiF_2, heat of form. mass spectrometric determ. 78−76900
SiF_2 transport, for purification of silicon 78−35316
SiF_3, bond polarisability and force constants 80−69260
SiF_3, heat of form. mass spectrometric determ. 78−76900
SiF_3, low-lying electronic states, ab initio HF calcs. 77−54512
SiF_4,($SiCl_4$), mol. force consts., parametric representation method 78−25503
SiF_4, ^{129}Xe chem. shift, chem. shielding 77−6707
SiF_4, ^{19}F chem. shielding, depend. on internal coords. 78−5249
SiF_4, ^{19}F NMR, chem. shielding, intermol. interactions and rovibr. motion effects 78−9171
SiF_4, ($SiCl_4$), ($SiBr_4$), X-ray absorpt. spectra struct. 80−37819
SiF_4, bond order and Raman intensity delta function eqn. 77−61693
SiF_4, CO_2 laser irrad., collision induced dissociation, visible fluoresc. 78−66613
SiF_4, CO_2 laser-irrad., dissoc. product fluoresc., wavelength depend. 80−11900
SiF_4, chemisorption on Si surface, chemistry, XPS and Auger spectra 80−81358
SiF_4, cryst. 78−23439
SiF_4, dissociation rate increase by red shift of nonresonant freq. under two freq. laser action *(Russian)* 77−58104
SiF_4, electronic struct., Xα SW calcs. 80−102447
SiF_4, energy threshold effects in collisionless dissociation by IR laser radiation 77−58096
SiF_4, interaction with strong IR field, instantaneous luminescence 79−18232
SiF_4, mol. cryst., coupled phonon modes and IR band shapes 78−26641
SiF_4, mol. cryst., giant anomaly of intensity of vibrs. of isotopic impurity, Raman spectrum 79−73276
SiF_4 molecule, saturated absorpt. of CO_2 laser radiation 80−37811
SiF_4, $\nu_3(F_2)$ IR band contour, isotopically pure cpds., mol. consts. 77−61746
SiF_4, perturber of HCl vibr.-rot. lines, broadening and shifting 77−23521
SiF_4, photoelectron spectra, bonding, MS Xα calcs. 79−18116
SiF_4, photon echoes, polarisation and amplitude decay meas. 77−88872
SiF_4, self-focusing and self-defocusing using IR laser 79−89978
SiF_4, sign of rot. g-factor, mol. beam expt. 79−59600
SiF_4, stella quadrangula as struct. building unit 80−15055
SiF_4, thermocyclic stress effects in corrosive-media, electrochem. polarization applic. *(Russian)* 78−11356
SiF_4, valence electron spectrum, vibr. struct. 77−75209
SiF_4, X-ray absorpt. spectra struct. 80−37819
SiF_4, XUV spectra, overlapping core-valence and core-Rydberg transitions and resons. 80−32735
SiF_4+H_2, SiF_xH_{4-x} heats of form., mass spectrometric determ. 78−7221
SiF_4+HCl, vibr.-rot. line broadening 77−27117
$SiF_4+O^+(Cl^+)$, Si highly stripped core ion outer shell rearrangement, Kα X-ray spectra 77−3451
SiF_6, saturation absorpt. spectra, evidence of tumbling multiplets 79−36637
SiF_6^{2-}, bond order and Raman intensity, delta function eqn. 77−61693
SiF_6^{2-}, octahedral complex, ionis. energy, SCF-Xα study 78−70967
SiF_6^{2-}, SCF Xα SW calcs., ionis. pot. 79−26887

silicon compounds continued
Si_2F_6, normal coord. analysis, vibr. freqs. and amplitudes, shrinkage and distortion consts., force consts. 80−27989
SiF_3Cl^-, radical anion struct. and ESR spectrum 78−25571
SiF_4Cl_{4-n} in γ-irradiated solid solution of tetramethysiline, EPR spectra obs. 80−80611
$SiF_3Cl^-(Br^-)(I^-)$ in γ-irradiated solid solution of tetramethysiline, EPR spectra obs. 80−80611
$SiFH_3$, heat of formation, mass spectrometric determ. 78−7221
SiF_2H_2, heat of formation, mass spectrometric determ. 78−7221
SiF_3H, heat of formation, mass spectrometric determ. 78−7221
$Si_{1-x}Ge_x$ amorphous, ESR centres, effect of annealing 77−55701
Si_xGe_{1-x}, ion beam synthesis for photodetector fabrication 79−46688
Si_xGe_{1-x}, vibr. props. 77−4176
$Si_{12}Ge_{10}As_{30}Te_{48}$, amorphous, energy controlled switching obs. *(Japanese)* 78−34867
$Si_{12}Ge_{10}As_{30}Te_{48}$, chalcogenide glasses, direct obs. of switching filaments 77−24595
$Si_{12}Ge_{10}As_{30}Te_{48}$, chalcogenide glass threshold switches, turn-on state maintenance *(Russian)* 77−85271
$Si_{12}Ge_{10}As_{30}Te_{48}$, chalcogenide glass film, switching delay time 78−26926
$Si_{12}Ge_{10}As_{30}Te_{48}$ chalcogenide glass threshold switch conductivity in high ohmic state *(Russian)* 78−43502
$Si_{12}Ge_{10}As_{30}Te_{48}$ chalcogenide glass, switching in thin layers with semicond. electrodes 79−4586
$Si_{12}Ge_{10}As_{30}Te_{48}$, conducting filaments and switching phenomena 79−87134
$Si_{12}Ge_{10}As_{30}Te_{48}$, dark cond. and thermoelec. power, thermal activation energies interpret. 78−23123
$Si_{12}Ge_{10}As_{30}Te_{48}$, energy-controlled switching obs. 77−35973
$Si_{12}Ge_{10}As_{30}Te_{48}$ glass, thermally stimulated depolarization current meas. *(Japanese)* 78−34875
$Si_{12}Ge_{10}As_{30}Te_{48}$ glass, nonlinear I-V characts. 79−99557
$Si_{12}Ge_{10}As_{30}Te_{48}$ surface, heat treatment and electron bombard. effects. SEM obs., rel. to switching filament form. 77−47700
$Si_{12}Ge_{10}As_{30}Te_{48}$, threshold switch, high resist. state 77−15924
$Si_{12}Ge_{10}As_{30}Te_{48}$, vitreous, localised states role in cond. in high elec. fields 77−76841
$Si_{0.5}Ge_{0.5}O_2$, band struct., photoemission spectra calc. and meas. 77−35865
$Si_xGe_{1-x}O_2$, $0\leq x\leq 1$, XPS and UPS, electronic struct. 77−48318
$Si_xGe_{1-x}O_2$, amorphous, electronic struct. in Bethe lattice approx. 80−44487
$Si_xGe_{1-x}O_2$, amorphous, electronic struct. 80−80166
SiH, A state new predissociations, improved dissoc. energy value from rot. level lifetimes 79−3496
SiH, emission spectroscopy, in H_2-SiH_4 glow discharge 80−69984
SiH, ground state, Λ-type doubling 80−23431
SiH, nucl. spin-spin coupling consts. to H, INDO calcs. 77−83621
SiH, optically derived lambda splitting rel. to interstellar existence 77−17657
SiH, rot. transition freqs. calc., rel. to search in interstellar space 78−93100
SiH, SiH^+, line positions and oscill. strengths of rot.-vibr. bands, interstellar medium appl. 78−58644
SiH_2, transition moments of $A^2\Delta$-$X^2\Pi$ band, 150-650 nm 79−45767
SiH^+, oscillator strengths and dissoc. energy determ. from time resolved precision spectroscopy 80−58272
SiH^+, PNO-CI and CEPA calcs. of electron correl. effects 77−34561
SiH^+, rot. transition freqs. calc., rel. to search in interstellar space 78−93100
SiH^++benzene, energy-rich collision complex. form. 77−9068
$SiH_{0.16}$ amorphous films, optical props. and photocond. near optical gap 80−50443
SiH_2, $1B_1$-state, geometry calcs., avoided crossings 80−53085
SiH_2, electron affinity, theoretical exam. 78−29863
SiH_3 radical, hyperfine coupling consts., vibr. depend., ab initio calcs. 80−87150
SiH_3 radical, in Ar(Kr)(N_2) matrix, anisotropic ESR spectroscopic parameters 80−63687
SiH_3-group containing mols., normal coord. anal. 80−9579
SiH_3^++benzene, energy-rich collision complex form. 77−9068
SiH_4, $1B_1(1T_2)$ pot. energy surface calcs. 80−53085
SiH_4, ab initio calcs. using FSGO, internal rot. 78−82639
SiH_4, ab initio Hartree-Fock SCF-LCAO-MO method 78−94195
SiH_4, appl. of NMR field cycling method for obs. of low temp. tunnelling in molecular solids 79−65755
SiH_4, avoided-crossing molecular-beam spectroscopy, hyperfine and spin rot. const. and rot. g factors determ. 80−78671
SiH_4, core Auger shifts, ab initio LCAO MO SCF calcs. 78−904
SiH_4, core-excited states, valence-Rydberg mixing and term values, XUV spectra and CI calc. 79−76444
SiH_4 discharge, low pressure, plasma parameters, relevance to Si film deposition 80−44030
SiH_4, Doppler-free optical double reson. spectroscopy using single-freq. laser and modulation sidebands 80−68274
SiH_4, electron binding energies, one-centre expansion method 77−6677
SiH_4, excitation energy, one-centre approx. calcs 78−70737
SiH_4, Gaussian basis sets, quality studies 79−59345
SiH_4, IR photochemistry 79−39185
SiH_4, IR spectra, ν_2 and ν_4 band anal. 78−9153
SiH_4, irrad. by CO_2 laser, Si film deposition 80−16190
SiH_4, $L_{II,III}$ continuous absorpt. spectrum of Si 80−95645
SiH_4, $L_{2,3}MM$ Auger spectrum, line width and intensities 80−58325
SiH_4, low temp. oxidation, film growth rates, IR absorption spectra 80−15399
SiH_4, low temp. pyrolysis, thin polycrystalline Si films 78−31342
SiH_4, magnetisation relax., appl. of theory of spin-lattice relax. 80−50214
SiH_4, mol., valence and core ionis. energy, RHF-SCF and PNO-CEPA calc. 79−85890
SiH_4, mol., XPS and KLL Auger effect, line shifts 79−31602
SiH_4, NMR linewidths and relax. times at 6.7 to 124K 77−85602
SiH_4, nucl. spin-spin coupling consts., ab initio calcs. 80−95647
SiH_4, nuclear mag. shielding of ^{29}Si, pseudopot. calcs. 79−6879
SiH_4, ν_3 and ν_1 IR bands, anal. 79−22704
SiH_4, ν_3 band assignment in IR and Raman spectra, ν_1-ν_3 vibr.-rot. coupling 77−75124
SiH_4, ν_4 fundamental, laser sideband direct freq. reading IR spectra, electro-optical, press. broadening 78−21920

silicon compounds continued
SiH_4, orbital valency force field 77−34779
SiH_4, photoelectron spectra, bonding, MS Xα calcs. 79−18116
SiH_4, plastic phase, rotational motion, quasi-elastic neutron scatt. study 79−51022
SiH_4, plastic phases I and II, neutron inelastic scatt. 79−7558
SiH_4, possible microwave interstellar maser lines 78−41020
SiH_4, props. of film obtained by oxidising in HF gas discharge plasma 77−11804
SiH_4, proton spin relax. rate, centrifugal distortion 77−75184
SiH_4 purification by selective photolysis using UV laser 78−31657
SiH_4 pyrolysis, at low temps. and atm. press., Si deposition kinetics 79−91595
SiH_4, relativistically parameterized extended Huckel theory 79−49924
SiH_4, SCF calcs. including polaris. functions 80−87034
SiH_4, second order mag. props., coupled Hartree-Fock perturbation theory 80−87042
SiH_4, second-order stark effects, RF-IR double reson. 78−58739
SiH_4, silane, decomp. kinetics under shock tube conditions 79−34292
SiH_4, solid, NMR direct detection of tunnel splittings 78−56396
SiH_4, Stark effect, rot. transitions in vibr. ground state, isotope shift 79−27029
SiH_4, tetrahedral mol., force field calcs. 78−29734
SiH_4, vertical excited states, CI calcs. 79−18127
SiH_4, vibr. energy transfer in pure SiH_4 and mixtures 77−524
SiH_4^+, struct, stability, ab initio calcs. 79−13632
$^{28}SiH_4$, analysis of ν_4 band interacting with ν_2 band *(French)* 78−9152
SiH_4-D_2, mixture, ion-mol. reactions, cross-sections 77−60061
SiH_4-He, reaction mechanisms of RF glow discharge deposition process 79−95944
SiH_4+F^{n+}, X-ray emission from gaseous target, q=4-9, 1 and 2 MeV/amu 79−83060
$SiH_4+O^+(Cl^+)$, Si highly stripped core ion outer shell rearrangement, Kα X-ray spectra 77−3451
$SiH_4+SF_6 \rightarrow S_2^*+SiF_4+HF+H_2$, laser augmented reaction, isotopic selectivity retention during detonation 78−48673
SiH_4+UF_6, IR laser single photon absorption reaction chemistry, solid state 79−66308
SiH_4+UF_6, photoinduced reaction in low temp. SiH_4 matrix 80−30256
SiH_x, amorphous, solar cells, short circuit-currents and collection efficiencies 80−94028
SiH_x amorphous films, internal photoemission, metal contacts 80−96964
SiH_x amorphous reactively sputtered films, in Pd Schottky barrier devices, photovoltaic props. 80−49910
SiH_x amorphous reactively sputtered films, optical props. 80−50444
SiH_x films, for microelectronics appls., plasma deposition and characterisation 79−78904
SiH_x polymer film, struct. rel. to amorphous solid 78−72048
SiH_x amorphous film, H content determ. by nuclear reaction analysis 80−59821
$Si_{1-x}H_x$ amorphous sputtered films, IR vibr. spectra 79−43051
$Si_{1-x}H_x$ film, amorphous, RF sputtered, pure and P(B) doped, optical consts. 79−95866
$Si_{1-x}H_x$, noncrystalline film, struct., interatomic distances, SRO 80−107053
$Si_{1-x}H_x$:Al, amorphous, co-sputtered Al modification, electronic and optical props. 80−100461
Si_2H_4 ground state struct., ab initio SCF calcs., singlet silylsilylene 80−27945
Si_2H_4, Si-Si double bond, ab initio GO calc. 78−94187
Si_2H_6, ab initio calcs. using FSGO, internal rot. 78−82639
Si_2H_6, barrier to internal rotation 78−66680
Si_2H_6, bond lengths, photoelectron spectrum, mol. orbitals calcs. 78−5132
Si_2H_6, nucl. spin-spin coupling, scanning MO HF LCAO calc. 79−50045
Si_2H_6, rot. barriers, MS-SCF-X$_\alpha$ calcs. 80−106267
Si_2H_6, tetrahedral edge sharing, distortions, MO calcs. 77−14380
Si_2H_6, valence electronic struct., model pot. in floating spherical GO formalism 78−74563
Si_3H_8, ab initio calcs. using FSGO, internal rot. 78−82639
Si_5H_{12} cluster, Si valence band Auger spectrum, cluster approach, comparison with experimental spectrum 80−40191
Si_6H_{12}, and Si_6D_{12}, Raman and IR spectra, vibr. force consts., config. *(German)* 79−22715
Si_nH_{2n+2}, silane, SCF Xα MO calc., appl. to amorphous hydrogenated Si 80−49580
Si_nH_{4-n}, enthalpies of formation, effusion mass spectrometric meas. 80−26043
$SiHBr_3$, heat of form., mass spectrometric determ. 79−20455
SiH_2Br_2, heat of form., mass spectrometric determ. 79−20455
SiH_3Br, heat of form., mass spectrometric determ. 79−20455
SiH_3Br, mol. ionis. and excitation energy, Xalpha calc. 79−41105
SiH_3Br, rot. Zeeman effect 79−54909
$SiH_3{}^{81}Br$, high resolution rot. microwave spectrum, 8-40 GHz, mol. consts. 78−21916
SiH_3Cl, mol. ionis. and excitation energy, Xalpha calc. 79−41105
SiH_3D, in polycryst. SiH_4, mol. motions and symmetries, IR obs. 78−48163
$^{28}SiH_3D$, IR spectrum ν_1 and ν_4 bands, rot. const. 77−83590
SiH_2DF, $SiHD_2F$, microwave spectra, harmonic force field, mol. struct. 77−18913
SiH_2F_2, ab initio Hartree-Fock SCF-LCAO-MO method 78−94195
SiH_2F_2, core Auger shifts, ab initio LCAO MO SCF calcs. 78−904
SiH_3F, ab initio Hartree-Fock SCF-LCAO-MO method 78−94195
SiH_3F, core Auger shifts, ab initio LCAO MO SCF calcs. 78−904
SiH_3F, microwave spectrum, rot.-vibr. interaction consts., Coriolis reson., E1 moment 77−6766
SiH_3F, mol. ionis. and excitation energy, Xalpha calc. 79−41105
SiH_3F, SiH_2F_2, valence ionisation pots., SCF-MS-Xα calcs., mol. space partitioning 79−36529
SiH_3F, total energy, MOs nonempirical minimum STO-4LGF calcs. 78−9074
$SiH_4(F_4)$, rot. mag. moment spectra, mol. beam mag. reson. obs. 77−14509
SiH_3I, mol. ionis. and excitation energy, Xalpha calc. 79−41105
$(SiH_3)_3N$, SCF calcs. including polaris. functions 80−87034
SiH_3NCO, geometric struct., ab initio MO calc. 79−13834
SiH_3NCS, microwave spectrum, mol. consts., isotope effects 77−46559
SiH_3NCS, microwave spectrum, struct., dipole moment, ^{14}N quadrupole coupling const. 77−46560
SiH_3NCS, microwave spectrum, rot. Zeeman effects 79−54847
SiH_3NH_2, total energy, MOs nonempirical minimum STO-4LGF calcs. 78−9074
$(SiH_3)_2O$, and d_6, Raman spectra, vibr. mode and config. 78−62940
$(SiH_3)_2O$, vibr. spectra, coupling of large amplitude vibrs. 78−37619
Si_2H_6O, geom. and electronic struct., ab initio MO calc. 79−97972
SiH_3OH, total energy, MOs nonempirical minimum STO-4LGF calcs. 78−9074
$SiH_3PH_2BD_3$, liquid and solid, vibr. analysis, spectra and structure of P-B compounds 78−84586
$SiH_3PH_2BH_3$, liquid and solid, vibr. analysis, spectra and structure of P-B compounds 78−84586
$(SiH_3)_2S$, rot. consts., internal rot. parameters, anal. of microwave spectra 78−46316
$(SiH_3)_2S$, microwave spectrum, r_0-struct., elec. dipole moment, internal rot. barrier 79−3439
$(SiH_3)_2S$, UV spectra, assignments 78−46359
$SiH_4(SiD_4)+F_2$, chemilum., at. absorption, and laser-induced fluoresc. obs. 80−3315
$SiH_4(SiF_4)$, electron rearrangement after inner shell ionisation by heavy charge particle impact 80−87043
$SiH_2(SiH_2^+)(SiH_2^-)$, electronic structure, ab initio LCAO MO SCF calcs. 79−10027
$SiHX_3$, (X=F,Cl,Br,I), force fields and consts., Redington's method calcs. 80−58130
SiH_3X (X=H, F, NH_2, OH), coord. bond calcs. 80−58129
$(SiH_3)_3Y$, (Y=As, P, Sb), vibr. force fields and amplitudes, zero point struct. 77−54551
SiL, neutron damage at 1200°C, fusion reactor first-wall appl. 79−93829
SiN film, elastic stiffness and thermal expansion coeffs. 80−107451
SiN film, on Si substrate, thermal stresses and cracking resist. 78−63958
SiN_x, interatomic interactions from XPS 80−49171
SiN^+, pot. curves, ab initio MRD-CI method 80−83293
SiN-Si mixtures, X-ray diffr. powder anal. method, integrated intensities peak height approx. 77−56323
SiN_x film, plasma deposited, comp. and characterisation, optical and elec. props. 80−15401
SiN_x, film by magnetron sputtering, composition, hardness and optical props. 78−3047
SiN_x film reactive plasma deposition enhancement 77−77405
SiN_x film reactive plasma deposition and characterisation 77−77406
SiN_x films, plasma enhanced CVD, props., meas. and interpretations 80−80987
SiN_x films, plasma-deposited, radial wafer-to-wafer uniformity 80−104073
SiN_x films plasma deposition, process and props. 80−80986
SiN_x, plasma deposited, H content meas. 78−63949
SiN_x, plasma deposited dielectric film, elec. props. 78−68103
Si_2N_4 powders, synthesis, charact. 79−33977
Si_3N_0 reaction bonded, strength parameters 77−1830
Si_3N_3, encapsulation of GaAs, surface effects, RHEED 77−1883
Si_3N_3, film growth by reactive sputtering, influence of electron-ion bombard. *(Russian)* 77−28717
Si_3N_4 78−64754
Si_3N_4, ^{15}N self-diffusion, isotope exchange meas. 77−11724
Si_3N_4, amorphous, CVD prep., struct. characts. by pulsed neutron diffr. 80−33891
Si_3N_4, amorphous, charge transport in band tails 78−76026
Si_3N_4 amorphous, crystallisation and sintering under pressure 79−87596
Si_3N_4, amorphous, in MIS struct., high field conductivity 78−23101
Si_3N_4, amorphous, ion implantation for radiation damage studies 77−80530
Si_3N_4, amorphous, $L_{2,3}$ threshold spectra 77−69934
Si_3N_4 amorphous film, CVD, core and valence electron excitations, low energy electron loss spectroscopy and AES 80−2365
Si_3N_4 amorphous film deposition by high rate DC reactive sputtering, passivation appl. 80−100784
Si_3N_4 amorphous films, CVD mech. and thermal props. *(Japanese)* 77−90280
Si_3N_4 amorphous films, struct., short-range order, and crystn. kinetics 79−28240
Si_3N_4, amorphous insulator film, high-field cond. 79−56320
Si_3N_4, and Si_3N_4-MgO, hot pressed, DC elec. props., 18-500°C, fields up to 1.1×10^4 V cm^{-1} 78−26860
Si_3N_4, aqueous suspension rheological and processing props. 77−23928
Si_3N_4, α to β transform., TEM and electron diffr. obs. 78−27507
Si_3N_4, α/β phase transform. 78−56632
Si_3N_4 based abrasive material for grinding unhardened steel 78−35529
Si_3N_4, bending strength, deformability, elastic moduli and brittleness 80−81191
Si_3N_4, biaxially stressed, exam. of localised impact damage 78−72846
Si_3N_4, CVD, chem. bond nature, Compton scatt. expts. 80−49539
Si_3N_4, CVD, chem. bound H, NH_3/SiH_4 ratio and annealing depend. 77−76680
Si_3N_4, CVD, plasma stream transport method 78−52684
Si_3N_4, CVD, struct., optical and mech. props. 77−1816
Si_3N_4, CVD, structural props., effect of deposition parameters 77−55272
Si_3N_4, CVD, Vickers microhardness, effect of deposition parameters 77−56079
Si_3N_4, CVD amorphous film, X-ray diffr. 79−87013
Si_3N_4, CVD anal. using hydrodynamics 77−40384
Si_3N_4, CVD film, elec. cond., film formation by pyrolysis of SiH_4-NH_3 79−91176
Si_3N_4 CVD film etching in acidic fluoride media 78−7071
Si_3N_4, CVD films, chemically trapped H reflection spectrometry 78−10081
Si_3N_4 CVD films, microstruct. and MNS struct. characts. 79−65339
Si_3N_4 CVD films on Si, dark currents 79−78240
Si_3N_4, CVD from $SiCl_4$ and NH_3, mass spectroscopic anal. of intermediates 79−43149
Si_3N_4, CVD on Si (111), EXAFS 79−95876
Si_3N_4 CVD thin film, multiple internal refl. IR spectroscopy 80−11499
Si_3N_4 capped GaAs, Ga precipitation 79−79127
Si_3N_4 ceramic, crack and inclusion detection, NDT microwave evaluation 78−95866
Si_3N_4 ceramic, high performance, for load-bearing engineering applics. 77−8785

silicon compounds continued
Si_3N_4 ceramic, surface and subsurface struct. by photoacoustic spectroscopy 78−68481
Si_3N_4, ceramic inclusions meas. and characterisation using US 80−76474
Si_3N_4, ceramic material fracture mechanics, review 80−45373
Si_3N_4 coated fibres for high-strength and improved fatigue 79−50470
β-Si_3N_4, combined X-ray and IR analyses 78−79579
Si_3N_4, conditions for thermal current runaway and breakdown 77−43760
Si_3N_4, consolidation by hot isostatic pressing 80−11605
Si_3N_4, containing MgO and Y_2O_3 additives, impurity effect on sintering 79−61543
Si_3N_4, corrosion resist. in residual fuel oil fired environment 79−39010
Si_3N_4, cracking characterisation by double torsion test *(French)* 80−104369
Si_3N_4, crystalline, N implant. in Si at high doses, buried insulating layer *(French)* 80−59498
Si_3N_4 degradation due to high-temp. processing 78−6454
Si_3N_4, densification, role of $Ce_{4.67}(SiO_4)_3O$ 79−61549
Si_3N_4, deposition by plasma stream transport method, use of charge exchange plasma source 79−15613
Si_3N_4, dielectric film, on Si. crysts. from amorphous state 79−28225
Si_3N_4 dielectric film on Ge, dislocation interactions 80−39472
Si_3N_4, dielectric films made by NH_3-silane reaction, TEM study 80−84413
Si_3N_4, dissolution rate in molten Si, Fick's law calc. 79−99319
Si_3N_4, effect of Al on oxidation behaviour *(German)* 78−31587
α-Si_3N_4, effect of excess Si under ionic implantation of N 79−86809
Si_3N_4, effect of oxide impurities on physicomechanical props. 80−16396
Si_3N_4, electronic struct., LCAO calc. 80−96776
Si_3N_4, encapsulant for annealing of GaAs, photolum. and AES evaluation 78−27657
Si_3N_4, end point detection in plasma etching by optical emission spectroscopy 80−50733
Si_3N_4, engng. ceramic, lattice resolution studies 78−27510
Si_3N_4, enhanced etching by ion beam, localised substrate heating effects 78−51573
Si_3N_4, etch rate loading effect and temp. depend. in CF_4 plasma 79−34167
Si_3N_4, etching charact. by plasma reactive sputter etching 78−27661
Si_3N_4, etching with CF_4 in diode system 79−61759
Si_3N_4, evidence for cavitation crack growth, SEM study 79−79086
α-Si_3N_4, exam. of chemical vapour deposition, and IR transmission and reflectance 79−19993
Si_3N_4, exam. of fracture resistance 78−76826
Si_3N_4 fabrication by rate-controlled react. sintering, nitridation react. control 79−24468
Si_3N_4 facet coating, GaAs-GaAlAs TJS lasers, high power density single mode operations 79−86186
Si_3N_4, factors affecting α, β phase formation, during nitridation of Si powders 78−52738
Si_3N_4 film, absorpt. meas. 79−78769
Si_3N_4, film, absorption, refr. index, freq. dispersion 78−48248
Si_3N_4 film, amorphous, AES and EELS characterisation 79−90905
Si_3N_4 film, amorphous, optical props., band gap and surface roughness 77−32396
Si_3N_4 film, CVD, etching in acidic fluoride media 78−39927
Si_3N_4 film, CVD, high-field dark currents 80−54791
Si_3N_4 film, CVD, ion implanted, compressive stress buildup 77−89456
Si_3N_4, film, cond. mechanism, double injection, trap SCL current 77−32099
Si_3N_4 film, deposition by pyrolysis of SiH_4-NH_3 mixture, struct. and props. of deposit *(French)* 77−40382
Si_3N_4 film, diffusion of Al, AES and depth profiling 78−51744
Si_3N_4 film, elastic stiffness and thermal expansion coeffs. 80−107451
Si_3N_4 film, grown by direct thermal reaction with N_2 78−52665
Si_3N_4 film, growth technique 79−43141
Si_3N_4, film, H_2 concentration profile, chem. bonding 79−33205
Si_3N_4 film, HF plasma deposition *(German)* 80−7507
Si_3N_4 film, high temp. annealing effect on struct. and comp. 77−15714
Si_3N_4 film, high-speed electron irradiation effect on charge storage 77−69430
Si_3N_4 film, in MNOS struct., mechanical stress and elec. props. as function of nitride deposition temp. 79−42651
Si_3N_4 film, in MNOS struct., kinetics of irreversible changes in cond. 79−73600
Si_3N_4 film, in MNS structures, dark conduction and photoconduction phenomena 78−30989
Si_3N_4 film, ion beam effects on opt. props. *(Russian)* 77−48265
Si_3N_4 film, laser coupling, new technique for refr. index and thickness meas. 77−88965
Si_3N_4 film, low press. CVD techniques, IC fabrication process anal. 79−100058
Si_3N_4 film, MNOS device, high temperature annealing, effect on Si_3N_4 stress, interface charge density and memory props. 79−87158
Si_3N_4 film, on Si, conc. profiles of ions and recoiled N after implantation through Si_3N_4 films 79−55764
Si_3N_4, film, on Si, hole conduction, shallow junction diode detection 77−8215
Si_3N_4 film, on Si, implantation effects on substrate hardening and film stress reduction 78−71748
Si_3N_4 film, on Si, influence of induced stresses on B diffusion in Si 80−29224
Si_3N_4 film, on Si, struct. stability 80−54564
Si_3N_4 film, on Si substrate, thermal stresses and cracking resist. 78−63958
Si_3N_4 film, on W-coated Si, photocond., 1.31-3.10 eV, mechanism 79−19679
Si_3N_4 film, plasma etching, role of chemisorpt. of CF_4, CF_3H, CF_3Cl, CF_2Cl_2 and CCl_4 79−11714
Si_3N_4 film, plasma-activated CVD, optical prop. depend. on growth conditions 77−55892
Si_3N_4 film, plasma-activated, passivation *(Japanese)* 80−85073
Si_3N_4 film, prep. by reaction of active N with SiI_4 vapour 77−24963
Si_3N_4 film, props., rel. to deposition conditions, appl. in semicond. devices 78−23612
Si_3N_4 film, pyrolytically deposited, AC cond. at low freq. 78−84334
Si_3N_4 film, reactive ion beam sputtering deposition, form. and characterisation 80−44452
Si_3N_4 film, self drifting of ionic charges, detection by surface potential decay method 78−72295
silicon compounds continued
Si_3N_4 film, synthesis mechanism 77−12538
Si_3N_4 film, thermal oxidation rate and masking effect against Si oxidation 78−64749
Si_3N_4 film, thickness measurements determ. using ellipsometer with nonmonochromatic source *(Russian)* 78−51862
Si_3N_4 film, with varying refr. index, AES and XPS 78−72029
Si_3N_4 film acousto-optical props. for integrated optical Bragg cell 79−55251
Si_3N_4 film deposited from SiH_2Cl_2 and NH_3, characterisation 79−11521
Si_3N_4, film deposition by ion beam methods 78−72728
Si_3N_4, film edge induced stress in Si substrate 78−30839
Si_3N_4 film formation by N ion implantation into Si 79−90692
Si_3N_4 film formation by $^{14}N_2^+$ ion implantation into Si 79−99455
Si_3N_4, film growth by reaction of NH_3 with Si (111) surface 79−100441
Si_3N_4 film in MNOS memory struct., distrib. and role of N-H and Si-H bonds 79−33358
Si_3N_4 film in MNOS struct., charge distribs. exam. 79−38184
Si_3N_4, film on Si substrate, stress meas., X-ray topography technique 78−5710
Si_3N_4 film on Si substrate, dislocation generation at film edge, suppression effect of SiO_2 80−2025
Si_3N_4 film on Si substrate, electrical properties *(Korean)* 80−55300
Si_3N_4 films, amorphous, CVD, IR spectra 77−21031
Si_3N_4 films, CVD in MNOS and MNS structs., elec. resist. 80−97019
Si_3N_4 films, elec. cond. 79−95499
Si_3N_4, films, ion-beam synthesis, IR spectra, struct., crystallisation on annealing 77−16705
Si_3N_4 films, plasma deposited over substrate steps, fast etching phenomenon 79−34168
Si_3N_4 films, plasma etching, MOS processing appl. 80−40577
Si_3N_4 films, prep., characterisation and appl. 80−40268
Si_3N_4 films, prep., props. and appls., bibliography 80−94939
Si_3N_4 films, prep. by thermal nitridation of Si in NH_3, comp. and oxidation resist. 80−3215
Si_3N_4 films, reactive plasma sputtering prep. 79−43147
Si_3N_4 films, struct. 80−54545
Si_3N_4 films, thermally stimulated depolarisation current meas. 80−88643
Si_3N_4 films for Si devices, surface and bulk elec. conduction obs. 77−43761
Si_3N_4 films grown by pyrolytic reaction between silane and ammonia, DC cond. 79−15243
Si_3N_4 films on Si, photocurrents 79−24092
Si_3N_4 films on Si wafers, O determ. by ^3He activation anal. 80−71981
Si_3N_4, finely dispersed, high-temp. synthesis 80−55331
Si_3N_4 first pressed, mixed mode fracture from controlled surface flaws 78−27603
Si_3N_4 form. by nitridation of SiO_2-C mixture 78−44068
α/β-Si_3N_4, formation during nitridation of Si 80−50609
Si_3N_4, fracture toughness meas. using Knoop indentation method *(German)* 80−25830
Si_3N_4, grain-boundary-crystallized, thermal shock resistance 78−11308
β-Si_3N_4, growth mechanism 79−55685
Si_3N_4, growth of α and β phases 78−95717
Si_3N_4, HS-130, dynamic mode I fracture toughness and flexural strength 77−21248
Si_3N_4, hard coating preparation by ion beam methods 80−25579
α-Si_3N_4, hardness anisotropy 78−95804
Si_3N_4, high temp. creep. 77−77530
Si_3N_4, high temp. thermal fatigue, role of activation energy of slow crack growth 77−44340
Si_3N_4, high-speed rolling bearings, fatigue strength 80−93655
Si_3N_4, highly insulating film, current cond., CV curves, and IR absorpt. 79−38208
Si_3N_4, hot press, high resolution electron microscopy 79−90501
Si_3N_4, hot pressed, crack healing *(German)* 79−24599
Si_3N_4, hot pressed, effect of powder composition and sintering temp., on phase transformation kinetics, microstructure and mech. strength *(German)* 79−4939
Si_3N_4, hot pressed, flawed plate under combined stresses, failure prediction 78−72884
Si_3N_4, hot pressed, fracture phenomenology, fracture surface energy, crack propagation 79−57090
Si_3N_4, hot pressed, high temp. compressive cracking, optical and electron microscopy exam. 78−76733
Si_3N_4, hot pressed, impurity phases, TEM obs. 79−8260
Si_3N_4, hot pressed, rate controlling process in oxidation 78−27659
Si_3N_4, hot pressed, slow crack growth from controlled surface flaws 78−80632
Si_3N_4, hot pressed, small surface cracks, size estimation using SAW 78−76793
Si_3N_4, hot pressed, strength and life prediction 80−3173
Si_3N_4, hot pressed, surface wave scatt. from elliptical cracks for failure prediction 80−55608
Si_3N_4, hot pressed, Y_2O_3 fluxed, microstruct. 78−64512
Si_3N_4, hot pressed with different grain struct., mech. props. 79−61700
Si_3N_4, hot pressing, effect of ZrO_2 *(Japanese)* 77−55929
Si_3N_4, hot pressing, starting powder requirements, review 79−33987
Si_3N_4, hot pressing with Mg-Si-N-O system additives *(Japanese)* 77−36437
Si_3N_4, hot pressing with Y_2O_3 and Li_2O additives 78−92220
β-Si_3N_4, hot-pressed, containing small amounts of Be and O in solid soln. 80−2985
Si_3N_4, hot-pressed, creep and strain recovery 80−100874
Si_3N_4, hot-pressed, dielec. props. 78−10822
Si_3N_4, hot-pressed, electrical props. 78−39136
Si_3N_4, hot-pressed, fracture in bending *(Japanese)* 79−79113
Si_3N_4, hot-pressed, fracture mech. parameters, indentation-precracking and double-torsion methods 80−104364
Si_3N_4, hot-pressed, fracture toughness determ. using specimens with chevron and straight through notches 80−108538
Si_3N_4, hot-pressed, impact resistance, instrumented drop weight test 78−11265
Si_3N_4, hot-pressed, proof-testing 78−80693
Si_3N_4, hot-pressed, strength anisotropy origins 80−89330
Si_3N_4, hot-pressed, thermal cond. by laser flash method 79−69302
Si_3N_4, hot-pressed with crystn. grain boundary phases, prep. 78−95715
Si_3N_4, impure, oxidation, phase equilibria 79−70045
Si_3N_4, in MNOS structure, V/I charcts. determ. *(Russian)* 77−8201

silicon compounds continued
Si_3N_4 inAl-Si_3N_4-Al thin-film cold cathode, electrical forming, expt. 78−76160
Si_3N_4, intermediates in CVD, mass spectrometric detect. 78−27411
Si_3N_4, investigation of gas phase of CVD reaction 78−52681
Si_3N_4, ion bombard. induced light emission 77−48257
Si_3N_4, kinetic model for RF plasma-activated CVD 78−27416
Si_3N_4, LVV Auger spectra 79−52055
α-Si_3N_4, lattice and atomic position parameters, neutron diffr. study 79−42040
Si_3N_4 layer form. by high dose implantation and annealing of Si:N wafers 80−70227
Si_3N_4 layer on Mo film, passivation against IR reflectance losses caused by oxidation 79−3758
Si_3N_4 layers, cond. process kinetics 77−76991
Si_3N_4 layers, on GaAs, encapsulation, low-energy ion beam sputtering 79−78882
Si_3N_4 layers, prep. by N_2 ion implantation into Si, TEM and IR absorpt. obs. 79−46974
Si_3N_4 layers, RF plasma deposition and props. 79−43155
Si_3N_4 layers deposition, high-temperature, in resistance furnace, temperature gradient and nitrogen flow influence obs. *(Bulgarian)* 80−80981
Si_3N_4 layers produced by ion implantation, oxidation inhibition and etching 80−103374
Si_3N_4, low press CVD film, steady-state electron and hole space charge distrib. 80−29493
Si_3N_4, low pressure CVD, thermochemical calcs. 80−108356
Si_3N_4, low temp. deposition using microwave-excited active N_2 78−84718
Si_3N_4, low-Z material, outgassing expts. 79−209
Si_3N_4 MIM cathode, fluctuation noise 78−2998
Si_3N_4, MIS struct. form. by reactive deposition on n-InSb substrates, C/V meas. 80−103752
Si_3N_4 mask, appl. in selective oxidation of Si in high press. steam 79−38997
Si_3N_4, meas. of critical stress intensity factor and subcritical crack propag. rates 78−72880
Si_3N_4, mechanical props. charact. by dynamic elastic modulus meas. up to 1400°C *(German)* 79−70101
Si_3N_4, mechanism of α-β transition under annealing 79−87629
Si_3N_4, MgO-fluxed, hot pressed, grain boundary phases 78−27464
Si_3N_4, N ion implantation synthesis, struct. and resonance mechanism of α-β transition during annealing 80−33981
Si_3N_4, N K-edge EXAFS, secondary electron yield meas. 79−47544
Si_3N_4, nitriding *(German)* 79−74414
Si_3N_4, non-stoichiometric films, struct. 79−42412
Si_3N_4 noncrystalline layers, CVD growth, encapsulant layers for annealing GaAs 79−19994
Si_3N_4 off-stoichiometric plasma-deposited layer, AES evaluation of comp. 78−26781
Si_3N_4 on Si, depth profiling, AES 77−40605
Si_3N_4, on Si, dissolution and corrosion in high temp. water and moisture 77−48564
Si_3N_4 on Si, optical monitoring of etching using grating 78−76775
Si_3N_4 on Si, optical waveguide, fabrication, propag. consts. 78−33826
Si_3N_4, optimization of props. as tool material, for high fracture toughness and hot pressing prod. 79−95987
Si_3N_4, oxidation, 1300 to 1500°C 77−8966
β- Si_3N_4, oxidation 77−56130
Si_3N_4, oxidation and hot corrosion resistance kinetics 80−25896
Si_3N_4, oxidised, with Y_2O_3 densification aid, temp. and compositional stability of $Y_6Si_6O_{21}$ 78−27664
Si_3N_4, oxidised ceramic, O_2 depth profiling using ^4He backscatt. 77−89463
Si_3N_4 passivation films, advances in deposition processes, review 78−23620
Si_3N_4, phase content determ., using X-ray diffr. anal. 78−44281
α/β-Si_3N_4, phase yields during form., influencing factors 80−108408
Si_3N_4, plasma deposition, optical absorption as control test 78−35314
Si_3N_4, plasma etching, mass spectroscopic exam. 78−72909
Si_3N_4, porous, reaction sintered, organosilicon infiltrated, decomposition, strength, density 79−29000
Si_3N_4 powder, high press. hot pressing 79−38772
α-Si_3N_4 powder, hot pressing, kinetics 77−55925
Si_3N_4, powder metallurgy recent developments, Sweden 80−93514
Si_3N_4 powders, laser synthesis using NH_3-SiH_4 gas mixtures 79−74119
Si_3N_4, prep. and charact. of ultrafine powders 80−2983
Si_3N_4, prep. by CVD, effect of raw gas flow rate *(Japanese)* 77−48348
Si_3N_4, preparation, effect of Fe and $FeSi_2$ on nitriding of Si powder 79−33985
Si_3N_4 protective coatings on Mo, RF reactive ion plating 78−3250
Si_3N_4, pyrolytic, amorphous and crystalline, chemical vapour deposited fracture surfaces rel. to struct. features 79−5038
Si_3N_4, pyrolytic, crystn. and amorphous, thermal diffusivity, thermal cond., specific heat 79−69303
Si_3N_4, pyrolytic, prep. by CVD, bulk and coatings, exam. of electrical, optical and physical props. 79−95935
Si_3N_4, pyrolytically-deposited, engng. significance 79−38746
Si_3N_4, RF-sputtered thin-film optical waveguide, effect of deposition parameters on optical loss 79−76881
α-Si_3N_4, Raman active modes, spectra 78−80326
Si_3N_4, rapid CVD, and struct. charcts. 77−28767
Si_3N_4, reaction bonded, bending strength meas., influence of loading conditions, proof testing and anal. methods *(German)* 78−31451
Si_3N_4, reaction bonded, creep, internal oxidation effects 78−56701
Si_3N_4, reaction bonded, exam. of strength as function of nitrided density, microstruct. design 78−68731
Si_3N_4, reaction bonded, effect of Si powder grain size on microstructure, and mech. props. *(German)* 79−4998
Si_3N_4, reaction bonded, exam. of Na_2SO_4 induced heat corrosion 79−20224
Si_3N_4, reaction bonded, fracture mech. pararucters, microstmet. amd temp. effect 79−24598
Si_3N_4, reaction bonded, ladder phase, interference phenomena explanation 78−72898
Si_3N_4 reaction bonded, microstructure, formation, properties, phase composition 79−56947
Si_3N_4, reaction bonded, Na assisted oxidation, exam. 78−56795
Si_3N_4, reaction bonded, pore size and distrib. effect on strength 79−29165

silicon compounds continued
Si_3N_4, reaction bonded, post-sintering, injection moulding applications 80−60807
Si_3N_4, reaction bonded and hot pressed. exam. of thermal shock behaviour *(German)* 78−64561
Si_3N_4, reaction bonded and hot pressed, compression creep, comparison with sialon and SiC 79−15728
Si_3N_4, reaction sintered, α- and β-phase form., effect on strength 77−21075
Si_3N_4, reaction sintered, time depend. strength degradation 79−29235
Si_3N_4, reaction sintered, H_2 in nitriding gas, effect on strength, struct., and composition 79−24478
Si_3N_4, reaction sintered, microstruct. charact. 80−35145
Si_3N_4, reaction sintered, thermal stress failure mode, effect of data scatter 80−60949
Si_3N_4, reaction-bonded, added oxides effect on strength after oxidation 79−39012
Si_3N_4, reaction-bonded, biaxial fracture strength 79−38969
βSi_3N_4, reaction-bonded, Fe-contaminant effects on Si nitridation 78−80496
Si_3N_4, reaction-bonded, gaseous boundary layer influence on oxidation at 1400°C 79−24638
Si_3N_4, reaction-bonded, hexagonal (wurtzite) form of Si 77−1112
Si_3N_4, reaction-bonded, internal oxidation processes role in high-temp. mech. props. 79−38915
Si_3N_4, reaction-bonded, microstructural analyses 77−8782
Si_3N_4, reaction-bonded, Na ion assisted oxidation, 800 to 1300°C 79−39011
Si_3N_4, reaction-bonded, pore struct. variations 79−24480
Si_3N_4, reaction-bonded, quantitative microstructural analysis 79−100092
Si_3N_4, reaction-bonded, struct., form. mechanisms and kinetics 77−4760
Si_3N_4, reaction-bonded, strength, effect of Si purity in production 80−100902
Si_3N_4, reaction-bonded, theoretical model of manufacture, effect of ambient reaction temp. and compact size 80−108379
Si_3N_4, reaction-bonded and hot pressed, hardness and wear behaviour 79−38970
Si_3N_4, reaction-bonded and hot pressed, deform. and fracture during creep 79−38916
Si_3N_4, reaction-sintered, non-axial dislocs. 77−19956
Si_3N_4, reaction-sintered, strength/nitrided density relationship 77−28891
Si_3N_4, reaction-sintered, effect of oxidation on thermal diffusivity 79−86933
Si_3N_4, reactively sputtered, MNS struct. hysteresis elimination 79−99633
Si_3N_4, recrystallisation during hot pressing 77−12587
Si_3N_4, rolling bearing materials, effects of high temp. operation 80−21124
Si_3N_4, room temp. CVD on InSb 80−71597
Si_3N_4, room temp. fracture strength data, statistical anal. 78−64619
Si_3N_4 sample substrates, high resoln. electron beam fabrication using STEM 80−104104
Si_3N_4, selective etching rel. to Si by plasma reactive sputter etching 80−81221
Si_3N_4, separation, effect of reactor geometry *(German)* 78−60583
Si_3N_4, Si rich, CVD film prep. and props. 78−76607
Si_3N_4, Si X-ray absorption K-edges, charact. parameters *(Russian)* 79−47541
Si_3N_4, Si(LVV) Auger spectra, ion bombardment, electron energy loss spectra 80−80911
β-Si_3N_4, single cryst., growth from Si melt in N_2 atmosphere, growth mechanism 79−24429
α-Si_3N_4 single crysts., growth, morphology, hardness and slip system 79−83112
Si_3N_4, sintering in powder bed with addition of MgO sintering aid 80−29910
Si_3N_4, sintering under high press., modulus of rupture tests 77−44202
Si_3N_4, sintering with Al_2O_3 and Y_2O_3 *(Japanese)* 78−19703
Si_3N_4, slip casting from aqueous suspension, reactions with HCl and NaOH 80−16259
β-Si_3N_4 solid soln., form. from SiO_2-AlN sintering 78−23655
β-Si_3N_4 solid soln. prod. by reaction sintering SiO_2-AlN mixture 80−25645
Si_3N_4, solid-solid reactions with Fe, Ni and Mo alloys 79−28151
Si_3N_4, sputtered deposit, encapsulation of preliminary heated GaAs *(French)* 77−32714
Si_3N_4, sputtered insulating film contouring over substrate topography 77−8752
Si_3N_4 sputtered layer, GaAs:Si encapsulation, photolum., annealing effects 80−20681
α-Si_3N_4, stable phase in Si-Al-O-N system, cryst. struct. obs. using TEM 80−108421
Si_3N_4, static fatigue, fitting of data to iterative trivariant analysis 78−76732
Si_3N_4, stress corrosion 77−8917
Si_3N_4, struct. of slow crack interface, light and electron microscope obs. 78−68770
Si_3N_4 substrate, nucleation of CVD Si in SiH_4-HCl-H_2 system at high temp. 80−49538
Si_3N_4, surface etching by laser-generated free radicals 80−71772
Si_3N_4, surface passivation of GaAs and interface props. 80−93005
Si_3N_4, swelling, blistering, 140 keV p, d and He ion irrads., porosity effects 77−35603
Si_3N_4, synthesis and props. of shapes 79−47650
Si_3N_4, synthesis in Cl_2 system 80−40308
Si_3N_4, tensile strength distrib. 80−40471
Si_3N_4, thermally grown films for high performance MNS devices 78−48322
Si_3N_4, thermodyn. props. and sp. ht. 77−80629
Si_3N_4 thin film, reactively sputtered, struct. and elec. props. 80−88656
Si_3N_4 thin films, Ga and As concentration measurement by CAMECA probe *(French)* 77−86411
Si_3N_4, thin intergranular phase, imaging by high-resolution electron microscopy 79−90895
Si_3N_4, thin sheets, reaction sintered, exam. of oxidation in damp air 78−48552
Si_3N_4 ultra-thin film composites of FET wafers and devices, thickness determ. by microprobe technique 77−36397
Si_3N_4, unsteady cond. in high elec. fields 78−76152
Si_3N_4, VDC, encapsulant for annealing of implanted GaAs:Se 78−83834
Si_3N_4 waveguide layer, as electro-optic phase modulator 79−23081

silicon compounds continued
Si_3N_4, Wiener filtering appl. to nondestructive evaluation, defect charact. 79−11732
Si_3N_4 with MgO, Al_2O_3 and/or spinel, pressureless sintering 77−25003
Si_3N_4 with Y_2O_3 and Al_2O_3 additions, hot pressed, exam. of mech. props., grain boundary crystallization 79−20009
β-Si_3N_4, X-ray cryst. struct. and refinement, struct. rel. to α-Si_3N_4 79−46605
Si_3N_4, Y_2O_3 doped, hot pressed, improved high temp. strength 79−61613
Si_3N_4, Zr-based hot pressing aids effect on oxidation resist. 77−8971
Si_3N_4:$(MgO+Al_2O_3)(Y_2O_3)$, hot-pressed and sintered, microstruct. and impurity distrib. 80−49261
Si_3N_4:C film struct., oxidation, defects 79−51455
Si_3N_4:Fe, α- and β-phases, Mossbauer and Raman obs. of state of Fe 79−33572
Si_3N_4:Ge films, intrinsic stress rel. to deposition conditions 80−39467
Si_3N_4:H, amorphous, ion induced H transfer from N to Si, band passivation, elec. props. 78−47439
Si_3N_4:H, film, impurity profile determ. by 1.2 MeV proton-proton scatt. 80−49256
Si_3N_4:MgO, hot-pressed, linear thermal expansion rel. to MgO content 80−70430
Si_3N_4:Si amorphous film, optical and electrical props. 77−76987
Si_3N_4/Al_2O_3, powder compact, electron microprobe investigation of reactions *(French)* 80−26009
Si_3N_4/Zr joint, solid state bonded, exam. of bond fracture strength 78−76826
Si_3N_4/Zr laminates, metal to ceramic joints, adherence props. 80−45386
Si_3N_4/ZrO_2, hot-pressed, compressive surface stresses developed by oxidation induced phase change 80−60992
Si_3N_4-Al_2O_3, hot-pressed with crystn. grain boundary phases, prep. 78−95715
Si_3N_4-Al_2O_3, hot-pressed with crystn. grain boundary phases 78−95716
Si_3N_4-Al_2O_3, Sialon, pressure sintering 77−55919
Si_3N_4-Al_2O_3-AlN, isothermal sections, free energy of formation 80−55363
Si_3N_4-Al_2O_3-AlN, Sialon, fabrication and reaction sintering 77−44201
Si_3N_4-Al_2O_3-SiO_2 systems, glass forming regions 80−84070
Si_3N_4-Al_2O_3-Y_2O_3, sintered, observation of a noncrystalline phase 78−64536
Si_3N_4-Al_2O_3(25.5, 37.0, 47.8 and 57.8 mol.%) thermal diffusivity 77−7913
β-Si_3N_4-AlN-Al_2O_3-MgO, insolubility of Mg in β-Si_3N_4 79−10953
Si_3N_4-AlN-Al_2O_3-SiO_2-Y_2O_3, phase equilibrium study by X-ray diffr. and optical microscopy 80−50614
Si_3N_4-AlN-SiO_2-Al_2O_3 solid-liquid equilibria 78−92247
Si_3N_4-based refractories, strength and microstruct. rel. to sintering 77−63610
Si_3N_4-CeO_2, surface stress development during oxidation 80−50736
Si_3N_4-CeO_2 additive, hot-pressing and oxidation behaviour 80−71618
Si_3N_4-ceramic, nondestructive evaluation, scanning photoacoustic microscopy 80−85115
Si_3N_4-GaAs, layer struct., electron-hole liq. at interface 79−69434
Si_3N_4-GaAs structure, photoluminesc. and collective effects 78−6727
Si_3N_4-InP, interface props., plasma deposited dielectrics, n-channel MOSFET action 80−93003
Si_3N_4-Mg_2SiO_4-Si_2N_2O, compressive creep, composition effect 80−50674
Si_3N_4-MgO, (5 wt.%), hot pressed, fracture toughness as function of initial α-phase content, SEM 80−3174
Si_3N_4-MgO, compressive creep, source of viscoelastic effect 80−50675
Si_3N_4-MgO, compressive creep, oxidation induced compositional change 80−50676
Si_3N_4-MgO, hot pressed, oxidation kinetics 79−29243
Si_3N_4-MgO, hot pressing and α-β phase transform. 78−27461
Si_3N_4-MgO, reaction with Fe to produce surface pitting 78−76778
Si_3N_4-MgO (2-5 wt.%) hot pressed, tensile creep testing 80−40423
α-Si_3N_4-MgO (5 wt.%), hot-pressed, mech. strength development 78−44195
Si_3N_4-MgO (5 wt.%), microstructural changes during gas pressure sintering *(Japanese)* 77−12589
Si_3N_4-Si_2N_2O-Mg_2SiO_4, melting and eutectic studies 80−45285
Si_3N_4-SiC-Y_2O_3 $(La_2O_3)(Ce_2O_3)(Eu_2O_3)(Gd_2O_3)$, reactively sintered, microstruct. and strength 80−25631
Si_3N_4-SiO_2, double dielec. layer on Si substrate, ellipsometric parameter meas. methodology 77−63474
Si_3N_4-SiO_2, interface, electron and hole cond. at moderate elec. fields 78−95376
Si_3N_4-SiO_2:As, graded and stepped energy band-gap MIS struct. 80−2473
Si_3N_4-SiO_2:N,Zn ion-implanted multiple layers, ion range distribs., secondary ion microprobe meas. 79−42129
Si_3N_4-SiO_2-AlN mixture, reaction sintering forming β-Si_3N_4 solid soln. 79−52145
Si_3N_4-SiO_2-AlN system, β-Sialon form. *(Japanese)* 80−45261
Si_3N_4-SiO_2-MgO, phase relations and interrelation with mech. strength, and oxidation 78−48386
Si_3N_4-SiO_2-Y_2O_2, subsolidus phase relations 80−60845
Si_3N_4-SiO_2-Y_2O_3 pseudoternary system, phase relations and stability 77−86015
Si_3N_4-SiO_2-ZrN-ZrO_2, X-ray diffr. phase anal. and reactions $Si_3N_4+ZrO_2$, SiO_2+ZrN 80−50613
Si_3N_4-Y_2O_3, hot-pressed, oxidation kinetics 80−16520
Si_3N_4-Y_2O_3 (8.0 wt.%), hot pressed, mech. props. 79−70134
Si_3N_4-Y_2O_3 ceramic, thermal degradation, C impurity effect 80−50708
Si_3N_4-Y_2O_3-Al_2O_3-SiO_2, X-ray diffr. exam., phase equilib. at 1400 degrees C *(Japanese)* 78−44113
Si_3N_4-Y_2O_3(CeO_2), hot pressed, sintered, microstruct., flexural strength and fractographic anal. 80−40293
Si_3N_4-Y_2O_4-Al_2O_3 (4-17, 4 wt.%), sintering 80−81009
Si_3N_4-ZrO_2, sintered and hot pressed, exam. of mech. props. 78−48509
Si_3N_4-ZrO_2, tetragonal to monoclinic transform. of ZrO_2 particles *(German)* 79−43240
α,β-Si_3N_4+C, powders, high temp. reactions *(Japanese)* 77−48685
Si_3N_4+MgO, hot pressing and effects 77−63614
Si_3N_4+MgO, reaction during hot pressing 78−68658
$Si_3N_4+XeF_2(Cl_2)(F_2)$, plasma etching, electron or ion bombardment, Ar^+ enhancement 79−82073
$Si_3N_4+ZrO_2$, X-ray diffr. phase anal. of reaction products 80−50613
Si_4N_4, coating for oxidation resistance 77−32704
silicon compounds continued
Si_4N_4, encapsulating material for GaAs:Si, ion-implanted As profiles 79−4319
Si_4N_4, ion-implanted, enhanced etching in buffered HF solns. 78−72903
Si_4N_5, reaction-bonded, Ar sintering stage 77−90306
Si_xN_y, amorphous, prepared by glow discharge method, elec. and optical props. 77−21035
Si_xN_y, film, chemical nonuniformity of films produced by ammonolysis of monosilane 77−1334
Si_xN_y films, for microelectronics appls., plasma deposition and characterisation 79−78904
Si_3N_4AlN-Al_2O_3 system, reaction sintering forming β-Si_3N_4 solid solns. 80−50585
SiNH films, thickness and refractive index meas., comparison of techniques 80−8957
$Si_xN_yH_z$, film, prep. from plasma-induced CVD from Si-NH_3 79−83132
Si_2NO_2, needle crystals, formation and growth rate, nitridation of Si-SiO_2 powder compacts *(Japanese)* 79−91574
Si_2N_2O, elastic props. 79−29122
Si_2N_2O, emissivity determ. by IR thermography 77−59130
Si_2N_2O, fast neutron irradiation, variation of lattice parameters 80−24504
Si_2N_2O, high-press. neutron diffr. exam. 77−51357
Si_2N_2O, sintered with MgO or BeO additives, effect on oxidation *(French)* 79−20233
Si_2N_2O, thermal decomp. 80−81311
Si_2N_2O-Al_2O_3, solid soln., prep., effect of Si_3N_4 powder reactivity 80−45256
$Si_xN_yO_z$, in MIM struct., electron microscope obs. of irreversible changes *(Russian)* 77−85342
$Si_xN_yO_z$, thin film MIM, use as non-heated source of electrons, review 80−84516
$Si_3N_4.Y_2O_3$ prepared by hot press, cryst. struct. 80−10534
$Si_3N_4.15Y_2O_3$, sintering under high N_2 pressure 80−29907
Si_3Ni_4, hot pressed, subcritical crack growth boundaries at internal fracture origins 80−11748
Si_3Ni_4, hot pressed MgO fluxed grain boundary impurity phases, lattice fringe imaging obs. 79−11540
SiO $^3\Pi$ valence states, struct. and perturbations 79−59369
SiO, 8 μm band obs. in circumstellar cloud around VY Canis Majoris 79−62840
SiO 86.2 GHz maser, astronomical sources polarisation props. 80−4449
SiO (A-X) system in sunspot UV umbral spectrum 79−75187
SiO, alumina surface deposited film, SiH bond form., inelastic electron tunnelling spectra 79−69375
SiO amorphous film, high freq. phonon scatt. 80−49328
SiO amorphous film, optical transmittance and reflectance, bulk optical props. determ. 80−88954
SiO, amorphous film, vac. evaporated, density meas., microcrystalline model of struct. 80−2313
SiO amorphous thin films prepared by vac. evaporation, density meas. 77−80714
SiO amorphous thin film capacitor, EPR, elec. cond. 78−68358
SiO, antireflection coatings for InP/CdS solar cells 78−50871
SiO circumstellar maser 78−16511
SiO coated MnCuBi film, Kerr readout charact. 77−85509
SiO condensate distrib. from extended aspherising source 79−52118
SiO, condensed amorphous, valence states, photoelectron spectra meas. 77−36353
SiO, core pseudopot. valence electron calc., orbital energy and bond length 79−72233
SiO, $d^2\Pi_r$-$b^3\Pi_r$ transition, 0-1 band rot. anal. 77−18961
SiO, doped, thermal stability of hole centres and hole recombination luminescence *(Russian)* 78−72614
SiO double deposition, homogeneous surface alignment of nematic liq. cryst., appl. to displays 79−4239
SiO, $E^1\Sigma^+$-$X^1\Sigma^+$ band system, transition moment 79−6970
SiO, elec. props. of Ag-SiO-Ag structures 79−87164
SiO emission, $A^1\Pi$, $b^3\Pi$ and $a^3\Sigma$ states, Si+N_2O flame chemiluminesc. 77−77767
SiO, evaporated film, AC cond meas. 80−20236
SiO evaporated film, dielec. function 8 to 33 μm, spectrophotometric and refl. meas. 80−80883
SiO, evaporation geometry for film deposition 78−48320
SiO film, Au coated, thickness meas. using stereo technique, TEM 77−30220
SiO film, binding energies, XPS meas. 77−7989
SiO, film, effect of ion implanted O_2 on optical props. 80−45027
SiO film, electrode effects in TSC and capacitance meas. 79−78203
SiO film, evap., for low tilt angle nematic alignment compatible with frit sealing 77−68910
SiO film, obliquely evaporated, topography rel. to liquid crystal orientation 77−69190
SiO, film, thickness influence on nematic MBBA orientation 80−59384
SiO film, vacuum evaporation on NaCl single cryst., IR absorption spectra 80−35098
SiO film and powder, effect of heat treatment on chemical and electronic struct., electron spectroscopy 77−48320
SiO film on Al, radiative cooling surface 80−50439
SiO, film prod. using large-capacity evaporator with filtering element 77−14819
SiO film structure exam., Raman microprobe-microscope appl. 80−62737
SiO films, adsorption of NO(N_2O)(NO_2)(O_2), infrared spectra exam. 79−45725
SiO grain formation in nova envelope 77−82254
SiO, identification in C star 78−93231
SiO in Ar matrix, vac. UV spectrum, vibr. progression 80−23432
SiO, in circumstellar shells, millimetre line emission obs. 78−49423
SiO in stars, equivalent widths of lines of (A-X) band 77−87368
SiO, interaction between $G^1\Pi$ and $I^1\Pi$ states 79−50040
SiO, interstellar, in $^1\Sigma$ state, collisional excitation by H_2 80−109508
SiO, interstellar abundances rel. to interstellar shocks mol. diagnostics 80−56899
SiO, interstellar grains, IR absorption features 78−49509
SiO interstellar line emission from Orion, shock chemistry 79−21391
SiO, isotopic lines in sunspots, $^{28}Si/^{29}Si/^{30}Si$ isotopic abundance ratio determ. 79−30044
SiO, low-lying electronic states, vib. assigned perturbations 77−27082
SiO, maser emission detect. at 7 mm wavelength in M- and S-type stars 78−4215

silicon compounds continued
SiO, maser emission from OH/IR sources 78−16432
SiO, maser emission from stellar sources, bright IR star monitoring at 2.7 μm 78−16433
SiO, maser emission from Mira variable stars, new sources 78−32467
SiO maser emission from late type stars, catalogue of objects 79−70965
SiO maser emission in OH/IR stars, new transition detect. 78−53954
SiO, maser emission obs. in long-period variable stars 78−4225
SiO maser in Orion-KL nebula VLBI obs. at 43 GHz 79−92836
SiO maser line evidence for circumstellar ring systems in supergiant stars 78−89195
SiO, maser luminosity in Mira variable stars correl. with spectral type 77−33512
SiO maser obs. in late-type stars at 43 GHz 77−74067
SiO maser pump mechanism and luminosity of long-period variable stars 79−92772
SiO maser sources, 43 GHz obs. 79−16942
SiO maser variability at 86 GHz of R Leonis, *o* Ceti and Orion A 80−41839
SiO masers in IR stars 79−71036
SiO masers in late-type stars, VLBI obs. at 43 GHz 79−92779
SiO mass loss and grain formation in expanding envelopes around evolved stars 79−48782
SiO, mol. binding states on clean and oxidised W surfaces 79−7750
SiO molecule, true potential energy curves for various states 77−6704
SiO, muonium and positronium form. 79−56679
SiO, nearly degenerate $G^1\Pi$-$I^1\Pi$ energy spectra, predissoc., extended virial theorem 79−22771
SiO, nonmaser emission lines from expanding envelopes around evolved stars 78−28650
SiO, obliquely coated on In_2O_3 coated substrate, TEM exam. of surface topology 77−39726
SiO obliquely evaporated film topography, effect on liq. cryst. orientation 78−38987
SiO, on liq. cryst. for surface alignment treatment 77−19871
SiO particles and 9.6 μ interstellar extinction feature 78−45378
SiO, population inversion mechanism for rot. levels, interstellar medium appl. 79−21406
SiO, reflective coatings, refr. index, UV polariser mirror coating appl. *(Russian)* 77−34928
SiO, rot. and vibr. consts., millimetre-wave spectrum 77−34619
SiO, rotational-level populations of interstellar molecule 79−97054
SiO, Si X-ray absorption K-edges, charact. parameters *(Russian)* 79−47541
SiO, single-layer vac. antirefl. coatings for near IR spectral region 80−33099
SiO, solar, equivalent widths of (A-X) band lines 77−17501
SiO substrate, struct. and internal stresses in Ag ultra-thin films 78−91572
SiO supermultilayer dielectric film, elec. strength *(Russian)* 77−85648
SiO surface, N_2^+ bombardment, 500 eV chem. reactions, XPS and UPS 78−48265
SiO, test of perturbation method for vibr. assignments, low lying electronic states 77−34645
SiO thin film, elec. breakdown voltage vs. thickness 78−2602
SiO thin films at 60 mK, high-freq. phonon propagation 79−19347
SiO, transition moment of $A^1\Pi$-$X^1\Sigma^+$ band, 260-290 nm 78−13552
SiO, VUV absorpt. spectra of mol., Rydberg, series and ionis. pot. 79−81213
SiO, valence ionis. energy, calc. including correl. effects 79−68185
SiO, valence-excited bound states, spectroscopic consts., radiative lifetimes 77−6752
SiO vapour, refractory silicates nonequilib. phases condensation 79−60497
SiO, vibr. struct. calcs. from photoelectron spectra 77−18973
SiO, vibr. wavefunctions, Franck-Condon factors, at low quantum numbers 78−55203
SiO vibration rotation bands in sunspots, equiv. widths at 8 μ 78−40903
SiO, $X^1\Sigma^+$, $A^1\Pi$, $C^1\Sigma^-$ and $E^1\Sigma^+$ states, SCF CI calcs. 79−45641
SiO^+, rot. spectrum, isotope shift, mol. consts. 79−59483
SiO^+, vac. UV photoelectron spectra, ab initio mol. orbital and Xα calcs., ($X^1\Sigma^+$) state 78−46395
SiO/BaO complex, new switching effect in MIM thin-film structures 78−80067
SiO-Al multilayer capacitors and inductors, heat treatment effect on elec. props. 77−32082
SiO-B_2O_3, amorphous composite dielec. film, AC conductivity 79−51703
SiO-B_2O_3 composite dielec. films, EPR, dangling bonds and dielec. loss 80−11246
SiO-CO gas phase, Si and C transfer to Fe-C liquid alloys 80−55655
SiO-Ge multilayer edge filter design, 3.2 to 4.9 μm range 78−87131
SiO-Permalloy multilayer flat ring cond., with circular anisotropy, mag. props. *(Russian)* 77−8366
$SiO+F_2$, matrix reaction, $OSiF_2$ prod., IR spectra and force consts. calcs. *(German)* 80−97718
SiO_2 (100), electronic struct., scattering-theory formulation 79−42607
SiO_2 (coesite), elasticity meas. on 100 μm cryst. 77−44978
SiO_2 (silicalite), new hydrophobic crystalline silica mol. sieve 78−30598
SiO_2, AES quantitative anal. of impurities *(Japanese)* 78−91356
SiO_2, action of plasma in capacitive electrode HF discharge *(Russian)* 78−95818
SiO_2 additive to Al_2O_3, effects on surface smoothness and densification 78−27462
SiO_2, adsorption of diketones, under carbon tetrachloride immersion, IR obs. 79−24821
SiO_2, adsorption of H_2O, surface treatment and methylation effects 78−84058
α-SiO_2, adsorption of H(H_2), microweighing and X-ray obs. *(German)* 78−51825
SiO_2, adsorption of pentan-3-one, under carbon tetrachloride immersion, IR obs. 79−24821
SiO_2, adsorption of water:Cu(II), EPR spectrum, freezing props. of water 77−4555
SiO_2 Aerosil, adsorpt. of cetyl pyridinium bromide, pH depend., mechanism 79−20466
SiO_2, amorphous, ^{30}Si diffusion *(French)* 80−59696
SiO_2, amorphous, chemical effects on freq. of Si-H vibrations 79−51227
SiO_2, amorphous, defect-controlled carrier transport 79−91049
SiO_2, amorphous, effect of second nearest neighbour forces on vibr. 78−59915

silicon compounds continued
SiO_2, amorphous, elec. cond. mechanism, review of developments 78−26854
SiO_2, amorphous, energy level schemes, Fermi level-electrochemical potential level coincidence, quantum yield spectrum 79−69400
SiO_2, amorphous, fast-time heat capacity, heat pulse propagation 78−51700
SiO_2, amorphous, high-field transport of excess electrons and holes 77−89767
SiO_2, amorphous, IR optical props. 79−56780
SiO_2, amorphous, in MOS struct., interface states 77−28254
SiO_2, amorphous, induced crystallisation exam. 78−6016
SiO_2, amorphous, intrinsic defects, photoluminesc. 79−78740
SiO_2, amorphous, intrinsic surface phonons, Raman scatt. and IR refl. 80−24728
SiO_2, amorphous, $L_{2,3}$ threshold spectra 77−69934
SiO_2, amorphous, local at. struct., XPS obs. 80−20042
SiO_2, amorphous, low temp. acoustic absorpt., 9 to 20K and 15 to 65 MHz, Anderson model interpret. 78−26633
SiO_2, amorphous, optical and elec. props., comparison with chalcogenide semiconds. 78−6721
SiO_2, amorphous, phonon scatt. by density fluctuations and thermal cond. 80−10626
SiO_2, amorphous, phonons, cluster-Bethe lattice approach 78−10150
SiO_2, amorphous, sp. ht., time-dependent, 0.1 to 1K 80−100338
SiO_2, amorphous, struct. and chem. bonding 78−51422
SiO_2, amorphous, struct. models 79−37628
SiO_2, amorphous, struct. model, surface struct. *(German)* 79−90859
SiO_2, amorphous, surface phonon theory 78−84044
SiO_2, amorphous, temp. below 1K, props., tunnelling 80−49576
SiO_2, amorphous, time-resolved hole transport, small polaron model 77−43598
SiO_2, amorphous, transient electrical transport, general and unified treatment 80−59977
SiO_2, amorphous, tunnelling models and thermal expansion below 4K 79−73326
SiO_2, amorphous, very small angle X-ray scatt. before and after thermal neutron irrad. 80−75270
SiO_2, amorphous and α-cristobalite cryst., band struct., photoelectron and X-ray spectra interpret. 80−24787
SiO_2, amorphous and cryst., XPS electronic band struct. interpret. 77−16454
SiO_2, amorphous and crystalline, with O vacancy, cathodolum. meas. 77−24901
SiO_2, amorphous and crystalline, surface polaritons and splitting of optical frequencies 78−72090
SiO_2, amorphous and cryst., Compton profile study 78−88378
SiO_2, amorphous and cryst., neutron irrad. and unirrad., intrinsic defect photolum. 80−50401
SiO_2, amorphous anodic layer on Si, MeV light ion multiple through-scatt., backscatt. obs. 79−86828
SiO_2, amorphous charge transport and storage 80−6864
SiO_2, amorphous diffusion of ^{30}Si, SIMS *(French)* 80−107482
SiO_2, amorphous electron transport and breakdown at high elec. fields 79−78108
SiO_2, amorphous estimate valence alternation pairs 80−54132
SiO_2 amorphous film, dye-sensitised steady-state photocond. in Au-dye-SiO_2-Au struct. 80−107924
SiO_2, amorphous film, form. by thermal oxidation of Si, struct., mechanism 77−12725
SiO_2 amorphous film, Si(LVV) Auger spectra, ion bombardment, electron energy loss spectra 80−80911
SiO_2 amorphous film, thermal, core and valence electron excitations, low energy electron loss spectroscopy and AES 80−2365
SiO_2, amorphous forms, surface struct. ESCA, X-ray line shift meas. *(Russian)* 77−66775
SiO_2, amorphous layer in multilayer target for channelled ion stopping power meas. 80−63431
SiO_2, and $SiO_{0.7}$, amorphous sputtered thin film, US anomalies, 0.5-300K 80−34145
SiO_2 and TiO_2, antireflection layers, on Al film, enhanced reflectance mirrors 77−42636
SiO_2 antireflection coating effect on CW laser annealing of ion implanted Si 80−49242
SiO_2, As diffusion , O_2 effects 78−43180
SiO_2 as high temp. stabiliser for Ag films 78−1319
SiO_2, As-implanted, electron trapping and detrapping characts. 80−65692
SiO_2, Auger line shapes, final state correlation effects 80−89095
SiO_2, Auger lineshapes Si $L_{23}VV$, Si $L_1L_{23}V$, O KVV, contributing factors 79−83064
SiO_2, avalanche injection of holes 78−26959
SiO_2, α-quartz structure, compression mechanism 79−23673
SiO_2, B_2O_3 glasses, struct. and phonon spectra 80−50324
SiO_2 based glasses, highly absorbing anomalous IR absorption at low temps. 78−43871
SiO_2 based optical fibre waveguides, water impurity 77−68270
SiO_2 based optical fibre rod preform, optical meas. of OH ion distrib. 78−87130
SiO_2, binary silica optical fibres, refr. index and profile dispersion meas. 77−19388
SiO_2 bricks, quartz estimation using IR spectra 78−48718
SiO_2, CVD anal. using hydrodynamics 77−40384
SiO_2, CVD coating on W-Re microelectrode 78−11752
SiO_2, CVD film, hydration props., ellipsometry meas. 78−22986
SiO_2 CVD layer, high current injection from Si rich SiO_2 film 80−80430
SiO_2, CVD of Ta film, struct., mech. props. 77−24965
SiO_2 CVD on Si producing near-ideal Si-SiO_2 interfaces, props. 80−80382
SiO_2 CVD thin film, multiple internal refl. IR spectroscopy 80−11499
SiO_2, calculated and measured Auger line shapes 79−83067
SiO_2 capsule, contamination effects on heat treatment of Zircaloy, vapour transport of Zr and Si 80−55437
SiO_2 charge transfer from metallic electrodes 80−15605
SiO_2, chem. bond and rel. props. 77−43199
SiO_2 chemical aspects of fluorocarbon plasma etching 79−83350
SiO_2, chemical bond and related props. 77−43171
SiO_2, clean film prep., use of poly-Si oxidation tubes 78−39924
SiO_2 clusters, CNDO/2 calc., appl. of cyclic boundary conditions 78−72110

silicon compounds continued
SiO_2, coalescence in Cu matrix 78−92271
SiO_2, coated silica fibres, tensile strengths of 1 km lengths 78−1384
SiO_2 coated TiO_2 powder, thickness meas. of coating, XPS and ion sputtering 79−88913
SiO_2 coating on $MoSi_2$, effect on oxidation, AES study *(German)* 79−74298
SiO_2 coatings on SiO_2 substrate, cathodoluminescence spectra, electron irrad. 80−76085
SiO_2, coesite, crystn. from soln. at high press. and temp. *(Japanese)* 77−72556
SiO_2, coesite, thermal cond. up to 40 kbar 79−1533
SiO_2 colloid, Brillouin scatt., particle size and density depend. 77−32844
SiO_2, colloidal, degrading effect on polymer fracture energy 78−52939
SiO_2 colloidal films, Cr^{6+}/Cr^{3+}, on Al, TEM/XPS study 80−85090
SiO_2 colloidal sol, particle size distrib., small-angle X-ray scatt. obs. 77−44516
SiO_2 concrete, elastic moduli meas. during heating and cooling 80−55451
SiO_2, condensed sol, electron microscopy and diffraction studies 77−29049
SiO_2 controlled electrode area ratio sputtering system operation and film props. 77−77382
SiO_2, core levels, chem. shift and relaxation energy, temp. dependence 80−39520
SiO_2, core levels, temp. depend. of conduction band and core exciton energies 80−24828
SiO_2 covered Si surface, scattering of keV H and He ions and neutrals 78−95638
SiO_2, cristobalites and topologically related structures, cryst. struct. 77−7688
SiO_2, critical surface tension anisotropy, liq. cryst. alignment 79−86676
SiO_2, cryst. and amorphous, laser-induced breakdown, electron avalanche damage mechanism 80−100711
SiO_2, cryst. and vitreous, struct. sensitive expansivity 78−22873
SiO_2 crystal and amorphous modifications, structural defect model 80−38915
SiO_2, crystal gyrotropy, meas. in IR region 80−88957
SiO_2, crystalline and amorphous density of states, bulk electronic struct., tight binding calcs. 80−44502
SiO_2, crystobalite form. in evacuated silica ampoules, cryst.-amorphous transform. 77−68933
SiO_2, D-impregnated, vitreous, radiation induced isotope exchange 79−99240
SiO_2, dangling bond states 80−24846
SiO_2 decomposition and reduction, in low temp. plasma jet *(German)* 80−45499
SiO_2 deposited on Ge, optical constants, reflection spectra by Kramers Kronig method 80−76099
SiO_2, deposition by plasma stream transport method, use of charge exchange plasma source 79−15613
SiO_2 deposition on InP by RF sputtering, surface damage 79−78879
SiO_2, depth profiling, AES 77−40605
SiO_2, detect. in subway air 78−36273
SiO_2, detection at interface of $In_{2-x}Sn_xO_{3-y}$-Si solar cells, Auger anal. 79−87991
SiO_2, dielectric breakdown, impact ionisation-recombination model 78−6633
SiO_2, dielectric film, on Si. crysts. from amorphous state 79−28225
SiO_2 dielectric film on Ge, dislocation interactions 80−39472
SiO_2, dielectric hard transparent coatings 77−36678
SiO_2 different modifications, chem. bonding, struct. *(German)* 78−30581
SiO_2 diffusion mask, stress enhanced diffusion of B in Si, photodiode fabrication 78−67865
SiO_2, diffusion of As, diffusivity and masking oxide thickness 80−39350
SiO_2, disperse, EPR, O_2 vacancy relax. rel. to substrate struct., gas adsorpt. *(German)* 79−95645
SiO_2 dispersed particulate in CVD reactor, correlations with film charcts. 80−76192
SiO_2, dissolution rate in molten Si, Fick's law calc. 79−99319
SiO_2 dissolution rate in molten Si 80−103481
SiO_2, dissolved, natural oceanic circulation tracer, Yucatan Strait 78−44830
SiO_2, doped, fibre-optic waveguide, effect of ionising radiation on optical attenuation 78−63170
SiO_2, dry etching induced surface contamination, SIMS, AES, and XPS obs. 80−11810
SiO_2, E′-centre model, IR absorption spectra 79−37634
SiO_2, effect on carbothermic reduction of Cr_2O_3, to metallic CR *(Japanese)* 78−48651
SiO_2, effect on high temp. creep of MgO 78−48450
SiO_2, effect on resistivity of $(Ba_{1-x}Y_x)TiO_3$ ceramic 79−65474
SiO_2, electroacoustic interaction obs. 77−11966
SiO_2, electron and ion emission from MOS field cathodes *(German)* 77−12499
SiO_2, electron beam induced charge carriers, MOS structs. *(German)* 77−12007
SiO_2, electron energy loss spectra, 0.02-2 eV 78−39642
SiO_2, electron-beam irrad., electron trapping, MOS capacitor expts. 78−72268
SiO_2, electron-beam-induced cond., appl. to obs. of voltage contrast in SEM 79−21856
SiO_2, electronic energy, structure calc. using tight binding approximation 77−69215
SiO_2, electronic struct., photoemission spectra calc. 77−35865
SiO_2, electronic struct., review of spectroscopic and theoretical data 77−76749
SiO_2, electronic struct. of point defects, surfaces and interfaces, Green's function scatt. theoretic method 79−33258
SiO_2, electronic structure, new interpretation 78−84120
SiO_2, electronic structure, theory 78−95260
SiO_2, ellipsometry of anodised layers on clean and ion bombarded Si surfaces *(Russian)* 79−24382
SiO_2, encapsulant for annealing of GaAs, photolum. and AES evaluation 78−27657
SiO_2, encapsulating material for GaAs:Si, ion-implanted As profiles 79−4319
SiO_2, etch rate loading effect and temp. depend. in CF_4 plasma 79−34167

silicon compounds continued
SiO_2 etching, DryOx process using anhydrous HF, microelectronic appls. 77−77606
SiO_2 etching by trifluoromethane plasma, optical spectroscopy appl. 80−87940
SiO_2, etching charcts. by plasma reactive sputter etching 78−27661
SiO_2, etching charcts. in trifluoromethane gas plasma 80−76392
SiO_2, etching charcts. using reactive ion etching with tetrafluoromethane-Cl_2 gas mixture 80−104313
SiO_2 etching in fluorocarbon glow discharge, chemical aspects 79−86631
SiO_2, etching in He-F_2 plasma, etch rates, mass spectra, direct ion sampling study 80−79510
SiO_2, etching with CF_4 in diode system 79−61759
SiO_2, evaporated film, Debye-type dielec. dispersion props. 78−56421
SiO_2, exciton study, luminescent centres as exciton detectors 80−66278
SiO_2 fabric, structural stability rel. to brittleness, X-ray diffr. and IR spectrosc. studies 80−96634
SiO_2, fabrication of surface relief struct. with linewidth below 2000 Å 78−42478
SiO_2 facet coating film effect on self-sustained pulsation suppression in GaAlAs DH lasers 80−95894
SiO_2, ferrobielastic poling 77−16102
SiO_2 fibre, CW tunable near IR Raman oscillator 78−1235
SiO_2 fibre, characterisation of physical props., $CaSiO_3$ production from xonolite slurry 78−39730
SiO_2 fibre near IR Raman laser, as universal fibre optic meas. system 79−23070
SiO_2 fibre reinforced Al, thermal degradation kinetics 77−44194
SiO_2, fibre waveguide, backward Raman amplification and pulse steepening 77−23740
SiO_2 fibres, freeze formed from polysilicic acid aq. soln. 80−71609
SiO_2 fibres, fused, drawn from rods, oxy-H_2 flame, prep., strength, dia. var. 80−102868
SiO_2 fibres, fused, load-elongation curves, elastic hysteresis, tensile testing machine 79−1891
SiO_2 fibres, LF optical phonons, Raman spectra 80−80789
SiO_2 fibres, plastic deformation and Young's modulus *(French)* 78−23746
SiO_2 fibres, reductions in static fatigue by hermetic jacketing with Al 79−43448
SiO_2 film, 10-22 Å, on Si wafer, production 77−76690
SiO_2 film, 1064 nm 150 ps laser pulse damage rel. to OH^- content and refr. index 79−14016
SiO_2 film, Al implanted, in MOS struct., electron traps charcts. obs. 79−15226
SiO_2 film, amorphous, shock crystn. obs. 80−10828
SiO_2 film, and TiO_2-SiO_2 film system, Rayleigh scatt., 441.6 nm, scatt. losses correl. with deposition parameters 79−78782
SiO_2 film, attenuated total reflectance study, impurity spectra 80−97311
SiO_2 film, bombardment by B^+ ions, waveguide layer form. 79−27454
SiO_2 film, CVD on GaAs using tetraethoxysilane oxidation 78−60582
SiO_2, film, charge effects at Al electrodes obs. 80−75625
SiO_2 film, dielectric breakdown and I-V characteristics 77−63368
SiO_2, film, drift mobilities of Na^+ and K^+ ions 78−10213
SiO_2 film, effect of oxidation on dielec. strength 77−16249
SiO_2 film, electric strength in MOS structures obs., under unidirectional, alternating and combined voltages *(Slovak)* 78−88034
SiO_2 film, electrical breakdown by impact ionisation, models compared with expt. 79−91373
SiO_2 film, electron-beam-induced cond. 80−20337
SiO_2 film, etching by conical beam of Ar ions *(Russian)* 80−76383
SiO_2 film, form. by reactive sputtering, effect of defects in Si wafer 77−89676
SiO_2, film, formation from tetraalkoxysilanes in O_2 current, props. 77−44170
SiO_2 film, from oxidation, in dry O_2 and H_2O ambients, initial oxidation regime obs. 79−29240
SiO_2 film, grown on Si surface in O_2-HCl mixture, Cl incorporation 79−70186
SiO_2 film, high-speed electron irradiation effect on charge storage 77−69430
SiO_2 film, IR spectra and elec. props., influence of prep. conditions 79−87176
SiO_2 film, in Al-SiO_2-Si struct., positive trapped charge location by internal photoemission 77−51820
SiO_2 film, in MIS struct., current-field charcts. 79−99623
SiO_2 film, ion beam effects on opt. props. *(Russian)* 77−48265
SiO_2 film, ion bombarded, attenuated total refl. method obs. of H capture 79−95863
SiO_2 film, laser coupling, new technique for refr. index and thickness meas. 77−88965
SiO_2 film, local defects detection by electrolytic decoration *(Bulgarian)* 78−60896
SiO_2 film, localised cond. regions, obs. by liq. cryst. technique 77−1507
SiO_2 film, localised states, low-temp. photocurrent spectroscopy 78−19090
SiO_2, film, low energy and high dose through-oxide P implantation into Si 77−15435
SiO_2 film, low press. CVD techniques, IC fabrication process anal. 79−100058
SiO_2 film, migration parameters of alkali ions, elec. meas. 80−39359
SiO_2 film, on GaP substrate, N ion implantation, optical refl. and EPR meas. 80−84197
SiO_2 film, on n-GaAs, Ga content after annealing at 730-940°C neutron activation anal. 78−43255
SiO_2 film, on semiinsulating GaAs:Cr,Si, annealing 79−4323
SiO_2 film, on Si, conc. profiles of P or (As) and recoiled O atoms after ion implantation, SIMS obs. 79−51138
SiO_2 film, on Si, influence of induced stresses on B diffusion in Si 80−29224
SiO_2, film, on Si, internal stresses 77−24499
SiO_2 film, on Si, radiation damage structures, EPR obs. 78−95097
SiO_2 film, on Si, range distrib. of implanted As, He^+ backscatt. obs. 77−39611
SiO_2 film, on Si, SiOH and SiH groups, IR absorpt. results 78−26779
SiO_2 film, on Si, structure determ. by electron diffr. anal. 79−15050
SiO_2 film, on Si, struct. stability 80−54564
SiO_2 film, on Si substrate, thermal stresses and cracking resist. 78−63958
SiO_2 film, on Si wafer, surface roughness by gas adsorption techniques 80−15398

silicon compounds continued
SiO_2 film, oxidation kinetics of Si in low O_2 partial press. *(Japanese)* 78−27665
SiO_2 film, penetration of As and P ions, 50 to 500 keV 77−76444
SiO_2 film, plasma grown, thermally stimulated depolarisation current meas. *(Russian)* 78−80082
SiO_2 film, preferential etching on Si substrate, plasma reactive sputter etching 77−20448
SiO_2 film, prep. using high press. O_2, residual stress, chemical etch rate, refr. index and density meas. 80−71768
SiO_2 film, prod. by oxid. of silane 78−3038
SiO_2 film, props., rel. to deposition conditions, appl. in semiconduct. devices 78−23612
SiO_2 film, quantitative secondary ion mass spectrometry of O isotopes and other light elements 77−9147
SiO_2 film, RF plasma deposition on glass or $In_{2-x}Sn_xO_{3-y}$, and liq. cryst. aligning props. 77−48350
SiO_2 film, refr. index and struct., deposition temp. depend. 79−4857
SiO_2 film, self drifting of ionic charges, detection by surface potential decay method 78−72295
SiO_2 film, spin-on oxide, phys. and cond. meas. 77−43762
SiO_2 film, thermally grown or sputtered, electrostriction and piezoelectricity 77−12010
SiO_2 film, thermally grown, pore size influence of punch-through voltage 78−6632
SiO_2 film, thermally grown, thickness, XPS obs. 80−11540
SiO_2 film, thermally stimulated depolaris. current, model *(Russian)* 79−56342
SiO_2 film, transient charge relax., continuous time random walk, simple approx. solns. 77−43584
SiO_2, film, transmission, photocond. and band gap meas. 79−73540
SiO_2 film covered Si:P, implanted, laser annealing behaviour 79−86808
SiO_2 film deposition by SiH_4 oxidation, kinetics and physicochemical model 79−42419
SiO_2 film deposition from SiH_2Cl_2 on Si 77−77407
SiO_2 film deposition on high-resistance Ge substrate by pyrolysis of tetraethoxysilane 77−1818
SiO_2 film electron beam induced conductivity theory and expts. 80−15640
SiO_2, film form. by reactive HF sputtering with voltage bias 78−3045
SiO_2 film formed by ion implantation, dielectric props. 78−35090
SiO_2 film grown by Si oxidation in O_2-H_2-HCl mixture, elec. props. 80−40569
SiO_2 film growth technology *(Japanese)* 77−40381
SiO_2 film on 6H-SiC substrate, ellipsometric meas., accuracy and sensitivity 80−77840
SiO_2 film on Cu substrate, surface EM wave absorpt., optical consts. *(Russian)* 80−108216
SiO_2, film on Si, electron beam damage, obs. using scanning AES 80−2070
SiO_2 film on Si, irradiation behaviour anal. 78−26957
SiO_2 film on Si, negative bias instability 78−91773
SiO_2, film on Si substrate, stress meas., X-ray topography technique 78−5710
SiO_2 film on Si substrate, reflectance and absorptance obs. 79−15542
SiO_2 film on Si substrate, Na transport caused by ion and atom impact 80−6682
SiO_2 film on Si surface, X-ray topographs 77−80396
SiO_2 film on thermally oxidised Si substrate, interface props., sputter deposition parameters effects *(German)* 80−40257
SiO_2, film thickness and field depend. of saturation defect density 78−56250
SiO_2 films, amorphous to cryst. transform. induced by diethyl ether vapour 79−55667
SiO_2 films, CVD at reduced press., optical props. 80−2957
SiO_2 films, DC plasma Si anodisation, dielectric const., O_2 pressure influence 80−70564
SiO_2 films, dehydroxylation, sintering, IR investig. *(Russian)* 78−75967
SiO_2 films, desorption from Si single cryst., ellipsometric obs. 80−100410
SiO_2 films, effect on mol. orientation of liquid cryst. *(French)* 79−10789
SiO_2 films, electron beam induced charge buildup, 80K 77−20440
SiO_2 films, grown in presence of O_2-trichloroethylene, room temp. negative bias instability 80−60102
SiO_2 films, growth on Si, role of defect structure 80−65403
SiO_2 films, microporous, sintering effects, IR ATR, transmission investigs. 79−66031
SiO_2 films, on Si, role of H_2 79−69376
SiO_2 films, plasma etching, MOS processing appl. 80−40577
SiO_2 films, prep. from tetraalkoxysilanes, by activation pyrolysis 79−87583
SiO_2 films, produced by thermal oxidation of Si, control of oxide defects 77−20477
SiO_2 films, RF-diode-sputtered, step coverage 80−80117
SiO_2 films, radiation induced charge transport and build-up, low temps. 77−20478
SiO_2 films, Si thermal oxidation, ^{18}O study 79−52400
SiO_2 films, Si-rich, amorphous Si region obs. 80−84400
SiO_2 films, spin-on diffusion sources, debris-induced effects 80−39465
SiO_2 films, stabilised by ion bombardment and heat treatment, crystn. and phase separation 79−77931
SiO_2 films, technology rel. to semicond. prod., bibliography 77−12038
SiO_2 films, thickness and dielectric const., elec. cond. mech. *(Japanese)* 79−8084
SiO_2 films, thickness and refractive index meas., comparison of techniques 80−8957
SiO_2 films, vac. thermal evaporation, parameter stabilisation 80−87571
SiO_2 films in poly-oxide poly Si structures, elec. cond. and charge distrib. 80−92984
SiO_2 films on Si, ellipsometric spectra, thickness determ. *(Chinese)* 80−86379
SiO_2 films on Si, mobile Na ion instability 79−82503
SiO_2 films sputtered in H-Ar mixed gas, enhanced step coverage 80−75470
SiO_2, fine powder, interstitial vac. thermal muonium production 78−42250
SiO_2, finite amplitude SAW distorted rippling profiles, optical probing obs. 80−34287
SiO_2, fluorocarbon ion beam etching charact. 80−35363

silicon compounds continued
SiO_2, form. by thermal oxidation in Cl-H-O ambient, gas phase comp. considerations 77−48562
SiO_2, formed by Si oxidation in trichloroethylene-O_2, Cl incorporation and elec. props. 79−91827
SiO_2, formed by trichloroethane oxidation of Si wafer, props. 79−70193
SiO_2, Fowler-Nordheim tunnel injection, Si surface pot. effect 79−91151
SiO_2, freq. and wavenumber depend. dielec. function, bond-charge approx. 79−56155
SiO_2, furnace drawn optical fibres, contamination reduction 78−33918
SiO_2, fused, absorption coeff. at 632.8 nm 78−8454
SiO_2, fused, absorption edge meas. 78−43887
SiO_2, fused, as-received and irrad., dielectric props. 79−65786
SiO_2, fused, broken bond defect generation mechanisms 80−88044
SiO_2, fused, bubble gas comp. rel. to furnace atm. 77−58402
SiO_2, fused, crack nucleation about pointed indentations 79−91779
SiO_2, fused, fibre Raman laser emitting over very large spectral region *(French)* 78−55405
SiO_2, fused, fibres, lifetime predictions, applicability of crack velocity date 77−52467
SiO_2, fused, filter in wide field-of-view SW radiometer for Earth radiation meas. 80−87473
SiO_2, fused, for sealed ampoule cryst. growth, thermal transmission function 80−84731
SiO_2, fused, γ-irrad., O-associated trapped-hole centres, optical absorpt. and ESR spectra obs. 79−65729
SiO_2, fused, He solubility and diffusion above transform. range 80−79965
SiO_2, fused, high transparency IR material 77−27326
SiO_2, fused, high-temp. darkening and absorption spectra meas. 77−36258
SiO_2, fused, ion beam induced luminescence 80−40166
SiO_2, fused, irrad., O_2^- radical defect centres, ESR obs. 79−61222
SiO_2, fused, isothermal compressibility to 20 kbar, inductance coil method 80−49302
SiO_2, fused, Lamb wave optical detect. 80−106690
SiO_2, fused, laser damage threshold rel. to surface roughness 77−40306
SiO_2, fused, laser damage threshold rel. to subsurface struct. 77−40307
SiO_2, fused, laser window material, refr. index, temp. and stress effects 77−46771
SiO_2, fused, optical elements, US cleaning, deleterious effects 77−42631
SiO_2, fused, photoelastic coeffs., freq. depend. 77−4619
SiO_2, fused, polymer coated optical fibre, static and dynamic fatigue 79−29244
SiO_2, fused, refractive index dispersion, thermal history depend. 80−25331
SiO_2, fused, shear-wave Brillouin scatt. intensity from photoelastic consts. 79−91454
SiO_2, fused, shock compressed, refractive index, density, and polarisability behaviour 80−50295
SiO_2, fused, single particle impact damage 80−40508
SiO_2, fused, stress optical coeff. 79−28713
SiO_2, fused, structural analysis, using fluorescence excitation *(German)* 80−38923
SiO_2, fused, surface charge in aqueous electrolyte soln. 79−29245
SiO_2, fused, surface crystn. by Li^+ ion implantation and annealing 80−89383
SiO_2, fused, surface damage threshold rel. to prep. and OH^- conc. 77−62026
SiO_2, fused, surface roughness rel. to prep. and treatment history 79−14058
SiO_2, fused, thermal expansion meas. at const. temp. 77−45824
SiO_2, fused, US cleaning effect on laser damage threshold 77−62024
SiO_2, fused, US study by harmonic generation, elastic consts., Gruneisen parameters 78−83735
SiO_2, fused, ultraprecise thermal expansion meas. 77−71290
SiO_2, fused, van der Waals forces between flat plate and spherical surface 79−37924
SiO_2, fused fibres, for linking very large astronomical telescope array 78−32342
SiO_2 fused fibres, radii determ. by multiwavelength laser light scatt. 80−22321
SiO_2 fused glass, coherent elec. echoes 79−61300
SiO_2, fused material removal mechanism by free abrasive grinding 77−52510
SiO_2, fused optical fibre, strength, appl. of Weibull type analysis 77−19418
SiO_2 fused powder, difference between white and black silica, devitrification rates 80−28918
SiO_2, fused silica, continuous inhomogeneities, refusing effect in H_2 77−50734
SiO_2, fused silica, isotopic CVD for low-loss optical waveguide prod. 77−72093
SiO_2, fused silica, KLR1, KLR2 and KU2, high-precision stability of end gauges 79−76778
SiO_2, fused silica, wetting by molten Al 77−15664
SiO_2, fused silica fibres, high-strength epoxy-acrylate coated, dynamic and static fatigue 78−1385
SiO_2, fused silica fibre lightguide, static fatigue transitions 80−58744
SiO_2, fused silica optical surface, ion polishing rel. to laser damage thresholds 77−75717
SiO_2, g-tensor and ^{29}Si hyperfine tensors of E_1'-centre for model of O^- vacancy 79−19777
SiO_2, g-tensor of interstitial O and broken Si-O bond, MO model calc. 79−78520
SiO_2 gate insulation on InP MIS inversion FETs, interface props. 80−93002
SiO_2 gate insulator MOS capacitors, hole transport, recovery charact. following electron beam irrad. 77−20439
SiO_2 gate insulators in radiation-hard MOS capacitors, charge relaxation 78−60206
SiO_2 gel, adsorpt. of ammonia, neutron scatt. investig., mol. vibrs., rots. 77−51608
SiO_2 gel, adsorption curves of O_2, EPR *(Russian)* 79−52776
SiO_2 gel, $BaMoO_4$ crysts. grown under influence of elec. field 80−93469
SiO_2 gel, hydrocarbon suspension, temp. depend. of electroviscous effect and dielectric parameters 79−79299
SiO_2 gel, internal and surface struct. by X-ray scatt. 80−84074
SiO_2 gel, irrad., adsorpt. of NH_3, neutron scatt. 79−33194
SiO_2 gel, macroporous, modification of surface by adsorption of thin layer of polymer 80−6624

silicon compounds continued
SiO_2 gel, meso-porous, SCI/IUPAC/NPL surface area standard, pore meas. 77−4941
SiO_2 gel, motion of NO_2 radicals adsorbed on surface, ESR spectrum averaging-out 77−60119
SiO_2, gel, pyrolysis, for low-temp. silica glass synthesis 79−43194
SiO_2 gel, $SiO_2Al_2O_3$, SiO_2MgO, pore structure influence on X-ray intensity in EPMA *(Japanese)* 80−26046
SiO_2 gel, sintering 77−85980
SiO_2 gel, steam treatment, struct. changes 80−35579
SiO_2 gel. struct., IR spectra obs. 78−88297
SiO_2 gels, heats of immersion, effects of pore narrowing 79−11833
SiO_2 geothermometer temp. of groundwater rel. to regional heat flow, United States 79−74876
SiO_2, glass, ^{29}Si hyperfine struct. of E′ centre, microwave saturation props. 80−7165
SiO_2 glass, AES anal. *(French)* 79−39236
SiO_2, glass, acoustic and thermal Gruneisen parameters 80−59608
SiO_2 glass, crystallinity positron annihilation study 78−72629
SiO_2 glass, electron microscopic determ. of struct. 79−90561
SiO_2 glass, electronic struct. and optical props. 80−2790
SiO_2 glass, formation by hydrolysis of $Si(OC_2H_5)_4$ with NH_4OH and HCl soln., and characterisation 80−71622
SiO_2, glass, HF phonon phase vel. meas., below 1K, tunnelling model 77−7818
SiO_2 glass, heat treatment study by positron annihilation 78−55812
SiO_2 glass, high rate MCVD of optical fibres 80−83671
SiO_2 glass, IR spectral emissivity and absorpt. coeff. at 600 to 1700K 80−16018
SiO_2, glass, ion implanted, radiation effect on chem. stability 77−1158
SiO_2, glass, irrad., EPR of Al E_1' centres 80−11268
SiO_2 glass, low loss optical fibre, radiation-induced IR absorpt. 80−87521
SiO_2 glass, low press. plasma treatment, paramag. defect form. *(German)* 78−23341
SiO_2 glass, molecular to band-like modes 77−66012
SiO_2 glass, monolithic, low temp. synthesis 80−40318
SiO_2 glass, optical props. of colour centres, intrinsic and modified defect states 79−60756
SiO_2 glass, phonon scatt., $>10^2$ GHz, by supercond. junction spectrosc. 80−10625
SiO_2 glass, porous, below-freezing pt. adsorbed layer, istohermal adsorption and dimensional changes obs. 78−75925
SiO_2 glass, Raman spectra of dissolved molecular H_2 and D_2 79−33707
SiO_2, glass, refractive index, effects of alkali oxide comp. changes *(Russian)* 78−22182
SiO_2 glass, sputter yield peak ang. var. 77−32484
SiO_2 glass, Suprasil I, electric dipole moment distrib. of values 79−61299
SiO_2 glass fibre, plastic-coated, liq. N_2 strength 80−58707
SiO_2 glass fibre drawing, caustic curves in solidified drawdown zones 77−39117
SiO_2 glass fibres, stimulated Raman scattering spectra 78−66869
SiO_2 glasses, opt. consts. in IR and vacuum UV 78−27238
SiO_2 glasses, radial distrib. functions 80−44136
SiO_2 glasses, spectral emittance at high temps. 80−96674
SiO_2, glassy, small-angle neutron scatt. obs. 77−7677
SiO_2, glassy-amorphous, light scatt. exam. 78−14281
SiO_2 glassy-amorphous system, struct. *(German)* 78−38626
SiO_2, glassy-amorphous structures, obs. by laser scatter light *(German)* 79−69015
SiO_2 grown anodically over Si, optical and electrophys. props. 77−72934
SiO_2 grown on polycrystalline Si, DC conduction obs. 77−76989
SiO_2 grown on polycryst. Si, surface asperity mechanism of cond., SEM obs. 78−19153
SiO_2, growth and thermal evaporation kinetics of oxide film on Si surface 78−3246
SiO_2, growth kinetics on Si by low-temp. oxidation of monosilane 77−8763
SiO_2 growth under deposited TiO_2 film on Si during postdeposition high temp. annealing 80−15400
SiO_2, HCl-grown oxides, characterisation of surface states using MOS transient currents 80−65696
SiO_2 HF plasma sputtered dielectric layer thickness and refractive index obs. 79−56931
SiO_2, HF vapour phase etching, prod. viability for semicond. manufacturing and reaction model 80−81219
SiO_2, heat of adsorption of various mols. by IR spectroscopy 77−55447
SiO_2, high field electronic props. 78−30930
SiO_2, high field electron capture by screened Coulomb attractive centre 79−56237
SiO_2, high press. supercooled liq., density max. 77−1162
SiO_2, high temp. amorphous film, transport props., prep. conditions effect 77−12040
SiO_2, high temp. compatibility with BN 77−24995
SiO_2, high temp. plasma, emissivity and opacity, photon group means 77−7573
SiO_2, high-field electron trapping, I-V characts. of MOS capacitor 78−6449
SiO_2 high-frequency sputtered optical coatings 79−76900
SiO_2, high-low cristobalite transitions, DTA meas. 79−82335
SiO_2, highly dispersed, produced by plasmochemical method, adsorption props. *(Russian)* 77−70275
SiO_2, homogeneously doped matrix, trace element standard prod. for neutron activation anal. 78−7289
SiO_2, hydrated vitreous, spectrum of low-energy dipolar states, dielec. const., dielec. losses and relax. 77−90098
SiO_2 hydrosols, diffusion coeffs. and characterisation by photon correl. spectrosc. *(German)* 79−29418
SiO_2, hydrotreating catalyst, oxidic precursory state of Co-Mo 79−61898
SiO_2, hydroxylated amorphous, small-particle dynamics, neutron scatt. 80−79899
SiO_2, ideal β-cristobalite struct., one-electron energy bands determ. 79−42452
SiO_2 implantation with Al, in MOS struct., trapped charge location, using photo I-V technique 79−15227
SiO_2, implanted, in MOS capacitor, direct current/voltage relns. as function of oxide doping 80−88635
SiO_2, implanted ^{222}Rn TIPAC measurements 78−43732

silicon compounds continued
SiO_2, impurity redistrib. in Si-SiO_2 during oxidation, numerical soln. including interfacial fluxes 80−25888
SiO_2, in diatoms, 20000 yr O isotope record in deep-sea sediments 78−32247
SiO_2 in FET, electron trapping due to electron beam deposited Al 78−80060
SiO_2, in IGFET struct., thermal reemission of trapped electrons 79−42650
SiO_2, in MIM struct., dye sensitisation of photocond., steady state and pulse photoelectric props. 78−6408
SiO_2, in MIS structures, polarisation hysteresis, ion motion *(Russian)* 80−54793
SiO_2 in MOS struct., electron trapping centres, photocurrent response 77−39947
SiO_2, in MOS struct., current and C-V instabilities at high fields 77−80841
SiO_2, in MOS struct., charge transport, TSD obs. 77−89870
SiO_2, in MOS struct., thermally stimulated ionic cond. 78−10565
SiO_2 in MOS struct., exciton transport rel. to surface states 78−34901
SiO_2 in MOS struct., room temp. cond., mobile Na^+ location 78−39217
SiO_2, in MOS struct., fast surface states density, electron irrad. effects 78−88042
SiO_2, in MOS structure, fast surface states and space charge, β-ray effects 77−55610
SiO_2 in MOS structure, Cl conc. effect on negative bias instability 77−59332
SiO_2, in MnZn ferrite, effect on mag. props. and microstructure, origin of core losses 78−64225
SiO_2, inclusion in steel, effect of high temp. heating on size, number and distrib. 78−44145
SiO_2, inhibitory additives, for anatase-rutile transition *(Japanese)* 78−95744
SiO_2, insulating films, neutron activation anal. and autoradiography 78−92574
SiO_2, interfacial chemistry with deposited Ba, AES obs. 80−44434
SiO_2, intrinsic luminescence 80−16098
SiO_2, ion implanted, fused, refr. index profiles 80−54272
SiO_2 ion implanted, radiation defects and optical props. 80−107293
SiO_2, ion irrad., H capture, absorpt. bands *(Russian)* 78−76505
SiO_2, ionicity dependence of defect reactions and negative-U states in glasses 80−88511
SiO_2 irradiated film, electron and hole trapping 80−11098
SiO_2 isolated GaAs-GaAlAs DH laser compared with O^+ isolation 80−74382
SiO_2, isotopically enriched target preparation using electron gun 80−23226
SiO_2, junction microresistor prepared by double ion implantation of ^{11}B and ^4He, ^{20}Ne, ^{40}Ar, ^1H 77−15432
SiO_2, LVV Auger spectra 79−52055
SiO_2 laser coating, UV damage obs. 80−33056
SiO_2, laser drawn fibers, tension rel. to drawing vel. and ultimate strength 78−74986
SiO_2, laser irradiated, in-depth and surface temp. meas. by Moire-Schlieren technique 80−53392
SiO_2, laser Raman spectra of adsorbed organic mols. 77−3367
SiO_2, laser-fusion microballoon, expansion density profile, 10.6 μm irrad. 78−86686
SiO_2 layer, on Si, XPS, data evaluation 79−65975
SiO_2 layer, thickness measurement by secondary electron emission 80−57435
SiO_2 layer anodically grown on high resistivity n-Si wafer, improved homogeneity 79−24642
SiO_2 layer formation on polycryst. Si, morphological aspects 80−76388
SiO_2 layer in Al-SiO_2-Si struct., mobile ion neutralisation, TSC and C-V characts. meas. 79−95503
SiO_2 layer laser annealing in Si 80−97505
SiO_2 layer of MOS structs., centroid location of implanted ions by photo I-V technique 79−24079
SiO_2 layer on Mo film, passivation against IR reflectance losses caused by oxidation 79−3758
SiO_2 layer on Si, effect on diffusion of Ga 78−51574
SiO_2 layer thickness effect, in MNOS capacitors, 'write' characteristics 78−34904
SiO_2 layer used for MOSFETs, electron trapping behaviour 80−92981
SiO_2 layers, anodic oxidation growth on p-Si, transmission electron diffr. obs. 79−28241
SiO_2 layers, crystallisation, structural props. rel. to annealing 78−34724
SiO_2 layers, DC current-voltage behaviour 77−85333
SiO_2 layers, dielectric strength, dislocation effect 78−31154
SiO_2 layers, in MOS struct., hole trapping induced by ion implantation and annealing at room temp. 80−54792
SiO_2, layers, on Si substrate, IR optical props. 79−56780
SiO_2 layers, passivating, deposition by plasma decomp. in planar reactor 78−88430
SiO_2 layers, room temp. transforms induced by diethyl ether vapour 79−99456
SiO_2 layers, thermally grown, undoped and ion implanted, elec. props. 78−23187
SiO_2 layers in LSI cct. device, cathodoluminesc. obs. 80−80867
SiO_2 layers on Si, ionis. thresholds of electron traps 80−92983
SiO_2, lifetime of carriers and excitons before self trapping 77−85236
SiO_2 light emission from sputtered O atoms or ions 80−58199
SiO_2 lightweight 370 mm mirror fabrication and testing 78−57447
SiO_2 liq. cryst. alignment films prod. by RF plasma beam technique 80−76198
SiO_2, low press. CVD production processes 77−77395
SiO_2, low pressure CVD, thermochemical calcs. 80−108356
SiO_2, low temp. CVD on n-InSb, surface quality improvement and characterisation 80−49932
SiO_2, low temp. vapour phase growth 79−95936
SiO_2, low tridymite, cryst. struct. 78−36150
SiO_2, low-pressure deposition from tetraethylorthosilicate, modelling 79−87582
SiO_2, MIS devices, radiation induced charge storage 80−6997
SiO_2 MOS capacitor, defect current obs. 80−92987
SiO_2, MOS gate insulator, mobile K ions 77−47623
SiO_2 MOS structure, Cl role in passivation 79−91150
SiO_2 MOS structures, removal of electron traps by RF annealing 80−44728
SiO_2 MOS system, current transport, T-D emission theory 79−91149

silicon compounds continued
SiO_2 MOST-transistor struct., breakdown-initiated negative resist. device 80−20314
SiO_2 magnetron sputtered film, oblique deposition effect on growth rate, etching rate, and struct. *(Japanese)* 80−54555
SiO_2, magnetron sputtering, compared with CVD 77−77381
SiO_2, masking film in alkaline etching 80−71771
SiO_2 massive dielectric target, 5-25 keV electrons penetration characts. 80−70260
SiO_2, melting curves at high press. 77−11672
SiO_2, microprobe state anal. by X-ray OK and BK emission band spectra *(Japanese)* 78−19606
SiO_2, mobility and trapping of ions, Si-SiO_2 interface states 80−92985
SiO_2, mobility of K^+ ions, triangular voltage sweep technique 79−95206
SiO_2, mol., ab initio SCF calcs., ground state stability, struct., vibr. freqs. 78−86781
SiO_2, molten, struct., X-ray radial distrib. anal. 78−67651
SiO_2, molten, viscosity, 2300 to 2600K 79−37863
SiO_2 monolayer, core excitons and inner well resonances in surface soft X-ray absorpt. spectra 80−40187
SiO_2 multimode fibre stimulated Raman scatt. obs. 78−1396
SiO_2, multiple trapping model and hole transport 78−6394
SiO_2, muonium and positronium form. 79−56679
SiO_2, negative muon capture, rel. probability meas. 77−50550
SiO_2, neutralisation of mobile ions, in Al-SiO_2-Si MIS diode *(Japanese)* 79−73591
SiO_2, new catalyst for CO-H_2O induced coal liquefaction 80−30335
SiO_2, new high-pressure modification 78−75825
SiO_2, Ni dispersed epitaxial layer, textural effects on catalyst, ferromag. reson. 78−23963
SiO_2, non crystalline, exam. of O_2 transport phenomena correlations 78−47581
SiO_2, nonaqueous dispersions stabilised by terminally-grafted polystyrene chains 79−39219
SiO_2, noncryst., in MOS struct., Na ion impurities motion 78−10223
SiO_2, noncryst., MOS structure, ionic impurities motion, trapping layers 78−30999
SiO_2 nonporous film, plasma deposition method, appl. to semicond. device manufacture *(Russian)* 80−16197
SiO_2, nucleating agent in isothermal crystn. of isotactic polystyrene 79−24807
SiO_2 nucleation of isotactic polystyrene, spherulite radial growth retardation 80−107066
SiO_2, numerical anal. of kinetics of space charge formation, rel. to irradiation *(Russian)* 79−78243
SiO_2, OH group interactions, IR and Raman spectra 78−80383
SiO_2, of albumin 80−10777
SiO_2 on BeO surface, effect on TSEE 80−76159
SiO_2 on Si, chem. stability of films produced by catalytic oxidation 77−86353
SiO_2 on Si, dissolution and corrosion in high temp. water and moisture 77−48564
SiO_2, on Si, H_2 and D_2 ion bombardment effects 80−34086
SiO_2 on Si, ion bombarded surface, de-excitation processes 77−16446
SiO_2 on Si, MOS interface states density, transient capacitance meas. eval. 80−92989
SiO_2 on Si, optical monitoring of etching using grating 78−76775
SiO_2, on Si, reduction by heating in Ga mol. beam at 800°C 80−50730
SiO_2, on Si, thermal growth kinetics, oxidation profile meas. 78−88551
SiO_2 on Si, thermally grown, breakdown, review 78−23172
SiO_2, on Si, viscous flow meas., 960 to 1075°C 77−39729
SiO_2, on Si (111), EXAFS 79−95876
SiO_2, optical absorpt. and external photoeffect, 6 to 40 eV 77−55802
SiO_2, optical coating in liquid, laser damage 77−61994
SiO_2, optical coatings, laser damage resist., spectral depend. 77−62022
SiO_2, optical constants at 5461 Å 78−92043
SiO_2, optical fibre, phys. behaviour of neck-down region during furnace drawing 78−83127
SiO_2 optical fibre, single-mode, CW three-wave mixing 79−10352
SiO_2, optical fibre, tensile strength distrib. and gauge length extrapolation 78−9434
SiO_2 optical fibre, three-wave stimulated Raman scatt. obs. *(French)* 80−78902
SiO_2 optical fibres, plastic-clad, short-term transient radiation effects 79−50420
SiO_2 optical fibres, self-phase modulation 78−66874
SiO_2 optical fibres intrinsic attenuation 78−30067
SiO_2, optical film cross sections, SEM and TEM 77−19387
SiO_2, optical waveguide form. by low energy electron irrad. 77−7189
SiO_2, orthosilicates, mica, soft X-ray spectra and photoelectric yield spectra 78−72640
SiO_2, oxide growth in HCl-O_2 mixture, ellipsometric meas. 78−7073
SiO_2, P-doped amorphous, porous and hydrophilic, water adsorpt. and IR spectra obs. 80−80061
SiO_2 particles, movement and heating in air plasma jet *(Russian)* 80−7522
SiO_2, particulate emission from calcining of clay, removal using electrostatic precipitator 79−24925
SiO_2 particulate filled polyurethane foam, mechanical props. 79−11666
SiO_2 particulates dispersed in CVD reactor, size distrib., semi-in situ obs. by light scatt. 78−27406
SiO_2 passivation films, advances in deposition processes review 78−23620
SiO_2, phase an amplitude relations between fundamental and second harmonic SAW 77−69157
SiO_2 phase equilibrium and microstructure interpretation 80−60847
SiO_2, phonon echos in SiO_2, ADP, KDP, and Rochelle salt *(Japanese)* 79−51213
SiO_2, phonon spectroscopy, amorphous versus crystalline material 78−83898
SiO_2, photoemission and X-ray emission spectra calc. 77−89866
SiO_2, picosecond laser induced breakdown at 5321 and 3547 Å, freq. depend. 77−63495
SiO_2, planarised sputter deposition 78−75959
SiO_2, plasma etching, control of relative etch rates 77−44390
SiO_2, plasma etching, effect of O_2 additions to CF_4 plasmas 78−72908
SiO_2, plasma etching, mass spectroscopic exam. 78−72909
SiO_2, plasma etching, using tetrafluoromethane plasma, O_2 addition effects 78−75363
SiO_2, plasma etching characts., effect of dark space in RF flow discharge 79−15830
silicon compounds continued
SiO_2, plasma etching with hexafluoroethane in radial flow reactor 80−76391
SiO_2, plasma-chemical etching, spectroscopy 80−85243
SiO_2, polymer clad optical fibre, ionising radiation effect 78−42405
SiO_2 polymerisation and deposition from dil. solns., kinetics, 5-180°C 80−7790
SiO_2 polymorphs, CNDO/2 MO calc. 80−6386
SiO_2, polymorphs (cristobalite and tridymite), vibr. normal modes, GVFF calcs. 78−51627
SiO_2 powder, positron annihilation quanta ang. distrib. 77−28642
SiO_2, powder, positronium fine struct. interval meas. by Zeeman transitions 78−95616
SiO_2 powder, surface modes, IR spectra 78−92063
SiO_2, powder support for MnO_2 catalyst, N adsorption obs. of dispersion modes 80−81363
SiO_2 precipitation in Si, effect on generation currents in MOS capacitor 79−78188
SiO_2, prep. by O_2 implantation into Si 77−80523
SiO_2 prepared in O_2-HCl and H_2O-HCl ambients, Cl conc. profiles using SIMS 79−65110
SiO_2, prop. of insulating film for tunnelling study on zero bias anomaly in Pb-SiO_2-$Pb_{0.8}Sn_{0.2}Te$ 79−15608
SiO_2 protective coating formation on SiC *(German)* 80−25885
SiO_2, proton induced ionisation, energy dépendence of K_β/K_α intensity ratio 80−60716
SiO_2, pseudopotential study of bonding and structure 78−75622
SiO_2, pyrolitic films, Ge substrate ellipsometry, TEM, electron diffr. studies of struct. 78−10297
SiO_2, pyrolytic, in MOS struct., C-V characts., non-equilib. lowering in inversion mode 77−55630
SiO_2 pyrolytic film, conduction process determ. 77−20479
SiO_2, quantitative anal. with SIMS 80−101052
SiO_2, quantity anal. of O ions, meas. of chemical shift in Si2p binding energy, using ESCA *(Japanese)* 78−48274
SiO_2 quartz glass sputtering by high frequency plasma, deposition products study *(Russian)* 77−21023
SiO_2, RF cosputtering with CeO_2 or TiO_2 optical film prep. and props. 78−6849
SiO_2 RF magnetron sputtered coatings for laser fusion targets 80−35089
SiO_2, RF plasma etching for IC processing, mechanistic considerations for selective etching 78−64754
SiO_2, RF sputtered, stoichiometry and atomic defects obs. 79−60647
SiO_2 RF sputtered film, Na^+ motion, small-voltage elec. response 79−90822
SiO_2, RF sputtered films, anomalous etching phenomenon 80−3226
SiO_2, RF sputtered films, AC conductivity and conduction mechanisms 80−20338
SiO_2, reaction cured glass insulation coating, space shuttle, combined load testing at 1100°C 79−34261
SiO_2 reactions with FeOOH crysts. prepared by hydrolysis 78−35678
SiO_2, reactive ion beam etching expts., selectivity, anisotropy 80−104308
SiO_2, reactive ion etching, reactant supply 79−83349
SiO_2, reactive ion etching damage, electron trapping characts. in MOS struct. 79−90704
SiO_2 reduction, with C and SiC, forming SiO vap. 79−79240
SiO_2, reduction by C using a plasma, thermodynamic computer anal. 77−40530
SiO_2, reduction by Mg vapour, reaction mechanism, SEM obs. 77−1944
SiO_2, reduction with C black in plasma reactor, feasibility of Si production 78−27426
SiO_2 reinforced decorative laminates, abrasion resistance, abrasive paper deterioration 77−16696
SiO_2, rel. to seawater Al concentration and distrib., control by biological activity 78−61437
SiO_2 relief, plasma etching, tapered wall prod. 80−97606
SiO_2, rippled deposits, form. in heat exchanger tubes 79−1087
SiO_2, SAW resonator transverse modes, effects of anisotropy 78−5609
SiO_2 samples with high specific surface areas, positron lifetime meas. 78−92141
SiO_2, seawater composition over opaline sediments 80−51419
SiO_2, selective etching, using reactive ion etching with CF_4-H_2 80−3224
SiO_2, selective etching rel. to Si by plasma reactive sputter etching 80−81221
SiO_2 separation below 500°C, state and tendency of chemical gas phase separation *(German)* 80−100794
SiO_2, shock compression at high press. *(Russian)* 80−92608
SiO_2, Si rich, CVD film prep. and props. 78−76607
SiO_2, Si X-ray absorption K-edges, charact. parameters *(Russian)* 79−47541
SiO_2, silica, amporphous, acoustic absorpt. in range 1 to 20K and 15 to 65 MHz 77−24357
SiO_2, silica, optical fibre-drawing, vac. furnace 78−66960
SiO_2, silica fibre, transmission of high power laser radiation, role of stimulated Raman scatt. 79−37011
SiO_2, silica fibres, contamination with furnace drawing, losses 77−42634
SiO_2, silica optical fibres, silicone clad, in flat cable form, characts. 78−66930
SiO_2, silica optical fibre preforms, OH-ion distribution 79−14121
SiO_2 single-mode optical fibre, wavelength dispersion characts. in low-loss region 80−53423
SiO_2, small amorphous particles, high resolution TEM 79−82157
SiO_2, smoke-particel aggregates, long-range correlations 79−46369
SiO_2, solid solubility in MgO 80−15247
SiO_2, solid state reaction with Ti film, backscatt. anal. 80−34257
SiO_2 sols and gels, low angle X-ray diffr., pore or particle size distrib., calc. 77−39512
SiO_2, space charged particle environment effect 80−69472
SiO_2, sputter deposition onto GaAs, and MIS struct. characts. 77−89864
SiO_2, sputtered, facet protection of (AlGa)As lasers 79−81444
SiO_2, sputtered, reactive ion etching in CF_4 plasma, competitive mech. 79−91816
SiO_2 sputtered film as Zn-diffusion mask for GaInAsP-InP planar stripe lasers 80−48249
SiO_2 sputtered film performance as acoustic antireflection coating at sapphire-H_2O interface 80−106686
SiO_2 sputtered films in thin film transistors, trapping centres 80−7014
SiO_2, sputtered insulator film contouring over substrate topography 77−8752
SiO_2 sputtered layers for semicond. devices, effect of impurities on elec. props. *(German)* 77−16495

silicon compounds continued
SiO_2, stacked-struct. improved quality by laser annealing of Si 80−65386
SiO_2, stishovite, electronic struct. determ. by X-ray spectroscopy 79−8210
SiO_2, stishovite, single cryst. anal. of struct. 78−53648
SiO_2, stishovite, synthetic polycrystalline, thermal diffusivity meas. 79−39706
SiO_2 stishovite, thermal cond. up to 40 kbar 79−1533
SiO_2, stoichiometric condensate form. during electron beam evaporation of quartz, electrophysical props. 77−16496
SiO_2, struct. of $L_{2,3}VV$-Auger line, rel. to soft X-ray spectra 78−2953
SiO_2, structural transforms., model, on chemically etched Si during thermal oxidation 78−79557
SiO_2 substrate, for interdigital transducer *(Czech)* 80−19201
SiO_2, substrate, glow discharge effect on surface props. and struct. 78−85201
SiO_2 substrate, nucleation of CVD Si in SiH_4-HCl-H_2 system at high temp. 80−49538
SiO_2 substrate, obliquely evaporated for cyano-biphenyl LC, alignment 80−79677
SiO_2 substrate for Pt-Ni vacuum condensates, X-ray anal. *(Russian)* 80−70559
SiO_2 substrate reaction with thin metal films obs. 78−51851
SiO_2 surface, adsorpt. pot. and electrophysical props. *(Russian)* 79−91123
SiO_2 surface, Ar plasma-treated, O_2 adsorption reactivity, EPR obs. 79−51418
SiO_2 surface, N_2^+ bombardment, 500 eV chem. reactions, XPS and UPS 78−48265
SiO_2, surface, NH_2 photodissoc., rate, mechanism *(Russian)* 78−53233
SiO_2, surface, plasma etching in CF_4-H_2 glow discharge, AES meas. 79−98922
SiO_2, surface and interface phonons in bonded solids 78−71931
SiO_2, surface characterisation by free radical spin labels 77−90701
SiO_2, surface charge, effect of doping with P+B, differing vacuum deposition conditions *(French)* 77−85286
SiO_2, surface defect studies, AES, theoretical model, and expt. 79−7738
SiO_2 surface defects, influence of adsorbed O_2 EPR spectra 80−7163
SiO_2, surface electronic struct., electron irrad. effects, EELS study 80−24985
SiO_2, surface etching by laser-generated free radicals 80−71772
SiO_2, surface pot. during ion implantation 80−19826
SiO_2, surface reactivity modification by Ar/O_2 plasma treatment 78−64890
SiO_2 surface reactivity with water and acid mols. *(French)* 79−79284
SiO_2, surface roughness effect on 1064 nm 150 ps laser pulse damage 79−14013
SiO_2 surfaces, bonding of Cu^{2+}, Cr^{3+}, Co^{2+} ions, EPR, optical spectroscopy investig. *(German)* 79−95266
SiO_2 surfaces, charging and dissociation, AES meas. 77−59650
SiO_2, surfaces, electronic struct. calc., scattering theoretic approach 80−6940
SiO_2, surfaces etched in CF_4 or CF_4-O_2 plasma morphology 80−93671
SiO_2, synthesized tridymite, thermal changes, X-ray and optical studies 79−65020
SiO_2 system, spatial-symmetry laws of cryst. lattices 80−19784
SiO_2 tapered layers for optical couplers, photolithographic fabrication processing sequence 79−41464
SiO_2, tensile and compressive strengths of fine powder bed *(Japanese)* 80−25780
SiO_2, tetrahedral glass, Raman studies 78−71823
SiO_2, thermal, elec. stressed film, dielec. breakdown 78−64322
SiO_2, thermal decomposition, appl. to solar energy storage 80−76656
SiO_2 thermal film, freon ion beam etching, IR study *(Russian)* 80−76095
SiO_2 thermal films, hole and electron trapping density reduction 80−2400
SiO_2 thermal growth, stress meas. 79−91812
SiO_2, thermal growth kinetics, in O_2/N_2 mixture, 950- 1100°C 77−86202
SiO_2, thermal oxide layer on Si, chemical shift meas. by ESCA *(Japanese)* 79−61761
SiO_2, thermal oxide layer on SiC, AES *(Japanese)* 79−96386
SiO_2, thermally grown film, optical absorption and photocond. 78−64421
SiO_2, thermally grown films, LF conductance 78−80081
SiO_2, thermally grown films, thicknesses-30-600 Å, defect density meas. 80−84412
SiO_2 thermally grown insulating film on Si, electron injection 78−23176
SiO_2 thermally-grown, highly stressed ultrathin films, cond. and trapped of electrons 77−66216
SiO_2, thermoluminescence, in H_2O vap. atm., temp. depend., time decay *(Russian)* 77−44074
SiO_2, thermophoretic deposition of small particles in MCVD process 79−52123
SiO_2 thin dielectric films in MOS structures, elec. props. with DC voltage *(Slovak)* 80−88634
SiO_2 thin film, elec. breakdown voltage vs. thickness 78−2602
SiO_2, thin film, obtained by oxidising SiH_4 in HF gas discharge plasma 77−11804
SiO_2, thin film, prep. from low-temp. oxidation of tetraisopropoxysilane, dielec. props. 77−8759
SiO_2 thin film capacitors using polycrystalline Si and Al electrodes, dielec. breakdown 79−69600
SiO_2, thin film coated sample, absorptive laser damage analysis by Weibull distrib. 80−33061
SiO_2 thin film grating for $LiNbO_3$:Ti waveguide mode convertor and reflector 80−64216
SiO_2 thin films, comparison of RI and IR spectra 80−11497
SiO_2 thin films, mobile Na ion passivation in HCl oxides 79−70187
SiO_2 thin films, oxide damage due to ion processing 79−24088
SiO_2 thin films, plasma deposition in prod. planar reactor 80−2966
SiO_2 thin films, radiation-induced trapping centres, rel. to MOS transistor technology 80−107804
SiO_2, thin films on rough polycryst. Si surfaces, oxide thickness and refractive index meas. 80−93422
SiO_2 thin films RF sputtering, homogeneity improvement using mag. quadrupole field, expt. *(Croatian)* 78−48316
SiO_2 thin thermally grown oxide layers etching in HCl, ellipsometric control of Si surface form. *(Russian)* 80−104315

silicon compounds continued
SiO_2, three-component glass, liq. phase separation, with two oxide modifiers 80−103250
SiO_2, transfer in quartz capsule 79−4902
a-SiO_2, transient photocond. simulations using multiple-trap model 80−49801
SiO_2, transparent film on Al, refr. index, thickness, ellipsometric meas. 77−52195
SiO_2, transport of electrons at high electric fields 80−20208
SiO_2, trapping level exam. by thermally stimulated discharge of capacitor *(Russian)* 78−34845
SiO_2, tridymite, non-integral phase from 150°-190° 79−99144
α-SiO_2, trigonal crystal, optical heterodyne detection using collinear acousto-optic interaction 78−66927
α-SiO_2, trigonal crysts., anisotropy of linear electrooptic effect 80−34894
SiO_2, tunnelable film form. using vap. O_2 source at liq. N_2 temp. 78−76774
SiO_2 tunnelling barrier asymmetry to electrons and holes in MOS struct., photocurrent 80−75645
SiO_2, UV visible absorpt. by laser calorimetry, wavelength modulation spectroscopy 78−66876
SiO_2 ultra-thin film composites of FET wafers and devices, thickness determ. by microprobe technique 77−36397
SiO_2, ultralow loss optical fibre material, loss mechanism 80−78920
SiO_2 ultrathin layers, refr. index meas. 80−103936
SiO_2, ultrathin layers on Ge substrate, ATR spectra, thickness depend., struct. obs. 80−55214
SiO_2 undoped film, cathodoluminescence *(Russian)* 80−40164
SiO_2, uniform film prep. by pyrolysis of tetraethoxysilane 77−40379
SiO_2, vacuum deposited, 7-10 μ, microhardness and structure 78−19669
SiO_2, valence band density of states from self-deconvolution of $L_{23}VV$ Auger spectrum 79−47561
SiO_2, vaporisation in steam atmosphere 80−44306
SiO_2, vitreous, band limits and vibrational spectra 79−73935
SiO_2, vitreous, charged defect centres 80−107745
SiO_2, vitreous, colour centres, dangling bond defects, radiation effects 78−71732
SiO_2, vitreous, compaction dependence on ionisation dose 78−67738
SiO_2, vitreous, D_2 diffusion and solubility, 0-800°C, interaction with structural OH 77−89585
SiO_2, vitreous, dielec. absorpt. saturation, 0.4-8K 78−23394
SiO_2, vitreous, effect of neutron irrad. on low temp. dielec. susceptibility 79−73878
SiO_2, vitreous, effect of high-dose X-rays and reactor radiation 80−19838
SiO_2, vitreous, electron irrad., vol., refr. index and stress changes 77−47482
SiO_2, vitreous, electron irrad. effect on sp. ht. 79−65212
SiO_2, vitreous, exam. of electron excitations and intrinsic defects 78−87905
SiO_2, vitreous, existence of gap in low-energy density of states 79−60769
SiO_2, vitreous, fast neutron irrad. effect on struct., interstitials role 78−26599
SiO_2, vitreous, fast neutron irrad., low temp. US meas., two-level systems role 78−30703
SiO_2, vitreous, grown from vapour, gamma ray irradiated, ESR and thermoluminescence exam. 78−88189
SiO_2, vitreous, H impregnated, Raman spectroscopy 77−36230
SiO_2, vitreous, H impregnated, γ radiation effects, hydride, hydroxyl formation 79−87874
SiO_2, vitreous, He solubility, 100 to 1350 atm., 5 to 80°C 79−4414
SiO_2, vitreous, heat treatment effect on viscosity and struct. 80−19714
SiO_2, vitreous, hydroxyl free, reaction with H, diffusion, absorpt. spectra 80−85210
SiO_2, vitreous, hypersound velocity meas. from Brillouin scatt. freq. 80−27349
SiO_2, vitreous, III-V analogues and bonding topology 79−73102
SiO_2, vitreous, impurity C determ. by isotopic spectral method 80−26093
SiO_2, vitreous, intrinsic radiation defects, nonbridging O 80−19837
SiO_2, vitreous, irradiated, EPR exam. of H_2 hyperfine spectra 79−28611
SiO_2, vitreous, LO vibrational modes, Raman and IR spectra 77−7819
SiO_2, vitreous, laser-annealed surface, characterisation by ellipsometry 80−103544
SiO_2, vitreous, low temp. sp. ht., effect of heat treatment 78−59955
SiO_2, vitreous, low temp. thermal props. and intrinsic defects 80−29057
SiO_2, vitreous, multiphonon IR absorpt. 80−25381
SiO_2, vitreous, neutron irrad. effects on heat capacity, thermal cond., US velocity temp. depend. 78−83851
SiO_2, vitreous, non-bridging O centre, optical props. and energetic struct. 80−34976
SiO_2, vitreous, O and Si diffusion-controlled processes 80−79981
SiO_2, vitreous, paramag. centres associated with bonding defects 80−80609
SiO_2, vitreous, photoelectric and photoluminescent props. in fundamental absorpt. region 78−39596
SiO_2, vitreous, polished surfaces, environment sensitive, ellipsometric obs. 77−48559
SiO_2, vitreous, pure and Ge doped, luminescence centres at 396 and 280 nm 80−103996
SiO_2, vitreous, quant. X-ray anal. of cristobalite 80−88049
SiO_2, vitreous, Raman active defects, thermal equilibration 80−55092
SiO_2, vitreous, Raman cross sections, rel. to appl. in fibre Raman lasers 78−31176
SiO_2 vitreous, Raman spectrum, bound OH, Si-O stretch vibr. 78−19462
SiO_2, vitreous, resist. to NaOH 80−21143
SiO_2, vitreous, spin-lattice relaxation times of paramag. hole and E_1'-centres 80−39871
SiO_2, vitreous, strengthening by coating application 77−32636
SiO_2, vitreous, struct. and phonon spectra 80−50324
SiO_2, vitreous, substrate for PbO film, interdiffusion reactions, UV spectroscopy obs. 78−51750
SiO_2, vitreous, Suprasil-I, spectral diffusion at 0.5K, acoustic hole burning expts. 79−60439
SiO_2, vitreous, Suprasil-W, short time scale transient temp. profiles, time-depend. sp. ht. 79−60519
SiO_2, vitreous, Suprasil-W, thermal diffusivity, 16 mK-2.3K 79−60563
SiO_2, vitreous, thermal expansion reference data: 1-1000K 80−96669
SiO_2, vitreous, US velocity, freq. and temp. depend. 78−63812

silicon compounds continued
SiO_2, vitreous, valence-attenuation pair defect, states, IR and Raman spectra 79−91442
SiO_2, vitreous, viscosity meas., review 80−103513
SiO_2, vitreous, X-ray compaction efficiency 80−65044
SiO_2, vitreous and cristobalite, interstitial struct. anal. from gas solubility data, review 79−23525
SiO_2, vitreous and neutron irrad., thermal cond., heat treatment effect 79−90837
SiO_2, vitreous Brillouin scatt., 35 GHz phonon vel. and absorpt. below 1K 80−100664
SiO_2 vitreous film on Si, defect struct. comparison with crystalline SiO_2 and Si-O bond nature 80−54557
SiO_2, vitreous films on Si, channel and network defects 80−54142
SiO_2, vitreous layers, thermal growth on Si 80−93675
SiO_2 wafers, Au contamination during plasma etching 80−19831
SiO_2, wettability of single crysts. by liq. metals *(Russian)* 77−43408
SiO_2 wideband dielectric mirror production, spectral transmission 79−76897
SiO_2, with embedded Au particles, thin film solar absorber 80−81490
SiO_2, with Ni overlayer, desorption of N and O, 200 to 400K *(German)* 78−30835
SiO_2:^{85}Kr, ion-implanted, impurity distrib. 80−15145
SiO_2:Ag, cryst. and glassy, X-ray induced EPR and luminesc. centre 80−65043
SiO_2:Ag, fused, crystalline, luminescence and colour centre props. 78−10954
SiO_2:Ag, implanted atom, X-ray photoemission obs. 78−39050
SiO_2:Al, vitreous state, EPR of Al defects 78−91951
SiO_2:Al film, ion-implanted, electron trapping behaviour 78−67729
SiO_2:Al gel, gamma rad. effects, depend. of H_2 adsorption and colour centre form. on Al content 79−69156
SiO_2:As, and Si_3N_4 encapsulation of GaAs:Se 79−11715
SiO_2:As^+ implanted layers in MOS struct., electron trapping and detrapping characts. 80−92982
SiO_2:Au, implanted atom, X-ray photoemission obs. 78−39050
SiO_2:Au(Ag)(Cu), XPS line broadening and extra-atomic relax. energies 80−71561
SiO_2:B, B segregation during dry, nearly dry and wet O_2 oxidation 79−66178
SiO_2:B, ion implanted, props. 79−65106
SiO_2:B film, on Si, AES meas. 77−39951
SiO_2:B implanted, thin films, props. *(Polish)* 80−39692
SiO_2:B_2O_3 doped, IR spectra 79−78664
SiO_2:B(P) film, high temp. deposition and evaluation 79−69989
SiO_2:Co(II), adsorption of H_2O, coord. lifetime, surface effect, NMR obs. 80−34299
SiO_2:Cs(B) film, implanted, electronic cond. mechanism in MOS struct. 77−15983
SiO_2:Cu(Ag)(Au), isolation matrix, XPS, atomic electronic struct. 79−89655
SiO_2:F, silica fibres, numerical aperture and attenuation, drawing from preforms 78−1449
SiO_2:F fibre preform plasma chemical deposition *(German)* 78−33926
SiO_2:F fibre preparation by plasma-activated CVD *(German)* 78−33927
SiO_2:F layers, deposition from $SiCl_4$-SiF_4-O_2 gas mixture by plasma CVD method 78−95699
SiO_2:F-ion implanted, mobile-ion drift compensation 79−19664
SiO_2:F(BF_2), ion implanted, F influence on oxidation-induced stacking faults 80−65011
SiO_2:Fe, vitreous and cryst., with or without Al_2O_3, Na_2O additions, exam. of Fe^{2+} coordination, IR spectroscopy 78−88344
SiO_2:Fe^{3+}, vitreous silica, absorpt. spectra and structural state 80−16071
SiO_2:Ga film, impurity distrib. after annealing, neutron activation anal. 80−24484
SiO_2:Ge silica-core fibre-optic waveguides, effect of B, P and OH on radiation response 79−50419
SiO_2:Ge single-mode fibres, dispersion meas., pulse synchronisation technique 80−48410
SiO_2:GeO_2 graded-index fibres, without index dip, fabrication by CVD method 78−9431
SiO_2:GeO_2 optical fibres, definitive profile-dispersion data over extended wavelength range 79−76828
SiO_2:GeO_2 single-mode optical fabre fabrication 79−46050
SiO_2:GeO_2-P_2O_5 graded-index, optical fibres, frequency characts. 80−58669
SiO_2:Ge(P) fibres, pulse delay meas. in zero-material-dispersion region 78−46769
SiO_2:Ge(P) optical fibre, single-polarisation single-mode, exposed cladding fabrication 80−58725
SiO_2:H(D), γ-irrad., hydroxyls and hydrides form., detect. by Raman scatt. 77−32817
SiO_2:Na, film, depth profiling by SIMS 78−79624
SiO_2:Na film, RF sputtered, low elec. field Poole-Frenkel effects in MIM struct. 79−95536
SiO_2:Na^+, heat treated, heat of immersion in H_2O, organic compds. 80−3396
SiO_2:Nd^{3+} films, cathodoluminesc. 80−20717
SiO_2:OH^-, vitreous, elec. dipolar echoes 78−52430
SiO_2:P, diffusion from spin-on source 80−44367
SiO_2:P film, spin-on, diffusion of P into Si 80−2050
SiO_2:P films, P content determ. by IR absorpt. and activation anal. 79−51139
SiO_2:P_2O_5, GeO_2 fibre, anomalous conc. profile of P_2O_5 and GeO_2 77−79943
SiO_2:P_2O_5, optical fibre, stimulated Raman scattering *(French)* 79−27324
SiO_2:TiO_2, prep., amorphous struct., effect of roasting, bonds 78−44061
SiO_2:W film electron trapping characts., obs. by avalanche injection techniques 77−89862
SiO_2:Xe, ion implanted, Xe retention, Rutherford backscatt., comparison with Si-O, Xe 79−4320
SiO_2/Al_2O_3 ratio in zeolite containing catalysts, IR spectra, struct. 79−42958
SiO_2/GaAs, interface reaction during high-temp. heat-treatments 80−88439
SiO_2/GeO_2 fibre, single-mode, numerical aperture effects on optical and mechanical props. 80−69548
SiO_2/InP film/substrate system, interface formation during CVD, modelling 80−24764
silicon compounds continued
SiO_2/InP interface formation, thermodynamic considerations 80−100529
SiO_2/$LiTaO_3$ SAW device, thermal stress effects of acoustic surface waves in layered media *(Japanese)* 79−98573
SiO_2/P_2O_5 fibre, single-mode, numerical aperture effects on optical and mechanical props. 80−69548
SiO_2/Si interface, obs. of chem. struct. 78−27654
SiO_2-Ag, coevaporated films, neutral density filters for near IR radiation 79−72673
SiO_2-Ag film, elect. and struct. props., ion beam sputtering 78−80071
SiO_2-Al and SiO_2-Si in MOS, interface electrochemical obs. 78−2381
SiO_2-Al interface, internal photoemission, phonon scatt. effects 77−85315
SiO_2-Al layered system, complete absorpt. of transverse mag. waves 78−39615
SiO_2-Al_2O_3, calculated thermodynamic data and metastable immiscibility 78−27495
SiO_2-Al_2O_3, coprecipitated gel, Si-Al spinel formation during transformation on heating 79−78958
SiO_2-Al_2O_3, minerals, phase equilibrium *(German)* 77−73261
SiO_2-Al_2O_3, mullite, sintering behaviour and microstruct. 80−20876
SiO_2-Al_2O_3, refractory fibrous heat insulating material 78−6990
SiO_2-Al_2O_3, sintering theoretical treatments and exp. procedure 78−44067
SiO_2-Al_2O_3, surface electron donor sites and acid-base props., adsorbed radical ESR 77−21417
SiO_2-Al_2O_3 (36.6 wt.%) plasma prep. powder, metastable immiscibility and microstruct. during sintering 80−35143
SiO_2-Al_2O_3 based minerals, phase equilib., struct., comp. *(French)* 78−60659
SiO_2-Al_2O_3 glaze, adhesive behaviour of metallic cation glaze exchanged on acid site struct. on steel *(Japanese)* 79−66216
SiO_2-Al_2O_3 melts, densities 79−99259
SiO_2-Al_2O_3 mixture, depend. of phase comp. on nuclei available 79−11584
SiO_2-Al_2O_3 porous catalysts, EPMA quantitative anal., new correction calc. method, modified ZAF method *(Japanese)* 80−93822
SiO_2-Al_2O_3 refractories, thermal shock props., fracture mech. appl. *(French)* 79−96109
SiO_2-Al_2O_3 system, location of metastable immiscibility gap 79−77521
SiO_2-Al_2O_3 system, phase equilibria 79−77724
SiO_2-Al_2O_3-CaO-MgO-TiO_2 system glasses, phase separation and crystn. 77−24384
SiO_2-Al_2O_3-CaO-MgO, liq. silicic and slag, struct, density, surface tension *(Polish)* 78−83711
SiO_2-Al_2O_3-CaO-MgO-NaO-K_2O-B_2O_3-ZrO_2, glaze, exam. of zircon crystallisation 79−19155
SiO_2-Al_2O_3-Fe_2O_3-K_2O, form. of Al-Fe leucite, inversion temp. *(Japanese)* 77−62481
SiO_2-Al_2O_3-MgO-CaO-$Fe_{(l)}$, heterogeneous equilib. calcs. *(Russian)* 77−59093
SiO_2-Al_2O_3-R_2O_3-MgO-TiO_2, T=rare earth of Ce group, glass-ceramic permittivity comp. depend. 77−43928
SiO_2-Al_2O_3-Si_3N_4, isothermal sections, free energy of formation 80−55363
SiO_2-AlN mixture sintering, form. of β-Si_3N_4 solid solns. 78−23655
SiO_2-$Al(OH)_3$, derived from metalalkoxides, sintering behaviour 79−29005
SiO_2-α-Al_2O_3, metastable phase equilib. diagram without mullite 79−4398
SiO_2-B_2O_3 glasses, Brillouin scattering meas. of attenuation and vel. of hypersounds 80−100309
SiO_2-based glassy layers, passivating Cu at 500°C 80−3246
SiO_2-basic oxide system, struct. model 80−54109
SiO_2-borosilicate glass, B diffusion from sputtered glass film into SiO_2 80−29040
SiO_2-C mixture, nitridation to form. Si_3N_4 additives effects, exam. 78−44068
SiO_2-carboxymethylcellulose suspension, filtration eqn. 78−55690
SiO_2-CdSe thin film transistors, slow states, trapping state densities and cross sections 80−15613
SiO_2-CeO_2, multilayer refractory oxide interf. coatings 79−7192
SiO_2-coated rutile, adsorption of N_2 and Ar, 77.4K, microcalorimetry obs. 80−80062
SiO_2-covered Si, ranges of implanted B^+ and B^{2+} 77−31687
SiO_2-encapsulated semi-insulating GaAs, Cr redistrib. during thermal annealing as function of encapsulant and implant fluence 80−84199
SiO_2-FeO_2 particulate mass transfer mechanism in modified CVD, thermophoresis 80−2955
SiO_2-GaAs MIS structures, fabrication and elec. props. 79−47166
SiO_2-$GaAs_{1-x}P_x$:N,Zn ion-implanted multiple layers, ion range distribs., secondary ion microprobe meas. 79−42129
SiO_2-GeO_2, synthetic, struct, IR spectra 79−42993
SiO_2-GeO_2 cored optical fibre, low loss 77−62072
SiO_2-GeO_2 glass, refr. index and density, comp. depend. 78−23424
SiO_2-GeO_2 particles, deposition props. in flame hydrolysis reaction for optical fibre fabrication 80−48470
SiO_2-GeO_2-P_2O_5,optical glass fibre, profile synthesis 77−27333
SiO_2-glass, high-temp. strain relax., optical correlation spectroscopy 77−65951
SiO_2-glass fibres, struct. anal. using X-ray diffr. and optical microscopy 77−65952
SiO_2-InP, interface props., plasma deposited dielectrics, n-channel MOSFET action 80−93003
SiO_2-InP, MIS struct., prod. by pyrolytic deposition resist., breakdown and interface states 77−15961
SiO_2-InP capacitor, carrier generation and trapping 80−49929
SiO_2-InP MOS struct., capacitance-voltage and surface photovoltage meas. 79−60931
SiO_2-InP system, interface and dielec. props. 80−49930
SiO_2-layers, charge transport induced by electron beam, simulation *(German)* 79−51702
SiO_2-Li_2O-Li_2SO_4, glass-forming region, struct. and ionic cond. 80−84320
SiO_2-$LiTaO_3$ structure, SAW propag. characts., thermal strain effects 79−19440
SiO_2-liquid heptane interface, adsorption of organic liqs., IR spectra obs. 79−57295
SiO_2-M_2O (M=Na,K) glasses, temp. depend. of elastic modulus 80−40410

silicon compounds continued
SiO_2-metal codeposited film, optical, elec., mechanical and corrosion props. 77−32708
SiO_2-MgO porous catalysts, EPMA quantitative anal., new correction calc. method, modified ZAF method *(Japanese)* 80−93822
SiO_2-MgO-BaO ceramic, steatite, glass-ceramics technology appl. 80−104097
SiO_2-MgO-CaO, melts, mixing enthalpy, 1700-1873K 78−79785
SiO_2-Mo-SiO_2 thin-film selective coatings for solar energy collectors 78−94422
SiO_2-Na_2CO_3, sodium Erevanit-25, sintering, struct. 79−43284
SiO_2-Na_2O surface, $Ca_3(PO_4)_2$ film form., bonding to bone 80−85212
SiO_2-Na_2O-BaO glass, rare earth doped, nonradiative decay and multiphonon relax. 77−85802
SiO_2-Na_2O-CaO (13, 11 wt.%) glass, phase separation, SiO_2 purity effect 80−44144
SiO_2-Na_2O-CaO:Fe(As)(Cr) glasses, optical absorpt. changes on heat treatment 78−31224
SiO_2-Na_2O-CaO-P_2O_5, BIOGLASS, surface, $Ca_3(PO_4)_2$ film form., bonding to bone 80−85212
SiO_2-Na_2O-Nd_2O_3 glass, magneto-optical props., absorpt. spectrum 80−88969
SiO_2-$Na_2O(Li_2O)$ glasses, bonding of Si-O exam. by X-ray emission spectra 78−52594
SiO_2-Ni granular metal films, minimum metallic cond. 78−56241
SiO_2-PSG-Si_3N_4 composite layer, on Si, crack occurrence, PSG film thickness and comp. effects 77−72806
SiO_2-PbO, interdiffusion layer optical waveguide, prep. and props. 80−43489
SiO_2-polystyrene, glass transition rel. to filler, cooling rate 79−4403
SiO_2-RO-Na_2O-Li_2O (RO=MgO, CaO, SrO) glass-ceramic coating, optimisation of props. by selective oxide action 80−55552
SiO_2-Si, cathodoluminesc. and AES rel. to struct. 78−43937
SiO_2-Si, effects of processing on radiation damage 78−39223
SiO_2-Si, electron photoemission from Si, band struct. effects 79−19977
SiO_2-Si, film-substrate, single reflection retarders for different Hg spectral lines 78−79122
SiO_2-Si, generation of interface states due to emission of leaky electrons 77−62972
SiO_2-Si, hot electron emission into SiO_2 78−30997
SiO_2-Si, influence of oxidation conditions on elec. props. of ultrathin SiO_2 layers 78−39226
SiO_2-Si, interface groups of states, C-V meas. 78−2541
SiO_2-Si, interface states from capacitance-voltage term spectra anal. 77−4446
SiO_2-Si, low-energy neutral particle bombardment of SiO_2 film, degradation 80−54790
SiO_2-Si, P ion implantation, electrical transport props. 80−39130
SiO_2-Si, separation boundary charact., surface oxidation after Ar^+ bombardment *(Russian)* 79−15028
SiO_2-Si, two-layer system, P^+-ion penetration tails, expt. and computer anal. 80−75249
SiO_2-Si (n-type) interface, electrochem. etching 77−11799
SiO_2-Si boundaries, insulator charges evaluation *(German)* 79−82682
SiO_2-Si film-substrate refl. polariser, operation at Hg spectral lines 77−75655
SiO_2-Si in MIS, interface states, thermally stimulated charge decay 77−12009
SiO_2-Si in MOSFETs inversion layer carrier mobility, theory 80−60094
SiO_2-Si interface, An influence studied using threshold voltage shift 79−82672
SiO_2-Si interface, broken symmetry states obs. in inversion layers 78−95125
SiO_2-Si interface, carrier mobility *(French)* 80−65601
SiO_2-Si interface, detection of SiO_2^- ions by SIMS 77−77848
SiO_2-Si interface, doping depend. of interface states and charges 80−92992
SiO_2-Si interface, evolution of surface states density during bias temp. treatment 78−14832
SiO_2-Si interface, hot electron capture process, expt. method for study 79−38180
SiO_2-Si interface, interaction of point defects, electron microscope exam. 77−7979
SiO_2-Si interface, N_2 gas reaction, elec. and structural charact. 77−39950
SiO_2-Si interface, new type of interfacial charge 78−23168
SiO_2-Si interface, quasistatic capacitance-voltage determ. of interface state density, sources of error 77−12011
SiO_2-Si interface, sputter profiling, ion knock-on mixing model 79−83081
SiO_2-Si interface, surface states and elec. defects obs. using ESR 78−23169
SiO_2-Si interface charge inhomogeneities effect on surface state density meas. by MOS AC cond. technique 78−14833
SiO_2-Si interface of hardened MOS capacitors, radiation effects 78−26958
SiO_2-Si interface states, effect on memory charact. of thin-oxide MNOS devices 79−82681
SiO_2-Si interface states, deposition of H containing layers and annealing 80−92991
SiO_2-Si interface state density in ion-controlled diodes, acid-base exposure effects 80−96984
SiO_2-Si interface thermally grown, surface pot. inhomogeneities after stress ageing 80−92993
SiO_2-Si interfaces, surface state form. during bias-temp. stress aging 79−78193
SiO_2-Si interfacial region, nature of fixed oxide charge 78−56047
SiO_2-Si interfacial regions obs., by XPS, ultrathin oxide films 79−15039
SiO_2-Si inversion layer solar cells, radiation effects 77−43244
SiO_2-Si layers, physics, electron and ion motion *(Dutch)* 80−60093
SiO_2-Si MOS capacitor, two-stage process for building up of radiation induced interface states 80−20313
SiO_2-Si MOS system, ion irrad. effects on struct. and electrophysical props. 80−6995
SiO_2-Si stratified system surface charges, adsorption and desorption effects *(Russian)* 80−49942
SiO_2-Si structure, scanning analyser of electrophysical parameters *(Polish)* 79−91145
SiO_2-Si structure P^+ bombardment damage, exoelectron emission obs. 78−95383

silicon compounds continued
SiO_2-Si system, implanted with N, P, and Te ions, reflectance spectra and interference fringes 79−23629
SiO_2-Si:A, effects of recoil-implanted O on elec. activation of As 79−99227
SiO_2-Si:P, P pile-up at interface 78−84303
SiO_2-Si_3N_4, double dielec. layer on Si substrate, ellipsometric parameter meas. methodology 77−63474
SiO_2-Ta_2O_5, plane optical waveguide, fabrication by reactive sputtering 78−71221
SiO_2-Ta_2O_5 film, refr.-index-adjustable, for integrated optical ccts., prep. and props. 78−63203
SiO_2-Ta_2O_5 film channel optical waveguide, fabrication using CO_2 laser 79−27386
SiO_2-TiO_2, multilayer dielec. mirrors, laser-induced damage resist. 79−10335
SiO_2-TiO_2, vitreous, US vel. and absorption 80−107380
SiO_2-TiO_2 antireflection coatings, 1064 nm 150 ps laser pulse damage rel. to barrier layering and smoothness 79−14018
SiO_2-TiO_2 antireflection coating, 1.064 μm laser damage, barrier 80−33059
SiO_2-TiO_2 films, obtained from $Si(OC_2H_5)_4$ and $TiCl_4$, exam. of props. 79−95934
SiO_2-TiO_2 glass phonons, IR and Raman spectra meas. 79−91447
SiO_2-TiO_2 interference filters, narrow band, 0.7 to 1.5 μm spectral region, from cathodic sputtering 79−7221
SiO_2-TiO_2 optical coatings, for Shiva laser optics 79−7135
SiO_2-TiO_2 stack reflector and antireflection coating, 1064 nm 180 ps laser pulse damage 79−14017
SiO_2-TiO_2 system, physicochem. props. of glasses with low thermal expansion coefficient 77−35718
SiO_2-TiO_2 system, true solid soln. existence obs. 77−36475
SiO_2-TiO_2-Al_2O_3-SrO(BaO), glasses, ceramic form. rel. to Al_2O_3 content 77−25005
SiO_2-TiO_2-Na_2O glass, optical absorption coeff., 2.1-3.3 eV 77−77240
SiO_2-$TiO_2(Al_2O_3)(ZrO_2)$, noncrystalline film form., IR study *(Japanese)* 77−59634
SiO_2-water system, inorg. polymer struct. form., globular crystn. 80−101042
SiO_2-ZnO interface, XPS and Auger LMM anal. 79−90893
SiO_2-ZnO-Na_2O-Li_2O, glass-ceramic coating, optimisation of props. by selective oxide action 80−55552
SiO_2-ZrO_2, protective antirefl. coatings, electron beam evaporation on glass 77−31143
SiO_2-ZrO_2 adsorbents, coprecipitated, porous struct. rel. to form. conditions 78−53263
SiO_2-ZrO_2-Li_2O-Na_2O based crystallisable glasses composition and properties 80−50731
SiO_2+F, heterogeneous reaction, discharge-flow tube meas. 80−21274
SiO_2+H_2 reactions, rate controlling processes for H_2 transport in vitreous silica 78−26733
SiO_2+$XeF_2(F_2)(Cl_2)$, plasma etching, electron or ion bombardment, Ar^+ enhancement 79−82073
SiO_2+ZrN, X-ray diffr. phase anal. of reaction products 80−50613
SiO_{2-x}, paramagnetic E centre, reply to comment on new concept of model 80−24445
SiO_{2-x}, paramagnetic E′-centre, comment on new concept of model 80−24444
SiO_{2-x} system, model for paramagnetic E′-centre 78−35034
SiO_{2-x}, vitreous, →β-cristobalite, polymorphic transformation with stoichiometry changes 77−43325
SiO_2:B, P films doped by pyrolisis and ion implantation, IR absorpt. obs. of impurity conc. 77−72802
SiO_2-$LiTaO_3$, temp. compensated SAW device fabrication 79−76923
SiO_2-Si, B ion implanted MOS struct., form. and annealing of radiation damage 79−56321
SiO_4 tetrahedra, mean Si-O bond lengths var. 78−63699
SiO_4 tetrahedra, semi-empirical molecular orbital model, radiation compaction application 79−73433
SiO_4^{4-} compounds, vibr. pot. function, force consts., isotopic shifts, mean vibr. amplitudes 80−23395
SiO_6 octahedra, var. of mean Si-O bond lengths 78−18577
SiO_x, amorphous, ESR and hopping cond., He^+ irrad. effects 79−61213
SiO_x, amorphous and recrystallised layer, optical props. 80−25474
SiO_x amorphous evaporated film with Al electrodes, threshold and memory switching 77−76945
SiO_x amorphous film, dispersion of refr. index and chem. comp. 80−7429
SiO_x amorphous films, acoustic study using Rayleigh waves 80−75312
SiO_x amorphous films, high energy electron diffr. study 80−38911
SiO_x, anodic, on SiC, IR spectra *(Russian)* 78−11376
SiO_x, antireflection coating, 100 ns pulsed laser damage at 2.7 and 3.8 μm 80−33057
SiO_x, chem. shift of Si 2p core level, relax. contrib. 79−47141
SiO_x, core level shifts, nature of bonding 77−84698
SiO_x, dielec. and optical props., chemical disorder effects 80−80815
SiO_x, electronic struct., mixed-crystal and random-bonding models 79−65029
SiO_x, electronic struct., random bonding model 79−82175
SiO_x, evaporated film, influence of electronic leakage current on meas. of ion polarisation 77−63014
SiO_x film, amorphous, AES and EELS characterisation 79−90905
SiO_x film, Cole-Cole diagrams of ionic hopping systems 77−66217
SiO_x film, durable optical, ion plating onto plastics, optical and mech. props. 80−38141
SiO_x film, in MIM sandwich, elec. props. 77−72933
SiO_x film, laser damage mechanisms 77−75592
SiO_x film, MIM struct., DC bias dependent dielectric dispersion props. 78−76178
SiO_x film, reactively evaporated, substrate temp. depend. of optical props. 77−70006
SiO_x film, vacuum evaporated, phase comp., electron spectroscopy obs. 78−60042
SiO_x films, for microelectronics appls., plasma deposition and characterisation 79−78904
SiO_x, freq. and wavenumber depend. dielec. function, bond-charge approx. 79−56155
SiO_x, grown in HCl/O_2 ambients, phase separation and Na passivation 80−3219
SiO_x inclusion formation on introduction of solid SiO into molten steel *(Russian)* 78−80530

silicon compounds continued
SiO_x layers, grown in HCl/O_2 ambients, struct. and comp. 79−42404
SiO_x, metal layer interdiffusion Rutherford backscatt. 77−85000
SiO_x, on Si exposed to O_2, phase comp., electron spectroscopy obs. 78−60042
SiO_x, powder and vac. deposited, amorphous struct., X-ray diffr. meas. 80−1931
SiO_x protected Al mirror, far UV refl., UV irrad. effect 79−7191
SiO_x, SIPOS, O determ. using differential thickness meas. 79−28228
SiO_x semi-insulating polycryst. films, AES and PES studies 80−107939
SiO_x, struct. and coalescence of oxide particles, during internal oxidation of Cu-Ti-Si *(Russian)* 79−90781
SiO_x substrate, growth and struct. of Au island film, effect of perp. elec. field *(German)* 77−76696
SiO_x system, cluster plus effective medium tight-binding study 79−33216
SiO_x thin film dielec., in MIM struct., interfacial props. rel. to non-stoichiometry 80−80399
SiO_x, thin film on YZ-$LiNbO_3$, SAW props. 80−84356
SiO_x thin films, deposition and characterisation study 80−80133
SiO_x thin films on Si, anal. by backscattering techniques 79−96385
SiO_x ultrathin oxide on Si, struct. obs. by high-resolution electron microscopy 80−103592
SiO_x-GaAs, vacuum evaporated system, acoustoelec. signal, interface props. 80−75646
Si_2O_2, tetrahedral edge sharing, distortions, MO calcs. 77−14380
Si_2O_3 smoke, nonequilib. phases condensation from SiO vapour 79−60497
$(Si_2O_7)^{6-}$ bitetrahedra, in silicates, total energy surface, ab initio calc. 78−23056
Si_3O_3, isotopically substituted, IR freq. and intensity patterns 78−21926
Si_3O_3, matrix isolated, IR isotope freq. and intensity patterns 78−46338
$Si_6O_{15}^{6-}$ double chain anion containing anhydrous silicates, synthesis, cryst. chem. 80−59444
Si_xO_{1-x} films, anal. of H ratios and profiling using nucl. techniques and Rutherford backscatt. 80−61202
Si_xO_y structures, $Si(OA)_4$ clusters, A=H,Li,K, HMO calcs., energy stability, charge distrib. *(German)* 79−89822
SiO_2(-Ag), CW CO_2 laser deposited dielect. thin film, optical and struct. props. 80−7506
SiO_2(-GeO_2)(P_2O_5)(B_2O_3), optical attenuation in IR region 77−75665
$((SiO_2)_{45}(CaO)_{55})_{65}$ $(Fe_2O_3)_{35}$ glass, effect of melt atmosphere on mag. props. 78−68299
$Si_2O(Cl_3)_2$, IR and Raman spectra, vibr. anal. 78−66552
$Si(OH)_4$, NO_3^-, PO_4^{3-}, ratios in Moroccan upwelling region 80−4045
SiON/GaAs film/substrate system, interface formation during CVD, modelling 80−24764
SiO_xN_y CVD thin film, multiple internal refl. IR spectroscopy 80−11499
SiO_xN_y, deposition kinetics in SiH_4-CO_2-NH_3-H_2 system 77−48346
SiO_xN_y film, ion beam effects on opt. props. *(Russian)* 77−48265
SiO_xN_y film, on Si, struct. stability 80−54564
SiO_xN_y films, for microelectronics appls., plasma deposition and characterisation 79−78904
SiO_xN_y films on Si, ^{16}O conc. profiles anal., using (d,p) and (d,α) reactions with mag. spectrom. 79−5215
SiO_xN_y, low temp. films, comp., chem. bonding and contamination 78−47676
Si_2ON_2, needle crystals, growth by nitriding process in powder compacts *(Japanese)* 78−76601
Si_2ON_2 needle crystals, growth by nitridation of Si-SiO_2 powder compacts *(Japanese)* 79−56921
Si_2ON_2, thermal diffusivity meas. by flash with negative pulse, plasma jet heating 79−37888
Si_2ON_2, thermodyn. props. and spt. ht. 77−80629
Si_2ON_2-Y_2O_3-Al_2O_3 phase relations at 1400°C *(Japanese)* 79−38811
Si_3ON_2 needle crystal growth by nitriding Si-SiO_2 system in powder compacts *(Japanese)* 78−68609
$Si_lO_mN_p$, CVD from SiH_4-CO_2-NH_3-H_2 system, physicochem. props. 78−38978
$Si_xO_yN_2$, dielectric film, on Si. crysts. from amorphous state 79−28225
$Si_xO_yN_2$ film, opt. props. rel. to reactive sputter prep. conditions 77−81165
$Si_xO_yN_2$ films, chemical struct. using AES 79−77945
$Si_xO_yN_z$ film, amorphous, shock crystn. obs. 80−10828
$Si_xO_yN_z$ film, on n-GaAs, C-V and I-V characts. 77−89863
$Si_xO_yN_z$, non-stoichiometric films, struct. 79−42412
$Si_xO_yN_z$, pyrolytic, on GaAs, evidence for growth-induced damage from photolum. expts. 78−75953
$SiO_{2-x}Nx$ thin CVD film processing and characteristaion 77−77413
$(SiO_2)_x(Si_3N_4)_{1-x}$ on GaAs, deposition method and props. 78−91796
$SiO_2.H_2O$, (x<1), cryst., IR spectra 79−51951
$SiO_2.6Bi_2O_3$, IR and Raman spectra, vibr. anal. 78−76464
SiO(g), enthalpy of formation and dissociation energy, time-of-flight mass spectra 77−16859
SiP, deterioration in air, product identification 77−36675
SiP, precipitation in Si:P concomitant with P predeposition 77−24326
SiP, thermodynamic characts. 10-300K, interatomic bond elasticity 80−59677
SiP_2, electron charge density calc., nature of bonding determ. 77−1098
SiP_2, pyrite structure, density of states 77−15733
SiP_2 with pyrite struct., Fermi surface calc. 80−65427
SiP_2O_7, AlV, cryst. struct. refinement, phase with six coordinated Si 79−42018
SiP_2O_7, active component of solid planar source for P diffusion 77−1139
SiS, and isotopes, microwave spectra and consts., review 77−23493
SiS, chemiluminescent flame spectra, electronic states and rot. struct. obs., vibr. assignments, Franck-Condon factors determ. 80−85179
SiS, core pseudopot. valence electron calc., orbital energy and bond length 79−72233
SiS, electronic spectra, parity nonconservation effects *(Russian)* 78−13488
SiS, Franck-Condon factors and r-centroids for ($D^1\Pi$-$X^1\Sigma^+$) transition using R-K-R-V 78−5293
SiS, matrix IR spectra, aggregation to Si_2S_2 77−83599
SiS molecule, true potential energy curves for various states, dissoc. energies 77−6704
SiS multiple collision chemiluminesc., intercombination systems from Si+OCS 80−45505
Si_2S_2, tetrahedral edge sharing, distortions, MO calcs. 77−14380
SiS*, collisional quenching from Si+OCS 80−45505

silicon compounds continued
SiTe:Ge(Sn), substitution of Si, thermoelectric props. *(Russian)* 80−11023
SiTe-ATe, A=Ga, In, Tl, solid solns., mag. suscept. meas., defects 78−43552
SiTe-GaTe, thermo-EMF, elec. cond. and solubility 77−20346
$SiTe_2$, dislocations and stacking fault energy 78−47378
Si_2Te_3, cryst., IR reflection, Raman spectra 77−12393
Si_2Te_3, fundamental absorption and Franz-Keldysh effect meas. 77−1694
Si_2Te_3, growth by Bridgman technique and sublimation, cryst. struct. 77−1106
Si_2Te_3, passivated single cryst., elec. conductivity 78−95299
p-Si_2Te_3, photoelectric props., luminesc., hole lifetime and trapping 77−39892
Si_2Te_3, prep. and growth, book contrib. 78−19651
Si_2Te_3, surface exam. by Auger spectroscopy 77−69150
Si_2Te_3 surface reaction, AES exam. 78−63931
Si_3Te_3, photoconductivity of cryst. with clean surface 77−4395
$(SiTe)_{1-x}(ATe)_x$, A=Ge, Sn, Pb, solid soln. with small substitution, mag. susceptibility *(Russian)* 80−70933
$Si_{12}Te_{48}As_{30}Ge_{10}$ amorphous film, high-field transient conduction 78−43500
$Si_{12}Te_{48}As_{30}Ge_{10}$, amorphous film, elec. cond. mechanisms, temp. depend. *(Japanese)* 78−80078
$Si_{12}Te_{48}As_{30}Ge_{10}$ amorphous film, current-voltage characts. 79−87104
$Si_{12}Te_{48}As_{30}Ge_{10}$ film, temp.-depend. of non-ohmic current and switching characts. 77−8158
$Si_{12}Te_{48}As_{30}Ge_{10}$ film, amorphous, transient cond. characts. in preswitching regime 77−32055
$Si_{12}Te_{48}As_{30}Ge_{10}$ film, amorphous, Poole-Frenkel cond. for centres with screened Coulomb pot. 78−19044
$Si_{12}Te_{48}As_{30}Ge_{10}$-Au, Schottky barrier props. 79−7897
$Si_{10}Te_{40}As_{30}P_{20}$, amorphous films, optically assisted mono-stable switching 77−11968
SiX_4, (X=Br,Cl), electron impact dissoc., low-energy reson. capture 78−9263
SiX_4 (X=Cl,H,F), chemical shifts, relax., X-ray spectra, SCF Xalpha calcs. 80−27928
SiX_n radical, (X=H,D; n=1,2,3), thermodynamic function in ideal gas state 80−14871
SiO_2 blazed holographic gratings, fabrication by reactive ion etching 80−53484
SiO_2 film, RF sputtered, stoichiometry and atomic defects obs. 79−90904
SiO_2:Ge, B, P, optical fibre, radiation induced optical absorpt. spectra, 0.4 to 1.7 μm region 80−58761
SiO_x deposition by reactive sputtering of Si in magnetron sputtering system, reaction kinetics 80−49553
^{29}SiO, mm emission lines obs. in Orion A 77−2477
SnO_2-SiO_2-n-Si heterojunction, cheap solar elements for ground-based appls. 80−40860
Su-SiO_2 interface states, exptl. study of charge model 79−65554
$Tb_2O_3.Si_3N_4$, prep. by sintering and X-ray diffr. data 79−77570
Te-Ge-As-Si amoprhous film, voltage controlled negative resistance type characts. 79−69614
Te-Si glassy alloys, IR transmission and sp. ht. changes in glass interval, vibr. modes, struct. models 78−23474
$Te_{40}As_{35}Ge_7Si_{18}$ film, threshold switching in relax. oscill. mode 77−69389
$Te_{40}As_{35}Ge_7Si_{18}$, amorphous, threshold switching, expt. 80−49830
$Te_{40}As_{35}Ge_7Si_{18}$ with pyrolytic graphite electrodes, threshold switching characts. 77−24593
$Te_{48}As_{18}Ge_6Si_{28}$ amorphous film, I-V curve, memory switching 79−69615
a-TeAsSiGe film with Mo contacts, AC performance *(German)* 77−63012
$Te_{39}As_{36}Si_{17}Ge_7P_1$ amorphous film, electroluminescence from on state 79−8188
$Te_{80}Si_{20-x}Pb_x$ glasses, phase separation, double T_g presence 80−88306
Ti-Si_3N_4 system, reactions under heating and plasma conditions 79−95988
Ti-Si-C system, complex carbide phase synthesis by crystallisation from gas phase 77−16526
TiO_2-SiO_2, semicond. glass, small polaron hopping cond. 78−60126
TiO_2-SiO_2, semicond. glass, optical props. 78−60412
TiO_2-SiO_2, submicron dispersion of impurity, chem. diffusivity and elec. cond. 79−1528
TiO_2-SiO_2 fibre, prep. from metal alcoholates, prep. of spinnable soln. *(Japanese)* 78−44071
TiO_2-SiO_2 mirror, dielectric, Rayleigh scatt. at 441.6 nm 80−97367
TiO_2-SiO_2 multilayer vacuum coatings, optical props. 80−97361
TiO_2-SiO_2 multilayered film striped optical filters, optical props. and fabrication of RF sputtering 80−10030
TiO_2-SiO_2 multilayers, laser damage, elec. field strength role 77−61993
TiO_2-SiO_2 powders, anatase-rutile transition, mechanism investigation *(Japanese)* 78−95746
TiO_2-SiO_2 reactive evaporation technique for multilayer coatings 77−10994
UO_2-SiO_2, 1000-1400°C, Ar solubility and diffusion 77−20130
V/SiO_2 composite film, optical props., rel. to solar collector appls. 78−72622
V-SiO_2 interface reaction, identification of diffusion species 78−75890
V_3Si-SiO_x-Mo_3Re_2, supercond. tunnel junctions 80−107961
W-SiO_2 cermet film, deposition by RF sputtering of powder target, elec. resist. and TCR 79−78890
$W_5(B,Si)_3$, stability of heatproof coating 77−86201
Y-Re-Si system, phase diagram at 800°C 79−38806
Y-Si-Al-O-N solid soln., based on α-Si_3N_4 struct., comp. and struct. 79−74136
Y_2O_3-SiO_2-Al_2O_3 system, composition depend. of refractive index in vitrification region 77−24812
$Y_x(Si,Al)_{12}(O,N)_{16}$, α'-Sialon ceramics, prep. and characterisation 78−84750
ZnO-PbF_2-SiO_2 glass, shear wave velocity and its temp. depend. *(Japanese)* 78−30702
ZnO-SiO_2 layered system, characts. of phase-velocity dispersion and struct. of surface waves 80−59775
ZnO-SiO_2 system, struct. and phase comp. of luminescent Zn orthosilicate 80−19951
ZnO-SiO_2-Si monolithic convolver, long time storage of surface-acoustic-wave signals 77−1287
ZnO-SiO_2-Si SAW device, interface transduction 80−102949

silicon compounds continued
ZnS-SiO_2 multilayer reflector, reflectance under slight absorpt. conditions 80−83655
ZnSiAs, electron irrad., defects, elec. and optical props. 79−19282
$ZnSiAs_2$, birefringence, effects on hydrostatic pressure and temp. 80−45033
p-$ZnSiAs_2$, electron irrad. elec. props. annealing, lattice defects 80−100465
$ZnSiAs_2$, photoelectron spin polarisations, electron level struct. 79−87557
p-$ZnSiAs_2$:Au(Tl)(S), photoluminesc., radiative recombination 77−24883
$ZnSiF_6.6H_2O$, dielec. props., 100-270K, rel. to $NiSiF_6.6H_2O$ 78−35088
Zn_2SiO_4-SiO_2 dielectric, struct. exam. by optical, photoemission electron and SEM 78−80706
$ZnSiP_2$, birefringence, effects on hydrostatic pressure and temp. 80−45033
$ZnSiP_2$, chem. inhomogeneities, X-ray lattice parameter meas. *(German)* 77−72693
$ZnSiP_2$ crysts., imperfect struct. anal. using divergent X-ray beam technique 77−76259
n-$ZnSiP_2$, deep impurity levels, Schottky TSC meas. 79−95419
$ZnSiP_2$, first- and second-order Raman scatt. 78−35151
$ZnSiP_2$, growth under nonstoichiometric conditions in gas phase, microanalytical investig. *(German)* 79−33909
$ZnSiP_2$ monocryst., impurity induced photoluminescence *(Russian)* 79−4850
$ZnSiP_2$, pseudodirect chalcopyrite semicond., electronic band struct. 80−20079
n-$ZnSiP_2$:Ga, elec. cond. and Hall meas., 77 to 1000K, scatt. mechanisms 79−11153
$ZnSiP_2$-Au(Ni) Schottky contact, production and props. 79−7901
$ZnSiP_2$-In Schottky diode, photovoltaic spectra 80−2423
ZrB_2-SiC-C(-V)(-Nb), refractory cermet, hot pressing and oxidation resist. 80−3231
ZrO_2-Al_2O_3-SiO_2 fusion cast ceramics, crystn., microstructures rel. to conditions 80−11638
ZrO_2-CaO-SiO_2, relationship between texture parameters, and sintering, elec. cond. and mech. strength props. *(German)* 79−24474
ZrO_2-SiO_2, liquid immiscibility, microstruct. of plasma dissociated $ZrSiO_4$ 80−107429
ZrO_2-SiO_2 (11 to 13 wt.%), X-ray phase anal. 80−35195
ZrO_2-SiO_2 glass fibre prep. form metal alcoholates 78−6886
ZrO_2-SiO_2 powder mixture for optical glass polishing 80−28367
ZrO_2-SiO_2, layer for dielectric mirror, for KrF excimer laser *(Japanese)* 79−72588
ZrO_2.SiO_2-αAl_2O_3 mixed powders, solid state reactions 80−40337
$ZrSiO_4$, sintering, effect of grinding and additives 78−48356
$ZrSiO_4$, zircon yellow pigment, synthesis *(Polish)* 80−66466
$ZrSiO_4$-SiO_2, suspensions for slip casting, prep. and props. 80−104103

silicon controlled rectifiers *see thyristors*

silicon integrated circuits *see monolithic integrated circuits*

silicon-on-sapphire integrated circuits *see field effect integrated circuits*

silicon reference diodes *see avalanche diodes; Zener diodes*

silicones
additive to polymeric electrophoretic coating *(Russian)* 79−15615
atmospheric radioactive gas monitoring by silicone oil absorbent scintillation counter 80−12044
dimethyl silicone oil, laser-induced breakdown mechanism *(Japanese)* 77−43935
double-layer coating with double cone nozzle in-line with optical fibre drawing 80−53488
elastomer, for teeth impressions, holographic interferometric meas. of dimens. variations 79−94195
elastomers, dental impression materials, dimens. stability, holographic and interferometric study 80−67204
film deposition, glow discharge polymerisation, elec. and thermal characts. 78−6467
fluid, discharge propag. 79−91362
fluid conductivity meas. under DC field 80−15533
fluoropropylmethylsiloxane fluids, viscoelastic relaxation 79−14361
fungicidal protection of optical components made of chem. unstable glass using Sn, Hg and As silicones 78−59107
haemolytic characteristics of polydimethylsiloxanes 77−60290
liquid, electrification during laminar flow in metal pipe 80−6954
liquid film, cond. currents obs. 79−91062
membrane progesterone release rate control by plasma polymerisation 77−60285
methyl chlorophenyl silicone, viscosity and density determ. up to 150°C and 150000 psig 77−59940
methylphenyl silicone oil, containing water drops, intermittent elec. field heat transfer augmentation 78−94872
mould for solid models, appl. to Pb Fermi surface modelling *(Japanese)* 77−26277
oil, behaviour under HV stress 79−91368
oil, props. determ. by harmonical shear vibr. *(German)* 78−67164
oil drop spreading on horizontal surfaces 80−2250
oils, thermal cond. 78−51752
optical compound glass fibres, silicone and glass clad, medium loss 80−69533
optical fibre cladding, in flat cable form, charact. 78−66930
optical fibre primary coat using modified silicone, transmission charact 80−38098
poly(vinyl pyrrolidone), silicone grafted, for contact lenses, surface props. and stability of thin tear film 80−17194
polydimethylsiloxane fluid permittivity and dielectric loss 78−6621
polyorganosiloxane fluids, temp. determ. in friction zone accompanying breakdown, using TV *(Russian)* 80−7688
prosthetic breast, dose obs. 80−98144
protective coating for optical fibres, pressure sensitivity meas. and limitation 80−106605
resin clad fibre technology, optical and mech. props. 80−28349
resin electret, thermally stimulated discharge meas. 79−87378
rubber, antithrombotic materials for artificial heart and devices for assisted blood circulation 78−36052
rubber, RTV 560, diffusion of outgassing species, kinetics data 79−15010
rubber, vulcanizing, possible substitute for damaged/diseased parts of eye 79−74788
rubber membrane, inert gases separation appl. 77−36791

silicones continued
rubber with radiation-grafted methacrylate, for burn wound dressing 79−29657
silastic strain gauge as in vivo muscle force transducer 79−29680
silicone oil surface, hot, Leidenfrost boiling of pentane drops, neutral stability line 78−94588
silicone-clad silica low-loss fibre radiation response obs. 78−1397
solar array repair, adhesive bonding, and interconnector developments 79−96455
torsional-vibration fluid damper design 77−71309
transparent silicone-glass hybrid Fresnel lens for solar energy concentration 80−61303
XEF-4-3561 as antitranspirant in forest catchment, streamflow effects 77−78272

silver
see also nuclei with .....
4d bandwidth influence on $M_{4,5}N_{4,5}N_{4,5}$ Auger spectra 79−100017
absorption of O_2^- catalytic oxidation mechanism 78−61046
activity determ. in molten Cu by two component method *(Japanese)* 78−11547
adsorbed amino acids, XPS and SIMS study 79−86986
adsorbed Cs and Cs-O, surface plasma waves, ATR study 80−39451
adsorbed ethylene, photon-induced field ionisation mass spectroscopy 80−6639
adsorbed I_2 on (111) surface, surface EXAFS study 80−40186
adsorbed layer, on Si (111), electronic and cryst. struct., Schottky barrier form. obs. 78−84091
adsorbed layer of Xe, lateral compression effects calc. 80−6641
adsorbed layers of $O_2(N_2)$(S), electronic props., XPS and UPS 78−10279
with adsorbed metal film, monolayer electronic states calc. 78−6318
adsorbed methanol, oxidation 78−88556
adsorbed methylpyridines, surface enhanced Raman spectra 80−83376
adsorbed on AgCl cryst., luminesc. fatigue 80−66281
adsorption, O_2-induced, and reaction of H_2, water, CO, and CO_2 on (110) surface 80−55714
adsorption, of aromatic hydrocarbons, heat of adsorption, coating and fine struct. *(German)* 79−23844
adsorption, of Cl_2 on low index surfaces, energetics and structures 79−82440
adsorption, of O_2, EPR of O_2^-, rate of angular reorientation 78−72413
adsorption, of O, dielec. perm., plasma surface vibr. modulation spectroscopy 77−48198
adsorption and desorption on W, mass spectra obs. *(German)* 79−46951
adsorption and early stages of condensation on W single cryst. surfaces 78−6212
adsorption and surface reaction of formic acid 80−40741
adsorption and surface structural chemistry of Na and Na+O_2 on (110) surface 77−31883
adsorption of acetic and propanoic acids on (111), LEED obs. 80−80073
adsorption of Ar, curved surface physisorption, small spherical particles or pores 77−7964
adsorption of Cl_2 on low index surfaces, energetics and structures 79−87000
adsorption of Cl, AgCl epitaxial layer form., RHEED 78−14642
adsorption of Hg, work function change 77−7966
adsorption of I_2, adsorption site and adsorbate-substrate bond length, EXAFS 78−84679
adsorption of I_2, surface EXAFS exam. 79−82446
adsorption of I on (111) surface, cluster calc. with Xα scattered wave method 77−31894
adsorption of inert gases, physisorption energies 78−71944
adsorption of mol. O_2 species on (110) surface 80−103578
adsorption of O_2, and coadsorpt. of Na and O_2 on Ag (110), XPS and UPS obs. 77−69183
adsorption of O_2, isosteric heat of adsorption determ. 77−55453
adsorption of O, surface species identification by XPS, high press. 79−28191
adsorption of organic dye, excited mol. decay near metal surface, energy transfer to plasmon surface polaritons 80−50440
adsorption of pyridine, UPS, AES and flash desorption meas. 80−92776
adsorption of S on (110) surface, equilib. segregation isotherm, selvedge model 79−90883
adsorption of Xe on Ag(111), structural and thermodynamic studies 80−6640
adsorption on C, scanning-transmission electron microscope obs. 77−51597
adsorption on W, substrate temp. effect on relation between work function and coverage, FEM obs. 80−2272
adsorption on W (011), LEED, AES, and work function meas. 79−86990
adsorption on W and Cu, pairwise interaction approach to adsorpt. of oriented overgrowths 77−62759
adsorption on W on (001), (011) and (111), work function changes 77−62757
AES, valence band spectra, solid-state and atomic features 78−72646
aggregated film, optical props., 0.35-1 μm 77−66548
aggregates, matrix isolation spectra 78−46476
air pollutant, trace analysis neutron activation technique 77−17215
alkali halide:Ag^+, high press. studies of luminesc. phenomena 79−43017
alkali halide:Ag^+, luminesc. spectra and lifetime, high-press. effects 78−35194
alkali halide:Ag film, EPR and optical exam. of Ag impurity centres 77−85562
analysis in electroplating solution, electrochemical, in presence of cyanide ions 77−1965
angle resolved photoemission from (111) surface, free electron final state model 78−72694
angular resolved photoemission from low index faces 78−48282
annealing twins rel. to stacking fault energy 79−33006
assay-activation analysis of rock, use of Au and Ag standards based on phenolformaldehyde resin 78−3419
atom, 4d level He II photoelectron spectra, energies and intensities 80−5511
atom, 4d-subshell absorpt. spectra, ab initio Hartree-Fock calcs. 79−18139
atom, effective ionisation cross section determ. for H, Li, Na, Cu, Ag, Au and Fr, classical theory *(Russian)* 77−30998
atom, electron (positron), impact, K- and L-shell ionisation, Kα and L X-rays meas. 80−99575

silver continued
atom, electron impact ionis., X-ray obs., 3000 to 6000 keV, measuring system 77−68116
atom, electron impact ionisation, K-shell, doubly differential cross section meas. 79−98226
atom, excitation by FKα and AlKα ESCA sources 78−53301
atom, integral Compton scatt. cross sections, of γ-rays from K-shell electrons 78−58643
atom, integral K-shell Compton scattering, cross-section, for 1250 keV photons 78−90128
atom, ionisation by proton-atom collisions, loss of K-electron calc. *(Russian)* 77−50523
atom, ionisation energies and oscill. strengths calcs. 80−5488
atom, isolated in mol. matrix, absorption spectra 79−22724
atom, $K\beta_3/K\beta_1$ and $K\beta_2/K\beta_1$ relative intensities 77−75088
atom, $K\beta/K\alpha$ rel. intensity obs. 80−32665
atom, K-fluorescence yield determ. from K-Auger electron emission rates 80−95569
atom, K-shell ionis. by electron impact, cross-sections, 300-600 keV 78−29853
atom, K-shell photoelectric cross section 79−22676
atom, K-shell X-ray prod. by H^+ and He^+ bombardment, cross sections, energy depend. 78−5337
atom, K-shell X-ray spectra, $K\beta_2/K\beta_1$ determ. 77−23456
atom, Lα X-ray spectra, $_{40}$Zr to $_{48}$Cd, linewidths 79−41131
atom, L-series X-ray spectrum, anal. Coster-Kronig calcs. 77−75091
atom, L-X-ray emission spectra, hypersatellite origin 79−89629
atom, matrix isolated, fluoresc. spectra. excimeric bond effects 78−50498
atom, oscillator strengths, relativistic HF, core-polarisation model pot. 78−86818
atom, photoelectric cross section, derived from total absorpt. cross sections 77−10646
atom, photoelectric cross sections, 5-40 keV photons, X-ray emission spectra 77−18866
atom, photoelectric cross sections for 323 keV gamma rays 77−88432
atom, photoionisation, photoelectron spectra 80−87086
atom, photoionisation cross sections, electron-impact inverse mean free paths, and stopping powers for each subshell 80−69113
atom, reson. Raman X-ray scatt., K-vacancy excited state widths 79−45661
atom, solvation in ice matrix, ESR and irrad. at 4.2 and 77K 79−8444
atom, solvation in ice matrix 79−5166
atom, stabilized, contact HFS const., matrix shifts 77−42254
atom, Sternheimer shielding functions calcs. 79−76352
atom, total to K-shell photoelectric cross section ratios, 145 to 662 keV γ-rays 77−54545
atom, VUV absorption spectrum autoionised level Fano parameters, photoionis. 79−49973
atom, XPS and XES, dynamical effects 80−52924
atom clusters, local density of states, Xα scattered wave calcs. 78−18989
atom K-shell ionis., X-ray prod. cross section for incident H^+, ^4He and ^{14}N ions 78−70923
atom solvation in methanol, geometrical model, electron spin-echo modulation obs. 80−63682
atomic N-shell vacancy state widths, X-ray photoelectron, Auger spectra 77−18875
atoms, in Kr matrix, isolation and aggregation 78−45723
atoms, polarised photoelectron yields in VUV region 80−106307
atoms, valence-core electron exchange interactions, local approx. 80−91416
Auger $M_{4,5}$-VV spectrum, quasi-atomic final states 78−72688
Auger spectra, 4d bandwidth effect 80−89093
Auger spectrum, $M_{4,5}$VV, analysis 77−59649
Auger spectrum, $M_{4,5}$VV, interpretation 78−23562
binding energies, stable phase and elastic constants calc., appl. of reson. model pot. 77−69263
Bordoni effect during recrystallisation 77−90388
boundary layer on seed cryst., role in hydrothermal growth mechanism of sodalite 78−30571
cascade energy density effect on isochronal recovery 78−47431
catalyst for oxidation of rubber, prep. of diene oligomers with hydroxyl groups *(German)* 80−85175
catalysts, multiply-twinned particles 80−15114
cathode, underpotential deposition of Pb 78−52692
cathode spots on vac. arc discharge electrodes, model 78−91179
cathodoluminescence, film and polycryst. samples, low energy electron irrad., visible and UV emission 78−2921
[CC] Ag−(100)InP, metal-semicond.cathode contact, metallurgical, physical, chemical processes 80−107911
CESR, influence of freq. and surface effects 79−51856
CESR, obs. using reflection technique 77−20702
CESR due to edge dislocations 78−19328
CESR line-width and g-shift anisotropy, singularities 77−20705
CESR linewidth and g-shift in presence of spin-orbit perturbation, spin-phonon scatt. 77−63285
channelling, reson. excitation of H- and He-like ions 78−43058
channelling of B^{4+}, C^{5+}, N^{6+}, O^{7+}, F^{8+} and F^{7+}, reson. coherent excitation 79−51178
chemically deposited layer, reflectivity rel. to heat treatment 79−27366
chemisorbed CN^- on (110), Raman scatt. 80−45075
chemisorption and oxidation of ethanol on (110) surface 78−61044
chemisorption and surface reactivity of NO on clean and Na dosed (110) surface 77−31882
chemisorption of Cl_2, XPS and UPS meas. 78−31293
chemisorption of CO, N_2, NO, semiempirical calcs. 78−14611
chemisorption of ethylene, IR refl. obs. 77−31903
cinefilm processing, effect of antifogging substances on Ag grain size *(Russian)* 79−67414
cluster 78−33646
cluster and microcrystal, matrix isolated, optical absorpt. spectra, photolysis and plasmon absorpt. 79−89820
cluster growth and nucleation on Mo (100), UHV-SEM, ASS/(RHEED or LEED) obs. comparison 78−63956
cluster growth on AgBr microcrystals after X-ray and low-temp. light exposure 79−83485
clusters, charge distrib., density of states, CNDO calcs. 78−70995
clusters, chemisorption of I, UPS obs. 80−84830
clusters on Si substrates, opt. spectra investig. of struct. *(German)* 80−25492

silver continued
coated Cu, corrosion by thermal degradation products of chloroprene and silicone rubber 79−47801
coating, sliding wear resistance 77−12708
coating, vapour deposited on Cu, defects and their effect on props. 80−39474
coating on refractory metals, energy struct. determ. at two monolayer thickness 80−100392
coating on steel for watch part finishing, ion plating *(French)* 78−23879
coating on Ti alloy, electrospark applied, friction and wear resistance obs. *(Russian)* 79−1916
coatings, specimen charging control for SIMS and AES 80−101875
coin Ag concentration meas. using small neutron source 79−79332
coincidence site lattice model, failure for grain boundaries 79−60384
coins, ancient Greek, neutron activation and at. absorpt. anal. 78−8489
cold rolled, weak beam method appl. to dislocation obs. *(German)* 77−84757
cold rolling, inhomogeneous texture 80−89251
colloidal, lattice defects, X-ray diffr. and electron microscopy exam. 78−51567
colloidal, reaction with photographic stabilisers, equilib. conditions *(German)* 78−61067
colour photographic paper, minimum surface conc. of Ag and colour components *(Russian)* 79−67409
compact, on H_2 permeated backing, precipitation *(Russian)* 78−27520
concentration in atmospheric sedimentable powder, in Vizcaya, Spain *(Spanish)* 78−57265
condensation on glass, temp. depend. *(Russian)* 77−32525
condensation on Mo(100) and W(100), early stage comparison 80−80072
conduction electron spin props., g-factor, de Haas-van Alphen oscill. amplitudes 77−35858
conduction-electron spin flip by phonons, expt. data anal. 79−61219
contact charge density, press. depend., trends for Ag-Te 78−39077
contact resistance with Ag and Pd, effect of surface roughness and surface films 78−10540
contact to InP(100) oriented substrate, conditions of fabrication that control interfacial microstruct. 79−42643
contacts on InP, TEM obs. of struct. 77−62765
convoy electrons from solids, ion vel. and Z and target material depend. 78−84692
core level binding energies 80−71564
corrosion, indoor, rate meas. 80−76404
corrosion in atmosphere, environmental test 79−66205
corrosion in marine atm., potentiometric technique, appls. 79−24693
coulostatic deposition at underpot., pot. relax., chem. effects 78−48335
critical temp. determ. by exploding wires method, liquid metal enthalpy 78−6149
crystal (100) faces, polynuclear growth mechanism during electrocrystallisation *(German)* 78−18562
crystal growth, oriented, by vacuum intake method *(Russian)* 77−4732
crystal growth from melt, distrib. of growth directions 79−33924
crystal growth on Si and W substrates, UHV-SEM studies of Stranski-Krastanov growth 80−79722
crystal structure stability, collinear three-ion interaction theory 80−49173
crystallites, surface migration on alkali halides 78−26783
curvature factor, interpretation of de Haas-van Alphen oscillation amplitudes 79−47000
CVD for appl in high temp. photothermal conversion 79−79403
cyclotron mass and Fermi velocity meas. by de Haas-van Alphen effect 77−76734
cyclotron wave dispersion and obs. of many body effects 77−28097
cylinder implosion plasma and vapour jet deposition recording 78−75400
Debye temp., X-ray diffr. determ., anharmonic parameters of pot. function 80−100320
Debye temperature correlations at high temp. 80−15210
Debye Waller determ. from modified Cheveau model 78−59918
Debye-Waller factor temp. parameter 78−30725
Debye-Waller factors, modified ang. force model 77−66013
deformation potentials for isotropic strains 79−42506
deformed, exoelectron emission and electron energy distrib. 80−7481
deformed bars, cold rolled, exam. of microstruct. by thin foil TEM 78−88502
dendrite growth from supercooled melt 77−51628
deposited on InP surfaces, Schottky barrier formation 80−39671
deposition on Si(100) surface, LEED and AES meas. 77−35833
desorption kinetics of two-dimens. condensed phases on Ge (111) 79−90882
desorption on Si (111), kinetics of two-dimens. phases on single cryst. substrate 78−14598
determ. in water and organic materials, flameless atomic absorpt. spectrometry with wire loop atomiser 80−45586
determination of Au in thin Ag objects by gamma ray differential absorpt. 80−85227
determination of sub-ppm levels by graphite furnace atomic absorption spectrometry in heat resistant Ni and Co alloys 78−48730
diffraction grating, concave, Ag-coated, polarisation anomalies 80−69519
diffusion, of ^{110}Ag in temp. gradient, local vacancy conc. determ. 78−87812
diffusion and electric transport in glassy As_2S_3, effect on elec. and opt. props. 77−76623
diffusion and electrodiffusion into Se, role of Ag in switching effect on amorphous Se 78−19163
diffusion bonding with Cu 77−62687
diffusion in β-AgI, quasielastic neutron scatt. study 78−83999
diffusion in $Ag_xV_2O_5$ 77−20120
diffusion in amorphous As_2Se_3 77−51549
diffusion in As_2S_3-Ag_2S, GeS_2-GeS-Ag_2S and P_2S_5-Ag_2S glasses 78−18828
diffusion in Cu, 759-1081°C 79−10982
diffusion in Cu, activation energy, form. enthalpy of vacancies 78−51736
diffusion in GaAs substrates, radiotracer profiles 80−24680
diffusion in Ge_2S_3 film, photoenhanced diffusion 79−65257
diffusion in InP at low temp. 78−75884
diffusion in InSe, GaSe and GaTe crystals, temp. depend. *(Russian)* 80−70467
diffusion in ion implanted GaAs, profiles 80−24681
diffusion in liq. TlSe, Tl_2Se and Tl_2Se_3 *(Russian)* 77−28030
diffusion in Na_2O-B_2O_3 glass 79−51300

silver continued
diffusion in Ni, volume and grain-boundary, diffusion parameter temp. depend. meas. *(Russian)* 78−67863
diffusion in PbTe, effect of gamma irradiation 80−59515
diffusion in polycrystalline Al in temp. gradient 77−76619
diffusion in PyC 77−24441
diffusion in quartz, for surface quality determ. 79−51401
diffusion in quartz, radiation stimulated diffusion *(Russian)* 77−39694
diffusion in semicond., B, temp. depend. of coeffs., mechanism 77−7898
diffusion of Cu, SIMS investigations 80−59717
diffusion of Fe 78−10225
diffusion of Ni, resistometric technique 78−38880
diffusion of S 78−47599
diffusion of Ti, V, Cr and Mn in Ag, 1051 to 1220K 80−15308
diffusion of Zn 79−77825
diffusion pyrocarbon and SiC by post irradiation annealing of coated 78−13247
diffusion through Se, effect on interferometric thickness meas. 80−96695
diffusion transfer systems, graphic arts appl. 80−37106
discontinuous film, light absorpt. spectra, dielec. function calcs. 79−51507
discontinuous film on (001) MgO, low energy electron spectrum 77−48288
dislocation core energy, core tension, Peierls model 79−27984
dislocation density decrease during reverse deform., obs. by etch-pit method, single crystals 77−7725
dislocation dynamics during strain rate changes *(German)* 78−18655
dislocation dynamics during stress rate changes, in single crystals 78−19813
dislocation recovery *(Russian)* 77−65980
dislocations, dynamic behaviour 77−4108
dislocations gliding on (001) planes, bright field and weak-beam images 80−107266
dispersed full-colour photosensitive glass, processing and struct. 79−10369
Doppler factor, comparison between calculated values and measured results 78−54811
doppleron propagation, Fermi surface characts. 77−51642
elastic constants, single cryst. 77−1164
elastic constants, third-order 79−51184
electric double layer of polycrysts. in NaF soln., diffuse capacitance minimum 79−91969
electric field gradient generated by nearest-neighbour impurity atoms 79−42510
electrical contact material with liquid lubricant, prod. and appl. 78−10559
electrical contacts appl., MgO-particles dispersion strengthening *(Slovak)* 78−31544
electrical resistivity, low temp., T^4 behaviour rel. to electron scatt. mechanisms 80−39552
electrical resistivity, low temp. 78−51964
electrical resistivity, low-temp. meas. 79−23944
electrical resistivity, press. variation 78−84193
electrical resistivity, pseudoharmonic effect of phonons 80−34414
electrical resistivity, temp. depend. data 80−51967
electrical resistivity at low temp., ultra high resolution meas. 79−60795
electrical resistivity increment due to low temp. plastic deform. *(Russian)* 77−31990
electrical resistivity meas., 293-908K 77−43559
electrochemical behaviour in nucl. reactor radiation field 77−52650
electrochemical electrode, photoemission-into-electrolyte 79−74390
electrocrystallisation, screw dislocation free (100) face growth kinetics 78−30557
electrode, adsorbed cyanopyridine isomers Raman scatt., orientational specificity 79−69822
electrode, adsorption of metal ions, kinetics, surface struct. 78−79873
electrode, adsorption of O_2 in KOH soln. 79−61871
electrode, emersed, electrorefl. spectra 79−28788
electrode, enhanced inelastic light scatt. caused by adatoms 80−89013
electrode, enhanced Raman effect from adsorbed cyanide 80−50348
electrode, evaporation rate from cathode spot in vac. arcs. 80−49024
electrode, intense Raman spectra in presence of Cl^- and pyridine 80−55076
electrode, preparation by sintering and by chemical method, performances comparison 79−87851
electrode, roughened, Raman band intensity of adsorbed pyridine 78−48160
electrode pot. effects on surface plasmon excitation 78−15149
electrode surface, adsorbed rhodamine B and Pb monomolecular film, anisotropy of optical props. 80−60534
electrode surface, adsorption of pyridine on graphitic C overlayer, Raman spectra obs. 80−103954
electrodeposited, role of stacking fault energy 77−29016
electrodeposition, influence of specific adsorpt. of S 79−20001
electrodeposition, of Pb and Tl, on (100) and (111) single cryst. surfaces *(German)* 79−15616
electrodeposition, on (111) face, habit modification caused by Cl^- 80−71600
electrodeposition on Pt film electrode, interface struct. 77−16512
electrodeposits, dendritic growth inhibition by tartaric acid and tartrates *(French)* 78−87894
electrodes, (111), electroreflectance spectra meas. 77−59591
electrodes, adsorbed pyridine, ang. resolved Raman spectra 80−16017
electrodes, AgCl deposition, properties, production, problems in biomedical appl. 77−40959
electrolytic plating of Fe powder 79−66017
electromigration, and diffusion of Ag^+ in Na_2WO_4 in $Ag/Na_2WO_4/Ag$ cell system 77−1255
electromigration in Pb 77−69116
electron backscattering by bulk target, theoretical model *(French)* 80−60722
electron beam irradiation, 2.3 MeV, positron annihilation exam. of radiation defects *(Russian)* 78−34542
electron beam plasma sputtered coatings on KCl substrate, islet struct. *(Russian)* 80−39460
electron density at nucleus, press. depend., Hartree SCF calcs. 78−56411
electron diffraction study, ECP contrast, Bloch wave model 80−96419
electron emission induced by low energy light ions 79−61482
electron emission spectra produced by exploding wire photon sources, yield and energy meas. 78−31299
silver continued
electron excited Lα emission spectra 80−102481
electron inelastic mean free paths and energy losses, electron gas statisitcal model 79−46733
electron irrad., elastic moduli and internal function *(French)* 78−87703
electron irradiated, exam. of vacancy migration energies, and annealing kinetics 78−47571
electron irradiated, stage I_E recovery 77−39616
electron irradiated, thermal variation of dislocation pinning by point defects 79−51150
electron mean free paths and stopping powers calc. using statistical model 77−19996
electron microscope specimens, noncyanide electropolishing method 80−100967
electron range, low-energies continuous-slowing-down approx. and range straggling calcs. 80−39183
electron scattering cross sections, 300 to 1200 keV 78−9922
electron-phonon collisions frequency, anisotropy on Fermi surface, RF size effect 77−15750
electron-phonon interaction determ. from current-voltage curve at 1.5K *(Russian)* 77−47789
electronic and mag. structure calcs. of mag. impurities 80−80213
electronic contribution to thermal cond. at low temps. 79−95384
electronic density of states, cluster approx., compared with photoemission spectra 79−60675
electronic props., pseudopotential calc. 78−51960
electronic stopping function for He^+ and Li^+, 50-300 keV 79−69169
electroplated lead frames, surface struct. rel. to bonding behaviour, IC prod. *(German)* 79−11010
electroplating, use in manufacture of semiconductor diodes 79−33952
electropolishing, cyanide-free solution 78−88603
electroreflectance exam. of CN^- bonding to surface 77−80700
electroreflectance of single cryst. electrodes, obs. in aqueous solns. 80−25342
electroreflectance spectroscopy, longitudinal surface plasmons 80−40137
electrostatic model for impurity diffusion 78−2300
ellipsoidal small particle assembly absorption spectra, optical model *(Russian)* 78−60483
emissivity, 335-1100K, polishing effect 77−39682
emissivity, total hemispherical, temp decay method meas. 78−26708
empirical parametrisation of electronic structure 78−91585
emulsion thickness, influence on amplitude reflective holograms *(Russian)* 77−54683
energy loss of fission fragments, Z_1 oscills. 77−76477
energy loss of heavy nonrelativistic ions in matter, semiclassical theory 80−84224
energy losses and straggling for H^+ and He^+ beams *(Russian)* 80−84226
energy reflection coefficient for 5 to 10 keV He ions 78−95639
epitaxial film, (111), grown on mica, surface defect struct., LEED study 80−80038
epitaxial film, cryst. orientation effect on EELS 78−80442
epitaxial film, twin boundaries of recrystn. type, electron microscope obs. *(Russian)* 79−4484
epitaxial film growth with ionised beams and surface imperfections 77−32529
epitaxial films, ang. depend. UPS 80−55270
epitaxial films, grain boundary struct. evolution during recrystn., interface energy effect *(Russian)* 80−15387
epitaxial growth, cluster mobilities, in-situ electron microscopes obs. 80−15407
epitaxial growth, on alkali halide substrates, role of phase interaction, TEM study 79−46979
epitaxial growth and reaction with SnTe substrates 78−14640
epitaxial growth on electron bombard. NaCl(111) surfaces, RHEED and AES 80−15419
epitaxial growth on InP (001) by at. beam deposition in ultrahigh vac. 77−59691
epitaxial layer, electron channeling pattern, large angle, generation and appl. 80−100296
epitaxially grown, on (001) Fe substrate, interface struct. 77−55470
epitaxially grown film, on Au (111) twin form., LEED detection 80−88442
epitaxy on W (001) 78−60041
epoxy, Ag powder filled, thermal cond. below 3K 78−51757
equation of state, low temp., appl. to thermal expansivity 79−60476
etching by graphite suspension method in 0.5 H_2SO_4 soln. *(Japanese)* 80−35406
evaporated coating on Al single crysts., surface strengthening effects 77−8972
evaporated film, adsorbed CO, enhanced Raman scatt. mechanism in ultrahigh vacuum 80−107645
evaporated film, density, adhesion, intrinsic stress, substrate temp. effects 77−15709
evaporated layer, secondary electron energy distrib. and work function *(French)* 79−99993
evaporated layer growth on V{100}, total current spectroscopy 77−36329
evaporated metal nuclei on C, SiO_2 films, atm. contamination, AES meas. 77−4264
excess noise energy scales 79−95458
extraction from fixing solutions, using sulphide-containing cellulose fibres *(Russian)* 79−58835
failure under hydrostatic press., kinetics 78−52944
fatigued, relationship between stress and point defect cluster density 80−10592
fatigued single crystal, annealing of deform. struct. 78−3204
FCC, dislocations, elastic instability 79−82235
FCC, dynamical study for Gruneisen parameters 77−47594
FCC, Gruneisen parameters, effect of temp. variation 78−22812
FCC, low stacking fault energy, nucleation phenomena 79−90681
FCC, polycrystalline, deformation-strain curve description using substruct. parameters *(Russian)* 79−87690
FCC, props. of vacancies and divacancies 80−10545
FCC, stacking fault, antiphase boundary energies, investig. methods, review *(French)* 79−42080
FCC(111) substrate, orientation relationship with Fe vac. deposits 80−59836
FCC crystal, stress-strain curve, stage I to stage II transition *(Japanese)* 78−19834

silver continued
FCC crystals, compressively activated slip, theoretical latent hardening 80−65128
Fermi surface and thermoelec. power, de Haas-van Alphen calc. 79−4503
Fermi surface anisotropy meas. by positron annihilation 77−20222
Fermi velocity from proximity effect tunnelling 78−51875
field desorbed ions, appearance pots. 79−24417
field evaporation, search for high ionic charges 78−35269
filament produced by glass coated melt spinning, mech. props. 77−86125
filaments, cryst., electrolytic growth in Teflon capillaries, differential-capacity meas. 77−40552
film, 1/f noise, role of substrate 79−28388
film, 1/f noise and its temp. depend. 79−60939
film, 1/f noise and its temp. depend. 79−60940
film, absolute work function meas. by field-emission retarding-pot. device 77−59322
film, adhesion changes on 10 MeV electron irrad. *(Russian)* 77−43460
film, aggregated, absorpt. peaks, collective oscills. of electrons 78−80428
film, angular depend. UPS, surface electronic struct. 79−83095
film, annealing study of elec. resist. and defect density 78−76167
film, bounded by dielectric slabs, attenuated total refl. angular spectra 78−92135
film, CESR linewidth exam., sample size effect 79−33536
film, chem. deposited, agglomeration, SEM and TEM obs. 80−59828
film, chemisorption effects on optical reflectance and elec. resistance 79−33361
film, condensate obtained in electric field, anisotropy of elec. props. 80−44743
film, continuous, 1/f noise, temp. and substrate depend. 79−24086
film, damping and vel. of longit. elastic waves at 9.4 GHz 80−10596
film, defect density, thickness depend., elec. resist. obs. 80−70568
film, deposited by cathodic sputtering using high-resolution electron microscopy, voids obs. 80−49557
film, deposited on substrates at 10K and 293K, specific stacking charcts. *(French)* 77−43459
film, discontinuous, adsorption of alkali halide mols., effect on elec. cond. 80−2487
film, dye monolayer effect on surface plasmons, ART obs. 79−87001
film, elec. cond., appl. of percolation theory 80−65712
film, electrolytic deposition on semicond. substrates 77−77425
film, electron bombarded, transition radiation 77−85828
film, electron inelastic scatt. mean free paths, synchrotron radiation photoelectron spectra meas. 78−76587
film, electronic stopping power on irrad. by He, Li, C ions, damage-rate measurements 79−77654
film, electroplated, stress meas. using holographic interferometry 80−20806
film, electroreflectance effects 79−43055
film, ellipsometric response to CO adsorption 80−103571
film, elongated epitaxial (111) island growth on Cu(001), interface misfit, dislocations 79−82493
film, energy depend. of defect production in displacement cascades 77−31700
film, energy losses of 20-40 keV electrons 78−92153
film, energy losses of electrons, microcalorimetric meas. 80−59543
film, energy transfer from excited dye mol. to surface plasmons 79−91119
film, enhancement of electron photoemission by excitation of surface plasmons *(French)* 77−63524
film, epitaxial growth, characterisation of [001] tilt boundaries 78−84097
film, epitaxial growth, effect of electron bombard. of NaCl substrate, TEM and AES obs. 79−90916
film, epitaxial growth on O_2 conditoined (001)MgO film, TEM obs. 79−82489
film, epitaxial growth on Pd, AES and LEED obs. of growth modes and substrate influences *(French)* 80−84408
film, epitaxial on Mo, S impurity segregation at interface 78−84076
film, evaporated, adhesion meas. 80−50822
film, evaporated, chemisorption effects on reflectance and elec. resist. 80−11495
film, evaporated, oxidation resistivity change meas. *(Japanese)* 79−11723
film, evaporated, sulphide formation 79−15874
film, excess (1/f) voltage noise 79−42598
film, FCC, on NaCl, electron diffr. pattern interpretation, appl. to Ag 77−1332
film, form. simultaneously on (111) and (100) NaCl 77−11826
film, Frenkel pair prod. by light energetic ions, elec. cond. changes 77−59050
film, friction and fear in ultrahigh vacuum, effects of speed, film thickness and substrate surface roughness 79−20202
film, granular, adhesion measurement 80−50807
film, granular, transmission and reflection spectra, validity of sum rule 80−97358
film, growth on C replica stripped from pure and doped NaCl single crysts., elec. memory expts. 77−76691
film, He^+ ion bombardment, radiation damage, ion entrapment, gas release and bubble formation 78−30679
film, high temp. stabilisation using SiO_2 78−1319
film, hole formation and hillock growth after heating in O_2 atmosphere 79−65345
film, in contact with dye, enhanced total refl. with surface plasmons 79−59694
film, in situ resistivity meas. 80−97008
film, in situ struct. determ. by internal stress meas. 80−54569
film, inert gas ion refl., semiempirical analysis, compared with expt., 10-30 keV 78−6823
film, inertialess glow induced by picosecond laser pulses *(Russian)* 80−100714
film, influence of target texture on backscatt. yield of 2 MeV ^4He particles 79−4875
film, initial stages of growth on Si (111) 7×7, LEED, AES and UPS expts. 78−38988
film, interaction with adsorbed dye mols., absorpt. and luminesc. 80−103981
film, intrinsic stress meas. 80−71696
film, ion deposition *(Japanese)* 77−36407
film, lifetimes of surface plasmons 79−47143
silver continued
film, Maxwell stresses at charged surface from elastoresistance 80−49957
film, MBE deposited on InP(001), struct. using TEM and RHEED 79−82492
film, modulated surface-plasmon reson. in situ meas., O_2 adsorpt. 77−77311
film, O_2 chemisorbed, modulated surface plasmon reson. method 79−82439
film, on Al, splitting of surface plasmon dispersion curves 78−60178
film, on amorphous C and Si substrates, dispersion force contrib. to adhesion *(French)* 80−59842
film, on Au substrate, monolayer overgrowth, quantitative AES method 80−10813
film, on Cu, ion-induced intermixing 80−15420
film, on MgF_2 and SiO substrates, internal stresses correl. with struct. 79−87026
film, on mica, microstruct. changes 78−72013
film, on Si, backscatt. spectrum edge determ., theory and expt. 77−8702
film, optical props. after thermal cycling, thickness and substrate temp. effects *(French)* 77−48263
film, optical props. as function of wavelength *(Russian)* 78−52591
film, optical props. in intermediate region between pure Drude and interband absorption 77−81170
film, photodissolution in amorphous As_2S_3 78−26737
film, plasma reson. radiation exam. *(German)* 79−69453
film, polycryst., singularities of recrystallisation *(Russian)* 78−2382
film, Raman scatt. from adsorbed CO 79−78672
film, reflection coeff. minima and surface plasma wave dispersion curve comparison *(French)* 78−80429
film, size effect in thermoelec. power, MFP and Fermi surface 77−69433
film, spike effects of heavy ion sputtering 80−35034
film, sputtered, hillock growth and agglomeration by annealing, SEM obs. 80−2309
film, sputtering, photon emission enhancement compared with sputtering rate 79−78815
film, stearic acid/Ag layer periodic structure, prep. and optical props. 77−69199
film, substrate surface structure effects on absorptance 78−19585
film, surface and volume plasmon light emission due to low energy electron scatt. 80−40177
film, surface plasmon wave excitation of dye mol. fluoresc. emission 79−89703
film, surface roughness, light scatt. meas. 80−107624
film, surface roughness determ. from light scatt. meas. 78−5541
film, surface-plasmon modulated reson. for adsorption studies 79−83045
film, temp. depend. of 1/f noise meas. 77−85277
film, thermal and elec. cond., Lorenz no. 78−43487
film, ultra-thin, deposited on MgF_2 and SiO substrates, struct. and internal stress 78−91572
film, underlayer effect on surface roughness, surface plasmon excitation meas. 79−51456
film, UV photostimulated oxidation, electron microscopy study *(Russian)* 78−95850
film, vac. deposited on V, Au or amorphous C substrates, surface pot. and work function 79−42672
film, vacuum deposited, defect density and activation energy depend. on deposition rate 80−29294
film, vacuum deposited, Ge coated, electrical resistance and ageing *(Russian)* 80−103759
film, vacuum deposited, internal friction vibr. reed technique 78−43276
film, vacuum deposited, internal stress and its depend. on gas adsorption 80−6683
film, vacuum deposited, orientation axis tilt rel. to vapour angle of incidence 80−88456
film, vacuum deposited, surface struct., HEED meas. 78−6234
film, vacuum deposited, thickness meas. using X-ray fluoresc. technique 79−90911
film, vacuum deposited, Young's modulus determ. by differential technique 77−1340
film, vacuum deposited on NaCl, microstructure and orientation, surface condition influence 79−82486
film, vacuum deposited onto SiO, C and mica, quantitative study of nucleation 79−77959
film, vacuum deposition on Pb (111), substrate diffusion effects, RHEED, LEED, AES 80−65410
film, vacuum-condensed films, on glass substrate, X-ray texture study 79−83226
film, vacuum-deposited, removed from substrate, internal strain *(Japanese)* 78−22872
film, vap.-deposited, lattice defects, convolution relations for X-ray line breadth calcs. 78−51394
film, vapour deposited on polymer, ageing, adhesion, elec. cond., electrochem. pot. *(Russian)* 79−33362
film, vapour-deposited on rotating substrate at oblique angle, X-ray struct. anal. 77−62775
film, void growth, TEM obs. 80−59833
film coated with dye monolayer, anomalous dispersion of surface plasma oscills. 79−8203
film deposition, thermal effects, influence on internal stress meas. 80−96767
film deposition by ion plating, on AT-cut quartz crystal, crystallographic structure obs. 80−2280
film for Ga liquid spreading, kinetic eqn. *(Russian)* 80−59376
film growth, initial stages, ion bombardment effects 78−14639
film growth on C, conductance meas. 79−82495
film growth on KCl, LEED, AES meas. 77−35834
film growth on Pd substrate, interface cpd. form., AES study *(French)* 80−80131
film growth on Si (111), nucleation and growth modes, SEM study 80−100423
film on Cu(111), plasma reson. absorption in interfacial photoemission 78−15289
film on Fe foil, EM excitation of sound, Mossbauer study *(Russian)* 79−99795
film vacuum deposition and ion plating, effects on surface topography 79−82427
film-liquid Ga interface, γ-phase interlayer growth, two-dimens. electron diffr. 79−19487

silver continued
films, effect of Ar- and N-ion bombardment on texture *(Russian)* 80−107338
films, electrodeposited and vac. deposited, AES depth profiling anal. 77−59232
films, on mica, graphite, and Si, early growth by ion-beam sputtering 77−44158
films, optical props., inverse problem of phenomenological theory 79−43053
films, thin evaporated, rel. between microstruct. and excess free energy, TEM 80−70427
films deposited from hot hollow-cathode source, adhesion rel. to ion pre-cleaning 77−8754
fine particles, adhesion and sintering, TEM exam. 78−44053
fine particles, prep. by gas evaporation technique, crystal habit 77−52239
fine particles, X-ray Debye temp. determ. using solid-state detector and continuous X-rays 79−50944
fine particles prep. by vacuum evap. onto running oil substrate 79−28925
finite dislocation elements, isostress contours 78−71735
foil, destruction by laser pulse in presence of plasma cloud *(Russian)* 77−80338
foil, electron scatt., appl. of Monte Carlo type calc. *(French)* 77−7636
foil, electron scattering, most probable transmitted scatt. angle calc. *(French)* 77−68901
foil, foils, polycryst. and bicrystals, grain boundaries, ^{119}Sn Mossbauer anal. 80−7229
foil, or film, conduction electron spin disorientation at surface 80−75855
foil, proton energy straggling determ., at 0.35, 1, and 1.75 MeV, γ-emission reactions 79−4354
foil, surface plasma-wave reflectance and roughness-induced scatt. 80−66228
foil, traversed by $H^+(He^+)$, energy loss and straggling meas. 78−95100
foil interface with liquid, oxide props. from reflectance and scatt. light spectroscopy 80−60702
foil-electrolyte boundary reactively formed oxide layers, differential reflectance 79−69856
foils, trapezoidal splitting of partial dislocations 77−51376
Frenkel defect production associated with He and light ion implantation, exam. 78−47443
frequency standard, Ag beam mag. resonance apparatus, features 78−89458
frictional behaviour, effect of mechanical properties 80−55548
galvanic coatings, corrosion by org. insulant thermal destruction products *(Ukrainian)* 77−52525
gamma-ray scattering, incoherent, total at. cross section 79−13679
gas bubble embrittlement mechanism 78−60824
gas phase, He I photoelectron spectra, photoionisation cross section meas. 79−98051
grain boundary cavity coalescence during tension creep 78−52894
grain boundary energy and struct., solute atom effects 77−47465
grain boundary energy misorientation, hydrostatic press. effect, press. induced struct. phase transformations 80−54257
grain growth in strained {110}<112> low stacking fault FCC crystals after artificial nucleation 79−91722
grains, comparison with colour image *(German)* 79−29380
granular film, anomalous light absorpt., oblique incidence 79−6205
granular film, plasma reson. absorpt. by incident light 79−28850
granular films, optical props., depend. on refractive index of surrounding medium 78−84672
granules and colloidal particles on Cs_2O film in Ag-O-Cs photocathode *(Chinese)* 80−2279
graphite/epoxy laminates, with Ag powder filler, stress meas. by X-ray diffr. from fillers 79−43331
grating, surface plasmons rel. to diffr. order intensity profile, higher harmonics influence 78−25981
grating, with LiF coating, p-polarised reflected light intensity, reson. anomalies 77−3665
growth in Ag-Bi and Ag-Pb melts, transition from round to face forms *(Russian)* 79−28906
growth on Si(111), cohesive energy and 2-dimens. phase diagram, AES exam. 78−43246
Gruneisen number and nonlinearity const., elastic moduli data, US attenuation 80−65165
Gruneisen parameters, 10-100K, phonon wave vector depend. 78−38801
Gruneisen parameters, dynamical study using modified Bhatia model 79−37797
hardness, temp. depend. 77−40440
heat pipe meas. of corrosion and vapour press. 80−23878
hollow cathode discharge population mechanism for highly-excited states *(Russian)* 78−63610
hollow cathode discharges, IR laser transitions, discharge conditions, excitation mechanisms 79−68383
holographic gratings, polystyrene coated, Raman spectra enhancement by plasmon surface polaritons 80−80885
holography, diffraction efficiency, depend. on size of developed Ag particles 78−78965
host, impurity effect on electric field gradient 78−23061
Hugoniots, third and fourth order, isotherms, Lagrangian and Eulerian strain measures 77−69068
implanted grain boundary cavities effect on cavity growth kinetics and creep fracture 78−52935
implanted Li atoms, depth profiles and sputtering anal. by optical spectra 77−35579
impregnated alumina, appl. in radioactive methyl iodide removal 79−85638
p-InSb:Cu, Ag, deep impurity centres, acceptor conc. effect on conduction type 80−44602
interatomic pair potential, phonon spectra 80−33927
interdiffusion in molten alkali metal chloride *(Japanese)* 79−60530
interdiffusion in SiO_2-B_2O_3-Al_2O_3-$Na_2O(K_2O)$, optical and NMR studies 80−24683
interdiffusion with SiO_x and Al_2O_3 films 77−85000
interface with ^{4}He, Kapitza cond. and enhanced power anomaly, 1-2K 80−88378
interface with liquid ^{3}He, thermal boundary resist. from 0.4 to 10 mK 79−56000
intraband optical conductivity, electron-electron scatt. 78−35166
ion bombardment, sputtering, re-emitted kinetic energy ang. distrib. 80−2910
silver continued
ion channelling, He^+, Okorokov effect 77−15468
ion exchange, of Na^+ in β.Al_2O_3 by Ag^+ and K^+ ions from the molten nitrates 79−24737
ion injection transport and grain boundary mobility in KBr bicryst. 80−2214
ion plated film on permalloy, Cu and Vicalloy substrate, AES, SEM and X-ray study *(Japanese)* 78−11128
ion scattering, energy spectrum of scattered Na^+ ions, double scatt. effect 78−92163
ion stopping power systematics, Z_1-oscills. 79−65130
ion-irradiation studies of damage function 79−37746
ions XI to XIX, relativistic Dirac-Fock-Slater orbital binding energies, one-electron transition energies 79−25778
IR absorption coefficient, temp. depend., 3 to 30 μm 78−74953
island film on Ni foil substrate, elec. props. 77−43745
island films, on W, growth and desorption kinetics, mass spectra obs. *(German)* 79−46978
islands, on Al_2O_3 substrate, adsorption of ethanol, inelastic electron tunnelling spectra and TEM obs. 79−90884
isoelectronic sequence, UV spectra, (60-600 Å), resonance line identifications 78−33455
isoelectronic series 79−54918
isothermal compression curves to 120 kbar, X-ray diffr. study 78−83876
K-edge photoabsorption spectra, linear APW calc. 78−43960
Kambalda (W.Australia) komatiite sequence, Au, Pd, Ir and Ag in interflow sedimentary rocks 79−20830
kinetic friction re-examination using modified pin and disc machine 80−55547
L shell prod. cross section of Zr, Mo, Ag, Cd and In for 75 to 150 keV p and e excitation 79−47552
laser unidentified transitions in Ag II as Lyman, spectrometer ghosts 78−5464
latent image particles, electronic effects 80−82840
lattice dynamics, energy wave number charact., by reson. model 80−10612
lattice dynamics, ion-ion and ion-electron interactions 80−49321
lattice dynamics, modified Bhatia model, phonon dispersion, Debye-Waller factor temp. depend. 77−31729
lattice dynamics, modified CGW model calcs., phonon dispersion, sp. ht. and equiv. Debye temp. 78−10135
lattice dynamics on Kreb's model 80−59594
lattice vibrations and ideal elec. resistivity 79−46770
layers, on W, scanning Auger microscopy, effect of backscatt. electrons on resolution 79−2898
layers, thickness determ. by laser microprobe and flame atomic absorpt. 80−27355
Lifshitz constant for calc. of van der Waals force between two solids *(French)* 80−107658
light diffraction from weakly modulated surface 77−31132
light ion (H, D, He, Li) irrad., defect prod. and electronic stopping power 80−34088
liquid, electrical resistivity and thermoelectric power using t matrix approach 77−31988
liquid, multiple scatt. calcs. of resist. 78−76039
liquid, neutron diffr. investig. of pair correl. function, coordination numbers 77−35467
liquid, surface tension temp. depend. 77−4248
liquid, viscosity, temp. depend. *(French)* 78−59964
liquid chromatography, electrochem. detect. and fraction collection system 78−35749
liquid metals, structure factor modelling using quasi-crystallised model *(Russian)* 80−54118
loosely packed powder, sintering SEM and dilatometry obs. 80−20843
low energy sputtering by Ar and Xe ion bombardment 78−15269
low field Hall coefficient determ at low temp. in pure and low density defect conc. samples 77−43568
luminescence spectra due to slow electron bombard. 78−10995
M shell prod cross section of Au, Pb and U for 75 to 150 keV p and e excitation 79−47552
magnetic susceptibility, Animalu transition metal model pot. invest. 80−75711
magnetoacoustic spin-orbit antireson. 78−26808
matrix isolated atoms, matrix influence, theory 78−46288
matrix isolated atoms, matrix influence, theory 78−46290
matrix-isolated, matrix-induced changes in opt. spectra 77−57913
MBE, ang. distrib. of beam from modified Knudsen cell 78−60586
mean excitation energies from α-particle stopping power meas. 79−13615
mean excitation energy based alpha particle stopping power meas. 78−30678
melting curve to 60 kbar press., reinvestigation 80−39260
melting theory for small particles, Helmholtz free energy 80−59629
membrane filters for sample collection for X-ray diffr. chem. anal. 77−63972
metal beam epitaxy, high temp. high purity sources 79−43156
metallography 78−3289
mica interface, Van der Waals forces, direct meas. 78−43461
microcrack propagation and plastic strain 80−81187
microcrystals, matrix isolation spectra 78−46476
microcrystals on C foil, size distrib. from electron micrograph obs., UV absorpt. spectra obs. 80−55121
microwave mag. resonance apparatus using Ag beam as freq. standard, features 79−21712
microwave size effect, open orbit, and obs. of solid state reson. 79−51621
microwave transmission, time-of-flight effects in Fermi vel. determ., calc. 80−20238
mirror, laser damage, temp. depend. of absorptance, vaporisation and vap. heating 79−81471
mirror, polarisation effects by overcoatings 77−72055
mirror, Y_2O_3 coated, for the 0.5 to 14 μm region 80−87456
mirror film, ultraclean DC sputtered, optical props. 77−50748
mirror formation by photolysis of high mol. wt. compounds 77−75720
mirror IR reflectance at 45° incidence, obs. 79−14074
molecule, dispersion absorption spectra, 1500 to 5300 Å, rot. anal. 78−42089
molecule, VB calcs., wave functions, interatomic distance and dissoc. energy values 77−57883
monolayer, on Au substrate, adsorbed pyridine giant Raman effect 80−63637

silver continued
monolayer adsorption of Xe, lateral struct. and Xe-Xe interactions 77−1311
Mossbauer resonance at 88 keV, temp. depend. 80−7213
multiphoton photoemission, expt. at 5° incidence of laser beam *(Hungarian)* 77−52214
multiply twinned particles, internal and surface struct. by electron microscopy 80−84189
muon diffusion, LAMPF results 80−71285
neutron irradiation, low temp. recovery, effect of plastic deform. 78−51588
neutron yield calcs., electron beam incidence 78−95622
optical functions, effect of surface roughness 78−56447
ore, leaching, effects of ultrasonics and their appls. 78−92214
oriented bicrystal, sintering prod. technique 80−108371
oriented crystallisation on active amorphous C centres 79−7762
oriented single crystal substrate for epitaxial growth of Sb electrodeposits 78−43267
overlayer on Cu laser mirror, microstruct. and 10.6 μm reflectivity 77−42543
pair potentials calc., appl. to point defect props. 80−19798
paramagnetic, conduction electron spin transmission 77−69693
particles, lattice defect influence on size effect 78−88329
particles, light scatt. spectra, size and shape effects 77−44015
particles, Mossbauer fraction from Gaussian potential 78−47489
particles, ultrafine, effect of truncation of size distrib. 80−49562
particles embedded in dielec. KCl medium, search for maximum metallic resist. 80−107756
particles on graphite, particle motion rel. to heating in gaseous environments 78−34695
particles prepared by evaporation in clean Ar atm., cryst. morphology 77−62494
passivation in 0.1 M Na_2SO_4, passive (Ag_2O, AgO and Ag_2SO_4) films properties obs. *(Japanese)* 79−8399
periodic precipitation, conc. depend. of diffusion coeffs. *(Russian)* 77−16584
phonon density of states determ. from thermodynamic functions *(Russian)* 77−7800
phonon dispersion, binding energy, compressibility, pseudopot. calc. 77−4164
phonon dispersion, model pseudopotential method 79−23685
phonon dispersion, transverse acoustic phonon branch, temp. depend., neutron scatt. *(German)* 78−71808
phonon dispersion 80−10611
phonon dispersion relation in resonant model potential 80−6473
phonon dispersion relations, screened shell model 78−83894
phonon dispersion relations and Debye-Waller factor calcs. 78−51630
phonon frequency determ. in noninteracting band scheme 78−47483
phonon limited electrical resistivity, temp. depend. 80−24876
phonon spectra, pseudopotential calc. 77−89508
phonon-limited elec. and thermal resistivity 79−42517
photocathode work function, decrease due to adsorbed alkali halides 79−78824
photodissolution in amorphous As_2S_3 film, struct. studies 77−11815
photodissolution in amorphous As_2S_3 films, elec. resist. meas. 77−62786
photoelectric cross section, total to K-shell ratios 78−5188
photoelectric cross section in region 187 to 662 keV 79−69952
photoelectric cross sections, from total absorption cross sections, 5 to 130 keV 79−26947
photoelectric cross-section at K-edge measurements 78−2983
photoelectron energy distribution curves from Ag(100), (110), (111) 77−28693
photoemission, (111) surface, failure of plane wave, OPW and APW final states 78−11080
photoemission, primary and secondary yields using low-energy monochromatic X-rays 80−35053
photoemission angular distrib., effects of transmission factors and matrix elements 77−44128
photoemission spectra and total primary yields for exploding wire radiator source 80−32773
photoemission spectrum from d-bands, ang. depend. obs. 77−12492
photoemission yield anomalies, quantitative analysis, dielec. response nonlocality *(French)* 79−61489
photographic autodoping of amorphous As_2S_3 films to produce negative relief image 80−59490
photographic development, determ. of charge sign of Ag particles *(Russian)* 79−100417
photographic emulsion, developed, X-ray emission microanal. for β-ray quantitative microautoradiography 78−20545
photographic emulsion microcrystals luminescence, effect of adsorbed Ag ions *(Russian)* 77−69912
photographic stabiliser reactions with colloidal Ag, decoloration reaction kinetics *(German)* 77−40563
photographic stabilisers, reaction with yellow colloidal Ag, semiconductor props. *(German)* 78−86369
photolytic, mass and distribution in the solarisation region 78−29185
photon absorption and photoelectric cross-sections calcs. 79−31486
photon activation analysis of coins and art objects 78−349
photoneutron yields released by incident electrons, improved calc. 80−27630
photoreactive diffusion in glassy As_2S_3 80−19991
photosurface deposition on $As_{15}S_{40}Ag_{45}$ glass 77−76650
pionic, Auger electron emission *(Russian)* 80−69271
planar channelling of α-particles, stopping power of solids 78−51602
plane, (111), specular refl. of He and H_2 beams, Debye-Waller factor and surface Debye temp. 79−47580
plasma, laser produced soft X-ray spectra, transitions 77−15171
plasma arc srapying, chem. reaction with plasma gases 80−66427
plasmon dispersion, d→f fine structure 77−11863
plasmons, influence of cryst. orientation on intensity, electron energy loss meas. *(German)* 79−23921
plastic deformation, energy storage efficiency 77−4807
plastically deformed at room temp., glide on {001} planes, TEM obs. 79−19257
plastically deformed crystal, exam. of dislocation by dynamics during strain rate changes 78−88506
plastically deformed crystals, exam. of dislocation dynamics during strain rate changes 78−88507
polycrystalline with artificial surface roughness, electrical resistivity temp. coeff. *(Russian)* 79−82688
polygonisation, impurity effects 77−63685
silver continued
porous metallic electrode, for determ. of Cl^- ions in nuclear reactor water coolant 80−89577
positron annihilation characteristics, effect of temp. 78−64427
positron annihilation radiation, ang. correl. shape, deform. effects 77−85831
positron annihilation rates, electron-electron and electron-positron correl. effects 78−76548
positron annihilation spectra, Doppler-broadened, temp. depend., 9 to 1098K 80−71510
positron trapping, temp. depend., vacancy form. energy 77−90215
positron trapping by vacancies using ^{19}Ne source 78−47341
positron-vacancy interactions, equilib. temp. depend. of positron annihilation 78−76547
positronium formation at (100) surface 79−82654
powder, sulphide coated, Fritt effect on appl. of DC voltage *(German)* 80−25599
powder, ultrafine, sintering, coalescence growth stage 80−89174
power law creep, exam. of whether creep is diffusion controlled 78−52890
in precipitation rel. to hail suppression seeding 78−65367
production and annealing of radiation defects 78−47362
proton diffusion, config. and activation energies 79−37878
proton irradiated, radiation-annealing effects in energetic displacement cascades, film resist. meas. 78−26603
pseudopotential nonlocal model 78−14659
α-quartz:Ag^{2+}, γ-irradiated, stabilisation of impurity atoms 79−8047
α-quartz:Ag, Ag atom paramagnetic centre, $A_{Ag\text{-}Si}$ 78−76308
quartz:Ag, paramagnetic centre formation after α-irradiation *(French)* 77−69690
quartz:Ag glasses, EPR of atomic Ag centres 79−15349
α-quartz:Al, Ag, EPR of Al-Ag centres 78−88186
radiation damage, interaction with recoil implanted ^{111}In impurities, TDPAC meas. 79−11362
radiation damage, TDPAC of ^{109}Cd and ^{113}Sn 78−43739
radiative electron capture by channelled O ions 79−77658
range of $^{27}Al^+$ ions, meas. by (p,γ) reson. broadening 79−46729
recovery and formation of mixed dumbbells after thermal neutron irradiation 79−69161
recovery from laboratory wastes, teaching appl. 79−84912
recrystallisation, nucleation and deformed struct. of high purity Ag, TEM study 79−29082
recrystallisation texture, rel. to rolling temp. 80−11664
recrystallisation texture development after plane-strain deform. 77−48448
reference standards for radiation pyrometry, silver and copper freezing points 78−57888
reflective coatings, refr. index, UV polariser mirror coating appl. *(Russian)* 77−34928
regeneration from cinefilm waste *(Russian)* 80−105734
resistance welding, apparatus using C rod electrodes 77−79077
resistivity and thermoelec. ratio, electron-electron scatt. contrib. 80−70670
resonance self-shielding factors, depend. of Doppler factor 78−17439
resonant and nonresonant conduction-electron-spin transmission 80−75857
resonant model potential, energy depend. 78−18952
rolled, dislocation struct. and recovery during annealing *(Russian)* 79−29084
rolled single crystal with defined solute content, stored energy and recrystallization temp. 79−96037
rough film, multiple light scatt. of surface plasmons 77−48262
saturation resistivity charges, ion and fission fragment irrad. induced 78−79643
scattering of light ions by Ag polycryst. 78−11048
second-order elastic consts., method of homogeneous deform. 79−55808
secondary electron low energy distrib. meas. using double-pass cylindrical mirror analyser 80−68293
self-diffusion, activation enthalpy determ., tracer diffusion method 79−28128
self-diffusion, low temp., comparison between microsectioning studes 79−19393
semiempirical, relativistic oscillator strengths including core polarisation for p-, s-, d-series 78−74609
shear band effects on rolling deformation, of (211){$\bar{1}$11} single crysts. 80−50651
shear modulus and internal friction under press., EM reson. technique 77−31709
single crystal, adsorption of metal ions on (111) and (100) surfaces *(German)* 78−68636
sintered electrode production for concentrating cell *(Portuguese)* 78−88637
sintering and grain growth, effect of Sb solute addition 78−84730
sintering of spherical powder, intermediate stage 78−52713
size effect, ballistic-type field penetration at 45 GHz, 3 MHz 80−44634
sliding charact., friction and wear *(Japanese)* 78−56778
solder strip continuity, US inspection 79−52605
solid metal embrittlement of Ti-Al-V-Sn (6,6,2 wt.%) 80−16551
solid state sintering, compact length change 80−11593
solid-state electro-thermal diffusion into glass to form low-loss optical waveguides 80−58792
solidification, adsorbing species in melt effect on solidification 78−23695
solvation in ice matrix, electron spin echo modulation 78−39396
sorption of pyridine, surface enhanced Raman scatt., mol.-surface separation depend. 80−92775
specific entropy, and surface heat determ. as function of temp. *(German)* 80−6619
specific volume meas., for ruby R_1 fluoresc. press. gauge calibration, 0.06-1 Mbar 78−70150
speck nucleation and phase formation in latent image 80−97716
spectral distrib. of X-ray braking radiation, due to electrons, calc. using Monte Carlo method 78−56538
spherical crystal, Bragg case, Kikuchi patterns 77−84599
spherical powder, sintering, study of initial stage 79−20004
spherical powder, struct. of sintering necks in compacts 80−11594
spin properties of conduction electrons 79−46999
spin rotation amplitudes for ^{107}Cd and ^{109}Cd, comparison of temp. depend. 78−43738
spin-orbit projected d density-of-states 78−38999
sputtered, angular distrib. during He^+ and Ar^+ ion bombardment 78−95624

silver continued
sputtered-deposited, damage-resistant high reflectivity material for high energy laser appl. 79−47181
sputtering, temp. depend. 80−2914
sputtering by 10 keV inert gas ions, angular distrib. 79−52061
sputtering by heavy atomic and molecular ion bombard. 80−71532
sputtering rate on Ar ion bombard. 80−55245
sputtering yields for ions over 15-135 keV 79−56899
stacking fault energy, temp. depend. 78−51565
stacking fault energy meas. by tensile deform. of polycrystalline samples 78−95060
standard specimen prep. 77−90680
steel/Al sliding system, tribological behaviour, effect of temp., atmos., load and geometry *(German)* 79−34158
stopping power for 0.3 to 2.0 MeV ^{4}He ions 79−60415
stopping power for 0.3-1.5 MeV protons 79−55801
stopping power for 28 MeV α-particles, re-evaluation 78−79651
stopping power for MeV H^+, D^+, $^4He^{2+}$, $^7Li^{3+}$ ions, deviations from Bethe formula 78−26612
stopping power meas. for 4-5 MeV/N ^{16}O, ^{40}Ar, ^{65}Cu, and ^{84}Kr 78−70720
stopping powers, low energy, determ. by TOF techniques 79−45594
stopping powers, projectile range for Z=8-20, 0.0125-12.0 MeV/nucleon 78−83856
stopping powers for 28.8 MeV α-particles 77−80556
stopping powers for 8.78 MeV α-particles 77−80557
stopping ratios of 50-300 keV H^+, He^+, $^7Li^+$, and $^8Be^+$ 80−42903
strained, anisotropic electron scatt. in elec. resist. 78−91656
structure of Ag (110) and effect of surface roughness on LEED intensities 77−24471
subcolloidal particle precipitation in full-colour photosensitive glass 79−47953
subcolloidal particles in light-sensitive glass with intensive staining, props. *(German)* 79−27350
substrate, electrodeposition of Au film 80−81329
substrate for solar selective surfaces, graphite coating props. 78−74952
surface, ^{4}He backscatt., Rutherford scatt. cross section correction test 80−66369
surface, (001), Cl adatom bonding effects from coverage-depend. angle-resolved photoemission 79−82436
surface, (100), (111) and polycryst. electrodes, adsorbed pyridine layer, intense Raman spectra 78−72492
surface, (100), angle-resolved Auger emission 78−72650
surface, (100) and (111), positronium form. due to slow positron trapping 80−107748
surface, (110), ethylene-O_2 interaction, LEED and AES obs. 80−89520
surface, (110), photoelectron spectroscopy and surface order, UPS and XPS obs. 78−56568
surface, (111), adsorbed I, geometry and bond length, surface EXAFS 78−71952
surface, (111), adsorbed I, photoelectron diffr. aximuthal patterns, struct. sensitivity 80−107644
surface, (111), Ar beam scatt., time of flight meas., 79−95894
surface, (111), Ar ion bombardment, effect in struct. and reactivity, ellipsometry and LEED meas. 77−59192
surface, (111), codeposited S and O layer, AES and photoelectron spectra 78−71957
surface, (111), diffr. of He 78−39651
surface, (111), diffr. of He and H_2 mol. beams 77−85880
surface, (111), dissociative chemisorpt. of S_2, surface layer struct. changes 79−42383
surface, (111), ethylene adsorption, XPS and UPS investigation 80−103573
surface, (111), He atom impact, energy transfer, isotropic Debye model 77−16443
surface, (111), ionic bombardment, diffr. effects in angular distrib. of emitted secondary electrons 79−15577
surface, (111), LEED of thin crysts. and monolayers of n-paraffins and cyclohexane 79−11014
surface, (111), obs. of surface plasmon splitting by electroreflectance spectroscopy 79−61338
surface, (111), ordered and damaged, O_2 adsorption, O_2+CO interaction 78−14583
surface, (111), Xe incommensurate overlayer, dynamical calc. of LEED 78−30828
surface, (111) and (100), crystallographic anisotropy in surface plasmon decay to photoelectrons 79−24052
surface, adsorbed isoquinoline, surface enhanced Raman spectrum 80−100400
surface, adsorbed pyridine, 210-243 cm^{-1} mode in surface enhanced Raman scatt. 80−89003
surface, adsorbed pyridine, enhanced Raman scatt., ultrahigh vac. study 80−88993
surface, adsorbed pyridine and CN^-, Raman active librational modes 80−65359
surface, adsorbed pyridine Raman intensity enhancement using surface plasmons 80−7334
surface, Auger depth profiling limitations 79−61473
surface, cadmium arachidate monolayer, reson. surface plasmon reflection 78−56536
surface, clean (111), absence of filled surface states in s-p gap, LCAO calc. 78−2543
surface, clean and oxidised, $M_{4,5}VV$ Auger spectra, anal. based on self-convolution of measured UPS 77−77332
surface, clean polycryst., low energy Na^+ scatt. 0.4-3.2 keV 79−87554
surface, CN monolayer, picosecond Raman gain spectroscopy 80−25351
surface, CO chemisorption, SIMS, XPS study 80−84382
surface, diffusion of labelled adsorbed Cl^-, I^- ions 80−39413
surface, electrochemically roughened, nature and role in promoting anomalous Raman scatt. intensity 78−84587
surface, enhanced Raman scatt. by physisorbed pyridine-d_5 thin film 80−20620
surface, H_2^+ and $^3He^+$ ion bombardment, H^+ and He^+ yields at elastic scatt. energy 78−88394
surface, He impact, generalised Langevin theory 77−8700
surface, Hg flow kinetics in temp. grad. *(Russian)* 78−6198
surface, intermediate UPS/XPS synchrotron radiation study 78−52633
surface, ion impact, mol. effects in electron emission 78−80446
surface, low-energy photoemission 78−60548
surface, mass analysed thermal desorption spectra of O_2-CO coadsorbed complexes 77−60121
silver continued
surface, nature of 3.8 eV plasmon in XPS 79−78838
surface, Ne scatt., rainbow effects and energy exchange, calc. 80−84825
surface, optical photoemission, high index faces, angle of incidence variation 79−100024
surface, optical props. of organic dye monolayers by surface plasmon spectroscopy 79−11480
surface, periodically modulated, radiative decay of surface plasmons excited by fast electrons 77−24599
surface, positronium emission 80−80897
surface, production of Na Auger electrons by Na^+ bombardment 77−63515
surface, rough, Raman scatt. by adsorbed pyridine molecules 79−15448
surface, scatt. of 30 keV He^+, verification of formula *(Russian)* 77−4706
surface, scatt. of He, H_2, Debye-Waller factors, expt. 80−60736
surface, SHG 80−83645
surface, single crystal, electrochem. grooving, gross linear defect obs. 78−67894
surface, sinusoidally modulated, light emission of nonradiative surface plasmons 77−1467
surface, time-resolved mol. electronic energy transfer interaction with pyrazine 80−92957
surface, vibr. spectrum of CN monolayer using picosec. Raman gain technique 80−91859
surface, X-ray prod. by 5 MeV/amu deuterons (oxygen ions), projectile Z depend. 80−42982
surface {110}, clean, re-exam. of struct. by LEED 77−85029
surface (001), photoemission, electron escape effect 79−1814
surface (100), underpotential adsorption of Tl and Pb, mean field theory and Monte Carlo simulation 79−60630
surface (110), adsorption of O_2 and CO-O_2 interaction, ellipsometry-LEED expts. 78−91542
surface (110), electroreflectance, surface state contrib. 80−80755
surface (110), relax., LEED results and anal. by convolution-transform method 77−89624
surface (110), struct. determ. by LEED, const. momentum transfer averaging 79−42350
surface (111), adsorpt., coadsorpt., and reactivity of Na and NO 78−38948
surface (111), adsorpt.-desorpt. props. and surface struct. chem. of Cl 77−89648
surface (111), adsorption of Cl, props., struct., AES study 78−72024
surface (111), angle-resolved photoemission, free-electron final state model 79−4896
surface (111), chemisorbed Rb struct., and NO reactivity on Rb-dosed Ag 79−28207
surface (111), clean or Na-covered, adsorpt.-desorpt. props. of Br_2 78−38944
surface (111), epitaxial growth of Pb and Tl, LEED, RHEED, AES study 78−84090
surface (111), Xe monolayer adsorption, LEED obs. 77−1307
surface (111) phonon dispersion, He atom scatt. meas. 80−75426
surface (111) surface Au decoration by chemical polishing and electrodeposits *(French)* 80−44445
surface (331), adsorpt.-desorpt. props., coadsorpt. and surface struct. chem. of O_3 and Cl_3 78−34711
surface analysis, by low energy Na^+ ion beam 77−40318
surface Landau level resonances, effect of k_H-broadening 79−65533
surface layers, reflectivity, contrib. of longit. polarisation waves 79−83046
surface layers on Au and Al substrates, reflectance spectroscopy 79−78780
surface phenomena, electron microscopy 80−103556
surface plasma oscills., sinusoidal surface 77−73179
surface plasma waves, dispersion curves, attenuated total reflection spectra 78−88015
surface plasma waves 79−47151
surface plasmon dispersion relation in presence of surface roughness 80−65650
surface plasmon light emission induced by fast electrons on modulated surface 78−80424
surface plasmons, coupled, in thin metallic layer structures 79−56873
surface polariton absorption and emission spectra, edge effects 78−10375
surface props. rel. to adsorbed O_2, H_2O vapour, work function determ. 78−60187
surface roughness induced electronic Raman scatt. 80−50347
surface scattering of Na^+ ions, energetic distrib. *(Russian)* 77−12482
surface self diffusion coefficient, O_2 pot. effect *(Japanese)* 78−60014
surface self-diffusion coeff., O_2 potential effect 80−15354
surface states, intrinsic, UV photoemission meas. 77−20983
surface with adsorbed Cl, enhanced Raman intensity 79−95766
surface with adsorbed pyridine and CN^-, giant Raman scatt. 79−95768
surface with thin transparent and absorbing coatings, surface plasma oscills. 78−43951
surface-plasmon resonance, roughness-induced wavelength corrections 80−108288
surfaces, dislocation climbing, etch pit investig. 79−19260
surfaces, Van der Waals forces computation 79−15204
TEM exam. of ion damage in FCC metals 78−87727
tensile deformed, dynamic recrystn. *(German)* 80−84959
tensile deformed single crystal, recrystallisation texture 79−91685
thermal conductivity at high press. meas. 78−95283
thermal emissivities and diffusivities, expt. transient technique and theory for foils 78−43353
thermal expansivity, simple eqn. of state appl. 77−27970
thermal resistivity, temp. depend calc., free electron approx. 77−66152
thermoelectric power at low temps. of pure samples 77−76798
thermoelectric power determ. 77−24549
thermomodulation spectra of high-energy interband transitions 80−108226
thermopower temp. depend. 79−65436
thermoreflectance spectrum at room temp. 77−8601
thin film, elec. resist., effect of annealing In electrodes 80−80416
thin film, on Al surface, surface plasmon ATR spectroscopy 79−78770
thin film, thickness meas., Hall effect and interferometric methods 77−5802
thin film, X-ray fluoresc. spectroscopy of surface using RHEED-solid state detector method 80−108760
thin film deposited on Si, work function *(French)* 80−80353

silver continued
thin films, discontinuous, thickness meas., electron mode microanalyser 79−2744
thin films, Ga spreading kinetics, influence of melt-support interaction *(Russian)* 79−37903
thin foil thickness meas. using ^{148}Gd and ^{241}Am alpha-particles 79−30417
thin sub-monolayer film, Auger emission coeffs. meas. 80−55236
thin targets, electron transmission below 3 keV *(French)* 80−60725
thin-film bicrystals, planar lattice defects and migrating grain boundaries interaction 80−79835
transition radiation from rough surface, surface plasmon light emission 78−60530
transport props. meas., 20 mK-4.2K 77−20292
transverse electron focusing and specular refl. from cryst. faces 80−6823
tropospheric fallout fluxes in Antarctica and Greenland 79−58007
two-parameter dynamical model appl., sp. ht. and Debye-Waller factor calc. 80−10597
ultrafine particle, sintering effect, study by positron annihilation 78−95615
ultrafine particles evaporated on glass, optical transmittance meas. 79−78772
ultrafine particles in glass matrix, retardation effects on optical props. 78−6677
ultrafine powder, role of evap. during sintering 78−64505
ultrafine spheres with dielectric cores, optical absorpt. 78−60455
underpotential deposition, on Pt substrate, XPS 77−59672
underpotential deposition on Pt electrodes, XPS and AES 77−77770
UPS, expt. methodology aspects 77−90245
vacancy and divacancy diffusion 79−82377
vacancy diffusion along single edge dislocations, computer modelling *(Russian)* 77−47612
vacancy formation energy, thermal expansion meas. 79−14798
vacancy model, electron statistical, formation energies determ. 77−76390
vacuum condensate, effect of Ge coatings on ageing kinetics *(Russian)* 77−59340
vacuum condensation on glass, temp. depends. *(Russian)* 77−32524
vacuum deposited on Al substrate, recrystallisation 78−60044
vacuum deposition of oriented coating on doped alkali halide substrates 80−2303
vacuum deposition on evaporated AgBr layers, growth mechanism 80−35095
vacuum deposition on GaAs (001), perfect and facetting growth 79−47632
vacuum-condensed film, structural changes under glow discharge *(Russian)* 79−15852
valence band Auger spectra 78−76563
valence band struct. along Λ, angle resolved photoemission spectra 79−95316
vaporization, thermodynamic props. determ. by mass spectroscopy 78−22841
vapour, field ion appearance potential spectroscopy, temp. effects 79−19978
vapour press. above different crystallographic planes *(Russian)* 78−18762
volume diffusion in Ni, activation energies, expt. and by Le Claire method *(Russian)* 79−99369
VPE on W (110), alignment of (111)FCC-(110)BCC epitaxial metal pairs 79−19488
wear coefficients determ. using pin-on-cisc apparatus 80−76366
wear recrystallisation as controlling process, FCC metal 77−56117
wear under reversed friction, temp. effect 80−108588
wire, ultrapure, cryst. forms of hillocks and voids formed by electromigration 77−31811
wires, polycryst., internal friction and rigidity modulus, O removal from grain boundaries 78−3160
X-ray absorption, discontinuities and limits, chem. combination effects 80−93435
X-ray Debye temp. and isobaric Gruneisen coeff., anharmonicity effects 77−62654
X-ray diffraction pattern recording on photographic film, student expt. 78−41130
X-ray emission analysis, particle induced, of Mercury Ag statuette 80−85228
X-ray photoelectron spectra, high resolution, 4d spectrum, comparison with APW calc. 77−1784
X-ray photoelectron spectra ang. depend. *(German)* 78−72679
X-ray photoemission, electron yield, 30-90 keV 77−8726
X-ray photoemission from valence bands, atomic cross-section effects 77−1783
X-ray production, K-shell, on N^+ impact 77−75090
XPS, electron level binding, energy determ., and spectrometer calibration method 77−16458
XPS and $M_{4,5}N_{4,5}N_{4,5}$ Auger spectra 79−61472
XPS core line asymmetries in muffin tin approximation 79−69953
yield point, 4.2 to 300K, depend. on cryst. purity *(Russian)* 79−20116
yield point, temp. depend., 2 to 300K *(Russian)* 80−45346
yield stress in single cryst., effects of impurities and prestraining, 2-300K *(Russian)* 77−47506
yield stress temp. variation hysteresis *(Russian)* 78−52905
Young's modulus depend. on temp. and mech. action *(Russian)* 80−92584
Z dependence of thick target β-ray backscattering 80−76118
zeolite-Y, continaing Ag atoms, ions and clusters, optical absorption spectra 79−36569
$^{107,109}Ag$, stopping power in Ni, (Au) 80−70284
Ag, adsorption of ethylene and propylene, enhanced Raman spectra obs. 80−95607
Ag, and Ag^+, solvation in deuterated-ice matrices, electron spin echo obs. 80−15780
Ag composite, SiC whisker-reinforced, prep. aboard Skylab. 78−84741
Ag electrodeposition, on (100) face of single crystal Ag in presence of sulphadiazine 80−89161
Ag epitaxial growth, on W-ribbon substrate, in UHV, cryst. orientation determ. by etching *(German)* 79−65994
Ag film, epitaxial growth on isolated Au patches covered with amorphous C layer 80−40270
Ag film, twin boundary faceted struct., struct. coarsening due to dislocations *(Russian)* 79−99215
Ag film-Pb sandwich, supercond., effective renormalisation interactions 79−56397
silver continued
Ag films, hillock form. hole growth and agglomeration 80−44455
Ag I, absorption spectrum, 1540-1850 Å 78−13453
Ag I, resonance level, radiative lifetime, dye laser excitation 78−46300
Ag II, 1 W multiline output power from 800.4, 825.5, 840.4 nm transitions 78−82953
Ag II, laser discharge in hollow cathode, new IR transitions 77−661
Ag, ion beam plating using mass analysed ions, SIMS and AES expts. 78−19673
Ag monolayer on (111)Si surface, Schottky barrier, interface electronic nature and epitaxy 79−77934
Ag surfaces, temp. defend. of sputtering based on thermal spike effect 80−50491
Ag, ultra-microhardness testing for vacuum deposited film and bulk specimen 78−79910
Ag vacuum condensates, on Cu substrate, struct. and substruct *(Russian)* 79−73412
Ag vacuum deposited coating on glass, strength 80−55505
Ag^+, addition to TiO_2 photographic layers for sensitivity enhancement during cuprous development *(Russian)* 80−62780
Ag^+, field emitted, crit. energy deficit, theory compared with expt. 77−73221
Ag^+, generation by laser ionis. source for ICR spectroscopy, chem. appls. 80−45597
Ag^+ impurity diffusion in molten alkali metal chlorides 80−59685
Ag^+, phosphoresc. and triplet yield enhancement of arene micellar assembly 78−95598
Ag^+ quenched aromatic hydrocarbons in ethanol, triplet state form. 79−11801
Ag^+, solvation in methyl cyanide-water (methanol), γ-irrad., ESR obs. 80−97726
Ag:^{111}Cd, hyperfine interaction, dose-rate depend. and annealing props. rel. to PAC obs. 77−27920
Ag:Al_2O_3:Al tunnel-junction struct., surface polariton mean free path, roughness 80−93008
Ag:Er(Dy), orbit-lattice coupling, nonuniform strain effects 78−88182
Ag:He, implanted films, solid solutions radiation induced polymorphism 79−86810
$Ag/Ag_2SO_4(WO_4)$ solid cell systems, interface form., intergrain contact growth 77−16827
Ag/AgI/Te thin film galvanic cell, shelf life determ. 78−35702
Ag/Al interface, interface energy and charge oscills. 77−62984
Ag/Al thin film couples, diffusional alloying, Kiessig X-ray interf. obs. 80−10713
Ag/Au thin film couple, interdiffusion mechanism 77−20132
Ag/α-Ag_2S, interface, electrochemical transfer across phase boundaries 78−73046
Ag/CN, coverage meas. using surface enhanced Raman scatt. and radioisotope meas., electrochemical treatments 80−29260
Ag/In/Ge ohmic contact to GaAs, solid phase epitaxy formation 79−60658
$Ag/Na_2SO_4(WO_4)$ solid cell systems interface form., intergrain contact growth 77−16827
$Ag/RbAg_4I_5$/Ta, solid electrolyte timing cell and coulometer 80−68216
Ag/Si (111), metastable 2D condensations, epitaxy, growth modes, exp. techniques, book contrib. 80−49558
Ag/Te double films, interdiffusion and struct. modifications *(French)* 77−62682
Ag-^4He interface, Kapitza conductance, proof of surface superfluidity in enhanced power anomaly 80−15359
Ag-(100)InP contacts, interface struct. 79−60922
Ag-AgCl emulsion, anisotropy induced by two coherent perpendicular light vibrs. 79−55196
Ag-AgCl films, photoinduced dichroism *(Russian)* 79−56878
Ag-AgCl reference electrode for high temp. eqn. environments, construction and performance 77−12803
Ag-AgCl reference electrode for high temp. and high press. electrochemistry 78−35693
Ag-AgCl/KCl/AgCl-Ag thermocell, and thermal liq. junction pot. for KCl solns. at high temp. 80−16819
Ag-AgI film, photoinduced dichroism *(Russian)* 77−1743
Ag-AgI island granular film, Weigert effect, anomalous dichroism 77−12455
Ag-AgI thin granular film, Herschel effect 78−82063
Ag-AgX films, (X=Br,Cl,I), Weigert effect 79−64298
Ag-Al polycryst. thin-film couples, interaction process 79−51443
Ag-Al_2O_3-Al junction, internal photoemission 79−82683
Ag-Al_2O_3-Al structure, photoinduced currents, UV detection charact., 325 nm 77−53979
Ag-Al_2O_3-Au structure, electrorefl. meas. *(French)* 80−50366
Ag-Al_2O_3(Al_2O_3-MgO) cermet selective surfaces for evacuated solar collectors 79−43785
Ag-As_2S_3 sandwich structure, holographic charact., recording kinetics 78−29913
Ag-Au, pseudoalloy behaviour at interfaces, grain boundary diffusion 80−6567
Ag-Au thin film couples, polycrystalline, low temp. diffusion, resist. obs. 79−4435
Ag-Au thin films, interdiffusion, pore formation, stress effects, adhesive effects *(Russian)* 79−82502
Ag-BN-Si-Al sandwich, humidity sensitive threshold switching 78−88046
Ag-CdO cermets, coprecipitated carbonates and hydroxides, physicomech. props. 80−25706
Ag-CdTe-Ag struct., negative differential resist. 78−19161
Ag-Cs_2O photocathode, light absorption and photoemission 80−50510
Ag-Cs-O photocathode, operation mechanism involving Cs_2O_2 80−66384
Ag-Cu, composite, fibre and layer structs., anomalous props. caused by internal phase boundaries 78−72754
Ag-Cu couple, grain boundary diffusion of Ag through Cu film, Rutherford backscattering obs. 80−34252
Ag-Cu flex leads, microstruct. study of corrosion 80−76406
Ag-Cu interface, interdiffusion, X-ray and electron microprobe data 77−4225
Ag-Cu_2O-Ag bistable switching devices, freq. distrib. of threshold voltage 77−32091
Ag-Cu-Ag, layered struct., proton induced X-rays, impurity atom depth determ. 77−11582
Ag-CuBr system, spectral distrib. of photosensitivity *(Russian)* 78−56535
Ag-electrolyte interface, enhanced Raman scatt. of adsorbed molecules, background continuum obs. 79−73926

silver continued
Ag-GaAs (InP) contact, surface stoichiometry and struct., and electronic surface states 78−95361
Ag-GaSb surface barrier struct., elec. and photoelec. props. 78−56229
Ag-Ge, amorphous, junction, current-voltage charact. 80−44725
Ag-Ge Schottky barrier photodetectors, near IR interband transitions and optical parameters 80−73449
Ag-H_2 electrochemical cell design using rolled stack configuration 80−101084
Ag-He CW mW-level laser source at 224 nm 80−43352
Ag-He discharges, new ion laser transitions in near IR region, CW excitation 79−59673
Ag-In (Sn) multilayers, vapour quenched, supercond. transition temp. 80−20346
Ag-In_2S_3-Si layered struct., Hall effect, I-V charact., surface states *(Russian)* 80−97001
Ag-InP contact in InP Gunn device, relationship between microwave efficiency and metallurgical state of cathode contact 80−6981
Ag-InP interface, AgP_2 formation during sintering 80−65309
Ag-InP Schottky barrier, hot electron attenuation length 80−49904
Ag-Li ion exchange effects on $LiNbO_3$ and $LiTaO_3$ optical waveguides 80−58791
Ag-Li ion exchange in $LiTaO_3$ optical waveguides 80−91888
Ag-LiF, alternating plasma-dielec. five layer system, ATR angular spectra 79−19943
Ag-liquid He interface, Kapitza conductance, dislocation depend. near acoustic mismatch 79−33172
Ag-metals thin film couples, room temp. interactions 80−2220
Ag-MgF_2 layered system, optical excitation of surface plasma waves 78−6803
Ag-MgF_2-Ag layered system bounding dielec., ATR ang. spectra, assoc. reson. EM oscills. 79−15541
Ag-Ni, composite, fibre and layer structs., anomalous props. caused by internal phase boundaries 78−72754
Ag-O-Cs cathode, photoemission mechanism *(Chinese)* 79−19966
Ag-O-Cs photocathode, Ag colloidal particles and long wavelength response *(Chinese)* 80−45195
Ag-O-Cs photocathode, role of Ag colloidal particles in photoemission *(Chinese)* 80−40215
Ag-O-Cs photocathodes, time resolution, contrast-time charact., calcs. 77−7208
Ag-O-Cs surface, oxidation, role of Cs suboxides in low work function surface layers, XPS 80−76131
Ag-Pb proximity effect sandwich, mag. field depend. of tunnelling characts. 77−20501
Ag-polystyrene powder mixture, hot-pressed, elec. resist. 77−32556
Ag-Si (111) interface, chemisorption, AES 78−14589
Ag-Si interfaces, solar cell contacts 80−92973
Ag-SiO_2, CW CO_2 laser deposited dielect. thin film, optical and struct. props. 80−7506
Ag-SiO_2, coevaporated films, neutral density filters for near IR radiation 79−72673
Ag-SiO_2 cermet film, optical props., comparison of effective medium theories 79−24379
Ag-SiO_2 composite film, optical props., appls. 77−754
Ag-SiO_2 film, elect. and struct. props., ion beam sputtering 78−80071
Ag-Sn, supercond. proximity-effect bridge, thermal effects 79−78265
Ag-Sn double films, high-speed superconducting bolometer appl. 80−57368
Ag-Sn proximity effect bridge, crit. current anomaly 78−76194
Ag-Sn proximity effect bridges, long, voltage anomaly 79−51725
Ag-Sn proximity effect bridges, nonequilibrium state, hysteresis of crit. current 79−56411
Ag-Sn proximity-effect bridges, crit. current hysteresis under phonon injection 79−87206
Ag-Sn proximity-effect bridges, T* anomaly under phonon injection 80−34566
Ag-Sn proximity-effect bridges, phonon-injection-induced first-order transition obs. 80−39718
Ag-zinc phthalocyanine-Ag junction, microstruct. characterisation by TEM method 78−95241
Ag^+-Na^+ ion-exchanged optical waveguide repeatability improved by melt dilution 80−53493
$Ag+{}^{208}Pb$, 5.8 MeV/amu, Pb K-shell excitation probability 78−5338
Ag+Ag symmetric collisions, MO-2pσ radiation anisotropy, quasimolecular nature 78−70924
$Ag+H^+$, 1 MeV, K-shell ionisation probability, ang. depend. 77−71859
$Ag+H^+$, 4 MeV beam-foil X-ray production cross-section 79−7003
$Ag+H^+$, characteristic X-ray emission polaris. *(Russian)* 79−59394
$Ag+H^+$, excited X-ray polarisation, Born approx. calcs. *(Russian)* 80−78566
$Ag+H^+$, K-shell ionisation, 7-15 MeV, relativistic effects 78−82830
$Ag+H^+$, K-shell ionisation cross-section determ. 80−48077
$Ag+H^+$, K-shell ionisation cross-section, 85 to 790 keV 80−106390
$Ag+H^+$, X-ray emission, optical transition radn. 78−58618
$Ag+H^+(O^{5+})$, L-shell X-ray prod. cross-section determ. 77−6913
$Ag+I^+$, impact parameter depend. of K X-rays 78−94308
Ag_2, Harris-Pohl selected valence electron split-shell MO calcs. 80−91439
Ag_2, Raman spectra, matrix isolated in Kr 78−46347
Ag_2^+/AlO_4 paramagnetic centre in X-irrad. α-quartz, EPR obs. 79−28612
Ag_3, Raman spectra, matrix isolated in Kr, linear config. 78−46347
Ag_6 cluster, quantum chemical model for latent image of Ag halide photography 79−24792
Ag_n, ($n<10$), uv-visible absorpt. spectra in Kr matrices 79−13858
AgBr-Ag light sensitive system, diffusion of excited states *(Russian)* 78−59101
$AgCl_xBr_{1-x}$, binary melt, Ag solubility, temp. and conc. depend. 80−10677
AgCuAg sandwich target, proton induced K-shell X-ray yield ratios 77−48724
Ag(I) ions, in methyl cyanide, electron loss and capture, ESR spectra 79−33531
AgI isoelectronic series, oscill. strengths, relativistic HF calcs. 79−98034
Ag(I) reduction by tartrate in HN_3 solns. *(Russian)* 79−47976
$Ag(T_1)/AgI/Ag(T_2)$ cell, thermo-EMF of highly conducting solid electrolytes 80−24659
Ag−S system, phase diagram, 100-600°C *(German)* 80−97471
^{107}Ag excesses in Santa Clara and Pinon Fe meteorites, meas. 80−85902
silver continued
^{107}Ag, hyperfine density splitting, density shifts meas. in inert gases 77−54540
^{110}Ag diffusion in β/γ_2 interphase boundary of Cu-Al alloy 80−79989
^{110m}Ag, diffusion coeff. in liq. Cu 79−95196
^{110m}Ag, diffusion in Cu 80−65301
^{110m}Ag, fission product, amount in burnt-up HTR fuel *(German)* 78−25298
Ag(111), desorption of Bi^{3+}, evidence of two-dimens. phase formation in monolayer 77−15680
$Ag(s)/Ag_2SO_4+Na_2SO_4(l)$ high temp. ref. electrode, study 80−76622
Al-Ag, struct. of two-layer film 79−23851
Al-Ag, thin-layered laminates, yield strength rel. to dislocation generation and motion 79−20137
Al-Ag alloy, dil., electron-irradiated, impurity-interstitial interaction 77−15449
Al-Al_2O_3-Ag structure, electron bombard, charge accumulation kinetics, exoelectron emission obs. 77−51825
Al-Al_2O_3-Ag tunnel junction, surface plasmon excitation 78−10578
Al-Al_2O_3-Ag tunnel junction, 4-pyridine carboxaldehyde-doped, surface enhanced Raman spectra, surface plasmons 79−98111
Al-CdSe-Ag dry air stabilised struct., elec. cond. mechanism, breakdown phenomena 80−34527
Al-copper phthalocyanine-Ag diode struct. with Schottky barrier 77−43740
Al-Mg, alloys, effect of Ag addition on ageing and related props. 77−36522
Al-octaethylporphin-Ag, electroluminesc. 77−59615
Al-Ox-Ag-Cu-Pb and Al-Ox-Cu-Ag-Pb trilayer junctions, tunnelling characts. 79−87208
$Al_xGa_{1-x}As$:Ag, LPE film, impurity levels, elec. and optical props. meas. 78−26862
β-Al_2O_3-Na_2O_3:Ag^{2+}, EPR measurements 78−95515
As-Se:Ag chalcogenide glass, effect of Ag electrodiffusion on volt-ampere characteristics 79−7869
$As_{10}Ge_{15}Te_{75}$:Ag glasses, elec. props. 79−91045
As_2S_3, vitreous, Ag, Cu, Sn and Ge impurities effect on electrophys. props. 77−76826
As_2S_3:Ag, AC conductivity determ. 77−66167
As_2S_3:Ag, amorphous, electrodiffusion profile meas. of Ag migration 78−87822
As_2S_3:Ag, amorphous US props. 78−51616
As_2S_3:Ag, vitreous, doping influence on photolum. at 77K 77−77293
As_2S_3:Ag film, Ag photodoping rate, localised struct. transform. effect, absorpt. meas. 77−31914
As_2S_3:Ag glassy films, optical transmission spectra, photodoping effect 80−66317
As_2S_3-Ag, light sensitivity for high exposure densities *(Russian)* 79−6212
As_2S_3-Ag, resistance meas. during form., supersensitivity *(Russian)* 77−80839
As_2S_3-Ag interface, photodissolution kinetics of Ag in amorphous films 77−15955
As_2S_3-Ag photosensitive film systems, hologram recording 78−1194
As_2S_3-Ag system, activation energy for photochem. conversion, 80-340K, radiation intensity depend. *(Russian)* 78−3356
As_2S_3-Ag system, photosensitivity depend. on As_2S_3 thickness *(Russian)* 80−54784
As_2S_3-Ag system, photosensitivity depend. on metallic layer thickness *(Russian)* 80−54785
$As_2S_3(Se_3)$:Ag glassy films, doped by photodiffusion and thermodiffusion, photocond. 80−29441
As_2Se_3, glassy, Cu, Ag and O impurities influence on electronic energy spectrum and mol. vibr. spectrum 77−90181
As_2Se_3:Ag, amorphous, doping effect of gap states and elec. cond., dielec. relax. and DC cond. meas. 79−47098
As_2Se_3:Ag, amorphous, US props. 78−51616
As_2Se_3:Ag amorphous, freq. depend. cond. 80−88565
As_2Se_3:X (X=Cu, Ag, Tl, I, Ge), effect of doping, NMR meas. 80−11282
As_2Se_3-Ag photosensitive semiconductor-metal systems, effect of AsS_3 barrier layer *(Russian)* 80−62777
Au (111)/Ag (111) thin film system, diffusion processes 79−77843
Au decoration, of individual Ag crysts. by ion bombardment *(German)* 79−69164
Au/Ag couple, diffusion induced stresses and plastic deform. 78−26736
Au/Si films, laser-irrad., phase transform. study 80−49536
Au-Ag, contact PD, electron interferometric meas. 77−32069
Au-Ag, thin film, double layer system electron beam effects during sputter profiling AES obs. 79−65347
Au-Ag bilayers, conc. profile by AES, interdiffusion coefficient determ. *(French)* 78−84077
Au-Ag film, diffusion of Ag along grain boundaries, scanning Auger microscopy obs. 78−22897
Au-Ag film system grain-boundary diffusion at low temp., meas. by surface accumulation method 79−77839
Au+Ag adsorbed layers on Si, dispersed struct. formation 78−22952
$Au+H^+$, atomic K-shell ionis., X-ray emission 79−18280
Au(111)/Ag(111) thin film system, diffusion processes, diffused Ag composition profile 79−90832
BaO-Al_2O_3-B_2O_3:Ag, X-ray irrad., atomic centre interactions, EPR spectra 80−25207
Bi:Ag, microhardness anisotropy 80−21079
CaO:Ag, electroluminesc. meas. 80−40162
CaO:Ag, thermoluminesc, following UV excitation, 290-500K 77−40292
CaO:Ag^{2+}, EPR spectrum, static, quasistatic and quasidynamic Jahn-Teller effect 77−85561
Cd^+ trapping on injection at various temps. 77−76436
$CdBr_2$:Ag^{2+}, strong Jahn-Teller coupling, EPR 79−28605
$CdCl_2$:Ag^{2+}, strong Jahn-Teller coupling, EPR 79−28605
$CdCr_2S_4$:Ag, mag. semicond., ferromagnet resonance angular and temp. depend. 79−69730
$CdCr_2S_4$:Ag magnetic semiconductor growth, structural defects, physical properties 80−60759
$CdCr_2Se_4$:Ag, effect of doping on exchange interaction 78−43579
$CdCr_2Se_4$:Ag, elec. props., vac. heat treatment effect 80−15518
p-$CdCr_2Se_4$:Ag, electrical props., 100-300K 80−54692
$CdCr_2Se_4$:Ag, ferromag. reson. meas. 77−8415
$CdCr_2Se_4$:Ag, ferromag. reson. field and linewidth anisotropy, Se vacancy effects 78−60338
$CdCr_2Se_4$:Ag, ferromag. linewidth and eddy current losses 79−33541

silver continued
$CdCr_2Se_4$:Ag, ferromag. reson. and ESR line widths 80−60413
$CdCr_2Se_4$:Ag, impurity contrib. to low temp. ferromag. reson. linewidth 79−65743
$CdCr_2Se_4$:Ag, mag. anisotropy, effect of annealing in vacuum 77−80929
$CdCr_2Se_4$:Ag, magneto-electrical props. temp. behaviour depend. on dopant conc. *(Russian)* 80−11006
$CdCr_2Se_4$:Ag, magneto-optical effects in impurity spectral region 80−97313
p-$CdCr_2Se_4$:Ag, oscillatory magnetoresist., temp. and mag. field depend. 78−52011
$CdCr_2Se_4$:Ga(Ag), and pure, photocond. and photomagnetoresist. spectra 77−80809
$CdGa_2S_4$:Ag, photoluminesc. and photocond. meas. 78−60159
$Cd_xHg_{1-x}Te$:Ag, impurity diffusion, gamma-ray effects 80−54441
$Cd_xHg_{1-x}Te$:Ag, solid soln., defect struct. model, Hg self-diffusion coeff. 79−95213
CdS:Ag, charge and transport mechanism of impurities, electrodiffusion doping 80−59725
CdS:Ag, induced impurity photocond. spectrum obs. 77−1447
CdS:Ag, orange luminesc. at 77K and induced impurity photoconductivity 79−43035
CdS:Ag, vaccuum deposited film, recrystn. by H_2S heat treatment 80−34328
CdS:Ag crystals, spectral shifts of induced impurity photocond. bands 80−39633
CdS:Ag phosphor, mechanism of trap ionisation by elec. field, Gudden-Pohl flashes 79−74007
CdSb-Ag, thermoelectric, thermal defect relax., elec. cond. and thermo-EMF effects *(Russian)* 78−14749
CdSe:Ag, In, cryst., photocurrent and electroreflection, 77 to 300K *(Russian)* 78−23136
CdTe:Ag, with microscopic p-n junction, photopolarisation in anomalous photovoltage 79−11175
CdTe:Ag film, photoelectret effect *(Russian)* 79−28676
CdTe-Ag diode, Schottky type, elec. and photoelec. props. 77−43719
$CdTl_2Se_4$:Ag, doping effect on surface tension of melt and cryst. microhardness 80−49464
CrFeCN epoxy resin-based membrane studies, Ag sensitive electrode 80−16726
CsCl:Ag phosphor, spectral characts., optical range 77−1724
Cu electrorefining process, quantitative evaluation of Ag transfer 80−30246
Cu, photoelectron spectra 77−73218
CuCl:Ag system, light sensitivity spectrum, exciton struct. *(Russian)* 79−51985
CuCl-Ag system, photosensitivity spectrum in region of CuCl exciton absorpt. *(Russian)* 79−78707
CuO-Ag film solar absorbers, mechanism of high-temp. instability 78−22971
Cu_2O, yellow exciton series, silver impurity influence on spectrum 78−64388
$Cu_2O:Ag^+$, exciton-neutral and exciton-charged impurity scatt. cross sections 80−70618
$Cu_2O:Ag^+$, yellow series line width, exciton-impurity scatt. 78−64386
F^{n+}+Ag foil, 10-40 MeV, Ag L-shell X-ray production 77−71856
$Fe(OH)_3$, coprecipitation with Cu, Ag, Au; Ge, Sn, Pb; Mn and Ca 79−70415
$GE_{40}S_{60}$-Ag glass, EPR exam. 78−23334
Ga, with 100 ppm Ag single cryst. growth by pulling, thermal parameters governing purity *(French)* 78−2046
Ga-Ag tunnel junction, evidence for existence of anisotropy of supercond. energy gap 80−20357
GaAs:Ag, diffusion of Ag at 1000°C, profiles, Schottky barrier and Hall effect meas. 80−54435
GaP-Ag, Schottky barrier, stress effects on elec. props. 80−34512
GaSb-Ag, phase diag. 77−90327
Ge:Ag, gamma ray effects on impurity states 80−96822
Ge:Ag, polycrystalline film, electron transport props. 79−99642
p-Ge:Ag, Sb, electron beam irradiation cond. characts. 80−19842
Ge-Ag, thermocouple, DTA under hydrostatic pressure, appl. to TMMC phase behaviour 79−65186
Ge-Ag film, polycryst., struct. props. determ. 79−4494
Ge_2S_3-Ag contact, photoinduced diffusion of Ag in amorphous semicond. film 80−49418
$Ge_{30}S_{70}$ glass film, Ag photodoping sensitivity 80−39121
$Ge_{40}S_{60}$:Ag, bond struct. and character in Ge-S system, EPR obs. 80−66014
$Ge_{42}S_{58}$:Ag, amorphous, bulk and film forms, doping effect on elec. props. 80−103691
$Ge_{42}S_{58}$:Ag, glass impurity effect on e.p.r., dangling bonds 77−4553
H, diffusion in Ag, using membrane permeability method 79−37879
$H_2(D_2)$+Ag(111), energy transfer, quantum mech. theory 77−8699
HgI_2:Ag, trapping effects, TSC, photocond. and photolum. meas. 77−32023
HgTe:Ag, impurity diffusion, gamma-ray effects 80−54441
p-$In_{0.77}Ga_{0.23}As$/Ag photocathode, field assisted photoemission to 2.1 microns 80−76130
InI:Ag, impurity behaviour during directional crystallisation, partition coeffs. 77−16491
InP-Ag contact system, evaluation of Auger depth profiling technique 79−56893
p-InSb:Ag, ionisation energy of multiply charged impurities, compensation effects 78−18996
KBr:Ag, formation of electron centres and self-localised holes, ESR exam. 78−91947
KBr:Ag, mag. field effect on luminesc. of paired Ag^- ions 78−27313
KBr:Ag, optical absorpt. spectra interpretation mol. orbital scheme 80−20671
KCl:Ag, Br, EPR spectra of $Ag^0(Br_1)$ paramag. centres *(French)* 79−11346
KCl:Ag, excitation in fund. absorpt. region, luminesc. and thermolum. 80−50433
KCl:Ag, formation of Ag atoms and self-localised holes by illumination, EPR meas. 78−31108
KCl:Ag, formation of electron centres and self-localised holes, ESR exam. 78−91947
KCl:Ag, hole capture radius, scintillation luminesc. obs. *(Russian)* 78−39582
KCl:Ag, luminescence induced by tunnelling recombinatior between neutral Ag atoms and V_k centres 79−61442
silver continued
KCl:Ag, optical absorpt. spectra interpretation mol. orbital scheme 80−20671
KCl:Ag, strong IR luminesc. obs. of Ag_F^0 centres 78−6736
KCl:Ag, thermoluminesc. meas. using high impedance DC amplifier 79−99955
KCl:Ag, UV irrad., anionic H and D atoms, ESR and optical absorpt. expts. 79−99187
KCl:Ag, X-irrad., thermoluminesc. study of Ag centres 80−80874
KCl:Ag,Tl, cryst. high-press. energy transfer, sensitised luminesc. 77−36281
KCl:Ag positron annihilation and impurity states 80−97375
$KCl:Ag^+$, entropy changes associated with point defect form. calc. 77−7741
$KI:Ag^+$, far IR props. of lattice resonant modes, hydrostatic press. effects 77−28574
Li ions stopping power and straggling 80−42908
$Li_2B_4O_7$:Cu, Ag, as thermoluminescence dosimeter *(Japanese)* 78−31906
LiCl:Ag, fluoresc. and UV absorpt. spectra 80−80844
LiCl:Ag, luminesc. anal. using synchrotron radiation 79−38639
LiF:Ag, electron spin-lattice relax. of V_k-centre 78−95518
$LiPO_3$-$Al(PO_3)_3$:Ag glass, ionic motions, thermally stimulated depolarisation study 79−65239
Mg-MgO-Ag, tunnel junction, potential barrier, equivalent rectangular shape 79−7906
Mg-MgO-Ag junction, stable room temp. light emission 78−31257
MgF_2-Ag film substrate tunable external-reflector retarder, computer based anal. 80−53407
$MgO:Ag^{2+}$, EPR spectrum, static, quasistatic and quasidynamic Jahn-Teller effect 77−85561
MgO-Ag porous layer, secondary electron emission from ion impact, gas discharge device appl. 78−68586
γ-Mn electrodeposition influence of Cu, Ag, and Be impurities *(Russian)* 79−47938
NaBr:Ag^+, UV absorption bands, temp. depend. 80−20672
NaCl:Ag, absorpt. spectra, influence of elec. field 80−2794
NaCl:Ag, diffusion parameters of hot holes created by ionising radiation 78−47800
NaCl:Ag, excitation in fund. absorpt. region, luminesc. and thermolum. 80−50433
NaCl:Ag, formation of Ag atoms and self-localised holes by illumination, EPR meas. 78−31108
NaCl:Ag, formation of electron centres and self-localised holes, ESR exam. 78−91947
NaCl:Ag, irrad. with synchrotron radiation, thermolum. light-sum spectrum of L absorpt. edge of Cl^- 79−15540
NaCl:Ag, luminescence induced by tunnelling recombination between neutral Ag atoms and V_k centres 79−61442
NaCl:Ag, positron annihilation and impurity states 80−97375
NaCl:Ag, thermolum. light sum storage by ultrasoft X-rays 77−20939
$NaCl:Ag^+$, lattice relaxation around tetragonal and rhombic defects 79−95110
$NaCl:Ag^+$, X-irrad., B-centres, thermal annealing, monomolecular and bimolecular sequence of kinetics 78−47373
$NaNO_2:Ag^+$, optical and MODR spectra, anion states spin-orbit perturbation 79−19908
Na_2O-Al_2O_3-B_2O_3-SiO_2:Ag, photochromic glass, EPR of Ag^0 and Ag_2^+ centres 77−24741
$Na_2Zn(SO_4)_2.4H_2O:Ag^{2+}$, EPR, Ag^{2+} dimeric struct., hyperfine and fine struct. tensors 77−51949
Ne scatt. from (111) surface, double rainbow scatt. distrib. 78−80443
Ne-Ag, UV ion laser, dominant transition at 318 nm 79−942
Ne-Ag UV laser, spectral range, threshold, power output 78−66809
Ni:Ag, ion-implanted, laser irrad. effect 80−108306
Ni-Ag, thin-film, elec. cond. depend. on substrate film thickness and condensation temp. 79−7911
Pb/Ag proximity effect sandwich, US surface wave attenuation 79−60994
Pb-Cu(Ag) double layers, intermetallic boundary effects, tunnelling 80−88692
Pb-In, containing Ag particles, flux pinning in superconducting matrix 80−2534
Pb-Zn-Ag, liquid system, 450-750°C, phase boundaries *(French)* 77−69081
Pb(Ag) alloys, effect of Ag content on yield strength 80−76322
PbBr(Cl)-Ag^+ IR absorpt. spectrum and vibr. of substitutional impurity 77−81135
PbI_2-Ag, light sensitive, internal photoelectric emission 80−107910
PbI_2-Ag system, effect of bound and free exciton states on light sensitivity *(Russian)* 78−71169
PbO:Ag film, X-ray stimulated diffusion, current-voltage characts. 77−80653
PbO_2-Ag electrode system for potentiometric titrations, semi-auto titrator, student experiment 79−84918
PbTe:Ag, thermoelec. props., thermal and elec. cond. 79−82616
α-quartz:Ge,Ag^+, Ag-compensated Ge centre, EPR meas. 77−77098
RbBr:Ag^+, press. tuning of motional behaviour in shallow off-centre pots. 79−78718
RbBr-Ag, mag. field effect on luminesc. of paired Ag^- ions 78−27313
RbBr(Cl):Ag^+, off to on centre defect transitions under hydrostatic press. 78−15199
RbCl:Ag, dynamic behaviour of off-centre Ag^+ defects, NMR study 79−28634
RbCl:Ag, phosphor, luminesc., absorpt. and excitation spectra 77−12424
RbCl:Ag, strong IR luminesc. obs. of Ag_F^0 centres 78−6736
$RbCl:Ag^+$, first-order impurity-induced Raman scatt. 77−77216
$RbCl:Ag^+$, off-centre system, quadratic-coupling phonon-assisted defect-tunnelling theory 79−55849
$RbCl:Ag^+$, press. tuning of motional behaviour in shallow off-centre pots. 79−78718
Sb_2S_3:Ag, sensitised photolysis and structure of latent photographic image 78−89574
Se:Te(Ag), amorphous film, elec. cond., 300 to 350K, transition 77−4454
Si:Ag, diffusion mechanism of fast impurities, distrib. in surface layers 77−11735
Si:Ag, photoexcitation of electrons from ionised AG acceptors 78−2519
Si:Ag, photoionisation cross-sections and energy levels 79−87060
Si:Ag, surface doped with metal impurities, water adhesion energy *(Russian)* 77−89620

silver continued
Si:Ag, surface layer, ellipsometry 78−19121
Si:Ag; ion bombardment enhanced mixing of Ag layers 80−65034
Si-Ag contacts, Schottky barrier heights and interface states 77−85317
n-Si-Ag evpoarated contact photoelectric props. *(Russian)* 78−43473
Si-Ag-Si heat mirror on plastic sheet for radiation insulation of visible windows 80−95985
SiO_2:Ag, cryst. and glassy, X-ray induced EPR and luminesc. centre 80−65043
SiO_2:Ag, implanted atom, X-ray photoemission obs. 78−39050
SiO_2:Ag, XPS line broadening and extra-atomic relax. energies 80−71561
Si(111)-$\sqrt{3}\times\sqrt{3}$-Ag structure, atomic arrangement, low energy ion scatt. spectroscopy 80−96724
Sn-Ag ohmic contacts, for InP, thin film epitaxy 79−38159
SnO_2-copper phthalocyanine-Ag systems, elec. and electroluminescent behaviour 80−80864
$SrF_2:Gd^{3+}$, Ag^+, EPR of orthorhombic Gd^{3+}-univalent metal ion complexes 80−11262
$SrO:Ag^{2+}$, EPR spectrum, static, quasistatic and quasidynamic Jahn-Teller effect 77−85561
Ta-Ta_2O_5-Ag junctions, polarity-depend. tunnelling cond. 80−70846
Te-Ag thin film system, stress-relief appearance conditions 80−65416
Ti/Ag metallisation system, corrosion inhibition using intermediary Pd layer 79−79155
TiO_2-Ag-TiO_2 heat mirror on plastic sheet for radiation insulation of visible windows 80−95985
Tl_2Te_3:Ag, effect of dopant on electrical props., density and viscosity, for solid or liquid states 79−95432
Xe^++Ag, quasimolecular L and Ag L X-ray excitation thresholds, electron correl., calc. and expt. 78−78793
ZnCdS:Ag, phosphor screen, electron beam excited, light ang. distrib., modulation transfer function 80−45150
(ZnCd)S:Ag phosphor, absolute efficiency under fluoroscopy conditions 78−73203
ZnCdS:Ag screen, electron beam excited, light emission spectra 80−25466
ZnCdS-Ag binder layers, electrophotographic characts. eval. for use in charge transfer electrophotography 77−41714
$Zn_xCd_{1-x}S:Cl$, $Cu^+(Ag^+)$, high pressure luminesc. 78−19533
ZnO:Er,Ag, photoluminescence and electroluminescence 78−27327
ZnS:Ag, Al, LV cathodoluminesc. 79−33844
ZnS:Ag, Al(Cu), trap parameters, thermostimulated luminesc. and cond. meas. *(Russian)* 77−72868
ZnS:Ag, cathodoluminesc. yield, calorimetric method determ. *(Russian)* 77−20938
ZnS:Ag, cathodoluminesc. investig., appl. to cathode ray tube screening 80−108282
ZnS:Ag, cryst. struct., electron traps and glow curves 79−61437
ZnS:Ag, electroluminesc., surface barriers *(Russian)* 78−2919
ZnS:Ag, luminesc. efficiency deterioration due to surface oxidation by $(NH_4)_2Cr_2O_7$ thermal decomp. 80−29810
ZnS:Ag, phosphor, luminesc. of surface glow centres 80−29782
ZnS:Ag, phospors, nature of fluorescent centres and traps 79−91484
ZnS:Ag, photon counting statistics of cathodoluminesc. light emission 79−24371
ZnS:Ag, single crystal, ionisation mechanism of field trapping centres 80−45156
ZnS:Ag, struct. and mech. props. 78−22753
ZnS:Ag, TSC and induced impurity photoconductivity, existence of two electron trapping centres 80−44655
ZnS:Ag, Tb phosphors, luminesc. props. 80−100690
ZnS:Ag,Al, computer calc. of band model for luminesc. and photocond. *(Russian)* 78−52542
ZnS:Ag,Al phosphors, luminesc. excitation spectra and exciton struct. 80−55164
ZnS:Ag,Cl, embedded in HBO_3-glass matrix, blue electrolum. 80−55195
ZnS:Ag,Sm, recomb. centre interaction, luminesc. quenching 78−10946
ZnS:Ag film, evaporated, IR quenching of photocapacitance, deep levels obs. 78−56180
ZnS:Ag film, photocapacitance IR quenching, hole photoionisation energy and spectral distrib. 79−87127
ZnS:Ag phosphor prep., physicochemical investigation of processes 78−11170
ZnS:Ag phosphors, luminesc. of glow surface centres *(Russian)* 79−28836
$ZnS:Ag^+$, $Cl^-(Al^{3+})(In^{3+})(Ga^{3+})$, interimpurity luminesc. at high press. 78−19532
$ZnS:Cl^-$, Ag^+, phosphor, high press. effect on thermoluminesc. 78−64419
ZnS-Ag, broad band visible heat reflecting mirror 77−39017
ZnS-Ag-ZnS coating on glass, structure, optical props. 77−46781
ZnS-CdS:Ag, cathodoluminesc. investig., appl. to cathode ray tube screening 80−108282
ZnS-CdS:Ag, cryst. struct., electron traps and glow curves 79−61437
ZnS-CdS:Ag, Ni, Co, thermoluminesc. glow curves 78−95611
ZnS-CdS:Ag, Ni, Co phosphor, thermoluminesc. 77−66547
ZnS-CdS:Ag, phospors, nature of fluorescent centres and traps 79−91484
ZnS-CdS:Ag electron-irradiated phosphors, void formation mechanism 79−55780
$ZnS(Se)(Te):Ag^{2+}$, absence of EPR spectra due to strong spin-lattice coupling of Kramers doublets 77−85181
ZnSe:Ag, low-temp. photolum. meas. 77−20912
ZnSe:Ag, melt growth, dopant partition coeffs. 79−14837
ZnTe:Ag, containing dislocation loops, optical absorption-edge fine struct. 78−43905
ZnTe:Ag, dislocation loops creation in region of interface 79−82210
ZnTe:Ag, doped during frowth and by diffusion, defect form. 80−15129
ZnTe:Ag, elec. field and impurity conc. effect on ionisation energy 80−88514
ZnTe:Ag, real structure effect on luminescence and absorption spectra, dislocations 80−16085
ZnTe:Ag high purity, acceptor bound and free exciton states 79−99941

silver alloys
α-Ag-Ge, superconducting transition temp. depend. on electron per atom ratio, lattice deform. 77−8222
Ag-Pd, surface comp. changes under ion bombardment, AES study 80−55250

silver alloys continued
ceramet contact, Brinell and Vickers hardness number comparison 79−38978
chemical analysis by low energy γ-rays and neutron transmission meas. 80−35591
dental amalgam, exam. of fracture toughness and critical strain energy release rate 78−48933
dental amalgams, Cu-rich, SEM and energy dispersive X-ray analysis 78−24184
dilute, containing rare earth impurities, magneto-transport props. 78−68015
dilute, cryst. growth from melt, distrib. of growth directions 79−33924
dilute, electric field gradients created at ^{111}Cd nuclei by near neighbour impurities 78−39450
dilute, electrical resistivity at low temp., ultra high resolution meas. 79−60795
dilute, transport props. 78−76046
dilute, virtual bound states due to 4d- and 5d-transition metal impurities 80−70667
electron microscope specimens, noncyanide electropolishing method 80−100967
electrospark alloying of steel and Cu substrates, residual stresses obs. *(Russian)* 77−56145
erosion, rate and props. of cathode spot 79−79119
ion-selective electrode membranes development, hot pressed *(Japanese)* 80−61203
LaAg, exchange coulombic contrib. of cond. electrons to cryst. elec. field 79−95376
magnetic susceptibility, correl. with lattice parameter for α-phase alloys 78−68154
mutual alloying behaviour of the elements straddling the line Li-Mg-Cu-Au in the long periodic table 78−84769
rare $earths_{50}Ag_{50}$, amorphous, bulk mag. props., field, time and temp. depends. 77−89932
rare earth alloys, RAg_2X_2 (X=Si,Ge), cryst. struct. 80−1964
rare earth intermetallic, RCu_4Ag, mag. props. and cryst. struct. 77−20562
rare earth intermetallic, RCu_4Ag, struct. 78−30587
rare earth-Ag alloy, amorphous, model calcs. of mag. props. 80−84616
wear resistance, internal oxide effect *(French)* 77−52503
yield stress temp. variation hysteresis *(Russian)* 78−52905
A-Mn, dil., mag. susceptibility and single impurity effects 78−64186
Ag brazing alloy, type BAg-3, supercond., props. 79−1639
Ag Zn system, β-β′ order-disorder phase transition 79−47678
Ag-^{112}In, dil., ^{112}In nucl. alignment, radiation damage, γ-ray spectra 78−19398
Ag-Al, dil., temp. depend. of elec. field gradient, impurity mass and conc. effects 78−48085
Ag-Al, dislocation interactions with migrating interphase boundary electron microscope obs. 77−55963
Ag-Al, plastic flow enhancement during massive transformations 78−48468
Ag-Al, short-range order, X-ray and electron diffr. study 80−54173
α-Ag-Al, superconducting transition temp. depend. on electron per atom ratio, lattice deform. 77−8222
Ag-Al, ζ-phase, short range order *(Japanese)* 80−15256
Ag-Al (26 at.%), massive transform, β→ζ, crystallography and morphology 80−97475
Ag-Al(Ga) electric field gradient temp. depend., nearest neighbour impurity mass effect, TDPAC meas. 78−6612
Ag-As, thermopower at low temp., Fe impurities 79−65440
Ag-Au, calibration line introduction for comp. determ. by AES 79−56892
Ag-Au, composition changes under ion bombardment, scanning Auger microprobe obs. 79−83076
Ag-Au, corrosion in HNO_3 80−85091
Ag-Au, determ. of surface versus bulk composition, low energy ion scatt. spectroscopy 77−1284
Ag-Au, dil., low temp. elec. resist. 78−51964
Ag-Au, ion irrad., surface segregation and selective sputtering, AES expts. 79−7740
Ag-Au, liquid, surface tension *(Japanese)* 79−19431
Ag-Au, nucleation and growth on substrates 79−77956
Ag-Au, order-disorder transforms., s-band model 79−60502
Ag-Au, sputtering, ion yield depend. on alloy comp. 77−20976
Ag-Au, sputtering by 6 keV Xe^+ ions, energy distribs. 78−43969
Ag-Au, surface comp. after sputtering, AES obs. 77−55858
Ag-Au, surface enrichment, AES meas. 77−1283
Ag-Au, surface layer, effect of Ar^+ bombardment, AES and SIMS 80−25504
Ag-Au, surface segregation, ion scatt. spectroscopy meas. 79−82423
Ag-Au, thermal conductivity, data anal. and synthesis 78−95284
Ag-Au, thermoelectric power determ. 77−24549
Ag-Au, vacuum-deposited monocryst., internal friction, 200-3000 Hz, 20-850°C *(Russian)* 77−21197
Ag-Au (50 at.%), thermal expansion and lattice parameters, temp. depend. 78−91456
Ag-Au alloy, Auger exam. of preferred sputtering 77−44106
Ag-Au alloy thin film electron microprobe analysis *(French)* 77−32856
Ag-Au alloys, EMF meas. employing Ag-β-Al_2O_3 *(German)* 80−104307
Ag-Au system, surface segregation 79−69330
Ag-Au-Ay thin films, diffusion induced grain boundary migration 79−77833
Ag-Au-Cu, sputtering and AES 80−50503
Ag-Au-Cu, surface composition change on sputtering with 2 keV Ar ions 80−66365
Ag-Au-Pd, liquidus and solidus surfaces 78−60649
Ag-Au(Bi), grain boundary energy and struct., solute atom effects 77−47465
Ag-Au(Cd), deviations from Matthiessen's rule 78−10420
Ag-Au(Cu), residual elec. resist., pseudopot. calc. 80−6813
Ag-Bi, discrete eutectic form. mechanism *(Russian)* 77−66634
Ag-Bi, liq. alloys, thermodynamic investigation 80−70428
Ag-Bi, metastable phases *(German)* 77−16543
Ag-Bi-Tl, system calculated from optimised binary boundary systems *(German)* 77−16545
Ag-Bi(Pb), melt, crystal growth of Ag, conditions for transition from round to face forms *(Russian)* 79−28906
Ag-Cd, α and β phase, XPS, effects of atomic order on band struct. 79−42440

silver alloys continued
Ag-Cd, behaviour of Cd d-bands, comparison with Hg and Au alloys 79−37972
α-Ag-Cd, chemical interdiffusion and Kirkendall shifts 78−87829
Ag-Cd, dil., DPAD meas. on ^{107}Cd and ^{109}Cd, nucl. Larmor precession meas., role of hyperfine interactions 79−47363
Ag-Cd, dil., electron irrad., stage I_E recovery 77−39616
α-Ag-Cd, dil., electronic struct. determ. from thermoreflectance and XPS 78−39011
β′-Ag-Cd (45 at.%), growth kinetics of bainite plates and Widmanstatten needles 77−36551
Ag-Cd (45 at.%), morphology and crystal struct. of stress-induced martensites 78−68693
Ag-Cd (45 at.%), morphology and struct. of bainite plates in β′ phase 79−52213
Ag-Cd (45 at.%) martensite, shape memory mech. and related phenomena 80−30009
Ag-Cd (47 at.%), crystal struct. and internal defects of thermoelastic martensite 77−48438
Ag-Cd (50 at.%), BCC β phase, high temp. creep, existence of master curve 80−55473
Ag-Cd (approx. 50 at.%), disordered hcp to ordered bcc transition, meas. of activation energy 78−72773
Ag-Cd alloys, internally oxidised, thermal stability of CdO, exam. of particle coarsening 78−76789
Ag-Cd dilute alloy, isotope effect and correlation factor for Cd diffusion 78−14501
Ag-Cd dilute α-phase alloys, optical gaps, thermoreflectance meas. 77−66520
Ag-Cd peritectic system, separate crystallisation of phases *(Russian)* 80−66497
Ag-Cd(-Nd), internally oxidised, oxide particle size control *(Japanese)* 80−89480
Ag-Co, dil., binding and caging of impurities and trapped interstitials 78−39462
Ag-Cr, dil., elec. cond. meas., 1.5 to 30K 77−62914
Ag-Cr, dil., negative magnetoresist. in pulsed fields up to 35T 77−62899
Ag-Cu, directionally solidified, obs. of cutting deform. zone *(Japanese)* 78−15422
Ag-Cu, highly deformed eutectic composite wire, anomalous props., fibre diameter and foreign atom effects *(German)* 77−36566
Ag-Cu, laser induced atomisation in graphite furnace, for at. absorption spectroscopy 77−44566
Ag-Cu, liquid, surface tension 78−43217
Ag-Cu, metastable alloy film, optical props. 77−12460
Ag-Cu, metastable solubility lines on Ag side 78−39737
Ag-Cu, optical spectra, 0.5-6 eV, d-band struct. 77−48168
Ag-Cu, surface comp. after sputtering, AES obs. 77−55858
Ag-Cu, surface segregation, electronic theory, density of states, cluster-Bethe-lattice approx. 80−49369
Ag-Cu (10 wt.%), contact material, contamination layer thickness, resist., ESCA study *(German)* 80−55561
Ag-Cu (39.9 at.%), eutectic composites, solidification and deform. *(Czech)* 77−59773
Ag-Cu (5 at.%) solid solution, pre-fatigued, strain hardening at high temp. 78−15426
Ag-Cu (50 at.%), splat-cooled, struct. of γ′ extended solid solution 78−3147
Ag-Cu (6.2 at.%), tricrystalline specimen, discontinuous precipitation, specific grain boundary energy *(German)* 77−86039
Ag-Cu (6.2 at.%), tricrystalline specimens, fine lamellar discontinuous precipitation *(German)* 78−52822
Ag-Cu (6.2 at.%), tricrystalline specimen, discontinuous precipitation, thermodynamics *(German)* 79−34043
Ag-Cu (6.2 at.%), with discontinuous precipitates, quantitative struct. anal. using SEM 79−43527
Ag-Cu (6.6% at.wt.), laser melt quenching and alloying 79−69919
Ag-Cu (8 wt.%), deformed, free energy changes in process of discontinuous precipitation 80−3054
Ag-Cu (8 wt.%), plastic deform. effect on discontinuous precipitation 80−3053
Ag-Cu alloy filaments, prod. by glass coated melt spinning, microstruct. and tensile strength 79−91667
Ag-Cu eutectic, mechanism of lamellar spacing adjustment 78−31395
Ag-Cu eutectic and off-eutectic alloys, thermal stability 77−25077
Ag-Cu metastable solid soln., form. by ion-beam mixing 80−75244
Ag-Cu solid soln., spectral determ. of comp. using UHF plasmotron as source 79−52812
Ag-Cu surface alloyed films, laser melt quenched, microstruct. 80−76423
Ag-Cu-Ni, phase diagram determ. 77−63634
Ag-Cu-Sn(Zn)(Au), effect of additions on eutectic and peritectic temp., of binary alloys 78−84801
Ag-Cu-Zn-Cd solid metal lubricant in self lubricating composite steels 78−11340
Ag-Cu-Zn-(Cd)(Mn), solder, UTS, room temp. to 4.2K 79−57064
Ag-Cu(Au)(Zn)(In)(Sn)(Bi), dil., elec. quadrupole interactions on ^{111}Cd probe nuclei, time differential PAC meas. 78−15066
Ag-Cu(Sn), dil. alloys, EFGs at impurities, ^{111}Cd TDPAC 77−16213
Ag-Cu(Zn)(Ga)(Ge)(As), α phase, thermopower at low temps. 78−84196
Ag-Cu(Zn)(In)(Sn)(Au), temp. depend. of elec. field gradient, TDPAC meas. 77−32304
Ag-Dy, dil., EPR linewidth anisotropy and mag. field depend., internal stress effects 79−33532
Ag-Dy, dil., Schottky effect, sp. ht. meas. 78−34633
Ag-Dy, dil., thin films, ESR spectra, stress effects 80−39866
Ag-Dy(Er), dil., cryst. field and spin exchange parameters, susceptibility and ESR expts. 77−40129
Ag-Dy(Ho)(Tm), dil., high field magnetoresist. 80−15503
Ag-Dy(Tb) alloy, dil., magnetoresistance meas., contrib. from quadrupole and exchange scatt. 79−78078
Ag-Er, dil., reflection EPR residual linewidth 77−81004
Ag-Er film, stress-induced g-anisotropy, EPR of Er 77−85566
Ag-Fe, dil., estimate of Kondo temp. from static mag. susceptibility meas. 78−19214
Ag-Fe, dil., ion implanted, phase comp., Mossbauer study 80−7244
Ag-Fe, implanted, Mossbauer conversion electrons spectroscopy, rel. to dose and annealing temp. 78−52397
Ag-Fe, Kondo system, magnetisation, Mossbauer expts. 71−77028
silver alloys continued
Ag-Fe, local moment system, low temp. susceptibility, Mossbauer effect meas. 77−43810
Ag-Fe alloy film, mag. susceptibility max. 79−24173
Ag-Ga, Ga spreading kinetics, influence of melt-support interaction *(Russian)* 79−37903
Ag-Ga, thermopower at low temp., Fe impurities 79−65440
Ag-Ga (0.42 to 2.09 at.%), internal oxidation *(Japanese)* 77−63908
Ag-Ga (27 at.%), cooling rate depend. of thermal arrest, transform. temp. 79−29053
Ag-Ga based contacts to GaAs alloyed in As_2 beam 79−95495
Ag-Ga solid soln., internally oxidised, hardness *(Japanese)* 78−60744
Ag-Ga(Ge)(In), α-phase, lattice sp. ht. calcs. 80−65246
Ag-Gd, dilute, thermoelec. power, crystal field and interaction effects 77−66158
α-Ag-Ge, cold-worked, lattice imperfections, X-ray diffr. study 78−38732
Ag-Ge, liq., thermodynamics and short range order, mass spectra meas. 79−52740
Ag-Ge, liq., viscosity, temp. depend. *(French)* 78−59964
Ag-Ge, liq. eutectic, neutron diffr. determ. of struct. 77−51302
Ag-Ge, liq. eutectic, struct. by neutron diffr. 78−18537
Ag-Ge, liquid, neutron diffr. investig. of pair correl. function, coordination numbers 77−35467
Ag-Ge, liquid, surface tension exam., sessile drop method *(French)* 77−20162
Ag-Ge, thermal expansion, X-ray determ. 78−26697
Ag-Ge, thermopower at low temp., Fe impurities 79−65440
Ag-Ge (4.5 at.%), FCC, vapour-deposited, lattice imperfections, X-ray diffr. 78−72032
Ag-Ge alloy, liq.-quenched, metastable phase formation and evolution 77−90338
Ag-Ge eutectic alloy, heat capacity meas. over temp. range 800-1200K *(French)* 80−88331
Ag-Ge eutectic alloys, unidirectional solidification, electron microscope study of twinning 79−61574
Ag-Ge liquid alloy, small angle neutron scatt. 79−64982
Ag-Ge system, atomic struct. and electronic props. *(Russian)* 77−20289
Ag-Ge(Si) eutectic alloy, X-ray spectral exam. *(Russian)* 77−63489
Ag-Hf(Ta)(Pt) film, optical absorption spectra meas. 77−85823
Ag-Hg alloys, thermopower, thermal cond., elec. resistivity 79−65439
Ag-Hg amalgam, lattice const., temp. depend., explained in terms of Hg evaporation 78−26704
Ag-Hg-Sn dental amalgams, non-γ_2 phase, transmission electron metallography 79−74162
Ag-In, dil., electron irrad., stage I_E recovery 77−39616
Ag-In, dil., interaction between recoil implanted impurities and lattice defects, TDPAC meas. 78−39467
Ag-In, dil., temp. depend. of elec. field gradient, impurity mass and conc. effects 78−48085
Ag-In, rapidly quenched from melt, stacking faults, TEM and X-ray diffr. meas. 77−59768
Ag-In, single cryst. elastic consts. 77−1164
Ag-In melt system, conc. depend. of component and impurity diffusion coeffs., radioactive isotope method *(Russian)* 80−107454
α-Ag-In solid solutions, lattice dynamics parameters *(Russian)* 80−96477
Ag-In-Ge alloyed contacts to GaAs 79−78174
Ag-In-Sn, internal oxidation, precipitation behaviour of oxide *(Japanese)* 80−66515
Ag-In-Sn, internal oxidation, solute element and O_2 behaviour *(Japanese)* 80−89479
Ag-In(Sn), HCP ζ-phase, magnetic susceptibility 78−47946
Ag-In(Sn)(Pb)(Bi)(Sb), liquid alloy, thermoelectric powder and magnetic susceptibility 77−8076
Ag-Li, solid and liquid alloys, calorimetric investigation of mixing enthalpy *(German)* 78−52773
α-Ag-Mg, disordered, shaft range order diffuse scatt., electron diffr., interpretation 77−84596
Ag-Mg, low temp. internal friction, 150 to 300K *(Polish)* 79−96077
Ag-Mg (15 at.%), disordered, short-range order, X-ray diffr. obs. 79−95176
Ag-Mg (18.5 wt.%), solid soln., rheological study of crystallographic order on creep *(French)* 80−97548
Ag-MgO, dispersion hardened, exam. of ductile fracture 79−34144
Ag-MgO, laws of plasticity of dispersion strengthened materials 78−84832
Ag-MgO (0.1 wt.%), intergranular cavity growth at elev. temps. 79−66068
Ag-Mn, annealing twins rel. to stacking fault energy 79−33006
Ag-Mn, conc. spin glasses, thermopower 80−65538
Ag-Mn, dil., anomalous thermal expansion below 50K 78−51710
Ag-Mn, dil., nuclear orientation expts. 78−43713
Ag-Mn, dil., spin glass, AC susceptibility 79−33490
Ag-Mn, dil., thin-film spin glass, mag. susceptibility and T_G meas., 1.2-60K 79−38346
Ag-Mn, dil., valence and core level spectra, XPS study 80−84838
Ag-Mn, dil. alloy, transverse magnetoresist. in spin glass regime 80−34417
Ag-Mn, dilute spin glass, AC susceptibility and ESR meas. 79−7968
Ag-Mn, spin glass, anomalous Hall effect 78−30908
Ag-Mn, spin glass, mag. susceptibility hydrostatic press depend., RKKY interaction 80−44845
Ag-Mn, spin glass alloy, elec. resist. 77−8067
Ag-Mn, spin-flip scatt. time, superconductive tunnelling 79−8003
Ag-Mn (20 at.%), mag. virtual bound state alloys, XPS of core states 79−47588
Ag-Mn alloys, dilute, low temp. elec. resist. *(Russian)* 78−68024
Ag-Mn dilute, magnetoresist. and Hall effect, field-depend. electron scatt. 77−43581
Ag-Mn film, supercond. proximity effect and pair breaking, normal state mag. interactions 77−63035
Ag-Nb-Ga, phase relations, A15 phase diffusion layer formation 78−52764
Ag-Nd, cryst. struct. *(German)* 78−51472
Ag-Ni, composite powder mixtures, compressibility and sinterability 77−63592
Ag-Ni, two ductile phase, exam. of rolling deformation 78−72819
Ag-Ni, two ductile phase alloy, exam. of softening behaviour after cold rolling 78−72847

silver alloys continued
Ag-Ni (10 wt.%) wire, plastically deformed, fracture struct. *(German)* 80−71744
Ag-Ni solid solution, reversible surface segregation, radioactive tracer, LEED, and AES expts. *(French)* 77−69155
Ag-Ni supersaturated metastable solid solns. formed by ion beam mixing 80−107425
Ag-O system, melt, blow hole form. during solidification 79−43238
Ag-Pb (30 wt.%), contact material, contamination layer thickness, resist., ESCA study *(German)* 80−55561
Ag-Pb-Hg system, DTA of phase diagram 77−12594
Ag-Pd, composition modulated foils, layer struct. and mech. props. 79−95300
Ag-Pd, dil., elec. field gradients due to Pd near neighbour configs., TDPAC obs. 78−19391
Ag-Pd, dil., elec. field gradient, conc. and temp. effects 78−68416
Ag-Pd, H mobility and solubility, appearance pot. spectra obs. 80−55231
Ag-Pd, investigation of mechanical props. and recrystallization process, for use as wire-spring relay contact material 79−52278
Ag-Pd, surface comp., AES expts., correl. with O_2 heat of chemisorpt. data 78−34684
Ag-Pd, thermal conductivity, data anal. and synthesis 78−95284
Ag-Pd, thermoelectric force meas., test of virtual bound d-state model 77−32001
Ag-Pd (20 at.%)/Pb, thin film reaction kinetics, X-ray diffr. expts. 77−89594
Ag-Pd alloys, inert gas ion bombardment, dynamic surface composition changes, AES obs. 80−60745
Ag-Pd film, thermal treatment and comp. depend. of resist., 273 to 700K *(French)* 77−76963
Ag-Pd system, low temp. resist., 1.5 to 40K 77−62887
Ag-Pd system, surface segregation 79−69330
Ag-Pd-Cu, contact-spring props., fatigue and spring limit *(Japanese)* 79−29117
Ag-Pd-Cu alloys, contact-spring props. and age hardening 78−88473
Ag-Pd-Cu-Au dental alloy, age-hardening characts. 79−87646
Ag-Pd-Ni, corrosion in marine atm., potentiometric technique, appls. 79−24693
Ag-Pd(Pt), dil., electric field gradient temp. depend., TDPAC meas. 78−39451
Ag-Pd(Pt), dil., electric field gradient meas. by TDPAC method 78−39452
Ag-Pd(Pt), dil., TDPAC exam. of radiation damage 78−39464
Ag-Pr, cryst. struct. *(German)* 78−51472
Ag-Pt, sintering, limited solid solubility, peritectic diagram 77−28754
Ag-Pu, metastable, high rate sputter deposition, annealing behaviour of deposits 77−21025
Ag-Pu (0.5 wt.%) deposited profiles, homogeneity, from hexagonal point source array 80−25559
Ag-rare earth alloys, Ag-rich, phase equilib. 80−45276
Ag-Ru(Rh)(Pd) film, valence band spectra, XPS meas. 78−52618
Ag-Sb (1.16 wt.%), Sb effect on sintering kinetics in early stages 79−52137
Ag-Sb alloy, reflectivity, effect of electrodeposition conditions 78−13784
Ag-Sb alloy coating, electrolytes for deposition *(Bulgarian)* 80−93763
Ag-Sm system, phase diagram, eutectic temps., microstruct. *(German)* 80−104119
Ag-Sn, dil., electric quadrupole interaction of ^{111}Cd probe nuclei, time depend. PAC 77−16229
Ag-Sn, dil., high perfection single cryst. growth, strain-anneal technique 78−44010
Ag-Sn, dil., temp. depend. of elec. field gradient, impurity mass and conc. effects 78−48085
Ag-Sn, liquid alloys, thermodynamic props. *(Japanese)* 80−108396
Ag-Sn, single cryst. elastic consts. 77−1164
Ag-Sn, splat-quenched, X-ray diffr. study 80−81094
Ag-Sn, UV photoelectron spectroscopy of valence bands 77−24924
Ag-Sn (In)(Sb), dil. alloys, single crystals, dynamic dislocation behaviour 77−4108
Ag-Sn (0 to 6 wt.%) exam. of bulk diffusion of ^{113}Sn and ^{110}Ag 78−75864
Ag-Sn (0 to 6%), equilibrium intergranular segregation and diffusion 78−43130
Ag-Sn (6,11 at.%) alloy, splat-quenched, X-ray diffr. study of microstruct. 77−8860
Ag-Sn (6(8.2)(11) wt.%), splat-quenched, X-ray line broadening 80−40397
Ag-Sn alloys and amalgams, electrochem. considerations, corrosion in physiological soln. 80−93760
Ag-Sn alloys containing Au, splat cooled ribbons, electron microscope exam. 78−39987
Ag-Sn liquid, optical reflectivity spectra of virtual bound states 80−89021
Ag-Sn system intermetallic formation rate, H_2 adsorption effect 79−90819
Ag-Sn-Au, dental amalgams, effect of small additions of Au, struct. and corrosion study 79−20718
Ag-Sn-Cu-Hg, constitution of quaternary amalgam at 37°C *(German)* 77−81250
Ag-Sn(In)(Cd), Zener relaxation, valency and dimensional effects *(Russian)* 78−19802
Ag-Sn(Sb), liquid alloys, anomalous behaviour of electrical resistivity and thermoelectric power 77−11901
Ag-Tb, dilute, thermoelec. power, crystal field and interaction effects 77−66158
Ag-Tb(Ho)(Dy)(Er)(Tm) dil., single and polycrystals, low temp. magnetostriction meas. 79−78501
Ag-Te, liq., struct. and elec. props. 80−49083
Ag-Te, liquid alloys, Ag_2Te solid compound, calorimetric, investigation at high temp. 79−61893
Ag-Te amorphous films, effect of annealing on elec. resist., phase transitions 79−11241
Ag-Tl, eutectic liquid alloy, structural features, interatomic interaction *(Russian)* 79−77494
Ag-Tm, dilute, thermoelec. power, crystal field and interaction effects 77−66158
Ag-transition metal, dil., mag. impurities, electronic struct., KKR-Green's function calc. 80−65783
α-Ag-Zn, atomic short-range order determ., X-ray scatt. and pseudopot. calc. 78−2067

silver alloys continued
Ag-Zn, cold-worked, lattice defects, convolution relations for X-ray line breadth calcs. 78−51394
α-Ag-Zn, electron irrad., atomic mobility enhancement by defects, dynamic characts. 79−37871
Ag-Zn, electron irrad. self-interstitials, migration and elimination characts. 79−37872
Ag-Zn, interdiffusion coeff. in ε phase *(Japanese)* 79−14969
Ag-Zn, internally oxidized, elec. contact characts., alloying additions effect *(Japanese)* 80−88619
Ag-Zn, liquid, thermodynamic props. *(German)* 79−87615
Ag-Zn, molten, EMF meas. of activities using ZrO_2 solid electrolytes *(Japanese)* 80−88339
Ag-Zn, negative muon capture ratios 80−55007
α-Ag-Zn, short-range order calc. by pseudopotential method *(Russian)* 77−43175
Ag-Zn, thermopower at low temp., Fe impurities 79−65440
Ag-Zn, vacancy prod. rate by displacement cascades, anelastic meas. during neutron irrad. 80−19794
Ag-Zn (2 to 12 wt.%) containing several metals, internal oxidation *(Japanese)* 80−16570
Ag-Zn (24 at.% Zn), γ-irradiated, freely migrating defects, rate of production *(French)* 79−10877
Ag-Zn (27-48 wt.%), interphase β′-ζ transform., thermal expansion exam. 77−63630
Ag-Zn (30 at.%), electron irrad., mobilities of self-interstitials and vacancies 77−84795
Ag-Zn (30 at.%), electron irrad. exam. of defect supersaturation by elasticity, and creep meas. 78−47366
Ag-Zn (30 at.%), electron irradiated, atomic mobility, elastic after-effect meas. *(French)* 78−63874
Ag-Zn (30 at.%), neutron irrad., at. mobility enhancement, Zener relax. meas. 77−1157
Ag-Zn (38 at.%), morphological and struct. studies of thermoelastic martensites 77−63669
Ag-Zn (50 at.%), BCC β phase, high temp. creep, existence of master curve 80−55473
Ag-Zn electrodeposition, controlled-potential, spontaneous transformations obs. 78−51853
Ag-Zn equiatomic, creep of β phase *(French)* 78−48477
Ag-Zn-Te(-Sn)(-In), internally oxidised, oxide particle size control *(Japanese)* 80−89480
Ag-Zn(Cd), production and annealing of radiation defects 78−47362
Ag-Zr(Nb)(Mo) film, dielec. const., optical props., DC resist. and thermoelec. power 77−85824
Ag_xAl_y, TDPAC meas. of ^{111}Cd 77−28492
AgAu, and AgCu, mols., VB calcs. 77−57883
AgAu, ion bombardment by alkali-metal sputter ion source *(Japanese)* 79−54734
AgAu, quenched, short range order effects on specific heat 80−29181
AgAu, recovery and formation of mixed dumbbells after thermal neutron irradiation 79−69161
AgAu, sputtered neutral mass spectrometry using post-ionisation in microwave plasma 78−92579
$Ag_3Au_{1-x}Cu_x$, phase relations, X-ray diffr. and differential thermal anal. 80−108395
$Ag_{0.6}Au_{0.4}Mn$, dil., effect of mean free path on strength of RKKY interaction 78−39291
$Ag_{1-x}Au_xYb_y$, thermopower and resistivity 79−65457
$Ag_xAu_{1-x}Zn$, resistivity and X-ray diffr. 78−47283
AgCd, charge transfer, core-electron binding-energy shift 80−2676
AgCd-AgMg(AgZn), quasibinary alloys, phase relations 79−8273
$Ag_{0.5}Cd_{0.5}$, Cd 4d band apparent splitting, cryst. field and d-d overlap influence XPS obs. 79−78825
Ag_xCd_y, TDPAC meas. of ^{111}Cd 77−28492
AgCr, dil., specific heat, impurity contrib. Kondo temp. 80−65903
AgH, electronic struct. and supercond., APW calc. 79−95318
Ag_2Hg_3, grain-boundary and volume diffusion coeffs. of Hg 77−55385
$Ag_{0.285}Li_{0.715}$, liq., partial interference functions, short range chem. order effects 79−7541
AgMg, B2 intermediate phase, slip system, ordering energy and atomic size ratio depend. 80−59471
β′-AgMg, de Haas-van Alphen effect, LMTO band struct. and Fermi surface 78−75984
AgMg, deform. at high temp., yield pts. 79−61674
AgMg single crystals, orientation and temp. depend. of slip 78−87682
AgMg two phase bicrystal growth, orientation, interface struct. 80−60773
Ag_3Mg, long-period alloy, ordered struct. 79−27949
Ag_3Mg, long-period ordered, struct., high resolution electron microscopy obs. 79−94960
Ag_3Mg, ordered, rational and irrational long period struct. 79−95175
Ag_3Mg, ordered alloy, projected pot. image of defect obs. 79−99176
Ag_3Mg, periodic antiphase boundaries, electron microscopy study *(French)* 80−59481
Ag_3Mg, structure of ordered alloy, electron diffraction, kinematical vs. dynamical diffraction calc. 80−10530
Ag_3Mg, two different types of long-period ordered alloys, characterisation by high resoln. electron microscopy 80−49181
$Ag_{83.3}Nd_{16.7}$ amorphous alloy, EPR of Nd^{3+} 79−65727
AgNi, dil., mag. susceptibility of isolated Ni atoms 80−65777
AgPd alloys with Mn and Fe impurities mag. susceptibility 79−73677
AgPd, dil. alloys, electronic states, virtual bound states model test *(French)* 77−62809
Ag_3Sn, containing Au, etching technique for alloys and amalgams 78−3291
Ag_3Sn-Hg, metallic powder-liquid system, correlation between hardness and evolution and sintering states 80−25614
AgZn, B2 intermediate phase, slip system, ordering energy and atomic size ratio depend. 80−59471
AgZn, β′ to ζ_0 and β to ζ_0 phase transform. 79−34026
AgZn, β′→ζ transformation, effect of additional elements 80−66507
AgZn-AgMg quasibinary alloy, phase relation and superlattice form. 78−3097
γ-Ag_5Zn_8, high pressure effect on brass struct. 80−107108
Ag_xZn_y, TDPAC meas. of ^{111}Cd 77−28492
Al-Ag, alloying effect on phonon spectrum and lattice heat cond. 77−62695
Al-Ag, dil., deviation from Matthiessen's rule at high temps. 77−69294
Al-Ag, dil., deviation from Matthiessen's rule at high temps. 78−64025

silver alloys continued
Al-Ag, dil., deviation from Mattheissen's rule, 4-OPW approx. calc. 79−19574
Al-Ag, dil., Dingle temp. calc. 78−39005
Al-Ag, dil., electron irrad., stage I_E recovery, interstitial trapping, 77−15405
Al-Ag, dil., Hall coeff. by OPW Fermi surface model 80−6816
Al-Ag, dil., radiation damage by channelled and random He^+ ion beams 79−46719
Al-Ag, discontinuous decomposition *(Polish)* 78−52808
Al-Ag, electrical resist. of Guinier-Preston zones during age hardening 77−72848
Al-Ag, electronic structure exam. by soft X-ray and X-ray photoelectron spectroscopy 77−85136
Al-Ag, force-and-mass disordered alloys, vibrs., average local-information transfer approx. 80−88290
Al-Ag, growth kinetics of plate precipitates 77−66649
Al-Ag, liquid alloys, exam. of Si diffusion *(Russian)* 79−28118
Al-Ag, low-conc. alloy, spinodal curve and metastable miscibility gap 77−63680
Al-Ag, nonhomogeneity of deform. 78−84888
Al-Ag, precipitate plate growth kinetics 79−15679
Al-Ag, precipitation kinetics and coarsening, effect of interfacial props. 79−91651
Al-Ag, precipitation study by internal friction *(French)* 80−35190
Al-Ag, rapid quenching, struct. and decomp. 80−76244
Al-Ag, resonance splitting of phonons 78−75759
Al-Ag, solute atom displacement in mixed dumbbell interstitials for FCC lattice 78−79631
Al-Ag, thin foil, X-ray microanalysis, surface film effect 78−44428
Al-Ag, type-II superconductor, torque oscillations in mag. field *(Russian)* 80−103800
Al-Ag (0.10 at.%), channelling meas. of trapping efficiencies of solute atoms for self-interstitials 79−86829
Al-Ag (12.6 wt.%), tensile ductility, effect of ageing and impact velocity *(Japanese)* 78−15465
γ′-Al-Ag (15 wt.%), dislocation splitting mechanism, cessation above critical temp. 78−26572
Al-Ag (15 wt.%), precipitate growth kinetics 77−28817
Al-Ag (15 wt.%), precipitation hardenend cyclic stress-strain response 78−35412
Al-Ag (16 wt.%), quenched, early stages of decomposition, small-angle X-ray scatt. meas. 77−59740
Al-Ag (1.03 at.%) alloy elec. resist. meas. above room temp., Ag atom configuration correlation 78−35534
Al-Ag (4 wt.%), scattering of conduction electrons, effect of size and internal struct. of GP zones *(Japanese)* 77−21149
Al-Ag (40 wt.%), deformed, free energy changes in process of discontinuous precipitation 80−3054
Al-Ag (40 wt.%), plastic deform. effect on discontinuous precipitation 80−3053
Al-Ag (5 wt.%), Guinier-Preston zone struct., correl. function *(Russian)* 77−12627
Al-Ag (7.27 wt.%), peculiarities exhibited during fatigue loading *(Chinese)* 80−71723
Al-Ag (up to 4 wt.%), creep, 570-630°C, influence of Ag addition *(Russian)* 79−5003
Al-Ag (up to 40 at.%), exam. of anelastic phenomena and structural state 78−76693
Al-Ag alloy, ageing exam. by X-ray electron spectroscopy and electron diffr. exam. *(Russian)* 78−60685
Al-Ag alloy, second ageing stage, diffuse electron and X-ray scatt. *(Russian)* 78−68711
Al-Ag alloy, thin foil, X-ray microanalysis 77−81439
Al-Ag alloy precipitation and heat of evolution, microcalometric obs. *(Japanese)* 78−15406
Al-Ag alloys, critical resolved shear stress 80−49296
Al-Ag alloys, dilute, electrical magnetoresist., temp. depend., mag. breakdown 79−99532
Al-Ag dil. alloys, Hall coeff., residual resist., and relax. times 79−11107
Al-Ag liquid alloys, diffusion of Ge, mechanism *(Russian)* 80−15276
Al-Ag mirror for use as solar reflector, co-sputtering 80−20789
Al-Ag_2Al, eutectic alloy, exam. of terminal solid solubility limits 78−76633
Al-Ag-Cu alloy precipitation and heat of evolution, microcalometric obs. *(Japanese)* 78−15406
Al-Ag-Mg, metastable T′ phase 77−21151
Al-Ag-Si alloys, phase equilibria at 500°C *(Russian)* 78−56612
Al-Ag-Zn, ring diffuse X-ray scatt. phenomena *(Russian)* 77−16538
Al-Ag(0.1 at.%), μ^+ depolarisation 79−56697
Al-Ag(10 at.%), supercond., flux pinning, torque meas., decomp. effect 77−1525
Al-Cu-Mg-Ag casting alloy, precipitation hardening in artificially aged condition 79−1874
Al-Cu-Mg-(Ag), effect of addition on fatigue microstructure relationships 80−40483
Al-Cu(Zn, Ag, Mg_2Si), intermediate precipitates, stability, X-ray, elec. resist. and hardness study 80−3063
Al-Mg-Ag, age effect on age hardening *(Japanese)* 78−52831
Al-Mg-(Ag), effect of addition on fatigue microstructure relationships 80−40483
Al-Zn, Ag effect on transport props., GP zones 77−16588
Al-Zn-Mg alloy, Ag addition and pre-precipitation treatment, influence on GP zone growth 80−71658
Al-Zn-Mg-Ag, detection of small amounts of Ag by energy dispersive X-ray anal. 77−60154
Al-ζ(AlAg) eutectic and off-eutectic alloys, thermal stability 77−25077
AlAg, Auger spectra, 4d bandwidth effect 80−89093
$Al_{0.965}Ag_{0.035}$, reson. splitting of phonons 77−59086
Au-3d transition metal alloys, UPS study, localised states 80−93449
Au-Ag, appl. of self-consistent cluster Bethe lattice study of two-band alloy model 80−29303
Au-Ag, bicryst. thin film couples, interphase interfaces, TEM 80−70540
Au-Ag, cold worked, impurity conc. rel. to internal friction Bordoni peak, solid soln. hardening mech. 80−16363
Au-Ag, deposition on alkali halide, kinetic nucleation model 77−85118
Au-Ag, dilute, low temp. thermoelec. power, electron diffusion and phonon drag 77−20301
Au-Ag, liquid alloy, surface energy meas. by const. temp. method on solid alumina 78−6208
Au-Ag, mech. damping 78−31444
silver alloys continued
Au-Ag, optical spectra, 0.5-6 eV, d-band struct. 77−48168
Au-Ag, plastic deformation, energy storage efficiency 77−4807
Au-Ag, radiation damage and diffusion 80−24645
Au-Ag, surface segregation 79−77873
Au-Ag, surface segregation, electronic theory, density of states, cluster-Bethe-lattice approx. 80−49369
Au-Ag, thin film struct., Rutherford backscattering spectrometry, signal overlap subtraction 80−50486
Au-Ag (13 at.%), thermopower standard in mag. field 79−78081
Au-Ag (35 at.%), dechannelling of energetic He ions at dislocations 80−70275
Au-Ag alloys, SRO and ordering energy *(Russian)* 77−65964
Au-Ag film, thermoelectric power and resist. meas., MFP and Fermi surface meas. 77−51826
Au-Ag single phase alloy, sputter yields 79−87546
Au-Ag-Cd, γ-ray PAC of ^{111}Cd, nearest neighbour contrib. to elec. field gradient 77−36161
Au-Ag-Cd, martensitic transformation, preceding struct. anomaly 78−68692
Au-Ag-Cd alloys, martensitic phase transition, elastic anomalies and mode softening 79−91647
Au-Ag-Cd pseudobinary alloys, thermodynamic study of order-disorder and martensitic transform. 78−48399
Au-Ag-Cu, chem. surface anal., low energy ISS compared with SIMS 78−64908
Au-Ag-Cu, optical props. study using automatic nulling spectroellipsometer 80−55058
Au-Cu alloy, internal oxidation, calorimetric meas. 79−43258
Au-Cu-Ag, phase precipitation on domain boundaries, effect of Ag *(Russian)* 78−39777
Au-Cu-Ag, phase transform. effect on mech. props. *(Russian)* 78−3122
Au-Cu-Ag dental alloy, age-hardened, struct. and morphology 78−92272
Au-Cu-Ag-Pd (35.4, 17.8, 9.7 at.%), dental alloy, age-hardenable, TEM obs. 77−21156
Au-Mg alloy, internal oxidation, calorimetric meas. 79−43258
Au-Pd-Pt-Ag, composition-property diagrams, mathematical models for diagrams *(Russian)* 79−11554
Au-Pt-Pd-Ag-Cu, commercial dental alloy, age-hardening charact. 80−89235
Au_xAg_{1-x}, density of states and resist., CPA calc. 80−24780
$Au_{52.5}Ag_xCd_{47.5}$, pseudoelastic behaviour associated with thermoelastic martensitic transform. 80−16304
$Au_3Cu_{1-x}Ag_x$, phase relations, X-ray diffr. and differential thermal anal. 80−108395
$Au_{0.77}Ge_{0.136}Si_{0.094}$, undercooled metallic melt, viscous behaviour 77−66037
Ca-Ag liquid alloy, thermodynamic exam. 78−75848
Cd-Ag, annealed, work softened, exam. of crystallographic texture, hardness 78−80559
Cd-Ag, polycryst. quenched foil, the influence of Ag on the recovery spectrum 78−76661
Cd-Ag, polycryst. wire, cold worked, resistivity changes 78−68827
Cd-Ag (0.015 to 0.25 at.%), critical resolved shear stress at low temp. 77−69035
Cd-Ag (3 wt.%), metallographic prep. at room temp. *(German, English)* 77−9026
Cd-Ag-Zn (96, 3, 1 wt.%.) soldering alloy powder, atomised, prod. and appl. 79−100073
Cd-Cd_3Ag, peritectic transform. 77−16564
CeAg, mag. and structural phase transition at hydrostatic press., elec. resist. meas. 79−61102
CeAg, magnetic struct. and cryst. field, neutron diffr. exam. 78−72328
$CeAg_xIn_{1-x}$, cubic to tetragonal phase transform., conc. dependence by resist. meas. 78−2252
$CeAg_2Si_2$, ^{29}Si NMR and mag. susceptibility 79−61246
Cs-Ag, dil., electronic struct., density functional approach 80−44492
Cu alloys purification of solid metals by electrotransport *(German)* 78−51745
Cu-Ag, Ag effect on stainless steel embrittlement during soldering 79−47773
Cu-Ag, alloys, activation vol. stress depend., single crysts. 77−48499
Cu-Ag, Auger spectroscopy, effect of composition on matrix parameters *(German)* 79−11489
Cu-Ag, biphase material X-ray stress determ. *(Russian)* 79−5097
Cu-Ag, deformed, recrystallization nucleation at second phase particles, electron microscope obs. 79−34059
Cu-Ag, dil., dose depend. of impurity detrapping stages after electron irradiation 78−51582
Cu-Ag, dil. molten alloy, Ag activity determ. by two-component evap. *(Japanese)* 77−48395
Cu-Ag, effective atomic number from β-ray produced bremsstrahlung meas. 78−22046
Cu-Ag, electron density change during Cu decay 79−99519
Cu-Ag, ion implantation as an ultrafast quenching technique for alloy production 77−55902
Cu-Ag, liquid alloy, solubility and activity of O_2 79−29028
Cu-Ag, metastable alloy layer formed by Ta^+ ion implantation 78−71709
Cu-Ag, order-disorder transforms., s-band model 79−60502
Cu-Ag, solid soln., nonhomogeneity of deform. 78−84889
Cu-Ag, surface segregation of S, Auger spectral study diffusion 80−76549
Cu-Ag (Ag-O), stirred at different speeds under press., evaporation of Ag 77−47555
Cu-Ag (0.1 wt.%), cold-worked, internal friction peaks in kHz range 80−89276
Cu-Ag (3 at.%), plastically deformed, lattice strain distrib. *(German)* 80−85012
Cu-Ag (8 wt.%), plastic deform. effect on discontinuous precipitation 80−3053
Cu-Ag film, amorphous resistivity, Hall coeff., thermopower and annealing kinetics 77−43744
Cu-Ag film, vac. deposited, thickness meas. using X-ray fluoresc. technique 79−90911
Cu-Ag film preparation with const. comp., by diffusion-limited evaporation from liquid 77−21038
Cu-Ag metastable alloy form. by ion implantation, combined TEM and ion channelling obs. 78−34530
Cu-Ag solder composite, plastic deform. below worn surfaces 77−36670
Cu-Ag-Au, coherent phase diagram, theoretical calc. 80−70373

silver alloys continued
Cu-Ag-Ge, Hume-Rothery glass form. 80−96449
Cu-Ag-O alloys, dil., O-metal interactions, activity coeff. meas. at 1423K 80−93792
Cu-Ag-P alloy wetting of Mo, Nb and Ta 79−82417
Cu-Ag-P amorphous alloys, strain gauge factor and elec. props. *(Japanese)* 79−79130
Cu-Ag-P(6-14, 11-14 wt.%) amorphous, crystn. and elec. props., X-ray diffr., elec. resist. and DTA meas. *(Japanese)* 80−84088
Cu-Ag-X, X=metals, P, S, Se, phase diagrams and thermodynamic props., iso-activity coeff. curves 77−81249
Cu-Ag-Zn, exam. of phase diagrams and thermodynamics props. 79−8275
Cu-Ag-(O), evaporation of Ag in vacuum induction melting 77−28742
Cu-Ag(-Se-Sn), Ag, Se, and Sn effects, singly and together, on recrystallisation 79−100164
Cu-Sn, Sn surface segregation in monolayer regime, model of kinetics and equilib., AES data explained 79−7739
Cu-Ti-Ag, wetting of Al_2O_3, alloying effects 80−107617
$Cu_3Ag_{1-x}Au_x$, phase relations, X-ray diffr. and differential thermal anal. 80−108395
$CuMnAg_x$, hysteresis, spin orbit scatt., effect on anisotropy in spin glass state, rel. to Ag impurity conc. 80−71095
$DyAg_{1-x}In_x$, elec. and Hall resist. 80−96844
Eu-Ag, amorphous, formation and mag. props. 79−91216
$EuAg_5$, cond. electron spin polarisation 77−63136
Fe-Ag, three-dimensional microstruct. analysis, appl. of basic topological concepts 77−59739
Fe-Ag (50 vol.%), two-phase system, plastic deformation *(French)* 78−39831
Fe-Ag (50 wt.%), plastic behaviour in compression, deform. rate effect *(French)* 80−71711
Fe-Ag-Cu melts, phase interface props., Cu influence *(Russian)* 79−51261
Gd-Ag, vap. quenched alloys, struct. and mag. props. 78−84461
Gd-Ag (0-16 at.%), vapour-quenched, struct. and mag. props. 78−38980
Gd-Ag alloy film, amorphous, struct. and mag. props. 78−52318
$Gd_{56}Ag_{46}$, amorphous, susceptibility and magnetisation, 6-300K *(French)* 77−36060
$GdAg_{1-x}In_x$, elec. and Hall resist. 80−96844
$GdAg_{1-x}In_x$, magnetic transition temp., effect of hydrostatic press. 78−76244
Ge-Ag, exam. of structure using electron microscope *(Russian)* 79−14738
Ge-Ag film, codeposited, amorphous and polycryst., struct. and elec. props. 80−24766
Hg-Ag-Sn, dental amalgams, corrosion penetration in crevices 80−3238
Ho-Ag, crystal field parameters from neutron spectra, rel. to mag. props. in ordered state 77−43546
In-Ag, dil., TDPAC technique appl. to diffusion model 79−78589
In_4Ag_9, γ-brass with P cell, struct. determ. 77−24290
La-Ag alloys, amorphous, elec. resist. and supercond. 80−70885
LaAg, band calcs., rel. to mag. and electronic props. and martensitic transform. 77−8014
LaAg, direct Coulomb contrib. of cond. electrons to crystalline elec. field 77−76784
LaAg, direct coulombic contrib. of cond. electrons to cryst. elec. field 79−91005
LaAg, electronic struct., susceptibility, sp. ht. and Knight shift meas. 77−43485
LaAg, electronic struct., NMR relax. times meas. 79−51871
LaAg, press. depend. of martensitic and supercond. transition temp. 79−19681
LaAg, Tb and Pr substituted, superconductors, cryst. field transitions linewidths 80−24854
LaAg, under hydrostatic press., supercond. and phase transform, elec. resist., 1-300K 78−10595
$LaAg_xIn_{1-x}$, crystal struct., neutron diffr. obs. 80−49187
$LaAg_xIn_{1-x}$, phonon dispersion, elastic consts. and struct. instability, soft mode behaviour 80−103436
$LaAg_xIn_{1-x}$, structural instability 78−79562
$LaAg_2Si_2$, ^{29}Si NMR and mag. susceptibility 79−61246
$La_{78}Au_{22}$, amorphous supercond., T_c and fluctuation cond. under high press. 79−7935
$La_{1-x}Gd_xAg$, antiferromagnet, spin echo NMR anal. 80−15821
$La_{1-x}Gd_xAg$, NMR ^{139}La 78−15038
$La_{1-x}Tb_xAg$, paramag. anisotropy of Tb^{3+} in cubic cryst. field 80−15687
$La_{1-x}Tb_xAg$, supercond., 0.6 meV cryst. field transitions, neutron spectroscopy 78−67991
$La_{1-y}Tb_yAg$, crystal field effects, normal and superconducting states 78−2621
$La_{1-y}Tb_yAg$, neutron spectroscopy of 0.6 meV cryst. field transitions 78−30894
Li-Ag, liq., density, compressibility and diffr. data 77−47336
$Li_2Ag_{2-x}In_x$, optical props., struct., energy bands, interband transitions 78−72539
Mg-Ag, anisotropic, dislocation interaction with tetragonal impurity, mobility 77−19953
Mg-Ag, dil., dislocation-point defect interactions in slip systems 78−47417
Mg-Ag, dil., ion irradiated, interaction between Ag and defects, channelling meas. 78−38766
Mg-Ag, ion implanted, recovery stage characterisation by electron irrad. 80−107295
Mg-Ag (0.18 at.%), channelling meas. of trapping efficiencies of solute atoms for self-interstitials 79−86829
Mg-Ag-Cd, X-ray diff. exam. of phase fields *(Russian)* 79−56957
Mg-Ag-Cu, phase comp. in Mg-rich region *(Russian)* 80−40331
MgAg, Auger spectra, 4d bandwidth effect 80−89093
$MgZn_2$-$MgAg_2$, Friauf-Laves phase, long-period stacking variants, electron conc. depend. 77−80444
Mn-Ag, XPS meas., Fermi level to 1000 eV below it 80−66389
MnAg alloys, XPS meas. 80−60751
$NdAg_2$, high temp. modification, thermal effects 78−38665
$NdAg_x$, low temp. mag. meas. 80−107989
$Nd_{21}Ag_{79}$, and $Nd_{50}Ag_{50}$, amorphous, mag. props. 80−60182
Ni-Ag, corrosion in marine atm., potentiometric technique, appls. 79−24693
Ni-Ag alloy, metallographic struct. and formability *(German, English)* 80−30201
silver alloys continued
Ni-Cu alloy, surface comp. and catalysis 80−54489
NiAg, dil., disordered, virtual bound states, reson. model pot. theory 79−23934
Pb-Ag, Ag precipitation kinetics 78−19758
Pb-Ag, diffusion of Au, de-enhancement by Ag impurities 80−19990
Pb-Ag, dil. alloys, dislocation motion and electron-dislocation interactions 77−7728
Pb-Ag, high shear technique for liquidus boundary meas. 79−61564
Pb-Ag, liquid alloy, exam. of thermodynamic props. using solid oxide galvanic cell 78−75851
Pb-Ag, solid soln. hardening due to metal interstials 77−52337
Pb-Ag (0.068 wt.%), Ag precipitation kinetics and activation energy 80−66517
Pb-Ag eutectic alloy, microstruct. coarsening under isothermal and temp. gradient conditions 79−20079
Pb-In-Ag, transport current distribution in longitudinal mag. field 80−25057
Pb(Ag) alloys, effect of Ag content on yield strength 80−76322
$Pb_{1-c}Ag_c$, liquid alloys, local fluctuations and quadrupolar relaxation 80−66060
Pd-Ag, alloys-H solid solutions, superconducting transition temp. behaviour *(Russian)* 80−70879
Pd-Ag, and Pd-Rh-Ag, effects of press. and alloying on Pd electronic struct., susceptibility meas. 78−91581
Pd-Ag, dilute, low temp. sp. ht. and mag. susceptibility 77−62650
Pd-Ag, disordered, extension of Taylor's theory of lattice vibr. 79−4387
Pd-Ag, elec. resist. meas., 300-900K 77−47792
Pd-Ag, electronic structure from annihilation quanta ang. distribs. 77−66107
Pd-Ag, Fermi energy influence on soln. behaviour of H, B and C *(German)* 80−44323
Pd-Ag, H-H interaction in dil. solns. 78−71862
Pd-Ag, influence of adsorbed H on positron lifetime spectra 80−25480
Pd-Ag, ion bombarded, surface segregation, XPES obs. 79−77885
Pd-Ag, positron annihilation, absorbed H_2 effect *(Russian)* 79−91528
Pd-Ag, surface segregation, Auger studies 78−87849
Pd-Ag, thin layer, deposited on glass or Si substrate, X-ray microanalysis *(French)* 80−50902
Pd-Ag (25 at.%) H_2 permeability and solubility, comparison with other Pd solid soln. alloys 79−23738
Pd-Ag alloy, asymmetry of XPS of shell electrons *(Russian)* 78−76579
Pd-Ag alloys, elec. resist. meas., density of states and Debye temp. 77−76715
Pd-Ag alloys, epitaxial growth and surface characterisation 78−14638
Pd-Ag alloys, photoelectron spectra of core electrons 79−100021
Pd-Ag electrical contacts in H_2S atmospheres, formation of contaminating layers *(German)* 80−71811
Pd-Ag electrical resistivity, thermo-EMF and thermal diffusivity at high temps. *(Russian)* 80−6808
Pd-Ag film on $BaTiO_3$ dielectric ceramic substrate, interaction between film and substrate during sintering 79−33958
Pd-Ag microwires, electrical resistance, influence of gaseous environment in heat treatment *(Russian)* 80−20146
Pd-Ag thin-walled tubes, for thermal diffusion apparatus H diffuser 80−100358
Pd-Ag-Au, lattice parameters and thermal expansion coeffs., X-ray diffr. meas. 79−99121
Pd-Ag-Au, temp. effect on lattice parameters and thermal expansion 78−51473
Pd-Ag-Cu (35,25 at.%), determ. of ageing transformations by resist. meas., metallography, TEM and X-ray diffr. 79−4967
Pd-Ag-D system, instability and superconductivity 78−39248
Pd-Ag-Fe, (0.5, 1.0, 2 at.% Fe), elec. resist. reduction near ferromag. and spin glass ordering 77−69299
Pd-Ag-H, alloys, 25-50% Ag, thermodynamic props., 555-700K 79−65216
Pd-Ag-H, band struct. and supercond. props., APW calc. 79−56354
Pd-Ag-H(D), elastic energy dissipation peak 80−60905
Pd-Ag-Si alloys, amorphous, crystn. kinetics, DSC meas. 80−1933
Pd-Au-Ag ternary system, isoparametric curves and Wegard's law plots 79−47657
Pd-Rh-Ag, mag. susceptibility, pressure effect up to 4000 atms. 77−16142
Pd-Rh-Ag, magnetic susceptibility press. depend., d-band deform. and exchange var. 77−47967
PdAg (4.7 at.%), effect of alloying on activation energy of H_2 diffusion 80−107571
PdAg, dil., disordered, virtual bound states, reson. model pot. theory 79−23934
PdAg surface, CO chemisorption, SIMS, XPS study 80−84382
PdAg wire, H_2 sorption, heat of adsorpt., sticking probabilities 78−43240
$Pd_{0.9}Ag_{0.1}$, H and D motion, thermodynamic data 79−65254
$Pd_{0.9}Ag_{0.1}$:H(D), free energy, enthalpies of soln. 78−15692
$Pd_{0.96}Ag_{0.04}$, phonon dispersion curves at 296K 80−24546
$Pd_{1-x}Ag_{1-x}$-Au, dil., electron density at Au, Mossbauer reson. 78−39473
$Pd_{70}Ag_{30}$, force-const. disorder system, obs. of reson.-like phonon mode 79−90745
Pd_cAg_{1-c}, possibility of superconductivity 80−10862
PdAgFe, ferromag., Curie temp. depend. on susceptibility, non-mean field theory 80−44829
$(Pd_{1-y}Ag_y)_{100-x}Fe_x$, exchange-enhanced alloys, mag. ordering 79−61050
$(PdAg_{0.2})H_2$, molar heat capacity, 2-6K, absence of supercond. transition 77−1516
$Pd_{1-x}Ag_xH_c$, superconducting transition temp. conc. var. 77−8221
$Pd_{1-x}Ag_xH_n$, positron annihilation examination of electronic structure *(German)* 77−69931
$Pd_{1-y}Ag_yH_x$, electronic struct. and supercond., APW calc. 79−95318
$Pd_{1-y}Ag_yH_x$, superconducting transition temp., APW band struct. calcs. 78−95393
$Pd_{0.91}Ag_{0.045}Rh_{0.045}H_x$, supercond. transition temp. rel. to optical phonon spectrum 79−56355
$Pd_{78}Ag_4Si_{18}$, amorphous, crystallisation kinetics 77−35487
$Pd_{82-x}Ag_xSi_{18}$, amorphous, roller-quenching conditions determ. 77−21051
$Pd_{0.775}Cu_{0.06}Si_{0.165}$, undercooled metallic melt, viscous behaviour 77−66037
$PrAg_2$, high temp. modification, thermal effects 78−38665
$PrAg_x$, low temp. mag. meas. 80−107989

silver alloys continued
$Pr_{21}Ag_{79}$, amorphous, sp. ht. at low temp. 80−75780
$Pr_{21}Ag_{79}$, $Pr_{50}Ag_{50}$, and $Pr_{10}Lu_{40}Ag_{50}$, amorphous, mag. props. 80−60182
$PrAl_{2-x}Ag_x$, cryst. field and exchange interactions 77−63076
Sc-Ag, electronic struct., susceptibility, sp. ht. and Knight shift meas. 77−43485
ScAg, electronic struct., NMR relax. times meas. 79−51871
ScAg, UPS exam. 78−48276
$Sm_{21}Ag_{79}$, amorphous, sp. ht. at low temp. 80−75780
Sn-Ag, liq., elec. resist. thermoelectric power using t matrix approach 77−31988
Sn-Ag liquid alloys, thermodynamic study by solid-oxide galvanic cell 79−20031
Sn-Pb-Ag, microduplex eutectic, cavitation during superplastic flow 78−48457
Sn-Sb-Ag, splat cooled foils, TEM study 80−40344
Tb-Cu-Ag, mag. props. *(Russian)* 77−51905
TbAg, hyperfine field exam. by NMR spin echo 78−23365
$Tb_{52}Ag_{48}$, amorphous, bulk magnetic props., evidence of strong local anisotropy 77−43830
$Tb_{52}Ag_{48}$, amorphous, mag. after-effect meas. 79−24200
$Tb_{52}Ag_{48}$, amorphous, mag. aftereffect 80−20435
$TbAg_{1-x}In_x$, elec. and Hall resist. 80−96844
$TbAg_{1-x}In_x$, mag. and transport props. 78−43572
$TbAg_{1-x}Zn_x$ solid solns., mag. props. *(Russian)* 77−77049
Te-Ag, dil. liq. alloy, elec. cond. at high temp. and press. 78−87959
Ti-Ag, existence of β to α_m phase transformation 78−44123
Ti-Ag, thermodynamics and kinetics of β to α_m transformation 78−84795
Ti-Ag (10 to 17.5 wt.%), eutectoid system, $\beta \rightarrow \alpha_m$ transform., nucleation kinetics 80−97474
YbAg, mag. susceptibility, thermally excited interconfiguration crossover 77−16042
YbPd-YbAg system, valency state, Yb behaviour *(French)* 80−45277
Zn-Ag, anisotropic, dislocation interaction with tetragonal impurity, mobility 77−19953
Zn-Ag, dil., dislocation-point defect interactions in slip systems 78−47417
Zn-Ag, dil., elec. field gradient, temp. depend. 78−39481
Zn-Ag, dil., polycryst., amplitude-depend. internal friction *(Polish)* 79−96079
Zn-Ag-Cu alloy powder, brazing solder, production using electrodeposition and heating in reducing atm. 79−100079
$Zr_3Co_{1-x}Ag_x$, phase stability and supercond. T_c 78−80519

silver compounds
Ag halides, photographic sensitivity, latent image centres, determ. of stability and dimens. *(Russian)* 80−90922
$AgBi(CrO_4)_2$, synthesis, thermolysis, crystallography *(French)* 80−33946
AgBr, thin layers, struct. and photographic characts. 78−49919
$AgGa_xIn_{1-x}Se_2$, X-ray diffr. cryst. data 80−84147
β-AgI, valence state and impurity-vacancy dipole formation, Mossbauer effect meas. 78−68435
α-$AgSbS_2$, X-ray diffr. study of phase transitions in quenched samples 77−15577
α-$AgSbS_2$ crystals, influence of external elec. field on elec. cond. 80−60056
β-Al_2O_3-Ag_2O, antiferroelectric transformation, Potts' model universality class 80−50277
borate glass, containing Ag_2O, ESR obs. of electron trap centres 77−20697
chalcogenide melts, changes in short-range order struct. during heating 79−50973
chalcogenides, single-phase, preparation 78−35293
chalcopyrite films, (112), lattice mismatch with (0001) CdS substrates 79−87012
chalcopyrites, refr. index dispersion 80−55057
complexes in fixing baths, math. model 77−34043
connection between the topography of luminescence centres and the latent image *(Russian)* 80−62785
dyed Ag halide powders and emulsions, light induced ESR signals 79−24211
glycine silver nitrate, and deuterated analogue, ferroelec. transition, hydrostatic press. effects 77−36185
glycine silver nitrate, dielec. relax. in paraelec. and ferroelec. phases 80−29678
glycine-$AgNO_3$, single cryst., X-irrad., oxidation product form. 77−48660
halide, Dember effect, photographic emulsion grain parameter depend. 78−16870
halide, exposed and unexposed grains, discrimination in photographic development 79−83447
halide, glass, kinetics of photochromic processes 80−103930
halide, grains, breakdown of $Na_2S_2O_3$, electron microscopy 78−21237
halide, photoelectronic glass, flash photolysis expts., metallic Ag formation on Ag halide surface 79−94310
halide, photographic material, sensitivity and struct. characts., review *(Russian)* 79−2868
halide, self-trapped holes, ESR *(Japanese)* 79−73811
halide bleached photographic plate, uniaxial medium generation 79−2848
halide bonding LCAO-MO treatment 79−23561
halide chemical development 79−20399
halide complexes electrodeposited on $In_{2-x}Sn_xO_{3-y}$ contacts, appl. to display struct. 79−15435
halide crystals, investigation of sensitizing and desensitizing action of cyanine dyes 79−20446
halide crystals, relative dissolution rates meas. by flow calorimetry 80−85220
halide crystn. during double-jet emulsification *(Russian)* 79−58826
halide crysts., dislocations, survey of post-war research 80−62449
halide diffusion transfer development chemistry 79−96340
halide doped photochromic glass absorption spectra *(Russian)* 78−60490
halide dry materials for laser printing appls. 80−13179
halide dyed powders and emulsions, nature of light induced ESR signal 79−2852
halide emulsion, mechanism of development 79−39169

silver compounds continued
halide emulsion, $Na_2S_2O_3$ digested, red-IR photoluminescence obs. at 77K 80−103982
halide emulsion and non-Ag halide sensitive materials in plate making 79−17541
halide emulsion colouring, k-value and sensitivity relationship *(German)* 80−7815
halide emulsion crystal growth, complex solubility computation 79−83516
halide emulsion grains, photographic effects of electron and positive hole traps 77−82635
halide emulsion microcrystals, mechanism of reduction by electrode 79−20404
halide emulsion props., Tl^+ ion influence 79−100413
halide emulsions, hot carriers multiplication and latent image formation 79−20408
halide emulsions, kinetics of fixation by thiosulphate and Ag ion 77−82634
halide emulsions, photomoment investigations of ionic and electronic props. 79−24782
halide emulsions, primitive and $AgNO_3$-digested, IR luminescence obs. at 77K 80−103983
halide emulsions, spectral sensitisation, review 78−4719
halide emulsions, ultra-fine-grain, spectral absorption 79−24793
halide film for nanosecond photography, 10.6 μm CO_2 laser pulse spatial distrib. recording 79−89016
halide film physical props., effect of gelatin structure 80−97715
halide grains, photographic sensitivity and response to charged particles, interstitial generation 77−10124
halide grains, restraining effects of adenine *(German)* 79−39175
halide grains, sulphide concentration specks, latent image formation 79−34334
halide high resolution materials, 3-D hologram recording, exposure characts. 78−17880
halide hydrosol models of photographic emulsions 79−20470
halide layers, ultimate sensitivity and resolving power 79−17546
halide microcryst., space charge characts. 78−15097
halide microcrystal, photoconductivity meas. by microwave technique 80−103719
halide microcrystal, sensitised and stabilised, concentration speck and development centre growth 79−83484
halide microcrystals, electron acceptoring props., chronovoltammetry 79−20441
halide microcrystals, low-temp. triboluminescence 77−87861
halide microcrystals, topography of latent image centres and ionic conductivity 79−20442
halide monodisperse emulsions, granularity prediction in processed coatings 79−26163
halide monodisperse photographic emulsion production methods, review of patents 1955-75 *(Russian)* 78−58084
halide optical fibres, extrusion, visible and IR transmission 80−58829
halide photochromic centres in glass, isothermal relax. kinetics 80−16072
halide photochromic glass:Cu^{2+}, characterisation of Cu ions 78−5530
halide photochromic glass, darkening mechanisms under pulsed laser excitation 78−25938
halide photochromic glass, optically induced anisotropy 80−1282
halide photochromic glasses, colour centres struct. 80−66254
halide photochromic glasses, darkening mechanisms, from flash photolysis and EPR studies 77−16156
halide photochromic glasses, flash photolysis expts. 79−20401
halide photochromic glasses, optical properties, effect of Cu ions 80−93364
halide photochromic glasses, props., effect of temp. 78−83057
halide photographic emulsion, fine grain, colloidal stability 79−20443
halide photographic emulsions, SEM investig. of grain props., specimen prep. technique 77−41715
halide photographic layers, 3D holograms recorded with short exposures, diffr. efficiency 79−55087
halide photographic materials for holography, book contrib. 78−25832
halide photography, semiconducting models 79−19630
halide photography and xerography compared *(Japanese)* 78−24876
halide photography in middle IR using laser sources 77−53997
halide polycrystalline fibre, 10.6 μm transmission loss obs. 80−64197
halide sensitised gelatin processing, phase volume hologram form. 80−78797
halide solvation, effect of restrainers in reversal first developer 79−24797
halide thin-film optical recording medium 80−102786
halide visible luminescence obs. at or below 77K 80−108263
halide-insulator interface, interfacial polarisation, dielec. loss meas. 77−2705
halides:Cu, in photochromic glass, formation and theoretical models, review 80−43418
halides, adsorpt. of water, mol. studies of ice-forming capabilities 77−31872
halides, anal. of cryst. binding and Anderson-Gruneisen parameters 80−15040
halides, correlation between electronic dielec. constant and ionic separation 79−4758
halides, cryst., van der Waals coeffs. calcs. 80−96459
halides, cryst. electronic polarisability and ion sizes 77−51341
halides, defect and impurity states, LCAO-MO treatment 78−16876
halides, dielectric behaviour and optic mode Gruneisen parameters 79−10907
halides, effects of ZnO, dyed ZnO and cyanine dyes on spectral sensitivity 79−20432
halides, electron-phonon interactions, review 78−63991
halides, energy transfer in spectral sensitization 79−20427
halides, EPR of triplet state of self-trapped excitons 78−43684
halides, evaporated layers for the study of the primary processes of photography 79−17540
halides, fundamental absorpt., nature and function of A-centres determ. the extra band at the long wave edge *(Russian)* 80−76060
halides, impurity ion migration 79−19406
halides, latent image formation 79−20395
halides, light scatt. ang. depend. and depolarisation, precip. defects 77−48141
halides, matter transport rel. to point defect parameters 80−107488
halides, NMR chemical shifts 80−74180

silver compounds continued
halides, Ostwald ripening in non-ionic surface active agent environment 79−20412
halides, photographic emulsions, latent image form. 77−5939
halides, photographic information recording and retrieval techniques *(German)* 77−26410
halides, photographic process as photoinduced phase transition 79−20402
halides, phys. props. and photographic sensitivity, review *(Japanese)* 77−54007
halides, physical props. rel. to photographic processes 79−19555
halides, sensitivity to multiply charged ionising particles, temp. depend. 79−80714
halides, sensitometric and thermodynamic properties of developable and sub-developable silver specks 79−20396
halides, spectral sensitivity of Herschel effect, photo- and thermostimulation photographic effects *(Russian)* 78−58082
halides, static dielec. constant, strain derivatives 80−100629
halides, strain derivatives of elastic and dielectric consts. 79−60421
halides, strain derivatives of static dielec. const. 79−56710
halides, surface defect struct. 79−19439
halides, surface microstructure of photographic emulsion layers *(Russian)* 79−58819
halides, temp. and press. depend. of transverse-optic modes and anharmonic self-energies 77−11649
halides, tetrahedrally coordinated, band struct. and optical props. 77−51655
halides, unsensitized photographic emulsion, quantitative interpretation of latent image distrib. data 79−20403
halides, valence and cond. states, UPS, temp. depend. 77−20997
halides calc. of heat of fusion using quantum mechanical relations 80−6491
halides van der Waals energy, cohesive energy calc. 77−51343
iodobromides, spectral absorpt. curves, density, wavelength and temp. depend. 78−16871
liquid chromatography, electrochem. detect. and fraction collection system 78−35749
organic acid salts, photolysis investig. for use as photosensitive material for PC forming 77−44496
photographic emulsions, preparation, explosion hazard of ammoniated silver salt solns. 78−4727
polyamine iodide-AgI solid electrolytes, elec. cond. and cryst. struct. 80−107537
proustite-pyrargyrite solid solns., thermal props. *(Russian)* 79−65227
pyridine-Ag_5I_6, superionic conductor, dynamical aspects 78−79695
pyridinium pentasilver hexaiodide, solid, far IR refl. spectra, incoherent neutron scatt., low freq. optical modes 78−2291
pyridinium silver iodide, fast ion conductor, phase transitions, thermoelec. power meas. 80−107540
rare earth silver tungstates, α,β and β' phases, cryst. struct. 77−31627
silver methanedisulphonate, cryst. struct. and information determ. 79−90633
soda lime glass, Ag^+ ion exchanged, planar optical waveguide, manufacturing tolerances 78−71212
stability increase during simultaneous photographic development and fixing *(Russian)* 80−95179
superionic conductors, transport props., review 77−62671
TCNQ salt, Ag.TCNQ, cryst. struct. 80−70186
tetraethylammonium iodide-Ag_nI_{n+1}, ionic conductors, electrochem., props. 77−31808
thioamides, precip., electron microscope and potentiometric studies, growth of photosensitive crysts. 80−33107
titration, amperometric, using thioxanthate 79−57326
trifluoroacetate, aq. soln., positronium form., quenching and inhibition 78−15690
zeolites, type 13X, acetylene adsorption, inelastic neutron scatt. 78−14584
(Ag,Na)Br, ionic transport numbers, polarization cell method 80−59705
(Ag,Na)Cl solid solns., ionic transport numbers, polarization cell method 80−59705
(Ag, Tl, Ca)NO_3, aqueous solutions, vapour press. meas. 80−6504
(Ag,Tl,Cd)NO_3, mixed aq. solns., vapour press., 98.5°C, Brunauer-Emmett-Teller isotherms 78−51655
Ag complex, DNA-Ag (I) in soln., theoret. interpret. of elec. dichroism obs. 80−85347
Ag complex, dioxane perchlorate, cryst. struct., phase transitions, X-ray study 80−59646
Ag complexes, Ag(II) porphyrins, picosec. flash photolysis, transient absorpt. 80−52976
Ag complexes in organic solns., ^{109}Ag NMR, solvent effects 77−16191
Ag complexes of 2-amino-5-methyl-1,3,4-thiadiazole and 2,5-dimethyl-1,3,4-thiadiazole, conductometric and IR meas. 80−87121
Ag halide, absorpt. and vac. photolysis 78−8458
Ag halide, crystals and photographic emulsions, luminescence parameters at 77K 79−24787
Ag halide, effect of Rh and other polyvalent ions on photographic props. 79−24785
Ag halide crystals, effect of redox potential on photosensitivity *(Russian)* 80−73507
Ag halide emulsions, induced sensitized photodichroism 80−9061
Ag halide emulsions, sensitivity calc. 79−21843
Ag halide gelatin emulsions, fixation and washing aspects 77−79176
Ag halide microcrystals, pulsed luminescence expts. 79−24786
Ag halide photochromic glass, darkening mech., temp. depend. 80−87449
Ag halide photochromic glasses, optical absorp. of Ag, optically induced dichroism 80−108177
Ag halide photographic materials, theory of supersensitisation, review *(Russian)* 80−62786
Ag halide system, high speed, for producing direct positives 79−20435
Ag halides, formation of metallic Ag on surface, optical absorpt. calcs. 79−24791
Ag halides, localised MO treatment of fractional bonding 77−58970
Ag halides, spectral sensitisation, estimation of rate constant 78−89575
Ag halides in thioamides, precip., electron microscope and potentiometric studies, growth of photosensitive crysts. 80−33107
Ag halogenide, grain form. and growth in metastable soln. *(Russian)* 77−34048
Ag I, monodispersed airborne particles, ice nucleation 79−20947
Ag I seeding for hail suppression, Ag occurrence analysis 78−65367
Ag photographic films, thermal development *(Russian)* 80−303

silver compounds continued
Ag^+ superionic conductors, US attenuation due to hopping of Ag^+ ions 78−22890
$Ag/Ag_2SO_4(WO_4)$ solid cell systems interface form., intergrain contact growth 77−16827
Ag/AgI/Te thin film galvanic cell, shelf life determ. 78−35702
Ag/α-Ag_2S, interface, electrochemical transfer across phase boundaries 78−73046
$Ag/RbAg_4I_5/I_2$ solid state battery, low temp. degradation 80−61331
$Ag/RbAg_4I_5$/Ta, solid electrolyte timing cell and coulometer 80−68216
Ag-AgCl emulsion, anisotropy induced by two coherent perpendicular light vibrs. 79−55196
Ag-AgCl films, photoinduced dichroism *(Russian)* 79−56878
Ag-AgCl reference electrode for high temp. eqn. environments, construction and performance 77−12803
Ag-AgCl reference electrode for high temp. and high press. electrochemistry 78−35693
Ag-AgCl reference electrode, construction and thermodynamic props., high temp. aq. environment appl. 80−21288
Ag-AgCl/KCl/AgCl-Ag thermocell, and thermal liq. junction pot. for KCl solns. at high temp. 80−16819
Ag-AgI film, photoinduced dichroism *(Russian)* 77−1743
Ag-AgI island granular film, Weigert effect, anomalous dichroism 77−12455
Ag-AgX films, (X=Br,Cl,I), Weigert effect 79−64298
Ag-As chalcogenide glass systems, reaction and diffusion 79−77826
Ag-As-S system glass, struct., props. and vibr. spectra 79−65901
Ag-As-Se system, glass-forming 79−65001
Ag-As-Se system glasses, soln. rate 79−43456
Ag-As-Te glasses, elec. props. *(Russian)* 77−85211
Ag-As-Te system, vitrification region, physiochem. props. 79−41960
Ag-B system, interactions, product chem., phase, struct. anal., book contrib. 78−47305
Ag-Bi-S, ternary phase diagram, DTA and X-ray diffr. investigation 80−84917
Ag-Br-I emulsion, high illumination, departure from reciprocity, intermittence effects, charact. curves *(French)* 78−79085
Ag-Cl-Br emulsion, high illumination, departure from reciprocity, intermittence effects, charact. curves *(French)* 78−79085
Ag-containing glasses, colour adaptation, photoinduced optical anisotropy 79−61331
Ag-Ge-S glasses, X-ray determ. of struct. *(Japanese)* 80−10501
Ag-Ge-Te, phase equilib. from Ag_2Te-GeTe mixture meas. *(German)* 78−84782
Ag-Ge-Te system, chalcogenide, phase equilibria and diagrams *(German)* 80−108418
Ag-halides, photoelastic const. calc. 77−76484
Ag-O-Cs photocathode structure 78−95661
Ag-Pb-Te, phase equilibrium *(German)* 79−34018
Ag-S, liq., mag. susceptibility meas., electron localisation and chem. bonding 80−60178
Ag-S solid solution, grain boundary segregation and S diffusion in Ag 80−25700
Ag-Sb-S, prep. and props. of glasses in the system 77−20053
Ag-Se, liq., mag. susceptibility meas., electron localisation and chem. bonding 80−60178
Ag-Se mixture, activity of Se *(German)* 78−27492
Ag-Se system, formation of FCC thin films *(French)* 77−4267
Ag-Si-Te, phase equilib. from Ag_2Te-SiTe mixture meas. *(German)* 78−84782
Ag-Sn-Te, phase equilib. from AgTe-SnTe mixture meas. *(German)* 78−84782
Ag-Sn-Te phase equilib. 79−29033
Ag-Te, liq., mag. susceptibility meas., electron localisation and chem. bonding 80−60178
Ag-Te-O, partial pressure diagrams 77−36681
(Ag-Cs)Br molten mixture, transport nos. and external mobilities *(French)* 79−77787
(Ag-M)Br, (M=Na, K, Rb, Cs) molten mixtures, molar vols. and molar conductivities *(French)* 79−77788
$AgAlS_2(Se_2)(Te_2)$, tetragonal distortion 79−32942
$AgAsS_2$, $AgSbS_2$ and $AgBiS_2$, cryst. and vitreous, refl. spectra, energy spectrum 77−8596
$AgAsS_2$, cryst. and amorphous, band struct., photoemission and refl. spectra obs. 77−66581
$AgAsS_2$, dissociation pressures and their temp. depend. 79−52640
$AgAsS_2$-$AgSbS_2$ system, thermal, microstructural X-ray phase anal. 77−32565
$AgAsS_3$, proustite, parametric upconvertor, temp. effects on tangential phase-matching condition 80−99804
Ag_3AsS_3, $CdGeAs_2$, freq. synthesis of 260 THz, 1.15 μm He-Ne laser 79−64263
Ag_3AsS_3, dissociation pressures and their temp. depend. 79−52640
Ag_3AsS_3, electroacoustic interaction obs. 77−11966
Ag_3AsS_3, low temp. struct. transition 79−69245
Ag_3AsS_3, phase transition near critical pt., spin-lattice relax. *(Russian)* 79−38397
Ag_3AsS_3, prod. and acoustooptic props. *(Russian)* 78−63158
Ag_3AsS_3, proustite, cryst., vibr. spectra 78−48172
Ag_3AsS_3, proustite, cryst., new trigonally oriented ferroelec. semiconductor 79−61317
Ag_3AsS_3, proustite, elec. cond. rel. to impurities, melt stoichiometry deviations 77−11914
Ag_3AsS_3, proustite, ferroelec. with no 180° polarisation reversal, ferroelec. phase transition 79−38465
Ag_3AsS_3, proustite, ferroelectric phase transition under continuous illumination *(Russian)* 79−61315
Ag_3AsS_3, proustite, ferroelectric transition, thermodynamic description 79−69787
Ag_3AsS_3, proustite, freq. conversion of CW chem. HF laser radiation 78−30023
Ag_3AsS_3, proustite, heat of melting 78−43106
Ag_3AsS_3, proustite, light effects on dielec. props., elec. resist. 80−49816
Ag_3AsS_3, proustite, multistage conversion of pump energy into low-freq. radiation 78−30022
Ag_3AsS_3, proustite, nonequilibrium carrier exam. 77−15912
Ag_3AsS_3, proustite, parametric oscillator with synchronous two-cascade interactions energy charcts. *(Russian)* 78−83032
Ag_3AsS_3, proustite, parametric conversion of single-pulse CO_2 laser for photographic recording 79−10357

silver compounds continued
Ag_3AsS_3, proustite, phonons and soft modes at ferroelec. transition 80−60524
Ag_3AsS_3, proustite, reflectivity and optical constants at 80K and 300K from 18 to 700 μm *(French)* 77−36235
Ag_3AsS_3, proustite, residual conductivity and low-temp. phase transitions 78−91729
Ag_3AsS_3, proustite, structural changes in low temp. phase transition, NQR study 80−19935
Ag_3AsS_3, proustite, thin cryst., difference freq. power generation, 6.7-10.5 micron 77−83926
Ag_3AsS_3, proustite, upconversion linearity for short CO_2 laser pulse diagnostics 79−27304
Ag_3AsS_3, proustite crystals, stoichiometric composition derivation influence on phase transition 79−95715
Ag_3AsS_3, proustite upconvertor, effect of temp. on phase match angle characts. 80−5799
Ag_3AsS_3, prustite ferroelectric order model in prustite type nonlinear crystals *(Russian)* 79−65807
Ag_3AsS_3, Raman spectra obs. of low-temp. phases 80−93327
Ag_3AsS_3, SHG, absorpt. coeffs. and temp. variation of refr. index difference 80−14390
Ag_3AsS_3, US absorpt. and vel., 4.2-100K 77−24361
Ag_7AsS_6, thermal, crystallographic and elec. props. *(French)* 80−40338
Ag_3AsS_3; NQR study of phase transitions, high press., tricrit. pt. determ. 79−77746
$AgAsSe_2$, X-ray diffr. exam. 77−7704
Ag_3AsSe, X-ray diffr. exam. 77−7704
Ag_3AsSe_3, synthesis and X-ray cryst. struct. anal. 79−4284
Ag_7AsSe_6, thermal, crystallographic and elec. props. *(French)* 80−40338
$AgBF_4$, ionic radii and chem. shifts, correl. with electronegativity 80−66054
AgBi, laser induced fluoresc., vibr. anal., rot. consts. *(French)* 77−18959
$AgBi(CrO_4)$, cryst. struct., neutron diffr. time-of-flight study *(French)* 80−15057
$AgBi(Cr_2O_7)$, cryst. struct. determ. by X-ray and neutron diffr. *(French)* 80−92492
$AgBiS(Se)_2$, polymorphism and defects, electron microscopy 78−2254
AgBr, (100) and (111) face, influence on aggregation of sensitising dyes 79−39202
AgBr (100) microcryst., dielectric loss meas., ionic conductivity 77−43931
AgBr absorption of gelatine *(Russian)* 79−100420
AgBr, activation parameters of mass transfer process by radiochemical meas. *(German)* 80−38974
AgBr, adsorption of cyanine, pH depend. 78−62254
AgBr, adsorption of gelatin on single crystals, ellipsometric investigations 79−24779
AgBr, Ag speck formation, ionic and electronic effects in photographic process 77−4917
AgBr, Ag^+ migration vol. for vacancy and interstitial motion, influence of anharmonicity 79−14965
AgBr and $AgBr:PbBr_2$, emulsion grains, dielec. loss, ionic cond. and surface space charge 77−28038
AgBr, and $AgBr_{1-x}I_x$, photolum. and X-ray luminesc. spectra *(Russian)* 79−2867
AgBr, Bose-Einstein condensation of triplet excitons 77−44057
AgBr, Br diffusion plot, anomalous curvature 79−60548
AgBr colloidal suspension radiolytic reduction obs. 79−91979
AgBr, connection between the topography of luminescence centres and the latent image *(Russian)* 80−62785
AgBr, crossed elec. and mag. fields, hot electrons, streaming motion and population inversion 80−44649
AgBr cryst. growth mechanism in gelatin solns. 77−54004
AgBr crystal face influence on aggregation of sensitizing dyes 79−20428
AgBr, crystal growth behaviour, influence of Gibbs-Thomson effect 78−24883
AgBr crystal produced by action of free radicals, developability 80−66838
AgBr crystals, electrical potential distrib. near interface, recording using automatic device 79−24759
AgBr crystals, positron lifetime *(German)* 78−19593
AgBr, curvature of conductivity plots, consequence of anharmonicity 78−79800
AgBr, cyclotron reson. of polarons at high microwave fields 78−67958
AgBr, cyclotron reson. of polarons at high microwave fields 79−61228
AgBr, cyclotron reson. of polarons at high density excitation 80−75859
AgBr, decay of proposed Bose-Einstein condensed excitons 78−15221
AgBr, decoration of sensitivity specks 79−24784
AgBr deformed crystals, positron annihilation, mean lifetimes *(German)* 77−11589
AgBr, determ. of ionic transport processes 77−89578
AgBr, dielectric behaviour under hydrostatic press. 78−52420
AgBr, diffusion of Fe^{3+}, vacancy migration evidence 78−47603
AgBr, diffusion of Na^+, NQR caused by vacancy diffusion of impurities, spectral density 78−68408
AgBr dispersion in gelatin, adsorbed S and Au, transient absorpt. spectra, latent image form. and decay 80−66837
AgBr, dispersive phonon modes, reson. Raman scatt. obs. 78−10896
AgBr, distrib. of Ag_2S on sensitised emulsion grains 78−62248
AgBr, doped, neutralisation of trapped photoholes 78−76108
AgBr, dye sensitized photo-process 79−20433
AgBr, EPR of excitons, detected in X-ray excited luminesc. spectra at 4K 77−55732
AgBr, effect on photographic characts. of subbing glass substrate *(Bulgarian)* 78−78016
AgBr, electron-hole kinetics 79−24005
AgBr, electron-hole liq. and biexciton pocket, luminesc. obs. 78−15216
AgBr, electron-hole liquid theory, generalised RPA 78−87914
AgBr, electron-hole liquid, RPA calcs. 80−6743
AgBr, electronic dielec. const., vol. depend., Clausius-Mossotti model 80−100630
AgBr emulsion, cubic, supersensitisation of microwave photocond. 77−41713
AgBr emulsion, desensitizing action of a secondary iodide *(Russian)* 79−58820
AgBr, emulsion, grain disorder and its influence on emulsion response 77−5940

silver compounds continued
AgBr emulsion, influence of iodide content on ripening behaviour 79−24794
AgBr emulsion, latent image speck size, characteristic curve anal. 79−34338
AgBr emulsion, latent image fading 79−34335
AgBr emulsion, low-intensity reciprocity failure *(French)* 78−37085
AgBr emulsion, model system, Ostwald ripening obs. 77−2707
AgBr, emulsion, sensitisation by hydroxy-tetraazaindenes 77−54006
AgBr emulsion, sub-image and latent image specks form. and props. 78−21245
AgBr emulsion crystal habit transitions 79−100447
AgBr emulsion grains, adsorbed dyes, light-induced ESR spectra 80−88862
AgBr emulsion grains, edge length dependence of ionic conductivity, space charge characteristics 80−88360
AgBr emulsion layer with gelatin, IR absorpt. spectra before and after laser exposure *(Russian)* 80−62776
AgBr emulsions, apparatus for studying reciprocity variations and intermittent effects *(French)* 77−71392
AgBr emulsions, effect of gelatin replacement with polyvinyl alcohol 79−20440
AgBr emulsions, ionic thermocurrents 79−19399
AgBr, enhanced defect form., mean field theory 80−107220
AgBr, epitaxial layer, ionic field effect 78−10588
AgBr, evaporated layer, vacuum deposition of Ag at room temp. 79−20409
AgBr, evaporated layer, influence of sublayer on stability and photographic characteristics *(Bulgarian)* 80−42281
AgBr evaporated layer chemical sensitisation 79−24766
AgBr evaporated layer response in ionisation semiconductor photographic system *(German)* 80−101859
AgBr, evaporated layers, high acuity development 79−24798
AgBr evaporated layers, spectral sensitization using cyanine dyes 80−26035
AgBr, evaporated layers, use as registrating system *(Bulgarian)* 80−52344
AgBr, evidence for population inversion of hot electrons 79−91085
AgBr, exchange charge polarisation 78−92016
AgBr, exciton absorpt. at high excitation rates 80−2343
AgBr, exciton relax. by intervalley scatt., reson. Raman meas. 79−33713
AgBr, exciton relaxation by intervalley scattering 80−20644
AgBr, excitonic mol. recomb., photoluminesc. 77−8633
AgBr excitonic mols., time-resolved luminesc. line obs. 77−69888
AgBr, far IR spectra, cond., cation local motion 79−1754
AgBr film, surface space charge region 77−1508
AgBr, film and microcrystal, interstitials and surface conductance thin films [CC AgBr, interstitials and surface conductance] surface conductance 79−23776
AgBr film coatings, luminesc. props. for H_2 and other reduction sensitisation 79−61886
AgBr, form. of mixed AgBr(J) phase during two-jet photographic emulsification *(Russian)* 79−44968
AgBr, formation vol. of Frenkel defect 78−79606
AgBr, free holes in spectral sensitisation 78−4720
AgBr, Frenkel defects, interstitials, neutron scatt. study 79−42059
AgBr, frequency dependent optical phonons contrib. to small radius excitons binding energy 77−69236
AgBr grains, photographic emulsion, sensitivity centre variation with grain size 80−9055
AgBr grains, photographic emulsion, grain diameter dependent development probability 80−9056
AgBr, Herschel effect, latent image centre struct. changes under laser irrad. 80−77900
AgBr, high-temp. ionic transport processes 79−23777
AgBr, high-temp. transport anomaly from Na tracer obs., mechanism 77−62669
AgBr, highly excited, time resolved luminesc., recomb. of excitonic mols. 77−69889
AgBr homogeneous emulsions, iodide influence on photographic props. 79−44959
AgBr, hot electron population inversion, in crossed elec.-mag. fields, 4.2K 79−38128
AgBr, hydrosol, latent-image stability, chem. sensitisation 78−21236
AgBr in gelatin films, effect of AgBr comp., aging, UV exposure *(Russian)* 79−67408
AgBr, indirect near edge emission, 1.5-50K 77−16380
AgBr, influence of Cd ions on crystal shape 79−19235
AgBr, ionic cond., dielec. loss meas. 79−23768
AgBr, ionic transport, defect form. and migration energies, quasiharmonic model 80−107538
AgBr large grain photographic emulsions, reciprocity errors and disturbance effects in high illuminations *(French)* 79−97452
AgBr, latent pre-image specks, investigations on temp. dependence of lifetimes by 'two-flash' method 79−20406
AgBr, lattice dynamics, 295K, three-body-force shell model 77−15517
AgBr, lattice dynamics, 4.4K, neutron scatt. expts. 77−39643
AgBr layer, model form. of latent image centres 78−62253
AgBr layer, sensitised, topography of developed centres 80−73491
AgBr layers, solubility and transport of Ag 79−23742
AgBr, localisation of polarons on (100) surface, rel. to photographic sensitivity *(Russian)* 77−35983
AgBr, luminesc. band shape of free excitons, at high exciton density, calc. 77−81148
AgBr, luminescence of photographic emulsions sensitised by 1,1′-diethyl-2,2′-cyanine with Ag_2S clusters *(Russian)* 80−73513
AgBr luminescence/wavelength relationship visible and near IR spectra *(Russian)* 80−50422
AgBr, magneto-optics, two-phonon pinning interaction 79−91411
AgBr melt, Raman spectra, rel. to sublattice melting in α-AgI 78−10882
AgBr melts, surface energy and surface tension coeffs., effect on photographic emulsion microcryst. growth rate *(Russian)* 80−47132
AgBr microcrystal dispersed in gelatin, effect of I^- on interstitial Ag ions 78−26726
AgBr, microcrystals, activation energy for ionic cond. 80−34237
AgBr microcrystals, Herschel effect, $Na_2S_2O_3$ etching soln. effects *(Russian)* 79−5167
AgBr microcrystals, influence of Pb^{2+} ions on ionic conductivity and space charge characts. 79−23778
AgBr microcrystals, photohole motion 78−26903

silver compounds continued
AgBr microcrystals, photocond. and luminesc. 78−26904
AgBr microcrystals, S sensitization effects on ionic conductivity 79−19398
AgBr microcrystals, sintered, photocurrent-inversion effect at room temp. 78−62246
AgBr microcrystals, spectrally sensitised, luminesc., effect of hydrophobic organic compounds 80−97331
AgBr microcrystals in dispersed photographic emulsions, dimens. determ., specific turbidity method *(Russian)* 79−26027
AgBr, molten, freq. depend. ionic cond. 77−7882
AgBr, molten, Monte Carlo computer simulation 78−26426
AgBr monocrystals, dimensioning rel. to light scatt. of highly dispersive photographic emulsions *(Russian)* 79−49327
AgBr monosize emulsion growth 79−79312
AgBr, multivalent impurities 79−19556
AgBr, NMR chemical shifts 80−74180
AgBr NaBr, thermodynamic props., metastable states and demixing 80−96660
AgBr, neutralisation of trapped photoholes 79−24788
AgBr, new shoulder in luminesc. spectra, triplet excitons 80−20706
AgBr, nucl. emulsion, latent image form., grain diameter depend. 80−9453
AgBr octahedral emulsion, reduction sensitization 79−20420
AgBr, optical absorpt. of indirect exciton in high mag. field 78−60486
AgBr, phonons at elevated temp. 78−79810
AgBr, photo-EMF relaxation, temp. depend. 230 to 316K *(Russian)* 80−73508
AgBr, photodielectric effect at low temp. *(Russian)* 80−96947
AgBr, photoexcited, dye sensitized bleaching of surface silver specks 78−308
AgBr, photoexcited electrons and holes in latest image form., review 80−73496
AgBr, photographic emulsions, dye spectral sensitization, latent image form., subcond. band events 78−32905
AgBr, photographic emulsions, sensitivity, fog rel. to treatment in redox-buffered solns. 78−32906
AgBr photographic emulsions, adsorpt. of thiolic antifoggants, chem. struct., ESCA investig. 78−32907
AgBr photographic emulsions, scale-up factors in batch precipitation 79−20410
AgBr, photographic gelatin dispersion, cryst. habit. rel. to Br^-, cyanine absorpt. 78−32908
AgBr, photographic monodisperse emulsions, Ag sub-specks 78−16875
AgBr, photoluminesc. study of excitons in high mag. fields 80−80843
AgBr, photolysis, diffusion and recombination processes 79−24789
AgBr, point defect form. energies, atomistic calc. and surface pot. meas. 80−107221
AgBr, polar semiconductor, electron-hole liquid, electron-phonon interactions 80−6739
AgBr polydispersed particles in unsensitised holographic emulsion, bulk attenuation and absorpt. *(Russian)* 79−2865
AgBr precipitates, phase boundary processes, quantum mech. law in mass transfer processes *(German)* 79−27937
AgBr, prep. of high purity cryst. with <3 ppb I 77−69982
AgBr, properties of Ag clusters 79−20397
AgBr, pure and doped, identification of shallow electron centres 77−59267
AgBr, quadrupolar deformability theory by tight binding method 80−10614
AgBr, radiative recomb. of indirect excitons at high concs. 78−6732
AgBr, Se sensitized, high intensity reciprocity failure 79−20421
AgBr, self-diffusion of ^{82}Br by both single vacancies and vacancy pairs 78−55978
AgBr sensitized photolayer, overall spectra of local electronic levels 79−23933
AgBr, shoulder in luminesc. spectra due to triplet excitons 79−15525
AgBr single crystals, adsorption and orientation of cyanine dyes 79−20431
AgBr single-crystal IR optical fibres, growth from melt 80−53449
AgBr, sol, electrophoresis of spectral sensitising dyes, dye layering obs. 77−56240
AgBr sols, kinetic exam. of halide conversion 77−82636
AgBr, Stark effect on I-bound exciton 79−28719
AgBr, streaming cyclotron motion of hot electrons, at intense microwave fields 80−6703
AgBr surface, vibr. freq. of adsorbed Ag atom, LCAO-MO calc. *(Russian)* 79−2866
AgBr, thin epitaxial layer, surface ionic cond., lattice disorder, space charge region 77−11730
AgBr thin film interstitials, Frenkel and space-charge contributions 79−18494
AgBr thin films, influence of bromine vapour on spectral props. 77−71393
AgBr, thin layers, evaporation conditions, photoresponse *(Bulgarian)* 78−78017
AgBr, time resolved luminesc. spectra at high excitation density 79−78751
AgBr track detectors, preparation, sensitivity, discrimination ability 78−94169
AgBr ultra fine grained photog. emulsions, impurity obs. spectra *(Russian)* 79−69871
AgBr undeveloped photographic layer, light scattering and absorption *(Russian)* 78−37090
AgBr, vacuum deposition of Ag, growth mechanism 80−35095
AgBr vacuum evaporated thin films, sensitometric obs. 78−78010
AgBr, vapour, photoelectron spectrosc., interpretation 80−95679
AgBr, vapour-deposited epitaxial film, surface structure 80−59814
AgBr, very fine grained emulsions, effect of hole and electron acceptors on photosensitivity *(Russian)* 80−73515
AgBr, X-ray diffraction pattern recording on photographic film, student expt. 78−41130
AgBr:AgCl, mixed crystals, first order reson. Raman scatt., momentum conservation relax. 79−56790
AgBr:Cd^{2+}(Sr^{2+}), single cryst., stress-induced migration and aggregation of solute ions, internal friction 79−51200
AgBr:Cl, exciton-phonon interaction, reson. Raman scatt. vs photolum. 80−29798
AgBr:Cl, impurity diffusion, vacancy pair and single vacancy contribs. 79−77830
AgBr:Cu^+(Cu^{2+}), luminesc., ion interactions 77−66534

silver compounds continued
AgBr:I, activator luminesc., energy model 79−28808
AgBr:I, isoelectronic trap 79−43016
AgBr:I, refilling of recombination centres during thermal stimulation 78−10464
AgBr:I emulsion, photocond. and luminesc. at −186°C, rel. to incident light intensity 78−64063
AgBr:I single jet precipitation, grain growth kinetics 79−20414
AgBr:I_3^- emission spectra at 4.2K 79−4841
AgBr:Li^+, time-depend. infrared absorpt. due to Li-localised mode 79−8133
AgBr:Li^+(Na^+), impurity induced IR absorpt. 80−7386
AgBr:Na^+(Li^+), correlated diffusion of impurities, nuclear spin relax. meas. 80−108094
AgBr:Ni^{2+}, low-temp. EPR 77−77091
AgBr:Pb_3 impurity distrib., ion scattering spectroscopy obs. 77−19979
AgBr:Pb^{2+}, cubic microcryst., ion influence on ionic cond. and space charge characts. 79−55928
AgBr:Pd, EPR of Pd^+ ions 78−27087
AgBr:Pd(II), photolysis-induced trapping behaviour, EPR study 80−54949
AgBr:Pt, photochemistry and role of Pt impurity ions 79−24783
AgBr:Sr, stress induced anomalies in internal friction, logarithmic decrement 79−66095
AgBr-Ag light sensitive system, diffusion of excited states *(Russian)* 78−59101
AgBr-Ag_2O-P_2O_5, glass formation and ionic conductivity 80−65290
AgBr-AgCl, mixed crystals, pure and I doped, lattice defect parameters, Frenkel defect form. energy, ionic cond. 80−44359
AgBr-AgCl, photographic emulsions, reciprocity errors and disturbance effects in high illuminations *(French)* 79−97452
AgBr-AgCl mixed crystal, elastic consts., temp. and press. derivatives 77−11620
AgBr-AgI, photographic emulsions, reciprocity errors and disturbance effects in high illuminations *(French)* 79−97452
AgBr-AgI emulsion sensitivity improved by AgCl shell crystallisation *(German)* 80−104453
AgBr-gelatin photographic composite film with high loading factor, extension of Maxwell-Garnett dielectric loss theory 79−19835
AgBr-Li^+(Na^+), local mode freqs., Green's function calc. 80−39237
AgBr-$Na_2S_2O_3$-H_2O system, thermodynamic and kinetic investigations 79−20444
AgBr-NaBr, phase diagram, miscibility, binodal curve and demixing kinetics, X-ray meas. 80−96659
AgBr-NaCl(Br) solutions, UV spectra 78−39560
AgBr-SiO_2, field effect potentiometric sensors 78−35691
$(AgBr)_3$, gas, He(I) photoelectron spectra 80−43103
AgBr(:Pb^{2+}), ionic conductivity, Frenkel defects 77−51542
AgBr(Cl):$Ru^{3+,2+}$, dopant vacancy config., EPR 79−91288
AgBr(Cl)-CuBr(Cl), photochromic film for hologram recording 79−64184
$AgBr_{1-x}Cl_x$, ESR of self-trapped holes, Jahn-Teller and reorientation effects 78−27092
$AgBr_{1-x}Cl_x$, Jahn-Teller type self-trapping of holes 79−65709
$AgBr_{1-x}Cl_x$, mixed cryst., formation of self-trapped holes 78−39399
$AgBr_{1-x}Cl_x$, self-trapped holes, ESR meas. 77−36131
$AgBr_{1-x}Cl_x$, self-trapped holes, Jahn-Teller and reorientation effects in ESR 78−64273
$AgBr_{1-x}Cl_x$:Cu^{2+}, EPR of $(AgBr_6)^{4-}$, Jahn-Teller effect 79−91294
AgBr(I) crystals, luminesc. of individual monocrystals *(Russian)* 80−301
AgBr(I), emulsion coating, H hypersensitisation to diminish recomb. and increase quantum efficiency 77−5942
AgBrI emulsions development, processing and DQE 79−24801
AgBrI, fine grain emulsion, spectral and reduction sensitization interaction 79−20430
AgBrI microcrystals, luminescence spectra 79−19935
AgBrI microcrystals, growth mechanisms 79−19171
AgBrI negative emulsions, sensitivity and fog centres with S sensitization 79−20418
AgBrI photographic emulsion prep., double-jet nucleation turbidimetry 79−100446
AgBrI photographic grains, TEM investig. of morphology and crystallography 77−57418
AgBrI, reduction sensitised emulsion by dyes, redox potentials, quantitative correlations 79−34298
AgBr(I), sensitization mechanism of a tetraazaindene stabilizer 79−20415
Ag_2BrNo_3, cryst. struct. 78−18594
$Ag(CN)_2$, adsorption on activated charcoal 79−82455
$Ag(CN)_2$, adsorption on activated charcoal, kinetics and thermodynamics 79−82456
AgCNS, mixed conductor, elec. cond. props. 80−65639
$Ag(CO)_2^+$, laser Raman spectra, CO stretching region 79−59469
Ag_2CO_3, high press. phase relations, DTA 77−43329
Ag_2CO_3, X-ray cryst. struct. determ. *(French)* 79−69071
Ag_2CdI_4, fast ionic cond. and order-disorder transition 79−99363
AgCdO, powder metallurgy production, for switchgear in power engineering 80−104094
AgCl, AgCl:AgBr, exciton creation, ODMR 78−79933
AgCl, activation parameters of mass transfer process by radiochemical meas. *(German)* 80−38974
AgCl, and Br doped, EPR of excitons, detected in X-ray excited luminesc. spectra at 4K 77−55732
AgCl bicrystal, grain boundary slip simulation 78−3176
AgCl, bond dissoc. energy, electronegativity pot. function, pot energy curves 77−10784
AgCl, colloid bands induced by reactor irradiation at low temps. 78−26567
AgCl, colloid centres by heavy ion implantation 78−63780
AgCl, colloid centres induced by reactor neutrons at 20K 78−72560
AgCl, crossed elec. and mag. fields, hot electrons, streaming motion and population inversion 80−44649
AgCl, cryst. growth by Stepanov's method 78−23600
AgCl, cryst. luminesc. and photovoltaic effect kinetics 78−64391
AgCl crystal growth in gelatin soln. 80−64942
AgCl, crystal growth modification in aq. gelatin by incorporation of Br^- and I^- ions 77−5946
AgCl crystal plate supersensitisation, photoelectrochemical obs. 79−83486
AgCl crystals, optically detected magnetic resonance 79−24233

silver compounds continued
AgCl, curvature of conductivity plots, consequence of anharmonicity 78−79800
AgCl, defects induced by energetic ion implantation 78−17518
AgCl deposition on Ag electrodes, properties, production, problems in biomedical appl. 77−40959
AgCl, determ. of ionic transport processes 77−89578
AgCl, dielectric behaviour under hydrostatic press. 78−52420
AgCl electrode, electrochem. dye spectral sensitization, gelatin addition *(Japanese)* 79−57262
AgCl, electronic contact charge density of ^{107}Ag, core and overlap contrib. 79−78064
AgCl, electronic dielec. const., vol. depend., Clausius-Mossotti model 80−100630
AgCl emulsion, anisotropy induced by two incoherent and perpendicular light vibrs. 79−41428
AgCl emulsion, spatial differentiation, of intensity distrib., using Weigert effect 79−81377
AgCl, enhanced defect form., mean field theory 80−107220
AgCl, epitaxial growth on TGS, model system for orientation mechanism determ. during epitaxy 79−11022
AgCl, epitaxial overgrowth on AgBr sheet crystals 79−19988
AgCl, epitaxy on Ag spherical cryst. by Cl adsorption 78−14642
AgCl, evidence for population inversion of hot electrons 79−91085
AgCl, exchange charge polarisation 78−92016
AgCl, excited states, optically detected EPR 79−8073
AgCl film, on complementary cleavage planes of TGS, morphology, electron microscope obs. 79−15031
AgCl, formation vol. of Frenkel defect 78−79606
AgCl, Frenkel defects, interstitials, neutron scatt. study 79−42059
AgCl, high-temp. ionic transport processes 79−23777
AgCl, hot electron population inversion, in crossed elec.-mag. fields, 4.2K 79−38128
AgCl in alkali chlorides aq. soln., absorpt. spectra 79−65895
AgCl, interionic forces, cohesive energy, bulk modulus calcs. 79−82176
AgCl, ionic mobility, diffusion coeffs., defect mobility energies 80−65284
AgCl, ionic space charge and dissolution 80−107431
AgCl, ionic transport, defect form. and migration energies, quasiharmonic model 80−107538
AgCl, irradiated, surface defect center, XPS study 79−28894
AgCl, light scatt. during photolysis 77−40565
AgCl, luminesc. excited by UV radiation at 80K *(Russian)* 78−31256
AgCl, luminescence, theory and measurement 79−19934
AgCl, luminescence fatigue, adsorbed Ag atoms 80−66281
AgCl, luminescence/wavelength relationship visible and near IR spectra *(Russian)* 80−50422
AgCl melts, surface energy and surface tension coeffs., effect on photographic emulsion microcryst. growth rate *(Russian)* 80−47132
AgCl microcrystals in sol., cryst. growth, optical absorpt. 77−12835
AgCl, molten, freq. depend. ionic cond. 77−7882
AgCl, molten and solid, visible absorption spectra *(Japanese)* 79−4816
AgCl monosized emulsions, S sensitization 79−20417
AgCl, multivalent impurities 79−19556
AgCl, NMR chemical shifts 80−74180
AgCl nuclear track detectors, track forming, stabilisation and development processes 78−17516
AgCl nucleation from aqueous solns., stopped-flow UV absorption spectrophotometry 79−20413
AgCl, optical absorpt. of indirect exciton in high mag. field 78−60486
AgCl, optically detected EPR of excited states rel. to luminesc. 77−12256
AgCl oriented single crystal, Kyropoulos growth using NaCl seed crysts. 78−11102
AgCl, paramagnetic S-centres, saturation props., ESR meas. 80−50181
AgCl particles suspended in photochromic glasses, shape rel. to photosensitivity 78−31223
AgCl photochromic glass, additional absorpt. spectrum, ellipsoidal model of colour centres 80−40142
AgCl, photoconductivity and photoluminesc., 6.8 to 80K, exciton and valence band states 77−43644
AgCl, photolum. and X-ray luminesc. spectra *(Russian)* 79−2867
AgCl photosensitive emulsion, Weigert effect appl. to contrast reversal of black and white transparency 79−26165
AgCl, piezo- and elasto-optic consts., temp. depend., 20-350°C 77−63392
AgCl, point defect form. energies, atomistic calc. and surface pot. meas. 80−107221
AgCl precipitates, phase boundary processes, quantum mech. law in mass transfer processes *(German)* 79−27937
AgCl, pure and dopded, identification of shallow electron centres 77−59267
AgCl, quadrupolar deformability theory by tight binding method 80−10614
AgCl, ratio of photoelastic constants 77−84828
AgCl, separation of neutron deficient Ru isotopes by gas thermochromatography 79−865
AgCl, single cryst., optical, acoustic and acousto-optical props. *(Czech)* 78−76417
AgCl single cryst. foil, photographic elementary process 78−17519
AgCl, single crystal, recovery controlled transient creep, substructural obs., phenomenological anal. 77−77526
AgCl, solid monodisperse aerosols, in He jet system, for unstable nuclide transportation 79−22507
AgCl sols, kinetic exam. of halide conversion 77−82636
AgCl, solubility in methanol+water mixtures 77−47579
AgCl, spectral absorpt. coeff. obs. rel. to published data 79−73963
AgCl, Stepanov growth, oriented plates, rods and tubes 78−3023
AgCl, surface crystallisation, due to colloid adsorption 80−54544
AgCl, surface layer stress distrib. after mech. treatment, polarisation-optical obs. 78−18887
AgCl, temp. fields during plastic deform., cholesteric liq. cryst. technique 79−82278
AgCl, thermal fields generated during plastic deform. 78−35457
AgCl track detector prep. and props. 78−17517
AgCl, US wave propagation, direct obs. 78−59864
AgCl ultra fine grained photog. emulsions, impurity obs. spectra *(Russian)* 79−69871
AgCl, vapour, photoelectron spectrosc., interpretation 80−95679
AgCl, vapour-deposited epitaxial film, surface structure 80−59814
AgCl:Cd, large sheet single cryst. prep. *(German)* 77−32516

silver compounds continued
AgCl:Cd^{2+}, heavily doped, free energy and point defect distrib., integral eqn. method 80−107219
AgCl:Cd^{2+}, Pb^{2+},Br^-, EPR anal., mechanism for photoinduced decomposition 78−80219
AgCl:Cd^{2+}(Pb^{2+})(Mn^{2+}), recombination processor, radioluminescence 78−2915
AgCl:$CdCl_2$, point defect model, free energy and radial distrib. functions 80−44201
AgCl:Cu^+(Cu^{2+}), luminesc., ion interactions 77−66534
AgCl:Hg^{2+}, effect of Hg^{2+} addition of photosensitivity *(Russian)* 79−67412
AgCl:Li^+(Na^+)(K^+)(Rb^+), impurities effect on plasticity, brittleness 78−14398
AgCl:Na^+, Frenkel defect formation energy, impurity diffusion and migration 79−99179
AgCl:Ni, double quantum EPR transition, superhyperfine struct. 80−7154
AgCl:Ni, optically detected double resonance, radiative recombination electron traps 80−20518
AgCl:Ni^{2+}, low-temp. EPR 77−77091
AgCl:OH^-, dielec. meas., defect reorientation 77−19947
AgCl:Pb^{2+}, ionic cond. and dielec. loss relax. vacancy-impurity complex. form. 77−1259
AgCl:Pd^+, ESR spectra, superhyperfine struct. lines 77−12197
AgCl:Pd^+, ESR spectrum, quasistatic Jahn-Teller effect 80−71170
AgCl:Pd^{2+}, EPR, role of vacancies in impurity based trapping 77−28439
AgCl:Pt, photochemistry and role of Pt impurity ions 79−24783
AgCl:Pt^{2+}(Pt^{4+}), single crystal EPR, substitution effects on photochemistry 79−15348
AgCl:Sr, effect of impurity doping on Sr^{2+} diffusion 78−84002
AgCl:X^{2+}, X=Mg, Ca, Sr, Cd, Ba, plasticity, impurity hardening effect 78−47466
AgCl-Ag_2O-P_2O_5, glass formation and ionic conductivity 80−65290
AgCl-AgBr, microcryst., halide comp. profiles, XPS 77−12850
AgCl-AgBr mixed crysts., elastic consts. and cryst. symm. 80−70290
AgCl-AgBr mixed system, third order elastic consts. 79−90713
AgCl-AgI, mixed cryst., trap distrib., thermolum. 78−68568
AgCl-$AgNO_3$, eutectic mixture, estimation of impurity distrib. coeffs. 80−55290
AgCl-KCl, solns., activity coeffs., surface tensions, 860 to 1000K 78−76897
AgCl-NaCl molten solns., activities and surface tension 80−10748
$(AgCl)_3$, gas, He(I) photoelectron spectra 80−43103
$(AgCl)_3$, photoelectron spectrum and valence shell struct. 78−62843
AgCl(:AgBr), intrinsic ODMR spectrum mechanism, doping effect 78−43682
AgCl(Br), activated photochromic glass, kinetics of thermal decolorisation 80−103931
AgCl(Br), fast Li^+ ion stopping, chem. bonding effects 77−27929
AgCl(Br), thermal shifts in energy level separations, ESCA 77−8723
$AgCl_xBr_{1-x}$, binary melt, Ag solubility, temp. and conc. depend. 80−10677
AgCl(Br)(I), static polaris. and effective charge parameters, Born-Mayer pot. 77−31628
AgCl(Br)(I), van der Waal dipole-dipole and dipole-quadrupole energies, Born and Slater-Kirkwood models 79−27947
Ag_2ClNO_3, X-ray cryst. struct. determ. and refinement 79−69073
$AgClO_3$, ^{35}Cl NQR spectrum under press. at 311K 80−11291
$AgClO_3$, ClO_2 spin Hamiltonian 78−60326
$AgClO_3$, γ-irrad., ESR of O_3^-, ClO_2 and $(ClO_2\text{-}Cl)^-$ paramag. centres 77−9102
$AgClO_3$, γ-irradiated, resonant Raman effect of O_3^- centres 78−48178
$AgClO_3$, mol. torsional oscills., cooperative study by NQR 80−25244
$AgClO_3$, NQR and thermal expansion investig. of phase transform. 77−12229
$AgClO_3$, NQR freq. of ^{35}Cl, temp. depend., phase transition 77−12228
$AgClO_3$, NQR press. depend. 77−12225
$AgClO_3$, NQR temp. depend., torsional mol. oscill. in solid 79−4743
$AgClO_3$, structural phase transition, ^{35}Cl NQR meas. 80−15819
$AgClO_4$, aq. soln., positronium form., quenching and inhibition 78−15690
$AgClO_4$ benzene, complex, heat capacity 78−75843
$AgClO_4$, solubilities and chem. reactions, comparison with $AgReO_4$ 79−15976
$AgCoPO_4$, crystalline struct. *(French)* 79−1422
Ag_2CrO_4, diffuse reflectance spectra 78−88326
$Ag_2Cr_2O_7$, X-ray cryst. structural anal. *(French)* 79−4288
$AgCrS_2$, mixed conductor props. 80−44675
$AgCrS_2(Se_2)$, superionic and electronic cond. meas. 77−89577
$AgCrX_2$, X=S, Se, EPR meas., g-factors, effective mag. moments, and dipolar shifts 79−8043
$Ag_{0.85}Cu_{0.15}Br$, far IR spectra, cond., cation local motion 79−1754
$Ag_{1-x}Cu_xI$-QI, Q=NH_4, $(CH_3)_4N$, $C_5H_5NCH_3$, elec. cond., −20 to 130°C 77−55387
AgCuSe, mixed conduction 79−78140
AgCuSe, X-ray photoelectron and Auger spectra 78−56561
AgF, -Z 79−78064
AgF, diffusion, elec. cond. and ^{19}F relax. $T_{1\rho}$ meas. 80−92718
AgF, heteronuclear spin coupling and decoupling dynamics 77−48066
AgF, interionic forces, cohesive energy, bulk modulus calcs. 79−82176
AgF, NMR chemical shifts 80−74180
AgF, polymorphic transition from NaCl to CsCl struct., thermodynamic anal. *(Russian)* 77−7860
AgF_2, high press. modification, cryst. and mag. props. 80−38988
Ag_2F, NMR of ^{109}Ag and ^{19}F, modified Korringa relation in two-dimens. metal 80−93199
AgF(Br), sputtering processes during 6 keV Xe ion bombard. 78−68590
$AgFeO_2$, EFG tensor, nucl. quadrupole coupling const., O^{2-} polarisability 77−72844
$AgFeSe_2$, thermographic investigation of phase transitions *(Russian)* 80−10661
$AgFeSe_2(S_2)(Te_2)$, elec. props., band gap *(Russian)* 79−11116
$AgFeTe_2$, Mossbauer parameters in phase-transition region 80−11308
$AgFeTe_2$, thermographic investigation of phase transitions *(Russian)* 80−10661
$AgGaCr_4S_8$, IR spectra obs. of ordering *(German)* 78−6669
$AgGaS_2$, up-conversion of 10.6 μm radiation into visible 78−33783
$AgGaS_2$ crystal, IR radiation conversion for nonlinear spectrograph 79−10360

silver compounds continued
$AgGaS_2$, deep level obs. by TSC meas. 80−65590
$AgGaS_2$, difference freq. generation for IR tunable radiation, 5.5 to 18.3 μm 77−10969
$AgGaS_2$, efficient up-conversion of 10.6 μm radiation into green spectral range 77−88838
$AgGaS_2$, elec. field influence on absorpt. spectrum, exciton parameters and energy of impurity levels *(Russian)* 77−69860
$AgGaS_2$, electroluminesc., mechanism *(Russian)* 77−69918
$AgGaS_2$, IR signal detection by mixing with dye laser radiation 77−88846
$AgGaS_2$, iso-index coupled-wave electrooptic filter 80−1324
$AgGaS_2$, $LiIO_3$, IR radiation two-stage conversion, high sensitivity detector appl. 79−59761
$AgGaS_2$, optical quality, grown from melt, EPR characterisation 78−64260
$AgGaS_2$, parametric up-conversion of IR radiation 77−79901
$AgGaS_2$, Raman spectrum, degenerate mods, temp. depend. 78−35150
$AgGaS_2$, thermal radiation recording by two-stage freq. conversion detects. 79−46002
$AgGaS_2$:Fe, EPR of Fe-associated defect 80−60412
$AgGaS_2$-$AgGaSe_2$ system, phase diagram, lattice consts., and IR spectra 80−60841
$AgGa_5S_8$, ionic cond., galvanic cell meas. 77−47616
$Ag_4Ga_2S_5$, formation mechanism, X-ray and isotope exchange anal. 79−87591
Ag_5GaS_4, form. in Ag-Ga-S system 79−87618
$AgGaS_2(Se_2)$, IR nonlinear material, laser induced surface damage 77−19266
$AgGaS_2(Se_2)$, ionic cond., galvanic cell meas. 77−47616
$AgGaS_2(Se_2)$, press. depend. of energy gap, absorption edge obs. 77−12401
$AgGaS_2(Se_2)(Te_2)$, tetragonal distortion 79−32942
AgGaSe, direct gap semicond., exciton energy at 300K from reabsorption of luminesc. 79−78728
AgGaSe, exciton energy determ., electron beam excited luminesc. 79−38680
$AgGaSe_2$, and Ag_9GaSe_6, XPS, Auger and direct electron spectra 78−52620
$AgGaSe_2$, down-conversion of $LiNbO_3$ optical parametric oscillator output, 4 to 18 μm 79−86215
$AgGaSe_2$, growth by Bridgman method, optical charcts. 77−69980
$AgGaSe_2$, optical phonons, IR reflectance meas. *(French)* 77−81095
$AgGaSe_2$, polarised IR refl. spectra, optical phonon modes 77−16304
$AgGaSe_2$, pressure-induced phase transformations 78−30748
$AgGaSe_2$, reabsorpt. of excitonic luminesc. in direct band gap semiconds. 77−63469
$AgGaSe_2$, SHG, absorpt. coeffs. and temp. variation of refr. index difference 80−14390
$AgGaSe_2$, Schottky diodes with tunnel device charcts. 78−39215
$AgGaSe_2$, seeded Bridgman growth of crack-free crysts., thermal expansion coeff. 78−11101
$AgGaSe_2$ single crysts., opt. quenching of photocond., temp. depend., slow centres activation energy *(Russian)* 77−69370
$AgGaSe_2$, ternary semiconductor crystals for nonlinear optical applics. 78−33782
$AgGaSe_2$, two-photon absorpt. and short pulse stimulated recombination 80−89054
$AgGaSe_2$ wavelength-modulated reflectance, optical electronic transitions, 1.5-5.5 eV 78−35170
Ag_9GaSe_6, crystn. in Ag_2Se-$GaSe_3$ system, lattice parameters *(French)* 77−51472
β-Ag_9GaSe_6, X-ray cryst. struct. determ. *(French)* 79−4277
$AgGa(Se_{1-x}S_x)_2$, crystal growth, phase studies, optical props. 78−48305
$AgGaSe_2(Te_2)$, phonons, far IR refl. obs. 78−60459
$AgGaTe_2$, Debye temp., standard entropies and enthalpies, sp. ht. meas. 78−30769
$AgGaTe_2$, optical phonons, IR reflectance meas. *(French)* 77−81095
Ag_8GeS_6, fundamental absorpt. edge changes due to polymorphic transitions 77−20240
$Ag_8GeS_6(Se_6)(Te_6)$, absorpt. edge investigs. at phase transitions 78−35149
n-Ag_8GeSe_6, elec. cond. and photoelec. props. 77−69380
Ag_8GeSe_6, forbidden energy gap changes under high press., polymorphic transitions 77−51649
Ag_8GeSe_6, fundamental absorpt. edge changes due to polymorphic transitions 77−20240
Ag_8GeSe_6, polymorphic transition, absorpt. coeff. meas. 78−2257
β′-Ag_8GeSe_6, X-ray cryst. struct. determ. *(French)* 80−39020
Ag_8GeTe_6, optical props. and polymorphism 80−45082
AgH, AgLi, AgAu and AgCu, VB calcs., wave functions, interatomic distance and dissoc. energy values 77−57883
AgH, bond dissoc. energy, electronegativity pot. function pot. energy curves 77−10784
AgH, electronic struct. and supercond., APW calc. 79−95318
AgH, gaseous, dissociation 79−91925
AgH, relativistic (non-relativistic) HF one-centre expansion calcs. 80−52908
$Ag_2H_3IO_6$, antiferroelec. phase transition investig., Landau anal. 77−1644
$Ag_2H_3IO_6$ crystal, growth, specific heat, antiferroelec. transition 77−69781
$Ag_2H_3IO_6$, paraelec. and antiferroelec. phases, IR vibrational study 77−85697
Ag_2HPO_4, X-ray cryst. struct. determ., Patterson method *(French)* 79−14755
$AgHg_2AsO_4$, cryst. struct. by X-ray diffr. *(French)* 78−34490
Ag_2HgI_4, disordered multicomponent solid solutions conc. fluctuation waves, microscopic theory 80−44327
Ag_2HgI_4, order-disorder transform. at 51°C, sound vels. and dielec. losses 78−10129
Ag_2HgI_4, ordered and disordered phases Raman spectra temp. depend., ion hopping 78−23438
Ag_2HgI_4, polycryst., Raman spectra, press. depend. 77−73137
Ag_2HgI_4, preparation, optical and luminescence spectra 80−104064
Ag_2HgI_4, Raman line shape and ionic cond., coupled mode model 80−66171
Ag_2HgI_4, superionic cond., cation disordering 77−84692
Ag_2HgI_4, valence electron spectrum, SRO and LRO effects 78−52639
Ag_2HgI_4, XPES, lattice instability 79−33904
$AgHg_2PO_4$, cryst. struct. by X-ray diffr. *(French)* 78−34490

silver compounds continued
$Ag_xHg_ySI_z$, prep. of mixed sulphide iodides, photochromism 77−36385
β-AgI, 2H and 4H polytypes, exciton refl. spectra at 4.2K 79−69860
β-AgI (4H), visible spectra, reflected light phase and amplitude, exciton resonance 80−45110
α-AgI, activation vol. for ionic cond. 80−59711
AgI, adsorption sites and dipole orientation of adsorbed water molecule in ice formation 79−48530
AgI aerosol, ice forming activity, UV irrad. effect 80−71950
AgI aerosol, studies of ice-forming activity, verification of theory 80−101406
AgI aerosol particle size, struct. rel. to ice forming activity 80−61164
AgI aerosol particles, influence of cryst. struct. on their ice-forming activity 79−16048
AgI, aerosols, ice nucleation at different supercooled fog temps. *(Russian)* 77−27983
AgI aerosols, particle size influence on cryst. struct. 80−2000
AgI, aerosols, preliminary tests of cumulus cloud seeding technique 78−57352
AgI, atmospheric ice forming props., impurities and surface state effects *(French)* 78−20459
AgI, α and melt phases, light scatt. from correl. ion fluctuations 79−95771
AgI, B1 phase, high press. elastic props., thermally activated rel. anomaly 80−44261
AgI based, superionic conductors, geometric struct. principles 77−89574
α-AgI, cation distrib. and anharmonic thermal vib. 77−66005
AgI, cation or anion doped, ionic cond. 79−46837
AgI, cloud seeding experiment, comparison of night-time and day-time seeding 79−88441
AgI, cloud seeding expts., Fujian province, China *(Chinese)* 80−46235
α-AgI, collective motion in superionic conductors, AC conductivity calc. 79−99368
AgI colloid, stability, dynamic theory 80−89544
α-AgI, cond. mechanisms in superionic phases, neutron diffr. obs. 80−59714
AgI, conductivity, hopping system, master equation 80−39348
α-AgI, current-current correlations 78−51732
AgI, density of states, IR cond., and Raman scatt., lattice dynamics calc. 78−30709
α-AgI, diffusion dynamics, quasielastic neut. scatt. expt. 80−107484
α-AgI, diffusive motion of Ag^+ ions, quasielastic neutron scatt. 77−11726
β-AgI, drift mobility of holes 77−47814
α-AgI, dynamic cage effect 80−107541
AgI, EXAFS investigation of struct. and ion motion 80−108302
AgI, elastic behaviour near phase transitions with negative dP/dT 78−83885
α-AgI electrolyte, degree of disorder of anion lattice 78−59975
β-AgI, exciton luminesc. of 2H and 4H polytypes 77−85783
β-AgI, exciton refl. spectra, optical activity *(Russian)* 78−64380
AgI, FCC and γ phase, electronic struct., relativistic KKR calc. 77−85140
α-AgI, fast ion conductor, phase transitions, thermoelec. power meas. 80−107540
AgI film, crystallisation, exciton absorption spectra meas. 77−35483
AgI film, light-induced changes, ellipsometric meas. 78−56537
AgI group superionic conductor, phase transition detection by thermoelectric power method 80−92669
AgI, growth, elec. and optical props. 79−77805
AgI hydrosols, appl. of radiometric method for particulate processes characterisation 80−45579
AgI hydrosols, kinetics and mechanics of colloid systems formation 80−101045
α-AgI, I_2 diffusion obs. using ^{131}I radiotracers 78−18830
AgI, ice-forming activity at −20°C, influence of aersol particle size 79−53465
AgI, interfacial electrochem., review 78−80748
AgI, iodyrite, ^{129}I concs. determ. by radiogenic ^{129}Xe meas. 77−63983
β-AgI, ion dynamics and transition to superionic state, nucl. spin-lattice relax. meas. 78−43179
β-AgI, ionic cond. and Frenkel pair form., dielec. loss meas. 79−33112
α-AgI, ionic cond. in 8-40 GHz range 80−44358
α-AgI, ionic motion, low freq. Raman scatt. 78−80354
α-AgI, ionic motions nature, mol. dynamics calcs. 80−107533
AgI, kinetic parameters of water drops crystn. *(Russian)* 77−81963
AgI large single crysts., gel and soln. growth and props. 80−35071
AgI, lattice dynamics of binary superionic conductors 80−107393
AgI, lattice instability, XPS 79−11500
β-AgI, low temp. electronic hopping 78−39111
β-AgI, luminesc. of 2H- and 4H-polytypes 80−2843
AgI microcrystal dispersed in gelatin, effect of I^- on interstitial Ag ions 78−26726
AgI microcrystals, photohole motion 78−26903
AgI microcrystals, photocond. and luminesc. 78−26904
AgI, mixed-polytype cryst. containing new 12H polytype 77−19911
AgI, molecular beam investig. of water vapour nucleation and condensation 77−52212
α-AgI, molecular dynamics exam. of Ag diffusion 78−55981
AgI, molten, freq. depend. ionic cond. 77−7882
AgI, NMR chemical shifts 80−74180
AgI nascent hydrosol absorption spectra and microcrystal growth 79−100449
β-AgI, neutron inelastic scatt., phonon dispersion curves 78−67786
α-AgI, neutron powder diffr. meas. interpretation 80−10533
α-AgI, neutron scatt. expts., Ag^+ ion motion 80−6552
AgI particles in seeded storms, detection 78−3884
AgI, phase transition, statics and local dynamics, mean field and Mori theory 80−39347
AgI, phase transitions and dynamics 78−59924
β-AgI, phonon-induced X-ray scatt. from lattice dynamical model 79−37790
β-AgI, piezoelectric ionic cryst., US investigation 79−77689
β-AgI, polariton dispersion curves, Raman spectra 80−29338
AgI, position and dynamics of Ag ions using EXAFS, jump-diffusion cond. model 77−59643
AgI precipitations, effects of pAg on crystal growth 79−19172
AgI pyrotechnic nucleant charcts., use in Florida Area Cumulus Expt. 79−100919
AgI, quadrupolar deformability theory by tight binding model 80−10614
β-AgI, self-diffusion of Ag, quasielastic neutron scatt. study 78−83999

silver compounds continued
AgI, single cryst. neutron diffr. meas., Ag distrib. determ. 78−10025
α-AgI, single particle and collective aspects of Ag^+ ion motion 80−6553
AgI, sol, water PMR meas., 3 to 60°C 78−76930
αAgI, solid electrolyte, contrib. of non-Brownian motion to transport props. 80−70453
AgI solid electrolyte α-phase stabilisation 80−29209
AgI solid electrolyte plastic deformation and thixotropy obs. 78−79660
α-AgI, state of order, config. model 80−6390
α-AgI, structural and dynamical behaviour 80−107544
AgI, structural model for superionic conduction 78−79797
α-AgI, structure, X-ray diffr. 77−84728
AgI substrates, growth of epitaxial cryst. growth, influence of saturation and elec. field 79−42408
α-AgI, superionic, anal. of Ag K-EXAFS data 80−97377
α-AgI, superionic, continuous order-disorder transition, Raman spectroscopic evidence 80−45070
α-AgI, superionic compound struct., cation distrib., powder neutron diffr. 77−72595
α-AgI, superionic cond., correlations in motion of particles, mol. dynamics calcs. 77−66043
AgI, superionic cond., cryst. struct., neutron diffr. study 79−42041
α-AgI, superionic cond., freq. depend. cond. 77−84973
AgI, superionic cond., lattice potential effects 80−65274
α-AgI, superionic cond., sublattice melting, Raman spectra, rel. to AgBr(Cl) melts 78−10882
α-AgI, superionic cond., statistical thermodynamic description *(French)* 80−65281
α-AgI, superionic cond. Raman spectra, compared with liquid like model 78−2855
α-AgI, superionic conductor, appl. of Brownian motion in polarisable lattice 77−76603
α-AgI, superionic conductor, Raman spectra, freq. depend. cond. exam. 78−10883
α-AgI, superionic conductor, microscopic model *(German)* 78−67861
AgI, superionic conductor, dynamical aspects 78−79695
α-AgI, superionic conductor, Raman scattering evidence for sublattice melting 78−80350
AgI, superionic conductor, Raman study 78−80353
αAgI, superionic conductor, hydrodynamic theory for collective excitations 79−1524
AgI, superionic conductor, lattice dynamics 79−95111
α-AgI, superionic conductor, microwave absorption spectrum 80−11515
AgI, superionic conductor, density of valence states, photoelectron spectra meas. 80−25523
α-AgI, superionic conductor, struct. and dynamics, two-dimens. mol. dynamics model 80−49413
α-AgI, superionic conductor, soft-core model, Monte Carlo study 80−54430
α-AgI, superionic phase, struct., X-ray scatt. anal. 80−28983
α-AgI, superionic. liquid-like Raman scatt. 79−95769
AgI surface, adsorption of water, effective pair pot. model 80−100394
AgI surface clusters, water molecule interaction, CNDO calc. 77−4254
AgI, surfactant adsorpt., electrokinetic investig. 80−3363
β-AgI, temp. depend. of anomalous and ordinary Raman scatt. 79−19890
β-AgI, thermal expansion, 4 to 270K 80−79961
AgI, thermal expansion under press. 80−92690
β-AgI thin film, exciton spectrum 80−55216
AgI type solid electrolytes, sp. ht. anomaly, theory *(Russian)* 78−10198
AgI type solid electrolytes, expt. props. 78−63877
α-AgI type superionic conductors, struct. and phase transition *(Japanese)* 79−65250
AgI ultrafine grained photog. emulsions, impurity obs. spectra *(Russian)* 79−69871
AgI, valence electron spectrum, SRO and LRO effects 78−52639
AgI, vapour, photoelectron spectrosc., interpretation 80−95679
B-AgI, X-ray diffuse scattering 80−14964
AgI, XPES, lattice instability 79−33904
AgI:Cd, polycrystalline, thermoelectric power meas. 80−59698
β-AgI:Cu, pure and doped, photoconductivity, band struct., trap nature 79−95449
AgI/Ag oxysalt system, vitreous solid electrolytes, conductance mechanism 80−107560
AgI/polyamine iodide solid electrolytes, conc. depend. of elec. cond. 80−24647
AgI/RbI quasibinary system, solid state reactions and transport props. 80−96700
AgI-Ag oxysalt high cond. glasses, struct. obs. 79−32908
AgI-Ag oxysalt ionic solids, thermoelec. power determ. 78−30947
AgI-Ag thin granular film, Herschel effect 78−82063
AgI-$Ag_2Cr_2O_7$ system, solid electrolyte stability 77−15619
AgI-$Ag_2Mo_2O_7$ system, solid electrolyte stability 77−15619
AgI-$Ag_2Mo_2O_7$($Ag_2Mo_4O_{13}$), solid, intermediate compounds with fast ion transport 77−43371
AgI-Ag_2MoO_4 pseudobinary system, superionic cond. glasses, comp. depend. of ionic cond. 80−75380
AgI-Ag_2O-MoO_3, comparison of ionic conductivity between glassy and crystalline solid electrolytes 78−30786
AgI-Ag_2O-MoO_3, superionic conducting glass, IR spectra and struct. 79−10804
AgI-Ag_2O-MoO_3 glass glass superionic cond., struct. and transport props. 80−88602
AgI-Ag_2O-MoO_3 system, glass form. with high ionic conductivity 77−89379
AgI-Ag_2O-P_2O_5, glass formation and ionic conductivity 80−65290
AgI-Ag_2O-P_2O_5 system, glass form. and superionic cond. characts. 78−26722
AgI-Ag_2O-P_2O_5(MoO_3) glassy electrolyte galvanic cells 80−104513
AgI-$Ag_2O.B_2O_3$ system, ionic cond., struct., electrochem. prop. in galvanic cell 78−95181
AgI-Ag_2WO_4 system solid electrolytes with glass-like struct., thermodynamic and electrochem. props. 79−10978
4AgI-Ag_2XO_4, (X=Cr, Mo, W), ionic cond., complex admittance 77−84969
AgI-Ag_3AsO_4 system, solid electrolyte stability 77−15619
AgI-AgBr emulsion, low-intensity reciprocity failure *(French)* 78−37085
AgI-AgCl, eutectic mixture, estimation of impurity distrib. coeffs. 80−55290
AgI-$AgNO_3$, eutectic mixture, estimation of impurity distrib. coeffs. 80−55290

silver compounds continued
AgI-AuI, pseudo-binary phase diagram 78−76637
AgI-based solid electrolyte cell discharge mechanism 80−35663
AgI-BiI_3, phase equilib. study *(French)* 79−66047
AgI-HgI_2, solid electrolyte, ionic and electronic cond., phase composition determ. 78−2296
AgI-I_2 system, isotope exchange study, 115 to 195°C 77−77756
AgI-PbI_2 molten mixtures, conductivity, thermodynamic excess props. 79−86914
AgI-piperazinium, (or N,N′-disubstituted piperazinium diiodides), binary salts, ionic cond. study *(French)* 78−2293
AgI-RbI films, vacuum deposited, cond. determ. 77−39689
AgI-type solid electrolytes, introductory survey 80−6549
AgI+$HgBr_2$, solid state reaction, kinetics and mechanisms 77−16790
AgI+$HgCl_2$ → $AgHgClI_2$($AgHgCl_2I$), solid state diffusion controlled reaction at 100°C 78−34659
$(AgI)_3$, gas, He(I) photoelectron spectra 80−43103
Ag_4I_5, ionic cond., effect of press. 78−51733
$(AgI)_x(Ag_2O\ B_2O_3)_{1-x}$, amorphous superionic compound, ^{11}B lineshape and relaxation 80−108107
$(AgI)_x(Ag_2O.B_2O_3)_{1-x}$ glass, ionic cond. and disorder modes 80−39344
$Ag_7I_4AsO_4$ vitreous electrolyte, ionic cond. 79−77807
$Ag_{11}I_{25}(C_5H_{24}N_2)_2$, solid electrolyte cryst. struct. determ. 77−7705
$Ag_{44}I_{53}(C_{11}H_{30}N_3)_3$, cryst. struct. determ. 78−26553
Ag_2INO_3, X-ray cryst. struct. determ. and refinement 79−32956
$AgIO_3$, chem. prep. and cryst. struct. 80−75207
$AgIO_4$, chem. shift, NMR obs. 80−48015
$AgIO_4$, dynamics of IO_4^- vibr. in lattice 79−42157
$Ag_7I_4PD_4$, superionic solid film, surface diffusion coeff. 80−92709
$Ag_7I_4PO_4$ film formation from electrolysis of HI-H_3PO_4 soln., electrocodepositional method 80−55315
$Ag_7I_4PO_4$, solid electrolyte, ionic cond. meas., 4-79°C 80−54433
$Ag_{26}I_{18}W_4O_{16}$, cryst. struct. and ionic conductivity 77−80647
$Ag_{26}I_{18}W_4O_{16}$, order-disorder type ferroelectric transitions, ionic conductivity meas. 80−66122
$Ag_{26}I_{18}W_4O_{16}$, solid electrolyte, anisotropic elec. cond., low temp. phase transitions 80−65289
$Ag_{26}I_{18}W_4O_{16}$, struct. phase transition, dielectric, cond. and Raman obs. 79−19368
$Ag_{1/2}In_{1/2}Cr_2S_4$, first order macro to microdomain transition 77−69562
$AgInCr_4S_8(Se_8)$, 1:1 ordering on tetrahedral sites, IR spectra obs. *(German)* 78−6669
$AgInS_2$, and $AgIn_5S_8$, spray pyrolysis, film struct., elec. and optical props. 80−71592
$AgInS_2$-SnS_2, spinel phase $Ag_xIn_xSn_{1-x}S_2$ obs., stoichiometry *(French)* 80−44326
$AgIn_5S_8$, cryst. growth and props. 78−39677
$AgIn_5S_8$, crystal growth by I_2 vapour transport, using temperature variation method 78−68610
$AgIn_5S_8$ thiospinel, space group assignment by X-ray diffractometry 79−99141
$AgInS_2(Se_2)$-$SnS_2(Se_2)$, degree of solid solubility and phases characts. 78−35377
$AgInS_2(Se_2)(Te_2)$, tetragonal distortion 79−32942
p-$AgInSe_2$, far IR props. 79−42976
$AgInSe_2$, far IR refl. spectra, polarised light 78−43870
$AgInSe_2$, far IR refl. spectra, ionic bonds 79−55695
$AgInSe_2$, press. depend. of energy gap, absorption edge obs. 77−12401
n-$AgInSe_2$, press.-induced compensation, resist. expts. 78−30919
$AgInSe_2$, reflectvvity and XPS meas. 78−35165
$AgIn_5Se_8$, optical gap and low temp. depend. 79−99907
$AgInSe_2(Te_2)$, phonons, far IR refl. obs. 78−60459
$AgInSe_2(Te_2)$, pressure-induced phase transformations 78−30748
$AgInTe_2$, Debye temp., standard entropies and enthalpies, sp. ht. meas. 78−30769
$AgInTe_2$, far IR refl. spectra, polarised light 78−43870
$AgInTe_2$, far IR refl. spectra, ionic bonds 79−55695
AgM (M=Mg, Ca, Sr, Ba, Zn, Hg) intermetallic mols., Ar matrix isolated, ESR investig. 79−811
Ag_8MSe_6, M=Ge,Sn,Si, absorpt. edge under hydrostatic press. 77−85740
AgMgO for LV switchgear contacts, properties, prep. *(Slovak)* 78−56603
Ag_2MoO_4, cathodic props. in Li primary batteries 80−3502
$Ag_xMo_3S_4$, chevrel phase, charge transfer and valence electron conc. 78−6029
$Ag_xMo_6S_8$, Chevrel phase, lattice instabilities, X-ray diffr. meas. 78−34491
AgN_3, dielec. breakdown by elec. induced chem. decomposition 80−20586
AgN_3, high-resist. explosive cpd., elec. and galvanomag. props., temp. depend. 80−103728
AgN_3, optical absorpt. spectra, and photoemission, electron band scheme 79−100015
AgN_3 pyrolysis, 513 to 558K 80−7787
$AgN(CN)_2$, cryst. struct. 77−35513
$Ag(NH_3)_2Ag(NO_2)_2$, and deuterate, proton and deuteron mag. reson., reorientation 79−11351
$Ag(NH_3)_2Ag(NO_3)_2$, phase transition, mol. motion, PMR obs. 78−88203
$AgNO_2$, high-pressure phase behaviour, crystal chemistry of univalent nitrites 78−30749
$AgNO_2$, single crystal, dielec. const., low temp. meas. 80−71290
$AgNO_3$, centre of symmetry and cryst. perfection *(French)* 80−107089
$AgNO_3$, cryst. and molten salt, Raman and IR spectra, vibr. anal. 77−16311
$AgNO_3$, differences between diffr. and vibr. spectroscopic results 79−69818
$AgNO_3$ digested AgBr(Cl) emulsions, IR luminesc. obs. at 77K 80−103983
$AgNO_3$, ESCA contrib. to X-ray struct. determ. *(French)* 77−62508
$AgNO_3$, electrolytic solution, sono-conductance rel. to temp. 77−15496
$AgNO_3$, external heavy atom effects on organic cpd. luminesc., donor-acceptor interaction *(German)* 78−84651
$AgNO_3$ in gelatin layers, phosphorescence kinetics curves *(Russian)* 80−62776
$AgNO_3$, influence on props. of semicond.-gelatin interfaces in MIS struct. 79−51684
$AgNO_3$ melt, contact with glass, conc. changes in surface layer 80−44372
$AgNO_3$ melt, diffusion of silver into $Na_2O.2SiO_2$ glass 80−44371

silver compounds continued
$AgNO_3$, melt, NO_3^- ion struct., pulsed neutron diffr. obs. 78−22631
$AgNO_3$, molten, Brillouin scatt. meas. 77−8592
$AgNO_3$, molten, refr. index and molar refractivity 80−93265
$AgNO_3$, molten, X-ray diffr. structural anal. 78−42887
$AgNO_3$, polymorphic structural relationships, X-ray diffr. and microscopy 77−19930
$AgNO_3$ soln., visible luminescence obs. at or below 77K 80−108263
$AgNO_3$, struct. at room temp. and press., perfect cryst. *(French)* 78−55846
$AgNO_3$-Ag_2S system, visible luminescence obs. at or below 77K 80−108263
$AgNO_3$-KF in ice matrix, γ-irrad., Ag at., form., solution, ESR 77−59454
$AgNO_3$-$NaNO_3$ mixed melts containing Na_2O-SiO_2-Ga_2O_3-Al_2O_3 glasses, ion exchange 80−21282
$AgNO_3$-$NaNO_3$ mixture, contact with glass, conc. changes surface layer 80−44372
$AgNO_3$-$TlNO_3$-$Cd(NO_3)_2$-H_2O mixtures, Henry's law, excess free energy 78−68908
AgNa mordenite, chemisorpt. of CO and H_2 80−2752
$AgNaNO_2$, ferroelectric transitions, one-mode model 80−29702
$AgNa(NO_2)_2$, ^{23}Na elec. field gradient tensor from NMR satellite lines near phase transition 80−71191
$AgNa(NO_2)_2$, complex piezoelectric constant, meas. by interferometric method, at frequencies up to 50 kHz 79−63270
$AgNa(NO_2)_2$, crit. dynamics, hydrostatic press. effect, dielec. props. meas. 80−71328
$AgNa(NO_2)_2$, crit. sp. ht. near ferroelec. transition 79−38474
$AgNa(NO_2)_2$, ferroelec. transition, ^{23}Na elec. field gradient tensor, NMR meas. 79−4777
$AgNa(NO_2)_2$, ferroelectric phase transition, theory 79−24272
$AgNa(NO_2)_2$, ferroelectric transitions, group theoretic comparison with $NaNO_2$ 80−7311
$AgNa(NO_2)_2$, ferroelec., Raman scatt. and phase transitions 80−71349
$AgNa(NO_2)_2$, ferroelec. cryst., Raman spectrum, phase transition, comparative anal. with $NaNO_2$ 80−88935
$AgNa(NO_2)_2$, Landau behaviour of sp. ht. close to nearly tricritical ferroelec. phase transition 78−10861
$AgNa(NO_2)_2$, order-disorder ferroelec., crit. dynamics, NMR data compared with dielec. data 78−76415
$AgNa(NO_2)_2$, order-disorder ferroelec., influence of hydrostatic press. on polarisation dynamics 80−103913
$AgNa(NO_2)_2$, Raman spectrum, NO_2^- bending vibr. 79−28737
$AgNa(NO_2)_2$, single cryst., specific heat anomaly, −90-55°C, ferroelec. transition entropy 77−77157
$AgNa(NO_2)_2$, triplet absorpt. polarised spectra, near ferroelec. phase transition 79−47473
$AgNa(NO_2)_2$, ultraslow crit. dynamics of order parameter, ^{23}Na spin relax. times obs. 78−76410
$Ag_xNa_{2-x}Te_2^{IV}Te_3^{VI}O_{14}$, (x=0,4), mixed tellurate, cryst. chem. and elec. cond. *(French)* 80−107150
$AgNbO_3$, cryst. growth and phase transitions 80−40243
$AgNbO_3$, single crysts. flux growth, space group determ. 80−55282
$AgNbO_3$-$AgTaO_3$ system, synthesis by exchange reaction 79−47625
$Ag_2Nb_2O_5F_2$, cryst. struct. determ. from single cryst. diffr. data *(French)* 78−95030
$AgNbO_3$.4AgI room temp. solid electrolyte and galvanic cell performance 78−79803
AgO, $A^2\Pi$-$X^2\Pi$ blue system, rot. anal. 77−38678
AgO and Ag_2O, ESCA spectra, Auger effect, initial and final states effect 78−15280
AgO, electronic spectra in rare gas matrix 78−996
Ag_2O, exciton luminesc. spectra, mag. field influence 80−80860
Ag_2O, film, photocond., annealing and time effects *(French)* 78−23135
Ag_2O film, prep. and effect of O_2, Ar and H_2 gases *(French)* 78−14637
Ag_2O, forbidden energy gap oxide semicond. crystals, review of spectroscopic props. 78−2876
Ag_2O, phase transitions at press. up to 39 kbar 77−31770
Ag_2O, photoconductivity of crystals grown under hydrothermal conditions 78−14765
Ag_2O, quadrupole exciton transition and struct. of optical absorpt. edge 79−38569
Ag_2O, thermal expansion, lattice parameter determ., 150-250K 78−2267
Ag_2O, X-ray absorption, discontinuities and limits, chem. combination effects 80−93435
Ag_2O-Al_2O_3-MgO-Na_2O, β″-alumina, structure, X-ray determ. 80−107148
Ag_2O-B_2O_3 glasses, electrical props. and dielectric relaxation *(Japanese)* 80−20199
Ag_2O-MgO-Al_2O_3, ionic cond. 80−107480
Ag_2O-Na_2O-B_2O_3 mixed cation glasses, electric conduction *(Japanese)* 77−24432
Ag_2O-P_2O_5, amorphous metaphosphate, memory cell with low switching fields *(German)* 79−19641
Ag_2O-P_2O_5 glass ESR of VO^{2+} ions 80−100610
Ag_2O-P_2O_5 system, electrical conductivity and dielectric relaxation *(Japanese)* 77−66455
Ag_2O-TeO_2 glass, struct. and props. *(Japanese)* 79−32917
Ag_2O-Tl_2O-B_2O_3, mixed-cation glass, electrical cond. 79−95210
Ag_2O-Tl_2O-B_2O_3 mixed cation glasses, elec. cond. 77−80644
AgP_2, d-electron participation in chem. bonds 77−28682
AgP_2 formation at Ag-InP interface during sintering 80−65309
$AgPO_3$-Ag_2SO_4, new Ag^+ and Li^+ ion glass conductors, glass transition, Raman spectra *(French)* 79−47094
$AgPO_3$-AgBr(Cl)(I) system glasses, soln. calorimetry obs., thermodynamic activity correl. with ionic cond. *(French)* 79−33102
$AgPO_3$-AgI glass system, solution calorimetry, enthalpy of formation *(French)* 78−64527
$AgPO_3$-AgX, X=I,Br,Cl, ionic conductivity *(French)* 78−79805
$AgPO_3$-CdI_2 glasses, ionic conductivity and structure *(French)* 78−67854
$AgPO_3$-PbI_2 system, elec. conductivity as function of composition and temp. *(French)* 77−69112
Ag_3PO_4, anhydrous, struct. relationships w.r.t. fast ion cond. 80−107188
Ag_3PO_4, cryst. struct. 78−42973
$AgPS_2$, single crystal, prep. and structure 77−35524
$Ag_2P_2S_6$, X-ray cryst. struct. determ. by direct methods *(French)* 79−14752
$Ag_4P_2S_7$, cryst. struct., X-ray diffr. meas. *(French)* 77−47412
silver compounds continued
$Ag_4P_2S_7$, single crystal, prep. and structure 77−35524
$Ag_4P_2Se_6$, cryst. struct. *(French)* 78−63703
$Ag_4P_2Se_6$, orthorhombic system, crystal parameters determ. *(French)* 78−34481
$(Ag_{x/2}Pb_{1-x}Bi_{x/2})Te$ solid solution, preparation and thermoelectric props. 77−47839
$(Ag_{x/2}Pb_{1-x}Sb_{x/2})Te$ solid solns., Hall coeff., thermoelec. power, and thermal cond., 100 to 500K 79−82614
Ag_4RbI_5, interfacial polarisation effects 79−60538
$Ag_3Rb(PO_4)_2$, struct., density and elec. cond. 80−33952
Ag_2Re films, galvanomag. props. and quantum size effects, obs. 80−70866
$AgReO_4$, external lattice vibr. modes and elastic wave vels., dispersion relations 79−33050
$AgReO_4$, NQR 77−20745
$AgReO_4$, solubilities and chem. reactions, comparison with $AgClO_4$ 79−15976
Ag_2S, Ag_2Se and Ag_2Te, TE properties, research obs. 77−28163
Ag_2S and Ag_2Se melts, electrotransfer, ionic component of elec. cond., Ag ion diffusion 79−51640
Ag_2S, α- to β-phase transform, phase boundaries effect 79−83179
Ag_2S, α-β transform., heterogeneous solid state reactions, role of phase boundaries, dynamic equilib. at interfaces 78−71848
Ag_2S, α-β transform., role of phase boundaries in heterogeneous solid state reactions 78−71849
Ag_2S, α⇌β transitions 78−22846
Ag_2S, bulk contact ice nucleation threshold under illum. 77−55343
Ag_2S, changes in elec. cond. and thermoelec. power at melting point 79−15147
Ag_2S, concentration specks, latent image formation 79−34334
β-Ag_2S, cond. mechanisms in superionic phases, neutron diffr. obs. 80−59714
α-Ag_2S, cryst. struct., X-ray scatt. determ. 79−46613
Ag_2S, d-electron participation in chem. bonds 77−28682
Ag_2S, distrib. on sensitised AgBr emulsion grains, X-ray microanalysis 78−62248
β-Ag_2S, electrogalvanic and elec. props., and range of existence *(French)* 78−43175
α-Ag_2S, electronic and electrogalvanic props. *(French)* 78−84237
Ag_2S, electronic struct. from X-ray emission spectra 77−28661
β-Ag_2S, fast-ion conductor, Ag ion density, neutron diffr. study 80−34234
Ag_2S, film, optical characterisation, inversion method 78−11008
Ag_2S film, oriented growth by vacuum evaporation 77−21028
Ag_2S film, tetragonal to cubic phase transform. kinetics, kinematic electron diffr. 77−4269
Ag_2S film, vacuum deposition and struct. 77−73233
Ag_2S film reduction, effect of Ag interdiffusion on the catalytic activity of Pt and Pd films 78−14519
Ag_2S, formation on evaporated Ag films 79−15874
α-Ag_2S, growth of single crysts. in solid/vapour system 77−85907
Ag_2S layers, quenching of photocond. by UV radiation 78−68047
Ag_2S, liquid, ionic and electronic cond., thermoelec. power 80−39329
Ag_2S, metal-nonmetal transition, crystallographic, optical, mag. and transport props. 78−6418
Ag_2S, nonlinear V-I characts. obs. at low temp. *(Japanese)* 78−34866
α-Ag_2S, single cryst. growth through capillary tube 80−108331
Ag_2S, solid and liquid, mass spectrometric obs. of VP, heats of form., comp. 79−42266
Ag_2S sols, red-IR photoluminescence obs. at 77K 80−103982
α-Ag_2S, struct., X-ray scatt. intensity anal. 78−38672
α-Ag_2S, structure, comment on coherent scattering intensity 78−95027
Ag_2S, thermodynamic props., growth of single cryst. by chem. transport reaction 77−36380
Ag_2S, transport props., 700-1500K 78−47796
α-Ag_2S whiskers, growth in VLS system, SEM and X-ray diffr. anal. 79−46989
Ag_2S, XPES, lattice instability 79−33904
Ag_2S-(As)(Sb)(Bi), temp.-comp. diagram 78−44105
Ag_2S-As_2S_3-AgI glasses, temp. and comp. depend. of ionic cond. *(French)* 80−34229
Ag_2S-Ga_2S system, phase diagram, DTA and X-ray diffr. meas. 77−15544
Ag_2S-In_2S_3-SnS_2 system quaternary and ternary sulphide spinels, solid solubility and struct. 78−35376
Ag_2S-K_2SO_4 mixtures, surface comp., AES and XPS obs. 80−81386
Ag_2S+Ln_2S_3, powdered mixtures, reaction rate, production of ionic semiconductors 80−93741
Ag_3SBr, ionic conductivity in temp. range 93-573K, X-ray diffr. and DTA 80−79988
Ag_3SBr, superionic conductor, phase transition, struct. 80−107144
$Ag_3SBr(I)$, Ag^+ ion mobility, appl. of Brownian motion theory 77−76607
βAg_3SI, anharmonic thermal vibr. of cations 80−65214
Ag_3SI, ionic conductivity in temp. range 93-573K, X-ray diffr. and DTA 80−79988
Ag_3SI, superionic conductor, dynamical aspects 78−79695
Ag_3SI, superionic conductor, ordered phase struct. 78−83792
Ag_3SI, superionic conductor, struct. and phase transition *(Japanese)* 79−65250
Ag_3SI, superionic cond., phase transition and cryst. structs., sp. ht., neutron and X-ray diffr. obs. 80−10662
Ag_2SO_4, anhydrous, struct. relationships w.r.t. fast ion cond. 80−107188
Ag_2SO_4, cryst. struct., form. 77−19928
Ag_2SO_4, enthalpies of transition and fusion 79−10925
Ag_2SO_4:CrO_4^{2-}, polarised electron spectrum assignments, red colour explained 77−85753
Ag_2SO_4-K_2SO_3 mixtures, surface comp., AES and XPS obs. 80−81386
$Ag_2S_2O_3$ solubility limit below 0°C 79−19376
$Ag_2SO_4.4NH_3$, mol. motion, proton mag. reson. 79−47349
$Ag_8S_3SO_4$, new cryst. data 79−37685
$Ag_2S(Se)$, ionic-electronic mixed conductor, solid state controlled growth using cryst. rotation 78−31338
$Ag_2S(Se)(Te)$, valence electron spectrum, SRO and LRO effects 78−52639
$Ag_2S.HgI_2$ and $Ag_2Se.HgI_2$ thin films, transmission spectra and photochromism 79−52032
$Ag_{14}Sb_{12}O_{36}F_2$, ionic conductivity, comparative study with pyrochlore phase $AgSbO_3$ *(French)* 80−103701
α-$AgSbS_2$ crystals, photoelectric props. 80−107861

silver compounds continued
$AgSbS_2$, synthetic crystals, monoclinic to cubic phase transition *(German)* 78−42943
Ag_2SbS_3, order-disorder phase transition, NQR and spin-lattice relax. expts. 78−47523
Ag_2SbS_3, Raman spectra obs. of low-temp. phases 80−93327
Ag_3SbS_3 film prep. 77−52250
Ag_3SbS_3, IR refl. spectra, permittivity, lattice vibrs. 79−65862
Ag_3SbS_3, ionic component of conductivity *(Russian)* 78−38870
Ag_3SbS_3, NQR elec. field effect, temp. depend. near ferroelec. transition 77−77121
Ag_3SbS_3, prod. and acoustooptic props. *(Russian)* 78−63158
Ag_3SbS_3, pyrargyrite, elec. cond. rel. to impurities, melt stoichiometry deviations 77−11914
Ag_3SbS_3, pyrargyrite, thermoelec. and photoelec. work functions, Fermi level and electron affinity *(Russian)* 77−15939
Ag_3SbS_3, pyrargyrite, electronic to ionic conductivity ratio *(Russian)* 77−80818
Ag_3SbS_3, pyrargyrite, order-disorder phase transition and elec. polarisation 79−38468
Ag_3SbS_3, pyrargyrite, US absorption, influence of illumination 79−42153
Ag_3SbS_4, dielec. and acoustic props. *(German)* 78−64335
Ag_3SbS_4, electron absorption and dispersion of ultrasound velocity 80−15197
$Ag_3SbS_3(AsS_3)$, electroacoustic echo, ultrasonic wave attenuation *(Russian)* 80−88280
Ag_3SbS_3. piezoelec. semicond., residual cond., ultrasound photoabsorpt. *(Russian)* 78−72465
$AgSbSe_2(Te_2)$, exam. of kinematic viscosity of melts, and short range ordering 79−1383
$Ag_{19}Sb_{29}Te_{52}$, single-phase, thermoelectric efficiency 80−107826
Ag_2Se, between metal electrodes, current-voltage charcts *(French)* 80−97005
Ag_2Se, changes in elec. cond. and thermoelec. power at melting point 79−15147
Ag_2Se, electronic and electrogalvanic props. in α-phase region *(French)* 80−107820
α-Ag_2Se, growth of single crysts. in solid/vapour system 77−85907
Ag_2Se, liquid, ionic and electronic cond., thermoelec. power 80−39329
Ag_2Se, metal-nonmetal transition, crystallographic, optical, mag. and transport props. 78−6418
Ag_2Se, polymorphic transition, DTA meas. 78−34620
α-Ag_2Se, single cryst. growth through capillary tube 80−108331
Ag_2Se, solid and liquid, mass spectrometric obs. of VP, heats of form., comp 79−42266
α-Ag_2Se, superionic cond., X-ray diffr. study 77−84719
Ag_2Se, thermodynamic props., growth of single cryst. by chem. transport reaction 77−36380
Ag_2Se, thermodynamics of phase changes *(Russian)* 77−73459
Ag_2Se thin film, switching and Ag movement, point contact technique 80−60107
Ag_2Se, X-ray determ. of inclusion function 77−76559
Ag_2Se, X-ray photoelectron and Auger spectra 78−56561
Ag_2Se-(As)(Sb)(Bi), temp.-comp. diagram 78−44105
Ag_2Se-Ga_2Se_3, phase diagram in rich Ag_2Se region *(French)* 77−51472
Ag_2Se-Ga_2Se_3, pseudobinary phase diagram determ., DTA, X-ray diffr., cryst. growth investigs. 77−70036
Ag_2SeO_4 single crystal growth in SiO_2 79−95915
$Ag_6Si_2O_7$, crystal atomic struct. determ. *(German)* 78−10007
Ag_8SiSe_6, absorpt. edge investigs. at phase transitions 78−35149
Ag_8SiSe_6, forbidden energy gap changes under high press., polymorphic transitions 77−51649
Ag_3Sn, dental alloy, prod. by melt extraction technique, exam. of mech. props. 78−48349
Ag_8SnS_6, fundamental absorpt. edge changes due to polymorphic transitions 77−20240
$Ag_8SnS_6(Se_6)$, absorpt. edge investigs. at phase transitions 78−35149
$Ag_2SnS_3(Se_3)(Te_3)$, Mossbauer effect, lattice dynamics obs. 77−43923
$Ag_{1-x}Sn_{1+x}Se_{2-y}$, supercond. and normal state props. 77−36008
Ag_8SnSe_6, cryst., Hall effect investigation of polymorphic transform. 80−39605
Ag_8SnSe_6, forbidden energy gap changes under high press., polymorphic transitions 77−51649
Ag_8SnSe_6, fundamental absorpt. edge changes due to polymorphic transitions 77−20240
Ag_8SnSe_6, phase transition, thermal expansion meas. 78−14466
$Ag(T_1)/AgI/Ag(T_2)$ cell, thermo-EMF of highly conducting solid electrolytes 80−24659
$AgTaO_3$, single crysts. flux growth, space group determ. 80−55282
Ag_2Te, Ag movements, X-ray microanal. by SEM *(French)* 79−42304
Ag_2Te, changes in elec. cond. and thermoelec. power at melting point 79−15147
α-Ag_2Te, diffusion of Ag^+, deviation from Einstein relation 77−76595
p-Ag_2Te, electrophysical props. 77−39842
Ag_2Te, growth by chem. transport *(Russian)* 79−38728
Ag_2Te, liq., elec. cond. at high temps. and pressures 79−11119
Ag_2Te, liquid, ionic and electronic cond., thermoelec. power 80−39329
Ag_2Te, low temp. thermal cond., thermoEMF 78−43423
Ag_2Te, polymorphic transition, DTA meas. 78−34620
Ag_2Te, solid and liquid, mass spectrometric obs. of VP, heats of form., comp. 79−42266
Ag_2Te, thermodynamic props., growth of single cryst. by chem. transport reaction 77−36380
Ag_2Te, thermodynamics of phase changes *(Russian)* 77−73459
Ag_2Te-(As)(Sb)(Bi), temp.-comp. diagram 78−44105
Ag_2Te-Ag_2S system, elec. and thermal props. at 300K 78−64044
$AgTe_2I$, Fermi surface meas. by Shubnikov-de Haas effect 77−39767
Ag_2TeO_3, chem. prep. and cryst. struct. *(French)* 80−79755
Ag_2TeO_4, cathodic props. in Li primary batteries 80−3502
Ag_2TeO_4, electrode for Li based primary cells, perform. data 79−52918
$Ag_2Te_xSe_{1-x}$ system, solid solns. of substitution existence, X-ray phase obs. 79−43217
$Ag_2Th(MoO_4)_3$, crystallographic data determ. *(French)* 78−10013
Ag_xTiS_2, intercalation cpd., Raman scatt. and electron diffr. meas. 79−24321
$Ag_2Tl_8I_{10}$, one-dimensional ionic conduction 79−7707
$AgTlSe_2$ and AgTlSe, elec. cond. and thermoelectric power, doping effects, rel. to pseudogap model 78−2506
AgTlTe(S)(Se), cryst. struct. 80−107156
$AgUO_2(NO_3)_3$, fluoresc. decay rates, temp. depend. 80−25429

silver compounds continued
$Ag_xV_{12}O_{30}$, oxygen bronze synthesis and thermal props. of single crysts. 77−84717
$Ag_xV_2O_5$, diffusion of Ag 77−20120
$Ag_xV_2O_5$, metallic, Raman scatt. 78−80358
$Ag_xV_2O_5$, thermodynamic, elec. and electrochem. props. 78−84265
β-$AgVO_3$.4AgI room temp. solid electrolyte and galvanic cell performance 78−79803
Ag_2WO_4, cathodic props. in Li primary batteries 80−3502
Ag_2WO_4, preparation and characterisation 79−99873
Ag_2WO_4-$In_2(WO_4)_3$, cpd. formation and polymorphism 77−86009
$Ag_2W_2O_7$, preparation and characterisation 79−99873
$Ag_2W_4O_{13}$, preparation and characterisation 79−99873
$Ag_8W_4O_{16}$, high temp. Raman spectra exam. 77−36236
Ag_xWO_3, atom motion 78−75874
β-$Ag_xW_yV_{2-y}O_5$ bronzes, β-phase existence range, elec. cond. and Ag diffusion 78−35373
AgX (X=halide) structure and stability of photographic sensitivity centres *(French)* 77−41708
AgX, selectivity of development of small aggregates of microcrystals in photographic layer *(Russian)* 79−58832
AgX, XX *(Russian)* 80−293
AgX, X=halide, form. and migration of catalytic nuclei *(Russian)* 79−70378
Ag_2ZnI_4, fast ionic cond. and order-disorder transition 79−99363
$AgZr_2(PO_4)_3$ system, phase charact. at different temps. 80−29936
β-Al_2O_3-Ag_2O, sp. ht. 0.1-1 K, evidence for localised low-energy excitations 78−34632
β-Al_2O_3-Ag_2O, cryst. structs. of stoichiometric and non-stoichiometric phases by X-ray diffr. *(French)* 80−28987
β-Al_2O_3-Ag_2O, far IR absorption and ionic cond. 78−72512
β-Al_2O_3-Ag_2O, Haven ratio, temp. depend., Ag diffusivity and ionic cond. 80−107503
β''-Al_2O_3-Ag_2O, ionic cond. at room temp. 80−107513
β-Al_2O_3-Ag_2O, low temp. dielec. susceptibility meas. 79−82911
β-Al_2O_3-Ag_2O, low-energy excitation spectra, localised modes 80−59606
β-Al_2O_3-Ag_2O, neutron diffr. obs. of struct. 80−107512
β-Al_2O_3-Ag_2O, Raman scatt., 12-400K, 2nd order phase transition 77−81091
β''-Al_2O_3-Ag_2O, Raman scatt. from mobile cations 80−11394
β''-Al_2O_3-Ag_2O, single cryst. Raman scatt., cond. mechanism and cryst. struct. 80−66209
β-Al_2O_3-Ag_2O, stoichiometric and nonstoichiometric, structure comparison, phase transitions in stoichiometric compound *(French)* 80−60856
β-Al_2O_3-Ag_2O, stoichiometric A phase, X-ray diffuse scatt. obs., sublattice phase transition 80−64944
β-$11Al_2O_3$-Ag_2O, sublattice phase transition, stoichiometric 79−42241
β-Al_2O_3-Ag_2O, superionic conductor, microwave absorption spectrum 80−11515
β-Al_2O_3-Ag_2O, thermal cond. below 300K 77−24454
β-Al_2O_3-Ag_2O, with mobile ion species, dielec. relax. 79−91351
β-Al_2O_3-Ag_2O, X-ray diffuse scatt. 78−71725
β-Al_2O_3-Ag_2O:Cu^{2+}, EPR of Cu^{2+} ions in conduction plane 77−69678
β-Al_2O_3-Ag_2O, low temp. sp. ht., tunnelling states and diffusion theory 77−43345
As-Te-Ag system glasses, absorpt. coeff. and optical band gap 79−65829
$As_{10}Ge_{15}Te_{75}Ag_x$ glass, elec. and dielec. props., Ag additions effect 80−65558
As_2S_3-Ag_2S glass, Ag diffusion, 50-120°C 78−18828
$As_{15}S_{40}Ag_{45}$ glass, photosurface deposition of metallic Ag discs 77−76650
$As_2S_{2.66}Se_{0.34}$, X-ray photoelectron spectra, electron binding energy, effect of Ag alloying 79−11499
$As_2Se_3Ag_x$ glassy semicond. film, prep. by photodiffusion of Ag, negative photocond. 80−92934
(Au, Ag)Te_2, calaverite, Te atom splitting and modulated struct. 79−99145
$Ba_2AgNb_5O_{15}$, $Ba_2AgTa_5O_{15}$, ferroelec. and ferroelastic props. *(French)* 79−24266
$BaAgP_3O_9.4H_2O$, cryst. struct. determ. *(French)* 77−80464
β-AgI, ionic cond. and dielec. meas., Frenkel defect formation energy 78−87814
$(C_5H_5NH)Ag_5I_6$, solid electrolyte, low-temp. phase transitions 77−72686
$Cd_{1-x}Ag_xCr_2S_4(Se_4)$, electronic struct., mixed valence 80−70612
$Cd_{1-x}Ag_xCr_2Se$, ferromag., magnetoresistance exam. *(Russian)* 78−84238
$Cd_{1-x}Ag_xCr_2Se_4$, Ag acceptor states effect on exchange interaction 80−20397
$Cd_{1-x}Ag_xCr_2Se_4$, ferromag. semicond., influence of strong elec. field on microwave absorption 77−28207
CdF_2:AgF, colour centres, IR absorpt. and photocond. after UV irrad. 80−79784
$CsAg_3Se_2$, crystal struct., X-ray study *(German)* 78−83795
CsCl-AgCl, spectral luminesc. charcts., optical range 77−1724
$(Cu,Ag)_2Se$, p-type, thermoelectric, vaporisation suppression, using inert and reactive coatings 79−48149
$(Cu,Ag)_2Se/(Bi,Sb)_2Te_3$, P type selenide segmented element fabrication, thermoelectric props. 80−107835
(Cu,Ag)X, (X=Cl, Br, I), molten, thermoelec. power determ. 78−26711
Cu-Ag-Se, computation of component activities from ternary miscibility gap data 79−11591
$CuAg_3I_4$, co-ionic cond. obs. 80−34231
$Cu_xAg_{1-x}I$ crystals, layer structs., X-ray diffr. studies 80−96457
$Cu_{1-y}Ag_yInS_{2-x}Se_{2x}$, for solar photovoltaic cells 80−10982
$Cu_{1-y}Ag_yInS_{2(1-x)}Se_{2x}$, lattice consts. and band gap variations 79−78000
$Cu_{1-y}Ag_yInS_{2(1-x)}Se_{2x}$ pentenary alloy system, appl. to photovoltaic solar-energy conversion 80−35680
CuBr-AgI system, ionic cond. and phase diagram 80−2198
Cu_2Se-$AgInSe_2$ heterojunction, photodetection props. 78−39195
Cu_2Te-Ag_2S, kinetic props. of solid solutions 79−7827
$ErAgSe_2$, cryst. struct. determ. *(French)* 77−47413
Ge-S-Ag, amorphous, props. and origin of paramagnetic defects 79−10801
Ge-S-Ag glasses, bulk and film, EPR study 78−43644
GeS_2-GeS-Ag_2S glass, Ag diffusion, 50-120°C 78−18828
$(GeTe)_x$-$(AgSbTe_2)_{1-x}$, thermoelectric props. of monolithic and pressed samples at 300K 78−80009
$(GeTe)_x$-$(AgSbTe_2)_{(1-x)}$, thermoelectric characts., temp. depend. 300 to 750K 79−78123
KAg_4I_5, phase transitions and dynamics 78−59924

silver compounds continued
KAg_4I_5, solid electrolyte, Raman spectra 79−73934
KAg_4I_5, superionic cond., pressure effect on phase transitions 80−70405
KAg_4I_5, superionic phase transition, dynamical and crit. pt. props. 80−107535
KAg_4I_5, superionic solid films, preparation and elec. cond. 79−82380
$K_2Ag_4Se_3$, crystal struct., X-ray study *(German)* 78−83795
KCl:AgCl, positron annihilation characts., positronium state form., X-irrad. effects 77−4700
KCl:AgCl, tunnelling-recombination luminesc. 78−88354
KCl-AgCl (0.5%), surface positron and positronium states, positron annihilation expts. *(Russian)* 78−39623
La_2O_2S-AgS-Ga_2S_3, ionic conducting glasses *(French)* 78−79804
La_2S_3-Ag_2S-Ga_2S_3 glass system, prep., thermal and elec. props. *(French)* 80−89192
Li-$AgCrO_4$ pacemaker cell construction 77−81739
$LiNO_3$-$NaNO_3$-$AgNO_3$, molten salt mixture, excess thermodynamic props. and US vel. *(French)* 77−31720
Mg-AgCl seawater battery, performance and EMF at great ocean depths 80−76623
$NH_4Ag_4I_5$, Raman spectra, internal vibrs. of NH_4^+ ions 78−72497
$NH_4Ag_4I_5$, solid electrolyte, Raman spectra 79−73934
$NH_4Ag_4I_5$, superionic cond., pressure effect on phase transitions 80−70405
$NH_4Ag_4I_5$, superionic solid film, surface diffusion coeff. 80−92709
$NH_4Ag_4I_5$, superionic phase transition, dynamical and crit. pt. props. 80−107535
NaCl:AgCl, positron annihilation characts., positronium state form., X-irrad. effects 77−4700
$NaNO_3$-$AgNO_3$, molten salt mixture, ionic and mol. mobilities, inter-diffusion and self-diffusion *(German)* 77−11720
Na_2O-Ag_2O-B_2O_3 glass, Ag^+ ion distrib., X-ray diffr. study 80−84076
Na_2O-Al_2O_3-B_2O_3-SiO_2-AgBr(Cl), photochromic glass, exam. of role of O and Cu ions, using luminescence spectra 79−4849
Na_2O-B_2O_3-SiO_2/$AgNO_3$ exam. of ion exchange equilibria 79−5178
Na_2O-B_2O_3-SiO_2/$AgNO_3$, thermodynamic characteristics of ion exchange process 79−8452
Na_2O-SiO_2/$AgNO_3$, exam. of ion exchange equilibria 79−5178
$Na_4[M^{II}(NH_3)_4][M^I(S_2O_3)_2]_2$.L, ($M^{II}$=Cu, Ni), ($M^I$=Cu, Ag), (L=$H_2O$, NH_3), IR spectra, vibr. anal. *(French)* 78−52477
P_2S_5-Ag_2S glass, Ag diffusion, 50-120°C 78−18828
$Pb_2AgNb_5O_{15}$, $Pb_2AgTa_5O_{15}$, ferroelec. and ferroelastic props. *(French)* 79−24266
PbI_2-Ag, photographic mat., photolysis, effect of PbI_2 photo-EMF effect *(Russian)* 80−92939
$RbAg_4I_5$, Ag^+ ion pot. energy calcs. 79−10828
$RbAg_4I_5$, cryst. growth from soln. 79−33916
$RbAg_4I_5$, crystal nonequilibrium thermodynamics, quasielastic light scatt., systematic anal. 79−61391
$RbAg_4I_5$, depolarisation of light by crit. fluctuations 79−61333
α-$RbAg_4I_5$, dynamic cage effect 80−107541
$RbAg_4I_5$ film, thermopower meas. temp. depend., correl. effects role 80−107539
$RbAg_4I_5$, ionic cond., effect of press. 78−51733
$RbAg_4I_5$, phase transitions and dynamics 78−59924
$RbAg_4I_5$, phase transition, statics and local dynamics, mean field and Mori theory 80−39347
$RbAg_4I_5$, single cryst., dielectric relax. *(German)* 79−4764
$RbAg_4I_5$, single particle excitations, inelastic neutron scatt. obs. 80−59599
$RbAg_4I_5$, solid electrolyte, compatibility with polyiodide cathodic materials of I_2-Ag current source 77−40555
$RbAg_4I_5$, solid electrolyte, cond., phase transitions 77−84972
$RbAg_4I_5$, solid electrolyte, electronic cond. meas. 78−2483
$RbAg_4I_5$, solid electrolyte, neutron scattering study 78−79696
$RbAg_4I_5$, solid electrolyte, thermodynamics and electrochem. behaviour of I_2 electrode 79−70348
$RbAg_4I_5$, solid electrolyte, Raman spectra 79−73934
$RbAg_4I_5$, solid electrolyte development, Ag^+ cond. 80−107532
$RbAg_4I_5$, static and dynamic NMR effects at 208K and 122K phase transitions 80−108105
$RbAg_4I_5$, superionic cond., US absorpt., ionic cond., relaxing sp. ht. 78−14505
$RbAg_4I_5$, superionic conductor, phase transition detection by thermoelectric power method 80−92669
$RbAg_4I_5$ superionic films, elec. cond. and optical absorpt. studies 79−99355
$RbAg_4I_5$, superionic phase transition, dynamical and crit. pt. props. 80−107535
$RbAg_4I_5$:AgI,Rb_2AgI_3, polycryst., ionic cond., impurity conc. effects 78−51734
$RbAg_4I_5$-metal interface, photocurrents, photoelectrochem. effects 78−34897
Rb_2AgI_3, cryst. struct. and polarised Raman spectrum 77−69813
$RbAg_3Se_2$, crystal struct., X-ray study *(German)* 78−83795
RbI:AgI, thermal reorientation kinetics of I_2^-, decay of optical anisotropy 77−52138
$(Rb_xK_{1-x})AgI_3$, cryst. struct. 77−51360
$(Rb_xK_{1-x})Ag_4I_5$, cryst. struct. 77−51360
$RbPO_3$-$AgPO_3$ system, phase diagram 77−25033
$SO_2(NHAg)_2$, disilver sulphamide, crystal atomic struct. *(German)* 78−10008
Se-Ag_2Se, heterojunction with memory, transient switching characteristics 80−44718
Se-Ag_2Se, heterojunction, electrically controlled negative differential conductance, mechanism 80−44720
Se-Ag_2Se, thin film polycrystalline heterostructure, exhibiting memory switching, noise level 78−84288
$SrAg_2I_4$, Raman and autocorrelation spectra, solid and soln. 79−38532
$SrAg_2I_4.8H_20$, cryst. struct. 79−23575
$Sr_2AgNb_5O_{15}$, $Sr_2AgTa_5O_{15}$, ferroelec. and ferroelastic props. *(French)* 79−24266
$Sr(PO_3)_2$-$AgPO_3$, phase diag., physicochem. characts. of $SrAg(PO_3)_3$ 77−52302
TeO_2-V_2O_5-Ag_2O, glass, IR spectra of crystalline phases 79−38536
Tl_2S-Ag_2S system, phase equil., DTA, X-ray and microhardness obs. 79−38803
Zn-AgO cell, Zn electrode slurry-paste fabrication optimisation 79−96430

SIMS *see secondary ion mass spectra; secondary ion mass spectroscopy*

simulation
see also aerospace simulation; analogue simulation; brain models; digital simulation; hybrid simulation; modelling; physiological models; plasma simulation; semiconductor device models
above knee prostheses, normal knee control in level walking using hydraulic simulator system 77−48955
accelerator magnetic field azimuthal variations, two-dimens. approx. calcs. 77−26908
accretion onto binary stars, numerical simulation 79−21358
acoustic ducts, finite element simulation 78−38115
acoustic filters, arbitrary profile, circular cross section, finite element simulation 77−11059
acoustic logging in cased wells, simulation rel. to excited wave freq. optimisation *(Russian)* 78−40707
acoustic multipath signal, individual pulse resolution, signal procesing, simulation results 78−83176
adsorbed molecular chains, config. props. effect on surface coverage 79−42371
aerosol formation, growth, general dynamic eqn., H_2SO_4/H_2O aerosol simulation appl. 79−47990
air pollution, smoke plumes visual effects, computer simulation 79−66429
air pollution effects on planetary boundary layer, one-dimens. numerical simulation 77−41143
air pollution reduction via bus lane network 79−52991
air quality, box models 79−70474
air-based solar heating systems with phase-change energy storage, performance anal. using computer simulation 80−35762
aircraft skin, lightning damage simulation 78−87575
alkaline earth halides, thermodynamic and structural props., computer simulation 78−75849
amorphous semiconductors, hopping conductivity in 3-D disordered systems 77−4336
amorphous semiconductors, simulation of elec. conductivity in one-dimens., temp. depend. 77−4334
amorphous semiconductors, simulation of elec. conductivity in two-dimens., temp. depend. 77−4335
antenna radiation effect on human body, 1/4 wave whip type *(Czech)* 79−43958
apodiser, optimum, simulation by binary filters 78−5539
aquifer mineralisation field dynamics simulation 77−56664
aquifer simulation of groundwater, Canterbury, New Zealand 77−53093
arterial system, elec. simulation 77−25501
Asian summer monsoon, hemispheric simulation 78−40629
Asian summer monsoon, simulation by general circulation models 78−40637
astronomical X-ray burster phenomenon, mathematical simulacrum 77−87570
atmosphere, large scale process simulation, conf., Hamburg (30 Aug.-4 Sept. 1976) 77−86961
atmosphere, urban, numerical simulation of mixing depths 80−105024
atmosphere frontal waves development, numerical simulation accounting for mountain ridges effect *(Russian)* 78−53701
atmosphere O_3 production transport and distribution, numerical simulations with global general circulation model 80−56544
atmosphere turbulent transport, Monte Carlo simulation and comparison with exptl. data 79−53479
atmospheric adiabatic boundary layer height vars., simulation in wind tunnel 78−7691
atmospheric air, temporal evolution of negative ions *(French)* 77−21869
atmospheric attenuation and turbulence simulation in pulsed laser Doppler velocimeter system 78−73513
atmospheric circulation flow patterns, laboratory simulation of abrupt changes, catastrophe theory appl. 78−40721
atmospheric wind simulation in wind tunnels, roughness element geometry anal. 78−47079
atomic orbital cross-sections, bonding interactions, spring model, teaching aid 78−93503
auditory and visual impairment simulator development project 79−83982
auroral arcs global formation, numerical simulation 80−67446
axisymmetric turbulence, return to isotropy, numerical simulation 79−32470
Baneberry nucl. explosion, numerical simulation 80−841
BCC structures, simulation of vacancy-thermotransport 78−47570
blood pressure monitoring systems simulator 79−83963
bond graph fluid line models for inclusion with dynamic systems simulations 80−27136
botany, transpiration from plant leaf, simulation expts. 79−48279
brass, simulation of rolling and shear texture, using an adapted Taylor theory 78−52835
Brattle Physiological Synchroniser, simulator for testing respiratory gating function 80−109055
brittle fibre reinforced composite, failure, mathematical simulation 78−3221
Brownian dynamics of ionic solutions 77−63921
bubble populations in a gas fluidised bed 78−22415
n-butane, skeletal alkane fluid simulation, vibr., rot., torsional gauche/trans relax., diffusion const. 79−1378
n-butane in tetrachloromethane, gauch-trans equilib. const., mol. dynamics and Monte Carlo anal. 79−70308
cardiac activity signal simulator 80−56230
cardiac pacemakers, diathermy interference, simulation models 79−84007
cardiovascular simulator for the undergraduate physics laboratory 79−84889
catalytic fluidised bed reactors, simulation by transient axial dispersion model 79−77289
cellular convection in liquids, numerical simulation *(Russian)* 78−34120
cellular system growing, graph generation by parallel rewriting 79−66458
centrifugal forces, simulation, on overhead projector, teaching appl. 77−41438
Cepheid variable stars, simulated, for introductory astronomy course 79−44664
ceramics, ion beam irradiation techniques for simulation of 14 MeV neutron irradiation 80−10584
chain molecule in solutions, finite concentrations, different solvent conditions, simulation 79−45872
channelling in solids, computer simulation of ion trajectories 77−80563

simulation continued
channels with single- or two-phase heat transfer fluid, computer simulation of transients 78−90969
chemical kinetics, teaching approach 77−13555
chemical reactors, Markov chains *(French)* 79−32706
chemical system far from equilibrium, stochastic simulation 80−3339
chromophores, model for simulation of EPR spectra, in partially oriented membrane multilayers 78−86894
climate and climatic change, numerical simulation 79−16643
climatic effects of large-scale thermal pollution, simulation with NCAR general circulation model 79−53478
clusters of galaxies, velocity dispersion profiles of N-body simulations 80−21908
clusters of galaxies compared with N-body simulations, masses and mass segregation 80−22091
coal conversion reactor environments, simulation 80−100831
coal pyrolysis, in entrained bed flow reactor, theoretical exam. with aid of physical models 79−48062
coherence, simulation expt. 78−73810
coherent optical adaptive Modal Wavefront Control System 77−19295
coil, AC loss meas. in superconducting wires 80−37050
comets, orbital evolution of short-period objects, Monte Carlo simulations 80−62073
comets type I tails, laboratory simulation rel. to ray struct. and electrodynamical forces *(Russian)* 79−101119
complex chemical systems, kinetic mechanisms simulation method 78−48622
composite fracture with bonding strength defects between components, computer simulation 80−11771
composite piezoelectric US transducer, finite element simulation 79−41541
computer films for research, review 79−21512
computer tomographic thermography, numerical simulation 79−83889
convection, natural, in closed container, numerical simulation 78−46969
cosmic gamma-ray burst sources, simulation rel. to location via periodic slot collimator 77−64647
cosmic rays, scatt. in simulated interplanetary mag. field fluctuations 80−51626
Coulomb friction in mechanical systems, overview 80−53723
coupline simulation, between chemical reactions and ion transport in brown adipose tissue using network thermodynamics 78−92606
critical phenomena, simulation, using Wien bridge oscillator, threshold instabilities 77−1211
crystal frequency distribution, simulation taking nuclei distrib. into account 80−100184
crystal-met interface of Lennard-Jones substance, Monte Carlo simulation 79−60622
cyclotron isochronous, bunch phase behaviour, Monte Carlo simulation 77−54382
cylindrical annulus phase-change energy storage simulation 79−57478
damage function anal., computer simulation 78−87721
Darrieus rotar windmill arrays, wake interaction, wind tunnel simulation 80−61245
daytime F_2-layer simulation, selection of aeronomic parameters system 78−45087
design storm selection for stormwater management simulation 77−37278
diatomic gas, molecular dissociation, recombination reactions simulation 78−23934
diatomic molecules, near saturated fluorescence, two-level model 79−50000
dielectric charge carrier drift simulation using stochastic graphs 80−15539
dielectric medium, co-sinusoidally modulated, simulation by artificial dielec. at microwave freqs. 78−78864
diesel engine pistons, simulation of slap at TDC 77−72222
differential interference contrast microscopy, computer simulation 77−53973
diffusion, chemical, highly defective solids, steady-state computer simulation method for lattice gas 80−49401
dilute aqueous solutions, Monte Carlo studies of struct., review 80−54101
dipolar lattice, 2-D, Monte-Carlo calc., lattice energy 78−14308
direct energy space charge based convertor, numerical simulator 77−35406
direct solar energy, Markov chain simulation with one minute binning *(French)* 80−61293
discharge, luminescent, in He, electrons energy distribution function evaluation, by Monte-Carlo type simulation *(French)* 77−19795
disturbed cell renewal systems, simulation by microprocessor system 80−35859
drag reduction by compliant wall, numerical simulation of turbulent boundary layer 78−26114
drift tube, parallel-plate, Monte Carlo simulation 77−58914
droplet growth and initial dew point temp. accuracy in cloud chamber on space shuttle 78−96268
dye laser pulse output, accurate numerical simulation 79−41380
dynamic faulting in half-space, three-dimens. numerical simulation 79−16376
dynamic simulation of the Gentilly-1 reboiler system 78−82439
dynamical astronomy numerical simulation, new Runge-Kutta algorithms 79−12387
earthquake simulator studies of cylindrical tanks 78−45027
earthquakes, centrifuge modelling 78−81429
EAS, electron-photon and muon components, simulation 77−49255
education, nuclear reactor dynamics, theory and computer simulation 77−45636
educational simulation involvement indices based on physiological responses 78−31760
electrocrystallisation, nucleation and growth mechanism, ohmic overpotential effects, simulation 78−51842
electron avalanche in gas under uniform electric field, Monte Carlo method appl. *(Japanese)* 77−39399
electron beam dose profiles, cumulative normal distrib. model 79−88199
electron behaviour in solids, Monte Carlo methods 79−33274
electron diffraction crystallography, multiple inelastic scatt. in thick crysts., Monte Carlo simulation 77−7637
electron diffusion and drift in gases Monte Carlo simulation 77−84392
electron drift tube, photon emission investig. 78−87566
electron interactions, low-energy, single and twin biological targets 80−12195
simulation continued
electron microdiffraction patterns of nucleation models, computer simulation *(French)* 77−62449
electron trajectory simulation in solids, Monte Carlo method, particle size anal. 79−43693
EM particle 3-dimens. simulation code 77−27230
emulsion chamber C-jets, computer simulation using conventional particle physics 79−58990
environmental systems planning, design and control, conf. Kyoto, Japan, (Aug. 1977) 79−52962
EPR, spectral simulation program, appl. to NO spin labels 78−78730
EPR spectra, of organic free radical crysts., simulation 77−1598
estuary and river sited power plants, water discharge and chlorination, simulation 78−96250
ethylene-propylene, synthetic rubber, mathematical simulation of kinetics of thermal expansion *(Russian)* 78−55958
exospheres of Moon and Mercury, Monte Carlo simulation methods 80−67588
exospheres of Moon and Mercury, Monte Carlo simulation methods 80−67589
fast breeder test reactor operator training simulator model development 80−91219
fault motion and earthquake occurrence, numerical and lab. simulation 79−100815
FBR blanket, integral neutron reaction rate meas., in FBBF facility 80−22887
FBR testing, sodium-cooled, blocking of cooling channels monitoring *(German)* 77−34372
fcc alloy, A_3B ordering process time evolution, Monte Carlo simulation 79−86869
ferromagnetics, conductive eddy current and hysteresis losses anal. 77−12153
FFTF, operator training simulator 78−5013
fibre, failure charact. determ. by electrical simulation, feasibility study 77−52597
finite amplitude sound wave, simulation of nonlinear propag. through circular pipe 78−13834
finite-size particle method, numerical criteria to test real system equivalence 77−11393
fission reactor cooling blockages, of LMFBR *(German)* 78−94044
fission reactor safety, two-phase flow, analytical simulations for safeguards design 78−46143
flow, annular, turbulent, with rot. core tube, numerical predictions 77−55010
flow simulation, vortex methods, review 80−106801
flowmeter, flux distortion, tests using analogue rig to simulate flow with boundary layer 78−38420
fluid, intermolecular potentials, coulombic and multipolar, 2-dimens. mol. dynamics simulation 78−75520
fluid dynamics, macroscopic relativistic approach to numerical simulation 79−9122
fluid with periodic boundary conditions, error in computer simulation determ. 77−15296
fluids, simple fluid shear depend. viscosity, central force interactions 80−79970
free electron storage ring laser, Boltzmann simulation 79−72547
free-shear plane stationary computer simulated turbulence struct., discretized Navier-Stokes eqns. 78−26111
fusion reactor air detritiation operations, computer modelling and bench-scale testing 79−85784
fusion reactor first wall, radiation damage simulation using fission reactor test facilities 80−57950
fusion reactor neutral beam injector vacuum system transient simulation anal. 80−95453
galactic models with variable spiral structure, computer simulations 78−32574
galaxies fields stochastic simulation 80−62295
galaxies in clusters, Monte-Carlo simulation of orientations 80−90528
galaxies redshift, numerical simulation test of cluster effect on Hubble Modulus 79−2569
galaxy clustering evolution, cosmological N-body simulations 78−96550
galaxy clustering N-body simulations, fraction in groups as function of density enhancement 80−67879
galaxy clustering N-point simulations, covariance function 80−31373
galaxy fields, stochastic simulation 80−90530
galaxy merging, cosmological N-body simulations 80−56922
Galerkin-finite element simulation of the effects of artificial recharge on flow and chemical quality in an alluvial aquifer 78−81263
games, for education, crit. anal. 78−49579
gas flow, Monte Carlo simulation, book contrib. 78−59365
gas laser kinetics simulation 79−59676
gas turbine combustion chamber flow three-dimens. calc. 80−79405
gas-discharge cathode region transfer process simulation, Monte Carlo method 78−71600
gas-liquid transient flow in horizontal pipes, flow pattern transitions 79−32629
geophysical fluid system, climate simulation 78−81353
geothermal problems, digital and analogue simulation *(Rumanian)* 77−29510
geothermal reservoir simulation, math. models 80−12446
geothermal reservoir simulation, numerical soln. techniques 80−12447
geothermal steam pipeline network, numerical simulation 80−40822
glass transition, empirical criterion, Monte Carlo simulation 79−1496
grain boundary dislocation structure, atomistic computer simulation 79−60383
grain growth, anomalous, mathematical simulation *(Russian)* 77−55972
graphite, tritium effects, first wall controlled thermonuclear reactor conditions, simulation 79−647
grass-covered ground, surface acoustic impedance modelling at oblique incidence angles 77−54848
graupel development, numerical simulation 79−5573
gravimeter, LaCoste and Romberg, simulation model rel. to vibr. charcts. *(Japanese)* 78−65400
gravitational system dynamics, two-dimensional simulation rel. to Universe large-scale struct. form. 80−98749
hail growth simulation, fresh and annealed accretions struct. 79−58034
hail growth simulation, rotation and mixed clouds effects 79−58033
hard-sphere liquid, glass transition, computer mol. dynamics simulation 77−11674
heat capacity evaluation, electrical analogy 79−10453
heat conduction, calc. via elec. analogue 77−72128

simulation continued
heat exchanger, thermal modelling for computer simulation 77−46904
heat storage in porous medium with circulating heat transfer fluid, solar system appl. *(French)* 80−40916
heat transfer in vertical thermal channels, interferometric simulation 79−17477
heated water jet impingement melting, cavity formation, expt. and simulation 78−95133
heavy isotope separation using nozzles, jets and channels, investig. 79−94097
heavy water production plants, process simulation 79−22396
helical turbulence, diffusion of passive-scalar and mag. fields, computer simulation 77−11272
heterogeneous flows of multi-component mixtures in porous media−review 78−59471
high current density magnet, thermal stability 80−37057
high irradiance solar simulator for thermal absorptive material evaluation 79−62063
high-current relativistic beam, bunching, 2-dimens. finite size particle model 78−9310
high-level radioactive waste storage, temp. distribution simulation expts. *(German)* 79−81015
homogeneous condensation, from supersaturated vapour, stochastic simulation 78−51657
hourly global radiation sequences, stochastic simulation 80−36382
HTGR core, 2-D vibr. test for vertical slice model, COLLAN 2-V simulation code *(Japanese)* 78−58328
HTGR Core Auxiliary Cooling System mathematical simulation 78−29570
human factor studies, conf., San Francisco, USA (Oct. 1977) 78−48742
hydrology, simulation procedures for Box-Jenkins models 79−79907
hypersonic rarefied flow past forward facing step 77−42872
hypervelocity particle-surface impact simulation, using high-power pulsed laser 77−44094
ice, hexagonal, lattice struct., computer simulation 78−14324
ideal fluid small oscillations, mass forces in elastic shell, simulation of blood vessels 79−77253
image phase conjugate laser adaptive control, isoplanatic effect simulation 77−19294
impact torsional test accuracy determ. using simulation *(Japanese)* 77−56198
induction type accelerator with steady focusing field, mag. system simulation 77−42198
inertial confinement fusion, LASNEX code simulation 78−58478
instrument CAD considerations *(Hungarian)* 79−93134
interplanetary shocks interaction with Earth's magnetosphere, computer simulation 78−16243
ion autoresonant acceleration, numerical simulation 78−21789
ion beams, transport, space charge effects, computer simulation 78−50328
ion-molecule reactions, in drift tube, reaction rates and cross-section determ. 77−60052
ionic motion, 3-D quadrupole electric field, charge exchange collisions 78−9315
ionograms, vertical incidence, simulation by ray tracing with replacement layer and ionospheric trough 77−78559
ionosphere, effect of upper boundary conditions 77−17272
ionosphere, electric fields of magnetospheric origin, simulation 79−62655
ionosphere modification, numerical simulation of artificially created equatorial spread-F 78−88972
ionosphere negative storms, numerical simulation using observed neutral comp. data 79−25393
ionosphere observations, numerical simulation rel. to thermospheric quantities determ. 77−53268
IR and submillimetric-wave antenna design and simulation 79−30552
Israeli coastal plain, weather year standardisation for solar heating simulations 79−84444
jet noise sources, shallow surface-wave simulator 77−80146
Josephson junction, penulum type mech. analogue *(Japanese)* 77−72948
Jupiter, atmosphere, subliming boundary layer flow, simulation 78−65545
Keplerian systems, computer simulations 80−26720
Keplerian systems, numerical simulations of collisional evolution 80−109342
kinetics of reacting solns., diffusional barrier crossing processes, trajectory simulation 80−81280
Kirchoff's laws of spectral analysis, computer laboratory exercises 78−73790
knee joint simulator, development 80−17190
laboratory experiments in chemical spectroscopy, computer-simulated, for teaching 79−40339
lake model 79−96767
lake vertical temp. profile determ. by one-dimensional heat transfer eqn. soln. 78−77290
laser beam, thermal self-action over path in medium moving at variable vel., expt. and numerical simulation 79−32003
laser low level pulse simulation and calibration, tracking system evaluation 78−59074
laser radar simulator for low scatter charcts., three-mirror design 78−59118
laser radiation simulator for 1.06 μm 77−38903
laser-supported detonation wave momentum transfer optimisation 78−30307
Lennard-Jones fluid in contact with Lennard-Jones wall, interfacial density profile 78−67901
Lennard-Jones system, cryst. nucleation kinetics 77−62615
lens mass production yield estimation by centering tolerance simulation 80−78941
lidar return, simulated, from one-dimensional stratospheric aerosol model 79−44247
light source coherence meas. and fibre modal noise simulation by Michelson interferometer 80−48324
light sources for simulating sunlight 80−87454
lightning return strokes, EM radiation simulation, tortuosity effects 79−8672
linac injection system beam dynamics 80−13989
linear molecule liquids, computer simulation and theory, review 78−38604
lipid monolayer, simulation using mol. dynamics 80−108838
liquid film, mol. dynamics simulation of surface struct. 77−15666
liquid/solid interface, mol. dynamics simulation of struct. 78−26764
simulation continued
liquids, mol. dynamics simulation, partial press. evaluation 78−71663
LMFBR, hypothetical core disruptive accident, molten fuel relocation dynamics, simulant fluids 79−30980
LMFBR debris bed simulation expt., in-reactor expt. 79−13404
LMFBR fuel assembly, 19 pin, simulation of flow blockage 80−582
LMFBR loss of piping integrity expt. 77−42027
LMFBR loss-of-flow accident, 28-pin cladding relocation simulation expt. 79−30979
LMFBR plant, thermohydraulic transient simulation 77−83001
LMFBRs, mixed Na convection problems, digital model simulation *(French)* 80−42737
local correlation schemes for autostereoscopic 3-D image synthesis from binocular stereoscopic images, 3-D displays appl. *(Japanese)* 79−31812
LSI circuits, appl. of electron beam meas. techniques for verification of computer simulations 79−21875
lumbar spine, human 79−83840
macromolecular chains, coordinated motion simulation 79−86721
macromolecular dynamics, constraint dynamics, computer simulation 78−9932
macromolecular structure, interactive model building program 77−52738
macromolecules, computer simulation techniques for mol. theory verification 78−13633
Magellanic Stream, simulation to estimate total mass of Milky Way 77−91622
magnetosphere, plasma dynamics in mag. field laboratory simulation 79−16757
magnetosphere boundary, mag. field from laboratory simulation data 78−57396
magnetospheric simulation expts. 80−46347
mammography, simulation of X-ray spectra 80−76826
Mars, Viking gas exchange reaction simulation on UV irradiated MnO_2 substrate 80−72831
mass spectrometric fragmentation, MO-model and simulation 77−417
mating simulation programs, functional gauging for plane, prismatic workpieces appl. *(German)* 78−77846
melting and freezing, molecular dynamics simulation, Gaussian core model 78−67811
membrane potentials, meas. in ionic environment, biological membrane simulation 80−3412
merging galaxies, numerical simulations 80−36716
metal, grain boundary slip simulation using AgCl 78−3176
metals, cubic struct., numerical simulation of cross-rolling textures *(French)* 79−20061
meteoric matter, evaporated, mass spectrum of particles formed in condensation 79−71005
MHD channel flow, averaging of EM fields by electromech. simulation 79−77277
microcanonical sampling method, simulation appls. 78−73917
microclusters, computer simulation of nucleation and thermodynamics, mol. dynamics and Monte Carlo 78−51656
micrometeoroid impact, laboratory simulation 78−57510
microstruct. damage, by simultaneous He H_2 and heavy ion bomardment 79−46723
microwave hyperthermia simulation *(French)* 80−3770
military training devices, visual simulation techniques 79−50413
mixed crystal, coexistence of different spin structures, computer simulation 77−8276
molecular crystals, thermal motion computer simulation 79−46577
molecular dynamics, collisional de-energisation 77−42378
molecular dynamics, computer simulation, orientation space representation 77−76276
molecular dynamics, fluctuation driven reson., hydrodynamic and kinetic theory simulation 77−55124
molecular dynamics computer simulation, multiple time-step methods 78−47220
molecular dynamics simulation, sp. ht., thermal press. coeffs., compressibilities 77−28013
molecular dynamics simulation of dense gases, test particle motion 78−9930
molecular dynamics simulation of rigid polyatomics, singularity free algorithm 77−76277
molecular EPR spectra 77−14460
Monte Carlo computer simulations, of cryst. surfaces and cryst. growth 79−14710
Monte Carlo simulation of Brownian dynamics, new method, convergence props. 79−12719
Monte-Carlo simulation of photon transport in a heterogeneous phantom 80−26257
Morishita neurons, modelling networks, cerebellum appl. 80−30703
multirow dry or wet heat exchangers, simulation 79−191
muscle contraction, simulation of thermophysical processes 78−96063
myotonia, Ca induced, computer simulation 79−57633
α-N_2, computer-simulation with atomic pair pot., plastic cryst., phonon dispersion 77−7679
N-particle system, Brownian dynamics with hydrodynamic interactions 78−91209
Navier-Stokes flow with suspended particles, mathematical modelling, numerical simulation 77−72348
Nb, simulation expts. for sputtering by 14 MeV neutrons 77−36320
neutrino transport, direct simulation and aspects of equilibration 78−89050
neutron activation anal., computer-simulated gamma-ray spectra 79−1985
Nimonic type PE-16, irradiated, numerical simulation of void nucleation 79−73208
noise analysis of power reactor, simulation using nucleate boiling noise generator 78−54840
noise stimuli, computer simulation of Poisson transduction 77−86512
nonelectrolyte solutions, liq. theory, review, book contrib. 77−39523
nonlinear magnetic field simulator for electromagnetic fields anal. *(Japanese)* 80−95756
W. North Atlantic Ocean circulation, quasi-geostrophic simulations comparison with primitive eqn. results 79−48493
nuclear event simulation, green LED, trigger circuit, wavelength matched to photomultiplier 77−3238
nuclear fuel cycle, USA policy in fuel reprocessing analysis 79−85737
nuclear fuel cycle Guard Tactics Simulation exercise facility safeguard 79−85742
nuclear plant design anal. tool 77−88222
nuclear power plant operator training, simulator 77−367

simulation continued
nuclear reactor accident, simulation of LMFBR molten fuel pool 77—61518
nuclear reactor control system design, Horowitz method 79—45338
nuclear reactor fluid dynamics, prospects for accurate computer simulation 77—79422
nuclear reactors, modular data based codes appl. *(German)* 78—17445
nuclear system with advanced reactors, feed and enrichment requirements 77—61624
nucleation in finite systems, theory and computer simulation 80—26038
ocean internal waves, wind-generated exptl. study *(French)* 79—62518
ocean storm surge simulation expts. 78—16052
oceanic mesoscale eddies generation, numerical simulations with two and three layer quasigeostrophic models 79—57950
opical element polishing simulation calc. and results *(German)* 80—87566
optical sensor system simulation and evaluation 80—96030
optical simulation of X-ray tube focal spot 77—26449
optical simulator, for UHF antennas 80—26742
orthorhombic rotating molecules, doublet-quartet transitions, Zeeman effect calcs. 78—94280
p-i-n photodetector under transient conditions, simulation and expts. 79—58793
pacemaker interference simulation by models 78—81069
N.Pacific Ocean, numerical simulation of anomalies, model and mean state 79—48494
particle simulation unit for counter circuitry testing 78—81002
particle transport phenomena, theory, book 79—63176
patch field, Maxwellian exoelectron energy distrib., simulation 77—85905
pattern generation in lobster stomatogastric ganglion, pyloric network simulation 80—12076
pattern identification, large-spatial, of air pollution by combined model of source-receptor matrix and revised GMDH 79—57543
percolation clusters, as teaching aid for Monte Carlo simulation and crit. exponents 78—12477
photochemical smog, rate parameters and computer simulation 78—48677
photograph simulations, on storage display, appls. to X-ray topography and TEM 79—14637
photographic brightness, two-dimensional field 77—79778
photographic sound recording, computer simulation 78—78022
photosynthesis, carbon fixation cycle, model, teaching appl. 78—73806
Pickering reactor, simulation of wire activation expts. with SORGHUM code 78—25310
piezoelectric resonator with vibrating wall, impacting oscills. simulation *(Japanese)* 78—9483
planet thermal radiation intensity field modelling; principles 80—62056
planetary accretion dynamics, computer simulation, sensitivity to initial conditions 77—82131
plasma collisionless shocks, simulation and laboratory expts. 80—87893
plume model simulation with curved trajectory on data of diffusion expt. 79—52986
pollutants releases in shallow sea, numerical simulation 77—78234
polymer, molecular dynamics simulation of struct. 80—28923
polymer, thermally stimulated discharge, thermal sampling technique 77—85645
polymer adsorption into surface pores, computer simulation, phase transition *(Russian)* 78—51824
polymer chains with excluded vol., molecular dynamics simulation 78—78845
polymer model, dynamic viscosity, simulation 78—58875
polymeric, insulating materials, partial discharges, simulation and meas. *(German)* 77—77146
polymeric networks, macromol. chain conforms., computer simulation, network form. process *(Russian)* 78—70994
polymers, adsorbed molecules, configurational behaviour, computerised dynamic display 79—874
polymers, by self-avoiding nonintersecting random chains, conc. effect 78—12639
positron scattering by atoms, computer simulations, review 77—79692
power line ground gradient simulation for biological effect exam. 77—86731
power station game for physics teaching appl. 79—62949
power system that includes wind energy generators, model based regulation 80—61256
practical air pollution model at signalised intersections in Tokyo metropolitan area 79—52987
press. by Monte Carlo computer simulation 78—4564
PWR power plant, primary cct. leakage, safety aspects *(German)* 78—33239
quadrupole mass spectrometry, numerical calcs., book contrib. 77—22611
radar, synthetic aperture system, coherent optical simulation 77—27260
radical species, tube electrode generation, laminar flow through EPR cavity 77—24746
rainfall, for evaluation of surface mine spoils area restoration, Wyoming 77—49094
rainfall, for lab. water erosion expts. 77—81931
rainfall simulation for surface coal mine spoils area restoration 77—33120
random coil polymer chain relax., lattice model with excluded vol., head movement rules 80—5642
random nonGaussian backgrounds, simulation, calc. spatial correl. function 78—79089
random vibrations, wide-band, automatic system 80—53730
rarefied hypersonic flow past flat-plate, numerical simulation 77—19626
reaction rate data evaluation and compilation, simulation and models 78—48621
reactor fuel pin heat transfer, digital transfer matrix 78—29548
reactor fuel pin simulators for thermodynamic expts. with nucl. fuel elements 80—37420
reactor operation and control simulation code 77—83006
relativistic electron beam deposition, field-enhanced, bremsstrahlung prod. 78—29677
remote sensing simulator for soil moisture meas. 78—49143
renal functions appl. 79—83841
respiratory control system simulation, state-of-the-art 78—53441
rimming flow, numerical simulation of free-surface flow with surface tension 78—22353
river flow prediction by multiplicative model 79—53399
riverine and coastal effluents, remote sensing of thermal alterations and circulation patterns 79—57524

simulation continued
rocks fabric development simulation, appl. to quartzite 78—49015
rolling texture control, theoretical and practical study 79—87656
rotation, contrib. from galaxy merging 80—4439
scintillation-camera simulator for remote-data acquisition testing 80—46020
sea ice dynamics in Arctic (May 1975), simulation 78—36192
seismic faulting, expt. thermal fragmentation 78—96160
semiconductor, math. simulation of zone melting process *(German)* 79—28913
sensitometer, Xe flash, for daylight, W illum. simulation 78—29192
separated flow with laminar mixing region, heat and mass transfer, math. simulation 78—59397
shedding from inclined flat plate in shear flow, simulation 77—80170
shock wave turbulent boundary layer interaction, numerical simulation, Navier-Stokes eqns. soln. 77—31332
simulated inductors, large voltage swing, used for oscillator and floating coupling cct. 78—69227
site percolation problem, numerical simulation *(French)* 79—44864
sky intensity and polarisation at right angles to solar direction, Monte Carlo simulation 78—81401
soft biological materials, nonlinear behaviour, numerical modelling 79—100642
soil, freezing processes, finite element simulation 79—16527
soil erosion, wind tunnel simulation, effects on fine dust production 79—20834
soil gas fluxes determination, chamber methods numerical evaluation 79—16700
solar air conditioning systems, using stochastic weather models 79—57415
solar central receiver plant, dynamic simulation of thermal-hydraulic characts. of Na-cooled plant 80—30400
solar collector 79—62056
solar collectors, tubular, computerised performance simulation 80—55903
solar concentration heliostat mirror field analysis and design 79—83570
solar diameter pulsations, phase coherence simulation rel. to significance 79—92747
solar energy thermal storage, numerical simulation of energy transfer by conduction and radiation *(French)* 79—24916
solar flares experimental simulation, merging of two current carrying plasma columns *(Japanese)* 80—94775
solar heating, of Japanese multi-family housing unit, comparison with expt. results 79—57455
solar input determination and irradiance maps, analytical model and simulation code 79—34426
solar power, heating systems, performance mathematical simulation for optimal dimensioning *(German)* 80—26110
solar radiation simulator, non-axial type, reflector profile calc. *(Russian)* 78—63169
solar radiation transmission through atmosphere, Monte Carlo simulation *(Russian)* 79—12265
solar simulation, for testing off-axis light attenuation in stellar sensor assembly 78—61714
solar simulator calibration photometer 79—26103
solar system collisions, basaltic bodies destruction by high-vel. impact 77—64704
solid, classical octopolar, temp. effect on struct., Monte Carlo calc. 78—75598
solid mixture charact. discrete fourier transform, spectroscopy, computer simulation 78—63859
solid-liquid coexistence, mol. dynamics simulation 78—67803
solid-liquid interface, optical methods of study *(French)* 80—7318
space conditions, simulation for isotope fractionation expts. 78—73623
Spacelab simulation, OH submicron air-glow bands correl. studies 79—25381
spark discharge, numerical simulation 77—89340
speech analysis, simulation rel. to error evaluation for linear predictive using small anal. segment *(Japanese)* 78—31824
spent nuclear fuel re-enrichment without reprocessing, calculation simulation 79—26660
SQUID, A/D conversion, conditions for countable pulse train 79—91191
star cluster high resolution imaging by speckle interferometry, simulation 78—77492
star clusters containing massive central black holes, dynamical simulations with self-consistent potentials 80—26915
star clusters containing massive central black holes, Monte Carlo simulations 79—8955
star formation process simulation, hydrostatic models evolution *(Polish)* 80—21998
star formation rate in external galaxies, numerical simulation 77—45555
star simulator lightguide test instrument and method 79—27422
stars rotating sphere, free collapse simulation 78—93325
steel, bright strip, light oil annealing, mathematical simulation 77—77512
steel, mag. anisotropy, magnetostatic fields, numerical simulation 77—27220
steel, stainless, in-pile irrad. effect simulation by Ni ion bombardment, dislocation density, swelling 77—347
steel, stainless AISI 316, fast neutron void swelling simulation dose and dose rate effects 77—15457
steel, stainless type 316, irradiated, numerical simulation of void nucleation 79—73208
stellar speckle interferometry, atmospheric effects, laboratory simulation 79—53730
stellar spectra simulation using optical filters, G- and F-type stars 77—37505
Stepanov method, liq. mixing in shaper hole, simulation device 78—3022
stored beam energy loss to vacuum components, particle bunch simulation meas. at PETRA 77—83258
stratosphere sulphate aerosol layer, processes, models, obs. and simulations 80—109212
streamflow, skewed annual flows generation using fast fractional Gaussian noise generator 79—53395
strong ground motions along principal axes, simulation, 1971 February 9 San Fernando earthquake appl. 80—3935
structural system, simulation anal. of reliability and maintenance *(Japanese)* 80—62453
subgrid modelling procedures, turbulence theory applications 79—50710
sunlight reflected from polygonal heliostat, optical simulation 79—29452
supernova remnants interaction, simulation rel. to interstellar hot tunnels 77—17645

simulation continued
surface roughness, mathematical models 79−82428
surveying underwater transducers by acoustic method, computer simulation model 79−32165
system aspects of electro-optics, seminar, Huntsville, AL, USA (May 1979) 80−94921
systems of soft diatomic mols., eqn. of state, Monte Carlo simulation 77−26262
temperature wave generator for diurnal temp. wave propag. simulation 78−85735
temporal sequence memory model studies 77−9181
texture anal. three dimensional, computer simulation of errors 78−64805
TFR 600 Tokamak, plasma equilib., numerical simulation of multitransformer eqns. 78−55760
thermal conduction and diffusion, electrical circuit analogue, for teachers 78−86089
thermal mixing layer development over water and heated land, lab. simulation 78−73449
thermal neutron monochromators, Monte-Carlo simulation of mechanical velocity selectors 78−24886
thermomagnetic gas analyser with internal convection 77−56296
tissue substitute materials formulation, effective atomic numbers 80−17169
tissue temperature simulation in cryosurgery 80−85355
Toda lattice, undamping of strongly nonlinear surface impurity localised mode, computer simulation 79−97315
tomography simulator, emission computed, design 80−61672
tornado vortex simulation at Purdue University 78−40677
tornadoes, numerical simulation of lab. vortex expts. 78−69411
traffic noise spectra, simulation model 77−46865
transonic flow simulation by tracking and blowing *(German)* 80−6081
transport coeff. numerical simulation of meas. by correlation method 78−8364
trigatron gap, transient glow discharge obs. and simulation *(Japanese)* 77−43097
tropical climate of ice age, simulation 78−16144
tropical cyclone development, latent heat release, numerical simulation 78−81309
tropical cyclones, landfall numerical simulation 78−81308
troposphere, urban photochemistry, computer simulation 78−49085
tsunami, island of Hawaii, 1979 November 25, numerical anal. by finite-element method 80−72449
tube banks, heat transfer, viscous flow, numerical anal. 79−55375
turbulence, laboratory-generated, simulating atm. turbulence effects on optical propag. 80−9803
turbulence, numerical simulation, intermittency effects 78−59375
turbulent compression corner flow, numerical simulation 77−62276
turbulent flow, numerical simulation of large eddies 78−9628
turbulent flow, subgrid-scale model evaluation 79−50709
turbulent flow in pipes, numerical anal. by finite element method 78−18341
turbulent shear flow computation, Navier-Stokes eqns., Reynolds stress modelling 78−46955
twilight observations, Monte Carlo simulation *(Russian)* 77−33186
two- and three-phase agitated systems, simulation model 77−11241
two-dimensional order-disorder phenomena, Monte Carlo simulation 78−67904
two-dimensional shear flow, viscosity effects, microscopic model 77−89085
two-phase flow through porous media, starting algorithm for numerical simulation 78−38388
typhoon movements expt. simulation *(Chinese)* 79−84449
underwater sound, simulation of phase modulation by first-mode directional internal wave 77−62089
underwater sound, simulation of reverberation from surface of sea *(French)* 77−14836
unsaturated porous media, heat and mass transfer, expt. and simulation *(French)* 78−94542
Uranus magnetosphere, plasma dynamics in mag. field laboratory simulation 79−16757
urban runoff pollution analysis, continuous and single event simulations compared 77−37271
vacuum gap breakdown initiation by microparticle impact 80−96413
variable star simulator 77−22357
vibration simulating system optimisation 80−53729
vibration-simulating systems optimisation, rel. to efficiency and cost 80−53728
vibrations, random, wide-band, simulators design optimisation 80−53731
Viking biology experiments simulation, possible surface reactions on Mars 78−7904
viscoelastic medium, numerical simulation of dynamic processes 79−46220
viscous incompressible fluid, two-dimensional turbulence in bounded region 78−30270
visual path neuron, analogue and digital electronic circuit appl. *(Spanish)* 78−27942
vocal cord vibration, computer simulation of pathological conditions 77−16940
volcanic activity dust veil index, stochastic simulation rel. to apparent periodicity 79−92514
voltage cell using Josephson junction, computer simulation 79−93089
vortex sheet evolution, buoyancy and surface tension effects 78−9643
wake, of circ. cylinders, in nearly homogeneous turbulent stream 79−1197
water, machine simulation, book contrib. 79−60249
water, simulation, Monte-Carlo method, 1 g cm^{-3}, 300K, using Rahman Stillinger ST2 pot. 77−51290
water, structure, theory based on quasi-component distrib. functions 78−38606
water organism, exptl. simulation of oscillatory motion by flexible plate *(Russian)* 77−32923
water pollution, nonpoint, continuous simulation 79−52967
wave supporting system, lossless, distributed parameters from boundary meas. 78−16658
Zeeman resonance lineshapes, motional narrowing, Monte Carlo simulation 77−38635
μ^+, nonadiabatic motion stability in mag. confinement system, numerical simulation 77−61646
π^+, nonadiabatic motion stability in mag. confinement system, numerical simulation 77−61646

simulation continued
Ar, electron avalanches at high E/N values, Monte Carlo simulation 77−35310
Au surface, high energy ion backscatt., computer simulation *(German)* 77−59664
Br+Br+Ar, photoinduced recombination, numerical simulation 79−16018
Cl_2, liquid-vapour surface, computer simulation 80−54478
$CuF_2.2H_2O$, X-band ESR powder spectrum and related magneto-microwave effects 79−24214
$^{18}F+H_2$, hot-atom reaction, nonequilib. vel. distrib. and reaction rate calcs. 77−63942
α-Fe, interaction of He with C impurities, computer simulation calc. 79−99235
Fe_3Al, ordered binary alloy, computer simulation of radiation effects 78−87709
H_2, electron swarms, motion, Monte Carlo simulation 77−39398
$HF(v_1=1)+HF(v_2=0)$, vibrational relaxation temperature dependence, laser-induced fluorescence simulation 79−50069
I_2, $(B^3\pi_{0+u})$, dissoc. reaction, computer simulation 78−48639
KCN, liq., mol. dynamics computer simulation 78−38609
KCl, (100) face, mol. dynamics computer simulation of surface props. 78−18880
Kr, near solidification, 50°C, up to 6500 bar, meas. and simulation using Lennard-Jones pot. *(French)* 78−67301
N_2, liq., computer-simulated ang. correlations and rot. motion 77−11461
N_2, liquid-vapour surface, computer simulation 80−54478
NaCl, evaporating surface, step motion obs. and simulation 78−26766
Ni, irradiated, numerical simulation of void nucleation 79−73208
Ni, Li ion scatt., expt. and computer simulation 77−63511
O and O_2, distrib. in lower thermosphere assuming tidal effects, one dimens. nonstationary diffusion-photochemical model 80−4160
O I 6300 Å nightglow, simulation rel. to neutral atmosphere parameters var. *(Portuguese)* 80−41584
Si, amorphous, implanted ion trajectory and spatial distrib., Monte Carlo simulation 77−11611
Si-C-O-Ar, high temp. plasma, prod. quenching mol. dynamics simulation 78−39711
UO_2 pellet compliance model based on out-of-pile simulation 80−42753
V_3Si, He irrad., computer simulation of channelling 79−55800
simulation, digital *see digital simulation*
simulators *see simulation*
Sinanoglu's theory *see atomic structure*
single phase rectifiers *see rectifiers*
sinks, heat *see heat sinks*
sintering
see also densification
activation energy error sources 79−95958
agglomeration techniques in powder technology, review 78−39713
air pollution control system options 77−66982
α-Al_2O_3, production rel. to props. of dense corundum refractories 80−25627
alloy, binary, vol. changes during sintering, inter-ion interaction influence 79−28982
alloy powder, two component, sintering 80−20847
alloys, binary, marker displacements as result of diffusion 80−92724
alumina based ceramics containing Mn and Ti compounds, sintering and paramag. props. 77−21069
atomised-Fe powder, friction of compaction process *(Japanese)* 77−59716
automated sintering and hot pressing system 79−33961
axisymmetric compacts from pressing in rigid discs, pressure and density distribs. 79−66022
bearing material, current state of prod. and development trends review 78−19902
borides, metallic, sintering, review, book contrib. 78−48359
borosilicate glass, phase separated and leached 77−85980
borosilicate glass, powder, sintering, foaming by chemical reactions 80−81017
brittle model mats., porous and nonporous, strength and struct. 77−4849
bronze, Al, electrode strip, short-time sintering 77−1824
bronze, Al and Ti, sintered frictional material, wear resistance, effect of matrix struct. 77−28911
bronze, sintered, mech. props. 77−28839
bronze, sintered, Zr addition effects on struct., hardness, wear resistance *(Russian)* 77−70019
bronze powder, granulated, porosity, compressibility and zinc stearate addition to starting mat. 77−63599
bronze powders, electric-pressure sintering onto cylindrical parts in fluidised bed 80−100960
bulk transport morphology relations 77−70015
calcinated simulated high level radioactive waste, prep. and characterisation of sintered glass-ceramics 77−28770
calculation of stress distrib. and X-ray elastic consts., of two-phase sintered material *(German)* 78−52883
$(CaO.6Fe_2O_3)_{97}(La_2O_3)_3$ compounds, effects of Nd_2O_3 substitution on magnetic props. *(Japanese)* 80−108010
$CaO-SiO_2$, wollastonaite, exam. of synthesis by hydrothermal sintering *(German)* 79−4934
carbide fuels, vibro-compacted, initial stages of sintering and hot-pressing 80−16254
[CC] Ag−(100)InP, metal-semicond.cathode contact, metallurgical, physical, chemical processes 80−107911
ceramic, compaction during pressing, green strength, effect of adsorbed layers *(German)* 78−6880
ceramic, firing in tunnel kiln, direct current and counter current in gases and waves 77−52264
ceramic, sintering kinetic laws with involvement of a liq. phase 80−55335
ceramic compounds, lyophilisation parameters, freeze-drying synthesis 80−97453
ceramic fuels, vibro-compacted, initial stages of sintering and hot-pressing 80−16254
ceramics, synthetic raw materials, sintered and fused, use in refractories industry, slagging, creep, thermal thick resistance *(German)* 79−4937
ceramics, technique for studying internal and external gas pressure within pores 80−11606
ceramics, US investigation, porosity, mech. and dielectric strengths *(Polish)* 79−52565
ceramics acid-resistant, based on Artemov clay and obsidian 80−20852

sintering continued
cermet, sintering, optimum conditions for electric heating elements 77−90287
chrome-forsterite-periclase refractory constitution and props., phase reactions during firing *(German)* 78−11175
clay, sintering tendency, effect of basalt and chemical-mineralogical composition 78−11177
coalescence of pores by dislocation mechanism, shape effect on charact. 77−73242
coke, effect of addition of borides on hot-pressing 80−40282
cold sintering under high pressures, correlation to plastic props. and diffusion 79−38757
complex diffusion alloying of sintered mats. 78−68650
computer simulation 79−61526
conf., Dubrovnik, Yugoslavia, (Sep. 1977) 80−17719
control by potentiometric level detector *(Russian)* 80−90813
cordierite, dense ceramic prep. with sintered condition over 300°C interval 79−33983
corundum ceramic, high-temp. treatment, powder medium effect on microstruct., comp., strength and dielec. props. 79−33984
Cr_2O_3, pure, hydrothermal reactive sintering 77−36431
crystal growth by solid state techniques review 77−85935
crystalline particles at sphere-plane contact, nondiffusional deform. under capillary forces 78−15329
diamond, polycryst. sintered under ultra high press., binary inclusion content effect on thermal stability *(Chinese)* 80−66453
diamond, polycryst. with Ni additives, sintering under ultrahigh pressure 80−84870
of diamond, polycrystal *(Chinese)* 77−59706
diamond, sintered compact, fracture and fatigue 79−52352
diamond, sintering under quasi-hydrostatic high press. *(Chinese)* 78−11141
diamond, temperature field dynamics during synthesis 79−38755
diamond polycrystal, sintering under high press., binary inclusion-diamond interaction *(Chinese)* 78−80484
diamond powder, ceramic prod. from H_2-saturated powder 79−15140
diamond powder, sintering with Co binder 78−27450
diamond powders, C metastable phases prod. during sintering 77−89404
diamond tool, metallic binder, microstruct. charact. by electron probe anal., SEM obs. *(Rumanian)* 79−74114
diamond-Co, sintered together, remanent magnetism 79−99731
diffusion controlled sphere-sphere sintering, simulation 80−20814
diffusion mechanisms, kinetics of contact form. 77−85956
diffusion models, steady state, for final stage sintering, testing of models by numerical simulation 79−4428
diffusion processes in ohmic sintering, temp. distrib. influence 80−92704
dilatometric method for study of dimensional anomalies in metallic materials rel. to crystal struct. *(French)* 79−52563
direct resistance, electric circuit components, breakdown voltage *(Ukrainian)* 77−70018
dolomite, powders sintering, decarbonisation cycle effect 80−104102
dunite-dolomite mixtures, sintering and minerogenesis 77−66613
electric discharge sintering, metal powder+punch electrode reactions 78−11148
electric discharge sintering of binary powder mixtures 77−63594
electric discharge sintering of metal powders, effect of diffusion coatings on steel electrode 77−63598
electric discharge sintering of oxidized metal powders 77−59719
electrical contact material, sintered, corrosion under tropical marine climate 78−11366
electrical contact materials, sintered materials based on powder metallurgy and powder composites 80−29902
electronic theory 77−63588
equations, statistical anal. of validity 79−95959
eucryptite-cordierite binary system, sintering of polycrystalline bodies *(Japanese)* 77−12588
FBR oxide fuels, dynamic response of grain boundary cavities to stress and temperature changes under conditions of continuous gas generation 80−66544
feldspar, sintering props. 79−29006
feldspars theoretical treatments and exp. procedure 78−44067
ferrite, grade 2000NM1, effect of CaO, MgO and SiO_2 impurities on props. 77−40412
ferrite, hard, fast firing in kilns with jet burners 78−64496
ferrite (Li-containing)-BiO_2, phase diagrams and sintering conditions 79−52141
ferrite core, strength improvement method, SiO_2 and Bi_2O_3 additions, mag. charact. 79−24484
ferrite powders, mag. props., explosive shock treatment effects 79−52395
ferrite spinel, DC resistivity depend. on substitutions 80−44565
ferrites, M type anisotropic, powder prep. and, sintered, effect of powder and pressing technology on alignment *(German)* 79−24472
ferrites, manufacture, modified technology development *(German)* 77−21073
ferrites, soft, spray firing for presintered powder prep. 80−89181
ferrites, strength and mag. props., vacuum effects 79−70028
ferromagnets, sintering theory and diffusion flow 79−28977
fibre reinforced composites with undeformable inclusions, densification kinetics prediction 77−63601
fibres, consolidation theory 77−73243
frictional electromagnetic clutch material, sintered, friction, hardness, wear props. 78−11339
frictional material, environment effects on props. 78−11338
furnace for remote nucl. fuel fabrication 79−89479
general theory on electronic level *(Russian)* 79−74111
glass, low density, sintering, expt. study 77−85980
glass, low density, sintering, pore size distrib. effect 77−85981
glass, low density, sintering theory 77−81246
glass powders, theoretical aspect of sintering 80−20883
grain and phase boundaries between crystals, conf., Konigstein, Germany (Oct. 1977) 78−72762
grain growth, chem. driven, during liq. phase sintering, computer simulation 80−55427
grinding powder *(Polish)* 78−6873
hard metal powders, electric-pressure sintering onto cylindrical parts in fluidised bed 80−100960
hardened metal, sintered, CVD of C rel. to atmosphere *(German)* 79−95966
hot pressing, reactive, identification of stages 79−11542
hot-pressing chamber, with US activation facility 77−59709
hydroxylapatite, sintered bioceramic, prep. and props. 79−43174
sintering continued
impurity segregation on sintering of technical purity powders 77−63586
Inconel 718, grain growth during sintering 80−97449
initial phase kinetics, model with diffusion *(French)* 78−35328
intermediate stage, powder compacts, anal. of surface area reduction kinetics 78−76614
isothermal, surface area reduction 77−8779
kaolinite, sintering mechanism at 900 and 1050°C, influence of mineralizers 77−90305
kyanite-sillimanite concentrate, sintering and mullitisation of basic minerals 77−59726
kyanite-sillimanite concentration, mullitisation and sintering, props. of refractory products 80−20867
liquid phase, microstructural evolution, coarsening 77−70014
liquid phase, microstructural evolution 77−70013
liquid phase, neck growth kinetics, analysis 77−70012
liquid phase, role of grain and phase boundaries 78−72747
liquid phase 80−16232
liquid phase sintered systems, particle coalescence probability estimation 80−104086
liquid phase sintering, elementary mechanisms, soln.-reprecipitation 80−50571
liquid phase sintering, expt. obs. of densification by sintering 80−11584
magnesite, powders sintering, decarbonisation cycle effect 80−104102
magnetic materials, sintering, structure and props., external mag. and elec. field influence 80−50570
material transport rate and stress distribution during grain boundary diffusion driven by surface tension 79−61525
mechanism diagram, computer program 79−28978
metal, packed powder, induction heating mechanism *(Japanese)* 79−59615
metal, plastic, work hardening, sintered, porous, irreversible deform. 78−19849
metal, sinter-forging process, powder charact. effects 77−59714
metal, sintered compacts, residual pore effect on grain size distrib. 77−85961
metal, sintering of solids containing several dissolved gases 80−20836
metal, solid state sintering, compact length change 80−11593
metal fibre materials, thermal and elec. conductivities 78−10419
metal gauze reinforced porous permeable mats. with prearranged struct., prep. 78−68652
metal powder, hot swaging test method for tensile testing 77−25235
metal powder, milling conditions effect on densification during pressing and sintering 78−11149
metal powder, with intense energy release of interparticle contacts 78−60615
metal powder density meas. by US velocity 77−32760
metal powders, at 1 to 10 MPa, melting mechanism *(German)* 80−35122
metal supported crystallites, wetting in sintering and redispersion 80−24751
metal systems, high-temp., conf., Helsinki, Finland, June 1975 77−52295
metal wick, sintered, effective thermal cond. meas. 78−94582
metal-glass material, relation between struct. and props., prod. by hot densification 78−11145
metallic fibre knitted gauze permeable materials, mech. props. 80−66607
metalloceramic materials, NDT of microstructure and porosity using mag. props. 77−73416
metals, sintering analysis using sintering maps 80−93513
metals, surface oxide layer effects, oxide dissolution process, anal. 80−11588
metals and alloys, sintered, hot pressing, effect on formation of struct. and props. during sintering 79−100088
mischmetal-Co-Cu-Fe-Mg, mag. props. 80−35353
mischmetal-Co-Cu-Mg, mag. props. 80−35353
Mo-Ni powder mixtures, form. using electric discharge sintering 77−12563
model system, theoretical consideration 77−85955
Na_2O-CaO sintering process, removal of S compounds for Al_2O_3 production *(Chinese)* 80−55323
NASICON solid electrolyte, processing and phys. props. 80−60820
nepheline containing ceramic masses, phase transform. during firing 77−66611
Ni powder 2JJ, porous, effect of sintering conditions in struct. and strength 80−20823
Ni-Cr alloy Kh20N80, sintered sheet material, stopping power and pore size relationship 78−19693
Nichrome wire, porous, strength charact. 78−6997
Nichrome/steel, porous metal-thread sheet materials, filteration, permeability and strength props. *(Russian)* 79−78915
nonisothermal, densification of powder compacts 78−60596
nonisothermal kinetics *(Russian)* 79−74112
nonisothermal method for sintering kinetics of materials controlled by two mechanisms 77−63580
optical graded-index fibre vapour-phase axial deposition method, fibre characteristics 80−58824
optical waveguides, inhomogeneous glass sintering, self stresses producing bulk flow 80−14448
oriented bicrystal, prod. technique 80−108371
oxide ceramics, dependence of props. on raw materials, exam. using ceramic magnets as model *(German)* 79−4936
oxide compounds, binary, solid-phase reactions of form., direction of diffusion 79−43179
oxide reactor fuel pellets, ammonium polyuranate precipitation, continuous, particle size distrib. and agglomeration control 79−93804
packing fraction effects *(German)* 78−64494
particle dimension and shape evaluation by SEM 80−40278
particle drag retardation, diffusion controlled sintering 77−12561
particle size effects *(German)* 79−91602
parts for frictional units 78−11342
paste, direct tensile tests and tied crack model 78−11178
perlite, low temp., processes occurring during firing 80−11607
Permalloy, pressing velocity effect on quality of compacts 80−20834
Permalloy 51N, powder metallurgy product. and props. 78−60603
Permalloy powders, electric pulse shaping and sintering 80−25605
permanent magnet alloys manufacture, Co-mishmetal alloys *(Polish)* 80−35132
permanent magnets, development history, magnetic and physical props., appl. 80−29901

sintering continued
physical and chemical phenomena, Fe, Al and W alloys charcts. *(Italian)* 79−83147
physico-geometrical explanation of deep dispersion of condensed substances 79−91603
piezoelectric ceramic, TsTBS-3, mech. strength, effect of glass powder addition 78−31370
piezoelectric ceramics, bimorph element for loudspeakers manufacture *(Japanese)* 80−53597
polymer filled ceramic, ZrO_2 stabilised, fracture mechanism *(Russian)* 80−100895
polyuranate gels, changes in pore structure during reduction and sintering 77−71685
porcelain, sintering, theoretical treatments and exp. procedure 78−44067
porcelain, sintering charact. 79−83156
porcelain body dynamic equation, during sintering process *(German)* 78−27455
porcelain wave, crazing resistance, glaze fitness *(Japanese)* 79−74278
porcelains, sintering props. 79−29006
porosity effect in sintered material on temp. generated during grinding 78−35530
porous material, role of gas in healing of isolated pore by volume vacancy diffusion 78−15330
porous materials, behaviour of pore filled with const. amount of gas 80−66450
porous materials, gas diffusion through pore during sintering 80−40281
porous materials, production method using stainless steel gauzes, exam. of hydraulic characteristics 80−16243
porous materials, sintered, mech. testing device for hydrostatic pressure conditions 80−40645
porous materials, sintering kinetics, superplasticity of polycryst. materials 79−100072
porous polycrystalline solids, mechanism hindering boundary sliding 79−95962
porous sintered materials, electrolytic preparation 79−52530
porous sintered metal, heat transfer in forced convection of fluid 77−55084
porous solid, effect of gases, healing of isolated pore accompanied by internal oxidation 77−90286
porous solids, gases influence, behaviour of assembly of pores filled with gas 80−84877
porous structure, shrinkage kinetics, boundary slip and superplasticity 77−36611
powder, apparatus for exam. sintering, electrical resistance 80−16217
powder, consolidation theory appl. 77−73243
powder, two component mixture, compact growth in liquid phase sintering 80−20835
powder compact densification charcts., non-isothermal sintering 79−28976
powder compacting, two-layer 79−47647
powder compacts, active shrinkage theory and mechanism 77−63579
powder consolidation process, exam. of quasimelt in pressing, sintering stages 80−20816
powder forging, review 79−43166
powder kinetics, variation of mechanism dependent exponent, with coordination number and neck size 80−20815
powder mixture electric-discharge sintering mass transfer and homogenization 80−20817
powdered metals, electric *(German)* 80−25598
powders, sintering, study of phase contacts formation in porous disperse structs. *(Russian)* 80−20811
powders, submicron, surface area reduction kinetics, model 78−44039
powders and sintered bodies, particle size distributions from chord and area distributions *(German, English)* 80−35126
prefired substrate, acid treatment, improvement in as-fired surface finish 79−24636
pressing dies, dimensions of hard-alloy inserts calc. 78−60593
pressure sintering, inhomogeneous flow and effective press. 80−93512
pressure sintering mapping, sintering mechanisms 79−28975
process characteristics 79−95961
PVC, sintered powder, elastic props. and porosity 77−63619
PVC, sintered powder, permeability and porous struct. 77−63620
PVC-chlorinated PVC mixtures, compatibility, mixing techniques, elastic modulus determ. 79−4943
quartz, ceramic, elastic property changes on sintering 77−90301
quartz glass-ceramics, atm. influence on sintering rate 79−38784
quartz porcelain, fast fired, development of microstruct. *(German)* 78−60625
random structures, volume diffusion and creep effects 80−35125
rare earth alloys, RCo_5, sintered magnets, texture determ. 79−100085
rare earth magnetic materials, in controlled atmosphere, permanent magnets flux stability enhancement, gyroscope-based guidance systems performance improvement 80−50144
rare earth RNb_3O_9, synthesis and physicochem. props. 77−90304
rare earth titanoniobates, $RTiNbO_6$, physicochem. investig. 77−47422
rare earth-Co, 2-17 comp., permanent magnet props. 77−8348
rare earth-Co alloys, powdered, fine grinding in gastight attrition mill 79−33967
rare earth-Co permanent magnets, processing and props., review *(Japanese)* 77−73049
rare earth-cobalt intermetallics, permanent magnet production and props. 78−52309
rare earth-Fe Laves phase alloys, sintering, magnetostrictive props. 77−16139
rare earth-iron intermetallic, O-stabilised, $R_{12}Fe_{33}O_2$, prep., struct. and mag. props. 77−8956
reactive, practical utilisation, theoretical and graphic interpretation 79−83150
refractories, multichamotte, sintering additives effect on props. 80−35147
refractories, sintered, X-ray diffraction method for assessing local stress levels 79−96265
refractories containing MgO, firing temp. effect *(French)* 79−38770
refractory, dense, sintered, role of isostatic pressing 79−28995
refractory films, stability, high temp. and electron irrad. effects 77−39747
refractory group VI metal, activated sintering mechanism 79−91605
refractory metal, generalised model for prediction of periodic trends in sintering activation 78−64498
refractory metals, enhanced diffusion model for activated sintering 80−25612
sintering continued
rehological and microscopical models relationship 79−95963
reinforced magnetically hard material, porosity and impact strength 77−55916
rel. to powder metallurgy 80−20841
rel. to powder metallurgy 80−25611
Samsonov electronic theory 77−90288
sciences 79−15621
SEM, qualitative and quantitative evaluation of void structures 80−16212
SEM obs., development of high temp. stage and appl. to sintering studies 79−21873
Si_3N_4-Ce_2O_3-SiO_2 materials: phase relations and strength 80−97465
β-Sialon, high strength, reaction sintering 80−7525
Sialon, reaction sintered, mech. props., effect of composition and X-phase 77−56013
β'-Sialon, sintering kinetics and rates of microstructural changes 79−100102
β'-sialon compositions, reaction sintering obs. 80−55337
sintered composite-liq. metal interaction, mass transfer eqn. approx. soln. 78−67262
sintered metal, cold forming with self aligning dies 78−11158
sintered metal parts and powders standardisation of quality control methods 79−96266
sintered parts, struct. stabilisation with C potential control of protective atmosphere 78−60614
sintering mechanism and sintered body anodization 79−95964
skinned sintering kinetics, cryst. surface calcs. *(Russian)* 80−40276
snow containing liq. water, sintering and compaction 79−62536
solid state sintering, models for kinetics 79−78912
soot preform, sintering 77−85980
spherical powder sintering by surface diffusion, computer simulation 78−48344
statistical data, 1958-1973 77−73245
steatite ceramic, sintering and crystn., depend. on original powder state 79−61527
steel, alloy hot forging for differential pinion gear 78−15337
steel, austenitic Kh18N9T, porous fibres, oriented struct., strength props. 78−3199
steel, austenitic stainless, porous fibre, sintered and compacted, mech. props. 79−15623
steel, austenitic stainless, powder, sintering behaviour 78−44051
steel, C, antifriction material, sintered, determination of elastic moduli 79−96070
steel, C, autectic, sintered, isothermal transformation behaviour, porosity effects 80−3031
steel, C, sintered, diffusional boronizing, exam. of process 79−96219
steel, Co, shrinkage kinetics of sintering and dependence on carbon content 79−100087
steel, Cr (13 wt.%), sintered, organometallic complex addition effects on mech. props. 80−25595
steel, Cr-Ni, rolled and sintered, to produce capillary structured filter material, exam. of mech. props., and production 80−16235
steel, Cr-W-Mo-Co, high-speed, from atomised powders, mech. and cutting props. 80−66556
steel, Cu-Ni-Mo (2, 2, 0.25 wt.%), sintering, kinetic charcts. 80−60805
steel, high speed, sintered, and wrought, type T6 strength and toughness 80−30102
steel, high speed, W-Mo-Co-Cr-V, production from atomized powder 80−20837
steel, high speed R6M5K5, excess carbide size and distrib. effect on grain size 77−90356
steel, high speed R8F8K7M6, cast, forged, sintered, struct. and props. 77−77516
steel, high-speed, sintered, refractory carbide additions effect on hardness and cutting performance 77−66608
steel, low alloy, sintered, isothermal transformations, porosity effects 80−3032
steel, mixed alloy, sintering, reaction kinetics of Fe and graphite powders 77−55907
steel, Mn-Cr-Mo, Mn-V-Mo, high-strength heat-treatable sintered 80−50575
steel, Ni, antifriction material, sintered, determination of elastic moduli 79−96070
steel, Ni, sintered, physical and mech. props. rel. to homogeneity 79−38762
steel, Ni, sintered, relation between microstruct., microchemistry and mech. props. 78−64504
steel, Ni-Cu, shrinkage kinetics of sintering and dependence on carbon content 79−100087
steel, Ni-Cu-Mo-C, powdered, influence of cooling rate after sintering on preps. 79−95969
steel, Ni-Mo, powder forged, as-forged props., effect of process variables 77−59715
steel, Ni-Mo, sintered, martensitic transformation due to cold working, metallographic study 78−44127
steel, Ni-Mo-C (2.0, 0.2, 0.4 wt.%) sintered, struct. transforms. and mech. props. after quenching 80−66557
steel, Ni-Mo-C (5, 0.5, 0.5 wt.%), sintered, effects of powder and sintering variables on props. 80−104093
steel, sintered, Cr-Mo, CaF addition effects on struct. heterogeneity 78−60611
steel, sintered, diffusion chromising 77−66607
steel, sintered, diffusion treatment with B, Si, Cr and C, corrosion and wear improvement 77−77642
steel, sintered, fracture of residual pores 80−76352
steel, sintered, high speed, with Ti(C,N) additions 78−11160
steel, sintered, mech. props., effect of small cold reduction 79−39048
steel, sintered, mech. props. 77−40439
steel, sintered, Ni-Cr-Mo additions, struct., props., thermomechanical treatment effects 77−12657
steel, sintered, oxidation in superheated steam, corrosion protection 79−39049
steel, sintered at various temps., isothermal decomposition of supercooled austenite 77−12617
steel, sintered bearing material, standardisation, wear and friction props. 78−19901
steel, sintered constructional, resistance to cyclic impact loads 77−77583
steel, sintered Cu, hardenability *(Japanese)* 77−48527
steel, sintered type M2 high speed, heat treatment response and cutting props. 78−15336

sintering continued
steel, stainless, 20Kh13, prep. by diffusion impregnation 80—60803
steel, stainless, atomised powder, effect of ultasonic refining on processing preps. 79—33972
steel, stainless, atomized 0Kh18N9 powder, activated sintering, US treatment 77—90291
steel, stainless, fibre reinforced porous coating, isostatically compressed for bone ingrowth 80—35134
steel, stainless, porous boronising sintering in BC packing material 78—60594
steel, stainless, prod. methods and props. for machine components, review 79—100082
steel, stainless, sintered sheet material, stopping power and pore size relationship 78—19693
steel, stainless 304L, sintering, effect of grain growth and boundaries on shrinkage rate 77—36419
steel, stainless-glass composite, sintered, corrosion resistance 77—77608
steel (alloy)-TiC (70, 30 wt.%) composite, sintered, wear resist. 80—100815
steel base composite, sintering, mech. props. 77—21061
steel fibre reinforced porous mat. prod., mat. props. 77—59723
steel W-Mo-V-TiC, powder, TiC effect on milling, pressing and sintering 78—60607
stereological charact. of interface interaction, appl. 77—63589
stress onset, first kind, mechanism *(Russian)* 78—80485
stresses generated during sintering of assemblages of real powder particles 77—63584
superalloy, hot consolidation of rapidly solidified powders, review 79—33965
surface area reduction kinetics during multiple mechanism sintering 79—100074
surface diffusion effect on sintering 79—74117
surface redistribution by grain boundary diffusion 80—84871
SYNROC-B ceramic for radwaste disposal, feasibility of subsolidus sintering 80—83198
SYNROC-B sintered ceramics for high-level radwaste fixation, comp. and phase charact. 80—106126
texture anal. of sinter struct., appl. to Ca ferrites in sinters of rich Fe ores 80—18009
transition metal borides, cryst. struct., prep. methods, chem., elec., mag. props., appls., book contrib. 78—47307
vacuum techniques' contribution to powder metallurgy 78—84736
Volume changes experienced by porous solids during nonisothermal liquid-phase sintering and self-propagating high-temperature synthesis 78—15328
YIG, hot spraying to give fine, free flowing, sinterable powder 80—20865
zeolites, synthetic, effect of sintering on elec. cond., porosity and microstruct. 79—29009
Zircon ceramic, exam. of development and fabrication 80—11608
Fe_2O_3-Bi_2O_3 sintered material, elec. switching effects due to thermal ionic breakdown *(Korean)* 80—70776
$3Y_2O_3.5Al_2O_3$, garnet, synthesis by firing mixed oxides 79—61545
ALN, O_2 effects on sintering 77—77451
Ag electrode preparation, performance comparison with chemically prepared electrode 79—87851
Ag, fine particles, adhesion and sintering, TEM exam. 78—44053
Ag, loosely packed powder, sintering SEM and dilatometry obs. 80—20843
Ag powder, ultrafine, sintering, coalescence growth stage 80—89174
Ag sintered electrode production for concentrating cell *(Portuguese)* 78—88637
Ag, sintering and grain growth, effect of Sb solute addition 78—84730
Ag, sintering of spherical powder, intermediate stage 78—52713
Ag, solid state sintering, compact length change 80—11593
Ag, spherical powder, sintering, study of initial stage 79—20004
Ag, spherical powder, struct. of sintering necks in compacts 80—11594
Ag, ultrafine particle, sintering effect, study by positron annihilation 78—95615
Ag, ultrafine powder, role of evap. during sintering 78—64505
Ag-InP interface, AgP_2 formation during sintering 80—65309
Ag-Ni alloy, composite powder mixtures, compressibility and sinterability 77—63592
Ag-Pt, sintering, limited solid solubility, peritectic diagram 77—28754
Ag-Sb (1.16 wt.%), Sb effect on sintering kinetics in early stages 79—52137
Ag-SiC, sintered, prep. of SiC whisker-reinforced Ag composite on Skylab 78—84741
Ag_3Sn-Hg, metallic powder-liquid system, correlation between hardness and evolution and sintering states 80—25614
Al alloy, powder, erosion resist. to hot propellant gases 77—56165
Al alloy, sintering of powder metallurgy parts, metallographic exam. and hardness testing 77—4752
Al, atomized powder, metallic contact for hot rolling in air 77—73294
Al contacts sintering in vacuum and O_2, room temp. 80—7512
Al, dispersion hardened with refractory carbides, sintering 79—74118
Al, powder, liquid phase sintering, solid-state solubility effect on vol. change 78—35332
Al powder, resist.-sintability *(Japanese)* 80—16228
Al powders, electric-pressure sintering onto cylindrical parts in fluidised bed 80—100960
Al, sintered powder, heat resistance increase method 77—90292
Al, sintering, activated, under thermal cycling 77—21053
Al sintering, low temp., form. of interparticle metallic contacts 80—20844
Al-Cu, electric discharge sintering of powder mixtures 78—60605
Al-Cu(0-10 wt.%) sintered alloys using composite powder 80—76210
Al-Ni-Si sintered SAS-1 alloy, struct. *(Russian)* 79—52135
AlB_{12}, powder, production of nitride materials by nitriding 77—12560
AlN, activating sintering process 80—25639
AlN powder, effect of O impurity on sintering and thermal cond. *(Japanese)* 79—20017
AlN powder, plasma synthesized, sintering behaviour, props. and struct. 79—100097
AlN, powder shock wave compression prior to sintering 77—66615
$Al_{2+x}O_3$, sintered, elec. cond. temp. and comp. depend., thermoelec. power 80—2438
Al_2O_2, sintering, rate contolled 80—20871
Al_2O_3 based ceramic sintering conditions effects on props. *(German)* 78—56604
Al_2O_3, calcined, exam. of morphological changes during calcination by SEM, exam. of sintering behaviour *(German)* 79—4931
α-Al_2O_3, ceramic, prod. from etching wastes of Al foils 80—108376
Al_2O_3 ceramic, vacuum compacted using $MgCl_2$ soln. moistener and MgO additive 79—61546
Al_2O_3 ceramics, sintering mechanism and kinetics, glass-forming additives effect 80—89187
β''-Al_2O_3, conductive, Li_2O stabilised, sintering and annealing 77—59724
Al_2O_3, corundum ceramic, effects of Na_2O, CaO additions on sintering struct., props. 79—15630
Al_2O_3, crystallite size and lattice distortion, determination using X-ray line broadening analysis, appl. to ceramic powders 79—8261
Al_2O_3, dense, effects of oxide sintering additions on strength *(German)* 77—1866
Al_2O_3, derived from gels, sintering behaviour, microstruct. 80—20875
Al_2O_3, derived from metalalkoxides, sintering behaviour 79—29005
β-Al_2O_3, effect of furnace atmosphere on sintering, and densification 79—20010
Al_2O_3, extraction from coal wastes, sinter process investigation 77—28769
Al_2O_3, high purity, sintering, impurity effects, analysis *(German)* 78—6881
Al_2O_3, $NH_4AlO(OH)HCO_3$ synthesis conditions effect *(Japanese)* 78—52710
Al_2O_3, $NH_4AlO(OH)HCO_3$ crystallinity effect *(Japanese)* 78—52711
β-Al_2O_3, new slip casting technique for fabrication of ceramics 78—84745
β''-Al_2O_3, polycrystn. electrolyte tubing, prepilot process for fabrication 79—87597
Al_2O_3 powder, active, sintering 80—20870
Al_2O_3, powder, phase composition, sintering, effect of explosive treatment 77—21079
Al_2O_3, powder sinterability, prep. history effects *(Japanese)* 77—66616
Al_2O_3, powder sintering, isochronal temp. depend. data interpreation 77—77453
Al_2O_3 pressing method, for the telecommunications industry *(Hungarian)* 78—52728
α-Al_2O_3, pure and doped, rapid sintering 79—74123
α-Al_2O_3, rapid firing, XPS study of cryst. struct. 78—68663
Al_2O_3, semisintered, shear strength at high press. 80—76308
α-Al_2O_3 sinterability, dependence on crystallinity of $NH_4AlO(OH)HCO_3$ parent salt *(Japanese)* 78—6883
Al_2O_3, sintered, containing $MgAl_2O_4$ precipitates, Mg distribution at grain boundaries 78—80498
Al_2O_3, sintered, electron microprobe anal. of impurity and additive distribs. 80—40359
Al_2O_3, sintered, MgO-enhanced densification, test of second phase and impurity segregation models 78—64511
Al_2O_3, sintered, residual stress meas., piezospectroscopic technique 78—52704
Al_2O_3, sintered, TEM ons. of K containing β'' precipitates 78—27522
α-Al_2O_3, sintered or hot-pressed, porosity effect on positron mean lifetime 78—27463
Al_2O_3, sintering, calcination cond. effect *(German)* 80—16251
Al_2O_3 sintering, effect of SrO, MgO and Y_2O_3 additives on α-Al_2O_3 mineralisation 80—89186
Al_2O_3 sintering, role of MgO 80—81010
Al_2O_3 sintering and props., glass forming additive effect 79—61544
Al_2O_3, sintering as function of phase comp. 80—66464
Al_2O_3, sintering behaviour and props. of 24 aluminas *(German)* 79—4932
Al_2O_3, sintering behaviour, effect of calcination with mineralisers *(German)* 80—25622
Al_2O_3 sintering in liq: phase presence, particle rearrangement 79—29004
Al_2O_3, sintering in reducing atmosphere, Na effect on density and strength 77—63613
Al_2O_3, sintering of single phase and multiphase components *(German)* 78—80494
Al_2O_3, sintering response with const. rate of heating, depend. on processing related pore distrib. 79—28992
Al_2O_3, sintering temperature effect of titanate additions 80—60808
Al_2O_3, sintering under press., survey *(Polish)* 78—31368
Al_2O_3, sintering with $SrTiO_3$ admixture *(Polish)* 78—19699
Al_2O_3 substrates, grain growth during sintering 80—40302
Al_2O_3 surface diffusion coefficient obtained by free sintering 77—72765
Al_2O_3, surface smoothness and densification, effects of SiO_2 additive 78—27462
Al_2O_3 suspensions, grinding method influence on rheology and suitability for high-density sintering 79—29001
Al_2O_3 targets manufacture, for vacuum thin film deposition *(German)* 80—11586
Al_2O_3, translucent, fabrication by high press. sintering 78—11167
Al_2O_3, transparent ceramic manuf., charcts. of powder and process 77—48383
Al_2O_3, wear and friction of MgO single crystal in vacuum 77—12710
Al_2O_3-Al, disordered, energy diagram model 79—56110
Al_2O_3-AlN phase diagram and reaction sintering of transparent cubic ALON spinel 80—25669
Al_2O_3-Cr cermet, Ti effect on sinterability 79—61552
Al_2O_3-glass mixture, microstructural changes and shrinkage during sintering 80—25640
Al_2O_3-MgO, MgO addition role in sintering 79—91608
Al_2O_3-$MgTiO_3$($CaTiO_3$)($BaTiO_3$), sintering *(Polish)* 79—100096
Al_2O_3-$MoSi_2$, for use as heating element, fabrication method and prop. *(Japanese)* 79—95989
β-Al_2O_3-Na_2O, MgO stabilised sintering *(German)* 78—19696
β-Al_2O_3-Na_2O, superionic anisotropic ceramic, prod. by microwave sintering *(French)* 78—52742
β-Al_2O_3-Na_2O, synthesis, ceramic form., sintering, cond. 79—11537
β''-Al_2O_3-Na_2O solid electrolyte, processing and phys. props. 80—60820
β-Al_2O_3-Na_2O:Fe, coordination site, oxidation state, Mossbauer, absorpt., emission spectra, mag. susceptibility meas. 78—68431
β-Al_2O_3-Na_2O:Mg, with and without Co co-doping, sintering behaviour rel. to ionic cond. 78—26723
β''- Al_2O_3-Na_2O-Li_2O (8.85, 0.75 wt.%) pressing powders, prep. by spray drying 80—40294
β-Al_2O_3-Na_2O-SiO_2, solid electrolytes, exam. of microstruct. ionic resistivity 78—80566
Al_2O_3-Pt metal-ceramic reaction, micro/macro obs. 80—66467
Al_2O_3-Si_3N_4 preparation, compressive strength 80—25634

sintering continued
Al_2O_3-SiO_2, derived from metalalkoxides, sintering behaviour 79−29005
Al_2O_3-SiO_2, mullite, powder, synthesis using silicic acid, clay and $AlCl_3$ *(German)* 79−4933
Al_2O_3-SiO_2-MgO, cordierite, powder, synthesis using silicic acid, clay and $AlCl_3$ *(German)* 79−4933
Al_2O_3-TiO_2-MgO.$2TiO_2$, exam. of solid solutions by X-ray phase analysis 79−95981
Al_2O_3-W cermet, sintered pressed compact, compressive and transverse rupture strength 78−19850
Al_2O_3-Y_2O_3, sintering kinetics, influence of minor additions of Y_2O_3 80−84868
Al_2O_3-$ZrSiO_4$ mixture, reaction sintering, correlation between densification and reaction 80−29911
Al_2O_3+TiO_2, reaction on sintering in reducing media 78−27457
$Al(OH)_3$, based ceramics containing Mn and Ti compounds, sintering and paramag. props. 77−21069
$Al(OH)_3$, derived from metalalkoxides, sintering behaviour 79−29005
β-Al_2O_3($Na_2O.11Al_2O_3$), prep. by diffusional transform. during sintering of Al_2O_3 in presence of $NaAlO_2$ 80−25637
β-Al_2O_3.Na_2O, ceramic tube fabrication, crystallite preferred orientation, ionic cond. 77−8781
$3Al_2O_3.2SiO_2$-ZrO_2 composites, sintered, in situ-reacted, fracture props. 80−81158
Al_2TiO_5, sinterability improvement by partial decomposition 79−28994
Al_2TiO_5, sintering and annealing effect on decomposition *(Japanese)* 79−87606
Au, fine particles, adhesion and sintering, TEM exam. 78−44053
Au powder, ultrafine, sintering, coalescence growth stage 80−89174
Au_8 particles, vacuum-deposited, degree of faceting during sintering 80−84411
B C powders, effect of C on sintering 80−40312
B fibre reinforced Al, prep. by reaction sintering 79−38769
B-Si alloys, B-rich, prep., anal. and cryst. growth *(French)* 80−104091
BC, sintered, struct. and props. 80−104181
BC, sintered and hot pressed, friction and wear, 20 to 1500°C 78−60844
$B_{12}C_3$, sintering and subsequent high temp. annealing, struct. and props. 80−20858
B_4C rings, Al bonded, exam. of fabrication techniques 78−72748
B_xC_y, pure and technical, sintering behaviour 77−63611
BN ceramic with organosilicon polymer additions, strength and oxidation resistance 80−20880
BN, cubic, sintering technology and cutting performance of tools 80−29919
BN powder, shock wave compression prior to sintering 77−66615
BN, turbostatic, hot pressing, struct. rearrangement, temp., residence time effects 77−8789
BN, wurtzite, chem. comp. and processing props. in prep. of Geksanit-R sinterings 80−25632
B_2O_3-SiO_2, optical waveguide glass, sintering kinetics 80−84898
(Ba,Sr)$Fe_{12}O_{19}$, Ferroxdure, developments and research 78−84455
Ba hexaferrite, Fe_2O_3-Fe_3O_4 equilibrium in BaO-B_2O_3 melt rel. to prep. 77−36428
$Ba_2Co_{2x}Zn_{2-2x}Fe_{12}O_{22}$, mechanically oriented, topotactic prod. technique, mag. props. 80−35140
$BaFe_{12}O_{19}$, effect of impurity concentrations, and sintering conditions on grain size *(German)* 79−23630
$BaFe_{12}O_{19}$ powders, fast reaction presintering 80−97445
BaO-Nd_2O_3-TiO_2-Bi_2O_3 system ceramics, high stability low loss dielectric preparation 80−81008
BaO-SiO_2-Fe_2O_3 permanent mag. ceramics, exam. of phase diagram, using X-ray analysis, optical microscopy, electron probe anal., and thermal analysis *(German)* 79−29012
BaO-TiO_2-Nd_2O_3, exam. of compositional and dielectric props. 79−33601
BaO.n Fe_2O_3, magnet, effect of SiO_2 on texture and densification behaviour *(German)* 79−24631
(Ba_xSb_{1-x})TiO_3, ferroelectric films, dielectric and semicond. props. 79−91388
$BaTiO_3$, acceptor doped, exam. of electrical conductivity 130 to 300°C 79−33286
$BaTiO_3$ ceramic, semiconductive sintering 77−36430
$BaTiO_3$ ceramics, calcination effects, TiO_2 powder eval. *(Japanese)* 78−64516
$BaTiO_3$, chemically precipitated, exam. of sintering behaviour by isothermal shrinkage *(German)* 79−4935
$BaTiO_3$, dielectric ceramic, interaction with metallic film during sintering 79−33958
$BaTiO_3$, doped-undoped ceramic composites, sintering behaviour 79−100094
$BaTiO_3$, powder compacts, sintered, physical and chem. inhomogeneities 79−87594
$BaTiO_3$, reduction inhibition by impurity ions 80−101018
$BaTiO_3$, thin film, obtained by modified doctor blade method grain orientation *(Japanese)* 77−77455
$BaTiO_3$:Al, 0.05-0.3 wt.%, ceramic dielectric, dielec. and mech. props. 79−8091
$BaTiO_3$:$BaTi_3O_7$, dielec. props. and microstruct. 80−60481
$BaTiO_3$:Dy ceramic, sintering, grain size, characterisation and props. 77−55923
$BaTiO_3$:Mn, polycrystn., annealing effect on transition temps. 80−3100
$BaTiO_3$-CuO(TiO_2)(ZrO_2) mixture, exam. of liquid phase sintering, densification 79−33979
$BaTiO_3$-Ni(Co, Mn)Fe_2O_4, ceramic, exam. of prep. and physical props. 78−68655
$BaTiO_3$-PbO-B_2O_3, liquid phase sintering, effect on props. *(German)* 79−33980
$BaTi_4O_9$ effect of chemical treatment on loss quality, at microwave wavelengths 79−34159
$Ba_2Ti_9O_{20}$, effect of chemical treatment on loss quality, at microwave wavelengths 79−34159
($Ba_{1-x}Y_x$)TiO_3 ceramic, resistivity rel. to donor dopant content 79−65474
$BaZrO_3$-$LaAlO_3$ systems, sintering conditions, elec. props. 79−43184
Be, plasma spray/sinter technique, Ar, satellite support structures, appls. 78−7079
Be, porous, shrinkage during sintering, kinetics, photographic method 79−15622
Be, sintered, physicomech. props. anisotropy, BeO inclusions effect 80−60804
sintering continued
BeO powder, sinterable and unsinterable, sintering processes, electron microscope exam. 79−33986
Bi powder, sintering in air, glycerol or vacuum 79−91604
$Bi_{12}GeO_{20}$, X-ray sensitive ceramic, sintering 80−25621
Bi_2O_3-CdO system, solid-state reaction, kinetics and mechanism 77−90303
C, dense hard-type solids prep. from petroleum coke powder by grinding 79−20002
C reinforced metal sintered composite materials, form of C present *(German)* 79−95978
CC TaC based hard metal, non-stoichiometric sintering, mech. props. 80−25616
C_2S, influence of polymorphic transform. on sinter stability *(Russian)* 80−66503
CaB_6-SmB_6 system complex borides, prep. and props. 78−52703
$CaCO_3$-$NaAlSiO_4$, micromechanism for phase formation during sintering *(Russian)* 80−16253
$CaIr_xRe_{1-x}O_3$, ($0<x<1$), sintered, exam. of mag. and electrical props. 78−80135
CaO based refractory from industrial lime, with 5% added electrocorundum 80−89184
CaO, determination of contents in sintering charge, using X-ray spectral anal., assessment of error 79−52823
CaO sintering, Cr_2O_3 addition effect *(Czech)* 80−45258
CaO-CaF, hot pressed, effects of CaF_2 addition, sintering behaviours and microstructs. investig. *(Japanese)* 78−95721
CaO-MgO-SiO_2, diopside, exam. of synthesis by hydrothermal sintering *(German)* 79−4934
CaO-SiO_2-Al_2O_3-Fe_2O_3 mix, liquid phase sintering 79−91610
$(CaO.nFe_2O_3)_{100-x}(La_2O_3)_x$ ferrite, permanent mag. material, mag. props. and preparation 79−83148
β-$Ca_2(PO_4)_2$ whitlockite ceramic fabrication for prosthetic applications 79−78924
$Ca_{10}(PO_4)_6(OH)_2$, synthesis and characterisation in dense polycryst. form 77−4749
$Ca_{10}(PO_4)_6(OH)_{2-2x}O_x\square_x$ polycryst. sintered bodies, prep. and thermal props. 80−25624
CaS discs, sintering method prep., ionic cond. meas., 650 to 900°C *(Japanese)* 78−75869
$CaTaRO_6$, (R=La, Nd, Gd, Sm, Er, Lu), synthesis and physicochem. props. 79−52139
$CaTiO_3$, perovskite, raw material activity and firing conditions as factors in sintering and grain growth 79−83161
$CaTiO_3$, protection against reduction during roasting in H_2 77−36426
$CaTiO_3$-$CaTiSiO_5$, sintering and dielectric props. 80−40307
$CaTiO_4$, perovskite, sintering during synthesis 77−36422
$Cd_xHg_{1-x}Te$ compressed sintered slabs, Hall coeff. and microstructure obs. *(Russian)* 78−10475
CdO, elec. cond. and IR refl. spectra after sintering and compaction 79−56945
CdS, effect of halide (NaCl, $CdCl_2$, $CdBr_2$, CdI_2) and polysulphide (Na_2S_x, K_2S_x) on recrystn. 78−11171
CdS:$CuCl_2$, sintered film, dopant conc. effects on carrier mobility 78−2484
CdS-CdTe sintered film, prep. and photocond. props. 77−28220
CdSe, effect of halide (NaCl, $CdCl_2$, $CdBr_2$, CdI_2) and polysulphide (Na_2S_x, K_2S_x) on recrystn. 78−11171
CdTe thick films, prep. by sintering and elec. props. 80−29451
Ce-Co-Cu-Fe-Ti, sintered magnet, prep. and mag. props. 77−73043
$CeO_2La_2O_3$, ceramic, thermal stability, sintering, deform., effect of La_2O_3 79−11532
(Co, Cu, Fe)$_5$Ce, sintered permanent magnets, magnetic charact. 78−60608
(Co,Cu,Fe)$_5$Ce, sintered, mag. props. 78−68302
Co-Ce Mischmetal powder, sintering 77−21055
Co-Cu-Fe-Ce, mag. characteristics of sintered permanent magnets 78−60312
Co-Cu-Fe-Ce alloys, sintered permanent magnets, mag. charact. 77−43855
Co-Mo, sintering, limited solid solubility, peritectic diagram 77−28754
Co-Sm magnets, H_2 atm. sintering effect on mag. props. 77−85504
Co-Sm-Gd(Ho) magnets, prep. and characterisation 77−8351
$CoFe_2O_4$ synthesis, chem., thermal histories rel. to fine cryst. struct. 79−43186
$Co_{3-x}Mn_xO_4$, solid soln., synthesis, effect of Bi_2O_3 admixture upon props., thermistor appl. 78−15325
CoO, pressure sintering densification model, computer program 78−44040
Co_2Z ferroxplana form. process peculiarities 80−89368
Cr-Al_2O_3 powder targets for plasma-ion spray deposition of resistance films 80−84897
CrC-Ni alloys, exam. of activated sintering 80−16241
CrC-Ni-(P), hard alloys, sintered, fracture props., P addition effects 78−60610
Cr_3C_2 electrophoretic alloy coatings on C steel, sintered, struct. form., Ni-P undercoat effect 80−61027
Cr_3C_2-(WC)-Ni, sintered, cavitation erosion resistance *(Japanese)* 77−52500
Cr_7C_3 electrophonetic coatings on steel, sintering 80−66707
Cr_2O_3, effect of oxide additions on sintering in air and reducing atm. 77−59729
Cr_2O_3, grain growth during sintering *(Japanese)* 80−16261
Cr_2O_3, influence of TiO_2 on sintering behaviour, densification as function of temp. 79−78919
Cr_2O_3 powder, activation and sintering 77−21078
Cr_2O_3, sintering behaviour, effect of TiO_2, C additions 80−66461
Cr_2O_3-Al_2O_3 solid soln., Vickers micro-hardness 80−66629
Cu alloys, reduction processes in sintering *(German)* 80−25597
Cu compact, exam. of anisotropic shrinkage as function of pressure 79−8257
Cu, compacted powder, thermal agglomeration, green strength 77−36417
Cu, dislocation form. during sintering *(German)* 78−31361
Cu, electrolytic powder, sintering, gas effects, finite size bodies 77−77447
Cu, hot forged powder compact 77−24981
Cu in contact, neck growth rate, mass transport mechanism, contact resist. expts. 77−55899
Cu, in contact with ^{3}He, thermal conductance, rel. to elec. resist., heat flow model calc. 80−10728

sintering continued
Cu, initial sintering, method for obtaining surface diffusion coeffs., appl. to shrinkage data 78−95713
Cu, loosely packed powder, sintering SEM and dilatometry obs. 80−20843
Cu, powder, electric discharge sintering, struct. changes 77−77446
Cu, powder, sprayed, effect of start props. in struct, and porosity of sintered products *(Czech)* 77−85960
Cu powder compacts, depend. of neck form. on particle size and sintering temp. 79−28988
Cu powder props. and sintered samples with Al_2O_3 77−55909
Cu, single crystal sintering model evaluation, Kossel interference and digital graphic simulation appl. *(German)* 80−2980
Cu, sintered, appl. of stereological charact. of interface interaction 77−63589
Cu, sintered, residual voids, quantitative anal. of morphological changes by metallography 79−47854
Cu, sintered, use for exchange of heat with flow of superfluid ^4He 77−82526
Cu, sintered preform, porous, ductile fracture criterion, rel. to forging process 77−56105
Cu, sintered strip, external friction of rolling 77−1845
Cu, solid state sintering, compact length change 80−11593
Cu spheres, rotation and translation during sintering onto a substrate, grain boundary energy SEM study 79−38759
Cu-Al, sintering, reduction processes, resist. meas. *(German)* 80−25597
Cu-Al powder mixture, elec. discharge reaction sintering 78−64507
Cu-Al-Ni, mixed powder compacts, Ni content influence in sintering behaviour *(Japanese)* 80−35130
Cu-Al-Ni (14, 8 wt.%), γ'-martensitic, sintered high damping 80−50577
Cu-Ni, powder, sintered, effect of cold and hot dynamic pressing, upon structure and props. 79−33970
Cu-Ni, powder mixture electric discharge sintering, struct. changes 77−77446
Cu-Ni, powder mixtures, form. using electric discharge sintering 77−12563
Cu-Ni, sintered, props. and degree of nonhomogeneity 80−20848
Cu-Ni, sintering, Kirkendall effect 80−93518
Cu-Ni composite formation by electric discharge sintering 77−63594
Cu-Ti, liquid phase sintering, metallographic electron beam microanalytical investigation 78−95888
Cu-TiC precipitation hardened composite, struct. effect on friction 78−11337
Cu-W sintered materials, porous, mech. and X-ray elastic const. *(German)* 77−81288
$Dy_3Fe_5O_{12}$, formation mechanism from metallic oxides 77−48376
$Dy_{0.7}Tb_{0.3}Fe_2$, magnetostrictive material, liq. phase sintering 78−64493
Er_2O_3 densely sintered and granular ceramics prep. physicomechanical props. 77−32548
Eu_2O_3, sintering kinetics 78−52731
Fe alloy electrodes, rolled from powders, sintering problems 80−25608
Fe alloy porous powder metallurgical components, gamma nitriding 79−20088
Fe and Fe alloy compacts, sintered, prod. directly from Fe_3O_4 powder *(Slovak)* 79−15626
Fe and Fe-C, (0.8 wt.%), sintered, hot forging ahd chemicothermal treatment, effect on wear resistance 80−25606
Fe atomised powder, sintering effect on recrystn., mech. props. 80−40292
Fe base composite, sintering, damping props. 77−21061
Fe, carbonyl pore struct. orientation, shrinkage anisotropy effect 80−20845
Fe, carburised sintered and pressed specimens, wear resistance 77−77590
Fe, cast, sintered, friction and wear 79−91806
Fe, cast powder, exam. of reaction between C and O, before and after annealing in converted gas 79−33973
Fe, compact, form. and growth of metal bridges during short sintering periods 77−1827
Fe effect of repressing and double sintering on impact strength *(Japanese)* 78−92217
Fe, exam. of graphite and cast Fe dissolution during sintering 79−33969
Fe, metallised pellet, factors influencing crushing strength after H_2 reduction 79−11531
Fe, operating performance, effect of polymer and graphite lubricant additives 80−11785
Fe ore, agglomeration charge layer shrinkage *(Russian)* 80−16224
Fe ore concentrate, sinter quality improvement *(Chinese)* 80−104089
Fe ore concentrates, two-layer charge, sintering conditions *(Russian)* 80−45248
Fe, oxidised powder, soft mag. props. oxide film-Fe composite material, magnetically soft, preparation, elec., mag. props. 77−8778
Fe, oxidised powder in prod. of soft mag. mat. 77−63813
Fe powder, plastic deformation, constitutive eqns. 79−61667
Fe powder, reduction annealing, comminution of sintered cakes 80−66456
Fe Powder, resist.-sintability *(Japanese)* 80−16228
Fe powder, sintered and hot pressed, effect of porosity, grain size on magnetic props. 79−96159
Fe, powder, sintering, effect of repeated allotropic transform. 77−40406
Fe powder, sponge and atomized types, steam oxidation, pore closure and surface hardness 80−45441
Fe powder, ZhGr1.0, optimisation of heat treatment in salt bath 77−28756
Fe powder based sintered porous permeable materials, diffusion chromising 80−100958
Fe powder compacts, pressed under static or vibr. load, shrinkage anisotropy during sintering 80−50574
Fe powder layers, sinter-bonded, hot-pressed, on steel, struct. and props 79−95976
Fe powder sintered compacts, mech. props. effect of powder type and processing conditions *(Czech)* 77−59830
Fe, powder-forged, elastic consts., density depend. 80−84987
Fe powders, exam. of production, props., and testing methods *(German)* 79−4927
Fe, sintered, austenitic nitriding and bainitic hardening 80−85084
Fe, sintered, fatigue, metallographic obs. 78−64646
Fe, sintered, fracture behaviour, microscopic obs. 79−47771
Fe, sintered, fracture mechanics *(German)* 77−8948
Fe, sintered, metallographic meas. of pore size, effect on mech. props. 78−19685
Fe, sintered, plastic deform., porosity effects 78−23801
sintering continued
Fe, sintered, porous, yield point *(Czechoslovakian)* 77−28748
Fe, sintered, produced by dynamic hot pressing, recrystn. diagram 79−70017
Fe, sintered, strength and elongation, rel. to density 80−30047
Fe, sintered and pressed, props., effect of atomised Fe powder particle size distrib. 80−11601
Fe sintered compact, shrinkage and mech. props., admixed zinc stearate lubricant effect 80−45402
Fe, sintered PZh1M, fracture resistance subject to thermomechanical treatment 77−77517
Fe, sintered parts, densification in burnishing process by rocking die method 78−35331
Fe-(Cr)-C alloys, sintered, successive impregnation with C and Cr 79−95979
Fe-(Cu)-C, sintered parts, struct. stabilisation with C potential control of protective atmosphere 78−60614
Fe-B, for infiltration of Fe compacts 80−60806
Fe-B_4C powder mixtures, phase changes and struct. of sintered materials *(Russian)* 78−6872
Fe-B_4C sintered material, mech. props. and struct. charcts. 79−100084
Fe-base fibres, extruded, heat treatment 78−35414
Fe-base wear resistant dispersion hardened electrolytic coating, annealed and sintered 78−35593
Fe-based powder PZh2K, porous struct., effect of diffusion chromising with sintering 79−66219
Fe-based sintered friction material, wear rate, depend. of phase struct. 79−15801
Fe-C (1.0 wt.%), mixed powder compact, sintering, C diffusion meas. 77−90293
Fe-C (2. wt.%), sintering shrinkage kinetics 80−20829
Fe-C (graphite, 0.3 wt.%), powder-forged, elastic consts., density depend. 80−84987
Fe-C-Ni-Cr(Cu), dynamically hot pressed, mech. props., additives effect 78−60620
Fe-C-O, sintered, ferritic struct. obtained by Ar_3 transform. *(Japanese)* 78−6874
Fe-C-Pb, sintered, antifriction props., Pb introduction effect 79−96155
Fe-Cr-Ni-Si, sintered, carbide coated, crack propag. energy in impact bending 79−66162
Fe-Cu, liquid phase sintering 80−16232
Fe-Cu, sintered compacts, cooling effect on strength 77−73293
Fe-Cu (2 wt.%), furnace cooled, ageing and steam oxidation 78−23744
Fe-Cu: graphite-$BaSO_4$-$CuSO_4$, friction material, solid state sintering kinetics 80−104096
Fe-Cu-C, mixed powder compact, sintering mechanism 78−15343
Fe-Cu-C sintered porous materials, machinability 80−66457
Fe-Cu-Ni-Cr_3C_2-C based sintered friction material, wear, surface geometry and struct. effects 80−25875
Fe-Cu(2, 4 and 6 wt.%), sintered, precipitation hardening 77−66653
Fe-glass-Cu sintered material, Cu effects on strength 77−77443
Fe-graphite, sintered, diffusion layer form. 79−100299
Fe-graphite porous sintered, determ. of impregnation depth with polycaprolactam-finely divided Cu metallic polymer 79−70272
Fe-Mo-CaF_2 sintered composite, struct. and mech. props., heat treatment effect 80−66526
Fe-Mo-(C)-(Ni), sintering 78−35333
Fe-Ni heterogeneous alloys, ferrite, martensite and austenite phase distrib., effect on mech. props. 80−45363
Fe-Ni mixed powders, effect of Ni particle size and unequal interdiffusion, on sintering process *(Japanese)* 78−84728
Fe-Ni system, Ni addition effects on activated sintering of Fe powder compacts 77−4756
Fe-Ni-Al-Co-Cu alloy, sintered single-crystal mag. prod., props. 77−66709
Fe-Ni-C, C effect on recrystallisation and reversion *(French)* 77−81282
Fe-P, sintered frictional material, friction and wear rubbing pair under moderate load 77−21208
Fe-P base frictional material, sintered, friction and wear under moderate load 77−12704
Fe-P(S) sintered materials, antifriction props. 79−24626
Fe-Pd (47 at.%) alloy, powders and powder compacts, mag. props. rel. to heat treatment *(Russian)* 79−15816
Fe-S-C (1,3 wt.%), sulphidised Fe-graphite bearing materials, sintering, struct. form. 78−60601
Fe-Si (1-5 wt.%), optimum sintering conditions and mag. props. 77−85958
Fe-Si (3 to 5 wt.%) sinters, mag. props., Si and Fe-Si additions effect 80−71104
Fe-Si-C mixed powder, cast Fe powder sintering study *(Japanese)* 80−108373
Fe-SiO_2-Al_2O_3 Lisakovskii concentrate mixture, sintering process, temp. thermal treatment *(Russian)* 80−55317
Fe-Si(6.5 wt.%) steel, core mat. development *(Korean)* 78−60852
Fe-VC-WC(TiC), sintering, densification 80−25615
Fe-WC-VC(TiC), sintering, densification 80−25615
β-Fe_5Ge_3 formation in isothermal sintering, phase transition kinetics 80−89197
Fe_2O_3 based catalysts for NH_3 synthesis, sintering of powders 79−61551
γ-Fe_2O_3, sat. moment *(French)* 77−85431
Fe_2O_3, semisintered, shear strength at high press. 80−76308
Fe_2O_3-Bi_2O_3 sintered material, elec. switching effects for temp. range 700-850°C *(Korean)* 80−70775
Fe_2O_3-FeO, sinter, heating and reduction effect of phase transform. and fracture *(Russian)* 78−15375
Fe_2O_3-FeO, sintered and pellets, reduction in H_2 *(Russian)* 78−15705
Fe_2O_y, powder, sintering, surface area reduction, exam. 78−44039
Fe_3O_4 briquettes, porous, struct. changes during reduction 77−21064
Fe_3O_4, low temp. sintering 78−92221
Fe_xO_y, sintered metallised compacts, pore struct. by Hg porosimetry 80−40280
$Fe_{1+x}V_{2-x}O_4$ spinels, prep. and negative resist. charcts. *(Korean)* 78−39119
GaAs substrate, Pd/Ge film sintering, Auger spectra, Schottky barrier energy 79−69581
$Gd_3Al_5O_{12}$ phase obtained by crystallisation of amorphous Gd_2O_3.5/3Al_2O_3 by quenching 78−92224
$Gd_3Fe_5O_{12}$, formation mechanism from metallic oxides 77−48376
Gd_2O_3 densely sintered and granular ceramics prep. physicomechanical props. 77−32548
Gd_2O_2S, compact specimen prep. 77−85951

sintering continued
$Ge_{30}Si_{70}$, hot press sintering 80−50572
HFO_2, powder, preparation technique for highly sinterable powder 78−39714
$HUO_2PO_4.4H_2O$, film fabrication and appl. as solid electrolyte in electrochromic displays 80−70462
HfC-$HfBr_2$, preparation and high temp. antifriction props. 79−1918
K triple orthoarsenates, $KM^{II}Cr_2(AsO_4)_3$, prep. by high temp. synthesis, and cryst. struct. 79−66028
β-K_2O-Al_2O_3, synthesis 77−81238
LaB_6, US comminution of refractory compound powders 78−23656
LaB_6-$SmB_6(YbB_6)$, exam. of secondary ion-ion emission, due to bombardment with 8 keV Ar ions 79−33882
La_2O_3-Mn_2O_3-Cr_2O_3, synthesis and properties of solid solutions 78−44038
$La(OH)_3$, thermal decomposition, TGA, DTA, X-ray diffr. study *(Japanese)* 77−36436
La_2O_2S, compact specimen prep. 77−85951
$La_{0.84}Sr_{0.16}CrO_3$, sintering 77−77440
$La_{1-x}Sr_xCrO_3$, densification 77−8780
Li-Na ferrite powders, props. rel. to Fe_2O_3 chem., thermal, mech. historical 79−11539
Li-Zn ferrite, magnetic props., effect of V_2O_5 addition *(Japanese)* 77−28415
LiF tile and sheet for thermal neutron shielding *(Japanese)* 78−74510
$Li_{0.5}Fe_{2.5}O_4$, effects of low-melting additive on struct. and dielec. props. 77−85494
$Li_{0.5}Fe_{2.5}O_4$ milled ferrite powder, substruct. and sinterability 80−84894
$Li_{0.5}Fe_{2.5}O_4$-$Bi_2O_3(V_2O_5)$ systems, phase diagrams, sintering conditions 78−35366
$Li_2K(IO_3)$ in $LiIO_3$-KIO_3 system, lattice parameter, equilib. and metastable phase diagram *(Chinese)* 80−7538
$Li_{0.5}Mn_{0.15}Fe_{2.35}O_4$ ferrite cores with rectangular hysteresis loops, pulse parameters, effect of Fe_2O_3 heat treatment 80−60370
Li_3N, Li ion conduction 80−70449
Li_3N, sinter prep. and Li ionic cond. props. 79−99361
LiNa ferrite, effect of sintering temp. on oxidation kinetics, conductivity meas. 77−21298
$Li_{0.04}Na_{0.1}Fe_{2.5}O_4$, $Li_{0.3}Na_{0.2}Fe_{2.5}O_4$, ferrites, form., X-ray, chem. and mag. anal. 77−36424
$LiNbO_3$-CdO, CdO addition effect on sintering 79−83157
$Li_{0.45}Ni_{0.1}$, $Fe_{2.45}O_4$, sintering, mag. props., rare earth oxide additive effects *(Japanese)* 77−66602
$Li_xNi_{1-x}0$ (x=0 to 0.03), solid soln. effect of Li on densification during sintering 80−25638
LiO_2 pellets, sintered, exam. of microstructure 78−72749
Li_2O pellets, sintered, reaction with Mo and Ho alloys 79−47913
Li_2S-Al_2S_3, prep., phase props. and elec. cond. 79−96010
$LiTi_2O_4$, prep., characterisation and supercond. props. 77−40010
$LiY_{1-x}Tb_xP_4O_{12}$, and $LiY_{1-x}Eu_xP_4O_{12}$ phosphors, prep. and fluoresc. 77−48219
$Li_{0.44}Zn_{0.09}Fe_{2.47}O_4$, ordering, elect. of V_2O_5 additions 77−35532
Mg ferrite, sintered, cation redistribution, microstructural effects 77−55356
Mg-Mn ferrite, finely divided, synthesis 77−28773
Mg-noble metal alloy, sintered, supercorroding for heat and H_2 gas generation, seawater reaction 78−15607
$MgAl_2O_4$, composition rel. to ceramic microstruct. form., light transmission 79−43188
$MgAl_2O_4$, powder effect of precursory sulphate solution anion on sintering 78−56605
MgB_4O_7:Dy, TLD phosphor development 79−79661
$MgFe_2O_4$, sintered, cation ordering, grain size effects 78−39763
$Mg_{0.8}Mn_{0.2}Fe_{1.8}Al_{0.2}O_4$, grade 6SChl ferrite, milling conditions effect on fine cryst. struct. and activity 79−24483
MgO (:CaO) powder compacts, sintering studies, SEM obs. 79−78918
MgO, effect of Cl^- and F^- ions on calcination and sintering *(Japanese)* 78−95719
MgO, fused periclase, sintering and struct. characts. 78−23652
MgO, lattice defects., calcination temp. effect 80−15091
MgO, pore distrib. and grain size in intermediated sintering stage *(Japanese)* 79−74124
MgO powder, active, sintering 80−20870
MgO, powder activation during grinding 77−90300
MgO, produced by thermal decomposition of Mg cmpds. to periclase refractory, sinter adhesion 79−83164
MgO, semisintered, shear strength at high press. 80−76308
MgO, sintered, refractories, props. after testing at over 2000°C 80−104317
MgO sintered-ceramic separator plate development, Li-Al/LiCl-KCl/FeS battery applications 80−61321
MgO, sintering, effect of Ca compound additions *(Japanese)* 80−55340
MgO, sintering by activating $3MgCo_3.Mg(OH)_2.3H_2O$ 80−89183
MgO, technical powder purity, of technical purity powders 77−63586
MgO/Ni-Cr (80, 20 wt.%) cermets, sintered, elec. resist. temp. effect 80−3206
MgO-Al_2O_3-SiO_2, sintered, cordierite, mineralogy and props. 80−60827
MgO-$Ca_3Mg(SiO_4)_2$($CaMgSiO_4$)-$NaPO_3$, phase conversions 77−66641
MgO-CaO-Fe_2O_3-Al_2O_3-SiO_2, clinker production from dolomite and magnesite 80−55339
MgO-Cr_2O_3, reaction sintering *(German)* 78−11174
MgO-NaCl refractory clinkers, Cr containing, densification, thermal treatment and phase composition effect *(French)* 80−76219
MgO-Pd metal-ceramic reaction, micro/macro obs. 80−66467
$Mg(OH)_2$, sintering, IR spectra, X-ray anal. 80−66452
$MgTiO_3$, Mg_2TiO_4, $MgTi_2O_5$, formation mechanism 77−48373
$MnCo_2O_4$ spinel, synthesis, effect of Bi_2O_3 admixture upon props., thermistor appl. 78−15325
Mn_2SiO_3, effect of vibration during sintering, on electrical resistivity 80−16258
MnZn ferrite, combined Sn-Ti substitutions, improved props. *(German)* 77−20644
MnZn ferrite, microstructure and initial permeability, presintering process effect 80−89367
MnZn ferrite, post sintering cooling rate effects on props. 77−63604
MnZn ferrite, props. rel. to raw materials *(German)* 77−21074
MnZn ferrite fabricated by hot isostatic pressing, recording head appl. 80−35139
MnZn ferrites, form. of comp. heterogeneity during high-temp. sintering 80−60818
MnZn ferrites, impurity induced exaggerated grain growth 78−92222
sintering continued
MnZn ferrites, post sinter-cooling rates effects 80−89369
Mo, powder, defective structure and activated sintering, exam. 80−16240
Mo powder, influence of powder reduction processes on props. 80−89175
Mo, powder sintering, transition metal activators, 1000-1350°C, heterodiffusion model 78−44044
Mo, sintered, fusion reactor blanket struct. material, low cycle fatigue behaviour 80−30073
Mo, sintered, gas evolution and degassing 80−100814
Mo, sintered, grain boundary segregation of S and N 79−56982
Mo, sintered, pure, work hardening 77−16607
Mo sintered composite, MoS_2 containing, friction and wear props. 80−11786
Mo, sintering, effect of Ni activator grain size 77−63590
Mo-Cr, powder mixture, activating effect of Group VIII metals on alloy form. during sintering 77−59728
Mo-Cr powder mixture, electric discharge sintering, struct. changes 77−77446
Mo-Fe alloy powders, densification and alloy formation on sintering 77−63597
Mo-Mn powder mixture, X-ray diffr. exam. of reaction between Mo and Mn, during sintering 80−16242
$MoSi_2$, ceramic additives effect on sintering, recrystallisation 80−40306
$MoSi_2$, self-propag. high-temp. synthesised, sintering and props. 80−11616
$Mo(ZrO_2.La_2O_3)$ structural changes during reduction and sintering 80−25636
N_2 purifier appl., 2.5 m^3/h *(Polish)* 79−12782
(Na,Li)NbO_3 ceramic, optimum prep. conditions and characterisation 78−3079
Na borosilicate glass microsphere material, sintering, struct., strength props. *(Russian)* 80−108383
Na triple orthoarsenates, $NaM^{II}Cr_2(AsO_4)_3$, prep. by high temp. synthesis, and cryst. struct. 79−66028
Na-βAl_2O_3 ceramics, synthesis 80−40305
NaCl monocrystal, sintering 77−59710
NaCl(:$CdCl_2$), sintering in air, densification kinetics and mechanism 77−4750
NaF, sintering, relation between densification and grain growth 77−12585
Na_2O-Ca glass powders, mixed with CO_3 compounds, cellular-struct. glass fabrication 80−108382
Na_2O-CaO glass phlogopite mica powders, composite fabrication, cellular struct. 80−84902
Na_2O-P_2O_5-SiO_2 glass, metastable liquid immiscibility 80−100331
$Na_2O.Li_2O.Al_2O_3$, comp. and props. for use in Na-S battery 79−87745
Na_2S-Al_2S_3, prep., phase props. and elec. cond. 79−96010
NbC, elastic modulus, porosity factor 77−21207
NbC_X powders, nonstoichiometric, sintering kinetics 79−100099
Nb_3Sn, powder metallurgically produced, microstruct. characts. 80−89233
Ni, carbonyl powder, dislocation density sintering 80−108372
Ni dispersions, semi-amorphous, on Al_2O_3-graphite, mag. characterisation 80−44876
Ni, electrolytic and carbonyl grades, sintered sheet material, stopping power and pore size relationship 78−19693
Ni, high temp. plasticity, oxide inclusion effect 80−50681
Ni powder, porous, relationships between mech., physical, and microstructural characts. 80−20846
Ni, powder, recrystallisation, effect of sintering atmosphere 77−12573
Ni powder, resist.-sintability *(Japanese)* 80−16228
Ni powder, sintered, use of extruded porous materials as fuel cell electrodes 80−40853
Ni, powder, subjected to vibratory milling, exam. of plastic deformation, recrystallisation, sintering 80−16234
Ni, powder charact. effects on sintering 77−1828
Ni, sintered carbonyl type and with dispersed ZrO_2 inclusions, struct. effect on high-temp. ductility 77−63757
Ni sintered permeable materials with bidisperse structure, pore-forming additions effect 80−84885
Ni, sintering kinetics, metallographic study 80−93519
Ni, surface diffusion effect on sintering 79−74117
Ni, volume strained, sintered, porous, physicomechanical props., electrical resistivity 77−12572
Ni, volume-strained sintered porous, physicomech. props., u.s. vibration propag. velocity 77−1823
Ni/Al_2O_3, catalysts, mag. and catalytic props. for methanation reaction 79−79296
Ni-Al, Raney nickel catalyst, surface texture studied by N_2 adsorption and ESCA *(French)* 79−69348
Ni-base wear resistant dispersion hardened electrolytic coating, annealed and sintered 78−35593
Ni-based alloys, binary, ternary, complex, TiC additions, effects 78−92305
Ni-based-Ta(Cn,N) hard metals, isostatic hot pressing influence on mechanical properties 78−92219
Ni-Co-Cr-Al-Ti-Mo superalloy IN738, casking porosity removal using hydrostatic press. sintering 80−55322
Ni-Cr (2 wt.%), role of hydrostatic pressure on sintering of creep cavities 79−28980
Ni-Cr-Al sintered alloy, hot vac. pressure, fracture and mech. characts. 80−66667
Ni-Cr-Al_2O_3 powder targets for plasma-ion spray deposition of resistance films 80−84897
Ni-Cr-Co-Ti, superalloy sintering thermochemical surface treatment 80−25617
Ni-Cr-MgO system, elec. resist. variation with comp. and prep. method 78−60637
Ni-Cr-ZrO_2, dispersion hardened, sintered, rupture 77−21272
Ni-Fe powder, effect of vibration and current pulses on shaping 79−95973
Ni-Mo, powder mixture, electric discharge sintering, struct. changes 77−77446
Ni-Mo, sintering limited solid solubility, peritectic diagram 77−28754
Ni-Re, sintering, limited solid solubility, peritectic diagrams 77−28754
Ni-W sintered powder pressings, intermetallic phases *(Russian)* 80−55349
Ni-Zn ferrites, comp., lattice imperfections, sintering 78−3080
Ni-Zn-Co ferrites, synthesis from solid solns. of schoenite-type salts 80−93511

sintering continued
NiCr-AlY sintered fibre metal struct. abradable seal material, friction and wear 78−56785
$NiFe_2O_4$, effect of sintering in air in range 1373-1773K on lattice parameter 79−19208
$NiFe_2O_4$ milled ferrite powder, substruct. and sinterability 80−84894
NiO-CaF_2 two-phase material, press. sintering, activation energy and compaction mechanism 79−47651
$Ni(OH)_2$, electrolytic precipitation into porous sintered plaques for Ni-Cd batteries *(Chinese)* 79−57237
NiZn ferrite, ZrO_2 additions influence on sintering and physicochem. props. 80−108369
NiZn ferrites, density and mag. props., isostatic pressure effect 80−60816
NiZnCo ferrites, temp. stability, effect of Fe content and processing conditions 79−28993
PLZT, exam. of grain growth in hot pressing, and liquid phase sintering 79−33981
PLZT, prep. by liquid phase sintering of oxides 79−38778
PLZT, transparent ferroelectric, ceramics obtained by hot pressing, optimum conditions *(German)* 79−43176
$(Pb,Sr)(Zr,Ti)O_3$, piezoceramic, effect of glass additions on props. during hot pressing 79−24475
Pb glass, secondary electron emission yield, reducing and heat treatment conditions *(German)* 79−56894
Pb, sintering, surface oxide layer effect 79−66024
$Pb_{0.94-x/2}Ba_{0.6}Nb_xZr_{1-x}O_3$, Nb dopant morphology effect on microstructure 80−81005
$Pb_5Ge_3O_{11}$ bonded $Pb(Zr,Ti)O_3$ composites, piezoelec. props. 79−78629
$PbMg_{1/3}Nb_{2/3}O_3$-$BiMg_{2/3}Nb_{1/3}O_3$, dielectric polarisation of solid solutions 78−43776
PbO, sintered, pure, prep. and props. 77−48361
PbS, hot-pressed compact, elec. behaviour, adsorbed atmos. gas effects 77−66601
$Pb_{1-x}Sn_xTe$ monocrystal and sinter thermoelec. inhomogeneity 78−91713
PbTe, effect of pressing and sintering, study of induced defects by SEM 80−59983
$Pb(Ti,Zr)O_3$, kinetics of initial stage of sintering 77−85973
$PbTiO_3$-$Pb(Fe_{1/2}Nb_{1/2})O_3$-$PbZrO_3$, with additions, exam. of electrical characteristics 80−2698
$Pb(Zr, Ti)O_3$ ceramics, low temp. sintering, elec. and mech. props. 80−71616
$Pb(Zr,Ti)O_3$ ceramics, DC field sintering preparation, piezoelectric props., ageing behaviour 80−81211
$Pb(Zr,Ti)O_3$ piezoelectric ceramic, CeO_2 additive effect on struct. and props. 79−52140
$Pb(Zr,Ti)O_3$ pyroelectric ceramics 79−47649
$Pb(Zr, Ti)O_3$, Sc modified, sintering 77−44204
$Pb(Zr,Ti)O_3$:Cr_2O_3 ceramics, reson. freq. comp. and temp. depend. 80−70413
$Pb(Zr,Ti)O_3$-$Pb_3Ge_5O_{11}$ ceramic, sintering conditions rel. to piezoelec., dielec. props., microstruct. 77−16252
$Pb(Zr_xTi_{1-x})O_3$, high density, sol-gel technique prep., piezoelec. props. 80−20596
Pd sponge powder, sintering shrinkage kinetics 80−29900
Pd-Ag(Au)(Cu) film on $BaTiO_3$ dielectric ceramic substrate, interaction between film and substrate during sintering 79−33958
$Pr_2O_3.Si_3N_4$, prep. by sintering and X-ray diffr. data 79−77570
$Pr_{0.75}Sm_{0.25}Co_5$ magnets, struct. and props. sintering temp. depend. *(Russian)* 79−82819
Pt on C, crystallite behaviour on sintering 78−7235
Pt-GaAs contacts, sintered, eval. of W, Ti, Mo and Hf barrier metals 77−8193
PuO_2, fuel prod. by powder techniques 79−9846
PuO_2-UO_2 mixed oxide fuel, plutonia particle behavior during sintering in Ar-H_2 (8%) atmosphere 79−8258
Re, activated sintering 77−52262
Re, sintered, preparation, thermal cond., linear expansion up to 1000K 79−61533
Sc_2O_3, heat treated, elec. cond. rel. to O_2 partial press. 77−15845
Se powder compacts, sintered, electrical cond. 80−70693
Si, powder compact, Ar-sintering, microstruct. changes 77−90306
Si, powder heap, thermal cond., effect of temp., press., and atmospheric composition, sintering appls. 78−80487
Si solar cells, low cost, Ni contacts 80−94017
p-Si-Al, ohmic contacts, Si dissoln. and recrystn. effects, computer calc. 80−103749
Si-Al-O-N sintered ceramic, microstruct., phase composition and transformation mech., mech. props. 80−40309
Si-Al-O-N system, exam. of compounds and properties 78−48387
Si-Al(Ti)C, sintered, exam. of props. 80−25644
Si-containing deposit layers on Ni alloys, appl. methods *(German)* 78−85025
Si-O_2-N_2 system, Si_2N_2O, corrosion in O_2, sintered in the presence of magnesia *(French)* 78−23837
SiAlON ceramic, pressureless sintering 78−27449
SiAlON, prepared from siliceous sand and Al powder, hot pressing, steatite contamination effects *(Japanese)* 80−93528
SiAlON, pressureless sintered with low amounts of sintering aid 79−66029
$Si_{6-z}Al_zO_zN_{8-z}$, β-Sialon, form. from Si_3N_4-SiO_2-AlN system *(Japanese)* 80−45261
SiC and Si_3N_4, hot pressed, comparison of high-temp. thermal fatigue resistance 77−36623
SiC and Si_3N_4 sintered bodies with polyborodiphenylsiloxane binder 77−40401
SiC base material, electrical props., heat treatment effect 77−12645
SiC, electrode and container material in Na/S cell 80−35355
SiC, high density, development for heating elements using planning method 77−12584
SiC, hot pressing, role of grain boundaries, addition of B, B_4C and Al_2O_3 77−24999
SiC, pellet, rise in temp. involving reaction sintering 77−12555
β-SiC, powder, synthesis by chemical vapour phase reaction from methylsilane, exam. of props. *(German)* 79−4938
SiC, powder mixtures, composition vs. apparent density diagrams construction, model 78−60633
β-SiC, prep. by siliconisation of C black, sinterability *(Japanese)* 79−78921
SiC, pressureless-sintered, high temp. strength *(Japanese)* 80−104299

sintering continued
SiC, reaction sintered, microstruct. *(Japanese)* 77−1825
SiC, reaction sintered, TEM exam. of recrystallisation, phase transformation 78−80567
SiC, reaction sintered transform. interface morphology 78−31364
SiC, self-bonded, fracture characts. and rupture strength, temp. effects 79−96136
SiC, self-bonded, microstruct., electrical props., sintering effects 77−1822
SiC, self-bonded, statistical distrib. of values of apparent density 78−68657
SiC, self-bonded polycryst., electrophys. props. 80−10980
α-SiC, sintered, influence of B, C additives on microstructure, SEM exam. 79−8262
SiC, sintered with three dimensional crosslinked polycarbosilane 78−56601
β-SiC, sintering, B transport and lattice parameter change 80−108370
SiC, US comminution of refractory compound powders 78−23656
SiC, uncommon mode of morphological development among coherent phases, optical and electron microscope exam. 78−80544
β-SiC/Si abrasive resistant material, prep. and props. 80−20878
α-SiC-Al_2O_3, sintering 80−11611
SiC-AlB_2 (0.61 to 1.2 wt.%), hot pressed, microstruct. 80−93563
SiC-B_4C (B+1 wt.% C), sintering 77−36432
Si_3N_4 amorphous, crystallisation and sintering under pressure 79−87596
Si_3N_4, containing MgO and Y_2O_3 additives, impurity effect on sintering 79−61543
Si_3N_4, densification, role of $Ce_{4.67}(SiO_4)_3O$ 79−61549
Si_3N_4 fabrication by rate-controlled react. sintering, nitridation react. control 79−24468
Si_3N_4, grain-boundary-crystallized, thermal shock resistance 78−11308
Si_3N_4, hot pressed, effect of powder composition and sintering temp., on phase transformation kinetics, microstructure and mech. strength *(German)* 79−4939
α-Si_3N_4 powder, hot pressing, kinetics 77−55925
Si_3N_4, reaction bonded, post-sintering, injection moulding applications 80−60807
Si_3N_4, reaction sintered, α- and β-phase form., effect on strength 77−21075
Si_3N_4, reaction sintered, H_2 in nitriding gas, effect on strength, struct., and composition 79−24478
Si_3N_4, reaction sintered, microstruct. charact. 80−35145
Si_3N_4, reaction-bonded, microstructural analyses 77−8782
Si_3N_4, reaction-bonded, struct., form. mechanisms and kinetics 77−4760
Si_3N_4, reaction-sintered, elastic moduli, fracture mechanics parameters, and strength 77−28889
Si_3N_4, reaction-sintered, strength/nitrided density relationship 77−28891
Si_3N_4, sintering in powder bed with addition of MgO sintering aid 80−29910
Si_3N_4, sintering under high press., modulus of rupture tests 77−44202
Si_3N_4, sintering with Al_2O_3 and Y_2O_3 *(Japanese)* 78−19703
β-Si_3N_4 solid soln. prod. by reaction sintering SiO_2-AlN mixture 80−25645
Si_3N_4, thin sheets, reaction sintered, exam. of oxidation in damp air 78−48552
Si_3N_4 with MgO, Al_2O_3 and/or spinel, pressureless sintering 77−25003
Si_3N_4/Al_2O_3, powder compact, electron microprobe investigation of reactions *(French)* 80−26009
Si_3N_4-Al_2O_3, Sialon, pressure sintering 77−55919
Si_3N_4-Al_2O_3-AlN, Sialon, fabrication and reaction sintering 77−44201
Si_3N_4-Al_2O_3-Y_2O_3, sintered, observation of a noncrystalline phase 78−64536
Si_3N_4-based refractories, strength and microstruct. rel. to sintering 77−63610
Si_3N_4-MgO (5 wt.%), microstructural changes during gas pressure sintering *(Japanese)* 77−12589
Si_3N_4-SiC-Y_2O_3 (La_2O_3)(Ce_2O_3)(Eu_2O_3)(Gd_2O_3), reactively sintered, microstruct. and strength 80−25631
Si_3N_4-SiO_2-AlN mixture, reaction sintering forming β-Si_3N_4 solid soln. 79−52145
Si_3N_4-Y_2O_3(CeO_2), hot pressed, sintered, microstruct., flexural strength and fractographic anal. 80−40293
Si_3N_4-Y_2O_4-Al_2O_3 (4-17, 4 wt.%), sintering 80−81009
Si_3N_4-ZrO_2, sintered and hot pressed, exam. of mech. props. 78−48509
Si_3N_4+MgO, reaction during hot pressing 78−68658
Si_3N_4AlN-Al_2O_3 system, reaction sintering forming β-Si_3N_4 solid solns. 80−50585
Si_2N_2O, sintered with MgO or BeO additives, effect on oxidation *(French)* 79−20233
$Si_3N_4.15Y_2O_3$, sintering under high N_2 pressure 80−29907
SiO_2 film deposition from SiH_2Cl_2 on Si 77−77407
SiO_2 films, dehydroxylation, sintering, IR investig. *(Russian)* 78−75967
SiO_2 films, microporous, sintering effects, IR ATR, transmission investigs. 79−66031
SiO_2 gel, sintering 77−85980
SiO_2 glass, formation by hydrolysis of $Si(OC_2H_5)_4$ with NH_4OH and HCl soln., and characterisation 80−71622
SiO_2-Al_2O_3, mullite, sintering behaviour and microstruct. 80−20876
SiO_2-Al_2O_3 (36.6 wt.%) plasma prep. powder, metastable immiscibility and microstruct. during sintering 80−35143
SiO_2-Al_2O_3-Cr_2O_3 system, KT-11 type, chromia-containing material production based on high-silica glass fabric 80−45266
SiO_2-Al_2O_3-RO-R_2O type glass additions, sintering of porcelain bodies 80−45265
SiO_2-AlN mixture sintering, form. of β-Si_3N_4 solid solns. 78−23655
SiO_2-$Al(OH)_3$, derived from metalalkoxides, sintering behaviour 79−29005
SiO_2-Na_2CO_3, sodium Erevanit-25, sintering, struct. 79−43284
Sm-Co, alloy powders and sintered magnets, effect of chem. treatment on mag. props. 78−60311
Sm-Co-Cu-Fe-Te magnets, comp. and sintering effects on coercivity 79−15326
Sm-Pr-Co, added Fe_2Sn, permanent magnets, demagnetisation curves, X-ray obs. 78−91900
Sm(-Pr)-Co, sintered, cryst. phases *(Russian)* 80−39004
$SmCO_5$ magnets, sintering time effect on props. 79−95977
$Sm_{1-u}Ce_u(Co_{1-x-y-w}Fe_xCu_yCr_w)_z$, permanent mag., improved mech. props. 79−87593
$SmCo_5$, mag. props., effect of phase and struct. transforms. during liq.-phase sintering 79−100086

sintering continued
$SmCo_5$ magnetic alloys, pressed, sintering rel. to mag. props., cryst. struct. 78−60600
$SmCo_5$, single cryst. and liq. phase sintered, magnetostriction, field depend. 77−63245
$SmCo_5$, single-cryst. and liq. phase sintered, elastic stiffness consts., US velocity obs. 77−73066
$SmCo_5$, sintered, high coercivity, microstruct. and mag. props. 77−69629
$SmCo_5$, sintered, orientation of particle easy axes, statistical model 77−8305
$SmCo_5$, sintered alloy permanent magnets, temp. depend. of domain struct. *(Russian)* 77−66380
$SmCo_5$ sintered magnets, periodic struct. and coercive force *(Russian)* 79−28554
$SmCo_5$ sintered magnets, struct. and magnetic characts., sintering temp. influence *(Russian)* 79−52397
$SmCo_5$, sintered permanent magnet manufacture 80−20838
$SmCo_5$ spheres, exam. of sintering in vacuum and Ar atmospheres 78−84738
$Sm(Co_{0.86-x}Cu_{0.14}Fe_x)_7$, permanent magnet, sintering and heat treatment effects 80−39817
Sm_2M_{17}, sintered magnet, hard mag. props. optimisation 77−8340
Sm_3NbO_7, grain growth kinetics 77−85969
$Sm_{0.5}Pr_{0.5}Co_5$, sintered alloy permanent magnets, temp. depend. of domain struct. *(Russian)* 77−66380
$Sm_{0.5}Pr_{0.5}Co_5$ sintered magnets, periodic struct. and coercive force *(Russian)* 79−28554
SnO_2, activated sintering 77−36415
SnO_2, activated sintering, mechanism and kinetics, additives role 79−38771
SnO_2 based ceramics, sintering qualities 79−61547
SnO_2 powders, specific area, granulation and sintering *(Polish)* 79−52146
SnO_2-NiO(ZnO)(Nb_2O_5), activated sintering mechanism 80−60810
$SrFe_{12}O_{19}$, ferrite, powder effect of SiO_2 during sintering, exam. of grain growth and phase diagram *(German)* 79−24473
$Sr_x(Na_{0.5}Bi_{0.5})_{1-x}$ solid solutions, piezoelec. and ferroelec. props. *(French)* 80−108158
$Sr_x(Na_{0.5}Bi_{0.5})_{1-x}TiO_3$ ferroelec. ceramic, hot pressing, numerical simulation *(French)* 80−76220
SrO-SiO_2-Fe_2O_3, permanent mag. ceramics, exam. of phase diagram, using X-ray analysis, optical microscopy, electron probe anal., and thermal analysis *(German)* 79−29012
SrO.HfO_2(ZrO_2), US comminution of refractory compound powders 78−23656
SrO.6Fe_2O_3, ultrafine, microstruct. development during sintering, mag. props. 79−70022
SrO.nFe_2O_3 isotropic ferrite magnets, manuf. process and mag. props. *(Japanese)* 80−29915
$SrTiO_3$ film, polycrystn., dielec. props. and struct. 77−81057
$SrTiO_3$, sintering kinetics rel. to added SrF_2, ZrO_2 78−44037
$SrZrO_3$, $NiTO_3$, sintering additive 78−23638
Ta, sintering with transition metal additions 78−15335
Ta-C-B system, mech. and physical props. 77−59731
Ta(C,N)-Ni-HfC(HfN)(Mo_2C)(VC), sintering, prod. of hard metals 78−11155
Ta(C,N)-Ni-VC, sintering behaviour, VC effect 80−93520
$Tb_{0.3}Dy_{0.7}Fe_2$, prep. by powder metallurgy, magnetostrictive props. 80−75826
$Tb_xDy_{1-x}Fe_2$, Laves phase alloy, magnetostriction depend. on powder orientation before sintering 78−76284
$Tb_2O_3.Si_3N_4$, prep. by sintering and X-ray diffr. data 79−77570
ThO_2 gel, morphology relations during bulk transport sintering 77−70015
(Ti,Cr)B_2, sintering kinetics and props. 80−100811
(Ti,V)C carbides, prep. and mech. props. 78−64518
Ti 78−60602
Ti base composite sintered bearing materials, metallic solid lubricant infiltrated, antifriction props. 80−60981
Ti, fatigue strength, oxidation effect 79−96137
Ti, porous structure, change in presence of liq. phase *(Russian)* 80−16223
Ti powder, resist.-sintability *(Japanese)* 80−16228
Ti, powder heap, thermal cond., effect of temp., press., and atmospheric composition, sintering appls. 78−80487
Ti sintered, struct. stability, effect of dispersed refractory compound inclusions 77−28825
Ti, sintered sheet material, stopping power and pore size relationship 78−19693
Ti, strip prod. by powder rolling 78−80493
Ti-Al (Sn), porous, effect of Al and Sn on sintering 80−20830
Ti-Al (14.7 wt.%), sintered, mech. props., effect of alloying and dispersed ZrO_2 phase 77−12636
Ti-Al (4 wt.%), sintered, long-time strength 80−40529
Ti-Al system, compact growth in liquid phase sintering 80−20835
Ti-Cr, sintered, friction and wear, structural factors 78−60843
Ti-Cr_3C_2 composite, TiC and struct. form. during sintering 79−29011
Ti-Cr-TiC, sintered, friction and wear, structural factors 78−60843
Ti-Mg-ZrC(HfC)(TiC)(TiB_2) sintered, friction and wear props. 79−70019
Ti-Mo (Zr) (Nb), sintered, manufacture and exam. of props. 79−95975
Ti-Si cosputtered films, silicide form., X-ray diffr. and resist. study 80−54546
Ti-TiC system, sintered, friction and wear, structural factors 78−60843
Ti-TiO_2-ZrO_2-Mo, sintered struct. and mech. props. 78−60618
TiAl, manufacture by extrusion of blended elemental powders 77−28750
TiB_2, hardness of sintered material 78−60636
TiB_2-(Ni) (20 wt.%), initial stage sintering under high press., lattice strain 77−55905
TiB_2-TiC powder mixtures, hydrostatic pressing 79−100098
TiB_2-TiC(20 wt.%), sintered, US machining 77−21325
TiC hard alloy prep., struct. during sintering 77−77448
TiC, sintering and grain growth, metallographic anal. 80−25642
TiC, wetting by Cr-Ni-Mo-Mn alloy steel, expt. planning investigation 80−60822
TiC-base alloys, anomalous phase flaky precipitation *(Japanese)* 78−48401
TiC-Cr_3C_2(Cr_3C_2-WC), powder mixture, steel bonded, exam. of sintering behaviour 78−52712
TiC-Fe-Cr powder mixture, exam. of milling condition effects 80−16237
sintering continued
TiC-Kh6V3M steel alloy, reaction during sintering and heat treatment 78−60617
TiC-Ni, reaction kinetics under simulated liq.-phase sintering 78−52746
TiC-Ni powder compact, wetting problems in sintering 80−11596
TiC-Ni-Co-Cr, sintered, mech. props. effect of processing factors 78−11159
TiC-Ni-Mo sintered hard alloy TN-20, fracture surfaces 80−7684
TiC-Ni-Mo(W), cemented carbides, grain growth, metallographic obs. 77−24982
TiC-steel alloy, struct. form. during sintering, strength, rel. to heat treatments 77−59717
TiC-steel alloys, structure formation during sintering 77−59732
TiC-steel compact prod. by sintering in vacuum and in Ar or H_2 atmos. 77−63616
TiC-steel composite, effect of method of Cr additions on props. 78−15341
TiC-TiB_2, preparation and high temp. antifriction props. 79−1918
TiC_x, nonstoichiometric, densification during sintering 80−84895
TiN, highly dispersed, metallic thermo-EMF 78−43363
TiN, powder defect struct., thermal and elec. props. 77−59286
TiN-Al_2O_3, exam. of sintering and densification kinetics, and physical props. 79−95986
TiN-Ni mixed powder compact, phase relations and denitrification during sintering *(Japanese)* 79−43167
TiN-Ni powder compacts, sintering, gas atm. and vac., shrinkage, solid solubility *(Japanese)* 78−72750
TiN_xO_y, cubic, concentration dependence of the degree of filling of unit cell 78−44063
TiO_2, sintered ceramic, props. rel. to additives, impurities 78−35329
TiO_2, sintering, hardness, density, elec. cond. and colour *(Japanese)* 78−68659
TiO_2, sintering, struct., pressing, atm., and doping effects 80−20873
TiO_2 slips and castings, rheological and technical props., firing and sintering effects 79−87599
TiO_2:Nb_2O_5, preparation method, effect on semiconductive props. and sintering temp. 77−16527
$TiSi_2$, crystal atomic struct., X-ray diffr. exam., lattice parameters and integrated intensities 78−75647
TIBS, synthesis, struct., optical, spectral props. 79−15631
(U,Pu)C, sintering, role of Ni as sintering additive 80−84892
U oxide, resistance furnace appl. and characteristics *(Italian)* 77−81239
UC FBR fuel fabrication by reaction sintering of UO_2 and UC_2 80−812
UC, sintering, role of Ni as sintering additive 80−84892
UC-based nuclear fuel materials, influence of parameters on sintering behaviour and properties 79−100100
UO_2, effect of H_2O vapour during sintering by sol-gel process *(Czech)* 79−31092
UO_2, grain boundary diffusion, sintering and creep correlation, reinterpretation of creep mechanism 79−66111
UO_2, green pellet with zinc stearate as additive, effect on sintering 80−68908
UO_2, initial stage kinetics 80−2987
UO_2 micropore sintering, irradiated below 1100°C, in Winfrith SGHWR 80−5255
UO_2 microspheres, prep. from UO_3 $(NH_3)_2$, exam. of mech. and physical preps. 79−6758
UO_2, modified Ashby's computer method for constructing sintering diagrams 79−43165
UO_2 pellets, sinterability, particle size effect 80−104098
UO_2 powder, effect of impurities on sinterability 79−49806
UO_2 powder, sintering charact. 78−35341
UO_2, powder, sintering effect of compaction 80−20874
UO_2 powders, cond. between sintering and agglomeration phenomena 79−9830
UO_2 powders, sintering characterisation 79−43189
UO_2, sintered, production by gel calcination and drying, thermal anal. *(Czech)* 80−45260
UO_2, sintered pellet, isothermal grain growth kinetics 77−18663
UO_2, sintered pellets, relationship between intercept length and grain diameter 78−52743
UO_2 sintering, effect of impurity 79−33962
UO_2, sintering, initial stage kinetics, diffusion coeff. 80−2987
UO_2 sintering, thermal anal., hexavalent uranium xerogel drying, thermal treatment modelling *(Czech)* 79−36378
UO_2, sintering, use of NH_3, grain size changes 77−55920
UO_2 sol-gel particles, low temp. sintering and props. 79−100101
UO_2, stoichiometric, sintering diagram *(Rumanian)* 79−87602
UO_2+Nd_2O_3, sintering, initial stage kinetics, diffusion coeff. 80−2987
$UO_{2+\alpha}$, ternary sintering diagram, grain boundary diffusion 79−59234
UO_{2+x}, sintering mechanism 77−21071
UO_2(−Nb_2O_3), kinetics of initial state of sintering stoichiometric and nonstoichiometric oxide 79−91609
VN powder, defect struct., thermal and elec. props. 77−59286
W, activated sintering, diffusion mech. *(Korean)* 77−73248
W alloys, sintered relation between density and sound velocity 78−53173
W, chemically activated sintering 77−1826
W, chemically driven grain growth during sintering in liquid Ni 79−61532
W, enhanced low temp. process using transition metal activators 77−36418
W fibre reinforced Ni, high temp. stability 77−48372
W fibre reinforced Ni-Cu composite, liquid phase sintering under press. 78−19695
W, porous, physicomechanical props. sintering effects 77−12575
W, porous, variation of open and closed porosity during sintering 78−15342
W powder, porous struct. rel. to powder props. 79−61540
W, powder, subjected to vibratory milling, exam. of plastic deformation, recrystallisation, sintering 80−16234
W, powders, defective structure and activated sintering, exam. 80−16240
W sintered rods, hot rolling with four roll passes, effect on struct. and mech. props. 79−100195
W, sintering, Ni activated, grain boundary diffusion mechanism 79−91606
W:K-Al-Si, state of bonding, distribution of impurities 78−92212
W:Ni compacts, optimum conc. of Ni for activated sintering, optical microscopy obs. 79−38758
W/Cu powders, liq. phase sintering, particle rearrangement 80−45253
W-Cr powder alloys, sintering in presence of Cu-Ni liq. phase 80−16246

sintering continued
W-Cu, porous material, skeletal type, produced by liquid phase sintering, exam. of mech. strength, determ. resistance 80−16245
W-Cu (92.8, 7.2 wt.%), liq.-phase sintered, embrittlement and interfacial impurity segregation 80−66647
W-Cu contact materials with Ni and Co dopants, sintering 77−55908
W-Cu permeable materials, development 77−28755
W-Cu powder, liquid phase sintering, stabilisation of porous structure and control of volume changes 79−95974
W-Cu sintered alloy, produced from coreduced powders, densification 78−11154
W-Cu-Ni powder, liquid phase sintering, stabilisation of porous structure and control of volume changes 79−95974
W-Cu-Ni(6), contact materials, activated sintering, Ni and Co effects 79−95967
W-Fe-Co, sintering and mechanical props. *(Japanese)* 80−21086
W-Mo, powder mixture, electric discharge sintering, struct. changes 77−77446
W-Mo powder mixture, activated sintering 77−21058
W-Mo powder mixtures, form. using electric discharge sintering 77−12563
W-Ni, liquid phase sintering, microstruct. meas. 78−44054
W-Ni, liquid phase sintering 80−16232
W-Ni, liquid phase sintering 80−25613
W-Ni (0.5, 2 and 5 wt.%), Ni effect on shrinkage anisotropy during sintering 77−21056
W-Ni compact, sintering behaviour and workability *(Japanese)* 80−20822
W-Ni liquid alloys, sintered, coarsening of W grains, exam. 78−56598
W-Ni sintered alloy, etching 79−29323
W-Ni system, grain growth and densification during liquid phase sintering 79−38760
W-Ni system, liq. phase sintering, 1640°C, solubility and vol. diffusion of Ni in W 79−86895
W-Ni-Fe, W-Ni-Fe-Mo (Mn), sintering and mechanical props. *(Japanese)* 80−21086
W-Ni-Fe (5(2), 5(2) wt.%) pore formation, effect on mech. props. 80−45396
W-Ni-Fe(Cu), liquid phase sintered, interfacial embrittlement 79−57101
W-Re alloys, sintered, preparation, thermal cond., linear expansion up to 1000K 79−61533
W-Re(Mo)(Cr), powder mixture, activating effect of Group VIII metals on alloy form. during sintering 77−59728
W-WC, activated sintering, mech. props. *(Korean)* 78−60622
W_2B_5, sintering rel. to prod. by boron carbide process 78−11184
WC, liquid phase sintering 77−4751
WC powder, processing conditions 80−11614
WC, sinterability of ultrafine powders obtained by CVD method 80−108378
WC vacuum sintering furnace systems 78−84737
WC-Co, β-SiC phase obs. on sintering 79−74150
WC-Co, cemented carbide sintered, appl. of dihedral angle meas. to microstruct. 78−39716
WC-Co, sintered, obs. of spinel particles by TEM 78−95714
WC-Co, sintered hard alloy, mechanism of penetration of liquid metals 78−60619
WC-Co (12 wt.%), sintering with various binding phases *(German)* 79−28984
WC-Co and WC-Co-TaC-TiC-NbC cemented carbides, microstructure, high temp. deformation, uniaxial plastic compression 80−40451
WC-Co cemented carbides, high temp. transverse rupture strength, effect of domain size of binder phase *(Japanese)* 78−92329
WC-Co compacts and sintered alloy, fine struct. of carbide phases, preforms re-pressing under high press. effect 79−28987
WC-Co from directionally carburized WO_3-C-Co_3O_4 mixtures, sinking *(Japanese)* 80−11589
WC-Co particles electrophoretic deposition, on metal surfaces, wear resistant coatings preparation *(German)* 80−2969
WC-Co powder, prep. by direct carburisation of WO_3 in presence of Co_3O_4 80−50573
WC-Co sintered carbide tips, microscopic stress anal. 78−5663
WC-Co-C based hard alloy VK6, densification kinetics in hot pressing 80−11600
WC-Co(TiC-Co), powder compacts, effect of additional pressing at hydrostatic pressures on props. 78−56596
WC-Ni hard alloy composite, sintered, void healing 80−60821
WC-Ni hard alloys, sintered, with uneven binder metal distrib., molten Ni migration 78−35336
WC-TaC-Co, cemented carbide, strength improvement by hot isostatic pressing 78−84969
$W(ZrO_2.La_2O_3)$, structural changes during reduction and sintering 80−25636
YAG, production of densely sintered ceramic, exam. of recrystallisation during sintering 80−11609
$YCrO_3$-$MgCr_2O_4$ sintered ceramics, elec. cond. 80−24927
$Y_3Fe_5O_{12}$, formation mechanism from metallic oxides 77−48376
YIG, permeability, domain rot. and wall displacement contrib. 80−80564
Y_2O_3 binder, sintering 79−24469
Y_2O_3, effect of roasting temp. of $Y_2(C_2O_4)_3$ on crushing, compressibility, sintering props. 77−8790
Y_2O_3, high temp. sintering *(Japanese)* 77−55928
Y_2O_3, hot cast ceramic, prod., used as dielectric 78−11181
Y_2O_3 powder, active, sintering 80−20870
Y_2O_3 sintered bodies, thermal cond. and diffusivity *(Japanese)* 79−55944
Y_2O_3 sintered body, blackness study thermoluminescence anal. *(Japanese)* 78−23541
Y_2O_3 sintered body, luminous pipe of high press. Na discharge lamp, corrosion resistivity *(Japanese)* 78−19915
Y_2O_3 sintered-ceramic separator plate development, LiAl/LiCl-KCl/FeS battery applications 80−61321
Y_2O_3, US comminution of refractory compound powders 78−23656
Y_2O_3-TiB_2, ceramic, production by sintering in vacuo, or hot moulding at 1500°C 78−60629
Y_2O_2S, compact specimen prep. 77−85951
$Y_{1-x}Tb_xP_3O_9$, and $Y_{1-x}Eu_xP_3O_9$ phosphors, prep. and fluoresc. 77−48219
Zn silicates:Mn, photocond. *(German)* 79−51627
$ZnFe_2O_4$, duplex struct. formation during sintering, grain growth study 79−11541
sintering continued
ZnMn ferrites, prepared by wet chemical and ceramic methods, comparison of struct. and mag. props. *(German)* 79−24470
$Zn_{1-x}Ni_xFe_2O_4$, heat treatment and sintering effect on porosity 80−25610
ZnO, additives effects on sintering and grain growth 78−80497
ZnO ceramics, nonohmic, cryst. phases 78−26530
ZnO electrode, for dye-sensitised solar photocell 80−16816
ZnO nonohmic ceramic, formation mechanism 80−60813
ZnO, powder, sintering, surface area reduction, exam. 78−44039
ZnO, segregation of Li_2O at grain boundaries 78−64513
ZnO, sintered, impurity ion effects on crystalline state *(Japanese)* 77−28768
ZnO-based ceramic microstructure and nonlinear props., B diffusion effects *(Russian)* 80−49423
ZnS, electroluminescent materials for low voltage excitation, props. *(Japanese)* 77−73169
ZnS, with CdS or Cu_2S addition, phase transform. during crystn., 850 or 1150°C 77−48362
ZnS-CdS system, solid soln. form. mechanism 79−43177
Zr and Hf, appl. *(Italian)* 78−4978
Zr, powder heap, thermal cond., effect of temp., press., and atmospheric composition, sintering appls. 78−80487
ZrB_2, prod., oxidation rate, corrosion resistance 77−52274
ZrB_2, pure, vacuum hot-press sintering and microstruct. *(Japanese)* 78−23649
ZrB_2-Ta composite, vacuum hot-press sintering and microstruct. *(Japanese)* 78−23649
ZrB_2-TiB_2 solid solns., prod., oxidation rate corrosion resist. 77−52274
ZrC, elastic modulus, porosity factor 77−21207
ZrC, isothermal sintering kinetics 79−66032
ZrC, sintering 78−19700
ZrC, sintering shrinkage, effect of struct. vacancies in interstitial phases 78−60630
ZrC, US comminution of refractory compound powders 78−23656
ZrC-ZrB_2, preparation and high temp. antifriction props. 79−1918
$ZrC_{0.91}$, sintered, strength charact. effect of struct. and substruct. 80−16260
ZrN, sintering in vacuum and in N_2 77−12586
ZrN, thermodynamic props. of vacancies 77−11539
ZrN-Al_2O_3, effect of N on sintering 79−33991
ZrN-Al_2O_3, exam. of sintering and densification kinetics, and physical props. 79−95986
ZrN-Al_2O_3, sintering reaction thermodynamics 80−2989
ZrN-Al_2O_3 composites, strength rel. to solid-, liquid-phase sintering 80−100823
ZrN-Mo, cermet, sintering reaction thermodynamics 80−2989
ZrO_2 ceramic, dense nonstabilized, fabrication by hydrothermal reaction sintering 80−97451
ZrO_2, destabilisation by phosphoric acid, cubic to monoclinic transition, effect of temp., grain size, chemical composition 79−20037
ZrO_2 electrolyte cells, elec. props. 79−24477
ZrO_2 electrolyte cells, sintering 79−24476
ZrO_2, optimum sintering characts., density, X-ray diffr., IR spectrum, UV spectrum obs. 78−76617
ZrO_2, partially stabilised ceramics, strengthening, post-sintering heat treatment 80−97518
ZrO_2, porous, sintered stabilised microspheres, strength and fracture studies 80−85019
ZrO_2, powder, preparation technique for highly sinterable powder 78−39714
ZrO_2, produced by coprecipitation with stabiliser, sintering 77−66614
ZrO_2 products from granules, props., prep. method effect 80−25628
ZrO_2, semisintered, shear strength at high press. 80−76308
ZrO_2, sintering of granular masses, stabilized with CaO and Y_2O_3 78−44064
ZrO_2, sintering response with const. rate of heating, depend. on processing related pore distrib. 79−28992
ZrO_2, stabilised, fabrication by hot petroleum drying method, X-ray diffr. and thermal anal. study 80−40297
ZrO_2, stabilized porous refractory, mech. strength 80−35322
ZrO_2, tetragonal polycryst., sintering and props. 79−29008
ZrO_2, wet vibro-grinding with surfactants, superhigh density sintering suitability 79−33989
ZrO_2, Y_2O_3 stabilised, hydrothermal growth 78−15302
ZrO_2-based solid solutions, effect of added B_2O_3 and Nb_2O_5 on sintering and stability 77−40410
ZrO_2-CaO (12-19 mole%), AC elec. behaviour, 300-900°C, grain size, electrode material, and sintering effects 78−34649
ZrO_2-CaO-SiO_2, relationship between texture parameters, and sintering, elec. cond. and mech. strength props. *(German)* 79−24474
ZrO_2-HfO_2, monoclinic solid soln., ceramic prep. and use 80−55338
ZrO_2-Y_2O_3-CaO(MgO), long term firing effect at 2100 to 2200°C on solid soln. conc. and microstruct. 77−90309
$ZrSiO_4$, sintering, effect of grinding and additives 78−48356
$ZrSiO_4$ zircon ceramic with glass-forming additives, sintering and mech. props. 80−60814

size, particle *see particle size*

size effect
alkali metal wire, low temp. elec. resist., size and temp. depend. 77−76958
brittle solids, particle compressive strength, size effects *(Japanese)* 79−51196
cermet film, elec. props. 77−66209
composite superconductor, granulated, superconducting transition, influence of particle size 79−69619
creep, size effect on time to rupture *(Czech)* 79−77024
crystalline films, dispersion law and struct. transition, Fermi line geometry, acoustic spectrum, resist. min. *(Russian)* 79−7764
Debye temperature, effect of size on acoustic phonon spectrum 77−72666
degenerate semiconductor film, quantized, screening of elec. field and Coulomb interaction in strong mag. fields 79−69611
dielectric crystal, small, size effect on thermal cond. 77−72724
disperse systems, solubility increase, phase composition, size effect calcs. 80−70418
electron-hole drops, size effects, work function determ. 78−72077
ferroactive fluids, advanced appls. 80−80714
ferroelectric crystal, thermodynamic potential of systems with size effects *(Russian)* 78−80297

size effect continued
ferrofluid, particle size distrib. parameters 79−1687
field-emission cathode peak current, size effect 80−29863
film, crystalline, band theory of size-quantised electron states 78−75976
film, electronic props. in longit. mag. field 79−73603
film, size quantised, thermomag. effects in strong mag. field *(Russian)* 77−63002
film with arbitary lattice potential, electron interference effects, theory 79−90934
granular materials, size effects in cond. and supercond. 80−77581
interactions due to static lattice displacements, continuum and lattice theory approach 80−39082
intermediate state, thermal cond., Fermi surface shape and topology effects *(Russian)* 78−72314
lattice percolation, in one-dimens. scaling theory 79−54064
linear chains, monatomic, anharmonicity in surface and size effects in sp. ht. 77−1236
liquid crystal phase transformations, size and surface effects 77−15555
magnetic resonance obs. of quantum size effects in small particles 77−20700
many-valley semicond., size-induced changes in valley populations in strong elec. fields 80−6855
matals, diffusion thermopower, boundary scatt. effect 80−6817
metal, electron-phonon and electron-impurity collision frequencies, RF size effect method 77−20227
metal, Gantmakher-Kaner effect in strong mag. field *(Russian)* 78−80015
metal, RF size effect, line shape, exactly solvable models 78−43429
metal, RF size effect, small-angle scatt., exactly solvable models 78−47821
metal, size-quantised, dielec. response 77−31968
metal, surface plasmons in thin films, circular cylinder and spherical void, RPA calcs. 77−80823
metal, surface scattering of conduction electrons and kinetic phenomena *(Russian)* 79−56210
metal, thermal cond. size effect in normal and supercond. states, and supercond. radiometric effect 78−60245
metal, transport coeffs. in strong mag. field, Wiedemann-Franz law and Mott rule 77−69303
metal discontinuous films, elec. props., effect of distrib. of particle size 77−66209
metal film, effect on temp. coeff. of resist. 78−43489
metal film, elec. cond. 78−76162
metal film, size effect, total resistance temp. coeff. 78−84318
metal film, size effect in Landau diamagnetism, surface pot. effect *(Russian)* 80−93012
metal film, size quantised, energies and Fermi level of electrons 77−15749
metal film, temperature coefficient of total resistance 80−70853
metal film, thermoelectric power and temp. coeff. of resistivity 78−91788
metal film, Umklapp processes of charge carriers and anomalous transmittance in RF range *(Russian)* 80−70851
metal films, strain coeffs. of resist., size effect 79−42673
metal thin wires, size effect correlation to longitudinal magnetoresistance 78−34824
metal wires, DC resistance, size effect correction 78−91679
metal-dielectric boundary, role of cond. electrons in form. of thermal resist. *(Russian)* 78−19149
metallic crystal, RF size effect, electron scatt. by impurities diffuse layer boundary *(Russian)* 78−91717
metallic film, electron transport effects and size effects *(Czech)* 77−47902
metallic films, metal-dielectric boundary thermal resistance, nonlinear elec. resistance *(Russian)* 80−65530
metallic films, monocrystalline, size and grain boundary effects in elec. cond. 78−76164
metallic films, polycryst., size effects and resist., approximate expressions 80−88645
metallic films, size effects, resistivity derivation 78−76163
metallic fine particles, tunnelling effects on props. 78−14704
metallic granules, electron work function interrelation with granule size 80−39660
metallic thin film, electrical conductivity measurement, thickness dependence, quantum size effect *(German)* 80−86344
metallic thin film, EM wave induced voltage 79−56330
metallic thin film, thermoelectric power 79−78210
metallic thin film, transverse electric quantum wave spectrum *(Russian)* 80−84517
metallic thin films, effect of pressure, case for in-situ meas. 78−39228
metallic thin films, low adsorption coverage, microscopic calc. of elec. cond. 79−15236
metallic thin films, size effect conductivity in transverse mag. field, Hall coeff. *(French)* 78−91787
metals, complex, RF size effect, mean free path depend. of reson. strength 79−56202
metals, RF size effect as tool for cond. electron scatt. investigations 79−23957
monolayer on graphite, sp. ht. and u.p., size and steric effects 77−85073
non-linear ultrasound absorption in an electromagnetic wave field under quantum size effect conditions 78−87745
parametrized model for obtaining electron scattering rates from radio-frequency size-effect data 79−69541
phase comparisons for Sondheimer size effect oscills. 78−34823
phonon transport in bounded systems, influence of size effect and surface roughness 79−46849
piezoelectric semiconductor film, mobility of hot electrons 78−56247
piezosemiconductors, second harmonics of acoustoelectric current 80−80329
point defect interactions due to static lattice displacements, continuum and lattice theory approach 80−39082
RF size effect, meas. via optimised marginal oscillator 77−26377
semiconductor, ambipolar hot-carrier size effect kinetics 80−107799
semiconductor, amorphous, tetrahedrally bonded, electronic density of states, size effect reduction 77−8002
semiconductor, bounded, transport effects when a current passes along an energy inhomogeneity 79−7845
semiconductor, nuclear polarisation due to anisotropic size effect in weak elec. field 80−71199
semiconductor, piezoelec., degenerate, transverse magnetoresist. in strong field, quantum effect 80−80299
size effect continued
semiconductor, size effect, influence of space-charge regions on boundary conditions 77−89790
semiconductor, size quantised, superlattice state 78−39142
semiconductor film, donor-acceptor pairs, polarisation of recomb. radiation in presence of quantum size effect 79−11462
semiconductor film, electron spin orientation in quantum size effect conditions 78−68575
semiconductor film, electron-phonon interactions in quantizing mag. field 79−69610
semiconductor film, inhomogeneous, transverse magnetoresist., size effects 78−72293
semiconductor film, phonon spectrum under one-dimens. quantisation conditions 77−66007
semiconductor film, quantised, indirect interband absorption rel. to surface irregularity 78−39618
semiconductor film, size-quantised, EM wave absorpt. coeff. in coherent hypersonic wave field 80−29819
semiconductor film, size-quantised with tilted valleys, two-photon absorpt. 79−95869
semiconductor film with impurity centres, light absorpt., quantum size effect 78−27274
semiconductor films, two-photon interband absorpt., quantum size effects 79−43054
semiconductor thin film, energy spectrum in mag. field, size effect, calc. 80−70865
semiconductor thin film, polaron near-threshold spectrum 80−65471
semiconductor thin films, degenerate one-valley and many-valley, photogalvanic effect calcs. 80−34487
semiconductor thin films, fabrication for device appls. 80−100418
semiconductor thin films, ferroelectric properties, quantum size effect 80−97201
semiconductor wire, quantised monochromatic wave absorpt., indirect transitions due to surface roughnesses *(Russian)* 79−91397
semiconductor wire, two-photon interband absorpt., quantum size effect *(Russian)* 79−95721
semiconductor wires, size-quartised, two-photon interband absorpt. 80−93256
semiconductors and semimetals, anisotropic size effects, review 77−32032
semimetal, electric current distribution, by diffusion size effect 79−23987
short range atomic order, size effect in electron theory, static conc. waves approximation *(Russian)* 78−39049
short-range order, size effect in electronic theory *(Russian)* 77−15339
small particles, cause of reduction in lattice spacing *(Russian)* 80−38967
small superconductor in magnetic field, first and second order phase transitions 80−2519
solids-^{3}He liquid boundary, size effect description of thermal boundary resistance 77−62698
steel, tufftrided, type S15CK, fatigue strength, estimation of size effect *(Japanese)* 80−81166
superconducting critical temperature increase due to size effect 78−88062
superconducting current carrying elements 79−61019
superconductor, intermediate state, magnetoacoustic size effect *(Russian)* 80−7047
surface magnetisation, size effect 78−15008
tetrafluoromethane, Kr diffusion, 243.15K, density depend., size effect 78−75859
thin crystal, interference spectra, size quantisation of excitons 78−47708
thin film heterostructure, energy spectrum study 80−70787
thin wire, negative longit. magnetoresist., kinetic theory 78−34821
transition metal alloy, dil., size effect 79−99508
type I superconductor, thermal cond. in intermediate state, size effect in longitudinal lamellar struct. 78−52153
Wannier-Mott exciton decay, on acoustic phonons, in thin semicond. wire *(Russian)* 78−72075
whisker blades, RF size effect, expt. technique and line shapes 79−65511
wire, elec. cond. theory 77−35907
wire, exciton energy spectrum and light absorption *(Russian)* 77−62832
X-ray crystallography, small-particle-size effect 77−31550
Ag, anisotropy of electron-phonon collision frequency on Fermi surface, RF size effect 77−15750
Ag film, size effect in thermoelec. power, MFP and Fermi surface 77−69433
Ag, microwave size effect, open orbit, and obs. of solid state reson. 79−51621
Ag particles, lattice defect influence on size effect 78−88329
Ag, size effect, ballistic-type field penetration at 45 GHz, 3 MHz 80−44634
Ag-Cu, composite, fibre and layer structs., anomalous props. caused by internal phase boundaries 78−72754
Ag-Cu composite wires, size effect and interface contribution to diamagnetism 77−69490
Ag-Ni, composite, fibre and layer structs., anomalous props. caused by internal phase boundaries 78−72754
Ag_2Re films, galvanomag. props. and quantum size effects, obs. 80−70866
Al alloys, dil., size effect, valency factor and point defect interactions 79−51143
Al, bicrystalline, RF size effect at intercryst. boundary *(Russian)* 80−29431
Al, electron-phonon collision frequencies, RF size effect, Fermi surface study 79−90945
Al film, epitaxial, resist. vs. grain diameter curves, theory and expt. 77−76961
Al, magnetoresistance size effect, effect of cyclotron orbit nature 78−47767
Al, small spheres, bulk plasmons damping 80−75561
Al, Sondheimer size effect, phonon-limited mean path, 1.8-12K 80−49698
Al, thin film, thermal cond. meas., size effect 80−65715
Al ultrafine particle film, size effects in optical absorption 79−99965
Al-Pb(Sn), liquid, surface tension, size effect *(French)* 80−15341
$Al_xGa_{1-x}As$-GaAs, CW 300k quantum-well heterojunction laser, optical and injection pumping operation 80−5735
Au clusters on alkali halide surface, size depend. of valence bands, XPS study 80−65647

size effect continued
Au film, annealing curves, size effect parameter determ. from Mayadas Shatzkes theory 77−76962
Au film, quantum size effect, field emission study 80−70849
Au, pure, small resistivities, size correction 77−43742
Au small particles, size effects studied by electron energy loss anal. 79−47567
Au, small particles, size-effect modifications of Debye-Waller factor 77−84877
(Ba, Sr)TiO_3 ferroelectric film, phys. props. in weak elec. fields 78−35098
Be wires and strips, elec. resist. at 77K, size factor *(Russian)* 80−24867
Bi, cylindrical thin crystal, size effect oscills. in longit. magnetoresist. *(Russian)* 77−69357
Bi, diffusion size effects 79−60824
Bi epitaxial films, size effect in elec. props. 80−54813
Bi filament, size-quantized, magnetoresist. oscills. 78−19062
Bi film, Hall effect, magnetoresist., resist. and TCR 78−2589
Bi film, high-mobility, quantum size effects, struct. and kinetic charact. improvement 79−91174
Bi film, kinetic props. of electrons 77−63011
Bi, film, quantum size effect, electric field effect, Thomas-Fermi approx. energy surfaces, cond. 78−47890
Bi film, quantum size effect and band struct. Bi-dielec.-metal system obs. 80−54811
Bi, film, size effect of carrier heating, surface scatt. *(Russian)* 80−100474
Bi, film, size effect on electrical cond. 78−84331
Bi thin film, structure and electronic props. 80−70562
Bi thin wire, resist. anomaly, possibility of one-dimensional quantum size effect 80−54809
Bi-Sb alloy film, elec. props. *(Russian)* 79−11245
Bi-Sb alloy film, elec. resist., magnetoresist., Hall coeff., 4.2K, conc. depend., anomalous size effect *(Russian)* 77−89884
Bi-Sb alloy films, quantum size effect *(Russian)* 77−85351
$Bi_{1-x}Sb_x$ epitaxial layers, effect of film thickness on elec. props. *(Russian)* 79−11244
$Bi_{1-x}Sb_x$ epitaxial thin films, galvanomag. props. in semimetal and semicond. regions 79−11254
$Bi_{1-x}Sb_x$ thin films, elec. props., 4.2-300K, size effect assoc. with film pot. *(Russian)* 79−24087
Cd, AF magnetic field penetration exam. using RF size effect 77−43635
Cd, electron-electron scatt., RF size effect meas. 79−60821
Cd film, elec. cond., classical size effect 77−89881
Cd foil, monocrystalline, anisotropy of size effect 79−38048
Cd, size oscillations in magnetocond. 77−4324
Cd_3As_2 film 78−2600
CdS, acoustoelectronic current SHG 80−6916
CdS, LO phonons, size effect reson., first order forbidden light scatt. 77−44002
CdS, size effect of dense electron hole systems 80−7413
Cr film, size effects on spin density waves, struct. and elec. props. 77−80973
Cs film, work function theory, size effect 78−43460
Cs wires, size effect and temp. depend. of resist. 79−51691
Cs wires, size effect and temp. depend. of resist. 79−51692
Cu alloys, dil., size effect, valency factor and point defect interactions 79−51143
Cu, electronic relax. time in Sondheimer size effect, temp. depend. 79−87086
Cu film, adsorption of CO, effect on resist., negative p-values 77−85083
Cu film, strain coeff. of resist., film thickness and grain size depend. 77−55620
Cu sandwiches, size effect 79−73604
Cu, screening charge density round $\Delta Z=-1$ impurities, vacancies, NQR study 80−103897
Cu, Sondheimer oscills. in elec. resist. and Hall effect meas. 77−11896
Cu wire, negative longitudinal magnetoresist. size effect 80−80252
Cu wire, residual elec. resist., size effect and grain boundary contribs., heat treatment effects *(Russian)* 78−56126
Cu, wire, residual resistivity reduction by internal oxidation 79−87747
Cu-Al (15 wt.%), residual resistivity, influence of short range order and size effect *(Ukrainian)* 79−99528
α- Cu-Al alloy, short range order structure 78−91303
Cu-Au, elec. resist., pseudopot. calc. *(Russian)* 78−2460
Cu-Fe, composite, fibre and layer structs., anomalous props. caused by internal phase boundaries 78−72754
Cu-Ni(Pd)(Pt), dil., screening charge density round $\Delta Z=-1$ impurities, vacancies, NQR study 80−103897
Cu-Pb, liquid, surface tension, size effect *(French)* 80−15341
Cu_xS, $1\leq x\leq 2$, quantum temp. size effect and magnetism *(Russian)* 80−103764
Fe alloys, amorphous, saturation magnetisation, Curie temp. and size effect 80−65815
Fe films, thickness variations in extraordinary and spontaneous Hall coeffs. 80−97013
Fe single crystals, size effect on slip deformation ability at very low temps. 80−21049
Fe whiskers, galvanomag. size effects 78−14709
$FeBO_3$, size effect during parametric spin wave excitations *(Russian)* 80−103824
FeNi-Cu, composite fibre and layer structs., anomalous props. caused by internal phase boundaries 78−72754
Ga film, monoclinic, elec. cond., classical size effect 77−89881
GaAs-$Ga_{1-x}Al_xAs$ heterostructures, quantum size effect in superlattices, electronic props. 80−29471
Ge, ambipolar hot-carrier size effect kinetics 80−107799
Ge, electron hole drop far IR absorpt., damping, size effects, Mie theory 79−78685
Ge, electron-hole drops, resonant power absorpt., Alfven wave anal. 79−42569
Ge, near intrinsic, negative differential cond., ambipolar size effect due to hot carriers 78−72185
Ge, nonuniformly deformed, electron-hole drop density depend. on size *(Russian)* 80−20092
Ge plate, anisotropic cond. thickness depend., intervalley scatt. *(Russian)* 77−85352
Ge, size effects in small electron-hole drops 79−82530
n-Ge thin plate, transverse magnetoresist. meas., size effect 78−72179
size effect continued
He film, mulilayer adsorbed, in restricted geometries, book contrib. 79−99391
Hg, solid, resistivity ratio, 1.65 to 234K 80−59952
In, electron scattering rates, RF size effect meas. under multiple-turn conditions 78−14654
In, Fermi surface dimensions, RF size effect meas., KKRZ calc. 77−89687
In, RF size effect signals, anomalous behaviour 79−4502
In sandwiches, size effect 79−73604
In-Au double layer, ultrathin In, quantum size effect *(French)* 77−20466
$In_{1-x}Ga_xP_{1-z}As_z$ LPE DH laser with multiple thin layer active region 77−83887
$In_{1-x}Ga_xP_{1-z}As_z$ single thin active layer visible spectrum heterostruct. lasers 78−63120
$In_{1-x}Ga_xP_{1-z}As_z$-InP, single and multiple layer heterostruct., LEDs and lasers 78−46626
InSb, film, E_0, E_1 absorption edge size quantisation, optical and electroreflectance spectra 80−34998
InSb film, quantum size effects, transport props. 78−76171
n-InSb, spherical samples, size resonances, magnetoplasma waves 79−11168
n-InSb, spin polarisation, anisotropic size effect, effect on CESR signal 80−70743
InSb, surface magnetoplasma waves, reson. spectrum and dispersion characts. 79−38148
InSb:NiSb, size reson. scatt. from hard cylindrical pot. obs. in magnetoresist. 79−95421
K, electrical resistivity below 2K, temp. depend. 78−51969
K, RF size effect, effect of modulation 78−91716
K wires, size effect and temp. depend. of resist. 79−51691
K wires, size effect and temp. depend. of resist. 79−51692
KCl:Li, 9.4 GHz pulse paraelec. reson. at zero elec. field 77−81076
Mg film, Fuchs Sondheimer theory, size effect, elec. cond., Fermi surfaces 79−99637
Mo, electron scatt. mech., RF size effect study *(Russian)* 79−37965
Mo, Fermi surface, precision investigation using RF size effect 79−77984
Mo, Fermi surface curvature *(Russian)* 79−87038
Mo, Fermi surface parameters, RF size effect meas. *(Russian)* 79−95311
Mo, film, specularity coefficient of conduction electrons, angular dependence *(Russian)* 79−87167
Mo, longwave dopplerons, nonlocal Hall effect, surface impedance, size effect *(Russian)* 80−80253
Na, size oscillations in magnetocond. 77−4324
Na wires, size effect and temp. depend. of resist., martensitic transform. effect 79−51691
Na wires, size effect and temp. depend. of resist. 79−51692
$NaNO_2$, size effect and spin-lattice relax. of ^{14}N 80−20480
Ni film, adsorption of CO, effect on resist., negative p-values 77−85083
Ni film, effects of finite size on crit. phenomena, resistivity anomaly 79−38192
$Ni_{65}Mo_2Fe$, O_2 effect on secondary recrystallisation and mag. props. 80−35201
PMMA, resonance size effect in space charge relaxation 80−75937
Pb, single and polytextured thin films, band struct., tunnelling spectroscopy 80−80169
PbS(Se), valence band struct. determ. by optical absorpt., size quantization effects 80−59871
$Pb_{0.82}Sn_{0.18}Te$ epitaxial films, surface transport of carriers at 77K 79−28419
PbTe epitaxial films, quantum size effect, optical meas. 80−11121
PbTe film, (001), two-photon transition rate calc. 79−95869
Pd film, quantum size effect, field emission study 80−70849
Pd sandwiches, size effect 79−73604
Pd, ultrafine particles, size effect on vibr. sp. ht. 78−10153
Pt film, quantum size effect, and its temp., tunnelling obs. 79−91160
Pt-SiO_2 granular sputtered film, size effects in electronic sp. ht. 77−43346
Rb wires, size effect and temp. depend. of resist. 79−51691
Rb wires, size effect and temp. depend. of resist. 79−51692
$RbHSO_4$, compressed powder, dielectric const. and particle size, 77-335K 78−76371
Re, Fermi surface, determ. from RF size effect 79−23889
Re, Fermi surface, RF size effect, temp. depend. 80−65424
Re, RF size effect, electron-electron scatt. 78−68025
Re, RF size effect, Fermi surface dimensions determ. 78−91598
Re, single crystal, size effect in elec. resistivity *(Russian)* 78−87961
Ru, single crystal, size effect in elec. resistivity *(Russian)* 78−87961
Sn film, polycrystn., elec. props., internal size effect rel. to annealing temp. 79−65560
Sn film, thermoelec. power, 3.7-8K 78−39231
Sn superconducting film bridge, obs. of operating conditions and shunting effects in small size supercond. 77−16005
Sn-Au double layer ultrathin Sn, quantum size effect *(French)* 77−20466
$SrCl_2:Gd^{3+}$, small dielec. particles, cryst. field size effects 80−44913
Te, hexagonal film vac.-evaporated at normal incidence, X-ray Fourier. line shape anal. 79−99454
Tl film, Fuchs Sondheimer theory, size effect, elec. cond., Fermi surfaces 79−99637
W, film, specularity coefficient of conduction electrons, angular dependence *(Russian)* 79−87167
W, longwave dopplerons, nonlocal Hall effect, surface impedance, size effect *(Russian)* 80−80253
W, low temp. transport props., phonon and impurity scatt. 78−10418
W, RF size effect, surface electron scatt. influence *(Russian)* 80−2414
W, RF size effect signal, anomalous behaviour 77−89788
Zn-Pb(Bi), liquid, surface tension, size effect *(French)* 80−15341

skin
abdominal, human, vol. compressibility 79−16238
acoustic impedance variations at burn-nonburn interfaces in porcine skin 79−21314
acupuncture points, elec. located, investigation of existence 79−43976
acupuncture points location using elec. impedance meas., statistical look 78−44628
alpha irradiation of the skin and the possibility of late effects 79−20584
artifacts in biopotential recording, reduction 77−40873

skin continued
artificial skin, integrated behaviour 77−81661
attenuation factors for certain tissues when the body is irradiated omni-directionally 79−92383
audio-visual heart monitor based on light transmission through the skin 79−53206
auditory impedance changes elicited by tactile and electrocutaneous stimulation 80−56066
beta-irradiated guineapig epidermis, cytokinetics of regeneration 78−15870
biofeedback control of skin potential level 80−21572
blood flow, reflex control by skin temp., role of core temp. 80−85427
blood flow clearance changes in pig skin after single doses of X-rays 79−29567
breast cancer thermograms, computer anal. *(Japanese)* 77−5099
burns, thermal conditions which cause 77−48758
burnt and healthy, human, determ. of Na, K and Cl by neutron activation 79−5343
burnt skin, heat and water losses 78−31790
cancer incidence due to UV radiation, modelling 78−77091
cancer induction by UV, evidence 80−35962
carcinomata, electron beam treatment obs. 79−62335
cell migration following irrad. of the skin in mice 78−24099
cell survival derivation method using tissue damage obs. after fractionated irrad. 80−36016
cellular survival kinetic parameters in rats after fractionated irradiation 80−21496
cetacean active swimming, self-regulation of skin damping and hydrodynamic drag reduction *(Russian)* 77−32918
Clinac 4, improvement of skin sparing characts. by leaded glass electron filters 78−31885
clinical thermograms, effect of obliquity 77−9286
cold urticaria, stable low temp. source for testing 78−61276
collagenous tissues, flat, struct. theory for homogeneous biaxial stress-strain rels. 80−3695
computer aided tomographic thermography, numerical simulation 79−83889
conductance, integrated circuit meas. 77−25566
cross-modal interactions, variations in punctuate press. sensitivity with skin surface temp. 78−3527
cryosurgical applicator for dermatology 77−78034
cumulative radiation effect, cell survival description 80−30771
cutaneous blood flow, meas. instrument using Doppler shifted laser light 78−28030
cutaneous receptors, multiple unit correl. anal. 79−100638
cutaneous receptors, on-line receptive field mapping technique 79−74797
cutaneous temperature of a living human body, accurate meas. 79−83976
depth-dose relationships near the skin resulting from parallel beams of fast neutrons 80−30902
dermal elastic fibres, new method for scanning electron microscopic visualisation 79−84036
dermal-resistance meter with high resolution *(German)* 79−84031
dermatologic laser treat ment successfully completed in Japan *(German)* 78−24177
dermatological practice, high-intensity laser therapy *(German)* 79−2117
dermatology research, appls. of photoacoustic spectroscopy 79−57823
dermus, collagen fibres, struct. and mech. characts. and natural interweaving 78−48824
dorsal epidermal cells, mouse regeneration and dose response characts. after irrad. 77−5031
dose fractionation effect on early and late skin responses to γ-rays and neutrons 79−20593
dose in ^{60}Co teletherapy, efficary of an Ag filter in reduction 79−79641
dose measurement using TLDs, implementation of the ICRP recommendation 78−92709
dose measurement with 1, 2 or 3 layers of lightcast 77−86635
dose-time relationships for post-irrad. cutaneous telangiectasia 78−3552
dosimetry in examinations carried out with the mammomat 78−73245
dosimetry of pion therapy beams 78−3606
dye lasers, investigation and therapy, in dermatology 78−35910
ear, mouse, fractionation effects in response to combined heat and X-rays 80−76805
ear, mouse, response to heat applied alone or combined with X-rays 78−27902
ECG recording, puncture method for reducing skin artifact 78−44672
effective temperature criterion for exercise heat stress prescription 79−92159
elasticity of living dolphins *(Russian)* 80−45926
electric field intensity distrib. in skin subject to an external pot. 77−73553
electrical burns caused by defibrillator ground-loop current, computer simulation 77−78039
electrical contacts, permanent, dry, generation by tattooing C into skin tissue 78−77122
electrical impedance dynamic meas. system 79−57744
electrical quantities, frog, method for in situ meas. 80−36208
electrical resistance, exam. with special regard to the galvanic skin reaction *(Hungarian)* 78−35982
electrocutaneous information transmission system using stimulus energy control device *(Japanese)* 80−101280
electrocutaneous nerve stimulation, model and expt. 79−11909
electrocutaneous nerve stimulation, stimulus waveform selection 79−48236
electrocutaneous stimulation, information transmission characts. *(Japanese)* 80−35872
electrocutaneous stimulus, effects of pulse height and pulse width on magnitude sensation *(Japanese)* 78−31998
electrocutaneous tracking, methodology for evaluating sensory feedback codes 79−25004
electrode for use in skin conductivity meas. *(German)* 78−85406
electrode motion artifact by skin abrasion, minimisation 77−40802
electron beam rotation therapy 79−88172
electrosurgical dispersive electrodes, thermal performance evaluation method 79−74735
electrotactile codes, evaluation 77−40932
environmental physiology and thermography 78−58043
epidemiologic monitoring, neutron activation anal. of trace elements in human skin lesions 80−17100
epidermal carcinoma in a sheep, probably radiation-induced 77−29180
skin continued
epidermal growth factor, human carcinoma cells A-431, visualisation by fluresc. 79−92189
epidermal mitotic activity, effect of head-irrad. during wound healing in the adrenalectomized mice 78−20220
epidermal mototic activity during wound healing x-irrad. effects, mouse 77−56436
epidermis, ultrastruct. stereology after X-irrad., rat tail expts. 80−36003
epithelia, low-noise amplification of voltage and current fluctuations 78−44741
epithelial stem cell survival parameters, considerations in use of mouse foot system 80−36017
equivalent circuit for skin impedance, ECG appl. 77−5101
evaporimeter, anal. of performance 80−56256
exercise thermoregulation after 14 days of bed rest 80−97865
exposure from radiography, anal. of film/screen combinations 78−73233
face, solar dosimetry, natural UV exposure rel. to basal cell carcinoma localisation 79−92382
fast neutron radiation therapy, skin-sparing effect 78−35923
fibreoptic light guides for phototesting in dermatological photobiology 78−53472
fibroblasts from D-deletion type retinoblastoma patient, abnormal X-ray sensitivity obs. 77−48848
freezing temperature of finger skin 77−21486
gamma ray therapy, acute rel. to late skin injury 79−34604
guinea pig keratinocytes and melanocytes in tissue culuture, influence of electron microscope obs. on results 80−21583
hand temperature self-regulation, assessment technique 80−16906
heat and H_2O migration through normal skin, steady state 79−88056
heat and H_2O migration through normal skin, unsteady state 79−92155
heat migration problems, unsteady state, appl. of similarity transformation 78−95990
heavy particle comparative study, acute and late reactions to irrad. 78−85338
hip radiography, bull, skin and gonadal dose reduction, Pb sheeting and Cu filtration 79−100743
histogenesis of abnormal epidermis, effects of X-rays, flesh fly 78−65084
homotransplanted, survival following total or partial irrad. 78−85335
hyperthermia combined with X-irrad, response of mouse 77−90857
immersion in various liquids, anal. of dynamic cold sensation *(Japanese)* 80−21448
impedance, anal. of change 77−81773
impedance, dispersion and correl. of parameters 79−29518
impedance, Laplace plane analysis 79−39458
impedance meter, AC, simple, battery-operated 78−81006
impedance of human skin, modelling 79−20607
imprinting by celloidine 79−25170
intensified minification cameras for low-dose radiography 78−20262
intercellular junctions of frog skin epithelial cells 77−12897
IR radiation, spectral anal. 79−88057
IR thermography in medicine 78−61279
keratinocytes, dose-dependent vol. changes after X-irrad. 80−61652
laser exposure limits development 79−66485
laser radiation effects, on wound healing, immunological aspects *(German)* 78−35917
lesion Mn, Cu and Zn conc. meas. by neutron activation 80−17063
light absorption and scatt., theoretical and expt. study, in vivo 80−101219
light therapy by argon laser *(German)* 78−35916
limb, mouse, early and late response to multifractionated X-irradiation 79−88123
lower resistance meridian, meridian distrib. in normal individuals *(Chinese)* 79−79717
lower resistance meridian investigation, method discussion *(Chinese)* 79−79716
malignant melanoma, thermal neutron capture therapy, in vitro radiobiological anal. 80−104657
mammalian epidermal keratin, organisation of polyreptide chains 77−4981
mammography, survey of radiation doses to patients 77−90901
material design criteria for the prevention of tissue breakdown 78−31964
mechanical properties, effects of split dose radiations 77−52842
mechanical properties, human skin, in vivo extensometer for meas. 77−44704
mechanical properties of human skin and subcutaneous tissue, influence of strain rate 79−20575
mechanical properties of living human skin 78−40237
mechanical properties variation in different areas of a healing wound 78−27984
mechanics, effects of some clinical treatments 79−100644
mechanoception, energy dependence in the human cutaneous system in masking conditions 78−20196
medical electrography, problem of skin-electrode processes 77−40828
medical thermography, quantitative 78−61280
melanoma therapy by laser irradiation *(German)* 80−12208
membrane channels of frog, Na specific, pores 77−36883
microwave heating combined with radiation therapy, skin and tumor thermal enhancement ratios 80−67192
mitochondrial Ca uptake and O_2 consumption in cystic fibrosis 79−43839
motion artefact of skin pot., reduction by skin abrasion 78−40361
mouse, ear, effect of prior heat treatment on thermal enhancement of radiation damage 79−48291
mycosis fungoides, whole body electron therapy 79−48322
mycosis fungoides lymphoma, advanced, evaluation and therapy recommendations 79−88157
neonatal jaundice detection, serum bilirubin conc. rel. to skin reflectance 79−92328
network thermodynamic approach to compartmental anal., Na+ transients in frog skin 79−24968
neutron irradiation, RBE of 50 MV neutrons in acute and late skin injury 79−34605
neutron teletherapy, effects of filters and wedges on skin sparing and γ/neutron dose ratios 80−46029
NMR of rat skin, ^{1}H and ^{13}C obs. 80−40965
optical rotatory dispersion and circular dichroism of enzyme-and alkaline-soluble collagen 77−70411
ouabain-like activity in toad skin rel. to endogenous regulation of ion transport 78−73147
percutaneous electrode systems, advances 77−5106

skin continued
percutaneous energy transmission system development 79−92433
perfusion, quantitative meas. with ^{133}Xe 80−81707
perspiration mass transfer coefficients and clothing models 79−92158
phospholipase A and the mechanism of action of aldosterone 78−24053
photoacoustic spectroscopy, dermatological appls. 78−31883
photobiologic phenomena in dermatology 78−35909
photochemotherapy of psoriasis vulgaris and mycosis fungoides 78−35908
pion-treated human skin nodules, investigation for therapeutic gain 79−20659
planarian, regeneration of epidermis and basement membrane after total-body X-irrad. 80−36022
plastic surgery, biomechanical aspects 80−56103
porcine, herniorrhaphic reinforcing prosthetic, mech. and struct. props., SEM study 79−74789
pressure meas., accuracy of elec. transducers 79−83959
radiation damage, early and late, effect of dose rate on production 77−70497
radiation damage in rodent skin, early rel. to late damage 77−25511
radiation dose to the fetus in obstetric radiography 79−92376
radiation effects on skin blood vol. pulse in humans 77−5029
radiation effects on visual appearance and mech. props. of mouse skin 77−12960
radiation fibrosis after β-irrad. and attempt at suppression, guinea pig expts. 80−72243
radiation injury, acute, caused by faulty X ray fluorescopy during cardiac procedures 77−9272
radiation therapy beams, physical factors affecting skin absorbed dose 79−83937
radiation-induced tumours in rat skin, split-dose recovery 77−90855
radioactive substances, transport through the skin, role of diffusion 77−81483
radioactive substances transport through the skin, role of diffusion 78−20158
radionuclide absorption through damaged and undamaged skins of guinea pigs 80−26383
radionuclide contamination, low-toxicity, calc. of derived working limits 79−66562
radiotherapy, relation between tolerance and dose and treatment field size 79−5359
ratio temperature thermography, results 77−40892
RBE of mouse skin damage, pions$^-$ rel. to X-rays 80−26272
RBE of pions in the acute response of human skin 79−20596
recoil characteristics of human skin, in vivo meas. apparatus 79−57698
reconstructive surgery, in-plane compressive strain limits prediction 80−41069
resistance during square-wave elec. pulses of 1 to 10 mA 78−31929
resistance measurements, collection and off-line processing *(German)* 80−67273
response to fractionated heat and X-rays 78−35887
response to selected cutting edges, pig 77−36980
rheological behaviour, expt. results and struct. model 80−16968
rheological properties of skin components under compressive load 80−35945
rheology of normal and maturing burn-scarred human skin, in vivo study 78−31935
safety and effect of UV and IR rays in skin *(Japanese)* 78−35882
safety considerations for lasers 77−77940
scopolamine permeation through human skin in vitro 77−21487
senescent, increased susceptibility to β-irrad., mouse obs. 80−104656
sensitivy meas., instrumentation for 79−74767
spectral emissivity, influence of cosmetics and ointments 77−9285
strain measurement in elastic thin membranes moire interferometry method, appl. to human skin 80−30828
stratum corneum, human, linear meas. of water content using microwave probe 80−21518
stratum corneum basic prtein and keratin filaments, assembly in macrofibrils 79−16142
stratum corneum intracorneal adhesion, meas. instrument 77−48819
stratum cornum, neonatal rat, diffusion and sorption phenomena 78−77007
stress-strain behaviour of living human skin, 2D, in plane method for determ. 77−37120
stress-strain curves, step phenomenon 79−70569
stress-strain relation, model calcs. 79−74705
subcutaneous tissue gas space pressure during superficial isobaric counter-diffusion 80−30968
surface temperature, effect on licalisation error and two-point threshold 78−77072
T content in organs, and DNA of rat liver cells, after doses of tritiated food, protein or water 80−56226
tactile hearing aid, portable with microprocessor control 79−84029
tactile sensation, mechanoreception physiology and psychophysics *(Japanese)* 80−16962
temperature, mean, simple device for meas. 79−2151
temperature change rate effect on local sweating rate 80−35848
temperature during sweating, estimation 77−48757
temperature measurements using a disc sensor, effect of press. 80−56259
temperature probe design, exptl. calibration results and numerical model predictions 80−56258
temperature rises, thermal props. of dry metal-foil dispersive electrosurgical electrodes 80−98171
temperature-increase of lighted objects as a result of lighting, skin sensation *(Japanese)* 78−44557
thermal effects of blood flow in human skin, modelling 79−24959
thermal recovery after cooling 79−53050
thermographic system model parameter calc. 79−79477
thermographics, classification by statistical filtering of spatial freqs. *(French)* 79−20610
thermoregulation investigation, passive subcutaneous temp. meas. 79−34721
thixotropy in human skin 79−39438
tissue mechanics 78−44521
tissue microelectrode design for skin pH meas. 79−100780
tissue pH electrodes for clinical applications 80−36175
tissue response to combined hyperthermia and X-rays 77−16955
transcutaneous electrical neurostimulation serial/parallel interface system 79−92321
transcutaneous O_2 and skin blood flow, laser system for simultaneous meas. 80−26321
skin continued
transducer for obtaining digital vol. pulse, skin-resistance response and ECG 77−86729
transient impedance between acupuncture points Li-4 and Li-12, Laplace plane anal. 79−43977
tumour incidence following single and fractionated exposures to proton radiation, rat skin 79−11982
tumour induction and hair follicle damage for different electron penetrations in rat skin 77−5052
tumours, human, selective heating at 27.12 MHz 78−24179
tumours, selective heating at 27.12 MHz 79−2123
undulation propagation rate, dolphin expts. *(Russian)* 80−45927
urophysis, transport across isolated skin of a marine teleost 79−74617
US heating in previously irrad. sites 79−62315
US pulse-echo determination of thermal injury in deep dermal burns 77−70511
UV irradiated human strain cells, herpes virus production as repair marker 80−30783
UV light therapy for skin diseases 80−36057
UV radiation hazards and protection standards 77−81588
UV radiation physics and the skin, review 80−81661
vasomotor thresholds, squirrel monkey, central and peripheral temp. effects 80−97866
veins temperature increase due to subcutaneous perpendicular to surface 80−40970
vibrotactile sense study for artificial visual machine *(Korean)* 79−66583
water exchange of reptile epidermis, the lipid barrier 80−97875
water exchange through skin, meas. method 77−81763
wheelchair cushion effect on skin temperature, heat flux, and relative humidity 79−83707
wheelchair sent evaluation by time-lapse and quantitative thermography of skin after sitting 80−51205
wrinkling of the human skin 77−52819
X-irradiated mouse skin, growth regulation, possible role of chalones 79−16168
X-irradiation, mech. and struct. response 80−35994
X-irradiation, response to single acute exposures, epidermal cell changes quantification, swine expts. 80−72245
X-irradiation and microwave heating, combined effects, pig 80−94290
X-irradiation combined with hyperthermia, fractionation studies 80−56138
X-irradiation combined with microwave heating, response of pig skin 80−61653
X-irradiation response, guinea-pig obs. 77−21566
X-irradiation response of mouse tumour and skin, effect of heating order 80−3738
X-ray and fast neutron damage, relationship between OER, RBE and no. of fractions 80−35978
xeromammography, absorbed dose obs. 80−41242
Ag/AgCl electrode, highly stable, for skin recordings 78−35989
Ar laser treatment of haemangiomas, teleangectasia, radiodermatitis and tatoos 78−35906
Cd distribution in bullfrog skin, determ. by electron probe X-ray microanalyzer 79−79707
^{137}Cs-irradiation, fractionated high dose-rate and continuous low dose-rate effect on pig skin 80−41127
^{137}Cs-irradiation, response of pig skin, various schedules of irrad. 80−72237
^{137}Cs-irradiation response, pig obs. 80−67161
Na^+ entry sites in fromg skin, irreversible inhibition by photosensitive amiloride analogue 78−69030
Na^+ flow model of frog skin epidermis, expt. varification 78−92607
Na^+ saturation kinetics in frog skin, compartmental aspects 80−67050
Na^+ washout rates in whole frog skin, numerical simulation 78−3456
^{210}Po intake into the body through damaged skin 77−25561
T radiation dose absorbed in rat organs, after feeding with organically bound T 80−51262

skin effect
see also anomalous skin effect
AC distribution in solid turns with skin effect, calc. *(German)* 80−69319
AC forces acting on conductors of bifilar lead *(German)* 79−41281
anisotropic metals in perpendicular mag. field, surface impedance behaviour *(Russian)* 78−39145
apparatus for demonstration of skin effect 77−27
conducting media, EPR line shape, magnetoresist. effect 80−84638
conductor, current carrying, finite element analysis 77−83785
conductor surface, calc. by Leontovitch boundary condition *(Russian)* 78−2508
current-carrying conductor, MHD instability suppression, skin effect in strong electric field 77−951
cyclotron resonance, retarded, effect of electron-phonon coupling *(Russian)* 79−8051
cylinder, anomalous skin effect 79−60866
difference between normal and abnormal skin effects *(Russian)* 77−11953
discharge, HF, stability under strong skin effect *(Russian)* 78−14242
doped conducting media, low-freq. props., EM wave reflection 80−103715
electroplasticity, skin effect 80−21046
EM wave penetration into plasma, permittivity sign changes *(Russian)* 80−100477
exploding foils, current distribution in LC circuit *(Russian)* 80−19628
ferromagnet, continuous EM-acoustic conversion, normal skin effect case, expt. *(Russian)* 77−59304
graphite, EPR, effect of motional averaging, anisotropy, skin effect rel. to heat treatment and neutron irradiation *(French)* 80−34752
impulsive field build-up, current skin-layer thickness anal. *(Russian)* 79−41285
inhomogeneous ferromagentic conductors *(Russian)* 77−47847
intermediate state dynamics in superconducting wire 80−88697
laminated cores with sectionally different material props. *(German)* 79−41280
magnetic circuit, pulsed, gap field geometry, numerical calc. 77−573
magnetic star polarity reversal, appl. of skin effect approx. 80−62010
metal, conduction electron distribution function and corrections to surface impedance for normal skin effect *(Russian)* 78−76100
metal, EM props., general lecture 78−26901
metal, EM to acoustic energy conversion, temp. depend. 77−51780

skin effect continued
metal, light refl., nonlinear thermo-optic effect at high intensity 80−93289
metal, surface impedance in mag. field, cyclotron waves 77−89787
metal, surface impedance in magnetic field, Azbel-Kaner cyclotron resonance 78−87901
metal film, surface impedance oscills. in perpendicular mag. field *(Russian)* 78−76165
metallic hydrides, solid echo amplitude and phase, skin effect 80−108115
metals, with open Fermi surfaces, galvanomag. effects, static skin effect *(Russian)* 80−29389
microwave cavity perturbation eqns. in skin depth regime 77−85253
microwaves and transverse pseudowaves in plasmas 78−59600
nuclear spin system, in spherical conductor, free induction decay and skin effect 80−2649
plasma, skin effect for microwaves and transverse pseudowaves 78−26297
polarity changes, skin effect of electrically conducting spherical shell 80−46389
powerful pulse discharge, form. and stability of fibrous struct. of current shell 77−31535
pyrocarbons, EPR, effect of motional averaging, anisotropy, skin effect rel. to heat treatment and neutron irradiation *(French)* 80−34752
RF discharge plasma skin effect counteraction by external mag. field 78−67543
semiconductor and semimetal powders, EPR, effect of mag. field depend. of elec. parameters 79−99749
semiconductor slice resistivity distrib., contactless meas. results *(Polish)* 77−89756
semimetals, anisotropic size effects, review 77−32032
surface impedance in mag. field 77−89786
theoretical interpretation *(Chinese)* 79−38118
thin metallic plate in strong mag. field, electron scatt. elec. cond. theory *(Russian)* 80−59974
thin plate, lateral mag. skin effect 77−10811
Tokamak toroidal field coil shielding calc. 79−31212
transients on hollow sphere in plane field of system of conductors *(German)* 80−37927
Ag-Cu eutectic composite wire, HF conductivity and skin effect 79−33305
Al, nonlinear skin effect at 4.2K, surface resist. determ. *(Russian)* 79−87122
Al wires, eddy current effects on NMR 80−2645
Au film, in mag. field up to 40 kOe, microwave skin effect 77−12032
Bi film, in mag. field up to 40 kOe, microwave skin effect 77−12032
Bi, static skin effect 78−56177
Bi, static skin effect *(Japanese)* 80−15555
Bi, transverse magnetoresistance, field depend., static skin effect 79−11149
CO_2-N_2-He laser, pulsed microwave discharge pump, skin effect and gain 79−13945
Cd film, surface RF impedance in strong mag. fields *(Russian)* 80−92920
Cu, surface spin-flip probability from TESR 78−91953
Ge, electron-hole drop interaction in stationary and alternating mag. field *(Russian)* 77−62845
Ge Schottky barrier diode, lightly doped, IR response and extended HF model 77−80836
Mo, skin effect, Gantmakher-Kaner effect peculiarities *(Russian)* 80−49796
$(SN)_x$, elec. cond., galvanomag. effects 79−91091
W atomically clean surface, static skin effect and transverse electron focusing *(Russian)* 79−91036
W film, surface RF impedance in strong mag. fields *(Russian)* 80−92920
W, magnetoresistance of size influenced samples, temp. depend. 79−28338
W, single cryst. plates, magnetoresistance, temp. depend. *(Russian)* 79−7820
W, surface, atomically conduction electron reflection, skin effect, transverse electron focusing, simultaneous meas. 78−76131
W, surface impedance and HF cond. in strong mag. field, thin single cryst. plates *(Russian)* 77−89831

sky
see also night sky; sky brightness
altazimuth sky scanner optical system, polarization characts. 80−77123
astronomical clear sky occurrence determ. for Middle Asia *(Russian)* 79−88472
clear daytime skies near Kitt Peak National Observatory, probability 80−12512
clear sky conditions, solar radiation and illumination simultaneous meas. 80−81985
cloud cover obs. for global solar radiation computation 77−25758
cloudless, diffuse solar irradiance 80−51505
cloudy or overcast days, max. temp. forecasts *(German)* 77−37311
daytime sky meas. of haze and aerosol characts. *(Russian)* 78−36276
direct solar transmittance for clear sky, model 79−74948
IR sky temp. computation and surface temp. comparison 79−34953
southern polar skies, star trails taken at Siding Spring 77−56906
starry sky simulator, optical system and cell unit 77−60575
twilight sky colours, modelling 79−100944

sky brightness
see also airglow; twilight
$\mu_H(\phi)$ indicatrix rel. to single scatt. optical depth, new formula *(Russian)* 78−11999
aerosol above Black Sea, spectral transmission and sky brightness obs. *(Russian)* 80−94603
aureole, photographic meas. and aerosol single scatt. 77−5448
auroral sky background elimination with stellar chopping photometer 80−72776
background brightness meas., 4500-10600 Å *(Chinese)* 80−12540
background estimation on starfield plate 80−67577
background radiation, brightness temp. from 2 mm meas. *(French)* 77−13503
background radiations in 0.03-4.1 MeV range, Kosmos 461 meas. *(Russian)* 77−33708
calibration via direct sensitometer, astronomical photographic photometry appls. *(French)* 77−13246

sky brightness continued
centimetre wavelengths, contribs. rel. to ionised gas detect. in X-ray galaxy clusters 78−89243
clear daytime sky, brightness rel. to aerosol scatt. indicatrices determ. in 0.55 to 2.4 μm region *(Russian)* 80−94600
clear sky normal incidence solar insolation measured with RG2 filter, charact. 78−69426
clear sky radiance, standard distribs. 77−87076
clouds, optically thick medium, asymptotic radiance and polarisation 77−21776
dark sky paradox and origin of universe 79−25770
day sky, intensity of direct and scattered UV radiation large air masses *(Russian)* 77−49166
daylight from north sky at Nagaoka, Japan, principal component anal., spectral distribs. *(Japanese)* 77−64433
dayside auroral emissions, obs. from Scandinavia of sky background 78−85755
daytime sky, brightness oscills. rel. to stellar extinction oscills. 80−56606
daytime sky, UV light polarisation as indicator of atmospheric turbidity 78−20517
daytime sky brightness fluctuations, due to aerosol layer *(French)* 80−81959
diffuse cosmic UV background, spectrum 80−17696
diffuse galactic light and Milky Way brightness fluctuations 78−61921
diffuse solar radiation below overcast sky, ang. distrib. 80−85719
direct solar radiation rel. to cloudiness and solar altitude 79−58073
dust loading of atmos., 1923-54, pyrheliometric and circumsolar sky radiation obs. 80−46240
extragalactic background light at 5115 Å, upper limit 79−101225
extragalactic background light intensity at 5100 Å wavelength 78−4414
far IR background, new balloon-borne meas. *(Italian)* 79−48965
far UV interstellar radiation field, prediction 77−64739
far UV radiation background at high galactic latits., D2B-Aura satellite obs. 79−17143
galactic 2 μm radiation, mean intensity in solar neighbourhood 80−36744
horizontal plane diffuse insolation from clear sky 79−83575
information content of sky intensity, polarisation meas. at right angles to solar direction 78−81401
IR emission, sky noise correl. for IR telescope focal plane *(French)* 78−53725
IR emission, statistical props. of sky noise *(French)* 78−53731
IR flux, meausurements over Atlantic Ocean *(Portuguese)* 79−2372
IR spectroradiometric meas., 7 to 14 μm, comparison with LOWTRAN-4 predictions 80−61897
light pollution, effect on astronomical obs. 78−3954
light pollution and possible measures 78−49139
light pollution over Jena, night sky brightening at Karl-Schwarzschild Observatory 80−51533
luminance and colour temperature of clear sky, in Rayleigh atmosphere *(Japanese)* 79−92594
Lyman α sky background, Copernicus high-resolution obs. 77−29963
meteoric nightglow, review of historical obs. 80−94761
Mt. Majdanak (1976 June-July), atmospheric extinction and night sky brightness *(Russian)* 79−39856
near IR nightglow, meas. rel. to galactic centre and Aquila region mapping 79−12514
neutron skyshine from nucl. facilities *(Japanese)* 79−18054
night natural illumination measurement in 0.4 to 1.2 μm spectral region, photometer 78−57367
night sky, effects of urban lighting 77−73853
night sky, Mitaka, Japan *(Japanese)* 80−82067
night sky model for artificial satellite search systems 77−73923
night sky zenithal brightness monitoring, light pollution rel. to astronomical observations 78−49141
normal incidence insolation measured with RG2 filter, charact. 77−29414
ocean surface with waves, radiance distrib. over surface, glitter and sky contrib. 77−21902
oscillations of daytime sky brightness 78−81406
phase problem in astronomy, sky brightness distrib. 80−46258
photographic astrometry against bright daylight sky, theory and appl. 79−8797
photomultiplier experiment, sky brightness and polarisation, for teachers 78−81768
photon, spectra of gamma rays backscattered by infinite air (skyshine) 80−101436
planetary atmosphere, zenithal brightness near terminator due to light scatt. by optically thin atmosphere 80−109382
polarising radiometer meas., skylight at South Pole station, Antarctica 78−57320
radiance during total solar eclipse, model 78−40652
radiation scattered by circumsolar parts of sky, parabolotoroidal focones and parabolocylindrical foclines assessment 78−83064
reflected light from Earth's surface in Rayleigh atmosphere, estimation *(Japanese)* 78−40663
Sacramento Peak Observatory, night sky brightness conditions 80−12545
Scorpius region, UBV surface brightness photometry of Milky Way from Helios 1 78−57634
shortwave diffuse radiation intensity over daytime sky calc., semiempirical method 77−70796
solar aureole rel. atm. aerosol props., photogrammetry 78−57315
solar eclipse, 26 February 1979, sky brightness meas., radiative transfer model 79−92588
solar radiation scatt. from gradient particulate atm., background noise in optical communication 79−62576
solar resonance radiation multiply scattered by nearby interstellar medium, backscattered intensity 80−41874
spatial var. obs. using intensified vidicon camera 77−70832
submillimetre sky emission and absorpt., freq. spectrum of fluctuations 77−41308
sunphotometer aperture effects on atmospheric turbidity meas. 79−84483
three dimensional spatial autocorrelation function meas. 80−67576
troposphere and low stratosphere, scattered solar radiation field meas. *(Russian)* 79−16667
UV, aerosol scattering albedo determ. using sky brightness meas. *(Russian)* 80−21822
zenith brightness radiometry, absorption altitude profile determ. at 2.53 mm 77−81979

sky brightness continued
zenith photoelectric measurements during annular solar eclipse (1976, April 29) 78−3900
zodiacal light UV observations by Astro 7 rocket expt., reddening 78−96427
sky surveys *see astronomical catalogues*
Slater-type orbital calculations *see STO calculations*
sliderules *see calculating apparatus*
sliding contacts, electrical *see electrical contacts*
slip
see also kink bands; plastic flow
acoustic emission during tensile tests, H_2 assisted fracture 79−100257
aggregate, polycrystalline, deform. 77−4816
alkali feldspar, deformation, plastic defects, TEM investig. 78−32066
alkali halide, deformed single cryst., dislocation struct. formation *(Russian)* 77−7733
alkali halide, doped single crystals, plastic anisotropy 78−26575
alkali halide crystals, dislocation internal friction, orientation depend. 78−48439
alkali halide doped angle crystals, latent hardening 78−51607
alloy, dispersion hardened, particle size effect on fracture 79−43418
alloy, formation of laminated martensitic structures *(Russian)* 78−39771
alloy, $L1_2$ ordered, yield stress 77−52392
alloy, ordered, conservative jog slip on superpartial screw dislocations, work hardening 77−7731
alloy, ordered, with LI_2 superstructure, plastic deform., slip system detection, phenomenological theory 79−7602
alloy, spinodally decomposed, interfacial energy effect on mech. strength, theoretical estimation 79−38790
alloy, strengthening mechanism anal. by thermal activation theory 79−78987
alloys, dislocation stress-velocity depend. 80−96537
alloys, $L1_2$-type superstruct., anomalous temp. depend. of deform. charcts. *(Russian)* 79−20109
alloys, LI_2, superstructure, dislocation link strength and strain hardening at high degrees of deform. *(Russian)* 78−39792
alumina, polycryst., compressive strength, microplasticity 77−36620
alumina, prismatic slip dislocations in single crystals, obs. *(French)* 77−59016
amorphous structure, computer simulation of deformation 79−7647
amorphous-crystalline substances, high temp. plastic deform. interpret. 77−35627
anisotropic body, slip planes 78−39874
anisotropic media, stress fields of dislocation arrays *(German)* 79−23615
anthracene, polymorphic forms, generation by repeated slip 78−34457
anthracene, slip planes, atom-atom pot. method 77−35569
anthracene, slip systems in deformed crysts. 79−42138
axially symmetric slip line fields, material press. depend. behaviour effects *(German)* 79−86360
axisymmetric plastic deformation, slip line model *(Russian)* 78−83261
band, action of dislocation sources in irregular stress field *(Russian)* 77−15426
Bauschinger effect, grain boundary contrib. 79−47759
BCC and FCC polycrystals, selection of active slip system 79−90665
BCC crystal, cyclic deformation, irreversible glide and shape changes 80−103356
BCC crystal, minimisation of shears for pencil glide 77−24319
BCC crystals in tension and compression, theoretical latent hardening 80−24459
BCC metals, plastic deform., computer simulation 80−40456
BCC metals and alloys, glide and work hardening, review *(German)* 79−34067
BCC metals and alloys, glide and work hardening review *(German)* 79−29089
biaxial, of mass on foundation subjected to earthquake motions 77−54915
binary, ternary oxides, dislocation motion and high temp. plasticity 80−59468
boundary value problems soln. *(Ukrainian)* 79−41588
α-brass, (211)[111] single crystal, rolling deform. 77−21174
α-brass, concentrated single crystal, yield region investigation, CRSS, slip 77−48478
α-brass, deformation mode during rolling *(Japanese)* 79−79001
α-brass, fractographic obs. of cracks in early stages of fatigue *(Japanese)* 78−7023
α-brass, prismatic glide, dislocation speed determ. 77−59867
β-brass, quenched single crystal, deform. and slip 79−79026
brass, rolling texture development and deform. struct., shear bands effect *(Japanese)* 80−84952
brass, shear band development during rolling, twinning, metallographic obs. *(Japanese)* 78−39849
α-brass, single crystal, deform. and ductility at elev. temps. *(Japanese)* 79−5012
α-brass, single crystal, obstacle strength variation during stress relaxation 78−68723
brass, stress corrosion cracking, effect of strain rate 79−20257
α-brass, stress corrosion cracking in single and bicrystals 77−4866
brass, two phase α/β bicrystal, transgranular slip and fracture across an interface 80−81150
α-β brass, two phase bicrystal, deform. and fracture at 450K 80−16409
α-β brass, two phase bicrystal, fatigue 80−108520
α-β-brass, two phase bicrysts., deform. and fracture at 150K 80−16388
α-β brass, two-phase bicrystals, plastic deform. and fracture mechanism 78−84898
β-brass, uniaxial tension and compression, cyclic stress-strain behaviour 80−97551
brass single crystal, intracrystalline slip bands in high temp. creep *(Czech)* 79−77604
α-β brass two-phase bicrystals, activated slip systems during yielding 78−84911
α-β-brass two-phase bicrystals, operative slip systems at 150K 79−70119
brittle fracture in ductile material, model and applic. to H embrittlement 78−23814
camphor, rhombohedral, polycryst., compressive deform. and dynamic recrystn. 80−71698
carbonate minerals, deform. twinning mechanisms 80−79814
cavity nucleation, by plastic deform. 79−29127
cementite, in white pig Fe, deform. and fracture 77−4827
slip continued
ceramic, polycrystn. creep stress exponents rel. to slip and ductility 77−90400
ceramic oxide, TEM study of deform., review 79−87686
circular fault, slip and stress drop 77−73641
climb process, of edge dislocation, effect of glide forces 80−70195
collective behaviour of dislocations, HVEM study *(French)* 80−65006
composite, lamellar, matrix strain hardening mechanism *(Russian)* 77−59801
composite dislocations, asymm. equilib. positions and line tensions 79−51108
computer modelling of broadening of slip bands 78−59808
computer simulation of thermally activated dislocation motion through random array of point obstacles 78−30636
continuum model of dislocation core 77−76399
β-copper phthalocyanine, dislocation detection *(German)* 78−63773
corundum, growth of large crystals of high opt. quality 77−34916
corundum, packing errors in structure, X-ray diffr. obs., charact. features 79−46655
crack, dislocation model of plastic zone 77−84837
crack behaviour, discrete dislocation analysis 78−22788
crack initiation notches, pure strain rate role, finite element computer program 77−70166
crack tips, blunting during conc. plastic flow *(Russian)* 78−7013
crack-tip slip band blocked by grain boundaries, simple model 79−50665
creep, irrad. induced in transient irrad. environments 80−92598
creep, irradiation induced, correlation of theory with expt. evidence 80−88255
creep, irradiation induced, dislocation glide enabled by preferred absorption of point defects 80−88250
creep and growth, radiation induced, fundamental mechanisms 80−92596
creep deformation model incorporating recovery and thermally activated glide 79−64534
creep model, based on dislocation climb at grain boundaries 79−37756
cross slip dislocation self-interaciton, Orowan loops 80−24453
cross-rolling and compression textures, numerical prediction 80−40382
β-succinic acid, cryst., slip system and dislocation detect. by etching 77−59015
crystal elastic and plastic anisotropy and dislocations *(Japanese)* 79−95069
crystal plasticity, hardening law for slip systems 79−33030
crystalline body, dislocation interaction between pores while being healed by external pressure *(Russian)* 77−19963
crystalline materials, in situ deform. by high voltage electron microscopy 80−103352
crystals, photogrammetric obs. method 80−100975
Cu, formation of double twist boundaries during plastic deform. *(Russian)* 77−81295
cubic crystal edge and screw dislocation−point defect elastic interactions 80−15151
cubic crystals, active slip systems in plastic deform. process *(French)* 78−35431
cubic crystals, compression test, double slip kinematics 80−65005
cubic crystals, scratch hardness, anisotropy 79−96130
cyclic creep, enhnaced, high temp. theory for polycrystalline materials 78−7018
deep circular notches, plane strain general yielding under loads and bending 79−18809
deformation, orientation changes accompanying slip and twinning 77−43273
deformation texture development and polycrystalline modelling 79−91671
diamond, synthetic, oxidized in fused salts, etch features 80−97604
discrete obstacle model, dislocation and stress field distrib. 80−79794
discrete obstacle model, dislocation pile-up kinetics dislocation mobility activation parameters 80−29022
dislocation behaviour, in fatigue, friction and back stress from hysteresis loops 80−3176
dislocation behaviour in fatigue 77−24352
dislocation ensembles, local heating at low temps., parallel glide planes, temp. distribution *(Russian)* 80−29020
dislocation glide plane with precipitates, work hardening and softening 78−83815
dislocation gliding, by-passing of hardened particles, coplanar Orowan loops form., stress-strain curves 80−49226
dislocation interaction, in intersecting slip planes 80−39087
dislocation interaction with point obstacle in non-uniform stress field, localised force approx. 80−15150
dislocation motion, thermal activation through random point obstacles 79−1434
dislocation motion through random array of short range barriers, digital simulation 78−30634
dislocation multiplication, double cross-slip mechanism 78−22720
dislocation multiplication, statistical approach 80−49230
dislocation pile-up dynamics, planar 78−6058
dislocation pile-ups, plane-parallel inertial mechanism of avalanche-like breakthrough 78−2121
dislocation segment oscillations, internal props., point obstacle collisions, glide plane motion *(Russian)* 80−39088
dislocation self-energy effect on choice of slip system 79−27982
dislocation substructure strengthening and thermomechanical processing, conf., Las Vegas, USA, Feb. (1976) 77−84760
dislocation unzipping, low temp., computer simulation *(Russian)* 79−86792
dislocation-phonon interaction in cryst. with anisotropic slip system 80−29137
dislocations, rate of piling up, rel. to average length of slip lines *(Russian)* 77−76416
dispersion-hardened single crystals, theory of high-temp. strength 77−48445
dispersion-strengthened alloys, threshold stress for creep 80−93626
double slip, general kinematical anal. for fcc and bcc crystals 79−18741
driving force and climbing force on dislocations 78−43017
ductile single crystal, geometric effects in inhomogeneous deform. 79−46741
ductile single crystals, exam. of strain localisation 78−52912
Duralumin, effect of alloy purity and ageing on fracture mechanism, and resultant toughness 79−5049
Duralumin 2017, superplasticity *(Korean)* 79−38902

slip continued
dynamic Peierls stress in cryst. model with slip anisotropy, screw dislocation motion 78−95056
dynamic stability of dislocation sub-boundaries during straining, computer simulation 78−30635
dynamic waves along dislocations overcoming local obstacles 80−29021
Earth crust, slip rel. to viscoelastic model of 1906 San Francisco earthquake 77−73671
earthflow slope formation in Hong Kong 80−109144
easy glide, computers modelling, range of permissible parameters *(Russian)* 78−47375
edge dislocation motion, glide and climb resist. due to dragging a Cottrell atm. 79−99194
elastic body, inhomogeneous yielding, slip plane intersection with stress free boundary 78−5667
elastic contact problems, in fracture mech., friction effects 78−67142
elastic layer pressed against substrate, separation and slip caused by tensile load 80−96536
elasto-diffusive solids, singularity movement, appl. to fracture propag. 78−30235
elastodynamic radiation from slip zone, ray method 78−73322
enstatite, wet polycrystalline, high temp. flow 78−32082
epitaxial island mobility, one-dimens. model sinusoidal pot. 80−44457
eutectics, single grained, directionally solidified, anisotropic yielding behaviour 80−103412
eutectoid thermomechanically treated, textural studies 80−29978
expansion of slip bands, steady-state, dislocation vel. theory 77−24320
fatigue, current aspects 77−86156
fatigue crack, dynamic treatment of growth *(Japanese)* 78−34084
fatigue crack initiation, rel. to grain boundaries, stress gradients and cross slip 77−27890
fatigue limit under combined stress 77−73314
fatigue striation form., three dimensional strain compatibility model 79−1908
faulted dipoles, formation and props. 77−72615
faulting analysis in three dimens., strain field 78−77225
f.c.c. alloy, rolling texture *(Russian)* 77−1843
FCC crystal, grip effect and bend gliding during uniaxial tensile deform. *(Japanese)* 79−52314
FCC crystal, homogeneous deform. by glide of dislocations with imposed stresses and strains *(French)* 77−7783
FCC crystal, transient effects during tensile tests in model of correlated dislocation motion 78−38715
FCC material, irradiation induced creep, climb induced glide model 80−89292
FCC metal, polycrystalline, computer simulation of rolling texture *(Japanese)* 77−63686
FCC metals and alloys texture transitions, computer simulation 79−90666
FCC to HCP transform., model and expt. evidence 77−44243
ferromagnetic crystal with dislocations, mag. anisotropy *(Russian)* 77−8377
finite distortional latent hardening in single crysts., perpetuation of slip 78−3144
finite element plasticity, slip model 79−32301
foam PS-4-40, microslip, effect of friction 77−77588
force plane diagrams for plane strain slip-line fields 78−63314
fracture, intergranular, low temp. mechanism 78−60795
fracture, plasticity model, dislocation based, geometrically consistent 78−30242
fracture along planar slip bands 80−107262
fracture mech. during creep, interference microscopy exam. of 12Kh18N9, 08Kh18N10T 78−56756
free boundaries, slip-line field solutions, matrix technique 80−53640
friction effects on microslip 77−77588
friction stress and back stress from hysteresis loop anal. during fatigue 79−42076
GaAs-$Ga_{1-x}Al_xAs$ DH crystals, <110> oriented dark line defects 77−80510
glide dislocation interaction with intrinsic boundary structure 78−87686
gliding dislocations, flexible, model of passage through plane dislocation accumulations 79−42066
grain boundaries, interfacial structure effects on high temp. mechanical behaviour 80−59480
grain boundary sliding, containing particles, during diffusional creep, dislocation bowing 79−37712
granular materials, intergrain slip in flowable zone, stress distrib., internal friction 79−99261
granular mats., stress-strain relations, intergrain slip 80−16374
graphite, irradiation induced creep, UKAEA reactor group studies 77−42065
HCP crystal, dislocation-point defect interactions, anisotropic elasticity theory, appl. to Zr 77−11588
HCP crystals, dislocation-point defect interactions in slip systems 78−47417
HCP metals and alloys, plastically deformed, electron microscopy *(French)* 77−44300
heating of slip lines and bands in thin crysts. at low temp. 79−69111
hexagonal crystals, intraction of flexible dislocations in intersecting slip planes 77−39592
hexagonal polycrystals, creep and plasticity, rel. to single crystal slip 78−13920
hexamine, BCC, dislocation slip initiation 77−43222
ice, dislocation vel. theory, glide plane influence 80−79805
ice Ih, dislocations, effect on physical and mechanical props. *(French)* 77−55287
II-VI compounds, charged dislocations and plastic deform. 80−107264
III-V compounds, dislocation half-loops, nucleation and generation 79−95009
interacting dislocation motion, resisted by point-like barriers, computer simulation 78−71742
interface of two solids, sliding mechanism without slipping 78−51136
interface slip, caused by plane horizontally polarised SH stress pulse 80−53648
irradiation creep, climb-enabled glide of dislocations resulting from preferred absorpt. of point defects 79−82280
irradiation creep due to dislocation and glide 77−69009
irradiation creep mechanisms, theoretical assessment 79−55817
isotropic solidification, plane slip line fields, construction by characteristic net method *(German)* 79−91640
kinematic hardening rule in single crystals 80−10551
slip continued
kyanite, deformed, defect struct. 77−31668
local heating in crystals during low-temperature deformation 78−67766
low temperature deform., heating of dislocation sources 78−18660
machine process, nonuniqueness 78−39932
martensitic transform. kinetics., strain induced, FCC to HCP 77−44249
martensitic transformations, thermodynamic stability of structural states *(Russian)* 79−43246
metal, BCC, appl. of results of computer simulation of screw dislocation motion 77−4102
metal, BCC, cryst. lattice change during deform., influence of boundary dislocations with different Burgers vectors *(Russian)* 77−21219
metal, BCC, deforming by {110} ⟨111⟩ and {112} ⟨111⟩ slip, lattice rotation calc. in axisymmetric flow *(Japanese)* 77−21225
metal, BCC, geometry of slip systems *(Hungarian)* 77−47463
metal, BCC, polycrystalline aggregate, prediction of plastic props., deformation by ⟨111⟩ pencil glide 80−11731
metal, BCC, relation between elastic energies of dislocations and choice of slip system *(Japanese)* 78−18656
metal, BCC, rolling texture, effect of critical shear stress ratio of {112} and {110} 79−91673
metal, brittle, ductility improvement by plating *(German)* 77−8954
metal, cleavage plane prediction, Ayres-Stein method 79−29214
metal, ductile fracture, crack initiation at dislocation cell boundaries 77−66692
metal, FCC, deformation mechanism under high hydrostatic pressure *(Ukrainian)* 80−25758
metal, FCC, dislocation behaviour at high strain rates, US detection method, data analysis basis 80−85136
metal, FCC, polycrystalline, quantitative anal. of cross-slip and twinning 79−90677
metal, FCC or BCC, dislocation annihilation during tensile and cyclic deform. and limits of dislocation densities 80−34007
metal, fracture under influence of high power US waves *(Russian)* 79−5034
metal, inhomogeneous dislocation struct., model 79−90655
metal, model of elastic-plastic deformation *(Russian)* 77−48484
metal, polycrystalline, strain hardening, dislocation link length model 80−84953
metal, recovered dislocation substructure, prod. and utility, review 77−84749
metal, shearing, scissors type, slip-line analysis 78−23761
metal, surface strain meas. by intensity of reflected light flux 77−17972
metal, thermo-inertial mechanism of plasticity enhancements normal to superconducting transition *(Russian)* 79−47183
metal, very thin foils, crack propag., electron microscope obs. 77−63792
metal and alloy surfaces, highly reflecting, pulsed laser stress phenomena 79−14015
metal mirrors, diamond turned, surface, optical and laser damage charcts. 77−50705
metal mirrors, for high-power appls., multithreshold damage analysis 77−88884
metallic glass, shear deform., mechanism involving dislocation glide 78−15462
metallic glasses, structures based on disclination-dislocation model 79−82159
metallic materials, fatigue life distrib. theoretical obs. near fatigue limit 80−59569
metallic polycrystals, deform. during cooling, revealed by deposited graphite layer *(Polish)* 80−25755
metallic thin film, polycryst., plastic flow, dislocation slip 79−82505
metals, BCC, dislocations, anisotropic elasticity theory *(Japanese)* 79−10853
metals, BCC, predicted rolled textures, influence of slip system and deform. model *(French)* 79−43309
metals, FCC, 'brass to copper' transition in rolling textures 80−76246
metals, FCC, hardened, plasticity, review 79−11683
metals, FCC, slip dislocation reactions at coherent twin boundaries, effect on work-hardening 79−1431
metals, FCC and CC, role of latent slip, computer simulation *(French)* 79−32998
metals, plastically deforming at high strain rates, distrib. of temp., strain rate and strain 79−19311
migration of steps on subboundaries 77−7721
misfit dislocations, Volterra-type model and relax. of nonequilibrium arrangements 80−2020
Mo, slip line study of pure single crystal compressively deformed at low temps. 79−43361
model crystal, thermally activated glide in strain rate change and stress relaxation expt. 77−36615
modelling of linear and surface defects 77−89450
morphology in dispersion hardened materials 77−4785
moving dislocations, low-temperature statistical charcts. *(Russian)* 79−90654
moving fluid interface on rough surface, slip coeffs. 77−3806
mullite, high temp. mech. props. in compression 77−56033
muscovite, exam. of dislocations and props. using elasticity theory *(German)* 79−10854
naphthalene single crysts., steady creep obs. 80−75296
naphthalene single crysts., surface active substances effect on plastic flow 80−44248
neutron damage simulation, using HVEM, state-of-the-art 77−51417
Nimanic 80A, inhomogeneity effect of cyclin strain on crack initiation 78−48532
Nimonic 80A, order hardening, comparison between revised theory and expt. 80−93565
non-crystallographic slip, in cubic cryst., algebraic determ. *(French)* 80−2112
nonlinear anisotropic strengthening model *(Ukrainian)* 78−67051
nonlinear model of anisotropically reinforced plane plastic medium based on slip concept *(Russian)* 77−35057
nuclear fuel-cladding interaction between cracked surfaces, mechanical and temp. contact 78−66341
octadecanol, normal, single cryst., lattice defects, X-ray topographic obs. 78−18650
olivine, hardness var. with temp., rel. to polycryst. yield stress 80−26500
olivine, plastic flow of oriented single crystals, dislocation struct. interpretation 78−36156
ordered alloy, noncoaxial dislocation loop behaviour 77−11549
ordered alloy, with $L1_2$ structure, dissociation of superdislocations and plastic deform. mech. *(Russian)* 78−52909

slip continued
ordering alloy, $L1_2$ superstruct., superdislocation dissoc. *(Russian)* 78−48451
orthotropic medium, strain localisability function 79−18743
oxides, dislocation climb model 80−100230
oxides, interaction between point defects and dislocations, cryst. plasticity 80−15149
oxides, plastic deform., TEM obs. *(French)* 77−44304
phthalic anhydride, single crystals growth and perfection 79−78869
phthalic anhydride spherulites, cryst. growth from melt, slip system identification 79−32930
piecewise homogeneous elastic medium, crack with finite branch, slip lines 80−38342
plagioclase feldspar, deformed in compression, dislocation substruct. and slip, TEM obs. 77−43221
planes, accumulated dislocations, diffr. effects obs. during X-ray transmission through cryst. 79−4310
plastic deformation, phenomenological theory, with mobile and immobile dislocations 78−75714
plastic failure, effect of deep wedge shaped notches of small flank angle 80−48593
plastic flow round crack under friction and combined stress 78−79280
plastic relaxation in shock wave, slip mechanism 79−41605
plastic slip concept, statistical approach *(Russian)* 78−18196
plastic slip line fields around elliptic holes, Riemann integral solns. 79−32303
plastic yielding, modelling at a crack tip by inclined slip planes 80−33472
plastic zone, direct meas. in side grooved fracture toughness specimens 78−68864
plastically deformed crystal, acoustic emission, bubble formation mechanism in liq. He *(Russian)* 78−85066
plasticity, polycrystalline, based on dislocation processes, probabilistic approach 78−26621
poly-[1,2-bis-(p tolylsulphonyloxymethylene)-1-butene-3-inylene], defect imaging 77−15418
polycrystal creep props., derivation from single crystal data 77−65696
polycrystalline materials, model of plastic deformation using slip 78−63802
polycrystals, constitutive relns. in elastic-plastic range 78−63801
polyethylene, crystal, elastic line energies and line tensions of dislocations 79−90656
polyethylene, high-density, oriented, deform. mechanisms 78−44171
polyethylene, high-density, semicryst., fold-surface morphology effect on deform. processes 78−34447
polyethylene, oriented, shear strain, effect on stuct., props. *(Russian)* 80−7656
polyethylene, roll oriented, superstructural change during uniaxial extension *(Japanese)* 77−52422
polyethylene, struct. changes on hot-rolling 77−86051
polyethylene, structural changes on hot-rolling 77−86052
polyethylene, ultradrawn linear, kink bands by compression, interfibrillar motion 79−24581
polymers, fracture, molecular interpretation 78−60769
polyoxymethylene, low-strain deform., transmission electron microscope exam. 79−5013
polyoxymethylene, rolled, prediction of yielding behaviour 77−73306
polystyrene, glassy, thermally activated deform. 79−20126
porous material, wedge indentation hardness, slip line field theory 77−86128
porous structure, shrinkage kinetics, boundary slip and superplasticity 77−36611
primary coplanar, role in deform. of FCC crystals *(Japanese)* 77−52412
punch identation with isolated slip line 78−79286
PVC, hard, flow zone effect on degradation, rigidity, deformation, under fatigue *(German)* 78−15471
quartz, ⟨a⟩ axes preferred orientations in tectonites, flow kinematics 78−96200
quartz, creep and mechanism by which water accommodates dislocation glide 77−90414
quartz, dislocations, elastic energy *(French)* 79−14807
quartz, dissociated a-dislocation, effect on plastic deformation 79−7610
quartz, microstruct. and fabric development in quartz-feldspar mylonite 78−96201
quartz, subgrain boundaries, theoret. predictions and microscopic obs. methods 80−84187
quartz, water saturated, plasticity, rel. to dislocation theory 79−34104
quartzite, deformation in Earth crust, dislocation climb mechanism 79−60425
quartzite, naturally deformed, textural and microstructural development, metallurgical approach 79−83228
recovery-creep, steady state, in pure materials, model 77−75815
recrystallisation nucleation, model for strain induced grain boundary migration 79−46675
refractory alloys, creep mechanism and struct. changes *(Russian)* 79−52299
refractory materials, group IVa and Va, slip, microhardness comments 78−84967
Rene 80, dislocation behaviour during plastic deform. *(Japanese)* 80−108504
Reynolds eqn., one-dimensional, with slip boundary conds., perturbation soln. 79−14372
rock, cracked, slip surface development 78−15480
rock, plane wave propag. in anisotropic jointed media 77−68501
rocks, slip propag. along frictional surfaces 79−25236
sand bodies, shear bands formation, bifurcation problem 78−73362
sandstone, fault development, deformation bands and slip surfaces 79−20819
sapphire, shaped single crystals, porosity, microstruct. 78−2125
sapphire, work hardening 77−16604
sapphire::Ti^{4+}, deformation history effects on precipitation hardening 79−83209
screw dislocation control of plastic deformation in crystals 78−51605
screw dislocations cross-slip processes in high temp. recovery-creep 77−19965
screw subboundaries as dislocation sources, creep 80−100234
semiconductor structures, defect obs. using stroboscopic SEM 79−9261
shear band formation models, in rolling and extrusion 80−3152
shear band formation models, in rolling and extrusion 80−11666
sheet, cold rolled, texture form., model *(French)* 78−68705
slip continued
sheet drawing, slip line field for mid-plane cracking or splitting 80−50648
sheet metals, strain-induced changes in mech. props. and press formabilities 78−19781
shift-type packing defects, involving dislocation representations, influence on diffr. pattern 80−107239
sign-reversing loading *(Russian)* 79−23224
siloxane rubber, energy investigation of softening during deform. 77−4819
Silumin, AlSi10Mn, struct. and mech. props., Na modification effects 77−63786
simulation of dislocation glide through fields of point obstacles 78−34521
single crystal deform., texture form. 79−87651
single crystal deformation, active slip system and orientation change determ. method 79−90664
single crystals, homogeneous plastic deform. by dislocation glide *(French)* 80−84232
slip and twinning relns. *(Russian)* 77−65982
slow viscous flow, slip-plane and slip-cylinder theorems 78−14046
solid free boundary, slip line initial development, elastic-plastic problem 80−96196
solid soln., flow stress, temp. plateau 79−14877
solid solution alloys, creep behaviour at intermediate stresses and creep power law breakdown 79−57058
solution hardening theory 77−36530
spinel oxide, dissociation of dislocations and plastic deform., temp. effects 79−7613
stainles steel, type 316, irrad. in simulated environment, tensile props. 80−34076
statistical theory, dislocation configs., in point obstacle random array 78−18645
steel, 12Kh1MF, fracture in creep at temp. near 0.5 MP *(Russian)* 77−32675
steel, austenitic, dislocation struct. formed by interstitial diffusion of C 77−4223
steel, austenitic, precipitation hardening, effect on fatigue strength 78−84829
steel, austenitic 03KhAG19, fatigue crack development at normal and low temps., struct. effects *(Russian)* 78−35480
steel, austenitic and martensitic, structural sensitivity of Bauschinger effect *(Russian)* 79−52303
steel, austenitic stainless, flow cavitation erosion, initial part of incubation period 78−44224
steel, austenitic stainless, interaction of grain boundary dislocations with precipitates during high temperature creep 80−16384
steel, austenitic stainless, irrad. creep of type 316 in HVEM 80−97523
steel, austenitic stainless, partial dislocation separation and dislocation substructure, effect of applied stress 78−22727
steel, austenitic stainless, plastically deformed, TEM obs. *(French)* 77−44302
steel, austenitic stainless, stress relaxation model, experimental confirmation of model 78−92293
steel, austenitic stainless, transgranular slip obs. 78−80595
steel, austenitic stainless 316, load relaxation data, comparison with Hart's deform. model 77−70091
steel, austenitic stainless tensile ductility in air and H_2 77−66687
steel, austenitic stainless type 304L, temp. depend. of acoustic emission accompanying plastic deform. 79−74217
steel, C, accelerated deform. by to H_2 absorption *(Japanese)* 79−70121
steel, C, fatigue crack exam. using slip initiation phenomena *(Japanese)* 77−8930
steel, C, type 45, crack form. mechanism during fatigue 79−38957
steel, C, yield point determ. rel. to grain size, deform., ageing and temp., dislocation theory *(Serbian)* 79−34120
steel, C(0.2 wt.%), explosively strengthened, cause of anomalous increase in H_2 of low cycle endurance *(Russian)* 77−16729
steel, cold-rolled, recovery of lattice defects in cementite 77−90370
steel, Cr (3.51, 3.74, 3.56 wt.%), bainite transform. of deformed austenite 77−32574
steel, Cr-C (3.74, 0.86 wt.%), stress assisted bainitic transform. *(Czechoslovakian)* 77−32573
steel, Cr-Ni (1.47, 1.48 wt.%), lath martensite microstruct. and props., cold rolling effect 80−55422
steel, Cr-V (1.5, 0.5 wt.%), ferritic, effect of temp. and microstruct. on creep damage 79−5023
steel, CrNi, etchability of austenite *(German, English)* 80−11860
steel, eutectoid, fatigue crack tip props. in rotary bending and cyclic torsion 77−32668
steel, ferritic stainless, embrittlement 80−85041
steel, ferritic-martensitic, fatigue crack tip plastic zone *(Japanese)* 80−71738
steel, hardness, tensile and impact props. correlation, at low temps. *(Japanese)* 77−52413
steel, high C, Burgers vector of dislocations in cementite crystal 77−27891
steel, high Mn, mech. props., strain induced martensitic transform., effect of austenite predeformation 77−16649
steel, high-C martensite, rel. to struct. transforms. during low temp. tempering *(Russian)* 77−59737
steel, low C, 10Kh2G3M, development of plastic deform., slip and dislocation struct. *(Russian)* 79−15722
steel, low C, alloy, structural transform. during deform. and annealing *(Russian)* 79−91707
steel, low C, initial stages of plastic deform. *(Japanese)* 80−93618
steel, low C, normalised, plastic deform., using microhardness and grain strain meas. 77−4810
steel, low C, orientation distribution function anal. in maximum shear planes 79−82172
steel, low C, plastic deformation by pencil glide, r-values and yield loci 80−7654
steel, low C, slip band expt. studies during fatigue process 80−45374
steel, low C, slip line development 78−15480
steel, low C, texture hardening in maximum shear planes during expansion 79−91704
steel, low C, under rotating bending and torsion, overstressing effects *(Japanese)* 77−8935
steel, low-alloy, plastic deform. mechanisms under dynamic loading 80−100883

slip continued
steel, low-alloy 12GN2MFAYu, heat treated, testing temp. influence on fatigue strength *(Russian)* 80−40501
steel, maraging, investigation with lower Ni and Co contents *(Chinese)* 78−84812
steel, martensitic, fatigue crack form. associated with cyclic slip deform. along prior austenite grain boundaries 78−60831
steel, microstructure of 0Kh16N15M3B after creep tests in BR-10 reactor, electron, microscope invest. *(Russian)* 80−92531
steel, mild, fractography study of shear mode fatigue crack growth by etch pits *(Japanese)* 80−108545
steel, mild, orientation distribution function, representation of texture and slip directions 80−11665
steel, Mn-Cr-B (1.46, 1.03, 0.003 wt.%) 80−55422
steel, Ni-Co-Mo (17.55, 8.02, 4.92 wt.%) maraging, lath martensite microstruct. and props., cold rolling effect 80−55422
steel, pearlite, deform. and fracture mechanisms, HV SEM obs. 80−104243
steel, pearlitic, deform. microstruct. and cementite fracture, −196 to 700°C 78−27576
steel, plastic deformation and cryst. texture in equibiaxial expsn. 80−7653
steel, spheroidised AISI 1095, U-notched bend specimens, hydrogen effect on fracture 79−52363
steel, spheroidized, Bauschinger effect and work hardening 78−64596
steel, spheroidized AISI 1095, ductile fracture of U-notched bend specimens 79−24616
steel, stainless, 18-8 type polycrystal, strain induced γ to α' transform. *(Japanese)* 78−11221
steel, stainless, 304, stress corrosion cracking in boiling $MgCl_2$ soln. *(Japanese)* 79−43476
steel, stainless, anelastic and nonlinear viscoplastic behaviour relations at low homologous temps. 77−63742
steel, stainless, ferritic and austenitic, fatigue crack propagation in single crysts., orientation depend. 79−29167
steel, stainless, fracture and crack tip plastic zones, in situ obs. 80−108686
steel, stainless, in-situ obs. of deform. in HVEM 80−103338
steel, stainless, laminated with Cu interlayers, mech. props. 77−48506
steel, stainless, martensite nucleation and growth, expt. study 78−3125
steel, stainless, martensite nucleation mechanisms, HVEM obs. 80−104157
steel, stainless, neutron irradiation effect on low cycle fatigue and tensile props. at 298K 80−30059
steel, stainless, single crystals, shear cracks, electron microscope study 80−40522
steel, stainless 304, crack propagation under intermittent overloading at elevated temperatures *(Japanese)* 79−38947
steel, stainless 304, stress corrosion cracking in boiling $MgCl_2$, crack growth rate study by SERT method *(Japanese)* 79−100290
steel, stainless 316, creep under high stress 78−52892
steel, stainless type 304 attack morphology of stress corrosion cracking, TEM study *(French)* 79−83368
steel, stainless type 316, in-situ HVEM studies under ion beam irradiation 80−103396
steel, structural, sharp notched bending specimens, fracture stress, temp. depend. anal. 77−56062
steel, tensile prestrained strength of anisotropic rolled steel, rot.-bending fatigue tests, slip bands 78−27590
steel, thermomechanical treatment effect on mech. props. and microstruct. *(French, German)* 79−66090
steel, tufftrided, fatigue strength under reversed torsion *(Japanese)* 79−61707
steel rolled, low-cycle torsional and push-pull fatigue anisotropy 78−27589
steel stainless, plastic deform. of single crystal, contribution of $\gamma \rightarrow \epsilon$ transform. 77−52394
steels, C and stainless, fatigue crack propag. and crystallographic orientation *(Japanese)* 78−7027
steels, structural St 37-2, cleavage fracture, report 80−25868
steels, ultrahigh C, superplastic, mech. behaviour at elevated temps 80−21028
stick-slip sliding dynamic props. appl. to earthquakes 78−48983
stress intensity factor for crack and nearby slip band, two-phase material 77−56097
stress-deformation diagram for materials without significant elastic section *(Russian)* 78−13923
superplasticity, mechanism rel. to hyperfine grain struct. 78−84930
superstructure, interaction between superdislocations of opposite signs gliding in parallel planes *(Russian)* 77−80506
Taylor model description of plastic deform. in polycrystals 79−90720
Taylor problem soln. for {111} <110> or {110} <111> 79−90663
teflon, microslip, effect of friction 77−77588
tetramethyl-p-silphenylenesiloxane-dimethylsiloxane block copolymer films, deformation 79−15739
thermal and thermoelastic fields around moving dislocations *(Russian)* 78−22731
thermal creep slip problem, rel. profiles, collision freq. effects 77−3738
thermoelectric materials, extruded materials with tetradymite struct., primary and in situ recrystn., elec. props. 79−43266
tilt grain boundaries, stress-induced migration in cubic crysts. 80−44252
transient sliding motion under idealized dry friction, earthquake faulting appl. 78−34093
transition metal refractory materials, slip and microhardness 78−3211
triglycine fluoberyllate, deuterated, dislocation line defect X-ray topographic analysis 80−59465
twinning and linear compressibility anisotropy under hydrostatic press. 78−51553
two phase alloy hardening by second phase particle coalescence 80−7591
two phase polycrystals, grain size stability and switching, dislocation climb and glide, computer model 78−75715
two-phase flow, frictional energy dissipation, appl. to nuclear fuel assemblies *(Japanese)* 77−55074
Udimet 520, γ' distribution in slip plane, dislocation loop form. during creep *(Japanese)* 79−42075
unilateral interface, elastic wave interactions, frictional slip effects 79−94542
α-W_2C, polycryst., plastic behaviour at ambient temp. *(French)* 79−1435
web dendrites, dislocations, stacking faults, X-ray topographic study *(Chinese)* 80−88148
slip continued
wedge shaped notches with large flank angles, plane strain general yielding under loads and bending 79−18808
wedge shaped object, elasticity theory 80−38294
work hardening, indentation hardness to yield stress ratio glide processes 77−40426
yielding on inclined slip planes at crack tip 77−42781
Zircaloy, micrograin superplasticity at 850°C 78−23758
Zircaloy, textured, interactive creep and growth, upper-bound evaluation 80−89293
Zircaloy-2, anisotropic irradiation creep 79−8333
Ag, (211)[$\bar{1}$11] single crysts., shear band effects on rolling deformation 80−50651
Ag, deformed at room temp., glide on {001} planes, TEM obs. 79−19257
Ag, dislocation dynamics during strain rate changes *(German)* 78−18655
Ag, dislocations gliding on (001) planes, bright field and weak-beam images 80−107266
Ag, FCC, dislocations, elastic instability 79−82235
Ag, FCC crystal, stress-strain curve, stage I to stage II transition *(Japanese)* 78−19834
Ag FCC crystals, compressively activated slip, theoretical latent hardening 80−65128
Ag, filament produced by glass coated melt spinning, mech. props. 77−86125
Ag halide crysts., dislocations, survey of post-war research 80−62449
Ag single crystal, dislocation dynamics during stress rate changes 78−19813
Ag, stacking fault energy meas. by tensile deform. of polycrystalline samples 78−95060
Ag, yield point, temp. depend., 2 to 300K *(Russian)* 80−45346
Ag-Mg (18.5 wt.%), rheological study of crystallographic order on creep *(French)* 80−97548
AgCl bicrystal, grain boundary slip simulation 78−3176
AgCl, temp. fields during plastic deform., cholesteric liq. cryst. technique 79−82278
AgMg, B2 intermediate phase, slip system, ordering energy and atomic size ratio depend. 80−59471
AgMg, deform. at high temp., yield pts. 79−61674
AgMg single crystals, orientation and temp. depend. of slip 78−87682
AgZn, B2 intermediate phase, slip system, ordering energy and atomic size ratio depend. 80−59471
Al alloy, slip deformation and low-cycle fatigue damage 77−73301
Al alloy, type 2024-T3, fatigue deformation and crack growth, holographic study 80−25836
Al alloy 7075, modified, fatigue and failure mechanisms 79−100252
Al alloys, fracture, grain size effect 78−60781
Al, alternating bending of single crysts., shear strain accumulation and microstrain distrib. *(Russian)* 78−60706
Al and Al alloy 5022, plastic anisotropy of textured sheet *(Japanese)* 79−34103
Al, bicrystal, ⟨100⟩ oriented, plastic deform. 78−19812
Al, bicrystal, fatigue crack initiation, crystal boundary effects *(Japanese)* 78−92328
Al, bicrystal, fatigue crack initiation along crystal boundaries *(Japanese)* 79−70163
Al bicrystal, plastically deformed, slip heterogeneities 80−79858
Al bicrystal, tensile and creep deform. obs. by holographic interferometry *(Japanese)* 77−56197
Al, bicrystal having Σ7 and Σ21 coincidence tilt boundary, plastic deform. *(Japanese)* 79−66116
Al bicrystals, fatigue crack initiation, cryst. boundary effect 80−55537
Al bicrystals, isoaxial, fatigue crack initiation in grain boundary affected regions *(Japanese)* 80−89338
Al, cold rolled, X-ray diffr. and optical microscope exam. of fatigue damage *(Japanese)* 78−84976
Al, crit. resolved shear stress, orientation depend. 80−21001
Al crystal, lattice rotation during tensile deform., X-ray diffr. meas. 80−49231
Al, deformation enhanced photoemission meas. 77−32511
Al, deformed in tension, elec. cond. changes at 78 and 283K, grain boundary effect *(Japanese)* 80−30029
Al, deformed in uniaxial and equibiaxial tension, dislocation arrangements 80−108516
Al, exoelectron photoemission enhanced by slip steps, plasmon reson. theory 78−15300
Al FCC crystals, compressively activated slip, theoretical latent hardening 80−65128
Al, fatigue crack initiation, pre-existing subgrain effect 80−97565
Al, flow mechanism in cutting, crystal orientation effects in single crystal 79−100300
Al, initial stages of plastic deform. *(Japanese)* 80−93618
Al, internal friction, dislocation glide and jog climbing *(French)* 78−11261
Al, internal friction at medium temps. *(French)* 78−39826
Al, laser pulse damage at 10.6 μm, single cryst. target in vac. 77−50706
Al, load relaxation, plastic deform. theory and plastic eqn. of state 78−27554
Al, oriented single crystal, plastic deform. *(Japanese)* 79−43336
Al, plastic deform. and prominent cross slip ⟨100⟩ oriented single crystal 78−19851
Al, plastic deform. of poly- and single-crystals, AE study 79−24579
Al, plastic deformation and prominent cross slip in ⟨100⟩ oriented single crysts. *(Japanese)* 77−8889
Al, plastically deformed single crystal, X-ray diffr. by defects 77−68976
Al, plastically deforming at high strain rates, distrib. of temp., strain rate and strain 79−19311
Al polycrystalline, exoelectron emission under tensile deform. and fracture *(Japanese)* 77−55870
Al, polycrystalline, fatigue damage detection by exoelectron emission meas. *(Japanese)* 77−55871
Al, prismatic displacement rings, plane normals determ. *(German)* 77−86118
Al, recrystallisation nuclei form. and well defined deform. band struct. 79−20136
Al single cryst., latent hardening in tension 80−60878
Al single crystal, Bauschinger effect, orientation depend. 77−21237
Al single crystal, high purity, unusual slip systems 78−47387
Al single crystals, ⟨100⟩ oriented, deform. temp. effect on stage IV deform. *(Japanese)* 80−66587

slip continued
Al single crystals, crystal orientation effect on their cutting mechanism 79−34193
Al single crystals, relation between axial orientation rotating and deform. banding 80−104206
Al, stationary creep in HVEM, cell struct. evolution 80−104242
Al, strained, localised corrosion on slip steps 79−20265
Al, surface strengthening of single crysts. on coating with evaporated films 77−8972
Al, tensile deformed single crystal, form. of recrystallisation textures 77−12647
Al, transient creep, effect of pre-torsional deform., dislocation glide and density 77−4147
Al, work of C. Crussard 80−62443
Al/Cu laminates, vapour deposited, strength enhancement 79−24576
Al-Ag (7.27 wt.%), peculiarities exhibited during fatigue loading *(Chinese)* 80−71723
Al-Ag alloys, critical resolved shear stress 80−49296
Al-Cu, Bauschinger effect 79−61646
Al-Cu, effect of alloy purity and ageing on fracture mechanism, and resultant toughness 79−5049
Al-Cu, single and two phase, superplastic behaviour 80−11709
Al-Cu (4 wt.%), precipitation hardened and fatigued alloys, solute loss at fracture surface, EPMA exam. 78−39893
Al-Cu (4 wt.%), supersaturated and aged conditions, high strain deform. 80−60907
Al-Cu-Mg-(Ag), effect of addition on fatigue microstructure relationships 80−40483
Al-Cu-Zr (6, 0.3 wt.%), superplastic, texture studies 79−83210
Al-Cu-Zr (6, 0.3 wt.%), superplastic, mech. anisotropy and deformation mechanisms 79−83254
Al-Cu(Zn-Mg), age hardening, conditions leading to localised plastic deform. and fracture in slip bands during fatigue 78−64670
Al-Ge (2 wt.%), averaged, plastic flow mechanism 77−48507
Al-Ge (2 wt.%), quenched and aged, deform. slip line obs. 78−51544
Al-Mg, creep behaviour in broad stress interval at 623K 80−30044
Al-Mg, discontinuous deform. under various conditions 77−63716
Al-Mg (0.3 wt.%) single cryst., dislocations obs. by high voltage electron microsc. 80−79796
Al-Mg (2 wt.%), exam. of Harper-Dorn creep 79−5026
Al-Mg (2 wt.%) subgrain formation at low stresses 78−84928
Al-Mg (2.2 at.%), creep at 573K 79−20145
Al-Mg (5.5 at.%), applied stress change effect in creep *(Czech)* 79−70126
Al-Mg single crystal, fatigue deform. 79−91747
Al-Mg-Si alloys, effects of dispersoids upon micromechanism of crack propagation 79−83286
Al-Mg-Si-Mn foil, planar defect spacing meas. by TEM 78−2135
Al-Mg-(Ag), effect of addition on fatigue microstructure relationships 80−40483
Al-SiO_2 interface, stress and microstruct. via TEM 78−26797
Al-Zn (6.5 at.%), fatigue props., effect of ageing and thermomech. treatment 78−27620
Al-Zn solid soln., controlling creep mechanisms, role of diffusion 78−31469
Al-Zn solid soln., controlling creep mechanisms role of diffusion 78−31470
Al-Zn-Mg, duplex ageing effect on tensile props. 79−91721
Al-Zn-Mg, fatigue crack propag., stage I 77−36653
Al-Zn-Mg, fractographic stage I fatigue facets 77−16680
Al-Zn-Mg (3,1.5 wt.%), precipitation hardened and fatigued alloys, solute loss at fracture surface, EPMA exam. 78−39893
Al-Zn-Mg (3.87, 1.79 wt.%), oriented growth of precipitates on dislocations, TEM obs. 80−108447
Al-Zn-Mg (6, 2.5 wt.%) alloy, ledge formation due to reaction with grain boundaries 79−57089
Al-Zn-Mg (9, 1 wt.%), superplastic flow, relative motion of grains 77−52426
Al-Zn-Mg-Cu, age hardened, effect of strain rate, temp. and environment on ductility 80−45368
Al-Zn-Mg-Cu type 7XXX, Cu effect and recrystallisation, low cycle corrosion fatigue 79−91852
Al-Zn-Mg-(Zr), low cycle fatigue, grain refinement effect 77−44345
Al-Zn-Mg-(Zr) alloy, microstruct. effect on fatigue crack growth 80−3164
Al-Zn-(Mg), age hardenable single crystal, fatigue and fatigue cracks *(German)* 77−16689
$Al_2Be_3(Si_6O_{18})$, beryl single crysts., dislocations obs., X-ray topography *(French)* 79−37709
AlCu-NiCo (5 at.%), θ′ hardened, creep mechanism 80−85013
Al_2O_3, alumina, deformed by prismatic slip, HV TEM obs. of dislocations 80−108517
Al_2O_3, fine grained, basal slip and nonaccommodated grain boundary sliding 80−60916
Al_2O_3, polycrystalline, slip band form. under fatigue stress, Schmid factor effect *(Korean)* 78−44199
α-Al_2O_3:Cr^{3+}(Ti^{3+})(Ti^{4+}), solid soln. hardening, yield stress conc. depend. 77−28823
Al_2O_3.Si kyanite, dislocation dissociation 77−76412
As, rhombohedral crystals, slip dislocations and slip systems 79−23617
AuCu II plates, growth mechanism 79−56976
AuMg, B2 intermediate phase, slip system, ordering energy and atomic size ratio depend. 80−59471
Be bronze BrB2, quenched deformed, substruct. and props., effect of prerecrystallisation annealing *(Russian)* 78−60677
Be, plastic strain mech., effect of impurities *(Russian)* 79−34101
Be, polycryst., yield strength, struct. factors effects 77−63749
Bi, crit. resolved shear stress of two slip systems, compression tests, 77-538K 80−59470
Bi, deformed cryst., phonon scatt. by lattice defects, thermal cond. calc. 78−22802
Bi, low temp. plasticity, temp. effect on strain hardening, slip *(Russian)* 77−31713
Bi, rhombohedral crystals, slip dislocations and slip systems 79−23617
Bi, strain hardening curve correlation with slip band nucleation stress spectra 80−70217
Bi, thermal cond. under plastic deform., phonon scatt. by dislocations and twin boundaries 77−11746
β-brass, nonisoaxial bicrystal, simultaneous hardening and softening 77−36606
$CaCO_3$, plastic deformation in compression parallel to (111) 78−38709

slip continued
$CaMg(CO_3)_2$, dolomite, partial dislocations and stacking faults obs. 78−3761
$Ca_5(PO_4)_3F$, dislocation struct. exam. *(Russian)* 78−63770
Cd crystals, X-ray topographic examination of basal dislocations during microplastic deformation 80−88156
Cd, dislocation internal friction, orientation depend., for single crysts. 78−52882
Cd, hardening resulting from pyramidal glide 77−48495
Cd, single crysts., plasticity study during deformation by twisting *(Russian)* 80−93597
Cd-Mg single crystals, exam. of critical resolved shear stress from 77 to 300K *(Czech)* 79−91741
Cd-Zn (up to 1.57 at.%), single cryst., precip. hardening, 77-300K 78−60675
Cd-Zn single crystal, plasticity, 4 to 50K 79−43362
$Cd_xHg_{1-x}Te$, determ. of slip planes by dislocation etching 79−82220
$Cd_xHg_{1-x}Te$, dislocation motion, effect of lattice defects on microhardness *(Russian)* 80−70220
$Cd_xHg_{1-x}Te$, thermally activated slip, microhardness temp. depend. *(Russian)* 78−34567
CdS, characts. of interaction of light with dislocations 78−2137
CdS, deformed, dislocation struct., TEM obs. 80−54250
CdS, dislocation charges determ. 78−2136
CdS, exciton optical and luminescence spectra characts. near dislocation slip bands 80−45111
CdS, plastically deformed cryst. with dislocation slip band, residual cond. 80−6839
CdSe, plastically deformed, luminescence line 0.96 eV 78−10950
CdTe, aB glide dislocations, dissociated into two Shockley partials, stacking fault energy 78−43024
Co base alloy, FCC, twin-slip interaction 77−51379
Co, glide ahead of terminating {10$\bar{1}$2} twins 80−96545
Co, single crystal, cavitation erosion, role of twinning 80−107272
Co, single crysts., {11$\bar{2}$1} twins, accommodation and form. 80−96540
Co-Fe alloys, transformation induced microstructs. extended total dislocations, TEM study 79−42073
Co-Ni (33 wt.%), FCC deform. twinning kinetics, relationship to stress-strain behaviour 78−52887
Co-Ni alloy, slip charact., and fatigue, FCC twinning and FCC to HCP martensite transform. effect 80−35182
$(Co_{1-x}Ni_x)O$, single crysts., morphology change during compressive creep testing 79−29144
CoO, polycrystalline, high temp. deform. 78−3174
CoO single crystal, compressive creep morphology 77−56034
CsCl type intermetallic compounds, correlation between dislocation character and operative slip system 79−10852
CsCl-type lattice, {111} superlattice screw dislocation motion, computer simulation 80−79793
CsI crystals, relation of struct. and bond type to slip geometry 80−88165
CsI, crysts., microplasticity mechanism 78−30696
Cu, ⟨100⟩ oriented single crystal plastic deform. and prominent cross slip 78−19852
Cu alloys, jog formation and glide on dissociated dislocations, direct obs. 77−68977
Cu and Cu-Al (8 wt.%) single crystal, surface dissolution effect on fatigue damage and crack nucleation 78−39936
Cu and Cu-Al alloys, effect of grain size, specimen thickness, on mech. props. 78−84945
Cu bicrystals, grain boundary sliding and intergranular fracture studies 78−75717
Cu, cold-rolled, microstruct. 79−83216
Cu, crack nucleation and stage I propag. in high strain fatigue, microscopic and interferometric obs. 78−52936
Cu, crack nucleation and stage I propag. in high strain fatigue, mechanism 78−52937
Cu, cracks in earlier stages of fatigue, fractography *(Japanese)* 77−8924
Cu, cross-slip at low stresses 77−11564
Cu, cyclically deformed, nucleation of persistent slip bands 78−72830
Cu, deform. of ⟨100⟩ single crystal *(Japanese)* 77−59864
Cu, deformation band, role in fatigue crack nucleation and propag. 79−24585
Cu, deformed at room temp., glide on {001} planes, TEM obs. 79−19257
Cu, dimple spacing on intergranular creep fracture surfaces with slip band spacing 80−76345
Cu, dislocations gliding on (001) planes, bright field and weak-beam images 80−107266
Cu, dispersion hardened, mobile dislocation density and length of slip lines 77−51387
Cu, ductile fatigue crack growth mechanism in single crystals, in situ SEM obs. 79−61695
Cu, FCC, dislocations, elastic instability 79−82235
Cu FCC crystal, stress-strain curve, stage I to stage II transition *(Japanese)* 78−19834
Cu, fatigue of single crystals and low const. plastic strain amplitude 79−20174
Cu, fatigued specimens, 'etch pit slip', SEM obs. 79−100258
Cu, flow stress of single crysts., strain rate sensitivity analysis 77−16645
Cu free electrolytic films, tensile creep for various film thicknesses calcs. *(Russian)* 80−11697
Cu, grain boundary character, revealed by etching and slip line continuity 79−33001
Cu, layered cell structures and slip lines in deformed cryst., TEM obs. 79−99209
Cu, mechanical twinning in (110)[$\bar{1}$12] single crystal under plane strain compression *(German)* 77−36616
Cu, near Σ9 grain boundary properties, boundary dissociation 80−100251
Cu, neutron irrad. cryst., slip band, growth rate, high-speed cinematographic recording 79−7607
Cu, plastic deformation, steady state, transients due to strain rate changes 77−81302
Cu plates, thin, dislocation-dislocation interaction inducing cross-slip, X-ray topographic anal. 80−49233
Cu polycrystal, fatigued, interior dislocation struct. 80−88147
Cu, polycrystalline, friction stress meas. during high temp. creep 79−1898

slip continued
Cu, polycrystalline, intracrystalline slip bands in high temp. creep, comparison with brass single crystal *(Czech)* 79−77604
Cu, pure, cross-slipping, stress orientation depend. 79−95022
Cu single cryst., latent hardening in tension 80−60878
Cu single crystal, stored energy meas. by new deform. calorimetry method 78−39834
Cu single crystals, neutron irradiated, secondary slip 80−88161
Cu, single crystals, neutron irradiated, stresses and secondary slip between overlapping and dislocation arrays 80−88162
Cu single crystals oriented along [100] and [111], exam. of slip line length 78−76664
Cu, single crysts., deformed in [001] and [111] axes, cell structs., TEM 80−70209
Cu single crysts., rel. to Bordoni peak, 10.2 and 30.6 MHz 80−66566
Cu, soft crystal, US irrad. induced dislocation distrib. 77−32584
Cu, strain hardening parameters, 4.2 to 300K *(Russian)* 79−20063
Cu, tensile deformed ⟨110⟩ orientated single cryst., recrystn., high voltage electron microscopy study 80−84958
β-Cu Zn, cross slip 78−26576
Cu-Al, faulted dipoles, geometry and form. 78−59809
α-Cu-Al, single crystal, low cycle fatigue 79−43405
α-Cu-Al (0.5 to 10 at.%), latent hardening and dislocation density 78−19853
Cu-Al (10, 16 at.%), influence of jogs on extension of dislocation nodes 80−84176
Cu-Al (10 at.%), single crystal, orientation depend. of work hardening near [111] axis 77−12646
Cu-Al (10 at.%) alloy, dislocation glide source, TEM obs. 77−19958
Cu-Al (10 at.%) alloy, work hardening at high temp. 77−32589
Cu-Al (10.5 at.%), dislocation generation and displacement in single crystal in bending 79−60368
Cu-Al (11 at.%) single cryst., dislocation reactions during deform. twinning 80−79795
Cu-Al (13 wt.%), polycrystn. rod specimens effect of diameter on slip mode, optical microscopy obs. 79−79051
Cu-Al (15 at.%), FCC, dislocations, elastic instability 79−82235
Cu-Al (15 at.%), single crystal, steady state deform. with ⟨001⟩ axis at high temp. *(Japanese)* 78−6980
Cu-Al (15 wt.%) single crystal, steady state deform. at high temps. *(Japanese)* 78−19833
Cu-Al (2.5 at.%), single crystal, steady state deform. at high temps. *(Japanese)* 77−52415
Cu-Al (5 wt.%), subjected to tension-compression fatigue, deform. and fracture strength *(Japanese)* 80−93644
Cu-Al (5.8 at.%) dislocation multipoles, weak-beam electron microscope obs. 79−73171
Cu-Al (7.5 at.%), single crystal, etched under load, slip bands 77−89446
Cu-Al (8 at.%), coplanar slip, related with specimen size and axis *(Japanese)* 78−34518
Cu-Al (<3 at.%), new type of discontinuous slip at low temps. 77−12676
Cu-Al alloy, low temp. deform., heating of dislocation sources 78−18660
Cu-Al alloys, strain hardening parameters, conc. and temp. depend., 4.2 to 300K *(Russian)* 79−20063
Cu-$Al_2O_3(SiO_2)(TiO_2)$ alloys, internally oxidised, plastically deformed, influence of particle form on primary loop nature *(French)* 80−103344
Cu-Al(Si), single crysts., latent hardening study by meas. of flow stress on secondary systems *(Japanese)* 79−24538
Cu-Al(8 at.%), single crystal, twinning deform. 77−21236
Cu-Bi (0.02 wt.%) alloy, intergranular fracture, Kossel X-ray diffrs. in SEM obs. 80−108579
Cu-Co, age hardenable single crystal., fatigue and fatigue cracks *(German)* 77−16689
Cu-Cr-SiO_2 system, age and dispersion strengthened, dislocation struct. around SiO_2 particles 80−108468
Cu-Cr(-SiO_2), single crysts., yield and pre-yield behaviour rel. to aging time 80−81103
Cu-Fe, single crystal with coherent γ-Fe particles, precipitation hardening 78−31416
Cu-Ge, primary coplanar slip, role in deform. of FCC crystals *(Japanese)* 77−52412
Cu-Ge (0.44 to 7.3 wt.%), concentrated single crystal, yield region investigation, CRSS, slip 77−48478
Cu-Ge (1 at.%), FCC crystal, stress-strain curve, stage I to stage II transition *(Japanese)* 78−19834
Cu-Ge(Zn), conc. single crystal, yield region investigation, flow stress and obstacle charact. 78−3173
Cu-Ni, Ni atom cluster break up, slip band formation, point defect motion 79−57096
Cu-Ni-Al (5, 2.5 at.%), precip. hardening *(Japanese)* 80−71663
Cu-Ni-Fe, age hardenable, dislocation interactions with internal coherency stresses 77−36528
Cu-Sb solid solution, dil., FCC, intergranular solid shortness mechanism *(Russian)* 79−5032
Cu-Si, stacking fault energy meas. by tensile deform. of polycrystalline samples 78−95060
Cu-Si (6.5 at.%) alloy, easy glide deform., obs. and mechanism 77−8887
Cu-Si (7 at.%), influence of jogs on extension of dislocation nodes 80−84176
Cu-SiO_2, in-situ deform. in HVEM 80−103338
Cu-SiO_2, low-temp. recovery creep, Orowan loop accumulation 80−81126
Cu-Zn, rheological study of crystallographic order on creep *(French)* 80−97548
Cu-Zn (30 wt.%), slip band growth, thermally activated 80−40457
α-Cu-Zn-Al (18, 7 at.%), deform. and mech. props. 79−29159
β-Cu-Zn(-Ni)(-Mn), order-disorder transformation temperature effect on quench hardening 78−95745
α-Cu-Zn(Al), solid soln., intermediate temp. embrittlement *(Japanese)* 79−20158
α-Cu-Zn(Al) fracture behaviour, effect of deform. temp. and alloying content *(Japanese)* 79−20159
Cu-Zr amorphous alloys, mech. props. *(Japanese)* 77−86179
CuAu-type superstructure, interaction of reacting dislocations *(Russian)* 78−83814
Cu_3Au, dislocation slip band mobility, critical stress 80−2032
Cu_3Au, disordered [001]-orientated single crysts., plastic deform., TEM and slip line studies 80−97541
Cu_3Au, ordered and disordered, cavitation induced erosion 77−16743
Cu_2MnAl, Heusler alloy, single crystal, plastic deform. 77−44308

slip continued
β(CuNi)Zn alloys, effect of normal stress on {112}⟨111⟩ slip 79−47760
β-(CuNi)Zn, anomalous strengthening 77−48503
β-(CuNi)Zn, cross slip 78−26576
Cu_2NiZn, characterisation of superlattice dislocations by TEM 79−55748
Cu_2O polycrystalline and single cryst. mech. behaviour 78−95777
Cu_2O, slip systems, Kroop hardness anisotropy meas. 77−31714
Cu_2O, thermal activation of plastic deform. *(French)* 80−16394
$Cu_2S(Te)$, microstructure, work hardening in polymorphic transform. and subsequent annealing effect 79−52199
Cu_2Te, microstructure, work hardening in polymorphic transform. and subsequent annealing effect 79−52199
β-CuZn, yield stress and operative slip systems, orientation depend. 77−48498
β-Cu(ZnMn), slip geometry, anomalous strengthening 78−10056
EuS, defect struct., etch pitting and electron microscopic obs. 79−27989
α-Fe, $(\bar{1}\bar{1}2)$ $[\bar{1}\bar{1}\bar{1}]$ anti-twinning slip system, low temp. strengthening, dislocation struct. 77−21164
Fe, [110] and [410] single crysts., push-pull fatigue 79−74257
Fe, Armco, crack and slip band form. during US fatigue 78−56723
Fe, Armco, cumulative fatigue damage at US freqs., thermal activation 77−70181
Fe, Armco, fatigue cracking under 23 kHz loading at 23°, 60° and 100°C 78−60763
α-Fe, crack initiation study at low-cycle fatigue using slip bands *(Slovak)* 79−38949
α-Fe, deformation induced intergranular creep cavitation 78−31473
Fe, deformed, dislocation structure determ. from magnetic props. 78−55874
Fe, effect of atm. corrosion on fatigue crack nucleation and fracture surface morphology, in air and vacuum *(Japanese)* 79−8387
α-Fe film, deform. in electron microscope, dislocation mechanism 79−82227
Fe, H_2, induced cracking, crystallographic and fractographic studies 79−5052
Fe, high purity single crysts., thermally activated slip deformation between 4.2 and 300K 80−25801
Fe, influence of H on slip process *(French)* 78−6965
Fe, microcracks formed by H_2 precipitation, SEM and TEM obs. *(Japanese)* 79−70071
Fe microcrystals, dislocation struct. singularities in early deform. stage *(Russian)* 77−55284
Fe, model for Luders band formation and plastic instability related with strain softening due to Johnston-Gilman-Hahn theory 79−61676
Fe, Ni-plated, surface film softening in single slip orientation 77−32719
Fe, plastic deform. and fracture, H_2 effect, studied by electron microscopy and Auger spectrography *(French)* 77−77545
Fe, plastic deform. of single crystal with shear tests in {110}⟨111⟩ and {112}⟨111⟩ slip system 77−48509
Fe, plastically deformed, dislocation arrangement exam. by ferromag. techniques 78−63774
Fe, pure, mech. props. at low temps. 78−44219
Fe single crystals, size effect on slip deformation ability at very low temps. 80−21049
Fe, single crystals, work hardening and behaviour and dislocation struct. during simple shear tests 78−95762
α-Fe, slip, rel. to screw dislocation core struct. in BCC lattice 79−82211
Fe, slip-initiation phenomenon by fatigue, appl. to stress meas. 80−45342
Fe, thermally activated slip deformation, 0.7 to 77K 79−91755
α-Fe whiskers, pure, ductile fracture initiation, macroscopic obs. of deform. history and failure 80−85043
Fe-Al, single crystals, deform. at high temps. 80−81125
Fe-Cr-Co, ductile magnet alloys, mech. props. 80−85001
Fe-Cr-Ni (18, 14 wt.%), single strain induced γ to α′ cryst. transform. *(Japanese)* 78−11221
Fe-Cr-Ni (25, 20 wt.%), single crystal, stress corrosion cracking 78−35553
Fe-Mn-C, austenitic, strain induced γ to ε transform., active slip systems 77−48427
Fe-Mn-C (0.7, 0.9 wt.%), pearlitic, deform. 77−86095
Fe-Mo (1.8 at.%), high temp. creep mech., use of stress exponent 79−5025
Fe-Mo(4.1 wt.%), steady state creep at high temps. 80−89316
Fe-N, single cryst., solid soln. softening, effect of interstitial N 80−97496
Fe-Ni, reversibility of crystal orientation in reverse martensitic transformation 79−83199
Fe-Ni, slip and twinning, SEM and optical obs. 79−71209
Fe-Ni (31%) alloy, deformed by slip, misaligned zones in $\{259\}_A$-martensite crysts. *(Russian)* 77−59850
Fe-Ni single crystals, stress induced martensite 77−8827
Fe-Ni-C, HVEM study of strain induced martensite 79−20047
Fe-Ni-C (26.4, 0.24 wt.%) martensite, partially twinned, slip lines obs. 78−84913
Fe-Ni-C alloys, obs. of banded struct. formed by deformation 79−79050
Fe-Ni-C austenitic single crysts., deform. props., martensitic transformation, SEM study 79−29143
Fe-Ni-Cr based alloy, KhN35VTYu, temp. depend. of energy of fracture, influence of γ′ phase *(Russian)* 80−81147
Fe-Ni-V-C alloy, reverse α to γ transformation, previous deformation influence on struct. and props. *(Russian)* 79−100139
Fe-Si, dynamically strained, temp. depend. of twinning charact. *(Russian)* 79−46673
Fe-Si, fatigue fracture fractography in broad strain-amplitude range, in air and vacuum 80−81186
Fe-Si, H_2, induced cracking, crystallographic and fractographic studies 79−5052
Fe-Si (2.4 wt.%), ductile fatigue crack growth mechanism in single crystals, in situ SEM obs. 79−61695
Fe-Si (3 at%), deformation and electron bombardment, influence on dislocation struct., 20-500°C *(Russian)* 80−92536
Fe-Si (3 wt.%), breaking stress grain size and grain boundary energy during onset of reversible temper brittleness *(Russian)* 77−32673
Fe-Si (3 wt.%), degeneration of slip on (211) planes *(Russian)* 78−80587
Fe-Si (3 wt.%), electron irradiated, yield strength and elongation 80−76325

slip continued
Fe-Si (3 wt.%), exam. of plastic deformation, slip band dislocation, under hydrostatic pressure 78−56695
Fe-Si (3 wt.%), single crystals, cyclic deformation oriented for single glide 79−100224
Fe-Si (3 wt.%), singularities in geometry of slip, point temp. depend. *(Russian)* 79−24574
Fe-Si (3.5 wt.%) plastic deform., slip initiation, X-ray topography study 79−47750
Fe-Si alloy, deformed by slip, polygonal boundary form. *(Russian)* 79−24534
Fe-Si(3.25 wt.%), crack nucleation depend. on twins during intense slip *(Russian)* 79−100239
Fe_3-Al, solid soln., rheological study of crystallographic order on creep *(French)* 80−97548
FeAl single crystal, compressed, dislocation arrangement 78−14354
Fe_3Al, roll magnetic anisotropy and dislocations *(Japanese)* 77−80930
Fe_3Al, slip geometry and pseudoelastic behaviour, effect of crystal orientation *(French)* 78−87681
$Fe_{40}Ni_{40}P_{14}B_6$, amorphous ribbon, cold rolling, annealing mag. props. 77−8958
FeS_2 (pyrite), glide elements study by electron microscopy and electron diffr. 78−83817
Fe_3Si, etching of slip produced antiphase domain boundaries 78−63769
$Ga_{1-x}Al_xAs$ epitaxial layers, spectroscopic technique for imaging spatial distrib. of nonradiative defects 78−23498
$Ga_xAl_{1-x}As$-GaAs DH laser, degraded, nature of ⟨110⟩ dark-line defects, TEM 77−89439
GaAs crystal growth, thermal and elastic const. evaluation 80−92586
GaAs, during deformation, acoustic emission rel. to cracks, dislocations 80−35441
GaAs laser material, secondary dislocation climb during optical excitation 78−75672
GaAs, pulled, dislocation generation, thermoelastic anal. 80−79787
GaAs-(GaAl)As, DH laser, injection enhanced dislocation glide under uniaxial stress 77−27885
GaAs-AlGaAs double heterostructure, optically induced dislocation glide, cooperative phenomena 78−74911
GaAs-$Ga_{1-x}Al_xAs$, DH, dark line defects induced by mech. bending 77−683
GaAs-GaAlAs DH lasers, optical studies of defects and degradation 78−18654
GaAs-GaAlAs DH material, dislocation glide and climb, electron diffr. 78−83824
GaAs$Ga_{1-x}Al_xAs$ DH laser material, rapid optical degradation obs. 77−75528
GaAsP epitaxial film, TEM obs. of misfit dislocation arrays, nucleation and multiplication 77−39742
GaP, birefringence observations of strain and plastic deform. 80−50678
GaP, crystal, growth conditions rel. to dislocation struct. 80−88151
GaP crystal, structure defect formation due to annealing and stress, dendrites, slip, dislocations 80−29026
Ge, cross-slip of single dissociated screw disclocations, double etching and X-ray topography studies 80−15104
Ge, dislocation mobility 77−76413
Ge, doubly deformed, dislocation interaction obs. 79−73172
Ge epitaxial layers, on GaAs substrate, misfit dislocation multiplication mechanism 78−87673
Ge monocrystal, dynamic interaction of screw dislocations with flat clusters of dislocations on other slip planes *(Russian)* 79−86800
Ge, screw dislocation loops, shrinkage vel. and cross slip freq., activation energies *(German)* 78−43028
Hg, rhombohedral crystals, slip dislocations and slip systems 79−23617
In, dislocation obs. by X-ray topography *(French)* 79−46661
InBi single crystal, deform. mode under dynamic indentation 80−88163
InP, damage induced during handling for TEM obs. 80−2024
InP, microstructs. assoc. with hardness indentations 78−80627
InP, plastic deform. and scratch microhardness meas. 78−27583
InP single crystals, uniaxial compression deform. characts. 80−84991
InP/$In_{1-x}Ga_xAs_yP_{1-y}$ heterostruct., optically induced degradation 79−86791
InSb, asymmetrical behaviour of 60° dislocation glide 79−7611
InSb, asymmetrical dislocation glide, expt. evidence for 79−82232
InSb, plastically bent single crysts., dislocation struct. obs. 78−59816
InSb, X-ray topographic evidence of asymmetrical pre-yield behaviour 80−75229
KBr, quench hardening related to dislocation density and slip 78−52855
KBr:divalent cations, minimum work-hardening rates in compression and shear 79−74175
KCl, cleaved slip step, Au surface decoration and depletion zone anal. 79−90868
KCl, cryst. isolated pore healing under press., dislocation struct. evolution *(Russian)* 80−100245
KCl:Sr, mechanical props. as function of dopant conc., dislocations 77−69027
KCl-KBr solid soln., highly conc., computer simulation of dislocation motion *(Japanese)* 77−68972
LiF bicrystal, high-angle tilt boundary and edge dislocation intersection effects 80−79836
LiF bicrystals, intergranular fracture due to single slip 78−34520
LiF crystal, plastically deformed, elec. field distrib. on surface meas. 77−31716
LiF crystals, relation of struct. and bond type to slip geometry 80−88165
LiF, crysts. containing rigid dislocation forest, mech. props. 79−99212
LiF, dislocation structure, influence of variable deform. temp. 80−70211
LiF, plasic deform., cleavage-crack propag., X-ray topography 77−39625
LiF, plastic strain accompanying local rise in surface temp., of natural shear *(Russian)* 80−6411
LiF, single crystal, dislocation generation, beneath static and rolling contact with sphere 78−87671
LiF single crystals, dislocation motion and generation on plate impact 79−95011
LiF single crystals, glide band sources, work hardening 80−34126
LiF, slip anisotropy under neutron irrad. and external stress, orientation of defects 77−31674
LiF, slip band steady-state expansion, dislocation vel. theory 77−24320
LiF, strain hardening curve correlation with slip band nucleation stress spectra 80−70217
LiF, stressed state and dynamics of dislocations near tip of fast growing crack 77−62541
slip continued
LiF:Mg, origin of dislocations *(Russian)* 77−15425
LiF:Mg, slip band struct. changes with temp. 78−47390
LiF(:Mg), shock waves in ⟨111⟩ direction, elastic precursor amplitudes 80−54314
Mg alloy MA12, thermally strengthened, fatigue cracking in air and vacuum *(Russian)* 78−35481
Mg crystal basal slip, anal. of pairwise dislocation interactions and contrib. to flow stress 78−35440
Mg, cyclic hardening of single crystal 78−64552
Mg, deformed single crysts., stacking faults and dislocation dissoc. 77−31681
Mg, dislocation internal friction, orientation depend., for single crysts. 78−52882
Mg, dislocation struct. after US deform. *(Russian)* 80−29027
Mg, pyramidal dislocation pair interactions contrib. to flow stress during slip 78−35441
Mg single crystal, anelastic internal stress field in easy glide region 78−48442
Mg-Ag(Cd), anisotropic, dislocation interaction with tetragonal impurity, mobility 77−19953
Mg-Al spinel, non-stoichiometric, climb dissociation of network dislocations 80−2031
Mg-Cd, single crysts., temp. depend. of crit. resolved shear stress *(Czech)* 80−29112
Mg-Mn-Ce, structural changes and deformation during superplastic flow 78−15472
Mg-Mn-Ce (1.5%, 0.3%) alloy, dislocation slip during superplastic deform. *(Russian)* 77−21214
Mg-Mn-Ce alloy, MA8, dislocations at grain boundaries and grain-boundary glide 78−64605
$MgAl_2O_4$, dislocations, sessile dissoc. 79−46663
$MgAl_2O_4$, microplasticity at room temp., dislocations, TEM study 80−19805
MgO bicrystal, fracture mechanism obs. 77−44339
MgO, compressive stress-strain behaviour at high temps. 80−25774
MgO, crack propagation during in-situ deform., plastic zone formation 80−16468
MgO, cryst. preliminary processing rel. to deform. curve parameters, slip line struct. 77−52421
MgO crysts., plastic deform. activation parameters, rel. between macroscopic and in-situ HVEM expts. 80−103355
MgO, fracture and crack tip plastic zones, in situ obs. 80−108686
MgO, lattice misorientation and displaced vol. for microhardness indentation 78−64617
MgO single cryst., impact wear characts. 80−76374
MgO, single cryst., tensile creep, stress induced dislocation structs. 80−96539
MgO single crystal, absorbed fluid effect on rolling contact deform. 78−64719
MgO single crystal, dislocation struct. of slip lines, TEM 79−27990
MgO, single crystals, compressed, SEM exam. of cathodoluminescence 78−56525
MgO, slip line struct. using replica electron microscope technique 79−7605
MgO:Li, mech. deformed crysts., imprinting of slip bands using Li impurities 80−59473
MgO:nAl_2O_3 spinel, plastic deformation at T<1000°C, slip systems 80−108505
MgO$(Al_2O_3)_n$ spinel, plastic deformation at 400°C 80−40453
MgO.1.1 Al_2O_3 spinel, high temp. deform., cryst. orientation effect 80−107263
Mg_2SiO_4, forsterite, decorated dislocations 80−54245
$MgZn_2$ Laves phase, deformation-mechanism maps 79−29150
$MgZn_2$, single cryst., yield strength 77−44318
Mn-Cu (25 wt.%) alloy, critical shear stresses of twinning and glide 79−87693
Mn-Cu alloy, plastic deform. mechanism and shape-memory effect, mag. struct. obs. *(Russian)* 78−60705
Mo alloys, intercryst. fracture in ductile-brittle transition region, local internal stresses effect 80−81200
Mo cold worked, dislocation struct. change during postdeform. at 493K 79−43271
Mo, dislocation structure, temp. depend., at crack tip, of fractured single cryst. 79−29210
Mo extinction length ζ_{200} meas., electron energy influence 80−90935
Mo, fatigue of single crystals, dislocation struct. and strain localisation *(Russian)* 80−71741
Mo film, deform. in electron microscope, dislocation mechanism 79−82227
Mo, plastic deform. by rolling at 293K, dislocation struct. *(Russian)* 77−48481
Mo, plastic deform. mechanism during hydrostatic extrusion *(Russian)* 77−8879
Mo, plastic deformation during rolling at 293K, crystallography of slip *(Russian)* 77−32588
Mo, powder specimens, fatigue and threshold behaviour under high cycle fatigue 80−40487
Mo, single and polycrysts., struct. change during work softening, HVEM 80−103336
Mo single crystal dislocation interactions during parallel shear in (011) plane *(French)* 78−43029
Mo single crysts., substruct. variation during fatigue, kinetics *(Russian)* 78−60742
Mo, slip geometry, HVEM straining 80−39207
Mo, strain localisation and fatigue, glide plane shearing stress 80−7683
Mo-W alloy, fatigue and threshold behaviour under high cycle fatigue 80−40487
Mo_2 single crysts., surface orientation effect as high temp. creep and fracture type 80−16403
NH_4Cl, order-disorder transition, slip bands 78−22848
NH_4Cl, order-disorder phase transform., effect of plastic deform. and electrooptic effect 79−33672
NH_4ClO_4:Cu^{2+}, dislocation etch pits exam., rel. to thermal decomp. 77−11555
NaCl, cross slip of screw dislocations during deform. at room temp. 77−84758
NaCl, damage process preceding semi-brittle fracture in depend. on deform. microcrack development 77−44272
NaCl, dislocation density in monocrystal deformed under high hydrostatic press. 80−70216

slip continued
NaCl, dislocation struct. of slip bands, hydrostatic press. effect 80−54249
NaCl, hydrostatically compressed crysts. in easy glide stage, plastic deformation 80−7630
NaCl, plastic deform., cleavage crack propag., X-ray topography 77−39625
NaCl, plastically deformed [001] orientated single crystal, glide props. and X-ray topography 77−21228
NaCl, plastically deformed [001] oriented single crystals, TEM 77−36579
NaCl, plastically deformed, glide on {111} planes 79−82234
NaCl, quench hardening related to dislocation density and slip 78−52855
NaCl, rock salt, quenched, residual stresses, optical study 80−55061
NaCl, single crystal, surface markings, left by unsteady cleavage crack propag. 79−46746
NaCl, single crystal, temp. anisotropy of plasticity and brittleness 78−3198
NaCl, strained in one glide system at 450°C, dislocation struct. 78−22728
NaCl, temp. fields during plastic deform., cholesteric liq. cryst. technique 79−82278
NaCl type crystal, dislocations due to high temp. stress relax. 78−2126
NaCl:Sr, mechanical props. as function of dopant conc., dislocations 77−69027
Na_2O-CaO glass, shear deform. under pyramidal indentations 80−84989
Na_xWO_3, hardness anisotropy, comp. depend. 79−29181
Nb, anomalous slip of single crystal, obs. 77−8900
Nb, catastrophic slip bands, fine struct. *(Russian)* 78−38718
Nb, deformation at 77-158K, slip and dislocation struct. 79−83277
Nb, dislocation-free single crystal, deformed at 180K, X-ray topographic obs. 79−24587
Nb, effect of electron irradiation on low temp. deform., tensile stress-strain curves 79−55784
Nb film, deform. in electron microscope, dislocation mechanism 79−82227
Nb, glissile dislocation interactions, TEM obs. 77−31666
Nb, local heating during abrupt strain, catastrophic slip band formation 80−7652
Nb, neutron bombarded, defect size distrib. influence on hardening *(Russian)* 80−10580
Nb single cryst., slip localisation during discontinuous plastic flow at 4.2K *(Russian)* 77−69029
Nb, single crystal, surface oxide softening, TEM obs. 77−40462
Nb, single crysts., plastic relaxation of internal stresses during mech. twinning at 4.2K, optical and SEM study *(Russian)* 79−66108
Nb, stress differential in surface oxide softening of single crystals 77−86116
Nb, surface oxide softening, anisotropy 78−60716
Nb-Mo alloy, single crysts. slip geometry on straining in tension *(Russian)* 77−66678
Nb-N (0.3 to 300 at. ppm), deform. 77−48477
Nb-O system, solid soln. hardening and softening 80−71665
NbB_2, single crysts., hardness anisotropy and slip 80−21085
NbC single cryst., Vickers microhardness, slip mechanism 80−71732
$NbC_{0.98}$ single crysts., rel. to creep, 1800-2700°C *(Russian)* 79−5005
NbC_x (x=0.868, 0.834, 0.766), single crysts., thermomech. behaviour during annealing 80−3104
β $NbH_{0.82}$, fracture, TEM obs. 80−108519
NbSn multifilamentary superconducting composites, micromechanics 79−38878
$(Ni,Co)_3Ge$, Co effect on temp. depend. of yield stress 78−31487
$(Ni,Co)_3Ge$, single cryst., Co effects on temp. depend. of yield stress 77−4812
Ni base superalloy, internal stresses due to dislocation walls around second phase particles 79−99210
Ni base superalloy, single crystal, apparent and effective creep parameters, incubation period 77−63715
Ni, creep, irrad. induced with 17 MeV deuterons 80−93607
Ni, deformed, coercivity and remanence anisotropy 78−31093
Ni, deformed, magnetic susceptibility anisotropic changes 78−27025
Ni, deformed, work-hardening, dislocation and mosaic struct., X-ray and electron microscopy 77−35625
Ni, deformed at room temp., glide on {001} planes, TEM obs. 79−19257
Ni, dislocation struct formed by C diffusion in single crystals, electron microscope obs. *(Japanese)* 78−10053
Ni, dislocations gliding on (001) planes, bright field and weak-beam images 80−107266
Ni, lattice defects, formation kinetics, work hardening and resistivity study *(Russian)* 80−10557
Ni, neutron irrad., slip bands, TEM and SEM obs. 78−51596
Ni plated Fe single crystal, deformed at 77K, surface obs. 78−19916
Ni single crystal foil, H_2 induced deform. during thinning, electron-optical obs. 79−57059
Ni, single crysts., strengthening, tested under compression at 293 and 77K *(German)* 80−50689
Ni, slip character, H effect 80−89287
Ni, structural changes, creep mechanism, multiple dislocation cross slip *(Russian)* 80−59476
Ni superalloy Mar-M200, slow fatigue crack propagation rate meas. using high freq. resonant technique 78−52983
Ni tensile-deformed single crystal glide step heights, latex sphere and SEM obs. *(German)* 77−59018
Ni, transient irrad.-induced creep under D bombardment, mechanism 78−80597
Ni, work hardening, grain size effects 77−16605
Ni/Ni_3Al-Ni_3Nb eutectic, directionally solidified, plastic deformation *(Russian)* 78−39843
Ni-Al, order hardening, comparison between revised theory and expt. 80−93565
Ni-Al, rheological study of crystallographic order on creep *(French)* 80−97548
Ni-Al_2O_3 alloy, electron beam evaporated, struct. and mech. props. 78−11114
Ni-Al-Cr, strain hardening, participation of various slip systems *(Russian)* 79−24536
Ni-Al-Cr-Co-Ti, Waspaloy, exam. of dislocation-precipitate interaction, cyclic stress-strain behaviour 78−84925

slip continued
Ni-base superalloy, ⟨111⟩ monocrystals under compression, inhomogeneous deformation 77−63736
Ni-Cr, movement and dislocations using SEM and diffr. contrast method *(Chinese)* 79−51110
Ni-Cr, partial dislocation, stacking fault TEM study *(Chinese)* 80−84174
Ni-Mo (14.4 wt.%) single crystals, ordered phase precipitates influence on deformation character, mechanical props. *(Russian)* 79−74155
Ni-Zn ferrites, polycrystalline, grain boundary slip *(Japanese)* 77−63764
Ni_2 (Al, Nb) single crystals, orientation and temp. depend. of yield stress 80−25791
γ'-Ni_3(Al,Ti), single crystal, dislocation movement, HVEM obs. *(Japanese)* 80−108503
Ni_3(Al,W), yield strength, temp. and orientation depend. 77−28857
Ni_3(Al,W), yield stress, orientation depend. 78−39830
Ni_3Al and Ni_3(Al,Ti), deformation characts., temp., strain rate and orientation depend. 77−44320
Ni_3Al, overshooting while testing in tension 78−44189
γ'-Ni_3Al-Fe (10 at.%) alloy, steady-state creep 78−15460
$Ni_3Al(\gamma')$-$Ni_3Nb(\delta)$, directionally solidified, deformation substruct. and slip systems 79−8326
$(Ni_xCo_{1-x})_3Ge$ single crysts., $L1_2$ struct., cross-slip 80−40459
Ni_2Cr, fine-domain ordered alloy, early deform. stages, dislocation struct. and motion *(Russian)* 77−81291
Ni_3Fe, dislocations, rate of piling up, rel. to average length of slip lines *(Russian)* 77−76416
Ni_3Fe, mono- and polycrysts., strain hardening, test temp. effects *(Russian)* 80−66531
Ni_3Fe, ordered and disordered states, strain hardening characts., temp. depend., multiple slip case *(Russian)* 78−15421
Ni_3Fe, polycrystalline alloy evolution of slip-line pattern during straining 80−107362
Ni_3Fe, roll magnetic anisotropy and dislocations *(Japanese)* 77−80930
Ni_3Fe, single crysts., long range order degree influence on strain hardening *(Russian)* 80−11660
Ni_3Fe, superlattice dislocations, compression induced mag. anisotropy 77−85442
Ni_3Fe, superlattice dislocations, compression induced mag. anisotropy 77−85443
$Ni_{0.33}Fe_{2.33}O_4$, {001} ⟨110⟩ glide system, room temp. TEM obs. 79−90660
Ni_3GA single crystals, anomalous temp. depend. of strength, dislocation struct., optical and TEM 79−74228
Ni_3Ga, form. mech. of superlattice intrinsic stacking faults 77−27897
Ni_3Ga, with $L1_2$ struct., dissociated struct. of superlattice dislocations 79−37706
Ni_3Ge single crystal, yield stress, temp. and orientation depend. 77−90432
Ni_3Ge single crystals, orientation and temp. depend. of flow stress 79−5008
NiO, polycrystalline, high temp. deform. 78−3174
NiO, single crysts., annealed, dislocation arrays in low angle tilt boundaries, TEM study 79−37707
NiO:Mn, microhardness, plasticity, ageing effects 79−43291
Ni_3V, dissociation of $^1/_2$⟨112⟩ perfect dislocations and nature of slip dislocations 78−43022
α-Np, deform. modes around hardness indentations 77−20009
Pb, crystal defect accumulation after plastic deform. in normal and supercond. state resist. meas. 77−85196
Pb, film, hillock formation by grain boundary sliding 80−107673
Pb film, thermal strain, depend. on cryst. orientation 78−10311
Pb film, thermal strain, strain relax. mech. 79−42427
Pb, film, thermal strain, strain relax. above room temp. 80−59841
Pb film, vac. deposited, thermal strain depend. on thickness and grain size 79−90926
Pb thin films, thermal strain, multiple cycling to 4.2K effects 79−90918
Pb-In-Au alloy, Josephson junction electrode materials, rel. to strain relax. 79−38255
Pb-Sn (62 wt.%), intercrystalline and interface boundary sliding, tensile tests, SEM obs. 79−38886
PbS, crystals, relation of struct. and bond type to slip geometry 80−88165
PbS, plastic deform. on compression along ⟨100⟩ direction 79−28036
Pd-Ce alloy, SRO determ. 77−7738
Pd-Cu-Si glass, cold drawn, serrated plastic flow, optical and SEM study 79−79052
$Pd_{80}Si_{20}$ amorphous alloy, skip deform. and crit. shear stress, using tensile testing machine 80−89321
Pt_2Mo-type superstructure, interaction of reacting dislocations *(Russian)* 78−83814
Re, metallo-ceramic, deform. and cold working by cold rolling *(Russian)* 78−56655
ReO_3, hardness anisotropy, comp. depend. 79−29181
$(SN)_x$ single crystal, mech. props. 79−24580
Sb, deformed in compression, secondary slip system *(French)* 79−66120
Sb, rhombohedral crystals, slip dislocations and slip systems 79−23617
Si, (111) surface, annealing of scratches 79−60609
Si, core structure of glide-set 90° and 30° partial dislocations 80−96523
Si, crack-tip dislocation pattern, X-ray topography *(French)* 80−107253
Si, critical resolved shear stress, 800 to 1050°C indentation dislocation rosettes 79−24577
Si cross-slip of isolated dislocations at surface and in bulk 80−70215
Si, cross-slip of single dissociated screw disclocations, double etching and X-ray topography studies 80−15104
Si, crystal, dislocation slip bands formation due to pores, nondestructive monitoring 79−55749
Si, crystal defects and impurities interaction obs. by electron microscopic methods 80−65003
Si crysts., dynamic processes associated with stacking faults and deform. twins, HVEM in-situ obs. 80−103369
n-Si, deformed, thermal treatment effect on elec. cond. and dislocation mobility 80−107265
Si, deformed crystal, Czochralski and float zone growth, Luder's bands 79−79025
Si, dislocation dynamics during plastic deform., stress-strain characts. 79−27996
Si, dislocation mobility 77−76413
Si, dislocation structure, effect of induction heating *(Russian)* 77−21180

slip continued
Si, extended glide dislocations, motion obs. by high voltage electron microscopy 80−10555
Si, initial stage of plastic flow 78−64602
Si, lattice damage, influence of laser annealing 79−23608
Si, low dislocation density, plastically deformed, electron mobility anisotropy anomaly *(Russian)* 77−80777
Si, low temp. relax. of local stresses, dislocation behaviour, X-ray obs. 79−69110
Si, near (III) surface, dislocation movement at annealed scratches, X-ray topography obs. 80−2029
Si, partial dislocation electron states 79−60760
Si, plastic deformation, dislocation density in yield point area *(German)* 78−38720
Si, plastically deformed monocrystal, X-ray topographical study *(German)* 78−59813
Si single crystals, plastic deformation, dislocation gliding *(German)* 79−52316
Si, slip, room temp., TEM obs. 80−79804
Si, slip dislocation nucleation during laser annealing 80−84179
Si wafer thermal gradient induced slip, effect of starting cooling temp. 78−10057
Si:B, with insulating coating, mechanical stress influence on B diffusion, strained surface layers 80−29224
Si:P, high dose implantation, outside dislocation generation 78−87672
SiC (6H), slip systems and plastic deform. at high temp., Knoop hardness meas. 79−87683
SiC, effect of crystallographic anisotropy on Knoop microhardness 80−66626
α-Si_3N_4, hardness anisotropy 78−95804
α-Si_3N_4 single crysts., growth, morphology, hardness and slip system 79−83112
SmS, single crystals, crystallographic slip 78−18659
Sn crystal, white, time-dependent internal friction 80−7610
β-Sn, impress creep of single crystal 79−91743
Sn, white, configurations, formation and Burgers vector of coupled dislocations straddling polygon wall 78−26569
Sn-Bi, eutectic, superplastic anisotropy *(German)* 80−25808
$SrTiO_3$, defects grown by Verneuil method 77−51390
TZM powder alloys, fatigue and threshold behaviour under high cycle fatigue 80−40487
Ta, between 0.7 and 40K 78−19808
Te, a-edge dislocated crystals, mobility anisotropy 80−107781
Te, c-slip, asymmetry and orientation depend. 77−27888
Te, deformed and annealed cryst., elec. props., directional depend. 79−7847
Te single crystals, glide struct. from pure shear deform. expts. 77−81367
β-Ti alloy, rolling orientation pattern form. *(Russian)* 77−21161
Ti, commercial-purity, Portevin-Le Chatelier effect, mechanism 77−8886
Ti, deform. mech. map 77−77546
Ti, fast neutron irrad., twinning deform. at room temp. 80−65061
α-Ti, fatigue crack growth, influence of grain orientation, SEM study 80−108550
Ti, fracture mechanism at different temps. 77−63785
Ti, martensitic transformation, strain energy minimisation 77−21140
α-Ti, plastically deformed by rolling, optical and electron microscope obs. 79−91666
Ti polycrystalline sheet, strain ratio prediction from the ODF, appl. of Taylor's model 79−91773
Ti, pure plate, silver band formation in ductile fracture process *(Japanese)* 80−16445
α-β Ti Widmanstatten alloy interfaces, elastic interact. stresses, effect on plastic flow onset 80−104218
α-Ti-Al, slip band spacing, correlation with β-Ti-Mn 79−99211
α-Ti-Al, stress/strain curves 77−63738
Ti-Al (6.6 wt.%), hydride habit planes, H_2 embrittlement, slip 77−36648
Ti-Al-Mo-V (8, 1, 1 wt.%), Widmanstatten colonies, fracture toughness 80−85031
Ti-Al-Sn (5, 2.5 wt.%), fracture mechanism at cryogenic temps. 78−64642
Ti-Al-Sn-Zr-Mo (6,2,45 wt.%), surface cracking under unidirectional loading 78−56753
Ti-Al-V (6, 4 wt.%), cavitation induced erosion, under mill annealed, soln. treated and aged, and beta annealed conditions 79−8371
Ti-Al-V (6, 4 wt.%), texture effect on fatigue crack path 78−27633
Ti-Al-V (6, 4 wt.%), textured, anisotropy of fracture toughness over various specimen orientations 79−8353
Ti-Al-V (6,4 wt.%), surface cracking under unidirectional loading 78−56753
Ti-Al-V-Sn (6, 6, 2 wt.%) weldments, heat treated, transangular fracture 80−40524
β-Ti-Mn, exam. of reloading yield points 78−72822
α, α+β, β-Ti-Mn alloys, Bauschinger effect during cyclic straining 79−43310
β-Ti-Mn slip band spacing, correlation with α-Ti-Al 79−99211
β-Ti-Mo, alloy, struct. changes during deformation and ageing *(Russian)* 78−39791
β−Ti-Mo, thermal instability, hardness and tensile deform. *(Japanese)* 80−71703
Ti-Mo (15 wt.%) alloy, metastable β-phase, deform. characts. 78−6975
Ti-Mo (16 at.%), effect of H impurities on lattice spacing, hardness, and plastic strain *(Russian)* 79−11664
Ti-V, cyclic stress-strain response 78−60700
Ti-V (27 and 30 wt.%), fatigue crack propag., in single and poly. crystals 79−5048
β-Ti-V (40 at.%), BCC, flow stress asymmetry and cyclic stress-strain response 77−36583
Ti-V (40 at.%), BCC, single crystal, fatigue and slip 78−19854
β-Ti-V metastable alloys, fatigue crack propag. 80−60964
α-β TiAl-Sn-Zr-Mo (6,2,4,6 wt.%), age hardening 79−61604
TiC, mech. props., 1073 to 2273K *(Japanese)* 79−15732
TiC single crystal, deformation behaviour, operative slip systems 79−100211
TiO_2, crystal dislocations, elastic parameters, elastic energy, stress field, anisotropic elasticity theory 79−95008
α-U, mech. behaviour, strain rate influence, 300 to 550°C 79−38907
UO_2, compressed, dislocation substructure obs. *(French)* 78−78461
V, anomalous slip, suppression by O interstitials 77−28875
V, high purity crystals, anomalous slip under compressive deform. 77−63737
V, purification and plastic props. 80−25810
slip continued
V, slip geometry and dislocation struct., rel. to degree and temp. of deform. *(Russian)* 78−38717
V, strain hardening, screw dislocations and microtwinning *(Russian)* 80−29971
V, zone-refined, deform. behaviour, stress relax. and slip plane patterns 79−29163
V-Ta (5 wt.%), strain hardening, screw dislocations and microtwinning *(Russian)* 80−29971
VC single cryst., Vickers microhardness, slip mechanism 80−71732
V_3Si, dislocations, obs. by TEM 77−59012
V_3Si, grown-in dislocations, diffr. contrast behaviour 79−86794
V_3Si single cryst., creep deform. 80−71695
W, BCC slip system geometry *(Hungarian)* 77−47463
W fibre reinforced Cu composite, work hardening 77−52341
W:Re, polygonisation in diffusion process, glide dislocation interactions 80−38998
W-Mo, vapour deposited, long-term strength and thermocyclic creep 80−16405
WC-Co, elastic and plastic charact. 80−35280
W_2C, slip systems, at ambient temp. *(French)* 78−84926
Y, polycrystn., plastic deform. at different deform. speeds, dislocation glide *(Russian)* 80−93598
Y_2O_3, dislocation and plasticity dissociation 80−107247
Y_2O_3, plastically deformed monocryst., HV electron microscopy obs. of dislocation config. *(French)* 79−55747
YSeF, orthorhombic polytype 140, struct. study *(French)* 80−88102
Zn, alternating bending of single crysts., shear strain accumulation and microstrain distrib. *(Russian)* 78−60706
Zn, basal dislocation−prismatic dislocation ring interactions by method of moments *(Russian)* 80−10550
Zn, basal forest dislocation as source of pyramidal, dislocations *(Russian)* 77−84759
Zn, basal slip, early stages in single crystal 77−72623
Zn bicrystals, $\langle 10\bar{1}0\rangle$ tilt, misorientation depend. of grain boundary sliding 80−15119
Zn bicrystals, grain boundary slip in deform. 80−34008
Zn, compatible bicrystal, plastic deform. *(Japanese)* 78−31460
Zn crystal, $\{11\bar{2}2\}\langle 11\bar{2}3\rangle$ slip system, deform. stress, dislocation density depend. *(Russian)* 80−103353
Zn crystals X-ray topographic examination of basal dislocations 80−88156
Zn, cutting mechanism of large crystals *(Japanese)* 77−48523
Zn, deformed, internal friction meas. 77−86067
Zn, deformed single crysts., stacking faults and dislocation dissoc. 77−31681
Zn, deforming stress under basal slip, contrib. of forest and primary dislocations 78−3186
Zn, density of basal dislocations, rel. to deforming stress, 1.5-300K *(Russian)* 80−29028
Zn, dislocation damping on $\{\bar{1}2\bar{1}2\}\{\bar{1}2\bar{1}\bar{3}\rangle$ slip system above Debye temp. 77−62538
Zn, dislocation interaction with 'forest' dislocation, TEM exam. 77−89440
Zn, dislocation internal friction, orientation depend., for single crysts. 78−52882
Zn, dislocation struct. stability, effect of deformational and thermal annealing 78−64567
Zn, glide dislocations, second order pyramidal band, etch pit obs. of pure single cryst. *(Japanese)* 78−38716
Zn, line energy of basal screw dislocation, exptl. determ. 80−88154
Zn, low-temp. thermal fatigue, causing fracture and plastic deform. 77−28837
Zn monocrystal, cavitation induced multiple slip, twinning and fracture 78−39872
Zn, oriented polycrystals, tensile behaviour under hydrostatic press. *(Japanese)* 77−52417
Zn particulate composite, mech. props., microstruct. correlation, at low and high temps. 77−32624
Zn, pure single cryst., fracture stress 80−104269
Zn, single cryst., contribution of basal dislocations to residual elec. resist. *(Russian)* 80−75539
Zn single crystal, rel. to discontinuous creep *(Russian)* 77−81292
Zn single crystals, temp. and strain rate effects on strength, slip and twinning 80−16373
Zn, twinning, influence of dislocation drag. mag. field effects 80−59472
Zn, work hardened crystal, jump-like plastic deform., dislocation struct. instability 79−96094
Zn-22 wt.% Al superplastic eutectoid alloy tensile deformation obs. *(Japanese)* 79−90714
Zn-Ag(Cd), anisotropic, dislocation interaction with tetragonal impurity, mobility 77−19953
Zn-Al, dislocation slip peculiarities during superplastic deform. 79−20102
Zn-Al (0.4 wt.%), intergranular slip during in situ superplastic deform. 80−96538
Zn-Al (10,22,50wt.%), low temp. mech. props. plastic deformation, glissile dislocation nucleation *(Russian)* 80−11695
Zn-Al alloys, comp. effects on intergranular slip during superplastic deform. *(Russian)* 77−32633
Zn-Al alloys, dislocations obs. in superplastic deformation 78−51549
ZnO, dislocation motion, in situ TEM obs. 77−19961
ZnS, glide plane of dislocations 79−46667
Zr alloys, creep and growth, irradiation induced, microstruct. depend. 80−93602
Zr, deformation texture during rolling in sequential passes 79−11674
Zr, neutron irradiated, twinning deformation 79−14848
α-Zr, polycrystalline, cyclic deformation *(Japanese)* 78−68757
Zr polycrystalline, low-temp. alternating deformation and annealing, yield stress, elec. cond. variation *(Russian)* 79−74199
Zr-Al (8.6 wt.%), neutron irradiation effect on tensile props., swelling 77−7768
Zr-base alloy as reactor core material, microstruct., deform. and fracture 78−4988
Zr-Nb (1 wt.%), static strain ageing between 295 to 773K, TEM obs. of plastic strain 79−38855
Zr_3Al, $L1_2$ phase, work hardening 78−23718
Zr_3Al, $L1_2$ phase yield strength 78−19811
$ZrH_{1.92}$, plasticity 77−36569
ZrO_2, CaO stabilised, preferred slip system 80−66585

slip (asynchronous machines)
deep slip motor starting characteristics, industrial cinefilm winder motor appl. *(Russian)* 78−29199

small electric machines
corneal mechanised trepan control 79−29659
sound reduction in small elec. appliances, investigation using time average holography *(German)* 79−37086
translation motors for position with micron precision *(German)* 80−86271

small polaron conduction
actinides, lattice vibrs. role in phys. props. determ. 77−28158
aromatic molecular crystal, electron-intramol. vibr. coupling, rel. to carrier mobility 77−15854
biphenyl, electron mobility and photogeneration temp. depend., polaron hopping 78−19033
disordered solids, electron-electron interaction effects on low temp. hopping 80−44584
disordered structure, deviations of polaron hopping mobility from Mott law 77−8095
disordered systems, theory of Hall effect in hopping region 77−47836
ferrites, electronic cond. mechanisms, review 77−20314
glass, high-field ionic and polaronic cond., dielec. relax., Poole-Frenkel theory 80−100351
glasses containing V_2O_5, small polaron cond. *(French)* 77−72867
hopping, reaction rate treatment, role of vibrational relaxation 78−72092
hopping conduction in small polaron model, review 77−15851
hopping conductivity in ordered and disordered solids, review 77−1420
ice film, low-temp. diffusion of electrons, evidence for polaron bands 77−1380
magnetic semiconductor, double exchange and small-polaron hopping 79−19591
magnetic semiconductor, small-polaron hopping, many-electron approach 79−95409
magnetic semiconductors, small polaron form. and motion 80−96882
metal, BCC, small-polaronic diffusion of light interstitials 79−42315
molecular crystals, electronic transport theory, local linear electron phonon coupling 80−65545
oxide glasses, elec. cond., polaronic hopping model 79−65479
Peierls-Frohlich state on many-phonon-coupling model, dynamical props. 78−47773
phonon-assisted hopping due to both acoustic and optical phonon interactions 77−66146
TTF-TCNQ, conductivity model 79−51557
tunnelling, thermally assisted, computer anal. 80−2391
vanadium phosphate glass, comp. depend. of elec. cond. 77−62922
As_2Se_3, amorphous, DC Hall effect, elec. cond. mechanism 78−23121
As_2Se_3, amorphous, transient electrical transport, general and unified treatment 80−59977
As_2Se_3-As_2Te_3 glass thermoelec. power, and transport mechanism 80−2408
$BaNb_xV^{III}Ti_{1-x}{}^{IV}O_3$, A and C-domain crysts., elec. cond. and absorption spectra 77−47805
BaO-B_2O_3-SiO_2:Ti^{3+}, elec. cond., struct. 78−72148
BaO-B_2O_3-V_2O_5 glasses, polaron hopping cond., optical absorpt. and ESR spectra 79−23966
BaO-B_2O_3-V_2O_5(Fe_2O_3)(Cu_2O), glass, resist. and activation energy, reduced valency 77−51749
BaO-K_2O-VO_2-SiO_2, glass, elec. cond. rel. to ion polarisability, polarons 80−49729
BaO-$La_{0.6}O$-VO_2-SiO_2, glass, elec. cond. rel. to ion polarisability, polarons 80−49729
n-$BaTiO_3$, elec. transport props., theoretical discussion and expt. 78−84215
$BaTiO_3$, transport and optical props., small polaron hopping theory 79−47096
CeO_{2-x}, conductivity and Seebeck coeff., small polaron and hopping mechanisms 77−76812
CeO_{2-x}, small polaron mobility, elec. cond. and nonstoichiometry meas. 78−47785
CoO, electronic cond., rel. to basic processes of Co corrosion 77−25198
Cu-Al_2O_3 cermet films, temp. depend. of AC and DC cond. 79−87166
CuO-CaO-P_2O_5 system glasses, DC cond., hopping transport, 300 to 620K 78−23096
Fe_2O_3-B_2O_3-PbO glass, semicond., elec. resist. meas. 78−95300
Fe_3O_4, magnetite, charge carriers, optical props. 80−34874
Fe_3O_4, magnetite, electronic cond. mechanisms, review 77−20314
Ge, sputtered hydrogenated amorphous, steady-state and transient photocond. meas. 78−10506
$KNbO_3$, elec. and thermoelec. singularities due to small polaron hopping motion cond. transition 79−42565
$La_{0.9}Ca_{0.7}CrO_3$ polar semiconductor, elec. props., slight reduction effect 80−20183
La_2CuO_4, high pressure phase transformation, small polaron cond. to semicond. transition 78−6156
$La_{1-x}Sr_xCoO_{3-y}$, Seebeck coeff. meas., small polaron hole conduction model 80−20233
$La_{1-x}Sr_xCrO_3$ ($0 \leq x \leq 0.4$), localised level hopping transport 80−10974
$La_{1-x}Sr_xCrO_3$, x=0-0.2, AC and DC cond., 77-1300K, hopping of polarons 78−2477
Mn ferrites, Fe-excess, charge carriers, optical props. 80−34874
MoO_3-P_2O_5, glass, polaron hopping DC conduction mechanism 78−6376
MoO_3-P_2O_5 glass, thermoelec. power meas. 78−84242
$NaNbO_3$, ferroelec. semicond., thermoelec. power for small polaron 77−89784
Na_2O-B_2O_3-SiO_2-As_2O_3(As_2O_5) glasses, DC and AC resist., bipolaronic hopping cond. 80−88558
Na_2O-TiO_2-SiO_2 glass, elec. props. and energy gap 78−26921
$Na_{1.9}V_{12}O_{29.7}$, press. depend. of elec. cond., semicond.-metal phase transition obs. 78−64072
$NbCl_4$, high press. elec. resistivity 80−29404
NbO_2, high press. elec. resistivity, phase transition 80−29404
$Ni_{1-x}Co_xS_2$, anomalous elec. props., polaron transport in highly correl. narrow bands 77−85222
$Ni_{1-x}Co_xS_2$, elec. cond., thermoelec. power and optical meas. 80−59986
NiO, electronic cond. rel. to basic processes of Ni corrosion 77−25198
$NiS_{2-x}Se_x$, elec. cond., thermoelec. power and Hall effect meas. 80−65561
P_2O_5-FeO glass, electrical cond., nonadiabatic hopping of small polaron 77−1417

small polaron conduction continued
$PbTiO_3$, ferroelec. semicond. thermoelec. power for small polaron 77−89784
$Pb(Ti_{0.47}Zr_{0.53})O_3$, small polaron cond. mechanism, elec. cond. and thermopower meas. point defects 78−43380
$PbZrO_3$, ferroelec. semicond., thermoelec. power for small polaron 77−89784
Pr_6O_{11}, mag. and transport props., multiphonon hopping conduction 78−19211
Sb_2S_3, cond. anomalies at phase transition pts. 77−43604
Se, amorphous, transient electrical transport, general and unified treatment 80−59977
Se-Te-Sb glasses, electronic transport 80−88579
Si, amorphous, AC cond., bipolaron hopping 79−23928
Si, amorphous, transient electrical transport, general and unified treatment 80−59977
SiO_2, amorphous, defect-controlled carrier transport 79−91049
SiO_2, amorphous, high-field transport of excess electrons and holes 77−89767
SiO_2, amorphous, time-resolved hole transport, small polaron model 77−43598
SiO_2, amorphous, transient electrical transport, general and unified treatment 80−59977
TiO_2-P_2O_5 reduced glasses, prep., elec. transport, chem. anal., DC, AC cond., seebeck coeff. 78−30924
TiO_2-SiO_2, semicond. glass, small polaron hopping cond. 78−60126
V_2O_5, amorphous hopping small polarons, effect of random glass struct. 79−23972
V_2O_5-As_2O_3-RO, R=Ba, Ca, Pb, semicond. glass, electronic props. 80−88557
V_2O_5-GeO_2-PbO glasses, memory and threshold switching 78−23142
V_2O_5-MoO_3 solid solns., small polaron cond., elec. resist. and thermoelec. power meas. 80−34447
V_2O_5-MoO_3-P_2O_5 glass, semicond., DC cond., dielec. props 79−91044
V_2O_5-P_2O_5 glass, splat-cooled, EPR of V^{4+}, polaron hopping and carrier localisation 77−28436
V_2O_5-P_2O_5 glass, thermoelec. power meas. 78−84242
$V_{1+x}P_{1-x}O_{5-c/2}$ glasses, structure, adiabatic hopping conduction model 77−43588
WO_3-B_2O_3-ZnO semiconducting glasses, DC cond. and optical absorpt. 80−107783
WO_3-P_2O_5 glass, DC elec. cond., 100-400K 78−39106
WO_3-P_2O_5 glass, thermoelec. power meas. 78−84242
YIG, elec. props. 79−99552
YIG, elec. props. meas., 600-1500K 77−8098

small-size generators *see small electric machines*

small-size motors *see small electric machines*

smectic liquid crystals
A→C second order phase transition, symm. changes and dipole orderings 78−2238
A and C phase and A-C phase transitions, diffuse-cone model 79−41952
A mesophase, spin-probe longitudinal relax. 79−94871
A phase, EHD instability and elec. cond. anisotropy *(Russian)* 78−59753
A phase, nucl. spin relax. by translational self diffusion 80−60442
A phase, scattering textures, appl. to display device 78−91236
A phase exhibiting positive and negative dielec. anisotropy 79−10793
A phases, mol. tilt, layer thickness and orientational disorder 79−32897
A to C phase transition, mean field model 78−95142
A to C phase transition, phenomenological model 79−1495
A-phase, impurity diffusion, appl. to TMS in BBOA 77−43140
A-phase, layer rigidity, stress relax. 78−18545
A-phase, oscillatory convective instabilities, caused by heating from below 80−103239
A-phase, sub-Rayleigh oscill. 80−87774
A-phase, thermooptical recording, echo images 80−91928
4-acetyl-4′-n-alkanoyloxy-azobenzenes, type A, B smectic, nematic phase, solid state polymorphism, preparation, melting behaviour 78−59745
acoustic emission, appl. to defect dynamics study 78−91232
acoustic props., US velocity and anisotropy in mag. fields *(Russian)* 79−90547
acoustical activity 78−83880
acousto-optical effect, instabilities generated by US field, review 78−91235
2-(4-n-alkylphenyl)-5(4-nalkoxyphenyl)-pyrimidines, smectic polymorphism, miscibility meas. 79−86678
4-alcanoyloxybenzoyloxy-4′-cyanoazobenzene series, influence of substituent on reentrant mesophases 80−88027
4-alcanoyloxybenzoyloxy-4′-cyanobiphenyl series, influence of substituent on reentrant mesophases 80−88027
4-alcanoyloxybenzoyloxy-4′-cyanostilbene series, influence of substituent on reentrant mesophases 80−88027
aligned rod system, nematic-smectic transition 79−77729
alignment, produced by RF plasma deposited films on glass or $In_{2-x}Sn_xO_{3-y}$ 77−48350
alignments of director using submicrometre periodicity gratings 78−63666
aliphatic compounds, trans, trans-cyclohexyl cyclohexanoates, synthesis, mesomorphic phases 80−44121
1-(4-alkoxy-benzoyloxy-phenyl)-2-(4′-pentylphenyl)-ethanes, synthesis and mesomorphic props. 79−90536
p-n-alkoxybenzoates of p-n-alkoxyphenyl, smectic A phases mol. struct. and elastic behaviour 80−59382
4(4′-n-alkoxybenzoyloxy)benzylidene-4″-aminophenols, synthesis and mesomorphic props. 79−90546
alkoxybenzylidenaminobenzonitriles, elec. field and press. induced transitions, transparency and texture 77−43317
N-(4-n-alkoxybenzylidene)-4′-alkylanilines, smectic-B to H transition, B-phase struct. 79−94896
L-p-alkoxybenzylidene p′-amino 2 methylbutyl cinnamate chiral smectic liq. cryst., dielec. and ferroelec. props. 79−91394
L-p- alkoxybenzylidene p′-amino 2 methylbutyl-cinnamate, dielec. props. in ferroelec. smectic phase *(Japanese)* 79−82154
N-4-n-alkoxybenzylidene-4′-n-alkylanilines, classification of polymorphic smectic phases 79−55661
N-4-alkoxybenzylidene-4′-n-alkylanilines, smectic F phases 79−94891
N-4-n-alkoxybenzylidene-4′-n-butylanilines, elec. cond. in nematic and smectic phases *(German)* 77−15860
p-alkoxybenzylidene-p-n-alkylanilines, thermotropic mesophases, proton spin-lattice relax. 78−91968

smectic liquid crystals continued
p-alkoxybenzylidene-p-n-butylanilines, optical and mag. anisotropies in liq. cryst. phase, thermal variations of order parameter *(French)* 79−82149
4-4′-n-alkoxybenzylideneamino-biphenyls, central Schiff's base linkage reversal effect on liq. cryst. props. 80−79683
4′-n-alkoxybiphenyl-4-carboxylic acids, 4-(2′-methylbutyl)phenyl esters, smectic phases 79−86684
4-n-alkoxyphenyl 4-n-alkylcyclohexanecarboxylates, smectic polymorphism, miscibility meas. 79−86678
p-alkoxyphenylazo-p-phenylesters, polymorphism, calorimetry *(French)* 78−51650
n-alkyl 4′-n-alkoxybiphenyl-4-carboxylates, smectic C and tilted smectic B phases 79−32888
n-alkyl 4′-n-alkoxybiphenyl-4-carboxylates, smectic polymorphism, X-ray diffr. and miscibility meas. 79−27912
alkyl cyanobiphenyls, pretransitional behaviour, alkal chain length depend., light scatt. in isotropic phase 80−44301
4,n-alkyl-4′-cyanotolanes, and related compds., homologous series, mesomorphic transition temps. 77−27991
4′-n-alkyl-4-cyanobiphenyls, press. effect on liq. cryst. phase transitions 79−95138
4′-n-alkylbiphenyl-4-carboxylic acids, 4-(2′-methylbutyl)phenyl esters, smectic phases 79−86684
alkylcyano-cyclohexyl-cyclohexanoates, nematic and smectic mesophases 80−19692
alkylcyclohexyl-cyclohexyl-cyclohexanoates, nematic and smectic mesophases 80−19692
trans-4-n-alkylcyclohexylbenzylamines, synthesis and mesomorphic props. 80−44116
4-alkyloxy-4′-cyanobiphenyls (nematic, smectic)-tetrabutylammonium picrate, elec. cond., temp. (conc.) depends. *(German)* 78−55966
4-4-n-alkyloxybenzoyloxy-benzylidene-4′-cyanoanilines, reentrant nematic and smectic phases 80−88308
n-(4-n-alkyloxybenzylidene)-4-n-alkylanilines, smectic polymorphism, miscibility meas. 79−86678
N-4-n-alkyloxybenzylidene-4-n-alkylanilines, smectic polymorphism, calorimetric study 80−88307
2-4-n-alkylphenyl-5-(4-n-alkyloxyphenyl)-pyrimidines, smectic polymorphism, calorimetric study 80−88307
2-[4-n-]alkylphenyl-5-[4-n-alkyloxyphenyl]-pyrimidines, X-ray study of smectic modifications 79−32882
aromatic esters derived from naphthalene, liqs. cryst. props. 78−47235
aryl p-fluoroalkoxybenzoates, synthesis and mesomorphism 78−91243
aryl p-fluoroalkylbenzoates, synthesis and mesomorphism 78−91243
p-p′-azoxy di-n-undecyl α-methylcinnamate, smectic C layer thickness meas. by X-ray scatt. 78−94986
azoxy-4,4′(di-undecyl α-methyl cinnamate), refr. index at 2nd order smectic A to C phase transition 79−19357
azoxy-4,4′-(di-undecyl α-methylcinnamate), smectic A to smectic C phase transition, optical tilt angle meas. 78−95141
B mesophase, series anal. of steric interaction models, X-ray scatt. calc. 79−86701
B phase, bond orientational order model 79−10790
B phases, interlayer correlations 79−77502
BBOA:Sn-BBA, liquid crystal glass, unresolved Mossbauer quadrupole doublet, orientation depend. 77−84645
BBOA, B phase, containing 4 ferrocene derivatives, ^{57}Fe Mossbauer study 78−27136
BBOA, pretransitional shear viscosity divergence near smectic A-smectic B transition 79−33077
BBOA, smectic B phase, fluidlike mol. dynamics, Raman scatt. study 80−20630
BBOA, smectic liq. cryst. glass-supercooled transition and Debye temp., ^{57}Fe Mossbauer effect 80−54999
BBOA, thermal diffusivity meas. by forced Rayleigh scatt. 78−76483
BBOA, uniaxial, polarized Raman scatt., orientational order 77−76296
benzylideneanilines, ordered smectic phases, X-ray diffr. meas. 77−89375
biaxial order parameters, NQR meas. 78−34432
binary mixtures, isobaric phase diagrams, non-ideal behaviour *(French)* 79−95141
binary mixtures, phase transitions, entropy, relation to smectic plane tilt angle 80−65203
biological membranes appl. 79−53051
biomembranes, electric and magnetic props. *(Russian)* 77−60190
biphenylbenzoates, synthesis, mesomorphic, and thermodynamic props. 80−44117
4-biphenylyl 4″-n-alkoxybenzoates, smectic liq. crysts., transition temps., DTA 78−75815
bis-(4,4′-n-alkoxybenzylidene)-1,4-phenylenediamines, smectic polymorphism up to 3 kbars, differential thermal anal. 79−55873
bis-(4′-n-heptyloxybenzylidene)-1,4-phenylenediamines, smectic phases, previously unclassified 79−77508
bis-heptyloxy-azoxybenzene, tilt angle in C-phase, dielectric measurements 78−63673
p-bis-octyloxyazoxybenzene, thermal diffusivity, Rayleigh scatt. obs. 78−94977
BPBAC, smectic B phase, neutron diffr. and X-ray obs. 78−94973
Brillouin scattering 77−8591
4-butoxybenzylidene-4′-alkylaniline, EHD instabilities in nematic and smectic A phases 79−90530
N-n-butoxybenzylidene-n-butylaniline, US propag. near nematic-smectic A transition, mag. field effect 80−39266
N-p-butoxybenzylidene-p-n-octylaniline, smectic A-B transition, birefringence pretransitional behaviour 80−15226
N-(p′-butoxybenzylidine)-p-n-octylaniline, order parameters in nematic and smectic phases, X-ray diffr. meas. 79−94874
4-n-butoxybenzylidine-4′-n-octylaniline, liquid cryst., smectic B phase lattice vibr. anisotropy, Mossbauer anal. 77−7666
n-butyl-4-(4′-phenylbenzylideneamino)cinnamate-d_9, smectic E, B and A phases, quasielastic neutron scatt. obs. 78−75539
butyloxybenzylidene octylaniline, liq. cryst. film, smectic B-A transition, mech. meas. 80−79918
butyloxybenzylidene octylaniline, two- and three-dimensional smectic B liq. cryst. film, long range order 80−96442
butyloxybenzylidene octylaniline film, freely suspended, smectic A layer spacing, optical determ. 80−64883
p-butyloxybenzylidene-p′-octylaniline, thermal diffusivity, Rayleigh scatt. obs. 78−94977
4-n-butyloxyphenyl-4′-nonyloxybenzoate, edge dislocations in smectic C mesophase 78−91231

smectic liquid crystals continued
butyloxyphenylnonyl oxybenzoate, smectic C layer thickness meas. by X-ray scatt. 78−94986
C phase, mol. director behaviour at domain EHD instability 80−15000
C phase, tilt angle determ. by field-induced Freedericksz transitions and X-ray meas. 79−94884
C phase, transition to A phase, exptl. evidence 77−89527
C phase, with second order transition to smectic A, molecular tilt, zigzag model 78−94986
C phase and smectic C-smectic A transition, induced dipole model 79−90527
C-phase, biaxial mol. order, NMR meas. 80−25227
C-phase, kinematic and dynamic light scatt. from periodic struct. 79−11427
C-phase, optical props. *(French)* 77−43959
caesium perfluorooctanate, thermodynamically independent nematic amphiphilic mesophase obs. 79−95126
carrier mobility and electro-optical effects anisotropy *(Japanese)* 77−43605
CBOOA:nitroxide, liq. cryst. phase transition study by electron spin relax. *(French)* 79−55874
CBOOA, acoustic emission at liq. cryst. transitions prod. by thermo-optically excited defects 79−95137
CBOOA, anisotropic shear viscosity meas. 77−15310
CBOOA, isotropic, nematic, smectic-A phases, Brillouin scatt. 80−11421
CBOOA, mag. aligned, smectic A-nematic transition, US absorpt meas. 78−95137
CBOOA, nematic to smectic A transition, high resolution X-ray scatt. exam. 78−94984
CBOOA, smectic A, nematic and isotropic phases, surface tension 77−39539
CBOOA, smectic A to nematic phase transition, crit. neutron scatt. 78−95135
CBOOA, smectic A-nematic transition, X-ray and light scatt. obs. 79−95129
CBOOA, smectic-A reentrant nematic transition under press., X-ray obs. 80−59637
CBOOA, smectic-A-nematic and nematic-isotropic transitions, vol. behaviour 77−39666
CBOOA, smectogenic, cryst. and mol. struct. determ. 78−2103
CBOOA, specific volume and layer spacing, X-ray diffr. and dilatometry meas. 79−55659
CBOOA, US absorpt. and dispersion at nematic-smectic-A transition 79−82287
CBOOA film, freely suspended, smectic A layer spacing, optical determ. 80−64883
4-n-cetyloxy-N-4′-cyanophenyl benzamide, thermotropic liq. cryst. behaviour, optical microscopy obs. 79−32895
chiral, electroclinic effect at A-C phase transition 77−39668
chiral, optics and electro-optics, kinematical diffr. theory 80−92461
chiral ferroelectric, flexoelectric effects, dielectric const. 80−33877
chiral polarised, electric field induced tricritical point 78−10176
chiral smectic C, distortion under shear, optical study 77−39536
chiral smectic C, ferroelec. props., dielec. meas. 78−52463
chiral smectic C phase, mol. theory 80−19695
chiral smectic C phases, defects induced by planar anchoring *(French)* 78−94978
chiral smectic critical behaviour near phase transformation point between two ferroelectric phases *(Russian)* 80−44124
chiral smectic liquid crystal, A-C phase change, electroclinic effect 79−42224
chiral structure in electric field, dielectric permeability, spontaneous polarisation *(Russian)* 80−75159
cholesteric helix period, mag. field strength depend. near phase transition to smectic A *(Russian)* 78−59754
cholesteryl 2-nitrobenzoate, mesophases, props. 77−11465
cholesteryl 4-nitrocinnamate, mesophases, props. 77−11465
cholesteryl capsylate and laurate, and their mixtures, elec. cond. *(Rumanian)* 79−64988
cholesteryl laurate-cholesteryl caprylate (75 wt.%), polymorphic behaviour, optical, elec. and dielec. meas. 80−65208
cholesteryl myristate, density of smectic, cholesteric, blue, isotropic phases 78−42897
cholesteryl myristate, smectic A-cholesteric transition, tricritical behaviour, DTA and DSC study 80−65206
classification system, based on symmetry and order 79−64985
COC, cholesteric-smectic-A transition, press. depend., optical meas. 77−47556
cofocal conics in smectic C phase 79−1395
collagen fibrils as examples of smectic A biological fibres 77−90721
conference, ferroelectric materials and their applications, Kyoto, Japan, Nov. 17-19, 1977 79−19846
conference on smectic and lyotropic liq. crysts., Trento, Italy (Jan. 1978) 78−91222
COOB, acoustic emission at liq. cryst. transitions prod. by thermo-optically excited defects 79−95137
COOB, sheared liq. crystal, near T_{A-N}, optical response 79−94895
COOB, smectic A-nematic transition, X-ray and light scatt. obs. 79−95129
COOB, solid state dimorphism and cryst.-smectic transition, Raman study 80−45063
COOB film, freely suspended, smectic A layer spacing, optical determ. 80−64883
critical dynamics near nematic-smectic A phase transition, renormalisation group approach 80−10646
critical dynamics of smectic A to nematic phase transition 79−1493
curvilinear defects in smectic C phase *(French)* 79−27908
cyano compounds, liq. cryst. phases, incommensurate coexistent density fluctuations 80−79691
cyano derivatives, smectic layer spacings 79−46561
cyano Schiff bases, high press. reentrant nematic bilayer smectic-*A* transition 79−28087
4-cyano-4′-n-octylbiphenyl, smectic A liq. cryst., electrically induced scatt. textures and elec. reversal 78−83725
4-cyano-4′-octylbiphenyl, dielec. props., 1 Hz-1 GHz, in smectic, nematic and liq. phases *(French)* 77−40168
4-cyano-4′-octylbiphenyl, dielectric relax. anal. in nematic and smectic phases 80−108153
4-cyano-4′-octylbiphenyl, smectic A phase, defect patterns induced by ultrasounds 79−86695

smectic liquid crystals continued
4-cyano-4′-octylbiphenyl, smectic A phase, ENDOR study of galvinoxyl radical 79−78567
4-cyano-4′-octyloxybiphenyl, nematic-smetic-A transition, optical birefr. temp. coeff. 78−47505
4-cyano-4-n-cyanobiphenyl, smectic A mesophase, plasticity anal., defects motion, Grandjean wall form. 78−91227
4-cyano-4-n-octylbiphenyl, focal conics motion and plasticity, stroboscope obs. 79−86692
cyano-biphenyl series, nematogens and smectogens, props. characterised by even-odd effect 80−107046
4-4′-cyano-octyl-biphenyl, smectic A phase, elec. field effects, capacitance meas. 78−91237
4-4′-cyano-octyloxy-biphenyl, smectic A phase, elec. field effects, capacitance meas. 78−91237
p-cyano-p′-pentylbiphenyl/p-pentylbenzoic acid, mixture, induced smectic phase, dielec. props. 80−6498
4-cyanobenzoyloxy-4′-pentylstilbene, nematic, smectic A, and orthogonal smectic B phases 80−64890
cyanobenzylidene octyloxyaniline, director bend mode behaviour near nematic to smectic-A phase transition 78−1985
N-p-cyanobenzylidene-p-n-octyloxyaniline, smectic-A liq. cryst., nematic pretransitional mech. effects 77−11481
cyanobiphenyls, 80CB and its mixtures with 7CB, orientational order and elastic consts. 78−91245
cyanobiphenyls, thermal diffusivity, Rayleigh scatt. obs. 78−94977
cyanooctylbiphenyl, X-ray diffr. study 80−79690
4-cyanophenyl 4-heptyloxybenzoate, nematic and smectic modifications, dielec. relax. meas. 77−69769
4-cyanophenyl-3-methyl-4-(4-n-alkylbenzoyloxy) benzoates, mesomorphic props. 79−94888
cyclohexane derivatives, mesophases obs. *(French)* 78−59747
trans-1,4-cyclohexane-di-4′-n-alkoxybenzenes, synthesis and mesomorphic props. 79−94887
trans-1,4-cyclohexane-di-n-octyloxybenzoate, struct. of smectic phases, X-ray diffr. meas. 79−86702
cylinder, instabilities under mech. tension 77−19868
de Gennes model, for nematic to smectic-A transition, anisotropic crit. props. 78−43110
p-decyloxbenzylidene p′-amino 2-methyl butyl cinnamate, smectic A to C transition, Landau theory 77−84906
p-n-decyloxybenzoic acid p-n-hexyloxyphenyl ester, dielec. permittivity in nematic and smectic phases 79−32899
L-p-decyloxybenzylidene-p′-amino-2-methylbutyl-cinnamate, ferroelec. smectic liq. cryst., electro-optical effect 78−39527
l-p-decyloxybenzylidene-p′-amino-2-methylbutylcinnamate, (l-DBC), liq. cryst., pyroelec. const. stationary value over ferroelec. temp. range 79−65801
l-p-decyloxybenzylidene-p′-amino-2-methylbutylcinnamate, ferroelec. liq. cryst., pulsed pyroelec. effect 79−15405
deuterated compounds, molecular order and conformation changes in phase transitions 78−47237
4,4′-di(p,n-alcoxybenzylideneamino) biphenyls, smectic polymorphism, dilatometric exam. *(French)* 77−51480
4,4′-di(p,n-alcoxybenzylideneamino)biphenyl series, smectic polymorphism, molecular area and tilt angle *(French)* 77−43139
4,4′-di(p,n-alcoxybenzylideneamino)diphenyls, X-ray diffr. study of smectic polymorphism *(French)* 77−76299
di-n-decyl azoxy methyl cinnamate, smectic-A liq. cryst., anisotropic US propag. 79−55829
diakyl-cyclohexyl-cyclohexanoates, nematic and smectic mesophases 80−19692
4,4′-dialkoxydiphenyldiacetylenes, synthesis and mesomorphic props. 79−32890
4,4′-dialkyldiphenyldiacetylenes, synthesis and mesomorphic props. 79−32890
dialkyloxyazoxybenzenes, synthesis of ferroelec. smectic B, smectic C, and nematic phases 78−94969
diarylethanes, bromo- or cyano-substituted, mesomorphic props. 79−90535
diazoxycinnamates, synthesis of ferroelec. smectic C and smectic A phases 78−94969
dibenzoate-TBBA, polar smectic A to non-polar smectic A transition line 79−82324
dielectric constant theory 79−78604
dielectric permittivity in smectic A phase 78−71673
dielectric relaxation at phase transitions 79−28090
diheptyloxyazoxybenzene, smectic-C phase, proton NMR 77−11474
dipole moments and smectic C phase 77−68917
disinclinations, rotation defects, topology *(French)* 80−79679
display devices, smectic classification, discotic phase *(French)* 78−91223
DOBAMBC, and DOBAMBCC, chiral smectic C liq. cryst., dielec. consts., electroclinic effect 78−94980
DOBAMBC, chiral smectic, ferroelec., press. and solute effects 80−103920
DOBAMBC, chiral smectic, flexoelectric effect and polarisation props. *(Russian)* 80−15002
DOBAMBC, chiral smectic C-phase ferroelectric liq. crystal film, classical X-Y system, props. 80−44123
DOBAMBC, chiral smectic phases, pyroelectric and dielec. props. 79−91380
DOBAMBC, dielec. dispersion at ferroelec. smectic A-smectic C transition 79−91385
DOBAMBC, dielec. props. near ferroelec. smectic A to C transition 80−45015
L-DOBAMBC, ferroelec. behaviour 77−43949
DOBAMBC, ferroelec. liq. crysts., elec. and optical props., appls. *(Japanese)* 80−88943
DOBAMBC, ferroelec. props. 79−32884
DOBAMBC, ferroelec. transition mechanism obs. by X-ray scatt. 79−77515
DOBAMBC, ferroelectric liquid crystal film, freely suspended, polarisation, elastic consts. and viscosity meas. 79−55663
DOBAMBC, polarized Raman scatt. and elec. field effects in aligned smectic phases 79−94873
DOBAMBC, smectic A and ferroelec. smectic phases, ^{13}C NMR study 80−75153
DOBAMBC, smectic A to C transform., birefringence and optical rotary power 78−75812
DOBAMBC, specific heat determ., temp. depend. 78−91250
DOBPC, smectic C phase, elasticity and defects 78−91233
smectic liquid crystals continued
p-dodecanoylbenzylidene-p′-aminoazobenzene, smectic A mesophase, self- and impurity diffusion, NMR spin echo obs. 78−94975
dodecylcyanobiphenyl, pretransitional behaviour of isotropic to smectic A phase transition 79−60487
p-ndodocyloxy benzylidene p-azophenyl aniline, smectic phases, mol. order, EPR study 80−79693
domain instabilities in elec. and mag. fields 79−94875
DOMBAMBC, ferroelectric, colour switching in elec. field 80−29719
dye laser, planar 77−3578
dyes, field-induced colour changes 80−25340
dynamic crit. neutron scatt. obs. near smectic-A nematic phase transition 78−79752
EABAC, liq. cryst., smectic and nematic, distrib. functions by X-ray diffr. 79−99072
EABAC, smectic A, nematic, and isotropic phases, NMR and quasielastic neutron scatt. obs. 80−88022
EABAC, smectic-A, mol. motions, incoherent quasielastic neutron scatt. obs. 78−59740
EABAC, smectic-A mesophase, bound motion and spatial disorder 78−59741
edge dislocations obs. by polaris. microscopy 79−7547
EEBAC-TBBA, mixed liq. cryst., layer thickness of smectic-B phases 78−38822
elastic deformation by external mag. fields 77−35477
electric field effects on structure and props. *(Russian)* 77−47340
electric field induced Lifshits point 78−71674
electric susceptibility and electroclinic coefficient, near A-C* transition 79−28088
electric susceptibility and electroclinic coefficient, near A-C* transition 79−28089
electro-optic effects 77−69801
electro-optical reversible memory effect *(Russian)* 78−31174
EOBC, liquid crystal phase transforms., Raman obs. 78−87774
erythrocyte membrane, phys. state of lipids, X-ray diffr. 78−80835
ESR observations, of anisotropic ordering, spin relax. and slow tumbling 79−95629
ester, smectic C phase liq. cryst., ferroelectricity and spontaneous polarisation *(Russian)* 79−8102
esters, incidence of smectic liq. cryst. phases, effects of mol. framework changes 77−27819
esters, SLC, ferroelectric behaviour, specific heat, spontaneous polarisation 80−75958
esters, smectic F materials 78−51651
ethyl p-methoxybenzilidene aminocinnamate, dimer, mesogenic, intermol. interactions 79−46564
ethyl-(methoxybenzylidene-amino)cinnamate, low freq. dielec. constant meas. 78−91226
ethyl-p-azoxybenzoate, far IR and Raman spectra, smectic polymorphism 80−76022
ferroelectric, chiral smectic C phase, phys. props., review 80−75150
ferroelectric, fundamentals and display appl. 80−79676
ferroelectric, linear electrooptic effect 80−11365
ferroelectric, new ordered smectic phases 78−51407
ferroelectric, submicrosecond bistable electro-optic switching 80−84051
ferroelectric, temp. depend. of elec. susceptibility and spontaneous polarisation *(Japanese)* 78−68467
ferroelectric chiral, direct elec. meas. of permanent polarisation 77−32331
ferroelectric film, two-dimensional X-Y crit. behaviour 79−77514
ferroelectric helicoidal smectic-C liq. cryst. dynamics 79−1396
ferroelectric liquid crystal, soft modes 79−55653
ferroelectric liquid crystals, kinetics of spontaneous polarisation *(Russian)* 79−8101
ferroelectric phenomena, symmetry and thermodynamic states, review 80−10493
ferroelectric properties, temp. depend. *(Russian)* 77−32332
ferroelectric smectic single C liquid cryst., electric field induced bend undulation instability 80−24351
ferroelectric smectic-C liquid crystal film, freely suspended, two-dimensional mol. orientation fluctuations, light scatt. meas. 78−47236
ferroelectric thin film, two-dimens. X-Y crit. behaviour 79−77497
ferroelectricity in nematic and smectic liquid crystals *(French)* 78−83729
film, dislocation-mediated theory of two-dimens. melting predictions, light scatt. use as probe 80−92651
focal conics energetics 78−22641
G and H phase code letters, recommendation for use 80−103241
HAB, dielectric and calorimetric investig. in solid, liq. cryst. and liq. phases 77−84639
HBHA, synthesis and smectic B-smectic B transition 77−15562
HBPA, smectic liq. cryst. glass-supercooled transition and Debye temp., ^{57}Fe Mossbauer effect 80−54999
HBT, mag. susceptibility and anisotropy, smectic, nematic, isotropic phases 78−18748
HBT, phase transitions, quenching effects, DSC, DTA, X-ray diffr. and microscopic obs. 78−22833
helicoidal ferroelectric smectic A-smectic C phase transition, low freq. polarisation fluctuation spectrum 79−95714
helixing crystal, dielec. props., temp. and freq. depends. *(Russian)* 78−60380
p,n-hepthyloxybenzoic acid, smectic C liq. cryst., coherent light diffr. 78−1999
4-n-heptyl-4′-β-cyanovinylbiphenyl, isotropic mechanism of mol. rot., dielec. permitt. meas. 80−10491
4-n-heptyl-d_{15}-oxybenzoic acid-d_1, nematic and smectic phases, mol. and relative segmental order 80−96439
heptylazoxybenzene, smectic liquid crystal, A phase, dielec. permittivity 78−71673
p-n-heptylhydroxybenzylidene-p′-n-butylaniline, phase transition study from 22 to 80°C 79−14679
4,4′-di-heptyloxyazoxybenzene, diffuse X-ray scatt. near smectic C-nematic transition 79−95139
heptyloxyazoxybenzene, filamentary structures 80−107051
heptyloxyazoxybenzene, liq. cryst., pretransition behaviour, volumetric study 77−69076
p-p′-heptyloxyazoxybenzene, smectic-C phase, mag. aligned, anisotropic US propag. 77−84630
p-heptyloxybenzylidene p′-heptylaniline, smectic C layer thickness meas. by X-ray scatt. 78−94986

smectic liquid crystals continued
4-n-heptyloxybenzylidene-4′-n-hexylaniline, nematic and smectic phases, long mol. axis reorientation, LF dielec. dispersion 80−70124
p-n-heptyloxybenzylidene-aminofluorenzone/COOB mixtures, dynamic twist viscosity near polycrit. points 79−95133
N-p-n-heptyloxybenzylidene-p′-n-pentylaniline, X-ray diffr. of smectic phases 77−51318
p-n-heptyloxybenzylidene-p-aminobenzoic acid, smectic C to nematic transition 79−33076
N-p-heptyloxybenzylidene-p-heptylaniline, dislocations obs. in smectic A and C mesophases 78−91230
4-n-heptyloxybenzylideneamino-4′-cyanobiphenyl, reentrant nematic phase and low temp. smectic phases 80−88031
herringbone packing and chain behaviour 79−73093
p-n-hexadecyloxycinnamic acid, liq. cryst., radiation stability 78−85184
p-hexanoylbenzylidene-p′-aminoazobenzene, smectic A mesophase, self- and impurity diffusion, NMR spin echo obs. 78−94975
HEXOAB/7CBP, mixed crystals, induced smectic A phases, elec. cond. 78−76068
n-hexyl 4′-n-decyloxybiphenyl-4-carboxylate, smectic C phase, tilt angle using electron reson. spectroscopy 80−33886
4-n-hexyloxybenzilidene-4′-n-propylaniline, liq. cryst. phases, thermal and structural studies 78−1989
4-n-hexyloxybenzylidene-4′-n-hexylaniline, liquid crystal, exam. of orientation order of dissolved molecules 80−44112
4-n-hexyloxybenzylidene-4′-n-propylanilene, smectic S_H and S_m phase structs. 79−14673
4-n-hexyloxybenzylidene-4-n′-hexylaniline, nematic and smectic phases, long mol. axis reorientation, LF dielec. dispersion 80−70124
N-p-hexyloxybenzylidene-p′-toluidene, positron lifetime meas. in solid and liq. cryst. phases 79−61460
p-n-hexyloxybenzylidene-p-aminobenzoic acid, phase transitions, X-ray diffr. and DSC meas. 79−86877
N-p-hexyloxybenzylidene-p-toluidine, optical props., density, and order parameter in liq. cryst. phases 79−55667
p,n-hexyloxybenzylideneamino-p′-chlorobenzene, liq. cryst., sp. ht. meas. 78−22831
HOAB, cryst. and mol. struct. rel. to smectic C phase struct. 79−55732
HOAB, effect of smectic C struct., on dielectric relax. 79−19140
HOAB, liq. cryst., smectic and nematic, distrib. functions by X-ray diffr. 79−99072
HOAB, liq. cryst. phase transitions, specific ht. meas. 79−33075
HOAB, molecular orientatioal order in uniaxial and biaxial phases by NMR 77−84629
HOAB, smectic, C-phase, magnetic instabilities studied by electron spin resonance spectroscopy 79−82147
HOAB, smectic C liquid crystal, spin label probe obs. 77−19867
HOAB, smectic C-phase pyroelectric effect 78−79522
HOAB-cholesteryl benzoate mixture, twisted smectic-C and twisted nematic phases, optical and X-ray investig. 77−84634
HOAB-d_{30}, biaxial liq. cryst., NMR of spinning sample 79−64987
HOAB-DOBAMBC nonchiral-chiral smectic C mixture, spontaneous polarization and induced circular dichroism 79−27910
HOBA, smectic C mesophase, EHD instabilities 78−91238
HOBA two dimensional diffr. grating due to AC electric field, pulsating diffr. 78−15148
HOBACPC, chiral smectic C liq. cryst., dielec. consts., electroclinic effect 78−94980
HOBHA, A to C transition, crit. biaxiality *(French)* 77−4039
homeotropic to confocal texture transformation *(Russian)* 78−18548
HxBPA, transitions, DSC and X-ray diffr., 170-380K 77−15314
HxBPA smectic phases, X-ray diffr. and Raman spectra 78−6012
hydrodynamic theory, near nematic-smectic A transition, acoustic props. 79−77731
IBPBAC, cryst. struct. and struct. of ordered smectic phases, X-ray diffr. obs. 79−86780
IBPBAC, dynamics of smectic phases, quasi-elastic neutron scatt. meas. 79−86700
IBPBAC, order parameters in nematic and smectic phases, X-ray diffr. meas. 79−94874
IBPBAC, smectic B phase, neutron diffr. and X-ray obs. 78−94973
IBPBAC, smectic phases, self-diffusion coeffs., radiotracer meas. 80−49394
n-indecyl-p-azoxy-α-methyl cinnamate, dislocations obs. in smectic A and C mesophases 78−91230
induced helical struct., ferroelectric props. and spontaneous polarisation, C→A transition 80−54123
induced smectic mesomorphism by incompatible nematogens 78−1983
interaction of injected macromolecules *(Russian)* 78−78848
internal field, dipole correlation factor 78−34428
lecithin, rheology and structure in conc. solns. and liquid crystalline state 77−64007
Lifshitz point, physical realisation 79−41957
Lifshitz point in H-T phase diagram between A, C and modulated C phases 77−84904
light propagation in chiral and cholesteric phases *(French)* 78−43836
light scattering in smectic-A phases, theory *(Russian)* 78−87618
lipid-water smectic phase, forced Rayleigh scatt. 78−14278
liquid crystal, smectic A and C phases, classification of defects 78−26433
liquid crystals, nematic and smectic, EPR and NMR relax., first-rank tensor component effects 78−14275
long range order excim. *(Russian)* 79−1392
MBBA, fluorinated analogues, mesomorphic props. 80−70118
MBBA-PCB (41 wt.%)+pleochroic dye, electrothermo-optic effect, optical storage device appl. 78−87611
mechanical instability under dilative or compressive stresses 77−31583
mercury carboxylates, phase transitions, DTA 79−90759
mesogenic compounds with smectic F phase, succession order of smectic mesophases *(French)* 79−19143
methoxy-benzylidene-alkyl-cinnamates, smectic mesophase, ESR of spin probes, nonunique ordering 77−47344
β-methyl-butyl-methoxybenzylidene amino cinnamate, smectic-B liq. cryst., US attenuation anisotropy 79−55828
4-2′-methyl-butylphenyl-4′-n-octyloxybiphenyl-4-carboxylate, smectic F phase, characterisation and struct. 79−86707
methylene-bridged, homologous series, mol. struct. effects on mesomorphism 77−47347
molecular conformation and orientational order, NMR studies, review 80−75151
molecular dynamical investigation 78−91252

smectic liquid crystals continued
molecular dynamics 79−19141
molecular ordering in E-phase, mol. field approximation calcs. 79−4406
molecular reorientation, incoherent quasielastic, coherent-quasielastic and coherent-inelastic neutron scatt. 78−63640
molecular statistical model, of rank two symmetry, for smectic A state 77−27814
molecular structure and occurrence of smectic A and smectic C phases 78−6008
molecular-statistical theory of translational transitions, taking account of short-range order *(Russian)* 77−15564
mosaic textures, mech. twinning obs. 77−11475
'nematic' amphiphilic liquid crystalline mesophases, thermodynamic stability 79−95126
nematic bend-splay elasticity near the nematic-smectic-A transition 80−24360
nematic mixtures, binary, induced smectic phases, X-ray diffr. obs. 78−94987
nematic to smectic C phase transition, renormalisation group anal. 80−34173
nematic-smectic A(C) phase transitions, contribs. to viscosities from order parameter fluctuations 79−60489
nematic-smectic A phase transition, sound attenuation and dispersion 79−82286
nematic-smectic A transition, orientational fluctuation effect 80−6496
nematic-smectic B mesophases, mutual orientation *(French)* 79−55660
nematic-smectic-A phase transition, mean field theory 77−24393
nematic-smectic-C phase transition fluctuatiops, ring model 77−24392
4-nitrophenyl 4′-decyloxybenzoate, mol. struct. rel. to mesomorphic props. 77−89372
4-nitrophenyl 4-octyloxybenzoate, smectic-A and nematic phases, dielectric meas. 79−23516
4-nitrophenyl-4′-alkoxybenzoates, incommensurate smectic A phase 80−10647
4-nitrophenyl-4-octyloxybenzoate, nematic and smectic-A phase, dielec. meas. 78−60392
NOBAMBC, chiral smectic phases, pyroelectric and dielec. props. 79−91380
nonlinear reversible hydrodynamics, external mag. field influence 80−75156
p′-nonylhydroxybenzoic acid, struct. characts., cylindrically symmetrical interatomic-distance function 77−11482
p-nonyloxy benzoate p-butyloxyphenol, smectic A to smectic C transition, crit. ang. fluctuations, Rayleigh scatt. obs. 79−95131
p-nonyloxybenzoate p-butyloxyphenol, smectic A to smectic C transition, crit. fluctuations, Rayleigh scatt. obs. 78−95140
p-n-nonyloxybenzoic acid, smectic C phase, electro-optical effect *(Russian)* 80−92458
nonyloxybenzoic acid/cholesteric liq. cryst. mixtures, helix pitch, temp. depend. 80−64895
p-n-nonyloxybenzylidene-p-aminobenzoic acid, phase transitions, X-ray diffr. and DSC meas. 79−86877
nuclear spin relax., effect of translational diffusion 78−63669
nuclear spin-lattice relax. due to layer sliding 77−36149
4-n-octyl-4′-cyano-diphenyl, appl. in detection of graphite powder particles by optical microscopy 80−9034
4-octyl-4′-cyanobiphenyl, dielec. relax. meas., short range interactions 78−94976
4-n-octyl-4′-cyanobiphenyl, smectic A and nematic liq. cryst., refr. indices and order parameters 78−22644
4-n-octyl-4′-cyanobiphenyl, smectic A phase, shear-induced textures and rheology 78−91228
4-n-octyl-4′-cyanobiphenyl, smectic A phase, stimulation of EHD instability 79−78656
4-n-octyl-4′cyanobiphenyl/4-n-decyl-4′cyanobiphenyl mixture, dynamic characts. of electrooptical effect with memory 80−108183
4′-n-octyl-4-cyanobiphenyl, interlayer elastic const. meas. close to smectic-A to nematic transitions 77−80606
4′-n-octyl-4-cyanobiphenyl, nematic and smectic A, elastic and optical props. 77−11613
4′-n-octyl-4-cyanobiphenyl, smectic bilayers, press. effects, phase diagrams *(French)* 78−10177
octyl-cyano-biphenyl, elastic props. near smectic-A nematic transition 79−23704
octyl-cyano-biphenyl, nematic and smectic-A phase, dielec. meas. 78−60392
octyl-cyano-biphenyl, smectic-A and nematic phases, dielectric meas. 79−23516
octyl-cyanobiphenyl, elastic props. near nematic-smectic A transition 78−59756
octyl-cyanobiphenyl, smectic A-nematic transition, X-ray and light scatt. obs. 79−95129
4-n-octyl-d_{17}-oxybenzoic acid-d_1, nematic and smectic phases, mol. and relative segmental order 80−96439
p-n-octyl-p′-cyanobiphenyl, thermally addressed liq. cryst. display, light scatt. and contrast 80−34892
octylcyanobiphenyl, crit. heat. capacity near nematic-smectic A transition 80−100323
octylcyanobiphenyl, orientation between different interface and induced struct. *(French)* 77−51310
octylcyanobiphenyl, second sound propag. and smectic response function, forced Rayleigh scatt. obs. 79−86693
octylcyanobiphenyl thin film, asymmetrical and symmetrical structure *(French)* 77−35473
p-n-octyloxy benzylidene-p-toluidine, mol. order, EPR VAAC probe 80−70114
4-octyloxy-4′-cyanobiphenyl, CN stretching in liq. cryst. phases, vibr. spectra 78−80325
4-n-octyloxy-4′-cyanobiphenyl, smectic A phase, elastic modulus determ., stress/strain relationships 78−91229
4-octyloxy-4′-heptyl-α-cyanstilbene liquid cryst., mag. props. 78−87615
4′-n-octyloxy-4-cyanobiphenyl, smectic bilayers, press. effects, phase diagrams *(French)* 78−10177
p-n-octyloxybenzoic acid, liq. cryst., radiation stability 78−85184
4-n-octyloxybenzoyloxy-4′-cyanostilbene, re-entrant polymorphism, nematic-smectic A-nematic-smectic A, X-ray study 80−34172
N-p-octyloxybenzylidene-p-toluidine, optical props., density, and order parameter in liq. cryst. phases 79−55657
octyloxycyanobenzylidene, smectic A, anomalous ordering, Landau-Peierls system 78−30538

smectic liquid crystals continued
octyloxycyanobenzylidene, smectic A liq. cryst., high resolution X-ray scatt. exam. 78−94984
octyloxycyanobiphenyl, nematic-smectic-A transition sp. ht. 79−42225
octyloxycyanobiphenyl, smectic-A phase, dislocation effects on viscoelastic props. 77−84633
4″-n-octylphenyl-4′-n-octylbiphenyl-4-carboxylate, orthogonal smectic B to tilted smectic B (smectic H) transition 79−94881
OOAB, liq. cryst., smectic and nematic, distrib. functions by X-ray diffr. 79−99072
OOBPD, DTA obs. of phase transitions to 3 kbar 79−23708
optical properties, diffraction nature, differences between cholesteric and chiral smectic liquid crystals 80−70123
ordered, structural classification, collective modes *(French)* 78−94971
organic doublet radicals in nematic and smectic liq. crysts., ENDOR obs. 80−91585
oxtyloxycyanobiphenyl, nematic-smectic-A transition, high-resolution 80−10649
p-alkoxybenzylidene-p′-amino-2-chloropropyl-cinnamate, chiral smectic, dielec. props. 80−96441
PAA, smectic-C and nematic long chain homologues, H-spin-lattice relax. *(German)* 78−87610
parabolic focal conic, smectic A defect 77−89374
paradiheptyloxyazoxybenzene, mol. cryst., characts. of mesomorphic transition to smectic phase 79−14920
paradiheptyloxyazoxybenzol-d, dynamics of smectic-nematic liq. cryst. phase transiton *(Russian)* 78−55938
PCB, nematic, smectic phases, dielec. and optical props. 78−60377
PEBAB/HEXOAB, mixed crystals, induced smectic A phases, elec. cond. 78−76068
p-pentoxy-benzylidene-alkylaniline series, smectic phases, dielec. anisotropy 80−55010
n-pentyl 4-(4-n-dodecyloxybenzylidene-amino)-cinnamate, X-ray studies in smectic I phase 80−70119
4-n- pentyl-phenylthiol-4′-alkoxybenzoate, homologous series, specific heat meas., nematic-smectic-A tricritical point 80−15227
4-n-pentyl-phenylthiol-4′-n-octyloxybenzoate, smectic A-smectic C phase transition, high-resolution X-ray study 80−79921
4-n-pentylbenzenethio-4′-n-alkoxybenzoates, birefr., crit. behaviour near smectic A-C transition 80−80745
4-n-pentylbenzenethio-4′-n-octyloxybenzoate, liq. cryst. phase transitions, press. and temp. depend. 79−77730
4,4′-di-n-pentyloxyazoxybenzene, anomalous smectic mesomorphism, calorimetric and optical texture obs. 79−77505
N-4-n-pentyloxybenzylidene-4-n-hexylaniline (50.6), unclassified smectic phase 80−75157
4-pentylphenyl-4′-benzoyloxybenzoate/TBBA system, smectic A_1-smectic A_2 transition, X-ray diffr. obs. 80−44303
4-n-pentylphenyl-4′-n-octylthiobenzoate, smectic-C phase, undulation instabilities, microscopic obs. 77−68919
4-n-pentylphenylthiol-4′-n-octyloxybenzoate, sp. ht. and crit. behaviour of liq. cryst. phases 78−67816
4-n-pentylphenylthiol-4-n′-octyloxybenzoate, birefringence, crit. suppression 78−76422
permeative flow around obstacle, extended boundary layers 78−67644
phase transition, A to C, mol. model 77−51478
phase transition, smectic A to smectic A 79−69229
phase transition, smectic A-nematic, liq. cryst. binary mixture, birefringence study 80−59638
phase transition of first kind, smectic A to smectic C 78−71844
phase transition smectic A to C, crit. behaviour, in mag. field 78−6148
phase transitions, B-E and H-VI, symmetry changes and crit. behaviour 78−2243
phase transitions and pretransition phenomena, book contrib. 79−60491
phenyl 4(4-alkylphenyl)cyclohexanecarboxylates, mesomorphism and dielec. props. 77−27810
phenyl 4-alkylbiphenyl-4′-carboxylates, mesomorphism and dielec. props. 77−27810
phenyl 5-alkoxypicolinates, synthesis, phase transition temps., and dielec. props. 79−86876
phenyl 6-alkoxynicotinates, synthesis, phase transition temps., and dielec. props. 79−86876
p-phenyl-benzylidene-p′-alkylaniline, ordered smectic B phase, mol. length, influence on characts. *(French)* 79−14671
4-phenylbenzylidene-4′-n-alkoxyanilines, central Schiff's base linkage reversal effect on liq. cryst. props. 80−79683
phenylcyclohexanes, alkylamino substituted, synthesis and mesomorphic props. 80−44120
p-phenylene-di-p-n-heptyloxybenzoate, liq. cryst., radiation stability 78−85184
phospholipid smectic phases, defect struct., freeze-fracture electron microscopy 77−21473
piezoeffects and ferroelectric phenomena 79−32883
piezoelectric domains, free energy minimisation and Euler eqns. calc. 77−51319
piezoelectric effect 78−6635
PNAOBA, type C smectic liq. crysts., electrohydrodynamic instability 80−1927
poly(azomethines), thermotropic mesophases *(French)* 79−77507
poly-Schiff bases, thermotropic smectic B mesophase *(French)* 79−27911
polymers, comb-like, with side groups modelling smectic type liq. cryst. *(Russian)* 79−32904
polymorphic phases, classification scheme 79−55661
polymorphism, mol. struct. effects 77−47348
di-n-propyl p-terphenyl-4,4″-dicarboxylate, biaxiality of smectic E mesophase 79−41949
reentrant nematic-smectic A phase transition, Landau theory 79−28084
reentrant-transition, nematic to bilayer smectic-A, under high press. 77−84905
refractive index near smectic-A/smectic-C transition, orientational order 80−24572
salicelidenanilines, SLC, ferroelectric behaviour, specific heat, spontaneous polarisation 80−75958
Schiff's base compounds, double axis, Siamese Twin type liq. crysts., thermal and X-ray obs. 80−39312
Schiff's bases, mesomorphic, two-component system, tricritical nematic-smectic A point 77−51482
Schiff base compounds, cholesteryl esters, mesomorphic behaviour 78−1994
smectic liquid crystals continued
Schiff base compounds, p-n-alkoxybenzaldehydes condensed with p-bromoaniline, transition temp. 78−42898
Schiff base esters, mesomorphic behaviour 78−1993
second sound excitation in insulating and conducting crystals 80−103244
self-diffusion meas. by multiple pulse NMR 78−76352
p-sexiphenyl, liq. cryst. phase transitions 79−82322
shear flow inducing smectic layer ordering, hydrodynamic theory 79−77731
shear wave attenuation 78−9944
shear waves in B_A, B_E and E_A smectics *(French)* 77−51309
SHG potential, phase-matched elec. field induced 79−86214
sitosteryl esters, mesomorphic props. 79−90539
smectic A to smectic C transition, separate order parameter for layer thickness and optical tilt angle 80−19923
smectic layers with tilted molecules, solid and fluid phases 80−96444
smectic-A phase, mol. model, steric effects 78−67646
smectic-A-smectic-C transition, model of tilted mols. in planar layer 78−79751
smectic-C, mol. orientation fluctuations in two-dimens., light scatt. obs. 80−93355
smectic-nematic phase boundary, elliptic, thermodynamic anal. 79−99300
sodium valerate, mesophase, self-diffusion and spin-lattice relax. 79−69008
solid-to-smectic B phase transition, defect model 77−7855
spontaneous polarisation meas. *(French)* 77−69765
storage effect, memorisation of oriented picture of EHD instability in smectic C phase 79−37615
striped patterns in thin droplet 78−26430
structural order effects of surface treatment, sample thickness, and cooling rate 78−63667
supercooled monotropic smectic-B liq. cryst., Mossbauer studies of ^{57}Fe bearing solute 77−81041
surface, statistical thermodynamics, local order parameter 80−88023
surface skin, on liq., periodic ripple form. 77−47352
surfactant vesicles, low-ang. light scatt. and photon correlation spectroscopy 79−79484
TBAA, synthesis and smectic B-smectic B transition 77−15562
TBAA homologous series, deform. vibrs. of alkyl chains, Raman spectra obs. 77−39531
TBACA, chiral, ^{14}N NQR of smectic phases 78−59749
TBACA, chiral, smectic C* and H* phases, mol. orientational ordering, ^{14}N NQR study 80−75152
TBBA, achiral, ^{14}N NQR of smectic phases 78−59749
TBBA, biaxial liq. cryst., orientational order, ^{14}N NQR meas. 77−32288
TBBA, biaxial smectic phases, orientational order, neutron scatt. and NQR results 78−91225
TBBA, cryst. phase, struct. at 20°C, butyl side chains disorder *(French)* 77−58998
TBBA, cryst. phase, struct. at 20°C, comparison with smectic B *(French)* 77−58999
TBBA, dielec. const. in cryst. and smectic phases 79−78607
TBBA, freq. dispersion of proton Zeeman relax. time and quadrupole reson. of ^{14}N 77−62468
TBBA, liq. cryst., orientational order in tilted smectic phases, high resolution neutron quasi-elastic scatt. 77−80413
TBBA, low temp. phase, inelastic coherent neutron scatt. exam. 78−26429
TBBA, mesophase identification by X-ray diffr., review 80−100166
TBBA, metastable phase, thermodynamic props., differential scanning calorimetry meas. 78−94985
TBBA, order parameters in nematic and smectic phases, X-ray diffr. meas. 79−94874
TBBA, phase transitions involving ordered biaxial phases, X-ray diffr. study 79−95136
TBBA, phonon dispersion curves in cryst. and smectic phases 79−86863
TBBA, proton ^{14}N nuclear double reson. 77−58947
TBBA, self diffusion coeffs., neutron diffr. and NMR study 80−19689
TBBA, self-diffusion and undulation modes, high resoln. neutron scatt. 77−11471
TBBA, smectic, spin-lattice relax., self-diffusion, mol. rot. 78−35055
TBBA, smectic A phase, incoherent neutron quasielastic scatt. exam. of molecular ordering 77−43143
TBBA, smectic A-nematic transition, cybotactic cluster form., X-ray obs. 78−95138
TBBA, smectic and cryst. phases, far IR absorpt., struct. and dynamical props. 77−84636
TBBA, smectic C layer thickness meas. by X-ray scatt. 78−94986
TBBA, smectic C to A phase transition, neutron diffr. exam. 78−91428
TBBA, smectic C to smectic A transition, crit. exponent, neutron diffr. obs. 78−95143
TBBA, smectic liq. cryst., crystalline at liq.-cryst. phases phonon modes, coherent neutron inelastic scatt. study *(French)* 79−51216
TBBA, smectic liq. cryst., polarised Raman spectra, 90-300K, 0-400 cm^{-1} 77−12383
TBBA, smectic phases, orientational order, ^{14}N NQR and double NMR obs. 78−94974
TBBA, smectic phases, rot. viscosity, phase transitions 77−80418
TBBA, smectic polymorphism *(French)* 77−35470
TBBA, smectic VI and H phases, orientational order, temp. depend. 79−46555
TBBA, smectic-A, self-diffusion, neutron incoherent scatt. law 78−83726
TBBA, temp. depend. of deuteron NMR splittings in nematic and smectic phases 79−32898
TBBA, US absorpt. and dispersion at nematic-smectic-A transition 79−82287
TBBA, VI and H phases, orientational order 77−84648
TBBA liquid crystal, monoclinic cell parameters of solid, smectic and metastable phases, temp. dependence 80−70122
TBBA mesophases, mol. orientational order 79−37619
TBBA/4-n-pentylphenyl-4-(4-cyanobenzoyloxy)benzoate, mixture, possibility of smectic A-smectic A transition 79−95132
TBBA/n-hexyl-4′-n-dodecyloxy-biphenyl-4-carboxylate, mixtures, orthogonal smectic B to tilted smectic B (smectic H) transition 79−94881
TBPA, liq. cryst., smectic F phase, X-ray diffr. obs. 80−44122
TCOOB, smectic A and C liq. cryst., A-C phase transition, diffuse-cone model description 79−86674
TDOBAMBCC, chiral smectic C liq. cryst., dielec. consts., electroclinic effect 78−94980

smectic liquid crystals continued
p-terephthal-bis-aminocinnamate, smectic phases, orientational order, ^{14}N NQR and double NMR obs. 78−94974
terephthal-bis-n-alkylaniline, homologous series, prep. and mesomorphic props. 78−26436
terephthal-bis-p-p'-butylaniline, pretransitional anomaly, US obs. 78−75818
terephthalates, vibr. spectra, vol. struct. 78−18547
terephthalylidene-bis-4-n-alkylanilines, smectic F planes 78−42902
terephthalylidene-bis-(4-n-alkylanilines), smectic polymorphism, calorimetric study 80−88307
terephthalylidenebis-4-n-pentylaniline, smectic F phase, characterisation and struct. 79−86707
terephtylidene-bis-(4-nalkylanilines), smectic polymorphism, miscibility meas. 79−86678
terphenyl, thermal diffusivity, Rayleigh scatt. obs. 78−94977
thermal conductivity anistropy, forced Rayleigh light scatt. meas. 78−94991
thermal parameters, transition temps. and latent heats 78−22832
thermodynamic phase diagram of smectic mixtures 77−62623
thermotropic, anomalous rheological responses, spectrometer study 80−6358
thermotropic, smectic phases formed by esters and cyanobiphenyls, smectic F materials 78−94968
thermotropic liquid cryst., diffusion and nucl. mag. relax. 80−24362
transition A to C state, effect of chiral solute 77−24389
transition from A to C phases, model 79−90762
transition to A-nematic phase, defect model 79−14916
trifluoromethyl liquid crystals, effect of mol. struct. on mesomorphism 78−51414
TTF derivatives, smectic and nematic, for liq. cryst. device appl. 80−54124
twist, absolute sense, determ. by contact method *(French)* 77−27827
two dimensional model, structure, transition to smectic and cryst. phases 77−7857
n-undecyl-p-azoxy-α-methylcinnamate, smectic C phase, domains, walls, and disclinations 79−86687
undecylazoxymethylcinnamate, crit. angular fluctuations above second order smectic-A to smectic-C transition 77−4190
undulation mode propag. in smectic A cryst. in mag. field 79−14672
unified Landau theory, for nematic, smectic-A and smectic-C phases 77−55238
unified model for bulk smectic-A, nematic and isotropic phases 80−79692
US propagation, mesophases and phase transitions 78−79667
variable tilt smectic A electro-optic effect giving stored colours 78−51415
vibrational IR and Raman spectra 79−73913
viscoelastic properties and field instabilities 79−27904
viscous and plastic behaviours 79−86686
X-ray analysis, induced phases of liq. cryst. mixtures *(German)* 78−94995
X-ray and light scattering obs., high resolution 80−92460
X-ray diffr. studies, review 80−100166
X-ray study under press. of smectic C* phase *(French)* 79−99061
CBOOA, smectic A order parameter meas. and crit. scatt. near smectic A⇌nematic phase transition 77−84649
Ni complexes, dithienes, nematic and smectic mesophases, synthesis and characts. 80−70120
Ni complexes, dithiolato complexes, smectic C phase, synthesis, isobaric phase diagrams 78−94970
Ni dithiene complexes, mesomorphic props. 80−88026
4n-octyl-4'-cyano-biphenyl, liq. cryst., density, and rel. change at phase transitions determ. 77−80605
Pt complexes, dithiolato complexes, smectic C phase, synthesis, isobaric phase diagrams 78−94970
Pt dithiene complexes, mesomorphic props. 80−88026

smell (physiological) *see chemioception*

smoke
see also air pollution; dust
acetylene, optoacoustic meas. of absorpt. at 0.5145, 10.6 μm 80−43060
acetylene smoke particles, agglomerated, optical extinction meas. at 0.5145 and 10.6 μm 80−48155
acetylene smoke particles, optoacoustic meas. 80−50895
aerosol microstruct. and refr. index, optical determ., inversion method 80−36399
aerosols, artificial, gravitational seidmentation, velocity *(Russian)* 78−85619
aerosols, optical absorption to extinction ratio, photoacoustic determ. 80−58459
atmosphere, long-term mean. conc. in England and Wales country areas 77−37360
atmosphere, solar radiation absorpt. by aerosol, spectrophone meas. 79−80027
atmospheric, optical probing, homogeneous particle model appl. *(Russian)* 78−77328
atmospheric particulate concentration, rise of smoke plumes, application of lidar 80−51026
atmospheric plume dispersion meas. at large distances from source 79−20998
atmospheric smoke and dust clouds, lidar observation at 0.7 μm, 10.6 μm 78−49181
atmospheric visibility rel. to surface wind at Gutersloh, Germany, smoke pollution effects 79−29853
chimney plume particulate and gaseous pollutant conc. and mass flow, IR radiometry 77−37393
cigarette, density changes during burning as obs. by β-source attenuation 78−11792
cigarette smoke, alpha radioactivity per smoke particle 77−29181
coal smoke particles, atmospheric natural radioactivity *(Rumanian)* 78−53723
coal smoke pollution, diurnal variation, harmonic anal. *(Rumanian)* 79−21009
combustion chemical and physical processes study *(Italian)* 77−66756
computerised rapid-scan spectroscopy, at NAVWPNSUPPCEN Crane 78−41362
concentrations, frequency of fog in Midlands, England 79−84458
condensation fume, nature and origin of particles 79−39221
density meter maximum sensitivity determination, flue gas optical density spectral analysis appl. 78−69500

smoke continued
detector design and smoke props. 79−63331
diesel smoke particles, optoacoustic meas. 80−50895
diffusion, steady state model, effect of terrain 79−92582
diffusion in atmosphere from small island and undisturbed ocean site 78−85647
dispersion modelling, meteorological methods appls. *(German)* 80−51496
dusty IR Test-1 lidar obs., transmission meas. 80−99625
flow structure, mixing region of laminar and turbulent flows 78−90863
gas velocity measurement by cross correlation of random thermal fluctuations 77−58812
gas-particle plumes from finite-size combustion sources, dynamics 78−30341
ground level concs. in urban areas of UK rel. to meteorology 79−12253
incinerator smog reduction by US vibration induced water mist 77−32845
industrial flare flames, smoke detection and control by electric fields 78−81360
IR extinction spectra of liquid droplet smokes and fogs 77−78416
laser velocimetry of distance smoke plume 78−28345
lidar obs. at 0.7 and 10.6 μm wavelength 78−69459
light extinction, absorption effects 78−33667
London, pollution control rel. to Global Solar Radiation Index vars. at Kew 77−17217
marine atmosphere, lightly polluted, dark smokes and acid pollution study 78−81376
metal oxide smoke particles prepared by gas evap., morphology and coalescence growth 80−97738
open field burning emissions and plume concs., depend. on meteorology, field conditions and ignition technique 78−36266
particle shape effect on low freq. absorpt. 80−99626
particle size and conc. meas., three-wavelength light transmission technique 79−79438
particle size determination by light scattering, unknown refractive index 78−95957
photochemical smog, transferred contaminant air pollution model *(Japanese)* 78−32217
plume associated with intense local fire, obs. 77−49148
plume concentration meas. by optical radar *(Chinese)* 78−58006
plumes, meas. of effective stack height with lidar *(German)* 77−9490
pollution, Greater London area, vehicular and domestic emissions relative importance 78−36269
pollution index system for rapid source-strength determ. 77−29450
retardation, Mo-containing formulations 77−77761
sedimentation, natural, visual, photographic and laser sonde obs. *(Russian)* 78−32216
sedimentation of sub-micron fractions, spontaneous, in confined space, expts. *(Russian)* 79−5182
shock wave structures, particle specific heat, Boltzmann eqn. 78−14072
silicate smokes, vapour-condensed, 800 to 130 nm extinction and interstellar extinction curve 80−82180
smoke-particle aggregates, long-range correlations 79−46369
smoke/dust cloud temporal analysis algorithm 80−98484
soot-gas mixture, in luminous flames and smoke, IR mean absorption coeffs. calc. procedure 78−91061
timber fires in Alaska, NOAA-5 images, of smoke 78−49079
C smokes, vapour-condensed, 800 to 130 nm extinction and interstellar extinction curve 80−82180
C sphere aerosol, black smoke opacity, calc. variation with particle size and refr. index 79−72488
Ge particles, homogeneously nucleated, production and props. 77−56252
K smoke particles, optical props. 480 to 620 nm, rel. light scatt. cross sections meas. 80−97293
MgO, particle size distrib. 80−104471
MoO_3, smoke particles, coalescence growth by gas-evaporation 78−47256
NO_2 and SO_2 pollution near industrial area, meas. and remote sensing equipment *(French)* 79−74928
Na smoke particles, nucleation and growth, light scatt. study 80−35580
SO_2 conversion in smoke plumes *(Dutch)* 77−70825
SiC smokes, vapour-condensed, 800 to 130 nm extinction and interstellar extinction curve 80−82180
Si_2O_3 smoke, nonequilib. phases condensation from SiO vapour 79−60497
WO_3, smoke particles, coalescence growth by gas-evaporation 78−47256

smoothing circuits
see also filters
bioelectric potentials, controlled filter 78−40357
filter for continuous radiometric monitoring, for material with fluctuating parameters 77−90553
nuclear medicine imagery data smoothing with digital filter 79−25070
ocean wave spectral density meas. with analogue filtering 77−41230
RC filters, for isotope flaw detector, choice of parameters and performance evaluation 79−15945
seismometer digital automatic amplitude controller with preliminary smoothing, parameter selection *(Russian)* 79−74985

snap off varactors *see varactors*

Snoek effect
anelastic relaxations and magnetic aftereffects in solids, conf., Katowice, Poland (Jan. 1978) *(Polish)* 79−96072
density matrix formalism for anelastic relaxation 79−14880
dislocation motion across transient Snoek atm. 79−73166
internal friction curves, numerical anal., program in ALGOL-1900 *(Polish)* 79−95079
metal, BCC, strain depend. elastic dipole tensor for interstitial impurities, nonlinear Snoek effect 79−8311
metal-H system, lattice strains, expt. methods, book contrib. 79−82202
metals, BCC, under elastic stress, Snoek peak height determ. 80−65153
steels, ferritic and martensitic, C and N migration at low temps., monograph 80−22149
transition metal alloy, ferromag., H-impurity complex obs. by magnetic aftereffect 78−72373
Zircaloy-4, quenched, strain ageing behaviour, ageing time and temp. effects 78−56657
Be, internal friction, temperature spectrum and dislocation damping, anelastic relaxation *(Russian)* 80−2118
Fe alloy, impurity-dislocation interaction and Snoek Koester relaxation *(Russian)* 78−59834
Fe, damping during and after deformation 79−43344

Snoek effect continued
Fe, impure, Snoek peak figures in various strain amplitude ranges 80−66562
α-Fe, neutron irradiated, mobile C atom trapping, anelastic and magnetic relaxations 80−100306
α-Fe, quenching, C atom pair form., isothermal mag. permeability disaccommodation meas. 77−36540
Fe, tetrahedral site occupation by C, study of possibility *(French)* 77−51508
Fe-C-Cu (0.21, 0.2 wt.%), neutron-irradiated, resolution of C atoms, internal friction meas. 78−31442
α-Fe-C(N), containing substitutional atoms, mag. permeability disaccommodation *(Polish)* 79−95612
Fe-H, deformed, internal friction 79−57041
Fe-H, Snoek-Koster peak of internal friction, Schoeck model *(Polish)* 79−96076
Fe-Ti, mag. permeability disaccommodation rel. to dissolved N migration *(Polish)* 79−95611
Fe-Ti, magnetic aftereffects of H isotopes, book contrib. 79−82835
KCl:Eu, flow stress 77−36577
NaCl:Ca, aggregation and precip. hardening in impurity vacancy, dipole decay 80−16322
Nb wire, neutron irrad., internal friction meas. 79−70077
Nb:H, lattice distortion and migration energy of H impurities 78−30796
Nb-O, Snoek mechanism and long distance diffusion under strain ageing *(French)* 77−81279
Ni-C, magnetic aftereffects of H isotopes, book contrib. 79−82835
Ni-Fe, magnetic aftereffects of H isotopes, book contrib. 79−82835
Ta:H, lattice distortion and migration energy of H impurities 78−30796
Ta-H alloy, absence of Snoek relax. 77−32610
Ta-O, BCC, Snoek type reordering during strain ageing *(French)* 79−8312
V, determination of effect of H on elastic moduli 80−75288
V:H, lattice distortion and migration energy of H impurities 78−30796
V-H single crysts., rel. to elastic consts., temp. depend., H effects 80−66563
V=O, lattice distortion and migration energy of O impurities 78−30796
Zr-Nb (1 wt.%), static strain ageing between 295 to 773K, TEM obs. of plastic strain 79−38855

Snoek-Koster relaxation *see anelastic relaxation; dislocation damping*

snow
β-activity of Antarctic and Greenland snows, stratospheric residence times 79−79421
ablation hollows on melting snow surface *(Japanese)* 80−36345
accumulation, distrib., melt and runoff 80−36338
acid precipitation in the Pittsburgh, Pennsylvania area 80−94129
acidity, release of S and nitrogen oxides by burning fossil fuels 80−26590
acidity of NW.Africa snowfields, 1977-79 obs. 80−98370
acoustic Doppler sounding of falling snow 79−53467
acoustic emission response 79−87801
aerodynamic roughness as function of wind direction over asymm. surface elements 78−92890
aggregation of falling flakes, theory 80−12491
air pollution accumulation 77−73841
albedo following dustfall, satellite remote sensing 80−17385
albedo of snow- and ice-covered regions, multiple reflections between clouds and surface 77−45131
alkaline snowfalls in Ottawa and Winnipeg, Canada 79−12175
alpine tundra habitats, effects of phys. habitat factors and plant morphology on ^{137}Cs contamination 77−37058
anions in snow cover of Adirondack Mountains, meas. 79−12149
Antarctic, surface dust contamination, climatonomical modelling of temp. response 78−24354
Antarctic snows, trace metals contents (1914 to 1974) 79−34867
Antarctica, snow accumulation rate vars. from 30000 yr isotope climatic record 79−92586
Arctic aerosol and snow compositional differences 79−88377
Arctic Canada, ice-sheet initiation and climatic influences of expanded snow cover 79−66724
Arctic Ocean sea ice, snow and ice cover conditions 80−26547
areal extent and water content estimate using LANDSAT imagery 77−78520
atmosphere snow and ice particles, influence on elec. field above Arctic Ocean *(Russian)* 79−48537
atmospheric surface layer above snow *(Russian)* 78−96264
auroral albedo profile over snow-covered ground, rocket obs. 78−77384
avalanche dynamics expt. study, Khibin Mountains 79−39783
avalanche forecasting in Khibins, model *(Russian)* 77−21812
avalanche motion, discontinuous solutions 77−67286
avalanche motion, hydraulic model for rectangular bed *(Russian)* 79−29804
avalanche release explosions, ionospheric effects 80−36451
avalanches, artificial, Lautaret Pass, French Alps *(French)* 77−37249
avalanches, critical condition prediction by statistical analysis *(French)* 77−33104
avalanches, critical factors *(French)* 77−33103
avalanches and landslides, reach and velocity *(German)* 77−53095
avalanches in conditions of limiting friction 79−66717
avalanches in Kurobe Canyon, Japan, study of high-speed events *(Japanese)* 78−88859
avalanches of freshly fallen snow, initial impulse role 79−39771
balance used as rain gauge *(German)* 77−33207
blizzard, 1978 February 18 to 19, in SW.England and S.Wales 80−12507
British Isles, catalogue of snowiness for last 100 winters 77−56719
calorimeter for measuring snow melt *(Japanese)* 78−88934
chemical composition of Norwegian snowpack, rel. to air pollution 79−20871
N.China, snowstorm, 1974 December 2, preliminary study *(Chinese)* 79−84451
cloud identification against snow background, aircraft obs. *(Russian)* 77−29392
clouds, water droplets size, density distrib. meas., laser remote sensing technique *(Japanese)* 78−49175
cohesion strength and compression resistance in snow cover 80−26560
collection and chemical anal. 78−57368
contamination of arctic snowfield, ion comp. and episodic var. 77−91159
cooling of snow and water surfaces, impact of atmospheric CO_2 79−92569

snow continued
cooling tower plumes, natural draught snowfall obs. 77−2215
cover of Yakutia (USSR), evap. and evolution 77−73768
Crete, evidence for glacial and nival formations *(German)* 77−64359
crystal conc. in air near ground, automatic meter 77−53242
crystal growth by droplet accretion 80−41495
crystalline forms rel. to cloud source thermodynamics *(Rumanian)* 77−33169
crystals and natural ice nuclei from Colorado winter storms 77−9475
depolarization at 11.6 GHz on a terrestrial radio link *(French)* 78−53687
depth, increase by snow fences rel. to permafrost amelioration near Schefferville, Quebec 77−33058
depth meas. using cosmic-ray snow gauge *(Japanese)* 77−5347
depth recorder using optical fibres *(Japanese)* 77−87112
depths in Birmingham, England 1917/18-1976/7 winters 78−44890
Devon Island ice cap, arctic Canada, $^{18}O/^{16}O$ climatic record from snow cores 77−41141
Devon Island ice cap, NWT, Canada, $\delta^{18}O$ vars. in snow 80−4050
dielectric breakdown characteristics *(Japanese)* 78−40669
dielectric relaxation and LF anomalous dispersion obs. *(Japanese)* 78−49056
drift meas. by radar *(Japanese)* 77−82032
drifts and drift density around obstruction *(Japanese)* 77−81946
dry slab avalanche release mechanism, shear fracture precipitated by strain softening 80−8338
education, snow and avalanche phenomena 80−57044
effect on lake P budget 79−62540
elemental abundances, natural enrichment 78−77303
energy budget of snow cover, energy flux meas. 78−92859
epitaxial relationship during three dimensional dendrite form. 79−23875
Eurasian winter snow cover rel. to Indian summer monsoon rainfall 77−41076
evaporation during chinooks along eastern slopes of Rocky Mountains, Alberta 79−79883
experimental device for measuring friction between ski and snow 78−92410
extraterrestrial matter in fresh snow, preliminary results 79−84302
falling crystals, attached aerosols direct obs. 80−17362
falling snow, occurrence over United Kingdom 77−41124
flood freq. model for snowmelt in northern subarctic basin 77−9454
flying snow caused by pressure drop in front of avalanches *(Japanese)* 77−87025
flying snow in front of avalanches, expansion flow out conditions *(Japanese)* 77−87026
flying snow in front of avalanches, snow cover descent *(Japanese)* 77−87027
forecasting, use of wet bulb pot. temp. charts 77−91232
friction vels. on snow surface *(Japanese)* 77−86949
gauge, cosmic ray, construction, characts., snow-water equivalent meas. *(Japanese)* 78−69498
Germany, weather forecast for New Year's Day 1978-9, moist baroclinic model *(German)* 80−77065
glide mechanism of snow cover on slope with bamboo bushes *(Japanese)* 78−88857
Great Britain, snow cover 79−12161
Greenland, NH_4^+, SO_4^{2-}, Cl^-, Ca and Na in snow and ice, natural and anthropogenic origins 79−70815
S. Greenland firn layers, transuranic nuclides, depositional history 77−86953
ground cover remotely sensed by radar, backscatter cross-section 80−46279
growth mechanism with specific grain boundary 79−23547
hailstone nuclei formation, role of giant aerosols *(Russian)* 80−56530
hardness and particle shape effects on drifting phenomena *(Japanese)* 78−88856
heat and mass flux through dry snow 79−57980
heat transfer, cond., radiation and water vapour diffusion model 78−94563
heat transfer in vacancy within snow *(Japanese)* 77−86952
Himalaya, snowfall during summer 80−72620
Himalayas, satellite snow cover obs. and estimates of seasonal streamflow 77−64349
induced airflow caused by wind blowing over snow cover *(Japanese)* 78−88854
induced snowfall, due to power plant plume 78−81284
Ishikari-Yufutsu plain, Hokkaido, snow cover characts. *(Japanese)* 77−81942
Japan, regional characts. of winter snow cover *(Japanese)* 78−88858
Kashmir region, study of chemical components 80−94594
Lake Leman area, precipitation trends, evidence for 50 year cycle *(French)* 77−21824
Lake Ontario induced snowfall systems, objective forecast method 80−51484
land basin with snow, radiative cooling 78−88872
LANDSAT snow mapping data 77−82061
laser beam, intensity fluctuations in snowfall *(Russian)* 80−94602
laser beam attenuation by snowfall, characts. 80−26611
laser beam propagation, intensity fluctuations during precip. *(Russian)* 77−29432
laser beam propagation through snowfall, characts. 79−74958
laser radiation transmission meas. at 10.6 μm 78−92977
lidar scattering from snow and ice crystals in atmosphere, polarization characts. 77−64430
light extinction at high densities *(Japanese)* 77−87028
light scattering effects on satellite aurora and nightglow obs. 78−77385
measurement of snowfall, dual-gauge and Wyoming shield systems 80−61928
melt of snowpack, two-dimens. turbulent diffusion model 77−78277
melting conditions, computer modelling *(French)* 77−33102
melting of prairie snowpack, energy budget approach 79−84310
melting on slopes of Mt. Asahidake, Hokkaido *(Japanese)* 80−36343
melting rate, urban/rural area comparison in Sapporo, Hokkaido *(Japanese)* 80−36342
melting rate and heat balance near building or board fence *(Japanese)* 77−86951
meltwater chemistry, conc. changes during melting 79−53388
metallic objects detection by passive mm wave radar systems, military appl. 79−84467
microwave attenuation at 36.8 GHz, meas. *(Russian)* 77−5209
microwave brightness spectra of layered media 77−81898

snow continued
microwave links, 11 GHz, fading due to rain, snow and multipath propag. 77−91206
microwave passive remote sensing, theory and expt. 80−26632
microwave radiometry determination of snow cover parameters 80−56652
microwave signatures rel. to snow state and wetness 78−57235
microwave spectroscopic imagery of Earth from Nimbus 6 satellite 78−12026
mountain ridge snow cover effect on ultrashort wave diffraction field 77−64395
mountain station, snow cover rel. to atmospheric electrode effect 79−25307
mountain watershed with ski basin, heavy metals concs. in snowpack and streams 79−20903
Mt. Asahidake, Hokkaido, snow accumulation and ablation *(Japanese)* 80−36344
Mt. Blanc, strong acidity of snow rel. to air pollution 78−81259
Mt. Teine, Hokkaido, deposition and melting of snow with altitude *(Japanese)* 80−36346
Mt Uenshiridake, Hokkaido, glaciological and meteorological studies of snowpatch *(Japanese)* 77−81943
Munich, snow cover from October 1887 to (April 1977) *(German)* 78−69421
New England, 1816, snow and frost in year without summer rel. to Tambora volcano eruption 80−4089
New York State, changes in local snowfall in four cities 80−105044
Ontario, east central, areal differentiation of snow cover 77−41086
organic micropollutants in precipitation in Norway 78−36262
pack, crystal orientation *(Japanese)* 77−86948
pack snow water on Mt. Everest, mass spectrometric chem. anal. of D, ^{17}O and ^{18}O *(Chinese)* 80−77016
passive microwave obs. from Nimbus satellites 80−101422
penetration and backscatter of millimetric waves 77−21877
permittivity and attenuation, 4-12 GHz 80−85692
persistence, runs and recurrence characts. of precip. 78−3865
pesticides and heavy metals in Bavarian snow 80−61488
pollution, atmospheric, metal and S content in deposited snow, effect of human activity compared to volcanoes *(French)* 80−67018
polycrystalline, twinning model with cubic struct. at junctions 77−1136
prediction of snow, with 10-level model 80−82025
radar backscatter in 1-8 GHz range, MAS expt. 77−86946
radar measurement of snowfall, accuracy assessment 79−12316
radiometry in 3 to 60 mm wavelength region, rel. to snow parameters investigation 80−72561
radiowave attenuation on SIRIO-1 Earth-satellite link *(French)* 80−56504
radiowave depolarisation due to snow at 11.6 GHz 78−57239
river drainage basins, snow estimated water equivalents and melting charcts. determ. 78−96249
rollers, form. at Coningsby, Lincolnshire (1979 January 2) 80−72568
roughness length and friction vel. in driftins snow *(Japanese)* 77−81941
satellite pictures and teledetection methods used for snow measurement and forecasting *(French)* 79−96770
Scotland, 1978 summer remaining snow beds 79−100882
Scotland, severe snowstorms, 1831-61 period 79−39839
E.-central Scotland, snow and sleet freq. var. in 1708-1975 period 78−44951
Scotland, snow survival during 1976 summer 77−91168
Scotland, snowstorms from (1729 to 1830) 77−25757
Scotland, summer 1977 snowbeds 79−2313
seasonal accumulation, melt and water input, New England model 77−2187
Sierra Nevadas, snowcover, satellite obs. during 1977 Californian drought 78−65352
sintering and compaction of wet snow 79−62536
SIRIO satellite link, 11.6 GHz, propag. meas. in Munich 79−84337
size spectra and snowflake aggregation efficiencies, theory and obs. 79−8660
sliding surface obs. within snow cover *(Japanese)* 77−81947
snow cover, correl. with upper atmosphere Na abundance 77−87140
snowfall detectors and automatic depth recorder *(Japanese)* 79−8700
snowfall intensity photometer theory *(Japanese)* 78−85736
snowfield assessment from Landsat 78−88941
snowflake, size and falling velocity meas. using laser Doppler velocimeter 80−68185
snowflakes, vapour deposition and aggregation growth, analytical model 78−73433
snowflakes rel. to cloud formation and Chinese name for mica 77−91195
snowgauge measurements, Canada, accuracy 79−70818
snowpack, model of planetary boundary layer above surface 80−41477
soil, seasonal freezing or thawing depth calc., eqns. eval. 77−78243
spectral reflectance, two-stream theory 79−88376
stone movement through snow creep, 1963-75 period, Mt. Twynam, Australia 78−69374
storage determ. for small high Arctic basins, error anal. 79−70817
stream temps. during melt period *(Japanese)* 78−88860
subarctic snowmelt, energy balance computations 77−5262
subarctic snowpacks, runoff generation 77−5261
thermal radiation polarisation, of permanent snow fields, from meas. obtained from the 'Meteor' satellite 78−88870
thermally stratified acid water in snowmelt 77−73770
undulations of snow cover on a mountain slope *(Japanese)* 77−86950
uniaxial tension, strain rate and fracture *(Japanese)* 78−88855
volumetric constitutive law based on neck growth model 80−48595
water content meas., calorimetric method *(Japanese)* 80−31142
water equiv. of dry snow, active and passive microwave response 80−72563
water equivalent measurement with standard densitometer, accuracy 79−29796
water pressure in ripe snowpacks 79−53384
water storage determ. using aircraft-borne gamma-ray surveys 78−16218
weather modification in USSR 77−64362
wet, grain clusters obs. 80−26553
wetness, active and passive microwave response 80−67382
wind and snow surface interaction 79−84356
wind interaction with dry snow and bare ice surface 80−109181
windblown, impact abrasion of minerals 77−70647
winter accumulation in Sapporo, Hokkaido *(Japanese)* 80−31071
winter weather in W.Fife in 18th century 77−29981
snow continued
Wisconsin driftless area, snowmelt rel. to small watersheds hydrology 77−91169
Yamadera area, Japan, snow survey (1973-1975) 79−12153
Ca excess in snow and rain samples, Japan, from calcite source 79−39766
D areal distribution in California and Nevada precipitation, 1968-1969 period 79−100918
N compounds exchange between ocean-atmosphere-continent system 78−3794
O isotopic composition of fallen snow in Antarctica, controlling factors 78−36237
O_3 meas. over snow surfaces 79−12281
Pb and S dry deposition onto snow surface 77−37288
Pb and sulphate dry deposition on snow surface 77−2231
Pb, Cd, Cu, Zn, Ag, tropospheric fallout fluxes in Antarctica and Greenland 79−58007
Pb, V, Cd, Zn, Cu, conc. in snow of Mt. Blanc rel. to air pollution 78−81258
^{210}Pb conc. or climatic changes at South Pole 78−7748
Pu isotopes in Antarctic snow layers, deposition and accumulation 79−70820
SO_2 deposition velocities to snow, N.Canada 79−70478
SO_4^{2-}, spatio-temporal distrib. in Antarctic snow 79−20870
T fallout at South Pole in 1954-1978 snow samples 80−16867

SNR *see supernova remnants*

social and behavioural sciences
see also demography; economic and sociological effects; ergonomics; psychology; teaching
aircraft noise, variation of community response with time of day 79−34462
animals unusual behaviour before earthquakes, positive and negative reports 80−26455
Askesian Society of London, 1796-1807, social and institutional context 77−41450
associated movement study, portable micro-system 80−51299
biological response to non-ionising EM radiation, research perspectives 79−48289
catastrophe theory application, claims and accomplishments 78−29
catastrophy theory appls., book 78−32665
cocktail parties, acoustical aspects 77−80008
Darwinian revolution, applicability of Planck's principle 79−62991
death statistics, Pade approximants used for sequential term prediction 78−57866
educational course, scientific method illustrated by paraphysical and neuroscience topics 78−24591
educational course in physics, history and society 77−41429
geodesy, an ordering factor in society *(German)* 77−60344
global problems and energy, nuclear power 78−45454
impulse noise annoyance, assessment via C-weighted L_{dn} 77−84068
intelligent life in Galaxy, significance of unsuccessful search 79−53736
Lotka's law, freq. distrib. of scientific performance 79−58524
man's effect on environment, natural resources 78−45455
marine animal biphasic constant current stimulator 78−48899
meteorite falls, science and social intelligence about anomalies 79−40346
motion online detection in digital video images, mice identification in labyrinth expts. *(German)* 78−92754
noise annoyance, social surveys 78−87189
nuclear power acceptance, public attitude formation 77−10496
research orientation differences reflected by allocation of grants 79−71218
road traffic noise, comment on survey method 79−37083
science statistics, inequality indices and skewed frequency distribs. 79−58523
scientific advance, measurement, objectivity vs. relevance techniques 79−58520
scientific collaboration, professional origins of co-authorship 79−58522
scientific growth, review of measurement indicators 79−58519
scientific research bureaucracy 79−97179
student and teacher perception of physicist's image 78−62030
subliminal communication for behaviour therapy and education, audiovisual technique 78−73293
tornado threat in United States, distrib. rel. to human attitudes 78−69397
visual behaviour modelling using catastrophe theory 79−83784
world science as input-output system 79−58521

social and behavioural sciences computing
see also educational computing; psychology
alcoholics, drinking consummatory response measuring device for automated aversion therapy 77−56510
animal communication, INFO program using information theory for anal. 77−90712
automated simulation of direct school/society interaction 79−35487
brightness perception nonlinearities, computer plotted luminance profiles 77−56380
microcomputer-based system for rat locomotor activities meas. 79−20722
movement-activated recording monitor for motor activity 77−25565
music perception, programmable tone generator presenting melodic and harmonic patterns 77−56381
neural spike trains rel. to physiology and behaviour, data acquisition system 77−13035
vocal cords vibratory behaviour in tension and mass imbalance 79−83803

social aspects of automation
robots and manipulators, symposium, Warsaw (Sept., 1976) 78−53574

social effects of automation *see social aspects of automation*

societies
ACS Tenth Biennial Education Conference on Safety and Health in Academic Lab., recommendations 79−80387
American Association of Physics Teachers, 1979 winter meeting 80−42042
Askesian Society of London, 1796-1807, social and institutional context 77−41450
Astronomical Society of Pacific (ASP), foundation by Edward S. Holden 79−75310
CODATA task group, high-temp. thermal transport props. 77−45818
European Communities' solar energy R&D programme 79−57360
European Physical Society, growth and struct. 77−5608
Illinois climate centre, review 80−77118

societies continued
International Energy Agency and NATO solar energy programme status 79−57362
International Union of Crystallography, early history 77−17738
optical standard test method development by ASTM 80−74528
Physics Manpower Panel of American Physical Society, employment and education trends 78−65735
Polish Physical Society, 1920 to 1939 *(Polish)* 78−54145
role of scientific and engineering societies in development 80−31480
Royal Astronomical Society, manuscript archives 78−32636
Royal Meteorological Society, history 79−2376
Royal Society in 17th century 77−26121
UNESCO solar energy programme 79−57358
UNIDO solar energy programme for developing countries 79−57359
United Kingdom Climatological Network, history and role of co-operating observers 79−5618
United Nations System solar energy programmes 79−57361
Webb Society handbook of double stars 80−8744
Webb Society handbook of planetary and gaseous nebulae 80−8743

sociological effects *see economic and sociological effects*

sociology *see social and behavioural sciences*

sockets (electrical) *see electric connectors*

sodar *see sonar*

sodium
see also nuclei with .....
abundance in M13 red giants, evidence for protocluster gas inhomogeneities 80−82439
accommodation coefficients, of Na, Rb and Cs on Ni, 658-1095K 77−47666
addition effects on Al_2O_3 sintering in reducing atmos. 77−63613
adion-surface interaction energy, density formalism calcs. for Al and W surfaces 78−68069
adsorbed c(2×2) overlayer on Ni (001), core level excitation effects, synchrotron radiation UPS study 80−40234
adsorbed film on Ni (100), plasmon losses in electron energy loss spectra 79−61480
adsorbed on Al, adatom valence-level position variation 80−88611
adsorbed on Cu (111), UPS study of surface electronic struct. 80−80350
adsorbed on Ni, hybridisation between s and p resons., jellium model 80−6932
adsorbed on Ni, photoemission, directional memory effects 80−100753
adsorbed on Ni(001), core-level photoelectron diffraction 78−95659
adsorbed on Ni(001), photoelectron diffr. effects in core-level photoemission 80−76144
adsorbed on Ni(100), photoelectron diffr. aximuthal patterns, struct. sensitivity 80−107644
adsorbed on Pt(III) surface, electronic struct. 78−19117
adsorbed on W (100), binding props. calc. 80−49522
adsorption, on W(110) plane, ordering, theoretical anal. 78−18892
adsorption and coadsorpt. with O_2, on Ag (110), XPS and UPS obs. 77−69183
adsorption on GaAs (InSb), LEED, AES, EELS study 78−68068
adsorption on V, effect on Br_2 chemisorption 80−101039
adsorption on ZnO (000$\bar{1}$) of alkali metals, anomalous behaviour of Na 78−79883
adsorption with O_2 on Ag (110) surface, LEED, thermal desorption and AES meas. 77−31883
aerosols and fires, expts., LMFBR safety anal. data 77−71650
AES, KLL spectra, and plasmon struct. 79−15592
arc, high pressure, plasma spectral change mechanism 79−82093
arc, high-pressure, time-depend. plasma temp. meas. 77−68866
arc lamp, high-press., tube temp., Al_2O_3 sublimation 78−5532
arc lamp, light-induced ignition method 80−77599
Ashcroft pseudopotential, unified study of props. 80−39239
atmosphere, enhanced Na and nightglow, space lidar obs. 80−101466
atmosphere Na layer in 80-105 km height range, lidar obs. of horizontal var. 78−36347
atmosphere Na layer wave-like structure, lidar obs. 78−88955
atom, $2s2p^63s^2$ term position and width 79−59347
atom, $3^2P_{1/2,3/2}$ reson. levels, electron impact excitation, differential cross-section calcs. 79−59584
atom, 3^2P-states, orientation and alignment relax. 79−76395
atom, 3^2S-4^2D two-photon transitions, isolated optical Ramsey fringes 77−83559
atom, 3S-4D and 3S-5S two-photon lines, broadening and shift by inert gases 77−75105
atom, 3s-5s transition, Doppler-free two-photon excitation by multiple light pulses 77−42306
atom, 5890/96 Å resonance emission lines, wing profile meas. 77−46534
atom, ^2D highly excited states, fine struct. splitting, field ionisation quantum interference 80−18835
atom, $^2P_{3/2}$-$^2S_{1/2}$ reson., light scatt. polarisation change 78−55144
atom, ^2P fine struct. splittings, Hartree-Fock calcs. 77−10606
atom, ^2P photodissoc. product, fine struct. anal. 80−78665
atom, ($4^2P_{1/2}$, $5^2_{1/2}$ states), mag. dipole interaction consts., RF spectroscopy 78−37577
atom, absolute photoabsorpt. cross section, 45-250 eV 77−88434
atom, absorption D-line shape, rel. to single-mode laser intensity 78−66491
atom, adsorption on B-Al_2O_3-Na_2O, surface electronic struct. 80−75431
atom, anomalous emission in blue wings 77−46517
atom, anomalous laser fluoresc. scatt. in shock tube 77−10627
atom, Auger effect transition energies calc. 79−18168
atom, Auger spectra, CI calcs., spin-orbit interactions 77−14558
atom, Autler-Townes effect in two-step optical resonance 77−38648
atom, backward-wave three-pulse echo in two-level system, Ar collisions effects 79−64289
atom, beam-foil populations, charge state distribs., independent electron model 77−19035
atom, coherent ground state transients, beat meas. 80−948
atom, Compton profiles using Gaussian expansion of at. orbitals 80−945
atom, core polarisation effect on oscillator strengths and energy level locations 78−82688
atom, core polarisation effects, influence on photoionisation cross sections, ground and excited states 78−46308
atom, cross section depend. of many-photon ionisation on light polarisation 77−42294
atom, cross-section meas. for five-photon ionisation 77−42297
atom, cyclic interaction with circularly polarised laser radiation 80−78581

sodium continued
atom, D_1 and D_2 reson. lines, intensity dependent polarisation change 78−5163
atom, D_1 line, optical coherent transients by laser freq. switching 78−42391
atom, D_1 line profile, Zeeman scanning 80−47928
atom, D doublet of nightglow, excitation and abundance determ. 80−98497
atom, D line broadening by inert gases, fluoresc. obs. 80−32663
atom, D-doublet in H_2-O_2-Ar flame, excitation profiles 77−88436
atom, D-line saturation, under high power laser illumination 80−32653
atom, D-lines, inert gas broadening, photon echo meas. 80−91475
atom, damping const. in acetylene-air flame, Lorentz collisions, mag. field effects 80−66805
atom, depolarisation obs. of near-resonant scattered light 80−52921
atom, detection of nF Rydberg levels by photoionisation *(French)* 77−71785
atom, diabatic field ionisation of highly excited at. states 80−43202
atom, Doppler-free two-photon linewidths, 3S-4D press. broadening coeffs. 78−25481
atom, doublet state, ionis. pots., electron affinities, using electron propagator 79−63933
atom, effective potentials, energy levels 80−106263
atom, ejected-electron spectrum of autoionis. levels excited by 35-400 eV electrons 77−14582
atom, electron affinity, model pot. CI and SCF calcs. 77−38609
atom, electron affinity, variation-perturbation approach 77−54513
atom, electron elastic and inelastic scatt. 80−91672
atom, electron impact excitation, 2nd order pots. method calcs. 78−13608
atom, electron impact excitation, combined classical theory and free fall model 79−98229
atom, electron impact excitation, ground-4s(5s)(6s) state cross-sections, Percival's combined classical theory 77−75301
atom, electron impact excitation, L-Auger and autoionis. spectra 78−5354
atom, electron impact excitation, polarised photon emission, delayed coincidence meas. 79−98225
atom, electron impact excitation cross sections, Vainshtein approx. 78−25721
atom, electron impact excitation of 3^2S-3^2P transition 77−58173
atom, electron impact ionisation, reson. and nonreson. electron distrib. 78−33615
atom, electron impact reson. transition excitation, unitarised distorted-wave polarised-orbit model 78−25710
atom, electron impact total excitation cross section, first order exchange approx. 79−31692
atom, electron ionis, ejected electrons ang. distrib. 77−50541
atom, electron scatt., elastic, differential cross sections, 12-140°, 54.4-150 eV optical model calcs. 78−74761
atom, electron scatt., theory 77−58172
atom, electronic excitation cross-section determ. method 77−540
atom, energy transfer between 3P excited atoms, fluoresc. 78−66498
atom, energy transfer with 3P-excited atom high density, mol. form., fluoresc. 77−88422
atom, excitation energy calc., improved virtual orbitals in extended basis function space 77−46491
atom, excited 4D and 5S state, absolute photoionisation cross-section 80−99488
atom, excited p-states radiative lifetimes, laser cascade fluoresc. meas. 77−27022
atom, excited state lifetime var. along isoelectronic series, HF cal. *(French)* 77−46538
atom, excited state photon echo relax. 78−37606
atom, excited states ionis. pot. calc., improved virtual orbitals 77−46491
atom, f-states collisional ang. momentum mixing by inert gas 78−58780
atom, field ionisation of highly excited states 78−17814
atom, fine-struct. of excited nd and nf states, at. core effect 78−58606
atom, first reson. doublet, anomalous dispersion meas. 77−71891
atom, flame absorption and fluorescence, laser saturation broadening 78−88661
atom, fluoresc., CW laser excitation appl. to flame diagnostics 77−79571
atom, fluoresc. in flame, saturation curves with pulsed tunable dye laser 79−36579
atom, four- and six-photon resonance spectra *(Russian)* 80−91527
atom, ground state, Li^+ electron capture cross sections 10-60 keV 80−48084
atom, ground state g_J factor, meas. from weak-field Zeeman spectra 78−33469
atom, Hanle effect for $3^2S_{1/2} \rightleftarrows 3^2P_{1/2}$ transition 77−42287
atom, high ang. momentum Rydberg states, quantum defect core polaris. depend. 77−18808
atom, high resolution inelastic electron scatt. at zero angle, oscillator strengths 78−9255
atom, high Rydberg states, quenching in strong 1.06 μm laser field 80−95559
atom, high-lying Rydberg states, field ionisation 79−45683
atom, high-resolution laser spectroscopy of at. beam *(Dutch)* 79−50166
atom, high-resolution laser spectroscopy with minute samples 78−17822
atom, highly excited, f-state fine struct., microwave reson. obs. 77−83535
atom, highly excited d states, elec. field ionisation 77−6658
atom, highly excited p and d states, fine struct. intervals and polarisabilities, RF reson. meas. 77−67999
atom, hyperfine interaction in $4D_{3/2}$ and $4D_{5/2}$ levels 78−37616
atom, in flames, laser-induced fluoresc. temp. meas. 80−11893
atom, in He buffer gas, collisional freq. redistrib. of scatt. laser light 77−30815
atom, in Xe matrix, 3s excitation, UV and vis. spectra 78−46291
atom, incoherent scatt. factors calc. by direct integration over impulse approx. Compton profiles 80−102475
atom, inner core neutral binding energies, relaxed orbital relativistic Hartree-Fock-Slater calc. 78−13433
atom, ionisation and energy pooling in laser-excited vapour 79−795
atom, ionisation of high-lying states by pulsed laser field *(Russian)* 77−75113
atom, ionisation of Rydberg state, depend. on $|m_l|$ 78−58856
atom, K-shell ionisation by ultrarelativistic electrons, density effect 80−99576

sodium continued
atom, L-Auger, autoionisation spectrum after electron impact excitation 77−14591
atom, laser excited fluoresc., saturation power, calc. and obs. 77−42276
atom, laser induced zero-field effect, non-optical obs. 78−37604
atom, laser oriented, refl. by non-disorienting surfaces, optical activity detect. 80−55252
atom, laser radiation highly excited at. states, Stark effect 79−13669
atom, laser temporal coherence effects in two-photon resonant three-photon ionisation 80−32686
atom, laser-excited, electron collision-induced alignment in 3P to nS transitions 77−19084
atom, long range and temp. depend. interaction with Re surface, theory 80−59802
atom, Lorentzian power broadening by optical pumping 78−17613
atom, mag. field quantum beats in two-photon free-induction decay 79−13692
atom, matrix isolated in Ne, absorpt. and emission spectra 80−99465
atom, multiphoton ionis., AC Stark effect 77−57948
atom, multiphoton ionisation, resonant, with intense monochromatic laser 80−32689
atom, multiphoton ionisation in third harmonic generation by mode locked Nd:YAG laser 78−94413
atom, narrowed optical lines, laser and accel. beam method 78−37770
atom, near-resonant Rayleigh scattering and atomic flame fluorescence spectroscopy 79−92033
atom, np radiative lifetimes, effect of blackbody radiation 79−41127
atom, one and two-photon ionis. of 3s and 3p states 78−50512
atom, optical amplification without population inversion 77−50645
atom, optical excitation function and polarisation meas. of spectral resolved D-lines 79−3575
atom, optical heterodyne spectra, hyperfine struct. 77−30841
atom, optical pumping, Hanle effect 78−33475
atom, oscill. strengths, Bates-Damgaard approx. calcs. 77−3311
atom, oscillator strength measurement using reson. Faraday effect in monochromatic light 80−23363
atom, outer-shell photoelectron ang. distrib. 80−37797
atom, overlapping autoionisation lines, interference effects 80−91677
atom, partial photoionis., cross sections $\sigma_{3p,s}$ and $\sigma_{3p,d}$, expt. separation and study 78−42020
atom, photoabsorpt. and photoionisation, RPA with exchange calcs. 77−54543
atom, photofragment of NaBr, non-Gaussian line shape, level shifting and velocity inversion 80−58182
atom, photoionis., one-electron pseudopotential calc. 79−18166
atom, photoionis. cross section resons., time-dependent HF theory 80−32684
atom, photoionisation and fluoresc. meas., reson. radiation illum. 80−83314
atom, photoionisation cross-section, electron correls. Brueckner-Goldstone calcs. 77−6742
atom, photon emissions, two-time correls. 79−22647
atom, photosensitized assoc. ionisation, excited from reson. levels 77−83710
atom, pionic X-ray transitions, strong interaction line widths and shifts 77−23586
atom, population change induced by laser radiation, hook method 78−33476
atom, quadrupole transition moment meas. 77−30830
atom, quantitative detect. of absorpt. by intracavity dye laser quenching 77−36817
atom, quantum beats of hyperfine levels observed in photoionisation 80−32690
atom, radioactive, spectrometer for meas. of isotopic, isomeric shifts and hyperfine structure 79−6191
atom, Raman transients obs. in Doppler free two-photon excitation 77−61728
atom, Rayleigh scatt. from vap. in flames with N_2 and Ar diluents 79−22627
atom, Rayleigh scatt. near $A^2P_{3/2,1/2}$-$^2S_{1/2}$ reson. doublet, polarisation reversal 77−10616
atom, rel. at. transition probabilities, by flame at absorption spectroscopy 79−89642
atom, reson. absorpt. transitions, laser saturation spectroscopy with optical pumping 80−47121
atom, reson. fluoresc., photon burst detection 78−42244
atom, reson. fluoresc. spectrum in intense monochromatic field 77−34585
atom, reson. light scatt., theory of correl. meas. 78−42014
atom, reson. multiphoton ionisation, broadband laser AC Stark splitting 78−70808
atom, reson. transition, laser saturation spectroscopy with optical pumping 80−52334
atom, reson. two-photon ionis., photoelectron ang. distrib. and polaris., nucl. spin influence 79−10083
atom, reson. two-photon ionisation via $3p^2P_{3/2}$ state, photoelectron ang. distrib. 80−43016
atom, resonance fluorescence, photon antibunching, quantisation of light 78−66791
atom, resonance fluorescence, photon antibunching obs. 77−83534
atom, resonance spectral lines, Stark broadening and shift 77−75097
atom, resonant collisions in laser beam 78−78782
atom, resonant three-photon ionis., saturation effects 78−58632
atom, rotation of plane of polarisation close to reson. 79−41129
atom, Rydberg levels, rel. to positron energy levels of $F^-.e^+$ and $CN^-.e^+$ 79−86089
atom, Rydberg levels mm resonances detected by field ionis., quantum defects, Stark shifts 77−42262
atom, Rydberg state quantum defects, semiclassical calc. 77−38621
atom, Rydberg states, collisional ang. momentum mixing theory 77−10748
atom, Rydberg states, diamag. struct. 78−50484
atom, Rydberg states, elec. field ionisation, sensitive detection of multiple thresholds 79−7026
atom, Rydberg states, fine struct. and Zeeman beats 79−14044
atom, Rydberg states, fine struct. splitting, quantum beat and double reson. spectroscopy 78−86979
atom, Rydberg states, high resolution spectroscopy 80−52901
atom, Rydberg states, high resolution two-photon mm spectroscopy, metrology appl. 80−43018

sodium continued
atom, Rydberg states, IR Stark spectra, term energy, fine struct. 77−57910
atom, Rydberg states, millmetre spectrosc. 80−99469
atom, Rydberg states, optically pumped, electric field ionis. *(Russian)* 79−27095
atom, SCF electron-gas local-spin-density model including correlation 80−9488
atom, seeded flames, excitation, laser radiation absorpt., sound vel., opto-acoustic effects obs. 80−43345
atom, seeded in acetylene-air flame, optoacoustic pulses, energy transfer from laser excited atoms 78−25490
atom, self-broadening of 3S-5S and 3S-4D two-photon transitions 79−26955
atom, single, detection by laser fluoresc. *(Russian)* 80−35620
atom, slow electron scatt., computer calcs. 77−50530
atom, spectra, emission and absorpt., inert gas matrix 78−90106
atom, spectral line breadth, total absorpt. of 3S→nP transitions 78−46306
atom, spin magnetic moment densities, spin density functional method calcs. 77−67969
atom, spin polarisation in flames by optical pumping, mag. reson. transitions 78−29762
atom, Stark effect study, S and D excited states struct., two-photon spectra 77−54547
atom, Stark shifts, absolute and differential, coherent optical transient meas. 80−37773
atom, three-photon ionisation, laser bandwidth and intensity effects 80−52956
atom, transient optical nutations in D_2 line 78−66507
atom, two-level, strongly driven, reson. fluoresc. and absorpt. spectra meas. 79−36581
atom, two-photon absorpt., detuning and polarisation selection rules 78−86836
atom, two-photon absorpt. processes, polarisation selection rules 80−9574
atom, two-photon absorption reson. in spatially separated fields 78−21890
atom, two-photon excitation in flame, saturation broadening, fluoresc. obs., broad-band excitation 78−74625
atom, two-photon optical free induction decay, Stark switching obs. 77−68024
atom, two-photon optical free-induction decay 78−90138
atom, two-photon polarisation rotation effect in vapour 77−68025
atom, two-photon transition, distinction of competing processes in non-linear resonant freq. mixing 80−33080
atom, two-photon transition broadened by Ar impact 79−22681
atom, vanishing electric dipole transition moment, fluoresc. obs. 79−59397
atom, wing profile of doublet lines, in flames at 1 atm. 79−22660
atom, X-ray spectra, K-absorpt. edge 79−81177
atom, XPS, free atom core binding energy 78−74699
atom+Ar, two-photon near-reson. light scatt. 77−30941
atom+He(Ar)(N_2), collision broadening and shift of 3S-4D and 3S-5S lines 79−3406
atom+He(Ne)(Ar), Rydberg transitions, excitation transfer cross-section calcs. 77−50520
atom+inert gas, fine struct. state changing cross-sections, crossed beam determ. 77−50496
atom+inert gas, quenching cross sections of alkali n^2P states, 5-100 eV 79−76505
atom beam, focusing and defocusing forces, radiation press. from CW dye laser 80−52944
atom beam deflection by reson. standing wave radiation 79−98056
atom detection by laser photoionisation *(Russian)* 78−33487
atom excited np states, fine struct., core electrons effect 77−18807
atom in oriented vapour, RF transitions and laser beat reson., expt. technique 77−27005
atom lines, flame locking of dye lasers 78−50795
atomic beam, absorpt. notch in spectrum of transform limited pulse 77−18817
atomic beam, AC Stark splitting of two-photon spectra 77−46551
atomic beam, Autler-Townes effect in double optical resonance 78−66499
atomic beam, fast, collinear laser spectroscopy 78−37078
atomic beam, focused with laser beam, Na beam and dipole forces 79−7066
atomic beam, laser beam irrad., reson. fluoresc. intensity, Bloch model calcs. 80−58206
atomic beam, velocity spectrum determ. from Doppler shifted fluoresc. meas. 77−3210
atomic beam focusing and defocusing using reson. radiation press. 80−47143
atomic beam intracavity, detect. by dye laser spectral narrowing 79−55159
atomic beam source, low-consumption, with recycling oven 78−5376
atomic concentration, in acetylene flame, meas. by laser saturation spectroscopy 79−29425
atomic D_2 line, fluoresc. freq. distrib. induced by monochromatic laser beam 78−942
atomic energy level ordering, in excited states 79−81162
atomic fluorescence, near resonant scatt. and collision induced *(Chinese)* 80−63582
atomic fluorescence detection in air-acetylene flame, harmonic saturated spectroscopy method 80−104472
atomic gas, polarisation spectroscopy and forward scatt. 80−52336
atomic hyperfine splitting, fluoresc. after two-photon excitation 79−18307
atomic jump processes, quasi-elast. neutron scatt. study 80−84317
atomic resonant lines, wing intensities after inert gas perturbation 78−37596
atomic Rydberg states, nd→(n+1)p intervals meas. 78−33629
atomic Rydberg transitions to detect far IR radn. 80−4763
atomic spectra, quantum defects and ionis. pots., graphical procedure for students 80−7
atomic vapour, Doppler-broadened system, degenerate four-wave mixing, line shape and strength angular depend. 80−43391
atomic vapour doublet, dispersion free point, cooperative phased-array radiation 80−53352
atomic vapours, three-level system, collisional effects in saturation spectroscopy 80−78579

sodium continued
atoms, $3^2S_{1/2}$-$3^2P_{3/2}$, spectral distrib. and collisional depolarisation of laser light, D_2-fluorescence 80−58209
atoms, Auger and autoionisation spectra, collisional excitation mechanisms 77−19042
atoms, excited, electron scatt. at low energy, total cross section 80−63821
atoms, fluoresc. excitation profile, laser saturation broadening in flames obs. 80−95568
atoms, fluoresc. selective detect. by laser radiation 80−83312
atoms, motion in optical freq. radiation trap 80−78818
atoms, saturation spectra, crossover signals, effect of atomic alignment, optical pumping 80−58202
atoms, spectroscopy, masers and superradiance study 80−53248
atoms+H(He)(Ne), D2 reson. linewidth 79−31647
atoms cooling by resonant laser radiation *(Russian)* 80−74155
attenuated total reflection minima, correlation with surface polariton modes, computational study 78−31265
Auger cross relaxation energy, SCF cluster model calc. 79−46945
Auger electron emission due to ion collisions with solid targets *(French)* 80−104031
Auger electron emission from ion-solid collision *(French)* 79−33876
Auger line, $KL_2L_3(^1D_2)$, lineshape 78−60535
Auger line shape, KLV, one-orthogonalised plane wave calc. 77−48316
Auger spectra, KLL and KLV, screening effects and plasmon gains 80−80913
Auger widths of core levels calc. using diagrammatic many-body technique 77−43544
Auger widths of core levels using renormalised many-body perturbation theory 79−74033
axon, squid, Na channel gates, interactions with quaternary lidocaine and tetrodotoxin 79−83745
axon, squid, Na channel inactivation, removed by high internal pH or tyrosine-specific reagents 79−20534
axon, squid giant, poisoned with quaternary strychnine, block of Na conductnace and gating current 79−83746
BCC, ang. forces in lattice dynamics 77−84870
BCC, anharmonicity and Debye-Waller factors 77−47533
BCC, modified tensor force model for lattice dynamics 77−35644
BCC crystal, elastic constants, thermal expansion and bulk modulus 80−6452
beam, deflection by reson. standing wave radiation 80−52945
binding energy and equilib. struct., pseudopot. calc. *(Russian)* 79−47037
biomembrane, electrogenesis in model of boundary transfer with Na pump 77−25401
biomembrane channels, inactivation delay 80−45872
biomembrane transport mediation by ionophore A23187 in absence of divalent cations 78−11623
boiling, LMFBR safety, flow rundown expts. in seven pin bundle 77−88240
boiling, LMFBR safety, seven pin bundle expts., flow patterns, two-phase press. drop 77−88241
boiling acoustic emission burst detection in parasitic noise 79−3214
boiling detection in LMFBR, power spectral density surveillance systems 80−68740
boiling detection technique tests, FFTF capabilities 79−13395
boiling in 7-pin bundle, LMFBR safety, KNK II driver zone 77−88246
boiling in heated annular channel with blockage, FBR core, partial failure 77−42108
boiling in LMFBR, acoustic detection using pulsed system 79−97839
boiling in tubes, heat transfer and pressure drop 80−28408
bound spin-helicon wave excitation, reson. refl. coeff. 79−95435
burning, aerosol release, temp., O conc. depend., LMFBR, safety anal. 77−83049
CaF_2:Na, Stark effect on Na disturbed F_2-centres 77−69279
cardiac Purkinje fibre, current model 79−43861
cardiac Purkinje fibres, rabbit, Na channels 79−43828
carotid artery Na kinetics 3-compartment model, incorporation of diffusion effects 78−27996
catalytic cycle, origin for luminosity of meteor trains, lifetimes 80−12711
CESR, influence of freq. and surface effects 79−51856
CESR linewidth and g-shift in presence of spin-orbit perturbation, spin-phonon scatt. 77−63285
charge-exchange continuous-action nuclear bombardment target 80−23205
chemisorption of H_2, calc. of adsorption sites and binding energy 79−46953
chemisorption of halogens, surface chemiluminesc., MO description 79−43048
chemisorption on Al_5, core hole induced electronic relax. 79−90874
classical plasma frequency in long-wavelength limit, quantum correction 80−107728
cloud around Jupiter's satellite Io, distrib. and intensity 78−36494
clouds on Io, form. by micrometeoroid impact 80−77330
cluster, density functional calcs. 77−8031
cluster and microcrystal, matrix isolated, optical absorpt. spectra, photolysis and plasmon absorpt. 79−89820
clusters, electronic relaxation energies in $KL_{2,3}L_{2,3}$ Auger transitions, SCF-Xα-SW calcs. 78−90334
coadsorption and reactivity with NO on Ag (111) 78−38948
coadsorption with Br_2 on Ag (111) 78−38944
cohesive properties, augmented-spherical-wave calcs. 79−94952
colon, turtle, active Na transport via an electrogenic Na-K exchange pump 80−108856
combustion of large pools in LMFBR, determ. of burning rate and flame struct. 80−47644
Compton profiles in liq. and solid states 79−87520
concentration in atmospheric sedimentable powder, in Vizcaya, Spain *(Spanish)* 78−57265
concrete-Na interactions, high-temp. nuclear materials consideration 77−50243
conductance in nerve, anomalous temp. dependence of rabbit rel. to frog 79−62235
conduction electron spin props. 77−8036
conduction-electron spin flip by phonons, expt. data anal. 79−61219
coolant in LMFBR, EBR II, Na purification by cold trapping, effectiveness 77−14225
core thresholds, inelastic electron scatt. spectra meas. 79−95359
corrosion of stainless steel at elevated temps. in nuclear reactors 79−24666
crystal, elec. cond., temp. depend. calcs. 77−59276
D_1-line, optical coherent transients by laser frequency switching: subnanosecond studies 79−46014
D_2 resonance line broadening in atom and molecule collisions *(Russian)* 80−14119
Debye-Waller factor, temp. variation, lattice dynamical calc. 78−55925
Debye-Waller factors, extended de Launay model calcs. 80−70352
Debye-Waller factors, temp. depend. calc. 78−22807
decarburisation effects on Cr-Mo steel 77−16619
deposition and sputtering of Jovian ionospheric Na on Io 79−44405
desorbed atoms, ang. and velocity distrib. 80−75428
desorption from Re, neutral and ionic rates meas. via surface ionisation detector with field reversal 77−2710
detection limit, using CW dye laser spectroscopy *(Japanese)* 78−44435
determination, in sweat, using elec. field method, for diagnosis of cystic fibrosis 77−73554
determination, in water, by neutron activation and X-ray fluoresc. analyses 78−3428
determination by (p,γ) reacts., target excitation yields determ., appls. 77−44545
determination in Greenland snow and ice, natural and anthropogenic origins 79−70815
determination in minerals, electron probe analysis with low temperature sample holder *(French)* 80−85248
determination in molten Al and Al-Si alloys using β-Al_2O_3 probe 77−48714
determination in rock, mineral samples, X-ray fluoresc. quantometer modification 78−61589
determination in small samples of healthy and burnt skin 79−5343
diffusion data under press., anal. 78−55975
diffusion in AgBr, NQR caused by vacancy diffusion of impurities, spectral density 78−68408
diffusion in Si, retarding action of radiation defects 77−1140
diffusion in single alkali silicate glass 77−84990
diffusion lateral, of ions at Si-SiO_2 interface, neutralisation in presence of Cl 80−92986
dimer, $B^1\Pi_u$-$X'^1\Sigma_g^+$ band system obs. 78−62837
distiller for purification, construction, operation 78−80490
distribution in Io Na cloud around Jupiter 80−46464
doped NH_3 frosts, reflectance spectra and implications for Io surface 78−84561
doubly occupied Wannier functions, constructive definition 80−75492
droplet, preignition oxidation process, rel. to LMFBR accident 79−30996
dynamical structure factor calc., High temp. 80−15047
in Earth mantle, $NaAlSiO_4$, with Ca ferrite struct. as Na host phase 77−64270
education, Rydberg states, anomalous fine struct., perturbation model 80−57035
elastic constants, appl. of model pseudopot. to elastic consts. 80−59845
elastic free energy meas., rel. to localised soft mode theory for martensitic transforms. 78−10159
elastic scattering amplitudes, for high energy electron scattering, by ionised atoms, numerical calcs. 80−49057
electrical and thermal resistivity determ. from first principles 79−69493
electrical conductivity, Toya's theory 78−51965
electrical resistivity, data tables, 1-2000K 79−78072
electrical resistivity, low-temp., electron-electron contrib., sample depend. 80−24875
electrical resistivity, temp. depend., anharmonic effects 78−76045
electron density redistribution on passing from atom to cryst. *(Russian)* 77−66103
electron inelastic scatt. in intense laser field 79−72427
electron potentials and wave functions *(Russian)* 78−47688
electron-phonon coupling const., calc., compared with expt. 79−99286
electronic charge density, OPW-based pseudopot. calc. 78−87896
electronic model of Na-channel gating current carriers 79−70542
electronic structure, optical absorption 79−38566
electrons around vacancies, electron density calc. 78−64003
EM pumps for liquid metal fast breeder reactor, review 78−94074
emission, anomalously intense, Na atomic lines in shock heated salt vapour 78−63089
emission and fixation during pressurised fluidised bed combustion of coal 80−30352
energy level calcs. for cryst. with vacancies or substitutional impurities, Green's function method *(Russian)* 78−56101
entropy change on melting of simple substances, thermal expansion, configurational entropy 80−59630
epithelium membrane permeability, effect of intracellular Na conc. 77−32882
equation of state meas. 80−19905
equations of state determ. 80−24564
equilibrium struct. and phys. props., pseudopot. method 80−96778
erythrocytes, rabbit, increased passive efflux of ^{22}Na and ^{86}Rb on microwave irrad. 80−108957
estimation in cotton clothing for use in neutron activation dosimetry 80−47729
evaporation from slot type capillary structs., crit. heat fluxes 80−74854
evaporation in Ar atm., fog formation, expt. theory comparison 77−55352
evaporative removal from LMFBR components 80−32348
fast reactors, Na purification system for primary and secondary loops 79−45344
fast reactors, Na-cooled, material corrosion problems 79−36328
fast reactors, track detector determ. of fuel contamination of primary Na coolant 80−32394
fast reactors Na cooled, core component material irradiation induced void swelling and creep, technological consequences summary 79−36327
Fermi surface distortion 80−2325
Fermi surface distortions, model pot. 80−80157
film, slow electron bombarded, light radiation 80−40168
film, XPS lineshapes, many body processes 78−39663
film for expendable filter in VUV, use and preparation technique 80−33193
filtration of Na-fire aerosols in LMFBR 80−68853
fire in LMFBR accident condition, theoretical anal. using SPOOL-FIRE code 77−14248
fire in nuclear reactor, anal. with SPOOL-FIRE code 77−46322

sodium continued
fires, expts. on extinguishing large quantities of burnina Na 79−41016
fires, origination and mechanism form. and sedimentation of Na aerosols, review *(Czech)* 79−30956
first excited states, non-resonant emission spectra *(Chinese)* 80−42971
fission reactor, evaporative removal of Na from components 79−93735
fission reactor fuel-coolant interaction, UO_2 fragmentation by thermal stress and pressurisation 77−88226
fission reactor primary coolant, effect of high reactivity with air and water *(French)* 79−26526
flame, excitation temperature meas. with spatial resolution, hook method 77−58200
flame, gain probing by intracavity dye laser spectroscopy 77−7092
flame, seeded H_2-O_2-Ar, population inversion, two-photon laser excitation 79−34307
free atom cooling in resonant laser field at scanning freq. *(Russian)* 79−72272
free electron metal, electron-phonon interact., comparison with metallic hydrogen 77−66125
gas diffusion induced by resonance light field 80−53918
GCFR cores, heat transfer with He and Na coolants, review 79−45331
glass-Na vap. interface, dye laser frequency locking by selective refl. 78−29992
granuloma pouch Na exchanges during initial and final stages of inflammatory process 77−77886
ground state of solids, spin density functional method, binding energy, compressibility 80−65477
Gruneisen parameter, press. depend. 80−65184
Gruneisen parameter temp. var. for BCC struct. 78−6137
Hall coefficient, quasiclassical Boltzmann eqn. calcs. 80−103678
hardfacing materials, friction characts. in high temp. Na *(Japanese)* 80−89356
heart muscle cells, Na current, electrophysiological studies, rat 79−43838
Heine-Abarenkov potential 78−6248
helicon-phonon interaction for parallel wave propagation 78−64054
high temperature, corrosion effect on austenitic stainless steel of different chem. comp. 78−80675
high-press. discharge lamp, theory and plasma diagnostics appl. 78−9829
hyperfine structure of P sequence, ^{23}Na, using quantum beat spectroscopy 79−89632
hyperthermal atoms, ionisation on W (110), temp. depend. 80−50504
ileum epithelial cells and intercellular spaces, microprobe meas. of Na, K and Cl conc. profiles, rabbit 78−35819
impurity at glass-metal seal interface, composition and conc. determ. by AES 80−76587
impurity effect on subboundary brittleness of Al-Mg-Li alloy *(Russian)* 77−21244
incipient boiling in the presence of a mag. field 79−37411
Incoloy 800, corrosion and carburization in liquid Na up to 973K 79−47841
interatomic function from phonon-dispersion curves and Heine-Abarenkov-Shaw optimised model pot. 79−19185
interatomic potentials from phonon spectra 80−19744
interface, Na(110)-Na(110), local and nonlocal contribs. to adhesive energies 77−85085
interface, Na (110)-Na (110), self-consistent electronic densities and adhesive energies 78−72005
interstellar Na I, quadratic depend. of column density on N_H 78−20872
interstellar Na I and/or Ca II lines, obs. towards 47 stars 79−25676
Io Na cloud, obs. rel. to Jupiter magnetosphere thermal electron density 79−40133
Io Na cloud, solar radiation press. as cause of east-west asymmetries 80−36560
Io Na D-line emission, comparison of observed and theoretical line profiles 78−93145
ion implantation in LiF, migration, segregation, effect on optical props. 80−100269
ion relaxation in skeletal muscle, evidence of Na ion binding inside a biological cell 78−88698
ion source, HF, proton yield increase, influence of various admixtures to H_2 obs. 80−57422
ion-selective membrane electrodes, Na ions selectivity *(Russian)* 79−96337
ionisation detector, aerosol effects on characts. 79−49243
ionisation interference, in Ebert spectrograph with 5 kW ICP unit 80−86453
ionophoretic model for Na-Ca counter transport 79−2017
ions, adsorbed on porous SiO_2 glass in distilled water medium, determ. 79−24814
ions, passage through nerve membranes, protein channels 77−4994
ions in liquid, Born-Oppenheimer pot. derivative, Monte Carlo calcs. 80−54117
IR and optical props., surface-plasmon-mediated absorpt. mechanism 80−93308
isoelectronic sequence, Bethe excitation cross-sections 78−82657
isoelectronic sequence, dielectronic recombination rate coeffs., 2-10^3 eV 80−10357
isoelectronic sequence, electron impact excitation, transition probabilities, oscill. and collision strengths 78−25718
isoelectronic sequence, hypervirial theorem, screening parameters and oscill. strengths 79−6882
isoelectronic sequence, theoretical f-values 78−37593
isoelectronic sequence, X-ray spectra 80−87071
isoelectronic series, Cu XIX-Br XXV, laser-produced at. spectra 79−49974
isoelectronic series, dipole polarisability, numerical Coulomb approx. 80−43199
isoelectronic series, hard-core pseudopotentials and struct. maps 80−44168
isoelectronic series, Hartree-Fock line strengths 78−9122
jellium model, appl. to X-ray spectra 80−39523
K_α X-ray satellite struct. and KLL Auger electron spectra, solid-state effects 80−89089
$K\alpha_1$ and $K\alpha_2$ wavelengths 80−50464
K-shell X-ray production, by 0.4 to 2.4 MeV ^{4}He and ^{1}H ions 79−47550
kidney, isolated, perfused in vitro, sugar reabsorpt. rel. to Na transport, rabbit 78−20155
kidney, medullary Na depletion during diuresis, digital computer simulation 77−60226

sodium continued
laser, 372 Å, travelling wave source pumping, numerical anal. 77−83864
lattice dynamics, angular force model 77−31735
lattice dynamics, electron fluid model, phonon dispersion 77−27954
lattice dynamics, model incorporating second neighbour shell-shell interactions 77−59082
lattice dynamics, modified Bhatia model 77−51455
lattice dynamics, phenomenological model 77−20017
lattice dynamics, sp. ht. and Debye temp., ang. force model 77−15509
lattice sp. ht. and thermal vibrs. 78−30768
light interstitials, thermodynamics, rel. to delocalised particles 79−46653
linear potential and phonons 79−82293
lipid-protein interaction in membrane bound Na^+, K^+-ATPase, spin label anal. 79−11902
liquid, anal. of temp. fluctuations for local flow velocity determ. *(Spanish)* 79−46405
liquid, atomic self-motions *(Rumanian)* 78−47226
liquid, boiling expts. ref. to fast reactor safety *(Italian)* 79−9764
liquid, boiling hazard in LMFBRs *(French)* 80−78402
liquid, compatibility with ceramics 77−44387
liquid, contaminated, packaging and storage 80−18468
liquid, contaminated, release of Pu compounds during burning, LMFBR safety evaluation 77−23224
liquid, coolant in fission reactor, degassing of Xe invest. using Na loop 77−34410
liquid, coordination numbers, calc. in microinhomogeneous struct. model *(Russian)* 80−38902
liquid, corrosion of V-Mo alloy, effect of ion plated Mo 78−53020
liquid, diffusion coefficient for model potentials through mean square displacement 80−70098
liquid, dynamic struct. factor, two body interaction pot. sensitivity 78−67638
liquid, effect on atomistic diffusion in alloys 77−7899
liquid, effect on corrosion and creep of stainless steels, 873 and 973K 77−57722
liquid, effective interionic interaction, many particle effects *(Russian)* 77−39530
liquid, elec. cond., role of multiparticle effects *(Russian)* 79−91015
liquid, elec. resistivity calcs. 78−79974
liquid, electrical resist. temp. depend. calc. 77−55507
liquid, electrical resistivity, effect of inter-electron interactions *(Russian)* 77−24546
liquid, electron correlations, evidence 78−55805
liquid, engineering handbook, purification, heaters, coolers, radiators 80−27045
liquid, entrainment and heat transfer with UO_2 vapour during HCDA 79−93775
liquid, entropy and enthalpy of solution of O(N)(C)(H) 78−51692
liquid, entropy calc. using phonon theory of liquids 80−39310
liquid, eqn. of state and thermodynamic props. at high temp. and density 79−55902
liquid, equation of state, press. and entropy along melting curve 77−47540
liquid, equation of state, vol. and compressibility meas. up to 22 kbar 77−47541
liquid, equilib. props., self consistent field methods calcs. 79−10767
liquid, evaporation from capillary-porous struct., capillary restriction in initial stages 80−107609
liquid, fast reactor coolant, boiling in circular pipe, single-bubble model 77−10466
liquid, flow in Na circuit surge tank, LMFBR cooling systems *(Czech)* 77−67792
liquid, heat transfer characteristics of flow field *(Japanese)* 78−54815
liquid, heating modular steam generators, pressure and temp. loading in breakdown situation *(Czech)* 78−50264
liquid, in EBR-II sodium systems, control of oxygen, hydrogen and tritium impurities 79−93696
liquid, in vert. pipe, hydraulic resistance under boiling conditions 78−90968
liquid, incipient superheat meas., expt. and physical parameter effects 78−18289
liquid, inelastic thermal neutron scatt., interatomic pots. calc. 78−42891
liquid, interaction with stainless steel fuel cluster sheath, effect on porosity development 77−71651
liquid, interionic interaction theory, pseudopotential calcs. *(Russian)* 80−79675
liquid, isothermal compressibility, harmonic pot. model calc. 79−14870
liquid, linear induction pump development *(Russian)* 78−94839
liquid, linear pot. and elec. resist., calcs. 80−65519
liquid, local boiling behind local flow blockage, simulated LMFBR fuel subassembly 78−54842
liquid, loop disposal system of sodium loop safety facility 80−18467
liquid, mean spherical approx. and effective pair pots. 80−70099
liquid, MHD induction machine, duct local flow charact. at large EM interaction parameter *(Russian)* 78−5818
liquid, molten chlinak extraction of I_2 in Na cooled fast reactor 80−27702
liquid, natural convection from plane surfaces, LMFBR design, review 80−37417
liquid, natural convection from vert. plate in fast breeder reactor 79−3202
liquid, new description of random stacks *(French)* 78−79512
liquid, nuclear reactor appl., high-temperature experimental plants *(German)* 77−10461
liquid, O_2 pot. and O_2 distrib. coeffs. between alkali and struct. metals 80−65231
liquid, optical conductivity 77−63425
liquid, paracrystalline BCC lattice evidence 79−41942
liquid, purification by mesh-packed cold traps, effect of shape on perform. 79−40986
liquid, radial distribution functions calc. at 100°C 78−22638
liquid, resist. and thermo-electric power using corrected parameters of Shaw model 79−19566
liquid, resistivity, thermoelectric power, Harrison nonlocal pseudopot. calcs. 78−23069
liquid, resistivity calc. 77−85190
liquid, self-diffusion coeff., 127°C, from mol. dynamics data 77−76585
liquid, shear waves, molecular dynamics 80−44096
liquid, short-wavelength density fluctuations 79−46550
liquid, small-leak Na+water reaction in LMFBR steam generator, dissolution rate of hydrogen 78−29545

sodium continued
liquid, solubility of NaH, and elec. resist. of Na-NaH and Na-Na_2O solns. 79−14934
liquid, square-well pot. mols., struct. factor, transport props. 78−22620
liquid, struct. factors, X-ray transmission diffr. expt. 77−47337
liquid, structure factors, higher order distrib. functions 77−51299
liquid, T_c, P_c, V_c, from eqn. of state 78−2228
liquid, thermocouple transfer function and flow velocity meas. by temp. noise 79−13394
liquid, thermodynamic activity of C, continuous method of determ. 77−56306
liquid, thermodynamic activity of C 77−83045
liquid, thermoelectric power, optimised model pot. calcs. 80−29391
liquid, thermophysical properties rel. to clustering 77−1065
liquid, transport coeffs., static struct. factor calcs. 77−7643
liquid, velocity autocorrelation from memory function, hard-sphere and square well pots. 80−28893
liquid, velocity autocorrelation function and freq. spectrum 79−27892
liquid, working fluid in AC cond. pump, performance characts., freq. depend. *(Japanese)* 80−13092
liquid and solid states, γ-ray Compton profiles 77−48269
liquid effect on austenitic stainless steel mech. props. 79−20150
liquid effect on fatigue crack growth in pressure vessel steel 77−8997
liquid metal boundary layer attenuation of temp. oscillations, appl. to LMBFR 77−83013
liquid metal slug flow, transfer function of temp. fluctuations 78−46133
liquid metals, structure factor modelling using quasi-crystallised model *(Russian)* 80−54118
liquid O_2 content determ. by ceramic probes, manufacture and props. 77−54308
liquid reactor coolant, effect of O_2 on H_2 permeability, partial pressure 80−614
liquid sphere, in infinite UO_2 bath, heat transfer problem temp. profile 77−75783
liquid-vapour transition at low press. 77−39669
liquids, optimised cluster expansion, struct. function evaluation 80−49085
LMFBR, accidental Na release as peroxide aerosol, effect on tomato and lettuce *(French)* 78−8997
LMFBR, coolant start of boiling detection by acoustic method 78−86646
LMFBR, core-disruptive accidents, neutronic and fuel element behaviour 80−32357
LMFBR, correl. meas. of Na flow rate using mag. detectors 79−71924
LMFBR, filtration of Na fire aerosols 79−30998
LMFBR, fire, statistical parametric anal. 79−30997
LMFBR, liquid Na-limestone concrete interaction following HCDA, US meas. 80−78412
LMFBR, long-term in-reactor corrosion of stainless steel cladding by liquid Na 80−16593
LMFBR, molten UO_2 fuel-Na coolant thermal interaction, characterisation of fragmented fuel 80−68774
LMFBR, Na flow meas. in main pipes, application aspects 80−22884
LMFBR, Na flow transient anal. using NATOF-2D code 80−47633
LMfBR, Na loop temp. control using 100 kW elect. heater *(Czech)* 80−5203
LMFBR, Na purification system, cold traps and plugging indicator 80−99209
LMFBR, Na-H_2O steam generator, calc. local heat fluxes in circular channels 79−36312
LMFBR, transient boiling of Na in 7-pin fuel bundle under loss-of-flow conditions 79−41007
LMFBR, transient boiling of sodium in seven-pin bundle under transient overpower conditions 79−76056
LMFBR, yield characts. of short-lived fission products in Na heat-transfer agent 78−66338
LMFBR accident, large scale Na/concrete reactions 79−30999
LMFBR containment response to postulated Na spills and fires, computer anal. 79−54480
LMFBR coolant, SAS-3D analysis of natural-convection boiling behavior in the sodium boiling test facility 80−47635
LMFBR coolant and Ar atmos., chemical comp. 79−71893
LMFBR coolant boiling under low heat flux condition during loss-of-heat sink accident 80−47636
LMFBR HCDA, appl. of acoustic agglomerators for suppression of Na-fire aerosols 79−54525
LMFBR HCDA, Na interaction with basalt concrete and silaceous firebrick 80−47638
LMFBR LOCA, use of temperature variance to detect sodium boiling 79−54527
LMFBR Na boiling, two-phase flow calculations in low-pressure systems 80−103068
LMFBR Na vapour bubble collapse detection by acoustic emission 79−13451
LMFBR Na/basalt concrete interactions following accident, chemical phenomenology 80−47639
LMFBR post-accident containment, time-resolved penetration of liquid Na into limestone concrete 79−93787
LMFBR rot. shield plug annulus, Na vapour, deposition rate, controlling factors 80−47591
LMFBR steam generator leak, meas. of sound produced during steam injection into Na 79−93782
LMFBR steam generators, leak detection of steam or water into sodium 79−13434
LMFBR structure materials in liquid Na, capsule type creep tester *(Japanese)* 80−108653
LMFBR wire-wrapped subassemblies, Na boiling behaviour 79−31031
low pressure depleted discharge, recomb. struct. 79−94837
magnetic property volume depend., Knight shifts, electron spin response 80−88729
magnetically perturbed gas, distortionless optical pulse propag. 78−22179
marine atmosphere particulate Na and Cl vertical distrib. 77−37304
martensitic phase transition energetics 79−99314
martensitic phase transitions, and phase diagrams at moderate press. 78−72775
martensitic transform. obs. neutron scatt. meas. 77−15581
mechanical ideal strength, pseudopot. model calcs. 79−77670
melting, pressure depend. 78−85517
mesenteric artery Na distrib. in early salt-induced hypertension 78−27999
sodium continued
mesenteric artery Na kinetics, digital simulation of 3 compartment model 77−44616
mesosphere, Na layer, extra-terrestrial source, evidence 79−12191
mesosphere CC Na layer, seasonal var. at low latits. 79−79964
mesosphere Na and K abundances, simultaneous nighttime lidar meas. 78−36239
metal impurity effect on residual elec. resistance *(Russian)* 80−84457
metallic compressibilities, general pseudopotential approach 80−54631
MHD generators, optimisation for maximum electrical efficiency, output and power factor *(Rumanian)* 80−64793
MHD laminar flow, longitudinal dynamic effects determination for Na *(Rumanian)* 80−64792
microelectrodes, Na-selective liquid ion-exchanger, for intracellular meas. 80−3888
microwave transmission modes at cryogenic temps. 79−42473
MIM struct., electron-phonon interaction function investigation by microcontact spectroscopy 79−95108
mobile ion passivation in HCl oxides, for SiO_2 thin film growth 79−70187
model pseudopotential, form factors, binding energy and compressibility calcs. 78−26486
molecular, diatomic, CW laser oscill. 77−38861
molecular beams ang. momentum polarisation 77−46635
molecular laser, optically pumped, review 80−58519
molecule, absorpt. and relax. const. determ. by optical laser pumping method 80−102550
molecule, form. by excited-unexcited atom collision, emission band 4160 to 4570 Å 77−88422
molecule, Franck-Condon factors direct meas. 78−25618
molecule, laser-induced dissoc., polarisation of atomic fluorescence obs. 80−78569
molecule, triplet satellite band obs. in self-broadened D-line very far blue wing 80−95688
molecule in free jet expansion, internal-state distribution 80−83403
molten UO_2-Na interaction, thermophysical behaviour of type 304 stainless steel impacted by jet of molten core debris 77−46319
monovacancy formation parameters, temp. depend. 78−75658
monovacancy thermodynamic parameter calcs., temp. dependence 78−2114
MOS structures, Na^+ neutralisation characteristics of HCl oxides 78−10572
muonic, $2s^1/_2$ level decay channel concurrence, neutral current effects observation *(Russian)* 80−83526
muonic K-shell X-ray transitions, nuclear charge radius 78−66195
muscle, skeletal, Na:K rel. to Na:Na exchange by Na pump 77−66807
muscle single fibres, Rb^+, Cs^+ and Na^+ localisation, autoradiographic demonstration at 77K 79−96726
Na_2, laser-excited, emission bands obs. in visible and IR 80−48036
Na-coloured intracavity flame, in dye laser, mode competition 78−46594
nerve channel potentiation by n-alkanols, squid giant axons 79−83744
nerve fibre Na permeab. inactivation in squid, review of exptl. work 78−73154
nerve impulse electro-diffusion model 79−53078
neuroblastoma cultured cells, membrane currents under volt. clamp 77−60193
neutral atom production by pulsed laser heating 77−85848
neutron flux integral meas., interactive graphic techniques 78−62590
neutron multigroup and point energy transport calcs. 77−50193
nonabsorption hyperfine resonances in dye laser irrad. vapour 79−93941
normal atom conc. determ. by resonance line broadening with Hg press. 80−43883
nuclear fuel-sodium interactions, effects of finite mixing time and noncondensable gas 78−17331
nuclear power station steam generators, Na-water type, design 77−50215
nuclear reactor coolant, impurity conc. meas. by automatic plugging indicator 78−17283
nuclear reactor stainless steel and Na shield radiation heating expt. 79−9903
oocytes, salamander, free and bound intracellular solutes, reference phase anal. 79−24966
oocytes, salamander, free and bound intracellular solutes, reference phase anal. 79−24967
optical parametric oscillator, resonantly enhanced four-wave, pump intensity 78−9412
optical properties by spectroscopic ellipsometry, review 80−103929
optical properties in generalised HF approximation 80−24825
optically excited vapour, evanescent light emission near interface, transient polarisation 78−25468
overlayer, c(2×2), on Ni (001), surface struct. effects via photoexcited core electron diffr. 79−74063
particle, consisting of ats., metallic Na, model, electronic levels 78−50673
Pauli susceptibility meas. by CESR method 79−42735
Pauli susceptibility meas. by CESR transmission 79−61217
phase comparisons for Sondheimer size effect oscills. 78−34823
phonon dispersion, modified de Launay model 78−34573
phonon dispersion curve crossing in (ζ00) direction 78−38795
phonon limited resistivity struct. depend., Umklapp scatt., elastic consts. 80−88532
phonon spectra, self-consistency condition for force const. models 80−44264
phonon spectral density, pseudopotential calcs. 80−39234
photoemission theory, book contrib. 80−16159
photon echo and self-induced transparency of vapour, picosec. range 79−46015
physiological pNa monitoring, by integrated FET micro ion sensor 78−44641
pituitary cell, Na and Ca action potential 77−48770
plasma, dense, high-temp., near-reson. light scatt., collision-induced fluoresc. 77−1019
plasma, dense, in arc, elec. and heat conds., two-probe diagnostics 80−38560
plasma, inhomogeneous, nonequilib. excited-level population 77−3917
plasma, optical props. 79−4115
plasmon satellite struct. in (e,2e) process 80−96809
plastic deformation 78−30693
point contacts, current-voltage characts. at liq. He temps. 80−39663
pool boiling heat transfer, liq. head effects 78−89951

sodium continued
positronium, formation in positron+alkali metal atom collisions, first Born approx. 80−83525
positronium formation in positron+alkali metal atom collisions, pseudopot. calcs. 80−83524
precipitation at Si-SiO_2 boundary, expt. *(Russian)* 80−49368
pressure generation, liquid UO_2 encapsulated Na *(Italian)* 78−82454
pseudopotential wavefunctions calc. 77−43542
radiation-induced changes in Na preference and fluid intake in the rat 80−35986
Raman scattering from atoms, two-photon reson. and coherence effects 79−45679
reaction between water droplets and molten sodium 78−71263
reactor containment leakage from Na fire anal., response surface method, SPOOL-FIRE code 79−18004
reactor coolant interactions with refractories and control materials at 850°C 77−83041
resonance line, laser excitation, combustion Rayleigh scatt., at. flame fluoresc. spectroscopy 80−42972
river water, Na determ. by flame emission meas. 77−36850
Rydberg atom, electron collisions 80−63833
Rydberg atom system, microwave superradiance and transient maser action 79−86153
Rydberg atoms, photoionisation, 300K background radiation effects 79−68271
Rydberg atoms, selective field ionisation, 300K blackbody radiation detect. 79−58787
Rydberg states, millimeter spectra, quantum defect, fine struct., polarisability, field ionis. obs. 78−82672
selective and counter transport through polyvinylbutyrolactonecoacrylonitrile membrane *(Japanese)* 78−31700
self-diffusion, quasielastic neutron scatt. obs. 79−90818
self-diffusion mechanism 78−51722
self-weldability of metals and alloys in high temp. Na *(Japanese)* 80−89392
serum automated electroanal. using ion-selective disc electrodes with neutral cation-carriers *(German)* 78−73269
single atom detection by saturated optical nonresonant emission spectroscopy 78−31741
size oscillations in magnetocond. 77−4324
skin, frog, Na^+ transients, network thermodynamic approach to compartmental anal. 79−24968
slow atoms, inverse scatt., semiclassical approx. calcs. 78−17747
small particle, model calc. of size depend. of CESR g-shift 79−61220
smoke particles, nucleation and growth, light scatt. study 80−35580
Soft X-ray emission edge self absorption and effect of exciting voltage 77−90220
soft X-ray L_{23} emission and absorpt. spectra 79−43064
soft X-ray spectra, phonon broadening calc. 77−63526
solid, at. migration 79−69279
solid, self-diffusion mech., NMR meas. 80−44356
solid and liquid eqns. of state, melting curve 80−103448
solubility and diffusion in Ge 77−89592
solubility in wustite and diagram Fe-Na-Ca-O at 1000°C *(French)* 78−31392
spin susceptibility and volume dependence 79−95569
sputtering, thermal and collisional effects influence on energy spectra 80−66370
sputtering from NaI target, velocity spectrum meas. by Doppler shift laser spectrometer 78−19621
stacking fault and twin boundary energies 77−76420
steel, austenitic stainless type 316, corrosion mechanism in hot flowing Na, computer simulation 80−3251
steel, stainless 304, metallurgical factors on the corrosion and mass transfer in liq. Na *(Japanese)* 80−71804
stratosphere, Na and minor constituents, meteoric origin 79−70835
structure factor determination, by X-ray and neutron diffr. 79−51046
submonolayer film, on W (011) or Mo (011), disordering, LEED obs. *(Russian)* 77−89655
superheated, LMFBR safety, formation of critical boiling nuclei 77−88242
superheated flow in pipe, single bubble slug expulsion 78−672
surface, (001), average pot., pseudopot. lattice model, bounded electron gas static semiclassical response 78−72221
surface, Cl_2 reaction, surface chemiluminesc. study 80−55708
surface, mol. chemisorption, self-consistent calc. 79−95260
surface (100), electronic states calc. by mixed-representation method 77−20399
surface (110), electron states in nearly-free-electron approx. *(French)* 79−33326
surface electronic struct., linear response theory 78−56197
surface energy, barrier height and work function, jellium model calc. rel. to fracture model 77−72907
surface energy, self-consistent calc. including ion pot. perturbation effect 77−8166
surface ionisation, on Re with adsorbed O_2, mol. beam surface ionisation detection 77−90232
surfaces, (100) and (111), electron energy states *(French)* 80−34496
surfaces, Van der Waals forces computation 79−15204
temperature fluctuation in single-pin-heated blocked annular channel 78−78439
test loop boiling, acoustic detection expts. 79−13487
thermal energy storage in a packed bed of iron spheres with liquid sodium coolant, thermocline broadening 80−45762
thermal expansion, temp. depend., vacancy effects 80−79962
thermal expansion calc. 77−11711
thermodynamic props., calc. for liq. and solid phases 77−43348
thermodynamic props. at high press. *(Russian)* 78−47536
thermodynamic props. for reactor safety analysis 79−13478
thermopower, high temp., first principles calc. 79−65447
thermopower and elec. cond., relationship at low temps. *(Russian)* 80−92882
Thomas-Fermi model, self-consistent central field potential and physical quantities 78−79956
tissue exchange, incorporating diffusion effects into multicompartment models using digital simulation 80−3611
trace detection in furnace atm., 1000°C, fluoresc. 77−4955
trace identification in neutral-beam research 80−95401
transepithelial current-voltage relationships of toad urinary bladder and colon 79−92195
sodium continued
transient boiling in single-pin annular channel under loss of flow 78−89933
trapping and desorption on clean and O_2 covered W (110) surface 77−11786
upper atmosphere, absorpt. studies of daytime abundance 77−87140
upper atmospheric layer, meas. by efficient forced oscillator dye laser 80−41563
UV absorpt. spectra 80−2780
vacancy, single, relax. energy 77−84741
vacancy double jumps and atomic diffusion 78−6175
vacancy electron density distrib. using Thomas-Fermi eqns. 77−15791
vacancy form. energy, math. model 77−51369
vacancy formation energies calc. 79−82197
vacancy formation energy calcs., electron density functional method 80−19801
vacancy formation energy value from phonon data 79−77592
vacancy formation volume, temp. depend. 78−47350
vacancy superlattice 77−7713
vacancy thermal expansion coeff., lattice statics calc. 79−37698
vaporisation from capillary-porous structs. (heat tubes, vap. chambers) crit. heat flux 78−90631
vapour, absorpt. spectra 79−21509
vapour, amplified refl. by degenerate four-wave mixing using Kerr nonlinearity 78−55413
vapour, assoc. ionis. by CW dye laser and applics. *(Japanese)* 80−5515
vapour, atomic, optical sum-freq.-generation interference 77−42569
vapour, CaF_2 coating apparatus for glass, Na-resistant cell 80−90874
vapour, conversion of He-Ne laser emission *(Russian)* 78−33776
vapour, CW optical wave-front conjugation by saturated absorption 78−71154
vapour, diffusion coeff. of oriented atoms in buffer gases 80−53908
vapour, direct ninth harmonic conversion of ps laser pulses 78−5526
vapour, effective freq. conversion of radiation 80−28278
vapour, efficient laser ionisation via superelastic collisions and reduced ionisation pot. 77−79588
vapour, electron and ion beam transportation channel form., reson. saturation based laser ionis. 79−77410
vapour, electron drift vel., expt. 78−30403
vapour, electron drift vel., momentum cross-section, theory 78−30404
vapour, fifth harmonic generation 77−65606
vapour, focusing and phase conjugation of photon echoes 79−23028
vapour, grating echoes, the temporally recurrent spatial ordering of at. population 79−98447
vapour, heat cond., temp. discontinuity for dissociating gas 78−94887
vapour, induced optical anisotropy *(Russian)* 80−38526
vapour, intracavity laser spectroscopy sensitivity, saturation absorpt. influence 79−63312
vapour, IR absorpt. bands 80−102507
vapour, laser beam photoionisation, cross-section obs. by absorpt. spectroscopy 77−71782
vapour, laser induced diffusion *(Russian)* 80−6195
vapour, laser induced population grating 80−69466
vapour, laser orientated, rotary power determ. 79−32737
vapour, magnetically induced SHG, intensity saturation 80−1273
vapour, nonuniform distrib., phase matching of 2-photon resonant 4-wave mixing processes 78−87104
vapour, optical SHG, quadrupole moment pot. by mag. field 77−46760
vapour, parametric amplification based on four-wave parametric processes in two-photon reson. 79−94296
vapour, particle size meas. using anemometer 80−13195
vapour, quantum counter, IR detection 78−30016
vapour, radiatively cooled, 3rd order nonlinear optics processes 79−81477
vapour, reson. freq. conversion by two-photon reson. pumping 80−28277
vapour, reson. refr. and dispersion, appl. to flow visualisation 79−41790
vapour, saturation holes meas. using FM spectrosc. 80−42262
vapour, saturation of transient reson. nonlinear processes 77−68243
vapour, seventh harmonic generation of light 78−18009
vapour, soliton interactions, self-induced transparency, numerical plane wave simulations 80−64117
vapour, spontaneous field induced optical SHG, multiphoton ionisation 80−14395
vapour, stimulated hyper-Raman emission obs. 77−79892
vapour, sum frequency generation, via reson. quadrupole transition, theory 78−42385
vapour, superradiance, quantum beat spectra 80−106311
vapour, thermal conductivity meas. in 900-1100K range by heated filament method 77−33990
vapour, third harmonic generation, four wave parametric mixing 77−737
vapour, tunable resonant third harmonic generation of ps pulses 77−42566
vapour, two and three photon resonances in strong nonmonochromatic field 77−34908
vapour, two-photon echo, quantum beats, superposition relax. 78−83041
vapour, two-photon reson. four-wave mixing 78−46716
vapour, two-photon reson. four-wave mixing process, phase matching 77−14772
vapour, two-photon resonant fifth harmonic generation 80−53374
vapour, two-photon resonantly pumped, upconversion of 3.39 μm He-Ne laser radiation 78−55409
vapour, viscosity meas., 1101-1186K, 0.2-0.8 bar 80−1723
vapour, viscosity meas., 727-1109K 78−71416
vapour, Zeeman coherence, transient and stationary, polarisation spectroscopy 80−58212
vapour cell, physically thin, phase-conjugate wave generation in forward direction 79−89957
vapour charge exchange cell development 77−83395
vapour condensation from rising bubble, effects of internal circulation velocity and noncondensable gas 78−50258
vapour delay line, temporal compression of dye laser 5890 Å CW output 78−46688
vapour deposition rates and gas flow patterns in LMFBR 80−68732
vapour diffusion in Ar(He), diffusion coeffs. meas. by Stefan method 79−41785
vapour flow in heat pipe *(Russian)* 77−80166
vapour heat pipe, performance rel. to nozzle discharge 78−75033
vapour in inert gas, effect of oxidant on optical props. 80−1736
vapour jet target, gating and pumping action 80−10281
vapour lamp reflector design *(Spanish)* 79−23042

sodium continued
vapour seeded He hypersonic flow, velocity profile visualisation 78−59530
vapour thin cell forward phase conjugation obs. 80−78917
variational cellular method, electronic struct. calcs. 80−54591
void reactivity anal., applicability of Benoist's diffusion coeff. 77−14218
wetting at high temps. in pure vapour atmos. 77−76645
wetting studies, heat pipe meas. with gas plug containment up to 720°C 80−23878
wire, low temp. elec. resist., size and temp. depend. 77−76958
wires, size effect and temp. depend. of resist., martensitic transform. effect 79−51691
wires, size effect and temp. depend. of resist. 79−51692
X-ray absorption and emission edges, one-electron and many-body effects 80−25484
X-ray edge shape, band struct. role 77−16425
X-ray emission, incomplete phonon relax. calc. 77−52202
X-ray emission spectra, double plasmon high energy satellites 80−29829
X-ray emission spectra, $L_{2,3}$ satellite, interpretation 80−20737
X-ray scattering, thermal diffuse, meas. in longitudinal and transverse branches 78−19598
X-ray spectra, temp. broadening 77−69936
X-ray spectrum, room temp. meas. using HgI_2 detector 78−78049
X-ray threshold anal. 78−31281
XPS, plasmon gains as monitor of incomplete relax., interference effects and sudden to adiabatic limits transition 80−66390
XPS, plasmon struct. of core lines 77−63530
XPS core line asymmetries in muffin tin approximation 79−69953
XPS from core levels, electron energy loss spectra, intrinsic and extrinsic plasmons 77−63532
XPS investigation of density of states 78−6829
XPS theory, core level spectra, plasmon creation 78−72701
XPS theory, valence band spectra band struct. 78−72702
zeolite, hydrated Na-Y, ^{23}Na pulsed NMR free induction decay 80−84660
Na leakage in reactor steam generators, solution kinetics of solid NaOH in Na 79−36365
Ag^+-Na^+ ion-exchanged optical waveguide repeatability improved by melt dilution 80−53493
AgBr:Na^+, correlated diffusion of impurities, nuclear spin relax. meas. 80−108094
AgBr:Na^+, impurity induced IR absorpt. 80−7386
AgBr:Na^+, local mode freqs., Green's function calc. 80−39237
AgCl:Na^+, Frenkel defect formation energy, impurity diffusion and migration 79−99179
AgCl:Na^+, impurity effect on plasticity 78−14398
Al:^{24}Na, diffusion of Na, determ. of diffusion coeff. and activation energy 78−51746
Al-Si, hypereutectic silumins, P and Na modification 78−84792
Al-Si-Mg alloys, Si content and Mg addition effect on mech. props., Na treatment *(Korean)* 79−38901
Al_2O_3-P_2O_5-Mg(Ca)(Sr)O glasses, Na^+, Sr^{2+} diffusion coeffs. rel. to temp. 78−30787
Ar, momentum density of electrons, two-gamma positron annihilation determ. 77−69211
a-As_2Se_3:Na, doped film, photoluminescence intensity and lineshape study 80−50448
BaF_2:Na^+, ionic conductivity meas., computer analysis, point defect parameters 80−54429
CAF_2:Na, natural fluorite colouring, effect of impurities on absorpt. spectra 79−56822
CSI:Na cryst., V_K-Na^0 centre pairs, tunnelling recomb. 78−91952
CaF_2:Na, pulsed DNMR exam. 78−35066
CaF_2:Na, single cryst., X-irrad., optical absorpt. and thermoluminesc. 80−34952
CaF_2:Na, tunable room temp. laser action of M-centres, luminesc. and absorpt. spectra 79−31907
CaF_2:Na, vacancy motion activation vol., complex dielec. const. meas. 80−39356
CaF_2:Na^+ cryst., thermal depolarisation 79−82912
CaF_2:Na^+,O^{2-} thermal depolarisation obs. of defect clusters 80−71299
CaF_2:U^{3+}, Na^+, EPR, orthorhombic U^{3+} centre 77−77100
$CaMoO_4$:Na, luminescence props., emission decay time 79−95835
CaS:Bi^{3+},Na^+ phosphor, luminescence of associated centres *(French)* 80−40155
CaS:Ce, Na, photon sidebands in emission and excitation spectra, pseudolocalised vibrs. 79−28800
CaS:Ce, Na phosphor, photoluminescence and excitation spectra 80−89049
$CaWO_4$:Na, luminescence props. 79−95835
CdF_2:Na, ionic cond. investigation by complex admittance method 80−100352
CdS:Na, Hagemark theory, green edge emission line intensity 80−75517
CdS:Na, thin film, dark- and photo-currents, annealing time effect 79−38199
CdS:Na film, chemical bath deposited, photothermoelectric effect 80−6906
CdS:Na thin film, photoconducting props. 80−39623
CsBr:Na^+, impurity induced IR absorpt. spectrum, breathing-shell model 77−77256
CsBr(Cl)(I):Na, optical absorpt. investig. of F_A-centres 77−44029
CsF:Na, F-centres, saddle-point configuration, molecular model parameter 80−107234
CsI:Na, crystal, kinetics of decay of surface solid soln. 79−23810
CsI:Na, elastically loaded, effect of annealing on optical absorption 77−44034
CsI:Na, electronic struct. and luminesc. 80−16080
CsI:Na, light yield under charged-particle bombardment 80−93409
CsI:Na, localised excitons, absorption and emission 77−32425
CsI:Na, photoluminescence spectra and lineshapes anal., exciton energies 77−77281
CsI:Na, self-trapped exciton emission polarisation 80−49607
CsI:Na, tunnelling recomb. of electron-hole pair, optical detection of ESR and circ. dichroism 79−47360
CsI:Na, UV irrad., thermoluminesc. 79−28846
CsI:Na, X-ray irradiated, optical and ESR studies in IR absorption band 80−80828
CsI:Na phosphor screen, absolute efficiency under fluoroscopy conditions 78−82084
CsI:Na^+, cryst., influence of impurities on yield stress 79−15748
CsI:Na^+, luminesc. processes 80−103989
sodium continued
CsI-Na, luminescence from bound excitons, UV absorpt. and EPR 77−77282
CsI(:Na), ionic cond. temp. depend. meas., effect of Na doping 78−18829
Cu:Na, positron source using Na^{22} ion-implantation for annihilation lifetime expts. 79−45489
Cu_2O:Na, ion-implanted, resonance Raman studies of annealing 79−55765
D+H^+(D^+)(He^+)(Ne^+)(Ar^+)(Kr^+), reson. charge charge transfer from photoexcited donor state 79−22820
GaAs:Na, impurity solubility and diffusion 79−55930
Ge:Na (111) surface, O_2 adsorpt., work function, surface cond. changes meas. 78−79875
Ge-Na interfaces, interdiffusion, electron states, EELS study 80−50484
H^++Cs(Rb)(K)(Na), charge exchange, H(2s) form. 79−64101
H_2-O_2-N_2 flame, photochem. reactions involving Na*, laser saturated conditions 78−80762
^3H meter for Na coolant systems 79−9690
He-Na mixture, low-pressure discharge, radial cataphoresis obs. 78−67507
He+Na_2, elastic scatt. and rot. excitation, model pot. energy surface 77−6895
He+Na_2, rotational inelastic scatt., uniform semiclassical sudden approx. 80−99544
He($^1S_0$)+Na(Li) radiative Penning ionis., photoionis. cross section depend. of continuum radiation 77−19034
Hg+Ne(Na)(K)(Rb), elastic scatt., interatomic pots. 77−58122
Hg(6^3P_0)+Na, energy transfer, rate consts. *(Russian)* 79−54952
I_2:Na, doping effect on elec. cond., semicond. props. 80−49732
I_2+Na(K)(Cs), ion-pair form., differential cross sections, I_2 internal energy effects 77−61840
K, Na, superthermal neutral beams impact on W surface, stimulated chemical reaction 77−9123
K/Na ratios in dew drops rel. to atmospheric aerosol comp. 77−91190
K+K(Na), excitation in slow collisions 78−70918
K^++Na, differential scatt. cross section, electronic excitation via. rot. coupling in NaK^+ 78−13579
KBr:Na, exciton-like state disturbance in radioluminesc. *(Russian)* 77−85805
KBr:Na, F_A centres, optical detection of ESR 79−99793
KBr:Na, low temp. radiation hardening mechanism, single halogen interstitials as hardening agent, Ha annealing 79−23634
KBr:Na, microcrystalline powders, isothermal decay of colour centres 80−2804
KBr:Na, U-centres, HFS and g-factor, EPR spectra 80−39869
KBr:Na, X-irrad., luminesc. from self-trapped excitons 77−28614
KBr:Na^+, electronic struct. of $(V_K e)_{Na}$ 78−95269
KCl cryst., Sr and Na impurities radial distrib., influence of form of crystn. front 80−107312
KCl:Na, absorption from relaxed excited state by F_A and F_B centres 77−44031
KCl:Na, electron trapping from α_A and F_A-centres, low temp. depend. 80−11444
KCl:Na, F_A reorientation and $F_A \rightleftarrows F'_A$ conversions, laser induced, kinetic studies 80−10547
KCl:Na, F_B centre energy levels 80−107738
KCl:Na, F_B centres, optical detection of ESR 79−99793
KCl:Na, K band of F_A centre, perturbation treatment 78−76016
KCl:Na, photodichroic holographic recording, polarisation sensitivity 78−29911
KCl:Na, photoinduced reorientation of A-centres near room temp. 78−64344
KCl:Na, thermoluminescence peaks cleaning using optical bleaching 77−81162
KCl:Na, tunable IR lasers with F_A(II) and F_B(II) colour centres 78−90420
KCl:Na, UV irrad., anionic H and D atoms, ESR and optical absorpt. expts. 79−99187
KCl:Na,Br, EPR of interstitial and diinterstitial $BrCl_2^{2-}$ centres 77−81007
KCl:Na and pure, hologram recording through F→X conversion 80−48190
KCl:Na^+, entropy changes associated with point defect form. calc. 77−7741
KCl:Na^+, F_B(II) colour centres, tunable CW laser action obs. 77−83877
KCl:Na^+, lattice relaxation around tetragonal and rhombic defects 79−95110
KCl:Na^+, OH^-, IR absorpt. spectra, Na^+ ions rel. to OH^- stretching vibr. 79−47442
KCl:Na^+, R-centre exam., uniaxial stress effects on zero-phonon lines 78−47371
KCl:Na^+, self trapped excitons, optical absorption and emission 77−43503
KCl:Tl^{2+}, Na, X-irrad., activator-impurity association *(Russian)* 77−85761
KCl-Na, F_A, F_B and F_C-centres, wave functions and energy level of bound states 77−8049
KCl;Na, F_A-centre optical absorpt., estimate using symmetry-adapted wave functions 80−11448
KF:Na^+, shape of pot. energy well of impurity 79−23692
KI:Na^+, lattice relaxation around tetragonal and rhombic defects 79−95110
Li^+,Na^+:KCl(RbCl), F_A(II) to F_B(II) centre crystals, CW laser oscill. with extended tuning range 80−32997
Li, one-electron calcs. of X-ray absorpt. and emission, jellium model 78−56543
Li^++Na, charge exchange, generalised Rosen-Zener model 77−50497
Li^++Na→Li+Na^+, electron transfer collisions time independ. quantum theory with nonorthogonal basis and R-matrix propag. 79−89769
LiF:Na^+ H_A-centre struct., hyperfine interaction 78−79611
$LiNbO_3$:Na structure field stability limits, LPE film growth, SAW velocity 80−80102
$LiNbO_3$:Na^+ film, improvement in temp. stability and SAW device appls. 80−75939
$LiNbO_3$:Na^+ films, LPE growth from Li_2O-V_2O_5 flux, X-ray and acoustic characterisation 80−15383
LiO:Na^+, finely divided catalyst, low-temp. doping 79−51128
Li_2SO_4:Na^+, monoclinic-cubic transform., effect of impurities 79−52744
MgO:Na^+, precipitation, dislocation obs. by TEM *(French)* 79−51163

sodium continued
N_2O+CO, Na catalysed, Na chemiluminesc., excitation mechanism, appl. chem. laser 77−63916
Na 4D level, relax. by inert gas collisions, expt. 79−68307
Na 4D level, relax. by inert gas collisions, theory 79−68308
Na (110), oxidation, LEED obs. of Na_2O (111) 77−72761
Na, (3s-4d), Doppler free spectra, 4d fine struct. splitting=1028±0.4 MHz 78−41356
Na $A^1\Sigma_u^+ \rightarrow X^1\Sigma_g^+$ system, transition moments and radiative lifetimes calcs. 77−34697
Na channel, fully coupled transient excited state model, action potential generation, threshold, accommodation and repetitive firing 79−57634
Na D-line nightglow, correl. with OH and O I 5577 Å emissions 79−80067
Na, energy and displacement field around edge dislocation, Ritz method 78−14344
Na I, atomic spectrum, series formulas 80−99466
Na I, even-parity autoionising states, photoabsorpt. 350 to 400 Å, laser excitation 79−59390
Na I, fine struct. splittings in some highly ionized n=3 doublets 80−43200
Na I, in W 51 region, possible detect. of 17 cm hyperfine emission 78−8139
Na I, interstellar, obs. in 30 Doradus nebula in LMC 80−46643
Na I, reson. line broadening in shock tube plasma 77−35393
Na I $3^2P_{3/2}$ meas. beyond natural linewidth by beam laser quantum beats 77−50399
Na I 5890-5896 Å, airglow in upper atmosphere, semi-annual vars. 78−28360
Na I 5893 Å nightglow and Na atoms distrib. in mesosphere, simultaneous obs. 78−88961
Na I 8190 Å absorption feature in M31 and M32, equivalent widths 80−51862
Na I D lines dayglow diurnal var. obs. at Poona 78−69558
Na I D_2-line at 5890 Å, laser obs. of ground-state hyperfine structure 80−931
Na I D-line, nightglow spectra correl. to atmos. Na density 80−41585
Na I D-line obs., Doppler width from intensity integral 80−41782
Na I D-lines, chromospheric formations beyond solar limb, filaments 79−96987
Na I emission from Jupiter Region C, attributed to terrestrial airglow 77−64696
Na I interstellar absorption in NGC 4321 galaxy 80−51847
Na I isoelectronic series, transition probabilities, oscill. strengths, lifetimes, branching ratios 78−33470
Na I lines in solar spectra, non-mag. polarisation, centre-to-limb var. 80−67678
Na I nightglow intensity vars. rel. to Na photochem. 79−70905
Na I reson. line broadening by collisions with dipolar mols. 80−941
Na I solar D-lines, non-mag. polarisation 80−63569
Na I twilight and nightglow, interferometric studies of D-line profiles 78−36353
Na II, radiative lifetimes calc. 79−98037
Na II, spectrum, config. superposition and transition probabilities calcs. 80−87082
Na isoelectronic series, oscill. strengths, effective orbital quantum no. method 80−9521
Na V(VI)(VII), beam-foil spectra, extreme UV mean lifes and oscillator strengths 79−31456
Na^-, electron affinity, model pot. CI and SCF calcs. 77−38609
Na^-, photodetachment cross-sections and multipole polarisabilities, extended asymptotic model 78−42028
Na^- positron complex, ground and excited states theoretical studies 80−42934
Na^+ activity of epithelial cells, liquid-ion exchanger microelectrode estimates, resistive artifacts 80−89909
Na^+ and Cl^-, interdependence of transport in dog tracheal epithelium 80−61519
Na^+ and Na layers in upper atm., meteor ablation-cluster ion theory 79−58138
Na^+, atomic core states, antishielding effects calcs. 80−83299
Na^+, autoionising $2s2p^6ns$, np states, electron reson. scatt. calc. 80−53142
Na^+, beam-tilted C foil interactions, charge-state distrib., photon emission, 100-400 keV 79−22814
Na^+ channel gating modifications in Myxicola giant axons 79−88072
Na^+, effect on extracellularly-recorded photoreceptor pots. of cephalopod retina 79−62245
Na^+ efflux from muscle, K^+ conc. effect obs. 79−79495
Na^+, electrogenic transport obs. in rat soleus muscle 80−21456
Na^+, electron scatt., reson. rel. to $2s2p^63s^2$ term position and width 79−59347
Na^+, flow through ion channels in nerve cell membrane 79−74644
Na^+, H_2O affinity, ab initio SCF calcs. 80−58125
Na^+ impurity effects on self-trapped hole in KBr *(Japanese)* 78−67982
Na^+ injection into cortical glia demonstrating glial-neural interaction 77−36905
Na^+ intracellular activity rel. to Na^+ transport across a tight epithelium 80−67051
Na^+ ion diffusion in β''-Al_2O_3, rel. to cond. 77−72715
Na^+ ion neutralisation in HCl grown SiO_2, TSIC method 79−38181
Na^+ ion solvation number determ. for sodium tetraethylaluminate-benzene (cyclohexane)-donor two-phase system 78−95987
Na^+, ionic size rel. to Koopmans' ionisation pot. 79−85892
Na^+, mass spectrometer quadrupole mass filter transmission 79−21851
Na^+ mobilities in gases *(Japanese)* 79−60101
Na^+, mobility and clustering in Ar gas 77−84389
Na^+, mobility and longit. diffusion coeffs. in Kr and Xe 80−106866
Na^+ multicompartment flow model of frog skin epidermis, experimental verification 78−92607
Na^+, NMR in lyotropic systems 79−22732
Na^+ pump, unphosphorylated, occlusion of K ions 79−88065
Na^+, red blood cell permeability repair after X-ray, fast-neutron damage 79−57615
Na^+, reson. line regularities in plasma Stark widths and shifts 80−43881
Na^+ saturation kinetics in frog skin, compartmental aspects 80−67050
Na^+, second order correl. energy, Z depend. of irreducible-pair energies 80−91417
Na^+ selective glass microelectrodes, electrochemical props. 79−91957
sodium continued
Na^+, X-ray microanal. of cultured skeletal muscle cells, calibration 79−100798
Na^{2+} interaction with Cl^- transport in canine tracheal mucosa 79−88060
Na:F^-, ground states and core hole states, self-consistent soln. using density functional formalism 79−69467
Na:O, evaluation of V wire equilibration method, for determining O content 78−79626
Na^+:KCl, CW laser action of $(F_2^+)_A$-centres, tunable from 1.62 to 1.91 μm 80−32998
Na/Li ratio upper limit for novae 79−101156
Na/Na_2 beam, diagnostics with internal selection, vel. distrib. and dimer form. 78−86968
Na/S batteries, load levelling and traction 80−21391
Na/S battery development program at GEC for utility lead levelling with beta alumina solid electrolyte 80−61327
Na/S cells operating with dissolved catholyte, elec. props. 80−101085
Na/S load levelling batteries, optimisation of fabrication process of beta Al_2O_3 solid electrolyte 80−72035
Na/S traction batteries, development progress and problems, review 80−61326
Na^+/Ca^{2+} extracellular ratio effect on photosensory membrane of Lumulus ventral nerve photoreceptor 78−69067
Na^+/K^+ intracellular ratio, rel. to protein synthesis control and cataract form. 78−11646
Na-(Ne)(He)(Ar)(Kr)(Xe), oscill. strengths, for induced dipole transitions, pot. energy curves 77−75100
Na-Ar, nonlinear optical 5th order susceptibility meas., VUV harmonic generation 78−42381
Na-Ar film, metal-nonmetal transition 77−62966
Na-Ar(Xe) phase-matched mixtures, seventh and ninth order nonlinear susceptibility meas. 79−55186
Na-D photoneutron sources, construction, yield 77−23347
Na-graphite intercalates, preparation, struct. 80−103307
Na-H, liq. and solid, mol. orbitals approach, solvation energies 77−4201
$Na-H_2-N_2$ jet, ignition and extinguishment in simulated LMFBR accident conditions 78−8932
$Na-H_2O$ reaction testing in large leak test rig 78−86577
Na-He model pot. calcs., fluoresc. line profile 79−36723
$Na-He-N_2$ dense vapour system, optical pumping, RF spectrum analyser appl. 79−76393
Na-Hg high-press. discharge, Na reson. radiation, self-reversed maxima shifts 80−92411
Na-Hg-Xe cylindrical high pressure arc discharge, acoustic resonance 78−67454
Na-ice condensate, EPR lineshape second moment, electron solvation struct. 78−3440
Na-K, rotationally stabilized liquid liner implosion for fusion plasma production 77−23274
Na-like ions, Kr-Mo, 2-3 transitions, plasma X-ray spectra classification 79−37544
$Na-NH_3$, nonmetal-metal transition, thermodynamics 78−18964
$Na-NH_3$, solns., US absorpt. and vel. near crit. point 79−28047
$Na-NH_3$ film, quench-condensed, anomalous elec. cond. obs. 77−32057
$Na-NH_3$ film, vapour deposited, elec. resistivity, metal-nonmetal transition 78−84317
$Na-NH_3$ solid mixture, cond., three component reactive percolation model 78−68003
$Na-NH_3$ solid solutions, phase comp., dissoc. *(Russian)* 77−35665
$Na-NH_3$ solns., elec. cond. and thermopower 77−1370
$Na-NH_3$ solns., metal-insulator transition 77−1369
$Na-NH_3$ solns., UV absorpt. *(German)* 77−24869
$Na-NH_3$ solution, small angle X-ray scatt. meas. 79−14667
Na-NaO-Na struct., inelastic tunnel effect, spectra, potential barrier parameters 79−95511
Na-Ne, gas phase, absorption, D-line profiles, dye laser meas. *(French)* 78−42007
Na-Ne, low press. discharge positive column, multistep ionisation 78−75446
Na-Ne plasma, near-reson. dye laser scatt. and two-photon absorpt. 77−39459
Na-Ne-Ar, low-pressure discharge, AC operated, time-resolved afterglow 77−43099
Na-Ne-Ar AC discharge, positive column 77−39487
Na-Ne-Ar discharge low-press., instability 78−9868
Na-S accumulator, electrical energy storage *(French)* 80−55835
Na-S batteries, load levelling and motive power appls. 77−86321
Na-S cells, S electrode potential distrib. model 79−96435
Na-Xe, high-pressure discharge, electron density, interferometric meas. 78−75415
Na-Xe discharge kinetic model for visible lasers 78−63088
Na-Xe excimer lasers, high-power discharges, models 80−69373
Na-Xe vapour, high power discharge, potential excimer laser 78−82957
Na^+-$(H_2O)_n$, complex struct., coord. numbers 79−7049
Na^+-gramicidin D emulsion, NMR obs. 79−43805
Na^+-solvated electron, reversible capture by 1,1-diphenylethylene, equilib., kinetics 78−7177
Na+Ar, collisional relax. by tri-level echo 78−17774
Na+Ar, differential cross-section at thermal energy, Na-Ar ground state pot. 78−58769
Na+Ar, fine structure transition cross-sections, emission spectra, NaAr form. 78−9085
Na+Ar, Na spectral lineshape, orientation and vel. relax. contribs., low press. region 80−5503
Na+Ar, scatt. cross-section, thermal energy, interaction pot. for $Na(3^2P)$ 79−27060
$Na+Ar^{2+}$, Ar^+ form, electron capture Ar^+ excited states relative population distrib. 80−23544
$Na+Ar^{2+}$ collision, single electron capture into Ar^+ excited states, 0.2-12 eV, emission cross section 80−48071
$Na+Ar^{2+}$ collision, single electron capture into Ar^+ excited states, relative population distrib. 80−48072
Na+Ar*, Penning, associative and total ionis. cross sections 77−79683
$Na+Ar(0_2)(N_2)(He)(H_2)$, total elastic cross sections meas. 77−30954
Na+Ar→NaAr, quasimol. form., laser spectroscopic obs. 77−57920
$Na+C^-(O^-)(F^-)(Cl^-)$, negative ion stripping, at. beam form. 77−6926
Na+CO velocity-changing collisions, stimulated photon echo obs. 79−81258
$Na+CO(NO)(CO_2)(C_2H_2)(CH_4)$, total cross sections 79−27064

sodium continued
Na+$Cl_2(Br_2)(I_2)(ICl)(IBr)$, negative ion prod. cross sections 77−531
Na+Cl^-, differential cross-section, small angle scatt. 79−98186
Na+Cl⇌Na^++Cl^-, chemi-ionis. and recomb. cross sections 78−33583
Na+ethanol, reaction rate determ., rel. to cleaning from LMFBR components 78−21689
Na+F^-, differential cross-section, small angle scatt. 79−98186
Na+F(Cl), quasiclassical charge transfer cross section, rel. vel. depend. 77−19073
Na+H, covalent and ionic states interaction, config. mixing 78−50613
Na+H_2, electronic to vibr. energy transfer, close coupling calcs. 79−98203
Na+H^+, $2p^53s^2{}^2P_{3/2}$ state alignment, collisionally induced, impact parameter calc. 80−83474
Na+H^+, charge transfer cross section and equilibrium fractions, 1-25 keV 80−5616
Na+H^+, charge transfer processes with plasma gun, Lyman-α radiation exam. 78−46573
Na+H^+, configuration interaction potentials and rainbow angle scatt. cross section 80−37745
Na+H^+, electron capture cross sections 79−86061
Na+H^+, K-shell ionisation cross sections for 15-65 keV protons 78−90284
Na+H^+ collisions, L-Auger electron emission, autoionising states, line broadening effects 77−14568
Na+H^+(H), single-electron capture total cross sections 80−91656
Na+H^+(He^+), excited state form. by inelastic processes, energy partitioning 78−82833
Na+H^+(He^+), Na $2p^53s^2{}^2P_{3/2}$ state alignment by 5-30 keV excitation 80−14200
Na+HX(J;ω)→NaX+H, (X=F,Cl), reaction rate, rot. excitation depend. 78−64818
Na+H(Ne)(Kr) vel.-changing collisions, effect on 2 photon and stepwise absorpt. line shape 80−87221
Na+He, Na ($3S_{1/2}$-$3P_{1/2}$) photon echo, collision vel. changes and dissimilar electronic states superposition 80−32803
Na+He (Ne), two-photon optical free induction decay meas. by broadband excitation in unidirectional beams 79−76489
Na+He^+, 25-90 keV, fast beam form., He(2^3S) population 79−31740
Na+He^+, 5-100 keV, electron capture form. of fast metastable He 78−74760
Na+He^+, crossed beams, l-changing collisions, n-depend. 80−58345
Na+He^+, single-electron capture cross-sections 78−37737
Na+He(Ar)(Ne), press. broadening coeffs. of Na 3S-4D transition 78−25481
Na+He(Ar)(Xe), excited state, collisional depopulation cross-sections meas. 79−86057
Na+He(Ne), 3s→3p excitation cross sections, model pot. calcs. 77−58152
Na+He(Ne), excitation cross sections, Na I resonance line emission and polarisation 77−61846
Na+He(Ne), Rydberg states, cross sections for collisional ang. momentum transfer 79−6997
Na+He(Ne)(Ar), 3^2P differential excitation, mechanism 79−86052
Na+He(Ne)(Ar), Na collision-induced alignment, reson.-line emission polaris. obs. 80−18912
Na+He(Ne)(Ar), Rydberg states, collisional angular momentum mixing meas. 77−68093
Na+He(Ne)(Ar), Rydberg S and D state relax., trilevel echo effect 79−72409
Na+He(2^3S_1), Penning ionis. in stationary afterglow 78−42184
Na+Hg, 15-1400 eV, electronic excitation, integral cross sections 80−43159
Na+Hg, collision processes, laser excitation, fluoresc. 79−94059
Na+I_2, ion-pair form. cross section, 15-120 eV, mol. props. depend. 77−28996
Na+I_2, ion-pair formation, energy transfer and differential scatt. 77−75272
Na+I_2, ionising collision, trajectory surface hopping calc. 77−50509
Na+inert gas, $4D_{3/2}$ and $4D_{5/2}$ levels relax. 78−50526
Na+inert gas, collisional redistrib., two-photon absorpt. with near-reson. intermediate state 80−23505
Na+inert gas, non-Lorentzian spectral line shape 80−106297
Na+inert gas, Rydberg states transitions, broadening cross-sections meas. 80−69110
Na+inert gas atom, 4^2D fine struct. transition 79−850
Na+inert gas atom collisions, optical emission cross section, reson. lines 78−13584
Na+Kr collisions in laser beam, transition probability 79−50120
Na+Kr(Xe), excimer bands, multiperturber interactions 78−66497
Na+Kr(Xe), reson. line broadening, press. depend. 78−66596
Na+Li^+, charge transfer and elastic scatt., two state model 78−58805
Na+Li^+, direct and charge exchange scatt., differential scatt. cross-sections meas. 78−42158
Na+methyl iodide, anisotropic interactions from double rainbow struct., interaction pot. meas. 80−99540
Na+Mg^+, charge exchange and excitation processes 78−17772
Na+molecule, vibr. or electronic excitation, prediction model 79−76496
Na+N_2, atom electronic excitation, vibr. to electronic energy transfer, seeded mol. beam studies 80−47919
Na+N_2, collisional deactivation of Na excited states, time resolved fluoresc. 78−42197
Na+N_2, higher Na s and manifold states deactivation cross sections 79−10176
Na+N_2, Na excitation in non-equilib. conditions behind shock wave 77−23539
Na+N_2, rot. excitation and fine struct.-changing collisions 78−42176
Na+N_2^+, 50-1000 eV, crossed beams, electron transfer and excitation 80−14226
Na+N_2O, Na chemiluminesc., excitation mechanism, appl. chem. laser 77−63916
Na+$N_2(H_2)(O_2)$, excited atom quenching, semi-empirical model 78−1065
Na+NO, energy transfer collisions via collision complex 77−83695
Na+Na, crossed-beam collision, laser-induced Penning and assoc. ionisation, struct. obs. 80−83476
Na+Na, electronic-field pot. curves determ. for large interatomic distances, excitation cross sections calc. 80−95704
Na+Na, excited atoms, coupling terms, asymptotic pot., excitation energy transfer 80−23530
sodium continued
Na+Na, excited atoms, electronic energy transfer, doublets obs. 77−3448
Na+Na, interatomic potential, pseudopot. method 79−68294
Na+Na, potential well depth estimation method 79−86034
Na+Na_2, reaction probability, energy transfer 77−28998
Na+Na_2→Na_2+Na, gas phase study 79−43568
Na+Na_2→Na_2+Na, simple model study of exchange reactions 79−43569
Na+Na* resonant collisions mechanisms, excitation transfer in strong mag. fields between Zeeman sublevels 77−83712
Na+Ne, autoionising Ne levels excited in 5-10 keV collisions 78−22017
Na+Ne, differential cross section at thermal energy, expt. and theoretical results comparison 80−37851
Na+Ne, electron excitation, multi-state impact parameter approx. 78−42200
Na+Ne, interaction model potential calcs. 79−86036
Na+Ne, Na(3p) excitation 80−1056
Na+Ne, Na(3s→3p) excitation, impact parameter depend. 78−58794
Na+Ne, potential curves from a model potential *(French)* 80−78685
Na+Ne(Ar)(Kr)(Xe)(N_2)(CO_2), fine struct. changing collisions, vel. depend. 79−22803
Na+Ne(Ar)(Xe), 3^2P-3^2D line broadening obs. 80−78684
Na+Ne(CO), 13d-13f transition, collisional dephasing, Ramsey method investig. 79−54791
Na+O_2, semiempirical pot. surfaces, dynamical considerations 79−11766
Na+O_3→NaO*+O_2, in upper atm., rel. to Na I nightglow intensity vars. 79−70905
Na+$SiCl_4(C(CH_3)_4)(Si(CH_3)_4)(Sn(CH_3)_4)$, rainbow scatt. at thermal energy, anisotropic pot. 78−29837
Na+t-butyl bromide, anisotropic interactions from double rainbow struct., interaction pot. meas. 80−99540
Na+t-butyl chloride, anisotropic interactions from double rainbow struct., interaction pot. meas. 80−99540
Na+t-butyl iodide, anisotropic interactions from double rainbow struct., interaction pot. meas. 80−99540
Na+Xe, nonreson. two-photon absorpt., 4s excited states and pot. energy curves, close coupled eqns. 80−48068
Na+Xe^{10+} depend. of charge transfer on ionisation pot. of atoms 79−64096
Na+Xe+ħw, collisions in presence of nonresonant lasers 80−99567
Na^++Cd, Cd(5^3P_1) and (5^1P_1) and mag. sublevels, excitation cross-sections 80−9710
Na^++Cu crystal, elastic scatt., ang. and energy relationships, 1-3 keV *(Russian)* 79−78802
Na^++ether(thioether)(amide) interaction, pair pots., ab initio SCF LCAO MO calc. 79−36721
Na^++HCN, rotational excitation, Stark shifted level transitions, energy transfer calcs. 79−98059
Na^++He, electron gas model, polarisation inclusion 78−37699
Na^++He, relative level excitation, orbital ang. momentum quantum number depend. 78−25688
Na^++He (Kr) thermal, two trajectory model from meas. cross-sections 77−75257
Na^++HeI, anisotropic collisions, direct meas. method 80−23498
Na^++He(Ne), slow collision, ionis. obs. 79−10194
Na^++Hg, low-energy collision, quantum mech. phase interference and optical polarisation 77−42385
Na^++Hg(6^3P_1), excitation, optical polarisation fractions and mag. sublevels obs. 78−50619
Na^++K, differential scatt. cross section, electronic excitation via. rot. coupling in NaK^+ 78−13579
Na^++Li, direct and charge exchange scatt., differential scatt. cross-sections meas. 78−42158
Na^++Ne, autoionising Ne levels excited in 5-10 keV collisions 78−22017
Na^++Ne, excitation and charge transfer, 0.2-12 keV collision 79−68314
Na^++Ne, nonadiabatic transitions, effective ionisation cross-section calcs. 79−10195
Na^++Ne, quasimolecular states, coherent population *(Russian)* 77−10718
Na^++Ne collisions, Na KK vacancy prod. 78−17781
Na^++Ti(Ni)(Zn)(Fe), 0.2-3.0 MeV, united-at. limits, mol.-orbital continua 77−19030
Na^{5+}+H^+, ^2P_J fine structure transitions 80−37864
Na_2, $^1\Sigma_g^+$-$^3\Sigma_u^+$ excimer emission, ab initio calcs. 80−91608
Na_2, 2-photon ionisation by Ar laser 78−55204
Na_2, A-X band intensity distrib., fluoresc. spectrum Franck-Condon calcs. validity 77−65511
Na_2, $A^1\Sigma_u^+$ state, spectroscopic consts. and RKR pot. calcs. 77−75130
Na_2, and anion, electronic struct., spin-unrestricted, spin-restricted SCF HF calc. 78−90331
Na_2, $B^2\Pi_u$ state, pot. energy curve, shape determ. 79−31432
Na_2, beam, multiphoton ionisation mass selective laser spectroscopy, vibronic, gyrovibronic states, clusters 78−21985
Na_2, beam anal. using detector based on lasers on optical fibres 79−54999
Na_2, continuous laser oscill., optical pumping 77−88706
Na_2, Doppler-free three-photon cross reson. obs. 77−58107
Na_2, electron impact, vibr.-rot. excitation by slow electrons, multiple scatt. calcs. 78−13617
Na_2, excited state identification by two-step polarisation labelling 79−76472
Na_2, form., collision-produced diffuse violet emission band obs. 79−27026
Na_2, Franck-Condon factors appl., rot. depend. 79−10154
Na_2, ground state, pot. curves, MTXα_R method 77−71762
Na_2, ground state, vibr.-rot. relax., optical pumping transients obs. 80−28067
Na_2, kinetic model of Na-Xe discharge for visible lasers 78−63088
Na_2, laser, continuous, optically pumped 78−87046
Na_2 laser action obs. in Na high press. discharge lamp 77−31091
Na_2, laser excited, atomic and molecular fluorescence with long radiative decay times 80−27976
Na_2, laser excited broadband violet emission, 420 to 457 nm 78−79006
Na_2, laser-induced atomic fluoresc., semiclassical intensity calc., transition moments 77−18838
Na_2, laser-induced photodisintegration *(Russian)* 79−89719
Na_2, long range mol., electronic and vibr. levels 78−94301

sodium continued
Na_2, mol. spectroscopy by photodeflection in supersonic nozzle beam 79−54995
Na_2 molecular beam, laser-induced alignment 77−31025
Na_2 molecular electronic struct. for lowest $^3\Sigma_u^+$, $^1\Sigma_u^+$, $^3\Sigma_g^+$, $^1\Pi_u$, $^1\Pi_g$, $^3\Pi_u$ and $^3\Pi_g$ states 80−63738
Na_2 molecule, Doppler-free two-photon transitions, $^1\Sigma_g^+$ state 77−3427
Na_2 molecules, magnetic shielding studies by NMR 77−42341
Na_2, optical orientation under circularly polarised laser excitation 77−65443
Na_2, optically aligned ground state, Hanle effect obs. 79−36707
Na_2, optically pumped CW dimer lasers 80−14322
Na_2 optically-pumped three-level dimer lasers, amplification profiles and dynamic Stark effect 79−41367
Na_2, photodissoc., ^2P products, at. fine struct. anal. 80−78665
Na_2, photodissoc. products of $C^1\Pi_u$ and $C^1\Sigma_u^+$ states 79−98171
Na_2, rot. level repopulation rate by laser-induced depopulation 77−65528
Na_2, rot. perturbed Morse oscillator eigenfunctions and Franck-Condon factors 77−42309
Na_2, Rydberg state, two-step polarisation labelling 80−87053
Na_2, spectroscopy and structure, triplet excimer continuum emission 80−32769
Na_2 supersonic beam rovibronic level population, anal. by laser spectroscopy 80−43118
Na_2, supersonic mol. beam, characterisation by multiphoton ionisation 78−23946
Na_2, two-photon transition, velocity tuned, polarisation depend. and Franck-Condon factors 78−90250
Na_2, two-photon transition, Doppler free vs. Doppler broadened absorpt. 79−13779
Na_2 vapour, near reson. two-photon absorption, polaris. depend. 77−79666
Na_2, vibrationally excited, photodissociation cross section 79−13777
Na_2^+, $^2\Sigma$ and $^2\Pi$ state pot. energy curves, two-centre model 79−26906
Na_2^+, adiabatic pot. curves, ground and excited state, Hellmann-type model pots. 78−78647
Na_2^+, core-core interaction potential calc. 78−25645
Na_2^+, FSGO calcs. with model pots. 78−33413
Na_2^+, form. from Na beam, resonance fluorescence 79−98215
Na_2^+, form. from Na vapour excitation, photodissoc. 79−795
Na_2^+, photodissoc., effective cross-section calcs. 79−31627
Na_2^+, photodissoc. and photoionisation in Na_2 multiphoton absorpt. 79−31628
Na_2^+, pot. energy curve, pseudopot. calc. 77−6703
Na_2^+ Simons-type pseudopots. calcs. 78−5120
Na_2^+-$(H_2O)_n$ clusters, gas phase, high press. mass spectrometry, atmospherical implications 80−58436
Na_2+Ar, differential cross sections meas. for rot. energy transfer process, obs. of halos 80−91643
Na_2+$Br_2(Cl_2)$, collisional ionisation reactions 77−50508
Na_2+He, optically pumped state to state differential cross sections for rot. transitions, rainbow phenomena 80−5609
Na_2+He, rot. excitation, rainbow oscills., coupled states and IOS approx. calcs. 80−23518
Na_2+He, rot. transitions differential cross sections, laser fluoresc. meas. 80−63771
Na_2+He, rotationally inelastic scatt., state-to-state differential cross sections 80−74234
Na_2+He(Ne), rot. transitions, state-resolved differential cross-sections 78−62887
Na_2+He(Ne)(Ar), collision induced dissoc. rate, vibr. distrib. depend. 79−22791
Na_2+Li→NaLi+Na, equilib. const., enthalpy change 78−25750
Na_2+Na, spin polarisation exchange via opt. pumping, NMR 77−14452
Na_2+Na(K), electron energy transfer from optically excited mols. 77−34742
Na_2+Xe, rot. energy transfer, scaling law 78−90272
Na_2+Xe, rot. inelastic collision, rate correls., scaling theory 79−36736
Na_2+Xe rate const., energy corrected scaling laws 80−69225
Na_3, absorpt. spectra, 405-690 nm, mol. beam expt. 79−50031
Na_3, EPR spectrum, Ar matrix, bonding models 77−14462
Na_3, electronic struct., pot. energy surface, ab initio CI study 78−70996
Na_n ($n \lesssim 8$), equilibrium geometries and ionization energies calcs. 80−1099
Na_x, matrix-isolated, formed in supersonic nozzle beam, 400-800 nm absorption and mass spectra obs. 79−76439
NaCl:Na, diffr. efficiency and self-amplification 79−7096
Na^+H_2O, supermolecule calcs. with additive procedure, intermolecular interactions and binding energy 80−52880
NaI isoelectronic sequence, 3s-3p and 3p-3d transitions, ionisation energy 78−70773
NaI night airglow, D-line excitation mechanism 79−84562
NaI-SVI isoelectronic series, radiative lifetimes calc. 79−72276
NaK+Na, spin polarisation exchange via opt. pumping, NMR 77−14452
NaKr, red wing radiation and pot. 80−87180
NaNe, $X^2\Sigma$, $A^2\Pi$ and $B^2\Sigma$ states, model pot. calcs. 78−78776
Na(^{2}P), quenching cross-sections, energy depend. 79−63952
Na(^{2}P)+Hg, differential cross section, orbiting backward peak, obs. 79−76482
Na($^3P_{1/2}$)+Ar→Na($^3P_{3/2}$)+Ar, angular scatt. distrib., Doppler spectrosc. obs. 78−94309
Na($^2P_{3/2}$)+Hg, differential scatt. cross sections 78−66644
Na($^2P_{3/2}$)+Hg, laser excited atoms, differential cross sections 78−62905
^{A}Na, A=21-31, hyperfine struct., mag. moments and isotope shifts, laser spectroscopy 79−10072
^{20}Na, D-line absorption, isotope shift determ. *(French)* 78−42008
^{22}Na and ^{23}Na, isotope shift, HFS, saturation spectroscopy 77−50409
^{22}Na, cosmogenic, in stony meteorites *(Russian)* 77−9719
^{22}Na injection, testis mass loss obs., mouse 80−67156
^{22}Na injection or X-irrad. of mice, sperm count reduction and abnormal sperm increase 80−108961
^{23}Na in heterogeneous system, nuclear mag. relaxation time determ., rel. with dimensions of colloidal particles 80−75876
^{23}Na, pionic 2p-1s X-ray transitions 79−18319
^{23}Na, relax. in polyelectrolyte solns. 79−20353
^{23}Na, S states, HFS optical double-reson. techniques 77−68023
^{23}Na spin-$^3/_2$ nuclei, double quadrupole resonance 80−32634
^{24}Na carrier-free production by 50-180 MeV protons on Si, P, S, Cl, Ar and K 79−83934
sodium continued
^{24}Na radioisotope investigation of Al-Si alloy modification by Na-containing agents *(Russian)* 77−40567
^{24m}Na, laser induced nuclear orientation 80−57680
Na*+N_2, differential quenching cross-section, polarisation effects 77−27019
Na_2*, fluoresc. red continuum emission, atom-mol. energy transfer 80−43086
Na_2*+Xe, rot. energy transfer, level-to-level dynamics, laser fluoresc. obs. 79−64029
Na_2*+Xe, rot. energy transfer, vel. depend. 80−95715
Na_2*(AΣ)+He(H_2)(N_2)(methane), rot. energy transfer, power law scaling 79−98204
Na*(^{2}P)+H_2(D_2)(O_2)(N_2)(CO)(CO_2)(N_2O)(C_2H_4), electronic to vibr.-rot. energy transfer, differential cross sections 77−38715
Na*(3p)+Na_2, collisional and radiative processes, fluoresc. decay obs. 78−66638
Na*(nd,nf)+He, ang. momentum mixing 79−10175
Na(110)-Na(110), metallic adhesion 79−73463
Na(1s), X-ray photoelectron spectrum, binding energy, at. compared with metal 78−70800
Na(^{2}P), electronic to vibrational energy transfer in collisions with simple molecules 80−63769
Na(^{2}P), in O_2-H_2-Ar flame, atm. press., lifetime obs. 79−39149
Na(^{2}P)+CO(X^2S^+), electronic-vibr. energy transfer reaction 79−64084
Na(^{2}P)+O_2(SO_2), near-threshold ionis. of Na* 77−88544
Na($^2P_{1/2,3/2}$), laser induced flame chemistry, saturated mode fluoresc. meas. 80−89491
Na($^2P_{3/2}$), electron total cross section, at. beam recoil technique 77−27186
Na(^3P_J)+Na($^3S_{1/2}$), collisional excitation transfer, pot. symm. rules and cond. function 80−9690
Na($3S_{1/2}$,$3P_{1/2}$)+He, total cross section, stimulated photon echo obs. 79−76503
Na($3p^2P_{3/2}$)+N_2(O_2)(CO)(NO), electronic energy quenching dynamics, crossed beam expt. 80−9683
Na^+.nH_2O+$PO_4H_2^-$, binding mechanisms, SCF ab initio calcs. 79−22586
Na(n^2D)+N_2(CO), collisional l-mixing, highly excited states, fluoresc. obs. 77−83686
Na(nd)+He(Ne)(Ar), l-changing Rydberg at. collisions, rel. to low-energy electron scatt. 79−50112
Ne+Na, inelastic scatt. differential cross-section calcs. 77−10730
Ne+Na^+, autoionising level excitation, electron spectra 77−14554
Ni-Na-di-2-ethylhexyl phosphoric acid-H_2O system, droplet phenomena 77−48697
O_2+Na(K)(Cs), negative ion pair form., total cross sections 79−3550
PbTe:Na, In, high temp. Fermi level position 79−90948
PuO_2-UO_2-Na aerosol, from LMFBR HCDA conditions, characterisation 78−94104
Rb+Na, spin exchange cross section 78−33637
RbCl:Na, F_A-centre optical absorpt., estimate using symmetry-adapted wave functions 80−11448
RbCl:Na, tunable IR lasers with F_A(II) and F_B(II) colour centres 78−90420
RbCl:Na, U-centres, HFS consts., g-factors, EPR spectra 80−39869
RbCl:Na^+, F_B(II) colour centres, tunable CW laser operation obs. 77−83877
RbF:Na, F-centres, saddle-point configuration, molecular model parameter 80−107234
Si:Na, amorphous, implantation effects on elec. props. 80−49716
Si:Na, amorphous, ion implanted, control of cond. 79−60835
p-Si:Na, control of diffusion profile of Na by radiation defects *(Russian)* 77−43386
Si:Na, quantitative analysis of residual impurities with SIMS 78−87688
Si:Na ion implanted, Hall effect temp. depend., electron surface density and mobility 80−11018
Si:Na^+, inversion layer, far IR optical spectroscopy 80−20680
Si:Na^+, variation of cond. in two-dimensional impurity band with Fermi level position 79−95510
Si-Na interface, barrier height anal. including virtual surface states 77−69416
Si-SiO_2 interface, Na^+ drifted, impurity bands in inversion layers 78−60211
Si-SiO_2:Na^+, physics, electron and ion motion *(Dutch)* 80−60093
SiO_2:Na, film, depth profiling by SIMS 78−79624
SiO_2:Na, ion trapping and mobility, energy levels 80−92985
SiO_2:Na film, RF sputtered, low elec. field Poole-Frenkel effects in MIM struct. 79−95536
SiO_2:Na^+, heat treated, heat of immersion in H_2O, organic compds. 80−3396
$SrCl_2$:Gd^{3+}, Na^+, elec. field gradient at nuclei on orthorhombic sites, vs. elec. zero-field splitting 79−87070
$SrCl_2$:Na^+, X-irradiated, recomb. luminesc. between trapped electrons and self trapped holes 77−73162
SrF_2:Gd^{3+}, Na^+, EPR of orthorhombic Gd^{3+}-univalent metal ion complexes 80−11262
SrF_2:Na, γ-irrad. cryst., spontaneous and induced colour centre emission 79−7131
SrF_2:Na, tunable room temp. laser action of M-centres, luminesc. and absorpt. spectra 79−31907
SrF_2:Na^+, cryst., thermal depolarisation 79−82912
$Sr_2Ta_2O_7$:Nd,Na, SHG, effect of dopants on Curie temp. 79−24267
TaS_2-Na intercalation compound, CDW's and superlattice patterns 77−47746
(U,Pu)C LMFBR fuel, Na-bonded, consequences of rapid Na loss on fuel behaviour 80−102238
UO_2/Na, fuel/coolant thermal interaction in FBR, out of pile preliminary tests *(Italian)* 78−54828
UO_2-Na contact interface temp., effect of internal radiation 79−13477
UO_2-Na thermal interaction, dropping experiments and subassembly test 78−82460
V_2O_5:Na, elec. cond. and thermoelec. power meas. 80−10987
α-V_2O_5:Na, far IR absorption spectra meas. 77−73158
WF_6+Na(K) electron transfer, WF_6^- form., dissoc. energies, electron affinity 77−19071
ZnO:Na, band-edge emission obs. 77−20933
ZnS:Na, and undoped, thermoemission of positive ions in simple gas atmos. *(Russian)* 77−28676
ZnSe:Li(Na)(Ga) doped and pure cryst., donor-acceptor bands 80−11465

sodium continued
ZnSe:Na, characterisation of edge emission 78−27312
p-ZnSe:Na, LPE layers, photocapacitance and photocond. meas. 79−99572
ZnSe:Na, shallow acceptor excited states, luminescence spectra, Rydberg energy 79−78750
ZnTe:Na, fluorescence spectra meas. 78−10949
ZnTe:Na, spin-flip acceptor scatt., transition selection rules gyromagnetic ratios 79−61380

sodium alloys
dilute, sp. ht. meas. close to melting point 78−47501
dilute binary alloy, residual resistivity 77−1406
Al-Na alloy, supercond. flux pinning by precipitates 77−47948
Al-Si-Na eutectic melts, struct. determ. *(Russian)* 77−80408
Cs-Na, liq., thermodynamic props. at high temps. 80−15262
Hg-Na, liquid, structure factors, X-ray scatt. *(Japanese)* 80−54122
Hg-Na (3 at.%), amalgam, thermodynamic and electron transport props. 79−23938
K-Na, dil., anisotropic scatt. of conduction electrons by impurities 78−18944
K-Na, dil., anisotropy of electron-impurity scatt., de Haas-van Alphen effect meas. 78−18943
K-Na, dil., dynamical props. of quasiparticle excitations, de Haas-van Alphen effect meas. 78−84128
KNa_2, binding energy and lattice const., nonparametric calc. *(Russian)* 78−51462
K_2Na^+, equilib. geom. and dissoc. energy, pseudopot. calc. 78−94329
Li-Na, liq., concentration fluctuation and structure factor 78−30534
Li-Na, liq., short-range order, neutron diffr. obs., near crit. composition 78−22639
Li-Na, liq. alloy, thermoelec. power and elec. resist. 77−47788
Li-Na liquid binary mixtures, phase separation under press. 80−34183
$LiNa_2$, ground and excited states, model pseudopot. calcs. 77−75069
$LiNa^+$, equilib. geom. and dissoc. energy, pseudopot. calc. 78−94329
Na amalgam-Na conductive glass interface, electrochem. obs. 78−76870
Na-Cd, liq., mag. susceptibility, diamagnetism 78−72326
Na-Cd(In), dil., magnetic susceptibility, impurities effect, free electron gas model 79−91206
Na-Cs, internal energy, heat of mixing, entropy, dielectric function 80−88340
Na-Cs, liq., conc. fluctuations, X-ray transmission meas. 77−47329
Na-Cs, liq., struct. factors, X-ray transmission diffr. expt. 77−47337
Na-Cs, liq., struct. factor, free energy of mixing, and electrochem. pot., thermodynamic calc. 80−96436
Na-Cs, liq., thermopower 78−23074
Na-Cs, liq. alloy, thermoelec. power and elec. resist. 77−47788
Na-Cs melt, density and molar volume *(Russian)* 78−15357
Na-Cs solution, saturated vapour pressure of Cs over solution 78−26688
Na-Ga, solid and liq., mag. susceptibility and elec. cond. *(Russian)* 80−29522
Na-Ga liquid alloy, thermodynamic props. 79−37854
Na-Ga liquid alloy, thermodynamic props. of mixing derivation method 80−54385
Na-H, liq. and solid, mol. orbitals approach, solvation energies 77−4201
Na-In, dilute soln., thermodynamic props. 77−89553
Na-K, internal energy, heat of mixing, entropy, dielectric function 80−88340
Na-K, liq., dynamical struct. factor calc. 78−22634
Na-K, liq., static struct. factors 78−63664
Na-K, liq., third-order partial struct. factors 77−47339
Na-K, liq. alloy, electronic correl. functions calcs. 78−63663
Na-K, liq. alloys, electromigration driving force expression 78−51714
Na-K, liquid, collective excitations, mol. dynamics calc. 80−28895
Na-K, liquid, electron theory of chemical potential and activity *(Japanese)* 77−72702
Na-K, liquid, resistivity calc. using general model pseudopot. 77−55506
Na-K, liquid alloy energy of soln. pseudopotential calcs. *(Russian)* 79−66330
Na-K, partial structure factors, square well pot. calcs. 77−51300
Na-K, surface tension theory for liquid mixtures 80−88404
Na-K alloys, liq., thermal conductivity, NaK_2 formation 78−10416
Na-K liq. alloy, Moelwyn-Hughes parameter calc. from US data 80−59375
Na-K liquid alloy, self and mutual diffusion coeff. 78−22877
Na-K liquid alloy, small angle X-ray scatt. study, conc.-fluctuation structure factors 80−54120
Na-K liquid alloys, struct., X-ray and neutron diffr. meas. 80−107041
Na-K liquid alloys, triplet correlation functions and thermodynamics, solute partial structure factor 80−64881
Na-K-Cs alloys, liquid contact material, phase diagram calcs. 78−6145
Na-K-H system, H influence on component interactions *(Russian)* 80−54383
Na-K(Cs), liq., form factors and transport coeffs., pseudopot. perturb. theory 80−44561
Na-K(Cs) liquid alloys as coolants, specific heat determination 79−86902
Na-K(Rb), liq. calc. of electromigration forces and resist. 79−82572
Na-K(Rb)(Cs), solute atom-grain boundary interaction energy, electron-statistical calcs. *(Russian)* 79−73175
Na-Li, liq., Knight shift calc. by multiple scatt. Xα method 80−54961
Na-Li (19.2 wt.%), elec. resistivity, immiscibility region 79−1593
Na-Rb, liq. alloys, electromigration driving force expression 78−51714
Na-Rb, liquid, resistivity calc. using general model pseudopot. 77−55506
Na-Se system, liq., thermodynamic props. 80−21319
Na-Sn, disordered, min. metallic cond. 79−95372
Na-Sn liq. alloys, thermodynamic props. by EMF meas. with β-Al_2O_3-Ba_2 electrolytes 79−19379
Na-Te, liq., chemical pot. and resist. 77−55232
Na-Te system, liq., electrochem. determ. of thermodynamic props. rel. to temp. 77−1245
Na-Tl, equiatomic, B-32 superstruct. instability in absence of many-particle interactions 77−58972
Na-Tl, liq., elec. resist. meas. 77−51717
Na-Tl, liq., mag. susceptibility, diamagnetism 78−72326
Na_3AlFe_6 coatings, transmission and refraction dispersion spectra *(Russian)* 77−48264
$Na_{1-x}Bi_x$ liq. alloys, metal-nonmetal transition, mag. susceptibility meas. 79−82525
Na_2Cs, OPW calc. of struct., bonding and stability 77−43169
NaIn, elastic moduli and Debye temp., US meas. 79−91724

sodium alloys continued
NaK, appearance pot., dissoc. energy, ionis. pot., mass spectra obs. 78−25750
NaK, liq., engineering handbook, purification, heaters, coolers, radiators 80−27045
Na_2K, OPW calc. of struct., bonding and stability 77−43169
Na_2K+, equilib. geom. and dissoc. energy, pseudopot. calc. 78−94329
Na_xK_{1-x}, solid-liquid transition 78−6144
NaLi, appearance pot., dissoc. energy, ionis. pot., mass spectra obs. 78−25750
$NaLi \rightarrow Na+Li$, equilib. const., enthalpy change 78−25750
Na_2Li^+, equilib. geom. and dissoc. energy, pseudopot. calc. 78−94329
NaPb alloy, compound-forming, vol. of mixing, conc. depend. 80−103484
$Na_{1-x}Sb_x$, liq., mag. susceptibility 78−14926
NaTl, elastic moduli and Debye temp., US meas. 79−91724
NaTl, pseudopotential method and ordering problem 77−35500
Nb-K melts, thermodynamic characts., elec. resistivity, single parameter rigid sphere calcs. *(Russian)* 80−34410
NiNaK, mol., intersection of pot. energy surfaces, ab initio calcs. 79−36557
Pb-Na, peak-effect supercond., flux pinning 78−95403
Pb-Na, with Pb_3Na precips., flux pinning, crit. currents obs. *(German)* 78−14907
Pb-Na (8.4 at.%), supercond., surface flux pinning, crit. state model 80−97044
PbNa, type-II superconductor, regularly ordered precipitates, peak effect, crit. current meas. *(German)* 78−19196
PnBa, supercond., flux density distrib. meas. differential magnetisation loop method 77−32129
Se-Na, and Se, liqs., elec. resistivity and phase separation 79−82573
Ti-Nb-Na (4 to 31, 8 to 38 at.%), with uniform distribution of refractory metal, prep. *(Russian)* 77−28747

sodium compounds
see also Rochelle salt; sodium alloys
β-spodumene, glass-ceramics, internal stresses 79−15770
acetate, molten mixtures, elec. cond., density 77−15613
acetate trihydrate, cryst. struct. and bonding 77−24309
acetate trihydrate, whisker growth on membrane in aq. soln. 78−30854
acetylacetonate, anomalous dielec. behaviour, evidence for ferroelectricity 79−91390
acid oscalate, neutron inelastic scatt. spectra in 2200-200 cm^{-1} range 80−70327
β-Al_2O_3-Na_2O, AE during breakdown under Na^+ transport 78−67860
β-Al_2O_3-Na_2O, diffusion and ionic cond. meas. 80−6542
β- and β″-Al_2O_3-Na_2O, fast ion conductors, TEM obs. 79−86920
β-Al_2O_3-Na_2O, geometrical aspects of breakdown, TEM study 79−79096
β-Al_2O_3-Na_2O, IR high temp. amplitude-phase spectroscopy 79−35860
β-Al_2O_3-Na_2O, mechanism of diffusion 80−2202
β-Al_2O_3-Na_2O, Monte Carlo calc. of Na diffusion 77−89579
alkanoates, phase relationships and thermal behaviour branching effects 78−43111
alunite-jarosite, spcae group refinement by means of vibr. spectroscopy 79−94981
amphiphilic-polymer liquid crystal, NaCl conc. influence on struct., X-ray diffr. study 80−44126
B_2O_3-Na_2O, thermal cond. of melt in region 900 to 1100°C, effect of convection 78−2309
benzoyalcetonate, piezoelectricity, transition of 70°C 79−8092
benzoylacetonate, dielec. props. and cryst. struct. 79−8099
benzoylacetonate, pyroelectric effect, peak near Curie temp. 79−8096
biphthalate, cryst. struct., X-ray diffr. meas. 77−39577
brine-kerosine system, horizontal layer, convective stability 77−7392
carnegieite, metastable cathodochromic, prep. by zeolite decomposition *(French)* 79−95719
CIDEP, examples of $S\text{-}T_{\pm 1}$ polarisation 78−86891
cryolite, hydrothermal synthesis of large synthetic single crystal, props. 78−19654
cryolite, in thin film polarising beam splitter 77−19422
cryolite, molten, struct. charact. by IR spectroscopy and splat cooling *(French)* 79−69835
cryolite melts saturated with alumina, interfacial tension between Al and melt 78−38913
decylsulphate-Li_2SO_4-decanol-H_2O system, lyotropic liq. cryst., high resolution NMR 79−4243
diemthyl sulphoxide-H_2O-NaCl system, DTA exam. of primary ice phase field 78−48382
dimethylsulphoxide-water-0.9 m $NaClO_4$, salt effect on vap.-liq. equilib. 79−51245
dodecane-sodium octylbenzene sulphonate phase diagram *(French)* 79−82339
dodecylsulphate, micellar system, 1-methylpyrene quenching by Cu^{2+}, general kinetic model 80−32753
ethanoate, solid, low energy photoelectron spectra 78−95656
fluor-richterite crystal, habit, growth in oxide-fluoride mixtures, statistical study *(German)* 78−38639
fluorescein-rhodamine B, energy transfer in luminescent mixed solutions 80−103976
formate, vibr. spectrum, lattice modes 79−28759
formate($-d_1$), far IR and IR absorpt. spectra, lattice mode assignment 77−85717
furan, adsorbed on NaCl, evidence of new condensed phase, IR spectra *(French)* 80−16028
germanate crystals and glasses, struct. and stability, IR spectra meas. 80−64911
graphite-Na-N-H intercalation compounds *(French)* 79−52633
halide, extended three-body shell-model dynamics 77−7797
halides, ^{23}Na NMR chem. shift meas. 77−71817
halides, absorpt., emission and lifetime data, temp. depend. 77−4671
halides, elastic constants, temp. derivatives at constant volume 80−59549
halides, shock generated plasmas, Na D line emission 77−47265
halides, vibrational surface modes of (001) unrelaxed face, shell model 77−43420
halosodalites, synthesis, cathodochromism, reflectivity spectra 77−40399
hexahalogeno compounds: $ReCl_6^{2-}$ ($ReBr_6^{2-}$), low symm. splittings in vibronic spectrum due to phase transitions 80−55161
HgI_2:NaI, cryst. growth from soln., doping rel. to elec. cond., phase transitions 77−55880
hydrogen oxalate, crystal growth in silicate gel, X-ray diffr. and i.r. spectrum 77−4724

sodium compounds continued
Hygroscopicity of double-condensed sodium potassium phosphates 77−84939
keratin-NaCl, Na Auger electron spectra 78−53339
leucosphere-tutualite-milarite, struct. series derived from α-celsian 79−19223
mordenite, dehydrated Na-exchanged, cation and molecular distrib. 79−90617
mullite-based dispersed refractory system, rheological props. at high temp. 77−16629
$Na_2V_2Ti_6O_{16}$, characterisation and mag. props., 90-800K, $Na_xTi_4O_8$ bronze isotypes *(French)* 80−39735
$Na_2[Fe(CN)_5NO]$, valence levels, X-ray photoelectron and X-ray spectra 77−88500
NaCl aqueous solutions, viscosity at high temps. and pressures, investigation 78−95175
NaCl crystals, air cleaved, anisotropy of round evaporation spirals, electron microscopy study 79−73300
NaCl substrate, epitaxial Au particles, high resolution dark field electron microscopy 77−85111
NaCN, lattice dynamics and order-disorder transitions, neutron scatt. expts. 78−14434
NASICON solid electrolyte, processing and phys. props. 80−60820
nepheline-kalsilite system, subsolidus phase relations at 0.5, 2.0, and 5.0 kbar 79−66041
octanoate-decanol-water system, liq. cryst. C phase, struct. determ. using electron microscopy 77−47341
octyl benzene sulphonate, micellar aq. soln., Cotton-Mouton effect in mag. field 79−16047
omphacite, Mossbauer spectra study 79−65771
omphacite, P2/n to C2/c transform. study 79−65183
orthophosphates, anhydrous, struct. relationships w.r.t. fast ion cond. 80−107188
oxalate:Cu^{2+}, EPR studies 80−60408
oxalate, cryst. struct. rel. to those of $Na_2Sn(C_2O_4)_2$, SnC_2O_4 *(French)* 80−2004
oxyacid salts, aq. electrolytes, apparent molar heat capacities and vols. 79−23744
plagioclase feldspar, deformed, elastic twinning, TEM obs. 77−62551
polyethylene:NaCl, internal field strength, Raman spectra obs. 80−40061
polysilicates, IR spectra, struct., crystallisation effects *(Russian)* 78−72528
proton bombardments, spectral refl. change and luminesc. with implications for Io 79−96950
pyrochlore, high temperature chlorination 78−11180
γ-quartz, reaction, with NaCl-kCl melt, exam. of struct., IR absorption spectra 80−55706
Rochelle salt, Cu and Zn plating appl., cyanide copper baths analysis *(German)* 77−25328
rocksalt, cleaving device for clean surface prep. 77−13738
salicylate, vac. UV scintillators, characteristic props. at 253.7 nm 79−71525
salt crystals in aqueous slurries, particle size distrib. determ. 79−61918
salt hydrates for heat storage in a solar heating system 80−67005
salt hydrates for heat storage in solar heating system, based on extra water principle 80−67006
salt solutions, freezing in cells, heat and mass transfer with phase change 80−6493
sheet phases $Na_x(L_xM_{1-x})O_2$, (L=In,Sc; M=Ti,Zr,Hf,Sn), ionic cond., influence of Na^+ environment *(French)* 79−65244
silicate glass temp. depend. of rate of nucleation of acicular crystals 77−19875
silicate glasses, Na ion mobility, OH content effect 79−99359
silicates, entropy estimates at 298K from molar vols. 77−1243
soda lime glass, Ag^+ ion exchanged, planar optical waveguide, manufacturing tolerances 78−71212
soda lime glass, microparticle impact, high speed photography obs. 78−44223
soda-lime glass, chemically modified, water contact angle, adhesional wetting 77−55426
soda-lime glass, depth profiles of Na and Ca by SIMS and AES 78−51805
soda-lime-silicate glass, dynamics of fracture mirror boundary formation 77−86132
sodalite, crystallisation process, effect of solid and liq. boundary layers, SEM 79−23544
sodalite, hydrothermal growth on seed crysts. covered with boundary layers, growth mechanism 78−30571
sodalite single crystals, exam. of growth mech. in hydrothermal method, using SEM 79−52105
sodalites, aluminogermanate- and aluminate-, IR spectra rel. to T-O bond length and T-O-T ang. 79−91445
sodium ammonium tartrate, crysts., temp. depend. of elastic compliances at phase transition 79−15409
sodium ammonium tartrate, ferroelec., thermodynamic theory of phase transitions 77−90112
sodium ammonium tartrate, improper ferroelec. transition anomalies 78−19430
sodium ammonium tartrate, polarisation, improper ferroelec. transition 78−72477
sodium bentonite, Wyoming suspension, comparison of optico-optical scattering and birefringence 80−85226
sodium benzoylacetonate, unit cell dimensions, X-ray determ. 79−69097
sodium biphthalate, water of crystn. detection, PMR 77−35546
sodium cholate-decanol, soln., aggregate form., comp. and dynamics 80−45575
sodium decanoate-n-decanol-water system, lamellar G-phase, orientational-order, EPR investigation 80−24355
sodium decyl sulphate/water/decanol/Na_2SO_4, lyotropic mesophase, mag.-oriented, X-ray diffr. obs. 80−1921
sodium dodecyl sulphate, polydisperse micellar solns., light scatt., size, shape and aggregation number calcs. 80−89531
sodium dodecylsulfate−H_2O system, X-ray anal. 80−1926
sodium dodecylsulphate micelle, intramicellar fluorescence quenching of $[1\text{-pyrenyl-}(CH_2)_n\text{-}N(CH_3)_3]^+Cl^-$ by cationic surfactant nitroxyl radical 80−9627
sodium hydrogen oxalate monohydrate, crystal struct. neutron diffr., deform. electron density analysis 78−10032
sodium hydrogen oxalate monohydrate, oriented single crvst., Raman spectra with very strong H-bonding 80−25359
sodium compounds continued
sodium iron fluorophosphate glasses, EPR and Mossbauer resonance study 80−39968
sodium lauryl sulphate micelles, chlorophyll-a, soln., dilution expts., solubilisation anal. 80−35587
sodium lauryl sulphate-3,3'-diethylthiacarbocyanine iodide-rhodamine-6G, soln., premicellar region, energy transfer 80−20685
sodium magnesium aluminium oxdate, elastic consts., Debye temp. 79−82275
sodium nitroprusside, isomeric molecular states generated by polarised light, Mossbauer resonance obs. 77−20781
sodium pentadecyl sulphonate, lyotropic liquid crysts., X-ray study of domain structure *(Russian)* 77−62469
sodium salicylate, UV convertor layer, fluoresc. props. *(French)* 77−4676
sodium salicylate-toluene, singlet-singlet energy transfer in Manoxol OT-cyclohexane-water 80−9531
sodium tetraborate glass, melt, temp. depend. of high viscosity property *(Russian)* 80−39336
sodium tetraethylaluminate-benzene (cyclohexane)-donor system, Na^+ ion solvation number 78−95987
sodium tetramethylborate, vibr. spectra and force constants *(German)* 79−26981
sodium tin oxalate, cryst. struct. rel. to those of $Na_2C_2O_4$, SnC_2O_4 *(French)* 80−2004
sodium uranyl acetate, absorpt. spectra, MCD and natural dichroism, UV and visible 79−69853
sodium uranyl acetate, fluoresc., circ. dichroism 79−38598
sodium uranyl acetate (deuteroacetate) 80−2830
sodium valerate, mesophase, self-diffusion and spin-lattice relax. 79−69008
stearate, Langmuir-Blodgett multilayers, comp. and transfer mechanism 80−80125
steel, low C, electroboronising by superimposed cyclic current, Na_2CO_3, B_4C, NaCl, NaOH activator studies 80−85081
steel, mild, in Na_2SO_4 soln., anodic polarisation study of corrosion by AC 80−40582
steel, stainless, type 304, corrosion fatigue and stress corrosion cracking, in boiling NaOH 80−7719
styrene-sodium methacrylate (9 mol.%) copolymer cond. relax. 78−38874
tartrate tetrahydrate, gel-grown single crysts., charact. 77−90261
TCNQ-Na, X-ray exam. of phase transitions 78−55933
tetraphenylboron sodium aq. soln., dielec. relaxation spectroscopy in microwave region, double-beam interferometry *(German)* 80−71309
thermal expansion measurement using X-ray powder diffractometer with polythermal attachment 80−311
tienshanite, cryst. struct. determ. 78−83800
tourmaline, elastic consts. by US phase-comparison method 80−2108
triple orthoarsenates, $NaM^{II}Cr_2(AsO_4)_3$, prep. by high temp. synthesis, and cryst. struct. 79−66028
trisoxalatoferrate complexes, Mossbauer studies of electronic relax. phenomena 80−44973
tuhualite-milarite-leucosopherite, struct. series derived from α-celsian 79−19223
ultramarine, catalyst struct., binding energies, ESCA 77−21420
undecanoate/water system, lyotropic liq. cryst. struct. change due to polymerisation of amphiphilic component 80−59386
uridine 5'-phosphate (Na salt), EPR study of PO_4^{2-} radical 79−57592
UV laser possible pumping by synchrotron radiation, NaCl:I(Br) luminesc. 78−66835
zeolite, adsorbed amino radical extra coupling with ^{23}Na 77−7963
zeolite, faujasite type, intermed. state of enhanced mobility of adsorbed H_2O mol. 78−60027
zeolite, Faujasite type, varied Si/Al ratio, absorption of H_2S 78−60029
zeolite, hydrated, partly exchanged with Ce ions, cation distrib. *(Spanish)* 77−4080
zeolite, molten salt inclusion in intracrystalline canals, spectrosc. charact. *(Rumanian)* 79−74463
zeolite, proton spin relax., adsorbed H_2O effect on Pt distrib. 78−88216
zeolite and Sc substituted zeolite, selective adsorption 79−90887
zeolite-S layers, high-temp. activated dipole moments in S clusters *(Russian)* 80−20575
zeolites, -A and -Y type, local coordination of Co(II) ions studied by X-ray absorpt. fine struct. spectroscopy 80−93434
zeolites, appl. in removing ^{137}Cs from nuclear power station liquid waste 79−6749
5A-zeolites, cation distrib. and diffusion *(German)* 78−64828
zeolites, Na, Cs, Sr types, processing radioactive waste soln., thermal transform. 77−10477
zeolites, radioactive waste soln. processing, Cs volatilization at high temp. *(Japanese)* 79−13441
zeolites, synthetic, effect of sintering on elec. cond., porosity and microstruct. 79−29009
zeolites, type 13X, acetylene adsorption, inelastic neutron scatt. 78−14584
zeolites, type Y, containg catalysts, cryst. struct., IR spectra 79−42958
zeolites, XPS, analytical and struct. information 77−90239
$16Na_2O.12CaO.72SiO_2$, self-diffusion of Ca^{2+} ions *(Japanese)* 78−6173
(Ag,Na)Br, ionic transport numbers, polarization cell method 80−59705
(Ag,Na)Cl solid solns., ionic transport numbers, polarization cell method 80−59705
Ag/$Na_2SO_4(WO_4)$ solid cell systems interface form., intergrain contact growth 77−16827
AgBr NaBr, thermodynamic props., metastable states and demixing 80−96660
AgBr-NaBr, phase diagram, miscibility, binodal curve and demixing kinetics, X-ray meas. 80−96659
AgBr-NaCl(Br) solutions, UV spectra 78−39560
$AgNO_3$-$NaNO_3$ mixed melts containing Na_2O-SiO_2-Ga_2O_3-Al_2O_3 glasses, ion exchange 80−21282
AgNa mordenite, chemisorpt. of CO and H_2 80−2752
$AgNa(NO_2)_2$, complex piezoelectric constant, meas. by interferometric method, at frequencies up to 50 kHz 79−63270
$AgNa(NO_2)_2$, crit. sp. ht. near ferroelec. transition 79−38474
$AgNa(NO_2)_2$, ferroelec. transition, ^{23}Na elec. field gradient tensor, NMR meas. 79−4777
$AgNa(NO_2)_2$, ferroelectric phase transition, theory 79−24272
$AgNa(NO_2)_2$, ferroelectric transitions, group theoretic comparison with $NaNO_2$ 80−7311

sodium compounds continued
$AgNa(NO_2)_2$, ferroelec., Raman scatt. and phase transitions 80−71349
$AgNa(NO_2)_2$, ferroelec. cryst., Raman spectrum, phase transition, comparative anal. with $NaNO_2$ 80−88935
$AgNa(NO_2)_2$, Landau behaviour of sp. ht. close to nearly tricritical ferroelec. phase transition 78−10861
$AgNa(NO_2)_2$, order-disorder ferroelec., crit. dynamics, NMR data compared with dielec. data 78−76415
$AgNa(NO_2)_2$, order-disorder ferroelec., influence of hydrostatic press. on polarisation dynamics 80−103913
$AgNa(NO_2)_2$, Raman spectrum, NO_2^- bending vibr. 79−28737
$AgNa(NO_2)_2$, single cryst., specific heat anomaly, −90-55°C, ferroelec. transition entropy 77−77157
$AgNa(NO_2)_2$, triplet absorpt. polarised spectra, near ferroelec. phase transition 79−47473
$AgNa(NO_2)_2$, ultraslow crit. dynamics of order parameter, ^{23}Na spin relax. times obs. 78−76410
$Ag_xNa_{2-x}Te_2{}^{IV}Te_3{}^{VI}O_{14}$, (x=0,4), mixed tellurate, cryst. chem. and elec. cond. *(French)* 80−107150
Ag_2O-Al_2O_3-MgO-Na_2O, β″-alumina, structure, X-ray determ. 80−107148
Ag_2O-Na_2O-B_2O_3 mixed cation glasses, electric conduction *(Japanese)* 77−24432
Al/$AlCl_3$-NaCl/FeS_2 secondary cell, preliminary study 80−108793
$AlCl_3$-NaCl melt, n-TiO_2 electrode, electrochem. and photoelec. props. 80−81328
β-AlO_3-$(Na,Li)_2O$, NMR, Raman and IR spectra, and X-ray diffr., heat treatment induced changes 80−107508
β-Al_2O_3, ^{22}Na labelled monocrystals, radiochemical anal. by isotope dilution method 80−11976
β-Al_2O_3-$(Na,K)_2O$, equil. distrib. of ionic species 80−107511
β-Al_2O_3-$(Na,K)_2O$, model calcs. of cond. anomalies, pot. energies of cation arrangements 80−107510
β-Al_2O_3-$(Na,Li)_2O$, first-order quadrupole NMR obs. of cation distrib. and ion motion 80−108113
β-Al_2O_3-$(Na,Li)_2O$, ionic cond. and Raman spectra 80−107509
β-Al_2O_3-$(Na,Li)_2O$, ionic motion obs. using NMR and internal friction 80−108099
β-Al_2O_3-$(Na,Li)_2O$ solid electrolyte, Li motion and activation obs. using ^7Li NMR 80−108100
β″-Al_2O_3-$H^+(H_2O)_n$, IR study 80−16037
β-Al_2O_3-Li_2O-Na_2O, solid electrolytes, elec. props., stability 77−84978
β-Al_2O_3-Li_2O-Na_2O, spin-lattice relaxation and Li motion 80−70451
β- Al_2O_3-Na_2-CaO, microstruct. and ionic resistivity 80−44357
β-Al_2O_3-Na_2O, ^{23}Na NMR spectrum, correl. effects 78−76324
β″-Al_2O_3-Na_2O, ^{23}Na NMR obs. of ionic diffusion, 180 to 800K, attempt freq. 80−108097
β-Al_2O_3-Na_2O, ^{23}Na NQR and two-dimens. diffusion, model analysis 80−108111
β-Al_2O_3-Na_2O, ^{23}Na nucl. spin-lattice relax., barrier height distribs. and diffusion processes 77−55720
β-Al_2O_3-Na_2O, ^{27}Al NMR obs., Na motion and cond. characts. 80−108096
β-Al_2O_3-Na_2O, AA 79−91351
β-Al_2O_3-Na_2O, AC impedance, microstruct. and strength 80−100349
β-Al_2O_3-Na_2O, AC ionic cond., dielec. and NMR relax. 80−59713
β″-Al_2O_3-Na_2O, absorbed water effect on NMR lineshape and spin-lattice relax. time 80−108098
B-Al_2O_3-Na_2O, adsorbed of Na, surface electronic struct. calcs. 80−75431
β-Al_2O_3-Na_2O, anomalous Na behaviour obs. using pulsed and CW NMR 80−108095
B″-Al_2O_3-Na_2O, bulk and grain boundary ionic cond. from conductance and capacitance meas. 80−2204
Al_2O_3-Na_2O, β and β″ phases, stability, cond., paramag. impurity effects obs. 77−84976
Al_2O_3-Na_2O, β and β″ phases, formation by solid state reaction between $NaAlO_2$ and γ-Al_2O_3 80−29912
Al_2O_3-Na_2O, β′ and β″ phases, engineering props. data compilation, rel. to energy storage 80−49415
β-Al_2O_3-Na_2O, calculation of simultaneous ionic cond. and tracer diffusion 78−43178
β-Al_2O_3-Na_2O, ceramic and powder specimens, various Na_2O content, NMR study 79−61240
β-Al_2O_3-Na_2O, colour centers, AES, electron energy loss, and optical spectroscopy obs. 78−35176
β-Al_2O_3-Na_2O, colour centre ESR by localised tunnelling states 80−108073
β″-Al_2O_3-Na_2O, computer simulation of ionic conductivity 77−89580
β-Al_2O_3-Na_2O, cond. plane struct. and energetics 80−92715
β-Al_2O_3-Na_2O, development for Na/S battery 80−71615
β-Al_2O_3-Na_2O, diffusion of Na^+, effect of path tortuosity and anisotropy 79−28140
β-Al_2O_3-Na_2O, ENDOR meas. of defects 80−66074
β-Al_2O_3-Na_2O, EPR and optical absorpt. studies of X-ray produced defects 78−95517
β-Al_2O_3-Na_2O, ESR of paramag. defects in cond. planes 80−29617
β-Al_2O_3-Na_2O, electrolytes, electric modulus spectroscopy 77−84974
β-Al_2O_3-Na_2O, far IR absorption and ionic cond. 78−72512
β-Al_2O_3-Na_2O, fracture stress, effect of microstruct. defects 77−44338
β-Al_2O_3-Na_2O, grain boundaries and ionic cond. 79−23620
β-Al_2O_3-Na_2O, H_2O intercalation effect on ionic cond. 79−99364
β-Al_2O_3-Na_2O, hot pressing and phys. props. 79−4940
β″-Al_2O_3-Na_2O, ionic cond. at room temp. 80−107513
β-Al_2O_3-Na_2O, ionic cond. temp. depend., comparison with NASICON 80−107520
β-Al_2O_3-Na_2O, layered material, contact free conductivity 80−2195
β″-Al_2O_3-Na_2O, Li_2O stabilised, electrolyte polarisation anal. by complex admittance method 80−2689
β-Al_2O_3-Na_2O, low freq. Raman scatt. from NH_4^+ ions 78−43878
β-Al_2O_3-Na_2O, low temp. dielec. susceptibility meas. 79−82911
β-Al_2O_3-Na_2O, low-energy excitation spectra, localised modes 80−59606
β-Al_2O_3-Na_2O, low-temp. ^{23}Na satellite spectra, Na ion motion 80−108112
β-Al_2O_3-Na_2O, MgO stabilised sintering *(German)* 78−19696
β-Al_2O_3-Na_2O, microwave absorpt., low-temp. dielectric props. anomalies, ion tunnelling states 78−92013
β-Al_2O_3-Na_2O, motion of charge carrying ions, mol. dynamics simulation 80−107506
β″-Al_2O_3-Na_2O, NMR of ^{23}Na, elec. quad. interaction, 185 to 419K, ion motion obs. 80−108110
β-Al_2O_3-Na_2O, non-stoichiometric, amorphous, US attenuation and velocity 80−39228
β″-Al_2O_3-Na_2O, nonstoichiometric, correl. effects in diffusion, Haven ratio, point defect interactions 80−107505
β-Al_2O_3-Na_2O, nucl. double reson. interferometry, satellite spectrum 78−31123
β-Al_2O_3-Na_2O, planar [00.l] disorder, TEM obs. 77−31680
β″-Al_2O_3-Na_2O, polycryst., Na^+ ion diffusion rel. to cond. 77−72715
β″-Al_2O_3-Na_2O, polycryst., ionic cond., 25-800°C 77−80645
β-Al_2O_3-Na_2O, potential energy distrib. and ionic motion 80−70455
β-Al_2O_3-Na_2O, preferable orientation for Na^+ cond. 80−35144
β-Al_2O_3-Na_2O, protonic, conductance and spectroscopy 80−70450
β-Al_2O_3-Na_2O, Raman scatt., 12-400K, 2nd order phase transition 77−81091
β″-Al_2O_3-Na_2O, Raman scatt. from mobile cations 80−11394
β″-Al_2O_3-Na_2O, rapid ion conductor, Na penetration 80−24653
β-Al_2O_3-Na_2O, single cryst. and polycryst., elec. props. 77−72714
β-Al_2O_3-Na_2O, single crystal ionic conductor, migration losses 77−80643
β″-Al_2O_3-Na_2O, single cryst. Raman scatt., cond. mechanism and cryst. struct. 80−66209
β-Al_2O_3-Na_2O, single cryst., non-Debye capacitance 80−107497
β-Al_2O_3-Na_2O, solid electrolyte, battery appl. *(Polish)* 80−12005
β″-Al_2O_3-Na_2O, solid electrolyte, behaviour at high current density, sodium heat engine mode 80−61330
β-Al_2O_3-Na_2O, sp. ht., 0.1-1 K, evidence for localised low-energy excitations 78−34632
β″-Al_2O_3-Na_2O, spinel formation, TEM obs. 77−76423
β″-Al_2O_3-Na_2O, struct. basis for superionic cond. 80−107498
β-Al_2O_3-Na_2O, superionic anisotropic ceramic, prod. by microwave sintering *(French)* 78−52742
β-Al_2O_3-Na_2O, superionic conductor, microwave absorption spectrum 80−11515
Al_2O_3-Na_2O, syntaxy between β and β″ structures, TEM 77−20075
β-Al_2O_3-Na_2O, synthesis, ceramic form., sintering, cond. 79−11537
β-Al_2O_3-Na_2O, synthesis by chem. methods 77−24993
β-Al_2O_3-Na_2O, thermal cond. below 300K 77−24454
β-Al_2O_3-Na_2O, thermal desorption of ions 77−7973
β-Al_2O_3-Na_2O, thermal etching *(German, English)* 78−60934
β-Al_2O_3-Na_2O, thermal expansion 79−55910
β-Al_2O_3-Na_2O, tunnelling states, electron spin relax. 79−78518
β-Al_2O_3-Na_2O, vacuum hot pressed, densification kinetics 78−72758
β-Al_2O_3-Na_2O, X-ray diffuse scatt. 78−71725
β-Al_2O_3-Na_2O, X-ray induced defects, EPR and ENDOR study 80−60456
β-Al_2O_3-Na_2O, Young's modulus and internal friction obs. 77−35624
β-Al_2O_3-Na_2O 79−19396
β-Al_2O_3-Na_2O ^{23}Na asymmetry parameter, temp. variations 80−6540
β-Al_2O_3-Na_2O doped with transition metal ions, complex plane anal. of impedance and admittance 80−70452
Al_2O_3-Na_2O solid electrolytes phase composition 77−36468
β″-Al_2O_3-Na_2O solid electrolyte, tube fabrication from cast ceramic tape 80−60819
β″-Al_2O_3-Na_2O solid electrolyte, processing and phys. props. 80−60820
β″-Al_2O_3-Na_2O solid electrolyte, strength degradation under electrolytic conditions 80−61329
β″-Al_2O_3-Na_2O solid electrolyte, heat treatment effects on ionic cond. and microstruct. 80−65293
β-Al_2O_3-Na_2O:Ba(Ti), dopant effect on ionic cond. and phase comp. 79−65242
β-Al_2O_3-Na_2O:Cr, absorpt. and emission spectra, mag. susceptibility 79−15495
β-Al_2O_3-Na_2O:Cu^{2+}, EPR of Cu^{2+} ions in conduction plane 77−69678
β-Al_2O_3-Na_2O:Fe, coordination site, oxidation state, Mossbauer, absorpt., emission spectra, mag. susceptibility meas. 78−68431
β-Al_2O_3-Na_2O:Mg, ionic cond., effect of microstruct. and phase composition 78−67859
β-Al_2O_3-Na_2O:Mg, with and without Co co-doping, ionic cond. and cryst. struct. 78−26723
β-Al_2O_3-Na_2O:Mn^{2+}, EPR of Mn^{2+} 78−6569
β-Al_2O_3-Na_2O:Mn^{2+}, ESR exam. 78−19313
β-″-Al_2O_3-Na_2O:Na^+,Ca^{2+}, charge compensation mechanism, Na^+ and Ca^{2+} ion movement 78−22891
β-Al_2O_3-Na_2O_3:Ag^{2+}, EPR measurements 78−95515
Al_2O_3-Na_2O-CaO-SiO_2(-B_2O_3) composite glasses, high strength, prod. by overlayering 80−89193
β-Al_2O_3-Na_2O-K_2O, cation interstitial pair modes in vibr. spectra 79−37788
β-Al_2O_3-Na_2O-Li_2O, ^7Li NMR 79−15361
Al_2O_3-Na_2O-Li_2O, phase transformations during firing 80−3036
β-Al_2O_3-Na_2O-Li_2O, struct. determ. by powder neutron diffr. 79−46623
β″- Al_2O_3-Na_2O-Li_2O (8.85, 0.75 wt.%) pressing powders, prep. by spray drying 80−40294
β-Al_2O_3-Na_2O-Li_2O membranes from Na-S cells, failure anal. 80−12003
Al_2O_3-Na_2O-LiO_2 (8.8, 0.75 wt.%) exam. of Na^+ resistivity as function of temp. grain size model 78−80654
β″-Al_2O_3-Na_2O-MgO, blocking defects observed by high resolution electron microscopy 78−55879
β-Al_2O_3-Na_2O-Rb_2O, cation interstitial pair modes in vibr. spectra 79−37788
β-Al_2O_3-Na_2O-SiO_2, solid electrolytes, exam. of microstruct. ionic resistivity 78−80566
β″-Al_2O_3-NaO-LiO_2, stabilised, effect of phase composition, grain size, on Na ion cond. 78−47582
Al_2O_3-SiO_2-Na_2O, coordination number study by AlK_α fluorescence X-ray spectra *(Japanese)* 77−73190
β-$Al_2O_3Na_2O$, H-exchanged, effect of moisture, on H_2 activity changes and thermal stability 78−47580
β-Al_2O_3(Na_2O.11Al_2O_3), prep. by diffusional transform. during sintering of Al_2O_3 in presence of $NaAlO_2$ 80−25637
β-Al_2O_3.$(K_xNa_{1-x})_2O$, anomalous behaviour in ionic cond. obs. 78−87818
β-Al_2O_3.Na_2O, low temp. sp. ht., tunnelling states and diffusion theory 77−43345
β-Al_2O_3.Na_2O:Cu, EPR, localisation of Cu^{2+} and linewidth effect 78−39395
$Al(PO_3)_3$-NaF system, glasses, IR spectra and struct. 79−65882
$Al(PO_3)_3$-NaF system glasses, microhardness and US vel. 79−99274
$Al(PO_3)_3$-NaF-LiF glasses, mixed-alkali effect 80−19715
n-alkanoates, long-chain, thermal and phase props. 77−62619

sodium compounds continued
B_2O_3-K_2O-Na_2O-Rb_2O-Cs_2O glass, small angle X-ray scatt. exam. of struct. 80−38922
B_2O_3-Na_2O glass, absorption spectra of S_2 mols. 79−24337
B_2O_3-Na_2O-Fe glass, mag. susceptibility 79−42733
B_2O_3-Na_2O-SiO_2-Al_2O_3, effect of alumina dispersions on the thermal cond./diffusivity/stress resist. 80−39368
B_2O_3-NaF-$NaBF_4$, crystalline compounds and glasses 78−11210
B_2O_3-NaKO glass, dielectric relaxation at low temp. 79−11384
$Ba_2Na(NbO_3)_5$, intracavity cryst., thermo-optical distortion, effect on freq. doubled Nd:YAG laser 77−71998
$Ba_2NaNb_3O_{15}$, struct. phase transitions, light scatt. meas. 79−95774
$Ba_2NaNb_5O_{15}$, birefr. material, thermal cond. determ. by optical method 78−18851
$Ba_2NaNb_5O_{15}$ crystal, high optical quality, and optical absorption coeff. meas. 78−30036
$Ba_2NaNb_5O_{15}$ crystals, in Nd^{3+}:YAG laser cavity, AM of optical second harmonic 80−78908
$Ba_2NaNb_5O_{15}$, dispersion of quadratic optical susceptibility *(Russian)* 77−3635
$Ba_2NaNb_5O_{15}$, effect of substituting Gd, Cr on lattice parameters 78−47291
$Ba_2NaNb_5O_{15}$, electrooptic coeffs. and refractive indices 79−33673
$Ba_2NaNb_5O_{15}$, electrooptical diffr. by periodic domain struct. 80−40090
$Ba_2NaNb_5O_{15}$, ferroelec. phase, thermally stimulated light flashes, surface elec. props. effects 79−73885
$Ba_2NaNb_5O_{15}$, Gd substitution, effect on linear thermal expansion, possible BSN replacement 78−43153
$Ba_2NaNb_5O_{15}$, high-pressure phase transitions, ferroelastic phase 79−7687
$Ba_2NaNb_5O_{15}$, low temp. ferroelectric transitions, birefr. and dielec. meas. 79−38499
$Ba_2NaNb_5O_{15}$, optical mode softenings, Raman scatt. meas., 1.5 to 600K 79−33631
$Ba_2NaNb_5O_{15}$, phase transition at high press., Raman scatt. obs. 79−55884
$Ba_2NaNb_5O_{15}$, Raman spectra in elec. field 79−1763
$Ba_2NaNb_5O_{15}$, Raman scatt. experiments in tetragonal tungsten bronze compounds 80−40113
$Ba_2NaNb_5O_{15}$, X-ray powder diffraction data determ. *(Chinese)* 80−70170
$Ba_{2.09}Na_{0.72}Nb_{5.02}O_{15}$, cryst. growth, monodomenisation, detwinning, optical homogeneity, composition, dielec., spectral props. 77−44151
$Ba_{4+2x}Na_{2-2x}Nb_{10}O_{30}$, tetragonal tungsten bronze structure ferroelec. mech. for ferroelec. transition 79−38481
$Ba_2NaNb_5O_{15}$ ferroelec. crystals for electrooptics and nonlinear optics, optical inhomogeneities, review *(Japanese)* 77−65613
$Ba_{2.09}Na_{0.72}O_{15}$, ferroelec., photocond. and optical absorpt. spectra. 77−8149
BaO-Fe_2O_3-Na_2O glass, mag. props. 78−88123
BaO-Fe_2O_3-Na_2O glasses, high Fe_2O_3 content, mictomagnetic props. 80−65916
BaO-Fe_2O_3-Na_2O glass, rapidly quenched, mag. and ferrimag. props. 80−75744
BaO-GeO_2-Na_2O-H_2O system, hydrothermal crystn., phase formation laws 79−46636
BaO-K_2O-Na_2O-ZnO-SiO_2, corrosion and microhardness, effect of detergents 80−16518
BeO-P_2O_5-Na_2O glass, gamma irrad., cation modifier effect on radiation centre formation 80−40720
BeO_2-Al_2O_3-SiO_2-NaF system glass, role of fluoride cations during crystn. 79−65176
CC $NaReO_4$, temp. depend. of nuclear quadrupole freq. of ^{23}Na, ^{187}Re, NMR and NQR meas., 78−95529
^{13}C, CIDNP, obs. in reactions of organic and inorganic radicals during pulse radiolysis 80−63660
Ca+NaCl, crossed beam reaction, collision complex lifetime internal state depend. fluoresc. 77−56217
$CaAl_2Si_2O_8$-$NaAlSi_3O_8$ (anorthite-albite) system, crystal growth rates and processes 80−4010
$CaCO_3$-$NaAlSiO_4$, micromechanism for phase formation during sintering *(Russian)* 80−16253
$CaCl_2$-NaCl-H_2O, conc. solns., vap. press. meas. 79−23713
$CaCu_3Ru_4O_{12}$, synthesis, cryst. struct., mag. and elec. props. *(French)* 80−107151
CaF_2-AlF_3-Na_3AlF_6-(Al_2O_3), phase equilibria, X-ray diffr. and DTA meas. 80−108409
CaF_2-NaF cryst., F_A centres, 385 and 435 nm absorpt. bands of electron irrad. crysts. 78−2889
$CaNH_4NaP_2O_7.3H_2O$, crystallographic data *(French)* 78−14316
$Ca_2NaHSi_3O_9$, pectolite, TEM obs., of microtwins and stacking faults 78−75677
CaO-MgO-$NaPO_3$ system, subsolidus struct. 79−43215
CaO-Na_2O-B_2O_3, Raman scatt. studies of glass struct. 77−90147
CaO-SiO_2-Al_2O_3-Na_2O-CaF_2 melts, surface tension and limit wetting angle in contact with C and CrNi steels *(Czech)* 79−37908
$ZCaO.SiO_2$-$2CaO.Na_2O.P_2O_5$ system, polymorphism and solid soln. 78−19731
$10CaO.15Na_2O.75SiO_2$ glass, thermal cond., temp. depend. at low temps. 80−65322
$CdCl_2$-NaCl, KCl molten salt mixtures, US velocity and adiabatic compressibility obs. 78−75730
CdF_2:NaF, colour centres, IR absorpt. and photocond. after UV irrad. 80−79784
CdF_2:NaF, formation and reorientation of Na^+-anion vacancy complexes 78−84516
CdF_2:NaF thin films, electroluminescence obs. at 77K *(French)* 80−80866
CdF_2-NaF, liquid mixture, enthalpy of mixing 78−48684
CdI_2-PbI_2-NaI, fusion diag. and thermodynamic calc. *(Russian)* 77−48417
$CdNH_4NaP_2O_7.3H_2O$, crystallographic data, crystal structure *(French)* 78−14316
$Cd_4Na(VO_4)_3$, X-ray single cryst. struct. determ. and refinement, Patterson synthesis 79−19196
$CoCl_2$-KCl-NaCl system, melting diagram investigation by thermographic anal. *(Russian)* 78−3111
$CoCl_2$-NaCl purification by H_2 reduction, of Co, exam. of conductivity *(Russian)* 79−28981
Cs-Na_2KSb, semitransparent photocathodes, UV response 77−167
CsCl+NaI→CsI+NaCl, solid-state displacement reaction 77−52635

sodium compounds continued
Cs_2NaAlF_6, cryst. struct. determ. 78−95036
$Cs_2NaBiCl_6$, optical props. 78−68549
$Cs_2NaEuCl_6$, luminescence Raman spectra, means for localisation of binding energy levels *(German)* 78−88304
$Cs_2NaEuCl_6$, mag. dipole transitions $^5D_3$→$^7F_4$, interpretation 79−42505
$Cs_2NaFe(CN)_6$, structural phase transformations 79−19178
$Cs_2NaM^{3+}Cl_6$, (M=Bi,Nd,Pr), struct. transitions, polarisation optical expts. 79−99318
$Cs_2NaMO_xF_{6-x}$, M=Ti, V, Nb, Mo, W, high press. transforms. *(German)* 77−89400
Cs_2NaRCl_6 (R=rare earth), low-temp. Raman spectra meas., cryst. field parameters calc. *(German)* 77−36228
Cs_2NaRCl_6, R=Pr^{3+}, Eu^{3+}, Tb^{3+}, Tb^{3+}, crystal field, ligand polarisability contributions 80−39536
Cs_2NaRCl_6:Er^{3+}(Gd^{3+}), R=lanthanide, EPR parameters and interpret. 77−59456
$Cs_2NaTbCl_6$, Tb^{3+} $^5D_4$→^7F_J transitions, mag. and elec. dipole intensities 78−76033
Cs_2NaTmF_6, mag. behaviour 2.9 to 251.3K, cryst. field levels, ang. overlap model *(German)* 80−29520
Cs_2NaYCl_6, Raman spectrum 77−59567
Cs_2NaYCl_6:Bi^{3+}, luminesc., cryst. growth, Stockberger method 79−8174
Cs_2NaYCl_6:Ce, ENDOR evidence of noncubic distortion 79−11357
$Cs_2NaYbCl_6$, electronic struct., paramag. susceptibility and electronic Raman spectrum, cryst. field parameters *(German)* 77−63072
$Cs_2NaYbCl_6$, Mossbauer relax. spectra, breakdown of white noise approx. 78−27141
$Cs_2NaYbF_6(Br)_6$, mag. behaviour, 3.5-251.3K *(German)* 80−50041
Cs_2O-SiO_2 glass, low temp. heat capacity 80−49373
D NaCl:Fe, defect struct., Mossbauer spectra and X-ray diffr. obs. 80−7237
$EuCl_3$-$NaPO_3$-H_2O system, Eu polyphosphates form. at 0°C 80−35515
$EuNa_2Mg_2(VO_4)_3$, disordered, thermal quenching of luminesc. 80−71472
Fe, influence of acid Na_3PO_4 soln. in tap water as a corrosion inhibitor 80−45424
Fe-Fe_2O_3-$NaFeO_2$, study of Na-containing wustite region *(French)* 77−73264
Fe_2O_3-Na_2O-BaO glass, mag. props. 4.2-295K, mictomagnetism *(French)* 80−39782
GaAs-NaOH interface, inversion layer form. and surface states 80−2465
β- and β''-Ga_2O_2-Na_2O, fast ion conductor, Na^+ self diffusion and Na-K exchange 79−28133
Ga_2O_3-Na_2O, β- and β''-phases, superionic conductors, Raman results 77−40234
Ga_2O_3-Na_2O, β- and β''-phases, ionic cond., room temp. to 350°C 77−43368
β''-Ga_2O_3-Na_2O, single cryst. growth by Na_2O evaporation from molten Na_2O-Ga_2O_3 77−44141
Ga_2O_3-Na_2O, syntaxy between β and β'' structures, TEM 77−20075
β''-Ga_2O_3-Na_2O-K_2O mixed crystals, cond. anomaly 79−46838
GeO_2-Na_2O, DC cond. rel. to dielectric loss peak freq. 79−78621
GeO_2-Na_2O, glass composition effect on solubility in H_2O 80−39303
GeO_2-Na_2O, Na^+ partial dissociation investigated by elec. meas. 80−92716
GeO_2-Na_2O borosilicate glass fibre prod. by phase separation and leaching 80−69558
GeO_2-Na_2O glass, Raman spectra, struct. and crystn. 80−92463
GeO_2-Na_2O glasses, equivalent cond., temp. depend., weak electrolyte theory appl. 80−107475
H_2O-NaCl-sucrose, phase diagram determ., appls. in cryobiology 78−15777
(K,Na) ($AlSi_3O_8$), feldspar, N^{2-} ESR spectrum parameters *(Ukrainian)* 79−38366
(K,Na)NbO_3 ceramic, hot pressed, dielec. props. 79−87375
KCN, Raman spectra, at very high press. 79−1759
KCl-$CaCl_2$-NaCl, ternary phase diagrams, interactive computer program 80−71629
KCl-NaCl, dislocation rosettes, diffusion origin 78−83820
KCl-NaCl mixed crystals, contact angles and free energies at solid/melt interface 80−64937
KCl-NaCl solid solns., equilib. decay curve *(Russian)* 79−90760
KCl-NaCl-$FeCl_3$ system, shape eutectics line calc. *(Russian)* 79−96016
KCl-NaCl-K_2NaVF_6, phase diagram 77−48416
KCl-NaCl-NaF-K_2NaVF_6 system, phase diagram 79−66049
KF-NaF-K_2NaVF_6, phase diagram 77−48416
KH II states and KH^+ ground state, pot. energy curves calc. 80−18812
$KMg_2LiSi_4O_{10}F_2$-$NaMg_2LiSi_4O_{10}F_2$, solid soln., solid solubility and swelling characts. 80−59660
KNO_2-$NaNO_2$-Na-NO_3 eutectic salt, use in indirect heating systems *(German)* 80−38233
$(K_xNa_{1-x})_2$ 0.58 Ga_2O_3, anomalous behaviour in ionic cond. obs. 78−87818
$K_{1-c}Na_cCl$, impurity centre local vibrs., comp. depend. of spectral parameters 80−79898
(KNa)NbO_3 ceramic, piezoelectric effect due to polarisation, expt. *(Polish)* 77−77151
$(K_xNa_{1-x})NbO_3$ single crystals, growth and phase transitions 79−33915
$K_3NaP_2O_7.4H_2O$, cryst. struct. *(French)* 78−42961
$KNaSO_4$, sulphate ion optical and spectroscopic props., cryst. environment effect 77−40224
$(K_{1-x}Na_x)_2SO_4$:Tl^+ phosphor, thermolum. characts. 77−90203
$K_{1-x}Na_xTaO_3$, quantum ferroelec., elastic compliance, impurity effects 79−99835
$K_{1-x}Na_xTaO_3$ quantum ferroelectric, dielec. susceptibility 80−103922
$K_xNa_{1-x}TaO_3$, press. depend. of impurity soft modes, low energy Raman scatt. meas. 78−2852
$KNa_3[AlSiO_4]_4$, nepheline, continuous laser emission effects on surface, spectroscopic obs. 79−94271
$K_2Na[Co(NO4d2)_6]$, single cryst., X-ray deffrs. determ. of electron density distrib. 79−14746
$KNa[Pt(CN)_4].3H_2O$, neutron diffr. cryst. struct. exam., refinement by least squares 78−2079
$KNa[Pt(CN)_4].3H_20$, energy band calcs. 77−39780
K_2O-Na_2O-BaO-SiO_2 glass, corrosion kinetics in aqn. KOH, transition metal oxide addition effects 77−56125
LaF_3-BaF_2-ZrF_4-NaF, glassy transition, refr. index, density and molar refr. 80−1937
$La_{1-x}Na_xFeO_{3-x}$, defect perovskite system, Mossbauer effect 77−36159
$(La_{0.5}Na_{0.5})RuO_3$, mag. props. 78−27027

sodium compounds continued
- La_2O_5-$Na_2Si_2O_5$ molten glasses, surface tension and density, 900-1500°C 80−15334
- (Li,Na,Cu,Zn) ferrites, nonceramic synthesis, electrochem. investig. 78−35339
- (Li,Na,K) $(Nb,Ta)O_3$, pseudo-binary and ternary systems quenched metastable glassy and cryst. phases 80−29935
- (Li, Na)NbO_3 ceramic, dielectric and electromechanical props. 77−40183
- (Li,Na)NbO_3, polycryst. disc, temp. and time dependent dielec. props. 77−81060
- (Li,Na)VO_3, struct. systematics 79−55719
- Li,Na/PO_3,F system, low melting point comp., solvent for InP electrodeposition 79−28079
- Li,Na/PO_3,F system, low melting-point comps. for electrodeposition appl. 79−43662
- Li-Na ferrite powders, props. rel. to Fe_2O_3 chem., thermal, mech. historical 79−11539
- LiAl-$NaAlCl_4$-$MoCl_5$ thermal battery test results 79−29459
- LiAl-$NaAlCl_4$-$MoCl_5$ thermal battery evaluation and optimisation 79−29458
- Li_2BeF_4-$NaBF_4$, phase diagrams 77−21119
- LiCl-NaCl-$AlCl_3$ melt, elec. cond., 800 to 1200K *(Japanese)* 80−24633
- LiCl-NaCl-$AlCl_3$ ternary melt, density as function of temp. and composition, meas. by macrometric method *(Japanese)* 79−42130
- LiCl+$NaNO_3$, apparent and partial molar volumes in aq. soln. 78−44396
- LiF-AlF_3-Na_3AlF_6-Al_2O_3 system, phase equilibrium, X-ray diffr., DTA, quenching, optical microscopy study 80−50610
- LiF-NaF, densities of binary molten salts *(Japanese)* 79−7644
- LiF-NaF binary molten salt, elec. cond. *(Japanese)* 77−76588
- LiF-NaF-KF molten mixture, diffusivity and solubility of H_2 78−34640
- LiF-NaF-KF-K_2GeF_6-GeO_2 fused mixture, for electrodeposition of Ge powder 80−2979
- LiF-$NaPO_3$-MeF_x (Me=Mg, Ca, Al) glasses, IR spectroscopy study 80−16042
- $LiNO_3$-$NaNO_3$-$AgNO_3$, molten salt mixture, excess thermodynamic props. and US vel. *(French)* 77−31720
- LiNa, and anion, electronic struct., spin-unrestricted, spin-restricted SCF HF calc. 78−90331
- LiNa ferrite, effect of sintering temp. on oxidation kinetics, conductivity meas. 77−21298
- $Li_{1-x}Na_xBr(I)$, intrinsic optical absorpt. spectra 78−23500
- $Li_{0.04}Na_{0.1}Fe_{2.5}O_4$, $Li_{0.3}Na_{0.2}Fe_{2.5}O_4$, ferrites, form., X-ray, chem. and mag. anal. 77−36424
- $Li_{0.5-x}Na_xFe_{2.5}O_4$, Na_2CO_3 effects on ferrite formation 78−27458
- $Li_{1-x}Na_xNbO_3$, LPE, growth and temp. coeff. of SAW velocity 78−43227
- $(Li_{0.63}Na_{0.37})_2O.2SiO_2$, short range struct. by pulsed neutron scatt. 80−59396
- LiO_2-Na_2O-CaO-SiO_2 glass-ceramic coating, high temp. effects on steel substrate 79−61776
- LiO_2-Na_2O-MgO-TiO_2-Al_2O_3-SiO_2, exam. of specific heat and thermal conductivity *(Russian)* 79−55898
- Li_2O-Na_2O-B_2O_3-Al_2O_3-SiO_2 glass, Young's modulus and density, ion exchange effects 80−84982
- Li_2O-Na_2O-B_2O_3-SiO_3, exam. of metastable phase separation region 78−88450
- Li_2O-Na_2O-P_2O_5, heat of soln. *(Japanese)* 79−34350
- $(LiO_{1/2}$-$NaO_{1/2})$-$2SiO_2$ glass, alkali motion ionic thermocurrent study, polarised impurity-vacancy dipole relaxation study 79−77806
- $100(Li_2O.2SiO_2).Na_2O$, directionally solidified, thermal and mech. props. *(Japanese)* 80−16295
- $LiTaO_3$-$NaTaO_3$-$KTaO_3$, quenched metastable glassy and crystalline phases 79−61568
- MgCl 2-NaCl, binary melts, surface tensions *(Japanese)* 78−10260
- $MgCl_2$-NaCl-H_2O, conc. solns., vap. press. meas. 79−23713
- $MgCl_2$-NaCl-H_2O, ionic diffusion theory, use of activity coeffs. in transition-state models 78−57224
- $Mg(NO_3)_2$-RNO_3 (R=Li, Na, K), thermogravimetric anal. of dehydration processes *(Japanese)* 80−66791
- $Mg_{0.7}Na_{0.9}K_{2.0}Ca_{2.4}Al_{9.1}Si_{26.9}O_{72}.xH_2O$, erionite, cryst. struct. exam., stacking faults 78−2083
- MgO-$Ca_3Mg(SiO_4)_2$($CaMgSiO_4$)-$NaPO_3$, phase conversions 77−66641
- MgO-CaO-SiO_2-Al_2O_3-$Na_2O.P_2O_5$, effect of $NaPO_3$ on phase composition rel. to basic refractories 78−80528
- MgO-Na_2O-B_2O_3, Raman scatt. studies of glass struct. 77−90147
- MgO-NaB_4O_7, melt, transport-controlled dissolution 79−90791
- MgO-NaCl, solution under hydrothermal conditions, exam. of phase equilibria 79−8292
- MgO-NaCl refractory clinkers, Cr containing, densification, thermal treatment and phase composition effect *(French)* 80−76219
- MgO-$NaSi_2O_5$, melt, transport-controlled dissolution 79−90791
- MgO-$NiVO_3$, melt, transport-controlled dissolution 79−90791
- (MgO-Fe_2O_3-Cr_2O_3-TiO_2):Na_2O, powder, prep., heat treatment, Na_2O impurity effect on props. 77−16528
- $Mg_2S_2O_3$-$Na_2S_2O_3$-H_2O system, 20°C isotherms *(French)* 78−52506
- $Mn_2NaSi_3O_8(OH)$, serandite, synthesis, struct., physicochem. props. 79−43187
- NH_3+NaSCN, coolant for solar refrigeration *(French)* 79−24911
- $(Na,Ca)_2Zr[Si_6O_{15}].3H_2O$, Mongolian elpidite, cryst. struct. 78−95038
- (Na,Cs)(F,Cl,I,) quaternary reciprocal system, calc. of phase diagrams 80−25666
- (Na,K)NbO_3 solid solns., struct. transitions, neutron powder diffr. 78−38649
- (Na,K)$(V,P)O_3$ system, cation substitutions, crystallographic studies 78−79581
- (Na,Li)NbO_3, ceramics, electrophys. and struct. props. near morphotropic transition 78−2816
- (Na,Li)NbO_3 ceramic, optimum prep. conditions and characterisation 78−3079
- Na,K/PO_3F system, low melting-point comps. for electrodeposition appl. 79−43662
- Na (111) surface, epitaxial film, electron induced dissociation 80−6646
- Na borate glass, nonradiative energy transfer from Sm^{3+}→Nd^{3+} 78−80394
- Na borosilicate glass microsphere material, sintering, struct., strength props. *(Russian)* 80−108383
- Na conductive glass-Na amalgam interface, electrochem. obs. 78−76870
- Na diethyldithiocarbamates, use in liquid-liquid extraction of corrosion and fission products 80−18459

sodium compounds continued
- β-Na, O-Al_2O_3, onset temp. of decomp. 77−81244
- Na salt of β-ketoaldehydes, configurations of anions in solutions studied by IR spectroscopy, H-bond form. 80−87117
- Na zeolite, adsorpt. of ethylene, uniaxial rot. and translational dynamics 78−91538
- Na zeolites, electronic struct., quantum chemical study 80−69058
- Na^+, interaction with purine and pyrimidine bases of nucleic acids, ab initio study 77−64005
- Na^+ ion complexes with HF, H_2O, and NH_3 solvent molecules, structural and electronic props. calc. 77−57873
- Na-A zeolite, struct. obs. by high-resolution electron microscopy 80−84175
- Na-βAl_2O_3 ceramics, synthesis 80−40305
- Na-C-O, thermodynamic computation of phase equilibria 77−63638
- Na-Co strip-chain silicates, structural-composition inhomogeneities 80−88122
- Na-Co-O system, synthesis and cryst. struct. determ. 80−107185
- Na-Cs, liquid, resistivity calc. using general model pseudopot. 77−55506
- Na-Cs silicate glass, thermal expansion 77−4186
- Na-Fe fluorophosphate glass, EPR and Mossbauer resonance study 80−15838
- Na-Fe fluorophosphate glass, Mossbauer study, mag. and optical props. 80−16065
- Na-K silicaalumo gels, crystn. and charact. of A-type zeolites 79−52780
- Na-K silicate glass, thermal expansion 77−4186
- Na-Mn-O system, synthesis of oxides 80−107185
- Na-NaO-Na struct., inelastic tunnel effect, spectra, potential barrier parameters 79−95511
- Na-NaOH-Na_2O-NaH, reciprocal ternary system 77−73263
- Na-Rb silicate glass thermal expansion 77−4186
- Na-V-O system, low O_2 potential 77−50238
- Na-zeolite, matrix, Te cluster superlattices, N and S type volt-ampere charact., elec. cond. *(Russian)* 80−70665
- Na^+-K^+-F^--SO_4^{2-}, asymmetrical reciprocal molten salt system, excess enthalpies 80−30268
- Na_2-B_2O_3 glass, pulsed EPR study of Cu 78−84479
- Na_2-β-Al_2O_3, far IR absorpt., Beevers-Ross sites, interstitials 80−66241
- Na_2-CaO-SiO_2, rain erosion mechanisms 79−34154
- Na_2-S-GeS_2 system, glass formation, struct. and ionic conduction 80−54138
- Na_2-SiO_2 glass, prep. by metallic-organic derived method, phase separation 78−56610
- Na_2-SiO_2-MgO glass, melt viscosity and IR meas. to study MgO behaviour *(Japanese)* 78−14495
- NaA and NaX zeolite crystals, crystn. study in presence of triethanolamine, Na_2O and SiO_2 content influence 79−65995
- NaA neolyte, Hg cluster transition to paramagnetic state due to mag. field *(Russian)* 80−60183
- NaA zeolite, dielectric polaris., cation distrib. *(French)* 79−51903
- NaA zeolite;S, optical spectra 78−88342
- $NaAl_2Br_7$, ^{81}Br NQR and ^{27}Al NMR 78−6597
- $NaAl(CO_3)(OH)_2$, cryst. struct., IR spectral investig. 77−8567
- $NaAlCl_4$, cryst. struct., charge distrib., X-ray, NMR and NQR meas. 77−11528
- $NaAlCl_4$, crystal struct. refinement 79−73145
- $NaAlCl_4$, Raman spectra, cryst. struct. *(French)* 80−60578
- $NaAlCl_4$, relative enthalpy to 573K and standard enthalpy of form., molar enthalpy of fusion 80−50878
- $NaAl(CrO_4)_2.2H_2O$, cryst. struct. *(French)* 77−80478
- $NaAlF_4$, dissoc. enthalpies, mass spectrometric determ., heat of form. 80−97720
- Na_3AlF_6, effect of temp. var. on light transmission 78−79136
- Na_3AlF_6 film, cryolite, struct., electron microscopy 77−59226
- Na_3AlF_6 film, evaporated, electron bombard. effect on secondary electron emission, Auger peak shifts 80−2903
- Na_3AlF_6 film, optical inhomogeneity, rel. to struct. 79−83047
- Na_3AlF_6, film on Si, fused quartz substrates, H_2O absorpt., IR anal. 80−75446
- Na_3AlF_6 flux for corundum cryst. growth 78−30563
- Na_3AlF_6, molten, structure *(French)* 77−51297
- Na_3AlF_6-AlF_3, liquid-solid and liquid-liquid enthalpy of mixing meas. 77−40569
- Na_3AlF_6-LiF-CaF_2-AlF_3-Al_2O_3, electrolyte, exam. of phase equilibria, review 79−11590
- Na_3AlF_6-MgF_2 thin film deposits, quenched ageing by chopping 80−97364
- Na_3AlF_6-PbF_2, interference filter prod. for near UV *(French)* 78−25974
- Na_3AlF_6-PbF_2, semitransparent wide band dielectric mirror synthesis using dispersive and absorbing materials 79−89986
- Na_3AlF_6-ZnS Fabry-Perot interference filter, neutron irrad. effects on props. 79−76867
- Na_3AlF_6-ZnS layer achromatic interference polarizers, design, fabrication 79−55222
- Na_3AlF_6-ZnS multilayer dielectric optical filter, irreversible thermal effect 77−7195
- $Na_8Al_6Ge_6O_{24}(CO_3).3H_2O$, water molecule dynamics and hydrogen bonds, PMR spectra 79−90577
- $Na_8Al_6Ge_6O_{24}(CO_3).3H_2O$, PMR anal. H_2O molecule orientation determ. 79−90631
- $Na_8Al_6Ge_6O_{24}.CO_3.2H_2$, cryst. struct. 78−83805
- $NaAlH_4$, ab initio calc. of geom. struct., charge distrib., bonding and pot. energy surfaces 80−18796
- $NaAlH_4$ and Na_3AlH_6, molar heat capacity and thermodynamic functions, 10 to 300K 80−65243
- $NaAlH_4$, X-ray cryst. struct. determ. 79−69081
- $Na_3Al_2Li_3F_{12}$, fluoride garnets, high press. form 77−76554
- $Na_3Al_2Li_3F_{12}$ garnet, cryolithionite, hydrothermal growth 79−43123
- $NaAl(MoO_4)_2$, domain struct., phase transition, and dielec. props. 79−56748
- $NaAl(MoO_4)_2$, ferroelastic, domain struct. obs. 77−15483
- $NaAlO_2$, electric field gradient tensor, dipolar contribs. 77−51707
- $NaAl_{11}O_{17}$, β-alumina, local electroneutrality 79−65054
- $Na_{56}(AlO_2)_{56}(SiO_2)_{136}:Eu^{3+}$, Y-type zeolite, luminesc. props. 79−83017
- $NaAl_3(PO_4)_2(OH)_4$, EPR of at. H caused by X-rays 79−28614
- $NaAlSi_2O_6$, elec. cond. meas. 78−47787
- $Na_{0.91}Al_2(Si_{3.09}Al_{0.91})O_{10}(OH)_2$, paragonite 1M, cryst. struct. determ., electron diffr. 78−26547

sodium compounds continued
$Na_6Al_6(Si_{0.99}Ge_{0.01})_6O_{24}.2NaBr$, Ge-doped sodalite powders, UV absorpt. band 80−71452
$NaAlSiO_4$ (nepheline), high-press. to transform. to first silicate Ca ferrite isotype 77−64270
$NaAlSiO_4$, carnegieite, cathodochromic props., storage CRT applic. 77−8604
$NaAlSi_2O_6$, jadeite, melt, changes in viscosity and struct. at high press. 77−29290
$NaAlSi_3O_8$, albite, melt, viscosity and struct. changes at high press. 79−29754
$NaAlSi_3O_8$, cryst., Al-Si order-disorder, electroneutrality effects in model 79−90593
$NaAlSi_3O_8$, radial distribution functions, quasi-crystalline model 80−1879
$Na_{1+x}Al_{1+x}Si_{1-x}O_4$, ionic cond. 79−65245
$Na_8Al_6Si_6O_{24}Cl_2$, radiolytic radiation damage, TEM obs. 79−7628
$Na_8(Al_6Si_6O_{24})Cl_2$, sodalite, photochromism, ESR and optical spectra obs. 77−32407
$Na_8(Al_6Si_6O_{24})Cl_2$, sodalite, electronic struct. of F-centre 80−2356
$Na_8Al_6Si_6O_{24}F_2(Cl)(Br)(I)$, sodalite, luminescence and coloration *(Russian)* 78−72578
$Na_6Al_6Si_6O_{24}(NaX)_{2n}$, X=Cl, Br or I, sodalites, thermal destruction of colour centres *(Russian)* 80−84169
$Na_9(Al_6Si_6O_{24})(OH)_2.6H_2O$, hydrosodalite, ferroelec. transition, pyro- and piezoelec. activity 79−15421
$Na_3Al_6Si_6O_{24}X_2$, optically erasable colouring and luminesc. *(Russian)* 77−85801
$Na_8Al_6Si_6O_{24}.Cl(Br)(I)$, cathodochromic sodalites, coloured crysts., tunnel and recomb. luminesc., temp. depend. *(Russian)* 80−66261
$NaAlSi_2O_6.H_2O$, synthetic analcite, optical and crystallographic props. *(French)* 77−43183
$(NaAl)_xSi_{2-x}O_6.H_2O$, analcite, polyhedral tilt transitions obs. at high press. 80−6515
$Na_6Al_6Si_6O_{24}.NaX_{(2-n)}$, (X=Cl, Br, I), X-ray irrad., thermal-erase cathodochromism and dihalide mol. centres *(Russian)* 80−66236
$Na_2Al_2Si_3O_{10}.2H_2O$, natrolite, cleavage etching in acidic and neutral media 80−6407
$Na_3Al_3Si_3O_{12}.2H_2O$, cryst. struct. determ. 79−90625
$NaAl_5Ti_2O_{12}$, form. in Na_2O-M_2O_3-TiO_2 ternary systems X-ray anal. 79−51067
$Na_2Al_2Ti_6O_{16}$ bronze, synthesis in $NaBO_2$, growth conditions *(French)* 78−43998
NaAr, ground and excited state pot. curves, dispersed fluoresc. spectrum 79−98140
NaAr, intramol. pot. functions of ground and excited state 79−54785
NaAr, $X^2\Sigma$, $A^2\Pi$ and $B^2\Sigma$ state, ab initio CI calcs. 78−9085
$NaAsO_2$ aq. solns., O exchange between $AsO_2(OH_2)^-$, and water 78−92459
$NaAsS_2$, cryst. struct., infinite chains 77−35523
Na_3AsS_3, cryst. struct. *(French)* 77−15347
NaAu(Ag), mol. dissoc. energy, third law enthalpy and heat of formation, mass spectra 78−40033
$NaAuCl_4.2H_2O$, ^{17}O and ^{23}Na pure quadrupole double reson., fine struct. 77−63323
NaB_6, prep., cryst. struct., thermal stability, phys. and chem. props., book contrib. 78−47304
Na_xB_{15}, x=0 to 1 prep., cryst. struct., thermal stability, phys. and chem. props., book contrib. 78−47304
$NaBD_4$, ^{11}B spin-lattice relax., struct. phase transition 78−84492
$NaBF_4$, electric field gradient, quadrupole coupling consts. 77−89740
$NaBF_4$, spin-spin coupling and T_1 in non-aq. solns. 77−23512
$NaBF_4$, static SIMS, mol. rearrangement, cluster formation 78−64440
$NaBF_4$, use in Al alloy manufacture, transfer efficiency of B 78−27453
$NaBF_4$-LiBF$_4$(KF)(LiF), phase diagram 77−21119
$NaBH_4$, ^{11}B spin-lattice relax., struct. phase transition 78−84492
$NaBH_4$, ab initio calc. of geom. struct., charge distrib., bonding and pot. energy surfaces 80−18796
$NaBH_4$, $NaBD_4$, first order struct. transition, NMR meas. 78−80240
$NaBH_4$, struct., pot. surface, ab initio calcs. 79−41092
$2NaBO_2$-B_2O_3 melt, thermodynamic props., mass spectra 80−65252
$Na_2B_4O_7$, borax, internal core catcher for GCFR 78−58372
$Na_2B_4O_7$, melt-crystal interface temp. meas. during crystallization of melts 79−44908
$Na_2B_4O_7$, nuclear spin lattice relax. in amorphous state, review 79−11354
$Na_3B_3O_6$, solid, low energy photoelectron spectra 78−95656
$NaB_3O_6(OH)_4$, cryst. struct. determ. 78−26511
$Na_3B_5O_8(OH)_2.H_2O$, synthetic, cryst. struct. 78−18591
$Na_2B_4O_5(OH)_4.8H_2O$, borax, neutron diffr. cryst. struct. determ. 79−14740
$NaBO_2.H_2O_2.3H_2O$, crystallisation from aq. soln., nucleation rates with surfactant 78−91276
$NaBO_2.2H_2O_2.3H_2O$, crystallisation from aq. soln., growth kinetics with surfactant 78−91277
$NaBSi_2O_6$, B=Mg, Fe^{3+}, Al, pyroxenes, order-disorder interpretation 80−38987
$Na_{2-2x}Ba_{3x}Ti_{6-x}O_{13}$, $0<x<0.2$, struct. evolution, tunnel struct. 79−65049
NaBaZn glass, Eu^{3+} centre symm. 80−100447
Na_2BeF_4, melting systematics at high press. 77−51475
$Na_2BeGe_2O_6$, crystal struct. by X-ray diffr. 77−1113
Na_2BeSiO_4, crystal struct. rel. to Na_2ZnSiO_4 77−1114
$Na_2Be[SiO_4]$, X-ray cryst. struct. determ., thermal vibration anisotropy allowance 80−92510
$NaBiMTeO_6$, M=Mg, Co, Cd, Ca, antiferroelectric, synthesis and charact. 77−55758
$NaBi(MoO_4)_2$, electrically induced optical activity 79−82942
$NaBi(MoO_4)_2$, low-temp. paraelectric, permittivity meas., 4.2-400K 79−95702
$NaBi(MoO_4)_2$, photoelastic props., acousto-optical figure of merit meas. 78−60420
$Na_{0.5}Bi_{4.5}Nb_2WO_{15}$, cryst. struct. 77−47428
$Na_{0.5}Bi_{0.5}TiO_3$, dielectric const. thermal hysteresis, ferroelectric-antiferroelectric transitions 80−50281
$Na_{0.5}Bi_{0.5}TiO_3$, phase transition, hysteretic behaviour 80−71330
$Na_{0.5}Bi_{4.5}Ti_4O_{15}$, hot-forged ferroelec. ceramic with layer struct. 79−43175
NaBr, ^{14}N impurities, molecular point defects, EPR isotropic hyperfine triplets 80−2636
NaBr, adsorbed on Ag photocathode, work function decrease 79−78824
sodium compounds continued
NaBr, adsorption pot. energies of Ar and Kr calc. 78−71993
NaBr, cohesive properties, analysis using density functional formalism 79−90592
NaBr, Compton profile, 59.54 keV γ-rays 78−64426
NaBr, Compton profile anisotropies 79−27044
NaBr, dispersion of phonons calc. 78−26646
NaBr, dissoc. energy by photofragmentation spectroscopic method 79−76527
NaBr, EXAFS at high press. 80−97376
NaBr, exciton mechanisms of electron sputtering 77−55857
NaBr, F-centre decay 79−11442
NaBr, far IR spectra, matrix isolated, monomers, dimers, trimers 78−66545
NaBr Frenkel pairs, interactions forming enrichment centres 80−96518
NaBr, gamma and additively coloured, dissolving in pure water, lyoluminesc. mechanism 80−100693
NaBr, heat capacity, Gruneisen parameters, 2 to 20K 80−29180
NaBr, high-temp. vapour, appl. of photographic plate for electron diffr. studies 77−39516
NaBr in hexantriol-1.2.6, structural relaxation shear and compressional viscous processes, electrolyte effects 79−94686
NaBr in hexantriol-1.2.6, shear relaxation 79−94687
NaBr, lattice dynamics and statics, three-body-force shell model 80−49323
NaBr, lifetime of colour centres 78−92115
NaBr, muonic X-ray intensities, Lyman series 80−23578
NaBr, n-propanol soln., cond. and transference no. meas., radioisotope method 77−35735
NaBr, optical breakdown, 1.06 to 0.172 μm 78−35089
NaBr, optically activated F→F′ centre conversion in mag. field 80−108253
NaBr, orbital g-factor and spin-orbit splitting of F-centre excited state, magnetoabsorpt. and MCD 78−2886
NaBr, oscillatory and diffusive regime, above and below melting point, IR thermal emission spectra 78−83985
NaBr photodissoc., Na non-Gaussian line shape, level shifting and velocity inversion 80−58182
NaBr powder coloured in electrodeless discharge, reflectance spectra, thermoluminescence props. 78−6796
NaBr, premelting elec. cond., heat capacity 78−91445
NaBr, self-trapped exciton and F-centre form. by picosecond laser pulses 80−10546
NaBr, shock adiabatic, nonparametric equation of state 78−10121
NaBr, spin-lattice relax. of F-centres, magneto-optical meas. 77−43884
NaBr, Stark effect of F-centre obs. 77−1707
NaBr, surface rumpling at finite temps, Verwey model 79−51402
NaBr, thermally processed cryst., optical absorption bands *(Russian)* 78−76513
NaBr, U_2 and U_1 centres, optical excitations 80−2803
NaBr, water preadsorbed, adsorption of organic vapours *(Japanese)* 78−18897
NaBr:Ag^+, UV absorption bands, temp. depend. 80−20672
NaBr:Cu^+, absorpt. spectra, pressure effects up to 6 kbar, comparison with NaCl:Cu^+ 79−4826
NaBr:Cu^+, luminesc. and lifetimes, press. depend. 79−33809
NaBr:Cu^+, off to on centre defect transitions under hydrostatic press. 78−15199
NaBr:Cu^+, press. tuning of motional behaviour in shallow off-centre pots. 79−78718
NaBr:Eu^{2+},Ho^{3+}, single cryst., cluster luminesc. centres *(Russian)* 77−20922
NaBr:Ho^{3+},Eu^{2+}, single cryst. synthesis, rel. to purification methods 77−8744
NaBr:Li^+, lattice relaxation around tetragonal and rhombic defects 79−95110
NaBr:Pb, absorpt. and emission spectra of Pb centres 79−78717
NaBr:Tl, emission spectra, press. effects 78−23509
NaBr:Tl, impurity segregation with Kyropoulos growth 78−9977
NaBr:Tl^+, absorption spectra meas. 78−15197
NaBr:Tl^+, emission spectra, excitation in A-band 78−15218
NaBr:V, covalency effects, EPR and optical spectra 77−85557
NaBr-H_2O, quick-frozen aq. soln., XPS 79−38713
NaBr-$MgBr_2$ system, thermochem. and struct. investigation *(German)* 79−1423
NaBr-U-centre containing cryst., X-ray radiation induced cation vacancy generation 80−39078
NaBr(I), exciton ionisation and decay, photoluminesc. in elec. field 77−44046
NaBr(Cl), F-centre formation, short-pulse optical exam. of exciton relax. 79−42061
$NaBrO_3$, ^{17}O NQR, spin echo double reson. method, electronegativity 80−54970
$NaBrO_3$, cryst., mechanoluminesc. spectra 80−97355
$NaBrO_3$, cryst. chirality and optical rotation sense 78−10026
$NaBrO_3$, crystal gyrotropy, meas. in IR region 80−88957
$NaBrO_3$, dislocation struct. inhomogeneity rel. to growth rate 77−47456
$NaBrO_3$, dispersion of Faraday effect 80−2731
$NaBrO_3$, IR and Raman spectra, vibrs., dipolar coupling effect 78−43852
$NaBrO_3$, in dioxane-water mixtures, ion-solvent interaction and conductance 79−34315
$NaBrO_3$, lattice energy, comparative computations using explicit minimisation procedures 79−32944
$NaBrO_3$, lattice parameters, thermal expansion, defect formation energy 78−79786
$NaBrO_3$, light polarisation, elec. field effect *(Russian)* 77−66480
$NaBrO_3$, NQR freq. temp. depend., phonon spectra interpretation 77−12226
$NaBrO_3$, optically active, crystal atomic struct. remeas. 78−10009
$NaBrO_3$, Raman spectra, intramolecular vibrs. and lattice vibrs. *(Russian)* 77−1683
$NaBrO_3$, Raman spectrum, temp. depend. *(Russian)* 78−23466
$NaBrO_3$, refr. index, temp. coeff., 285-700 nm, 320-500K *(Russian)* 77−66473
$NaBrO_3$, single crystals, thermolum., optical absorpt., X-ray effect 79−95858
$NaBrO_3$, surface polariton spectroscopy, frustrated total reflection method *(Russian)* 80−49628
$NaBrO_3$, X-ray Debye temp. 80−103440

sodium compounds continued
- $NaBrO_3$:IO_3^-, Raman spectra, fundamental vibr. modes of halate ion 78−78711
- $NaBr.2H_2O$, lattice energy, electrostatic, multipole expansion method 79−99107
- $NaBr.2H_2O$, polycryst. hydrates, librational motion of H_2O mols., neutron diffr. exam. 80−10604
- $NaBr.2H_2O$, single cryst. struct. anal. by neutron diffr. 79−77561
- NaCN, aq. solns., IR spectral reflectance meas., Kramers-Kronig anal. 77−4633
- NaCN, Brillouin backscatter spectra of (100) LA phonons, elastic consts. determ. 79−65886
- NaCN, cryst., struct., phase transition, 6-300K, neutron diffr. obs. 77−76347
- NaCN, cryst. phases at press. up to 55 kbar, Raman spectra obs. 79−82975
- NaCN, crystal props., log potential model calc. 78−63829
- NaCN, cubic, KCN-type anomalous thermoelastic behaviour 77−84823
- NaCN, cubic, third-order elastic consts., nonlinear behaviour 79−28026
- NaCN, diffuse scatt., hard-core correl., weak-graph method 80−49137
- NaCN, disordered, Brillouin scatt. 77−48181
- NaCN, elastic const. temp. depend., Brillouin and US exam. 77−80572
- NaCN, FCC, orientational anisotropy of CN^- ions, Raman spectra meas. 77−36247
- NaCN, He I photoelectron spectra 79−64046
- NaCN, lattice dynamics in disordered cubic phase 78−38794
- NaCN, lattice dynamics calc. 79−77705
- NaCN, librational and phonon sidebands of IR CN^- stretching mode 79−15457
- NaCN, multidomain birefr. solid, light scatt. and IR transmission spike 80−60587
- NaCN, optical F centres and phase transitions 78−56504
- NaCN, order-disorder transition, press. and temp. depend. of soft elastic const. 78−79769
- NaCN, plastic phase, Raman scatt. spectra *(French)* 80−11379
- NaCN, polymorphic transitions, lattice energies calc. 77−1092
- NaCN, Raman diffusion spectra, IR absorpt. in phases II and III *(French)* 80−84741
- NaCN, Raman spectra, at very high press. 79−1759
- NaCN, Raman spectrum, hydrostatic press. effects 78−6663
- NaCN, single cryst., orientationally disordered, Brillouin scatt., elastic consts. 77−85732
- NaCN, struct. domains, NMR determ. 80−50204
- $NaCN.2H_2O$, cryst. struct. determ. 78−75635
- $NaCN.2H_2O$, electron density, 150K, X-ray crystallography expts. 77−24295
- $NaCO_3$, enthalpies of dilution 79−57284
- $NaCO_3$+ZrC, flame, optical and temp. characts. meas. method, light scatt. ZrO_2 particles *(Russian)* 78−56894
- Na_2CO_3, disordered struct., 400°C neutron and X-ray powder diagrams 79−46625
- Na_2CO_3, elec. cond., 270-830°C, and transition points 78−10216
- Na_2CO_3 electrolyte, silent discharges elec. characts., expt. *(Korean)* 78−40057
- Na_2CO_3, incommensurate structural phase transform., neutron diffr. obs. 79−86886
- Na_2CO_3, modulation wave form, tenfold supercell approx. 79−95157
- Na_2CO_3, molten, IR emission spectra *(Japanese)* 78−19469
- Na_2CO_3, molten, of O_2 and CO_2, manometric technique 79−69251
- Na_2CO_3, new catalyst for CO-H_2O induced coal liquefaction 80−30335
- Na_2CO_3, phys. props. related to phase transitions 80−96643
- Na_2CO_3, quasicrystalline state, incommensurate phase transformation 79−99310
- Na_2CO_3, single cryst. growth from melt, thermal expansion meas. 79−4913
- Na_2CO_3, struct. changes at incommensurate phase transition 79−95158
- Na_2CO_3, structural modulation, theory 77−35535
- Na_2CO_3+$CaCO_3$ solid state reactions, Hedvall effect 79−96300
- $Na_2C_2O_4$ $(SbF_3)_2$, growth from soln. and X-ray diffr. study *(French)* 77−80481
- $Na_2CO_3.1^1/_2H_2O_2$, cryst. struct. 78−18588
- $Na_2CO_3.1.5D_2O_2$, neutron profile refinement and deuterium positions 79−90602
- $Na_2CO.2CaCO_3$, shortite, cryst. struct. and space group, pyroelec. effect 79−23573
- Na_2CO_3(s), $NaHCO_3$(s), standard enthalpies of solution and formation, standard Gibbs energies of formation and standard entropy 79−57285
- $Na_{0.5}Ca_{0.5}Al_{1.5}Si_{2.5}O_8$, labradorite feldspars, lattice parameter determ. of exosolution structs. 77−84704
- $Na_{7.5}Ca_{0.5}(AlSiO_4)CO_3.2H_2O$, cancrinite, proton-containing groups, PMR meas. 78−2094
- $Na_6Ca_4(BeF_4)_6F_2$, cryst. struct. by X-ray diffr., cation distrib. *(German)* 78−43001
- $NaCa_2Cu_2V_3O_{12}$, crystal struct. distortion due to cooperative Jahn-Teller effect *(Russian)* 77−1119
- $NaCa_2Mn_2V_3O_{12}$, antiferromag., spin wave contrib. to sp. ht., λ-anomaly at 25.05K T_N 77−77068
- $NaCa(NH_2)_3$, cryst. struct. and cryst. chemistry *(German)* 79−51080
- $Na_x(Ca_{3-x}Na_x)Al_2O_6$ series, powder diffr. data 79−94975
- $NaCaPO_4$-Ca_2SiO_4 partial system, phase diagram 78−35364
- $NaCaPO_4$-$Ca_3MgSi_2O_8$(CaO) systems, phase diagrams of partial system 78−35369
- $NaCaPO_4$-Ca_3SiO_5 partial system, phase diagram 78−35365
- $NaCaPO_4$-$CaMgSiO_4$ system, phase diagram 78−35370
- $NaCaPO_4$-MgO, $NaCaPO_4$-$NaMgPO_4$, $NaCaPO_4$-Mg_2SiO_4, $Na_2CaMg(PO_4)_2$-MgO, partial systems, phase diag. 77−86005
- $Na_4Ca(SO_4)_3$, cryst. data and IR spectra 78−42986
- $(Na_xCa_y)_2SO_4$, cryst. struct., form. 77−19928
- $NaCa_2Sb_2Fe_3O_{12}$, mag. ordering and bond geometry rel. to tetrahedral Fe^{3+} 77−32163
- $NaCa_2Sb_2Fe_3O_{12}$, neutron diffr. patterns, group theory approach for determ. of mag. struct. *(Russian)* 79−51749
- $NaCa_2Si_4O_{10}F$, agrellite, new type of silicate double chain 78−51514
- $Na_8Ca_3SiO_{1.5}[Si_2O_7][PO_4]_3$, synthesis conditions, cryst. struct. and IR spectra characts. 80−108335
- $NaCaVO_4$, luminesc. spectra in visible region, vanadate group 78−43921
- NaCaX zeolite, ion migration and $Ni(CO)_n^+$ form., EPR obs. 79−33522
- $(Na_{1-x}Cd_x)Cd_2(PO_4)(PO_{3+x}(OH)_{1-x})$, cryst. struct. determ. 79−23589
- $(Na_{1-x}Cd_x)Cd_2[PO_4][PO_{3+x}(OH)_{1-x}]$, cryst. struct. determ. 77−15387
- $Na_2Cd_3Si_3O_{10}$, cryst. struct. 78−83801

sodium compounds continued
- $Na_4Cd_2[Si_3O_{10}]$, cryst. struct. determ. 79−14778
- $NaCeS_2$, mag. susceptibility, 3.7 to 297K, extended mol. field model 79−87227
- $Na_3Ce_{1-x}Tb_x(PO_4)_2$, UV excitation, emission spectra 79−38595
- $Na_2Ce_2TiO_2[SiO_4](CO_3)_2$, tundrite, new crystal. struct. and formula 77−31648
- NaCl, ^{14}N impurities, molecular point defects, EPR isotropic hyperfine triplets 80−2636
- NaCl, $^4He^+$ ion scatt. spectrometry below 5 keV 80−108313
- NaCl 46 cm window optical evaluation facility 80−74526
- NaCl (Br) aqueous solutions, IR absorpt. ν_1 (CN) band parameter temp., conc. study *(Russian)* 80−80801
- NaCl (001), surface relax. influence on surface vibr. modes, bulk shell model calcs. 78−71927
- NaCl (001) substrate, preferential epitaxy of evaporated films induced by electron bombard. or elec. field 80−10824
- NaCl (001) surface, relax. and rumpling effects on point ion potential 77−72770
- NaCl, (100), (110) and (111) surfaces annealed in vac. 400-800°C, evap. struct. 77−15572
- NaCl (100), adsorption of Xe, AES and LEED meas. 77−11792
- NaCl (100), elec.-mech. coupling of dislocations 78−75676
- NaCl (100) face, angle-resolved photoemission 78−56567
- NaCl (100) surface perturbations during LEED investig. *(French)* 77−28069
- NaCl, (111) surfaces, electron bombard. effects and subsequent Ag epitaxial growth, RHEED and AES 80−15419
- NaCl, absorpt. spectra, influence of elec. field 80−2794
- NaCl, absorption coeff. determ. in 10.6 μm region, laser calorimetry method 79−7186
- NaCl, acoustic non-linearity parameter in cubic crysts. 77−51444
- NaCl, activation coefficients and solvation numbers in mixed methanol solvents 80−81334
- NaCl, activation energy for mass transfer, quantum theory calc. *(German)* 79−51031
- NaCl, additively coloured, sensitised with O, photochromic props. 79−28792
- NaCl, additively coloured, SHG 80−1274
- NaCl, adsorbed on Ag photocathode, work function decrease 79−78824
- NaCl, adsorbed Xe on stepped and disordered surfaces, two-dimens. phase transformations 80−103580
- NaCl, adsorpt. of CO, N_2 and H_2, electrostatic interaction energies 79−23831
- NaCl, adsorption heat of Ar, variation 77−85049
- NaCl, adsorption heat of Ar variation 78−26772
- NaCl, adsorption of Ar, gas-solid virial anal. 77−55444
- NaCl, adsorption of Ar and Kr, energy distrib. using numerical algorithm HILDA 77−55443
- NaCl, adsorption of CO, electrostatic interaction energy 78−74592
- NaCl, adsorption of CO_2, atomic interaction pot. on (100) face *(German)* 80−15380
- NaCl, adsorption of CO_2, gas-solid interaction potential, adsorption sites and surface migration 80−24738
- NaCl, adsorption of methane, adsorpt. pot., localised and mobile phases, hopping adsorbates 80−24739
- NaCl, adsorption of N_2, electrostatic interaction energy 78−74592
- NaCl aerosols, charge and size distrib., appl. of four-parameter distrib. model 78−85213
- NaCl aerosols, density rel. to formation by condensation 78−7244
- NaCl, alkali halide crystals, defect state change during electrolysis 78−95057
- NaCl, amplitude phase hologram recording on colloid type centres *(Russian)* 80−69347
- NaCl, anharmonic cryst. of order λ^4, self-energy of phonons, approximate numerical results 79−55843
- NaCl, aq. soln., Cl^- self-diffusion, using β-active tracers, plastic capillary method 77−50333
- NaCl, aq. soln., isothermal compressibility, hydration parameters, up to 350°C and 10^3 kg cm^{-2} 78−10112
- NaCl, aq. soln., pipe flow heat and mass transfer, Polyox WSR 301 addition effect 79−46309
- NaCl, aq. soln., pulsed limiter discharge, nonideal plasma chem. composition 80−19657
- NaCl, aq. soln., thermal cond. meas., 20-330°C, 5, 10, 15, 20 and 25% solns. 77−47629
- NaCl aq. soln., vel. correls., time integral calcs. 80−59360
- NaCl, aq. solns., laser induced breakdown 79−87530
- NaCl, aq. solns. hypersonic sound vel. and absorpt. meas. 78−30699
- NaCl aqueous aerosols, fixation and microscopic sizing 80−16734
- NaCl, aqueous soln., direct calorimetric meas. of enthalpies, at high temp. and pressure 79−57286
- NaCl, aqueous soln., high precision viscosity meas. 80−10695
- NaCl, aqueous soln., Lennard-Jones parameters, mol. dynamics and X-ray obs. 78−9939
- NaCl aqueous soln., mol. dynamics simulation, central force model 80−49077
- NaCl as natural sea salt nuclei and laboratory controlled recrystallization 78−24337
- NaCl, automated scan of X-ray powder diffraction pattern 80−22492
- NaCl, band struct. calc. by mixed LCAO and OPW method 77−8019
- NaCl, barrier instability in strong elec. fields 79−69522
- NaCl beam thermal decomposition, Na time-of-flight spectrum using laser fluoresc. 77−49804
- NaCl, bent single crystal, equilib. face, surface relief form. during annealing 78−47651
- NaCl, bi-exciton luminescence possibility 80−40167
- NaCl bicrystal, grain boundary segregation, Au decoration obs. 77−68982
- NaCl, binding energy of F_{c+}', M_{c+}' and R_{c+}' centres, positron trapping 79−69460
- NaCl, bonding characts. of powders mixed with Mg stearate, SEM 78−84731
- NaCl, Born-Mayer parameters of He and Ar, interstitial interaction with neighbouring ions 80−100228
- NaCl, Bragg diffraction, anharmonic contributions, Mossbauer study 78−76359
- NaCl, bulk and (001)-surface equal-time vibr. correlation function 78−47655
- NaCl, bulk and surface absorpt., 2 to 10 μm, calorimetric meas. 78−71160

sodium compounds continued
NaCl, bulk and surface absorpt. in 9.2-10.8 μm region 79−95808
NaCl, bulk and surface absorption comparison, 9.2 to 10.85 μm 80−33051
NaCl, CO_2 laser pulse transmission, breakdown dynamics near surface in gaseous media 79−45986
NaCl, calc. of migration volume of vacancies 78−75872
NaCl, calc. of third- and fourth-order elastic constants 79−10891
NaCl, capacitance determination of area thermal expansion and dielectric constant 79−80573
NaCl, cation defects creation mechanism 80−75224
NaCl, cation motion energy parameters, dielectric relax. meas. 78−30784
NaCl, changes in internal friction and discharge following plastic deform. 79−99191
NaCl, channelling of MeV H^+ and He^+, zero dose meas. 78−18689
NaCl, cleavage faces, evaporation pattern determ. by decoration method in electron microscopy *(German)* 80−107626
NaCl, cleavage ledges and interface dislocations on Suzuki phases 79−90659
NaCl, cleavage of single crystals, investigation of fast electrical processes 79−24045
NaCl cleavage step decoration, nucleation and growth of metallic thin films 77−69200
NaCl cleaved surface, growth of Au island film, effect of perp. elec. field *(German)* 77−76697
NaCl cleaved surface structure, electron microscope 79−7735
NaCl, cohesive props., augmented-spherical-wave calcs. 79−94952
NaCl, Compton profile, 59.54 keV γ-rays 78−64426
NaCl, Compton profile anisotropies, charge and momentum distrib., LCAO-SCF-MO calc. 79−3500
NaCl, con. effect on pitting corrosion of martensitic cutlery steel 80−100962
NaCl, conduction band struct. from first principles 79−65379
NaCl, containing Na colloids, first-order Raman spectra 79−73943
NaCl, Coulombic energy calcs. 79−99104
NaCl, cross slip of screw dislocations during deform. at room temp. 77−84758
NaCl cryst., $KCaCl_3$ impurity precipitation and dissolution 79−42259
NaCl, cryst., laser irrad., electron emission 80−80948
NaCl cryst., laser pulse breakdown freq. depend., self-focusing elimination 77−55855
NaCl, cryst., optical breakdown plasma effects 77−66558
NaCl, cryst., plasma prod. by laser impact, effect on surface 78−1866
NaCl, cryst., triboluminesc. spectra 80−66312
NaCl, cryst., ultrasonic attenuation along (111) and (110) directions 78−63813
NaCl crystal, annealed near thermodynamic equilib. of cryst. and vapour, {110} surface struct. and coarsening 77−28067
NaCl, crystal, electron emission under uniaxial compresssion 80−7483
NaCl crystal, radiation coloured by electron beam, holographic lattice recorded by He-Ne laser 78−58950
NaCl crystal rough surface smoothing, during evaporation or condensation 80−103470
NaCl crystal surface struct., effect of ionic bombardment *(German)* 80−24507
NaCl crystal with aggregate colour centres, photocond. kinetics 78−19100
NaCl crystals, config. of screw dislocation halfloops *(Russian)* 77−89436
NaCl crystals, electronic and hole centres and surface, quantum-chemical calcs. 80−65489
NaCl crystals irrad. by high electron doses, annealing, colour centre prod. 80−2074
NaCl crystals with dipole O colour centres, radiation colouring and holographic recording 80−48187
NaCl, crysts., X-ray irradiated, luminescence during release of pressure 79−65939
NaCl, cubic cryst., temp. depend. of third-order elastic consts. 78−18699
NaCl cubical 4 μm particles, 0.627 μm light scatt. meas. 80−9804
NaCl, current oscills. in elec. fields of $\sim 10^6$ Vm^{-1} *(Russian)* 77−20334
NaCl Czochralski crystal growth for large CO_2 laser windows 80−74525
NaCl, Czochralski growth, temp. distrib. near crystn. front 78−2036
NaCl, damage caused by CO_2 laser radiation 77−90222
NaCl, damage induced by $CaF_2:Er^{3+}$ laser radiation at 2.76 μm 79−91539
NaCl, damage process preceding semibrittle fracture, plastic strain depend. 77−32692
NaCl, damage process preceding semi-brittle fracture in depend. on deform. microcrack development 77−44272
NaCl, defect fermion properties, ionic cond. calcs. 80−59457
NaCl, defect modes due to substitutional anion-pair and cation-pair impurities in ionic crystals 80−92540
NaCl, defects of electron irradiated single crystals *(Russian)* 77−47488
NaCl, deform. mech. map. 77−81298
NaCl, deform. process, exoemission and desorption meas. *(Russian)* 78−75708
NaCl, deformed, dislocation densities, TEM 77−43219
NaCl, deformed, influence of surface on density of edge components of dislocations 77−31670
NaCl, deformed by conc. loading, X-ray beam scattering *(Russian)* 78−35430
NaCl, deformed surface layer, block misorientation 79−99405
NaCl, dielec. band struct. calc. 79−47034
NaCl, dielectric polarisation calcs., microscopic local fields 80−20582
NaCl, dielectric properties, mean point value calc. 78−87930
NaCl dilute solution, US vel. meas. by differential velocimeter 77−78065
NaCl dimer, electron diffr. study of mol. struct. 80−28951
NaCl, dipole polarisation, depend. on AC and DC voltage superposition 80−20577
NaCl, dislocation charge photostimulated variation kinetics *(Russian)* 80−79806
NaCl, dislocation density, laser beam effect, electron microscopy of etch pits 77−11553
NaCl, dislocation density in monocrystal deformed under high hydrostatic press. 80−70216
NaCl, dislocation distrib. on surface parallel to Burgers vector 79−65090
NaCl, dislocation half loop mobility 78−59817
sodium compounds continued
NaCl, dislocation internal friction, orientation depend. 78−48439
NaCl, dislocation microplasticity, internal friction expts. 78−47388
NaCl, dislocation mobility under high press., temp. depend. 80−75235
NaCl, dislocation motion in micro-plastic region 78−91341
NaCl, dislocation movement, effects of adsorpt. of octadecylamine *(Russian)* 77−51372
NaCl, dislocation ordering influence on integrated X-ray coeff. 80−103357
NaCl, dislocation rosettes around Vickers diamond pyramid indents, quenching effect 80−11740
NaCl, dislocation struct. of slip bands, hydrostatic press. effect 80−54249
NaCl, dislocation velocity determ. by nuclear spin-lattice relax. meas. 77−35566
NaCl, doped, secondary ion emission, at. and mol. processes 78−68588
NaCl, doped by Ca^{++} and OH^-, thermal conductivity in 5-190K range 78−14520
NaCl, doped substrate for vac. deposition of Ag oriented films 80−2303
NaCl, doubly rotating coordinate system, NMR multiple-quantum transitions 77−81019
NaCl, dynamic dislocation retardation, impurities effect 78−26577
NaCl, edge dislocation, core struct. and props., theory 80−70194
NaCl, edge dislocation dissoc. energy, atomistic calc. 77−27883
NaCl, edge dislocation displacement 77−62540
NaCl, edge dislocation dissoc., computer simulation of core struct. 79−37703
NaCl, effect of annealing and neutron irrad. on block struct. 80−29061
NaCl, effect of dislocation density on viscous drag dislocation coeff. *(Russian)* 77−80512
NaCl, effect of surface cond. on crystal bulk elec. cond. 78−6177
NaCl, effect on diffusion saturation of W by Si in vacuum 79−15859
NaCl, effect on high temp. hot corrosion 78−48563
NaCl, effective Debye temp., press. and temp. depend. 78−18728
NaCl, efficiency of creation of X_3^- centres in X-rayed alkali halides *(Russian)* 78−71731
NaCl, elastic moduli, quadratic fit against temp. 78−14397
NaCl, elastic props. at press. up to 9 GPa, ultrasonic wave velocities 79−95073
NaCl, elastic X-ray scatt., effect of dynamic deform. calc. 78−26378
NaCl, elec. cond. and distrib. of Ni^{2+} ions 79−33010
NaCl, electric field gradients near dislocations, resulting NMR lineshapes 80−75225
NaCl, electric field induced by homogeneous stresses 80−11343
NaCl, electron and ion beam excited luminesc. spectra 79−52026
NaCl, electron beam excited, luminesc. and cond. of nonideal degenerate electron-hole plasma 78−10488
NaCl, electron beam irrad., formation of colour centres *(Russian)* 77−7716
NaCl electron excited luminescence yield orientational depend. 80−40169
NaCl, electron impact, colour centre distrib., channelling 79−14866
NaCl, electron irrad., secondary electrons and radiation defects 79−55782
NaCl, electron irradiated, electrotransport 79−69526
NaCl, electron irradiation, energies greater than 1 MeV, defect form. and secondary electron emission *(Russian)* 77−55304
NaCl, electron momentum distrib. and Compton profiles 79−13631
NaCl, electron trapping by alkali ion impurities 78−47809
NaCl, electronic struct., SCF cryst. cluster model 80−24792
NaCl, electronic structure calculation, CNDO semi-empirical methods *(Russian)* 80−10909
NaCl, electrostatic energy calc. by planewise summation method 79−23564
NaCl, electrostriction consts. calc. 77−36178
NaCl, emission band of F-centre 80−76071
NaCl, emission of Cl atoms during V_k centre decomposition 80−10578
NaCl, energy of form. of Schottky defects 77−7714
NaCl, energy of migration of Cl^-, Br^-, I^- and F^- ions 77−43380
NaCl, energy spectra of sputtered Na atoms from 20 keV rare gas ion bombard. 79−52068
NaCl, energy struct. determ. by electron absorpt. spectra 78−11040
NaCl, enthalpy calc. for solid and liq. phases 77−43349
NaCl, eqn. of state, effect of Gruneisen parameter 79−51233
NaCl, eqn. of state to 32 kbar and 500°C, length change meas. 80−70361
NaCl etalon used to control modelocked multiline TEA CO_2 laser 80−23713
NaCl, etch pits on cleaved surfaces, oriented overgrowths 77−73359
NaCl, etched cleavages, moisture effect on spiral and terraces steps 77−4251
NaCl, evaluation of ionic thermocurrent technique in monitoring relaxation behaviour of impurity-vacancy dipoles 78−43778
NaCl, evaporating cryst. surfaces, successive monatomic step trains with different density 80−29254
NaCl, evaporating surface, step motion obs. and simulation 78−26766
NaCl, evaporation coeff. meas. by TEM 78−18909
NaCl, exciton luminesc. obs. 77−12449
NaCl, excitons at $L_{II,III}$ absorption edge of Cl^-, decay characts. thermolum. meas. 77−28121
NaCl, exposed to high-current electron beam pulses, min. size of excited region for crack initiation *(Russian)* 78−84961
NaCl, exposed to US waves, dislocation multiplication in original stage 78−47383
NaCl, exposed to ultrasoft X-rays, thermal luminesc. and electron emission 79−8192
NaCl, F_3-centre quartet state, IR emission spectra 78−43930
NaCl, F^--centres, thermal and photolytic decay processes 78−95053
NaCl, F-centers, laser irrad. optical bleaching kinetics 80−66244
NaCl, F-centre, wave functions and spin densities, pseudopot. calc. 79−4533
NaCl, F-centre aggregation, initial stage study by Raman scatt. 79−56791
NaCl, F-centre interactions and local distortions *(French)* 78−43016
NaCl, F-centre space distrib., pair correl. function 79−60361
NaCl, F-centres near monoenergetic proton stopping region, space charge effect 78−18640
NaCl, far IR complex refr. indices, dispersive Fourier transform 78−80322
NaCl, far IR dispersive-reflection meas. at room temp., comparison with calc. 78−35139

sodium compounds continued
NaCl, far IR spectra, matrix isolated, monomers, dimers, trimers 78−66545
NaCl, filamentary crystal, vacancy-enriched surface layers 78−51536
NaCl film, electron emission under metastable He and Ne atom impact 80−20747
NaCl film, UPS linewidth, phonon broadening of core levels 77−36371
NaCl, finite strain isotherm and vels. for single crystal and polycrystalline samples 78−53646
NaCl, for thermoelectrochemical prod. of H_2 80−55946
NaCl, frozen soln., NMR study of phase transitions 79−56617
NaCl, fundamental luminescence at high ionisation levels *(Russian)* 80−103985
NaCl, gamma and additively coloured, dissolving in pure water, lyoluminesc. mechanism 80−100693
NaCl, gamma irradiated, optical bleaching of colour centres, F-aggregate centre form. 79−95813
NaCl, gamma irradiation, optical and thermal bleaching of colour centres, trapped electron centre form. 79−95814
NaCl, gamma-irradiated, aquoluminescence spectra in presence of activators 77−69913
NaCl gas-droplet counterflow heat exchanger, numerical model *(French)* 80−61396
NaCl, gaseous, effect on oxidation of NiAl 78−95853
NaCl, growth and composition of Al clusters 77−89677
NaCl, Gruneisen coeff. press. depend. up to 33 kbar 77−35714
NaCl, Gruneisen γ and other thermodynamic props., vol. depend. 77−76577
NaCl, γ-irrad., C-centres, position ang. correl. obs. 78−22712
NaCl, γ-irrad., F-centres form., energy storage 79−82264
NaCl, γ-irrad., F-stimulated inversion of sign of dislocation charge 80−59475
NaCl, γ-irrad., photoplastic effect and internal friction aftereffect 80−24529
NaCl, γ-irrad. and doped, lattice relax., cold neutron scatt. obs. 77−7715
NaCl, γ-irradiated, F→M phototransformation, effect on aquoluminescence 80−7418
NaCl, γ-radiation effect on 10.6 μ absorpt. coeff. assoc. with F-aggregate centres 77−4661
NaCl, halite, dynamic recrystn. during compression creep, geophys. appl. 80−25772
NaCl, hardness increase mode, effect on dislocation mobility 79−51114
NaCl, high density of dislocations meas., new etchant 78−43019
NaCl, high hydrostatic press. effects on dislocation mobility 78−14358
NaCl, high press. eqn. of state and sound vels. to fourth order elastic consts., 270 kbar 79−37806
NaCl, high press. metallic modification, superconduction obs. *(Russian)* 79−65576
NaCl, high resolution TEM and radiation sensitivity, dislocation obs. on deformed crysts. 80−107260
NaCl, high-temp. deformed, dislocation grain subboundaries *(Russian)* 80−96534
NaCl, high-temp. vapour, appl. of photographic plate for electron diffr. studies 77−39516
NaCl, hologram recording, F-centre bleaching by 633 nm light 79−22922
NaCl, hydrostatically compressed crysts. in easy glide stage, plastic deformation 80−7630
NaCl, IR transparent materials, bulk and surface absorpt., calorimetric meas. method 79−27347
NaCl, illuminated over large area, optical strength 77−75593
NaCl, impurities, divalent, existence of charged aggregates 77−84790
NaCl, impurity precipitation and grain boundary diffusion 80−107567
NaCl, inelastic light scattering of localised vibration of interstitial H atom in alkali halides 80−88998
NaCl, influence of coloration on intrinsic luminesc. 78−80399
NaCl, integrated intensity of X-ray diffr. by polygonization walls 77−89447
NaCl, interatomic Auger processes 77−85892
NaCl, interfaced polarisation and losses, superimposed AC and DC voltage study 80−25276
NaCl, internal damage threshold for CO_2 laser pulses rel. to absorption 77−75594
NaCl, internal stresses and dislocation mobility 78−48440
NaCl, interpolational eqn. of state with allowance for melting, vaporis., dissoc. and ionis. processes 80−24566
NaCl, interrupted neutron irrad. expts. involving dislocations 79−99208
NaCl, intrinsic defects at (001) and (011) surfaces 77−47443
NaCl, ion and electron emission following ion impact 80−100729
NaCl, ionic clusters, struct., thermodynamic functions, energy surfaces and SIMS 80−63881
NaCl, ionic mobilities in cellulose acetate membranes 80−45550
NaCl, irradiated, at 80K, thermolum. processes 80−34990
NaCl, irradiated, determ. of molar extinction coeff. and oscillator strength of V_2-centre *(Russian)* 78−80384
NaCl, irradiated at room temp., thermolum. and F-centre thermal stability 78−84669
NaCl, irradiation-induced energy transfer from bulk to surface, luminesc. meas. 78−92132
NaCl, isothermal diffusion of ^{54}Mn 77−47625
NaCl, isothermal eqn. of state, length change meas. technique 77−1210
NaCl, kinetic energies of sputtered excited atoms 80−66373
NaCl, kinetics and morphology of lamellar-spiral growth hillocks 78−18566
NaCl, Knoop microhardness anomaly on (001) planes 79−38942
NaCl large window continuous polishing 80−74527
NaCl, laser damage, phenomenological theory 80−19836
NaCl, laser damage simulation, optical breakdown probability at 6943 Å 77−12470
NaCl, laser damage threshold at 10.6 μm, up to 10^{10} W/cm^2 77−50707
NaCl, laser irradiated, electron emission, surface layer electric discharge effects 79−74032
NaCl laser-induced breakdown fields rel. to wavelength and focal spot radius 80−35019
NaCl, laser-induced damage threshold variations 80−14380
NaCl, lattice dynamics and statics, three-body-force shell model 80−49323
NaCl lattice investigations, start stresses of ensemble leading dislocations 80−92530
NaCl, lattice thermal and optical phonon contrib. 79−14971
sodium compounds continued
NaCl, liq., Brillouin scatt. determination of hypersonic vel. 79−82288
NaCl, liq. surface, Fowler model, electroneutrality correction 79−28174
NaCl, load relaxation studies 79−79016
NaCl, local field, microscopic electronic polarisation 80−25283
NaCl, low temp. space charge polarisation 78−43789
NaCl, luminesc. induced by ion-impact, −160 to 200°C 77−8654
NaCl, luminesc. singlet from triplet self-trapped excitons 79−99936
NaCl, luminesc. under 10.6 μm laser pulse irrad. *(Russian)* 77−16381
NaCl, luminescence excited by vacuum UV lasers 78−10941
NaCl, luminescence induced by tunnelling recombination between neutral Ag atoms and V_k centres 79−61442
NaCl, M-centre prod. processes, in-beam studies, 15-95°C 79−55737
NaCl, M-centre statistical prod. meas. 80−15097
NaCl, m-crocryst. powders coloured in electrodeless discharge, reflectance spectra, thermolum. 78−15238
NaCl, Madelung pot. determ. by Ewald method 80−92475
NaCl, mass transfer from sedimentary deposit layer to stationary water region *(Japanese)* 77−25700
NaCl, mechanoluminesc. peaks, microbreakdown mechanism, generation of ionisation waves 79−33032
NaCl melt, effect of cooling rate upon glass transition, X-ray analysis 79−27920
NaCl, microcrack propagation and plastic strain 80−81187
NaCl, microcryst. powder, isothermal stability of colour centres, thermolum. glow curve 79−15535
NaCl, microcrystallites, sp. ht. calc. 77−72696
NaCl, microindentation, dislocation rosette generation 77−27936
NaCl, migration of nonrelaxed holes, self-trapping, ESR and luminesc. obs. *(Russian)* 80−66033
NaCl, Mn^{2+}-□ reorientation, ESR elec. field effect meas. 79−8050
NaCl, mol. beam, on hot W(Re), surface, Na_2Cl^+ ion form. 79−56907
NaCl, mol. beam condensation on Ir and Pt substrates, adsorbed C effects 77−66593
NaCl, molecular versus atomic secondary ion emission, rel. to quantitative analysis 79−61481
NaCl, molten, diffusion of Li^+ ion *(Japanese)* 78−14489
NaCl, molten, dynamical struct. factors 78−47228
NaCl, molten, dynamical correlations, fourth moment of current and appl. 79−14664
NaCl, molten, surface tension calcs., Fowler model modification 78−67888
NaCl molten salt, collective dynamical props., mol. dynamics calc. 77−76292
NaCl molten salt, nucl. quadrupolar spin-lattice relax., microscopic liq. dynamics 79−91313
NaCl, molten salt, thermodynamic function, Brillouin spectroscopy, hypersonic vel. *(French)* 78−35161
NaCl, monatomic step struct., decoration technique 80−103554
NaCl monocrystal, sintering 77−59710
NaCl, monocrystalline, defect struct. and intrinsic ionic cond. relationship 79−95211
NaCl, monodisperse aerosol, preparation and growth 77−86389
NaCl monodisperse aerosols, appl. in cloud droplet nucleation expts. 80−82003
NaCl, monoelectrolyte, highly mineralised salt soln., dielec. and radiation characts. 80−97184
NaCl, monomer/dimer vapour equilib. mixture, flow through porous barrier 77−31383
NaCl, motion of individual surface dislocation semi loops *(Russian)* 78−51542
NaCl, moving dislocations, interaction with defects, elec. effects meas. in plastic deformation *(Hungarian)* 80−10572
NaCl, muonic X-ray intensities, Lyman series 80−23578
NaCl, Ne^+, Ar^+, Kr^+ bombard., sputtering and ionoluminescence 80−96583
NaCl nearly cubic particles, Mueller scatt. matrices 78−90366
NaCl, neutron irradiated, induced flow stress and optical absorpt. 77−62569
NaCl, Ni-based superalloys, mechanical integrities of surface scales, contaminant corrosion 78−95845
NaCl, nuclei in atm., optical props. 78−11995
NaCl, occlusion formation during dendritic crystal growth, expt. 78−38993
NaCl, optical breakdown, 1.06 to 0.172 μm 78−35089
NaCl, optical breakdown threshold, illuminated spot dimension effects 78−68582
NaCl, optical breakdown from 0.53-10.6 μm 80−7292
NaCl, optical conversion, luminesc. and colour centre formation 79−24354
NaCl, optical strength, effect of irrad. in mechanically stressed state 80−80695
NaCl, optically bleached and X-irrad., relation between F- and C-centres 77−72613
NaCl, orbital g-factor and spin-orbit splitting of F-centre excited state, magnetoabsorpt. and MCD 78−2886
NaCl, oscillatory and diffusive regime, above and below melting point, IR thermal emission spectra 78−83985
NaCl particle, luminesc. duration rel. to time in CO_2 laser beam focal zone 80−34983
NaCl particle generation 79−16606
NaCl particles, laser irradiated, white light flash obs. 79−15565
NaCl, phase transformation due to high press. and shear stress 80−75357
NaCl, phonon dispersion curves calc. 77−39648
NaCl, phonon freqs. in off-symm. directions, neutron inelastic scatt. 79−46767
NaCl, photoemission exam. of Na^+-2p core excitons 78−43982
NaCl, photofragment spectra, bond energies and excited state symmetries 80−87190
NaCl, photoluminescence under pulsed UV laser excitation 77−77289
NaCl, photoplastic effect *(Japanese)* 79−82279
NaCl, picosecond laser-induced breakdown at 5321 and 3547 Å, freq. depend. 77−63495
NaCl, piezoelectric effect 79−69779
NaCl plasma, acoustic wave-coherent CO_2 light scatt. 78−34325
NaCl, plasma, dense, nondegenerate, electron transport, thermal cond. *(Russian)* 79−98865
NaCl, plastic deform., cleavage crack propag., X-ray topography 77−39625
NaCl, plastic deform. and dielec. losses 78−19410

sodium compounds continued
NaCl, plastic deformation influence on shape recovery effects 80−6684
NaCl, plastically deformed [001] orientated single crystal, glide props. and X-ray topography 77−21228
NaCl, plastically deformed, recovery of work hardening *(German)* 77−35626
NaCl, plastically deformed [001] oriented single crystals, TEM 77−36579
NaCl, plastically deformed, containing dislocation distribs., X-ray diffr. broadening 77−43218
NaCl, plastically deformed, integrated X-ray reflection coeff. determ. 77−65981
NaCl, plastically deformed, glide on {111} planes 79−82234
NaCl, plate, distortions due to 10.6 μm laser irrad., interferometric obs. 78−46697
NaCl plates, γ-irrad., hologram recording, He-Cd laser radiation 78−17878
NaCl, point defect interaction with dislocations, internal friction meas. 79−90662
NaCl, polarisation caused by charged dislocation motion 80−59463
NaCl, polarisation mechanism and lattice mechanics, microscopic approach 78−59888
NaCl, polishing of single crystals, kinetics of defect formation *(Russian)* 78−95819
NaCl polycryst. containing Al_2O_3 dispersion, diffusive creep 80−97531
NaCl, polycrystalline, acoustic vels. at 300K from 2.5 to 270 kbar 77−27945
NaCl polydisperse aerosol number and mass conc. meas. by elect. aerosol anal. 80−108753
NaCl Polytran laser windows, for CO_2 lasers, fusion appls. 78−59067
NaCl, positron ang. correl., cryst. orient. depend., positron states and ionic distortion 77−63484
NaCl, positron annihilation in colour centres 77−73185
NaCl, positron source, temp. depend. 80−93426
NaCl, positron trapping by X-ray produced defects, A-centre form. 77−48273
NaCl, positron-trapping colour centre dynamics, positron annihilation study 80−108294
NaCl, positronic atom scatt. on optical phonons, positron thermalisation 80−50457
NaCl, positronium-like states, ang. correlation of photons from positron annihilation 77−36310
NaCl, powder diffr. using synchrotron radiation, energy-dispersive technique 77−24245
NaCl preirradiation effect on proton channelling, thermoluminescence study 80−19860
NaCl, premelting due to thermal form. of dislocations 77−11671
NaCl, premelting elec. cond., heat capacity 78−91445
NaCl, prep., 5-30 μ thick single cryst., for channellography appl. 78−80658
NaCl, prep. of fine crysts. demonstrated by electron microscopy 78−48302
NaCl, press. effect on ionic cond. at 300K 77−7895
NaCl, press. shifts of F-centre hyperfine interaction parameters 78−79957
NaCl primary press. gauge, failure of central force model 77−15492
NaCl prism IR spectrometer, calibration curve, non-min. deviation effect 77−13809
NaCl, pulsed dielectric breakdown, mech. stress photoelasticity obs. *(Russian)* 78−2800
NaCl, pulsed Rf radiation produced by scratching *(Russian)* 78−19607
NaCl, pulsed-laser-induced damage, role of avalanche multiplication and multiphoton absorpt. 80−48316
NaCl, pure, indoped, luminesc. obs. 77−32412
NaCl, pure and doped, 20K X-ray irradiation, thermolum. and recovery processes 80−93412
NaCl, pure and doped, nucl. acoustic reson. 79−69746
NaCl, pure and Mn-doped, CESR of dendritic metal phase precip. 77−24744
NaCl, pure and Sr doped crystals, strengthening effects rel. to IV-dipoles and aggregates 78−55907
NaCl, quantum-chem. calcs. of electronic and hole centres and surface 80−20118
NaCl, quench hardening of single crystals 79−43261
NaCl, quench hardening related to dislocation density and slip 78−52855
NaCl, radiation damaged, proton and $^4He^+$ channelling, F-centre production, optical absorpt. meas. 78−79656
NaCl, radiation from axially-channelled relativistic electrons *(Russian)* 77−84813
NaCl, reduction of dislocation density during isothermal annealing *(Russian)* 79−4303
NaCl, rock salt, average electron range in dielec., 20-50 keV, precise meas. 79−14868
NaCl, rock salt, progressively mined soln. cavities, struct. behaviour 78−61409
NaCl, rock salt, quenched, residual stresses, optical study 80−55061
NaCl, rocksalt (h10) faces, terrace like step trains, evaporation, TEM obs. 77−35801
NaCl, rot. excitation by electron impact, calc. cross sections 78−66670
NaCl, Schottky defect, formation enthalpy, entropy, temp. effects, correction 78−10039
NaCl, screw dislocation mobility under high hydrostatic press. 79−69109
NaCl, screw dislocations, atomistic calc. of core config. 79−23606
NaCl, sea water relaxation and sound absorption 79−68466
NaCl, search for IR absorption by triplet self-trapped excitons 78−56473
NaCl, second relaxed excited state of F-centre, optically detected EPR 79−87335
NaCl, secondary electron emission, appearance of collective and individual interactions of slow electrons 77−69948
NaCl, self trapped exciton, optical detection of spin relax. processes 78−60358
NaCl, self-trapped exciton form. via thermally induced defect reactions 80−60687
NaCl, shock compressed, thermal energy relaxation 77−69043
NaCl, shock compressed, vel. of sound meas. 78−10123
NaCl, single cryst., crack healing at low temp. 77−36622
NaCl, single cryst., for IR dispersive refl. meas., low temp., rel. to anharmonicity calcs. 80−11371
sodium compounds continued
NaCl, single cryst., lattice structure distortion on freshly formed surface, electrification 77−51582
NaCl, single cryst., shock wave compression, flash X-ray diffr. obs. 78−83877
NaCl single cryst., stress birefr. 80−60542
NaCl, single cryst. expt. on distension of gas-filled cavity 80−49286
NaCl, single cryst. in vac., influence of dislocations on evaporation 79−10935
NaCl single crystal, plasticity, effect of alternating electric field 78−15481
NaCl, single crystal, recovery controlled transient creep, substructural obs., phenomenological anal. 77−77526
NaCl single crystal, stained by abrasion, struct. defects *(Russian)* 79−74262
NaCl single crystal, surface relief obs. using PbS epitaxial replicas 77−51577
NaCl, single crystal, surface markings, left by unsteady cleavage crack propag. 79−46746
NaCl, single crystal, temp. anisotropy of plasticity and brittleness 78−3198
NaCl single crystal-electrode interface, anomalous transient currents 78−22886
NaCl single crystals, screw dislocations, influence of interionic potentials on core configs. 80−34000
NaCl single crystals, thermomigration of brine inclusions, eval. of radioactive waste repositories 80−99251
NaCl, single cubic particles, suspended in laser beam, optical size determ. 78−33673
NaCl, Sn film, vapour-deposited on NaCl single cryst., nucleation, growth, microstruct. 78−91561
NaCl, solid monodisperse aerosols, in He jet system, for unstable nuclide transportation 79−22507
NaCl, soln., electrolysis, surface deposit on Ti anode anal. 78−73117
NaCl soln., nebulized aerosol, droplet size distrib., evaporation effect, medical appl. 78−24084
NaCl soln., no particle fragmentation during evaporation 77−91189
NaCl, soln., sp. ht. capacity at high press., temp. jump method 77−69092
NaCl solns. containing radiosensitisers and radioprotectors, effect on mammalian cell radiosensitivity 78−69146
NaCl, solution, apparent molar heat capacity and volume, at 298.15K 80−29179
NaCl, solution, droplet evaporation in laminar gaseous stream *(French)* 77−51102
NaCl solution, electrochemical corrosion of metals and alloys *(Russian)* 79−52445
NaCl solution, ionic hydration for cations 77−62460
NaCl, solution, seawater, with trace quantities of Cs, adsorption behaviour on paper *(Russian)* 77−73766
NaCl solution, thermodynamic driving force, for crystallisation at 298K 79−37643
NaCl, solution in ethyl alcohol using uncommon complexes 77−25356
NaCl, solution of $ZnCl_2$, solubility of Co_2 79−90785
NaCl solutions, anodic dissoln. of Ni-Cr steels and alloys in, at high current densities *(Russian)* 80−76396
NaCl solutions, of Zn-nucleotide triphosphate complexes ^{35}Cl NMR obs. 80−63661
NaCl, sound speed as function of conc., temp., and press. 78−79668
NaCl, sp. ht., thermal cond. and thermal diffusivity, meas. by pulse method, influence of press. 79−7701
NaCl, spectrum of intrinsic oscills., allowance for quadrupole deform. of ions 77−7810
NaCl, spin-lattice relax. of F-centres, magneto-optical meas. 77−43884
NaCl, spiral dislocation mobility depend. on elec. field, relaxation time 80−39105
NaCl, sputtering by Ar ion bombardment, temp. depend. of sputtering rate *(Japanese)* 78−88389
NaCl, sputtering of atoms by 540 eV electrons, delay times 80−35025
NaCl, strain ageing exam. 78−56661
NaCl, strained in one glide system at 450°C, dislocation struct. 78−22728
NaCl, stratified solutions, elec. cond. meas. instrument 77−52718
NaCl, strength under confining press. of 250 kbar, brittle-ductile transition 77−47510
NaCl, stress-induced birefringence meas., 1-12 μm 77−24818
NaCl, struct. refinement at 32 kbar, using single-crystal diamond cell 78−67610
NaCl structure, evaluation of finite strain eqns. of state using lattice models 80−96620
NaCl structure ionic cryst., high temp. dynamics, var. approach 80−29130
NaCl, sublimation struct., back force effect 77−15571
NaCl substrate, elec. memory in C replicas, Au and Ag deposition expts. 77−76691
NaCl substrate, role of surface steps in nucleation of VPE Au 78−79902
NaCl substrate for condensed Au film, ion bombarded, thermally stimulated exoelectron emission 80−50537
NaCl, substrate with colloidal centre, vacuum deposition of Au particles *(Rumanian)* 78−60579
NaCl, supersaturated soln., H_2O activity prediction 79−23713
NaCl surface, residence times of Au atoms, time-of-flight meas. 80−10788
NaCl, surface and bulk absorpt. at 10 μm, temp. depend. 77−28576
NaCl, surface charge meas. in ultra high vac. 80−20287
NaCl surface conditions of step decoration 80−15349
NaCl, surface lattice dynamics, Green function approach 77−31865
NaCl, surface self-diffusion const. from growth or evaporation spiral evolution kinetics 79−65301
NaCl, surface states, detection by photocharging spectroscopy 77−66193
NaCl surface with adsorbed water layer, absorpt. and thickness meas. 80−16001
NaCl, temp. fields during plastic deform., cholesteric liq. cryst. technique 79−82278
NaCl, thermal and athermal plasticity *(Russian)* 79−11685
NaCl thermal cond. press. depend. 77−15641
NaCl, thermal cond. under press. meas. 78−30802
NaCl, thermal cond. up to 40 kbar 79−1533
NaCl, thermal conductivity at high temperature 79−55857
NaCl, thermal expansion, rapid increase near melting point 77−51521

sodium compounds continued
NaCl, thermal expansion, compressibility and melting calcs. 79−33069
NaCl, thermal expansion coefficients temp. depend., anharmonic effects 79−99290
NaCl, thermal expansion meas. after X-ray irrad., F-centre bleaching 80−44338
NaCl, thermal fields generated during plastic deform. 78−35457
NaCl, thermal focusing of elliptically shaped optical beams 79−18489
NaCl, thermal phonon scatt. by low angle grain boundaries 78−67795
NaCl, thermodynamic equilib. vapourisation, transpiration mass spectrometry 80−52356
NaCl, thermodynamic props., lattice-dynamical calc. 77−35715
NaCl, thermoluminesc. and optical absorpt., simultaneous DC field and X-irrad. 79−99956
NaCl, thin film, crystal-vacuum (100) surface, mol. dynamics computer simulation 80−34288
NaCl, thin single-crystal film, hot electron emission 79−15244
NaCl, transient infrared absorption of bound polarons 78−91642
NaCl, transparent, plasma form. at surface due to CO_2 laser irrad. 78−60534
NaCl transverse optic mode anharmonic self-energy meas. by dispersive Fourier transform spectroscopy 77−39642
NaCl, transverse optical mode anharmonic self energy, far IR spectrum 78−6131
NaCl, tricrystal, crack propag. 77−70177
NaCl type crystal, binding energy of ion on unrelaxed (100) and (110) faces, Madelung and dispersion contrib. 79−77550
NaCl type crystal, dislocations due to high temp. stress relax. 78−2126
NaCl type crysts., elastic consts., Cauchy discrepancy, three-body force shell model 77−20004
NaCl type ionic crystals, statistical theory calcs. of surface energy and surface tension 80−17894
NaCl, U_2 and U_1 centres, optical excitations 80−2803
NaCl, UPS, expt. methodology aspects 77−90245
NaCl, US deformation, stress anal. by polarised light method *(Russian)* 77−11641
NaCl, US vel., Poisson's ratio and shear modulus meas., 9 GPa 77−4140
NaCl, UV visible absorpt. by laser calorimetry, wavelength modulation spectroscopy 78−66876
NaCl, uniform deformation and birefringence in nonuniform elec. field *(Russian)* 79−87396
NaCl, V- and X-centres accumulation *(Russian)* 80−54228
NaCl, vacancy comaplex formation and binding energies in zeroth approx. 80−24441
NaCl, valence electron distrib., pseudopotential calcs. 80−2335
NaCl, valence-electron charge density along nearest-neighbour axis 79−27944
NaCl vapour, and Na_2SO_4, hot corrosion of Co-Cr-Al-Y turbine blade coatings 78−19941
NaCl, vapour, effect on oxidation of Ni-Cr-Al alloy 78−44274
NaCl, vibrational contribution to surface thermodynamic functions 77−47659
NaCl, viscous drag of dislocations, internal friction, 4.2-300K 77−11566
NaCl, water-HMPT soln., ionic diffusion coeffs. meas. *(French)* 80−65265
NaCl whiskers, plastically deformed, internal friction amplitude depend. 77−15727
NaCl whiskers, plastification in elec. field *(Russian)* 80−21010
NaCl whiskers, X-irrad., stress oriented dislocation loop nucleation 79−33213
NaCl window production for Antares CO_2 laser system 80−74524
NaCl, with dispersed Au particles, age hardening of surface, double decoration obs. 79−11634
NaCl with divalent impurities, lattice relax. from density meas. 80−70226
NaCl with $K_3(Fe(CN)_6)$, in aq. soln., electrolyte for porosity determ. of Cu platings on C steel filaments 79−70239
NaCl, work hardening, acoustic emission 79−100167
NaCl, X-centres thermal decay process, activation energy *(Russian)* 79−90651
NaCl, X-irrad., F-thermal bleaching 77−89433
NaCl, X-irrad. dose depend. of dislocation charge 77−47464
NaCl, X-ray irrad., F-centre accumulation and rad. hardening *(Russian)* 78−51538
NaCl, X-ray irrad., vacancy conc., thermal expansion meas. 80−6431
$NaCl^-$, mol. orbital calcs., diffuse functions for basis sets, electron affinity 78−25436
$NaCl^-$, $NaBr^-$, NaI^-, photodetachment cross section resons., 2-2.3 eV 79−54922
$^{22}NaCl$, tracer diffusion meas. in aq. NaCl soln., closed capillary method 78−14491
NaCl:$^{63}Cu^+$, resonant bandmode, stress spectroscopy with far IR laser 78−2847
NaCl:$(Mn^{2+}$-□$)_{Fanion}$, F^- assoc. complex, ionic thermocurrent and EPR 79−8086
NaCl:Ag, absorpt. spectra, influence of elec. field 80−2794
NaCl:Ag, diffusion parameters of hot holes created by ionising radiation 78−47800
NaCl:Ag, electroluminescence spectra 78−2918
NaCl:Ag, excitation in fund. absorpt. region, luminesc. and thermolum. 80−50433
NaCl:Ag, formation of Ag atoms and self-localised holes by illumination, EPR meas. 78−31108
NaCl:Ag, formation of electron centres and self-localised holes, ESR exam. 78−91947
NaCl:Ag, irrad. with synchrotron radiation, thermolum. light-sum spectrum of L absorpt. edge of Cl^- 79−15540
NaCl:Ag, positron annihilation and impurity states 80−97375
NaCl:Ag, thermolum. light sum storage by ultrasoft X-rays 77−20939
NaCl:Ag film, EPR and optical exam. of Ag impurity centres 77−85562
NaCl:Ag^+, X-irrad., B-centres, thermal annealing, monomolecular and bimolecular sequence of kinetics 78−47373
NaCl:AgCl, positron annihilation characts., positronium state form., X-irrad. effects 77−4700
NaCl:Au, EPR and optical absorpt. 78−39397
NaCl:Ba, Ba precipitation at dislocations, kinetics, ionic cond. meas. 79−60510
NaCl:Ba^{2+}, dopant aggregation and precipitation 80−107306
NaCl:$BaCl_2$, oriented growth of $BaCl_2$ phases, platelet-matrix interface structure and energy 78−87793

sodium compounds continued
NaCl:Bi^{3+}, complex form. in soln., absorpt. spectra 77−28591
NaCl:Br, host-sensitized luminesc., energy transfer due to excitons and holes 79−38590
NaCl:Ca, aggregation and precip. hardening in impurity vacancy, dipole decay 80−16322
NaCl:Ca, hologram recording on R-centres 80−1157
NaCl:Ca, holographic appls., diffr. efficiency 77−54679
NaCl:Ca, light scattering coeff., effect of growing condition 78−55418
NaCl:Ca, microhardness and thermoluminescence, hardness-quenching temp. variation 80−29813
NaCl:Ca, precipitate form., transform. after annealing, critical flow stress 78−38848
NaCl:Ca, reflection holograms recording 79−98320
NaCl:Ca, single cryst., vaporisation kinetics meas. 78−18763
NaCl:Ca, surface segregation and diffusion 77−43416
NaCl:Ca, X-irradiated, Z_1-centre form. kinetics, thermolum. investig. 77−4693
NaCl:Ca, Z_1 centre thermoluminescence study 80−16109
NaCl:Ca crystals, optimum temp. for holographic recording *(Russian)* 80−1163
NaCl:Ca crystals, surface recrystn., moisture effect 80−84950
NaCl:Ca^{2+}, cryst., hydrolysed, IR absorpt. bands 77−32404
NaCl:Ca^{2+}, dipole concs. determ. considering aggregation, expt. and theoretical comparison 80−59512
NaCl:Ca^{2+}, highly doped, aggregation of point defects, NMR and dielec. loss meas. 79−10847
NaCl:Ca^{2+}, spin-lattice relax. meas., 160 to 360°C, vacancy contrib. 77−28477
NaCl:Ca^{2+}, X-ray induced luminescence 78−23516
NaCl:Ca^{2+},Mn^{2+}, EPR of Mn^{2+}, effect of Ca^{2+} on Mn^{2+} vacancy dipole decay 78−56371
NaCl:Ca^{2+} crystals, influence of dipoles and dipole complexes on yield point 80−39208
NaCl:$CaCl_2$, quenched, aggregation process of Ca^{2+} ion-vacancy dipole, elec. cond. and dielec. loss meas. 77−80535
NaCl:Ca(K), impurity state from heat treatment on microhardness 77−80532
NaCl:Ca(Mg), X- and gamma-irrad., thermostimulated electrons and luminesc. 79−91505
NaCl:Cd, EPR of anisotropic Cd_F^+ centres, similarity to Z-centres 77−77101
NaCl:Cd^{2+}, dielectric loss following plastic deform. 80−84690
NaCl:Cd^{2+}, superstructure obs. by ionic thermal current meas. 78−39499
NaCl:Co^{2+}, dynamic braking of dislocations *(Russian)* 78−6068
NaCl:Cu, UV absorpt., emission, excitation spectra, Cu^- centres 77−81127
NaCl:Cu, X-irrad., thermoluminesc., F-centres 79−33849
NaCl:Cu^+, electrolytically coloured, electron trapping, optical absorpt. 80−100672
NaCl:Cu^+, far IR props. of lattice resonant modes, hydrostatic press. effects 77−28574
NaCl:Cu^+, luminesc. and lifetimes, press. depend. 79−33809
NaCl:Cu^+, X-irrad., anisotropic Cu centre anal. 79−78714
NaCl:Cu^+, X-irrad., thermoluminesc. centre, EPR anal. 79−43045
NaCl:Cu^+, X-irrad. at room temp., ESR of Cu^{2+} centres 78−52343
NaCl:Cu^+, X-ray irrad., role of Cu^+ in thermoluminesc. 78−56526
NaCl:Cu^{++}, EPR spectra anal. spin-Hamiltonian parameters determ. *(Spanish)* 77−69673
NaCl:Eu, secondary Eu phase dissolution, EPR and optical absorpt. study 80−96655
NaCl:Eu^{2+}, optical absorpt. meas. for Eu^{2+} conc. determ. 79−51137
NaCl:Eu^{2+}, oriented growth and cryst. struct. of precipitated phases 80−24303
NaCl:Eu^{2+}, reorient. of Eu^{2+}-vacancy complexes, ESR method using elec. field effect 79−99768
NaCl:Eu^{2+}, single cryst. optical absorpt. spectra 80−45117
NaCl:Eu^{2+}, spin Hamiltonian cryst. field consts. calcs. 79−38035
NaCl:Eu^{2+}, spin Hamiltonian, cryst. field consts. calcs. 79−51537
NaCl:Eu^{2+}(Mn^{2+}), ESR and elec. field effects 77−28441
NaCl:F^-(Br^-)(I^-), anion impurities substitution, energies of soln., association and migration 78−83831
NaCl:F^-(Li^+)(Ag^+), lattice relaxation around tetragonal and rhombic defects 79−95110
NaCl:Fe(Mn), nucleation of Au, surface imperfection effects 77−15699
NaCl:Ga, optically detected EPR in relaxed excited states of Ga^+ 78−72437
NaCl:Ga^+, polarisation of Ga^+ centre A_T emission, temp. depend. 80−80842
NaCl:Ga(In), ESR of impurity centres, impurity optical absorpt. bands 80−29618
NaCl:Ga(Tl,Pb), EPR spectra 79−28613
NaCl:H (Cl) interstitials repulsive parameters from electronic charge density overlap, diffusion 77−59006
NaCl:H^-, defect pairs of F-centres and U-centres, Raman meas. 79−7599
NaCl:H^-, U-centre absorpt. band shape, piezodichroism dispersion curve and electron-phonon interaction 77−24873
NaCl:Hg^+, X-irradiated, ESR meas. 77−1588
NaCl:I, UV laser generation by optical pumping 78−82973
NaCl:K_3IrCl_6 electron irrad., ligand field anal., EPR obs. 80−29612
NaCl:Li, U-centres, HFS consts., g-factor, EPR spectra 80−39869
NaCl:LiCl, melt, semiperiodic closed growth lamellae on crystal-melt interface 78−67668
NaCl:Mg^{2+}, dopant aggregation and precipitation 80−107306
NaCl:Mg^{2+}(Ca^{2+})(Sr^{2+})(Ba^{2+}), defect struct., Mott-Littleton technique study 80−59487
NaCl:Mg^{2+}(Mn^{2+})(Ni^{2+})(Cd^{2+})(Pb^{2+}), Z_4-like centre, absorpt. spectra obs. 78−76498
NaCl:$MgCl_2$ (0.1 mol.%), thermoluminesc. glow curves, temp. distrib. and trapping centres 78−48241
NaCl:Mn, impurity-vacancy dipole aggregation, role of dimers and trimers, reanal. of dielec. and cond. data 79−1458
NaCl:Mn^{++}, Mg^{++}, doubly doped, ionic thermocurrent study of linear dimer 80−79977
NaCl:Mn^{2+}, CN^-, EPR spectrum rel. to Mn^{2+}-vacancy-CN^- complex 80−54942
NaCl:Mn^{2+}, dimer detection, EPR and ITC expts. 78−59833
NaCl:Mn^{2+}, elastic wave damping, 300-1800 MHz, acousto-optical obs. 79−69198

sodium compounds continued
NaCl:Mn^{2+}, ionic thermocurrents, comparison between microscopic and phenomenological anal. 79−51302
NaCl:Mn^{2+}, radiation-induced colouring, room temp. kinetics 79−55736
NaCl:Mn^{2+}, thermolum. spectra, mechanisms 80−80873
NaCl:Mn^{2+}, X-irrad., thermoluminesc. and EPR 79−61444
NaCl:Mn^{2+}, X-ray irradiated, thermolum. and EPR 77−81161
NaCl:Mn^{2+} crysts., electrolysis, dendrite form., mechanism 77−1934
NaCl:Mn^{2+}(Zn^{2+})(Sn^{2+}), electrolytically coloured, CESR 77−16174
NaCl:$MnCl_2$, Suzuki phase precip. obs. by TEM, misfit dislocations 77−31776
NaCl:Na, diffr. efficiency and self-amplification 79−7096
NaCl:NaBr crysts., dislocation motion under work hardening, transmission electron microscopy 77−51381
NaCl:NaOH, $NaNO_3$, oxygen-colour centres, thermo-optical transform. 77−69862
NaCl:NaOH($NaNO_3$), absorpt. spectra and dielectric losses 78−19524
NaCl:Ni single crystals, VUV spectrum, ionic conductivity, X-ray diffr. 78−92097
NaCl:Ni^{2+}, kinetics of impurity precipitation 77−69090
NaCl:O, hologram recording, colloidal type centre transformation *(Russian)* 80−55147
NaCl:O, photographic recording in far-UV, colour-centre formation 79−23035
NaCl:O_2^-, excitation and absorpt. spectra at 2K, O_2^- excited state field 79−56843
NaCl:OH^-, additively coloured, form. and decay of defect clusters and elec. double layers, Au decoration obs. 79−10850
NaCl:OH^-, UV and IR absorpt. spectra, colour centres transformation 79−28791
NaCl:Pb, colouring, room temp., influence of conc. and aggregation state of Pb 78−14339
NaCl:Pb, γ-irrad., centres in thermoluminescent emission 77−85816
NaCl:Pb, luminesc. spectra obs. 78−95604
NaCl:Pb, Pb determ. by optical absorpt. in aq. soln. 78−85232
NaCl:Pb, precipitation of Pb impurity 78−48415
NaCl:Pb^{2+}, activation energy for clustering of Pb^{2+} vacancy pairs 77−72610
NaCl:Pb^{2+}, decay of luminescence emission 78−39593
NaCl:Pb^{2+}, emission spectra obs., and luminesc. centre model 77−36286
NaCl:Pb^{2+} crystals, grown from aq. soln., flotation study 80−39144
NaCl:$PbCl_2$ crysts., melt grown, Pb distrib. determ., UV spectrochem. anal. 78−40101
NaCl:Pr^{3+}(Sm^{3+}), absorption spectra at 4.2 K, anal. 80−7378
NaCl:Ru, optical absorption bands, complex form. 77−1705
NaCl:S^{2-}, enthalpy of anion vacancy migration 80−15309
NaCl:Sn^{2+}, thermally stimulated space charge decay 78−48111
NaCl:Sr, dimer and trimer aggregate formation by NMR, ionic cond. and dielectric losses 80−15094
NaCl:Sr, high temperature phenomena, Cottrell effect, thermal decomp. 79−20351
NaCl:Sr, mechanical props. as function of dopant conc., dislocations 77−69027
NaCl:Sr, positron annihilation and trapping in A-centres 80−84802
NaCl:Sr, solubility of free and assoc. Sr by elec. cond. and ionic thermocond. meas. 77−62645
NaCl:Sr deformation control by thermally activated processes 195 to 300K 79−24570
NaCl:Sr^+, ionic thermocurrent exam. 78−10833
NaCl:Tl, deformed phosphors, thermoluminesc., impurity conc. effects 77−63473
NaCl:Tl, emission spectra, press. effects 78−23509
NaCl:Tl, luminesc. yield, effect of fast electron channelling 78−84646
NaCl:Tl^+, γ-irrad., aquoluminesc. obs. 80−2856
NaCl:V^{2+}, EPR and optical absorpt. spectrum temp. depend., crystal field theory 77−16163
NaCl:V^{2+}, EPR spectra above 300K 80−34765
NaCl:V^{2+}, elec. field effect on Z-like centres spectrum 80−2802
NaCl:V^{2+}, phonon induced zero field splitting 78−39073
NaCl:V^{2+}, spin-lattice relaxation 78−91941
NaCl:V^{2+}, X-irrad. and unirrad., EPR of isolated V^{2+} ions 79−15347
NaCl:V^{2+}(Ca^{2+})(Mn^{2+}), X-irrad. effects on divalent metal aggregates, EPR and ionic cond. meas. 79−82263
NaCl:X (X=Ca, Sr, Ba, Mg, K, Li, Tl, Ag), impurity conc. effect on mech. and elec. props. 78−47469
NaCl:Zn^+, interpretation of optical absorption spectra 79−51993
NaCl:Zn^+, X-irrad., EPR and optical absorpt. 78−43642
NaCl-AgCl molten solns., activities and surface tension 80−10748
NaCl-Al_2O_3, threshold stress in particle inhibited diffusive creep 79−38922
NaCl-$AlCl_3$, molten mixture, vap. pres. meas. 78−87779
NaCl-$AlCl_3$, phase diagram determ. by DTA and X-ray anal. *(Japanese)* 78−92250
NaCl-$AlCl_3$ melt mixtures, viscosity meas. 79−82368
NaCl-$AlCl_3$-$CrCl_3$, molten, electrochemical exam. of Cr 78−56939
NaCl-$BaCl_2$ 1%, oriented growth of $BaCl_2$ phases, morphology 77−80627
NaCl-Ca, single crysts., load-microhardness curves, heat treatment, impurity effects obs. 78−30694
NaCl-$CaCl_2$, dislocation struct., etch pit obs. 78−43020
NaCl-$CaCl_2$, electrolyte mixture, evaporation from multi-component droplets, in stream of air 77−56255
NaCl-CdO heterojunction form. in cathode-plasma dyeing, temp. depend. *(Russian)* 78−67710
NaCl-CsCl-$CrCl_3$ system, melting diagram determ. by DTA, phase comp. *(Russian)* 77−63645
NaCl-CsCl-$CrCl_3$ system, phase struct. anal. by X-ray method *(Russian)* 78−3112
NaCl-CsCl-$MnCl_2$, molten salt system, molar volume and elec. cond. meas. 80−34217
NaCl-CsCl-$MnCl_2$, molten salt system, molar volume and elec. cond. meas. 80−34218
NaCl-Cu^-, absorpt. and emission spectra, $3d^{10}4s^2 \rightarrow 3d^9 4s^2 4p$ bands 79−24343
NaCl-gas reactions, atmospheric, in situ TEM studies 80−104544
NaCl-graphite interface, elec. cond. 78−52060
NaCl-H_2O, quick-frozen aq. soln., XPS 79−38713
NaCl-induced accelerated oxidation of Ti alloys 77−21322
NaCl-KCl, aq. solns., isopiestic studies, 383 to 474K 80−21320
NaCl-KCl, interdiffusion and demixing, electron microprobe anal. *(French)* 80−54444
sodium compounds continued
NaCl-KCl, molten, alkaline earth oxides solubility products, potentiometric determ. 80−76488
NaCl-KCl electrolyte mixtures, in aq. soln., viscosity, individual electrolyte effects *(German)* 78−22881
NaCl-kCl melt, reaction with LiO_2-$2SiO_2$ X-ray, IR exam. 80−55706
NaCl-KCl mixed aq. solns., viscosity meas. 79−82370
NaCl-KCl mixed crystal, growth, X-ray exam. and microstruct. 78−44001
NaCl-KCl mixture, electrical, electromag., and acoustic props. *(Russian)* 78−30759
NaCl-KCl novel encapsulant for LEC growth of GaSb single crystals 80−93475
NaCl-KCl system, interdiffusion, miscibility, Kirkendall effect 80−107568
NaCl-KCl-$CaCl_2$, solid soln., X-ray examination of final decomp. stage *(Russian)* 77−63681
NaCl-KCl-CuCl system diagram investig. *(Russian)* 79−96015
NaCl-KCl-H_2O, ionic diffusion theory, use of activity coeffs. in transition-state models 78−57224
NaCl-KCl-$NiCl_2$ system diagram investig. *(Russian)* 79−96014
NaCl-KCl(CsCl) melts, X-ray diffr. struct. determ. 79−41925
NaCl-KCl($MgCl_2$)-H_2O mixed electrolyte solns., elec. transport 80−3355
NaCl-K(Al) adhesion 78−18914
NaCl-LiCl mixed crystals, Au decoration study of solid-melt interface, phase separation 80−15026
NaCl-metal system, sliding and rolling electrification 78−14796
NaCl-MgO mixture, high pressure uniaxial stress component effect on eqns. of state, opposed anvil X-ray determ. 80−49301
NaCl-NH_3-CO_2-H_2O system, $NaHCO_3$ crystn. 80−100771
NaCl-NaBr, elastic wave damping, 300 to 1500 MHz, impurity effects 80−92602
NaCl-NaBr, mixed crysts., microhardness, theory 80−75298
NaCl-NaBr, solid soln., negative muon capture ratios 80−55007
NaCl-NaBr mixed crysts., ionic cond., 42-450°C, cation vacancy migration 78−59970
NaCl-NaBr-$CaCl_2$, dislocation struct., etch pit obs. 78−43020
NaCl-NaBr-TeO_2, condition diagram, thermographic obs. *(Russian)* 80−55377
NaCl-NaF:Pb^{2+}, point defects, ionic thermal current and optical meas. 80−6403
NaCl-NaF-Na_3VF_6, phase diagram 77−21123
NaCl-$NaNO_3$-H_2O, apparent and partial molal volumes in mixed salt solns. 77−9114
NaCl-O^{2-} X-ray irrad., defect generation during radiolysis 80−7831
NaCl-OH^-, electron irrad., F_2^+ centre stabilisation and tuneable laser operation 80−54231
NaCl-oil boundary, formation of discharge in system of electrodes *(Russian)* 79−8089
NaCl-RbCl(KCl) fused binary mixtures, electrocapillary phenomena on liq. Bi 77−40553
NaCl-water-tetrahydrofuran system, heat. of soln. meas. using Calvet microcalorimeter *(French)* 77−44504
NaCl-$ZnCl_2$, molten, US velocity, thermodynamic quantities and struct. *(Japanese)* 80−88270
NaCl-$ZnCl_2$, molten, US absorption coeffs. and bulk viscosity coeffs. *(Japanese)* 80−88271
NaCl+Ar, dissoc.-ionis. process rates in shock tube 78−35674
NaCl+cosmic ray muons, photonuclear cross section, nuclear muon losses 77−64581
NaCl+HCl/membrane/HCl isotonic osmotic system, inversion 79−52775
NaCl+K, prior statistical distribs., collinear reactions 78−35670
NaCl+K, three dimens. collision, exponentiating trajectories and statistical behaviour 80−5595
NaCl+KF→NaF+KCl, solid state reaction mechanism 79−61857
NaCl+muonium in aq. soln., rate const. 77−38752
NaCl+Pb, Pb aggregation effect on yield stress, incoherent precipitates, solubility determ. method 80−50645
$NaCl_4$ on Pt and Ir surfaces, adsorption kinetics 80−84393
$(NaCl)_n$ (n=1-7) equilib. configs., total energy calcs., far IR spectra 78−29872
Na_2Cl^+ ion form., by NaCl beam impact on hot W(Re) surface 79−56907
Na_2Cl^+, mass spectra, struct., stability, expt. and theory 77−554
NaCl(:Ca) cryst., radiation colouring, amplitude-phase hologram appls., diffraction efficiency 77−68191
NaCl(:Ca), irrad. at room temp., stored energy rel. to thermolum. 80−10574
NaCl(:$CdCl_2$), sintering in air, densification kinetics and mechanism 77−4750
NaCl(:Mn^{2+}), influence of elec. field on flow stress 79−51193
NaCl(Br) aqueous solutions, tetrahedral hydration of ions, Raman obs. 78−55804
NaCl(Br):Eu, Eu^{2+} ESR meas. 78−80209
$NaCl_{1-x}Br_x$, mixed cryst., vibr. and optical props. 80−29133
NaCl(F), permittivity and polarisation behind shock wave front 77−52013
NaCl(I), acoustic radiation generated by ionising particles 78−87726
$NaClO_2$ based reagent from NO_x removal, from highly polluted air *(Japanese)* 79−52976
$NaClO_3$, ^{17}O NQR, spin echo double reson. method, electronegativity 80−54970
$NaClO_3$, ^{35}Cl NQR meas. 77−66435
$NaClO_3$, ^{35}Cl NQR appl. in thermometry below 77K 80−66067
$NaClO_3$, acoustic activity, inelastic neutron scatt. obs. *(French)* 80−103431
$NaClO_3$, cryst., mechanoluminesc. spectra 80−97355
$NaClO_3$, cryst. chirality and optical rotation sense 78−10026
$NaClO_3$, cryst. growth from soln., selective etching technique for observation of dislocations 79−19251
$NaClO_3$, cryst. growth from soln., convection phenomena 79−74074
$NaClO_3$, crystal gyrotropy, meas. in IR region 80−88957
$NaClO_3$, crystallisation, composition of heat carrier heating aqueous solution system 77−12513
$NaClO_3$, dislocations rel. to growth mechanism from aq. soln., X-ray topography 80−59464
$NaClO_3$, dispersion of Faraday effect 80−2731
$NaClO_3$, electrogyration and piezogyration meas. 79−28716

sodium compounds continued
$NaClO_3$, growth and dissolution kinetics, diffusion and convection regimes 78−63684
$NaClO_3$, growth from solution, effect of i.r. radiation on growth rate 77−1794
$NaClO_3$, I^--irrad. defects, ^{35}Cl NQR, 77 and 300K 78−91981
$NaClO_3$, γ-irradiated, metastable O_2 reson. Raman scatt.,, excitation profile, polarisation meas. and decay kinetics 77−14437
$NaClO_3$, γ-irradiated, ESR of trapped O_3^- 79−29381
$NaClO_3$, IR and Raman spectra, vibrs., dipolar coupling effect 78−43852
$NaClO_3$, lattice energy, comparative computations using explicit minimisation procedures 79−32944
$NaClO_3$, lattice vibrations and sp. ht., neutron spectroscopic study 80−107388
$NaClO_3$, magnetoelectric susceptibilities, phenomenological rules for computation 80−55068
$NaClO_3$, melting pressure curves up to 5 kbar 77−15547
$NaClO_3$, metastable-stable phase transition mechanism *(French)* 80−15031
$NaClO_3$, mol. torsional oscills., cooperative study by NQR 80−25244
$NaClO_3$, molten, electrolytic cond. at pressures up to 6 kbar 77−15609
$NaClO_3$, optically active, crystal atomic struct. remeas. 78−10009
$NaClO_3$, radiation damage, XPS obs. 80−29844
$NaClO_3$, Raman spectroscopy exam. of high-pressure phase transform. 78−10186
$NaClO_3$, reson. Raman scatt. from metastable O_2 produced by γ-irrad. 78−60432
$NaClO_3$, shift of Na NQR freq. by nonreson. RF photon dressing 78−43674
$NaClO_3$ single crystals, change of elastic constants by gamma radiation 78−63800
$NaClO_3$ temperature variation in bulk moduli in solids 79−73237
$NaClO_3$, trapped O species in irradiated samples, low-temp. X-ray photoelectron spectroscopy 78−27799
$NaClO_3$, X-irrad., thermal stability of radiation damage products 79−34324
$NaClO_3$, X-ray diffr. determ. of ClO_3^- ion dimensions and libration correction 77−80462
$NaClO_3$, Zeeman NQR powder spectra 80−20502
$NaClO_3$:BrO_3^- (IO_3^-), Raman spectra, fundamental vibr. modes of halate ions 78−78711
$NaClO_3$:O_3^-, form. by γ-irrad., reson. Raman scatt., temp. depend. 78−92062
$NaClO_3$-$CsClO_3$, NQR, mag. susceptibility meas. 78−35059
$NaClO_3$-$NaBrO_3$, Raman spectra, mode coupling and ^{79}Br-^{81}Br isotope effects 79−19873
$NaClO_3$-$NaBrO_3$ mixed crystals, internal optic modes, Raman and IR spectra meas. 79−95746
$NaClO_4$, anhydrous, Raman, IR and FIR spectra, 90 to 600K *(German)* 79−78687
$NaClO_4$, aq. glass, formation of trapped H-atoms and electrons on X-irrad. 80−35559
$NaClO_4$ aqueous soln., IR absorpt. spectra, band profile temp. depend. 77−30869
$NaClO_4$, Brewster type surface mode dispersion, IR refl. meas. 80−11415
$NaClO_4$, diamag. ion solvation in methanol soln., NMR relax. obs. 78−56389
$NaClO_4$ electrolyte influence on lasing props. of rhodamine G solutions 80−91788
$NaClO_4$, frozen soln., acidic, X-irrad., H atom scavenger effects 79−39163
$NaClO_4$, frozen soln., EPR of trapped H-atoms produced by UV and X-irrad. 80−3369
$NaClO_4$ glass, radiation induced trapped electrons, photobleaching, H form. 77−44494
$NaClO_4$, isoelectronic series, negative muon capture, rel. probability meas. 77−50550
$NaClO_4$, Raman spectra temp. depend. near 581K phase transition 78−56477
$NaClO_4$, single ion props. by lattice energy minimisation 78−83769
$NaClO_4$:Fe^{2+}, frozen soln., photo- and radiation-produced H-atoms obs. 79−39162
$NaClO_4$/$Mn(ClO_4)_2$ in aq. soln., interaction between Mn^{2+} and ClO_4^-, NMR studies 80−71212
$NaClO_4$-D_2O, glass, 4.2K, trapped electron photocond. and optical spectra following radiolysis 79−29378
$NaClO_4$-D_2O, glassy matrix, absorpt. spectra after X-irrad., solvated electrons 79−65903
$NaClO_4.D_2O$, H bonding, D NMR 77−34664
$NaClO_4.H_2O$, ^1H NMR second moment, H_2O dynamic disorder 80−25221
$NaClO_4.H_2O$, cryst. struct. deform. refinement 80−107123
NaCl. deform. in steel band, X-ray investig. *(Russian)* 78−68727
6NaCl.$CdCl_2$, 60 wt.% powders, Suzuki phases prep. and stability 80−35123
$NaCo(CO)_4$, soln., ion sites, cryptand C221 doping effects 80−70102
Na_2CoCl_4, cryst., chrysoberyl struct., neutron diffr. 77−19919
Na_2CoGeO_4, cryst. struct. determ. 79−90626
Na_2CoGeO_4, hydrothermal growth from CoO-GeO_2-NaOH-H_2O 77−48329
Na_2CoGeO_4 hydrothermal single crystals, X-ray topographic study of growth defects rel. to growth conds. 79−19166
Na_2CoGeO_4, single cryst. growth and study of their piezoelec. and elastic props. 79−4906
$Na_2Co_2Ti_6O_{14}F_2$, characterisation and mag. props., 90-800K, $Na_xTi_4O_8$ bronze isotypes *(French)* 80−39735
$Na_xCr(Mn)(Co)O_2$, layer struct., elec. cond. behaviour *(French)* 78−26542
$NaCrO_2$, electric field gradient tensor, dipolar contribs. 77−51707
$NaCrO_2$, thermodynamic props. 77−69099
$NaCrO_2$, two-dimens. mag. order, neutron powder diffr. obs. 80−44805
$NaCrO_2$, two-dimens. mag. props. rel. to cryst. struct. 80−75776
$NaCrO_2$, two-dimensional antiferromag., mag. props. *(French)* 78−23251
Na_2CrO_4-MoO_3-Cr_2O_3 system, phase diag. 77−86007
$Na_3Cr_2(PO_4)_3$, crystallographic data, ionic conductivity *(French)* 80−88077
$Na_3Cr_2(PO_4)_3$, $Na_3Fe_2(PO_4)_3$, $Na_3Ti_2(PO_4)_3$ and $Na_3V_2(PO_4)_3$, synthesis and cryst. struct. *(French)* 79−32964
sodium compounds continued
$Na_3Cr_3(PO_4)_4$, crystallographic data, ionic conductivity *(French)* 80−88077
$NaCrS_2$ antiferromag. reson. meas. 77−69705
$NaCrS_2$, antiferromag. semicond., Raman and far-IR spectra 79−47454
$NaCrS_2$, intercalation cpd., NMR 77−90048
$NaCrS_2$, rhombohedral, antiferromag. reson. meas. 77−20717
$NaCrS_2(Se_2)$, EFG tensor, S and Se dipolar contribution 77−31984
$Na_2Cr_2Ti_6O_{16}$, characterisation and mag. props., 90-800K, $Na_xTi_4O_8$ bronze isotypes *(French)* 80−39735
$NaCrX_2$, X=S, Se, EPR meas., g-factors, effective mag. moments, and dipolar shifts 79−8043
$NaCs^+$, adiabatic pot. curves, ground and excited state, Hellmann-type model pots. 78−78647
$NaCu_3Ru_4O_{12}$, synthesis, cryst. struct., mag. and elec. props. *(French)* 80−107151
$Na_2Cu(Si_2O_7)_2.5H_2O$, polymorphism of infinite Si_2O_7 radicals in layered stacks 79−60301
NaD, nightglow spectral intensity changes, correl. with O_2 spectra 80−61932
NaD+K, prior statistical distribs., collinear reactions 78−35670
$NaD_2AsO_4.D_2O$, crystal struct. determ. 77−80460
$Na(D_xH_{1-x})_3(Se_3)_2$, ferroelec. dispersion 80−40069
$NaD_{3x}H_{3(1-x)}(SeO_3)_2$, ferroelec. dispersion 80−66129
$Na(D_xH_{1-x})_3(SeO_3)_2$, Raman spectra and nature of phase transitions 78−80341
$Na_{0.6}(D_2O)_2VX_2$, X=S,Se, struct., chem. reactions, and hydration/dehydration process 79−46616
$NaD_2PO_4.2D_2O$, Raman spectra, phonon freqs. 79−61370
$NaD_3(SeO_3)_2$, ^{23}Na NQR, second-order quadrupole shift, temp. depend. 78−15055
$NaD_3(SeO_3)_2$, ^{23}Na resonance line temp. depend., of first order quadrupole shift and spontaneous polarisation 79−8069
$NaD_3(SeO_3)_2$, polarised Raman spectra, lattice vibrs., ferroelec. transition 77−24851
$NaEr(SO_4)_2$, cryst. struct. by X-ray diffr. *(French)* 78−42990
$Na_2Eu_3(NH_2)_8$, cryst. struct. and cryst. chemistry *(German)* 79−51080
$Na_3Eu(PO_4)_2$, synthesis and IR spectra 80−16019
$NaEu(PO_3)_7.12H_2O$ and $Na_3Eu(PO_3)_6.6H_2O$, form. in $EuCl_3$-$NaPO_3$-H_2O system at 0°C 80−35515
NaF, ^4He scattering, selective adsorption effects on diffr. beam intensity 77−12480
NaF, $^4He^+$ ion scatt. spectrometry below 5 keV 80−108313
NaF (001), H and D beam scatt., specular bound state reson. struct. 79−52069
NaF, ab-initio calc. of cohesion energy, compressibility and density 78−71782
NaF, anharmonicity of lattice vibrations, neutron scatt. study, rel. to melting 77−84862
NaF, antireflection coating, 100 ns pulsed laser damage at 2.7 and 3.8 μm 80−33057
NaF antireflection coating, multithreshold damage meas. at HF and DF laser wavelengths 80−33058
NaF, aq. soln., in contact with single cryst. (100) Au electrode, differential-pot. *(French)* 79−47932
NaF, band struct. and charge densities, intersecting spheres model 80−49591
NaF, binding energy of F_{c+}', M_{c+}' and R_{c+}' centres, positron trapping 79−69460
NaF, CW lasing of F_2^+-centres, 0.9-2 μm 78−29957
NaF, channelling of MeV H^+ and He^+, zero dose meas. 78−18689
NaF coating defects and impurities affecting damage threshold and absorptance 79−14065
NaF, coherent optical computing elements using photodichroism 77−71962
NaF, Compton profile, 59.54 keV γ-rays 78−64426
NaF, Compton profiles, anisotropies 80−20730
NaF, computer generated polarisation hologram 77−61923
NaF, cryst., ultrasonic attenuation along (111) and (110) directions 78−63813
NaF crystal M-centre storage element, photosensitive characteristics 79−14067
NaF, DNMR cross relaxation modes 78−10803
NaF, deformed, influence of surface on density of edge components of dislocations 77−31670
NaF, delocalised positronium existence at room temp. 78−76546
NaF, dislocation microplasticity, internal friction expts. 78−47388
NaF, dislocation velocity determ. by nuclear spin-lattice relax. meas. 77−35566
NaF, ESR study of interstitial atomic H centres 79−56609
NaF, elastic moduli, quadratic fit against temp. 78−14397
NaF, elastic X-ray scatt., effect of dynamic deform. calc. 78−26378
NaF, electron momentum distrib. and Compton profiles 79−13631
NaF, enthalpy calc. for solid and liq. phases 77−43349
NaF, excess electron colour centre obs. 77−16343
NaF, F_2^- mag. reson. absorpt. spectrum 77−73079
NaF, F_2^+-like colour centre, room temp. stable, CW laser, 0.99-1.22 μm tunable 80−69399
NaF, F_3^+ centre zero-phonon line, photochem. and population hole burning 79−42997
NaF, F_3^+-centre decay by optical free induction 78−68555
NaF, F^--centres, thermal and photolytic decay processes 78−95053
NaF, F-centre, wave functions and spin densities, pseudopot. calc. 79−4533
NaF, far IR complex refr. indices, dispersive Fourier transform 78−80322
NaF, far IR spectra, matrix isolated, monomers, dimers, trimers 78−66545
NaF, fast Li^+ ion stopping, chem. bonding effects 77−27929
NaF film, electron emission under metastable He and Ne atom impact 80−20747
NaF film on CaF_2, interface and bulk absorption meas. 80−35001
NaF film on ZnSe plate, absorption coeff. ATR spectroscopy 80−35000
NaF filter material interaction mechanism with Al melt *(Russian)* 80−108743
NaF, fluorine K absorpt. spectra using APS technique 79−99986
NaF, gamma irrad., colour centre stimulated emission, threshold pump power, tuning range 79−73971
NaF, γ-irradiated cryst., relaxational damping of elastic waves and activiation energy of motion of defects 79−14891

sodium compounds continued
NaF, H-surface bound states, surface averaged pot. energy function 77−11789
NaF, He and H bean scatt., semiempirical determ. of atom-surface interaction 78−72676
NaF, He atom scatt., Debye Waller effects 79−8218
NaF, He atomic beam refl., selective adsorpt. transitions, band-struct. effects 77−11781
NaF, He atomic beam scatt. by surface and bulk phonons 77−73209
NaF, heat capacity, Gruneisen parameters, 2 to 20K 80−29180
NaF, high-temp. behaviour of elastic moduli, comparison with MgO and CaO 77−11621
NaF, high-temp. vapour, appl. of photographic plate for electron diffr. studies 77−39516
NaF, IR window coating, prep. and optical props. 77−50736
NaF IR window refractive index var. with temp., −180° to +200°C obs. 79−14052
NaF, interatomic Auger transitions, XPS exam. 77−8692
NaF, irradiated at room temp., thermolum. and F-centre thermal stability 78−84669
NaF, irradiated at room temp., stored energy 80−79839
NaF, isothermal compressibility calc., 0-1000K 77−7784
NaF, isothermal compression at 673K, up to 10 GPa, X-ray diffr. study 80−59565
NaF laser coating, UV damage obs. 80−33056
NaF, laser window coating material, damage at 10.6 μm 77−61991
NaF, lattice dynamics and statics, three-body-force shell model 80−49323
NaF, lattice thermal cond., 2-10K 79−90834
NaF, lattice thermal conductivity, point defects effects at low temp. 79−90836
NaF, load relaxation studies 79−79016
NaF, low temperature, role of point defect scatt. in lattice thermal cond. 77−76631
NaF, luminesc. induced by ion impact, −160 to 200°C 77−8654
NaF, M-centre vibronic absorpt. spectra, elec. field, method of moments 78−27186
NaF, M-centres, dichroim absorpt., appl. to optical waveguide polariser 79−995
NaF, M-centres, quadratic Stark effect, differential electroabsorption spectra 77−66526
NaF, measurement of thermal expansivity at low temp. using Si cell 80−37027
NaF, muon Coulomb capture ratio 78−62959
NaF oligomers, struct., stability SCF and CEPA-PNO calcs. 78−78640
NaF, one electron props., SCF-Xalpha scattered wave method 80−83279
NaF, phonon conductivity correction due to three phonon normal processes in presence of dislocations 80−15318
NaF, phonon linewidths at high temps. 77−62594
NaF, photodichroic, as optical processing elements 78−83056
NaF, photodichroic, direct-writing M-centre, Hurter-Driffield curves 77−4662
NaF, photodichroic crystals use for coherent opt. data processing 77−68248
NaF photodichroic crystals, hologram synthesis in in-line scheme 77−88670
NaF, piezo-birefringence, piezo-optical properties, temperature dependence 78−92050
NaF, piezooptical coeffs., 200-600 mμ 77−69800
NaF, positronium-like states, ang. correlation of photons from positron annihilation 77−36310
NaF powder, porous, of skeleton struct., grain size effect on strength *(Russian)* 77−24991
NaF, pulsed-laser-induced damage, role of avalanche multiplication and multiphoton absorpt. 80−48316
NaF, quadrupole coupling, vibr. and rot. effects, Morse oscill. calcs. 77−6805
NaF, quasimolecular struct. characts. of $NaL_{II,III}$ absorpt. edge 80−93436
NaF, radiation damaged, proton and $^4He^+$ channelling, F-centre production, optical absorpt. meas. 78−79656
NaF, relaxation rate calculation 78−15060
NaF, reversible optical storage element using M-centre polarisation 78−94416
NaF, selective adsorption of ^3He and ^4He, atomic beam scatt. meas., binding energies 78−63935
NaF, self-trapped exciton, ODMR spectra 79−28286
NaF, single crystal, TSEE by electron bombardment 78−6836
NaF single-layer film 2.8 μm, 3.8 μm absorpt. meas. 78−90463
NaF, sintering, relation between densification and grain growth 77−12585
NaF, Stark effect, M-centre absorpt. bands 78−84614
NaF, static SIMS, mol. rearrangement, cluster formation 78−64440
NaF surface absorption regions on KCl crystals, photoacoustic detect. 79−87466
NaF, surface rumpling at finite temps, Verwey model 79−51402
NaF, thermal cond. meas. at high press. 80−75392
NaF, thermal expansivity determ. at high press. 78−79787
NaF, thin insulating film, lattice parameter meas. by electron microscope 77−65940
NaF, two-photon absorpt. cross sections of N_1 and F_3^+ centres 79−73991
NaF, UPS, expt. methodology aspects 77−90245
NaF, US vel., Poisson's ratio and shear modulus meas., 9 GPa 77−4140
NaF UV visible absorpt. by laser calorimetry, wavelength modulation spectroscopy 78−66876
NaF, vibrational contribution to surface thermodynamic functions 77−47659
NaF, with colour centres, laser stimulated luminesc. 78−6749
NaF, X-irrad., colour centres and thermolum. 80−84790
NaF, X-ray diffr., electron distrib. determ. 77−84706
NaF, X-ray intensity, extinction wavelength depend. 79−27956
NaF: Mn^{2+}, VUV absorpt. spectrum and EPR 80−55142
NaF:Ca, migration enthalpy and entropy, TSC obs. 80−54716
NaF:$Ca^{2+}(K^+)(Li^+)$, substitutional impurities, defect props. of (001) and (011) surfaces 77−47443
NaF:Fe, dispersed ions, absorber Mossbauer spectra 78−15077
NaF:Fe, Mossbauer study of Fe precipitates 79−91327
NaF:Fe^{2+}, ENDOR associated with Na^+ vacancy 79−61264
NaF:Hg^{2+}, electrolytic colouration 78−75665
NaF:K^+, γ-irradiated, $H_A(K)$ centres, EPR obs. 77−69689
sodium compounds continued
NaF:Li, combined suppressive and extinction writing, using $M(M_A)$ centres 77−7164
NaF:Li, pulsed double nucl.-nucl. reson. *(Russian)* 78−10804
NaF:LiF, γ-irrad., colour centre form., reflectance and thermolum. meas. 79−55739
NaF:LiF, M/M_A-centre photodichroic props., for holographic spatial filter 77−7011
NaF:Mn_3 role of Mn^{2+} in thermolum. 80−97353
NaF:Mn^{2+}, two-step photoionisation, laser-active F_2^+ centre form. 79−963
NaF:OH, mag. field-independent capacitance thermometers 78−4623
NaF:OH^-, electron irrad., F_2^+ centre stabilisation 80−54231
NaF:U, luminesc. spectra, Vibr. struct. 80−80840
NaF:U, single crystals, luminescence and electrical conductivity 78−72588
NaF:U, X- and γ-irrad., EPR of U^{5+} centre, charge compensation mechanism 77−90030
NaF:U^{5+}, U isotope abundance determ. by EPR hyperfine struct. 79−91296
NaF:U^{6+} luminesc. spectrum obtained using chronospectroscopic method and phase spectra 79−54199
NaF/GeSe, IR multilayer partial mirrors effective from 1.3 to 16 μm 80−9978
NaF-^4He liquid interface, phonon propagation 78−14526
NaF-$3Na_2O.2SiO_2$, freezing point depression meas., effect of silica compound additions 77−28797
NaF-Al adhesion 78−18914
NaF-Al_2O_3, β-Al_2O_3 form. *(Japanese)* 78−6912
NaF-AlF_3, ion-molecule equilibria studied by mass spectrometric method, heats of dissoc. and form. calc. 80−104479
NaF-AlF_3 binary melt, density and elec. cond. *(Japanese)* 78−18814
NaF-AlF_3 melt mixture, viscosity meas. 79−82369
NaF-AlF_3 system, thermodynamics, solid soln. in cryolite 79−52183
NaF-BeF_2, and CaO-SiO_2 systems, complex ionic liquids, corresponding-state principle *(Japanese)* 77−56245
NaF-BeF_2, molten corresponding state principle with CaO-SiO_2 and appl. 79−11589
NaF-BeF_2 glass, anion conductivity, transport number radiometric meas. 79−86923
NaF-H_2O, quick-frozen aq. soln., XPS 79−38713
NaF-He interface, absence of anomalous Kapitza resistance 78−63923
NaF-liq. He interface, phonon transmission in both directions 79−28164
NaF-liquid ^4He interface, phonon ang. distrib. after refl. 79−55979
NaF-liquid He interface, freq. of emitted phonons 79−55978
NaF-LnF_3 (Ln=Y, La, Yb) binary liquid mixtures, thermochemistry 80−45538
NaF-MgF_2-MgO-SiO_2, phase formation 78−27460
NaF-ScF_3 system, ionic equilib., mass spectra 78−7222
NaF-SrF_2-CrF_3, glass transition, crystn. and melting temps., optical transmission *(French)* 80−64910
NaF-UF_4, ion-molecule equilibria, heat of form. and dissoc. and electron affinities determ. 80−104480
NaF-YF_3 system, fusibility diagram, quasibinary section of NaF-YF_3-YOF system characts. 80−55371
NaF-ZnF_2-CrF_3, solid-liquid equilib. diagram *(French)* 77−1216
NaF+Eu^{2+}, cryst., hyperfine splitting, EPR 78−2733
NaF+HF, V-V energy transfer collisions, 'triple beam' expt. 79−98197
NaF_2, picosecond laser-induced breakdown at 5321 and 3547 Å, freq. depend. 77−63495
Na_2F^+, mass spectra, struct., stability, expt. and theory 77−554
NaF(Cl), (100) surface, potential energy of isolated Au atom above surface 77−89650
NaF(Cl) substrate, epitaxial crystn. of isotactic polypropylene 78−26787
$NaF(NaF^-)$, electron affinity and dipole moment, ab initio calc. 78−41938
$Na_2(Fe,Mg)_5Si_8O_{22}(OH)_2$, riebeckite, low temp. Mossbauer obs. of oriented single cryst. behaviour and mag. props. 80−84674
$Na_2(Fe,Mn)_5(PO_4)_4$, arrojadite, X-ray cryst. struct. determ. 80−39058
$Na_2Fe(CN)_5NO.2H_2O$, new isomeric mol. state, Mossbauer data 77−23513
$Na_2Fe(CN)_5NO.2H_2O$, absolute Mossbauer fraction of ^{57}Fe nuclei 80−80648
$Na_2(Fe(CN)_5.NO).2H_2O$, powder, Mossbauer absorption in mag. field 78−68418
$NaFeF_2$, Mossbauer and low-temp. dilatometry study *(French)* 80−80662
$NaFeF_4$, amorphous, mag. props. and Mossbauer spectra, speromagnetism and mictomagnetism 80−75778
$NaFeF_4$, amorphous, Mossbauer study 80−39970
$NaFeF_4$, two-dimens. antiferromagnetism 77−66444
$Na_3Fe_2Li_3F_{12}$, fluoride garnets, high press. form 77−76554
$NaFe(MoO_4)_2$, domain struct., phase transition, and dielec. props. 79−56748
α-$NaFeO_2$, EFG tensor, nucl. quadrupole coupling const., polarisability 77−72844
$NaFeO_2$, solubility in CaO, meas. *(French)* 78−31392
α-$NaFe_2O_3$, Na-Ca substitution *(French)* 79−43576
β-$NaFe_2O_3$, struct. of single cryst. *(French)* 78−6033
α-$NaFe_2O_3$:$Mg^{2+}(Co^{2+})(Zn^{2+})$, substitution of Fe^{2+} *(French)* 78−95034
$Na_2Fe_3(PO_4)_3$, synthetic alluaudite, cryst. struct. 78−83802
$Na_3Fe_2(PO_4)_3$, crystallographic data, ionic conductivity *(French)* 80−88077
α-$Na_3Fe_2(PO_4)_3$ orthophosphate, cryst. and vitreous, Mossbauer spectroscopy and mag. susceptibility *(French)* 80−80657
$Na_3Fe_2(PO_4)_3$, polymorphism and ionic conduction *(French)* 78−67678
$NaFeS_2$, cryst. struct. by X-ray diffr., isolated from colloid 79−43635
$NaFeS_2$, mag. hyperfine fields and covalency, Mossbauer effect meas. 77−90077
$NaFeTiO_4$, form. in Na_2O-M_2O_3-TiO_2 ternary systems X-ray anal. 79−51067
$Na_{0.56}Fe_{0.28}Ti_{1.72}O_4$, non stoichiometric, X-ray cryst. diffr. determ., heavy atom method 79−4293
$Na_2FeTi_6O_{16}$, characterisation and mag. props., 90-800K, $Na_xTi_4O_8$ bronze isotypes *(French)* 80−39735
$Na_2Fe_2Ti_6O_{16}$ bronze, synthesis in $NaBO_2$, growth conditions *(French)* 78−43998
$Na_2Fe_2Ti_6O_6$, freudenbergite, cryst. struct. determ. 78−26519
$Na_{0.70}Ga_{4.72}Ti_{0.29}O_8$, one-dimens. Na^+ ion cond., cryst. struct. and cond. meas. 80−107521

sodium compounds continued
$NaGdO_2:Bi^{3+}$, luminesc., vibr. struct. 79−33790
$NaGdO_2:Tb^{3+}$, obs. of efficient luminesc., UV excitation 78−43922
$NaGdSiO_4$, single cryst. data and ionic cond. 80−84158
$Na_5GdSi_4O_{12}$, ionic conductivity and struct. 78−18826
$Na_8(Ge_6Al_6O_{24}).CO_3.nH_2O$, linear pyroelectric, temp. depend. of polarisation 79−99821
Na_2GeF_6, A=Si, Ge, Sn, IR absorpt. spectra, integrated intensity 79−73944
Na_2GeF_6, IR absorpt. spectra, integrated intensity, 100-300K 79−73945
Na_2GeO_3, cryst. struct. 78−51489
$Na_2Ge_2O_5$, crystn., from Na_2O-GeO_2 glasses, lattice constants 79−77527
$Na_4Ge_9O_{20}$, $Na_2GeO_3.H_2O$, hydrothermal growth from CoO-GeO_2-NaOH-H_2O 77−48329
NaH, $A^1\Sigma^+$ states radiative lifetime in HF discharge 77−6841
NaH, $A^1\Sigma^+$-$X^1\Sigma^+$ electronic transition, spectroscopic anal. and potential energy curves 80−48102
NaH, ground state, pot. curves, MTXα_R method 80−5482
NaH, ground state dipole moment, elec. quadrupole state selector meas. 79−98243
NaH in diffuse interstellar clouds 78−93361
NaH, interstellar, search in diffuse clouds 78−4325
NaH oligomers, struct., stability SCF and CEPA-PNO calcs. 78−78640
NaH Π states and NaH^+ ground state, pot. energy curves calc. 80−18812
NaH solution in liq. Na, elec. resist. and solubility 79−14934
NaH, variational time-dependent H-F calcs. in pseudopot. framework 77−10588
NaH, $X^1\Sigma^+$ states, many body effects, diagrammatic perturbation theory 77−79547
NaH^-, mol. orbital calcs., diffuse functions for basis sets, electron affinity 78−25436
NaH^+, FSGO calcs. with model pots. 78−33413
NaH^+, PNO-CI and CEPA calcs. of electron correl. effects 77−34561
NaH^+, Σ state pot. energy, Hellman pseudopot. calcs. 78−70764
Na_2H^+, equilib. geom. and dissoc. energy, pseudopot. calc. 78−94329
$NaHAs_2O_6$, cryst. struct., and new type of bidimensional infinite anion $(As_2O_6)_n^{2n-}$ *(French)* 79−14757
Na_2HAsO_4, ^{75}As NQR, phase transition mechanism 78−52375
Na_2HAsO_4, hydrogen bonded, ^{75}As NQR study 79−38399
$Na_2HAsO_4.7H_2O$:Cu^{2+}, ESR, Cu lattice location 78−52342
$NaHCO_3$, $^1H/^2H$ quadrupole reson. freqs. detected by double reson. with level crossing 78−84497
$NaHCO_3$, crystn. in system NaCl-NH_3-CO_2-H_2O 80−100771
$NaHCO_3$, enthalpies of dilution 79−57284
$NaHCO_3$, sea water relaxation and sound absorption 79−68466
$NaHCO_3$ solution, oxygenated, electrochemical studies of Pt electrode 78−85026
$NaHCO_3$, thermal conductivity thermal decomposition 78−2310
$NaH^{14}CO_3$, scintillation counting problems 79−3283
$NaHCd_4(Ge_5O_{15})$, cryst. struct., comparison with natural rhodonite 78−30600
$NaHCd_2(Si_2O_9)$, synthetic cryst., refined struct. 79−86763
$Na(H_{1-x}D_x)_3(SeO_3)_2$, ferroelectric, dielectric behaviour at RF and microwave freq. 79−33640
$NaHF_2$, IR refl. spectra 78−80324
$Na_5HMo_5P_2O_{23}(H_2O)_{11}$, mol. and cryst. struct., X-ray diffr. anal. 79−32951
NaH^-(NaH), ab initio ground-state pot. energy curves, electron affinities 78−41946
$Na(H_2O)(I(OH)_3O_2)$, pyroelec., cryst. struct. at room temp. 79−10835
$Na_x^+(H_2O)_y[CrS_2]^{x-}$, form. and reactions 79−91961
$Na(H_3O)[I(OH)_3O_3]$, piezoelec. and pyroelec. ionic displacements 79−38456
$Na^+(H_2O)n$ (n=1,2,4,6), FSGO-pair-pot. calcs. *(German)* 80−74278
NaH_2PO_2-$NaHPO_3$, quantitative anal. of $H_2PO_2^-$ and HPO_3^{2-}, by relative Raman intensities obs. *(Japanese)* 78−23991
NaH_2PO_4-NH_4Cl-$NiCl_2$, soln., Ni yield, factors affecting, pot. use as radiographic media 79−52702
$Na_xH_2P_xO_{3x+1}$, conversion products in presence of orthophosphate effect on melt props. 77−25355
β-$Na_2HPO_4.12H_2O$, dosorder of HPO_4^{2-} and H bonds 78−34471
$NaH_2PO_4.2H_2O$, Raman spectra, phonon freqs. 79−61370
$Na_2HPO_4.2H_2O$, crystal struct., coordination and H bond competition 78−14315
$NaH_2PO_2.4/5H_2O$, X-ray cryst. struct. determ., pseudo-symmetry and H_2 bonding 79−60315
$Na_2HPO_4.7H_2O$:KH_2AsO_4, EPR of arsenic and phosphorus oxyradicals 77−77102
α-$NaHSO_4$, cryst. struct. and hydrogen bonding 79−99128
$NaHSO_4$, struct. of new modification 78−34477
$NaHSO_4$:Mn^{2+}, EPR 79−24215
$Na_3H(SO_4)_2$, cryst. struct. refinement, short asymmetrical H bond, S-OH vs. O-H...O correlation 79−37663
$NaHSO_4.H_2O$ pseudo-symmetric crystal struct., hydrogen bonding 77−55258
$NaHSeO_3$, ^{77}Se Fourier transform NMR 78−95528
$NaHSeO_3$, and deuterated analog, vibr. spectra 79−24311
$NaHSeO_3$, and $NaDSeO_3$, NMR of ^{23}Na and ^2D, hydrogen bonding 80−44190
$NaH_3(SeO_3)_2$, β to δ ferroelec. transition under press. Raman spectra study 80−80725
$NaH_3(SeO_3)_2$, central mode, spin lattice relaxation dispersion 78−15108
$NaH_3(SeO_3)_2$, dielec. props. 78−43764
$NaH_3(SeO_3)_2$, domain struct. realignment and Barkhausen effect 80−71361
$NaH_3(SeO_3)_2$, dynamics of α-β transition, Brillouin scatt. meas. 77−8526
$NaH_3(SeO_3)_2$, ferroelec. crystal, Barkhausen effect study 79−38507
$NaH_3(SeO_3)_2$, ferroelectric, electromechanical props. near Curie point 80−29690
$NaH_3(SeO_3)_2$, ferroelec., proton motion within H bonds, neutron scatt. study 80−75986
$NaH_3(SeO_3)_2$, high-pressure phase transform., ^{23}Na NMR obs. 77−63380
$NaH_3(SeO_3)_2$, IR and Raman spectra, internal modes, intra- and inter-H-bond tunnelling 78−43853
$NaH_3(SeO_3)_2$, $NaD_3(SeO_3)_2$, IR and Raman spectral interpretation of ferroelectric phases 79−24312
$NaH_3(SeO_3)_2$, paraelec., neutron diffr. refinement of struct. 77−72584
$NaH_3(SeO_3)_2$, phase transition, pyroelec. current meas. 79−82934

sodium compounds continued
$NaH_3(SeO_3)_2$, proton behaviour in H-bonding, neutron spectroscopy obs. *(German)* 78−22816
$NaH_3(SeO_3)_2$, proton spin lattice relaxation 79−78557
$NaH_3(SeO_3)_2$:Cr^{3+}, deuterated, phase transitions, EPR 77−48135
$NaH_3(SeO_3)_2$:Mn^{2+}, single crystal, EPR 78−72396
$NaH_3(SeO_3)_2$:VO^{2+}, ESR spectra 79−4718
$Na_3HZr[GeO_4]_2$, hydrothermal crystn. 79−47604
$Na_4Hf(C_2O_4)_4.nH_2O$, electric field gradient at metal site, γ-ray perturbed ang. correlation meas. 78−52380
NaI (001), surface relax. influence on surface vibr. modes, bulk shell model calcs. 78−71927
NaI additives in Hg discharge, high-pressure, line broadening and radiative transport 80−74199
NaI and NaI:Tl^+, intrinsic and impurity induced luminesc., exciton diffusion 77−16367
NaI, aq. solns., laser induced breakdown 79−87530
NaI, continuous slowing down approx., range difference for 0.2 to 10 MeV electrons 80−39187
NaI crystals, used in nuclear medicine, determ. of cause of breakage 80−98077
NaI, diamag. ion solvation in methanol soln., NMR relax. obs. 78−56389
NaI, dil. aq. solns., conductance at 25°C 77−69105
NaI, dissoc. energy by photofragmentation spectroscopic method 79−76527
NaI, exciton luminesc., characteristics near absorption edge 78−88363
NaI, exciton mechanisms of electron sputtering 77−55857
NaI, exciton-phonon polarisation interaction *(Russian)* 78−35195
NaI, far IR spectra, matrix isolated, monomers, dimers, trimers 78−66545
NaI, free exciton reson. luminesc. lines 77−77272
NaI, impurity in AC metal halide discharge, atomic plasma characts., a priori method 80−44034
NaI in acetone, press. effects on Walden products, ion-solvent interactions 80−3398
NaI, inversion and superfluoresc. emission of Na reson. line by selective photodissoc. 78−87040
NaI, isothermal compressibility calc., 0-1000K 77−7784
NaI, lattice dynamics and statics, three-body-force shell model 80−49323
NaI, long wave phonon modes, IR absorpt. 78−79686
NaI, luminesc. polarisation for free and bound excitons 78−10942
NaI, motion of free excitons and their self-localisation 80−2342
NaI, n-propanol soln. cond. and transference no. meas., radioisotope method 77−35735
NaI opposed detector/turntable γ counter for voluminous samples 79−100706
NaI, optically activated F→F' centre conversion in mag. field 80−108253
NaI, photodissoc., perpendicular transition leading to ground state atoms 77−58097
NaI, refr. index, 300-700 nm., temp. coeff., 100-580K *(Russian)* 78−15142
NaI, resonant Raman scattering in crystals with self-trapping excitons 80−7344
NaI scintillation detectors, efficiency values, point and extended volume source geometries 78−13387
NaI scintillation spectrometer, gamma-ray energy released from fission products, response matrix *(Japanese)* 80−42888
NaI, scintillator props. in temp. range 125 to 293K 80−58047
NaI, self-trapped exciton and F-centre form. by picosecond laser pulses 80−10546
NaI, single cryst., reson. zero-phonon exciton luminesc., polariton emission 78−52564
NaI, surface lattice dynamics, Green function approach 77−31865
NaI, surface rumpling at finite temps, Verwey model 79−51402
NaI, temp. varying Mossbauer spectra, isomer shift 80−4726
NaI, thermal dissoc. of photoproduced excitons at UV band edge, recomb. luminesc. obs. 80−50412
NaI, transport processes, test of validity of Arrhenius law *(French)* 79−77808
NaI, U_2 and U_1 centres, optical excitations 80−2803
NaI, vibrational contribution to surface thermodynamic functions 77−47659
NaI, X- or γ-irrad., colour centre formation and accumulation *(Russian)* 77−65978
NaI, Xe^+ ion bombard., sputtering processes, time of flight meas. 78−88392
$Na^{125}I$ tracer telemetric detection for biological rhythms in renal study 77−86586
NaI:Ca^{2+}, pure and doped, ionic thermocurrents meas. 80−80677
NaI:Ca^{2+}, pure and doped, lattice defects, entropy and enthalpy of formation and migration 80−96687
NaI:Cl^-, anharmonic effects on low-frequency impurity phonon resonances 78−75771
NaI:Cl^-, local vibr. exam. by neutron scatt. 77−24373
NaI:Cu^+, luminesc. of iolated V_K-centres 78−84641
NaI:F, electron-lattice coupling of F-centres, optical props. 80−60641
NaI:H^-, U-centres, force consts. using Green's functions 79−46775
NaI:Pb, absorpt. spectra of Pb^{++} centres 80−76058
NaI:Tl, and unactivated NaI, scintillation response to random and channelled ions 77−48255
NaI:Tl, fluoresc. excited by γ-rays, a student laboratory expt. 79−97143
NaI:Tl, scintillation excitation mechanism for γ-rays *(Russian)* 78−92126
NaI:Tl, scintillation excitation mechanism 80−2857
NaI:Tl, triple-peaked scintillation pulse height spectra for MeV channelled ions 77−48254
NaI:Tl scintillation crysts., analytic calc. of photofractions to monoenergetic γ-rays 79−52038
NaI:Tl scintillator response, γ-ray, (X-ray) rel. $^1/_2$-width energy depend., undergrad. expt. 78−49600
NaI:Tl^+, luminescence spectrum, excited states of monomer centre 77−66536
NaI-H_2O, quick-frozen aq. soln., XPS 79−38713
NaI-KI(RbI) binary molten mixture, surface tension meas. 79−65294
NaI-LiI, phase diagram 77−21119
NaI-polyethylene oxide complexes, order-disorder transformations 78−47251

sodium compounds continued
$NaIO_3$, crystal struct. determ., anisotropic thermal vibr. parameters 80−88123
$NaIO_3$, in dioxane-water mixtures, ion-solvent interaction and conductance 79−34315
$NaIO_3$, XPS, binding energies and bond orders 77−18976
$NaIO_4$, normal coord. anal., internal and external modes 79−23684
$NaIO_4$, nuclear electric hexadecapole interactions of ^{121}I 79−1722
$NaIO_4$, nuclear electric hexadecapole interactions 80−65513
$NaIO_4$, XPS, binding energies and bond orders 77−18976
NaI(Tl) decay time constant temp. depend., influence on detector appls. 77−54417
NaI(Tl) detectors, response functions to terrestrial γ-radiation, computer program 80−83233
NaI(Tl) scintillation cameras, image artifacts and counting losses 80−94345
NaI(Tl), well-detector, low-background γ-spectrometry, comparison with CsI(Tl) 78−86724
NaI(Tl) well-type detectors, photopeak efficiency values, expts. and calcs. 80−63454
$NaInO_2$, electric field gradient tensor, dipolar contribs. 77−51707
$NaInO_2$, prep., props. and struct. 80−35517
$NaInS_2$, prep., props. and struct. 80−35517
$Na_3In(SO_4)_3.3H_2O$, cryst. struct. by X-ray methods 80−6393
$NaInS_2(Se_2)$, EFG tensor, S and Se dipolar contribution 77−31984
$NaIn(SeO_4)_2.6H_2O$, cryst. struct. by X-ray diffr., symm. 78−43004
$NaIn(SeO_4)_2.6H_2O$, X-ray cryst. struct. determ., H bond system 80−92511
$Na_xIn_xSn_{1-x}S_2$ (1>x>0), intercalation-substitution system, NMR study *(French)* 79−69095
$Na_xIn_xSn_{1-x}S_2$, intercalation-substitution compounds, NMR study 80−44952
$Na_xIn_xSn_{1-x}S_2$, ionic conductivity, activation energies, NMR study 79−28138
$Na_xIn_xSn_{1-x}S_2$, ionic conductors, ^{23}Na NMR and complex impedance meas. 79−91314
$Na_xIn_xZr_{1-x}S_2$, ionic conduction of phases *(French)* 77−47620
$Na_xIn_xZr_{1-x}S_2$, ionic conductivity, activation energies, NMR study 79−28138
NaK, $^1\Pi$ state perturbations, circular polarisation fluoresc. meas. 79−76462
NaK, $a^3\Sigma^+$ state, laser induced fluorescence, $D^1\Pi$ to $a^3\Sigma^+$ transition, molecular constants, dissociation energies 79−98143
NaK, $a^3\Sigma^+$ state, $X^1\Sigma^+$ state, fluorescence, visible spectrum 79−98114
NaK, ab initio and pseudopot. energy curves 78−90068
NaK, $C^1\Pi$ state, spectroscopic consts., vibr.-rot. struct., K fluoresc. obs. 77−18901
NaK, detailed spectroscopic study, sub-Doppler spectroscopic techniques 80−52339
NaK dimer formed in supersonic beam, laser-induced emission 80−9636
NaK, laser induced $D\,^1\Pi$-$a^3\Sigma$ fluorescence, mol. vibr. 80−87160
NaK, laser-induced fluoresc. in supersonic nozzle beams 78−25593
NaK, mol. transition dipole moment, from laser-induced fluoresc. spectra 79−94034
NaK, sub-Doppler laser spectrosc., high resolution 80−52320
NaK^+, adiabatic pot. curves, ground and excited state, Hellmann-type model pots. 78−78647
NaK+K collisions studied using circularly polarised laser fluorescence, molecular reorientation obs. 80−69215
NaK+K reactive collisions studied using circularly polarised laser fluorescence 80−69215
NaK+Na, spin polarisation exchange via opt. pumping, NMR 77−14452
$NaK_3(MO_4)_2$, (M=Mo, Se, W), cryst. struct., form. 77−19928
$NaKMg_3Cu_2Si_{12}O_{30}$, cryst. struct., X-ray diffr. and IR spectra *(French)* 80−107158
$NaKMg_8Si_{12}O_{30}$, cryst. struct., X-ray diffr. and IR spectra *(French)* 80−107158
$Na_{0.5}K_{0.5}NbO_3$, piezoelectric ceramic solid soln. *(Polish)* 77−55755
$Na_{1-x}K_xNbO_3$, solid soln., crystal lattice parameters, conc. depend. calc. 78−95041
Na_2KSb, evaluation as photocathode material 78−11072
Na_2KSb photocathodes, prep. and props. 78−84693
$Na_2KSb(Cs)$, photocathode, optical props. 79−78827
$Na_{0.5}K_{3.5}(Te_2O_6(OH)_4).6H_2O$, cryst. struct. determ. 78−26520
$(Na_xKy)_2CO_3$, non-stoichiometric, cryst. struct. *(French)* 80−79761
$NaLO_3$, disorder of NO_3^- ions, rel. to Raman spectrum temp. depend. *(Russian)* 78−2099
$Na_3La(AsO_4)_2$, allotropes, prep. and cryst. struct. *(French)* 78−63724
$Na_xLa_{1-x}B_6$, electrodeposition 79−47643
$(Na_{0.5}La_{0.5})_xBa_{1-x}TiO_3$, dielec. and IR spectra exam., ferroelec. transition 78−23418
$Na_3La_{1-x-y}Ce_xTb_y(PO_4)_2$, optical props. *(French)* 80−103991
$Na_3La_{0.98}Eu_{0.02}(VO_4)_2$, luminesc. spectrum 77−4673
$Na_3La_{1-x}Gd_x(PO_4)_2$, UV excitation, nonradiative transfer 79−38595
$Na_2LaGeO_4(OH)$, cryst. struct. and refinement 77−65970
$NaLa(MoO_4)_2$, luminesc. centres, EPR meas. *(Russian)* 77−28442
$NaLaO_2:Bi^{3+}$, luminesc., vibr. struct. 79−33790
$NaLaO_2:Pr^{3+}$, obs. of efficient luminesc., UV excitation 78−43922
$Na_3La(PO_4)_{1.9}(VO_4)_{0.1}$, luminesc. spectrum 77−4673
$Na_3La(VO_4)_2$, luminesc. spectrum 77−4673
NaLi, ground state, pot. curves, $MTX\alpha_R$ method 77−71762
$Na_{5-x}Li_xErSi_4O_{12}$, solid electrolytes for Na/TiS_2 cells, synthesis, charact. and utilisation 80−107518
$Na_{1-x}Li_xNbO_3$, dielec. const. and X-ray diffr., for Curie temp. and phase diagrams 78−72768
$Na_{1-x}Li_xNbO_3$ mixture, ferroelec.-paraelec. transitions, dielec. props. meas. 80−66125
$NaLiSO_4$, anhydrous, struct. relationships w.r.t. fast ion cond. 80−107188
$Na_{2-x}Li_xSiO_3$, long-period superstructure 77−55269
$NaLiZrSi_6O_{15}$; zektzerite, silicate mineral with six-tetrahedral-repeat double chains 78−63719
$Na_5LuSi_4O_{12}$, cryst. struct. 79−32979
NaM natural mordenite, Se thread lattice, optical absorpt., cond. *(Russian)* 80−89022
$Na_3M_2Li_3F_{12}$, M=Sc, Ti, V, Cr, Mn, Fe, Ce, Ni, IR spectra 79−38544
$Na_3M_2^{3+}Li_3F_{12}$ garnets, M=Al,Cr,Fe, synthesis from aq. soln., props. 77−44184
Na_xMS_2 (M=Ta,Ti), Na chem. pot. and free energy of intercalation, electrochemical meas. 79−100396

sodium compounds continued
NaMgA zeolites, diffusion anomaly of n-alkanes *(German)* 79−77817
$NaMgF_3$, defects induced by X- and vacuum UV irrad., optical and elec. study 80−107319
$NaMgF_3$, extreme UV spectra, 9-30 eV 78−23486
$NaMgF_3$, optical absorpt. of radiation produced defects 77−28604
$NaMgF_3$, orthorhombic perovskite, contribution to crystal chem. 80−19777
$NaMgF_3:Eu^+$, Zeeman absorpt. and luminesc. spectra *(Russian)* 77−69872
$NaMgF_3:Sm^{2+}$, absorpt. spectra and Zeeman effect, 3000-12000 Å, 4.2-295K 79−24341
$NaMgF_3:Sm^{2+}$, luminesc. spectra 4.2, 77 and 295K and Zeeman spectra, 4.2K 77−81146
$Na_3Mg_4LiSi_{12}O_{30}$, cryst. struct., X-ray diffr. and IR spectra *(French)* 80−107158
$Na_2Mg_3M_2Si_{12}O_{30}$ (M=Cu, Fe, Zn, Mg), cryst. struct., X-ray diffr. and IR spectra *(French)* 80−107158
$NaMgPO_4$-MgO, $NaMgPO_4$-$NaCaPO_4$, partial systems, phase diag. 77−86005
$Na_3Mg_2P_5O_{16}$, cryst. and X-ray powder data 79−51072
$Na_3Mg_2P_5O_{16}$, new type of phosphate radical P_5O_{16} 79−94978
$Na_2Mg_1SiO_4$, ionic cond. meas. 80−6545
$Na_4Mg_2Si_3O_{10}$, ionic cond. meas. 80−6545
$Na_4Mg_2Si_3O_{10}$, powder diffr. cryst. data 80−19765
$Na_2Mg_6Si_8O_{22}F_2$, fluoramphibole, fibrous, crystn. from gas phase, mechanism 78−34451
$Na_2Mg_2Ti_6O_{14}F_2$, α and β forms, ionic conductivities *(French)* 77−43373
$NaMnCl_2$, mag. susceptibility, 4.2-350K, quasi-two-dimens. antiferromagnetism 77−59399
$NaMnCl_3$, antiferromagnet, exciton self-localisation luminesc. and excitation spectra *(Russian)* 80−11456
$NaMnCl_3$, antiferromag. insulator, self-trapping of excitons 80−70619
$NaMnCl_3$, mag. props., 2-25K, antiferromag.-paramag. transition *(Russian)* 78−88125
$NaMnCl_3$, mag. struct. and spin-flip transition, powder neutron diffr. exam. 80−60210
$NaMnCrF_4$, cryst. struct. *(French)* 77−47402
$NaMnCrF_6$, ferrimagnetic, magnetic props. *(French)* 79−1668
$NaMnCrF_6$, mag. struct., neutron Laue diffr. method 80−70951
$NaMnCrF_6$, magnetic struct., neutron Laue diffr. study *(French)* 79−99682
Na_2MnFeF_7, trigonal weberite variant, X-ray and neutron diffr. *(German)* 78−51508
$Na_2MnP_2O_7.4H_2O$, physicochem. characts. 77−39562
$Na_2Mn(SiO_3)_2$, X-ray diffr. anal. of cryst. struct. 77−35538
$NaMnTiO_4$, form. in Na_2O-M_2O_3-TiO_2 ternary systems X-ray anal. 79−51067
$Na_{0.5}Mn_{0.5}TiO_3$, form. in Na_2O-M_2O_3-TiO_2 ternary systems X-ray anal. 79−51067
$Na_6Mn(Ti[Si_6O_{18}])$, Kazakovite, cryst. struct. determ. 80−19782
$Na_4Mo_{12}GeO_{40}(H_2O)_8$, X-ray diffr. cryst. struct. exam. 78−2075
Na_2MoO_4 based melt, crystn. from $Cl_2(MoO_4)_3$ and $La_2(MoO_4)_3$ 80−20920
Na_2MoO_4, corrosion inhibition of low C steel 77−86221
Na_2MoO_4-$MMoO_4$, M=Ca, Sr or Ba , phase diagrams 77−36467
Na_2MoO_4-Na_2SO_4, phase diag. and isomorphism 78−27486
$Na_2Mo_2O_7$, heat of melting and activities using cryoscopic data 77−40573
$Na_2MoO_4(S_4)(Se_4)$ crystals, charge transfer spectra of MoX_4^{2-} complexes 80−54658
$Na_6Mo_5P_2O_{23}(H_2O)_{14}$, X-ray diffr. cryst. struct. determ., refinement 78−2074
$Na_6Mo_6V_2O_{26}(H_2O)_{16}$, X-ray cryst. struct. determ. 79−99132
NaN_3, dynamic electron density distribution, calc. from static mol. wave functions 77−27776
β-NaN_3, dynamic electron densities, anharmonic contribs. from large molecular librations 79−97971
NaN_3, electron density distrib., X-ray diffr. data 77−84705
NaN_3, exptl. electron density distribs. cf. theoret. density distribs. of N_3^- 77−46489
NaN_3, lattice dynamics and phase transition, theory 77−76501
NaN_3, NMR, Na nuclear quadrupole moment, phase transition 77−73092
NaN_3, orientational motion and elastic anomaly 79−46803
NaN_3, phase transitions and N_3^- librational motion 77−4178
NaN_3, polycryst., IR active lattice vibr., optical consts. 77−77185
NaN_3, solid, CO_2 laser radiation decomposition, for high-press. chem. laser 79−34326
NaN_3, struct. phase transform., microscopic model 79−65022
NaN_3, thermal decomp., N_3 generation 79−100351
NaN_3, UV irradiated, F-centre ESR 77−28444
NaN_3, UV irradiated, polarised optical absorpt. of F_2^+-, F-centres 77−28605
NaN_3, X-irrad., EPR of N_2^- 77−66421
NaNCO, val. band electronic struct., XPS meas., MOC and INDO calc. 80−95520
$NaND_4SeO_4.2D_2O$, nonlinear electromechanical props. above Curie temp. 79−33610
$NaNH_4SO_4.2H_2O$, nonlinear opt. props. including SHG 78−76396
$NaNH_4SO_4.2H_2O$, ferroelec. and thermal props. 78−83968
$NaNH_4SeO_4.2H_2O$ ferroelectric crystal optical SHG and pulse modulation *(Russian)* 77−14771
$NaNH_4SeO_4.2H_2O$, crystal struct. in ferroelec. phase, nature of transition 77−43946
$NaNH_4SeO_4.2H_2O$, model of ferroelec. phase transition 78−19433
$NaNH_4SeO_4.2H_2O$, ferroelectric phase transition mechanism 78−31162
$NaNH_4SeO_4.2H_2O$, ferroelectric crystal, effect of hydrostatic pressure on phase transition 78−52453
$NaNH_4SeO_4.2H_2O$, nonlinear opt. props. including SHG 78−76396
$NaNH_4SeO_4.2H_2O$, polarisation effect in piezoelectric executing longitudinal vibs. 79−1741
$NaNH_4SeO_4.2H_2O$, atomic struct. exam. and phase transition 79−37678
$NaNH_4SeO_4.2H_2O$, neutron-diffr. investigation 79−46638
$Na^{15}N_x{}^{14}N_{1-x}O_3$ mixed crystal, Raman spectra determ. of phonon density of states *(Russian)* 80−93313
$Na^{15}N_x{}^{14}N_{1-x}O_3$, reflection spectra, Kramers-Kronig anal. with preliminary dispersion anal. 78−49915
$NaNO_2$, ^{14}N NQR, multiple spin echoes 78−19365

sodium compounds continued
$NaNO_2$, ^{23}Na elec. field gradient tensor from NMR satellite lines near phase transition 80−71191
$NaNO_2$, 163°C phase transition, thermal history effects on range of modulated struct. 78−95563
$NaNO_2$, adiabatic and isothermal elastic compliances, critical behaviour 78−92031
$NaNO_2$ and $NaNO_3$, muonic X-ray intensities, Lyman series 80−23578
$NaNO_2$, antiferroelec. phase, struct. anal. by neutron diffraction 80−24410
$NaNO_2$ aqueous solutions, differential diffusion coeffs. determ. diaphragm cell method 79−95193
$NaNO_2$, band struct., polarisation and piezoelec. consts. calc. 78−52448
$NaNO_2$, complex dielectric constant, sinusoidal phase in ferroelectric material 79−11376
$NaNO_2$, compressed powder, dielec. props., surface layer effects 78−76413
$NaNO_2$, crit. dynamics, nuclear relax. 78−75805
$NaNO_2$, cryst., delayed fluoresc., triplet excitons, dopant effects 78−10963
$NaNO_2$, cryst., Stark shift of visible absorpt. of NO_2^- 78−19499
$NaNO_2$, cryst., triplet excitons, localised states, zero-field ODMR, dopant effects 78−15062
$NaNO_2$, elastic constants and US attenuation coeffs., anisotropic charact. 78−63809
$NaNO_2$, electric field gradient, quadrupole coupling consts. 77−89740
$NaNO_2$, electrostrictive constants, isothermal and adiabatic, in antiferroelec. transition region 77−12317
$NaNO_2$, enthalpy of soln. and dilution, obs. 78−80781
$NaNO_2$, ferroelec., ang. dispersion of internal phonon modes, Raman meas. 79−51211
$NaNO_2$, ferroelec., crit. X-ray scatt. 79−33636
$NaNO_2$, ferroelec., dielec. and thermal behaviour 80−80680
$NaNO_2$, ferroelec., electric field gradient *(Korean)* 79−15419
$NaNO_2$, ferroelec., electron distrib., X-ray and neutron diffraction study 80−24411
$NaNO_2$, ferroelec., lattice dynamics, two-phonon Raman scatt. and IR absorpt. 79−33684
$NaNO_2$, ferroelec., X-ray diffr. topographic study of polarisation reversal 79−38441
$NaNO_2$, ferroelec., X-ray obs. during polarisation reversal 79−51921
$NaNO_2$, ferroelec. nuclear quadrupole coupling const. and spontaneous polarisation 80−71229
$NaNO_2$, ferroelec. thin crysts., struct. investig. 79−27962
$NaNO_2$, ferroelec. transitions into inhomogeneous modulated phase, Landau theory analysis 77−8527
$NaNO_2$, ferroelectric, NMR of ^{23}Na small particles 79−28629
$NaNO_2$, ferroelectric, second-order vibr. spectra and dispersion of phonon branches 79−69847
$NaNO_2$, ferroelectric transitions, based on model thermodynamic pot. 78−80295
$NaNO_2$, ferroelectric transitions, group theoretic comparison with $AgNaNO_2$ 80−7311
$NaNO_2$, ferroelectric transitions, one-mode model 80−29702
$NaNO_2$, fine struct. in luminesc. spectra in UV region 77−59607
$NaNO_2$, high-pressure phase behaviour 78−30749
$NaNO_2$, hot luminesc. 78−6722
$NaNO_2$, hot luminescence 78−10976
$NaNO_2$, incommensurate phase transitions 78−26653
$NaNO_2$, incommensurate phase transition, Bethe-Peierls and mol. field approx. 80−20599
$NaNO_2$, incommensurate-and-antiferroelectric phase transition, amplitude mode, ultrasonic study 80−39227
$NaNO_2$, incommensurate antiferroelec. phase, Brillouin scatt. freq. shift 80−93349
$NaNO_2$, investigation of switching characts. using cct. containing bipolar square pulse generator 80−62687
$NaNO_2$, linear compressibility to 27 kbar, X-ray diffr. obs. 80−34125
$NaNO_2$, mechanism of ordering type ferroelec. transition, vibr. spectroscopy 78−76402
$NaNO_2$, mechanism of order-disorder transition, opt. spectra 78−76403
$NaNO_2$, melting curve maximum 77−43311
$NaNO_2$, melting pressure curves up to 5 kbar 77−15547
$NaNO_2$, modulation of intermediate antiferroelectric phase 79−38462
$NaNO_2$, molten, electrolytic cond. at pressures up to 6 kbar 77−15609
$NaNO_2$, NQR of ^{14}N at ferroelec. transition, order-disorder fluctuations 77−63311
$NaNO_2$, nonlinear dielec. anomaly in paraelec. phase 78−39495
$NaNO_2$, nuclear fuel processing solutions 78−78487
$NaNO_2$, ν_1 Raman linewidth and reorientation of NO_2^-, temp. depend. 78−72522
$NaNO_2$, optical harmonic generation near ferroelec. transition 80−91858
$NaNO_2$, order-disorder ferroelec., crit. dynamics, NMR data compared with dielec. data 78−76415
$NaNO_2$, phase transitions accompanied by noncommensurate superstruct. form. 77−32336
$NaNO_2$, phonon side bands of triplet absorption 78−76488
$NaNO_2$, polarisation reversal by time-resolved X-ray diffr., NO_2 radical rot. 77−63382
$NaNO_2$, positron lifetimes, ferro-paraelectric transition 79−74017
$NaNO_2$ powder, surface layer effects on dielec. props. 77−1631
$NaNO_2$, Raman and IR spectra, destructive Fermi reson. 77−16309
$NaNO_2$, rot. behaviour of NO_2 radicals in order-disorder transition, Fourier synthesis study of neutron data 79−56739
$NaNO_2$, second order phase transition prod. by strain 79−15420
$NaNO_2$, size effect and spin-lattice relax. of ^{14}N 80−20480
$NaNO_2$, vacuum UV spectra and electro-optical prop. *(Japanese)* 79−65900
$NaNO_2$, vibr. spectrum, interference effects 78−87752
$NaNO_2$, with adsorbed film of soln., NMR investig. 77−8426
$NaNO_2$, X-irradiated IR, UV and visible absorption 79−95811
$NaNO_2$, X-ray crit. scatt. 78−52461
$NaNO_2$:Ag^+, optical and MODR spectra, anion states spin-orbit perturbation 79−19908
$NaNO_2$:Mn^{2+}, ferroelectric phase metastable struct., EPR obs. 78−60328
$NaNO_2$:Mn^{2+}, zero-field splitting, ferroelec. soft-mode contrib., phase transition, EPR obs. 79−15344
$NaNO_3$, ^{23}Na spin-lattice relax., orientation depend. 78−23372
$NaNO_3$, aq. soln., heat capacity at 298.15K 78−3364
sodium compounds continued
$NaNO_3$, aq. soln., pulsed limiter discharge, nonideal plasma chem. composition 80−19657
$NaNO_3$, aqueous soln., X-ray diffraction, radial functions and positional correl. 80−79665
$NaNO_3$, cryst., ^{23}Na transitions, two-photon transient effects, NMR obs. 77−85588
$NaNO_3$, crystallite boundary structural instability during solidification *(Russian)* 78−95738
$NaNO_3$ crystals, determination of permittivity 79−97403
$NaNO_3$, dielec. loss anal., Debye type loss peaks 80−50260
$NaNO_3$, disordered, temp. depend. of Raman spectra, Rayleigh wing scatt. 78−31209
$NaNO_3$, double quantum nuclear magnetic resonance of ^{23}Na by double resonance, line shape 80−75886
$NaNO_3$, electric field gradient, quadrupole coupling consts. 77−89740
$NaNO_3$, electron density distrib. *(German)* 80−92481
$NaNO_3$ floating zone melting, surface tension driven flow 78−48313
$NaNO_3$, γ-irrad., electron trap depth, ESR 79−66317
$NaNO_3$, IR spectra study of shear-stress-induced phase transitions at high press. 77−32368
$NaNO_3$, in liq. NH_3, Raman spectra, curve resolution anal. 77−82610
$NaNO_3$ in N,N-dimethylacetamide, Raman, IR and US relaxation studies 80−50315
$NaNO_3$ infrared spectroscopic study of structural transformations, electronic structure characteristic features 79−47436
$NaNO_3$, isotopically mixed, vibr. spectra, IR and Raman spectra 79−28770
$NaNO_3$, lattice vibration neutron diffusion study *(French)* 80−103429
$NaNO_3$, lattice vibrs., order-disorder transform., IR spectra study 80−65176
$NaNO_3$, linear compressibility to 27 kbar, X-ray diffr. obs. 80−34125
$NaNO_3$, low temp. struct. changes, elec. props. 79−87377
$NaNO_3$ melt, Marangoni number, critical, for the onset of oscillatory flow in crystal growth melts 79−23555
$NaNO_3$, melt, NO_3^- ion struct., pulsed neutron diffr. obs. 78−22631
$NaNO_3$, melt, Tl^+ high dilution diffusion, interferometry 78−47546
$NaNO_3$ melts, ion exchange reaction with Na silicate glasses 80−16673
$NaNO_3$, molten, thermal diffusivity meas. at 320-80°C 77−82525
$NaNO_3$, molten, X-ray diffr. structural anal. 78−42887
$NaNO_3$ molten salt, nucl. quadrupolar spin-lattice relax., microscopic liq. dynamics 79−91313
$NaNO_3$, N atom velocity, NO_3^- vib. and orientation, nucl. reson. photon scatt. 78−68433
$NaNO_3$, Nd laser second harmonic stimulated Raman scatt., efficiency in calcite, nitrate crysts. 80−95949
$NaNO_3$, occupation waves, displacive modulation, struct. using superspace-group concept 80−79726
$NaNO_3$, order-disorder transition point, hyper-Rayleigh scatt. due to rotation of NO_3^- 78−52520
$NaNO_3$, press. induced ferroelec. transition, soft mode dynamics, Raman scatt. meas. 78−72475
$NaNO_3$, pure and Ca^{2+} doped, γ-irrad., damage species annealing 79−66324
$NaNO_3$, pure cryst., NO_3^- singlet-triplet absorption, Stark effect obs. 79−8153
$NaNO_3$, Raman scatt. band lineshape, orientational disorder of NO_3^- ion in pre-transition region 77−8589
$NaNO_3$, Raman spectroscopic study of NO_3^- component with temp. 78−76458
$NaNO_3$, single cryst. growth using zone melting furnace 79−52110
$NaNO_3$, single cryst. cleavage, Bi film deposition by vacuum evaporation 80−35091
$NaNO_3$, soft mode dynamics at ferroelec. transition 78−80308
$NaNO_3$ soln., Raman spectral studies of NO_3^- motion and interaction 78−92067
$NaNO_3$ solution cathodic gas evolution rate rel. to electrode material *(Russian)* 80−26020
$NaNO_3$, spin-lattice relax. time of ^{23}Na −75.5 to +320°C *(Japanese)* 77−43897
$NaNO_3$, vibrations of isotopic impurities, IR reflection and Raman spectra meas. 77−51465
$Na^{14}NO_3$, $Na^{15}NO_3$, polarised IR reflection spectra, surface damage effects 79−19872
$Na^{14}NO_3$, $Na^{14}NO_3$, multiphonon transitions in microcryst. reflectivity 78−72499
Na^ANO_3, (A=14,15), anomalous IR reflectivity min. in transverse-longitudinal band gap 79−56796
$NaNO_3$-$AgNO_3$, molten salt mixture, ionic and mol. mobilities, interdiffusion and self-diffusion *(German)* 77−11720
$NaNO_3$-$AgNO_3$ mixture, contact with glass, conc. changes in surface layer 80−44372
$NaNO_3$-$Cd(NO_3)_2$ molten mixtures, electrical conductance, non-Arrhenian behaviour 78−43158
$NaNO_3$-$CsNO_3$-$Pb(NO_3)_2$, fusion diag. *(Russian)* 77−48418
$NaNO_3$-H_2O, quick-frozen aq. soln., XPS 79−38713
$NaNO_3$-KNO_3-$Ca(NO_3)_2.4.09H_2O$ melt, mixed alkali effect 80−34219
$NaNO_3$-$LiNO_3$ (urea), solid eutectic mixtures, Raman IR spectra, line shifts, widths 77−55793
$NaNO_3$-$Pb(NO_3)_2$, ht. of crystn. *(Russian)* 77−48418
$NaNO_3$-$RbNO_3$-$Pb(NO_3)_2$, crystn. heat of eutectic, thermodynamic anal. *(Russian)* 77−63644
$NaNO_3$-$TlNO_3$-$Ca(NO_3)_2.4.09H_2O$ melt, mixed alkali effect 80−34219
$NaNO_3$+muonium in aq. soln., rate const. 77−38752
$NaNO_{3(2)}$, precipitation from mixed aq. solns. 80−100191
$Na_2N_2O_3$, vibr. spectra, assignments 77−38670
$(NaNO_3$-$Mg(NO_3)_2)$:Nd^{3+}, glass, cryst., absorpt. luminesc. spectra, term struct. of Nd^{3+}, bonding 77−8624
$NaN0_3$, fine structure changes on interaction with weak shock waves *(Russian)* 80−54313
$Na_3Na(PO_4)_2$, synthesis and IR spectra 80−16019
$NaNbF_6$, NMR, quadrupole effects and struct. distortion 80−15809
$NaNbO_3$, antiferroelec., primary order parameter, X-ray scatt. 79−51919
$NaNbO_3$, birefr., temp. depend., behaviour at P⇄N struct. transition 78−64331
$NaNbO_3$, cubic to tetragonal transition, inelastic neutron scatt. study *(French)* 79−60469
$NaNbO_3$, elec. and photoelec. props. near ferroelec.-antiferroelec. phase transition 80−15989
$NaNbO_3$, elec. and thermoelec. props., influence of O defects 80−29401

sodium compounds continued
$NaNbO_3$, elec. cond., Hall mobility, thermoelec. coeff. 79−82584
$NaNbO_3$, elect. cond. mech., resist., Hall coeff. and thermoelec. power meas. 80−65603
$NaNbO_3$, ferroelec., local field determ., phase transition study by EPR 79−38471
$NaNbO_3$, ferroelec. semicond., thermoelec. power for small polaron 77−89784
$NaNbO_3$, hydrostatic press. effect on permittivity, phase transition, hysteresis 80−80670
$NaNbO_3$, memory effect, in ferroelec. phase, ESR meas. 79−28696
$NaNbO_3$, perovskite structure, semiconductor props. *(Polish)* 78−56437
$NaNbO_3$, photoconductivity and TSC 78−2520
$NaNbO_3$, photoferroelectric effect 78−35108
$NaNbO_3$, thermoelec. effect and phase transitions 78−48123
$NaNbO_3$, X-ray and Mossbauer γ-ray scatt., near phase transition, energy width of central peak 78−79724
$NaNbO_3$:Mn^{2+}, ESR, temp. depend., −269-750°C, fine splitting 77−51948
$NaNbO_3$:Mn^{2+}, T_2 phase, EPR spectra 78−88179
$NaNbO_3$-$BaTiO_3$, ferroelec. Curie temp., theory 80−7313
$NaNbO_3$-$BaTiO_3$, unidirectionally solidified transparent ceramics 80−25677
$NaNbO_3$-$BaTiO_3$ solid soln. form. and props. *(Russian)* 78−48378
$NaNbO_3$-based ferroelec. solid solns., morphotropic transitions and elec. props., enhanced vacancy conc. 80−55048
$NaNbO_3$-$LiNbO_3$-$SrNb_2O_6$ pseudo-ternary system, DTA, heat treatment and X-ray diffr. obs. *(Chinese)* 79−52175
$NaNbO_3$-$PbTiO_3$, ferroelec. Curie temp., theory 80−7313
$NaNbO_3$-$SrNb_2O_6$, phase diagram, props. meas. 79−11576
$Na_{0.5}NbS_2$, supercond. props., alkali cation and topotactic solvation influences 79−87180
$NaNbTiO_5$, high temp. chlorination kinetics 79−61765
$Na_3Nd(AsO_4)_2$, allotropes, prep. and cryst. struct. *(French)* 78−63724
$NaNdP_4O_{12}$, CW laser oscill., near 1.32 μm 77−61957
$NaNdP_4O_{12}$, laser emission cross sections, fluorescence spectra, radiative lifetimes, quantum efficiency 80−23694
$Na_3Nd(PO_4)_2$, laser mat., cryst. struct. 78−79582
$Na_2NdPb_6(PO_4)_6Cl_2$, self-activated mini-laser material, quantum yield determ. 79−33773
$Na_2Nd_2Pb_6(PO_4)_6Cl_2$, laser material, flux growth *(French)* 78−35288
$Na_2Nd_2Pb_6(PO_4)_6Cl_2$, high-Nd conc. laser material, oscillator strengths and laser effect 79−55140
$NaNd(SO_4)_2$, cryst. struct. by X-ray diffr. *(French)* 78−42990
$NaNdSi_6O_{14}$, CC Si_3O_7 layered stacks, polymorphism, cryst. chem. anal. 79−60301
$NaNdSi_6O_{14}$, cryst. struct., X-ray diffr. meas. 77−15385
$NaNdSi_6O_{13}(OH)_2.nH_2O$, cryst. struct. determ. 78−63738
$(Na_{5-x}Nd_x)(W_{3-2x}Nb_{2x})O_9F_5$, ferroelastic-ferroelectric material *(French)* 79−99834
NaNdX, zeolite hydrated, ion exchange of Na for Nd, cryst. structs. 80−33979
NaNe, intramol. pot. functions of first excited state 79−54785
NaNe, laser spectroscopy, interat. pot. curves 78−86871
NaNe, van der Waals mol., form., laser spectroscopy 78−29797
$NaNiF_3$, cryst. struct. 77−76362
$NaNiF_3$, electronic UV laser excited Raman, scatt. by mag. excitons 78−68492
Na_2NiFeF_7, weberite struct. refinement *(German)* 78−47294
$Na_{2.4}Ni_{0.8}(MoO_4)_2$, paramag. props., 90-800K *(French)* 80−39734
Na_2NiO_2, thermodynamic props. 77−69099
Na_5NiO_4, crystallographic data *(German)* 78−63736
Na_4NiPO_4, X-ray diffr. spectra *(French)* 80−93546
$Na_4Ni(PO_4)_2$, double phosphate, X-ray diffr. spectra *(French)* 80−93546
$Na_2Ni_3(P_2O_7)_2.nH_2O$, thermal dehydration 80−35513
$Na_2NiTi_7O_{16}$ bronze, synthesis in $NaBO_2$, growth conditions *(French)* 78−43998
$Na_2Ni_2Ti_6O_{14}F_2$, characterisation and mag. props., 90-800K, $Na_xTi_4O_8$ bronze isotypes *(French)* 80−39735
$NaNo_2$, correlation between experimental and theoretical diffusion coeffs. 77−24421
$NaNo_3$, ^{23}Na satellites in nuclear double resonance interferometric spectroscopy 79−4745
$NaNo_3$, aq. soln., Raman spectra, vibr., orient. relaxation *(French)* 78−62808
$Na_4NpO_2(O_2)_3.9H_2O$, structure and bonding study 77−27868
$NaO-B_2O_3-SiO_2$, phase separated glass, viscosity and microstruct., heat treatment effect 79−99343
NaO-CaO glass, melting speed, effect of struct. and grain shape *(Polish)* 79−29002
$NaO-CaO-SiO_2$ glasses, fluorinating agents effect on comp. and surface struct. 80−35364
$NaO-SiO_2$, glass, distrib. of different O ions, molar refractivity meas. 80−33897
NaO+O, nightglow, excitation and abundance of Na 80−98497
$NaO_{0.5}$-$CaO-SiO_2$ liquid, heat capacity of mixing at 1000K 79−77765
$NaO_{0.5}$-SiO_2 liquid, anal. expressions for heat capacities 79−77765
NaO_2, elastic interaction, role in disordered-pyrite to ordered-pyrite phase transition 80−19739
NaO_2, non-isothermal decomp. kinetics 80−16649
NaO_2, physical mechanisms of phase transitions 80−6381
NaO_2, thermal decomp. macrokinetics, differential thermal anal. 80−16650
$NaO_2-B_2O_3$ glass melts, fluctuations 79−94865
Na_2O (111) on Na (110), LEED 77−72761
Na_2O, additive, effect on sintering struct., props. of corunudm ceramic 79−15630
Na_2O, aerosol behaviour in closed chamber under thermal convection flow in LMFBR accident 77−57723
Na_2O aerosol gravitational fallout rate, validation of computer code for fast reactor accident anal. 80−18535
Na_2O aerosols, aerodynamic props. 80−23011
Na_2O agglomerate props., rel. to aerosol behaviour in LMFBR containment vessels 79−36368
Na_2O, cation diffusion NMR investigation up to 800°C 80−108092
Na_2O, determination of enthalpy of solution in $PbO-B_2O_3$ mixture 79−95166
Na_2O, effect of admixture on props. of $MgFe_{2-y}Al_yO_4$ with added Co 77−36423
Na_2O, effect on corundum ceramic comp. and phase struct. 77−81244
sodium compounds continued
Na_2O, effect on props. of PbO containing cryst. glass 80−24637
Na_2O glasses, partially leached, dehydrated surface reaction with water 80−3406
Na_2O impurity in commercial alumina, removal method and modifier incorporation 79−43183
Na_2O, in phosphate or silicate glass, effect on thermooptics props. 78−18029
Na_2O, in porcelain raw material, determ. by ion exchange chromatography 78−7272
Na_2O particles, effect on optical props. of Na vapour 80−1736
$Na_2O-2B_2O_3$ glass, numerical optimisation of ESR V^{4+} spectra 79−38370
$Na_2O-2B_2O_3$ molten glass, reactions with conducting materials 80−85186
$Na_2O-2CaO-3SiO_2$ glass, cryst. nucleation and growth, viscosity, thermodynamic props. 80−84079
$Na_2O-2SiO_2$, melt, effect of cooling rate upon glass transition, X-ray analysis 79−27920
$Na_2O-2SiO_2$ glass, alkali motion ionic thermocurrent study, polarised impurity-vacancy dipole relaxation study 79−77806
$Na_2O-2SiO_2$ high expansion glass, chemical durability improvement by ion exchnage 78−48361
$Na_2O-3SiO_2$ glass, high-temp. thermolum., colour centre absorpt. 80−16110
$Na_2O-3SiO_2$:Fe^{2+}, Fe^{3+} glasses, Mossbauer and ESR spectra and internal friction 80−100865
$Na_2O-(BaO)-SiO_2$ glass, chemical durability of surface, heat treatment effect 79−52405
$Na_2O-(CaO)-SiO_2$, corroded, quantitative anal. by IR frequency shifts 78−19909
$20Na_2O-(80-x)B_2O_3-xSiO_2$ glass system, structure toughness-composition relationship 80−104257
$Na_2O-Ag_2O-B_2O_3$ glass, Ag^+ ion distrib., X-ray diffr. study 80−84076
β-$Na_2O-Al_2O_3$, isomorphous replacement of Al^{3+}, solubility of Cr^{3+}, Ti^{3+}, Fe^{3+} 77−85926
β-$Na_2O-Al_2O_3$, single cryst. Czochralski growth 77−77367
$Na_2O-Al_2O_3$ (CaO)-SiO_2 glass, surface charge in aqueous electrolyte soln. 79−29245
β-$Na_2O-Al_2O_3$ low temp. ultrasonic vel. meas., temp. depend. 80−79885
$Na_2O-Al_2O_3-B_2O_3$ glasses, kinetic study of Cu^+-Cu^{2+} equilib. 79−8448
$Na_2O-Al_2O_3-B_2O_3-SiO_2$ photochromic glass, $AgCl_{1-x}Br_x$ activated, comp. optimisation by Box-Wilson method 77−50741
$Na_2O-Al_2O_3-B_2O_3-SiO_2$, glass, ESR exam. of paramagnetic centres formed during mech. destruction by grinding 78−88188
$Na_2O-Al_2O_3-B_2O_3-SiO_2$-AgBr(Cl), photochromic glass, exam. of role of O and Cu ions, using luminescence spectra 79−4849
$Na_2O-Al_2O_3-B_2O_3-SiO_2$-AgCl(Br), photochromic glass, kinetics of thermal decolorisation 80−103931
$Na_2O-Al_2O_3-GeO_2-H_2O$ system, hydrothermal synthesis 77−36388
$Na_2O-Al_2O_3-P_2O_5$, exam. of subsolidus structure 79−4954
$Na_2O-Al_2O_3-P_2O_5$ glass, low-temp. viscosity 80−39198
$Na_2O-Al_2O_3-P_2O_5$:Eu glasses, fluorescence line narrowing meas. *(French)* 80−34975
$Na_2O-Al_2O_3-SiO_2$, glass, nucleation, crystn., ceramic form. 80−84082
$Na_2O-Al_2O_3-SiO_2$, porous glass, crack shape, US fractography obs. 77−44336
$Na_2O-Al_2O_3-SiO_2$ glass, He migration 77−7902
$Na_2O-Al_2O_3-SiO_2$ glasses, elec. cond. and cation mobility 78−59973
$Na_2O-Al_2O_3-SiO_2$ glass, formation from alkoxides, phys. and chem. evolution 78−80503
$Na_2O-Al_2O_3-SiO_2$ glass, diffusion of Ca and Mg, SIMS study 79−82387
$Na_2O-Al_2O_3-SiO_2$ glass, leaching in HCl solns., Na conc. distrib. in surface layers 80−21141
$Na_2O-Al_2O_3-SiO_2$ glass, interaction with aq. salt solns., alkali ions distrib. in surface layers 80−21142
$Na_2O-Al_2O_3-SiO_2$ system glass melts, alkali ions interdiffusion coeffs., conc. depend. 79−65231
$Na_2O-Al_2O_3-SiO_2-TiO$, effect of Cr_2O_3, NiO, and MgO additions on crystallisation 78−87626
$Na_2O-Al_2O_3-SiO_2-TiO_2$-NiO glass, paramagnetic centres, form. during crystn., ESR study 79−65710
$Na_2O-Al_2O_3-SiO_2(-K_2)$ glasses, ion exchange kinetics and interdiffusion mechanisms 80−80003
$Na_2O-Al_2O_3-SiO_2.xH_2O$, fibrous crystal growth in silica gel, X-ray, electron probe and IR spectra obs. 80−25541
$Na_2O-Al_2O_3-SnO_2-SiO_2$ glass, chemical stability in NaOH and Na_2CO_3 solns. 80−16532
$Na_2O-Al_2O_3-ZrO_2-SiO_2$ glass, chemical stability in NaOH and Na_2CO_3 solns. 80−16532
$Na_2O-B_2O_3$, ferroelectric glass, phase transition, permittivity, electrochromism, photochromism 80−80719
$Na_2O-B_2O_3$, microhardness and boric oxide anomaly 77−36624
$Na_2O-B_2O_3$, vitreous and cryst., enthalpy of form., calorimetric study 80−66861
$Na_2O-B_2O_3$ glass, absorptivity of OH determ. 79−52763
$Na_2O-B_2O_3$ glass, covered with PbO film, deep penetration of Pb^{2+} ions 78−79535
$Na_2O-B_2O_3$ glass, Eu^{3+}→Nd^{3+} diffusion-limited energy transfer, quantum efficiency 78−31238
$Na_2O-B_2O_3$ glass, γ- or UV-irrad., laser and thermal bleaching of colour centre, absorpt. spectra 79−33744
$Na_2O-B_2O_3$ glass, mag. susceptibility, annealing and base comp. effect 79−91811
$Na_2O-B_2O_3$ glass, Na and Ag diffusion, elec. cond. 79−51300
$Na_2O-B_2O_3$ glass, negative thermal expansion, LF Guneisen parameter, numerical analysis 77−11707
$Na_2O-B_2O_3$ glass, PbO interdiffusion layer form. 79−51318
$Na_2O-B_2O_3$ glass, struct. interpretation of ^{10}B and ^{11}B NMR spectra 78−80241
$Na_2O-B_2O_3$ glass, wetting and adherence on Au 80−24714
$Na_2O-B_2O_3$ glass struct. study using ^{10}B NMR 80−84658
$Na_2O-B_2O_3$ glass-forming melts, thermodynamic functions 80−25673
$Na_2O-B_2O_3$ glasses, electrical props. and dielectric relaxation *(Japanese)* 80−20199
$Na_2O-B_2O_3$ melt, crystallisation of $Na_2B_8O_{13}$ 78−59763
$Na_2O-B_2O_3$:Au glasses, Au solubility, oxidation state and opt. absorpt. 80−44321
$Na_2O-B_2O_3$:Cu^{2+}, ESR and optical absorption 80−34760
$Na_2O-B_2O_3$:Cu^{2+}, Mn^{2+} glasses, Cu^{2+}-Mn^{2+} interaction studied by ESR 80−93166

sodium compounds continued
Na_2O-B_2O_3:Fe_2O_3 glass, $Fe^{2+/(3)}$ impurity ions struct.-chem. state, Mossbauer data 80−40028
Na_2O-B_2O_3:Mn^{2+} glass, fine struct. parameter distribs., EPR meas. 80−11256
Na_2O-B_2O_3:$PbBr_2$ glasses luminescence damping kinetics *(Russian)* 77−16393
Na_2O-B_2O_3:Se, EPR, γ-ray effects *(Russian)* 78−31109
Na_2O-B_2O_3-B_2O_3, glass with metallic Bi granules, elec. cond. 80−84493
Na_2O-B_2O_3-CoO, Co^{2+} ions activated, magneto-opt. study 79−65844
Na_2O-B_2O_3-Cr_2O_3 glass, Raman spectra obs. of Cr^{VI} 77−52076
Na_2O-B_2O_3-CuO, γ-irrad., CuO effects on EPR 80−84645
Na_2O-B_2O_3-Fe_2O_3, and Na_2O-Al_2O_3-B_2O_3-Fe_2O_3 glass, Mossbauer expts., 85-500K 78−80260
Na_2O-B_2O_3-GeO_2 glass-forming melts, thermodynamic props. and vaporisation processes, mass spectrometric study 80−79926
Na_2O-B_2O_3-GeO_2 system glass-forming melts, mass spectrometry obs. of thermodynamic props. 80−97468
Na_2O-B_2O_3-GeO_2 vitreous melts, thermodynamic props. from mass spectra 80−65253
Na_2O-B_2O_3-Na_2SO_4, glass, exam. of chemical differentiation, using Cu ion segregation 78−87625
Na_2O-B_2O_3-NiO melts, NiO activity and solubility meas. by EMF method *(Japanese)* 80−92677
Na_2O-B_2O_3-P_2O_5 glass, mech. and elec. props 80−84228
Na_2O-B_2O_3-SiO_2, containing halogens glass formation 80−103254
Na_2O-B_2O_3-SiO_2 glass, ^{11}B NMR obs. of struct. 78−38625
Na_2O-B_2O_3-SiO_2 glass, type DB-1, exam. of distrib. of rare earth activators, by absorption study 79−4832
Na_2O-B_2O_3-SiO_2 glass, phase separated, HCl leaching rate and microstruct. 79−29242
Na_2O-B_2O_3-SiO_2 glass fibre, prep. with low loss 79−59850
Na_2O-B_2O_3-SiO_2 glass, phase-separated, leaching 79−66394
Na_2O-B_2O_3-SiO_2 glass, NMR, struct. 79−87325
Na_2O-B_2O_3-SiO_2 glass, Rayleigh scattering losses 79−99893
Na_2O-B_2O_3-SiO_2 glass fibre, plastic coating influence on strength 80−58697
Na_2O-B_2O_3-SiO_2 glass fibre, plastic-coated, liq. N_2 strength 80−58707
Na_2O-B_2O_3-SiO_2 glass, low-loss GRIN fibres, double-crucible prod., loss and bandwidth meas. 80−69559
Na_2O-B_2O_3-SiO_2 glass-Ni compact, indented, strength and fracture toughness 80−93636
Na_2O-B_2O_3-SiO_2 glasses, phase-separated, leaching rate 80−104131
Na_2O-B_2O_3-SiO_2 glass, fracture toughness, effect of microheterogeneous struct. 80−104256
Na_2O-B_2O_3-SiO_2 low-loss optical fibre prep. by double crucible technique *(German)* 78−33929
Na_2O-B_2O_3-SiO_2:Fe_2O_3, effect of liquid phase separated structure on transparency in near UV and visible regions 79−4823
Na_2O-B_2O_3-SiO_2:GeO_2 medium-loss graded-index preform fabrication by phase separation and leaching *(German)* 78−33930
Na_2O-B_2O_3-SiO_2:Yb(Tb), luminesc. cooperative processes, glass struct. and comp. effect 80−16101
Na_2O-B_2O_3-SiO_2/$AgNO_3$ exam. of ion exchange equilibria 79−5178
Na_2O-B_2O_3-SiO_2-As_2O_3(As_2O_5) glasses, DC and AC resist., bipolaronic hopping cond. 80−88558
Na_2O-B_2O_3-SiO_2-Fe glass, near IR optical absorption of Fe (II) 78−84616
Na_2O-B_2O_3-SiO_2-MoO_3 glass containing high level radioactive waste, phase separation 80−25683
Na_2O-B_2O_3-Bi_2O_3-SiO_2, heterophase glass, diffusion and elec. cond. 78−67858
Na_2O-B_2O-SiO_2 glasses, high temp. mech. relax. 79−96071
Na_2O-B_2O_3-SiO_2, mechanical strength and swelling in liq. 80−85024
Na_2O-BaO-Al_2O_3-SiO_2, glass, nucleation, crystn., ceramic form. 80−84082
Na_2O-BaO-SiO_2, metastable two liquid tie line calc. 78−92246
Na_2O-BaO-SiO_2 based oxide glasses, ion-bombarded, optical line intensities 80−35037
Na_2O-BaO-SiO_2:Nd^{3+} glasses, absorption and fluoresc. spectra, density 80−25417
Na_2O-Bi_2O_3-TiO_2, subsolidus phase equilibrium at 1000 degrees C 78−48384
Na_2O-Ca_2O-SiO_2 glass, crack nucleation about pointed indentations 79−91779
Na_2O-CaO glass, (K_I,V) diagram determ. *(French)* 80−108558
Na_2O-CaO glass, atomic absorption spectroscopy 79−43656
Na_2O-CaO glass, crack nucleation during indentation, micromechanics 80−30069
Na_2O-CaO glass, impacted with sharp SiC particles, strength degradation of annealed surfaces 79−61760
Na_2O-CaO glass, shear deform. under pyramidal indentations 80−84989
Na_2O-CaO glass, strength and failure predictions 77−21256
Na_2O-CaO glass, wettability, effect of cleaning procedures 80−65336
Na_2O-CaO glass phlogopite mica powders, composite fabrication, cellular struct. 80−84902
Na_2O-CaO glass tube, fracture by field assisted ion exchange 78−68771
Na_2O-CaO_2-SiO_2 glass, stressed, chemical reaction in water vapour 79−91819
Na_2O-CaO-Al_2O_3-SiO_2-Cr_2O_3 glass, Raman spectra obs. of Cr^{VI} 77−52076
Na_2O-CaO-Al_2O_3-SiO_2 glass, exam. of liquid phase separation phenomena 79−4417
Na_2O-CaO-Al_2O_3-SiO_2-F-B_2O_3-ZrO_2 glaze, crystallisation, MgO, ZnO, BaO and SrO effects 79−60279
Na_2O-CaO-Al_2O_3-SiO_2 glass, crystn. for the purpose of obtaining vitroceramics *(French)* 80−75163
Na_2O-CaO-B_2O_3-Fe_2O_3 glass, Mossbauer expts., 85-500K 78−80260
Na_2O-CaO-MgO-Al_2O_3-SiO_2 glasses, ternary and quaternary, struct., Raman spectra obs. 77−36229
Na_2O-CaO-MgO-Al_2O_3-SiO_2, corrosion and microhardness, effect of detergents 80−16518
Na_2O-CaO-P_2O_5:Co glass, bonding, symmetry meas. 79−46572
Na_2O-CaO-SiO_2, Al-coated glass, electron bombarded, SIMS analysis 79−66376
Na_2O-CaO-SiO_2, corroded glasses, electron microprobe analysis 77−4956
Na_2O-CaO-SiO_2, double torsion specimens, compliance and fracture load as crack length function 78−48508
Na_2O-CaO-SiO_2, dynamic hardness testing, pendulum attenuation, yield stress obs. 79−24699
sodium compounds continued
Na_2O-CaO-SiO_2, expt. errors in estimating time to failure 77−16666
Na_2O-CaO-SiO_2, foil, exam. of surface plasticity, and cracks, by electron microscopy 78−68733
Na_2O-CaO-SiO_2, for optical fibres, high purity glass production methods 78−87176
Na_2O-CaO-SiO_2, glass, elastic moduli meas., laser-target technique, for wide temp. range 77−27497
Na_2O-CaO-SiO_2, glass, transition from slow to fast crack propag., effect of different liquids 78−23828
Na_2O-CaO-SiO_2, glass, surface indentation effect on mech. strength, and thermal stress resistance 78−48463
Na_2O-CaO-SiO_2, glass, light scatt. rel. to heat treatment *(German)* 78−84598
Na_2O-CaO-SiO_2, glass, formation of colour centres, linear absorption of UV radiation 80−103328
Na_2O-CaO-SiO_2, multicomponent liq. state diffusion 78−55962
Na_2O-CaO-SiO_2, proof testing 80−108654
Na_2O-CaO-SiO_2, refining in glassmelting process 78−27467
Na_2O-CaO-SiO_2, soda-lime glass, hydration 79−87877
Na_2O-CaO-SiO_2 glass, optical props. characteris. in 0.006 to 22 eV region 77−16328
Na_2O-CaO-SiO_2 glass, Na surface conc. determ., by $^{23}Na(p,\alpha)^{20}Ne$ reaction 77−20171
Na_2O-CaO-SiO_2 glass, K_{IC} eval. by double torsion technique 77−90444
Na_2O-CaO-SiO_2 glass, Hertzian fracture characts., comp. influence 78−31522
Na_2O-CaO-SiO_2 glass, crack nucleation around plastic indents 78−92327
Na_2O-CaO-SiO_2 glass, water content effect on crystal nucleation and growth 79−55670
Na_2O-CaO-SiO_2 glass, SIMS anal. of aq. corrosion profile 79−66182
Na_2O-CaO-SiO_2 glass, surface viscous flattening kinetics, sinusoidal profile decay method 79−79139
Na_2O-CaO-SiO_2 glass, mm wavelength absorpt. 79−82978
Na_2O-CaO-SiO_2 glass, annealed and tempered, fracture strength studies under dynamic conditions 79−96132
Na_2O-CaO-SiO_2 glass, corrosion in alkaline soln. *(Japanese)* 79−96174
Na_2O-CaO-SiO_2 glass, sharp contact cracking, residual stress effects 79−100245
Na_2O-CaO-SiO_2 glass, electronic struct. and optical props. 80−2790
Na_2O-CaO-SiO_2 glass, microprobe anal. of corroded surface 80−7704
Na_2O-CaO-SiO_2 glass, effect of phase on liquids and gas diffusion *(German)* 80−38931
Na_2O-CaO-SiO_2 glass, grain-cleaning procedures effect on crushed glass chem. durability tests 80−66678
Na_2O-CaO-SiO_2 glass, vol. relaxation and thermal history during forming process 80−70130
Na_2O-CaO-SiO_2 glass, leaching studies by sputter-induced photon spectrometry 80−80004
Na_2O-CaO-SiO_2 glass, molten, metal ion diffusion and redox behaviour, electrochemical studies 80−81332
Na_2O-CaO-SiO_2 glass, redox phenomena evaluation in melting-fining process, SO_2 evolution 80−84900
Na_2O-CaO-SiO_2 glass, high-vel. liq. impact, oblique impact anomaly 80−89329
Na_2O-CaO-SiO_2 glass, hot erosion plastic flow and fracture 80−89354
Na_2O-CaO-SiO_2 glass microbubbles, permeation eccentricities of He, Ne and D-T 78−47598
Na_2O-CaO-SiO_2 glass foils, HVEM in-situ straining expts. 80−104216
Na_2O-CaO-SiO_2 glass:Fe, Mossbauer spectra of Fe^{2+}, Fe^{3+} impurities *(French)* 79−51893
Na_2O-CaO-SiO_2 glasses, ion-exchanged, mixed alkali effect rel. to elec. cond. 78−34653
Na_2O-CaO-SiO_2 glasses, Auger analysis, alkali signal decrease 80−61189
Na_2O-CaO-SiO_2 molten glass, electrolysis reactions 80−89496
Na_2O-CaO-SiO_2 sheet glass, pristine and scratched, fracture behaviour during bending 78−23829
Na_2O-CaO-SiO_2:Cr^{3+} glass, absorpt. spectra, Fano antireson. and vibronic Lamb shift 80−71458
Na_2O-CaO-SiO_2-Cr_2O_3 glass, Raman spectra obs. of Cr^{VI} 77−52076
Na_2O-CaO-SiO_2-Cr_2O_3 glass, redox equilibria of Cr ions, impurity effects 80−89477
Na_2O-CaO-SiO_2-Fe_2O_3 molten glass, optical props., temp. depend. *(French)* 80−100667
Na_2O-CaO-SiO_2-H_2O system gels, metastable nature 80−71952
$2Na_2O$-CaO-$XSiO_2$ glass, He mobility, interconnectivity, miscibility limits, effect of morphology 78−67864
$2Na_2O$-CaO-$3SiO_2$ glass, cryst. nucleation rate, viscosity, heat treatment 80−84081
Na_2O-CaO(Al_2O_3)-SiO_2 glass, composition-density relationship 77−90326
Na_2O-Cs_2O-SiO_2 glasses, thermal diffusivity, heat capacity and thermal cond., laser flash method study 80−65310
Na_2O-Fe_2O_3-SiO_2, Mossbauer spectra, crystallisation study *(Russian)* 79−19816
Na_2O-Fe_2O_3-SiO_2 glass, partially crystallised, mag. props. 78−23302
Na_2O-Fe_2O_3-SiO_2 glass and crystals, leucite type, Mossbauer ESR study of Fe^{3+} distrib. 79−65774
Na_2O-Fe_2O_3(Al_2O_3)(Cr_2O_3)(Mn_2O_3)-TiO_2, ternary systems, X-ray investigation 79−51067
Na_2O-Fe_xO_y, (where x=1,2,3, y=1,3,4), thermodynamic props. 77−69099
Na_2O-FeO-Fe_2O_3-SiO_2, chemical durability at different pH values 78−72902
Na_2O-FeO-P_2O_5 metaphosphate glass, internal friction *(Polish)* 79−96078
Na_2O-Ga_2O_3 system, new superionic conductor *(French)* 78−14504
Na_2O-Ga_2O_3 system β and β″ phases, fast ion cond., prep. and phase comp. 80−59716
Na_2O-GeO_2, and Na_2O-K_2O-GeO_2 glasses, He permeability, diffusivity and solubility 79−51308
Na_2O-GeO_2, electric cond. and dielec. relaxation *(Japanese)* 78−19905
Na_2O-GeO_2, glass, thermolum. rel. to coordination number 77−16405
Na_2O-GeO_2 glass, struct., Raman scatt. obs. 80−1936
Na_2O-GeO_2 glass, X-ray diffr. study of Ge coordination number 80−10503
Na_2O-GeO_2 glasses, low temp. viscosity, as function of composition 78−38865

sodium compounds continued
Na_2O-GeO_2 glasses, neutronographic study of Ge^{4+} struct. state 80−19711
Na_2O-GeO_2 glasses, struct. changes, X-ray diffr. study *(Japanese)* 78−91254
Na_2O-GeO_2:Fe_2O_3 glass, $Fe^{2+(3)}$ impurity ions struct.-chem. state, Mossbauer data 80−40028
Na_2O-GeO_2-CoO, Co^{2+} ions activated, magneto-opt. study 79−65844
Na_2O-GeO_2-SiO_2, refractive index and density 79−51926
Na_2O-GeO_2-Yb_2O_3, glass struct., Yb^{3+} ion segregation 78−87620
Na_2O-GeO_2(SiO_2), thermal expansion at low temperatures 78−83982
Na_2O-GeO_2(SiO_2) glasses, structure toughness-composition relationship 80−104257
Na_2O-K_2O-Al_2O_3-SiO_2 glasses, effect of Al_2O_3 on elec. cond. 77−8104
Na_2O-K_2O-Al_2O_3-SiO_2 glass, mixed alkali effect, nonbridging O content effects 78−18827
Na_2O-K_2O-Al_2O_3-SiO_2, structure of modified surface layer, internal friction method 80−103258
Na_2O-K_2O-$Al_2O_3SiO_2$-H_2O system A-type zeolites, crystn. from Na-K silicaalumo gels, and characts. 79−52780
Na_2O-K_2O-B_2O_3-SiO_2, glass, character of elec. cond. 80−103516
Na_2O-K_2O-CaO-SiO_2 glasses, chemical durability, mixed alkali effect 79−8377
Na_2O-K_2O-SiO_2, Na diffusion 78−26724
Na_2O-K_2O-SiO_2 glasses, optical absorption of Ni (II) complex, complex co-ordination change, annealing effects 79−69870
Na_2O-K_2O-SiO_2 glass melt, interdiffusion coeffs. of Na^{2+}, K^{2+}, temp. depend. 80−44348
Na_2O-K_2O-SiO_2 melts, Na^+ and K^+ diffusion and interdiffusion processes 80−34221
Na_2O-Li_2O-Al_2O_3, local electrode current density and flow decoration 80−100935
Na_2O-Li_2O-B_2O_3:Fe_2O_3, Mossbauer spectra, isomer shift and quadrupole splitting *(Korean)* 79−51889
Na_2O-Li_2O-NiO-Fe_2O_3-B_2O_3-SiO_2 glasses, thermally stimulated cond. studies of trapping centres 79−78113
Na_2O-Li_2O-β-Al_2O_3.H_2O, water mol. vibrs., IR and Raman spectra 80−89006
Na_2O-Li_2O(K_2O)-SiO_2 glass, heat of mixing *(Japanese)* 78−10195
Na_2O-MgO-Al_2O_3, β''-alumina, high-resolution electron microscopy 80−75208
Na_2O-MgO-Al_2O_3, ionic cond. 80−107480
Na_2O-MgO-Al_2O_3-SiO_2, chemical durability at different pH values 78−72902
Na_2O-MgO-B_2O_3:Cu^{2+}, micro-inhomogeneities, EPR and Raman study 80−84080
Na_2O-MgO-P_2O_5, subsolidus struct. 77−63640
Na_2O-MoO_3, melt, EMF meas., rel. partial molar thermodynamic props. 80−6526
Na_2O-NaF-B_2O_3 glass, nature of conductivity 78−63876
Na_2O-NaF-CaO_xZnO_{1-x}-Al_2O_3-SiO_2, opal glasses, strength, surface composition 80−30066
Na_2O-P_2O_5, metaphosphate glass, active solute doped, absorpt. spectra of radiation products 78−64865
Na_2O-P_2O_5 and Li_2O-Na_2O-P_2O_5 glasses with oxide additions, eval. as membranes for chem. sources of current *(Russian)* 79−96338
Na_2O-P_2O_5 glass, elastic and viscoelastic props. by Brillouin scatt. 79−51972
Na_2O-P_2O_5 glass, numerical optimisation of ESR V^{4+} spectra 79−38370
Na_2O-P_2O_5 glass, XPS quantitative struct. anal. 80−2917
Na_2O-P_2O_5 glass ESR of VO^{2+} ions 80−100610
Na_2O-P_2O_5:Cr^{3+} glass, absorpt. spectra, Fano antireson. and vibronic Lamb shift 80−71458
Na_2O-P_2O_5:Cu II, glass, O basicity, ESR study 78−80199
Na_2O-P_2O_5-CuO, γ-irrad., CuO effects on EPR 80−84645
Na_2O-P_2O_5-SiO_2 glass, metastable liquid immiscibility 80−100331
Na_2O-P_2O_5-SiO_2 glass, substitution of Li^+, Mg^{2+}, Sr^{2+}, Ba^{2+}, Zn^{2+} for Na^+ 80−100332
Na_2O-P_2O_5-Y_2O_3-Tb_2O_3 glass, conc. quenching of luminesc. in disordered system with dipolar interaction 80−89059
Na_2O-PbO-B_2O_3-SiO_2, homogeneous melt formation rate, exam. 78−64520
Na_2O-PbO-SiO_2, activity of PbO, EMF meas. 77−47595
Na_2O-PbO-SiO_2, molten glass, reactions with conducting materials 80−85186
Na_2O-PbO-SiO_2, PbO activity 78−44112
Na_2O-PbO-SiO_2 glass-ceramic composite, directionally crystallised 80−107058
Na_2O-PbO-SiO_2 system glasses, radiative paramag. and optical absorpt. centres 77−8402
Na_2O-Si_2O glass, high-temp. peak of internal friction 80−39218
Na_2O-SiO_2, (5.3, 94.7 wt.%) glass, liq.-phase separated, struct., heat treatment effect 80−16359
Na_2O-SiO_2, and Na_2O-K_2O-SiO_2 based glasses, high field cond. and ionic jump processes 78−38873
Na_2O-SiO_2, aqueous solns., Raman and IR spectra, pH depend., species at equilib. identification 79−87866
Na_2O-SiO_2, crack front shape corrections for crack velocities in double torsion specimens 79−91778
Na_2O-SiO_2, disilicate glass, reaction with Fe, Mossbauer effect 78−11190
Na_2O-SiO_2, disilicate glass, Fe ion introduction, Mossbauer effect 78−11191
Na_2O-SiO_2, effect of annealing on absorbed H_2O action on temp. spectra of internal friction 78−88487
Na_2O-SiO_2, glass, devitrification with ageing 78−79536
Na_2O-SiO_2, melt, EMF meas., partial molar enthalpy and entropy 80−6525
Na_2O-SiO_2, Na_2O-CaO-SiO_2 glasses, thermal capacity meas. at low temps. 80−44334
Na_2O-SiO_2 glass, acoustic and thermal Gruneisen parameters 80−59608
Na_2O-SiO_2 glass, bridging to non-bridging ratio and correl. to glass density and refr. index, ESCA study 80−84832
Na_2O-SiO_2 glass, bubble gas comp. change 80−79946
Na_2O-SiO_2 glass, conduction and dielec. loss mechanisms, paired interstitialcy model 80−107468
Na_2O-SiO_2 glass, effect of high-dose X-rays and reactor radiation 80−19838
Na_2O-SiO_2 glass, electronic struct. and optical props. 80−2790
Na_2O-SiO_2 glass, evaporation by high temp. mass spectrometry 80−79927
sodium compounds continued
Na_2O-SiO_2 glass, fusion process study, EMF meas. *(French)* 80−89190
Na_2O-SiO_2 glass, IR reflection spectra change due to moisture corrosion *(Japanese)* 78−19914
Na_2O-SiO_2 glass, influence of $p(O_2)$ on Na vaporisation at 1345°C 80−6502
Na_2O-SiO_2 glass, internal and surface struct. by X-ray scatt. 80−84074
Na_2O-SiO_2 glass, microcracking about NiS inclusions, fracture mech. description 80−89333
Na_2O-SiO_2 glass, molten, metal ion diffusion and redox behaviour, electrochemical studies 80−81332
Na_2O-SiO_2 glass, OH^- content effect on mech. and other props. 80−89337
Na_2O-SiO_2 glass, pulsed EPR study of Cu 78−84479
Na_2O-SiO_2 glass, scoring, deform. and fracture mech. approach 80−89332
Na_2O-SiO_2 glass, sp. ht., 2-20K and expansion coeff., 2-30K, comp. effects 77−20097
Na_2O-SiO_2 glass, stability at high press., X-ray diffraction obs. *(German)* 78−92251
Na_2O-SiO_2 glass, suitability of small angle neutron scatt. for struct. determ. 78−22663
Na_2O-SiO_2 glass, tunnelling recomb. luminesc. 80−2875
Na_2O-SiO_2 glass containing halogens glass formation 80−103254
Na_2O-SiO_2 glass drops, quenched from liq. state, thermally treated, density profile 80−81085
Na_2O-SiO_2 glass melt, dissoln. of O_2 and CO_2 gas bubbles 80−79945
Na_2O-SiO_2 glass surface anal., effect of electron bombardment during AES on composition 79−83065
Na_2O-SiO_2 glass waveguides, low loss, new fabrication method, exam. 78−55481
Na_2O-SiO_2 glasses, Auger analysis, alkali signal decrease 80−61189
Na_2O-SiO_2 glasses, elementary electronic excitations, refl., luminesc., and photoemission meas. 80−84778
Na_2O-SiO_2 glasses, Na_2O effect on Si-O bonds *(Japanese)* 78−42918
Na_2O-SiO_2 glasses, water reactions at elevated temps. and press. 80−81312
Na_2O-SiO_2 melt, diffusion coeffs., electron microanal. meas. of Na and Si concs. 77−31790
Na_2O-SiO_2 melts, cryoscopic struct. study 80−14994
Na_2O-SiO_2 system glasses, ionic cond. correl. with chem. pot. 77−89581
Na_2O-SiO_2 vitreous system with relaxating structure, spinodal decomposition 78−75553
Na_2O-SiO_2:Au+CeO_2, Au particle nucleation 80−81066
Na_2O-SiO_2:Ce photochromic glass absorption centres 79−27352
Na_2O-SiO_2:CeO_2, photochromic glass, form. and decay kinetics of absorpt. centres 78−13774
Na_2O-SiO_2:Cu^{2+} glass ESR and optical absorption 79−77526
Na_2O-SiO_2:CuO glass, gamma-irradiated, EPR and optical spectra 80−103885
Na_2O-SiO_2:Fe_2O_3 glass, $Fe^{2+(3)}$ impurity ions struct.-chem. state, Mossbauer data 80−40028
Na_2O-SiO_2/$AgNO_3$, exam. of ion exchange equilibria 79−5178
Na_2O-SiO_2/$AgNO_3$, thermodynamic characteristics of ion exchange process 79−8452
Na_2O-SiO_2-B_2O_3 glasses, phase separation meas. by optical absorption spectra of VO^{2+} *(Japanese)* 79−70414
Na_2O-SiO_2-B_2O_3-Al_2O_3, comp. changes as evidence for spinodal decomposition 79−11549
Na_2O-SiO_2-CaO:Fe_2O_3, Mossbauer spectra, isomer shift and quadrupole splitting *(Korean)* 79−51889
Na_2O-SiO_2-CoO, Co^{2+} ions activated, magneto-opt. study 79−65844
Na_2O-SiO_2-Cr_2O_3 glass, Raman spectra obs. of Cr^{VI} 77−52076
Na_2O-SiO_2-CuO, γ-irrad., CuO effects on EPR 80−84645
Na_2O-SiO_2-Fe_2O_3, glass, X-ray absorpt. spectra, effective co-ordination charges 80−84805
Na_2O-SiO_2-Ga_2O_3-Al_2O_3-B_2O_3-SnO_2 glasses, ion exchange reactions with $NaNO_3$ and KNO_3 melts 80−16673
Na_2O-SiO_2-Ga_2O_3-Al_2O_3 glasses in mixed $AgNO_3$-$NaNO_3$ melts, ion exchange 80−21282
Na_2O-SiO_2-GeO_2 digermanosilicate glass, Raman study of structure 79−77524
Na_2O-SiO_2-GeO_2 metagermanosilicate glass, Raman study of structure 79−77523
Na_2O-SiO_2-H_2O-FeO system, 'heavy phase', recrystallisation and struct. 78−2089
Na_2O-SiO_2-MgO melt, elec. cond. meas., MgO behaviour *(Japanese)* 78−75857
Na_2O-SiO_2-MgO(CaO)(BaO) glasses, elec. cond., room temp. to 450°C 80−107473
Na_2O-SiO_2-NaCl system glass, phase relationships and diagrams 79−66048
Na_2O-SiO_2-NaF, elec. cond. of melt, and IR absorpt. spectra of glassy phase *(Japanese)* 77−62657
Na_2O-SiO_2-NaF system glass, phase relationships and diagrams 79−66048
Na_2O-SiO_2-NiO melt, viscosity and elec. cond., effect of NiO conc. *(Japanese)* 79−23760
Na_2O-SiO_2-NiO systems Ni ions anal. by ESCA *(Japanese)* 80−40787
Na_2O-SiO_2-Pr_2O_3(Ho_2O_3) glass, magneto-optical props. 79−65894
Na_2O-SiO_2-SnO_2 (TiO_2) glass, exam. of Na^+ self diffusion, elec. conductivity, and viscosity 78−87819
Na_2O-SiO_2(-B_2O_3) glass, torsional deform. above Tg under low stresses 80−25804
Na_2O-SnO_2-ZrO_2-SiO_2 glass, chemical stability in NaOH and Na_2CO_3 solns. 80−16532
Na_2O-SrO-Nb_2O_5 system, solid state equil., 800°C *(Italian)* 77−47549
Na_2O-TeO_2 glass, radiational EPR centres, struct. model *(Russian)* 77−28426
Na_2O-TeO_2 glass, struct. and props. *(Japanese)* 79−32917
Na_2O-TeO_2:Ho^{3+}(Er^{3+})(Yb^{3+}) glass, luminesc. quenching by OH and OD *(Russian)* 79−28839
Na_2O-TiO_2-Al_2O_3-SiO_2 glass, γ-irrad., struct. position of Ti, EPR study 80−84644
Na_2O-TiO_2-SiO_2, phase relations 79−61567
Na_2O-TiO_2-SiO_2 glass, IR refl., Raman and EPR spectra, struct. *(Russian)* 78−2860
Na_2O-TiO_2-SiO_2 glass, elec. props. and energy gap 78−26921
Na_2O-TiO_2-SiO_2 glass, Si-O bonding, SiKβ X-ray fluorescence and IR spectra 80−10500

sodium compounds continued
Na_2O-TiO_2-SiO_2 glass, co-ordination of Ti, X-ray emission spectra study 80−84072
Na_2O-Tl_2O-B_2O_3, mixed-cation glass, electrical cond. 79−95210
Na_2O-V_2O_5-Al_2O_3 melts, soln. of Al_2O_3 single crystals 80−20910
Na_2O-V_2O_5-$(VO_2)_2$-V_2O_5, phase comp. and equilib. 80−35172
Na_2O-WO_3 glass containing transition metal ions optical absorption 78−27254
Na_2O-ZnO-P_2O_5, exam. of chemical durability, glass transformation temp. 79−20221
Na_2O-ZrO_2-SiO_2 glass, treated with 2 N solns. of $NaCO_3$ and NaOH, surface layer comp. 80−35366
Na_2O-ZrO_2-SiO_2 glass fibres, prep. from metal alkoxides, resistance to NaOH soln. 80−97454
Na_2O-ZrO_2-SiO_2 system, glass, corrosion in NaOH and Na_2CO_3 solns. at 90-150°C 79−66187
Na_2O+GeO_2, molten mixture, EMF measurements 78−43144
Na_2O_3-Al_2O_3-SiO_2 effect of composition on mechanical props. 78−48435
Na_2O_3-B_2O_3-SiO_2, glass, effect of composition on mech. props. 78−48435
$(Na_2O)(Al_2O_3)x(SiO_2)$, zeolites, thermonic emission of alkali ions, desorption mechanism 79−4887
NaOBr, solns., as reagents in enthalpimetric determs. 78−68954
NaOD solution in D_2O, collective excitations in liquid and amorphous state, 77 to 300K 80−92636
NaOD-D_2O, glass, 4.2K, trapped electron photocond. and optical spectra following radiolysis 79−29378
NaOH aqueous glassy systems, 77K, γ-irrad., struct. stabilisation 79−91976
NaOH, aqueous system, LET depend. of transient yields in deuteron and alpha pulse radiolysis 77−63940
NaOH, cubic, reorientational motion of OH^- ion, neutron scatt. 79−51017
NaOH, electron tunnelling to NO_3^- scavenger sites 77−52655
NaOH, etchant for fission fragment track visualisation in crysts. 78−66454
NaOH, frozen soln., EPR of trapped H-atoms produced by UV and X-irrad. 80−3369
NaOH, fused, H_2 prod. by H_2O electrolysis 80−76660
NaOH fusion for heat storage, heat utilisation for turbo-alternator unit *(French)* 80−40915
NaOH gas-crystal system, isotopic equilibrium near phase transition points *(Russian)* 80−91697
NaOH glass, radiation induced trapped electrons, photobleaching, H form. 77−44494
NaOH glass: tryptophan (tyrosine), γ-irrad., electron traps, stimulated luminesc. 78−11536
NaOH ice, γ-irrad, ESR and absorpt. spectra of trapped electrons 79−66318
NaOH ice, γ-irrad., electron trap depth, ESR 79−66317
NaOH ice, trapped electrons, photostimulated decay, time-depend. rate const. 79−52692
NaOH, in water, apparent molar vel. determ., dilatometry with pressure transducing instrumentation 78−75702
NaOH, liq., thermal storage, steel corrosion, appl. in accumulation type steam generator *(French)* 80−40914
NaOH, melt, preferential dissolution of Mg_2SO_4, etching obs. 78−34513
NaOH, UPS, expt. methodology aspects 77−90245
NaOH water solution, struct. props. of disordered systems, Raman spectral study 77−4631
NaOH:CrO_4^{2-}(NO_2^-), electron tunnelling, pulse radiolysis 80−108722
NaOH:$Fe(Cn)_6^{3-}$, electron tunnelling, pulse radiolysis 80−108722
NaOH-8% $NaNO_3$ phase change thermal storage for solar total energy system 79−57481
NaOH-D_2O, glassy matrix, absorpt. spectra after X-irrad., solvated electrons 79−65903
NaOH-KOH eutectic molten mixture, elec. cond. and sp. mass 79−82365
NaOH+muonium in aq. soln., rate const. 77−38752
$NaOH_2^+(H_2O)_n(NaOH)_m$ cluster in stratosphere 79−34895
$Na_2O(K_2O)$-P_2O_5 glasses, P K-band X-ray emission spectra, state anal. 80−40190
Na_2O; SiO_2, use as US transducer bond 79−83437
β-$Na_2O.Al_2O_3$, high-field ^{23}Na NMR 78−64284
$Na_2O.Al_2O_3.10TiO_2$, crystallized bronze, chem. comp., morphology, optical and thermal props. *(Japanese)* 80−16172
$5Na_2O.Fe_2O_3.8SiO_2$, glass crystallisation study by Fe^{3+} EPR and Mossbauer spectra 80−64904
β″-$Na_2O.Ga_2O_3$, reaction with water, particle size effect 77−21379
$Na_2O.Li_2O.Al_2O_3$, comp. and props. for use in Na-S battery 79−87745
$Na_2O.SiO_2$ fibre, reactivity to atmospheric moisture below annealing range, internal friction measurement 78−92288
$Na_2O.SiO_2$, prep. from film forming soln. 80−60811
$Na_2O.SiO_2$-Tb_2O_3 glass magnetooptical study 80−88976
$Na_2O.11Al_2O_3$, conversion to β-$H_2O.11Al_2O_3$ 78−3069
$Na_2O.11Al_2O_3$, Cr, impurity ion struct., ESR study 80−80605
$Na_2O.11Al_2O_3$, polycrystalline with preferably orientated grains, preparation *(Japanese)* 80−81012
$Na_2O.2Al_2O_3.5SiO_2$:Fe^{3+}, Mossbauer effect and magnetometric exam. 78−6613
$Na_2O.2B_2O_3$-Fe_2O_3 glass, Fe_2O_3 crystallite formation, Mossbauer obs. 78−68429
$Na_2O.2SiO_2$ glass, diffusion of Ag into surface layer from $AgNO_3$ melt 80−44371
$Na_2O.2SiO_2$, short range struct. by pulsed neutron scatt. 80−59396
$Na_2O.3B_2O_3$, effect of Fe_2O_3 conc. and temp. on UV absorption 77−16340
$Na_2O.4SiO_2$, glass, behaviour of VO^{2+} as spectroscopic probe 79−78510
$25Na_2O.75SiO_2$ glass, thermal cond., temp. depend. at low temps. 80−65322
$Na_2O.nB_2O_3$ (n=6, 4 or 3), heats of soln. *(Japanese)* 77−77802
$Na_2O.nAl_2O_3$, polycrystalline, Na^+ ion exchange rates with Ag^+ and K^+ ions from the molten nitrates 79−24737
$Na_2O.xSiO_2.yH_2O$, x71, y71, cryst., IR spectra 79−51951
$Na_2O.y(Al_{1-x}Fe_x)_2O_{3-m}$ β″-Al_2O_3 phase stability, lattice constants 80−45283
$Na_3PCr_3O_{13}.3H_2O$, cryst. struct. 80−107154
$NaPF_6$, high press. phase diagram, vibr. spectra 78−60446
$NaPF_6.H_2O$, IR and Raman spectra 77−61749
$NaPF_6.H_2O$, Raman spectra 79−19875
$NaPO_2$, mol. identification by matrix isolation IR spectrosc. 80−104485

sodium compounds continued
$NaPO_3$ coating on Fe_xO_y powders, coercivity increase 77−89980
$NaPO_3$ crystal, P K-band X-ray emission spectra, state anal. 80−40190
$NaPO_3$ glass, Na diffusion 78−63875
$NaPO_3$, Graham's, Kurrol's and Maddrell's salts, cryst. struct. and crystallinity 79−55721
$NaPO_3$, He(I) photoelectron spectra, UTARC calc., assignments 79−72357
$NaPO_3$, heat content between 300.05 and T (T from 400 to 1000K) drop calorimetry *(French)* 80−10682
$NaPO_3$, mol. identification by matrix isolation IR spectrosc. 80−104485
$NaPO_3$, vitreous, microhardness 80−25864
$NaPO_3$:Eu^{3+}, luminesc. of Eu^{3+}, transition probabilities 80−80845
$NaPO_3$-AlF_3(-NH_4HF_2) glasses, synthesis, chem. thermal and optical anal. *(French)* 79−100104
$NaPO_3$-$Mn(PO_3)_2$, cpd. formation 77−52307
$NaPO_3$-$NaAsO_3$ system solid solutions, four-mode type IR spectra 79−51942
$(NaPO_3)_x$ glass ceramic, transient heterogeneous nucleation 80−88042
Na_3PO_4, aq. soln., elec. cond. and Raman spectra at high-press., 25°C 79−56220
Na_3PO_4 crystal, P K-band X-ray emission spectra, state anal. 80−40190
Na_3PO_4, high temp. fast ion cond. phases, neutron diffr. obs. of struct. 80−107512
Na_3PO_4, pure and doped ionic cond., doping effect 78−51725
Na_3PO_4-$M_3(PO_4)_2$, M=Ca, Sr, Ba, Zn, Cd, high temp. stabilisation of phases *(French)* 77−44235
Na_3PO_4-$Mg_3(PO_4)_2$, phase diag. and $NaMgPO_4$ and $NaMg_4(PO_4)_3$ formation 77−48412
Na_3PO_4-$Ni_3(PO_4)_2$ system, phase equilibrium diagrams, crystallographic study, double orthophosphates *(French)* 80−93546
$Na_4P_2O_7$ crystal, P K-band X-ray emission spectra, state anal. 80−40190
$Na_4P_2O_7$, heat of melting and activities using cryoscopic data 77−40573
$Na_5P_3O_{10}$, γ-irrad., PO_3^{2-} EPR obs. 78−27091
$NaPO_3.Al(PO_3)_3$:U, vibronic excitation, absorption and emission spectra 78−52524
$Na_6Pb_4(BeF_4)_6F_2$, cryst. struct. by X-ray diffr., cation distrib. *(German)* 78−43001
$Na_2Pb_{11}F_{18}Br_6$, cryst. struct. determ., X-ray study 79−60320
$Na_3Pr(AsO_4)_2$, allotropes, prep. and cryst. struct. *(French)* 78−63724
$Na_3Pr(C_4H_4O_5)_3.2NaClO_4.6H_2O$, single cryst., forbidden $A_1 \rightarrow A_1$ transition, mag. field induced intensification 80−50302
$Na_3Pr(C_4H_4O_5)_3.2NaClO_4.6H_2O$, absorpt., circular dichroism, and mag. circular dichroism spectra 80−97243
$NaPrSi_6O_{14}$, CC Si_3O_7 layered stacks, polymorphism, cryst. chem. anal. 79−60301
$NaPrSi_6O_{14}$, cryst. struct., X-ray diffr. meas. 77−15385
$Na_2PrSiO_4(OH)$, cryst. struct. 77−65970
$Na_2Pt(CN)_4Br_2.2H_2O$, cryst. struct., neutron diffr. determ. 77−24296
$Na_2(Pt(CN)_4)3H_2O$, transition energy tuning from 3.3 to 1.4 eV 79−61436
NaPtY zeolite, proton spin relax., adsorbed H_2O effect on Pt distrib. 78−88216
$NaRSi_6O_{14}$, R=La, Ce, Pr, Nd, new crystal-chemical group of rare-earth silicates 77−7703
$Na_5RSi_4O_{12}$ (R=Sm to Lu, Y, Sc), solid electrolytes, struct. characts. 80−1997
$Na_5RSi_4O_{12}$, superionic conductors, Na conductivity paths 78−91482
$Na_4R(WNb_2)O_9F_5$, (R=Y, Nd, Eu, Gd, Dy, Lu), synthesis, cryst.-chem. and dielec. study *(French)* 80−108164
$Na_3R(XO_4)_2$ (R=rare earth; X=P, As, V), pressure synthesis *(French)* 80−93509
$NaRb^+$, adiabatic pot. curves, ground and excited state, Hellmann-type model pots. 78−78647
$NaReO_4$, ^{23}Na and ^{187}Re NMR and NQR temp. depend. 80−54973
$NaReO_4$, EPR spectra of paramag. centres and free radicals 80−108072
$NaReO_4$, external lattice vibr. modes and elastic wave vels., dispersion relations 79−33050
$NaReO_4$, matrix isolated, IR spectra 80−28012
$NaReO_4$, NQR 77−20745
$NaReO_4$, NQR and thermal expansion investig. 77−12229
$NaReO_4$, quadrupole coupling, cation electric field gradients 78−35060
NaRhY zeolite, Rh complexes with CO and methyl iodide ligands, spectrosc. obs. 80−85159
Na_3RuO_4, ^{99}Ru Mossbauer spectra, antiferromag. order, mag. relax. 80−50234
Na_3RuO_4, mag. props., isolated tetranuclear cluster model 79−24180
Na_3RuO_4, tetranuclear cluster, eigenvalues spectrum of spin Hamiltonian calc., thermodynamic props. *(French)* 77−35902
Na_2S, cation diffusion NMR investigation up to 800°C 80−108092
Na_2S, dielectric const., transverse and longitudinal optical mode, static dielectric const., effective charge 79−73892
Na_2S, muonic X-ray intensities, Lyman series 80−23578
Na_2S, phonon dispersion curves, inelastic neutron scatt. obs. *(German)* 78−14414
Na_2S single cryst. grown by Bridgman-Stockbarger method 79−100044
Na_2S:Gd^{3+}, EPR and ENDOR meas., spin-stress Hamiltonian 77−63278
Na_2S:Gd^{3+} crystal field splitting, parametrisation of temperature dependence 78−91652
Na_2S:Mn^{2+}, polycrystalline, EPR and luminesc. of Mn^{2+} 78−27082
Na_2S:Mn^{2+} single crystal, EPR expts. and interpretation 79−1708
Na_2S-Al_2S_3, prep., phase props. and elec. cond. 79−96010
Na_2S-GeS_2, glass, synthesis, elec. cond., Raman spectra, temp. and composition depends. *(French)* 79−14962
Na_2S-P_2S_5, glass forming region, struct. and ionic cond. 80−88358
Na_2S-$SiS_2(GeS_2)(P_2S_5)$, synthesis, structure and ionic conduction *(French)* 80−65291
Na_2S-XS_2, X=Si, Ge, glass forming region, struct. and ionic cond. 80−88358
Na_2S_5-molten S interface, mass transport phenomena, rel. to Na/S battery 80−72026
NaSCN, and similar salts, Na atomic charge determ. by numerical integration 80−28944
NaSCN, cryst., Raman spectral lines, temp. depend., anion disorientation *(German)* 78−52514
NaSCN, cryst. struct. and electron density determ., X-ray and neutron diffr. meas. 77−47414
NaSCN, diamag. ion solvation in methanol soln., NMR relax. obs. 78−56389

sodium compounds continued
NaSCN in N,N-dimethylacetamide, Raman, IR and US relaxation studies 80−50315
Na_2SO_3 and Na_2SO_4, muonic X-ray intensities, Lyman series 80−23578
Na_2SO_3, solvated electron, ESR, time profile meas. and anal. 77−5878
Na_2SO_4, and vaporous NaCl, hot corrosion of Co-Cr-Al-Y turbine blade coatings 78−19941
Na_2SO_4 aq. soln. droplets, nucleation by $Na_2B_4O_7.10H_2O$ in emulsion *(French)* 79−1492
Na_2SO_4, aq. solns., isomorphous salts viscosity investig. 78−95173
Na_2SO_4, high temp. phase, DTA and dielec. meas. 79−82333
Na_2SO_4, IR absorpt. spectra, polymorphism, site group approx. and SO_4 stretching mode 78−52510
Na_2SO_4, IR and Raman spectra of vap. over heated matrices 78−25525
Na_2SO_4 in aqueous soln., diffusion coeffs. and Onsager-Fuoss theory disagreement 80−40729
Na_2SO_4, in dioxane-water mixtures, ion-solvent interaction and conductance 79−34315
Na_2SO_4, inhibitory additives, for anatase-rutile transition *(Japanese)* 78−95744
Na_2SO_4, liq., standard free energy of formation from 1160 to 1220K 78−56911
Na_2SO_4, melting point determ., DTA method 80−218
Na_2SO_4, molten, and molten Li_2SO_4-Na_2SO_4 mixtures, struct. anal. by X-ray diffr. 78−63660
Na_2SO_4, molten, corrosion of Ni, at 1173K, E-pO^{2-} diagram 78−44247
Na_2SO_4, molten, of O_2 and SO_2, manometric technique 79−69251
Na_2SO_4, Ni-based superalloys, mechanical integrities of surface scales, contaminant corrosion 78−95845
Na_2SO_4, pure and K-doped, phase transforms., X-ray, DSC and elec. cond. obs. 79−33082
Na_2SO_4, role as charge compensator in X-irradiated $CaSO_4$:Dy thermoluminesc. 79−78764
Na_2SO_4, sound speed as function of conc., temp., and press. 78−79668
Na_2SO_4, sulphate ion optical and spectroscopic props., cryst. environment effect 77−40224
Na_2SO_4, thermodynamic equilib. vapourisation, transpiration mass spectrometry 80−52356
Na_2SO_4, topotaxic phase change obs. 77−51340
Na_2SO_4:XO_4^{2-}, X=Cr, Se, Mo, W, lattice-impurity interactions, IR spectra 78−19522
Na_2SO_4-$CoSO_4$-H_2O, phase equilib., activities, Pitzer eqn. calcs. *(Russian)* 80−65190
Na_2SO_4-H_2O, quick-frozen aq. soln., XPS 79−38713
Na_2SO_4-NaCl, melt, reactions, polarisation at interface with Pt electrode 78−68898
Na_2SO_4-$Y_2(SO_4)_3$, solid solution, effect of defect concentration on ionic conductivity 78−75870
$Na_2S_2O_3$, effect on image microgranularity during photographic development and fixation *(Russian)* 79−100419
$Na_2S_2O_3$, breakdown on Ag halide grains, electron microscopy 78−21237
$Na_2S_2O_3$ digested AgX emulsions, red-IR photoluminescence obs. at 77K 80−103982
$Na_2S_2O_5$-picric acid-ethanol-H_2O etchant for high-strength dual-phase steel 80−100951
$Na_2S_2O_8$, thermal transitions, catalytic effects of CuO and ZnO 79−15983
$Na_2S_2O_35H_2O$, glass transition, anal. of large stable supercooling 77−51477
$Na_2SO_4.10H_2O$, solid-liq. transform., solar energy conversion applicability 78−60155
$Na_2SO_4.10H_2O$, thermal energy storage for solar heating systems 80−101134
$Na_2SO_4.10H_20$, Glauber's salt, neutron diffr. cryst. struct. determ. 79−14740
$Na_2SO_4.12H_2O$ aq. soln., dodecanol additive effect near critical micelle conc. 77−73472
$Na_2S_2O_6.2D_2O$, bonding in $[S_2O_6]^{2-}$, X-ray diffr. refinement and pictorial representation 80−54177
$Na_2S_2O_6.2D_2O$, X-ray diffr. cryst. struct. redeterm. 80−39014
$Na_2S_2O_4.2H_2O$ hydrogenase-catalysed decomposition for biologically-assisted H_2 prod. 80−61460
$Na_2S_2O_6.2H_2O$, bonding in $[S_2O_6]^{2-}$, X-ray diffr. refinement and pictorial representation 80−54177
$Na_2S_2O_6.2H_2O$, cryst. struct. 78−42969
$Na_2S_2O_6.2H_2O$, X-ray diffr. cryst. struct. redeterm. 80−39014
$4Na_2SO_4.2H_2O_2.NaCl$, cryst. struct. determ. 78−55841
$Na_2S_2O_3.5H_2O$, cryst. struct. 77−47400
$Na_2S_2O_3.5H_2O$, cryst. struct. determ. by neutron diffr. 78−63714
$Na_2S_2O_3.5H_2O$, glass transition, theory 77−84890
$Na_2S_2O_3.5H_2O$, solid-liq. transform., solar energy conversion applicability 78−60155
$Na_2S_2O_3.5H_2O$, solidification, heat transfer processes *(Japanese)* 80−6372
$Na_2S_2O_3.5H_2O$, use in polishing of lead glass 80−33258
$Na_2S.9H_2O$-NaOH-H_3BO_3, glass, IR and Raman spectra of boro-ultramarine, exam. of S_3^- presence 78−68502
Na_3Sb, and Na_2KSb, photocathode materials, band struct., empirical pseudopotential calc. 78−10346
$NaSbBrF_3.H_2O$, cryst. struct. *(French)* 78−18589
$NaSbClF_3.H_2O$, cryst. and mol. struct. *(French)* 77−43200
Na_2SbF_5, linear and nonlinear optical props., hyperpolarisability 78−30010
$Na_2Sb_4O_7$, cryst. struct., X-ray diffr. meas. *(French)* 77−47386
$NaSbO_3$.1/6NaF, dielec. spectroscopy study, 100 Hz to 10 MHz, 238 to 417K *(German)* 80−108144
α-$NaSbS_2$, cryst. struct. and $\beta \rightarrow \alpha$ phase transform. features 80−33961
Na_3SbS_4, vibrational spectra, internal SbS_4 vibr. assignments 80−66199
$Na_3SbS_4.9D_2O$, Schlippe's salt, H bonds and cryst. struct. refinement, by neutron diffr. 79−19191
$Na_3SbS_4.9H_2O$, Schlippe's salt, H bonds and cryst. struct. refinement, by X-ray diffr. 79−19191
$Na_3SbS_4.9H_2O(D_2O)$, vibrational spectra, internal SbS_4 and $H_2O(D_2O)$ vibr. assignments 80−66199
$NaSbSe_2$ films, struct., photoelec. and opt. props. 78−51834
$NaScO_2$, electric field gradient tensor, dipolar contribs. 77−51707
$Na_3Sc_2(PO_4)_3$, ferroelectric props., X-ray diffr. study 79−69789
$Na_3Sc_2(PO_4)_3$, X-ray cryst. struct. determ. 79−60341
$Na_3Sc_2P_3O_{12}$, fast-ion conductor, struct. phase transition 80−88362
sodium compounds continued
$Na_3Sc_2P_3O_{12}$, superionic cond. synthesis, cryst. struct. and ionic cond. 80−107519
$NaScS_2$, crystal struct. determ. by X-ray powder diffr. 80−49205
$Na_3Sc_2V_3O_{12}$:(Fe^{3+}, Mn^{2+}), spin Hamiltonian parameters, g-factors, temp. depend. EPR obs. 77−48038
$Na_3Sc_2V_3O_{12}$:Yb^{3+}, EPR of Yb^{3+} in octahedral sites 80−54948
Na_2Se, muonic X-ray intensities, Lyman series 80−23578
Na_2SeO_3, ^{77}Se Fourier transform NMR 78−95528
Na_2SeO_3 and Na_2SeO_4, muonic X-ray intensities, Lyman series 80−23578
Na_2SeO_4, ^{77}Se Fourier transform NMR 78−95528
Na_2SeO_4, aq. solns., isomorphous salts viscosity investig. 78−95173
Na_2SeO_4, cryst. struct., form. 77−19928
$Na_{1+x}Si_x\ Zr_2\ P_{3-x}\ O_{12}$; monoclinic to rhombohedral phase transformation 80−29950
Na_2SiF_6, A=Si, Ge, Sn, IR absorpt. spectra, integrated intensity 79−73944
Na_2SiF_6, precipitation from H_2SiF_6 soln., mechanism, kinetics, habit 77−44142
Na_2SiF_6, struct. of continuous X-ray absorpt. near $L_{2,3}$(2p) ionisation threshold of Si 79−99983
Na_2SiO_2-CaO glass, thermostimulated and tunnel luminesc. 80−45157
Na_2SiO_3 aqueous soln., ^{29}Si NMR expts. 78−15051
Na_2SiO_3 glass pH meter electrode performance *(German)* 80−40695
Na_2SiO_3-K_2SiO_3, molten, thermodynamics of mixing at 1100°C, CaO addition effects 77−47581
α-$Na_2Si_2O_5$, laminated cryst., IR spectra, dispersion anal. 77−1675
$Na_2Si_3O_7$ melt, changes in viscosity at high press. 77−29290
$Na_2Si_3O_7$, polymorphism of infinite Si_3O_7 radicals in layered stacks 79−60301
$Na_2Si_3O_7.xH_2O$, amorphous, pulsed NMR study 79−78555
$Na_{4-x}(Si_{1-x}P_x)O_4$, (O≤x≤0.25), exam. of Na ion conductivity by impedance meas. *(French)* 78−51731
Na_2SnF_6, A=Si, Ge, Sn, IR absorpt. spectra, integrated intensity 79−73944
$Na_2Sr(CO_3)_2$, phase diagrams *(French)* 78−95033
$Na_2Sr_3(NH_2)_8$, cryst. struct. and cryst. chemistry *(German)* 79−51080
Na^+TCNQ^-, optical absorpt. spectra of small particles 78−19505
$NaTaO_3$, electric field gradients and isomer shift ^{181}Ta 78−39453
$NaTaO_3$, high temp. structs. neutron powder diffr., comparison with $SrZrO_3$ and $NaNbO_3$ 80−88094
$NaTaO_3$, struct., X-ray powder diffr. 77−19912
$NaTaO_3$-$AgTaO_3$ system, synthesis by exchange reaction 79−47625
$Na_{5-x}Ta_{11+x/5}O_{30}$, synthesis, non-stoichiometry, density and ionic cond. meas. *(French)* 78−52741
$Na_{0.33}TaS_2$, supercond. props., alkali cation and topotactic solvation influences 79−87180
$Na_{1+\alpha}(Ta_{1+\alpha}W_{1-\alpha})O_6$, exam. of ionic conductivity *(French)* 78−51729
$Na_{1+x}Ta_{1+x}W_{1-x}O_6$ pyrochlore system, comp. depend. of ionic cond. 80−107517
$Na_xTa_yW_{1-y}O_3$, substitution of W with Ta, Anderson type transition *(French)* 79−60879
$Na_{1+\alpha}(Ta_{1+\alpha}W_{1-\alpha})O_6$, synthesis by cation exchange, stability and struct. *(French)* 77−1110
$NaTb(MoO_4)_2$, lattice thermal expansion, rel. to temp., X-ray method 79−77782
$Na^{99m}TcO_4$, imaging for diagnosis of deep-vein thrombosis 77−16971
$Na^{99m}TcO_4$ solution, special chambers for production *(Hungarian)* 80−93785
$Na_3Te_2Fe_3O_{12}$, mag. ordering and bond geometry rel. to tetrahedral Fe^{3+} 77−32163
$Na_3Te_2Fe_3O_{12}$, neutron diffr. patterns, group theory approach for determ. of mag. struct. *(Russian)* 79−51749
Na_2TeO_3, chem. prep. and cryst. struct. *(French)* 80−79755
Na_2TeO_3, D_2O soln., ^{123,125}Te Fourier transform NMR 78−15046
Na_2TeO_4, 3-dimens. X-ray struct. anal., Te(VI) and cation coord. *(French)* 78−18610
Na_2TeO_4, X-ray cryst. struct. determ. 77−80455
$Na_2Te^{IV}O_3.5H_2O$, crystallographic study *(French)* 79−69069
Na_2TiF_6, use in Al alloy manufacture, transfer efficiency of Ti 78−27453
$Na_{0.9}Ti_{1.1}Fe_{0.9}O_4$, short period β-alumina type cpds., cryst. struct. and superionic cond. 80−107499
$NaTiO_2$, electric field gradient tensor, dipolar contribs. 77−51707
$Na_{16}Ti_{10}O_{28}$ structure determ. *(French)* 77−1108
$Na_2Ti_4O_9$, preparation, cryst. struct. determ. 78−75646
$Na_2Ti_9O_{19}$, cryst. struct. anal. by 1 MV high-resolution electron microscopy 79−73137
$Na_2Ti_9O_{19}$, cryst. struct. 79−77573
$Na_2Ti_9O_{19}$, orthorhombic, unit-cell twinning of monoclinic $Na_2Ti_9O_{19}$, cryst. struct. 80−107155
$Na_xTi_4O_8$ bronze, hydrothermal prep., Na ion arrangement 80−75209
$Na(TiO)[SiO_4]$, revised cryst. struct. 79−32978
$(Na_2Ti_6O_{13})_n.(BaTi_4O_9)_m$, tunnel struct. intergrowth, electron, microscopy investigations 80−100218
Na_xTiS_2, alkali ion ordering, X-ray study 80−107165
Na_xTiS_2, electrochemically intercalated, ion ordering, X-ray diffr. meas. 80−44177
Na_xTiSe_2 intercalation cpd., struct. and phase limits *(French)* 77−35536
Na_2TiSiO_5, cryst. struct. 78−42976
$Na_2Ti_2Si_2O_9.Na_3PO_4$, lomonosovite, cryst. struct. determ. 78−51520
$Na_2TiZn_2(SiO_4)O_3$, cryst. struct. determ. 77−11522
$Na_2TiZn_2[GeO_4]O_3$, cryst. struct. determ. 78−63734
$NaTlO_2$, electric field gradient tensor, dipolar contribs. 77−51707
$NaTl_3(SO_3)_2$, crystallograms, cryst. struct. determ. method 80−103286
$NaTl_3(SO_3)_2$, heat capacity and thermodynamic functions, 10 to 300K 80−65244
Na_2UBr_6, phase transformations, elec. cond. and entropy meas., synthesis *(French)* 78−79763
δ-Na_2UF_6, X-ray single cryst. struct. determ. 79−55704
$NaUO_3$, anomaly in mag. susceptibility-temp. curves 77−32152
$NaUO_3$, ht. capacity and thermodyn. props., 5-350K 77−43343
$Na_2UO_2Cl_4$ melts and mixtures, thermogravimetric determ. of uranyl cation state 80−101050
$Na_3UO_2F_5$, IR and Raman spectra, struct. *(French)* 79−11409
$Na_4UO_2(O_2)_3.9H_2O$, structure and bonding study 77−27868
$NaVO_2$, polycryst., quadrupole coupling const., asymmetry parameter, chem. shift, NMR computer calcs. 78−6584
$NaVO_3$, cryst. struct. 78−6043

sodium compounds continued
$NaVO_3$, flux for YVO_4 growth, solubility 78−95687
$NaVO_3$, heat of melting and activities using cryoscopic data 77−40573
$NaVO_3$, thermal expansion and ferroelec. phase transition 79−38482
$NaVO_3$:Cr^{3+}, study of ESR spectra 80−80601
$NaVO_3$-BaV_2O_6-SrV_2O_6, phase diagrams, simple eutectic system 78−48379
$NaVO_3$-KVO_3-Al_2O_3, melts soln. of Al_2O_3 single crystals 80−20910
NaV_6O_{15} monocrystal, electronic struct. and X-ray emission spectra anisotropy 80−84807
β-$Na_{0.27}V_2O_5$, heat of form. and sp. ht., 450 to 900K 80−61129
$Na_{0.33}V_2O_5$, dielec. const. and microwave cond. 78−60378
$Na_{0.33}V_2O_5$, quasi-one-dimensional conductor, anisotropic cond. meas., 18-400K 77−85204
β-$Na_{0.33}V_2O_5$, quasi-one-dimensional conductor, NMR studies 80−93204
$Na_{1.9}V_{12}O_{29.7}$, phase transitions, elec. cond., susceptibility and sp. ht. meas. 78−14776
$Na_{1.9}V_{12}O_{29.7}$, press. depend. of elec. cond., semicond.-metal phase transition obs. 78−64072
Na_3VO_4, X-ray Lα emission spectra, excited states calcs. 79−59488
$Na_4V_2O_7$, heat of melting and activities using cryoscopic data 77−40573
β-$Na_xV_2O_5$, antiferromag. props. and weak ferromagnetism 79−78337
β-$Na_xV_2O_5$, Bridgman and Czochralski single cryst. growth 79−47618
$Na_xV_2O_5$ β-phase single cryst., phase transitions EPR meas. 78−95514
$Na_xV_2O_5$, catalytic behaviour in decomp. of isopropanol, 186-300°C 78−11553
β-$Na_xV_2O_5$, EPR evidence of Na clustering 78−43630
$Na_xV_2O_5$, metallic, Raman scatt. 78−80358
$Na_xV_2O_5$, nonmetallic bronze, low field sp. ht. and mag. suscept. 78−72357
$Na_6V_{10}O_{28}.18H_2O$, X-ray cryst. struct. determ. *(French)* 80−54191
$NaVS_2$, intercalation cpd., NMR 77−90048
Na_xVS_2, intercalation cpd., mag. phase transitions 77−69558
Na_xVS_2, mag. and elec. props. rel. to struct. transitions 78−91848
Na_xVS_2, Na_xVSe_2, charge density waves, electron localisation 79−47038
$Na_xVS_2(Se_2)$, intercalation compounds, phys. props. 80−44179
Na_xVSe_2, intercalation cpd., mag. and structural phase transitions 77−69558
Na_xVSe_2, mag. and elec. props. rel. to struct. transitions 78−91848
Na_xVSe_2, synthesis and struct. determ. 78−26537
$NaWO_3$, electronic density of states calc. for perovskite struct. cryst. 77−76720
$Na_{0.8}WO_3$, model for X-ray photoelectron distrib. of d-band perovskites 79−61491
Na_2WO_4 and $Na_2W_2O_7$, thermal expansion, X-ray diffr. obs. 77−43353
Na_2WO_4, cationic transport props. and struct. 77−76601
Na_2WO_4, liq. mixture, mixing enthalpy with WO_3 at 801, 950°C 79−10949
Na_2WO_4, molten, struct. by X-ray radial distribution anal. 78−83717
Na_2WO_4, solid electrolyte, diffusion, electromigration of Ag^+ ions in $Ag/Na_2WO_4/Ag$ cell 77−1255
Na_2WO_4-$CsWO_4$-WO_3, system form., melting point 79−43222
Na_2WO_4-K_2WO_4-WO_3 ternary system, phase diagram investig. 77−12608
Na_2WO_4-Pb_2WO_4-WO_3 system investigation, crystn. from melt, coordination compounds form. 79−52189
$Na_2W_2O_7$, molten, struct. anal. 79−41927
$Na_2W_2O_7$, Raman and IR spectra 80−25356
Na_xWO_3, $0.22<x<0.84$, low temp. struct., press. effects, NMR study 80−59443
Na_xWO_3, $(0.22\leq x\leq 0.84)$, ^{183}W NMR, electronic struct. near metal-semicond. transition, Knight shift 78−48063
Na_xWO_3, anomalous supercond. transition temp., electron pairing by acoustic plasmon exchange 79−56358
Na_xWO_3, atom motion 78−75874
Na_xWO_3, band struct., XPS meas. 77−59667
Na_xWO_3, band struct. calcs. 77−62824
Na_xWO_3, bronze, composition-dependent microhardness, rel. to bonding 79−24606
Na_xWO_3 bronze, oxidation state of W, oxidation by air exposure 77−8719
Na_xWO_3 bronze, XPS of W 4f levels 78−95648
Na_xWO_3 bronzes, electroreflectance vs. bulk dielectric behaviour, classical model 77−66479
Na_xWO_3 bronzes, reaction with Fe powder, reaction mechanism and reactivity 80−108712
Na_xWO_3 bronzes $(0.4<x<1)$, domain, surface and substrate structs. 80−34281
Na_xWO_3, core level photoelectron spectra, final state effects 80−50509
Na_xWO_3, cubic, final-state effects in XPS 77−90251
Na_xWO_3, cubic single cryst., LEED/Auger obs. 78−19614
Na_xWO_3, degenerate electron gas, Friedman effect, review 77−20242
Na_xWO_3, domain struct., optical microscope obs. 79−19436
Na_xWO_3, elastic consts., composition depend. Brillouin scatt. meas. 79−61388
Na_xWO_3 enhanced T_c, interband coupling 78−91804
Na_xWO_3 films, chem. pot. variation of Na, free electron gas model 80−16698
Na_xWO_3, hardness anisotropy, comp. depend. 79−29181
Na_xWO_3, intra- and interband plasmons, inelastic electron scatt. exam. 78−72098
Na_xWO_3, Knight shift, spin-lattice and spin-spin relax., high press. NMR obs. 80−50211
Na_xWO_3, local struct. states in supercond. Tl phase, lattice props. 78−26981
Na_xWO_3, metallic, light-scatt. studies 80−45071
Na_xWO_3, metallic, optical and electronic props. 80−24398
Na_xWO_3, metallic, transport props. near metal-insulator transitions 77−24596
Na_xWO_3, metallic, XPS, initial and final states, WO_3 binding energy 79−95898
Na_xWO_3 microscopic inhomogeneity rel. to electronic transport props. 77−24518
Na_xWO_3, optical props., analysis of free- and bound-electron contribs. 77−77248
Na_xWO_3, optical props. 79−38515
Na_xWO_3, struct. phase transition sequence 78−22852
Na_xWO_3, struct. transitions and lattice dynamics 78−79771
Na_xWO_3, supercond. crit. temp., semiempirical model lor lattice instabilities in nonstoichiometric materials 78−14442
Na_xWO_3, surface props. 80−71767

sodium compounds continued
Na_xWO_3, vacuum UPS exam. 78−84700
Na_xWO_3, x=0.6 and 0.8, surface characts. 80−39392
Na_xWO_3, X>0.5, temp. depend. of Raman active soft modes, tetragonal-tetragonal transition 78−48180
Na_xWO_4, cluster model 78−10351
$Na_5W_3O_9F_5$, phase transitions obs. *(French)* 80−6516
$Na_5W_3O_9F_5$, single cryst., prep., optical and dielec. studies *(French)* 80−15994
$Na_6W_7O_{24}.14H_2O$, crystal and molecular struct. X-ray determ. 79−82188
NaX, (X=Br,Cl,F,I), X-ray absorpt. near Na^+ K edge 79−99982
NaX, (X=F, Cl, Br), photoelectron spectra using Zr Mζ, Al Kα and other X-ray lines, photoionis. cross sections ratios 77−90246
NaX zeolite, hydrated, cryst. struct. at t=20 and −165°C 80−33978
NaX:Tl^{2+}, (X=Br, Cl, I), F-centres energy levels change 79−65075
NaX-Se semiconductor superlattice absorpt. edge, light scatt. *(Russian)* 80−71438
Na_2XO_4, (X=S, Cr, Mo, W), anal. and calc. of binary and ternary phase diagrams 80−88299
NaXe, kinetic model of Na-Xe discharge for visible lasers 78−63088
$NaYF_4$:Ho, Yb, two photon anti-Stokes effect, excited by 2 μm radiation 78−50852
$Na_6YSc[SiO_7]_2$, crystal struct., atom coordinates, X-ray study 80−59446
$NaYSiO_4$, crystal structure refinement, X-ray anal. 80−79764
$NaYSiO_4$, $Na_3YSi_2O_7$, $Na_3YSi_3O_9$ and $Na_3YSi_4O_{12}$, single cryst. data and ionic cond. 80−84158
$Na_5YSi_4O_{12}$, high Na^+ ion conduct. 78−91479
$NaY_{1-x}Sm_xF_4$, luminesc. expt. suggesting Sm^{3+} ion pairing 80−76065
$Na_xY_xZr_{1-x}S_2$, ionic conductivity, activation energies, NMR study 79−28138
$Na_xY_xZr_{1-x}S_2$, ionic cond. and NMR mobility obs., comp. depend. *(French)* 80−70459
$Na_{3(1+x)}Yb_{(2-x)}(PO_4)_3$, single cryst. preparation and X-ray cryst. struct. determ. 79−42028
$NaZn_{13}$, stella quadrangula as struct. building unit 80−15055
$NaZnCl_4$, cryst., chrysoberyl struct., neutron diffr. 77−19919
$Na_2ZnCl_4.3H_2O$, NQR of ^{23}Na and ^{35}Cl, single-cryst. study 78−91983
$Na_{2-x}Zn_xFe_3(PO_4)_2(OH)_{2-x}O_x$, x=0.1, X-ray struct. anal. 77−84733
$NaZnGeO_4$:Mn, electrolum., ionisation domains 80−84787
$(Na_xZn_y)_2SO_4$, cryst. struct., form. 77−19928
$Na_2Zn(SO_4)_2.4H_2O$:VO^{2+}, EPR spectra at X-band, spin-Hamiltonian parameters 79−56606
$Na_2Zn(SO_4)_2.4H_2O$:Ag^{2+}, EPR, Ag^{2+} dimeric struct., hyperfine and fine struct. tensors 77−51949
$Na_2Zn(SO_4)_2.4H_2O$:Ni, optical absorpt. and EPR. obs. 78−76501
Na_2ZnSiO_4, crystal struct. rel. to Na_2BeSiO_4 77−1114
$Na_2ZnSi_3O_8$, cryst. struct. 77−47396
$Na_2Zn_2Si_2O_7$, cryst. struct. refinement 78−87652
$Na_2Zn_3(SiO_4)_2$, cryst. struct. anal. 79−19222
$Na_3ZnTh_6F_{29}$, X-ray cryst. struct. determ. *(French)* 80−19761
$Na_2Zn[SiO_4]$, X-ray cryst. struct. determ., thermal vibration anisotropy allowance 80−92510
$Na_2Zn[Si_3O_8]$ crystal, phase A, refined cryst. struct. 79−19220
Na_2ZrGeO_5, hydrothermal crystn. 79−47604
$Na_2ZrGe_3O_7$ hydrothermal crystn. 79−47604
$Na_4Zr_2Ge_3O_{12}$, cryst. struct., X-ray diffr. 79−19224
$Na_4Zr_2Ge_3O_{12}$, hydrothermal crystn. 79−47604
$Na_{1+x}Zr_{2-x}In_x(PO_4)_3$, three-dimens. solid soln., comp. depend. of ionic cond. *(French)* 80−34230
$Na_2Zr(MoO_4)_3$, synthesis and cryst. struct. 80−39059
$Na_4Zr(MoO_4)_4$, synthesis and cryst. struct. 80−39059
$NaZr_2O_5H$ ion exchange material, use in ^{137}Cs separation from nucl. waste 80−27760
$Na_3Zr_2PSi_2O_{12}$, NASICON, ^{23}Na NMR obs. of ionic diffusion, 180 to 800K 80−108097
Na_2ZrSiO_5, scintillation props., excited by α particles 80−29809
Na_2ZrSiO_5:Ln^1,Ln_2, scintillation, α-excited *(Russian)* 79−28841
$Na_4Zr_2Si_3O_{12}$, struct. analysis at 300 and 600°C, rel. to ionic cond. 80−107189
$Na_{1-x}Zr_2Si_xP_{3-x}O_{12}$, press. and comp. effect on fast Na^+ ion transport 80−107516
$Na_3Zr_2Si_2PO_{12}$, NASICON, phase transition, X-ray diffr., ionic cond. and sp. ht. meas. 80−19979
$Na_3Zr_2Si_2PO_{12}$, NASICON, ionic cond. temp. depend., comparison with β-Al_2O_3-Na_2O 80−107520
$NaZr[Si_2O_6OH]$, keldyshite, X-ray structural anal. 79−14779
Na0, surface rumpling at finite temps, Verwey model 79−51402
$Na_20.2SiO_2$, nucleation kinetics 78−26467
$Na_20.3B_2O_3.xFe_2O_3$, borate glass, Fe^{3+} spin state and distrib. meas. 80−39966
$Na_20.3MoO_3$, nucleation of fibrillar crystals, effect of surface layer, growth on air bubbles 78−60559
$Na_20.3MoO_3.3H_2O$, nucleation and growth from soln. 77−84682
$25Na_20.75SiO_2$ glass, ionic cond. meas. 79−33110
Na*H_2, potential energy surfaces 80−74215
Na(4S)Xe, Na(4S)Kr, excimer, visible emission band, exptl. results relative to theory 78−82779
$Na_2[B_4O_6(OH)_2]$, cryst. struct. 78−51479
$Na_8[B_{12}O_{20}(OH)_4]$, X-ray cryst. struct. determ. and refinement 80−19753
$Na_2[B_2(O_2)_2(OH)_4].6H_2O$, X-ray cryst. struct. refinement 79−14749
$Na_2[B_4O_6(OH_4)].8H_2O$, differential thermal X-ray anal. of phase transitions in non isothermal conditions 79−52205
$Na_3[Co(NO_2)_6]$, X-ray Co K absorpt. edge struct. meas. 77−20956
$Na_2[Fe(CN)_5(NO)]$ powder, Mossbauer spectroscopic study of ultrasonic anharmonicity 78−52411
$Na[Fe(CN)_5NO].2H_2O$, X-ray spectroscopy of single crysts., use of polarised radiation 78−8481
$Na_2[Fe(CN)_5NO].2H_2O$, powder, Mossbauer spectra, acoustic-excitation-induced asymmetry of quadrupole splitting 78−27145
$Na_2[Fe(NO)_2(S_2O_3)]_2$, valence levels, X-ray photoelectron and X-ray spectra 77−88500
$Na_4[M^{II}(NH_3)_4][M^I(S_2O_3)_2]_2.L$, ($M^{II}$=Cu, Ni), ($M^I$=Cu, Ag), (L=$H_2O$, NH_3), IR spectra, vibr. anal. *(French)* 78−52477
$Na_2[MoO_{1-x}(OH)_{2x}(H_2O)_{1-x}O(MoO_4)_2].2H_2O$, proton NMR for chem. comp. at −195°C 78−38651
$Na[Mo_2O_5(O_3(OH)C_6H_8(OH)_2)].2H_2O$, struct. determ. and refinement 78−2073
$Na_2[Pt(CN_4)].3H_2O$, cryst. struct. 77−58990
$Na_2[Pt(CN)_4].3H_2O$, energy band calcs. 77−39780

sodium compounds continued
$Na_8[Si_6Al_6O_{24}](OH)_2.1:7H_2O$, hydrosodalite, cryst. struct. by neutron diffr. 78−95039
$Na_6[Ti(Ti_{0.9}Nb_{0.1})_4(Si_6O_{17})_2(O,OH)_5].11H_2O$, zorite, X-ray cryst. struct. determ. 80−92513
$Na_4[UO_2(CO_3)_3]$, vibr. and low temp. optical spectra, rel. to U recovery from oceans 79−73939
$Na_3[V(NCS)_6].12H_2O$, single crysts., X-ray diffr. cryst. struct. anal. 78−95021
$Na_2[ZnSi_3O_8]$, synthetic cryst. struct. 77−65968
NbO_2-Na_2O-SiO_2, amorphous films, characteristics of monostable switching 77−80817
Nb_2O solution in liq. Na, elec. resist. 79−14934
Nb_2O_5-semicond. oxide interface, electron injection and reactions 77−76936
Ni-ferrite powders, form. in presence of Li_2SO_4-Na_2SO_4 molten salts, prep. and characts. 80−84869
$NiNa_2H_8(PO_4)_4.4H_2O$, cryst. struct. determ. *(French)* 78−26504
P_2O_5-Al_2O_3-Na_2O-K_2O-Li_2O-(CaO+MgO) glass system, ion exchange effect on mech. props. 80−30229
P_2O_5-K_2O-CdO-Na_2O glass:Nd^{3+}, highly doped, spectroscopic props. and CW laser action *(French)* 79−41385
$PbCl_2$:NaCl, trapped exciton states, absorption spectra 80−50383
$PbNb_2O_6$-$NaNbO_3$, DTA *(French)* 77−44234
PbO-B_2O_3-Na_2O melt, activity of PbO 77−11708
$Pb_{1.8}Zn_{0.15}Na_{0.05}Nb_2O_{6.95}F_{0.05}$, electric cond. and dielect. props. of cathodic-sputtered films *(French)* 79−33371
PuO_2-Na_2O, biological solubility of aerosols in rats 78−96096
RbO_2-Na_2O-P_2O_5 glasses, Raman and far IR spectra, vib. at cation site, struct. 78−60435
Sb_2O_3-Na_2O-B_2O_3-SiO_2 glass, elec. cond. meas., −160 to 200°C 80−20190
Sb_2O_3-$SiO_2(GeO_2)$-Na_2CO_3-H_2O, crystallisation 77−12605
Sb_2O_4-$NaSbO_3$-(NaF), phase equilibria and crystal growth 77−70035
Sb_2O_4-$NaSbO_3$($KSbO_3$)-NaF, phase equilibria and crystal growth 77−70035
$(Sb_2S_3)_{0.95}(Na_2S)_{0.05}$, condensate, local states and switching effect 80−20336
$ScCl_3$-NaCl-CsCl ternary system, cpd. form., thermographic investig. *(Russian)* 80−66490
Si-$NaNO_3$ aq. soln., anodic polarisation of semicond. electrode 77−11999
SiO_2-Al_2O_3-B_2O_3 $LiO_2.Na_2O$, exam. of optical props. 78−88277
SiO_2-Al_2O_3-B_2O_3-Na_2O, exam. of optical props. 78−88277
SiO_2-Al_2O_3-B_2O_3-MgO-CaO-Na_2O, strengthened by ion exchange, exam. of internal stresses using polarising microscope 78−88549
SiO_2-Al_2O_3-B_2O_3-CaO-Na_2O-K_2O system glasses, relax. of struct. stresses rel. to forming process 79−34088
SiO_2-Al_2O_3-CaO-BaO-SrO-ZnO-Na_2O-K_2O-B_2O_3, glaze effect of P_2O_5 additions 80−60824
SiO_2-Al_2O_3-CaO-MgO-Na_2O (1.58, 7.16, 3.59, 14.9 mole.%), polished sheet, strength in commercial state and after strengthening by ion exchange 79−1904
SiO_2-Al_2O_3-CaO-MgO-Na_2O, ion exchange and electrodiffusion of Li ions in surface layer 79−20227
SiO_2-Al_2O_3-CaO-MgO-Na_2O-K_2O effect of partial substitution of Na_2O by K_2O, on crystallisation 80−10499
SiO_2-Al_2O_3-CaO-Na_2O:Fe^{3+}, optical absorpt. due to Fe^{3+} ligand field and charge transfer 80−89020
SiO_2-Al_2O_3-Fe_2O_3-CaO-MgO-Na_2O-SO_3 glass, thermophysical props. 78−18849
SiO_2-Al_2O_3-Fe_2O_3-CaO-MgO-Na_2O-B_2O_3-SO_3, exam. of white flaky inclusions, causes and formation time 79−29237
SiO_2-Al_2O_3-Fe_2O_3-Na_2O-K_2O-CaO-MgO glasses, Mossbauer spectra study 80−39967
SiO_2-Al_2O_3-K_2O-Na_2O, exam. of leucite crystal growth 79−19496
SiO_2-Al_2O_3-Na_2O-BaO-TiO_2, glass ceramic interaction with Pb borosilicate glaze 80−84398
SiO_2-B_2O_3-Al_2O_3-NaO, Ag interdiffusion, optical and NMR studies 80−24683
SiO_2-B_2O_3-Na_2O glass, high silica, conductivity behaviour, Na ion dependence 80−24652
SiO_2-B_2O_3-Na_2O-K_2O system glass, phase separated, loss of oxides during acid leaching, atomic absorpt. anal. 79−11716
SiO_2-CaO-Na_2O, glass, layers near surface, anal. using SIMS 80−88041
SiO_2-CaO-Na_2O-M_mO_n systems, M=Zr, Sn, Ti, Al, La, Ta, P, Mn, Fe, Pb, Cr, water, alkali, acid resist., chem. durability 79−34162
SiO_2-CaO-ZnO-B_2O_3-Na_2O-S, SrO effect on crystallisation 80−54135
SiO_2-K_2O-Na_2O-BaO-SrO-ZnO system glass, props. optimisation 79−91611
SiO_2-M_2O (M=Na,K) glasses, temp. depend. of elastic modulus 80−40410
SiO_2-Na_2CO_3, sodium Erevanit-25, sintering, struct. 79−43284
SiO_2-Na_2O, phase separation detection 77−1890
SiO_2-Na_2O, thermodynamic approach to ionic conds., statistical model of chem. potential 79−46833
SiO_2-Na_2O alkali glass, grain-cleaning procedures effect on crushed glass chem. durability tests 80−66678
SiO_2-Na_2O glass, bonding of Si-O exam. by X-ray emission spectra 78−52594
SiO_2-Na_2O glass, fracture initiating flaws, depth meas., crack propag., SEM exam. 78−48494
SiO_2-Na_2O glass, Na^+ diffusion 78−91478
SiO_2-Na_2O surface, $Ca_3(PO_4)_2$ film form., bonding to bone 80−85212
SiO_2-Na_2O-$CaCO_3$ sheet glass, rupture upon local contact loading 80−50725
SiO_2-Na_2O-CaO (13, 11 wt.%) glass, phase separation, SiO_2 purity effect 80−44144
SiO_2-Na_2O-CaO glass, phase separation characts., melting atmosphere effect 80−44141
SiO_2-Na_2O-CaO:Fe(As)(Cr) glasses, optical absorpt. changes on heat treatment 78−31224
SiO_2-Na_2O-CaO-MgO-Al_2O_3, toughening by electrochemical treatment in Sn melt 80−11800
SiO_2-Na_2O-CaO-MgO-Fe_2O_3-Al_2O_3-SO_3-Sn thermally polished, exam. of strength of surfaces 80−25887
SiO_2-Na_2O-CaO-MgO float glass, surface SnO_2 distrib., ellipsometry and XPS study 80−84346
SiO_2-Na_2O-CaO-P_2O_5, BIOGLASS, surface, $Ca_3(PO_4)_2$ film form., bonding to bone 80−85212

sodium compounds continued
SiO_2-Na_2O-K_2O water glass with polyethylene filler, thermogravimetric and thermomechanical anal. 79−20020
SiO_2-Na_2O-K_2O-CaO-MgO-Al_2O_3 glass melt, anodic dissolution of Ti 80−19949
SiO_2-Na_2O-Nd_2O_3 glass, magneto-optical props., absorpt. spectrum 80−88969
SiO_2-NaAlSiO_4 glasses and devitrificates, prep. and vibr. spectroscopy study *(Polish)* 80−93530
SiO_2-NaO-K_2O-CaO-MgO-Al_2O_3 melt, anodic dissolution of Co and Ni in melt 78−88582
SiO_2-PbO-B_2O_3-Al_2O_3-CaO-Na_2O-K_2-O glaze, interaction with aluminosilicate glass-ceramics 80−84398
SiO_2-RO-Na_2O-Li_2O (RO=MgO, CaO, SrO) glass-ceramic coating, optimisation of props. by selective oxide action 80−55552
SiO_2-TiO_2-Na_2O glass, optical absorption coeff., 2.1-3.3 eV 77−77240
SiO_2-TiO_2-Na_2O(−CaO), thermal diffusivity in range 0-600°C, influence of TiO_2 80−29233
SiO_2-ZnO-Na_2O-Li_2O, glass-ceramic coating, optimisation of props. by selective oxide action 80−55552
SiO_2-ZrO_2-Al_2O_3-CaO-Na_2O-K_2O-Li_2O, chemical resistant glass for glass fibres 80−21128
SiO_2-ZrO_2-Li_2O-Na_2O based crystallisable glasses composition and properties 80−50731
SiO_3-Na_2O-CaO-MgO-Al_2O_3 charge, silicate formation during heating 80−55342
$SnCl_2$-AlkAlCl_4 melts (Alk=Li, Na or Cs) 79−99874
SrBaNaNb_5O_{12}, X-ray powder diffraction data determ. *(Chinese)* 80−70170
$SrCu_3Ru_4O_{12}$, synthesis, cryst. struct., mag. and elec. props. *(French)* 80−107151
$Sr_x(Na_{0.5}Bi_{0.5})_{1-x}$ solid solutions, piezoelec. and ferroelec. props. *(French)* 80−108158
$Sr_x(Na_{0.5}Bi_{0.5})_{1-x}TiO_3$ ferroelec. ceramic, hot pressing, numerical simulation *(French)* 80−76220
$Sr_4NaLiNb_{10}O_{30}$, electro-optic, pyroelec., dielec. and piezoelec. props. *(Chinese)* 79−69810
$Sr_4NaLiNb_{10}O_{30}$, single cryst. growth, Czochralski method *(Chinese)* 79−74078
$Sr_2NaNb_5O_{15}$, Raman scatt. experiments in tetragonal tungsten bronze compounds 80−40113
$Sr_{2.05}Na_{0.90}Nb_5O_{15}$, X-ray powder diffraction data determ. *(Chinese)* 80−70170
TeO_2-V_2O_5-Na_2O, glass, IR spectra of crystalline phases 79−38536
$Te(OH)_6.Na_2HAsO_4.H_2O$, synthesis and cryst. data *(French)* 80−33948
$Th_{0.25}NbO_3$-xNaNbO_3 solid soln., cryst. struct., perovskite-type phases, X-ray diffr. obs. *(French)* 79−1413
TiS_2-Na_2S(K_2S) systems, synthesis of Na_2TiS_3, K_2TiS_3, K_4TiS_3 and K_8TiS_5 *(French)* 79−52636
$TlNO_3$-$NaNO_3$, melt, cationic self-diffusion coeffs., temp. and conc. depends. 78−22879
$Tl_3Na(SO_3)_2$, α-phase, IR and Raman spectra, order of cryst. struct. *(French)* 77−85718
V_2O_5-P_2O_5-Na_2O glasses, enhanced secondary electron emission yield 80−93441
Zn-Ti, environmental factors affecting pitting corrosion potential in NaOH solns. 80−45423
$ZnCl_2$-KCl-NaCl, molten system, containing Ni^{2+} ions, appl. to electrorefining, polarographic study 80−66810
$ZnCl_2$-NaCl, molten, density meas. *(Japanese)* 79−19383
$ZnCl_2$-NaCl, molten, viscosity, 260 to 560°C *(Japanese)* 77−51537
$ZnCl_3$-NaCl, melt, viscosity meas. by oscillating cylinder method *(Japanese)* 80−10696
$Zn_2NaP_3O_{10}.9H_2O$, cryst. struct. determ. *(French)* 77−47406
ZnS:Cu, Er, Na, phosphor, mechanism of sensitisation effect of Cu and Na ions 77−16369
ZnS-Na_3O-K_2O-SiO_2, form. using electric furnace, furnace design 80−11620
ZnS-Na_3AlF_6 multilayer films, thermally evaporated, dispersion characts. 77−59629
ZrF_4-BaF_2-NaF, vitreous phases, network formers, modifiers and stabilisers *(French)* 80−64909
ZrF_4-BaF_2-ThF_4-NaF(RF_3) (R=rare-earth) glass system, anion cond. 80−70460
$ZrNa_xH_{2-x}(PO_4)_2$, Na^+ transport, gas-solid and solid-solid reaction kinetics in $Zr(HPO_4)_2.H_2O$ 80−61086

sodium potassium tartrate tetrahydrate *see Rochelle salt*

sofar *see sonar*

soft modes
see also displacive transformations; lattice phonons
A15 compounds, coherence length and phonon softening 78−34587
A15 compounds, high supercond., T_c, attributed to linear chains or cubic symmetry 79−38221
A15 compounds, mode softening and high supercond. crit. temp. 78−14851
A15 superconductors, electronic instabilities and phonon softening 79−95115
A15 superconductors, supercond. and phonon softening in unstable systems 79−65587
A-15 compounds, struct. transformations and soft phonon modes, microscopic theory *(Chinese)* 79−37803
alkali-alkaline earth ceramic solid solutions, with tetragonal tungsten bronze struct., low freq. optical modes 78−76477
alkaline trihydrogen selenites, ferroelec. phase transitions, Raman spectra 77−8525
alkylammonium compounds with perovskite-type layer struct., symmetry of lattice vibrs. 78−22797
anharmonic crystal, lattice dynamics and stability 78−6129
aniline hydrobromide, ferroelastic, acoustic softening near transition temp. 80−96617
aniline-HBr, ferroelasticity, orthorhombic to monoclinic phase transition, X-ray scatt. 80−39276
arsenates, ferroelec. phase, E-mode splitting 78−15163
benzil, phase transition, far IR spectroscopy meas. 80−71407
benzil, phase transition study be simultaneous Raman-scatt. and domain-struct. investigations 79−60504
benzil, structural transition model, cryst. symm. spontaneous strain components 80−2161
binary compound, Kohn anomaly in optical phonon branch 80−92626

3 8198 307 019 883
THE UNIVERSITY OF ILLINOIS AT CHICAGO

THIS BOOK IS FOR USE
ONLY IN THE LIBRARY
IT DOES NOT CIRCULATE